

Q  
1  
S3  
V.83  
1980  
N/C

Sa.

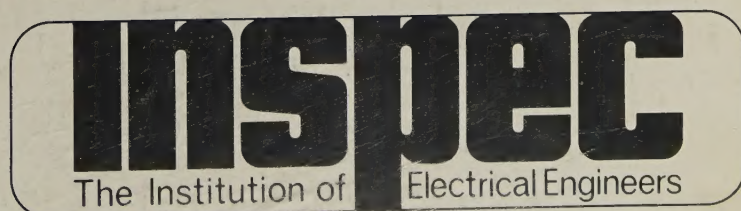
# Physics Abstracts

Science Abstracts Series A  
January-June 1980

Subject Index (M - Z)

PAMPHLET BOX

U.I.C.C.  
OCT 2 1980  
LIBRARY





# CONTENTS

Title page	i	Subject index	S863
Abbreviations and acronyms	iii		

---

## SIX-MONTHLY INDEXES TO SCIENCE ABSTRACTS

Cumulative indexes to Science Abstracts are published twice a year covering the period January-June and July-December. They comprise author and subject indexes and some specialised or 'small' indexes. For Physics Abstracts and Electrical & Electronics Abstracts the Author Index and Subject Index are published as separate volumes. In this case the Small Indexes are included in the Author Index volume.

Cumulative author and subject indexes for preceding years are also available. For details please see inside back cover.

### Subject Index

The Subject index provides an alphabetical subject key to the articles included in the abstracts journal. Some general guidance on its use is given below:

1. Look in the index for the name of the specific subject in which you are interested. In most cases this name will be a heading in the index and you will find relevant articles listed under it. The majority of the subject headings fall into the following categories: property, phenomena, substance or named objects, instrument, device, theory, method, process, application, event.
2. Occasionally you will be directed from the subject heading chosen to a different heading under which the relevant or additional articles are listed.
3. If you do not find the subject heading you first chose, try a more general heading.
4. Each entry under the heading relates to an article appearing in the abstracts journal and gives the serial number of that article in the journal preceded by the last digit of the current year, e.g. 0-12345; i.e. Abstract number 12345 in the abstracts journal for 1980.

The language of the article, if it is not in English, is also indicated. e.g. digital frequency meter jamming, distribution function determ. (Russian) 0-41575.

Each entry starts with a Keyword or Keyphrase considered to be most relevant to the heading. On sorting these Keywords, the qualifying prefixes are usually ignored. (e.g.  $\alpha$ -brass, 5-sulphosalicylic, 31 Cygni, n-Ge are sorted under brass, sulphosalicylic, Cygni, Ge respectively).

There are three main Keyword lists; alphabetical A-Z, elementary particles, and chemical symbols (organic substances are written and not given as chemical formula). More than one Keyword list may be present under each subject heading.

For document on, say, 'photoemission of germanium' at least two access points 'photoemission' and 'Germanium' are provided. Under the heading 'photoemission' the Keyword will be 'Ge' and under 'germanium' the Keyword will be 'photoemission'.

In a case like this, it is advisable and quicker to use the heading 'photoemission' and go straight to the chemical symbol list for 'Ge'.

Intermetallic compounds are indexed under the appropriate alloy headings. The chemical formula is used as Keyword. However, it is important to realise in searching the chemical symbol list that, at present, alloys and intermetallic compounds are sorted separately. For example FeCo is sorted at the end of the Fe- list e.g. Fe-Al, ... Fe-Co, ... Fe-Si, ... Fe-Si-B, ... FeCo, ... FeSi and so on in this order.



# Physics Abstracts

Science Abstracts Series A

January-June 1980

## Subject Index (M - Z)

Physics Abstracts is published twice monthly by the Institution of Electrical Engineers. Twice-yearly subject and author indexes covering the period January-June and July-December are included in the subscription. Printed by Unwin Brothers Ltd., Old Woking, Surrey, England. Second class postage paid at Piscataway, NJ 08854 USA.

© 1980: THE INSTITUTION OF ELECTRICAL ENGINEERS







# Abbreviations and Acronyms

Abbreviations and acronyms are used in the modifiers in all INSPEC Cumulative Subject Indexes. Individual terms should be readily understood in the context of the subject headings. **Inorganic substances** are usually given by their chemical formulae. Iron and aluminium garnets appear in the formulae lists as MIG and MAG (where M is metal element, e.g. YIG and YAG);  $(\text{Pb},\text{La})(\text{Zr},\text{Ti})\text{O}_3$  and  $\text{Ce}_2\text{Mg}_3(\text{NO}_3)_{12}$  appear as PLZT and CMN respectively. **Organic substances** including **liquid crystals** are not given as formulae but common abbreviations are used.

ABS resin	acrylonitrile-butadiene-styrene	CRO	cathode ray oscilloscope
AC	alternating current	CRT	cathode ray tube
ACV	air cushion vehicle	CS	coupled states
A/D	analogue-to-digital	CSM	continuous slowing down models
ADP	administrative data processing	CTR	controlled thermonuclear reactor
AES	Auger electron spectra(oscopy)	CVD	chemical vapour deposition
AF	audio frequency	CW	continuous wave
AFC	automatic frequency control		
AFL	abstract family of languages	D/A	digital-to-analogue
AGC	automatic gain control	DBR	distributed Bragg reflector
AGR	advanced gas-cooled reactor	DC	direct current
AM	amplitude modulation	DDC	direct digital control
ANS	Astronomical Netherlands Satellite	DDL	diode-diode logic
APACHE	accelerator for physics and chemistry of heavy elements	DECENT	distribution of exact classical energy transfer
APR	acoustic paramagnetic resonance	DESY	Deutsches Electron Synchrotron
APS	appearance potential spectra(oscopy)	DF	Dirac-Fock
APW	augmented plane wave	DFB	distributed feedback
ATR	attenuated total reflection	DH	double heterostructure
ATS	applications technology satellite	DIL	dual-in-line
ATWS	anticipated transients without scram	DITE	divertor in torus experiment
AVC	automatic volume control	DLTS	deep level transient spectra(oscopy)
		DM	delta modulation
BARITT	barrier injection transit time	DMSO	dimethyl sulphoxide
BBEA	4-butoxybenzal-4'-ethylaniline	DMSS	Defence Meteorological Satellite System
BCC	body centred cubic	DOBAMBC	p-decyloxybenzylidene p'-amino 2-methyl butyl cinnamate
BCD	binary-code decimal		
BFO	beat-frequency oscillator	DODS	different orbitals for different spins
BWO	backward wave oscillator	DORIS	Dopple-ring-Speicher
BWR	boiling water reactor	DOVETT	double velocity transit time
BWT	backward wave tube	DP	data processing
		DPCM	differential pulse code modulation
CAD	computer aided design	DPPH	diphenylpicrylhydrazyl
CAI	computer assisted instruction	DPSK	differential phase shift keying
CARS	coherent antiStokes Raman scattering (spectra)	DSC	differential scanning calorimetry
CATV	community antenna TV	DTA	differential thermal analysis
CB	citizen band	DV-X $\alpha$	discrete variational X $\alpha$ method
CBOOA	cyanobenzylidene octyloxyaniline		
C-CD	charge-coupled device	E1,E2	electric dipole, quadrupole
CDI	collector diffusion isolation	EAS	extensive air shower
CDM	code division multiplexing	EB	exponential Born
CDW	charge-density wave	EBBA	4-ethoxybenzylidene-4'-n-butylaniline
CEM	channel electron multiplier	EBR	experimental breeder reactor
CEPA	coupled electron pair approximation	EBT	Elmo Bumpy Torus
CERN	Conseil Européen pour la Recherche Nucléaire	ECC	emergency core cooling
CESR	conduction electron spin resonance	ECELR	epithermal critical experiment laboratory reactor
CGTO	contracted Gaussian-type orbital	ECG	electrocardiography (-gram)
CHF	coupled Hartree-Fock	EDA	ethylene diamine
CI	configuration interaction	EDP	electronic data processing
CIEH	charge iterated extended Huckel	EDTA	ethylene diamine tetra-acetic acid
CIHY	configuration interaction Hylleras	EEBAC	ethyl-4-(4'-ethoxy-benzylidene-amino) cinnamate
CNDO	complete neglect of differential overlap		
COC	cholesteryl oleyl carbonate	EEG	electroencephalography (-gram)
COM	computer output to microform (fiche or film)	EELS	electron energy loss spectra
COOB	4,4'-cyano-octyloxy-biphenyl	EFM	extended Flygare method
CP	charge, parity	EHD	electrohydrodynamics
CPA	coherent potential approximation	EHF	extremely high frequency
CPSK	coherent phase shift keying	EHP	electron-hole potential method
CPT	charge, parity, time	EHT	extended Huckel theory
		EHV	extra high voltage
		ELDOR	electron electron double resonance



ELF	extremely low frequency	HOMO	highest occupied molecular orbitals
EM	electromagnetic	HORM	hybrid orbital rehybridisation method
EMC	electromagnetic compatibility	HTGR	high temperature gas-cooled reactor
EMF	electromotive force	HV	high voltage
EMG	electromyography(-gram)	HVEM	high voltage electron microscopy
ENDOR	electron nuclear double resonance	HWR	heavy water reactor
EOS	earth observatory satellite	IAEA	International Atomic Energy Authority
EPEN	empirical potential energy function based on interactions of electrons and nuclei	IBPBAC	Agency isobutyl-4-(4'-phenylbenzylideneamino) cinnamate
EPMA	electron probe microanalysis	IC	integrated circuit
EPR	electron paramagnetic resonance	ICDF	intermediate coupling Dirac-Fock
ERG	electroretinography(-gram)	IDT	interdigital transducer
ERPS	extramolecular relaxation polarisation shift	IEPA	independent electron pair approximation
ERTS	earth resources technology satellite	IF	intermediate frequency
ESCA	electron spectroscopy for chemical analysis	IGFET	insulated gate field effect transistor
ESCAR	experimental superconducting accelerating ring	IKO	Institute v. Kernph Ouder Amsterdam
ESFI	epitaxial silicon film on insulator	I <sup>2</sup> L	integrated injection logic
ESS	electronic switching system	I <sup>3</sup> L	isoplanar I <sup>2</sup> L
EUV	extreme ultraviolet	ILS	instrument landing system
EXAFS	extended X-ray absorption fine structure	IMPATT	impact avalanche transit time
FBR	fast breeder reactor	INDO	intermediate neglect of differential overlap
FCC	face centred cubic	INDOR	internuclear double resonance
FDM	frequency division multiplex(ing)	ING	intense neutron generator
FDNC	frequency dependent negative conductance	INO	iterative natural orbital
FDNR	frequency dependent negative resistance	INTELSAT	international telecommunications satellite consortium
FEM	field emission microscopy	I/O	input/output
FET	field effect transistor	IOC- $\omega$	inclusion of the overlap charges in the omega
FFHR	fusion-fission hybrid reactor	IR	infrared
FFT	fast Fourier transform	IRDO	intermediate retention of differential overlap
FFTF	fast flux test facilities	ISABELLE	intersecting storage and acceleration
FIM	field ion microscopy	ISR	intersecting storage ring
FM	frequency modulation	ISX	impurity study experiment
FPT	finite perturbation theory	ITEP	Institute of Theoretical and Experimental Physics
FSK	frequency-shift keying	IU	Indiana University
FSGO	floating spherical Gaussian orbitals	IVO	improved virtual orbitals
FTR	fast test reactor	JET	Joint European torus
GAMBIT	gate modulated bipolar transistor	JAERI	Japan Atomic Energy Research Institute
GANIL	grand accélérateur national a ions Lourds	JINR	Joint Institute for Nuclear Research
GARP	global atmospheric research programme	KEK	Japan National Laboratory for High Energy Physics
GATE	GARP Atlantic tropical experiment	KKR	Korringa-Kohn-Rostoker
GCFR	gas-cooled fast breeder reactor	LAMPF	Los Alamos meson physics facility
GCM	generator coordinate method	LC	inductance-capacitance
GHF-NO-CI	generalised Hartree-Fock/natural orbital/configuration interactions	LCAO	linear combination of atomic orbitals
GIAO	gauge-invariant atomic orbitals	LCBO	linear combinations of (semi-localised) band orbitals
GO	Gaussian orbitals	LCGO	linear combination of Gaussian orbitals
GOO	generalised Overhauser orbitals	LCP	large coil program
GPM	ground potential model	LCRO	linear combination of Rydberg orbitals
GSO	general spin orbitals	LEC	liquid encapsulated Czochralski
GTO	Gaussian-type orbitals	LED	light emitting diode
GVB	generalised valence bond	LEED	low energy electron diffraction
HAM	hydrogenic atoms in molecules	LEP	large electron positron
HBAB	hexyloxybenzylidene-p' aminobenzonitrile	LET	linear energy transfer
HBT	N-(p-hexyloxybenzylidene)-p-toluidene	LF	low frequency
HCDA	hypothetical core disruptive accident	LMC	Large Magellanic Cloud
HCP	hexagonal close packed	LMFBR	liquid metal fast breeder reactor
HEED	high energy electron diffraction	LMTO	linear combination of muffin tin orbitals
HF	high frequency or Hartree-Fock	LOCA	loss of coolant accident
HFB	Hartree-Fock-Bogoliubov	LOCE	loss of coolant experiment
HFER	hot fuel examination facility	LOFT	loss of flow test facility
HFIR	high flux isotope reactor	LPE	liquid phase epitaxy
HFO	Hartree-Fock-Overhauser	LSA	limited space charge accumulation
HFS	hyperfine structure		
HLW	high level waste (radioactive)		
HMO	Huckel molecular orbitals		
HOAB	heptyloxyazoxybenzene		
HOBHA	p-n-heptyloxy-benzylidene-p-n heptylaniline		



LSD	local spin density	ODMR	optical detection of magnetic resonance
LSI	large-scale integration	OER	oxygen enhancement ratio
LTE	local thermodynamic equilibrium	OGO	orbiting geophysical observatory
LUMO	lowest unoccupied molecular orbitals	OPHF	orbital polarised Hartree-Fock
LV	low voltage	OPW	orthogonal plane wave
LWR	light water reactor	OR	operations research
MADO	Mulliken approximation for differential overlap	ORELA	Oak Ridge electron linear accelerator
M1,M2	magnetic dipole, quadrupole	ORNL	Oak Ridge National Laboratory
MBBA	4-methoxybenzylidene-4'-n-butyl-aniline	OSO	orbiting solar observatory
MBE	molecular beam epitaxy	OTF	optical transfer function
MBPT	many body perturbation theory	PAA	paraazoxyanisole
MCD	magnetic circular dichroism	PABX	private automatic branch exchange
MCPESCF	multiconfiguration paired excitation SCF	PAC	perturbed angular correlation
MCZDO	multi-centre zero differential overlap	PAHR	post accident heat removal
MEDO	multipole expansion of diatomic overlap	PAM	pulse amplitude modulation
MESFET	metal-semiconductor field effect transistor	PAMPUS	photons for atomic and molecular processes and universal studies
MF	medium frequency	PAP	paraazoxyphenetole
MFP	mean free path	PBF	power bursts facility
MHD	magnetohydrodynamics	PBR	pebble bed reactor
MIC	microwave integrated circuit	PBX	private branch exchange
MIEHM	modified iterative extended Huckel method	PC	printed circuit
MIM	metal-insulator-metal	PCAC	partially conserved axial currents
MIS	metal-insulator-semiconductor or management information system	PCB	printed circuit board
MIT	Massachusetts Institute of Technology	PCGVB	pairwise correlated generalised valence bond
MMF	magnetomotive force	PCILOCC	perturbative configuration interaction using localised orbitals for crystal calculation
MNOS	metal-nitride-oxide-semiconductor	PCM	pulse code modulation
MO	molecular orbitals	PCX	plasma confinement experiment
MOCIC	molecular orbital constraint of interaction coordinates	PDX	poloidal divertor experiment
MODPOT	model potential	PEP	positron electron proton
MOS	metal-oxide-semiconductor	PETRA	positron electron tandem ringbeschleuniger anlage
MOSFET	metal-oxide-semiconductor field effect transistor	PF	power factor
MOST	metal-oxide-semiconductor transistor	PFM	pulse frequency modulation
MRD	multi-reference double excitation	PHWR	pressurised heavy water reactor
MRINDO	modified Rydberg INDO	PID(PI,PD)	proportional+integral+differential (derivative)
MSI	medium scale integration	PLA	phase locked arrays
MSR	molten salt reactor	PLC	programmable logic control
MSU	Michigan State University	PLL	phase locked loops
MTBF	mean-time between failures	PLT	Princeton Large Torus
MTF	modulation transfer function	PM	pulse modulation
MTX $\alpha$	muffin-tin X $\alpha$	PMMA	polymethylmethacrylate
MUF	maximum usable frequency	PMDR	phosphorescence microwave double resonance
MWH	Mulliken-Wolfsberg-Helmholz-semi-empirical method	PNDO	partial neglect of differential overlap
NAL	National Accelerator Laboratory	PNO-CI	pair natural orbital configuration interaction
NAND	not-and(logic)	POL	pair orthogonalised Lowdin
NC	numerical control	POP AE	protons on protons and electrons
NCMET	non-closed shell many electron theory	POPOP	phenyl-oxazolyl-phenyl-oxazolyl-phenyl
NDDO	neglect of diatomic differential overlap	POS	point of sale
NDT	nondestructive testing	PPDP/S	Pariser-Parr-Del Bene-Pople/Segal calculations
NEMO	non-empirical molecular orbitals	PPI	plan position indicator
NEVE	non-empirical valence-electron	PPM	pulse position modulation or parts per million
NIC	negative impedance convertor	PPP	Pariser-Parr-Pople
NMR	nuclear magnetic resonance	PRDDO	partial retention of diatomic differential overlap
NNNDO	neglect of non-neighbour differential overlap	PRF	pulse recurrence (repetition) frequency
NOR	not-or(logic)	PROM	programmable read-only-memory or Pockels readout optical modulator
NPOST	non-perturbative open-shell theory	PS	proton synchrotron (CERN)
NPSO	non-paired spatial orbitals	PSK	phase shift keying
NQR	nuclear quadrupole resonance	PTFE	polytetrafluoroethylene
NRC	nuclear regulatory committee	PTM	pulse time modulation
NRM	natural remanent magnetisation	PVC	polyvinyl chloride
NTO	natural transition orbitals	PWM	pulse width modulation
OAQ	orbiting astronomical observatory	PWR	pressurised water reactor
OCR	optical character recognition		



QCD	quantum chromodynamics	TCR	temperature coefficient of resistance
QDMBPT	quasi-degenerate many-body perturbation theory	TDHF	time dependent Hartree-Fock
QED	quantum electrodynamics	TDM	time division multiplex(ing)
QPSK	quaternary phase shift keying	TDMA	time division multiple access
RAM	random access memory	TDPAC	time differential perturbed angular correlation
RBE	relative biological effectiveness	TE	transverse electric
RC	resistance-capacitance	TEA	transversely excited atmospheric
RCNDO	Rydberg CNDO	TEM	transverse electromagnetic or transmission electron microscopy
R & D	research and development	TEXT	Texas Experimental Tokamak
RF	radio frequency	TFTR	Tokamak fusion test reactor
RFI	radio frequency interference	TGFB	triglycine fluoroberyllate
RHEED	reflection high energy electron diffraction	TGS	triglycine sulphate
RINDO	Rydberg INDO	TGSe	triglycine selenate
RKKY	Rudermann-Kittel Kasuya-Yosida	TJS	transverse junction stripe
RLC	resistance-inductance-capacitance	TLD	thermoluminescent dosimeter(-ry)
RMS	root-mean-square	TM	transverse magnetic
ROM	read-only memory	TMMC	tetramethylammonium manganese chloride
RPA	random phase approximation	TOP	transient overpower accident
RPM	relaxation potential model	TNS	The next step
SAMO	simulated ab initio molecular orbitals	TRAPATT	trapped plasma avalanche triggered transit
SAS	small astronomy satellite	TREAT	transient reactor test facility
SAW	surface acoustic waves	TRM	thermoremanent magnetisation
SCF	self consistent field	TSC	thermally stimulated currents
SCL	space charge limited	TSEE	thermally stimulated exo-electron emission
SCPT	self consistent perturbation theory	TTF	tetrathiofulvalinium
SCR	silicon controlled rectifier	TTL	transistor transistor logic
SDM	space division multiplexing	TTT	tetrathiotetracene
SDO	shielded diatomic orbitals	TUCA	transient undercooling accident
SEHF	spin extended Hartree-Fock	TV	television
SEM	scanning electron microscope	TW	travelling wave
SFE	solar-flare effect	TWT	travelling wave tube
SGHWR	steam generating heavy water reactor		
SHF	superhigh frequency	UCHF	uncoupled Hartree-Fock
SHG	second harmonic generation	UHF	ultra high frequency unrestricted Hartree-Fock
SIMS	secondary ion mass spectrometer		
SIN	Swiss Institute of Nuclear Research	UHV	ultra high voltage
SINDO	scaled INDO	UKAEA	United Kingdom Atomic Energy Authority
SISAM	spectrometer with interference selective amplitude modulation	ULF	ultra low frequency
		UMD	unitised microwave devices
SMC	Small Magellanic Cloud	UPS	ultraviolet photoelectron spectra
SMS	synchronous meteorological satellite	US	ultrasonic
S/N	signal-to-noise	UV	ultraviolet
SOG	strongly orthogonal geminal		
SOS	silicon on sapphire	VB	valence bond
SPA	separated pair approximation	VCR	video cassette recorder
SPC	stored program control	VDM	vector dominance model
SPEAR	Stanford positron electron asymmetric ring	VDU	visual display unit
		VHF	very high frequency
SPHF	spin polarised Hartree-Fock	VLBI	very long base line interferometry
SPIN-CIPSI	spin symmetry adapted generalisation of CIPSI	VLF	very low frequency
SPS	super proton synchrotron (CERN)	VLSI	very large scale integration
SQUID	superconducting quantum interference device	VOR	VHF omnidirectional range
SRMCASE	symmetry-restricted-multiconfiguration annihilation of single excitations	VPE	vapour phase epitaxy
		VRC	visual record computer
SSB	single sideband	VRDDO	variable retention of diatomic differential
SSC	sudden storm commencement	VSF	vestigial sideband
SSI	supersonic transport	VSEPR	valence shell electron pair repulsion
STD	salinity-temperature-depth or subscriber trunk dialling	VSWR	voltage standing wave ratio
		VTOL	vertical take-off and landing
STEM	scanning transmission electron microscopy	VTR	voltage transformation ratio or video tape recorder
STO	Slater-type orbitals		
STOL	short take-off and landing	VUV	vacuum ultraviolet
STP	Slater-transfer Preuss	VVER	water moderated water cooled reactors
SUHFC	spin unrestricted Hartree-Fock with local approximation for correlations		
		WWER	water moderated water cooled reactors
SW	short wave		
SWR	standing wave ratio	XPS	X-ray photoelectron spectra
SXAPS	soft X-ray appearance potential spectrum		
		ZEBRA	zero energy breeder reactor assembly
TBBA	terephthal-butylaniline	ZGS	zero gradient synchrotron
TCNE	tetracyanoethylene	ZPPR	zero power plutonium reactor
TCNQ	tetracyanoquinodimethane		



# Subject Index

## M-centres

- alkali metal halides, F-centre luminesc. rel. to cryst. chemical parameters 0-29780
- alkaline earth oxides and fluorides, F-centre luminesc. rel. to cryst. chemical parameters 0-29780
- ionic cryst. positron-containing M-centre, struct. 0-49220
- optical waveguides, slab-type, mode coupling via dichroic absorpt. of M-centres 0-33178
- BaF<sub>2</sub>, undoped and U-doped, neutron irradi., absorpt. band attributed to F<sub>2</sub><sup>+</sup> centres 0-7380
- BaF<sub>2</sub>:U, absorption band spectra following neutron irradi. 0-29763
- CaF<sub>2</sub>:Dy crystal with M-centre, antiresonance line, mag. field effect 0-55138
- KBr photochromic materials, F→M transform., electrostatic field control of optical information recording (*Russian*) 0-48370
- KCl, radiative tunnel transitions in negatively charged colour centre systems 0-49655
- KCl:Na<sup>+</sup>, CW laser action of (F<sub>2</sub><sup>+</sup>)<sub>A</sub>-centres, tunable from 1.62 to 1.91 μm 0-32998
- KCl(Br):OH<sup>-</sup>, electron irradi., F<sub>2</sub><sup>+</sup> centre stabilisation 0-54231
- KCl(Br)(I) with alkali and halogen impurities, colour centre deformation induced nonradiative decay 0-7387
- KF, F<sub>2</sub><sup>+</sup>-centre excited-state absorption spectrum, rel. to H<sub>2</sub><sup>+</sup> model 0-16066
- LiF crystal with F<sub>2</sub><sup>+</sup> centres, periodic pulsed tunable laser, Nd laser second harmonic excited 0-38021
- LiF OH-stabilised F<sub>2</sub><sup>+</sup>-centre laser, appl. to intracavity laser spectroscopy 0-32999
- LiF with stable F<sub>2</sub> centres, F<sub>2</sub><sup>+</sup> colour centre generation accumulation, tunable laser production (*Russian*) 0-28238
- LiF:OH<sup>-</sup>, electron irradi., F<sub>2</sub><sup>+</sup> centre stabilisation 0-54231
- NaCl, γ-irradiated, F→M phototransformation, effect on aquoluminescence 0-7418
- NaCl, M-centre statistical prod. meas. 0-15097
- NaF(Cl):OH<sup>-</sup>, electron irradi., F<sub>2</sub><sup>+</sup> centre stabilisation 0-54231
- ZnS, luminescence of M-centre 0-29779

## M-regions see Sun

## Mach number

- see also *acoustic wave velocity; shock waves*
- hypersonic blunt-slender cones, artificially induced boundary layer transition 0-28496
- shock tube flows, unsteady non-equilibrium, discretisation of boundary layer terms, computation at Mach 10 0-14742
- shock tubes, use of fast-acting valves, shock wave formation, max. Mach number 0-24052
- subsonic base pressure fluctuations on axisymmetric blunt-based body, Mach no. depend. 0-19423

## Mach principle see cosmology; space-time configurations

## machine bearings

- air bearing and diamond machine design for optics 0-1365
- flywheels, development of low loss magnetic bearings, for energy storage appls. 0-30566
- flywheels, performance of retainerless bearings for vehicular energy storage appls. 0-30567
- journal bearing, hydrodynamic lubrication including surface tension free boundary problem 0-19542
- linear motion gas bearing for Fourier spectrometers 0-31893
- optical diamond turning air-bearing spindle and eddy-current motor 0-5851

## machine insulation

- bar insulation in stator winding of large turbogenerator, inspection using microwave defectoscope 0-35474

## machine testing

- vibration testing and dynamic balancing 0-23971

## machine tools

- see also *numerical control*
- computer-controlled machine tool for diamond-turned surface accuracy improvement 0-1367
- cutting fluids testing rel. to tool wear, thin layer activation technique 0-55619
- length meas. international standards compared (*German*) 0-36977
- noise, determ. of sound performance for multi-position machines (*German*) 0-43523
- noise control, conf., W.Lafayette, IN, USA (Apr/May 1979) 0-43526
- positioning system using laser interferometer (*German*) 0-9022
- precision, floor vibration isolation 0-43522
- vibration-damping plug for noise reduction 0-43525
- wear resistance, accelerated testing (*Russian*) 0-40543

## machine windings

- see also *rotors; stators*
- wound wires, enamel insulated, elongation plus flexibility 0-20999

## machines, electric see electric machines

## machining

- see also *cutting; electrolytic polishing; electron beam machining; grinding; laser beam machining; spark machining*
- brass, magnetoabrasive machining, optimum conditions 0-30172
- diamond machined optical surface specification 0-48472
- ion beam sputtering, appl. to surface machining 0-30129
- linear motor slide drive system for optical machining 0-1366
- metal cutting, separation process tool tip, fracture detection, acoustic emission method (*Japanese*) 0-1388
- metals, abrasive finishing with refractory carbide micropowders, surface struct. 0-11842
- NC diamond turning system evolution 0-1369
- ophthalmic lens surface working machinery 0-28363

## machining continued

- optical diamond turning and precision engineering 0-1364
- optical precision machining, seminar, San Diego, USA (Aug. 1978) 0-1363
- optical precision machining commercialisation for military economy 0-1371
- roughness of machined surfaces, on-line meas. technique using He-Ne laser (*German*) 0-33014
- Ni plated aspheric metal mirror fabrication for IR optical systems 0-14497
- WC-Co hard alloys, machined with polycryst. superhard materials, surface struct. using X-ray photoelectron spectroscopy 0-25919

## macromolecular configurations

- acrylonitrile Na methallylsulphonate copolymer electrolytes in dimethylformamide, gel permeation chromatography appl. 0-21345
- adenovirus hexon, three dimensional structure from electron microscopy, computer modelling 0-35833
- anthramycin-DNA adduct, proposed struct. 0-30658
- bacteriorhodopsin, anomalous amide I IR absorpt. rel. to alpha helices distorted struct. 0-12058
- biomembrane, phase changes and determination methods (*Czech*) 0-3599
- biopolymer, electronic-conformation interactions 0-3588
- biopolymer chain, uniform, elastic, possible conformational states 0-37913
- biopolymer chains, intramol. reacts., enzyme catalysis appl., review 0-40953
- cellulose, conform. states and IR dichroism calcs. 0-55986
- cellulose, nitrated, strength, deform. and disintegration, influence of stable free nitroxyl radicals 0-11717
- chain networks, static and dynamic entanglements, contrib. to equilib. shear modulus 0-28126
- collagen structures, piezoelec. effect, in rel. to mol. struct. 0-41100
- collagen fibrils, rat tail tendon, quasi-hexagonal mol. packing model 0-30660
- computer modelling of matter, conf., Anaheim, USA (March 1978) 0-51954
- copolymer model with alternating spins, kinetics 0-9768
- deoxy ferrous haemoglobin, Fe atom distortion, pseudo-Jahn-Teller effect 0-55984
- DNA, conformation of native molecule, influence of solvent struct. 0-30655
- DNA, phase transition, ψ transition of single coils 0-26200
- DNA, X-ray diffr. from side-by-side model 0-35835
- DNA conformation, influence of intermol. interactions 0-16900
- DNA hydrate, stability studied by thermogravimetry 0-30650
- DNA in chromatin, stereochem. model for superfolding 0-35829
- DNA packing in fibrils of DNP of polytene chromosomes 0-30649
- DNA structure of left-handed double helical DNA fragment 0-30659
- DNA with irreversible cross-links and low counterion conc., helix-coil transition 0-32860
- DNA-adduct systems, binding geometry, determ. by induced circ. dichroism 0-55988
- DNA-type macromolecule, melting, low mol. wt. impurity effect 0-12050
- electron microscopy, high resolution, mol. struct. determ. 0-21595
- epoxy resins, struct. changes under mag. field action 0-40516
- (ethylene-co-vinyl alcohol)-g-ethylene oxide graft copolymers, sol. behaviour 0-19682
- fibres, natural, Brillouin scatt. shifts, comparison with synthetic polypeptide obs. 0-55991
- glass fibre reinforced plastics, coupling agent/matrix interface investigation by Fourier transform IR spectroscopy 0-20884
- glass transition temperature, rel. to mol. wt. 0-34176
- gramicidin A in biomembrane channel, IR spectroscopic obs. 0-16901
- haemoprotein, fine structure of Fe ions 0-30661
- histones, H2a and H4, aggregation ionic strength effect (*Russian*) 0-55697
- lysozyme, binding to bacterial cell wall trisaccharide NAM-NAG-NAM, X-ray cryst. struct. anal. 0-35834
- multichain polymer system, simulating dynamic and equilib. props. 0-53179
- nucleic acid components, pyrimidine and purine, electronic struct. 0-30654
- nucleic acid-dye complexes, energy transfer obs. using laser-induced fluorescence 0-12054
- oligoesters, effect of mol. architecture on dispersion props of TiO<sub>2</sub> in non-aqueous liquids 0-40751
- ovalbumin aqueous soln., macromol. gel layer formed on ultrafiltration tubular membrane, charact. 0-14260
- Pf1 filamentous bacterial virus, macromolecular structural transitions 0-3584
- phosphates, cellular, heteronucleic. two-dimens. NMR as conform. probe 0-3590
- piperylene-acrylonitrile copolymers, polymerisation, monomer composition rel. to copolymer struct. (*Russian*) 0-5651
- plasma protein interaction with polyanion complex studied by circular dichroism and UV spectroscopy (*Japanese*) 0-12316
- plasmid DNA and DNA-histone chromatin-like complexes, conform. and soln. props. by laser light scatt. 0-55987
- PMMA, partial draining of low-molecular weight polymers with flexible chains 0-23592
- poly(α-methylvinyl alkyl ether)s, <sup>1</sup>H-, <sup>13</sup>C-NMR spectra, stereoregularity 0-48112
- poly(ethylene oxide), partial draining of low-molecular weight polymers with flexible chains 0-23592
- poly-β-substituted vinyl ethers, cationic polymeris., stereochem. 0-21284
- poly-thio-1-N,N-diethylaminomethylethylene, optically active samples, <sup>13</sup>C NMR spectra 0-28127



## macromolecular configurations continued

- polyacetylene, bond length alternation and energy gap, intermediate excitation formalism 0-29305
- polyacetylene, dynamic nuclear polarisation of protons (*French*) 0-43217
- polyacetylene, nascent morphology obs. 0-24379
- cis-polyacetylene, static lattice calcs. for crystals 0-10509
- polyacetylene, thin film, ESR study, effects of O<sub>2</sub>, NO and halogens 0-25186
- polyacrylonitrile, copolymerisation with poly-2-hydroxyethyl methacrylate rel. to crystallinity 0-38935
- polyamides, 1,3-cyclohexanediis(methylamine) based, thermal props. and glass transition temp. 0-39264
- polybutyl acetate-polyvinyl acetate crosslinked compositions, proton mag. relax., forced compatibility (*Russian*) 0-44950
- polydimethyl siloxanes, cyclic and linear, neutron scatt. meas. of dimensions 0-18952
- all-trans polyene, ab initio studies 0-43222
- polyethylene, conform. stability, 1-electron levels, long-range effects calcs. 0-28123
- polyethylene, crystalline, steric struct. modelling of end defects 0-6371
- polyethylene, linear, melt props. correl. with chain length distrib. (*Russian*) 0-37920
- polyethylene, partial draining of low-molecular weight polymers with flexible chains 0-23592
- polyethylene, rapid crystn. from melt rel. to struct. 0-44152
- polyethylene, ultra-high modulus, drawing behaviour, effect of drawing temp. 0-35232
- polyglycine, IR spectra calc. for helix and  $\beta$  configs. 0-45853
- polyisoprenes, partly deuterated, <sup>1</sup>H-NMR spectra, struct. 0-50202
- polymer, amorphous, chain conform., small-angle neutron scatt. obs. (*Polish*) 0-10511
- polymer, crosslinked, probabilistic theory of structural and physical characteristics 0-5649
- polymer athermal self avoiding chains, configurational props. 0-18950
- polymer chain, frequency dependent energetics, Orwells-Stockmayer hopping model 0-24346
- polymer chain cyclisation, lattice embedded model, discrete scatt. series representation 0-48109
- polymer chains 0-3116
- polymer crystal, conformational energy calcs., appl. to defect props. 0-54154
- polymer linear self interacting chains, configurational props. 0-23586
- polymer linear self interacting chains, internal distrib., radius of gyration 0-23587
- polymer model equivalent to the Ising model 0-37914
- polymer network, crosslinks and trapped entanglements, two-network model 0-38962
- polymer network, permanently crosslinked, topological struct. and macroscopic behaviour 0-37919
- polymer network, Riemann's metric degeneration to graph metric demonstration, chain entanglement problems 0-38963
- polymer network, small-angle neutron scatt. obs. of mol. behaviour 0-37918
- polymer network formation, pre-gel intramol. reaction and gelation, shear moduli and glass transition 0-45501
- polymer network formation, relaxational props. variation 0-38961
- polymer network formation, struct. and mech. props., computer simulation 0-38965
- polymer network in solution, free energy of deform. 0-38900
- polymer networks and semi-crystalline polymers, diffusion mechanism and model, local conform. change 0-15288
- polymer single chain, coil-globule transition obs. 0-1098
- polymer solution, second virial coeff., segment cloud model, chain length and branching study 0-24559
- polymer solution and bulk state, partially labelled chains, neutron scatt. obs. 0-38899
- polymeric macromolecules, with structure regularity, description and design 0-23591
- polymers, electrical phenomena, nature and appl., review 0-50254
- polymers, specific heat, conform. effects 0-24607
- polymers, stereochemical definitions, IUPAC nomenclature 0-23593
- polymers, stereoregularity distortions, local oscill. freqs., eqn. (*Russian*) 0-5653
- polynucleotide, double-stranded, conform. inhomogeneity of sugar-phosphate chain rel. to compact particle optical activity 0-35839
- polynucleotides, double helical, conformation, pairwise pot. function calcs. 0-53173
- polyoxymethylene, rapid crystn. from melt rel. to struct. 0-44153
- polypropylene-alt-1,4-butadiene and hydrogenated derivative, mol. relaxations in glassy state 0-53177
- polypropylene sulphide, atactic chains, dipole moments, dielec. const. meas. 0-23584
- polypropylene sulphide in athermal solvent, viscosity-temp. coeffs. 0-39333
- polyquinones, ladder, partially-ladder, synthesis, struct., props., review (*Russian*) 0-7529
- polyriboxanthic acid, spatial struct., H bonding 0-53086
- polystyrene, chem. shift, conformational struct. (*Russian*) 0-5652
- polystyrene, cyclohexane soln., coil-globule transition 0-54110
- polystyrene, isotactic, conformation in bulk crystallised state 0-43221
- polystyrene, partial draining of low-molecular weight polymers with flexible chains 0-23592
- polystyrene, soln. ion cyclohexane, mol. dimens. near theta point 0-54105
- polystyrene and model cpds., conformational struct. influence on normal modes of benzene ring, Raman study 0-14144
- polystyrene-*b*-isoprene and hydrogenated derivative, mol. relaxations in glassy state 0-53177
- polystyrene-polyisoprene two-block copolymer soln., conformation, small angle neutron scattering, X-ray diffraction, review (*Rumanian*) 0-6348
- polyvinyl acetate, partial draining of low-molecular weight polymers with flexible chains 0-23592
- polyvinylalcohol, macromol. gel layer formed on ultrafiltration tubular membrane, charact. 0-14260
- polyvinylpyrrolidone, conformational states investig. by atom-atom function method (*Russian*) 0-53178
- polyvinylpyridines, atactic, chem. shift, conformational struct. (*Russian*) 0-5652
- protein secondary structure determ. by circular dichroism spectra 0-30653
- proteins, coiling and topology of the antiparallel  $\beta$ -struct. 0-40956
- proteins, coiling and topology of the parallel  $\beta$ -struct. 0-40957

## macromolecular configurations continued

- proteins, conformations, quantitative approach 0-30652
- pseudoisocyanine bound by sulphated polysaccharides, dil. aq. soln., visible and circular dichroism spectra 0-45107
- recent advances in polymer characterization by GPC 0-16740
- ribose phosphate backbone, effective partial charges calc. 0-8013
- rubber, network, highly swollen, long time dynamics 0-38291
- rubber, network entanglement contrib. to elasticity 0-39203
- rubber network elasticity, mol. theory 0-38290
- saturated hydrocarbon polymers, conform. stability, 1-electron levels, long-range effects calcs. 0-28123
- semicrystallised chains, small-angle neutron scatt., mean dimension evaluation 0-43220
- sphere radii moments, size distrib. 0-21329
- styrene-isoprene triblock copolymer, mol. relax. in glassy state 0-53177
- teacher resource paper on entropy an rubbery elasticity 0-17777
- three-dimensional cubic lattice, random walk of particle, polymer chain config. approach 0-22294
- ribosomal RNA interacting sequences, expt. determ., method and results 0-3586
- triblock copolymer, model for rheology 0-23979
- $\alpha$ -tropomyosin, specific splitting at cysteine-190, physicochem. study of fragments 0-30647
- twisted stiff chains theory 0-1093
- vinyl alcohol-vinyl acetate copolymers, mol. architecture and physicochem. props. 0-44103
- xanthane, dilute solns., viscosity rel. to temp., shear rate (*French*) 0-39332
- H<sup>+</sup>-ATPase, soluble mitochondrial, thermal stability obs. 0-55992

## macromolecular dynamics

- biopolymers, conditions of liquid crystal formation 0-30642
- Brownian particles, k-dependence of long-time diffusion 0-5645
- chain networks, static and dynamic entanglements, contrib. to equilib. shear modulus 0-28126
- chymotrypsin-like proteins,  $\gamma$ -irrad. rel. to UV irrad., unfolding obs. 0-35984
- coil, dynamical polymer coil overlap, NMR model 0-23583
- copolymer model with alternating spins, kinetics 0-9768
- critical branching a statistical theory 0-3413
- deformed networks, equilibrium props. from thermomechanical anal. (*German*) 0-37917
- DNA, backbone vibrational mode displacements of A-DNA and B-DNA 0-8000
- DNA, soln., phase transitions, light absorption oscils. obs. 0-26197
- DNA-type macromolecule, melting, low mol. wt. impurity effect 0-12050
- E. coli, light scatt., ribosomal subunit diffusion coeffs. 0-21438
- enzyme dynamics, statistical phys. 0-21439
- flexibility, detect. by time-depend. diffusion coeffs. obs. 0-23585
- fluorescence depolarisation, E-type delayed, rotational motion probe techniques 0-36207
- G 0-44099
- hard disc necklaces, rigid and nonrigid models, mol. dynamics 0-43219
- helical wormlike chain, dipole moment, elec. birefringence, elec. dichroism, statistical mech. calcs. 0-14262
- light scattering in dynamical props. study, principles spectra derivation and applies. 0-53218
- lipid bilayer head group, orientational order and rotational diffusion, NMR obs. 0-21451
- lipid bilayers, D relax. rates and mol. dynamics 0-26206
- metmyoglobin, dynamics study using Rayleigh scatt. of Mossbauer radiation 0-40963
- multichain polymer system, simulating dynamic and equilib. props. 0-53179
- myelin lattice swelling kinetics study, X-ray diffr. obs. 0-21436
- myoglobin, static and dynamic structure of biomolecules, Mossbauer effect 0-40952
- nucleic acid subunits, simulation of inter- and intra-molecular interactions 0-30643
- nucleic acids, H<sub>2</sub> exchange kinetics and internal motions 0-21440
- phospholipids, <sup>31</sup>P NMR, slow-motional lineshapes for very anisotropic rot. diffusion 0-5644
- plasma protein interaction with polyanion complex studied by circular dichroism and UV spectroscopy (*Japanese*) 0-12316
- plasmid DNA and DNA-histone chromatin-like complexes, conform. and soln. props. by laser light scatt. 0-55987
- PMMA, C-H stretching and bending vibs., IR spectra, selective deuteration 0-23582
- poly-1,6-di-p-toluenesulphonyloxy-2,4-hexadiene, thermal polymerisation, Raman spectra 0-35531
- polyacrylamide-fluorescein conjugates, fluoresc. polarisation, high press. obs. 0-20683
- polybutadiene, mol. motion in solid and soln., <sup>13</sup>C NMR relaxation meas. (*Japanese*) 0-2666
- polyethylene, linear, nuclear relaxation, mol. motion (*Russian*) 0-44949
- polyethylene crystals, plastic deformation, molecular mech., TEM obs. 0-21022
- polyisobutene solns., X-ray scatt., Kratky cone collimation 0-19681
- polyisobutylene soln., NMR, chain segment motions 0-20475
- polymer, branched and crosslinked molecules, mol. description of dynamics 0-9767
- polymer, crosslinked, probabilistic theory of structural and physical characteristics 0-5649
- polymer, soln., freely jointed chain, with excluded vol. interaction, Monte Carlo studies 0-10475
- polymer athermal self avoiding chains, configurational props. 0-18950
- polymer chain, frequency dependent energetics, Orwells-Stockmayer hopping model 0-24346
- polymer chain dynamics, ang. correl. function decay by multiple rot. pot. diffusion 0-3569
- polymer chain dynamics, review of Brownian motion theory 0-23589
- polymer chain in solution, mol. dynamics obs. 0-5643
- polymer dynamics including side group motion, free draining limit 0-48111
- polymer linear chains, excluded vol. problem 0-5650
- polymer linear self interacting chains, configurational props. 0-23586
- polymer linear self interacting chains, internal distrib., radius of gyration 0-23587
- polymer network formation, struct. and mech. props., computer simulation 0-38965



**macromolecular dynamics continued**

- polymer off-lattice chains, Monte Carlo anal. of excluded vol. problem 0-5647  
 polymer solns., dilute, Hartree self-consistent field analysis 0-5648  
 polymer solution, dilute, chain mol. dynamics and transport processes 0-14989  
 polymer solution, dynamical scaling, neutron spin echo obs. 0-14990  
 polymer solution, flexible chain, entanglement effects in segmental motion, dielec. obs. 0-40050  
 polymer solutions and gels, dynamic behaviour obs. using light scatt. 0-55727  
 polymers, electrical phenomena, nature and appl., review 0-50254  
 polymers, rectilinear on square lattice, series expansion 0-5646  
 polymers, stereoregularity distortions, local oscill. freqs., eqn. (*Russian*) 0-5653  
 polymethylene coils in solution, dimension and shape, computer simulation (*Russian*) 0-54111  
 polypeptides, in aq. poly(L-glutamic acid) soln., helix-coil transition, US relax. times 0-45849  
 polysiloxane dizwitterionomers, mech., dielec. relax., effect of H<sub>2</sub>O sorpt., thermal history 0-50261  
 polystyrene, end group modified, chain dynamics studied by fluorescence depolarization 0-19724  
 polystyrene, glassy state, relax., free vol. fluctuations effect 0-19722  
 polystyrene, isotactic crystals, plastic deformation, molecular mech., TEM obs. 0-21022  
 polystyrene, molecular motion obs. during thermal polymerisation of styrene, PMR 0-3342  
 polystyrene, monosubstituted, US relaxation, dynamics of mol. chains 0-29124  
 polystyrene, soln., macromol. dynamics, us relax. 0-19882  
 polystyrene, soln. ion cyclohexane, mol. dimens. near theta point 0-54105  
 polytetrahydrofuran, H bonding effects on skeletal optical and longitudinal acoustical modes 0-34914  
 proteins, H<sub>2</sub> exchange kinetics and internal motions 0-21440  
 PTFE, peroxy radical labelled, temp. dependent rots., EPR obs. 0-28125  
 random coil polymer chain relax., lattice model with excluded vol., head movement rules 0-5642  
 ribose phosphate backbone, effective partial charges calc. 0-8013  
 t-RNA, rot. relax. time, 10<sup>-9</sup>s range Fabry-Perot and photoelectron time of arrival method 0-21437  
 rubber, network, highly swollen, long time dynamics 0-38291  
 solution, diffusion and self-diffusion phenomena, review 0-15273  
 solutions, light scattering, polydispersity and internal modes of motion 0-20651  
 2,4,6,8-tetraphenylnonane soln., macromol. dynamics, us relax. 0-19882  
 thermodynamics and its possible relevance to physiology 0-53176

**macromolecular energy levels**

- biopolymer, electronic-conformation interactions 0-3588  
 copolymer model with alternating spins, kinetics 0-9768  
 deoxyhaemoglobin, high mag. field Mossbauer spectra, electronic states 0-35845  
 deoxymyoglobin, high mag. field Mossbauer spectra, electronic states 0-35845  
 electrostatic isopotential maps for large biomolecules, STO transferable bond calc. 0-3571  
 energy migration in one-dimensional structures with resonance interaction 0-1092  
 epoxy resins, correlation between valence energies and low temp. flexibility 0-25815  
 finite size polymer chain, collective excited state (*Russian*) 0-9769  
 heart cytosol, aspartate transaminase, electron density map interpretation 0-55990  
 large molecule, electronic struct., photoemission and optical absorpt. spectrum, CNDO/S3 model 0-53172  
 NMR estimation of equilib. const., intermediate exchange processes effect 0-1094  
 polyacetylene, undoped, thermally activated mobile defect, temp. EPR line broadening 0-43218  
 polyethylene, correlation between valence energies and low temp. flexibility 0-25815  
 polymer chains, Coulombic contributions, LCAO-SCF-CO method, Fourier representations 0-32862  
 polymethine-cyanine molecular aggregate, band struct. 0-53174  
 protein, electron-transport type, H-bonding, ab initio MO 0-51039  
 protein model chain, aperiodic, electronic spectra, hopping cond. 0-5641

**macromolecular spectra**

- see also spectra of organic molecules and substances*  
 bacteriorhodopsin, reson. Raman evidence for secondary protein-Schiff base interactions, primary excitation mechanism 0-55981  
 benzene, plasma polymerisation in glow discharge, thin film IR and free radical EPR obs. 0-2964  
 cellulose, conform. states and IR dichroism calcs. 0-55986  
 coupled spin systems, selective nucl. Overhauser effects calc., use in struct. chem. 0-23588  
 deoxyhaemoglobin high spin ferrous ion, low lying electronic states; far IR mag. reson. 0-48110  
 deoxymyoglobin high spin ferrous ion, low lying electronic states, far IR mag. reson. 0-48110  
 dilute solution of macromols., electrically induced fluorescence polarised component change meas. 0-32863  
 DNA, soln., phase transitions, light absorption oscils. obs. 0-26197  
 DNA bases, selective electronic excitation using dye lasers 0-8012  
 DNA bases, theoretical study of electronic spectra 0-30665  
 DNA conformation, influence of intermol. interactions 0-16900  
 elastomer, segmented block, morphology, pulsed proton NMR study 0-33907  
 fibres, natural, Brillouin scatt. shifts, comparison with synthetic polypeptide obs. 0-55991  
 field desorption mass spectrometry, appl. to biochemistry, medicine, and environmental science 0-35592  
 fluorescence depolarisation, E-type delayed, rotational motion probe techniques 0-36207  
 glass fibre reinforced plastics, coupling agent/matrix interface investigation by Fourier transform IR spectroscopy 0-20884  
 helical wormlike chain, dipole moment, elec. birefringence, elec. dichroism, statistical mech. calcs. 0-14262  
 IR linear dichroism of oriented nucleic acid films 0-8013  
 $\beta$ -lactoglobulin, absorpt. spectra for complexes formed with vitamin-A 0-30664

**macromolecular spectra continued**

- methacrylate polymer, carbazoyl substituted, excimer and charge transfer complex trapping of excitons 0-34367  
 NADH coenzyme, two photon absorpt. cross section meas., reaction rate modification 0-51043  
 NMR estimation of equilib. const., intermediate exchange processes effect 0-1094  
 nuclear Overhauser effect, truncated driven, in presence of spin diffusion 0-1095  
 nucleic acid-dye complexes, energy transfer obs. using laser-induced fluorescence. 0-12054  
 oxymetalloproteins, electronic spectroscopic data review 0-52977  
 phosphates, cellular, heteronuc. two-dimens. NMR as conform. probe 0-3590  
 phospholipids, <sup>31</sup>P NMR, slow-motional lineshapes for very anisotropic rot. diffusion 0-5644  
 plasmid DNA and DNA-histone chromatin-like complexes, conform. and soln. props. by laser light scatt. 0-55987  
 PMMA, atactic, FT IR spectrum, <sup>18</sup>O substitution effects 0-23581  
 PMMA, C-H stretching and bending vibs., IR spectra, selective deuteration 0-23582  
 poly-1,6-di-p-toluenesulphonyloxy-2,4-hexadiyne, thermal polymerisation, Raman spectra 0-35531  
 poly-2-vinylnaphthalene, soln., lowest triplet props., flash photolysis and radiolysis obs. 0-32861  
 poly- $\gamma$ -benzyl-L-glutamate helices, optical activity 0-48113  
 poly-N-vinylcarbazole, soln., picosecond time-resolved fluoresc. by pulse radiolysis 0-28122  
 poly-thio-1-N,N-diethylaminomethylethylene, optically active samples, <sup>13</sup>C NMR spectra 0-28127  
 polyacetylene, dynamic nuclear polarisation of protons (*French*) 0-43217  
 polybutadiene, mol. motion in solid and soln., <sup>13</sup>C NMR relaxation meas. (*Japanese*) 0-2666  
 polyethylene, H bonding effects on skeletal optical and longitudinal acoustical modes 0-34914  
 polyglycine, IR spectra calc. for helix and  $\beta$  configs. 0-45853  
 polyisocyanides, solns., struct. and acidification 0-19915  
 polymer band structure, symposium contrib., Florida, USA (March 1979) 0-51946  
 polymer solns. and gels dynamic behaviour by light scatt. 0-55727  
 polystyrene, end group modified, chain dynamics studied by fluorescence depolarization 0-19724  
 polystyrene, molecular motion obs. during thermal polymerisation of styrene, PMR 0-3342  
 polystyrene film, Fourier-transformed IR photoacoustic spectra 0-34993  
 polytetrahydrofuran, H bonding effects on skeletal optical and longitudinal acoustical modes 0-34914  
 porphyrins, reson. Raman spectra, selection rules, normal coord. treatment 0-53175  
 protein model chain, aperiodic, electronic spectra, hopping cond. 0-5641  
 PTFE, peroxy radical labelled, temp. dependent rots., EPR obs. 0-28125  
 rhodopsin, picosecond spectroscopy obs. of primary events 0-56312  
 t-RNA, rot. relax. time, 10<sup>-9</sup>s range Fabry-Perot and photoelectron time of arrival method 0-21437  
 styrene, plasma polymerisation in glow discharge, thin film IR and free radical EPR obs. 0-2964  
 vinylidene fluoride-trifluorochloroethylene copolymers, <sup>19</sup>F NMR (*Russian*) 0-7181  
 (CD)<sub>x</sub>, polymer, heavily doped, IR spectra, vibronic intensity enhancement 0-28124  
 (CH)<sub>x</sub>, polymer, heavily doped, IR spectra, vibronic intensity enhancement 0-28124  
 (SN)<sub>x</sub>, radicals polymerisation to (SN)<sub>x</sub> in thin films, optical spectra 0-16656
- macromolecules**  
*see also DNA; macromolecular configurations; macromolecular dynamics; macromolecular energy levels; macromolecular spectra; polymers; proteins*  
 bioelectrets, occurrence of electret state and appl. in mol. biophysics and bioengineering 0-8007  
 biopolymer chains, intramol. reacts., enzyme catalysis appl., review 0-40953  
 biopolymer soln. heat capacity, conformational props. temp. depend. 0-8009  
 carbonic anhydrase, active site substrate binding, environmental effects, CNDO and SCF LCAO calcs. 0-8002  
 DNA-acridine dye complex, fluorescence studies 0-37921  
 dumbbell-shaped, alternating electric field light scatt. 0-1130  
 eukaryotic ribosomes, 2 step binding to brome mosaic virus RNA3 0-3580  
 heart cytosol, aspartate transaminase, electron density map interpretation 0-55990  
 interactions when introduced into liq. cryst. 0-30639  
 Kerr effect of charged dipolar macromolecules without condensed counterions in conducting solution 0-53171  
 ligand binding to macromolecules, allosteric and sequential models of cooperativity 0-12870  
 liquid, translational friction coeffs. of rigid, symm. top mols. 0-6003  
 myosin, interaction with adenosine 5'-diphosphate, intermolecular spin diffusion study 0-18951  
 myosin, interactions with HDO, intermolecular spin diffusion study 0-18951  
 net repulsive van der Waals forces between different particles, macromolecular, or biological cells in liqs., appls. 0-34274  
 nucleic-protein interactions in tobacco mosaic virus, spin label and fluorescence obs. 0-40949  
 solution, gel conc. and diffusivity at gelling determ. by ultrafiltration 0-21325
- Madelung constant** *see lattice energy*  
**magamps** *see magnetic amplifiers*  
**Magellanic Clouds** *see galaxies*  
**Maggi-Righi-Leduc effect** *see thermomagnetic effects*  
**magnesium**  
*see also nuclei with .....*  
 abundance gradient for gaseous Mg in NGC 7027 planetary nebula 0-41875  
 AES, backscattering factor, Monte Carlo method calc. 0-7449  
 atom, correlation energies, second-order, by variational-perturbation study 0-908  
 atom, electron scatt., effective pot. calcs. 0-53131



**magnesium continued**

- atom, electron scatt. cross sections, close coupling calc. with CI 0-43180  
 atom, free, electron-excited, K-Auger spectrum, including K-LM and K-MM transitions 0-5519  
 atom, optical beam foil spectra, relative level populations 0-23540  
 atom, SCF electron-gas local-spin-density model including correlation 0-9488  
 atomic vibr. and fermion behaviour of HCP metals 0-6474  
 atoms, cooling to broad band reson. light press. 0-48835  
 Auger electron prod. by  $\text{Ne}^+$  bombard., origin of Ne Auger peaks (French) 0-7461  
 Auger electron prod. by  $\text{Ne}^+$  bombard. 0-7460  
 cluster, multibody expansions, convergence 0-23594  
 cold rolling texture development 0-25720  
 discharge, hollow cathode, excitation mechanisms of triplet state atoms and decay obs. 0-44015  
 dislocation structure, after US deform. (Russian) 0-29027  
 film, defect energy distrib., elec. resist. meas. during annealing 0-54808  
 galactic cosmic rays, Ne, Mg and Si isotopes high resolution meas. 0-51631  
 GK-type dwarf stars, Mg isotopic abundances 0-51757  
 grain boundary struct., Kikuchi electron diffr. obs. 0-15116  
 graphite, spheroidal, presence of magnesium studied with electron probe microanalyser (Ukrainian) 0-26072  
 HCP metals, K-emission valence bands, structure and bonding 0-7438  
 ions, foil-excited, EUV spectrum 0-42976  
 $K\alpha_1$  and  $K\alpha_2$  wavelengths 0-50464  
 K $\alpha$  radiation, X-ray photoelectron spectroscopy resolution 0-18888  
 nitridation in HF discharge, temp. effect 0-3399  
 Orion nebula, C and Mg abundances from UV spectrum 0-41882  
 partial molar thermodynamic data from EMF and calorimetric meas. of Mg-In liquid solns. 0-55359  
 phonon density of states determ. from heat capacity (Russian) 0-29131  
 photoemission theory, book contrib. 0-16159  
 plasmon-loss intensities in XPS, EELS and Auger spectra 0-10902  
 polycrystals with axial texture, heterogeneity of props. (Russian) 0-29192  
 pure, Bordoni relax. behaviour after plastic deformation 0-20997  
 rolling texture formation, computer simulation in HCP and orthorhombic metals 0-3095  
 shock wave compression, reduced Hugoniot curve and eqn. of state (Chinese) 0-44259  
 soft X-ray emission and absorpt. edges, self-absorpt. studies 0-40183  
 spectrochemical analysis of biological solns. using wall stabilised arc source 0-41343  
 steel fibre reinforced Mg, fibre-matrix interfacial reactions 0-20043  
 surface, small angle scatt. of low energy  $\text{K}^+$  ions 0-20752  
 twin boundaries, computer simulation 0-39109  
 US hardening kinetics rel. to dislocations 0-50644  
 X-ray absorption and emission edges, one-electron and many-body effects 0-25484  
 X-ray emission spectra, K, double plasmon high energy satellite 0-11510  
 Al-oxide-Mg-Al, thin proximity effect sandwiches, spin-polarised tunnelling obs. 0-50007  
 B fibre reinforced Mg, exam. of fatigue props. and corrosion 0-11751  
 B fibre reinforced Mg, fibre-matrix interfacial reactions 0-20043  
 $\text{CaO:Mg}^{2+}$ , g-shift anal. 0-29313  
 GaAs:Mg, impurity conc. profile by glow-discharge optical spectroscopy 0-49258  
 GaAs:Mg, ion-implanted, capless anneal, effect of As partial press. 0-29038  
 GaP:Mg,Te, donor-acceptor pair luminesc., excitation spectroscopy 0-25440  
 Ge:Mg, diffusion and p-type cond. 0-6419  
 Ge:Mg, energy level behaviour, Hall coeff. and elec. cond. meas. 0-34396  
 Ge:Mg, positron annihilation angular distrib. 0-45165  
 InGaAsP-InP:Mg LEDs, for high-bit-rate optical communication systems 0-5823  
 KCl:Mg microcrystalline powders, role of Z-centres in stabilizing coloration 0-54227  
 KCl:Mg, thermolum. of Z-centre, optical absorpt. 0-55203  
 $\text{LiD:Mg}^{2+}$ , X-irrad., dielec. loss 0-55024  
 LiF:Mg, Maxwell-Wagner relax. induced by impurity clouds around dislocations, ionic thermocond. meas. 0-7281  
 LiF:Mg, shock waves in  $\langle 111 \rangle$  direction, elastic precursor amplitudes 0-54314  
 LiF:Mg, X-ray irrad., trapping processes, Z-centres and dipoles, two models 0-49222  
 LiF:Mg,Ti crystals,  $Z_1$ -centres, correlation of thermoluminescence and optical absorption 0-45154  
 Mg I,  $^3\text{F}^0$  Rydberg series, energy levels, multiconfigurational HF procedure 0-47882  
 Mg I,  $^3\text{p}$  triplet system, lifetime meas. 0-47946  
 Mg I, Mg II autoionisation state radiative decay (Russian) 0-5509  
 Mg I to Mg III, beam-foil excitation, Rydberg states, relative populations 0-14208  
 Mg II flux profiles in cool stars, obs. rel. to chromospheric radiative loss rates 0-36611  
 Mg IX, wavefunctions and oscill. strengths, CI calcs. 0-23317  
 Mg positron trapping and bound states 0-2367  
 Mg XII, resonance line, atomic parameters calc. for dielectronic satellite lines 0-42983  
 $\text{Mg}^+$ , Penning trap, laser cooling, optical spectrum from laser freq. sweep- ing 0-52916  
 $\text{Mg}^+$ , reson. line regularities in plasma Stark widths and shifts 0-43881  
 $\text{Mg}^{2+}$ , marine sediment content, western continental shelf, India 0-8289  
 $\text{Mg}^{2+}$ , beam-foil excited, spin orbit-forbidden X-ray transition obs. 0-23537  
 Mg/Cr ratio in achondrites and mesosiderite silicate fraction 0-51704  
 Mg-I cycle for thermochem. decomposition of  $\text{H}_2\text{O}$  for H prod. 0-35786  
 Mg-inert gas, Mg reson. lines broadening, absorpt. cross sections anal. 0-32642  
 $\text{Mg}+\text{F}_2$ , crossed beam chemilum., kinetics and mechanisms 0-21264  
 $\text{Mg}+\text{H}^+$ , electron capture and impact ionisation cross sections, CI calc. 0-23343  
 $\text{Mg}+\text{O}_2=\text{MgO}+\text{O}$ , shock-tube study of evap. and oxidation kinetics 0-16651  
 $\text{Mg}^++\text{He}(\text{Ne})(\text{Ar})$ ,  $\text{Mg}^+$  collision-induced alignment, reson.-line emission polaris. obs. 0-18912  
 $\text{Mg}^{6+}+\text{H}^+$ ,  $^3\text{P}$ , fine structure transitions 0-37864  
 $\text{Mg}_2$ , empirical pot. curves, Pade approximant calcs. 0-14184

**magnesium continued**

- $\text{Mg}_2^++\text{H}$ , electron capture by slow ions, pseudo-crossing 0-43176  
 $\text{Mg}_2\text{SiO}_4:\text{Mg}^{2+}$ , elec. field gradients, asymmetry parameters 0-54660  
 $\text{MgVII}$ , solar emission lines, density dependence 0-21963  
 $^{25}\text{Mg}$ ,  $^3\text{P}$ , and  $^1\text{P}$ , levels, quadrupole coupling consts. 0-23434  
 $^{28}\text{Mg}$ , intestinal absorpt. obs. in man 0-36217
- magnesium alloys**  
 see also magnesium compounds  
 Br.AZHNMTs 7-2.5-1.5-9 bronze, Mg-Al, type, fatigue and stress corrosion cracking, welding effects 0-3233  
 fatigue of alloy MA12, low temp. effect 0-55529  
 mischmetal-Co-Cu-Fe-Mg, mag. props. 0-35353  
 mischmetal-Co-Cu-Mg, mag. props. 0-35353  
 $\text{Ag}_3\text{Mg}$ , structure of ordered alloy, electron diffraction, kinematical vs. dynamical diffraction calc. 0-10530  
 $\text{Ag}_3\text{Mg}$ , two different types of long-period ordered alloys, characterisation by high resolu. electron microscopy 0-49181  
 Al-Cu-Mg, acoustic emission during tensile testing 0-7632  
 Al-Cu-Mg, aged, stress corrosion cracking in NaCl soln. 0-7709  
 Al-Cu-Mg, alloy 2124-T351, crack tip closure assessment by electronfractography 0-16427  
 Al-Cu-Mg, rolled plate fatigue charact. (Russian) 0-16437  
 Al-Cu-Mg, type 2036, deformation at ageing temp., effect on struct. and props. 0-7605  
 Al-Cu-Mg (2.6, 0.4 wt.%), Fe, Si, Mn and Ti addition effects on age-precipitation (Japanese) 0-20937  
 Al-Cu-Mg (4.1 wt.%), behaviour during ductile fracture, SEM (Rumanian) 0-21062  
 Al-Cu-Mg-Fe-Ni, Hiduminium RR58, crack propag. rates in air and salt soln. 0-21063  
 Al-Cu-Mg-Mn-Si-Fe, endurance with cyclic bending, effect of loading conditions 0-50724  
 Al-Cu-Mg-Mn-Si-Fe, subcritical crack growth under static plane stress 0-55528  
 Al-Cu-Mg-(Ag), effect of addition on fatigue microstructure relationships 0-40483  
 Al-Cu-Mn-Mg-Fe-Si, corrosive environment effect on fatigue crack growth rate 0-55584  
 Al-Cu(Zn, Ag, Mg, Si), intermediate precipitates, stability, X-ray, elec. resist. and hardness study 0-3063  
 Al-Mg, AMg6 alloys, effect of chem. comp. on strength and ductility at low temps. 0-3148  
 Al-Mg, acoustic emission during tensile testing 0-7632  
 Al-Mg, ageing process, effects of Ag additions and pressure (Russian) 0-45321  
 Al-Mg, cast, chilled zone composition and thickness obs. (Japanese) 0-7541  
 Al-Mg, creep behaviour in broad stress interval at 623K 0-30044  
 Al-Mg, determ. of distortion field, induced by substitutional defect 0-44536  
 Al-Mg, oxidation induced stresses, dislocation network form., HVEM obs 0-14978  
 Al-Mg, subcritical crack growth under static plane stress 0-55528  
 Al-Mg, type AMg6, cryogenic welded vessels, structural strength 0-16477  
 Al-Mg, vapour press. temp. depend., 1104 to 1637K 0-24576  
 Al-Mg (1 wt.%), behaviour during ductile fracture, SEM (Rumanian) 0-21062  
 Al-Mg (13 wt.%), aged single crystals, small angle neutron scattering 0-1961  
 Al-Mg (2 wt.%), steady creep characts., precip. effect 0-35189  
 Al-Mg (7wt.%), corrosion fatigue crack propag. 0-30145  
 Al-Mg alloy, AL24M, decomp. kinetics and ageing mechanism (Russian) 0-45269  
 Al-Mg alloy, crystallisation front form. props., casting in EM field (Russian) 0-55384  
 Al-Mg foil, alloying effect on strength characts. and weldability 0-55475  
 Al-Mg solid solns., decomposition studied by ultrasonic meas. of elastic props. 0-35184  
 Al-Mg spherical shell with reinforced holes, local stability 0-50686  
 Al-Mg/ $\text{Al}_2\text{O}_3$  composites, interface phase, Auger and electron diffr. study 0-25646  
 Al-Mg:Si (1 wt.%), precipitation reactions 0-11652  
 Al-Mg:Si(1.42 wt.%), aged, dislocation structs. caused by plastic deformation 0-25786  
 Al-Mg-Li alloy 01420, riveted, low-cycle fatigue strength 0-30097  
 Al-Mg-Si, DTA exam. after small and medium deform. 0-21002  
 Al-Mg-Si, dil. alloy, Mn additions and heat treatment effect on  $\beta-\alpha$  transformation 0-7566  
 Al-Mg-Si, heterogeneous precipitation studies using differential scanning calorimetry 0-3062  
 Al-Mg-Si, nucleation and precipitation growth on dislocations, electron microscope studies 0-3064  
 Al-Mg-Si core, deformation behaviour contrib. in rod drawing (German) 0-11684  
 Al-Mg-Zn, granulated, degassing atm. effect on mech. props. of semifinished products 0-7720  
 Al-Mg-Zn,  $\text{O}_2^+$  ion bombard., SIMS and photon emission spectra, local thermodynamic equilib. model 0-20751  
 Al-Mg-Zn alloy 7179-T651, reduced ductility under tensile after exposure to water 0-11835  
 Al-Mg-Zn alloys, liq./solid phase equilibria determ. (German) 0-50601  
 Al-Mg-(Ag), effect of addition on fatigue microstructure relationships 0-40483  
 Al-Si-Cu-Mg-Ni, piston, depend. between min. creep rate and time of beginning of secondary creep (Czech) 0-35267  
 Al-Zn-Cu-Mg (V95T1), subcritical crack growth under static plane stress 0-55528  
 Al-Zn-Mg, acoustic emission meas. during tensile testing, reproducibility of results 0-50782  
 Al-Zn-Mg, decomp. kinetics and ageing mechanism (Russian) 0-45269  
 Al-Zn-Mg, Guinier-Preston zones, comp. and contrib. to elec. resist. 0-16316  
 Al-Zn-Mg, plastic deform. influence on structural transform. and mechanical props. (Russian) 0-7623  
 Al-Zn-Mg, polygonized struct. in extrusions, thermal stability and mech. props. 0-50659  
 Al-Zn-Mg, stress conversion cracking based on micromech. surface reactions 0-7716  
 Al-Zn-Mg, type 7075, strain rate effects on H embrittlement 0-3190



## magnesium alloys continued

- Al-Zn-Mg, welded section stress in rolled plate edges, mechanical surface treatment and environment effects 0-21193  
 Al-Zn-Mg (2.1, 1.3 wt.%), single crystals, fatigued age-hardenable, dislocation structure (*German*) 0-54247  
 Al-Zn-Mg (4.5, 2 to 3 at.%) solid state reactions by interrupted continuous heating 0-25737  
 Al-Zn-Mg (4.5 at.%, 2 or 3 at.%), decomposition behaviour during continuous cooling, XSAS and TEM examination 0-16264  
 Al-Zn-Mg (4.5 at.%, 2 to 3 at.%), decomp. behaviour during continuous heating 0-29922  
 Al-Zn-Mg (4.8, 1.2 wt.%), quenched, Guinier Preston zones formation 0-45273  
 Al-Zn-Mg (5.9, 2.9 wt.%), ageing effects on microstruct. 0-16306  
 Al-Zn-Mg (6.3 wt.%), hydrogen embrittlement and trapping 0-55490  
 Al-Zn-Mg alloys, extra-resistivity of coherent precipitates calc. using X-ray small angle scattering intensities 0-3050  
 Al-Zn-Mg alloys stress corrosion 0-35395  
 Al-Zn-Mg plasma sputtered, mech. props. rel. to heat treatment (*Russian*) 0-40387  
 Al-Zn-Mg powder, selected-area electron diffraction patterns 0-50642  
 Al-Zn-Mg-B fibre reinforced composite, packet rolling, thermodeform. process parameters (*Russian*) 0-55433  
 Al-Zn-Mg-Co, crazing tendency (*Russian*) 0-30068  
 Al-Zn-Mg-Cu, age hardened, effect of strain rate, temp. and environment on ductility 0-45368  
 Al-Zn-Mg-Cu, type 7075, microstruct. role in hydrogen assisted fracture 0-30091  
 Al-Zn-Mg-Cu (6.76, 2.37, 1.80 wt.%), cyclic SCC in salt water (*Japanese*) 0-45435  
 Al-Zn-Mg-Cu age-hardened alloys, fatigue crack propagation rel. to grain size in vac. and NaCl soln. 0-16538  
 Al-Zn-Mg-Cu-Co (6.5, 2.5, 1.5, 0.4 wt.%), fatigue crack propag. 0-55521  
 Al-Zn-Mg-Cu-Co-Fe-Si, powder alloy, fatigue crack tip plasticity, from load interactions 0-21066  
 Al-Zn-Mg-(Zr) alloy, microstruct. effect on fatigue crack growth 0-3164  
 Al<sub>2</sub>Mg<sub>3</sub>Mn, H impurity detection by <sup>1</sup>H(<sup>15</sup>N,  $\alpha$ ) reaction 0-55767  
 Au-Mg, charge transfer, Mossbauer effect <sup>197</sup>Au isomer shifts, XPS valence-band spectra 0-2676  
 Au-Mg, high resolution electron microscope and electron diffraction investigation, obs. of Au<sub>13</sub>Mg<sub>4</sub> monoclinic phase 0-1968  
 B fibre reinforced Al-Mg, calc. of thermodynamic interaction potential between B fibre and matrix 0-11627  
 B fibre reinforced Al-Mg, heat treatment effect on struct., tensile strength 0-55487  
 Ba-Mg, liq. alloys, thermodynamic activities determ. 0-50604  
 CC Al-Zn-Mg (4.5, 1(2)(3) at.%), decomposition during ageing, preageing and cooling rate influence 0-20938  
 Ca-Mg, liq. alloys, thermodynamic activities determ. using modified Ruff method (*German*) 0-11631  
 Cd-Mg, mag. susceptibility near 2<sup>1/2</sup>th order electron transition, non-linear magnetisation anal. (*Russian*) 0-44859  
 Cd<sub>1-x</sub>Mg<sub>x</sub>, magnetic susceptibility anisotropy, press. effects, electronic phase transitions (*Russian*) 0-54869  
 CeMg, V(Cr)(Mn)(Fe)(Co), hydriding and appl. in H<sub>2</sub> storage 0-51009  
 Cu-Be-Ni-Ti-Mg bronze, alloying element influence on minimum thermo EMF, cold working (*Russian*) 0-34426  
 EuMg<sub>3</sub>, Mossbauer effect, effective moments, mag. ordering temp. and isomer shifts 0-34833  
 Eu<sub>2</sub>Mg<sub>17</sub>, Mossbauer effect, effective moments, mag. ordering temp. and isomer shifts 0-34833  
 Fe, cast, spheroidizing effect of Mg and Ce modifiers 0-35193  
 Fe-Mg, cast ferrite-based, graphite nucleation on surface (*Russian*) 0-40360  
 In-Mg, ordered equiatomic, lattice specific heat meas., Debye temp., superconducting transition 0-54396  
 Li-Al electrode, Mg surface additives effect on performance 0-40698  
 Mg/Mg<sub>2</sub>Cu eutectic, hydriding and dehydriding kinetics obs. by press. sweep method 0-35765  
 Mg-Ag-Cu, phase comp. in Mg-rich region (*Russian*) 0-40331  
 Mg-Al (0.8 wt.%), grain-boundary sliding component in high temp. fatigue 0-50706  
 Mg-Al single crystal growth, specimen for tensile testing in corrosive medium (*Russian*) 0-20774  
 Mg-Al-Zn (9wt.%Al), sand cast, preferred orientation and mechanical props. (*Japanese*) 0-20979  
 Mg-Bi melt; X-ray and neutron diffraction, conc. depend., correl. number and nearest neighbours 0-49091  
 Mg-Cd, single crystals, temp. depend. of crit. resolved shear stress (*Czech*) 0-29112  
 Mg-Ce, workability, aging characts. and tensile strength 0-55416  
 Mg-Fe film, defect energy distrib., elec. resist. meas. during annealing 0-54808  
 Mg-Ga-In(Tl) and Mg-In-Tl, phase diagrams and electrochem. props. (*Russian*) 0-40330  
 Mg-Gd(Ho), dil., magnetoresist., anomalous Hall effect 0-15502  
 Mg-In liquid solns., EMF and calorimetric meas. 0-55359  
 Mg-La, workability, aging characts. and tensile strength 0-55416  
 Mg-Li-Al (31, 1 at.%), heat treated, precipitation 0-40364  
 Mg-Li-Ga(Ge)(In)(Ti)(Pb), phase diagram, isothermal cross section (*Russian*) 0-20900  
 Mg-Mg<sub>17</sub>Y<sub>13</sub>, high temp. hydrides for vehicular H storage 0-45793  
 Mg-Mg<sub>2</sub>Ni, high temp. hydrides for vehicular H storage 0-45793  
 Mg-Mg<sub>2</sub>Ni eutectic alloy and Mg<sub>2</sub>Ni, catalytic effect in hydrogenation, surface analysis 0-30283  
 Mg-Ni-W-Co-Al-Cr alloy KhN56VMKYu, Al effect on excess Mg phase 0-29926  
 Mg-rare earth dilute alloy, mag. susceptibility and magnetisation 0-15689  
 Mg-Sm, phase diagram and mech. props. (*Russian*) 0-20892  
 Mg-Sr, liq. alloys, thermodynamic activities determ. 0-50604  
 Mg-Tb, (up to 45 wt.%), phase diagram, and mech. props. 0-16277  
 Mg-Y-Al alloys, phase equilib. (*Russian*) 0-20890  
 Mg-Y-Cd, phase equilibria and mech. props. (*Russian*) 0-20894  
 Mg-Y-Zn alloys, phase equilib. (*Russian*) 0-16271  
 Mg-Y-Zn-Nd-Cd alloys, influence of Zr addition on struct. and mech. props. (*Russian*) 0-40370  
 Mg-Yb, dil., Kondo scatt. from Yb, low temp. elec. resist. meas. 0-44578  
 Mg<sub>2</sub> Ni metal hydrides, numerical physical property data for H storage 0-40929

## magnesium alloys continued

- Mg<sub>2</sub>Cd, order-disorder transformation kinetics 0-2138  
 Mg<sub>2</sub>Cu, industrial hydride reservoir, characts., technological aspects 0-45792  
 Mg(Cu<sub>0.535</sub>Al<sub>0.465</sub>)<sub>2</sub>, 2D lattice images of Friedel-Laves phase and defect type 0-24324  
 MgCu<sub>2-x</sub>Ni<sub>x</sub>, X-ray and neutron diffraction investigation of Laves phases of MgCu<sub>2</sub>-type (*German*) 0-15050  
 MgCu<sub>2-x</sub>Zn<sub>x</sub>, X-ray and neutron diffraction investigation of Laves phases of MgCu<sub>2</sub>-type (*German*) 0-15050  
 Mg<sub>1-x</sub>Er<sub>x</sub>, dil., cryst. field interactions, neutron scatt. spectra 0-50048  
 Mg<sub>2</sub>(Ni,Cu) cubic metal binary alloys for H energy storage 0-45787  
 MgNi<sub>2-x</sub>Zn<sub>x</sub>, X-ray and neutron diffraction investigation of Laves phases of MgCu<sub>2</sub>-type (*German*) 0-15050  
 MgSi<sub>2</sub>, laser irradi. induced form., cryst. microstruct. 0-35011  
 Nb/Cu-Sn-Mg, superconductor, effect of Mg addition to Cu-Sn matrix 0-25028  
 SiC fibre reinforced Al-Mg, heat treatment effect on struct., tensile strength 0-55487  
 Tb-Mg, mag. ordering temps., susceptibility meas. 0-25136  
 U/Magnox fuel element materials performance 0-47580

## magnesium compounds

- see also magnesium alloys  
 MgO:Cr<sup>3+</sup>, single crystal, ESR linewidth 0-29605  
 MgO, high temperature interactions with Re 0-16665  
 MgO, temp. depend. of int. angles for proton axial channelling 0-10586  
 MgO-ZrO<sub>2</sub> ceramic reinforced with filamentary crystals, mech. and thermal props. 0-45262  
 MgSiO<sub>3</sub>, Mg<sub>2</sub>SiO<sub>4</sub>, vapour condensed, mid IR optical props. 0-31337  
 periclase-spinel refractories, phase conversions up to 1720°C 0-25670  
 platino-oxalate, one-dimens. conductors, prep., struct. and elec. cond. 0-24900  
 symmetry anal. in neutron diffraction studies 0-25091  
 talc, <sup>57</sup>Fe Mossbauer analysis 0-40006  
 vermiculite, firing temp. depend. of Mossbauer parameters 0-15837  
 AlMgB<sub>14</sub>, prep. and electrothermal props. 0-20863  
 $\beta$ -Al<sub>2</sub>O<sub>3</sub>:MgO, strength and delayed fracture behaviour 0-35290  
 $\beta$ -Al<sub>2</sub>O<sub>3</sub>-MgO ceramic, formation and structure of atomic scale cracks 0-45395  
 Al<sub>2</sub>O<sub>3</sub>-SiO<sub>2</sub>-Fe<sub>2</sub>O<sub>3</sub>-CaO-MgO-TiO<sub>2</sub>, refractory, corrosion and mech. behaviour correlations 0-40563  
 BaGeO<sub>3</sub>-(0.25MgF<sub>2</sub>·0.75YF<sub>3</sub>)-Ga<sub>2</sub>O<sub>3</sub> glass, synthesis and props. 0-25648  
 BaGeO<sub>3</sub>-CaF<sub>2</sub>MgF<sub>2</sub>-Ca<sub>2</sub>Al<sub>2</sub>GeO<sub>7</sub>(CaTiGeO<sub>5</sub>) systems, glass forming and props. 0-19717  
 BaO-Al<sub>2</sub>O<sub>3</sub>-GeO<sub>2</sub>-MF<sub>2</sub> (M=0.45 CaF<sub>2</sub>+0.55MgF<sub>2</sub>), MgF<sub>2</sub> and CaF<sub>2</sub> effect on physicochem. props. 0-34876  
 BaO-PbO-GeO<sub>2</sub>-MF<sub>2</sub> (M=0.45CaF<sub>2</sub>+0.55MgF<sub>2</sub>), MgF<sub>2</sub> and CaF<sub>2</sub> effect on physicochem. props. 0-34876  
 Ba(PO<sub>3</sub>)<sub>2</sub>-MgF<sub>2</sub>, IR absorption spectra exam. of hydrolytic stability 0-39291  
 Ca-Mg-Zr combustion sensor, pipe-form ceramics appl. (*Japanese*) 0-55761  
 CaF, excited state spectroscopic consts., dissociation, chemilum. obs. 0-21264  
 CaMgSiO<sub>4</sub> (monticellite), high-pressure phase transforms. and implications for upper mantle mineralogy 0-17255  
 CaMgSi<sub>2</sub>O<sub>6</sub>, diopside, elasticity, Brillouin scatt. meas. 0-6454  
 CaO-MgO-Al<sub>2</sub>O<sub>3</sub>-SiO<sub>2</sub>, quartz sand-dolomite-magnesia-clay based glasses, crystn. 0-20915  
 CaO-MgO-Al<sub>2</sub>O<sub>3</sub>-SiO<sub>2</sub>, glass formation, at molar ratio CaO: MgO=1 (*Russian*) 0-39269  
 CaO-MgO-ZrO<sub>2</sub>-SiO<sub>2</sub> refractories, phase diagram 0-11634  
 CaO-SiO<sub>2</sub>-NiO-MgO glass melt, interaction of NiO and MgO, elec. cond. and IR spectra obs. (*Japanese*) 0-24632  
 Ca<sub>2</sub>SiO<sub>4</sub>-MgO, conditions and mechanism in crystal-chemical stabilisation of unstable phases 0-39302  
 CaY<sub>2</sub>Mg<sub>2</sub>Ge<sub>2</sub>O<sub>12</sub>Nd<sup>3+</sup>, optical absorpt. and fluoresc. intensities 0-29793  
 Co<sub>2</sub>Mg<sub>1-x</sub>O, solid solution, EPR of Co<sup>2+</sup> (*Russian*) 0-11251  
 CoO-MgO-Cr<sub>2</sub>O<sub>3</sub>-Fe<sub>2</sub>O<sub>3</sub>-TiO<sub>2</sub>, form. and colour of spinel solid soln. (*Japanese*) 0-16059  
 Cr-Ti/MgO-NbC(TaC) dispersion-strengthened, high temp. wear and oxidation resist. 0-25877  
 Cu-MgO, dispersion hardened alloys, prep. and props. 0-40291  
 (Fe,Mg)O<sub>4</sub>, magnetostriiction calcs. (*Dutch*) 0-2619  
 Fe<sub>2</sub>Mg<sub>1-x</sub>Cl<sub>2</sub>, Ising metamagnet, dilute, tricritical point calcs. 0-50099  
 Fe<sub>3-x</sub>Mg<sub>x</sub>O<sub>4</sub>, Verwey transition, Mossbauer study 0-39942  
 Fe<sub>0.55</sub>Mg<sub>0.45</sub>SiO<sub>3</sub>, orthopyroxene, electron irradi. effects, Mossbauer study 0-40016  
 Fe<sub>2(1-y)</sub>Mg<sub>1+y</sub>Ti<sub>2</sub>O<sub>4</sub>, Mossbauer spectra anal., model 0-20560  
 La<sub>1-x</sub>Mg<sub>x</sub>CrO<sub>3</sub>, electronic struct. study by XPS 0-25518  
 La<sub>2</sub>Mg<sub>3</sub>(NO<sub>3</sub>)<sub>12</sub>·24H<sub>2</sub>O:Nd<sup>3+</sup>, polarised neutron diffraction from dynamically and statically polarised protons 0-44078  
 La<sub>2</sub>Mg<sub>3</sub>(NO<sub>3</sub>)<sub>12</sub>·24H<sub>2</sub>O:Nd<sup>3+</sup>, proton raser, self-radiating nuclear spin system (*German*) 0-53298  
 LiF-NaPO<sub>3</sub>-MgF<sub>2</sub> glasses, IR spectroscopy study 0-16042  
 100(Li<sub>2</sub>O·2SiO<sub>2</sub>)·3Na<sub>2</sub>O, directionally solidified, thermal and mech. props. (*Japanese*) 0-16295  
 (Mg, Fe)SiO<sub>3</sub>, orthopyroxenes, cation distrib., electronic and Mossbauer spectra 0-7370  
 Mg complex, bis-pyridyl-Mg-tetrabenz-porphyrin, disagreement with diffuse interstellar bands 0-56905  
 Mg F<sub>2</sub>, vibr. anal., kinetic consts. method 0-18838  
 Mg-Al spinel, non-stoichiometric, climb dissociation of network dislocations 0-2031  
 Mg-Al spinel ceramics, mech. strength, non-stoichiometry and microstruct. (*Japanese*) 0-21054  
 Mg-Fe-O ferrite system, thermodynamic stability, dissociation and phase relations (*Japanese*) 0-55378  
 Mg(AlH<sub>4</sub>)<sub>2</sub>, prep., thermal decomposition, molar heat capacity, heat of form. 0-3325  
 MgAl<sub>2</sub>O<sub>4</sub>, microplasticity at room temp., dislocations, TEM study 0-19805  
 MgAl<sub>2</sub>O<sub>4</sub> spinel, single crystal, fracture behaviour, temp. depend. 0-40503  
 MgAl<sub>2</sub>O<sub>4</sub> spinel, space group 0-28937  
 MgAl<sub>2</sub>O<sub>4</sub> transparent ceramic, transmittance, grain size and dopant effects (*Japanese*) 0-19083  
 (MgAl<sub>2</sub>O<sub>4</sub>)<sub>x</sub>(AMn<sub>2</sub>O<sub>4</sub>)<sub>1-x</sub>, A=Mn,Zn,Cd, 0<x<1, mixed oxide spinels, chemical shifts of Mn K-absorpt. edge 0-29828  
 MgB<sub>2</sub>H<sub>2</sub>·10H<sub>2</sub>O, struct. dehydration, intermediate phases and thermooxidative degradation 0-33951



## magnesium compounds continued

- MgB<sub>2</sub>O<sub>3</sub>·5H<sub>2</sub>O = Mg[B<sub>2</sub>O<sub>3</sub>(OH)<sub>2</sub>]<sub>2</sub>, cryst. synthesis and struct., bonding, X-ray study 0-33973
- MgBSi<sub>2</sub>O<sub>6</sub>, B=Mg, Fe<sup>3+</sup>, Al, pyroxenes, order-disorder interpretation 0-38987
- MgCl<sub>2</sub>, enthalpies of formation and of soln. 0-7844
- MgCl<sub>2</sub>, mol. struct. parameters, average values, geom. config., gaseous electron diff. obs. 0-37904
- MgCl<sub>2</sub> solution, stainless steel (304) stress corrosion cracks initiation (Japanese) 0-10593
- MgCl<sub>2</sub>:Co, spectroscopic studies of interactions 0-29769
- MgCl<sub>2</sub>:TiCl<sub>4</sub>, high activity catalyst for polyethylene, struct. and mechanism investig. 0-11951
- MgCl<sub>2</sub>·nH<sub>2</sub>O, cryst. struct. (German) 0-1987
- MgF, excited state spectroscopic consts., dissociation, chemilum. obs. 0-21264
- MgF<sub>2</sub>, band struct., tight-binding calc. 0-24796
- MgF<sub>2</sub>, CW CO<sub>2</sub> laser deposited dielect. thin film, optical and struct. props. 0-7506
- MgF<sub>2</sub> coated thick Fe films, surface magnetism 0-7196
- MgF<sub>2</sub>, complex dielec. const. at audio freqs., 5.5 to 380K 0-25272
- MgF<sub>2</sub>, cryst., atomic vibr., anisotropy parameters, bonding 0-54195
- MgF<sub>2</sub>, electronic struct. and densities of states, tight-binding calcs. 0-15447
- MgF<sub>2</sub> laser coating, UV damage obs. 0-33056
- MgF<sub>2</sub>, nonactivated, X-ray luminesc. 0-2832
- MgF<sub>2</sub>, transparent, multiphonon IR absorption spectra 0-7348
- MgF<sub>2</sub>, vacuum deposited, destruction props. obs., suitability for integrated optics assessment (Slovak) 0-33224
- MgF<sub>2</sub>, X-ray luminesc. polarisation 0-11462
- MgF<sub>2</sub>:Co<sup>2+</sup>(Mn<sup>2+</sup>), Coulomb and exchange interaction consts. optical spectra line assignment, new technique 0-45124
- MgF<sub>2</sub>:Co(Ni), laser, broadly tunable CW operation, output powers, optical pumping 0-32995
- MgF<sub>2</sub>-Ag (Al)(Cu)(Au) film substrate tunable external-reflector retarder, computer based anal. 0-53407
- MgF<sub>2</sub>-ZnS multilayers, high vacuum deposition for cold light mirror prod. (German) 0-53486
- MgFe<sub>2</sub>O<sub>4</sub>, epilayer, perpendicular anisotropy 0-39769
- MgFe<sub>2</sub>O<sub>4</sub>-Co<sub>2</sub>O<sub>3</sub> solid soln. spinels, domain wall formation inhibition, effect on bulk mag. props. 0-11220
- MgGeO<sub>3</sub>, HP phase transform. 0-19941
- MgGeO<sub>4</sub>, reduction processes by C, kinetic analysis, reaction products (Russian) 0-55644
- MgH<sup>+</sup>, CI pot. curves and cross sections for lowest singlet states 0-23343
- MgH(D), spectra in 230-235 nm region 0-48012
- MgHPO<sub>4</sub>·3H<sub>2</sub>O, newberyite, struct. refinement and H bonding 0-15058
- MgIn<sub>2</sub>S<sub>4</sub>, cation distrib. and deform. parameter using Bertaut, Furuhashi and Baltzar methods 0-15041
- MgIn<sub>2</sub>S<sub>4</sub>:Co(Cr), EPR powder spectra 0-25197
- (MgMn<sub>2</sub>O<sub>4</sub>)<sub>1-x</sub>(MgAl<sub>2</sub>O<sub>4</sub>)<sub>x</sub>, 0 < x < 1, mixed oxide spinels, chemical shifts of Mn K-absorpt. edge 0-29828
- Mg<sub>1-x</sub>Mn<sub>x</sub>Te<sub>2</sub>, random dil. antiferromagnet, mag. props. 0-54870
- MgMnZn ferrite, ultrafine powder, prod. by cryochemical, freeze drying, spray drying or soln. techniques 0-55336
- Mg(NH<sub>4</sub>)<sub>2</sub>(SO<sub>4</sub>)<sub>2</sub>·6H<sub>2</sub>O:Cr<sub>2</sub>O<sub>7</sub><sup>2-</sup>, optical absorption study, Cr<sub>2</sub>O<sub>7</sub><sup>2-</sup> and CrO<sub>4</sub><sup>2-</sup> centres 0-55128
- Mg(NO<sub>3</sub>)<sub>2</sub>·6H<sub>2</sub>O, crystal structure changes due to substitution of Mg<sup>2+</sup> by Co<sup>2+</sup> or Ni<sup>2+</sup> (German) 0-24428
- MgNbF<sub>7</sub>, polymorphism, X-ray powder diff. data (French) 0-19779
- MgO (100), chain method of LEED/MEED intensity anal. 0-20018
- MgO (100), surface struct., LEED study 0-39396
- MgO, adsorbed <sup>3</sup>He, nucl. mag. relax. props. 0-49457
- MgO, adsorpt. of CO, IR spectra 0-2751
- MgO, adsorption of Cs and Li, AES, LEED, work function, and secondary electron emission meas. 0-44407
- MgO and MgO-dolomite, crack detection caused by thermal shock, AE technique (Japanese) 0-21248
- MgO, chemisorption of O<sub>2</sub>, adsorboluminescence from surface F-centres 0-20723
- MgO coated thick Fe films, surface magnetism 0-7196
- MgO, coating on Fe film, Mossbauer study 0-7221
- MgO, compressive stress-strain behaviour at high temps. 0-25774
- MgO, crack propagation during in-situ deform., plastic zone formation 0-16468
- MgO, critical voltage effect, effect of temp. (French) 0-10463
- MgO, crystal, electron emission under uniaxial compression 0-7483
- MgO crystals, dislocation core energy from etching data 0-39100
- MgO crystals, etching and polishing, inorganic or organic acids effect 0-40573
- MgO crystals, etching behaviour rel. to chem. reactions 0-3229
- MgO, crystals, adsorption processes in selective etching 0-39098
- MgO, dielec. const., 5.5 to 400K 0-50249
- MgO dielectric detector characteristics 0-27898
- MgO, dielectric polarisation calcs., microscopic local fields 0-20582
- MgO, displacement function calc. 0-34047
- MgO, dissolution mechanism in acids 0-39296
- MgO, effect on props. of PbO containing cryst. glass 0-24637
- MgO, effect on viscosity of PbO containing crystal glasses 0-19973
- MgO, electron irradiated, luminescence, radiative recombination kinetics 0-7421
- MgO, electrophoretic deposition on stainless steel mandrel 0-11580
- MgO, exciton luminesc. spectrum, fine struct. 0-20715
- MgO, F centre luminesc., effects of uniaxial stress and ODMR 0-20690
- MgO, film, dissociation under heat and electron bombardment 0-7834
- MgO film, graphitic C detected by surface Raman spectra 0-2297
- MgO, fusion cast compounds, crystn., microstructures rel. to conditions 0-11638
- MgO, GCFR shielding material, anal. of shielding effectiveness 0-47746
- MgO, γ-irrad. polycryst., isothermal luminesc., recomb. of electron from F<sub>2</sub><sup>+</sup> centres 0-34985
- MgO, hot-pressed, elasticity props. of polycrystals and single crystals 0-54301
- MgO, IR absorpt. spectra, 2300K, elec. furnace appl. (French) 0-27311
- MgO, interference electron microscopy using electron holography 0-32929
- MgO, lattice defects., calcination temp. effect 0-15091
- MgO, local field, microscopic electronic polarisation 0-25283
- MgO, neutron irradiated, Huang diffuse scattering of neutrons 0-10544
- MgO, plasmachemical synthesis, oxidised from metals, exam. of props. 0-2984

## magnesium compounds continued

- MgO polycrystals, ultrafine-grained, creep microstruct. 0-35246
- MgO powder, active, sintering 0-20870
- MgO powders, hot pressing, mechanisms 0-40300
- MgO, precipitate morphology, strain energy effects 0-40358
- MgO, red and near UV bands calc., rel. to sunspot spectra 0-12736
- MgO single cryst., γ-irrad. in presence of O<sub>2</sub>, H<sub>2</sub> and H<sub>2</sub>O adsorbates, thermostimulated surface cond. 0-34499
- MgO single cryst., internal stresses and dislocation mobility, stress relaxation method 0-6413
- MgO, single cryst., order hardening by large precipitated vol. fraction of spinel particles 0-3085
- MgO, single crystal, thermal and optical stimulation processes of V-centres (Japanese) 0-11485
- MgO single crystals, crack formation process, micro-deformation and fracture (Japanese) 0-24530
- MgO, sintering, effect of Ca compound additions (Japanese) 0-55340
- MgO, solid solubility of Se<sub>2</sub>O<sub>3</sub>, Al<sub>2</sub>O<sub>3</sub>, Cr<sub>2</sub>O<sub>3</sub>, SiO<sub>2</sub> and ZrO<sub>2</sub> 0-15247
- MgO surface, mobile (CO<sub>2</sub>-O<sub>2</sub>)<sup>-</sup> radical, ESR spectrum 0-43076
- MgO, tensile and compressive strengths of fine powder bed (Japanese) 0-25780
- MgO, valence electron distrib., pseudopotential calcs. 0-2335
- MgO, X-ray determ. of electron density distrib., atomic scatt. factors 0-15078
- MgO:Be epitaxial layers, vacuum UV luminescence 0-11480
- MgO:CaO(SiO<sub>2</sub>)(B<sub>2</sub>O<sub>3</sub>)(Cr<sub>2</sub>O<sub>3</sub>), effective of impurities on high temp. creep 0-40455
- MgO:Cr, Co, optical and ESR studies 0-50175
- MgO:Cr<sup>3+</sup> (Mn<sup>2+</sup>) spin Hamiltonian parameters, lattice expansion and vibr. effects 0-24851
- MgO:Cr<sup>3+</sup>(V<sup>2+</sup>), <sup>4</sup>A<sub>2g</sub>→<sup>4</sup>T<sub>2g</sub> spectra, new expt. results 0-11441
- MgO:Li, enhancement of elec. cond. by oxidation 0-44600
- MgO:Li, internal friction, mech. and dielec. relax. (German) 0-34135
- MgO:Mn<sup>2+</sup>, clustering of mag. ions, study method 0-11155
- MgO:Ni<sup>2+</sup> laser system, optical parameters 0-48260
- MgO:Pt<sup>3+</sup>, Jahn-Teller effect in EPR spectrum 0-7160
- MgO:S, cathodoluminesc. spectrum (Russian) 0-55197
- MgO/Ni-Cr (80, 20 wt.%) cermets, sintered, elec. resist. temp. effect 0-3206
- MgO-Al<sub>2</sub>O<sub>3</sub>-P<sub>2</sub>O<sub>5</sub> irradiated electret glasses, relax. of external field intensity on heating 0-25282
- MgO-Al<sub>2</sub>O<sub>3</sub>-SiO<sub>2</sub>, glass ceramics, phase transformation processes 0-3025
- MgO-Al<sub>2</sub>O<sub>3</sub>-SiO<sub>2</sub>, glass ceramic, structure and props. (German) 0-38927
- MgO-Al<sub>2</sub>O<sub>3</sub>-SiO<sub>2</sub> based cordierite glass-ceramic, strength and thermal shock, surface treatment effect 0-25884
- MgO-Al<sub>2</sub>O<sub>3</sub>-SiO<sub>2</sub> glass/polysulphone adhesive failure, ISS and SIMS obs. 0-55626
- MgO-Al<sub>2</sub>O<sub>3</sub>-SiO<sub>2</sub>:ZrO<sub>2</sub>, TiO<sub>2</sub>, glass, phase separation (German) 0-38932
- MgO-Al<sub>2</sub>O<sub>3</sub>-TiO<sub>2</sub>-SiO<sub>2</sub>, glass formation, structure of cations (Russian) 0-38933
- MgO-C in melts, corrosion resist., rel. to oxidation, porosity, content 0-40578
- MgO-CaMgSiO<sub>4</sub>-(Al<sub>0.5</sub>Cr<sub>0.5</sub>)<sub>2</sub>O<sub>3</sub>(Al<sub>2</sub>O<sub>3</sub>)(Cr<sub>2</sub>O<sub>3</sub>), spinel phase, phase equilibrium relations and spinel bonding 0-55376
- MgO-CaO-Fe<sub>2</sub>O<sub>3</sub>-Al<sub>2</sub>O<sub>3</sub>-SiO<sub>2</sub>, clinker production from dolomite and magnesite 0-55339
- MgO-CoO, high surface area, O<sub>2</sub> adsorpt., EPR, volumetric investigs. 0-10782
- MgO-MgAl<sub>2</sub>O<sub>4</sub>(FeCr<sub>2</sub>O<sub>4</sub>), thermoplastic and thermophys. props. for steel vacuuming installations 0-35281
- MgO-P<sub>2</sub>O<sub>5</sub>:Fe<sub>2</sub>O<sub>3</sub> glass, Fe<sup>2+</sup>(<sup>3</sup>) impurity ions struct.-chem. state, Mossbauer data 0-40028
- MgO-spinel concrete, cast, hardening by elec. heating 0-21258
- MgO-ZnO-Fe<sub>2</sub>O<sub>3</sub>, sintered ferrite, preparation, mag. susceptibility, DC resistivity 0-34598
- MgO(Al<sub>2</sub>O<sub>3</sub>)<sub>n</sub> spinel, plastic deformation at 400°C 0-40453
- MgO-Al<sub>2</sub>O<sub>3</sub> surface, crystalline, mass transport mechanisms at high temperatures (Japanese) 0-54479
- Mg(PO<sub>3</sub>)<sub>2</sub>, vitreous, microhardness 0-25864
- MgS:Eu<sup>2+</sup> emission and excitation spectra obs. 0-55162
- MgS:Eu<sup>2+</sup> phosphors, anal. of absorption spectra 4f<sup>n</sup>+1→4f<sup>n</sup>5d-6s 0-7383
- MgSO<sub>4</sub>, soln., electrolytic cond. dispersion, 1-6 MHz, caused by US prop. 0-44343
- MgSiF<sub>6</sub>·6H<sub>2</sub>O, orientational periodic antiphase (French) 0-15053
- MgSiO<sub>3</sub>, kinetics of dislocation etching 0-6409
- MgSiO<sub>3</sub>, elec. cond. under defined thermodynamic activities up to 20 kbar, 340-1100°C 0-6832
- MgSiO<sub>3</sub>, HP phase transform. 0-19941
- MgSiO<sub>3</sub>, orthorhombic perovskite, contribution to crystal chem. 0-19777
- MgSiO<sub>3</sub>:Dy, thermolum. induced by 254 nm UV photons 0-55204
- Mg<sub>2</sub>SiO<sub>4</sub> crystals, morphology and dislocation etch pits, (010) surface 0-24457
- Mg<sub>2</sub>SiO<sub>4</sub>, forsterite, decorated dislocations 0-54245
- Mg<sub>2</sub>SiO<sub>4</sub>, forsterite, ion scatt. spectrometry, atom shielding effect of O 0-50493
- Mg<sub>2</sub>SiO<sub>4</sub>, microhardness variation, exam. using Vicker indenter 0-25849
- Mg<sub>2</sub>SiO<sub>4</sub>:Fe<sup>3+</sup>(Mn<sup>2+</sup>)(Cr<sup>3+</sup>)(Mg<sup>2+</sup>) elec. field gradients, asymmetry parameters 0-54660
- Mg<sub>2</sub>SiO<sub>4</sub>:Tb, TLD phosphor response, heating rate effect 0-26359
- Mg<sub>2</sub>Si<sub>2</sub>O<sub>10</sub>(OH)<sub>2</sub>, talc, for hydrothermal crystn. of fibrous amphiboles 0-20810
- 2Mg<sub>2</sub>SiO<sub>4</sub>·3Mg(OH)<sub>2</sub>, new high-pressure struct. type, cryst. struct. 0-39028
- MgTiO<sub>3</sub>, ESR study of Fe<sup>3+</sup> 0-50173
- MgTiO<sub>3</sub>, HP phase transform. 0-19941
- Mg<sub>2</sub>U<sub>1-x</sub>O<sub>2+x</sub>, thermodynamic props., EMF meas. 0-29187
- Mg<sup>2+</sup>Y<sup>3+</sup>O<sub>7</sub>, quadrupole coupling tensor of <sup>51</sup>N nucleus 0-11290
- Mg<sub>3</sub>(VO<sub>4</sub>)<sub>2</sub>, determination of enthalpies of formation, from heats of solution 0-2182
- MgX<sub>2</sub> (X=F, Cl, Br, I), 2Z 0-43021
- MgO bicrystals, electron microscope exam. of secondary grain boundary dislocations in high angle twist boundaries 0-6415
- MgO, vol. eqn. of state under static press. conditions, rel. to Earth core-mantle models 0-19904
- Mn-Si, liq. alloys, equilibria between MnO-SiO<sub>2</sub>-CaO-MgO slags 0-10639
- Mn<sub>2</sub>Mg<sub>1-x</sub>O, solid solution EPR, mag. interactions (Russian) 0-44908
- NaCl-MgCl<sub>2</sub>-H<sub>2</sub>O mixed electrolyte solns., elec. transport 0-3355
- NaCl-MgO mixture, high pressure uniaxial stress component effect on eqns. of state, opposed anvil X-ray determ. 0-49301
- NaMgF<sub>3</sub>, orthorhombic perovskite, contribution to crystal chem. 0-19777



**magnesium compounds continued**

- Na<sub>2</sub>Mg<sub>2</sub>SiO<sub>4</sub>, ionic cond. meas. 0-6545  
 Na<sub>4</sub>Mg<sub>2</sub>Si<sub>3</sub>O<sub>10</sub>, ionic cond. meas. 0-6545  
 Na<sub>2</sub>O-CaO-MgO-Al<sub>2</sub>O<sub>3</sub>-SiO<sub>2</sub>, corrosion and microhardness, effect of detergents 0-16518  
 Ni<sub>1-x</sub>Mg<sub>x</sub>O, EPR in magnetoconcentrated solid solution (*Russian*) 0-39856  
 PbO-SiO<sub>2</sub>-NiO-MgO glass melt, interaction of NiO and MgO, elec. cond. and IR spectra obs. (*Japanese*) 0-24632  
 RbMgF<sub>3</sub>Mn<sup>2+</sup>, EPR obs. and struct. interpret. (*French*) 0-50167  
 Rb<sub>2</sub>Mn<sub>2</sub>Mg<sub>1-x</sub>F<sub>4</sub>, spin dynamics near percolation threshold, EPR study 0-39859  
 Si<sub>3</sub>N<sub>4</sub>(MgO+Al<sub>2</sub>O<sub>3</sub>)(Y<sub>2</sub>O<sub>3</sub>), hot-pressed and sintered, microstruct. and impurity distrib. 0-49261  
 Si<sub>3</sub>N<sub>4</sub>-Mg<sub>2</sub>SiO<sub>4</sub>-Si<sub>2</sub>N<sub>2</sub>O, compressive creep, composition effect 0-50674  
 Si<sub>3</sub>N<sub>4</sub>-MgO, (5 wt.%), hot pressed, fracture toughness as function of initial  $\alpha$ -phase content, SEM 0-3174  
 Si<sub>3</sub>N<sub>4</sub>-MgO, compressive creep, source of viscoelastic effect 0-50675  
 Si<sub>3</sub>N<sub>4</sub>-MgO, compressive creep, oxidation induced compositional change 0-50676  
 Si<sub>3</sub>N<sub>4</sub>-MgO (2-5 wt.%) hot pressed, tensile creep testing 0-40423  
 Si<sub>3</sub>N<sub>4</sub>-Si<sub>2</sub>N<sub>2</sub>O-Mg<sub>2</sub>SiO<sub>4</sub>, melting and eutectic studies 0-45285  
 SiO<sub>2</sub>-Al<sub>2</sub>O<sub>3</sub>-CaO-MgO-Na<sub>2</sub>O-K<sub>2</sub>O effect of partial substitution of Na<sub>2</sub>O by K<sub>2</sub>O, on crystallisation 0-10499  
 SiO<sub>2</sub>-Al<sub>2</sub>O<sub>3</sub>-CaO-MgO-FeO-Fe<sub>2</sub>O<sub>3</sub> glasses, struct. transforms during heating 0-15014  
 SiO<sub>2</sub>-Al<sub>2</sub>O<sub>3</sub>-Fe<sub>2</sub>O<sub>3</sub>-Na<sub>2</sub>O-K<sub>2</sub>O-CaO-MgO glasses, Mossbauer spectra study 0-39967  
 SiO<sub>2</sub>-Al<sub>2</sub>O<sub>3</sub>-FeO-CaO-MgO pyroxene glasses, phase changes 0-15013  
 SiO<sub>2</sub>-Al<sub>2</sub>O<sub>3</sub>-MgO-CaO-Fe<sub>2</sub>O<sub>3</sub>, glass ceramic, crystn., microstructures rel. to conditions 0-11638  
 SiO<sub>2</sub>-Al<sub>2</sub>O<sub>3</sub>-MgO-(K<sub>2</sub>O-F), glass ceramics, crystn., microstructures rel. to conditions 0-11638  
 SiO<sub>2</sub>-Na<sub>2</sub>O-CaO-MgO-Al<sub>2</sub>O<sub>3</sub>, toughening by electrochemical treatment in Sn melt 0-11800  
 SiO<sub>2</sub>-Na<sub>2</sub>O-CaO-MgO-Fe<sub>2</sub>O<sub>3</sub>-Al<sub>2</sub>O<sub>3</sub>-SO<sub>3</sub>-Sn thermally polished, exam. of strength of surfaces 0-25887  
 SiO<sub>2</sub>-Na<sub>2</sub>O-K<sub>2</sub>O-CaO-MgO-Al<sub>2</sub>O<sub>3</sub> glass melt, anodic dissolution of Ti 0-19949  
 SiO<sub>2</sub>-Na<sub>2</sub>O-CaO-MgO-Al<sub>2</sub>O<sub>3</sub> charge, silicate formation during heating 0-55342  
 Sn<sub>2</sub>Li<sub>1-x</sub>Mg<sub>1-x</sub>O<sub>8</sub>, four layer close packing, cryst. struct. determ. (*French*) 0-28999  
 YCrO<sub>3</sub>-MgCr<sub>2</sub>O<sub>4</sub> sintered ceramics, elec. cond. 0-24927  
 Y<sub>2</sub>WO<sub>7</sub>-MgO, polycryst., elec. cond., 800-7400°C 0-15517  
 Zn<sub>1-x</sub>Mg<sub>x</sub>Te alloys, high purity, metallurgical and analytical methods of prep. 0-40247  
 Zn<sub>1-x</sub>Mg<sub>x</sub>Te alloys, luminesc. and elec. props. 0-2813

**magnetic aftereffect**

- disaccommodation measurement in Rayleigh range using semi-automatic equipment (*Polish*) 0-31812  
 CdCr<sub>2</sub>Se<sub>4</sub> films, mag. hysteresis, domain struct., mag. viscosity 0-25169  
 Co<sub>2</sub>R-H(D) system, R=rare earth, mag. orientation aftereffect 0-50148  
 Cu-Co, superparamagnetic, mag. aftereffects, dynamic neutron depolarisation study 0-50147  
 $\alpha$ -Fe, magnetic aftereffect disaccommodation between 30 and 300K after low-temp. neutron-irrad. 0-29585  
 Fe-C, neutron irradiated at low temp., mag. disaccommodation 0-44881  
 Fe-Co-Si-B alloy, amorphous, mag. heads appl. (*Japanese*) 0-54922  
 Ni-Fe-Cu, Mu-metal, mag. aftereffects, dynamic neutron depolarisation study 0-50147  
 $\beta'$ -NiAl B2 phase, in 15 kOe field 0-34700  
 Tb<sub>52</sub>Ag<sub>48</sub>, amorphous, mag. aftereffect 0-20435

**magnetic amplifiers**

- linear movement transducers, magnetic amplifier principles 0-22341  
 space applications of LF supercond. sensors inc. SQUID devices 0-56691

**magnetic anisotropy**

- see also induced anisotropy (magnetic)  
 , 0-29395  
 advances in basic magnetism during past twenty-five years 0-36791  
 amorphous ferromagnets with random anisotropy axes, spin waves 0-7096  
 amorphous magnetic layers, SAW device appl. 0-28389  
 amorphous magnetic system, microwave absorption spectra, calc. 0-50469  
 antiferromagnet, cluster approximation, Neel temp. and specific heat calc. 0-54901  
 antiferromagnet, magnetic dislocation domains, mag. moment distribution 0-2601  
 austenitic stainless steel weld metal, US propag. 0-45452  
 bubble domain film, growth induced order parameter, estimation from coercive force meas. 0-39828  
 canted magnetic struct. crystn., magnetoacoustic resonance, elastic vibrations 0-29599  
 Co-Ni, magnetic anisotropy induced by mag. annealing and cold rolling, calc. 0-7696  
 contiguous disc bubble patterns utilising intrinsic crystalline anisotropy 0-2611  
 current threshold sensor, struct. and operational features 0-34689  
 cyanobiphenyls, nematic, dialec. consots. and diamag. anisotropies 0-7253  
 cyanocyclohexylcyclohexanes, nematic, dialec. consots. and diamag. anisotropies 0-7253  
 cyanophenylcyclohexanes, nematic, dialec. consots. and diamag. anisotropies 0-7253  
 dialkylammonium copper tetrachloride, ferromagnetic layer compound, magnetostatic mode excitation 0-29538  
 dislocated ferromagnet, inhomogeneous magnetisation near dislocation effect on FMR linewidth 0-25213  
 domain lattices, parallel stripe susceptibility, uniaxial anisotropy field 0-54930  
 ferrimagnet, uniaxial two-sublattice, energy spectrum, magnetisation, and crit. field, Green function method 0-25060  
 ferrite, epilayers for bubble appl. 0-39829  
 ferrogarnets, monocrystalline films, mag. anisotropy 0-2609  
 ferromagnet, amorphous, magnetisation, temp. depend. effect of nonrandom anisotropy 0-39773  
 ferromagnet, anisotropic, instantons 0-7066  
 ferromagnet, anisotropic Landau-Lifshitz, quasiclassical spectra (*Russian*) 0-15678

**magnetic anisotropy continued**

- ferromagnetic, anisotropic, in random longitudinal field, multicrit. point, theory 0-54903  
 ferromagnetic fine particles, stability of magnetisation curling mode and magnetisation helicoid struct. 0-11227  
 ferromagnetic nonmetallic film, stand exchange mode determ. 0-2565  
 ferromagnetic phase transitions, nucl. spin dynamics in anisotropic systems 0-11205  
 ferromagnetic resonance in anisotropic Heisenberg model, magnon-magnon, phonon-magnon interactions (*Russian*) 0-11274  
 ferromagnetic superconductor, mag. domain struct., sample thickness effects 0-39704  
 ferromagnetic superconductor, uniaxial, domain struct. parameters 0-39705  
 ferromagnets, anisotropic, HF magnon energy renormalisation, kinematic consistency 0-29539  
 garnet epitaxial film, damage prod. by multiple ion implantation, ferromag. reson. obs. 0-34703  
 garnet film, orthorhombic anisotropy, fast bubble devices 0-25168  
 garnet films, (111)-oriented, cubic anisotropy meas. 0-54924  
 group velocity, four-dimensional, electromagnetic waves in electrically and magnetically anisotropic media 0-17814  
 guanidinium vanadium sulphate hexahydrate, singlet ground state system, low temp. mag. props. 0-44843  
 Heisenberg ferromagnet, anisotropic, with biquadratic exchange interaction and uniaxial anisotropy, Curie temp. 0-7118  
 Heisenberg magnet, classical, with layer structure, mag. phase transitions, anisotropic lattice, theory 0-29557  
 intrinsic anisotropy constants from mag. props., book contrib. 0-11191  
 iron formate dihydrate, higher order term of uniaxial anisotropy (*Japanese*) 0-2571  
 Ising ferromagnet, high-freq. props. quantum theory, susceptibility tensor calcs. (*Russian*) 0-11143  
 measurement of microwave freq., experimental results 0-52279  
 metamagnetism, temperature induced, caused by mag. anisotropy 0-11195  
 Metglas 2826 ribbons, ferromagnetic resonance and SEM obs. 0-15804  
 model, temp. and field dependence, anisotropy constant meas., review (*Rumanian*) 0-25125  
 one-dimensional magnetic system, spin anisotropy and exchange alternation 0-34644  
 one-spin ferromagnet, high temp. series expansion for mag. susceptibility and sp. ht. 0-25148  
 orthoferrites, weak ferromagnetism, single ion anisotropy contrib. 0-25126  
 paramagnet, statistical mechanics using second order Green's function theory 0-25074  
 Permalloy, FCC, mag. anisotropy induced by cold rolling 0-11188  
 Permalloy film, domain wall mass and energy, wall vel. depend. calc. 0-2614  
 Permalloy RF sputtered films, struct.-sensitive mag. props. 0-34705  
 random quenched site model, competing exchange energies and competing anisotropy energies 0-29552  
 rare earth alloys, Curie temperature, high press. effects (*Japanese*) 0-20444  
 rare earth alloys, RFe<sub>2</sub>, magnetostriction studies, book contrib. 0-39846  
 rare earth aluminium Laves phase cpds., RAl<sub>2</sub>, anisotropic magnetostriction, temp. depend. 0-39841  
 rare earth amorphous alloys, random anisotropy antiferromag. model 0-20399  
 rare earth amorphous alloys, random mag. anisotropy 0-20398  
 rare earth amorphous alloys, transport props. 0-20152  
 rare earth garnet thin films, macroscopic magn. props., magneto-optical expts. 0-46764  
 rare earth garnets, prep. and props. book contrib. 0-44193  
 rare earth Laves phase compounds, R<sub>2</sub>R<sub>1-x</sub>Fe<sub>2</sub>, magnetostriction, anisotropy energy 0-25177  
 rare earth permanent magnets, physics and technology 0-20433  
 rare earth-Cu intermetallic compds. single crystn., mag. props. 0-54892  
 rare earth-gold amorphous alloys, R<sub>4</sub>Au, anisotropy versus exchange 0-34624  
 rare earth-transition metal (4f-3d) intermetallic cpds., mag. moment and mag. anisotropy 0-25107  
 rare-earth orthoferrite, cubic anisotropy constns. 0-11190  
 single-ion anisotropy, magnetic systems, high temp. series expansion 0-34576  
 soft ferromagnetic film, theoretical wall mobility 0-34677  
 steel, induced anisotropy influence on mag. props., thermomagnetic working (*Russian*) 0-55549  
 sublattice metamagnet, temp. dependent anisotropy, magnetisation curves, mag. transitions, classical approx. 0-39795  
 superconducting cable, magnetisation anisotropy meas. in hysteresis loss using Hall sensors 0-17966  
 surface and interface magnetism by Mossbauer spectroscopy 0-7218  
 TANOL, free radical, spin flopping transition, temp. depend., mag. anisotropy energy 0-54890  
 thin films, magnetic anisotropy rel. to columnar microstruct., calc. 0-39822  
 transition metal alloys, Curie temperature, high press. effects (*Japanese*) 0-20444  
 transition metal-rare earth intermetallics, two sublattice system with high competing single ion anisotropies, model 0-39767  
 transition metals, theory of ferromagnetism rel. to mag. anisotropy 0-2541  
 trimethylammonium cobalt trichloride dihydrate, Ising-like system, nucl. spin-lattice relax. of <sup>1</sup>H and <sup>51</sup>Cr 0-29638  
 uniaxial ferromagnetic crystal, irreversible rotation processes 0-39768  
 uniaxial Heisenberg antiferromagnet, phase diagrams 0-15730  
 X-Y quasi-one-dimens. system anisotropic, spin-Peierls phase transition, tricritical point 0-25142  
 Zn-Mn(Cr), dil., mag. anisotropy below 1K, low field magnetisation meas. 0-20382  
 Au<sub>4</sub>V single crystal, ordered, mag. props., domain models 0-39770  
 Ba<sub>2</sub>NiF<sub>6</sub>, specific heat capacity, critical amplitude, cross-over from 2-D Ising to Heisenberg behaviour 0-39791  
 (BiTm)<sub>3</sub>(FeGa)<sub>2</sub>O<sub>12</sub>, monocrystalline films, mag. anisotropy 0-2609  
 Ca<sub>2</sub>Mn<sub>2</sub>Ge<sub>2</sub>O<sub>12</sub>, mag. struct. study 0-2554  
 CdCr<sub>2</sub>Se<sub>4</sub>, ferromag. semicond., photoinduced mag. anisotropy 0-50086  
 Cd<sub>1-x</sub>Mg<sub>x</sub>, magnetic susceptibility anisotropy, press. effects, electronic phase transitions (*Russian*) 0-54869  
 CeBi, magnetoelastic effects, anisotropic mag. behaviour 0-25176



## magnetic anisotropy continued

- CeFe<sub>2</sub>, magnetostriction and magnetisation 0-39844  
 CeSb, magnetoelastic effects, anisotropic mag. behaviour 0-25176  
 Co film, ion beam sputtering prep., struct. and mag. props. 0-35085  
 Co, magnetic anisotropy induced by mag. annealing and cold rolling, expt. 0-7695  
 Co, magnetic anisotropy induced by mag. annealing and cold rolling, calc. 0-7696  
 Co-Ni, magnetic anisotropy induced by mag. annealing and cold rolling, expt. 0-7695  
 Co-P, amorphous, ferromag. antireson. 24 GHz microwave transmission, mag. props. 0-34778  
 Co-P amorphous alloys, electrodeposited, mag. anisotropy 0-15713  
 Co-Pt film, electrodeposited, saturation mag. induction, mag. anisotropy and coercive field meas. (French) 0-2610  
 Co-Zr, dil., mag. annealing effect, depend. of uniaxial mag. anisotropy on Zr conc. 0-39772  
 Co-Zr-Er alloys, mag. annealing effect, effect of Er on induced uniaxial mag. anisotropy 0-39771  
 Co<sub>90</sub>B<sub>10</sub>, amorphous metal ribbon, stresses, magnetoelastic anisotropy and zero-field mag. domain struct. 0-44896  
 CoBr<sub>2</sub>, magnetic excitations, neutron scatt. investigation 0-39761  
 CoCl<sub>2</sub>·2H<sub>2</sub>O-FeCl<sub>2</sub>·2H<sub>2</sub>O, random mixture with competing spin anisotropies, tetracrit. transition, neutron diffr. obs. 0-2575  
 (CoFeB)<sub>100-x</sub>Crx thin films, magnetic props. and corrosion resist. 0-34709  
 Co<sub>35</sub>P<sub>65</sub>, amorphous, strip domains, anisotropy const. effects 0-29571  
 Co<sub>1-x</sub>Ti<sub>x</sub>, ferromag. props., Ti conc. effect 0-54872  
 Cr, magnetic phase diagram in external mag. field, spin reorientation curve, critical point coordinates (Russian) 0-29548  
 Cr-Co-Fe permanent magnet anisotropic alloys, plastic deform., ageing, particle alignment temp. 0-35254  
 CsNiF<sub>3</sub>, demagnetising effects on antiferromag. reson. 0-15803  
 CuMn, magnetisation processes below freezing temp. 0-15748  
 CuMn, spin glass, mag. hysteresis meas. 0-34691  
 CuMn, spin glass, remanence, new approach from zero field NMR 0-34785  
 dimethylammonium manganese tetrachloride, 2D Heisenberg antiferromag., spin wave anal. 0-54879  
 Dy-Th, single cryst., mag. susceptibility, transitions, anisotropy 0-54873  
 DyFe amorphous film, Mossbauer and mag. meas. 0-15844  
 DyFe<sub>3</sub>, Mossbauer spectra, easy magnetisation axis temp. rot. 0-15859  
 Er, magnetisation and susceptibility in basal plane in strong mag. field (Russian) 0-50145  
 ErB<sub>4</sub>, mag. and elec. props., metallic character 0-20386  
 Er<sub>2</sub>Fe<sub>3</sub>, lower critical field 0-20414  
 Er<sub>3-x</sub>Fe<sub>3+x</sub>O<sub>12</sub>, garnet, mag. anisotropy and magnetostriction 0-11189  
 EuIG:Pb film saturation magnetisation improved by Sb<sup>3+</sup> substitution 0-54926  
 EuIG:Sb(Ca)(Ti), growth from PbO-B<sub>2</sub>O<sub>3</sub> based flux, prop. depend. on Pb content 0-39824  
 Eu<sub>3-x</sub>Ga<sub>x</sub>Fe<sub>5-x</sub>O<sub>12</sub>, epitaxial garnet films, props. at compensation points 0-39823  
 EuYIG:Sb, growth from PbO-B<sub>2</sub>O<sub>3</sub> based flux, prop. depend. on Pb content 0-39824  
 Fe complex, Fe(Br)[S<sub>2</sub>CN(C<sub>2</sub>H<sub>5</sub>)<sub>2</sub>]<sub>2</sub>, 3-D Ising ferromag., cryst. susceptibility, 1.5-20K 0-20390  
 Fe complex, Fe(Cl)[S<sub>2</sub>CN(C<sub>2</sub>H<sub>5</sub>)<sub>2</sub>]<sub>2</sub>, 3-D Ising ferromag., cryst. susceptibility, 1.5-20K 0-20390  
 Fe complex, tetraphenylporphyrinate iron III bromide, mag. props., zero-field splitting 0-34584  
 Fe film, evaporated at oblique incidence, optical and mag. anisotropies 0-7134  
 Fe, film, ion beam sputtering prep., struct. and mag. props. 0-35085  
 Fe film, on Cu and Ag substrates, mag. props., Mossbauer spectra meas. 0-11233  
 Fe film coated by MgO, Mossbauer spectra, mag. hyperfine field 0-7221  
 Fe whiskers, magnetisation and temp. depend. near T<sub>c</sub> 0-39766  
 Fe-B amorphous alloy, mag. anisotropy temp. depend. 0-15846  
 Fe-B-Si amorphous ribbons, effect of annealing conditions on magneto-mechanical props. 0-34740  
 Fe-Co-Si-B sputtered amorphous thin film, coercivity, galvanomagnetic props., resistivity 0-29578  
 Fe-Cr-Co, mechanism of coercive force 0-34674  
 Fe-Ni-Al, magnetic anisotropy form. and struct. changes by annealing, Mossbauer obs. 0-39994  
 Fe-Ni-Al-Cu (25, 14, 4 wt.%), alloy YuND4, effect of Ti addition on structure, mag. props. 0-15714  
 Fe-P amorphous alloys, electrodeposited, mag. anisotropy 0-15713  
 Fe-Pt Invar alloy, magnetocryst. anisotropy energy, itinerant electron model 0-54884  
 Fe<sub>78</sub>B<sub>22</sub>Si<sub>10</sub>, amorphous, Mossbauer study of hyperfine interaction and mag. anisotropy 0-40027  
 Fe<sub>80</sub>B<sub>15</sub>Si<sub>5</sub>, metallic glass, large uniaxial magnetostrictive anisotropy, magnetisation reversal 0-34736  
 Fe<sub>81</sub>B<sub>14</sub>Si<sub>4</sub>, amorphous metal ribbon, stresses, magnetoelastic anisotropy and zero-field mag. domain struct. 0-44896  
 (Fe<sub>1-x</sub>Co<sub>x</sub>)<sub>78</sub>Si<sub>10</sub>B<sub>12</sub>, amorphous alloys, magnetic anisotropy meas. 0-2570  
 FeGe<sub>2</sub>, canted antiferromagnet, mag. susceptibility anisotropy and temp. dependence 0-25112  
 Fe<sub>40</sub>Ni<sub>38</sub>Mo<sub>4</sub>B<sub>18</sub>, metallic glass, mag. and transport props. 0-39752  
 Fe<sub>40</sub>Ni<sub>38</sub>Mo<sub>4</sub>B<sub>18</sub> ribbon, magnetic characterisation 0-34680  
 Fe<sub>40</sub>Ni<sub>40</sub>P<sub>14</sub>B<sub>6</sub>, amorphous, strip domains, anisotropy const. effects 0-29571  
 Fe<sub>40</sub>Ni<sub>40</sub>P<sub>14</sub>B<sub>6</sub>, amorphous ribbon, influence of torsion on mag. props. 0-7138  
 Fe<sub>40</sub>Ni<sub>40</sub>P<sub>14</sub>B<sub>6</sub> metallic glass, ferromag. reson., spin waves, thermal ageing and long-range order effects 0-25214  
 Fe<sub>40</sub>Ni<sub>40</sub>P<sub>14</sub>B<sub>6</sub>, amorphous, kinetics of induced mag. directional order 0-44824  
 α-Fe<sub>2</sub>O<sub>3</sub>:Sn<sup>4+</sup>, antiferromag. reson. (Russian) 0-7175  
 Fe<sub>3</sub>O<sub>4</sub>, magnetite, magnetoec. effect at 77K, elec. field depend. of mag. anisotropy 0-29594  
 Fe<sub>7</sub>Si<sub>3</sub>B<sub>10</sub>, mag. behaviour rel. to magnetostatic interactions 0-11224  
 Fe<sub>1-x</sub>Ti<sub>x</sub>, ferromag. props., Ti conc. effect 0-54872  
 Ga<sub>1-x</sub>In<sub>x</sub>Se, magnetic susceptibility anisotropy, chemical bonds, electron density distribution (Russian) 0-50073  
 GaSe<sub>1-x</sub>S<sub>x</sub>, magnetic susceptibility anisotropy, chemical bonds, electron density distribution (Russian) 0-50073  
 Gd alloys, amorphous, mag. props. and ferromag. reson. 0-54952

## magnetic anisotropy continued

- Gd-Co amorphous films, annealed, short-range order and perpendicular mag. anisotropy 0-15765  
 Gd-Co amorphous films, correlation between struct. and mag. props. (Chinese) 0-54532  
 Gd-Co amorphous films, RF sputtered, magnetisation ripple effects 0-11232  
 Gd-Co amorphous films, struct. and mag. anisotropy 0-20438  
 Gd-Co amorphous sputtered film, magnetostriction and anisotropy 0-39821  
 Gd-Fe(Co) amorphous films, O<sub>2</sub> adsorption, effect on perpendicular anisotropy 0-34713  
 Gd<sub>37</sub>Al<sub>63</sub> amorphous film, spin glass, microwave mag. resonance, freq. dependence 0-39798  
 GdCl<sub>3</sub>, crystn. field parameter of Gd<sup>3+</sup> 0-10930  
 GdCo films, deposited on simple-crystal substrates (Russian) 0-24747  
 GdFe amorphous film, Mossbauer and mag. meas. 0-15844  
 GdFe films, deposited on single-crystal substrates (Russian) 0-24747  
 GdFe<sub>2</sub>, easy direction of magnetisation 0-20535  
 Ho<sub>0.5</sub>Dy<sub>0.5</sub>FeO<sub>3</sub> orthoferrite, domain wall struct., stability conditions, Morin transition, anisotropy const. 0-34684  
 K<sub>2</sub>CoF<sub>4</sub>, specific heat capacity, critical amplitude, cross-over from 2-D Ising to Heisenberg behaviour 0-39791  
 K<sub>2</sub>FeCl<sub>4</sub>(H<sub>2</sub>O), phase diagram, antiferromag., paramag. and spin flop phases 0-44831  
 K<sub>2</sub>MnF<sub>4</sub>, specific heat capacity, critical amplitude, cross-over from 2-D Ising to Heisenberg behaviour 0-39791  
 K<sub>2</sub>Mn<sub>2</sub>F<sub>7</sub>, two magnon Raman scatt., magnon dispersion, susceptibility, Green's function methods 0-50340  
 K<sub>2</sub>NiF<sub>4</sub>, specific heat capacity, critical amplitude, cross-over from 2-D Ising to Heisenberg behaviour 0-39791  
 La-Sm-Lu iron garnet film grown as NdGaG substrates, mag. props. 0-44888  
 La<sub>1-x</sub>Tb<sub>x</sub>Ag(Sn<sub>3</sub>)(Al<sub>2</sub>), paramag. anisotropy of Tb<sup>3+</sup> in cubic cryst. field 0-15687  
 LiH, mag. domains and nucl. mag. ordered phases, antiferromag. and ferromag. neutron diffr. obs. 0-50051  
 MgFe<sub>2</sub>O<sub>4</sub>, epilayer, perpendicular anisotropy 0-39769  
 Mn-substituted garnet film, growth characts. and mag. props. 0-39826  
 Mn-Zn ferrite single crystals, mech. polishing effect on mag. props. (Japanese) 0-16569  
 Mn<sub>2</sub>Fe<sub>3-x</sub>O<sub>4</sub> epitaxial films, mag. and reson. props. 0-50149  
 MnP, anisotropic, ferromagnetic microwave resonance relations 0-15805  
 MnZn ferrite, mag. anisotropy, effect on recording head characts. 0-39765  
 (Nd<sub>0.95</sub>Sm<sub>0.05</sub>)<sub>1-x</sub>(Co<sub>0.7</sub>Fe<sub>0.3</sub>)<sub>0.7</sub>, mag. anisotropy 0-34622  
 Ni film, ion beam sputtering prep., struct. and mag. props. 0-35085  
 Ni, magnetic surface anisotropy of transition metals, model calc. 0-34625  
 Ni-SiO<sub>2</sub> supported catalysts, particle size, H<sub>2</sub> chemisorption, Mossbauer study 0-7219  
 Ni<sub>0.95</sub>S Fe, spin glass, spin flop in exchange field 0-34640  
 NiFe, magnetic surface anisotropy of transition metals, model calc. 0-34625  
 Ni<sub>2</sub>FeC, mag. anisotropy depend. on C content, magnetometric study (Russian) 0-54887  
 (Ni<sub>1-x</sub>Fe<sub>x</sub>)<sub>1-δ</sub>S, anisotropic spin glass, mag. props. 0-39793  
 NiO (111) platelets, antiferromag. S domains, optical obs., spin flop 0-54915  
 NiO (111) platelets, magnetic torque and susceptibility meas. 0-54885  
 NiO, thin films with spinel-type defect structure, FMR study 0-39877  
 Ni<sub>1-x</sub>Ti<sub>x</sub>, ferromag. props., Ti conc. effect 0-54872  
 NiWO<sub>4</sub> monoclinic antiferromagnet, orientational phase transition and intermediate state (Russian) 0-15725  
 O, solid, magnetic props. theory for Heisenberg system (Russian) 0-54900  
 PbFe<sub>12-x</sub>Ga<sub>x</sub>O<sub>19</sub> ferrite, single cryst., ferromag. reson. 0-50193  
 Pr compounds, Van Vleck paramagnets, mag. props., anisotropy from NMR anal. 0-54862  
 Pr, magnetic excitations, exchange, crystal field and magnetoelastic interactions 0-2563  
 PrB<sub>4</sub>, mag. and elec. props. 0-20386  
 PrCo<sub>5</sub>, uniaxial ferromag. cryst., irreversible rotation processes 0-39768  
 Rb<sub>2</sub>MnCl<sub>4</sub>, 2D Heisenberg antiferromag. spin wave analysis 0-54879  
 Rb<sub>2</sub>NiF<sub>4</sub>, specific heat capacity, critical amplitude, cross-over from 2-D Ising to Heisenberg behaviour 0-39791  
 Rh based ferromag. Heusler alloys, peaks in low field AC susceptibility 0-50071  
 Ru based ferromag. Heusler alloys, peaks in low field AC susceptibility 0-50071  
 Tb-Y(Gd) alloys, contrib. from single-ion cryst. anisotropy and anisotropic exchange (Russian) 0-29546  
 TbB<sub>2</sub>, mag. struct., ferromag. ordering, neutron diffr. study 0-15692  
 TbBe<sub>13</sub>, magnetic structure at low temps., antiferromagnetic, neutron diffraction study (French) 0-39743  
 Tb(OH)<sub>3</sub>, powder and single crystal, mag. props. 0-2558  
 Tb<sub>x</sub>Y<sub>1-x</sub>Co<sub>0.5+0.1x</sub>, exchange interactions and magnetocrystalline anisotropy 0-34618  
 (Ti<sub>1-x</sub>V<sub>x</sub>)<sub>2</sub>O<sub>3</sub>, spin-glass props., 0.05-300K 0-25149  
 UAs, anisotropic susceptibility 0-7087  
 U<sub>3</sub>As<sub>4</sub>, mag. anisotropy, magnetisation meas. 0-50085  
 U<sub>3</sub>As<sub>4</sub>, magnetisation in strong fields, 4.2 to 200K anisotropy and exchange forces 0-54886  
 UGa<sub>2</sub>, mag. and magnetoelastic props. 0-15775  
 UP, anisotropic susceptibility 0-7087  
 USB, anisotropic susceptibility 0-7087  
 USB, neutron inelastic scatt. meas., phonon spectra, mag. response, anisotropy 0-50065  
 (U,Th<sub>1-x</sub>)Sb, magnetisation, U valence change 0-7089  
 V<sub>2</sub>O<sub>5+x</sub>, 0≤x≤0.08, mag. and elec. props. 0-49833  
 (Y,Sm,Lu,Ca)<sub>3</sub>(Fe,Ge)<sub>2</sub>O<sub>12</sub> bubble magnetic garnet film, LPE grown, props., CaCO<sub>3</sub>/GeO<sub>2</sub> molar ratio influence 0-50152  
 Y(Co<sub>1-x</sub>Ni<sub>x</sub>)<sub>5</sub>, spontaneous magnetisation mag. anisotropy, spin reorientation transformation (Russian) 0-7082  
 Y<sub>2</sub>Er<sub>1-x</sub>Al<sub>2</sub>, paramag. anisotropy 0-39737  
 (YEuYbCa)<sub>3</sub>(GeFe)<sub>2</sub>O<sub>12</sub> bubble film with ion-implanted layer, FMR study 0-2643  
 Y<sub>3</sub>Fe<sub>5-x</sub>Ga<sub>x</sub>O<sub>12</sub> garnet, spin wave parametric excitation threshold anisotropy in second region 0-29542  
 YFeO<sub>3</sub>:Co<sup>2+</sup>, weak ferromagnetism, single ion anisotropy contrib. 0-25126



**magnetic anisotropy continued**

- $Y_{1-x}Gd_xCo_5$ , exchange interactions and magnetocrystalline anisotropy 0-34618  
 YIG bubble films, light scatt. from spin waves, hysteresis meas. by Voigt effect 0-15770  
 YIG substrates, magnetoelastic surface waves, magnetostatic reson. anal. 0-20441  
 $Y_{1-x}Nd_xCo_5$ , exchange interactions and magnetocrystalline anisotropy 0-34618  
 $Y_{1.62}Sm_{0.21}Lu_{0.27}Cu_{0.9}Ge_{0.9}Fe_{4.1}O_{12}$ , implanted bubble garnet, anisotropy profile, FMR study 0-7103  
 $Y_{1-x}Tb_xCo_5$ , spontaneous magnetisation anisotropy, spin reorientation transforms. (Russian) 0-7082  
 Zn-Mn(Cr), dil. mag. anisotropy, Hartree-Fock calcs. 0-11162  
 $Zn_xCo_{1-x}Fe_{2.9}O_4$ , Cu, Zn substituted magnetite, domain wall resonance, mag. props. 0-15756  
 $ZnCr_2Se_4Mn_{1-x}$  paramagnetic, giant cubic anisotropy 0-7073  
 $ZnGa_2O_4Fe^{3+}(Mn^{2+})$ , EPR, spin Hamiltonian parameters 0-25195  
 Zr(Fe,Al), weak itinerant ferromag., mag. anisotropy effects on mag. isotherms 0-11187

**magnetic annealing**

- see also induced anisotropy (magnetic)  
 Co, magnetic anisotropy induced by mag. annealing and cold rolling, expt. 0-7695  
 Co, magnetic anisotropy induced by mag. annealing and cold rolling, calc. 0-7696  
 Co-Ni, magnetic anisotropy induced by mag. annealing and cold rolling, expt. 0-7695  
 Co-Ni, magnetic anisotropy induced by mag. annealing and cold rolling, calc. 0-7696  
 Co-Zr, dil., mag. annealing effect, depend. of uniaxial mag. anisotropy on Zr conc. 0-39772  
 Co-Zr-Er alloys, mag. annealing effect, effect of Er on induced uniaxial mag. anisotropy 0-39771  
 $Co_{75}Fe_{6.5}B_{14.5}$  amorphous thin films, zero magnetostriction, high magnetisation 0-34708  
 Cr-Co-Fe, chromindur alloy, field heat treatment, and mag. props. 0-35354  
 Fe-Al(4 wt.%), ferromag. alloy, mag. anisotropy induced by cold rolling 0-30114  
 Fe-B-C amorphous alloys, effect of Si addition on mag. props. 0-34694  
 Fe-Co-Si-B alloy, amorphous, rapidly quenched, mag. heads appl. (Japanese) 0-54922  
 Fe-Cr-Co(Mo), mag. props. after isothermal thermomag. treatment (Russian) 0-25159  
 Fe-Si(3 wt.%), ferromag. alloy, mag. anisotropy induced by cold rolling 0-30114  
 $Fe_5Co_{70}Si_{10}B_{15}$  amorphous magnetic alloy, decrease of permeability after demagnetisation, disaccommodation 0-39814  
 $Fe_{40}Ni_{16}P_{16}B_6$ , amorphous, kinetics of induced mag. directional order 0-44824  
 Ni-Co (25 wt.%), single crystals, mag. annealing effect on magnetostriction and magnetisation (Japanese) 0-34744

**magnetic bays** see geomagnetic variations**magnetic bottles**

- see also magnetic mirrors  
 No entries

**magnetic breakdown**

- (Russian) 0-44859  
 diamagnetic band structure, second order calc. using Landau functions, mag. breakdown determ. 0-24784  
 Cr, antiferromag., electron interference oscills. and spin-density-wave energy gaps at Fermi surface 0-49574  
 $Hg_{1-x}As_xF_6$ , linear chain cpd., open orbits, induced torque meas. 0-29309  
 Ru, thermo-EMF and Nernst effect under mag. breakdown conditions (Russian) 0-24878

**magnetic bubble devices**

- contiguous disc structs., bubble propag. dynamics 0-34718  
 garnet film, mag. bubble domain, annealing by laser pulse 0-15769  
 garnet thin films for fast bubble devices 0-25168  
 ion-implanted propag. patterns, cryst. symm. effects, roof-top designs 0-15768  
 memories, amorphous thin film materials, review (Polish) 0-34715  
 Permalloy, conductor crossing effect on bubble propagation margins 0-29588  
 Permalloy-SiO<sub>2</sub>-Schott glass, bubble propagation struct. 0-34719  
 Gd-Co influence of gaseous phase on mag. props. (Polish) 0-39820  
 Gd-Fe influence of gaseous phase on mag. props. (Polish) 0-39820  
 YEuLuCaGe garnets, 7  $\mu$ m-period bubble devices 0-44887  
 YEuLuGa garnets, 7  $\mu$ m-period bubble devices 0-44887  
 YEuTmCaGe garnets, 7  $\mu$ m-period bubble devices 0-44887  
 YEuTmGa garnets, 7  $\mu$ m-period bubble devices 0-44887  
 YSmLuCaGe garnets, 7  $\mu$ m-period bubble devices 0-44887  
 YSmLuGa garnets, 7  $\mu$ m-period bubble devices 0-44887  
 YSmTmCaGe garnets, 7  $\mu$ m-period bubble devices 0-44887  
 YSmTmGa garnets, 7  $\mu$ m-period bubble devices 0-44887

**magnetic bubbles**

- see also magnetic bubble devices  
 contiguous disc bubble patterns utilising intrinsic crystalline anisotropy 0-2611  
 cylindrically symmetric bubbles, static and dynamic props. 0-39835  
 domain film, growth induced order parameter, estimation from coercive force meas. 0-39828  
 domain wall states, discrimination by bubble collapse time 0-39830  
 ferrite, epilayers for bubble appl. 0-39829  
 ferrite garnet film, ion-implanted, hard mag. bubble suppression mechanism 0-44890  
 garnet, epitaxial film, mag. bubble props., permanent local modification by laser annealing 0-2612  
 garnet, Permalloy-coated film, bubble vel. and stability, influence of planar domains 0-39831  
 garnet film, 180° capped double layer LPE film, bubble wall states coding 0-34716  
 garnet film, mag. bubble domain, annealing by laser pulse 0-15769  
 garnet film for fast bubble devices 0-25168  
 garnet layers, ion-implanted, domain-wall behaviour for 1- $\mu$ m bubble devices 0-2613  
 garnet thin film, bubble domain lattice collapse characts. in alternating mag. field 0-54932  
 hard bubbles, static and dynamic props., micromagnetic struct. 0-11236

**magnetic bubbles continued**

- horizontal Bloch line motion 0-11237  
 ion-implanted bubble garnet film, vel. asymmetry during stripe head propag. 0-39834  
 ion-implanted propag. patterns, cryst. symm. effects, roof-top designs 0-15768  
 materials, prep. of memory element, review 0-50153  
 motion of bubble domain Bloch lines, computer simulation 0-54916  
 Permalloy, conductor crossing effect on bubble propagation margins 0-29588  
 Permalloy-SiO<sub>2</sub>-Schott glass, bubble propagation struct. 0-34719  
 pure chirality, discrimination between right and left handed bubbles 0-34723  
 rare earth garnet thin films, macroscopic magn. props., magneto-optical expts. 0-46764  
 static and kinetic parameters of bubble walls having horizontal Bloch line pair 0-39836  
 static spin config. in cylindrical coordinates 0-54928  
 transverse mass in rotating gradient 0-39832  
 unichiral magnetic bubbles, radial motion in in-plane field 0-34724  
 $DyFe_{0.998}Co_{0.002}O_3$ , orthoferrite, domain struct. near mag. transitions 0-2599  
 (Eu,Lu)<sub>3</sub>(Fe<sub>2</sub>O<sub>7</sub>)<sub>2</sub>·Ga(Al)(Ca,Ge), bubble material, dynamic characterisation, comparison between transport and FMR methods 0-39833  
 EuGaYIG:Cr, epitaxial garnet film, interaction pot. of domain walls with localised stress fields 0-44889  
 EuIG:Pb film saturation magnetisation improved by Sb<sup>5+</sup> substitution 0-54926  
 Eu<sub>3-x</sub>Ga<sub>x</sub>Fe<sub>5-x</sub>O<sub>12</sub>, epitaxial garnet films, props. at compensation points 0-39823  
 GdTmGa garnet bubble film, ion implanted, pot. wells under charged wells 0-34717  
 La-Sm-Lu iron garnet film grown as NdGaG substrates, mag. props. 0-44888  
 Mn-substituted garnet film, growth characts. and mag. props. 0-39826  
 NiFe stripes, mag. props. and domain struct. 0-44886  
 (Y,Sm,Lu,Ca)<sub>3</sub>(Fe,Ge)<sub>2</sub>O<sub>12</sub> bubble magnetic garnet film, LPE grown, props., CaCO<sub>3</sub>/GeO<sub>2</sub> molar ratio influence 0-50152  
 (Y,Sm,Lu,Cu)<sub>3</sub>(Fe,Ge)<sub>2</sub>O<sub>12</sub>, ion implanted, hard bubble suppression 0-11238  
 (Y,Sm,Lu,Tm,Ca)<sub>3</sub>(Fe,Ge)<sub>2</sub>O<sub>12</sub>, epitaxial garnet film, temp. depend. mag. props. 0-39825  
 (Y,Sm)<sub>3</sub>(Ga,Fe)<sub>2</sub>O<sub>12</sub>/(Eu,Er)<sub>3</sub>(Ga,Fe)<sub>2</sub>O<sub>12</sub> double-layer self-biasing garnet films, dynamic behaviour of domain walls 0-34722  
 (YEuTm)<sub>3</sub>(FeGa)<sub>2</sub>O<sub>12</sub> film, dynamic props. of bubble domains by high speed photography 0-15771  
 (YEuTm)<sub>3</sub>(FeGa)<sub>2</sub>O<sub>12</sub> garnet film, bubble domain steady state motion on a circle 0-29589  
 YEuTmGa garnet bubble film, dynamic diffuse wall deform. 0-54927  
 (YEuYbCa)<sub>3</sub>(GeFe)<sub>2</sub>O<sub>12</sub> bubble film with ion-implanted layer, FMR study 0-2643  
 (YGdYbBi)<sub>3</sub>(FeAl)<sub>2</sub>O<sub>12</sub> epitaxial film, diffuse domain wall, bubble domain expansion 0-25170  
 YIG bubble films, light scatt. from spin waves, hysteresis meas. by Voigt effect 0-15770  
 YIG, double layer struct., LPE growth from molybdate and Pb borate fluxes 0-39827  
 YIG epitaxial films, substituted, floating bubble domains, effect of structural stratification 0-2615  
 $Y_{1.62}Sm_{0.21}Lu_{0.27}Cu_{0.9}Ge_{0.9}Fe_{4.1}O_{12}$ , implanted bubble garnet, anisotropy profile, FMR study 0-7103  
 (YSmCaLu)<sub>3</sub>(FeGe)<sub>2</sub>O<sub>12</sub>, bubble film inhomogeneity, spin wave reson. meas. 0-44439  
 (YSmLuCa)<sub>3</sub>(FeGe)<sub>2</sub>O<sub>12</sub>, double layer struct., LPE growth from molybdate and Pb borate fluxes 0-39827  
 (YSmLuCa)<sub>3</sub>(FeGe)<sub>2</sub>O<sub>12</sub>, bubble material, dynamic characterisation, comparison between transport and FMR methods 0-39833  
 (YSmLu)<sub>3</sub>(FeGaSc)<sub>2</sub>O<sub>12</sub>, submicron mag. bubble garnet 0-54929

**magnetic circuits**

- electrotechnical steel, quality significance on energy and materials savings in magnetic circuits (Czech) 0-20947  
 low permeability or saturated parts with permanent magnet, analytical calc. (German) 0-23596

**magnetic circular dichroism**

- alkali halides, doped, optical absorption and MCD spectra, Gaussian quadrature calc. 0-7367  
 benzene, and methyl derivatives, <sup>1</sup>E<sub>u</sub> N-V state mag. moments, MCD obs. 0-23575  
 bromomethane, mol. Rydberg transitions mag. circular dichroism 0-43081  
 chromophores, semiempirical rules in circular dichroism, Cotton effect sign correl. with stereochem. 0-1006  
 coronene, excited state Faraday values mag. circular dichroism spectra and MO CI calcs. 0-18877  
 cyclopentadienyl Ho(III), cyclooctadienyl sandwich compound, mag. circular dichroism and absorption spectra, anal. 0-23449  
 group theoretical techniques, one-electron reduced matrix elements 0-45048  
 heavy atom, parity violation in forbidden mag. transitions, chiral absorpt. of polarized light and circular dichroism in crossed DC fields 0-23370  
 di-(tetraethylammonium)tetrahalomanganate, mag. circular and linear dichroism obs. 0-29725  
 transition metal complexes, ligand field spectroscopy, selection rules, intensity enhancement of forbidden transitions 0-45049  
 triphenylene, excited state Faraday values mag. circular dichroism spectra and MO CI calcs. 0-18877  
 CS<sub>2</sub>, <sup>3</sup>A<sub>2</sub> state, triplet bands, MCD spectrum, near UV absorpt. spectrum 0-48010  
 CS<sub>2</sub>, <sup>3</sup>A<sub>2</sub>-state, MCD and UV spectrum, theoretical anal. 0-48011  
 CaF<sub>2</sub>:Dy crystal with M centre, antiresonance line, mag. field effect 0-55138  
 Cs<sub>3</sub>NaTmCl<sub>6</sub>, UV absorpt. spectra, mag. circular dichroism spectra, vibr. obs. 0-29758  
 Eu-Fe garnet, light mag. linear birefringence and dichroism near absorption band (Russian) 0-55063  
 I<sub>2</sub>, N<sub>2</sub> and Ar matrix isolated, magnetic circular dichroism spectrum 0-5567  
 I<sub>2</sub>-benzene mixture, N<sub>2</sub> and Ar matrix isolated, magnetic circular dichroism spectrum 0-5567



**magnetic circular dichroism continued**

- KBr:In<sup>+</sup>, B-band, optical absorpt. and mag. circular dichroism calcs. 0-29765  
 KBr:In<sup>+</sup>, optical absorption and MCD spectra, Gaussian quadrature calc. 0-7367  
 KBr(Cl)(I), electron-spin memory and magnetic-circular-dichroic effects in F-centre luminesc. 0-29794  
 KCl:Ti<sup>3+</sup> cryst., A band, mag. field effect 0-34897  
 KI:Pb<sup>2+</sup>, UV absorpt. and mag. circular dichroism spectra 0-25418  
 KZnF<sub>2</sub>:Ni<sup>2+</sup>, Mn<sup>2+</sup>, interference transition electric dipole mechanism 0-34896  
 Pr<sup>3+</sup> aquo ion spectra, MCD of <sup>3</sup>P<sub>0</sub>→<sup>3</sup>H<sub>4</sub> transition 0-7331  
 YIG, MCD meas. by retardation modulation technique 0-16014

**magnetic cooling**

- nuclear demagnetisation refrigerator, double range, microkelvin range 0-31769  
 nuclear demagnetisation refrigerator, two stage (*Japanese*) 0-47063  
 nuclear demagnetisation refrigerator, two-stage 0-52244  
 reciprocating magnetic refrigerator for 2-4K operation 0-2577  
 S=1, singlet ground state systems, mag. props. 0-11157  
 LiH, mag. domains and nucl. mag. ordered phases, antiferromag. and ferromag. neutron diff. obs. 0-50051  
 LiH, nuclear ordered ferromag. and antiferromag. phases, neutron diff. study 0-50052  
<sup>17</sup>O, NQR at natural isotope abundance, double reson. new techniques using adiabatic demagnetisation, review 0-53013

**magnetic cores**

- Permalloy thin film cores, domain wall motion and flux patterns, Kerr magneto-optic effect obs. 0-34721  
 tape cores carrying current, torsional stress effects 0-34742  
 Fe, three dimensional arbitrarily shaped cores, eddy currents calc. (*German*) 0-18956  
 Fe-Ci, high permeability, mag. props., applied stress effects 0-34726  
 Fe-Ci (3 wt.%), commercially produced, grain-oriented, mag. props., stress coating effects 0-34727  
 Fe-Co-Si (4.15 wt.%), textured, mag. props. 0-35200  
 Fe-Ni-Co-Mo-Ge alloy 40NKM, excess mag. noise after various thermo-mag. treatments (*Russian*) 0-29575  
 Fe-Si (3 wt.%), mag. props., stress coating effects 0-34728  
 Fe-Si (3 wt.%) steel, oriented, stress depend. mag. props., coating effects 0-34729

**magnetic devices**

- see also ferrite devices; magnetic amplifiers; magnetic lenses; magnetic storage devices; magnetic thin film devices; magnetostrictive devices  
 brush development characteristics for xerography 0-4798  
 discharge manometric convertor 0-31779  
 EM flowmeter, for industrial appl. 0-1701  
 ferromagnetic plate, surface magnetostatic wave excitation 0-25119  
 imaging magnetic energy filters free of second-order aberrations, optimization 0-4816  
 magnetographic flaw detector for monitoring cylindrical articles 0-35478  
 thermomagnetic gas analysers, for use in power stations (*Russian*) 0-3445  
 thin rolled sheet, IMA-4 impulse magnetic analyser 0-35470

**magnetic dipoles** see magnetic moments**magnetic domain walls**

- amorphous ferromagnetic alloys, domain struct. and mag. microstruct., review 0-15751  
 Bloch wall bound spin waves, equations of motion 0-34612  
 bubble, static spin config. in cylindrical coordinates 0-54928  
 bubble, transverse mass in rotating gradient 0-39832  
 bubbles, horizontal Bloch line motion 0-11237  
 charged, zigzag form 0-44852  
 chevron stacks, stroboscopic meas. of strip domain expansion 0-39810  
 cylindrically symmetric bubbles, static and dynamic props. 0-39835  
 domain wall states, discrimination by bubble collapse time 0-39830  
 dynamic shift of NMR freq. of nuclei located in domain walls 0-15823  
 eddy current contrib. to effective mass 0-29570  
 ferromagnet, domain wall retardation by spin waves (*Russian*) 0-25154  
 ferromagnet, narrow domain wall, localised modes 0-34681  
 ferromagnet, spin waves with moving domain wall 0-39764  
 ferromagnetic crystal, pinning and nucleation of mag. domain walls at antiphase boundaries 0-11216  
 ferromagnetic domain wall, soliton theory and dynamics 0-29569  
 ferromagnetic metals, domain wall motion, voltage generation 0-34679  
 ferromagnetic superconductor, mag. domain struct., sample thickness effects 0-39704  
 ferromagnetic superconductor, uniaxial, domain struct. parameters 0-39705  
 ferromagnets, domain struct. effects on dynamic props., review 0-34678  
 ferromagnets, solitary domains, Bloch and Neel stability, calcs. 0-25157  
 ferromagnets and antiferromagnets, EM and acoustic energy attenuation in many-domain magnets 0-7140  
 film, charged domain walls, variational method calc. 0-11235  
 frustration network, phase transitions 0-2596  
 garnet layers, ion-implanted, domain-wall behaviour for 1-μm bubble devices 0-2613  
 Heisenberg ferromagnet, spin configurations near singularities in micro-magnetism 0-54908  
 intrinsic coercivity in narrow magnetic domain wall material 0-2597  
 ion-implanted bubble garnet film, vel. asymmetry during stripe head propagation 0-39834  
 Ising model with competing interactions, solitons and phasons 0-34653  
 magnetic sheet with simple bar-like 180° domain structs., eddy current losses 0-39808  
 mass at high vel., numerical anal. 0-11217  
 metallic glasses, mag. props., effect of mech. deform. 0-39840  
 motion of bubble domain Bloch lines, computer simulation 0-54916  
 orthoferrites, struct. of domain walls 0-34684  
 orthorhombic ferrimagnets, domain wall motion at near sonic velocity, magnetoelastic interactions 0-34683  
 Permalloy film, coercive force associated with domain boundary displacement (*Russian*) 0-50151  
 Permalloy film, domain wall mass and energy, wall vel. depend. calc. 0-2614  
 Permalloy I-bar elements, magnetostatic effects, unifying overview of domain and continuum results 0-44853  
 Permalloy thin film cores, domain wall motion and flux patterns, Kerr magneto-optic effect obs. 0-34721

**magnetic domain walls continued**

- porous ferromagnet, with Bloch walls and self-consistent magnetisation, energy and coercive field 0-15760  
 rare earth-transition metal amorphous thin films, mag. potential distribution and wall velocity meas. 0-34725  
 SEM, magnetic contrast, type-2, isolation by lock-in technique, domain wall movement 0-13184  
 soft ferromagnetic film, theoretical wall mobility 0-34677  
 spinels, domain wall formation inhibition, effect on bulk mag. props. 0-11220  
 static and kinetic parameters of bubble walls having horizontal Bloch line pair 0-39836  
 superdiamagnetic and ferromagnetic state struct., gradient invariant free energy functional (*Russian*) 0-7143  
 thermally activated domain wall motion and coercive field in materials with extremely narrow domain walls 0-25156  
 uniaxial crystal, with narrow domain boundaries, coercive force (*Russian*) 0-50140  
 unichiral magnetic bubbles, radial motion in in-plane field 0-34724  
 velocity, damping parameter meas. from low field microwave excitations 0-34676  
 Ca<sub>2</sub>Mn<sub>2</sub>Ge<sub>2</sub>O<sub>12</sub>, antiferromagnetic garnet, neutron diff. study in mag. field 0-50060  
 CdCr<sub>2</sub>Se<sub>4</sub>, ferromag. semicond., photoinduced mag. anisotropy 0-50086  
 Co<sub>2</sub>Sm, magnetic domains, nucleation and pinning, magneto-optical Kerr effect 0-39811  
 DyFe<sub>0.998</sub>Co<sub>0.002</sub>O<sub>3</sub>, orthoferrite, domain struct. near mag. transitions, domain wall bending 0-2599  
 ErCo<sub>3</sub>, ErCo<sub>6</sub> and Er<sub>2</sub>Co<sub>17</sub>, Kerr effect determ. of domain structure, Bloch wall energy 0-39805  
 Er<sub>2</sub>Fe<sub>2</sub>Co<sub>4</sub>, Kerr effect determ. of domain structure, Bloch wall energy 0-39805  
 EuGaYIG:Cr, epitaxial garnet film, interaction pot. of domain walls with localised stress fields 0-44889  
 EuTe, mag. semicond., antiferromag. reson. meas. 0-44926  
 Fe, polycryst., rel. to magnetostriction sign change under compressive stress 0-29596  
 Fe-Si (3 wt.%), domain struct. rel. to cryst. size (*Russian*) 0-29568  
 Fe-Si (4 at.%), Bloch wall thickness determ. by neutron small-angle scatt. 0-15754  
 Fe-Si single crystals, interaction of {110} 90° walls with lattice imperfections 0-39807  
 Fe-Si (4 wt.%), (110) and (100)[001] oriented, simulation of domain wall bowing 0-44854  
 Fe<sub>30</sub>B<sub>70</sub>Si<sub>2</sub>, metallic glass, large uniaxial magnetostrictive anisotropy, magnetisation reversal 0-34736  
 Fe<sub>2</sub>Co<sub>10</sub>Si<sub>10</sub>B<sub>13</sub>, amorphous magnetic alloy, decrease of permeability after demagnetisation, disaccommodation 0-39814  
<sup>57</sup>Fe powder, NMR excitation function, drumhead model of Bloch walls 0-15810  
 Fe-Fe-Nb, cold-worked and aged, mag. props. and microstruct. 0-34690  
 Gd-Co amorphous film 0-34725  
 HoCo<sub>3</sub>, Ho<sub>2</sub>Co<sub>7</sub>, HoCo<sub>5.5</sub> and Ho<sub>2</sub>Co<sub>7</sub>, Kerr effect determ. of domain structure, Bloch wall energy 0-39806  
 Ho<sub>2</sub>Dy<sub>0.5</sub>FeO<sub>3</sub>, orthoferrite, domain wall struct., stability conditions, Morin transition, anisotropy const. 0-34684  
 Ho<sub>2</sub>Fe<sub>2</sub>Co<sub>4</sub>, Kerr effect determ. of domain structure, Bloch wall energy 0-39806  
 La-Sm-Lu iron garnet film grown as NdGaG substrates, mag. props. 0-44888  
 Li<sub>0.5</sub>Fe<sub>2.5</sub>O<sub>4</sub>, magnetic domain walls, mobility 0-2600  
 MnFe<sub>2</sub>O<sub>4</sub>, ferrite, dynamic shift of NMR freq. of nuclei located in domain walls 0-15823  
 Mn<sub>2</sub>Sb, domain and domain wall resons. in <sup>55</sup>Mn NMR spectrum 0-25219  
 MnZn ferrite, wall topography change induced by external press. 0-34734  
 Ni (100), Bloch wall meas. by neutron small-angle meas. 0-15753  
 Ni-Fe film, low field domain wall mobility 0-25167  
 Ni<sub>0.81</sub>Fe<sub>0.17</sub> films, reson. oscills. of mag. domain walls and Bloch lines, stroboscopic electron microscopy 0-54931  
 NiO (111) platelets, antiferromag. S domains, optical obs., spin flop 0-54915  
 NiZn ferrite, wall topography change induced by external press. 0-34734  
 Sm(Co, Cu) alloys, coercivity mech. 0-44862  
 V1<sub>2</sub>, antiferromag., zone-boundary phonon Raman scattering, modulation of exchange interaction 0-11386  
 (Y, Gd, Yb, Bi)<sub>3</sub>(Fe, Al)<sub>2</sub>O<sub>12</sub> epitaxial film, domain wall motion and oscill. 0-2616  
 (Y,Sm)<sub>3</sub>(Ga,Fe)<sub>2</sub>O<sub>12</sub>/(Eu,Er)<sub>3</sub>(Ga,Fe)<sub>2</sub>O<sub>12</sub> double-layer self-biasing garnet films, dynamic behaviour of domain walls 0-34722  
 YEuTmGa garnet bubble film, dynamic diffuse wall deform. 0-54927  
 (YEuYbCa)<sub>2</sub>(FeGe)<sub>2</sub>O<sub>12</sub>, garnet film, isolated straight stripe domain, dynamic behaviour 0-39809  
 YFeO<sub>3</sub>, weak ferromagnet, domain wall motion and velocity (*Russian*) 0-54917  
 (YGdYbBi)<sub>3</sub>(FeAl)<sub>2</sub>O<sub>12</sub> epitaxial film, diffuse domain wall, bubble domain expansion 0-25170  
 (YGdYbBi)<sub>3</sub>(FeAl)<sub>2</sub>O<sub>12</sub>, epitaxial film, 360° domain walls with periodically distrib. Bloch lines 0-7127  
 YIG, dilute, magnetoacoustic surface wave excitation by RF field on Bloch walls 0-25178  
 YIG, domain boundary nuclear spin echo excitation, NMR domain freq. capture effect (*Russian*) 0-44955  
 Zn,Cu<sub>0.1</sub>Fe<sub>2.9</sub>O<sub>4</sub>, Cu, Zn substituted magnetite, domain wall resonance, mag. props. 0-15756

**magnetic domains**

- see also magnetic bubbles; magnetic domain walls  
 amorphous ferromagnetic alloys, domain struct. and mag. microstruct., review 0-15751  
 antiferromagnet, magnetic dislocation domains, mag. moment distribution 0-2601  
 bubble domain film, growth induced order parameter, estimation from coercive force meas. 0-39828  
 colloid patterns interference colours associated with mag. domains 0-2598  
 dialkylammonium copper tetrachloride, ferromag., static and dynamic mag. props. 0-50074  
 ferromagnet, domain struct. study by time depend. neutron depolarisation 0-50138



**magnetic domains continued**

- ferromagnet, elec. resist., just below crit. temp., effect of mag.-domains 0-39557  
 ferromagnetic materials, phase transition, mathematical bifurcation process 0-29572  
 ferromagnetic metal, dragging of domains by temp. gradient 0-34425  
 ferromagnetic superconductor, mag. domain struct., sample thickness effects 0-39704  
 ferromagnetic superconductor, supercond. Bloch wall 0-20349  
 ferromagnetic superconductor, uniaxial, domain struct. parameters 0-39705  
 ferromagnetic uniaxial particles, domain struct. and crit. size (Russian) 0-25153  
 ferromagnets, domain struct. effects on dynamic props., review 0-34678  
 ferromagnets, domain structure image obtained by SEM (Polish) 0-34682  
 ferromagnets, solitary domains, Bloch and Neel stability, calcs. 0-25157  
 film, resonance props. in network of cylindrical mag. domains (Russian) 0-50194  
 garnet, Permalloy-coated film, bubble vel. and stability, influence of planar domains 0-39831  
 lattices, parallel stripe susceptibility, uniaxial anisotropy field 0-54930  
 magnetic sheet with simple bar-like 180° domain structs., eddy current losses 0-39808  
 neutron depolarisation studies of ferromagnetic domain structures 0-25155  
 Permalloy film, domain nucleation using low intensity US 0-34731  
 regular domain structs., magneto-optical characts., optoelectronics appls. 0-40098  
 rocks, domain state depend. of uniaxial stress effect upon remanent magnetisation 0-26505  
 steel, induced anisotropy influence on mag. props., thermomagnetic working (Russian) 0-55549  
 steel, Si, highly-oriented domain and grain obs. methods, using ferromagnetic colloid technique 0-11856  
 Au<sub>4</sub>V single crystal, ordered, mag. props., domain models 0-39770  
 BaO-Fe<sub>2</sub>O<sub>3</sub>, chemically coprecipitated, mag. props., orientation 0-15763  
 (BiTm)<sub>3</sub>(FeGaTm)<sub>2</sub>O<sub>12</sub>, layer separation of domain struct. 0-44857  
 CdCr<sub>2</sub>Se<sub>4</sub> films, mag. hysteresis, domain struct., mag. viscosity 0-25169  
 Co-Pt, atomic ordering props. and domain growth in strong pulsed mag. field (Russian) 0-54918  
 Co<sub>80</sub>B<sub>20</sub>, amorphous metal ribbon, stresses, magnetoelastic anisotropy and zero-field mag. domain struct. 0-44896  
 CoF<sub>2</sub>, 180-degree antiferromag. domain obs. by new magnetooptical effect 0-44855  
 Co<sub>35</sub>P<sub>15</sub>, amorphous, strip domains, anisotropy const. effects 0-29571  
 DyFe<sub>0.999</sub>Co<sub>0.002</sub>O<sub>3</sub>, orthoferrite, domain struct. near mag. transitions 0-2599  
 (Er,Tb,Gd)<sub>3</sub>Fe<sub>2</sub>O<sub>12</sub> plate, pseudouniaxial, domain struct., magneto-optical obs. 0-11221  
 ErCo<sub>3</sub>, ErCo<sub>6</sub> and Er<sub>2</sub>Co<sub>17</sub>, Kerr effect determ. of domain structure, Bloch wall energy 0-39805  
 Er<sub>2</sub>Fe<sub>2</sub>Co<sub>14</sub>, Kerr effect determ. of domain structure, Bloch wall energy 0-39805  
 Fe whiskers, elastically and plastically deformed, mag. domain structs. 0-15752  
 Fe-B amorphous alloy, mag. anisotropy temp. depend. 0-15846  
 Fe-Co-V, Vicalloy, magnetisation reversal by stretching and twisting 0-34733  
 Fe-Si, coated, effective domain and grain obs. methods and Fe losses 0-34675  
 Fe-Si, maze domains upon appl. of horizontal mag. field or mech. tension 0-11218  
 Fe-Si (2.5%), mag. stray fields above stripe domains, electron optic meas. 0-15755  
 Fe-Si (3 wt.%), domain struct. rel. to cryst. size (Russian) 0-29568  
 Fe-Si (3 wt.%), polycrystal in mag. field, stress induced magnetisation, synchrotron Bragg refl. topography obs. 0-50139  
 Fe-Si (3 wt.%) laminations, isotropic and cube-on-face, magnetostriction behaviour 0-39843  
 Fe-Si (3 wt.%) locally deformed, EM loss depend. on cryst. struct. and orientation (Russian) 0-7694  
 Fe<sub>81</sub>B<sub>14</sub>Si<sub>4</sub>, amorphous metal ribbon, stresses, magnetoelastic anisotropy and zero-field mag. domain struct. 0-44896  
 FeGe<sub>2</sub>, canted antiferromagnet, mag. susceptibility anisotropy and temp. dependence 0-25112  
 FeI<sub>2</sub>, neutron inelastic scatt. from mag. excitations 0-50078  
 Fe<sub>40</sub>Ni<sub>38</sub>Mo<sub>2</sub>B<sub>18</sub> ribbon, magnetic characterisation 0-34680  
 Fe<sub>40</sub>Ni<sub>40</sub>P<sub>14</sub>B<sub>6</sub>, amorphous, strip domains, anisotropy const. effects 0-29571  
 Fe<sub>2</sub>O<sub>4</sub>, magnetite, grain size limits for pseudosingle domain behaviour, rel. to palaeomagnetism 0-11215  
 Fe<sub>25</sub>Pd<sub>50</sub>Au<sub>25</sub>, atomic ordering influence on mag. props. and elec. resistance (Russian) 0-7551  
 FeSi, domain struct. and magnetisation reversal, time depend. neutron depolarisation 0-50138  
 Fe<sub>2</sub>Ti<sub>0.6</sub>O<sub>4</sub>, TRM acquired by multi-domain single cryst. 0-36293  
 Gd-Co amorphous films, struct. and mag. anisotropy 0-20438  
 Gd-Co amorphous thin films, crystn. process and domain struct. (Chinese) 0-54533  
 HoCo<sub>3</sub>, Ho<sub>2</sub>Co<sub>7</sub>, HoCo<sub>5.5</sub> and Ho<sub>2</sub>Co<sub>17</sub>, Kerr effect determ. of domain structure, Bloch wall energy 0-39806  
 Ho<sub>2</sub>Fe<sub>2</sub>Co<sub>14</sub>, Kerr effect determ. of domain structure, Bloch wall energy 0-39806  
 LiH, mag. domains and nucl. mag. ordered phases, antiferromag. and ferromag. neutron diffr. obs. 0-50051  
 LiH, nuclear ordered ferromag. and antiferromag. phases, neutron diffr. study 0-50052  
 Mn<sub>2</sub>Sb, domain and domain wall resons. in <sup>55</sup>Mn NMR spectrum 0-25219  
 MnZn ferrite, mag. permeability accommodation depend. on mag. field (Russian) 0-34685  
 (NH<sub>4</sub>)<sub>2</sub>CuBr<sub>4</sub>·2H<sub>2</sub>O, ferromag., static and dynamic mag. props. 0-50074  
 Ni film, single cryst., domain width from ferromag. reson. 0-39879  
 Ni-Fe films, magnetisation reversal in narrow strips, TEM study 0-34720  
 NiWO<sub>4</sub> monoclinic antiferromagnet, orientational phase transition and intermediate state (Russian) 0-15725  
 NiWO<sub>4</sub>, monoclinic antiferromag., domain struct. induced by strong mag. field 0-44856  
 Rb<sub>2</sub>CuBr<sub>4</sub>·2H<sub>2</sub>O, ferromag., static and dynamic mag. props. 0-50074  
 Si-Fe, domain and grain obs. using ferromag. colloid technique 0-11219

**magnetic domains continued**

- Sm-Co-Cu-Fe-Zr alloy, reversible changes in coercive force and struct. state during heat treatment 400-800°C (Russian) 0-29574  
 Sm(Co<sub>0.84</sub>Cu<sub>0.16</sub>)<sub>6.9</sub>, microstruct. and domain struct., mag. reversal (Russian) 0-20429  
 (Tb<sub>0.77</sub>Dy<sub>0.23</sub>)Fe<sub>2</sub>, magnetisation, ferromag. domains 0-25162  
 Tb<sub>0.3</sub>Er<sub>1.3</sub>Gd<sub>1.0</sub>Al<sub>0.2</sub>Fe<sub>4.8</sub>O<sub>12</sub>, garnet plate, domain struct. 0-2602  
 TbFe<sub>2</sub>, magnetisation, ferromag. domains 0-25162  
 YIG substrates, magnetoelastic surface waves, magnetostatic reson. anal. 0-20441  
**magnetic double refraction** *see magneto-optical effects*  
**magnetic double resonance**  
*see also CIDEP; double nuclear magnetic resonance; dynamic nuclear polarisation; ELDOR; ENDOR; microwave-optical double resonance; nuclear polarisation*  
 p-dichlorobenzene, in p-dibromobenzene, optical detection of Cl NQR in mag. field 0-50228  
 NMR under optical pumping conditions 0-25253  
 quartz, muonium EPR transitions by muon-spin rot. 0-29668  
 spin polarisation torsional spectroscopy, four time domains 0-20510  
 Ta, NMR-Mossbauer double reson. 0-40019  
 Tl atomic beam tubes, freq. pulling effect with mag. double reson. 0-37802  
**magnetic epitaxial layers**  
 ferrite, epilayers for bubble appl. 0-39829  
 ferrite spinel films, LPE growth and props., SIMS, X-ray diffr., and spin wave reson. obs. 0-34323  
 ferrogarnets, monocrystalline films, mag. anisotropy 0-2609  
 garnet, 180° capped double layer LPE film, bubble wall states coding 0-34716  
 garnet, mag. bubble props., permanent local modification by laser annealing 0-2612  
 garnet, magnetic bubble materials, review 0-50153  
 garnet, technique for magnetostriction coeff. meas. 0-243  
 garnet films, damage prod. by multiple ion implantation, ferromag. reson. obs. 0-34703  
 garnet films, isolated steps, rate analysis of growth parameters 0-10805  
 rare earth garnets, prep. and props. book contrib. 0-44193  
 (BiTm)<sub>3</sub>(FeGa)<sub>2</sub>O<sub>12</sub>, monocrystalline films, mag. anisotropy 0-2609  
 EuGaYIG:Cr, epitaxial garnet film, interaction pot. of domain walls with localised stress fields 0-44889  
 Eu<sub>2</sub>Y<sub>3</sub>Ga<sub>2</sub>Fe<sub>2</sub>O<sub>12</sub>, epitaxial garnet films, props. at compensation points 0-39823  
 Fe epitaxial film, Mossbauer effect, depth profiling of mag. hyperfine field 0-11295  
 Fe epitaxial film, Mossbauer effect, interface magnetism 0-11297  
 γ-Fe<sub>2</sub>O<sub>3</sub>:Co acicular powder epitaxially doped, coercivity increase, surface anisotropy (Chinese) 0-7130  
 (Gd,Bi)<sub>3</sub>(Fe,Ga)<sub>2</sub>O<sub>12</sub> epitaxial garnet film, nucl. tracks effect on mag. props. 0-11234  
 La-Sm-Lu iron garnet film grown as NdGaG substrates, mag. props. 0-44888  
 MgFe<sub>2</sub>O<sub>4</sub>, epilayer, perpendicular anisotropy 0-39769  
 Mn-substituted garnet film, growth characts. and mag. props. 0-39826  
 Mn<sub>2</sub>Fe<sub>2</sub>O<sub>4</sub> epitaxial films, mag. and reson. props. 0-50149  
 (Y, Gd, Yb, Bi)<sub>3</sub>(Fe, Al)<sub>2</sub>O<sub>12</sub> epitaxial film, domain wall motion and oscill. 0-2616  
 (Y,Sm,Lu,Ca)<sub>3</sub>(Fe,Ga)<sub>2</sub>O<sub>12</sub> bubble magnetic garnet film, LPE grown, props., CaCO<sub>3</sub>/GeO<sub>2</sub> molar ratio influence 0-50152  
 (Y,Sm,Lu,Cu)<sub>3</sub>(Fe,Ga)<sub>2</sub>O<sub>12</sub>, ion implanted, hard bubble suppression 0-11238  
 (Y,Sm,Lu,Tm,Ca)<sub>3</sub>(Fe,Ga)<sub>2</sub>O<sub>12</sub>, epitaxial garnet film, temp. depend. mag. props. 0-39825  
 (Y,Gd)<sub>3</sub>(Ga,Fe)<sub>2</sub>O<sub>12</sub>, nonlinear magnetoelastic effects (French) 0-34745  
 (YGdYbBi)<sub>3</sub>(FeAl)<sub>2</sub>O<sub>12</sub> epitaxial film, diffuse domain wall, bubble domain expansion 0-25170  
 (YGdYbBi)<sub>3</sub>(FeAl)<sub>2</sub>O<sub>12</sub>, epitaxial film, 360° domain walls with periodically distrib. Bloch lines 0-7127  
 YIG bubble films, light scatt. from spin waves, hysteresis meas. by Voigt effect 0-15770  
 YIG, double layer struct., LPE growth from molybdate and Pb borate fluxes 0-39827  
 YIG epitaxial films, substituted, floating bubble domains, effect of structural stratification 0-2615  
 YIG ferromagnetic film, quasi surface spin wave giant oscills. (Russian) 0-15767  
 YIG, high energy heavy ion irradi., lattice strain 0-49278  
 YSmCaFeGe, mag. garnet films, segregation of Ca and Ge in LPE growth 0-29959  
 (YSmCaLu)<sub>3</sub>(FeGe)<sub>2</sub>O<sub>12</sub>, bubble film inhomogeneity, spin wave reson. meas. 0-44439  
 (YSm)<sub>3</sub>(FeGa)<sub>2</sub>O<sub>12</sub> film, LPE on Gd<sub>2</sub>Ga<sub>2</sub>O<sub>12</sub>, interface processes, horizontal dipping obs. 0-49552  
 (YSmLuCa)<sub>3</sub>(FeGe)<sub>2</sub>O<sub>12</sub>, double layer struct., LPE growth from molybdate and Pb borate fluxes 0-39827  
**magnetic field effects**  
*see also biomagnetism; galvanomagnetic effects; magnetic levitation; magnetic properties of substances; magnetic separation; magneto-optical effects; magnetoacoustic effects; magnetocaloric effects; magnetolectric effects; magnetohydrodynamics; magnetomechanical effects; particle optics; Scott effect; Senftleben-Beenakker effect; thermal magnetoresistance; thermomagnetic treatment*  
 arc (electric) in transverse aerodynamic and mag. fields, approx. model 0-24285  
 bacteria, effect of mag. field on recomb. fluoresc. 0-35856  
 biomolecular effects of 50 Hz EM fields, mechanism of effect (Russian) 0-51158  
 bituminous pitch oils, flow curves, mag. field effect 0-33553  
 black hole in external mag. field, relativistic particle radiation 0-22035  
 capillary-porous bodies, internal mass transfer, influence of inhomogeneous elec. and mag. fields 0-6138  
 catalyst surface mag. field effect on mol. dissociation rate 0-16721  
 conference, Munster, Germany (March 1979) 0-12843  
 diamond, electrolytic grinding, magnetic field effect 0-11790  
 disordered anisotropic antiferromagnet, random field effects 0-2580  
 drift instability, current-driven, sheared mag. field, finite-beta effect on transport 0-28617  
 electric breakdown in long tube 0-24120  
 electrolysis, annulus flow, solenoidal mag. field effect on ionic mass transport 0-26021



**magnetic field effects continued**

- electron gas, dielectric transition temp. in strong mag. field 0-24813  
 electron solid in superstrong mag. field, bifurcation theory approach 0-4640  
 epoxide compound, polymerisation in non-uniform magnetic field, exam. of structural changes 0-7791  
 epoxy resins, struct. changes under mag. field action 0-40516  
 excited nuclei moving through ferromag. media, transient mag. field effect, mag. moment meas. 0-37325  
 ferroelectric semiconductor, magnetic field influence, ferroelectric transitions 0-55049  
 field emitter vacuum breakdown, external mag. field effects, transition period 0-38824  
 fluids, conducting, dynamics under rotational mag. forces 0-48820  
 gauge variance for particles in an external magnetic field 0-47167  
 Gribble Limnoria tripinctata, reaction to intensity gradient of mag. fields (German) 0-56074  
 interplanetary magnetic field Z-components, variations causing magnetic storm main phase 0-4200  
 IV-VI compounds, mag.-field-induced displacive phase transition 0-50278  
 low melting, metals, on Cu surface, spreading kinetics 0-10742  
 lymphocytes, living and dead, mag. props. and mag. sedimentation 0-35925  
 magneto-rheological suspensions, elec. cond. 0-11960  
 plasma simulation, heat transport 0-28817  
 plasma transverse Cherenkov mode nonlinear stabilisation by external mag. field 0-38642  
 plasmas, magnetically confined, modes and ballooning 0-28650  
 positive column, deflection of radiation intensity by transverse mag. field 0-28866  
 relativistic theory of H atom in superstrong magnetic field 0-23320  
 stability of conductor suspended in alternating mag. field, theory and expt. 0-32869  
 thermomagneto-phoresis of particles in magnetic suspensions 0-35581  
 Ar+CO<sub>2</sub>, drift properties of tubular drift chambers in high magnetic fields 0-53917  
 Ar+isobutane+methylal, drift properties of tubular drift chambers in high magnetic fields 0-53917  
 CdMnTe, exciton ground state, magnetic field influence 0-54616  
 Ge resistive sensing devices, temp. calibration and reproducibility, high mag. field effect (Czech) 0-37029  
 H atom in mag. field, Schrodinger eqn., Monte Carlo soln. 0-31545  
 H, relativistic, in strong mag. field 0-9518  
 H<sub>2</sub><sup>+</sup>, high (10<sup>5</sup> G) mag. fields, dissociation energy, electron binding energy and equilib. separation 0-52910  
<sup>3</sup>He, solid, possible explanation for recently obs. phase transition in high mag. fields 0-20006  
 Pb<sub>1-x</sub>Ge<sub>x</sub>Te, degenerate semiconducting ferroelectric, structural phase transition temp., mag. field effects 0-45017

**magnetic field measurement**

- see also field plotting; fluxmeters; magnetometers  
 amplitude of alternating magnetic fields, EPR method 0-52277  
 compact preset SQUID for total field measurement 0-22392  
 distribution rapid meas. using NMR 0-27322  
 gaussmeter, Hall-probe adapter cct. for use with digital multimeter, leakage detect. 0-37014  
 geomagnetic surveys, field difference method with noise reduction 0-21850  
 Hall-effect magnetic field detection, for fields down to 10<sup>-3</sup> T 0-244  
 HF magnetic field standards, calibration field strength meters, biologically active, RF interference fields appl. (Polish) 0-51311  
 IC Hall generator appl. (German) 0-52276  
 magnetic pickup for spontaneous magnetic fields meas. near laser plasma 0-24246  
 microfields, quantitative registration on solid surface, using raster electron microscope 0-31790  
 optical fibre magnetostrictive perturbation for possible mag. field detect. 0-53450  
 plasma magnetic field determ. from charged particle beam defl. 0-28825  
 quantum devices appl., Rb maser, threshold sensitivity and short-term fluctuations determ. 0-22394  
 RF industrial heaters, elec. and mag. field strengths meas. 0-52175  
 solenoid, superconducting, magnetic field inhomogeneity measurement method, Hall probe appl. (Czech) 0-13107  
 visualisation based on narrow light beam reflection at inclined liquid surfaces (German) 0-31817

**magnetic field variations, earth** see geomagnetic variations**magnetic fields**

- see also electromagnetic fields; geomagnetism; interplanetary magnetic fields; interstellar magnetic fields; magnetic field effects; magnetic field measurement; solar magnetism; superconducting critical field  
 air coils, magnetostatic field FFT calcs., linear system theory 0-32868  
 charged particles in single wave fields, adiabatic and stochastic motion 0-9795  
 circuits with low permeability or saturated parts with permanent magnet, analytical calc. (German) 0-23596  
 computer methods, MHD and finite elements method 0-32879  
 cosmological magnetic fields and the Faraday rotation from QSOs 0-22087  
 cyclootron, one parameter function representation 0-18725  
 dipole, charged particle beam linear transformation coeffs. 0-5681  
 eddy currents force effects calc., induced in thin plate by cylindrical magnetic field 0-14269  
 external physical fields of sources investigation, modelling devices construction 0-17817  
 flowmeter, MHD type, with circ. cross section, inhomogeneous mag. field effect on signal 0-33709  
 high energy accelerators, superconducting dipole magnets with high field uniformity, development and investigation (Russian) 0-5416  
 homogeneous magnetic field synthesis in internal region of cylindrical solenoid (German) 0-37923  
 hybrid magnets for high mag. field generation, polyhelix coils, optimization calcs. 0-240  
 intergalactic magnetic fields and Faraday rotation of extragalactic radio sources 0-22086  
 inverse problems, soln. (Russian) 0-1102  
 Jupiter Galilean satellites, intrinsic mag. fields and magnetospheres props. 0-46465  
 Jupiter magnetic field, influence on Galilean satellites volcanism and rot. 0-31247

**magnetic fields continued**

- Jupiter magnetic field studies by Voyager 1, preliminary results 0-26793  
 lightning return stroke elec. and mag. fields, obs. in Florida 0-31096  
 lunar far-side magnetised regions, correl. with ringed impact basins 0-36521  
 magnetisation curve analytic functions, numerical parameter calc., variational methods appl. (Russian) 0-14267  
 magnetosphere model, particle (electric current) approach 0-17442  
 magnetosphere reconnection, substorms and energetic particle acceleration 0-31169  
 magnetostatic problems, soln. by MAGGY2 problem package 0-28134  
 megagauss fields, macroparticle acceleration 0-47789  
 MHD convector channel and regions, eddy current losses due to magnetic field variations 0-40874  
 Moon, anisotropic mag. fluctuations rel. to elec. cond. anomaly beneath Mare Serenitatis 0-56730  
 multipole DC electromagnet, working gap field analysis (Russian) 0-28142  
 non-stationary, calc. for current filament over conducting layer (Czech) 0-52283  
 numerical techniques in field calcs. 0-32878  
 permanent magnet and current-carrying conductor fields, Fe filing pictures, theory (German) 0-28145  
 permanent multipole magnets of oriented rare earth cobalt materials 0-37925  
 plane permanent magnet system field distrib. model (Russian) 0-28133  
 principles and appls., book 0-32866  
 reciprocity theorem for corrugated surfaces used in conical diffraction mountings 0-1333  
 solid state physics, high mag. fields, generation and application 0-27321  
 stellarator toroidal field production by modular systems 0-10441  
 superconducting systems, calculation method from boundary conditions (Ukrainian) 0-34545  
 synchronous machines, slot-less, armature and excitation field, analytical calc. method using polar coordinates (German) 0-32870  
 synchronous machines, slot-less, winding reactances and inductances determ. under stationary conditions (German) 0-32871  
 teaching w.r.t. chemistry, guide to units 0-12871  
 turbulent dynamo, dynamic eqn. of magnetic field 0-32880  
 Uranus, struct. and mag. field theory using two-layer model 0-4298  
 Fe, in magnetostatic field prod. by toroidal conductor 0-1104

**magnetic film stores**

- see also magnetic bubble devices  
 bubble materials, review 0-50153  
 Ni-Fe polycrystalline film cross-tie memory for shipborne radar/sonar 0-42204

**magnetic films** see magnetic thin films**magnetic fluids**

- ferrofluid constitution examination by rotating test tube method 0-33693  
 ferrofluid devices, magnetostatic and centrifugal, nonmagnetic body motion 0-33700  
 ferrofluid droplet, interphase boundary hydrostatic characts. in uniform mag. field 0-33692  
 ferrofluid flow in circular pipe, uniform mag. field effects 0-43782  
 ferrofluid patterns on thin film materials, zigzag form of charged domain wall 0-44852  
 ferromagnetic colloids, domain and grain obs. of highly-oriented Si steel 0-11856  
 ferromagnetic suspension, magnetorheological characts. meas., errors 0-33550  
 ferrosuspensions, internal rotations and the other transport phenomena 0-28573  
 flow in rotating vessel, homogeneous mag. field effect 0-33691  
 layer, thermocapillary instability with thermally insulated boundary 0-33595  
 loudspeaker design parameter dependence on props. 0-38206  
 magnetisation, absence of anisotropy effects 0-50146  
 motion in rotating homogeneous mag. field 0-28572  
 superparamagnetic particles, mutual attraction 0-29581  
 temperature-sensitive magnetic fluid, use in instrument for temp. meas. 0-31745  
 thermomagneto-phoresis of particles in magnetic suspensions 0-35581  
 waves, nonstationary, one-dimens., in fluid with intrinsic ang. momentum 0-33690  
 CrO<sub>2</sub> acicular particle suspensions, mag. props., optical meas. 0-44874  
 Fe colloidal dispersion, mag. props., struct. and oxidation 0-34699  
 Fe<sub>2</sub>O<sub>3</sub>, flocculated suspension in ethylene glycol, intrinsic viscosity rel. to shear rate 0-1502  
 γ-Fe<sub>2</sub>O<sub>3</sub>/Cr, pure and doped, acicular particle suspensions, mag. props., optical meas. 0-44874  
 Fe(OH)<sub>3</sub>-Fe(OH)<sub>2</sub> suspension system, potential-pH diagram 0-55728  
 Si-Fe, domain and grain obs. using ferromag. colloid technique 0-11219

**magnetic flux**

- see also flux creep; flux flow; flux-line lattice; flux pinning; fluxmeters; skin effect  
 ferromagnet, vortex lines, Heisenberg model calc. 0-50026  
 field measurement in toroidal plasma systems 0-49004  
 permanent magnets flux stability enhancement, by thermomechanical treatment, gyroscope-based guidance systems performance improvement 0-50144  
 plasma-β measurements in high-β fusion experiments from magnetic flux and luminosity profiles 0-49007  
 quantisation, topology theory appl. (Russian) 0-8770  
 skin effect transients on hollow sphere in plane field of system of conductors (German) 0-37927  
 superconducting round wire, flux distribution and hysteresis loss 0-34570  
 thermomagnetic motor, dynamic characts. and stable operation (Japanese) 0-16840

**magnetic flux jumping** see Meissner effect**magnetic glasses** see spin glasses**magnetic hardness** see ferromagnetic properties of substances**magnetic heads**

- Permalloy, magnetic head wear resistance and surface charact. against magnetic tape (Japanese) 0-35335  
 Permalloy, solid bonding for mag. head appl., wear resist. and microhardness 0-21172  
 Sendust alloy, magnetic head wear resistance and surface characts. against mag. tape (Japanese) 0-35335  
 CoNiB, corrosion-resistant amorphous mag. thin films 0-54923



**magnetic heads continued**

- Fe-Co-Si-B alloy appl., amorphous, rapidly quenched (*Japanese*) 0-54922  
 FeAl-Pr (16 wt.%), resist. depend. on rolling process, thermal treatment, tape recording appl. (*Polish*) 0-39555  
 FeCoB, corrosion-resistant amorphous mag. thin films 0-54923  
 FeTiB, corrosion-resistant amorphous mag. thin films 0-54923  
 MnZn ferrite, mag. anisotropy, effect on recording head characts. 0-39765  
 MnZn ferrite fabricated by hot isostatic pressing, recording head appl. 0-35139  
 Ni-Fe-Nb-Al(-Mo), wear resisting mag. head material, mag. props. and struct. 0-35350

**magnetic hysteresis**

- ferrites, hysteresis loops, formation processes 0-39813  
 ferrites, square hysteresis loop magnetisation mechanism and conditions 0-29577  
 ferromagnet, soft, hysteresis rel. to irreversible phase transition 0-34693  
 ferromagnetic alloy, transition to spin glass ordering 0-34628  
 ferromagnetic alloys, amorphous, sputter-deposited, soft mag. props., magnetostriction 0-34696  
 ferromagnetic fine particles, stability of magnetisation curling mode and magnetisation helicoid struct. 0-11227  
 ferromagnetic materials in strong fields, determination using equipment with Hall transducer 0-4745  
 ferromagnetic thin film magnetometer, development and performance 0-31808  
 ferromagnets and antiferromagnets, EM and acoustic energy attenuation in many-domain magnets 0-7140  
 hydrostatic pressure effect on ferrite props. of pressure sensors (*Polish*) 0-31707  
 loop tracer for mag. phase detection 0-22393  
 particles, interacting, switching behaviour, dipole and Stoner-Wohlfarth models 0-44870  
 Permalloy, conductor crossing effect on bubble propagation margins 0-29588  
 Permalloy RF sputtered films, struct.-sensitive mag. props. 0-34705  
 rare earth garnet thin films, macroscopic magn. props., magneto-optical expts. 0-46764  
 relays inductance measurement to TGL 24961 specification methods for Fe-cored coils (*German*) 0-4736  
 soft magnetic materials, hysteresis model 0-2606  
 spinels, domain wall formation inhibition, effect on bulk mag. props. 0-11220  
 steel, austenitic stainless, neutron irradi., mag. props. 0-29067  
 Stoner-Wohlfarth particle, two-component, hysteretic props. 0-11228  
 superconducting cable, magnetisation anisotropy meas. in hysteresis loss using Hall sensors 0-17966  
 superconducting composite, multifilamentary, AC losses in transverse AC mag. field 0-34568  
 superconducting round wire, flux distribution and hysteresis loss 0-34570  
 TlF-CuS<sub>4</sub>C<sub>4</sub>(CF<sub>3</sub>)<sub>4</sub>, spin-Peierls system, high-field phase 0-39816  
 CdCr<sub>2</sub>Se<sub>4</sub>, ferromag. semicond., photoinduced mag. anisotropy 0-50086  
 CdCr<sub>2</sub>Se<sub>4</sub> films, mag. hysteresis, domain struct., mag. viscosity 0-25169  
 Co film, ion beam sputtering prep., struct. and mag. props. 0-35085  
 Co-Ni-P, film, props. independent of mag. hysteretic and anhyseretic remanences (*French*) 0-2604  
 Co-P films, electrodeposited, magnetic recording media (*Japanese*) 0-29587  
 (Co<sub>1-x</sub>Fe<sub>x</sub>Ni<sub>y</sub>)<sub>80</sub>(Si<sub>1-x</sub>B<sub>2</sub>)<sub>20</sub>, amorphous films, spin wave spectra 0-34777  
 CoS<sub>2</sub>-Se, magnetism and metamagnetic transition, neutron diff. and NMR meas. 0-15717  
 Cu-Mn spin glass, hysteresis loops, temp. and field depend. 0-15742  
 CuMn, spin glass, mag. hysteresis meas. 0-34691  
 CuMn, spin glass, remanence, new approach from zero field NMR 0-34785  
 Eu<sub>1-x</sub>Gd<sub>x</sub>S films, mag. and elec. props. 0-15766  
 Fe colloidal dispersion, mag. props., struct. and oxidation 0-34699  
 Fe, film, ion beam sputtering prep., struct. and mag. props. 0-35085  
 Fe-Al alloys, rapidly quenched, mag. props. 0-29579  
 Fe-Co-B powders, synthesis and mag. props., appl. to mag. recording 0-20432  
 Fe-Co-Si-B sputtered amorphous thin film, coercivity, galvanomagnetic props., resistivity 0-29578  
 Fe<sub>40</sub>Ni<sub>38</sub>Mo<sub>2</sub>B<sub>18</sub> amorphous alloys, compatibility of DC and AC mag. props. 0-34695  
 α-Fe<sub>2</sub>O<sub>3</sub>-Li<sub>2</sub>O, structural and thermal phase behaviour from mag., spectral and thermal studies 0-2673  
 Fe<sub>2</sub>O<sub>3</sub>-Na<sub>2</sub>O-BaO glass, mag. props. 4.2-295K, micromagnetism (*French*) 0-39782  
 Fe<sub>3</sub>O<sub>4</sub>, magnetite particles, interaction fields effect on hysteretic props. 0-54921  
 Fe<sub>3</sub>O<sub>4</sub>, metallic phase, photocond. and mag. permeab., photoinduced changes 0-15566  
 Fe-Fe-Nb, cold-worked and aged, mag. props. and microstruct. 0-34690  
 Gd alloys, amorphous, mag. props. and ferromag. reson. 0-54952  
 Gd-Co amorphous films, struct. and mag. anisotropy 0-20438  
 Mn-Zn ferrite single crystals, mech. polishing effect on mag. props. (*Japanese*) 0-16569  
 MnZn ferrite, mag. loss accommodation depend. on freq. and amplitude of mag. field (*Russian*) 0-34686  
 MnZn ferrite, mag. permeability accommodation depend. on mag. field (*Russian*) 0-34685  
 Nb-Ti, single core conductor, carrying DC transport current, alternating field losses 0-34550  
 Ni film, ion beam sputtering prep., struct. and mag. props. 0-35085  
 (Ni<sub>0.75</sub>Mn<sub>0.25</sub>)<sub>52</sub>Si<sub>10</sub>B<sub>38</sub>, amorphous, exchange anisotropy, mag. susceptibility meas., 4.2K to room temp. 0-11186  
 (Pd<sub>0.965</sub>Fe<sub>0.0035</sub>)Mn<sub>0.05</sub>, ferromag. and spin-glass props. 0-2590  
 SmCo<sub>5</sub>, permanent magnet stability, during long-term ageing (*Chinese*) 0-55428  
 SrFe<sub>12</sub>O<sub>19</sub>, hysteresis loops, formation processes 0-39813  
 TbFe<sub>2</sub>, magnetoelastic props., magnetostriction hysteresis (*Russian*) 0-29590  
 YIG bubble films, light scatt. from spin waves, hysteresis meas. by Voigt effect 0-15770

**magnetic impurity interactions**

- Anderson impurities, interacting, pair, Fermi-liq. theory 0-44803  
 Anderson model, direct interaction between impurities 0-54681  
 critical temperature for Ising systems with regularly arranged impurities 0-44785

**magnetic impurity interactions continued**

- dilute alloy, appl. of low temp. nucl. orientation 0-15825  
 dilute ferromagnet, slow neutron inelastic scatt. by spin excitations, cluster approx. 0-11168  
 dilute rare earth in metal, effective exchange interaction model 0-25127  
 ferromagnet, impurity spin critical dynamics 0-2593  
 ferromagnet, metallic, correl. of temp. anomalies of hyperfine field and thermal expansion of lattice 0-20400  
 ferromagnetic nondegenerate semiconductor, magnetoresistance 0-11019  
 ferromagnetic transition metal, Fano effect and hyperfine field of non-transition impurity 0-25128  
 ferromagnets and antiferromagnets, mag. impurity levels, standard basis operator method (*Russian*) 0-11192  
 Heisenberg, impure classical chain, dynamic props. using local-moment pair correl. functions 0-15728  
 Kondo alloy, low temp. props. 0-2569  
 linear conductor, localized mag. moment formation and one and two impurity sites 0-50087  
 metal with magnetic impurity, appl. of low temp. nucl. orientation, book 0-3  
 metals, localised moment interaction, Alexander-Anderson model, perturbation expansion 0-29524  
 one-dimensional Hubbard model, Friedel oscills. around a nonmagnetic impurity 0-25073  
 one-dimensional systems, impurity effects on ordered phases 0-24905  
 semiconductor, doped with mag. impurity, ordering mechanism 0-2572  
 spin systems with quenched random impurities, dynamics, replicas and frustration approaches 0-34673  
 superconducting amorphous metals, mag. impurity interactions 0-44777  
 superconductor with mag. impurities, Shiba theory consequences beyond s-wave scatt., sp. ht. discontinuity 0-2516  
 TMMC:Cu, dynamic props. using local-moment pair correl. functions 0-15728  
 TMMC:Cu, EPR linewidth freq. depend., spin dynamics 0-15794  
 Cd<sub>1-x</sub>Mg<sub>x</sub>, magnetic susceptibility anisotropy, press. effects, electronic phase transitions (*Russian*) 0-54869  
 Co<sub>1-x</sub>Mn<sub>x</sub>F<sub>2</sub>, antiferromagnet mag. impurities, spin excitation spectrum collective rearrangement in external mag. field 0-50199  
 Cr alloys, localised magnetic moments in band antiferromagnets, impurity interactions (*Russian*) 0-54888  
 Cr-Fe, dilute, localised moment cluster model, ferromagnetic exchange coupling 0-39774  
 Cr-Fe<sub>x</sub> (x=0.5, 1.5 and 3.5 at.%), antiferromag., Kondo anomaly 0-11163  
 Cr-Ru, dil. absence of mag. hyperfine field, TDPAC meas. 0-50237  
 EuB<sub>2-x</sub>C<sub>x</sub>, magnetisation, effects of C 0-25163  
 Fe, hyperfine field at nonmagnetic impurities 0-25129  
 Fe-Ti, mag. moment distrib. and environmental effects around Ti impurity 0-7092  
 Fe-V(Cr)(Mn), dil., local mag. moments, polarised neutron elastic diffuse scatt. 0-50088  
 Fe:P:Cu, Mossbauer spectra, mag. transition 0-50240  
 FeS<sub>2</sub> (marcasite), temp. depend. mag. susceptibility 0-20391  
 InSb:Mn<sup>2+</sup> nondegenerate semicond., mag. impurity indirect interaction (*Russian*) 0-34591  
 K<sub>2</sub>CoF<sub>4</sub>Mn<sup>2+</sup>, impurity induced mag. excitations, magnon gap mode, far IR spectra obs. 0-44821  
 Nb<sub>78</sub>Ga<sub>22-x</sub>Mn<sub>x</sub>, supercond. props., influence of Mn mag. impurities 0-54825  
 Nb<sub>80</sub>Ga<sub>20-x</sub>Mn<sub>x</sub>, supercond. props., influence of Mn mag. impurities 0-54825  
 Ni-Ti, mag. moment distrib. and environmental effects around Ti impurity 0-7092  
 Ni<sub>0.95</sub>S Fe, spin glass, spin flop in exchange field 0-34640  
 β-NiAl, self consistent embedded cluster model for Fe, Co, Ni mag. impurities 0-2549  
 Ni<sub>1-x</sub>Au<sub>x</sub>-Co, dil., Mossbauer effect, mag. hyperfine field 0-20528  
 (Ni<sub>1-x</sub>Fe<sub>x</sub>)<sub>1-x</sub>Sn, anisotropic spin glass, mag. props. 0-39793  
 Ni<sub>2</sub>Mn<sub>2</sub>Ti<sub>1-x</sub>Sn, Mossbauer spectra, mag. hyperfine field 0-15857  
 Pb<sub>1-x</sub>Sn<sub>x</sub>Te: Mn, Mn mag. and elec. active states, mag. impurity behaviour 0-44627  
 PdAgFe, ferromag., Curie temp. depend. on susceptibility, non-mean field theory 0-44829  
 PdFeRh, ferromag., Curie temp. depend. on susceptibility, non-mean field theory 0-44829  
 PrEu(Gd), magnetic interactions, Mossbauer spectra quadrupole splitting, crystal field parameters 0-39907  
 (SN)<sub>x</sub>, thermopower from 0.15 to 4.2K 0-34427  
 Tb-Sr(Y)(La)(Lu)(Yb)(Mg)(Th), mag. ordering temps., susceptibility meas. 0-25136  
 Te-Fe alloy, Mossbauer spectra, hyperfine field 0-20526  
 Y(Fe<sub>1-x</sub>Ir<sub>x</sub>)<sub>2</sub>, magnetisation, mag. hyperfine field 0-20531  
 ZnTe:Mn, ordering mechanism 0-2572

**magnetic inks see magnetic fluids****magnetic leakage**

- amorphous magnetic alloys, ferromagnetic props. and appl. 0-50143  
 charged particles, multiple times for nonadiabatic leakage from mag. mirror traps 0-33806  
 composite superconductor, effect on losses in variable mag. field of mag. props. 0-34549  
 electrical steel sheets, specific core loss meas. using analogue wattmeter (*German*) 0-13099  
 electrotechnical steel, quality significance on energy and materials savings in magnetic circuits (*Czech*) 0-20947  
 gaussmeter, Hall-probe adapter cct. for use with digital multimeter, leakage detect. 0-37014  
 Fe-Ci, high permeability, mag. props., applied stress effects 0-34726  
 Fe-Ci (3 wt.%), commercially produced, grain-oriented, mag. props., stress coating effects 0-34727  
 Fe-Co-Si (4.1.5 wt.%), textured, mag. props. 0-35200  
 Fe-Si, coated, effective domain and grain obs. methods and Fe losses 0-34675  
 Fe-Si (3 wt.%), mag. props., stress coating effects 0-34728  
 Fe-Si (3 wt.%) locally deformed, EM loss depend. on cryst. struct. and orientation (*Russian*) 0-7694  
 Fe-Si (3 wt.%) steel, oriented, stress depend. mag. props., coating effects 0-34729  
 MnZn ferrite, mag. loss accommodation depend. on freq. and amplitude of mag. field (*Russian*) 0-34686



**magnetic leakage continued**

- MnZn soft ferrites, commercial grade, microstruct. rel. to mag. props. 0-34009  
 Nb-Ti, single core conductor, carrying DC transport current, alternating field losses 0-34550  
 Nb-Ti-Zr, superconducting wire, coil simulation meas. of losses and instabilities 0-37050  
 Nb<sub>3</sub>Sn, multifilament superconductor, pulsed mag. field losses and critical current densities 0-54853  
 V<sub>3</sub>Ga, multifilament superconductor, pulsed mag. field losses and critical current densities 0-54853

**magnetic lenses**

- see also aberrations*  
 deflection systems combined with mag. lenses, optical props. 0-31938  
 developments at the Cavendish Laboratory 0-37948  
 quadrupole lenses with sector magnets, nonzero emittance beam focusing conditions 0-23612  
 sextupole system for spherical aberration correction 0-43246  
 superconducting, bright-field imaging of single heavy atoms in an electron microscope with superconducting lens system 0-10472  
 two-lens projection systems, reduction of third-order distortion 0-48134  
 Fe-free ribbon type multipole magnetic lens 0-42300

**magnetic levitation**

- metals prep. by electromagnetic levitation in ultrahigh vac. 0-29899  
 Nb-Ti, sheet, flux trapping, appl. to mag. shielding and levitation 0-31806

**magnetic lines of force** *see magnetic flux***magnetic liquids** *see magnetic fluids***magnetic losses** *see magnetic leakage***magnetic materials**

- see also ferrites; garnets; magnetic fluids; magnetic thin films; permalloy; permanent magnets*  
 bibliography of William Fuller Brown, Jr 0-8751  
 conference, 2nd joint INTERMAG-MMM, New York, USA (July 1979) 0-27031  
 conference, Munster, Germany (March 1979) 0-12843  
 experimental magnetism, book 0-8747  
 halide, crystals, method of growing low-dimensional single crystal (Japanese) 0-50539  
 high-energy, props., treatment procedures and testing (Italian) 0-54914  
 layer magnetic properties meas. on saturated substrate 0-13108  
 magnetism research, materials development and appl. during past 25 years 0-36792  
 rare earth metals, alloys, and cpds., book 0-36785  
 recording on particulate media, conference, Gardone Riviera, Italy (Sep. 1979) 0-41930  
 sintering, structure and props., external mag. and elec. field influence 0-50570  
 soft magnetic materials, hysteresis model 0-2606  
 B and borides, conference, Varna, Bulgaria (Oct. 1978) 0-12842

**magnetic materials, amorphous** *see magnetic properties of amorphous substances***magnetic memories** *see magnetic storage systems***magnetic mirrors**

- bumpy torus, NBT-I, effective toroidal curvature, error field, electron beam diagnostics 0-24237  
 bumpy torus plasma, weak vertical mag. field effect on fluctuation induced transport 0-48946  
 bumpy torus reactor, beam driven 0-42859  
 charged particles, multiple times for nonadiabatic leakage from mag. mirror traps 0-33806  
 drift loss cone instability in inhomogeneous mag. field 0-48934  
 drift-cone instabilities in mirror-confined plasma 0-28630  
 drift-cone instability, nonlocal hybrid-kinetic stability anal. 0-24230  
 driven magnetic fusion reactors, conf., Erice-Trapani, Italy (Sept. 1978) 0-41948  
 EBT expts., simple annulus power balance 0-48947  
 electron cloud confinement, radial and longitudinal distrib. determ. 0-14928  
 enhanced plasma confinement by MHD oscillation 0-24205  
 field reversal studies 0-27802  
 field reversed mirror configuration, sustaining a toroidal current 0-28804  
 field reversed mirrors, fusion product energy distrib. 0-37595  
 fusion and hybrid reactors, plasma models 0-6273  
 fusion energy program, mirror approach 0-42855  
 fusion reactions, measuring MeV ions in magnetic mirror experiments 0-6281  
 fusion reactor, field-reversed mirror 0-42857  
 fusion reactor, time-dependent tandem mirror confinement, start-up and alpha particle build-up 0-10419  
 fusion reactor, using toroidally-linked mirrors 0-42858  
 fusion reactors, differences between mirror and toroidal fusion systems, superconducting magnets 0-32429  
 fusion reactors, field reversed mirrors 0-43961  
 fusion research, philosophy 0-42854  
 GAMMA 6, tandem mirror confinement expt. 0-28786  
 Hamiltonians of particle motion, canonical transforms. 0-33748  
 high density plasma in multiple mirror, low freq. instability 0-48870  
 hollow axisymmetric mirror, MHD stable, multipole field stabilization (Russian) 0-33801  
 hybrid tandem mirror reactors, design, fissile fuel production 0-27811  
 injected plasma particle refl. (trapping), quiescent (turbulent) plasma 0-48955  
 ion motion, superadiabatic and stochastic, in mirror-machine plasma, in presence of electrostatic wave 0-53933  
 linear gasdynamic confinement system 0-48957  
 mirror fusion test facility 0-43962  
 mirror hybrid reactors 0-42860  
 mirror machine, fusion reactors, survey 0-47721  
 mirror machine diagnostics 0-48958  
 mirror reactors, economic significance of Q 0-47722  
 multiple-mirror plasmas, MHD stabilisation 0-6244  
 Ogra-3 mirror device, loss mechanism due to cyclotron instabilities 0-28788  
 Ogra-3B, ECR as a diagnostic for mirror trap plasma 0-38709  
 Ogra-3B, open mag. mirror trap, with min. B, LF oscils. 0-38708  
 quasi steady high beta plasma in multiple mirror machine, density oscill., stability obs. 0-28663  
 superconducting magnets, mirror fusion test facility 0-42862

**magnetic mirrors continued**

- tandem mirror, passive generation of ambipolar pot. barriers 0-24203  
 tandem mirror confinement studies 0-28785  
 tandem mirror hybrid; <sup>233</sup>U prod. 0-47708  
 tandem mirror physics, fusion plasma confinement 0-43960  
 tandem mirror reactor, plasma parametric studies and appl. 0-42865  
 Tandem mirror reactors, anomalous and classical transport effect 0-13862  
 tandem mirror reactors, fusion power reactor and fusion-fission hybrid reactor 0-42856  
 tandem mirrors, analytic approx. to resonant plateau transport coeff. 0-32486  
 toroidal collective focusing accelerator for heavy ion acceleration 0-14015  
 transverse confinement of high press. plasma in corrugated mag. field 0-48944  
 Twin Beam Mirror, effect of hot beam injection angle 0-48939

**magnetic moments**

- see also atomic magnetic moment; hyperon magnetic moment; local moments in dilute systems; meson magnetic moment; molecular moments; nuclear magnetic moment; proton magnetic moment*  
 actinide metallic systems, magnetism 0-7076  
 alkali metal-transition metal double molybdates, paramag. behaviour (French) 0-39734  
 alloy with two ferromagnetic components, surface excitations 0-25179  
 amorphous magnet, magnetisation, mag. moment temp. distrib. 0-15848  
 amorphous magnetic layers, SAW device appl. 0-28389  
 anisotropic paramagnet with exchange-bond dilution, sixth freq. moments 0-44789  
 antiferromagnet, magnetic dislocation domains, mag. moment distribution 0-2601  
 arbitrary moving magnetic dipole, EM field calc. (Russian) 0-9772  
 baryon, incorrect value from static compound quark models 0-9169  
 baryon magnetic moments, implications for quark model 0-13290  
 baryons, current status, additional symmetry breaking assumptions 0-4995  
 baryons, mag. moment calcs. in quark models 0-27505  
 baryons, ordinary and charmed, magnetic moments in broken SU(4) 0-18136  
 borate glass: Ni, absorption spectra, mag. props., coordination behaviour (German) 0-40147  
 composite models, mag. moments of quarks, leptons and hadrons 0-32081  
 current density and electric and magnetic multipole-moment operators in quantum mechanics 0-27433  
 dimethylammonium copper chloride bromide, mag. props., pulsed NMR expts. 0-11292  
 education, Dirac delta function, appl. elec. current and mag. multipole distrib. 0-17740  
 ferrofluids, magnetisation, absence of anisotropy effects 0-50146  
 ferromagnetic alloys, amorphous, sputter-deposited, soft mag. props., magnetostriiction 0-34696  
 ferromagnetic alloys, disordered crystalline and amorphous, dipole field distribution 0-25101  
 ferromagnetic nondegenerate semiconductor, magnetoresistance 0-11019  
 ferromagnetic transition metal alloys, mag. props. review 0-44823  
 ferromagnetism and ferroelectricity, coexistence in systems with electron-hole pairing 0-7310  
 ferromagnets, solitary domains, Bloch and Neel stability, calcs. 0-25157  
 frequency-dependent electric and magnetic multipole moments and Siegert's theorem 0-27432  
 hamiltonian for the nonrelativistic two-fermion bound state 0-13273  
 Heisenberg paramagnet, exchange bond dilution, freq. moments of spin correl. function 0-50030  
 high-field solenoid field gradient appl. 0-31813  
 induced moment systems, effect of spin fluctuations 0-2585  
 Invar, magnetic and thermal anomalies 0-34603  
 itinerant-electron ferromagnetic film on nonmagnetic metallic substrate, mag. props. 0-20371  
 Lee model in EM field, mag. moment calc. using Schwinger source theory 0-42350  
 light emission by mag. and elec. dipoles, radiation patterns 0-32886  
 low lying baryons, anomalous mag. moment contrib. from quarks 0-42462  
 magnetic structure elastic polarised neutron scatt. atomic mag. moments 0-29531  
 metal hydrides, rare earth and intermetallic, electronic and mag. props., Mossbauer study 0-34830  
 metal-H systems at high H press., physicochemical props., book contrib. 0-24535  
 metals, ferromagnetic, point contact spectroscopy, electron-magnon interactions (Russian) 0-54766  
 metastable polarised crystals, decay kinetics, exchange magnon-phonon interactions (Russian) 0-7060  
 neutron, electric and magnetic dipole moments 0-4993  
 neutron magnetic moment meas., separated oscillatory-field magnetic resonance technique 0-22613  
 neutron resonances, polarised neutron expts., spin depend. of neutron cross-sections, mag. moments, radiation capture of neutrons (Russian) 0-52654  
 non-stoichiometric phase, physico-chemical props. 0-29532  
 one-spin ferromagnet, high temp. series expansion for mag. susceptibility and sp. ht. 0-25148  
 orthoferrites, weak ferromagnetism, single ion anisotropy contrib. 0-25126  
 periodic lattice, theory of coexistence of supercond. and magnetism, supercond. transition temp. 0-34543  
 Permalloy-Rh, film, influence of Rh on corrosion resist. and mag. props. 0-3235  
 phosphate glass: Ni, absorption spectra, mag. props., coordination behaviour (German) 0-40147  
 planetary magnetic moments, two predictions from scaling law test 0-21934  
 polyarylenealkyls, colour, EPR, electron density delocalisation degree determ. (Russian) 0-7152  
 quark colour magnetic moment 0-42400  
 rare earth compounds, binary, regression eqns., for calc. props. from electron struct. 0-39498  
 rare earth dihydrides and dideuterides, electronic and mag. props. 0-25260  
 rare earth intermetallic cpds., mag. props., book contrib. 0-39759



## magnetic moments continued

rare earth metasilicates,  $R_2(\text{SiO}_3)_3$ , mag. susceptibility, temp. depend., 77-800K 0-20372  
 rare earth mixed valence compounds, charge dominated fluctuation props. comparison, mag. moments and ordering 0-54659  
 rare earth perovskites, prep. and props. book contrib. 0-44193  
 rare earth-Au(Cu), amorphous, mag. and transport props. 0-34605  
 rare earth-Cu intermetallic compds. single crystals, mag. props. 0-54892  
 rare earth-transition metal (4f-3d) intermetallic cpds., mag. moment and mag. anisotropy 0-25107  
 rotating coordinate system with quadrupole splitting, paramag. susceptibility 0-11178  
 spin system, absorpt. of energy under parallel pumping conditions 0-2592  
 spin wave damping, magnetic materials with canted mag. struct., thermodynamic and high freq. props. 0-11184  
 steel, Cr-Ni-Mo-V, Mossbauer austenitometry and mag. props. 0-40003  
 superconductor, critical temperature mag. field depend., strong diamagnetism (*Russian*) 0-7022  
 superparamagnetic particles, Mossbauer spectra, magnetisation vector precession 0-15872  
 surface and interface magnetism by Mossbauer spectroscopy 0-7218  
 transition metal alloys, ferromag., high-field susceptibility 0-7083  
 transition metal amorphous alloys, mag. props. 0-29576  
 transition metal surfaces, mag. props. 0-44861  
 3d-transition metal-metalloid cryst. and glassy alloys, electronic struct. from magnetisation and Mossbauer meas. 0-29363  
 Wigner crystal, lattice quantum oscills. in mag. field, specific heat, mag. moments (*Russian*) 0-49636  
 D and F meson spectra, electromagnetic interactions effect 0-47293  
 $\mu$ , anomalous mag. moment, finite QED 0-47222  
 $\mu$  magnetic moment, weak coupling contribution, Weinberg-Salam model 0-22607  
 $\mu$  magnetic moment form factor 0-18138  
 n, anomalous magnetic moment in struct. model using phions 0-18134  
 BaVSe<sub>3</sub>, one-dimensional, struct. and mag. props. 0-28993  
 CaB<sub>6</sub>-SmB<sub>6</sub>, mag. props., comp. depend. 0-50034  
 CdS, press. quenched, mag. moment, semicond.-conducting transition 0-15683  
 CeAl<sub>2</sub>, Anderson lattice system, mag. moment reduction, press. effects 0-7093  
 CeFe<sub>2</sub>, ferromagnetic cpds., mean field exchange const., Stoner itinerant model calcs. 0-50084  
 CeX (X=P, As, Sb, Bi), neutron inelastic scatt. expts. 0-19674  
 (Co<sub>1-x</sub>M<sub>x</sub>)B, M=Mn or Fe, ferromag., internal fields meas. by NMR spin echo 0-29646  
 CoMnP, ferromagnetism and metamagnetism, polarized neutron diff. study 0-44809  
 CoS<sub>2</sub>-Se, magnetism and metamagnetic transition, neutron diff. and NMR meas. 0-15717  
 CoS<sub>2</sub>-Se<sub>x</sub>, conc. and temp. effects on metamagnetic transition 0-15716  
 Co<sub>1-x</sub>Ti<sub>x</sub>, ferromag. props., Ti conc. effect 0-54872  
 CoU<sub>2</sub>S<sub>3</sub>, mag. struct. and props. 0-11166  
 Cr alloys, localised magnetic moments in band antiferromagnets, impurity interactions (*Russian*) 0-54888  
 Cr, electronic structure model, Invar effect, antiferromagnetic-non mag. transitions 0-20370  
 Cr-Fe, antiferromagnetic, effect of press. on hyperfine mag. fields at Fe nuclei (*Russian*) 0-15936  
 Cr-Fe, disordered, polarised neutron diffuse scatt. meas., 4.6-110K 0-34592  
 CrB<sub>2</sub>, CrB, and Cr<sub>3</sub>B<sub>3</sub>, mag. and thermal props. at low temps. 0-20385  
 Cr<sub>x</sub>Mn<sub>1-x</sub>As, antiferromagnetic-ferromagnetic transition, mag. moment and elec. resist. meas. 0-15718  
 Cr<sub>x</sub>Mn<sub>1-x</sub>As, antiferromag. to ferromag. transitions, superexchange-double exchange mag. coupling, susceptibility and resist. obs. 0-50070  
 Cr<sub>1-x</sub>Ti<sub>x</sub>N, cryst. and mag. struct., at low temps. (*French*) 0-29005  
 Cs<sub>2</sub>K<sub>2</sub>TmBr<sub>6</sub>(Cl<sub>6</sub>)(F<sub>6</sub>), Cs<sub>2</sub>NaTmF<sub>6</sub> and Cs<sub>2</sub>RbTmF<sub>6</sub>, mag. behaviour 2.9 to 251.3K, cryst. field levels, ang. overlap model (*German*) 0-29520  
 Cs<sub>2</sub>NaTmCl<sub>6</sub>, UV absorpt. spectra, mag. circular dichroism spectra, vibr. obs. 0-29758  
 CsNiF<sub>3</sub>, demagnetising effects on antiferromag. reson. 0-15803  
 CsYbO<sub>2</sub>, normal-temp. form, mag. props. (*German*) 0-54864  
 CuCr<sub>2</sub>Se<sub>4</sub>(S<sub>4</sub>)(Te<sub>4</sub>), binary and ternary solid solns., mag. and elec. props. 0-2407  
 $\alpha$ -Cu<sub>2</sub>V<sub>2</sub>O<sub>7</sub>, EPR and mag. susceptibility meas., mag. moment calc. 0-2627  
 Dy, liq., mag. susceptibility, elec. resistivity 0-20377  
 Dy-Sm, magnetic moment growth due to Sm addition (*Russian*) 0-34608  
 Dy<sub>6</sub>Mn<sub>23</sub>, magnetic moments, magnetisation 0-25094  
 ErFe<sub>2</sub>H<sub>8</sub>, mag. props. 0-25095  
 ErFe<sub>2</sub>Mn<sub>23</sub>, magnetic moments, magnetisation 0-25094  
 ErVO<sub>3</sub>, produced by Er<sub>2</sub>O<sub>3</sub>+VO<sub>2</sub> high-press. reaction, cryst. struct. and mag. props. meas. 0-19773  
 EuCrO<sub>3</sub>, long term mag. ordering, antiferromagnetic resonance study (*Russian*) 0-54953  
 EuMg<sub>2</sub>, Mossbauer effect, effective moments, mag. ordering temp. and isomer shifts 0-34833  
 Eu<sub>2</sub>Mg<sub>17</sub>, Mossbauer effect, effective moments, mag. ordering temp. and isomer shifts 0-34833  
 EuO(S)(Se)(Te), cryst. and electronic struct., mag., elec., and optical props., book contrib. 0-39760  
 Eu<sub>x</sub>Sr<sub>1-x</sub>S, dil. insulator spin-glass versus blocking 0-34641  
 Fe alloys, BCC, Mossbauer spectra, local mag. moments 0-15861  
 Fe alloys, FCC, Invar effect, model 0-25105  
 Fe base amorphous alloys, Invar and Elinvar characts. 0-29592  
 Fe colloidal dispersion, mag. props., struct. and oxidation 0-34699  
 Fe complexes, 2- or 3-pyridyl imine complexes of FeCl<sub>2</sub>, Mossbauer and mag. props. 0-15896  
 Fe complexes with dimethylformamide, dimethylthioformamide, Mossbauer and mag. props. 0-39974  
 Fe epitaxial film, Mossbauer effect, interface magnetism 0-11297  
 Fe powder, BH<sub>4</sub> reduced, coercive force and remanence ang. variation 0-44879  
 Fe powders, prep. by BH<sub>4</sub> process, comp. and stability 0-44878  
 Fe pyrophoric powders, stabilising layer form. during passivation, saturation moment meas. 0-44865  
 Fe-Al, Mossbauer spectra, local mag. moments 0-15861  
 Fe-Al-Fe, phase diagram, microscopic model 0-34630  
 Fe-B amorphous alloys, Mossbauer spectra, mag. moment conc. depend. 0-15847  
 Fe-Cr-B, amorphous, Elinvar and Invar charact. (*Japanese*) 0-11832

## magnetic moments continued

Fe-Ni(Cr), Invar, exchange interactions between ferromag. and antiferromag. components 0-29545  
 Fe-P-B, amorphous alloy, Mossbauer effect and short-range order 0-2675  
 Fe-P-C, amorphous alloy, Mossbauer effect and short-range order 0-2675  
 Fe-SiO multilayer film, interface magnetisation 0-7135  
 Fe-Ti, mag. moment distrib. and environmental effects around Ti impurity 0-7092  
 Fe<sub>2</sub>Al, mag. moment determ., role of local environment, self consistent calcs. 0-44815  
 FeGe<sub>2</sub> canted antiferromagnet, mag. susceptibility anisotropy and temp. dependence 0-25112  
 Fe<sub>12</sub>, cyclodextrin, quasi-one-dimens. cpd., synthesis, elec. and mag. props. 0-2380  
 Fe(N<sub>3</sub>)<sub>5</sub><sup>2-</sup>, paramag. relax. in trigonal bipyramidal environment, Mossbauer spectra 0-15871  
 (Fe<sub>1-x</sub>Ni<sub>x</sub>)<sub>77</sub>Si<sub>10</sub>B<sub>13</sub> amorphous alloy system, saturation mag. moment, Curie temp., mag. susceptibility 0-39753  
 FeO-FeS, mag. susceptibility, eutectic phase diagram (*Russian*) 0-15682  
 $\alpha$ -Fe<sub>2</sub>O<sub>3</sub>, haematite, substituted, Morin transition, neutron diff. study 0-54897  
 Fe<sub>2</sub>Pt, non-linear local environment effect, Mossbauer effect of <sup>57</sup>Fe and <sup>195</sup>Pt 0-39910  
 Fe<sub>1-x</sub>Ti<sub>x</sub>, ferromag. props., Ti conc. effect 0-54872  
 Gd, liq., mag. susceptibility, elec. resistivity 0-20377  
 Gd(Co<sub>2</sub>Ni<sub>1-x</sub>)<sub>2</sub>, Mossbauer spectra, mag. props. 0-20563  
 Gd(Fe<sub>2</sub>Ti<sub>1-x</sub>)<sub>2</sub>, Mossbauer spectra, mag. props. 0-20563  
 Gd<sub>2</sub>Mn<sub>23</sub>, magnetic moments, magnetisation 0-25094  
 Gd(Rh<sub>1-x</sub>Fe<sub>x</sub>)<sub>2</sub>,  $x \leq 0.15$ , magnetisation and EPR studies 0-34767  
 Hf(Fe<sub>1-x</sub>Co<sub>x</sub>)<sub>2</sub>, mag. props., Mossbauer spectra and magnetisation meas. 0-39948  
 Ho, liq., mag. susceptibility, elec. resistivity 0-20377  
 Ho-Dy-Sm, magnetic moment growth due to Sm addition (*Russian*) 0-34608  
 Ho-Sm, magnetic moment growth due to Sm addition (*Russian*) 0-34608  
 HoFe<sub>2</sub>H<sub>8</sub>, mag. props. 0-25095  
 Ho<sub>2</sub>Ge<sub>4</sub>, mag. struct., neutron diff. study 0-25093  
 InSb:Mn<sup>2+</sup> nondegenerate semicond., mag. impurity indirect interaction (*Russian*) 0-34591  
 LaNi<sub>1-x</sub>Fe<sub>x</sub>O<sub>3</sub>, Mossbauer spectra, mag. hyperfine field 0-20537  
 Li-transition metal dioxide intercalation compounds, mag. props., decomposition effects 0-25075  
 LuFe<sub>2</sub>, ferromagnetic cpds., mean field exchange const., Stoner itinerant model calcs. 0-50084  
 $\alpha$ -Mn, electronic structure model; Invar effect, antiferromagnetic-non mag. transitions 0-20370  
 x.MnO<sub>2</sub>(1-x)[19TeO<sub>2</sub>.PbO], glass, antiferromag. behaviour, mag. props. 0-50072  
 Nd<sub>2</sub>Eu<sub>1-x</sub>B<sub>6</sub> solid solution, mag. susceptibility, lattice parameters, Weiss temp. 0-29535  
 Ni film, few atomic layers thick, transition from Pauli paramag. to band ferromag. 0-44885  
 Ni, rectilinear screw dislocation, magnetisation distrib., mag. moment anal. 0-44897  
 Ni-Fe-Pd thin films, mag., surface and corrosion props. 0-34707  
 Ni-Mn, mag. moment and asphericity of spin density distrib., polarised neutron scatt. obs. 0-44813  
 Ni-Pt, magnetic moment distrib., diffuse neutron scatt. meas. 0-34593  
 Ni-SiO multilayer film, interface magnetisation 0-7135  
 Ni-SiO<sub>2</sub> supported catalysts, particle size, H<sub>2</sub> chemisorption, Mossbauer study 0-7219  
 Ni-Ti, mag. moment distrib. and environmental effects around Ti impurity 0-7092  
 Ni<sub>2</sub>Al, electronic, mag., and cohesive props. 0-44491  
 Ni<sub>2</sub>Fe, non-linear local environment effect, Mossbauer effect of <sup>57</sup>Fe 0-39909  
 Ni<sub>1-x</sub>Ti<sub>x</sub>, ferromag. props., Ti conc. effect 0-54872  
 NpFe<sub>2-x</sub>Co<sub>x</sub>Si<sub>2</sub>, mag. and hyperfine props. 0-7247  
 Pd-Mn, dil. alloy, very temp. magnetisation 0-34692  
 PrEu(Gd), magnetic interactions, Mossbauer spectra quadrupole splitting, crystal field parameters 0-39907  
 PrSb, pressure-induced antiferromag., neutron scatt. study 0-39750  
 Pt<sub>1</sub>Mn<sub>1</sub>Cr<sub>1-x</sub> alloys, mag. props. 0-2562  
 RbCoCl<sub>3</sub>2D<sub>2</sub>O, metamagnetic phase transition, crystallographic and mag. struct., neutron diff. meas. 0-44174  
 SmFe<sub>2</sub>, ferromagnetic-ferri-mag. cpds., mean field exchange const., Stoner itinerant model calcs. 0-50084  
 SmN, magnetic props., neutron diff. and mag. susceptibility meas. 0-50036  
 SrF<sub>2</sub>:Tb<sup>3+</sup>, mag., thermal and hyperfine props. 0-29368  
 SrFe<sub>12</sub>O<sub>19</sub>, hysteresis loops, formation processes 0-39813  
 Sr<sub>2</sub>Zn<sub>2</sub>Y(Y=Ba<sub>2-x</sub>Fe<sub>2</sub>O<sub>22</sub>),  $x=0, 1, 1.6$ , mag. moments reorientation 0-44851  
 Tb, liq., mag. susceptibility, elec. resistivity 0-20377  
 Tb-Sm (*Russian*) 0-34608  
 TbP, singlet-groundstate magnetism, static mag. props. 0-7109  
 Tb<sub>2</sub>Y<sub>1-x</sub>Co<sub>0.5+0.1x</sub>, exchange interactions and magnetocrystalline anisotropy 0-34618  
 TiBe<sub>2</sub>, neutron diff. study of mag. ordering 0-44811  
 TiO<sub>2</sub> and (Ti<sub>1-x</sub>V<sub>x</sub>)<sub>2</sub>O<sub>7</sub>, metal-insulator transitions, EPR, elec. and mag. props. 0-2336  
 (Ti<sub>1-x</sub>V<sub>x</sub>)<sub>2</sub>O<sub>3</sub>, spin-glass props., 0.05-300K 0-25149  
 TmFe<sub>2</sub>H<sub>8</sub>, mag. props. 0-25095  
 Tm<sub>2</sub>Fe<sub>2</sub>O<sub>12</sub>, mol. field coeffs., mag. moment/temp. relations 0-50067  
 TmSe, mag. props. and struct. 0-25109  
 UGa<sub>2</sub>, mag. and magnetoelastic props. 0-15775  
 US(Se)(Te), photoelectron energy distrib. and spin polarisation, electronic and mag. props. 0-16146  
 USb, neutron inelastic scatt. meas., phonon spectra, mag. response, anisotropy 0-50065  
 USb<sub>0.8</sub>Te<sub>0.2</sub>, magnetisation and neutron meas., mag. moments 0-15703  
 UTe, magnetisation and neutron meas., mag. moments 0-15703  
 V<sub>2</sub>S<sub>5</sub>, paramag. cryst., struct. factors using polarised neutron diff. 0-15691  
 YFe<sub>2</sub>, ferromagnetic cpds., mean field exchange const., Stoner itinerant model calcs. 0-50084  
 Y(Fe<sub>2</sub>Al<sub>1-x</sub>)<sub>2</sub>, Mossbauer spectra and mag. props. 0-39950  
 Y(Fe<sub>1-x</sub>Mn<sub>x</sub>)<sub>2</sub>, Mossbauer spectra and mag. props. 0-39952  
 YFeO<sub>2</sub>:Co<sup>2+</sup>, weak ferromagnetism, single ion anisotropy contrib. 0-25126  
 Y(Fe<sub>2</sub>Ti<sub>1-x</sub>)<sub>2</sub>, Mossbauer spectra, mag. props. 0-20563



**magnetic moments continued**

- $Y_{1-x}Gd_xCo_2$ , exchange interactions and magnetocrystalline anisotropy 0-34618  
 ( $Y_{1-x}Gd_x$ ) $Co_2$ , spin echo NMR of mag. states 0-7190  
 YIG, polariser neutron study of covalency effects 0-2552  
 $Y_6Mn_{21}$ , magnetic moments, magnetisation 0-25094  
 $Y_{1-x}Nd_xCo_5$ , exchange interactions and magnetocrystalline anisotropy 0-34618  
 Yb-Eu alloys, mag. ordering, magnetisation meas. 0-7081  
 Zn-Mn(Cr), dil, mag. anisotropy, Hartree-Fock calcs. 0-11162  
 $Zr_{1-x}Nb_xZn_2$ , microscopic mag. props., NMR investigation 0-15807

**magnetic monopoles**

- (2+1) dimensional Georgi-Glashow model, critical Higgs mass, clustering, monopoles 0-52441  
 Bogomolny-Prasad-Sommerfield monopole, multiinstanton ADHM generalisation 0-52407  
 charmed baryons, elec. and mag. quarks rel. to Dirac mag. monopoles 0-402  
 classical field eqns. with a mag. charge 0-4872  
 conference on hadron struct. and lepton-hadron interactions, Cargèse, France (July 1977) 0-4473  
 cosmic, behaviour in geomagnetic field (*Chinese*) 0-46358  
 Dirac's monopole and the Hopf map 0-27402  
 Dirac monopoles and the Hopf map  $S^3 \rightarrow S^2$  0-32042  
 Dirac string Lagrangian in  $A^0_0$  gauge, path integral quantisation 0-32007  
 duality invariance, simple gauge theories including EM-type fields with sources 0-27440  
 duality rotations in EM charge space, secondary symmetry, magnetic current conservation 0-27431  
 energy tension and gravitational field (*French*) 0-52075  
 Euclidean manifolds, N-dimensional instantons and monopoles 0-42321  
 instantaneous Coulomb interaction in SU(2) Yang-Mills QCD 0-22574  
 linear deformations of the Prasad-Sommerfield monopole 0-52419  
 long range interactions in non-Abelian gauge fields 0-22520  
 monopoles with no strings, action principle and canonical quantisation 0-31990  
 path group appl. to gauge theory and quarks 0-31985  
 Prasad-Sommerfield dyon (monopole) soln. of SU(2) Yang-Mills field with Higgs multiplet 0-339  
 PT-invariant theory of massive dually charged particles, Dirac-like eqn. 0-52429  
 QFT of mag. charges, one pot. formulation 0-22512  
 relativistic classical eqns. of motion, electric dipole moment case 0-37195  
 spin 1/2 particle, motion in field on mag. monopole 0-18097  
 stability analysis, Yang-Mills equations 0-31987  
 stationary charged C-metric 0-17849  
 SU(2) magnetic monopole solns., parameter counting in Prasad Sommerfield limit 0-352  
 SU(N) gauge theory, current synchrospherical symmetrical monopole in multisynchrospherical symmetrical case (*Chinese*) 0-22527  
 superfluid flow analogy to Dirac's monopole 0-6575  
 superheavy magnetic monopoles, cosmological prod. in grand unified models 0-8884  
 supersymmetric point particles and monopoles with no strings 0-52432  
 tachyon + bradyon interactions, superluminal and subluminal EM fields 0-12902  
 unitarity and renormalized 't Hooft identities 0-13205  
 very early Universe, phase transitions and mag. monopole prod., grand unification 0-51934  
 Yang-Mills fields, equivalence with equation of motion of monopole system, 't Hooft monopolar solution 0-9084  
 Yang-Mills theory, magnetic monopoles in the presence of quark sources 0-13213  
 zero energy fermions in U(1) pointwise monopole field (*Chinese*) 0-42345

**magnetic permeability**

- composite superconductor, effect on losses in variable mag. field of mag. props. 0-34549  
 dialkylammonium copper tetrachloride, ferromagnetic layer compound, magnetostatic mode excitation 0-29538  
 electrotechnical steel, quality significance on energy and materials savings in magnetic circuits (*Czech*) 0-20947  
 heterogeneous matrix system, generalised conductivity and loss, tangent 0-7289  
 magnetization curve and Gaussian error function (*German*) 0-50137  
 metal powders, packed, complex mag. permeability calcs. 0-29583  
 metallic glasses, characts. and appls. (*French*) 0-39815  
 steel, austenitic stainless, neutron irradiat., mag. props. 0-29067  
 steels, ferritic and martensitic, C and N migration at low temps., monograph 0-22149  
 transition metal amorphous alloys, mag. props. 0-29576  
 $Ca_{0.9}Ni_{0.1}Fe_2O_4$ , initial permeability and Curie temp. 0-25130  
 $CdCr_2Se_4$ , ferromagnetic low anisotropy semicond., spontaneous magnetisation RF determ. 0-22396  
 $CdCr_2Se_4$ , spin system heating by drifting current carriers, magnon-phonon system energy transfer (*Russian*) 0-29541  
 ( $Co, Fe, Mn$ ) $_2Si_2B_{14}$  amorphous alloys ( $M = V, Nb, Ta, Cr, Mo, W, Mn$  or  $Ni$ ), zero magnetostriction and low field mag. props. 0-34741  
 $Co-Ni(Ti)(Cu)(Mn)$ , cryst. struct. and stacking fault influence on mag. props. (*Russian*) 0-25164  
 $Co_{70}Fe_{30}B_{14.5}$  amorphous thin films, zero magnetostriction, high magnetisation 0-34708  
 $CuCr_2Se_4$ , crystal growth from melt, exam. of props. 0-55283  
 $EuO$ , spin system heating by drifting current carriers, magnon-phonon system energy transfer (*Russian*) 0-29541  
 Fe-Al alloys, rapidly quenched, mag. props. 0-29579  
 Fe-B-Si amorphous ribbons, effect of annealing conditions on magneto-mechanical props. 0-34740  
 Fe-Ci, high permeability, mag. props., applied stress effects 0-34726  
 Fe-Ci (3 wt.%), commercially produced, grain-oriented, mag. props., stress coating effects 0-34727  
 Fe-Co-Si-B alloy, amorphous, rapidly quenched, mag. heads appl. (*Japanese*) 0-54922  
 Fe-Ni-Si-Mn-Cr(Co-Mo), effect of prolonged aging on mag. props. 0-16513  
 Fe-P amorphous alloys, initial permeability, time depend. 0-15759  
 Fe-Si (3 wt.%), mag. props., stress coating effects 0-34728  
 Fe-Si (3 wt.%) steel, high permeability, magnetostriction, stress inducing coating effects 0-34730  
 Fe-Si-B, melt C content effect on grain growth and induction 0-35351

**magnetic permeability continued**

- Fe-Si-B amorphous films, mag. props. 0-34710  
 $Fe_{50}Co_{70}Si_{10}B_{15}$  amorphous magnetic alloy, decrease of permeability after demagnetisation, disaccommodation 0-39814  
 $Fe_{40}Ni_{38}Mo_2B_{18}$  amorphous alloys, compatibility of DC and AC mag. props. 0-34695  
 $Fe_2O_4$ , metallic phase, photocond. and mag. permeab., photoinduced changes 0-15566  
 $Fe(OH)_3$ - $Fe(OH)_2$  suspension system, potential-pH diagram 0-55728  
 MnZn ferrite, mag. permeability accommodation depend. on mag. field (*Russian*) 0-34685  
 MnZn ferrite fabricated by hot isostatic pressing, recording head appl. 0-35139  
 MnZn soft ferrites, commercial grade, microstruct. rel. to mag. props. 0-34009  
 Ni-Al-Ti ferromagnetic non-homogeneous alloy, composition determination by Curie temp. meas. 0-11196  
 Ni-Fe-Nb (Mo), magnetic alloy, TEM and X-ray obs. (*Chinese*) 0-24401  
 Ni-Fe-Nb-Al-(Mo), wear resisting mag. head material, mag. props. and struct. 0-35350  
 Ni-Zn ferrites 600 NN and M450 NNI, Curie point radiative shift due to neutron irradiat. (*Russian*) 0-39775  
 $Ni_{0.5-x}Co_xZn_{0.5}Fe_2O_4$  ferrosilical solid solutions, cryst. lattice defects and props. 0-19796  
 $Ni_{45}Mo_2Fe_{55}O_2$  effect on secondary recrystallisation and mag. props. 0-35201  
 ( $Sc, Lu_{1-x}$ ) $_2V_2O_7$  0-29547  
 ( $Y, Lu_{1-x}$ ) $_2V_2O_7$  semiconducting ferromag. pyrochlore, mag. props. 0-29547  
 $Zn_{0.9}Co_{0.1}Fe_{0.9}O_4$ , Cu, Zn substituted magnetite, domain wall resonance, mag. props. 0-15756

**magnetic permeability measurement**

- RF method of determining spontaneous magnetisation of ferromag. with low anisotropy 0-22396  
 sensors, shrinking and thermal tension estimations in epoxy resins appl. (*Polish*) 0-35456

**magnetic pinch see pinch effect****magnetic properties of amorphous substances**

- alloys, bulk amorphous, prep. by high rate sputter deposition (*Japanese*) 0-29906  
 disordered anisotropic antiferromagnet, random field effects 0-2580  
 ferromagnet, amorphous, magnetisation, temp. depend. effect of nonrandom anisotropy 0-39773  
 ferromagnet, Ising amorphous, crit. temp. 0-11207  
 ferromagnet, Ising model, Curie temp., exchange integral fluctuation effects 0-50121  
 ferromagnetic, developments and appl. 0-50143  
 ferromagnetic alloys, amorphous, sputter-deposited, soft mag. props., magnetostriction 0-34696  
 ferromagnetic alloys, disordered crystalline and amorphous, dipole field distribution 0-25101  
 ferromagnetic alloys, domain struct. and mag. microstruct., review 0-15751  
 ferromagnetic alloys, micromagnetic eqns. for case of dipolar and magnetocryst. fluctuations 0-11171  
 ferromagnets, Curie temp. depend. on nearest neighbour fluctuations 0-50120  
 ferromagnets, localised spin excitations 0-15708  
 ferromagnets with random anisotropy axes, spin waves 0-7096  
 film, SAW device appls. 0-28389  
 Heisenberg ferromagnet, spin disorder resist., force-force correl. function method 0-24918  
 Heisenberg ferromagnet, variational cluster method 0-39728  
 Ising model, bond-diluted, percolation-thermal crossover index calc. 0-11145  
 magnetisation, mag. moment temp. distrib. 0-15848  
 mathematical models of disordered systems, book 0-1878  
 metallic amorphous films for mag. bubble memories, materials review (*Polish*) 0-34715  
 metallic glass, bulk and surface properties, review 0-44147  
 metallic glasses, characts. and appls. (*French*) 0-39815  
 metallic glasses, structure, stability and prod., elec., mag. and mech. props., review 0-44134  
 metallic glasses props., development and appl. 0-19710  
 Metglas 2826 ribbons, ferromagnetic resonance and SEM obs. 0-15804  
 microwave absorption spectra of amorphous magnetic system 0-50469  
 pyrite structured 3d-transition metal chalcogenide mag. props. from Mossbauer effect obs. (*Japanese*) 0-15933  
 rare earth alloys, mag. props., Mossbauer spectra 0-7225  
 rare earth alloys, random anisotropy antiferromag. model 0-20399  
 rare earth alloys, spin glasses, bulk mag. props. in amorphous and cryst. systems 0-20415  
 rare earth alloys, transport props. 0-20152  
 rare earth amorphous alloys, random mag. anisotropy 0-20398  
 rare earth compounds,  $RFeO_3$ , amorphous films for mag. bubble memories, materials review (*Polish*) 0-34715  
 rare earth-Au(Cu), amorphous, mag. and transport props. 0-34605  
 rare earth-gold amorphous alloys,  $R_2Au$ , anisotropy versus exchange 0-34624  
 rare earth-transition metal alloys, amorphous, struct. and mag. props., book contrib. 0-39818  
 rare earth-transition metal amorphous thin films, mag. potential distribution and wall velocity meas. 0-34725  
 rare earth-transition metal amorphous thin films for thermomag. recording 0-20403  
 rare earth-transition metal garnets,  $R_3M_2O_{12}$ , amorphous films for mag. bubble memories, materials review (*Polish*) 0-34715  
 ribbon materials manufacture, props. improvement and appl. 0-7693  
 Sendust ribbon, mag. props. 0-15761  
 superconducting amorphous metals, mag. impurity interactions 0-44777  
 tape cores carrying current, torsional stress effects 0-34742  
 transition metal amorphous alloys 0-29576  
 3d-transition metal-metalloid cryst. and glassy alloys, electronic struct. from magnetisation and Mossbauer meas. 0-29363  
 $Al_2O_3$ - $CoO$ - $SiO_2$  glasses, spin correls., neutron diff. meas. 0-15694  
 $Al_2Mn_2Si_2O_{12}$  spin glasses, spin dynamics, neutron scatt. meas. 0-15741  
 $Al_2O_3$ - $MnO$ - $SiO_2$  glasses, spin correls., neutron diff. meas. 0-15694  
 B-Fe (16 at.%), magnetisation in high mag. field, Arrott-Noakes plot 0-54919



**magnetic properties of amorphous substances continued**

- BaO-Fe<sub>2</sub>O<sub>3</sub>-B<sub>2</sub>O<sub>3</sub> glass, struct. and mag. props., Mossbauer spectra 0-7226
- BaO-Fe<sub>2</sub>O<sub>3</sub>-B<sub>2</sub>O<sub>3</sub> glass, splat cooled, low temp. micromagnetism 0-34660
- C, char, amorphous, mag. interactions between localised spins 0-34587
- (Co,Fe,M)<sub>78</sub>Si<sub>8</sub>B<sub>14</sub> amorphous alloys (M=V,Nb,Ta,Cr,Mo,W,Mn or Ni), zero magnetostriction and low field mag. props. 0-34741
- Co-Ni-Fe-Si(B), amorphous ribbon, magnetostriction meas. 0-15778
- Co-P, amorphous, ferromag. antireson. 24 GHz microwave transmission, mag. props. 0-34778
- Co-P alloys, electrodeposited, mag. anisotropy 0-15713
- Co<sub>1-x</sub>B<sub>x</sub>, polycrystalline and amorphous sputtered films, Brillouin spectra 0-2775
- Co<sub>80</sub>B<sub>20</sub>, amorphous metal ribbon, stresses, magnetoelastic anisotropy and zero-field mag. domain struct. 0-44896
- (CoFeB)<sub>100-x</sub>Cr<sub>x</sub> thin films, magnetic props. and corrosion resist. 0-34709
- (Co<sub>1-x</sub>Fe<sub>x</sub>Ni<sub>1-x/2</sub>)(Si<sub>1-x/2</sub>B<sub>x/2</sub>)<sub>20</sub>, amorphous films, spin wave spectra 0-34777
- CoNiB, corrosion-resistant amorphous mag. thin films 0-54923
- Co<sub>50</sub>Ni<sub>20</sub>Fe<sub>6</sub>Si<sub>12</sub>B<sub>12</sub>, amorphous, mag. props., effects mech. deform. 0-39840
- Co<sub>85</sub>P<sub>15</sub>, strip domains, anisotropy const. effects 0-29571
- CrO<sub>2</sub>, amorphous thin films, Mossbauer and magnetisation data 0-34712
- CuCl, disordered, diamag. transition 0-34636
- DyFe amorphous film, Mossbauer and mag. meas. 0-15844
- Fe base amorphous alloys, Invar and Elinvar charact. 0-29592
- Fe-Al alloys, rapidly quenched, mag. props. 0-29579
- Fe-B, (16.3 at.%) amorphous, coercive force temp. depend. 0-25158
- Fe-B amorphous alloy, mag. anisotropy temp. depend. 0-15846
- Fe-B amorphous alloys, Mossbauer spectra, soft ferromag. props. 0-11302
- Fe-B amorphous alloys, Mossbauer spectra, mag. moment conc. depend. 0-15847
- Fe-B-C amorphous alloys, effect of Si addition on mag. props. 0-34694
- Fe-B-Si, amorphous ferromag. alloys, mag. struct., Mossbauer study 0-39746
- Fe-B-Si ribbon, strain induced anisotropy, and toroid diam. effect on mag. props. 0-34623
- Fe-Co-B powders, synthesis and mag. props., appl. to mag. recording 0-20432
- Fe-Co-Si-B alloy, rapidly quenched, mag. heads appl. (*Japanese*) 0-54922
- Fe-Co-Si-B sputtered amorphous thin film, coercivity, galvanomagnetic props., resistivity 0-29578
- Fe-Cr-B, amorphous, Elinvar and Invar charact. (*Japanese*) 0-11832
- Fe-Gd amorphous film, struct. and mag. props. 0-20439
- Fe-Ni base amorphous alloys, effect of annealing on Curie temp. 0-34632
- Fe-Ni-P-B, amorphous ferromag. alloys, mag. struct., Mossbauer study 0-39746
- Fe-P alloys, electrodeposited, mag. anisotropy 0-15713
- Fe-P alloys, initial permeability, time depend. 0-15759
- Fe-Si amorphous film, struct. and crystallisation, Mossbauer study 0-11300
- Fe-Si-B amorphous films, mag. props. 0-34710
- Fe<sub>1-x</sub>B<sub>x</sub>, polycrystalline and amorphous sputtered films, Brillouin spectra 0-2775
- Fe<sub>80</sub>B<sub>20</sub>, amorphous, transverse magnetoresist., stress effect 0-15501
- Fe<sub>80</sub>B<sub>20</sub>, amorphous ferromag. metallic glass, stress-induced rot. of magnetisation, Mossbauer study 0-20445
- Fe<sub>80</sub>B<sub>20</sub>, metallic glass, low temp. specific heat, metalloid effects 0-34654
- Fe<sub>80</sub>(B<sub>1-x</sub>C<sub>x</sub>)<sub>20</sub>, saturation magnetostriction, comp. effects 0-34735
- Fe<sub>80</sub>(B<sub>1-x</sub>P<sub>x</sub>)<sub>20</sub> amorphous alloys, isothermal crystallisation kinetics 0-33895
- Fe<sub>78</sub>B<sub>12</sub>Si<sub>10</sub>, amorphous, Mossbauer study of hyperfine interaction and mag. anisotropy 0-40027
- Fe<sub>80</sub>B<sub>15</sub>Si<sub>5</sub> metallic glass, large uniaxial magnetostrictive anisotropy, magnetisation reversal 0-34736
- Fe<sub>80</sub>(B<sub>1-x</sub>Si<sub>x</sub>)<sub>20</sub>, saturation magnetostriction, comp. effects 0-34735
- Fe<sub>81.5</sub>B<sub>4.5</sub>Si<sub>4</sub>, amorphous metal ribbon, stresses, magnetoelastic anisotropy and zero-field mag. domain struct. 0-44896
- Fe<sub>82</sub>B<sub>15</sub>Si<sub>3</sub>, metallic glass, low temp. specific heat, metalloid effects 0-34654
- FeCoB, corrosion-resistant amorphous mag. thin films 0-54923
- (Fe<sub>2</sub>Co<sub>0.8</sub>)<sub>80</sub>P<sub>17</sub>Al<sub>3</sub>, Mossbauer spectra, isomer shift, mag. hyperfine field 0-11301
- (Fe<sub>100-x</sub>Co<sub>x</sub>)<sub>79</sub>P<sub>13</sub>B<sub>8</sub>, amorphous, hyperfine field distrib., <sup>59</sup>Co NMR spin-echo meas. 0-34818
- (Fe<sub>1-x</sub>Co<sub>x</sub>)<sub>78</sub>Si<sub>10</sub>B<sub>12</sub>, amorphous alloys, magnetic anisotropy meas. 0-2570
- Fe<sub>5</sub>Co<sub>70</sub>Si<sub>10</sub>B<sub>15</sub> amorphous magnetic alloy, decrease of permeability after demagnetisation, disaccommodation 0-39814
- Fe<sub>5</sub>Co<sub>70</sub>Si<sub>15</sub>B<sub>10</sub>, amorphous, crystn. effect on mag. props. (*Russian*) 0-44858
- (Fe<sub>1-x</sub>Mn<sub>x</sub>)<sub>75</sub>P<sub>15</sub>B<sub>6</sub>Al<sub>3</sub>, amorphous, spin-glass-ferromag. multicritical point, AC susceptibility meas. 0-50117
- (Fe,Mn<sub>1-x</sub>)<sub>75</sub>P<sub>15</sub>B<sub>6</sub>Al<sub>3</sub>, amorphous, mag. ordering temp., hyperfine field distrib., elec. resist. 0-34633
- (Fe<sub>1-x</sub>Mn<sub>x</sub>)<sub>75</sub>P<sub>15</sub>C<sub>10</sub>, amorphous, mag. ordering, Mossbauer study 0-39747
- (Fe<sub>1-x</sub>Mn<sub>x</sub>)<sub>75</sub>P<sub>15</sub>C<sub>10</sub>, amorphous pair radial distrib. functions, neutron scatt. study 0-49128
- Fe<sub>78</sub>Mo<sub>2</sub>B<sub>20</sub>, amorphous, transverse magnetoresist., stress effect 0-15501
- Fe<sub>40</sub>Ni<sub>38</sub>Mo<sub>2</sub>B<sub>18</sub> amorphous alloys, compatibility of DC and AC mag. props. 0-34695
- Fe<sub>40</sub>Ni<sub>40</sub>B<sub>20</sub>, amorphous, casting conditions effect on mag. props. (*Japanese*) 0-34698
- Fe<sub>40</sub>Ni<sub>40</sub>B<sub>20</sub>, amorphous, mag. props., effects mech. deform. 0-39840
- Fe<sub>40</sub>Ni<sub>40</sub>B<sub>20</sub>, high-field magnetisation curve, spin wave spectrum and microstructural inhomogeneities 0-15702
- Fe<sub>40</sub>Ni<sub>40</sub>B<sub>20</sub>, metallic glass, low temp. specific heat, metalloid effects 0-34654
- (Fe,Ni<sub>1-x</sub>)<sub>80</sub>B<sub>20</sub>, amorphous, Mossbauer spectra, mag. props. 0-15843
- Fe<sub>40</sub>Ni<sub>33</sub>Mo<sub>4</sub>B<sub>18</sub>, metallic glass, mag. and transport props. 0-39752
- (Fe<sub>0.6</sub>Ni<sub>0.96</sub>)<sub>80</sub>P<sub>10</sub>B<sub>10</sub>, amorphous magnetisation, field and temp. depend. 0-39755
- Fe<sub>77</sub>Ni<sub>5</sub>P<sub>14</sub>B<sub>6</sub>, amorphous, Hall resist. and mag. props., short range order effects 0-34422
- Fe<sub>40</sub>Ni<sub>40</sub>P<sub>14</sub>B<sub>6</sub>, strip domains, anisotropy const. effects 0-29571
- Fe<sub>40</sub>Ni<sub>40</sub>P<sub>14</sub>B<sub>6</sub>, amorphous, transverse magnetoresist., stress effect 0-15501
- Fe<sub>40</sub>Ni<sub>40</sub>P<sub>14</sub>B<sub>6</sub>, amorphous, mag. props., effects mech. deform. 0-39840

**magnetic properties of amorphous substances continued**

- Fe<sub>40</sub>Ni<sub>40</sub>P<sub>14</sub>B<sub>6</sub> metallic glass, ferromag. reson., spin waves, thermal ageing and long-range order effects 0-25214
- Fe<sub>40</sub>Ni<sub>40</sub>P<sub>14</sub>B<sub>6</sub>, amorphous, kinetics of induced mag. directional order 0-44824
- Fe<sub>2</sub>Ni<sub>1-x</sub>P<sub>4</sub>B<sub>6</sub>, amorphous, spin-glass regime, magnetoresist. meas. 0-34418
- (Fe<sub>x</sub>Ni<sub>1-x</sub>)<sub>75</sub>P<sub>15</sub>B<sub>6</sub>Al<sub>3</sub>, magnetisation temp. depend., spin wave theory 0-44927
- (Fe<sub>1-x</sub>Ni<sub>x</sub>)<sub>77</sub>Si<sub>10</sub>B<sub>13</sub> amorphous alloy system, saturation mag. moment, Curie temp., mag. susceptibility 0-39753
- Fe<sub>2</sub>O<sub>3</sub> amorphous film, Mossbauer spectra, mag. props. 0-15851
- Fe<sub>2</sub>O<sub>3</sub> amorphous RF sputtered thin films, Mossbauer and mag. study 0-34711
- Fe<sub>2</sub>O<sub>3</sub> amorphous thin films, Mossbauer and magnetisation data 0-34712
- Fe<sub>2</sub>O<sub>3</sub>-Na<sub>2</sub>O-BaO glass, mag. props. 4.2-295K, micromagnetism (*French*) 0-39782
- Fe<sub>2</sub>O<sub>3</sub>-PbO-B<sub>2</sub>O<sub>3</sub> glass, X-ray and electron microscope studies, mag. and Mossbauer effect meas. 0-28919
- FeOOH gels, Mossbauer spectra, mag. props. 0-11303
- Fe<sub>80</sub>P<sub>20</sub>, binary amorphous ferromagnet, Mossbauer study 0-34829
- Fe<sub>82-x</sub>Si<sub>18</sub>, amorphous, magnetisation, magnetoresist., spin glass and ferromag. phases 0-34697
- Fe<sub>2</sub>Pd<sub>82-x</sub>Si<sub>18</sub> metallic glass, mag. phase diagram, weak ferromagnet-spin glass transition 0-54893
- Fe<sub>2</sub>Sn<sub>1-x</sub>, amorphous alloy, Mossbauer spectra, charge transfer and atomic vol. effects 0-39959
- FeTiB, corrosion-resistant amorphous mag. thin films 0-54923
- Gd alloys, mag. props. and ferromag. reson. 0-54952
- Gd-Co amorphous films, correlation between struct. and mag. props. (*Chinese*) 0-54532
- Gd-Co amorphous films, RF sputtered, magnetisation ripple effects 0-11232
- Gd-Co amorphous films, struct. and mag. anisotropy 0-20438
- Gd-Co amorphous ribbons, mag. props. and Invar effects 0-2574
- Gd-Co amorphous sputtered film, magnetostriction and anisotropy 0-39821
- Gd-Co films, annealed, short-range order and perpendicular mag. anisotropy 0-15765
- Gd-Co sputtered amorphous films, resistivity anomalies, 42 to 300K (*Chinese*) 0-7001
- Gd-Fe(Co) amorphous films, O<sub>2</sub> adsorption, effect on perpendicular anisotropy 0-34713
- Gd-Ni, amorphous, Mossbauer spectra 0-25262
- Gd<sub>37</sub>Al<sub>63</sub> amorphous film, spin glass, microwave mag. resonance, freq. dependence 0-39798
- GdCo amorphous sputtered film mag. props. from Mossbauer effect obs. (*Japanese*) 0-15933
- GdCo film structure, dependent on substrate type (*Russian*) 0-24747
- GdCo, thin film, for thermomagnetic recording (*Japanese*) 0-11562
- GdCoMo amorphous alloy films, mag. cobalt alloys susceptibility, uniaxial anisotropy field 0-54930
- GdFe amorphous film, Mossbauer and mag. meas. 0-15844
- GdFe film structure, dependent on substrate type (*Russian*) 0-24747
- GdFe homogeneous amorphous films, compensation point switching, magneto-optical Kerr signal anal. 0-15726
- (Gd<sub>1-x</sub>Fe<sub>x</sub>)<sub>1-x</sub>Bi<sub>x</sub> amorphous films, saturation magnetisation, Kerr and Faraday rotation 0-40093
- GdIG, amorphous, Mossbauer spectra, mag. props. 0-15849
- Ge powder, diamag., strong mag. particle form., mag. props., EPR (*Russian*) 0-54863
- x.MnO.(1-x)[19TeO<sub>2</sub>.PbO], glass, antiferromag. behaviour, mag. props. 0-50072
- MnSi, amorphous magnetisation meas. 0-34599
- MnSi, sputtered, mag., elec., struct. and thermal props., spin glass behaviour 0-50124
- Ni dispersions, semi-amorphous, on Al<sub>2</sub>O<sub>3</sub>-graphite, mag. characterisation 0-44876
- Ni-Co amorphous alloys, magnetostriction 0-34738
- Ni-P, amorphous electrodeposited alloys, phase-separation (*Japanese*) 0-54140
- (Ni<sub>0.75</sub>Mn<sub>0.25</sub>)<sub>82</sub>Si<sub>10</sub>B<sub>8</sub>, exchange anisotropy, mag. susceptibility meas., 4.2K to room temp. 0-11186
- PbFe<sub>12</sub>O<sub>19</sub> hexagonal ferrite amorphous films for mag. bubble memories, materials review (*Polish*) 0-34715
- RuS<sub>2</sub> amorphous, preparation at ambient temp., magnetic susceptibility meas. 0-35119
- Tb<sub>52</sub>Ag<sub>48</sub>, amorphous, mag. aftereffect 0-20435
- TbFe<sub>2</sub>, amorphous, Mossbauer spectra (*French*) 0-25261
- YFe<sub>2</sub>, amorphous concentrated spin glass, susceptibility, Mossbauer and neutron scatt. meas. 0-39783
- YIG, amorphous, ionic glass, hard-sphere random-packing model 0-24369
- Y<sub>2</sub>Ni<sub>1-x</sub>, amorphous, high press. magnetisation and Curie temp. 0-20442
- (Zr<sub>1-x</sub>Er<sub>x</sub>)<sub>3</sub>Rh, amorphous, influence of mag. ordering on supercond. props. 0-29511

**magnetic properties of dilute alloys see magnetic properties of dilute systems****magnetic properties of dilute systems**

- see also local moments in dilute systems; magnetic impurity interactions
- dilute Heisenberg magnet, cluster expansion 0-15734
- elastic properties of magnetic materials, review 0-7142
- ferromagnet, slow neutron inelastic scatt. by spin excitations, cluster approx. 0-11168
- ferromagnetism of disordered systems, review 0-29513
- frustrated lattice, spin-glass ordering, triangle and FCC lattices, Monte Carlo simulation 0-15746
- Heisenberg, spin 1/2 dil. magnet, crit. props. 0-15733
- Heisenberg ferromagnet, dil., spin wave localisation near percolation threshold 0-25120
- Ising, internally dil. film, surface enrichment as possible source of surface magnetism 0-15731
- Ising, spin 1/2 dil. magnet, crit. props. 0-15733
- Ising and Heisenberg magnets with competing interactions, phase diagrams and mag. props. 0-34672
- Ising metamagnet, dilute tricritical point calcs. 0-50099
- mag. props. from Mossbauer effect obs. (*Japanese*) 0-15933
- manganese zinc formate dihydrate, two-dimens. antiferromag., anomalous crit. phenomena, neutron scatt. and PMR obs. 0-50104
- metals, ferromagnetic, nonmagnetic impurity hyperfine field temp. depend. 0-34402



**magnetic properties of dilute systems continued**

- rare earth alloys, magnetic properties, impurity effects, CPA calc. 0-44784  
 rare earth intermetallics,  $\text{RAl}_2\text{-Gd(Er)(Dy)(Nd)}$ , dil., (R=La, Yb, Lu), EPR and mag. susceptibility 0-15797  
 reverse Kondo effect, magneto-transport theory 0-15509  
 spin glasses, mean field theory, replica method 0-34658  
 transition metal compounds and dil. alloys, mag. ordering phenomena in high mag. fields 0-50075  
 Au-Er, cold-worked, EPR expts. 0-39864  
 Au-Fe (3.1-10.4 at.%) spin glass alloys, high field magnetisation curves 0-11213  
 $\text{Cd}_{1-x}\text{Ag}_x\text{Cr}_2\text{Se}_4$ , Ag acceptor states effect on exchange interaction 0-20397  
 Cr antiferromagnetic with nonmagnetic impurities, mag. susceptibility using two band model 0-2559  
 Cr-Co (4.0 at.%) alloy, antiferromag., disappearance of resist. min. under press., and press. coeff. of  $T_N$  0-10960  
 Cr-Co-V alloys, dil., elec. resist. min. 0-54680  
 Cr-Ni(V), dil., mag. susceptibility, 77 to 400K (*Russian*) 0-50066  
 $\text{Cr}_1\text{-xFe}_x$ , Mossbauer spectra, mag. behaviour 0-20532  
 Cu-Fe, dilute, low temp. heat capacity in mag. field, superparamagnetism 0-39804  
 $\text{Er}_x\text{Ce}_{1-x}\text{Pd}_3$ , cryst. field spectra, neutron scatt. study 0-50047  
 $\text{Eu}_x\text{Sr}_{1-x}\text{S}$ , dilute Heisenberg magnet, complex susceptibility of blocked spins 0-15740  
 $\text{Eu}_x\text{Sr}_{1-x}\text{S}$ , ferromagnet-spin glass transition, mag. ordering, mag. susceptibility and neutron scatt. meas. 0-50135  
 $(\text{Fe}_{100-x}\text{Co}_x)_{70}\text{P}_{13}\text{B}_8$ , amorphous, hyperfine field distrib.,  $^{59}\text{Co}$  NMR spin-echo meas. 0-34818  
 $\text{Fe}_x\text{NbSe}_2$  (2H), mag. susceptibility meas., 1.3-300K 0-39740  
 $\text{FeP(Ga)(As)(Sb)}$ , short-range order, neutron diffuse scatt. and spin echo NMR 0-50106  
 $\text{Gd(Rh}_{1-x}\text{Fe}_x)_2$ ,  $x \leq 0.15$ , magnetisation and EPR studies 0-34767  
 $\text{K}_2\text{Cu}_x\text{Zn}_{1-x}\text{F}_4$ , two-dimens. ferromag., spin correls. near percolation limit 0-44840  
 $\text{LaNi}_2\text{-Gd}$ , dil., ESR spectra, fine struct. and random stresses 0-25203  
 Mg-rare earth dilute alloy, mag. susceptibility and magnetisation 0-15689  
 $\text{Mg}_{1-x}\text{Mn}_x\text{Te}_2$ , random dil. antiferromagnet, mag. props. 0-54870  
 Ni-Fe, dil., temp. depend. of Mossbauer absorpt. near Curie point (*French*) 0-11305  
 $\text{Ni}_{1-x}\text{Au}_x\text{-Co}$ , dil., hyperfine field and isomer shift, precip. process, Mossbauer expts. 0-25267  
 $\text{Ni}_2\text{Fe-Sn}$ , dil., atomic order detection by  $^{119}\text{Sn}$  spectroscopy 0-39993  
 $\text{Ni}_2\text{Mn}_x\text{M}_{1-x}\text{Sn}$  (M=Ti,V) mag. hyperfine fields,  $^{119}\text{Sn}$  Mossbauer spectra study 0-55003  
 $(\text{Ni}_{1-x}\text{X}_x)_{99}\text{Mn}$ , X=Rh, Fe, Mn, ferromagnetic, NMR study of local environment effect, relaxation mechanism 0-7193  
 Pd-Co, very dil., Mossbauer emission spectra of  $^{57}\text{Co}$ , relax. effects 0-29656  
 Pd-Fe resist. min. 0-11050  
 Pd-Fe-Mn, dil. alloy, high press. study 0-34600  
 Pd-Mn, dil. alloy, very temp. magnetisation 0-34692  
 Pd-Mn(Fe), mag. ordering phenomena, neutron scatt. obs. 0-44812  
 Pd-Ni, resist. min. 0-11050  
 PdAgFe, ferromag., Curie temp. depend. on susceptibility, non-mean field theory 0-44829  
 PdFeRh, ferromag., Curie temp. depend. on susceptibility, non-mean field theory 0-44829  
 Pr-Eu, dil., magnetisation, Mossbauer spectra 0-15928  
 $\text{Rb}_2\text{Co}_x\text{Mg}_{1-x}\text{F}_4$ , dilute antiferromag. two dimens. Ising system, phase boundary effective medium theory 0-50130  
 $\text{ScAl}_2\text{-Er(Dy)(Nd)}$ , dil., EPR and mag. susceptibility 0-15797  
 $(\text{Ti}_x\text{Al}_{1-x})_2$ , disordered alloys, cryst. field transitions, inelastic neutron scatt. obs. 0-50055  
 $\text{YAl}_2\text{-Er(Dy)(Nd)}$ , dil., EPR and mag. susceptibility 0-15797  
 $\text{ZrZn}_2$ ,  $^{57}\text{Fe}$  mag. props. from Mossbauer effect obs. (*Japanese*) 0-15933

**magnetic properties of fine particles**

- see also superparamagnetism*  
 Fe particles in glass-like C matrix, identification and props. 0-11229  
 ferromagnetic particles, quantum effects (*Russian*) 0-29584  
 ferromagnetic particles, stability of magnetisation curling mode and magnetisation helicoid struct. 0-11227  
 ferromagnetic particles, thermal fluctuations, Brownian motion theory 0-11226  
 ferromagnetic uniaxial particles, domain struct. and crit. size (*Russian*) 0-25153  
 interacting, switching behaviour, dipole and Stoner-Wohlfarth models 0-44870  
 metal powders, packed, complex mag. permeability calcs. 0-29583  
 recording on particulate media, conference, Gardone Riviera, Italy (Sep. 1979) 0-41930  
 remanent loop measurement, single magnetic particles 0-17967  
 Stoner-Wohlfarth particle, two-component, hysteretic props. 0-11228  
 tapes, static and antihysteretic mag. props. 0-44868  
 $\text{BaO-Fe}_2\text{O}_3$ , chemically coprecipitated, mag. props., orientation 0-15763  
 $\text{CrO}_2$ , oxidative prep. method, mag. props. 0-44863  
 $\text{CrO}_2$  powders, print through values and mag. characts. 0-44871  
 $\text{Cr}_{1-x}\text{Rh}_x\text{O}_2$ , oxidative prep. method, mag. props. 0-44863  
 Fe aerosoled fine particles, Mossbauer spectra 0-7223  
 Fe clusters, supported, Mossbauer spectra 0-7220  
 Fe, fine particles, chemisorption of  $\text{CO}$ ,  $\text{H}_2$ , Mossbauer study 0-39415  
 Fe, Mossbauer spectra, demagnetising field effect on magnetic splitting 0-39932  
 Fe powders, Co- or Cu-plated, prep. by rad. and chem. plating, mag. props. 0-44867  
 Fe powders, prep. by  $\text{BH}_4$  process, comp. and stability 0-44878  
 Fe pyrophoric powders, stabilising layer form. during passivation, saturation moment meas. 0-44865  
 $\text{Fe-Al}_2\text{O}_3$  granular film, interface props., Mossbauer spectroscopy 0-34336  
 Fe-Co-B powders, synthesis and mag. props., appl. to mag. recording 0-20432  
 $\text{Fe-SiO}_2$  granular film, interface props., Mossbauer spectroscopy 0-34336  
 $\text{Fe-ZrO}_2$  granular film, interface props., Mossbauer spectroscopy 0-34336  
 $\gamma\text{-Fe}_2\text{O}_3$  acicular particles, coercivity increase by Co ferrite surface crystn. 0-44866  
 $\gamma\text{-Fe}_2\text{O}_3$ , densified, rheological and mag. props. 0-44873  
 $\gamma\text{-Fe}_2\text{O}_3$ , magnetisation distribution in isolated transitions 0-29580

**magnetic properties of fine particles continued**

- $\gamma\text{-Fe}_2\text{O}_3$ , microstruct. and magnetisation 0-44875  
 $\gamma\text{-Fe}_2\text{O}_3$  particles, mag. props. rel. to mag. tape appl. 0-15762  
 $\gamma\text{-Fe}_2\text{O}_3$  small particles, noncollinearity as crystallite-size effect, Mossbauer study 0-39939  
 $\gamma\text{-Fe}_2\text{O}_3\text{-Co}$  acicular powder epitaxially doped, coercivity increase, surface anisotropy (*Chinese*) 0-7130  
 $\gamma\text{-Fe}_2\text{O}_3$ -organic interfaces, mag. struct., Mossbauer effect, IR absorpt., and magnetisation meas. 0-44869  
 $\text{Fe}_3\text{O}_4$ , magnetite particles, interaction fields effect on hysteretic props. 0-54921  
 $\text{Fe}_3\text{O}_4$  particles, nonstoichiometric, morphology and enhanced coercivity, Mossbauer meas. 0-7132  
 $\text{Fe}_3\text{O}_4$  powder, oxidation to  $\gamma\text{-Fe}_2\text{O}_3$ , coercivity changes 0-44864  
 $\text{Fe(OH)}_3\text{-Fe(OH)}_2$  suspension system, potential-pH diagram 0-55728  
 $\text{FeOOH}$  gels, Mossbauer spectra, mag. props. 0-11303  
 $\alpha\text{-FeOOH}$  ultrafine particle NGR spectra, size distrib. and surface effects 0-11299  
 $^{57}\text{Fe}$  powder, NMR excitation function, drumhead model of Bloch walls 0-15810  
 Ge powder, diamag., strong mag. particle form., mag. props., EPR (*Russian*) 0-54863  
 Ni, single-domain particles, LF mag. susceptibility, 2K up to Curie point 0-29582  
 Ni-SiO<sub>2</sub> supported catalysts, particle size, H<sub>2</sub> chemisorption, Mossbauer study 0-7219  
 Pd, confined geometry, p-wave supercond. or itinerant ferromag. 0-11129  
 $\text{SmCo}_5$  powder, comminution temp. effect on mag. props. 0-39819  
 $\text{Sm}(\text{Co}_{0.81}\text{Cu}_{0.15}\text{Fe}_{0.04})_{6.9}$  and  $\text{Sm}(\text{Co}_{0.84}\text{Cu}_{0.16})_{6.9}$  powders, mag. props. (*Russian*) 0-20434
- magnetic properties of substances**  
*see also antiferromagnetic properties of substances; demagnetisation; diamagnetic properties of substances; ferrimagnetic properties of substances; ferromagnetic properties of substances; magnetic permeability; magnetic properties of amorphous substances; magnetic properties of dilute systems; magnetic properties of fine particles; magnetic structure; magnetic surface phenomena; magnetic susceptibility; magnetic transitions; magnetisation; magnetocaloric effects; paramagnetic properties of substances*  
 actinide compounds, structure, mag. and related props., review 0-6389  
 EM NDT phenomena, fissile element modelling 0-40633  
 neutron scattering and magnetism, conference, Julich, Germany (Aug. 79) 0-41934  
 rare earth alloys and compounds, book 0-36785  
 $\text{Tb}^{57}\text{Fe}_{1-x}\text{Cr}_x\text{O}_3$  mag. props. from Mossbauer effect obs. (*Japanese*) 0-15933
- magnetic read/write heads** *see magnetic heads*
- magnetic recording**  
*see also tape recorders; thermomagnetic recording*  
 digital, magnetisation distribution in isolated transition 0-29580  
 ECG, long-term recording on mag. tape 0-56243  
 on particulate media, conference, Gardone Riviera, Italy (Sep. 1979) 0-41930  
 tape material, gyromagnetic magnetisation in anisotropic mag. material 0-50142  
 Co-P films, electrodeposited, magnetic recording media (*Japanese*) 0-29587  
 Cr-Co-Ni hard film on Mo substrate 0-2608  
 Fe-Co-Cr film RF sputtering 0-2947  
 $\text{Fe}_2\text{O}_3$ , Co modified, synthesis with autoclave in H<sub>2</sub> atm. 0-35117
- magnetic relaxation**  
*see also ferromagnetic relaxation; magnetic resonance; spin-lattice relaxation; spin-spin relaxation*  
 diamine oxidase solutions, proton mag. relax. dispersion obs. 0-51136  
 NMR relaxation processes, macroscopic evolution eqns. and virtual spins importance (*French*) 0-32739  
 one-dimensional semi-infinite chain, enhanced surface exchange interaction, mag. relax. 0-29558  
 spin glasses, magnetisation relaxation time near freezing temp., HF calc. 0-34665  
 $(\text{Al}_2\text{O}_3\text{-Fe}_2\text{O}_3)\text{:Cr}^{3+}$ , (0.04 mol.%  $\text{Fe}_2\text{O}_3$ ), paramag., cross relax., annealing temp. effect from Mossbauer meas. 0-44983  
 Au-Fe spin glass, energy flux associated with remanent magnetization relaxation (*French*) 0-7110  
 Fe complex, Fe(III) Schiff-base complexes, mag. relax., Mossbauer spectra 0-15897  
 $\text{Na}_3\text{RuO}_4$ ,  $^{99}\text{Ru}$  Mossbauer spectra, antiferromag. order, mag. relax. 0-50234  
 Pd-Co, very dil., Mossbauer emission spectra of  $^{57}\text{Co}$ , relax. effects 0-29656  
 $(\text{Ti}_{0.9}\text{V}_{0.1})_2\text{O}_3$ , spin glass, dynamic mag. susceptibility meas. 0-39792
- magnetic resonance**  
*see also acoustic magnetic resonance; antiferromagnetic resonance; atomic beam magnetic resonance; ferrimagnetic resonance; ferromagnetic resonance; laser magnetic resonance; magnetic double resonance; magnetic relaxation; molecular beam magnetic resonance; nuclear magnetic resonance; paramagnetic resonance*  
 atom spin transition, nonadiabatic, in time-depend. mag. field 0-9576  
 atomic RF spectroscopy, nonlinear and parametric effects, review 0-18816  
 conference on magnetism, Munster, Germany (March 1979) 0-12843  
 deoxyhaemoglobin high spin ferrous ion, low lying electronic states, far IR mag. reson. 0-48110  
 deoxymyoglobin high spin ferrous ion, low lying electronic states, far IR mag. reson. 0-48110  
 Magnetic dipolar Hamiltonian 0-25181  
 many-spin system, group approach in dynamics (*Russian*) 0-44900  
 muonic radicals, muon spin resonance frequency spectra, theory 0-1088  
 rare earth metals, alloys, and cpds., book 0-36785  
 rotating coordinate system with quadrupole splitting, paramag. susceptibility 0-11178  
 InSb, charact. and phys. props., review (*Japanese*) 0-39576  
 $\text{ND}_2(\text{NH}_2)_2$ ,  $\nu_2$  band, laser mag. reson., 9-10 micron 0-9601  
 Ne,  $2p^3s^2P_0$  state, optical pumping, g-factor, metastability exchange cross section 0-947  
 SO, and isotopic forms,  $\text{X}^3\Sigma^-$  state,  $\text{CO}_2$  laser mag. reson. spectroscopy 0-9602
- magnetic resonance spectrometers**  
 amplifier-generator for nuclear acoustic resonance spectrometer 0-27324



**magnetic resonance spectrometers continued**

- APR investigation by low-temp. spectrometer using Bragg diffraction of laser light 0-27326  
 bridge RF spectrometer, high freq. preamplifier 0-22380  
 ENDOR, low impedance design 0-246  
 EPR/ENDOR, modified Ka-band spectrometer, obs. of electron spin echoes at 35 GHz 0-13113  
 FT NMR sensitivity improvement for spectrometer using double-tuned receiver coil 0-31824  
 laser magnetic resonance spectrometers, sensitivity improvement using laser properties 0-13115  
 magnetic field modulator, EPR radiospectrometer having discrete set of modulation frequencies 0-52285  
 magnetic flux stabiliser, resonance conditions stabilisation 0-52286  
 NMR, automatic system, for recording, processing and summation 0-27327  
 NMR, commercial spectrometer modification for rot. frame spin-lattice relax. meas. 0-22407  
 NMR, for quantitative analysis, microprocessor-controlled digital integrator 0-11971  
 NMR, for simultaneous multinucl. NMR by alternate scan recording of  $^{31}\text{P}$  and  $^{13}\text{C}$  spectra 0-26426  
 NMR, Fourier transform, standard spectrometers use for multicomponent self-diffusion meas. by spin echo 0-22401  
 NMR, magnetic field in superconducting solenoid meas. method (Czech) 0-13107  
 NMR, programming device for control of frequency synthesizers 0-22400  
 NMR, pulse type, programmable pulse sequence generator 0-17979  
 NMR in internal fields of ferromagnets for freq. range 10 to 230 MHz 0-27325  
 NMR in undergrad. instruction, general purpose microcomputers use for hypothetical spectra synthesis 0-42009  
 NMR probe assembly, He-cooled, for proton-enhanced  $^{13}\text{C}$  reson. 0-17978  
 NMR probe for high-pressure and high-temp. expts. 0-22403  
 NMR spectrometer, transverse AC component of magnetisation detected by transverse SQUID 0-37064  
 NMR spectrometer-computer interface, demonstration expt., signal averaging influences on S/N ratio 0-36813  
 NQR, programming device for a spin-echo installation 0-17972  
 NQR, small sample enhanced coupling using ferrite coils 0-52287  
 NQR, weak signal relax. meas. with Sigma type digital storage device, pulse-train program blocks 0-17970  
 NQR injection and phase locked spectrometer for Zeeman NQR studies 0-54979  
 NQR pulse spectrometer modulator 0-17971  
 NQR short range remote spectrometer for anal. 0-55742  
 NQR spectrometers for precision measurement of temp., optimisation (Russian) 0-22412  
 ODMR spectrometer system, use of signal averager with minicomputer facilities for control, data recording and evaluation 0-31825  
 pulsed NQR-FFT radiofrequency spectrometer for  $^{14}\text{N}$ , description and operation 0-17982  
 single channel two freq.  $^{14}\text{N}$  NQR pulse spectrometer, multiplet spectra 0-17968  
 stroboscopic integrator for studying NQR relax. processes 0-17969  
 superconducting NMR, efficient decoupler coil design to reduce heating in conductive samples 0-31828  
 UHF spectrometer for NQR studies at liquid  $\text{N}_2$  temp. 0-13114  
 variable temperature probe, magic angle rot. H NMR spectra meas., polymer gel appl. 0-31830  
 X-band cavity for electron spin resonance experiments 0-248  
 CI NQR spectrometer with exact reading of resonant freq. 0-42247  
 $^{14}\text{N}$  NQR, observation equipment and techniques 0-22399

**magnetic resonance spectroscopy**

- anisotropic motion, and reson. line shape 0-7144  
 autotype detector, spin resonance detection 0-22397  
 current filament over conducting layer, non-stationary magnetic field calc. (Czech) 0-52283  
 2,6-dimethylbenzoic acid,  $^1\text{H}$  chem. shift recovery from combined multiple pulse NMR and sample spinning 0-32738  
 EPR, instrument cavities,  $\text{TE}_{011}$  and  $\text{TE}_{020}$ , inhomogeneous static fields, spurious line feature obs. 0-31833  
 EPR, ns time-resolved, in pulse radiolysis, via spin echo method 0-43075  
 ferromagnetic-resonance linewidth meas. method and apparatus 0-22411  
 fluorite lattices,  $^{19}\text{F}$ , self-diffusion, spin lattice relax., NMR techniques 0-34801  
 Fourier transform multiple quantum NMR 0-31819  
 modified pulsed gradient technique for measuring diffusion in the presence of large background gradients 0-31831  
 molecular spectroscopic laboratory strategies, queuing theory and digital simulation use 0-30299  
 nematic liquid cryst., one-deuteron system, multiple quantum spin-echo spectroscopy 0-31832  
 neutron spin-echo integral transform spectroscopy 0-4748  
 NMR, Fourier transform, standard spectrometers use for multicomponent self-diffusion meas. by spin echo 0-22401  
 NMR, group theory, independent-particle Hamiltonian 0-43074  
 NMR, high-resolution, broadband decoupling and scaling of heteronucl. spin-spin interactions 0-17980  
 NMR, J-resolved, two-dimensional, spin decoupling, appl. to 2,3,4-trichlorophenol 0-31823  
 NMR, measurement of nuclear spin-lattice relaxation times based on null method 0-22402  
 NMR, multiple-quantum coherence, selective excitation, appl. to benzene 0-23439  
 NMR, phase-modulated spin echoes, derivation of pure absorpt. spectra 0-22410  
 NMR, pulse Fourier transform, commercial waveform analyser use 0-17977  
 NMR, rot. frame,  $^{13}\text{C}$  spin-lattice relax. using proton decoupled Fourier transform spectra, errors origin 0-18945  
 NMR, selective excitation with single-freq. off-reson. decoupling 0-17981  
 NMR, simultaneous multinucl., by alternate scan recording of  $^{31}\text{P}$  and  $^{13}\text{C}$  spectra 0-26426  
 NMR, solid, 'magic angle' spinning apparatus 0-17983  
 NMR, two-dimens. spin-echo spectra, anomalous spinning sidebands 0-17976  
 NMR data bank,  $^{13}\text{C}$  DARC PLURIDATA system 0-30298

**magnetic resonance spectroscopy continued**

- NMR detector, transistorised marginal oscillator, for student lab. 0-27078  
 NMR in undergrad. instruction, general purpose microcomputers use for hypothetical spectra synthesis 0-42009  
 NMR J cross-polarisation in liquids, refocusing method 0-22406  
 NMR limb blood flowmeter, clinical appls. 0-17178  
 NMR medical imaging, resolution and S/N ratios 0-26406  
 NMR probe assembly, He-cooled, for proton-enhanced  $^{13}\text{C}$  reson. 0-17978  
 NMR probe heating furnace for high mag. field use 0-247  
 NMR pulsed, automatic trigger pulse logic for pulse programmer 0-47084  
 NMR spectroscopy, appl. to organic compounds anal. 0-16756  
 NMR spectroscopy, resolution enhancement, effective sample volume restriction effects 0-31836  
 NMR-NQR double resonance, two-freq. methods, resonance spectrometers 0-20512  
 NMR, multiple pulse, of solids, accurate phase adjustment 0-22404  
 nonlinear absorption method in magnetic field for spectral line width and shift meas. 0-37066  
 NQR, quantum kinetic theory 0-52288  
 NQR  $T_1$  relax. time meas., steady state pulse method, master eqn. 0-54975  
 nuclear magnetism of liquid systems in the Earth field range, review 0-50206  
 nuclear spin-lattice relaxation measurement, variable perturbation method 0-22408  
 PMR, tunable notch filter for solvent elimination 0-22405  
 pulsed NMR in solids, survey 0-34782  
 solid state NMR, selection of nonprotonated  $^{13}\text{C}$  resons. 0-50201  
 solid torsional oscillators, rotating frame, nucl. spin polarisation losses, torsional spectroscopy 0-31821  
 solution NMR, enhanced selection of non protonated C resonances,  $^{13}\text{C}$  spin echo obs. 0-31835  
 super-regenerative NQR spectrometric obs. of apparent spin-spin time 0-54963  
 TGS, proton and deuteron NMR anal. of temp. depend. 0-33919  
 transversely polarised deuteron target for kaon-nucleon interaction studies 0-37669  
 two dimensional  $^{13}\text{C}$  NMR spectroscopy, high sensitivity 0-31826  
 two-centre integrals involving one-electron dipolar coupling and Slater AOs, computational procedure 0-23291  
 CI NQR spectroscopy, parametric superregenerator with phase quantisation application 0-22398  
 $^{14}\text{N}$  NMR, single cryst., separation of dipolar and quadrupolar splittings, new technique 0-25217  
 $^{14}\text{N}$  NQR, observation equipment and techniques 0-22399  
 $^{15}\text{N}$  NMR heteronuclear spectroscopy, two dimensional Fourier transform technique 0-31818  
 $^{17}\text{O}$ , NQR at natural isotope abundance, double reson. new techniques 0-53013

**magnetic screening see magnetic shielding****magnetic semiconductor materials see magnetic semiconductors****magnetic semiconductors**

- antiferromagnet, spin-magnetomagnon resonance 0-2566  
 antiferromagnetic Faraday light depolarisation in mixed mag. states 0-29726  
 antiferromagnetic resonance rel. to surface impedance, magnetoelastic contrib. 0-50200  
 antiferromagnetic semiconductor, spin-wave amplification 0-7099  
 antiferromagnetic semiconductors, magnetoelc. effect, magnetization and ferroelc. props. 0-25180  
 chalcogenide spinel-type, crystal growth using closed tube vapour transport method (Japanese) 0-25539  
 $\text{CoCr}_2\text{S}_4$  films, galvanomagnetic and thermoelec. props. 0-54717  
 dichalcogenides, pyrite-type,  $^{57}\text{Fe}$  isomer shift, quadrupole splitting, Mossbauer study 0-15832  
 electron spectrum, light absorpt. spectrum, calcs. 0-2793  
 electron struct. and indirect exchange mechanisms 0-25123  
 ferromagnet, CESR line width, two-magnon exchange splitting 0-29621  
 ferromagnet, magnon coupling to plasmons and LA phonons, s-d model 0-29536  
 ferromagnet, refr. index variation in strong alternating mag. field 0-23741  
 ferromagnet s-d model, electronic struct. from lowest six momenta 0-39732  
 ferromagnetic, acoustic plasmons 0-7098  
 ferromagnetic, anomalous carrier density mag. field depend., EuSe appl. 0-49774  
 ferromagnetic, dielectric function depend. on magnetisation, light absorpt. coeff. (Russian) 0-15467  
 ferromagnetic, electronic spectra, s-d model, method of moments 0-7070  
 ferromagnetic, theory review 0-20369  
 ferromagnetic nondegenerate semiconductor, magnetoresistance 0-11019  
 ferromagnetic semiconductor, electronic excitation spectrum 0-11149  
 ferromagnetic semiconductors, parametric amplification of coupled spin, helical and acoustic waves (Russian) 0-2621  
 magnetoelectric effect, classical and quantum theory, magnon drag effect 0-34746  
 many-valley, electron fluctuon states spin direct interactions 0-29364  
 Raman scattering of light on plasmon excitations 0-2738  
 s-f system, excitation spectrum, temp. and band occupation depend. 0-49588  
 semimagnetic semiconductors, mixed crystal, review 0-49702  
 small-sample mag. semiconductor thermoelectric power meas. installation 0-31795  
 static magnetic properties, mean field approach 0-7090  
 $\text{tC FeCr}_2\text{S}_4\text{-xSe}_x$  chalcospinel, ESR spectrum and paramag. susceptibility 0-15789  
 $\text{Cd}_{1-x}\text{Ag}_x\text{Cr}_2\text{Se}_4$ , Ag acceptor states effect on exchange interaction 0-20397  
 $\text{CdCr}_2\text{S}_4$ , magnetic semicond., resonance Raman scatt., mag. circular polarisation props. 0-50341  
 $\text{CdCr}_2\text{S}_4(\text{Se}_x)$ , electron spectrum, light absorpt. spectrum, calcs. 0-2793  
 $\text{CdCr}_2\text{Se}_4$ , ferromag. semicond., photoinduced mag. anisotropy 0-50086  
 $\text{CdCr}_2\text{Se}_4$ , ferromagnetic low anisotropy semicond., spontaneous magnetisation RF determ. 0-22396  
 $\text{CdCr}_2\text{Se}_4$  films, mag. hysteresis, domain struct., mag. viscosity 0-25169



**magnetic semiconductors continued**

- CdCr<sub>2</sub>Se<sub>4</sub>, magnetic red shift origin, specular reflectivity, band struct. 0-40127  
 CdCr<sub>2</sub>Se<sub>4</sub>, refr. index variation in strong alternating mag. field 0-23741  
 p-CdCr<sub>2</sub>Se<sub>4</sub>, resistivity anomalies at mag. transitions, sp.ht. 0-39785  
 CdCr<sub>2</sub>Se<sub>4</sub>, single cryst. growth by chem. transport reactions 0-16163  
 CdCr<sub>2</sub>Se<sub>4</sub>, spin system heating by drifting current carriers, magnon-phonon system energy transfer (*Russian*) 0-29541  
 CdCr<sub>2</sub>Se<sub>4</sub>/Ag, magneto-electrical props. temp. behaviour depend. on dopant conc. (*Russian*) 0-11006  
 CdCr<sub>2</sub>S<sub>4</sub>(se<sub>4</sub>), ferromag. semicond., band struct., EHT calc. 0-54608  
 Cd<sub>1-x</sub>In<sub>x</sub>Cr<sub>2</sub>Se<sub>4</sub>, electric, photoelectric and mag. props., metal-semicond. transition (*Russian*) 0-54738  
 Cd<sub>1-x</sub>Mn<sub>x</sub>Te, EPR, mag. crit. point 0-39851  
 Cd<sub>1-x</sub>Mn<sub>x</sub>Te mixed crystals, excitonic magnetoabsorption 0-40095  
 Cd<sub>1-x</sub>Mn<sub>x</sub>Te, spin-orbit coupled bands, indirect exchange interaction via electrons 0-34407  
 Co<sub>1-x</sub>Cu<sub>x</sub>Cr<sub>2</sub>S<sub>4</sub>, paramag. susceptibility 0-20373  
 Co<sub>0.7</sub>Cu<sub>0.3</sub>Cr<sub>2</sub>S<sub>4-x</sub>Se<sub>x</sub>, ferrimag. chalcospinel, paramag. susceptibility 0-15681  
 CuCr<sub>2</sub>Se<sub>4</sub>(S<sub>4</sub>)(Te<sub>4</sub>), binary and ternary solid solns., mag. and elec. props. 0-2407  
 CuFeS<sub>2</sub>, single crystal, optical reflectivity spectrum 0-40129  
 EuB<sub>6</sub>, mag. and transport props. 0-54689  
 EuB<sub>6-x</sub>C<sub>x</sub>, Mossbauer spectra, cond. electrons effect 0-20545  
 EuO film for thermomagnetic recording, anisotropy of resolving power 0-20404  
 EuO, piezoresistance effect, 4.2 to 300K 0-34450  
 EuO, spin system heating by drifting current carriers, magnon-phonon system energy transfer (*Russian*) 0-29541  
 EuO(S)(Se)(Te), cryst. and electronic struct., mag., elec., and optical props., book contrib. 0-39760  
 EuS films, ferromag., optical spectra and light scatt. from spin waves 0-16116  
 EuSe, annealed, AC conductivity and dielectric anomaly 0-34445  
 EuSe, polarisability of shallow donors, permittivity meas. 0-24833  
 EuTe, mag. semicond., antiferromag. reson. meas. 0-44926  
 Eu<sub>1-x</sub>X<sub>x</sub>S (X=Sr,Gd), spin-disorder-induced Raman scatt. from phonons, expt. investigation 0-20635  
 Eu<sub>1-x</sub>X<sub>x</sub>S (X=Sr,Gd), spin-disorder-induced Raman scatt. from phonons, theory 0-20636  
 EuX (X=O,S,Se) 0-20635  
 EuX (X=O,S,Se), spin-disorder-induced Raman scatt. from phonons, theory 0-20636  
 FeSb<sub>2</sub>, quasi-magnetic semicond., mag. susceptibility 0-39757  
 Gd<sub>2</sub>S<sub>3</sub> with excess Gd, magnetoresist. meas. 0-49777  
 GeFe<sub>2</sub>O<sub>4</sub>, single crystals, elec. and mag. props, optical absorpt. spectra 0-54719  
 n-HgCr<sub>2</sub>Se<sub>4</sub>, plasmon refl., 86 to 320K 0-50346  
 Hg<sub>1-x</sub>Mn<sub>x</sub>Se, band struct. from anomalous Shubnikov-de Haas effect 0-20080  
 Hg<sub>1-x</sub>Mn<sub>x</sub>Se, spin-orbit coupled bands, indirect exchange interaction via electrons 0-34407  
 Hg<sub>1-x</sub>Mn<sub>x</sub>Te, mag. props., self-consistent two spin cluster model 0-54874  
 Hg<sub>1-x</sub>Mn<sub>x</sub>Te, mag. susceptibility, 2.4 to 300K 0-20379  
 Hg<sub>1-x</sub>Mn<sub>x</sub>Te, spin-orbit coupled bands, indirect exchange interaction via electrons 0-34407  
 Mg<sub>1-x</sub>Mn<sub>x</sub>Te<sub>2</sub>, random dil. antiferromagnet, mag. props. 0-54870  
 Mn<sub>2</sub>Fe<sub>2-x</sub>O<sub>4</sub> ferrite film, exchange interaction depend. on conduction electrons (*Russian*) 0-34621  
 MnP, elec. resist. of different mag. phases, temp. depend. 0-54691  
 MnTe, resistivity anomalies at mag. transitions, sp.ht. 0-39785  
 MnZn ferrites, elec. cond. mechanism in paramag. and ferrimag. phases 0-15524  
 (Sc<sub>1-x</sub>Lu<sub>1-x</sub>)<sub>2</sub>V<sub>2</sub>O<sub>7</sub> 0-29547  
 Sn<sub>1-x</sub>Mn<sub>x</sub>Te, degenerate mag. semicond., thermoelec. power meas. 0-29392  
 SnTe-MnTe, degenerate semicond., anomalous Hall effect 0-29420  
 Ti<sub>2</sub>Mn<sub>2</sub>O<sub>7</sub>, synthesis, mag. and elec. props. and cryst. struct. 0-33963  
 (Y<sub>1-x</sub>Lu<sub>1-x</sub>)<sub>2</sub>V<sub>2</sub>O<sub>7</sub> semiconducting ferromag. pyrochlore, mag. props. 0-29547

**magnetic separation**

- ferrofluid devices, magnetostatic and centrifugal, nonmagnetic body motion 0-33700  
 high gradient magnetic separation at moderate Reynolds number 0-38500  
 paramagnetic particle trajectories in a lattice of parallel magnetized fibers 0-53204

**magnetic shielding**

- closed cylindrical vol., characts. of shield 0-43244  
 eddy current losses in semi-infinite shielded/unshielded mag. solid due to AC in parallel conductors (*Polish*) 0-37929  
 eddy-current losses in shielded magnetic solid, due to AC in parallel conductors (*Polish*) 0-32873  
 electron ring accelerators, shielding effect on ring motion 0-13991  
 EM pulse shielding of soft mag. materials 0-28143  
 photomultiplier array in strong external field 0-32573  
 Nb-Ti, sheet, flux trapping, appl. to mag. shielding and levitation 0-31806  
 Nb-Ti/Cu sheet composite, flux trapping and shielding capabilities in transverse fields 0-15667  
 Nb<sub>3</sub>Sn, flux trapping and shielding capabilities in transverse fields 0-15667

**magnetic shielding, nuclear see nuclear screening****magnetic stars**

- Am-type stars, envelopes circulation 0-4370  
 Am-type stars with known spectral types, second catalogue 0-36514  
 ET Andromedae (HR 8861), Ap star, light vars. and period 0-46571  
 Ap, Am stars, among composite spectrum stars of Hynek's (1938) list (*French*) 0-56876  
 Ap and Am stars, numerical taxonomy 0-22015  
 Ap stars, angular diameters, radii, and effective temps. 0-26870  
 Ap- and Bp-stars, 206-287 nm UV spectra 0-51776  
 Ap-stars, photometry and surface magnetic fields 0-56847  
 56 Arietis, spectrophotometry of Ap star, continuum features vars. 0-36638  
 53 Camelopardalis, photometric vars. 0-4367  
 49 Cancr, spectrophotometry of Ap star, continuum features vars. 0-36638  
 β Coronae Borealis, H I Paschen lines and Ca II triplet study 0-26869

**magnetic stars continued**

- δ Delphini stars in Michigan Spectral Catalogue, uvbyβ photometry rel. to spectral types 0-4377  
 equatorially symmetric rotator model, inhomogeneous element distrib. 0-4371  
 γ Equulei, magnetic field obs. of Ap-star 0-51782  
 Feige 86, UV high-resolution spectrum 0-41834  
 HD 184927, He variable star, spectroscopic props. 0-51790  
 HD 215441 (Babcock's star), magnetic vars., non-axisymmetric eccentric dipole model 0-51779  
 HD 221568, Ap star, light var. period 0-56856  
 HD 3980, late Ap star, photometric and mag. variability obs. 0-56845  
 HD 64740, He rich star, UV spectral vars. 0-22016  
 HR 1217, Ap star, spectrum and light vars. relationship 0-26878  
 NGC 2287, open cluster, spectral classification of brightest stars 0-26919  
 oblique rotator with irrotational axisymmetric mag. field surface distrib., effective mag. field 0-26872  
 21 Persei, spectrophotometry of Ap star, continuum features vars. 0-36638  
 polarity changes, skin effect of electrically conducting spherical shell 0-46389  
 Przybylski's star (HD 101065), β photometry and period determ. 0-41835  
 CQ Ursae Majoris, line identification list and radial vel. 0-41841  
 78 Virginis, Ap star, mag. field geometry, oblique rotator model 0-51773  
 78 Virginis, magnetic Ap star, high resolution polarisation obs. inside spectral lines 0-51772  
 Dy III lines in spectra of Ap and Bp stars 0-12764  
 H deficient and He weak stars, uvby photometry, variability 0-46579  
 He abundance anomalies, radiative forces calcs. in stellar envelopes 0-31291  
 Hg-Mn stars, absolute magnitude 0-46564  
 Hg-Mn stars, chemical abundances 0-56838  
 HgMn stars, spectrophotometry 0-26867

**magnetic storage devices**

- disc memory recording heads, investigation of dynamic mechanical props. that appear as stresses during small motions 0-22422

**magnetic storage systems**

- see also magnetic film stores; magnetic tape storage  
 recording on particulate media, conference, Gardone Riviera, Italy (Sep. 1979) 0-41930

**magnetic stores see magnetic storage systems****magnetic storms**

- see also micropulsations  
 1969 November 8-9, thermospheric response 0-12574  
 1970 December 10 to 20, electron temp. behaviour meas. in main ionosphere valley 0-4170  
 1974 June 30, polar substorms rel. to midlatit. thermosphere neutral wind meas. 0-31153  
 1976, December 8 substorm, magnetic and ionospheric disturbances features, morphology study 0-4201  
 auroral bulge expansion features during substorms 0-41597  
 auroral E-region fine structure obs. in substorm 0-36452  
 auroral substorm, assoc. mag. variation and auroral motion 0-51593  
 BDI position and plasmopause position during Feb. 1972 mag. storm 0-56666  
 chorus VLF and ELF emission, plasmopause origin model 0-41608  
 currents generated, delineation of cosmic ray flux, Earth mag. field (*German*) 0-51609  
 D<sub>st</sub> variation asymmetry, as function of local time 0-41643  
 D<sub>st</sub> variations analyses, comparison using distortion free filter 0-17419  
 F-region effects at magnetic field line L=4, electron data anal. 0-8472  
 F-region response to storm of June 1972, thermosphere-ionosphere coupling 0-41617  
 field changes, ionospheric-magnetospheric contribs. 0-12612  
 HF radio noise study during auroral substorms, freq. range 8 to 25.5 MHz 0-41670  
 high-energy protons produced by substorms, interplanetary conditions 0-51615  
 influences on man-made technologies 0-12887  
 interplanetary magnetic field changes correl. to geomag. storms 0-41642  
 interplanetary magnetic field Z-components, variations causing magnetic storm main phase 0-4200  
 ionosphere, electric fields and currents in substorms, simulation 0-12601  
 ionosphere, lower, storm-produced disturbances in long-distance mid-latit. VLF transmission 0-8485  
 ionosphere polar electric field, horizontal transmission to equator 0-8478  
 ionosphere total electron content, storm-time changes at nearby mid-latit. locations 0-31164  
 magnetosphere, magnetic energy conversion in substorms 0-56682  
 magnetosphere, magnetic field models 0-41640  
 magnetosphere, substorms and solar flares, similar plasma processes 0-41671  
 magnetosphere disturbances, effects on high-latit. ionospheric absorpt., riometer meas. 0-8488  
 magnetosphere reconnection, substorms and energetic particle acceleration 0-31169  
 magnetosphere substorms, ionosphere elec. fields determ. from Doppler sounding 0-4169  
 magnetosphere substorms, prediction of occurrence by solar wind and IMF obs. 0-41648  
 magnetotail, plasma flow during substorm 0-51616  
 magnetotail neutral sheet southward mag. field rel. to energetic electrons distrib. and substorms 0-26695  
 midlatitude disturbances, assoc. VLF radio wave phase anomalies 0-56671  
 Pc 4.5 geomagnetic pulsations generation, influence of bounce effects 0-4197  
 plasma dynamics, vertical displacement during substorms 0-4184  
 prediction by multivariate statistical anal. (*Chinese*) 0-12614  
 radiowave propag. errors due to troposphere and ionosphere during mag. storms 0-4077  
 search for interplanetary quantity controlling development of magnetospheric storms, review 0-17447  
 solar 146 MHz C-type bursts correl. with mag. storms (*Chinese*) 0-4321  
 SSC magnitudes, equatorial enhancement 0-31174  
 substorm activity, rel. to rapid subauroral ion drifts obs. by Atmosphere Explorer C 0-4188



**magnetic storms continued**

- substorm auroras, pot. and inductive elec. fields on magnetosphere 0-21878
- substorm electric fields in plasmasphere, model based on whistler data 0-41661
- substorm inhomogeneities affected by ionosphere, experimental verification proposed 0-4199
- substorms, Alfvén waves excitation by bouncing electron beams rel. to nightside mag. pulsations 0-4203
- sudden commencement, uniform ionosphere transient response rel. to preliminary reverse impulse 0-8477
- sudden commencement in equatorial region, 1958 to 1972 period (*French*) 0-51606
- thermosphere heating during magnetic storm, dynamic energy transport from high to low latits. 0-26657
- whistlers, meas. of occurrence rate during geomagnetic magnetosphere storms 0-12621
- $O^+$  energetic ions precip. during mag. storms and magnetosphere-thermosphere coupling 0-26665

**magnetic structure**

- see also *canted spin arrangements*
- cubic spinels, appl. of determinant method (*French*) 0-54854
- di-(2,2,6,6-tetramethyl-4-piperidinyl-1-oxyl)-suberate, spin densities, polarised neutron diff. meas. 0-50037
- 1,5-dinitronaphthalene, diamag. cryst., mag. axis, struct. interpretation 0-50039
- elastic polarised neutron scatt. atomic mag. moments 0-29531
- exciton ferromagnet, incommensurate mag. structs., inhomogeneous magnetisation (*Russian*) 0-29566
- finite sample, mag. rearrangements near surface 0-11240
- GdH<sub>3</sub>, mag.-ordering at 1.8K 0-50062
- group theory description, single irreducible group representation (*Russian*) 0-44804
- Heisenberg-Mattis model, long-wavelength dynamic response 0-20409
- Invar, magnetic structure, absorbed H<sub>2</sub> effect 0-20534
- isotropic three-sublattice ferrimagnet, magnetisation 0-2605
- manganese aluminosilicate glass, insulating spin glass, exchange dipole optical transition 0-40136
- neutron diff., integrated intensity heats, crystal and mag. struct. determ. 0-44079
- neutron diffraction, symmetry anal., group theoretical group anal. of exchange Hamiltonian 0-29527
- neutron diffraction studies of mag. materials, book contrib. 0-11169
- nuclear orientation and NMR of oriented nuclei, appl. to solid state magnetism 0-44928
- paramagnetic metal, polarised neutron inelastic and quasi-elastic scattering 0-50045
- paramagnetic metals, polarised neutron studies of field induced magnetisation 0-25084
- polarisation analysis of diffuse neutron scattering 0-25098
- polarised neutron diffraction, determ. of magnetic form factors, pioneering work 0-24321
- polarised neutrons in condensed matter [conference, Zaborow, Poland (Sept. 1979)] 0-22136
- powder least-squares program, POWLS 0-1892
- rare earth amorphous alloys, mag. props., Mossbauer spectra 0-7225
- rare earth cpds., RRh<sub>2</sub>B<sub>3</sub> and RM<sub>2</sub>X<sub>8</sub> (X=S, Se), mag. order and supercond., neutron scatt. studies 0-44807
- rare earth intermediate valence systems, neutron scatt., review 0-49674
- rare earth intermetallic cpds., mag. props., book contrib. 0-39759
- rare earth intermetallics, mag. struct. 0-15698
- rare earth intermetallics, neutron scatt., induced moment magnetism, high press. 0-15699
- rare earth mixed valence compounds, spin dynamics, mag. neutron scatt., Mossbauer effect, XPS studies 0-39786
- rare earth perovskites, prep. and props., book contrib. 0-44193
- rare earth pnictides, prep. and props., book contrib. 0-54212
- rare earth-Cu intermetallic compds. single crystals., mag. props. 0-54892
- rare earth-transition metal alloys, amorphous, struct. and mag. props., book contrib. 0-39818
- rare-earth metal, semi-infinite surfaces with mag. struct., density of states calc. 0-10851
- semiconductor, doped with mag. impurity, ordering mechanism 0-2572
- semiconductors, many-valley, magnetic electron fluctuation states spin direct interactions 0-29364
- singlet ground state system, mag. props. 0-44850
- solitons, mag., obs. in one-dimensional mag systems (*Japanese*) 0-2555
- spinel, symmetry anal. in neutron diff. studies 0-25091
- superconductor, magnetic, spin-spiral ordering 0-2517
- TCNQ salt, quinolinium, electron spin location, elec., mag., and thermal props. 0-25189
- 5d-transition metal antiferromagnetic crystal, struct. props. and lattice dynamics, mag. struct. 0-44268
- transition metal elements and alloys, spin distribution, neutron diffraction expts. 0-25097
- transition metal magnetic clusters, neutron inelastic scatt., review 0-50083
- Al<sub>2</sub>O<sub>3</sub>-CoO-SiO<sub>2</sub> glasses, spin correls., neutron diff. meas. 0-15694
- Ag-Mn, dil. alloy, transverse magnetoresist. in spin glass regime 0-34417
- Al<sub>2</sub>Ce and Al<sub>2</sub>Ce<sub>3</sub>, Kondo cpds., mag. behaviour obs. by neutron diff. 0-50049
- Al<sub>2</sub>O<sub>3</sub>-MnO-SiO<sub>2</sub> glasses, spin correls., neutron diff. meas. 0-15694
- Au-Fe, dil. alloy, transverse magnetoresist. in spin glass regime 0-34417
- BaCo<sub>2</sub>(AsO<sub>4</sub>)<sub>2</sub>, magnetic field effect on mag. ordering neutron diff. obs. 0-50053
- BaFe<sub>12</sub>-M<sub>2</sub>O<sub>19</sub> (M=Al, Ga, Sc, In) ferrites, mag. props. and struct. 0-15690
- Ca<sub>3</sub>Fe<sub>2</sub>Cr<sub>2-x</sub>Ge<sub>3</sub>O<sub>12</sub>, antiferromagnetic order below 12K, Mossbauer study 0-39945
- Ca<sub>3</sub>Mn<sub>2</sub>Ge<sub>2</sub>O<sub>12</sub>, antiferromagnetic garnet, neutron diff. study in mag. field 0-50060
- Ca<sub>3</sub>Mn<sub>2</sub>Ge<sub>2</sub>O<sub>12</sub>, mag. struct. study 0-2554
- CeAl<sub>2</sub>, multiple-q mag. struct. 0-25100
- CeAl<sub>2</sub>, neutron diff. at low temp., magnetism 0-20383
- (Ce<sub>1-x</sub>Ho<sub>x</sub>)Ru<sub>2</sub>, superconducting, mag. props., neutron scatt. study 0-44808
- Ce<sub>1-x</sub>Pr<sub>x</sub>Al<sub>3</sub>, mag. struct., comp. depend., neutron diff. and mag. susceptibility meas. 0-50054
- CoMnP, ferromagnetism and metamagnetism, polarized neutron diff. study 0-44809

**magnetic structure continued**

- CoNb<sub>2</sub>O<sub>6</sub>, magnetic struct., neutron diff. and mag. susceptibility meas. 0-15693
- Co<sub>2</sub>Ni<sub>1-x</sub>O, antiferromagnet, neutron diff. study of mag. struct. 0-34595
- CoU<sub>2</sub>S<sub>8</sub>, mag. struct. and props. 0-11166
- Cr, incommensurate antiferromag., inelastic neutron scatt. meas. 0-25088
- Cr<sub>2</sub>Te<sub>1-x</sub> (x=0 to 0.2), magnetic props. study 0-11194
- Cr<sub>1-x</sub>Ti<sub>x</sub>N, cryst. and mag. struct., at low temps. (*French*) 0-29005
- CsCrCl<sub>3</sub>, mag. structure and excitations, neutron diff. and susceptibility meas. 0-44806
- Cu<sub>2</sub>FeGeS<sub>4</sub>, crystallographic and magnetic structure (*French*) 0-28998
- Cu<sub>2</sub>MnSnS<sub>4</sub>, mag. struct. discussed rel. to Cu<sub>2</sub>FeGeS<sub>4</sub> (*French*) 0-28998
- Cu(NO<sub>3</sub>)<sub>2</sub>·2/3H<sub>2</sub>O, singlet ground state system, mag. props. 0-44850
- Cu(NO<sub>3</sub>)<sub>2</sub>·2.5 D<sub>2</sub>O, magnetic ordering, neutron diff. meas., 0.08-0.25K 0-39749
- DyB<sub>4</sub>, cryst. and mag. struct., neutron diff. meas. 0-15692
- Dy<sub>2</sub>O<sub>2</sub>SO<sub>4</sub>, magnetic struct. in antiferromag. and ferrimag. states 0-15695
- ErB<sub>4</sub>, cryst. and mag. struct., neutron diff. meas. 0-15692
- EuO, magnetic semiconductor, piezoresistance effect, 4.2 to 300K 0-34450
- Fe complex, Fe(II) oxalato-bridged chain compounds, Mossbauer spectra 0-15890
- γ-Fe, mag. struct. Mossbauer studies 0-39917
- Fe-Bi, amorphous ferromag. alloys, mag. struct., Mossbauer study 0-39746
- Fe-Ni alloys, mag. state of austenite and γ-α transform. (*Russian*) 0-40350
- Fe-Ni-P-B, amorphous ferromag. alloys, mag. struct., Mossbauer study 0-39746
- Fe<sub>80</sub>B<sub>20</sub> metallic glass, spin texture determ. 0-15842
- FeI<sub>2</sub>, first order mag. phase transition, neutron scatt. study 0-50090
- (Fe<sub>1-x</sub>Mn<sub>x</sub>)<sub>2</sub>P<sub>15</sub>C<sub>10</sub>, amorphous, mag. ordering, Mossbauer study 0-39747
- (Fe<sub>1-x</sub>Mn<sub>x</sub>)<sub>2</sub>P<sub>15</sub>C<sub>10</sub>, amorphous pair radial distrib. functions, neutron scatt. study 0-49128
- α-Fe<sub>2</sub>O<sub>3</sub>:Al<sup>3+</sup>(Ga<sup>3+</sup>)(Cr<sup>3+</sup>)(In<sup>3+</sup>), substitution effect on Morin transition, neutron diff. study 0-44827
- γ-Fe<sub>2</sub>O<sub>3</sub>-organic interfaces, Fe<sub>2</sub>O<sub>3</sub>, mag. struct., Mossbauer effect, IR absorpt., and magnetisation meas. 0-44869
- Fe<sub>2</sub>O<sub>3</sub>, crit. exponents meas. by polarized neutron scatt. 0-44828
- Fe<sub>2</sub>(PO<sub>4</sub>)Cl, Mossbauer study of mag. ordering and local co-ordination 0-39972
- GaMn<sub>2</sub>(C<sub>1-x</sub>N<sub>x</sub>) phase transition, rel. to valence instabilities in rare earth compounds (*French*) 0-34596
- GdAl<sub>2</sub>, hyperfine fields, ferromagnetic coupling between rare earth spins, NMR study 0-39880
- HgCr<sub>2</sub>S<sub>4</sub>, spinel, symmetry anal. in neutron diff. studies 0-25091
- Ho, Hall effect, field and temp. depend., 4.2-150K, singularities (*Russian*) 0-29387
- Ho-Sm alloy, Hall effect, field and temp. depend., 4.2-150K, singularities (*Russian*) 0-29387
- Ho<sub>2</sub>O<sub>2</sub>SO<sub>4</sub>, magnetic struct. in antiferromag. and ferrimag. states 0-15695
- HoP, fopside mag. struct. to ferromag. transition, elastic neutron scatt. obs. 0-50058
- KCrO<sub>2</sub>, two-dimens. mag. order, neutron powder diff. obs. 0-44805
- KFeS<sub>2</sub>, cryst. struct. and mag. ordering, neutron diff. and mag. susceptibility meas. 0-54867
- KMnCl<sub>3</sub>, magnetic spiral struct., neutron diff. study 0-39748
- La<sub>1-x</sub>Gd<sub>x</sub>Ag, antiferromagnet, spin echo NMR anal. 0-15821
- La<sub>2</sub>MnZnS<sub>5</sub>, antiferromag., neutron diff. study 0-25099
- LiCrO<sub>2</sub>, two-dimens. mag. order, neutron powder diff. obs. 0-44805
- LiH, nuclear ordered ferromag. and antiferromag. phases, neutron diff. study 0-50052
- LiTi, substituted ferrite, cation distribution, Mossbauer, X-ray, neutron diff. study 0-28975
- LiZn, substituted ferrite, cation distribution, Mossbauer, X-ray, neutron diff. study 0-28975
- Mg<sub>1-x</sub>Mn<sub>x</sub>Te<sub>2</sub>, random dil. antiferromagnet, mag. props. 0-54870
- MgV<sub>2</sub>O<sub>4</sub>, spinel, symmetry anal. in neutron diff. studies 0-25091
- Mn-Bi alloy, melting and solidification under microgravity, mag. props. (*German*) 0-45296
- γ-Mn-Ni (15 at.%), antiferromag. defect scatt., neutron polarisation anal. 0-50056
- Mn<sub>4</sub>F, non-collinear component in mag. struct. 0-25089
- Mn<sub>1-x</sub>Fe<sub>x</sub>Pt<sub>3</sub>, noncollinear mag. structs., neutron diff. anal. (*Russian*) 0-25087
- MnP, appl. of method for study of mag. structs. (*Russian*) 0-39741
- Mn<sub>2</sub>TeO<sub>6</sub>, magnetic structure, stability of mag. modes, neutron diffraction study (*French*) 0-39744
- NaCrO<sub>2</sub>, two-dimens. mag. order, neutron powder diff. obs. 0-44805
- NaMnCl<sub>3</sub>, antiferromagnet, exciton self-localisation luminesc. and excitation spectra (*Russian*) 0-11456
- Nd, magnetic form factors, polarised neutron diff. meas. 0-50057
- Nd, magnetic structure, 2D modelled 0-15697
- Nd, magnetoresistance, mag. struct., elec. resistance at low temps. (*Russian*) 0-54936
- Ni-Mn, mag. moment and asphericity of spin density distrib., polarised neutron scatt. obs. 0-44813
- Ni-Pd, mag. form. factor, polarised neutron diff. meas. 0-29525
- NiF<sub>2</sub>, magnetisation and antiferromagnetic resonance freq. in mag. field (*Russian*) 0-34781
- Ni<sub>2</sub>Mn<sub>2</sub>M<sub>1-x</sub>Sn (M=Ti,V) mag. hyperfine fields, <sup>119</sup>Sn Mossbauer spectra study 0-55003
- NpFe<sub>2-x</sub>Co<sub>x</sub>Si<sub>2</sub>, mag. and hyperfine props. 0-7247
- Pd-Mn(Fe), mag. ordering phenomena, neutron scatt. obs. 0-44812
- Pd<sub>2</sub>MnIn<sub>1-x</sub>Sb<sub>x</sub>, Heusler alloy, mag. order obs. 0-29528
- Pr, antiferromagnetic ordering 0-15709
- Pr, magnetic form factors, polarised neutron diff. meas. 0-50057
- Pr, magnetic ordering, stress induced 0-15776
- Pr, quasielastic mode damping, dynamic susceptibility 0-15705
- PrSb, neutron scatt., press. induced antiferromag. 0-15699
- PrSb, pressure-induced antiferromag., neutron scatt. study 0-39750
- RbCoCl<sub>2</sub>·2D<sub>2</sub>O, metamagnetic phase transition, crystallographic and mag. struct., neutron diff. meas. 0-44174
- RuF<sub>3</sub>, mag. props. 0-15707
- SmAl<sub>2</sub>, hyperfine fields, ferromagnetic coupling between rare earth spins, NMR study 0-39880



**magnetic structure continued**

- Sm<sub>1-x</sub>Gd<sub>x</sub>Al<sub>3</sub>, hyperfine fields, ferromagnetic coupling between rare earth spins, NMR study 0-39880  
 SmN, magnetic props., neutron diffr. and mag. susceptibility meas. 0-50036  
 SrCoO<sub>3</sub>, Fe<sup>4+</sup>, ferromag., sign of Fe<sup>4+</sup> hyperfine field, spin struct., Mossbauer study 0-39933  
 SrLaFeO<sub>4</sub>, mag. and cryst. struct. determ. (*French*) 0-54866  
 Sr<sub>1-x</sub>Zn<sub>x</sub>Y(Y = Ba<sub>2-x</sub>Fe<sub>12</sub>O<sub>22</sub>), x=0, 1, 1.6, mag. moments reorientation 0-44851  
 steel, Cr-Ni, ferrite precip. (*Japanese*) 0-35187  
 TbB<sub>2</sub>, mag. struct., ferromag. ordering, neutron diffr. study 0-15692  
 TbBe<sub>13</sub>, magnetic structure at low temps., antiferromagnetic, neutron diffraction study (*French*) 0-39743  
 TbD<sub>3</sub>, non-stoichiometric, complex antiferromag. struct., neutron diffr. study 0-50061  
 Tc, paramagnetic form factor, polarised neutron diffr. study 0-39745  
 ThCo<sub>5</sub>, itinerant electron metamagnetism, polarised neutron study 0-39742  
 TiBe<sub>2</sub>, neutron diffr. study of mag. ordering 0-44811  
 TmAl<sub>3</sub>, ferromagnetic structs., elastic neutron scatt. obs. 0-50055  
 TmSe, mag. neutron scatt. 0-25096  
 TmSe, mag. props. and struct. 0-25109  
 α-U, electronic band struct. and props. 0-10861  
 UAs, magnetic struct. in high mag. fields, neutron diffr. study 0-34597  
 UAs, magnetisation, ferrimag. spin struct. 0-7088  
 U<sub>3</sub>As<sub>4</sub>, magnetisation in strong fields, 4.2 to 200K anisotropy and exchange forces 0-54886  
 UGe<sub>3</sub>, induced magnetisation density and f-d bonding, polarised neutron diffr. study 0-50063  
 UGe<sub>3</sub>, magnetisation density, neutron scatt. meas. 0-50038  
 UN, mag. inelastic scatt. 0-7079  
 UPb<sub>3</sub>, crystal field energy levels, magnetisation and susceptibility, neutron spectra obs. 0-50064  
 USB, neutron inelastic scatt. from collective excitation 0-7080  
 USB<sub>9</sub>Te<sub>0.1</sub>, multiaxial mag. structure 0-15696  
 USB<sub>9</sub>-Te<sub>9</sub>, mag. struct. and mag. phase diagram, neutron diffr. study 0-50059  
 V<sub>1-x</sub>Cr<sub>x</sub>Si, x=0 to 3, struct., supercond. and mag. props. 0-1962  
 V<sub>2</sub>S<sub>8</sub>, paramag. cryst., struct. factors using polarised neutron diffr. 0-15691  
 V<sub>2</sub>WO<sub>6</sub>, magnetic structure, stability of mag. modes, neutron diffraction study (*French*) 0-39744  
 Y(Co<sub>1-x</sub>Ni<sub>x</sub>)<sub>5</sub>, mag. heterogeneities and coercive force, neutron scatt. study 0-2553  
 YFe<sub>2</sub>, amorphous concentrated spin glass, susceptibility, Mossbauer and neutron scatt. meas. 0-39783  
 Y<sub>3</sub>Fe<sub>5-x</sub>Ga<sub>x</sub>O<sub>12</sub>, garnet, magnetically inequivalent positions of cations in external mag. field 0-11307  
 YFeO<sub>4</sub>, two-dimensional spin ordering, neutron diffr. study 0-29530  
 Y<sub>1-x</sub>Gd<sub>x</sub>Rh<sub>2</sub>B<sub>4</sub>, mag. supercond., anomalous temp. depend. of upper crit. fields 0-29510  
 YIG, polariser neutron study of covalency effects 0-2552  
 Yb-Eu alloys, mag. ordering, magnetisation meas. 0-7081  
 Zr, magnetic form factor, field-induced, polarised neutron scatt. meas. 0-50044  
 Zr(Fe<sub>1-x</sub>Al<sub>x</sub>)<sub>2</sub>, transition region, spin glass or long range mag. order 0-44841  
 Zr(Fe<sub>1-x</sub>Co<sub>x</sub>)<sub>2</sub>, transition region, spin glass or long range mag. order 0-44841

**magnetic surface phenomena**

- alloy with two ferromagnetic components, surface excitations 0-25179  
 binary alloys, magnetic interface struct. 0-29564  
 dipolar magnet, surface effects on phase transitions, local spontaneous polarisation 0-2708  
 ferrite rods, magnetised longitudinally, surface mode propag. 0-54878  
 ferromagnet, itinerant electron, surface spin waves, tight-binding Hubbard model 0-39763  
 ferromagnetic films, spin correl. functions, crit. indices 0-7133  
 ferromagnetic plate, surface magnetostatic wave excitation 0-25119  
 ferromagnetic plate, with anisotropic surface discontinuities, spectrum and damping of quasi-surface spin waves 0-11185  
 ferromagnets, exchange and dipolar coupled, spin wave renormalisation, Damon-Eshbach surface spin waves 0-2564  
 film, complex surface pinning parameter and quasi-localised surface spin wave modes 0-50150  
 finite sample, mag. rearrangements near surface 0-11240  
 Invar, Fe-Ni-C, spin pinning effect in RF collapse studies, Mossbauer spectroscopy 0-44971  
 Ising, internally dil. film, surface enrichment as possible source of surface magnetism 0-15731  
 magnetisation profile, in crit. region by  $\epsilon$ -expansion, Wilson perturbation theory calc. 0-50100  
 magnetite, spin polarisation, effect of temp. and photon energy 0-45221  
 Mossbauer spectroscopy and surface phenomena study 0-39916  
 Mossbauer spectroscopy of surface and interface magnetism 0-7218  
 nonexchange surface spin waves at interface between two ferromagnets 0-29544  
 one-dimensional semi-infinite chain, enhanced surface exchange interaction, mag. relax. 0-29558  
 one-magnon states in BCC Heisenberg antiferromag., spectral density near stepped surfaces 0-20396  
 ordering temps. determ. by Bethe-Peierls-Weiss (BPW) method 0-54912  
 photoemission, spin energy analysed, feasibility anal. 0-55271  
 Schottky barrier, mag. surface levels in presence of depletion-type band bending 0-20285  
 sublimation current and vapour press. of mag. solids 0-34182  
 thin surface layer, interactions between nondegenerate electrons, effect on cyclotron resonance, mag. cond. (*Russian*) 0-15802  
 transition metal, FCC, semi-infinite, susceptibilities near (001) surface 0-15701  
 transition metals, review 0-44861  
 Fe epitaxial film, Mossbauer effect, interface magnetism 0-11297  
 Fe, ferromagnetic, chemisorption of H, spin-spin interactions, UPS spectra calc. 0-6630  
 Fe film coated by MgO, MgF<sub>2</sub> and Sb, surface mag. 0-7196  
 Fe film coated by MgO, Mossbauer spectra, mag. hyperfine field 0-7221  
 γ-Fe<sub>2</sub>O<sub>3</sub>/Co acicular powder epitaxially doped, coercivity increase, surface anisotropy (*Chinese*) 0-7130

**magnetic surface phenomena continued**

- γ-Fe<sub>2</sub>O<sub>3</sub>/organic interfaces, mag. struct., Mossbauer effect, IR absorpt., and magnetisation meas. 0-44869  
 α-FeOOH ultrafine particle NGR spectra, size distrib. and surface effects 0-11299  
<sup>3</sup>He, liq., in contact with dielec. surface, mag. susceptibility enhancement, thermodynamics 0-54460  
 Ni, ferromagnetic, chemisorption of H, spin-spin interactions, UPS spectra calc. 0-6630  
 Ni, magnetic surface anisotropy of transition metals, model calc. 0-34625  
 NiFe, magnetic surface anisotropy of transition metals, model calc. 0-34625  
 NiO (111) surfaces, antiferromag., mag. scattering by polarised LEED, spin polarisation effect in theory 0-29529  
 Pd, film with defects, field-induced resist. min. 0-11050  
 YIG, dilute, magnetoacoustic surface wave excitation by RF field on Bloch walls 0-25178  
 YIG ferromagnetic film, quasi surface spin wave giant oscills. (*Russian*) 0-15767  
 YIG film, magnetostatic surface and forward volume wave oblique incident at shallow groove 0-34704  
 YIG film tangentially magnetised, magnetostatic surface wave excitation 0-29586  
 YIG, magnetised in raised cosine profile magnetostatic surface wave propag. 0-2567  
 YIG periodic film layer, magnetostatic surface wave propag. 0-2607  
 YIG substrates, magnetoelastic surface waves, magnetostatic reson. anal. 0-20441

**magnetic susceptibility**

- see also molecular magnetic susceptibility; photomagnetic effect  
 0-29395  
 AC, depend. on magnitude meas. field 0-241  
 achondrite meteorites, brecciation and shock effects on mag. susceptibility and NRM 0-8603  
 actinides, susceptibility meas. using micro-mag. susceptometer 0-13112  
 alkali metal-transition metal double molybdates, 90-800K, paramag. behaviour (*French*) 0-39734  
 Anderson impurities, interacting, pair, Fermi-liq. theory 0-44803  
 Anderson model, direct interaction between impurities 0-54681  
 Anderson model for dilute magnetic alloys, static suscept., functional integral approach 0-50050  
 anisotropic Heisenberg ferromag., inhomogeneous dynamic susceptibility tensor 0-39729  
 anisotropic paramagnet, statistical mechanics using second order Green's function theory 0-25074  
 anthracene, mag. susceptibility anisotropies, high field <sup>2</sup>H NMR quadrupolar effects obs. 0-25225  
 antiferromagnetic chain, random, quantum spin-1/2 Heisenberg soln. 0-11148  
 antiferromagnetism in system if itinerant electrons 0-2547  
 α-B, rhombohedral, magnetic props. and ESR spectra 0-20452  
 biphenyl, mag. susceptibility 0-25076  
 charge-density-wave metal, mag. susceptibility of cond. electrons 0-44523  
 Chevrel phase compounds, bonding and phys. props. rel. to struct., book contrib. 0-49209  
 chromium phosphinate polymer, one-dimensional antiferromagnet, spin-flop 0-50131  
 chrysene, mag. susceptibility anisotropies, high field <sup>2</sup>H NMR quadrupolar effects obs. 0-25225  
 classical planar spin model, two-dimens., Monte Carlo study 0-25147  
 copolymer model with alternating spins, kinetics 0-9768  
 copper complex CuBr<sub>2</sub> (pyrimidine)<sub>2</sub>, mag. susceptibility and magnetisation curve, 1.2-4.2K 0-11177  
 coronene, mag. susceptibility anisotropies, high field <sup>2</sup>H NMR quadrupolar effects obs. 0-25225  
 critical point, complementary expressions for scaling function 0-34656  
 crystal with strong s-d exchange, mag. susceptibility and Curie-Weiss law (*Russian*) 0-25068  
 cubic metal binary alloys for H energy storage 0-45787  
 demagnetisation eigenfunctions anal. of linear transverse magnetisation in long, thin stripes 0-34687  
 dialkylammonium copper tetrachloride, ferromag., static and dynamic mag. props. 0-50074  
 diamagnetic susceptibility calculation using Pascal's consts., BASIC program 0-37717  
 dilute magnetic alloys, asymmetric Anderson model, renormalisation-group approach, static props. 0-44802  
 dilute magnetic alloys, symm. Anderson model, renormalisation-group approach, static props. 0-44801  
 diluted Ising and Heisenberg magnets with competing interactions, phase diagrams and mag. props. 0-34672  
 dimethyl ammonium copper chloride, spin dynamics near crit. pt. 0-7112  
 dimethylammonium manganese tetrachloride-d<sub>4</sub>, structural and mag. phase transitions, neutron scatt. and AC susceptibility meas. 0-44825  
 1,5-dinitronaphthalene, diamag. cryst., mag. axis, struct. interpretation 0-50039  
 dipropylammonium manganese tetrachloride, and tetrabromide, two-dimens. antiferromagnet, spin canting and exchange 0-34620  
 disordered anisotropic antiferromagnet, random field effects 0-2580  
 disordered one-dimensional conductors, interacting electron thermodynamics (*Russian*) 0-54679  
 domain lattices, parallel stripe susceptibility, uniaxial anisotropy field 0-54930  
 Earth crust, mag. susceptibility, meas. at Yerington mine, Nevada 0-51323  
 electron gas, metallic densities, dynamical dielectric function and paramagnetic spin susceptibility 0-39514  
 epoxy resin, mag. susceptibility, constant mag. field effect 0-11154  
 ferredoxin, from Clostridium pasteurianum, Mossbauer effect, ESR, and mag. susceptibility meas. 0-40961  
 ferrimagnet, polaritons, mag. susceptibility 0-7095  
 ferroelectric semiconductor, spin susceptibility near ferroelec. transition 0-2710  
 ferromagnet, spin wave nonresonant excitation by varying mag. field, nonequilibrium states (*Russian*) 0-34616  
 ferromagnet, uniaxial dipolar, crossover behaviour, theory 0-29559  
 ferromagnetic alloy, transition to spin glass ordering 0-34628  
 ferromagnetic film, transverse bioped susceptibility, two-dimens. micro-magnetism 0-11231



**magnetic susceptibility continued**

ferromagnetic films, spin correl. functions, crit. indices 0-7133  
 first row elements, ground state, self-consistent orbitals with uniform long-range behaviour 0-9485  
 frustrated two-dimensional planar model, spin-spin correl. 0-11212  
 frustrationless models, rel. to spin glasses 0-29561  
 graphite intercalation cpds., mag. susceptibility, tight-binding model 0-44796  
 graphite intercalation cpds. with alkali metal, interlayer screening and mag. susceptibility 0-44794  
 graphite-alkali metal intercalation cpds., electronic props. 0-45202  
 graphite-alkali metal intercalation cpds., large anisotropy and stage depend. 0-44795  
 HCP metals, mag. susceptibility near  $2\frac{1}{2}$ th order electron transition, non-linear magnetisation anal. (*Russian*) 0-44859  
 Heisenberg antiferromagnetic chain, random, low temp. thermodynamic props. in zero mag. field 0-34657  
 Heisenberg ferromagnet, longitudinal static spin susceptibility at  $T < T_c$  0-50114  
 Heisenberg linear chain, alternating spin quantum numbers, mag. and thermodynamic props. 0-34578  
 p-heptyl-p'-cyanobiphenyl, refractive index, dielec. const., mag. susceptibility, orientational ordering (*Dutch*) 0-33884  
 high-field solenoid field gradient appl. 0-31813  
 Hubbard model, doubly degenerate, long range order 0-50029  
 Hubbard model calc., isothermal longitudinal susceptibility of strongly correlated electrons 0-25069  
 II-VI semiconductors, mag. susceptibility, effect of physical parameters 0-44793  
 III-V semiconductor effect of covalent bonding on mag. susceptibility 0-11153  
 ilvaite, Mossbauer spectra and mag. features 0-7248  
 induced moment systems, effect of spin fluctuations 0-2585  
 intermediate valence, mag. susceptibility and mag. instabilities 0-39532  
 intermediate valence, phase diagram and Kondo behaviour 0-29366  
 intermediate valence, three-site, six-electron, even-parity model 0-20125  
 Invar, magnetic and thermal anomalies 0-34603  
 iron (III) salicylates, Mossbauer and IR spectra, mag. susceptibility 0-50242  
 Ising ferromagnet, high-freq. props. quantum theory, susceptibility tensor calcs. (*Russian*) 0-11143  
 Ising ferromagnets, correlation decay, zero-field susceptibility, mass gap 0-50116  
 Ising model, adiabatic susceptibility and specific heat at const. magnetisation 0-7114  
 Ising model, kinetic with triplet interactions, Monte Carlo anal. 0-7061  
 Ising model, one-dimens., wavevector depend. of fluctuations in cluster approx. 0-12999  
 Ising model, three-dimens. mag. susceptibility and sp. ht., high temp. series anal. 0-22295  
 Ising model with free surface, series anal. 0-25062  
 Ising O(2), O(3) and O(4) spin systems, Hamiltonian string-coupling expansions 0-20426  
 Ising square lattice, phase transitions, next nearest neighbour interactions 0-50128  
 Ising systems of different spin values, random system 0-11144  
 liquid metals, spin-orbit interactions effect on mag. susceptibility, effective pseudohamiltonian 0-29299  
 long wavelength spin susceptibility from particle-particle scattering, logarithmic temp. control 0-7124  
 low-temperature materials props. and appl. (*German*) 0-3081  
 lymphocytes, living and dead, mag. props. and mag. sedimentation 0-35925  
 lyotropic nematic liquid crystals, mag. susceptibility, mol. aggregation meas. 0-19690  
 manganese zinc formate dihydrate, two-dimens. antiferromag., anomalous crit. phenomena, neutron scatt. and PMR obs. 0-50104  
 MBBA, refractive index, dielec. const., mag. susceptibility, orientational ordering (*Dutch*) 0-33884  
 measurement system, for student laboratory 0-4491  
 metal borides,  $MM_2B_4$  ( $M=Y, R$ ;  $M'=Os, Ir$ ), mag. meas., Curie Weiss behaviour 0-20375  
 mixed valence cpds., mag. susceptibility and sp. ht., periodic Anderson model, CPA alloy analogue method 0-15474  
 mixed valence state, electronic structure, spin-orbit interaction effects, mag. susceptibility 0-54657  
 molecules, rigid-body, librating mag. susceptibility 0-25076  
 $Na_3V_2Ti_6O_{16}$ , characterisation and mag. props., 90-800K,  $Na_3Ti_4O_8$  bronze isotypes (*French*) 0-39735  
 negative ion, singly-charged, Thomas-Fermi-Amaldi eqn., approx. variational soln. 0-52870  
 nematic liquid crystals, temp. depend. of mag. susceptibility 0-25103  
 neptunium cyclopentadienyl compounds,  $(C_5H_5)_3NpX$ , ( $X=F, Cl, Br, I, (SO_4)_{1/2}$ ), mag. susceptibility 0-11152  
 non-stoichiometric phase, physico-chemical props. 0-29532  
 one-dimensional disordered systems, magnetism 0-25152  
 one-spin ferromagnet, high temp. series expansion for mag. susceptibility and sp. ht. 0-25148  
 PAA, refractive index, dielec. const., mag. susceptibility, orientational ordering (*Dutch*) 0-33884  
 pion condensate props. in mag. field, superconductivity, mixed state (*Russian*) 0-49974  
 polyethylene mag. susceptibility, constant mag. field effect 0-11154  
 polysulphur nitride:Br mag. susceptibility, linear temp. depend. 0-25114  
 Potts model, Monte Carlo simulation in three dims. 0-163  
 pseudo one-dimensional kinetic Ising model, dynamic susceptibility 0-50025  
 PVC magnetoelectrets, mag. susceptibility 0-2687  
 random exchange Heisenberg antiferromagnetic chain, exchange-coupled pair model 0-20423  
 random Ising ferromagnet, upper bounds 0-34663  
 random spherical model, crit. dynamics 0-44844  
 rare earth alloys,  $R(Fe, Rh)_{1-x}$ , mag. props., Mossbauer spectra 0-25108  
 rare earth alloys,  $RZn_{12}$  and  $RCu_2Al_8$ , mag. struct. and interactions 0-25092  
 rare earth complexes, formation and props., book contrib. 0-43204  
 rare earth compounds,  $R_2MoO_5$ , cryst. struct., IR spectra, elec. and mag. props. 0-33954  
 rare earth dodecaborides, mag. susceptibility temp. depend., 90-1200K 0-20374

**magnetic susceptibility continued**

rare earth intermetallic cpds., mag. props., book contrib. 0-39759  
 rare earth intermetallics,  $Al_2-Gd(Er)(Dy)(Nd)$ , dil., ( $R=La, Yb, Lu$ ), EPR and mag. susceptibility 0-15797  
 rare earth intermetallics,  $RGa_2$ , ordering and exchange interactions 0-39779  
 rare earth intermetallics, RPt, ( $R=Gd, Tb, Dy, Ho, Er, Tm$ ), structs. and mag. props. 0-50069  
 rare earth metasilicates,  $R_2(SiO_3)_3$ , mag. susceptibility, temp. depend., 77-800K 0-20372  
 rare earth oxides, binary, struct. and props., book contrib. 0-45292  
 rare earth tetraborides, mag. and elec. props., metallic character 0-20386  
 rare earth-Cu intermetallic compds. single crystals, mag. props. 0-54892  
 rare earth-iron,  $RFe_2$ , Laves phase intermetallics, ordered and paramagnetic phases, mean field exchange consts. 0-50084  
 rotating coordinate system with quadrupole splitting, paramag. susceptibility 0-11178  
 $S=1$ , singlet ground state systems, mag. props. 0-11157  
 $S=1$  generalised Ising model, stability conditions 0-20427  
 semiconductor, diamagnetic susceptibility of excitonic molecules (*Russian*) 0-7074  
 semiconductors, magnetic, static magnetic properties, mean field approach 0-7090  
 single-ion anisotropy, magnetic systems, high temp. series expansion 0-34576  
 spin glass, EPR frequency and mag. transverse susceptibility with remanent magnetisation (*French*) 0-7145  
 spin glass, relaxation times, influence of spectral distrib. on freq. depend. of freezing temp. 0-44848  
 spin glasses, phase transition, mag. susceptibility, specific heat, Ising model calcs. (*Russian*) 0-34671  
 spin glasses, sp. ht. and susceptibility, random series method 0-44542  
 spin glasses, susceptibility, wave-vector-depend., theory 0-11209  
 spin systems, coupled itinerant localised systems, dynamic magnetic response 0-34583  
 spin wave theory of spin  $1/2$  X-Y model, phase transition, susceptibility 0-7068  
 spin-glass, one-dimens., sp. ht. and mag. susceptibility calcs. 0-7120  
 spin-glass, two-dimensional Ising model, low temp. dynamic props. 0-20425  
 spin-phonon system, transition to self-trapping 0-10606  
 spinels, domain wall formation inhibition, effect on bulk mag. props. 0-11220  
 steel, austenitic stainless, magnetic susceptibility and magnetisation, low temp. 0-25102  
 steel, induced anisotropy influence on mag. props., thermomagnetic working (*Russian*) 0-55549  
 superconducting small metal particles ground state energy and orbital mag. susceptibility 0-49983  
 superconductor, magnetic, Fermi surface nesting effect on mag. instability 0-54831  
 superconductor, magnetic, spin-spiral ordering 0-2517  
 superconductor, thermodynamics of magnetism and supercond., mol. field theory 0-34668  
 $tCFeCr_2S_4-xSe_x$  chalcospinel, ESR spectrum and paramag. susceptibility 0-15789  
 TCNQ complexes with ferrocenes, charge transfer type, struct. and mag. props. 0-24439  
 TCNQ salt, (N-methylphenazinium) $_x$ (phenazine) $_{1-x}$ , 1 band filling, carrier mobility and disorder effects 0-24904  
 TCNQ salt, (NMP) $_{0.5}$ (phenazine) $_{0.5}$  TCNQ, transport props. 0-24891  
 TCNQ salt, (TSeF) $_x$ (TTF) $_{1-x}$ -TCNQ, struct., elec. and mag. props., review 0-20158  
 TCNQ salt, MEM(TCNQ) $_2$ , phase transition electronic struct. interpretation 0-24781  
 TCNQ salt, MEM(TCNQ) $_2$ , phase transitions, elec. cond., ESR, mag. susceptibility study 0-24981  
 TCNQ salt, N-propyl-quinolinium(TCNQ) $_2$ , defect conc. depend. phase transition 0-44577  
 TCNQ salt, NMP $_{0.63}$ phenazine $_{0.37}$ TCNQ, mag. susceptibility, 0.03-4.2K 0-25191  
 TCNQ salt, NPQn (TCNQ) $_2$ , neutron irradi. induced defect concentration depend. phase transition 0-29449  
 TCNQ salt, pyridinium (TCNQ) $_2$ , low temp. mag. phase transition, ESR study 0-25139  
 TCNQ salt, quinolinium, electron spin location, elec., mag., and thermal props. 0-25189  
 TCNQ salt, quinolinium (TCNQ) $_2$ , mag. chain double resonance study, deuteration 0-25250  
 TCNQ salt, quinolinium (TCNQ) $_2$ , transport props. 0-24891  
 TCNQ salt, tetramethylhexamethylenediammonium-TCNQ-iodine, elec. and mag. props., struct., specific heat 0-24898  
 TCNQ salt, TMTSF-DMTCNQ, mag. susceptibility meas. under press. 0-29521  
 TCNQ salts, aminopyridinium (TCNQ) $_2$ , elec. and mag. props., 4.2 to 300K 0-24889  
 TCNQ salts, n-methylacridium (TCNQ) $_2$ , 2,2'-bipyridinium (TCNQ) $_2$  and Qn(TCNQ) $_2$ , with asymmetric donors, mag. susceptibility, 0.035-4.2K 0-25190  
 TCNQ- $\phi_4$ DTP, chemisorbed  $O_2$  effects on mag. susceptibility 0-15679  
 TCNQ-NMP, transport props. 0-24891  
 TCNQ-TTF, chemisorbed  $O_2$  effects on mag. susceptibility 0-15679  
 transition metal, FCC, semi-infinite, susceptibilities near (001) surface 0-15701  
 transition metal alloys, ferromag., high-field susceptibility 0-7083  
 transition metal compounds and dil. alloys, mag. ordering phenomena in high mag. fields 0-50075  
 transition metal hydrides and deuterides, conc.-temp. depend. of mag. susceptibility 0-29523  
 transition metal intercalates of Ni and Ta dichalcogenides, magnetic susceptibility, function of temp. 0-39756  
 $\alpha$ TTF:Br, transport and mag. props., effect of doping 0-24934  
 TTF(MBDT) spin-Peierls transition, mag. exchange interactions, mag. props. 0-25138  
 TTF-TCNQ, deuterated, isotope effect on mag. susceptibility 0-25080  
 TTF-TCNQ, divergent mag. responses at  $2k_F$  and structural phase transitions 0-20376  
 TTF-TCNQ, elec. cond. and spin susceptibility, press. and temp. depend. 0-24894  
 TTF-TCNQ, phase transitions and CDW state, controlled disorder effects 0-15507



## magnetic susceptibility continued

- TTF-TCNQ, phase transitions and CDW state, induced defect depend., transport and mag. studies 0-24980  
 TTT<sub>2</sub>(I<sub>3</sub>)<sub>1+x</sub>, physical props., elec., mag. and optical meas. 0-24908  
 vibronic ferroelectric semiconductor, mag. susceptibility calc. 0-2711  
 Ag-Mn, spin glass, mag. susceptibility hydrostatic press depend., RKKY interaction 0-44845  
 Al-Ni alloys, solid and liq. mag. susceptibility, 600-1650°C (*Russian*) 0-15685  
 Al<sub>0.5</sub>V<sub>2</sub>O<sub>5</sub>, spin glass phase, low temp. mag. susceptibility meas. 0-29565  
 As<sub>2</sub>S<sub>3</sub>-Te<sub>2</sub>, ternary chalcogenide glassy system, optical absorpt., mag. susceptibility and AC cond. meas. 0-55125  
 α-B, rhombohedral, temp. depend. 0-34585  
 B<sub>2</sub>O<sub>3</sub>-Fe<sub>2</sub>O<sub>3</sub>-nMO (M=Fe, Co, Ni, Cu, Mg), synthesis and mag. props. 0-20384  
 BaO-Fe<sub>2</sub>O<sub>3</sub>-B<sub>2</sub>O<sub>3</sub> glass, splat cooled, low temp. micromagnetism 0-34660  
 BaTiO<sub>3</sub>(X=Cr, Mn, Fe, Co, Ni, Zn, Ga), annealed in H<sub>2</sub> and O<sub>2</sub>, valence change in phase stability 0-20600  
 BaVSe<sub>3</sub>, one-dimensional, struct. and mag. props. 0-28993  
 Ba<sub>2</sub>XRuO<sub>6</sub>(X=La, Eu), <sup>99</sup>Ru Mossbauer spectra and other techniques 0-29659  
 Bi-Sn, maximum diamagnetism rel. to electron density 0-54865  
 β<sup>2</sup>-Cu<sub>2</sub>V<sub>2</sub>O<sub>7</sub>, mag. and spectroscopic study, semiconductor to metal transition 0-2628  
 C, char, amorphous, mag. interactions between localised spins 0-34587  
 C<sub>6</sub>K, intercalation cpd. with graphite, supercond. props. 0-44755  
 CaB<sub>6</sub>-SmB<sub>6</sub>, mag. props., comp. depend. 0-50034  
 Ca<sub>2</sub>MnO<sub>4-x</sub>F<sub>x</sub>, antiferromagnetic props. and elec. cond. (*French*) 0-29526  
 Ca<sub>2</sub>XRuO<sub>6</sub> (X=Y, La, Eu), <sup>99</sup>Ru Mossbauer spectra and other techniques 0-29659  
 Cd-Mg, mag. susceptibility near 2<sup>1/2</sup>th order electron transition, non-linear magnetisation anal. (*Russian*) 0-44859  
 Cd<sub>1-x</sub>Ag<sub>x</sub>Cr<sub>2</sub>Se<sub>4</sub>, Ag acceptor states effect on exchange interaction 0-20397  
 Cd<sub>1-x</sub>Mg<sub>x</sub>, magnetic susceptibility anisotropy, press. effects, electronic phase transitions (*Russian*) 0-54869  
 CdPS<sub>3</sub>, layered, organometallic intercalates, X-ray diffr., optical absorpt. and mag. props. 0-45103  
 CdS, powder, mechanically induced localised states in energy gap 0-2354  
 Ce binary and pseudobinary intermetallics, struct. and mag. data 0-20129  
 Ce cubic intermetallics, interconfig. fluctuations 0-20130  
 Ce, liq., 4f electron susceptibility temp. depend. 0-20378  
 CeAl<sub>2</sub>, Anderson lattice system, mag. moment reduction, press. effects 0-7093  
 CeAl<sub>2</sub>, low temp. mag. props., Kondo effect 0-20381  
 CeIn<sub>3</sub>, Neel temp., hydrostatic press. depend. 0-29549  
 CeIn<sub>3-x</sub>Sn<sub>x</sub>, scaling behaviour near valence instability, mag. susceptibility and mag. transitions 0-25111  
 Ce<sub>1-x</sub>La<sub>x</sub>Sn<sub>3</sub> (x=0 to 1), mag. susceptibility and magnetisation, lattice parameters, X-ray and neutron diffr. meas. 0-49675  
 Ce<sub>1-x</sub>Pr<sub>x</sub>Al<sub>2</sub>, mag. struct., comp. depend., neutron diffr. and mag. susceptibility meas. 0-50054  
 CeRu<sub>2</sub>, H absorption induced Ce valence change, mag. and supercond. props. 0-50042  
 CeSn<sub>3</sub>, polarised neutron study of induced magnetisation 0-34594  
 C<sub>60</sub>, ground and first excited bending, vibr. state, props., mol. beam elec. reson. 0-37823  
 Co-V, solid and liq., mag. susceptibility and electronic struct. 0-39738  
 Co<sub>1-x</sub>Cu<sub>x</sub>Cr<sub>2</sub>S<sub>4</sub>, paramag. susceptibility 0-20373  
 Co<sub>0.5</sub>Cu<sub>0.5</sub>Cr<sub>2</sub>S<sub>4</sub>-Se<sub>x</sub>, ferrimag. chalcospinel, paramag. susceptibility 0-15681  
 Co<sub>5</sub>Ga<sub>46</sub>, superparamag. response to low DC fields 0-44860  
 Co<sub>2</sub>Ga<sub>1-x</sub>β-phase, spin glass behaviour 0-44837  
 Co<sub>2</sub>Ga<sub>1-x</sub> cluster spin glass, AC susceptibility in DC mag. fields, 77 to 500K 0-34670  
 CoNb<sub>2</sub>O<sub>6</sub>, magnetic struct., neutron diffr. and mag. susceptibility meas. 0-15693  
 Co<sub>1-x</sub>Ni<sub>x</sub>Al, Knight shift and mag. susceptibility study, electron struct. peculiarities (*Russian*) 0-15814  
 CoU<sub>2</sub>S<sub>8</sub>, mag. struct. and props. 0-11166  
 Cr antiferromagnetic with nonmagnetic impurities, mag. susceptibility using two band model 0-2559  
 Cr-Fe, dilute, localised moment cluster model, ferromagnetic exchange coupling 0-39774  
 Cr-Fe<sub>x</sub> (x=0.5, 1.5 and 3.5 at.%), antiferromag., Kondo anomaly 0-11163  
 Cr-Ni(V), dil., mag. susceptibility, 77 to 400K (*Russian*) 0-50066  
 CrB<sub>2</sub>, CrB, and Cr<sub>2</sub>B<sub>3</sub>, mag. and thermal props. at low temps. 0-20385  
 Cr<sub>2</sub>Mn<sub>1-x</sub>As<sub>x</sub>, antiferromag. to ferromag. transitions, superexchange-double exchange mag. coupling, susceptibility and resist. obs. 0-50070  
 Cr<sub>0.5</sub>Nb<sub>0.5</sub>, cryst. struct., metallic cond., mag. and phys. props. (*French*) 0-33956  
 CrSe<sub>2</sub>, layered, phys. and elec. props. 0-44594  
 CrVO<sub>4</sub>, Neel temp., mag. susceptibility meas. 0-29550  
 Cs, fluid, metal-nonmetal transition and mag. interactions 0-49602  
 Cs fluid, metallic and nonmetallic, mag. props. 0-44799  
 Cs-Ag, dil., electronic struct., density functional approach, appl. to elec. and mag. props. 0-44492  
 Cs<sub>2</sub>CoCl<sub>4</sub>, mag. susceptibility and magnetisation curve meas. 0-11176  
 CsCrCl<sub>3</sub>, mag. structure and excitations, neutron diffr. and susceptibility meas. 0-44806  
 Cs<sub>2</sub>KTMBr<sub>6</sub>(Cl<sub>6</sub>)(F<sub>6</sub>), Cs<sub>2</sub>NaTmF<sub>6</sub> and Cs<sub>2</sub>RbTmF<sub>6</sub>, mag. behaviour 2.9 to 251.3K, cryst. field levels, ang. overlap model (*German*) 0-29520  
 Cs<sub>2</sub>KYbF<sub>6</sub>, mag. behaviour, 3.5-251.3K (*German*) 0-50041  
 Cs<sub>2</sub>NaYbF<sub>6</sub>(Br<sub>6</sub>), mag. behaviour, 3.5-251.3K (*German*) 0-50041  
 Cs<sub>1-x</sub>Rb<sub>x</sub>MF<sub>3</sub> (M=Mg, Co, Ni, Zn), hexagonal fluoride perovskite structural evolution by cationic substitution (*French*) 0-24430  
 Cs<sub>2</sub>RbYbF<sub>6</sub>, mag. behaviour, 3.5-251.3K (*German*) 0-50041  
 CsYbO<sub>2</sub>, normal-temp. form, mag. props. (*German*) 0-54864  
 Cu complex, 1,2-ethanediammonium tetrachlorocuprate, layered struct. mag. susceptibility 0-7094  
 Cu complex, chloride monodimethylsulfoxide, spin 1/2 ferromag. Heisenberg linear chain, cryst. struct. and mag. susceptibility 0-15706  
 Cu complex, chloride tetramethylsulfoxide, spin 1/2 ferromag. Heisenberg linear chain, cryst. struct. and mag. susceptibility 0-15706  
 Cu complex, dichloro(dimethylnitrosamine)copper(II), magnetic phase transition, <sup>15</sup>N NQR obs. 0-11289  
 Cu complex, dichloro(dimethylnitrosamine) Cu II, mag. props., <sup>14</sup>N NQR obs. 0-54988

## magnetic susceptibility continued

- Cu complex, halocuprates, ferromagnetic insulator, two-dimens. Heisenberg layers, mag. susceptibility 0-50068  
 Cu complex with L-phenylalanine amino acid, ESR spectra and magnetic susceptibility measurement 0-34761  
 Cu, spin density wave fluctuations in nuclear spins, susceptibility, internal energy 0-50115  
 Cu-Co heterobinuclear complex, cryst., mag. susceptibility of Cu-Co(fsa)<sub>2</sub> en, 3H<sub>2</sub>O 0-2556  
 Cu-Mn, spin glass, meas. of order parameter 0-34642  
 Cu-Pd, mag. susceptibility and electronic struct. of ordering (*Russian*) 0-11161  
 CuAu, mag. susceptibility and electronic struct. of ordering (*Russian*) 0-11161  
 Cu<sub>3</sub>Au, mag. susceptibility and electronic struct. of ordering (*Russian*) 0-11161  
 CuCrS<sub>2</sub>, single cryst., spectral study and phys. props. (*French*) 0-29002  
 CuK<sub>2</sub>Cl<sub>2</sub>·2H<sub>2</sub>O, Heisenberg ferromag., mag. field effect on susceptibility near crit. point 0-39758  
 CuMn, spin glass, remanence, new approach from zero field NMR 0-34785  
 Cu<sub>2</sub>MnAl, dynamical mag. susceptibility, spin waves, calc. from band struct. 0-54871  
 Cu(NH<sub>4</sub>)<sub>2</sub>Br<sub>4</sub>·2H<sub>2</sub>O Heisenberg ferromagnet, mag. props. in mag. field 0-34637  
 CuO-CdO-Fe<sub>2</sub>O<sub>3</sub>, sintered ferrite, preparation, mag. susceptibility, DC resistivity 0-34598  
 CuO-ZnO-Fe<sub>2</sub>O<sub>3</sub>, sintered ferrite, preparation, mag. susceptibility, DC resistivity 0-34598  
 Cu<sub>2</sub>O-CuO-MoO<sub>3</sub>, subsolidus phase diagram, mag. props. 0-50615  
 Cu<sub>2</sub>Si-Ti<sub>2</sub>S system, phase diagram 0-20906  
 α-Cu<sub>2</sub>V<sub>2</sub>O<sub>7</sub>, EPR and mag. susceptibility meas. 0-2627  
 dimethylammonium manganese tetrachloride, 2D Heisenberg antiferromag., spin wave anal. 0-54879  
 Dy, Curie-Weiss law anisotropy, paramag. susceptibility meas. 0-15686  
 Dy, liq., mag. susceptibility, elec. resistivity 0-20377  
 Dy-Th, single cryst., mag. susceptibility, transitions, anisotropy 0-54873  
 Dy<sub>2</sub>Ga<sub>2</sub>O<sub>12</sub>, crystal field effect on paramag. props. of Dy<sup>3+</sup> ion 0-50040  
 Er, magnetisation and susceptibility in basal plane in strong mag. field (*Russian*) 0-50145  
 (Er<sub>1-x</sub>Ho<sub>x</sub>)Rh<sub>2</sub>B<sub>4</sub>, superconductive and mag. interactions, hydrostatic press. effect 0-49973  
 Er<sub>2</sub>Te<sub>3</sub>, magnetic susceptibility meas., cryst. field interpretation 0-11156  
 Er<sub>1-x</sub>Al<sub>x</sub>, mag. props. meas. and neutron diffr. data 0-7126  
 EuB<sub>6</sub>, ferromag., mag. props. 0-2561  
 EuB<sub>6</sub>, pure single crystals, magnetic and electric props. 0-11260  
 EuB<sub>6</sub>-C<sub>60</sub>, pure and doped, mag. and transport props. 0-54689  
 Eu<sub>2</sub>O<sub>3</sub>Cl(Br), synthesis and characterisation 0-39039  
 EuO(S)(Se)(Te), cryst. and electronic struct., mag., elec., and optical props., book contrib. 0-39760  
 Eu<sub>2</sub>Sb<sub>3</sub>, cryst. struct., elec. and mag. props. 0-33958  
 Eu<sub>2</sub>Sr<sub>1-x</sub>S<sub>x</sub>, dilute Heisenberg magnet, complex susceptibility of blocked spins 0-15740  
 Eu<sub>2</sub>Sr<sub>1-x</sub>S<sub>x</sub>, ferromagnet-spin glass transition, mag. ordering, mag. susceptibility and neutron scatt. meas. 0-50135  
 Eu<sub>2</sub>Sr<sub>1-x</sub>S<sub>x</sub>, insulating spin glass, mag. props. 0-2589  
 Fe base amorphous alloys, Invar and Elinvar chars. 0-29592  
 Fe complex, Fe<sub>2</sub>M<sub>1-x</sub>(1,10-phenanthroline)<sub>2</sub>(NCS)<sub>2</sub>, M=Mn, Co, Ni, spin crossover, Mossbauer and magnetism study 0-44980  
 Fe complex, Fe(Br)[S<sub>2</sub>CN(C<sub>2</sub>H<sub>5</sub>)<sub>2</sub>]<sub>2</sub>, 3-D Ising ferromag., cryst. susceptibility, 1.5-20K 0-20390  
 Fe complex, Fe(Cl)[S<sub>2</sub>CN(C<sub>2</sub>H<sub>5</sub>)<sub>2</sub>]<sub>2</sub>, 3-D Ising ferromag., cryst. susceptibility, 1.5-20K 0-20390  
 Fe complex, Fe(II) oxalato-bridged chain compounds, Mossbauer spectra 0-15890  
 Fe complex, tetraphenylporphyrinate iron III bromide, mag. props., zero-field splitting 0-34584  
 Fe complexes, FeO[Co(cyclopentadienyl)<sub>2</sub>]<sub>0.16</sub> and FeOCl[Fe(cyclopentadienyl)<sub>2</sub>]<sub>0.16</sub>, Mossbauer and mag. susceptibility meas. 0-44176  
 Fe complexes with dimethylformamide, dimethylthioformamide, Mossbauer and mag. props. 0-39974  
 Fe, paramagnetic, orbital magnetic susceptibility calc. 0-7075  
 Fe particles in glass-like C matrix, identification and props. 0-11229  
 Fe-Ni-Cr, Elinvar, struct. and mag. props., singularities during tempering (*Russian*) 0-50627  
 Fe-Ni(Co), solid and liq., paramag. susceptibility and electron struct., 800-1800°C (*Russian*) 0-25081  
 Fe-Ni(Cr), Invar, exchange interactions between ferromag. and antiferromag. components 0-29545  
 Fe<sub>2</sub> magnetism, randomised exchange field theory 0-39733  
 FeBMO<sub>4</sub>, M=Mg, Cu, Co, Ni, mag. props. meas. 0-34607  
 Fe<sub>1-x</sub>Co<sub>x</sub>Al, Knight shift and mag. susceptibility study, electron struct. peculiarities (*Russian*) 0-15814  
 Fe<sub>1-x</sub>Co<sub>x</sub>Cl<sub>2</sub>, mag. phase diagram 0-11198  
 Fe<sub>2</sub>Cu<sub>1-x</sub>Cr<sub>x</sub>Se<sub>4</sub>, crystallographic and mag. props. 0-39049  
 FeGe, canted antiferromagnet, mag. susceptibility anisotropy and temp. dependence 0-25112  
 Fe<sub>1</sub>, cyclodextrin, quasi-one-dimens. cpd., synthesis, elec. and mag. props. 0-2380  
 (Fe<sub>1-x</sub>Mn<sub>x</sub>)<sub>75</sub>P<sub>15</sub>B<sub>6</sub>Al<sub>3</sub>, amorphous, spin-glass-ferromag. multicritical point, AC susceptibility meas. 0-50117  
 Fe<sub>2</sub>NbSe<sub>2</sub> (2H), mag. susceptibility meas., 1.3-300K 0-39740  
 (Fe<sub>0.5</sub>Ni<sub>0.5</sub>)-Co, solid and liq., paramag. susceptibility and electron struct., 800-1800°C (*Russian*) 0-25081  
 Fe<sub>1-x</sub>Ni<sub>x</sub>Al, Knight shift and mag. susceptibility study, electron struct. peculiarities (*Russian*) 0-15814  
 FeNiBO<sub>4</sub>, FeNi<sub>2</sub>BO<sub>3</sub>, Mossbauer spectra, mag. relax. 0-15889  
 Fe<sub>40</sub>Ni<sub>38</sub>Mo<sub>2</sub>B<sub>18</sub>, metallic glass, mag. and transport props. 0-39752  
 (Fe<sub>0.04</sub>Ni<sub>0.96</sub>)<sub>80</sub>P<sub>10</sub>B<sub>10</sub>, amorphous magnetisation, field and temp. depend. 0-39755  
 Fe<sub>27</sub>Ni<sub>53</sub>P<sub>14</sub>B<sub>6</sub>, amorphous, Hall resist. and mag. props., short range order effects 0-34422  
 (Fe<sub>1-x</sub>Ni<sub>x</sub>)<sub>75</sub>Si<sub>10</sub>B<sub>13</sub>, amorphous alloy system, saturation mag. moment, Curie temp., mag. susceptibility 0-39753  
 FeO-FeS, mag. susceptibility, eutectic phase diagram (*Russian*) 0-15682  
 Fe<sub>2</sub>O<sub>3</sub> amorphous film, Mossbauer spectra, mag. props. 0-15851  
 Fe<sub>2</sub>O<sub>3</sub> amorphous RF sputtered thin films, Mossbauer and mag. study 0-34711  
 α-Fe<sub>2</sub>O<sub>3</sub>-Li<sub>2</sub>O, structural and thermal phase behaviour from mag., spectral and thermal studies 0-2673



## magnetic susceptibility continued

- $\text{Fe}_2\text{O}_3\text{-PbO-B}_2\text{O}_3$  glass, X-ray and electron microscope studies, mag. and Mossbauer effect meas. 0-28919  
 $\text{Fe}_2\text{O}_4$  (magnetite), mag. susceptibility under hydrostatic press. and implications for tectonomagnetism 0-26504  
 $\text{Fe}_3\text{O}_4$ , magnetite, magnetoelc. effect at 77K and cryst. symm. 0-29593  
 $\text{Fe}_3\text{O}_4$ , magnetite particles, interaction fields effect on hysteretic props. 0-54921  
 $20\text{Fe}_2\text{O}_3\cdot 80[3\text{B}_2\text{O}_3\cdot (1-x)\text{PbO}\cdot x\text{GeO}_2]$  glass, phys. props. 0-49119  
 $\alpha\text{-FeP}_4$ , diamag., semicond., Mossbauer study 0-50243  
 $\text{Fe}_{25}\text{Pd}_{50}\text{Au}_{25}$ , atomic ordering influence on mag. props. and elec. resistance (Russian) 0-7551  
 $\text{FeS}_2$  (marcasite), temp. depend. mag. susceptibility 0-20391  
 $\text{FeS}_2$ , pyrite, Van Vleck susceptibility, temp. depend. 0-34589  
 $\text{FeSb}_2$ , quasi-magnetic semicond., mag. susceptibility 0-39757  
 $(\text{Fe}_{1-x}\text{V}_x)_2\text{Ge}$ , magnetic and X-ray studies 0-1966  
 $\text{FeVO}_4$ , Neel temp., mag. susceptibility meas. 0-29550  
 $\text{Fe}_{0.35}\text{V}_{0.65}\text{O}_5$ , spin glass phase, low temp. mag. susceptibility meas. 0-29565  
 $\text{Ga}_{0.67}\text{Cr}_{0.33}\text{S}_4$ , semiconducting thiospinelide, spin glass type mag. ordering (Russian) 0-50123  
 $\text{Ga}_{1-x}\text{In}_x\text{Se}$ , magnetic susceptibility anisotropy, chemical bonds, electron density distribution (Russian) 0-50073  
 $\text{GaSe}_{1-x}\text{S}_x$ , magnetic susceptibility anisotropy, chemical bonds, electron density distribution (Russian) 0-50073  
Gd alloys, amorphous, mag. props. and ferromag. reson. 0-54952  
Gd, liq., mag. susceptibility, elec. resistivity 0-20377  
Gd-Co amorphous films, RF sputtered, magnetisation ripple effects 0-11232  
 $\text{GdCl}_3$ , crystn. field parameter of  $\text{Gd}^{3+}$  0-10930  
 $\text{Gd}(\text{Cu}_{1-x}\text{Gd}_x)$ , pseudobinary alloy, mag. susceptibility and elec. resist. at low temp. 0-34602  
GdS, meas. of opto-magnetic interactions at low mag. fields 0-2735  
 $\text{GdSn}_3$ , Neel temp., hydrostatic press. depend. 0-29549  
 $(\text{Ge,Pb})_{1-x}\text{Mn}_x\text{Te}$ , mag. and elec. props. meas. 0-29534  
 $\text{GeFe}_2\text{O}_4$ , single cryst., elec. and mag. props, optical absorpt. spectra 0-54719  
 $^3\text{He}$ , liq., in contact with dielec. surface, mag. susceptibility enhancement, thermodynamics 0-54460  
 $^3\text{He}$ - $^4\text{He}$ , superfluid, osmotic and mag. props., review (French) 0-10733  
 $\text{Hf-C-N-O-H}$ , solid solns. of H, exam. of props. 0-29172  
 $\text{HfSe}_{2-x}\text{Te}_x$ , and  $\text{HfTe}_{2-x}\text{Se}_x$ , elec. resist. and mag. suscept. studies 0-44599  
 $\text{Hg}_{1-x}\text{Mn}_x\text{Te}$ , mag. props., self-consistent two spin cluster model 0-54874  
 $\text{Hg}_{1-x}\text{Mn}_x\text{Te}$ , mag. susceptibility, 2.4 to 300K 0-20379  
 $\text{Hg}_{1-x}\text{Mn}_x\text{Te}$ , zero-gap semicond., indirect-exchange interactions 0-29370  
 $\text{Ho}$ , liq., mag. susceptibility, elec. resistivity 0-20377  
 $\text{HoAlGa}_{2-x}$ , mag. props. and phase transitions 0-25133  
 $\text{HoNi}_5$ , ferromag., magnetisation and paramag. susceptibility 0-25082  
 $\text{Ho}_2\text{O}_3\text{SO}_4$ , magnetic phase diagram, magnetisation and mag. susceptibility meas. 0-15720  
 $\text{Ho,Y}_{1-x}\text{Sb}_x$ , mag. props. 0-34634  
K, Pauli susceptibility and Knight shift meas., electron wave functions 0-44937  
 $\text{K}_2\text{FeCl}_4(\text{H}_2\text{O})$ , phase diagram, antiferromag., paramag. and spin flop phases 0-44831  
 $\text{KFe}_2\text{O}_3$ ,  $\beta''$  phase, mag. props., hyperfine interactions, Mossbauer study 0-20524  
 $\text{KFeS}_2$ , cryst. struct. and mag. ordering, neutron diffr. and mag. susceptibility meas. 0-54867  
 $\text{K}_3\text{Mn}_2\text{F}_7$ , two magnon Raman scatt., magnon dispersion, susceptibility, Green's function methods 0-50340  
 $(\text{La,Gd})\text{Al}$ , spin glasses, reversible and irreversible mag. susceptibility 0-15738  
La, FCC, NMR 4.2 to 296K, mag. susceptibility and sp. ht. 0-15813  
 $\text{La}_{1-x}\text{Eu}_x\text{B}_6$  solid solutions, cryst. lattice defectiveness, mag. susceptibility and elec. conductivity 0-15083  
 $(\text{LaNd})\text{Sn}_3$ , containing Nd impurities, supercond. and normal state props. 0-49967  
 $\text{LaNi}_5$ , crystal field investigation from inelastic slow neutron scatt. expts. 0-39538  
 $\text{LaRu}_2$ , H absorption induced Ce valence change, mag. and supercond. props. 0-50042  
 $\text{La}_{1-x}\text{Sr}_x\text{CrO}_3$  ( $0 \leq x \leq 0.4$ ), localised level hopping transport 0-10974  
Li-transition metal dioxide intercalation compounds, mag. props., decomposition effects 0-25075  
 $\text{LiBO}_2\text{-In}_2\text{O}_3$ , phase composition, mag. props, elec. cond. 0-55365  
 $\text{LiFeS}_2$ , magnetic hyperfine interactions, Mossbauer spectra and mag. susceptibility meas. 0-29658  
 $\text{LiTbF}_4$ , mag. props., crit. behaviour at marginal dimensionality 0-54906  
 $\text{LiTb}_{0.5}\text{Y}_{0.5}\text{F}_4$ , mag. susceptibility, dilution effect on critical behaviour of dipolar uniaxial ferromagnet 0-34635  
 $\text{LuB}_{12}$ , 90-1200K 0-50032  
Mg-rare earth dilute alloy, mag. susceptibility and magnetisation 0-15689  
 $\text{Mg}_{1-x}\text{Mn}_x\text{Te}$ , random dil. antiferromagnet, mag. props. 0-54870  
 $\text{MgO}$ , lattice defects, calcination temp. effect 0-15091  
 $\text{MgO-ZnO-Fe}_2\text{O}_3$ , sintered ferrite, preparation, mag. susceptibility, DC resistivity 0-34598  
MnBi, (micromag. alloys, elastic props. (Russian) 0-7141  
 $\text{MnO}(1-x)[\text{I}9\text{TeO}_2\cdot\text{PbO}]$ , glass, antiferromag. behaviour, mag. props. 0-50072  
MnSi, amorphous, sputtered, mag., elec., struct. and thermal props., spin glass behaviour 0-50124  
MnSi, amorphous magnetisation meas. 0-34599  
 $\text{Mn}_{23}\text{Y}_4\text{D}_8$ , D atom location, neutron diffr. study, and magnetism (French) 0-24426  
MnZn ferrite, wall topography change induced by external press. 0-34734  
Mo-Al-Ge, new compounds, structure and props. 0-39003  
 $\text{Mo}_2\text{B}_5$  and  $\text{MoB}_4$ , thermal, elec., and mag. props. 0-20187  
 $(\text{Mo}_2\text{V}_{1-x})\text{O}_5$ , mag. and spectroscopic investigation 0-25206  
 $(\text{NH}_4)_2\text{CuBr}_4\cdot 2\text{H}_2\text{O}$ , ferromag., static and dynamic mag. props. 0-50074  
Na-Fe fluorophosphate glass, Mossbauer study, mag. and optical props. 0-16065  
Na-Ga alloy, solid and liq., mag. susceptibility and elec. cond. (Russian) 0-29522  
 $\text{Na}_2\text{Co}_2\text{Ti}_6\text{O}_{14}\text{F}_2$ , characterisation and mag. props., 90-800K,  $\text{Na}_x\text{Ti}_4\text{O}_8$  bronze isotypes (French) 0-39735  
 $\text{Na}_2\text{Cr}_2\text{Ti}_4\text{O}_{16}$ , characterisation and mag. props., 90-800K,  $\text{Na}_x\text{Ti}_4\text{O}_8$  bronze isotypes (French) 0-39735

## magnetic susceptibility continued

- $\text{Na}_2\text{FeTi}_6\text{O}_{16}$ , characterisation and mag. props., 90-800K,  $\text{Na}_x\text{Ti}_4\text{O}_8$  bronze isotypes (French) 0-39735  
 $\text{Na}_2\text{Ni}_2\text{Ti}_6\text{O}_{14}\text{F}_2$ , characterisation and mag. props., 90-800K,  $\text{Na}_x\text{Ti}_4\text{O}_8$  bronze isotypes (French) 0-39735  
 $\text{Na}_2\cdot 3\text{B}_2\text{O}_3\cdot x\text{Fe}_2\text{O}_3$ , borate glass,  $\text{Fe}^{3+}$  spin state and distrib. meas. 0-39966  
Nb, NMR study up to 1700K, Knight shift and spin-lattice relax. time 0-2653  
Nb, spin fluctuations effect on  $T_c$ , from sp. ht. and mag. suscept. 0-7030  
Nb-C-N-O-H, solid solns. of H, exam. of props. 0-29172  
Nb-H, exam. of electron structure 0-29306  
Nb-Hf (38 at.%) superconductor, peak effect, summation problem, mag. history flux pinning force 0-20362  
Nb-S system, phase relations at high temp., elec. and mag. props. 0-29932  
 $\text{Nb}_{78}\text{Ga}_{22-x}\text{Mn}_x$ , supercond. props., influence of Mn mag. impurities 0-54825  
 $\text{Nb}_{80}\text{Ga}_{20-x}\text{Mn}_x$ , supercond. props., influence of Mn mag. impurities 0-54825  
 $\text{NbS}_2(\text{Se}_2)$  intercalation complexes with 3d transition metals, mag. and metallic transport props. 0-44814  
 $\text{NbSe}_3$ , mag. anomalies at CDW transitions 0-11158  
 $\text{Nd}_2\text{Eu}_{1-x}\text{B}_6$  solid solution, mag. susceptibility, lattice parameters, Weiss temp. 0-29535  
NdO, mag. props., lattice const., and X-ray absorpt. spectra 0-44798  
 $\text{NdSn}_3$ , Neel temp., hydrostatic press. depend. 0-29549  
 $\text{NdTiO}_3$ , physicochem. props. 0-25625  
Ni film, few atomic layers thick, transition from Pauli paramag. to band ferromag. 0-44885  
Ni, magnetic susceptibility, generalised, neutron scatt. meas. 0-34606  
Ni, single-domain particles, LF mag. susceptibility, 2K up to Curie point 0-29582  
Ni-Co, solid and liq., paramag. susceptibility and electron struct., 800-1800°C (Russian) 0-25081  
Ni-Fe, 79 NM alloy, gamma and neutron influence on mag. susceptibility comparative study (Russian) 0-39751  
Ni-Pt disordered alloy, off-diagonal, T-matrix itinerant electron ferromagnetism calcs. 0-25067  
Ni-V, solid and liq., mag. susceptibility and electronic struct. 0-39738  
 $\text{Ni}_{0.95}\text{S}$  Fe, spin glass, spin flop in exchange field 0-34640  
 $\text{Ni}_3\text{Mn}$ , thermoremanent magnetisation and blocking temp. 0-34601  
 $(\text{Ni}_{0.75}\text{Mn}_{0.25})_8\text{Si}_{10}\text{B}_8$ , amorphous, exchange anisotropy, mag. susceptibility meas., 4.2K to room temp. 0-11186  
 $\text{Ni}(\text{NO}_3)_2\cdot 6\text{H}_2\text{O}$ , susceptibility and specific heat meas., spin ordering, antiferromag. spin pair coupling 0-7084  
NiO (111) platelets, magnetic anisotropy investigation by torque and mag. susceptibility meas. 0-54885  
NiO:Cr, effect of Cr additives on structure parameters (Bulgarian) 0-44319  
 $\text{Ni}_3(\text{VO}_4)_2$ , Neel temp., mag. susceptibility meas. 0-29550  
 $\text{NiWO}_4$  monoclinic antiferromagnet, orientational phase transition and intermediate state (Russian) 0-15725  
NiZn ferrite, wall topography change induced by external press. 0-34734  
 $\text{Ni}_2\text{Zn}_{1-x}\text{Fe}_x\text{O}_4$ , catalytic oxidation of CO, mag. props., kinetic parameters and composition depend. 0-16723  
 $(\text{Np}_{1-x}\text{U}_x)\text{Fe}$ , Mossbauer spectra, magnetism and hyperfine interactions 0-20529  
O, solid,  $\alpha$ - $\beta$  transition, mag. susceptibility (Russian) 0-6592  
P-Se-Te system glasses, mag. susceptibility and opt. props. 0-25079  
 $2\text{PbFe}_{1/2}\text{Nb}_{1/2}\text{O}_3\text{-Pb}_2\text{FeReO}_6$ , comp., struct., dielec. and mag. props. 0-2704  
 $2\text{PbFe}_{1/2}\text{Ta}_{1/2}\text{O}_3\text{-Ba}_2\text{FeReO}_6$ , comp., struct., dielec. and mag. props. 0-2704  
 $2\text{PbFe}_{1/2}\text{Ta}_{1/2}\text{O}_3\text{-Pb}_2\text{FeReO}_6$ , comp., struct., dielec. and mag. props. 0-2704  
PbSe, electron gas magnetisation, energy band parameters determ., use of Faraday effect 0-45047  
PbSe, Faraday effect and electron gas magnetisation, Kane two band model calcs. (Russian) 0-34899  
 $\text{Pb}_{1-x}\text{Sn}_x\text{Te}$ , Faraday effect and electron gas magnetisation, Kane two band model calcs. (Russian) 0-34899  
 $\text{Pb}_{1-x}\text{Sn}_x\text{Te}$ , mag. and kinetic props. near ferroelec. transition 0-11160  
 $\text{Pb}_{1-x}\text{Sn}_x\text{Te}$ : Mn, Mn mag. and elec. active states, mag. impurity behaviour 0-44627  
Pd, confined geometry, p-wave supercond. or itinerant ferromag. 0-11129  
Pd-Fe-Mn, dil. alloy, high press. study 0-34600  
Pd-Mn(Fe), mag. ordering phenomena, neutron scatt. obs. 0-44812  
PdAgFe, ferromag., Curie temp. depend. on susceptibility, non-mean field theory 0-44829  
PdF<sub>2</sub> flourite-type form, mag. props., structure studies (French) 0-34187  
 $(\text{Pd}_{0.995}\text{Fe}_{0.005})\text{Mn}_{0.05}$ , ferromag. and spin-glass props. 0-2590  
PdFeRh, ferromag., Curie temp. depend. on susceptibility, non-mean field theory 0-44829  
 $\text{Pd}_2\text{MnIn}_{1-x}\text{Sb}_x$ , Heusler alloy, mag. order obs. 0-29528  
Pr, quasielastic mode damping, dynamic susceptibility 0-15705  
Pr-Ce(Tm), mag. order onset, elec. resistivity 0-20416  
PrEu(Gd), magnetic interactions, Mossbauer spectra quadrupole splitting, crystal field parameters 0-39907  
PrNi<sub>5</sub>, crystal field investigation from inelastic slow neutron scatt. expts. 0-39538  
PrNi<sub>5</sub>, metallic Van Vleck paramag., nucl. interactions, NMR meas. 0-44953  
PRO, mag. props., lattice const., and X-ray absorpt. spectra 0-44798  
 $\text{PrSn}_3$ , Neel temp., hydrostatic press. depend. 0-29549  
 $\text{RM}_2\text{Al}_3$  (M=Cr, Mn, Fe, Cu), magnetism and hyperfine interactions 0-25256  
 $\text{RbCoCl}_3\cdot 2\text{D}_2\text{O}$ , metamagnetic phase transition, crystallographic and mag. struct., neutron diffr. meas. 0-44174  
 $\text{Rb}_2\text{CuBr}_4\cdot 2\text{H}_2\text{O}$ , ferromag., static and dynamic mag. props. 0-50074  
 $\text{Rb}_2\text{MnCl}_4$ , 2D Heisenberg antiferromag. spin wave analysis 0-54879  
 $\text{RbNi}_2\text{Mn}_{1-x}\text{Fe}_x$ , powder, mag. props. 0-2560  
Rh based ferromag. Heusler alloys, peaks in low field AC susceptibility 0-50071  
Ru based ferromag. Heusler alloys, peaks in low field AC susceptibility 0-50071  
RuF<sub>5</sub>, mag. props. 0-15707  
RuS<sub>2</sub> amorphous, prep. at ambient temp., magnetic structure 0-35119  
S-Se(Te)(Ti), liq. semicond., bonding energies and entropies, mag. susceptibility meas. 0-49082  
 $(\text{SN})_x$ , Meissner effect, mag. susceptibility meas. 0-20351



## magnetic susceptibility continued

- Sc-H, conc.-temp. depend. at room temp. of elec. resist. thermo-EMF, mag. susceptibility, and Hall coeff. 0-29382  
 ScAl<sub>2</sub>-Er(Dy)(Nd), dil., EPR and mag. susceptibility 0-15797  
 (Sc<sub>1-x</sub>Lu<sub>x</sub>)<sub>2</sub>V<sub>2</sub>O<sub>7</sub> 0-29547  
 ScSi, paramag. susceptibility 0-50035  
 Sc<sub>2</sub>(SiO<sub>3</sub>)<sub>3</sub>, mag. susceptibility, temp. depend., 77-800K 0-20372  
 Si, diamagnetism of excitons and biexcitons, recomb. spectra (*Russian*) 0-7412  
 Si:B, heavily doped, paramagnetic props., anomalous hole spin susceptibility (*Russian*) 0-54861  
 SmN, magnetic props., neutron diffr. and mag. susceptibility meas. 0-50036  
 SmO, mag. props., lattice consts., and X-ray absorpt. spectra 0-44798  
 SmRh<sub>2</sub>B<sub>4</sub>, coexistence of supercond. and antiferromag. order 0-11140  
 Sm<sub>2</sub>S<sub>4</sub>, mag. susceptibility meas., valence state of Sm 0-15684  
 SmS<sub>1-x</sub>P<sub>x</sub>, intermediate valence cpd., lattice parameter and mag. susceptibility 0-7091  
 SrF<sub>2</sub>:Tb<sup>3+</sup>, mag., thermal and hyperfine props. 0-29368  
 Sr<sub>2</sub>YRuO<sub>6</sub>, <sup>99</sup>Ru Mossbauer spectra and other techniques 0-29659  
 TTF-TCNQ, pure and irradi., nonlinear transport, ESR study, 1.2-4.2K 0-20167  
 TaS<sub>2</sub>, intercalation complexes with 3d transition metals, mag. and metallic transport props. 0-44814  
 Tb, critical magnetic studies 0-15745  
 Tb, liq., mag. susceptibility, elec. resistivity 0-20377  
 Tb-Sc(Y)(La)(Lu)(Yb)(Mg)(Th), mag. ordering temps., susceptibility meas. 0-25136  
 TbAlGa<sub>2-x</sub>, mag. props. and phase transitions 0-25133  
 TbAsO<sub>4</sub>, ferromag., static and AC susceptibility meas. 0-29533  
 TbNi<sub>2</sub>, ferromag., magnetisation and paramag. susceptibility 0-25082  
 Tb(OH)<sub>3</sub>, powder and single crystal, mag. props. 0-2558  
 TbP, singlet-groundstate magnetism, static mag. props. 0-7109  
 TbPO<sub>4</sub>, phase transitions at low temp. 0-15237  
 Tc film, supercond. transition, complex susceptibility 0-29495  
 ThCo<sub>5</sub>, itinerant electron metamagnetism, polarised neutron study 0-39742  
 Ti alloys, data handbook of low temp. mech. and phys. props. 0-22153  
 Ti, high purity, data handbook of low temp. mech. and phys. props. 0-22153  
 Ti-C-N-O-H, solid solns. of H, exam. of props. 0-29172  
 Ti-Fe, magnetic susceptibility depend. on phase composition (*Russian*) 0-54875  
 Ti-H exam. of electron structure 0-29306  
 Ti-Ni, electron phase transition XPS, optical spectra and mag. susceptibility meas. 0-19943  
 TiC-VC, mag. susceptibility, elec. cond. and thermoelec. props. 0-50033  
 TiC-ZrC, mag. susceptibility, elec. cond. and thermoelec. props. 0-50033  
 TiC-ZrC, solid soln., conc. and temp. dependence of props. 0-39736  
 TiC<sub>2</sub>O<sub>4</sub>, are TiC<sub>2</sub>O<sub>4</sub>H<sub>m</sub>, cubic phases, mag. susceptibility 0-15680  
 Ti<sub>1-x</sub>Co<sub>x</sub>, electronic struct. and anomalies of elec. and mag. props. 0-6710  
 Ti<sub>0.9</sub>NbSe<sub>2</sub>, cryst. struct., metallic cond., mag. and phys. props. (*French*) 0-33956  
 Ti<sub>1-x</sub>Ni<sub>x</sub>, electronic struct. and anomalies of elec. and mag. props. 0-6710  
 Ti<sub>4</sub>O<sub>7</sub> and (Ti<sub>1-x</sub>V<sub>x</sub>)<sub>4</sub>O<sub>7</sub>, metal-insulator transitions, EPR, elec. and mag. props. 0-2336  
 (Ti<sub>0.9</sub>V<sub>0.1</sub>)<sub>2</sub>O<sub>3</sub>, spin glass, dynamic mag. susceptibility meas. 0-39792  
 (Ti<sub>1-x</sub>V<sub>x</sub>)<sub>2</sub>O<sub>3</sub>, spin-glass props., 0.05-300K 0-25149  
 TiCoF<sub>3</sub>, paramagnetic, nonmagnetic atomic nuclei spin density, NMR study 0-29633  
 TiGaSe<sub>2</sub>-TiGaSe<sub>2</sub>, phase and composition-property diagrams 0-55366  
 TiInS<sub>2</sub>-TiInSe<sub>2</sub>, phase and composition-property diagrams 0-55366  
 Ti<sub>2</sub>Se<sub>1-x</sub>, liquid semiconductor, diamagnetism and paramagnetism, dangling bond paramag. centres, mag. susceptibility obs. 0-44797  
 TmSe, mag. props. and struct. 0-25109  
 TmSe, susceptibility, Tm<sup>2+</sup> and Tm<sup>3+</sup> characts. 0-25110  
 TmSe, valence instabilities, antiferromag. order 0-20128  
 TmVO<sub>4</sub>, Jahn-Teller distortion, RF susceptibility and NMR meas. 0-44930  
 Tm<sub>2</sub>Y<sub>1-x</sub>Se<sub>2</sub>, Kondo effect, Van Vleck behaviour 0-25085  
 U tetragonal compounds, mag. props. 0-15704  
 UAl<sub>2</sub>, transport props., susceptibility and sp. ht. 0-11174  
 UAs, anisotropic susceptibility 0-7087  
 U(Co<sub>2</sub>Ni<sub>1-x</sub>), cryst. struct. and mag. props. at 4.2K 0-54175  
 β-U<sub>2</sub>, electronic props., metallic character 0-6693  
 UFe<sub>2</sub>, nonstoichiometry effects on Curie temp., susceptibility obs. 0-25131  
 UN, mag. susceptibility under press. 0-7086  
 UNi<sub>5-5.5</sub>Cu<sub>0.5</sub>, NMR and press. effects 0-25230  
 U(OH)<sub>2</sub>SO<sub>4</sub>, mag. susceptibility, heat capacity anomalies at 21K 0-11151  
 UP, anisotropic susceptibility 0-7087  
 UPb<sub>3</sub>, crystal field energy levels, magnetisation and susceptibility, neutron spectra obs. 0-50064  
 US, ferromag., AC mag. susceptibility at high press. 0-7085  
 USb, anisotropic susceptibility 0-7087  
 U<sub>1-x</sub>Th<sub>x</sub>Al<sub>2</sub>, mag. susceptibility, low temp. depend. 0-11173  
 V, orbital magnetic susceptibility calc. 0-7075  
 V, spin fluctuations effect on T<sub>c</sub>, from sp. ht. and mag. suscept. 0-7030  
 V-H, effect of neutron irradi. on electrical resistance, magnetic susceptibility 0-29063  
 V-H, exam. of electron structure 0-29306  
 (V<sub>1-x</sub>Cr<sub>x</sub>)<sub>2</sub>Si, mag. susceptibility, 4.2 to 320K, density of states model 0-7035  
 V<sub>3-x</sub>Cr<sub>x</sub>Si, x=0 to 3, struct., supercond. and mag. props. 0-1962  
 V<sub>1-x</sub>Fe<sub>x</sub>O<sub>2-x</sub>F<sub>x</sub>, 0<x<0.20, magnetic susceptibility and electron cond. (*German*) 0-39754  
 V<sub>0.5</sub>NbSe<sub>2</sub>, cryst. struct., metallic cond., mag. and phys. props. (*French*) 0-33956  
 V<sub>2</sub>O<sub>3+x</sub>, 0≤x≤0.08, mag. and elec. props. 0-49833  
 V<sub>2</sub>O<sub>7</sub>, microscopic mag. props., NMR 0-7177  
 V<sub>0.2n-1</sub> (3≤3≤9), Magneli phases, mag. susceptibilities at low temp. 0-20389  
 V<sub>0.2n-1</sub>, insulating Magneli phases, mag. susceptibility and sp. ht. meas. 0-34604  
 W-Fe alloys, spin glass props., DC susceptibility and remanence meas., 1.6 to 295K 0-29560  
 W<sub>2</sub>B<sub>5</sub> and WB<sub>4</sub>, thermal, elec., and mag. props. 0-20187  
 Y, magnetic and elec. props., 100 to 900K (*Russian*) 0-25077

## magnetic susceptibility continued

- Y-H, exam. of electron structure 0-29306  
 YAl<sub>2</sub>-Er(Dy)(Nd), dil., EPR and mag. susceptibility 0-15797  
 YB<sub>12</sub>, 90-1200K 0-50032  
 YFe<sub>2</sub>, amorphous concentrated spin glass, susceptibility, Mossbauer and neutron scatt. meas. 0-39783  
 YFe<sub>2</sub>O<sub>3</sub>, low temp. phase transitions and mag. props. 0-7106  
 Y<sub>3-x</sub>Gd<sub>x</sub>Fe<sub>5</sub>O<sub>12</sub>, mag. phase diagrams, mag. transitions, exchange interaction (*Russian*) 0-54896  
 YH<sub>x</sub> (x=1.92 to 1.98), magnetic and elec. props., 100 to 900K (*Russian*) 0-25077  
 (Y<sub>1-x</sub>Lu<sub>x</sub>)<sub>2</sub>V<sub>2</sub>O<sub>7</sub>, semiconducting ferromag. pyrochlore, mag. props. 0-29547  
 YM<sub>4</sub>Al<sub>8</sub> (M=Cr, Mn, Fe, Cu), magnetism and hyperfine interactions 0-25256  
 YNi<sub>3</sub>, loss of ferromagnetism after H<sub>2</sub> absorpt., Pauli paramag. props. 0-34588  
 YbB<sub>12</sub>, valence state and mag. props. 0-50031  
 YbB<sub>6</sub>, mag. and transport props. 0-54689  
 YbS<sub>1.387</sub>, magnetic and thermal props. 0-34586  
 Zn<sub>0.9</sub>Fe<sub>0.1</sub>O<sub>3</sub>, Cu, Zn substituted magnetite, domain wall resonance, mag. props. 0-15756  
 Zr-C-N-O-H, solid solns. of H, exam. of props. 0-29172  
 Zr-H, effect of neutron irradi. on electrical resistance, magnetic susceptibility 0-29063  
 Zr-H, exam. of electron structure 0-29306  
 Zr-Hf-ZZ (*Russian*) 0-39551  
 Zr-Ti, alloy, mag. susceptibility, elec. cond., Hall conc. thermoEMF conc. depend. (*Russian*) 0-39551  
 Zr(Hf<sub>1-x</sub>V<sub>x</sub>)<sub>2</sub>, polycrystalline superconductor, resist. and mag. susceptibility, transition temp., temp. depend. 0-25113  
 ZrZn<sub>2</sub>, phonon contrib. to Stoner enhancement factor, ferromag. and possible superconductivity 0-25070
- magnetic switching**  
 particles, interacting, switching behaviour, dipole and Stoner-Wohlfarth models 0-44870  
 Wiegand effect and applications (*Spanish*) 0-31735  
 CrO<sub>2</sub> acicular particle suspensions, mag. props., optical meas. 0-44874  
 γ-Fe<sub>2</sub>O<sub>3</sub>:Cr, pure and doped, acicular particle suspensions, mag. props., optical meas. 0-44874
- magnetic tape recorders** see *tape recorders*
- magnetic tape storage**  
 NMR spectra, automatic system, for recording, processing and summation 0-27327  
 unsupervised data gathering, operation of receiving stations (*Italian*) 0-4692
- magnetic tape stores** see *magnetic tape storage*
- magnetic tapes**  
 see also *magnetic tape storage*  
 gyromagnetic magnetisation in anisotropic mag. material 0-50142  
 particle dispersion and particle orientation 0-15762  
 recent magnetic sound recording tape (*Japanese*) 0-33406  
 recording on particulate media, conference, Gardone Riviera, Italy (Sep. 1979) 0-41930  
 static and antihysteretic mag. props. 0-44868  
 CrO<sub>2</sub> powders, print through values and mag. characts. 0-44871
- magnetic thin film devices**  
 see also *magnetic bubble devices*  
 ferromagnetic thin film magnetometer, development and performance 0-31808  
 measurement transducers appls. (*Polish*) 0-4700
- magnetic thin film stores** see *magnetic film stores*
- magnetic thin films**  
 see also *magnetic epitaxial layers*  
 anisotropy, magnetic, rel. to columnar microstruct., sputtered and vapour deposited films 0-39822  
 antiferromagnetic, two dimens. spin-wave theory, spontaneous magnetisation parameter depend. 0-34714  
 bubble domain film, growth induced order parameter, estimation from coercive force meas. 0-39828  
 charged domain walls, variational method calc. 0-11235  
 complex surface pinning parameter and quasi-localised surface spin wave modes 0-50150  
 dialkylammonium copper tetrachloride, ferromagnetic layer compound, magnetostatic mode excitation 0-29538  
 dipolar magnet, surface effects on phase transitions, local spontaneous polarisation 0-2708  
 ferrite garnet, ion-implanted, hard mag. bubble suppression mechanism 0-44890  
 ferrofluid patterns, zigzag form of charged domain wall 0-44852  
 ferromagnetic, elliptical spin precession correction factor in spin-wave reson. theory 0-20464  
 ferromagnetic, nonlinear spin wave parametric resonance 0-2642  
 ferromagnetic, two dimens. spin-wave theory, spontaneous magnetisation parameter depend. 0-34714  
 ferromagnetic film, shift of ant. temp. as result of Raman scatt. 0-54909  
 ferromagnetic film, transverse bioped susceptibility, two-dimens. micro-magnetism 0-11231  
 ferromagnetic films, spin correl. functions, crit. indices 0-7133  
 ferromagnetic films, spin wave excitation by microwave antenna field 0-44816  
 ferromagnetic nonmetallic film, stand exchange mode determ. 0-2565  
 garnet, magnetic bubble materials, review 0-50153  
 garnet, Permalloy-coated film, bubble vel. and stability, influence of planar domains 0-39831  
 garnet film, mag. bubble domain, annealing by laser pulse 0-15769  
 garnet films, (111)-oriented, cubic anisotropy meas. 0-54924  
 garnet films, domain lattices, parallel stripe susceptibility, uniaxial anisotropy field 0-54930  
 garnet films for a fast bubble devices 0-25168  
 garnet thin film, bubble domain lattice collapse characts. in alternating mag. field 0-54932  
 heavy ion-solid surface collision cascade theory and expt. (*Japanese*) 0-11527  
 ion-implanted bubble garnet film, vel. asymmetry during stripe head prog. 0-39834  
 itinerant-electron ferromagnetic film on nonmagnetic metallic substrate, mag. props. 0-20371  
 magnetic properties meas. on saturated substrate 0-13108



## magnetic thin films continued

- metallic amorphous films for mag. bubble memories, materials review (Polish) 0-34715
- Permalloy, conductor crossing effect on bubble propagation margins 0-29588
- Permalloy, domain wall mass and energy, wall vel. depend. calc. 0-2614
- Permalloy, films, Faraday rotation effect dispersion 0-40092
- Permalloy film, coercive force associated with domain boundary displacement (Russian) 0-50151
- Permalloy film, domain nucleation using low intensity US 0-34731
- Permalloy film, multi- and single-layer, reson. curves subjected to tangential mag. reversals (Russian) 0-50195
- Permalloy films, oxidation effects on atmospheric corrosion, AES, XPS and ion sputtering anal. 0-11829
- Permalloy RF sputtered films, struct.-sensitive mag. props. 0-34705
- Permalloy thick film coercivity control 0-15764
- Permalloy thin film cores, domain wall motion and flux patterns, Kerr magneto-optic effect obs. 0-34721
- pulse magnetic reversal in high freq. field in ferromag. reson. range (Russian) 0-11230
- rare earth compounds,  $\text{RFeO}_3$ , amorphous films for mag. bubble memories, materials review (Polish) 0-34715
- rare earth garnet thin films, macroscopic magn. props., magneto-optical expts. 0-46764
- rare earth-transition metal amorphous thin films, mag. potential distribution and wall velocity meas. 0-34725
- rare earth-transition metal amorphous thin films for thermomag. recording 0-20403
- rare earth-transition metal garnets,  $\text{R}_3\text{M}_2\text{O}_{12}$ , amorphous films for mag. bubble memories, materials review (Polish) 0-34715
- resonance props. in network of cylindrical mag. domains (Russian) 0-50194
- soft ferromagnetic film, theoretical wall mobility 0-34677
- surface and interface magnetism by Mossbauer spectroscopy 0-7218
- time-magnifier, IR-range, construction 0-13139
- transition metal surfaces, mag. props. 0-44861
- $\text{CdCr}_2\text{Se}_4$  films, mag. hysteresis, domain struct., mag. viscosity 0-25169
- Co, ferromag. film, magnetoresistance parameter meas. (Spanish) 0-2485
- Co film, ion beam sputtering prep., struct. and mag. props. 0-35085
- Co-Ni-P electrolytic layers, partial anhyseretic remanent magnetisation, additivity prop. (French) 0-44882
- Co-P films, electrodeposited, magnetic recording media (Japanese) 0-29587
- Co-Pt, electrodeposited, saturation mag. induction, mag. anisotropy and coercive field meas. (French) 0-2610
- Co-Pt alloy, electrolytic deposition conditions over large comp. range (French) 0-45242
- $\text{Co}_{70}\text{Fe}_{30}\text{B}_{14.5}$  amorphous thin films, zero magnetostriction, high magnetisation 0-34708
- (CoFeB) $_{100-x}\text{Cr}_x$  thin films, magnetic props. and corrosion resist. 0-34709
- ( $\text{Co}_{1-x}\text{Fe}_x\text{Ni}_x$ ) $_{80}(\text{Si}_{1-x}\text{B}_x)_20$ , amorphous films, spin wave spectra 0-34777
- CoNiB, corrosion-resistant amorphous mag. thin films 0-54923
- $\text{CoPt}_3$ , electrolytic films, saturation mag. induction, coercive fields, thickness depend. (French) 0-44883
- Cr-Co-Ni hard film on Mo substrate for magnetic recording 0-2608
- $\text{CrO}_2$  amorphous thin films, Mossbauer and magnetisation data 0-34712
- DyFe amorphous film, Mossbauer and mag. meas. 0-15844
- DyIG, noncrystalline, Mossbauer and magnetisation data 0-34828
- $\text{Eu}_{1-x}\text{Gd}_x\text{S}$  films, mag. and elec. props. 0-15766
- $\text{EuIG}$ , noncrystalline, Mossbauer and magnetisation data 0-34828
- EuO film for thermomagnetic recording, anisotropy of resolving power 0-20404
- EuS films, ferromag., optical spectra and light scatt. from spin waves 0-16116
- Fe, evaporated at oblique incidence, optical and mag. anisotropies 0-7134
- Fe, ferromag. film, magnetoresistance parameter meas. (Spanish) 0-2485
- Fe, film, ion beam sputtering prep., struct. and mag. props. 0-35085
- Fe film, on Cu and Ag substrates, mag. props., Mossbauer spectra meas. 0-11233
- Fe film, vacuum deposited, resist. minimum 0-44741
- Fe film coated by  $\text{MgO}$ ,  $\text{MgF}_2$  and Sb, surface mag. 0-7196
- Fe film coated by  $\text{MgO}$ , Mossbauer spectra, mag. hyperfine field 0-7221
- Fe multilayer films stability, Mossbauer spectra 0-29651
- Fe, ultra-thin Mossbauer spectroscopic studies of mag. props. 0-44970
- Fe-Co-Cr film RF sputtering for magnetic recording 0-2947
- Fe-Co-Si-B sputtered amorphous thin film, coercivity, galvanomagnetic props., resistivity 0-29578
- Fe-Gd amorphous film, struct. and mag. props. 0-20439
- Fe-Si amorphous film, crystallisation, Mossbauer studies 0-33900
- Fe-Si amorphous film, struct. and crystallisation, Mossbauer study 0-11300
- Fe-Si-B amorphous films, mag. props. 0-34710
- Fe-SiO multilayer film, interface magnetisation 0-7135
- FeCoB, corrosion-resistant amorphous mag. thin films 0-54923
- $\text{Fe}_2\text{O}_3$  amorphous film, Mossbauer spectra, mag. props. 0-15851
- $\text{Fe}_2\text{O}_3$  amorphous RF sputtered thin films, Mossbauer and mag. study 0-34711
- $\text{Fe}_2\text{O}_3$  amorphous thin films, Mossbauer and magnetisation data 0-34712
- FeSb alloy films, vapour-deposited, formation of metastable phase 0-44437
- FeTiB, corrosion-resistant amorphous mag. thin films 0-54923
- Gd-Co amorphous film 0-34725
- Gd-Co amorphous films, annealed, short-range order and perpendicular mag. anisotropy 0-15765
- Gd-Co amorphous films, correlation between struct. and mag. props. (Chinese) 0-54532
- Gd-Co amorphous films, RF sputtered, magnetisation ripple effects 0-11232
- Gd-Co amorphous films, struct. and mag. anisotropy 0-20438
- Gd-Co amorphous sputtered film, magnetostriction and anisotropy 0-39821
- Gd-Co amorphous thin films, crystn. process and domain struct. (Chinese) 0-54533
- Gd-Co rare earth-transition metal alloy, influence of gaseous phase on mag. props. (Polish) 0-39820
- Gd-Co sputtered amorphous films, resistivity anomalies, 42 to 300K (Chinese) 0-7001
- Gd-Fe rare earth-transition metal alloy, influence of gaseous phase on mag. props. (Polish) 0-39820

## magnetic thin films continued

- Gd-Fe(Co) amorphous films,  $\text{O}_2$  adsorption, effect on perpendicular anisotropy 0-34713
- GdCo, amorphous, for thermomagnetic recording (Japanese) 0-11562
- GdCo film structure, dependent on substrate type (Russian) 0-24747
- GdCoMo amorphous alloy films, susceptibility, uniaxial anisotropy field 0-54930
- GdFe amorphous film, Mossbauer and mag. meas. 0-15844
- GdFe film structure, dependent on substrate type (Russian) 0-24747
- GdFe homogeneous amorphous films, compensation point switching, magneto-optical Kerr signal anal. 0-15726
- ( $\text{Gd}_{1-x}\text{Fe}_x$ ) $_{1-x}\text{Bi}_x$  amorphous films, saturation magnetisation, Kerr and Faraday rotation 0-40093
- MnBi, ionized-cluster beam and reactive ionized-cluster beam deposition 0-16202
- $\text{Mn}_x\text{Fe}_{3-x}\text{O}_4$  ferrite film, exchange interaction depend. on conduction electrons (Russian) 0-34621
- Ni, chemisorption of  $\text{H}_2$ , isothermal desorption near Curie temp., rate meas. 0-29268
- $\text{Nd}_{0.35}\text{Co}_{0.65}$ , vacuum evaporated, magnetisation ripple struct., TEM and defocused Lorentz microscopy 0-7136
- Ni, ferromag. film, magnetoresistance parameter meas. (Spanish) 0-2485
- Ni, few atomic layers thick, transition from Pauli paramag. to band ferromag. 0-44885
- Ni film, ion beam sputtering prep., struct. and mag. props. 0-35085
- Ni film, multi- and single-layer, reson. curves subjected to tangential mag. reversals (Russian) 0-50195
- Ni film, single cryst., domain width from ferromag. reson. 0-39879
- Ni films, Faraday rotation effect dispersion 0-40092
- Ni-Co thin films, spin-wave reson. obs., exchange stiffness const. 0-44924
- Ni-Fe, electrodeposition, role of buffers and anions 0-25583
- Ni-Fe, low field domain wall mobility 0-25167
- Ni-Fe films, magnetisation reversal in narrow strips, TEM study 0-34720
- Ni-Fe-Pd thin films, mag., surface and corrosion props. 0-34707
- Ni-Fe-Rh, magnetic and corrosion props. 0-34702
- Ni-SiO multilayer film, interface magnetisation 0-7135
- NiFe stripes, mag. props. and domain struct. 0-44886
- $\text{Ni}_{0.83}\text{Fe}_{0.17}$  films, reson. oscils. of mag. domain walls and Bloch lines, stroboscopic electron microscopy 0-54931
- Ni, Fe,  $\text{Cr}_{1-x-y}$  films, struct., mag. props., and corrosion resist. 0-34706
- NiO, thin films with spinel-type defect structure, FMR study 0-39877
- NiS, electrolytically deposited, mag. props., S content influence 0-44884
- $\text{PbFe}_{12}\text{O}_{19}$  hexagonal ferrite amorphous films for mag. bubble memories, materials review (Polish) 0-34715
- SmCo, films, struct. transformations effect on coercive force and mag. reversal (Russian) 0-20436
- SmCo, thin film, hydride form., kinetics, mag. monitoring 0-35571
- Ti-Permalloy films, interdiffusion, Auger anal. and X-ray diffr. obs., degradation of mag. props. 0-34251
- W/EuS field emitters, electron emission current depend. on annealing temp., mag. props. 0-16160
- (Y,Sm) $_2(\text{Ga,Fe})_2(\text{Eu,Er})_3(\text{Ga,Fe})_2\text{O}_{12}$  double-layer self-biasing garnet films, dynamic behaviour of domain walls 0-34722
- (YEuTm) $_3(\text{FeGa})_2\text{O}_{12}$  film, dynamic props. of bubble domains by high speed photography 0-15771
- (YEuTm) $_3(\text{FeGa})_2\text{O}_{12}$  garnet film, bubble domain steady state motion on a circle 0-29589
- YEuTmGa garnet bubble film, dynamic diffuse wall deform. 0-54927
- (YEuYbCa) $_3(\text{GeFe})_2\text{O}_{12}$  bubble film with ion-implanted layer, FMR study 0-2643
- YIG dielectric layered struct. magnetostatic bulk wave steering 0-25166
- YIG film, magnetostatic surface and forward volume wave oblique incident at shallow groove 0-34704
- YIG film tangentially magnetised, magnetostatic surface wave excitation 0-29586
- YIG film-dielectric layer-conductor struct., magnetostatic bulk wave propag. dispersion relations 0-54925
- YIG, magnetostatic surface wave propag. in nonuniform mag. field, anal. 0-20437
- YIG periodic film layer, magnetostatic surface wave propag. 0-2607
- YIG substrates, magnetoelastic surface waves, magnetostatic reson. anal. 0-20441
- YSmCaFeGe, mag. garnet films, segregation of Ca and Ge in LPE growth 0-29959
- (YSmLu) $_3(\text{FeGaSc})_2\text{O}_{12}$ , submicron mag. bubble garnet 0-54929

## magnetic transition temperature

- see also Curie temperature; Morin temperature; Neel temperature
- critical temperature for Ising systems with regularly arranged impurities 0-44785
- ferromagnet, Ising amorphous, crit. temp. 0-11207
- Heisenberg ferromagnet mixed crystal, mag. props. 0-34579
- Ising model, randomly diluted, on honeycomb lattice, thermodynamic props. 0-54902
- Ising pair-quartet interactions, PAD approx. 0-11202
- metal hydrides, rare earth and intermetallic, electronic and mag. props., Mossbauer study 0-34830
- mixed magnets, competing spin glass and mag. order, phase diagrams, crit. points 0-39802
- rare earth intermetallic cpds., mag. props., book contrib. 0-39759
- spin glass, relaxation times, influence of spectral distrib. on freq. depend. of freezing temp. 0-44848
- spin-Peierls transition in mag. field, phonon freq., Heisenberg model calcs. 0-25151
- TTCuBDT, spin-Peierls transition in spin 1/2 Heisenberg chains, RPA calcs. 0-25150
- X-Y quasi-one-dimens. system anisotropic, spin-Peierls phase transition, tricritical point 0-25142
- $\text{Ca}_2\text{MnO}_{4-x}\text{F}_x$ , antiferromagnetic props. and elec. cond. (French) 0-29526
- $\text{Cd}_{1-x}\text{Mn}_x\text{Te}$ , EPR, mag. crit. point 0-39851
- $\text{CsNiF}_3$ , one-dimensional magnet, dynamics, mol. field theory approach 0-34614
- $\text{Cs}_{1-x}\text{Rb}_x\text{MF}_3$  (M=Mg, Co, Ni, Zn), hexagonal fluoride perovskite structural evolution by cationic substitution (French) 0-24430
- EuMg, Mossbauer effect, effective moments, mag. ordering temp. and isomer shifts 0-34833
- $\text{Eu}_2\text{Mg}_{17}$ , Mossbauer effect, effective moments, mag. ordering temp. and isomer shifts 0-34833
- Fe complex,  $\text{Fe}(\text{Br})[\text{S}_2\text{CN}(\text{C}_2\text{H}_5)_2]_2$ , 3-D Ising ferromag., cryst. susceptibility, 1.5-20K 0-20390



**magnetic transition temperature continued**

- ( $\text{Fe}_x\text{Mn}_{1-x}$ )<sub>2</sub>P<sub>16</sub>B<sub>6</sub>Al<sub>3</sub>, amorphous, mag. ordering temp., hyperfine field distrib., elec. resist. 0-34633  
 FeOCl, Mossbauer spectra, lattice dynamics, hyperfine interactions 0-44985  
 $\text{K}_2\text{FeCl}_4(\text{H}_2\text{O})$ , phase diagram, antiferromag., paramag. and spin flop phases 0-44831  
 MnBi, mictomag. alloys, elastic props. (*Russian*) 0-7141  
 MnCoSi, effect of press on mag. transition temp. (*Russian*) 0-25137  
 $\text{NbS}_2(\text{Se}_2)$  intercalation complexes with 3d transition metals, mag. and metallic transport props. 0-44814  
 $\text{Ni}(\text{NO}_3)_2 \cdot 6\text{H}_2\text{O}$ , susceptibility and specific heat meas., spin ordering, antiferromag. spin pair coupling 0-7084  
 $\text{TaS}_2$  intercalation complexes with 3d transition metals, mag. and metallic transport props. 0-44814

**magnetic transitions**

- see also critical fluctuations; ferromagnetic-antiferromagnetic transitions; ferromagnetic-paramagnetic transitions; magnetic transition temperature; paramagnetic-antiferromagnetic transitions  
 actinide compounds, specific heat meas., review 0-6524  
 antiferromagnet, disordered spin-flop, random-field effects 0-11208  
 antiferromagnetic Ising model, triangular, with transverse field, zero temp., ground-state props. 0-7115  
 antiferromagnets,  $n=4$  type II, phase transitions, Landau Ginzburg Wilson Hamiltonian 0-15735  
 atom + diatom, rot. inelastic scatt., mag. transitions, time reversal symm. 0-48066  
 BCC Ising model with competing interactions, fluctuation-induced first-order transition 0-20424  
 binary alloys, magnetic interface struct. 0-29564  
 Bose glass, marginal fluctuations 0-2586  
 classical planar spin model, two-dimens., Monte Carlo study 0-25147  
 critical fluctuations obs. using Mossbauer spectroscopy 0-39955  
 crossover, field-induced, in mag. chain, scaling theory 0-54904  
 dimethylammonium copper chloride bromide, mag. props., pulsed NMR expts. 0-11292  
 dimethylammonium manganese tetrachloride- $d_6$ , structural and mag. phase transitions, neutron scatt. and AC susceptibility meas. 0-44825  
 dipolar magnet, surface effects on phase transitions, local spontaneous polarisation 0-2708  
 disordered anisotropic antiferromagnet, random field effects 0-2580  
 elastic properties of magnetic materials, review 0-7142  
 ferrimagnet, uniaxial two-sublattice, energy spectrum, magnetisation, and crit. field, Green function method 0-25060  
 ferromagnet, elec. resist., just below crit. temp., effect of mag.-domains 0-39557  
 ferromagnet, Ising model, nonuniform mag. field method, crit. correlation function approximations, calc. 0-20407  
 ferromagnet, Ising model, transition point calc. 0-20408  
 ferromagnet, random uniaxial, dipolar interactions, crossover behaviour, renormalisation group equations numerical soln. 0-50136  
 ferromagnet, soft, hysteresis rel. to irreversible phase transition 0-34693  
 ferromagnet, uniaxial dipolar, crossover behaviour, theory 0-29559  
 ferromagnetic, anisotropic, in random longitudinal field, multicrit. point, theory 0-54903  
 ferromagnetic alloy, transition to spin glass ordering 0-34628  
 ferromagnetic film, shift of ant. temp. as result of Raman scatt. 0-54909  
 ferromagnetic films, nonlinear spin wave parametric resonance 0-2642  
 ferromagnetic films, spin correl. functions, crit. indices 0-7133  
 ferromagnetic materials, phase transition, mathematical bifurcation process 0-29572  
 ferromagnetic phase transitions, nucl. spin dynamics in anisotropic systems 0-11205  
 ferromagnetic phase transitions, nucl. spin dynamics in isotropic systems 0-11204  
 ferromagnetic superconductor, vortex structure 0-25055  
 ferromagnetism, itinerant electron model, spin quantization direction fluctuations, short range order. 0-34582  
 ferromagnets and antiferromagnets, EM and acoustic energy attenuation in many-domain magnets 0-7140  
 first-order, intrinsic volume magnetostriction concept 0-29562  
 frustration network, phase transitions 0-2596  
 Ginzburg-Landau-Wilson model,  $n$ -component, derivation of nonlinear  $\sigma$ -model, in low temp. limit 0-44787  
 Heisenberg model, magnetic transitions 0-25141  
 Heisenberg model, three dimensional, crit. exponents and corrections to scaling 0-7117  
 Heisenberg spin system, one-dimensional, dynamical behaviour 0-29567  
 high-temperature representation of anisotropic rotator, XY and Heisenberg models for dimensions  $D \geq 2$  0-11146  
 ilvaite, Mossbauer spectra and mag. features 0-7248  
 incommensurate phase transition, Bethe-Peierls and mol. field approx. 0-20599  
 insulator, mag. transition sp. ht. anomaly, photoacoustic meas. 0-4773  
 Ising, quenched dil. random-bond model, CPA difference eqn. and crit. curves 0-2584  
 Ising ferromagnet and spin glass systems, random, crit. dynamics 0-34666  
 Ising ferromagnet with two- and four-spin interaction, improved product average decomposition method 0-20406  
 Ising frustration pots., phase transition 0-52142  
 Ising metamagnet, dilute tricritical point calcs. 0-50099  
 Ising model, looped tree-like lattice, phase transition 0-7113  
 Ising model, one dimensional, with infinite radius of interaction in transverse magnetic field 0-2587  
 Ising model, one-dimensional, long range, metastability 0-42166  
 Ising model with competing interactions, solitons and phasons 0-34653  
 Ising replica magnets, phase struct. 0-39777  
 Ising square lattice, phase transitions, next nearest neighbour interactions 0-50128  
 Ising type model, elastically coupled, effects of dipolar forces on crit. sound attenuation in uniaxial systems 0-50158  
 magnetic ordering in antiferromagnets without spatial struct., phase transitions (*Russian*) 0-50134  
 magnetic system with cryst. field pots., Green's function theory and high temp. series expts. 0-15673  
 magnetisation theory, of slab of finite thickness, role of positive surface energy 0-15724  
 manganese zinc formate dihydrate, two-dimens. antiferromag., anomalous crit. phenomena, neutron scatt. and PMR obs. 0-50104

**magnetic transitions continued**

- metamagnetism, temperature induced, caused by mag. anisotropy 0-11195  
 Migdal transformation, renormalisation group, recursion relations 0-34647  
 mixed magnets, competing spin glass and mag. order, phase diagrams, crit. points 0-39802  
 Monte Carlo simulation of model spin systems 0-20421  
 Neel ferrimagnet, field-induced spin-orientational phase transitions 0-2576  
 one-dimensional electron system, with attractive interaction in mag. field, paramag. transition 0-7072  
 one-dimensional magnetic system, spin anisotropy and exchange alternation 0-34644  
 one-dimensional semi-infinite chain, enhanced surface exchange interaction, mag. relax. 0-29558  
 ordering temps. determ. by Bethe-Peierls-Weiss (BPW) method 0-54912  
 planar spin two-dimens. model, mag. correlation function, self-consistent calc. 0-29563  
 Potts model, first order phase transitions, Monte Carlo renormalisation group method 0-34645  
 Potts model, Monte Carlo simulation in three dims. 0-163  
 random Ising magnet, phase diagrams 0-7065  
 randomly distributed interaction centres, mol. field distrib. function (*Russian*) 0-44834  
 rare earth alloys,  $\text{RCO}_2$ , elec. resistivity, thermopower, X-ray struct. meas. 0-24874  
 rare earth compounds,  $\text{RMO}_2\text{X}_8$ , ( $\text{X}=\text{S}, \text{Se}$ ), supercond. and long range mag. order coexistence 0-15642  
 rare earth compounds,  $\text{RRh}_2\text{B}_4$ , supercond. and long range mag. order coexistence 0-15642  
 rare earth dihydrides and dideuterides, electronic and mag. props. 0-25260  
 rare earth metal, magnetic properties, nonlinear s-f exchange interaction effect 0-15711  
 rare earth mixed valence compounds, charge dominated fluctuation props. comparison, mag. moments and ordering 0-54659  
 rare earth molybdenum sulphides, supercond. and magnetism coexistence (*Japanese*) 0-7025  
 rare earth trihydrides, light, low-temp. sp. ht., mag., elec., and cryst. field splitting effects 0-49379  
 rare earth-transition metal (4f-3d) intermetallic cpds., mag. moment and mag. anisotropy 0-25107  
 rotationally inelastic scattering, mag. transitions, time reversal symm. 0-53105  
 scaling function near mag. critical point, complementary expressions 0-34656  
 second order phase transitions, superspace group description (*Chinese*) 0-8942  
 small superconductor in magnetic field, first and second order phase transitions 0-2519  
 solitons in condensed matter physics, theory 0-50122  
 solitons near critical point, neutron scattering observation 0-34650  
 spin glasses, order parameter for replica symmetry breaking 0-44835  
 spin glasses, phase transition, fluctuations of local spins, mean-field theory 0-34661  
 spin glasses, phase transition, mag. susceptibility, specific heat, Ising model calcs. (*Russian*) 0-34671  
 spin glasses, susceptibility, wave-vector-depend., theory 0-11209  
 spin Peierls transition, gap eqns. 0-24801  
 spin system, cubic model, Monte Carlo simulation, phase transitions 0-34646  
 spin wave damping, magnetic materials with canted mag. struct., thermodynamic and high freq. props. 0-11184  
 spin wave theory of spin 1/2 X-Y model, phase transitions 0-7068  
 spin-Peierls transition in mag. field, phonon freq., Heisenberg model calcs. 0-25151  
 surface magnetisation profile, in crit. region by  $\epsilon$ -expansion, Wilson perturbation theory calc. 0-50100  
 TANOL, free radical, spin flopping transition, temp. depend., mag. anisotropy energy 0-54890  
 TCNQ salt, N-propyl-quinolinium( $\text{TCNQ}$ )<sub>2</sub>, defect conc. depend. phase transition 0-44577  
 TCNQ salt, pyridinium ( $\text{TCNQ}$ )<sub>2</sub>, low temp. mag. phase transition, ESR study 0-25139  
 tensor order parameters for magnetic-structural phase transitions in strong spin-lattice coupled crystals. 0-50125  
 TMMC, XY-Ising crossover transition, quasi-elastic neutron scatt. obs. 0-44826  
 TTF(MBDT) spin-Peierls transition, mag. exchange interactions, mag. props. 0-25138  
 (TTF) $\text{Cu}_2\text{C}_4(\text{CF}_3)_4$ , spin Peierls system, mag. field effects 0-7123  
 TTF- $\text{Cu}_2\text{C}_4(\text{CF}_3)_4$ , spin-Peierls system, high-field phase 0-39816  
 TTFcubDT, spin-Peierls transition in spin 1/2 Heisenberg chains, RPA calcs. 0-25150  
 two-dimensional Ising antiferromagnet, neutron scatt., review 0-50103  
 uniaxial antiferromagnet, crit. dynamics at bicritical points 0-15321  
 uniaxial Heisenberg antiferromagnet, phase diagrams 0-15730  
 X-Y model, spin 1/2, anal. of high temp. series expansions of some thermodynamic quantities in four dimensions 0-50098  
 $\text{Al}_2\text{La}_2\text{Ce}_{1-x}$ , low temp. mag. props. 0-20564  
 $\text{B}_2\text{O}_3\text{Fe}_x\text{O}_{3-n}\text{MO}$  ( $\text{M}=\text{Fe}, \text{Co}, \text{Ni}, \text{Cu}, \text{Mg}$ ), synthesis and mag. props. 0-20384  
 $\text{BaVSe}_3$ , one-dimensional, struct. and mag. props. 0-28993  
 Bi, vapour, optical activity, Faraday effect, parity nonconservation, mag. transitions (*Russian*) 0-55070  
 $\text{Ca}_3\text{Mn}_2\text{Ge}_2\text{O}_{12}$ , mag. struct. study 0-2554  
 $\text{Cd}_{1-x}\text{Mg}_x$ , magnetic susceptibility anisotropy, press. effects, electronic phase transitions (*Russian*) 0-54869  
 Ce monochalcogenides, cryst. field effects, phase transitions 0-24853  
 Ce mononitrides, cryst. field effects, phase transitions 0-24853  
 $\text{CeAl}_2$ , Anderson lattice system, ground state props. 0-20443  
 CeBi, phase diagram in mag. field, hydrostatic press. effect 0-25132  
 $\text{Ce}_{0.7}\text{Ho}_{0.3}\text{Ru}_2$ , superconductors, mag. correlations and crystal-field levels 0-34547  
 $\text{CeIn}_3$ - $\text{Sn}_x$ , scaling behaviour near valence instability, mag. susceptibility and mag. transitions 0-25111  
 $\text{Ce}_{1-x}\text{La}_x$ , thermoelectric power, mag. transition temps. 0-20154  
 $\text{CoCl}_2 \cdot 2\text{H}_2\text{O}$ , antiferromag., light scatt. from phonons and magnons 0-40104



## magnetic transitions continued

- Co<sub>1-x</sub>Mn<sub>x</sub>F<sub>2</sub>, antiferromagnet mag. impurities, spin excitation spectrum collective rearrangement in external mag. field 0-50199  
 Co<sub>3</sub>Ni<sub>1-x</sub>Cl<sub>2</sub>·6H<sub>2</sub>O, solid solution, mag. props. and phase diagram, calc. 0-7104  
 CoS<sub>2-x</sub>Se<sub>x</sub>, magnetism and metamagnetic transition, neutron diffr. and NMR meas. 0-15717  
 CoS<sub>2-x</sub>Se<sub>x</sub>, conc. and temp. effects on metamagnetic transition 0-15716  
 Cr, electronic structure model, Invar effect, antiferromagnetic-non mag. transitions 0-20370  
 Cr, magnetic phase diagram in external mag. field, spin reorientation curve, critical point coordinates (Russian) 0-29548  
 Cr-Os, magnetic transition T-P-C diagram, triple points (Russian) 0-54895  
 Cr<sub>1-x</sub>Fe<sub>x</sub>, Mossbauer spectra, mag. behaviour 0-20532  
 CrS<sub>2</sub>Te<sub>1-x</sub> (x=0 to 0.2), magnetic props. study 0-11194  
 CsCoCl<sub>3</sub>, Ising like antiferromag., mag. phase transition, <sup>133</sup>Cs NMR 0-7184  
 CsCuBr<sub>3</sub>, quasi-1-dimens., NQR obs. 0-54987  
 CsCuCl<sub>3</sub>, quasi-1-dimens., NQR obs. 0-54987  
 CsMn<sub>3</sub> (M=V, Cr, Mn), Mossbauer spectra, struct., electronic and mag. props. 0-15908  
 CsMnCl<sub>2</sub>·2H<sub>2</sub>O, quasi-one-dimensional antiferromag., phase diagram (French) 0-20405  
 CsMnF<sub>3</sub>, mag. phase boundaries, XY to Ising crossover, virtual bicritical point 0-50095  
 CsNiF<sub>3</sub>, demagnetising effects on antiferromag. reson. 0-15803  
 Cu complex, 1,2-ethanediammonium tetrachlorocuprate, layered struct. mag. susceptibility 0-7094  
 Cu complex, dichloro(dimethylnitrosamine)copper(II), magnetic phase transition, <sup>14</sup>N NQR obs. 0-11289  
 Cu complex, dichloro(dimethylnitrosamine) Cu II, mag. props., <sup>14</sup>N NQR obs. 0-54988  
 Cu-Mn, spin glass, meas. of order parameter 0-34642  
 CuBr<sub>2</sub>, quasi-1-dimens., NQR obs. 0-54987  
 CuCl, disordered, diamag. transition 0-34636  
 CuCl<sub>2</sub>, quasi-1-dimens., NQR obs. 0-54987  
 CuK<sub>2</sub>Cl<sub>2</sub>·2H<sub>2</sub>O, Heisenberg ferromag., mag. field effect on susceptibility near crit. point 0-39758  
 DyIG, noncrystalline, Mossbauer and magnetisation data 0-34828  
 ErB<sub>3</sub>, mag. and elec. props., metallic character 0-20386  
 ErB<sub>4</sub>, mag. phase diagram, neutron diffr. study 0-50091  
 Er<sub>1-x</sub>Al<sub>x</sub>, mag. props. meas. and neutron diffr. data 0-7126  
 Er<sub>1-x</sub>Rh<sub>x</sub>B<sub>4</sub>, supercond. phase transitions, recentring temp. to normal ferromag. state 0-7024  
 EuB<sub>3-x</sub>C<sub>x</sub>, Mossbauer spectra, cond. electrons effect 0-20545  
 EuIG, noncrystalline, Mossbauer and magnetisation data 0-34828  
 EuS<sub>1-x</sub>Se<sub>x</sub>, mag. phase diagram, from temp. depend. of magnetisation 0-7105  
 Eu<sub>1-x</sub>Sr<sub>x</sub>S, ferromagnet-spin glass transition, mag. ordering, mag. susceptibility and neutron scatt. meas. 0-50135  
 Fe complex, FeM<sub>1-x</sub>(1,10-phenanthroline)<sub>2</sub>(NCS)<sub>2</sub>, M=Mn,Co,Ni, spin crossover, Mossbauer and magnetism study 0-44980  
 Fe-Al, spin glass transition, Monte Carlo study 0-39801  
 Fe-Al (0.27 to 0.50 at.%), spin glass behaviour, microscopic model, Ising lattice, exchange and superexchange 0-39800  
 Fe-Al-Fe, phase diagram, microscopic model 0-34630  
 Fe-Mn, Mossbauer spectroscopy of temp. hysteresis of phase transformations (Czech) 0-29949  
 Fe-Ni-Al, type YuN14DK25BA, thermomag. treatment 0-16512  
 FeCl<sub>2</sub>·2H<sub>2</sub>O-CoCl<sub>2</sub>·2H<sub>2</sub>O, random mixture with competing spin anisotropies, tetracrit. transition, neutron diffr. obs. 0-2575  
 Fe<sub>1-x</sub>Co<sub>x</sub>Cl<sub>2</sub>, mag. phase diagram 0-11198  
 Fe<sub>2</sub>, magnetic phase transitions, Mossbauer spectra in high mag. fields 0-39936  
 (Fe<sub>1-x</sub>Mn<sub>x</sub>)<sub>75</sub>P<sub>15</sub>B<sub>6</sub>Al<sub>3</sub>, amorphous, spin-glass-ferromag. multicritical point, AC susceptibility meas. 0-50117  
 α-Fe<sub>2</sub>O<sub>3</sub>, hematite, Morin transition, Mossbauer mag. diffr. spectra 0-20562  
 Fe<sub>2</sub>O<sub>4</sub>, magnetite Mossbauer spectra, mag. dipolar and elec. quadrupole effects 0-20544  
 Fe<sub>2</sub>O<sub>4</sub>, typical spontaneous symmetry breakdown in solid state 0-34737  
 Fe<sub>2</sub>(PO<sub>4</sub>)<sub>2</sub>(OH)<sub>2</sub>, synthetic barbosaltite, temp. depend. quadrupolar and mag. hyperfine interactions 0-25255  
 Fe<sub>2</sub>Pd<sub>2-x</sub>Si<sub>x</sub>, metallic glass, mag. phase diagram, weak ferromagnet-spin glass transition 0-54893  
 Fe<sub>2</sub>S<sub>10</sub>, polytypism, Fe diffusion near antiferromag. to ferrimag. transition 0-44830  
<sup>3</sup>He, liquid, EPR of negative ions, antiferromagnetic transition possibility (Russian) 0-15322  
<sup>3</sup>He, solid, mag. ordering, NMR study 0-54470  
<sup>3</sup>He, solid, nuclear antiferromag. reson. 0-54471  
 Ho, magnetic phase diagrams, helicoid-ferromag. transform. (Russian) 0-50089  
 Ho-Sm, magnetic phase diagrams, helicoid-ferromag. transform. (Russian) 0-50089  
 HoAlGa<sub>2-x</sub>, mag. props. and phase transitions 0-25133  
 Ho<sub>2</sub>O<sub>3</sub>SO<sub>4</sub>, magnetic phase diagram, magnetisation and mag. susceptibility meas. 0-15720  
 HoP, flopside mag. struct. to ferromag. transition, elastic neutron scatt. obs. 0-50058  
 K<sub>2</sub>CuF<sub>4</sub>, two-dimensional planar ferromagnet, giant fluctuation of spins (Japanese) 0-54894  
 La<sub>0.5</sub>Sr<sub>0.5</sub>CoO<sub>3</sub>, ferromagnetic phase transition obs. at 230K, heat capacity meas. (Japanese) 0-54898  
 LiTb<sub>0.5</sub>Y<sub>0.5</sub>F<sub>4</sub>, mag. susceptibility, dilution effect on critical behaviour of dipolar uniaxial ferromagnet 0-34635  
 α-Mn, electronic structure model, Invar effect, antiferromagnetic-non mag. transitions 0-20370  
 Mn-Al-C, ferromag., transform. kinetics 0-34627  
 MnAs, orthorhombic, low temp. magnetic transitions (Russian) 0-11193  
 Mn<sub>1-x</sub>Fe<sub>x</sub>As, magnetic transition under high press., exchange striction model calcs. (Russian) 0-50096  
 Nd, magnetic structure, 2D modulated 0-15697  
 Nd<sub>1-x</sub>La<sub>x</sub>, thermoelectric power, mag. transition temps. 0-20154  
 Ni<sub>2</sub>Mg<sub>1-x</sub>O, EPR in magnetocentrated solid solution (Russian) 0-39856  
 NiWO<sub>4</sub>, monoclinic antiferromagnet, orientational phase transition and intermediate state (Russian) 0-15725  
 NiWO<sub>4</sub>, monoclinic antiferromag., domain struct. induced by strong mag. field 0-44856

## magnetic transitions continued

- O, solid, magnetic props. theory for Heisenberg system (Russian) 0-54900  
 Pb compounds, perovskites, polymorphic transformations possibility, mag. anal. elec. ordering effects 0-55389  
 Pr-Ce(Tm), mag. order onset, elec. resistivity 0-20416  
 Pr<sub>2</sub>Ti, critical fluctuations temp. depend. 0-25160  
 Pr<sub>2</sub>Ti, transition temp. and magnetisation 0-25161  
 RbCoCl<sub>3</sub>·2D<sub>2</sub>O, metamagnetic phase transition, crystallographic and mag. struct., neutron diffr. meas. 0-44174  
 Rb<sub>2</sub>Co<sub>2</sub>Mg<sub>1-x</sub>F<sub>4-x</sub>, dilute antiferromag. two dimens. Ising system, phase boundary effective medium theory 0-50130  
 RbCuCl<sub>3</sub>, quasi-1-dimens., NQR obs. 0-54987  
 RbFeCl<sub>3</sub>·2H<sub>2</sub>O, 2D Ising system, crit. fluctuations, Mossbauer spectra study 0-44842  
 Rb<sub>2</sub>Mn<sub>2</sub>Mg<sub>1-x</sub>F<sub>4-x</sub>, two-dimens. antiferromag., spin fluctuations, neutron diffr. study 0-44846  
 Tb, critical magnetic studies 0-15745  
 Tb, ferromagnet, field depend. of elastic const. c<sub>66</sub> 0-15181  
 Tb, magnetic phase diagram, US meas. of elastic const. 0-15721  
 TbAlGa<sub>2-x</sub>, mag. props. and phase transitions 0-25133  
 TbAsO<sub>4</sub>, ferromag., static and AC susceptibility meas. 0-29533  
 TbIG, Faraday rotation and transition of spin config. at high mag. fields 0-39776  
 TbP, singlet-groundstate magnetism, static mag. props. 0-7109  
 TbPO<sub>4</sub>, linear optical birefr. meas. near bicritical point 0-15719  
 TmCd(Zn), quadrupolar phase transitions, magnetoelastic and quadrupolar coupling consts. 0-15744  
 TmSe, mag. props. and struct. 0-25109  
 UAs, magnetisation, ferrimag. spin struct. 0-7088  
 UAs, sp. ht. meas., 5-300K, mag. transition obs. 0-50101  
 UO<sub>2</sub>, mag. ordering lattice internal rearrangement transition, theory 0-20402  
 UP, vol. changes at mag. transitions 0-7107  
 Y(Co<sub>1-x</sub>Ni<sub>x</sub>)<sub>5</sub>, spontaneous magnetisation mag. anisotropy, spin reorientation transformation (Russian) 0-7082  
 YFe<sub>2</sub>O<sub>4</sub>, low temp. phase transitions and mag. props. 0-7106  
 Y<sub>3-x</sub>Gd<sub>x</sub>Fe<sub>2</sub>O<sub>4</sub>, mag. phase diagrams, mag. transitions, exchange interaction (Russian) 0-54896  
 Y<sub>1-x</sub>Tb<sub>x</sub>Co<sub>5</sub>, spontaneous magnetisation anisotropy, spin reorientation transforms. (Russian) 0-7082  
 Yb, FCC phase, low temp. mag. props., impurity effects 0-20387  
 Zr(Fe<sub>1-x</sub>Al<sub>x</sub>)<sub>2</sub>, transition region, spin glass or long range mag. order 0-44841  
 Zr(Fe<sub>1-x</sub>Co<sub>x</sub>)<sub>2</sub>, transition region, spin glass or long range mag. order 0-44841

## magnetic traps

see also magnetic bottles

- 2XIIB magnetic mirror device, neutral beam injection 0-28782  
 adiabatic, drift cone instability suppression by electron heating (Russian) 0-53959  
 ambipolar trap, transverse loss reduction method (Russian) 0-10417  
 current sheet generation in rarefied plasma, mag. flux plasma trap appls. 0-38698  
 divertor fluxes in stellarators and torsatrons, azimuthal distrib. 0-6216  
 electrostatic bounce modes in mirror plasmas 0-1790  
 EM trap confinement, microwave investig. (Russian) 0-10416  
 Engineering Test Facility work on magnetic confinement 0-52787  
 glass-CO<sub>2</sub>-hybrid laser system for plasma prod. and heating in mag. traps 0-24196  
 helical magnetic axis trap, plateau and banana diffusion regimes 0-10425  
 Heliotron D, RF heating, equilibrium and stability 0-28777  
 high beta MHD theory, stellarator equilibrium and stability, mirror traps and reverse field machines 0-28778  
 laser produced plasma in cusp field, RF plugging 0-28783  
 magneto-electrostatic reactor, power gain factor 0-48933  
 microwave heating of plasma in EM trap (Russian) 0-10400  
 mirror configuration for heating of K plasma with hot W filament array 0-33789  
 multipole mag-field for surface trapping of primary electrons 0-33810  
 non-axisymmetric open trap, longit. plasma losses (Russian) 0-33799  
 open traps, axially symmetric, transverse particle losses 0-28784  
 proboktron plasma stabilisation system, automatic, against flute oscills. (Russian) 0-24211  
 RF heating of magnetized rarefied plasma 0-24195  
 RF intense heating, energy confinement 0-38674  
 tearing instability in cylindrical plasma configurations (Russian) 0-10370  
 Tokamak magnetic fusion R+D, ISX and PDX programs 0-37586  
 Tormac, confinement system, magnetoacoustic heating studies 0-24217

## magnetic variables control

- plasma flute oscillation suppression, regulator synthesis (Russian) 0-24212  
 proboktron plasma stabilisation system, automatic, against flute oscills. (Russian) 0-24211

## magnetic variables measurement

- see also fluxmeters; magnetic field measurement; magnetic permeability measurement; magnetometers  
 anisotropy meas. at microwave freq., experimental results 0-52279  
 Curie temp., pressure cell with cubic-anvil press 0-13109  
 disaccommodation measurement in Rayleigh range using semi-automatic equipment (Polish) 0-31812  
 domain patterns obs., of highly-oriented Si steel, using ferromagnetic colloid technique 0-11856  
 electrical steel sheet, magnetostriction meas. using Hall effect transducer (German) 0-13111  
 epitaxial garnet films, technique for magnetostriction coeff. meas. 0-243  
 ferromagnetic materials in strong fields, equipment using Hall transducer 0-4745  
 ferromagnetic sphere in nonuniform mag. field, magnetisation meas. arrangement 0-42242  
 ferromodulation meas. transducers, with increased temp. stability 0-52281  
 galvanomagnetic effects, at pressures up to 27 kbar, using low-temperature hydrostatic pressure chamber 0-47069  
 hysteresis loop tracer for mag. phase detection 0-22393  
 layer magnetic properties meas. on saturated substrate 0-13108  
 magnetisation of small ferrite samples, extraction method 0-242  
 magneto-microwave Kerr effect in semiconductors and ferrites using K-band interferometer 0-52263



**magnetic variables measurement continued**

- magnetoresistance and Hall EMF, of low-resistance materials, by AM method 0-52278  
 magnetoresistance of semiconductors, automatic device for temperature dependence determ. 0-52270  
 magnetostrictive vibration meas., laser interferometric technique 0-37059  
 magnets testing, permanent, test parameters selection w.r.t. errors 0-52280  
 micro-magnetic susceptometer for actinides 0-13112  
 single magnetic particles, remanent loop measurement 0-17967  
 SQUID using Nb thin film microbridge (*Japanese*) 0-31816  
 superconducting cable, magnetisation anisotropy meas. in hysteresis loss using Hall sensors 0-17966  
 susceptibility, AC, depend. on magnitude meas. field 0-241  
 susceptibility, demonstration system for student laboratory 0-4491  
 temperature dependences, of permanent magnets, automated apparatus for -150 to 300°C range 0-31809  
 Wiegand effect, influence on magnetic sensors (*Spanish*) 0-31735

**magnetic wells** *see magnetic traps***magnetisation**

*see also Barkhausen effect; coercive force; demagnetisation; magnetic aftereffect; magnetic anisotropy; magnetic domains; magnetic hysteresis; magnetisation reversal; magnetostatic waves; remanence; spontaneous magnetisation*

- amorphous alloys, ferromagnetic props. and appl. 0-50143  
 amorphous magnet, magnetisation, mag. moment temp. distrib. 0-15848  
 antiferromagnet, magnetisation, crit. spin-flop angle, temp. and field depend. (*Russian*) 0-7111  
 ballistic instrument, errors associated with circuit magnetisation parameters 0-22391  
 Bloch equations solution in presence of varying  $B_1$  field, selective pulse analysis 0-25222  
 Bloch wall bound spin waves, equations of motion 0-34612  
 boson magnetised ideal gas, effect of confinement, anal. 0-12987  
 composite superconductor, effect on losses in variable mag. field of mag. props. 0-34549  
 copper complex  $\text{CuBr}_2$  (pyrimidine) $_2$ , mag. susceptibility and magnetisation curve, 1.2-4.2K 0-11177  
 cubic Ising ferromagnet, three spin interaction effect on mag. props. 0-54910  
 cylindrically symmetric bubbles, static and dynamic props. 0-39835  
 dilute local moment local magnetisation, Kondo-like deviations from free spin behaviour 0-44800  
 dimethyl ammonium copper chloride, spin dynamics near crit. pt. 0-7112  
 distribution in isolated transition, digital magnetic recording 0-29580  
 electron gas, relativistic, spin-polarised, Bloch theory 0-15465  
 electron-hole pairing systems, current states and domains 0-54614  
 exchange processes, two-dimensional NMR spectrosc. investig. 0-25218  
 ferredoxin synthetic analogues,  $[\text{Fe}_2\text{S}_4(\text{SR})_4]^{3-}$  clusters, Mossbauer effect, EPR, and mag. props. 0-41057  
 ferrite, light diffr. by magnetisation inhomogeneities, multiple refl. 0-2733  
 ferrite spinels, normal and inverse, solid state chem. expts. for students 0-36815  
 ferrites, wave beam propagation in longitudinally magnetised gyrotropic media (*Russian*) 0-23607  
 ferrofluids, magnetisation, absence of anisotropy effects 0-50146  
 ferroinsulators, spin waves and uniform transverse magnetization, oscillatory eigenstates (*Russian*) 0-11181  
 ferromagnet, amorphous, magnetisation, temp. depend. effect of nonrandom anisotropy 0-39773  
 ferromagnet, uniaxial, magneto-dipole interaction influence on one dimensional magnetisation soliton (*Russian*) 0-54880  
 ferromagnetic alloy, transition to spin glass ordering 0-34628  
 ferromagnetic film, transverse biopole susceptibility, two-dimens. micro-magnetism 0-11231  
 ferromagnetic semiconductors, dielectric function depend. on magnetisation, light absorpt. coeff. (*Russian*) 0-15467  
 ferromagnetic sphere in nonuniform mag. field, magnetisation meas. arrangement 0-42242  
 ferromagnetic thin film magnetometer, development and performance 0-31808  
 ferromagnetism, itinerant electron model, spin quantization direction fluctuations, short range order. 0-34582  
 ferromagnets, exchange and dipolar coupled, spin wave renormalisation, Damon-Eshbach surface spin waves 0-2564  
 ferromagnets, magnetic vortex as topological soliton in Landau-Lifshitz eqns. (*Russian*) 0-7097  
 garnet, epitaxial film, mag. bubble props., permanent local modification by laser annealing 0-2612  
 HCP metals, mag. susceptibility near  $2^{1/2}$ th order electron transition, non-linear magnetisation anal. (*Russian*) 0-44859  
 Heisenberg ferromagnet, low temp. behaviour in spectral density method 0-50028  
 Heisenberg ferromagnet mixed crystal, mag. props. 0-34579  
 high-energy magnetic materials, props., treatment procedures and testing (*Italian*) 0-54914  
 intermetallic compounds, containing d-transition metal, hydrogenated, magnetism 0-34609  
 Invar, magnetic and thermal anomalies 0-34603  
 Invar, thermal expansion coeff. relationship to magnetisation 0-15269  
 Ising disordered chains, ferromag., long-time relax. 0-34652  
 Ising model, 1-D, energy conserving relax. 0-20420  
 Ising model, cubic lattice, high temp. expansion at magnetisation of ninth order (*Russian*) 0-54858  
 Ising model, kinetic with triplet interactions, Monte Carlo anal. 0-7061  
 Ising model, magnetisation probabilities and metastability 0-29516  
 Ising quadratic two-dimensional ferromagnet with three spin interactions 0-2542  
 isotropic three-sublattice ferrimagnet, magnetisation 0-2605  
 linear transverse in long thin stripes, demagnetisation eigenfunctions anal. 0-34687  
 magnetisation curve analytic functions, numerical parameter calc., variational methods appl. (*Russian*) 0-14267  
 magnetization curve and Gaussian error function (*German*) 0-50137  
 micromagnetism, numerical calcs. 0-11222  
 neutron studies of magnetic densities and magnetic excitations, book contrib. 0-11170  
 nonexchange surface spin waves at interface between two ferromagnets 0-29544  
 magnetisation continued  
 obsidian, Lipari and Teotihuacan origin, Mossbauer, magnetisation, X-ray diffr. and fluoresc. study 0-46173  
 one-dimensional planar magnets, low temp. NMR 0-44943  
 one-dimensional semi-infinite chain, enhanced surface exchange interaction, mag. relax. 0-29558  
 orthorhombic ferrimagnets, domain wall motion at near sonic velocity, magnetoelastic interactions 0-34683  
 paramagnet, classical, wavelength-depend. fluctuations in mag. field 0-7069  
 Permalloy I-bar elements, magnetostatic effects, unifying overview of domain and continuum results 0-44853  
 Permalloy-Rh, film, influence of Rh on corrosion resist. and mag. props. 0-3235  
 phase transition thermodynamics, theory of magnetisation, role of positive surface energy 0-15724  
 phase transitions in quantum X-Y and Heisenberg models 0-25141  
 plane Ising lattice, local magnetisation depend. on linear defects (*Russian*) 0-2595  
 polyethylene, linear, melt props. correl. with chain length distrib. (*Russian*) 0-37920  
 Potts model, Monte Carlo simulation in three dims. 0-163  
 random exchange Heisenberg antiferromagnetic chain, exchange-coupled pair model 0-20423  
 random spherical model, crit. dynamics 0-44844  
 rare earth alloys, Curie temperature, high press. effects (*Japanese*) 0-20444  
 rare earth alloys,  $\text{RZn}_{12}$  and  $\text{RCu}_4\text{Al}_8$ , mag. struct. and interactions 0-25092  
 rare earth amorphous alloys, random anisotropy antiferromag. model 0-20399  
 rare earth garnets, prep. and props. book contrib. 0-44193  
 rare earth intermetallic cpds., mag. props., book contrib. 0-39759  
 rare earth intermetallics,  $\text{RAl}_2\text{-Gd(Er)(Dy)(Nd)}$ , dil., ( $\text{R}=\text{La, Yb, Lu}$ ), EPR and mag. susceptibility 0-15797  
 rare earth intermetallics,  $\text{RGa}_2$ , ordering and exchange interactions 0-39779  
 rare earth intermetallics,  $\text{RPt}$ , ( $\text{R}=\text{Gd, Tb, Dy, Ho, Er, Tm}$ ), structs. and mag. props. 0-50069  
 rare earth permanent magnets, physics and technology 0-20433  
 rare earth tetraborides, mag. and elec. props., metallic character 0-20386  
 rare earth-gold amorphous alloys,  $\text{R}_4\text{Au}$ , anisotropy versus exchange 0-34624  
 rare earth-iron,  $\text{RFe}_2$ , Laves phase intermetallics, ordered and paramagnetic phases, mean field exchange consts. 0-50084  
 rare earth-transition metal alloys, amorphous, struct. and mag. props., book contrib. 0-39818  
 rare-earth, mag. supercond., appl. of boson theory to mixed state 0-7050  
 semi-infinite Heisenberg ferromagnet, macroscopic theory of response functions and appl. to light scatter. 0-20410  
 semiconductors, magnetic, static magnetic properties, mean field approach 0-7090  
 Sendust ribbon, mag. props. 0-15761  
 solid torsional oscillators, rotating frame, nucl. spin polarisation losses, torsional spectroscopy 0-31821  
 spin glasses, magnetisation relaxation time near freezing temp., HF calc. 0-34665  
 spin system, transient phenomena, soln. using eigen-coordinate system of magnetisation vector 0-25116  
 spin- $1/2$  XY model, thermodynamic quantities, high-temp. series expansions anal. 0-7067  
 spin-glass, two-dimensional Ising model, low temp. dynamic props. 0-20425  
 spin-Peierls transition in mag. field, phonon freq., Heisenberg model calcs. 0-25151  
 steel, austenitic stainless, magnetic susceptibility and magnetisation, low temp. 0-25102  
 steel, Cr-Ni-Mo-V, magnetic induction, struct. dependence (*Czech*) 0-50141  
 steel, stainless, cold plastic deform. effect on struct. and props. 0-29113  
 steel, types 45 and U8, plastically deformed, magnetoelastic props. (*Russian*) 0-44893  
 steel fibres, polycrystalline, Mossbauer spectroscopy 0-44959  
 sublattice metamagnet, temp. dependent anisotropy, magnetisation curves, mag. transitions, classical approx. 0-39795  
 superconducting slab, type I, first stage magnetisation and metastable migration field 0-15655  
 superconductor, type-II, magnetisation, rel. to anisotropy of upper crit. field 0-54832  
 superparamagnetic particles, Mossbauer spectra, magnetisation vector precession 0-15872  
 surface and interface magnetism by Mossbauer spectroscopy 0-7218  
 transition metal alloys, Curie temperature, high press. effects (*Japanese*) 0-20444  
 transition metal compounds and dil. alloys, mag. ordering phenomena in high mag. fields 0-50075  
 transition metal surfaces, mag. props. 0-44861  
 3d-transition metal-metalloid cryst. and glassy alloys, electronic struct. from magnetisation and Mossbauer meas. 0-29363  
 transition metal-rare earth intermetallics, two sublattice system with high competing single ion anisotropies, model 0-39767  
 transition metals and alloys, magnetisation in high mag. field, Arrott-Noakes plot 0-54919  
 trimethyl ammonium cobalt chloride, magnetisation temp. depend. 0-7128  
 $(\text{TTF})\text{Cu}_2\text{S}_4(\text{CF}_3)_4$ , spin Peierls system, mag. field effects 0-7123  
 $\text{TTF-Cu}_2\text{S}_4(\text{CF}_3)_4$ , spin-Peierls system, high-field phase 0-39816  
 type II superconductor, giant-vortex state, temp. depend. 0-7051  
 uniaxial ferromagnetic crystal, irreversible rotation processes 0-39768  
 Au-Fe (3.1-10.4 at.%) spin glass alloys, high field magnetisation curves 0-11213  
 $\text{Ba}_2\text{Co}_2\text{Zn}_{1-2}\text{Fe}_{1/2}\text{O}_{22}$ , mechanically oriented, topotactic prod. technique, mag. props. 0-35140  
 $\text{BaO-Fe}_2\text{O}_3$ , chemically coprecipitated, mag. props., orientation 0-15763  
 BeCu pressure clamp cell, for low temp. specific heat and magnetisation meas. 0-17956  
 Bi-MnBi, directionally solidified composite, processing parameter role on mag. props. 0-35352  
 $\text{Bi}_{0.6}\text{Mn}_{0.4}$ , magnetisation of ferromag. precipitates, effect of ultrasonic pulses 0-2121  
 C, char, amorphous, mag. interactions between localised spins 0-34587



## magnetisation continued

- $\text{Ca}_3\text{Mn}_2\text{Ge}_3\text{O}_{12}$ , mag. field induced transition 0-50094  
 $\text{Cd-Mg}$ , mag. susceptibility near  $2^{1/2}$ th order electron transition, non-linear magnetisation anal. (*Russian*) 0-44859  
 $\text{Cd}_{1-x}\text{Ag}_x\text{Cr}_2\text{Se}_4$ , Ag acceptor states effect on exchange interaction 0-20397  
 $\text{Cd}_{1-x}\text{In}_x\text{Cr}_2\text{Se}_4$ , electric, photoelectric and mag. props., metal-semicond. transition (*Russian*) 0-54738  
 $\text{CeAl}_2$  and  $\text{CeAl}_3$ , magnetisation and sp. ht. 0-20418  
 $\text{CeBi}$ , phase diagram in mag. field, hydrostatic press. effect 0-25132  
 $\text{CeFe}_2$ , magnetostriction and magnetisation 0-39844  
 $\text{CeIn}_3$ , magnetisation and sp. ht. 0-20418  
 $\text{Ce}_{1-x}\text{La}_x\text{Sn}_2$  ( $x=0$  to 1), mag. susceptibility and magnetisation, lattice parameters, X-ray and neutron diff. meas. 0-49675  
 $\text{CeRu}_2$ , H absorption induced Ce valence change, mag. and supercond. props. 0-50042  
 $\text{CeSn}_3$ , polarised neutron study of induced magnetisation 0-34594  
 $\text{CeX}$  ( $X=\text{P, As, Sb, Bi}$ ), neutron inelastic scatt. expts. 0-19674  
 $\text{Co}$ , itinerant ferromag., Fermi surface and single particle excitations 0-34350  
 $\text{Co}$ , Kerr equatorial effect freq. spectra anisotropy, dielectric permeability tensor (*Russian*) 0-55072  
 $\text{Co-Ni-Fe-Si(B)}$ , amorphous ribbon, magnetostriction meas. 0-15778  
 $\text{Co-Ni(Ti)(Cu)(Mn)}$ , cryst. struct. and stacking fault influence on mag. props. (*Russian*) 0-25164  
 $\text{Co-P}$ , amorphous, ferromag. antireson. 24 GHz microwave transmission, mag. props. 0-34778  
 $\text{Co-Pt}$ , atomic ordering props. and domain growth in strong pulsed mag. field (*Russian*) 0-54918  
 $\text{Co-Ti}$  (9 at.%), decomp. kinetics, elec. resist., hardness, and saturation magnetisation during ageing (*Russian*) 0-50587  
 $\text{Co}_{100-x}\text{B}_x$ , amorphous alloys, saturation magnetostriction and annealing behaviour 0-34739  
 $\text{CoCl}_2 \cdot 2\text{H}_2\text{O}$ , magnetisation temp. depend. 0-7128  
 $\text{CoCl}_2 \cdot 2\text{NC}_2\text{H}_5$ , magnetisation temp. depend. 0-7128  
 $\text{Co}_{70}\text{Fe}_{30}\text{B}_{14.5}$ , amorphous thin films, zero magnetostriction, high magnetisation 0-34708  
 $(\text{CoFeB})_{100-x}\text{Cr}_x$  thin films, magnetic props. and corrosion resist. 0-34709  
 $\text{Co}_2\text{Ga}_{1.95}\text{Fe}_{0.05}$ , mag. behaviour, Mossbauer effect and DC magnetisation meas. 0-50244  
 $(\text{Co}_{1-x}\text{Mn}_x)_2\text{B}$ ,  $0 \leq x \leq 1$ , magnetisation, lattice consts., press. depend. of Curie temp. 0-7137  
 $\text{Co}_2\text{Ni}_{1-x}\text{Cl}_2 \cdot 6\text{H}_2\text{O}$ , solid solution, mag. props. and phase diagram, calc. 0-7104  
 $\text{CoPt}_3$ , electrolytic films, saturation mag. induction, coercive fields, thickness depend. (*French*) 0-44883  
 $\text{CoS}_2$ , ferromagnet, elec. resist. and thermal expansion anomalies 0-15542  
 $\text{CoS}_2-x\text{Se}_x$ , magnetism and metamagnetic transition, neutron diff. and NMR meas. 0-15717  
 $\text{CoS}_2-x\text{Se}_x$ , conc. and temp. effects on metamagnetic transition 0-15716  
 $\text{CoU}_2\text{S}_5$ , mag. struct. and props. 0-11166  
 $\text{Cr-Fe}$ , spin-glass phase, magnetisation curve test for mag. ordering 0-11201  
 $\text{CrO}_2$ , amorphous thin films, Mossbauer and magnetisation data 0-34712  
 $\text{CrS-FeS}$ , sulphorspinel, struct. and elec. props. 0-49834  
 $\text{CrS}_2\text{Te}_{1-x}$  ( $x=0$  to 0.2), magnetic props. study 0-11194  
 $\text{Cs}_2\text{CoCl}_4$ , mag. susceptibility and magnetisation curve meas. 0-11176  
 $\text{Cs}_2\text{NaRCl}_6$  ( $R=\text{Ce, Nd}$ ), tetragonal distortion from cubic symm., magnetisation and NMR meas. 0-34403  
 $\text{Cu-Al-Mn}$ , partial decomp. of  $\beta_1$  phase, effect on mag. props. and martensitic transform. (*Russian*) 0-45306  
 $\text{Cu-Mn}$  spin glass, magnetisation curves, time depend. 0-15743  
 $\text{CuCl}_2 \cdot 2\text{H}_2\text{O}$ , magnetoelastic props. under press., antiferromagnetic resonance, lattice parameters 0-29598  
 $\text{CuMn}$ , magnetisation processes below freezing temp. 0-15748  
 $\text{Cu}(\text{NH}_4)_2\text{Br}_4 \cdot 2\text{H}_2\text{O}$  Heisenberg ferromagnet, mag. props. in mag. field 0-34637  
 $\text{dimethylammonium manganese tetrachloride}$ , 2D Heisenberg antiferromag., spin wave anal. 0-54879  
 $\text{Dy}$ , elastic constants, magnetoelastic contrib. 0-15777  
 $\text{DyGa}_3\text{O}_{12}$ , crystal field effect on paramag. props. of  $\text{Dy}^{3+}$  ion 0-50040  
 $\text{DyIG}$ , non-cryst., Mossbauer and magnetisation studies 0-44979  
 $\text{DyIG}$ , noncrystalline, Mossbauer and magnetisation data 0-34828  
 $\text{DyIn}_3$ , magnetisation 0-25106  
 $\text{Dy}_6\text{Mn}_{23}$ , magnetic moments, magnetisation 0-25094  
 $\text{Dy}_2\text{O}_3\text{SO}_4$ , magnetic struct. in antiferromag. and ferrimag. states 0-15695  
 $\text{Er}$ , elastic constants, magnetoelastic contrib. 0-15777  
 $\text{Er}$ , magnetisation and susceptibility in basal plane in strong mag. field (*Russian*) 0-50145  
 $\text{ErCrO}_3$ , magnetisation, NMR freq. temps. depend. weak ferromagnetic-antiferromagnetic spin reorientation transition 0-29631  
 $\text{Er}(\text{Fe}_{1-x}\text{Co}_x)_3$ , spin reorientation, easy axis of magnetisation 0-25144  
 $(\text{Er}_{0.6}\text{Ho}_{0.4})\text{Rh}_4\text{B}_4$ , reentrant supercond., magnetisation meas. near lower crit. temp. 0-25043  
 $\text{Er}_x\text{La}_{1-x}\text{Cu}$ , and  $\text{Er}_x\text{Y}_{1-x}\text{Cu}$ , antiferromag., mag. and resist. behaviour 0-34412  
 $\text{Er}_6\text{Mn}_{23}$ , magnetic moments, magnetisation 0-25094  
 $\text{Er}_x\text{Y}_{1-x}\text{Al}_2$ , mag. props. meas. and neutron diff. data 0-7126  
 $\text{Er}_x\text{Y}_{1-x}\text{FeO}_2$ , garnet, mag. anisotropy and magnetostriction 0-11189  
 $\text{EuB}_6$ , ferromag., mag. props. 0-2561  
 $\text{EuB}_6-x\text{C}_x$ , magnetisation, effects of C 0-25163  
 $\text{EuIG}$ , non-cryst., Mossbauer and magnetisation studies 0-44979  
 $\text{EuIG}$ , noncrystalline, Mossbauer and magnetisation data 0-34828  
 $\text{EuS}_{1-x}\text{Se}_x$ , mag. phase diagram, from temp. depend. of magnetisation 0-7105  
 $\text{Eu}_x\text{Sr}_{1-x}\text{S}$ , insulating spin glass, mag. props. 0-2589  
 $\text{Fe}$  complex, tetraphenylporphyrinate iron III bromide, mag. props., zero-field splitting 0-34584  
 $\text{Fe}$  film, ultra-thin Mossbauer spectroscopic studies of mag. props. 0-44970  
 $\text{Fe}$  film coated by  $\text{MgO}$ ,  $\text{MgF}_2$  and  $\text{Sb}$ , surface mag. 0-7196  
 $\text{Fe}$ , grade EA, plastically deformed, magnetoelastic props. (*Russian*) 0-44893  
 $\text{Fe}$ , itinerant ferromag., Fermi surface and single particle excitations 0-34350  
 $\text{Fe}$  particles in glass-like C matrix, identification and props. 0-11229  
 $\text{Fe}$  whiskers, magnetisation in small mag. fields, investigation using Kerr magneto-optic effect 0-2603

## magnetisation continued

- $\text{Fe-B}$  amorphous alloys, Mossbauer spectra, soft ferromag. props. 0-11302  
 $\text{Fe-B-C}$  amorphous alloys, effect of Si addition on mag. props. 0-34694  
 $\text{Fe-Cr-Co}$ , mechanism of coercive force 0-34674  
 $\text{Fe-Gd}$  amorphous film, struct. and mag. props. 0-20439  
 $\text{Fe-Ni}$  (23 wt.%), struct., composition changes during  $\alpha$  to  $\gamma$  transform., martensite plastic deformation influence (*Russian*) 0-11642  
 $\text{Fe-Si}$  (3 wt.%), polycrystal in mag. field, stress induced magnetisation, synchrotron Bragg refl. topography obs. 0-50139  
 $\text{Fe-Si-B}$  amorphous films, mag. props. 0-34710  
 $\text{Fe-SiO}$  multilayer film, interface magnetisation 0-7135  
 $\text{Fe}_{1-x}\text{B}_x$ , polycrystalline and amorphous sputtered films, Brillouin spectra 0-2775  
 $\text{Fe}_{100-x}\text{B}_x$ , amorphous alloys, saturation magnetostriction and annealing behaviour 0-34739  
 $\text{Fe}_{30}\text{B}_{70}$ , amorphous ferromag. metallic glass, stress-induced rot. of magnetisation, Mossbauer study 0-20445  
 $\text{FeBMO}_4$ ,  $M=\text{Mg, Cu, Co, Ni}$ , mag. props. meas. 0-34607  
 $\text{FeF}_3$ , canted antiferromag., spin echo spectra of  $^{57}\text{Fe}$  and  $^{19}\text{F}$  nuclei 0-2662  
 $\text{FeGe}_2$ , antiferromag., biquadratic exchange 0-2371  
 $\text{Fe}_{40}\text{Ni}_{38}\text{Mo}_4\text{B}_{18}$  ribbon, magnetic characterisation 0-34680  
 $(\text{Fe}_{0.04}\text{Ni}_{0.96}\text{Sb}_{0.30}\text{P}_{0.10}\text{B}_{10})$ , amorphous magnetisation, field and temp. depend. 0-39755  
 $\text{Fe}_{40}\text{Ni}_{40}\text{P}_{14}\text{B}_6$ , amorphous ribbon, influence of torsion on mag. props. 0-7138  
 $(\text{Fe}_{0.9}\text{Ni}_{1-x})_{75}\text{P}_{16}\text{B}_6\text{Al}_3$ , magnetisation temp. depend., spin wave theory 0-44927  
 $\text{Fe}_2\text{O}_3$  amorphous thin films, Mossbauer and magnetisation data 0-34712  
 $\gamma\text{-Fe}_2\text{O}_3$ , microstruct. and magnetisation 0-44875  
 $\text{Fe}_2\text{O}_4$  (magnetite), piezomag. response depth depend. rel. to tectonomagnetism as earthquake precursor 0-26465  
 $\text{Fe}_3\text{O}_4$ , magnetite, magnetoelc. effect at 77K, elec. field depend. of mag. anisotropy 0-29594  
 $\text{Fe}_{25}\text{Pd}_{50}\text{Au}_{25}$ , atomic ordering influence on mag. props. and elec. resistance (*Russian*) 0-7551  
 $\text{Fe}_2\text{Pd}_{82-x}\text{Si}_{18}$ , amorphous, magnetisation, magnetoresist., spin glass and ferromag. phases 0-34697  
 $\text{FeS}_2$ , oxidation, Mossbauer spectroscopic and magnetokinetic studies, 400-500°C 0-44880  
 $\text{Fe}_3\text{S}_4$ , galvanomagnetic props., resist. and Hall effect meas., 4.2-300K 0-54673  
 $\text{FeS}_{10}$ , polytypism, Fe diffusion near antiferromag. to ferrimag. transition 0-44830  
 $(\text{Fe}_{1-x}\text{V}_x)_2\text{Ge}$ , magnetic and X-ray studies 0-1966  
 $(\text{Gd,Bi})_3(\text{Fe,Ga})_3\text{O}_{12}$  epitaxial garnet film, nucl. tracks effect on mag. props. 0-11234  
 $\text{Gd-Co}$  amorphous ribbons, mag. props. and Invar effects 0-2574  
 $\text{GdFe}_2$ , easy direction of magnetisation 0-20535  
 $(\text{Gd}_{1-x}\text{Fe}_x)_1-x\text{Bi}_x$  amorphous films, saturation magnetisation, Kerr and Faraday rotation 0-40093  
 $\text{GdIn}_3$ , magnetisation 0-25106  
 $\text{Gd}_6\text{Mn}_{23}$ , magnetic moments, magnetisation 0-25094  
 $\text{Gd}(\text{Rh}_{1-x}\text{Fe}_x)_2$ ,  $x \leq 0.15$ , magnetisation and EPR studies 0-34767  
 $\text{H}$ , spin-polarised, density, magnetisation, compression and thermal leakage 0-44391  
 $^3\text{He}$ , adsorbed on Vycor glass under press., nature of phases, entropy and magnetisation expts. 0-49458  
 $^3\text{He}$ , solid, mag. ordering, NMR study 0-54470  
 $^3\text{He}$  superfluid, A-phase, transverse magnetisation relaxation and superfluid spin flows (*Russian*) 0-34265  
 $\text{Hf}(\text{Fe}_{1-x}\text{Co}_x)_2$ , mag. props., Mossbauer spectra and magnetisation meas. 0-39948  
 $\text{Hg}$ , liquid, ferromag., containing Fe particles, time depend. magnetisation 0-44877  
 $\text{Hg}_{3-x}\text{AsF}_6$ , linear chain compound, mag. field induced residual resist., anisotropic supercond. 0-24897  
 $\text{Hg}_{1-x}\text{Fe}_x\text{Te}$  mixed crystals, zero gap, magneto-optical evidence of exchange interactions 0-45045  
 $\text{Hg}_{1-x}\text{Mn}_x\text{Te}$ , mag. props., self-consistent two spin cluster model 0-54874  
 $\text{Ho-YIG}$ , magnetic props. in strong fields at low temp., Ising approx. calcs. (*Russian*) 0-54920  
 $\text{HoFe}_2\text{O}_4$ , magnetic props., 77-300K 0-11225  
 $\text{HoNi}_3$ , ferromag., magnetisation and paramag. susceptibility 0-25082  
 $\text{Ho}_2\text{O}_3\text{SO}_4$ , magnetic phase diagram, magnetisation and mag. susceptibility meas. 0-15720  
 $\text{Ho}_2\text{O}_3\text{SO}_4$ , magnetic struct. in antiferromag. and ferrimag. states 0-15695  
 $\text{Ho}_x\text{Y}_{1-x}(\text{Fe}_{0.1}\text{Co}_{0.9})_2$ ,  $^{57}\text{Fe}$  hyperfine interaction, mag. props., Mossbauer study 0-39951  
 $\text{Ho}_x\text{Y}_{1-x}\text{Sb}$ , mag. props. 0-34634  
 $\text{Ir}_3\text{Cr}$ , yield stress and saturation magnetisation 0-16389  
 $\text{La-Sm-Lu}$  iron garnet film grown as  $\text{NdGaG}$  substrates, mag. props. 0-44888  
 $\text{LaNi}_{1-x}\text{Mn}_x\text{O}_3$ ,  $^{55}\text{Mn}$  NMR study, magnetisation meas., ferromag. and Pauli paramag. components 0-7191  
 $\text{LaRu}_2$ , H absorption induced Ce valence change, mag. and supercond. props. 0-50042  
 $\text{La}_2\text{S}_4$ , high crit. mag. field supercond., elec. resist., sp. ht. and magnetisation 0-2532  
 $\text{LiTi}$ , substituted ferrite, cation distribution, Mossbauer, X-ray, neutron diff. study 0-28975  
 $\text{LiZn}$ , substituted ferrite, cation distribution, Mossbauer, X-ray, neutron diff. study 0-28975  
 $\text{Mg-rare earth dilute alloy}$ , mag. susceptibility and magnetisation 0-15689  
 $\text{MnAs}$ , generalised P-T phase diagram, mag. and structural phase transition 0-39780  
 $\text{Mn}_{1-x}\text{Fe}_x\text{As}$ , magnetic transition under high press., exchange striction model calcs. (*Russian*) 0-50096  
 $\text{Mn}_2\text{Fe}_{3-x}\text{O}_4$  ferrite film, exchange interaction depend. on conduction electrons (*Russian*) 0-34621  
 $\text{Mn}_{1+x}\text{Sb}$ , ferromag., mag. disturbance around Mn interstitials 0-54868  
 $\text{Mn}_{23}\text{Y}_6\text{D}_x$ , D atom location, neutron diff. study, and magnetism (*French*) 0-24426  
 $\text{Na-Fe}$  fluorophosphate glass, Mossbauer study, mag. and optical props. 0-16065  
 $\text{NaMnCl}_3$ , antiferromagnet, exciton self-localisation luminesc. and excitation spectra (*Russian*) 0-11456



**magnetisation continued**

- Nb-Hf (38 at.%) superconductor, peak effect, summation problem, mag. history flux pinning force 0-20362  
 Nb<sub>7</sub>Ga<sub>22-x</sub>Mn<sub>x</sub>, supercond. props., influence of Mn mag. impurities 0-54825  
 Nb<sub>80</sub>Ga<sub>20-x</sub>Mn<sub>x</sub>, supercond. props., influence of Mn mag. impurities 0-54825  
 Nd<sub>0.35</sub>Co<sub>0.65</sub> film, vac. evaporated, magnetisation ripple struct., TEM and defocused Lorentz microscopy 0-7136  
 NdFe<sub>2</sub>, preparation and mag. props. 0-25259  
 NdIn<sub>3</sub>, magnetisation 0-25106  
 NdO, mag. props., lattice consts., and X-ray absorpt. spectra 0-44798  
 (Nd<sub>0.5</sub>Sm<sub>0.5</sub>)<sub>2</sub>(Co<sub>0.7</sub>Fe<sub>0.3</sub>)<sub>17</sub>, mag. anisotropy 0-34622  
 Ni, band structure, rel. to lattice const., spin polarised APW calc., magnetisation meas. 0-20073  
 Ni crystals in strong mag. field, EM excitation and vel. dispersion of sound (*Russian*) 0-39837  
 Ni dispersions, semi-amorphous, on Al<sub>2</sub>O<sub>3</sub>-graphite, mag. characterisation 0-44876  
 Ni film, few atomic layers thick, transition from Pauli paramag. to band ferromag. 0-44885  
 Ni, hyperfine field and magnetisation, press. and temp. depend. 0-6795  
 Ni, itinerant ferromag., Fermi surface and single particle excitations 0-34350  
 Ni-Co (25 wt.%), single crystals, mag. annealing effect on magnetostriction and magnetisation (*Japanese*) 0-34744  
 Ni-Cr-Mo-Mn alloy 02KhN40MB, corrosion-resist, heat-resist., phys. and mech. props. 0-35411  
 Ni-Fe conductor, EM pulse shielding, magnetisation curves 0-28143  
 Ni-Fe-Cr, extraordinary Hall effect, elec. and mag. meas. at 77 and 300K 0-34421  
 Ni-Mn, hydrogenation kinetics, magnetisation, interstitial H influence 0-35528  
 Ni-SiO multilayer film, interface magnetisation 0-7135  
 Ni-Ti (9.6 wt.%), mag. study on phase decomposition (*Japanese*) 0-15758  
 Ni<sub>0.95</sub>S Fe, spin glass, spin flop in exchange field 0-34640  
 Ni<sub>3</sub>Al, itinerant ferromag., Fermi surface and single particle excitations 0-34350  
 NiF<sub>2</sub>, magnetisation and antiferromagnetic resonance freq. in mag. field (*Russian*) 0-34781  
 Ni<sub>1-3x</sub>Fe<sub>2+3x</sub>Vac<sub>0.2-0.3</sub> (Vac=cation vacancy), solid solns., cryst. lattice imperfections 0-39069  
 NiMn, high field magnetisation 0-2557  
 Ni<sub>3</sub>Mn, thermoremanent magnetisation and blocking temp. 0-34601  
 NiO (111) surfaces, antiferromag., mag. scattering by polarised LEED, spin polarisation effect in theory 0-29529  
 NiS film, electrolytically deposited, S content influence 0-44884  
 NiWO<sub>4</sub>, monoclinic antiferromag., domain struct. induced by strong mag. field 0-44856  
 NpFe<sub>2-x</sub>Co<sub>x</sub>Si<sub>2</sub>, mag. and hyperfine props. 0-7247  
 (Np<sub>1-x</sub>U<sub>x</sub>)Fe, Mossbauer spectra, magnetism and hyperfine interactions 0-20529  
 Pb-In-Ag, transport current distribution in longitudinal mag. field 0-25057  
 PbSe, electron gas magnetisation, energy band parameters determ., use of Faraday effect 0-45047  
 PbSe, Faraday effect and electron gas magnetisation, Kane two band model calcs. (*Russian*) 0-34899  
 Pb<sub>1-x</sub>Sn<sub>x</sub>Te, Faraday effect and electron gas magnetisation, Kane two band model calcs. (*Russian*) 0-34899  
 Pd-Fe-Mn, ferromag. and spin-glass props; comment 0-2591  
 Pd-Mn, Curie temp. and magnetisation, vol. depend. 0-34629  
 Pd-Mn, dil. alloy, very temp. magnetisation 0-34692  
 (Pd<sub>0.9965</sub>Fe<sub>0.0035</sub>)Mn<sub>0.05</sub>, ferromag. and spin-glass props. 0-2590  
 Pd<sub>2</sub>MnIn<sub>1-x</sub>Sb<sub>x</sub>, Heusler alloy, mag. order obs. 0-29528  
 Pr-Eu, dil., magnetisation, Mossbauer spectra 0-15928  
 PrCo<sub>5</sub>, uniaxial ferromag. cryst., irreversible rotation processes 0-39768  
 Pr(Co<sub>0.7</sub>Cu<sub>0.3</sub>)<sub>5</sub>, anomalous magnetisation curves 0-15757  
 PrFe<sub>2</sub>, preparation and mag. props. 0-25259  
 PrO, mag. props., lattice consts., and X-ray absorpt. spectra 0-44798  
 Pr<sub>2</sub>Ti, critical fluctuations temp. depend. 0-25160  
 Pr<sub>2</sub>Ti, transition temp. and magnetisation 0-25161  
 RM<sub>2</sub>Al<sub>8</sub> (M=Cr, Mn, Fe, Cu), magnetism and hyperfine interactions 0-25256  
 Rb<sub>2</sub>MnCl<sub>4</sub>, 2D Heisenberg antiferromag. spin wave analysis 0-54879  
 ScAl<sub>2</sub>Er(Dy)(Nd), dil., EPR and mag. susceptibility 0-15797  
 (ScLu<sub>1-x</sub>)<sub>2</sub>V<sub>2</sub>O<sub>7</sub> 0-29547  
 SiH<sub>4</sub>, magnetisation relax., appl. of theory of spin-lattice relax. 0-50214  
 SmCO<sub>3</sub>, based permanent magnets, props. and cryst. orientation (*Russian*) 0-20431  
 Sm(Co<sub>0.86-x</sub>Cu<sub>0.14</sub>Fe<sub>x</sub>)<sub>7</sub>, permanent magnet, sintering and heat treatment effects 0-39817  
 SmO, mag. props., lattice consts., and X-ray absorpt. spectra 0-44798  
 Sm<sub>0.4</sub>R<sub>0.4-x</sub>M<sub>0.2</sub>Co<sub>5</sub> (R=Gd, Dy, M=Pr, Nd), temp. coeff. of magnetisation 0-34688  
 Tb, critical magnetic studies 0-15745  
 Tb, elastic constants, magnetoelastic contrib. 0-15777  
 Tb, ferromagnet, field depend. of elastic const. c<sub>66</sub> 0-15181  
 (Tb<sub>0.27</sub>Dy<sub>0.73</sub>)Fe<sub>2</sub>, magnetisation, ferromag. domains 0-25162  
 TbFe<sub>2</sub>, magnetisation, ferromag. domains 0-25162  
 TbFe<sub>2</sub>, magnetoelastic props., magnetostriction hysteresis (*Russian*) 0-29590  
 TbNi<sub>5</sub>, ferromag., magnetisation and paramag. susceptibility 0-25082  
 Tb<sub>1-x</sub>Co<sub>0.5+0.1x</sub>, exchange interactions and magnetocrystalline anisotropy 0-34618  
 ThFe<sub>2</sub>H<sub>14.2</sub>, Mossbauer spectra, mag. props. 0-15852  
 Tm<sub>2</sub>Y<sub>1-x</sub>Se, Kondo effect, Van Vleck behaviour 0-25085  
 UAl<sub>2</sub>, high field, high press. mag. props. 0-11172  
 UAs, magnetisation, ferrimag. spin struct. 0-7088  
 U<sub>3</sub>As<sub>4</sub>, mag. anisotropy, magnetisation meas. 0-50085  
 UGe<sub>3</sub>, magnetisation density, neutron scatt. meas. 0-50038  
 UPb<sub>3</sub>, crystal field energy levels, magnetisation and susceptibility, neutron spectra obs. 0-50064  
 USb<sub>0.8</sub>Te<sub>0.2</sub>, magnetisation and neutron meas., mag. moments 0-15703  
 USb<sub>0.9</sub>Te<sub>0.1</sub>, multiaxial mag. structure 0-15696  
 UTe, magnetisation and neutron meas., mag. moments 0-15703  
 (U<sub>1-x</sub>Th<sub>x</sub>)Sb, magnetisation, U valence change 0-7089  
 V<sub>3-x</sub>Cr<sub>x</sub>Si<sub>3</sub>, x=0 to 3, struct., supercond. and mag. props. 0-1962  
 V<sub>3</sub>O<sub>7</sub>, microscopic mag. props., NMR 0-7177

**magnetisation continued**

- V<sub>2</sub>S<sub>8</sub>, paramag. cryst., struct. factors using polarised neutron diff. 0-15691  
 YAl<sub>2</sub>Er(Dy)(Nd), dil., EPR and mag. susceptibility 0-15797  
 YCrO<sub>3</sub>, magnetisation, NMR freq. temps. depend. weak ferromagnetic-antiferromagnetic spin reorientation transition 0-29631  
 Y<sub>2</sub>Er<sub>1-x</sub>Al<sub>2</sub>, paramag. anisotropy 0-39737  
 Y<sub>2</sub>Fe<sub>5-x</sub>Ga<sub>x</sub>O<sub>12</sub>, substituted garnet, floating zone grown, FMR line width, saturation magnetisation 0-29626  
 Y(Fe<sub>1-x</sub>Ir<sub>x</sub>)<sub>2</sub>, magnetisation, mag. hyperfine field 0-20531  
 Y(Fe<sub>1-x</sub>Mn<sub>x</sub>)<sub>2</sub>, mag. order onset 0-25135  
 Y(Fe<sub>1-x</sub>Mn<sub>x</sub>)<sub>2</sub>, Mossbauer spectra and mag. props. 0-39952  
 Y<sub>2</sub>(Fe<sub>1-x</sub>Mn<sub>x</sub>)<sub>23</sub>, struct. and mag. props. 0-25083  
 Y<sub>1-x</sub>Gd<sub>x</sub>Co<sub>5</sub>, exchange interactions and magnetocrystalline anisotropy 0-34618  
 Y<sub>1-x</sub>Gd<sub>x</sub>Fe<sub>3-x</sub>Al<sub>3</sub>O<sub>12</sub>, solid solns., IR absorpt. spectra, physical props. 0-55082  
 Y<sub>1-x</sub>Gd<sub>x</sub>Fe<sub>3</sub>O<sub>12</sub>, solid solns., IR absorpt. spectra, physical props. 0-55082  
 YIG, distrib. of easy magnetisation axes near edge dislocation (*Russian*) 0-44891  
 YIG, ferromagnetic resonance and magnetostatic waves in inhomogeneous internal field (*Russian*) 0-54954  
 YIG film-dielectric layer-conductor struct., magnetostatic bulk wave propagation dispersion relations 0-54925  
 YIG, polariser neutron study of covalency effects 0-2552  
 YIG-rare earth garnet solid solutions, magnetisation temp. depend. calcs. 0-20388  
 (Y<sub>1-x</sub>Lu<sub>1-x</sub>)<sub>2</sub>V<sub>2</sub>O<sub>7</sub>, semiconducting ferromag. pyrochlore, mag. props. 0-29547  
 YM<sub>2</sub>Al<sub>8</sub> (M=Cr, Mn, Fe, Cu), magnetism and hyperfine interactions 0-25256  
 Y<sub>6</sub>Mn<sub>23</sub>, magnetic moments, magnetisation 0-25094  
 Y<sub>1-x</sub>Nd<sub>x</sub>Co<sub>5</sub>, exchange interactions and magnetocrystalline anisotropy 0-34618  
 YNi<sub>3</sub>, loss of ferromagnetism after H<sub>2</sub> absorpt., Pauli paramag. props. 0-34588  
 Y<sub>2</sub>Ni<sub>1-x</sub>, amorphous, high press. magnetisation and Curie temp. 0-20442  
 YRh<sub>2</sub>B<sub>4</sub>, supercond., anomalous cond.-electron polaris. 0-25047  
 Yb, FCC phase, low temp. mag. props., impurity effects 0-20387  
 Yb-Eu alloys, mag. ordering, magnetisation meas. 0-7081  
 YbBe<sub>3</sub>, mag. props. and EPR meas. 0-11175  
 YbFe<sub>2</sub>, preparation and mag. props. 0-25259  
 Zr(Fe,Al)<sub>2</sub>, weak itinerant ferromag., mag. anisotropy effects on mag. isotherms 0-11187  
 (Zr<sub>1-x</sub>Nb<sub>x</sub>)Fe<sub>2</sub>, magnetovolume effects and Invar characters 0-15773  
 Zr<sub>1-x</sub>Nb<sub>x</sub>Zn<sub>2</sub>, microscopic mag. props., NMR investigation 0-15807

**magnetisation reversal**

- current threshold sensor, struct. and operational features 0-34689  
 ferromagnetic fine particles, stability of magnetisation curling mode and magnetisation helicoid struct. 0-11227  
 film, pulse magnetic reversal in high freq. field in ferromag. reson. range (*Russian*) 0-11230  
 soft ferromagnetic cylinder, point singularities and magnetisation reversal 0-11223  
 Co<sub>5</sub>Sm, magnetic domains, nucleation and pinning, magneto-optical Kerr effect 0-39811  
 CuMn, spin glass, mag. hysteresis meas. 0-34691  
 CuMn, spin glass, remanence, new approach from zero field NMR 0-34785  
 Fe-Co-V, Vicalloy, magnetisation reversal by stretching and twisting 0-34733  
 Fe-Ni-Co-Mo-Ge alloy 40NKM, excess mag. noise after various thermomag. treatments (*Russian*) 0-29575  
 Fe<sub>80</sub>B<sub>10</sub>Si, metallic glass, large uniaxial magnetostrictive anisotropy, magnetisation reversal 0-34736  
 FeSi, domain struct. and magnetisation reversal, time depend. neutron depolarisation 0-50138  
 Fe-Fe-Nb, cold-worked and aged, mag. props. and microstruct. 0-34690  
 Ni-Fe films, magnetisation reversal in narrow strips, TEM study 0-34720  
 SmCo<sub>5</sub> films, struct. transformations effect on coercive force and mag. reversal (*Russian*) 0-20436  
 Sm(Co<sub>0.84</sub>Cu<sub>0.16</sub>)<sub>6.9</sub>, microstruct. and domain struct., mag. reversal (*Russian*) 0-20429

**magnetism**

- see also antiferrimagnetism; antiferromagnetism; band model of magnetism; diamagnetism; electromagnetism; ferrimagnetism; ferromagnetism; geomagnetism; Heisenberg model; Ising model; magnetic moments; magnetic monopoles; metamagnetism; paramagnetism; rock magnetism; stellar magnetism; superparamagnetism; weak ferromagnetism; X-Y model  
 bibliography of William Fuller Brown, Jr 0-8751  
 conference, 2nd joint INTERMAG-MMM, New York, USA (July 1979) 0-27031  
 conference, Munster, Germany (March 1979) 0-12843  
 David Ausubel learning theory as reference system for content organisation in physics 0-22172  
 developments during past 25 years, personal reminiscences 0-36829  
 experimental magnetism, book 0-8747  
 magnetostatic problems, soln. by MAGGY2 problem package 0-28134  
 neutron scattering and magnetism, conference, Julich, Germany (Aug. 79) 0-41934  
 periodic lattice, theory of coexistence of supercond. and magnetism, supercond. transition temp. 0-34543  
 renormalisation group anal. 0-17838  
 superconductor, thermodynamics of magnetism and supercond., mol. field theory 0-34668  
 teaching w.r.t. chemistry, guide to units 0-12871  
 theoretical developments from 1949-1974, personal memories 0-31438

**magneto-optical devices**

- bounce-cavity modulator, direct AM 0-5769  
 circulator, polarisation independ., for optical fibre transmission systems 0-23779  
 circulator, polarization-independent, configuration method 0-38095  
 Faraday rotation isolator, fibre-optic communication applications 0-48408  
 Faraday rotator and Glan-Taylor prisms, circulator for optical fibre transmission 0-23769  
 isolator, based on Faraday rotator, for diode laser, struct. simplification 0-1209  
 meas. of Kerr and Faraday effects, with accuracy up to 0.001° 0-47087



**magneto-optical devices continued**

modulators, switches and deflectors, physical principles and Czechoslovak developments (*Czech*) 0-19090  
ring laser gyroscope, Raytheon four freq., mag. mirror, Faraday and Zeeman biasing 0-1269

**magneto-optical effects**

see also Faraday effect; Kerr magneto-optical effect; magnetic circular dichroism; magnetoabsorption; magnetorefractance; optical constants; Zeeman effect  
alkoxy-cyanobiphenyls, isotropic phase, Cotton-Mouton effect 0-16013  
alkyl-cyanobiphenyls, isotropic phase, Cotton-Mouton effect 0-16013  
atomic system, hydrogenlike, polarised monochromatic laser radiation absorption in electronic transitions, DC mag. field effects 0-9563  
benzene, magneto-optic rotatory dispersion curves 0-45040  
cubic ferrite garnet, diffracted light polarisation characts., spin and magnetoelastic waves 0-20614  
EM wave, stimulated Brillouin scatt., transverse static mag. field effect 0-50355  
Fabry-Perot spectrometer instrumental function determ., Voigt function assignation (*Spanish*) 0-52322  
Faraday rotation, and mag. field dependence of exciton absorption lines in semiconductors, high mag. fields 0-27321  
ferrite, light diffr. by magnetisation inhomogeneities, multiple refl. 0-2733  
ferromagnet, light scatt. by spin waves 0-45086  
ferromagnetic semiconductor, refr. index variation in strong alternating mag. field 0-23741  
fluids, polarisation state of light scatt. in elec. and mag. fields, symmetry indications 0-29751  
garnet films, (111)-oriented, cubic anisotropy meas. 0-54924  
garnet films, susceptibility of parallel stripe domain lattices, magneto-optical study 0-54930  
gas laser, theory of polarisation effects 0-23660  
ground state Zeeman splittings, reson. Raman spectra and mag.-optical activity 0-5579  
light scattering, space-time symmetry rel. to light scatt. in elec. and mag. fields 0-29750  
liquid, of chiral mols., magnetorefractive effect, linear 0-25343  
liquid short chain molecules, optical investig. of mol. motions 0-40123  
magnetolectric susceptibilities, phenomenological rules for computation 0-55068  
naphthalene, triplet exciton annihilation and triplet spin relax. 0-29792  
narrow band gap semiconductors, conference, Warsaw, Poland (Sept. 1977) 0-49703  
nematic layers, optical phase difference and capacitance, elec. and mag. field depend. 0-28911  
nematic liquid cryst., Fredericksz transition in mag. field, domain struct. 0-33880  
nematic-isotropic transition, correlation functions, Cotton-Mouton coeffs. 0-15228  
nonmutual optical effects, in an external mag. field 0-40097  
perfluorocarbons,  $\gamma$ -irrad. solns., mag. field effect on fluorese. 0-55677  
rare earth garnets, prep. and props. book contrib. 0-44193  
reabsorption method at high optical densities for two identical tubes 0-38528  
regular domain structs., magneto-optical characts., optoelectronics appls. 0-40098  
ring laser, nonreciprocal effects on appl. of transverse mag. field to active medium 0-53341  
ring laser placed in longit. mag. field, nonlinear nonreciprocity effects 0-43377  
scattering of light by crystals, in book 0-2774  
semiconductor plasma, magnetised, stimulated Brillouin scatt. 0-33085  
semiconductors, p-type, mag. oscills. of momentum distribution of hot photoexcited electrons (*Russian*) 0-2854  
semiconductors, relax. and reson. struct. in magneto-optical spectra 0-29723  
steel, austenitic, thermonuclear reactor walls, ferromagnetic layer form. magneto-optical testing method 0-35465  
p-terphenyl, triplet exciton annihilation and triplet spin relax. 0-29792  
vibrational magneto-optical effect in cryst. 0-45043  
Voigt contour of spectral line, nomogram for parameters determ. 0-52321  
zero gap semiconductor, magneto-optical and impurity effects 0-6721  
AgBr, new shoulder in luminesc. spectra, triplet excitons 0-20706  
 $\text{Al}_x\text{Ga}_{1-x}\text{As}$ , optically magnetised, luminescence polarisation anisotropy, hysteresis effect symmetry props. 0-34982  
 $\text{Cd}_{1-x}\text{Mn}_x\text{Te}$ , exchange interaction, magneto-optical spectra 0-25348  
 $\text{CdBr}_2\cdot\text{Co}$ , spectroscopic studies of interactions 0-29769  
 $\text{CdCl}_2\cdot\text{Co}$ , spectroscopic studies of interactions 0-29769  
 $\text{CdCr}_2\text{Se}_4$ , magnetic red shift origin, specular reflectivity, band struct. 0-40127  
 $\text{CdCr}_2\text{Se}_4$ , refr. index variation in strong alternating mag. field 0-23741  
 $\text{CoF}_2$ , 180-degree antiferromag. domain obs. by new magneto-optical effect 0-44855  
 $\text{CoF}_2$ , linear and quadratic mag. birefr. 0-16005  
 $\text{CrO}_2$ , acicular particle suspensions, mag. props., optical meas. 0-44874  
 $\text{CsBr}$ , self-trapped excitons, magneto-optical props., 1.3-50K 0-49606  
 $\text{CsI}$ , self-trapped exciton electronic struct., semi-empirical mol. orbital method 0-49605  
 $\text{CsI}$ , self-trapped excitons, magneto-optical props., 1.3-50K 0-49606  
 $\text{CsPbCl}_3$ , exciton states, magneto-optical investigation 0-29328  
 $\text{Cu}$ , fine interaction of surface electrons, IR spectra 0-16041  
 $\text{CuBr}_2$ ,  $^1\text{S}$  exciton triplet state, magneto-optical props. 0-25345  
 $\text{CuBr}_4^{2-}$ , ground state Zeeman splittings, reson. Raman spectra and mag.-optical activity 0-5579  
 $\text{Eu-Fe}$  garnet, light mag. linear birefringence and dichroism near absorption band (*Russian*) 0-55063  
 $\text{EuO}$ , light scatt. by spin waves 0-45086  
 $\text{EuO}(\text{S})(\text{Se})(\text{Te})$ , cryst. and electronic struct., mag., elec., and optical props., book contrib. 0-39760  
 $\text{EuS}$  films, ferromag., optical spectra and light scatt. from spin waves 0-16116  
 $\text{EuTe}$ , antiferromagnet, phonon Raman scatt. from spin superstructures 0-16030  
 $\text{Fe}$ , light scatt. by spin waves 0-45086  
 $\text{Fe}$ , light scatt. from surface and bulk thermal magnons 0-45087  
 $\text{FeF}_2$ , one-magnon Raman scatt., anomalous behaviour of anti-Stokes-Stokes intensity ratio 0-40115

**magneto-optical effects continued**

$\gamma\text{-Fe}_2\text{O}_3\cdot\text{Cr}$ , pure and doped, acicular particle suspensions, mag. props., optical meas. 0-44874  
 $\text{GaAs}$ , donor van der Waals interactions, spectral lineshapes 0-11450  
 $\text{GaAs}$ , hot photoluminescence depolarisation in mag. field, 0.4 eV energy state electron lifetime (*Russian*) 0-16086  
 $\text{GaAs-AlGaAs}$  DH injection laser, emission energy, wavelength depend. in strong mag. fields 0-48248  
 $\text{GaSe}$ , exciton magneto-optical spectra 0-25347  
 $\text{GdAlO}_3\cdot\text{Cr}^{3+}$ , mag. field effects on fluorese. 0-2850  
 $\text{GdCoMo}$  amorphous films, susceptibility of parallel stripe domain lattice, magneto-optical study 0-54930  
 $\text{GdS}$ , meas. of opto-magnetic interactions at low mag. fields 0-2735  
 $\text{Ge}$ , electron-hole drop and exciton atmosphere 0-6748  
 $\text{Ge}$ , electron-hole drop luminesc., phonon wind induced anomalous depend. at low mag. fields 0-34980  
 $\text{Ge}$ , electron-hole drops, IR magnetoplasma absorptions 0-6728  
 $\text{Ge}$ , electron-hole liq. thermalisation between mag. field split, valleys 0-25444  
 $\text{Ge}$ , magnetoluminescence of electron-hole liq. 0-29790  
 $\text{H}$ , in strong magnetic field,  $\text{so}(4,2)$  algebra use in perturbation theory 0-47845  
 $\text{H}$ , strongly bound states in intense mag. field 0-37721  
 $\text{He-Ne}$  laser, simultaneous oscillation at 0.63 and 3.39  $\mu\text{m}$ , output power depend. on loss in mag. fields (*Japanese*) 0-32959  
 $\text{He-Ne}$  ring laser placed in longit. mag. field, nonlinear nonreciprocity effects 0-43377  
 $\text{Hg}_{1-x}\text{Cd}_x\text{Te}$ , magneto-optical and impurity effects 0-6721  
 $\text{n-HgCr}_2\text{Se}_4$ , ferromagnetic semiconductor, plasmon refl., 86 to 320K 0-50346  
 $\text{Hg}_{1-x}\text{Mn}_x\text{Te}$ , magneto-optical and impurity effects 0-6721  
 $\text{HgSe}$ , Fermi surface anisotropy parameters, magneto-optical effect 0-25350  
 $\text{HgSe}$ , magneto-optical and impurity effects 0-6721  
 $\text{HgTe}$  type semiconductors, spin-flip transitions in magneto-optics and magneto-transport 0-50306  
 $\text{In}_{1-x}\text{Ga}_x\text{Sb}$ , band parameter variations 0-20084  
 $\text{n-InSb}$ , magneto-optical transitions from deep levels, photocond. obs. 0-55069  
 $\text{n-InSb}$ , optical phonon emission in intraband magneto-optical transitions, photocond. meas. 0-34481  
 $\text{InSb}$  type semiconductor, spin-flip transitions in magneto-optics and magneto-transport 0-50306  
 $\text{InSb}$  type semiconductors, shallow donor states in magneto-optical props. 0-6785  
 $\text{IrCl}_6^{2-}$ , ground state Zeeman splittings, reson. Raman spectra and mag.-optical activity 0-5579  
 $\text{KBr:Ti}$ , Jahn-Teller system, negative mag. circular polarisation in emission spectrum 0-20694  
 $\text{KCl:Ti}$ , Jahn-Teller system, negative mag. circular polarisation in emission spectrum 0-20694  
 $\text{Kl:Ti}^{3+}$ ,  $A_1$  emission, mag. circular polarisation, WKB approx. for non-radiative transition rate 0-55180  
 $\text{Kl:Ti}$ , Jahn-Teller system, negative mag. circular polarisation in emission spectrum 0-20694  
 $\text{KMgF}_3\cdot\text{Ni}$ , Ni-Ni pair optical spectra 0-45042  
 $\text{LaF}_3\cdot\text{Pr}^{3+}$ , ultrahigh resolution photon echo spectroscopy 0-28285  
 $\text{MgCl}_2\cdot\text{Co}$ , spectroscopic studies of interactions 0-29769  
 $\text{MnF}_2$ , magnetic, thermal, elastic refraction of light, mag. order influence on refractive index (*Russian*) 0-34880  
 $\text{Na}_3\text{Pr}(\text{C}_4\text{H}_9\text{O}_5)_3\cdot 2\text{NaClO}_4\cdot 6\text{H}_2\text{O}$ , single cryst., forbidden  $A_1 \rightarrow A_1$  transition, mag. field induced intensification 0-50302  
 $\text{Ni}$ , light scatt. from surface and bulk thermal magnons 0-45087  
 $\text{Ni}_3\text{Fe}_2\text{Cr}_{1-x-y}$  films, struct., mag. props., and corrosion resist. 0-34706  
 $\text{Pb}_{1-x}\text{Ge}_x\text{Te}$ , n- and p-type, effective masses 0-44481  
 $\text{PbI}_2$ , exciton magneto-optical spectra 0-25347  
 $\text{Pb}_{1-x}\text{Sn}_x\text{Te}$ , inter- and intraband magneto-optical transitions 0-25346  
 $\text{TbPO}_4$ , linear optical birefr. meas. near bicritical point 0-15719  
 $\text{Ti}$ , photo-excited carriers, far IR magneto-spectroscopy 0-50343  
 $\text{Vl}_2$ , antiferromagnet, phonon Raman scatt. from spin superstructures 0-16030  
 $\text{YAlO}_3\cdot\text{Pr}^{3+}$ , ultrahigh resolution photon echo spectroscopy 0-28285  
 $\text{YIG}$  bubble films, light scatt. from spin waves, hysteresis meas. by Voigt effect 0-15770  
 $\text{YIG}$ , spin and magnetoelastic waves on longit. mag. pumping, optical obs. (*Russian*) 0-29727

**magnetoabsorption**

disordered-semiconductors, optical magnetoabsorption coeff. calc. in strong mag. field 0-16011  
ferromagnetic semiconductors, dielectric function depend. on magnetisation, light absorpt. coeff. (*Russian*) 0-15467  
ruby,  $\text{Cr}^{3+}$  ion doped, R-line region, absorpt. spectrum, dispersion rel. to mag. field 0-2732  
semiconductor, interband absorpt. in strong parallel mag. and elec. fields 0-6799  
semiconductor, optically anisotropic, effect of modulation of mag. field on absorption 0-34898  
semiconductors, nondegenerate, free carrier absorpt. in quantising mag. fields 0-45044  
Voigt effect, reson. absorpt. description 0-30302  
 $\text{Bi}_{1-x}\text{Sb}_x$ , far IR magnetoabsorption, band struct. study 0-50351  
 $\text{CaF}_2\cdot\text{Dy}$  crystal with M centre, antiresonance line, mag. field effect 0-55138  
 $\text{Cd}_{1-x}\text{Mn}_x\text{Te}$  mixed crystals, excitonic magnetoabsorption 0-40095  
 $\text{CdTe}$ , oscillatory magnetoabsorpt. spectra 0-40096  
 $\text{DyIG}$ , magneto-optical absorption, near IR 0-40094  
 $\text{Hg}_{1-x}\text{Cd}_x\text{Te}$ , n-surface inversion layers study 0-25017  
 $\text{Hg}_{1-x}\text{Fe}_x\text{Te}$  mixed crystals, zero gap, magneto-optical evidence of exchange interactions 0-45045  
 $\text{HgTe}$ , long-wavelength magneto-absorptions 0-11397  
 $\text{HgTe}$ , zero-gap semicond., absorpt. spectrum in mag. field 0-11370  
 $\text{InSe}$ , high field magnetoabsorpt. of hydrogenic excitons at second direct gap 0-6729

**magnetoacoustic effects**

see also magnetoacoustic resonance  
elastic properties of magnetic materials, review 0-7142  
ferromagnet, planar, US attenuation, spin-phonon coupling, magnons and magnetostriction contrib., calc. 0-34611  
ferromagnet, pure and random uniaxial with dipolar interaction, US attenuation 0-11239



**magnetoacoustic effects continued**

- graphite, giant quantum attenuation of sound waves 0-54741  
 Ising type model, elastically coupled, effects of dipolar forces on crit. sound attenuation in uniaxial systems 0-50158  
 liquid-solid interface, plane sound wave reflection and refraction in mag. field 0-38150  
 many-domain magnetism, phenomenological theory of EM and sound energy attenuation 0-7140  
 metallic film, conduction electron surface scatt. process, magnetoacoustic oscillations (*Russian*) 0-15575  
 metals, anomalous sound propag. by cond. electrons 0-11048  
 oscillation excitation in strongly inhomogeneous plasma 0-38641  
 Permalloy film, domain nucleation using low intensity US 0-34731  
 plasma, cold, bounded and cylindrical, viscous damping of magnetoacoustic oscillations 0-24151  
 plasma, weakly inhomogeneous, nonlinear magnetoacoustic waves 0-48867  
 semiconductor subjected to mag. and US fields, EM radiation gain 0-48201  
 semiconductors, ferromagnetic, parametric amplification of coupled spin, helical and acoustic waves (*Russian*) 0-2621  
 steel, Cr, EM excitation and recording of US 0-34748  
 superconductor, intermediate state, magnetoacoustic size effect (*Russian*) 0-7047  
 underwater explosions and implosion, generation of sonomagnetic pulses 0-43510  
 Bi, magnetoacoustic attenuation, line shape anal. 0-2429  
 Bi, US attenuation in strong mag. fields, electron-hole correlation effects 0-11049  
 BiMn, with ferromag. inclusions, magnetisation changes by US pulses 0-34732  
 Bi<sub>1-x</sub>Sb<sub>x</sub>, magnetoacoustic attenuation 0-2428  
 Bi<sub>1-x</sub>Sb<sub>x</sub>, magnetoacoustic attenuation, line shape anal. 0-2429  
 CsNiF<sub>3</sub>, planar ferromagnet, US attenuation, spin-phonon coupling, magnons and magnetostriction contrib., calc. 0-34611  
 Cu, carrier scattering rate, temp. dependence, magnetoacoustic experiments 0-44671  
 In, helicon resonance acoustic satellites, flexural acoustic wave spectrum (*Russian*) 0-2415  
 In, US velocity dispersion in external mag. field 0-20446  
 n-InSb, non-degenerate semicond., magnetoacoustic effect 0-20257  
 Ni crystals in strong mag. field, EM excitation and vel. dispersion of sound (*Russian*) 0-39837  
 Sn, sound absorption giant resonance, produced by coherent mag. breakthrough (*Russian*) 0-6700  
 Sn, sound attenuation and velocity depend. on mag. field (*Russian*) 0-29446  
 Tb<sub>0.1</sub>Dy<sub>0.9</sub>Fe<sub>2</sub>, sound velocity mag. field and temp. depend. elastic moduli calcs. 0-39839  
 V<sub>2</sub>Si, US anomaly when cooled below martensitic and supercond. transition temps. 0-20354  
 YIG, dilute, magnetoacoustic surface wave excitation by RF field on Bloch walls 0-25178  
 YIG substrates, magnetoelastic surface waves, magnetostatic reson. anal. 0-20441

**magnetoacoustic resonance**

- see also *ferroacoustic resonance*  
 canted magnetic struct. crystals, magnetoacoustic resonance, elastic vibrations 0-29599  
 ferrite, magnetoacoustic reson. in strong mag. field 0-11309  
 metals and alloys, EM acoustic reson. for elastic moduli meas. 0-15573

**magnetoacoustics** see *magnetoacoustic effects***magnetocaloric effects**

- see also *magnetic cooling; thermomagnetic recording; thermomagnetic treatment*  
 Al<sub>2</sub>O<sub>3</sub>:V<sup>3+</sup>, magnetocaloric effect in high magnetic fields 0-25140  
 Br-graphite, intercalation cpd., magnetothermal oscill. and charge-density waves 0-11199  
 CrB<sub>2</sub>, CrB, and Cr<sub>2</sub>B<sub>3</sub>, mag. and thermal props. at low temps. 0-20385  
 EuO, magnetocaloric effect in high magnetic fields 0-25140  
 Fe-Ni(Cr), Invar, exchange interactions between ferromag. and antiferromag. components 0-29545  
 HoFe<sub>2</sub>O<sub>4</sub>, magnetic props., 77-300K 0-11225  
 Ni complex, Ni(C<sub>2</sub>H<sub>5</sub>NO)<sub>6</sub>(ClO<sub>4</sub>)<sub>2</sub>, field induced antiferromag., magnetocaloric effect 0-29551  
 Tb, magnetocaloric effect in high magnetic fields 0-25140

**magnetocrystalline anisotropy** see *magnetic anisotropy***magnetoelastic effects**

- amorphous ferromagnetic alloys, micromagnetic eqns. for case of dipolar and magnetocryst. fluctuations 0-11171  
 diethylammonium manganese chloride, antiferromag., low temp. luminesc. spectra, magnetoelastic effect 0-2810  
 dimethylammonium manganese chloride, antiferromag., low temp. luminesc. spectra, magnetoelastic effect 0-2810  
 elastic properties of magnetic materials, review 0-7142  
 ferromagnet, cubic, elastic props., group theoretical approach 0-29600  
 ferromagnetic beams, prismatic elastic, deformation by external mag. field 0-34749  
 magnetothermoelastic interactions in cylindrical conductor, mechanocaloric effect 0-7139  
 many-domain magnetism, phenomenological theory of EM and sound energy attenuation 0-7140  
 orthorhombic ferrimagnets, domain wall motion at near sonic velocity, magnetoelastic interactions 0-34683  
 rare earth alloys, RFe<sub>2</sub>, magnetostriction studies, book contrib. 0-39846  
 rare earth alloys and intermetallic cpds., US attenuation, temp. and mag. field depend. 0-15195  
 rare earth compounds, hexagonal, cryst. field effect in thermal expansion 0-49390  
 rare earth intermetallics, quadrupole interactions, magnetoelasticity 0-15489  
 rare earth intermetallics, structural instabilities 0-24587  
 rare earth-Co alloys, ferromag., first and second order transitions 0-34631  
 semiconductors, antiferromagnetic resonance rel. to surface impedance, magnetoelastic contrib. 0-50200  
 steel, types 45 and U8, plastically deformed, magnetoelastic props. (*Russian*) 0-44893  
 Al, fluxural oscillations in longitudinal mag. field, sound attenuation, magnetoelasticity (*Russian*) 0-54844

**magnetoelastic effects continued**

- CeBi, magnetoelastic effects, anisotropic mag. behaviour 0-25176  
 CeSb, magnetoelastic effects, anisotropic mag. behaviour 0-25176  
 Co<sub>90</sub>B<sub>10</sub>, amorphous metal ribbon, stresses, magnetoelastic anisotropy and zero-field mag. domain struct. 0-44896  
 Er, elastic constants, magnetoelastic contrib. 0-15777  
 ErCu, magnetic excitations 0-25115  
 Fe, grade EA, plastically deformed, magnetoelastic props. (*Russian*) 0-44893  
 Fe-Cr-B, amorphous, Elinvar and Invar charact. (*Japanese*) 0-11832  
 Fe<sub>81.5</sub>B<sub>14.5</sub>Si<sub>4</sub>, amorphous metal ribbon, stresses, magnetoelastic anisotropy and zero-field mag. domain struct. 0-44896  
 Fe<sub>40</sub>Ni<sub>40</sub>B<sub>20</sub>, amorphous, high-field magnetisation curve, spin wave spectrum and microstructural inhomogeneities 0-15702  
 Fe<sub>40</sub>Ni<sub>40</sub>P<sub>14</sub>B<sub>6</sub>, amorphous ribbon, influence of torsion on mag. props. 0-7138  
 HoZn, magnetic excitations 0-25115  
 La<sub>1-x</sub>Tb<sub>x</sub>Ag(Sn<sub>3</sub>)(Al<sub>2</sub>), paramag. anisotropy of Tb<sup>3+</sup> in cubic cryst. field 0-15687  
 MnBi, mictomag. alloys, elastic props. (*Russian*) 0-7141  
 Ni crystals in strong mag. field, EM excitation and vel. dispersion of sound (*Russian*) 0-39837  
 Ni, magnetoelastic and magnetostrictive sensitivities, reversible and irreversible components (*Russian*) 0-25172  
 Ni, phonon generation and attenuation at FMR 0-39875  
 NpFe<sub>2</sub>, lattice distortions in ferromag. phase, X-ray obs. 0-15774  
 NpNi<sub>2</sub>, lattice distortions in ferromag. phase, X-ray obs. 0-15774  
 Pb, fluxural oscillations in longitudinal mag. field, sound attenuation, magnetoelasticity (*Russian*) 0-54844  
 Pr, antiferromagnetic ordering 0-15709  
 Pr, magnetic excitations, exchange, crystal field and magnetoelastic interactions 0-2563  
 Pr, soft mode excitation behaviour under press., long range order 0-39838  
 PuP, lattice distortions in ferromag. phase, X-ray obs. 0-15774  
 Tb, elastic constants, magnetoelastic contrib. 0-15777  
 Tb, magnetic phase diagram, US meas. of elastic const. 0-15721  
 Tb<sub>0.1</sub>Dy<sub>0.9</sub>Fe<sub>2</sub>, sound velocity mag. field and temp. depend. elastic moduli calcs. 0-39839  
 TbFe<sub>2</sub>, magnetoelastic props., magnetostriction hysteresis (*Russian*) 0-29590  
 (Ti<sub>1-x</sub>V<sub>x</sub>)<sub>2</sub>O<sub>3</sub>, spin-glass props., 0.05-300K 0-25149  
 TmCd(Zn), quadrupolar phase transitions, magnetoelastic and quadrupolar coupling consts. 0-15744  
 UAl<sub>2</sub>, elastic consts., temp. and mag. field depend. 0-55450  
 V, fluxural oscillations in longitudinal mag. field, sound attenuation, magnetoelasticity (*Russian*) 0-54844  
 Y-Co, ferromagnet, first and second order transitions 0-34631  
 (Y<sub>2</sub>Gd)(GaFe)<sub>2</sub>O<sub>12</sub> epitaxial film, nonlinear magnetoelastic effects (*French*) 0-34745  
 YIG, distrib. of easy magnetisation axes near edge dislocation (*Russian*) 0-44891

**magnetoelastic waves**

- asymmetric elastic medium, electrically conducting, magneto-thermo-elastic waves anal. 0-15772  
 canted magnetic struct. crystals, magnetoacoustic resonance, elastic vibrations 0-29599  
 cubic ferrite garnet, diffracted light polarisation characts., spin and magnetoelastic waves 0-20614  
 elastic properties of magnetic materials, review 0-7142  
 ferrite-semiconductor hybrid struct., magnetoelastic wave interaction with drifting carriers 0-54934  
 Love magnetoelastic surface wave propagation in laminates 0-38322  
 magnetoelastodynamics problem with mixed boundary conditions 0-1466  
 magnetoelastodynamic Rayleigh waves with thermal relaxation in uniform magnetostatic field 0-2617  
 magnetoelastoviscous waves reflection at semi-infinite solid boundary 0-48633  
 orthorhombic ferrimagnets, domain wall motion at near sonic velocity, magnetoelastic interactions 0-34683  
 shell, orthotropic, axisymmetric vibr. in mag. field, asymptotic solns. 0-2620  
 CoCl<sub>2</sub>·2H<sub>2</sub>O, magnon-phonon interactions and two-magnon Raman scatt., magnetoelastic waves and selection rules 0-34917  
 FeCl<sub>2</sub>·2H<sub>2</sub>O, magnon-phonon interactions and two-magnon Raman scatt., magnetoelastic waves and selection rules 0-34917  
 YIG, spin and magnetoelastic waves on longit. mag. pumping, optical obs. (*Russian*) 0-29727  
 YIG substrates, magnetoelastic surface waves, magnetostatic reson. anal. 0-20441

**magnetolectric effects**

- advances in basic magnetism during past twenty-five years 0-36791  
 anisotropic media, piezomagnetolectric effects 0-25174  
 magnetic materials, review (*Japanese*) 0-50159  
 magnetic semiconductor, classical and quantum theory, magnon drag effect 0-34746  
 nonlinear susceptibility, three-dimens. model 0-39845  
 phenomenological rules for computation, magnetolectric susceptibilities 0-55068  
 polyvinylidene fluoride magnetoelctret, AF and RF charge and dielectric characts. 0-40038  
 PVC magnetoelctrets, mag. susceptibility 0-2687  
 semiconductors, antiferromagnetic, magnetoelc. effect, magnetization and ferroelc. props. 0-25180  
 toxic air ion effects due to tachyon magnetoelctric dipoles and beta rays 0-35999  
 BaTiO<sub>3</sub>, Fe-Co-Ti-Ba-O, composites ferroelectric, idealised analysis (*Russian*) 0-20440  
 BiFeO<sub>3</sub>-Pb(Fe<sub>0.5</sub>Nb<sub>0.5</sub>)O<sub>3</sub>, ferroelc., magnetoelc. obs. temp. and conc. depend. 0-50156  
 CdTe, nonlinear magnetoelc. susceptibility, three-dimens. model 0-39845  
 Cr<sub>2</sub>O<sub>3</sub>, magnetoelctric effect mechanism, magnetoelc. susceptibility and antiferromag. reson. elec. shift meas. 0-44894  
 Fe<sub>2</sub>O<sub>4</sub>, magnetite, magnetoelc. effect at 77K and cryst. symm. 0-29593  
 Fe<sub>3</sub>O<sub>4</sub>, magnetite, magnetoelc. effect at 77K, elec. field depend. of mag. anisotropy 0-29594  
 Fe<sub>3</sub>O<sub>4</sub>, typical spontaneous symmetry breakdown in solid state 0-34737  
 GaAs, magnetoelctric susceptibility, nonlinear, three-dimens. model 0-39845  
 ZnTe, nonlinear magnetoelc. susceptibility, three-dimens. model 0-39845



**magnetofluidynamics** *see magnetohydrodynamics*

**magnetogasdynamics** *see magnetohydrodynamics*

**magnetohydrodynamic conversion**

- air heater operability and materials testing 0-35703
- baseload power plant for intermediate and peaking duty 0-35702
- closed cycle MHD power generation, history of development and physics research need 0-45717
- coal-fired MHD power generation, plant development in United States, present status 0-16818
- commercial viability of MHD/steam power generation systems 0-35701
- end effects with a slowly varying magnetic field in a MHD channel with segmented electrodes 0-45716
- environmental assessment of a coal-fired open-cycle MHD power plant 0-35795
- MHD power generation, future prospects 0-35700
- open-cycle coal-fired liquid-metal MHD 0-40875
- pollutants, emissions and controls 0-30613
- power generation cycles 0-16817
- principle, research and 1979 development trends (*German*) 0-7949
- Cs applicability, owing to low ionisation potentials (*Hungarian*) 0-3526
- Rb applicability, owing to low ionisation potentials (*Hungarian*) 0-3526

**magnetohydrodynamic convertors**

- air-core magnetic system, induced fields in conducting medium 0-43796
- blow-down experiment, Eindhoven (*Dutch*) 0-33827
- channel and regions, eddy current losses due to magnetic field variations 0-40874
- channel with Hall and ion slip currents, forced convective heat transfer 0-33823
- characteristics improvement, using current parallel to magnetic field 0-1751
- closed cycle MHD power generation, history of development and physics research need 0-45717
- coal-fired, high-temp. plasma, mol. beam mass spectrometric sampling system 0-52358
- combustion products plasma characterisation, generator channel flow, diagnostic techniques 0-43993
- conductivity and power output ionization stability, and boundary layer effects 0-1752
- constant velocity Faraday-type generator, transient characteristics 0-10440
- duct potential and current distribution, two- and three-dimensional analysis, finite element method appl. 0-24259
- equivalent networks, for convertors with non-uniform gas (*Italian*) 0-3525
- fusion reactors, MHD decelerators for removal of fuel pellet microexplosion energy 0-13801
- isothermal expansion of a two-phase fluid in a magnetohydrodynamic generator duct 0-1695
- liquid metal MHD generator, wall-jet gas injection 0-28830
- liquid-metal, two-phase, power generation cycle, interfacial heat and mechanical energy transfers 0-1409
- local charact., transverse current inhomogeneity in MHD channel 0-24146
- metal electrodes erosion 0-24260
- MHD power generation, future prospects 0-35700
- open cycle generator channels, interelectrode strength (*Ukrainian*) 0-49016
- open cycle MHD generator, theory of nonuniform electrical conduction 0-28831
- performance optimization of an MHD generator with physical constraints 0-40876
- principle, research and 1979 development trends (*German*) 0-7949
- series channels characteristics with diminishing electrode commutation angle 0-48818
- series MHD generators, performance characteristics, loading factor influence 0-43790
- single-load, in combined steam power stations, performance and efficiency obs. (*Italian*) 0-26148
- structural analysis of power losses in liquid-metal slip contacts 0-43795
- U-25, flow in channel 0-24261
- variable operation, Faraday machine appl. 0-35699

**magnetohydrodynamic generators** *see magnetohydrodynamic convertors*

**magnetohydrodynamic waves**

- Alfven pulse-excited instability in neutral sheet, mag. field lines reconnection dynamics (*Russian*) 0-1768
- Alfven wave heating in toroidal plasma 0-28740
- Alfven waves, accelerated particles distrib. function, self-similar soln. 0-56702
- Alfven waves, circular polarisation, propagation in mag. field, spiky soliton 0-28662
- Alfven waves, circularly polarised, spiky soliton soln. to nonlinear evolution eqn. 0-38590
- Alfven waves, exact, nonlinear, existence of solitons 0-24159
- Alfven waves, Landau damping in solar wind 0-21885
- Alfven waves, parametric excitation in cylindrical plasma 0-24157
- Alfven waves in ionosphere/magnetosphere, rel. to coherent anomalous resist. assoc. with electrostatic shocks 0-4189
- Alfven waves in sunspots, prod. by convective overstability in mag. field in downdraft 0-21960
- finite amplitude solitary Alfven waves 0-53973
- helical system, MHD instabilities 0-1829
- helical waves in tail of Comet Morehouse (1908 III), WKB approximation theory 0-4305
- interplanetary shock waves in turbulent medium, energetic particles interaction 0-4210
- ionized medium, technique for rot. freq. meas. 0-41730
- magnetosphere, Alfven waves excitation by bouncing electron beams rel. to nightside mag. pulsations 0-4203
- magnetosphere, toroidal line resons. rel. to continuous (Pc 3,4) pulsations in European sector 0-21877
- plasma, Alfven wave nonlinear self-precession and wavenumber shift 0-10389
- plasma, compressible magnetic-field reconnection 0-6226
- plasma, hydrodynamic wave description including electron spin 0-38643
- plasma, in Tokamak thermonuclear reactor, MHD modes drift phenomena, kinetic method (*Russian*) 0-1827
- plasma, magnetoacoustic disturbance, hydrodynamic instability in nonuniform plasma flow (*Russian*) 0-1766
- solar corona, loop heating by fast mode waves 0-41801
- solar wind, MHD solitons theory 0-4217

**magnetohydrodynamic waves continued**

- solar wind large amplitude Alfven waves propag. direction rel. to average interplanetary mag. field 0-26709
- surface hydromagnetic waves, dissipation 0-21904
- vertically propagating, in isothermal atm. with horizontal mag. field 0-6162

**magnetohydrodynamics**

- see also magnetohydrodynamic conversion; magnetohydrodynamic convertors; magnetohydrodynamic waves; plasma magnetohydrodynamics*
- anti-dynamo theories, compressible flow effect 0-56361
- axial flow in triangular pipe, transverse mag. field effects 0-53870
- axisymmetric convection in presence of mag. field, solar granulation and sunspots appl. 0-12724
- axisymmetric jet of magnetisable fluid, stability 0-14835
- BN-600 reactor first loop, MHD phenomena 0-37421
- boundary layer transition and turbulence, mag. field as investig. tool 0-1696
- cavitation in nonuniform mag. fields 0-19518
- channel, annular, finite length (*Chinese*) 0-43781
- channel, elec. cond. fluid in mag. field with incident EM wave, mag. press. 0-33698
- channel, vertical, round, in nonuniform mag. field, steady-state MHD convection 0-33696
- comet tails, hydromagnetic models 0-56773
- cometary plasma acceleration, role of mag. structs. 0-46486
- compressible finitely conducting rotating fluid in mag. field, Rayleigh-Taylor instability 0-10228
- conducting fluid in cylindrical MHD induction pump, laminar flow 0-43788
- conducting fluids, dynamics under rotational mag. forces 0-48820
- conduction pump for filling casting mold 0-43798
- conductor, MHD kink instability 0-6307
- Couette flow with porous boundary 0-53876
- discontinuity surface stabilisation in magnetisable media by mag. field 0-48806
- discrete mathematical model construction from principle of least action 0-38502
- double radiosources, magnetogasdynamics 0-26999
- duct, nonconducting walls, MHD volumetric flow rate under uniform mag. field 0-1691
- Earth global dynamics, Canadian contribs., 1971-79 period 0-8262
- Ekman layer on free convection past infinite porous flat plate 0-14830
- electrically conducting rarefied gas near accelerated porous plate, MHD flow 0-14836
- electrically-conducting fluid, mag. flux linkage, planetary dynamo theory 0-8536
- electrically-conducting fluid, mag. flux linkage, relativistic case, planetary dynamo theory 0-12655
- electromagnetic field anal., computer methods, MHD and finite elements method 0-32879
- exact soln., generalised procedures 0-14838
- ferrofluid, permeability in alternating mag. field 0-48808
- ferrofluid constitution examination by rotating test tube method 0-33693
- ferrofluid droplet, interphase boundary hydrostatic charact. in uniform mag. field 0-33692
- ferrofluid flow in circular pipe, uniform mag. field effects 0-43782
- ferromagnetic convection in crossflow over a cylinder, heat transfer rate 0-1558
- ferromagnetic fluid in inhomogeneous mag. field, thermal convection 0-1559
- ferromagnetic suspension, magnetorheological charact. meas., errors 0-33550
- ferrosuspensions, internal rotations and the other transport phenomena 0-28573
- flat plate, MHD unsteady flow of Maxwell fluid, relaxation parameter 0-24101
- flow near oscillating porous flat plate under body force action 0-24102
- flow past solid spherical drop at low Reynolds and Hartmann numbers 0-6158
- flowmeter, with circ. cross section, inhomogeneous mag. field effect on signal 0-33709
- flowmeter, with circ. cross section, symmetry conditions effect on signal, arbitrary vel. profile 0-33708
- fluctuating free convection flow on horizontally magnetised plate 0-33683
- Fokker-Planck equatn. numerical solutn. 0-18622
- forced flow through horizontal channel, Hall effect, buoyancy force effects 0-53871
- free boundary capillary MHD flows 0-43794
- free convection effects on MHD accel. flow past vertical porous limiting surface 0-23996
- free shift stationary flow, in strong field, of viscous fluid 0-28576
- fusion reactor blankets, MHD coolant flows, 3-D model 0-23119
- gas, boundary layer swirling nozzle and diffuser flows with mag. field 0-1693
- general relativity conformal groups, appl. (*French*) 0-101
- Hartmann MHD flow, radiative transfer 0-6161
- heat transfer, effects of pressure gradient, suction, injection 0-53872
- heat transfer between porous discs, one rotating one at rest 0-28561
- heat transfer in rarefied MHD laminar channel flow 0-48687
- heat transfer in two-dimens., parallel plane channel flow 0-14833
- heavy liquid, free surface equilibrium and stability between charged and bent vertical surfaces 0-48812
- high gradient magnetic separation at moderate Reynolds number 0-38500
- hydromagnetic penetration in a rotating fluid 0-14839
- induction machines in DC breaking mode, operating anal. 0-48816
- induction MHD pump, active zones, effective forces, EHDA integrator study 0-43797
- ingot forming from melt, liq. containment by EM field 0-35120
- interplanetary shock waves interaction with bow shock-magnetopause system 0-26712
- interstellar clouds, mag. fields influence on OB associations subgroups sequential form 0-4408
- interstellar magnetised gaseous discs, gravitational instability 0-4424
- isothermal expansion of a two-phase fluid in a magnetohydrodynamic generator duct 0-1695
- Jupiter, lower atmosphere MHD rel. to atmosphere differential rot. 0-46467



**magnetohydrodynamics continued**

- Kelvin-Helmholtz hydromagnetic instability, of streaming layer in unbounded self-gravitational field 0-53878  
 kinematic dynamo action, helical symm. in unbounded fluid conductor 0-10315  
 kinematic dynamo action, helical symm. in unbounded fluid conductor 0-10316  
 Knudsen molecular gas in mag. field, transport phenomena 0-33684  
 linear induction machines, performance characteristics from longitudinal edge effect 0-48817  
 linear induction motor, fluid flow induced in liquid metals, investigation 0-43800  
 liquid, undergoing inhomogeneous Poiseuille flow, spin echo signal shape (Russian) 0-50225  
 liquid jets, behaviour in electric and mag. fields 0-43783  
 liquid metal flow in curved channels, transversely applied mag. field 0-14829  
 liquid metal flow rate meas. method 0-43793  
 liquid metal high Hartmann number flows in ducts with conducting walls 0-33689  
 liquid metal rectangular duct flow with opposite walls conducting and insulating 0-33688  
 liquid metal transient flow at electrode in linear cond. motor 0-43792  
 lubricant in gap in journal bearing 0-10319  
 magnetic fluid in rotating vessel, flow in homogeneous mag. field 0-33691  
 magnetic fluid with intrinsic ang. momentum, one-dimensional nonstationary waves 0-33690  
 magnetisable fluid, motion in rotating homogeneous mag. field 0-28572  
 magnetisable suspensions, hydrodynamic in travelling mag. field 0-48807  
 magneto-acoustic wave stability in thermally conducting compressible fluid 0-48803  
 magnetoatmospheric instabilities, Hilbert space approach to max. growth rate 0-31172  
 magneto-electrolytic convection, accuracy of estimation method 0-14691  
 magnetogasdynamics, reciprocal type transformations 0-48804  
 magnetohydroelectric interaction, realisability 0-53874  
 materials, review 0-40240  
 moving ribbon conductor, interaction with field of ferromag. inductor 0-48815  
 multiple MHD throttle with annular duct 0-43789  
 nematic liquid cryst., Fredericksz transition in mag. field, domain struct. 0-33880  
 neutron star magnetosphere, plasma dynamics and accretion, fate of sinking filaments 0-51798  
 neutron stars, rotating, magnetic, accretion torques rel. to pulsating X-ray sources period changes 0-31320  
 non-Newtonian incompressible fluid with pressure gradient and fluid injection, MHD flow 0-33686  
 nonlinear wave propagation in relativistic continuum mechanics, limiting cases of relativistic magnetohydrodynamics 0-22203  
 nonsteady turbulent MHD flows in plane channels and circular tubes 0-48810  
 oscillatory flow, free convection effects 0-53865  
 paramagnetic particle trajectories in a lattice of parallel magnetized fibers 0-53204  
 perturbations for finite magnetic Reynolds number 0-1757  
 Phase V, nematic, transient response to redirected mag. field, EPR study 0-33879  
 pipe flow, single and two phase 0-53869  
 plane interface between two viscoelastic superposed cond. fluids, instability in mag. field 0-1694  
 plane stagnation point flow in the presence of transverse magnetic field 0-14834  
 point force in a stratified fluid in a cylinder under a magnetic field 0-14776  
 Poiseuille perturbed pipe flow in nonuniform axisymmetric mag. field, anal. 0-24104  
 power-law non-Newtonian conducting fluid, laminar boundary layer in transverse mag. field 0-33694  
 pressure surface in magneto-gas dynamics (German) 0-14841  
 pulsar magnetosphere models, interior and exterior struct., pair prod. 0-46594  
 pulsar magnetospheres, relativistic MHD wind or plasma wave 0-31317  
 pump, AC conduction type, for ferrous metal 0-33701  
 pumps for Hg transfer in chlorine and caustic soda production 0-43787  
 radiative magnetogasdynamic Couette flow with variable parameters 0-14840  
 radiative MHD, with planar symmetry, invariant solns. 0-24099  
 radio sources, extended, extragalactic, MHD instabilities and electron accel. 0-27000  
 radio sources, superluminal, mag. dipole model 0-56959  
 rarefied gas channel flow, effects of external cct. 0-33630  
 Rayleigh-Taylor instability of a conducting viscous fluid in a magnetic field 0-43785  
 rectangular duct flow with opposite walls conducting and insulating 0-33688  
 relativistic Boltzmann eqn. and MHD eqns. with radiative reaction 0-36956  
 relativistic EM fluid flows 0-52094  
 relativistic fluid, infinite thermal conductivity, Cauchy problem solutions, existence and uniqueness (Italian) 0-48821  
 relativistic magnetofluid flows, geometry 0-46895  
 rigid ellipsoidal particles in external field, dil. suspension, rheological eqns. (Ukrainian) 0-48661  
 rotating Hall plasma, self gravitational instability, MHD stability 0-14890  
 Saturn, lower atmosphere MHD rel. to atmosphere differential rot. 0-46467  
 shear inviscid flow, vortex sheet stability 0-28571  
 singular hypersurfaces, asymptotic regularisation as alternative to distrib. 0-36923  
 slow viscous flow in rectangular cavity 0-19517  
 solar atmosphere, thin magnetic tube instability rel. to network struct. 0-12725  
 solar corona, turbulent heating role 0-12715  
 solar coronal loops, thermal instabilities in magnetically confined plasmas 0-36600  
 solar flares, mag. structs. models and predictions of flux rope theory 0-21955  
 solar type III radio bursts, electron exciters obs. near 1 AU 0-46513

**magnetohydrodynamics continued**

- space-times, family of contracted Ricci collineations symmetry mappings 0-51650  
 sphere, nonconducting, slowly rotating in steady MHD flow, exact soln. 0-33695  
 sphere motion in infinite conductive fluid, variable mag. dipole located within sphere case 0-19519  
 steady and nondissipative flows, geometric results 0-48819  
 steady-state MHD convection in a vertical annular duct in a radial magnetic field 0-48809  
 stellar convection in rot. magnetic star, toroidal field effect 0-41816  
 stochastic particle accel. by MHD turbulence 0-31203  
 Stokes problem, boundary layers and skin friction 0-14837  
 Stokes problem for infinite vert. plate, hydromagnetic free convection effects 0-10318  
 stratified flow between oscillating disks, boundary layers 0-28570  
 Sun, eruptive prominences and coronal transients 0-56809  
 Sun expanding mag. arch, MHD oscill. rel. to moving type IV radio bursts modulation 0-26833  
 sunspot cycle morphology, theory (Chinese) 0-12722  
 sunspots and magnetic flux tubes physics, umbral dots and longitudinal overstability 0-26825  
 supercritical Taylor-Couette flow 0-33702  
 supernovae, MHD model 0-46588  
 Taylor column irregularity in rapidly rotating MHD fluid, mag. field effects 0-43786  
 temp. distrib. for flow between coaxial cylinders with wall temp. discontinuity 0-1690  
 thermal instability of an internally heated fluid layer in a magnetic field 0-53875  
 transient phenomena, simultaneous solns. to coupled gasdynamic-EM equations of motion 0-6157  
 turbulent boundary layers in rot. circ. vessel, drag 0-33697  
 turbulent MHD flows, residual disturbances after laminarisation, entry effects 0-6160  
 turbulent thermal convection in presence of rot. and mag. field, stellar and planetary dynamos appl. 0-6042  
 two channel DC EM pump, expt. study 0-43791  
 unsteady Couette flow through porous wall in presence of mag. field 0-53856  
 unsteady laminar flow of elastic viscous fluid through porous channel, applied mag. field effects 0-38499  
 unsteady MHD flow in rotating system, Hall current effects 0-33704  
 Uranus magnetic dynamo, implications for mantle struct. and comp. 0-4298  
 viscoelastic free convection boundary layer flow past porous plate 0-10317  
 viscous electrically cond. fluid, laminar free shear flow, transverse mag. field effect 0-48811  
 viscous fluid, electrically conducting, flow between rotating and stationary porous coaxial discs 0-43799  
 vortex sheet stability in compressible perfectly conducting fluids 0-14831  
 water, MHD free convection flow past infinite porous plate 0-33703  
 weak discontinuities in a conducting magnetizable medium 0-48805

**magnetomechanical effects**

- see also *gyromagnetic effect*; *magnetoelastic effects*; *magnetoelastic waves*; *magnetostriction*  
 amorphous ferromagnetic alloys, domain struct. and mag. microstruct., review 0-15751  
 Invar, Mossbauer effect at high press. 0-15858  
 metallic glass, Fe Mossbauer effect at high press. 0-15858  
 pole effect, theory 0-25175  
 rare earth alloys, Curie temp. (Japanese) 0-20444  
 rare earth intermetallics, neutron scatt., induced moment magnetism, high press. 0-15699  
 rocks, piezomagnetic effect due to lake ground loading 0-8346  
 rocks remanent magnetisation, uniaxial stress effects, stress cycling and domain state depend. 0-26505  
 shock compression of solids, review 0-24534  
 steel, stainless, Mossbauer effect at high press. 0-15858  
 stiffness of conducting bodies config. in time-varying mag. field 0-43230  
 TCNQ salt, TMTSF-DMTCNQ, mag. susceptibility meas. under press. 0-25521  
 transition metal alloys, Curie temp. (Japanese) 0-20444  
 Ag-Mn, spin glass, mag. susceptibility hydrostatic press. depend., RKKY interaction 0-44845  
 CeBi, phase diagram in mag. field, hydrostatic press. effect 0-25132  
 CeIn<sub>3</sub>, Neel temp., hydrostatic press. depend. 0-29549  
 (Co<sub>1-x</sub>Mn<sub>x</sub>)<sub>2</sub>B, 0 ≤ x ≤ 1, magnetisation, lattice const., press. depend. of Curie temp. 0-7137  
 Cr, spin density wave Q-vector, temp. and press. depend. 0-11167  
 Cr-Co (4.0 at.%) alloy, antiferromag., disappearance of resist. min. under press., and press. coeff. of T<sub>N</sub> 0-10960  
 (Er<sub>1-x</sub>Ho<sub>x</sub>)Rh<sub>2</sub>B<sub>4</sub>, superconductive and mag. interactions, hydrostatic press. effect 0-49973  
 EuGaYIG:Cr, epitaxial garnet film, interaction pot. of domain walls with localised stress fields 0-44889  
 Fe, Mossbauer effect at high press. in α-, ε- and γ-phases 0-15858  
 Fe whiskers, elastically and plastically deformed, mag. domain structs. 0-15752  
 Fe:C(N), small concs. determ., mag. and mech. relax. methods 0-7879  
 Fe-B-Si amorphous ribbons, effect of annealing conditions on magnetomechanical props. 0-34740  
 Fe-Co-V, Vicalloy, magnetisation reversal by stretching and twisting 0-34733  
 Fe-Pt, plastic deform. effect on struct. singularities and mag. props. (Russian) 0-44892  
 Fe-Si, maze domains upon appl. of horizontal mag. field or mech. tension 0-11218  
 Fe<sub>80</sub>B<sub>20</sub>, amorphous, transverse magnetoresist., stress effect 0-15501  
 Fe<sub>80</sub>B<sub>20</sub>, amorphous ferromag. metallic glass, stress-induced rot. of magnetisation, Mossbauer study 0-20445  
 Fe<sub>78</sub>Mo<sub>2</sub>B<sub>20</sub>, amorphous, transverse magnetoresist., stress effect 0-15501  
 Fe<sub>40</sub>Ni<sub>40</sub>P<sub>14</sub>B<sub>6</sub>, amorphous, transverse magnetoresist., stress effect 0-15501  
 Fe<sub>3</sub>O<sub>4</sub> (magnetite), mag. susceptibility under hydrostatic press. and implications for tectonomagnetism 0-26504  
 Fe<sub>3</sub>O<sub>4</sub> (magnetite), piezomag. response depth depend. rel. to tectonomagnetism as earthquake precursor 0-26465  
 GdSn<sub>3</sub>, Neel temp., hydrostatic press. depend. 0-29549



**magnetomechanical effects continued**

- $\alpha$ -Mn, electronic structure model, Invar effect, antiferromagnetic-non mag. transitions 0-20370
- MnAs, orthorhombic, low temp. magnetic transitions (*Russian*) 0-11193
- MnCoSi, effect of press on mag. transition temp. (*Russian*) 0-25137
- $\gamma$ -MnCu, antiferromag., stressed, mag. defects meas. by neutron polarisation anal. 0-50076
- MnZn ferrite, wall topography change induced by external press. 0-34734
- Mo, mechanical props. and dislocation struct., mag. field effect 0-54935
- Nb, mechanical props. and dislocation struct., mag. field effect 0-54935
- NdSn<sub>3</sub>, Neel temp., hydrostatic press. depend. 0-29549
- Ni Curie temp., press. depend., using press. cell developed for meas. with cubic-anvil press 0-13109
- Ni, deformation in const. mag. field, 4.2K (*Russian*) 0-29591
- Ni-Mn (up to 32 at.%), Curie temp., press. depend., using press. cell developed for meas. with cubic-anvil press 0-13109
- NiZn ferrite, wall topography change induced by external press. 0-34734
- Pr, magnetic ordering, stress induced 0-15776
- PrSb, neutron scatt., press. induced antiferromag. 0-15699
- PrSn<sub>3</sub>, Neel temp., hydrostatic press. depend. 0-29549
- Pr<sub>2</sub>Ti, critical fluctuations temp. depend. 0-25160
- UA1<sub>2</sub>, high field, high press. mag. props. 0-11172
- UN, mag. susceptibility under press. 0-7086
- US, ferromag., AC mag. susceptibility at high press. 0-7085
- Y, Ni<sub>1-x</sub>, amorphous, high press. magnetisation and Curie temp. 0-20442

**magnetometers**

- see also *magnetic field measurement*
- alkali metal-He quantum magnetometer 0-17965
- ferromagnetic thin film magnetometer, development and performance 0-31808
- ferromodulation meas. transducers, with increased temp. stability 0-52281
- fluxgate, interference of signal (*Japanese*) 0-37060
- Hall, system of calibration and checking in 0.3 to 6.0 T range 0-17964
- induction magnetometer, high permeability metal core solenoid sensor absolute sensitivity 0-31133
- multichannel, using galvanomagneto-recombination convertors 0-31810
- narrow line <sup>87</sup>Rb magnetometers, sensitivity to local geomag. field changes, and noise reduction 0-26636
- quantum, threshold sensitivity and short-term fluctuations determ. 0-22394
- sea floor temporal mag. variation measurement, fluxgate system 0-51581
- sensor measuring articulatory characteristics of tongue and jaw point movements in connected sounds of Japanese 0-26243
- space applications of LF supercond. sensors inc. SQUID devices 0-56691
- SQUID, biomagnetic instrumentation and meas. 0-36181
- SQUID, DC, circuits, optimisation 0-13056
- torque magnetometer for vacuum-to-high-pressure H<sub>2</sub> environments 0-4746
- UHF SQUID magnetometer using coded (4.2K) GaAs FET preamplifier, biased at 430 MHz 0-52282
- UHF SQUID magnetometer using varactor-tuned 4.2K GaAs FET amplifier 0-31814
- <sup>4</sup>He, optically pumped (*Japanese*) 0-8434

**magneto-optics** see *magneto-optical effects***magnetoplasma** see *plasma***magnetoplasma dynamics** see *plasma magnetohydrodynamics***magnetorefectance**

- graphite, magnetoreflexion under press., Landau level transitions 0-50303
- graphite intercalation cpds., K-point effective masses and Fermi level shifts, magnetorefl. study 0-50305
- Bi, magnetorefectance, L-pt. band parameters 0-25344
- Cd<sub>1-x</sub>Mn<sub>x</sub>Te, exchange interaction, magneto-optical spectra 0-25348
- GaAs, exchange interaction, analytical and nonanalytical parts, from polariton spectra in mag. fields 0-50367
- InP, exchange interaction, analytical and nonanalytical parts, from polariton spectra in mag. fields 0-50367
- InSb, Landau level struct., magneto-electroreflectance 0-25349
- Pb<sub>1-x</sub>Sn<sub>x</sub>Te, inter- and intraband magneto-optical transitions 0-25346
- p-PbTe, MIS struct. inversion layer sub-bands, IR magnetorefectance obs. 0-44731
- ZnTe, valence band parameters and free exciton reduced mass, free exciton magnetorefectance 0-45046

**magnetoresistance**

- see also *Corbino effect*
- charge carrier with anisotropic energy spectrum, cond. oscills. in quantised mag. field (*Russian*) 0-6886
- CoCr<sub>2</sub>S<sub>4</sub> films, galvanomagnetic and thermoelec. props. 0-54717
- cubic crystals, weak field magnetoresistance skewness imposed by mag. field 0-34416
- degenerate semiconductor, electron g-factor determ., Shubnikov-de Haas type oscills. 0-20070
- degenerate semiconductors, hot electron transport in parabolic energy bands, kinetic theory, transport coeffs. 0-29412
- ferromagnetic nondegenerate semiconductor, magnetoresistance 0-11019
- finite fibre, fluctuation magnetocond. 0-24956
- graphite, anisotropic elec. cond. rel. to stacking disorder 0-34437
- graphite, carrier mobility, temp. depend. determ. from magnetoresist. expts. 0-11009
- graphite, galvanomagnetic and thermomagnetic effects at low temp. 0-44618
- graphite, neutron irradiation, electron transport, annealing study 0-39165
- graphite, pyrolytic, galvanomag. effects, effect of fast neutron irradiation 0-34465
- graphite, with small-sized blocks, negative magnetoresist. (*Russian*) 0-49779
- heavily doped semiconductor, magnetoconductivity, effect of resonant phonon-plasmon coupling 0-24954
- metal-insulator-semiconductor structure, DC cond. and Shubnikov-de Haas effect 0-11012
- metallic rare earths, conference, St. Pierre-de-Chartreuse, France (Sept. 1978) 0-12844
- Permalloy-Rh, film, influence of Rh on corrosion resist. and mag. props. 0-3235
- polyacetylene film, doped, transport props. 0-24913
- rare earth amorphous alloys, random anisotropy antiferromag. model 0-20399
- rare earth amorphous alloys, transport props. 0-20152

**magnetoresistance continued**

- rare earth metal, conduction electron interactions, anisotropic 0-15492
- semiconductor, antiferromagnetic, spin-magnetomagnon resonance 0-2566
- semiconductor, cubic, Seitz coefficients calc. for resistivity 0-6880
- semiconductor, effect of pot. fluctuations induced by cryst. inhomogeneities 0-49780
- semiconductor materials temperature dependence meas., using automatic device 0-52270
- semiconductor with charged defects, elec. cond. and magnetoresist. 0-20225
- semiconductors, superoperator theory 0-49776
- semiconductors temperature dependences meas., automated installation 0-31792
- TCNQ-HMTSF, de Haas-Shubnikov oscills. 0-10956
- thin films, superconducting fluctuation influence on magnetoresistance (*Russian*) 0-54815
- thin surface layer, interactions between nondegenerate electrons, effect on cyclotron resonance, mag. cond. (*Russian*) 0-15802
- TMTSF-DMTCNQ, metallic state, transport props. 0-24974
- TTT<sub>2</sub>(I<sub>3</sub>)<sub>2</sub>, physical props., elec., mag. and optical meas. 0-24908
- Ag-Dy(Ho)(Tm), dil., high field magnetoresist. 0-15503
- Ag-Mn, dil. alloy, transverse magnetoresist. in spin glass regime 0-34417
- Al alloy, dilute, Matthiessen's rule deviations in strong mag. field 0-44571
- Al, Sondheimer size effect, phonon-limited mean path, 1.8-12K 0-49698
- Al, stabiliser for fusion reactor supercond. mag., neutron irradiation effects on magnetoresistance 0-34062
- Au-Fe, dil. alloy, transverse magnetoresist. in spin glass regime 0-34417
- Bi film, carrier conc., mobility and 1/f noise 0-44748
- Bi, in high mag. fields (*Japanese*) 0-54720
- Bi, Shubnikov-de Haas effect in high mag. fields 0-2404
- Bi thin wire, resist. anomaly, possibility of one-dimensional quantum size effect 0-54809
- Bi whiskers, electron transition on simple extension, elec. resist. and magnetoresist. meas. (*Russian*) 0-29422
- Bi-Sb, Shubnikov-de Haas effect and semimetal-semicond. transition in high mag. fields 0-44674
- Bi<sub>0.925</sub>Sb<sub>0.075</sub>, semiconductor-semimetal transition under tensile strain, Shubnikov-de Haas oscills. obs. 0-44678
- Bi<sub>2</sub>Sb<sub>2</sub>Te<sub>3</sub>Se, solid solution, density-of-states effective mass, carrier mobility temp. depend. 0-24931
- Bi<sub>2</sub>Te<sub>3</sub>Se<sub>0.3</sub>, magnetoresistance and Hall EMF meas., using AM method 0-52278
- C disordered, variable-range hopping cond. and negative magnetoresist. 0-34436
- C, glassy and fibrous, density of states, magnetoresistance theory appl. 0-44620
- C pregraphitic, negative magnetoresist. 0-34466
- C resistance thermometers, determination of magnetoresistance in liquid He temp. range 0-31752
- Cd<sub>3</sub>As<sub>2</sub>, anisotropy of electronic g\*-factor 0-44483
- Cd<sub>3</sub>As<sub>2</sub>, band struct. and g-factor, Shubnikov-de Haas oscills. meas. 0-49598
- Cd<sub>3</sub>As<sub>2</sub>, band struct. from Shubnikov-de Haas and de Haas-van Alphen effects 0-49597
- Cd<sub>3</sub>As<sub>2</sub>, Shubnikov-de Haas effect 0-11020
- CdCr<sub>2</sub>Se<sub>4</sub>Ag, magneto-electrical props. temp. behaviour depend. on dopant conc. (*Russian*) 0-11006
- Cd<sub>x</sub>Hg<sub>1-x</sub>Te, influence of nonparabolicity on transverse magnetoresist. near transition to zero gap 0-20228
- Cd<sub>x</sub>Hg<sub>1-x</sub>Te, photomagnetic and galvanomagnetic effects in quantising mag. fields 0-20223
- Cd<sub>1-x</sub>In<sub>x</sub>Cr<sub>2</sub>Se<sub>4</sub>, electric, photoelectric and mag. props., metal-semicond. transition (*Russian*) 0-54738
- CeCoSi<sub>2</sub> film, Hall effect and magnetoresist. (*Russian*) 0-11109
- Co, ferromag. film, magnetoresistance parameter meas. (*Spanish*) 0-2485
- (Co<sub>1-x</sub>Ni<sub>x</sub>)<sub>75</sub>(PBAI)<sub>25</sub>, amorphous, high-field magnetoresist. meas. 0-34423
- CoS<sub>2</sub>, ferromagnet, elec. resist. and thermal expansion anomalies 0-15542
- Cr, antiferromag., electron interference oscills. and spin-density-wave energy gaps at Fermi surface 0-49574
- Cu, stabiliser for fusion reactor supercond. mag., neutron irradiation effects on magnetoresistance 0-34062
- CuCr<sub>2</sub>Se<sub>4</sub>(S<sub>2</sub>)(Te<sub>4</sub>), binary and ternary solid solns., mag. and elec. props. 0-2407
- EuSe, giant negative magnetoresistance, anomalous carrier density mag. field depend. 0-49774
- Fe, ferromag. film, magnetoresistance parameter meas. (*Spanish*) 0-2485
- Fe-Co-Si-B sputtered amorphous thin film, coercivity, galvanomagnetic props., resistivity 0-29578
- Fe<sub>80</sub>B<sub>20</sub>, amorphous, transverse magnetoresist., stress effect 0-15501
- Fe<sub>78</sub>Mo<sub>2</sub>B<sub>20</sub>, amorphous, transverse magnetoresist., stress effect 0-15501
- Fe<sub>40</sub>Ni<sub>38</sub>Mo<sub>2</sub>B<sub>18</sub>, metallic glass, mag. and transport props. 0-39752
- Fe<sub>40</sub>Ni<sub>40</sub>P<sub>14</sub>B<sub>6</sub>, amorphous, transverse magnetoresist., stress effect 0-15501
- Fe<sub>2</sub>Ni<sub>1-x</sub>P<sub>14</sub>B<sub>6</sub>, amorphous, spin-glass regime, magnetoresist. meas. 0-34418
- (Fe<sub>1-x</sub>Ni<sub>x</sub>)<sub>75</sub>(PBAI)<sub>25</sub>, amorphous, high-field magnetoresist. meas. 0-34423
- Fe<sub>2</sub>Pd<sub>82-x</sub>Si<sub>18</sub>, amorphous, magnetisation, magnetoresist., spin glass and ferromag. phases 0-34697
- 1T-Fe<sub>2</sub>Ta<sub>1-x</sub>S<sub>2</sub>, Anderson localisation, elec. resist. and magnetoresist. meas. 0-44596
- GaAs, electrical and optical props. at low temps. 0-39636
- n-GaAs, heavily doped, impurity-band cond., DC cond., Hall mobility, and magnetoresist. meas. 0-49733
- n-GaAs, hot electron magnetophonon resonance, Fourier anal. 0-54718
- GaAs, influence of strong transverse mag. field on Gunn effect 0-6854
- GaAs-Al<sub>0.1</sub>Ga<sub>0.9</sub>As, heterojunction and superlattice, magnetophonon reson., polaron mass 0-44715
- GaAs-Al<sub>0.1</sub>Ga<sub>0.9</sub>As superlattice, electronic props. 0-11080
- GaAs-GaAlAs, superlattice, subband related anisotropy in negative magnetoresistivity 0-11082
- Ga<sub>1-x</sub>In<sub>x</sub>As<sub>1-y</sub>P<sub>y</sub>, conduction band and phonons, Shubnikov-de Haas effect, magnetophonon resonance, Raman scattering 0-24795
- GaP, electrical and optical props. at low temps. 0-39636
- Gd<sub>67</sub>Co<sub>33</sub>, amorphous, elec. resist. and magnetoresist. 0-49693
- Gd<sub>2</sub>S<sub>3</sub> with excess Gd, magnetoresist. meas. 0-49777
- Ge, amorphous, anomalous magnetoresistance 0-6877



**magnetoresistance continued**

- Ge amorphous films, high elec. field cond. and magnetoresist. at 4.2K 0-49748  
 Ge bicrystal, cond., Hall effect and Shubnikov-de Haas oscills. 0-10984  
 Ge, electrical and optical props. at low temps. 0-39636  
 Ge, neutron irradi., Hall effect and magnetoresist. meas. 0-6883  
 Ge, photoconcurrent magneto-oscillations 0-6911  
 Hg<sub>1-x</sub>AsF<sub>6</sub>, linear chain compound, mag. field induced residual resist., anisotropic supercond. 0-24897  
 Hg<sub>1-x</sub>AsF<sub>6</sub>, quasi one-dimensional, anomalous magnetoresistance 0-24884  
 Hg<sub>1-x</sub>Cd<sub>x</sub>Ge, quantum oscillations of magnetoresistivity (*Russian*) 0-11007  
 HgCdTe, Magneto transport anomalies at low carrier densities, Wigner crystallisation 0-20222  
 n-Hg<sub>0.8</sub>Cd<sub>0.2</sub>Te, microwave bolometer heterodyne receiver based on magnetic field induced phase transition 0-13135  
 Hg<sub>1-x</sub>Cd<sub>x</sub>Te, semiconducting phase, acceptor states and galvanomagnetic effects 0-11017  
 Hg<sub>1-x</sub>Cd<sub>x</sub>Te, ( $x < 0.16$ ), semimetallic phase, acceptor states and galvanomagnetic effects 0-6882  
 Hg<sub>1-x</sub>Mn<sub>x</sub>Se, band struct. from anomalous Shubnikov-de Haas effect 0-20080  
 Hg<sub>1-x</sub>Mn<sub>x</sub>Te, acceptor reson., states in high mag. field 0-49668  
 Hg<sub>1-x</sub>Mn<sub>x</sub>Te, energy levels at  $\Gamma$ -point in intense mag. fields, Shubnikov-de Haas effect meas. 0-24951  
 Hg<sub>1-x</sub>Mn<sub>x</sub>Te, Shubnikov de Haas effect and quantum oscills. of thermoelec. power 0-49781  
 HgSe, Shubnikov-de Haas determ. of electron  $g$  factors 0-6704  
 HgTe, acceptor reson., states in high mag. field 0-49668  
 HgTe, magnetophonon oscills. of thermoelec. power 0-49789  
 HgTe type semiconductors, spin-flip transitions in magneto-optics and magneto-transport 0-50306  
 InAs, longitudinal magnetoresistance in extreme quantum limit (*Russian*) 0-11008  
 n-InAs, Shubnikov-de Haas transverse kinetic coeffs., quantum oscills. 0-49778  
 InAs-GaSb superlattice, semiconductor-semimetal transition obs. 0-44710  
 InAs-GaSb superlattices, semicond.-semimetal transition obs. 0-49882  
 InAs<sub>1-x</sub>P<sub>x</sub>, electron effective mass cyclotron reson. and magnetophonon effect 0-24786  
 InP, electrical and optical props. at low temps. 0-39636  
 InSb, charact. and phys. props., review (*Japanese*) 0-39576  
 n-InSb, freq. depend. cond. tensor in quantising mag. fields (*German*) 0-29419  
 n-InSb, Hall effect and magnetoresist. in extreme quantum limit, stress depend. 0-11021  
 n-InSb, longitudinal magnetoresistance in extreme quantum limit (*Russian*) 0-11008  
 p-InSb, magnetoconductivity and cyclotron reson. in inversion layers 0-49946  
 N-InSb, magnetophonon resonance, damping factor by mag. field modulation technique 0-6878  
 p-InSb, magnetophonon resonance due to non-equilib. electron injection 0-6881  
 InSb magnetoresistive elements, fundamental effects (*Japanese*) 0-11013  
 n-InSb, magnetotransport experiments, surface treatment induced effects 0-34468  
 n-InSb, narrow gap, appl. of effect of pot. fluctuations induced by cryst. inhomogeneities 0-49780  
 p-InSb, negative magnetoresist. under press. 0-20224  
 n-InSb, Shubnikov-de Haas effect 0-11015  
 n-InSb, Shubnikov-de Haas transverse kinetic coeffs., quantum oscills. 0-49778  
 InSb type semiconductor, spin-flip transitions in magneto-optics and magneto-transport 0-50306  
 KTaO<sub>3</sub>In, two-phase polycryst. films, negative magnetoresist. 0-11011  
 p-TaO<sub>3</sub>, Shubnikov-de Haas effect, cond. band struct. 0-10875  
 Mg-Gd(Ho), dil., magnetoresist., anomalous Hall effect 0-15502  
 Mo-B<sub>2</sub> and MoB<sub>3</sub>, thermal, elec., and mag. props. 0-20187  
 NbSe<sub>2</sub>:Fe (2H), pure and doped, magnetoresist. and elec. resist. temp. depend. rel. to CDW form. 0-44574  
 NbSe<sub>3</sub>, Fermi surface, press. effects, Shubnikov-de Haas effect meas. at 1.5K 0-20068  
 NbSe<sub>3</sub>, two band model and galvanomagnetic study 0-20176  
 NbTi/In granular composite, resistivity mag. field depend. 0-15654  
 Nd, magnetoresistance, mag. struct., elec. resistance at low temps. (*Russian*) 0-54936  
 NdSn<sub>3</sub>, magnetoresistance 0-24877  
 Ni, ferromag. film, magnetoresistance parameter meas. (*Spanish*) 0-2485  
 Ni-Co films, electron-beam evaporated, magnetoresist. anisotropy, deposition temp. effect 0-34528  
 Ni-Fe-Pd thin films, mag., surface and corrosion props. 0-34707  
 Pb<sub>1-x</sub>Ge<sub>x</sub>Te, n- and p-type, effective masses 0-44481  
 PbO<sub>2</sub> compressed powder magnetoresistance and apparent carrier mobility 0-35669  
 Pb<sub>1-x</sub>Sn<sub>x</sub>Se, band struct. and transport props., hydrostatic press. effects 0-15452  
 PbSnTe, Magneto transport anomalies at low carrier densities, Wigner crystallisation 0-20222  
 Pb<sub>1-x</sub>Sn<sub>x</sub>Te:In, carrier spectroscopic  $g$ -factors, magnetoresistance, temp. depend. 0-6705  
 Pb<sub>1-x</sub>Sn<sub>x</sub>Te:In, energy spectra modifications due to comp. changes and press. appl. 0-10915  
 PbTe, Magneto transport anomalies at low carrier densities, Wigner crystallisation 0-20222  
 PbTe, resonant scattering, photocond. 0-6910  
 Pd<sub>80</sub>Si<sub>20</sub>, amorphous, elec. resist. and magnetoresist. 0-49693  
 PrSn<sub>3</sub>, magnetoresistance 0-24877  
 (SN)<sub>x</sub>, halogenated derivatives, cond. and magnetoresist., 4.2-300K 0-24915  
 Sb, carrier transport, magnetoresistivity, field-dependent tensor study 0-39609  
 Sb-Ge (1.2 to 2.2 at.%), carrier transport, magnetoresistivity, field-dependent tensor study 0-39609  
 Sb-Sn (0.5 to 1.0 at.%), carrier transport, magnetoresistivity, field-dependent tensor study 0-39609  
 Si (100) MOST, comparison of Shubnikov-de Haas effect and cyclotron reson. under uniaxial stress 0-20320  
 Si, amorphous, anomalous magnetoresistance 0-6877  
 n-Si, impurity-assoc. magnetophonon reson. 0-20221

**magnetoresistance continued**

- Si, inversion layers, resolution of Shubnikov-de Haas paradoxes 0-39648  
 Si MOS inversion layers, negative magnetoresist. 0-49922  
 n-Si, magnetoresistance, growth layer influence, effect of randomly distributed inhomogeneities 0-20229  
 Si, neutron irradi., Hall effect and magnetoresist. meas. 0-6883  
 Si, on sapphire, MOS inversion layer, magnetoconductance oscillations 0-20325  
 Si, recomb. centre study by spin-depend. photocond. 0-49805  
 a-Si, resonant and non-resonant photoconductivity changes 0-49814  
 a-Si, resonant and non-resonant luminesc. changes theory 0-50410  
 Si:In amorphous films, EPR, elec. cond., and magnetoresist. 0-50160  
 Si-SiO<sub>2</sub> (111) interfaces, sixfold valley degeneracy in electron inversion layers 0-49936  
 (TSeT)<sub>2</sub>Cl, one-dimens. conductor, metallic phases 0-20159  
 1T-TaS<sub>2</sub> and 1T-TaS<sub>2-x</sub>Se<sub>x</sub>, Anderson localisation, elec. resist. and magnetoresist. meas. 0-44596  
 Te inversion layers in mag. fields 0-44690  
 Ti<sub>1-x</sub>Co<sub>x</sub>, electronic struct. and anomalies of elec. and mag. props. 0-6710  
 Ti<sub>1-x</sub>Ni<sub>x</sub>, electronic struct. and anomalies of elec. and mag. props. 0-6710  
 Ti<sub>0.99</sub>V<sub>0.01</sub>Se<sub>2</sub>, negative magnetoresist. and nonlinear cond. 0-44617  
 W, RF size effect, surface electron scatt. influence (*Russian*) 0-2414  
 W-Re, amorphous wire, elec. resist., 2-20K, dimens. and mag. field depend., quantum localisation 0-39547  
 W<sub>2</sub>B<sub>3</sub> and WB<sub>3</sub>, thermal, elec., and mag. props. 0-20187  
 Zn,Hg<sub>1-x</sub>Se, galvanomagnetic effects, Shubnikov-de Haas oscill. determ. of band struct. 0-6884
- magnetoresistance, thermal** *see thermal magnetoresistance*  
**magnetoresistivity** *see magnetoresistance*  
**magnetosphere**  
*see also magnetospheric electromagnetic wave propagation; radiation belts*  
 ATS-6 radio beacon studies, review 0-56677  
 aurora primary ions, above diffuse midnight aurora 0-41595  
 aurora quiet-time patterns rel. to magnetospheric convection 0-17433  
 auroral electric field, description based on plasma interaction with geomag. field 0-46342  
 auroral electrons, bounce periods rel. to latitude effect in pulsating patches periodicity 0-31155  
 auroral zone, Kosmos 721 obs. of relativistic electrons 0-8492  
 Birkeland currents, primary sources 0-31176  
 bow shock ion acceleration, upstream region obs., review 0-31168  
 bow shock-magnetopause system, interplanetary shock waves interaction 0-26712  
 chorus VLF and ELF emission, plasmopause origin model 0-41608  
 coherent anomalous resistivity, in region of electrostatic shocks 0-4189  
 conf. Tokyo, Japan, 1978, AEROS and TAIYO satellite results 0-46340  
 conference, June 1979, Alpach, Austria 0-36776  
 conjugate electron precipitation, high time resolution riometer and X-ray meas. 0-41666  
 continuous (Pc 3,4) pulsations, complex demodulation rel. to magnetosphere toroidal line resons. 0-21877  
 convection of magnetosphere plasma affecting ionosphere electron density disturbance spatial struct. 0-41606  
 convection rel. fields, dynamics and interrelations with polar ionosphere struct. 0-4176  
 current instability on short wave drift oscills., nonlinear theory (*Russian*) 0-53981  
 current sheet in compressible plasma, self-similar resistive decay 0-1755  
 current systems, N.polar cap mag. variations associated with interplanetary field 0-41645  
 D<sub>st</sub> variation asymmetry, as function of local time 0-41643  
 dayside cleft emission, Dec. 1976 obs., 6300 Å photometry 0-46332  
 dayside cleft region, photometric obs. at 6300 Å 0-41586  
 dayside plasmopause position, Pc 3 and 4 spectral analysis 0-56681  
 double layers and electrostatic shocks in space, review 0-36460  
 downward flowing ions and ionospheric ions injection into plasma sheet 0-26694  
 drift boundary approximations in simple magnetospheric convection models 0-26693  
 electric field, plasma density and temp., field-aligned currents, S3-3 satellite obs. 0-26699  
 electric field model used to predict ionosphere plasma convection at high latitude 0-41612  
 electric field power spectra, double probe meas., Doppler shift effects 0-26634  
 electric fields, potential and inductive during auroras 0-21878  
 electric fields absence rel. to particle entry 0-41669  
 electric fields and currents influence on thermospheric circulation and comp. 0-17446  
 electric fields of magnetospheric origin in ionosphere, simulation 0-4177  
 electric fields penetration along geomag. force lines, electrostatic approach applicability 0-4178  
 electron cyclotron plasma instability, multiharmonic, numerical calc. 0-41659  
 electron densities determinatoin, whistler inversion via spectral expansion 0-8495  
 electron distribution function, assoc. with electrostatic emissions, dayside 0-17445  
 electrons of energy 0.3-3.0 MeV, satellite obs. 0-51632  
 electrostatic emissions and cold plasma densities 0-26696  
 electrostatic ion cyclotron waves, nonlinear steepening 0-31175  
 electrostatic waves near upper hybrid resonance freq. 0-12616  
 energetic electrons in polar cusp and high latit. plasma sheet, source regions 0-41667  
 energetic heavy ions from Jupiter, possible detect. at Skylab orbit 0-26684  
 energetic particle precipitation, Kosmos 484 polar meas. 0-8491  
 energetic protons near Earth's bow shock, pitch angle distrib. 0-26683  
 equatorial region bays, interplanetary mag. field sector polarity influence 0-8489  
 ether drag theory and the reference frames of relativistic physics 0-12905  
 geomagnetic coordinate system, high latitude station location, error determination 0-4202  
 geomagnetic field meas. from near-Earth orbit, review of obs. 0-56347  
 geomagnetic indices impulse response to interplanetary mag. field 0-51622



**magnetosphere continued**

- geomagnetic micropulsations 0-41638  
 geomagnetic storm sudden commencement, uniform ionosphere transient response rel. to preliminary reverse impulse 0-8477  
 geomagnetic variations correl. with interplanetary mag. fields 0-41642  
 geomagnetic variations in N. polar cap region, rel. to interplanetary field 0-41644  
 Geos 1 and 2 satellites, keV plasma expt., magnetospheric electrons and ions distrib. 0-41695  
 heat energy equations, time-depend., numerical soln. 0-21875  
 high-energy protons produced by substorms, interplanetary conditions 0-51615  
 hydromagnetic phenomena described by elec. currents 0-36495  
 inert gas precipitation, gases of solar and terrestrial origin, Skylab foil obs. 0-41653  
 International Magnetosphere Research programme, review (*Russian*) 0-17467  
 International Magnetospheric Study, data management 0-4206  
 interplanetary magnetic field interaction, diurnal and seasonal vars. of Y-component effect on low-latit. geomag. field 0-56354  
 inverted V event, scale of elec. field along mag. field, satellite obs. 0-41662  
 ion cyclotron wave turbulence, nonlinear effects, lab. expt., magnetosphere appl. 0-24170  
 ion cyclotron waves and high-energy protons, nonlinear interaction in Earth's magnetosphere (*Russian*) 0-17444  
 ion flux oscillations of ultralow frequency, particle obs. 0-41657  
 ions, ionospheric source with transverse acceleration 0-12604  
 irregularities, formation and evolution by mag. flux tubes interchange 0-21876  
 laboratory and space plasmas, conference, Nagoya, Japan (1977 December 8 to 9) 0-4470  
 LF radiation source located at 2.5  $R_E$ , satellite elec. field data 0-41656  
 magnetic disturbances, effects on high-latit. ionospheric absorpt., riometer meas. 0-8488  
 magnetic field models 0-41640  
 magnetic field variations by axisymmetrical magnetospheric current systems (*German*) 0-51609  
 magnetospheric instabilities, Hilbert space approach to max. growth rate 0-31172  
 magnetopause, energetic particle obs. and boundary motion 0-41650  
 magnetopause, plasma acceleration evidence for reconnection 0-26701  
 magnetopause, plasma wave turbulence obs. 0-51610  
 magnetopause, theory based on rotational shock wave 0-41641  
 magnetopause at dawn, plasma flow obs. by Voyager 1 0-41655  
 magnetopause configuration in two dimens. (*German*) 0-31167  
 magnetopause surface fluctuations, Voyager 1 obs. 0-51613  
 magnetosheath, dawnside,  $H^+$  and  $He^{++}$  mass and energy anals. 0-4204  
 magnetotail, energetic particle activity rel. to auroral activity 0-51614  
 magnetotail, mag. reconnection causing shock wave plasma accel. 0-51618  
 magnetotail, plasma flow during substorm 0-51616  
 magnetotail, self-consistent theory, general soln. for quiet tail with vanishing field-aligned currents 0-26689  
 magnetotail neutral sheet southward mag. field rel. to energetic electrons distrib. and substorms 0-26695  
 magnetotail particle acceleration, satellite obs. 0-31170  
 micropulsations at magnetospheric equator, Pc 3, 4, 5 observed by geosynchronous satellite 0-41647  
 micropulsations with long period, global electric circuit model 0-41646  
 model, based on phenomenological mag. field 0-12619  
 near-Earth plasma, 0 to 100 keV, quantitative models review 0-36459  
 neutral current layer, cosmic ray spectrum (*Russian*) 0-4211  
 particle (electric current) model 0-17442  
 particle acceleration in auroral magnetosphere 0-31171  
 particle dynamics in low freq. EM waves, magnetosphere particle flux in inhomogeneous plasma 0-1804  
 Pc 1 pulsation signal causing horizontal propag. 0-51604  
 Pc 1-2 wave obs. in outer magnetosphere 0-12618  
 Pc 3 to 5 nightside pulsations origin, Alfvén waves excitation by bouncing electron beams 0-4203  
 Pc 4.5 geomagnetic pulsations generation, influence of bounce effects 0-4197  
 perturbed Stormer problem, long periodic solns. families 0-17440  
 Pi 2 pulsations, initial movements arrival at conjugate stations 0-31173  
 plasma acceleration caused by shocks resulting from mag. reconnection 0-51618  
 plasma convection, high-latit., and ionospheric depletion, effect of displaced geomag. and geographic poles 0-26680  
 plasma convection system 0-41651  
 plasma dynamics, vertical displacement during substorms 0-4184  
 plasma entry into magnetosphere, role of irregularities 0-56680  
 plasma injection and time depend. convection electric fields 0-8494  
 plasma parameters along satellite trajectories 0-8490  
 plasma sheet dynamics, satellite obs. 0-26687  
 plasma sheet origin of electrons precipitating in assoc. with diffuse aurora 0-41614  
 plasma sheet outer boundary, particle struct. obs. 0-41654  
 plasma simulation expts., similarity laws 0-46347  
 plasma trough of dayside, warm plasma obs. at geosynchronous orbit 0-51611  
 plasmopause, spontaneous polarization of a turbulent magnetized plasma 0-19580  
 plasmopause and BDI positions during magnetic storm of 1972, Feb. 13-17th 0-56666  
 plasmopause location from Orel 2 data 0-8473  
 plasmasphere, horiz. inhomogeneities, whistler obs. 0-4168  
 plasmasphere, mid-latit., He ions behaviour 0-41630  
 polar cap electron acceleration regions rel. to interplanetary mag. field direction 0-26698  
 polar cleft, position and motion rel. to F-lacuna distrib. and occurrence freq. 0-4193  
 proton-cyclotron harmonics, instability due to anti-loss cone proton distrib. 0-56678  
 pulsar magnetosphere model, cylindrical, with particle inertia but no dissipative forces 0-51796  
 radar observation method, meas. of auroral zone elec. field 0-51573  
 reconnection, substorms and energetic particle acceleration 0-31169  
 search for interplanetary quantity controlling development of magnetospheric storms, review 0-17447

**magnetosphere continued**

- solar wind interaction, Chapman-Ferraro image method graphs correction 0-12620  
 stationary turbulence regions and anomalous resist. in magnetosphere plasma 0-38649  
 storm-time magnetic field changes, ionospheric-magnetospheric contribs. 0-12612  
 substorm, ionospheric disturbance, location and development study 0-4185  
 substorm electric fields in plasmasphere, model based on whistler data 0-41661  
 substorm inhomogeneities affected by ionosphere, experimental verification proposed 0-4199  
 substorms, ionosphere elec. fields determ. from Doppler sounding 0-4169  
 substorms, magnetic energy conversion 0-56682  
 substorms and solar flares, similar plasma processes 0-41671  
 tail, interplanetary mag. field interaction, Alfvén pulse-excited instability (*Russian*) 0-1768  
 tail region mag. field configuration, obs. 0-41649  
 tangential magnetopause structure, unified kinetic model 0-41652  
 trapping boundary at midnight, sharply defined L depend. energy threshold for anisotropy 0-41649  
 upstreaming energetic ions and electrostatic  $H^+$  cyclotron waves 0-51620  
 VLF saucer source region 0-41664  
 whistlers, meas. via remote unmanned ELF/VLF goniometer receiver in Antarctica 0-21854  
 $O^+$  energetic ions precip. during mag. storms and magnetosphere-thermosphere coupling 0-26665
- magnetospheric electromagnetic wave propagation**  
 auroral kilometeric radiation coherent generation by nonlinear beatings between electrostatic waves 0-26691  
 auroral kilometeric radiation correl. with inverted-V electron precip. 0-26692  
 circumterrestrial plasma faraday inverse effect (*Russian*) 0-4190  
 electron-coherent whistler wave interaction, rel. to precipitation 0-46349  
 ELF emissions, geographic control search 0-12615  
 examination of VLF whistler pulse analysis 0-17441  
 generation, comparative obs. 0-26685  
 HF radio noise study during auroral substorms, freq. range 8 to 25.5 MHz 0-41670  
 HF signals, magnetospheric propag. mechanism 0-4196  
 HF signals magnetospheric propag. on Earth-Earth path, exptl. investigations 0-4195  
 parametric decay of non-ducted whistler-mode signal 0-6239  
 plasma temperature anisotropy instability affecting propagation 0-46350  
 plasmopause, sounder design using ray tracing studies from geostationary satellite 0-4191  
 plasmasphere, horiz. inhomogeneities, whistler obs. 0-4168  
 plasmaspheric ELF hiss, origin, importance of wave propag. and plasmopause 0-26672  
 radio signal transmission, long-delay echoes generation, models 0-26670  
 radiowave propagation, HF and VLF propag. between mag. conjugate pts. on Earth surface 0-41639  
 super whistler, theory and anal. 0-26688  
 ULF or VLF emissions, apparent and real fine struct. 0-26697  
 VLF cross meridian refraction at 500-600 km height, electron density 0-46339  
 VLF pulse propagation and distortion, fast Fourier transform investig. 0-56679  
 VLF saucer source region 0-41664  
 VLF signal interruption causing emission triggering 0-51617  
 whistler damping near electron gyrofreq. due to cold-plasma injection, rel. to magnetosphere 0-28659  
 whistler mode instability, parallel elec. field effect 0-26700  
 whistler propagation in thermal plasma, elec. field parallel to geomag. field 0-41663  
 whistler propagation times eqn., inversion via spectral expansion 0-8495  
 whistler wave modulation, nonlinear theory 0-26686  
 whistlers, Dowden-Alcock approximation generalisation and comparison with Bernard approximation 0-51607  
 whistlers, meas. of occurrence rate during geomagnetic magnetosphere storms 0-12621  
 whistlers, nature, types and observations, review 0-36458
- magnetostatic wave devices**  
 ferrite-semiconductor structure with volume magnetostatic waves, effect of convolution 0-54761  
 status report of SAW and magnetostatic wave devices, transversal filters appl. 0-28394
- magnetostatic waves**  
 dialkylammonium copper tetrachloride, ferromagnetic layer compound, magnetostatic mode excitation 0-29538  
 ferrimagnetic materials 0-39878  
 ferrite rods, magnetised longitudinally, surface mode propag. 0-54878  
 ferrite-semiconductor structure with volume magnetostatic waves, effect of convolution 0-54761  
 ferromagnetic plate, surface magnetostatic wave excitation 0-25119  
 Permalloy I-bar elements, magnetostatic effects, unifying overview of domain and continuum results 0-44853  
 YIG dielectric layered struct. magnetostatic bulk wave steering 0-25166  
 YIG, ferromagnetic resonance and magnetostatic waves in inhomogeneous internal field (*Russian*) 0-54954  
 YIG film, dielec. layered struct., magnetostatic bulk wave power flow and energy distrib. 0-34610  
 YIG film, magnetostatic surface and forward volume wave oblique incident at shallow groove 0-34704  
 YIG film, surface wave propag. in nonuniform mag. field, anal. 0-20437  
 YIG film tangentially magnetised, magnetostatic surface wave excitation 0-29586  
 YIG film-dielectric layer-conductor struct., magnetostatic bulk wave propag. dispersion relations 0-54925  
 YIG, magnetised in raised cosine profile magnetostatic surface wave propag. 0-2567  
 YIG periodic film layer, magnetostatic surface wave propag. 0-2607  
 YIG slab, partially magnetised, expt. obs. of group delay 0-7100  
 YIG, subsidiary absorpt. spin-wave instability threshold, anomalous struct. 0-34776  
 YIG substrates, magnetoelastic surface waves, magnetostatic reson. anal. 0-20441
- magnetostriction**  
 amorphous magnetic layers, SAW device appl. 0-28389



**magnetostriction continued**

dislocated ferromagnet, inhomogeneous magnetisation near dislocation effect on FMR linewidth 0-25213  
 elastic properties of magnetic materials, review 0-7142  
 electrical steel sheet, magnetostriction meas. using Hall effect transducer (German) 0-13111  
 epitaxial garnet films, technique for magnetostriction coeff. meas. 0-243  
 ferrite, epilayers for bubble appl. 0-39829  
 ferrite, magnetoacoustic reson. in strong mag. field 0-11309  
 ferromagnet, cubic, elastic props., group theoretical approach 0-29600  
 ferromagnet, inhomogeneous, Landau's theory of second-order phase transition 0-50092  
 ferromagnet, planar, US attenuation, spin-phonon coupling, magnons and magnetostriction contrib., calc. 0-34611  
 ferromagnet, rectilinear screw dislocation, magnetisation distrib. 0-44897  
 ferromagnet, soft, non-zero magnetostriction, hysteresis rel. to irreversible phase transition 0-34693  
 ferromagnetic alloys, amorphous, sputter-deposited, soft mag. props., magnetostriction 0-34696  
 Invar, dislocation motion anomaly 0-10554  
 magnetic transitions, first-order intrinsic volume magnetostriction concept 0-29562  
 magnetostrictive ferrites, energy dissipation in high-freq. cyclic loading 0-15779  
 mathematical models for direct and reverse magnetostriction (Rumanian) 0-25171  
 measurement of magnetostrictive vibr., laser interferometric technique 0-37059  
 metallic glasses, characts. and appls. (French) 0-39815  
 metallic glasses, mag. props., effect of mech. deform. 0-39840  
 optical fibre magnetostrictive perturbation for possible mag. field detect. 0-53450  
 pulse-producing wire plating 0-2618  
 rare earth alloys, RFe<sub>2</sub>, magnetostriction studies, book contrib. 0-39846  
 rare earth alloys for magnetostrictive underwater sound transducers 0-19204  
 rare earth aluminium Laves phase cpds., RAl<sub>2</sub>, anisotropic magnetostriction, temp. depend. 0-39841  
 rare earth garnets, prep. and props. book contrib. 0-44193  
 rare earth intermetallics, quadrupole interactions, magnetoelasticity 0-15489  
 rare earth Laves phase compounds, R<sub>x</sub>R<sub>1-x</sub>Fe<sub>2</sub>, magnetostriction, anisotropy energy 0-25177  
 rare earth-Al Laves phase intermetallics, RAl<sub>2</sub>, R=Gd, Ho, Dy, Tb, cubic Laves phase compounds, exchange striction determ. 0-44895  
 rare earth-Fe rod, US resonance with large eddy currents 0-54933  
 review (Rumanian) 0-34747  
 steel, induced anisotropy influence on mag. props., thermomagnetic working (Russian) 0-55549  
 tape cores carrying current, torsional stress effects 0-34742  
 theory and measurement techniques, book contrib. 0-11241  
 transition metal amorphous alloys, mag. props. 0-29576  
 CeAl<sub>2</sub>, Anderson lattice system, ground state props. 0-20443  
 CeFe<sub>2</sub>, magnetostriction and magnetisation 0-39844  
 (Co,Fe,M)<sub>78</sub>Si<sub>8</sub>B<sub>14</sub> amorphous alloys (M=V,Nb,Ta,Cr,Mo,W,Mn or Ni), zero magnetostriction and low field mag. props. 0-34741  
 Co-Ni-Fe-Si(B), amorphous ribbon, magnetostriction meas. 0-15778  
 Co<sub>100-x</sub>B<sub>x</sub>, amorphous alloys, saturation magnetostriction and annealing behaviour 0-34739  
 Co<sub>80</sub>B<sub>20</sub>, amorphous metal ribbon, stresses, magnetoelastic anisotropy and zero-field mag. domain struct. 0-44896  
 Co<sub>79</sub>Fe<sub>6.5</sub>B<sub>14.5</sub> amorphous thin films, zero magnetostriction, high magnetisation 0-34708  
 Co<sub>35</sub>P<sub>15</sub>, amorphous, strip domains, anisotropy const. effects 0-29571  
 Co<sub>1-x</sub>Ti<sub>x</sub>, ferromag. props., Ti conc. effect 0-54872  
 CuCl<sub>2</sub>·2H<sub>2</sub>O, magnetoelastic props. under press., antiferromagnetic resonance, lattice parameters 0-29598  
 CuCr<sub>2</sub>Se<sub>4</sub>, crystal growth from melt, exam. of props. 0-55283  
 Er<sub>3-x</sub>Fe<sub>2</sub>O<sub>12</sub>, garnet, mag. anisotropy and magnetostriction 0-11189  
 (Fe,X)O<sub>4</sub>, (X=Ti, Co, Mg, Mn, Ni), magnetostriction calcs. (Dutch) 0-2619  
 Fe base amorphous alloys, Invar and Elinvar characts. 0-29592  
 Fe, polycryst., magnetostriction sign change under compressive stress 0-29596  
 Fe-Al alloys, rapidly quenched, mag. props. 0-29579  
 Fe-Ci, high permeability, mag. props., applied stress effects 0-34726  
 Fe-Cr-B, amorphous, Elinvar and Invar charact. (Japanese) 0-11832  
 Fe-Pd crystalline alloy, positive large linear magnetostriction 0-25173  
 Fe-Si (3 wt.%), mag. props., stress coating effects 0-34728  
 Fe-Si (3 wt.%) laminations, isotropic and cube-on-face, magnetostriction behaviour 0-39843  
 Fe-Si (3 wt.%) steel, high permeability, magnetostriction, stress inducing coating effects 0-34730  
 Fe-Si single crystals, interaction of {110} 90° walls with lattice imperfections 0-39807  
 Fe-Si-B amorphous films, mag. props. 0-34710  
 Fe<sub>2</sub>Al, ordered, magnetostriction and thermal expansion 0-39842  
 Fe<sub>100-x</sub>B<sub>x</sub>, amorphous alloys, saturation magnetostriction and annealing behaviour 0-34739  
 Fe<sub>80</sub>(B,C<sub>1-y/20</sub>)<sub>20</sub>, amorphous, saturation magnetostriction, comp. effects 0-34735  
 Fe<sub>80</sub>B<sub>15</sub>Si<sub>5</sub> metallic glass, large uniaxial magnetostrictive anisotropy, magnetisation reversal 0-34736  
 Fe<sub>80</sub>(B,Si<sub>1-y/20</sub>)<sub>20</sub>, amorphous, saturation magnetostriction, comp. effects 0-34735  
 Fe<sub>81.5</sub>B<sub>14.5</sub>Si<sub>4</sub>, amorphous metal ribbon, stresses, magnetoelastic anisotropy and zero-field mag. domain struct. 0-44896  
 Fe<sub>40</sub>Ni<sub>40</sub>P<sub>14</sub>B<sub>6</sub>, amorphous, strip domains, anisotropy const. effects 0-29571  
 Fe<sub>1-x</sub>Ti<sub>x</sub>, ferromag. props., Ti conc. effect 0-54872  
 Fe<sub>2</sub>TiO<sub>4</sub>, cooperative Jahn-Teller effect, neutron scatt. study 0-49678  
 Gd-Co amorphous sputtered film, magnetostriction and anisotropy 0-39821  
 NH<sub>3</sub> halides, acoustic anomalies above critical temps., volume magnetostriction type terms 0-2123  
 Ni, forced magnetostriction at 4.2K 0-50155  
 Ni, magnetoelastic and magnetostrictive sensitivities, reversible and irreversible components (Russian) 0-25172  
 Ni, rectilinear screw dislocation, magnetisation distrib., mag. moment anal. 0-44897

**magnetostriction continued**

Ni, spontaneous magnetostriction determ. method, molecular field theory study (Russian) 0-50157  
 Ni-Co (25 wt.%), single crystals, mag. annealing effect on magnetostriction and magnetisation (Japanese) 0-34744  
 Ni-Co amorphous alloys, magnetostriction 0-34738  
 Ni-Fe-Cr, extraordinary Hall effect, elec. and mag. meas. at 77 and 300K 0-34421  
 Ni<sub>1-x</sub>Ti<sub>x</sub>, ferromag. props., Ti conc. effect 0-54872  
 TbCo<sub>2</sub>, rhombohedral distortion at low temp. 0-34743  
 TbFe<sub>2</sub>, magnetoelastic props., magnetostriction hysteresis (Russian) 0-29590  
 UGa<sub>2</sub>, mag. and magnetoelastic props. 0-15775  
 V<sub>3</sub>Si, US anomaly when cooled below martensitic and supercond. transition temps. 0-20354  
 Y<sub>1.62</sub>Sm<sub>0.21</sub>Lu<sub>0.27</sub>Cu<sub>0.9</sub>Ge<sub>0.9</sub>Fe<sub>4.1</sub>O<sub>12</sub>, implanted bubble garnet, anisotropy profile, FMR study 0-7103  
 Zr(Fe<sub>1-x</sub>Co<sub>x</sub>)<sub>2</sub>, magnetovolume effects, thermal expansion and forced vol. magnetostriction meas. 0-29595  
 (Zr<sub>1-x</sub>Nb<sub>x</sub>)Fe<sub>2</sub>, magnetovolume effects and Invar characters 0-15773

**magnetostrictive devices**  
 mobility analogy equivalent cct. of magnetostrictive transducer in presence of eddy currents 0-48540  
 radiation reactance of magnetostrictive transducer, spherical scatterer effect 0-48531  
 reactor diagnosis by acoustic meas. methods, magnetostrictive and piezoelec. high-temp.-resistant sensors 0-32411

**magnetostrictive microphones** *see microphones*  
**magnetostrictive transducers** *see magnetostrictive devices; transducers*  
**magnetothermal effects** *see magnetocaloric effects*

**magnetrons**  
 discharge, DC, Ar filled diode, spectroscopic obs. 0-44010  
 helical electron beam shaping using synthesis of axially symmetrical systems 0-309  
 ion sputtering, thin film layers deposition uniformity investigation (Russian) 0-20787  
 manometer, magnetic-discharge open-type, with inhomogeneous mag. field 0-31730  
 reactive DC sputtering, magnetron-plasmatron processing and instrumentation, review 0-35090

**magnets**  
*see also electromagnets; permanent magnets; superconducting magnets*  
 hybrid magnets for high mag. field generation, polyhelix coils, optimization calcs. 0-240  
 SrO.nFe<sub>2</sub>O<sub>3</sub> isotropic ferrite magnets, manuf. process and mag. props. (Japanese) 0-29915

**magnons**  
*see also phonon-magnon interactions; spin waves*  
 amorphous solids, low-energy excitations of phonons, magnons, electrons rel. to struct. factor 0-44488  
 antiferromagnet, high frequency properties, spin wave spectra corrections magnon interactions (Russian) 0-54876  
 antiferromagnets, magnon parametric generation with impulses at Brillouin zone boundary (Russian) 0-29540  
 antiferromagnets, spin waves, microwave and optical expts., review 0-50081  
 Bose expansion for general spin, exact 0-31662  
 dilute ferromagnet, slow neutron inelastic scatt. by spin excitations, cluster approx. 0-11168  
 dislocated ferromagnet, inhomogeneous magnetisation near dislocation effect on FMR linewidth 0-25213  
 electron-magnon interaction effects on Ward-Takahashi identities in itinerant electron ferromag. 0-39730  
 ferrimagnet, polaritons, mag. susceptibility 0-7095  
 ferromagnet, light scatt. by spin waves 0-45086  
 ferromagnet, planar, US attenuation, spin-phonon coupling, magnons and magnetostriction contrib., calc. 0-34611  
 ferromagnet, spin wave nonresonant excitation by varying mag. field, nonequilibrium states (Russian) 0-34616  
 ferromagnetic alloys, itinerant electron model, spin wave stiffness const. calc. 0-34613  
 ferromagnetic chain, anisotropic, kink excitations, nonlinear model 0-54881  
 ferromagnetic chain, characts. of soliton-like mag. excitations 0-39762  
 ferromagnetic metal, magnon and cond. electron relax. processes (Russian) 0-7102  
 ferromagnetic resonance in anisotropic Heisenberg model, magnon-magnon, phonon-magnon interactions (Russian) 0-11274  
 ferromagnetic semiconductor, CESR line width, two-magnon exchange splitting 0-29621  
 ferromagnetic semiconductor, magnon coupling to plasmons and LA phonons, s-d model 0-29536  
 ferromagnetic semiconductor, refr. index variation in strong alternating mag. field 0-23741  
 ferromagnetic semiconductors, dielectric function depend. on magnetisation, light absorpt. coeff. (Russian) 0-15467  
 ferromagnetic semiconductors, Raman scattering of light on plasmon excitations 0-2738  
 ferromagnetic semiconductors, self-consistent electron-magnon oscillations 0-7098  
 ferromagnets, anisotropic, HF magnon energy renormalisation, kinematic consistency 0-29539  
 ferromagnets, conducting, magnon spectra and magnetoacoustic reson. singularities (Russian) 0-50154  
 ferromagnets, magnetic vortex as topological soliton in Landau-Lifshitz eqns. (Russian) 0-7097  
 ferromagnets, magnon relaxation, spin-orbit interaction, itinerant electron ferromagnets 0-11179  
 Ising model, one dimensional, with infinite radius of interaction in transverse magnetic field 0-2587  
 kinetic eqns. in parametric ultrasonically excited ferromagnets 0-44820  
 localisation in condensed matter, electrons, phonons and magnons 0-10905  
 magnetic semiconductors, magnetoelectric effect, classical and quantum theory, magnon drag effect 0-34746  
 manganese aluminosilicate glass, insulating spin glass, exchange dipole optical transition 0-40136  
 metals, ferromagnetic, point contact spectroscopy, electron-magnon interactions (Russian) 0-54766  
 one-dimensional planar magnets, low temp. NMR 0-44943



**magnons continued**

- one-magnon states in BCC Heisenberg antiferromag., spectral density near stepped surfaces 0-20396  
 periodic lattice, theory of coexistence of supercond. and magnetism, supercond. transition temp. 0-34543  
 semiconductor, antiferromagnetic, spin-magnetomagnon resonance 0-2566  
 spin system, mag. excitations, polarised neutron inelastic and quasi-elastic scattering 0-50045  
 spin waves, space disordered media phenomenological Lagrangian, exchange, relativistic interactions (*Russian*) 0-29537  
 superconductivity-ferromagnetism coexistence, transition temp., magnon freq., indirect exchange 0-44757  
 transition metal alloys, ferromagnetic, low temp. resist. calc. 0-24919  
 trimethylammonium cobalt trichloride dihydrate, Ising-like system, nucl. spin-lattice relax. of  $^1\text{H}$  and  $^{35}\text{Cl}$  0-29638  
 $\text{CdCr}_2\text{Se}_4$ , refr. index variation in strong alternating mag. field 0-23741  
 $\text{Co}_{1-x}\text{B}_x$ , polycrystalline and amorphous sputtered films, Brillouin spectra 0-2775  
 $\text{CoCO}_3$  light scatt. from parametric magnons and phonons (*Russian*) 0-34937  
 $\text{CoCO}_3$ , spin wave spectra light scatt. expts., review 0-50081  
 $\text{CoCO}_3$ , weak ferromagnet, antiferromag. reson. and two-magnon absorpt. (*Russian*) 0-29627  
 $\text{Co}_{75-x}\text{Fe}_x\text{Si}_{15}\text{B}_{10}$ , quenched ferromag. ribbon, Brillouin spectra 0-2776  
 $\text{CsCoBr}_3$ , quasi one dimensional antiferromag., magnon Raman scatt. 0-11395  
 $\text{CsMnCl}_2 \cdot 2\text{H}_2\text{O}$ , nonequilibrium magnon population obtained by optical pumping (*Russian*) 0-11457  
 $\text{CsMnF}_3$ , magnon absorption and luminesc. 0-7400  
 $\text{CsMnF}_3$ , RF modulation effect on parallel microwave pumping threshold (*Russian*) 0-29628  
 $\text{CsMnF}_3$ , spin wave spectrum obs., review 0-50081  
 dimethylammonium manganese tetrachloride, 2D Heisenberg antiferromag., spin wave anal. 0-54879  
 $\text{EuO}$ , light scatt. by spin waves 0-45086  
 $\text{Eu}_{1-x}\text{X}_x\text{S}$  ( $\text{X}=\text{Sr}, \text{Gd}$ ), spin-disorder-induced Raman scatt. from phonons, expt. investigation 0-20635  
 $\text{EuX}$  ( $\text{X}=\text{O}, \text{S}, \text{Se}$ ) 0-20635  
 $\text{Fe}$ , elec. resist. between 2 and 30K, deviations from Matthiessen's rule 0-10944  
 $\text{Fe}$ , light scatt. by spin waves 0-45086  
 $\text{Fe}$ , light scatt. from surface and bulk thermal magnons 0-45087  
 $\text{Fe}_{1-x}\text{B}_x$ , polycrystalline and amorphous sputtered films, Brillouin spectra 0-2775  
 $\text{Fe}_{100-x}\text{B}_x$ , quenched ferromag. ribbon, Brillouin spectra 0-2776  
 $\text{FeF}_2$ , one-magnon Raman scatt., anomalous behaviour of anti-Stokes-Stokes intensity ratio 0-40115  
 $\text{FeF}_2 \cdot \text{Co}^{2+}$ , impurity-induced magnon, influence of localisation 0-11182  
 $\text{Fe}_2$ , neutron inelastic scatt. from mag. excitations 0-50078  
 $\text{Fe}_2\text{Mo}_2\text{B}_{20}$ , quenched ferromag. ribbon, Brillouin spectra 0-2776  
 $\text{Fe}_2\text{Ni}_{80-x}\text{B}_{20}$ , quenched ferromag. ribbon, Brillouin spectra 0-2776  
 $\text{Gd}$ , microcontact magnon spectra, electron-magnon interaction (*Russian*) 0-54768  
 $\text{GdIG}$ , spin wave intrinsic relaxation, magnon damping at low temps. 0-29543  
 $^3\text{He}$ , superfluid, A-phase, viscosity tensor, generalised paramagnon model 0-39379  
 $\text{Ho}$ , microcontact magnon spectra, electron-magnon interaction (*Russian*) 0-54768  
 $\text{K}_2\text{CoF}_4$ , pseudo Ising antiferromag., inelastic light scatt. by mag. excitons 0-11377  
 $\text{K}_2\text{CoF}_4 \cdot \text{Mn}^{2+}$ , impurity induced mag. excitations, magnon gap mode, far IR spectra obs. 0-44821  
 $\text{K}_2\text{CuF}_4$ , microwave excitation, optical detection of ferromagnetic reson. 0-50197  
 $\text{K}_2\text{MnF}_4$ , nucl. spin-magnon relax. time, temp. depend., NMR study 0-25117  
 $\text{K}_2\text{MnF}_7$ , two magnon Raman scatt., magnon dispersion, susceptibility, Green's function methods 0-50340  
 $\text{K}_2\text{NiF}_4$ , nucl. spin-magnon relax. time, temp. depend., NMR study 0-25117  
 $\text{KNi}_2\text{Mn}_{1-x}\text{F}_3$ , mixed antiferromagnet, light scatt. meas. 0-16025  
 $\text{MnCO}_3$ , RF modulation effect on parallel microwave pumping threshold (*Russian*) 0-29628  
 $\text{MnCO}_3$ , spin wave spectrum obs., review 0-50081  
 $\text{Nb}$ , spin fluctuations effect on  $T_c$ , from sp. ht. and mag. suscept. 0-7030  
 $\text{Ni}$ , light scatt. from surface and bulk thermal magnons 0-45087  
 $\text{O}$ , solid, magnetic props. theory for Heisenberg system (*Russian*) 0-54900  
 $\text{PdAg}_{1-x}$ , possibility of superconductivity 0-10862  
 $\text{Rb}_2\text{CoF}_4$ , pseudo Ising antiferromag., inelastic light scatt. by mag. excitons 0-11377  
 $\text{Rb}_2\text{MnCl}_4$ , 2D Heisenberg antiferromag. spin wave analysis 0-54879  
 $\text{RbMnF}_3$ , antiferromagnetic resonance, optical detection, luminescence 0-7174  
 $\text{Rb}_2\text{NiF}_4$ , planar antiferromagnet, cluster-Bethe-lattice method 0-22306  
 $\text{Tb}$ , magnon lifetimes at 4.2K 0-15710  
 $\text{Tb}$ , microcontact magnon spectra, electron-magnon interaction (*Russian*) 0-54768  
 $\text{V}$ , spin fluctuations effect on  $T_c$ , from sp. ht. and mag. suscept. 0-7030  
 $\text{YIG}$ , spin and magnetoelastic waves on longit. mag. pumping, optical obs. (*Russian*) 0-29727

**Magnus effect** see fluid dynamics

**mail** see postal services

**maintenance** see maintenance engineering

**maintenance engineering**

- aluminium plants electrolytic baths, power consumption limitation method (*Russian*) 0-3366  
 BWR control rod drive hydraulic return nozzle repair 0-23043  
 Indian Point Unit No.2 reactor vessel, detection and identification of loose object 0-18553  
 Millstone power plant, Unit 3 design 0-22922  
 nuclear medicine instruments maintenance, IAEA programme in Southeast Asia 0-46082  
 nuclear power conf., Chicago, United States, July 1979 0-794  
 nuclear stations, maintenance optimization through trend monitoring 0-18552  
 PWR steam generator repair options 0-22923  
 reactor fluid systems, program for initial cleaning 0-23047

**maintenance engineering continued**

- Tokamak fusion reactor, design modifications to simplify remote maintenance 0-18613  
 Tokamak fusion test reactor, in-vessel maintenance remote manipulator system 0-18611

**Majorana forces** see nuclear forces

**majority algebra** see algebra

**Malter effect** see secondary electron emission

**management**

- see also research and development management  
 high-level radioactive waste management 0-37470  
 nuclear power in developing countries, regulatory capability transfer 0-13634  
 peat resource management policy formulation, systems approach 0-30324  
 radioactive waste management practices in selected European countries 0-37471

**management information systems**

- see also database management systems  
 microprocessor, in industry (*French*) 0-17729

**Mandelstam representation**

- nuclear fission, Mandelstam-Sommerfeld-Watson transformation (*Rumanian*) 0-47463

**manganese**

- see also nuclei with .....  
 antiferromagnetic, spin wave mode, wave function calcs. 0-20098  
 atom, electronic spectra of 3s and 3p levels and X-ray K spectra, many-config approx. 0-32615  
 charged particle prod. cross sections for 14 MeV neutrons, Ti, V, Cr, Mn 0-42648  
 corrosion, at high temp. in pure  $\text{SO}_4$  0-50774  
 deep sea nodules deposits, telemetering methods (*German*) 0-26623  
 deep-sea Mn nodules, quant. distrib. and metal content (*Japanese*) 0-8292  
 determ., in seawater, graphite furnace atomic absorption spectroscopy 0-40768  
 determ. in water and organic materials, flameless atomic absorpt. spectrometry with wire loop atomiser 0-45586  
 diffusion characteristics in Ag, 1051 to 1220K 0-15308  
 electronic structure model, Invar effect, antiferromagnetic-non mag. transitions and  $\alpha$ -phase 0-20370  
 estuarine river water, particulate heavy metal content, Cochin backwater, India 0-7964  
 extended X-ray finestructure observation 0-25482  
 film, refractive index determ. using Rayleigh-Lowe refractometer 0-7427  
 lithium potassium tartrate monohydrate:  $\text{Mn}^{2+}$ , isomorphism with lithium ammonium tartrate monohydrate, EPR obs. 0-29607  
 molten, contact reaction with graphite 0-15342  
 nickel acetate tetrahydrate:  $\text{Mn}^{2+}$ , EPR spectra, angular var. calc. 0-54940  
 Pacific Ocean, Mn distrib. 0-56494  
 phosphate glass  $\text{Mn}^{2+}$ , luminesc. colour change 0-7392  
 potassium oxalate,  $\text{Mn}^{2+}$  EPR spectra 0-39858  
 river water solution with Fe and organic material, estuarine mixing implications 0-17296  
 Si:Mn, surface characterised by negative electrochemical pot., electronic props. 0-44695  
 skin lesion Mn, Cu and Zn conc. meas. by neutron activation 0-17063  
 spectrochemical analysis of biological solns. using wall stabilised arc source 0-41343  
 strontium acetate hemihydrate:  $\text{Mn}^{2+}(\text{Cu}^{2+})$ , EPR, spin Hamiltonian anal. and unit cell symmetry 0-29603  
 vapour laser, self-terminating, max. pulse repetition freq. 0-23677  
 $\text{BaAl}_2\text{O}_{19}$ :Mn, phosphor, vac. UV excitation spectra, appl. to gas discharge display 0-2816  
 $\text{BaTiO}_3$ :Mn, annealed in  $\text{H}_2$  and  $\text{O}_2$ , valence change in phase stability 0-20600  
 $\text{BaTiO}_3$ :Mn, polycrystn., annealing effect on transition temps. 0-3100  
 $\text{CaF}_2 \cdot \text{Mn}^{2+}$ , fluoride, radiation and thermal redox processes 0-55678  
 $\text{CaI}_2$ :Mn, recomb. processes, luminesc. characts. (*Russian*) 0-25450  
 $\text{Ca}_2\text{P}_2\text{O}_7$ :Sb, Mn, luminesc., colouration 0-2828  
 $\beta\text{-Ca}_3(\text{PO}_4)_2$ :Sb, Mn, luminesc., colouration 0-2828  
 $\text{Ca}_3(\text{PO}_4)_2 \cdot \text{OH}$ : $\text{Mn}^{2+}$ , thermolum. props. 0-2877  
 $\text{CaS}$ :Mn,Ce, phosphor, fluoresc. spectrum, fine struct.,  $^4\text{T}_{1g}({}^4\text{G})$ - $^6\text{A}_1({}^6\text{S})$  transition 0-45130  
 $\text{Cs}_2\text{SiF}_6$ : $\text{Mn}^{4+}$ , Jahn-Teller effect in  $^4\text{T}_{2g}$  state, Zeeman meas. 0-29367  
 $\text{Fe-Mn}$  powders, reactions with  $\text{NH}_4\text{Cl}$  and  $(\text{NH}_4)_2\text{CO}_3$  0-11597  
 $\text{I}_2$ :Mn, doping effect on elec. cond., semicond. props. 0-49732  
 $\text{InSb}$ : $\text{Mn}^{2+}$  nondegenerate semicond., mag. impurity indirect interaction (*Russian*) 0-34591  
 $\text{In}_{2-x}\text{Sn}_x\text{O}_{3-y}\text{ZnS}$ :Mn thin film structure, surface morphology and electro-optical props. (*Russian*) 0-49554  
 $\text{K}_2\text{CoF}_4 \cdot \text{Mn}^{2+}$ , impurity induced mag. excitations, magnon gap mode, far IR spectra obs. 0-44821  
 $\text{K}_2\text{O-B}_2\text{O}_3$ : $\text{Mn}^{2+}$  glass, fine struct. parameter distribs., EPR meas. 0-11256  
 $\text{KZnF}_3$ : $\text{Ni}^{2+}$ ,  $\text{Mn}^{2+}$ , interference transition electric dipole mechanism 0-34896  
 $\text{LiCl}(\text{Br})$ : $\text{Mn}^{2+}$ , optical absorpt., charge transfer spectra 0-2797  
 $\text{Li}_2\text{O-B}_2\text{O}_3$ : $\text{Mn}^{2+}$  glass, fine struct. parameter distribs., EPR meas. 0-11256  
 $\text{MgF}_2$ : $\text{Mn}^{2+}$ , Coulomb and exchange interaction consts. optical spectra line assignment, new technique 0-45124  
 $\text{MgO}$ : $\text{Mn}^{2+}$ , clustering of mag. ions, study method 0-11155  
 $\text{MgO}$ : $\text{Mn}^{2+}$ , spin Hamiltonian parameters, lattice expansion and vibr. effects 0-24851  
 $\text{Mg}_2\text{SiO}_4$ : $\text{Mn}^{2+}$ , elec. field gradients, asymmetry parameters 0-54660  
 $^{54}\text{Mg}$ , removal from waste water by oxine-impregnated activated charcoal 0-9344  
 $\gamma$ -Mn, enthalpy of fusion at 1386K 0-6490  
 Mn XIV, level struct. and predicted intercombination lines 0-14098  
 Mn XVII to Mn XXII ions spectrum emitted by Tokamak produced plasma 0-10437  
 $\text{Mn}^{2+}$ , effect on sodium polyelectrolyte impedance parameters in electrochem. cell 0-21296  
 $\text{Mn}^{2+}$ , crystalline spherical pot., effect on Fermi-contact term 0-20140  
 $\text{Mn}^{2+}$ , cubic spin-Hamiltonian parameters in inorganic compounds, superposition model anal. 0-20367  
 $\text{Mn}^{2+}$  EPR spectra in glasses with  $g_{\text{eff}}=4.29$  computer simulation 0-34764



**manganese continued**

- Mn<sup>2+</sup>, effects on prolonged depolarising afterpot. in barnacle photoreceptor 0-8051  
 Mn<sup>2+</sup>, impurities in CaCO<sub>3</sub>, magonite EPR, orthorhombic spin-Hamiltonian parameters 0-2631  
 Mn<sup>2+</sup>, in nearly tetrahedral clusters, <sup>4</sup>E levels, orbit-lattice interaction and Jahn-Teller effect, spectra obs. 0-24860  
 Mn<sup>2+</sup>, in soln., non-radiative transitions as Forster's energy transfer to solvent vibrations 0-1014  
 Mn-SiO cermet films, DC and AC resist. 0-54804  
 Mn-SiO cermet films, elec. resist., annealing behaviour 0-54803  
 Mn-substituted garnet film, growth characts. and mag. props. 0-39826  
 Mn<sup>2+</sup>-Cu<sup>2+</sup> coupled pair, ESR spectrum, strong isotropic exchange model 0-29606  
 Mn<sup>2+</sup>-F<sup>-</sup>, overlap and covalency contrib. to zero field splitting, LCAO-MO calc. 0-24850  
 Mn<sup>2+</sup>-KBrO<sub>3</sub>-H<sub>2</sub>SO<sub>4</sub>-KBr system, chem. automat with three steady states 0-7769  
 Mn<sup>2+</sup>-O<sup>2-</sup>, overlap and covalency contrib. to zero field splitting, LCAO-MO calc. 0-24850  
<sup>55</sup>Mn, uptake of gamma-emitting activation products in plants 0-30614  
 NaCl:Mn<sup>2+</sup>, CN<sup>-</sup>, EPR spectrum rel. to Mn<sup>2+</sup>-vacancy-CN<sup>-</sup> complex 0-54942  
 NaCl:NaF:Mn<sup>2+</sup>, point defects, ionic thermal current and optical meas. 0-6403  
 NaF:Mn<sup>2+</sup>, VUV absorpt. spectrum and EPR 0-55142  
 Na<sub>2</sub>O-B<sub>2</sub>O<sub>3</sub>:Mn<sup>2+</sup> glass, fine struct. parameter distrib., EPR meas. 0-11256  
 Ni-Mn multilayer for monochromators and supermirrors, neutron reflectivities 0-22880  
 Ni<sub>2</sub>MnSn, ferromag. Heusler alloy, electronic struct., spin polarisations, theory 0-54598  
 Ni(NH<sub>4</sub>)<sub>2</sub>(SO<sub>4</sub>)<sub>6</sub>H<sub>2</sub>O, Mn<sup>2+</sup> doped, EPR study 0-34763  
 NiSO<sub>4</sub>·7H<sub>2</sub>O, Mn<sup>2+</sup> doped, EPR study 0-34763  
 Pb<sub>1-x</sub>Sn<sub>x</sub>Te, Mn, Mn mag. and elec. active states, mag. impurity behaviour 0-44627  
 RbCaF<sub>3</sub>:Mn<sup>2+</sup>, overlap and covalency contrib. to zero field splitting, LCAO-MO calc. 0-24850  
 RbMgF<sub>3</sub>:Mn<sup>2+</sup>, EPR obs. and struct. interpret. (French) 0-50167  
 p-Si:Mn, giant residual cond. 0-20250  
 Si:Mn amorphous films, ESR and elec. cond. 0-50171  
 p-Si-Mn contact, barrier height 0-34510  
 SnO<sub>2</sub>-ZnS:Mn thin film structure, surface morphology and electro-optical props. (Russian) 0-49554  
 SnTe:Mn, EPR as probe of phase transitions 0-15790  
 SnTe:Mn, NMR study 4.2 to 300K (French) 0-54960  
 TiO<sub>2</sub>:Mn, impurity levels, photocurrent and ESR meas. 0-29346  
 ZnCr<sub>2</sub>Se<sub>4</sub>:Mn, paramagnetic, giant cubic anisotropy 0-7073  
 ZnF<sub>2</sub>:Mn, thin films, electroluminescence, brightness voltage characts. hysteresis 0-20709  
 ZnGa<sub>2</sub>O<sub>4</sub>:Mn<sup>2+</sup>, EPR, spin Hamiltonian parameters 0-25195  
 ZnS:Mn, dopant conc. effect on stacking fault energy 0-2041  
 ZnS:Mn, self-activated and Mn<sup>2+</sup> emission, high press. action 0-16093  
 ZnS:Mn AC thin film electrolum. device, filament behaviour 0-20712  
 ZnS:Mn co-deposited electrolum. thin film device, phys. and elec. characterisation 0-20713  
 ZnS:Mn Schottky diodes, reverse-biased, electroluminescence, hot electron impact excitations 0-25005  
 ZnS:Mn<sup>2+</sup>, <sup>4</sup>T<sub>2</sub> level, Zeeman splittings, Jahn-Teller effect 0-40141  
 ZnS:Mn<sup>2+</sup>, spin-lattice relaxation, EPR, optical phonons 0-39852  
 ZnS:Mn<sup>2+</sup> phosphors, luminesc. excitation spectra and exciton struct. 0-55164  
 ZnSiF<sub>6</sub>·6H<sub>2</sub>O:Mn<sup>2+</sup>, ESR spectrum, effect of uniaxial compression 0-29609  
 Zn<sub>2</sub>SiO<sub>4</sub>:Mn film, electron beam depth-dose functions, cathodoluminesc. 0-2867  
 Zn<sub>2</sub>SiO<sub>4</sub>:Mn phosphor, efficiency enhancement by AlPO<sub>4</sub> substitution 0-11452  
 ZnTe:Mn, exciton refl. spectra 0-2806  
 ZnTe:Mn, ordering mechanism 0-2572

**manganese alloys**

- see also *Elinvar*; *Invar*; *manganese compounds*  
 intermetallic compounds, containing d-transition metal, hydrogenated, magnetism 0-34609  
 manganese stress gauges, low-impedance, for precision measurement in severe shock-wave environments 0-38367  
 manganin thin film microtransducers for elastohydrodynamic lubrication studies 0-37048  
 steel, austenitic, Cr-Mn, martensitic transform. effect on hardening kinetics and fracture resist. of friction surface (Russian) 0-50727  
 steel, austenitic, Cr-Mn, metastable, plasticity, contrib. of martensitic transform. during deform. (Russian) 0-30018  
 steel, austenitic, type 110G13, martensitic transform. effect on hardening kinetics and fracture resist. of friction surface (Russian) 0-50727  
 steel, austenitic Cr-Mn, M<sub>23</sub>C<sub>6</sub> carbide precipitates comp., heat and thermomech. treatment influence (Russian) 0-40361  
 steel, austenitic stainless, biphasic, ferritic, ageing and thermomech. treatment effects on struct. and props. 0-35226  
 steel, Co-Cr-Ni-Mo-Mn (39.65, 20.25, 15.33, 7.08, 1.9 wt.%) carbide formation during tempering after plastic deformation 0-16330  
 steel, Cr, carbide form. depend. on Mn, Cr, V additions, cementite stabilisation, microstruct. (Russian) 0-55399  
 steel, Cr-Mn, metastable constitution diagram and phase transforms. (Russian) 0-50590  
 steel, Cr-Mn-C-Si (20, 14, 0.2, 0 to 3 wt.%), high-temp. oxidation (Russian) 0-25904  
 steel, fine grained C-Mn-V-Al-N, relationship between ferrite and austenite grain size 0-3001  
 steel, low C, Mn effect on recrystallisation and texture (French) 0-3110  
 steel, low-alloy, case carburised, retained austenite effect on contact fatigue strength 0-30096  
 steel, low-alloy, V effect on mech. props. 0-35312  
 steel, Mn-Ni-Mo low alloy steels for nuclear appl., toughness and heat treatment 0-5239  
 steel, Mn-Si, St 52-3, cleavage fracture toughness, temperature and notch sharpness influence (German) 0-35291  
 steel, Mn-Si, St 52-3, fracture toughness determ. from yield strength and cleavage fracture strength (German) 0-35292  
 Ag-Mn, dil. alloy, transverse magnetoresist. in spin glass regime 0-34417

**manganese alloys continued**

- Ag-Mn, spin glass, mag. susceptibility hydrostatic press depend., RKKY interaction 0-44845  
 Al-Cu-Mg-Mn-Si-Fe, endurance with cyclic bending, effect of loading conditions 0-50724  
 Al-Cu-Mg-Mn-Si-Fe, subcritical crack growth under static plane stress 0-55528  
 Al-Cu-Mn-Mg-Fe-Si, corrosive environment effect on fatigue crack growth rate 0-55584  
 Al-Cu-Mn-Zr, type 2219, particle, coarsening of disk shaped  $\theta'$  particles 0-45315  
 Al-Mn, direct chill-cast, struct. changes during heat treating (German) 0-40408  
 Al-Mn, liq., dissoln. and diffusion of alloying components, 700-1000°C (Russian) 0-15275  
 Al-Mn, metastable L1<sub>0</sub> phase, transformations, mag. struct., TEM study 0-3029  
 Al-Mn,  $\mu^+$  localisation temp. depend. 0-44993  
 Al-Mn, quenched, thermal stability (Russian) 0-20976  
 AlMg<sub>2</sub>Mn, H impurity detection by <sup>1</sup>H(<sup>15</sup>N, $\alpha$ ) reaction 0-55767  
 Al<sub>3</sub>Mn<sub>5</sub>, rhombohedral  $\gamma$ -brass, direct imaging of struct. and structural defects 0-15115  
 Au-Mn, band profile, density of states, quantum defect-Green's function calcs. 0-54599  
 Au-Mn, orthorhombic struct., electron diffr. and electron microscopy obs. 0-15052  
 Au-Mn, spin glass, residual resistivity conc. depend. 0-2382  
 Au-Mn, spin-orbit coupling and electron scatt. 0-2370  
 B fibre reinforced Al-Mn, calc. of thermodynamic interaction potential between B fibre and matrix 0-11627  
 Bi-MnBi, directionally solidified composite, processing parameter role on mag. props. 0-35352  
 BiMn, with ferromag. inclusions, magnetisation changes by US pulses 0-34732  
 Bi<sub>50</sub>Mn<sub>44</sub>, magnetisation of ferromag. precipitates, effect of ultrasonic pulses 0-2121  
 CdGeAsMn, glass, recrystallisation 0-44133  
 Ce-Mn-Cu systems, phase equilibria at 600 and 400°C (Ukrainian) 0-11625  
 CeMn<sub>2</sub>(Si<sub>1-x</sub>Ge<sub>x</sub>)<sub>2</sub>, Ce(Mn<sub>1-x</sub>B<sub>x</sub>)<sub>2</sub>Si<sub>2</sub>, (B=Fe, Cu) mag. props. 0-25134  
 Ce-Mn, cryst. struct. and stacking fault influence on mag. props. (Russian) 0-25164  
 Co-Mn (0 to 45 wt.%), high temp. oxidation 0-35371  
 (Co<sub>1-x</sub>Mn<sub>x</sub>)B, ferromag., internal fields meas. by NMR spin echo 0-29646  
 (Co<sub>1-x</sub>Mn<sub>x</sub>)B, paramag., spin echo NMR spectra, ferromag. transition, spin-lattice relax. 0-29645  
 CoMnP, ferromagnetism and metamagnetism, polarized neutron diffr. study 0-44809  
 Cu-Al-Mn, duplex shape memory effect after nonuniform plastic deform. (Russian) 0-25759  
 Cu-Al-Mn, partial decomp. of  $\beta_1$  phase, effect on mag. props. and martensitic transform. (Russian) 0-45306  
 Cu-Mn, dil., oxide film form. in ammoniacal Cu(II) solns., AES obs. 0-45415  
 Cu-Mn, molecular field distribution function in disordered Ising model (Russian) 0-54859  
 Cu-Mn, spin glass, meas. of order parameter 0-34642  
 Cu-Mn (15 at.%), micromagnetic, short-range ordering, neutron scatt. polarisation anal. 0-50110  
 Cu-Mn spin glass, hysteresis loops, temp. and field depend. 0-15742  
 Cu-Mn spin glass, magnetisation curves, time depend. 0-15743  
 Cu-Mn spin glass alloy, spin correl. function, combined neutron spin echo and polarisation anal. 0-50107  
 Cu-Mn-P alloys, phase diagram (Russian) 0-20891  
 Cu-Mn-S, Mn surface segregation and Mn/S cosegregation 0-40367  
 CuMn, magnetisation processes below freezing temp. 0-15748  
 CuMn, spin glass, mag. correls., neutron scatt. study 0-50105  
 CuMn, spin glass, mag. hysteresis meas. 0-34691  
 CuMn, spin glass, remanence, new approach from zero field NMR 0-34785  
 Cu<sub>0.95</sub>Mn<sub>0.05</sub>, spin glass, inelastic neutron scatt., time-of-flight and three-axis techniques 0-50108  
 Cu<sub>0.95</sub>Mn<sub>0.05</sub>, spin glass, low temp. mag. excitation spectrum, inelastic neutron scatt. obs. 0-50109  
 $\gamma$ -Cu<sub>15</sub>Mn<sub>85</sub>, antiferromag., neutron diffr. 0-2550  
 Cu<sub>2</sub>MnAl, dynamical mag. susceptibility, spin waves, calc. from band struct. 0-54871  
 Cu<sub>2</sub>MnAl, Heusler alloy, decomposition at 360°C 0-7536  
 DyMn<sub>2</sub>, H<sub>2</sub> absorpt., Mossbauer study 0-44987  
 Dy<sub>2</sub>Mn<sub>17</sub>, magnetic moments, magnetisation 0-25094  
 DyMn<sub>2</sub>Si<sub>2</sub>, Mossbauer spectra 0-20558  
 Er<sub>6</sub>Mn<sub>23</sub>, magnetic moments, magnetisation 0-25094  
 Fe-As-Mn, Mn additions to Fe-As melts, influence on surface tension and density (Russian) 0-15337  
 Fe-As-Sn-Mn, melts, As and Sn distrib., Si, Cr, and Mn influence (Russian) 0-16274  
 Fe-C-Mn (0.5, 0.6 wt.%), powder forged, mech. props. 0-21096  
 Fe-C-Mn-Si (4, 2, 1.5 wt.%), cast wire, influence of B addition on struct. and elec. cond. (Russian) 0-55391  
 Fe-Cr-Mn, influence of alloying with Ni, Mo, N on defect conc. energy (Russian) 0-54241  
 Fe-Mn, dil., local mag. moments, polarised neutron elastic diffuse scatt. 0-50088  
 Fe-Mn, electron state density and elec. resist. 0-39558  
 Fe-Mn, high-temp. sulphidation, scale struct., corrosion kinetics 0-50777  
 Fe-Mn, Mossbauer spectroscopy of temp. hysteresis of phase transformations (Czech) 0-29949  
 $\alpha$ -Fe-Mn, singularities of martensite struct. (Russian) 0-28948  
 Fe-Mn, struct. defects effect on interdiffusion 0-15314  
 Fe-Mn, unlimited component solubility, intercrystallite internal adsorption (Russian) 0-39294  
 Fe-Mn 8%, type K1525 thermal cycling, effect on impact toughness 0-7608  
 Fe-Mn (-C), Mn influence on martensitic transform in presence of strain (Russian) 0-20934  
 Fe-Mn (15(24)(30)wt.%), high hydrostatic pressure influence on stress-strain curve 0-25805  
 Fe-Mn (2 to 8 wt.%) alloys, phase transformations, tempering influence (Russian) 0-25735



# manganese alloys continued

Fe-Mn (9 to 20 wt.%),  $^{57}\text{Fe}$  Mossbauer spectroscopy in phase transformations 0-29948  
Fe-Mn (up to 8 wt.%), microstructure, mech. props. and fracture (Japanese) 0-35304  
Fe-Mn alloys,  $\alpha$ ,  $\epsilon$  and  $\gamma$ , brittleness 0-35314  
Fe-Mn mag. contributions to  $\gamma$ - $\epsilon$  phase transformations 0-25694  
Fe-Mn-C, anomalous changes in austenite and martensite lattice parameters 0-50636  
Fe-Mn-C, lattice parameters of cementite, annealing effect 0-29007  
Fe-Mn-C, variation of martensite morphology with Mn and C composition 0-50635  
Fe-Mn-O melts, formation of oxide inclusions, cryst. pulling, Bridgman tests (German) 0-35074  
Fe-Mn-Sb, phase comp. 0-16267  
Fe-Mn-Ti alloys, austenitic, precipitation strengthened 0-25714  
Fe-Mn-V-C austenitic steel, discontinuous precipitation, morphological changes 0-3078  
Fe-Ni-Mn, concentration ferromag. antiferromag. phase transition and mag. state diagram. (Russian) 0-20401  
Fe-Ni-Mn (20, 5 wt.%), surface martensite, crystallography and morphology 0-40354  
Fe-Ni-Mn-C (5.9, 4.4, 0.48 wt.%) alloy, elastic moduli near martensitic transform. 0-7619  
Fe-Ni-Si-Mn-Cr(Co-Mo), effect of prolonged aging on mag. props. 0-16513  
Fe-Sb-Mn, dil., interactions and precip., Mossbauer study 0-39997  
Fe<sub>3</sub>Mn-Fe<sub>3</sub>Si, slow neutron polariser, by single cryst. (111) refl. 0-49052  
(Fe<sub>1-x</sub>Mn<sub>x</sub>)<sub>75</sub>P<sub>16</sub>B<sub>9</sub>Al<sub>3</sub>, amorphous, spin-glass-ferromag. multicritical point, AC susceptibility meas. 0-50117  
(Fe<sub>1-x</sub>Mn<sub>x</sub>)<sub>75</sub>P<sub>16</sub>B<sub>9</sub>Al<sub>3</sub>, amorphous, mag. ordering temp., hyperfine field distrib., elec. resist. 0-34633  
(Fe<sub>1-x</sub>Mn<sub>x</sub>)<sub>75</sub>P<sub>15</sub>C<sub>10</sub>, amorphous, mag. ordering, Mossbauer study 0-39747  
(Fe<sub>1-x</sub>Mn<sub>x</sub>)<sub>75</sub>P<sub>15</sub>C<sub>10</sub>, amorphous pair radial distrib. functions, neutron scatt. study 0-49128  
Fe<sub>0.65</sub>(Ni<sub>1-x</sub>Mn<sub>x</sub>)<sub>0.35</sub>, Mossbauer spectra,  $^{57}\text{Fe}$  hyperfine field distrib. 0-20533  
Gd<sub>2</sub>Mn<sub>23</sub>, magnetic moments, magnetisation 0-25094  
In-Mn, dilute alloy, local excited states, electron tunnelling observation 0-34565  
Mg-Ni-Si, electroforming, mech. props. rel. to heat treatment 0-35133  
 $\beta$ -Mn- $^{57}\text{Fe}$ - $^{119}\text{Sn}$  alloy mag. props. from Mossbauer effect obs. (Japanese) 0-15933  
Mn-Al-C, ferromag., transform. kinetics 0-34627  
Mn-Bi alloy, melting and solidification under microgravity, mag. props. (German) 0-45296  
Mn-Cr-Mo-C, master alloys, development for low alloyed PM steel 0-50576  
Mn-Cu, alloying behaviour and high damping capacity 0-35160  
Mn-Cu (9.3 wt.%), cryst. struct. at FCC to FCT transform. (Russian) 0-11643  
Mn-Cu alloy, local premartensitic instability in FCC phase 0-40355  
Mn-Cu alloy, volume effect, paramagnetic-antiferromagnetic and structural transition, lattice consts. 0-39007  
Mn-Fe-C, melts, activities of Mn at 1673K 0-50597  
Mn-Fe-C, phase instability 0-11628  
Mn-Fe-Si-C, melts, activities of Mn at 1673K 0-50597  
Mn-Ge amorphous films, short-range order, electron diffr. obs. 0-39473  
 $\gamma$ -Mn-Ni (15 at.%), antiferromag. defect scatt., neutron polarisation anal. 0-50056  
Mn-Si, liq. alloys, equilibria between MnO-SiO<sub>2</sub>-CaO-MgO slags 0-10639  
Mn-Si (62.5 to 63.8 wt.%), phase anal. and cryst. struct. (Japanese) 0-15049  
Mn-Si-C, melts, activities of Mn at 1673K 0-50597  
Mn-Si(C), melt, activation determ. by vapour press. meas. 0-16279  
Mn-Tb, dil., hyperfine interactions, nuclear orientation 0-15929  
Mn-Ti-Fe, ternary phase diagram, computer calculations 0-45274  
Mn-V-Mo-C master alloys, development for low alloyed PM steel 0-50576  
Mn-Y-Zn-Cd alloy, phase equilibria, plastic deformation, microhardness (Russian) 0-40334  
Mn-Zn ferrite single crystals, mech. polishing effect on mag. props. (Japanese) 0-16569  
Mn<sub>2</sub>Al<sub>11</sub>, X-ray cryst. struct. 0-38999  
MnAu<sub>2</sub>, helical antiferromagnetic compound, optical props. and electronic struct., visible and IR obs. (French) 0-45101  
MnBi, ionized-cluster beam and reactive ionized-cluster beam deposition. 0-16202  
MnBi, mictomag. alloys, elastic props. (Russian) 0-7141  
MnCoSi, effect of press on mag. transition temp. (Russian) 0-25137  
 $\gamma$ -MnCu, antiferromag., stressed, mag. defects meas. by neutron polarisation anal. 0-50076  
Mn<sub>1-x</sub>Fe<sub>x</sub>As, magnetic transition under high press., exchange striction model calcs. (Russian) 0-50096  
Mn<sub>1-x</sub>Fe<sub>x</sub>Pt<sub>3</sub>, noncollinear mag. structs., neutron diffr. anal. (Russian) 0-25087  
Mn<sub>2</sub>Ge<sub>7</sub>, high-temp. phase, X-ray powder cryst. struct. (German) 0-39005  
Mn<sub>2</sub>Sb, domain and domain wall resons. in  $^{55}\text{Mn}$  NMR spectrum 0-25219  
MnSi, amorphous, sputtered, mag., elec., struct. and thermal props., spin glass behaviour 0-50124  
MnSi, amorphous magnetisation meas. 0-34599  
Mn<sub>2</sub>Si<sub>3</sub>-Mn<sub>2</sub>Ge<sub>3</sub>, electrical resistivity meas., order-disorder transition 0-10945  
Mn<sub>23</sub>Y<sub>6</sub>D<sub>3</sub>, D atom location, neutron diffr. study (French) 0-24426  
Mo-Mn alloy, plasticity, fracture, strength depend. on C content (Russian) 0-35257  
Mo-Mn metalloceramic alloy, brittle fracture investigation, segregation, morphology, struct. (Russian) 0-55503  
Mo-Mn powder mixture, X-ray diffr. exam. of reaction between Mo and Mn, during sintering 0-16242  
Monel, Norton-Bailey parameters, from creep rupture data 0-30098  
Nb<sub>78</sub>Ga<sub>22-x</sub>Mn<sub>x</sub>, supercond. props., influence of Mn mag. impurities 0-54825  
Nb<sub>80</sub>Ga<sub>20-x</sub>Mn<sub>x</sub>, supercond. props., influence of Mn mag. impurities 0-54825  
Ni-Cr-Mn-Fe-Nb (20,3,3,2.5 wt.%), short-range order effects on tensile behaviour 0-25793

# manganese alloys continued

Ni-Cr-Mo-Mn alloy 02KhN40MB, corrosion-resist, heat-resist., phys. and mech. props. 0-35411  
Ni-Mn, hydrogenation kinetics, magnetisation, interstitial H influence 0-35528  
Ni-Mn, mag. moment and asphericity of spin density distrib., polarised neutron scatt. obs. 0-44813  
Ni-Mn (up to 32 at.%), Curie temp., press. depend., using press. cell developed for meas. with cubic-anvil press 0-13109  
Ni-Mn-Al-Si-Co, Almel, Ettingshausen-Nernst coeff. and transport props. from 200 to 473K 0-44573  
Ni-Zn-Mn-Fe spinel, crystn. from soln. in melt 0-2945  
(Ni<sub>1-x</sub>Fe<sub>x</sub>)<sub>99</sub>Mn, ferromagnetic, NMR study of local environment effect, relaxation mechanism 0-7193  
NiMn, high field magnetisation 0-2557  
Ni<sub>1-x</sub>Mn<sub>x</sub>, ferromagnetic, NMR study of local environment effect, relaxation mechanism 0-7193  
Ni<sub>2</sub>Mn, partially ordered, spin-wave dispersion relation, inelastic neutron scatt. meas. 0-20394  
Ni<sub>3</sub>Mn, thermomagnetic magnetisation and blocking temp. 0-34601  
Ni<sub>2</sub>Mn<sub>2</sub>M<sub>1-x</sub>Sn (M=Ti,V) mag. hyperfine fields,  $^{119}\text{Sn}$  Mossbauer spectra study 0-55003  
NiMnSb, hyperfine mag. field at Cd impurity, TDPAC study 0-39906  
(Ni<sub>0.75</sub>Mn<sub>0.25</sub>)<sub>92</sub>Si<sub>10</sub>B<sub>8</sub>, amorphous, exchange anisotropy, mag. susceptibility meas., 4.2K to room temp. 0-11186  
Ni<sub>2</sub>Mn<sub>2</sub>Ti<sub>1-x</sub>Sn, Mossbauer spectra, mag. hyperfine field 0-15857  
(Ni<sub>1-x</sub>Rh<sub>x</sub>)<sub>99</sub>Mn, ferromagnetic, NMR study of local environment effect 0-7192  
(Ni<sub>1-x</sub>Ru<sub>x</sub>)<sub>99</sub>Mn, ferromagnetic, NMR study of local environment effect 0-7192  
Pd-Fe-Mn, dil. alloy, high press. study 0-34600  
Pd-Fe-Mn, ferromag. and spin-glass props; comment 0-2591  
Pd-Mn, Curie temp. and magnetisation, vol. depend. 0-34629  
Pd-Mn, dil. alloy, very temp. magnetisation 0-34692  
Pd-Mn, mag. ordering phenomena, neutron scatt. obs. 0-44812  
(Pd<sub>0.9965</sub>Fe<sub>0.0035</sub>)Mn<sub>0.05</sub>, ferromag. and spin-glass props. 0-2590  
Pd(M<sub>1</sub>Co), giant moments, Mossbauer study of  $^{57}\text{Fe}$  0-44969  
Pd<sub>2</sub>Mn, disordered, mag. correls., neutron scatt. study 0-50105  
Pd<sub>2</sub>MnIn<sub>1-x</sub>Sb<sub>x</sub>, Heusler alloy, mag. order obs. 0-29528  
Pd<sub>2</sub>MnSn, ferromag. Heusler alloy, electronic struct., spin polarisations, theory 0-54598  
Pd<sub>2</sub>Mn<sub>0.95</sub>Sn<sub>1.05</sub>, hyperfine mag. fields, Mossbauer spectra 0-15870  
Pd<sub>2</sub>MnSn<sub>1-x</sub>Sb<sub>x</sub>, Mossbauer spectra, mag. hyperfine field 0-15868  
Pt<sub>2</sub>Mn, mag. excitation dispersion relation 0-25090  
Pt<sub>2</sub>Mn<sub>2</sub>Cr<sub>1-x</sub> alloys, mag. props. 0-2562  
Pt<sub>2</sub>Mn<sub>2</sub>Cr<sub>1-x</sub>, electronic specific heat meas. comparison with band model calcs. 0-54400  
PtMnSb, hyperfine mag. field at Cd impurity, TDPAC study 0-39906  
Rh<sub>2</sub>MnGe(Pb), hyperfine mag. field at Cd impurity, TDPAC study 0-39905  
Ti-Al-Mn, endurance with cyclic bending, effect of loading conditions 0-50724  
 $\alpha$ - $\beta$  Ti-Mn (8 wt.%), calcs. of stress-strain curve, stress and strain distrib., discussion 0-7637  
 $\alpha$ - $\beta$  Ti-Mn (8 wt.%), stress-strain curve and stress and strain distrib. calcs., reply to discussion 0-7638  
Ti-Zr-Cr-Mn/LaNi<sub>5</sub> hydriding alloy mixtures for H energy storage 0-45788  
TiMn, faceted parent martensite interface 0-6417  
V-Mn, equiatomic, ordering kinetics and antiphase domain coarsening 0-7559  
Y(Fe<sub>1-x</sub>Mn<sub>x</sub>)<sub>2</sub>, mag. order onset 0-25135  
Y(Fe<sub>1-x</sub>Mn<sub>x</sub>)<sub>2</sub>, Mossbauer spectra and mag. props. 0-39952  
Y<sub>6</sub>(Fe<sub>1-x</sub>Mn<sub>x</sub>)<sub>23</sub>, struct. and mag. props. 0-25083  
Y<sub>6</sub>Mn<sub>23</sub>, magnetic moments, magnetisation 0-25094  
Zn-Mn, dil. mag. anisotropy, Hartree-Fock calcs. 0-11162  
Zn-Mn, dil., mag. anisotropy below 1K, low field magnetisation meas. 0-20382  
Zr-Mn-H, synthesis at high H pressure exam. of props. 0-29924

# manganese compounds

see also manganese alloys  
aluminosilicate glass, insulating spin glass, exchange dipole optical transition 0-40136  
diethylammonium manganese chloride, planar Heisenberg magnet, spin diffusion, EPR study 0-15793  
dimethylammonium manganese tetrachloride, phonon density of states, expt. and calc. 0-54323  
dimethylammonium manganese tetrachloride-d<sub>2</sub>, structural and mag. phase transitions, neutron scatt. and AC susceptibility meas. 0-44825  
dipropylammonium manganese tetrachloride, and tetrabromide, two-dimens. antiferromagnet, spin canting and exchange 0-34620  
ethylammonium tetrachloromanganate, dielec. props. in phase transition region 0-55011  
ferrites, Fe-excess, charge carriers, optical props. 0-34874  
ferrites, photogalvanomagnetic effects 0-34483  
manganese zinc formate dihydrate, two-dimens. antiferromag., anomalous crit. phenomena, neutron scatt. and PMR obs. 0-50104  
di-(tetraethylammonium)tetrahalomanganate, mag. circular and linear dichroism obs. 0-29725  
TMMC:Cu, EPR lines, dynamic effect of low-symmetric spin distrib. 0-39854  
TMMC:Cu, EPR linewidth freq. depend., spin dynamics 0-15794  
TMMC, classical Heisenberg antiferromagnet, one-dimens., dynamic props., review 0-15737  
TMMC, EPR lines in one-dimensional mag. systems, dynamic effect of low-symmetric spin distrib. 0-39853  
TMMC, linear Heisenberg antiferromagnet, EPR half-field transitions 0-15792  
TMMC, one dimensional antiferromagnet, EPR expts. 0-20454  
TMMC, quasi-1D antiferromag., mag. phase diagram 0-2573  
TMMC, XY-Ising crossover transition, quasi-elastic neutron scatt. obs. 0-44826  
Al<sub>2</sub>Mn<sub>2</sub>Si<sub>2</sub>O<sub>12</sub> amorphous spin glass, spin dynamics, neutron scatt. meas. 0-15741  
(Ca<sub>0.15</sub>Mn<sub>0.85</sub>Fe<sub>0.05</sub>)SiO<sub>3</sub>, rhodonite lattice imaging of struct. defects 0-49240  
CaO-MnO system, solid soln. form. and analysis 0-28996



## manganese compounds continued

- CaO-SiO<sub>2</sub>-MnO molten mixtures, struct. and phys. props. (French) 0-24635
- CaX-MnX, X=S, Se, Te, solubility limits 0-44320
- Cd<sub>1-x</sub>Mn<sub>x</sub>Te, exchange interaction, magneto-optical spectra 0-25348
- CdMnTe, exciton ground state, magnetic field influence 0-54616
- Cd<sub>0.6</sub>Mn<sub>0.4</sub>Te crystals, Mn(3d<sup>5</sup>) band, photoemission evidence 0-11535
- Cd<sub>1-x</sub>Mn<sub>x</sub>Te, EPR, mag. crit. point 0-39851
- Cd<sub>1-x</sub>Mn<sub>x</sub>Te, Faraday rot. meas. up to 150 T 0-29722
- Cd<sub>1-x</sub>Mn<sub>x</sub>Te mixed crystals, excitonic magnetoabsorption 0-40095
- Cd<sub>1-x</sub>Mn<sub>x</sub>Te, spin-orbit coupled bands, indirect exchange interaction via electrons 0-34407
- (Co<sub>1-x</sub>Mn<sub>x</sub>)<sub>2</sub>B, 0≤x≤1, magnetisation, lattice consts., press. depend. of Curie temp. 0-7137
- Co<sub>1-x</sub>Mn<sub>x</sub>F<sub>2</sub>, antiferromagnet mag. impurities, spin excitation spectrum collective rearrangement in external mag. field 0-50199
- Cr<sub>1-x</sub>Mn<sub>x</sub>As, antiferromagnetic-ferromagnetic transition, mag. moment and elec. resist. meas. 0-15718
- Cr<sub>1-x</sub>Mn<sub>x</sub>As, antiferromag. to ferromag. transitions, superexchange-double exchange mag. coupling, susceptibility and resist. obs. 0-50070
- CsMnCl<sub>3</sub>(Br<sub>3</sub>), rare earth doped, energy transfer, emission spectra obs. 0-20684
- CsMnCl<sub>3</sub>·2H<sub>2</sub>O, quasi-one-dimensional antiferromag., phase diagram (French) 0-20405
- CsMnF<sub>3</sub>, mag. phase boundaries, XY to Ising crossover, virtual bicritical point 0-50095
- CsMnF<sub>3</sub>, NMR saturation, nuclear spin wave excitation, large freq. shifts (Russian) 0-50207
- CsMnI<sub>3</sub>, Mossbauer spectra, struct., electronic and mag. props. 0-15908
- (Fe,Mn)O<sub>4</sub>, magnetostriction calcs. (Dutch) 0-2619
- Fe<sub>1-x</sub>Mn<sub>x</sub>Cl<sub>2</sub>, disordered, Mn spin excitations by microwave absorption at high freqs. 0-34759
- Fe<sub>1-x</sub>Mn<sub>1-x</sub>(1,10-phenanthroline)<sub>2</sub>(NCS)<sub>2</sub>, spin crossover, Mossbauer and magnetism study 0-44980
- GaMn<sub>2</sub>(C<sub>1-x</sub>N<sub>x</sub>), mag. struct., phase transition, rel. to valence instabilities in rare earth compounds (French) 0-34596
- (Ge,Pb)<sub>1-x</sub>Mn<sub>x</sub>Te, mag. and elec. props. meas. 0-29534
- GeTe-MnTe, heat treatment effect on struct., elec. props. 0-54725
- GeTe-MuTe, temp. characts. of phase transition, MnTe influence 0-20926
- Hg<sub>1-x</sub>Mn<sub>x</sub>S, EPR, order-disorder transition temp. 0-50176
- Hg<sub>1-x</sub>Mn<sub>x</sub>Se, band struct. from anomalous Shubnikov-de Haas effect 0-20080
- Hg<sub>1-x</sub>Mn<sub>x</sub>Se, EPR, order-disorder transition temp. 0-50176
- Hg<sub>1-x</sub>Mn<sub>x</sub>Se, spin-orbit coupled bands, indirect exchange interaction via electrons 0-34407
- Hg<sub>1-x</sub>Mn<sub>x</sub>Te, acceptor reson., states in high mag. field 0-49668
- Hg<sub>1-x</sub>Mn<sub>x</sub>Te, EPR, order-disorder transition temp. 0-50176
- Hg<sub>1-x</sub>Mn<sub>x</sub>Te, energy levels at Γ-point in intense mag. fields, Shubnikov-de Haas effect meas. 0-24951
- Hg<sub>1-x</sub>Mn<sub>x</sub>Te, mag. field induced microwave transparency 0-49797
- Hg<sub>1-x</sub>Mn<sub>x</sub>Te, mag. props., self-consistent two spin cluster model 0-54874
- Hg<sub>1-x</sub>Mn<sub>x</sub>Te, mag. susceptibility, 2.4 to 300K 0-20379
- Hg<sub>1-x</sub>Mn<sub>x</sub>Te, magnetooptical and impurity effects 0-6721
- Hg<sub>1-x</sub>Mn<sub>x</sub>Te, Shubnikov de Haas effect and quantum oscills. of thermoelec. power 0-49781
- Hg<sub>1-x</sub>Mn<sub>x</sub>Te, spin-orbit coupled bands, indirect exchange interaction via electrons 0-34407
- Hg<sub>1-x</sub>Mn<sub>x</sub>Te, zero-gap semicond., indirect-exchange interactions 0-29370
- KClO<sub>4</sub>:MnO<sub>4</sub><sup>-</sup>, reson. Raman excitation profiles for totally symmetric mode, vibronic struct. 0-50309
- KMnCl<sub>3</sub>, rare earth doped, energy transfer, emission spectra obs. 0-20684
- K<sub>1</sub>Mn<sub>2</sub>F<sub>7</sub>, two magnon Raman scatt., magnon dispersion, susceptibility, Green's function methods 0-50340
- K<sub>2</sub>SO<sub>4</sub>:MnO<sub>4</sub><sup>2-</sup>, electronic struct. by ESR 0-44906
- LaNi<sub>5</sub>H<sub>6</sub> sponges, Mn substitution, neutron diff. 0-24427
- LaNi<sub>1-x</sub>Mn<sub>x</sub>O<sub>3</sub>, <sup>55</sup>Mn NMR study, magnetisation meas., ferromag. and Pauli paramag. components 0-7191
- Mg<sub>1-x</sub>Mn<sub>x</sub>Te<sub>2</sub>, random dil. antiferromagnet, mag. props. 0-54870
- MgMnZn ferrite, ultrafine powder, prod. by cryochemical, freeze drying, spray drying or soln. techniques 0-55336
- Mn bi-univalent cpds, soln., activity and osmotic coeffs., H<sub>2</sub>O activity, Gibbs energy, molality depend. 0-51964
- Mn-Fe-O ferrite system, thermodynamic stability, dissociation and phase relations (Japanese) 0-55378
- Mn-Si, liq. alloys, equilibria between MnO-SiO<sub>2</sub>-CaO-MgO slags 0-10639
- Mn-Zn ferrosilicates, carrier transfer phenomena 0-54727
- Mn<sub>3</sub>Al<sub>2</sub>(SiO<sub>4</sub>)<sub>2</sub>, Mossbauer spectra and absorpt. bands 0-55144
- MnAs, generalised P-T phase diagram, mag. and structural phase transition 0-39780
- MnAs, orthorhombic, low temp. magnetic transitions (Russian) 0-11193
- MnAs, PTH phase diagram of mag. transitions, Curie point 0-44832
- MnAs<sub>0.88</sub>P<sub>0.12</sub>, excitonic absorpt., derivative refl. spectra 0-25406
- MnAs<sub>0.96</sub>P<sub>0.04</sub>, latent ferromagnetism 0-11197
- MnB<sub>12</sub>, growth from melt and phys. props. 0-20782
- MnBi holographic film, reduction of thermomag. recording energy threshold (Russian) 0-43302
- MnCO<sub>3</sub> crystals, gel. grown, Ca<sup>2+</sup>, Ni<sup>2+</sup> impurity influence, SEM study 0-20778
- MnCO<sub>3</sub>, NMR saturation, nuclear spin wave excitation, large freq. shifts (Russian) 0-50207
- MnCO<sub>3</sub>, RF modulation effect on parallel microwave pumping threshold (Russian) 0-29628
- MnCO<sub>3</sub>, spin wave spectrum obs., review 0-50081
- Mn<sub>2</sub>(CO)<sub>10</sub>, extended CNDO calc. 0-918
- Mn(CO)<sub>4</sub>(NO), appl. of HF and CI calcs. 0-9513
- (Mn<sub>2</sub>(CO)<sub>8</sub>)<sub>2</sub>(GeMn(CO)<sub>2</sub>I<sub>2</sub>), X-ray cryst. struct. determ. 0-54190
- MnCl<sub>2</sub>-tetra-n-butylammonium halide melts, density, elec. cond., and viscosity 0-24631
- MnCo<sub>2</sub>O<sub>4</sub> DC sputtered films, struct. and elec. props. 0-54812
- Mn<sub>2</sub>Cr<sub>3</sub>-O<sub>4</sub>, dilute Jahn-Teller system, simple model 0-44547
- MnD<sub>3</sub>, synthesized at high pressures, neutron diff. anal. of struct. 0-28977
- MnF<sub>2</sub>, EM and acoustic energy attenuation in domain magnets 0-7140
- MnF<sub>2</sub>, magnetic, thermal, elastic refraction of light, mag. order influence on refractive index (Russian) 0-34880
- MnF<sub>2</sub>, piezo-optical effect, birefringence variation on uniaxial compression (Russian) 0-34887
- Mn<sub>4</sub>F, non-collinear component in mag. struct. 0-25089

## manganese compounds continued

- Mn<sub>1-x</sub>Fe<sub>x</sub>Cr<sub>2</sub>S<sub>4</sub>, Fe II electronic struct., Mossbauer spectra 0-15876
- MnFeO<sub>2</sub>·Co, Mossbauer spectrum, 4s covalent bonding 0-20540
- MnFe<sub>2</sub>O<sub>4</sub>, ferrite, dynamic shift of NMR freq. of nuclei located in domain walls 0-15823
- Mn<sub>2</sub>Fe<sub>3</sub>-O<sub>4</sub> epitaxial films, mag. and reson. props. 0-50149
- Mn<sub>2</sub>Fe<sub>3</sub>-O<sub>4</sub> ferrite film, exchange interaction depend. on conduction electrons (Russian) 0-34621
- Mn<sub>2</sub>Fe<sub>3</sub>-O<sub>4</sub>, optical props. 0-20606
- MnFe<sub>2</sub>(PO<sub>4</sub>)<sub>2</sub>(OH)<sub>2</sub>·6H<sub>2</sub>O, strunzite, cryst. chem., Mossbauer study 0-39975
- MnGeO<sub>3</sub>, HP phase transform. 0-19941
- Mn<sup>II</sup>(H<sub>2</sub>PO<sub>4</sub>)<sub>2</sub>·2H<sub>2</sub>O, cryst. and powder diff. data (French) 0-24419
- Mn<sub>2</sub>Mg<sub>1-x</sub>-O<sub>4</sub>, solid solution EPR, mag. interactions (Russian) 0-44908
- MnNO, appl. of HF and CI calcs. 0-9513
- MnO (100), surface struct., LEED study 0-39396
- MnO, alpha-particle irradi., Mossbauer study of nucl. reaction aftereffects 0-40015
- MnO, antiferromagnetic-paramagnetic phase transition at high press. 0-39778
- MnO based pigments, willemite struct., synthesis 0-20855
- MnO, cubic NaCl-type cryst., Debye temp. 0-54333
- MnO, dielec. behaviour, Dick and Overhauser shell model calcs. 0-45001
- MnO, EPR spectra of ceramic and epitaxial monocrystalline thin film samples (Russian) 0-11252
- MnO, X-ray determ. of electron density distrib., atomic scatt. factors 0-15078
- MnO-H<sub>2</sub>, interaction with surface, quantum chemical study 0-45549
- MnO<sub>2</sub>, β and γ conductivity meas. by new method 0-45517
- MnO<sub>4</sub><sup>-</sup> ion, <sup>18</sup>O enriched, matrix isolated IR spectra, force consts. 0-52985
- Mn<sub>2</sub>O<sub>3</sub> film, form. on glass surface from Mn<sup>2+</sup> ions in water (Japanese) 0-45411
- Mn<sub>2</sub>O<sub>3</sub>:Li(Cr)(Al)(S), and pure Mn<sub>2</sub>O<sub>3</sub>, elec. cond. and thermo-EMF 0-20231
- Mn<sub>2</sub>O<sub>3</sub>:S, defect struct. and elec. props., electron, hole conc. 0-44601
- Mn<sub>2</sub>O<sub>3</sub>-Co<sub>2</sub>O<sub>3</sub> spinels, phase diagram anal., thermodynamic props. 0-3009
- (Mn<sub>2</sub>O<sub>3</sub>)<sub>1-x</sub>(MgAl<sub>2</sub>O<sub>4</sub>)<sub>x</sub>, 0<x<1, mixed oxide spinels, chemical shifts of Mn K-absorpt. edge 0-29828
- MnOOH, α- and γ-phase, thermal decomp., 20 to 670°C 0-35521
- x.MnO.(1-x)[19TeO<sub>2</sub>.PbO], glass, antiferromag. behaviour, mag. props. 0-50072
- MnP, anisotropic, ferromagnetic microwave resonance relations 0-15805
- MnP, elec. resist. of different mag. phases, temp. depend. 0-54691
- MnP, method for determ. of successive mag. struct. (Russian) 0-39741
- Mn<sub>3</sub>(PO<sub>4</sub>)<sub>2</sub>, coating on steel, wear resistant appl. 0-16609
- MnS, cubic NaCl-type cryst., Debye temp. 0-54333
- Mn<sub>1-x</sub>Sb<sub>x</sub>, ferromag., mag. disturbance around Mn interstitials 0-54868
- MnSe, and MnSe<sub>2</sub>, thermodynamic props. 0-19958
- Mn<sub>2</sub>SiO<sub>3</sub>, effect of vibration during sintering, on electrical resistivity 0-16258
- Mn<sub>1/3</sub>TaS<sub>2</sub>, Hall coefficient and resistivity 0-39610
- Mn<sub>1/3</sub>TaS<sub>2</sub>, magnetic susceptibility, function of temp. 0-39756
- Mn<sub>1/4</sub>TaS<sub>2</sub>, Hall coefficient and resistivity 0-39610
- Mn<sub>1/4</sub>TaS<sub>2</sub>, magnetic susceptibility, function of temp. 0-39756
- MnTe, resistivity anomalies at mag. transitions, sp.h. 0-39785
- MnTe<sub>2</sub>, Mossbauer spectra, hyperfine field 0-15866
- (MnTe)<sub>1-x</sub>(Bi<sub>2</sub>Te<sub>3</sub>)<sub>x</sub> (x≤0.05) solid solution, electrophys. props. 0-24925
- Mn<sub>2</sub>TeO<sub>6</sub>, magnetic structure, stability of mag. modes, neutron diffraction study (French) 0-39744
- MnTiO<sub>3</sub>, HP phase transform. 0-19941
- MnX<sub>2</sub> (X=F, Cl, Br), discrete variational Xα cluster calcs. 0-15444
- Mn<sub>2</sub>Y<sub>2</sub>D<sub>2</sub>, D atom location, neutron diff. study (French) 0-24426
- MnZn ferrite, combined Bridgman-zone levelling cryst. growth technique 0-35076
- MnZn ferrite, mag. anisotropy, effect on recording head characts. 0-39765
- MnZn ferrite, mag. loss accommodation depend. on freq. and amplitude of mag. field (Russian) 0-34686
- MnZn ferrite, mag. permeability accommodation depend. on mag. field (Russian) 0-34685
- MnZn ferrite, O<sub>2</sub> stoichiometry effect on fracture 0-25826
- MnZn ferrite, Ti substituted, vacancy contents and phase equilibria 0-29012
- MnZn ferrite, wall topography change induced by external press. 0-34734
- MnZn ferrite fabricated by hot isostatic pressing, recording head appl. 0-35139
- MnZn ferrites, elec. cond. mechanism in paramag. and ferrimag. phases 0-15524
- MnZn, pressing powders, spray dried, pressing behaviour and props. 0-11617
- MnZn soft ferrites, commercial grade, microstruct. rel. to mag. props. 0-34009
- MnZn-ferroferrites, sintered, microstruct., TEM study (Dutch) 0-2036
- MnO<sub>2</sub> powders with admixed fine materials, density and conductivity under pressure 0-54682
- Mn<sub>4</sub>[AsSi<sub>2</sub>O<sub>2</sub>(OH)], cryst. struct. determ. and refinement 0-1970
- MuCl<sub>2</sub>·nH<sub>2</sub>O, cryst. struct. (German) 0-1987
- NaCl-CsCl-MnCl<sub>2</sub>, molten salt system, molar volume and elec. cond. meas. 0-34217
- NaCl-CsCl-MnCl<sub>2</sub>, molten salt system, molar volume and elec. cond. meas. 0-34218
- NaMnCl<sub>3</sub>, antiferromagnet, exciton self-localisation luminesc. and excitation spectra (Russian) 0-11456
- Na<sub>6</sub>Mn(Ti<sub>2</sub>Si<sub>6</sub>O<sub>18</sub>), Kazakovite, cryst. struct. determ. 0-19782
- Rb<sub>2</sub>MnCl<sub>4</sub>, rare earth doped, energy transfer, emission spectra obs. 0-20684
- RbMnF<sub>3</sub>, antiferromagnetic resonance, optical detection, luminescence 0-7174
- RbMnF<sub>3</sub>, nuclear spin waves spectra, relaxation, parametric excitation, NMR dynamic shift (Russian) 0-11180
- Rb<sub>2</sub>Mn<sub>2</sub>Mg<sub>1-x</sub>F<sub>4</sub>, spin dynamics near percolation threshold, EPR study 0-39859
- Sn<sub>1-x</sub>Mn<sub>x</sub>Te, degenerate mag. semicond., thermoelec. power meas. 0-29392
- SnTe-MnTe, degenerate semicond., anomalous Hall effect 0-29420
- ZnMn<sub>1-x</sub>Cr<sub>x</sub>FeO<sub>4</sub>, Mossbauer effect, quadrupole splitting 0-29664
- ZnO-Bi<sub>2</sub>O<sub>3</sub>-CoO-MnO-Sb<sub>2</sub>O<sub>3</sub> (97.5, 0.5, 0.5, 1.0 mole%), exam. of elec. props. at different annealing temps. 0-3099



**manganese compounds continued**

ZnO-GeO<sub>2</sub>-MnO-B<sub>2</sub>O<sub>3</sub> wideband cathodoluminescent phosphor 0-55196  
 ZnS-MnS-CuInS<sub>2</sub>, subsolidus equilib., phase diagrams 0-3016

**manometers**

see also pressure measurement

magnetron-type, with inhomogeneous mag. field 0-31730  
 membrane, differential, for low pressures meas. 0-31777  
 U-shaped, Hg for 1300 to 2300 torr range 0-31784  
 U-tube, fluid free oscillation, Navier-Stokes equations solution and expt. verification (Japanese) 0-6142  
 U-tube water manometer, for water injection dew point hygrometer (Japanese) 0-8998  
 vacuum valve construction, mounted on pressure pickup 0-47066

**manufacture**

see also electron device manufacture; electronic equipment manufacture; steel manufacture  
 1200 MWe FBR steam generators, Creys-Malville in France, manufacture 0-27797  
 fission reactor pressure vessel and circuit development, conf. report 0-47541  
 solar energy paraboloid concentrator fabrication, simplified method 0-16837  
 terrestrial solar generators, design, fabrication, testing and economic power generation 0-45672

**manufacturing ADP** see manufacturing data processing**manufacturing computer control**

see also computerised numerical control; manufacturing data processing; process computer control  
 optical systems, aspherical, manufacturing and testing techniques development (Italian) 0-48467

**manufacturing data processing**

see also manufacturing computer control  
 NDT, data processing and acquisition for product quality control 0-11862  
 solar cell arrays, economics modelling of photovoltaic module manufacturing, SAMICS methodology developments 0-55860

**manufacturing industries**

powder metallurgical parts, development, and manufacture of semifinished products 0-50578

**manufacturing processes**

see also cold working; cutting; drawing (mechanical); extrusion; forging; forming processes; hot pressing; hot working; joining processes; machining; manufacture; rolling; sintering  
 industrial visual testing, photographic methods as technical aid (German) 0-31923  
 non-Gaussian distribution laws for statistical error theory generalisation (German) 0-22315  
 powder metallurgical parts, development, and manufacture of semifinished products 0-50578  
 single crystal permanent magnet, industrial technology and equipment for manufacturing process 0-35075  
 Si solar cells, crystal growth, heat exchanger method, fixed abrasive slicing technique 0-35082

**many-body problems**

see also BCS theory; quantum statistical mechanics; renormalisation  
 3-body problem with one infinite mass particle, integral and Schrodinger eqn. equivalence 0-18255  
 A=15-18, effective interaction from coupled cluster many-body method extension 0-22701  
 applications, review of development 0-46968  
 atom, heavy, parity non-conserving E1 matrix elements, many body calcs. 0-47924  
 atom surface scatt., reflection and sticking coeffs., short range forces, low energy limit 0-40208  
 atomic electron scattering, second-order many-body theory 0-32832  
 atomic systems, collisions and interactions calc. method 0-46726  
 atomic systems, many-electron autoionisation states, transition probability and autoionisation rate, perturbation theory Z-expansion 0-52863  
 atoms, collective dynamics, hydrodynamic approach and many body approach based on RPA calcs. 0-47855  
 atoms, correl. problem for open and closed shell system, coupled cluster approach 0-47842  
 atoms, MBPT appl., comparison with problem for nuclei 0-47406  
 atoms, nucl. vol. isotope shift theory, many electron effects 0-47851  
 atoms, photoionisation cross sections, electron correl. reson. struct., relax. effects many body perturbation calcs. 0-47852  
 atoms, Schrodinger eqn. standard solns. 0-47863  
 atoms, Z=46-54, L<sub>γ2,3</sub> emission spectra, breadth, dynamical effects 0-32645  
 Baer-Kouri-Levin-Tobocman many body scatt. theory, Feshbach projection operator method 0-508  
 BBG theory developments, hole and particle lines, dispersion effects and healings 0-22719  
 benzene, π electron system, excitation energy, appl. of MBPT 0-52876  
 Bogolyubov method, equilibrium system many body correlation function contracted description (Russian) 0-38888  
 boson, nonrelativistic, potentials, attractive discreteness of ground state 0-46957  
 Brueckner-Bethe calculations of nuclear matter 0-22718  
 charged three body problems with Coulomb pots. 0-18256  
 chemical dynamics, generalised Langevin theory, formulation and equiv. harmonic chain representation 0-35504  
 collective Hamiltonian subdynamics and collective states, geometric approach 0-8904  
 commutation symmetry for system of identical particles (Russian) 0-12944  
 conference on many-body theories, Trieste, Italy (Oct. 1978) 0-22135  
 Coulomb off shell two body amplitudes, numerical computation 0-46858  
 covalent semiconductor, valence band calc. using many-electron theory 0-15434  
 density matrix, harmonic oscill. approx. 0-13391  
 diagrammatic many-body perturbation theory applicable to arbitrary model spaces 0-47844  
 diatomic molecules, excitation energies, oscillator strengths, many body approach, eqns. of motion method 0-47969  
 direct energy minimisation methods in self-consistent nuclear fields, ground state props. 0-22702  
 dominant partition method 0-47455  
 equations of state in many body theory 0-42183

**many-body problems continued**

exchange effects in direct reactions, antisymmetrisation and three body models 0-13446  
 Faddeev equations, two-potential formula, three-body scattering 0-4893  
 Faddeev integral eqns. for three charged particles (Russian) 0-8830  
 fermion hypernetted chain approx., optimal correlation functions for liquid <sup>3</sup>He, electron gas 0-24822  
 Friedrichs model unitary regularisation for many particle system 0-32039  
 generalised optical potentials, four-body problems 0-22781  
 Green's function method for many-body problem for relativistic meson field theory, book contrib. 0-357  
 Hamiltonian, zero-order, for many-body perturbation theory 0-9483  
 infinite nuclear matter ambiguities, harmonic oscillator and infinite well solns. 0-22742  
 inhomogeneous many-body system integral equations for quantum liquids and solids 0-22732  
 ionisation potentials, sum rule, Manne Åberg theorem connection, many body Green's function formalism 0-27930  
 isobar degrees of freedom, binding energy from BHF approx. 0-22734  
 isobar degrees of freedom in nuclear matter, binding, NN interactions and 2π exchange 0-22735  
 K-harmonic solution for three bound unequal particles 0-12940  
 linear response and Hartree-Fock, coordinate space representation and gradient iteration 0-18216  
 Lippmann-Schwinger eqns. for three charged particles 0-4580  
 Maxwell-Boltzmann statistical distrib. function of ideal gaseous assembly 0-17858  
 Mayer cluster function and quantum two-body t matrix 0-17859  
 metal, with stored H, electronic struct., many electron theory 0-49667  
 molecular dynamics method in statistical physics, review 0-18895  
 molecular polarisability, scaling and Pade approximants, many-body perturbation theory 0-42952  
 molecules, Fokker-Planck eqns., stochastic modeling 0-43128  
 molecules, ground state props., coupled cluster and MBPT methods appl. 0-47881  
 molecules, valence and core photoionisation, spectral lines, many body effects 0-47853  
 Molien function of a symmetric group 0-8857  
 Monte Carlo methods in quantum many-body problems, nuclear physics 0-22727  
 multichannel scattering, exact and Glauber amplitudes 0-13421  
 Muskhelishvili-Omnès equation and final state interactions 0-17821  
 N identical particles, Rayleigh-Ritz principle complement for energy spectrum 0-5074  
 N-dimensional systems, exact time-depend. invariants 0-8824  
 neutron, alpha and nuclear matter, ground vacuum states 0-22738  
 neutron and nuclear matter, variational calc. models 0-22724  
 neutron distribution in nuclei, elastic and inelastic proton scattering, review 0-22649  
 neutron matter, spin and tensor correlations, cluster expansion hypernetted chain eqns. 0-22728  
 neutron or nuclear matter, spin depend. correlations, variational method 0-22726  
 nonrelativistic supersymmetry, relevance to many-body problems 0-22537  
 nuclear matter, Brueckner Bethe and variational calcs. review, nuclear saturation problem 0-22745  
 nuclear matter, constrained variational calcs., three body and N\* (1234) contribs., cluster energy 0-22743  
 nuclear matter, fermion hypernetted chain variational calc. 0-22725  
 nuclear matter, three-body problem, variational and Bethe-Faddeev methods 0-27586  
 nuclear matter, variational techniques, review 0-22748  
 nuclear matter BBG theory, auxiliary single particle field for binding energy 0-22723  
 nuclear matter binding energy from low density expansions, Brueckner-Hartree-Fock approx. 0-22720  
 nuclear medium, solid like aspect with alternating layer spin and π condensation 0-22733  
 nuclear system, total energy, static Hartree-Fock calcs. 0-47414  
 open shell RPA unitary group formulation, Hartree Fock stability eqns. 0-52860  
 orbit-orbit interaction, new tensor expansion, matrix and graphical forms 0-14064  
 pairing rotations and quadrupole modes, many-quasiparticle excitations 0-18165  
 paramagnet, electron state density for narrow-band model with Coulomb interaction 0-10852  
 path integrals and time-dependent mean-field theories, many-body problem, Hartree-Fock eqns., Slater determinants 0-37342  
 perturbation theory, many-body, arbitrary point group symmetry, wave operator matrix elements 0-23311  
 pion condensation, field theoretic many-body system 0-22703  
 plasma, one-component, virial pressure 0-38536  
 polyatomic molecules, excitation energies, oscillator strengths, many body approach, eqns. of motion method 0-47969  
 probability amplitudes of transitions between not necessarily stationary states, coupling const. 0-36902  
 programmable procedure for generating many-particle states 0-27169  
 quantum chemistry, many body perturbation theory fourth order calc. of correl. energy 0-14087  
 quantum three-body problem, distorted Faddeev eqns. with coupled channel approach 0-52635  
 realistic NN pot. construction for three body systems and nuclear matter 0-22699  
 relativistic Hamiltonian mechs., position variables 0-27123  
 relativistic RPA determ. of oscill. strengths and excitation energies 0-47925  
 relativistic two-body forces in many-body systems, Weinberg and Yukawa interactions 0-32203  
 ring diagrams in nuclear matter, many-body forces contrib., ρ and π exchange 0-22740  
 rubbers, swollen, low-freq. dynamics, optical and mech. props. 0-43626  
 scalar meson field and many-body forces, book contrib. 0-359  
 Schrodinger eqn., complete exact solution to the translation-invariant N-body harmonic oscillator problem 0-31558  
 semiconductor, Raman scatt., one-phonon final states and many-body effects 0-34913  
 simple fluid, one-component, liquid-vapour phase coexistence, surface tension determ. from many body pot. 0-49465  
 simple quantum liquids, Jastrow variational wave functions, for nuclear matter, liquid <sup>3</sup>He and <sup>4</sup>He 0-22729



**many-body problems continued**

- Skyrme-type interactions, spectroscopy of light nuclei, density dependent Hartree-Fock 0-22717  
 solid dielectric loss peak, many-body interpretation 0-15953  
 solid universal dielectric response law, many-body interpretation 0-15952  
 spatial correlations and elementary excitations in many-body systems 0-22730  
 superconductivity and elementary particles theory, review 0-4911  
 three body phase space distrib., Monte Carlo calcs. 0-37393  
 three body problem for hyperbolic and Coulomb potentials 0-22223  
 three body scatt., spline function moment methods 0-505  
 three particle Coulomb problem for two electron systems, hyperspherical coords. framework 0-52875  
 three particle systems with Coulomb interaction, scatt. and breakup eqns. exact solns. 0-504  
 three particles with Coulomb interaction, binding energy and scatt. states (Russian) 0-5051  
 three-body scatt. problem, cluster expansions, effective intercluster pots. 0-5082  
 three-body systems, number of bound states and Efimov's effect 0-31536  
 three-particle relativistic kinematics 0-27602  
 transition metals, 3d, electron impact excited soft X-ray spectra, resonances and many body effects 0-50468  
 unitary group approach to molecular electronic structure 0-5467  
 Universe, high density matter, many body treatment, pulsars 0-26738  
 variational principles for true three- and four-particle scatterings 0-18254  
 weakly coupled mixtures of charged particles at zero temperature 0-140  
 Wigner's (2n+1) rule in MBPT 0-42095  
 ( $\gamma, \pi$ ), few body pion photoprod. in  $\Delta$ -resonance, region 0-42636  
 $N\pi\pi$  dynamics, medium energy, dispersion relations, isobar expansion for  $\pi N$  0-4917  
 ( $\pi, \pi$ ) many body QFT framework anal., final state particle-hole correlations 0-13508  
 Al, positron annihilation studies using high-density proportional chambers 0-25478  
 Be-like system, numerical many-body perturbation calcs. using multiconfig. model space 0-47907  
 CO<sub>2</sub>, lattice energies, non-additive three body contributions, triple-dipole term 0-54168  
 Ca+Ca, classical many-body model for heavy ion collisions 0-536  
 Cu, positron annihilation studies using high-density proportional chambers 0-25478  
 Ge, ion bombarded, radiation defect formation, atom-atom collision cascades modelling 0-10582  
 H<sub>2</sub><sup>+</sup> three lower states, three body problems, separations of variables 0-36903  
 H<sub>2</sub>O, ground state correlation energy, diagrammatic perturbation theory 0-18774  
 H<sub>2</sub>O, many body perturbation theory fourth order calc. of correl. energy 0-14087  
<sup>3</sup>H binding energy, 3N bound state with separable interactions, Faddeev theory corrections 0-13388  
<sup>3</sup>H( $\mu, \nu$ )3n, transitions from bound to continuum three nucleon states 0-5128  
 He, electron scatt., ionisation, elastic and inelastic collisions, many body theory appl. 0-48093  
 He, many electron system, photoionisation and photoexcitation, at. transition strong config. interaction effect 0-47909  
<sup>3</sup>He charge form factor, 3N bound state with separable interactions, Faddeev theory corrections 0-13388  
<sup>4</sup>He, liq., ground and low excited state struct., pair-pair correlation function 0-24694  
<sup>4</sup>He, liq., ground state from HNC and BBGKY eqns., elementary diagram effects 0-24693  
 La, electron impact excited soft X-ray spectra, resonances and many body effects 0-50468  
 Li<sup>+</sup>+CO<sub>2</sub>, rot. vibr. energy transfer, 1 to 10 eV, many body theory 0-28093  
 LiH, many body perturbation theory fourth order calc. of correl. energy 0-14087  
 $\alpha$ -N<sub>2</sub>, lattice energies, non-additive three body contributions, triple-dipole term 0-54168  
 Ne+Ne, classical many-body model for heavy ion collisions 0-536  
<sup>16</sup>O and Sd shell nuclei, binding energy from realistic Hamiltonians and spectral distrib. theory 0-22678  
<sup>16</sup>O, energy calcs., Jastrow variational method extension, FAHT cluster expansion 0-22677  
<sup>208</sup>Pb and neighbouring nuclei, shell model calcs. with correlated pairs basis 0-22712  
 Si, ion bombarded, radiation defect formation, atom-atom collision cascades modelling 0-10582
- many-particle systems** *see statistical mechanics*
- many-valley semiconductor materials** *see many-valley semiconductors*
- many-valley semiconductors**  
 antiferromagnetic or atomic ordering effects on conduction electrons 0-2329  
 conductivity, electron-electron scatt., memory function 0-10967  
 films, photogalvanic effect calcs., electron mean free path, size effect 0-34487  
 free-electron screening of short-range scatt. pot. 0-49704  
 high field transport, inter-valley scatt., intra-collisional field effect 0-34455  
 hot electron distrib. function, response to step changes in elec. field 0-24937  
 impurity electron states, localised, with low binding energy 0-24835  
 inelastic light scattering, single particle excitation 0-29749  
 inversion layer, transient response of hot electrons, calc. 0-49747  
 magnetic, electron fluctuation states spin direct interactions 0-29364  
 metal-insulator transition at finite temp., calc. 0-49603  
 size-induced changes in valley populations in strong elec. fields 0-6855  
 space charge, contrib. of different charge carriers (French) 0-34458  
 thermoelectric power, depend. of longitudinal mag. field 0-39618  
 valley-splitting without effective-mass approx. 0-15586  
 AgBr, exciton relaxation by intervalley scattering 0-20644  
 GaAs, influence of strong transverse mag. field on Gunn effect 0-6854  
 n-GaAs, three valley band struct., high temp. Hall mobility 0-29318  
 Ga<sub>1-x</sub>In<sub>x</sub>P<sub>1-y</sub>As<sub>y</sub>, electron transient drift vel., influence of effective mass and alloy scatt. 0-2384  
 GaP, scatt. mech., mobility tensor 0-6826

**many-valley semiconductors continued**

- GaSb, space charge, contrib. of different charge carriers (French) 0-34458  
 Ge, cyclotron reson. in strong elec. fields, classical theory 0-7172  
 Ge, deep donor character of muons and protons 0-10911  
 Ge, electron-hole liq. thermalisation between mag. field split valleys 0-25444  
 n-Ge, IR absorption by hot carrier 0-40087  
 Ge:As(P)(Sb), impurity photocond. spectra under uniaxial compression 0-44656  
 n-Ge:As piezoresistance in presence of deep levels, stress anisotropy 0-10979  
 Pb<sub>1-x</sub>Ge<sub>x</sub>Te, n- and p-type, effective masses 0-44481  
 Pb<sub>1-x</sub>Sn<sub>x</sub>Te films, size quantisation, optical orientation of free carriers 0-20725  
 Si (001)-SiO<sub>2</sub>, n-inversion layer, valley splitting without effect mass approx. 0-15586  
 Si, deep donor character of muons and protons 0-10911  
 Si inversion layer, transient response of hot electrons, calc. 0-49747  
 Si inversion layers, resolution of Shubnikov-de Haas paradoxes 0-39648  
 n-Si, shear deformed, Smith-Herring and mobility change piezoresistance 0-6842  
 Si, two-dimensional inversion layer on surface, minigap and conductivities 0-20267  
 n-Si:O, charge carrier scattering on neutral centres 0-49762  
 Si(100), inversion layer, interaction induced transition at low density 0-15581

**manybody problems** *see many-body problems***map drawing** *see cartography***marine systems***see also ships*

- magnetometer for sea floor temporal mag. variation meas. 0-51581  
 NAVSTAR Global Positioning System, sea trials results 0-12645  
 offshore surveys, accurate positioning at distances to 400 km 0-12328  
 radio teletype communication system, satellite based, INMARSAT 0-26614  
 radiofacsimile weather chart receiver and recorder 0-46297  
 resources and meas. techniques, conference, San Diego (1979) 0-41943  
 seismology hydrophone system for ocean bottom deployment 0-51582  
 thermal imaging system material and design considerations 0-42259  
 tow system with depth control, hydrographic and current meas. 0-17403  
 two stroke compression ignition engines, heat exchange modelling 0-30529  
 LiSOCl<sub>2</sub>, battery undersea applications 0-45658

**mark scanning equipment**

- resonant cantilevered fibre-optic scanner 0-53428

**marketing***see also commerce*

- camera market, status and growth prospects, USSR 0-27367  
 fibre-optic technical innovations and market development 0-10008  
 fission reactor fuel, for PWR, French status (French) 0-627

**Markov chains** *see Markov processes***Markov processes**

- asymptotic phase enlargement of weak inhomogeneous Markov processes (Ukrainian) 0-46973  
 atom in strong EM field, characts. calc. using quantum theory of Markovian processes 0-32943  
 beam on nonlinear spring support, random vibr. 0-33515  
 Brownian motion, generalised Einstein theory for nonequilibrium fluctuations 0-31672  
 Brownian motion, velocity field, generalised Langevin equation 0-147  
 chain reversibility (Chinese) 0-46971  
 chemical reactions, complex, kinetics, Markov chain appl., teaching 0-27085  
 class construction for processes invariant under a time change (French) 0-17869  
 comets, short-period orbital evolution 0-46484  
 corrosion under random exposure conditions 0-40579  
 coupled-core nuclear reactors, irreversible circulation of fluctuation 0-27700  
 critical dynamics, real-space renormalisation group approach 0-31699  
 denumerable state infinite horizon contracted Markov decision processes, finite state approx. 0-46974  
 deterministic dynamics, relationship to probabilistic description 0-4646  
 dielectrics, electron multiplication, phonon scatt., ionisation rate calcs., Markov processes 0-50267  
 diffusion product (French) 0-8909  
 Dirichlet forms, construction of stochastic processes 0-8921  
 disequilibrium theory applied to two-spin Glauber model 0-31669  
 disordered chains, electronic props. 0-2363  
 embedding problem for Markov chain with three states, Bang-Bang representation 0-31673  
 EPR spectra of stable radicals, slow molecular motion study, review 0-25212  
 Fenyes-Nelson stochastic model of quantum mechanics 0-86  
 fission reactors, coupled core system, noise sources in coupling medium, stochastic study 0-22962  
 fission reactors, CRBR shutdown system, Markovian reliability anal. 0-27761  
 fission reactors, supervised protective systems, probability level of readiness anal., four-state Markov process 0-27762  
 fluid, Monte Carlo calculations, optimisation of sampling algorithms 0-54099  
 Fokker-Planck equation derivation for system interacting weakly with heat bath 0-17900  
 Fokker-Planck-Kolmogorov type equations (Russian) 0-145  
 Gaussian generalised stochastic fields, Markov property 0-22287  
 hourly global radiation sequences, stochastic simulation 0-36382  
 inclinable pipe, suspension in turbulent flow, Markovian model, eddies 0-48790  
 laminated composites, mechanics of homogenisation and random evolutions 0-28423  
 Lie group, central limit theorem (French) 0-52127  
 localization of eigenstates in one-dimensional infinite disordered systems with off-diagonal randomness 0-17876  
 Markovian nature of the two-dimensional self-avoiding random walk problem 0-4648  
 master equations, Langevin description 0-31676  
 molecules, Fokker-Planck eqns., stochastic modeling 0-43128



**Markov processes continued**

- neural automaton model I/O characteristic for semi-Markov impulse sequences (*Japanese*) 0-16917  
 non-Markov processes, memory effects, elimination by transform. 0-42146  
 one-dimensional Markov processes, transition probability densities calc. using Fokker-Planck eqn. 0-42047  
 optic tract fibers, cat, Markov properties of nonstationary spike trains 0-51077  
 organic compounds, complex, nuclear relaxation influence on stimulated emission 0-48019  
 particle motion through matter, fluctuations in cascade processes 0-5456  
 particulate material deformation mechanism as Markov process (*Japanese*) 0-14562  
 powder particle motion and segregation by density difference in V-type mixer 0-45250  
 probabilistic methods for stationary problems of linear transport theory 0-167  
 PWR nuclear reactor, Markov model for quantitative systems interactions anal. of system unavailability 0-22898  
 QCD jets, Markov branching processes 0-27463  
 radiative transfer, adding algorithm for Markov chain formalism 0-21902  
 radiative transfer in diatomic gas, vibr. nonequil., probabilistic modelling 0-33434  
 random walks with Markovian steps (*French*) 0-17868  
 Reggeon field theory on a lattice, critical behaviour, Monte Carlo calc. 0-18126  
 relaxation process as contraction of Markovian type multidimensional one 0-31671  
 reservoir storage, distrib. of max. deficit of partial sums of variables 0-4651  
 River Nile, Kalman forecasting model 0-31081  
 sedimentation of monodisperse suspension of solid particles in viscous fluid, Markov model 0-28551  
 semiconductors, electron multiplication, phonon scatt., ionisation rate calcs., Markov processes 0-50267  
 subsystem interacting with thermal bath, kinetic eqn., Markov approx. 0-47006  
 transition operator for Markov and non-Markov processes, interpolation model 0-8910  
 turbulence fully developed, quasi-normal Markovian approx. 0-53756  
 turbulent dynamo, dynamic eqn. of magnetic field 0-32880  
 zero-two laws, recurrent process characterisation (*French*) 0-27217

**Mars**

- aeolian sedimentation on Earth and Mars, comparisons 0-31042  
 angular momentum of seasonally condensing atmospheres, appl. to Mars 0-26735  
 atmosphere, chemical composition deduced from twilight glow obs. 0-56739  
 atmosphere, N atom loss rate, calc. 0-46452  
 atmosphere, photoelectrons caused by solar photons of less than 80 Å 0-56744  
 atmosphere, thermal radiative transfer, numerical modelling 0-8574  
 atmosphere, travelling thermal wave effect on circulation 0-8388  
 atmosphere modelling, multilayer radiative transfer 0-46451  
 atmosphere opacity, 1977 obs. from Viking 0-41753  
 brightness distribution over planetary disc, determ. from light refl. meas. 0-17512  
 crater ejecta emplacement, atmos. effects 0-56747  
 crater ejecta-emplacement in Coprates quadrangle 0-56745  
 cusp of magnetosphere, to explain Mars 5 mag. and plasma obs. 0-51685  
 Deimos, spectral evidence for carbonaceous chondrite surface comp. 0-41754  
 Deimos, surface features map and props. 0-31224  
 dust deposits in Martian north polar region, evolution 0-31225  
 eccentricity origin in secular resonances 0-46449  
 equatorial flattening 0-4282  
 geological evolution data from Viking probes (*French*) 0-8578  
 gravitational spectrum, determ. from Mars Mariner 9 orbiter tracking 0-41744  
 gravity anomalies due to topography, comparison with Earth 0-21939  
 gravity field, comparison of results obtained from Viking 1 and 2 and Mariner 9 0-8577  
 heavy ions in solar wind plasma flow 0-8576  
 ice-covered rivers 0-17526  
 lithosphere global TRM in presence of central dipole field, theory 0-31223  
 magnetic field, measurements of Mars 2, 3 and 5 spacecraft 0-36538  
 magnetosphere, effect of Deimos 0-41752  
 palaeoclimate and enhanced atmospheric CO<sub>2</sub> 0-46450  
 Phobos, surface features map and props. 0-31224  
 Phobos, Viking 1 Orbiter, encounter, trajectory analysis 0-12641  
 Phobos and Deimos orbital evolution 0-26770  
 Phobos surface grooves, hybrid origin 0-31229  
 radio brightness, longit. depend. confirmation 0-21937  
 regolith, as reservoir of volatiles 0-17524  
 rotation model, including precession and nutation 0-21938  
 rotation theory in Euler angles 0-51684  
 soil transport by winds 0-31228  
 solar wind interaction region, ion flux meas. interpretation 0-8575  
 south polar region, eolian features rel. to polar vortex, seasonal var. 0-31227  
 surface morphology, review 0-56748  
 Tharsis province, isostatic model 0-12701  
 Tiu Vallis, longit. grooving origin, responsible fluid types 0-26769  
 upper atmosphere absorption of solar UV, interaction model 0-56746  
 Viking Lander tracking contributions to Mars mapping 0-12702  
 watery past of Mars, implications of Mariner and Viking obs. 0-17527  
 wind blown deposits, silt-clay electrostatic aggregates 0-21940  
 windblown particle abrasion, erosion of quartz and basaltic sand 0-17525  
 CO<sub>2</sub> frost streaks in south polar cap 0-31226

**martensitic steel**

- age hardening with Cu, Nb additions, exam. of hardness 0-7681  
 corrosion cracking in chloride and alkaline solutions, 07Kh16N4B 0-55576  
 duplex ferrite, microstructure resistance optimisation to fracture 0-40482  
 fatigue crack propag., effect of intercrystalline fracture associated with temper brittleness (*French*) 0-16463  
 fatigue damage, development rate by exoelectron meas. 0-25835  
 fusion reactor first wall/blanket material 0-32451

**martensitic steel continued**

- heat-resistant, martensitic, Kh12NMFB weldability 0-20987  
 low C, development and props. (*Russian*) 0-20933  
 low C, packet martensite struct. and localisation of residual austenite, electron microscope obs. (*Russian*) 0-25695  
 low C without Ni, for deep-well sucker rods, corrosion fatigue 0-55588  
 microcrack growth, in ferrite grain in two-phase martensitic-ferritic steel 0-21070  
 nitriding in metastable condition 0-30167  
 stainless, CrMoV, stress effect on pitting susceptibility 0-16542  
 stainless types 403 and 616, temp. depend. of low cycle fatigue behaviour 0-7667  
 steels, ferritic and martensitic, C and N migration at low temps., monograph 0-22149  
 strain hardened martensite, resist. to tempering, exam. 0-16348  
 strength and embrittlement, early stages of martensite decomp. effect 0-35227  
 structure, <sup>57</sup>Fe Mossbauer spectra 0-15051  
 tempered martensite embrittlement of type SAE 4340 0-30084  
 void swelling response after fast reactor irradiation 0-6437  
 C, tempering induced decomposition and segregation, atom probe study 0-3112  
 low-C martensitic, Ni addition influence on toughness and ductile-brittle transition 0-30099

**martensitic transformations***see also shape memory effects*

- A-15 type compounds, relation between martensitic and supercond. phase transition 0-29497  
 alloy, austenitic, mechanical changes after electrolytic quenching (*Russian*) 0-50653  
 alloy steels, ferrite and alloy carbide interrelation 0-3040  
 conference, phase transformations in metallurgy, York, England (Apr. 1979) 0-2994  
 martensite crystal, dislocation representations of development kinetics 0-39086  
 metals and alloys, martensitic transitions accompanied by interactions between phases (*Russian*) 0-7568  
 nucleation of martensite at dislocations, elasticity model 0-55393  
 nucleation time, estimate in martensitic transformation 0-29954  
 premartensitic phenomena, nucleation, shape memory effect, review 0-3041  
 review 0-3037  
 shape-memory alloys, props. and appl. 0-30049  
 steel, 50N29 type, self-consistent junctions and spatial relative organisation 0-19750  
 steel, alloy, type AISI 4340, martensitic transformation, TEM study 0-3043  
 steel, alloy 40Kh, sulphide cracking resistance, strengthening method influence 0-55577  
 steel, austenitic, Cr-Mn, metastable, plasticity, contrib. of martensitic transform. during deform. (*Russian*) 0-30018  
 steel, austenitic, martensitic transform. effect on hardening kinetics and fracture resist. of friction surface of 45Kh12G8 and 110G13 (*Russian*) 0-50727  
 steel, austenitic, type En58B, martensite formation and reversion, effect on void swelling 0-11641  
 steel, austenitic, type M316, martensite formation and reversion, effect on void swelling 0-11641  
 steel, austenitic stainless, 18-8, effect of H on martensitic transformation (*Chinese*) 0-55394  
 steel, austenitic stainless, fatigue and cyclic stress-strain characts. austenite-martensite transform. effect 0-21109  
 steel, austenitic stainless, stacking fault effect on martensitic transform. during plastic deform. (*Russian*) 0-25696  
 steel, austenitic-martensitic, phase comp., struct. and mech. props. 0-29974  
 steel, C, martensitic by quenching 0-3038  
 steel, C, transform. kinetics, heat cond. and elastic-plastic stresses during quenching (*Japanese*) 0-25688  
 steel, carburised, transform. of residual austenite, mag. field effects (*Russian*) 0-29952  
 steel, complex alloy, Cr (12-18 wt.%), transformation behaviour (*German*) 0-40349  
 steel, Cr, stress relaxation, superplasticity and thermal cycling (*Russian*) 0-21019  
 steel, Cr-Ni (18%, 12(8)%), martensite formation and reversion, effect on void swelling 0-11641  
 steel, Kh18N9T, strengthening by vibrational stirring effect 0-40405  
 steel, low C, packet martensite struct. and localisation of residual austenite, electron microscope obs. (*Russian*) 0-25695  
 steel, low or medium alloy, work hardening effect on martensitic transform. cond. (*French*) 0-16329  
 steel, maraging, effect of thermal cycling ( $\gamma$  to and from  $\alpha$ ) on props. 0-20986  
 steel, martensitic low C, development and props. (*Russian*) 0-20933  
 steel, Mn, Mn influence on martensitic transform in presence of strain (*Russian*) 0-20934  
 steel, stainless, martensite formation, in situ obs. 0-25692  
 steel, stainless, martensite nucleation, in situ electron microscope obs. 0-7572  
 steel, stainless, martensite nuclei obs., role of defects in nucleation 0-25693  
 steel, stainless type 03Kh13AG19, deformation temp. influence on dislocation struct (*Russian*) 0-11698  
 steels, high strength stainless, types 1Kh15N5AM3 and 1Kh16N4AB, phase transformations 0-20931  
 steels 2Kh13 and 20Kh1M1FTR, sulphide cracking resistance, strengthening method influence 0-55577  
 stress induced, STEM study 0-47155  
 Al-Ni, thermoelastic phase transform., acoustic emission 0-3039  
 Al<sub>2</sub>O<sub>3</sub> phase transformations,  $\gamma$  to  $\alpha$ , produced by shock wave working 0-16305  
 Au<sub>52.5</sub>Ag<sub>47.5</sub>, pseudoelastic behaviour associated with thermoelastic martensitic transform. 0-16304  
 Ce, critical isomorphous  $\gamma \rightleftharpoons \alpha$  transition, phase equilibrium curve (*Russian*) 0-55397  
 Co-Ni alloy, slip charact., and fatigue, FCC twinning and FCC to HCP martensite transform. effect 0-35182  
 Cu-Al-Mn, partial decomp. of  $\beta_1$  phase, effect on mag. props. and martensitic transform. (*Russian*) 0-45306



**martensitic transformations continued**

- Cu-Al-Ni, long period martensite phases, X-ray diff. obs. 0-7571  
 Cu-Zn-Al, martensitic phase transformation effect on low cycle fatigue behaviour 0-7666  
 Cu-Zn-Al, single cryst., stress induced martensitic transformation 0-45308  
 Fe alloy type G18, martensitic  $\gamma \rightarrow \epsilon$  transformation, dislocation pile-ups,  $\epsilon$  phase nucleation (*Russian*) 0-55396  
 Fe, morphology and transition temp. 0-3042  
 $\alpha$ -Fe, struct. after polymorphic transform. under press. (*Russian*) 0-29946  
 Fe-C, martensitic transformation, thermodynamical study (*Chinese*) 0-55395  
 Fe-Co-Mo ternary system, phase diagram (*Russian*) 0-16269  
 Fe-Cr-C, crystallography of austenite-ferrite/carbide transformation 0-16303  
 Fe-Cr-C, isothermal transformations 0-16302  
 Fe-Mn (-C), Mn influence on martensitic transform in presence of strain (*Russian*) 0-20934  
 Fe-Mn mag. contributions to  $\gamma \rightarrow \epsilon$  phase transformations 0-25694  
 Fe-Mn-C, anomalous changes in austenite and martensite lattice parameters 0-50636  
 $\alpha$ -Fe-Ni, struct. after polymorphic transform. under press. (*Russian*) 0-29946  
 Fe-Ni (29 wt.%), martensite nucleation at dislocations, elasticity model 0-55393  
 Fe-Ni (31 wt.%), thermoelastic martensite obs. 0-3052  
 Fe-Ni alloys, mag. state of austenite and  $\gamma \rightarrow \alpha$  transform. (*Russian*) 0-40350  
 Fe-Ni-C, austenite cryst. volume effect on martensitic transformation temp. 0-40352  
 Fe-Ni-C (25, 0.02 wt.%), thermal stabilisation role in martensitic transformations 0-25697  
 Fe-Ni-C (31, 0.1 wt.%), pre-deformation and temp. effect on transformation-deformation behaviour 0-3127  
 Fe-Ni-Co-C (29.6, 10.7, 0.009 wt.%), thermal stabilisation role in martensitic transformations 0-25697  
 Fe-Ni-Co-Mo phase diagram and structure (*Russian*) 0-20899  
 Fe-Ni-Mn (20, 5 wt.%), surface martensite, crystallography and morphology 0-40354  
 Fe-Ni-Mn-C (5.9, 4.4, 0.48 wt.%) alloy, elastic moduli near martensitic transform. 0-7619  
 Fe-Ni(-Mn)(Cr)(V), concentration ferromag. antiferromag. phase transition and mag. state diagram. (*Russian*) 0-20401  
 Fe-Pt (22-24 at.%) austenite, long range order parameter, temp. depend. 0-40353  
 Mn-Cu (9.3 wt.%), cryst. struct. at FCC to FCT transform. (*Russian*) 0-11643  
 Mn-Cu alloy, local premartensitic instability in FCC phase 0-40355  
 Mn-Cu alloy, volume effect, paramagnetic-antiferromagnetic and structural transition, lattice consts. 0-39007  
 Ni-Al system, ordering and instability of  $\beta$  phase near martensitic transform. (*Russian*) 0-45304  
 Ni-Ti, martensitic phase transformation effect on low cycle fatigue behaviour 0-7666  
 Ni-Ti, structural instability, deform. effects on electron energy spectrum 0-39284  
 Ni-Ti shape memory alloy processing and medical applications (*German*) 0-17203  
 Ti-Al-Mo-Sn-Si (2.25, 4, 11, 0.25 wt.%), type IM1 680, internal friction study of martensitic transformations 0-7573  
 Ti-Al-Mo-Sn-Si (2.25, 4, 11, 0.25 wt.%), type IM1 680, stability of martensitic phases 0-7574  
 Ti-Al-Mo-Sn-Si (4, 4, 4, 1/2 wt.%), type IM1 551, internal friction study of martensitic transformations 0-7573  
 Ti-Al-Mo-Sn-Si (4, 4, 4, 1/2 wt.%), type IM1 551, stability of martensitic phases 0-7574  
 Ti-Al-V (6, 4 wt.%), type IM1 318, internal friction study of martensitic transformations 0-7573  
 Ti-Al-V (6, 4 wt.%), type IM1 318, stability of martensitic phases 0-7574  
 Ti-Cr-Zr, martensite formation, chemical composition effect 0-50634  
 Ti-Mo-Fe (3, 0.13 at.%), metastable phases, Mossbauer study 0-7243  
 Ti-Ni, effect of alloying on crit. points and martensitic transform. hysteresis 0-20935  
 Ti-Ni, electron phase transition XPS, optical spectra and mag. susceptibility meas. 0-19943  
 Ti-Ni, martensite transform. B2-B19', optical props. and electron struct. (*Russian*) 0-34878  
 Ti-Ni, thermoelastic phase transform., acoustic emission 0-3039  
 Ti-Ni alloys, absorpt. of  $H_2$ , press.-composition-temp. relationships, enthalpy, entropy 0-2267  
 TiH<sub>2</sub>, band model of martensitic phase transition 0-29953  
 TiMn, faceted parent martensite interface 0-6417  
 V<sub>3</sub>Si, d-spacing fluctuations above Martensitic phase transition 0-7570

**maser clocks** *see* **atomic clocks****masers**

- alkali metal, Rydberg states and microwaves, spectroscopy, masers and superradiance study 0-53248  
 atomic freq. standards, transfer of freq. stability to quartz-crystal resonator 0-17927  
 VY Canis Majoris, OH/IR star, 1612 MHz OH maser multibaseline VLBI obs. 0-12766  
 cyclotron maser, relativistic, high-current, exptl. characts. 0-9844  
 cyclotron maser instability, quasi-linear theory, calc. of microwave generation efficiency 0-1783  
 cyclotron maser instability in intense hollow electron beams, effect of energy and axial momentum spreads 0-1782  
 cyclotron resonance maser, high power MM wave source-gyrotron (*Japanese*) 0-23654  
 cyclotrons resonance maser, Vlasov-Maxwell eqns., guided wave field theory 0-14309  
 V1057 Cygni, OH obs. 0-36629  
 NML=V1489 Cygni, OH/IR star, 1612 MHz OH maser multibaseline VLBI obs. 0-12766  
 Dicke maser model, equilibrium states for mean field models 0-46961  
 Dicke model, dynamical struct. 0-37985  
 diffraction radiation pulses, spectral characts. 0-32946  
 electron cyclotron maser as high power travelling wave amp. of MM waves 0-1176

**masers continued**

- fluctuating intensity regimes in lasers and masers 0-19015  
 galactic masers, role of plasma effects in generating high-vel. and symmetric spectral features 0-31378  
 W Hydrae, long-period variable, suspected Zeeman splitting in OH masers 0-36632  
 interstellar H II/OH maser regions, heating by ion streams 0-56912  
 interstellar masers,  $\Lambda$ -doublet population inversion in OH, OD, CH, CD and NH<sup>+</sup> collisions 0-22065  
 interstellar masers membership in star form. regions rel. to population categories 0-17645  
 interstellar OH maser sources, accurate position meas. 0-46646  
 MCR monoton synchronization by external harmonic signal applied to resonator 0-43312  
 Orion A, 22 GHz water line giant outburst 0-8703  
 U Orionis, Mira variable, relation between 1612 MHz flare and light curve 0-56844  
 parametric instability in a stream of phased oscillators, nonlinear theory 0-5719  
 quantum amplifiers and their application in space research, review 0-36503  
 ruby, research and development 0-27094  
 ruby maser with wide tuning band 0-53247  
 semiconductor subjected to mag. and US fields, EM radiation gain 0-48201  
 spherical open resonator, approx. theory (*French*) 0-48301  
 stellar SiO masers,  $J=1-0$   $\nu=1$  and 2 masers relative intensity and vel. 0-4339  
 W51 Main, H<sub>2</sub>O maser emission 0-8701  
 C stars, search for HCN and CH maser emissions 0-51856  
 Fe<sup>3+</sup>:Al<sub>2</sub>SiO<sub>5</sub>, andalusite travelling wave maser in 40 to 46 GHz freq. range (*Ukrainian*) 0-53246  
 Fe<sup>3+</sup>:TiO<sub>2</sub>, low noise travelling wave maser, noise temp. 0-32945  
 H<sub>2</sub>O maser features, high-velocity, in W3(OH), obs. 0-31339  
 H<sub>2</sub>O maser sources in different stages of evolution, new VLBI maps 0-26954  
 H<sub>2</sub>O maser in S252 (NGC 2175) star forming complex, discovery 0-4411  
 NH<sub>3</sub>  $J=K=1$  line mol. beam maser emission, ring-type focusing 0-28119  
 NH<sub>3</sub> molecular beam maser with semi-confocal cavity, output power spectral distrib. 0-43311  
 OH 1612 MHz masers, unsuccessful search in symbiotic stars 0-12774  
 OH, interstellar, new main line maser obs. with probable Zeeman pattern 0-56908  
 OH maser emission, rot. states, hyperfine states, microwave spectra, interstellar appl. 0-32694  
 OH maser sources, interstellar, radiative transport effects on inversion 0-17681  
 OH type I source G 109.7+2.2 near Herbig-Haro object (*Russian*) 0-17684  
 Rb, magnetometric devices appl., threshold sensitivity and short-term fluctuations determ. 0-22394  
 SiO 86.2 GHz maser, astronomical sources polarisation props. 0-4449  
 SiO maser variability at 86 GHz of R Leonis,  $\alpha$  Ceti and Orion A 0-41839

**masking (acoustic)** *see* **hearing; speech intelligibility****masks**

- see also semiconductor device manufacture*  
 diffraction grating form. on optical waveguide surface, ion-beam etching through photoresist mask 0-14492  
 interleaved glass layer prism for semiconductor mask testing 0-43425  
 ion implantation, semiconductor device processing 0-34031  
 sapphire, etching of arrays of orifices using Pt-Cr composite layer mask 0-3216  
 Cr film, reversal etching in gas plasma, reaction mechanism, AES and XPS obs. 0-16564  
 GaAs film optical components, prep. by MBE using Si shadow masking technique 0-28358  
 Si:B,As selective area simultaneous doping 0-34015  
 Si<sub>3</sub>N<sub>4</sub>/Ge films, intrinsic stress rel. to deposition conditions, use as Si oxidation mask 0-39467

**masonry dams** *see* **dams****mass**

- see also atomic mass; elementary particle mass; molecular weight*  
 double galaxies, data anal. and galaxian mass (M/L) determ. 0-4428  
 galaxy systems, virial mass estimation 0-17678  
 spiral galaxies, local mass-to-light ratio radial var. 0-31361  
 standards for industry 0-42198

**mass analyzers** *see* **mass spectrometer components and accessories****mass differences**

- see also baryon mass; lepton mass; mass formulae; meson mass*  
 b-mesons, mass splitting, SU<sub>3</sub> nonet of SU<sub>c</sub> 0-47288  
 Gelfand pattern, charmed hadrons and magnetic moment 0-398  
 hadron EM mass differences and struct. 0-27502  
 isospin violating mass differences and mixing angles, quark mass and QCD 0-52505  
 isospin-violating mixing in meson nonets, dd-u $\bar{u}$ (s $\bar{s}$ ) mass differences 0-32096  
 meson mass spectrum, planar bootstrap, and Regge approach 0-22581  
 nonlocal quark model in SU(3) $\times$ SU<sup>c</sup>(3) $\times$ U(1), meson decay and mass correction (*German*) 0-27456  
 pseudoscalar mesons, EM mass shifts, quark-parton model, SU<sub>3</sub> quark triplet 0-42459  
 QCD, asymptotic freedom, energy levels J/ $\psi$  and T mass difference (*Chinese*) 0-52480  
 quark-quark interactions, Bjorken scaling law violation 0-9160  
 quarkonium systems, binding energy effect on mass spectra 0-37229  
 quarks, third and fourth generation, mass prediction using quantised magnetic self-energy 0-18133  
 B<sup>0</sup>-B<sup>-</sup>, EM mass difference, some phenomenological estimates about heavy quark (b,t) bound states 0-47262  
 c-u quark mass difference, baryon mag. moments 0-37240  
 D<sup>0</sup>, D<sup>+</sup>, decays, charm changing neutral current limits, QCD depend., mass differences 0-32062  
 $\Delta^{++}$ - $\Delta^0$  pole parameter determ. 0-13303  
 e- $\nu$ , finite QED 0-47222  
 $\eta_c$  and  $\eta'_c$ , mass prediction using QCD 0-22590  
 K<sub>L</sub>-K<sub>S</sub>, Kobayashi-Maskawa six quark model, mixing angles, mass matrix and CP violation 0-13284  
 n-p, finite QED 0-47222



**mass differences continued**

- $\rho$ - $\omega$  mixing, quark mass differences 0-37243  
 $\Delta(1236)$ -N(939) mass difference from deep inelastic scatt. quark wave functions, hyperon masses 0-47289  
 $^2\text{H}$  neutron binding energy and n, mass excess from  $^1\text{H}(n,\gamma)$  0-47362

**mass filters** *see mass spectrometer components and accessories***mass formulae**

- see also baryon mass; lepton mass; mass differences; meson mass*  
 b-mesons, mass splitting, SU, nonet of  $\text{SU}_6$  0-47288  
 electron theory, chronon, charged-lepton mass formula 0-47224  
 hadron masses and current algebra quark masses 0-42436  
 hadron multiplets, realisations in SU(3) from stable particles 0-9159  
 hadronic matter exponential mass spectrum, incompatibility with weakly interacting quark phase 0-37219  
 heavy mesons, polynomials approximating sequence of masses (*Russian*) 0-407  
 Higgs bosons, masses, gauge hierarchies,  $\text{SU}_3$  model 0-47236  
 leptons, charged, new quantum number n 0-13244  
 meson isosinglets, mixing angles, non-relativistic quark model, Schwinger-type mass relations for  $\text{SU}_4$  and  $\text{SU}_3$  0-18125  
 meson isosinglets, mixing angles, non-relativistic quark model,  $\text{SU}_3$  and  $\text{SU}_n$  0-22591  
 meson mass spectrum and unitarity in quark model 0-18115  
 relativistic oscillator formalism for hadron struct. and props. 0-9144  
 relativistic quark models, cc and bb singlet triplet splitting, mass formulae (*Russian*) 0-37232  
 SU(4)  $\times$  SU(4) symmetry breaking, Cabibbo angle, nonlinear hadronic Lagrangian, PCAC (*Russian*) 0-42360  
 SU(4) 16-plet boson mass formulas, flavour symmetry breaking 0-37250  
 SU(5), broken, meson mass formulae 0-47267  
 unified gauge model with a nonlinear chiral hadron Lagrangian,  $\text{SU}_4$  hadron multiplets 0-42378

**mass measurement**

- see also weighing*  
 periodic mass variations obs., using electromechanical vibrating system 0-47020  
 resistive transducers, normalisation (*Rumanian*) 0-4699

**mass spectra**

- see also mass spectrometers; mass spectroscopic chemical analysis; mass spectroscopy; secondary ion mass spectra; time of flight mass spectra*  
 adhesive bonds breaking under high vacuum, light and electron emission, spectral comp. obs. 0-55190  
 benzene,  $^{13}\text{C}$  substituted, mass selective two-photon ionis., mass spectroscopy obs. 0-9651  
 carbon tetrachloride, charge exchange mass spectra 0-43177  
 chloroform, charge exchange mass spectra 0-43177  
 chloromethane, charge exchange mass spectra 0-43177  
 dichloromethane, charge exchange mass spectra 0-43177  
 electrolyte, aq. soln., field-induced ion evap. from liq. surface at atm. press. 0-29859  
 ethanol, ion internal energy selection by angle-resolved mass spectrometry 0-53164  
 ethylene, ion ejection mass resolution test of wideband freq.-swept marginal oscillator detector for ion cyclotron reson. spectrometer 0-9069  
 ethylene, line selective excitation with  $\text{CO}_2$  laser light and vibr. relax. 0-9705  
 ethylene, mol. ion, mass spectra ion intensity internal energy depend., quasi equilibrium theory calcs. 0-53163  
 hexafluoro ethyl cation fragmentation, mass spectrometry 0-53070  
 n-hexane, mass selective storage mass spectra by quadrupole ion storage mass spectrometer 0-52351  
 metal layer growth by sputtering, corpuscular diagnostics of hollow cathode discharge 0-16180  
 metastable atoms, charge permutation, appl. of reversed geometry mass spectrometers 0-37118  
 methane, ion internal energy selection by angle-resolved mass spectrometry 0-53164  
 methanol, ion internal energy selection by angle-resolved mass spectrometry 0-53164  
 organic ion, excited electronic state correlation with mass-spectral fragmentation pattern 0-45482  
 polyacetylene:  $\text{AsF}_5$ , thermal decomp. kinetics, elec. cond., ESCA and mass spectra 0-50830  
 polyatomic ions, energy deposition on high-energy collision, angle-resolved mass spectrometry obs. 0-32825  
 propan-1-ol, ion internal energy selection by angle-resolved mass spectrometry 0-53164  
 propane, ion internal energy selection by angle-resolved mass spectrometry 0-53164  
 propane, mol. ion, mass spectra ion intensity internal energy depend., quasi equilibrium theory calcs. 0-53163  
 sym-tetrazine, isotope selective mol. spectroscopy and isotopically pure mol. prod. with dye laser 0-11926  
 $\text{pp}-\Delta^{++}\text{pr}^-$ , 4 GeV/c, mass spectra, ang. distrib. and momentum transfer (*Russian*) 0-42489  
 Bi film, on Si(111) substrate, MBE deposition kinetics 0-10817  
 $\text{CO}$ , chemisorption on AgNa mordenite 0-2752  
 $\text{CO}_2^-$ , hydrated anion stable gas phase heteronuclear clusters, mass spectra, autodetachment rates 0-14266  
 Co, pure surfaces, adsorp. of water and decomp. (*German*) 0-26054  
 Cu mirror, surface defect layer form. on mech. polishing 0-33122  
 $\text{H}_2$ , chemisorption on AgNa mordenite 0-2752  
 HCl, charge exchange mass spectra 0-43177  
 $\text{He}_2^+$  form. in pulsed afterglow, mass spectroscopic obs. 0-54046  
 Hf-H, diffusion in hydride phase, exam. 0-29204  
 $\text{Hg}_2$ , Cd, Te, vaporisation under Knudsen effusion conditions 0-2154  
 $\text{K}_2\text{SO}_4$ , mass spectrum obs. of vaporisation, vapour comp. and press., transition and form. heats 0-19933  
 Li-Pb, thermodynamic study using Knudsen effusion mass spectrometry 0-24578  
 $\text{LiReO}_4$ , thermodynamic activity in  $\text{LiReO}_4$ - $\text{CsReO}_4$  system, mass spectra meas. 0-2174  
 $\text{NO}_2^-$ ,  $\text{NO}_2$ ,  $\text{H}_2\text{O}$ , and peroxy isomers, photodissoc. and photodetachment 3500-8250 Å, rel. to ionosphere 0-35554  
 $\text{NO}_3^-$ ,  $\text{NO}_3$ ,  $\text{H}_2\text{O}$ , and peroxy isomers, photodissoc. and photodetachment 3500-8250 Å, rel. to ionosphere 0-35554  
 $\text{NO}_2^-$ - $\text{HNO}_2$ - $\text{H}_2\text{O}$  clusters, gas phase, thermodynamic quantities, mass spectra obs. 0-50875  
 Na (111) surface, epitaxial film, electron induced dissociation 0-6646

**mass spectra continued**

- $\text{Rh}^+$ ,  $\text{Rh}^{2+}$ , field evaporation, field ion mass spectra and field ion appearance spectra study 0-7479  
 Ti-H, diffusion in hydride phase, exam. 0-29204  
 ZnO powders, electron-beam-induced desorption, phase-sensitive detection 0-54502  
 Zr-H, diffusion in hydride phase, exam. 0-29204

**mass spectrometer applications**

- see also isotope separation; mass spectroscopic chemical analysis*  
 ionosphere, positive ion detection with rocket-borne mass spectrometer 0-8459  
 isobar nuclei, separation of alkali and alkaline earth elements using surface ion source 0-37688  
 isotope fractionation, controllable, in thermal-ionis. mass spectrometry, SRM 987 standard test (*German*) 0-42299  
 laser microprobe mass analyser (LAMMA) appl. 0-18041  
 planetary atmospheric composition determ. 0-8518  
 $\text{O}_2$  inhalation automatic control for patients with respiratory failure 0-17181  
 $\text{SiO}_2$ , comparison of depth profiling techniques 0-29048

**mass spectrometer components and accessories**

- see also ion sources*  
 bakeable hollow cathode, ion-molecule reaction study in discharge gas mixtures 0-37117  
 capillary device construction for liquid introduction into analytic mass spectrometer 0-4805  
 effusive beam source, heterogeneous reaction type, chem. equil. 0-52362  
 electron multiplier three-state time delay switch 0-37116  
 EM analyser control, automatic registration of the back-scattered ions 0-18042  
 focusing lens system, quadrupole, for beam of mass-separator 0-47801  
 gas mass spectrometer, ion source numerical simulation (*German*) 0-47141  
 ion detector, electro-optical, for spark source mass spectrometry 0-42246  
 ion source, cold cathode 0-42293  
 ion source, high sensitivity for quadrupole mass spectrometers 0-52353  
 ion source, TOF spectrometer, electron beam collimation, rel. to resolution and sensitivity 0-42294  
 Knudsen effusion cell, high temp. mass spectroscopy, thermodynamic and physicochemical behaviour, review 0-52354  
 laser ionisation source for ICR spectroscopy, metal at. ion chem. appl. 0-45597  
 magnet power supply, programmable, to allow rapid scanning with min. reset time 0-37121  
 mass analyser, two-stage, with vel. filter, using sector mag. 0-4808  
 mass analyzer using electron-beam-guiding type ion source 0-31933  
 plasma chromatograph/mass spectrometer column overload prevention valve 0-16748  
 pump, orbitron ion-getter, small non-cooled and low power consumption 0-52352  
 quadrupole ion storage mass spectrometer, cylindrical geometry and operational characts., QUISTOR comparison 0-52351  
 quadrupole ion store, simultaneous positive-negative ion mass spectrometry, scanning techniques and systems description 0-52350  
 quadrupole ion store, three-dimensional, ion motion, charge exchange reactions effect, two-ion model 0-55738  
 quadrupole mass filter, computer simulation of ion trajectories in quadrupole field 0-52349  
 quadrupole mass filter, operation and theory 0-52348  
 turbomolecular pump, miniaturized for space appl. 0-52254  
 wideband freq.-swept marginal oscillator detector for ion cyclotron reson. spectrometer 0-9069

**mass spectrometers**

- see also ion optics; mass spectra; mass spectroscopy*  
 computerised data acquisition and processing system, gas chromatograph input 0-13181  
 double collecting, device for automatic digital measurement of isotopic ratios 0-31932  
 gas chromatography/mass spectroscopy system, computer-controlled, DP-102 0-22470  
 instrumentation for chemists and biologists 0-42297  
 interface module for multichannel analyser ADC input 0-27916  
 multiplexed exit slits and field scan, improved sensitivity, speed and S/N ratio 0-31930  
 quadrupole, 3-dim., with elliptical electrodes 0-31931  
 quadrupole, 3-dimens. theory 0-4806  
 quadrupole, on 'Vertical-7' geophysical rocket 0-31935  
 quadrupole ion storage mass spectrometer, cylindrical geometry and operational characts., QUISTOR comparison 0-52351  
 quadrupole RF trap, temporal invariance and energetic and spatial statistical properties of confined ions (*French*) 0-22471  
 quartz tube orifice leaks for local, fast-response gas sampling 0-35609  
 resonance mass spectrometer with a coaxial helical undulator 0-9071  
 reversed geometry mass spectrometer for organic compound identification 0-50913  
 reversed geometry mass spectrometers, charge permutation 0-37118  
 stratospheric composition investigation using gas expansion and mass spectrometer beam system 0-31934  
 tandem double focusing mass analyser, uncoupled E+M system 0-18043  
 three-dimensional quadrupole type, ion beam struct. 0-9070  
 time of flight spectrometer, 3-dimens., asymmetric quadrupole lens 0-4807  
 triple quadrupole mass spectrometer and technique, direct mixture analysis and struct. elucidation 0-35583  
 vacuum extraction device, with mass spectrum analyser, gas-forming admixture in metals determ. 0-22371

**mass spectrometry** *see mass spectroscopy***mass spectroscopic chemical analysis**

- see also atom probe field ion microscopy; ion microanalysis; ion microprobe analysis; isotope separation; mass spectra; secondary ion mass spectra; secondary ion mass spectroscopy*  
 aliphatic perfluorocarbons, electron attachment, fragmentation 0-12 eV 0-5618  
 alkali halides, cluster ions and mol. ions in salt field desorption 0-40238  
 trans-2-butene, charge transfer mass spectra and photoelectron spectra 0-40778  
 chondrite Kirin H, inert gas content interpretation (*German*) 0-46505  
 chondrite Yamato-74191, inert gas composition and neutron capture effects 0-46504



**mass spectroscopic chemical analysis continued**

- collisional activation mass spectra 0-48106  
 computer data search system, based on catalogue of compressed mass spectra (*Russian*) 0-30292  
 computer-aided classification of mass spectra, pattern recognition techniques, decision-tree approach 0-40774  
 data bases, information content of retrieval procedures calc. 0-30297  
 depth profiles obtained by ion-beam sputtering, edge-effects correction 0-55757  
 DNA, intact, modified bases characterisation by mass-analysed ion kinetic energy spectrometry 0-3591  
 EBR, dissolver soln. fission product determ. by spark source mass spectroscopy 0-32422  
 field desorption mass spectrometry, appl. to biochemistry, medicine, and environmental science 0-35592  
 fly ash and trace organic compounds anal., from municipal incinerators 0-45584  
 Fourier transform ion reson. spectrometry of ions undergoing collisions with mols. 0-35598  
 gas chromatography mass spectrometry technique 0-26094  
 gas chromatography-mass spectrometry, integrated analytical systems, applics. in biomed. and related sciences, review 0-36200  
 gas chromatography-mass spectrometry data system, research-oriented, principles and applics. 0-40770  
 high temperature, Knudsen effusion cell, thermodynamic and physico-chemical behaviour, review 0-52354  
 high temperature gas phase species, IR spectral meas., mol. beam mass spectrometry 0-52235  
 high temperature molecules, high pressure molecular beam mass spectrometric sampling, review 0-52355  
 high temperature vapour, charact. by angular distrib. mass spectrometry 0-55769  
 high temperature vapours, photoionisation mass spectrometry 0-52238  
 human disease study using mass spectrometry and metabolite profiling 0-51289  
 hydrocarbons, normal, mass-spectrometric fragmentation processes, quantum field theory 0-40782  
 involatile molecule thin films, electrospray deposition for  $^{252}\text{Cf}$  plasma desorption obs. 0-35584  
 ion cyclotron resonance spectroscopy, interpretive expt. 0-36814  
 ion kinetic energy spectrum peaks, collision gas sensitive 0-40679  
 ion-molecule equilibria in solvolysis, secondary  $\beta$   $^3\text{H}$  isotope effects, hyperconjugation 0-50874  
 ion-molecule reactions, bakeable hollow cathode for sampling 0-37117  
 ions, multiple dissociation probabilities 0-40678  
 laser ionisation source for ICR spectroscopy, metal at. ion chem. appl. 0-45597  
 low-resolution spectra identification using combined forward-reverse library search system 0-30296  
 LPE, molecular beam mass spectrometry, in situ anal. of minor gaseous species 0-52357  
 lubrication, spectroscopic methods for surface anal. (*French*) 0-26095  
 LWR, dissolver soln. fission product determ. by spark source mass spectroscopy 0-32422  
 meteorites, iron, elements distrib. between metal and phosphide phases 0-46508  
 MHD plasma, coal-fired, molecular beam mass spectrometric sampling system 0-52358  
 molecular spectroscopic laboratory strategies, queueing theory and digital simulation use 0-30299  
 monoterpene hydrocarbons in rural atmospheres, gas chromatography/mass spectrometric anal. 0-17336  
 oligomers, polymer-derived, mass spectral charact. 0-37916  
 organic compound identification using reversed geometry mass spectrometer 0-50913  
 peptide analysis by field desorption mass spectrometry using pretreated Si emitter 0-55751  
 polymer matrix composites, component interaction mass spectrometry investigation (*Russian*) 0-35511  
 propyl halides, photoionisation mass spectrometry 0-40779  
 propylene, electron impact ionisation and dissociation 0-37894  
 rare earth oxides, determ. by mass spectrometric complexometric method 0-3442  
 selected fragment scans in direct mixture analysis, active computer monitoring and control 0-35597  
 SIMS, solid surface investig. applications (*Rumanian*) 0-49510  
 space plasma, mass discrimination effects in mass spectrometers ion and neutral extraction 0-4230  
 spark source sensitivity factors for elements in graphite matrix 0-16760  
 surface anal. by photon-induced field ionisation mass spectroscopy 0-40780  
 surface ionisation, elemental anal. of sputtering products (*French*) 0-50905  
 surface ionisation meas. after ion sputtering (*French*) 0-27374  
 thin film surface anal. and depth profiling by spark-source mass spectroscopy, discharge model 0-40781  
 transpiration mass spectrometry, of high temp. vapours 0-52356  
 triple quadrupole mass spectrometer and technique, direct mixture analysis and struct. elucidation 0-35583  
 vacuum extraction device, with mass spectrum analyser, gas-forming admixture in metals determ. 0-22371  
 Wien-Thompson modern mass spectrometer review 0-45613  
 Al, condensed film, phase and struct. nonuniformity (*Russian*) 0-54536  
 Al, surface ionisation, elemental anal. of sputtering products (*French*) 0-50905  
 $^{26}\text{Al}/^{26}\text{Mg}$  isobars, separation via negative ion mass spectroscopy 0-31146  
 Ar-hexamethyldisiloxane, glow discharge positive column ion mass spectra identification 0-38834  
 B,  $\beta$ -rhombohedral, purification by electron beam melting and CVD 0-20781  
 BaBr<sub>2</sub>-BaCl<sub>2</sub>, vap. mixture, ion-mol. equil., heat of form. of ions 0-26039  
 BaCl<sub>2</sub>-BaBr<sub>2</sub>, vap. mixture, ion-mol. equil., heat of form. of ions 0-26039  
 CO<sub>2</sub>, ion drift velocities and mobilities 0-43834  
 (CO<sub>2</sub>)<sub>2</sub><sup>+</sup>, ion-mol. reaction product distrib. and rate coeffs. 0-50852  
 $^{13}\text{C}/^{12}\text{C}$ , ratio analysis in carbonates by mass spectrometry (*Portuguese*) 0-7875  
 CaCl<sub>2</sub>, cluster ions and mol. ions in salt field desorption 0-40238

**mass spectroscopic chemical analysis continued**

- Ca<sub>2</sub>O:Bi, positive ion nonequilibrium emission in heterogeneous chemical reaction, mass spectra 0-55277  
 CdTe, gas, identification by high-temp. mass spectrometry 0-45593  
 CdTe, trace anal. by heavy ion induced X-ray emission and SIMS 0-55755  
 CeO<sub>2</sub>, plasma deposition of crystals and their characterisation 0-20800  
 CsAlSi<sub>3</sub>O<sub>8</sub> and CsAlSi<sub>5</sub>O<sub>12</sub>, cryst. evap., mass spectral investig. 0-49353  
 Cu, surface ionisation, elemental anal. of sputtering products (*French*) 0-50905  
 Cu-Al, surface ionisation, elemental anal. of sputtering products (*French*) 0-50905  
 Fe-TiB<sub>2</sub>, phase composition, secondary ion-ion emission study (*Russian*) 0-20896  
 G<sub>2</sub>-B<sub>2</sub>O<sub>3</sub>, melt, thermodynamic props. from mass spectroscopy 0-39318  
 GaAs epitaxial layer, Be, O, Si, S, Zn and Sn impurity concentrations 0-49260  
 Gd<sub>0.27</sub>Co<sub>0.64</sub>Kr<sub>0.09</sub>, amorphous film, thermal release of Kr and H, meas. using UHV mass spectrometric technique 0-3439  
 HfO<sub>2</sub>, plasma deposition of crystals and their characterisation 0-20800  
 HgSe, gas, identification by high-temp. mass spectrometry 0-45593  
 LaI(r), thermodynamic stability, high-temp. mass spectra obs. 0-7781  
 NO, state selective step-wise photoionisation, with mass spectroscopic ion detect. 0-43119  
 NaCl, thermodynamic equil. vapourisation, transpiration mass spectrometry 0-52356  
 Na<sub>2</sub>SO<sub>4</sub>, thermodynamic equil. vapourisation, transpiration mass spectrometry 0-52356  
 Ni, electrolytic, O, H, N liberation during vacuum heating, Mossbauer spectra (*Russian*) 0-35594  
 $^{18}\text{O}/^{16}\text{O}$  ratio analysis in carbonates by mass spectrometry (*Portuguese*) 0-7875  
 SF<sub>6</sub>, photon-enhanced dissociative electron attachment, isotope selectivity 0-18939  
 Sb<sub>2</sub>Se<sub>3</sub> (x=0 to 4; y=1 to 4) molecular species formed in vaporisation of solid Sb<sub>2</sub>Se<sub>3</sub>, thermodynamic props. 0-11943  
 SeS gas, thermodynamic props., quadrupole mass filter study 0-16716  
 Si whisker field desorption ion source, Cu, Sn, Ag, Te, Cd and Sb isotope abundance ratios 0-11975  
 Si:As sputter rate meas. SIMS combination with Rutherford backscatter 0-21334  
 Sn film, reactively sputtered, discharge produce evaluation, mass spectrometer obs. 0-6668  
 ThO<sub>2</sub>, plasma deposition of crystals and their characterisation 0-20800  
 Ti-Ir alloys, Ti-rich, thermodynamic study at high temp. using Knudsen cell mass spectrometry 0-45539  
 TiO<sub>2</sub>-(Cr<sub>2</sub>O<sub>3</sub>)<sub>2</sub>, rutile, Cr<sub>2</sub>O<sub>3</sub> effects on O<sub>2</sub> tracer diffusivity, depth profile meas. by SIMS 0-24651  
 W, zonal electronic purification, mass spectra of contaminants (*Polish*) 0-25552  
 ZnS, gas, identification by high-temp. mass spectrometry 0-45593  
 ZnTe, gas, identification by high-temp. mass spectrometry 0-45593  
 ZrO<sub>2</sub>, plasma deposition of crystals and their characterisation 0-20800

**mass spectroscopy**

- see also atom probe field ion microscopy; mass spectra; mass spectrometers; secondary ion mass spectroscopy  
 $^{81}\text{Br}$  isotope enrichment by laser photodissociation of HBr 0-1075  
 acetic acid, ionised, pot. energy profiles for unimol. reactions 0-43210  
 angle resolved mass spectrometry, ion internal energy selection 0-53164  
 angle resolved technique, applics. 0-304  
 angular distribution, charact. of high temp. vapours 0-55769  
 application to in situ atmospheric measurements 0-17388  
 bioactive compound structural studies 0-51305  
 collisional activation mass spectra 0-48106  
 data bases, information content of retrieval procedures calc. 0-30297  
 digital system for cancer research 0-22469  
 elemental composition determination low resolution magnetic mass spectrometers 0-42296  
 epitaxy, growth modes, exp. techniques, book contrib. 0-49558  
 Fourier transform ICR spectrometry, error estimates 0-37061  
 high temperature, Knudsen effusion cell, thermodynamic and physico-chemical behaviour, review 0-52354  
 ion cyclotron resonance spectroscopy, interpretive expt. 0-36814  
 ion probe mass spectrometry microanalysis, basic physics (*Chinese*) 0-42311  
 ion-sensitive photographic plate evaluation using optical wedge microdensitometer (*German*) 0-42298  
 laser fusion target pellets, mass spectrometer determ. of AR contents 0-32442  
 low-resolution spectra identification using combined forward-reverse library search system 0-30296  
 mechanistic studies 0-47142  
 molecular beam mass spectrometric sampling, high press., high temp. mols., review 0-52355  
 molecular beam mass spectrometry, in situ anal. in crystal growth ambients 0-52357  
 molecular beam mass spectrometric sampling system, ion concs. in coal-fired MHD plasmas 0-52358  
 molecular photoionisation mass spectroscopy, reson. peak shapes 0-42295  
 molecular spectroscopic laboratory strategies, queueing theory and digital simulation use 0-30299  
 molecule+negative ion, thermochemical data, gas phase acidity scale, mass spectroscopic techniques 0-30234  
 monitoring chemicals, description of technique 0-4803  
 negative ions 0-43211  
 organic ion, excited electronic state correlation with mass-spectral fragmentation pattern 0-45482  
 organic ions, pot. energy profiles for unimol. reactions 0-43210  
 peptide and glycopeptide research methods 0-51307  
 photoionisation, of high temp. vapours 0-52238  
 porphyrins and related tetrapyrroles 0-51306  
 propane, vapour-liquid and vapour-solid equil., data, mass spectroscopic tracer pulse chromatography 0-37115  
 quadrupole ion store, simultaneous positive-negative ion mass spectrometry, scanning techniques and systems description 0-52350  
 review, applications (*Japanese*) 0-27373  
 review of current status 0-55665  
 steroid research 0-51308  
 transpiration mass spectrometry, of high temp. vapours 0-52356  
 Wien-Thompson modern mass spectrometer review 0-45613



## mass spectroscopy continued

- CO<sub>2</sub>, vapour-liquid and vapour-solid equilib. data, mass spectroscopic tracer pulse chromatography 0-37115  
 CdI<sub>2</sub> crystals, photolysis obs. (*Russian*) 0-7833  
 nC(graphite)+U(g)→UC<sub>n</sub> (n=1 to 6), enthalpy changes obs. 0-7842  
 Cu-Ge, liq. alloy, thermodynamic activity meas. by Knudsen-cell mass spectrometry (*French*) 0-10684  
 Cu-H, evolution of gas during heating, mass spectroscopic exam. 0-30221  
 He-Ar mixture, mass separation during molecular beam sampling process 0-31937  
 Ir (110), desorption of H, thermal desorption mass spectrometry, order plots 0-44409  
 Sb<sub>2</sub>Se<sub>3</sub> (x=0 to 4; y=1 to 4) molecular species formed in vaporisation of solid Sb<sub>2</sub>Se<sub>3</sub>, thermodynamic props. 0-11943  
 Si<sub>4</sub>H<sub>4-n</sub>, enthalpies of formation, effusion mass spectrometric meas. 0-26043  
 TiO<sub>2</sub>, photodesorption of H<sub>2</sub>O, pulsed-laser-dynamic-mass-spectrometer study 0-35568  
 ZnO, photodesorption of CO<sub>2</sub>, pulsed-laser-dynamic-mass-spectrometer study 0-35568

## mass standards see measurement standards

## mass transfer

- accretion disks, theoretical review (*Polish*) 0-26739  
 accretion onto rapidly moving gravitating centre, self-similar soln. 0-17609  
 air-water surfaces, turbulence characts., mass transfer and eddies 0-14665  
 analog solution of free convection mass transfer from downward-facing horizontal plates 0-43706  
 annulus with non-Newtonian fluids, mass transfer to inner wall, Leveque soln. adaptation 0-10267  
 AE Aquarii, cataclysmic variable, rapid light oscills. obs. rel. to mass transfer rate 0-36634  
 atmospheric aerosols, particle size distrib. evolution via Brownian coagulation, num. simulation 0-41513  
 bibliography of Soviet works on heat and mass transfer 0-41972  
 binary stars, equipotential surfaces, modification due to pressure of radiation of component (*French*) 0-56880  
 black hole accretion discs, boundary-layer behaviour of flow at disc inner edge 0-46598  
 black hole X-ray sources in galactic bulge, disk model 0-17691  
 black holes, electron-positron pair production in hot unsaturated Compton accretion models 0-36658  
 black holes, nonsymmetric disc accretion (*Russian*) 0-36661  
 black holes in binary stellar systems, gamma emission during spherically symmetric accretion 0-17608  
 blackholes, accretion contrib. to background radiation density 0-4461  
 blunt-body boundary layers, three dimensional, surface curvature effects 0-1520  
 i Bootis, light curve and period vars. of W Ursae Majoris type star 0-4398  
 capillary-porous bodies, internal mass transfer, influence of inhomogeneous elec. and mag. fields 0-6138  
 cataclysmic binaries, mass transfer rel. to evolution and origin 0-56885  
 cataclysmic variables, accretion discs models rel. to emission line spectra 0-51774  
 catalyst granular bed, static, flow transfer processes 0-45554  
 SV Centauri, early-type contact binary, evolutionary models and mass exchange rate 0-4403  
 U Cephei, eclipsing binary, gas stream effects in UV spectrum, IUE obs. 0-26898  
 Z Chamaeleontis, cataclysmic binary, mass exchange due to gravit. radiation 0-4386  
 combined heat and mass exchange processes, model eqns. and techniques (*German*) 0-27236  
 condensing mixed vapors, suction effects heat and mass transfer (*German*) 0-33609  
 conical nozzle and diffuser, laminar compressible boundary layer swirling flow 0-48768  
 conservation equation, numerical soln. by variational approach, mass transfer problem appl. (*French*) 0-19317  
 contact binary stars, solar type, ang. momentum controlled evolution and mass transfer 0-36670  
 convective, stationary, inside drop, influence of chemical volume reaction at large Peclet numbers (*Russian*) 0-28508  
 convective heat and moisture transfers with const. heat flux (*French*) 0-33582  
 correlations for flow between fluidised spheres and liquid 0-14805  
 corrosion pit, convective diffusion 0-40601  
 creeping flow mass transfer in size distrib. cloud drops, high Schmidt number 0-14783  
 SS Cygni, dwarf nova, spectrophotometry rel. to accretion disc models in eruption and at min. light 0-36635  
 32 Cygni, IUE obs. rel. to late-type supergiant mass loss rate 0-22036  
 59=V832 Cygni, variable mass flux from spectroscopic obs. 0-41840  
 Cygnus X-1, model of neutron star surrounded by massive disc 0-36736  
 Cygnus X-3, 4.8 hour modulation period meas. rel. to high mass loss binary models 0-8713  
 cylindrical channel with evaporation and condensation at walls, model kinetic eqn. 0-6101  
 dielectric drop in electric field, low Peclet number heat and mass transfer 0-6050  
 differential transfer equations for multiphase, multicomponent media 0-14794  
 disc accretion in soft potential well, excess surface density ring form. 0-8532  
 dissociating gas in pipes, heat and mass transfer 0-24105  
 dust transport on lunar surface 0-8558  
 electrically conducting fluid, laminar flow mass transfer at high Peclet numbers 0-43784  
 electrochemical mass transfer between rough surfaces and solutions containing drag-reducing polymers 0-19447  
 electrochemical phase formation 0-55309  
 electrogenerated chromophores, electrochemical conc. profiles, mass transfer, charge transfer, laser absorpt. spectroelectrochem. obs. 0-40765  
 electrolysis, annulus flow, solenoidal mag. field effect on ionic mass transport 0-26021  
 electrolysis, mass transfer to stacked net electrode 0-11896
- mass transfer continued  
 evaporation, quasisteady half-space problem, gas kinetics theory and expt. 0-6106  
 evaporation, quasisteady one-dimens. problem, entropy-balance relation 0-6168  
 evaporation with natural convection, simultaneous heat and mass transfer in laminar boundary layer, numerical anal. (*French*) 0-53778  
 evaporation-condensation two-surface problem, in presence of noncondensable gas 0-6169  
 evaporation-effusion problem, rarefied regime, nonlinear numerical soln. 0-6167  
 flame, mass streamline, vel. and density fluctuations correlation (*Japanese*) 0-6164  
 flame, round jet type, mass exchange between recirculation zone and outer flows, stabilisation 0-14842  
 fluctuating flow, mass transfer near front stagnation point of axisymmetric body 0-48675  
 fluid flow, use of dispersion model 0-48784  
 fluid interfaces, isothermal and deformable, mass transfer and surface tension, review 0-33564  
 fluid interfaces, Marangoni instability, dissipative structures and nonlinear kinetics 0-33565  
 fluid interfaces dynamics and instability, conf., Lyngby, Denmark (May 1978) 0-31423  
 fluidised bed, random pulsations 0-24089  
 forced and free convective heat and mass transfer (*French*) 0-48689  
 forced convection in two-phase flow from jets, mass transfer near interface (*German*) 0-53782  
 free binding liquid film, mean velocity distrib. meas. by laser Doppler velocimeter 0-38508  
 free convection in Stokes' problem for infinite vertical limiting surface, mass transfer effects 0-28501  
 galaxies early-type, accretion phenomena, role of gas-rich dwarfs 0-31349  
 gas diffusion through surfactant films, interfacial resistance 0-39385  
 gas flow to liquid jet mass transfer 0-53827  
 gas mixture, multicomponent, transport equations near catalytic surfaces 0-43821  
 gas-dust clouds, rotation, mass transport processes rel. to solar system origin 0-8556  
 glacial ice, melting in sea water, heat and mass transfer (*German*) 0-33606  
 HD 44179 (Red Rectangle), precessing jets model 0-4422  
 heat and mass transfer between turbulent flowing fluid and solid wavy surface 0-14681  
 heat pipe, 2-component, heat and mass transfer 0-24021  
 heated body in perfect incompressible fluid, convective heat and mass transfer 0-43698  
 Helmholtz layer model diffuse layer, discreteness of charge effect calcs. 0-26030  
 Hercules X-1 (HZ Herculis), periodic mass transfer rel. to X-ray light curve 0-51911  
 DQ Herculis (Nova 1934), high time resolution spectrophotometry rel. to mass transfer rate 0-22017  
 DQ Herculis (Nova 1934), short-period oscills. modulation and pulsed emission lines asymmetry interpretation 0-22044  
 hot massive stars, stellar wind mass loss, evolution study 0-17578  
 Hubble-Sandage variables, mass accretion model 0-26877  
 HV evaporation, mass transfer in evaporating space (*Japanese*) 0-50558  
 VW Hydri, cataclysmic variable, mass transfer modulation rel. to light curve superhumps model 0-4381  
 impulse plasma centrifuge with circulation, theory (*Russian*) 0-38553  
 interfacial cellular convection, effect on mass transfer enhancement 0-14690  
 internal flows with initial swirl, generated heat and mass transfer law 0-24025  
 irradiated stars in active galactic nuclei, mass loss and evolution 0-56949  
 isotropic turbulent flowfield, smoke downstream diffusion, mass transfer characts. 0-14668  
 jet entering fluidised bed, aerodynamics and mass transfer 0-14809  
 Krogh tissue cylinder, transient convective mass transfer 0-3598  
 Lewis number, heat and mass transfer coeff. derivation 0-14698  
 limiting relative law of heat and mass transfer and friction, permeability parameter effect 0-23999  
 local mass/heat transfer distribution on surfaces roughened with small square ribs 0-19506  
 macromolecular solution, gel conc. and diffusivity at gelling determ. by ultrafiltration 0-21325  
 magnetoelectrolytic convection, accuracy of estimation method 0-14691  
 massive binary stars, effects of mass transfer on heavy elements prod. 0-46534  
 membrane transport, monosubstrate inhibited enzymes, conc. response, multiplicity and memory 0-30679  
 methanol-H<sub>2</sub>O mixture, evaporating droplets in air, temp. modelling (*German*) 0-2243  
 Mira variables, envelope instability and mass loss rel. to planetary nebula form. 0-26928  
 multicomponent condensation, simplified mass transfer anal. 0-10675  
 multiperforate laminae, mass transfer of chem. species by diffusion, plate and associated boundary layer case 0-40736  
 neutron star, interaction between accretion disc and mag. field (*Russian*) 0-51799  
 neutron stars, disk accretion, transition zone radial and vertical structure 0-4393  
 neutron stars, H rich material accretion rel. to thermonuclear runaways 0-22032  
 neutron stars, magnetised, accretion, fate of sinking filaments 0-51798  
 neutron stars, rotating, magnetic, accretion torques rel. to pulsating X-ray sources period changes 0-31320  
 noninertial particle transfer to rotating in laminar flow under external force field 0-10250  
 nonlinear heat and mass transfer in porous media 0-1577  
 nozzle, two phase, efficiency at high rates of heat and mass transfer 0-48767  
 nozzle expansion in turbulent flow, downstream heat and mass transfer 0-1669  
 nuclear reactor, interfacial mass and momentum transfer in two-phase flow 0-27725  
 numerical solution of transfer theory problems by the direct reduction method 0-22309



**mass transfer continued**

ocean, mass conservation calculations in natural coordinates with example from Baltic Sea 0-51433  
 one dimensional heat and mass transfer, Stefan flow and Lewis number influence (*German*) 0-1590  
 ovalbumin aqueous soln., macromol. gel layer formed on ultrafiltration tubular membrane, charact. 0-14260  
 packed bed, mass transfer time domain evaluation from chromatograph peaks 0-19496  
 particle in fluid with steady linear ambient vel. distrib., mass and heat transfer 0-19385  
 particles in a fluid, convective diffusion and mass transfer, wakes, chemical reactions 0-38394  
 $\beta$  Persei type systems, orbital period changes and evolutionary status 0-4396  
 polystyrene suspension, laminar flow, augmentation of heat and mass transfer, correl. of data 0-53840  
 polyvinylalcohol, macromol. gel layer formed on ultrafiltration tubular membrane, charact. 0-14260  
 porous bodies, stresses induced by drying, elastoviscoplastic model, finite element anal. 0-23904  
 porous electrode diffusion controlled operation, mass transport with memory 0-21298  
 pseudoplastic fluid crossflow around circular cylinder, heat and mass transfer 0-19370  
 Roche lobe formation in highly eccentric X-ray binary systems 0-41858  
 rotating disc, convective mass transfer 0-43707  
 rotating disc electrode mass transfer, appl. of pulsed voltage and pulsed current 0-21292  
 WZ Sagittae, cataclysmic variable, mass transfer modulation rel. to light curve superhumps model 0-4381  
 WZ Sagittae, recurrent nova, accretion disc brightening during 1978 outburst, spectroscopic obs. 0-26862  
 XZ Sagittarii, Algol system, UVB photometry rel. to circumstellar matter 0-22041  
 salt solutions, freezing in cells, heat and mass transfer with phase change 0-6493  
 sand tracer dispersion under progressive water waves, laboratory and field obs. 0-46170  
 saturated porous wedge with impermeable boundaries, heat and mass transfer 0-19375  
 Schwarzschild black hole, gas accretion 0-56871  
 Schwarzschild black hole stationary spherical accretion, stability 0-51800  
 solar prominence condensation, horizontal temp. gradient meas. 0-26832  
 solidifying melt thermal gravitational convection, impurity distrib. and transfer processes 0-19367  
 soluble flat surface stability in turbulent flow 0-14676  
 Soret driven convective instability, mass diffusion and boundary effects 0-53776  
 sorption processes, formation of new crystalline phases 0-6625  
 southern peculiar emission-line stars, observational data rel. to mass ejection 0-41843  
 spherical particle in free-fall, time-to-complete-dissolution prediction 0-15245  
 spontaneous condensation processes, classification 0-6500  
 SS 433, accreting mag. neutron star model (*Russian*) 0-36647  
 SS 433, early-type star plus neutron star model 0-56843  
 SS 433, mass accel. and collimation mechanisms 0-4368  
 SS 433, ultra-close black hole-degenerate dwarf binary system model 0-4384  
 staggered tube bundle, pressure and friction drag, mass transfer effects 0-38388  
 stars, asymptotic giant branch evolution with steady mass loss 0-26846  
 stars, constraints on mass loss rates from white dwarf data 0-46548  
 stars, massive, effect of mass loss on chemical yields 0-36614  
 stars, massive, He burning, mass loss by stellar wind rel. to evolution and Wolf-Rayet binaries 0-36615  
 stars of high mass, stellar wind effects on evolution 0-21982  
 steam condensation in moving two-phase film, heat transfer, volumetric coefficient 0-48696  
 steam-water annular flow, moisture exchange, salt method 0-24078  
 steel-Si alloy formation kinetics at solid cathodes, metal electrodeposition from molten salt electrolytes 0-26028  
 steel, carburisation, calc. of mass transfer in diffusional saturation 0-24676  
 stellar surfaces, accretion of interstellar matter 0-51734  
 stellar systems, effect of mass loss on dynamical evolution, analytic approximations 0-51815  
 stellar wind flow past compact object, hydrodynamic eqns. and X-ray intensities 0-22116  
 Sun, mass loss rel. to meteoroid swarm evolution 0-8592  
 sunspot, Evershed flow in complex region 0-51732  
 supercritical accretion discs winds struct. and appearance, numerical models 0-21984  
 supernova explosion from shock heating, collapse of massive star cores 0-56863  
 supersonic gas particle flows over wedge (*German*) 0-43731  
 ternary gas mixture, natural convection, naphthalene sublimation appl. 0-6511  
 thermogravimetric method for recording mass transport of materials under action of radiant fluxes 0-17944  
 thermomagnetoforesis of particles in magnetic suspensions 0-35581  
 turbulent Prandtl and Schmidt numbers from modelled transport eqns. 0-19373  
 4U 1626-67, X-ray pulsar, X-ray and optical obs. rel. to accretion disc optical emission 0-51914  
 unsteady state heat transfer through the interface of spherical particles (*German*) 0-1412  
 vapourisation of particles in high temp. gas, Sherman eqn. calcs. (*Russian*) 0-39270  
 wall region heat and mass transfer in turbulent Newtonian and viscoelastic flow 0-14680  
 X-ray bursters 0-4460  
 X-ray sources, steady accretion discs general struct. with mag. field 0-8714  
 Cs, vapour in Ar, fog condensation in MHD generator, heat and mass transfer 0-1410  
 Cu electrodeposition at vertical electrode, current distrib.,  $H_2$  evolution effect 0-35543  
 Cu:Be, alloy formation kinetics at solid cathodes, metal electrodeposition from molten salt electrolytes 0-26028

**mass transfer continued**

$D_2O+H_2$ , isotope exchange and separation with Pt hydrophobic catalyst (*Japanese*) 0-37901  
 Fe anode in  $H_2SO_4$ , passivation, dissolution model 0-35545  
 Fe-Co, compositional diffusionally bonded alloy, mass transfer investigation (*Russian*) 0-39342  
 H-O electrochemical matrix-type cells, transport effects study 0-26027  
 $LaMnO_3$ , solid phase synthesis mechanism 0-21268  
 $N_2O_4$  flowing in axisymmetric channels, mass and heat transfer calcs. 0-1570  
 NiO, grain boundary thermal grooving, mass transport, self-diffusion coeffs. 0-44217  
 Si-Ge-Br system, diffusion mass transfer 0-33911  
 $YMoO_3$ , solid phase synthesis mechanism 0-21268

**master equation**

Brusselator, dynamic correl. functions, Mori-Zwanzig formalism 0-25988  
 chemical metastable and unstable states relax., analytical theory of extrema 0-50829  
 chemical systems, non-equilib., mol. dynamics studies of long range and short range fluctuations 0-21318  
 dilute atomic gas, weak at.-at. interaction pot. from master eqn. for coupled radiation 0-23484  
 dissociation, unimolecular, master eqns., analytic theory of extrema 0-50841  
 dynamical renormalisation group transform., Ginzburg-Landau model, kinetic Ising model 0-42170  
 electrical circuit, power conversion of energy fluctuations, rel. to 2nd law of thermodynamics 0-17911  
 hopping transport theory, master eqn. approach (*German*) 0-27237  
 kinetic Ising chain, renormalisation group transform. for master eqn. 0-11214  
 laserlike systems, stochastic master equation description 0-53243  
 linear response theory, master eqn. approach 0-31663  
 Malthus-Verhulst process, crit. point calcs. 0-42176  
 Markovian integro-differential master eqns., Langevin description 0-31676  
 molecular crystal, multicomponent, energy migration master eqn. 0-16075  
 nonequilibrium systems, cluster expansions with contraction for homogeneous systems 0-46964  
 photon statistics, unsaturated k-photon absorption, exact soln. of master eqn. 0-37984  
 quantum damped oscillator, master equation and pure state representations 0-8823  
 semiconductor, hot electron fluctuations with displaced Maxwellian distrib. 0-29418  
 statistical mechanics, foundations 0-22271  
 Sterman-Weinberg formula for quark jets and gluon jets, leading log version, master equation 0-22552  
 three two-level atoms system, continuously incoherently-pumped, radiation rate, spectrum 0-5716  
 transition operator for Markov and non-Markov processes, interpolation model 0-8910  
 unimolecular reactions, nonequil. time-depend., model calc., single collision approx. 0-25987  
 unimolecular reactions induced by monochromatic IR radiation, intensity and laser energy fluence influence 0-11903  
 AgI, conductivity, hopping system, master equation 0-39348  
 H, recombining atomic plasmas, population inversion 0-32679  
 N, recombining atomic plasmas, population inversion 0-51040  
 O, recombining atomic plasmas, population inversion 0-32679

**matched filters**

narrowband matched SAW filters realisation (*Russian*) 0-23850  
 optical, pattern recognition by means of holography (*Japanese*) 0-5699  
 SAW slanted device technology for radar system appl. 0-19181  
 SAW/CCD programmable matched filter 0-5896

**materials**

see also individual materials, e.g. ceramics  
 bitumen, diffusion of  $^{13}C$  and  $^{90}Sr$ , radioactive waste treatment (*Russian*) 0-52771  
 bituminous surfaces, review of aggregate selection criteria for improved wear and skid resist. 0-7689  
 orchard leaves, metals, determ., in water and organic materials, flameless atomic absorpt. spectrometry with wire loop atomiser 0-45586  
 tissue substitute materials formulation, effective atomic numbers 0-17169  
 tooth enamel, human cryst. struct. refinement, Rietveld method 0-51040  
 tyres, used, pyrolysis to produce organic raw materials (*German*) 0-3307

**materials handling**

see also computerised materials handling; crushing; fission reactor fuel preparation and reprocessing; fluidised beds; grinding; transportation; winding (process)  
 biomedical target, water-cooled pion-production, remote exam. and disassembly 0-25975  
 cutting laser beam appl. in material-cutting, processing optimisation (*German*) 0-43384  
 FBR, alternative fuel recycling technology search 0-5303  
 FFTF fuels and materials exam. facility and materials handling systems design 0-18421  
 fission reactor fuel, mixed oxide, suitability of spent fuel shipping casks 0-27757  
 fission reactor irradiated cladding, in-cell facility for mechanical testing 0-21244  
 glove box for sealed manipulator maintenance 0-18684  
 glove boxes, Pu-contaminated, size reduction and waste packaging 0-18469  
 hot cell liners, removable, design 0-18685  
 hot fuel examination facility, auxiliary equipment for remote handling systems 0-18686  
 isotope induction at LAMPF, fabrication, cladding, handling of irradiated targets 0-23231  
 liquefied natural gas, safe handling, measurement system, prediction of roll-over 0-27269  
 LMFBR fuel elements, remote exam. of shroud tubes 0-18470  
 LNG, transport and storage hazards 0-45620  
 loop disposal system of sodium loop safety facility 0-18467  
 LWR, alternative fuel recycling technology search 0-5303  
 metal surface radioactive waste chemical decontamination 0-37530  
 mixed-oxide fuel pellets, remote encapsulation for transient testing 0-18422



**materials handling continued**

- nuclear material transportation, ORNL Nuclear Legislative Data Base program 0-37539  
 nuclear power stations, fuel circuit review, radioactive conditioned waste final storage (*German*) 0-799  
 nuclear spent fuel shipping cask licensing 0-37545  
 nuclear waste transportation, DOE transportation technology centre 0-37537  
 postirradiation examination facility 0-18682  
 PWR assemblies, pool-site fuel inspection and exam. techniques 0-18567  
 radioactive contact-handled transuranic waste transportation 0-37538  
 radioactive fuel storage, air-cooled, Canadian canister program 0-5253  
 radioactive fuel storage, dry, with air cooling 0-675  
 radioactive waste, packaging containers, a survey 0-23097  
 radioactive waste management, dismantling of PWR 0-27756  
 slab tanks for criticality control, neutron multiplication calc. 0-13606  
 solid neutron shield development, materials eval. for spent fuel shipping cask 0-13939  
 temporary confinement structures, design criteria and guidelines 0-18683  
 Tokamak fusion test reactor, in-vessel maintenance remote manipulator system 0-18611  
 tree form energy plantations, woodchip transport and handling 0-30327  
 Zircaloy-UO<sub>2</sub> fuel rods, eddy-current testing of claddings using encircling and probe coils 0-21245  
 H<sub>2</sub>, cryogenic storage and refuelling for automobiles 0-30604  
<sup>85</sup>Kr, pressurised cylinder storage tests 0-5269  
 Na, contaminated, packaging and storage 0-18468  
 Pu, high burnup fuels, shielding and handling problems 0-27833  
 Pu, transportation, effect on environment, evaluation study (*French*) 0-27785  
 Pu(NO<sub>3</sub>)<sub>4</sub> solution concentrator equipment for criticality safety 0-18432  
 PuO<sub>2</sub> air transportable package PAT-1, dose rate and criticality calcs. 0-13938  
 (U,Th)O<sub>2</sub> fuel rods, analytical stressing in hot cell 0-18566  
 U refining and decay processes, radioactive waste (*Dutch*) 0-21418  
 U-Al, storage of unirradiated fuel in borated concrete, criticality safety anal. 0-13608  
 UO<sub>2</sub>(NO<sub>3</sub>)<sub>4</sub>, secondary criticality control, use of chlorinated PVC piping 0-13607  
<sup>A</sup>UO<sub>2</sub>(NO<sub>3</sub>)<sub>2</sub>, a=233, 235, slab tanks for criticality control, neutron multiplication calc. 0-13606

**materials preparation**

- see also *crystal growth; hot pressing; powder metallurgy; powder technology; sintering; vulcanisation*  
 actinide metals and their refractory cpds., synthesis from oxides and single cryst. growth 0-16229  
 ceramic, quartz glass based, organosilicon binder, spalling-resistant, prod. 0-40313  
 ceramics, manufacture using waste glass fibres 0-40304  
 chlorination of Cu and Zn in Cu converter slag 0-20840  
 composite materials preparation under microgravity conditions, stability during melting, thermal soak, solidification (*German*) 0-7521  
 condensation of highly conc. dispersions, to give strong materials 0-40274  
 diamond, synthesis and characterisation 0-50580  
 diamond production by C shock compression 0-11613  
 dispersion hardened metallic materials, production (*German*) 0-50646  
 dispersion-hardened materials, production (*German*) 0-45316  
 dynamic stabilization of multiphase media subjected to vibrations under low gravitation conditions 0-7511  
 ferromagnetic thin film magnetometer, development and performance 0-31808  
 GFRP sheet moulding compound, influence of cure time restrictions, on minimum weight design of double layer panels 0-11623  
 glass fibres, strength, forming conditions influence 0-20882  
 PAN graphite-Al composites, liquid metal infiltration process and interface barrier coatings 0-11779  
 graphite-alkali metal lamellar cpd., reversible intercalation of tetrahydrofuran 0-16211  
 metals, prep. by electromagnetic levitation in ultrahigh vac. 0-29899  
 niobate based ceramics, synthesis, struct., elec. cond., mag. props. (*Czech*) 0-45259  
 plasmochemical synthesis, powdered infusible compounds, props. 0-55330  
 polyethylene filaments, ultrahigh-strength, from soln. spinning and hot drawing 0-45268  
 polypropylene rods, prep. by die-drawing 0-45327  
 radiation processing, conf., Miami, FL, USA (Oct. 1978) 0-36772  
 rare earth oxyphosphates, x Ln<sub>2</sub>O<sub>3</sub>.y P<sub>2</sub>O<sub>5</sub>, synthesis, characterisation and thermal stability 0-16256  
 rare earth perovskites and garnets, prep. and props. book contrib. 0-44193  
 rare earth pyrochlores, R<sub>2</sub>(V<sub>4/3</sub>W<sub>3/3</sub>)O<sub>7</sub>, (R=Gd, Tb, Dy, Ho, Er, Tm, Xb, Lu), synthesis and elec. props. 0-29914  
 refractory borides, carbides, nitrides, manufacture and appl. in electronic and electrotechnic field (*French*) 0-40311  
 refractory compound fibre reinforced cpd. materials, diffusional reaction, effect of alloying calc. 0-20851  
 sitalls, synthesis based on elec. power plant residues 0-40314  
 TCNQ salts with heterocyclic amines and hydroquinone form. via redox reaction 0-26013  
 tetraphenylthiadiapiranylidene-iodine, synthesis and cond. props. 0-24910  
 transition metal hydrides, synthesis and physicochemical props., conf., Moscow, USSR (Jan. 1978) 0-27032  
 transition metals processing and appl., using vacuum technology (*Hungarian*) 0-55318  
 transuranic chalcogenides and pnictides, prep. and cryst. chem. 0-16255  
 Vycor glass, manufacture, struct., physical and chem. props. 0-7527  
 AlN powders, synthesis and impurities 0-55329  
 Al<sub>2</sub>O<sub>3</sub> ceramics, with thermoplastic bond, prep. 0-45254  
 Al<sub>2</sub>O<sub>3</sub> porous refractories, production 0-35149  
 3Al<sub>2</sub>O<sub>3</sub>.2SiO<sub>2</sub>, mullite, synthesis by freeze drying 0-16252  
 B fibre reinforced Al VKA-1 composite, fibre/matrix interface reaction during prep. 0-25619  
 B-Si compounds, thermoelec. material, prep. by pyrolysis of BBBr<sub>3</sub>-SiBr<sub>4</sub> mixture 0-20862  
 B<sub>4</sub>C, synthesis in HF EM field 0-20864  
 BN composites, polymer impregnated 0-7526  
 Be<sub>2</sub>Ti<sub>2</sub>O<sub>7</sub>, grain oriented ferroelectric ceramic, prep. by molten salt synthesis-tape casting method 0-40296

**materials preparation continued**

- Bi<sub>2</sub>Te<sub>3</sub>-Bi<sub>2</sub>Se<sub>3</sub> thermoelectric alloys, diffusion and evaporation of volatile component during prep. 0-35118  
 Bi<sub>2</sub>WO<sub>6</sub> grain oriented ferroelectric ceramic, prep. by molten salt synthesis-tape casting method 0-40296  
 Ca<sub>3</sub>(PO<sub>4</sub>)<sub>2</sub>.OH, prep. from sulphate, X-ray diff. and IR spectrosc. 0-29893  
 β-Ca<sub>2</sub>SiO<sub>4</sub>-CaO-SiO<sub>2</sub> paste, hydration, compression strength and composition 0-50584  
 CeO, high press. synthesis, struct. and lattice const. (*French*) 0-29913  
 Co<sub>2</sub>Zr<sub>2</sub>S<sub>8</sub>, (0<x≤0.50), intercalation compounds, ordered phases obs. 0-33962  
 Cr, high-purity, production by bis(ethylbenzene) chromium thermal degradation (*Russian*) 0-35128  
 CrO<sub>2</sub>, oxidative prep. method, mag. props. 0-44863  
 Cr<sub>1-x</sub>Rh<sub>x</sub>O<sub>2</sub>, oxidative prep. method, mag. props. 0-44863  
 Cs<sub>3</sub>R<sub>2</sub>X<sub>9</sub> (=Sc,Y,Ho-Lu, X=Cl and R=Sc,Sm-Lu, X=Br), prep. and Guinier-Simon X-ray study 0-49204  
 Cu-Ga porous solid formed by shock compression 0-29905  
 Cu<sub>x</sub>MS<sub>2</sub>, (0<x≤0.50) (M=Zr, Hf), intercalation compounds, ordered phases obs. 0-33962  
 Cu(Mo<sub>2</sub>Re<sub>2</sub>)S<sub>8</sub>, synthesis and electrical props. of mixed tetrahedral cluster phases 0-2971  
 CuO-CdO-Fe<sub>2</sub>O<sub>3</sub>, sintered ferrite, preparation, mag. susceptibility, DC resistivity 0-34598  
 CuO-ZnO-Fe<sub>2</sub>O<sub>3</sub>, sintered ferrite, preparation, mag. susceptibility, DC resistivity 0-34598  
 Dy<sub>2</sub>B<sub>4</sub>, prep. and props., DTA study 0-20859  
 Eu<sub>2</sub>(PO<sub>4</sub>)<sub>3</sub>.OH, prep. from sulphate, X-ray diff. and IR spectrosc. 0-29893  
 Fe complex, FeOCl[(ethyltetramethylcyclopentadienyl)<sub>2</sub>Fe]<sub>0.16</sub> synthesis and struct. 0-44176  
 Fe(Mo<sub>2</sub>Re<sub>2</sub>)S<sub>8</sub>, synthesis and electrical props. of mixed tetrahedral cluster phases 0-2971  
 Fe<sub>2</sub>O<sub>3</sub>, Co modified, synthesis with autoclave in H<sub>2</sub> atm. 0-35117  
 δ-Fe(OH) and its solid solns. synthesis, X-ray diff. and TEM studies 0-29891  
 FeTiO<sub>3</sub>, ilmenite, prep. at focus of solar furnace (*French*) 0-29908  
 Fe<sub>x</sub>Zr<sub>2</sub>S<sub>8</sub>, (0<x≤0.50), intercalation compounds, ordered phases obs. 0-33962  
 Ga(Mo<sub>2</sub>Re<sub>2</sub>)S<sub>8</sub>, synthesis and electrical props. of mixed tetrahedral cluster phases 0-2971  
 Ge-S-Cu, phase separation in melt centrifugal quenching 0-25701  
 KHgC<sub>8</sub> and KHgC<sub>9</sub>, intercalation cpds., synthesis and struct. 0-44183  
 LiAlO<sub>2</sub>, fine particle size, heat treatment synthesis, molten carbonate fuel cell appl. 0-21395  
 LiTi<sub>2</sub>O<sub>4</sub>, single-phase, prep., crystal struct. and superconducting transition characts. 0-50583  
 MgO-ZnO-Fe<sub>2</sub>O<sub>3</sub>, sintered ferrite, preparation, mag. susceptibility, DC resistivity 0-34598  
 Mo-Re, prep. from reduction in Mo-Re-O system (*Russian*) 0-16225  
 MoS<sub>3</sub>, prep., use as Li battery cathode 0-29892  
 Nb-Mo, prod. by simultaneous carbothermic reduction of oxides/electron beam melting method (*Japanese*) 0-11590  
 Nb<sub>2</sub>Si, metastable A-15 struct. synthesis by ion implantation, supercond. transition temp. 0-55319  
 Nd<sub>2</sub>PO<sub>7</sub>, prep. and luminesc. props. 0-34964  
 Ni(Mo<sub>2</sub>Re<sub>2</sub>)S<sub>8</sub>, synthesis and electrical props. of mixed tetrahedral cluster phases 0-2971  
 Ni<sub>0.38</sub>Zn<sub>0.62</sub>Fe<sub>2</sub>O<sub>4</sub>, preparation, Mossbauer study 0-50231  
 Ni<sub>x</sub>Zr<sub>2</sub>S<sub>8</sub>, (0<x≤0.50), intercalation compounds, ordered phases obs. 0-33962  
 Pb bullion production, elec. smelting of PbSO<sub>4</sub> residues 0-11592  
 Pb-Se-As-Ge, phase separation in melt centrifugal quenching 0-25701  
 PbF<sub>2</sub>-AlF<sub>3</sub> glass, optical props., crystn. and thermal expansion 0-48367  
 Pb<sub>2</sub>MoO<sub>6</sub>, form. conditions 0-20853  
 Pb<sub>3</sub>(PO<sub>4</sub>)<sub>2</sub>.OH, prep. from sulphate, X-ray diff. and IR spectrosc. 0-29893  
 Pb<sub>2</sub>TaMoO<sub>6</sub>, reaction of form. from oxides, ferroder. props. 0-55326  
 PrO, high press. synthesis, struct. and lattice const. (*French*) 0-29913  
 RbHgC<sub>4</sub> and RbHgC<sub>8</sub>, intercalation cpds., synthesis and struct. 0-44183  
 RuS<sub>2</sub> amorphous, prep. at ambient temp., magnetic structure 0-35119  
 Si, solar grade, prod., using Dow Corning process 0-29894  
 SiAlON powder, prod. by reaction clay+C+N<sub>2</sub> 0-40295  
 SiC fibres obtained from polycarbosilane fibre 0-50582  
 Si<sub>3</sub>N<sub>4</sub>, finely dispersed, high-temp. synthesis 0-55331  
 Si<sub>3</sub>N<sub>4</sub>, synthesis in Cl<sub>2</sub> system 0-40308  
 Sr<sub>5</sub>(PO<sub>4</sub>)<sub>3</sub>.OH, prep. from sulphate, X-ray diff. and IR spectrosc. 0-29893  
 Sr<sub>2</sub>Pb<sub>1-x</sub>(Zr<sub>0.545</sub>Ti<sub>0.455</sub>)O<sub>3</sub>, piezoelec. resonator, preparation and props. (*Rumanian*) 0-28402  
 Ti complex, TiOCl[Co(cyclopentadienyl)<sub>2</sub>]<sub>0.16</sub>, synthesis and struct. 0-44176  
 Ti-Cr-B system, self-propagating high temp. synthesis, crystallochemical and mech. props. 0-20861  
 Ti-H, deposited on carriers, synthesis, structure and catalytic props. 0-29890  
 TiB<sub>2</sub>, electric arc melting prep. and oxidation props. 0-20860  
 TiB<sub>2</sub>, preparation method rel. to compressive strength 0-55327  
 TiN, self-propag. high-temp. synthesis under high N<sub>2</sub> pressures 0-25630  
 TiP, TiP<sub>2</sub>, iodide synthesis, and catalytic props. of TiP 0-55316  
 Ti<sub>2</sub>Cr<sub>2</sub>O<sub>7</sub>, Ti<sub>2</sub>Mn<sub>2</sub>O<sub>7</sub>, pyrochlore type, synthesis and physical props. 0-33963  
 (U,Pu)O<sub>2</sub>, FBR fuel pellets, gel-supported precipitation conversion and prep. 0-813  
 U<sub>16</sub>-alkali metal halide system, prep. 0-50568  
 V complex, VOCL[Co(cyclopentadienyl)<sub>2</sub>]<sub>0.16</sub>, synthesis and struct. 0-44176  
 Y<sub>2</sub>Cr<sub>2</sub>O<sub>7</sub>, Y<sub>2</sub>Mn<sub>2</sub>O<sub>7</sub>, pyrochlore type, synthesis and physical props. 0-33963  
 Y<sub>2</sub>(V<sub>4/3</sub>W<sub>3/3</sub>)O<sub>7</sub> pyrochlore, synthesis and elec. props. 0-29914  
 Zn(Mo<sub>2</sub>Re<sub>2</sub>)S<sub>8</sub>, synthesis and electrical props. of mixed tetrahedral cluster phases 0-2971  
 ZnS-Na<sub>2</sub>O-K<sub>2</sub>O-SiO<sub>2</sub>, form. using electric furnace, furnace design 0-11620  
 Zr-Cr-B system, self-propagating high temp. synthesis, crystallochemical and mech. props. 0-20861  
 Zr-H, deposited on carriers, synthesis, structure and catalytic props. 0-29890  
 ZrB<sub>2</sub>, electric arc melting prep. and oxidation props. 0-20860  
 ZrB<sub>2</sub> powders, synthesis and impurities 0-55329



**materials preparation continued**

ZrC powders, synthesis and impurities 0-55329  
 ZrO<sub>2</sub>, Y<sub>2</sub>O<sub>3</sub> stabilized, heat-resistant granular artifacts, procedure for making 0-35148

**materials properties**

*this heading is restricted to those properties which are not covered by other specific headings*

*see also dielectric properties of substances; electrical properties of substances; magnetic properties of substances; mechanical properties of substances; optical properties of substances; thermal properties of substances; thermodynamic properties*

annual review of materials science, book 0-46740

practicing scientist's handbook 0-2

rare earth compounds, handbook 0-41957

rare earth non-metallic compounds, handbook 0-51972

**materials testing**

*see also acoustic applications; corrosion testing; creep testing; dynamic testing; electron beam applications; fatigue testing; fracture toughness testing; hardness testing; insulation testing; mechanical testing; nondestructive testing; notch testing; ultrasonic materials testing*

acoustic emission analysis for vibration and shock testing of industrially produced substances (German) 0-3279

acrylic, denture base, tensile testing 0-16621

adhesion measurement, locus of failure, bond failure in adhesive joints 0-50801

adhesion measurement, of thin films, thick films and bulk coatings, conf. Philadelphia, USA (Nov. 1976) 0-46729

adhesion measurement, of thin films, thick films and coatings 0-50817

alloys for coal gasifiers, susceptibility to stress corrosion cracking determ. 0-7726

antifriction materials, device for wear testing 0-21223

autoradiography on thin foils, high resolution, anal. of technique characts. (French) 0-55598

Bauschinger effect, temp. influence, combined tension-torsion testing machine, appl. to Al 0-45453

bonded joints, device for automatically recording internal stresses 0-25963

brittle materials, load-transmitting medium to measure strength 0-40652

brittle materials, normal elasticity modulus, strain gauge meas. 0-55601

brittle rod, optimum specimen shape for compression tests, gluing technique effects 0-50797

brittle rod, optimum specimen shape for compression tests, struct. and technological parameters 0-50798

building product, nonmetallic, first crack determ. device, during load test (Czech) 0-45471

castings, economic testing by mag. powder method (German) 0-3277

coherent-optical materials testing for vibration pattern and defect discrimination (German) 0-30181

COMECON standard reference-data system 0-45469

composite materials under complex stress-state conditions, mech. props., method for studying 0-50799

composite structures, fracture initiation prediction 0-11870

composites, thermal stresses investigation, using polymer models 0-40639

condensation chamber, for flame photometric analysis, exam. of design 0-21342

creep tests, machine, conditions of plane state of stress 0-21232

CRISP-E, use in a phase-in mode 0-40654

cutting fluids testing rel. to tool wear, thin layer activation technique 0-55619

cutting oil performance, test machine 0-11848

deposit-substrate systems, adhesion testing 0-50814

destructive, advances in servo-hydraulic test machines 0-35453

dynamic stress strain relations in combined tension and torsion, testing device 0-21197

electrodeposit, on metallic substrate, peel test for determ. adhesion 0-50815

electrodeposits, multilayer, thickness meas., instrument based on destructive coulombmetric method (Czech) 0-8980

electronics materials, possible applications of laser microanalysers (Polish) 0-33008

electroplated coatings (German) 0-2967

facilities available at Altrincham Laboratories 0-35454

fibre composites, impetus of composite mechanics on test methods 0-11868

fibre-glass plastics, fatigue lifetime prediction based on cumulative damage 0-11776

fibre-glasses, long-term strength evaluation, parametric methods efficiency 0-40662

film, adhesion measurement 0-50819

filmed structures, hardness and adhesion meas., scratch technique 0-50805

films and tissues multiple bending testing device 0-21225

fission reactor materials testing, General Electric Test Reactor appls. 0-565

fission reactors, LOCA simulation, armature testing (German) 0-42785

flame-sprayed coatings, adhesion testing 0-50812

fluorescent penetrant inspection, heat assisted 0-45466

foil strain gauges, use on materials with heat constraints during heat treatment 0-25938

gels, swelling kinetics device 0-21210

glass, elastic moduli, device for temp. depend. meas. at low pressures 0-30183

glass fibre, tensile strength meas. using chain-loading fibre tensometer (Japanese) 0-55610

glass fibre reinforced plastics, design criteria 0-25970

granular materials shear deformation, simulation by Al rods (Japanese) 0-11691

graphitic materials deformation, crack and fracture behaviour, SEM exam 0-11706

high temp. inner press.-tensile test device (Japanese) 0-25972

high temp.-high flux material testing, solar power station appls. 0-40668

historical development, Instron Ltd., product range since 1946 0-35452

Inconel 718, environment effect on high temp. fatigue crack growth 0-30090

ion exchange resins, macroporous rapid method of rating total void volume 0-21208

laser microprobe mass analyser (LAMMA) appl. 0-18041

liquid penetrant testing, continuum fluid mechanics aspects 0-43818

lubricant evaluation, using four ball friction machine 0-25951

**materials testing continued**

lubricants, ester-type, thin-film test for meas. of oxidation and evaporation 0-40626

magnetic particle inspection oxides, evaluation 0-40657

metals, positron annihilation, localised probe of lattice defects 0-55224

metals, working, method of applying fusion thermal indicators to surfaces, including heated surfaces 0-17937

microscope photometry appls. 0-21236

Mossbauer effect appl., conference, Kyoto, Japan (Aug.-Sept. 78) 0-7199

nuclear reactor materials, apparatus to meas. thermophysical props. at high temps. 0-37458

opposed-anvil high-press. devices, material strength effect 0-47068

optical glass, K8, bending strength, sample dimension effects 0-9975

photoelastic load meas. and testing (German) 0-19297

plastics, tensile and flexural testing device, incorporating an impactor (German) 0-3276

plastometer, electronically controlled, for tensile and compression tests (German) 0-3273

polarographic sensor with microwire indicator electrode, exam. of design 0-21340

polybutadienes, use of high modulus inclusion gauge, in stress analysis 0-21254

polymer material bending strain, strain gauge to meas. reliably 0-25948

polymer melts, quasistatic bulk strength meas., specially built apparatus 0-7737

polymer viscoelasticity and strength characterisation, advanced light scatt. techniques 0-11857

polymers, automatic recording device for thermomechanical and linear dilatometric testing 0-11858

polymers, microtoming for structure analysis 0-40665

polymers, stress-state meas. using chemiluminesc. system 0-40628

porous material, gas diffusion technique for pore struct. investigation 0-30185

porous sintered materials, mech. testing device for hydrostatic pressure conditions 0-40645

positron measurements, for NDT of metals and alloys 0-55222

powder dustiness, determ. method 0-45455

radiography, effect of stress on crack detection 0-40653

reference materials for COMECON member countries 0-45468

rubber mixtures, device for determining wear 0-21226

semiconductor domain instability and resistivity profile meas., universal capacitive probe 0-31796

shear resistance of finely dispersed bulk material 0-21224

soldered thick-film conductor, adhesion meas. technique 0-50811

steel, cast, equipment for thermal shock resistance determ. 0-55614

steel, cold-rolled sheet, St10 kp, St10 sp, mag. inspection of ferroprobe coercimeters 0-21234

steel, high strength low alloy, acoustic emission meas. from crack opening displacements 0-7732

steel, non-metallic inclusions changes due to heating obs., influence on ductile fracture (Spanish) 0-25744

steel, pressing die X45 CrNiWMoVCo 9.9, test results (German) 0-50785

steel, punch, for blanking tools, method of wear resist. determ. 0-55600

steel, sheet, rapid test for props. assessment 0-40650

steel, stainless, pipes, electro-thermal method for NDT of welds 0-35447

steel, thermal props. meas. (French) 0-25977

steel, wear resistance, determ. using MI-IM machine 0-25943

steel pressure vessel plates, destructive examination, PISC trial 0-52745

steels, stainless, accelerated test for susceptibility to Cl<sub>2</sub> stress corrosion cracking 0-21199

strain gauge measurements on plastic models, instrumentation, accuracy 0-21255

stress/strain diagram, instrument for displaying on TV screen 0-21222

subsurface stress meas. 0-21252

textures materials, residual stress evaluation by X-rays (German) 0-40670

thermal analysis system, Du Pont 1090, microcomputer-controlled 0-16613

thermography, NDI method for damage detection 0-35445

thick film, adhesion to ceramic, destructive and nondestructive meas. 0-50809

thick film terminations on chip components, adhesion meas. methods 0-50810

US equipment, selection of material for concentrator-instrument section 0-21242

vacuum extraction device, with mass spectrum analyser, gas-forming admixture in metals determ. 0-22371

wires, thin, fatigue testing 0-25834

X-ray stress measurement method, appl. to practical materials (Japanese) 0-52379

Zircaloy-UO<sub>2</sub> fuel rods, eddy-current testing of claddings using encircling and probe coils 0-21245

Ag-Cu-Pb coin chem. anal. by low energy  $\gamma$ -rays and neutron transmission meas. 0-35591

Al alloys, stress-strain state after treatment by pressure, moire strip method appl. (Russian) 0-40648

Al, thin film on fused quartz, threshold adhesion failure, meas. by stylus method 0-50806

Al-Zn-Mg, acoustic emission meas. during tensile testing, reproducibility of results 0-50782

Al<sub>0.9</sub>Ga<sub>0.1</sub>As DH laser, rake-line form. in LPE growth, scanning photocurrent technique 0-2287

Co enamel, vitreous, objective colour evaluation, rel. to firing parameters (Czech) 0-42252

Fe, grey cast, tensile testing of mechanical props., from room temp. to liquidus (Japanese) 0-7728

Mg-Al single crystal growth, specimen for tensile testing in corrosive medium (Russian) 0-20774

Ni-In alloy, deposited on Kovar, vacuum seal for borosilicate glass appl. (Italian) 0-40621

Pt-Au, thick film, adherence meas. and evaluation 0-50813

Sn plate, rapid test for props. assessment 0-40650

Ti alloys, metallurgical characterisation using thermoelec. power meas. (French) 0-45462

UO<sub>2</sub> ceramic fuel fabrication, simulation of thermal processes by emanation thermal anal. 0-811

ZnCl<sub>2</sub>-oil system, simulation of steel-slag, macrophotographic method of diagnosing disperse system 0-25952

ZnO fibre reinforced elastomer, X-ray diffr. exam. of filamentary crystal distrib. 0-7738



**mathematical analysis**

- see also approximation theory; Bessel functions; calculus; catastrophe theory; differential equations; eigenvalues and eigenfunctions; Fourier analysis; integral equations; numerical analysis; series (mathematics); spectral analysis; transforms
- acoustic wave propagation, review of techniques for soln. of problems 0-53514
- global climate, mathematical model appl. to CO<sub>2</sub>-climate sensitivity study 0-31117
- conference, Tokyo, Japan (June 1979) 0-31412
- convection driven by non-uniform surface tension 0-10116
- geophysics, analytic construction for two-dimensional gravimetric and magnetometric problem 0-21846
- geothermal power plants flash cycle optimisation, analytical expression in terms of temp. only 0-40894
- heat conduction problems, extended domain solns. 0-19209
- interstellar shocks, analytical results for post-shock gas temp., density, vel. and comp. 0-56911
- inverse theory, appl. to geostrophic ocean currents determ. independently of reference level 0-51574
- meteorology, isentropic objective anal. (Polish) 0-51546
- minimum Entropy Deconvolution with an exponential transformation 0-17407
- multilayer cylindrical shells with fillers, analysis of stability 0-7643
- radiant-convective heat exchange problems, nonstationary, analytical soln. method 0-33432
- US atomization, cavitation-induced capillary waves 0-33328

**mathematical logic** see formal logic**mathematical programming**

- see also linear programming; nonlinear programming
- elastoplastic structures, stresses and strains during loading, mathematical programming, pivoting procedure 0-53641

**mathematics**

- see also algebra; combinatorial mathematics; convergence; digital arithmetic; duality (mathematics); equations; formal logic; functions; geometry; mathematical analysis; number theory; probability; statistics; topology
- No entries

**matrices** see matrix algebra**matrix algebra**

- see also S-matrix theory
- astrometry, overlapping plate method appls. 0-36479
- Casimir invariants and characteristic identities for generators of graded Lie algebras 0-13227
- combined transfer matrix and finite element techniques, analysis of static and dynamic structural problems 0-53619
- crystal vacancy modelling, topological approach 0-10543
- crystallographic orientation, distribution function generalisation using rotation matrix 0-11665
- cylindrical lenses, rotation of parallel fan of light, matrix representation 0-38089
- Davidson's algorithm with and without perturbation ocrrections 0-27570
- discrete Gauss transform, inversion of  $\{\rho^{(r-s)2}\}$  matrix 0-4505
- elliptic polarisation, Stokes parameters, vector trihedron, optical element evaluation 0-53209
- equations of state, search procedure, based on step-wise least-squares technique 0-19900
- fractional-parentage coefficients, reduced in quasi-spin space, submatrix elements of tensor operators 0-4578
- G, F and  $\Sigma$  matrices for XY<sub>8</sub> molecules of D<sub>2d</sub> symmetry (French) 0-970
- gyroscopic systems eigenvalue problems solution, with real symmetric matrix of same dimension 0-12895
- Hadamard and M-sequence transforms are permutationally similar 0-32921
- Hermitian matrix, disorder effect on spectrum 0-31547
- HF approximations, thermodynamic Fermi systems 0-4642
- hologram interferometry, use of projection matrices 0-37965
- Huckel matrix reduction, graphical method 0-14085
- isotropic media, linear dynamical equations of state 0-22314
- kinetic theory differential operator, matrix representation 0-14867
- linear transport relaxation equations, matrices, variational principle 0-17785
- matrix diagonalisations via involutorial transforms. 0-17827
- matrix diagonalisations via reduced characteristic eqns., appl. to ang. mom. coupling 0-17828
- neutron spin-echo integral transform spectroscopy 0-4748
- octahedral group, symmetry-adapted functions, calc. of rotation matrices using recursion relation 0-31482
- perturbation theory, many-body, arbitrary point group symmetry, wave operator matrix elements 0-23311
- polar semiconductor, nonlinear transport, field-dependent relaxation time 0-6866
- precession theory, vector-matrix notation 0-51642
- ray transfer matrix, for 90 degree reflector 0-33184
- sparse system of linear equations, solution 0-23
- spin system, ABC type, matrix elements of tensor operators calc., transition probability matrix 0-25182
- SU(3) in SO(3) basis, sum rules for matrices of generators 0-13226
- surface potentials of stratified spheroidal volume conductors excited by electric dipole source 0-32867
- tops and d-functions in even spaces (Russian) 0-4508
- U(p+q) and U(p,q) in U(p)×U(q) basis, matrix elements for infinitesimal operators 0-12928
- U(p+q) and U(p,q) in U(p)×U(q) basis, matrix elements of infinitesimal operators 0-12929
- vibrating beam, multiplicity of solns. of inverse problem 0-28462
- H<sub>2</sub><sup>+</sup>, exponentially small part of wave function (Russian) 0-9497

**matrix isolation spectra**

- see also Shpol'skii spectra
- alkali atom, in inert-gas solid, at level struct. calc. pseudopot. method 0-9532
- alkali tetrafluoroaluminates, matrix isolated IR spectra 0-985
- anharmonic molecules in low temp. matrices, vibronic dephasing 0-6469
- aromatic esters, phosphoresc. and fluoresc. spectra in organic matrices 0-32756
- 1,2-benzanthracene in polystyrene films, delayed luminesc. decay kinetics 0-43088
- benzil, excited electronic states; conformational relax., time resolved matrix isolation spectral obs. 0-32701

**matrix isolation spectra continued**

- 2,2'-bipyrimidine, in nematic solvent, conformation, ab initio and PMR determ. 0-47869
- trans-2-butene, Ar matrix, TEA CO<sub>2</sub> laser irradi. photoisomerisation study 0-21303
- cis-butene, ozonolysis, radical form., matrix ESR spectrosc. 0-16653
- diatomic molecules, matrix isolated, vibr. relax., rot.-translational coupling 0-53102
- 1,2-dichloroethane, conformer equilibrium by effusive beam-matrix IR spectroscopy 0-48100
- trans-1,2-dichloroethylene, Ar matrix, TEA CO<sub>2</sub> laser irradi. photoisomerisation study 0-21303
- 1,2-difluoroethane, internal rotation temp. frozen in supersonic jet, matrix IR spectroscopy 0-9594
- dihydrophenazine derivatives, in 3-methylpentane (ethanol) (PMMA), radiationless processes, temp. depend. 0-43087
- ethylene, ozonolysis, radical form., matrix ESR spectrosc. 0-16653
- fluorobenzene radical cations, matrix laser fluoresc. spectra 0-1009
- fluoromethane+HCl, IR spectra, intermol. interactions 0-9605
- fluoromethane-d<sub>2</sub>, matrix isolated, vibr. energy transfer at low temps. 0-37860
- fluoromethane-d<sub>3</sub>, vibr. energy transfer at low temps., inert gas and N<sub>2</sub> matrix obs. 0-9706
- formaldehyde, solid soln. in Xe, precipitation, IR spectra obs. 0-45059
- methane in condensed inert gas matrices, optical excitation of rotational transition, far IR absorption spectra 0-37808
- methyl nitrite, internal rotation temp. frozen in supersonic jet, matrix IR spectroscopy 0-9594
- naphthyl, excited electronic states; conformational relax., time resolved matrix isolation spectral obs. 0-32701
- pentacene in naphthalene, intersystem crossing rates following single-mode laser excitation 0-43085
- perdeuterobenzophenone, in 4,4'-dibromodiphenylether, cross-relax., microwave pulse obs. 0-53031
- perylene in n-heptane cryst., polarised fluoresc. 0-1017
- perylene-tetracene in liquid crystal, absorption, fluorescence and polarisation, temp. depend. study (German) 0-18887
- photochemistry in solid state, IR lasers appl. 0-11929
- photoexcited triplet state molecules, in cryst., cross-relax., variable freq. ODMR obs. 0-53031
- pyridine cation radical in trichlorofluoromethane matrix, gamma irradi., EPR and optical obs. 0-23442
- scandium octaethylporphyrin,  $\mu$ -oxo bridged dimer, triplet states and geometrys, ODMR obs. 0-9625
- scandium octaethylporphyrin, triplet states and geometrys, ODMR obs. 0-9625
- tetracene in liquid crystal, absorption, fluorescence and polarisation, temp. depend. study (German) 0-18887
- tetrafluoromethane, bond length and chemical shielding, NMR lineshape anal. of multispin system 0-32741
- tetraphenylporphyrin, free base in PVC matrix, excited state props., electrochromism obs. 0-37815
- thiirene and deuteroderivatives, Fourier transform IR spectra using Ar matrix isolation, vibr. band assignments 0-14142
- transition metal, bimetallic cluster, photoselective bimetallic aggregation, review 0-53182
- trapped electrons in glassy hydrocarbons, gamma ray irradi., relax., spectral obs. 0-23416
- 1,3,5-trichloro-2,4,6-trifluorobenzene radical cation, B<sup>2</sup>A<sub>2</sub>'→X<sup>2</sup>E" laser-induced fluoresc. spectra 0-14172
- trichloromethane glass:O<sub>2</sub>, <sup>17</sup>O, NQR by proton double reson., broad reson. assignments 0-53014
- trifluoromethylperoxy radical, in Ar:O<sub>2</sub> matrix, IR spectra 0-50845
- tropolone vibr. spectra and proton tunneling 0-28014
- AlH<sup>+</sup> radical cation, EPR matrix isolation obs., hyperfine components calcs. 0-14158
- ArS, photoluminesc. in rare gas matrices 0-5568
- BCl<sub>3</sub>, high-resolution IR Ar matrix-isolation spectra, 10K 0-32708
- BiN, form., IR matrix spectra, comparison with group V nitrenes 0-18853
- CB<sub>2</sub>, emission in solid Ar, laser excitation spectra and lifetimes 0-48034
- CB<sub>2</sub>Cl emission in solid Ar, laser excitation spectra and lifetimes 0-48034
- CO, isotopically enriched, Ar matrix isolation, laser-included vibr. fluoresc. 0-9707
- CO, matrix-isolated, librational relax., IR line broadening 0-978
- CO-NO mixtures, Ar matrix isolation, laser-included vibr. fluoresc. 0-9707
- Cl<sub>2</sub>, Ar matrix, vibronic dephasing 0-6469
- CoO, matrix isolated IR spectra, ground state vibr. freqs. 0-28015
- Fe complex, FeCl<sub>3</sub>-tetraphenylporphyrin in PVC matrix, excited state props., electrochromism obs. 0-37815
- FeCo molecules, matrix-isolation Mossbauer spectra 0-23448
- FeO, matrix isolated IR spectra, ground state vibr. freqs. 0-28015
- Ge, matrix isolated cluster, optical absorpt. 0-16045
- GeTe, matrix isolated absorpt. and emission visible spectra, electronic states 0-28026
- H bonding molecules, self assoc., intermolecular interactions, matrix isolation vibr. spectra obs. Raman and IR spectra 0-52995
- H<sub>2</sub>O, in D<sub>2</sub>O ice I<sub>c</sub>, decoupled vibr. spectra 0-52984
- H<sub>2</sub>O-formaldehyde complex, IR spectrum in solid Ar, N<sub>2</sub> matrix 0-43042
- HPO, in Ar matrix, IR and UV absorpt. spectra 0-47985
- I<sub>2</sub>, N<sub>2</sub> and Ar matrix isolated, magnetic circular dichroism spectrum 0-5567
- I<sub>2</sub>-benzene, N<sub>2</sub> and Ar matrix isolated, magnetic circular dichroism spectrum 0-5567
- <sup>127</sup>I atoms in Xe matrices, ESR spectrum 0-1005
- KReO<sub>4</sub>, matrix isolated, IR spectra 0-28012
- KrS, photoluminesc. in rare gas matrices 0-5568
- MnO<sub>4</sub><sup>-</sup> ion, <sup>18</sup>O enriched, matrix isolated IR spectra, force consts. 0-52985
- Mo<sub>2</sub>, matrix isolated visible absorpt. spectra, electronic, vibronic and vibr. states 0-28027
- MoN, matrix isolated visible absorpt. spectra, electronic, vibronic and vibr. states 0-28027
- MoO, matrix isolated visible absorpt. spectra, electronic, vibronic and vibr. states 0-28027
- N<sub>2</sub>, matrix isolated, fundamental vibr. Raman spectra 0-272
- N<sub>2</sub>, solid and matrix isolated mol., triplet state spectra (Russian) 0-5574
- NBr, in solid Ar, b<sup>1</sup> $\Sigma^+$ →X<sup>3</sup> $\Sigma^-$  transitions 0-32702



**matrix isolation spectra continued**

- NCl, in solid Ar,  $b^1\Sigma^+ \rightarrow X^3\Sigma^-$  transitions 0-32702  
 NI, in solid Ar,  $b^1\Sigma^+ \rightarrow X^3\Sigma^-$  transitions 0-32702  
 NaReO<sub>4</sub>, matrix isolated, IR spectra 0-28012  
 Ni atoms, Xe matrix isolation, photoemission 0-27987  
 Ni<sub>2</sub>, A-X system, Ar matrix isolation fluoresc. spectrosc. obs. 0-9628  
 NiO, matrix isolated IR spectra, ground state vibr. freqs. 0-28015  
 OH radical, matrix-isolated, from H<sub>2</sub> oxidation on Pt, laser diagnostics 0-5572  
 O<sub>2</sub>(c<sup>2</sup> $\Sigma_u^-$ ), in Ar(Kr)(Ar-Kr) matrices, multiphonon vibr. relax. time-resolved emission obs. 0-18861  
 PO, in Ar matrix, IR and UV absorpt. spectra 0-47985  
 Pr<sup>3+</sup> aquo ion spectra, MCD of <sup>3</sup>P<sub>0</sub> → <sup>4</sup>F<sub>4</sub> transition 0-7331  
 SCl(Br), unstable radicals, matrix-isolated, IR spectra force const. (*German*) 0-43053  
 SF<sub>6</sub>, high-resolution IR Ar matrix-isolation spectra, 10K 0-32708  
 Si, matrix isolated cluster, optical absorpt. extended Huckel calcs., electron energy levels 0-16045  
 SiGe, matrix isolated cluster, optical absorpt. 0-16045  
 SiO in Ar matrix, vac. UV spectrum, vibr. progression 0-23432  
 Xe: <sup>57</sup>Co, solid, ion implantation for rare gas matrix isolation, Mossbauer spectroscopy study 0-54271  
 XeF<sub>2</sub>, photodissoc. yield in solid Xe and Kr, time-resolved photolum. excitation obs. 0-3372  
 XeS, photoluminesc. in rare gas matrices 0-5568

**matrix isolation spectroscopy**

- cryophotoaggregation, bimetallic cluster, transition metal atom nucleation, review 0-53182  
 high pressure cell for matrix isolation Raman spectroscopy 0-272  
 molecular spectroscopy book 0-27052  
 Raman, toxic organic substances detection in water 0-30616

**Matteucci effect**

- Fe<sub>40</sub>Ni<sub>40</sub>P<sub>14</sub>B<sub>6</sub>, amorphous ribbon, influence of torsion on mag. props. 0-7138

**maximum principle**

- aeroelastic vibr. elimination, optimal control method 0-33514  
 Dirac operator, essential self adjointness anal. 0-18794  
 solar heating system optimal controllers 0-45739

**maximin technique** *see minimax techniques***Maxwell-Boltzmann distribution** *see statistical mechanics***Maxwell effect** *see flow birefringence***Maxwell equations** *see electromagnetism***MBE** *see molecular beam epitaxial growth***mean free path, carrier** *see carrier mean free path***measurement**

- see also specific measurements, e.g. frequency measurement*  
*see also instruments; measurement by laser beam; recording; testing; units (measurement)*  
 data processing, automation of meas. equipment state-inspection results, USSR Krasnodar territory 0-52152  
 diffusion coefficient of gases in liquids, bubble evolution method using crit. size concept. 0-4828  
 dust control, measurement methods (*Hungarian*) 0-35810  
 electronic measurements, book 0-31805  
 long-range metrological plans, USSR Comprehensive Production Efficiency Improvement System, Kuban region 0-52150  
 metrology, scope and relationship with physics 0-52153  
 metrology in industry and government, seminar, Daeduk, Korea (Sept. 1978) 0-27259  
 National Bureau of Standards time code relay to western hemisphere by satellite 0-47039  
 plan programs for instrument development in the Ministry of Instrumentation 0-183  
 quality control management, metrological support 0-184  
 state control of measuring equipment in the USSR 0-52151  
 technical term translation problems (*German*) 0-36965

**measurement by laser beam**

- see also laser velocimeters; plasma diagnostics by laser beam*  
 absolute acceleration due to gravity, meas. using laser ballistic gravimeter 0-12569  
 acousto-optical modulator, metrological certification of photodetection devices 0-23727  
 aerosol meas. by lidar, error analysis and simulation 0-26617  
 air pollution monitoring, spectrophone measurement of absorpt. coeffs. at CO<sub>2</sub> laser wavelengths 0-26193  
 airborne laser scanner, modulation techniques 0-5770  
 airborne particle distributions, inertial sizing using laser velocimeter method 0-53901  
 angular measurement, errors 0-42196  
 atmospheric-turbulence-structure parameter meas. using space-limited laser beam 0-46285  
 autocollimator, photo-electric, calibration with laser interferometer system and microcomputer 0-1304  
 ballistic expt. using diffraction interferometer 0-47093  
 biological cells laser Doppler meas., scattering characts. of intersecting beams (*Russian*) 0-3874  
 biological material, laser stereometry light-scatt. technique, cardiac images 0-56310  
 body motion, quantitative meas. by Schottky barrier Si photodiode and laser beam 0-12207  
 calorimetric absorption coefficient measurements using pulsed CO<sub>2</sub> lasers 0-9918  
 CANDU type 19 rod bundle, velocity distrib. in peripheral subchannel 0-32328  
 CdSe two-photon absorption, laser calorimetric obs. 0-33076  
 celestial bodies range measurements, atmospheric correction determ. (*Russian*) 0-12674  
 clock comparison by laser in the nanosecond range 0-47035  
 correlator, Malvern, based on photon correlation and laser scattering spectroscopy, development and appl. 0-5741  
 diffuse reflectance rel. to partial coherence and IR laser photogoniometric meas. 0-14283  
 diffusely reflecting objects, deformation meas. by lasers, appl. of holography and speckle, review (*Japanese*) 0-9832  
 Doppler vibr. meas. system using bispectral anal. 0-38357  
 dye laser, for metrological interference measurements 0-28250  
 dye laser appl., CW, technology developments influence 0-43383  
 Earth-Moon system laser ranging meas. 0-21933

**measurement by laser beam continued**

- elasto-optical constants and refractive index, thermo-optical method for meas. 0-7327  
 electro-optics, conference, Utrecht, Netherlands (Oct. 1978) 0-31420  
 electrophoretic mobility, measurement using wide-angle, crossed-beam laser Doppler scattering configuration 0-33011  
 fatigue damage, development rate by exoelectron meas. 0-25835  
 fission reactor fuel element in-cell laser profilometer 0-22955  
 flowfield diagnostics using lasers 0-14853  
 fluorescence temperature measurement of Na in flames 0-11893  
 fluorescence temperature measurements in flames 0-11892  
 gas complex analysis method, resonance absorption with pulsed laser light (*Japanese*) 0-36421  
 gas trace anal. by laser-induced Schlieren technique 0-9929  
 general relativity test, precision ring laser interferometry technique 0-52117  
 gyrometer, accuracy increase by automatic output signal correction (*Russian*) 0-215  
 heat capacities of La<sub>1-x</sub>Sr<sub>x</sub>CoO<sub>3</sub>, at 80 to 950K, phase transitions obs. (*Japanese*) 0-54898  
 high accuracy distance measurement by two-wavelength pulsed laser sources 0-192  
 holographic interference microscope, MGI-1 0-5706  
 interferometer, for accurate positioning, built-in system for machine tools (*German*) 0-9022  
 interferometer, NBS system designed for seismology appl. 0-13125  
 interferometer application to length meas. in production (*German*) 0-18007  
 interferometer for precision linear displacement meas. 0-27285  
 interferometric system, double-freq., with automatic compensation (*Chinese*) 0-27340  
 interlocked solid-state lasers, radiation intensity modulation for precision meas. 0-1250  
 IR laser interferometer, length measuring, alignment using laser feedback 0-37075  
 LAMMA (laser microprobe mass analyser) appl., materials testing and thin film microprocessing 0-18041  
 light beating spectroscopic instrument for continuous meas. of tissue blood flow 0-41160  
 light velocity and wavelength determ. 0-42190  
 mechanical vibrations of small amplitude using multiple-beam interferometer 0-4759  
 methane-air flames, meas. of temp. and OH conc. 0-16687  
 neutron flux energy spectrum meas. from luminesc. line freq. change 0-23272  
 object dimension meas. by computer-controlled laser beams 0-31715  
 ocular tonometry through sonic excitation and laser Doppler velocimetry 0-56152  
 ophthalmology and vision research, appl. of lasers, holography 0-12210  
 optical coating absorption meas. by 1.06  $\mu$ m laser calorimeter calorimeter 0-33066  
 optical fibres, baseband freq. response meas. by modulated InGaAsP laser beam, dispersion characts. 0-1308  
 optophysical and physicochemical meas. instrum. 0-13121  
 particle and spray sizing, using laser diffraction 0-17925  
 photoelastic method of thermal stress determ. circumferentially grooved cylinder 0-38363  
 photographic pulp quality control using He-Ne laser scanning system (*German*) 0-3272  
 plane mixing layer, two-point LDV meas., vorticity distrib. 0-38506  
 polarimeter for e<sup>+</sup> e<sup>-</sup> beam polarisation meas. in storage ring 0-14019  
 rate calorimetry analysis with coating absorption 0-33050  
 retinal resolving power meas. by laser interferometry 0-36066  
 roughness measurement using laser scanning analyser 0-36992  
 roughness of periodically shred surfaces, on-line meas. technique using He-Ne laser (*German*) 0-33014  
 scanning laser acoustic microscope applications (*German*) 0-3271  
 single atom detection in particle tracks 0-9475  
 single pulse formation from measurement laser 0-23734  
 small angle scattering meas. from streaming particles, laser heterodyne apparatus 0-1261  
 solid laser, measurement, radiation pulses formation and stabilisation 0-23735  
 solid-state measurement laser, radiation pulse width meas. 0-23736  
 solid-state measurement lasers, single-pulse with uniform distribution of energy density, correction equipment 0-23703  
 Special Theory of Relativity, expt. 0-27118  
 spherical particle velocity and size meas., crossed-beam light scatt. interferometry 0-47011  
 submillimetric waveguide laser for gas spectroscopy 0-33022  
 supersonic chemical laser flowfield, laser induced I<sub>2</sub> fluorescence meas. 0-38008  
 surface planarity, by interference pattern assessment 0-31711  
 surface structure influence on image speckle pattern contrast 0-17985  
 thin layer absorption loss meas. by CW dye laser intra-cavity technique (*German*) 0-16113  
 time and frequency, conf., Helsinki, Finland (Aug. 1978) 0-46728  
 transcutaneous O<sub>2</sub> and skin blood flow, laser system for simultaneous meas. 0-26321  
 transient chemical events measurement using laser-based methods 0-40801  
 vacuum evaporation, substrate temp. meas. 0-20794  
 vapour pressure, high temperature vapours, phase transitions, equations of state, appl. of laser pulse heating 0-52230  
 vibrations testing, in precision units, by real-time holography (*German*) 0-38366  
 video disk pit geometry, control, optical techniques 0-5775  
 As<sub>2</sub>S<sub>3</sub> film, vacuum deposited, selective etching characts. obs. (*Russian*) 0-3207  
 As<sub>2</sub>Se<sub>3</sub> film on CaF<sub>2</sub>, interface and bulk absorption meas. 0-35001  
 C particulate, airborne, photacoustic and absorption spectrum using tunable dye laser 0-4102  
 CO<sub>2</sub>/<sup>192</sup>OsO<sub>4</sub> laser, absolute light oscill. freq., universal const. variation meas. possibilities (*Russian*) 0-5723  
 CdTe two-photon absorption, laser calorimetric obs. 0-33076  
 He-Ne laser stabilisation and performance for dimensional meas. 0-19049  
 He-Ne laser wavelength stability, calibration and traceability 0-19050  
 KCl, bulk and surface absorption comparison, 9.2 to 10.85  $\mu$ m 0-33051  
 NaCl, bulk and surface absorption comparison, 9.2 to 10.85  $\mu$ m 0-33051  
 NaF film on CaF<sub>2</sub>, interface and bulk absorption meas. 0-35001



## measurement by laser beam continued

- Nz pulsed laser stroboscopic fluorimeter 0-35593
- Si, CVD, underlying oxide layer thickness effect on in-process thickness monitoring 0-6679
- UO<sub>2</sub>, liquid, reactor safety research (*German*) 0-42787

## measurement errors

- Aanderaa Ni-coated current meter, pressure-induced direction error 0-4121
- aberrant values, recognition and elimination (*Rumanian*) 0-22316
- aberrant values elimination, from series of repeated meas. (*Rumanian*) 0-47008
- acid-base titrations, logarithmic diagrams for pH value and error estimation 0-35619
- analytical correction in meas. results, probabilistic method 0-13030
- anemograph data quality control 0-56642
- angular meas., testing instrument for errors 0-42186
- angular measurement, digital method using photoelectric angular transducer with unstable datum, increasing accuracy 0-17920
- angular measurement using laser interferometer 0-42196
- astronomical observations errors, optimum linear estimation of mathematical expectation and standard deviation (*Russian*) 0-12673
- beam-foil lifetime measurement, cascading problem, ANDC method use and error limits 0-14249
- biomedical pulse echo US, intensity meas. errors assess. when using miniature hydrophones 0-3743
- buoy wave data analyses noise correction functions and error sources 0-46302
- cartography, point transfer error determ. 0-17227
- chemical composition, error analysis of analytical results 0-21341
- corrected measurement result, error description and confidence limit calc. (*German*) 0-27262
- dielectric constant meas. by cavity method, freq. and mode errors 0-13103
- dielectrophoretic measurement of permittivity, effects of sample size 0-13094
- diffusion furnace temp. profile meas. systematic errors, theoretical model (*German*) 0-8989
- diffusion furnaces, temp. profile meas., systematic errors (*German*) 0-37030
- direct loading, equipment used in standard force measuring machine 0-17934
- electrochemical measurement transducers, actual distribution of errors 0-45605
- EM flowmeters with large-area electrodes, performance anal. of three models 0-1706
- error separation processes, roundness meas. appl. (*German*) 0-31701
- faradimeters, errors checking with aid of tables 0-52271
- ferromagnetic suspension, magnetorheological characts. meas., errors 0-33550
- ferromagnetic-resonance linewidth meas. method and apparatus 0-22411
- ferromodulation meas. transducers, with increased temp. stability 0-52281
- flow sensor using annular-averaging, error in discharge coeff. 0-38509
- flowmeter, MHD type, with circ. cross section, inhomogeneous mag. field effect on signal 0-33709
- flowmeter, MHD type, with circ. cross section, symmetry conditions effect on signal, arbitrary vel. profile 0-33708
- flowmeter converging devices, effect of aeration on error 0-10327
- Fourier transform IR spectrometry, absorbance subtract, wedging errors diagnosis and correction 0-11967
- freely sinking probe horizontal velocity meas. interpretation 0-46321
- frequency meter, digital, accuracy and noise rejection increase, weighting method (*Russian*) 0-27281
- galaxy redshifts, uncertainty cross correl. data reduction techniques 0-22074
- gas microconcentrations in air determ., metrological certification of meas. methods 0-55972
- geodesy, gravimetric geoids comparison with Geos 3 altimetric geoid 0-3898
- Geos 3 altimetric data, bias due to ephemeris error rel. to sea surface topography 0-3908
- Geos 3 altimetry, orbited bias error rel. to NW.Atlantic oceanic geoid and tides determ. 0-3901
- Geos 3 tracking systems, intercomparison for meas. and time biases determ. 0-4227
- graphite ionisation chamber, ionisation error due to porosity 0-52829
- gyrooptical compass, signal measurement time (*Russian*) 0-33007
- high-performance telescope aspheric mirror test error budget 0-48386
- images aberrated by turbulence, undersampling errors in moments meas. 0-1137
- indicators accuracy categories (*Croatian*) 0-13063
- inertial meas. systems, basic eqns. and error models (*German*) 0-56655
- laser interferometer appl. to positioning, built-in system for machine tools (*German*) 0-9022
- laser interferometer application to length meas. in production (*German*) 0-18007
- laser interferometer system, Doppler, error sources analysis, meas. volume structure (*Russian*) 0-27336
- laser range measurements, atmospheric correction determ. (*Russian*) 0-12674
- lecture demonstration for chem. course 0-17773
- length meas. international standards compared (*German*) 0-36977
- level of material arranged in arbitrary fashion in tank, measurement using acoustic methods 0-17921
- magnets testing, permanent, test parameters selection 0-52280
- Moire strain measurement method using diffraction beams, compensation of errors 0-13068
- monochrome photographic film densitometry errors and standards (*German*) 0-37102
- NMR, rot. frame, <sup>13</sup>C spin-lattice relax. using proton decoupled Fourier transform spectra, errors origin 0-18945
- non-Gaussian distribution laws for statistical error theory generalisation (*German*) 0-22315
- nonGaussian error limits, distribution and probability curves (*German*) 0-36967
- nonplanarity of surface plates using optical planarity meter 0-17919
- ocean geoid near Blake Escarpment, undulation values errors from Geos 3 satellite altimetry data 0-3902
- ocean vertical temperature gradients, moored instrument accuracy 0-12561

## measurement errors continued

- ohmmeter, relative-error determination in checking 0-17961
- optical coating requirements in United States military specifications 0-48365
- optical rate sensor, discrete component Sagnac effect, error sources 0-1342
- optical rotation sensor, passive ring cavity, drift performance 0-1343
- optical system aperture, effect on measurements in thermophysical research 0-17992
- path difference measurement on anisotropic materials 0-4758
- periodic variables meas., multi-scale cyclical, meas. analysis (*Russian*) 0-187
- photographic astrolabe at Turku observatory, errors 0-36499
- pneumatic press. transducer for corrosive media, error and sensitivity 0-22345
- polarisation torque-measuring system (*Russian*) 0-52191
- power and energy meas., digital, errors sources and suppression (*Rumanian*) 0-47078
- pressure transducer measurements, thermal transient effects 0-31700
- quantitative IR spectral analysis, background and overlapping of absorpt. bands influence on accuracy 0-55748
- radial velocity spectrometer at McDonald Observatory, meas. uncertainty 0-51667
- Rankine-type capillary viscometer, for gases (*Japanese*) 0-14859
- resistance thermometry review, error sources 0-52206
- sea temperature gradient meas., errors in stepwise stratified ocean 0-31149
- sea-surface temperatures, satellite-determined, in tropical Pacific, climatological usefulness 0-31044
- seismic refractor velocity determ., cause and nature of errors 0-56621
- semiconductor, capacitive profilometry, accuracy 0-9005
- semiconductor volume and contact parameter determ. from V-I characteristic (*Russian*) 0-49912
- shock tube measurements of elem. gas reaction rate coeffs., review 0-3299
- sound velocity measuring instrument, digital electronic, comments 0-14528
- space plasma, mass discrimination effects in mass spectrometers ion and neutral extraction 0-4230
- stellar spectra, line equivalent width errors due to photon statistics, calc. formalism 0-8625
- stochastic processes, mean values and standard deviations fundamentals (*German*) 0-13031
- strain-gauge measurements in heat-resistance tests, error estimation 0-4703
- surface waves meas., using resistance wave gauge, accuracy and calibration 0-24110
- temperature meas. accuracy, additive and multiplicative meas. errors influence (*German*) 0-8985
- thermal radiation sources, high-temp., for calibrating radiometers 0-17946
- thermocouple, 3-channel corrector of dynamic errors 0-17939
- thermogravimetric system for investigating gas-metal reactions at elevated temps. 0-229
- thermophysical properties, standardisation of meas. methods 0-52197
- thermostat metals, influence of specimen curvature on thermal sensitivity (*German*) 0-27291
- triple point determination, of O<sub>2</sub> at low temp. (*Japanese*) 0-31749
- UK 1.2-m Schmidt telescope, alignment, pointing accuracy and field rot. 0-4252
- US flowmeter, propagation time of acoustic signal 0-6175
- US vel. meter using sing-around technique, IC 0-38198
- Vaisala-Brunt frequency vertical fine struct. meas. in Mediterranean Sea 0-26537
- vibration meas., errors evaluation due to pulse signals 0-23972
- voltage divider calibration, inductive, between 10 kHz and 100 kHz, international comparison of calibration methods 0-13100
- voltmeters, error estimation 0-22381
- voltmeters and milliammeters, installation for determining freq. error over side range 0-4734
- weighing, balances accuracy class increase, using several standard weights of equivalent mass (*Rumanian*) 0-47022
- X-ray stress measurement, error caused by side declining angle of counter scanning plane (*Chinese*) 0-52373

## measurement standards

- see also atomic clocks; temperature scales
- AC voltages, small, combined meter checking 0-13057
- accelerometer base strain sensitivity test device 0-52173
- astronomical photometry, Cousins VRI system, temp. and absolute flux calibration, appls. 0-26750
- ATA standard time broadcast, synchronisation methods 0-47024
- blackbody radiators, effect of surface roughness 0-52228
- British Calibration Service 0-22319
- British trade weights and measures activities 0-27267
- calibration methods for primary and secondary standards, in Hungary 0-5357
- cells, development of reference group with microcomputer-controlled inter-comparisons 0-22384
- coaxial mutual-inductance, computation of parameters 0-4735
- colour reproduction, of images obtainable by two-primary colour projections 0-12125
- COMECON standard ST SEV 1052-78 for establishing units of physical quantities 0-42189
- convergent nozzles incorporated into gas flowmeter, comparison with standard 0-6126
- cresyl violet, luminesc. quantum yield standard for red, calorimetric obs. 0-190
- definitions, of units, standards and measurement methods (*French*) 0-27264
- development trends, length, press., mass, electrical and photometric standards 0-191
- didymium glass filters for spectrophotometer wavelength scale calibration 0-43417
- dielectric constant, class 1 standard specimens, certification methods 0-13036
- DIN 45 635 Part 1, envelope meas. method for sound power level, multi-position machines (*German*) 0-43523
- dosimetric primary and secondary standardization within the European Communities 0-9415



## measurement standards continued

- dosimetry, calibration and meas. standards at Austrian Dosimetry Laboratory 0-5362
- dosimetry, primary standard for determination of absorbed dose in water for X-rays generated at potentials of 7.5 to 30 kV 0-5354
- dosimetry, primary standards for industrial radiation processing 0-5356
- dosimetry, Regional Calibration Laboratory, Cleveland, USA 0-5364
- dosimetry, secondary standard laboratory organisation in India 0-5366
- dosimetry, secondary standards laboratory, role in a nuclear power utility 0-5365
- dosimetry calibration problems in connection with radiation protection around nuclear facilities 0-9422
- dosimetry of electrons and photons, standardisation in Germany 0-5353
- dosimetry standardisation in Japan, review 0-5359
- dosimetry standardisation in UK, review 0-5358
- eddy current testing of tubes, rods and wires (*German*) 0-25971
- electrical measuring instruments, new CEI standards (*Italian*) 0-31789
- EM flowmeter type ERO-1, calibration use 0-43812
- exoelectron dosimeters, reference dosimeter bank, storage, exposure and reading 0-5360
- exposure standards for U mining 0-46055
- extragalactic reference frame, for stellar absolute proper motion catalogue (*Russian*) 0-51747
- faint stars, spectral-type standards for objective prism plates 0-46539
- flow, volumetric and mass, development of COMECON standard 0-43809
- flow rate equipment calibration and testing with load ring equipment, noncorrosive gases appl. 0-43813
- flowmeter generators for calibration and checking of standard flowmeters 0-43814
- fluorescent measuring equipment, selection of standard testing substances 0-7882
- force standards for industry 0-42198
- free air chamber for X-ray exposure standardisation at high quantum energies 0-14053
- frequency, atomic standards, transfer of freq. stability to quartz-crystal resonator 0-17927
- frequency, relativistic Doppler shift in satellite tracking 0-46951
- Fricke dosimetry, determ. of molar extinction coeffs. of  $\text{Fe}^{3+}$  0-13949
- gamma sources, secondary standard preparation for low activity gamma spectrometry 0-18701
- gamma-ray standard sources using complex decay schemes 0-9081
- global coordinate time scale, practical implications of relativity 0-47030
- gravity new system, changes in international gravity base values and anomaly values 0-51317
- HD 14969, IAU radial-velocity standard star, orbit from photoelectric radial vels. 0-56884
- IAU Radial Velocity Standard stars, radial vels. meas. (*French*) 0-51743
- Indian Secondary Standards Dosimetry Laboratory, development and functions 0-41244
- inductive voltage divider, calibration between 10 kHz and 100 kHz, international comparison of calibration methods 0-13100
- International Bureau of Weights and Measures, 1978 activities and news 0-188
- international radiation standards, role of ICRU 0-9414
- international standard reference radiations and their application to the type testing of dosimetric apparatus 0-9416
- international time standard coordination (*German*) 0-52171
- ionisation chambers, radiation exposure intercomparison 0-5363
- ionising radiation, metrology and calibration, French system (*French*) 0-5351
- ionising radiation, primary standards and transfer methods in France, review (*French*) 0-5352
- ionising radiation, traceability in meas. systems 0-5355
- ionising radiation calibration, meas. standards, CNEN, Italy 0-12273
- ionizing radiations, comparison of standards within COMECON framework 0-42899
- IR and optical frequency standards 0-47027
- IR file searching, ASTM, algorithm using peak intensity data 0-30295
- IR reference spectra, for GC-IR, presentation specifications 0-31908
- isotope fractionation, controllable, in thermal-ionis. mass spectrometry, SRM 987 standard test (*German*) 0-42299
- Krasnodar Centre of Standardisation and Metrology, regularisation of DP 0-52152
- laboratory discharge lamp source, for O I 5577 and 6300 Å lines of known width 0-4148
- laser power and energy meters, calorimeter system for calibration 0-38024
- laser radiation pulse meas., based on semiconductor radiators 0-23710
- laser wavelengths comparison, interference circuits analysis 0-23737
- length meas. 0-194
- length meas. international standards compared (*German*) 0-36977
- light sources, suitability of W strip lamps as secondary sources below 1064 degrees C 0-27297
- light sources props. meas., photometric laboratory equipment (*Slovak*) 0-17990
- low level radiation monitors, calibration accuracy and precision 0-9428
- low vel. airflow facility for calibration of wind-speed measuring instrums. 0-1718
- mass, force and weight 0-27273
- materials testing, COMECON standard reference-data system 0-45469
- medical dosimetry standards programme of the National Bureau of Standards, USA, review 0-8187
- melting point standards, secondary, for temp. range 2000-3000°C, chemical aspects of choice 0-52226
- microwave radiation hazard monitors, calibration 0-26374
- microwave time and frequency standards 0-47026
- monitored parameters for quality control in instrument production 0-186
- monochrome photographic film densitometry errors and standards (*German*) 0-37102
- national time and frequency standards of Finland 0-47031
- neutron, intermediate energy, standard field, neutronics anal. 0-27692
- neutron dosimeter and monitoring instrumentation calibration using  $^{252}\text{Cf}$  and  $^{238}\text{PuBe}$  sources 0-13946
- neutron dosimetry, meas. standardisation for biological and biomedical appl. 0-12271
- NGC 3379, elliptical galaxy as luminosity distrib. standard 0-22073
- noise emission measurements for computer and business equipment 0-53589
- noise evaluation of portable air tools 0-23855

## measurement standards continued

- nuclear gamma transition energy standard value and accurate determ. (*Czech*) 0-22755
- nuclear medicine and metrology of ionising radiations (*French*) 0-17057
- optical surface quality standards based on total integrated scatt. 0-48391
- optical physical measurements, metrological provisions 0-8953
- personal dosimeter calibration, US NBS standard reference neutron fields 0-9417
- personal dosimeter design and use, physical requirements for dose meas. 0-9424
- personal dosimetry, criteria for testing of performance 0-23169
- personal dosimetry performance, testing standard 0-9421
- personal dosimetry photon calibrations, use of phantom 0-9425
- pollution, trace amounts of toxic substances, meas. techniques and standards 0-26188
- powder diffraction data, American Crystallographic Association recommendations (*Czech*) 0-24306
- precise  $\gamma$ -ray standards 0-36973
- precise time dissemination via OMA-50 kHz 0-47032
- pressure gauges, secondary standard, for measurement up to 1 GPa 0-27289
- pressure meas., primary standards comparison, mercury barometer vs. gas-operated pressure balance 0-13090
- primary dosimetric standards at the Memorial Sloan-Kettering Cancer Center, NY, USA 0-8190
- quick calibration checks, devices to calibrate commonly used meas. instruments 0-47010
- radial-velocity standard stars, list of 200 stars 0-26849
- radiation dosimetry standardisation, conf., Atlanta, GA, USA, Dec. (1977) 0-4469
- radiation protection instrumentation test and calibration 0-9420
- radiation standard, continuous bremsstrahlung emission from inert gas HF discharge 0-1856
- radiation therapy, calibration and meas. standards in USA 0-8188
- radioactive,  $^{14}\text{C}$  and  $^3\text{H}$ , miniature, liquid scintillation counter appl. to colorimetric analysis 0-21346
- radioactivity standards programme of the National Bureau of Standards, USA 0-18700
- radiological instrumentation calibration by British Calibration Service 0-8186
- reference materials for COMECON member countries 0-45468
- reference temperature, 0.015 to 0.21K, based on superconducting phase transitions 0-17948
- relative dielectric constant, USSR state standard for 0.2-1 GHz range 0-9004
- relative dielectric constant for insulators in range 1-10 GHz, State Special Standard 0-13037
- rock deformability, determ. by in situ methods 0-17411
- ruled steel grating system for length meas. 0-13039
- Rutherford backscatt. standard for ion beam expts. 0-50496
- saturated water vapour pressure standardization 0-26596
- Secondary Standards Dosimetry Laboratory, review of role 0-5361
- SEM magnification standard reissue 0-27375
- SI system, need for periodic recalibration of laboratory equipment 0-31705
- SI system, Swiss legislation (*French*) 0-13032
- SI-system, physical standards and units 0-17915
- socialist economic integration, COMECON standardization 0-42188
- solar standards and testing activities in developed and developing countries 0-55819
- solid density, liquid density meas., single-pan analytical balances (*German*) 0-52167
- South African standard SABS 572 1973, meas. real-ear attenuation of hearing protectors 0-53581
- southern standard stars, monochromatic flux from 3200 Å to 8800 Å 0-51742
- Soviet, for linear and angular quantities meas., exhibition survey 0-52161
- specific heat meas., modulation method with SOTS-2 standard specimen 0-8988
- specific heat standards choice and certification, for liquids and vapours in 90 to 273.15K range 0-23877
- spectral analysis, correlation of signals, internal standardisation 0-55749
- spectroscopic reference frequencies in OCS 9.5  $\mu\text{m}$  band, heterodyne freq. meas. 0-18850
- stellar photoelectric UVB sequences, in fields of eight low-red shift quasars (*French*) 0-51904
- strain gauge transducers in testing machine and as force standards 0-42215
- stretched wires as standards of straightness (*German*) 0-36976
- surface profile monitors for thin film thickness meas., calibration standards 0-17918
- surface roughness parameters meas., Soviet development, All-Union test scheme 0-22328
- surface transportation vehicles, sound meas. standards 0-14531
- technique, congress, Moscow (1979) (*German*) 0-36964
- TEM cell for electromag. interference investigations, large 0-238
- temperature reference standard for use below 0.5K, SRM 768 0-27303
- thermocouples and meas. line inspection, using computer-controlled capacitor discharging method (*German*) 0-13079
- thermometry,  $\text{N}_2$ ,  $\alpha$ - $\beta$  transition applicability 0-13076
- thermophysical properties, conf., Dubrovnik, Yugoslavia (June 1978) 0-51944
- thermophysical properties, standardisation of meas. methods 0-52197
- time, South African measuring standard, national and international role 0-36971
- time and frequency, conf., Helsinki, Finland (Aug. 1978) 0-46728
- time and frequency, establishing common scale for COMECON member countries 0-42200
- time scale generation by international organizations 0-47028
- TLD, calibration procedures in the Studsvik standardized personnel dosimetry system, Sweden 0-9418
- TLD, dose intercomparison for orthovoltage X-ray therapy 0-12272
- total luminous flux scale using precision goniophotometer 0-42250
- tribometry metrological provisions, Soviet installations and instruments development 0-23974
- UBVRI standard stars, faint, photometric obs. 0-51813
- units of physical quantities, standard for unification within COMECON framework 0-42187
- UV, at Australian Nat. Meas. Lab. 0-31704
- UV and VUV high-temp. luminance standard, plasma source 0-19084
- UV measurement, accurate techniques 0-47103



**measurement standards continued**

- UV radiometric standards, gas discharges, plasma diagnostics appls. 0-47088
- VLBI, improvement of freq. stability of local oscillators (*Japanese*) 0-17504
- Washington Photometric System, props. and standard stars 0-31213
- weighing, balances accuracy class increase, using several standard weights of equivalent mass (*Rumanian*) 0-47022
- weights and measures, conference, Washington (1978) 0-27260
- X-ray fluorescence spectrometry with incoherent scattered radiation as internal standard trace elements determ. 0-11970
- X-ray fluorescence thin film calibration standards 0-22496
- X-ray powder diffractometer, APD3600, file searching techniques 0-24319
- Ar arc, new cathode shape for UV spectral radiance transfer standard (*French*) 0-38082
- C with Au and Al implants, Rutherford backscatt. standard 0-50496
- <sup>60</sup>Co radiation therapy, eval. of dosimetric accuracy and uniformity 0-12269
- Cs beam freq. standard, servo-control system anal. 0-42201
- H bulk standards, appl. to calibration of ion beam surface anal. 0-7884
- H high power arc, standard source of continuum radiation, 53-92 nm 0-44054
- He-Ne laser stabilised by methane E-component saturated absorpt., quantum freq. standard 0-9901
- Mo, temperature standard reference material, USA National Bureau of Standards 0-47009
- <sup>14</sup>N(n,γ), γ-ray energies, calibration standards 0-52613
- Pt-alloy thermocouples, reference-standard testing apparatus 0-13077
- Si photodetector, shallow junction type, internal quantum efficiency meas. model fits, visible quantum yield 0-267
- X-ray dosimetry, intercomparison and standardisation 0-12270

**measurement systems**

- analogue versus digital measuring instruments (*Italian*) 0-37015
- control of mechanical guides displacement, using speckle interferometry (*Czech*) 0-31852
- dragline bucket angular inclination system (*Russian*) 0-22325
- electronic measurements, book 0-31805
- flow meter for liquids (*Spanish*) 0-6181
- frequency-fluctuation characts. 0-22333
- gas turbine rotor vibration contactless system (*Russian*) 0-8982
- heat exchanger measurement systems, one and two loop measurement systems (*Hungarian*) 0-31702
- industrial, thermography appl. (*German*) 0-13072
- magnetoresistance and Hall EMF meas., of low-resistance materials, using AM method 0-52278
- measuring instruments as tools of knowledge and control, book 0-41968
- oscillating ball device measures ultra low flows 0-6171
- ultrasonic flow transmitter 0-1710

**measurement theory**

- aberrant values, recognition and elimination (*Rumanian*) 0-22316
- aberrant values elimination, from series of repeated meas. (*Rumanian*) 0-47008
- balances accuracy class increase, using several standard weights of equivalent mass (*Rumanian*) 0-47022
- contribution to measuring process intensification (*German*) 0-36966
- dimensional analysis 0-27263
- Einstein, quantum mechanics, conceptual problems 0-46783
- expt. data analysis, normal distribution verification algorithm (*Bulgarian*) 0-27261
- function segmentation from discrete readouts (*Russian*) 0-42185
- Gleason's theorem generalisation 0-36889
- information amount determ. approach 0-8949
- information propagation in a quantum-mechanical system between 2 physical parts 0-17832
- Mason topological formula (*Russian*) 0-13029
- measuring cycle improvement, correction of measurement path (*Polish*) 0-22318
- null circuit balancing by Radishev draft procedure (*Russian*) 0-13028
- periodic variables meas., multi-scale cyclical meas. analysis (*Russian*) 0-187
- profile deviation from circular, invariant props. determ. 0-22326
- quantum mechanical measurement process, argument against superluminal transmission 0-52055
- quantum mechanics, meas. problem 0-12948
- quantum mechanics and relativity, interrelations between truth space and time space, holistic analysis of theory of measurement 0-27177
- reliability in metrology, statistical approach (*Russian*) 0-22317
- stochastic processes, mean values and standard deviations fundamentals (*German*) 0-13031
- technique, congress, Moscow (1979) (*German*) 0-36964

**mechanical birefringence**

- see also photoelasticity*
- constitutive relations in photomechanics 0-43251
- germanosilicate optical fibres, single polarisation, strain birefringence 0-1314
- glass, thermally tempered sheet and plate, surface stress meas. using optical waveguide effect 0-25967
- measurement using photoelastic modulator 0-31838
- nonlinear photomechanics, birefringence in polymers, stress anal. appl. 0-33545
- optical fibre, elliptically clad borosilicate single-mode, strain birefringence 0-33148
- PMMA, glassy, photoelasticity 0-45034
- PMMA, piezobirefringence, optical and mech. relaxations, temp. depend. 0-34885
- polymer, brittle photoelastic, use of gelatin gels in prep. for optical polarization stress study 0-40325
- polymer film between two rigid or quasirigid bodies, memorised mechanical birefringence (*French*) 0-43677
- polymer network, crosslinks and trapped entanglements, two-network model 0-38962
- polystyrene, crazed, orientation and struct., optical meas. 0-30121
- rotating birefringent and achromatic quarter wave plates, appl. to ellipsometry and photoelasticimetry (*French*) 0-14278
- rubber under biaxial strain, nonGaussian theory, optical props. 0-16367
- sapphire, shock compressed, refractive index, density, and polarisability behaviour 0-50295
- single mode optical fibre polarisation stabilisation 0-33154
- surface stress meas. by optical waveguide effect 0-43681

**mechanical birefringence continued**

- GaAs, birefringence, photoelastic constns. dispersion 0-11361
- GaP, birefringence, photoelastic constns. dispersion 0-11361
- GaP, birefringence observations of strain and plastic deform. 0-50678
- MgO:Cr<sup>3+</sup>(V<sup>2+</sup>), <sup>4</sup>A<sub>2g</sub>-<sup>4</sup>T<sub>2g</sub> spectra, new expt. results 0-11441
- NaCl, rock salt, quenched, residual stresses, optical study 0-55061
- Nd doped (fluoro) phosphate laser glass piezo-optic coeffs. meas. at 0.6328 and 1.15 μm 0-34888
- SiO<sub>2</sub>, fused, shock compressed, refractive index, density, and polarisability behaviour 0-50295

**mechanical contact**

- see also abrasion; friction; lubrication; wear*
- annulus, circular, elastic contact problems, approx. soln. 0-38349
- beam, cracked, transverse loading by stamp, stress and fracture anal. 0-10187
- bimaterial interface, wave propagation in non-uniform motion of displacement discontinuities 0-19264
- coaxial cylinders, contact problem, iterative soln. technique (*Russian*) 0-23963
- colloids, linear elasticity, soft contact problems 0-48653
- contact force interactions between deformed solids (*Ukrainian*) 0-10214
- Coulomb friction, elastic theory 0-33539
- cylindrical shell and belt, interaction contact stresses, elastic layer model 0-33543
- cylindrical tubes or shells, mild steel, quasi-static piercing 0-45351
- discs, photoelastic obs. of static and dynamic contact conditions (*Japanese*) 0-23970
- drag reduction of an oscillating flat plate with an interface film 0-10268
- dynamical contact problem, shock waves in elastic layer after impact (*Russian*) 0-23964
- elastic contact between flexible plate and isotropic halfspace 0-43679
- elastic cylinders, approx. soln. of Shtaerman's eqn. 0-38355
- elastic half space, ring shaped punch contact stress determ. 0-38356
- elastic incompressible body, contact problems involving forces and moments, rigid punch problems 0-53719
- elastic layer on substrate, frictional slip caused by normal load 0-33541
- elastic ring indentation by rigid roller system 0-36854
- elastic surface waves on interface of pre-stressed elastic bodies (*Ukrainian*) 0-10176
- elastomers, tackiness, fracture mechanics theory (*French*) 0-38344
- fatigue, rolling contact, fracture mech. approach 0-23961
- ferrite and ceramic joining, bulk interaction (*Russian*) 0-40277
- fission reactor, FEM anal. of pellet-clad bonding 0-42765
- fission reactor fuel performance anal. by finite element method 0-42750
- fission reactor fuel rod deformation code FEMAXI-II and its application 0-37446
- glass segment, resting on elastic ring, structural strength 0-14630
- granular materials, packing parameters, calc. from particle size anal. results 0-19294
- Griffith crack, stress distrib. at interface of elastic layer bonded to half plane 0-23955
- guillotining materials, mechanics, fracture and burr formation 0-14619
- impact vibrations, steady, of body having hysteresis collision characteristics 0-14602
- impulse load effects, EPIC-3 code anal. 0-19293
- interfacial waves in pre strained neo-Hookean body, biaxial strain states 0-48630
- interfacial waves in pre-strained neo-Hookean body, triaxial strain states 0-48631
- joints, double adhesive bonded, loaded in shear tension (*French*) 0-23968
- lamination, hydrodynamic analogy, utilisation of current function (*French*) 0-19292
- linear elastic half space, frictional unloading problem 0-33542
- linearly deformable base reinforced with finitely large cover plates 0-14631
- moving load on elastic strip on elastic half plane, steady soln. 0-10215
- multilayered packet, contact elastic-plastic problem 0-5997
- nonplanar stamps, contact area determ., variational aspects 0-36855
- penny-shaped crack in elastic cylinder bonded to elastic surrounding material 0-19285
- planar thermoelastic contact problems, Green's function for exterior contact 0-38350
- planar thermoelastic contact problems, Green's function for interior contact 0-38351
- plates with pressed in solid discs, contact stresses (*Russian*) 0-43678
- polymer film between two rigid or quasirigid bodies, memorised mechanical birefringence (*French*) 0-43677
- Prandtl punch problem for case with eccentric forces (*Russian*) 0-23965
- punch, axisymmetric, contact with semi-infinite transversely isotropic elastic body (*French*) 0-23969
- rigid disc inclusion embedded in isotropic elastic medium, displacements for external force 0-48652
- rigid perfectly plastic strip, plane strain compression between parallel dies with slipping friction 0-48603
- rigid punch problems, forces and moments by reciprocal variational techniques 0-23967
- rolling, critical line nature in multiple-roll passes (*Russian*) 0-38347
- rolling, determ. of stress distrib. in rolled material 0-48651
- rolling, inhomogeneous deformation model 0-48650
- rough curved surfaces, elastic contact stresses calc. 0-10213
- rough materials, stressed state on contact 0-38352
- rough surface, plastic deformation in mechanical contact 0-14583
- shear contacting displacements of mating surfaces (*Russian*) 0-23962
- shell, supported cylindrical, interaction pressure variation 0-38354
- shell wall on fluid, impact problems (*Ukrainian*) 0-38345
- sliding fit, stick-slip phenomena 0-5996
- slip friction characteristics in nonstationary motion (*Russian*) 0-43652
- smooth circular plates, axisymmetric elastic contacts 0-19291
- soldered layer on half-plane, rigid stamp impression 0-38353
- steel, austenitic stainless, friction in vac. at elevated temps. 0-55542
- steel, C and Ni-Cr surface hardened, rolling contact fatigue failure 0-16608
- steel, mild, ground/sandblasted interfaces, tangential displacement, contact press. and lubricating film distrib. effect 0-16484
- steel, mild, two sandblasted interfaces, tangential displacement, contact press. and lubricating film distrib. effect 0-16484
- strip rolling, kinetostatics (*Russian*) 0-38348
- surface analysis, appl. to lubrication problems, review (*French*) 0-45616
- thin elastic layer, bending by rigid die 0-14627



**mechanical contact** continued

- three-part contact problem, Chebyshev polynomials and elliptic integrals 0-33540
- transversally isotropic plate, bending by smooth stamp, contact problem (Ukrainian) 0-38346
- uniformly loaded plate, interaction with isotropic elastic halfspace 0-23966
- unilateral contact problem integral eqn. approach 0-8798
- Cu, virgin surface, contact formation and cohesion, influence of multiple contacting (Russian) 0-40548
- Fe, Armco, friction in vac. at elevated temps. 0-55542
- Pb, virgin surface, contact formation and cohesion, influence of multiple contacting (Russian) 0-40548
- SiC single crystal, friction and fracture in contact with itself and Ti 0-11780

**mechanical engineering**

- machine noise transmission, device for meas. and comparison with computation 0-28380
- thermoplastic beams, constant stress, design 0-38248

**mechanical engineering computing**

see also computerised control

- conference, computational methods in nonlinear problems in mechanics and engineering, Austin, Texas, USA (March 1979) 0-51945
- dielectric parts, stress patterns and deformation characts., computer anal. 0-17787
- dislocation groups, of opposite sign emitted from a stressed source, computer simulation of dynamic behaviour 0-6406
- elastic deformation of continuous flexible member, shooting method with Newton-type iteration 0-48575
- metals, dynamic compression testing, mech. behaviour 0-40464
- noise environment modelling at General Motors Corporation 0-43542
- non-uniform pipe gas flow simulation model 0-33682
- nonstationary stochastic process, computer programme for statistical characts. 0-22283
- pressure vessels, axisymmetric, with structural discontinuities, elastic stress analysis (Japanese) 0-38265
- rock fracture in uniaxial compression, computer modelling (Japanese) 0-12379
- rolling process, math. model based on plasticity theory (Russian) 0-16335
- rotating systems, steady motions, computational anal. 0-53618
- structural design, using 'moment schema' of finite elements, convergence (German) 0-14563
- structural dynamics analyser development, microcomputer-based 0-53733
- tension test, computer simulation, effect of testing conditions 0-7729
- transonic potential flow, finite element method programme 0-24045
- vibration installations certification results processing 0-22336
- vibration modal anal. (French) 0-42216

**mechanical impact** see impact (mechanical)**mechanical interfaces** see mechanical contact**mechanical organs** see artificial organs**mechanical permeability** see permeability**mechanical properties of liquids**

see also elasticity of liquids

- polymer melts, quasistatic bulk strength meas., specially built apparatus 0-7737
- viscoelastic props. meas. using torsion resonator, 20-1200 KHz (Russian) 0-52196
- water, free surface, metastable effects associated with press. pulse refl. 0-6463

**mechanical properties of solids** see mechanical properties of substances**mechanical properties of substances**

- see also anelasticity; bending; brittleness; creep; deformation; elastic aftereffect; elastic moduli; elasticity; fracture; hardness; internal stresses; mechanical properties of liquids; mechanical strength; photoelasticity; photoplasticity; plasticity; slip; stress relaxation; stress/strain relations; tribology; viscoelasticity
- acrylonitrile-methylacrylate-acrylamide latexes graft copolymerised onto PVA, for haemodialysis membranes (Japanese) 0-12297
- elements, monotonous series based on atomic bond energy, for mech. and phys. props. calc. (Russian) 0-19740
- epoxy resin cross linked with aliphatic polyamines, struct. and dynamic mech. props. (Japanese) 0-38956
- gradient index material models and exptl. verification 0-16002
- low-temperature materials props. and appl. (German) 0-3081
- materials science, phys. and mech. props. 0-25538
- metallic glasses, structure, stability and prod., elec., mag. and mech. props., review 0-44134
- metallic glasses props., developments and appl. 0-19710
- polyether-urethane elastomers, crosslinked, three dimensional polymerisation, kinetics, gel. form., mech. props. (Russian) 0-7792
- polyethylene films, fibres, radiation initiated graft polymerisation of acrylonitrile, initiation rate rel. to props. (Russian) 0-7531
- polyimides, oriented cycloaliphatic, thermomech. props., synthesis (Russian) 0-55443
- prosthetic material mech. props., effects of physiological environment, cardiovascular appls. 0-8212
- PVC, chlorinated, fibres, radiation initiated graft polymerisation of acrylonitrile, initiation rate rel. to props. (Russian) 0-7531
- refractory metals, mech. props. and diffusion figures (Russian) 0-40436
- steel, complex alloy, Cr (12-18 wt.%), transformation behaviour (German) 0-40349
- structural materials, radiation effects, review 0-49267
- Al-Mg-Zn, granulated, degassing atm. effect on mech. props. of semifinished products 0-7720
- Cr pyrolytic coating, effect of support metal mech. props. on formation (Russian) 0-7713
- Mg-Y-Zn-Nd-Cd alloys, influence of Zr addition on struct. and mech. props. (Russian) 0-40370
- Mo-Zr-B, porosity and mech. props. after neutron bombard., 780-1080°C (Russian) 0-24502
- T, metal and alloys, mechanical props., electrochemistry, oxidation and corrosion resist., conference, Nantes, France (Nov. 1978) 0-41932

**mechanical relaxation** see anelastic relaxation**mechanical strength**

- for fatigue strength, see fatigue; for creep strength see creep fracture
- see also bending strength; compressive strength; fracture toughness; impact strength; notch strength; shear strength; tensile strength; yield strength

**mechanical strength** continued

- adhesion testing, use of fracture mechanics concepts 0-50802
- alloy, austenitic, mechanical changes after electrolytic quenching (Russian) 0-50653
- brittle materials specimen prep. for strength determ. 0-40632
- cellulose, nitrated, strength, deform. and disintegration, influence of stable free nitroxyl radicals 0-11717
- composite material strength criteria 0-10208
- composite materials, reliability, exam. of mech. strengths and fatigue characts., review 0-11762
- composites, reinforced in two directions, strength 0-19288
- composites, strength criteria, stress anal. (Russian) 0-1482
- composites, three-dimensional structure, mech. characts. 0-38266
- corundum, grinding material, review (Polish) 0-29917
- corundum, mech. strength rel. to tension intensity factor (Polish) 0-11725
- creep analysis of thin wall structures, subject to transient heating and loading 0-33486
- diamond, mechanical strength depend. on thermal working parameters, microcracks (Russian) 0-55501
- diamond, synthetic, N impurity effect on strength characts. and thermal stability 0-11726
- fatigue crack growth dependence on loading parameters, phenomenological model 0-38340
- Fe, Armco, long-term strength, H effect 0-55581
- ferrites, 2000NM and 2BA, effect of temp. 0-7753
- fibre reinforced composites, conf. Moscow, USSR (Nov. 1978) 0-8733
- fibre reinforced composites, zonal winding pattern analysis, thin spherical shells 0-38253
- fibre reinforced thermoplastic, mechanical strength, depend. on fibre morphology (German) 0-30043
- fibreboard, made from Asplund pulp-PMMA composite, props. (Japanese) 0-7664
- fibrous materials, NDT determ. of mech. strength anisotropy using radio-wave method 0-25969
- filament reinforced hypoeutectoid C steel, strength characts. after deform. and quenching 0-35271
- girder, circ-arc bow type, ultimate strength, plasticity (Japanese) 0-43631
- glass, rupture behaviour, long-term strength, thermofluctuation theory (Russian) 0-40536
- glass, silicate, ultimate strength, and max. breaking rate 0-25863
- glass fibre reinforced plastic wound struct., scale factor rel. to strength 0-3135
- glass fibre reinforced plastics, coupling agent/matrix interface investigation by Fourier transform IR spectroscopy 0-20884
- glass fibres, forming conditions influence 0-20882
- glass plastics, strength criteria 0-10208
- glass segment, resting on elastic ring, structural strength 0-14630
- glass workability rel. to melting history, microstruct., apparent liquidus temp., mechanical props. 0-11633
- joint, glued permanent in spherical shell of brittle material, structural strength 0-3293
- laminate cylindrical shells, prepared by continuous filament winding calc. of strength and reliability 0-10194
- laminated composites, effective length of reinforcing component 0-25797
- layered thin composites, optimum design and strength 0-10210
- long-term strength prediction by stepwise loading based on theory of damage accumulation 0-48644
- metal heat resistant power installation elements, estimating strength, ductility, heat resistance diagrams 0-25770
- metal-polymer joint, meas. of temp. dependence of joint strength 0-50824
- metallic glass, composition, mech. props., simulation 0-49117
- metals radiation damaged long term strength curve forecasting (Russian) 0-34040
- multilayer cylindrical shell, theory in inhomogeneous temp. field 0-1434
- mylonites, grainsize reduction and grain boundary sliding rel. to flow strength 0-21721
- Ni powder 2JJ, porous, effect of sintering conditions in struct. and strength 0-20823
- opposed-anvil high-press. devices, material strength effect 0-47068
- optical fibre, mechanical strength, fractographical analysis, review (Japanese) 0-35319
- optical fibre cable transmission and strength improvement technology 0-28347
- organic fibre reinforced plastics, failure 0-11774
- organicfibre reinforced epoxy, temp. dependence of strength under plane stress state 0-7642
- plasma sprayed materials, control of mech. props. 0-11560
- p-polyamide based organic fibres, effect of temp. and deform. time, on deform. strength props. 0-11720
- polyamide mixtures, thermodynamically incompatible, composition-prop. relationship (Russian) 0-7872
- polyimide substrate foils for nuclear targets 0-18739
- polymer viscoelasticity and strength characterisation, advanced light scatt. techniques 0-11857
- PVA-fibre-reinforced composites, thermal fluctuation dimensional effect on strength 0-16476
- refractory multiphase systems, infusible, some novel effects, rel. to practical appls. 0-55460
- reinforced composites, strength and deformation anisotropy, numerical characts. 0-38285
- reinforced concrete, cracking strength and max. rack width (Chinese) 0-5988
- silicone resin clad fibre technology, optical and mech. props. 0-28349
- stainless steel, type 316, irradi. in simulated environment, tensile props. 0-34076
- stainless steel, ferritic SUS 410 type, coated with organometallic complexes and Ti alkoxides 0-34078
- steel, alloy cast, optimal alloying, carburising effect 0-50771
- steel, austenitic Mn-Ni ageing, alloying element influence on struct. and mechanical props. (Russian) 0-35256
- steel, austenitic-martensitic, phase comp., struct. and mech. props. 0-29974
- steel, C, corrosion cracking by sulphide, effect on props. 0-55587
- steel, C, isoforming and warm rolling, effect of mech. props. 0-11673
- steel, C, natural reinforced composite 0-30039
- steel, C content effect on annealing texture, plastic anisotropy and mechanical props. 0-29976
- steel, C type 45, martensitic needle size, effect on mech. props. after induction hardening 0-11672



# mechanical strength continued

steel, Cr-Al (12, 6 wt.%), ferritic stainless, high temp. treated, strengthening mechanisms 0-3106  
steel, Cr-W-V-Mo (3.9 to 4.5, 1.5 to 2, 0.9 to 1.2, 3.9 to 4.4 wt.%), heat resistant, type 8Kh4M4V2F1-Sh, mech. props. 0-16464  
steel, electric field effect on strength, hardness 0-50714  
steel, high-temp. isothermic combined heat treatment and mech. working influence on struct. and mech. props. of 60S2 (*Russian*) 0-20969  
steel, long-term strength, H effect 0-55581  
steel, low alloy, brittle fracture, quenched and tempered 0-11677  
steel, maraging, effect of thermal cycling ( $\gamma$  to and from  $\alpha$ ) on props. 0-20986  
steel, Mn-Si, for springs, metallographic study, present phases rel. to mech. props. (*French*) 0-21090  
steel, rail, AE use for mech. tests 0-35467  
steel, stainless, Cr-Ni (18, 10 wt.%), long-term strength in H at high pressure 0-55485  
steel, stainless, durability in  $H_2$  up to 500°C 0-30170  
steel, stainless, Ni-Cr-Mo-W (29, 13, 3, 2 wt.%), long-term strength in H at high pressure 0-55485  
steel, stainless, nickelless, low cycle fatigue 0-35326  
steel, stainless, type 304, BWR coolant pipe, critical strength under stress corrosion cracking 0-52743  
steel, tempering effect on struct. and mech. props. of types 70, U8, and U12 (*Russian*) 0-50655  
steel, ultra high strength, historical 0-7609  
steel fibre reinforced  $Al_2O_3$ -Al, production and mech. props. 0-11619  
steels, ultrahigh C, superplastic, mech. behaviour at elevated temps 0-21028  
vegetable fibre reinforced cement sheets, strength 0-21024  
viscoelastic structures, strength and stability, a method of solving integral eqns. used 0-10167  
window, composite vacuum-tight, for IR and visible observations, strength and IR transmission 0-48406  
Ag-CdO cermets, coprecipitated carbonates and hydroxides, physicomach. props. 0-25706  
Al alloys, electric field effect on strength, hardness 0-50714  
Al substitutional solid solution alloys, volumetric effect and props. (*Russian*) 0-39293  
Al, vacuum condensate, struct. and mech. props. depend. on deposition conditions 0-15417  
Al wire, hot and cold deformation drawing strengthened, thermal EMF study (*Russian*) 0-54674  
Al-Mg, AMg6 alloys, effect of chem. comp. on strength and ductility at low temps. 0-3148  
Al-polymer joint, temp. depend. meas. of joint strength 0-50824  
Al-W(Mo)(Nb), struct. and props. of alloys obtained from granules 0-50717  
B fibre reinforced Al-Zn-Mg, packet rolling, thermodeform. process parameters (*Russian*) 0-55433  
B fibre reinforced  $AlB_2$  and  $TiB_2$  fibre coating effect on strength (*Russian*) 0-40426  
BN ceramic with organosilicon polymer additions, strength and oxidation resistance 0-20880  
C fibre reinforced Al, interaction between components and compatibility, mech. props. effect 0-11761  
C fibre reinforced polyphenylsiloxane composites, long-time strength, and influence of protective coatings 0-3133  
CC TaC based hard metal, non-stoichiometric sintering, mech. props. 0-25616  
Cu, vacuum condensate, struct. and mech. props. depend. on deposition conditions 0-15417  
Cu-Al, vacuum condensate, struct. and mech. props. depend. on deposition conditions 0-15417  
Cu-plated C fabric, plasma sputtering influence on strength and elec. cond. (*Russian*) 0-21008  
 $Cu_2O$ -Al $_2$ O $_3$ -SiO $_2$  glasses, strengthening by alkali-Cu ions exchange 0-55467  
 $Cu_{60}Zr_{40}$ , metallic glass, composition, mech. props., simulation 0-49117  
Fe, sintered and pressed, props., effect of atomised Fe powder particle size distrib. 0-11601  
Fe solid solution, substitution strengthening by Cr and Mo (*Czech*) 0-30080  
Fe-refractory compound, dispersion strengthened, thick vacuum condensate, control of struct. and mech. props. 0-16324  
 $La_{0.003}Ba_{0.66}Sr_{0.34}TiO_3$ , water absorpt., mech. strength, stability, TCR (*Russian*) 0-16511  
Mg-Tb, (up to 45 wt.%), phase diagram, and mech. props. 0-16277  
Mg-Y-Al alloys, phase equilib. (*Russian*) 0-20890  
MgO-Al $_2$ O $_3$ -SiO $_2$ , glass ceramic, structure and props. (*German*) 0-38927  
MgO-Al $_2$ O $_3$ -SiO $_2$  based cordierite glass-ceramic, strength and thermal shock, surface treatment effect 0-25884  
Mo alloys, fusion reactor first-wall and blanket material, mech. props. 0-34074  
Mo-Hf (0.3 wt.%), strength, plasticity and microhardness, internal nitriding effect (*Russian*) 0-40433  
Mo $_2$ B $_3$ , monocryst., grain size, abrasive and strength props. 0-11787  
Mo $_2$ B $_3$ -based alloys, mech. props., rel. to appl. as electrodes in electros-park machining 0-21174  
Nb alloys, fusion reactor first-wall and blanket material, mech. props. 0-34074  
Nb-Mo-Al-(Cr) eutectic directionally crystallised alloy, heat resistance, alloy struct. (*Russian*) 0-40481  
Nb-W-Mo-Zr, long-term strength props., vac. level effect 0-55484  
Nb-W-Mo-Zr-C, strength and ductility, prolonged high-temp. soaking effect 0-55483  
Nb-W-Zr-Ta, long-term strength props., vac. level effect 0-55484  
Ni-Al $_2$ O $_3$ (ZrO $_2$ ), dispersion strengthened, thick vacuum condensate, control of struct. and mech. props. 0-16324  
Ni-Al-Ti(Nb), heat-resisting dispersion-hardening alloys, props. and struct.,  $\gamma$ -phase comp. influence (*Russian*) 0-20943  
Ni-Ce-Fe-Ti (77, 20, 4, 2.5 wt.%), long-term strength in H at high pressure 0-55485  
Ni-Cr-Mo (74, 20, 4 wt.%), long-term strength in H at high pressure 0-55485  
Pd alloys, controllable hydrogen phase naklep, hardening and phase-strengthening 0-16323  
Pd $_{80}Si_{20}$ , metallic glass, composition, mech. props., simulation 0-49117  
PtRh5 alloy, phosphate glass addition effect on high temp. strength (*German*) 0-25807

# mechanical strength continued

Si, mechanical strength, origin of difference in Czochralski grown and float-zone-grown cryst. 0-44212  
SiC, chem. stability, mech. and thermal props. rel. to appls. 0-21103  
SiC fibre reinforced Al interaction between components and compatibility, mech. props. effect 0-11761  
Si $_3$ N $_4$ , effect of oxide impurities on physicomachanical props. 0-16396  
Si $_3$ N $_4$ , hot pressed, strength and life prediction 0-3173  
SiO $_2$ -Li $_2$ O-K $_2$ O-ZnO glass ceramic, prep., phase transformations and physical props. 0-45299  
Ti alloy, disc, rotating notched, strength in quasibrittle fracture 0-55533  
Ti alloys, fusion reactor first-wall and blanket material, mech. props. 0-34074  
Ti-Al-Mo(Cr)(Fe), thermomechanical treatment effect on mech. props., strengthening mechanisms 0-55441  
Ti-W-(Al), mech. props. and heat treatment 0-35274  
Ti-C-Ni-Mo sintered hard alloy TN-20, fracture surfaces 0-7684  
V alloys, fusion reactor first-wall and blanket material, mech. props. 0-34074  
V, plasticity and strength change in temp. range 20 to 1000°C impurity effects 0-35235  
W fibre reinforced, Co powder alloys, reactions and recryst. 0-11603  
W-Cu, porous material, skeletal type, produced by liquid phase sintering, exam. of mech. strength, determ. resistance 0-16245  
W-Cu-(Ti)(Zr), exam. of mech. props. as function of temp., composition, and oxidation props. 0-16472  
W-Mo, vapour deposited, long-term strength and thermocyclic creep 0-16405  
W $_2$ B $_5$ , monocryst., grain size, abrasive and strength props. 0-11787  
W $_2$ B $_5$ -based alloys, mech. props., rel. to appl. as electrodes in electros-park machining 0-21174  
WC-Co hard alloy composite, calc. of weakest link in struct. 0-11730  
YCrO $_3$ -MgCr $_2$ O $_4$  sintered ceramics, elec. cond. 0-24927  
ZrC $_{0.91}$ , sintered, strength charact. effect of struct. and substruct. 0-16260

# mechanical testing

see also creep testing; dynamic testing; fatigue testing; fracture toughness testing; hardness testing; materials testing; mechanical variables measurement; notch testing  
acoustic microscopy, with microwave freq., determ. of mech. props. of materials 0-48535  
acrylic, denture base, tensile testing 0-16621  
adhesion measurement, locus of failure, bond failure in adhesive joints 0-50801  
adhesion measurement, of thin films, thick films and bulk coatings, conf. Philadelphia, USA (Nov. 1976) 0-46729  
adhesion measurement, of thin films, thick films and coatings 0-50817  
adhesion testing, use of fracture mechanics concepts 0-50802  
blood vessels, medium sized, mech. characts. 0-41101  
brittle materials, load-transmitting medium to measure strength 0-40652  
ceramic rods, arrangement type 2037/ZT-10 for testing flexural resistance (*Polish*) 0-35455  
ceramics, impact toughness testing device 0-25941  
coatings, adhesion strength, meas. using microindentation method 0-40640  
composite materials under complex stress-state conditions, mech. props., method for studying 0-50799  
creep tests, machine, conditions of plane state of stress 0-21232  
curved specimens, elastic and strength characts., universal clamping device 0-25960  
deposit-substrate systems, adhesion testing 0-50814  
dry strength determinations, testing conditions influence (*German*) 0-25928  
elastic contact problems, mixed approach using finite element methods (*Chinese*) 0-5995  
electrodeposit, on metallic substrate, peel test for determ. adhesion 0-50815  
EM tensile adhesion test method 0-50804  
fatigue testing, of thin wires 0-25834  
fibre reinforced composites, unidirectional, tensile testing 0-40664  
filamentary crystals, complex stressed state, method of investigating mech. props. 0-3264  
film, adhesion measurement 0-50819  
filmed structures, hardness and adhesion meas., scratch technique 0-50805  
films and foils, mechanical testing methods, review 0-40637  
flame-sprayed coatings, adhesion testing 0-50812  
foam plastic, device for compression tests at different temps. 0-25947  
fracture monitoring with simultaneous recording of acoustic emission signals 0-55599  
friction machine SMTs-2, self adjusting fixture for block specimens 0-25944  
furnace, heating specimens to 1400°C 0-3265  
glass fibre, tensile strength meas. using chain-loading fibre tensometer (*Japanese*) 0-55610  
glass-fibre reinforced plastic specimens, prep. of three-layer cylindrical with syntactic foam base 0-3267  
gripping attachment for wire and strip specimens on dividing machine type PTA 0-40647  
heat energy relaxed due to deform., thermocouples obs. 0-21214  
heat-resistant alloys, installation for mech. tests under superplasticity conditions 0-55603  
hydrostatic pressure testing device, tensile, upsetting tests 0-25959  
impact tester attachment, for bending impact tests, method of obtaining asymmetric cycles 0-16628  
impression fatigue test 0-25861  
J integral and its components, determ. method 0-45458  
mechanical oscillations amplifier 0-13069  
metal electroplastic deformation meas. pulse generator (*Russian*) 0-25931  
metal fatigue, eddy current sensors, tuning method 0-21231  
microprocessor applications in deformation processes (*German*) 0-40627  
optical fibres and cables 0-3285  
optical glass, K8, bending strength, sample dimension effects 0-9975  
plastics, for transmission media, thermomech. reliability 0-40666  
plastics, tensile and flexural testing device, incorporating an impactor (*German*) 0-3276  
plastometer, electronically controlled, for tensile and compression tests (*German*) 0-3273  
polymer testing by dynamic mech. anal. 0-16626



**mechanical testing continued**

- polymers, automatic recording device for thermomechanical and linear dilatometric testing 0-11858  
 polymers, relaxation props., photometric transducer method of meas. 0-3268  
 power transmission cables, pipe-type, low-cycle fatigue tests 0-7731  
 SEM attachment to record stress-strain diagram 0-25961  
 soldered thick-film conductor, adhesion meas. technique 0-50811  
 steel, Cr-Ni-Mo-V, ductile fracture during tensile loading 0-45381  
 steel, high strength low alloy, acoustic emission meas. from crack opening displacements 0-7732  
 steel, industrial tests for determining lamellar tearing susceptibility (French) 0-21250  
 steel, low alloy, elastoplastic strain evaluation in crack weakened cross sections by fracture mechanics 0-45380  
 steel, pressing die X45 CrNiWMoVCo 9.9, test results (German) 0-50785  
 steel, sheet, rapid test for props. assessment 0-40650  
 steel, wear resistance, determ. using MI-IM machine 0-25943  
 strain gauge application on compact bone 0-3883  
 stress intensity factors, photoelastic meas. correlation, for various specimen and defect geometries (German) 0-53727  
 supersonic gas jet, penetration into the ground (Russian) 0-28544  
 tensile, plotting device for stress-strain diagrams 0-3269  
 tensile and flexural testing device, incorporating an impactor (German) 0-3276  
 tension test, computer simulation, effect of testing conditions 0-7729  
 thick film, adhesion to ceramic, destructive and nondestructive meas. 0-50809  
 thick film conductor, adhesion meas. 0-50808  
 thick film terminations on chip components, adhesion meas. methods 0-50810  
 thin walled pipes, device for gripping in tests with complex stress state 0-25945  
 torsional strain curves plotting 0-40638  
 wear due to impulse friction, device 0-25957  
 wear of specimens on friction machine, device for continuous recording 0-55604  
 wire in torsion, installation for automated determination of yield strength 0-21221  
 Al, Bauschinger effect, temp. influence, combined tension-torsion testing machine 0-45453  
 Al, thin film on fused quartz, threshold adhesion failure, meas. by stylus method 0-50806  
 Al-Zn-Mg, acoustic emission meas. during tensile testing, reproducibility of results 0-50782  
 Cu alloy, ductile fracture during tensile testing 0-45381  
 Fe, grey cast, tensile testing of mechanical props., from room temp. to liquidus (Japanese) 0-7728  
 Ni coatings on Al alloy substrates, adhesion strength, meas. using microindentation method 0-40640  
 Pt-Au, thick film, adherence meas. and evaluation 0-50813  
 Sn plate, rapid test for props. assessment 0-40650

**mechanical variables measurement**

- see also elastic moduli measurement; force measurement; pressure measurement; shock measurement; strain measurement; stress measurement; torque measurement; vibration measurement*  
 adhesion, locus of failure, bond failure in adhesive joints, experimental methods 0-50801  
 adhesion, locus of failure 0-50818  
 adhesion, of evaporated thin films 0-50822  
 adhesion, of preformed film to solid 0-50819  
 adhesion, of thin films, adhesive failure, rel. to interfacial structure 0-50820  
 adhesion, of thin films, thick films and coatings 0-50817  
 adhesion measurement, of thin films, thick films and bulk coatings, conf. Philadelphia, USA (Nov. 1976) 0-46729  
 adhesive energy, meas. techniques, in metal/ceramic systems 0-50803  
 compressibility of solids, optical method (Slovak) 0-37023  
 deposit-substrate systems, adhesion testing 0-50814  
 electrodeposit, on metallic substrate, peel test for determ. adhesion 0-50815  
 EM tensile adhesion test method 0-50804  
 film-substrate bond strength, meas. by laser spallation 0-50821  
 filmed structures, hardness and adhesion meas., scratch technique 0-50805  
 flame-sprayed coatings, adhesion testing 0-50812  
 holographic interferometry, deformation analysis of opaque bodies, book 0-27050  
 internal friction, measurement using automated Marx's composite oscillator method 0-37151  
 internal friction measurement (Spanish) 0-6002  
 metal-polymer joint, meas. of temp. dependence of joint strength 0-50824  
 metals, determ. of yield strength 0-25937  
 sapphire fibres, meas. of bending strength 0-25964  
 soldered thick-film conductor, adhesion meas. technique 0-50811  
 stretch measurement of ribbons in industrial processes, digital instrument (Polish) 0-42194  
 thick film, adhesion to ceramic, destructive and nondestructive meas. 0-50809  
 thick film conductor, adhesion meas. 0-50808  
 thick film terminations on chip components, adhesion meas. methods 0-50810  
 tribometry development, friction reduction and meas. 0-23973  
 tribometry metrological provisions, Soviet installations and instruments development 0-23974  
 viscoelastic properties of liqs. meas. using torsion resonator, 20-1200 KHz (Russian) 0-52196  
 Ag, granular thin film, adhesion measurement 0-50807  
 Al, thin film on fused quartz, threshold adhesion failure, meas. by stylus method 0-50806  
 Cu, on thermally oxidised Si, EM tensile adhesion test method 0-50804  
 Pt-Au, thick film, adherence meas. and evaluation 0-50813

**mechanical waves** *see elastic waves***mechanics**

- see also bending; biomechanics; celestial mechanics; classical mechanics; damping; density; dynamics; fluid mechanics; intermolecular mechanics; kinematics; momentum; relativistic mechanics; statics; statistical mechanics; wave mechanics*  
 No entries

**mechanics of fluids** *see fluid mechanics***mechanoreception**

- auditory impedance changes elicited by tactile and electrocutaneous stimulation 0-56066  
 digit-wrist sensory compound nerve action pot. obs. in patients with focal nerve injuries 0-3655  
 electrophysiological responses of Didinium nasutum to Paramecium capture and mechanical stimulation 0-56001  
 equilibrium reception in an insect, mediation by giant interneurons 0-45925  
 evoked giant sensory nerve pots., EMG in quadriparetics and quadriplegics 0-3653  
 intramuscular nerve action pot. derived from sensory fibres 0-56071  
 ipsilateral vibrissae in adult rodents, projections on cortical somatic I barrel subfield 0-8074  
 lateral line, onset of neural function in South African clawed frog 0-21480  
 lingual tactile sensory system, automated instrumentation for research 0-8205  
 lumbosacral spinal cord and cauda equina, evoked pots. recording 0-17147  
 matching information to brain, problems 0-51114  
 peripheral nervous system multichannel data anal., frog sartorius muscle mechanoreceptor transducer characts. (Japanese) 0-3656  
 proprioceptors with central cell bodies, in locust 0-51132  
 prosthetic hand pinch force, sensory-feedback system compatible with myoelectric control 0-41324  
 receptors sensitive to muscle length in the horseshoe crab 0-12167  
 sensory nerve conduct. vel. of medial antebrachial cutaneous nerve 0-3654  
 somatosensory evoked potential, extended sources assessment method 0-26244  
 somatosensory evoked potentials, abnormalities due to brainstem lesions 0-56070  
 somatosensory evoked potentials, in man, cerebral, subcortical, spinal and peripheral nerve pots. 0-16961  
 somatosensory evoked potentials, short latency, stimulus intensity effect 0-35924  
 spatial orientation of animals, role of auditory mechanisms (Russian) 0-45915  
 tactile sensation, mechanoreception physiology and psychophysics (Japanese) 0-16962  
 tactual vocoder, max. information transmission, time-invariant stimulation (Japanese) 0-41317

**medical administrative data processing**

- see also medical computing*  
 automated TLD processing and dose record keeping service 0-12267  
 cardiology data processing system 0-56236  
 intracavity radiotherapy, interactive treatment planning using CT 0-8145  
 obstetric computer system for intensive care of mother and foetus during labour (German) 0-3857  
 radiotherapy treatment planning using microcomputer 0-8191  
 review, computer applications in biomedical engineering (Japanese) 0-12289  
 treatment planning, three dimensional model for CT radiotherapy 0-8192

**medical computing**

- see also medical administrative data processing; medical diagnostic computing*  
 anatomy, 3D display for radiotherapy treatment planning 0-3773  
 angiography, computerised, anal. and visualisation of blood dynamics and motion of organs 0-8170  
 atherosclerosis detection, computerised electronic radiographs appl. 0-8169  
 cardiac disc mitral valve in left ventricle, computer model of motion 0-8214  
 cardiac US data, moving heart surfaces extraction 0-8114  
 cardiology data processing system 0-56236  
 conditioning EEG activity, computerised laboratory 0-30912  
 curvilinear view generation from CAT scanned data 0-8149  
 deaf people, computer generated speech training patterns 0-51290  
 dosage selectivity by planning 3-D radiation treatment using computer 0-41178  
 echocardiogram, automatic anal. and VTR recording 0-8112  
 EEG alternations, power spectral analysis 0-30924  
 EEG data acquisition and data processing system, peripheral equipment 0-41270  
 EEG data processing, discrete Fourier transformation 0-26385  
 EEG photic flash response, quantitative approach 0-30923  
 EEG wave duration anal., microcomputer implementation 0-21558  
 electronic radiography 0-8162  
 EMG, single fibre, microcomputer-based jittermeter 0-46078  
 external beam radiotherapy, isodose planning, new suite of programs 0-41243  
 gait analysis subsystem for smoothing and differentiation of human motion data 0-35953  
 gastrointestinal signals, quantitative analysis 0-41339  
 head and neck 3-D mapping derived from computed tomographic serial scans 0-8148  
 human disease study using mass spectrometry and metabolite profiling 0-51289  
 image reconstruction formulae, computer implementation 0-52179  
 image reconstruction from projections, book 0-51961  
 image reconstruction from projections 0-52178  
 limbs motion analysis using goniometers, prosthesis microcomputer control appl. 0-51138  
 lung tissue micrograph computer processing approach 0-8123  
 magnetoencephalogram and electroencephalogram, comparison of spatial response 0-26245  
 mammary carcinoma conservative radiotherapy, computer assisted dosimetric soln. (Dutch) 0-36139  
 mammary lymphoscintigraphy in radiation treatment planning, minicomputer technique 0-12223  
 microcomputer, use in ventilatory function testing 0-41291  
 microcomputer-based data acquisition and analysis system for CO<sub>2</sub> rebreathing studies 0-36161  
 microprocessor appl. developments 0-51285  
 microprocessor-controlled cardiac output meter 0-36162  
 microprocessors in bioscience, review 0-21557  
 Monte Carlo computer code for calc. of radiation dose from syringes 0-41246



**medical computing continued**

- MORPHOQUANT automatic microscope image analyser, universal program system 0-56160  
 movement dynamics, human, investigation using a computer 0-51284  
 myocardial perfusion imaging using  $^{201}\text{Tl}$ , algorithm for background activity calc. 0-56195  
 myocardium of human left ventricle, stiffness distrib. rel. to shape change in diastole 0-41095  
 nuclear angiocardigram anal. program for radiology trainees 0-8143  
 nuclear medicine, appl. of computers, review (*German*) 0-41214  
 nuclear medicine, history of computer appls. 0-42037  
 nuclear medicine, image processing system 0-41174  
 nuclear medicine studies, automated interpretation 0-8164  
 obstetric computer system for intensive care of mother and foetus during labour (*German*) 0-3857  
 oculomotor function analysis 0-46092  
 perimetry standards 0-46084  
 pion<sup>-</sup> radiation, uniform depth-dose distrib. technique and cell survival obs. 0-17139  
 pneumoconiosis, small lesions, computer aided identification 0-30887  
 pulmonary artery press. estimation using pulse wave velocity 0-12203  
 radiation dose deposition calcs. in human marrow 0-26365  
 radiation therapy, computer program for negative pion beam calcs. 0-46061  
 radiation therapy planning programs development for SIN pion applicator 0-26339  
 radiological images, conf. Newport Beach, CA, USA (June 1979) 0-8141  
 radionuclide cardiac output determination, automated computer program 0-56196  
 radiotherapy treatment planning, inter-hospital interactive computerised system 0-36068  
 review, computer applications in biomedical engineering (*Japanese*) 0-12289  
 scintigraphic joint imaging, technical aspects 0-56197  
 skeletal muscle motor unit contractile characts. determ. through twitch characts. 0-17159  
 spatial image processing, research projects at IROE Institute (Firenze) (*Italian*) 0-56668  
 spectral estimates of auditory brainstem responses 0-30913  
 tomography, resource sharing computer hierarchy for 3D image reconstruct. 0-26345  
 tomography depth-dose distribution, effect of slice thickness 0-46038  
 tumour detection, computer processing of microwave enhanced thermographic images 0-8125  
 US computerised tomography, improvements in data acquisition and pre-processing 0-26309  
 ventricle excitation spread, simulation (*Japanese*) 0-3847  
 ventricular arrhythmias, intraoperative mapping system 0-56242  
 versional eye movement control 0-46090  
 visual fields, computer appls. 0-45892  
 vocal tract, computer representation of geometrical configuration (*Russian*) 0-46111

**medical diagnostic computing**

- see also computerised signal processing*  
 automated patient testing 0-46088  
 bone, disease diagnosis, automatic texture anal. methods 0-8156  
 cardiology data processing system 0-56236  
 chest radiograph nodule detection system 0-8140  
 chest radiographs, computed detection of nodules 0-8172  
 computer graphics for red cell anal. 0-21597  
 dyslexia, detect. by computerised brain mapping 0-36185  
 ECG pattern classification from complete computer descriptions 0-56265  
 heavy particle computed tomography 0-8146  
 imaging system, new, in computed radiography 0-8147  
 nuclear medicine display algorithms evaluations 0-8144  
 radiological digital image processing facility 0-36127  
 review, computer applications in biomedical engineering (*Japanese*) 0-12289  
 strabismus and amblyopia, eye movement analysis by computerised ocular motility test system 0-41299  
 tomography principles, realisations and results interpretation (*Czech*) 0-36085

**medical effects of radiation** *see biological effects of radiation***medical electronics** *see biomedical electronics***medical information processing** *see medical administrative data processing; medical computing***medical sciences** *see medicine***medicine**

- see also biomedical engineering; cardiology; health hazards; patient diagnosis; patient monitoring; patient treatment; physiology*  
 aeronautical and space medicine, conf., Brussels, Belgium (Jan. 1979) 0-41944  
 Berson, Solomon A., biography, achievements in nuclear medicine 0-42028  
 conference, Stockholm, Sweden (Dec. 1979) 0-31410  
 education, physical sciences in medicine diploma 0-31444  
 laser beam appls. (*French*) 0-41165  
 nuclear medicine in the UK, history 0-42039  
 optical instrumentation in medicine, conf., Toronto, Canada, (Mar. '79) 0-36777  
 physics and its methods in medicine (*Polish*) 0-12048  
 technological advances, rigorous assessments of benefits and costs 0-17163

**Meissner effect**

- core radius of current-carrying supercond. cylinder in intermediate state 0-11134  
 metals, triplet supercond. transition in strong mag. field 0-25040  
 semimetal, mixed superconducting-excitonic insulator phase, diamagnetism, virtual intraband transitions 0-2520  
 $\text{Hg}_{1-x}\text{AsF}_6$ , linear chain compound, mag. field induced residual resist., anisotropic supercond. 0-24897  
 $\text{Hg}_{1-x}\text{AsF}_6$ , supercond., absence of surface Hg 0-20350  
 $(\text{SN})_x$ , Meissner effect, mag. susceptibility meas. 0-20351  
 $(\text{Y,Lu})\text{B}_6$ , superconducting transition temps., impurity effects 0-20341

**Meissner-Ochsenfeld effect** *see Meissner effect***melting**

- see also melting point; zone melting*  
 adsorbed monolayer of orientable molecules, lattice fluid model, real-space renormalisation group method 0-17882  
 alkali halides, mol. dynamics study 0-15220  
 basaltic achondrite meteorites, rare earth element abundance patterns rel. to origin 0-36581  
 behaviour induced by horizontal row of heating cylinders 0-33442  
 biomembrane phase transition studied by positron annihilation energy spectrometry 0-35854  
 butanethiol, volume change on melting and reduced Lindemann's relation 0-29151  
 caesium propanoate, solid state transitions and melting process, diff. and conductometric meas. 0-10670  
 chondrules origin, primordial melting mechanism 0-4310  
 closed form solution to problem with heat generation by viscous friction (*Japanese*) 0-19225  
 computer simulation, using array processor 0-54353  
 cylinder, stable conditions for phase change problem with internal heat generation 0-10130  
 diamond, 'melting' to solid metallic C phase above graphite triple point 0-15236  
 1,2-dibromoethane, volume change on melting and reduced Lindemann's relation 0-29151  
 p-dichlorobenzene, expansivity, determ. by calorimetric compression from 0 to 400 MPa 0-44339  
 1,2-dichloroethane, volume change on melting and reduced Lindemann's relation 0-29151  
 DNA-type macromolecule, melting, low mol. wt. impurity effect 0-12050  
 electron solid, two-dimens., defects and implications for melting 0-39076  
 electron solid, two-dimens., shear modulus and melting, temp. depends. 0-158  
 ethane submonolayer on graphite, struct. and melting, elastic neutron scatt. 0-29266  
 ethyleneterephthalate-ethylene glycol copolyester/15% polyglycol, semicryst. melting and glass transitions 0-49346  
 finite medium freezing (melting), variational anal., radiation and convection effects 0-38244  
 geothermal well logging, temp. meas. utilising melting props. of materials 0-56659  
 glacial ice, melting in sea water, heat and mass transfer (*German*) 0-33606  
 glass devitrification, heat treatment parameters determ. from viscosity changes (*Polish*) 0-40404  
 glass workability rel. to melting history, microstruct., apparent liquidus temp., mechanical props. 0-11633  
 graphite, interfacial tension determ. between C saturated liquid Fe by buoyancy meas. (*German*) 0-34273  
 high melting particle heating, melting and vaporisation in hot gas 0-6201  
 hydrometeor precipitation from anvil clouds, melting and evaporation 0-17323  
 ice cubes, melting time, water film thickness, interface temp., weight var. 0-29153  
 ice melting model, appl. to Antarctic ice shelf and icebergs 0-4036  
 ionic crystals, structurally modulated, elasticity and its limits, yielding and melting 0-49295  
 lake ice cover, dissipation, effect of surface meltwater accumulation, heat flow 0-8364  
 latent heat storage materials, high temp. corrosion resistance and thermodynamic stability 0-30582  
 latent heat-of-fusion energy storage: experiments on heat transfer from cylinders during melting 0-6492  
 latent-heat thermal energy storage materials, energy density and materials cost (*Japanese*) 0-26168  
 Lennard-Jones two-dimensional system, Monte Carlo study 0-49338  
 Lindemann's criterion and necessary condition for melting curve maximum 0-2145  
 metal, effect of fusible-metal deform. on contact-melting kinetics 0-49339  
 metal powders, sintering at 1 to 10 MPa (*German*) 0-35122  
 metallic fine particles, theory of melting in the Percus-Yevick limit, appl. to particles on  $\text{SiO}_2$  and C substrates 0-20060  
 metals, contact melting process kinetics, investigation method 0-39259  
 metals, enthalpy and average mass temp. on plasma-arc melting (*Russian*) 0-54405  
 metals, heat capacity near melting point, vacancy mechanism of melting 0-10641  
 methane adsorbed on graphite basal plane, first order melting transition, triple point 0-2269  
 methylcyclohexane, dense liq., self-diffusion and viscosity 0-15278  
 minerals (petrurgy) (*Czech*) 0-44298  
 minor planets, melting by EM heating in early solar system 0-36555  
 molecular crystal, action of external forces on mesogenic struct. form. 0-2147  
 naphthalene, melting of rotational degrees of freedom near cryst.-liq. transition 0-54352  
 octaphenylcyclotetrasiloxane, phase behaviour and nucleation kinetics 0-29168  
 n-paraffin, crystals, phase transitions, statistical theory 0-44290  
 paraffin plate heat storage element, fusion, periodic solidification, heat transfer kinetics (*French*) 0-40913  
 paraffin wax, two-phase Stefan problem solns. 0-43594  
 particles in nonisothermal plasma jet, trajectory and temp. calcs. (*Russian*) 0-7514  
 permanent magnet alloys manufacture, Co-mishmetal alloys (*Polish*) 0-35132  
 planar melting front stability in two-phase thermal Stefan prob. 0-43600  
 plasma furnaces, mineralogy and extractive metallurgy appls. (*French*) 0-28849  
 poly(ethylene-oxide), isothermal growth, thickening, melting, bilayer crystals, and chain end effects 0-38939  
 poly-ε-caprolactum, semicryst. melting and glass transitions 0-49346  
 1,4-cis-polybutadiene, stereoregular, recrystn. in partial melting temp. region (*Russian*) 0-6495  
 polyethylene, drawn, ultrahigh modulus, linear, melting behaviour 0-19916  
 polyethylene, ultra-high-strength filaments, soln. spun/drawn, mech. and thermal props. 0-40440



**melting continued**

- polyethylene crystal, longitudinal growth in flowing soln., melting of continuous fibrillar crystal 0-19917  
 polyethylene terephthalate-p-oxybenzoate, nematic-isotropic transition loss 0-44300  
 polyethylene-isostatic polypropylene mixture, melting anal. 0-29150  
 polymers, model equivalent to Ising model 0-37914  
 polyoxyethylene-glutaric acid eutectic, melting and crystn. 0-28924  
 polypropylene, Halen and Daplen, semicryst. melting and glass transitions 0-49346  
 polystyrene, isotactic and static cold-crystallised blends, thermal transitions 0-24381  
 power overdistribution to AC and DC arcs for melting metals (*Russian*) 0-54055  
 PTFE, annealing effect on melting and crystallisation (*Japanese*) 0-20980  
 rare earth metals, heat capacity near melting pt., vacancy mechanism of melting 0-15221  
 rare gas solids, Debye Waller factors from unpaired elastic force model, Lindemann's melting criterion 0-19896  
 restoration, evaporation and melting of materials in high temp. gas flow (*Russian*) 0-39271  
 rubidium propanoate, solid state transitions and melting process, diff. and conductometric meas. 0-10670  
 slab, melting in contact with fluid, heat cond. prob. (*Japanese*) 0-53612  
 slab with heat generation by friction, approx. anal. (*Japanese*) 0-14555  
 snow, deposition and melting with altitude on Mt. Teine, Hokkaido (*Japanese*) 0-36346  
 snow melting rate, urban/rural area comparison in Sapporo, Hokkaido (*Japanese*) 0-36342  
 snow on slopes of Mt. Asahidake, Hokkaido (*Japanese*) 0-36343  
 solid surfaces, ablation in impingement region of water jet 0-14766  
 solid-liquid transition, optical reflectance spectra 0-24569  
 soliton lattice melting, functional integral method 0-17883  
 spherical end faced coupling fibre fabrication by selective etching/melting 0-53492  
 sputtered particles-substrate, temp. overaging (*Russian*) 0-40385  
 steel, alloy, electroslog remelting effect, an impact-abrasive wear resistance 0-55541  
 steel, austenitic stainless, high N, plasma arc remelting, processing parameters and props. 0-16336  
 steel, diffusion melting in Fe-C melts, heat transfer correl. 0-54348  
 surface dynamics, phase boundary configuration calcs., moving heat source (*Russian*) 0-54342  
 surface theory 0-10644  
 terrestrial planets, melting rel. to core formation 0-17514  
 vacancy cell model and BGY integral eqn. 0-38887  
 Al powder, liq.-solid phase transforms. (*French*) 0-45294  
 Al sputtered coating development, porosity, durability temp. depend., electric arc metallisation regime (*Russian*) 0-39402  
 Al<sub>2</sub>O<sub>3</sub>-Dy<sub>2</sub>O<sub>3</sub>, phase diagram at high temps. (*Japanese*) 0-50619  
 B,  $\beta$ -rhombohedral, purification by electron beam melting and CVD 0-20781  
 B<sub>2</sub>C, melting and phase homogeneity range 0-20911  
 Ba I-Ba II phase boundary, Ba I fusion curve peak at high press. (*Russian*) 0-2165  
 BiH(PO<sub>3</sub>)<sub>4</sub>, condensed, thermal behaviour and IR spectra 0-19912  
 BiP<sub>2</sub>O<sub>14</sub>, condensed, thermal behaviour and IR spectra 0-19912  
 CaCl<sub>2</sub>·6H<sub>2</sub>O heat of fusion system for solar energy storage 0-16846  
 Cd, atomic vibr. and fermion behaviour of HCP metals 0-6474  
 CdTe, Hall and thermo-EMF coeffs., in solid, liquid states 0-54704  
 Co melt, struct. charact. time depend. in X-ray studies (*Russian*) 0-24350  
 Cu, molten surface layer thickness, emissivity and AES meas. 0-39261  
 Fe, diffusion melting in Fe-C melts, heat transfer correl. 0-54348  
 Fe-base samples, for working curves, HF induction melting and centrifugal casting 0-22340  
 Fr, properties from melting point to 7500K, prediction (*Russian*) 0-44296  
 Ge, laser irradiation, photoacoustic detection 0-2901  
 Ge-Si:Sb, prepared in Universal Furnace expt. in Soyuz-Apollo programme, melting and crystn. 0-19737  
<sup>3</sup>He, solid, low temp. thermal cond., structural crystalline defects 0-2240  
<sup>3</sup>He, solid, melting curve shifts due to pore condensation 0-54469  
<sup>3</sup>He, two-dimens. solid, melting mechanism 0-10643  
 KMg<sub>2</sub>(AlSi<sub>3</sub>O<sub>10</sub>)F<sub>2</sub>·KMg<sub>2</sub>Si<sub>4</sub>O<sub>10</sub>F<sub>2</sub>, solid soln., melting and crystn., quenching and DTA study 0-39263  
 Li-Pb, thermodynamic study using Knudsen effusion mass spectrometry 0-24578  
 LiNO<sub>3</sub>·3H<sub>2</sub>O(D<sub>2</sub>O), crystals, and melts, density, mol. vol., thermal coeff. of expansion, rel. to struct. 0-15270  
 Mg, atomic vibr. and fermion behaviour of HCP metals 0-6474  
 Mn-Bi alloy, melting and solidification under microgravity, mag. props. (*German*) 0-45296  
 Mo-Cr, fusibility diagram (*Russian*) 0-20897  
 NaCl, interpolational eqn. of state with allowance for melting, vaporis., dissoc. and ionis. processes 0-24566  
 NaF-YF<sub>3</sub> system, fusibility diagram, quasibinary section of NaF-YF<sub>3</sub>-YOF system characts. 0-55371  
 Nb-Mo, prod. by simultaneous carbothermic reduction of oxides/electron beam melting method (*Japanese*) 0-11590  
 Nb-Si diagram of state, melting temp., polymorphic transform. temp. (*Russian*) 0-50594  
 Ni melt, struct. charact. time depend. in X-ray studies (*Russian*) 0-24350  
 Ni, spreading kinetics of Al 0-24717  
 Os, atomic vibr. and fermion behaviour of HCP metals 0-6474  
 Pb melting curve, high press. effect, and Pb diffusion in Cu 0-49337  
 Pb, melting studies by temperature wave anal. method 0-15217  
 Pd-Cu-Si, laser melting and splat quenching to form foils for TEM obs. 0-29986  
 Re, atomic vibr. and fermion behaviour of HCP metals 0-6474  
 Ru, atomic vibr. and fermion behaviour of HCP metals 0-6474  
 Se, monoclinic to trigonal conversion, thermodynamic stability and associated investigs. 0-24592  
 (Se)<sub>n</sub>, crystn. and melting 0-40241  
 Si, defect annihilation depth by pulse laser annealing 0-16128  
 Si, dislocation growth during laser melting and solidification 0-2022  
 Si, laser annealed ion implanted, elec. props., melting threshold 0-10969  
 Si on sapphire, laser annealing dynamics epitaxial regrowth, optical reflectivity 0-29285

**melting continued**

- Si<sub>3</sub>N<sub>4</sub>-Si<sub>2</sub>N<sub>2</sub>O-Mg-SiO<sub>4</sub>, melting and eutectic studies 0-45285  
 SiO<sub>2</sub>-Na<sub>2</sub>O-CaO (13, 11 wt.%) glass, phase separation, SiO<sub>2</sub> purity effect 0-44144  
 SiO<sub>2</sub>-Na<sub>2</sub>O-CaO glass, phase separation characts., melting atmosphere effect 0-44141  
 SiO<sub>2</sub>-(TiO<sub>2</sub>) glass prep., melting (*Polish*) 0-40316  
 Sn, melting studies by temperature wave anal. method 0-15217  
 ThO<sub>2</sub>, simultaneous freezing and melting in finite media 0-620  
 Ti-Ni, laser melting and splat quenching to form foils for TEM obs. 0-29986  
 Ti<sub>2</sub>Te<sub>3</sub>, exam. of electrical props., in solid, liquid state 0-54686  
 UO<sub>2</sub>, simultaneous freezing and melting in finite media 0-620  
 V-Ni-Mo, structure in alloy crystallisation region, peritectic equilibria (*Russian*) 0-50622  
 W, heat resistant particles in low temp. Ar plasma, heating, melting, vapourisation (*Russian*) 0-40384  
 Zn, atomic vibr. and fermion behaviour of HCP metals 0-6474  
 Zn-Sn-Hg, diagram of state, melting temp., peritectic and eutectic phases (*Russian*) 0-55350  
 ZrC-W (75 wt.%) eutectic refractory alloys, smelting in suspended states, components distrib. (*Russian*) 0-19913

**melting point**

- classical quadrupole solids, correl. effects 0-10628  
 diamond-like solids, laser irradi. effect on cohesion 0-50470  
 glass, photochromic, thermo-optic transitions 0-50307  
 halobenzenes, aqueous molar solubilities and partitioning, 25°C obs., rel. to melting pts. 0-40803  
 high-pressure liquid MP determ. centrifuge cell 0-31783  
 ice, Ih, thermal resist. near melting point meas. 0-44375  
 inorganic crystals, glasses, thermal expansion coeff. rel. to phys. props. 0-49389  
 Lindemann hypothesis and size depend. 0-15222  
 metals, heat capacity near melting point, vacancy mechanism of melting 0-10641  
 polyethylene, solid-state extruded, exam. of props. 0-11669  
 polyethylene fibres, high density, ultra oriented, physical, mech. props. 0-25649  
 polyethylene melt, lightly crosslinked, crystn. under uniaxial compression, stretching 0-38957  
 polyethylene oxide, peculiarities of struct. form. near below the melting point 0-54150  
 rare earth borides, higher types, phys. props. and electronic struct., group orbitals-LCAO calcs. 0-20077  
 rare earth compounds, binary, regression eqns., for calc. props. from electron struct. 0-39498  
 rare earth metals, elastic props., connection with electron struct. (*Russian*) 0-19895  
 sputtered particles-substrate, temp. overaging (*Russian*) 0-40385  
 standards, secondary, for temp. range 2000-3000°C, chemical aspects of choice 0-52226  
 terephthalate copolyester, heat treatment effect on melting point (*Japanese*) 0-40400  
 transition metal borides, higher types, phys. props. and electronic struct., group orbitals-LCAO calcs. 0-20077  
 Ag, melting curve to 60 kbar press., reinvestigation 0-39260  
 Ag<sub>2</sub>Rb(PO<sub>3</sub>)<sub>2</sub>, struct., density and elec. cond. 0-33952  
 Al, Fermi momentum, for solid and liq. phases, temp. variation, Compton scatt. obs. 0-50451  
 Au, melting curve to 60 kbar press., reinvestigation 0-39260  
 B, liq., thermoelastic props. near melting point 0-19862  
 CdS(Se), reaction with Sn chalcogenides, thermodynamic anal. 0-40728  
 Cu, melting curve to 60 kbar press., reinvestigation 0-39260  
 Fe<sub>3</sub>O<sub>4</sub>-FeAl<sub>2</sub>O<sub>4</sub>-FeTiO<sub>3</sub> titaniferous magnetite, chlorination, 1273 to 2273K 0-55752  
 HgS(Se), reaction with Sn chalcogenides, thermodynamic anal. 0-40728  
 Na<sub>2</sub>SO<sub>4</sub>, melting point determ., DTA method 0-218  
 Nd<sub>2</sub>Zr<sub>2</sub>O<sub>7</sub>-Nd<sub>2</sub>Hf<sub>2</sub>O<sub>7</sub>, struct., elec. cond. and melting point 0-54197  
 Pd, effect of surrounding O<sub>2</sub> 0-27299  
 (Se)<sub>n</sub>, crystn. and melting 0-40241  
 W-Hf-C, phase equilb. 0-55348  
 ZnS(Se), reaction with Sn chalcogenides, thermodynamic anal. 0-40728

**membranes**

- see also *biomembranes; lipid bilayers; osmosis*  
 adsorbed, use of Si-SiO<sub>2</sub> as electrode for elec. and ellipsometric meas. 0-15366  
 anisotropic fluid, diffusion, EPR spin exchange and nuclear spin relax., theory 0-34753  
 bile salt micelles as liquid membranes 0-21327  
 cation binding to membranes, modified Gouy-Chapman equation 0-55998  
 cation exchange membrane, counterion interdiffusion 0-26044  
 cellophane membrane, polarised, electret transport props., permeability coeff. 0-7860  
 cellulose acetate, granulocyte growth enhancement on peritoneal cell-coated membranes following irradiation 0-21504  
 cellulose acetate, reverse osmosis membranes, ion mobility, diffusion coeff., elec. resist. obs. 0-45550  
 cellulose acetate-g-polyacrylamide, radiation grafted, appl. in water desalination by reverse osmosis 0-45548  
 choline phosphate calcium chloride tetrahydrate, struct., conformation, metal coordination, model for membrane surface interactions 0-15085  
 corrugated, with rigid centre, free axisymmetric oscillations (*Russian*) 0-38302  
 coupled transport of electrons and metal cations 0-3403  
 electrode, rotated disc, for membrane mass transport evaluation 0-26069  
 ethylene-vinyl alcohol copolymer membranes for haemodialysis, prep. conditions and props. (*Japanese*) 0-12299  
 flexing, appl. of displacement meas. by holographic interferometry 0-8962  
 Fourier transform IR transmission spectroscopy, appl. to natural and model membrane study 0-17218  
 haemodialysis membranes, permeability and rejection coeffs. 0-26207  
 haemodialysis membranes prepared from acrylonitrile-methylacrylate-acrylamide latexes graft copolymerised onto PVA (*Japanese*) 0-12297  
 haemodialysis with hollow fibre membranes, flow maldistribution effect on performance 0-26248  
 inflated, thin walled elastic circular cylinder under axial loading, bifurcations, membrane theory 0-19246  
 inviscid shear flow over flexible membranes, stability 0-14658  
 ion exchange membrane selectivity w.r.t. dialysis prospects 0-45560



**membranes continued**

- kaolinite membranes, anion permeation 0-11952  
 light optical imaging, of focused US field (*German*) 0-3275  
 macrocyclic receptor mols., chem. reactivity, mol. catalysis, transport processes 0-21280  
 model using millipore-DOPH membrane, increase in elec. resist. with  $\text{Ca}^{2+}$  ions and its oscill. 0-40745  
 phosphatidylcholine bilayers, artificial, interaction with C-reactive protein 0-3579  
 photochemical H prod. from  $\text{H}_2\text{O}$  using sunlight and asymmetric membranes 0-45776  
 poly-n-hexyl L-glutamate, sorption and permeation mechanism 0-26048  
 polyelectrolyte solution, thermodynamic props. determ. from Donnon equil. obs. 0-7846  
 polyethylene, permeation of hydrocarbons 0-30281  
 polymer, transport of organic liqs., review 0-16720  
 polyphenylquinoxaline-cellulose acetate, battery separator membrane, diffusion meas. 0-35574  
 porous, filtration characts., pore and particle size distrib. correl. (*Japanese*) 0-3418  
 porous hydrophobic membrane, anomalous gas mixture flow into liqs. 0-40744  
 potentials, meas. in ionic environment, biological membrane simulation 0-3412  
 potentials measurements 0-3411  
 regenerated cellulose-activated charcoal membrane adsorpt. characts. for haemoperfusion (*Japanese*) 0-12298  
 rotating circular cylindrical elastic membranes bifurcation 0-33494  
 selectivity, influence of particle/pore size ratio 0-11946  
 smectic lipid bilayer, in cryst. matrix, phase transition 0-21453  
 spatial light modulator with CCD address 0-48445  
 steady nonionic countergradient transport through membranes by coupled diffusion [dialysis application] 0-16718  
 synergetics, chemical processes far from equilb., conf. Bordeaux, France (Sept. 78) 0-3334  
 thick membrane strip, effect of shearing prestress, static case 0-10137  
 thick membrane strip, effect of shearing prestress on response, dynamic case 0-10138  
 thin circular membrane, forced symmetric vibrs. 0-10181  
 vibration, functionals method for lateral vibr. freqs. determ. (*Japanese*) 0-12918  
 Au thin films, with nm-sized pores, prep. from Au-Ge eutectic films by etching 0-16227  
 CrFeCN epoxy resin-based membrane studies, Ag sensitive electrode 0-16726  
 H production, electrolytic, using inorganic ion exchange membrane 0-45804

**memories see digital storage****memory devices see storage devices****mendelevium**

see also nuclei with .....

No entries

**mendelevium compounds**

No entries

**mercury (metal)**

see also nuclei with .....

- atom, 6D levels excited by dye laser, lifetimes 0-42996  
 atom, electron impact ionisation cross-sections for excited states 0-9742  
 biological material analysis, As and Hg determ. by neutron activation anal. 0-36216  
 cathode,  $\text{H}^+$  ( $\text{D}^+$ ) discharge activation energies in  $\text{H}_2\text{O}$  ( $\text{D}_2\text{O}$ ) 0-40707  
 cathode, motion of cathode spot of vacuum arc 0-54069  
 concentration meas. in South Atlantic Bight 0-4046  
 diffusion of Al, diffusion coeff. meas. 0-24627  
 distribution in Gulf Stream waters 0-7965  
 dropping Hg electrode, synchronisation in natural drop expts., high speed device 0-37049  
 electrical and thermodynamic props. in metal-semicond. transition range 0-20144  
 flow, unsteady stagnation heat transfer through laminar, incompressible boundary layer 0-1584  
 flow of liquid metals in curved channels laminar, transversely applied mag. field 0-14829  
 intercalation with graphite and alkali metal 0-44183  
 liquid, ferromagnetic, containing Fe particles, time depend. magnetisation 0-44877  
 liquid, sound vel. near metal-nonmetal transition, up to 1600°C and 2000 kg/cm<sup>2</sup> 0-39222  
 liquid structure, X-ray diff. obs., 173-473K 0-14997  
 S.New England coastal rain, Hg flux 0-41508  
 partial vapour pressure, determ. for volatile component by static method 0-37150  
 photoemission, transition from ordered solid to disordered liquid 0-45217  
 plasma, optically pumped positive column, E-I characts. 0-44035  
 plasma flow, electron temp. determ. from partial LTE populations 0-24248  
 pollution of Mediterranean sediments around Alexandria, Egypt 0-3538  
 pool boiling heat transfer in mag. field 0-33584  
 radiochemical neutron activation anal. of environmental matrices for Hg and noble metals 0-16889  
 sediment pollution by Hg and As, instrumental neutron activation and atomic abs. spectrometric anal. 0-16890  
 self-diffusion coeffs. by radioactive tracer technique 0-49392  
 superconducting transition temp., perturbative corrections, direct and indirect ladder diagrams 0-49979  
 surface tension, in Rankine-type capillary viscometer (*Japanese*) 0-14859  
 Townsend discharge, electron swarm props. Boltzmann eqn. anal. 0-19648  
 turbulent flow on stabilising thermal section, temp. fields and heat transfer 0-19366  
 valence band spectra by PES study 0-4822  
 vapour, viscosity and thermal cond. meas., data anal., 694-1054K 0-19545  
 vapours, viscosity meas. by vibr. disc method, 620-800K 0-19530  
 volatilisation losses during neutron irradiation in a reactor 0-13596  
 volatility, in NAA from samples and standards (*Russian*) 0-41128  
 Au/Hg probe for C-V meas., work function difference between probe and Si 0-2450  
 $\text{Bi}_2\text{Se}_3$ -Hg point defects in crystal lattice, Hall coefficient and IR spectra determ. 0-55129

**mercury (metal) continued**

- $\text{DyI}_3$ -Hg arc discharge plasma, spectroscopic study 0-54033  
 Ge:Hg, S-type diode, elec. props. 0-20299  
 Ge:Hg S-type diodes, photoelec. props. 0-6964  
 $^3\text{He}$ -Hg ( $-\text{Kr}$ ) +  $^3\text{He}$ (n,p)T, high press. plasma excitation, luminesc. spectra 0-38719  
 Hg 6  $^1\text{S}_0$ -Hg 6  $^1\text{P}_1$ , Van der Waals term in interaction, blue satellite line (*French*) 0-37848  
 Hg 6  $^3\text{P}_1$  collisional transfer rate between m-sublevels mag. field depend. 0-32802  
 Hg vapour, absorpt. spectrum, 1849 Å line, self-broadening, interatomic interaction (*French*) 0-32661  
 Hg/electrolyte contacts, adsorption model for double-layer capacitance 0-44706  
 Hg/ $\text{Na}_2\text{B}_4\text{O}_7 \cdot 10\text{H}_2\text{O}$  contacts, double-layer capacitance, temp. depend. 0-44707  
 Hg-Ar, HF discharge, electron energy distrib. and atom ionisation processes 0-44048  
 Hg-Ar mixture, RF discharge, frequency characts. investig. 0-38761  
 Hg-I ANL-4 cycle for thermochem. H prod. 0-35785  
 Hg-in-glass thermostat 0-22359  
 Hg-KI solution interface, specific adsorption of I ions, electrical double layer, interface excess activity coeff. 0-49523  
 Hg-Tl-I discharges, 50 H<sub>2</sub>, Tl atoms axial segregation 0-38781  
 Hg-Xe film, random mixtures, superconducting transition temp. and metal-nonmetal transition 0-29498  
 Hg + halomethane,  $^3\text{P}_1$ -state total quenching 0-52927  
 Hg + Hg, gas discharge plasma, collision cross section anal. 0-33735  
 Hg + Hg<sup>+</sup>, combination into ugrader dimer states 0-55633  
 Hg + Na(K)(Rb), 15-1400 eV, electronic excitation, integral cross sections 0-43159  
 Hg + Tl, excitation energy transfer, excitation rate consts. 0-37772  
 Hg<sub>2</sub>, dissociative recomb. and optical transmissions meas. in high press. discharge 0-37816  
 Hg<sub>2</sub>, emission and form. kinetics, sequential two-photon absorpt. expt. 0-32767  
 Hg<sub>2</sub> excimers, photoassoc., spectroscopy and kinetic processes of high-lying vibronic states, laser applics. 0-9649  
 Hg<sub>2</sub>, quenching and predissociation, possible excimer laser 0-32770  
 Hg<sub>2</sub> vapour, high-press., selective refl. meas. up to 700 bar 0-28031  
 Hg<sub>2</sub><sup>+</sup>, electronic struct. and photoabsorpt. calcs. 0-27932  
 $^{199}\text{Hg}^m$  and  $^{190m-185m}\text{Hg}$ , nucl. spins, on-line quantum beat spectrosc. determ. 0-9562  
 $^{197}\text{Hg}$ , labelling of human albumin microspheres 0-51251  
 $^{199}\text{Hg}$  optically oriented atom interaction with cell wall paramag. centres 0-37762  
 $^{203}\text{Hg}$ , tracer for Hg conc. in seawater expts.  $^{75}\text{Se}$  tracer 0-21420  
 Hg( $6^1\text{P}_1$ ) + Hg( $6^1\text{S}_0$ ), collisional excitation transfer in high mag. fields, fluoresc. obs. 0-9689  
 n-InP-Hg, Schottky barrier height and stability characterisation 0-54786  
 liquid, polyvalent, electrical resistivity by harmonic model potential 0-54668

**Mercury (planet)**

- charged particle fluxes, electron calibration of Mariner 10 instrumentation 0-12628  
 cometary collision, origin of swirl patterns on surface 0-51675  
 EM heating, EM heating in early solar system 0-36555  
 lithosphere global TRM in presence of central dipole field, theory 0-31223  
 magnetic field and magnetosphere, Mariner 10 obs. and theory 0-36530  
 magnetic moment, deduction methods using limited data 0-36532  
 magnetosphere model 0-36531  
 orbital motion, Lorentz-covariant model of the system of two gravitating particles 0-8865  
 reflectance meas. in thermal emission region, thermal component removal 0-17497  
 regolith containing  $\text{Fe}^{2+}$ , refl. spectra, 0.65-2.5  $\mu\text{m}$  0-56736  
 surface features and internal structure, post-Mariner 10 assessment 0-12697  
 swirl patterns produced by comet collision 0-51675

**mercury alloys**

see also mercury compounds

- Wood's alloy, liq. enthalpy effects when solute is added 0-39314  
 Ag-Sn-Hg, metallic powder-liquid system, correlation between hardness and evolution and sintering states 0-25614  
 $\text{Cd}_3\text{Hg}_{45}$ , X-ray study of cryst. struct. and thermal expansion 0-24405  
 $\text{Cd}_3\text{Hg}_{35}$ , X-ray study of cryst. struct. and thermal expansion 0-24405  
 Hg-Ag-Sn, dental amalgams, corrosion penetration in crevices 0-3238  
 Hg-Cd-(Te), partial vapour pressure, determ. for volatile component by static method 0-37150  
 Hg-K, liquid, structure factors, X-ray scatt. (*Japanese*) 0-54122  
 Hg-Na, liquid, structure factors, X-ray scatt. (*Japanese*) 0-54122  
 Hg<sub>2</sub>-Pt,  $^{199}\text{Hg}$  Mossbauer meas., isomer shift and quadrupole splitting calcs. 0-28039  
 Ni amalgam, anodic polarisation in alkaline soln. 0-11823  
 UHg prep. from uranyl ion using two-compartment electrolyser 0-802  
 Zn-Sn-Hg, diagram of state, melting temp., peritectic and eutectic phases (*Russian*) 0-55350

**mercury compounds**

see also mercury alloys

- halide electrically excited dissociation laser, kinetic processes 0-38013  
 halide electronic transition laser, quantum chem. 0-32971  
 hexaphenylene mercury, bright-field imaging of single heavy atoms in an electron microscope with superconducting lens system 0-10472  
 $\alpha$ -HgS, cryst. growth from soln. at low temps. 0-7487  
 plasmon refl., 86 to 320K 0-50346  
 Ag<sub>2</sub>HgI<sub>4</sub>, disordered multicomponent solid solutions conc. fluctuation waves, microscopic theory 0-44327  
 (Cd,Hg)Te, photoconductive detector, uncooled, for 8-14  $\mu\text{m}$  region 0-31868  
 Cd-Hg-Te, phase diagram, computer estimation 0-20903  
 CdHg, excimer kinetics and transmission meas. 0-37832  
 CdHg, fluoresc. kinetics, optical excitation, energy spacings and equilb. consts. 0-43090  
 Cd, Hg<sub>1-x</sub>Se, narrow band gap semicond., electron scatt., and transport phenomena 0-49706  
 n-Cd<sub>0.2</sub>Hg<sub>0.8</sub>Te, fundamental absorption edge, influence of temp. 0-20640  
 Cd, Hg<sub>1-x</sub>Te, band struct. and optical props. 0-15450  
 n-Cd, Hg<sub>1-x</sub>Te, conduction band struct., IR refl. spectra obs. 0-39502



## mercury compounds continued

- Cd,Hg<sub>1-x</sub>Te, correlation between structural and chemical inhomogeneity (*Russian*) 0-49484  
 Cd,Hg<sub>1-x</sub>Te, current-voltage charact., pinch effect, mag. field effects 0-6858  
 Cd,Hg<sub>1-x</sub>Te, effects of electron heating at low temps. 0-49823  
 Cd,Hg<sub>1-x</sub>Te, influence of nonparabolicity on transverse magnetoresist. near transition to zero gap 0-20228  
 Cd,Hg<sub>1-x</sub>Te, low temp. piezoresistance, Hall effect, elec. cond., plastic flow 0-6844  
 Cd,Hg<sub>1-x</sub>Te photoconductive detectors, 77 to 300K, normalised thermal figure of merit 0-31878  
 Cd,Hg<sub>1-x</sub>Te, photomagnetic and galvanomagnetic effects in quantising mag. fields 0-20223  
 Cd,Hg<sub>1-x</sub>Te, photothermomag. effect and photocond. in millimetre wavelength range 0-44657  
 n-Cd,Hg<sub>1-x</sub>Te, single crystal, scattering mechanism on intensity of 1/f noise 0-39642  
 Cd,Hg<sub>1-x</sub>Te, variable-gap structures, galvanomagnetic effects 0-11014  
 Cd,Hg<sub>1-x</sub>Te, zero gap semiconductor, interband optical-phonon scattering 0-6846  
 Cd,Hg<sub>1-x</sub>Te:(Ag), impurity diffusion, gamma-ray effects 0-54441  
 p-(Hg,Cd)Te, carrier lifetime, dominant Auger transitions comparison 0-49768  
 (Hg,Cd)Te n<sup>+</sup>-p photodiodes, 8 to 12  $\mu$ m IR imaging appls. 0-9044  
 (Hg,Cd)Te photodiode IR detectors, planar technology 0-9043  
 (Hg,Cd)Te photodiodes, wide-bandwidth 10.6  $\mu$ m IR heterodyne detect. 0-9042  
 Hg<sub>3-6</sub>AsF<sub>6</sub>, linear chain compound, mag. field induced residual resist., anisotropic supercond. 0-24897  
 Hg<sub>3-6</sub>AsF<sub>6</sub>, one dimens. fluctuations and chain ordering transform 0-24593  
 Hg<sub>3-6</sub>AsF<sub>6</sub>, one dimensional phonons and chain ordering 0-24544  
 Hg<sub>3-6</sub>AsF<sub>6</sub>, quasi one-dimensional, anomalous magnetoresistance 0-24884  
 Hg<sub>3-6</sub>AsF<sub>6</sub>, space group symmetry and phase ordering 0-6396  
 Hg<sub>3-6</sub>AsF<sub>6</sub>, theory of phase transitions 0-6486  
 Hg<sub>3-6</sub>AsF<sub>6</sub>, linear chain metallic cpd., square Fermi surface model for conduction 0-6822  
 Hg<sub>3-6</sub>AsF<sub>6</sub>, linear chain cpd., open orbits, induced torque meas. 0-29309  
 Hg<sub>3-6</sub>AsF<sub>6</sub>, supercond., absence of surface Hg 0-20350  
 HgBr electrically excited dissociation laser, kinetic processes 0-38013  
 HgBr emission intensity, HgBr<sub>2</sub> dissociative excitation by inert gas and N<sub>2</sub> metastables 0-40687  
 HgBr, laser photolysis prep., laser induced fluoresc., collisional quenching processes 0-38014  
 HgBr laser using dissociative excitation of HgBr<sub>2</sub>, extraction efficiency increased by N<sub>2</sub> addition 0-38012  
 HgBr, polarised photofluoresc. spectroscopy, HgBr<sub>2</sub> photodissociation by ArF laser 0-37841  
 HgBr<sub>2</sub> dissociation laser, elec. excited, kinetic processes 0-48231  
 HgBr<sub>2</sub>, dissociative excitation for HgBr laser, extraction efficiency increased by N<sub>2</sub> addition 0-38012  
 HgBr<sub>2</sub>, dissociative excitation by inert gas and N<sub>2</sub> metastables, HgBr emission intensity 0-40687  
 HgBr, photodissociation by ArF laser, characterisation of transition prod. HgBr(B<sup>2</sup> $\Sigma^+$ ) 0-37841  
 HgBr<sub>2</sub>/HgBr dissociation laser, oscillator and oscillator-amplifier expts. 0-48232  
 HgBr<sub>2</sub>+K, laser irr., HgBr\* form., chemiluminescence 0-55658  
 HgBr\*, collisional quenching by inert gas (molecule) 0-42986  
 HgBr\*, collisional quenching by inert gas (molecules) 0-43091  
 HgBr\* form. from laser irr., K+HgBr<sub>2</sub>, chemiluminescence 0-55658  
 Hg<sub>1-x</sub>Cd<sub>x</sub>Ge, quantum oscillations of magnetoresistivity (*Russian*) 0-11007  
 Hg<sub>1-x</sub>Cd<sub>x</sub>Se, IR absorpt. spectra, band struct., refr. index 0-50337  
 Hg<sub>1-x</sub>Cd<sub>x</sub>Se, zinc blende structure, optical and electronic properties 0-6723  
 HgCdTe, Magneto transport anomalies at low carrier densities, Wigner crystallisation 0-20222  
 HgCdTe, narrow band gap semiconductor IR devices, advances 0-48464  
 n-HgCdTe, photocond., Hall mobility and resist. 0-34478  
 HgCdTe Schottky barrier diode and n-p diffused junction IR detectors, comparison 0-9039  
 HgCdTe-CdTe IR detector arrays, 3 to 11  $\mu$ m, fabrication techniques 0-9041  
 Hg<sub>0.60</sub>Cd<sub>0.40</sub>Te, LPE growth from Te-rich soln. 0-7508  
 Hg<sub>0.75</sub>Cd<sub>0.25</sub>Te, single crystal, reflection spectra 0-40140  
 Hg<sub>0.75</sub>Cd<sub>0.25</sub>Te, thermoref. spectra, effect of excitons on E<sub>1</sub> and E<sub>1</sub>+ $\Delta_1$  structs. 0-16057  
 Hg<sub>0.79</sub>Cd<sub>0.21</sub>Te, ion implanted, elec. props. 0-20184  
 n-Hg<sub>0.4</sub>Cd<sub>0.6</sub>Te, microwave bolometer heterodyne receiver based on magnetic field induced phase transition 0-13135  
 Hg<sub>1-x</sub>Cd<sub>x</sub>Te, acceptor bound exciton Auger and radiative transition rates, radiative recomb. 0-6733  
 Hg<sub>1-x</sub>Cd<sub>x</sub>Te, acceptor impurity band form. 0-20119  
 Hg<sub>1-x</sub>Cd<sub>x</sub>Te, anodic oxide films, formation and props. 0-3212  
 Hg<sub>1-x</sub>Cd<sub>x</sub>Te, carrier conc., Hall effect, photocond., IR spectra meas. 0-49771  
 Hg<sub>1-x</sub>Cd<sub>x</sub>Te, for appl. in IR detector arrays, comp. control 0-31872  
 Hg<sub>1-x</sub>Cd<sub>x</sub>Te IR photodetectors for night vision appl. 0-22429  
 Hg<sub>1-x</sub>Cd<sub>x</sub>Te interface with native oxide, elec. props. 0-20318  
 Hg<sub>1-x</sub>Cd<sub>x</sub>Te, LPE current controlled 0-40272  
 Hg<sub>1-x</sub>Cd<sub>x</sub>Te, LPE growth and characterisation 0-50565  
 Hg<sub>1-x</sub>Cd<sub>x</sub>Te, magneto-optical and impurity effects 0-6721  
 Hg<sub>1-x</sub>Cd<sub>x</sub>Te, mixed crystals, crystn. by chemical transport 0-20775  
 Hg<sub>1-x</sub>Cd<sub>x</sub>Te, n-surface inversion layers study 0-25017  
 Hg<sub>1-x</sub>Cd<sub>x</sub>Te, narrow-gap semiconductor, high intensity IR transmission limit 0-7361  
 Hg<sub>1-x</sub>Cd<sub>x</sub>Te, nonlinear optical effects 0-14389  
 Hg<sub>1-x</sub>Cd<sub>x</sub>Te photodiodes, for IR detection 0-13144  
 Hg<sub>1-x</sub>Cd<sub>x</sub>Te photodiodes, implanted n<sup>+</sup>-p, improved performance using insulated field plates 0-52309  
 Hg<sub>1-x</sub>Cd<sub>x</sub>Te, photolum. and optical pumping 0-50424  
 Hg<sub>1-x</sub>Cd<sub>x</sub>Te, semiconducting phase, acceptor states and galvanomagnetic effects 0-11017  
 Hg<sub>1-x</sub>Cd<sub>x</sub>Te, two-photon absorpt. spectra 0-20660  
 Hg<sub>1-x</sub>Cd<sub>x</sub>Te, vaporisation under Knudsen effusion conditions 0-2154  
 Hg<sub>1-x</sub>Cd<sub>x</sub>Te-oxide interfaces, MIS capacitance charact. 0-49926  
 Hg<sub>1-x</sub>Cd<sub>x</sub>Te, (x<0.16), semimetallic phase, acceptor states and galvanomagnetic effects 0-6882

## mercury compounds continued

- Hg,Cd<sub>1-x</sub>Te, zero-gap props. correlated to  $\Gamma_8$  symmetry, review 0-6717  
 HgCl, photodissociation cross section, laser extraction efficiency 0-32972  
 HgCl, photodissociation calcs., laser efficiency 0-48047  
 HgCl photolytically pumped laser system, quantum chem. 0-32971  
 HgCl<sub>2</sub>, <sup>35</sup>Cl powder Zeeman NQR, injection and phase locked NQR spectrometer 0-54979  
 HgCl<sub>2</sub>, deformation densities, relativistic effect 0-42928  
 HgCl<sub>2</sub>-PbCl<sub>2</sub>, Raman spectra, solid and melt, species identification (*German*) 0-45083  
 HgCl\*, collisional quenching by inert gas (N<sub>2</sub>) 0-42986  
 HgCr<sub>2</sub>S<sub>4</sub>, spinel, mag. struct., symmetry anal. in neutron diffr. studies 0-25091  
 HgCr<sub>2</sub>Se<sub>4</sub>, Cd, precipitations during growth by chem. transport method 0-55409  
 HgF<sub>2</sub>, electronic structure of outermost levels, UPS study 0-7468  
 Hg<sub>2</sub>F<sub>2</sub>, <sup>199</sup>Hg Mossbauer meas., isomer shift and quadrupole splitting calcs. 0-28039  
 Hg<sub>1-x</sub>Fe<sub>x</sub>Te mixed crystals, zero gap, magneto-optical evidence of exchange interactions 0-45045  
 HgGa<sub>2</sub>S<sub>4</sub>, melt growth, optical props. and SHG, HgS-HgGa<sub>2</sub>S<sub>4</sub> phase diagram 0-50548  
 HgGa<sub>2</sub>S<sub>4</sub>, energy band struct. calc., empirical pseudopot. method 0-24793  
 HgGa<sub>2</sub>Se<sub>4</sub>, energy band struct. calc., empirical pseudopot. method 0-24793  
 HgH<sup>+</sup>, HgH<sub>2</sub>, relativistic (non-relativistic) HF one-centre expansion calcs. 0-52908  
 HgI<sub>2</sub>, cryst. growth by multiple vacuum sublimation 0-7485  
 $\alpha$ -HgI<sub>2</sub>, Raman scatt. at room temp., improved polarisation spectra 0-25368  
 HgI<sub>2</sub>, red anisotropic polariton dispersion, reson. Brillouin scatt. 0-7366  
 HgI<sub>2</sub>, relativistic effects, photoelectron spectra, Hartree-Fock-Slater method, perturbation theory approach 0-27962  
 $\alpha$ -HgI<sub>2</sub>, single cryst. growth from iodomercurate complexes 0-35069  
 $\alpha$ -HgI<sub>2</sub>, single cryst. growth from dimethylsulfoxide complexes 0-35070  
 HgI<sub>2</sub> thin sections with Peltier-cooled preamplification for X-ray spectrosc. 0-324  
 Hg<sub>2</sub>I<sub>2</sub>, cryst. growth by multiple vacuum sublimation 0-7485  
 HgI\*, collisional quenching by inert gas (N<sub>2</sub>) 0-43091  
 Hg<sub>1-x</sub>Mn<sub>x</sub>S, EPR, order-disorder transition temp. 0-50176  
 Hg<sub>1-x</sub>Mn<sub>x</sub>Se, band struct. from anomalous Shubnikov-de Haas effect 0-20080  
 Hg<sub>1-x</sub>Mn<sub>x</sub>Se, EPR, order-disorder transition temp. 0-50176  
 Hg<sub>1-x</sub>Mn<sub>x</sub>Se, spin-orbit coupled bands, indirect exchange interaction via electrons 0-34407  
 Hg<sub>1-x</sub>Mn<sub>x</sub>Te, acceptor reson., states in high mag. field 0-49668  
 Hg<sub>1-x</sub>Mn<sub>x</sub>Te, EPR, order-disorder transition temp. 0-50176  
 Hg<sub>1-x</sub>Mn<sub>x</sub>Te, energy levels at  $\Gamma$ -point in intense mag. fields, Shubnikov-de Haas effect meas. 0-24951  
 Hg<sub>1-x</sub>Mn<sub>x</sub>Te, mag. field induced microwave transparency 0-49797  
 Hg<sub>1-x</sub>Mn<sub>x</sub>Te, mag. props., self-consistent two spin cluster model 0-54874  
 Hg<sub>1-x</sub>Mn<sub>x</sub>Te, mag. susceptibility, 2.4 to 300K 0-20379  
 Hg<sub>1-x</sub>Mn<sub>x</sub>Te, magneto-optical and impurity effects 0-6721  
 Hg<sub>1-x</sub>Mn<sub>x</sub>Te, Shubnikov de Haas effect and quantum oscills. of thermoelec. power 0-49781  
 Hg<sub>1-x</sub>Mn<sub>x</sub>Te, spin-orbit coupled bands, indirect exchange interaction via electrons 0-34407  
 Hg<sub>1-x</sub>Mn<sub>x</sub>Te, zero-gap semicond., indirect-exchange interactions 0-29370  
 HgS, cinnabar, photoelectron X-ray spectroscopy study 0-29858  
 $\alpha$ -HgS, cinnabar, reson. Raman effect and luminesc. meas. 0-50338  
 $\alpha$ -HgS, electronic energy level calcs. 0-6718  
 $\gamma$ -Hg<sub>2</sub>S<sub>2</sub>Cl<sub>2</sub> order-disorder structures, desymmetrisation 0-38986  
 HgSO<sub>4</sub>·H<sub>2</sub>O, X-ray and neutron diffr. study of struct. 0-33936  
 HgS(Se), reaction with Sn chalcogenides, thermodynamic anal. 0-40728  
 HgSe, Fermi surface anisotropy parameters, magneto-optical effect 0-25350  
 HgSe, gas, identification by high-temp. mass spectrometry 0-45593  
 HgSe, magneto-optical and impurity effects 0-6721  
 HgSe, narrow band gap semicond., electron scatt., and transport phenomena 0-49706  
 HgSe, Shubnikov-de Haas determ. of electron g factors 0-6704  
 HgSe, zero-gap props. correlated to  $\Gamma_8$  symmetry, review 0-6717  
 HgSe:In, enrichment of doping substances at pseudo phase boundaries (*German*) 0-29036  
 HgSe/CdSe lattice-matched heterostructs. as Schottky barriers, CVD epitaxial growth and elec. props. 0-49877  
 HgTe, acceptor reson., states in high mag. field 0-49668  
 HgTe, and ternary compounds, mag. field induced microwave transparency 0-49797  
 HgTe, electron conc. temp. depend., 1.6 to 32K, Hall effect and cond. meas. 0-24952  
 HgTe film, vac. deposited, elec. props. 78-420K 0-11119  
 HgTe, long-wavelength magneto-absorptions 0-11397  
 HgTe, magnetophonon oscills. of thermoelec. power 0-49789  
 HgTe, narrow band gap semicond., electron scatt., and transport phenomena 0-49706  
 HgTe, pressure-induced polymorphic transition 0-10667  
 HgTe, quantum galvanomag. effects 0-49782  
 HgTe thin film Hall sensor fabrication 0-2951  
 HgTe type semiconductors, spin-flip transitions in magneto-optics and magneto-transport 0-50306  
 HgTe, VPE growth control by EM irr., (*Russian*) 0-34338  
 HgTe, vacancy mech. of resorption of Hg droplets 0-39070  
 HgTe, zero gap semiconductor, resonant acceptor states 0-6772  
 HgTe, zero-gap props. correlated to  $\Gamma_8$  symmetry, review 0-6717  
 HgTe, zero-gap semicond., absorpt. spectrum in mag. field 0-11370  
 HgTe:In, enrichment of doping substances at pseudo phase boundaries (*German*) 0-29036  
 HgTe-CdTe ideal superlattice, electronic props. calc. 0-49885  
 (HgTe)<sub>1-x</sub>(CdTe)<sub>x</sub>, diamond-type semiconductor, Mossbauer spectra, quadrupole interaction of <sup>125</sup>Te 0-44992  
 HgTe:(Ag), impurity diffusion, gamma-ray effects 0-54441  
 HgTl optically excited excimers, upper state kinetics 0-37831  
 Hg<sub>2</sub>X<sub>2</sub> (X=Cl, Br, I), calomel family, single crystals, microhardness using Vickers method 0-25848  
 NH<sub>4</sub>HgCl<sub>3</sub>, high resolution heat capacity meas. (*Japanese*) 0-52218  
 $\alpha$ -NH<sub>4</sub>HgCl<sub>3</sub> quasioctahedral dimensional type cryst., phase transition statistics, molecular field approx. calcs. 0-34190  
 $\alpha$ -NH<sub>4</sub>HgCl<sub>3</sub>, Raman study of phase transition (*French*) 0-11378  
 Pb<sub>1-x</sub>Hg<sub>x</sub>S electroless-deposited films, optical and elec. props. 0-7011



**mercury compounds continued**

$\text{Zn}_2\text{Hg}_{1-x}\text{Se}$ , band struct. from Shubnikov-de Haas effect and hydrostatic press. meas. 0-49599  
 $\text{Zn}_2\text{Hg}_{1-x}\text{Se}$ , galvanomagnetic effects, Shubnikov-de Haas oscill. determ. of band struct. 0-6884

**mercury lamps** *see mercury vapour lamps***mercury vapour lamps**

No entries

**m.e.s.f.e.t.** *see Schottky gate field effect transistors***mesic atoms**

atomic negative meson capture, nuclear giant resonance excitation (*Russian*) 0-42623  
 conference on high energy physics and nuclear struct. Vancouver, Canada (Aug. 1979) 0-41936  
 mesoatoms in static electromagnetic fields, excited state lifetimes and population, nuclear moments (*Russian*) 0-53170  
 nuclear bound states of  $k^-$ ,  $p$  and  $\Sigma$  0-13399  
 pionic atom, X-ray intensity, at. no. variation,  $Z=5-90$  0-43212  
 pionic atoms, nuclear and atomic research review 0-43216  
 relativistic  $\pi$ -mesic atom, eigenfunctions and eigenenergies, N-space dimensions calcs. 0-41988  
 stimulated production, photoassociation, induced, in field of strong EM wave (*Russian*) 0-1091  
 strongly bound  $\pi^-$  nuclear states, vel. depend. pot. binding, pionic atoms 0-37331  
 $Z=8-50$  kaonic atoms, X-rays, strong interaction effects 0-9763  
 C, pionic X-ray intensities in graphite 0-32858  
 $^{40}\text{Ca}$ ,  $A=40$ , 42-44, 48, pionic X-rays, strong interaction and isotope shifts,  $\pi$ -nuclear optical pot. 0-53169  
 $\text{Cd}+\text{Te}$ ,  $\pi^-$  capture, radioactivity meas. 0-47831  
 H, kaonic, strong interaction effects,  $K^-p$  scatt. length Coulomb corrections 0-14257  
 H, mesonic primary population, formation cross section by Born approx. 0-43214  
 $\text{H}_2\text{-D}_2\text{-T}_2$  mixtures, mesic at. and mol. processes 0-23580  
 $^4\text{He}$ ,  $A=3,4$ , pionic 1s state energy shift and line broadening (*German*) 0-48107  
 $^{16}\text{O}$ ,  $A=16,18$ , pionic 1s state energy shift and line broadening (*German*) 0-48107  
 $^{48}\text{Ti}$ ,  $A=46, 48, 50$ , pionic X-rays, strong interaction and isotope shifts,  $\pi$ -nuclear optical pot. 0-53169  
 $\text{Zn}+\text{Se}$ ,  $\pi^-$  capture, radioactivity meas. 0-47831

**mesic molecules**

stimulated production, photoassociation, induced, in field of strong EM wave (*Russian*) 0-1091  
 $\text{H}_2\text{-D}_2\text{-T}_2$  mixtures, mesic at. and mol. processes 0-23580

**mesomorphic state** *see liquid crystals***meson absorption**

$\text{Cd}+\text{Te}$ ,  $\pi^-$  capture, radioactivity meas. 0-47831  
 $\text{Zn}+\text{Se}$ ,  $\pi^-$  capture, radioactivity meas. 0-47831

**meson-baryon interactions**

*see also kaon-baryon interactions; meson-baryon scattering; pion-baryon interactions*  
 meson spectra in forward jets, hadron cascade model anal. 0-32103  
 resonance-nucleon and particle beam-nucleon scatt. cross sections (*Russian*) 0-32115

**meson-baryon scattering**

*see also kaon-baryon scattering; meson-baryon interactions; pion-baryon scattering*  
 bag model  $Q^2Q$  states, meson-nucleon low-energy S-wave scatt., P-matrix formalism 0-13271  
 data amalgamation technique 0-37293  
 gauge-dual-topological approach to soft hadronic reactions, trajectory slopes 0-18142  
 QCD, heavy-vector meson-nucleon scatt., cross section suppression, T and  $\psi$  0-22564

**meson capture**

*see also mesic atoms; mesic molecules; radioactivity*  
 $\text{CH}_2(\text{CD}_2)$ , pionic X-ray intensities in polyethylene( $-d_n$ ) 0-32858  
 $^{16}\text{O}(\pi,\gamma n)$ , direct and resonance reaction unified shell model, n,  $\gamma$  spectra 0-52696

**meson decay**

*see also kaon decay; meson hadronic decay; meson leptonic decay; pion decay*  
 hadronic charmed particle decays, quark and particle helicities, charm changing current chirality 0-37256  
 neutral charmed particle decay, direct observation in  $\nu$ -emulsion interactions 0-9165  
 nonlocal quark model in  $\text{SU}(3)\times\text{SU}^c(3)\times\text{U}(1)$ , meson decay and mass correction (*German*) 0-27456  
 orthoquarkonium decay, Dalitz plot population and thrust ang. distrib., scalar gluon nonexistence 0-27470  
 P-wave radial mixing, effect on E1 radiative decays, charmonium mass 0-37271  
 resonances, strong and EM decays, particle mixing and meson pole dominance 0-18127  
 b-quark meson, decay, weak mass mixing, CP violation 0-32086  
 $\text{B}^0\text{B}^0$  mixing in six quark model, decay, mass mixing and CP nonconservation 0-42406  
 c $\bar{c}$  and b $\bar{b}$  states, spectra and strong decays 0-52502  
 $\text{D}^0, \bar{\text{D}}^0$  decays, charm changing neutral current limits, QCD depend., mass differences 0-32062  
 $\text{D}^0-\text{D}^{\pm}$  lifetime difference, possible mechanism  $\text{D}^0\rightarrow s+\bar{d}+\text{gluon}$  0-37255  
 $\text{D}^+\text{D}^0$  decays and lifetimes assuming sextet dominance and colour clustering 0-32094  
 $\eta$ , vacuum symmetry, decay consts., mixing consts. in  $\text{SU}(3)\times\text{SU}(1)$  QCD 0-27483  
 $\eta\rightarrow\pi^0\gamma\gamma$  decay width and processes in chiral QFT (*Russian*) 0-32099  
 $\text{F}^+$  lifetime,  $\delta$  dominance and  $\text{W}^+$  exchange dominance 0-37254  
 $\psi, \psi'$ , DASP results on  $e^+e^-$  annihilation 0-42483  
 $\psi(3684)$  radiative decays, energy correlation 0-13307  
 x-boson, mass and asymmetric decay rel. to cosmological baryon asymmetry 0-4464

**meson detection and measurement**

high LET radiation therapy beams, expt. microdosimetry 0-12280  
 $\pi^-$  and  $\pi^+$ , stopping density distrib. in 1 and 2 dimensions 0-26340  
 $\pi^-$  broad therapeutic beams, microdosimetric characterisation 0-12277

**meson detection and measurement continued**

$\pi^-$  capture at rest, exptl. method for pion discrimination and absolute counting 0-5432  
 $\pi^-$  radiotherapy, biological effect prediction, star distrib. for high LET dose determ. 0-12248  
 $\pi^0\pi^0$  correlations determ. in  $pp\rightarrow\pi^0\pi^0$  0-5011

**meson-deuteron interactions**

*see also meson-deuteron scattering*  
 $K^-d\rightarrow\pi\Delta p$ ,  $\Sigma N$  bound state and  $\Delta p$  enhancement 0-47326  
 $\pi^-d$ , 15 MeV, charged multiplicity distrib. and rescatter probabilities 0-52545  
 $\pi^-d\rightarrow\pi^-pn$ , 438 GeV/c, break up process, kinematic variables, np final state interaction (*Russian*) 0-52701  
 $\pi^-d\rightarrow\pi^-pn$  final state interactions and d breakup for 438 MeV/c  $\pi^-$  impulse (*Russian*) 0-18145  
 $\pi^-d\rightarrow\pi^0nn$ , transition rate of charge exchange process 0-435  
 $\pi^-d\rightarrow\rho^0\pi^-d$ , 9 GeV exchange Deck model anal. 0-47322  
 $\pi^+d$ , 15 GeV/c, many-pion prod. and resonant prod. cross sections 0-22642

**meson-deuteron scattering**

*see also meson-deuteron interactions*  
 $K_L^0K_S^0$  transmission regeneration on deuterons and neutrons, 10 to 50 GeV/c 0-4985  
 $\pi d$ , microscopic theory, review 0-47511  
 $\pi d$  elastic scatt., 142-256 MeV, dibaryon resonance interference with Faddeev amplitudes 0-32123  
 $\pi^-d$ , 552 MeV/c, elastic differential cross section Glauber theory anal. (*Russian*) 0-52700  
 $\pi^-d$  1.57, 1.66 and 1.76 GeV/c elastic back scatt. cross section energetic shape struct. (*Russian*) 0-47510

**meson effects**

biomedical experiences with  $\pi^-$ , conf., Brugg-Windisch, Switzerland (Dec. 1978) 0-22138  
 Ehrlich ascites carcinoma cells, effects of pions $^-$  rel. to electrons and X-rays 0-26267  
 pion $^-$  radiation, uniform depth-dose distrib. technique and cell survival obs. 0-17139  
 radiosensitivity of CHO cells, negative pions rel. to X-rays at various cell stages 0-17021  
 RBE of mouse skin damage, pions $^-$  rel. to X-rays 0-26272  
 $\pi^-$ , cell survival over the depth profile after irradiation 0-26268  
 $\pi^-$ , chromatid breaks induced in Chinese hamster cells, rel. to X-irradiation 0-26270  
 $\pi^-$ , effect on brain vascular permeability of neonatal rats 0-26275  
 $\pi^-$ , effects on monolayers and spheroids of Chinese hamster cells 0-26269  
 $\pi^-$ , effects on mouse embryo pronuclear zygote stage 0-26274  
 $\pi^-$ , long-term effects on female mice rel. to X-rays 0-26273  
 $\pi^-$ , pre-clinical studies at TRIUMF 0-26264  
 $\pi^-$ , RBE and OER values from Vicia Faba root growth inhibition obs. 0-26271  
 $\pi^-$ , radiobiological data for clinical dosimetry in pion tumour therapy 0-26266  
 $\pi^-$ , suitability for use in radiotherapy, radiobiological obs. 0-26338

**meson field theory**

*see also nuclear forces*  
 $\sigma$  model,  $\text{SU}_2\times\text{SU}_3$ , modified Goldberger-Treiman relation, pseudoscalar form factor 0-27421  
 $A=16$  to 40, mag. moments, shell model calcs, mesonic exchange current effects, book contrib. 0-479  
 baryonium dual S-matrix approach 0-52526  
 chiral symmetry and pion condensation, review book contrib. 0-437  
 conference on interacting bosons in nuclear physics, Erice, Italy (June '78) 0-27042  
 deuteron wave functions, relativistic,  $\pi$ -NN coupling 0-22595  
 direct energy minimisation methods in self-consistent nuclear fields, ground state props. 0-22702  
 Green's function method for many-body problem for relativistic meson field theory, book contrib. 0-357  
 hadrons, extended, second-quantisation of strongly interacting fields 0-13270  
 isotopic spin and coherent states 0-4843  
 Kerr-Schild's gravitational fields, quantisation 0-31653  
 large amplitude collective motion, field theory, excitation, energies 0-22665  
 many-phonon monopole pairing vibrs. interaction in nuclear field theory, IBM 0-27578  
 massless boson, unified nonlinear theory 0-376  
 meson exchange, relativistic corrections, book contrib. 0-475  
 meson exchange currents, configuration mixing, role in nucl. mag. moment, beta decay, review, book contrib. 0-478  
 meson exchange currents, conservation principles, symmetries, book contrib. 0-473  
 meson exchange currents, effect in electron inelastic scatt., book contrib. 0-480  
 meson theory of nuclear vector and axial vector exchange currents, review, book contrib. 0-474  
 mesonic effects in photonuclear sum rules, book contrib. 0-476  
 mesonic exchange effect on nuclear mag. moment, expt. study, book contrib. 0-477  
 mesonic processes and quarks in nuclei 0-42564  
 mesons in nuclei, exchange current effects on nuclear mag. moments, book 0-471  
 mesons in nuclei, field theoretical aspects, book 0-481  
 multilocal field theory description of hadron struct. 0-9148  
 nuclear critical opalescence, pion field and condensation 0-42559  
 nuclear Dirac phenomenology, consistency with meson-nucleon interactions 0-9272  
 nuclear Dirac phenomenology and the  $\Lambda$ -nucleus potential, anomalous mag. moment 0-37344  
 nuclear exchange mag. moments, meson exchange currents, field theoretical approach 0-52574  
 nuclear field theory, Dyson boson expansion and Faddeev-Watson resummation technique 0-13385  
 nuclear field theory treatment of the interacting boson model 0-27577  
 nuclear pion field struct., book contrib. 0-482  
 nuclei, description in relativistic field theory, book contrib. 0-358  
 nucleon-nucleon interaction and nuclear forces, meson exchange 0-32195  
 parity violating nucl. force, unified treatment 0-47400  
 pion condensation, field theoretic many-body system 0-22703



## meson field theory continued

- pion condensation and the pion-nuclear interaction, book contrib. 0-485  
 pion condensation in nuclear matter, book contrib. 0-484  
 pion condensation threshold in finite nuclei 0-18218  
 pion excitations and phase transitions in nuclear matter, review, book contrib. 0-483  
 quantised gravitational interaction with meson field 0-31652  
 relativistic two-body forces in many-body systems, Weinberg and Yukawa interactions 0-32203  
 S-matrix for interaction of gravitational and Yang-Mills fields 0-42315  
 scalar meson field and many-body forces, book contrib. 0-359  
 virtual mesons effect on hadron-nucleus reactions, book contrib. 0-472  
 Yukawa<sub>2</sub> QFT, Lorentz invariance of CPT invariant states 0-52381  
 Yukawa quantum field theory, Matthews-Salam integral representations 0-327  
 Yukawa quantum field theory in 2D space-time, linear  $N_f$  bound, locally Fock property 0-326  
 $(\pi, \pi')$  many body QFT framework anal., final state particle-hole correlations 0-13508  
 $\pi$  form factor, expt. behaviour, influence of left-hand cut on second Riemann sheet 0-13304  
 $\pi N$  scattering amplitude in nuclear matter, quantum field theory approach 0-42570  
 $\pi NN$  form factor,  $\Delta(1236)$  contrib., calc. 0-22609  
 $^{12}\text{C}$  M1 (15.11 MeV) form factor, evidence for nuclear pion field critical opalescence 0-32232  
 $^9\text{Nb}$  B(EA) transitions, quasiparticle-phonon multiplet, nuclear field theory for superfluid nuclei 0-47427

## meson hadronic decay

- see also kaon hadronic decay  
 bottom meson weak hadronic decays, Kobayashi-Maskawa weak current model 0-42456  
 Cabibbo-suppressed nonleptonic D decays,  $\Delta I = 1/2$  rule 0-52501  
 charmed meson decay, interference effects, 2nd order suppressed amplitudes 0-4987  
 gluon observation in P-wave quarkonium decay 0-32068  
 heavy meson hadroproduction, QCD effect on scale breaking 0-37239  
 meson strong decay, 2 quark-antiquark pair model 0-52496  
 pseudoscalar and vector meson decays, triangular quark diagram anomalies,  $\psi$ ,  $\eta$  and  $\eta'$  appl. (Russian) 0-42455  
 quarkonia, S- and P-wave, gluon jets, perturbative QCD anal. 0-32070  
 quarkonia states, heavy, strong decay into other heavy flavours, and triple-gluon vertex 0-47279  
 Zweig rule in two-dimensional QCD,  $\psi$  and  $T$  decays 0-52479  
 $B \rightarrow J/\psi + \text{hadrons}$ , branching ratio, b quark decay calcs. 0-32095  
 $B \rightarrow \psi K^-$ , search for b flavoured baryons 0-42450  
 b quark- $\psi(\eta_c) + X$ , B branching ratios assuring colour suppression 0-37259  
 B-meson decays, Cabibbo patterns, QCD effects, Kobayashi-Maskawa model 0-42451  
 D meson decay,  $SU_4$  20-plet dominance model, inclusive branching ratios 0-13299  
 D mesons, anomalous Cabibbo suppressed decay ratios, simple model 0-42452  
 D to 2 body nonleptonic decays, quark model predictions 0-9164  
 $D^0 \rightarrow K^0 \pi^0$ , branching ratio from final state soft gluon exchange 0-52498  
 $D^0 \rightarrow K^+ K^-$ , Cabibbo suppressed decays, Penguin diagram contribution, mixing angles 0-22604  
 $D^0$  nonleptonic exclusive and semi-inclusive decays, pole model test 0-37258  
 $D^0$  prod. and decay in high energy photon interaction, mass and decay time 0-42478  
 $D^0 \rightarrow \pi^+ \pi^-$ , Cabibbo suppressed decays, Penguin diagram contribution, mixing angles 0-22604  
 $D^+$ ,  $D^0$  nonleptonic decays, vectorial colour octet qq annihilation 0-52500  
 $D^+$  decay, Cabibbo suppression, strong 20-plet dominance and W exchange 0-42453  
 $D^+$  nonleptonic decays, uniformly populated Dalitz plot, soft  $\pi$  theorem appl. 0-52503  
 $\eta \rightarrow 3\pi^0$ , chiral  $SU(4) \times SU(4)$  breaking and tadpole term 0-22532  
 $\eta \rightarrow \gamma \gamma (\pi^0 \gamma \gamma) (\pi^0 \pi^0 \pi^0)$ , neutral decay channels, possible  $3\pi^0$  system (Russian) 0-42454  
 $\eta \rightarrow \pi^+ \pi^- \gamma$ , rare decay modes near production threshold from  $\pi^- p \rightarrow \eta n$  reaction 0-9171  
 $F^+$  decay,  $SU_4$  20-plet dominance model, inclusive branching ratios 0-13299  
 $F^+$  decay widths and branching ratios, quark recombination widths, free quark model 0-27500  
 $\gamma(10.0)$ , two-body hadronic and radiative decays, pseudo-dimension rule,  $\pi\pi$  and  $KK$  suppression,  $SV_3$  singlet 0-52495  
 $J/\psi$  decay, gluon source, search for scalar gluonium, QCD 0-47296  
 $J/\psi \rightarrow \eta(\eta') \gamma$  decay rate, QCD sum rules 0-52497  
 $\omega(1670) \rightarrow B\pi$ , decay mode cross section from  $K^- p$  backward prod. 0-37257  
 $\phi \rightarrow \pi^+ \pi^-$ ,  $\pi$  form factor,  $\phi$  peak, unitarity and gluonic corrections 0-22615  
 $\psi$ , radiative decay, gluonic bound state  $O^-$  width 0-37272  
 $\psi(4.03) \rightarrow DD$ , suppression problems, model-independent approach 0-52494  
 $\psi(4.42) \rightarrow DD$ , suppression problems, model-independent approach 0-52494  
 $\psi(4.42) \rightarrow FF$ , suppression problems, model-independent approach 0-52494  
 $\psi(3100)$  decay, inclusive  $\gamma$  and  $\pi^0$  momentum spectra, direct  $\gamma$  prod. at large  $x$  0-42466  
 $\psi$  decay, high energy direct photons,  $\gamma$ ,  $\pi^0$  momentum distrib., QCD calcs. 0-32098  
 $\psi \rightarrow \eta(\eta') \gamma$ ,  $SU_3$  violation, symmetry breaking and decay amplitudes 0-52499  
 $\psi \rightarrow \eta(\eta') \gamma$ , Ward identity anal.,  $\eta, \eta'$  quark-gluon struct. 0-42449  
 $\psi(3685) \rightarrow P_c/\chi \rightarrow \gamma \gamma J/\psi(\pi^+ \pi^-) (\gamma K^+ K^-)$ , investig. of  $\gamma \gamma \mu^+$  final state 0-18132  
 $\psi \rightarrow \eta J/\psi(\pi^0 J/\psi)$ , investig. of  $\gamma \gamma \mu^+$  final state 0-18132  
 $\psi \rightarrow \psi \eta$ , Ward identity anal.,  $\eta, \eta'$  quark-gluon struct. 0-42449  
 $\psi \rightarrow \psi \pi(\eta)$ ,  $SU_2$  violation, symmetry breaking and decay amplitudes 0-52499  
 $\psi' \rightarrow (4.42) \rightarrow DD$ , FF, decay suppression, pseudo-dimension selection rule 0-9163  
 $D^0$ ,  $D^+$  decay widths and branching ratios, quark recombination widths, free quark model 0-27500

meson interactions see lepton-hadron interactions; meson-baryon interactions; meson-deuteron interactions; meson-meson interactions; meson-nucleus reactions; photon-hadron interactions

## meson leptonic decay

- see also kaon leptonic decay  
 charmed meson  $\rightarrow l^+ l^- X$ , model for charm fragmentation function 0-37237  
 meson weak and EM decays, relativistic confined quarks, MIT bag model 0-47277  
 multilepton configurations in b and t decays from  $t\bar{t}$  and  $b\bar{b}$  0-18130  
 quark bag model with finite potential barrier, S-wave mass spectra of QQ and leptonic widths 0-47242  
 quarkonium leptonic decay rates for 1S and 2S states, constraints 0-37252  
 vector mesons, leptonic decays, six-quark sequential model 0-52490  
 $e^+ e^- \rightarrow \gamma V \rightarrow \gamma \nu \bar{\nu}$ , neutral vector meson radiative prod. and decay (Russian) 0-52492  
 $\eta \rightarrow \gamma + (e^+ e^-)$ , EM bound states, approx. Bethe-Salpeter wave function (Chinese) 0-42448  
 $\eta \rightarrow \gamma + (\mu^+ \mu^-)$ , EM bound states, approx. Bethe-Salpeter wave function (Chinese) 0-42448  
 $\eta \rightarrow \mu^+ \mu^- \gamma$ , in  $\pi$  p interactions at 25 and 33 GeV/c, form factors (Russian) 0-4984  
 $F^\pm \rightarrow \pi^\pm \nu(\bar{\nu})$ , beam-dump experiment, observation of  $\nu$ , interactions 0-22601  
 from  $\pi^- p$  mass spectrum 0-27498  
 $\pi \rightarrow e \nu \gamma$ , isospin violation in form factor, induced by current quark mass 0-32069  
 $\pi^+ \rightarrow \mu^+ \nu_\mu$ , muon momentum meas. 0-37253  
 $\psi$  decay width calc. in one parameter pot. 0-13279  
 $\psi \rightarrow e^+ e^-$ , quarkonium, quantum mechanical applications, masses and leptonic widths of  $\psi$  and  $T$  0-27484  
 qq resonance energy spectrum, leptonic and radiative decay widths, QCD pot. calcs. 0-52491  
 $T$  decay width calc. in one parameter pot. 0-13279  
 $T \rightarrow e^+ e^-$ , quarkonium, quantum mechanical applications, masses and leptonic widths of  $\psi$  and  $T$  0-27484  
 $T'$  leptonic width, some phenomenological estimates about heavy quark (b,t) bound states 0-47262  
 $Z^0 \rightarrow \mu^+ \mu^- \gamma$ , Weinberg model anal. of  $Z^0$  decay ang. distrib. 0-47275

## meson magnetic moment

- composite models, mag. moments of quarks, leptons and hadrons 0-32081  
 topped and bottomed hadrons, mag. moments in additive quark model 0-52478

## meson mass

- b-mesons, mass splitting,  $SU_3$  nonet of  $SU_6$  0-47288  
 baryonium masses in a quark model 0-37241  
 bootstrap, QCD, meson mass spectrum 0-22581  
 charmed hadron masses, from effective quark masses, sum rules 0-4965  
 charmed meson mass splitting in universal confining potential model 0-4967  
 charmonium psion states, confining pots. and inverse scatt. problem, T mass 0-4946  
 dynamically broken chiral symmetry and the gauge technique for Ward identities 0-47211  
 grand unified theories, vector meson mass restrictions 0-32058  
 hadron spectroscopy with covariant Coulomb and confining interactions 0-32090  
 heavy mesons, polynomials approximating sequence of masses (Russian) 0-407  
 linear  $SU(4)$  meson  $\sigma$ -model, one-loop approx., spin zero mass spectrum and leptonic-decay 0-47278  
 MIT bag model, coloured quark and gluon constituents of mesons 0-4929  
 mixing angles, non-relativistic quark model, Schwinger-type mass relations for  $SU_4$  and  $SU_3$  0-18125  
 mixing angles, non-relativistic quark model,  $SU_5$  and  $SU_n$  0-22591  
 P-wave radial mixing, effect on E1 radiative decays, charmonium mass 0-37271  
 pseudoscalar mesons, EM mass shifts, quark-parton model,  $SU_3$  quark triplet 0-42459  
 quarkonium mass spectra, one gluon exchange corrections, gauge invariance and choice 0-52483  
 quarkonium systems, binding energy effect on mass spectra 0-37229  
 reggeisation in theories with broken global symmetries, nondegeneracy of vector meson masses, non-trivial mixing 0-13236  
 $SU(4)$  16-plet boson mass formulas, flavour symmetry breaking 0-37250  
 $SU(5)$ , broken, meson mass formulae 0-47267  
 symmetry-breaking, current algebra quark masses 0-42436  
 unitarity and spectrum in quark model 0-18115  
 b-quark meson, decay, weak mass mixing, CP violation 0-32086  
 $B^0 B^0$  mixing in six quark model, decay, mass mixing and CP nonconservation 0-42406  
 D and F meson spectra, electromagnetic interactions effect 0-47293  
 $D^0$  prod. and decay in high energy photon interaction, mass and decay time 0-42478  
 $\eta_c$  and  $\eta'_c$ , mass prediction using QCD 0-22590  
 $\eta'$ , QCD sum rules for mass, possible pseudoscalar gluonium, instanton effects 0-388  
 $J/\psi$  meson mass spectra, quasipotential calcs. (Russian) 0-47268  
 $K_L - K_S$  mass difference, Kobayashi-Maskawa six quark model, mixing angles, mass matrix and CP violation 0-13284  
 $\omega/N$ , mass ratio in QCD lattice gauge theory 0-4928  
 $\phi$ , mass compilation study 0-52552  
 $\pi/N$ , mass ratio in QCD lattice gauge theory 0-4928  
 $\psi$ , quarkonium, quantum mechanical applications, masses and leptonic widths of  $\psi$  and  $T$  0-27484  
 QQ mass, approx. scheme is QCD 0-42398  
 qq potential, asymptotic freedom, linear confinement 0-13279  
 $\rho/N$ , mass ratio in QCD lattice gauge theory 0-4928  
 $T$ , quarkonium, quantum mechanical applications, masses and leptonic widths of  $\psi$  and  $T$  0-27484  
 $v$  p-wave ground state, mass scaling inequalities for quarkonium levels 0-32071  
 T-meson mass spectra, quasipotential calcs. (Russian) 0-47268  
 x-boson, mass and asymmetric decay rel. to cosmological baryon asymmetry 0-4464



**meson-meson interactions**

see also *meson-meson scattering; pion-pion interactions*  
cross sections in QCD (*Russian*) 0-4968

**meson-meson scattering**

see also *meson-meson interactions; pion-pion scattering*  
gauge-dual-topological approach to soft hadronic reactions, trajectory slopes 0-18142  
high energy meson elastic scatt. amplitude, leading term approx. in SU(2) Yang-Mills theory 0-5017  
 $K\pi$  elastic scatt., asymptotic total cross sections and positivity 0-13334  
 $\pi K$ , low energy cross sections (*Chinese*) 0-52535  
 $\pi\omega \rightarrow \pi\omega$ ,  $\rho'(1250)$  meson and two channel  $\pi\pi$ ,  $\pi\omega$  problem, N/D method (*Russian*) 0-37297

**meson-nucleus reactions**

for inelastic meson-nucleus scattering, see "meson-nucleus scattering"  
see also *kaon-nucleus reactions; meson-baryon interactions; meson capture; pion-nucleus reactions*  
emulsion nuclei, 20 TeV, balloon-borne chamber, Monte Carlo simulation 0-9309

**meson-nucleus scattering**

see also *kaon-nucleus scattering; meson-baryon scattering; pion-nucleus scattering*  
No entries

**meson photoproduction**

$e^+e^- \rightarrow e^+e^- \rho$ , bremsstrahlung production of neutral vector mesons 0-5006  
 $\gamma d \rightarrow \pi^0 d$ , meson-exchange currents in photomesic reactions, relativistic many-body theory 0-422  
 $\gamma d \rightarrow \pi^+ nN$ , off-energy shell photoprod. amplitudes for reactions on bound neutrons 0-421  
 $\gamma N \rightarrow K^+ \Sigma$ , meas. of asymmetries and cross sections using 16 GeV linearly polarised photons 0-13318  
 $\gamma N \rightarrow \pi^+ n$ , meas. of asymmetries and cross sections using 16 GeV linearly polarised photons 0-13318  
 $\gamma N \rightarrow \pi \Delta$ , meas. of asymmetries and cross sections using 16 GeV linearly polarised photons 0-13318  
 $\gamma N \rightarrow \psi(3.1) + \text{anything}$ , cross section and N charmed quark composition 0-423  
 $\gamma p \rightarrow K^+ \Lambda$ , meas. of asymmetries and cross sections using 16 GeV linearly polarised photons 0-13318  
 $\gamma p \rightarrow \pi \pi^+$ , multipole anal. in region of first reson. 0-22622  
 $\gamma p \rightarrow \pi \pi^0$ , multipole anal. in region of first reson. 0-22622  
 $\gamma p \rightarrow \pi^+ p$ , 1.4 GeV, differential cross section meas. 0-42476  
 $\nu p \rightarrow \pi$ , threshold to 450 MeV, energy depend. multipole anal. 0-32110  
 $\rho\alpha$ , 1300 to 2300 MeV,  $\pi^0$  photoproduction, double polarisation parameters 0-13317  
 $\rho\gamma$ , one-gluon exchange, quark loop contrib. to photon total cross sections 0-4999  
 $\pi$ , photoproduction in  $E < 450$  MeV region, dispersion relations, CT invariance, review, book contrib 0-47311  
 $\pi$  photoproduction in large cosmic-ray showers 0-4214  
 $\rho'(1600)$  diffractive photoprod. in two pion final state 0-22624  
 $^3H(\gamma, \pi^0)$ , polarisation effects 180 to 700 MeV, impulse approx. calcs. (*Russian*) 0-37368  
 $^3H(\gamma, \pi^0)^3H$ , polarisation effects 180 to 700 MeV, impulse approx. calcs. (*Russian*) 0-37368  
 $^3He(\gamma, \pi^+)$ , polarisation effects 180 to 700 MeV, impulse approx. calcs. (*Russian*) 0-37368  
 $^3He(\gamma, \pi^0)^3He$ , polarisation effects 180 to 700 MeV, impulse approx. calcs. (*Russian*) 0-37368  
 $^4He(\gamma, \pi^0)$ , polarisation effects 180 to 700 MeV, impulse approx. calcs. (*Russian*) 0-37368  
 $^6Li(\gamma, \eta)^6Li^*(3.56 \text{ MeV})$ , partial photoproduction reactions, large momentum transfer anal., form factor choice 0-22808  
 $^6Li(\gamma, \pi^0)^6Li^*(3.56 \text{ MeV})$ , partial photoproduction reactions, large momentum transfer anal., form factor choice 0-22808

**meson production**

see also *kaon production; meson photoproduction; pion production*  
 $\pi^- p \rightarrow \delta^- p$ ,  $\pi^+ \pi^- \pi^- \gamma\gamma$  backgrounds produced near the  $\delta^-$  mass region 0-9182  
beauty and charm photoprod. in QCD,  $q\bar{q} \rightarrow b\bar{b}$  or  $c\bar{c}$  mechanism 0-32079  
heavy meson hadroproduction, QCD effect on scale breaking 0-37239  
quark recombination model, meson and baryon prod. sum rules 0-4922  
strange axial vector meson non-diffractive prod. in Kp and  $\pi p$  interactions 0-32122  
t-flavoured meson production in photonuclear and pp collision 0-22623  
vector meson production in pp interactions, constituent-interchange model 0-22579  
 $\chi_c$  radiative decay,  $\psi$  and  $\psi'$  prod., straton coupling constants (*Chinese*) 0-42467  
 $e^+e^- \rightarrow$  hadrons, quark existence and theory 0-37234  
 $e^+e^- \rightarrow F^*F^* \rightarrow F_1F_2$ , photon ang. correlations and prod. amplitudes 0-47319  
 $e^+e^- \rightarrow$  quarkonium state, D, F, T mesons, importance as experimental tool in new particle searches 0-42425  
F-meson production,  $F^+ \rightarrow \pi^+ \nu_\mu(\bar{\nu}_\mu)$ , beam-dump experiment, observation of  $\nu_\mu$  interactions 0-22601  
 $\gamma^* N \rightarrow \psi N$ , gluon momentum, spin, parity and coupling 0-42395  
 $\mu^+ N$ , 280 GeV/c in Fe,  $\psi$  virtual photoprod. 0-37279  
pN in Fe, 400 GeV/c, bottom meson prod. search in multimeson final states 0-47334  
pp, ISR energies, inclusive high  $p_T \omega^0$  and  $\eta'$  prod. 0-42504  
pp, pp, 540 GeV, T and  $\psi$  transverse momenta from QCD 2 $\rightarrow$ 3 processes, gluon subprocesses 0-52546  
pp inclusive interaction, 30 to 50 GeV  $\eta$  meson prod. 0-5023  
pp $\rightarrow$ meson+lepton pair, transverse momentum distrib. and branching ratios, proton gluon distribution 0-52537  
 $\pi^+ \pi^-$  U interaction at 55 GeV/c, search for long lived heavy mesons (*Russian*) 0-5029  
 $\pi^- p \rightarrow \phi n$ , quark line rule, violations 0-52530  
 $\psi(4.03) \rightarrow DD$ , suppression problems, model-independent approach 0-52494  
 $\psi(4.42) \rightarrow DD$ , suppression problems, model-independent approach 0-52494  
 $\psi(4.42) \rightarrow FF$ , suppression problems, model-independent approach 0-52494  
 $\psi$  hadronic prod., lepton pair ang. distrib., cross section  $\chi$  contribution from  $\pi N$ , pN, pN 0-42487  
 $\rho^0$  electroproduction, parity violating effects 0-9178  
pp $\rightarrow D^+ X$ , 53 GeV,  $D^+ \rightarrow K^- \pi^+ \pi^+$  (*Polish*) 0-9187

**meson resonances**

see also *D mesons; eta meson resonances; omega mesons; phi mesons; psi mesons; rho mesons*  
0 $^-$  meson, EM form factor in straton model (*Chinese*) 0-22616  
 $\pi^- p \rightarrow \delta^- p$ ,  $\pi^+ \pi^- \pi^- \gamma\gamma$  backgrounds produced near the  $\delta^-$  mass region 0-9182  
additive quark model with six flavours 0-27455  
axial vector meson model, quasi-renormalisation using BPHZ approach 0-13208  
baryonium, empirical evidence and theoretical interpretation review 0-42394  
baryonium, molecular model, quark-diquark picture of baryon 0-27462  
baryonium, S-matrix representation 0-399  
baryonium and nonexotic hadron trajectories from a color-dependent potential 0-13286  
baryonium dual S-matrix approach 0-52526  
baryonium masses in a quark model 0-37241  
beauty and charm photoprod. in QCD,  $q\bar{q} \rightarrow b\bar{b}$  or  $c\bar{c}$  mechanism 0-32079  
beautyonium bound states, T, T', T'', dispersion sum rules (*Russian*) 0-13235  
charmonium model and the  $\psi$  and T families 0-47253  
charmonium quark-antiquark pots., flavour independ.,  $\gamma$ ,  $\gamma'$ ,  $\psi$  and  $\psi'$  appls. 0-47254  
dynamion Hamiltonian on  $S^3$  sphere, gauge invariant formalism 0-27460  
flavour independence of forces between quarks,  $\psi$  and T spectra 0-22569  
hadron lepton model interpretation of particle resonance states 0-4957  
hadronic coupling constants and the nonrelativistic quark model with charmonium potential 0-37207  
heavy neutral mesons, parity determ. 0-37264  
heavy vector meson annihilation rate to lepton pairs, hadronic corrections 0-4943  
high energy meson elastic scatt. amplitude, leading term approx. in SU(2) Yang-Mills theory 0-5017  
isospin-violating mixing in meson nonets,  $d\bar{d}-u\bar{u}(s\bar{s})$  mass differences 0-32096  
leptonic decays, six-quark sequential model 0-52490  
mass spectrum, planar bootstrap and Regge approach 0-22581  
mixing angles, non-relativistic quark model, Schwinger-type mass relations for  $SU_4$  and  $SU_5$  0-18125  
mixing angles, non-relativistic quark model,  $SU_5$  and  $SU_6$  0-22591  
multiple quark configurations in b and t decays from tt and b $\bar{b}$  0-18130  
multi-quark states, obs. in pp formation and prod. expts. 0-9153  
nucleon-nucleon interaction and nuclear forces, meson exchange 0-32195  
orthoquarkonium decay, Dalitz plot population and thrust ang. distrib., scalar gluon nonexistence 0-27470  
P-wave radial mixing, effect on E1 radiative decays, charmonium mass 0-37271  
QCD, asymptotic freedom, energy levels J/ $\psi$  and T mass difference (*Chinese*) 0-52480  
QCD, heavy-vector meson-nucleon scatt., cross section suppression, T and  $\psi$  0-22564  
QCD, spin-dependent forces in heavy-quark systems 0-4937  
QCD and dual resonance model vertices, string prod. operators, singlet colour states (*Russian*) 0-42410  
quark bag model with finite potential barrier, S-wave mass spectra of QQ and leptonic widths 0-47242  
quark jet,  $q\bar{q}$  pair production mechanism, average transverse momenta 0-18118  
quarkonia, S- and P-wave, gluon jets, perturbative QCD anal. 0-32070  
quarkonia states, heavy, strong decay into other heavy flavours, and triple-gluon vertex 0-47279  
quarkonium leptonic decay rates for 1S and 2S states, constraints 0-37252  
quarkonium mass spectra, one gluon exchange corrections, gauge invariance and choice 0-52483  
quarkonium radiative transition amplitudes, QCD dispersion sum rules 0-52511  
reggeisation in theories with broken global symmetries, nondegeneracy of vector meson masses, non-trivial mixing 0-13236  
relativistic quark models,  $c\bar{c}$  and  $b\bar{b}$  singlet triplet splitting, mass formulae (*Russian*) 0-37232  
Schrödinger eqn. with logarithmic pot., soln. for quark model particle spectroscopy 0-32065  
strange axial vector meson non-diffractive prod. in Kp and  $\pi p$  interactions 0-32122  
strong and EM decays, particle mixing and meson pole dominance 0-18127  
 $SU_3$  couplings of scalar mesons to two pseudoscalars,  $S^*$  to  $\pi\pi$  and  $\epsilon$  to  $KK$  0-22580  
 $SU(4) \otimes SU(3)'$  model, T particles and  $SU(3)'$  colour space (*Chinese*) 0-42409  
 $SU(5)$ , Clebsch-Gordan series, quark model appl. 0-47256  
T' (10040) as an I=1 vector meson resonance 0-47241  
t-flavoured meson production in photonuclear and pp collision 0-22623  
vector meson production in pp interactions, constituent-interchange model 0-22579  
very high energy cosmic ray-nuclear interactions, new particle search, X particles 0-8508  
Yang-Mills theory, IR divergences and zero mass limit 0-32025  
Zweig rule in two-dimensional QCD,  $\psi$  and T decays 0-52479  
 $A_1$ , spectral function sum rules and  $A_1$ -W coupling const. 0-27429  
 $B \rightarrow \psi(\eta_c) + X$ , branching ratio 0-37259  
B-meson decay, partial unification of strong, weak and EM interactions 0-18106  
 $B^0 \rightarrow B^-$ , EM mass difference, some phenomenological estimates about heavy quark (b,t) bound states 0-47262  
 $B^0 \bar{B}^0$  mixing in six quark model, decay, mass mixing and CP nonconservation 0-42406  
 $c\bar{c}$  and  $b\bar{b}$  states, spectra and strong decays 0-52502  
 $\chi_c$  radiative decay,  $\psi$  and  $\psi'$  prod., straton coupling constants (*Chinese*) 0-42467  
 $\chi_{12} \rightarrow \gamma\psi$ , charmonium states radiative and hadronic widths, gluon spin 0-4998  
 $\chi_1$  P-wave charmonium states, hadronic prod. cross section in  $K^- p$ ,  $\bar{p}p$ , and  $\pi^- p$  0-37292  
 $e^+e^- \rightarrow$  hadrons, scaling and quark struct. 0-425  
 $e^+e^- \rightarrow$  jets, in T and T' region, sphericity and charged multiplicity 0-428  
 $e^+e^-$  annihilation, fine energy scan for narrow states between 29.9 and 31.46 GeV 0-22627



## meson resonances continued

- $e^+e^-$  annihilation, gluon jets and heavy quarkonium prod., QCD test,  $\psi$  prod. 0-42479  
 $e^+e^- \rightarrow \gamma V \rightarrow \gamma \nu \bar{\nu}$ , neutral vector meson radiative prod. and decay (Russian) 0-52492  
 $e^+e^- \rightarrow$  hadron jet, 3 to 17 GeV, including charm threshold and upson resonances, review 0-47321  
 $e^+e^- \rightarrow \mu^+\mu^-$ , Pauli type interaction, vector meson role 0-4974  
 $e^+e^- \rightarrow$  quarkonium state, D,F,T mesons, importance as experimental tool in new particle searches 0-42425  
F-mesons, DASP results on  $e^+e^-$  annihilation 0-42483  
 $F^+$  decay,  $SU_4$  20-plet dominance model, inclusive branching ratios 0-13299  
 $\gamma(10.0)$ , two-body hadronic and radiative decays, pseudo-dimension rule,  $\pi\pi$  and  $KK$  suppression,  $SV_1$  singlet 0-52495  
 $K^-d \rightarrow \pi^- \Delta p$ , three body Faddeev formalism, unstable dibaryon bound state search 0-32130  
 $KN$ , below 1 GeV/c,  $Y^*$  states,  $SU(6) \otimes O(3)$  quark model classification 0-27523  
 $K^-p \rightarrow (K\pi\pi)^- p$ , 4.2 GeV/c, partial wave anal. in Q region 0-13330  
 $K^-p \rightarrow K^*(890) \Delta(1236)$ , 10 GeV/c, multidimens. anal., reaction sub-channel separation 0-32127  
 $K^+p$ , 32 GeV/c,  $\rho, K^*, \phi$  inclusive prod., quark fusion model 0-32135  
 $K_L^0 p \rightarrow K_S^0 \pi^+ \pi^- p$ , up to 17 GeV/c,  $Q^0, Q^0$  prod., cross sections 0-32129  
 $\mu N \rightarrow \mu \chi$ ,  $\chi = 2$  or 3, charm muoprod. with small angle veto 0-47306  
 $NN$  cross-sections and resonances in nonstatic OBEP 0-13386  
 $NN$  narrow meson resonances near threshold, theoretical approaches 0-9157  
 $NN$  potential, imaginary part 0-32118  
 $NN$  spectrum in pot. models, meson exchange forces 0-9156  
 $pp$ , 373-734 MeV/c, total cross section enhancement, 1936 MeV narrow resonance 0-13324  
 $pp$ , 62.4 GeV,  $e^+e^-$  massive pair prod., continuum and T resonance cross sections 0-18153  
 $pp$ , 93 GeV,  $pp$  narrow enhancement at 1940 MeV,  $S(1936)$  mass 0-52542  
 $pp$ ,  $pp$ , 540 GeV, T and  $\psi$  transverse momenta from QCD 2-3 processes, gluon subprocesses 0-52546  
 $pp$  elastic scatt., FESR constraint on baryonium resonances, S, T, U, contrib. 0-27520  
 $pp$  scatt., exchange degeneracy violating  $A_1$ -Z Regge amplitude and dibaryon resonances 0-4971  
 $\pi d$  elastic scatt., 142-256 MeV, dibaryon resonance interference with Faddeev amplitudes 0-32123  
 $\pi d$  polarised scatt., dibaryon resonance signals in excitation functions 0-9181  
 $\pi^+d$ , 15 GeV/c, many-pion prod. and resonant prod. cross sections 0-22642  
 $\pi N \rightarrow \pi^+ \pi^- N$ , 4-17 GeV/c,  $\rho^0$  and f prod. mech. 0-436  
 $\pi^-p \rightarrow KKN$ , S-wave anal., scalar mesons and branching ratios 0-13328  
 $\pi^-p \rightarrow p p n$ , 18 GeV,  $p p$  resonant state partial wave anal. 0-32134  
 $\pi^-p \rightarrow \pi^+ \pi^- \pi^+ p$ , 63, 94 GeV/c,  $A_2$  meson prod. from partial wave anal. 0-37303  
 $\pi^-p \rightarrow \pi^+ \pi^- \pi^+ p$ , 63, 94 GeV/c,  $A_1$  meson existence from partial wave anal. 0-37304  
 $\pi^-p \rightarrow \pi^+ \pi^- \pi^+ p$ , 63, 94 MeV/c,  $A_3$  meson,  $3\pi$  resonances in  $2^-$  partial waves 0-37305  
 $\pi^-p \rightarrow \pi^+ \pi^- n$ ,  $\pi\pi$  scatt. partial wave anal. f, g and h mesons 0-5015  
 $\pi^+p$ , 11.46 GeV/c, search for new meson resonance prod. in  $\mu$  channel 0-22641  
 $\pi^+p \rightarrow (\pi^+ p) p$ , 50 GeV/c, narrow baryonium states, diffractive prod. cross sections 0-442  
 $\psi$  hadronic prod., lepton pair ang. distrib., cross section  $\chi$  contribution from  $\pi N$ ,  $pN$ ,  $\bar{p}N$  0-42487  
 $q\bar{q}$  resonance energy spectrum, leptonic and radiative decay widths, QCD pot. calcs. 0-52491  
 $S(1935)$ , reson. parameters determ., finite energy resolution effects, folding problem 0-32673  
 $\tau \rightarrow \nu \mu \pi$  decay parameters from PCAC and current algebra,  $A_1$  characts. 0-37314  
T, heavy quark bound states in potential model with relativistic corrections 0-37247  
v, masses and leptonic-decay widths, one-parameter potential 0-13279  
T, quixotic interpretation as QQ bound state 0-13280  
T family, EM transition rates, geometrodynamical quark model 0-47295  
v p-wave ground state, mass scaling inequalities for quarkonium levels 0-32071  
T-meson mass spectra, quasipotential calcs. (Russian) 0-47268  
 $T''$  leptonic width, some phenomenological estimates about heavy quark (b,t) bound states 0-47262  
 $X(2.82)$  DASP results on  $e^+e^-$  annihilation 0-42483  
x-boson, mass and asymmetric decay rel. to cosmological baryon asymmetry 0-4464  
 $^2H(\pi, \pi)$ , polarised d, dibaryon resonance signals in excitation functions 0-9181  
 $S^*-8^0$  scalar meson mixing as threshold phenomenon from coupling constants 0-27477

meson scattering see lepton-hadron scattering; meson-baryon scattering; meson-deuteron scattering; meson-meson scattering; meson-nucleus scattering; photon-hadron scattering

## meson spin and parity

- charged pseudoscalar meson photoprod. from H and D with 16 GeV linearly polarised photons 0-13318  
field equation for arbitrary hadrons and parity operators 0-37263  
heavy neutral mesons, parity determ. 0-37264  
 $\pi^+$ , negative parity assignment from  $pp \rightarrow \pi d$  0-32117  
 $\rho^0$ -electroproduction, parity violating effects 0-9178

mesonic atoms see mesic atoms

mesonic molecules see mesic molecules

## mesons

- for  $\mu$  mesons see muons  
see also cosmic ray mesons; eta mesons; kaons; meson resonances; pions  
electric and magnetic confinement schemes for mesons and baryons 0-4960  
form factors, relativistic covariant quark model (Russian) 0-9140  
light scalar, pion, in neutron struct. theory 0-18134  
MIT bag model, coloured quark and gluon constituents of mesons 0-4929  
pion spectrom. for meas. electro- and photo-pion spectra in high background environment 0-27868

## mesons continued

- quark masses and structure functions,  $0^-, 1^-$  mesons 0-22585  
strong PCAC appls., axial vector current 4-divergence, meson fields (Chinese) 0-42364

## mesosphere

- composition of middle atm., in situ meas. 0-17339  
dynamics of middle atmosphere, review 0-17338  
W.Europe, atmos. temp. 20-110 km altitude, 1975/6 winter anomaly 0-36356  
W.Europe, ion production obs., 50-120 km altitude, 1975/6 winter anomaly 0-36439  
W.Europe, mesosphere and lower thermosphere temp. and density, 1975/6 winter anomaly 0-36357  
W.Europe, mesosphere and lower thermosphere trace constituents, 1975/6 winter anomaly 0-36433  
ion mobility and concentration, and conductivity, 10-70 km altitude 0-36358  
Joule heating at high-latitude 0-41500  
Kelvin waves, struct. and behaviour from Nimbus 5 IR meas. 0-8394  
mesopause, radiative cooling 0-26660  
meteor trail diffusion, radio refl. determination 0-46329  
planetary waves, struct.-correction 0-8403  
planetary waves at 20-80 km altitude rel. to ionospheric absorpt. winter anomaly 0-36359  
positive in composition and chemistry of high-latitude mesopause 0-46224  
radar signal detection, VHF, complementary code and digital filtering 0-46274  
Sardinia (40°N), comp. and temp. during D-region winter anomaly 0-21871  
satellite observations of middle atmosphere processes 0-21803  
structure in presence of noctilucent clouds 0-8412  
temperature waves of annual and semiannual period, radiometer obs. 0-51500  
wind and thermal structure, W.Europe 1975/6 winter anomaly obs. 0-36438  
wind determination by meteor track movement (French) 0-51589  
wind measurement at 60-120 km, radiowave drifts technique 0-31137  
winds and turbulence continuous meas. using VHF Doppler radar, preliminary results 0-8444  
winds and waves over Jicamarca, 1974 May 23-24 VHF radar obs. 0-12497  
 $H_2O$  cluster ions at cold mesosphere, rocket borne expt. 0-17429  
 $NO$ , photodissoc. in mesosphere and stratosphere, theory 0-41580  
 $NO$ , photodissoc. rate, calc. 0-51498  
 $NO$  predissociation, photochemistry 0-21802  
Na layer, mesosphere, meas. by efficient forced oscillator dye laser 0-41563  
O concentration, inference from positive ion comp. data 0-8405  
 $O_2$ , photodissoc. and spectral absorpt. in stratosphere and mesosphere 0-51497  
 $O_3$  content in tropics, during March-April 1976 stratospheric warming 0-12494  
 $O_3$  number density profile of lower mesosphere 0-41579  
OH emissive layer, waves, near IR photographic studies 0-51545  
 $O(^3P)$  translationally hot, energy distrib. function 0-21811

metal castings see castings

## metal clusters

- energy spread of cluster ion from molten metal, charge exchange 0-37922  
isomer shift of  $^{57}Fe$ , nearest neighbour effect 0-44988  
structure and properties 0-39304  
transition metal, bimetallic cluster, photoselective bimetallic aggregation, review 0-53182  
transition metal clusters, particle size rel. to bulk metallic props. 0-44490  
Wolfsberg-Helmholz relation analysis, reson. integral approx. 0-49566  
Ag, on Si substrates, opt. spectra investig. of struct. (German) 0-25492  
 $Co(CO)_4^-$ , extended CNDO calc. 0-918  
 $Co_2(CO)_8$ , extended CNDO calc. 0-918  
 $Co_4(CO)_{12}$ , extended CNDO calc. 0-918  
Fe clusters, supported, Mossbauer spectra 0-7220  
 $Li_2$ , ( $n=1, 2, 3$ ), stable cluster configs., ionisation pots., binding energies, vibr. freqs., al initio SCF and CEPA calcs. 0-14265  
 $Mn_2(CO)_{10}$ , extended CNDO calc. 0-918  
Ni, chemisorptive binding of O, CNDO calc. of potential energy curves (German) 0-44431  
Ni-Cu alloys, short-range atomic clustering, residual resist. meas. 0-29386  
Pt cluster, conduction electron density oscils., NMR spin-echo meas., indirect exchange interaction 0-44954  
 $Re_3Cl_8$  metal cluster complexes, He(I) photoelectron spectrum, SCC DV X $\alpha$  calcs.,  $Re_3Cl_8^{2-}$  comparison 0-28063

metal corrosion see corrosion

## metal-insulator boundaries

- see also metal-insulator-metal structures  
band gap closure in insulator near metal-insulator interface 0-11086  
bulk states in semiconductors and insulators in contact with metals, charging 0-54781  
catalytic reactions studied by work function meas. 0-55711  
dielectric space charge distrib., carrier mobility and interface injection mechanism identification 0-15974  
electron tunnelling, its role in contact electrification 0-2453  
electrostatic interaction of charges with metal-insulator interface 0-24996  
interfacial polarisation effect on dielectric props., sandwich capacitor model 0-15614  
PET, ionic cond. current rel. to neutralisation at polymer-metal interface at elevated temps. 0-24664  
polyethylene terephthalate charge transfer from metallic electrodes 0-15605  
polymonochloro-p-xylylene,  $\gamma$ -ray-induced cond., hole injection effects 0-34452  
polystyrene,  $\gamma$ -ray-induced cond., hole injection effects 0-34452  
polystyrene films on metal substrates, electrode effect on carrier injection, TSC, I-V characts. 0-34463  
PVE, charge injection from metallic electrode, obs. 0-15947  
 $Al-SiO_2$ , surface reactions and interdiffusion, photoemission study 0-49532  
 $Al-SiO_2$  interface, internal photoemission and photon-assisted tunnelling 0-6982



**metal-insulator boundaries continued**

- Au-sapphire interface, effect on shear strength of adsorbed species 0-49485
- Cr/polymer interface, electronic struct., XPS study 0-45204
- Cu/polymer interface, electronic struct., XPS study 0-45204
- Cu-sapphire interface, effect on shear strength of adsorbed species 0-49485
- Ni/polymer interface, electronic struct., XPS study 0-45204
- Ni-sapphire interface, effect on shear strength of adsorbed species 0-49485
- SiO<sub>2</sub> charge transfer from metallic electrodes 0-15605

**metal-insulator-metal devices**

- diodes, metal whisker point contact junctions, tunnelling and rectification characts. 0-6955
- diodes, negative differential resistance, stimulated inelastic tunnelling theory 0-49951
- electrical hygrometer with thin layer of LiF (*Czech*) 0-231
- MOM diodes fabrication, two-level e-beam resist process with 1000 Å resolution 0-49996
- Ni-Nichrome, MOM diode, breakdown effect in visible and near-IR regions 0-6999
- Ti-TiO<sub>2</sub>-Au diode, spectral photoresponse and I-V characts. 0-15617
- W-Ni, MOM diode, breakdown effect in visible and near-IR regions 0-6999

**metal-insulator-metal structures**

- DC conductivity and Shubnikov-de Haas effect 0-11012
- dielectric diode, Joule instability under space-charge-limited current conditions 0-15618
- electrical transport, influence of mech. modulation 0-2481
- electron emission modelling (*Czech*) 0-2479
- injection current enhancement at metal insulator interface, theory 0-49953
- nonequilibrium states, kinetic eqns. (*Russian*) 0-11101
- p 0-40062
- [p]-quinquaphenyl film between metal electrodes, memory switching 0-2484
- paper cellulose sandwiched between metal electrodes, thermo-induced elec. current 0-25021
- PET, in MIM struct., injection current enhancement at metal insulator interface, theory 0-49953
- polyethylene, electrical capacitance under high DC elec. field 0-54705
- polymer, charge carrier species determ. using interfacial phenomena 0-24978
- polymer films, electron irradi. controlled form., elec. props. 0-15635
- polypropylene film, in MIM struct., electroforming 0-25019
- polystyrene, atactic, bulk and surface elec. props., contact charging obs., dielec. const. 0-15615
- polystyrene film, in MIM struct., elec. conduction and free radicals 0-20340
- polytetrahydrofuran films, electrochemically prepared between metal electrodes, DC elec. props. 0-39695
- polyvinylacetate film, in MIM struct., DC cond. phenomena 0-25020
- PVC film, soln.-grown, between Al electrodes, AC elec. props. 0-15619
- shellac, electrical cond. mechanisms, Schottky and Poole-Frenkel processes and work function 0-29402
- stearic acid film, in MIM struct., AC cond. and dielec. props., freq. depend. 0-55030
- thin disordered film, electronic energy spectrum calcs. extended Halpern Green's function technique 0-20066
- tunnel junctions, roughened, photon emission, calc. 0-44738
- tunnelling, elastic, in MIM structures, zero bias anomaly calc. 0-2483
- vinyl chloride-vinyl acetate copolymer film between metal electrodes, depolarisation current studies 0-2691
- Ag-Al<sub>2</sub>O<sub>3</sub>-Au structure, electrorrefl. meas. (*French*) 0-50366
- Al/(Al<sub>2</sub>O<sub>3</sub>)-BaS<sub>2</sub>/Sn struct., internal voltage temp. variation 0-20326
- Al/SiO<sub>2</sub>-B<sub>2</sub>O<sub>3</sub>/Au (*French*) 0-39681
- Al-Al oxide-Pd tunnel junctions, exposed to H<sub>2</sub>, inelastic electron tunnelling spectra 0-20327
- Al-Al<sub>2</sub>O<sub>3</sub>-Au, electron trapping due to neutron irradiation 0-2505
- Al-Al<sub>2</sub>O<sub>3</sub>-Pb(Au), solid-state anodisation of Al by vapour infusion, oxide growth rate 0-11830
- Al-Al<sub>2</sub>O<sub>3</sub>-(SN)<sub>x</sub> structure, tunnelling spectroscopy study of electronic struct. of (SN)<sub>x</sub> (*Japanese*) 0-49954
- Al-Al<sub>2</sub>O<sub>3</sub>-metal capacitors, elec. props. interrelations 0-54801
- Al-Al<sub>2</sub>O<sub>3</sub>-metal capacitor, capacitance and power factor rel. to voltage and temp. changes 0-54802
- Al-Al<sub>2</sub>O<sub>3</sub>-Pb tunnel junction, thermal annealing effects 0-49952
- Al-AlF<sub>3</sub>-Al, dielec. props. temp. irreversibility (*Czech*) 0-15616
- Al-CeF<sub>3</sub>-Al(Au), dielec. props. temp. irreversibility (*Czech*) 0-15616
- Al-polyacrylonitrile-Al films, current-voltage characteristics 0-11125
- Al-Sb<sub>2</sub>O<sub>3</sub>-In films, negative resistance characts. 0-11103
- Al-SiO<sub>2</sub>-Al evaporated film anomalous dielectric dispersion under high DC field 0-15620
- Au-Al<sub>2</sub>O<sub>3</sub>-Al system, influence of mech. modulation on elec. transport 0-2481
- Au-SiO<sub>2</sub>-Au evaporated thin film sandwich, circulating and emission currents 0-11102
- Au-SiO<sub>2</sub>-Au structure AC conductivity, bulk and interface effects 0-54798
- Bi-NbO<sub>3</sub>-Bi system, Schottky barrier effects in transport and dielec. props. 0-29486
- Bi<sub>2</sub>O<sub>3</sub>, thermally-grown capacitor-film, dielec. props. 0-2480
- CeF<sub>3</sub> film, in MIM struct., dielec. props. (*Czech*) 0-25309
- Cu-GeO<sub>2</sub>/BaO-Cu thin film, amorphous, effect of electroforming on conductance and capacitance 0-34537
- Cu-SiO<sub>2</sub>/B<sub>2</sub>O<sub>3</sub>-Cu thin film, amorphous, conductance and capacitance, effect of electroforming 0-34537
- FeF<sub>3</sub> film, localised electronic states effect on elec. cond., MIM struct. meas. 0-20328
- GeS film, between Al(Zn)(Sn) electrodes, Schottky and Poole-Frenkel cond. mechanisms 0-54799
- Pt/polymer/metal capacitors, electroforming and elec. cond. 0-54800
- Ta<sub>2</sub>O<sub>5</sub> films, Poole-Frenkel effect and cond., effect of heat treatment in oxygen and in vacuum 0-39693
- W-Ni, MBM diode, resist. depend. of detected signals 0-2482
- Y-Y<sub>2</sub>O<sub>3</sub>-Au thin film capacitors, self-healing dielec. breakdown 0-11104

**metal-insulator-semiconductor devices**

- see also charge-coupled devices
- AlSiO<sub>2</sub>-Si photodiode, experimental verification of theoretical predictions 0-29485

**metal-insulator-semiconductor devices continued**

- MOS devices, interfacial and bulk trap props., expt. characterization techniques 0-49950
- MOS devices, inversion layer, pot. and carrier distrib., quantum mechanical determ. 0-29483
- MOS diodes, Al-SiO<sub>2</sub>-Si, defects due to electron beam lithography, obs. (*Japanese*) 0-54787
- MOS diodes, minority carrier lifetime determ. from photocurrent spectra 0-49920
- solar cells, basic principles of operation theoretical characts. 0-50986
- solar cells, fabrication and performance characts. 0-45707
- solar cells, low-temp. CVD of SiO<sub>2</sub> to form inversion layer 0-12019
- solar cells, optimal interface design using computer simulation and expt. meas. 0-16805
- solar cells, spectral response characts. and meas. of effective diffusion lengths 0-16804
- switching voltage criteria for metal-insulator-Si(n)-Si(p<sup>+</sup>) device 0-15610
- Al-SiO<sub>2</sub>-Si MIS solar cells, I-V characts. temp. depend. 0-7935
- Al-SiO<sub>2</sub>-p-Si MIS solar cells with back surface fields 0-12006
- CdS, Au deposition, Schottky diodes and MIS devices, surface treatment effects, SEM obs. 0-54794
- CdTe/Langmuir film photovoltaic structures for solar cells 0-49918
- Cr-SiO<sub>2</sub>-Si MIS solar cell, current cond. 0-7936
- GaAs MIS diodes, interface states determ., by deep-level transient spectroscopy (*Japanese*) 0-49917
- GaAs polycryst. tunnel MIS solar cells, grain boundary problem 0-16809
- Ge MIS photocapacitive IR detector 0-47106
- Si MOS device, electron optical identification of precipitations 0-16309
- Si-P, time dependence of depletion region formation at cryogenic temp. 0-34522
- SiO<sub>2</sub>-Si, low-energy neutral particle bombardment of SiO<sub>2</sub> film, degradation 0-54790
- SnO<sub>2</sub>-Si solar cells, stability and degradation mechanisms 0-16806

**metal-insulator-semiconductor integrated circuits** see field effect integrated circuits**metal-insulator-semiconductor structures**

- capacitance, high- and low-freq. steady state 0-54796
- capacitance meas. for Schottky barrier 0-39678
- capacitance-voltage characts., built-in charge fluctuation effects, negative surface state density 0-6992
- charge distrib., optoelectric determ. methods (*Polish*) 0-39675
- deep centres investigation using capacitance method 0-39677
- deep level parameters determ. in surface layer of semiconductor of MIS struct. 0-15612
- graded and stepped energy band-gap MIS structures 0-2473
- interface states and deep level impurities, DLTS, charge storage and charge release modes 0-49923
- inversion layer, hot electron effects in Landau levels 0-6998
- inversion layer, transient response of hot electrons, calc. 0-49747
- metal-gelatin-n-GaAs struct., C-V characts. and gelatin-semiconductor interaction rel. to photographic process (*Russian*) 0-49944
- metal-ZnO-SiO<sub>2</sub>-Si structures, charge injection 0-49919
- MM wave modification by surface carrier scatt., surface pot. depend. 0-44736
- MNOS capacitors, simple technique for charge centroid meas. 0-34521
- MNOS P-channel switch, accelerated reliability testing (*German*) 0-6988
- MNOS structure, model for degradation mechanisms 0-29477
- MNOS structures, new technique for determ. of charge centroid 0-6990
- MNOS structures, transport processes of electrons 0-34523
- mobile charges determ., using triangular voltage sweep methods (*German*) 0-4740
- MOS capacitor, TSC meas., suppression of meas. interferences from interface states and mobile ions 0-29479
- MOS capacitors, charge distrib. for large electron beam irradi. doses 0-34518
- MOS inversion layer, hot electron effects in Landau levels 0-20315
- MOS inversion layers, electron-phonon interaction and cyclotron reson. 0-25014
- MOS structs., Schottky barrier characterisation by scanned internal photoemission 0-49915
- MOS structure, distrib. of interface states conc., method for determ. 0-44733
- MOS structure, model for ion-electron (configurational) interface states 0-29478
- MOS structure, p-channel, effect of isotropic stress on Si valence band struct., press. transducer appl. 0-25011
- MOS structures with superthin gate dielectric, hole mobility in inversion layers 0-29482
- MOS surface states, DLTS spectra synthesis and anal. 0-11090
- nonuniformly doped MOS devices with lateral symmetry 0-15606
- optical image recording, As<sub>2</sub>Se<sub>3</sub> as photosensitive element 0-42286
- optical phonon-electron gas interaction, high freq. cond. 0-6888
- photosensitive MIS structure in contact with nematic liq. cryst., light spatial modulation 0-48436
- photovoltaic effects (*Japanese*) 0-54737
- plasmon-acoustic wave interactions due to deformation potential (*Russian*) 0-15356
- polarisation hysteresis, ion motion, on thermal SiO<sub>2</sub> (*Russian*) 0-54793
- polymer, in MIS struct, charge movement study using capacitance-voltage characts. (*French*) 0-39575
- potential barrier height determ. using photoelectric methods (*Polish*) 0-20317
- pulsed MOS capacitor, recombination lifetime meas. 0-25012
- radiation induced charge storage 0-6997
- semiconductor surface states, capacitance, admittance, freq. depend. 0-49940
- spectral characteristics of MIS struct. with variable-gap semicond. 0-44735
- surface electron states in band gap, calc. by Green's function method 0-15611
- tunnel diodes, photoionisation of states 0-11099
- Al-Al<sub>2</sub>O<sub>3</sub>-GaAs MOS struct., mol. beam reaction growth of Al<sub>2</sub>O<sub>3</sub> film, C-V characts. 0-11095
- Al-Al<sub>2</sub>O<sub>3</sub>-SnTe, junction, tunnelling, Fermi level depend. on carrier conc., influence of surface states 0-25046
- Al-Al<sub>2</sub>O<sub>3</sub>-SnTe, tunnelling characts., model anal. 0-29480
- Al-Al<sub>2</sub>O<sub>3</sub>-(a-Ge)-Al, electron tunnelling into a-Ge, press. effect 0-49938
- Al-rare earth oxide-Si, elec. props. of oxide thin film, oxide-Si interface props. 0-7013



**metal-insulator-semiconductor structures continued**

- Al-Si<sub>3</sub>N<sub>4</sub>-Si struct., surface energy bands under step function illumination 0-49840  
 Al-SiO<sub>2</sub>-Si, void form. in Al interconnection lines at Si-SiO<sub>2</sub> boundaries 0-2476  
 Al-SiO<sub>2</sub>-Si structure, positive interface charge, exciton and H diffusion models 0-2471  
 Al-SiO<sub>2</sub>-Si system with reactively sputtered SiO<sub>2</sub>, work functions difference 0-6987  
 Al-silicide-Si systems with CoSi<sub>2</sub>, Pt<sub>3</sub>Ni<sub>1-x</sub>Si, and MoSi<sub>2</sub> as silicide, diffusion, compound form., and microstructure 0-34253  
 Al-silicide-n-Si systems with CoSi<sub>2</sub>, MoSi<sub>2</sub>, and Pt<sub>3</sub>Ni<sub>1-x</sub>Si as silicide, Schottky-barrier height 0-34520  
 Al<sub>2</sub>O<sub>3</sub> plasma anodised film on Si, elec. resist. 0-7722  
 Au/Se(As<sub>2</sub>Se<sub>3</sub>)(CdS)-liquid insulator interface, carrier injection 0-24970  
 Au-oxide-GaAs struct., steady-state and transient photocurrents 0-6994  
 Au-oxide-n-GaAs structs., reverse-bias depend. photocurrent, photoionisation of surface states 0-20323  
 BaTiO<sub>3</sub>/SiO<sub>2</sub>-Si charge storage memory films for IGFETs 0-11566  
 Bi film, quantum size effect and band struct. Bi-dielectric-metal system obs. 0-54811  
 CdS<sub>1-x</sub>Se<sub>x</sub> multilayered struct., charge pattern formation during recharging 0-47129  
 CdSe MIS thin film solar cell 0-45688  
 CdTe/Langmuir film photovoltaic structures for solar cells 0-49918  
 p-Ga<sub>1-x</sub>Al<sub>x</sub>As crystals, spectral characts. of photosensitivity, mechanism 0-44735  
 GaAs anodic MIS system, dynamic props. of interface state bands 0-49933  
 GaAs anodic MOS structs., interface-state band model 0-11093  
 GaAs MIS structs., nitride-based passivation for reduced surface state density 0-16537  
 In-GaAs, MOS capacitor struct., elec. props., annealing effects 0-34519  
 GaAs MOS diodes, interface states, deep-level: transient spectroscopy 0-44727  
 GaAs MOS structure, small signal admittance study 0-2478  
 GaAs MOS structures, props. of capacitance transient 0-25013  
 GaAs, oxidation in multiple plasma, MOS elec. props. 0-44737  
 GaAs, thermal oxide film growth and characterisation 0-11808  
 GaAs-Al<sub>2</sub>O<sub>3</sub> anodic oxide interface, elec. props., rel. to MESFET passivation 0-49934  
 GaP anodic MOS structs., interface-state band model 0-11093  
 Ge-GeO<sub>2</sub> MIS structure, growth of GeO<sub>2</sub> from liq. phase (*Russian*) 0-40273  
 Hg<sub>1-x</sub>Cd<sub>x</sub>Te-oxide interfaces, MIS capacitance characts. 0-49926  
 InAs surface accumulation layers, magneto-transconductance study 0-49948  
 InP MIS capacitor surface states 0-49931  
 n-InP-SiO<sub>2</sub> capacitor, carrier generation and trapping 0-49929  
 n-InP-SiO<sub>2</sub> system, interface and dielec. props. 0-49930  
 InSb based MIS structs., charge accumulation in insulator layers 0-6993  
 InSb MIS capacitors, gamma-ray radiation effects at cryogenic temps. 0-34517  
 n-InSb MIS device interfaces, low-temp. CVD of SiO<sub>2</sub>, characts. 0-16196  
 InSb, MIS struct., background radiation effect on photoelec. processes 0-25015  
 InSb, MISS struct., surface electron and hole mobility and conc. (*Russian*) 0-44701  
 InSb MOS structure, props. 0-49947  
 p-InSb, magnetoconductivity and cyclotron reson. in inversion layers 0-49946  
 n-InSb, surface quality improvement by low temp. CVD of SiO<sub>2</sub>, and characterisation 0-49932  
 Pb/oxide/InAs structure, effective mass determ. by tunnelling spectroscopy (*Russian*) 0-44482  
 Pb-SiO<sub>2</sub>-Pb<sub>1-x</sub>Ge<sub>x</sub>Te, semicond. band struct., tunnelling obs. 0-54795  
 p-PbTe, MIS struct. inversion layer sub-struct., IR magnetoreflectance obs. 0-44731  
 PbTe-oxide-Pb(Sn) junctions, quantum levels obs. 0-49945  
 PbTe-ZrO<sub>2</sub> (SiO<sub>2</sub>), epitaxial MIS struct., fabrication and elec. props. 0-2472  
 Si (100) MOST, comparison of Shubnikov-de Haas effect and cyclotron reson. under uniaxial stress 0-20320  
 Si inversion layer, transient response of hot electrons, calc. 0-49747  
 Si inversion layer in MOS struct., carrier-phonon interaction, nonohmic transport 0-49943  
 Si MIS switch diode, charge storage effects, threshold depend. on driving voltage pulse freq. 0-49939  
 Si, MOS capacitor, nondestructive of P<sup>+</sup> and He<sup>+</sup> induced damage, doping profiles 0-34087  
 Si MOS capacitors, on Czochralski-grown wafers, lifetime improvement by two-step annealing 0-49916  
 n-Si MOS inversion layers, Hall cond. meas. 0-39676  
 Si MOS struct., space-charge generation props. of Au 0-2475  
 Si, on sapphire, MOS inversion layer, magnetoconductance oscillations 0-20325  
 Si oxides, grown in Cl-containing ambients, correl. between elec. and material props. 0-39479  
 Si, under stress, density functional calc. of subband struct. 0-20321  
 Si:Ar ion implant gettering obs. by MOS and Rutherford backscatt. techniques 0-39119  
 Si:H, amorphous, density of states determ. using field effect 0-49937  
 a-Si:H MIS junction, electronic struct. study by tunnelling 0-44729  
 Si:In, MIS structure, determ. of deep level parameters in surface layer of semiconductor 0-15612  
 Si-Al<sub>2</sub>O<sub>3</sub>, from UV irradiation converted metalorganic compounds (*Russian*) 0-45245  
 Si-SiO<sub>2</sub>, SiO<sub>2</sub> layer charging in UV irradiation of MISS struct., photoinjection currents (*Russian*) 0-39680  
 Si-SiO<sub>2</sub> interface, effect of hot electron injection on interface charge density 0-49921  
 Si-SiO<sub>2</sub> interface, radiation damage coeffs. for fission neutron and gamma-ray irradiation 0-34058  
 Si-SiO<sub>2</sub> interface, radiation hardness eval. using elec. meas. technique 0-34516  
 Si-SiO<sub>2</sub> interface, surface states characterization, expt. techniques review 0-49949  
 Si-SiO<sub>2</sub> interface state spectroscopy using MOS tunnelling structures 0-6991

**metal-insulator-semiconductor structures continued**

- Si-SiO<sub>2</sub> MOS capacitors, two-dimens. calc. of avalanche breakdown voltage 0-11096  
 Si-SiO<sub>2</sub> structures, electron trapping, donor state generation, photo I-V study 0-20210  
 Si<sub>3</sub>N<sub>4</sub> film, CVD, high-field dark currents 0-54791  
 Si<sub>3</sub>N<sub>4</sub>-SiO<sub>2</sub>-As, graded and stepped energy band-gap MIS struct. 0-2473  
 SiO<sub>2</sub> film, migration parameters of alkali ions, elec. meas. in MOS capacitor 0-39359  
 SiO<sub>2</sub> layers, in MOS struct., hole trapping induced by ion implantation and annealing at room temp. 0-54792  
 SiO<sub>2</sub> MOS structures, removal of electron traps by RF annealing 0-44728  
 SiO<sub>2</sub>-Si, irradiated SiO<sub>2</sub> film electron and hole trapping 0-11098  
 SiO<sub>2</sub>-Si MOS capacitor, two-stage process for building up of radiation induced interface states 0-20313  
 SiO<sub>2</sub>-Si MOS system, ion irradiation effects on struct. and electrophysical props. 0-6995  
 Si(100) inversion layers, effects of uniaxial stress on cyclotron reson. 0-20322  
 TiO<sub>2</sub>/SiO<sub>2</sub>-Si charge storage memory films for IGFETs 0-11566  
 TiO<sub>2</sub>-SiO<sub>2</sub>-Si structure, SiO<sub>2</sub> growth under TiO<sub>2</sub> film during postdeposition high temp. annealing 0-15400  
 ZnO-Ti transparent type MIS solar cells 0-45662

**metal-insulator transition**

- see also electrical conductivity transitions; minimum metallic conductivity*  
 adamantane ceramic, structural, thermophysical and electrophysical props. 0-6918  
 Anderson localisation problem, cond. numerical studies 0-49673  
 Anderson transition, electron localisation in disordered systems, review 0-29361  
 Anderson transition in mag. field, weak field cond. and Hall effect 0-6726  
 conducting liquid, effect of metal-insulator transition on crit. state 0-20089  
 diamond, 'melting' to solid metallic C phase above graphite triple point 0-15236  
 dielectrics, transfer processes, theoretical model review 0-15529  
 disordered one-dimensional system, electron density of states and Peierls transition (*Russian*) 0-29304  
 disordered system, Anderson localised states, intra- and inter-state interactions 0-44543  
 disordered systems, one dimensional, nonvanishing zero temp. static cond., Anderson transition 0-29396  
 doped semiconductors, metal-insulator transition pretransition range anal., screening model 0-6724  
 education, electrochromism in WO<sub>3</sub>, advanced lab. expt., colour centres, proton diffusion 0-17738  
 electron gas, dielectric transition temp. in strong mag. field 0-24813  
 electronic Peierls transition, gap eqns. 0-24801  
 extrinsic semiconductors, impurity interaction and metal-nonmetal transition 0-29325  
 Fermi surface topological transition, electron-phonon interaction contrib. calc. 0-6697  
 Hubbard model, cluster-variation method in two-site approx. at high temp. 0-7071  
 impurity conduction phenomena, review of exptl. work (*Japanese*) 0-49737  
 intermediate valence, phase diagram and Kondo behaviour 0-29366  
 liquid semiconductors, data and model densities of states 0-50364  
 many-valley semiconductor, metal-insulator transition at finite temp., calc. 0-49603  
 mixed valence states, excitation mechanism in tight-binding approx., metal-insulator transition 0-10925  
 mixed-valence compounds, dielectric-metal phase transition (*Russian*) 0-6788  
 mobility edge, classical solns. and crit. exponents 0-10936  
 mobility edge problem, continuous symmetry 0-10939  
 model Hamiltonian 0-34361  
 Mott transition in the presence of impurities, Hubbard model and SCF anal. 0-10878  
 Mott transitions, temperature induced, Hubbard model theory 0-29326  
 one-dimensional organic semiconductors, resonant states, mag. excitations and impurities 0-24839  
 orientational metal-insulator phase transitions in quadrupolar strands with itinerant electrons 0-15455  
 plasma, three-component, weakly-ionised, ionis. equilib. instability 0-10877  
 rare earth perovskites, prep. and props. book contrib. 0-44193  
 rare earth trihydrides, light, low-temp. sp. ht., mag., elec., and cryst. field splitting effects 0-49379  
 semiconductor, electric field induced nonequilibrium phase transitions 0-10879  
 semiconductor melts, metallic cond. at high temp. 0-49832  
 semiconductor-metal transition, struct. changes 0-34360  
 semiconductors, doped, dielec. const. enhancement on insulating side 0-20087  
 semiconductors, doped, insulator-metal transition, dielec. constant enhancement on insulating side 0-20088  
 semimetal-exciton phase transition, microwave cond. 0-29430  
 superconductors, effect of insulating pairing of electrons on mag. props. 0-15651  
 TCNQ salt, MEM(TCNQ)<sub>2</sub>, phase transition electronic struct. interpretation 0-24781  
 TCNQ salt, tetramethylhexamethylenediammonium-TCNQ-iodine, elec. and mag. props., struct., specific heat 0-24898  
 thermochromic material, vanadium oxides mixture, appl. to laser beam indicator/visualiser 0-9976  
 TMTSF-DMTCNQ, metallic state, transport props. 0-24974  
 transport processes, isothermal method for static cond. of electrons 0-29373  
 TTF and derived cpds., intramolecular vibr. and vibronic effects, IR and Raman spectra 0-25387  
 TTF-TCNQ, electron-molecular distortion coupling near Peierls transition, IR spectra obs. 0-25390  
 TTF-TCNQ, impurity effects on CDW fluctuations 0-44576  
 TTF-TCNQ, phase transitions and CDW state, controlled disorder effects 0-15507  
 TTT<sub>1/3+δ</sub>, thermoelec. power and metal-semicond. transition 0-34431



**metal-insulator transition continued**

- two-dimensional system, phase transitions and metal-insulator transitions 0-2143
- Al-Al<sub>2</sub>O<sub>3</sub>-(a-Ge)-Al, electron tunnelling into a-Ge, press. effect 0-49938
- AlSb film, laser-induced metal-semicond. transition in Al-Sb mixed film 0-6661
- B<sub>2</sub>Cy, metal-insulator transition, elec. cond. and thermoelec. power, 80 to 700K 0-44673
- Bi, Shubnikov-de Haas effect in high mag. fields 0-2404
- Bi-Sb, Shubnikov-de Haas effect and semimetal-semicond. transition in high mag. fields 0-44674
- $\beta$ -Cu<sub>2</sub>V<sub>2</sub>O<sub>5</sub>, mag. and spectroscopic study, semiconductor to metal transition 0-2628
- Cd<sub>1-x</sub>In<sub>x</sub>Cr<sub>2</sub>Se<sub>4</sub>, electric, photoelectric and mag. props., metal-semicond. transition (*Russian*) 0-54738
- CdS, press. quenched, mag. moment, semicond.-conducting transition 0-15683
- CdSe:Au impurity light absorpt. for current control in negative resistance region 0-11052
- Co<sub>0.83</sub>[Pt(C<sub>2</sub>O<sub>4</sub>)<sub>2</sub>].6H<sub>2</sub>O, quasi-one-dimens. conductor, Peierls distortion and superlattice, X-ray study 0-29397
- Cs, fluid, metal-nonmetal transition and mag. interactions 0-49602
- Cs fluid, metallic and nonmetallic, mag. props. 0-44799
- Cs-Au, liquid, metal-insulator transition, mag. susceptibility, Knight shift, theory 0-44672
- CuCl, optical microscopic, X-ray diffr. and elec. resist. studies at high press. 0-11051
- donor polarisability, enhanced, below insulator-metal-transition, self-consistent calc. 0-7262
- Fe<sub>3-x</sub>Mg<sub>x</sub>O<sub>4</sub>, Verwey transition, Mossbauer study 0-39942
- Fe<sub>3</sub>O<sub>4</sub>, Coulomb gap and hopping cond., effects on thermopower and Verwey ordering 0-44583
- Fe<sub>3</sub>O<sub>4</sub>, magnetite, Verwey transition temp., isotope effect, elec. resist. and DTA meas. 0-24976
- Fe<sub>3</sub>O<sub>4</sub>, magnetite Mossbauer spectra, mag. dipolar and elec. quadrupole effects 0-50544
- Fe<sub>3</sub>O<sub>4</sub>, optical cond. anisotropy calcs. below Verwey transition 0-50289
- Fe<sub>3</sub>O<sub>4</sub>, Verwey transition, electron-phonon versus Coulomb interaction effects 0-39280
- Fe<sub>3</sub>O<sub>4-x</sub>F<sub>x</sub> substituted magnetite, low temp. resistivity, Seebeck coeff., thermopower 0-20234
- Fe<sub>x</sub>V<sub>2-x</sub>O<sub>4</sub> solid solutions, specific heat near semiconductor-metal transition 0-24612
- Ge, plastically deformed low temp. cond. (*Russian*) 0-6831
- Ge, stressed, metal-insulator transition, luminesc. 0-20695
- GeSb, low-freq., low temp. dielec. behaviour below metal-insulator transition 0-50250
- Hg, electrical and thermodynamic props. in metal-semicond. transition range 0-20144
- Hg, liq., sound vel. near metal-nonmetal transition, up to 1600°C and 2000 kg/cm<sup>2</sup> 0-39222
- Na<sub>2</sub>WO<sub>3</sub>, Knight shift, spin-lattice and spin-spin relax., high press. NMR obs. 0-50211
- (Ni<sub>1-x</sub>Fe<sub>x</sub>)<sub>2</sub>S, anomalous thermal hysteresis in metal-semicond. transition 0-39640
- Ni<sub>1-x</sub>S, metal-semimetal transition, lattice dynamics and thermodynamic props. 0-29324
- S, shock wave method observation of transition to highly conducting state 0-4738
- n-Si, EPR linewidth, Orbach relax. process, conc. depend. 0-44901
- Si, electronic structure at high press. near semicond.-metal transition 0-49586
- Si:P, heavily doped, mag.-field depend. of sp. ht., rel. to metal-nonmetal transition 0-29183
- Si-H, amorphous, struct. and press. induced transition 0-44131
- SmB<sub>6</sub>, mixed valence cpd., EPR and heat capacity obs., metal-semicond. behaviour 0-20456
- Sm<sub>0.8</sub>Gd<sub>0.2</sub>S, valence transition, positron annihilation study 0-15454
- Sm<sub>1-x</sub>Gd<sub>x</sub>S system, semicond. to metallic isomorphous phase transition mechanism 0-2338
- SmS (001) surface, mixed valency and phase transitions 0-39658
- SmS, and Sm<sub>0.8</sub>Tb<sub>0.2</sub>S, resistivity and thermopower 0-20260
- SmS, defect struct., TEM obs., semicond.-metal transition in surface layer 0-44214
- SmS, electronic phase transition, mechanism, trivalent metal impurity effects 0-49604
- SmS, metallic phase, compressibility anomalous behaviour 0-29114
- SmS, valence fluctuation phenomena 0-24800
- SmS, valence transition, positron annihilation study 0-15454
- (TSeT)<sub>2</sub>Cl, one-dimens. conductor, metallic phases 0-20159
- Ta<sub>2</sub>S<sub>3</sub>, phase transitions and elec. props. 0-20178
- Ta<sub>2</sub>S<sub>3</sub>, transport props. 0-20175
- Te, high pressure metallic phase, cryst. struct. 0-49161
- Te, trigonal, <sup>129</sup>I Mossbauer obs. at high press. 0-55005
- Te:Sb, impurity states and impurity conduction, hydrostatic pressure 0-39521
- Te-Se mixtures, liquid, semiconductor to metal transition, high temps. and pressures 0-39639
- Ti-Ni, electron phase transition XPS, optical spectra and mag. susceptibility meas. 0-19943
- Ti<sub>2</sub>O<sub>3</sub>, metal-semicond. transition, refl. spectra study 0-10880
- Ti<sub>4</sub>O<sub>7</sub> and (Ti<sub>1-x</sub>V<sub>x</sub>)<sub>4</sub>O<sub>7</sub>, metal-insulator transitions, EPR, elec. and mag. props. 0-2336
- (Ti<sub>1-x</sub>V<sub>x</sub>)<sub>4</sub>O<sub>7</sub> order-disorder and metal-insulator transition theory 0-24802
- (Ti<sub>1-x</sub>V<sub>x</sub>)<sub>4</sub>O<sub>7</sub>, elec. cond. and phase diagram near metal-insulator transition 0-11054
- (Ti<sub>1-x</sub>V<sub>x</sub>)<sub>4</sub>O<sub>7</sub>, order-disorder and metal-insulator transitions 0-39504
- Tm<sub>1-x</sub>Eu<sub>x</sub>Se, valence changes, semicond.-metal transition 0-20086
- TmSe<sub>1-x</sub>Te<sub>x</sub>, valence changes, semicond.-metal transition 0-20086
- V oxides, XPS and AES study, electron correl. effects, semicond.-metal transition 0-7467
- V<sub>0.966</sub>Fe<sub>0.014</sub>O<sub>2</sub>, metal-insulator phase transition, effect of hydrostatic press. 0-6725
- V<sub>1-x</sub>Fe<sub>x</sub>O<sub>2-x</sub>F<sub>x</sub>, 0 < x < 0.2, phase diagrams, <sup>57</sup>Fe-Mossbauer spectra, X-ray diffr. studies (*German*) 0-29663
- VO<sub>2</sub>, cylindrical specimen, thermal switching 0-44679
- VO<sub>2</sub>, film, visualisation of microwave and IR radiation 0-5839
- VO<sub>2</sub>, nonstoichiometry influence on electron struct. and metal-insulator phase transition 0-44507

**metal-insulator transition continued**

- VO<sub>2</sub> single cryst. film, ion-irrad., 'splitting' of semicond.-metal transition 0-11053
- VO<sub>2</sub>, single crystal and polycrystalline, synthesis and resist. near metal-semicond. phase-transition 0-44680
- VO<sub>2</sub> thin film semiconductor-metal transition applications 0-49835
- VO<sub>2</sub>, V<sub>2</sub>O<sub>5</sub>, V<sub>2</sub>O<sub>3</sub>, metal-insulator transitions, effect of isotopic substitution 0-2337
- V<sub>5</sub>O<sub>9</sub>, metal-insulator phase transition temp. depend. on press. 0-29327
- V<sub>6</sub>O<sub>11</sub>, metal-insulator phase transition temp. depend. on press. 0-29327
- V<sub>6</sub>O<sub>13</sub>, optical props. in metallic and semicond. phase 0-40135
- WO<sub>3</sub> films on Si, sapphire, glass and metal substrates, colour intensity dependence obs. (*Russian*) 0-2430
- Yb, FCC phase, low temp. mag. props., impurity effects 0-20387
- metal-oxide-semiconductor devices** *see metal-insulator-semiconductor devices*
- metal-oxide-semiconductor field effect transistors** *see insulated gate field effect transistors*
- metal-oxide semiconductor structures** *see metal-insulator-semiconductor structures*
- metal-semiconductor boundaries** *see semiconductor-metal boundaries*
- metal semiconductor field effect transistors** *see Schottky gate field effect transistors*
- metal-semiconductor-metal structures**
- metal/PbI<sub>2</sub>/metal struct. reson. and inelastic tunnelling 0-44739
- p-quaterphenyl, polycryst. thin layer-metal sandwich, elec. cond. 0-34526
- superconducting metal contacts, anal. of conductivity of Si 0-15621
- tunnelling phenomena in terms of exact method and WKBJ approximation 0-20329
- Al-CdSe-Ag dry air stabilised struct., elec. cond. mechanism, breakdown phenomena 0-34527
- Al-Si-Al contact current response to 100 keV neutron irrad. (*Russian*) 0-49956
- Al-TeO<sub>2</sub>-Al, field-assisted cond. mechanism 0-11105
- As<sub>50</sub>Te<sub>50</sub>, amorphous films, metal and semicond. contacts, threshold switching, IR emission 0-49831
- Au-B-Au systems, elec. field effect on B film struct. 0-20050
- Au-PbTe-Au, semiconductor thin films, random noise measurements 0-15629
- GaSe MSM struct., inelastic tunnelling investigation of lattice dynamics, electron-phonon interaction 0-20330
- GeS film, between Al(Zn)(Sn) electrodes, Schottky and Poole-Frenkel cond. mechanisms 0-54799
- In-PbTe-In semiconductor thin films, random noise measurements 0-15629
- Mo-Si-Mo structure, non-volatile memory switching 0-54814
- TiInS<sub>2</sub>(Se<sub>2</sub>), electrical cond. of single crystals with symm. and asymm. Ag-In contacts 0-6835
- V<sub>2</sub>O<sub>5</sub>-P<sub>2</sub>O<sub>5</sub> (70-30), electrical cond. and thermoelectric meas., Au-glass-Au sandwich 0-29403
- ZnS-metal interface in MIM struct., photoexcitation level assignment (*French*) 0-15622
- metal theory**
- see also band structure of crystalline metals; electron gas; lattice dynamics of metallic crystals*
- 1/f noise, temp. fluctuations as source, theory 0-11059
- alkali metal, Ashcroft pseudopotential, unified study of props. 0-39239
- APS, multiple scatt. approach using muffin-tin pot. 0-25490
- charge-density-wave metal, mag. susceptibility of cond. electrons 0-44523
- cluster model theory and its application to metal surface-adsorbate systems, book contrib. 0-24991
- conduction electron photoemission spectrum, effect of recoil on shake-up spectra, infinite summation method 0-50526
- conduction electron spin echo modulation in small metal particles 0-39872
- core level binding energy shifts between free and condensed atoms 0-20136
- cubic metals, intra-atomic correl. energies with canonical d bands, Hubbard interaction calc. 0-39518
- disorder systems, conduction electron surface scatt. (*Russian*) 0-24917
- electron gas, correlation effects on polarisation 0-54628
- electron gas, local density functional for kinetic energy near defect, metal surface 0-20105
- electron gas, metallic densities, dynamical dielectric function and paramagnetic spin susceptibility 0-39514
- electron gas, optical props. in generalised HF approx. 0-24825
- electron gas, semi-infinite, nonlocal cond. tensor calc., effective optical surface region 0-20283
- electron-lattice interaction effect on equilib. struct. form. (*Russian*) 0-34380
- FCC metal, covalent component of electron density and energy (*Russian*) 0-28945
- Fermi surface topological transition, electron-phonon interaction contrib. calc. 0-6697
- ferromagnetic metals, dislocation drag by conduction electrons 0-24451
- Friedel sum rule, high conc. extension, appl. to coherent pot. approx. 0-44462
- Gruneisen parameters, interatomic forces, pseudopot. calc. for simple metals 0-44165
- jellium metal, surfaces props., statistical calc. 0-24987
- jellium model, impurities and photoexcited ions in metal 0-39523
- light impurities, electronic struct. 0-34394
- metals, degenerate electron gas, collective props. using electron knock-out processes 0-6758
- microwave transmission, time-of-flight effects in Fermi vel. determ., calc. 0-20238
- noble metals, Krasko-Gurskii model potential, test of validity for Cu 0-39485
- photoemission, ultrasoft XPS, plasmon satellite intensity 0-35058
- positron trapping rate into vacancy clusters in metals 0-2890
- positron-phonon interaction through cond. electrons (*Russian*) 0-29126
- Raman scattering by adsorbed molecules on metal surface, intensity enhancement, theory 0-54518
- resonant photoemission, mech. 0-50524
- simple metal, Knight shift, single-ion approach 0-44935
- simple metals, photoemission theory, book contrib. 0-16159
- simple metals, plasmon dispersion anal. from electron gas dielectric response 0-6761
- simple metals, X-ray absorpt. and emission edges, one-electron and many-body effects 0-25484
- single-particle density matrix, perturbation expansion 0-54635



**metal theory continued**

- spin scattering and spin-orbit coupling 0-29369  
 surface, density functional theory, review 0-44698  
 surface, dynamic image pot. for tunnelling electrons 0-49874  
 surface, electrodynamics, microscopic effects (*Russian*) 0-6936  
 surface, electron-phonon coupling in image-potential bound states 0-54752  
 surface, electron-plasmon interaction 0-39649  
 surface, influence of submonolayer films on props., calc. (*Russian*) 0-2273  
 surface, integro-differential eqn. for electron density and formula for surface tension of jellium 0-44689  
 surface, interaction with  $H_2$  0-29259  
 surface, positron-electron correlations, RPA calc. 0-40181  
 surface, theory, book 0-36787  
 surface bonding, book contrib. 0-24990  
 surface dipole barrier, semi-empirical calc. 0-39659  
 surface electronic barrier, elec. field effect in presence of adsorbate, Thomas-Fermi model 0-49864  
 surface energy, gradient corrections in interpolation formulae, surface plasmons 0-2441  
 surface impedance, extreme anomalous limit, diffuse refl. from boundary 0-29460  
 surface plasmon dispersion 0-2440  
 surface problems in microwave region, theory and meas. (*Chinese*) 0-44704  
 surfaces, exchange and correlation energy, wave vector anal. 0-20273  
 work function, nonideal terraced surface, calc. 0-6950  
 Cu, Krasko-Gurskii model potential, test of validity 0-39485  
 H storage, electronic struct., many electron theory 0-49667  
 H-impurity, energy and electron density of states 0-34398  
 Na, liquid, entropy calc. using phonon theory of liquids 0-39310  
 Nb, band effective mass, Animalu TMMP theory 0-29312  
 V, band effective mass, Animalu TMMP theory 0-29312

**metal vapour lamps**

- see also *mercury vapour lamps*  
 film lighting appl. luminance fluctuations assessment 0-4796  
 halide, filler composition, physico-chemical studies (*Russian*) 0-48373  
 Cs vapour, nearly saturated, prebreakdown elec. cond. 0-48841

**metallic epitaxial layers**

- large misfit systems, epitaxy and misfit dislocations 0-24767  
 Ag (100) and (111) epitaxial films, ang. depend. UPS 0-55270  
 Ag epitaxial films, grain boundary struct. evolution during recrystn., interface energy effect (*Russian*) 0-15387  
 Ag film, epitaxial growth on isolated Au patches covered with amorphous C layer 0-40270  
 Ag, growth on electron bombard. NaCl(111) surfaces, RHEED and AES 0-15419  
 Ag, vac. deposition of oriented coating on doped alkali halide substrate 0-2303  
 Ag-Dy, dil., thin films, ESR spectra, stress effects 0-39866  
 Al epitaxial films, grain boundary struct. evolution during recrystn., interface energy effect (*Russian*) 0-15387  
 Al, epitaxial growth on GaAs (001) 0-24757  
 Al-GaAs interface, struct. study by X-ray total-external-refl.-Bragg diffr. 0-34321  
 Au, epitaxial films, grain boundary struct. evolution during recrystn., interface energy effect (*Russian*) 0-15387  
 Au film, on NaCl, preferential epitaxy induced by electron bombard. or elec. field 0-10824  
 Au, on NaCl substrate, electrotransport inferred from void growth rate (*German*) 0-10699  
 Cr film, on NaCl, preferential epitaxy induced by electron bombard. or elec. field 0-10824  
 Fe film, on NaCl, preferential epitaxy induced by electron bombard. or elec. field 0-10824  
 Fe, VPE on W tip, depositing direction depend. 0-10812  
 Hf, oxidation, microstructural study (*French*) 0-45436  
 Nb heteroepitaxial layers on sapphire, residual mechanical stress and strain influence on superconductivity 0-15644  
 Ni electrodeposition, surface-stress phenomena at start 0-35542  
 Ni solar collector coating, microstruct., FIM and SEM obs. 0-26166  
 NiSi<sub>2</sub>, epitaxial film on Si, <sup>4</sup>He ion channelling meas. and RHEED anal. 0-10834  
 Pd<sub>2</sub>Si, epitaxial film on Si, <sup>4</sup>He ion channelling meas. and RHEED anal. 0-10834  
 Pt, on Au, crit. thickness of pseudomorphic film growth, substrate size depend. (*Russian*) 0-29286  
 PtSi, epitaxial film on Si, <sup>4</sup>He ion channelling meas. and RHEED anal. 0-10834  
 Sn film, on NaCl, preferential epitaxy induced by electron bombard. or elec. field 0-10824  
 Ta epitaxial layers, formation conditions influence on struct. (*Russian*) 0-20045  
 W/ $\alpha$ -Al<sub>2</sub>O<sub>3</sub>, heteroepitaxial structs., refined formulation of relative orientation criteria 0-44448  
 W-Os system films, condensation temp., conc., and phase comp. effect on struct. and props. (*Russian*) 0-24749

**metallic glasses**

- amorphous, ribbon samples, Young's modulus, using impulse induced resonance method 0-30008  
 amorphous magnetic alloys, characts. and appls. (*French*) 0-39815  
 bulk and surface properties, review 0-44147  
 Cl (Co<sub>100-x</sub>Fe<sub>x</sub>)<sub>83</sub>B<sub>17</sub>,  $1 \leq x \leq 30$ , annealing embrittlement and crystn. 0-45329  
 continuous cooling versus isothermal transformation diagrams, critical cooling rate 0-15012  
 continuous-biased sputter-deposited, Kr entrapment 0-24603  
 electrical resistance min. at low temp., mixed conduction model 0-44560  
 ferromagnetic, sputter-deposited, soft mag. props., magnetostriction 0-34696  
 ferromagnetic alloys, amorphous, domain struct. and mag. microstruct., review 0-15751  
 film, SAW device appls. 0-28389  
 formation prediction with bond parametric diagram (*Chinese*) 0-11587  
 metal-metalloid amorphous alloys produced by ion implantation, TEM 0-15128  
 metallic glasses, structure and formation, thermodynamic props., cluster relaxation approx. 0-54143  
 Metglas 2826 ribbons, ferromagnetic resonance and SEM obs. 0-15804

**metallic glasses continued**

- Mossbauer spectra, hyperfine field distrib. determ. 0-39965  
 Mossbauer studies 0-39917  
 polymer model 0-6361  
 properties and development review, scientific and industrial appl. 0-19710  
 resistivity due to two-level systems 0-10941  
 ribbons, manufacturing magnetic and physical props. 0-29898  
 ribbons, quenching stabiliser to improve geometrical uniformity and cross-section 0-55343  
 Sendust ribbon, mag. props. 0-15761  
 steel, stainless, alloyed with C, magnetron-sputtered, microstruct., and cryst.-amorphous transition 0-19719  
 structure, stability and prod., elec., mag. and mech. props., review 0-44134  
 structure direct obs. by bright field TEM 0-10502  
 structure of simple inorganic amorphous solids, review 0-15004  
 transition metal alloyed with metalloids, glass transition temp. 0-24371  
 transition metal-metalloid, short-range order, hyperfine field distrib. determ. by Mossbauer spectroscopy 0-39962  
 3d-transition metal-metalloid cryst. and glassy alloys, electronic struct. from magnetisation and Mossbauer meas. 0-29363  
 transition metal-metalloid glasses, struct., elec., supercond., and mech. props. 0-6365  
 transport properties and thermopower of amorphous alloys 0-34411  
 Young's modulus meas. by impulse induced resonance technique 0-40411  
 Al-Fe<sub>70</sub>Mo<sub>20</sub>B<sub>10</sub> wire composite, mech. props. 0-40441  
 Au<sub>81.4</sub>Si<sub>18.6</sub>, glass forming alloy, Gibbs free energy change on crystallisation 0-25676  
 B-transition metal thin films, amorphous to cryst. transformation 0-7563  
 CdGeAsMn, glass, recrystallisation 0-44133  
 (Co,Fe,M)<sub>78</sub>Si<sub>14</sub>B<sub>8</sub> amorphous alloys (M = V, Nb, Ta, Cr, Mo, W, Mn or Ni), zero magnetostriction and low field mag. props. 0-34741  
 (Co,Fe)<sub>0.75</sub>B<sub>0.25</sub> metallic glasses, annealed, equilb. crystalline phases 0-3019  
 Co-B-Mo-Cr, amorphous, Mo and Cr addition effect on corrosion behaviour 0-16568  
 Co-Ni-Fe-Si(B), amorphous ribbon, magnetostriction meas. 0-15778  
 Co-P, amorphous, ferromag. antireson. 24 GHz microwave transmission, mag. props. 0-34778  
 Co<sub>1-x</sub>B<sub>x</sub>, polycrystalline and amorphous sputtered films, Brillouin spectra 0-2775  
 Co<sub>100-x</sub>B<sub>x</sub>, amorphous alloys, saturation magnetostriction and annealing behaviour 0-34739  
 Co<sub>80</sub>B<sub>20</sub>, amorphous metal ribbon, stresses, magnetoelastic anisotropy and zero-field mag. domain struct. 0-44896  
 Co<sub>35</sub>Dy<sub>65</sub>, metallic glass, internal friction peaks 0-25753  
 Co<sub>79</sub>Fe<sub>6.5</sub>B<sub>14.5</sub> amorphous thin films, zero magnetostriction, high magnetisation 0-34708  
 (CoFeB)<sub>100-x</sub>Cr<sub>x</sub> thin films, magnetic props. and corrosion resist. 0-34709  
 (Co<sub>1-x</sub>Fe<sub>x</sub>Ni<sub>1-80</sub>(Si<sub>1-x</sub>B<sub>x</sub>)<sub>20</sub>) amorphous films, spin wave spectra 0-34777  
 Co<sub>75-x</sub>Fe<sub>15</sub>Si<sub>10</sub>B<sub>0</sub>, quenched ferromag. ribbon, Brillouin spectra 0-2776  
 Co<sub>50</sub>Ni<sub>20</sub>Fe<sub>6</sub>Si<sub>12</sub>B<sub>12</sub>, amorphous, mag. props., effects mech. deform. 0-39840  
 Co<sub>85</sub>P<sub>15</sub>, strip domains, anisotropy const. effects 0-29571  
 Co<sub>78</sub>P<sub>18</sub>B<sub>8</sub>, amorphous, photoemission and electronic struct. 0-2926  
 Co<sub>35</sub>Y<sub>65</sub>, metallic glass, internal friction peaks 0-25753  
 Cu-Fe<sub>78</sub>Mo<sub>20</sub>B<sub>20</sub> wire composite, mech. props. 0-40441  
 Cu-Zr, metallic glasses, valence band struct. investigation 0-11533  
 Cu<sub>66</sub>Ti<sub>34</sub>, metallic glass, neutron diffr. meas. of struct. factor 0-24367  
 Cu<sub>46</sub>Zr<sub>54</sub>, devitrification effect on mech. props. 0-30082  
 Cu<sub>46</sub>Zr<sub>54</sub>, metallic glass, dynamical struct. factor and freq. distrib. meas. 0-54136  
 Cu<sub>50</sub>Zr<sub>50</sub>, metallic glass, internal friction peaks 0-25753  
 Cu<sub>56</sub>Zr<sub>44</sub>, metallic glass, devitrification and its effect on mech. props. 0-33893  
 Fe base amorphous alloys, Invar and Elinvar characts. 0-29592  
 Fe-Al alloys, rapidly quenched, mag. props. 0-29579  
 Fe-B, (16.3 at.%) amorphous, coercive force temp. depend. 0-25158  
 Fe-B, amorphous, elec. resist., temp. depend. 0-44563  
 Fe-B, amorphous, short-range order, Mossbauer meas. 0-44986  
 Fe-B, amorphous paramag. alloys, hyperfine field distrib., Mossbauer study 0-39958  
 Fe-B amorphous alloy, mag. anisotropy temp. depend. 0-15846  
 Fe-B amorphous alloys, Mossbauer spectra, soft ferromag. props. 0-11302  
 Fe-B amorphous alloys, Mossbauer spectra, mag. moment conc. depend. 0-15847  
 Fe-B amorphous alloys, valence band spectrum, XPS study 0-50534  
 Fe-B-C amorphous alloys, effect of Si addition on mag. props. 0-34694  
 Fe-B-Mo-Cr, amorphous, Mo and Cr addition effect on corrosion behaviour 0-16568  
 Fe-B-Si, amorphous ferromag. alloys, mag. struct., Mossbauer study 0-39746  
 Fe-B-Si amorphous ribbons, effect of annealing conditions on magneto-mechanical props. 0-34740  
 Fe-B-Si ribbon, strain induced anisotropy, and toroid diam. effect on mag. props. 0-34623  
 Fe-B(Si) amorphous alloys, Mossbauer spectra, struct. 0-15840  
 Fe-based, Mossbauer effect at high press. 0-15858  
 Fe-based, Mossbauer spectroscopy, effect of neighbours on hyperfine field 0-39931  
 Fe-Co-Si-B sputtered amorphous thin film, coercivity, galvanomagnetic props., resistivity 0-29578  
 Fe-Cr-B, amorphous, Elinvar and Invar charact. (*Japanese*) 0-11832  
 Fe-Ni-Cr-P-B amorphous alloy, localized corrosion 0-16559  
 Fe-Ni-P-B, amorphous ferromag. alloys, mag. struct., Mossbauer study 0-39746  
 Fe-Ni-P-B, amorphous paramag. alloys, hyperfine field distrib., Mossbauer study 0-39958  
 Fe-Ni-Si-B, amorphous paramag. alloys, hyperfine field distrib., Mossbauer study 0-39958  
 Fe-P-C amorphous alloys, Mossbauer spectra, struct. 0-15840  
 Fe-Si amorphous film, struct. and crystallisation, Mossbauer study 0-11300  
 Fe-Si-B amorphous films, mag. props. 0-34710  
 Fe<sub>1-x</sub>B<sub>x</sub>, polycrystalline and amorphous sputtered films, Brillouin spectra 0-2775  
 Fe<sub>100-x</sub>B<sub>x</sub>, amorphous alloys, saturation magnetostriction and annealing behaviour 0-34739  
 Fe<sub>100-x</sub>B<sub>x</sub>, quenched ferromag. ribbon, Brillouin spectra 0-2776



## metallic glasses continued

- $\text{Fe}_{80}\text{B}_{20}$ , amorphous, elec. and mag. hyperfine field distrib., Mossbauer study 0-39964  
 $\text{Fe}_{80}\text{B}_{20}$ , amorphous, fast neutron and fission fragment irradi., effect on elec. resist. 0-19846  
 $\text{Fe}_{80}\text{B}_{20}$ , amorphous, transverse magnetoresist., stress effect 0-15501  
 $\text{Fe}_{80}\text{B}_{20}$ , amorphous ferromag. metallic glass, stress-induced rot. of magnetisation, Mossbauer study 0-20445  
 $\text{Fe}_{80}\text{B}_{20}$ , high-resolution XPS study, electronic state struct. 0-29846  
 $\text{Fe}_{80}\text{B}_{20}$ , metallic glass, spin texture determ. 0-15842  
 $\text{Fe}_{80}\text{B}_{20}$ , metallic glass, low temp. specific heat, metalloid effects 0-34654  
 $\text{Fe}_{80}\text{B}_{20}$ , metallic glass, triplet correlation, field-ion microscopy study 0-38921  
 $\text{Fe}_{83}\text{B}_{17}$ , metallic glass, struct. from neutron diff. study 0-6363  
 $\text{Fe}_{100-x}\text{B}_x$ , amorphous, stress relax. after annealing 0-55447  
 $\text{Fe}_{80}(\text{B}_{1-x}\text{C}_x)_{20}$ , saturation magnetostriction, comp. effects 0-34735  
 $\text{Fe}_{84}\text{B}_{16-x}\text{C}_x$ , amorphous alloys, short range order, Mossbauer and DSC study 0-39960  
 $\text{Fe}_{80}(\text{B}_{1-x}\text{P}_x)_{20}$ , amorphous alloys, isothermal crystallisation kinetics 0-33895  
 $\text{Fe}_{78}\text{B}_{12}\text{Si}_{10}$ , amorphous, Mossbauer study of hyperfine interaction and mag. anisotropy 0-40027  
 $\text{Fe}_{80}\text{B}_{15}\text{Si}_5$ , metallic glass, large uniaxial magnetostrictive anisotropy, magnetisation reversal 0-34736  
 $\text{Fe}_{80}(\text{B}_x\text{Si}_{1-x})_{20}$ , saturation magnetostriction, comp. effects 0-34735  
 $\text{Fe}_{81.5}\text{B}_{14.5}\text{Si}_4$ , amorphous metal ribbon, stresses, magnetoelastic anisotropy and zero-field mag. domain struct. 0-44896  
 $\text{Fe}_{82}\text{B}_{15}\text{Si}_3$ , metallic glass, low temp. specific heat, metalloid effects 0-34654  
 $(\text{Fe}_{92}\text{Co}_{0.8}\text{P}_{1.2})_{80}\text{P}_{1.2}\text{Al}_3$ , Mossbauer spectra, isomer shift, mag. hyperfine field 0-11301  
 $(\text{Fe}_{100-x}\text{Co}_x)_{79}\text{P}_{13}\text{B}_8$ , amorphous, hyperfine field distrib.,  $^{59}\text{Co}$  NMR spin-echo meas. 0-34818  
 $(\text{Fe}_{1-x}\text{Co}_x)_{77}\text{Si}_{10}\text{B}_{13}$ , amorphous magnetic alloys, density meas. 0-1934  
 $(\text{Fe}_{1-x}\text{Co}_x)_{78}\text{Si}_{10}\text{B}_{12}$ , amorphous alloys, magnetic anisotropy meas. 0-2570  
 $\text{Fe}_5\text{Co}_{70}\text{Si}_{15}\text{B}_{10}$ , amorphous, crystn. effect on mag. props. (Russian) 0-44858  
 $\text{Fe}_x\text{Ge}_{1-x}$ , amorphous, conversion electron Mossbauer spectra down to 4.2K 0-7205  
 $(\text{Fe}_{1-x}\text{Mn}_x)_{75}\text{P}_{16}\text{B}_6\text{Al}_3$ , amorphous, spin-glass-ferromag. multicritical point, AC susceptibility meas. 0-50117  
 $(\text{Fe}_x\text{Mn}_{1-x})_{75}\text{P}_{16}\text{B}_6\text{Al}_3$ , amorphous, mag. ordering temp., hyperfine field distrib., elec. resist. 0-34633  
 $(\text{Fe}_{1-x}\text{Mn}_x)_{75}\text{P}_{15}\text{C}_{10}$ , amorphous, mag. ordering, Mossbauer study 0-39747  
 $(\text{Fe}_{1-x}\text{Mn}_x)_{75}\text{P}_{15}\text{C}_{10}$ , amorphous pair radial distrib. functions, neutron scatt. study 0-49128  
 $\text{Fe}_{76}\text{Mo}_4\text{B}_{20}$ , quenched ferromag. ribbon, Brillouin spectra 0-2776  
 $\text{Fe}_{78}\text{Mo}_2\text{B}_{20}$ , amorphous, transverse magnetoresist., stress effect 0-15501  
 $\text{Fe}_{78}\text{Mo}_2\text{B}_{20}$ , amorphous, fast neutron and fission fragment irradi., effect on elec. resist. 0-19846  
 $\text{Fe}_{78}\text{Mo}_2\text{B}_{20}$ , metallic glass, triplet correlation, field-ion microscopy study 0-38921  
 $\text{Fe}_{78}\text{Mo}_2\text{B}_{20}$ , thermal expansion, glass transform. and crystn. temps. 0-2183  
 $\text{Fe}_{40}\text{Ni}_{38}\text{Mo}_4\text{B}_{18}$ , amorphous alloys, compatibility of DC and AC mag. props. 0-34695  
 $\text{Fe}_{1-x}\text{Ni}_x$ , amorphous film, growth stress and structure factor, stabilisation by conduction electrons 0-38920  
 $(\text{Fe}_{1-x}\text{Ni}_x)_{75}\text{B}_{25}$ , amorphous and cryst., short range order, Mossbauer study 0-39961  
 $(\text{Fe}_{100-x}\text{Ni}_x)_{100-y}\text{B}_y$ , metallic glass, embrittlement and crystn. 0-7685  
 $\text{Fe}_{40}\text{Ni}_{20}\text{B}_{20}$ , metallic glassy ribbon, casting conditions (Japanese) 0-55386  
 $\text{Fe}_{40}\text{Ni}_{40}\text{B}_{20}$ , amorphous, high-field magnetisation curve, spin wave spectrum and microstructural inhomogeneities 0-15702  
 $\text{Fe}_{40}\text{Ni}_{40}\text{B}_{20}$ , amorphous, casting conditions effect on mag. props. (Japanese) 0-34698  
 $\text{Fe}_{40}\text{Ni}_{40}\text{B}_{20}$ , amorphous, mag. props., effects mech. deform. 0-39840  
 $\text{Fe}_{40}\text{Ni}_{40}\text{B}_{20}$  glass,  $^{10}\text{B}$  self-diffusion, meas. by SIMS 0-49406  
 $\text{Fe}_{40}\text{Ni}_{40}\text{B}_{20}$ , metallic glass, low temp. specific heat, metalloid effects 0-34654  
 $\text{Fe}_{40}\text{Ni}_{40}\text{B}_{20}$ , molten, jet streaming, planar and cylindrical, instabilities rel. to glassy alloy casting 0-35129  
 $(\text{Fe}_{1-x}\text{Ni}_x)_{80}\text{B}_{20}$ , amorphous, Mossbauer spectra, mag. props. 0-15843  
 $\text{Fe}_{78}\text{Ni}_{80-x}\text{B}_{20}$ , quenched ferromag. ribbon, Brillouin spectra 0-2776  
 $\text{Fe}_{32}\text{Ni}_{36}\text{Cr}_{14}\text{P}_{12}\text{B}_6$ , thermal expansion, glass transform. and crystn. temps. 0-2183  
 $\text{Fe}_{32}\text{Ni}_{36}\text{Cr}_{14}\text{P}_{12}\text{B}_6$ , high-resolution XPS study, electronic state struct. 0-29846  
 $\text{Fe}_{40}\text{Ni}_{38}\text{Mo}_4\text{B}_{18}$ , metallic glass, mag. and transport props. 0-39752  
 $\text{Fe}_{40}\text{Ni}_{38}\text{Mo}_4\text{B}_{18}$  ribbon, magnetic characterisation 0-34680  
 $\text{Fe}_{27}\text{Ni}_{53}\text{P}_{14}\text{B}_6$ , amorphous, Hall resist. and mag. props., short range order effects 0-34422  
 $\text{Fe}_{40}\text{Ni}_{40}\text{P}_{14}\text{B}_6$ , strip domains, anisotropy const. effects 0-29571  
 $\text{Fe}_{40}\text{Ni}_{40}\text{P}_{14}\text{B}_6$ , amorphous ribbon, influence of torsion on mag. props. 0-7138  
 $\text{Fe}_{40}\text{Ni}_{40}\text{P}_{14}\text{B}_6$ , amorphous, transverse magnetoresist., stress effect 0-15501  
 $\text{Fe}_{40}\text{Ni}_{40}\text{P}_{14}\text{B}_6$ , amorphous, mag. props., effects mech. deform. 0-39840  
 $\text{Fe}_{40}\text{Ni}_{40}\text{P}_{14}\text{B}_6$ , high-resolution XPS study, electronic state struct. 0-29846  
 $\text{Fe}_{40}\text{Ni}_{40}\text{P}_{14}\text{B}_6$ , metallic glass, cryst., isothermal annealing behaviour 0-6367  
 $\text{Fe}_{40}\text{Ni}_{40}\text{P}_{14}\text{B}_6$ , metallic glass, ferromag. reson., spin waves, thermal ageing and long-range order effects 0-25214  
 $\text{Fe}_{40}\text{Ni}_{40}\text{P}_{14}\text{B}_6$ , metallic glass, isothermal viscosity and crystn. 0-49395  
 $\text{Fe}_{40}\text{Ni}_{40}\text{P}_{14}\text{B}_6$ , thermal expansion, glass transform. and crystn. temps. 0-2183  
 $\text{Fe}_{40}\text{Ni}_{40}\text{P}_{16}\text{B}_6$ , amorphous, kinetics of induced mag. directional order 0-44824  
 $\text{Fe}_{44}\text{Ni}_{40}\text{P}_{14}\text{B}_6$ , homogeneous deformation effect on crystn. and Curie temp. 0-21045  
 $\text{Fe}_x\text{Ni}_{1-x}\text{P}_{14}\text{B}_6$ , amorphous, spin-glass regime, magnetoresist. meas. 0-34418  
 $\text{Fe}_x\text{Ni}_{80-x}\text{P}_{14}\text{B}_6$  ( $x=0, 20, 40, 60, 80$ ), metallic glass, low temp. sp. ht. 0-2588  
 $(\text{Fe}_{1-x}\text{Ni}_x)_{75}\text{P}_{16}\text{B}_6\text{Al}_3$ , magnetisation temp. depend., spin wave theory 0-44927  
 $(\text{Fe}_{1-x}\text{Ni}_x)_{77}\text{Si}_{10}\text{B}_{13}$ , amorphous magnetic alloys, density meas. 0-1934

## metallic glasses continued

- $\text{Fe}_{80}\text{P}_{20}$ , binary amorphous ferromagnet, Mossbauer study 0-34829  
 $\text{Fe}_{82-x}\text{Si}_{18}$ , amorphous, magnetisation, magnetoresist., spin glass and ferromag. phases 0-34697  
 $\text{Fe}_{82-x}\text{Si}_{18}$  metallic glass, mag. phase diagram, weak ferromagnet-spin glass transition 0-54893  
 $\text{Fe}_{81-x}\text{Si}_{19}$ , amorphous alloy, Mossbauer spectra, charge transfer and atomic vol. effects 0-39959  
 $\text{Gd-Fe}(\text{Co})$ , thin amorphous system, resistance and hardness, chemical comp. and temp. effect 0-15625  
 $\text{Hf-Ni}(\text{Co})$ , amorphous, formation, decomposition and elec. transport props. 0-20143  
 $\text{Hf-V}$  foil, rapidly quenched and heat treated, supercond. props. 0-54852  
 $(\text{Mo}_{0.6}\text{Ru}_{0.4})_{82}\text{B}_{18}$ , supercond. metallic glass, neutron irradi. effects 0-29060  
 $\text{Nb-Ni}$  glasses, struct. factor temp. depend. 0-28920  
 $\text{Nb}_{0.55}\text{Ti}_{0.45}$  metallic glass, Young's modulus meas. by impulse induced resonance technique 0-40411  
 $\text{Nb}_{0.4}\text{Ni}_{0.6}$ , pair distrib. function, temp. depend., rel. to glass transition 0-24368  
 $\text{Ni-C-W-Cr}(\text{Mo})$ , Vickers hardness and crystallisation temp. 0-16361  
 $\text{Ni-Mo-C}(\text{Cr})(\text{W})$ , Vickers hardness and crystallisation temp. 0-16361  
 $\text{Ni-P}$ , amorphous electrodeposited alloys, phase-separation (Japanese) 0-54140  
 $\text{Ni}_{50}\text{Co}_{40}\text{P}_{10}$  amorphous film, spin wave excitation, ferromagnetic resonance study 0-50198  
 $\text{Ni}_{36}\text{Fe}_{32}\text{Cr}_{14}\text{P}_{12}\text{B}_6$ , amorphous, electrochem. corrosion in chloride solns. 0-50763  
 $\text{Ni}_{49}\text{Fe}_{29}\text{P}_{14}\text{B}_6\text{Si}_2$  glass, flow and failure 0-40438  
 $(\text{Ni}_{0.75}\text{Mn}_{0.25})_{82}\text{Si}_{10}\text{B}_8$ , amorphous, exchange anisotropy, mag. susceptibility meas., 4.2K to room temp. 0-11186  
 $\text{Ni}_{62}\text{Nb}_{38}$ , metallic glass, struct., neutron diff. study 0-54148  
 $\text{Ni}_{76}\text{P}_{24}$ , thermopower and resist. meas. 0-20145  
 $\text{Ni}_{100-x}\text{Zr}_x$  ( $x=34-40$ ) metallic glass, cryst., isothermal annealing behaviour 0-6367  
 $\text{Ni}_{64}\text{Zr}_{36}$  and  $\text{Ni}_{62}\text{Ti}_{29}\text{Zr}_{31}$ , H-sorption, X-ray and DSC obs. 0-49526  
 $\text{Pd-Ag-Si}$  alloys, amorphous, crystn. kinetics, DSC meas. 0-1933  
 $\text{Pd-Si}$  glasses, changes in density of states with alloys comp., UPS obs. 0-50531  
 $\text{Pd-Si-Fe}$  amorphous alloy, Mossbauer spectra, struct. and bonding 0-7224  
 $\text{Pd-Zr}$ , metallic glasses, valence band struct. investigation 0-11533  
 $\text{Pd}_{0.775}\text{Cu}_{0.06}\text{Si}_{0.165}$  glass, optical props. in energy range 0.67 to 5.6 eV 0-34872  
 $\text{Pd}_{77.5}\text{Cu}_2\text{Si}_{16.5}$ , metallic glass, composition, mech. props., simulation 0-49117  
 $\text{Pd}_{77.5}\text{Cu}_2\text{Si}_{16.5}$  metallic glass wire, cold drawing 0-50650  
 $\text{Pd}_{77.5}\text{Cu}_2\text{Si}_{16.5}$ , ternary miscibility gap, simulation, dispersed phase composite form. 0-54379  
 $\text{PdSi}$ , amorphous, structural relaxation enhancement following stress reduction 0-3118  
 $\text{Pd}_{80}\text{Si}_{20}$ , amorphous, structural changes with neutron irradi., X-ray scatt. obs. 0-33898  
 $\text{Pd}_{80}\text{Si}_{20}$ , high-resolution XPS study, electronic state struct. 0-29846  
 $\text{Pd}_{80}\text{Si}_{20}$ , metallic glass, composition, mech. props., simulation 0-49117  
 $\text{PdSiCu}$ , amorphous, US attenuation and vel. studies 0-19881  
 $\text{Pd}_{18}\text{Si}_{14}\text{Cu}_6$ , glass, changes in density of states with alloys comp. UPS obs. 0-50531  
 $\text{Pd}_{80}\text{Si}_{17}\text{Cu}_3$ , glass, changes in density of states with alloys comp., UPS obs. 0-50531  
 $\text{Pd}_{82-x}\text{V}_x\text{Si}_{18}$ , metallic glasses, effect of press. on elec. resist. 0-6805  
 $\text{Th-Fe}$  (20 to 70 at.%), amorphous alloy, electrical resistivity and thermal stability 0-33901  
 $\text{Ti-Be}$ , metallic glass form. and props. 0-16219  
 $\text{Ti}_{0.60}\text{Ni}_{0.40}$  metallic glass, Young's modulus meas. by impulse induced resonance technique 0-40411  
 $\text{W-Ru}$  based refractory transition metal-metalloid glass, struct. 0-1938  
 $\text{Zr-Be}$ , metallic glass form. and props. 0-16219  
 $\text{Zr-V}$  foil, rapidly quenched and heat treated, supercond. props. 0-54852  
 $\text{Zr}_{0.3}\text{Cu}_{0.65}$  metallic glass, Young's modulus meas. by impulse induced resonance technique 0-40411

## metallic thin films

- see also discontinuous metallic thin films; electronic conduction in metallic thin films; metallic epitaxial layers; metallic glasses; metallisation  
 adhesion, locus of failure, bond failure in adhesive joints, experimental methods 0-50801  
 adsorbed molecules, surface plasmon enhanced light absorption 0-40176  
 amorphous metal-metalloid alloys production by ion implantation, TEM study 0-15128  
 atomic absorption analysis with laser atomisation 0-30308  
 carrier density, evaluation from transverse elec. field and cond. meas. (French) 0-39682  
 coated Mo tips characterised by atom probe FIM, atomic clusters, voids 0-33863  
 condensate, anisotropy in electric field 0-15624  
 conduction electron surface scatt. process, magnetoacoustic oscillations (Russian) 0-15575  
 conversion electron scatt. processes anal. 0-45181  
 diffusion thermopower, boundary scatt. effect 0-6817  
 electrocrystallisation, soln. component interaction 0-20055  
 electrostatic interaction of charges with metal surface in size-quantised film 0-24996  
 EM wave transmission under resonance conditions (Russian) 0-54805  
 failure processes due to powerful light pulses (Russian) 0-7443  
 free-electron films, optical props., theory including electron surface scatt. 0-29817  
 growth by sputtering, corpuscular diagnostics of hollow cathode discharge 0-16180  
 laser-surface impact, on metal surface, atom vel. distrib. 0-5637  
 microcontacting in thin metallic layers (German) 0-55624  
 noble metal contact, substrate material diffusion and corrosion film formation, model 0-2312  
 nucleation, controlled interaction with Si substrate, silicide form. 0-10711  
 nucleation and growth on alkali halide substrates, surface study techniques, review 0-10809  
 one-dimensional, electronic states 0-54758  
 optical absorption due to particle-hole excitations 0-45160  
 optical properties, review 0-45106



## metallic thin films continued

- Permalloy-Rh, film, influence of Rh on corrosion resist. and mag. props. 0-3235
- powders, SAW interactions, for various directions of propagation 0-49486
- rare earth impurities and struct., general review 0-54556
- refractory metal, electron beam evaporator for in situ deposition studies in UHV electron microscope 0-40264
- scanner laser marking 0-43385
- soft, role in reducing friction between metal surfaces 0-55592
- solid-liquid transition, optical reflectance spectra 0-24569
- sputtered, deposited by cylindrical magnetron sputtering, internal stresses 0-24773
- superconducting state realisation 0-49977
- surface plasmon light emission due to low energy electron irradiation 0-34997
- surfaces, catalytic reactions studied by work function meas. 0-55711
- unlike surface properties, transport coeffs., diffuse surface scatt. 0-20331
- vacuum deposition, early stage obs. using microbalance technique and electron microscopy (Japanese) 0-54554
- valve metal thin films, deposited on dielectric supports, exam. of anodisation kinetics (Russian) 0-7702
- wet-chemical etching, galvanic effects 0-25915
- Ag, adhesion meas. 0-50822
- Ag, condensate obtained in electric field, anisotropy of elec. props. 0-44743
- Ag, contact material, contamination layer thickness, resist., ESCA study (German) 0-55561
- Ag, damping and vel. of longit. elastic waves at 9.4 GHz 0-10596
- Ag, deposited by cathodic sputtering using high-resolution electron microscopy, voids obs. 0-49557
- Ag, electroplated, stress meas. using holographic interferometry 0-20806
- Ag, evaporated, chemisorption effects on reflectance and elec. resist. 0-11495
- Ag film, epitaxial growth on isolated Au patches covered with amorphous C layer 0-40270
- Ag film, in situ struct. determ. by internal stress meas. 0-54569
- Ag film, sputtering mechanism, SEM 0-29839
- Ag films, hillock form. hole growth and agglomeration 0-44455
- Ag, ion plating on AT-cut quartz crystal, crystallographic structure obs. 0-2280
- Ag, on Au substrate, monolayer overgrowth, quantitative AES method 0-10813
- Ag, on Cu, ion-induced intermixing 0-15420
- Ag, spike effects of heavy ion sputtering 0-35034
- Ag, sputtered, hillock growth and agglomeration by annealing, SEM obs. 0-2309
- Ag, surface and volume plasmon light emission due to low energy electron scatt. 0-40177
- Ag, thin sub-monolayer film, Auger emission coeffs. meas. 0-55236
- Ag, vacuum deposited, internal stress and its depend. on gas adsorption 0-6683
- Ag vacuum deposited coating on glass, strength 0-55505
- Ag, vapour deposited on Cu, defects and their effect on props. 0-39474
- Ag-Cu couple, grain boundary diffusion of Ag through Cu film, Rutherford backscattering obs. 0-34252
- Ag-metals thin film couples, room temp. interactions 0-2220
- Al, adhesion to substrate, meas. 0-50822
- Al and Al-alloy films, struct. induced electromigration failure, Monte Carlo calcs. 0-49405
- Al, appl. of current noise technique for dislocation processes during plastic deform. 0-35442
- Al caesiated thin film, surface plasma wave excitation by polarised light, photoemission obs. 0-50518
- Al clean films, O<sub>2</sub> interaction study using synchrotron-radiation-induced-photoemission 0-55709
- Al, colour anodised, selective surfaces for solar collectors (Japanese) 0-55893
- Al, condensate obtained in electric field, anisotropy of elec. props. 0-44743
- Al, condensed film, phase and struct. nonuniformity (Russian) 0-54536
- Al, electron transmission, ang. aspects (French) 0-49284
- Al film, vacuum evaporation growth, impurity presence, effects (Hungarian) 0-7495
- Al, film integral radiation ability determ. by electron diffr. (Russian) 0-54413
- Al films, N<sub>2</sub><sup>+</sup> and O<sub>2</sub><sup>+</sup> ion bombardment, structural and phase changes 0-2094
- Al, ion plating deposition system using electron beam evaporation (French) 0-20802
- Al, plasma etching, MOS processing appl. 0-40577
- Al sputtered coating development, porosity, durability temp. depend., electric arc metallisation regime (Russian) 0-39402
- Al thin films, HF induction plasma treatment, effect on phys. props. (Russian) 0-24961
- Al thin films, vacuum deposited, crystal growth in presence of O<sub>2</sub> and Ni 0-15409
- Al, threshold adhesion failure, meas. by stylus method 0-50806
- Al vacuum deposited coating on glass, strength 0-55505
- Al, vapour deposited on NaCl, defects and their effect on props. 0-39474
- Al-Cu, prep. by planar magnetron sputtering (Japanese) 0-16184
- Al-Cu alloy layer, photolithographically patterned, separation from substrate using plasma etching (Slovak) 0-45405
- Al-Cu thin film couple, interdiffusion, AES obs. 0-6569
- Al-Cu thin films, microstruct. rel. to electromigration 0-44355
- Al-Sb, laser-induced metal-semicond. transition 0-6661
- Au condensed films on NaCl, ion bombarded, film growth, thermally stimulated exoelectron emission 0-50537
- Au, damping and vel. of longit. elastic waves at 9.4 GHz 0-10596
- Au, effect of high DC density stressing on pre-existing voids 0-24770
- Au, electrodeposit, Co-hardened, state of Co in as-deposited material, Mossbauer obs. 0-15397
- Au, film, evaporated, DC elec. resist. 0-29487
- Au film, work function changes upon water contamination 0-44705
- Au film (001) surface, computer modelling of high resolution TEM images 0-6330
- Au, film on (100) Si, meas. of SAW dispersion and thickness using acoustic microscopy 0-53575
- Au film on Si, SAW dispersion and film thickness meas. 0-10769
- Au films, (111), sputtering in high voltage electron microscope 0-35027
- Au, films, optical props. meas. rel. to electron surface scatt. theory 0-29818

## metallic thin films continued

- Au fine particles, vacuum deposited, morphological features using TEM weak-beam dark-field technique 0-15410
- Au, interface reaction with n-type Ga<sub>0.7</sub>Al<sub>0.3</sub>As and GaAs 0-39482
- Au, ion plated, defect growth structs., SEM obs. 0-24768
- Au, material transport instabilities accompanying ageing (German) 0-7601
- Au, on Cu, ion-induced intermixing 0-15420
- Au, spike effects of heavy ion sputtering 0-35034
- Au, surface step structure imaging by dark field electron microscopy 0-15346
- Au thin films, cryst. ripening rel. to heat treatment (German) 0-3109
- Au thin films, with nm-sized pores, prep. from Au-Ge eutectic films by etching 0-16227
- Au, vac. deposited thin film, Auger spectroscopy 0-2952
- Au, vacuum deposited, internal stress and its depend. on gas adsorption 0-6683
- Au vacuum deposited coating on glass, strength 0-55505
- Au/Si films, laser-irrad., phase transform. study 0-49536
- Au/Sn, evaporated, microstructure and texture, TEM obs. 0-39481
- Au/Ti thin films, effect of Cl<sub>2</sub> on elec. resistance, Ti atom migration and preferred orientation 0-34530
- B-transition metal thin films, amorphous to cryst. transformation 0-7563
- Ba film, on SiO<sub>2</sub>, interfacial chemistry, AES obs. 0-44434
- Be, on Cu substrate, monolayer overgrowth, quantitative AES method 0-10813
- Bi, refractive index determ. using Rayleigh-Lowe refractometer 0-7427
- Bs, laser beam hole machining 0-30207
- Ca, vac. deposited, struct. and photoemission meas. 0-11538
- Cd, nucleation and growth, props. 0-29878
- Cd, vacuum evaporated, HCP, microstruct., X-ray obs. 0-10827
- CeCoSi<sub>3</sub> film, Hall effect and magnetoresist. (Russian) 0-11109
- Co evaporated film, X-ray diffr. study 0-6663
- Co film, evaporated, columnar struct. depend. on degree of texture 0-54567
- Co film, evaporated, texture and columnar struct. 0-54566
- Co film, on Si substrate, laser irradiation, cellular struct. and silicide form. 0-10710
- Co film, optical props. by self-consistent photometric technique 0-55217
- Co film, work function changes upon water contamination 0-44705
- Co-Ni-P, film, props. independent of mag. hysteretic and anhysteretic remanences (French) 0-2604
- Co<sub>1-x</sub>B<sub>x</sub>, polycrystalline and amorphous sputtered films, Brillouin spectra 0-2775
- Cr, damping and vel. of longit. elastic waves at 9.4 GHz 0-10596
- Cr, defects and mechanical stability, different deposition methods (Bulgarian) 0-44438
- Cr film, effect of substrate temp. on formation, electron microscope obs. 0-39469
- Cr, film, sputtering yields, proton-induced X-ray meas. 0-50488
- Cr films, on Al<sub>2</sub>O<sub>3</sub>, quartz and glass, electron-beam deposition techniques improvement 0-7496
- Cr, fine particle solar absorber, effective medium theory 0-21396
- Cr, overlayers on polymer, electronic struct., XPS study 0-45204
- Cr, reversal etching in gas plasma, reaction mechanism, AES and XPS obs. 0-16564
- Cr vacuum deposited coating on glass, strength 0-55505
- Cr, vapour deposited on low temp. KCl substrates, struct. obs. 0-10826
- Cr-C, hard coating preparation by ion beam methods 0-25579
- Cu, adhesion meas. 0-50822
- Cu, damping and vel. of longit. elastic waves at 9.4 GHz 0-10596
- Cu, EXAFS meas. by total refl. 0-55228
- Cu, electrodeposit on Al and Fe, defects and their effect on props. 0-39474
- Cu film, effect of thermal strain on orientation 0-49294
- Cu film, in situ struct. determ. by internal stress meas. 0-54569
- Cu, film, sputtering mechanism, SEM 0-29839
- Cu film, valence bands, XPS excited by Zr M<sub>5</sub> radiation 0-40236
- Cu film, work function changes upon water contamination 0-44705
- Cu film on Mo substrates, film stability on reinforced fibre substrates (Russian) 0-39462
- Cu film on Ni substrate, EXAFS in photoelectron yield spectra 0-16123
- Cu free electrolytic films, tensile creep for various film thicknesses calcs. (Russian) 0-11697
- Cu, ion plated, defect growth structs., SEM obs. 0-24768
- Cu, on Ni, recrystallisation and interdiffusion, electron microscope obs., 450-600°C 0-39363
- Cu, on thermally oxidised Si, EM tensile adhesion test method 0-50804
- Cu, overlayers on polymer, electronic struct., XPS study 0-45204
- Cu thin layers, thickness meas. by proton-induced X-ray emission 0-4690
- Cu, transport prop. investig. 0-13011
- Cu, vac. deposited thin film, Auger spectroscopy 0-2952
- Cu-Au thin films after accelerated ageing, failure by Kirkendall porosity 0-6675
- Es film, preparation and characterisation 0-15405
- Fe, and Fe-Cr, film, sputtering yields, proton-induced X-ray meas. 0-50488
- Fe film, vacuum deposited, resist. minimum 0-44741
- Fe film, work function changes upon water contamination 0-44705
- Fe multilayer films stability, Mossbauer spectra 0-29651
- Fe, thermally evaporated, contamination effects obs. 0-49545
- Fe, vacuum deposited on Au (111), interaction layer formation mechanism 0-54559
- Fe-Ge, characteristic energy losses and optical props. 0-29834
- Fe<sub>1-x</sub>B<sub>x</sub>, polycrystalline and amorphous sputtered films, Brillouin spectra 0-2775
- Fe<sub>0.9</sub>Ni<sub>0.1-x</sub>, amorphous films, crystallisation, effect of codeposited O<sub>2</sub>, N<sub>2</sub> or Kr gases 0-10807
- Ga amorphous film, elec. field gradient 0-25264
- Gd-Co thin films sputtered from mosaic target, thickness and composition distrib. 0-6676
- Ge, inelastic mean free path, 700 to 1200 eV, bulk method 0-20763
- Hf, oxidation, microstructural study (French) 0-45436
- Hf, RF sputter deposition, ion bombardment and ion implantation 0-25564
- In, damping and vel. of longit. elastic waves at 9.4 GHz 0-10596
- In film, oxidation, XPS excited by Zr M<sub>5</sub> radiation 0-40236
- In film, vacuum evaporation growth, impurity presence, effects (Hungarian) 0-7495
- In, RF plasma oxidised, surface analysis using ESCA 0-50742
- Ir, evaporated, CO adsorption, IR refl.-absorpt. spectroscopy 0-34925



**metallic thin films continued**

- Li, film, adsorption on Mo (112) surface, LEED and contact pot. method 0-10794
- Mg clean films, O<sub>2</sub> interaction study using synchrotron-radiation-induced-photoemission 0-55709
- Mn, refractive index determ. using Rayleigh-Lowe refractometer 0-7427
- Mn-Ge, amorphous, short-range order, electron diff. obs. 0-39473
- Mo, amorphous thin films, for photothermal conversion, CVD fabrication 0-7503
- Mo, CVD, with high IR refl. and large solar absorpt., prep. and props. 0-26163
- Mo, energy loss function, Kramers-Kronig anal., reflectivity, optical props., EELS 0-40194
- Mo film, on Si substrates, laser irradi., cellular struct. and silicide form. 0-10710
- Mo thin film fabrication for photothermal solar converters using CVD 0-11573
- Na film, slow electron bombarded, light radiation 0-40168
- Nb CVD coatings on graphite, grain struct. depend. on temp. 0-25574
- Nb film on Si, Ar ion bombard., NbSi<sub>2</sub> form. 0-10709
- Nb, H absorption rate, metallic film effect 0-49525
- Nb thin films on Si substrate, intermixing, ion induced silicide formation 0-34101
- Nb thin foils, surface segregation during sputtering at elevated temps., Auger study 0-54386
- Nb-Ge film, phase transformations due to annealing, electron diff. study 0-54551
- Ni, damping and vel. of longit. elastic waves at 9.4 GHz 0-10596
- Ni, electrodeposit on Cu, defects and their effect on props. 0-39474
- Ni electrodeposited film, appl. of stereomicroscopic method for obs. of organic molecule incorporation 0-2288
- Ni, epitaxial growth, on NiO(100), by low pressure hydrogen reduction (French) 0-11578
- Ni film, work function changes upon water contamination 0-44705
- Ni foil, crystal struct. as function of substrate temp. during deposition 0-18742
- Ni, growth on Au (001) substrates (French) 0-44446
- Ni, HCP and amorphous, RF sputtered, O<sub>2</sub> incorporation, ESCA obs. 0-10832
- Ni, layer mode growth on Fe (001) surface, AES study 0-49540
- Ni monolayer and submonolayer films, on ZnO, UPS study 0-7472
- Ni, overlayers on polymer, electronic struct., XPS study 0-45204
- Ni, phonon transport into SrF<sub>2</sub> substrate, diffusive scatt. at impurities 0-49487
- Ni solar collector coating, microstruct., FIM and SEM obs. 0-26166
- Ni, sputter deposited on Cu, induced stresses 0-24774
- Ni-B, amorphous, electronic transport and crystn. activation energies (French) 0-6807
- Ni<sub>66</sub>B<sub>34</sub>, morphological, structural and phys. props. (French) 0-44444
- Ni<sub>50</sub>Co<sub>40</sub>P<sub>10</sub> amorphous film, spin wave excitation, ferromagnetic resonance study 0-50198
- Pb, film, sputtering mechanism, SEM 0-29839
- Pb, inelastic mean free path, 700 to 1200 eV, bulk method 0-20763
- Pb, vapour deposited FCC, normal and oblique incidences, microstructure, X-ray diff. study 0-20048
- Pd film, high dose Si<sup>+</sup> ion implantation, silicide phases, backscatter spectra 0-19820
- Pd film, on Si substrate, laser irradi., cellular struct. and silicide form. 0-10710
- Pd film on Si, Xe ion beam induced form. of PdSi 0-10800
- Pd, film with defects, field-induced resist. min. 0-11050
- Pd films, catalytic reactions studied by work function meas. 0-55711
- Pd, on Si, ion-induced intermixing 0-15420
- Pd overlayers, on Nb, form. of Pd (111) surface states and reson. d-levels, photoemission obs. 0-50523
- Pd, two-dimens. nucleus form. on Ag (111), UHV electron microscope obs. 0-10760
- Pd-amorphous Si thin film interaction, metal rich Pd-silicide formation 0-2284
- Pd-H thin film system, phase diagrams using quartz crystal thickness monitor 0-7537
- PdH<sub>x</sub> layer, galvanostatic desorption of hydrogen, quantitative theory 0-40694
- Pt film, work function changes upon water contamination 0-44705
- Pt films, optical props. and radiation stability 0-34999
- Pt foil, crystal struct. as function of substrate temp. during deposition 0-18742
- Pt, nucleate and film boiling in travelling wave regime 0-19231
- Pt, on Si, ion-induced intermixing 0-15420
- Pt, spike effects of heavy ion sputtering 0-35034
- Pt, vapour deposited on Ir and W, defects and their effect on props. 0-39474
- Rh-Si thin film interaction, interdiffusion, temp. depend. 0-54443
- Se, film, obliquely deposited, elec. resist. anisotropy 0-2486
- Se, laser beam hole machining 0-30207
- Sm, ion plating deposition system using electron beam evaporation (French) 0-20802
- Sn, inelastic mean free path, 700 to 1200 eV, bulk method 0-20763
- Sn, superconducting, paraconductivity 0-54845
- Ta, H absorption rate, metallic film effect 0-49525
- Ta, planar-magnetron-sputtered, phys. and elec. props. 0-6673
- $\beta$ -Ta sputtered film, stabilisation by Ta-Si interlayer, SIMS depth profiling 0-54568
- Ta<sub>2</sub>N film, high temp. nitriding kinetics depend. on press. (Russian) 0-50838
- Ti (0001) film, electronic struct., Fermi level, surface states, GO calcs. 0-6927
- Ti film, ion stimulated N<sub>2</sub> sorption, TiN<sub>x</sub> form., sorption ratio, capture coeff. anal. 0-39411
- Ti, films, implanted inert gas desorption, reemission process 0-39453
- Ti films on Al<sub>2</sub>O<sub>3</sub>, quartz and glass substrates, electron-beam deposition techniques improvement 0-7496
- Ti, interaction with O<sub>2</sub>, resist. and work function changes obs. 0-45431
- Ti, interference enhanced Raman scatt. 0-40105
- Ti, RF sputter deposition, ion bombardment and ion implantation 0-25564
- Ti, solid state reaction with Si or SiO<sub>2</sub> substrates backscatt. anal. 0-34257
- Ti-Al alloy, evaporated, anodisation, anodic voltage-time dependence obs. (Polish) 0-55574

**metallic thin films continued**

- Ti-Cu thin films, oxidation kinetics in air at 100 to 300°C, meas. 0-40590
- TiO<sub>2</sub>, reactive DC sputtering deposited films with magnetron-plasmatron, mechanical elec., optical props. 0-25566
- V, fluxural oscillations in longitudinal mag. field, sound attenuation, magnetoelasticity (Russian) 0-54844
- V thin film-amorphous Si interface, V silicide formation, backscattering diffraction meas. 0-2285
- W films, (010), energy band calc. including spin-orbit interactions 0-20274
- W, ion plating deposition system using electron beam evaporation (French) 0-20802
- Y, ion plating deposition system using electron beam evaporation (French) 0-20802
- Zn, film, sputtering mechanism, SEM 0-29839
- Zr, RF sputter deposition, ion bombardment and ion implantation 0-25564
- metallisation** see also electrodeposition
- electrode surface prep. for excimer lasers metallisation techniques 0-19048
- MBE, device appls. 0-25570
- SAW devices, use of Cu-doped Al 0-23856
- substrates, compensating work holder for coating two sides uniformly 0-22372
- vacuum seals, Cu-ceramic, metallisation process 0-37046
- Al sputtered coating development, porosity, durability temp. depend., electric arc metallisation regime (Russian) 0-39402
- Al-Cu alloy, deposition from RF induction source, onto laminated polyimide substrates and characterisation 0-16535
- Al-SiO<sub>2</sub>-Si, void form. in Al interconnection lines at Si-SiO<sub>2</sub> boundaries 0-2476
- n-Al<sub>1-x</sub>Ga<sub>x</sub>As, Au-based ohmic contacts TEM obs. 0-34509
- Al<sub>2</sub>O<sub>3</sub> (Russian) 0-50552
- Au thick film surface, Cu and Ag contamination, AES obs. 0-24763
- Au/Ti thin films, effect of Cl<sub>2</sub> on elec. resistance, Ti atom migration and preferred orientation 0-34530
- Au-Fe-Ni layer coating, Fe and Ni conc. meas. by X-ray diff. (German, English) 0-34330
- Cr films, on Al<sub>2</sub>O<sub>3</sub>, quartz and glass, electron-beam deposition techniques improvement 0-7496
- Ga<sub>1-x</sub>Al<sub>x</sub>As, ohmic contacts, metallisation systems 0-25010
- GaAs, review of ohmic contacts fabrication 0-49901
- GaAs, shallow-homojunction solar cell by MBE, conversion efficiency 0-30476
- Si-Al interface in semiconductors, electronic parts, electromigration aspects 0-39355
- Ti films on Al<sub>2</sub>O<sub>3</sub>, quartz and glass substrates, electron-beam deposition techniques improvement 0-7496
- Ti-Cu thin films, oxidation kinetics in air at 100 to 300°C, meas. 0-40590
- Ti-Pt-Au, nonalloyed ohmic contacts to n-GaAs by pulse-electron beam annealed Se implants 0-2466
- Ti-Si cosputtered films, silicide form., X-ray diff. and resist. study 0-54546
- Ti-Si film thin film interaction, metallisation, X-ray diff. and sheet resist. 0-54442
- Ti-W, bias-sputtered, resist. and comp. 0-25023
- Ti-W magnetron sputtered films 0-45231
- W CVD for thin film passive components fabrication for high temp. instrumentation 0-40266
- ZrO<sub>2</sub> particles, influence of ionic treatment on formation of Al coatings (Russian) 0-50552

**metallising** see metallisation**metallo-organic compounds** see organometallic compounds**metallocenes** see organometallic compounds**metallography**

- see also electron diffraction examination of materials; electron microscopy; optical microscopy
- autoradiography on thin foils, high resolution, anal. of technique characts. (French) 0-55598
- bimetallic welded joints, heterogeneous, metallographic anal., etchants and etching regimes 0-40635
- biomedical target, water-cooled pion-production, remote exam. and disassembly 0-25975
- boride coatings, method of revealing structural components 0-21228
- brass, 70/30, rolled, nucleation and annealing texture development 0-45320
- $\alpha$ -brass, metallographic and fractographic study of void formation during creep 0-16449
- CANDU irradi. fuel bundles, sheathed in Zircaloy-4, long term stability investig. 0-13774
- carbides, sintered, sample prep. for metallographic structural anal. 0-13048
- cast iron, white, high Cr-Mo, fracture toughness 0-50726
- Cunial MNA13-3, Mn addition effect on props. 0-21035
- deformed solids under tensile loads, automated installation of metallographic and exoemission obs. 0-50792
- electron microscope appl. transmission type, steel microstructure determ. (German) 0-15089
- EPIQUANT automatic structure analyser for inclusion investigs. in free-cutting steel 0-55609
- gases in metals, trends in modern anal. (Russian) 0-15123
- hard and brittle materials, microsection prep. technonon and polishing systems (German, English) 0-11859
- Hastelloy X, grain size effect. creep and creep-rupture (Japanese) 0-16382
- low temperature modified installation IMASH-5S-65 0-21229
- metallic polycrystals, deform. during cooling, revealed by deposited graphite layer (Polish) 0-25755
- metallographic specimens, automatic machine and procedure for prep. 0-13050
- rapid heating attachment, for IMASH-5S installation 0-21230
- Rene 95, as hot isostatically pressed (HIP) and HIP+forged, low cycle fatigue 0-25854
- review, quantitative metallography (French) 0-30205
- spinodal alloys characterisation techniques, props. and appls., review 0-50588



**metallography continued**

- steel, 0.2 to 0.8% C, ferrite-pearlite transformation, tensile strength, cooling rate effect 0-7549
- steel, alloy, type 11Kh18M, eutectic carbide composition change due to heating 0-16353
- steel, alloy, type ST.5, structural and phase changes after high temp. heating (*Russian*) 0-55439
- steel, alloy structural, anomalous grain growth 0-20984
- steel, austenite grain size eval. technique 0-25933
- steel, austenitic, martensitic transform. effect on hardening kinetics and fracture resist. of friction surface of 45Kh12G8 and 110G13 (*Russian*) 0-50727
- steel, austenitic stainless, 18-8, effect of H on martensitic transformation (*Chinese*) 0-55394
- steel, austenitic stainless, Ni-alloyed, Cr<sub>2</sub>N precipitation, interface struct. and morphology 0-11644
- steel, austenitic stainless, precipitates and grain orientation by non aqueous electrolyte potentiostatic etching method (*Japanese*) 0-15102
- steel, C1020, dual phase, mech. behaviours and structs. (*Korean*) 0-25779
- steel, C, cementite formation and properties 0-45313
- steel, carbide struct., quantitative analysis using Epiquant analyser (*German*) 0-3284
- steel, carbonitrided, case struct. investigation by warm electrolytic etching 0-35414
- steel, Cr, exam. of surface layer after electrochemical treatment, effect on mech. props. (*Russian*) 0-7727
- steel, Cr-Al (12, 6 wt.%), ferritic stainless, high temp. treated, strengthening mechanisms 0-3106
- steel, Cr-Mn, metastable constitution diagram and phase transforms. (*Russian*) 0-50590
- steel, Cr-Mo (2.25, 1 wt.%), small changes effect in impurity elements, creep life 0-25790
- steel, dual phase, improved etching technique for percent martensite determ. 0-16624
- steel, ferritic, base material for powder flame spraying process, intercrystn. corrosion (*Czech*) 0-30158
- steel, fully killed, nonmetallic inclusions, microprobe and metallographic exam. 0-30196
- steel, heat-resist., C replica method of investigating creep damage in TEM 0-21012
- steel, high Si dual-phase, mech. props and microstruct. anal. 0-40444
- steel, hot deformed austenite, transition from discontinuous to continuous formation of pearlite (*German*) 0-35214
- steel, low-C-Si, LS1.2, LS1.5, phase transformation 0-45302
- steel, maraging, heated to high temperatures,  $\gamma$  to  $\delta$  transformations 0-20930
- steel, medium C, Nb addition, effect on transformation and strength 0-7607
- steel, Mn (16 to 20 wt.%) metallographic analysis method 0-50791
- steel, Mn-Si, for springs, metallographic study, present phases rel. to mech. props. (*French*) 0-21090
- steel, Ni and W, recrystallisation mech. during laser treatment 0-50658
- steel, rolled products, H flaking 0-50719
- steel, stainless, martensite nucleation, in situ electron microscope obs. 0-7572
- steel, stainless, Type 304, pitting corrosion in Na<sub>2</sub>SO<sub>4</sub> soln. (*French*) 0-40581
- steel, stainless type 304, evaluating tendency for sensitization using Jominy bar test 0-16337
- steel, stainless type 316 welds, post weld heat treatments on struct., composition and ferrite amount 0-29992
- steel, tool, low alloy, methods of revealing austenitic grain 0-25949
- steel, tool, martensitic hardened, reagent for revealing austenitic grain size 0-21207
- steel, type 1Kh17N2, white zone formation and props. during friction in vac. (*Russian*) 0-40542
- steel, unskilled deep drawing sheets, influence of N content on recrystn. (*German*) 0-40376
- steel, W-Mo, types R6M5 and R6M5K5, decarburising layer evaluation 0-21164
- steel fibre reinforced Mg, fibre-matrix interfacial reactions 0-20043
- steels, free-machining, fractography and X-ray photoelectron spectroscopy 0-7673
- steels, high-purity and commercially based, containing 10 wt.%W or 5 wt.%Mo, tempering behaviour 0-7600
- steels, structural St 37-2, cleavage fracture, report 0-25868
- Technotron system for specimen prep. (*German, English*) 0-30199
- textured material, X-ray quantitative phase anal. (*Chinese*) 0-21195
- textured sheet metals, X-ray diffr. anal. 0-6316
- wear test specimen, metallographic technique 0-35496
- wear theory, metallography of worn surfaces 0-35346
- Zircaloy-2, effect of simulated fission products on elongation fractography and metallography 0-649
- Zircaloy-2, neutron irradiated, inhomogeneous deformation behaviour 0-50679
- Ag, (211)[111] single crysts., shear band effects on rolling deformation 0-50651
- Al alloy, type 2024-T3, fatigue deformation and crack growth, holographic study 0-25836
- Al-alloy plates, type VAD23, thermomech. parameters effect on struct. and props. 0-20988
- Al-Cu-Zn system, solid-phase reactions, phase diagram 0-50603
- Al-Pd eutectic, microstruct. morphology 0-3018
- Al-W(Mo)(Nb), struct. and props. of alloys obtained from granules 0-50717
- Al-water vapour reaction, stress corrosion susceptibility STEM study, Mg addition effect 0-3247
- Al-Zn-Mg/Al-Mg filler welds, weld fusion boundary structure 0-39459
- Al<sub>2</sub>O<sub>3</sub>-glass mixture, microstructural changes and shrinkage during sintering 0-25640
- Au thin films, with nm-sized pores, prep. from Au-Ge eutectic films by etching 0-16227
- Au-Ni-Cu-Zn, white gold, metallographic struct., heat treatment and plastic working effect 0-40403
- B fibre reinforced Mg, fibre-matrix interfacial reactions 0-20043
- B films, prep. by H reduction of BCl<sub>3</sub>, struct. and hardness 0-54543
- B-C system, electron probe microanalysis and destructive chem. methods of study (*French*) 0-11982
- B<sub>4</sub>C, melting and phase homogeneity range 0-20911

**metallography continued**

- Bi<sub>2</sub>CoO<sub>3.7</sub>, in Bi<sub>2</sub>O<sub>3</sub>-CoO system, X-ray diffr., thermal anal. and metallography obs. 0-24598
- Bi<sub>2</sub>O<sub>3</sub>-CoO system, X-ray diffr., thermal anal. and metallography obs. 0-24598
- cast Fe, grey and ductile, subsurface defects, SEM and EDAX study grey and ductile, subsurface defects, SEM and EDAX study 0-44400
- Ce-Ga system, phase equilib. and cryst. struct. of phases 0-35159
- Co, corrosion in Ar-SO<sub>2</sub> atmospheres, scale struct. obs. (*Japanese*) 0-55568
- Cr, interaction with dense stream of N ions, metallography, microhardness, specific volume (*Russian*) 0-15169
- Cu-Al-Ni-Fe system, corrosion behaviour in sea water 0-45421
- Cu-B(25 wt.%) (*Japanese*) 0-55402
- Cu-Be (2 wt.%), alloying addition effects on grain boundary reaction (*Japanese*) 0-49236
- Cu-Be-Co, cuboid (Co, Cu, Ni, Fe)Be inclusions, metallography, ageing effects 0-11645
- Cu-Be-Co(0.1,0.2 wt.%), discontinuous precipitation (*Japanese*) 0-55402
- Cu-Ni-Be-(Al) (30,0.5,(0.2-2) wt.%), Al addition effect on grain boundary reaction (*Japanese*) 0-54254
- Fe, Armco, borided surface layers, Mossbauer and metallographic anal. 0-50769
- Fe, cast, spheroidizing effect of Mg and Ce modifiers 0-35193
- Fe, ductile, with different secondary struct., abrasive wear (*German*) 0-25871
- Fe, interaction with dense stream of N ions, metallography, microhardness, specific volume (*Russian*) 0-15169
- Fe pellets, re-oxidation at high temp., growth of needle-like haematite crystals 0-35431
- Fe, pure, initial grain boundaries effect on cold-rolling and annealing textures (*Japanese*) 0-35205
- Fe/ZrB<sub>2</sub>, metal-like cpd. form. in diffusion layer during solid phase saturation 0-19994
- Fe-base amorphous alloys, embrittled by H and heat-treatment 0-55518
- Fe-Mn (15(24)(30)wt.%), high hydrostatic pressure influence on stress-strain curve 0-25805
- Fe-Mn-C, variation of martensite morphology with Mn and C composition 0-50635
- Fe-Mn-Ti alloys, austenitic, precipitation strengthened 0-25714
- Fe-Ni (23 wt.%), struct., composition changes during  $\alpha$  to  $\gamma$  transform., martensite plastic deformation influence (*Russian*) 0-11642
- Fe-Ni (31 wt.%), thermoelastic martensite obs. 0-3052
- Fe-Ni-Al system, multiphase diffusion at 1000°C, diffusion structs. and props. 0-19995
- Fe-Si, etch figure method appl. (*Chinese*) 0-21194
- FeTi, H storage alloy, prep. for TEM (*German, English*) 0-30197
- HfB<sub>2</sub>, oxidation in O<sub>2</sub> atmosphere, exam. 0-11814
- Mg-Ni-S, electroforming, mech. props. rel. to heat treatment 0-35133
- Mn-Si (62.5 to 63.8 wt.%), phase anal. and cryst. struct. (*Japanese*) 0-15049
- Mo-low alloys, C enrichment mechanism of intercrystalline zones (*Russian*) 0-20963
- Nb, pure, reaction with gas residual in vacuum, physicomach. props. effect 0-16587
- Nb-alloys, reaction with gas residual in vacuum, physicomach. props. effect 0-16587
- NbC, deformation behaviour during rubbing in wide temp. range 0-16486
- Ni alloy Ehl698, new etchant for revealing microstructure 0-25934
- Ni, C precipitation 0-29958
- Ni, inner layer of high temp. oxide scale, metallographic obs. 0-3240
- Ni, pure, anomalous grain growth 0-20984
- Ni, single crysts., H and liq.-Hg embrittlement 0-25862
- Ni wire plasma sputtering with W particles, coagulation, struct. and particle size (*Russian*) 0-40260
- Ni-Ag alloy, metallographic struct. and formability (*German, English*) 0-30201
- Ni-C-Ce, overmodification (*Russian*) 0-40432
- Ni-Ta-Al system, phase equilibria and diagram, electron probe, X-ray diffr. anal. 0-29927
- Ni-Ti (1.6, 7.64 wt.%), monophasic high temp. scaling, metallography study 0-21159
- Ni<sub>3</sub>Al-Ni<sub>3</sub>Nb eutectic, directionally solidified, high-temp. oxidation mechanism 0-16544
- Pb, Pb alloys, metallographic preparation using pH controlled silica gel and superior microetchant 0-16623
- Pd sponge powder, sintering shrinkage kinetics 0-29900
- SiC-Ni based superalloy reaction, at elevated temps. 0-3287
- Sn droplets, on Bi, Zn and Al, heterogeneous nucleation 0-44294
- Ta-O supersaturated solid solution, precipitation processes, hardness change meas. 0-25712
- $\alpha$ -Ti, recrystallised commercial purity, Fe-rich precipitates obs. (*French*) 0-50637
- Ti-Al-H, H effect on mech. props. and lattice constants 0-21036
- Ti-Al-Mo-Sn-Si (2.25, 4, 11, 0.25 wt.%), type IMI 680, internal friction study of martensitic transformations 0-7573
- Ti-Al-Mo-Sn-Si (2.25, 4, 11, 0.25 wt.%), type IMI 680, stability of martensitic phases 0-7574
- Ti-Al-Mo-Sn-Si (4, 4, 4, 1/2 wt.%), type IMI 551, internal friction study of martensitic transformations 0-7573
- Ti-Al-Mo-Sn-Si (4, 4, 4, 1/2 wt.%), type IMI 551, stability of martensitic phases 0-7574
- Ti-Al-Sn (5, 2.5 wt.%), annealing of near-basal hydrides 0-20989
- Ti-Al-Sn-Zr-Mo (6.2,4.6 wt.%),  $\alpha$ - $\beta$  type 6246, fusion zone fracture behaviour in weldments 0-30093
- Ti-Al-V (6, 4 wt.%), type IMI 318, internal friction study of martensitic transformations 0-7573
- Ti-Al-V (6, 4 wt.%), type IMI 318, stability of martensitic phases 0-7574
- Ti-Al-V (6.4 wt.%),  $\alpha/\beta$  interface phase influence on tensile props. 0-30034
- Ti-Al-V (6.4 wt.%), to H effect on fracture props. and microstruct. 0-40512
- Ti-Al-V-Sn (6.6,2 wt.%),  $\alpha$ - $\beta$  type 662, fusion zone fracture behaviour in weldments 0-30093
- TiC, deformation behaviour during rubbing in wide temp. range 0-16486
- TiC, sintering and grain growth, metallographic anal. 0-25642
- U-UNi<sub>2</sub>-UCO<sub>2</sub> system, phase equilibria, lattice constants (*German*) 0-50598
- (V,Ti)C+Ni cermet, binder grain size 0-44401



**metallurgy continued**

V-H(D), metallographic and thermal differential anal., potential for H energy storage appls. 0-45281  
W fibre reinforced Cu, interface porosity formation, on thermal cycling 0-30092  
W spheres, in liq. Ni, sintered, coalescing, crystallographic orientation, SEM study 0-45249  
WC, deformation behaviour during rubbing in wide temp. range 0-16486  
Zn, stacking faults, plastic deformation, due to laser beam irradi., X-ray metallography study (*Russian*) 0-15121  
 $\alpha$ -Zr, H terminal solid solubility, optical metallographic study 0-34195  
ZrB<sub>2</sub>, oxidation in O<sub>2</sub> atmosphere, exam. 0-11814

**metallurgical industries**

see also *forging; rolling mills*  
aluminium plants electrolytic baths, power consumption limitation method (*Russian*) 0-3366  
high-temperature materials, technological requirements, R and D, report 0-45222  
microwave appl., w.r.t. economics and safety 0-3754  
rare earth industry review 0-25537  
steelmaking, heat transfer correl. during diffusion melting of Fe, steel in Fe-C melts 0-54348  
tensoresistors, measuring force 0-17930

**metallurgy**

see also *ageing; alloys; crystal microstructure; deformation; electrical properties of substances; hardening; heat treatment; magnetic properties of substances; materials testing; mechanical properties of substances; metallography; metallurgical industries; metals; metalworking; phase diagrams; phase transformations; physical chemistry; powder metallurgy; precipitation; recrystallisation; surface treatment; zone refining*  
chalcopyrite, electrooxidation in ACL, stoichiometry and reaction mechanism, Cu extraction appl. (*French*) 0-16231  
chlorination of Cu and Zn in Cu converter slag 0-20840  
extractive, developments in basic principles and phys. chem., review 0-20819  
extractive metallurgical processes, thermodynamic evaluations 0-11591  
high-temperature materials, technological requirements, R and D, report 0-45222  
hydrometallurgy, developments, review 0-45252  
pyrometallurgy, process developments, review 0-25596  
Cu production and extractive metallurgy, developments, review 0-20821  
Pb, extractive metallurgy, developments, review 0-20820  
Sn, extractive metallurgy, developments, review 0-20820  
Zn, extractive metallurgy, developments, review 0-20820

**metallorganic compounds** see *organometallic compounds*

**metals**

see also *actinides; alkali metals; alkaline earth metals; aluminium; bimetallic; cadmium; gallium; indium; lattice dynamics of metallic crystals; lead; mercury [metal]; metallic thin films; rare earth metals; thallium; thermoelectric effects in metals and alloys; tin; transition metals; zinc*  
abrasive finishing with refractory carbide micropowders surface struct. 0-11842  
AC anodic dissolution rate, effect of H<sup>+</sup> evolution (*Russian*) 0-16693  
acoustoelectric current for conductivity electron arbitrary dispersion law (*Russian*) 0-49829  
adhesion theory for two surfaces 0-20270  
adsorption of S, thermodynamics of two-dimen. and three-dimen. sulphides 0-20036  
air pollution control, activation analysis for 14 volatile heavy metals as constituents of aerosol particles 0-16891  
ammonia-metal soln., ionis. equilib. instability of weakly-ionised 3-component plasma 0-10877  
Anderson model, local moments and localised states (*Czech*) 0-2353  
anharmonic parameter,  $\gamma$ BT, interpretation (*French*) 0-34160  
anisotropic, description of history dependent plastic flow behaviour 0-11732  
anisotropic normal metal, thermopower calc. 0-24879  
anodic activation of passive metals, theory 0-25918  
antiwear action of Zn di-n-butyl phosphate 0-11782  
atomic displacements near impurities and many-particle interactions (*Russian*) 0-24553  
atomic interaction force characts., association with struct., mech. props. 0-49172  
Bauschinger effect, in metals, review 0-21025  
BCC, dislocation (100) stability, field stress effects (*Russian*) 0-10558  
BCC, dislocation processes, straining expts., electron microscope obs. 0-29025  
BCC, polycrystalline aggregate, prediction of plastic props., deformation by {111} pencil glide 0-11731  
BCC, quantum diffusion model of light interstitial atoms 0-2212  
BCC, solid solution hardening, crystal resolved shear stress depend. on dislocations 0-40373  
BCC metals, plastic deform., computer simulation 0-40456  
BCC single crystals, plastic deformation localisation 0-54303  
BCT, electron-ion interactions 0-10527  
bicrystals, residual resistance theory, diffusivity, disorientation effects (*Russian*) 0-49875  
brittle and plastic, energetic strength theories (*Bulgarian*) 0-38296  
catalysts for C graphitisation 0-3401  
cavitation erosion resist., increase by case hardening, possible mechanism 0-11845  
chemicothermal treatment, process kinetics 0-35415  
chemisorption energetics, book contrib. 0-24740  
clad fibre reinforced composites, debonding risk 0-3132  
clean polycrystalline metal surfaces, ion-induced electron emission, review 0-35032  
coal gasification, demands made on materials used in process (*German*) 0-45438  
coated abrasive belt grinding, relation between wear of grain cutting edge and material removal 0-16507  
cohesion and Cauchy discrepancy 0-54170  
collective modes of void-surface coupled systems, surface plasmons 0-49642  
combustion under CW CO<sub>2</sub> laser radiation action 0-30241  
composite shell, three-layer, stochastic formulation of optimisation using heuristic methods 0-38268  
composite spherical pressure vessels with hardening metal liners 0-7655  
contact melting process kinetics, investigation method 0-39259  
corrosion and passivation, ion selectivity effects 0-35377

**metals continued**

corrosion in electrolytes, pit growth 0-21186  
corrosion pit initiation and growth, salt film form. 0-16563  
crystallisation process, X-ray fluoroscopic obs. 0-50620  
crystallites, orientation and shape determ. by TEM 0-1907  
cubic, Debye temp., elastic const. averaging 0-54332  
cubic lattice, inverse pole figures, calc. method on digital computer 0-20950  
cutting rel. to plasticity theory 0-16610  
cyclotron resonance in weak mag. fields surface impedance, current density asymptotic (*Russian*) 0-2641  
cyclotron wave excitation, diffuse boundary scatt. (*Russian*) 0-54729  
deformation process, stage-by-stage nature investigation using acoustic emission (*Russian*) 0-40434  
deformation resistance, rel. between uniaxial stress state and breaking stresses in shear 0-3147  
deformed in pressing process, temp. field modelling (*Russian*) 0-53602  
diffusion coefficient of H in metal with low adsorption activity, steady-state flow method 0-10795  
diffusion coefficients of H, appl. of H and He quenching methods (*Japanese*) 0-7604  
diffusion in presence of high diffusivity paths, random walk model 0-24640  
diffusion of H, complex jump diffusion model rel. to quasi-elastic neutron scatt. by H 0-24638  
diffusion of H, random walk model with correlated jumps 0-24639  
diffusion of H(D), slow neutron scatt. obs., review 0-34248  
dislocation annihilation during tensile and cyclic deform. and limits of dislocation densities 0-34007  
dislocations in metals, residual elec. resist., one-electron approx. (*German*) 0-39568  
disordered, conductivity electrons and elastic scatt. by static inhomogeneities (*Russian*) 0-29375  
disordered surface, multiple scatt. of cond. electrons 0-10959  
Drucker postulate verification at high temp. 0-30025  
ductile fracture, void growth stress/strain relations (*French*) 0-19280  
ductile metals, spontaneous void growth in elastic and elastic/plastic media 0-48567  
ductile-brittle transition temperature evaluation, as function of thickness 0-3261  
dynamic compression testing, mech. behaviour 0-40464  
dynamic hardness testing of metallic materials 0-21241  
elastic-plastic vector props. at normal and low temps. 0-16406  
electric resistance, temp. depend., qualitative anal. by audible demonstration 0-46775  
electrodeposition, chemical factors 0-16207  
electron drag of dislocations 0-10961  
electron field emission (*Polish*) 0-35063  
electron spectroscopy of crystals, book 0-36786  
electron-dislocation scatt. anisotropy effect on electron-electron scatt. contrib. to elec. resist. 0-29398  
electronic transport eqns., optical cond., number conserving relaxation time approx. calcs. 0-49681  
EM acoustic reson. for elastic moduli meas. 0-15573  
EM waves near cyclotron reson. in inclined mag. field (*Russian*) 0-29625  
emissivity angular dependence, meas. in IR spectral region 0-34214  
enthalpy and average mass temp. on plasma-arc melting (*Russian*) 0-54405  
epoxy-metal joints, environmental fracture and effects of shrinkage stresses 0-16635  
erosion accompanying simultaneous action of laser emission and ultrasound (*Russian*) 0-7442  
erosion by high speed particles, temp. effects 0-40556  
fatigue analysis, inversion of strain-life, and strain-stress relationships 0-16428  
fatigue analysis, inversion of strain-life and strain-stress anal. 0-19289  
fatigue behaviour of metals and alloys, vacuum effect, review 0-35309  
fatigue crack propag. life, statistical study on distrib. characts. (*Japanese*) 0-25847  
fatigue damage accumulated by combination of alternately applied over- and under-stresses (*Japanese*) 0-35306  
fatigued, relationship between stress and point defect cluster density 0-10592  
FCC, coincidence-site lattice interfaces 0-15381  
FCC, props. of vacancies and divacancies 0-10545  
FCC, single phase FCC, cyclic deform. long range stress changes 0-54308  
FCC, small vacancy clusters, structures and energies, computer simulation 0-39073  
FCC, under H<sub>2</sub> press., crit. phenomena and isomorphic transitions 0-49367  
FCC, vacancy migration near twin boundaries and stacking faults 0-39075  
FCC, yield threshold at 4.2K, effect on strain-hardening curve (*Russian*) 0-50671  
FCC metals, polycrystn., fatigued, behaviour model during plastic deformation (*German*) 0-21023  
FCC nonhomogeneous sheet, orientational distrib. function calc. of mean texture 0-11659  
FCC polycrystals, deform. during cooling, revealed by deposited graphite layer (*Polish*) 0-25755  
FCT, electron-ion interactions 0-10527  
ferromagnetic, dragging of domains by temp. gradient 0-34425  
ferromagnetic, nonmagnetic impurity hyperfine field temp. depend. 0-34402  
ferromagnetic, point contact spectroscopy, electron-magnon interactions (*Russian*) 0-54766  
ferromagnetic metal, magnon and cond. electron relax. processes (*Russian*) 0-7102  
ferromagnetic resonance linewidth, interaction of spin waves with conduction electron current 0-25216  
ferromagnetic slab, transmission of 24 GHz radiation, effect of diffuse surface scatt. of carriers, calc. 0-34780  
ferromagnetism quantitative criterion correlation calcs. (*Russian*) 0-2540  
forming limit curve for bending processes 0-7627  
fracture due to laser irradi. and shock compressed plasma (*Russian*) 0-55500  
fracture during laser working, depend. on physico-chem. props., heat cond. (*Russian*) 0-55432  
free atoms of metals [and their chemistry] (*French*) 0-21281  
friction and wear rel. to comp., struct. and props., review 0-25872



## metals continued

- friction pair with polymer, temp. calc. under severe friction 0-40550  
 frictional electrification between metal and polymer, depend. on temp. and friction speed, contrib. of mol. motion to electrification 0-6953  
 fusible-metal deformation, effect on contact-melting kinetics 0-49339  
 fusion reactor metals, He embrittlement, grain boundary cavity model 0-34075  
 grain boundary relax., model (*Russian*) 0-39107  
 granules, electron work function interrelation with granule size 0-39660  
 hard, roll deform. effect on separating forces in cold strip rolling 0-35212  
 hard metal, tensile strength meas., bend test-piece geometry effect 0-30184  
 HCP metals, mag. susceptibility near  $2\frac{1}{2}$ th order electron transition, non-linear magnetisation anal. (*Russian*) 0-44859  
 HCP polycrystals, deform. during cooling, revealed by deposited graphite layer (*Polish*) 0-25755  
 heat capacity near melting point, vacancy mechanism of melting 0-10641  
 heat resistant power installation elements, estimating strength, ductility, heat resistance diagrams 0-25770  
 heating by concentrated energy sources, simple analytical expressions (*Russian*) 0-38215  
 heating by laser emission, spatial nonlinear problems (*Russian*) 0-7440  
 hexagonal, twin refl. indexing in four-axis hexagonal reciprocal lattice 0-14970  
 high temperature species, absorpt. and fluoresc., high temp. fast flow reactor technique 0-42231  
 hot plastic deformation, stress/strain/time relations (*Russian*) 0-20968  
 hydriding and dehydriding kinetics,  $H_2$ -diffusion-rate-limited 0-35764  
 hydrogen embrittlement effects from acoustic emission meas. 0-11742  
 impurity atoms, diffusion in region of dislocations (*Russian*) 0-24670  
 inhomogeneous circular cylinders, non-radiative surface plasmon-polariton modes 0-29455  
 ion etching, dispersion coeff. determ. (*German*) 0-40597  
 ion-implanted, friction and wear, review 0-40555  
 irradiation-induced creep, transient stage, vacancy loop contrib. (*Russian*) 0-29115  
 isotope compounds, conversion to metals by reduction-distillation methods 0-23223  
 laser and nuclear radiation induced emission anomalies, current sources (*Russian*) 0-25536  
 laser heating kinetics, influence of oxide film interf. effects 0-11841  
 laser irradiated, optical and electronic emissions (*French*) 0-2919  
 lattice surface relaxation, electrostatic model 0-49488  
 LEED intensity and image pot. above beam threshold 0-44084  
 liquid metal embrittlement, review 0-3257  
 localised magnetic moment magnitudes of transition or rare earth impurity, Anderson model 0-25086  
 martensitic transitions accompanied by interactions between phases (*Russian*) 0-7568  
 mechanical props., testing and modelling 0-25811  
 mechanical treatment in aq. salt soln., material transport rel. to wear 0-16506  
 metal-rare earth, effective exchange interaction model 0-25127  
 metal-electrolyte boundary, elec. refl. and photoemission relationship 0-45211  
 metal-electrolyte boundary, electrostatics in visible and near UV range, microscopic effects 0-45521  
 metal-electrolyte boundary, photoemission effect on elec. refl. 0-45212  
 metal-H systems, appl. oriented props., book 0-22154  
 metal-H systems, heat transformer for energy cascading, book contrib. 0-26151  
 metal-metal contacts, use as prevention H escape from metals 0-24595  
 metal-polymer friction pairs, triboelec. effects 0-11784  
 metal-semimetal system, local and total density of states determ. (*Russian*) 0-54586  
 metals, diffusion alloying conditions, deep chemical-heat treatment (*Russian*) 0-40393  
 metals, noble, dilute alloys, solute vacancy binding energy, Dingle temp. 0-49177  
 meteorites, iron, elements distrib. between metal and phosphide phases 0-46508  
 microstructure, effect on bulk material props. 0-34004  
 mirror design and mounting specifications 0-48388  
 Mossbauer spectra of implanted  $^{83}\text{Kr}$ , line widths, isomer shifts 0-39899  
 muon trapping by defects and impurities 0-20573  
 noble-metal tubes, cold-weld sealing 0-41556  
 nonferrous metals, unlubricated wear data 0-16510  
 normal crystal growth, fluctuation theory, modelling of melt-growth interface motion 0-15025  
 notched, fatigue under alternately over- and under-stresses (*Japanese*) 0-35307  
 optical reflector metal specifications 0-48387  
 optoacoustic phase angle meas. for subsurface struct. 0-28388  
 oxides, diffusion activation process, interatomic bonding energy (*Russian*) 0-54428  
 oxides, used as battery cathodes or electrocatalysts, electrochemical behaviour 0-45516  
 oxidising metal heating by periodically pulsed  $\text{CO}_2$  laser 0-7445  
 particle surface tension depend. on size, vapourisation time (*Russian*) 0-34290  
 particulates, theory of melting in the Percus-Yevick limit, appl. to particles on  $\text{SiO}_2$  and C substrates 0-20060  
 passivity, in metals and alloys 0-50750  
 phase analysis by Mossbauer spectra 0-15922  
 phase transformations in metals and alloys, thermodynamic and mechanistic classification, review 0-2995  
 phonon limited resistivity, anharmonicity, Debye Waller factors, multiphonon terms 0-49691  
 photoelectrochemical cells, metal, electrodes in contact with fluorescent dye solns., photovoltage generation, comprehensive model 0-40871  
 photoemission in solids, book 0-12860  
 plasmon dispersion effect in (e,2e) process with atomic electron knockout 0-2904  
 plastic clad, corrosion charact. by electrical resist. and capacitance meas. (*German*) 0-30171  
 plastic impact, energy absorbed by elastic waves 0-5972  
 point defect relaxation volumes, dipole tensors and Kanzaki forces 0-54222  
 polyvalent, Matthiessen's rule deviation crit. resist. 0-6811  
 porous, mean principal stress in rolling without lateral expansion 0-25803

## metals continued

- porous, yield stress variation during cold deformation 0-16395  
 porous gauze materials, struct. and hydraulic characts. 0-11729  
 porous strip, metal pressure in cold rolling in elastic aftereffect zone 0-40421  
 porous trip, elastic aftereffect in cold rolling 0-11689  
 positron annihilation, localised probe of lattice defects 0-55224  
 positron annihilation experiments, electronic struct. and Fermi surface studies 0-54594  
 powder compacts, elec. resist., surface layer effect 0-34415  
 powders, fundamentals of compaction 0-40279  
 powders, packed, complex mag. permeability calcs. 0-29583  
 power overdistribution to AC and DC arcs for melting metals (*Russian*) 0-54055  
 preparation by electromagnetic levitation in ultrahigh vac. 0-29899  
 proper EM radiation on inelastic electron tunnelling with photon emission, cond. (*Russian*) 0-54765  
 PTFE+metal, fluoride prod., DSC and XPS anal., rel. to polymer wear 0-11889  
 PTFE-metal interaction, X-ray photoelectron spectroscopy obs. 0-11788  
 radiation blistering developments, review 0-44239  
 radiation damaged long term strength curve forecasting (*Russian*) 0-34040  
 radiation effects on elasticity and elastic moduli, yield stress 0-2078  
 radiation induced creep, fundamental mechanisms (*Italian*) 0-55457  
 radiation-induced creep and swelling, radiation dose depend. (*Russian*) 0-29050  
 radioactive waste, decontamination by smelting 0-13741  
 refractory, heat treatment and zone melting installation 0-20959  
 refractory, mech. props. and diffusion figures (*Russian*) 0-40436  
 refractory, nitriding reactions and processing conditions, thermodynamic approach (*Russian*) 0-21169  
 refractory, water vapour attack, immersion heater appl. in vacuum radiation furnace (*German*) 0-21184  
 refractory metals, enhanced diffusion model for activated sintering 0-25612  
 residual stresses, determ. using internal boring technique 0-3263  
 rolling, critical line nature in multiple-roll passes (*Russian*) 0-38347  
 rolling of complex sections, unified anal. function of surface of strain focus (*Russian*) 0-21017  
 rough dielectric and rough metallic surface discrimination, specular scatter depolarisation 0-32911  
 shear waves, rotary activity under helicon-phonon interaction 0-2412  
 simple metals, dynamical calcs. of X-ray absorption and emission spectra 0-55227  
 simple metals, effect of core hole on X-ray emission spectra 0-20737  
 single electron excitation damping, conduction electron scatt. (*Russian*) 0-15510  
 sintered strip rolling, algorithm for force and geometric parameters calc. 0-11727  
 slow positron studies 0-55223  
 Snoek-Koster relaxation, theory 0-16369  
 soft film, initial wear rate 0-11795  
 solar water heating system, corrosion 0-30131  
 solid solution hardening theories, review (*Czech*) 0-3084  
 sound propagation, anomalous, by cond. electrons 0-11048  
 space lattice types  $A_1$ ,  $A_2$  and  $A_3$ , strain hardening function (*German*) 0-20955  
 spatially dispersive, EM waves and plasmons, propagation 0-15549  
 specific heat meas. method at low temperatures and high pressures 0-52246  
 sputtering, effects of adsorbed Cs on photon and secondary ion emission 0-35038  
 static and dynamic isothermal elasticity moduli (*Russian*) 0-24524  
 static skin effect in metals with open Fermi surfaces, galvanomag. effects (*Russian*) 0-29389  
 strengthening by electroplastic strain, surfactant effect (*Russian*) 0-20953  
 strip, high-speed compression, force parameters determ. (*Russian*) 0-21016  
 strip rolling, kinetostatics (*Russian*) 0-38348  
 structure and thermodynamic properties at high temperatures, microscopic theory (*Japanese*) 0-29191  
 substitutional impurities in solids, entropy and volume of solution 0-15253  
 sulphidation mechanisms, review (*Polish*) 0-45413  
 superconductors, polyvalent Brillouin zone boundary influence on Coulomb interactions 0-24827  
 supported crystallites, wetting in sintering and redispersion 0-24751  
 surface, adsorbed benzene, obs. of vibrational modes 0-6649  
 surface, adsorbed O and CO, sputtering effects, combined analytical techniques 0-35047  
 surface, anisotropic contrib. to optical pot., in electron spectroscopy, theory 0-44086  
 surface, atomic and mol. beam scatt., review 0-40203  
 surface, electron density depend. on modulation, adsorption, diffusion 0-54526  
 surface, fast ion scatt. by plasmons, theory 0-45190  
 surface, high-intensity laser beam interaction 0-19600  
 surface, interaction with molecules and reactivity, theoretical description 0-39652  
 surface, luminesc. due to equilb. excitation of electrons by laser radiation 0-7399  
 surface, microalloy layer formation by ion implantation 0-16600  
 surface,  $\text{N}_2^+(\text{Ar}^+)$  energy accommodation coeffs. meas. in rarefied plasma stream by thermoanemometric sounding 0-16722  
 surface, perturbative calc. of elec. field 0-45108  
 surface, plasmon mechanism for energy loss, dissoc. and orientation of fast ions excited by grazing collisions 0-11523  
 surface, sticking coeff. and transmission problem, quadratic phonon coupling effects 0-39424  
 surface, sticking probability, correl. with adsorbate-induced electron struct. 0-39425  
 surface adatom pair interaction asymptotics, degenerate electron gas permittivity 0-29281  
 surface cleanliness control by photoemission recording (*Russian*) 0-49839  
 surface energies and work function, simple analytic model 0-49862  
 surface free energy for BCC, FCC and HCP structs. etch pit depend. 0-29258  
 surface photoemission, spatially-varying photon field effects 0-2921  
 surface reconstruction, physical realisation of two-dimensional Ising and X-Y model 0-15351



**metals continued**

- surface self-diffusion of single atoms and diffusion of adatoms, activation energies calc. 0-24732  
 surfaces, and interfaces, slow exchange processes study using SIMS 0-55653  
 surfaces, catalytic reactions studied by work function meas. 0-55711  
 synthetic, anisotropy of elec. props. rel. to chem. bond struct. 0-24888  
 thermal conductivity model, during hot descaling (*Russian*) 0-24869  
 thermal fatigue testing, installation for -180 to 1100°C 0-3266  
 thermal vision systems, theoretical basis of use to monitor boundary stratification in hot metals 0-7748  
 thermionic electron emission anisotropy 0-20757  
 thermodynamic equations of state, complete 0-24561  
 thermoelastic distortion in machining metals 0-5939  
 thermoelectromagnetic waves in conductors in a mag. field (*Russian*) 0-49695  
 thermomechanical deformation, analytical description 0-49391  
 trace analysis in jet engine oils by atomic emission/fluoresc. spectrometer system, computer controlled 0-45587  
 trapping of H, book contrib. 0-24491  
 triplet supercond. transition in strong mag. field 0-25040  
 two atom surface coupling, double reson. at plasmon freq., collective effects 0-34934  
 two-way polishing, thermal stresses and surface quality (*Russian*) 0-30151  
 US generation by EM radiation, surface scatt. effects 0-24973  
 vapour, partial pressure meas. (*Japanese*) 0-34179  
 viscoplastic behaviour, anal. 0-6457  
 volumetric plastic deform., kinematic and static parameter calcs. (*Russian*) 0-34124  
 welded joints, pore formation mechanism evaluation, rel. to solidification 0-3017  
 wire and bar NDT, electrical and EM methods 0-11865  
 X-ray spectra, final state pot., one-electron theory 0-55230  
 yield criterion, rheological interpretation (*Russian*) 0-21014  
 yield strength determ. 0-25937  
 C content determ., isotope-spectral method (*Russian*) 0-55766  
 C high sensitivity meas. using nuclear microprobe 0-50908  
 H diffusion, and solubility in solid metals 0-49422  
 H permeability, general transport eqn. 0-54426

**metalworking**

- see also bending; cold working; forging; hot working*  
 electro-optics, conference, Utrecht, Netherlands (Oct. 1978) 0-31420  
 forging in closed dies, deformation parameters determ., theory and expt. comparison (*German*) 0-25745

**metamagnetism**

- Ising metamagnet, dilute tricritical point calcs. 0-50099  
 rare earth alloys, RM<sub>2</sub>, (M=Fe, Co, Ni), magnetism, review 0-20365  
 rare earth-Cu intermetallic compounds, single crystals, mag. props. 0-54892  
 sublattice metamagnet, temp. dependent anisotropy, magnetisation curves, mag. transitions, classical approx. 0-39795  
 temperature induced, caused by mag. anisotropy 0-11195  
 Ca<sub>3</sub>Mn<sub>2</sub>Ge<sub>3</sub>O<sub>12</sub>, mag. field induced transition 0-50094  
 CoMnP, ferromagnetism and metamagnetism, polarized neutron diffr. study 0-44809  
 CoS<sub>2</sub>-Se, magnetism and metamagnetic transition, neutron diffr. and NMR meas. 0-15717  
 ErB<sub>4</sub>, mag. phase diagram, neutron diffr. study 0-50091  
 FeCO<sub>3</sub>, metamagnetic insulator Neel temp. anal. by model including spin fluctuations (*Russian*) 0-15715  
 RbCoCl<sub>3</sub>·2D<sub>2</sub>O, metamagnetic phase transition, crystallographic and mag. struct., neutron diffr. meas. 0-44174  
 ThCo<sub>5</sub>, itinerant electron metamagnetism, polarised neutron study 0-39742  
 Tm<sub>3</sub>Sc<sub>2</sub>Te<sub>1-y</sub>, magnetic ordering studies (*German*) 0-54882

**meteor trails** *see meteors***meteorites**

- see also meteors; micrometeorites*  
 Abe meteorites, mobile element transport in heated sample 0-36586  
 achondrite meteorites, mag. effects of brecciation and shock 0-8603  
 achondrites, Mg-Cr relationship 0-51704  
 achondrites, petrogenetic model 0-4312  
 acoustic-gravity waves generated in atmosphere (*Russian*) 0-21795  
 Allan Hills 77005, achondrite petrological study 0-21949  
 Allan Hills 77005, new meteorite type found in Antarctica 0-26824  
 Allende, amoeboid olivine aggregates, trace element anal. 0-17553  
 Allende, chem. props. reveal condensation sequence in presolar nebula 0-26758  
 Allende, evidence for supernova trigger for solar system form., description 0-12683  
 Allende, normal <sup>39</sup>K/<sup>40</sup>K ratio for inclusions confirmed 0-26820  
 Allende, superheavy element search 0-21752  
 Allende chondrule magnetisation and solar nebula mag. field 0-36520  
 Allende meteorite, isotopic anomalies rel. to cosmochemistry 0-4462  
 Allende meteorite, Sr fractionation in Ca-Al inclusions 0-46503  
 Antarctic meteorites, review of discoveries and significance 0-8597  
 Antarctic meteorites, trace element contents, weathering effect 0-56784  
 Atlantic, stone, inert gas content, isotopic composition 0-46506  
 basaltic achondrite meteorites, rare earth element abundance patterns rel. to origin 0-36581  
 Bencubbin meteorite, metal clast origin, evolution model 0-8599  
 Binda howardite, <sup>87</sup>Rb-<sup>87</sup>Sr chronology 0-26819  
 C3 carbonaceous chondrite (Ornans), noble gas component of minerals 0-51698  
 Canon City meteorite, <sup>37</sup>Ar and <sup>39</sup>Ar radioactivities 0-36582  
 carbonaceous chondrite groups, refractory elements fractionations obs. 0-36595  
 carbonaceous chondrite material on Deimos, spectral evidence 0-41754  
 carbonaceous chondrite origin and classification, review 0-56781  
 carbonaceous chondrites, H/D ratio study 0-46497  
 carbonaceous chondrites, parent bodies form. 0-36580  
 carbonaceous chondrites, reduction kinetics, Mossbauer obs. 0-41777  
 carbonaceous chondrites, <sup>15</sup>N/<sup>14</sup>N ratios, isotope fractionations in Fischer-Tropsch and Miller-Urey reactions 0-46496  
 Chainpur LL3 chondrite, and H isotope study 0-36518  
 chondrite, fluid drop chondrule size freq. distrib. 0-36588  
 chondrite magnetisation meas. 0-36599  
 chondrites, Fe-Ni superstructure in metal particles 0-12713  
 chondrites, kinetics of volatile loss 0-4311

**meteorites continued**

- chondrites, remanent magnetisation rel. to shock and metamorphic history 0-36598  
 chondrites, thermoluminescence 0-51706  
 chondrites of H-group, thermal history by orthopyroxene struct. 0-46499  
 chondrules, origin 0-4310  
 CI carbonaceous meteorites, magnetite morphology and form. in parent body 0-51707  
 Copiapo group IA Fe meteorite, cooling history 0-36578  
 craters, geophysical and geomechanical aspects 0-17265  
 Dhajala meteorite, <sup>37</sup>Ar and <sup>39</sup>Ar radioactivities 0-36582  
 Djerma (H) chondritic breccia, preirradiation history 0-36579  
 enstatite chondrite, mineralogy and petrology rel. to solar nebula composition 0-51699  
 enstatite chondrites, <sup>87</sup>Rb-<sup>87</sup>Sr chronology 0-8596  
 eucrite parent asteroid, bulk composition, planetary evolution bearing 0-56786  
 eucrites, major and trace elements, preliminary modelling 0-51704  
 Farmington chondrite, U-Pb abundances and Pb isotopic studies 0-56778  
 gas-rich meteorites, volatile element trends 0-51701  
 Grefsheim meteorite, Norway, mineralogy of L5 chondrite 0-36591  
 Haviland meteorite crater site, location and photograph 0-51399  
 Homewood hypersthene chondrite, chemistry and mineralogy 0-51703  
 howardite parent body, layered crust model 0-36554  
 howardites and mesosidrites petrography and neutron activation anal. 0-8598  
 Indarch enstatite chondrite, cathodoluminescence of clinoenstatites 0-36596  
 inert gas content, solubility in serpentine 0-12712  
 inert gas isotope and element anomalies, He and Xe 0-56779  
 IR spectra, comparison with astrophysical IR features 0-26728  
 irons of group IA and IIA, phosphide morphology revealed by Cl<sub>2</sub> etching 0-36593  
 isotope abundance anomalies, astrophysical implications 0-46511  
 isotope abundance anomalies, cosmological implications 0-46510  
 isotope abundance ratios, determ. with Si whisker field desorption ion source 0-11975  
 isotopic anomalies, rel. to supernovae and solar system origin 0-17509  
 isotopic anomalies, role of grains as carriers in early solar nebula 0-26757  
 isotopic anomalies from neutron reactions during stellar explosive C burning 0-12651  
 Jilin, organic compounds 0-17557  
 Kamiomi olivine bronzite chondrite; mineralogy, petrography and chemistry 0-51702  
 Kapoeta howardite, <sup>40</sup>Ar/<sup>39</sup>Ar chronology of lithic clasts 0-46501  
 Karoonda meteorite, classified as Vigarano type carbonaceous chondrite by chem. composition 0-36590  
 Kirin H chondrite, inert gas content interpretation (*German*) 0-46505  
 Krymka LL-chondrite carbonaceous inclusion, noble gas and trace element anal. 0-17555  
 L chondrites, <sup>87</sup>Rb-<sup>87</sup>Sr dating, shock and brecciation effects 0-51705  
 L-6 chondrite, petrogenesis evidenced by mineral chemistry 0-41775  
 Lance carbonaceous chondrite, basalts 0-56783  
 Landes group IA Fe meteorite, cooling history 0-36578  
 Lappajarvi impact melt crater projectile 0-56785  
 LL-chondrite, noble gas isotope anomalies 0-51697  
 lunar and planetary science, ninth conference, Houston, Texas, (1978 March 13 to 17) 0-17711  
 magnetic field origin, conf., Nov. 1978, Texas USA 0-36234  
 magnetisation and early solar system 0-36597  
 mass loss and shape change with radiative heating 0-31198  
 mesosiderites, silicate fraction, Mg-Cr relationship 0-51704  
 Mezo Madaras, L3 chondrite, <sup>87</sup>Rb-<sup>87</sup>Sr dating, shock and brecciation effects 0-51705  
 Moore County meteorite, geochem. study and genesis 0-36587  
 Morasko, Poland, soil anal. near crater lakes 0-8605  
 Mt. Baldr (a,b), rel. to ten stone Antarctic meteorite inert gas contents 0-46506  
 Murchison carbonaceous chondrite, monocarboxylic acid isomer struct. 0-26823  
 Murchison chondrite, noble gases isotopic anomalies, evidence for stellar condensates 0-41772  
 noble gases, isotopic anomalies origin, comment 0-26818  
 ordinary chondrites, Ga, Ge, Cu, Sb, moderately volatile siderophiles content 0-8595  
 Orgueil, type C-1, IR spectra, comparison with serpentine minerals 0-17556  
 Orgueil chondrite, <sup>22</sup>Ne anomalous abundance, evidence for presolar grains 0-41773  
 pallasites origin, role of minor planets EM heating in early solar system 0-36555  
 primordial condensation of components, expt. evidence of source medium state 0-26816  
 refractory lithophile elements, condensation and fractionation 0-36517  
 regmaglyptic relief index, meas. 0-56782  
 Rica Aventura Fe meteorite, petrology 0-36585  
 Richardson chondrite, U-Pb abundances and Pb isotopic studies 0-56778  
 Ries impact crater, siderophile and volatile element anal. 0-17552  
 Sena stone, bronzite chondrite formation conditions (*French*) 0-26817  
 Serra de Mage meteorite, geochem. study and genesis 0-36587  
 shergottite meteorites, petrology and origin 0-51700  
 Shergotty achondrite, <sup>40</sup>Ar/<sup>39</sup>Ar age and post-shock thermal history 0-46502  
 Shergotty achondrite, mineralogy, petrography and minor elements 0-36592  
 Shergotty achondrite, Rb-Sr age and isochron age resetting 0-41774  
 Siberia, Outer Mongolia and Indochina Peninsula, geographical distrib. pattern (*Japanese*) 0-31263  
 Slate Island impact site, shock remanent magnetisation 0-30986  
 St. Severin LL-chondrite, Fe-Ni ordered phase Llo superstruct., Mossbauer spectrum Debye-Scherrer pattern 0-50241  
 superheavy element composition of irons, fission track study 0-26821  
 clear taenite, identification as ordered FeNi FeNi 0-8604  
 tektite, Muong Nong-type indochinites, mineral inclusions 0-36301  
 tektites, fission-track plateau dating evidence of australites older than indochinites 0-56780  
 tektites and natural glasses, Mossbauer anal. 0-21952  
 tektites and natural glasses, N concs. 0-41446  
 tektites from Australasia, possible origin in Zhamanshin impact struct. 0-51358



**meteorites continued**

- tektites of Australasia, possible origin crater in Cambodia 0-36302
- terrestrial cratering history, theory incorporating galactic modulation 0-31043
- thermoluminescence, rel. to orbit, pre-impact history and Earth residence time 0-31262
- thermoluminescence as measure of irradi. history, validity of method 0-36584
- thermoluminescence of meteorites of known age 0-46498
- Toluca octahedrite, Mossbauer spectra petrological study 0-36589
- Tunguska catastrophe, computational modelling 0-41779
- Unter-Massing Fe-meteorite, cosmic-ray exposure age and preatmospheric size (*German*) 0-46507
- uracil in carbonaceous chondrites, Murchison, Murray and Orgueil meteorites 0-31261
- ureilite meteorites, mag. effects of brecciation and shock rel. to strong nebular mag. fields 0-8602
- vaporisation of lithophile elements, vac. conditions 0-36583
- Yamamoto carbonaceous chondrite, amino acid content 0-26822
- Yamato-74191 chondrite, inert gas composition and neutron capture effects 0-46504
- Zaisho, Japanese pallasite, mineralogical and petrographical study 0-46509
- Zhamanshin impact structure, USSR, impact glass chemically similar to tektites 0-51358
- <sup>36</sup>Cl content of Antarctica meteorites, cosmic irradi. histories 0-21950
- Fe group, thermodynamic model evidence for asteroid belt origin 0-36577
- Fe meteorites, group IAB, silicate and troilite dating by Xe-I method 0-17554
- Fe meteorites, group IIICD, plessite struct., electron microscopy study 0-8600
- Fe meteorites, nuclides formed by cosmic ray exposure 0-21951
- Fe meteorites chemical classification, role of Ga, Ge and Sb nebular condensation 0-36594
- Fe-meteorites, elements distrib. between metal and phosphide phases 0-46508
- Fe-Ni ordered phase in meteorites, Mossbauer studies 0-41776
- Pa abundance, mass spectroscopy 0-8601
- <sup>187</sup>Re-<sup>187</sup>Os systematics in meteorites, rel. to solar system early chronology and Galaxy age 0-41778

**meteoroids**

- see also meteorites; meteors*
- micrometeoroid hazard of Comet Halley probe, workshop proceedings (Noordwijk, Netherlands, 18-19 April 1979) 0-36782
- Perseid shower meteoroids, evidence for progressive fragmentation from television obs. 0-4309
- properties and deionisation processes rel. to radio echo characteristics 0-17550
- Quadrantid meteor stream, effect of orbital evolution on meteoroids influx 0-56776
- Quadrantid meteor stream, long-term orbital evolution 0-17551
- Quadrantid meteor stream, orbital evolution between (AD 1830 and 2030) 0-21948
- swarm evolution, solar mass reduction link 0-8592

**meteorological instruments**

- see also anemometers; barometers; hygrometers*
- aircraft dropwindsonde system 0-17393
- aircraft meteorograph, design, appls., accuracy (*Chinese*) 0-17387
- anemometer, CSIRO liquid water probe, hot wire, freq. response 0-12562
- anemometer for medium and high winds, Gill propeller instrument 0-26618
- cold-wire thermometers used for atmospheric turbulence meas. in marine environment, freq. response 0-56650
- data acquisition and processing, computerised data collection system (*German*) 0-37007
- fog, quantitative meas. of precipitation onto surfaces 0-56654
- hair hygrometer, technique to linearise hair extension (*German*) 0-46284
- laser radar system, mobile computerised meteorological phenomena observation 0-56644
- lightning flash counters, for ground flash density meas. 0-51552
- Meteosat data collecting platform (*Danish*) 0-12637
- Meteosat-1, observational history (*French*) 0-8513
- microwave radiometry for precipitable water vap. and liq., dual-channel method 0-51564
- ocean surface meteorological buoy and aircraft VHF link 0-46298
- optical array precipitation probe, small-particle response 0-51577
- rain rate and drop size distribution, with fast-response optical sensor 0-31135
- raingauge corrections, mountain meas. accuracy 0-26597
- shipboard meteorological data system 0-46299
- thermometry in range 253-318K, resistance thermometer 0-46291
- wind and turbulence meas. with propeller vane devices, dynamic props. 0-31138
- wind meter, with speed and direction indication 0-207
- wire temperature sensors, frequency response meas. by internal and acoustic heating 0-31123

**meteorological optics *see atmospheric optics*****meteorology**

- see also climatology; wind*
- advection equation, numerical study (*Chinese*) 0-46233
- Africa, southern east coast rainfall rel. to southern oscill. and subtropical high press. belt 0-12518
- agricultural weather service, New Jersey, user survey 0-4065
- air-sea interaction at large scale, math. modeling 0-41535
- aircraft-to-satellite data relay system 0-17380
- airports, recurrence probabilities of weather events 0-51491
- S.America and Antarctica, synoptic climatology and mountains 0-12532
- annual rainfall records, comparison methods for climatology 0-51587
- Antarctica, polar desert pond dynamic chemical equilib., as sensitive index of meteorological cycles 0-12441
- atmosphere physics, book 0-51976
- atmospheric numerical model (*French*) 0-21814
- atmospheric pollution modelling appls. (*German*) 0-51496
- atmospheric stability, rel. to S dry deposition vels. over E United States 0-56507
- automatic weather stations, network in Switzerland, computerised monitoring appl. (*German*) 0-17356
- available potential energy over uneven topography, theory 0-51514

**meteorology continued**

- balloon tethering system, for very low altitude meteorological obs. 0-36430
- baroclinic instability of zonal flow, modified quasi-geostrophic eqns. 0-56574
- barotropic primitive equation model using splines for typhoon prediction (*Chinese*) 0-4063
- Bay of Bengal, forecasting tropical storm movements 0-41531
- Bay of Bengal, tropospheric structure during Aug. 1977 active and break monsoon 0-56570
- beach atmosphere, microclimate of sandy shoreline 0-8417
- biometeorology, plants, animals, human beings, weather change effects (*French*) 0-17360
- blizzard, 1978 February 18 to 19, in SW.England and S.Wales 0-12507
- blocking weather systems, atmosphere multiple flow equilibria theory 0-56536
- S.Britain, 1978 warm dry autumn 0-4093
- Britain, max. rainfall in few hours 0-4091
- Britain, N.Pennines, altitudinal temp. gradients 0-4094
- British Isles, 1968 and 1977 summers, comparison 0-41538
- Carpathian meteorology, conference, Tatranska Lomnica, Czechoslovakia (1975 September 21 to 25) (*French, German, Russian*) 0-46739
- chimney height for optimal air pollution reduction 0-26588
- Chinese chronicles, 2187 BC-AD 3 meteorological record 0-46213
- chronology of air pollution events (up to 1970) 0-7975
- circulation, by two-level quasi-geostrophic model 0-56546
- circulation characts. forecasting rel. to autumn low temp. over Yangtze basin 0-12531
- cloud dynamics and modelling, appl. to forecasting 0-8375
- cloud motion wind data, meas. improvement 0-8386
- cloud seeding, ice 0-12489
- cloud seeding devices, AgI nuclei formation efficiency 0-41552
- cloud seeding experimental results analysis 0-8389
- cloud seeding experiments, statistics appl. 0-8438
- cloud seeding with AgI and metaldehyde, Fujian province, China (*Chinese*) 0-46235
- Cochin Harbour mouth, India, monsoons rel. to hydrographic characts. and tidal prism 0-41452
- cold-frontal rainband, cellular struct. obs. 0-51512
- computer applications (*German*) 0-36363
- computer weather prediction, 1950 ENIAC computations 0-42030
- computer worded forecasts, description of input and usage 0-17310
- conjugate equations use in calc. meteorological fields, inclusion of a priori information (*Russian*) 0-4136
- convective mixed-layer entrainment, for realistic capping inversion layer 0-12487
- cyclogenesis, asymmetric jets instability theory 0-56537
- cyclones, unstable baroclinic waves downstream and upstream development 0-56540
- depression life-cycle as function of latitude, rel. to meridional transport 0-51508
- diagnostic analysis in weather forecasting, appl. to storms (*Chinese*) 0-12467
- Doppler radar weather surveillance near airports 0-46272
- Doppler weather radar, development of weather echo props. 0-26645
- Earth annual wobble, affected by wind stressed sea level 0-36221
- effects of solar thermal electric conversion plant, numerical modelling 0-35794
- EM Waves refraction in atmospheric boundary layer, expt. investigation 0-36400
- empirical orthogonal functions of 500 mb height, truncation of series 0-56581
- empirical orthogonal functions of 500 mb level, N.hemisphere 0-56580
- E.England, meteorological situation rel. to storm surge (1978 January 11 to 12) 0-12419
- equatorial wave mean-flow interaction, role of latitudinal shear 0-51461
- equatorial wave resonant interaction, nonlinear dynamics 0-56550
- E.Europe, tropospheric wind variance spectrum 0-8397
- European air temperature band-pass filtered series, correls. and phases 0-26579
- Everglades Agricultural Area, USA, soil temp. obs. in winter nighttime 0-56559
- extratropical cyclone, enhancement after separation from polar front (*French*) 0-56517
- FGGE observing system, data system tests 0-56610
- First GARP Global Experiment, introduction 0-12550
- fluid dynamics conference, Aug. 1978, Strasbourg, France 0-36764
- forecast accuracy for rain, limit due to spatial variability of rainfall 0-56510
- forecast model with 10 levels, lower boundary condition 0-51494
- forecasting, satellite technology development, (1960 to 1979) (*Dutch*) 0-12559
- forecasting, stochastic-dynamic system, asymptotic behaviour 0-12474
- forecasting for Ninian Field drilling platform construction 0-41522
- forecasting of daily pressure by statistical method 0-56528
- forecasting skill, daily precipitation and temp. 1966-78, Boston, USA 0-56509
- forecasting with non-hydrostatic mesoscale model including orography 0-51507
- freeze-thaw cycles causing road potholes in USA, 1977-8 obs. 0-56560
- frontal rainband, conditional symm. instability explanation 0-56584
- GARP Winter Monsoon Expt., Dec. 1978 field phase report 0-46262
- general circulation, models with lower boundary condition and energy consistency 0-56547
- general circulation model, Earth rot. increased or decreased 5 times 0-56545
- geopotential values retrieved by objective anal. methods 0-36386
- NW.Georgia, monthly rainfall spatial correls. rel. to climatology and weather modification expts. 0-51479
- German Bight, meteorological parameters rel. to trilateration distance meas. (*German*) 0-8248
- Global Weather Experiment, observational phase through first special observing period 0-51543
- Global Weather Expt., roles played by METEOSAT and TIROS-N 0-26714
- global weather model, thermodynamic, with turbulent transport (*Spanish*) 0-36372
- Great Britain, northerly gales of (1978 January 11 to 12) 0-12508
- W.Gulf of Maine, meteorological data rel. to gulf winter circulation 0-51430



## meteorology continued

- historical meteorological data, appl. to hourly mixing depths estimation 0-51482
- ice nucleation by fluid-breaking metaldehyde particles (*Chinese*) 0-12468
- Indian Ocean, sea levels in western equatorial region rel. to tides, meteorology and ocean circulation 0-4018
- Indian sea areas, 1976 cyclonic storms and depressions 0-56533
- information retrieval publications, comparative study hydrometeorology in USSR 0-36401
- intertropical convergence zone cloud cluster, wind field behaviour 0-17322
- irradiance, seminumerical method accounting for atmos.  $H_2O$  (*Spanish*) 0-36373
- isentropic and sigma coord. hybrid numerical model 0-12485
- isentropic objective analyses, theory and appl. to meteorology (*Polish*) 0-51546
- Kansas, storm and tornado watches compared to observed tornadoes, rel. to weather modification 0-12505
- kinetic energy balance of large-scale motion over British Isles 0-56578
- Kitt Peak National Observatory, probability of clear daytime skies 0-12512
- lapse rate regimes and parameterisation 0-12486
- light refraction calc. in three-dimensional model atmosphere, meteorological data requirements 0-46260
- linear prediction models, review 0-56590
- SE.Louisiana, forecast model 0-46216
- central Mali, rainfall comparison between Kabara and Tombouctou 0-4092
- marine radiofacsimile weather chart receiver and recorder 0-46297
- mathematical analysis of cloud seeding expts., physically meaningful covariates 0-56522
- mathematical analysis of weather modification and meteorological data 0-56521
- mesoscale structure of line convection at surface cold fronts 0-12514
- Meteosat project MISS IDA, interactive image system 0-36404
- Meteosat system, wind vector calculation from cloud motion 0-46270
- Middle East, monthly temps./rainfall relation appl. to palaeoclimates evaluation 0-31091
- moist available energy, numerical procedure 0-46241
- Monsoon Experiment, Monex, GARP subprogram 0-8428
- monsoon seasons at old Mangalore port, rel. to waters hydrographic conditions 0-41451
- Monte Capellino, ice formation, meteorological conditions statistical analysis (*Italian*) 0-12471
- Munster, minimum ground temperatures, var. (*German*) 0-4083
- National Weather Service information, external user survey 0-4064
- natural orthogonal components of meteorological fields calc. (*Russian*) 0-4137
- Navstar global positioning system, meteorological appl. 0-17396
- Negev rainfall diurnal variation, climatological and meteorological implications 0-17344
- New England, 1816, snow and frost in year without summer rel. to Tambora volcano eruption 0-4089
- numerical weather prediction, finite element method appl. 0-12526
- numerical weather prediction, modified forward-backward scheme for two-grid-interval noise 0-26575
- numerical weather prediction model with momentum boundary layer 0-51451
- numerical weather prediction using GATE data 0-56586
- ocean passive radiometry, radio meteorology colloquium, Victoria, British Columbia, Canada (1978 June 14 to 21) 0-46724
- ocean topographic Rossby waves, meteorological generation rel. to kinetic energy on continental shelf 0-51425
- Oklahoma hail falls and storms charact. 0-12504
- S.Ontario weather pattern rel. to suspended particulate nitrates 0-17365
- optimum interpolation analysis, role of obs. errors 0-8383
- Oviedo, Spain, global solar radiation and air temp. (*Spanish*) 0-36377
- Oxford, 1682 May 31, point deluge and tornado 0-51521
- Oxford, cold winters (1767-8, 1776 and 1814) 0-51520
- tropical Pacific, ITCZ and atmospheric fronts 0-41509
- planetary boundary layer processes, incorporation into numerical forecasting models 0-17312
- polar air outbreaks, cyclone-anticyclone couplet construction, vorticity budget computation 0-8391
- polar low as extratropical CISK disturbance 0-51502
- precipitation forecasting 0-6 hours ahead, radar and satellite imagery, FRONTIERS plan 0-12509
- precipitation over ocean, quantity rel. to precipitation freq. 0-31105
- prediction methods (*Japanese*) 0-31095
- radar measurement of clouds and precipitation, correl. and spectral anal. 0-12529
- radar observation of lower atmos., VHF pulsed Doppler method 0-46277
- radar remote sensing, optimal positions of multiple-Doppler system 0-31140
- radar system appls. 0-26651
- rainfall in England and Wales, long-period records spectral and filter anal. 0-4080
- remote sensing by two satellites, radio illumination method 0-51550
- ridge regression-time extrapolation of short records of rainfall 0-51489
- Sahel rainfall 1975-6, D, T and  $^{18}O$  evidence and regional winds (*French*) 0-21809
- satellite communication systems, weather sensitive economic activities appl. 0-46244
- satellite data uses, ESA conf. (Lannion, France, 17-21 September 1979) 0-36783
- satellite observations, their contribution to FGGE 0-36403
- satellite telemetering system, NOAA 0-56592
- seasonal climate model on global scale 0-41544
- shipboard automated information processing system, for hydrometeorological data 0-41553
- shipboard sounding system for GWE 0-17394
- snowfall systems induced by Lake Ontario, objective forecast method 0-51484
- solar radiation data, statistical correl. between daily and monthly averages 0-8409
- South Polar Plateau, meteorological transport of particulate material 0-51481
- Soviet progress 0-26598
- spectral energetics, determ. via numerical filtering anal. 0-26577
- spectral transmittance sensitivity to line and meteorological parameters 0-26610

## meteorology continued

- spectrum width estimates for weather echoes 0-12477
- squall line, formation from boundary layer forcing and temp. gradient, model 0-8396
- statistical analysis of weather modification projects 0-56520
- stochastic weather algorithms for predictions of solar cooling performance 0-35642
- storm spotting, National Weather Service's training programme 0-8382
- stratosphere data compatibility used in meteorological analysis, empirical study 0-17308
- subtropical high in N.Pacific rel. to sea surface temp. anomaly (*Chinese*) 0-46237
- summer monsoon circulation aspects 0-8413
- Sun-weather connections 0-51467
- Sun-weather relation, vorticity area index to interplanetary mag. sector struct. 0-46222
- sunlight intensity, data rehabilitation, SOLMET-2 procedures criticised 0-4071
- surface weather charts for wind speed over drifting pack ice 0-41476
- synoptic and mesoscale mechanisms for heavy rainfalls causing flash floods 0-8385
- synoptic windfinding, NCAR aircraft dropwindsonde system 0-17393
- technical meteorology, technical and commercial appls. (*German*) 0-46231
- temperature forecasts, case for an operational programme 0-17311
- thermal wind-field disturbances in sea coastal zone, statistical forecasting of frequency 0-36371
- thermally driven flow in beta-plane channel, regime diagrams 0-56552
- time-averaged data, variance by simple approx. 0-31139
- Transcaucasia rainless periods, 1966-75 obs. 0-26603
- TROPEX-74, USSR meteorology expedition, consistency of shipboard meas. with 'Meteor' buoy 0-36402
- tropical air-sea interaction at large scale, numerical study 0-56549
- tropical boundary layer over ocean, turbulence closure model for BOMEX data 0-56583
- tropical cloud cluster, struct. and evolution 0-12488
- typhoon Ora, form. in intertropical convergence zone under influence of midlevel jets 0-12527
- United Kingdom, regional units, wet and dry periods defined 0-51522
- E.United States, meteorological control of sulphates diurnal var. at rural sites 0-30621
- USA, National Severe Storms Forecast Centre, 1970-9, predictive success 0-46214
- vertical precipitation structure recording, meteorological radar appl. (*German*) 0-17358
- visibility probed with lidar 0-31141
- water vapour images from Meteosat, comparison to tropical streamline analyses 0-8384
- weather, severe convective event numerical simulation and prediction, Navier-Stokes eqns. initialisation 0-31111
- weather and climate, definitions 0-41540
- weather and climate, solar-terrestrial influences, symposium/workshop proceedings (Columbus, Ohio, 1978 August 24-28) 0-27037
- weather changes and air pollution, meteorological meas., brief survey (*French*) 0-17359
- weather conditions occupying a line or area, probability model 0-56558
- weather experimentation, statistical issues 0-8439
- weather forecasting, analysis method (*Chinese*) 0-46238
- weather forecasting, assessment of model initial conditions using satellite imagery 0-31084
- weather forecasting, complexing of alternative forecasts 0-41530
- weather forecasting, dynamic statistical model of complex stable processes 0-26599
- weather forecasting and general circulation, finite element models 0-51504
- weather forecasting in USSR, short-term predictions since 1920 0-41529
- weather forecasting nonlinear evolutionary problems, finite element methods appl. 0-21865
- weather forecasting skill of beginners 0-4066
- weather forecasts, economical and optimal combination method (*Russian*) 0-21792
- weather maps, for present weather, wind, and ceiling, examples, forecasting use (*German*) 0-4081
- weather modification, prospects and problems, book 0-36790
- weather modification, statistical anal. of cloud seeding expts. 0-56519
- weather modification expts., bibliography 0-56523
- weather prediction by finite difference scheme (*Chinese*) 0-46234
- weather radar, Doppler, estimation of echo spectral moment 0-51563
- weather radar, signal anal. (*French*) 0-36418
- weather rel. to solar and interplanetary mag. sector struct. 0-17340
- weather station operation, management practices on USAF stations 0-46215
- weather variations, of forced or free nature 0-56596
- weather-solar activity relationships, possible mechanisms 0-17341
- wind, beaufort scale data, conversion to wind vel. study (*German*) 0-8407
- wind shear detection radar, for airport use 0-51565
- winter lower atmosphere, influence of interplanetary mag. field sector struct. 0-8510
- zonal and meridional large scale flow over British Isles 0-56579
- $H_2O$  dimer, meteorological implications 0-8418
- Rn evolution in neutral atmospheres, correl. with meteorological parameters (*Spanish*) 0-4058

## meteors

- see also meteorites; meteoroids
- Brno fireball (1977 Sept. 14), photographic data 0-41771
- counts, test for registration independence 0-8594
- drift due to tidal winds at 80-100 km altitude, poleward momentum transport 0-12581
- $E_c$ -layer, occurrence rel. to meteor metallic ions 0-46336
- fireball luminous efficiency, theory 0-21947
- Geminids, flux in 1974, magnitude ratio and mass index 0-4307
- luminosity of meteor trains, lifetimes, Na catalytic cycle 0-12711
- nonequilibrium thermodynamic model 0-4308
- Orionids 1975, radar echo rates, long-baseline obs. 0-36576
- Perseid meteor shower, television obs. 0-4309
- Perseids, meteoritic aerosols, twilight optical charact. modification (*French*) 0-46255
- photographic altitudes, observational-theoretical comparison 0-8593
- Quadrantid meteor stream, long-term orbital evolution 0-17551



**meteors continued**

- Quadrantid meteor stream, orbital evolution between (AD 1830 and 2030) 0-21948
- Quadrantid meteors influx, effect of meteoroid stream orbital evolution 0-56776
- radar meteor echo rates, correl. with zonal winds at 95 km altitude 0-56775
- radar obs. of neutral wind gradients 0-41575
- radio echo characteristics, rel. to deionisation processes and meteoroid props. 0-17550
- radio waves scattering by meteor trails, trapping by ionospheric ducts 0-4172
- radiometeor characts. assessment, statistical analysis of time-dependent series (*Russian*) 0-56777
- radiowave reflection from meteor trail, ambipolar diffusion coeff. 0-46329
- stream disintegration, solar radiation and planetary perturbation effects (*Russian*) 0-46495
- trail maximum ionisation height, detect. method 0-8487
- tribo-induced discharge luminesc. 0-25471
- upper atmosphere winds at 95 km altitude, meteor obs. at 45°N 0-46330
- upper atmosphere winds observed by radio meteor drift, 80-100 km altitude 0-46328
- wind height structure determination, statistical method (*French*) 0-51589

**metering**

- see also *ammeters; electrometers; frequency meters; galvanometers; level meters; ohmmeters; phase meters; volt-ampere meters; voltmeters; watt-hour meters; wattmeters; wavemeters*
- analogue or digital differences and basis for rational choice 0-52184
- analogue versus digital, analogue meter advantages 0-13053
- digital capacitance meter (*Spanish*) 0-13062
- sound-level meter, innovative high school teaching project 0-4495

**meters** see *metering***metrology** see *measurement***metrosils** see *varistors***MHD** see *magnetohydrodynamics***MHD converters** see *magnetohydrodynamic converters***mica**

- biotite stress corrosion cracking, seen in grandiorite 0-36299
- glauconites, Mossbauer anal.,  $\text{Fe}^{3+}/\text{Fe}^{2+}$  ratio 0-17252
- mica, metamorphic white, surface microtopography 0-54493
- nuclear tracks, etched, statistical distrib. of quadratic holes on planar surface, computer simulation 0-37705
- surfaces, interaction forces at small separations in polar and non-polar liquids 0-39458

**Micelle systems** see *colloids***microcalorimeters** see *calorimeters***microchemical analysis** see *chemical analysis***microcircuits** see *integrated circuits***microcomputers**

- for microcomputer applications see under relevant applications e.g. *computerised control; natural sciences computing*
- see also *microprocessor chips*
- Culham fusion expts., distributed control systems using microcomputers 0-13909
- Culham fusion expts., integrated data network for microcomputer based diagnostics 0-13910
- Culham fusion studies, appl. of microcomputer to data acquisition and control 0-13908
- disturbed cell renewal systems, simulation by microprocessor system 0-35859
- fusion experiments, microprocessor applications in data acquisition and control 0-13918
- general purpose, use for hypothetical spectra synthesis in NMR underground. instruction 0-42009
- industrial service, of microprocessor (*French*) 0-17729
- Intel MDS-800, DMA interface for Biomation 8100 recorder 0-203
- ion-selective electrode analysis use of microprocessor-based millivoltmeter 0-16752
- laboratory data acquisition and control system based on Commodore PET microcomputer 0-204
- medical application, ventilatory function testing 0-41291
- nonvocal communication aid improvement by microprocessor technology 0-8217
- physics teachers and students guide to calculator choice 0-4494
- Pickier FACS-I diffractometer, microprocessor-controlled optical incremental angle encoder system 0-18058
- portable microcomputer system, associated movement study 0-51299
- potentiometric analyser, automated, with selective electrodes, microcomputer control 0-40773
- rehabilitation of severely disabled, microcomputer environmental control and communication system 0-8216
- single-chip, architecture and operation, use in instruments design and meas. techniques (*German*) 0-27276
- TFR Tokamak, microcomputer data acquisition system 0-13916
- visual stimuli generation for psychology experiments, Z-80 based system 0-41328
- X-ray double crystal spectrometer, microcomputer automatic control (*Polish*) 0-32563

**microcopying** see *microphotography***microelectrodes**

- bioelectrode methods (*Japanese*) 0-30919
- endocardial electrode lead and pacemaker failure, actuarial analysis 0-30945
- glass microelectrode, for pH meas. 0-21291
- implantable pair for recording from intact small nerves 0-36204
- metal biomedical microelectrodes, noise characts. (*Japanese*) 0-3846
- motion artifacts in surface applied bioelectrodes, quantification (*German*) 0-3829
- moving-coil microelectrode puller 0-30964
- multi-microelectrode system characts., neuron single-unit pots. recording appl. (*Japanese*) 0-21581
- reference microelectrode sterilizable with ethylene oxide 0-17153
- tissue measurements of local  $\text{PO}_2$ , local flow and local ion activity 0-51287
- tissue pH electrodes for clinical applications 0-36175
- $\text{Ca}^{2+}$  intracerebral transients, photoelectrode for recording 0-30961
- Na-selective liquid ion-exchanger, for intracellular meas. 0-3888

**microelectronics** see *integrated circuits***microfarad meters** see *capacitance measurement***microfiche** see *microforms***microfilm** see *microforms***microfilming** see *microphotography***microforms**

- see also *computer output to microfilm*
- electrophotographic process of contact copying of microfiches and microfilms 0-47127
- spatial filter correlator, coherent optical matched, for microfilm data base word recognition 0-43279

**microhardness** see *hardness***micromanometers** see *manometers***micrometeorites**

- ablation spheres in deep-sea sediments 0-46500
- micrometeoroid hazard of Comet Halley probe, workshop proceedings (Noordwijk, Netherlands, 18-19 April 1979) 0-36782

**micrometeoroids** see *meteoroids***micrometers** see *micrometry***micrometry**

- see also *interferometry; strain gauges*
- No entries

**microphones**

- array microphone, const. beamwidth, wideband, near field use 0-14535
- calibration at depth in dry hyperbaric chambers 0-38205
- cardioid microphones, transmission props. in LF region (*Czech*) 0-43584
- coincident, for triphonic sound reproduction system 0-28405
- condenser, arrangement for precision reciprocity calibration 0-19203
- coupler for noise source location, BOTSEAR 0-43576
- electroacoustic transducers using piezoelectric polyvinylidene fluoride films for diaphragm material 0-10100
- miniature probe microphone using optical fibre 0-48534
- noise cancelling microphone with piezoelectric plastic diaphragm, coupled oscillator theory 0-43581
- nonlinear US fields in air, numerical representation, microphone signal example (*French*) 0-53521
- polychlorotrifluoroethylene, electret, TSC 0-7266
- radio, receiver for parallel operation in film, TV studios, theatres (*German*) 0-4787
- sound-controlled flashlamp trigger circuit (*Spanish*) 0-13175
- techniques for recording or broadcasting symphonic music 0-5885

**microphonics** see *microphones***microphotography**

- see also *microforms*
- chromosome-classification system based on banding technique 0-36199
- electrophotographic process of contact copying of microfiches and microfilms 0-47127
- equipment to improve microscope photography 0-22460
- fundamentals and practical use 0-13166
- low-power, critical focusing, use of auxiliary telescope 0-13165
- neurosecretory cell IR photomicrography 0-30959
- TV microscopy and cinephotomicrography with Zeiss Axiomat 0-27343

**microphotometers** see *densitometry; photometers***microprobe analysis, electron** see *electron probe analysis***microprobe analysis, ion** see *ion microprobe analysis***microprocessor chips**

- programmable fast logic unit 0-52842

**microprocessor systems** see *microcomputers***microprocessors** see *microcomputers; microprocessor chips***micropulsations**

- continuous (Pc 3,4) pulsations in European sector, high resolution study 0-21877
- high-latitude Pc1-2 in rel. to dayside polar cusp 0-51623
- ionosphere propagation of Pc 1 pulsation signals 0-51604
- IPDP pulsation polarisation, correl. with particle precipitation 0-51612
- latitude dependence of power spectra, ssc and si excited near  $L=4$  0-51619
- long-period, global electric circuit model 0-41646
- magnetospheric equator, Pc 3, 4, 5 pulsations obs. by synchronous satellite 0-41647
- morphology and physical processes 0-41638
- Pc 1 pulsation polarisation, correl. with particle precipitation 0-51612
- Pc 1-2 wave obs. in outer magnetosphere 0-12618
- Pc 3 and 4, Dodge satellite and ground-based obs., correlated effects 0-12617
- Pc 3 and 4 spectral analysis rel. to dayside plasmopause position 0-56681
- Pc 3 and energetic electron precipitation 0-8493
- Pc 3 to 5 nightside pulsations origin, Alfvén waves excitation by bouncing electron beams 0-4203
- Pc 4,5 geomagnetic pulsations generation, influence of bounce effects 0-4197
- Pc 4 giant pulsations in morning sector, magnetometer obs. 0-26690
- Pc 5 waves, latitudinal struct. by satellite obs. 0-51621
- Pi2 propagation at low latitude, longitudinal range 0-51624
- Pi 1 to 2, appl. to geomag. induction study of seismically active fault along SW Japan Sea coast 0-26475
- Pi 2 pulsations, initial movements arrival at conjugate stations 0-31173
- Pi pulsations, assoc. with VLF radio waves phase anomalies in midlatitudes 0-56671
- power spectra and Stokes vector representations of LULF micropulsation states 0-51608
- solar wind speed correl. with Pc 3, 4 and 5 activity 0-41665

**microrecording** see *microphotography***microreduction** see *microphotography***microscopes**

- see also *acoustic microscopes; electron microscopes; ion microscopes; optical microscopes*
- X-ray microscopy of biological specimens, flash X-ray method 0-51310

**microscopy**

- see also *electron microscopy; ion microscopy; optical microscopy*
- powders microscopic quantitative analysis 0-22475
- projection microradiography, historical development and applications 0-37138
- publications concerning microscopic equipment, methods, appls. and related topics 0-22167



**microstructure, crystal** *see crystal microstructure*

**microtext** *see microforms*

**microtomes** *see laboratory apparatus and techniques*

## microtrons

- Mainz microtron project, MAMI A status report 0-23197
- MUSL-Z, 6 pass microtron using superconducting linac, operating experience 0-23196
- tuning of coupled-cavity structs., nondimensional 0-32546

**microwave acoustic devices** *see acoustic microwave devices*

## microwave antenna arrays

- solar power satellite, appl. of solid state microwave technology 0-40870
- solar power satellite ground station rectifying antenna, basic design concepts 0-16782
- tumour irradiation using focused array system 0-21521

## microwave antennas

- see also waveguide antennas*
- atmospheric water vapour and liquid monitoring using radiometry at 21 and 32 GHz 0-26628
- microstrip antennas for biomedical applications of microwaves 0-3762
- spin wave excitation in ferromag. films by antenna field 0-44816

## microwave detectors

- automatic nulling radiometer for the 3-4-mm band 0-18016
- breast cancer 30 GHz and 68 GHz telethermography (*French*) 0-3765
- conference, Zurich, Switzerland (Mar. 1979) 0-4783
- InSb subMM detector, fast response, for use in measuring electron cyclotron emission 0-27347
- Josephson junctions mounted in a waveguide, wide-band detect. characts. 0-4767
- Josephson video-detector, optimisation for mm wavelengths 0-4768
- mm waves video detection by capsule type point-contact Josephson junctions 0-13141
- PAM microwave field dosimetric device 0-3818
- plasma detector system for gas chromatography/emission spectroscopy in environmental pollution studies 0-26070
- remote sensing from space, synthetic-aperture radar systems and Spacelab expts. 0-36409
- semiconductor superlattice microwave/infrared detectors 0-13138
- superconductivity, space applications 0-41694
- thermography, principle and biomedical appls. (*French*) 0-30957
- tunnel junction mixers, quantum limited detection 0-18015
- n-Hg<sub>0.8</sub>Cd<sub>0.2</sub>Te, microwave bolometer heterodyne receiver based on magnetic field induced phase transition 0-13135
- TiO<sub>2</sub>:Fe<sup>3+</sup>, microwave second harmonic generation and freq. conversion 0-50166
- VO<sub>2</sub>, film, visualisation of microwave and IR radiation 0-5839

## microwave devices

- see also acoustic microwave devices; Gunn devices; masers; microwave parametric devices; solid-state microwave devices; waveguides*
- 4-port, transmission charact. utilizing total reflection, wave transmission matrix (*Czech*) 0-37937
- accelerator, linear, transient behaviour of high-current relativistic electron beam 0-32541
- exposure system for marine animals, dosimetry and reflectometric obs. 0-56319
- interferometer, improved Michelson-type operating at 140 GHz 0-31854
- Josephson junctions in self-pumping mode of operation 0-54839
- K-band interferometer for measuring the magneto-microwave Kerr effect in semiconductors and ferrites 0-52263
- power symposium, Monaco (1979) 0-3758
- scanner for soft tissue tumour detect. 0-17054
- waveguide system for chronic exposure of small animals to microwaves 0-56318

## microwave filters

- interference filter for submillimetre astronomy 0-48393

## microwave generation

- see also microwave oscillators; relativistic electron beam tubes*
- circular waveguide, microwave generation by relativistic electron beam 0-48128
- cyclotron maser instability, quasi-linear theory, calc. of microwave generation efficiency 0-1783
- high power MM wave source-gyrotron (*Japanese*) 0-23654
- intense microwave radiation, generation by relativistic electron beam introde 0-14887
- GaAs devices and their use for generation and freq. conversion of microwave oscillations 0-15534
- p-InSb, high resist. compensated, generation of microwave radiation 0-34476

**microwave heaters** *see radiofrequency heating*

**microwave heating** *see radiofrequency heating*

## microwave holography

- data processing using Fermat number transform 0-43298
- developments, review 0-23645
- imaging, influence of wave polarization and surface discontinuities 0-14305
- imaging, real-time camera prospects 0-53241
- lens for holographic imaging 0-48183
- multifrequency, improved image reconstruction 0-1159
- quadratically spaced linear antenna array 0-32938

**microwave induced delayed phosphorescence** *see MIDP*

**microwave-infrared double resonance** *see optical double resonance*

## microwave links

- attenuation of signals under adverse dust-storm conditions 0-46247
- over-the-sea propag. hops in Republic of Indonesia 0-46245
- rain attenuation, estimation of duration time distribution (*Japanese*) 0-21788
- rain attenuation meas., microwave radio link projected design appls. (*Slovenian*) 0-46217
- satellite to Earth path, effect of rain on crosspolarization 0-21789
- SIRIO radiowave propag. data for earth-space rain-cell modelling 0-36352
- Voyager Project, spacecraft communication system 0-26718

## microwave measurement

- see also microwave reflectometry*
- 9 GHz radiometry of tumours (*French*) 0-3767
- 22.75 GHz microwave attenuation characts. at high elevation (*Japanese*) 0-27346
- absorption by water in heterogeneous organic materials 0-15998
- anisotropy meas. at microwave freq., experimental results 0-52279

## microwave measurement continued

- application survey, non-conventional (*Italian*) 0-13093
- aqueous soln. reaction kinetics meas. microwave apparatus 0-3470
- atmospheric temperature-pressure profile meas. by microwave remote sensing (*Chinese*) 0-4116
- biological effects determ., contactless meas. of temp. and absorbed energy, using fluorescent screens 0-36186
- cancerous mouse hyperthermia meas., microwave, IR and thermocouple methods (*French*) 0-3768
- Cicoil personal RF radiation hazard detector, evaluation 0-5337
- clinical microwave focusing thermography 0-3771
- conference, Zurich, Switzerland (Mar. 1979) 0-4783
- conference on microwave power appls., London, England (Nov. 1979) 0-21520
- dielectric const. measurement using cavity perturbation technique 0-31802
- dielectric constant of liquids, complex, with high dielectric losses, 300 MHz to 6 GHz (*German*) 0-13106
- dielectric parameters meas. by cavity perturbation technique 0-9002
- digital freq. counters and counter-timers, new range using MSI 0-27318
- electric field intensity meas. using Ne gas-discharge tube 0-9006
- Fabry-Perot interferometer, inhomogeneous, dielectric loading and general phase-frame shaping, analysis 0-13197
- forest fire sources, microwave radiation spectra 0-52314
- frequency counter, LSI design 0-213
- Gulf of Alaska SeaSat Experiment 14.6 GHz scatterometer surface wind obs. 0-46200
- high permittivity measurement using waveguide measuring line 0-47080
- human thorax, mapping of transmitted microwave power 0-3756
- kidney, canine, isolated, microwave scattering parameter imagery 0-3755
- microwave detection of third-order nonlinearities 0-55594
- MM and subMM wave appl. in 100-1000 GHz range 0-17962
- ocean passive radiometry, radio meteorology colloquium, Victoria, British Columbia, Canada (1978 June 14 to 21) 0-46724
- oceanographic microwave remote sensing 0-56612
- open resonator methods for microwave permittivity meas. 0-15942
- passive microwave remote sensing of snowpacks, theory and expt. 0-26632
- permittivity measurement for human sera and erythrocytes 0-26424
- permittivity of liquids using modified microwave cavity perturbation technique 0-42239
- phase measurement of microwave interference signals from 0 to n.360° for plasma density meas. (*German*) 0-6278
- power symposium, Monaco (1979) 0-3758
- radiation power density measurement, used in formulation of dosimetry standards 0-26377
- radiometer measurements, microwave brightness temperature (*Danish*) 0-26625
- radiometers for ice movement measurement (*Danish*) 0-26624
- refractive index of isotropic and anisotropic media, meas. at 35 GHz 0-256
- remote sensing and profiling of lower atmosphere using radiowaves, ground-based 0-56628
- remote sensing atmospheric sounding of cloudy atmospheres (*Chinese*) 0-51549
- SeaSat scanning multichannel microwave radiometer 0-46248
- skin stratum corneum, human, linear meas. of water content using microwave probe 0-21518
- small liquid biological sample microwave complex permittivity meas. 0-17222
- thermometer with automatic balancing, for liquid streams temperature meas. 0-47055
- tissue equivalent bolus, 1 to 10 GHz electrical prop. characterisation 0-3763
- trilateration distance measurement in German Bight (*German*) 0-8248
- troposphere, temp. profiles from ground-based angular microwave meas. 0-51551
- Si wafer, nondestructive method for meas. of spatial distrib. of minority carrier lifetime 0-13098

## microwave-optical double resonance

*see also PMDR*

- anthracene-tetracyanobenzene cryst., triplet exciton annihilation, time correlated delay fluoresc., ODMR 0-39895
- <sup>3</sup>π\*benzaldehyde, zero field splitting and sublevel decay rates, deuteration and host effect 0-37750
- (biphenol)<sup>+</sup>/(biphenol)<sup>-</sup> ion-radical pair, ODMR, hyperfine struct. (*Russian*) 0-15829
- chlorophyll-a (b), dimerisation, fluoresc. and ODMR study 0-18876
- cyanogen fluoride, fund., hot bands, laser microwave two photon and double reson. spectroscopy 0-32752
- dibenzofuran, cryst., phosphoresc. spectra and ODMR meas. 0-11470
- dibenzofuran-fluorene, mixed cryst., phosphoresc. spectra and ODMR meas. 0-11470
- 1,4-dibromonaphthalene, substitutionally disordered, energy localisation, optical and ODMR spectra of triplet Frenkel excitons 0-54996
- fluorene, cryst., phosphoresc. spectra and ODMR meas. 0-11470
- fluoroacetylene, fund. and hot bands, laser microwave two-photon and double reson. spectroscopy 0-32752
- fluoromethane, excited state rot. spectroscopy and kinetics, appl. of tunable sub-MM sources 0-14162
- formaldehyde, microwave-microwave double resonance 0-53029
- high temperature molecules, rotational spectroscopy 0-52236
- II-VI semiconductor, recombination radiation, ODMR study, detrimental effects of high excitation intensities 0-44958
- methyldichlorosilane, Stark effect and microwave-microwave double reson., struct. (*German*) 0-47975
- modern aspects, theoretical and further developments, book contrib. 0-53029
- molecular planar structure, double reson. signals depend., appl. to microwave spectra 0-32751
- perdeuterobenzophenone, in 4,4'-dibromodiphenylether, cross-relax., microwave pulse obs. 0-53031
- phenazine, substitutionally disordered, energy localisation, optical and ODMR spectra of triplet Frenkel excitons 0-54996
- pheophytin-a (b), dimerisation, fluoresc. and ODMR study 0-18876
- photoexcited triplet state molecules, in cryst., cross-relax., variable freq. ODMR obs. 0-53031
- scandium octaethylporphyrin, μ-oxo bridged dimer, triplet states and geometrys, ODMR obs. 0-9625



**microwave-optical double resonance** continued  
 scandium octaethylporphyrin, triplet states and geometrys, ODMR obs. 0-9625  
 solid, molecular fluoresc., phosphoresc., and ODMR line narrowing 0-43084  
 spectroscopy, modern aspects, book 0-51973  
 1,2,4,5-tetrachlorobenzene, excited triplet state dimer, intermol. exchange integral, isotope effect 0-15826  
 1,2,4,5 tetrachlorobenzene, triplet excitons, high. mag. field, spin-lattice relax. study 0-20517  
 triplet state broadening, inhomogeneous and homogeneous, of optical and ODMR transitions in solids 0-32750  
 AgCl:Ni, optically detected double resonance, radiative recombination electron traps 0-20518  
 As<sub>2</sub>S<sub>3</sub>, amorphous, luminesc. and optically detected ESR, photoinduced struct. change 0-50399  
 As<sub>2</sub>Se<sub>3</sub>, amorphous and single cryst., ODMR expts. 0-50230  
 CaF<sub>2</sub>,  $^2S_{1/2}$  ground state, spin-rot. and hyperfine splittings rot. depend., mol. beam laser-RF double reson. 0-43079  
 CaO, relax. in  $^1T_{1u}$  state of F centres 0-24443  
 CsBr, self-trapped excitons, magneto-optical props., 1.3-50K 0-49606  
 CsI, self-trapped excitons, magneto-optical props., 1.3-50K 0-49606  
 GaAs:Cr, far IR EPR spectroscopy, mag. field-modulation technique 0-15830  
 GaAs-Al<sub>x</sub>Ga<sub>1-x</sub>As multilayer, photoluminesc., electron spin orientation 0-25453  
 GaP:O<sup>-</sup>, two-electron O<sup>-</sup> state evidence, ODMR, IR emission, phonon replicas 0-15828  
 GaS, optical detection of triplet excitons 0-29650  
 GaSe, triplet excitons ODMR 0-25252  
 HCN, microwave-microwave double resonance 0-53029  
 InSb, electron spin levels resonant excitation, photolum. 0-25454  
 KCl:PO<sub>2</sub><sup>-</sup>, triplet state, level anticrossing and pseudonuclear Zeeman effect, microwave ODMR 0-39896  
 K<sub>2</sub>CuF<sub>4</sub>, microwave excitation, optical detection of ferromagnetic reson. 0-50197  
 Kr, g-factors meas. by optical pumping and mag. reson. 0-14246  
 MgO, F centre luminesc., effects of uniaxial stress and ODMR 0-20690  
 NH<sub>3</sub>, microwave-microwave double resonance 0-53029  
 OCS, microwave-microwave double resonance 0-53029  
 RbMnF<sub>3</sub>, antiferromagnetic resonance, optical detection, luminescence 0-7174  
 Si, amorphous, glow-discharge deposited, ODMR spectrum, deposition temp. and annealing effects 0-50229  
 Si, amorphous, time-resolved ODMR and luminesc. 0-25254  
 Si amorphous film, glow-discharge, optically detected mag. reson., annealing and substrate temp. effects 0-20519  
 TI, in gas discharge, optical self pumping, hyperfine struct., microwave-optical spectroscopy 0-32680  
 Xe, g-factors meas. by optical pumping and mag. reson. 0-14246

#### microwave oscillators

*see also Gunn oscillators; microwave parametric oscillators; parametric oscillators; tunnel diode oscillators*  
 stabilizing resonator of high-power klystron self-oscillator for microwave supply system of linear accelerator 0-42878

#### microwave parametric amplifiers

No entries

#### microwave parametric devices

*see also microwave parametric amplifiers; microwave parametric oscillators*  
 n-GaAs, parametric interaction of HF waves, anal. 0-15554

#### microwave parametric oscillators

No entries

#### microwave reflectometry

*see also swept-frequency reflectometry; time-domain reflectometry*  
 dual six-port automatic network analyser, performance 0-47074  
 human serum and erythrocyte microwave complex permittivity meas. 0-3889  
 K-band interferometer for measuring the magneto-microwave Kerr effect in semiconductors and ferrites 0-52263  
 solid dielectric complex and power reflectivity determ., 100 GHz to 3 THz 0-15999  
 thru reflect line, improved technique for calibrating dual six-port automatic network analyser 0-47073

#### microwave region *see microwaves*

#### microwave spectra

*see also molecular rotation; molecular vibration; radiofrequency and microwave spectra of diatomic inorganic molecules; radiofrequency and microwave spectra of organic molecules and substances; radiofrequency and microwave spectra of polyatomic inorganic molecules*  
 atmospheric transparency, 3-13 cm<sup>-1</sup>, rel. to water vapour conc. 0-12476  
 forest fire sources, microwave radiation spectra 0-52314  
 K-band interferometer for measuring the magneto-microwave Kerr effect in semiconductors and ferrites 0-52263  
 magnetic system, amorphous, microwave absorption spectra 0-50469  
 $\alpha$ -AgI, superionic conductor, microwave absorption spectrum 0-11515  
 $\beta$ -Al<sub>2</sub>O<sub>3</sub>-Ag<sub>2</sub>O, superionic conductor, microwave absorption spectrum 0-11515  
 $\beta$ -Al<sub>2</sub>O<sub>3</sub>-Na<sub>2</sub>O, superionic conductor, microwave absorption spectrum 0-11515  
 CuTeBr, superionic conductor, microwave absorption spectrum 0-11515  
 Hg<sub>1-x</sub>Cd<sub>x</sub>Te, n-surface inversion layers study 0-25017  
 KD<sub>2</sub>PO<sub>4</sub>, microwave spectra, temp. depend. mode rel. to proton subsystem 0-24548  
 SiO<sub>2</sub>, glass, <sup>29</sup>Si hyperfine struct. of E' centre, microwave saturation props. 0-7165

#### microwave spectrometers

*see also magnetic resonance spectrometers*  
 absorption spectrometer with automatic tuning 0-270  
 acousto-optical radio astronomy spectrometer for processing of MM-wave signals 0-4253  
 interferometric microwave spectroscopy, modern aspects, book contrib. 0-52330  
 intrinsic sensitivity limitations, optimum attainable parameters, methods of realisation 0-37087  
 modern aspects, book 0-51973  
 modern aspects, book contrib. 0-52328  
 modulation technique, high temp. mols. 0-52236

#### microwave spectrometers continued

scanning spectrometry, submillimetre, modern aspects, book contrib. 0-52329  
 Stark effect spectrometer, with electric molecular modulation (Russian) 0-9003

#### microwave spectroscopy

*see also magnetic resonance spectroscopy; microwave spectrometers; paramagnetic resonance*  
 1-butanol, permitt., dielec. time domain spectroscopy, total transmission method study 0-27323  
 computer acquisition, simultaneous, of IR, microwave and Raman spectral data (Japanese) 0-4776  
 dielectric relaxation spectroscopy, liquids, frequency and time domain expt. methods 0-40044  
 Fabry-Perot resonator for CESR studies at 34 GHz 0-37065  
 high resolution spectroscopy in alkali metals 0-53248  
 high temp. molecules, modulation technique 0-52236  
 interferometric microwave spectroscopy, modern aspects, book contrib. 0-52330  
 interstellar molecules, microwave astronomy, modern aspects, book contrib. 0-56921  
 modern aspects, book 0-51973  
 modern aspects, book contrib. 0-52328  
 molecular spectroscopy book 0-27051  
 molecular spectroscopy book 0-27052  
 molecule energy barrier to internal rotation 0-28117  
 multilayer dielectric microwave reflectance and transmittance, characteristic matrix formalism 0-239  
 2-propanol, dielec. time domain spectroscopy, total transmission method study 0-27323  
 scanning spectrometry, submillimetre, modern aspects, book contrib. 0-52329  
 time delay spectroscopic imagery of isolated canine kidney 0-46109  
 TI, in gas discharge, optical self pumping, hyperfine struct., microwave-optical spectroscopy 0-32680

#### microwave tubes

*see also electron-wave tubes; relativistic electron beam tubes*  
 fusion machine application, review 0-23151  
 gyrotron, new milliwatt power tube 0-53198  
 gyrotron for electron-cyclotron heating in large Tokamaks 0-28751  
 gyrotron power source development in MM wavelength range 0-28852  
 O-type relativistic electron devices, linear theory 0-43242  
 O-type relativistic electron devices, nonlinear theory 0-43243

#### microwaves

applications, in industry, science and medicine, w.r.t. economics and safety 0-3754  
 biological effects and medical applications (Spanish) 0-26260  
 brain tissue, dog, dielectric props. between 0.01 and 10 GHz 0-16915  
 dielectric relaxation in muscle 0-51146  
 rain effects, drop-size and temp. effects on forward and backward scattering 0-17317  
 remote probing for wind and struct. const., line-of-sight method 0-36426  
 remote sensing of Earth, radiative transfer eqns. 0-21855  
 soil, surface roughness effect on microwave emission 0-17264  
 solar power satellite, microwave power transmission technology 0-40868  
 solar power satellite, microwave system perform. during startup/shutdown 0-40869

#### micromagnetism

*see also spin glasses*  
 BaO-Fe<sub>2</sub>O<sub>3</sub>-B<sub>2</sub>O<sub>3</sub> glass, splat cooled, low temp. micromagnetism 0-34660  
 Cu-Mn (15 at.%), short-range ordering, neutron scatt. polarisation anal. 0-50110  
 EuB<sub>6-x</sub>C<sub>x</sub>, magnetisation, effects of C 0-25163  
 EuB<sub>6-x</sub>C<sub>x</sub>, Mossbauer spectra, cond. electrons effect 0-20545  
 Fe<sub>2</sub>Ni<sub>1-x</sub>F<sub>1+x</sub>B<sub>6</sub>, amorphous, spin-glass regime, magnetoresist. meas. 0-34418  
 Fe<sub>2</sub>O<sub>3</sub>-Na<sub>2</sub>O-BaO glass, mag. props. 4.2-295K, micromagnetism (French) 0-39782  
 Fe<sub>2</sub>O<sub>3</sub>-PbO-B<sub>2</sub>O<sub>3</sub> glass, X-ray and electron microscope studies, mag. and Mossbauer effect meas. 0-28919  
 Ho<sub>x</sub>Y<sub>1-x</sub>(Fe<sub>0.1</sub>Co<sub>0.9</sub>)<sub>2</sub>, <sup>57</sup>Fe hyperfine interaction, mag. props., Mossbauer study 0-39951  
 MnBi, micromag. alloys, elastic props. (Russian) 0-7141  
 $\beta$ -NiAl B2 phase, mag. aftereffect 0-34700  
 Y(Fe<sub>2</sub>Al<sub>1-x</sub>)<sub>2</sub>, Mossbauer spectra and mag. props. 0-39950  
 Zr(Fe<sub>1-x</sub>Al<sub>x</sub>)<sub>2</sub>, transition region, spin glass or long range mag. order 0-44841  
 Zr(Fe<sub>1-x</sub>Co<sub>x</sub>)<sub>2</sub>, magnetovolume effects, thermal expansion and forced vol. magnetostriction meas. 0-29595  
 Zr(Fe<sub>1-x</sub>Co<sub>x</sub>)<sub>2</sub>, micromagnetism 0-15863  
 Zr(Fe<sub>1-x</sub>Co<sub>x</sub>)<sub>2</sub>, transition region, spin glass or long range mag. order 0-44841

#### MIDP

<sup>13</sup>C\*benzaldehyde, zero field splitting and sublevel decay rates, deuteration and host effect 0-37750

#### Mie theory *see electromagnetic wave scattering*

#### military equipment

*see also aircraft; military systems; ships*  
 acousto-optic parallel channel wideband receiver 0-48447  
 optical coating requirements in United States military specifications 0-48365  
 optical diamond turning and precision engineering 0-1364  
 optical glass fibre development, large-core, for military apps. 0-48451  
 optical precision machining commercialisation for military economy 0-1371  
 optical rotation rate sensors, Air Force apps. 0-9932  
 portable US warning tape, perimeter warning device for combat troops 0-19200

#### military systems

*see also military equipment*  
 hydroacoustic sources of locally generated sound in towed arrays, hose material 0-23822  
 NAVSTAR Global Positioning System, sea trials results 0-12645  
 signal processing activities of United States Army 0-48172  
 signal processing research programme of United States Air Force 0-48171  
 sonar horizontal array shape measurement using active/passive acoustic techniques 0-23824  
 towed arrays, hydrodynamics 0-23823



**Milky Way** see the *Galaxy*

**millimeters** see *ammeters*

**mills, rolling** see *rolling mills*

**m.i.m. devices** see *metal-insulator-metal devices*

**m.i.m. structures** see *metal-insulator-metal structures*

# MINDO calculations

- ethane, localised molecular orbitals, orthogonal transformations calcs. 0-47892
- lactam-lactim tautomeric equilibria, quantum chem. calcs. 0-50833
- 3-methyleneoxetane, electron structure, orbital-O interaction, MO calcs., UV photoelectron spectra 0-28058
- 3-oxetanone, electron structure, orbital-O interaction, MO calcs., UV photoelectron spectra 0-28058
- trans-polyacetylene, electronic energy band struct., extended Huckel and MINDO studies 0-20065
- $\beta$ -propiolactone, electron structure, orbital-O interaction, MO calcs., UV photoelectron spectra 0-28058
- radical, small, isotropic hyperfine coupling consts., MINDO/3 calcs. 0-52894

**mineral oil industry** see *petroleum industry*

**mineralogy** see *minerals*

# minerals

see also *lunar rocks and minerals*

- albite, radial distribution functions, quasi-crystalline model 0-1879
- albite porphyroblasts, growth rel. to deform. in Sambagawa schist, Central Shikoku, Japan 0-26509
- allophane, synthetic, amorphous mineral struct. obs. using  $^{57}\text{Fe}$  Mossbauer effect 0-34836
- amalcite, X-ray cryst. struct. determ. 0-28961
- amethysts of E.Siberia, form. conditions and history (*Russian*) 0-12393
- amphibole, electrical resist., up to 60 kbar (*German*) 0-31032
- analcite, polyhedral tilt transitions obs. at high press. 0-6515
- andalusite, shock-loaded, deform. 0-19873
- andalusite+sericite+sillimanite, cyclic reactions in Willyama Complex, New South Wales 0-26508
- anhydrite, phonon spectroscopy, lattice dynamical calc. 0-19889
- anhydrite, radioactive waste storage, anion effect on sorption of trivalent actinides 0-13717
- apatite, fission track retention as functions of heating time during isothermal expts. 0-36420
- apatite radioactive waste storage, anion effect on sorption of trivalent actinides 0-13717
- aragonite, Sr/Ca ratio for ocean temp. 0-12568
- arroyadite, X-ray cryst. struct. determ. 0-39058
- aubertite, X-ray cryst. struct. determ. (*French*) 0-33932
- augite, influence on plagioclase fractionation in igneous rocks 0-12390
- baddeleyite, high-press. phase transform., Earth mantle appl. 0-8296
- barite, deposits at deep-sea hydrothermal site on strike-slip fault 0-21710
- barite rare earth composition rel. to formation conditions 0-41439
- biotite, deform. and recrystallisation in Woodroffe Thrust mylonite zone 0-21739
- biotite, excess  $^{40}\text{Ar}$ , mobility in metamorphic terrain 0-17260
- biotite at Fleurieu Peninsula, South Australia, deform. rel. to slaty cleavage development 0-21735
- biotite deformation, comparison with muscovite from optical microstruct. 0-26507
- biotite stress corrosion cracking, seen in granodiorite 0-36299
- bismuthinite, superheavy element search using neutron multiplicity counter 0-4011
- bulk modulus-volume relationship, for cation-anion polyhedra 0-41434
- calcite, elec. cond., 300 to 1200°C at  $\text{CO}_2$  pressure of 40 bars 0-20195
- calcite, I-II phase transition interrelation with flow or fracture in carbonate rock deform. 0-51389
- calcite, thermoluminesc. spatial distrib. using image intensifier technique 0-47115
- E.China Sea sediments, mineral comp. and distrib. (*Chinese*) 0-8293
- chlorite,  $^{57}\text{Fe}$  Mossbauer analysis 0-40006
- clinopyroxenes from deep-sea basalts, statistical anal. of chemistry 0-41437
- compressional wave velocity and damping, minerals and rocks at high-press. (*German*) 0-31031
- cordierite, Brazilian, giant halos, superheavy element search 0-21752
- dating, EPR method 0-36415
- determination of C and  $\text{O}_2$ , ZAF correction procedure (*French*) 0-11983
- diamond with garnet inclusion, expt. crystallisation conditions study 0-46172
- diagenesis, plate tectonic controls 0-12387
- diopside, elasticity 0-6454
- dispersion staining method for refr. index meas. of a thin crystal section 0-8433
- dolomite, radioactive waste storage, anion effect on sorption of trivalent actinides 0-13717
- dolomite (Magneta), migration of  $^{137}\text{Cs}$ , effect on radioactive waste storage 0-13718
- elbaite, ferrihydrous,  $\gamma$ -irradiated, Mossbauer study 0-44990
- electron microprobes and scanning electron microscopy, conf., Orsay, France, Dec. (1978) 0-11979
- enorthite-albite system, crystal growth rates and processes 0-4010
- feldspar stress corrosion cracking, seen in granodiorite 0-36299
- feldspars from Mt. Rokko granites, electron probe X-ray microanalysis 0-31038
- felsic and mafic mineral separates from an Abitibi dike,  $^{40}\text{Ar}/^{39}\text{Ar}$  dating 0-17237
- fission fragment range and closing time. for track retention 0-41566
- fission track dating technique 0-36417
- fission track retention as function of heating time during isothermal expts. 0-36420
- fluorite,  $\text{CaF}_2$ , radiation and thermal redox processes of Mn ions 0-55678
- fluorite, Gruneisen parameter at high press. 0-8299
- forsterite, decorated dislocations 0-54245
- garnet inclusion in diamond 0-46172
- garnets, fluid inclusion data rel. to thermal history around Grassy granodiorite, Tasmania 0-4012
- glaucophane group, Norwegian-Greenland basin, age determ. by EPR and Mossbauer spectra 0-26467
- glaucophane, Mossbauer anal.,  $\text{Fe}^{3+}/\text{Fe}^{2+}$  ratio 0-17252
- gratonite, single crystal, photoelectric props. 0-49822
- gypsum, phonon spectroscopy, lattice dynamical calc. 0-19889

# minerals continued

- gypsum, powder Jeener-Broekaert three-pulse sequence, inhomogeneous lineshapes, second rank spin interactions 0-39891
- haematite-magnetite-fayalite nodule, stressed state parameters, stress zones, phase compositions (*Russian*) 0-40336
- halite, dynamic recrystn. during compression creep, geophys. appl. 0-25772
- hemimorphite, phase angle determ., by four-circle diffractometer (*Japanese*) 0-1897
- Hildebrand equation of state, appl. to Earth interior geophysics 0-56464
- hornblende, Cumberland Peninsula, Baffin Island, grain etching, age and palaeoclimate indicator 0-8307
- hydrogen embrittling effects from acoustic emission meas. 0-11742
- ilvaite, Mossbauer spectra and mag. features 0-7248
- jadeite, electrical resist., up to 60 kbar (*German*) 0-31032
- jarosite,  $\text{NH}_4\text{Fe}_3(\text{SO}_4)(\text{OH})_6$ , decomposition 0-11624
- kaersutite, sound vels. and anisotropy, rel. to upper mantle seismic struct. 0-26501
- kaolinite, hydration, lattice deform., vol. expansion due to adsorbed  $\text{H}_2\text{O}$  0-45555
- Kazakovite, cryst. struct. determ. 0-19782
- kyanite-sillimanite concentration, multistage and sintering, props. of refractory products 0-20867
- lower mantle, thermodynamically based eqn. of state 0-26473
- magnetite, grain size limits for pseudosingle domain behaviour, rel. to palaeomagnetism 0-11215
- magnetite, in Lake Tahoe, California-Nevada, sediments, palaeomag. and sedimentological studies 0-41371
- magnetite, oxidation mechanism during roasting of nodules (*Russian*) 0-40567
- magnetite, partial thermal remanent magnetisation additivity 0-26498
- magnetite, spin polarisation, effect of temp. and photon energy 0-45221
- magnetite ( $\text{Fe}_3\text{O}_4$ ), mag. susceptibility under hydrostatic press. and implications for tectonomagnetism 0-26504
- magnetite ( $\text{Fe}_3\text{O}_4$ ), piezomag. response depth depend. rel. to tectonomagnetism as earthquake precursor 0-26465
- magnetite in Bushveld Complex upper zone, Cr content vars. rel. to magma chambers heterogeneity 0-56421
- magnetite nodules with fayalite additives, stressed state parameters (*Russian*) 0-45352
- manganese (II) arsenatotrisilicate, cryst. struct. determ. and refinement 0-1970
- marble, LF dielectric props. 0-34843
- marble, radioactive waste storage, anion effect on sorption of trivalent actinides 0-13717
- melting (petrurgy) (*Czech*) 0-44298
- meteorite Zaisho, Japanese pallasite, mineralogical and petrographical study 0-46509
- mica, metamorphic white, surface microtopography 0-54493
- microcline, maximum, room temp. phase transition, heat capacity meas. 0-54373
- microcline, maximum room temp. phase transition, unit cell parameters, thermal expansion 0-54208
- monazites, search for superheavy elements 0-36297
- monticellite ( $\text{CaMgSiO}_4$ ), high-press. phase transforms. and implications for upper mantle mineralogy 0-17255
- montmorillonite clay sols, structure determ. by neutron diffr. and small angle scatt. 0-40748
- montmorillonite group, Norwegian-Greenland basin, age determ. by EPR and Mossbauer spectra 0-26467
- mulite, X-ray diffr. structural model 0-49191
- muscovite deformation, comparison with biotite from optical microstruct. 0-26507
- natrolite, cleavage etching in acid and neutral media 0-6407
- obsidian glass, Lipari and Teotihuacan origin, Mossbauer, magnetisation, X-ray diffr. and fluoresc. study 0-46173
- Oklo fossil nuclear reactors, radiation damage of minerals 0-21751
- Oklo natural fission reactors, temp. of mineral phase assemblages and rock textures 0-21722
- olivine, hardness var. with temp., rel. to polycryst. yield stress 0-26500
- olivines, elec. cond. meas. under defined thermodynamic activities, up to 20 kbar, 340-1100°C 0-6832
- opal, Spor Mountain, Utah, U-Pb age systematics 0-46149
- opals, crystal struct. and IR spectra 0-40117
- orthopyroxenes, electron irradi. effects, Mossbauer study 0-40016
- petroleum generation in SW block of Los Angeles Basin, rel. to thermal subsidence 0-3967
- phyllosilicates, dioctahedral and trioctahedral, calc. of electrostatic energy relations 0-19743
- plagioclase feldspars, banding, calcs., nonlinear partial differential eqns. appls. 0-4510
- plagioclase fractionation in igneous rocks, influence of augite 0-12390
- plasma furnaces, mineralogy and extractive metallurgy appls. (*French*) 0-28849
- pseudoboehmite, exam. of structure, using radial electron distrib. method, and X-ray diffraction 0-1977
- pyrope-almandine garnets, elastic consts. temp. depend. 0-17251
- pyroxene, containing trivalent cations, lab. meas. of elec. cond., rel. to lunar temp. profile 0-31033
- pyroxene, electrical resist., up to 60 kbar (*German*) 0-31032
- pyroxenes, elec. cond. meas. under defined thermodynamic activities, up to 20 kbar, 340-1100°C 0-6832
- pyroxenes, order-disorder interpretation 0-38987
- quartz, Dauphine twinning, stress-induced, acoustic emissions 0-6414
- quartz, defects growth, study by X-ray diffr. topography (*French*) 0-39095
- quartz, formation in closed seams, inferences from expts. on hydrothermal crystn. 0-10516
- quartz, Gruneisen parameter at high press. 0-8299
- quartz, high-low transition, effect on compressional and shear wave vel. in rocks under high press. 0-12380
- quartz, natural, gamma-irradiated, stress effect on thermolum. sensitivity 0-11482
- quartz, natural, virgin ( $\gamma$ -irradiated), polarisation effect on thermolum. sensitivity 0-11483
- quartz c-axis orientation in Saxony Granulites, petrofabric anal. by optical and X-ray diffr. studies 0-21740
- quartz distribution in Atlantic sediments, relation to climate, last glaciation 0-8308
- quartz in granites, cathodoluminescence rel. to granites microcracking and healing 0-51391



**minerals continued**

- quartz radioactive waste storage, anion effect on sorption of trivalent actinides 0-13717  
 rare earth geochemistry and mineralogy, book contrib. 0-46157  
 release-adiabat measurements, effect of viscosity 0-51388  
 rhodonite, lattice imaging of struct. defects 0-49240  
 rhodulite, electrical resist., up to 60 kbar (*German*) 0-31032  
 rutile, isothermal compression under hydrostatic press. to 106 kbar 0-31035  
 serpentine, solubility of inert gases, meteoritic abundance 0-12712  
 serpentine minerals, IR spectra, comparison with Orgueil, type C-1 chondrite 0-17556  
 shale investigation as radioactive waste repository, vermiculite role 0-32354  
 silica, determ. respirable dust from steelmaking, silicosis 0-45832  
 silicate, identification and asbestiform varieties, electron optical and X-ray techniques 0-8446  
 silicate dust condensation processes investigation, expt. techniques 0-26940  
 silicate minerals, Mossbauer anal. of Fe chem. state 0-20547  
 silicates, elec. field gradient at  $\text{Fe}^{3+}$  sites, Mossbauer spectra 0-15484  
 silicates, heat capacities rel. to simple lattice vibrational models 0-4005  
 silicates, IR spectra compared with astrophysical IR features 0-26728  
 silicates in Fe meteorites group IAB, I-Xe dating 0-17554  
 sillimanite-andalusite-kyanite ( $\text{Al}_2\text{SiO}_5$  polymorphs) thermal expansion and high-temp. cryst. chemistry 0-39319  
 staurolite, chem. decomp., ESR obs. 0-15788  
 strunzite,  $^{57}\text{Fe}$  Mossbauer study of crystal chemistry 0-39975  
 suspensions, dielectric separation of solid particles 0-16213  
 clear taenite in meteorites, identification as ordered  $\text{FeNi}$  0-8604  
 talc,  $^{57}\text{Fe}$  Mossbauer analysis 0-40006  
 thermal conductivity and thermal expansion, conference, Chicago, USA (Nov. 79) 0-31425  
 threadgoldite, X-ray cryst. struct. determ. 0-28969  
 titanomagnetite, TRM acquired by multi-domain single cryst. 0-36293  
 titanomagnetite in Waipipi iron sands, New Zealand, mag. assessment technique 0-17254  
 titanomagnetites of oceanic basalts, low-temp. oxidation rel. to mag. anomalies statistical anal. 0-36233  
 torbermorite study by X-ray line profile anal. (*Japanese*) 0-33984  
 tourmaline, elastic consts. by US phase-comparison method 0-2108  
 tourmaline, Mossbauer spectra, struct. 0-20566  
 tourmaline, proton jumps, NGR obs. 0-15921  
 tourmalines of dravite-schorl series, Mossbauer anal. 0-15920  
 troilite in Fe meteorites group IAB, I-Xe dating 0-17554  
 twin composition plane as extended defect, structure-building entity 0-44218  
 uraninite, Oklo phenomenon, isotopic abundances, long-term radioactive waste storage information 0-52769  
 uraninite from Oklo natural fission reactors, comp., evidence for mode of deposition and metamorphism 0-21747  
 uraninite grains, U solubility in the Oklo reactor 0-21756  
 uraninite in Oklo natural fission reactors, geochemistry of insoluble organic material (*French*) 0-21748  
 USA developments, by means of technological innovations, federal regulations influence 0-16763  
 vermiculite, firing temp. depend. of Mossbauer parameters 0-15837  
 voglite, cryst. and powder diffr. data 0-24421  
 X-ray anal. of microcrystallite nucleation and detection threshold 0-890  
 zircon, element distrib. from proton multiprobe and fission track techniques 0-17261  
 zircon, high-pressure phase transform., Earth mantle appl. 0-8296  
 zircon in Uivak II gneiss from Saglek area, Labrador, age meas. 0-3958  
 $(\text{Ca},\text{Fe})\text{SiO}_3$ , intracryst.  $\text{Fe}^{2+}$ - $\text{Ca}^{2+}$  exchange, Mossbauer spectra 0-20548  
 $\text{CaHPO}_4$ , monetite, low-temp. ordering of H atoms, X-ray and neutron diffr. study at 145K 0-39022  
 Fe, concretions origin of Hepworth carboniferous sediment, geochemistry 0-17262  
 Fe containing minerals, basalt rocks, Mossbauer spectroscopy identification 0-8302  
 Fe ore concentrates, two-layer charge, sintering conditions (*Russian*) 0-45248  
 $\text{Fe}_3\text{O}_4$ - $\text{FeAl}_2\text{O}_4$ - $\text{FeTiO}_3$  titaniferous magnetite, chlorination, 1273 to 2273K 0-55752  
 haematite nodules with fayalite and Ca ferrite additives, stressed state parameters (*Russian*) 0-45352  
 $\text{Mg}_3\text{Si}_2\text{O}_5(\text{OH})_2$ , talc, for hydrothermal crystn. of fibrous amphiboles 0-20810  
 $2\text{Mg}_3\text{Si}_2\text{O}_5\cdot 3\text{Mg}(\text{OH})_2$ , new high-pressure struct. type, cryst. struct. 0-39028  
 $\text{SiO}_2$ - $\text{Al}_2\text{O}_3$ , mullite, sintering behaviour and microstruct. 0-20876  
 Ti garnets, Mossbauer spectroscopic anal. of chem. state of Fe 0-20547  
 U are at Oklo, appl. of Ep-pH diagrams to problems of retention and migration of fissionogenic elements 0-21757  
 U, nature and exploration in US sandstone deposits, educational module 0-36799  
 U ore, Ru isotopic anal. 0-21764  
 U, world resources, effect on development of nuclear power 0-55826

**mines (coal) see mining****mines (mineral) see mining****minicomputers**

- for minicomputer applications see under relevant applications; administrative data processing; computerised control; natural sciences computing see also electronic calculators  
 real-time portable minicomputer system, for dynamic ocean data acquisition and display 0-12552  
 Royco aerosol particle counter 225, data processing system and modified system props. 0-37005

**minimax techniques**

- neutron flux, collision probability integrals, annular geometry, evaluation using analytic expansions 0-32317

**minimisation**

- see also minimisation of switching nets; minimum principle  
 beam-columns, optimal design 0-10142  
 free energy minimisation method in aqueous multicomponent multiphase equil. comput. 0-40724

**minimisation of switching nets**

- see also logic design  
 No entries

**minimum metallic conductivity**

- Anderson transition, electron localisation in disordered systems, review 0-29361  
 disordered materials, thin films and wires, resist. and localisation 0-44537  
 disordered solids, electronic props., numerical methods 0-44538  
 disordered systems, Anderson localisation theory in two dims., real space scaling method 0-44540  
 disordered systems, localisation using random series, Anderson transition for extended states 0-44542  
 localised electronic system, sp. ht., singularity at Anderson-Mott transition 0-34381  
 semiconductor melts, metallic cond. at high temp. 0-49832  
 transport processes, isothermal method for static cond. of electrons 0-29373  
 Fe film, vacuum deposited, resist. minimum 0-44741  
 Pd, film with defects, field-induced resist. min. 0-11050  
 $\text{Sb}_2\text{S}_3$ , mixed valent, large low-temp. Hall effect and resist. 0-39611  
 W-Re, amorphous wire, elec. resist., 2-20K, dims. and mag. field depend., quantum localisation 0-39547

**minimum principle**

- viscoelasticity, linear theory (*Japanese*) 0-48599

**mining**

- Boksburg, S. Africa, dyke strain relief meas. near mine working 0-17263  
 coal, deep-level seams, bed rocks instability obs., by monitoring acoustic emission activity (*Japanese*) 0-10071  
 coal and U, mining, processing and transportation, in Western US, impact 0-45621  
 diesel-powered underground mining equipment, noise control 0-53557  
 flame sensor-trigger device for explosion barrier in underground mines 0-52313  
 HF EM induction profiling, of boreholes in underground mines (*Polish*) 0-51547  
 long-hole drilling machine, noise reduction 0-53559  
 Lubin Cu mine, source study of mining tremor 0-41377  
 mobile equipment noise control in surface mining 0-53558  
 noise, characterization of environment, control methods 0-53556  
 Oklo natural reactors, mining, geology and tectonics (*French*) 0-21743  
 production in New Mexico, constraints 0-42843  
 radioactive waste disposal, Dutch policy (*Dutch*) 0-671  
 stoper drills for coal mines, total noise-control systems 0-53560  
 Szombierki coal mine, Upper Silesia, Poland, mining tremors, freq.-mag. relation 0-41378  
 ventilation fan acoustic noise spectral anal. (*Russian*) 0-53584  
 Mn nodules deposits, deep sea telemetry (*German*) 0-26623  
 U and coal, mining, processing and transportation, in Western US, impact 0-45621  
 U, CEA and Cogema activities (*French*) 0-626  
 U, in situ leach mining, environmental considerations rel. to water quality 0-3543  
 U mines, radiological evaluation 0-42806  
 U mining, U refining and decay processes, radioactive mining waste disposal (*Dutch*) 0-21418

**minimax technique see minimax techniques****minor planets see asteroids****minority carrier conduction see minority carriers****minority carriers**

- lifetime profile measurements in heavily doped emitter structures using electron beams 0-15538  
 MOS diodes, minority carrier lifetime determ. from photocurrent spectra 0-49920  
 p-n junction minority carrier diffusion length meas. by short-circuit current ratio 0-31849  
 p-n junctions, partially opened, three-frequency parameter systems, equivalent conductivities (*Russian*) 0-24998  
 recombination lifetime measurement using pulsed MOS capacitor 0-25012  
 semiconductor, spatial resolution of SEM electron beam induced conductivity images 0-6327  
 semiconductor crystals, with high quantum efficiency, minority carrier lifetime meas. (*Japanese*) 0-54711  
 solar cell, interaction of electron beam, minority carrier diffusion length 0-7943  
 $\text{Al-SiO}_2$ -Si, experimental verification of theoretical predictions 0-29485  
 $\text{Ga}_{1-x}\text{Al}_x\text{As}$   $n$ - $p_1$ - $p_2$ - $p_3$ - $p_0$  struct., degradation electrolum. 0-50428  
 p-GaAs, electron minority carrier diffusion lengths 0-29807  
 n-GaAs epitaxial films, residual cond. meas., struct. perfection rel. to photomemory 0-7010  
 GaAs MOS structures, props. of capacitance transient 0-25013  
 GaAs, minority carrier lifetime at high temp., solar cell performance appl. 0-24947  
 GaAs, VPE, hole diffusion lengths, surface prep. and heat treatment effects, etchant evaluation 0-15627  
 GaAs, VPE, hole diffusion lengths, effect of transition metal diffusional doping 0-15628  
 GaAs:Si p-n light-emitting structs., soln. of general minority carrier transport eqn. 0-15597  
 $\text{GaAs}_{0.8}\text{P}_{0.2}$ , VPE, hole diffusion lengths, surface prep. and heat treatment effects, etchant evaluation 0-15627  
 $\text{GaAs}_{0.8}\text{P}_{0.2}$ , VPE, hole diffusion lengths, effect of transition metal diffusional doping 0-15628  
 n-Ge, minority-carrier injection and extraction 0-49767  
 p-InGaAsP, on InP surface, diffusion coeff. and surface recombination velocity 0-39598  
 InSb p-n junction, minority carrier injection in mag. field, recomb. radiation obs. 0-11078  
 $\text{Pb}_{1-x}\text{Sn}_x\text{Te}$  DH laser, minority carrier lifetimes and lasing thresholds 0-19031  
 Si, amorphous, solar cells, efficiency, transport props. 0-50961  
 Si, diode, minority-charge-carrier lifetime rel. to abrasion of surface (*Russian*) 0-11805  
 Si, epitaxial, minority carrier lifetime and impurity conc. meas. (*Japanese*) 0-25025  
 Si epitaxial layer, minority carrier lifetime obs. (*Russian*) 0-49765  
 n-Si, heavily doped, meas. of minority carrier transport parameters 0-15537  
 Si, minority carrier lifetime, effect of  $\text{SiO}_2$  coating deposited by sputtering 0-11003  
 Si, minority carrier lifetime in neutron doped samples 0-20218



**minority carriers continued**

- p-Si, minority carrier lifetime, effect of low dose ion implantation (Japanese) 0-54715  
 Si, neutron transmutation doping, annealing, deep defect levels 0-20123  
 Si p-n junction, charge carrier recomb. at dislocations, combined SEM and TEM study 0-15105  
 Si, polycryst. films, transport props. and grain boundary charact. by TEM 0-50980  
 Si, temporary trap characteristic after heat treatment (German) 0-34459  
 Si wafer, nondestructive method for meas. of spatial distrib. of minority carrier lifetime 0-13098  
 Si:H, amorphous, surface activated, photoemission spectra, minority carrier diffusion length 0-40235  
 Si:P(B) solar cells, minority carrier lifetime mobility rel. to impurity conc. 0-55848  
 Zn,Cd,S/GaAs heterojunction solar cells, meas. of minority carrier diffusion length 0-26158

**mirages** *see atmospheric optics; light refraction***mirrors**

- adaptive optics technology status and prospects 0-33132  
 animal eye technology use in better lens and mirror design 0-28295  
 aspheric reflecting systems, geometrical design 0-38083  
 aspherical planoidal surface, autocollimation apparatus for testing manufacturing quality 0-10053  
 astronomical mirror suspended on belt, deforms. during horizontal control 0-17494  
 astronomical telescope concave mirrors, design of lens compensators for testing 0-28305  
 beam divider and mirror expt., amplitude correlation method for optical polarisation meas. 0-53206  
 Bragg mirror reflectance, dielectric waveguide inhomogeneity effect 0-28356  
 Brillouin, pump wave wavefront reversal, influence of certain radiation parameters 0-9961  
 catoptric objective design, testing (German) 0-53400  
 Cherenkov counter, ellipsoidal mirrors, fabrication and use 0-47818  
 coatings, selective reflectors, and antireflection coatings for nonlinear optics, chemical method 0-28300  
 cold light production by high vacuum deposition of multilayer interference coatings (German) 0-53486  
 compound elliptical concentrator, geometrical vector flux field 0-33119  
 compound parabolic concentrator solar collector design 0-3532  
 compound spherical mirror for space radio telescope 0-41720  
 computer-controlled polisher for small-tool fabrication of mirrors 0-14496  
 corrosion resistance (Polish) 0-11811  
 cylindrical mirror analyser, design and use with synchrotron radiation, autoionisation obs. 0-18049  
 cylindrical parabolic mirror utilisation as solar receiver (Rumanian) 0-7914  
 cylindrical-mirror confocal resonator design with high transmissivity region (Russian) 0-14361  
 deformable mirror, integrated imaging irradiance sensor for real-time wavefront measurement 0-33138  
 deformable mirrors with bimorph actuators 0-33135  
 dichroic multilayer mirror for 16  $\mu$ m region, design and fabrication 0-5808  
 dielectric laser mirror production with variable transmissivity (Russian) 0-14362  
 dielectric mirror, temp. field during laser radiation absorpt. 0-19063  
 differential ball screw actuator driven deformable mirror design and performance 0-33137  
 dihedral corner reflector, effective scattering area calculation, radiation balance method 0-48380  
 discrete actuator deformable mirror 0-33133  
 discrete component Sagnac optical rate sensor, error sources 0-1342  
 dye laser, short constructional length with folded mirror beam expansion system 0-53328  
 fast aspheric mirror figure control by profile monitor, wire tester and null lens 0-14419  
 fixed mirror solar concentrator for application to a 100 MW(e) electric generating plant 0-30393  
 flatness of mirror surfaces by group of line light sources (Japanese) 0-1294  
 Fresnel formula for dielectric multilayer mirrors 0-33118  
 Fresnel mirror interference method for diff. grating generation 0-48460  
 gas laser cavity light intensity optimisation for three-mirror system utilising Fabry-Perot resonators 0-48305  
 gas laser resonator, simple method of adjusting mirrors 0-19054  
 grating mirror, loss of periodic mode in IR laser resonator 0-28254  
 heat mirrors, spectral selectivity of conducting micromeshes 0-26160  
 heliostat facets, optical characterisation 0-53485  
 high-energy laser mirror thermal distortion test facility 0-14348  
 high-performance telescope aspheric mirror test error budget 0-48386  
 holographic Pancake Window reflective system 0-1165  
 imaging polarizer with spherical mirrors for VUV radiation 0-48375  
 inhomogeneous interface laser mirror coatings, durability improvement 0-1252  
 ion polishing for diamond-turned mirror dielectric coating adhesion 0-1370  
 IR multidither deformable-mirror COAT system expts. 0-1289  
 IR multilayer partial mirrors effective from 1.3 to 16  $\mu$ m, GeSe/KRS-6 and GeSe/NaF 0-9978  
 laser, sputtered films production and props. (Hungarian) 0-53483  
 laser beam scanning using rotating mirrors, specifications and tolerances 0-9979  
 laser gyros, low-scatter low-loss mirror prod. 0-1272  
 laser resonator mirrors, optimal refl. coeffs. for intracavity Q-switching 0-48302  
 laser system, high energy, thermally induced optical distortion 0-38051  
 light reflection by rough surface 0-18996  
 linear echelon refractor/reflector solar concentrators 0-7929  
 linear focusing solar reflector, production by elastic deformation of flat sheet 0-30391  
 long fibre, mirror and hollow dielec. lightguides, photometric characts. 0-33201  
 magneto-optic bounce-cavity modulator, direct AM 0-5769  
 metal mirror design and mounting specifications 0-48388  
 metal optics, reflective system specifications 0-48387  
 metallic mirror as complex rough surface, light scatt. 0-1293

**mirrors continued**

- metallic mirrors for laser fusion reactors, neutron and gamma irradiation response calc. 0-23121  
 monolithic deformable mirror/heat exchanger unit evaluation 0-33139  
 multiactuator deformable mirror evaluations 0-14416  
 multibeam modular interferometer design 0-18004  
 multidither adaptive optical system, 69-channel hybrid controller 0-33136  
 multidither adaptive optics system operation 0-33141  
 neutron reflectivities, Ni-Mn and Ni-Ti multilayers for monochromators and supermirrors 0-22880  
 nonimaging concentrator design as second stages with image-forming first-stage concentrators 0-50933  
 nonlinear holographic gratings for high energy laser beam sampling 0-14476  
 nonlinear media, phase distortion compensation by phase conjugation 0-43392  
 nonorthogonal resonators, fund. mode props. w.r.t. rotating Gaussian beams 0-53336  
 objective using a planoidal mirror 0-28297  
 off-axis parabolic mirror fabrication for laser function expt. 0-1374  
 optical design of two-mirror systems, coupling props. 0-53396  
 optical fibre-laser transverse coupling and front-mirror monitoring for feedback control of laser transmitters 0-33151  
 optical materials, laser induced damage, symposium, Boulder, USA (Sep. 1978) 0-31417  
 optical scatter meas. specification proposal 0-48390  
 oscillating beam spectrometer for organic thin film transmission 0-18022  
 para-ellipsoid mirrors for fan shaped beams, calc. method 0-33117  
 parabolic solar reflector for accurate and economic producibility 0-7930  
 paraboloid epimirror for microscope illuminator, design 0-28304  
 phase compensation of thermally bloomed laser beam, mirror deform. 0-8423  
 phase conjugate mirror, dynamic interferometry, differential holography of irregular phase objects 0-37969  
 phase conjugate mirror for optical resonator, longit. and transverse modes 0-14392  
 phase-conjugate mirrors for optical resonators, degenerate four-wave mixing 0-43393  
 phase-conjugate reflection using TEM<sub>00</sub> pump beam 0-48327  
 piezoelectric mirror translator, stabilisation of narrow-bandwidth CW dye laser 0-33036  
 plane mirror system synthesis using biquaternions 0-9982  
 position, in Michelson interferometer, form. of bands of equal thickness 0-52298  
 Prony method for symmetric matrix in scalar resonator calc. 0-5807  
 quarter-wave dielectric reflector, spectral absorptance approximation 0-33131  
 ray-optical analysis of unstable resonators with spherical mirrors 0-14415  
 reference mirror for alignment of optical instruments 0-10054  
 reflectors, deep paraboloid, light intensity curves with transverse cylindrical light source, calc. (Russian) 0-38090  
 resonator, spherical optical, mirror misalignment sensitivity 0-53334  
 resonator with wavefront reversing mirror, oscillator modes 0-53345  
 reversing, laser beam spatial struct. reproduction inaccuracy in amplifying medium 0-14379  
 ring optical cavity, nearly confocal, with spatially inhomogeneous medium, threshold gain 0-43373  
 Ronchi test, fringe sharpening 0-53480  
 rotationally symmetrical reflector, physical modelling (Slovak) 0-38088  
 scanning IR microscope, photodetector field of view correction using additional mirror 0-52304  
 scanning rate restrictions in monochromators 0-48430  
 scanning system with multifaceted mirror, tracking sweep 0-33123  
 semireflecting lossless, transmitted and reflected optical fields phase shift 0-46769  
 simulated multiple mirror telescopes, speckle interferometry, meas. of astronomical objects 0-56716  
 solar cells test facility using plane mirror heliostat 0-45668  
 solar collector, fixed spherical, optical simulation 0-7912  
 solar collectors, mirror configurations for flat plate double-exposure panels 0-50999  
 solar compound parabolic concentrator collectors, prediction of thermal performance 0-55905  
 solar concentrator, fixed-mirror-distributed focus, optical-thermal performance anal. 0-30392  
 solar concentrator image characteristics, non-uniform intensity distrib. 0-55816  
 solar concentrators, design variables, optical efficiency, heat loss coefficient and heat removal factor 0-7927  
 solar concentrators, reflector shapes for truncation of nonimaging cusp concentrators 0-21385  
 solar energy, photo-optical instrumentation, [Conf. San Diego, CA, USA Aug. 1978] 0-7926  
 solar energy collecting system, cylindrical absorbers, sun following reflectors, semi-parabolic reflector (Korean) 0-21380  
 solar energy collector, reflector and absorber design, spherical stationary mirror, and automatic tracking absorber 0-50997  
 solar energy concentrators design, American and Australian practices (Italian) 0-50935  
 solar focusing collectors, cylindro-parabolic mirrors (Rumanian) 0-50934  
 solar reflector concentrator, Fresnel geometrical design 0-45636  
 spherical, radii, seventh-order design of a reflecting optical system 0-48378  
 spherical wide angle mirror under oblique illumination, diffraction in focal region 0-1108  
 stigmata using two curved Fresnel surfaces 0-38084  
 stimulated Raman scatt. and optical freq. mixing, simultaneous occurrence using three-mirror config. 0-48342  
 student experiment in mirror prep., electroless plating of Cu on treated glass 0-36817  
 thin film Kapton mirror for concentrator enhanced solar arrays for spacecraft appls. 0-30501  
 three-actuator deformable water-cooled mirror 0-33134  
 three-mirror image rotator use in laser produced plasma expt. 0-33814  
 toroidal mirror optical polisher 0-5848  
 two-sided photovoltaic solar cell static concentrators 0-35684  
 underground beam-guide lines with periodic light beam corrections 0-33196  
 vector transformation by system of four plane mirrors 0-9981  
 Al, diamond-turned, surface reflectivity meas. 1 to 12  $\mu$ m 0-1298  
 Al reflective coating, reflectance in UV and visible 0-28307



**mirrors continued**

- Al spherical mirror generation with single point diamond cutting tool 0-33249
- Al-Ag alloy mirror for use as solar reflector, co-sputtering 0-20789
- AlGaAs DH laser mirror degradation mechanism and lasing characts. changes 0-9919
- Al<sub>2</sub>O<sub>3</sub>-Si-Te-Al<sub>2</sub>O<sub>3</sub> layered apertured facet reflector, for lateral mode stabilisation of diode lasers 0-23708
- Be mirrors, props. and fabrication procedures 0-38138
- Be substrate for lightweight mirror, surface quality and thermal props. 0-23762
- CO<sub>2</sub> laser, 10 ns pulse generation, rotating mirror technique 0-33042
- CO<sub>2</sub> laser bimetallic mirror coating vacuum sputtering technology 0-35086
- Cu plated substrates for Antares CO<sub>2</sub> laser mirrors 0-14349
- Cu, surface defect layer form. on mech. polishing 0-33122
- Cu vapour deposited mirror on SiC substrate, pulsed laser damage characts. 0-48314
- In<sub>2</sub>O<sub>3</sub>, transparent heat mirror formation by ion plating on ambient temp. substrates and props. 0-25578
- Mo laser mirror, optical and metallurgical characterisation 0-33129
- Mo sputtering for laser mirror refurbishment 0-14498
- Ni plated aspheric metal mirror fabrication for IR optical systems 0-14497
- VO<sub>2</sub> variable-reflectance mirror for CO<sub>2</sub>-N<sub>2</sub>-He 10.6  $\mu$ m scan laser 0-38026

**m.i.s. devices** *see metal-insulator-semiconductor devices***m.i.s. integrated circuits** *see field effect integrated circuits***m.i.s. structures** *see metal-insulator-semiconductor structures***miscibility** *see solubility***missiles**

No entries

**mixed conductivity**

- metallic glasses, electrical resistance min. at low temp., mixed conduction model 0-44560
- polymer, charge carrier species determ. using interfacial phenomena 0-24978
- superionic conducting oxides, review 0-49414
- superionic-electronic solid solution electrodes, partial cond. meas. technique 0-44360
- AgCrS<sub>2</sub>, mixed conductor props. 0-44675
- BaF<sub>2</sub>, solid electrolyte, n-type electronic cond., 700-900°C 0-29448
- CaF<sub>2</sub> crystals, elec. cond., O<sup>2-</sup> effect 0-2431
- CaMoO<sub>4</sub>, electrical cond. and ionic transport number meas., defect struct. model 0-2388
- Cu<sub>1-x</sub>Te, x<0.22, phase diagram, electronic and ionic cond. meas. 0-6917
- Cu<sub>2</sub>VS<sub>4</sub>, conducting ions as mobile donors 0-11055
- Se, nanosecond switching investigation 0-20263
- Si-Al-O-N system, ionic cond. from 850 to 1400°C 0-2203
- TiO<sub>2</sub>, stoichiometric single crystals, anisotropy of ion transport 0-2206
- Y<sub>2</sub>O<sub>3</sub>:HfO<sub>2</sub>, elec. cond. and O ion mobility 0-34490

**mixed state**

- see also flux creep; flux flow; flux-line lattice; flux pinning*
- dirty superconductor, thermal cond. anisotropy 0-7036
- film, resistive transition 0-7049
- magnetic field response, intensity, and direction-varying, nonrot. vortices 0-2535
- pion condensate props. in mag. field, superconductivity, mixed state (*Russian*) 0-49974
- resistive layer microstructure on superconducting Al surface (*Russian*) 0-34567
- ring with low capacitance Josephson point contact junction, flux transition mechanisms 0-44770
- superconducting composite, endurance in mixed state, fatigue failure (*Russian*) 0-44778
- superconductors, tilted vortices, mixed state features in surface layers (*Russian*) 0-29512
- type II superconductor, giant-vortex state, temp. depend. 0-7051
- Al, superconducting thin film, evidence for Kosterlitz-Thouless transition 0-39721
- Nb, plastic deformation effects on superconducting specific heat transition 0-20352
- Nb<sub>3</sub>Ge, amorphous nongranular thin superconducting film, thermodynamic and resistive transitions 0-34571
- Pb-In (5%), supercond. mobile dislocation density, instantaneous flux change meas. 0-15670
- V-Ti (42 at.%), US attenuation meas. at 4.14K 0-15657
- V<sub>3</sub>Si, normal, mixed and supercond. state, specific heat meas., thermodynamic and superconducting props. 0-49987

**mixed valence compounds**

- actinide, compounds, f-electron systems with fluctuating valence, phase transitions 0-6789
- actinide alloys, valence fluctuation model, physical prop. response 0-6791
- atomic limit approach to intermediate valence 0-39531
- dielectric-metal phase transition (*Russian*) 0-6788
- electron-hole symmetry, phase diagrams, and lattice props., periodic Anderson model 0-15481
- electronic structure, spin-orbit interaction effects, mag. susceptibility 0-54657
- exchange coupled ions, electron transfer, optical intervalence transition 0-44556
- excitation mechanism in tight-binding approx., metal-insulator transition 0-10925
- Falicov-Kimball model, mag. short- and long-range order 0-15480
- Hubbard regime, at. and nearly free state hybridisation 0-44546
- impurity model, Fermi liq. theory, Ward identities 0-34401
- inorganic compounds with inequivalent atoms, XPS 0-2918
- magnetic susceptibility and mag. instabilities 0-39532
- magnetic susceptibility and sp. ht., periodic Anderson model, CPA alloy analogue method 0-15474
- phase diagram and Kondo behaviour 0-29366
- phonon effect on press.-temp. phase diagram 0-24849
- rare earth compound, valence fluctuation type, replicate core level XPS probe 0-25521
- rare earth compounds, charge dominated fluctuation props. comparison, mag. moments and ordering 0-54659
- rare earth compounds, spin dynamics, mag. neutron scatt., Mossbauer effect, XPS studies 0-39786

**mixed valence compounds continued**

- rare earth compounds, valence changes, book contrib. 0-39533
- rare earth compounds, valence fluctuations, electron-phonon coupling effect 0-20134
- rare earth compounds, valence instabilities rel. to electronic structure of GaMn<sub>3</sub>(C<sub>1-x</sub>N<sub>x</sub>) (*French*) 0-34596
- rare earth Cu<sub>2</sub>Si<sub>2</sub>, interconfiguration fluctuation system, NMR meas. 0-15817
- rare earth systems, neutron scatt., review 0-49674
- three-site, six-electron, even-parity model 0-20125
- three-site, six-electron model, variational calc. 0-20126
- TTT salts, IR spectra, mixed-valence salts 0-40121
- Ba<sub>2</sub>Ru<sub>2</sub>MO<sub>12</sub>, (M=Ta, Nb), Ru oxidation state, Mossbauer study 0-44965
- CaFe<sub>2</sub><sup>2+</sup>Fe<sup>3+</sup>Si<sub>2</sub>O<sub>7</sub>(OH), Mossbauer spectra, temp. depend. electron delocalisation 0-20567
- Ce cubic intermetallics, interconfig. fluctuations 0-20130
- Ce-based alloys, valence transition, scaling studies 0-20135
- CeAl<sub>2</sub>, press.-induced electronic transition 0-20147
- CeIn<sub>3-x</sub>Sn<sub>x</sub>, scaling behaviour near valence instability, mag. susceptibility and mag. transitions 0-25111
- CeIn<sub>3-x</sub>Sn<sub>x</sub>, electrical resist. and thermal expansion meas., 1.5-300K 0-34400
- Ce<sub>1-x</sub>La<sub>x</sub>Sn<sub>3</sub> (x=0 to 1), mag. susceptibility and magnetisation, lattice parameters, X-ray and neutron diff. meas. 0-49675
- Ce<sub>1-x</sub>Sc<sub>x</sub>Al<sub>2</sub>, fluctuating valence system, quadrupole interaction temp. depend. 0-54972
- CeSn<sub>3</sub>, induced magnetic form factor, polarised neutron studies 0-25078
- CeSn<sub>3</sub>, polarised neutron study of induced magnetisation 0-34594
- Ce<sub>0.74</sub>Th<sub>0.26</sub>, induced magnetic form factor, polarised neutron studies 0-25078
- CoM<sub>2</sub>O<sub>4+x</sub> (M=Rh,Mn), anomalous <sup>57</sup>Fe<sup>m</sup> charge states, Mossbauer study 0-40017
- DyCoO<sub>3</sub>, anomalous <sup>57</sup>Fe<sup>m</sup> charge states, Mossbauer study 0-40017
- Er<sub>2</sub>Ce<sub>1-x</sub>Pd<sub>x</sub>, cryst. field spectra, neutron scatt. study 0-50047
- EuCoO<sub>3</sub>, anomalous <sup>57</sup>Fe<sup>m</sup> charge states, Mossbauer study 0-40017
- EuCu<sub>2</sub>Si<sub>2</sub>, fluctuating valence system, quadrupole interaction temp. depend. 0-54972
- FeF<sub>3</sub>·3H<sub>2</sub>O,  $\alpha$  and  $\beta$  phase, <sup>57</sup>Fe Mossbauer study of local struct. 0-39973
- Fe<sub>2</sub>F<sub>6</sub>·7H<sub>2</sub>O and oxidation products, <sup>57</sup>Fe Mossbauer study of local struct. 0-39973
- Fe<sub>2</sub>O<sub>4</sub>, magnetite, valence instabilities, Mossbauer effect 0-20543
- K<sub>2</sub>Pt(CN)<sub>4</sub>Br<sub>0.3</sub>·3H<sub>2</sub>O, spin-lattice model for elastic anomalies 0-15179
- La<sub>1-x</sub>Ce<sub>x</sub>Sn<sub>3</sub>, electrical resist. and thermal expansion meas., 1.5-300K 0-34400
- LaCoO<sub>3</sub>:Ca(Sr), anomalous <sup>57</sup>Fe<sup>m</sup> charge states, Mossbauer study 0-40017
- (MgAl<sub>2</sub>O<sub>4</sub>)<sub>x</sub>(AMn<sub>2</sub>O<sub>4</sub>)<sub>1-x</sub>, A=Mg,Mn,Zn,Cd, 0<x<1, mixed oxide spinels, chemical shifts of Mn K-absorpt. edge 0-29828
- Pd complex, linear ionic mixed valence cpd., IR and resonance Raman spectra rel. to lattice modes 0-25393
- Pt complex, linear ionic mixed valence cpd., IR and resonance Raman spectra rel. to lattice modes 0-25393
- RM<sub>4</sub>Al<sub>8</sub> (M=Cr, Mn, Fe, Cu), magnetism and hyperfine interactions 0-25256
- Sm compounds, mixed valence, metals or small gap insulators, two-band Hubbard Hamiltonian 0-34399
- SmB<sub>6</sub>, EPR and heat capacity obs., metal-semicond. behaviour 0-20456
- SmB<sub>6</sub>, mixed valent, large low-temp. Hall effect and resist. 0-39611
- SmB<sub>6</sub>, valence fluctuating state, sp. ht. 0-20127
- SmB<sub>6</sub>, valence fluctuation system, ground state and elementary excitations, Anderson lattice model Hamiltonian, dense Kondo problem 0-54656
- Sm<sub>2</sub>Bi<sub>3</sub>, press.-induced valence instability 0-20261
- Sm<sub>0.4</sub>Gd<sub>0.6</sub>S, valence transition, positron annihilation study 0-15454
- Sm<sub>1-x</sub>M<sub>x</sub>S, M=transition metal, valence charges, band struct. 0-20131
- SmN, magnetic props., neutron diff. and mag. susceptibility meas. 0-50036
- SmO, intermediate valence state (*French*) 0-20132
- SmO, mag. props., lattice consts., and X-ray absorpt. spectra 0-44798
- SmS (001) surface, mixed valency and phase transitions 0-39658
- SmS, and Sm<sub>0.9</sub>Tb<sub>0.1</sub>S, resistivity and thermopower 0-20260
- SmS, electronic phase transition, mechanism, trivalent metal impurity effects 0-49604
- SmS, induced magnetic form factor, polarised neutron studies 0-25078
- SmS, metallic phase, compressibility anomalous behaviour 0-29114
- SmS type cpd., fd mixing effect on impurity levels, local valence transition 0-24831
- SmS, valence fluctuation phenomena 0-24800
- SmS, valence fluctuation system, ground state and elementary excitations, Anderson lattice model Hamiltonian, dense Kondo problem 0-54656
- SmS, valence transition, positron annihilation study 0-15454
- SmS:P, neutron irradi., semiconductor-metal transition 0-24975
- Sm<sub>2</sub>S<sub>4</sub>, mag. susceptibility meas., valence state of Sm 0-15684
- SmS<sub>1-x</sub>P<sub>x</sub>, intermediate valence cpd., lattice parameter and mag. susceptibility 0-7091
- Sm<sub>0.25</sub>Y<sub>0.75</sub>S, phonon anomalies and electron-lattice coupling 0-39490
- Sm<sub>0.75</sub>Y<sub>0.25</sub>S, intermediate valence compound, phonon investigation by neutron scatt. 0-6476
- Sm<sub>0.75</sub>Y<sub>0.25</sub>S, mixed valence, phonon dispersion theory 0-34153
- Sm<sub>0.76</sub>Y<sub>0.24</sub>S, induced magnetic form factor, polarised neutron studies 0-25078
- TeSe, valence fluctuation system, ground state and elementary excitations, Anderson lattice model Hamiltonian, dense Kondo problem 0-54656
- Tm<sub>1-x</sub>Eu<sub>x</sub>Se, valence changes, semicond.-metal transition 0-20086
- TmSe, intermediate valent, Raman scatt. 0-16038
- TmSe, mag. neutron scatt. 0-25096
- TmSe, mixed valence state, ferromag. alignment 0-20133
- TmSe, susceptibility, Tm<sup>2+</sup> and Tm<sup>3+</sup> characts. 0-25110
- TmSe, valence instabilities, antiferromag. order 0-20128
- TmSe<sub>1-x</sub>Te<sub>x</sub>, mixed-valent cpd., spontaneous magnetisation 0-20392
- TmSe<sub>1-x</sub>Te<sub>x</sub>, phase relationships and press. induced transitions 0-19771
- TmSe<sub>1-x</sub>Te<sub>x</sub>, valence changes, semicond.-metal transition 0-20086
- TmY<sub>1-x</sub>Se<sub>x</sub>, Kondo effect, Van Vleck behaviour 0-25085
- UCu<sub>5</sub>, core and valence band spectra, XPS obs. 0-50530
- UNi<sub>0.5</sub>Cu<sub>0.5</sub>, core and valence band spectra, XPS obs. 0-50530
- V<sub>0.20-1</sub> (3 $\leq$ 3 $\leq$ 9), Magneli phases, mag. susceptibilities at low temp. 0-20389
- YCoO<sub>3</sub>, anomalous <sup>57</sup>Fe<sup>m</sup> charge states, Mossbauer study 0-40017
- YM<sub>4</sub>Al<sub>8</sub> (M=Cr, Mn, Fe, Cu), magnetism and hyperfine interactions 0-25256



**mixers (circuits)**

see also frequency converters; radio receivers

MM-wave and sub MM-wave receiver elements, Schottky-barrier resistive mixer devices 0-11558

**mixes** see mixtures**mixing**

see also blending; dissolving; heat of mixing; mixtures; solubility; solutions

atmosphere, critical evaluation of mixed-layer model with penetrative convection 0-51483

atmosphere, urban, local mixing and turbulence effects on CO<sub>2</sub> concs. 0-16870

atmospheric boundary layer, hourly mixing depths estimation from historical meteorological data 0-51482

Baltic Sea horizontal mixing, Lagrangian and Eulerian meas. 0-17290

tert-butyl alcohol in nonpolar solvents, liq. struct. from dielectric studies 0-38894

chemical stirred-tank reactor, homogeneous p-order reactions, mixing effects, two parameters model 0-14843

chemically reacting turbulent shear layer between two streams obs. 0-6163

dilution refrigerator, multiple mixing chamber 0-37042

FFTF upper-plenum mixing and stratification, comparative studies 0-583

flame, round jet type, mass exchange between recirculation zone and outer flows, stabilisation 0-14842

flames, turbulent, calc. in one-dimensional approach 0-30236

flow, separating boundary layer, subsonic, integral prediction method 0-1623

gas-liquid systems, vibs. stabilisation of dynamic equilb. and mixing (Ukrainian) 0-10291

indices for multicomponent solid mixtures 0-39300

liquid-liquid mixing analysis, lamellar model 0-15246

liquids of different density, turbulent mixing at an accelerating interface 0-6030

magma convective mixing, implications of density var. among mid-ocean ridge basalts 0-56460

methane tracers, single-jet mixing in turbulent tube flow, similarity and scaling law 0-14765

non-proportionality between flux and reservoir content 0-46261

petrogenetic mixing models and Nd-Sr isotopic patterns 0-3965

photographic emulsion production, effect of mixing on diffusion rate (Russian) 0-3388

plate, flat, with suction, boundary layer eddy viscosity, mixing length, Von Karman's constant 0-1680

polymer melt, particulate mixing, fluid dynamics, rheological and energetic considerations 0-43686

polymer solutions, free energy of mixing, modelling, critical exponents 0-44106

powder particle motion and segregation by density difference in V-type mixer 0-45250

power-law fluid, two-stream mixing along flat plate, variational solns. 0-53817

stars, convective, force mixing theory 0-56818

stratified fluid, reinterpretation of entrainment process in laboratory expts. 0-51405

suction-induced asymptotic boundary layers, exptl. and predicted props. 0-1553

suspensions, fluid dynamical aspects of operating conditions of suspension stirrers (German) 0-26058

thermosphere, lower, turbulent mixing rel. to O and O<sub>2</sub> distrib. simulation 0-4159

turbulence formation in parallel blast mixing (Ukrainian) 0-6033

Cd-In-Sb, liq. alloy, Cd thermodynamic activities, Gibbs free mixing enthalpy (German) 0-45279

Cu substrate, ion induced intermixing of Au or Ag surface film 0-15420

Fe/zinc stearate, compacts, admixing, effect on mech. props. 0-45402

Fe/Zn stearate powder compacts, admixing effect on apparent density, mixing, compaction 0-45403

HF chemical laser, CW, influence of mixing effects on energy characts. 0-9875

N<sub>2</sub>-Ar corona discharge, convection and mixing, atm. press., mass spectra obs. 0-1853

NaCl-KCl, interdiffusion and demixing, electron microprobe anal. (French) 0-54444

Pu binary alloys, periodical depend. of equilibrium distrib. coeffs. of Pu admixtures on atomic number of admixture 0-18419

Si substrate, ion induced intermixing of Pd or Pt film 0-15420

**mixing, heat of** see heat of mixing**mixing circuits** see mixers (circuits)**mixtures**

see also critical mixtures; mixing; solutions

adsorption, competitive, from binary liquid mixtures, adhesive hard sphere model 0-2265

aerodynamic isotope separation technique based on vel. slip in freejet expansions 0-19441

air-H<sub>2</sub> (methane), ignition energy by capacitive discharge (French) 0-10446alkali fluoride-LnF<sub>3</sub> (Ln=Y, La, Yb) binary liquid mixtures, thermochemistry 0-45538

alkali metal halides, molten binary mixtures, excess enthalpies calc. 0-3397

n-alkanes, liq. mixtures, thermodynamics 0-55700

N-alkylpyridium halides-AlCl<sub>3</sub>, molten, density, elec. cond. and viscosity meas. 0-24630

bases, mixtures, potentiometric titrations, computer-calc. curves, learning machine appl. 0-3426

benzene-p-dioxan, mixtures, mol. reorientation and assoc., depolarised Raman scatt. obs. 0-7341

benzene-p-xylene, excess vol., enthalpies, Gibbs free energies 0-44335

benzene-tetrahydrofuran, soln., excess thermodynamic props. and interactions, US vel. and density meas. 0-39288

binary, close to vaporisation, hydrostatic and external field effect, anal. 0-19929

binary, excess isentropic compressibilities and isochoric heat capacities 0-21313

binary dielectric mixture relative permittivity formulae compared 0-15939

binary gas systems, thermal diffusion factors meas. 0-10344

binary liquid mixture, horizontal layer, surface tension driven instability in presence of Soret effect 0-10227

**mixtures continued**

binary liquid mixtures adsorption onto solid surface, effect of surface heterogeneity 0-44411

binary liquid systems, apolar-apolar and polar-apolar, significant structure theory, appl. 0-1909

binary mixture of hard spheres and square-well molecules, quantum corrections to eqn. of state 0-6338

binary mixtures, liquid-vapour equilb. data, internal consistency, automatic checking method 0-54364

binary polymeric mixtures, soln. viscosities meas. 0-54423

binary system forming simple association complexes, liq. diffusivities prediction 0-34216

butanol-methylethyl ketone, soln., excess thermodynamic props. and interactions, US vel. and density meas. 0-39288

characterisation of ordered mixes using X-ray microanal. 0-16215

chemically reacting, microfluids theory 0-14777

chloroform-p-dioxan and chloroform-benzene mixtures, mol. reorientation and assoc., depolarised Raman scatt. obs. 0-7341

cholesteric positive dielectric anisotropy mixture, helix pitch increase below 20 kHz 0-15997

cholesteric-nematic mixtures, helix inversion 0-24358

clay soil/sand mixtures, reflectance 0-56475

compressed powder mixture electrical conductivity calc. (German) 0-10940

curved shock waves in ideal fluid mixtures with multiple temps., theory of singular surfaces 0-28533

p-cyano-p'-pentylbiphenyl/p-pentylbenzoic acid, induced smectic phase, dielec. props. 0-6498

electrolyte mixtures in aq. soln., viscosity contrib. coeffs. (German) 0-15287

flow rate meas. ultrasound propagation and scatt. approach 0-43806

fluid, molecular basis of activity coeff., isobaric-isothermal ensemble approach 0-55690

fluid, of hard convex bodies, accurate eqn. of state 0-6484

fluid, simple, dense, bulk viscosity, hard spheres appl. 0-14982

fluid mixtures, thermophysical properties prediction 0-48563

fluorocarbon-hydrocarbon mixtures press. second virial coeff., graph theory prediction 0-43823

gas, binary, moderate density diffusive creep along flat surface 0-43822

gas, disparate mass, double sound propag., theory 0-33724

gas mixture, multicomponent, transport equations near catalytic surfaces 0-43821

gas mixtures, IR absorpt. theory using hard sphere model (Russian) 0-14879

gas-solid, hydrodynamics, use of relative velocity of gas to solids (Croatian) 0-14799

gaseous, ignition energy by capacitive discharge and through discharge of person charged with static elec. (French) 0-10446

gaseous mixtures, equilb. at high temp., Raman scatt. obs. 0-45619

hard sphere mixtures, finite angle light scatt., Percus-Yevick approx. calcs. 0-7363

hard spheres, dipolar, dielec. props. 0-24335

hard spherocylinders and spheres mixtures, Monte Carlo study 0-49073

heterogeneous solid surface, adsorption from multicomponent gas and liq. mixtures (German) 0-44430

hydrocarbon-fluorocarbon, press. second virial coeffs., walks on graphs method 0-7841

inert gases, liquid phase mixtures, dipole autocorrelation function, IR absorpt. spectra obs. 0-28903

inert gases, mixtures, dipole moments, IR absorpt. spectra obs. 0-28903

ionised mixture, dense, binary, dynamical props., statistical mechs. 0-43895

Ising lattice, thermal relaxation, nonideal behaviour, stochastic theory 0-22312

liquid binary mixtures of optically anisotropic molecules, depolarized Rayleigh scatt. 0-40122

liquid mixture, shallow, laser separation, thermal mechanism 0-5925

liquid-liquid mixing analysis, lamellar model 0-15246

methane-Ar, cryogenic fluid mixture, transport phenomena, shear viscosity (Russian) 0-29198

methane-ethane liq. mixture, phase equilb., heat of mixing, vol. change, data evaluation 0-15233

methylethyl ketone-butanol, soln., excess thermodynamic props. and interactions, US vel. and density meas. 0-39288

molecular volume effects in the excess functions of binary mixtures (Spanish) 0-15261

multicomponent vapours-condensed phases, equilb., computer modelling 0-44288

nematic solution, hard rigid/flexible mols. mixture, unathermal, lattice model (Russian) 0-54129

Newtonian fluids, mean velocity and vol. flow rate for steady 1-D flow 0-6132

nitroethane-isooctane mixture, depolarised Rayleigh scatt. near crit. point 0-45089

nonpolar binary mixture, partial molar vol. prediction from Lee-Kesler eqn. of state 0-10632

nylon 6-inorganic salts, glass transition temp. 0-19921

organic, second virial coeff. meas. using new apparatus 0-44289

organic binary liquid mixtures, excess free vol. calcs. 0-34202

organic binary mixtures, with weak charge transfer interactions, thermodynamic props. 0-54360

organic liquid mixture separation by hyperfiltration and pervaporation through polymer membrane 0-16720

pigment associations, conc. effects, luminesc., absorpt. spectra and dichroism obs. 0-1007

polymer blends, two-component, glass transition, calorimetric investig. (Russian) 0-39268

precipitation of aerosol particles on a fixed evaporating droplet 0-7869

precipitation of aerosol particles on an evaporating droplet in a turbulent gas flow 0-7870

radionuclide corrosion and fission products, ion exchange separation 0-18460

radionuclide corrosion and fission products, liquid-liquid extractions with metal diethyldithiocarbamates 0-18459

Raman spectroscopy and liq. chromatography anal. (French) 0-45595

saturated densities of liqs. and mixtures, new correlation method 0-15174

sedimentation of binary particle mixtures 0-40757

soft spheres binary mixtures, equilb. and non-equilib. radial distrib. functions 0-49074

soft-sphere mixture viscosity, nonequilibrium. mol. dynamics 0-19680



**mixtures continued**

- solids, multicomponent mixing index and contact number estimation by spot sampling 0-16214  
 supersonic blunt body flow of viscous perfect gas and nonequilib. gas mixture 0-28578  
 tetrafluoromethane-trifluoromethane-chlorotrifluoromethane, vapour-liq. equilib. compositions, calc. 0-19925  
 tetrahydrofuran-benzene, soln., excess thermodynamic props. and interactions, US vel. and density meas. 0-39288  
 vapour-liquid equilibria, mixing rules in equations of state 0-19902  
 water-ethanol(methanol), nonlinear acoustic coeff. meas., 0-50°C (*French*) 0-34142  
 water-methanol(ethanol)(acetic acid), liq., Verdet const., pulsed mag. field meas. 0-16012  
 water-methanol (n-propanol), binary mixtures, nucleation 0-44305  
 water-nigrosin black dye-Teflon spheres dispersion, laser backscatt., turbidity 0-1129  
 $\text{AgCl}_2\text{Br}_{1-x}$ , binary melt, Ag solubility, temp. and conc. depend. 0-10677  
 $\text{AlCl}_3\text{-LiCl}$ , molten, specific cond. meas., comp. and temp. depend. 0-15279  
 $\text{Ar-NH}_3$ , viscosity under press., density depend. and mol. assoc. 0-1727  
 $\text{BaBr}_2\text{-BaCl}_2$ , vap. mixture, ion-mol. equilib., heat of form. of ions 0-26039  
 $\text{BaCl}_2\text{-BaBr}_2$ , vap. mixture, ion-mol. equilib., heat of form. of ions 0-26039  
 $\text{Bi-Bi}_2(\text{BiBr}_3)$  liquid binary mixtures, phase separation under press. 0-34183  
 $\text{Bi}_2\text{O}_3\text{-CoO}$  system, X-ray diffr., thermal anal. and metallography obs. 0-24598  
 $\text{CO-N}_2\text{-He}$ , nucl. reactor active zone, plasma and sustained discharge props. 0-5729  
 $\text{CO}_2\text{-N}_2\text{-He}$ , vol. discharge, negative ions effect 0-14956  
 $\text{CuCl}_2\text{Br}_{1-x}$ , binary melt, Cu solubility, temp. and conc. depend. 0-10677  
 $\text{D}_2\text{-DT-T}_2$  fusion fuel, estimated physical and chem. props. 0-8746  
 $\alpha\text{-Fe}_2\text{O}_3\text{-Li}_2\text{O}$ , structural and thermal phase behaviour from mag., spectral and thermal studies 0-2673  
 H, thermochemical production, irreversibility anal. of separation schemes from binary gas mixtures 0-35767  
 $\text{H}_2\text{-Ar}$ ,  $\text{H}_2$  separation in thermogravitational column 0-45561  
 $\text{H}_2$ -methane mixture properties for hydrogen supplementation of natural gas 0-45781  
 $\text{HI-H}_2\text{-I}_2$ ,  $\text{H}_2$  separation in thermogravitational column 0-45561  
 $\text{HNO}_3\text{-HNO}_2$ , aq. soln., N isotope exchange in presence of NO 0-16662  
 $\text{He-Ar}$ , gas mixtures, thermal cond. meas. in the range 0.5-15 MPa 0-14874  
 $\text{He-Ar(N}_2\text{)(O}_2\text{)(CO}_2\text{)}$ , binary diffusion coeffs., press. depend., 300 and 323K, Thorne's eqn. 0-1724  
 $\text{He-Ne}$ , disparate mass, double sound propag., theory 0-33724  
 $\text{He-D}_2$  mixture, binary diffusion coeff. near phase separation line (*Russian*) 0-6191  
 $\text{In}_{1-x}\text{Sn}_x$ , molten mixture, NMR, reson. shifts, relax. rates, quadrupole relax. 0-2654  
 $\text{KBr-LiBr}$ , liq. mixture, struct. and diffusion 0-24344  
 $\text{KNO}_3\text{-RbNO}_3$ , liq., electromigration cation and mobility and isotope effect 0-10691  
 $\text{Kr-He(Ne)(Ar)(Xe)}$ , gas, diffusion coeffs. meas., 350-1200K 0-14869  
 $\text{N}_2\text{-H}_2\text{O}$  mixtures, two-phase pressure drops in the low flowrate region 0-19480  
 $\text{N}_2\text{-Kr-Xe}$ , liquefaction, retention of  $^{85}\text{Kr}$  from fission exhaust gases, separation technique (*German*) 0-27753  
 $\text{N}_2\text{O}$ , pure and in mixtures, electron attachment near 1 atm., microeave cond. meas. 0-1063  
 $\text{Ne-Ar}$ , gas mixtures, thermal cond. meas. in the range 0.5-15 MPa 0-14874  
 $\text{Ne-Ar-Kr}$ , gas mixtures, thermal cond. meas. in the range 0.5-15 MPa 0-14874  
 $\text{Ne-H}_2$  mixture, liquid vapour phase equilib., sound vel., compressibility, thermodynamic perturbation theory obs. (*Russian*) 0-39306  
 $\text{Ne-Kr}$ , time-dependent props. near crit. mixing point, 2000 bar, mol. dynamics calcs. 0-24580  
 $\text{Ne-Kr}$  Penning mixtures, Townsend ionisation coeffs. and breakdown pot. meas. 0-19641  
 $\text{O}_2\text{-}^{85}\text{Kr-Xe}$ , liquefaction, retention of  $^{85}\text{Kr}$  from fission exhaust gases, separation technique (*German*) 0-27753  
 $\text{O}_2\text{-CO}_2$  (ethylene)(neopentane), thermal electron attachment meas., microwave cond., pulse radiolysis 0-28592  
 $\text{SF}_6\text{-N}_2(\text{He})$ , dielec. props., ionisation and attachment coeffs. 0-33726  
 $\text{TiCl}_4\text{-SiCl}_4(\text{SnCl}_4)$ , liq., beat effects, neutron diffr. studies 0-38897  
 $\text{UF}_6\text{-H}_2$ , near UV and visible excitation, quantum yield from photodissociation 0-35549  
 $\text{Xe-He(Ne)}$ , gas mixture, element and isotope separation in impulse plasma centrifuge (*Russian*) 0-38725

mm waves see microwaves

MO calculations see molecular orbitals calculations

**mobile radio systems**

- INMARSAT marine system, satellite radio teletype communication 0-26614  
 marine radiofacsimile weather chart receiver and recorder 0-46297  
 selective paging systems, noise disturbance considerations 0-40944

mobility, carrier see carrier mobility

**modelling**

- see also brain models; catastrophe theory; identification; physiological models; semiconductor device models; simulation  
 acoustic noise propagation, railway lines 0-48500  
 acoustic signal, pulsed, representation by ordered sequence of uniform information elements magnitudes (*Russian*) 0-38180  
 adenovirus hexon, three dimensional structure from electron microscopy, computer modelling 0-35833  
 atmosphere vertical diffusion from ground-level source, Lagrangian similarity modelling 0-51480  
 atmospheric models, contrast attenuation factors calc., for remote sensing 0-4135  
 atmospheric motion, wind tunnel characts. review (*Italian*) 0-4156  
 atmospheric pollution, photochemical numerical model 0-40943  
 atomic independent particle pots. comparison 0-52846  
 biomedical signal modelling and recognition, system identification approach 0-51286  
 ceramics, high temp. failure mechanisms, statistical model 0-39210  
 chemical reactions, diffusion-controlled, continuous-time random walk modelling 0-3297

**modelling continued**

- coal liquefaction preheaters and reactors, modelling of heat transfer characts. 0-30337  
 cold rolling force model, and its adaptive control (*Chinese*) 0-55418  
 combined photovoltaic/thermal flat plate collectors, extended Hottel-Whillier model 0-3520  
 composite materials, failure predictions 0-10200  
 composites, thermal stresses investigation, using polymer models 0-40639  
 convection, turbulent, numerical models based on unsteady Navier-Stokes eqns. 0-38415  
 cooling tower plumes and drift 0-45836  
 crystal-size distribution, population models, review 0-49153  
 dielectric relaxation processes, simulation using network model 0-40046  
 disordered systems, mathematical models, book 0-1878  
 dissolved  $\text{O}_2$  in rivers, reliability parameter in probabilistic programming models 0-26179  
 dose-rate model testing with *Chlamydomonas reinhardtii* 0-21543  
 double cantilever beam model, for  $K_{IC}$  determ. (*Chinese*) 0-54306  
 Earth atmosphere, lower, temp. skewness budget, turbulence modelling implications 0-21816  
 earthquake, stick slip, rupture propag. and energy focusing in foam rubber model 0-3947  
 elasticity, rel. to rubber microscopic structure, small angle neutron scattering appl. 0-3113  
 elastoplastic fracture modelling 0-35303  
 energy demand and conservation in USA, in residential and commercial buildings, National Energy Plan impact 0-26121  
 energy planning in Arab world, with aid of computer 0-26122  
 finite element, acoustic absorption models 0-53497  
 fixed collector, optimised design, radiation collection study 0-40839  
 flow, axisymmetric body, pot. flow/boundary layer interaction models 0-1546  
 flow, free shear layer, Reynolds stress closures systematic modelling rules 0-1552  
 flow, recirculating, behind backward-facing step, mean vel. and Reynolds stresses 0-19355  
 flow, Reynolds stress transport eqns. 0-19320  
 flow, separating boundary layer, subsonic, integral prediction method 0-1623  
 flow, subgrid modelling with classical closures and Burgers' eqn. 0-19332  
 flow, subgrid scale modelling 0-17808  
 flow, turbulent, developing, in square duct 0-19351  
 flow, turbulent wall jet, algebraic Reynolds stress model calc. 0-1668  
 flow of viscous electroconducting fluid in strong mag. field, free shift stationary type 0-28576  
 forced vibration model, rail/wheel noise generation 0-48496  
 fracture mechanics, elastic-plastic, finite element method appl. 0-1489  
 geothermal reservoirs, mathematical modelling of heat and mass transfer 0-55802  
 glass fibre reinforced plastic, time depend. probabilistic failure model 0-40477  
 gradient index material models and exptl. verification 0-16002  
 ground motion simulation and spectral representation using non-stationary amplitude modulated mathematical model (*Spanish*) 0-56397  
 horizontal surface solar irradiance prediction models compared 0-36384  
 hot strip rolling simulation, by hot torsion technique 0-29990  
 interfacial polarisation effect on dielectric props., sandwich capacitor model 0-15614  
 interferometer, two-channel, based on prismatic dividers, with aid of coupled multi-terminal networks (*Russian*) 0-52302  
 Johnson-Mehl and cellular microstructure, comparative analysis, computer simulation 0-54392  
 lattice packing of spheres, in 3D space 0-49166  
 LMFBR, HCDA exptl. modelling 0-32366  
 LMFBR safety, scale modelling 0-32367  
 LMFBR simulation, parameter estimation 0-47597  
 LWR fuel assemblies, coolant channel closure modelling using pattern recognition techniques 0-42835  
 machined surface time series modelling 0-36998  
 magnetosphere, particle (electric current) approach 0-17442  
 Mars atmosphere, thermal radiative transfer, numerical modelling 0-8574  
 metallic thin films, discontinuous, field effect of electrical conductance (*Japanese*) 0-11107  
 multilayered media, layer-indexed acoustic reflection model 0-43517  
 multiphoton absorption modelling, using  $\text{SF}_6$  energy-dependent absorption cross sections 0-32789  
 municipal wastewater treatment plants, electrical energy consumption and heating requirements 0-26194  
 natural philosophy, scientific models, catastrophe theory 0-8772  
 natural sciences, mathematical models role (*Afrikaans*) 0-8771  
 noise transmission between dwellings, partitions and flanking structures 0-43545  
 nuclear fuel cycle environmental impact assessment, oceanic and geological disposal, use of box model method (*Japanese*) 0-9346  
 nuclear power engineering development 0-7901  
 nuclear reactor noise analysis, time series modelling methods, comparative eval. (*Japanese*) 0-13552  
 ocean currents, Gauss-Markov models for error analysis of inertial navigation system 0-36411  
 ocean currents, synoptic-scale, numerical model 0-12424  
 ocean currents generated by heat and momentum fluxes through surface, numerical simulation 0-26535  
 ocean thermal anomalies numerical study with dynamic model 0-17271  
 ocean wave imaging and wavelength meas. by aerial photography 0-46323  
 ocean waves, currents and sediments transport, near breakwater 0-51401  
 optical element contamination modelling, photometric characts. estimation 0-48429  
 optical fibre communication systems, computer design aids 0-28350  
 order-disorder structures, layer stacking 0-38981  
 N.Pacific mesoscale phenomena, oceanographic model and acoustic survey comparison 0-46195  
 passive solar building thermal performance modelling by passive solar test boxes, expt. 0-3494  
 passive solar building thermal performance modelling by passive solar test boxes, theory 0-7921  
 photographic development process, mathematical modelling of growth of spherical metallic particles (*Russian*) 0-50871  
 physics models, nature and purpose 0-42023  
 plastic yielding, modelling at a crack tip by inclined slip planes 0-33472  
 proteins, model building procedure 0-51036



**modelling continued**

- PWR reactor dismantling, model scheme to meet West German regulations 0-825  
 quantum-chemical  $\pi$ -electron system, molecules-in-molecule model (*German*) 0-5490  
 quasi stationary short arc, anode spot mathematical model temp. field calcs. (*Polish*) 0-19664  
 radioactive waste management, mathematical modelling 0-701  
 reflector, rotationally symmetrical physical modelling (*Slovak*) 0-38088  
 scale models, incoherent jet noise line source (*Japanese*) 0-33337  
 scale models of buildings, acoustical performance of self-protecting buildings 0-23839  
 semiconductor film, polycrystalline, modified carrier model (*German*) 0-7012  
 semiconductors, high-resistivity, carrier transport (*Japanese*) 0-6850  
 slit and crack type leaks, calc. model and results of its use 0-35490  
 sound sensation varying with time 0-41053  
 spectra, IR and Raman, of disordered solids, analytical models 0-7336  
 structures under impact loading, finite element modelling as tool for noise analysis and control 0-43535  
 student experiment, evolution of theoretical models (*Polish*) 0-36819  
 sucrose, mathematical model of crystn. rate in pure solns. 0-49151  
 surface waveguide electrooptical deflector, high-resolution, prism model 0-48454  
 thermal fluid selection for long-distance heat transmission, theoretical model 0-35761  
 tidal waves, finite element method appl. (*French*) 0-21782  
 train induced ground vibration, propagation pathways 0-48491  
 tuition process, cybernetic principles appl., comparison with other educational methods (*Croatian*) 0-12866  
 Tunguska catastrophe, computational modelling 0-41779  
 turbulence, inhomogeneous, simulation, clipping approx. 0-19331  
 turbulent flow separation, review 0-1543  
 turbulent shear stress generation models, three-dimens. boundary layers 0-19360  
 two-dimensional space isothermal and nonisothermal turbulent flow (*German*) 0-28505  
 two-phase flow of particles during crystallisation in gaseous stream, modelling by aerothermochemistry of suspension eqns. (*French*) 0-53844  
 US transducers for medical imaging (*French*) 0-26302  
 Vancouver Island region, analogue model study of EM induction 0-56356  
 Venus atmosphere, thermal radiative transfer, numerical modelling 0-8574  
 Cu, single crystal sintering model evaluation, Kossel interference and digital graphic simulation appl. (*German*) 0-2980  
 GaAs structures, charge accumulation and transmission (*Bulgarian*) 0-6947  
 Zn-Cl<sub>2</sub> batteries for electric vehicles, battery design modelling 0-30452

**modelling, computer** *see computer-aided analysis*

**models** *see modelling*

**modems**

- DC microvoltmeter based on modem 0-31798  
 DC nanovoltammeter based on modem 0-31797

**moderation (neutron)** *see neutron moderation*

**moderators**

- see also beryllium; graphite; heavy water*  
 graphite, neutron effects on shrinkage 0-37456  
 graphite moderator structure design and manufacturing specification 0-23110  
 graphite oxidation and coolant chemistry of CEBG gas-cooled reactors 0-42774  
 heavy atom moderator, resonance capture of neutrons 0-14310  
 HTR, pyrocarbon coated fuel, C density determ. by X-ray absorpt. 0-5301  
 light atom moderators, resonance capture of neutrons 0-14310  
 neutron maximum density and capture rate, pulsed sources 0-13522  
 PWR, appl. of moderator temp. for enhancement of operating flexibility 0-695  
 PWR assemblies, spectral and density components of moderator temp. coeff. 0-9356  
 Be, anisotropy in thermal neutron scatt., anal. 0-552  
 D<sub>2</sub>O thermal column irradiation facility, in Penn State Breazeale Reactor, D<sub>2</sub>O thermal column irradiation facility 0-9339  
 ZrH rethermaliser for IVV-2 reactor hot neutron flux increase 0-37676

**modes, laser** *see laser modes*

**modes, lattice vibrations** *see lattice dynamics*

**modes, vibration** *see vibrations*

**modular circuits** *see modules*

**modulation**

- see also amplitude modulation; demodulation; demodulators; modulation spectroscopy; modulators; optical modulation; pulse modulation; Schwarz-Hora effect*  
 aurora, latitude effect in pulsating patches periodicity 0-31155  
 Cygnus X-3, 4.8 hour modulation period change disproved 0-8713  
 solar moving type IV bursts, gyro-synchrotron modulation obs. 0-26833  
 sunspot, Wolf number amplitude and phase modulation from freq. anal. 0-56797  
 US Doppler flowmeter, new modulation method 0-45989

**modulation factor** *see modulation*

**modulation index** *see modulation*

**modulation spectroscopy**

- see also appearance potential spectroscopy; electroabsorption; electroreflectance; magnetoabsorption; magnetorelectance; piezorelectance; thermorelectance*  
 circular differential photoacoustic spectroscopy 0-47114  
 echo spectroscopy in double reson. mode 0-1284  
 frequency-modulation spectroscopy: a new method for measuring weak absorptions and dispersions 0-42262  
 IR laser Stark spectroscopy, RF elec. field modulation effects 0-52989  
 polarisation, relaxation characts. of degenerate states obs. (*Russian*) 0-27348  
 solid state spectroscopy using synchrotron radiation, book contrib. 0-7375  
 BaF<sub>2</sub>:Pr<sup>3+</sup>, wavelength and temp.-modulated UV absorpt. 0-2799  
 CaF<sub>2</sub>:Ce<sup>3+</sup>, absorpt. peaks in the lowest 4f-5d band, effect of conc. 0-2798  
 CaF<sub>2</sub>:Pr<sup>3+</sup>, wavelength and temp.-modulated UV absorpt. 0-2799  
 Cu-Al, optical composition modulation spectra, dielec. const. var., Fermi surface and electronic level shifts 0-6707

**modulation spectroscopy continued**

- Cu-Zn, optical composition modulation spectra, dielec. const. var., Fermi surface and electronic level shifts 0-6707  
 Fe-Cr alloys, passivation films, modulation spectroscopy study 0-3244  
 SrF<sub>2</sub>:Pr<sup>3+</sup>, wavelength and temp.-modulated UV absorpt. 0-2799  
 ZnTe, reflectivity meas., double beam wavelength modulated technique (*Korean*) 0-50365  
 ZrS<sub>3</sub>, thermomodulated reflectivity and transmission 0-50357

**modulation transfer function** *see optical transfer function*

**modulator-demodulators** *see modems*

**modulators**

- see also demodulators; modems; modulation*  
 accelerator modulator charging system upgrade for 5 MeV electron accelerator 0-23182  
 broadband optical modulator for laser range finder (*Russian*) 0-53424  
 coherent OCR system using spatial light modulator (*Japanese*) 0-14291  
 electrochromic ATR prism modulator 0-43440  
 magnetic field, EPR radiospectrometer having discrete set of modulation frequencies 0-52285  
 multibeam acousto-optic modulator efficiency stabilisation 0-43439  
 two-phase PSK modulator employing SAW delay line, fundamental performance 0-33398

**modules**

- see also CAMAC*  
 instruments based on standard units, mathematical aspects of design (*Russian*) 0-37021  
 low-cost encapsulation materials for terrestrial solar cell modules 0-3522  
 plastic modular solar energy collector with reticulated foam 0-16833  
 solar energy conversion, use of flat-type Si chips (*German*) 0-55840

**modulus, Young's** *see Young's modulus*

**moire fringes**

- Airy profile interferometric grilles, moire fringe analysis (*Spanish*) 0-27354  
 automatic pattern processor for simple and complex interference patterns 0-13129  
 contour plotting, moire technique 0-42002  
 convex cylindrical surfaces, deformation anal. using moire fringes 0-14636  
 corneal topography using moire contour fringes 0-26316  
 curved surface, deform. meas. by dynamic moire method 0-14634  
 deflection measurement from moire fringes and holograms 0-32936  
 difference detection by digitised moire pattern processing 0-52156  
 Fabry Perot spectrom., transformation of interference orders 0-263  
 Fabry-Perot interferometer as refractometer 0-264  
 gloss appearance by means of moire patterns (*German*) 0-52300  
 gratings optical imaging, embedded, Fourier optics methods appl. (*German*) 0-23805  
 historical review of moire topography 0-9024  
 idiopathic scoliosis, adolescent, monitoring with Moire fringe photography 0-17047  
 image moire method for determination of partial slopes in fixed plates 0-14645  
 image processing of additive-obtained moire patterns (*German*) 0-47017  
 location of optical interf. fringes by digital scanning methods 0-13128  
 multicomponent assemblies, moire inspection 0-35434  
 optical stress analysis using moire fringe and laser speckles 0-10217  
 quasiregular rasters in moire techniques 0-31857  
 refractive index measurement using image-moire technique 0-22420  
 scintillation camera/high energy collimator system, misleading results with a bar phantom image 0-12237  
 sensitivity in deformation meas. (*Rumanian*) 0-48654  
 spiral gratings, regular interval, fringe properties and appls. (*Japanese*) 0-53434  
 steel, thread rolled, Moire fringe method for examining local deform. zones 0-21220  
 strain analysis 0-28476  
 strain analysis by multipurpose optical moire processor 0-9028  
 strain meas., long time high temperature applications 0-38361  
 strain measurement in elastic thin membranes moire interferometry method, appl. to human skin 0-30828  
 strain measurement method using diffraction beams, compensation of errors 0-13068  
 stress analysis interferometer with microprocessor 0-31858  
 strip method application, stress-strain state of Al alloys (*Russian*) 0-40648  
 temperature measurement of laser irradiated transparent materials, Moire-Schlieren technique 0-53392  
 topography appl., real-time and time-resolved, in microseconds region 0-52154  
 tunable moire grating for optical mapping 0-5832  
 two-crystal system with non-diffracting zone, X-ray interferogram fine struct. 0-1887  
 white light moire interferometry using auxiliary compensator grating 0-31847  
 C fibre reinforced plastics, fatigue behaviour visualised by moire fringe method 0-21110  
 Cu film, on Ni, recrystallisation and interdiffusion, electron microscope obs., 450-600°C 0-39363  
 Pb, SO type, commercial purity, local deform. meas., using Moire method 0-21219

**moistening** *see wetting*

**moisture**

- see also humidity*  
 acrylic fibres, oxidative stabilisation, moisture sensitivity 0-16524  
 cellulose film, moisture effect on phys. and mech. props. 0-40450  
 fibre reinforced plastic laminates, US evaluation of hygrothermal effects 0-7730  
 graphite reinforced epoxy composites, moisture detection by nuclear reaction anal. 0-30306  
 microwave absorption by water in heterogeneous organic materials 0-15998  
 nylon 66, fatigue crack propagation, effect of moisture 0-3166  
 polyamide 6 (polycapromide), temp. depend. of complex permittivity rel. to moisture content 0-50251  
 radiative forcing of atmosphere, sensitivity to variable cloud and moisture 0-56553  
 sands, poorly graded, moisture distrib. in capillary crack (*German*) 0-31066  
 soil, pore size distrib. estimation from moisture charact. 0-12454



**moisture continued**

- soil moistening, one-dimensional, surface water effects (*Russian*) 0-46209  
 soil moisture, heat and salt transport, math. model 0-26563  
 soil-water system, thermodynamic state functions (*German*) 0-4056  
 tetraglycidyl 4,4' diaminodiphenyl methane, diaminodiphenyl sulphone cured, failure and tensile mech. props., moisture effect 0-50735  
 troposphere moisture, temp., IR soundings anal. by statistical struct. and correl functions 0-8398  
 Al alloys, H impurities, improving productivity and detection threshold, by removing moisture with light pulse 0-26076

**moisture content** *see* **moisture****moisture measurement**

- see also* **humidity measurement**  
 AF3 unit replacement for Karl Fischer units using peristaltic pump 0-22376  
 passive neutron activation for environmental transuranic and moisture assay 0-21431  
 soil moisture and geology mapping, thermal inertia method 0-8344  
 soil moisture content by microwave radiometry 0-17425  
 soil surface, remote sensing by visible and false colour IR photography 0-56653

**molar volume** *see* **density****molecular alignment** *see* **molecular orientation****molecular beam electric resonance**

- halogen dimers, mol. beam. elec. deflection obs. 0-53080  
 inert gas complexes spectroscopic data, geometry, pot. energy curve, dis-  
 soc. energy, equilib. internuclear distance, determ. 0-53018  
 interhalogen dimers, mol. beam. elec. deflection obs. 0-53080  
 interhalogen trimers, mol. beam. elec. deflection obs. 0-53080  
 Ar-methyl chloride, mol. beam elec. reson. spectrosc. 0-23477  
 Ar.HBr(DBr), van der Waals complexes, rot. spectra and struct. 0-48055  
 ClCN, ground and first excited bending, vibr. state, props., mol. beam  
 elec. reson. 0-37823  
 KrHCl, van der Waals complexes, struct., RF and microwave spectra,  
 isotope effects 0-37806  
 TIF, P- and T-violating interactions in hyperfine struct., mol. beam reson.  
 expt. 0-53019

**molecular beam epitaxial growth**

- device applications 0-25570  
 GaAs MBE growth, deep levels effect on electron and hole trap densities  
 0-49652  
 III-V compounds and alloys, MBE process and problem areas, review  
 0-10815  
 III-V semiconductors, p-n heterostructures, epitaxial growth techniques,  
 appl. to optoelectronics, review 0-54770  
 microscopic mechanism of film growth from non-condensed phases, kinetic  
 anal. 0-54565  
 semiconductor films, superlattices control 0-2283  
 semiconductors (*Japanese*) 0-55305  
 Al, epitaxial growth on GaAs (001) 0-24757  
 Al-Ge (100) interfaces, MBE prep. and geometrical struct., total refl.  
 X-ray diffr. study 0-49531  
 Al<sub>0.1</sub>Ga<sub>0.9</sub>As-GaAs, heterojunction, interface width, AES obs. 0-20290  
 AlN, epitaxial film growth by MBE, physical and optical props. 0-2293  
 Bi film, on Si(111) substrate, MBE deposition kinetics 0-10817  
 CdSe films, growth kinetics and cryst. struct. during vacuum condensation  
 0-2305  
 GaAl<sub>0.27</sub>Ga<sub>0.73</sub>As DH lasers grown by MBE, growth conditions influ-  
 ence on threshold current density 0-32984  
 GaAlAs based heterojunctions, integrated optics appl., technology  
 advancements (*Slovak*) 0-33226  
 GaAs (110), surface struct., LEED and AES study, comparison of MBE  
 and ion bombard. surface prep. 0-54496  
 GaAs, epitaxial layers, MBE grown, Hall mobilities, substrate temps.  
 0-20335  
 GaAs film on GaAs substrate, uncontrolled doping obs. (*Russian*) 0-2276  
 GaAs film optical components, prep. by MBE using Si shadow masking  
 technique 0-28358  
 GaAs, MBE, undoped, growth and characterisation 0-10836  
 GaAs, shallow-homojunction solar cell by MBE, conversion efficiency  
 0-30476  
 GaAs, thin layers, growth conditions and phys. props. (*German*) 0-55307  
 GaAs:Cr, epitaxial layers, MBE grown, Hall mobilities, substrate temps.  
 0-20335  
 GaAs:Ge, MBE layers, complex free-carrier profile synthesis 0-54266  
 GaAs:Ge, mol. beam epitaxy of n- and p-types 0-10839  
 GaAs:Si layers, MBE growth, elec. and optical props., doping characts.  
 0-10819  
 GaAs:Sn films 0-50563  
 p-GaAs:Zn, luminescent, ion doped MBE growth 0-44436  
 GaAs-Al<sub>0.1</sub>Ga<sub>0.9</sub>As current injection multi-quantum-well heterostructure  
 lasers, MBE grown 0-19042  
 GaAs-Al<sub>0.1</sub>Ga<sub>0.9</sub>As DH lasers, very low current threshold, MBE grown  
 0-43353  
 GaAs-Al<sub>0.1</sub>Ga<sub>0.9</sub>As DH lasers, MBE grown, substrate temp. effect on  
 current threshold 0-48243  
 n-GaAs-n<sup>+</sup>-Al<sub>0.1</sub>Ga<sub>0.9</sub>As heterostructure production, by MBE (*German*)  
 0-44711  
 InAs, epilayer, MBE growth parameters, relationship with elec. props.  
 0-2296  
 In<sub>0.1</sub>Ga<sub>0.9</sub>As layers, on GaAs substrate, MBE fabrication and laser opera-  
 tion 0-10820  
 InP, MBE from In and P<sub>2</sub> beams, substrate temp. limits 0-15385  
 InP(100) undoped homoepitaxial films grown by MBE, photoluminesc.  
 props. 0-2809  
 InSb film, heteroepitaxial, MBE growth and elec. props. 0-2301  
 Si from ion-molecular beams, growth mechanism 0-2299  
 Si, MBE growth and surface struct. 0-10816  
 Si MBE layer resistivity and carrier mobility obs. (*Russian*) 0-49962  
 Si:As(Sb), n-type doping techniques 0-15126  
 Si:Sb, epitaxial film, growth by mol. beam technique 0-2292  
 ZnS, epitaxial growth, appl. to electronic devices, review (*Japanese*)  
 0-55281  
 ZnSe:In films, MBE growth, doping effect on photoluminesc. 0-10818

**molecular beam magnetic resonance**

- isotope separation, supersonic molecular beam technique using RF spectro-  
 scopy, mag. reson. 0-47725

**molecular beams**

- see also* **molecular beam electric resonance**; **molecular beam magnetic resonance**; **molecule-surface impact**; **particle velocity analysis**  
 benzene, <sup>13</sup>C substituted, mass selective two-photon ionis., mass spectro-  
 scopy obs. 0-9651  
 cluster beam, nozzle flow formation and detection, high energy beam  
 0-5638  
 continuum source particle beam properties, comput. modelling 0-26062  
 education, effusive flow, vector flux density distrib. calc. for any aperture  
 0-22165  
 electrostatic space focusing 0-28118  
 ethylene dimer, CO<sub>2</sub> laser induced photodissoc., pulsed mol. beam obs.,  
 van der Waals bond 0-9660  
 linear laser spectroscopy in collimated mol. beams, single mode tunable  
 lasers appl. to small mols. 0-52339  
 mass spectrometric sampling system, ion concs. in coal-fired MHD plasmas  
 0-52358  
 mass spectrometric sampling, high press., high temp. mols., review  
 0-52355  
 mass spectrometry, in situ anal. in crystal growth ambients 0-52357  
 mass spectrometry, IR spectral meas. of gas phase species, at high temp.  
 0-52235  
 multichannel counter for molecular beam time-of-flight experiments  
 0-37119  
 rotational temp. meas. by CARS 0-23423  
 state selection and focusing, appl. to NH<sub>3</sub> hyperfine spectrum 0-28119  
 supersonic mol. beam, CARS rot. temp. meas. 0-23423  
 supersonic nozzle beam, high temp. and press. device 0-37907  
 CH<sub>2</sub> molecular beam source 0-37908  
 CO<sub>2</sub> free jet, rarefied flow, homogeneous condensation scaling law  
 0-6121  
 Cu<sub>2</sub>, in supersonic free jet expansion, laser induced excitation spectrum  
 obs. 0-14151  
 H<sub>2</sub> cluster beam formation, from nozzle flow, isotope effect 0-6127  
 H<sub>2</sub><sup>+</sup>+CO→H+HCO<sup>+</sup>, 1.89 eV crossed beam study 0-21287  
 He-Ar mixture, mass separation during molecular beam sampling process  
 0-31937  
 I<sub>2</sub>, in seeded supersonic beams, vibr. and rot. relax., laser-induced fluoresc.  
 obs. 0-23522  
 KOH, beam, formed at 300-800°C, electron elastic scatt. obs., species  
 identification 0-14231  
 NO<sub>2</sub>, dissociative limit, mol. beam characts. determ. by fluoresc. excita-  
 tion spectra 0-53074  
 NaK dimer formed in supersonic beam, laser-induced emission 0-9636  
 SF<sub>6</sub>, resonant single-photon dissociation route using prelim. electron excitation  
 0-9662  
 W, catalytic decomp. of NH<sub>3</sub> single pulses, mol. beam relax. spectrometry  
 0-21321

**molecular biophysics**

- see also* **biomembrane transport**; **biomolecular effects of radiation**; **DNA**;  
**lipid bilayers**; **proteins**  
 absorption spectra for the complexes formed from vitamin-A and β-  
 lactoglobulin 0-30664  
 N-acetyl-L-phenylalanine methyl ester, model for amino acid side chains  
 internal motions in peptides and proteins 0-48017  
 acetylcholine receptor from Torpedo Californica, struct. anal., low-angle  
 neutron scatt. obs. 0-30651  
 actomyosin kinetic anal., review 0-21441  
 adenine tautomers, relative stabilities, nonempirical MO calcs. 0-21442  
 adenovirus hexon, three dimensional structure from electron microscopy,  
 computer modelling 0-35833  
 β-adrenergic receptor, molecular interactions with agonists and antagonists  
 0-8005  
 albumin, adsorption on SiO<sub>2</sub> 0-10777  
 albumin denaturation, investigation by PMR 0-3582  
 amino acid residues, contacting, ligand binding rate dependence on specific  
 microdynamics 0-51031  
 amino acid side chains, internal motions in peptides and proteins, N-  
 acetyl-L-phenylalanine methyl ester model 0-48017  
 anthramycin-DNA adduct, proposed struct. 0-30658  
 L-arginine L-ascorbate, X-ray cryst. struct. determ. 0-35826  
 B-DNA helix, guanine-cytosine base pair, electrostatic pot. 0-8003  
 bacterial catalase, <sup>57</sup>Fe enriched, active centre, Mossbauer spectra meas.  
 0-8024  
 bacteriochlorophyll a, triplet state energy and lifetime 0-30682  
 bacteriopheophytin a, triplet state energy and lifetime 0-30682  
 bacteriorhodopsin, anomalous amide I IR absorpt. rel. to alpha helices  
 distorted struct. 0-12058  
 bacteriorhodopsin, reson. Raman evidence for secondary protein-Schiff  
 base interactions, primary excitation mechanism 0-55981  
 bacteriorhodopsin Br570, bathochromic shift of absorpt. band in external  
 elec. field 0-35838  
 bathoproducts of rhodopsin, isorhodopsin I, and isorhodopsin II 0-51088  
 bilirubin in neonatal jaundice, chemistry, biosynthesis, transport, excretion,  
 photodecomposition and elimination 0-3578  
 bimolecular rate constant ionic strength dependence, effect of a molecular  
 dipole 0-55977  
 bioelectrets, occurrence of electret state and appl. in mol. biophysics and  
 bioengineering 0-8007  
 biological systems, nonequilib. mol. vibr. excitation, electron mechanism  
 0-55979  
 bioluminescence spectra of fireflies 0-35821  
 biopolymer, electronic-conformation interactions 0-3588  
 biopolymer soln. heat capacity, conformational props. temp. depend.  
 0-8009  
 biopolymers, conditions of liquid crystal formation 0-30642  
 biotin, NMR of <sup>13</sup>C, spectrum assignment 0-26204  
 bipyridines, torsional isomerisation of biologically active bicyclic molecules  
 0-27996  
 blood proteinpolymer interfacial behaviour, influence of hydrophilic-  
 hydrophobic type of microphase separated struct. (*Japanese*) 0-12051  
 bone, hydrazine deproteinated, rat, UV induced thermolum. glow peak  
 obs. 0-29814  
 Bose condensation of phonons in biological systems 0-30641  
 C-reactive protein, interaction with artificial phosphatidylcholine bilayers  
 0-3579  
 cancer receptor sites, proof by MO method for interstrand guanine bind-  
 ing of DNA 0-30656  
 capsular polysaccharide antigen, structure investig. by <sup>13</sup>C NMR  
 0-35828



**molecular biophysics continued**

carbonic anhydrase, active site substrate binding, environmental effects, CNDO and SCF LCAO calcs. 0-8002  
 carbonmonoxymyoglobin, frozen soln., recoilless fraction, Mossbauer spectra meas. 0-8025  
 cell surface receptors, molecular movements 0-45866  
 cellulose, conform. states and IR dichroism calcs. 0-55986  
 chemical reactions with inner sphere complex charge redistrib., polar solvent reorganisation energy 0-40730  
 chlorophyll, photosystem 2, activation energy and lifetime of fluoresc. 0-35842  
 chlorophyll special pair models, reaction centres 0-3574  
 chlorophyll-a, conc. quenching rel. to functional charge transfer 0-30666  
 chlorophylls a and b and pheophytins, fluoresc. and phosphoresc. 0-12057  
 chloroquine-biopolymer binding interactions, PMR effects 0-55982  
 chromophores, biochemical, in cosmic dust, contrib. to interstellar UV extinction 0-26945  
 cofacial diporphyrins, electron transfer reactions following picosecond excitation, CT state lifetimes, optical difference spectra 0-25995  
 collagen structures, piezoelec. effect, in rel. to mol. struct. 0-41100  
 collagen fibrils, rat tail tendon, quasi-hexagonal mol. packing model 0-30660  
 conformational analysis, solvent effects 0-3583  
 coupled spin systems, selective nucl. Overhauser effects calc., use in struct. chem. 0-23588  
 cross-peptide bond  $^{13}\text{C}$ - $^{15}\text{N}$  coupling constant, NMR obs. 0-55980  
 $\beta$ -crystallin, lens protein, prep. 0-16921  
 cytochrome oxidase reaction, semiconduction as mechanism 0-55983  
 cytochrome P-450, non-equilib. states formed by low-temp-reduction, absorpt. spectra 0-35837  
 dense phase chem. reaction theory 0-3575  
 deoxyhaemoglobin, high mag. field Mossbauer spectra, electronic states 0-35845  
 deoxymyoglobin, frozen soln., recoilless fraction, Mossbauer spectra meas. 0-8025  
 deoxymyoglobin, high mag. field Mossbauer spectra, electronic states 0-35845  
 deoxymyoglobin single crystals, Mossbauer study with polarised  $\gamma$ -rays 0-40962  
 diamine oxidase solutions, proton mag. relax. dispersion obs. 0-51136  
 dichelated protohaeme, model haemoglobin cpd., Mossbauer spectra 0-16904  
 1,3-dimethyluracil, non-hydrogen bonding crystal, radical formation 0-35552  
 dipalmitoyl phosphatidylcholine vesicles, appl. of depolarised light scatt. theory from hollow spherical particles 0-45946  
 dipalmitoylphosphatidylcholine/glucagon (cardiolipin/insulin) systems, Raman spectra study 0-16903  
 DNA, backbone vibrational mode displacements of A-DNA and B-DNA 0-8000  
 DNA, calf-thymus, diffusion coeff. meas. using quasielastic light scatt. apparatus (German) 0-12314  
 DNA, circular superhelical, X-ray scatt. calcs. 0-56109  
 DNA, conformation of native molecule, influence of solvent struct. 0-30655  
 DNA, hydrodynamic shearing simulation 0-16895  
 DNA, intact, modified bases characterisation by mass-analysed ion kinetic energy spectrometry 0-3591  
 DNA, phase transition,  $\psi$  transition of single coils 0-26200  
 DNA, soln., phase transitions, light absorption oscils. obs. 0-26197  
 DNA, sorption and desorption of water, thermal-stimulated press. and thermogravimetric anal. 0-8008  
 DNA, X-ray diffr. from side-by-side model 0-35835  
 DNA bases, selective electronic excitation using dye lasers 0-8012  
 DNA bases, theoretical study of electronic spectra 0-30665  
 DNA conformation, influence of intermol. interactions 0-16900  
 DNA film, dehydration and conform. state, differential scanning microcalorimetry 0-35830  
 cDNA for human chorionic gonadotropin  $\alpha$ -subunit, isolation, cloning and sequence anal. 0-3587  
 DNA hydrate, stability studied by thermogravimetry 0-30650  
 DNA in chromatin, stereochem. model for superfolding 0-35829  
 DNA packing in fibrils of DNP of polytene chromosomes 0-30649  
 DNA structure of left-handed double helical DNA fragment 0-30659  
 DNA-type macromolecule, melting, low mol. wt. impurity effect 0-12050  
 DNA-water interaction, single and double helix DNA 0-30646  
 E. coli, light scatt., ribosomal subunit diffusion coeffs. 0-21438  
 E. coli cells, iron-storage protein, Mossbauer spectra obs. 0-8022  
 electron micrographs, computer-aided anal. 0-4813  
 electron microscopical analysis of macromolecular 3D struct. 0-35836  
 electron microscopy, high resolution, mol. struct. determ. 0-21595  
 electron transport over large distance in biol. systems, medium as mediator 0-35820  
 electronic structural props. of mols. relevant to photosynthesis 0-16902  
 electrostatic isopotential maps for large biomolecules, STO transferable bond calc. 0-3571  
 elementary biological function, localised electron subsystem interaction process theory 0-55978  
 energy migration in one-dimensional structures with resonance interaction 0-1092  
 enzyme dynamics, statistical phys. 0-21439  
 eukaryotic ribosomes, 2 step binding to brome mosaic virus RNA3 0-3580  
 excitons and Bose-Einstein condensation in living systems 0-30640  
 eye lens low molecular weight protein obs. and prep. 0-16921  
 ferredoxin, from *Clostridium pasteurianum*, Mossbauer effect, ESR, and mag. susceptibility meas. 0-40961  
 ferredoxin, soluble, investigation of 2 forms from pea leaves, EPR obs. 0-45851  
 ferredoxin synthetic analogues,  $[\text{Fe}_4\text{S}_4(\text{SR})_4]^{3-}$  clusters, Mossbauer effect, EPR, and mag. props. 0-41057  
 ferredoxin-like centres, membrane bound, in photosystem I of blue-green algae, Mossbauer and EPR study 0-40974  
 ferric haeme complex of low spin, Mossbauer spectra, crystal field parameters 0-26203  
 ferric myoglobin cpds., single cryst., Mossbauer studies 0-8016  
 ferrichrome A, selective excitation double Mossbauer meas. 0-8015  
 fibres, natural, Brillouin scatt. shifts, comparison with synthetic polypeptide obs. 0-55991  
 fireflies, bioluminesc. spectra 0-35821

**molecular biophysics continued**

firefly chemiluminescence emissions, time-resolved spectra 0-35822  
 fluorescence, nonexponential decay, method of moments for data anal. 0-55975  
 fluorescence depolarisation, E-type delayed, rotational motion probe techniques 0-36207  
 fluorescence picosec. kinetics in chromatophores and reaction centres from *R.sphaeroides*, 295 to 80K 0-35857  
 Forster energy transfer problem in 2D, analytic soln. 0-26195  
 genes, mouse, heavy chain immunoglobulin, nuclear transcripts 0-26208  
 $\gamma$ -glycine, cryst. struct. by neutron diffr. at 83K and 298K 0-35825  
 gramicidin A in biomembrane channel, IR spectroscopic obs. 0-16901  
 guanine tautomers, relative stabilities, nonempirical MO calcs. 0-21442  
 haeme proteins and metalloporphyrins, redox chem. and oxygen binding 0-3573  
 haemoglobin, dielectric props. under UV excitation 0-6912  
 haemoglobins and chlorocruorins, extracellular respiratory, physicochemical and functional props. 0-3581  
 haemoproteins, Fe-ligand binding and electronic struct., Mossbauer studies 0-8021  
 heart cytosol, aspartate transaminase, electron-density map interpretation 0-55990  
 histones, H2A and H4, effect of molecular interactions on fluorescence intensity 0-51032  
 histones H<sub>2</sub>A and H<sub>4</sub>, mixed solns., oligomer structs. 0-30648  
 homopolymer, theory of 1D adsorpt. on to 0-51034  
 horseradish peroxidase cpd. II, high-field Mossbauer spectra, 4.2 to 120K 0-8026  
 hyaluronate solns., cooperative phase transitions, review 0-45850  
 hydrocarbon chain tilt differences between hydrated bilayers 0-51038  
 3-hydroxyflavone, excited state proton transfer, luminesc. 0-35818  
 immunoglobulin (Ig)  $\kappa$  chain m RNAs, identical 3' non-coding sequences favour unique C<sub>g</sub> gene in mouse 0-8010  
 indole soln. containing histidine, fluoresc. rel. to soln. pH 0-2826  
 IR linear dichroism of oriented nucleic acid films 0-8013  
 isoelectric focusing method for human globin chain separation 0-17219  
 Kerr effect of charged dipolar macromolecules without condensed counterions in conducting solution 0-53171  
 kidney, tissue water freezing study,  $^1\text{H}$  NMR obs. 0-8027  
 L-amino acids, weak neutral currents and biological stereoselection 0-26196  
 lecithin-deoxycholate mixed micelles, surface curvature and mobility, PMR study 0-21452  
 ligand binding to macromolecules, allosteric and sequential models of cooperativity 0-12870  
 lipid bilayer, paraffin chain dynamics, ang. correl. function decay by multiple rot. pot. diffusion 0-3569  
 lipid bilayers, D relax. rates and mol. dynamics 0-26206  
 lipid function in excitable membranes 0-12095  
 lipid membranes, molecular forces between and within 0-51051  
 lipid-rhodopsin interactions in photoreceptor membranes 0-12094  
 lysozyme, binding to bacterial cell wall trisaccharide NAM-NAG-NAM, X-ray cryst. struct. anal. 0-35834  
 lysozyme, sorption and desorption of water, thermal-stimulated press. and thermogravimetric anal. 0-8008  
 lysozyme complex with substrate-inhibitors, photosensitised electron transfer, role of  $\text{Cu}^{2+}$  0-30638  
 macromolecular thermodynamics and its possible relevance in physiology 0-53176  
 macromolecule behaviour when introduced into liq. cryst. 0-30639  
 macromolecule liquid, translational friction coeffs. of rigid, symm. top mols. 0-6003  
 macromolecules, nonpolar groups, solvation, correl. function anal. 0-30644  
 macromolecules buoyant density determ. by analytical density gradient equilb. centrifugation 0-17217  
 mammalian DNA, viscoelastic behaviour, rat obs. 0-8078  
 mass spectrometry appls. in struct. studies of bioactive compounds 0-51305  
 membranes, radial autocorrelation function, significance in X-ray diffr. patterns 0-51048  
 metalloenzymes and carriers, hydration effect on mobility of Mossbauer atoms 0-35819  
 methanol dehydrogenase, enzyme, electron spin echo, 35 GHz 0-13113  
 methionine sulfoxide in protein,  $^{13}\text{C}$  NMR anal., method and expt. obs. 0-56305  
 metmyoglobin, dynamics study using Rayleigh scatt. of Mossbauer radiation 0-40963  
 microemulsions, struct. aspects, using dielec. relax. and spin label techniques 0-26199  
 microwave absorption by biological material, role of water 0-17004  
 monomer self-associating systems, nonideal, graphical anal. by equilibrium ultracentrifugation 0-41335  
 muscle, mouse, NMR multiwindow anal. and proton local fields and magnetisation distrib. 0-21444  
 muscle contraction, time-resolved X-ray diffr., data-collection system (Japanese) 0-46108  
 muscle water, mouse,  $^1\text{H}$  NMR anal. above and below freezing 0-56073  
 muscle water, study of spin-lattice and spin-spin relax. times of  $^1\text{H}$ ,  $^2\text{H}$ , and  $^{17}\text{O}$  0-21443  
 myelin lattice swelling kinetics study X-ray diffr. obs. 0-21436  
 myoglobin-H<sub>2</sub>O<sub>2</sub>, high-field Mossbauer spectra, 4.2 to 120K 0-8026  
 myoglobin-O<sub>2</sub>(CO), elec. field gradient tensor, Mossbauer meas. 0-8017  
 myosin helical fragments, stepwise pattern of thermal denaturing 0-40966  
 myosin kinetic anal., review 0-21441  
 NADH coenzyme, two photon absorpt. cross section meas., reaction rate modification 0-51043  
 net repulsive van der Waals forces between different particles, macromolecular, or biological cells in liqs., appls. 0-34274  
 nitrogenase, cofactor centres, Mossbauer spectra obs. 0-8023  
 nitrogenase active site, Mossbauer spectra of Mo-Fe-S clusters 0-45852  
 NMR of rat skin,  $^1\text{H}$  and  $^{13}\text{C}$  obs. 0-40965  
 NMR studies of water in biological systems 0-3886  
 nuclear Overhauser effect, truncated driven, in presence of spin diffusion 0-1095  
 nuclear spin-lattice relaxation meas., variable nutation WEFT, biochemical appl. 0-20482  
 nuclei acid base stacked dimer, origin of excimer states in extended Hucklel method 0-35832



**molecular biophysics continued**

- nucleic acid bases,  $^{14}\text{N}$  relax. and N-proton spin coupling, NH-proton spin-lattice relax. 0-26202  
 nucleic acid bases,  $\text{Zn}^{2+}$  binding, ab initio SCF (pseudopot.) calcs. 0-12052  
 nucleic acid components, pyrimidine and purine, electronic struct. 0-30654  
 nucleic acid subunits, simulation of inter- and intra-molecular interactions 0-30643  
 nucleic acid-dye complexes, energy transfer obs. using laser-induced fluorescence. 0-12054  
 nucleic acid-TCNQ complex, charge transfer interaction 0-3576  
 nucleic acids, electronic absorpt. and emission spectra 0-55989  
 nucleic acids,  $\text{H}_2$  exchange kinetics and internal motions 0-21440  
 nucleic acids, nucleosides and nucleotides, metal ions interaction, review 0-3577  
 nucleic bases, interactions and self-organisation, ionisation and solvent salt comp. effects 0-55985  
 nucleotide bases, electronic absorpt. and emission spectra 0-55989  
 nucleotides, interactions and self-organisation, ionisation and solvent salt comp. effects 0-55985  
 origin of life 0-4111  
 oxymyoglobin, frozen soln., recoilless fraction, Mossbauer spectra meas. 0-8025  
 paddy leaves, spectrochem. anal., mineral constituents rel. to brown spot disease resistance 0-12055  
 paracrystal disorder, in biological systems 0-51035  
 pentofuranosyl nucleosides, isomeric,  $^1\text{H}$  NMR coupling consts., SCF FPT INDO approx. calc. 0-14156  
 peptide and glycopeptide research methods 0-51307  
 peptides, charge transfer, 1-electron reactions, pulse radiolysis obs. 0-45848  
 peptides and derivatives, mol. electron acceptor groups 0-30637  
 perdeuterio-N-1-oxyl-2,2,6,6-tetramethyl-4-piperidinyI maleimide, spin label, biological EPR 0-32746  
 Pfl filamentous bacterial virus, macromolecular structural transitions 0-3584  
 phosphamides, carcinostatic,  $^{14}\text{N}$  NQR, electron distrib. and bonding configs. 0-48018  
 phosphates, cellular, heteronuclei. two-dimens. NMR as conform. probe 0-3590  
 phosphatidylcholine-cholesterol vesicles interacting with lucensomycin, PMR obs. 0-40954  
 phospholipid inter- and intra-molecular interactions, PCILOCC and pot. function calc. 0-3570  
 phospholipid membrane, polar head motion, NMR and EPR linewidth study using TCNQ $^-$  ion-radical (*French*) 0-45865  
 phospholipids,  $^{31}\text{P}$  NMR, slow-motional lineshapes for very anisotropic rot. diffusion 0-5644  
 photosynthesis, redox conversion kinetics in the electron transport chain 0-40950  
 physical and biological science conf., Japan (Feb. 1979) 0-12846  
 pigment associations, conc. effects, luminesc., absorpt. spectra and dichroism obs. 0-1007  
 pigment molecule organisation and interaction in reaction centres of *Rhodospseudomonas viridis* 0-35843  
 pigment-protein complexes oriented, of photosynthetic bacterium *Chromatium minutissimum*, linear dichroism 0-35841  
 plant tissues, adsorbed water, detection of OH groups for adsorption centres, dielectric relaxation (*Japanese*) 0-7999  
 plasma protein interaction with polyanion complex studied by circular dichroism and UV spectroscopy (*Japanese*) 0-12316  
 plasma proteins adsorbed on polymer surface, Fourier transform IR spectrometry 0-16899  
 plasmid DNA and DNA-histone chromatin-like complexes, conform. and soln. props. by laser light scatt. 0-55987  
 poly ( $\text{N}^{\alpha},\text{N}^{\epsilon}$ -terephthaloyl-L-lysine) membrane for artificial red blood cells, interaction with serum proteins (*Japanese*) 0-12061  
 poly- $\gamma$ -benzyl-L-glutamate helices, optical activity 0-48113  
 polyelectrolyte + physiologically active substance complexation, stability, kinetics (*Russian*) 0-8006  
 polyelectrolyte solution, polyion-polyion interaction effects, computer simulation 0-35817  
 polyglycine, IR spectra calc. for helix and  $\beta$  configs. 0-45853  
 polymer chain, uniform, elastic, possible conformational states 0-37913  
 polymer chains, intramol. reacts., enzyme catalysis appl. review 0-40953  
 polymers, aqueous, solns., IR spectra 0-2761  
 polymers solns., cooperative phase transitions, review 0-45850  
 polynucleotide, double-stranded, conform. inhomogeneity of sugar-phosphate chain rel. to compact particle optical activity 0-35839  
 polynucleotides, double helical, conformation, pairwise pot. function calcs. 0-53173  
 polynucleotides, interactions and self-organisation, ionisation and solvent salt comp. effects 0-55985  
 polyoma virion and capsid crystal structures 0-8011  
 polypeptides, in aq. poly(L-glutamic acid) soln., helix-coil transition, US relax. times 0-45849  
 polyurethanes, linear, in physiological soln., in vivo, degradation by ester hydrolysis (*Russian*) 0-40690  
 porphyrins, reson. Raman spectra, selection rules, normal coord. treatment 0-53175  
 porphyrins orientation in n-alkane Shpol'skii hosts, spectra 0-48035  
 porphyrins and related tetrapyrroles, mass spectrometry appls. 0-51306  
 protein, electron-transport type, H-bonding, ab initio MO 0-51039  
 protein, globular, compressibility in water at 25°C 0-40951  
 protein secondary structure determ. by circular dichroism spectra 0-30653  
 protein structures, Fourier refinement 0-51037  
 protein-nucleic interactions in tobacco mosaic virus, spin label and fluorescence. obs. 0-40949  
 protein-substrate binding, linear differential equations in chemical equilibrium calculations 0-30279  
 proteins, adsorbed at interfaces, fluorescence spectroscopy study 0-12315  
 proteins, coiling and topology of the antiparallel  $\beta$ -struct. 0-40956  
 proteins, coiling and topology of the parallel  $\beta$ -struct. 0-40957  
 proteins, conformations, quantitative approach 0-30652  
 proteins, globular, cryst. growth kinetics 0-35823  
 proteins, globular, crystalline, intermol. interactions, denaturation, DSC and X-ray diff. obs. 0-16897  
 proteins,  $\text{H}_2$  exchange kinetics and internal motions 0-21440

**molecular biophysics continued**

- proteins, kinetic constants of association and dissociation, theoretical determ. 0-51033  
 proteins, minimisation of functions of many variables appl. to X-ray struct. anal. 0-3589  
 proteins, model building procedure 0-51036  
 proteins, resolution of components of complex spectra by Alentsev-Fok method 0-1097  
 proteins, solid, NMR, detection of individual C resonances, appls. 0-51042  
 proteins, solid, PMR spin-lattice relax., mol. dynamics 0-51041  
 proteins, UV fluorescence spectra, resolving of components, Alentsev-Fok method 0-1096  
 quercetin, excited state proton transfer, luminesc. 0-35818  
 rare earth bone uptake, Mossbauer study 0-8019  
 red blood cells of thalassemia, sickle-cell anaemia, and haemoglobin Ham-mersmith, ferritin-like Fe, Mossbauer study 0-8018  
 redox enzyme, Fe-, Cu-, or Mo-containing, electron transfer peculiarities 0-16896  
 retinal chromophore transition dipole moment, orientational changes obs. 0-41023  
 rhodopsin, picosecond spectroscopy obs. of primary events 0-56312  
 rhodopsin, vertebrate, chromophore orientation obs. 0-40959  
 rhodopsin thermal stability in photoreceptor membrane, role of lipids, PMR spectroscopy 0-35874  
 ribonuclease-A, solid, PMR spin-lattice relax., mol. dynamics 0-51041  
 ribose phosphate backbone, effective partial charges calc. 0-8013  
 t-RNA, rot. relax. time,  $10^{-9}$ s range Fabry-Perot and photoelectron time of arrival method 0-21437  
 rubredoxin, frozen soln., recoilless fraction, Mossbauer spectra meas. 0-8025  
 semiconducting biopolymers and their part in biochemical phenomena 0-12053  
 L-serine-L-ascorbic acid, X-ray cryst. struct. determ. 0-35827  
 small molecules in protein solns., spin-lattice relax. times, inversion recovery spin-echo sequence 0-21446  
 smectic lipid bilayer, in cryst. matrix, phase transition 0-21453  
 solitons in molecular systems, biophys. effects 0-51044  
 spectrochemical analysis of biological solns. using wall stabilised arc source 0-41343  
 static and dynamic structure of biomolecules, Mossbauer effect 0-40952  
 steroid research using mass spectrometry 0-51308  
 structural determinations using synchrotron X-rays 0-46112  
 substrate, small, binding to large biomolecule, fast kinetics studied by NMR, review 0-55662  
 subtilisin charge-relay system, electrostatic pot. map, STO transferable bond calc. 0-3571  
 tail structure of temperate phage no.1 of *Bacillus megaterium*, electron micrograph 3-D reconstruction 0-35831  
 testosterone, dielectric props. under UV excitation 0-6912  
 tetrabutylammonium iodide, in aq. proline soln., elec. conductance investigation 0-10692  
 tetramethylammonium iodide, in aq. proline soln., elec. conductance investigation 0-10692  
 thromboxane, evidence against prostaglandin hairpin conformation 0-3585  
 ribosomal RNA interacting sequences, expt. determ., method and results 0-3586  
 tomato bushy stunt virus crystals, appl. of oscillation method to data collection 0-14961  
 tooth enamel, human cryst. struct. refinement, Rietveld method 0-51040  
 $\alpha$ -tropomyosin, specific splitting at cysteine-190, physicochem. study of fragments 0-30647  
 tryptophan soln. containing histidine, fluoresc. rel. to soln. pH 0-2826  
 urea, electro-optical coeffs. meas., rel. to nonlinear optics calcs. 0-34889  
 valinomycin conformation in a phospholipid bilayer,  $^1\text{H}$  NMR obs. 0-40958  
 vascular walls, physical theory of permeability rel. to atherogenesis, mech. effects 0-16908  
 vision, molecular mechanism for initial process 0-51089  
 visual pigments, resonance Raman studies of the primary photochemical event 0-41020  
 water diffusion in wheat grain endosperm tissue,  $^1\text{H}$  NMR obs. 0-8001  
 water molecules in biological systems, relax. rel. to vol., pulse NMR obs. 0-40960  
 water sorbed on DNA, temp. anomaly, IR spectroscopic obs. 0-51046  
 $[\text{Fe}_2\text{S}_2(\text{SH})_2]^{2-3-}$ , HFS-LCAO calcs., 4-Fe active site model in high pot. Fe protein and ferredoxin 0-42929  
 $\text{CH}_3^+$ , carcinogen, attack on guanine, symposium contrib., Florida, USA (March 1979) 0-51946  
 Co(II)-octaethylporphyrin, Mossbauer emission spectra 0-8020  
 FHF ion, H-bond excited electronic states, CI calc., dissoci. and autoionising states 0-5489  
 Fe(III) Laeme complex, EPR g-value anal. 0-30657  
 $^{57}\text{Fe}$ , isomer shift calibration const. rel. to biological cpds. 0-7227  
 H-bonded model systems, intermolecular charge transfer, biological implications 0-3572  
 $\text{H}^+$ -ATPase, soluble mitochondrial, thermal stability obs. 0-55992  
 $\text{H}_2^+$ , 6 MeV, PIXE anal. of organic materials 0-26087  
 $^{39}\text{K}$  pulsed NMR obs. of whole body live and dead newborn mice 0-40964  
 $\text{N}_2$  fixation, semiempirical INDO study 0-16898  
 NO-Fe(II)haemoproteins, orbit-orbit interaction, low temp. mag. circular dichroism obs. 0-30645  
 $\text{PO}_4$  electron structure rel. to synthesis and utilisation of ATP 0-40955

**molecular bonds see bonds (chemical)****molecular clusters**

- alkali halides, cluster ions and mol. ions in salt field desorption 0-40238  
 carbon tetrachloride, clusters, collision induced polarisability, mol. frame distortion 0-32798  
 carbon tetrafluoride, clusters, collision induced polarisability, mol. frame distortion 0-32798  
 cluster beam, nozzle flow formation and detection, high energy beam 0-5638  
 diatomic clusters, break-up in thin films, particle energy distrib., central peak nature 0-50490  
 ion clusters, 3-body pots., SCF energy partitioning calcs. 0-18953  
 ions, mol. clustering, gaseous-condensed state, nucleation and solvation 0-28129



**molecular clusters continued**

- linear aggregates, small, polarisability determ., CNDO method and analytical models (*French*) 0-29298  
 methane, clusters, collision induced polarisability, mol. frame distortion 0-32798  
 microemulsions, aerosol OT, inhomogeneous interior, fluoresc. and polarisation decay probes 0-50891  
 nozzle flowfield, cluster form., reservoir temp. scaling 0-5639  
 nucleation, homogeneous kinetic steady state solns. 0-50873  
 nucleation in finite systems, theory and computer simulation 0-26038  
 polar molecule clusters, 3-body pots., SCF energy partitioning calcs. 0-18953  
 polymethine-cyanine molecular aggregate, band struct. 0-53174  
 suspension concentrates, physical stability criteria, review 0-45562  
 transition metal-carbonyl cluster molecules, electronic struct., localised orbital pseudopot. method 0-39653  
 CO, adsorbed on Ni (100), freq. and amplitude of localised vibrs., cluster calc. 0-6616  
 CO<sub>2</sub> free jet, rarefied flow, homogeneous condensation scaling law 0-6121  
 CO<sub>2</sub><sup>-</sup>, hydrated anion stable gas phase heteronuclear clusters, mass spectra, autodetachment rates 0-14266  
 CaCl<sub>2</sub>, cluster ions and mol. ions in salt field desorption 0-40238  
 F<sup>-</sup>(H<sub>2</sub>O)<sub>2</sub>, 3-body pots., SCF energy partitioning calcs. 0-18953  
 H<sub>2</sub>, cluster beam formed from nozzle flow, isotope effect 0-6127  
 (HF)<sub>3</sub>, 3-body pots., SCF energy partitioning calcs. 0-18953  
 H<sub>2</sub>O-HNO<sub>3</sub>-NO<sub>3</sub><sup>-</sup> clusters, gas phase, thermodynamic quantities, mass spectra obs. 0-50875  
 (H<sub>2</sub>O)<sub>n</sub>, n=2 to 8, correlation energies, ab initio and SCF calcs. semiempirically corrected 0-43223  
 H<sub>2</sub>O<sub>4</sub><sup>2-</sup>, cluster anion tetrahedral struct. and stability, polarisation model 0-53181  
 Li<sup>+</sup>(OH)<sub>2</sub>, 3-body pots., SCF energy partitioning calcs. 0-18953  
 MoO<sub>4</sub><sup>6-</sup>, electronic struct., discrete variation and scatt. wave X<sub>α</sub> methods 0-917  
 NO<sub>2</sub><sup>-</sup>, NO<sub>2</sub><sup>-</sup>-H<sub>2</sub>O, and peroxy isomers, photodissoc. and photodetachment 3500-8250 Å, rel. to ionosphere 0-35554  
 NO<sub>3</sub><sup>-</sup>, NO<sub>3</sub><sup>-</sup>-H<sub>2</sub>O, and peroxy isomers, photodissoc. and photodetachment 3500-8250 Å, rel. to ionosphere 0-35554  
 NbO<sub>2</sub>, rutile phase, energy levels, momentum density, and Compton profile, embedded cluster model 0-50453  
 SF<sub>6</sub>, clusters, collision induced polarisability, mol. frame distortion 0-32798  
 Si (111), chemisorption of H, localised model, ab initio HF-LCAO calc. 0-6930  
 Si<sub>3</sub>H<sub>7.2</sub>, silane, SCF X<sub>α</sub> MO calc., appl. to amorphous hydrogenated Si 0-49580  
 UO<sub>6</sub><sup>6-</sup>, electronic struct., discrete variation and scatt. wave X<sub>α</sub> methods 0-917  
 WO<sub>6</sub><sup>6-</sup>, electronic struct., discrete variation and scatt. wave X<sub>α</sub> methods 0-917  
 Zn<sup>2+</sup>-H<sub>2</sub>O clusters, solvation, Monte Carlo simulation 0-44102  
 Zn<sup>2+</sup>-CO<sub>2</sub>-H<sub>2</sub>O clusters, solvation, Monte Carlo simulation 0-44102

**molecular collision processes** *see elastic scattering of atoms and molecules; molecular inelastic collisions*

**molecular configuration interactions** *see molecular electron correlations*

**molecular configurations**

- see also bond angles; bond lengths; inorganic molecule configurations; isomerism; macromolecular configurations; molecular orbitals calculations; organic molecule configurations; X-ray diffraction examination of molecular structure*  
 charge distribution, quantum topology, bonding theory and molecular structure 0-5463  
 chiral molecules, prochiral centres, electronic and structural chirality 0-30220  
 chiral representations in one-centre mol. and field models, symmetry rules 0-14095  
 contracted Gaussian basis set for correl. wave functions, appl. struct. and energies 0-52881  
 diatomic systems, reln. between internuclear distances and force constants 0-43205  
 dynamical groups in atomic and molecular physics 0-42362  
 electron distribution anal. ab initio calcs. 0-47866  
 electron-density maps of bent bonds, in non-cyclic mols., flexible-spring model 0-1084  
 flexible molecules, chain end diffusion 0-23569  
 geometry optimisation with explicit inclusion of electron correl. 0-37748  
 ground state props., coupled cluster and MBPT methods appl. 0-47881  
 high temperature gas and vapour characterisation, conf., Gaithersburg, USA (Sept. 1978) 0-53910  
 high temperature species, molecular shape determination 0-52233  
 homeomorphism, structural, between nuclear pot. and electronic charge density 0-42968  
 icosahedral cage, symmetry coords. and vibration freq. 0-47966  
 image formation, electron holographic method, optical spatial domain filter appl. 0-10016  
 internuclear parameters measurement method using total scatt. of fast electrons 0-32857  
 ion+molecule, intramolecular selectivity, stereochemistry, gas phase ionic chemistry techniques 0-35529  
 mass spectrometry, mechanistic studies 0-47142  
 model molecule, skeleton-ligand interactions, algebraic invariant investig. 0-52853  
 molecular crystals, optimum packing in atom-atom approx., algorithm and computer program 0-1960  
 NMR in undergrad. instruction, general purpose microcomputers use for hypothetical spectra synthesis 0-42009  
 non-rigid molecules in condensed phases, liquid struct. effects on chem. reactions and conform. changes 0-40725  
 nonlinear symmetric XY<sub>2</sub> type molecules, isotopic invariants, Coriolis coupling constants, centrifugal distortion constants 0-923  
 oriented molecules, NMR spectra, vibr. correction study 0-18840  
 planar structure, double reson. signals depend., appl. to microwave spectra 0-32751  
 quantum mechanics, mol. struct. defn. 0-52843  
 Raman spectra of gases, high-resolution, mol. struct. and orops. 0-53000  
 simple fluid, mol. dynamics simulation, including three-body interactions 0-54100  
 sparse s and p type Gaussian basis set LCAO MO SCF calc., mol. props. 0-23306

**molecular configurations continued**

- stereoisomer generation, algorithm and implementation 0-1080  
 supersonic jet spectroscopy, appls., teaching approach 0-41996  
 symmetry coordinates, description of mol. distortions 0-10517  
 symmetry properties of non-rigid molecules, unified approach 0-1083  
 transition metal complexes, O containing, coordinate bonding, charge transfer electronic bands, complex struct. determ. 0-52977  
 vibrational spectroscopy, high pressure, and conformational analysis 0-9758  
 WINIMAX weighting factor, for isotope chem. and mol. struct. calcs. 0-27940

**molecular conformations** *see molecular configurations*

**molecular dissociation**

- see also heat of dissociation; molecular dissociation energies; molecular electron impact dissociation; molecular photodissociation; molecular predissociation*  
 acetic acid, ionised, pot. energy profiles for unimol. reactions 0-43210  
 acid dissociation consts., computer programs 0-26005  
 actinide oxides, preparation of metals and refractory cpds. 0-16229  
 aliphatic perfluorocarbons, electron attachment, fragmentation 0-12 eV 0-5618  
 alkyl substituted diacetylene radical cations, optical emission and photoelectron spectra, fragmentation decay 0-53004  
 benzene, doubly charged ion fragmentation, ion kinetic energy spectrum peaks, collision gas sensitive 0-40679  
 trans-2-butene, charge transfer mass spectra and photoelectron spectra 0-40778  
 cis-butene, ozonolysis, radical form., matrix ESR spectrosc. 0-16653  
 catalyst surface mag. field effect on mol. dissoci. rate 0-16721  
 chloroacetylene decomposition, unimolecular lifetime and relative translational energy distrib. 0-25994  
 chlorobenzene ion fragmentation, kinetic shift and phenyl ion heat at formation, photoelectron-photoion coincidence meas. 0-25998  
 cyclobutene, strong collision and thermal decomp. on surface, variable encounter method calcs. 0-50885  
 cyclopropane+inert gas, reactant decomp., rot.-vibr. energy transfer, relax. analytic soln. 0-55650  
 diatom dissociation and recombination mechanisms, bound complex and triple collision mechanisms 0-23478  
 p-diazoquinone, photodecomp. 0-7827  
 DNA-Au (III) interaction, rate consts., activation energies, pH, spectrophotometric obs. 0-30228  
 electron gas, dissociative recombination 0-36940  
 ethane, shift of electronic spectrum during dissoci., CNDO calc. 0-37759  
 ethanol, ion internal energy selection by angle-resolved mass spectrometry 0-53164  
 ethyl radical decomposition, mol. dynamics, trajectory studies 0-7780  
 ethylene, ozonolysis, intermediate struct., multiconfig. SCF CI calcs. 0-18803  
 ethylene, ozonolysis, radical form., matrix ESR spectrosc. 0-16653  
 ethylene, planar dissociation, electronic rearrangement, states, bonds, ab initio multiconfigurational SCF calcs. 0-27937  
 fast molecular ion+solid (gas), excited electronic states effects 0-9687  
 fluoroethyl radical, unimol. dissoci., pot. energy characts. and energy partitioning calcs. 0-45488  
 formaldehyde<sup>+</sup>, excited state dissoci., nonadiabatic interactions, conical and Jahn-Teller intersections, classical trajectory method 0-25997  
 formaldehyde→H<sub>2</sub>+CO, reaction path and activation energy, potential energy surface for ground state of formaldehyde 0-42967  
 formaldehyde decomposing to H<sub>2</sub>+CO, reaction path Hamiltonian 0-45486  
 formic acid, chemisorption and decomp. on Cu (100), EELS study 0-16729  
 hexafluoro ethyl cation fragmentation, mass spectrometry 0-53070  
 hydrocarbons decomposition reaction, with Ta and α-Hf, surface segregation influence of O<sub>2</sub> or N<sub>2</sub> 0-55654  
 interstellar molecules, collision-induced dissociation 0-17632  
 ions, multiple dissoci. probabilities 0-40678  
 lysozyme complex with substrate-inhibitors, photosensitised electron transfer, role of Cu<sup>2+</sup> 0-30638  
 mass spectrometry, mechanistic studies 0-47142  
 methane, ion internal energy selection by angle-resolved mass spectrometry 0-53164  
 methanol, ion internal energy selection by angle-resolved mass spectrometry 0-53164  
 methanol, laser-induced decomp., comparative obs. using pulsed HF and CO<sub>2</sub> lasers 0-11888  
 micelle dissociation-recombination kinetics, stochastic model 0-30291  
 Morse oscillator collinear collision induced dissoci., vibr. enhancement, quasiclassical trajectory study 0-28089  
 nonadiabatic interactions, conical and Jahn-Teller intersections, classical trajectory method 0-25997  
 nonequilibrium dissoci., Morse oscill. rigid rotator system, master eqn. soln. 0-40682  
 organic ion, excited electronic state correlation with mass-spectral fragmentation pattern 0-45482  
 organic ions, pot. energy profiles for unimol. reactions 0-43210  
 phenoxyl radical dimer, reversible diffusion controlled dissoci., detailed equilib. principle 0-7770  
 polyatomic ions, energy deposition on high-energy collision, angle-resolved mass spectrometry obs. 0-32825  
 polyatomic molecule dissociation, thermochemical study of thermal negative ion production (*Japanese*) 0-50495  
 polyatomic molecule under nonequilibrium conditions, dissoci. kinetics, unimol. decomp. rates 0-11886  
 polyatomic mols., dissoci. reaction path Hamiltonian 0-45486  
 polyatomics, restricted intramolecular vibr. relax. and laser selective effects 0-27992  
 polymer matrix composites, component interaction mass spectrometry investigation (*Russian*) 0-35511  
 polymers, oligomer mass spectral charact. 0-37916  
 propan-1-ol, ion internal energy selection by angle-resolved mass spectrometry 0-53164  
 propane, ion internal energy selection by angle-resolved mass spectrometry 0-53164  
 toluene, 91<sup>2+</sup> ion fragmentation, ion kinetic energy spectrum peaks, collision gas sensitive 0-40679  
 trifluoromethane, D ultrahigh single-step enrichment by CO<sub>2</sub> laser photolysis 0-45527



**molecular dissociation continued**

- $\alpha$ -tropomyosin, specific splitting at cysteine-190, physicochem. study of fragments 0-30647
- unimolecular, master eqns., analytic theory of extrema 0-50841
- unimolecular decay dynamics, pole approx. calcs. 0-35501
- unimolecular dissoc. kinetic energy distrib., photoelectron-photoion coincidence spectrometer for the study of translational energy release distributions 0-11974
- CO, chemisorbed on Rh (111), dissociation probability, isotopic exchange and AES meas. 0-40743
- CO<sup>+</sup>, exploding fast mol. ions, Auger spectra 0-32781
- CO<sub>2</sub>, C 1s<sup>-1</sup>,  $\pi^*$ -state decay, fragment ion relative abundance by electron-ion coincidence technique 0-9743
- CO<sub>2</sub>, valence shell ionic photofragmentation, oscill. strengths, EELS and electron-ion coincidence meas. 0-37879
- CO<sub>2</sub><sup>-</sup>, dissoc.,  $^2\Sigma^+$  state, Wall Porter pot. surface, autodetachment and vibr. level population inversion 0-21275
- CO<sub>2</sub>-N<sub>2</sub>-He, vol. discharge, negative ions effect 0-14956
- CO<sub>2</sub>+inert gas, reactant decomp., rot.-vibr. energy transfer, relax. analytic soln. 0-55650
- CO<sub>2</sub>-(He) discharge, UV-initiated, electron ion recomb. and CO<sub>2</sub> dissoc. 0-44068
- Cr<sub>2</sub>O<sub>3</sub> dissociation in presence of C in Ar, CO and vac. atm., Cr<sub>3</sub>C<sub>2</sub> form. (Russian) 0-35570
- FHF ion, H-bond excited electronic states, CI calc., dissoc. and autoionising states 0-5489
- Fe(CO)<sub>5</sub>+inert gas, dissoc. energy transfer, chemiluminesc. 0-55647
- Fe<sub>2</sub>O<sub>3</sub> phase comp. on equilb. heating to 3300K (Russian) 0-16285
- Gal, AO<sup>+</sup>-XO<sup>+</sup> and BI-XO<sup>+</sup> transitions, isotope shifts, UV and visible spectra obs. 0-53005
- H<sub>2</sub><sup>+</sup> and H<sub>2</sub><sup>+</sup> interactions with thin foils, electronic polarisation wake effects, dissoc. of mol. ions 0-16135
- H<sub>2</sub><sup>+</sup>, collisional dissoc., excited electronic states effects 0-9687
- H<sub>2</sub><sup>+</sup>, ion beam surface interaction, H<sup>+</sup> formation by reson. electron capture 0-40691
- H<sub>2</sub>-H-Ne mixture, positive column characts. and comparison with approx. diffusion theory 0-44025
- H<sub>2</sub>+He<sup>+</sup>, DIM approx. pot. energy surfaces and nonadiabatic coupling 0-23330
- H<sub>2</sub>+He(Ne), gas discharge plasma, H<sub>2</sub> dissoc. excitation, cross section anal. 0-33735
- H<sub>2</sub><sup>+</sup>+CO excited products dissoc., proton transfer dynamics, correl. diagram anal., crossed beam obs. 0-48079
- HCC→H+C=C dissoc., trajectory calcs., random vibr. excitation 0-45491
- HCl, in nonequilb. plasma, electron energy distrib. function and dissoc. kinetics 0-11882
- H<sub>2</sub>O adsorbed on pure Co surfaces, decomp. phenomena (German) 0-26054
- H<sub>2</sub>O dissociation by polynaphthoquinone-SO<sub>2</sub>-I<sub>2</sub> system for H<sub>2</sub> prod. 0-16825
- H<sub>2</sub>O, on Pt(111), identification of adsorbed OH species 0-49509
- H<sub>2</sub>O, Sb-I-Ca process for thermochem. prod. of H<sub>2</sub> 0-16824
- H<sub>2</sub>O, thermochem. prep. of H<sub>2</sub> using S-I cycle 0-16823
- H<sub>2</sub>O, 0-34826
- He-CO<sub>2</sub> atomic C nuclear pumped laser collision processes, output delay 0-38002
- He<sup>+</sup>+CO<sub>2</sub>, dissociative charge exchange kinematics 0-3318
- He<sub>2</sub><sup>2+</sup>, bound excited states, potential energy curves and rovibronic energy, dissociation 0-23327
- HeH<sup>+</sup>, collisional dissoc., excited electronic states effects 0-9687
- Hg halide electrically excited dissociation laser, kinetic processes 0-38013
- Hg<sub>2</sub>, dissociative recomb. and optical transmissions meas. in high press. discharge 0-37816
- HgBr<sub>2</sub>, dissociation laser, elec. excited, kinetic processes 0-48231
- HgBr<sub>2</sub>, dissociative excitation for HgBr laser, extraction efficiency increased by N<sub>2</sub> addition 0-38012
- HgBr<sub>2</sub>, dissociative excitation by inert gas and N<sub>2</sub> metastables, HgBr emission intensity 0-40687
- HgBr<sub>2</sub>/HgBr dissociation laser, oscillator and oscillator-amplifier expts. 0-48232
- I<sub>2</sub>, adsorption on ZnO,  $\gamma$ -irrad. induced centres 0-54513
- I<sub>2</sub>, hydrolysis, reaction rate const. 0-11883
- I<sub>2</sub> fluoresc., Ar<sup>+</sup> laser excited, high resolution and sub-Doppler Fourier transform spectroscopy 0-43089
- InCl disproportionation under influence of high pressure 0-16660
- InX(X<sub>2</sub>)(X<sub>1</sub>), InAlX<sub>4</sub>, X=Cl, Br, Raman spectra, up to 1200K 0-48003
- Kr-Cl<sub>2</sub> mixture, glow discharge positive column, electron energy distrib. and rates of inelastic processes, negative Cl ions form. 0-19632
- LiCl molecular dissoc., obs. by interference method 0-40684
- N<sub>2</sub> adsorbed on W, effect of SIMS sputtering induced recomb. anal. 0-55243
- N<sub>2</sub> adsorbed on W(110) vicinals, step sites as dissoc. centres 0-6642
- N<sub>2</sub><sup>+</sup>, dissociative recombination in ionosphere, rate cont. 0-17435
- N<sub>2</sub><sup>+</sup>, exploding fast mol. ions, Auger spectra 0-32781
- NH<sub>3</sub>, catalytic decomposition of single pulses on W, mol. beam relax. spectrometry 0-21321
- N<sub>2</sub>O, N 1s<sup>-1</sup>,  $\pi^*$ -state decay, fragment ion relative abundance by electron-ion coincidence technique 0-9743
- N<sub>2</sub>O, valence shell ionic photofragmentation, oscill. strengths, EELS and electron-ion coincidence meas. 0-37879
- N<sub>2</sub>O+inert gas, reactant decomp., rot.-vibr. energy transfer, relax. analytic soln. 0-55650
- N<sub>2</sub>O<sub>4</sub>, sound dispersion and velocity mol. dissoc. effects (Russian) 0-1730
- N<sub>2</sub>O<sub>4</sub>→2NO<sub>2</sub>→2NO+O<sub>2</sub>, precipitation of corrosion products in a fractionating column (Russian) 0-25707
- N<sub>2</sub>O<sub>4</sub>→2NO<sub>2</sub>→2NO+O<sub>2</sub>, working fluid for power-producing thermodynamic cycles 0-13536
- Ni(Co)<sub>4</sub>+inert gas, dissoc. energy transfer, chemiluminesc. 0-55647
- NiO-H<sub>2</sub>, interaction with surface, quantum chemical study 0-45549
- O<sub>2</sub>, glow discharge, DC, particle concs. calc. 0-1859
- O<sub>2</sub>, thermal decomposition, vibr.-rot. state depletion, Monte Carlo calc. 0-35506
- O<sub>2</sub><sup>+</sup>, dissociative recombination in auroral region 0-41581
- O<sub>2</sub>+inert gas, reactant decomp., rot.-vibr. energy transfer, relax. analytic soln. 0-55650
- O<sub>2</sub><sup>+</sup>AsF<sub>6</sub><sup>-</sup>, thermal decomposition, Raman spectra study, free radical mechanism 0-55652
- Re<sub>2</sub>(CO)<sub>10</sub> vapour decomposition, for plasma deposited Re films 0-20799
- SF<sub>6</sub>, multiphoton absorpt., energy transfer, dissoc. probability, laser field interaction, classical trajectory approx. 0-37730

**molecular dissociation continued**

- SF<sub>6</sub>, multiple-photon excited, double reson. spectroscopy 0-53030
- SF<sub>6</sub>, photon-enhanced dissociative electron attachment, isotope selectivity 0-18939
- SF<sub>6</sub>+X<sup>-</sup>→SF<sub>5</sub><sup>-</sup>+F+X (X=O, S, F, Br, I), electron affinity of SF<sub>5</sub> radical 0-45495
- Si (111), 7×7 surface, chemisorption of H<sub>2</sub>O 0-10792
- SiH<sub>4</sub>, 1B(1T<sub>2</sub>) pot. energy surface calcs. 0-53085
- SiO<sub>2</sub>, decomposition and reduction, in low temp. plasma jet (German) 0-45499
- UH<sub>3</sub>, UD<sub>3</sub>, dissoc., isotope effect 0-26174

**molecular dissociation energies**

- ab initio effective core pot. method appl. to F<sub>2</sub>, Cl<sub>2</sub> and LiCl 0-32625
- alkali halides, bond order correl. with dissoc. energy 0-32596
- t-butyl cyanide-HF, hydrogen bonded heterodimer, spectroscopic consts. from IR and microwave spectra 0-43039
- chloropentafluoroethane, multiphoton dissoc., crossed laser and mol. beam obs. 0-11908
- cyanomethane-HF, hydrogen bonded heterodimer, spectroscopic consts. from microwave spectrum 0-43038
- diatom product, from diatom+atom, dissoc. energy from reaction cross section 0-16655
- diatomic molecules, Simon-Parr-Finlan potential appls. 0-18785
- diatomic molecules, universal dissoc. energy relationships 0-5493
- formaldehyde, atomisation and bond energies, LMO calc., conjugation contrib. 0-9496
- formyl radical, -d<sub>0</sub>, (-d<sub>1</sub>), first ionis. pot., photoelectron spectrosc. determ. 0-48039
- formyl radical, electronic struct., dissoc. energy and pot. energy surface many body perturbation theory and couple cluster doubles calc. 0-23296
- ground state props., coupled cluster and MBPT methods appl. 0-47881
- Group IA element halides, bond order correl. with dissoc. energy 0-32596
- Group IIIA element halides, bond order correl. with dissoc. energy 0-32596
- inert gas complexes spectroscopic data, geometry, pot. energy curve, dissoc. energy, equilb. internuclear distance, determ. 0-53018
- infrared multiphoton dissociation of molecules, review (Japanese) 0-11885
- AlO radical, ground state dissoc. energy 0-53159
- AsF<sub>3</sub>, pot. energy curves and dissoc. energy, Hulbert-Hirschfelder calc. 0-30210
- Ca<sub>2</sub>, new ground state, photolum. obs. vibr. consts., dissoc. energy 0-5576
- CuO, ab initio HF-MC-SCF with GTO basis set, dissoc. energy and bond length 0-47890
- H<sub>2</sub>, Compton profile, electronic energy calc. 0-37822
- H<sub>2</sub><sup>+</sup>, high (10<sup>9</sup> G) mag. fields, dissoc. energy, electron binding energy and equilb. separation 0-52910
- H<sub>2</sub><sup>+</sup>, SCF multiple scatt. calc. 0-916
- HCN...HF, hydrogen bonded heterodimer, spectroscopic consts. from microwave spectrum 0-43037
- HN<sub>3</sub>, ground 'A' state, SCF and CI calcs., conform., geom., vibr. freqs. and dissoc. 0-18806
- H<sub>2</sub>O, Compton profile, electronic energy calc. 0-37822
- Hg<sub>2</sub><sup>+</sup>, electronic struct. and photoabsorpt. calcs. 0-27932
- LaIr(g), thermodynamic stability, high-temp. mass spectra obs. 0-7781
- LiAlH<sub>4</sub>, LiBH<sub>4</sub>, ab initio calc. of geom. struct., charge distrib., bonding and pot. energy surfaces 0-18796
- NF, pot. energy curves and dissoc. energy, Hulbert-Hirschfelder calc. 0-30210
- NO<sup>+</sup> ground state mol. consts., from NO X<sup>2</sup>Π( $\nu$ "=0) UPS obs. 0-14177
- NOH, groundstate electronic struct., MRD CI calc., dissoc. energy, isomerisation energy 0-14088
- NaAlH<sub>4</sub>, NaBH<sub>4</sub>, ab initio calc. of geom. struct., charge distrib., bonding and pot. energy surfaces 0-18796
- Ne<sub>2</sub><sup>+</sup> formation and destruction in Townsend discharges 0-38747
- OH, Simon-Parr-Finlan potential appls. 0-18785
- OH<sup>+</sup>, Simon-Parr-Finlan potential appls. 0-18785
- P<sub>2</sub><sup>+</sup>, electronic states pot. energy curves, dissoc. energy, ionisation pot., curve fitting 0-32796
- PF, (PF<sup>+</sup>), pot. energy curves and dissoc. energy, Hulbert-Hirschfelder calc. 0-30210
- SbF<sub>3</sub>, pot. energy curves and dissoc. energy, Hulbert-Hirschfelder calc. 0-30210

**molecular electron correlations**

- ab initio CI pot. curves, mol. wavefunctions and vibr. freqs. comparison of methods 0-27956
- acetylene, core ionised, core-excited and shake-up states, ab initio MRD-CI methods 0-42950
- adiabatic CI pot. surface LCAO calc., gradient determ., mol. dynamics 0-48056
- benzene, noncrossing and degeneracy in Hubbard models 0-14096
- benzene, UV photoelectron spectra, valence electron shake up approx. methods 0-18788
- carbenes, triplet state g-tensors and hyperfine coupling tensors 0-52895
- carbonyls, electric polarisability, in excited singlet and triplet states (Bulgarian) 0-52897
- chain molecule excitation correlator at local relaxation (Russian) 0-14090
- chemical bonds, RPA calcs., ground state correlation energies 0-47847
- CI methods for improving unrestricted Hartree-Fock spin densities 0-32617
- cluster expansion, electron correlations, SAC and SAC CI calcs. 0-18802
- cluster expansion electron correlations, SAC and SAC CI theories 0-18801
- complete active space method, comparison of super CI and Newton Raphson scheme 0-47904
- complex electron configurations, quasispin method, mixing configurations 0-42953
- configuration interaction calc., atoms and atomic complexes confined in spherical boxes, Hartree-Fock-Slater potential 0-47898
- configuration interactions, appl. of unitary group methods 0-27958
- coronene, excited state Faraday values mag. circular dichroism spectra and MO CI calcs. 0-18877
- correlated II-electron systems, mol. interactions, linear response theory 0-53090



## molecular electron correlations continued

correlation energy, many-body Rayleigh-Schrodinger perturbation theory calcs., exclusion principle violation 0-52890  
 coupled cluster approach, open (closed) shell systems 0-47842  
 coupling constants in direct CI method 0-9516  
 cyclobutadiene, noncrossing and degeneracy in Hubbard models 0-14096  
 cyclopentadienyl radical, pot. surface and vibronic states, ab initio CI calcs. 0-47897  
 density functional calculations for atoms, molecules and clusters 0-47850  
 dihydrophenazine derivatives, in 3-methylpentane (ethanol) (PMMA), radiationless processes, temp. depend. 0-43087  
 dihydroxycarbene, singlet and triplet state rot. pot. surfaces 0-32627  
 direct CI method, Hartree-Fock interacting space for doublets, quartets and open-shell singlets 0-52889  
 direct CI method generalisation, graphical unitary group approach 0-47900  
 electric dipole allowed transitions, amplified sector rule based on electron correlation 0-5523  
 equations of motion, Green's function methods and config. interaction methods, comparison, appl. and anal. 0-47841  
 equations of motion Green's function methods, higher order terms, ionisation pots. 0-52891  
 equations of motion Green's function methods, higher order terms, ionisation pots., CI comparison 0-52892  
 ethane, nuclear spin-spin coupling consts., vicinal proton-proton coupling calcs. 0-32737  
 ethylene, core ionised, core-excited and shake-up states, ab initio MRD-CI methods 0-42950  
 ethylene, planar dissociation, electronic rearrangement, states, bonds, ab initio multiconfigurational SCF calcs. 0-27937  
 ethylene, quasidegeneracy and effective Hamiltonians, canonical transformation cluster expansion formalism 0-52888  
 ethylene, UV photoelectron spectra, valence electron shake up approx. methods 0-18788  
 ethylene V state, ab initio study of spatial extension 0-27952  
 formaldehyde, adiabatic CI pot. surface LCAO calc., gradient determ., mol. dynamics 0-48056  
 formaldehyde, triplet state g-tensors and hyperfine coupling tensors 0-52895  
 free radicals, RHF CI INDO spin density calc. 0-919  
 geometry optimisation with explicit inclusion of electron correl. 0-37748  
 ground state,  $n\pi^*$ -excited states (Bulgarian) 0-32614  
 ground state props., coupled cluster and MBPT methods appl. 0-47881  
 Group IV-VI diatomic molecules, He(I) photoelectron spectra, calcs. 0-1023  
 hydrocarbons, electric polarisability, in excited singlet and triplet states (Bulgarian) 0-52897  
 hyperpolarisabilities, HF calc. with correlation method, appl. to HF mol. 0-23342  
 intermolecular forces, ab initio calcs. applicability and accuracy 0-18898  
 local force densities and stress tensors, density functional theory 0-18781  
 local-density theory of multiplet structure 0-18776  
 many body perturbation theory fourth order calc. of correl. energy 0-14087  
 many electron correl. problem, unitary group approach via spin algebra graphical methods 0-47902  
 MCSCF method improvement 0-52857  
 metalloporphyrins, reson. Raman spectra, intra- and inter-manifold couplings interference 0-28020  
 methane, elastic and inelastic electron scatt. differential cross section, obs. and calc., struct., binding energy 0-28110  
 methyl formate( $-d_1, d_3, d_4$ ), mol. vibr. spectrum, struct., beginning with PCIO calc. (French) 0-23401  
 methylene +  $H_2$  → methane, ab initio CI calc. on SCF level, insertion reaction min. energy path 0-7774  
 methylene peroxide, multiconfig. SCF CI calcs. 0-18803  
 MNDO semiempirical calcs. accuracy rel. to current MO methods 0-47893  
 molecules, natural orbitals, Brillouin-Levy-Berthier theorem, multiconfigurational SCF optimisation 0-27936  
 nitrosomethane, ground state and nonvertical  $n\pi^*$  excitation energy calcs. 0-18804  
 nuclear spin-spin coupling consts., finite perturbation-CI calcs. 0-5563  
 orbit-orbit interaction, new tensor expansion; matrix and graphical forms 0-14064  
 organic system, nonlinear second-order optical susceptibility 0-9947  
 ozone,  $^1A_1$  ground state, dipole moment function, ab initio SCF and CI calcs. 0-32628  
 perturbation theory, diagrammatic, triply excited state contrib., water appl. 0-18774  
 phospholipid inter- and intra-molecular interactions, PCIOCC and pot. function calc. 0-3570  
 photosynthetically relevant mols., electronic structural props. 0-16902  
 polar mol. anion ab initio ground state pot. energy surfaces calc. 0-47923  
 polar molecule, excited state MCSCF wave functions, BeO appl. 0-47916  
 polarisability, scaling and Pade approximants, many-body perturbation theory 0-42952  
 polarization Green's function with multiconfiguration self-consistent-field reference states 0-37724  
 polymeric chains and Mott insulators, similarities w.r.t. electronic correl., AMO method (French) 0-24775  
 scaling and Pade approximants, rel. to perturbation series higher-order terms 0-5487  
 TCNQ dimers, extended Huckel hamiltonian supermol. CNDOS calcs. 0-27953  
 tetrafluoromethane, elastic and inelastic electron scatt. differential cross section, obs. and calc., struct., binding energy 0-28110  
 transition metal dihydrides, gas phase geometrical struct. calcs. 0-42951  
 transition metal nitrosyls, appl. of HF and CI calcs. 0-9513  
 triphenylene, excited state Faraday values mag. circular dichroism spectra and MO CI calcs. 0-18877  
 truncated CI calcs. 0-27954  
 two-electron ions, ground state, quadratic Stark effect 0-37775  
 UHFS model, CI, CC, and MBPT approaches, appl. to weak  $\delta$ - $\delta^*$  bonds and  $\delta$ - $\delta^*$  excitation 0-32585  
 unitary group generators and permutations, CI matrix elements, algebraic method 0-37725  
 unitary group generators and permutations, CI matrix elements, graphical method 0-37726  
 unitary group irreducible representation subduction coeffs. 0-37723

## molecular electron correlations continued

variational description, loop driven graphical unitary group approach 0-47903  
 water, liq., structure and props., minimal basis set description 0-6347  
 $AlH^+$  radical cation, EPR matrix isolation obs., hyperfine components calcs. 0-14158  
 Ar XV, wavefunctions and oscill. strengths, CI calcs. 0-23317  
 $BH_3^+$   $^1\Sigma^+$  ground state, mag. susceptibility, paramag. contrib., large config. interaction wave function calcs. 0-47899  
 $BH_3$  PE curve, spectroscopic consts., perturbation theory appl. 0-23341  
 BeH radical, hyperfine splitting const., electronic energy, UHF-type, CCI calcs. 0-52909  
 $C_2$ ,  $^3\Pi_u$  states, large CI wavefunctions, non-adiabatic coupling matrix elements 0-37744  
 $CH_2^+$ ,  $^4A_2$  states, large CI wavefunctions, non-adiabatic coupling matrix elements 0-37744  
 $CN^+$ , lower states, pot. energy curves, equilib. distances SCF CI calcs. 0-27957  
 $C_2N_2$ , satellite struct. of electron spectra, CI and vibronic coupling, dynamical calc. 0-53044  
 CO, one-electron props., SCF and CI calcs. 0-27951  
 $CO+N_2$ , electronically inelastic collision, distorted wave calc. and pot. energy curve 0-9709  
 $CO_2$ , elastic and inelastic electron scatt. differential cross section, obs. and calc., struct., binding energy 0-28110  
 Ca XVII, wavefunctions and oscill. strengths, CI calcs. 0-23317  
 $D_3^+$ , ab initio vibr. intervals and vibr. freq. refinement 0-47968  
 $F_2$ , PE curve, spectroscopic consts., perturbation theory appl. 0-23341  
 FHF ion, H-bond excited electronic states, CI calc., dissoci. and autoionising states 0-5489  
 Fe XXIII, wavefunctions and oscill. strengths, CI calcs. 0-23317  
 $H_2$ , atoms-in-molecules theory, non-Hermitian formulation 0-9517  
 $H_2$ , electron correl. as rot. polarisation, Heitler-London-Rosen calc., for teacher 0-4492  
 $H_2$ , second order props., dipole polarisability nucl. coupling, fast CI method 0-27950  
 $H_3^+$ , ab initio vibr. intervals and vibr. freq. refinement 0-47968  
 HCCN, a cyanocarbene, geom. struct., electron correl. effects 0-1077  
 $HCN^+$ , A and B  $^2\Sigma^+$  states, pot. surfaces, ab initio SCF calcs. 0-27959  
 HF, Auger spectra, correl. effects, energies and wavefunctions, ab initio CI calc. 0-14125  
 $HN_3$ , ground  $^1A'$  state, SCF and CI calcs., conform., geom., vibr. freqs. and dissoci. 0-18806  
 HNO, low-lying states, pot. energy curves 0-9533  
 $H_2O$ , ground state ionis. pots., generalized Mo theory 0-52907  
 $H_2O$ , KLL Auger electron spectrum, semi-internal correl. 0-48038  
 $H_2O$ , many body perturbation theory fourth order calc. of correl. energy 0-14087  
 $HeH^+$ , excited states, variable screening models, natural spin orbital analysis of wave functions 0-37747  
 $Li_3$ , second virial coeffs., Konowalow MCSCF potential calcs. 0-23312  
 $LiF^+$ , ground and excited states, ab initio calcs. single config. and multiconfig. SCF calcs. 0-52873  
 $LiH$ , many body perturbation theory fourth order calc. of correl. energy 0-14087  
 $LiH$ , one electron props.,  $X\alpha$  multiple scattering wave functions 0-42945  
 Mg IX, wavefunctions and oscill. strengths, CI calcs. 0-23317  
 $MgH^+$ , CI pot. curves and cross sections for lowest singlet states 0-23343  
 $N_2$ , correlated electron density using AHF GTO wavefunctions 0-23313  
 $N_2$ , elastic and inelastic electron scatt. differential cross section, obs. and calc., struct., binding energy 0-28109  
 $N_2$ , ground state ionis. pots., generalized Mo theory 0-52907  
 $N_2$ , one-electron props., polarisabilities and polarisability derivatives, SCF and CI calcs. 0-37746  
 $N_2$ , PE curve, spectroscopic consts., perturbation theory appl. 0-23341  
 $NH_3$ , first triplet state, photodissoc. and Rydbergisation investig. 0-53067  
 $NH_3$ , lowest triplet state geometry, SCF and CEPA-PNO calc. 0-914  
 $NH_3+2H_2$ , triplet  $n3S$  Rydberg state, ab initio UHF CI SCF calc. 0-53095  
 $N_2H_2$ , model rearrangement system, electron correlation and basis set effects 0-3317  
 $NH_4Cl$ , gas  $^1A_1$  ground state, pot. surface 0-32626  
 $NH_2(X^2B_1)$  radical, and  $ND_2$ , ionisation pot., vibr. anal., ab initio calcs. and vacuum UPS obs. 0-53047  
 $NO_2$ , direct CI calcs. 0-52889  
 $NO_2^-$ , direct CI calcs. 0-52889  
 $NOH$ , groundstate electronic struct., MRD CI calc., dissoci. energy, isomerisation energy 0-14088  
 $O_2$ ,  $^3\Pi_u$  states, large CI wavefunctions, non-adiabatic coupling matrix elements 0-37744  
 $O_2^+$ , electron impact dissoci. recomb., pot. energy curves calcs. 0-53150  
 $OH+H_2$ , pot. energy surface, barrier heights and transition state geometry, POL-CI calc. 0-55649  
 $O(^1P, ^1D)+H_2(^1\Sigma_g^+)-H_2O$ , potential energy surfaces, extended basis first-order CI study 0-7776  
 $O(^1P)+H_2-OH+H$ , potential energy surface, theory 0-45492  
 $SH_3^+$  geometry and inversion barrier, basis set depend. 0-921  
 $SO$ , low lying bound mol. electronic states, SCFCI calc. 0-23314  
 $SO_2$ ,  $2^1A'$  state, electron correl. variational description, loop driven graphical unitary group approach 0-47903  
 Si XI, wavefunctions and oscill. strengths, CI calcs. 0-23317

## molecular electron impact dissociation

aliphatic perfluorocarbons, electron attachment, fragmentation 0-12 eV 0-5618  
 alkali halides, electron stimulated dissoci. 0-34301  
 discharge, dissoci. on bombardment by low energy electrons 0-43845  
 ethane,  $H^+$ ,  $H_2^+$ , and  $H_3^+$  kinetic energy distrib., electron impact dissoci. ionisation, time of flight mass spectra 0-32843  
 ethanol,  $H^+$ ,  $H_2^+$ , and  $H_3^+$  kinetic energy distrib., electron impact dissoci. ionisation, time of flight mass spectra 0-32843  
 inert gas-halide lasers, halide mol. negative ion prod. rates 0-18938  
 metal oxides, electron stimulated dissoci. 0-34301  
 methane,  $H^+$ ,  $H_2^+$ , and  $H_3^+$  kinetic energy distrib., electron impact dissoci. ionisation, time of flight mass spectra 0-32843  
 methane and methane- $d_4$ , low energy electron impact dissoci. autoionisation 0-9744  
 methanol and deuterates,  $H^+$ ,  $H_2^+$ , and  $H_3^+$  kinetic energy distrib., electron impact dissoci. ionisation, time of flight mass spectra 0-32843



**molecular electron impact dissociation continued**

- propylene, dissoc. on bombardment by low energy electrons 0-43845  
 propylene, electron impact ionisation and dissoc. 0-37894  
 CO discharge plasma, electron energy distrib. and kinetic coeffs., vibr. excited mols. 0-43868  
 CO<sub>2</sub>, electron swarm parameters for high E/N, Monte Carlo simulation 0-19548  
 D<sub>2</sub>, electron dissociative attachment rates, rot. (vibr.) excitation depend., in plasma 0-43848  
 D<sub>2</sub>, electron impact, threshold excitation and predissoc., electron-photon coincidence meas. 0-18941  
 D<sub>2</sub>, electron impact dissociative ionisation near  $2\Sigma_g^+$  state dissoc. threshold 0-43197  
 F<sub>2</sub>, electron dissociative attachment rate consts. at 300 and 500K, in discharge plasma 0-43849  
 H<sub>2</sub>, electron dissociative attachment rates, rot. (vibr.) excitation depend., in plasma 0-43848  
 H<sub>2</sub>, electron impact, threshold excitation and predissoc., electron-photon coincidence meas. 0-18941  
 H<sub>2</sub>, electron impact dissoc. excitation, cross sections, mechanisms 0-37895  
 H<sub>2</sub>, electron impact dissociative ionisation near  $2\Sigma_g^+$  state dissoc. threshold of H<sub>2</sub> 0-43197  
 H<sub>2</sub> glow discharge with variable degrees of dissoc., diffusion theory of positive column 0-44018  
 H<sub>2</sub><sup>+</sup>, electron cooling through resonant collisions 0-32845  
 H<sub>2</sub><sup>+</sup>, H<sup>-</sup> production cross section 0-5628  
 H<sub>2</sub>(-He), H production at 10 torr in pulsed discharge 0-9748  
 HCN, and DCN, electron impact dissoc., product H(n=4) kinetic energy distrib., emission obs. 0-28106  
 HCl, controlled electron impact, excited H product translational energy distrib. 0-14238  
 H<sub>2</sub>(D<sub>2</sub>), dissociative electron attachment and vibr. excitation, low-energy 0-23565  
 H<sub>2</sub>O, slow electron scatt., rigid mol. model with exchange and polarisation, vibr. excitation, dissoc. attachment 0-43194  
 H<sub>2</sub>O vapour, ionis. coeffs. and dissociative electron attachment 0-43833  
 H<sub>2</sub>S, slow electron scatt., rigid mol. model with exchange and polarisation, vibr. excitation, dissoc. attachment 0-43194  
 N<sub>2</sub>, low energy electron impact dissociative ionis., N<sup>2+</sup> form. and energy distrib. 0-5626  
 N<sub>2</sub>, rel. to O<sub>3</sub> generation in air-fed ozonisers 0-3323  
 NF<sub>3</sub>, electron dissociative attachment rate consts. at 300 and 500K, in discharge plasma 0-43849  
 NH<sub>3</sub>, ionis. coeffs. and dissociative electron attachment 0-43833  
 Ne<sub>2</sub><sup>+</sup>, dissoc. recomb. in afterglow, prod. of Ne 2p atoms 0-43855  
 O<sub>2</sub>, discharge, conditions, self-consistent electron energy distrib. functions calc. 0-38746  
 O<sub>2</sub>, low energy electron impact dissociative ionis., O<sup>2+</sup> form. and energy distrib. 0-5626  
 O<sub>2</sub>, rel. to O<sub>3</sub> generation in air-fed ozonisers 0-3323  
 O<sub>2</sub><sup>+</sup>, electron impact dissoc. recomb., pot. energy curves calcs. 0-53150  
 O<sub>3</sub> generation in air-fed ozonisers 0-3323  
 SF<sub>6</sub>, photon-enhanced dissociative electron attachment 0-9749  
 SF<sub>6</sub>, photon-enhanced dissociative electron attachment, isotope selectivity 0-18939  
 SO<sub>2</sub>, electron attachment processes investig. and mobility of negative ions 0-38518

**molecular electron impact excitation**

- see also electron spectra*  
 alkyl substituted diacetylene radical cations, optical emission and photoelectron spectra, fragmentation decay 0-53004  
 benzene, elec. dipole forbidden states, high resolution electron impact obs. 0-43195  
 Born partial wave amplitude for any electrostatic multipole field 0-53128  
 diatomic molecule electron scatt., iterative static exchange method 0-53155  
 electron impact spectroscopy, low-energy aspects, book contrib. 0-14243  
 electronic-rotational molecular states, electron-impact excitation, cross sections and rate consts. 0-14241  
 ethylene(-d<sub>4</sub>), Rydberg states assignments, electron energy loss spectra 0-53153  
 glow discharge in diatomic molecular gas, electronic excitation rate, vibr. temp. influence 0-19633  
 haloacetylene cations, electron impact excitation A—X band system assignment 0-32766  
 high-energy electron impact spectroscopy, book contrib. 0-14244  
 inert gas excited molecules formation, rate const. determ. 0-9859  
 ion+electron scatt., static exchange approx. Schwinger variational principle, photoionisation cross section 0-43192  
 K-shell electrons excitation with high energy resolution, review 0-37899  
 methane, elastic and inelastic electron scatt. differential cross section, obs. and calc., struct., binding energy 0-28110  
 methane, large angle elastic and inelastic electron scatt. differential cross section, exchange corrections 0-28111  
 methane, slow electron scatt., rigid mol. model with exchange and polarisation 0-43194  
 molecular vibration excitation on resonant electron scatt., time-perturbation method (Russian) 0-14242  
 molecules, rot. and vibr. excitation, methods for calcs. 0-17721  
 partial resonance widths, Siegert eigenvalues, basis-set calc. 0-37880  
 polar molecule electron scatt. at intermediate J, closed-form treatment 0-32846  
 polar molecule electron scattering, exam. of models 0-37898  
 positive column of glow discharge of electronegative gas, molecular excitation and ionisation by electron collisions 0-49031  
 rotated coordinate method use, rel. to stabilisation method 0-37845  
 tetrafluoromethane, elastic and inelastic electron scatt. differential cross section, obs. and calc., struct., binding energy 0-28110  
 vibrational and rotational excitation, review 0-32847  
 vibrational excitation, shape-reson.-enhanced, 10-40 eV, appl. to CO<sub>2</sub> 0-5629  
 water vapour electron stopping power and energy degradation 0-23276  
 CH<sup>+</sup> polar molecular ion, electron vibr.-rot. excitation (Russian) 0-1053  
 CO, b<sup>2</sup> $\Sigma^+$  state excitation, low-energy electron impact,  $\nu=3$  level lifetime 0-1072  
 CO discharge plasma, electron energy distrib. and kinetic coeffs., ground-state mols. 0-43867  
 CO discharge plasma, electron energy distrib. and kinetic coeffs., vibr. excited mols. 0-43868

**molecular electron impact excitation continued**

- CO, electron impact vibrational excitation, 1-4 eV 0-9747  
 CO, K-shell, excitation and ionisation, vibr. struct., electron energy loss spectra obs. 0-18943  
 CO+ZZ 0-9745  
 CO<sub>2</sub>, elastic and inelastic electron scatt. differential cross section, obs. and calc., struct., binding energy 0-28110  
 CO<sub>2</sub>, large angle elastic and inelastic electron scatt. differential cross section, exchange corrections 0-28111  
 CO<sub>2</sub>, low energy electron (positron) collisions, ab initio adiabatic polarisation pots. 0-14240  
 CO<sub>2</sub>, low energy electron scatt. cross sections, vibr. excitation, Boltzmann eqn. 0-18942  
 CO<sub>2</sub>, vibr. excitation threshold struct., low-energy electron scatt. 0-5625  
 CO<sub>2</sub>+ZZ 0-9745  
 D<sub>2</sub>, electron impact, threshold excitation and predissoc., electron-photon coincidence meas. 0-18941  
 F<sub>2</sub>, electron energy loss spectra, 0-17 eV, 5-140°, repulsive valence states excitation 0-32844  
 H<sub>2</sub> (D<sub>2</sub>) mol. bands, electron impact excitation, rot. transitions, cross sections in plasma 0-37896  
 H<sub>2</sub>, elastic and rot. excitation, effective pot. theory 0-5627  
 H<sub>2</sub>, electron impact, threshold excitation and predissoc., electron-photon coincidence meas. 0-18941  
 H<sub>2</sub>, electron impact dissoc. excitation, cross sections, mechanisms 0-37895  
 H<sub>2</sub>, electron impact excitation,  $\nu \leq 4$  vibr. levels, theory 0-18940  
 H<sub>2</sub>, electronic stopping power calcs. 0-2104  
 H<sub>2</sub>, metastable level electron impact excitation, resonances (Russian) 0-43198  
 H<sub>2</sub><sup>+</sup>, electron cooling through resonant collisions 0-32845  
 H<sub>2</sub><sup>+</sup>, electron scatt., Schwinger variational principle appl. 0-48086  
 HF, electron scatt. cross section, vibr. and rot. excitation, close coupling calc. 0-53154  
 HN<sub>3</sub> IR multiphonon dissociation with electronic excitation 0-11934  
 H<sub>2</sub>O, slow electron scatt., rigid mol. model with exchange and polarisation 0-43194  
 H<sub>2</sub>S, slow electron scatt., rigid mol. model with exchange and polarisation 0-43194  
<sup>2</sup>HN<sub>3</sub> IR multiphonon dissociation with electronic excitation 0-11934  
 KrF, electron impact deexcitation cross sections and rate consts. calcs. 0-32848  
 KrF, excimer, electron impact deexcitation, low energy cross-sections and rate consts. 0-1071  
 KrF linac-excited gas mixture, UV fluoresc. meas. 0-28216  
 Li-like ion, in plasma, ion electron collisional radiative recomb. coeffs., bottleneck calc. 0-53942  
 N<sub>2</sub>, C<sup>2</sup> $\Pi_u$ -state, electron impact excitation, low energy 0-9746  
 N<sub>2</sub>, diffuse plasma, population densities of triplet states, correl. with electron impact processes 0-43966  
 N<sub>2</sub>, discharge, excitation efficiency of rot. and vibr. levels, heating due to elastic collisions and relax. 0-38751  
 N<sub>2</sub>, elastic and inelastic electron scatt. differential cross section, obs. and calc., struct., binding energy 0-28109  
 N<sub>2</sub>, electron impact, reson. vibr. excitation, ab initio R matrix calc. 0-32842  
 N<sub>2</sub>, electron impact enhanced vibr. excitation, continuum multiple scatt. model with Hara exchange approx. 0-43196  
 N<sub>2</sub>, electron impact excitation cross-sections for B<sup>3</sup> $\Pi_g$ , C<sup>3</sup> $\Pi_u$  and E<sup>3</sup> $\Omega_g^+$  states 0-1073  
 N<sub>2</sub>, electron impact rot. and vibr. excitation, elastic scatt., close coupling and Born approx. 0-28108  
 N<sub>2</sub>, electron scattering, local-exchange approx. for intermediate-energy-differential cross sections 0-48094  
 N<sub>2</sub>, K-shell, excitation and ionisation, vibr. struct., electron energy loss spectra obs. 0-18943  
 N<sub>2</sub>, large angle elastic and inelastic electron scatt. differential cross section, exchange corrections 0-28111  
 N<sub>2</sub> laser UV-IR pulse time lag theory (Japanese) 0-14325  
 N<sub>2</sub>, low energy electron (positron) collisions, ab initio adiabatic polarisation pots. 0-14240  
 N<sub>2</sub>, metastable level electron impact excitation, resonances (Russian) 0-43198  
 N<sub>2</sub>, N K-shell excitation, high-resolution electron energy loss spectra 0-53152  
 N<sub>2</sub> plasma, electronic excitation levels in gas-discharge 0-24280  
 N<sub>2</sub><sup>+</sup>, A- and B-states interactions, time-resolved obs. 0-18862  
 N<sub>2</sub>+Ar+POPOP, electron beam excited, energy transfer mechanisms 0-23497  
 N<sub>2</sub>+H<sup>+</sup>(e), vibrational N<sub>2</sub><sup>+</sup> excitation (Russian) 0-53156  
 NO, N K-shell excitation, high-resolution electron energy loss spectra 0-53152  
 N<sub>2</sub>O, N K-shell excitation, high-resolution electron energy loss spectra 0-53152  
 O<sub>2</sub>, electron impact vibr. excitation, direct and stepwise, rate coeffs. 0-5630  
 O<sub>2</sub>, K-shell, excitation and ionisation, vibr. struct., electron energy loss spectra obs. 0-18943  
 O<sub>2</sub>, metastable level electron impact excitation, resonances (Russian) 0-43198  
 SF<sub>6</sub>, electronic props., (e,2e) spectrosc. obs. 0-5527  
 SF<sub>6</sub>, resonant single-photon dissoc. route using prelim. electron excitation 0-9662  
 Xe<sub>2</sub>, e-beam excited, 193 nm absorpt. studies 0-43323  
 Xe<sub>2</sub>, electron beam excited, 193 nm absorpt. meas. rel. to 172 nm laser pulse termination 0-28200  
 Xe<sub>2</sub>, laser performance for atm. press. and microsecond electron beam excitation 0-28199  
 Xe<sub>2</sub>, performance as photolytic driver at low electron beam excitation rates 0-32963  
 XeCl molecule excited by electron beam, stimulated emission obs. 0-32966  
 XeF, electron impact deexcitation cross sections and rate consts. calcs. 0-32848  
 XeF, excimer, electron impact deexcitation, low energy cross-sections and rate consts. 0-1071  
 XeF linac-excited gas mixture, UV fluoresc. meas. 0-28216



**molecular electron impact ionisation***see also electron spectra*

- acetylene, electron momentum distribns. in  $\pi$  orbitals from (e,2e) expts. 0-14239
- air, electron backscattering coeffs., 100 eV to 5 keV 0-9750
- butadiene, electron momentum distribns. in  $\pi$  orbitals from (e,2e) expts. 0-14239
- cyclopropane, electron momentum distribns. in  $\pi$  orbitals from (e,2e) expts. 0-14239
- electron attachment, high temperature processes, chemical modelling 0-18937
- ethylene, electron momentum distribns. in  $\pi$  orbitals from (e,2e) expts. 0-14239
- methane, electron transmission function and mean energy per ion pair, obs. 0-23566
- positive column of glow discharge of electronegative gas, molecular excitation and ionisation by electron collisions 0-49031
- propylene, electron impact ionisation and dissociation 0-37894
- tissue equivalent gas electron transmission function and mean energy per ion pair, obs. 0-23566
- transient species, vacuum UPS, book contrib. 0-14178
- water vapour electron stopping power and energy degradation 0-23276
- Ar, electron transmission function and mean energy per ion pair, obs. 0-23566
- AsBr<sub>3</sub>, electron impact positive ion form., appearance energy obs. 0-53151
- AsCl<sub>3</sub>, electron impact positive ion form., appearance energy obs. 0-53151
- AsF<sub>3</sub>(AsF<sub>5</sub>), electron impact positive ion form., appearance energy obs. 0-53151
- CO discharge plasma, electron energy distrib. and kinetic coeffs., vibr. excited mols. 0-43868
- CO, K-shell, excitation and ionisation, vibr. struct., electron energy loss spectra obs. 0-18943
- CO<sub>2</sub>, electron impact, 50-400 eV, secondary electrons double differential cross section 0-37897
- CO<sub>2</sub>, electron swarm parameters for high E/N, Monte Carlo simulation 0-19548
- CO<sub>2</sub>, electron transmission function and mean energy per ion pair, obs. 0-23566
- D<sub>2</sub>, electron impact dissociative ionisation near  $2\Sigma_g^+$  state dissociation threshold 0-43197
- H<sub>2</sub>, electron impact dissociative ionisation near  $2\Sigma_g^+$  state dissociation threshold of H<sub>2</sub> 0-43197
- H<sub>2</sub><sup>+</sup>, electron cooling through resonant collisions 0-32845
- HF, valence orbitals momentum distribns., (e, 2e) binding energy spectra 0-14237
- H<sub>2</sub>O vapour, ionis. coeffs. and dissociative electron attachment 0-43833
- H<sub>2</sub>S, valence electron ionisation and momentum distribns. 0-28107
- He flow discharge, intermediate press., positive column conc. of ions and metastables 0-44017
- N<sub>2</sub>, electron backscattering coeffs., 100 eV to 5 keV 0-9750
- N<sub>2</sub>, electron impact, electron distrib. function in laser radiation field, vibr. excitation influence 0-28112
- N<sub>2</sub>, electron swarm parameters for high E/N, Monte Carlo simulation 0-19548
- N<sub>2</sub>, K-shell, excitation and ionisation, vibr. struct., electron energy loss spectra obs. 0-18943
- N<sub>2</sub>, low energy electron impact dissociative ionis., N<sub>2</sub><sup>2+</sup> form. and energy distrib. 0-5626
- NH<sub>3</sub>, ionis. coeffs. and dissociative electron attachment 0-43833
- Nz, electron transmission function and mean energy per ion pair, obs. 0-23566
- O, discharge plasma, metastable states role, two-step ionisation, electron densities and transition pts. 0-44019
- O<sub>2</sub>, electron backscattering coeffs., 100 eV to 5 keV 0-9750
- O<sub>2</sub>, K-shell, excitation and ionisation, vibr. struct., electron energy loss spectra obs. 0-18943
- O<sub>2</sub>, low energy electron impact dissociative ionis., O<sub>2</sub><sup>2+</sup> form. and energy distrib. 0-5626
- SF<sub>6</sub>, pure and mixtures, dielec. props., ionisation and attachment coeffs. 0-33726

**molecular electron scattering** *see elastic scattering of electrons by atoms and molecules; molecular electron impact dissociation; molecular electron impact excitation; molecular electron impact ionisation*

**molecular electronic states***see also charge transfer states; molecular metastable states; triplet state*

- ab initio CI pot. curves, mol. wavefunctions and vibr. freqs. comparison of methods 0-27956
- acetophenone enolate anion radicals, substituted, electron photodetachment cross sections, reson. states 0-1030
- adenine tautomers, relative stabilities, nonempirical MO calcs. 0-21442
- alkali bromides, photofragment spectra, 266 nm, bond energies and excited state symmetries 0-53072
- alkali iodides, photofragment spectra, bond energies and excited state symmetries 0-5589
- aromatic hydrocarbon in soln., excited electronic state vibr. relax., time resolved fluoresc. 0-48024
- aromatic hydrocarbons, singlet-triplet conversion at low temp. 0-43094
- azobenzene, derivatives, photoelectron spectra, ionisation pot., electronic struct. determ. 0-1024
- benzene,  $\pi$  electron system, excitation energy, appl. of MBPT 0-52876
- benzene, and methyl derivatives, <sup>1</sup>E<sub>1u</sub> N-V state mag. moments, MCD obs. 0-23575
- benzene, elec. dipole forbidden states, high resolution electron impact obs. 0-43195
- benzenetricarbonylchromium, neutron inelastic scatt. spectrum and valence force field 0-48096
- broadening, inhomogeneous and homogeneous, of optical and ODMR transitions in solids 0-32750
- chiral molecules, prochiral centres, electronic and structural chirality 0-30220
- chlorophyll photo-oxidation, role of singlet-excited and triplet states 0-51156
- CO, in glow flow discharge, electronic states, excitation mechanism 0-53040
- Combination of Atomic Boxes MO model, development and testing 0-32592
- complex molecules appl. to electronics, liquid crystals and plastics 0-6355

**molecular electronic states continued**

- conjugated cpds., aromaticity determ. by topological reson. energy method 0-42915
- cyanogen fluoride, fund., hot bands, laser microwave two photon and double reson. spectroscopy 0-32752
- d-orbital basis functions role in electronic struct. description of systems containing Si, P, S and Cl 0-9484
- degenerate electron states, electron interaction with doubly degenerate vibr., optical transitions, semiclassical approx. 0-27927
- density functional calculations for atoms, molecules and clusters 0-47850
- diatomic representation of one-dimens. diatomic mols. 0-23285
- diatomic fragments, from triatomic mol. photodissoc., fluoresc. polarisation excitation spectroscopy 0-28054
- diatomic molecule, overtone intensities in reson. Raman scatt. 0-48001
- diatomic molecules, excitation energies, oscillator strengths, many body approach, eqns. of motion method 0-47969
- diatomic systems, interactions, long-range dipoles, quadrupoles and hyperpolarisabilities 0-53161
- diatomic molecules, Stark effect variational and perturbational calcs. 0-1022
- diene-iron tricarbonyl complexes,  $\pi$ -orbital perturbation energies, ionisation energies; UV photoelectron spectra 0-32775
- dihydroxycarbene, singlet and triplet state rot. pot. surfaces 0-32627
- dimethyl ether, review of microwave spectrum, tabulated data 0-51965
- 1,6-diphenylhexatriene, lower excited states fluoresc. quenching 0-1016
- donor-acceptor pairs, electron transfer, theory 0-27918
- electron distribution anal. ab initio calcs. 0-47866
- equations of motion, Green's function methods and config. interaction methods, comparison, appl. and anal. 0-47841
- ethanol, ion internal energy selection by angle-resolved mass spectrometry 0-53164
- ethylene, planar dissociation, electronic rearrangement, states, bonds, ab initio multiconfigurational SCF calcs. 0-27937
- ethylene, quasidegeneracy and effective Hamiltonians, canonical transformation cluster expansion formalism 0-52888
- ethylene(-d<sub>4</sub>), Rydberg states assignments, electron energy loss spectra 0-53153
- ethylene cation, state geometries, electronic vibr. coupling consts., HF calcs., comparison with Xalpha calcs. 0-27946
- ethylene V state, ab initio study of spatial extension 0-27952
- excited state dissociation, nonadiabatic interactions, conical and Jahn-Teller intersections, classical trajectory method 0-25997
- exponential transformation, quadratically convergent SCF procedure, appl. to closed shell ground states 0-47875
- fast molecular ion+solid (gas), excited electronic states effects 0-9687
- ferrous porphyrin, intermediate (S=1) spin state, PMR characterisation 0-48014
- fluoroacetylene, fund. and hot bands, laser microwave two-photon and double reson. spectroscopy 0-32752
- fluorobenzene cations, fluoresc. quantum yields and lifetimes, electronic state relax. processes 0-48027
- formaldehyde<sup>+</sup>, excited state dissociation, nonadiabatic interactions, conical and Jahn-Teller intersections, classical trajectory method 0-25997
- formic acid, H bonding, electronic struct., geometries, moments, dimerisation energies, charge distrib., pseudopotential calcs. 0-27942
- formyl radical, electronic struct., dissociation energy and pot. energy surface many body perturbation theory and couple cluster doubles calc. 0-23296
- gas phase reaction consts. for electronically excited species, relax. processes, data tables 0-16644
- glyoxal, singlet-triplet coupling, double reson. and level-anticrossing spectroscopy 0-48053
- ground state props., coupled cluster and MBPT methods appl. 0-47881
- Group IIA hydrides and halides, ionic bonds 0-18789
- guanidine tautomers, relative stabilities, nonempirical MO calcs. 0-21442
- haloacetylene cations, electron impact excitation A→X band system assignment 0-32766
- hexafluoro ethyl cation fragmentation, mass spectrometry 0-53070
- homonuclear coupled NMR spectra, pulses applied to multiplets, mutual coupling determ. 0-18873
- hydrocarbons, conjugated, heat of formation and reson. energies 0-7839
- ortho-hydroxybenzophenone, soln., intramol. proton transfer and energy relax. photostability, transient absorption obs. 0-28032
- inorganic species, vibr. and electronic props., reson. Raman spectra appl. 0-52996
- integrated spatial electron populations using projection function method 0-23299
- ion+molecule, electronic states, kinetic energy, molecular beams obs. 0-30230
- isocyanic acid, molecular structure and centrifugal distortion constants 0-47974
- isothiocyanic acid, H<sup>15</sup>NCS, HN<sup>13</sup>CS and HNC<sup>34</sup>S, ground state spect. constants and molecular struct. 0-47973
- large molecule, electronic struct., photoemission and optical absorpt. spectrum, CNDO/S3 model 0-53172
- ligand fields calcs., strong and intermediate fields, tensor algebra 0-42922
- local density functional theory of atomic and mol. ground electronic states 0-23286
- local-density theory of multiplet structure 0-18776
- Manoxal OT-cyclohexanewater reversed micellar system, singlet-singlet energy transfer 0-9531
- methane, electronic density, multiple scatt. method, muffin-tin approx. 0-27924
- methane, ion internal energy selection by angle-resolved mass spectrometry 0-53164
- methanol, H bonding, electronic struct., geometries, moments, dimerisation energies, charge distrib., pseudopotential calcs. 0-27942
- methanol, ion internal energy selection by angle-resolved mass spectrometry 0-53164
- methanol (d<sub>3</sub>), OH stretch fund., torsion-rot. levels, IR spectra obs. 0-32711
- 3-methylenoxetane, electron structure, orbital-O interaction, MO calcs., UV photoelectron spectra 0-28058
- molecular photoexcited excited states, dynamics, advances using synchrotron radiation 0-37836
- MS potential from a set of overlapping densities 0-52850
- nitrosomethane, ground state and nonvertical n- $\pi^*$  excitation energy calcs. 0-18804
- omega like technique, Hartree Fock formalism 0-18792



## molecular electronic states continued

one-electron Hamiltonian method applied in SCF theory to states with open shell 0-23302  
open shell RPA unitary group formulation, Hartree Fock stability eqns. 0-52860  
open shells, RHF treatment without Lagrange multipliers 0-32589  
organic compounds, complex, nuclear relaxation influence on stimulated emission 0-48019  
organic compounds, low freq. anharmonic vibr., pot. function determ., Raman and IR spectra obs. 0-52997  
organic ion, excited electronic state correlation with mass-spectral fragmentation pattern 0-45482  
organic molecules, quadrupole moments, dipole quadrupole A and C polarisabilities, perturbation theory anal. 0-27934  
ovalene, isolated ultra cold mol., intermediate level structure of  $S_2$  state 0-28048  
3-oxetanone, electron structure, orbital-O interaction, MO calcs., UV photoelectron spectra 0-28058  
ozone,  $^1A_1$  ground state, dipole moment function, ab initio SCF and CI calcs. 0-32628  
phosphamides, carcinostatic,  $^{14}N$  NQR, electron distrib. and bonding configs. 0-48018  
photochemical reactions, isomerisation, complexing, proton transfer, initiation of internal conversion processes 0-40713  
photoelectron spectroscopy, charact. of vapours oven heated inorganic solids 0-52239  
photosynthetically relevant mols., electronic structural props. 0-16902  
pinacyanol dye, adsorbed on CdS substrate, aggregation effect on mol. electronic states 0-37757  
point groups, continuous, characters and representations 0-36809  
point groups, continuous, reduction of representations 0-36808  
point groups, continuous, reduction of representations 0-36810  
polar mol. anion ab initio ground state pot. energy surfaces calc. 0-47923  
polar molecule, excited state MCSCF wave functions, BeO appl. 0-47916  
polyatomic molecule, vibr. struct. of electronic spectra, FORTRAN programs 0-32699  
polyatomic molecules, excitation energies, oscillator strengths, many body approach, eqns. of motion method 0-47969  
polyatomic molecules, two-parameter intramol. distrib. and props. 0-47967  
polyatomic radical cations, excited states, decay processes 0-28055  
polyethylene molecule, fractured, local electron level calc. 0-14263  
propan-1-ol, ion internal energy selection by angle-resolved mass spectrometry 0-53164  
propane, ion internal energy selection by angle-resolved mass spectrometry 0-53164  
 $\beta$ -propiolactone, electron structure, orbital-O interaction, MO calcs., UV photoelectron spectra 0-28058  
pseudopotentials, reliability criteria 0-49563  
pyrazine, triplet-triplet absorpt. related to state splitting 0-47917  
pyridazine,  $\pi$  bond order calc. using U(3) basis algebra 0-18810  
pyridine and salts, deuterium NQR, double reson. method, ring charge distrib. 0-53015  
quantum mechanics, mol. struct. defn. 0-52843  
quantum-chemical  $\pi$ -electron system, molecules-in-molecule model (*German*) 0-5490  
quasi-linear molecules, low frequency anharmonic vibrations, pot. function determ., Raman and IR spectra obs. 0-52997  
Raman spectroscopy, in high temp. chem., review 0-52234  
relativistic corrections, estimation method 0-14091  
relativistic corrections, review 0-47914  
rhodamine, CARS spectroscopy, vibr. spectra of electronic states 0-27964  
ring current theories in NMR 0-53020  
Rydberg states, quantum defect theory applic. 0-32700  
satellite struct. of electron spectra, CI and vibronic coupling, dynamical calc. 0-53044  
solvent effects, rel. to polarisation structure 0-43062  
symposium, Florida, USA (March 1979) 0-51946  
TCNQ salt, NMP-TCNQ, electronic struct., SCF calc., total energy polarisation effects 0-15469  
tetraphenylporphyrin, free base in PVC matrix, excited state props., electrochromism obs. 0-37815  
Tokamak impurity problems, atomic and mol. struct. and collision data, review 0-43959  
transition metal complexes, ligand field spectroscopy, selection rules, intensity enhancement of forbidden transitions 0-45049  
transition metal complexes, mol. dissymmetry, book 0-27057  
transition metal dihydrides, gas phase geometrical struct. calcs. 0-42951  
transition metal-carbonyl cluster molecules, electronic struct., localised orbital pseudopot. method 0-39653  
triatomic isoelectronic molecules, electronic struct., one-electron props. 0-42935  
triply excited state contrib. to correlation energy, diagrammatic perturbation theory, water appl. 0-18774  
two-centre integrals calculation in semi-empirical INDO method 0-32611  
two-particle states, Talmi transformation theory, kinematic consts., appl. to mol. electronic states 0-32588  
U(3) symmetric matrices algebra applic. to  $\pi$  bond order calc. 0-18810  
UHFS model, CI, CC, and MBPT approaches, appl. to weak  $\delta$ - $\delta$  bonds and  $\delta$ - $\delta^*$  excitation 0-32585  
unimolecular decay, nonadiabatic interactions, transition probability as function of Massey parameter 0-35503  
unimolecular reactions, laser-induced, by multiphoton IR excitation, theory 0-9664  
unitary group approach to molecular electronic structure, review 0-5467  
vibronically coupled electronic states, radiationless decay, non-Condon effects 0-52966  
 $\pi$  electronic states and transitions, interpretation 0-52862  
[BH $_2$ ] $_n$  energy band structure 0-5478  
[BeH $_2$ ] $_n$  energy band structure 0-5478  
[Fe $_2$ (SH) $_4$ ] $^{0.2-3-}$ , HFS-LCAO calcs., 4-Fe active site model in high pot. Fe protein and ferredoxin 0-42929  
AcH,  $^1\Sigma$  state, Dirac-Fock one-centre calcs. 0-23301  
Al $_n$ H $_n$ , electron density distrib., reaction channels and bonding characts., electrostatic mol. pot. CNDO/2 calc. 0-23309  
AlO radical, ground state dissociation energy 0-53159  
Ar, liq., recomb. and self-trapped exciton luminesc., free electron dynamics, excited states 0-25463  
ArBr, emission spectrum and chemiluminesc. 0-45508  
ArBr, pot. curves, population distrib. and chemiluminesc. for B(1/2) and C(3/2) electronic states 0-45509

## molecular electronic states continued

ArO $^+$ ,  $X^1\Sigma^+$  state, pot. energy curves and correl. effects, elastic scatt. cross sections 0-23502  
BH,  $^1\Sigma^+$  ground state, mag. susceptibility, paramag. contrib., large config. interaction wave function calcs. 0-47899  
BaH( $N^2\Sigma$ ), perturbations, 3800 Å absorption band obs. 0-14154  
BeH radical, hyperfine splitting const., electronic energy, UHF-type, CCI calcs. 0-52909  
BiBr,  $A^3(0^+)$  and  $X^3\Sigma^-(0^+)$  states, pot. energy functions comparison 0-43133  
BiF, spectrum, 5800-6600 Å, vibr. anal., electronic transition assignment 0-992  
BrCN, vacuum UV photodissociation spectroscopy, quantum yield, fluorescence polarisation 0-32736  
BrHe,  $X^2\Sigma$  and  $A^2\Pi$  states, SCF calcs. 0-23503  
BrHe $^+$ ,  $X^1\Sigma$  state, SCF calc. 0-23503  
C $_2$ ,  $^3\Pi$ , states, large CI wavefunctions, non-adiabatic coupling matrix elements 0-37744  
C( $A^3\Pi$ ) vibr. relax. in He 0-53106  
CH,  $B^1\Sigma^+$  state predissoc., calcs. and time resolved spectrosc. 0-23576  
CH $_2^+$ ,  $^4A_2$  states, large CI wavefunctions, non-adiabatic coupling matrix elements 0-37744  
CN $^+$ , ground state, identity, ab initio CI calcs. 0-5468  
CN $^+$ , lower states, pot. energy curves, equilib. distances SCF CI calcs. 0-27957  
C $_2$ N $_2$  and C $_2$ N $_2^+$ , electronic struct. UV and PE spectra 0-23304  
C $_2$ N $_2$ , C $^1\Pi$ , state predissoc., vibronic effects 0-28078  
C $_2$ N $_2$ , satellite struct. of electron spectra, CI and vibronic coupling, dynamical calc. 0-53044  
CO discharge plasma, electron energy distrib. and kinetic coeffs., ground-state mols. 0-43867  
CO, electronic struct., binding energy and interatomic distance, SCF variational cellular calc. 0-9498  
CO, vibr. struct., core and valence ESCA spectra, Frank-Condon and HF anal. 0-32602  
CO $_2^-$ , dissociation,  $^2\Sigma_g^+$  state, Wall Porter pot. surface, autodetachment and vibr. level population inversion 0-21275  
CO $_2$ -N $_2$ -He discharge, electron distrib. relax., numerical study 0-54070  
CO $^+$ ( $A^1\Pi$ ) vibr. relax. in He 0-53106  
CS, vibr. states in RF discharge plasma, microwave spectrosc. obs. 0-14133  
CS $_2$ ,  $^3A_2$  state, triplet bands, MCD spectrum, near UV absorpt. spectrum 0-48010  
CS $_2$ ,  $^3A_2$ -state, MCD and UV spectrum, theoretical anal. 0-48011  
CS $_2$ , photoelectron spectrum, spin-orbit splitting, excited state form. 0-43102  
CS( $A^1\Pi$ ) vibr. relax. in He 0-53106  
Ca $_2$ , new ground state, photolum. obs. vibr. consts., dissociation energy 0-5576  
CaH, low lying electronic states, ab initio SCF-CI calcs. 0-52893  
CeO, C $_1$ -X $_1$  and D $_2$ -X $_2$  systems, fluorescence, vibr. spectra, laser spectroscopy obs. 0-32761  
Cl $_2$ , semi-empirical INDO calc. of electronic struct. 0-32611  
CICN, ground and first excited bending, vibr. state, props., mol. beam elec. reson. 0-37823  
CICN, vacuum UV photodissociation spectroscopy, quantum yield, fluorescence polarisation 0-32736  
Cl $_2$ CS, excitation, singlet and triplet states, two photon absorpt., singlet-singlet energy pooling, fluorescence obs. 0-48032  
ClF(CIF $_2$ )(CIF $_3$ ), localised MO ab initio calc., Gaussian orbital ab initio calc. 0-14083  
CoCl $_n$ , electronic struct., INDO theory 0-42948  
CrCl $_4$ , ligand field states, multiple scatt. Alpha calcs. 0-47891  
Cu complex, Cu(II) dimers, temp. depend. PMR relax., singlet-triplet separation determ. 0-43073  
CuCl $_n$ , electronic struct., INDO theory 0-42948  
 $^{63}Cu_2$ ,  $B^1\Sigma_u^+-X^1\Sigma_u^+$  transition, Franck-Condon factors, r-centroids and pot. curves 0-43114  
D $_2$ , electron impact dissociative ionisation near  $^2\Sigma_g^+$  state dissociation threshold 0-43197  
D $_3^+$ , ab initio vibr. intervals and vibr. freq. refinement 0-47968  
F $_2$ , electron energy loss spectra, 0-17 eV, 5-140°, repulsive valence states excitation 0-32844  
Fe complex, FeCl $_3$ -tetraphenylporphyrin in PVC matrix, excited state props., electrochromism obs. 0-37815  
FeCl $_n$ , electronic struct., INDO theory 0-42948  
FeCo molecules, matrix-isolation Mossbauer spectra 0-23448  
Gal, A $0^+$ -X $0^+$  and B $1$ -X $0^+$  transitions, isotope shifts, UV and visible spectra obs. 0-53005  
GeTe, matrix isolated absorpt. and emission visible spectra, electronic states 0-28026  
H-bonded model systems, intermolecular charge transfer, biological implications 0-3572  
H $_2$  (D $_2$ ) mol. bands, electron impact excitation, rot. transitions, cross sections in plasma 0-37896  
H $_2$ , diabatic and reson. states, dissociative photoionisation calcs. 0-47883  
H $_2$ , electron impact dissociative ionisation near  $^2\Sigma_g^+$  state dissociation threshold of H $_2$  0-43197  
H $_2$ , ground state, vibr. eigenenergies, functional form 0-27998  
H $_2$ , metastable level electron impact excitation, resonances (*Russian*) 0-43198  
H $_2$  ortho-para transition as means of observing weak interaction parity nonconservation (*Russian*) 0-900  
H $_2$ , predissociation of  $^1\Pi_u^-$  state vibr. and rot. levels, dissociation yields meas. 0-32784  
H $_2$  predissociation probabilities of  $4p\pi^1\Pi_u+\nu'\geq 1$  levels, dissociation channels interference 0-28074  
H $_2^+$ , high (10 $^9$  G) mag. fields, dissociation energy, electron binding energy and equilib. separation 0-52910  
H $_2^+$ , spontaneous emission lifetimes in ground electronic states 0-32810  
H $_2^+$ +He $^+$ , DIM approx. pot. energy surfaces and nonadiabatic coupling 0-23330  
H $_3$ , interat. pot. energy matrix elements, generalised DIM calc., ZDO approx. 0-52864  
H $_3$ , Rydberg spectrum, theory 0-5528  
H $_3$ , Rydberg states, Jahn-Teller calcs. 0-9494  
H $_3$ , Rydberg states energies and equilib. geometry calcs. 0-9493  
H $_3^+$ , ab initio vibr. intervals and vibr. freq. refinement 0-47968  
HCN $^+$ , A and B  $^2\Sigma^+$  states, pot. surfaces, ab initio SCF calcs. 0-27959  
HCl, semi-empirical INDO calc. of electronic struct. 0-32611  
HD $^+$ , spontaneous emission lifetimes in ground electronic states 0-32810



## molecular electronic states continued

- $\text{H}_2(\text{D}_2)$ , Rydberg states, nonadiabatic effects, elec. field ionis. 0-9528  
 HF, valence orbitals momentum distrib., (e, 2e) binding energy spectra 0-14237  
 $\text{HF}_2$  ion, H-bond excited electronic states, CI calc., dissoci. and autoionising states 0-5489  
 $\text{HNO}$ , low-lying states, pot. energy curves 0-9533  
 $\text{H}_2\text{O}$ , ESCA and soft X-ray emission, vibr. excitation 0-23433  
 $\text{H}_2\text{O}$ , ground state ionis. pots., generalized MO theory 0-52907  
 $\text{H}_2\text{O}$ , H bonding, electronic struct., geometries, moments, dimerisation energies, charge distrib., pseudopotential calcs. 0-27942  
 $\text{H}_2\text{O}^+$ , states geometries, electronic vibr. coupling consts. HF calcs., comparison with  $\text{X}\alpha$  calcs. 0-27946  
 $\text{HPO}$ , emission system, rot. anal. of vibr. bands 0-47957  
 $\text{H}_2\text{S}$ , semi-empirical INDO calc. of electronic struct. 0-32611  
 $\text{He}_2^+$ , possibility of existence, Lennard-Jones pair potential 0-52869  
 $\text{He}_2^+$ , bound excited states, potential energy curves and rovibronic energy, dissociation 0-23327  
 $\text{He}_2(\Sigma_g^+)$ , general-model-space diagrammatic perturbation theory appl. 0-47844  
 $\text{Hg}_2^+$ , electronic struct. and photoabsorpt. calcs. 0-27932  
 $\text{ICN}$ , vacuum UV photodissociation spectroscopy quantum yield, fluoresc. polarisation vacuum UV photodissociation spectroscopy, quantum yield, fluoresc. polarisation 0-32736  
 $\text{I}_2\text{X}^+\Sigma^+$ , collisional relax. of highly excited vibr. levels, using  $\text{I}_2$  optically pumped laser 0-43155  
 $\text{InCl}$ , discharge excited spectrum 4100-3900 Å, vibr. anal. 0-27372  
 $\text{K}_2(\text{A}\Sigma_u^+)$ , form. by  $\text{K}(4\text{P})$  at. in K discharge 0-44013  
 $\text{Kr}$ , liq., recomb. and self-trapped exciton luminesc., free electron dynamics, excited states 0-25463  
 $\text{KrF}$  discharge pumped laser, energy extraction, collisional coupling between B, C and D-states 0-28213  
 $\text{KrO}^+$ ,  $\text{X}^4\Sigma$  state, pot. energy curves and correl. effects, elastic scatt. cross sections 0-23502  
 $\text{LaH}$ ,  $^3\Sigma$  state, Dirac-Fock one-centre calcs. 0-23301  
 $\text{Li}_2(\text{A}\Sigma_u^+)$ , state multiplets transfer following rot. inelastic He collisions, polarised emission obs. 0-5608  
 $\text{LiAlH}_4$ ,  $\text{LiBH}_4$ , ab initio calc. of geom. struct., charge distrib., bonding and pot. energy surfaces 0-18796  
 $\text{LiF}$ , ground and excited states, ab initio calcs. single config. and multi-config. SCF calcs. 0-52873  
 $\text{LiNC}$  type molecules, Born-Oppenheimer approx. applicability 0-32603  
 $\text{LrH}$ ,  $^3\Sigma$  state, Dirac-Fock one-centre calcs. 0-23301  
 $\text{LuH}$ ,  $^3\Sigma$  state, Dirac-Fock one-centre calcs. 0-23301  
 $\text{MgH}^+$ , CI pot. curves and cross sections for lowest singlet states 0-23343  
 $\text{Mo}_3$ , matrix isolated visible absorpt. spectra, electronic, vibronic and vibr. states 0-28027  
 $\text{MoN}$ , matrix isolated visible absorpt. spectra, electronic, vibronic and vibr. states 0-28027  
 $\text{MoO}$ , matrix isolated visible absorpt. spectra, electronic, vibronic and vibr. states 0-28027  
 $\text{N}$ ,  $3\text{p}^4\text{S}^0$ -state quenching in low-press. glow discharge 0-23355  
 $\text{N}_2$ ,  $\text{C}^3\Pi_u$ -state, electron impact excitation, low energy 0-9746  
 $\text{N}_2$ , electronic density, multiple scatt. method, muffin-tin approx. 0-27924  
 $\text{N}_2$ , electronic struct., binding energy and interatomic distance, SCF variational cellular calc. 0-9498  
 $\text{N}_2$ , metastable level electron impact excitation, resonances (Russian) 0-43198  
 $\text{N}_2$ , N K-shell excitation, high-resolution electron energy loss spectra 0-53152  
 $\text{N}_2$  triplet-triplet transitions, Einstein-A coeffs., oscill. strengths, lifetimes, theory and experiment comparison 0-47876  
 $\text{N}_2$ , vibr. struct., core and valence ESCA spectra, Franck-Condon and HF anal. 0-32602  
 $\text{N}_2^+$ , A- and B-states interactions, time-resolved obs. 0-18862  
 $\text{N}_2\text{-CO}_2(\text{-He})$  volume discharge,  $\text{N}_2$  vibr. levels, stepwise excitation, effect on electron energy balance 0-54071  
 $\text{N}_2 + \text{H}^+$  (e), vibrational  $\text{N}_2^+$  excitation (Russian) 0-53156  
 $\text{NBr}$ , in solid Ar,  $\text{b}^1\Sigma^+ \rightleftharpoons \text{X}^1\Sigma^+$  transitions 0-32702  
 $\text{NCl}$ , in solid Ar,  $\text{b}^1\Sigma^+ \rightleftharpoons \text{X}^1\Sigma^+$  transitions 0-32702  
 $\text{NH}_2(\text{X}^2\text{A}_1)$ , excited state dynamics and bimol. quenching processes 0-9681  
 $\text{NH}_3$ , ESCA and soft X-ray emission, vibr. excitation 0-23433  
 $\text{NH}_3$  inverse level doubling mol., space and combined parity nonconservation (Russian) 0-52879  
 $\text{NH}_3$ , mol. beam state selection and focusing, hyperfine spectrum 0-28119  
 $\text{N}_2\text{H}_3$  radical, lowest two electronic states 0-925  
 $\text{NH}_2(\text{A}^2\text{A}_1)$ , IR emission detection in UV laser photodissoc. of  $\text{NH}_3$  0-11901  
 $\text{NH}(\text{A}^2\Pi, \text{b}^1\Sigma)$ , two-photon generation in  $\text{NH}_3$  UV laser photodissoc. 0-11901  
 $\text{NH}_4\text{Cl}$ , gas  $^1\text{A}_1$  ground state, pot. surface 0-32626  
 $\text{NHD}$  radical,  $\text{A}^2\text{A}'$  state transitions, Stark effect contribs. 0-23455  
 $\text{NH}_2(\text{X}^2\text{B}_1)$ , laser-induced fluoresc. obs. in UV laser photodissoc. of  $\text{NH}_3$  0-11901  
 $\text{NH}(\text{X}^2\text{B}_1)$  radical, and  $\text{ND}_2$ , ionisation pot., vibr. anal., ab initio calcs. and vacuum UPS obs. 0-53047  
 $\text{NI}$ , in solid Ar,  $\text{b}^1\Sigma^+ \rightleftharpoons \text{X}^1\Sigma^+$  transitions 0-32702  
 $\text{NO}$ , and isotopic forms,  $\nu=0$  electronic states, spin-rot. doubling 0-5540  
 $\text{NO}$ , N K-shell excitation, high-resolution electron energy loss spectra 0-53152  
 $\text{NO}$ , state selective step-wise photoionis. with mass spectroscopic ion detect. 0-43119  
 $\text{NO}$ , UV fluorescence, IR laser induced 0-53032  
 $\text{NO}^+$  ground state mol. consts., from  $\text{NO X}^2\Pi(\nu=0)$  UPS obs. 0-14177  
 $\text{NO}^+$ , pot. energy curves calcs. 0-5602  
 $\text{NO}_2$ , Hanle effect, nonstationary states in molecular spectroscopy, level splitting 0-23465  
 $\text{NO}_2$ , visible spectrum simplification, rot.-vibr. levels, excitation, polarisation labelling spectroscopy 0-32730  
 $\text{N}_2\text{O}$ , N K-shell excitation, high-resolution electron energy loss spectra 0-53152  
 $\text{NOH}$ , groundstate electronic struct., MRD CI calc., dissoci. energy, isomerisation energy 0-14088  
 $\text{NO}_2^*$ , multiple IR photon fluoresc. excitation and dissoci., isomerically excited 0-48050

## molecular electronic states continued

- $\text{Na}_2$ , ground state, vibr.-rot. relax., optical pumping transients obs. 0-28067  
 $\text{NaAlH}_4$ ,  $\text{NaBH}_4$ , ab initio calc. of geom. struct., charge distrib., bonding and pot. energy surfaces 0-18796  
 $\text{Ni}_2$ , A-X system, Ar matrix isolation fluoresc. spectrosc. obs. 0-9628  
 $\text{O}^+ + \text{Ne}$ , pot. energy curves, nonadiabatic coupling matrix elements 0-53110  
 $\text{O}_2$ ,  $^3\Pi_u$  states, large CI wavefunctions, non-adiabatic coupling matrix elements 0-37744  
 $\text{O}_2$ ,  $\text{b}^1\Sigma_g^+ \rightleftharpoons \text{X}^1\Sigma_g^+$  electronic transition, absorpt. coeffs. and transition moments 0-43061  
 $\text{O}_2$ , electronic struct., self-consistent pseudopot. calc. 0-9508  
 $\text{O}_2$ , metastable level electron impact excitation, resonances (Russian) 0-43198  
 $\text{O}_2$ , multiconfig. Hartree-Fock calcs. convergence 0-47901  
 $\text{O}_2$ , singlet states, quenching by  $\text{O}_2(\text{N}_2)$ , shock tube study 0-23511  
 $\text{O}_3$ , open-shell SCF secular eqn., iterative algorithm soln. 0-52868  
 $\text{O}_3$ , photolysis, primary products electronic and vibr. state distrib. 0-50865  
 $\text{OCS}$ , rot.-vibr. levels and semiclassical energy levels 0-37804  
 $\text{OCl}_2^+$ , radical cation, struct. and electronic props., ab initio RHF SCF MO calc. 0-52883  
 $\text{OH}$ ,  $\text{A}^2\Sigma^+ \rightleftharpoons \text{X}^2\Pi$  system, vibrational and rotational levels, transition probability determ. 0-43034  
 $\text{OH}$ , prod. by photolysis, A-doublets, population, rot. states, hyperfine struct., microwave spectra 0-32694  
 $\text{OH}(\text{A}^2\Sigma^+) + \text{N}_2(\text{O}_2)(\text{H}_2\text{O})(\text{air})$ , quenching rates and fluoresc. efficiency, rel. to atmosphere 0-14199  
 $\text{O}_2^* + \text{O}_3$ , UV photolysis,  $\text{O}^3\text{P}$  prod., rate const. determ. 0-55636  
 $\text{P}_2$  radical,  $\text{b}^1\Sigma_g^+ \rightleftharpoons \text{a}^3\Sigma_u^+$  transition, perturbed by  $1^5\Sigma_g^+$  state (French) 0-18855  
 $\text{P}_2^+$ , electronic states pot. energy curves, dissoci. energy, ionisation pot., curve fitting 0-32796  
 $\text{PH}_3$ , X-ray K-fluoresc. obs. of electronic struct. 0-37818  
 $\text{Re}_3\text{Cl}_9$  metal cluster complexes,  $\text{He(I)}$  photoelectron spectrum, SCC DV  $\text{X}\alpha$  calcs.,  $\text{Re}_2\text{Cl}_7^{2-}$  comparison 0-28063  
 $\text{S}_2$ ,  $^1\Delta_g$  and  $^3\Sigma_g^+$  states, near IR emissions 0-18852  
 $\text{S}_8^{2+}$ , electronic struct. and localised MOs, bonding nature and geom. struct. 0-18798  
 $\text{SF}_6$  molecule absorption of IR laser radiation (Russian) 0-986  
 $\text{SF}_6$ ,  $\nu_3$  bands, rot. fine struct., HFS spectroscopic consts. determ., saturation spectroscopy obs. 0-53008  
 $\text{SF}_6$ , vibr. spectra, rot. consts., IR spectra, Raman spectra obs. 0-32719  
 $\text{SO}$ , low lying bound mol. electronic states, SCF CI calc. 0-23314  
 $\text{SO}_2$ ,  $2^1\text{A}'$  state, electron correl. variational description, loop driven graphical unitary group approach 0-47903  
 $\text{SO}_2$ ,  $\text{X} \rightarrow \text{A}$  electronic absorpt. band system, non Condon effects study 0-18837  
 $\text{Si}^6\text{O}_2(\text{Si}^18\text{O}_3)$ ,  $^1\text{B}_2(\text{'A'})$  state, force field for large amplitude motions 0-43023  
 $\text{SiH}$ ,  $^1\Sigma$  state, Dirac-Fock one-centre calcs. 0-23301  
 $\text{Se}_8^{2+}$ , electronic struct. and localised MOs, bonding nature and geom. struct. 0-18798  
 $\text{SiH}$ , ground state, A-type doubling 0-23431  
 $\text{SiH}_2$ ,  $1\text{B}_1$ -state, geometry calcs., avoided crossings 0-53085  
 $\text{SiH}_4$ ,  $1\text{B}_1(1\text{T}_2)$  pot. energy surface calcs. 0-53085  
 $\text{Ti}_2$ , electronic structure of five and ten atom chains SCF-X $\alpha$ -SW calcs. 0-5483  
 $\text{TiH}$ , electronic structure of five and ten atom chains SCF-X $\alpha$ -SW calcs. 0-5483  
 $\text{TmH}$ ,  $^3\Sigma$  state, Dirac-Fock one-centre calcs. 0-23301  
 $\text{UF}_6$ , photophysical props., laser study 0-28040  
 $\text{UO}_2^{2+}$  (aq) +  $\text{UO}_2\text{NO}_3^+$  (aq), ground and excited state interaction, struct., thermodynamic functions, photochemistry obs. 0-32779  
 $\text{VCl}_4(\text{Br}_4)$ , vibronic systems, degenerate ground states, statistical sums, thermodynamic func. calcs. 0-27997  
 $\text{Xe}$ , liq., recomb. and self-trapped exciton luminesc., free electron dynamics, excited states 0-25463  
 $\text{XeCl}$  avalanche discharge laser, D and B state coupling, population depletion 0-28214  
 $\text{XeF}$ , (B,C) state prod. and kinetics,  $\text{XeF}_2$  photolysis with VUV radiation 0-32975  
 $\text{XeF}$ , B and C-state kinetics with self-sustained discharge pumping 0-28212  
 $\text{XeF}_2$ , photodissoc. yield in solid Xe and Kr, time-resolved photolum. excitation obs. 0-3372  
 $\text{XeO}^+$ ,  $\text{X}^4\Sigma^+$  state, pot. energy curves and correl. effects, elastic scatt. cross sections 0-23502  
 $\text{YH}$ ,  $^1\Sigma$  state, Dirac-Fock one-centre calcs. 0-23301

## molecular electronic structure see molecular electronic states

## molecular energy level calculations

- see also molecular electron correlations; molecular orbitals calculations; molecular rotation calculations; molecular rotation-vibration calculations; molecular vibration calculations; VB calculations  
 6d metal superheavy hexafluorides, relativistic mol. calcs. 0-5484  
 covalent bonding from superposition of one-centre charge densities 0-37722  
 d-orbital basis functions role in electronic struct. description of systems containing Si, P, S and Cl 0-9484  
 diatomic systems, correl. diagrams, Thomas-Fermi calcs. 0-23294  
 diatomic systems, Thomas-Fermi and Thomas-Fermi-Dirac-Weizsacker eqns., solns. 0-23293  
 electronic structures comparison, arbitrary electronic state, distance and similarity measures appl. 0-9487  
 formaldehyde, atomisation and bond energies; LMO calc., conjugation contrib. 0-9496  
 formaldehyde, bond polarity effect on other bonds and lone pairs, LMO calc. 0-9495  
 hydrides, single-centre perturbation theory calcs. 0-5470  
 inner-shell vacancy system, saddle point calcs. 0-23292  
 local-density theory of multiplet structure 0-18776  
 many-electron systems, excitation energies, linear response function theory, coupled-cluster framework 0-42936  
 multicentre potential,  $\text{X}_n$  scattered waves method and Schrödinger eqn. soln. 0-37740  
 multidimensional interpolation by polynomial roots 0-18778  
 non-Hermitian operators, self-adjoint matrix equations 0-42916  
 nonadiabatic transitions, linear curve crossing problem, generalised Stueckelberg method 0-28085



**molecular energy level calculations continued**

- open shell polarisation propagator, for doublet-doublet transitions calcs. 0-27939  
 potentials at nuclei of atoms in molecule, relation with total energy of molecule 0-42917  
 $\text{Co}_3\text{O}_4\text{-H}_2$ , interaction with surface, quantum chemical study 0-45549  
 $\text{CrCl}_4$ , ligand field states, multiple scatt. Xalpha calcs. 0-47891  
 $\text{Cr}_2\text{O}_3\text{-H}_2$ , interaction with surface, quantum chemical study 0-45549  
 $\text{Fe}_2\text{O}_3\text{-H}_2$ , interaction with surface, quantum chemical study 0-45549  
 HD, spin-spin coupling const., convergence of calc. 0-9506  
 LiNC type molecules, Born-Oppenheimer approx. applicability 0-32603  
 $\text{LiO}_2$ , molecule, vibronic interaction in low-lying states, model calc. 0-32603  
 $\text{MnO-H}_2$ , interaction with surface, quantum chemical study 0-45549  
 N-N, correl. diagrams, Thomas-Fermi calcs. 0-23294  
 Ne-Ne, correl. diagrams, Thomas-Fermi calcs. 0-23294  
 $\text{NiO-H}_2$ , interaction with surface, quantum chemical study 0-45549  
 OCS, rot.-vibr. levels and semiclassical energy levels 0-37804  
 $\text{PtCl}_2(\text{NH}_3)_2$ , cis- and trans-isomers, electronic struct., SCF-Xa study 0-18795  
 $\text{Si}_2\text{H}_4$  ground state struct., ab initio SCF calcs., singlet silylsilylene 0-27945  
 $\text{THH}_4$ , Dirac-Fock one-centre expsn. calc. 0-5485  
 $\text{UF}_5$ , electronic struct. and geometry, ab initio calcs. using relativistic ECP 0-32606  
 $\text{UH}_6$ , Dirac-Fock one-centre expsn. calc. 0-5485  
 $\text{V}_2\text{O}_5\text{-H}_2$ , interaction with surface, quantum chemical study 0-45549

**molecular energy levels**

- see also macromolecular energy levels; molecular electronic states; molecular energy level calculations; molecular fine structure; molecular hyperfine structure; molecular libration; molecular polarisability; molecular reorientation; molecular resonant states; molecular rotation; molecular rotation-vibration; molecular vibration; molecular vibronic states; nuclear screening  
 alkali metal molecular, laser radiation absorpt., at. excitation processes 0-32785  
 anthracene dimer anion, charge reson. transition anal. 0-42931  
 $^3\pi^*\text{benzaldehyde}$ , zero field splitting and sublevel decay rates, deuteration and host effect 0-37750  
 charge distribution in ions and mols., inductive effect 0-47837  
 clustering, qualitative theory of irreducible tensor operators spectra 0-28001  
 conjugated molecules eigenvalue polynomials 0-14078  
 electronic distribution and electronegativity, theory 0-23283  
 fluorobenzenes, negative ion states, comments and reply 0-32599  
 ion-molecule equilibria in solvolysis, secondary  $\beta$   $^3\text{H}$  isotope effects, hyperconjugation 0-50874  
 isocyanates, nonbonding and  $\pi$ -orbital interactions, photoelectron spectra 0-32774  
 isothiocyanates, nonbonding and  $\pi$ -orbital interactions, photoelectron spectra 0-32774  
 methane, electron pair interactions calcs. 0-23298  
 nonadiabatic transitions, 1-dimens. model, mol. prop. appls. 0-52861  
 orbital pairs, transformation into localised pairs, use of FORTRAN for angle selection 0-27922  
 organic chemistry courses, unified approach to teaching of struct. and bonding 0-17732  
 sandwich complexes, mag. props., effective Hamiltonian method 0-37731  
 spontaneous symmetry breaking, induced representations 0-5464  
 thiocyanates, nonbonding and  $\pi$ -orbital interactions, photoelectron spectra 0-32774  
 triethylamine-perfluoro-T-butanol, photoelectron and Rydberg bands, UV spectra study 0-18865  
 valence shell electron pair repulsion model, geometry variations, ab initio calc. 0-5472  
 van der Waals molecules, pot. functions, level spacings and thermodynamic props. 0-14185  
 WINIMAX weighting factor, for isotope chem. and mol. struct. calcs. 0-27940  
 $\text{BaTiO}_3$ , XPS satellite spectra, mol. orbital study 0-43100  
 $\text{CH}^+$ , predissociated levels obs. 0-37838  
 CO, K-shell, excitation and ionisation, vibr. struct., electron energy loss spectra obs. 0-18943  
 $\text{CeFe}_2\text{Si}_2$ , charge state of 3d shell, state of Fe atoms, atomic bonds (Russian) 0-47884  
 Cu complexes, Cu(I)-P tetrahedral,  $^{63}\text{Cu}$  FT-NMR 0-53021  
 H like molecule ion, chemical pot. asymptotic scaling, homonuclear diatomic total energy 0-47885  
 $\text{H}_2\text{O}$ , electron pair interactions calcs. 0-23298  
 $\text{H}_2\text{S}$ , electron pair interactions calcs. 0-23298  
 $\text{N}_2$ , K-shell, excitation and ionisation, vibr. struct., electron energy loss spectra obs. 0-18943  
 $\text{NH}_3$ , electron pair interactions calcs. 0-23298  
 $\text{O}_2$ , K-shell, excitation and ionisation, vibr. struct., electron energy loss spectra obs. 0-18943  
 $\text{TiO}_2$ , XPS satellite spectra, mol. orbital study 0-43100

**molecular excitation** see beam-foil spectra; chemical reactions; Davydov splitting; discharges (electric); molecular fluorescence; optical pumping; photoionisation; radiation quenching

**molecular fine structure**

- 2-benzoylpyridine crystals, lowest triplet state, optically detected EPR 0-15827  
 ethyl radical,  $^{13}\text{C}$ , and  $\text{H}^+$  hyperfine interactions, EPR spectra, vibr. anal. 0-23443  
 fluorene: acridene, radical pair form. from excited states, optical nucl. polarisation obs. 0-14155  
 fluorene:pyrene- $\text{d}_{10}$  cryst., magnetic resonance absorpt. of host-guest triplet paired centres 0-34750  
 $\text{Br}_2$ , extended X-ray absorption fine struct. amplitude attenuation, rel. to XPS satellites 0-37821  
 CO, X-ray K-absorpt. spectra, reson. obs., near fine struct. 0-37817  
 FO free radical, detection by  $\text{CO}_2$  laser mag. reson. 0-45594  
 $\text{H}_2$  3s, 3d:  $^2\Sigma$ ,  $^3\Pi$ ,  $^3\Delta$  complex, fine struct., Doppler-free laser spectroscopy 0-1087  
 $\text{N}_2$ , X-ray K-absorpt. spectra, reson. obs., near fine struct. 0-37817  
 $\text{O}_2$ , photofragment spectroscopy using fast ion beams 0-9755  
 $\text{OsO}_4$ , HFS and fine struct., saturation spectroscopy obs. visible spectra 0-53008  
 $\text{PH}_2$ ,  $\text{X}^2\text{B}_1$ -state, rot. laser mag. reson. spectrosc. 0-28038  
 $\text{SF}_6$ , IR double reson. with tunable diode laser 0-14160

**molecular fine structure continued**

- $\text{SF}_6$  molecule, resonant energy absorpt. struct. in IR laser field (Russian) 0-5592  
 $\text{SF}_6$ ,  $\nu_3$  bands, rot. fine struct., HFS spectroscopic consts. determ., saturation spectroscopy obs. 0-53008  
 $\text{ZrO}^+$ ,  $^2\Pi$ - $^2\Sigma$  system 0.0 band spin-split components 0-23413

**molecular fluorescence**

- [1-pyrenyl-( $\text{CH}_2$ ) $_n$ -N( $\text{CH}_3$ ) $_3$ ] $^+\text{Cl}^-$ , intracellular fluorescence quenching 0-9627  
 3-amino- and 4-amino-N-methylphthalimide, effect of orientational-relax. processes in fluoresc. kinetics 0-18886  
 acetic anhydride, multiphoton dissoc.,  $\text{CH}_2$  and  $\text{C}_2$  prod., fluence depend. meas. 0-5586  
 acetonitrile molecule dissociation in IR field, laser-induced fluoresc. obs. 0-53075  
 acetophenone, highly purified, luminesc. props. 0-32764  
 acetylene, multiphoton vacuum UV photodissoc. obs. and interpret. 0-11939  
 acetylenic hydrocarbons, cyclohexane soln., structureless fluoresc. 0-5575  
 acrylonitrile, multiple photon dissoc., photofragment spectroscopy by laser-induced fluoresc. 0-11937  
 alkali metal molecular, laser radiation absorpt., at. excitation processes 0-32785  
 alkyl benzenes, jet-cooled, intramol. vibr. relax., reson. fluoresc. and excitation obs. 0-14152  
 anthracene, vapour, fluoresc. spectra, mol. vibr. freq. reson. laser IR irradiation, quenching 0-18883  
 anthracene intramolecular excimer in 1,3-dianthrylpropane, direct obs. 0-48029  
 4-(9-anthryl)-N,N-dimethylaniline, fluoresc., dipole moments and polarisabilities 0-1019  
 aromatic compounds, absolute fluorescence quantum yield, calorimetric determ. 0-43092  
 aromatic esters, phosphoresc. and fluoresc. spectra in organic matrices 0-32756  
 aromatic hydrocarbon, centrosymmetric, two photon excited upper state fluoresc. spectra, reson. fluoresc. and vibr. mode selectivity 0-18878  
 aromatic hydrocarbon in soln., excited electronic state vibr. relax., time resolved fluoresc. 0-48024  
 aromatic isolated mol. nonradiative conversion, internal and S-T conversion, vibr. excitation and fluoresc. quantum yield 0-43095  
 atom + molecule reaction rate meas. 0-16676  
 7-azaindole dimers, photoautomerisation by double proton transfer, fluoresc. kinetics 0-11880  
 trans-azobenzene,  $\text{S}_1 \rightarrow \text{S}_0$  fluoresc. 0-28044  
 azulene-fluoranthene, soln., triplet energy transfer, delayed fluoresc. study of  $\text{S}_2 \rightarrow \text{S}_0$  0-23331  
 BBO dye, vapour phase, optical props. (Japanese) 0-9879  
 benzaldehyde, electronic spectra, Cl and F substitution effects 0-23456  
 1,2-benzanthracene in polystyrene films, delayed luminesc. decay kinetics 0-43088  
 chlorofluoromethylene radical, gas phase laser-induced fluoresc. spectroscopy 0-14173  
 chloromethanes, VUV fluoresc., UV multiphoton dissoc. 0-28076  
 chlorophyll-a (b), dimerisation, fluoresc. and ODMR study 0-18876  
 chlorophylls a and b and pheophytins, fluoresc. and phosphoresc. 0-12057  
 chlorotetracycline fluorescence, use in demonstrating  $\text{Ca}^{2+}$  release from cardiac cells 0-3612  
 CO, in glow flow discharge, electronic states, excitation mechanism 0-53040  
 colliding particle system, two-photon transition, stimulated Raman scatt. 0-9663  
 combustion diagnostics, laser appls. 0-16688  
 concanav A, light irradi. causing membrane damage 0-56123  
 copperporphyrin, metastable quartet state radiative decay 0-23453  
 coronene, luminesc., spin-orbit coupling perturbation by metal chlorides (German) 0-1021  
 cresyl violet, rot. diffusion, picosec. saturation spectrosc. obs. 0-5634  
 cryptoleurine derivatives, absorpt. and fluoresc. obs. of photodecomp. processes, dye laser relevance 0-55686  
 cyclohexane+toluene, energy transfer, pulse radiolysis obs. 0-16714  
 cyclopropane, partial vibr. energy transfer map 0-32760  
 decay, nonexponential, method of moments for data anal. 0-55975  
 dialkylaniline derivatives, twisted intramol. charge transfer states, dual fluoresc. obs. and form. dipole moments 0-18881  
 diatomic fragments, from triatomic mol. photodissoc., fluoresc. polarisation excitation spectroscopy 0-28054  
 dibromodifluoromethane, UV laser fluoresc. and photochem.,  $\text{CF}_2$ , CF and  $\text{Br}_2$  fluoresc. obs. 0-16703  
 dichlorodifluoromethane, UV photolysis, free radical emission 0-30263  
 dielectric cylinder embedded mols., Raman and fluoresc. scatt. 0-37949  
 3,3'-diethylthiacarbocyanine iodide-rhodamine-6G-sodium lauryl sulphate, soln., premicellar region, energy transfer 0-20685  
 difluorocarbene,  $\text{A}^1\text{B}_1$ - $\tilde{\text{X}}^1\text{A}_1$  system spectrosc. and photophysics 0-5577  
 dihydrophenazine derivatives, in 3-methylpentane (ethanol) (PMMA), radiationless processes, temp. depend. 0-43087  
 1,5-dimethylnaphthalene, fluoresc. quenching by cyclic azoalkanes, micelle system probe 0-35578  
 1,8-diphenyl-1,3,5,7-octatetraene, high press. fluoresc. studies of radiative and nonradiative processes 0-1011  
 1,6-diphenyl-1,3,5-hexatriene, high press. fluoresc. studies of radiative and nonradiative processes 0-1011  
 1,6-diphenylhexatriene, lower excited states fluoresc. quenching 0-1016  
 4-diphenylphosphorylstilbenes, fluoresc., photodimerisation 0-1015  
 2,5-distyrylpyrazine, absorpt., Raman and fluoresc. spectrosc. 0-28049  
 DNA dye complex, spectral changes observed using microfluorometer and cryostat 0-17949  
 DNA packing in fibrils of DNP of polytene chromosomes 0-30649  
 DNA-acridine dye complex, fluorescence studies 0-37921  
 Doppler-free Raman spectroscopy and suppression of laser-induced mol. Doppler broadened transitions 0-9638  
 dye solution, nonlinear fluoresc. meas., two-photon pumping by low power laser 0-48037  
 dye solutions, picosecond flash photolysis and very fast processes 0-30249  
 energy transfer dye lasers and laser induced intermol. and intramol. energy transfer processes 0-9647  
 ethylene, excited with parametric oscillator, vibr. relax. obs. and interpret. 0-9702



**molecular fluorescence continued**

- ethylene, multiphoton dissociation,  $\text{CH}_2$  and  $\text{C}_2$  prod., fluence depend. meas. 0-5586
- fluorobenzene cations, fluoresc. quantum yields and lifetimes, electronic state relax. processes 0-48027
- fluorobenzene radical cations, matrix laser fluoresc. spectra 0-1009
- fluoroethanes, IR multiphoton dissociation, HF vib. energy distrib. 0-53073
- fluoroethylenes, IR multiphoton dissociation, HF vib. energy distrib. 0-53073
- fluoromethane, laser pumped, vibr. states collision dynamics fluoresc. obs. 0-53104
- fluoromethane- $\text{d}_3$ , vibr. energy transfer at low temps., inert gas and  $\text{N}_2$  matrix obs. 0-9706
- fluorometric system, nanosec. time-resolved spectrometry with tunable dye laser and pulse-gated photon counter 0-11968
- formaldehyde+O, absolute rate consts., discharge flow and flash photolysis reson. fluoresc. meas. 0-55648
- formaldehyde- $\text{d}_1$  ( $-\text{d}_2$ ), single vibronic levels, fluoresc. emission, radiative lifetimes and vibr. relax 0-23521
- formaldehyde- $\text{d}_2$  vapour, IR-UV double resonance 0-43078
- glyoxal, singlet-triplet coupling, double reson. and level-anticrossing spectroscopy 0-48053
- glyoxal, vibr. energy redistrib. following internal conversion 0-23452
- glyoxal ( $\text{A}_1$ ), fluoresc. quantum yields, radiative and nonradiative lifetimes 0-32759
- haloacetylene cations, electron impact excitation  $\text{A} \rightarrow \text{X}$  band system assignment 0-32766
- halomethanes, UV multiphoton dissociation, photofragment fluoresc. 0-14165
- heteroaromatic molecules, planar, orientation and phosphoresc. polarisation in stretched film 0-14169
- histones, H2A and H4, effect of molecular interactions on fluorescence intensity 0-51032
- 3-hydroxyflavone, excited state proton transfer, luminesc. 0-35818
- inert gas afterglow, excimer form., VUV emission obs. at low press. 0-38755
- inert gas halides, UV emission spectra, pressure and temp. depend. 0-28209
- 9-iodoanthracene, picosecond fluoresc. lifetimes, thermally activated  $\text{S}_1 \rightarrow \text{T}_1$  intersystem crossing 0-28045
- IR multiple-photon dissociation, laser induced fluoresc. photofragment detect. 0-37840
- isotropic solutions, fluorescence emission anisotropy, time depend. 0-7391
- ketene, multiphoton dissociation,  $\text{CH}_2$  and  $\text{C}_2$  prod., fluence depend. meas. 0-5586
- ketcyanines alcohol solns., spectral-luminesc. props. 0-2835
- laser dyes, photochemical quantum yield determ. using fluorescence data 0-55685
- laser studies of relaxation and reaction of species in defined quantum states 0-11918
- liquids, two-pulse spectroscopy with ps laser pulses 0-53041
- luminescence decay, exchange mechanism, parameters 0-28051
- macromolecules in dilute soln., electrically induced fluorescence polarised component change meas. 0-32863
- Manoxol OT-cyclohexane-water reversed micellar system, singlet-singlet energy transfer 0-9531
- methacrylate polymer, carbazoyl substituted, excimer and charge transfer complex trapping of excitons 0-34367
- methane, energy transfer obs. using excitation of fund., overtone and combination bands 0-9704
- methanol, UV multiphoton dissociation, photofragment fluoresc. 0-14165
- methylamine, multiple-photon dissociation, laser induced fluoresc. photofragment detect. 0-37840
- 2-methylPOPOP, soln., anisotropic fluoresc. of prolate mol. (German) 0-1018
- 1-methylpyrene, fluoresc. quenching by  $\text{Cu}^{2+}$  in micellar system, general kinetic model 0-32753
- micelles, inverted containing water, hydrodynamic vol. determ. by fluoresc. polarisation 0-50892
- microemulsions, aerosol OT, inhomogeneous interior, fluoresc. and polarisation decay probes 0-50891
- molecular excited state relaxation processes, oscillatory versus dissipative limits, education appl. 0-31468
- molecular X-rays from heavy-ion collisions, superheavy quasi-molecule spectroscopy 0-23509
- multiphoton ionisation dynamics, rate eqn. modelling 0-48046
- $\text{Na}_2$ , laser-excited, emission bands obs. in visible and IR 0-48036
- naphthalene, adsorbed on silica gel surface, biphasic photochemistry, time-resolved spectra 0-30252
- naphthalene, fluorescence and absorpt. spectra, deviations from Condon approx. 0-28004
- naphthalene, triplet exciton annihilation and triplet spin relax. 0-29792
- naphthalimide derivatives, solutions, lasing characts. in green spectral region, photostability 0-32978
- neutron flux energy spectrum meas. from freq. change of luminesc. line 0-23272
- nitromethane molecule dissociation in IR field, laser-induced fluoresc. obs. 0-53075
- $\alpha$ -NPO, fluoresc. spectrum light quenching factor wavelength depend. 0-18882
- nucleic acid-dye complexes, energy transfer obs. using laser-induced fluoresc. 0-12054
- organic compounds, IR fluorescence under  $\text{CO}_2$  laser radiation 0-37830
- organic dyes, absolute fluorescence quantum yield, calorimetric determ. 0-43092
- ovalene, isolated ultra cold mol., intermediate level structure of  $\text{S}_2$  state 0-28048
- ovalene, vibrational quasicontinuum threshold, spectrosc. criterion 0-52972
- palladium-octaethylporphyrin, gas phase delayed fluoresc. and phosphoresc., triplet excimer formation 0-18884
- pentacene, vibrational quasicontinuum threshold, spectrosc. criterion 0-52972
- perylene in n-heptane cryst., polarised fluoresc. 0-1017
- perylene-tetracene in liquid crystals, temp. depend. of absorption and fluoresc. (German) 0-18887
- phase fluorometry as a probe of diffusion-controlled molecular encounters in dense fluids 0-32799
- pheophytin-a (b), dimerisation, fluoresc. and ODMR study 0-18876
- phthalimide derivatives, hidden vibr. band determ. method, fluorescence and excitation spectra meas. 0-40158
- phthalimide derivatives, solutions, lasing characts. in green spectral region, photostability 0-32978

**molecular fluorescence continued**

- picosecond time-resolved fluorescence techniques using mode-locked laser system 0-27359
- polarised fluorescence, polymeric noncrystalline chain orientation evaluation (Japanese) 0-6368
- poly (ar-methylstyrene)s, steric effects on excimer formation, fluorescence spectra exam. 0-25430
- poly-N-vinylcarbazole, in polymer film, excimer fluoresc., high press. effects 0-34966
- poly-N-vinylcarbazole, soln., picosecond time-resolved fluoresc. by pulse radiolysis 0-28122
- polyatomic molecule, ultrafast vibr. using laser light pulses 0-9699
- polyatomic mols., quantum beats 0-37826
- polyatomic radical cations, excited states, decay processes 0-28055
- polyatomics, absorpt. and luminesc. spectra, higher electronic states effect 0-9586
- polymethine cyanine dyes, viscosity depend. fluoresc. lifetime using synchronously operated ps streak camera 0-28041
- polystyrene, steric effects on excimer formation, fluorescence spectra exam. 0-25430
- polystyrene microspheres, dye impregnated, fluoresc. spectra struct. resonances 0-50914
- POPOP, fluoresc. spectrum light quenching factor wavelength depend. 0-18882
- POPOP, soln., anisotropic fluoresc. of prolate mol. (German) 0-1018
- POPOP laser, bleaching of vapour 0-19027
- porphyrin in host n-alkane crystals, phototautomerism, IR spectral obs. 0-34963
- porphyrins orientation in n-alkane Shpolskii hosts, spectra 0-48035
- prolate molecules, anisotropic fluoresc. in soln. (German) 0-1018
- propynal, energy dispersion and relax., laser IR-visible double reson. 0-48023
- proteins, adsorbed at interfaces, fluoresc. spectroscopy study 0-12315
- proteins, resolution of components of complex spectra by Alentsev-Fok method 0-1097
- proteins, UV fluorescence spectra, resolving of components, Alentsev-Fok method 0-1096
- pyrazine, excited and  $\text{N}_1$  ionised states, ab initio calcs. broken orbital symm. 0-27931
- pyrazine ( $-\text{d}_2$ ), single vibronic level fluoresc. spectra, rel. to vibronic coupling 0-28043
- pyrazine ( $-\text{d}_2$ ) vapour, single vibronic level fluoresc. from n,  $\pi^*$  0-37827
- pyrene, adsorbed on silica gel surface, biphasic photochemistry, time-resolved spectra 0-30252
- pyrene-sodium 5-[1-pyrenyl]pentanoate intramolecular excimer formation in CTAC and SDS micelles, fluoresc. probe 0-16733
- quercetin, excited state proton transfer, luminesc. 0-35818
- radicals, laser fluoresc. detection with high time resolution 0-9632
- rare earth complexes, formation and props., book contrib. 0-43204
- resonance fluoresc., probe of intramolecular relax., density matrix formalism, lifetimes and quantum beats 0-32757
- resonance interactions of atomic and molecular systems driven by strong laser field, theory 0-14097
- retinyl acetate, high press. fluoresc. studies of radiative and nonradiative processes 0-1011
- rhodamine 4C, in ethanol soln., rot. relax. time using ps. spectroscopy technique 0-1013
- rhodamine 6G, fluoresc. polarisation, solvent effects 0-32755
- rhodamine 6G, orientated relax. times, streak camera meas. 0-14168
- rhodamine 6G and rhodamine B adsorbed on  $\text{AlH}_3$ , luminesc. spectra during  $\text{AlH}_3$  photolysis 0-55171
- rhodamine B and 6G, fluoresc. decay time meas. in different solns. 0-9637
- rhodamine dyes in soln., bleaching, electronic and vibr. absorpt. spectra, fluoresc. 0-42960
- rhodamine-6G-3,3'-diethylthiacyanocarbonyl iodide-sodium lauryl sulphate soln., premicellar region, energy transfer 0-20685
- rotational motion probe technique using E-type delayed fluorescence depolarisation 0-36207
- rubrene, sensitised photooxidation of 1,3-diphenylisobenzofuran solns.,  $\text{S}_1$  excited state  $\text{O}_2$  quenching 0-45529
- solid, molecular fluoresc., phosphoresc., and ODMR line narrowing 0-43084
- stilbene, cis-trans photoisomerisation rate const., direct meas. 0-30250
- trans-stilbene, time resolved fluoresc. in ps. regime 0-14164
- p-terphenyl, triplet exciton annihilation and triplet spin relax. 0-29792
- tetracene, vibrational quasicontinuum threshold, spectrosc. criterion 0-52972
- tetracene in liquid crystals, temp. depend. of absorption and fluoresc. (German) 0-18887
- tetracyanobenzene+methylated benzene, fluorescent exciplex form., electronic relax. 0-5573
- s-tetrazine in n-hexane, picosecond time-resolved fluoresc., vibr. relax. 0-48025
- thiophosgene,  $\text{B}^1\text{A}'$ -state, photophys., fluoresc. lifetime meas. 0-53033
- three-level molecular system, cooperative evolution, transient effects of dephasing and relax. 0-28184
- time-correlated picosecond laser pulses generation, rapid sampling of optical relax. phenomena 0-9969
- time-resolved laser fluorescence spectroscopy for atomic and mol. excited states obs., review, book contrib. 0-9760
- TOPOT, 1,4-bis[2-(5-p-tolylloxazolyl)]benzene laser, bleaching of vapour 0-19027
- TOPOT, fluoresc. spectrum light quenching factor wavelength depend. 0-18882
- 1,3,5-trichloro-2,4,6-trifluorobenzene radical cation,  $\text{B}^2\text{A}_2' \rightarrow \text{X}^2\text{E}^*$  laser-induced fluoresc. spectra 0-14172
- tryptophan, stereoselective energy transfer induced by circularly polarised light 0-1010
- two-level molecular systems, optically pumped, increased inversion efficiency 0-23657
- two-photon excited molecular fluorescence technique in chem. analysis 0-40799
- two-photon fluorescence, contrast ratio decrease depend. on laser pulse intensity 0-1255
- 2-vinylanthracene, conform. conversion kinetics, fluoresc. 0-9631
- xanthene dyes, hidden vibr. band determ. method, fluorescence and excitation spectra meas. 0-40158
- xanthene dyes, internal heavy atom effect on radiative and non-radiative rate consts. 0-32765
- Ar, condensed electron beam excited, exciton radiative lifetimes 0-6727



## molecular fluorescence continued

- ArCl\*, excimer formation rate consts., B state radiative lifetimes, quenching, VUV excitation 0-55631  
 ArF, Ar<sub>2</sub>F, time depend. emission meas., Ar-Kr-F<sub>2</sub> laser mixture kinetics 0-32768  
 ArF, electron quenching rate consts. meas. by fluoresc. anal., laser implications 0-32969  
 BO<sub>2</sub>, Doppler free spectra, backscatter fluoresc. line narrowing, theory and obs. 0-53034  
 Ba+SO<sub>2</sub>→BaO+SO reaction, laser-induced fluoresc. obs., vibronic distrib. of BaO, collisional energy depend. 0-11917  
 Br+NOBr, primary and secondary photochemistry, vibrationally excited NO, IR fluoresc. obs. 0-48030  
 Br<sub>2</sub>, fluoresc. obs. in UV laser photochem. of dibromodifluoromethane 0-16703  
 BrCN, vacuum UV photodissociation spectroscopy, quantum yield, fluoresc. polarisation 0-32736  
 C<sub>2</sub>, laser fluoresc. detection with high time resolution 0-9632  
 C<sub>2</sub>, low lying a<sup>1</sup>Π<sub>g</sub> state produced in intense IR field, fluoresc. and quenching obs. 0-11931  
 CBr<sub>2</sub>, emission in solid Ar, laser excitation spectra and lifetimes 0-48034  
 CBrCl emission in solid Ar, laser excitation spectra and lifetimes 0-48034  
 CF, fluoresc. obs. in UV laser photochem. of dibromodifluoromethane 0-16703  
 CF<sub>3</sub>, fluoresc. and radiative lifetime obs. in dibromodifluoromethane UV laser photolysis 0-16703  
 CF<sub>3</sub>NO→CF<sub>3</sub>NO, photodissociation dynamics, two-photon laser-induced fluorescence study 0-43122  
 CH<sub>2</sub>, photoprod. from ketene, singlet-triplet energy separation and rovibronic level obs. 0-11936  
 CN radicals, time behaviour in laser-initiated thermal isomerisation of CH<sub>3</sub>CN 0-11887  
 CO, A<sup>1</sup>Π(ν=1), vibr. relax. by reversible intersystem crossing, fluoresc. obs. 0-14170  
 CO, isotopically enriched, Ar matrix isolation, laser-included vibr. fluoresc. 0-9707  
 CO, multiphoton UV photolysis, isotope effects obs. 0-55679  
 CO, two-photon spectroscopy with tunable ArF laser 0-37843  
 CO-NO mixtures, Ar matrix isolation, laser-included vibr. fluoresc. 0-9707  
 CO+<sup>14</sup>N<sub>2</sub> (<sup>14</sup>N<sup>15</sup>N<sub>2</sub>), (<sup>15</sup>N<sub>2</sub>), vibr. energy transfer, laser fluoresc. obs. 0-28050  
 CO+CO<sub>2</sub>, vibr. level depend. quenching of CO(ν=1-16) 0-32808  
 CO<sub>2</sub> IR Zeeman spectra utilizing copropag. wave reson., diagm. shift obs. 0-53055  
 CS+He, Penning ionisation, CS<sup>+</sup>(B<sup>2</sup>Σ<sup>+</sup>→A<sup>2</sup>Π<sub>g</sub>) fluoresc., flowing afterglow 0-14197  
 Ca+CCl<sub>4</sub>→CaCl+CCl<sub>3</sub> reaction, laser-induced fluoresc. obs. 0-11916  
 Ca<sub>2</sub>, new ground state, photolum. obs. vibr. consts., dissoc. energy 0-5576  
 CaCl, laser excitation and fluorescence spectra, rotational anal. of A<sup>2</sup>Π=X<sup>2</sup>Σ transition 0-43098  
 Cd<sub>2</sub>(Cd<sub>3</sub>), fluoresc. kinetics, optical excitation, energy spacings and equilib. consts. 0-43090  
 CdHg, excimer kinetics and transmission meas. 0-37832  
 CdHg excimer system, absorpt. meas. 0-48007  
 CdHg, fluoresc. kinetics, optical excitation, energy spacings and equilib. consts. 0-43090  
 CeO, C<sub>1</sub>-X<sub>1</sub> and D<sub>3</sub>-X<sub>3</sub> systems, fluoresc., vibr. spectra, laser spectroscopy obs. 0-32761  
 Cl+NOCl, primary and secondary photochemistry, vibrationally excited NO, IR fluoresc. obs. 0-48030  
 Cl<sub>2</sub>, and isotopic forms, B<sup>2</sup>Π(0<sub>g</sub><sup>+</sup>) state, laser-induced fluoresc., collisional energy transfer rates 0-53038  
 Cl<sub>2</sub>, B-X transition, predissoc., laser-induced fluoresc. obs. 0-43093  
 ClCN, vacuum UV photodissociation spectroscopy, quantum yield, fluoresc. polarisation 0-32736  
 Cl<sub>2</sub>CS, excitation, singlet and triplet states, two photon absorpt., singlet-singlet energy pooling, fluoresc. obs. 0-48032  
 ClFCS, second excited singlet state photophysics, laser excitation obs. 0-32758  
 Cl(<sup>2</sup>P)+CH<sub>3</sub>→CH<sub>3</sub>+HCl, reaction rate const., laser flash photolysis-resonance fluoresc. kinetic study 0-45485  
 Eu chelate, fluoresc. lifetime, depend. on optical environment 0-9630  
 F+CH<sub>3</sub>(CF<sub>3</sub>)(ICl) reactions, product state analysis using laser-induced fluoresc. 0-11915  
 H<sub>2</sub>, density meas. by resonance fluoresc. (X<sup>1</sup>Σ<sub>g</sub><sup>+</sup>→B<sup>1</sup>Σ<sub>u</sub><sup>+</sup> transition) 0-5570  
 H<sub>2</sub>, two-photon spectroscopy with tunable ArF laser 0-37843  
 H<sub>2</sub>, vibr. population relax. in gas and fluid 0-29775  
 HCl-Br<sub>2</sub>-Ar, flash photolytically produced Br\* to HCl electronic to vibr. and rot. energy transfer 0-48069  
 HF, time resolved fluoresc., IR energy deposition in laser irradiated SF<sub>6</sub>-H<sub>2</sub> mixture 0-23454  
 HF+HF(H<sub>2</sub>)(D<sub>2</sub>)(CO<sub>2</sub>)(isobutene), vibr. relax. dye laser pumping effects 0-9703  
 HNO, vibronic state perturbative and predissoc. mechanisms, fluoresc. excitation spectra obs. 0-9658  
 He-N<sub>2</sub>, de excitation rate consts., energy transfer, pulse radiolysis obs. 0-30303  
 He-N<sub>2</sub> plasma, N<sub>2</sub> B<sup>3</sup>Π<sub>g</sub> state excitation, role of long lived states, luminesc. 0-37829  
 He<sub>2</sub>, 600 Å emission continuum 0-1012  
 He<sub>2</sub>, metastable states, laser excitation spectra 0-5578  
 Hg<sub>2</sub>, dissociative recomb. and optical transmissions meas. in high press. discharge 0-37816  
 Hg<sub>2</sub>, emission and form. kinetics, sequential two-photon absorpt. expt. 0-32767  
 Hg<sub>2</sub> excimers, photoassoc., spectroscopy and kinetic processes of high-lying vibronic states, laser applics. 0-9649  
 HgBr emission intensity, HgBr<sub>2</sub> dissociative excitation by inert gas and N<sub>2</sub> metastables 0-40687  
 HgBr, laser photolysis prep., laser induced fluoresc., collisional quenching processes 0-38014  
 HgBr laser using dissociative excitation of HgBr<sub>2</sub>, extraction efficiency increased by N<sub>2</sub> addition 0-38012  
 HgBr, polarised photofluoresc. spectroscopy, HgBr<sub>2</sub> photodissociation by ArF laser 0-37841  
 HgBr\*, collisional quenching by inert gas (molecule) 0-42986  
 HgBr\*, collisional quenching by inert gas (molecules) 0-43091

## molecular fluorescence continued

- HgCl\*, collisional quenching by inert gas (N<sub>2</sub>) 0-42986  
 HgI\*, collisional quenching by inert gas (N<sub>2</sub>) 0-43091  
 HgI<sup>+</sup> optically excited excimers, upper state kinetics 0-37831  
 I<sub>2</sub>, blue-green fluoresc., ArF laser excitation 0-14166  
 I<sub>2</sub>, CW intracavity dye laser spectroscopy 0-13155  
 I<sub>2</sub>, coherent optical transients and optical dephasing in mol. collisions 0-9966  
 I<sub>2</sub>, in CCl<sub>4</sub> (cyclohexane) soln., ps dye laser excitation, fluoresc. and resonance Raman emission 0-28021  
 I<sub>2</sub>, in seeded supersonic beams, vibr. and rot. relax., laser-induced fluoresc. obs. 0-23522  
 I<sub>2</sub>, predissociation, electric-field induced 0-37839  
 ICN, vacuum UV photodissociation spectroscopy quantum yield, fluoresc. polarisation vacuum UV photodissociation spectroscopy, quantum yield, fluoresc. polarisation 0-32736  
 IF internal vibr.-rot. product distrib., formed in F+CH<sub>3</sub>I(CF<sub>3</sub>I), fluoresc. obs. 0-48078  
 I<sub>2</sub>, Ne, He, van der Waals complexes photodissoc. 0-50864  
 I<sub>2</sub> fluoresc., Ar<sup>+</sup> laser excited, high resolution and sub-Doppler Fourier transform spectroscopy 0-43089  
 KXe, dye laser induced emission, excimer bands and uses 0-9650  
 Kr<sub>2</sub>, prod. and decay of 0<sub>g</sub><sup>+</sup> and 1<sub>g</sub> states, synchrotron excited 0-43109  
 KrCl\*, excimer formation rate consts., B state radiative lifetimes, quenching, VUV excitation 0-55631  
 KrCl\*+Xe, substitution efficiency during excitation in transverse AC electric discharge 0-50850  
 KrF discharge pumped laser, energy extraction, collisional coupling between B, C and D-states 0-28213  
 KrF, electron quenching rate consts. meas. by fluoresc. anal., laser implications 0-32969  
 KrF, Kr<sub>2</sub>F, time depend. emission meas., Ar-Kr-F<sub>2</sub> laser mixture kinetics 0-32768  
 KrF laser, collisional coupling between B, C, D states from fluoresc. meas., influence on energy extraction 0-1189  
 KrF linac-excited gas mixture, UV fluoresc. meas. 0-28216  
 Kr<sub>2</sub>F, absorpt. in near UV wing of 410 nm band, fluoresc. efficiency 0-14323  
 Li<sub>2</sub>, circular polarisation of emission, influence of nucl. hyperfine interactions and elastic collisions 0-9635  
 Li<sub>2</sub>, collisional depolarisation and rot. energy transfer, laser-induced fluoresc. obs. 0-9698  
 Li<sub>2</sub>, spectroscopy and structure, triplet excimer continuum emission 0-32769  
 Li<sub>2</sub>+inert gas, collision induced transition rate consts., two-laser spectrosc. 0-9629  
 N<sub>2</sub>, electrical discharge excitation, vibr. level population distrib., electron beam fluoresc. obs. 0-48031  
 N<sub>2</sub> plasma, non-equilib., excited species, vibr.-rot. anal. fluoresc. obs. 0-54034  
 N<sub>2</sub>, rarefied fluid dynamics, flow meas. by electron beam-body interactions 0-6186  
 N<sub>2</sub><sup>+</sup>, UV spectral line width in rarefied free jet, for rot. temp. 0-6184  
 N<sub>2</sub>-CO, electrical discharge excitation, vibr. level population distrib., electron beam fluoresc. obs. 0-48031  
 N<sub>2</sub>+Ar+POPOP, electron beam excited, energy transfer mechanisms 0-23497  
 N<sub>2</sub>+C<sup>+</sup> collisions, luminesc. 0-1055  
 NH<sub>2</sub> (A<sup>2</sup>A<sub>1</sub>), excited state dynamics and bimol. quenching processes 0-9681  
 NH<sub>2</sub> fragments, multiple photon dissoc. of CH<sub>3</sub>NH<sub>2</sub> and NH<sub>3</sub>, laser-excited fluoresc. obs. 0-11938  
 NH<sub>2</sub>+NO<sub>2</sub>, reaction rate const. meas. 0-7772  
 NH<sub>2</sub>(X<sup>2</sup>B<sub>1</sub>), laser-induced fluoresc. obs. in UV laser photodissoc. of NH<sub>3</sub> 0-11901  
 NO, UV fluorescence, IR laser induced 0-53032  
 NO+O, vibr. relaxation of NO, laser induced IR fluoresc. study 0-9626  
 NO<sub>2</sub>, dissociative limit, mol. beam characts. determ. by fluoresc. excitation spectra 0-53074  
 NO<sub>2</sub>, excited, fluoresc. spectrum, IR multiphoton vibr. pumping, photon absorpt. probability distrib. study 0-18854  
 NO<sub>2</sub>, inter and intramolecular radiationless transitions, relax., time resolved excitation and fluoresc. spectra 0-27966  
 NO<sub>2</sub>, laser and flash lamp fluoresc. monitors, comparison 0-17367  
 NO<sub>2</sub>, laser-induced fluoresc. quenching rate const. and lifetimes 0-11930  
 N<sub>2</sub>O quadrupole hyperfine struct., vibr. depend. obs. using twin-laser spectrometer 0-43097  
 NO<sub>2</sub>\*, multiple IR photon fluoresc. excitation and dissoc., electronically excited 0-48050  
 Na<sub>2</sub>, ground state, vibr.-rot. relax., optical pumping transients obs. 0-28067  
 Na<sub>2</sub>, laser excited, atomic and molecular fluorescence with long radiative decay times 0-27976  
 Na<sub>2</sub>, spectroscopy and structure, triplet excimer continuum emission 0-32769  
 Na<sub>2</sub> supersonic beam rovibronic level population, anal. by laser spectroscopy 0-43118  
 NaK dimer formed in supersonic beam, laser-induced emission 0-9636  
 Na\*, fluoresc. red continuum emission, atom-mol. energy transfer 0-43086  
 Ni<sub>2</sub>, A→X system, Ar matrix isolation fluoresc. spectrosc. obs. 0-9628  
 O<sub>2</sub> in chloroform and carbon tetrachloride solns., sensitized luminesc. 0-32762  
 OH, A-X system, rot. transition probabilities 0-43027  
 OH concentration profile in methane-air flames 0-35534  
 OH, produced in CH<sub>3</sub>+O<sub>2</sub>, 368K, rate const. upper limit 0-7771  
 OH radical, matrix-isolated, from H<sub>2</sub> oxidation on Pt, laser diagnostics 0-5572  
 OH(A<sup>2</sup>Σ<sup>+</sup>)+N<sub>2</sub>(O<sub>2</sub>)(H<sub>2</sub>O)(air), quenching rates and fluoresc. efficiency, rel. to atmosphere 0-14199  
 PrO, 0-0 band in XVII system, hyperfine splitting, visible excitation spectra 0-28028  
 SF<sub>6</sub> gas, CO<sub>2</sub> TEA laser-excited, slow intermol. redistrib. of vibr. energy 0-53039  
 SF<sub>6</sub>, multiphoton excited, IR fluoresc. spectrum meas. 0-37828  
 SO<sub>2</sub>, laser-induced phosphoresc.-excitation spectra of vibr. bands of (<sup>3</sup>B<sub>1</sub>)-(X<sup>1</sup>A<sub>1</sub>) transition 0-18879  
 SO<sub>2</sub>F, laser fluoresc. spectrum 0-28047  
 Se<sub>2</sub>, photolytic dissoc. obs. using inert gas halide lasers 0-11935  
 SiF<sub>4</sub>, CO<sub>2</sub> laser-irrad., dissoc. product fluoresc., wavelength depend. 0-11900



**molecular fluorescence continued**

- UF<sub>6</sub>, photophysical props., laser study 0-28040  
 UF<sub>6</sub>, UV photophysics, energy balance through quantum efficiency meas. 0-9634  
 UF<sub>6</sub>-H<sub>2</sub>, near UV and visible excitation, quantum yield from photodissociation 0-35549  
 Xe, condensed electron beam excited, exciton radiative lifetimes 0-6727  
 Xe<sub>2</sub>, laser performance for atm. press. and microsecond electron beam excitation 0-28199  
 Xe<sub>2</sub>, performance as photolytic driver at low electron beam excitation rates 0-32963  
 Xe<sub>2</sub><sup>+</sup> excimer form. in pulsed discharge, visible emission obs. 0-38754  
 XeBr, emission and form. kinetics, sequential two-photon absorpt. expt. 0-32767  
 XeCl avalanche discharge laser, D and B state coupling, population depletion 0-28214  
 XeCl, energy curves and transition moments 0-28210  
 XeCl, relax. and quenching rate consts., emission spectra modelling 0-28211  
 XeCl\*+Kr, substitution efficiency during excitation in transverse AC electric discharge 0-50850  
 XeF, (B,C) state prod. and kinetics, XeF<sub>2</sub> photolysis with VUV radiation 0-32975  
 XeF, B and C-state kinetics with self-sustained discharge pumping 0-28212  
 XeF, broadband emission origin 0-38007  
 XeF, electron beam pumped laser, gain, fluoresc. and laser output at 351, 488 nm 0-28215  
 XeF, electron quenching rate consts. meas. by fluoresc. anal., laser implications 0-32969  
 XeF, energy curves and transition moments 0-28210  
 XeF, ground state dissoc. vibr. equilibrium 0-9652  
 XeF laser using XeF<sub>2</sub> photodissociation, fluoresc. and laser performance 0-32976  
 XeF linac-excited gas mixture, UV fluoresc. meas. 0-28216  
 XeF, relax. and quenching rate consts., emission spectra modelling 0-28211  
 XeF, supersonic expansion jet, B-X system rot. and vibr. anal., isotope intervals, fluoresc. spectra 0-14174  
 XeO, luminesc. meas. of O(<sup>1</sup>S) absolute quantum yield in photolysis of CO<sub>2</sub>, N<sub>2</sub>O 0-35561  
 ZrO, B<sup>2</sup>II state radiative lifetimes, transition rates and oscillator strengths, reson. fluoresc. decay 0-28053

**molecular force constants**

see also *Coriolis force*

- 3,3,3-trifluoropropene, struct. and vibr. spectra, IR, Raman polarisation study 0-18845  
 acetaldehyde, Coriolis resonance bands in IR spectrum 0-47995  
 acetonitrile, quadratic force fields, MOCIC pot. functions calcs. 0-5475  
 alkali metal tetrafluoroborates, intramol. force fields and mean vibr. amplitudes 0-2743  
 alkenes, IR absorpt. curves calc. using standard fragments computer library 0-982  
 boron trihalides, mol. force field using parametric represent. method 0-27991  
 bromotrifluoromethane, E-species force consts., using L-F approx. method, HLFS applicability 0-962  
 C<sub>3</sub>, symmetry excited vibr. state mol. consts., graphical method 0-52969  
 chlorotrifluoromethane, E-species force consts., using L-F approx. method, HLFS applicability 0-962  
 cyclopentene, mol., pot. functions of bending modes 0-9753  
 diatomic molecules, spectrosc. consts., rel. to electronegativity 0-28007  
 diatomic systems, reln. between internuclear distances and force constants 0-43205  
 2,5-dihydrofuran, mol., pot. functions of bending modes 0-9753  
 N,N-dimethyl acrylamide (-d<sub>3</sub>,d<sub>6</sub>,d<sub>9</sub>), force field, IR and Raman spectra obs. 0-47979  
 dimethyl di(trifluoromethyl) germanium, and perdeuterated analogues, vibr. spectra, normal coord. anal. (*German*) 0-5547  
 N,N-dimethylselenourea, deuterated forms and methyl derivatives, fundamental IR vibr. assignments 0-961  
 N,N-dimethylthiourea, deuterated forms and methyl derivatives, fundamental IR vibr. assignments 0-961  
 1,4-dioxadiene, mol., pot. functions of bending modes 0-9753  
 fluoroform, quadratic force fields, MOCIC pot. functions calcs. 0-5475  
 force field determination, Green's function method, ambiguities 0-960  
 formic acid, H bonding, electronic struct., geometries, moments, dimerisation energies, charge distrib., pseudopotential calcs. 0-27942  
 ground state props., coupled cluster and MBPT methods appl. 0-47881  
 heavy metal diatomic halides, Wasastjerna pot. function, force consts. internuclear separations and binding energies 0-14187  
 hexafluoropropene, struct. and vibr. spectra, IR, Raman polarisation study 0-18845  
 inert gas complexes spectroscopic data, geometry, pot. energy curve, dissoc. energy, equilib. internuclear distance, determ. 0-53018  
 iodotrifluoromethane, E-species force consts., using L-F approx. method, HLFS applicability 0-962  
 ion-molecule equilibria in solvolysis, secondary β<sup>2</sup>H isotope effects, hyperconjugation 0-50874  
 isostructural molecules and ions, force const. set calcs. 0-23390  
 JWKB phase integrals, to high-order 0-5632  
 L-F approx. method for symmetrized force consts., XY<sub>n</sub> mols. 0-14128  
 light atom molecules, general quadratic force fields, semiempirical MOCIC calcs. 0-5474  
 methanol, H bonding, electronic struct., geometries, moments, dimerisation energies, charge distrib., pseudopotential calcs. 0-27942  
 methyl chloride, charge distrib., substituents effect 0-905  
 methyl fluoride, charge distrib., substituents effect 0-905  
 methyl formate(-d<sub>1</sub>,d<sub>3</sub>,d<sub>4</sub>), mol. vibr. spectrum, struct., beginning with PCIO calc. (*French*) 0-23401  
 methyl halides, force consts. evaluation using gp. vibrs. and centrifugal distortion consts. 0-9580  
 methyl halides, mol. force fields, IR intensities, and vibr. props. 0-47879  
 methyl tri(trifluoromethyl) germanium, and perdeuterated analogues, vibr. spectra, normal coord. anal. (*German*) 0-5547  
 methyl vinyl sulphide, syn-gauche equilib., force field and ab initio calcs., microwave and Raman spectra 0-23573  
 methylacetylene, quadratic force fields, MOCIC pot. functions calcs. 0-5475  
 N=3 eigenvalue problem, appl. to XYZ bent mols. (*German*) 0-14131

**molecular force constants continued**

- normal co-ordinates through coriolis coupling constants 0-28005  
 phenanthrene, planar normal vibrs. calcs. 0-5525  
 polyatomic molecule, anharmonic force consts., vibr.-rot. interaction consts. 0-966  
 polyatomic molecule, crit. consts. evaluation from intermol. force consts. 0-37844  
 polyatomic mols., nuclear charge model and valence force consts. prediction 0-43022  
 polyatomic XY<sub>5</sub> type molecules, vibr. assignment using Redington's method 0-23410  
 porphins, reson. Raman spectra, selection rules, normal coord. treatment 0-53175  
 relaxed force constants, generalised approach 0-23409  
 tetrahalides of Gp.IV elements, M-X bond flexibility, by compliance scheme 0-37805  
 s-tetrazine, mol., pot. functions of bending modes 0-9753  
 thiirene and deuteroderivatives, Fourier transform IR spectra using Ar matrix isolation, vibr. band assignments 0-14142  
 trifluoromethyl trimethyl germanium (tin)(lead), and perdeuterated analogues, vibr. spectra, normal coord. anal. (*German*) 0-5547  
 XY<sub>2</sub>-type bent symmetric mols., vibr. anal., kinetic consts. method 0-18838  
 XY<sub>3</sub> pyramidal-type mols., mol. consts., kinetic consts. and L-approx. methods 0-18839  
 XY<sub>8</sub> molecules of D<sub>2d</sub> symmetry, G, F and Σ matrices (*French*) 0-970  
 BI<sub>3</sub>, mol. force field using parametric represent. method 0-27991  
 CO, vibr. struct., core and valence ESCA spectra, Frank-Condon and HF anal. 0-32602  
 C<sub>2</sub>O, mol., pot. functions of bending modes 0-9753  
 COF<sub>2</sub>, force field analysis using parametric represent. method 0-27990  
 COS, mol. potential surface, evaluation from spectroscopic observations 0-43207  
 ClO, UV spectra of C<sup>2</sup>Σ<sup>+</sup>-X<sup>2</sup>II system, rot. anal. 0-996  
 ClO<sub>2</sub>F, pyramidal type mol., force field comput. using Green's function procedure 0-23407  
 FH-OH<sub>2</sub>(dimethyl ether), H-bonded complexes, cubic force consts. calcs. 0-47868  
 GeCl<sub>4</sub>, mol., UV spectra, band assignments and rot. consts. 0-997  
 GeH<sub>3</sub>-group containing mols., normal coord. anal. 0-9579  
 GeO<sub>4</sub><sup>4-</sup> compounds, vibr. pot. function, force consts., isotopic shifts, mean vibr. amplitudes 0-23395  
 H<sub>2</sub><sup>+</sup>, SCF multiple scatt. calc. 0-916  
 HBS, and isotopic forms, force consts., coriolis consts., vibr. amplitudes, shrinkage effects 0-43021  
 H<sub>2</sub>O, ESCA and soft X-ray emission, vibr. excitation 0-23433  
 H<sub>2</sub>O, H bonding, electronic struct., geometries, moments, dimerisation energies, charge distrib., pseudopotential calcs. 0-27942  
 HPO, emission system, rot. anal. of vibr. bands 0-47957  
 ICl, <sup>35</sup>Cl and <sup>37</sup>Cl, B<sup>2</sup>Π<sub>g</sub>+ state IR spectra, mol. consts. 0-28016  
 KrHCl, van der Waals complexes, struct., RF and microwave spectra, isotope effects 0-37806  
 KrHCl, weak complex, rot. spectra 0-52980  
 Li<sub>2</sub>, optical-optical double reson., <sup>1</sup>Σ<sub>g</sub><sup>+</sup> state mil. consts. 0-53027  
 MgX<sub>2</sub> (X=F, Cl, Br, I), 2Z 0-43021  
 MnO<sub>4</sub><sup>-</sup> ion, <sup>18</sup>O enriched, matrix isolated IR spectra, force consts. 0-52985  
 N<sub>2</sub>, solid, α- and γ-forms, Raman spectra, vibron and lattice freq. shifts, libration 0-16020  
 N<sub>2</sub>, vibr. struct., core and valence ESCA spectra, Franck-Condon and HF anal. 0-32602  
 NH<sub>2</sub>, ground state mol. consts., absorption spectra 0-28030  
 NH<sub>3</sub>, ESCA and soft X-ray emission, vibr. excitation 0-23433  
 NH<sub>3</sub>, predissociation of A<sup>2</sup> state, force constants calc. 0-1034  
 OCS in Ar soln., IR spectra, solvent shifts, vibr. band assignment and anharmonic force consts. 0-9607  
 PH<sub>3</sub>, equilibrium structure and harmonic force field, ab initio calc. 0-9502  
 PH<sub>3</sub>, equilibrium structure and harmonic force field, ab initio calc. 0-9502  
 (SCN)<sub>2</sub><sup>-</sup>, and (SCN)<sub>2</sub>, vibr. anal., bond strengths 0-9582  
 SCI(Br), unstable radicals, matrix-isolated, IR spectra force const. (*German*) 0-43053  
 Si<sub>2</sub>F<sub>6</sub>, normal coord. analysis, vibr. freqs. and amplitudes, shrinkage and distortion consts., force consts. 0-27989  
 SiH<sub>3</sub>-group containing mols., normal coord. anal. 0-9579  
 SiO<sub>4</sub><sup>4-</sup> compounds, vibr. pot. function, force consts., isotopic shifts, mean vibr. amplitudes 0-23395  
 TiF<sub>4</sub>, equilib. config., force field, Coriolis consts., vibr. freqs. and amplitudes 0-32835  
 UO<sub>2</sub>(NO<sub>3</sub>)<sub>2</sub> complexes, IR spectra, normal coordinate anal., vibr. assignments, force consts. and ligation effects 0-9608  
 WO<sub>3</sub>, vibr. anal., mol. consts., kinetic consts. method 0-23393

**molecular force fields** see *molecular force constants***molecular hyperfine structure**

- bromomethyl methyl ether, microwave spectra, quadrupole computing effect 0-18848  
 bromomethyl methyl ether, microwave spectra, quadrupole coupling effect 0-14135  
 bromomethylsilane, microwave spectra, quadrupole computing effect 0-18848  
 bromomethylsilane, microwave spectra, quadrupole coupling effect 0-14135  
 carbenes, triplet state g-tensors and hyperfine coupling tensors 0-52895  
 deoxyhaemoglobin, high mag. field Mossbauer spectra, electronic states 0-35845  
 deoxymyoglobin, high mag. field Mossbauer spectra, electronic states 0-35845  
 diatomic mol., hyperfine struct. transitions, quantum theory for undergraduate demonstration 0-17762  
 ferrous porphyrin, intermediate (S=1) spin state, PMR characterisation 0-48014  
 fluorene: acridene, radical pair form. from excited states, optical nucl. polarisation obs. 0-14155  
 formaldehyde, triplet state g-tensors and hyperfine coupling tensors 0-52895  
 hyperfine coupling, constants, nucl. spin spin coupling const., NDDO MO calcs. 0-23310  
 imidazoles, reaction with photochemically generated α-hydroxyalkyl radicals, EPR study 0-35558



**molecular hyperfine structure continued**

- methane, line profile of coherent radiation in separated fields due to  $F_2^{(2)}$  transition 0-37835  
 methyl radical in sodium acetate, EPR spectra, anisotropic hyperfine interaction, rot. tunnelling 0-34775  
 saturation spectroscopy, hyperfine component intensities 0-31886  
 scandium octaethylporphyrin,  $\mu$ -oxo bridged dimer, triplet states and geometrys, ODMR obs. 0-9625  
 scandium octaethylporphyrin, triplet states and geometrys, ODMR obs. 0-9625  
 transition metal complex, ligand field problems, group theory 0-42920  
 $AlH^+$  radical cation, EPR matrix isolation obs., hyperfine components calcs. 0-14158  
 BeH radical, hyperfine splitting const., electronic energy, UHF-type, CCI calcs. 0-52909  
 $^{79}BrF$ ,  $(^{81}BrF)$ , hyperfine struct., elec. dipole moment, rot. transitions, microwave spectral obs. 0-32695  
 $COCl_2$ , phosgene,  $Cl_2$  nuclear quadrupole coupling tensor, microwave spectra 0-52982  
 $CaF$ ,  $^2\Sigma_{1/2}^+$  ground state, spin-rot. and hyperfine splittings rot. depend., mol. beam laser-RF double reson. 0-43079  
 $CICN$ , ground and first excited bending, vibr. state, props., mol. beam elec. reson. 0-37823  
 Cu complex, catena- $\mu$ -isothiocyanato- $(N'$ -pyridylmethylene- $N''$ -salicyloylhydrazinato- $NN'O$ ) copper (II), EPR and visible spectra 0-5566  
 $CuBr$ , rot. spectrum hyperfine struct., coupling consts., microwave spectroscopy study 0-18844  
 FO free radical, detection by  $CO_2$  laser mag. reson. 0-45594  
 $(H_2)_2$ ,  $(D_2)_2$ ,  $(HD)_2$  and  $H_2$ - $D_2$ , Van der Waals complexes, mol. symmetry 0-42963  
 $Hg_2$ -Pt,  $^{199}Hg$  Mossbauer meas., isomer shift and quadrupole splitting calcs. 0-28039  
 $Hg_2F_2$ ,  $^{199}Hg$  Mossbauer meas., isomer shift and quadrupole splitting calcs. 0-28039  
 $I_2$ , folded Doppler broadened system, interaction with two reson. laser fields 0-53007  
 $I_2$ , hyperfine transition saturation intensities, saturated absorpt. technique 0-43208  
 $I_2$ , line near 520 THz, HFS, direct freq. meas. 0-53266  
 $^{127}I$ , hyperfine structure components, stabilization of doubly resonant intracavity SHG of 1153 nm radiation 0-33077  
 $Li_2$ , circular polarisation of emission, influence of nucl. hyperfine interactions and elastic collisions 0-9635  
 $NH_3$ , hyperfine quadrupole coupling, ro-inversional levels, inversional depend. 0-27961  
 $NH_3$ , mol. beam state selection and focusing, hyperfine spectrum 0-28119  
 $N_2O$  quadrupole hyperfine struct., vibr. depend. obs. using twin-laser spectrometer 0-43097  
 OH, prod. by photolysis, A-doublets, population, rot. states, hyperfine struct., microwave spectra 0-32694  
 $OsO_4$ , HFS and fine struct., saturation spectroscopy obs. visible spectra 0-53008  
 $PH_3$ ,  $X^2B_1$ -state, rot. laser mag. reson. spectrosc. 0-28038  
 PRO, 0-0 band in XVII system, hyperfine splitting, visible excitation spectra 0-28028  
 $SF_6$ ,  $\nu_3$  bands, rot. fine struct., HFS spectroscopic consts. determ., saturation spectroscopy obs. 0-53008  
 $ScS$ ,  $B^2\Sigma^+X^2\Sigma^+$  system, rot. struct. and hyperfine effects near IR spectrum 0-5544  
 TIF, electric dipole hyperfine struct. calc. 0-53162  
 TIF, P- and T-violating interactions in hyperfine struct., mol. beam reson. expt. 0-53019

**molecular inelastic collisions**

- see also atom-molecule collisions; atom-molecule reactions; ion-molecule collisions; ionisation of molecules; molecular rotational-vibrational energy transfer; molecule-molecule reactions  
 acetaldehyde +  $H_2(N_2)(CO_2)$ , rot. line broadening, mol. quadrupole moments calc. 0-28065  
 alkali metal dicarboxylates, H bonding and motion, incoherent inelastic neutron scatt. spectroscopy 0-48095  
 atomic and molecular collisions, book 0-27058  
 benzenetricarbonylchromium, neutron inelastic scatt. spectrum and valence force field 0-48096  
 bimolecular, time delay, multichannel spectral theorem 0-43144  
 binary collisions, time correlation functions, influence of bounded trajectories 0-43143  
 bound states, semiclassical study 0-9693  
 collinear scattering, information content, dynamical approach 0-23500  
 collision reorientation in resonant light field (*Russian*) 0-14192  
 critical molecules, neutron scatt., 'optical activity' 0-23567  
 cyclohexane + toluene, energy transfer, pulse radiolysis obs. 0-16714  
 diatom + diatom, vibr. energy transfer, collinear and 3-dimens. rate consts. 0-48065  
 diatomic mol. scatt., Tietz phase shift differences, semi-empirical relations, Varshni and Hulbert-Hirschfelder pots. 0-9673  
 direct chemical reactions in fast molecule collisions, eikonal approx. calcs. (*Russian*) 0-3332  
 DODCI + malachite green (DQOCI), electronic energy transfer obs. 0-5633  
 energy level transitions, Doppler broadening, phase-destroying collisions 0-9561  
 fast molecular ion + solid (gas), excited electronic states effects 0-9687  
 fluoromethane + fluoromethane, collisionally induced relax. processes and vibr. energy transfer 0-53107  
 fluoromethane +  $SO_2$ , collisionally induced relax. processes and vibr. energy transfer 0-53107  
 gas mixture, laser irradiated, anisotropy of inelastic scatt. and selective diffusion 0-53907  
 gaseous relax. phenomena, few-level approx. validity 0-53097  
 inert gas excimer lasers, at. and mol. collision processes 0-53263  
 inert gas halide lasers, at. and mol. collision processes 0-53263  
 isotropic tetrahedrally and octahedrally symmetric molecules, clusters, collision induced polarisability, mol. frame distortion 0-32798  
 laser spectroscopy, atom and mol. interactions, conf., Zaragoza, Spain (June 1979) 0-27041  
 light scatt., near-reson., from collisionally perturbed atoms and molecules, theory 0-1045  
 light scattering, collision-induced and multiple, by simple fluids 0-53919

**molecular inelastic collisions continued**

- many channel scattering model, exactly soluble 0-43127  
 microphysics to macrochemistry, discrete simulations, review 0-54102  
 nonadiabatic transitions, linear curve crossing problem, generalised Stueckelberg method 0-28085  
 phase fluorometry as a probe of diffusion-controlled molecular encounters in dense fluids 0-32799  
 quasi-classical and quantum moments of distrib. of states, semiclassical comparison 0-23480  
 radiative transitions in collision processes in presence of picosecond laser pulses 0-23479  
 resonance transfer rate of electron excitation, model of convergent terms, effect of diffusional motion of particles 0-8936  
 tetracyanobenzene + methylated benzene, fluorescent exciplex form., electronic relax. 0-5573  
 three body problems with Coulomb interaction, adiabatic representation, two-level approx. 0-47861  
 Tokamak impurity problems, atomic and mol. struct. and collision data, review 0-43959  
 translation factor, parameter-free, semiclassical approach 0-23482  
 two-photon transition in colliding particle system, stimulated Raman scatt. 0-9663  
 $CO_2$ - $N_2$ -He discharge, electron distrib. relax., numerical study 0-54070  
 $COF_2$  +  $COF_2$ , collisionally induced relax. processes and vibr. energy transfer 0-53107  
 $D_2$  +  $D_2$ , collision effect on depolarised light scatt. linewidths 0-53059  
 $H_2$ ,  $D_2$  and HD, intermol. collision process obs. using light scatt. expts. 0-53001  
 $H_2$  in Seyfert, galaxy NGC 1068 nucleus, collisional excitation 0-12816  
 $H_2^+$ , collisional dissoci., excited electronic states effects 0-9687  
 $H_2$  + H, rot. excitation in diffuse interstellar clouds rel. to  $CH^+$  prod. by shock waves 0-56898  
 $H_2$  +  $H_2$ , collision effect on depolarised light scatt. linewidths 0-53059  
 $H_2$  +  $H_2$ , quadrupolar  $S_1(J) + S_0(J)$  double transitions, IR fundamental band, 77K 0-52986  
 HD, gas, fundamental band, R and P line shapes 0-23461  
 $HeH^+$ , collisional dissoci., excited electronic states effects 0-9687  
 $Hg_2$  excimers, photoassoc., spectroscopy and kinetic processes of high-lying vibronic states, laser applics. 0-9649  
 $N_2$ , rotational collision number from thermal cond., 700-2500K 0-23526  
 $N_2$  + CO, electronically inelastic collision, distorted wave calc. and pot. energy curve 0-9709  
 $NH_3$  +  $2H_2$ , triplet n3S Rydberg state, ab initio UHF CI SCF calc. 0-53095  
 NO, press. broadening coeffs., spin-flip Raman laser spectrosc. 0-43147  
 $NO_2$ , inter and intramolecular radiationless transitions, relax., time resolved excitation and fluoresc. spectra 0-27966  
 $O_2$ , microwave spectrum, press. broadening 0-23412  
 OH collisional broadening parameter in  $H_2$ -NO flame, curve of growth calcs. 0-53052  
 $OH + H_2O(NO_2)(CH_3Cl)(N_2)(H_2)(He)$ , mean collision cross sections from microwave spectroscopy 0-1046  
 $SF_6$ , collisions, laser spectroscopy investig. 0-9697  
 $SF_6$ , multiphoton dissoci., collision effects 0-23467

**molecular internal conversion** see nonradiative transitions**molecular internal mechanics** see molecular vibration**molecular internal rotation** see rotational isomerism**molecular intersystem crossing** see nonradiative transitions**molecular libration**

## see also macromolecular dynamics

- alkali halide:  $NH_4^+$ , hindered rot. energy levels calc. 0-10514  
 anthracene-pyromellitic dianhydride, mol. charge transfer cryst., Raman scatt. meas. 0-29743  
 biphenyl, diamagnetism and thermal motion 0-25076  
 bipyridines, torsional isomerisation of biologically active bicyclic molecules 0-27996  
 cyclobutane- $d_6(d_8)$ , cryst. modifications, low. freq. Raman and IR spectra 0-7342  
 diatomic molecular crystal, librational force constants, appl. to  $\alpha$ - $N_2$  and  $\gamma$ - $N_2$  0-16020  
 malononitrile, displacive phase transition, 294.7K, Raman and Brillouin-Rayleigh scatt. obs. 0-16047  
 one-dimensional conductor, phenomenological eqns. of motion for electrons, phonons and librins 0-10955  
 potassium hydrogen oxalate, oriented single cryst., Raman spectra with very strong H-bonding 0-25359  
 propenyl chloride, IR bands, torsional struct. 0-28018  
 isopropyl chloride, torsional pot. function, far IR and Raman obs. 0-28022  
 1,3-propylenediammonium manganese tetrachloride, vibr. study of phase transitions, IR and Raman spectra 0-40103  
 rigid molecules, dil. soln. in decalin, mean librational freqs. 0-6479  
 rigid-body molecules, diamagnetism and thermal motion 0-25076  
 sodium hydrogen oxalate monohydrate, oriented single cryst., Raman spectra with very strong H-bonding 0-25359  
 TTF-TCNQ, anharmonic props., temp. (press.) depend., rel. to naphthalene and anthracene 0-15200  
 TTF-TCNQ, Landau free energy function, CDW-libron interaction, sp. ht. near phase transitions 0-19963  
 $B_2H_6$ , cryst., mol. charge distrib. anal., using struct. factors from mol. densities 0-15068  
 $BaCl_2 \cdot 2H_2O$ , polycryst. hydrates, librational motion of  $H_2O$  mols., neutron diffr. exam. 0-10604  
 CO, matrix-isolated, librational relax., IR line broadening 0-978  
 $D_2$ , solid, phonon absorption line shape as function of density 0-50329  
 $D_1$ , crystalline, Raman and IR spectra, mol. vibr., libration and translation 0-2757  
 $H_2$ , phonon absorption line shape as function of density 0-50329  
 $p$ - $H_2$ , solid, rotation-libration transition under press., Monte Carlo study 0-49460  
 HI, crystalline, Raman and IR spectra, mol. vibr., libration and translation 0-2757  
 $KBr:CN^-$  0-49316  
 KCN, plastic phase, Raman scatt. spectra (*French*) 0-11379  
 $KCl:CN^-$ , coherent admixtures of phonons with impurity libronic excitations, neutron scatt. study 0-49316  
 $K(TCNQ)$ , Raman spectra from 30 to 2300  $cm^{-1}$  0-11392  
 methane, solid, librational tunnelling and proton relax. temp. 0-38969  
 $N_2$ , solid,  $\alpha$ - and  $\gamma$ -forms, Raman spectra, vibron and lattice freq. shifts, libration 0-16020



**molecular libration continued**

- N<sub>2</sub>, solid,  $\beta$ -phase, for IR absorption spectra 0-11385  
 N<sub>2</sub>, solid, mol. libration and  $\alpha$ - $\gamma$  phase transition, Kihara pot. calcs. 0-44312  
 ND<sub>3</sub>ClO<sub>4</sub>, librational tunnelling and proton relax. temp. 0-38969  
 NH<sub>4</sub>Br and NH<sub>4</sub>I, Raman scatt., 1 bar-7 kbar, 86-295 K 0-34909  
 (NH<sub>4</sub>)<sub>2</sub>PbCl<sub>6</sub>, librational tunnelling and proton relax. temp. 0-38969  
 NaBr·2H<sub>2</sub>O, polycryst. hydrates, librational motion of H<sub>2</sub>O mols., neutron diff. exam. 0-10604  
 NaCN, plastic phase, Raman scatt. spectra (French) 0-11379  
 NaO<sub>2</sub>, physical mechanisms of phase transitions 0-6381  
 SrCl<sub>2</sub>·2(H<sub>2</sub>D)<sub>2</sub>O, IR and Raman spectra, force fields 0-2753

**molecular librational states** *see molecular libration***molecular magnetic susceptibility**

- acetylene, magnetic susceptibility, frost model wavefunctions with p-type Gaussians 0-5477  
 aromatic hydrocarbons, proton chemical shifts, localised  $\pi$ -bond model calcs. 0-43070  
 ethylene, magnetic susceptibility, frost model wavefunctions with p-type Gaussians 0-5477  
 ferrous porphyrin, intermediate (S=1) spin state, PMR characterisation 0-48014  
 molecules or clusters, interpretation of data from Mossbauer, ESR, susceptibility, optical and XPS meas. 0-37825  
 sandwich complexes, mag. props., effective Hamiltonian method 0-37731  
 triatomic isoelectronic molecules, electronic struct., one-electron props. 0-42935  
 BH,  $\Sigma^+$  ground state, mag. susceptibility, paramag. contrib., large config. interaction wave function calcs. 0-47899  
 Cu-Co heterobinuclear complex, cryst., mag. susceptibility of Cu-Co(fsa)<sub>2</sub> en, 3H<sub>2</sub>O 0-2556  
 Fe complexes, tetraphenylporphyrins, mag. susceptibility, hyperfine mag. field value Mossbauer spectra 0-37824  
 H<sub>2</sub>, nucl. mag. shielding and susceptibility, elec. field depend., SCF-Hartree Fock method 0-18791  
 HF, NMR shielding consts. and mag. susceptibilities, coupled HF with extended GTO basis 0-5480  
 HF, nucl. mag. shielding and susceptibility, elec. field depend., SCF-Hartree Fock method 0-18791  
 LiH, NMR shielding consts. and mag. susceptibilities, coupled HF with extended GTO basis 0-5480  
 PH<sub>3</sub>, NMR shielding consts. and mag. susceptibilities, coupled HF with extended GTO basis 0-5480

**molecular mass** *see molecular weight***molecular metastable states**

- copperporphyrin, metastable quartet state radiative decay 0-23453  
 p-dichlorobenzene, in p-dibromobenzene, optical detection of Cl NQR in mag. field 0-50228  
 negative ion lifetimes, review, book contrib. 0-9529  
 properties, energy transfer mechanisms and expl. techniques 0-27921  
 Cd<sup>2+</sup>, 470 nm absorber, multiconfiguration SCF calcs. 0-27963  
 HCOH, prediction, potential energy surface for ground state of formaldehyde 0-42967  
 He flow discharge, intermediate press., positive column conc. of ions and metastables 0-44017  
 He<sub>2</sub>, metastable states, laser excitation spectra 0-5578  
 HgBr\* form. from laser irradi. K+HgBr<sub>2</sub>, chemiluminescence 0-55658  
 N<sub>2</sub>, ionisation current increase, metastable mol. induced cathode secondary electron emission 0-38830  
 NH<sub>3</sub>, obs. in Orion Molecular Cloud 0-36687  
 NO<sup>+</sup> + molecule, reaction rate consts. meas. 0-7782  
 NO<sup>+</sup>, ( $\alpha^2\Sigma^+$ ), prod. from N<sup>+</sup>+O<sub>2</sub> reaction 0-7784  
 NO<sup>+</sup>+Ar, reaction product ratios, 300K 0-7783  
 O<sub>2</sub>, discharge plasma, metastable states role, two step ionisation, electron densities and transition pts. 0-44019  
 O<sub>2</sub>, laser-induced photolysis of ozone reactions 0-11928  
 O<sub>2</sub><sup>-</sup>, first negative system, high-resolution photofragment spectroscopy 0-47971  
 O<sub>3</sub>, Hartley band during formation, metastable states, vibr. excitation and relax. 0-55632  
 O<sub>2</sub>(<sup>1</sup> $\Delta_g$ ), sensitisation of SO(<sup>1</sup> $\Delta_g$ , <sup>1</sup> $\Sigma_g^+$ ) chemiluminescence 0-26016  
 O<sub>2</sub>(<sup>1</sup> $\Delta_g$ )+O<sub>3</sub>, UV photolysis, O(<sup>1</sup>P) prod., rate consts. determ. 0-55636

**molecular moments**

- 1,3-butadiene-1-one, spectroscopic consts., IR and microwave spectra, prep. 0-18859  
 AB system, molecular calcs., electric dipole moments and electronic valence population, CNDO study 0-37742  
 acetylene, multipole moments and polarisabilities, SCF calcs. 0-5471  
 acetylene-(d<sub>1</sub>,d<sub>2</sub>), integrated IR intensities 0-23457  
 AH system, molecular calcs., electric dipole moments and electronic valence population, CNDO study 0-37742  
 anilines, substituted, in nonpolar solvent, dielec. relax. obs. 0-55022  
 4-(9-anthryl)-N,N-dimethylaniline, fluoresc., dipole moments and polarisabilities 0-1019  
 benzene, and methyl derivatives, <sup>1</sup>E<sub>1u</sub> N-V state mag. moments, MCD obs. 0-23575  
 $\Delta^6$ -bicyclo[3.2.0]heptene, microwave spectrum and dipole moment 0-9591  
 bromal, in benzene soln., dielec. relax., loss, and dipole moment 0-2692  
 tert-butyl alcohol in nonpolar solvents, liq. struct. from dielectric studies 0-38894  
 t-butyl cyanide-HF, hydrogen bonded heterodimer, spectroscopic consts. from IR and microwave spectra 0-43039  
 2-chloro-p-nitroaniline, in benzene soln., dipole moment from solute relax. time-solvent viscosity relation 0-37905  
 chloroform-(d<sub>1</sub>), Raman and IR intensity anal. 0-18857  
 cyanomethane-HF, hydrogen bonded heterodimer, spectroscopic consts. from microwave spectrum 0-43038  
 dialkylaniline derivatives, twisted intramol. charge transfer states, dual fluoresc. obs. and form., dipole moments 0-18881  
 diatomic molecules, homonuclear, molecular dynamics, translation-rotation coupling 0-44094  
 diatomic systems, interactions, long-range dipoles, quadrupoles and hyperpolarisabilities 0-53161  
 difluoromethylborane, microwave spectra and struct. obs. 0-43036  
 dipole properties and dispersion energies additivity, using atoms and small mol. models 0-53091  
 ethane, multipole moments and polarisabilities, SCF calcs. 0-5471  
 ethylene, multipole moments and polarisabilities, SCF calcs. 0-5471  
 fluoromethane,  $\nu_3$  band Lamb dips, effects of RF elec. field modulation on Stark spectra 0-52989

**molecular moments continued**

- formic acid, H bonding, electronic struct., geometries, moments, dimerisation energies, charge distrib., pseudopotential calcs. 0-27942  
 formyl chloride, equilib. geometries and one-electron props., ab initio calcs. 0-47878  
 formyl fluoride, equilib. geometries and one-electron props., ab initio calcs. 0-47878  
 helical wormlike chain, dipole moment, elec. birefringence, elec. dichroism, statistical mech. calcs. 0-14262  
 hydrocarbons, dipole moments, NDDO calcs. 0-47894  
 iodomethane-d<sub>3</sub>, Stark tuned level crossings and saturated absorpt., RF elec. field modulation effects 0-52989  
 IR absorption band integrated intensities, ab initio and LMO studies 0-23458  
 methane,  $\nu_3=1$  state, dipole moment and IR-radiofrequency double reson. spectra 0-14161  
 methanol, H bonding, electronic struct., geometries, moments, dimerisation energies, charge distrib., pseudopotential calcs. 0-27942  
 methyl chloride, charge distrib., substituents effect 0-905  
 methyl fluoride, charge distrib., substituents effect 0-905  
 methyl formate, microwave spectra, rot. consts., moments and struct., radio astronomy appl., review 0-17637  
 MNDO semiempirical calcs. accuracy rel. to current MO methods 0-47893  
 3-nitro-o-anisidine, in benzene soln., dipole moment from solute relax. time-solvent viscosity relation 0-37905  
 organic solids, charged excitonic complexes, coupled states, exciton interaction with charge carriers study 0-20050  
 ozone, <sup>1</sup>A<sub>1</sub> ground state, dipole moment function, ab initio SCF and CI calcs. 0-32628  
 p-nitroaniline, in benzene soln., dipole moment from solute relax. time-solvent viscosity relation 0-37905  
 polypropylene sulphide, atactic chains, dipole moments, dielec. const. meas. 0-23584  
 small mol. electro-optical parameters, dipole moment derivatives, vibr. calc. valence-optical theory 0-23406  
 sparse s and p type Gaussian basis set LCAO MO SCF calc., mol. props. 0-23306  
 thioketen, microwave spectrum, substitution structure and dipole moment 0-975  
 o(m)-toluidine+o-chlorophenol, H-bonded mol. complex, microwave absorpt., dipole moment and relax. times 0-14134  
 triatomic isoelectronic molecules, electronic struct., one-electron props. 0-42935  
 vinyl mercaptan -d<sub>0</sub>, -d<sub>1</sub>, anti rotamer, conform., microwave spectrum 0-9592  
 vinyl mercaptan -d<sub>0</sub>, -d<sub>1</sub>, synrotamer, conform., microwave spectrum 0-5535  
 XY<sub>2</sub> molecules, nonlinear, inertia defects and dipole moments by kinetic consts. method 0-928  
 [<sup>13</sup>NH<sub>3</sub>], modulated coherent Raman beats 0-23464  
 Ar-O<sub>2</sub>, Van der Waals complex, struct. and props., RF and microwave obs. 0-32704  
 ArH<sup>+</sup>,  $\Sigma^+$  ground state, molecular consts. calc. from pot. curves 0-9680  
 Ar.HBr(DBr), van der Waals complexes, rot. spectra and struct. 0-48055  
 BF(OH)<sub>2</sub>, identification, rot. and centrifugal consts., mol. struct., microwave spectra obs. 0-32705  
<sup>79</sup>BrF, (<sup>81</sup>BrF), hyperfine struct., elec. dipole moment, rot. transitions, microwave spectral obs. 0-32695  
 CO, one-electron props., SCF and CI calcs. 0-27951  
 CO, total X $\alpha$  energy, LCAO calc., rel. to local density models 0-32607  
 CO<sub>2</sub>,  $\Pi_u$  symmetry transition probabilities, dipole moment and electro-optical consts. calc. 0-43115  
 CO<sub>2</sub>+ZZ 0-28065  
 CS<sub>2</sub>, symmetric stretch mode, moments and polarisability derivatives, SCF calcs. 0-901  
 ClCN, ground and first excited bending, vibr. state, props., mol. beam elec. reson. 0-37823  
 Cu complex, Cu(II) dimers, temp. depend. PMR relax., singlet-triplet separation determ. 0-43073  
 Eu(III) complexes, f-f transition probabilities, ligand polarisation model, anisotropic contribs. 0-53049  
 H<sub>2</sub>, quadrupole moments calcs. from line broadening collision with acetaldehyde 0-28065  
 H<sub>2</sub>, second order props., dipole polarisability nucl. coupling, fast CI method 0-27950  
 (H<sub>2</sub>)<sub>2</sub>, (D<sub>2</sub>)<sub>2</sub>, (HD)<sub>2</sub> and H<sub>2</sub>-D<sub>2</sub>, Van der Waals complexes, mol. symmetry 0-42963  
 HCN...HF, hydrogen bonded heterodimer, spectroscopic consts. from microwave spectrum 0-43037  
 HD, gas, fundamental band, R and P line shapes 0-23461  
 HF, hyperpolarisabilities, dipole moment, HF calc. with correlation 0-23342  
 H<sub>2</sub>O, H bonding, electronic struct., geometries, moments, dimerisation energies, charge distrib., pseudopotential calcs. 0-27942  
 KF, ab initio SCF MO energy, dipole moment and polarisability 0-1085  
 LiF, ab initio SCF MO energy, dipole moment and polarisability 0-1085  
 N<sub>2</sub>, multiple moments, polarisabilities and anisotropic long range interaction coeffs. 0-43206  
 N<sub>2</sub> quadrupole moment calc. from N<sub>2</sub>+OH collision cross section 0-1046  
 N<sub>2</sub>, quadrupole moments calcs. from line broadening collision with acetaldehyde 0-28065  
 N<sub>2</sub> triplet-triplet transitions, Einstein-A coeffs., oscill. strengths, lifetimes, theory and experiment comparison 0-47876  
<sup>14</sup>NH<sub>3</sub>, <sup>15</sup>NH<sub>3</sub> and <sup>14</sup>NH<sub>3</sub>D, IR laser Stark spectroscopy 0-47978  
 NHD radical, dipole moment determ., optical Stark spectroscopy 0-23455  
 O-containing compounds, dipole moments, NDDO calcs. 0-47894  
 PH<sub>3</sub>, dipole moment in ground and excited states, submm. spectrum obs. 0-28056  
 SF<sub>6</sub>, gas, thermodynamical and spectral props., effect of angle-dependent part of dispersion forces 0-43138  
 TlF, electric dipole hyperfine struct. calc. 0-53162

**molecular nuclear coupling**

- bromomethyl methyl ether, microwave spectra, quadrupole computing effect 0-18848  
 bromomethyl methyl ether, microwave spectra, quadrupole coupling effect 0-14135



**molecular nuclear coupling continued**

- bromomethylsilane, microwave spectra, quadrupole computing effect 0-18848  
 bromomethylsilane, microwave spectra, quadrupole coupling effect 0-14135  
 carbonanes, small cage, antipodal H-H coupling 0-1003  
 chlorinated compounds,  $^{13}\text{C}$  T<sub>1</sub> meas. and scalar coupling consts. 0-18945  
 difluoromethylborane, microwave spectra and struct. obs. 0-43036  
 elastomer, segmented block, morphology, pulsed proton NMR study 0-33907  
 ethane, nuclear spin-spin coupling consts., vicinal proton-proton coupling calcs. 0-32737  
 ethyl-trimethyl phosphines,  $(\text{C}_2\text{H}_5)_3\text{P}[\text{E}^{\text{IVB}}(\text{CH}_3)_3]_n$  ( $\text{E}^{\text{IVB}}=\text{C}; \text{Si}; \text{Sn}; n=0,1,2,3$ ),  $(^1\text{H}, ^{13}\text{C}, ^{29}\text{Si}, ^{31}\text{P}, ^{119}\text{Sn})$  NMR 0-32744  
 homonuclear coupled NMR spectra, pulses applied to multiplets, mutual coupling determ. 0-18873  
 hyperfine coupling, constants, nucl. spin spin coupling const., NDDO MO calcs. 0-23310  
 liquid crystal, chain ordering model 0-24357  
 liquid crystal, thermotropic mesophase, DMR chain segments assignment 0-24356  
 methane, nuclear spin-spin coupling consts., finite perturbation-CI calcs. 0-5563  
 methanol, mol., nucl. spin-spin coupling const., Hartree-Fock calc. 0-9618  
 methylmercury nitrate, in nematic and lyotropic liq. crystals,  $r_\alpha$ -struct. and anisotropy of Hg-C coupling const. 0-43071  
 multiple-quantum coherence, selective excitation, appl. to benzene NMR 0-23439  
 NMR parameters, chem. shielding,  $^{13}\text{C}$  chem. shifts 0-23435  
 pentofuranosyl nucleosides, isomeric,  $^1\text{H}$  NMR coupling consts., SCF FPT INDO approx. calc. 0-14156  
 phosphates, cellular, heteronucl. two-dimens. NMR as conform. probe 0-3590  
 polyisoprenes, partly deuterated,  $^1\text{H}$ -NMR spectra, struct. 0-50202  
 solid state NMR, selection of nonprotonated  $^{13}\text{C}$  resons. 0-50201  
 spin-spin coupling consts., mol. vibr. contrib., calc. methods comparison 0-23402  
 succinic acid, partially deuterated,  $^1\text{H}$  and  $^2\text{H}$  distant ENDOR obs. of mol. struct. parameters 0-23445  
 1,2,3-trichlorobenzene, oriented mols.,  $^{13}\text{C}$  satellites use in proton spectra,  $r_\alpha$ -structure 0-18872  
 2,3,4-trichlorophenol, AX spin system, two-dimens. J-resolved NMR, spin decoupling 0-31823  
 vibrationally coupled electronic states, radiationless decay, non-Condon effects 0-52966  
 $\text{COCl}_2$ , phosgene,  $\text{Cl}_2$  nuclear quadrupole coupling tensor, microwave spectra 0-52982  
 $^{13}\text{C}$ - $^{13}\text{C}$  spin-spin coupling consts., data compilation, meas. and appls. review 0-17725  
 C<sub>6</sub>H<sub>6</sub>, ground and first excited bending, vibr. state, props., mol. beam elec. reson. 0-37823  
 Cu complexes, Cu(I)-P tetrahedral,  $^{63}\text{Cu}$  FT-NMR 0-53021  
 H<sub>2</sub>, nucl. mag. shielding and susceptibility, elec. field depend., SCF-Hartree Fock method 0-18791  
 H<sub>2</sub>, nuclear spin-spin coupling consts., finite perturbation-CI calcs. 0-5563  
 H<sub>2</sub>, second order props., dipole polarisability nucl. coupling, fast CI method 0-27950  
 HD, nucl. spin coupling const., MBPT theory calcs. 0-28035  
 HF, nucl. mag. shielding and susceptibility, elec. field depend., SCF-Hartree Fock method 0-18791  
 HF, nuclear spin-spin coupling consts., finite perturbation-CI calcs. 0-5563  
 HNCS, ground state spectroscopic const., microwave, millimeter and IR spectra 0-28010  
 H<sub>2</sub>O, nuclear spin-spin coupling consts., finite perturbation-CI calcs. 0-5563  
 KrHCl, van der Waals complexes, struct., RF and microwave spectra, isotope effects 0-37806  
 KrHCl, weak complex, rot. spectra 0-52980  
 KrHF,  $^{83}\text{Kr}$  nucl. quadrupole coupling, charge transfer 0-53012  
 $^{83}\text{Kr}$ ,  $^3\text{P}_1$  and  $^1\text{P}_1$  levels, quadrupole coupling consts. 0-23434  
 $^{25}\text{Mg}$ ,  $^3\text{P}_1$  and  $^1\text{P}_1$  levels, quadrupole coupling consts. 0-23434  
 NH<sub>3</sub>, nuclear spin-spin coupling consts., finite perturbation-CI calcs. 0-5563  
 N<sub>2</sub>O dissolved in liq. cryst., NMR, relax. times 0-25233  
 $^{14}\text{N}$  NMR, single cryst., separation of dipolar and quadrupolar splittings, new technique 0-25217  
 $^{15}\text{N}$ - $^{13}\text{C}$  spin-spin coupling constants calc. using SCF and INDO method 0-32609  
 $^{67}\text{Zn}$ ,  $^3\text{D}$ ,  $^1\text{D}$ ,  $^3\text{P}_1$  and  $^1\text{P}_1$  levels, quadrupole coupling consts. 0-23434

**molecular orbitals** see molecular energy levels**molecular orbitals calculations**

- includes calculations of electronic and geometric molecular structure  
 see also APW calculations; EHT calculations; GO calculations; GTO calculations; HMO calculations; KKR calculations; LCAO calculations; NDO calculations; OPW calculations; PNO calculations; PPP calculations; STO calculations  
 ab initio CI pot. curves, mol. wavefunctions and vibr. freqs. comparison of methods 0-27956  
 acetaldehyde, first triplet state geometry, fragmentation into free radicals 0-47915  
 acetic acid-formic acid, 'dimer', tritium  $\beta^-$ -decay causing H<sup>+</sup> transfer, ab initio MO calc. 0-3391  
 acetonitrile, quadratic force fields, MOCIC pot. functions calcs. 0-5475  
 acetylene, electron momentum distribs. in  $\pi$  orbitals from (e,2e) expts. 0-14239  
 acetylene, LMO population calc. method appl., from given SCF eigenvector matrix 0-14063  
 acetylene, mol. and cluster Auger spectrum calc., SCF core-valence-valence spectra 0-48045  
 addition theorems of spatial functions, multicentre integrals of arbitrary atomic functions, symmetry and analytical struct. (German) 0-37729  
 aromatic hydrocarbons,  $\pi$ -ionisation energies correl. with free electron MO energies 0-14073  
 atom+ion slow collisions, K-shell excitation of relativistic atoms 0-48073  
 atom+multiply charged ion, slow collisions, MO calcs. 0-23504

**molecular orbitals calculations continued**

- benzene, LMO population calc. method appl., from given SCF eigenvector matrix 0-14063  
 biomolecule conformational anal., solvent effects 0-3583  
 biopolymer, electronic-conformation interactions 0-3588  
 bond orbitals and intramolecular interactions, barriers to rotation and non-bonded interactions 0-32855  
 borazine, triplet instability, RPA calculations 0-27938  
 Born-Oppenheimer Hamiltonian, resolvent matrix elements complex coord. calc. 0-52878  
 butadiene, electron momentum distribs. in  $\pi$  orbitals from (e,2e) expts. 0-14239  
 butadiene, LMO population calc. method appl., from given SCF eigenvector matrix 0-14063  
 1-butanethiol, simulated ab initio MO method calcs. 0-47867  
 cancer receptor sites, proof by MO method for interstrand guanine binding of DNA 0-30656  
 chromium formate, mol., Hartree-Fock instability of SCF wavefunctions 0-9492  
 chromophores, semiempirical rules in circular dichroism, Cotton effect sign correl. with stereochem. 0-1006  
 Combination of Atomic Boxes MO model, development and testing 0-32592  
 conference, group theory and application to spectroscopy, Nova Scotia, Canada (Aug. 1978) 0-41947  
 configuration interactions, appl. of unitary group methods 0-27958  
 conjugated molecules eigenvalue polynomials 0-14078  
 conservation of molecular orbital symmetry, construction of energy correl. diagrams (Chinese) 0-910  
 contracted Gaussian basis set for correl. wave functions, appl. struct. and energies 0-52881  
 contracted Gaussian-type orbital basis sets, test with and without outer orbital splitting 0-47872  
 core-valence approx. scheme 0-42927  
 coronene, excited state Faraday values mag. circular dichroism spectra and MO CI calcs. 0-18877  
 Coulomb interaction integrals bounds 0-52856  
 coupled cluster many electron theory, unitary group formulation 0-52859  
 coupling constants in direct CI method 0-9516  
 crystal field theory connections 0-29514  
 cyclopropane, 3e-orbital, electron momentum distribs., mol. distortions effects 0-18773  
 cyclopropane, electron momentum distribs. in  $\pi$  orbitals from (e,2e) expts. 0-14239  
 diagrammatic many-body perturbation theory for general model spaces 0-18780  
 diatomic molecule electron scatt., iterative static exchange method 0-53155  
 diatomic system, pair polarisability curve shape, rel. to chem. bonding 0-42930  
 dibutyl-phenyl-benzoyloxy-benzoate, nematic liq. cryst., rot. barrier, PCIO and CND0/2 calcs. 0-33874  
 doubly charged molecular ions, energy calc. by HAM/3 method 0-9512  
 dynamical damping in ab initio MO SCF calcs., energy minimisation method 0-18777  
 electron density calc., approx. differential eqn. 0-47864  
 electron momentum distribs., mol. distortions effects 0-18773  
 electronic structures, omega like technique, Hartree Fock formalism 0-18792  
 electrostatic isopotential maps for large biomolecules, STO transferable bond calc. 0-3571  
 equations of motion Green's function methods, higher order terms, ionisation pots. 0-52891  
 equations of motion Green's function methods, higher order terms, ionisation pots., CI comparison 0-52892  
 ethane, localised molecular orbitals, orthogonal transformations calcs. 0-47892  
 ethylene, electron momentum distribs. in  $\pi$  orbitals from (e,2e) expts. 0-14239  
 ethylene, Hartree-Fock energy and Moller-Plesset perturbation energy, harmonic vibr. freq. 0-52852  
 ethylene, mol. and cluster Auger spectrum calc., SCF core-valence-valence spectra 0-48045  
 ethylene, quasidegeneracy and effective Hamiltonians, canonical transformation cluster expansion formalism 0-52888  
 exponential transformation, quadratically convergent SCF procedure, appl. to closed shell ground states 0-47875  
 ferrocene, metal to ring distance, ab initio MO SCF calcs. 0-47870  
 fluoroethyl radical, unimol. dissoci., pot. energy characts. and energy partitioning calcs. 0-45488  
 fluoroform, quadratic force fields, MOCIC pot. functions calcs. 0-5475  
 formaldehyde, triplet instability, RPA calculations triplet instability, RPA calculations 0-27938  
 formamide dimer, tritium  $\beta^-$ -decay causing H<sup>+</sup> transfer, ab initio MO calc. 0-3391  
 formic acid dimer, tritium  $\beta^-$ -decay causing H<sup>+</sup> transfer, ab initio MO calc. 0-3391  
 geminal product approx., optimisation of molecular wavefunction 0-37733  
 group theory applications to physical and chemical systems in relation to struct. and substructs. 0-42921  
 H-bonded complexes-first row hydrides, ab initio calcs. (French) 0-5479  
 Hamiltonians, effective, appl. to atomic pot. transferability in hydrocarbons 0-42933  
 harmonic oscill., excited states, hypervirial relations, off-diagonal 0-37728  
 hydrides,  $\text{MH}^+$ ,  $\text{MH}_2$ , M=alkaline earths: Zn, Cd, Hg, Yb, No, relativistic (non-relativistic) HF one-centre expansion calcs. 0-52908  
 hydrocarbons, bond functions, for ab initio calcs. 0-5469  
 hydrocarbons, conjugated, heat of formation and reson. energies 0-7839  
 hydrocarbons, effective Hamiltonians for atomic pot. transferability 0-42933  
 hydrocarbons, normal, mass-spectrometric fragmentation processes, quantum field theory 0-40782  
 hydroxymethylene radical cation stability,  $\text{CH}_2\text{O}^+$  isomers, ab initio MO study 0-42965  
 hyperfine coupling, constants, nucl. spin spin coupling const., NDDO MO calcs. 0-23310  
 incomplete basis set problem, virtual orbitals and CIBS expansion of HF energies 0-52844  
 inert gas diatomic molecule, excited state pots., fast calc. 0-9490



**molecular orbitals calculations continued**

- integrated spatial electron populations using projection function method 0-23299
- intermolecular energies calculation from delocalised pictures, artifacts and elimination 0-18899
- ion-molecule equilibria in solvolysis, secondary  $\beta$   $^2\text{H}$  isotope effects, hyperconjugation 0-50874
- isocyanates, nonbonding and  $\pi$ -orbital interactions, photoelectron spectra 0-32774
- isothiothiocyanates, nonbonding and  $\pi$ -orbital interactions, photoelectron spectra 0-32774
- large molecular systems, local pot. surface and charges, parametrisation scheme for quantum mechanical computation (*German*) 0-18793
- ligand fields calcs., strong and intermediate fields, tensor algebra 0-42922
- light atom molecules, general quadratic force fields, semiempirical MOCIC calcs. 0-5474
- local force densities and stress tensors, density functional theory 0-18781
- localised molecular orbitals, orthogonal transformations calcs. 0-47892
- magnetic circular dichroism, group theoretical techniques 0-45048
- metal cluster, Wolfsberg-Helmholz relation analysis, reson. integral approx. 0-49566
- methane, bonding, electron pairs, size and shape parameters, Gaussian basis set MO calcs. 0-27935
- methane, elastic and inelastic electron scatt. differential cross section, obs. and calc., struct., binding energy 0-28110
- methane, large angle elastic and inelastic electron scatt. differential cross section, exchange corrections 0-28111
- methane, mol. and cluster Auger spectrum calc., SCF core-valence-valence spectra 0-48045
- method of optimal relax., eqns. of motion method, k lowest or highest solns. 0-37727
- methylacetylene, quadratic force fields, MOCIC pot. functions calcs. 0-5475
- methylene +  $\text{H}_2$  → methane, ab initio CI calc. on SCF level, insertion reaction min. energy path 0-7774
- 3-methyleneoxetane, electron structure, orbital-O interaction, MO calcs., UV photoelectron spectra 0-28058
- mol. and cluster Auger spectrum calc., SCF core-valence-valence spectra 0-48045
- molecular solid, electron tunnelling, long-range electron transfer processes, orbital overlap model 0-7813
- molecules or clusters, interpretation of data from Mossbauer, ESR, susceptibility, optical and XPS meas. 0-37825
- molybdenum formate, mol., Hartree-Fock instability of SCF wavefunctions 0-9492
- natural orbitals, Billouin-Levy-Berthier theorem, multiconfigurational SCF optimisation 0-27936
- one-dimensional molecular crystals, electronic struct., mol. orbital theory 0-54588
- one-electron Hamiltonian method applied in SCF theory to states with open shell 0-23302
- open shell RPA unitary group formulation, Hartree Fock stability eqns. 0-52860
- open shells, RHF treatment without Lagrange multipliers 0-32589
- organic chemistry courses, unified approach to teaching of struct. and bonding 0-17732
- 3-oxetanone, electron structure, orbital-O interaction, MO calcs., UV photoelectron spectra 0-28058
- PAA, nematic liq. cryst., rot. barrier, PCILO and CNDO/2 calcs. 0-33874
- phospholipid inter-and intra-molecular interactions, PCIOCC and pot. function calc. 0-3570
- photoionisation cross sections, at. extrapolation, ground state inversion method appl. 0-18787
- point charge model approach to intermol. interaction coeffs. 0-18897
- point charge model approach to mol. elec. polarisability 0-18797
- point group coupling, coeffs., props. and application 0-43033
- polarization Green's function with multiconfiguration self-consistent-field reference states 0-37724
- polyacetylene, band struct. valence Hamiltonian minimal STO-3G basis calc., nonempirical model pot. 0-54596
- polyatomic molecules, bond functions, for ab initio calcs. 0-5469
- polyethylene, band struct. valence Hamiltonian minimal STO-3G basis calc., nonempirical model pot. 0-54596
- polymeric chains and Mott insulators, similarities w.r.t. electronic correl., AMO method (*French*) 0-24775
- polymethine-cyanine molecular aggregate, band struct. 0-53174
- $\beta$ -propiolactone, electron structure, orbital-O interaction, MO calcs., UV photoelectron spectra 0-28058
- protein, electron-transport type, H-bonding, ab initio MO 0-51039
- pyrazine, excited and  $\text{N}_1\text{s}$  ionised states, ab initio calcs. broken orbital symm. 0-27931
- satellite struct. of electron spectra, CI and vibronic coupling, dynamical calc. 0-53044
- semiempirical MO theory, modified NDO model 0-52887
- simulated ab initio MO method, appl. to second row elements in mols. 0-47867
- Singer polymal tempering methods 0-52845
- sparse s and p type Gaussian basis set LCAO MO SCF calc., mol. props. 0-23306
- spin-orbit formalism of Hartree-Fock energy and Moller-Plesset perturbation energy 0-52852
- subtilislin charge-relay system, electrostatic pot. map, STO transferable bond calc. 0-3571
- supermolecule calcs. with additive procedure, intermolecular interactions and binding energy 0-52880
- TCNQ salt, NMP-TCNQ, electronic struct., SCF calc., total energy polarisation effects 0-15469
- tetrafluoromethane, elastic and inelastic electron scatt. differential cross section, obs. and calc., struct., binding energy 0-28110
- thiocyanates, nonbonding and  $\pi$ -orbital interactions, photoelectron spectra 0-32774
- transition metal, bimetallic cluster, photoselective bimetallic aggregation, review 0-53182
- transition metal complex, ligand field problems, group theory 0-42920
- transition metal surface atom interaction with ethylene and acetylene, MO calc. 0-6623
- triatomic isoelectronic molecules, electronic struct., one-electron props. 0-42935
- s-triazine, triplet instability, RPA calculations 0-27938

**molecular orbitals calculations continued**

- triphenylene, excited state Faraday values mag. circular dichroism spectra and MO CI calcs. 0-18877
- two centre and three centre integrals for attraction of Slater type orbitals to nucleus, coord. systems 0-14068
- unitary group generators and permutations, CI matrix elements, algebraic method 0-37725
- unitary group generators and permutations, CI matrix elements, graphical method 0-37726
- unitary group irreducible representation subduction coeffs. 0-37723
- variational cellular method, electronic struct. calcs. 0-54591
- X-ray emission spectra, techniques and spectral interpretation, rel. to XPS, book contrib. 0-11514
- $\text{Ar}_2^+$ , excited state pots., fast calc. 0-9490
- $\text{B}_2\text{H}_6$ , LMO population calc. method appl., from given SCF eigenvector matrix 0-14063
- $\text{Br}(\text{H}_2\text{O})_n$ , hydration energies, orientation, ab initio-LCAO SCF MO calcs. 0-27944
- $\text{C}_2$ , pot. curves, binding and ionisation energies and config. variational cellular method 0-32597
- $\text{C}_2\text{N}_2$ , satellite struct. of electron spectra, CI and vibronic coupling, dynamical calc., equil. geometry 0-53044
- $\text{CO}$ , electronic struct., binding energy and interatomic distance, SCF variational cellular calc. 0-9498
- $\text{CO}$ , nonempirical PRDDO scheme and calcs. 0-37739
- $\text{CO}$ , pot. curve, variational cellular method, electronic struct. calcs. 0-54591
- $\text{CO}$ , pot. curves, binding and ionisation energies and config. variational cellular method 0-32597
- $\text{CO}_2$ , elastic and inelastic electron scatt. differential cross section, obs. and calc., struct., binding energy 0-28110
- $\text{CO}_2$ , large angle elastic and inelastic electron scatt. differential cross section, exchange corrections 0-28111
- $\text{CO}_2$ , nonempirical PRDDO scheme and calcs. 0-37739
- $\text{CO}_3^{2-}$ , molecular orbital anal., anisotropic X-ray emission obs. of components 0-18786
- $\text{Cl}(\text{ClF}_2)^-(\text{ClF}_3)$ , localised MO ab initio calc., Gaussian orbital ab initio calc. 0-14083
- $\text{CrCl}_4$ , ligand field states, multiple scatt. Xalpha calcs. 0-47891
- $\text{CsI}$ , self-trapped exciton electronic struct., semi-empirical mol. orbital method 0-49605
- $\text{CsI:Na}$ , electronic struct. and luminesc. 0-16080
- $\text{Cu-Co}$  heterobinuclear complex, cryst., mag. susceptibility of  $\text{Cu-Co}(\text{fsa})_2$ , en,  $3\text{H}_2\text{O}$  0-2556
- $\text{Cu}_2$ , contracted Gaussian-type orbital basis sets, test with and without outer orbital splitting 0-47872
- $\text{CuO}$ , ab initio HF-MC-SCF with GTO basis set, dissoci. energy and bond length 0-47890
- $^{63}\text{Cu}_2$ ,  $\text{B}'\Sigma_u^+ - \text{X}'\Sigma_g^+$  transition, Franck-Condon factors, r-centroids and pot. curves 0-43114
- $\text{F}_2$ , MSX $\alpha$  calc., partial wave expansion, binding energy and orbital energy 0-37738
- $\text{F}_2$ , photoexcitation and ionisation cross sections, Stieltjes -Chebyshev static exchange calc. 0-53060
- $\text{F}_2$ , pot. curves, binding and ionisation energies and config. variational cellular method 0-32597
- $\text{FCIO}^+$ , radical cation, struct. and electronic props., ab initio RHF SCF MO calc. 0-52883
- $\text{FH-OH}_2$  (dimethyl ether), H-bonded complexes, cubic force consts. calcs. 0-47868
- Fe complex, Fe (alkyldithiocarbamate) $_2\text{X}$ ,  $\text{X} = \text{Cl, I}$ , mol. orbital calc., hyperfine fields, elec. field gradient 0-39981
- $\text{H} + \text{H}^+$ , low energy, optimised translation factors 0-18813
- $\text{H}_2$ , atoms-in-molecules theory, non-Hermitian formulation 0-9517
- $\text{H}_2$ , electron correl. as rot. polarisation, Heitler-London-Rosen calc. for teachers 0-4492
- $\text{H}_2$ , photoionisation Born-Oppenheimer Hamiltonian, resolvent matrix elements complex coord. calc. 0-52878
- $\text{H}_2$ , pot. curves, binding and ionisation energies and config. variational cellular method 0-32597
- $\text{H}_2^+$ , exponentially small part of wave function (*Russian*) 0-9497
- $\text{H}_2^+$ , high ( $10^5$  G) mag. fields, dissoci. energy, electron binding energy and equil. separation 0-52910
- HF, Auger spectra, correl. effects, energies and wavefunctions, ab initio CI calc. 0-14125
- HF, NMR shielding consts. and mag. susceptibilities, coupled HF with extended GTO basis 0-5480
- $\text{H}_2\text{O}$ , bonding electron pairs, size and shape parameters, Gaussian basis set MO calcs. 0-27935
- $\text{H}_2\text{O}$ , many body perturbation theory fourth order calc. of correl. energy 0-14087
- $\text{H}_2\text{O.H}_2\text{O}$  and  $\text{H}_2\text{O.Ne}$ , excited, first order interaction energy, ab initio calc. 0-32598
- $\text{H}_2\text{S}$ , valence electron ionisation and momentum distrib. 0-28107
- He pair, dispersion interaction, independent particle model, polarisabilities 0-37732
- $\text{HeH}^+$ , excited states, variable screening models, natural spin orbital analysis of wave functions 0-37747
- $\text{Hg-Pt}$ ,  $^{199}\text{Hg}$  Mossbauer meas., isomer shift and quadrupole splitting calcs. 0-28039
- $\text{Hg-F}_2$ ,  $^{199}\text{Hg}$  Mossbauer meas., isomer shift and quadrupole splitting calcs. 0-28039
- $\text{KCl:Ti}$ , energy level scheme, mol. orbital model 0-10912
- KF, ab initio SCF MO energy, dipole moment and polarisability 0-1085
- $\text{Li}_n^+$  ( $n = 1, 2, 3$ ), stable cluster configs., ionisation pots., binding energies, vibr. freqs., al initio SCF and CEPA calcs. 0-14265
- $\text{LiAlF}_4$ , struct. pot. energy surface,  $\text{Li}^+$  migration, ab initio LCAO SCF calcs. 0-23305
- $\text{LiF}$ , ab initio SCF MO energy, dipole moment and polarisability 0-1085
- $\text{LiH}$ , many body perturbation theory fourth order calc. of correl. energy 0-14087
- $\text{LiH}$ , NMR shielding consts. and mag. susceptibilities, coupled HF with extended GTO basis 0-5480
- $\text{MoS}_3$ , struct., XES and XPS obs. 0-43105
- $\text{N}_2$ , elastic and inelastic electron scatt. differential cross section, obs. and calc., struct., binding energy 0-28109
- $\text{N}_2$ , electronic struct., binding energy and interatomic distance, SCF variational cellular calc. 0-9498
- $\text{N}_2$ , large angle elastic and inelastic electron scatt. differential cross section, exchange corrections 0-28111



**molecular orbitals calculations continued**

- $N_2$ , MSX $\alpha$  calc., partial wave expansion, binding energy and orbital energy 0-37738  
 $N_2$ , pot. curves, binding and ionisation energies and config. variational cellular method 0-32597  
 $NF_3$ , mol. orbital calcs. core-valence approx. scheme 0-42927  
 $NH_3$ , bonding electron pairs, size and shape parameters, Gaussian basis set MO calcs. 0-27935  
 $NH_3$ , LMO population calc. method appl., from given SCF eigenvector matrix 0-14063  
 $NH_3$ , lowest triplet state geometry, SCF and CEPA-PNO calc. 0-914  
 $NOH$ , groundstate electronic struct., MRD CI calc., dissociation energy, isomerisation energy 0-14088  
 $NbO_2$ , rutile phase, energy levels, momentum density, and Compton profile, embedded cluster model 0-50453  
 $Ne_2$ , excited state pots., fast calc. 0-9490  
 $O_2$ , MSX $\alpha$  calc., partial wave expansion, binding energy and orbital energy 0-37738  
 $O_2$ , multiconfig. Hartree-Fock calcs. convergency 0-47901  
 $O_2$ , photoexcitation and photoionisation cross sections, HF Gaussian method 0-53064  
 $OCl_2^+$ , radical cation, struct. and electronic props., ab initio RHF SCF MO calc. 0-52883  
 $OH+H_2$ , pot. energy surface, barrier heights and transition state geometry, POL-CI calc. 0-55649  
 $PCl_3$ , mol. orbital calcs. core-valence approx. scheme 0-42927  
 $PH_3$ , NMR shielding consts. and mag. susceptibilities, coupled HF with extended GTO basis 0-5480  
 $SO$ , low lying bound mol. electronic states, SCFCI calc. 0-23314  
 $Si_4H_{2n+2}$ , silane, SCF X $\alpha$  MO calc., appl. to amorphous hydrogenated Si 0-49580

**molecular orientation**

- 2,4-hexadiyne-1, 6-diol, bis(p-toluene sulphonate), dark-current meas. 0-15520  
 3-amino- and 4-amino-N-methylphthalimide, effect of orientational-relax. processes in fluoresc. kinetics 0-18886  
 adamantane, Ising, diffuse scatt., hard-core correl., weak-graph method 0-49137  
 adsorbed layer, classical octupoles on triangular lattice, orientational phases 0-2263  
 adsorbed monolayer of orientable molecules, lattice fluid model, real-space renormalisation group method 0-17882  
 amorphous solids, diffusion of nonspherical particles, correl. effects 0-39337  
 anisotropic impurity centres, local relaxational phase transitions (*Russian*) 0-44220  
 1,2-benzanthracene in polystyrene films, delayed luminesc. decay kinetics 0-43088  
 m-chloronitrobenzene, molecular crystals, translational and orientational vibr. determ. 0-55103  
 cholesteric liquid crystal, molecular polarisability, arrangement order calc. (*Polish*) 0-10495  
 4-cyano-4'(n-amy)-diphenyl, isotropic phase, induced molecular orientation relaxation time, Kerr effect (*Russian*) 0-19699  
 diatomic molecules, homonuclear, molecular dynamics, time-dependent statistical props. 0-44093  
 diatomic molecules, homonuclear, molecular dynamics, translation-rotation coupling 0-44094  
 4,4-dihexyloxybenzene, nematic liq. cryst., alignment on surfactant treated obliquely evaporated surfaces 0-49092  
 dimethyl tin difluoride, solid, methyl group motion, neutron scatt. study 0-10607  
 disordered crystal, diffuse scatt., hard-core correl., weak-graph method 0-49137  
 DOBAMBC, ferroelec. liq. cryst., helical struct., elec. field depend. (*Japanese*) 0-38910  
 epoxide compound, polymerisation in non-uniform magnetic field, exam. of structural changes 0-7791  
 ethoxyhexyltolan, Raman spectra, molecular conformational instability, internal field effects 0-54127  
 ethoxyoctyltolan, Raman spectra, molecular conformational instability, internal field effects 0-54127  
 fluid with nearly spherically symmetric molecules, thermodynamic perturbation theory 0-14985  
 furan, adsorbed on NaCl, evidence of new condensed phase, IR spectra (*French*) 0-16028  
 hard rod system, improved lattice model, nematic and isotropic phases 0-33882  
 4-heptyl-4'-cyanobiphenyl, nematic liq. cryst., alignment on surfactant treated obliquely evaporated surfaces 0-49092  
 p-heptyl-p'-cyanobiphenyl, refractive index, dielec. const., mag. susceptibility, orientational ordering (*Dutch*) 0-33884  
 n-hexyl 4'-n-decyloxybiphenyl-4-carboxylate, smectic C phase, tilt angle using electron reson. spectroscopy 0-33886  
 ion-water interactions, survey of diff. studies 0-24347  
 lattice energy, minimisation, singularity-free, static 0-10525  
 liquid, coupling of vel. gradients to molecular orientation, light scatt. and flow birefringence anal. 0-25398  
 liquid crystal, order parameter measurement, phys. chem. lab. expt. 0-36818  
 liquid crystal, theoretical foundations of chain ordering props. 0-38907  
 liquid crystal symmetry and thermodynamic states, review 0-10493  
 liquid crystals, deuterated, dueteron mag. resonance mol. ordering, conformational changes 0-34789  
 liquid crystals, static and dynamic props., time depend. fluoresc. depolarisation obs. 0-29786  
 liquid crystals, surface alignment using polynuclear metal complexes 0-1924  
 lyotropic mesophase, mag.-oriented, X-ray diff. obs. 0-1921  
 MBBA, refractive index, dielec. const., mag. susceptibility, orientational ordering (*Dutch*) 0-33884  
 MBBA/EBBA binary liquid crystal mixture, US absorpt. and vel. dispersion, phase transition and alignment effects (*Korean*) 0-29121  
 molecular crystals, chem. shielding, spin-lattice, quadrupole interactions,  $^2D$  NMR spin echo spectroscopy 0-34817  
 nematic bend-splay elasticity near the nematic-smectic-A transition 0-24360  
 nematic liquid cryst., Fredericksz transition and anchoring effects for general config. 0-33875

**molecular orientation continued**

- nematic liquid cryst. display devices, with twisted and tilted arrangements, guest-host interactions 0-34891  
 nematic liquid crystal, ionic conduction-induced flow alignment angle, NMR evidence 0-44125  
 nematic liquid crystal, thermal instabilities in layer with oblique orientation at boundaries 0-44110  
 nematic liquid crystals, molecular mechanisms of dielec. polarisation and relaxation 0-34846  
 nematic liquid crystals, behaviour in inhomogeneous elec. fields 0-44118  
 nematic-cholesteric mixtures, spiral pitch temp. depend. (*Russian*) 0-19700  
 nematic-smectic A transition, orientational fluctuation effect 0-6496  
 NMR spectra, vibr. correction study 0-18840  
 non-random orientation distribution functions with random pole figures 0-6320  
 PAA, refractive index, dielec. const., mag. susceptibility, orientational ordering (*Dutch*) 0-33884  
 perylene in n-heptane cryst., polarised fluoresc. 0-1017  
 PMMA, glassy, photoelasticity 0-45034  
 poly- $\gamma$ -benzyl-L-glutamate, monolayers, struct. studies, IR, ATR, and TEM obs. 0-44396  
 polycapraamide, oriented, molecular rearrangements during deformation, IR spectra exam. 0-7644  
 polyethylene, doubly oriented, low density, deformation and structure, exam. 0-11705  
 polyethylene, lightly crosslinked, processed under mol. orient., struct., props., review 0-38957  
 polymer film, noncrystalline chain orientation evaluation, with polarised fluorescence method (*Japanese*) 0-6368  
 polymer matrix, decreased stabilisation energy of excimers and exciplexes 0-25431  
 polypeptide liquid crystal, electric field-induced phase transition 0-24571  
 polystyrene, isotactic, orientation of remaining amorphous chains during crystallisation 0-10506  
 porphyrin in host n-alkane crystals, phototautomerism, IR spectral obs. 0-34963  
 N-p-propoxybenzylidene-p-pentylaniline, Williams domains, interference study 0-44114  
 simple cubic lattice, orientational ordering of quadrupoles 0-44157  
 smectic C phase, mol. director behaviour at domain EHD instability 0-15000  
 smectic-C liquid crystals, biaxial mol. order, NMR meas. 0-25227  
 succinonitrile, plastic, diffuse scatt., hard-core correl., weak-graph method 0-49137  
 thermotropic systems of rodlike molecules with orientation-depend. interactions 0-33883  
 1,2,3-trichlorobenzene, oriented mols.,  $^{13}C$  satellites use in proton spectra,  $r_e$ -structure 0-18872  
 water interface, mol. orientation and surface pot. at 4°C 0-15339  
 $H_2$ , solid, quadrupolar glass, relax. time and low temp. sp.ht., computer simulations 0-49377  
 $N_2$  dissolved in Ar, mol. orientation, Raman spectrosc. obs. 0-52994  
 $N_2$  liquid, mol. correl. functions, effective pair pot. evaluation 0-10476  
 $N_2$  overlayer on graphite, orientational ordering, neutron scatt. meas. 0-10783  
 $NH_4$  Br single cryst., low temp. PMR lineshapes of tunnelling  $NH_4^+$  ions 0-25223  
 NaCN, diffuse scatt., hard-core correl., weak-graph method 0-49137  
 $O_2$  dissolved in Ar, mol. orientation, Raman spectrosc. obs. 0-52994  
 $O_2$  liquid, mol. correl. functions, effective pair pot. evaluation 0-10476  
 $SO_2$  liquid, short range orientation effects, vibr. Raman spectra 0-2759

**molecular photodissociation**

- acetic anhydride, multiphoton dissociation,  $CH_2$  and  $C_2$  prod., fluence depend. meas. 0-5586  
 acetone- $d_6$ , multiphoton dissociation, recomb. to ethane 0-3371  
 acetonitrile molecule dissociation in IR field, laser-induced fluoresc. obs. 0-53075  
 acetylene, multiphoton vacuum UV photodissoc. obs. and interpret. 0-11939  
 acrylonitrile, IR multiphoton dissociation,  $C_2$  prod. and quenching obs. 0-11931  
 acrylonitrile, multiple photon dissociation, photofragment spectroscopy by laser-induced fluoresc. 0-11937  
 alkali bromides, photofragment spectra, 266 nm, bond energies and excited state symmetries 0-53072  
 alkali iodides, photofragment spectra, bond energies and excited state symmetries 0-5589  
 alkali metal molecular, laser radiation absorpt., at. excitation processes 0-32785  
 alkyl iodides, UV photodissoc., time-resolved obs. of  $I(^2P_{1/2})$  reactions 0-11940  
 biomethylfluoromethane, multiphoton dissociation, isotopically selective 0-28113  
 bromomethane, multiphoton vacuum UV photodissoc. obs. and interpret. 0-11939  
 chlorodifluoroethane, CW laser-induced reaction, vibr. rate enhancement obs. 0-11922  
 chloroethane, reson. multiphoton dissociation 0-53077  
 chlorofluoroethane, multiphoton dissociation under  $CO_2$  laser irradi., decomposing mol. energy distrib. 0-30251  
 chloromethanes, VUV fluoresc., UV multiphoton dissociation 0-28076  
 chloropentafluoroethane, multiphoton dissociation, crossed laser and mol. beam obs. 0-11908  
 chlorotrifluoroethane, IR photoreaction (*Japanese*) 0-11885  
 complex molecules, laser induced dissociation, thermal energy effects 0-53071  
 complex molecules, photostability and quenching effect on laser generation kinetics 0-3390  
 diatomic molecule, vibr. Green's function and two-photon dissociation 0-28075  
 diatomic molecules, form. and dissociation in interstellar medium 0-23471  
 dichlorodifluoroethane, infrared multiphoton processes, apparent step cross-sections, pulse spatial structure, irradiation techniques 0-32792  
 dichlorodifluoroethane, threshold multiphoton dissociation.  $Cl_2$  elimination 0-9653  
 dimethyl s-tetrazine, two-photon laser photochem., hole burning appls. 0-21304  
 N-ethylcarbazole, soln., laser induced ionic photodissoc., transient polyelectrolyte form. 0-53068  
 ethylene, multiphoton dissociation,  $CH_2$  and  $C_2$  prod., fluence depend. meas. 0-5586



**molecular photodissociation continued**

ethylene dimer, CO<sub>2</sub> laser induced photodissoc., pulsed mol. beam obs., van der Waals bond 0-9660  
 fluoroethanes, IR multiphoton dissoc., HF vib. energy distrib. 0-53073  
 fluoroethylenes, IR multiphoton dissoc., HF vib. energy distrib. 0-53073  
 formaldehyde, multiphoton dissoc. by CO<sub>2</sub> laser, intensity/fluence depend. 0-11913  
 formaldehyde, multiphoton dissoc. intensity depend. 0-28073  
 formaldehyde-d<sub>2</sub>, reson. multiphoton dissoc. 0-53077  
 halides, aryl and aryl-alkyl 193 nm photodissoc., fragment translational energy distrib. 0-48048  
 halomethanes, UV multiphoton dissoc., photofragment fluoresc. 0-14165  
 HeH<sup>2+</sup>, photodissoc., rel. to UV flux deficiency of stellar spectra 0-9654  
 heptafluorodopropane, photodissoc., appl. in I ring laser 0-48236  
 hexafluoroacetone, IR multiphoton decomposition, press., fluence, wavelength, temp. depend. 0-7809  
 hexafluoroacetone, IR multiphoton dissociation, isotopic selectivity and yield, temp. effect 0-53069  
 inert gas dimer ions, A<sup>2</sup>Σ<sub>1/2u</sub><sup>+</sup> → D<sup>2</sup>Σ<sub>1/2g</sub><sup>+</sup> system, theoretical absorption spectrum 0-32734  
 infrared multiphoton dissociation of molecules, review (*Japanese*) 0-11885  
 infrared multiphoton processes, apparent step cross-sections, pulse spatial structure, irradiation techniques 0-32792  
 infrared multiphoton processes, reaction rate, scale factors, pulse structure 0-32791  
 iodotrifluoromethane, IR multiphoton dissoc., source of trifluoromethyl radicals 0-26036  
 ion fragmentation mechanisms and photoelectron spectroscopy, book contrib. 0-14179  
 IR multiple-photon dissociation, laser induced fluoresc. photofragment detect. 0-37840  
 IR multiple-photon photolysis, fluence-depend. dissociation probabilities calc. 0-32786  
 isotope separation by pulse-periodic CO<sub>2</sub> laser, multiphoton process 0-9931  
 ketene, multiphoton dissoc., CH<sub>2</sub> and C<sub>2</sub> prod., fluence depend. meas. 0-5586  
 laser induced reactions, activation energies, temps. and rate consts. 0-40710  
 laser radiation, selective action on matter, review 0-7832  
 laser specific and thermal reactions classifications 0-11919  
 laser-controlled unimolecular and bimolecular processes, field-depend. rate const. 0-11906  
 laser-induced, effective manifold reduction, criteria 0-43123  
 linear triatomic mol. photodissociation, fragment ang. distrib., theory 0-23468  
 metal-triiodide vapour two-photon dissociation for atomic transition lasers 0-23679  
 methanol, UV multiphoton dissoc., photofragment fluoresc. 0-14165  
 methyl amine, photodissoc. products, Doppler spectroscopy 0-53124  
 methyl isocyanide, laser initiated thermal isomerisation, time behaviour of CN radicals 0-11887  
 methylamine, multiphoton dissoc., N isotope separation 0-35553  
 methylamine, multiple photon dissoc., NH<sub>2</sub> fragments, laser-excited fluoresc. obs. 0-11938  
 methylamine, multiple-photon dissociation, laser induced fluoresc. photofragment detect. 0-37840  
 molecular photoselected excited states, dynamics, advances using synchrotron radiation 0-37836  
 multiphoton absorption modelling, using SF<sub>6</sub> energy-dependent absorption cross sections 0-32789  
 nitromethane molecule dissociation in IR field, laser-induced fluoresc. obs. 0-53075  
 photofragment spectroscopy of mol. ions using fast ion beams 0-9755  
 poly N-vinylcarbazole, soln., laser induced ionic photodissoc., transient polyelectrolyte form. 0-53068  
 polyatomic molecule, anharmonic model for mol. photoexcitation 0-9669  
 polyatomic molecule, collisionless multiphoton dissoc., threshold behaviour, nonthermal theory 0-11905  
 polyatomic molecule, laser photochem. dissoc., isotope effect rel. to dissoc. probability 0-23472  
 polyatomic molecule, multiphoton absorpt. resons., dynamic Stark splitting 0-9670  
 polyatomic molecule, multiphoton dissoc. dynamics, classical model 0-11904  
 polyatomic molecule radiative dissociation model 0-43124  
 polyatomic molecules, IR laser sensitised chem. reactions 0-11910  
 polyatomic mols., multiple photon IR processes, reviews 0-43125  
 polyatomic symmetric molecules, collisionless dissoc. and vibr. spectrum of degenerate modes 0-18893  
 polyatomic symmetric molecules, selective multistep IR dissoc. 0-23473  
 population trapping during laser induced molecular excitation and dissociation 0-1035  
 propenal, IR photochem. in electronically excited state 0-11923  
 pyrimidine N<sub>2</sub>O aq. solns., dimer formation in γ-radiolysis, chromatographic obs. 0-7785  
 resonant photocatalytic effect, in laser induced uni-mol. dissoc. 0-3377  
 rotational heating during IR multiphoton excitation, dynamical effects on dissoc. products 0-18892  
 s-tetrazine, two-photon laser photochem., hole burning appls. 0-21304  
 simple molecules, two-photon dissoc., spectrosc. obs. 0-32787  
 sub-Doppler laser spectroscopy of mol. ions in fast ion beams 0-9655  
 tetrafluorodihietane, IR photolysis, multiphoton dissoc. models 0-30253  
 sym-tetrazine, isotope selective mol. spectroscopy and isotopically pure mols. prod. with dye laser 0-11926  
 triatomic molecules photodissociation to diatomic fragments, fluoresc. polarisation excitation spectroscopy 0-28054  
 triatomic van der Waals complex, vibr. predissoc. and photodissoc. lifetimes 0-9661  
 trifluoriodomethane, isotopic sensitivity of IR laser photodissociation 0-7805  
 trifluoriodomethane, multiphoton dissoc., isotopically selective 0-28113  
 trifluoriodomethane, multiphoton IR excitation and dissoc. (*Russian*) 0-35562  
 trifluoriodomethane, multiple IR photon excitation and dissoc., primary characts. 0-11909  
 trifluoriodomethane, UV absorpt. spectrum broadening by laser-induced vibr. excitation 0-53050  
 trifluoromethyl chloride, IR multiphoton dissociation, isotopic selectivity and yield, temp. effect 0-53069

**molecular photodissociation continued**

unimolecular reactions, laser-induced, by multiphoton IR excitation, theory 0-9664  
 unimolecular reactions induced by monochromatic IR radiation, intensity and laser energy fluence influence 0-11903  
 uranyl hexafluoroacetylacetonate tetrahydrofuran, IR laser photodissoc., O and U isotope selective 0-50868  
 water solar photodecomposition, redox reaction thermodynamics 0-35697  
 Br+NOBr, primary and secondary photochemistry, vibrationally excited NO, IR fluoresc. obs. 0-48030  
 Br<sub>2</sub>, photolytic cage effect in high-press. gases, laser wavelength depend. 0-11925  
 BrCN, vacuum UV photodissociation spectroscopy, quantum yield, fluoresc. polarisation 0-32736  
 CF<sub>3</sub>NO → CF<sub>3</sub>NO, photodissociation dynamics, two-photon laser-induced fluorescence study 0-43122  
 CO, UV photodissoc., O I 1304 angstrom emission 0-32652  
 CO<sub>2</sub>, photolysis, O(<sup>1</sup>S) absolute quantum yield spectral depend. meas. using XeO luminesc. 0-35561  
 CO<sub>2</sub>, UV photodissoc., O I 1304 angstrom emission 0-32652  
 CO<sub>2</sub>-O<sub>2</sub>-H<sub>2</sub>O, photodissoc. and photodetachment of negative ions 0-14182  
 CS<sub>2</sub><sup>+</sup>, photodissociation cross section, UV and visible spectral obs. 0-28077  
 Cl+NOCl, primary and secondary photochemistry, vibrationally excited NO, IR fluoresc. obs. 0-48030  
 ClCN, vacuum UV photodissociation spectroscopy, quantum yield, fluoresc. polarisation 0-32736  
 Cs<sub>2</sub>, two-photon dissoc., spectrosc. obs. 0-32787  
 H<sub>2</sub>, diabatic and reson. states, dissociative photoionisation calcs. 0-47883  
 H<sub>2</sub><sup>+</sup>, vibr. Green's function and two-photon dissociation 0-28075  
 HBr, laser photodissociation, <sup>81</sup>Br isotope enrichment 0-1075  
 HD<sup>+</sup>, vibr.-rot. transitions, using new two-photon IR photodissoc. technique 0-23405  
 HF dissociation with one and two IR lasers, classical mech. treatment 0-23470  
 H<sub>2</sub><sup>+</sup> (HD<sup>+</sup>), IR photodissoc. cross sections, calc. and simulation expt. 0-9659  
 HN<sub>3</sub>, IR multiphoton dissociation with electronic excitation 0-11934  
 H<sub>2</sub>O, solar photochemical decomposition for H<sub>2</sub> prod. 0-16822  
<sup>2</sup>HN<sub>3</sub>, IR multiphoton dissociation with electronic excitation 0-11934  
 HgBr<sub>2</sub> photodissociation by ArF laser, characterisation of transition prod. HgBr(B<sup>2</sup>Σ<sup>+</sup>) 0-37841  
 HgCl, photodissociation cross section, laser extraction efficiency 0-32972  
 HgCl, photodissociation calcs., laser efficiency 0-48047  
 I<sub>2</sub>, photolytic cage effect in high-press. gases, laser wavelength depend. 0-11925  
 I<sub>2</sub>-aromatic complexes, photodissociation, I-aromatic complex in soln. formation ps laser studies 0-40711  
 IBr:CO<sub>2</sub> photolysis, electron-vibr. pumping, 2.7 μm Br and 4.3, 10.6 μm CO<sub>2</sub> laser transitions 0-28196  
 ICN, vacuum UV photodissociation spectroscopy quantum yield, fluoresc. polarisation vacuum UV photodissociation spectroscopy, quantum yield, fluoresc. polarisation 0-32736  
 I<sub>2</sub>Ne<sub>4</sub>He<sub>6</sub>, van der Waals complexes photodissoc. 0-50864  
 NH<sub>3</sub>, first triplet state, photodissoc. and Rydbergisation investig. 0-53067  
 NH<sub>3</sub>, multiple photon dissoc., NH<sub>2</sub> fragments, laser-excited fluoresc. obs. 0-11938  
 NO, photodissoc. in mesosphere and stratosphere, theory 0-41580  
 NO, stratospheric and mesospheric photodissoc. rate, calc. 0-51498  
 NO<sub>2</sub>, one-photon dissoc. to NO+O, Doppler spectroscopy 0-53124  
 NO<sub>2</sub><sup>+</sup>, NO<sub>2</sub><sup>+</sup>.H<sub>2</sub>O, and peroxy isomers, photodissoc. and photodetachment 3500-8250 Å, rel. to ionosphere 0-35554  
 NO<sub>3</sub><sup>+</sup>, NO<sub>3</sub><sup>+</sup>.H<sub>2</sub>O, and peroxy isomers, photodissoc. and photodetachment 3500-8250 Å, rel. to ionosphere 0-35554  
 N<sub>2</sub>O, atmospheric, instantaneous global photochemical reaction rates 0-17335  
 N<sub>2</sub>O, O prod. and props. in liq. Ar and N<sub>2</sub> 0-43063  
 N<sub>2</sub>O, photolysis, O(<sup>1</sup>S) absolute quantum yield spectral depend. meas. using XeO luminesc. 0-35561  
 NO<sub>2</sub><sup>+</sup>, multiple IR photon fluoresc. excitation and dissoc., electronically excited 0-48050  
 O<sub>2</sub><sup>+</sup>, first negative system, high-resolution photofragment spectroscopy 0-47971  
 O<sub>2</sub><sup>+</sup>, predissociated b<sup>4</sup>Σ<sub>g</sub><sup>-</sup> state, high resolution laser spectroscopy in fast ion beam 0-9656  
 O<sub>3</sub>, multiphoton dissoc. dynamics, classical model 0-11904  
 O<sub>3</sub>, UV photodissoc. rate, expt. and theory 0-40722  
 O<sub>3</sub>+O<sub>2</sub>(<sup>1</sup>Δ<sub>g</sub>)(O<sub>2</sub><sup>+</sup>), UV photolysis, O(<sup>1</sup>P) prod., rate consts. determ. 0-55636  
 O<sub>3</sub>+O(<sup>1</sup>D), UV photolysis, O(<sup>3</sup>P) prod., rate consts. determ. 0-55636  
 OCS photodissociation, S(<sup>1</sup>S) prod. and props. in liq. Ar and N<sub>2</sub> 0-43064  
 OCS<sup>+</sup>, photodissociation cross section, UV and visible spectral obs. 0-28077  
 S isotope separation, multiphoton process using high-power CO<sub>2</sub> laser radiation 0-9657  
 SF<sub>5</sub><sup>+</sup> ion-molecules, IR multiple-photon dissoc., lifetime meas. 0-28072  
 SF<sub>6</sub> cooled gas, multiphoton dissociation with CO<sub>2</sub> laser, enrichment with <sup>35</sup>S 0-14245  
 SF<sub>6</sub>, infrared multiphoton processes, apparent step cross-sections, pulse spatial structure, irradiation techniques 0-32792  
 SF<sub>6</sub>, isotope separation, TEA CO<sub>2</sub> laser irradiation (*Japanese*) 0-11885  
 SF<sub>6</sub>, laser-irrad., high-resolution double-reson. spectroscopy, collisionless multiphoton dissoc. 0-9623  
 SF<sub>6</sub>, multiphoton dissoc., unified dynamical model 0-5587  
 SF<sub>6</sub>, multiphoton dissoc., collision effects 0-23467  
 SF<sub>6</sub>, multiphoton dissoc., classical model 0-53076  
 SF<sub>6</sub>, multiple photon excitation, collisionless 0-53079  
 SF<sub>6</sub>, resonant single-photon dissoc. route using prelim. electron excitation 0-9662  
<sup>32</sup>SF<sub>6</sub>, infrared multiphoton processes, reaction rate, scale factors, pulse structure 0-32791  
 SF<sub>6</sub>-H<sub>2</sub> mixtures, laser irradiated, IR energy deposition and HF fluoresc. 0-23454  
 Se<sub>2</sub>, photolytic dissoc. obs. using inert gas halide lasers 0-11935  
 SiH<sub>4</sub>, irrad. by CO<sub>2</sub> laser, Si film deposition 0-16190  
 Ti photodissociation, Ti atomic fluorescence, pressure and Doppler broadening 0-5504



**molecular photodissociation continued**

- U complex, bis-hexafluoroacetylacetonate uranyl tetrahydrofuran, laser-induced dissociation 0-53071  
 UF<sub>6</sub>-H<sub>2</sub>, near UV and visible excitation, quantum yield from photodissociation 0-35549  
 XeF, ground state dissociation, equilibrium 0-9652  
 XeF<sub>2</sub>, for XeF laser 0-32976  
 XeF<sub>2</sub> photodissociation forming XeF, laser action due to bound-free C(3/2)-A(3/2) transition 0-14334

**molecular polarisability**

see also *molecular moments*

- acetic acid amides, polarisabilities and  $\pi$ - $\pi^*$  transitions, dipole interaction calcs. 0-23411  
 acetylene, multipole moments and polarisabilities, SCF calcs. 0-5471  
 4-(9-anthryl)-N,N-dimethylaniline, fluoresc., dipole moments and polarisabilities 0-1019  
 aromatic hydrocarbons, mol. polarisability, INDO calc. 0-52886  
 benzene, SCF-EHT polarisability calc. 0-47895  
 benzyl bromide and chloride, bond orders estimation, bond polarisability derivative 0-32594  
 bounds on van der Waals coeffs., oscillator strength sum rules 0-27941  
 carbon tetrachloride, clusters, collision induced polarisability, mol. frame distortion 0-32798  
 carbon tetrafluoride, clusters, collision induced polarisability, mol. frame distortion 0-32798  
 carbonyls, electric polarisability, in excited singlet and triplet states (*Bulgarian*) 0-52897  
 charge distribution in ions and mols., inductive effect 0-47837  
 chloroform-d<sub>0</sub>(-d<sub>1</sub>), Raman and IR intensity anal. 0-18857  
 cholesteric liquid crystal, molecular polarisability, arrangement order calc. (*Polish*) 0-10495  
 classical fluid, collision-induced and multiple light scatt. 0-53919  
 crystal, molecular lattice vibr. IR intensities, mol. polarisability calc. 0-11372  
 diatomic molecules, polarisability correl. with mol. dims. 0-23288  
 diatomic system, pair polarisability curve shape, rel. to chem. bonding 0-42930  
 diatomic systems, interactions, long-range dipoles, quadrupoles and hyperpolarisabilities 0-53161  
 dielectric friction in plasma, harmonic oscillator and rigid dipole dielectrics 0-53928  
 dipolar molecular lattice, dielec. absorpt. of disordered mol. solids, electrodynamic influences 0-40040  
 dipolar molecules, zero-THz liq. phase dielec. absorpt. and rot. Langevin eqn. 0-40032  
 disordered media, LF spectrum study from Raman scattering cross section 0-25363  
 electron+molecule, scatt., polarisation pot. determ. 0-17721  
 ethane, multipole moments and polarisabilities, SCF calcs. 0-5471  
 ethylene, multipole moments and polarisabilities, SCF calcs. 0-5471  
 formic acid amides, polarisabilities and  $\pi$ - $\pi^*$  transitions, dipole interaction calcs. 0-23411  
 ground state props., coupled cluster and MBPT methods appl. 0-47881  
 homonuclear diatomic ions, static polarisabilities, internuclear separation effects 0-5494  
 hydrocarbons, electric polarisability, in excited singlet and triplet states (*Bulgarian*) 0-52897  
 hydrocarbons, mol. Raman intensities calcs. 0-52993  
 hyperpolarisabilities, HF calc. with correlation method, appl. to HF mol. 0-23342  
 liquid structure and dynamics from light scatt. spectra 0-55105  
 methane, clusters, collision induced polarisability, mol. frame distortion 0-32798  
 methane, slow electron scatt., rigid mol. model with exchange and polarisation 0-43194  
 olefins, zwitterionic states, polaris. and vibronic interactions 0-32620  
 organic molecules, quadrupole moments, dipole quadrupole A and C polarisabilities, perturbation theory anal. 0-27934  
 organic solids, charged excitonic complexes, coupled states, exciton interaction with charge carriers study 0-20090  
 organic system, nonlinear second-order optical susceptibility 0-9947  
 oscillating electric dipole contrib. to light scatt. and interpret. in terms of polarisability and hyperpolarizability 0-53212  
 (+)-(S)-2-phenyl-3,3-dimethylbutane, optical activity, circular dichroism, polarisability model 0-43082  
 PMMA, piezobirefringence, optical and mech. relaxations, temp. depend. 0-34885  
 point charge model approach to mol. elec. polarisability 0-18797  
 polyatomic molecule, crit. consts. evaluation from intermol. force consts. 0-37844  
 polypeptides,  $\alpha$ -helical,  $\pi$ - $\pi^*$  absorpt. and circular dichroism spectra 0-23398  
 pyrazine absorbed on electrode, surface enhanced Raman spectra, symmetry and polarisability changes 0-50310  
 pyridine iodine complexes, charge transfer complexes, vibr. spectra, laser Raman obs. 0-52990  
 di- $\alpha$ -pyridyl hydroperchlorates, intramol. H bonds, steric conditions and polarisability obs. 0-53160  
 Raman scatt. theory, vibr. state summation, polarisability tensor upper and lower bounds 0-48000  
 Raman spectra of gases, high-resolution, mol. struct. and orps. 0-53000  
 scaling and Pade approximants, many-body perturbation theory 0-42952  
 TCNQ salt, NMP-TCNQ, electronic struct., SCF calcs., total energy polarisation effects 0-15469  
 vapour-liquid equilibria, and intermol. forces, semi-empirical approach 0-54359  
 CO<sub>2</sub>, low energy electron (positron) collisions, ab initio adiabatic polarisation pots. 0-14240  
 CS<sub>2</sub>, symmetric stretch mode, moments and polarisability derivatives, SCF calcs. 0-901  
 Eu(III) complexes, f-f transition probabilities, ligand polarisation model, anisotropic contrbs. 0-53049  
 H halides, polarisability, correl. with mol. dims. 0-23288  
 H<sub>2</sub>, polarisabilities, higher, static, calc., wave-function quality depend. 0-18814  
 H<sub>2</sub>, polarisability, finite field MC SCF calcs. 0-14075  
 H<sub>2</sub>, second order props., dipole polarisability nucl. coupling, fast CI method 0-27950  
 H<sub>2</sub><sup>+</sup>, hyperpolarisabilities, quadrupole and field-gradient quadrupole polarisabilities 0-1086

**molecular polarisability continued**

- H<sub>2</sub>+H<sub>2</sub>, interaction polarisability comparison with the He diatom, ab initio SCF calcs. 0-27943  
 H<sub>2</sub>+H<sub>2</sub>, quadrupolar S<sub>1</sub>(J)+S<sub>0</sub>(J) double transitions, IR fundamental band, 77K 0-52986  
 HF, hyperpolarisabilities, dipole moment, HF calc. with correlation 0-23342  
 H<sub>2</sub>O, polarisability tensor components, virial theorem calcs. 0-53087  
 H<sub>2</sub>O, slow electron scatt., rigid mol. model with exchange and polarisation 0-43194  
 H<sub>2</sub>S, slow electron scatt., rigid mol. model with exchange and polarisation 0-43194  
 He pair, dispersion interaction, independent particle model, polarisabilities 0-37732  
 He<sub>2</sub>, polarisability and collision induced Raman spectra 0-48005  
 KCl, charge transfer and pair polarisability anisotropy 0-43173  
 KF, ab initio SCF MO energy, dipole moment and polarisability 0-1085  
 LiCl, charge transfer and pair polarisability anisotropy 0-43173  
 LiF, ab initio SCF MO energy, dipole moment and polarisability 0-1085  
 N<sub>2</sub>, electron-mol. adiabatic polarisation pots. and ab initio SCF polarisabilities 0-9499  
 N<sub>2</sub>, light polarisability parameters, Raman scatt. ang. meas. 0-37814  
 N<sub>2</sub>, low energy electron (positron) collisions, ab initio adiabatic polarisation pots. 0-14240  
 N<sub>2</sub>, multiple moments, polarisabilities and anisotropic long range interaction coeffs. 0-43206  
 N<sub>2</sub>, one-electron props., polarisabilities and polarisability derivatives, SCF and CI calcs. 0-37746  
 N<sub>2</sub>, polarisability tensor anisotropy, Raman spectra differential scatt. cross section 0-18860  
 N<sub>2</sub>, Raman intensity, ab initio calc. 0-1028  
 N<sub>3</sub>, polarisability correl. with mol. dims. 0-23288  
 O<sub>2</sub>, light polarisability parameters, Raman scatt. ang. meas. 0-37814  
 O<sub>2</sub>, polarisability tensor anisotropy, Raman spectra differential scatt. cross section 0-18860  
 Pd complex, Pd<sup>II</sup>(CNCH<sub>3</sub>)<sub>6</sub>(PF<sub>6</sub>)<sub>2</sub>, vibr. spectra, M-M bonds. (*French*) 0-47997  
 Pt complex, Pt<sup>II</sup>(CNCH<sub>3</sub>)<sub>4</sub>(PF<sub>6</sub>)<sub>2</sub>, Pt<sup>I</sup>(CNCH<sub>3</sub>)<sub>3</sub>(PF<sub>6</sub>)<sub>2</sub>, and Pt<sup>IV</sup>(CNCH<sub>3</sub>)<sub>6</sub>(PF<sub>6</sub>)<sub>2</sub>, vibr. spectra, M-M bonds. (*French*) 0-47997  
 SF<sub>6</sub>, clusters, collision induced polarisability, mol. frame distortion 0-32798

**molecular positron scattering** see *elastic scattering of electrons by atoms and molecules; molecular electron impact dissociation; molecular electron impact excitation; molecular electron impact ionisation*

**molecular potentials** see *potential energy functions*

**molecular predissociation**

- alkali metal molecular, laser radiation absorpt., at. excitation processes 0-32785  
 diatomic molecules, form. and dissociation in interstellar medium 0-23471  
 formaldehyde predissoc., from reson. multiphoton dissociation of small mols. 0-53077  
 harmonic oscillator, relative line widths and level shifts 0-23469  
 laser-induced of diatomic and polyatomic mols., photocatalytic effect 0-11907  
 methane+Ar, rot. compound state resons. 0-28090  
 photorecombination emission reaction mechs. during atomic collisions 0-18914  
 resonant photocatalytic effect, in laser induced uni-mol. dissociation 0-3377  
 sub-Doppler laser spectroscopy of mol. ions in fast ion beams 0-9655  
 triatomic van der Waals complex, vibr. predissoc. and photodissoc. lifetimes 0-9661  
 Van der Waals cluster, gas phase, vibr. predissoc., rel. to matrix-isolated O<sub>2</sub> multiphonon vibr. relax. 0-18861  
 van der Waals dimers, intramolecular vibr. dynamics, vibr. predissociation 0-28083  
 van der Waals molecules, vibrationally excited, lifetimes, momentum gap 0-5601  
 CH, B<sup>2</sup> $\Sigma^-$  state predissoc., calcs. and time resolved spectrosc. 0-23576  
 CH<sup>+</sup>, predissociated levels obs. 0-37838  
 C<sub>2</sub>N<sub>2</sub>, C<sup>1</sup> $\Pi_u$ -state predissoc., vibronic effects 0-28078  
 Cd<sub>2</sub>, quenching and predissociation, possible excimer laser 0-32770  
 Cl<sub>2</sub>, B-X transition, predissoc., laser-induced fluoresc. obs. 0-43093  
 D<sub>2</sub>, electron impact, threshold excitation and predissoc., electron-photon coincidence meas. 0-18941  
 D<sub>2</sub>, predissoc. linewidths and shapes for 3 $\pi$ D<sup>1</sup> $\Pi_u$  state 0-53066  
 H<sub>2</sub>, electron impact, threshold excitation and predissoc., electron-photon coincidence meas. 0-18941  
 H<sub>2</sub>, predissoc. linewidths and shapes for 3 $\pi$ D<sup>1</sup> $\Pi_u$  state 0-53066  
 H<sub>2</sub>, predissociation of  $\Pi_u^+$  state vibr. and rot. levels, dissociation yields meas. 0-32784  
 H<sub>2</sub> predissociation probabilities of 4 $\pi$ <sup>1</sup> $\Pi_u$  +  $\nu \geq 1$  levels, dissociation channels interference 0-28074  
 HD, predissoc. linewidths and shapes for 3 $\pi$ D<sup>1</sup> $\Pi_u$  state 0-53066  
 HNO, vibronic state perturbative and predissoc. mechanisms, fluoresc. excitation spectra obs. 0-9658  
 Hel<sub>2</sub>, Van der Waals mol. vibr. predissoc. anharmonicity effects 0-52971  
 Hg<sub>2</sub>, quenching and predissociation, possible excimer laser 0-32770  
 I<sub>2</sub>, predissociation, electric-field induced 0-37839  
 I<sub>2</sub>, vibr.-translational relax., collisional predissoc., opto-acoustic effect obs. 0-43157  
 I<sup>35</sup>Cl, predissociations in B<sup>3</sup> $\Pi_{0+}$  state 0-1033  
 I<sup>37</sup>Cl, predissociations in B<sup>3</sup> $\Pi_{0+}$  state 0-1033  
 I<sub>2</sub><sup>+</sup>He, vibrational predissociation, van der Waals molecules, vibration-translation scaling theory 0-43135  
 NH, lower valence states, predissociations, Franck-Condon anal. 0-5590  
 NH<sub>3</sub>, predissociation of A<sub>2</sub> state from UHF calcs. of potential energy surface 0-1034  
 NO predissociation in mesosphere and stratosphere, photochemistry 0-21802  
 NO<sub>2</sub>, dissociative limit, mol. beam characts. determ. by fluoresc. excitation spectra 0-53074  
 O<sub>2</sub>, predissoc. of B<sup>2</sup> $\Sigma_u^-$  state, Rydberg-valence crossing model 0-1032  
 O<sub>2</sub><sup>+</sup>, first negative system, high-resolution photofragment spectroscopy 0-47971  
 O<sub>2</sub><sup>+</sup>, photofragment spectroscopy using fast ion beams 0-9755  
 O<sub>2</sub><sup>+</sup>, predissociated b<sup>2</sup> $\Sigma_g^-$  state, high resolution laser spectroscopy in fast ion beam 0-9656  
 O<sub>2</sub>(b<sup>2</sup> $\Sigma_g^-$ ,  $\nu=4$ , N', F') predissociation fragments, ang. distrib., separation energies 0-5588



**molecular predissociation continued**

$O_2^+(b^2\Sigma^-)$  predissociation, branching ratio determ. 0-14181  
 $Zn_2$ , quenching and predissociation, possible excimer laser 0-32770

**molecular quadrupole moments** *see molecular moments*

**molecular relaxation** *see chemical reactions; molecular fluorescence; molecular inelastic collisions; molecular spectra; time resolved spectra*

**molecular reorientation**

*see also macromolecular dynamics*

acetic acid,  $-d_1(=d_4)$  liquid, molecular motion, proton spin echo study (Russian) 0-32745  
 acetonitrile, soln., high press., mol. reorientation, correl. times, depolarised Rayleigh scatt. obs. 0-29748  
 alcohols, OH-stretching vibr. band in overtone region, IR-Fourier spectral investig. (German) 0-976  
 alkali halide:  $NH_4^+$ , hindered rot. energy levels calc. 0-10514  
 alkane chains in liquids, rot. and torsional dynamics, Riemann tensor theory 0-54084  
 alkanes, liquid, chain reorientation, Brownian dynamics simulation, comparison of models 0-49067  
 ammonium compounds, rotational tunnelling, temp. dependence 0-38970  
 anilines, substituted, in benzene soln., dielectric relax. time, dipole moment 0-50259  
 anilines, substituted, in nonpolar solvent, dielec. relax. obs. 0-55022  
 anilinium halides, and anilinium sulphate, proton mag. relax. obs. 0-34800  
 anisotropic liq. ang. correl. functions, memory function approach, Mori theory and extended diffusion eqn. 0-10489  
 BBOA, smectic B phase, fluidlike mol. dynamics, Raman scatt. study 0-20630  
 benzene-p-dioxan, mixtures, mol. reorientation and assoc., depolarised Raman scatt. obs. 0-7341  
 biradical metal chelates, rot. motion in polar solvents, rel. to ESR line-shape 0-27994  
 2-chloro-2-nitropropane, far IR-microwave estimation of binary collision approx. 0-55095  
 chloroform-He(Ar)(N<sub>2</sub>) gaseous compressed mixture, mol. reorientation, Raman spectra 0-23422  
 chloroform-p-dioxan and chloroform-benzene mixtures, mol. reorientation and assoc., depolarised Raman scatt. obs. 0-7341  
 classical quadrupole solids, correl. effects 0-10628  
 cresyl violet, rot. diffusion, picosec. saturation spectrosc. obs. 0-5634  
 cyclohexane, plastic and liquid crystal phase, rot. correl. func. by Raman spectroscopy 0-23403  
 cyclohexane- $d_6(d_8)$ , plastic crystal phase transition, mol. reorientation, Raman scatt. phonon spectra 0-20631  
 dibutyl-phenyl-benzoyloxy-benzoate, nematic liq. cryst., rot. barrier, PCIL0 and CNDO/2 calcs. 0-33874  
 N,N-dimethyltrichloroacetamide, two-site exchange system, total line shape anal. 0-35519  
 dipolar molecular lattice, dielec. absorpt. of disordered mol. solids, electrodynamic influences 0-40040  
 dipolar molecules, zero-THz liq. phase dielec. absorpt. and rot. Langevin eqn. 0-40032  
 dipole-dipole coupling, inertial effect 0-40049  
 dyes, rot. diffusion of prolate, oblate mols. from absorpt. relax. 0-1008  
 electrostatic space focusing of molecular beam 0-28118  
 N-p-ethoxybenzylidene-p'-cyanoaniline, nematic, mol. reorientation in DC elec. field, IR ATR spectra study 0-45064  
 p-p-ethoxyphenylazophenyl hexanoate, dielec. relax. in stable and metastable solid phases 0-34851  
 p-fluorani,  $^{19}F$  NMR and spin-lattice relax. meas., pot. profile calc., mole. reorientation 0-29634  
 glassy polar matrix, electron trap relaxation model 0-15470  
 glycerol- $d_3(-d_4)$ , compressed viscous liq., reorientational motion, NMR obs. 0-7183  
 4-n-heptyl-4'- $\beta$ -cyanovinylbiphenyl, liq. cryst., isotropic mechanism of mol. rot., dielec. permitt. meas. 0-10491  
 hexafluorobenzene-benzene, liq., mol. interactions, IR and Raman line-shape obs. 0-28907  
 4-n-hexyl-4-cyanobiphenyl, liq. cryst., isotropic mechanism of mol. rot., dielec. permitt. meas. 0-10491  
 liquid, IR and Raman studies, model 0-11390  
 liquid crystal display, with dichroic dye guest, field-induced colour switching 0-1327  
 liquid crystals, static and dynamic props., time depend. fluoresc. depolarisation obs. 0-29786  
 liquid short chain molecules, optical investig. of mol. motions 0-40123  
 liquid structure and dynamics from light scatt. spectra 0-55105  
 lithium acetate dihydrate, nearly free methyl rotors, rot. energy states, nucl. reson. props. 0-34784  
 luminescent system, orientation factor in conc. effects due to nonradiative energy transfer 0-25425  
 magnetic relaxation depend. on internal motion in solid, correlations 0-25239  
 magnetic resonance line shape, effect of anisotropic motion 0-7144  
 MBBA/EBBA, nematic, mol. interaction energy 0-33881  
 methane, solid, high press. NMR obs. 0-50214  
 $^{13}C$ -methane- $d_3$ , annealed, spin conversion and proton 2nd moment time-depend. 0-11283  
 methyl compounds, rotational tunnelling, temp. dependence 0-38970  
 methyl groups in solids, reorienting and tunnelling, spin-lattice relax. 0-50217  
 methyl groups in solids, tunnelling freq. for internal rotation in pot. function 0-49134  
 methylcyclohexane, dense liq., self-diffusion and viscosity 0-15278  
 molecular crystals, rot. and sp. hf. anomalies 0-28932  
 molecule, tetrahedral, in cryst. field, torsional ground state splitting, appl. to methane and  $(NH_4^+)_2SnCl_6$  0-15019  
 Mossbauer spectroscopic studies of mol. motion in solids 0-39915  
 naphthalene, melting of rotational degrees of freedom near cryst.-liq. transition 0-54352  
 naphthalene in nonpolar solvent, vibr. and reorientational relax., correl. function 0-45065  
 neutron scattering studies of mol. rotational motion in solid state 0-24384  
 nitrobenzene, oscill. optically induced Kerr kinetics 0-1286  
 nonlinear symmetric  $XY_2$  type molecules, isotopic invariants, Coriolis coupling constants, centrifugal distortion constants 0-923  
 NQR, molecular reorientations between unequal potential wells 0-54989

**molecular reorientation continued**

NQR, NMR and EPR, spectral parameters, influence of mol. motion dynamics, review 0-20486  
 NQR spin-lattice relax. due to mol. fragments reorientation (Russian) 0-7189  
 organic reactions in solid state 0-21309  
 organic surfactant molecules reorientation on electrode surface, electrochem. kinetics 0-45522  
 PAA, nematic liq. cryst., rot. barrier, PCIL0 and CNDO/2 calcs. 0-33874  
 Phase V, nematic, transient response to redirected mag. field, EPR study 0-33879  
 phenylene sulphides, NMR relaxation for mol. motions (German) 0-11288  
 phospholipids,  $^{31}P$  NMR, slow-motional lineshapes for very anisotropic rot. diffusion 0-5644  
 phthalimide acetyl derivatives in polar solvents, luminesc. kinetics and phosphoresc. quenching 0-18885  
 polar molecule, dielec. friction effect on reorientation in liq. 0-40048  
 poly(L-histidine), molecular motions in solid state, NMR and dielec. meas. 0-11332  
 poly-p-phenylene sulphide, NMR relaxation for mol. motions (German) 0-11288  
 polyatomic fluid, local dynamics, spectroscopic studies, summer school lecture series 0-6343  
 polybutadiene, mol. motion in solid and soln.,  $^{13}C$  NMR relaxation meas. (Japanese) 0-2666  
 polyethylene, linear, nuclear relaxation, mol. motion (Russian) 0-44949  
 polyethylene crystals, plastic deformation, molecular mech., TEM obs. 0-21022  
 polypropylene, TSC meas. of relax. modes, apparent double glass transition 0-11323  
 polystyrene, end group modified, chain dynamics studied by fluorescence depolarization 0-19724  
 polystyrene, glassy state, relax., free vol. fluctuations effect 0-19722  
 polystyrene, isotactic crystals, plastic deformation, molecular mech., TEM obs. 0-21022  
 polystyrene, molecular motion obs. during thermal polymerisation of styrene, PMR 0-3342  
 polyvinylidene fluoride, TSC and thermoluminescence, reln. to molecular motion (Japanese) 0-55200  
 resorcin, Raman line intensity as function of mol. orientation 0-11383  
 rhodamine 4C, in ethanol soln., rot. relax. time using ps. spectroscopy technique 0-1013  
 ribonuclease-A, solid, PMR spin-lattice relax., mol. dynamics 0-51041  
 sodium decanoate-n-decanol-water system, lamellar G-phase, orientational-order, EPR investigation 0-24355  
 solid torsional oscillators, rotating frame, nucl. spin polarisation losses, torsional spectroscopy 0-31821  
 stability constraints on potential function and rotational invariance in external mode formalism 0-24543  
 o-terphenyl, dipolar solutes, reorientational motions, dielectric relax. below glass transition 0-19706  
 tetraalkylammonium halides, mol. reorientation, spin lattice relax. time study 0-18875  
 tetrahedral four spin  $1/2$  systems, Zeeman and tunnel system reson., coupled and uncoupled relax. 0-50214  
 time-dependent distribution functions, pictorial representation, correlation functions 0-55021  
 5d-transition metal antiferroite cryst., struct. props. and lattice dynamics, mag. struct. 0-44268  
 trichlorophosphazoperfluoro-1,1-dimethylethane, cryst.,  $^{19}F$  NMR and mol. mobility, fluorination influence 0-34809  
 trifluoroacetates, methyl and ethyl, intramol. relax. at microwave freqs. 0-55020  
 Ag, and  $Ag^+$ , solvation in deuterated-ice matrices, electron spin echo obs. 0-15780  
 CO, collision-induced reorientation, direct meas. by IR double reson. 0-32800  
 CS<sub>2</sub>, liq., props. from allowed light scatt. spectra 0-25364  
 Cd(NH<sub>3</sub>)<sub>2</sub>X<sub>2</sub>, X=Br, Cl, I, orientational phase transitions, Raman spectra 0-11382  
 Cl<sub>2</sub>PNCCI(CF<sub>3</sub>)<sub>2</sub>, cryst.,  $^{35}Cl$  NQR obs. of molecular reorientations between unequal potential wells 0-54989  
 D<sub>2</sub>, solid, quadrupolar glass ordering NMR adsorption line shapes 0-7178  
 DCl, liquid, on coexistence line, light scatt., orientational correlation function 0-20632  
 p-H<sub>2</sub>, solid, rotation-libration transition under press., Monte Carlo study 0-49460  
 HBr, liquid, on coexistence line, light scatt., orientational correlation function 0-20632  
 HCl, liquid, on coexistence line, light scatt., orientational correlation function 0-20632  
 KCN, plastic phase, Raman scatt. spectra (French) 0-11379  
 methane, solid, librational tunnelling and proton relax. temp. 0-38969  
 MoF<sub>3</sub>, mol. and electronic struct., vitreous, liq., and tetrameric states,  $^{19}F$  NMR obs., mol. mobility 0-34787  
 ND<sub>3</sub> dissolved in poly- $\gamma$ -benzyl-L-glutamate-chloroform, NMR study 0-34805  
 ND<sub>3</sub>ClO<sub>4</sub>, librational tunnelling and proton relax. temp. 0-38969  
 NG<sub>4</sub>HgCl<sub>3</sub>, NQR freq. anomalous temp. depend., reorientation 0-54976  
 NH<sub>4</sub>HF<sub>2</sub>, powder, proton and fluorine 2nd moments meas., 77-395K 0-34803  
 NH<sub>4</sub>I<sub>3</sub>, NQR freq. anomalous temp. depend., reorientation 0-54976  
 (NH<sub>4</sub>)<sub>2</sub>PbCl<sub>6</sub>, inelastic neutron scatt. and pot. shape 0-1946  
 (NH<sub>4</sub>)<sub>2</sub>PbCl<sub>6</sub>, librational tunnelling and proton relax. temp. 0-38969  
 (NH<sub>4</sub>)<sub>2</sub>PbCl<sub>6</sub>, temp. depend. of tunnel freq. 0-1947  
 (NH<sub>4</sub>)<sub>2</sub>PdCl<sub>6</sub>, inelastic neutron scatt. and pot. shape 0-1946  
 (NH<sub>4</sub>)<sub>2</sub>PtCl<sub>6</sub>, inelastic neutron scatt. and pot. shape 0-1946  
 NH<sub>4</sub>ReO<sub>4</sub>, NQR freq. anomalous temp. depend., reorientation 0-54976  
 (NH<sub>4</sub>)<sub>2</sub>SnCl<sub>6</sub>,  $^{35,37}Cl$  NQR, Raman spectra and spin lattice relax., hindered rot. 0-54974  
 (NH<sub>4</sub>)<sub>2</sub>SnCl<sub>6</sub>, inelastic neutron scatt. and pot. shape 0-1946  
 (NH<sub>4</sub>)<sub>2</sub>TeCl<sub>6</sub>, inelastic neutron scatt. and pot. shape 0-1946  
 NO<sub>2</sub>, impurity in alkali halide, linear dichroism (Russian) 0-45127  
 N<sub>2</sub>O, pure liq., mol. motion, anisotropic interaction 0-24345  
 NaCN, plastic phase, Raman scatt. spectra (French) 0-11379  
 NaClO<sub>4</sub>·H<sub>2</sub>O,  $^1H$  NMR second moment, H<sub>2</sub>O dynamic disorder 0-25221



**molecular reorientation continued**

O<sub>2</sub>, impurity in alkali halide, linear dichroism (*Russian*) 0-45127  
ZnSe:Cr, piezodichroism due to reorientation of Jahn-Teller centres 0-11363

**molecular reorientational states** *see molecular reorientation***molecular resonant states**

*see also Fermi resonance; molecular vibronic states*  
acetaldehyde, Coriolis resonance bands in IR spectrum 0-47995  
acetophenone enolate anion radicals, substituted, electron photodetachment cross sections, reson. states 0-1030  
aliphatic perfluorocarbons, electron attachment, fragmentation 0-12 eV 0-5618  
alkali homonuclear dimers, quasi-static wing profiles of self-broadening reson. lines 0-48042  
alkali metal molecular, laser radiation absorpt., at. excitation processes 0-32785  
C<sub>2v</sub> molecules, l-reson. perturbations in overtone and combination vibr. systems 0-52962  
chloroethane, reson. multiphoton dissoc. 0-53077  
diatomic molecule, resonance multiphoton processes of laser radiation interaction 0-37800  
electron impact shape-reson.-enhanced vibr. excitation, 10-40 eV, appl. to CO<sub>2</sub> 0-5629  
electron scattering from ats.(mols.), partial resonance widths, Siegert eigenvalues, basis-set calc. 0-37880  
formaldehyde-d<sub>2</sub>, reson. multiphoton dissoc. 0-53077  
metalloporphyrins, reson. Raman spectra, intra- and inter-manifold couplings interference 0-28020  
methane, narrow reson., elastic scatt., spectroscopic studies 0-53094  
methane, saturated absorpt. reson. shape, geometry and field intensity effects (*Russian*) 0-32778  
methane+Ar, rot. compound state resons. 0-28090  
methyl bromide, l-reson. perturbations in overtone and combination vibr. systems 0-52962  
molecule-photon interaction, techniques and calcs. for reson. determ. 0-17721  
multiphoton ionisation dynamics, rate eqn. modelling 0-48046  
polyatomic molecule, multiphoton absorpt. resons., dynamic Stark splitting 0-9670  
Raman gain spectroscopy, stimulated, Doppler broadening at electronic resonance 0-38065  
resonant energies and width from discrete states in spherical box 0-47918  
rhodamine B, 6G, resonance CARS line shape, scatt. processes in ground or excited states 0-48043  
rotated coordinate method use, rel. to stabilisation method 0-37845  
rotational coherence, reson. collisional exchange, time-resolved microwave obs. 0-23525  
sub-Doppler laser spectroscopy of mol. ions in fast ion beams 0-9655  
CO, X-ray K-absorpt. spectra, reson. obs., near fine struct. 0-37817  
CO<sub>2</sub> IR Zeeman spectra utilizing copropag. wave reson., diamag. shift obs. 0-53055  
CO<sub>2</sub>, narrow reson., elastic scatt., spectroscopic studies 0-53094  
H<sub>2</sub>, autoionising states, complex scaling method calcs. 0-9527  
H<sub>2</sub>, diabatic and reson. states, dissociative photoionisation calcs. 0-47883  
H<sub>2</sub>, autoionising states, complex scaling method calcs. 0-9527  
H<sub>2</sub>(D<sub>2</sub>), dissociative electron attachment and vibr. excitation, low-energy 0-23565  
H<sub>2</sub>(D<sub>2</sub>), electron dissociative attachment rates, rot. (vibr.) excitation depend., in plasma 0-43848  
HF, electron scatt. cross section, vibr. and rot. excitation, close coupling calc. 0-53154  
N<sub>2</sub>, 3σ<sub>g</sub> photionis., shape-reson.-induced non-Franck-Condon vibr. intensities 0-43120  
N<sub>2</sub>, elastic electron scatt. from 0 to 1000 eV, energy dependent exchange pots., continuum multiple scatt. method 0-43182  
N<sub>2</sub>, electron impact enhanced vibr. excitation, continuum multiple scatt. model with Hara exchange approx. 0-43196  
N<sub>2</sub>, X-ray K-absorpt. spectra, reson. obs., near fine struct. 0-37817  
O<sub>2</sub><sup>+</sup>, predissociated b<sup>2</sup>Σ<sub>g</sub><sup>-</sup> state, high resolution laser spectroscopy in fast ion beam 0-9656  
SF<sub>6</sub>, narrow reson., elastic scatt., spectroscopic studies 0-53094  
SF<sub>6</sub>, resonant single-photon dissoc. route using prelim. electron excitation 0-9662  
SiF<sub>4</sub>, XUV spectra, overlapping core-valence and core-Rydberg transitions and resons. 0-32735

**molecular rotation**

*see also macromolecular dynamics; molecular force constants; molecular reorientation; molecular rotation calculations; molecular rotational-vibrational energy transfer; molecular spectra; rotational isomerism*  
acetaldehyde+H<sub>2</sub>(N<sub>2</sub>)(CO<sub>2</sub>), rot. line broadening, mol. quadrupole moments calc. 0-28065  
alkali hydrides, Woodcock pot. calcs. 0-43136  
benzene in solution, rotational motion, Raman study 0-44104  
Δ<sup>6</sup>-bicyclo[3.2.0]heptene, microwave spectrum and dipole moment 0-9591  
biralical metal chelates, rot. motion in polar solvents, rel. to ESR line-shape 0-27994  
chlorofluoromethylene radical, gas phase laser-induced floresc. spectroscopy 0-14173  
chloromethyl oxirane, microwave spectra and conformations of cis and gauche-2 forms 0-5534  
N-cyanoformimine-d<sub>2</sub>, struct., microwave transitions 0-973  
diatom-atom gas mixture, infrared line shape, rotational lines, influence of collision duration 0-43110  
diatomic molecules, homonuclear, molecular dynamics, time-dependent statistical props. 0-44093  
diatomic molecules, homonuclear, molecular dynamics, translation-rotation coupling 0-44094  
diatomic molecules, spectrosc. consts., rel. to electronegativity 0-28007  
1,2-difluoroethane, internal rotation temp. frozen in supersonic jet, matrix IR spectroscopy 0-9594  
dimethyl ether, review of microwave spectrum, tabulated data 0-51965  
dyes, rot. diffusion of prolate, oblate mols. from absorpt. relax. 0-1008  
ethyl formate, microwave rot. spectrum, centrifugal distortion effects 0-52979  
ethylene oxide, <sup>13</sup>C and D variants, T<sub>2</sub>-relax., 2<sub>0</sub>-2<sub>1</sub> rot. transition by microwave pulse spectrometer 0-47976  
fluorescence depolarisation, E-type delayed, rotational motion probe technique 0-36207

**molecular rotation continued**

fluoromethane, ν<sub>3</sub> band Lamb dips, effects of RF elec. field modulation on Stark spectra 0-52989  
fluoromethane, excited state rot. spectroscopy and kinetics, appl. of tunable sub-MM sources 0-14162  
formaldehyde, microwave-microwave double resonance 0-53029  
formaldehyde-<sup>13</sup>C, A<sup>1</sup>A<sub>2</sub>-X<sup>1</sup>A<sub>1</sub> system, UV absorpt. spectra, rot. anal. 0-9614  
G 0-44099  
gases, high resolution rotational Raman spectra, review 0-23425  
glyoxal, internal conversion, energy redistrib. 0-53036  
Hamiltonian of a molecular type system with internal rotation 0-18842  
hydrogen, and isotopic forms, cryogenic data rel. to mag. fusion energy 0-8746  
interstellar masers, Λ-doublet population inversion in OH, OD, CH, CD and NH<sup>+</sup> collisions 0-22065  
iodomethane-d<sub>3</sub>, Stark tuned level crossings and saturated absorpt., RF elec. field modulation effects 0-52989  
IR and Raman studies in liqs. and gases 0-11390  
IR multiphoton excitation, rot. heating, dynamical effects on dissoc. products 0-18892  
isocyanic acid, molecular structure and centrifugal distortion constants 0-47974  
isothiocyanic acid, H<sup>15</sup>NCS, HN<sup>13</sup>CS and HNC<sup>34</sup>S, ground state spect. constants and molecular struct. 0-47973  
linear triatomic mol. photodissociation, fragment ang. distrib., theory 0-23468  
methane-d<sub>1</sub>, laboratory rotational spectrum and upper limits on abundance in (OMC-1) 0-56705  
methane-d<sub>4</sub>, ν<sub>2</sub> and ν<sub>4</sub> IR bands meas. and anal. 0-18851  
methanol (d<sub>3</sub>), OH stretch fund., torsion-rot. levels, IR spectra obs. 0-32711  
methanols, labelled, proton T<sub>1</sub> in presence of intramol. rots., intermol. relax. rate 0-2656  
methyl formate, microwave spectra, rot. consts., moments and struct., radio astronomy appl., review 0-17637  
methyl nitrite, internal rotation temp. frozen in supersonic jet, matrix IR spectroscopy 0-9594  
methyl radical in sodium acetate, EPR spectra, anisotropic hyperfine interaction, rot. tunnelling 0-34775  
methylene radicals, rotational transitions, laser mag. resonance spectra 0-5538  
microwave rotational spectroscopy, of high temp. mols. 0-52236  
molecular fluids, coupling of rotation and translation 0-38892  
morpholine, centrifugal distortion consts., microwave spectrum 0-5531  
OCS, submillimetre rot. lines, press. shifts 0-23463  
n-p-octyloxybenzylidene-p-toluidine, dielectric behaviour in nematic mesophase at RF 0-34842  
parity-violating effects of weak interactions 0-52455  
picosecond intramolecular dynamics in solution, Fokker Planck eqn. 0-28891  
planar structure, double reson. signals depend., appl. to microwave spectra 0-32751  
polar molecule electron scatt. at intermediate J, closed-form treatment 0-32846  
polyatomic molecules, high intensity IR absorpt. 0-14183  
premixed H<sub>2</sub>-O<sub>2</sub>-N<sub>2</sub> laminar flames, temp. profiles, Raman, absorpt. and line reversal obs. 0-42227  
propenyl chloride, IR bands, torsional struct. 0-28018  
Raman spectra of gases, high-resolution, mol. struct. and orops. 0-53000  
symmetric top molecule, radiationless processes, angular momentum constraints 0-28052  
tertiarybutylisocyanide-borane, vibr., rot. consts., moment of inertia, microwave spectra obs. 0-32706  
thioformaldehyde-d<sub>0</sub>, -d<sub>2</sub>, A<sup>1</sup>A<sub>2</sub>-X<sup>1</sup>A<sub>1</sub> vis. absorpt. system, rot. anal. 0-5559  
thioketen, microwave spectrum, substitution structure and dipole moment 0-975  
triatomic molecules, rotating, semiclassical eigenvalues 0-9588  
Ar-O<sub>2</sub> Van der Waals complex, struct. and props., RF and microwave obs. 0-32704  
BF(OH)<sub>2</sub>, identification, rot. and centrifugal consts., mol. struct., microwave spectra obs. 0-32705  
BF<sub>3</sub>, spectrum, 5800-6600 Å, vibr. anal., electronic transition assignment 0-992  
Br<sub>2</sub>-Ar system, mol. rot. effects on V-T energy transfer 0-14195  
<sup>79</sup>BrF, (<sup>81</sup>BrF), hyperfine struct., elec. dipole moment, rot. transitions, microwave spectral obs. 0-32695  
CO, collision-induced reorientation, direct meas. by IR double reson. 0-32800  
CO discharge plasma, electron energy distrib. and kinetic coeffs., ground-state mols. 0-43867  
<sup>12</sup>CO, pure rot. far IR spectra, rot. consts. 0-47996  
CO<sub>2</sub>, and isotopic forms, bending fund. region, IR spectra, rot. consts. 0-47988  
CO<sub>2</sub> multiatmosphere UV preionized laser, elec. and gain characts. 0-14313  
CO<sub>2</sub>, pure rotational stimulated Raman photoacoustic spectroscopy 0-32724  
CO<sub>2</sub>-N<sub>2</sub>-He discharge, electron distrib. relax., numerical study 0-54070  
C<sub>2</sub>O<sub>2</sub>, ν<sub>7</sub> vibrational states, rigid-bender model 0-47964  
C<sub>2</sub>O<sub>2</sub>, vibr. IR spectra anal. 0-47984  
COCl<sub>2</sub>, phosgene, Cl<sub>2</sub> nuclear quadrupole coupling tensor, microwave spectra 0-52982  
CS<sub>2</sub>, <sup>3</sup>A<sub>2</sub> state, triplet bands, MCD spectrum, near UV absorpt. spectrum 0-48010  
CS<sub>2</sub>, <sup>3</sup>A<sub>2</sub>-state, MCD and UV spectrum, theoretical anal. 0-48011  
CaCl<sub>2</sub>, laser excitation and fluorescence spectra, rotational anal. of A<sup>2</sup>Π=X<sup>2</sup>Σ<sup>+</sup> transition 0-43098  
CaF, <sup>2</sup>Σ<sub>1/2</sub><sup>+</sup> ground state, spin-rot. and hyperfine splittings rot. depend., mol. beam laser-RF double reson. 0-43079  
CaH, D<sup>2</sup>Σ<sup>+</sup>-X<sup>2</sup>Σ<sup>+</sup> band system 0-18847  
ClO, UV spectra of C<sup>2</sup>Σ<sup>+</sup>-X<sup>2</sup>Π system, rot. anal. 0-996  
CrO molecule, B<sup>2</sup>Π and X<sup>2</sup>Π states, potential energy curves 0-42962  
Cs<sub>2</sub>, rot. consts., Doppler-free polarisation spectrosc. 0-5555  
Cu<sub>2</sub>, in supersonic free jet expansion, laser induced excitation spectrum obs. 0-14151  
CuBr, rot. spectrum hyperfine struct., coupling consts., microwave spectroscopy study 0-18844  
D<sub>2</sub>, electron dissociative attachment rates, rot. (vibr.) excitation depend., in plasma 0-43848



**molecular rotation continued**

- F+I<sub>2</sub>→IF+I, energy partitioning, vibr. populations and rot. temp., population inversion 0-50832  
 FO free radical, detection by CO<sub>2</sub> laser mag. reson. 0-45594  
 GaI, A<sup>0</sup>-X<sup>0</sup> and B<sup>1</sup>-X<sup>0</sup> transitions, isotope shifts, UV and visible spectra obs. 0-53005  
 GeCl<sub>4</sub> mol., UV spectra, band assignments and rot. consts. 0-997  
 H<sub>2</sub> 3s, 3d: <sup>3</sup>Σ<sub>g</sub><sup>+</sup>, <sup>3</sup>Π<sub>g</sub>, <sup>3</sup>Δ complex, fine struct., Doppler-free laser spectroscopy 0-1087  
 H<sub>2</sub> (D<sub>2</sub>) mol. bands, electron impact excitation, rot. transitions, cross sections in plasma 0-37896  
 H<sub>2</sub>, electron dissociative attachment rates, rot. (vibr.) excitation depend., in plasma 0-43848  
 H<sub>2</sub>, predissociation of <sup>1</sup>Π<sub>u</sub><sup>+</sup> state vibr. and rot. levels, dissociation yields meas. 0-32784  
 H<sub>2</sub> predissociation probabilities of 4pπ<sup>1</sup>Π<sub>u</sub><sup>+</sup>ν≥1 levels, dissociation channels interference 0-28074  
 HCP, ν<sub>3</sub> band, high-resolution IR absorption spectrum 0-47994  
 HCl, intermol. partial struct. factors, isotopic substitution and neutron diff. obs. 0-53157  
 HCl+Ar(Xe), infrared line shape, rotational lines, influence of collision duration 0-43110  
 HNO, low-lying states, pot. energy curves 0-9533  
 HNO<sub>2</sub>, trans and cis, ν<sub>2</sub> fundamental vibrational bands, intracavity CO laser Stark spectroscopy 0-47992  
<sup>1</sup>H<sup>3</sup>H and <sup>2</sup>H<sup>3</sup>H, pure rot. and vibr.-rot. Raman spectra 0-14145  
 He+Na<sub>2</sub>, optically pumped state to state differential cross sections for rot. transitions, rainbow phenomena 0-5609  
 ICl, A<sup>2</sup>Π(1)-X<sup>2</sup>Σ<sup>+</sup> emission spectrum, near-IR, rotational analysis 0-47991  
 IF internal vibr.-rot. product distrib., formed in F+CH<sub>3</sub>I(CF<sub>3</sub>I), fluoresc. obs. 0-48078  
 I<sub>2</sub> fluoresc., Ar<sup>+</sup> laser excited, high resolution and sub-Doppler Fourier transform spectroscopy 0-43089  
 InX(X<sub>2</sub>)(X<sub>3</sub>), InAlX<sub>4</sub>, X=Cl,Br, Raman spectra, up to 1200K 0-48003  
 KrHCl, van der Waals complex, prod. and rot. spectra assignments 0-5532  
 KrHCl, van der Waals complexes, struct., RF and microwave spectra, isotope effects 0-37806  
 KrHCl, weak complex, rot. spectra 0-52980  
 MgH(D), spectra in 230-235 nm region 0-48012  
 N<sub>2</sub>, diffuse plasma, population densities of triplet states, correl. with electron impact processes 0-43966  
 N<sub>2</sub>, gaseous, density behaviour of rototranslational spectrum, IR spectra obs. 0-28002  
 N<sub>2</sub>, polarisability tensor anisotropy, Raman spectra differential scatt. cross section 0-18860  
 N<sub>2</sub>, rotational collision number from thermal cond., 700-2500K 0-23526  
 N<sub>2</sub>, supersonic mol. beam, CARS rot. temp. meas. 0-23423  
 NF<sub>2</sub>, IR spectra, ν<sub>1</sub> and ν<sub>2</sub> bands, vibr. excitation and spin-rot. interaction, doublet splitting 0-28011  
 NH<sub>2</sub> (A<sup>1</sup>A<sub>1</sub>), excited state dynamics and bimol. quenching processes 0-9681  
 NH<sub>2</sub> fragment internal energy distrib. in NH<sub>3</sub> UV laser photodissoc. 0-11901  
 NH<sub>2</sub>, ground state mol. consts., absorption spectra 0-28030  
 NH<sub>3</sub>, hyperfine quadrupole coupling, ro-inversional levels, inversional depend. 0-27961  
 NH<sub>3</sub>, microwave-microwave double resonance 0-53029  
<sup>14</sup>NH<sub>3</sub>, <sup>15</sup>NH<sub>3</sub> and <sup>14</sup>NH<sub>2</sub>D, IR laser Stark spectroscopy 0-47978  
 NH<sub>2</sub>D, dipole moments effects of RF elec. field modulation on IR Stark spectroscopy 0-52989  
 NO, and isotopic forms, ν=0 electronic states, spin-rot. doubling 0-5540  
 NO, state selective step-wise photoionis. with mass spectroscopic ion detect. 0-43119  
 N<sub>2</sub>O, pure rotational stimulated Raman photoacoustic spectroscopy 0-32724  
 N<sub>2</sub>O, submillimetre rot. lines, press. shifts 0-23463  
 O<sub>2</sub>, polarisability tensor anisotropy, Raman spectra differential scatt. cross section 0-18860  
 O<sub>2</sub><sup>+</sup>, first negative system, high-resolution photofragment spectroscopy 0-47971  
 O<sub>2</sub><sup>+</sup>, photofragment spectroscopy using fast ion beams 0-9755  
 OH, A<sup>2</sup>Σ<sup>+</sup>-X<sup>2</sup>Π<sub>2</sub> system, vibrational and rotational levels, transition probability determ. 0-43034  
 OH, band oscill. strength, rot. excitation effects 0-23460  
 OH maser sources, interstellar, radiative transport effects on inversion 0-17681  
 OH, prod. by photolysis, A-doublets, population, rot. states, hyperfine struct., microwave spectra 0-32694  
 OH rotational temp. determ., successive approx. 0-23389  
 OSC, N<sub>2</sub>O, submillimetre rot. lines, press. shifts 0-23463  
 P<sub>2</sub>, intersystem transition obs. in absorpt. spectrum 0-48008  
 P<sub>2</sub> radical, b<sup>3</sup>Π<sub>g</sub>-a<sup>3</sup>Σ<sub>u</sub><sup>+</sup> transition, perturbed by <sup>1</sup>Σ<sub>g</sub><sup>+</sup> state (French) 0-18855  
 PH<sub>2</sub>, X<sup>2</sup>B<sub>1</sub>-state, rot. laser mag. reson. spectrosc. 0-28038  
 PH<sub>3</sub>, liq. and solid, Raman spectra, vibr. correl. functions, rot. motions 0-55087  
 PbCl, rot. analysis of A-X<sub>1</sub> system 0-32703  
 SF<sub>6</sub>, highly excited, time-resolved IR absorpt. obs. 0-9666  
 SF<sub>6</sub>, multiphoton dissociation, classical model 0-53076  
 SF<sub>6</sub>, ν<sub>3</sub> bands, rot. fine struct., HFS spectroscopic consts. determ., saturation spectroscopy obs. 0-53008  
 SF<sub>6</sub>, vibr. spectra, rot. consts., IR spectra, Raman spectra obs. 0-32719  
 SF<sub>6</sub>Cl, pure rot. spectra, 300 GHz, isotope effects 0-5533  
 SeS<sub>2</sub>, B<sup>2</sup>Σ<sup>+</sup>-X<sup>2</sup>Σ<sup>+</sup> system, rot. struct. and hyperfine effects near IR spectrum 0-5544  
 ThO, L<sup>1</sup>Π-Σ<sup>+</sup> and N<sup>1</sup>Π-X<sup>2</sup>Σ<sup>+</sup> systems, spectra, rot. anal. 0-23430  
 XeF, supersonic expansion jet, B-X system rot. and vibr. anal., isotope intervals, fluoresc. spectra 0-14174

**molecular rotation calculations**

- bipyridines, torsional isomerisation of biologically active bicyclic molecules 0-27996  
 bond orbitals and intramolecular interactions, barriers to rotation and non-bonded interactions 0-32855  
 carbon tetrafluoride laser, emission spectrum in 16 micron range, CO<sub>2</sub> laser stimulation 0-9870  
 diatomic molecule, pots. superposition, rel. to lattice dynamics, mol. consts. calcs. 0-5598

**molecular rotation calculations continued**

- diatomic molecule, Stark effect calcs., rigid rotator rotational levels in asymmetric potential well 0-5580  
 diatomic molecules, rot. line strengths in multiphoton transitions 0-48051  
 electric dipole <sup>4</sup>Σ(int)-<sup>4</sup>Σ(int) transitions, rot. intensities 0-9642  
 electronic-rotational molecular states, electron-impact excitation, cross sections and rate consts. 0-14241  
 energy level clustering, qualitative theory of irreducible tensor operators spectra 0-28001  
 9H-fluorene, soln., correl. times from <sup>13</sup>C relax. 0-23438  
 methane, rotational partition function, isotope effects 0-14130  
 molecular fluid, computer simulation of liquid-vapour surface 0-54478  
 monomer self-associating systems, nonideal, graphical anal. by equilibrium ultracentrifugation 0-41335  
 polyatomic molecule, anharmonic force consts., vibr.-rot. interaction consts. 0-966  
 pyramidal XY<sub>3</sub> molecules, mol. geometry calcs. using centrifugal distortion const. 0-18841  
 triptycene, soln., correl. times from <sup>13</sup>C relax. 0-23438  
 AsF<sub>3</sub>, mol. geometry calcs. using centrifugal distortion const. 0-18841  
 CO, rot. line strengths in multiphoton transitions 0-48051  
 COS, mole. potential surface, evaluation from spectroscopic observations 0-43207  
 Cl<sub>2</sub>, liquid-vapour surface, computer simulation 0-54478  
 H<sub>2</sub>, electron cooling through resonant collisions 0-32845  
 Li<sup>+</sup>+H<sub>2</sub>, rot. inelastic scatt., body frame partitioning approx. calcs. 0-23527  
 N<sub>2</sub>, electron impact rot. and vibr. excitation, elastic scatt., close coupling and Born approx. 0-28108  
 N<sub>2</sub>, electron scattering, local-exchange approx. for intermediate-energy-differential cross sections 0-48094  
 N<sub>2</sub>, liquid-vapour surface, computer simulation 0-54478  
 N<sub>2</sub>, rot. line strengths in multiphoton transitions 0-48051  
 NH<sub>3</sub>, rot.-inversion Raman spectra, K-splitting 0-9611  
 NO, rot. line strengths in multiphoton transitions 0-48051  
 OH, A-X system, rot. transition probabilities 0-43027  
 PF<sub>3</sub>, mol. geometry calcs. using centrifugal distortion const. 0-18841  
 PtH(D), pot. energy curves, r-centroids, Franck Condon factors, rot. depend. 0-28082

**molecular rotation in solids** *see molecular reorientation; nuclear magnetic resonance; plastic crystals*

**molecular rotation-vibration**

- see also macromolecular dynamics; molecular force constants; molecular rotation-vibration calculations*  
 allene(d<sub>4</sub>), IR absorption intensities 0-1026  
 benzenetricarbonylchromium, neutron inelastic scatt. spectrum and valence force field 0-48096  
 chlorotrifluoromethane, IR rovibr. spectrum (German) 0-47998  
 correlation spectroscopy, rotational and vibrational relaxation autocorrelation functions 0-32856  
 cyclohexane, plastic and liquid crystal phase, rot. correl. func. by Raman spectroscopy 0-23403  
 diatomic molecules, spectrosc. consts., rel. to electronegativity 0-28007  
 diatomic mols., internal partition functions for O<sub>2</sub>, N<sub>2</sub>, NO and their ions, max. summation indices 0-27995  
 electron+ molecule, rot. and vibr. excitation 0-17721  
 formaldehyde, T<sub>2</sub>-relax., rot. transitions, time resolved spectra, microwave pulsed spectrometer study 0-18846  
 formaldehyde-d<sub>3</sub> vapour, IR-UV double resonance 0-43078  
 formic acid, vibr. states, rot. and Coriolis parameters IR Fourier transform spectra 0-32709  
 formyl radical, laser mag. reson. spectrum at 5.3 micron 0-47981  
 Freon 14, roto-vibr. mol. laser, low-temp. performance 0-9871  
 laser scaling, CO<sub>2</sub>-TEA laser pumped 0-5728  
 line broadening by monatomic gas 0-9643  
 methane, narrow reson., elastic scatt., spectroscopic studies 0-53094  
 methane, solid, Raman spectra and II-III phase transition 0-2745  
 methane in condensed inert gas matrices, optical excitation of rotational transition, far IR absorption spectra 0-37808  
 methanol, rot.-torsional-vibr. quantum nos. for FIR laser action 0-14320  
 polyatomic molecules, vibr.-rot. coupling, modified Eckart conditions 0-27993  
 propenal, energy dispersion and relax., laser IR-visible double reson. 0-48023  
 Raman spectroscopy, in high temp. chem., review 0-52234  
 rotation vibration emission turbulent flowfield spectral absorpt. coeff., temp. depend. 0-52987  
 spectroscopy, finite symmetry adaptation 0-43032  
 C<sub>3</sub>, linear, high temp., rot.-vibr., anharmonicity, thermodynamic function calcs. 0-43830  
 CD<sup>+</sup>, A<sup>1</sup>Π, rot.-vibr. population distrib. 0-23396  
 CH<sup>+</sup>, A<sup>1</sup>Π, rot.-vibr. population distrib. 0-23396  
 CH<sub>2</sub>, photoproduct from ketene, singlet-triplet energy separation and rovibronic level obs. 0-11936  
 CO, hole burning in single quantum power spectrum due to Autler-Townes splitting 0-9671  
 CO laser, multiphoton amplification, HF removal of forbiddenness (Russian) 0-53262  
 CO, rovibr. multiphoton spectra comput., hole burning effect 0-9672  
 CO-Ar(N<sub>2</sub>), C<sub>2</sub> and CN form. by optical pumping, room temp. 0-16701  
 CO-N<sub>2</sub> and CO lasers, energy and spectral characteristics 0-14327  
 CO<sub>2</sub>, 201μm-000 band, press. broadened coeffs. and absolute intensities, temp. depend., IR obs. 0-53054  
 CO<sub>2</sub> and isotopic species, high-resolution Fourier spectra near 4.3 micron 0-47982  
 CO<sub>2</sub> laser, multiphoton amplification, HF removal of forbiddenness (Russian) 0-53262  
 CO<sub>2</sub>, linear, high temp., rot.-vibr., anharmonicity, thermodynamic function calcs. 0-43830  
 CO<sub>2</sub>, narrow reson., elastic scatt., spectroscopic studies 0-53094  
 CO<sub>2</sub>, optically pumped laser, simultaneous lasing in bands of sequence 0-5725  
 CO<sub>2</sub>, turbulent flow field, mol. vibr.-rot. bands, spectral absorpt. coeff., temp. depend. 0-52987  
 CO<sub>2</sub>, vibr.-rot. band shape calcs. 0-969  
 C<sub>3</sub>O<sub>2</sub>, bending pot. function, vibr. depend. 0-48058  
 C<sub>3</sub>O<sub>2</sub>, vibr. IR spectra anal. 0-47984  
 C<sub>3</sub>O<sub>2</sub>, vibr.-rot. band, microwave, spectrum obs. 0-5536  
 Cl<sub>2</sub>, and isotopic forms, B<sup>2</sup>Π(0<sub>g</sub><sup>+</sup>) state, laser-induced fluoresc., collisional energy transfer rates 0-53038



**molecular rotation-vibration continued**

- ClO radical, 2-0 vibrational overtone band, laser magnetic resonance spectroscopy study 0-48021  
 FO free radical, detection by CO<sub>2</sub> laser mag. reson. 0-45594  
 GeH<sub>4</sub>,  $\nu_2$  fundamental, isotope effect 0-43024  
 H<sub>2</sub>, electron impact excited singlet-g states, optical and time resolved spectra, radiative lifetimes, quenching rates for rovibronic levels 0-23564  
 HD<sup>+</sup>, vibr.-rot. transitions, using new two-photon IR photodissoc. technique 0-23405  
 H<sub>2</sub>(D<sub>2</sub>), Rydberg states, nonadiabatic effects, elec. field ionis. 0-9528  
 HNO<sub>3</sub>, high resolution spectral meas. of 5.9  $\mu$ m band using tunable diode laser 0-32707  
 H<sub>2</sub>O, 4 $\nu_2$  band, hot vap., Fourier transform spectrum, rot. consts. 0-32712  
 H<sub>2</sub>O-H<sub>2</sub>, cooling in supersonic nozzle, submillimetre wave generation 0-48229  
<sup>1</sup>H<sup>1</sup>H and <sup>2</sup>H<sup>3</sup>H, pure rot. and vibr.-rot. Raman spectra 0-14145  
 He<sub>2</sub><sup>2+</sup>, bound excited states, potential energy curves and rovibronic energy, dissociation 0-23327  
<sup>4</sup>HeH<sup>+</sup>, IR rot.-vibr. spectrum obs. 0-23420  
 I<sub>2</sub>, high-dispersion polarisation-labelled spectrum 0-990  
 I<sub>2</sub>+I<sub>2</sub>, collisional energy transfer, ground and excited states, polarisation spectra 0-32805  
 IC<sub>1</sub>, A<sub>2</sub><sup>+</sup>(1)-X<sup>1</sup> $\Sigma^+$  absorption spectrum, rotational analysis 0-47990  
 InX(X<sub>2</sub>)(X<sub>1</sub>), InAlX<sub>4</sub>, X=Cl,Br, Raman spectra, up to 1200K 0-48003  
 N<sub>2</sub> plasma, non-equilib., excited species, vibr.-rot. anal. fluoresc. obs. 0-54034  
 N<sub>2</sub>, Raman spectra, intermol. torques and orientational correlation times 0-48006  
 NH<sub>3</sub>, Coriolis and l-type interactions,  $\nu_2$ , 2 $\nu_2$  and  $\nu_4$  states, IR spectra 0-47993  
 NO, photofragment of NO<sub>2</sub>, Doppler spectroscopy 0-53124  
 NO<sub>2</sub>, (101) band, line strengths, spin-splittings and forbidden transitions 0-47987  
 NO<sub>2</sub>, visible spectrum simplification, rot.-vibr. levels, excitation, polarisation labelling spectroscopy 0-32730  
 N<sub>2</sub>O, 40°00'-00°00' band, IR high press. absorpt. spectra profiles 0-52988  
 N<sub>2</sub>O, as mol. probe in MBBA, solute solvent interaction, IR spectra vibr.-rot. fundamental 0-29155  
 Na<sub>2</sub>, supersonic beam rovibronic level population, anal. by laser spectroscopy 0-43118  
 O<sub>2</sub>, thermal decomposition, vibr.-rot. state depletion, Monte Carlo calc. 0-35506  
 OCS, roto-vibr. mol. laser, low-temp. performance 0-9871  
 SF<sub>6</sub>, collisions, laser spectroscopy investig. 0-9697  
 SF<sub>6</sub>, molecule absorption of IR laser radiation (*Russian*) 0-986  
 SF<sub>6</sub>, multiple-photon excited, double reson. spectroscopy 0-53030  
 SF<sub>6</sub>, narrow reson., elastic scatt., spectroscopic studies 0-53094  
 SO, and isotopic forms, X<sup>1</sup> $\Sigma^+$  state, CO<sub>2</sub> laser mag. reson. spectroscopy 0-9602  
 SO<sub>2</sub>, T<sub>2</sub>-relax., rot. transitions, time resolved spectra, microwave pulsed spectrometer study 0-18846  
 TiO, X(<sup>2</sup> $\Delta$ ) state, vibrational IR spectrum using microwave powered molecular source, rotational analysis 0-9596  
 XeF, supersonic expansion jet, B-X system rot. and vibr. anal., isotope intervals, fluoresc. spectra 0-14174  
 ZrO, X(<sup>1</sup> $\Sigma$ ) state, vibrational IR spectrum using microwave powered molecular source, rotational analysis 0-9596

**molecular rotation-vibration calculations**

- acetaldehyde, Coriolis resonance bands in IR spectrum 0-47995  
 diatomic molecule, electronic pot. rot.-vibr. eigenfunction, analytic expression 0-52964  
 diatomic molecule, pots. superposition, rel. to lattice dynamics, mol. consts. calcs. 0-5598  
 diatomic molecules, vibr. relaxation, vibr.-rot. levels, population relationships (*Spanish*) 0-959  
 formyl fluoride, and isotopic forms, mol. struct., from electron diff. and microwave data 0-23570  
 inhomogeneous molecular gas radiation calc. using spectral comp. modelling 0-32697  
 methane, vibration-rotation energies, 2 $\nu_2$  and  $\nu_2$ + $\nu_4$  bands 0-47963  
 methane, vibration-rotation energies of harmonic and combination levels 0-47962  
 methyl halides, force consts. evaluation using gp. vibrs. and centrifugal distortion consts. 0-9580  
 molecular gas, laser-stimulated cooling 0-5594  
 polyatomic molecule, anharmonic force consts., vibr.-rot. interaction consts. 0-966  
 polyatomic molecule, semirigid, Watson hamiltonian expansion 0-23404  
 polyatomic molecules, forbidden rotation-vibration transitions (*Russian*) 0-5593  
 silylacetylene, centrifugal distortion consts., thermodynamic functions 0-47959  
 symposium contrib., Florida, USA (March 1979) 0-51946  
 triatomic linear mol., parallel bands, band model parameters 0-43026  
 vibrational-rotational line profiles, theory 0-1029  
 vinyl bromide, mol. struct., from gas-phase electron diff. and microwave data 0-23571  
 XY<sub>4</sub> molecules, tetrahedral, vibration-rotation energies of harmonic and combination levels 0-47962  
 Ar.HBr(DBr), van der Waals complexes, rot. spectra and struct. 0-48055  
 C<sub>2</sub>, Swan band system, vibr.-rot. interaction on pot. energy curves 0-27965  
 CH<sup>+</sup>,  $\pi$ - $\Sigma$  band systems, vibr.-rot. interaction on pot. energy curves 0-27965  
 CN violet system, rotational and vibrational analysis 0-52961  
 CO pulsed laser emission with line selection, analytical theory 0-53277  
 CO<sub>2</sub>, rot.-vibr. bands, absorpt. coeff. calc. method, Fermi reson. effect on spectral lines 0-32696  
 Cl<sub>2</sub>, B-X transition, predissoc., laser-induced fluoresc. obs. 0-43093  
 (H<sub>2</sub>)<sub>2</sub>, (D<sub>2</sub>)<sub>2</sub>, (HD)<sub>2</sub> and H<sub>2</sub>-D<sub>2</sub>, Van der Waals complexes, mol. symmetry 0-42963  
 HD,  $\nu=0$  to  $\nu=5$  rot.-vibr. band, photoacoustic spectrosc. obs. 0-9589  
 H<sub>2</sub>O, dimer config., vib.-rot. band intensities, rel. to 8-13  $\mu$ m atmospheric extinction 0-9610  
 HPO, emission system, rot. anal. of vibr. bands 0-47957  
 N<sub>2</sub>, electron impact rot. and vibr. excitation, elastic scatt., close coupling and Born approx. 0-28108  
 N<sub>2</sub>, Raman intensity, ab initio calc. 0-1028  
 OCS, rot.-vibr. levels and semiclassical energy levels 0-37804  
 molecular rotational energy transfer *see* molecular rotational-vibrational energy transfer  
 molecular rotational states *see* molecular rotation  
 molecular rotational-vibrational coupling *see* molecular rotation-vibration  
 molecular rotational-vibrational energy transfer  
*see also* atom-molecule reactions; molecule-molecule reactions  
 anharmonic oscillators, two-component system, diffusion description of vibr. relax. 0-23528  
 Ar+SO<sub>2</sub>, vibr. relax., shock tube study 0-48062  
 aromatic hydrocarbon in soln., excited electronic state vibr. relax., time resolved fluoresc. 0-48024  
 atom+diatom, rot. inelastic scatt., mag. transitions, time reversal symm. 0-48066  
 atom+harmonic oscillator, vibrational excitation, sudden approx. theory 0-53103  
 benzene and deuterates, highly vibr. excited intramolecular V-V transfer, visible and photoacoustic spectra 0-32729  
 bromomethane, vibr., rot. and translational energy exchange, semiclassical theory 0-48067  
 catalysis, heterogeneous, vibr. excitation, classical trajectory calcs. 0-26045  
 2-chloro-2-nitropropane, far IR-microwave estimation of binary collision approx. 0-55095  
 chlorofluoromethanes, laser photolysis, product vibr. relax. rates and diffusion coeffs. 0-55680  
 chloromethane, vibr., rot. and translational energy exchange, semiclassical theory 0-48067  
 chlorotrifluoroethylene, multiphoton dissoc., fragment energy partitioning 0-55681  
 classical versus quantum calcs., forced quantum oscillator and moment methods 0-28095  
 competitive decomposition and stabilisation models for collisional efficiency in external activation systems 0-25989  
 cyclobutane-t, chem. activated by nucl. recoil reaction, energy transfer interpret. 0-25985  
 cyclopropane, partial vibr. energy transfer map 0-32760  
 cyclopropane, thermal unimol. isomerisation, vibr. energy transfer, diffusion cloud method 0-26001  
 cyclopropane+inert gas, reactant decomp., rot.-vibr. energy transfer, relax. analytic soln. 0-55650  
 1,1-cyclopropane-d<sub>3</sub>, isomerisation transient vibr. energy distrib., collisional relax., variable encounters method 0-50836  
 diatom+diatom, vibr. energy transfer, collinear and 3-dimens. rate consts. 0-48065  
 diatomic molecules, matrix isolated, vibr. relax., rot.-translational coupling 0-53102  
 diatomic molecules, vibr. relaxation, vibr.-rot. levels, population relationships (*Spanish*) 0-959  
 diatomic molecules, vibr.-translation relax. calcs., classical vs. quantum diffusion 0-14196  
 1,1-difluoroethane, rot. relax., anharmonic shifts and excited state absorpt. 0-43154  
 donor-acceptor transition kinetics, with allowance for vibr. struct. 0-144  
 electron-vibration system, nonequib. first-order type phase transition 0-9633  
 ethylene, excited with parametric oscillator, vibr. relax. obs. and interpret. 0-9702  
 ethylene, line selective excitation with CO<sub>2</sub> laser light and vibr. relax. 0-9705  
 fluoromethane, laser pumped, vibr. states collision dynamics fluoresc. obs. 0-53104  
 fluoromethane, molecular pumping, thermal lens phenomena 0-9708  
 fluoromethane+fluoromethane, collisionally induced relax. processes and vibr. energy transfer 0-53107  
 fluoromethane+SO<sub>2</sub>, collisionally induced relax. processes and vibr. energy transfer 0-53107  
 fluoromethane-d<sub>2</sub>, matrix isolated, vibr. energy transfer at low temps. 0-37860  
 fluoromethane-d<sub>3</sub>, vibr. energy transfer at low temps., inert gas and N<sub>2</sub> matrix obs. 0-9706  
 form-factors, l-dominant, analytical formulae, appl. to Ar+N<sub>2</sub> 0-1052  
 formaldehyde-d<sub>1</sub> (-d<sub>2</sub>), single vibronic levels, fluoresc. emission, radiative lifetimes and vibr. relax 0-23521  
 gas phase reaction consts. for electronically excited species, relax. processes, data tables 0-16644  
 glyoxal, vibr. energy redistrib. following internal conversion 0-23452  
 interstellar masers,  $\Lambda$ -doublet population inversion in OH, OD, CH, CD and NH<sup>+</sup> collisions 0-22065  
 iodomethane, vibr., rot. and translational energy exchange, semiclassical theory 0-48067  
 kinetically controlled chemical activation, multistep deactivation processes applic. in energy transfer interpret. 0-25985  
 laser studies of relaxation and reaction of species in defined quantum states 0-11918  
 laser-controlled unimolecular and bimolecular processes, field-depend. rate const. 0-11906  
 metal vapours, excitation energy transfer, sensitised fluoresc. 0-23358  
 methane, (methane-Xe)(methane-NH<sub>3</sub>), mol. relax., optoacoustic reson. meas. 0-27351  
 methane, energy transfer obs. using excitation of fund., overtone and combination bands 0-9704  
 methane+CO, vibr. relax. rates, energy transfer 0-37862  
 methane+d<sub>2</sub>, Ar vibr.-vibr. energy transfer process diagnostics 0-32807  
 methane-d<sub>4</sub>, selectively excited, cooling, vibr.-vibr., vibr.-translational relax. 0-33723  
 methyl iodide, liq., A<sub>1</sub> modes, vibr. relax., temp. depend. Raman spectra obs. 0-32806  
 molecule+ion,  $\Lambda$ -doublets transitions 0-14132  
 monofluoromethane+Ar, vibr.-vibr. energy transfer process diagnostics 0-32807  
 multiphoton absorption modelling, using SF<sub>6</sub> energy-dependent absorption cross sections 0-32789  
 naphthalene in nonpolar solvent, vibr. and reorientational relax., correl. function 0-45065  
 nucleic acid-dye complexes, energy transfer obs. using laser-induced fluoresc. 0-12054  
 plasma, nonequib., diat. mols. vibr. excited state population, rel. to plasma chem. 0-19553  
 polar molecular ion, charged particle vibr.-rot. excitation (*Russian*) 0-1053



**molecular rotational-vibrational energy transfer continued**

- polyatomic fluid, nonassociated, vibr. relax. density depend., simple model 0-32809
- polyatomic molecule, multiple-photon IR laser pumping, collisional effects 0-9668
- polyatomic molecule, ultrafast vibr. using laser light pulses 0-9699
- polyatomic molecules, applic. of classical perturbation theory of good action-angle variables 0-23481
- polyatomic molecules, IR laser sensitised chem. reactions 0-11910
- polyatomic molecules, vibr., rot. and translational energy exchange, semiclassical theory 0-48067
- polymethine cyanine dyes, vibronic energy relax., picosec. spectrosc. obs. 0-5526
- potential well depths, intermolecular, effect on molecular vibration energy transfer 0-43156
- propynal, energy dispersion and relax., laser IR/visible double reson. obs. 0-53028
- propynal, internal energy distrib., collisional effects, IR-vis. double reson. obs. 0-14159
- reaction product rot. distrib., relax. rates and chem. laser threshold times 0-28222
- resonant electronic-vibrational energy transfer and use in pumping IR mol. lasers 0-9700
- resonant exchange of molecular rotational coherence 0-23525
- rotationally inelastic collisions, tensorial factorisation 0-28096
- rotationally inelastic scattering, mag. transitions, time reversal symm. 0-53105
- scaling of energy and quantum no. for nonreactive collisions 0-9695
- self-sustained gas discharge, mol. vibr. relax. effect on thermal stability 0-10358
- semiclassical model of vibr. energy relax. in simple liqs. and compressed fluids 0-33865
- sonic nozzle expansions, rot. relax. theory 0-43827
- state change collisions, attractive intermolecular forces, temp. depend. 0-23515
- tetracyanobenzene+methylated benzene, fluorescent exciplex form., electronic relax. 0-5573
- tetrafluoromethane+CO, vibr. relax. rates, energy transfer 0-37862
- s-tetrazine in n-hexane, picosecond time-resolved fluoresc., vibr. relax. 0-48025
- thermal lens phenomena in mol. pumping expts., time-resolved geom. optics approach 0-9708
- triatomic exchange reactions, exothermic, semiclassical dynamics calcs. 0-25999
- triatomic mol. in solvent, rot. induced vibr. energy relax., Coriolis effect 0-47921
- unimolecular reactions, nonequil. time-depend., model calc., single collision approx. 0-25987
- unimolecular reactions induced by monochromatic IR radiation, intensity and laser energy fluence influence 0-11903
- V-V energy transfer, perturbed wave eqn. soln.  $H_2+H_2$  appl. 0-1051
- vibrational relaxation, scaling theoretical anal., rot. effects, long-range collisions 0-14194
- Ar+ $H_2$ , vibr. transition rates, thermally averaged, Monte Carlo trajectory calcs. 0-23519
- Ar+N $_2$  rotational excitation, differential cross sections and orientation effects, classical trajectory method 0-23523
- Ar $^+$ +N $_2$ →Ar+N $_2^+$ , electronic to vibr. energy transfer, time depend. theory 0-23514
- Br $_2$ -Ar system, mol. rot. effects on V-T energy transfer 0-14195
- Br $_2$ -CO $_2$  IR laser with Br $^+$ →CO $_2$  electronic-vibr. energy transfer as pump mechanism 0-53260
- C $_2$ , low lying  $a^3\Pi_u$  state produced in intense IR field, fluoresc. and quenching obs. 0-11931
- C $_2$ +He, C $_2$ ( $A^3\Pi_u$ ) vibr. relax. 0-53106
- CH+p-H $_2$ (He), collisional pumping of  $\Delta$ -doublet transitions, pot. energy surface 0-23516
- CO, collision-induced reorientation, direct meas. by IR double reson. 0-32800
- CO, isotopically enriched, Ar matrix isolation, laser-included vibr. fluoresc. 0-9707
- CO, vibr. excitation using steady state chemical reaction between CO and N $_2$ O 0-50851
- CO-Ar(N $_2$ ), C $_2$  and CN form. by optical pumping, room temp. 0-16701
- CO-NO mixtures, Ar matrix isolation, laser-included vibr. fluoresc. 0-9707
- CO+ $^{14}N_2$  ( $^{14}N^{15}N$ ), ( $^{15}N_2$ ), vibr. energy transfer, laser fluoresc. obs. 0-28050
- CO+CO, vibr. energy transfer, collinear and 3-dimens. rate consts. 0-48065
- CO+CO, vibr.-vibr. energy transfer, rot. effects and long-range collisions 0-14194
- CO+N $_2$ O, CO $_2$  vibr. temps. under gasdynamic laser conditions 0-21276
- CO $^+$ +He collisions, CO $^+$ ( $A^2\Pi$ ) vibr. relax. 0-53106
- CO $_2$ +inert gas, reactant decomp., rot.-vibr. energy transfer, relax. analytic soln. 0-55650
- COF $_2$ +COF $_2$ , collisionally induced relax. processes and vibr. energy transfer 0-53107
- CO( $\Sigma^+$ )+O( $D_2$ ), collisional quenching, energy transfer processes 0-23501
- CS+He, CS( $A^1\Pi$ ) vibr. relax. 0-53106
- Cd+N $_2$ ,  $A^3\Sigma_u^+$  state, vibr. excitation 0-1054
- Cl $_2$ , and isotopic forms, B $^3\Pi(0^+)$  state, laser-induced fluoresc., collisional energy transfer rates 0-53038
- Cl $_2$ -HI-He chemical laser system, rot. nonequilibrium, kinetic modelling, three model comparison 0-53281
- CsF, rot. inelastic collisions, mol. beam meas. 0-1049
- DF+DF(HF), DF vibr. deactivation, semiclassical calcs. 0-48061
- D $_2$ O, far IR absorpt. coeffs. meas., press. broadening 0-9599
- D $_2$ O, vibrational and rotations meas. by laser spectrosc. 0-43050
- H+F $_2$ →HF+F, vibr. adiabatic and static distorted wave Born approx. calcs. 0-7768
- H $_2$ , interstellar, rot. excitation rel. to CH $^+$  prod. by interstellar shocks 0-56898
- p-H $_2$ , rotational 0-2 transaction cross-sections (Russian) 0-32812
- H $_2$ , vibr. population relax. in gas and fluid 0-29775
- H $_2^+$ , spontaneous emission lifetimes in ground electronic states 0-32810
- H $_2$ +H $_2$ , quadrupolar S $_1$ (J)+S $_0$ (J) double transitions, IR fundamental band, 77K 0-52986
- o-, p-H $_2$ +Li $^+$ , rot. excitation and ang. depend. transition probabilities, time of flight spectra 0-23517

**molecular rotational-vibrational energy transfer continued**

- H $_2^+$ +H $^+$ →H $_2$ +H recombination react., calcs. (Russian) 0-55659
- HCN (001)+HCN(Ar)(N $_2$ )(CO $_2$ )(CO), relax. rate consts., using Cs vap. IR source 0-9696
- HCO $^+$ +H $_2$ , J=0-1 transition press. broadening, microwave absorpt. 0-52981
- HCl, in nonequilib. plasma, electron energy distrib. function and dissoc. kinetics 0-11882
- HCl+H $_2$ , vibr. energy transfer, collinear and 3-dimens. rate consts. 0-48065
- HCl+HCl, rot. energy transfer, quasiclassical trajectory calc. 0-23524
- HD $^+$ , spontaneous emission lifetimes in ground electronic states 0-32810
- HD+HD( $^4He$ )(D $_2$ ), vibr. relax., 80 to 400K 0-5607
- H $_2$ (D $_2$ ), dissociative electron attachment and vibr. excitation, low-energy 0-23565
- HF laser, H $_2$ +F $_2$  chain reaction, rotational nonequilibrium mech. vibr.-rotational energy exchange effect 0-48230
- HF+DF, DF vibr. deactivation, semiclassical calcs. 0-48061
- HF+HF(H $_2$ )(D $_2$ )(CO $_2$ )(isobutene), vibr. relax. dye laser pumping effects 0-9703
- H $_2$ O, far IR absorpt. coeffs. meas., press. broadening 0-9599
- H $_2$ O, relaxation by IR and microwave coherent transients 0-28092
- H $_2$ (1)+H $_2$ (1)→H $_2$ (2)+H $_2$ (0), V-V energy transfer temp. and rot. depend., semi-empirical pot. calc. 0-28094
- He+H $_2$ ( $\mu$ H), interaction pots. and rot. scatt. calcs. 0-43158
- He+N $_2$ , rot. excitation, rainbow oscills., coupled states and IOS approx. calcs. 0-23518
- He+SO $_2$ , vibr. relax., shock tube study 0-48062
- I+methane d $_0$ (-d $_3$ ), (-d $_4$ ), excited atoms, quenching, isotope effects, time resolved reson. fluoresc. 0-32656
- I $_2$ , coherent optical transients and optical dephasing in mol. collisions 0-9966
- I $_2$ , in seeded supersonic beams, vibr. and rot. relax., laser-induced fluoresc. obs. 0-23522
- I $_2$ , vibr.-translational relax., collisional predissoc., opto-acoustic effect obs. 0-43157
- I $_2$ +CO $_2$ , collisional energy transfer, quenching effects 0-14193
- I $_2$ +He, energy transfer, centrifugal sudden approx., classical infinite order sudden approx. 0-27933
- I $_2$ +I $_2$ , collisional energy transfer, ground and excited states, polarisation spectra 0-32805
- IBr-CO $_2$  IR laser with Br $^+$ →CO $_2$  electronic-vibr. energy transfer as pump mechanism 0-53260
- I $_2$ X $^1\Sigma_g^+$ , collisional relax. of highly excited vibr. levels, using I $_2$  optically pumped laser 0-43155
- K+N $_2$ (CO), rot. inelastic scatt., quantum effects, simple model surfaces 0-48064
- Kr+CO $_2$ , collisional energy transfer, anharmonicity effects 0-28097
- KrF discharge pumped laser, energy extraction, collisional coupling between B, C and D-states 0-28213
- KrF laser, collisional coupling between B, C, D states from fluoresc. meas., influence on energy extraction 0-1189
- KrF $^+$ , oscillatory bound-free emission spectra, semiclassical anal. method 0-7799
- Li $^+$ +CO $_2$ , rot. vibr. energy transfer, 1 to 10 eV, many body theory 0-28093
- Li $^+$ +H $_2$ , rot. inelastic scatt., body frame partitioning approx. calcs. 0-23527
- Li $_2$ , collisional depolarisation and rot. energy transfer, laser-induced fluoresc. obs. 0-9698
- Li $_2$ +inert gas, collision induced transition rate consts., two-laser spectrosc. 0-9629
- Li $_2$ ( $A^1\Sigma_u^+$ ), state multipoles transfer following rot. inelastic He collisions, polarised emission obs. 0-5608
- N $_2$ , discharge, excitation efficiency of rot. and vibr. levels, heating due to elastic collisions and relax. 0-38751
- N $_2$ , V-V and V-T/R energy transfer rate coeffs. by semiclassical collision model 0-9694
- N $_2$ , vibr. excitation using steady state chemical reaction between CO and N $_2$ O 0-50851
- N $_2$ +Cu, preferential energy transfer from N $_2$  to specific Cu energy levels 0-43152
- N $_2$ +K collision, electronic excitation and energy transfer, time of flight spectra 0-43151
- N $_2^+$ +He, vibronic excitation, curve-crossing trajectories 0-23520
- N $_2^+$ +Li(Na)(K), 50-1000 eV, crossed beams, electron transfer and excitation 0-14226
- NH $_2$  ( $A^1A_1$ ), excited state dynamics and bimol. quenching processes 0-9681
- NH $_2$ +H rot. energy transfer in vibronic levels, absolute transfer rates 0-9701
- NH $_3$ , relaxation by IR and microwave coherent transients 0-28092
- NH $_3$  sensitizer, excitation in MW region using CO $_2$  laser, pumping models 0-11911
- NO+O, vibr. relaxation of NO, laser induced IR fluoresc. study 0-9626
- NO $_2$ , laser-induced fluoresc. quenching rate const. and lifetimes 0-11930
- N $_2$ O+inert gas, reactant decomp., rot.-vibr. energy transfer, relax. analytic soln. 0-55650
- Na $_2$ , ground state, vibr.-rot. relax., optical pumping transients obs. 0-28067
- Ne+CO $_2$ , energy transfer, anharmonic coupling terms, semiclassical calcs. 0-37861
- Ne+HD, j=0 to 1 rot. excitation, differential cross sections, time of flight obs. 0-48104
- Ne $_2^+$ +He, pot. energy surface, reaction cross sections, ab initio calcs. 0-11881
- O $_2$ , discharge, conditions, self-consistent electron energy distrib. functions calc. 0-38746
- O $_2$ , relaxation by IR and microwave coherent transients 0-28092
- O $_2$ +inert gas, reactant decomp., rot.-vibr. energy transfer, relax. analytic soln. 0-55650
- O $_2$ +O $_2$ (H $_2$ ), vibr. energy transfer, collinear and 3-dimens. rate consts. 0-48065
- O $_3$ +inert gas, rot. energy transfer, centrifugal sudden approx. 0-27933
- OCS in n-alkane, rot. relax., solvent hydrodynamic props., Raman and IR spectra 0-45055
- OCS, relaxation by IR and microwave coherent transients 0-28092
- OCS+H $_2$ (CO $_2$ ) (fluoromethane), rot. relax. parameters, microwave spectra linewidth parameters 0-28009
- OCS+N $_2$ , 0-48063



**molecular rotational-vibrational energy transfer continued**

- OCS+nongray perturbation,  $J=1 \rightarrow 2$  microwave line press. broadening 0-9644  
 OH+P-H<sub>2</sub>(He), collisional pumping of  $\Lambda$ -doublet transitions, pot. energy surface 0-23516  
 PHD<sub>2</sub>, vibr. dephasing in liq. and solid PD<sub>3</sub>, calcs. 0-19884  
 SF<sub>6</sub> and S<sub>2</sub>F<sub>10</sub>, multiple-photon IR laser pumping, collisional effects 0-9668  
 SF<sub>6</sub> gas, CO<sub>2</sub> TEA laser-excited, slow intermol. redistrib. of vibr. energy 0-53039  
 SF<sub>6</sub>, highly excited, time-resolved IR absorpt. obs. 0-9666  
 SO<sub>2</sub>, liq., vibr. relax., US absorpt. and vel. meas. 0-34147  
 SO<sub>2</sub>+SO<sub>2</sub>, vibr. relax., shock tube study 0-48062  
 Sr+N<sub>2</sub>, A<sup>3</sup> $\Sigma_u^+$  state, vibr. excitation 0-1054  
 UF<sub>6</sub> vibrational relaxation, ultrasonic meas. in UF<sub>6</sub>-Ar-N<sub>2</sub> mixtures 0-1050  
 U(<sup>3</sup>ds<sup>2</sup>)+molecule, collisional relax. of <sup>5</sup>K<sub>5</sub><sup>0</sup> and <sup>5</sup>L<sub>7</sub><sup>0</sup> states, laser-induced fluoresc. obs. 0-52925  
 Zn+N<sub>2</sub>, A<sup>3</sup> $\Sigma_u^+$  state, vibr. excitation 0-1054

**molecular rotational-vibrational states** *see* molecular rotation-vibration**molecular spectra**

- see also* macromolecular spectra; molecular fluorescence; molecular rotation; molecular spectral line breadth; molecular vibration; multiphoton spectra; optical double resonance; radiative corrections; spectra of inorganic molecules; spectra of organic molecules and substances  
 active Raman spectroscopy, high resolution molecular methods 0-52998  
 bound states, semiclassical study 0-9693  
 chemisorbed molecules, on metal surface, spectrosc., electron gas effects 0-54504  
 chiral representations in one-centre mol. and field models, symmetry rules 0-14095  
 classical model for vibr. transition dynamics, absorpt. of IR radiation 0-52965  
 Condon approximation deviation in fluoresc. and absorption spectra, appl. to naphthalene 0-28004  
 conference, group theory and application to spectroscopy, Nova Scotia, Canada (Aug. 1978) 0-41947  
 crystal field theory, finite symmetry adaptation in spectroscopy 0-43032  
 data analysis, phenomenological and theoretical 0-52963  
 degenerate electron states, electron interaction with doubly degenerate vibr., optical transitions, semiclassical approx. 0-27927  
 diatomic molecules, excitation energies, oscillator strengths, many body approach, eqns. of motion method 0-47969  
 diatomic molecules, spectrosc. consts., rel. to electronegativity 0-28007  
 electric dipole allowed transitions, amplified sector rule based on electron correlation 0-5523  
 electronic and magnetic structure, interpretation of data obtained from Mossbauer, ESR, susceptibility, optical and XPS meas. 0-37825  
 energy level clustering, qualitative theory of irreducible tensor operators spectra 0-28001  
 energy level transitions, Doppler broadening, phase-destroying collisions 0-9561  
 Fourier transform IR spectroscopy, use in atm. chem. 0-55743  
 Franck-Condon effects in resonance Raman spectra and excitation profiles, appl. to CrO<sub>2</sub><sup>2-</sup> and  $\beta$ -carotene 0-14129  
 gas lasers, computer modelling, at. and mol. processes 0-23661  
 gas-pressure shifts, Stark displacements 0-23463  
 generator coordinate theory, nonadiabatic effects 0-23391  
 inner level spectroscopy with synchrotron radiation, theoretical aspects, book contrib. 0-4778  
 intramolecular hydrogen bond, calc. of electronic absorption spectra 0-42949  
 inverse Raman scattering spectroscopy and chem. appls. 0-37094  
 IR and Raman vibrational intensity changes due to long-range interactions 0-53084  
 IR Doppler free molecular spectroscopy, two photon coherence and pumping 0-48052  
 IR radiation, interaction with molecular system, classical/semiclassical theory challenged 0-43117  
 isotopic isomers, spectroscopic obs. 0-53009  
 lanthanide (III) complex, octahedral, f-f transitions, mag. dipole intensities, vibronic coupling model 0-25404  
 laser-induced processes in molecules, conf., Edinburgh, Scotland (Sept. 1978) 0-9577  
 molecular crystals, spectroscopy, bibliography (1977) 0-7317  
 molecular spectroscopy using synchrotron radiation, book contrib. 0-4780  
 molecule+ion,  $\Lambda$ -doublets transitions 0-14132  
 nongrey molecular gases, total IR band absorption, anal. and approx. models 0-14141  
 organic chemistry courses, unified approach to teaching of struct. and bonding 0-17732  
 oscillating electric dipole contrib. to light scatt. and interpret. in terms of polarisability and hyperpolarizability 0-53212  
 partially ordered ensembles, spectrosc. props., theory, 1-vector problems 0-42261  
 photofragment spectroscopy of mol. ions using fast ion beams 0-9755  
 point group coupling, coeffs., props. and application 0-43033  
 polyatomic molecule, vibr. struct. of electronic spectra, FORTRAN programs 0-32699  
 polyatomic molecules, excitation energies, oscillator strengths, many body approach, eqns. of motion method 0-47969  
 polyatomic molecules, mol. parameters isotopic depend. 0-9522  
 polyatomic molecules, multiple-photon absorption, quantitative comparison 0-32790  
 polyatomics, absorpt. and luminesc. spectra, higher electronic states effect 0-9586  
 quantum intramolecular dynamics: criteria for stochastic and nonstochastic flow 0-53082  
 Raman scatt. time depend. theory 0-28023  
 Raman spectra of gases, high-resolution, mol. struct. and orops. 0-53000  
 Raman spectroscopy, high-resolution, using tunable spin flip Raman laser, review 0-55762  
 random velocity fields, radiative transfer and line form., intensity moment transfer eqn. derivation 0-52967  
 resonance interactions of atomic and molecular systems driven by strong laser field, theory 0-14097  
 resonance Raman scatt. from mols., temp. effect, displaced harmonic oscillator model 0-23424  
 rotational coherence, reson. collisional exchange, time-resolved microwave obs. 0-23525

**molecular spectra continued**

- rotational intensities in <sup>2</sup> $\Sigma$ (int)-<sup>4</sup> $\Sigma$ (int) transitions 0-9642  
 Rydberg states, quantum defect theory applic. 0-32700  
 selection rules for spectra and photochemical reactions (*Chinese*) 0-21308  
 solvated electrons, optical spectra and model potentials 0-30318  
 spectroscopic data analysis, phenomenological and theoretical 0-52963  
 spectroscopy, conf. Frankfurt, Germany (Sept. 1979) 0-51948  
 spectroscopy and crystal physics, generating function techniques 0-44162  
 sub-Doppler laser spectroscopy of mol. ions in fast ion beams 0-9655  
 synchrotron radiation, techniques and appls., book 0-5668  
 tensorial calculations 0-18836  
 tetrahedral molecules, vibr., charge and charge flux 0-47961  
 time-resolved resonance Raman spectroscopy and vidicon Raman spectrography, vibr. spectra on nsec scale 0-37095  
 transition metal complexes, O containing, coordinate bonding, charge transfer electronic bands, complex struct. determ. 0-52977  
 triatomic molecules, motion, regular and irregular spectra, theory 0-9590  
 valence and core photoionisation, spectral lines, many body effects 0-47853  
 vibrational spectroscopy, high pressure, and conformational analysis 0-9758  
 H bonded  $\nu_{X-H}$  band, dynamic theories survey 0-52983  
 O<sub>2</sub> (0-0) atmospheric band, laboratory discharge lamp source 0-4148

**molecular spectral line breadth**

- absorption line variation across planetary disc with inhomogeneous atm. 0-8569  
 acetaldehyde+H<sub>2</sub>(N<sub>2</sub>)(CO<sub>2</sub>), rot. line broadening, mol. quadrupole moments calc. 0-28065  
 acetone, liq., C-C stretching mode relax., Fermi reson. influence 0-25352  
 acetonitrile, in liq. phase, Ramon band profiles, calc. using IR intensities 0-2741  
 alcohols, OH-stretching vibr. band in overtone region, IR-Fourier spectral investig. (*German*) 0-976  
 alkali homonuclear dimers, quasi-static wing profiles of self-broadening reson. lines 0-48042  
 alkyl benzenes, jet-cooled, intramol. vibr. relax., reson. fluoresc. and excitation obs. 0-14152  
 benzene, molecule translational mobility in depolarised Raman spectra 0-14150  
 benzene and deuterates, highly vibr. excited intramolecular V-V transfer, visible and photoacoustic spectra 0-32729  
 benzene in solution, rotational motion, Raman study 0-44104  
 biradical metal chelates, rot. motion in polar solvents, rel. to ESR line-shape 0-27994  
 cyanodiacetylene (HC<sub>3</sub>N) is Heiles's cloud 2, line widths and relative intensities 0-22054  
 cyanogen fluoride, fund., hot bands, laser microwave two photon and double reson. spectroscopy 0-32752  
 dense polyatomic molecular systems, vibr. correl., HF band exchange dephasing 0-37803  
 diatom-atom gas mixture, infrared line shape, rotational lines, influence of collision duration 0-43110  
 dimer triplet state line shape, small excitons, appl. to phenazine, naphthalene, tetrachlorobenzene 0-48041  
 energy level transitions, Doppler broadening, phase-destroying collisions 0-9561  
 fluoroacetylene, fund. and hot bands, laser microwave two-photon and double reson. spectroscopy 0-32752  
 formaldehyde-d<sub>2</sub>, 733  $\mu$ m line, Autler-Townes effect in laser interacting with RF field 0-53269  
 Franck-Condon effects in resonance Raman spectra and excitation profiles, appl. to CrO<sub>2</sub><sup>2-</sup> and  $\beta$ -carotene 0-14129  
 hexafluorobenzene-benzene, liq., mol. interactions, IR and Raman line-shape obs. 0-28907  
 hexafluorobutene, vibrational broadening, dense fluid region, Raman and NMR study 0-43056  
 hole burning into molecular velocity distribution due to monochromatic radiation and molecular elastic collision 0-43116  
 inhomogeneous molecular gas radiation calc. using spectral comp. modelling 0-32697  
 intermolecular forces Raman scatt. obs., review 0-23427  
 line profile, spectral absorption coeff. calc., statistical modeling in semiclassical approx. 0-52865  
 liquids, and dense gases IR and Raman spectra 0-11390  
 malononitrile, dispersive phase transition, 294.7K, Raman and Brillouin-Rayleigh scatt. obs. 0-16047  
 methane,  $\nu_1$  line contour anomalous behaviour on pressure changes (*Russian*) 0-43052  
 methane, line profile of coherent radiation in separated fields due to F<sub>2</sub><sup>(2)</sup> transition 0-37835  
 molecular crystals, two particle exciton-phonon interactions, optical absorpt. line shapes theory 0-55120  
 nitrobenzene, in acetone-isopropanol soln., Rayleigh scatt. and viscosity 0-5550  
 nongrey molecular gases, total IR band absorption, anal. and approx. models 0-14141  
 organic compounds, complex, nuclear relaxation influence on stimulated emission 0-48019  
 polyene chromophones, band broadening in electronic-vibr. absorpt. spectra 0-28003  
 predissociating harmonic oscillator, relative line widths and level shifts 0-23469  
 radiative transfer in real spectrum, calc. using integration over freq. method 0-33430  
 resonance fluoresc., probe of intramolecular relax., density matrix formalism, lifetimes and quantum beats 0-32757  
 resonance Raman spectra lineshapes, first order, rel. to optical absorpt. lineshapes 0-5548  
 rhodamine B, 6G, resonance CARS line shape, scatt. processes in ground or excited states 0-48043  
 scattered light spectrum Rayleigh lines, density fluctuations in two component reacting fluid 0-25397  
 self reversal contours, use in determ. of line broadening and shift consts. 0-52940  
 solid, molecular fluoresc., phosphoresc., and ODMR line narrowing 0-43084  
 solvated electrons, Raman spectrum modification, polarisation CARS obs. 0-5549  
 solvent effects, rel. to polarisation structure 0-43062



**molecular spectral line breadth continued**

- spherical top molecules, fluid vibr. spectra, repulsive force depend. line broadening (*Russian*) 0-47970
- tetrabromomethane, in disordered phases, IR active mode Raman line shape, dipole-dipole interaction 0-9603
- tetrachloromethane, fluid vibr. spectra, repulsive force depend. line broadening (*Russian*) 0-47970
- tetrafluoromethane, in disordered phases, IR active mode Raman line shape, dipole-dipole interaction 0-9603
- toluene, molecule translational mobility in depolarised Raman spectra 0-14150
- triatomic linear mol., parallel bands, band model parameters 0-43026
- trichlorofluoromethane, 8-12  $\mu\text{m}$  band model calcs. 0-43112
- trifluoriodomethane, UV absorpt. spectrum broadening by laser-induced vibr. excitation 0-53050
- triplet state broadening, inhomogeneous and homogeneous, of optical and ODMR transitions in solids 0-32750
- two-dimensional spectra, eval. of peak volume, position and width, computer program 0-18890
- vibrational-rotational line broadening by monatomic gas 0-9643
- vibrational-rotational line profiles, theory 0-1029
- $^{10,11}\text{B}_2\text{H}_6$  gas (liq.) phase, vibr. dephasing and Raman spectra 0-48101
- $\text{BO}_2$ , Doppler free spectra, backscatter fluoresc. line narrowing, theory and obs. 0-53034
- CO in IR C star CIT 6 (IRC+30219), line profile rel. to mass outflow 0-12761
- CO, matrix-isolated, librational relax., IR line broadening 0-978
- CO, rovibr. multiphoton spectra comput., hole burning effect 0-9672
- $\text{CO}_2$ ,  $10^00\text{-}00^0_{1,11}$  absorpt. band profile temp. depend., integral and spectral binary absorpt. coeffs. 0-43049
- $\text{CO}_2$ ,  $201_{11}\text{-}000$  band, press. broadened coeffs. and absolute intensities, temp. depend., IR obs. 0-53054
- $\text{CO}_2$ , band model parameters prediction, 4.3 micron, 200-3000K 0-43047
- $\text{CO}_2$  induced absorpt., 3-4 $\mu\text{m}$ , temp. depend. 0-983
- $\text{CO}_2$  pulsed laser with continuously tunable radiation frequency 0-48292
- $\text{CO}_2$ , rot-vibr. bands, absorpt. coeff. calc. method, Fermi reson. effect on spectral lines 0-32696
- $\text{CO}_2$  vibr.-rot. band shape calcs. 0-969
- $^{113}\text{Cd}_2$ , two-level system, absorpt. spectrum, subradiative struct. (*Russian*) 0-28008
- $\text{D}_2$ , predissoc. linewidths and shapes for  $3p\pi\text{D}^1\Pi_u^+$  state 0-53066
- $\text{D}_2+\text{D}_2$ , collision effect on depolarised light scatt. linewidths 0-53059
- $\text{D}_2\text{O}$ , far IR absorpt. coeffs. by  $\text{H}_2\text{O}$  laser meas., foreign gas and self broadening 0-9599
- $\text{H}_2$ ,  $\text{D}_2$  and HD, intermol. collision process obs. using light scatt. expts. 0-53001
- $\text{H}_2$ , predissoc. linewidths and shapes for  $3p\pi\text{D}^1\Pi_u^+$  state 0-53066
- $\text{H}_2+\text{H}_2$ , collision effect on depolarised light scatt. linewidths 0-53059
- $\text{HCO}^++\text{H}_2$ ,  $J=0-1$  transition press. broadening, microwave absorpt. 0-52981
- $\text{HCl}+\text{Ar}(\text{Xe})$ , infrared line shape, rotational lines, influence of collision duration 0-43110
- HD, gas, fundamental band, R and P line shapes 0-23461
- HD, predissoc. linewidths and shapes for  $3p\pi\text{D}^1\Pi_u^+$  state 0-53066
- HF, pressure broadened linewidths in 2.5  $\mu\text{m}$  band, influence of polymer form. 0-32777
- $\text{HNO}_3$ , high resolution spectral meas. of 5.9  $\mu\text{m}$  band using tunable diode laser 0-32707
- $\text{H}_2\text{O}$ , far IR absorpt. coeffs. by  $\text{H}_2\text{O}$  laser meas., foreign gas and self broadening 0-9599
- $\text{H}_2\text{O}$ , interstellar, in Orion Nebula, 183 GHz emission line vel. profile 0-41869
- $\text{H}_2\text{O}$  vapour, line shape functions in absorpt. coeff. calc. 0-9600
- $\text{H}_2\text{O}$ -formaldehyde complex, IR spectrum in solid Ar,  $\text{N}_2$  matrix 0-43042
- $\text{I}_2$  vapour, absorpt. lines meas. using FM spectrosc. 0-42262
- $^{135}\text{Cl}$ , predissociations in  $\text{B}^1\Pi_{0+}$  state 0-1033
- $^{137}\text{Cl}$ , predissociations in  $\text{B}^1\Pi_{0+}$  state 0-1033
- $\text{I}_2$  fluoresc.,  $\text{Ar}^+$  laser excited, high resolution and sub-Doppler Fourier transform spectroscopy 0-43089
- KrF, 25 J unstable resonator oscillator, injection locking 0-28218
- $\text{MgO}$ , red and near UV bands calc., rel. to sunspot spectra 0-12736
- $\text{N}^{2+}$ , spectral line breadth in molecular nonequilibrium plasma (*Russian*) 0-48044
- $\text{N}_2^+$ , UV spectral line width in rarefied free jet, for rot. temp. 0-6184
- $\text{NF}_2$ , IR spectra,  $\nu_1$  and  $\nu_2$  bands, vibr. excitation and spin-rot. interaction, doublet splitting 0-28011
- $\text{NH}_3$  in benzene( $\text{CCl}_4$ )(pentane) Fermi resonance, solvent and phase depend. 0-47960
- $\text{NH}_3$ , magnetic relaxation rates for microwave spectrum and contributions to linewidth 0-5564
- $\text{NH}_3$ , optical band strengths and curves of growth rel. to spatial distrib. on Jupiter 0-46386
- NO, intracavity Zeeman modulation detect., passive Q-switching, CO IR laser obs. 0-9597
- NO, press. broadening coeffs., spin-flip Raman laser spectrosc. 0-43147
- $\text{N}_2\text{O}$ ,  $40^00\text{-}00^0$  band, IR high press. absorpt. spectra profiles 0-52988
- $\text{N}_2\text{O}$ , pure liq., mol. motion, anisotropic interaction 0-24345
- $\text{O}_2$ , microwave spectrum, press. broadening 0-23412
- $\text{O}_2$ , Schumann-Runge band system in sunspots UV spectrum 0-12735
- $\text{OCS}+\text{H}_2(\text{CO}_2)$ (fluoromethane) rot. relax. parameters, microwave spectra linewidth parameters 0-28009
- $\text{OCS}+\text{nonpolar}$  perturbation,  $J=1\rightarrow 2$  microwave line press. broadening 0-9644
- $\text{POF}_3$ , level anticrossing effects, vibr., laser Stark spectra obs. 0-32771
- $\text{SF}_6$ , IR double reson. with tunable diode laser 0-14160
- S0 in Orion Molecular Cloud, line profile rel. to rotational explanation of high-vel. mol. emission 0-36688

**molecular structure (electronic)** see *molecular electronic states*

**molecular structure (geometrical)** see *molecular configurations*

**molecular vibration**

- see also *Fermi resonance; macromolecular dynamics; molecular force constants; molecular rotational-vibrational energy transfer; molecular spectra; molecular vibration calculations; molecular vibration in solids; potential energy curves and surfaces of molecules; potential energy functions*
- 1,3-butadiene-1-one, spectroscopic consts., IR and microwave spectra, prep. 0-18859
- 3,3,3-trifluoropropene, struct. and vibr. spectra, IR, Raman polarisation study 0-18845

**molecular vibration continued**

- acetaldehyde, adsorbed on  $\text{Al}_2\text{O}_3$ , inelastic electron tunnelling spectra, surface vibr. struct. determ. 0-35572
- acetamide, IR spectra, amino group inversion transitions and pot. functions 0-43041
- acetic acid, adsorbed on  $\text{Al}_2\text{O}_3$ , inelastic electron tunnelling spectra, surface vibr. struct. determ. 0-35572
- acetone, liq., C-C stretching mode relax., Fermi reson. influence 0-25352
- acetonitrile, in liq. phase, Raman band profiles, calc. using IR intensities 0-2741
- acetylene( $-d_1, d_2$ ), integrated IR intensities 0-23457
- acetylene- $d_1$ , vibr. bands, IR spectrum in region of bending fundamental  $\nu_4$  0-23418
- alkyl benzenes, jet-cooled, intramol. vibr. relax., reson. fluoresc. and excitation obs. 0-14152
- alkyl substituted diacetylene radical cations, optical emission and photoelectron spectra, fragmentation decay 0-53004
- 1-alkynes+ $\text{O}^+(\text{P})$ , CO prod., vibr. population distrib., rate consts., laser reson. absorpt. technique 0-40676
- 2-amino-5-chloropyridine, IR absorption, vibr. assignments 0-979
- $\gamma$ -aminobutyric acid, aq. soln., low freq. vibrs. Raman spectra obs. 0-987
- anthracene, vapour, fluoresc. spectra, mol. vibr. freq. reson. laser IR irradiation, quenching 0-18883
- aromatic hydrocarbon, centrosymmetric, two photon excited upper state fluoresc. spectra, reson. fluoresc. and vibr. mode selectivity 0-18878
- aromatic isolated mol. nonradiative conversion, internal and S-T conversion, vibr. excitation and fluoresc. quantum yield 0-43095
- benzaldehydes, para-halogenated, IR and Raman spectra, vibr. assignments, thermodynamic functions 0-14139
- benzene, local mode combination bands and local mode mixing 0-27999
- benzoic acid, IR absorpt. spectra, fundamental assignments 0-5542
- biological systems, nonequilib. mol. vibr. excitation, electron mechanism 0-55979
- biphenyl, vibr. level classification by Longuet-Higgins group 0-43030
- $\text{C}_3$  molecules, I-reson. perturbations in overtone and combination vibr. systems 0-52962
- chloroethane, reson. multiphoton dissociation 0-53077
- chloroform- $\text{He}(\text{Ar})(\text{N}_2)$  gaseous compressed mixture, mol. reorientation, Raman spectra 0-23422
- chloromethyl formate( $-d_1, d_2, d_3$ ), gas, solid and liq., IR spectra assignments and struct. 0-32715
- coherent interaction with strong monochromatic laser light, classical calc. 0-28079
- complex molecules, vibr. spectra, stochastic description, appl. to optically active Brownian oscillator 0-52974
- coupled vibration systems, eigenvalues, semi-classical SCF calcs. 0-27929
- cryogenic liquids, vibr. kinetics, nonlinear optics appls. 0-13082
- crystal violet, prereson. Raman spectra 0-32721
- cyanoacetylene, vibrational excitation in Orion molecular cloud 0-22067
- cyanogen fluoride, fund., hot bands, laser microwave two photon and double reson. spectroscopy 0-32752
- cyclobutene, strong collision and thermal decomp. on surface, variable encounter method calcs. 0-50885
- chloroheptatriene, and substituted forms, vibr. highly excited, steady-state photoionisation 0-16704
- cyclopropane, partial vibr. energy transfer map 0-32760
- cyclopropyl bromide, IR absorption, Raman scatt., assignments, thermodynamic functions 0-984
- degenerate electron states, electron interaction with doubly degenerate vibr., optical transitions, semiclassical approx. 0-27927
- dense polyatomic molecular systems, vibr. correl., HF band exchange dephasing 0-37803
- diatomic molecules, spectrosc. consts., rel. to electronegativity 0-28007
- diatomic mols., internal partition functions for  $\text{O}_2$ ,  $\text{N}_2$ , NO and their ions, max. summation indices 0-27995
- meso-2,3-dibromo-1,4-dichlorobutane, rot. isomerism, IR and Raman spectra 0-981
- dichloroanilines, vibr. assignments, Raman spectra obs., thermodynamic functions 0-52992
- 3,4-dichlorobromobenzene, liq., laser Raman spectrum, LF band assignments 0-48002
- dichloromethane, high press. and temp. IR absorpt. spectra, stretching fundamentals (*German*) 0-47999
- 3,6-dichloropyridazine, liq. and solid soln. spectra, fundamental freqs. and assignments 0-5541
- dicyanodiacetylene radical cation, photoelectron and emission spectra 0-5558
- 1,2-diiodobenzene, vibr. spectra, packing calcs. and crystal structure investigation 0-28938
- dimethyl ether, review of microwave spectrum, tabulated data 0-51965
- dimethylsulphoxide, effects on water struct., Raman and IR spectral study 0-14143
- electron impact shape-reson.-enhanced vibr. excitation, 10-40 eV, appl. to  $\text{CO}_2$  0-5629
- ethanol, adsorbed on  $\text{Al}_2\text{O}_3$ , inelastic electron tunnelling spectra, surface vibr. struct. determ. 0-35572
- ethyl formate, microwave rot. spectrum, centrifugal distortion effects 0-52979
- ethyl methyl sulphide, low freq. vibr. spectra, methyl torsional pot. functions and internal rot. 0-5543
- ethyl radical,  $^{13}\text{C}_\alpha$  and  $\text{H}^+$  hyperfine interactions, EPR spectra, vibr. anal. 0-23443
- ethylene, autoionisation and photoemitted electron ang. distrib., cylindrical mirror analyser study 0-18049
- ethylene( $-d_1$ ), Rydberg states assignments, electron energy loss spectra 0-53153
- ethylene cation, state geometries, electronic vibr. coupling consts., HF calcs., comparison with Xalpha calcs. 0-27946
- fluoroacetylene, fund. and hot bands, laser microwave two-photon and double reson. spectroscopy 0-32752
- fluoroanilines, isomers, thermodynamic functions and fundamental vibr. freqs. 0-9581
- fluoroethanes, IR multiphoton dissociation, HF vib. energy distrib. 0-53073
- fluoroethylenes, IR multiphoton dissociation, HF vib. energy distrib. 0-53073
- fluoroethylenes, variable angle photoelectron spectra, ionisation pot. asymmetry parameter 0-28064
- fluoromethane, excited state rot. spectroscopy and kinetics, appl. of tunable sub-MM sources 0-14162
- formaldehyde- $d_2$ , reson. multiphoton dissociation 0-53077
- formamide, IR spectra, amino group inversion transitions and pot. functions 0-43041



**molecular vibration continued**

- Fourier transform IR spectroscopy, use in polymer research as vibr. spectroscopy tool 0-55744
- free radicals, photolysis, excimer laser UV obs. 0-16711
- glow discharge in diatomic molecular gas, electronic excitation rate, vibr. temp. influence 0-19633
- glyoxal, vibr. energy redistrib. following internal conversion 0-23452
- haloacetylene cations, electron impact excitation A $\rightarrow$ X band system assignment 0-32766
- halomethanes, synchrotron radiation photoabsorption cross sections, Rydberg states 0-28033
- hexafluoroacetone, IR multiphoton dissociation, isotopic selectivity and yield, temp. effect 0-53069
- hexafluorobutene, vibrational broadening, dense fluid region, Raman and NMR study 0-43056
- hexafluoropropene, struct. and vibr. spectra, IR, Raman polarisation study 0-18845
- high temperature electron diffraction, review 0-52237
- homonuclear molecules, vibr. excitation by IR radiation 0-28068
- inorganic species, vibr. and electronic props., reson. Raman spectra appl. 0-52996
- intermolecular triplet excitation transfer in diffusive limit 0-28046
- ion+molecule, charge transfer, energy disposal and reaction mechanisms 0-28103
- IR and Raman vibrational intensity changes due to long-range interactions 0-53084
- isotopically tagged molecules, normal vibr. freq. calc., eigenvalue behaviour, perturbation theory obs. 0-52973
- level classification by Longuet-Higgins group 0-43030
- liquid, vibr. dynamics using picosecond Raman techniques 0-52325
- liquid structure and dynamics from light scatt. spectra 0-55105
- liquids, two-pulse spectroscopy with ps laser pulses 0-53041
- methane,  $\nu_3=1$  state, dipole moment and IR-radiofrequency double reson. spectra 0-14161
- methane,  $\nu_4$  band, high resolution spectrosc. 0-5529
- methane,  $\nu_4$  band Q-branch spectrum 0-5530
- methane,  $\nu_4$  fundamental, Q and R branch absolute line intensities 0-5539
- methane, CW vibr. photchem. for D enrichment, economic aspects 0-11920
- methane- $d_4$ , selectively excited, cooling, vibr.-vibr., vibr.-translational relax. 0-33723
- methyl bromide, l-reson. perturbations in overtone and combination vibr. systems 0-52962
- methyl thionine chloride, intramol. vibr. spectra 0-977
- methylmercuric halides, partially oriented,  $^1\text{H}$  and  $^{13}\text{C}$  NMR obs. 0-23437
- methoxy radical, electronic absorpt. spectra, visible, vibr. freqs., vibronic intensities and oscill. strengths 0-28025
- Morse oscillator collinear collision induced dissoci., vibr. enhancement, quasiclassical trajectory study 0-28089
- multiphoton absorption modelling, using  $\text{SF}_6$  energy-dependent absorption cross sections 0-32789
- $\text{MX}_2$  and  $\text{MX}_3$  mols., vibr. freq. and geom. struct. 0-1081
- organic compounds, IR fluorescence under  $\text{CO}_2$  laser radiation 0-37830
- organic compounds, low freq. anharmonic vibr., pot. function determ., Raman and IR spectra obs. 0-52997
- organo-arsenic compounds,  $(\text{CF}_3)_2\text{AsSCH}_3$  and  $(\text{CF}_3)_2\text{AsSeCH}_3$ , gas phase IR and liq. Raman spectra, normal coord. anal. (German) 0-32725
- organophosphorus compounds,  $(\text{CF}_3)_2\text{PSCH}_3$  and  $(\text{CF}_3)_2\text{PSeCH}_3$ , gas phase IR and liq. Raman spectra, normal coord. anal. (German) 0-32725
- oriented molecules, NMR spectra, vibr. correction study 0-18840
- ovalene, vibrational quasicontinuum threshold, spectrosc. criterion 0-52972
- parity-violating effects of weak interactions 0-52455
- pentacene, vibrational quasicontinuum threshold, spectrosc. criterion 0-52972
- perhalonitrosomethanes, gas phase IR spectra, assignments, isomerism 0-28017
- phenacyl halides, IR spectra,  $\delta(\text{CH}_2)$  vibr. correlation with structs. (French) 0-23417
- phthalic acid, IR absorpt. spectra, fundamental assignments 0-5542
- phthalimide derivatives, hidden vibr. band determ. method, fluorescence and excitation spectra meas. 0-40158
- picosecond spectroscopy, anal. using polarisation method 0-13152
- plasma, atomic ion-electron recomb. in presence molecules, appl. to HCl 0-28601
- polyatomic molecule, collisionless multiphoton dissoci., threshold behaviour, nonthermal theory 0-11905
- polyatomic molecules, high intensity IR absorpt. 0-14183
- polyatomic molecules, laser-induced energy distrib. 0-5591
- polyatomic molecules, vibrations, anharmonic problem, soln. by direct diagonalisation of Hamiltonian 0-52975
- polyatomic rarefied gases, vibrational modes, energy exchange (Russian) 0-32811
- polyatomic symmetric molecules, collisionless dissoci. and vibr. spectrum of degenerate modes 0-18893
- polydeoxyribonucleotides, poly(dA).poly(dT) and poly(dAT).poly(dAT), HF vibr. modes, Raman and IR spectra 0-32698
- polymer, branched and crosslinked molecules, mol. description of dynamics 0-9767
- polymethylene, extended chain, C-H stretching band struct., Fermi reson., Raman spectrum 0-5552
- polystyrene and model cpds., conformational struct. influence on normal modes of benzene ring, Raman study 0-14144
- premixed  $\text{H}_2\text{-O}_2\text{-N}_2$  laminar flames, temp. profiles, Raman, absorpt. and line reversal obs. 0-42227
- propenyl chloride, IR bands, torsional struct. 0-28018
- pyrazine ( $-d_4$ ) vapour, single vibrational level fluoresc. from n,  $\pi^*$  0-37827
- pyridine iodine complexes, charge transfer complexes, vibr. spectra, laser Raman obs. 0-52990
- pyridine- $l_2(\text{Br}_2)$  charge transfer complexes, vibr. spectra, vibronic contrib., intensity enhancement 0-53048
- quasi-linear molecules, low frequency anharmonic vibrations, pot. function determ., Raman and IR spectra obs. 0-52997
- quasicontinuum threshold, spectrosc. criterion for large mols. 0-52972
- Raman spectra of gases, high-resolution, mol. struct. and orops. 0-53000
- rhodamine, CARS spectroscopy, vibr. spectra of electronic states 0-27964
- molecular vibration continued**
- rhodamine dyes in soln., bleaching, electronic and vibr. absorpt. spectra, fluoresc. 0-42960
- salicylic acid, IR absorpt. spectra, fundamental assignments 0-5542
- selective excitation using stimulated Raman scatt. Cs vap. source, appl. to HCN (001) 0-9696
- 1-silabicyclo 2,2,2 octane, double-min. skeletal torsion, microwave spectroscopy 0-47972
- spin-spin coupling consts., mol. vibr. contrib., calc. methods comparison 0-23402
- succinic acid and its alkaline salts in aqueous soln., Raman and IR spectra (French) 0-32723
- tertiarybutylisocyanide-borane, vibr., rot. consts., moment of inertia, microwave spectra obs. 0-32706
- meso-1,2,3,4-tetrabromobutane, IR and Raman spectral studies 0-32722
- tetracene, vibrational quasicontinuum threshold, spectrosc. criterion 0-52972
- meso-1,2,3,4-tetrachlorobutane, IR and Raman spectral studies 0-32722
- tetracyanobenzene+methylated benzene, fluorescent exciplex form., electronic relax. 0-5573
- s-tetracyanobenzene+p-xylene, photoassoc. exciplex form., excitation energy and isotope depend., vibr. effects 0-55634
- tetramethylsilane, IR and visible spectral intensity data and the universal intensity concept 0-28066
- tetramethylsilane, local mode combination bands and local mode mixing 0-27999
- tetrazine-Ar, van der Waals bond, nonstatistical vibr. energy distrib., photochemical reaction effects 0-30255
- thiirene and deuteroderivatives, Fourier transform IR spectra using Ar matrix isolation, vibr. band assignments 0-14142
- thioacetamide, IR spectra, amino group inversion transitions and pot. functions 0-43041
- thioketen, microwave spectrum, substitution structure and dipole moment 0-975
- thiomethoxyl anion, and deuterate, electron photodetachment, affinities, vibr. freq. and spin-orbit splitting 0-53063
- third row element mols., general harmonic force field, SCF-MO-MNDO and freq. calc., MOCIC pot. 0-27948
- toluene, electronic-vibr. spectra calcs., Franck-Condon and Herzberg-Teller approx. 0-37735
- toluene, two-photon ionisation spectrum, of  $^1\text{L}_b\text{-S}_0$  transition 0-14180
- transition metal complexes, vibronic coupling and spin relax. NMR decay rate study 0-18870
- tri-*i*-propylgermylamine, and isotopomers, IR and Raman spectra, normal coord. anal. (German) 0-32716
- tri-*t*-butylstannylamine, and isotopomers, IR and Raman spectra, normal coord. anal., Mossbauer spectrum (German) 0-32716
- triatomic van der Waals complex, vibr. predissoc. and photodissoc. lifetimes 0-9661
- tribromotrifluoroethane, IR and Raman spectra, normal coord. anal. (German) 0-32726
- 1,3,5-trichloro-2,4,6-trifluorobenzene radical cation,  $\text{B}^2\text{A}_2'\text{-X}^2\text{E}''$  laser-induced fluoresc. spectra 0-14172
- trichlorotrifluoroethane, IR and Raman spectra, normal coord. anal. (German) 0-32726
- triethylsilylamine, and isotopomers, IR and Raman spectra, normal coord. anal. (German) 0-32716
- trifluoroethane ( $-d_3$ ), IR and Raman spectra, normal coord. anal. (German) 0-32726
- trifluoroiodomethane, molecular vibration energy stochastization in intense IR laser field by Raman spectroscopy (Russian) 0-14149
- trifluoroiodomethane, multiphoton IR excitation and dissoci. (Russian) 0-35562
- trifluoroiodomethane, UV absorpt. spectrum broadening by laser-induced vibr. excitation 0-53050
- trifluoromethyl chloride, IR multiphoton dissociation, isotopic selectivity and yield, temp. effect 0-53069
- trifluoromethylperoxy radical, in Ar: $\text{O}_2$  matrix, IR spectra 0-50845
- trifluorotriiodoethane, IR and Raman spectra, normal coord. anal. (German) 0-32726
- trimethylene sulphoxide, ring puckering vibr., IR spectra obs. 0-32710
- tropolone vibr. spectra and proton tunneling 0-28014
- unimolecular reactions, laser-induced, by multiphoton IR excitation, theory 0-9664
- van der Waals molecules, vibrationally excited, lifetimes, momentum gap 0-5601
- vibrational spectroscopy, high pressure, and conformational analysis 0-9758
- vibronically coupled electronic states, radiationless decay, non-Condon effects 0-52966
- water, adsorbed on Pt(100), bonding, electron energy loss spectra 0-34311
- water-carbon tetrachloride soln., fundamental  $\text{H}_2\text{O}$  IR spectrum, liq. struct. 0-23419
- p-xylene, electronic-vibr. spectra calcs., Franck-Condon and Herzberg-Teller approx. 0-37735
- $^{15}\text{NH}_3$ , modulated coherent Raman beats 0-23464
- Ar- $\text{O}_2$  Van der Waals complex, struct. and props., RF and microwave obs. 0-32704
- $\text{BCl}_3$ , high-resolution IR Ar matrix-isolation spectra, 10K 0-32708
- $^{10,11}\text{B}_2\text{H}_6$  gas (liq.) phase, vibr. dephasing and Raman spectra 0-48101
- BiF, spectrum, 5800-6600 Å, vibr. anal., electronic transition assignment 0-992
- Br+NOBr, primary and secondary photochemistry, vibrationally excited NO, IR fluoresc. obs. 0-48030
- $\text{CBr}_2$  emission in solid Ar, laser excitation spectra and lifetimes 0-48034
- $\text{CBrCl}$  emission in solid Ar, laser excitation spectra and lifetimes 0-48034
- $\text{CO}$ , A  $\Pi(\nu=1)$ , vibr. relax. by reversible intersystem crossing, fluoresc. obs. 0-14170
- $\text{CO}$ , adsorbed on Pt, low temp. vibr. mode, site occupation, electron energy loss spectra 0-29263
- $\text{CO}$ ,  $\text{CO}^+$ , emission spectra, 2100-5600 Å, electronic band systems and assignments 0-5560
- $\text{CO}$  discharge plasma, electron energy distrib. and kinetic coeffs., ground-state mols. 0-43867
- $\text{CO}$  discharge plasma, electron energy distrib. and kinetic coeffs., vibr. excited mols. 0-43868
- $\text{CO}$ , K-shell, excitation and ionisation, vibr. struct., electron energy loss spectra obs. 0-18943
- $\text{CO}$ , matrix-isolated, librational relax., IR line broadening 0-978



## molecular vibration continued

- CO, one-electron props., SCF and CI calcs. 0-27951  
 $\text{CO}^+$ ,  $^{14}\text{C}$  and  $^{18}\text{O}$  isotope shifts, vibr. anal. of first negative, comet-tail and Baldet Johnson systems 0-28029  
 $\text{CO-Ar}(\text{N}_2)$ ,  $\text{C}_2$  and CN form. by optical pumping, room temp. 0-16701  
 $\text{CO} + ^{14}\text{N}_2$ , ( $^{14}\text{N}^{15}\text{N}$ ), ( $^{15}\text{N}_2$ ), vibr. energy transfer, laser fluoresc. obs. 0-28050  
 $\text{CO}_2$ , 201<sub>11</sub>-000 band, press. broadened coeffs. and absolute intensities, temp. depend., IR obs. 0-53054  
 $\text{CO}_2$ , Fermi reson. effect on vibr. bands relative intensities 0-965  
 $\text{CO}_2$  gasdynamic laser, IR spectroscopic determ. of vibr. level populations 0-32952  
 $\text{CO}_2$  gasdynamic laser, vibr. temp. meas. method 0-9854  
 $\text{CO}_2$  IR Zeeman spectra utilizing copropag. wave reson., diamag. shift obs. 0-53055  
 $\text{CO}_2$  multatmosphere UV preionized laser, elec. and gain characts. 0-14313  
 $\text{CO}_2$ , vibr. excitation threshold struct., low-energy electron scatt. 0-5625  
 $\text{CO}_2$  vibrational temps. in reaction products of  $\text{CO} + \text{N}_2\text{O}$  under gasdynamic laser conditions 0-21276  
 $\text{CO}_2\text{-N}_2\text{-He}$  discharge, electron distrib. relax., numerical study 0-54070  
 $\text{C}_2\text{O}_2$ , vibr. IR spectra anal. 0-47984  
 $\text{CS}$ , vibr. states in RF discharge plasma, microwave spectrosc. obs. 0-14133  
 $\text{CS}_2$ , liq., props. from allowed light scatt. spectra 0-25364  
 $\text{Ca}_2$ , new ground state, photolum. obs. vibr. const., dissoc. energy 0-5576  
 $\text{CaH}$ ,  $\text{D}^2\Sigma^+ - \text{X}^2\Sigma^+$  band system 0-18847  
 $\text{CeO}$ ,  $\text{C}_1\text{-X}_1$  and  $\text{D}_3\text{-X}_3$  systems, fluoresc., vibr. spectra, laser spectroscopy obs. 0-32761  
 $\text{Cl} + \text{NOCl}$ , primary and secondary photochemistry, vibrationally excited NO, IR fluoresc. obs. 0-48030  
 $\text{ClCN}$ , ground and first excited bending, vibr. state, props., mol. beam elec. reson. 0-37823  
 $\text{ClO}_2$ , laser-microwave double reson. of  $\nu_1$  band 0-48022  
 $\text{Co}$  complex,  $\text{Co}(\text{l-sparteine})\text{Cl}_2$ , IR circular dichroism spectra, vibr.-electronic interaction 0-55074  
 $\text{CoO}$ , matrix isolated IR spectra, ground state vibr. freqs. 0-28015  
 $\text{Cu}_2$ , in supersonic free jet expansion, laser induced excitation spectrum obs. 0-14151  
 $\text{D}_2$ , electron dissociative attachment rates, rot. (vibr.) excitation depend., in plasma 0-43848  
 $\text{D}_2$ , predissoc. linewidths and shapes for  $3p\pi\text{D}^1\Pi_u^+$  state 0-53066  
 $\text{DF}$ , form., initial vibr. energy distrib., IR chemiluminescence. obs. 0-45497  
 $\text{Dy}^{3+}$ , in soln., non-radiative transitions as Forster's energy transfer to solvent vibrations 0-1014  
 $\text{Eu}^{3+}$ , in soln., non-radiative transitions as Forster's energy transfer to solvent vibrations 0-1014  
 $\text{F} + \text{I}_2 \rightarrow \text{IF} + \text{I}$ , energy partitioning, vibr. populations and rot. temp., population inversion 0-50832  
 $\text{FHF}^+$ , H bonds, vibr. dynamics calcs. 0-23397  
 $\text{FeO}$ , matrix isolated IR spectra, ground state vibr. freqs. 0-28015  
 $\text{GaI}$ ,  $\text{A}^0\text{-X}^0$  and  $\text{B1-X}^0$  transitions, isotope shifts, UV and visible spectra obs. 0-53005  
 $\text{GeO}_4^{4-}$  compounds, vibr. pot. function, force const., isotopic shifts, mean vibr. amplitudes 0-23395  
 $\text{GeS}$ , band system vibr. anal. 0-48009  
 $\text{H}$  bonded  $\nu_{\text{X-H}}$  band, dynamic theories survey 0-52983  
 $\text{H}$  bonding molecules, self assoc., intermolecular interactions, matrix isolation vibr. spectra obs. Raman and IR spectra 0-52995  
 $\text{H}_2$ , electron dissociative attachment rates, rot. (vibr.) excitation depend., in plasma 0-43848  
 $\text{H}_2$ , many electron systems, chem. binding, local stresses and force densities 0-27920  
 $\text{H}_2$ , predissoc. linewidths and shapes for  $3p\pi\text{D}^1\Pi_u^+$  state 0-53066  
 $\text{H}_2$ , predissociation of  $^1\Pi_u^+$  state vibr. and rot. levels, dissoc. yields meas. 0-32784  
 $\text{H}_2$  predissociation probabilities of  $4p\pi^1\Pi_u^+ \nu \geq 1$  levels, dissoc. channels interference 0-28074  
 $\text{H}_2 + \text{He}$  (metastable), Penning ionisation (French) 0-1060  
 $\text{HCC} \rightarrow \text{H} + \text{C} \rightarrow \text{C}$  dissoci., trajectory calcs., random vibr. excitation 0-45491  
 $\text{HCP}$ ,  $\nu_3$  band, high-resolution IR absorption spectrum 0-47994  
 $\text{HCl-He}$ , discharge, possible laser action on vibr. transitions 0-14332  
 $\text{HClO}_4\text{-H}_2\text{O}$ , aq. soln., IR and Raman spectra, conc. depend. (Russian) 0-53002  
 $\text{HD}$ , predissoc. linewidths and shapes for  $3p\pi\text{D}^1\Pi_u^+$  state 0-53066  
 $\text{H}_2^+(\text{HD}^+)$ , IR photodissoc. cross sections, calc. and simulation expt. 0-9659  
 $\text{HNCS}$ , ground state spectroscopic const., microwave, millimeter and IR spectra 0-28010  
 $\text{HNO}_2$ , trans and cis,  $\nu_2$  fundamental vibrational bands, intracavity CO laser Stark spectroscopy 0-47992  
 $\text{H}_2\text{O}$ , ESCA and soft X-ray emission, vibr. excitation 0-23433  
 $\text{H}_2\text{O}^+$ , form. in  $\text{Ar}^+ + \text{H}_2\text{O}$ , kinetic and vibr. energy distrib. 0-16654  
 $\text{H}_2\text{O}^+$ , states geometries, electronic vibr. coupling const., HF calcs., comparison with X $\alpha$  calcs. 0-27946  
 $\text{HOCl}$ , photolysis product of  $\text{Cl}_2\text{-O}_3\text{-H}_2$  dil. mixtures, absolute integrated IR band intensities 0-26033  
 $\text{HOD}$ , IR spectra in  $\text{D}_2\text{O}$ , combination vibr. 0-9609  
 $\text{HPO}$ , in Ar matrix, IR and UV absorpt. spectra 0-47985  
 $\text{HfF}_4$ , mol. struct. and vibr. freqs., gaseous electron diff. obs. 0-32836  
 $\text{I}_2$ , predissociation, electric-field induced 0-37839  
 $\text{IBr-CO}_2$  photolysis, electron-vibr. pumping, 2.7  $\mu\text{m}$  Br and 4.3, 10.6  $\mu\text{m}$  CO<sub>2</sub> laser transitions 0-28196  
 $\text{IF}$  internal vibr.-rot. product distrib., formed in  $\text{F} + \text{CH}_3\text{I}(\text{CF}_3\text{I})$ , fluoresc. obs. 0-48078  
 $\text{I}_2\text{Ne}$ ,  $\text{He}$ , van der Waals complexes photodissoc. 0-50864  
 $\text{I}_2\text{X}^+\Sigma_g^+$ , collisional relax. of highly excited vibr. levels, using  $\text{I}_2$  optically pumped laser 0-43155  
 $\text{I}_2^*\text{He}$ , vibrational predissociation, van der Waals molecules, vibration-translation scaling theory 0-43135  
 $\text{InCl}$ , discharge excited spectrum 4100-3900 Å, vibr. anal. 0-32732  
 $\text{Kr}_2$ , prod. and decay of  $\text{u}^+$  and  $\text{l}_u$  states, synchrotron excited 0-43109  
 $\text{KrHCl}$ , van der Waals complexes, struct., RF and microwave spectra, isotope effects 0-37806  
 $\text{KrHCl}$ , weak complex, rot. spectra 0-52980  
 $\text{Li}_2$ , optical-optical double reson.,  $^1\Sigma_g^+$  state mil. const. 0-53027  
 $\text{Mn}^{2+}$ , in soln., non-radiative transitions as Forster's energy transfer to solvent vibrations 0-1014

## molecular vibration continued

- $\text{Mo}_2$ , matrix isolated visible absorpt. spectra, electronic, vibronic and vibr. states 0-28027  
 $\text{MoN}$ , matrix isolated visible absorpt. spectra, electronic, vibronic and vibr. states 0-28027  
 $\text{MoO}$ , matrix isolated visible absorpt. spectra, electronic, vibronic and vibr. states 0-28027  
 $\text{Mo}_2[(\text{CH}_2)_2\text{P}(\text{CH}_3)_2]_2$ ,  $\delta\text{-}\delta^*(^1\text{A}_{2u}\text{-}^1\text{A}_{1g})$  transition, vibr. struct. anal. 0-53006  
 $\text{N}^{2+}$ , spectral line breadth in molecular nonequilibrium plasma (Russian) 0-48044  
 $\text{N}_2$ ,  $3\sigma_g$  photolysis, shape-reson.-induced non-Franck-Condon vibr. intensities 0-43120  
 $\text{N}_2$  arc plasma, stabilised by gas injection, thermochem. nonequil., particle excitation, vibr. temps. 0-19634  
 $\text{N}_2$ , electrical discharge excitation, vibr. level population distrib., electron beam fluoresc. obs. 0-48031  
 $\text{N}_2$ , electron impact, electron distrib. function in laser radiation field, vibr. excitation influence 0-28112  
 $\text{N}_2$ , electron impact, reson. vibr. excitation, ab initio R matrix calc. 0-32842  
 $\text{N}_2$ , electron impact enhanced vibr. excitation, continuum multiple scatt. model with Hara exchange approx. 0-43196  
 $\text{N}_2$ , K-shell, excitation and ionisation, vibr. struct., electron energy loss spectra obs. 0-18943  
 $\text{N}_2$ , light polarisability parameters, Raman scatt. ang. meas. 0-37814  
 $\text{N}_2$ , matrix isolated, fundamental vibr. Raman spectra 0-272  
 $\text{N}_2$ , N K-shell excitation, high-resolution electron energy loss spectra 0-53152  
 $\text{N}_2$  positive column, superelastic collisions and electron distrib. function 0-1858  
 $\text{N}_2$ , vibr. temp. meas. in  $\text{CO}_2$  fast flow laser 0-32955  
 $\text{N}_2$ , vibration stimulated Raman scatt., four photon parametric effects 0-33087  
 $\text{N}_2\text{-CO}$ , electrical discharge excitation, vibr. level population distrib., electron beam fluoresc. obs. 0-48031  
 $\text{N}_2\text{-CO}_2\text{-(He)}$  volume discharge,  $\text{N}_2$  vibr. levels, stepwise excitation, effect on electron energy balance 0-54071  
 $\text{N}_2 + \text{H}^+(\text{e})$ , vibrational  $\text{N}_2^+$  excitation (Russian) 0-53156  
 $\text{ND}_2(\text{NH}_2)$ ,  $\nu_2$  band, laser mag. reson., 9-10 micron 0-9601  
 $\text{NF}_2$ , IR spectra,  $\nu_1$  and  $\nu_2$  bands, vibr. excitation and spin-rot. interaction, doublet splitting 0-28011  
 $\text{NH}_2$  ( $\text{A}^2\text{A}_1$ ), excited state dynamics and bimol. quenching processes 0-9681  
 $\text{NH}_2$  fragment internal energy distrib. in  $\text{NH}_3$  UV laser photodissoc. 0-11901  
 $\text{NH}_3$ , ESCA and soft X-ray emission, vibr. excitation 0-23433  
 $\text{NH}_3$ , inversion spectra,  $\nu_4$  state 0-47965  
 $\text{NH}_4(\text{NH}_3)_n^+$ ,  $n=0$  to 4, gas phase IR spectra 0-43044  
 $\text{NH}_2(\text{X}^2\text{B}_1)$  radical, and  $\text{ND}_2$ , ionisation pot., vibr. anal., ab initio calcs. and vacuum UPS obs. 0-53047  
 $\text{NO}$ , N K-shell excitation, high-resolution electron energy loss spectra 0-53152  
 $\text{NO}$ , Q-branch spectra, external-resonator controlled Raman laser pumped by CW CO laser 0-9624  
 $\text{NO}$ , UV fluorescence, IR laser induced 0-53032  
 $\text{NO}$ ,  $\text{X}^2\Pi(\nu=0)$ , ionis. energies to  $\text{NO}^+ \text{X}^1\Sigma^+(\nu=0-34)$ ,  $\text{NO}^+$  mol. const., UPS obs. 0-14177  
 $\text{NO}_2$ , excited, fluoresc. spectrum, IR multiphoton vibr. pumping, photon absorpt. probability distrib. study 0-18854  
 $\text{NO}_2$ , aq. soln., vibr. width and dephasing, conc. depend. 0-43029  
 $\text{N}_2\text{O}$ , N K-shell excitation, high-resolution electron energy loss spectra 0-53152  
 $\text{N}_2\text{O}$  quadrupole hyperfine struct., vibr. depend. obs. using twin-laser spectrometer 0-43097  
 $\text{NaH}$ ,  $\text{A}^2\Sigma^+ - \text{X}^2\Sigma^+$  electronic transition, spectroscopic anal. and potential energy curves 0-48102  
 $\text{Ni}$  complex,  $\text{Ni}(\text{l-sparteine})\text{Cl}_2$ , IR circular dichroism spectra, vibr.-electronic interaction 0-55074  
 $\text{Ni}_2$ , A-X system, Ar matrix isolation fluoresc. spectrosc. obs. 0-9628  
 $\text{NiBr}$ , band system in near UV, vibr. analysis 0-32733  
 $\text{NiO}$ , matrix isolated IR spectra, ground state vibr. freqs. 0-28015  
 $\text{O} + \text{O}_2$  reaction, vibr. enhancement 0-30215  
 $\text{O}_2$ ,  $\text{C}^3\Delta_u - \text{a}^1\Delta_g$  band system, vibr. anal. 0-5556  
 $\text{O}_2$ , electron impact vibr. excitation, direct and stepwise, rate coeffs. 0-5630  
 $\text{O}_2$ , K-shell, excitation and ionisation, vibr. struct., electron energy loss spectra obs. 0-18943  
 $\text{O}_2$ , light polarisability parameters, Raman scatt. ang. meas. 0-37814  
 $\text{O}_2^+$ , electron impact dissoci. recomb., pot. energy curves calcs. 0-53150  
 $\text{O}_3$ , photolysis, primary products electronic and vibr. state distrib. 0-50865  
 $\text{OCS}$  in Ar soln., IR spectra, solvent shifts, vibr. band assignment and anharmonic force const. 0-9607  
 $\text{OH}$ ,  $\text{A}^2\Sigma^+ - \text{X}^2\Pi$  system, vibrational and rotational levels, transition probability determ. 0-43034  
 $\text{O}_2(\text{c}^3\Sigma_u^-)$ , in  $\text{Ar}(\text{Kr})(\text{Ar-Kr})$  matrices, multiphonon vibr. relax. time-resolved emission obs. 0-18861  
 $\text{PF}_2\text{H}(\text{D})$ , vibr. spectra and normal coordinate anal., Raman and IR spectra 0-14147  
 $\text{PO}$ , in Ar matrix, IR and UV absorpt. spectra 0-47985  
 $\text{POF}_3$ , level anticrossing effects, vibr., laser Stark spectra obs. 0-32771  
 $\text{Pd}$  complex,  $\text{Pd}^{\text{II}}(\text{CNCH}_3)_4(\text{PF}_6)_2$ , vibr. spectra, M-M bonds. (French) 0-47997  
 $\text{Pt}$  complex,  $\text{Pt}^{\text{II}}(\text{CNCH}_3)_4(\text{PF}_6)_2$ ,  $\text{Pt}_2^{\text{II}}(\text{CNCH}_3)_6(\text{PF}_6)_2$ , and  $\text{Pt}^{\text{II}}\text{Pd}^{\text{II}}(\text{CNCH}_3)_6(\text{PF}_6)_2$ , vibr. spectra, M-M bonds. (French) 0-47997  
 $\text{SF}_6$  and  $\text{S}_2\text{F}_{10}$ , absorpt. of intense laser radiation, vibr. excitation 0-9667  
 $\text{SF}_6$ , high-resolution IR Ar matrix-isolation spectra, 10K 0-32708  
 $\text{SF}_6$ , highly excited, time-resolved IR absorpt. obs. 0-9666  
 $\text{SF}_6$ , intramode anharmonicity const., vibr. linear absorpt. spectrum 0-18893  
 $\text{SF}_6$ , laser-irrad., high-resolution double-reson. spectroscopy, collisionless multiphoton dissoci. 0-9623  
 $\text{SF}_6$ , molecular vibration energy stochasticization in intense IR laser field by Raman spectroscopy (Russian) 0-14149  
 $\text{SF}_6$ , multiphoton absorpt., pulsed  $\text{CO}_2$  laser radiation absorpt., press., freq., fluence depend. 0-28080  
 $\text{SF}_6$ , multiphoton dissoci., classical model 0-53076  
 $\text{SF}_6$ ,  $\nu_3$  bands, rot. fine struct., HFS spectroscopic const. determ., saturation spectroscopy obs. 0-53008  
 $\text{SF}_6$ , photon-enhanced dissociative electron attachment 0-9749



**molecular vibration continued**

- $\text{SF}_6$ , photon-enhanced dissociative electron attachment, isotope selectivity 0-18939  
 $\text{SF}_6$ , vibr. spectra, rot. consts., IR spectra, Raman spectra obs. 0-32719  
 $(\text{SN})_n^*$  radicals polymerisation to  $(\text{SN})_x$  in thin films, optical spectra 0-16656  
 $\text{SO}_2$ , laser-induced phosphoresc.-excitation spectra of vibr. bands of  $(^3\text{B}_1)-(X, ^1\text{A}_1)$  transition 0-18879  
 $\text{SiO}$  in Ar matrix, vac. UV spectrum, vibr. progression 0-23432  
 $\text{SiO}_4^{4-}$  compounds, vibr. pot. function, force consts., isotopic shifts, mean vibr. amplitudes 0-23395  
 $\text{TiF}_4$ , equilib. config., force field, Coriolis consts., vibr. freqs. and amplitudes 0-32835  
 $\text{UF}_6$ , room temp., IR absorpt. obs., isotope shift of fund. band and combination bands, freq. depend. 0-23421  
 $\text{XeF}$ , ground state dissociation, vibr. equilibrium 0-9652  
 $\text{XeF}$ , supersonic expansion jet,  $\text{B}_2-X$  system rot. and vibr. anal., isotope intervals, fluoresc. spectra 0-14174  
 $\text{Yb}^{3+}$ , in soln., non-radiative transitions as Forster's energy transfer to solvent vibrations 0-1014  
 $\text{Zn}$  complex,  $\text{Zn}(\text{l-sparteine})\text{Cl}_2$ , IR circular dichroism spectra, vibr.-electronic interaction 0-55074  
 $\text{ZrF}_4$ , mol. struct. and vibr. freqs., gaseous electron diffraction obs. 0-32836  
 $\text{ZrO}$  bands, integrated intensity meas. and effective vibr. temp. 0-43111

**molecular vibration calculations**

- ab initio CI pot. curves, mol. wavefunctions and vibr. freqs. comparison of methods 0-27956  
 acetylene, core ionised, core-excited and shake-up states, ab initio MRD-CI methods 0-42950  
 alkali metal dicarboxylates, H bonding and motion, incoherent inelastic neutron scatt. spectroscopy 0-48095  
 n-alkanes, longitudinal acoustic modes, Raman intensities 0-32718  
 alkenes, IR absorpt. curves calc. using standard fragments computer library 0-982  
 atom+triatomic collisional energy transfer, ergodicity in mol. vibr., Henon-Heiles pot. 0-18906  
 p-benzoquinones, chlorinated, transferable force field for in-plane vibrs. 0-964  
 biphenyl, diamagnetism and thermal motion 0-25076  
 boron trihalides, mol. force field using parametric represent. method 0-27991  
 $\text{C}_{3v}$  symmetry excited vibr. state mol. consts., graphical method 0-52969  
 cellulose macromolecule, conform. states and IR dichroism calcs. 0-55986  
 chemisorbed molecule, vibr. freq. rel. to interaction with surface 0-54519  
 1-chloro-2-methylbutane, conformer depend. C-Cl stretching vibrs., Raman optical activity spectrum simulation 0-14146  
 classical model for vibr. transition dynamics, absorpt. of IR radiation 0-52965  
 coupled isotope effects in exchange reactions, vibr. freq. and atomic masses 0-18843  
 cyclopentene, mol., pot. functions of bending modes 0-9753  
 1,1-cyclopropane- $\text{d}_2$ , isomerisation transient vibr. energy distrib., collisional relax., variable encounters method 0-50836  
 diatomic molecule, vibr. Green's function and two-photon dissociation, appl. to  $\text{H}_2^+$  0-28075  
 diatomic molecule, vibrational transitions, Franck-Condon matrix elements 0-9645  
 2,5-dihydrofuran, mol., pot. functions of bending modes 0-9753  
 N,N-dimethyl acrylamide ( $-\text{d}_3, \text{d}_6, \text{d}_9$ ), force field, IR and Raman spectra obs. 0-47979  
 dimethyl di(trifluoromethyl) germanium, and perdeuterated analogues, vibr. spectra, normal coord. anal. (German) 0-5547  
 N,N-dimethylselenourea, deuterated forms and methyl derivatives, fundamental IR vibr. assignments 0-961  
 N,N-dimethylthiourea, deuterated forms and methyl derivatives, fundamental IR vibr. assignments 0-961  
 1,4-dioxadiene, mol., pot. functions of bending modes 0-9753  
 DNA, backbone vibrational mode displacements of A-DNA and B-DNA 0-8000  
 energy level clustering, qualitative theory of irreducible tensor operators spectra 0-28001  
 energy transfer, classical versus quantum calcs., forced quantum oscillator and moment methods 0-28095  
 ethane ( $-\text{d}_4, \text{d}_3, \text{d}_1$ ), electro-optical parameters from IR intensities, least-squares calc. 0-9584  
 ethylene, core ionised, core-excited and shake-up states, ab initio MRD-CI methods 0-42950  
 ethylene, Hartree-Fock energy and Moller-Plesset perturbation energy, harmonic vibr. freq. 0-52852  
 fluorinated ethylenes, valence bond polar parameters, IR intensities, MO calc. 0-28013  
 fluoromethane- $\text{d}_2$ , matrix isolated, vibr. energy transfer at low temps. 0-37860  
 force field determination, Green's function method, ambiguities 0-960  
 formaldehyde, adiabatic CI pot. surface LCAO calc., gradient determ., mol. dynamics, vibr. freqs. 0-48056  
 formaldehyde, vibrational band intensities of  $^1\text{A}_2-^1\text{A}_1$  transition, ab initio calc. 0-43028  
 formyl fluoride, and isotopic forms, mol. struct., from electron diffraction and microwave data 0-23570  
 four centre elimination reactions, HX vibr. state distrib., surprisal anal. and synthesis 0-25993  
 Franck-Condon effects in resonance Raman spectra and excitation profiles, appl. to  $\text{CrO}_4^{2-}$  and  $\beta$ -carotene 0-14129  
 homonuclear molecular ions, adiabatic pot. curves 0-929  
 hydrocarbons, vibr. intensities, G sum rule appls. 0-32776  
 icosahedral cage, symmetry coords. and vibration freq. 0-47966  
 inert gas dimer ions,  $\text{A}^2\Sigma_{1/2u}^+ \rightarrow \text{D}^2\Sigma_{1/2g}^+$  system, theoretical absorption spectrum 0-32734  
 inversion splitting, generalised WKB method 0-9585  
 isostructural molecules and ions, force const. set calcs. 0-23390  
 L-F approximation method extension HLFS applicability, appl. to  $\text{CF}_3\text{Cl}$ ,  $\text{CF}_3\text{Br}$  and  $\text{CF}_3\text{I}$  0-962  
 linear molecule in reson. light field, bending vibr. 0-968  
 methane ( $-\text{d}_1, \text{d}_3, \text{d}_4$ ), electro-optical parameters from IR intensities, least-squares calc. 0-9584  
 methyl formate ( $-\text{d}_1, \text{d}_3, \text{d}_4$ ), mol. vibr. spectrum, struct., beginning with PCILO calc. (French) 0-23401

**molecular vibration calculations continued**

- methyl halides, force consts. evaluation using gp. vibrs. and centrifugal distortion consts. 0-9580  
 methyl torsion modes, vibrational optical activity, inertial contrib. 0-5524  
 methyl tri(trifluoromethyl) germanium, and perdeuterated analogues, vibr. spectra, normal coord. anal. (German) 0-5547  
 methylene radical, classical stretching dynamics 0-23400  
 molecular spectroscopy book 0-27051  
 molecular spectroscopy book 0-27052  
 molecular vibration excitation on resonant electron scatt., time-perturbation method (Russian) 0-14242  
 multicomponent polyanions,  $\text{PMo}_3\text{O}_{14}$  model vibr. freqs. 0-23408  
 N=3 eigenvalue problem, appl. to XYZ bent mols. (German) 0-14131  
 nonequilibrium dissociation, Morse oscill. rigid rotator system, master eqn. soln. 0-40682  
 normal coordinate calcs., computer program for Z-matrix determ. 0-23388  
 NQR freq. anomalous positive temp. coeff., vibr. depend. 0-53016  
 phenanthrene, planar normal vibrs. calcs. 0-5525  
 point groups, continuous, characters and representations 0-36809  
 point groups, continuous, reduction of representations 0-36808  
 point groups, continuous, reduction of representations 0-36810  
 polyatomic molecule, SCF-SI theory applic. to coupled vibr. motion 0-23399  
 polyatomic molecule, vibr. struct. of electronic spectra, FORTRAN programs 0-32699  
 polyatomic molecules, applic. of classical perturbation theory of good action-angle variables 0-23481  
 polyatomic molecules, two-parameter intramol. distrib. and props. 0-47967  
 polyatomic mols., nuclear charge model and valence force consts. prediction 0-43022  
 polyatomic  $\text{XY}_3$  type molecules, vibr. assignment using Redington's method 0-23410  
 polyatomics, restricted intramolecular vibr. relax. and laser selective effects 0-27992  
 polyatomics, Wilson GF matrix method 0-9578  
 porphyrins, reson. Raman spectra, selection rules, normal coord. treatment 0-53175  
 predissociating harmonic oscillator, relative line widths and level shifts 0-23469  
 pyramidal  $\text{XY}_3$  molecules, mol. geometry calcs. using centrifugal distortion const. 0-18841  
 Raman scatt. theory, vibr. state summation, polarisability tensor upper and lower bounds 0-48000  
 rigid-body molecules, diamagnetism and thermal motion 0-25076  
 small mol. electro-optical parameters, dipole moment derivatives, vibr. calc. valence-optical theory 0-23406  
 spherical top molecules, fluid vibr. spectra, repulsive force depend. line broadening (Russian) 0-47970  
 statistical mechanics, flexible vs. rigid constraints 0-31658  
 symmetry group of nonrigid molecules, completely reduced representation 0-9587  
 symmetry properties of non-rigid molecules, unified approach 0-1083  
 tetrachloromethane, fluid vibr. spectra, repulsive force depend. line broadening (Russian) 0-47970  
 tetrahalides of Gp.IV elements, M-X bond flexibility, by compliance scheme 0-37805  
 tetrahedral molecules, vibr., charge and charge flux 0-47961  
 s-tetrazine, mol., pot. functions of bending modes 0-9753  
 transition moments, vibrational, of diatomic and polyatomic mols., elec. and mech. anharmonicity influences 0-23459  
 triatomic nonlinear mols., stretching vibrs., partial Morse oscills. 0-967  
 trifluoromethyl trimethyl germanium (tin)(lead), and perdeuterated analogues, vibr. spectra, normal coord. anal. (German) 0-5547  
 van der Waals dimers, intramolecular vibr. dynamics, vibr. predissociation 0-28083  
 wave functions, semiclassical Gaussian basis set method 0-9583  
 $\text{XY}_2$  molecules, nonlinear, inertia defects and dipole moments by kinetic consts. method 0-928  
 $\text{XY}_2$ -type bent symmetric mols., vibr. anal., kinetic consts. method 0-18838  
 $\text{XY}_3$  pyramidal-type mols., mol. consts., kinetic consts. and L-approx. methods 0-18839  
 ZXF $_5$ , heavy central atom, vibr. mean amplitudes and mol. geometry, charact. vibr. method 0-5522  
 $[\text{B}_{12}\text{H}_{12}]^{2+}$ , icosahedral cage, symmetry coords. and vibration freq. 0-47966  
 $\text{AlCl}$ , A-X system, vibr. anal. 0-23394  
 $\text{ArBr}$ , pot. curves, population distrib. and chemiluminesc. for  $\text{B}(1/2)$  and  $\text{C}(3/2)$  electronic states 0-45509  
 $\text{ArH}^+$ ,  $\Sigma^+$  ground state, molecular consts. calc. from pot. curves 0-9680  
 $\text{Ar}^+ + \text{N}_2 \rightarrow \text{Ar} + \text{N}_2^+$ , electronic to vibr. energy transfer, time depend. theory 0-23514  
 $\text{AsF}_3$ , mol. geometry calcs. using centrifugal distortion const. 0-18841  
 $\text{BI}$ , mol. force field using parametric represent. method 0-27991  
 $\text{CO}$  in Ar matrix, vibr. freq. shift and interaction pot., force-field calcs. 0-47958  
 $\text{CO}$ , vibr. struct., core and valence ESCA spectra, Franck-Condon and HF anal. 0-32602  
 $\text{CO}_2$  conc. and temp. in flames, Raman spectroscopy 0-32720  
 $\text{CO}_2$  laser resonator, gasdynamic, optimal parameters determ. from vibr. energy exchange kinetics 0-14317  
 $\text{CO}_2$ , low energy electron scatt. cross sections, vibr. excitation, Boltzmann eqn. 0-18942  
 $\text{CO}_2$ , nonbending, vibr. motion calc. using SCF-SI theory 0-23399  
 $\text{C}_2\text{O}_2$ , mol., pot. functions of bending modes 0-9753  
 $\text{C}_2\text{O}_2$ ,  $\nu_7$  vibrational states, rigid-bender model 0-47964  
 $\text{COF}_2$ , force field analysis using parametric represent. method 0-27990  
 COS, mole. potential surface, evaluation from spectroscopic observations 0-43207  
 $\text{CS}_2$ , symmetric stretch mode, moments and polarisability derivatives, SCF calcs. 0-901  
 $\text{ClO}_2\text{F}$ , pyramidal type mol., force field comput. using Green's function procedure 0-23407  
 $\text{D}_3^+$ , ab initio vibr. intervals and vibr. freq. refinement 0-47968  
 $\text{GeH}_3$ -group containing mols., normal coord. anal. 0-9579  
 $\text{H}_2$ , ground state, vibr. eigenenergies, functional form 0-27998  
 $\text{H}_2^+$ , electron cooling through resonant collisions 0-32845  
 $\text{H}_3^+$ , ab initio vibr. intervals and vibr. freq. refinement 0-47968



**molecular vibration calculations continued**

- HBS, and isotopic forms, force consts., coriolis consts., vibr. amplitudes, shrinkage effects 0-43021  
 HN<sub>3</sub>, ground 'A' state, SCF and CI calcs., conform., geom., vibr. freqs. and dissoc. 0-18806  
 H<sub>2</sub>O, energy levels, triat. large amplitude vibrs. model appl. 0-23392  
 H<sub>2</sub>O, slow electron scatt., rigid mol. model with exchange and polarisation, vibr. excitation, dissoc. attachment 0-43194  
 H<sub>2</sub>O, vibr. motion, local- vs. normal-mode description 0-5521  
 H<sub>2</sub>S, slow electron scatt., rigid mol. model with exchange and polarisation, vibr. excitation, dissoc. attachment 0-43194  
 HeI<sub>2</sub>, Van der Waals mol. vibr. predissoc. anharmonicity effects 0-52971  
 Li<sub>2</sub>n<sup>+</sup> (n=1, 2, 3), stable cluster configs., ionisation pots., binding energies, vibr. freqs., ab initio SCF and CEPA calcs. 0-14265  
 MgX<sub>2</sub> (X=F, Cl, Br, I), 2Z 0-43021  
 N<sub>2</sub>, electron impact rot. and vibr. excitation, elastic scatt., close coupling and Born approx. 0-28108  
 N<sub>2</sub>, vibr. struct., core and valence ESCA spectra, Franck-Condon and HF anal. 0-32602  
 ND<sub>3</sub>, inversion splitting, generalised WKB method 0-9585  
 NH<sub>3</sub>, IR absorption band integrated intensities, ab initio and LMO studies 0-23458  
 NH<sub>3</sub>, inversion splitting, generalised WKB method 0-9585  
 NH<sub>4</sub>Cl, gas 'A<sub>1</sub>' ground state, pot. surface 0-32626  
 Ne<sub>2</sub>, vibr. spectra, calc. from pot. curve 0-1040  
 OH, A-X system, rot. transition probabilities 0-43027  
 PF<sub>3</sub>, mol. geometry calcs. using centrifugal distortion const. 0-18841  
 (SCN)<sub>2</sub>, and (SCN)<sub>3</sub>, vibr. anal., bond strengths 0-9582  
 S<sup>16</sup>O<sub>2</sub>(S<sup>18</sup>O<sub>2</sub>), 'B<sub>2</sub>'('A') state, force field for large amplitude motions 0-43023  
 Si<sub>2</sub>F<sub>6</sub>, normal coord. analysis, vibr. freqs. and amplitudes, shrinkage and distortion consts., force consts. 0-27989  
 SiH<sub>3</sub> group containing mols., normal coord. anal. 0-9579  
 WO<sub>3</sub>, vibr. anal., mol. consts., kinetic consts. method 0-23393

**molecular vibration in solids**

- adipic acid crystals, H bonds, harmonic couplings, IR vibr. modes, isotope effect origin 0-34902  
 adsorbed molecules on solid surface, effect on electron capture by deep levels 0-29458  
 alkali hexahalogeno compounds: ReCl<sub>6</sub><sup>2-</sup>(ReBr<sub>6</sub><sup>2-</sup>), low symm. splittings in vibronic spectrum due to phase transitions 0-55161  
 alkali metal tetrafluoroborates, intramol. force fields and mean vibr. amplitudes 0-2743  
 alkali tetrafluoroaluminates, matrix isolated IR spectra 0-985  
 anharmonic molecules in condensed media, vibronic dephasing, intra- and intermolecular processes 0-2127  
 anharmonic molecules in low temp. matrices, vibronic dephasing 0-6469  
 L-ascorbic acid, cryst. isolated OH oscillators, IR absorption, temp. and H-bond effects 0-7351  
 chloromethyl formate(-d<sub>1</sub>,d<sub>2</sub>,d<sub>3</sub>), gas, solid, and liq., IR spectra assignments and struct. 0-32715  
 m-chloronitrobenzene, cryst., low freq. vibrs., polarised Raman and IR spectra study (French) 0-16029  
 m-chloronitrobenzene, molecular crystals, translational and orientational vibr. determ. 0-55103  
 cyclobutane-d<sub>0</sub>(d<sub>8</sub>), cryst. modifications, low. freq. Raman and IR spectra 0-7342  
 gamma-ray resonant scatt. cross section frequency of normal modes 0-18060  
 α-glycine, deuterated, low freq. intermol. modes, neutron diffr. obs. 0-15086  
 ice, IV, 4000-400 cm<sup>-1</sup> IR spectra, H-bonding and assignments, orientational disorder 0-16022  
 ice VI, OH stretching peak freq. press. depend., Raman spectra using diamond anvil cell 0-16023  
 inorganic molecular crystals, metal complexes electronic spectra and intermolecular interactions 0-55137  
 magneto-optical effect in cryst. 0-45043  
 malononitrile, dispersive phase transition, 294.7K, Raman and Brillouin-Rayleigh scatt. obs. 0-16047  
 methane, solid, Raman spectra and II-III phase transition 0-2745  
 methyl ammonium chloride, Raman spectra, 70 to 300K, H stretching vibrs. 0-20628  
 molecular crystals, two particle exciton-phonon interactions, optical absorpt. line shapes theory 0-55120  
 [n]-Jalkanes, cryst., vibr. correl. splitting and chain packing 0-7338  
 naphthalene, vibr. dephasing and Raman active localised internal mode temp. depend. 0-45060  
 NQR, NMR and EPR, spectral parameters, influence of mol. motion dynamics, review 0-20486  
 palladium porphyrin, in n-alkane crystal, Zeeman and crystal field effects, absorpt. vibr. anal. 0-7372  
 perovskite, ordered, A<sub>2</sub>BMO<sub>6</sub> type, MO<sub>6</sub> octahedra, mean vibr. amplitudes (German) 0-54320  
 phenol, cryst., mol. vibrs., factor group splittings 0-16021  
 polyacetylene, doped and neutral, resonance Raman scatt. 0-55107  
 polystyrene amorphous film, cyclically fatigued, molecular behaviour 0-35310  
 polystyrene and model cpds., conformational struct. influence on normal modes of benzene ring, Raman study 0-14144  
 potassium hydrogen oxalate, oriented single cryst., Raman spectra with very strong H-bonding 0-25359  
 potassium oxalate, anhydrous, phase II, vibr. spectra and cryst. struct. 0-34901  
 radiative electronic transitions of impurities, effects of hydrostatic press. 0-11446  
 resonance Raman scattering, appl. to ultrafast dephasing and relax. obs., phonon scatt. effects 0-7337  
 sodium acetate trihydrate, press. depend. of methyl tunnelling motion 0-10603  
 sodium hydrogen oxalate monohydrate, oriented single cryst., Raman spectra with very strong H-bonding 0-25359  
 stability constraints on potential function and rotational invariance in external mode formalism 0-24543  
 stearyl alcohol, H bonding effects on skeletal optical and longitudinal acoustical modes 0-34914  
 surface vibrational spectroscopy using stimulated Raman scatt. 0-38062  
 TCNQ salt, MTPA (TCNQ)<sub>2</sub>, IR refl., dielec. function and cond. 0-34924

**molecular vibration in solids continued**

- TCNQ salts, anomalous infra-red activity and the determination of electron-molecular vibration coupling constants 0-25389  
 TEA(TCNQ)<sub>2</sub>, elec. cond. and thermoelec. power under hydrostatic press. 0-11024  
 tetrabromomethane, in disordered phases, IR active mode Raman line shape, dipole-dipole interaction 0-9603  
 tetrafluoromethane, in disordered phases, IR active mode Raman line shape, dipole-dipole interaction 0-9603  
 thiourea, phonon modes near phase transitions, IR and Raman spectra 0-45084  
 TTF and derived cpds., intramolecular vibrs. and vibronic effects, IR and Raman spectra 0-25387  
 TTF halides, charge transfer effect on internal modes, Raman scatt. 0-25392  
 TTF-Cu bis-dithiolene, dimer, mol. displacements at 4.2K 0-10539  
 TTF-TCNQ, anharmonic props., temp. (press.) depend., rel. to naphthalene and anthracene 0-15200  
 TTF-TCNQ, charge transfer determ. from spectral line shift using Raman scatt. 0-25392  
 TTF-TCNQ, electron-molecular distortion coupling near Peierls transition, IR spectra obs. 0-25390  
 xanthene dyes, hidden vibr. band determ. method, fluorescence and excitation spectra meas. 0-40158  
 AgClO<sub>3</sub>, mol. torsional oscills., cooperative study by NQR 0-25244  
 AgNa(NO<sub>2</sub>)<sub>2</sub>, ferroelectric transitions, group theoretic comparison with NaNO<sub>2</sub> 0-7311  
 β-Al<sub>2</sub>O<sub>3</sub>, stoichiometric, Raman and IR spectra, Frenkel defects, order-disorder transition and cation cond. 0-55086  
 BaTiO<sub>3</sub>, OH<sup>-</sup> impurity IR spectra obs. 0-20679  
 Ca(ClO<sub>4</sub>)<sub>2</sub>, mol. torsional oscills., cooperative study by NQR 0-25244  
 CdS<sub>1-x</sub>Se<sub>x</sub> film, resonance between Se atom dipole vibr. and interference modes, IR spectra obs. (Russian) 0-2888  
 Cl<sub>2</sub>, Ar matrix, vibronic dephasing 0-6469  
 CsUO<sub>2</sub>(NO<sub>3</sub>)<sub>3</sub>, <sup>15</sup>N isotope shifts in electronic spectrum, internal mode identification 0-55098  
 Cu(ClO<sub>4</sub>)<sub>2</sub>, mol. torsional oscills., cooperative study by NQR 0-25244  
 DF, cryst., Raman spectra 0-55075  
 DI, crystalline, Raman and IR spectra, mol. vibr., libration and translation 0-2757  
 Dy<sub>2</sub>(SeO<sub>4</sub>)<sub>3</sub>·8H<sub>2</sub>O, thermal decomp. and IR spectra 0-3319  
 Er<sub>2</sub>(SeO<sub>4</sub>)<sub>3</sub>·8H<sub>2</sub>O, thermal decomp. and IR spectra 0-3319  
 Fe hexacyanoferrates, M<sub>4</sub>Fe(CN)<sub>6</sub>·nH<sub>2</sub>O, Mossbauer and IR spectra 0-2739  
 FeCO<sub>3</sub>, vibronic coupling at Neel temp. 0-15491  
 H<sub>2</sub>Co(CN)<sub>6</sub>, strong NHN hydrogen bond, vibr. lattice and mol., incoherent inelastic neutron scatt. 0-39232  
 HF, cryst., Raman spectra 0-55075  
 HI, crystalline, Raman and IR spectra, mol. vibr., libration and translation 0-2757  
 Ho<sub>2</sub>(SeO<sub>4</sub>)<sub>3</sub>·SH<sub>2</sub>O, thermal decomp. and IR spectra 0-3319  
 KClO<sub>4</sub>·MnO<sub>4</sub><sup>-</sup>, reson. Raman excitation profiles for totally symmetric mode, vibronic struct. 0-50309  
 K<sub>2</sub>Co(CN)<sub>6</sub>, <sup>59</sup>Co quadrupole coupling const., temp. depend. 0-44557  
 K<sub>4</sub>Fe(CN)<sub>6</sub>·3H<sub>2</sub>O, C-N vibrs., Raman study 0-40106  
 KReO<sub>4</sub>, vibr. spectrum, Raman and IR spectra obs. 0-55104  
 K<sub>3</sub>(UO<sub>2</sub>)<sub>2</sub>F<sub>7</sub>·2H<sub>2</sub>O, single cryst., polarised Raman spectra, vibr. modes assignment (French) 0-29728  
 Lu<sub>2</sub>(SeO<sub>4</sub>)<sub>3</sub>·8H<sub>2</sub>O, thermal decomp. and IR spectra 0-3319  
 N<sub>2</sub>, solid, Raman spectroscopy up to 374 kbar 0-7353  
 NaClO<sub>3</sub>, mol. torsional oscills., cooperative study by NQR 0-25244  
 NaNO<sub>2</sub>, ferroelectric transitions, group theoretic comparison with AgNaNO<sub>2</sub> 0-7311  
 O<sub>2</sub>(c'<sup>2</sup>Σ<sub>u</sub><sup>-</sup>), in Ar(Kr)(Ar-Kr) matrices, multiphonon vibr. relax., time-resolved emission obs. 0-18861  
 PF<sub>3</sub>H(D), Raman and IR spectra 0-14147  
 PH<sub>3</sub>, liq. and solid, Raman spectra, vibr. correl. functions, rot. motions 0-55087  
 PHD<sub>2</sub>, vibr. dephasing in liq. and solid PD<sub>3</sub>, calcs. 0-19884  
 Pd-Au:H<sub>2</sub>(D<sub>2</sub>), thermodynamic props. at 555 and 700K, vibr. freqs. and excess entropies 0-29186  
 Pt complex, [Pt(en)]<sub>2</sub>[Pt(en)<sub>2</sub>Cl<sub>2</sub>](ClO<sub>4</sub>)<sub>4</sub>, reson. Raman spectra 0-2760  
 ReBr<sub>6</sub><sup>2-</sup> doped K<sub>2</sub>PtCl<sub>6</sub> type crystals, vibronic side band intensity distrib., Γ<sub>7</sub>(<sup>2</sup>T<sub>2g</sub>)→Γ<sub>8</sub>(<sup>4</sup>A<sub>2g</sub>) transition 0-10609  
 ReCl<sub>6</sub><sup>2-</sup> doped K<sub>2</sub>PtCl<sub>6</sub> type crystals, vibronic side band intensity distrib., Γ<sub>7</sub>(<sup>2</sup>T<sub>2g</sub>)→Γ<sub>8</sub>(<sup>4</sup>A<sub>2g</sub>) transition 0-10609  
 α-S, zone-centre lattice vibrs., including hydrostatic press. effects 0-49314  
 SnS<sub>2</sub>, Mossbauer spectra, vibr. amplitudes anisotropy 0-15904  
 SnSe<sub>2</sub>, Mossbauer spectra, vibr. amplitudes anisotropy 0-15904  
 Sr(ClO<sub>4</sub>)<sub>2</sub>, mol. torsional oscills., cooperative study by NQR 0-25244  
 SrCl<sub>2</sub>·2(H<sub>2</sub>D)<sub>2</sub>O, IR and Raman spectra, force fields 0-2753  
 SrCl<sub>2</sub>·2H<sub>2</sub>O, IR and Raman spectra, force fields 0-2753  
 Tb<sub>2</sub>(SeO<sub>4</sub>)<sub>3</sub>·8H<sub>2</sub>O, thermal decomp. and IR spectra 0-3319  
 Tm<sub>2</sub>(SeO<sub>4</sub>)<sub>3</sub>·8H<sub>2</sub>O, thermal decomp. and IR spectra 0-3319  
 Y<sub>2</sub>(SeO<sub>4</sub>)<sub>3</sub>·8H<sub>2</sub>O, thermal decomp. and IR spectra 0-3319  
 Yb<sub>2</sub>(SeO<sub>4</sub>)<sub>3</sub>·8H<sub>2</sub>O, thermal decomp. and IR spectra 0-3319

**molecular vibrational energy transfer** *see* **molecular rotational-vibrational energy transfer**

**molecular vibrational relaxation** *see* **molecular rotational-vibrational energy transfer**

**molecular vibrational states** *see* **molecular vibration**

**molecular vibronic states**

- alkali metal hexahalogenostannate: ReBr<sub>6</sub><sup>2-</sup>, vibronic transition Γ<sub>7</sub>(<sup>2</sup>T<sub>2g</sub>)→Γ<sub>8</sub>(<sup>4</sup>A<sub>2g</sub>), intensity distrib. 0-45142  
 anharmonic molecules in condensed media, vibronic dephasing, intra- and intermolecular processes 0-2127  
 anharmonic molecules in low temp. matrices, vibronic dephasing 0-6469  
 anthracene, soln. and melt, second vibronic transition, spectroscopic characts., effective field dispersion calcs. 0-55102  
 benzaldehyde, electronic spectra, Cl and F substitution effects 0-23456  
 benzene, T<sub>1</sub>-S<sub>0</sub> intersystem crossing vibronic interactions IR absorpt. spectrum obs. 0-28042  
 benzene(-d<sub>1</sub>,d<sub>2</sub>,d<sub>4</sub>), two-photon <sup>1</sup>B<sub>2u</sub>→<sup>1</sup>A<sub>1g</sub> spectrum, deuterium effect 0-32788  
 benzonitrile, vibronic spectrum, semiempirical method 0-43031  
 chlorofluoromethylene radical, gas phase laser-induced fluores. spectroscopy 0-14173  
 complex molecules, vibr. spectra, stochastic description, appl. to optically active Brownian oscillator 0-52974



**molecular vibronic states continued**

coronene, luminesc., spin-orbit coupling perturbation by metal chlorides (*German*) 0-1021  
 cyclopentadienyl radical, pot. surface and vibronic states, ab initio CI calcs. 0-47897  
 diatomic molecule, semiempirical methods of calculating electron-transition moments 0-52970  
 difluorocarbene,  $A^1B_1-X^1A_1$  system spectrosc. and photophysics 0-5577  
 dimer triplet state line shape, small excitons, appl. to phenazine, naphthalene, tetrachlorobenzene 0-48041  
 exciton-phonon interaction, molecular crystal, one-dimensional model 0-24542  
 formaldehyde- $d_1$  ( $-d_2$ ), single vibronic levels, fluoresc. emission, radiative lifetimes and vibr. relax 0-23521  
 formaldehyde- $d_2$  vapour, IR-UV double resonance 0-43078  
 glyoxal ( $A_{g_g}$ ), fluoresc. quantum yields, radiative and nonradiative lifetimes 0-32759  
 haloaceneophthenes in n-heptane, quasi-line phosphoresc. spectra, vibronic spin-orbit interaction 0-43096  
 heteroaromatic molecules, planar, orientation and phosphoresc. polarisation in stretched film 0-14169  
 heterocyclic N compounds, radiationless transitions, isotope effects 0-48033  
 induced electronic transitions, radiative lifetimes, non-Condon effects 0-53051  
 inverse electronic relaxation, theory 0-23474  
 lanthanide (III) complex, octahedral, f-f transitions, mag. dipole intensities, vibronic coupling model 0-25404  
 level mixing, under electronic coupling operator 0-52968  
 metalloporphyrins, reson. Raman spectra, intra- and inter-manifold couplings interference 0-28020  
 methylene radical, vibronic bands obs. in pulsed supersonic jet 0-28024  
 methoxy radical, electronic absorpt. spectra, visible, vibr. freqs., vibronic intensities and oscill. strengths 0-28025  
 multimode Jahn-Teller effect for E-term with strong vibronic coupling, local and resonant states 0-24858  
 naphthalene, fluorescence and absorpt. spectra, deviations from Condon approx. 0-28004  
 naphthalene, soln. and melt, second vibronic transition, spectroscopic characts., effective field dispersion calcs. 0-55102  
 naphthalene, triplet state time evolution after radiationless transition, initial vibronic distrib. effects 0-23450  
 olefins, zwitterionic states, polaris. and vibronic interactions 0-32620  
 palladium porphyrin, in n-alkane crystal, Zeeman and crystal field effects, absorpt. vibr. anal. 0-7372  
 phonon-impurity interaction, molecular crystal, one-dimensional model 0-24542  
 polydiacetylene, cryst., one-dimens. conjugated semicond., vibronic coupling, Fano interference effects 0-34939  
 polyene chromophones, band broadening in electronic-vibr. absorpt. spectra 0-28003  
 polymethine cyanine dyes, vibronic energy relax., picosec. spectrosc. obs. 0-5526  
 population inversion during chemiluminesc. 0-3351  
 pyrazine, vibronic and spin-orbit coupling interaction 0-14126  
 pyrazine ( $-d_4$ ), single vibronic level fluoresc. spectra, rel. to vibronic coupling 0-28043  
 pyridine- $I_2(Br_2)$  charge transfer complexes, vibr. spectra, vibronic contrib., intensity enhancement 0-53048  
 radiationless transition rate constants, effect of geometry change in molecular vibrational promoting modes 0-5569  
 rare earth ions, ligand-induced pseudoquadrupole absorpt., vibronic contribs. 0-52978  
 satellite struct. of electron spectra, CI and vibronic coupling, dynamical calc. 0-53044  
 semiconductor, conjugated, one-dimens., vibronic coupling, Fano interference effects 0-34939  
 toluene, two-photon ionisation spectrum, of  $^1L_b-S_0$  transition 0-14180  
 transition metal complexes, ligand field spectroscopy, selection rules, intensity enhancement of forbidden transitions 0-45049  
 1,3,5-trichloro-2,4,6-trifluorobenzene radical cation,  $B^2A_2'-X^2E''$  laser-induced fluoresc. spectra 0-14172  
 triphenylene( $-d_{12}$ ), lowest  $T_1[A_2'(\pi\pi^*)]$  state vibronic coupling 0-47955  
 two-electron level with quasidegenerate levels, local phase transitions and temp. effects in lattice dynamics 0-10666  
 vibrationally coupled electronic states, radiationless decay, non-Condon effects 0-52966  
 BaO produced in Ba+SO<sub>2</sub> reaction, vibronic distrib., collisional energy depend., laser-induced fluoresc. obs. 0-11917  
 C<sub>3</sub>, Renner effect, vibronic levels and wavefunctions, ab initio variational method 0-14127  
 (CD)<sub>2</sub>, polymer, heavily doped, IR spectra, vibronic intensity enhancement 0-28124  
 CH<sub>2</sub>, photoproduct from ketene, singlet-triplet energy separation and rovibronic level obs. 0-11936  
 (CH)<sub>2</sub>, polymer, heavily doped, IR spectra, vibronic intensity enhancement 0-28124  
 C<sub>2</sub>N<sub>2</sub>, C<sup>1</sup> $\Pi_u$ -state predissoc., vibronic effects 0-28078  
 C<sub>2</sub>N<sub>2</sub>, satellite struct. of electron spectra, CI and vibronic coupling, dynamical calc. 0-53044  
 CO, A<sup>1</sup> $\Pi(\nu=1)$ , vibr. relax. by reversible intersystem crossing, fluoresc. obs. 0-14170  
 Cl<sub>2</sub>, Ar matrix, vibronic dephasing 0-6469  
 CIFCS, second excited singlet state photophysics, laser excitation obs. 0-32758  
 FeBr<sub>4</sub><sup>-</sup>, in various solvents,  $^4A_1$ ,  $^4E$  d-d band reson. Raman spectra, solvent depend., vibronic coupling 0-55085  
 FeCO<sub>3</sub>, vibronic coupling at Neel temp. 0-15491  
 H<sub>2</sub>, electron impact excited singlet-g states, optical and time resolved spectra, radiative lifetimes, quenching rates for rovibronic levels 0-23564  
 HNO, vibronic state perturbative and predissoc. mechanisms, fluoresc. excitation spectra obs. 0-9658  
 Hg, excimers, photoassoc., spectroscopy and kinetic processes of high-lying vibronic states, laser applics. 0-9649  
 KClO<sub>4</sub>MnO<sub>4</sub>, reson. Raman excitation profiles for totally symmetric mode, vibronic struct. 0-50309  
 LiO<sub>2</sub>, molecule, vibronic interaction in low-lying states, model calc. 0-32603  
 Mo<sub>2</sub>, matrix isolated visible absorpt. spectra, electronic, vibronic and vibr. states 0-28027

**molecular vibronic states continued**

MoN, matrix isolated visible absorpt. spectra, electronic, vibronic and vibr. states 0-28027  
 MoO, matrix isolated visible absorpt. spectra, electronic, vibronic and vibr. states 0-28027  
 N<sub>2</sub>, diffuse plasma, population densities of triplet states, correl. with electron impact processes 0-43966  
 N<sub>2</sub>, solid and matrix isolated mol., triplet state spectra (*Russian*) 0-5574  
 N<sub>2</sub>+He collisions, vibronic excitation, curve-crossing trajectories 0-23520  
 NH<sub>2</sub>+H rot. energy transfer in vibronic levels, absolute transfer rates 0-9701  
 PH<sub>2</sub>, X<sup>3</sup>B<sub>1</sub>-state, rot. laser mag. reson. spectrosc. 0-28038  
 SO<sub>2</sub>, nonradiative transitions and intersystem crossing rates in gas phase, theory 0-23451  
 SO<sub>2</sub>, X<sup>1</sup>A<sub>1</sub> electronic absorpt. band system, non-Condon effects study 0-18837  
 TeF, chemiluminesc. from oxidation in F<sub>2</sub>+H<sub>2</sub>Te(D<sub>2</sub>Te) emission spectrum obs. 0-43058  
 VCl<sub>4</sub>(Br<sub>4</sub>), vibronic systems, degenerate ground states, statistical sums, thermodynamic func. calcs. 0-27997  
 ZnS:Co Mossbauer source, Fe<sup>2+</sup> abnormal populations and vibronic props. 0-15912

**molecular weight**

*see also mass spectra; molecular weight determination*  
 diepoxide-diamine network polymers, chem. props. and average mol. wt. 0-37915  
 isocyanate polymers, partitioning between isotropic and anisotropic phases 0-24343  
 $\alpha$  methyl styrene-acrylonitrile, molecular mass determ., solubility studies (*German*) 0-23590  
 nylon 6, oriented glassy, mol. wt. influence on cryst. rate 0-44156  
 PMMA, partial draining of low-molecular weight polymers with flexible chains 0-23592  
 poly(aminophosphate)s, mol. wts., and cond. studies 0-14264  
 poly(ethylene oxide), partial draining of low-molecular weight polymers with flexible chains 0-23592  
 poly(N-vinylcarbazole), glass transition temp., mol. wt. relation 0-19922  
 polyazomethines, dil. soln. props. 0-19972  
 polycarbonate, effect of mol. weight on craze shape and fracture toughness 0-25858  
 polyelectrolyte complexes, nonstoichiometric water-soluble structure (*Russian*) 0-54112  
 polyethylene, partial draining of low-molecular weight polymers with flexible chains 0-23592  
 polyethylene, ultra-high modulus, drawing behaviour, effect of drawing temp. 0-35232  
 polyisobutylene, undiluted, mol. wt. influence on creep behaviour 0-45370  
 polymer, adhesion phenomena and influence of various factors, work of adhesion (*Polish*) 0-3292  
 polymer, dil. soln., light scattering charact. of thermodynamic props., solvent and mol. wt. effect 0-16717  
 polymer, glass transition temperature, rel. to mol. wt. 0-34176  
 polymer semicrystallised chains, small-angle neutron scatt., mean dimension evaluation 0-43220  
 polymer solution, intrinsic viscosity, mol. wt. and temp. dependence 0-34222  
 polymer solutions viscosity rel. to mol. mass (*Russian*) 0-2190  
 polymeric systems, fluid, rheology, characterised by mol. int. distrib., review 0-1504  
 polymers, semi-crystn., radius of gyration variation rel. to mol. wt. 0-38936  
 polysaccharide gel, anomalous behaviour of PMR line width of water (*Russian*) 0-11962  
 polystyrene, isotactic, conformation in bulk crystallised state 0-43221  
 polystyrene, partial draining of low-molecular weight polymers with flexible chains 0-23592  
 polystyrene-co-divinylbenzene microgels in dimethylformamide, diffusion coeff., viscosity and mol. wt. meas. 0-30286  
 polyvinyl acetate, partial draining of low-molecular weight polymers with flexible chains 0-23592  
 recent advances in polymer characterization by GPC 0-16740

**molecular weight determination**

*see also mass spectra*  
 acrylonitrile Na methallylsulphonate copolymer electrolytes in dimethylformamide, gel permeation chromatography appl. 0-21345  
 DNA, sedimentation constants, direct meas. by analytical ultracentrifugation (*French*) 0-8004  
 heterodisperse polymers, mol. wt. distribution and viscosity average mol. wt. 0-35530  
 mass spectrometry, current status and future trends 0-55665  
 polymer, absolute mol. wt. and mol. heterogeneity determ. from sedimentation vel. in ultracentrifugation (*German*) 0-14261

**molecule-atom collisions** *see atom-molecule collisions***molecule-ion collisions** *see ion-molecule collisions***molecule-ion reactions** *see ion-molecule reactions***molecule-molecule reactions**

*see also molecular rotational-vibrational energy transfer*  
 competitive decomposition and stabilisation models for collisional efficiency in external activation systems 0-25989  
 cosmic dust condensation onset, role of association reactions 0-26931  
 esterification kinetic study by monitoring pitch changes in cholesteric liq. cryst. solvent 0-7786  
 four centre elimination reactions, HX vibr. state distrib., surprisal anal. and synthesis 0-25993  
 intermolecular triplet excitation transfer in diffusive limit 0-28046  
 interstellar synthesis of cyanopolynes and related molecules, gas-phase form. pathways 0-12793  
 laser specific and thermal reactions classifications 0-11919  
 laser-controlled unimolecular and bimolecular processes, field-depend. rate const. 0-11906  
 metastable and unstable states relax., analytical theory of extrema 0-50829  
 methylene+H<sub>2</sub>-methane, ab initio CI calc. on SCF level, insertion reaction min. energy path 0-7774  
 micellar diffusion-controlled reaction kinetics 0-30213  
 microphysics to macrochemistry, discrete simulations, review 0-54102  
 POPOP+Ar+N<sub>2</sub>, electron beam excited, energy transfer mechanisms 0-23497



**molecule-molecule reactions continued**

- reversible bimolecular diffusion-controlled reactions, detailed equilib. principle 0-7770  
 state change collisions, attractive intermolecular forces, temp. depend. 0-23515  
 s-tetracyanobenzene+p-xylene, photoassoc., exciplex form., excitation energy and isotope depend., vibr. effects 0-55634  
 thionine triplet+haloanilines, electron transfer reaction, radical yield meas. 0-3330  
 toluene+OH, rate constant under simulated atmospheric conditions 0-50846  
 translationally driven reactions, transition state theory, cross section curve 0-26000  
 BCl<sub>3</sub>+methane reaction, laser-induced, vibr. excitation influence on reactivity, isotope selectivity 0-11921  
 Br<sub>2</sub>+acetylene, laser-induced photochemistry 0-45498  
 CO+N<sub>2</sub>O, CO<sub>2</sub> vibr. temps. under gasdynamic laser conditions 0-21276  
 Cl<sub>2</sub>+H<sub>2</sub>(H<sub>2</sub>S)(methanethiol), laser-initiated chain reactions, rates, mechanisms, chemiluminesc. obs. 0-55651  
 Fe(CO)<sub>5</sub>+O<sub>3</sub>, modulated chemiluminesc. by CO addition 0-40692  
 H<sub>2</sub>+F, collinear trajectories, statistical behaviour and detailed dynamics 0-16664  
 H<sub>2</sub>+F<sub>2</sub> chain reaction, rotational nonequilibrium mech. vibr.-rotational energy exchange effect 0-48230  
 H<sub>2</sub>+N<sub>2</sub>, nitrogen fixation, semiempirical INDO study 0-16898  
 H<sub>2</sub><sup>+</sup>+CO excited products dissociate, proton transfer dynamics, correl. diagram anal., crossed beam obs. 0-48079  
 HO<sub>2</sub>+NO laser-induced fluoresc. of NO<sub>2</sub>, quenching rate consts. and lifetimes 0-11930  
 H<sub>2</sub>O+Cl<sub>2</sub>O=HOCl, equilib. const., Fourier transform IR determ. 0-7765  
 HgBr<sub>2</sub>+N<sub>2</sub> metastables, dissociative excitation, HgBr emission intensity 0-40687  
 NO+BrO, temp. depend. kinetic study, stratospheric Br photochemistry implication 0-50866  
 NO+O<sub>3</sub>→NO<sub>2</sub><sup>\*</sup>+O<sub>2</sub>→NO<sub>2</sub>+hν+O<sub>2</sub>, chemiluminesc., translational and rot. energy effects 0-30218  
 NO<sub>2</sub>+OH+M→HNO<sub>3</sub>+M, rate constant under simulated atmospheric conditions 0-50846  
 N<sub>2</sub>O+CO, use of steady state chemical reaction for vibr. excitation of CO<sub>2</sub> and N<sub>2</sub> 0-50851  
 Ni(CO)<sub>4</sub>+O<sub>3</sub>, modulated chemiluminesc. by CO addition 0-40692  
 O<sub>2</sub>+O<sub>3</sub>, laser-induced photolysis of ozone reactions 0-11928  
 O<sub>3</sub>+O<sub>2</sub>(<sup>1</sup>Δ<sub>g</sub>)(O<sub>2</sub><sup>\*</sup>), UV photolysis, O(<sup>1</sup>P) prod., rate consts. determ. 0-55636  
 OH+H<sub>2</sub>, pot. energy surface, barrier heights and transition state geometry, POL-CI calc. 0-55649  
 OH+H<sub>2</sub>→H<sub>2</sub>O+H, rate constant, ab initio calc. 0-45478  
 SO(<sup>1</sup>Δ<sub>g</sub>), (<sup>2</sup>Σ<sub>g</sub><sup>+</sup>)+O<sub>2</sub>(<sup>1</sup>Δ<sub>g</sub>), chemiluminescence and energy pooling 0-26016  
 SiH<sub>4</sub>(SiD<sub>4</sub>)+F<sub>2</sub>, chemilum., at. absorption, and laser-induced fluoresc. obs. 0-3315  
 UF<sub>6</sub>+SiH<sub>4</sub>, photoinduced reaction in low temp. SiH<sub>4</sub> matrix 0-30256

**molecule-surface impact**

- see also sputtering  
 cyclobutene, strong collision and thermal decomp. on surface, variable encounter method calcs. 0-50885  
 metal surface, thermal negative ion production through polyatomic mol. dissociation, thermochemical study (*Japanese*) 0-50495  
 metals, atomic and mol. beam scatt., review 0-40203  
 reflection and sticking coeffs., short range forces, low energy limit 0-40208  
 vacuum system, rate of molecular impact on surface or orifice, possible conflict with second law of thermodynamics 0-46954  
 Pd (111), scattering, adsorption, and absorpt. of H<sub>2</sub> and D<sub>2</sub>, mol. beam study 0-29277  
 SiO<sub>2</sub>-Si, low-energy neutral particle bombardment of SiO<sub>2</sub> film, degradation 0-54790  
 W, catalytic decomp. of NH<sub>3</sub> single pulses, mol. beam relax. spectrometry 0-21321  
 W, clean and H<sub>2</sub>-covered, Cl<sub>2</sub> scatt. 0-20743

**molecules**

- see also excimers; hydrogen neutral molecules; macromolecules; mesic molecules; muonic molecules; quasimolecules  
 excitation processes by fluctuating light 0-9646

**Mollier diagrams** see thermodynamic properties**molten metals** see liquid metals**molten polymers** see polymer melts**molybdenum**

- see also nuclei with .....  
 adsorbed layer of Ba on (011) face, surface diffusion (*Russian*) 0-6658  
 adsorption of CO<sub>2</sub> and trimethylamine on (100), adsorbed O effect, LEED and AES obs. 0-39443  
 adsorption of CO, O<sub>2</sub>, metastable He de-excitation spectroscopy and UPS study 0-34314  
 adsorption of Cs and O<sub>2</sub>, work function and thermal stability 0-44427  
 adsorption of O<sub>2</sub> on (100) surface, AES, LEED, work function, and desorption meas. 0-6654  
 adsorption of Sr on (112) face 0-2271  
 adsorption sites of CO on Mo (100), electron stimulated desorption and LEED meas. 0-49516  
 amorphous, reflection of D and T, Monte Carlo study 0-40197  
 BCC, void nucleation following electron irradiation 0-29054  
 boriding, Cu influence 0-21165  
 candidate refractory for Tokamak, thermal fatigue failure testing 0-32454  
 cathodes arced in vacuum, erosion structs. 0-1872  
 CESR, prediction of obs. 0-29369  
 combustion under CW CO<sub>2</sub> laser radiation action 0-30241  
 CVD, thin film fabrication for photothermal solar converters 0-11573  
 CVD thin films for solar photothermal conversion 0-7503  
 deformation in fatigue loading of single crystal 0-35328  
 deformed single crystals, struct. state and dislocation splitting (*Russian*) 0-29029  
 desorption kinetics of halogens, pulsed ion beam method 0-34300  
 determ. by atomic absorption, using low temp. flames 0-30307  
 dislocation (100) density variation, deformation effects, dislocation stability (*Russian*) 0-15108  
 dislocation structure inhomogeneity in electromachining crater zone (*Russian*) 0-16326

**molybdenum continued**

- doped rod, surface tension driven flow in electron beam floating zone expts. 0-19731  
 electron beam melted, C charge effect on ductility (*Japanese*) 0-35264  
 electron irradiation, anisotropic damage prod. 0-2071  
 electronic and struct. props., nonlocal pseudopot. calc. 0-34349  
 fatigue charact., effect of Ni and Re surface doping on mech. props. (*Russian*) 0-7660  
 fibre, brittle to tough transition, impact strength meas. 0-40527  
 film, CVD, with high IR refl. and large solar absorpt., prep. and props. 0-26163  
 film, electron beam evaporator for in situ deposition studies in UHV electron microscope 0-40264  
 film, evaporated, optical props., rel. to struct. 0-55211  
 film, polycryst., energy loss function, Kramers-Kronig anal., reflectivity, optical props., EELS 0-40194  
 film on Si substrate, laser irradiation, cellular struct. and silicide form. 0-10710  
 flame sprayed coatings, comp., microstruct. and mech. props. 0-16598  
 foil, electron energy loss spectra 0-7452  
 fracture and crack propag. tested in tension along [001] axis (*Russian*) 0-50697  
 grain boundary segregation of O, atom probe FIM study 0-37134  
 Hall effect, effect of electron-phonon scatt. anisotropy (*Russian*) 0-10947  
 impurity diffusion in JIPP T-II tokamak plasma during H<sub>2</sub> gas puffing 0-28602  
 interatomic pair potential, phonon spectra 0-33927  
 ion irradiated, dislocation loops and stacking fault tetrahedra, electron microscope image contrast 0-6326  
 ions, beam-foil spectra from 20 to 238 MeV energy, 5 to 60 nm, lifetime meas. problems 0-9722  
 irradiated between 425 and 1000°C, ductility in bending 0-39164  
 isomer shift values of implanted <sup>133</sup>Xe/<sup>133</sup>Cs, Mossbauer spectra 0-7240  
 isotopically enriched target preparation using electron gun 0-23226  
 laser mirror, optical and metallurgical characterisation 0-33129  
 mechanical props. and dislocation struct., mag. field effect 0-54935  
 microhole working by laser irradiation, accuracy increase (*Russian*) 0-55434  
 microstructure, swelling induced by ion bombardment, He injection effects 0-29083  
 microvoid form., gaseous impurity atom effects, positron annihilation study 0-49275  
 neutron activation analysis of Mo content in 12-molybdophosphoric acid 0-15148  
 neutron bombardment, radiation damage, electron microscopy obs. (*Russian*) 0-44235  
 neutron irradiated, radiation softening and hardening 0-34083  
 neutron low energy interaction cross sections, gravitational spectrometer meas. 0-24521  
 nitriding, kinetics 0-35415  
 orientation distrib. function depend. on deform. during cold rolling (*Russian*) 0-50647  
 oxidation kinetics, Mossbauer study 0-40005  
 pair potentials calcs., elastic props. calc. 0-49176  
 phonon density of states determ. from heat capacity (*Russian*) 0-29131  
 plasma impurity, flux on wall of DITE Tokamak 0-28688  
 plasma impurity, from Tokamak neutraliser plate, recycling effect in scrape-off plasma 0-10421  
 plastic strain mechanism, in single crystals, in hydroextrusion (*Russian*) 0-21009  
 positron annihilation and vacancy formation 0-16119  
 powder metallurgy prep. 0-29904  
 powders, defective structure and activated sintering, exam. 0-16240  
 production by MoO<sub>3</sub> reduction reaction kinetics 0-16230  
 proton energy loss, 0.1-1.0 MeV 0-42909  
 reactions with LiO<sub>2</sub> in fusion blanket feasibility tests 0-26055  
 sintered, fusion reactor blanket struct. material, low cycle fatigue behaviour 0-30073  
 sintered composite, MoS, containing, friction and wear props. 0-11786  
 skin effect, Gantmakher-Kaner effect peculiarities (*Russian*) 0-49796  
 slip geometry, HVEM straining 0-39207  
 sputtering for laser mirror refurbishment 0-14498  
 steel, ferritic (17 wt.% Cr), influence of Mo on intergranular corrosion 0-30139  
 steel, maraging, 0Kh6N8M7S, effect of Cr, Ni and Mo on hardness 0-21093  
 steel, Ni-Cr low alloy, effect of Mo on tempered martensite embrittlement 0-3187  
 steels, high-purity and commercially based, containing 10 wt.%W or 5 wt.%Mo, tempering behaviour 0-7600  
 strain localisation and fatigue, glide plane shearing stress 0-7683  
 substrate, film coated characterisation by atom probe FIM, atomic clusters, voids 0-33863  
 substrate for W-Al<sub>2</sub>O<sub>3</sub> composite films, oxide evaporation deposited, struct., props. 0-25581  
 superconducting transition temp., perturbative corrections, direct and indirect ladder diagrams 0-49979  
 superconducting transition temperature, ab initio calc. 0-25036  
 surface, (001), electronic origin of reconstruction 0-11065  
 surface, (100), adsorbed H<sub>2</sub>, photoemission rel. to surface resonances and surface reconstruction 0-44417  
 surface, Ar<sup>+</sup>-bombarded, 40 keV, excited at emission 0-11481  
 surface, metastable He atom beam contamination by fast neutral atoms, effect on secondary emission 0-55253  
 surface, SiC coatings, deposition by RF sputtering 0-25563  
 surface (001), H chemisorbed, self-consistent electron struct. 0-44693  
 surface (001), struct., LEED anal. 0-34282  
 surface (001) with saturated H adsorption, band structure self-consistent calc. 0-15585  
 surface (100), clean, electron struct., positron annihilation obs. 0-24988  
 surface (112), adsorption of Li, LEED and contact pot. method 0-10794  
 surface impurities, depend. on prep. method, ion scatt. spectroscopy 0-40200  
 surface orientation effect as high temp. creep and fracture type 0-16403  
 surface reconstruction, physical realisation of two-dimensional Ising and X-Y model 0-15351  
 surface thermoelectrotransport of atoms 0-2448  
 temperature standard reference material, USA National Bureau of Standards 0-47009  
 TFTR protective plate, sputtering and surface damage by D<sup>+</sup> irradiation 0-18645



**molybdenum continued**

- Tokamak impurity in fusion reactor, at. (mol.) struct. and collision data, review 0-43959
- Tokamak limiter, surface observation, infrared techniques 0-38693
- twin and stacking fault energies calc. 0-2038
- whisker crystal growth incorporated with field electron emission 0-44458
- work hardening and softening in cyclic strain 0-20957
- X-ray  $M\beta$  energy, revised values 0-14102
- $Al_2O_3$ , Mo-refined single crystals, fabrication 0-16250
- $Al_2O_3:Mo^{3+}$ , zero field splitting study by ESR 0-7159
- $Al_2O_3$ -Mo (20 wt.%) cermet,  $ZrO_2$  crystal addition effect on thermal fatigue resistance 0-40528
- $BaO-Al_2O_3-SiO_2-Ta_2O_5$ -Mo glass ceramic metal composites, cermet prep. 0-11618
- $Bi_2W_2O_{12}$ -Mo, energy transfer and luminesc. props. 0-55177
- C content determ., isotope-spectral method (Russian) 0-55766
- $CaMoO_4:Mo^{3+}$ , g-factor, ground state, line broadening, EPR obs. 0-39863
- Fe-Cr-Mn-Mo, influence of Mo on defect conc. energy (Russian) 0-54241
- Mo VX-XIV, transition array and energy level distrib. variance 0-37767
- Mo XIV, ionisation energy, multiplet strengths, diagrammatic MBPT theory calcs. 0-9500
- Mo XXXIII, dielectronic recombination rate calc. 0-14232
- Mo XXXIII, XXXIV, XXXV, transition identification X-ray spectra 0-32648
- $Mo^{3+}$ , determination of spectrum using low-inductance spark and laser-produced plasma 0-19610
- $Mo^{29+}$  to  $39+$  photoionis. cross sections, radiative recomb. rate coeffs., rel. to plasma diagnostics 0-52953
- $Mo^{32+}$ , dielectronic recomb. rate coeffs. in plasma 0-43853
- $Mo^{32+}$ , Na like ions, dielectronic recombination rate, scaling props. 0-32668
- $Mo^{38+}$ , dielectronic recomb. rate coeffs. in plasma 0-43852
- $Mo^{39+}$ , partial photoionis. cross-sections and radiative recomb. rate coeffs. 0-52951
- Mo:He, accumulation and distrib., monolayer conc. by sputtering quantitative anal. 0-49253
- Mo-Si-Mo and Mo-Si structs., non-volatile memory switching 0-54814
- Mo+Nb, K-shell vacancy prod., impact parameter depend. 0-14225
- $Mo_2$ , matrix isolated visible absorpt. spectra, electronic, vibronic and vibr. states 0-28027
- $^A Mo$ ,  $A=92, 94-98, 100$ , muonic atom X-ray transitions, nuclear charge radii 0-27545
- $^{99}Mo$  impurities in  $^{99m}Tc$ , gamma camera array 0-36100
- $Nb_2O_5:Mo^{5+}$ , ESR obs. on B-form single crystals. 0-54946
- Ni-Fe-Cr-Nb-Ta-Mo alloy, fatigue crack growth, stress ratio and hold time effects 0-40531
- SiC coating 0-7500
- ZrN-Mo, cermet, sintering reaction thermodynamics 0-2989

**molybdenum alloys**

see also molybdenum compounds

- cast iron, white, high Cr-Mo, fracture toughness 0-50726
- dispersion-strengthened, plastic deform. and hardness, temp. depend. 0-3087
- fusion reactor first wall and blanket material, props. for struct. appl. 0-30071
- fusion reactor first-wall and blanket material, mech. props. 0-34074
- Hastelloy C-276 and G, accelerated  $H_2$  charging in aq.  $H_2SO_4$  at 0.2% yield stress 0-30144
- Hastelloy C-4, loaded at high temp., useful life 0-40523
- Hastelloy X, carburisation and dimens. stability in HTGR, He environment 0-45366
- Hastelloy X, thermal fatigue props. 0-21071
- mag. props. after isothermal thermomag. treatment (Russian) 0-25159
- steel, alloy, V-W-Mo-Cr, exam. of carbide transformation 0-16299
- steel, alloy, W-Mo-Cr-V, blanks welded to steel 45, optimal high temp. tempering 0-16351
- steel, austenitic, high-temp. crack resist., B and Mo influence (Russian) 0-16435
- steel, Co-Cr-Mo, maraging, age hardening, Mossbauer study 0-40002
- steel, Co-Cr-Ni-Mo-Mn (39.65, 20.25, 15.33, 7.08, 1.9 wt.%) carbide formation during tempering after plastic deformation 0-16330
- steel, Cr, ferritic, corrosion morphology, electrochem. pot. and Mo additions effect (French) 0-45439
- steel, Cr (17 wt.%), influence of Mo on intergranular corrosion (French) 0-21182
- steel, Cr-Mo, kinematic hardening models, use in multi-axial cyclic plasticity 0-25717
- steel, Cr-Mo, materials specifications for AGR steam generators 0-42772
- steel, Cr-Mo, toughness of heat treated steels of equal tensile strength (German) 0-25727
- steel, Cr-Mo (2.25, 1 wt.%), exposed to  $H_2$ - $H_2O$ - $H_2S$  environment, fatigue crack growth 0-40623
- steel, Cr-Mo (2.25, 1.0 wt.%), thermally aged and Na decarburised, stress-rupture props. 0-21102
- steel, Cr-Mo (2.25, 1 wt.%), strain hardening shakedown load during bending 0-20958
- steel, Cr-Mo low alloy ferritic, meas. of alloy and impurity elemental distrib. using STEM 0-35601
- steel, Cr-Mo-V, austenite to bainite transformation under cooling conditions, effect on creep 0-3033
- steel, Cr-Mo-V, biaxial cyclic deformation behaviour 0-16431
- steel, Cr-Mo-V, high temp. main steam pipe, residual stresses in butt welds 0-21059
- steel, Cr-Mo-V, high temp. steam pipe weld, defect distrib. and growth 0-25979
- steel, Cr-Mo-V, stress rupture strength at high temps. (German) 0-40474
- steel, Cr-Mo-V-W, crack-growth and thermal-mech. fatigue 0-21072
- steel, Cr-Ni-Mo, dynamic and static softening behaviour at hot forming temp. (German) 0-25728
- steel, Cr-Ni-Mo, for boiler tubes, austenisation conditions effects obs., on structure and mechanical props. 0-3151
- steel, Cr-Ni-Mo-V, magnetic induction, struct. dependence (Czech) 0-50141
- steel, Cr-Ni-Mo-V, Mossbauer austenitometry and mag. props. 0-40003
- steel, Cr-W-V-Mo (3.9 to 4.5, 1.5 to 2, 0.9 to 1.2, 3.9 to 4.4 wt.%), heat resistant, type 8Kh4M4V2F1-Sh, mech. props. 0-16464
- steel, Mn-Ni-Mo low alloy steels for nuclear appl., toughness and heat treatment 0-5239
- steel, Mo and Cr-Mo, X-ray elasticity constants at high specimen temp. (German) 0-35239
- steel, Mo-Cr (3 wt.%), CrC formation in isochronal tempering, electron microscope study 0-7584
- steel, Mo-Nb (2.5, 0.035 wt.%) Mo content effect on sulphide stress cracking resistance 0-21157
- steel, Ni-Co-Mo-Ti, maraging, electron diffraction obs. of second phase (Chinese) 0-11655
- steel, Ni-Cr-Mo, cleavage fracture toughness, temperature and notch sharpness influence (German) 0-35291
- steel, Ni-Cr-Mo, fracture toughness determ. from yield strength and cleavage fracture strength (German) 0-35292
- steel, Ni-Cr-Mo, quenched and tempered, notched bar tensile tests (German) 0-35247
- steel, Ni-Cr-Mo (11, 5, 3 wt.%), maraging, corrosion cracking in chloride and alkaline solutions 0-55576
- steel, Si-Cr-Mo-W-V (2.4, 1.3, 2 wt.%), heat treatment and props. 0-16349
- steel, solubility of W and Mo in Ti(C,N)<sub>x</sub> 0-16276
- steel, stainless, Cr-Ni-Mo-N, phase diagrams 0-35161
- steel, stainless, Ni-Cr-Mo-W (29, 13, 3, 2 wt.%), long-term strength in H at high pressure 0-55485
- steel, stainless complex alloy, hot ductility, B effect 0-30038
- steel, tool, W-Mo, heat treatment effect on props. 0-50656
- steel, W-Mo, sintered high-speed, naphthalenelike grain form., quenching effect on fracture toughness 0-30103
- steel, W-Mo, tool, hydrostatic extrusion and tempering, wear resistance effect 0-50728
- Al-Mo, struct. and props. of alloys obtained from granules 0-50717
- Al-MoSi<sub>3</sub>-Si system, diffusion, compound form., and microstructure 0-34253
- Al-MoSi<sub>3</sub>-n-Si system, Schottky-barrier height 0-34520
- Co-B-Mo-Cr, amorphous, Mo and Cr addition effect on corrosion behaviour 0-16568
- Co-Cr-Mo shoulder prosthesis, wear and fatigue tests 0-26415
- Co-Mo catalyst, Mossbauer spectra 0-7222
- Cr-Ni-Mo-Cr<sub>2</sub>C<sub>3</sub>, wear resistant coating prep. by laser beam melting, and props. 0-40607
- Fe solid solution, substitution strengthening by Cr and Mo (Czech) 0-30080
- Fe-B-Mo-Cr, amorphous, Mo and Cr addition effect on corrosion behaviour 0-16568
- Fe-Co-Mo ternary system, phase diagram (Russian) 0-16269
- Fe-Cr-Mo, (30.2 wt.%) Bridgman-type, unexpected embrittlement phenomena, hydrostatic tensile test (Japanese) 0-55517
- Fe-Cr-Mo, passivated single crystal, selective dissolution and surface enrichment 0-16543
- Fe-Cr-Mo, sputtering effect on surface comp., AES obs. 0-6601
- Fe-Cr-Mo (26, 1 wt.%), single crystals and polycrystals, strain rate influence on low cycle fatigue props. 0-3126
- Fe-Mo (5 wt.%), Auger anal. of passive films in neutral aq. soln. 0-16605
- Fe-Mo alloys, pitting 0-16549
- Fe-Mo catalyst, Mossbauer spectra 0-7222
- Fe-Mo-C, lattice parameters of cementite, annealing effect 0-29007
- Fe-Mo-P, P-induced temper embrittlement, Mo role 0-35316
- Fe-Ni-Co-Mo phase diagram and structure (Russian) 0-20899
- Fe-Ni-Co-Mo-Ge alloy 40NKM, excess mag. noise after various thermomag. treatments (Russian) 0-29575
- Fe-Ni-Cr-Mo superalloy, mech. props.,  $\eta$ -phase form. effect (Chinese) 0-20925
- Fe-Ni-Mo (16.4, 8.1 wt.%), effect of substituting Mo by W during ageing 0-29991
- Fe-Ni-Si-Mn-Co-Mo, effect of prolonged aging on mag. props. 0-16513
- $Fe_{76}Mo_{24}B_{20}$ , quenched ferromag. ribbon, Brillouin spectra 0-2776
- $Fe_{78}Mo_{22}B_{20}$ , amorphous, transverse magnetoresist., stress effect 0-15501
- $Fe_{78}Mo_{22}B_{20}$ , amorphous, fast neutron and fission fragment irradi., effect on elec. resist. 0-19846
- $Fe_{78}Mo_{22}B_{20}$  glass, thermal expansion, glass transform. and crystn. temps. 0-2183
- $Fe_{78}Mo_{22}B_{20}$ , metallic glass, triplet correlation, field-ion microscopy study 0-38921
- $Fe_{40}Ni_{38}Mo_{2}B_{18}$  amorphous alloys, compatibility of DC and AC mag. props. 0-34695
- $Fe_{40}Ni_{38}Mo_{2}B_{18}$ , metallic glass, mag. and transport props. 0-39752
- $Fe_{40}Ni_{38}Mo_{2}B_{18}$  ribbon, magnetic characterisation 0-34680
- GdCoMo amorphous alloy films, mag. cobalt alloys susceptibility, uniaxial anisotropy field 0-54930
- Mn-Cr-Mo-C, master alloys, development for low alloyed PM steel 0-50576
- Mn-V-Mo-C master alloys, development for low alloyed PM steel 0-50576
- Mo alloy:Re, effect of Re on mechanical props. 0-35196
- Mo-Al-Ge, new compounds, structure and props. 0-39003
- Mo-B, Mo-B-Fe(Ni), microalloying influence on mechanical props., cold rolling, plasticity (Russian) 0-40502
- Mo-Cr, fusibility diagram (Russian) 0-20897
- Mo-Fe metalloceramic alloy, brittle fracture investigation, segregation, morphology, struct. (Russian) 0-55503
- Mo-Hf (0.3 wt.%), strength, plasticity and microhardness, internal nitriding effect (Russian) 0-40433
- Mo-Hf-C-Ni, electrochemical phase composition anal., precip. of HfC phase (Russian) 0-20901
- Mo-low alloys, C enrichment mechanism of intercrystallite zones (Russian) 0-20963
- Mo-Mn alloy, plasticity, fracture, strength depend. on C content (Russian) 0-35257
- Mo-Mn metalloceramic alloy, brittle fracture investigation, segregation, morphology, struct. (Russian) 0-55503
- Mo-Mn powder mixture, X-ray diffraction exam. of reaction between Mo and Mn, during sintering 0-16242
- Mo-N, nonporous metal production accompanying arc plasma nitriding (Russian) 0-7712
- Mo-Nb, dil., impurity diffusion and vacancy-impurity binding energy 0-15307
- Mo-Nb solid solutions, enthalpy of soln. of H meas. 0-2166
- Mo-O system, grain boundary segregation and intergranular fracture 0-55516
- Mo-O-C system, grain boundary segregation and intergranular fracture 0-55516



**molybdenum alloys continued**

- Mo-Re, prep. from reduction in Mo-Re-O system (*Russian*) 0-16225  
 Mo-Re,  $\sigma$  phase alloy, critical mag. field, elec. resistance 0-54850  
 Mo-Re-C (0.3, 0.2 at.%) time-of-flight atom-probe expts. 0-55741  
 Mo-Si-Cu, struct. and supercond., Cu influence 0-50592  
 Mo-Ti, irradi. between 425 and 1000°C, ductility in bending 0-39164  
 Mo-Ti-Zr, alloy TZM, polycrystalline, anal. of elastic anisotropy and microyielding 0-30050  
 Mo-Ti-Zr, D trapping in fusion reactor materials, temp. dependence 0-37577  
 Mo-Ti-Zr, fusion reactor first wall material, compatibility with impure He 0-32469  
 Mo-Ti-Zr (0.5, 0.1 wt.%), neutron irradiated, void swelling and shrinkage, TEM study 0-34079  
 Mo-Ti-Zr (0.5, 0.7 wt.%) alloy TZM, props. and appl. (*German*) 0-21040  
 Mo-TiC-Ni phase equilibria, subsolidus temp., metallographic and X-ray anal. 0-16278  
 Mo-TiC(ZrC)(HfC), thermionic emission, surface structural characts. after prolonged use, work function variation 0-20758  
 Mo-V-C, hot-worked, substructural hardening and high-temp. strength (*Russian*) 0-25731  
 Mo-W, fatigue and threshold behaviour under high cycle fatigue 0-40487  
 Mo-W-C, phase equilibria calc., line compounds 0-10638  
 Mo-Zr, heavy ion irradiated, void swelling, phase instability 0-29084  
 Mo-Zr-B, neutron irradi. at 780-1080°C, porosity, hardening and embrittlement (*Russian*) 0-29062  
 Mo-Zr-B, porosity and mech. props. after neutron bombard., 780-1080°C (*Russian*) 0-24502  
 Mo<sub>2</sub>B<sub>5</sub>-based alloys, mech. props., rel. to appl. as electrodes in electros-park machining 0-21174  
 MoC coatings, produced by plasma flux deposition in vacuum, exam. (*Russian*) 0-11567  
 (Mo<sub>0.6</sub>Ru<sub>0.4</sub>)<sub>82</sub>B<sub>18</sub>, supercond. metallic glass, neutron irradi. effects 0-29060  
 Mo<sub>2</sub>Si<sub>3</sub> based coating, interaction (*Russian*) 0-21167  
 Nb-Mo, electronic struct., thermoreflectance meas. 0.5-5.0 eV 0-45050  
 Nb-Mo, nitriding, diffusive saturation, lattice spacing and activation coeffs. (*Russian*) 0-21168  
 Nb-Mo, prod. by simultaneous carbothermic reduction of oxides/electron beam melting method (*Japanese*) 0-11590  
 Nb-Mo steel, HSLA, low temp. fatigue props. 0-40490  
 Nb-Mo system, electron-phonon coupling const. and supercond. transition temp., average T-matrix approx. 0-39707  
 Nb-Mo-Al-(Cr) eutectic directionally crystallised alloy, heat resistance, alloy struct. (*Russian*) 0-40481  
 Nb-Mo-Ti-Zr-C, work function temp. and phase depend. (*Russian*) 0-2449  
 Nb-W-Mo-Zr, long-term strength props., vac. level effect 0-55484  
 Nb-W-Mo-Zr-C, strength and ductility, prolonged high-temp. soaking effect 0-55483  
 Nb<sub>0.5</sub>Mo<sub>0.5</sub>, soft X-ray spectra, theoretical considerations 0-11511  
 Ni-Al-Mo, heat resist., solidification range 0-35177  
 Ni-Co-Cr-Al-Ti-Mo superalloy IN738, caskings porosity removal using hydrostatic press. sintering 0-55322  
 Ni-Cr-Co-Mo alloy MP35N, accelerated H<sub>2</sub> charging in aq. H<sub>2</sub>SO<sub>4</sub> at 0.2% yield stress 0-30144  
 Ni-Cr-Co-Mo-(Ti), oxidation depend. on alloying element, cohesion strength (*Russian*) 0-40587  
 Ni-Cr-Mo, creep parameters, high temp. 0-50685  
 Ni-Cr-Mo (74, 20, 4 wt.%), long-term strength in H at high pressure 0-55485  
 Ni-Cr-Mo-Mn alloy 02KhN40MB, corrosion-resist., heat-resist., phys. and mech. props. 0-35411  
 Ni-Cr-Mo-Ti (19.1, 1.3 wt.%) for TiC reactively sputtered coatings, adherence, XPS and wear study 0-25565  
 Ni-Cr-W-C-Mo, Vickers hardness and crystallisation temp. 0-16361  
 Ni-Cr-W-Mo-Al-Ti (15.6, 3.2, 2.2, wt.%), wrought, Si effect on transition brittleness (*Chinese*) 0-55491  
 Ni-Fe-Mo, K-effect, Mossbauer study 0-39998  
 Ni-Fe-Mo, magnetic alloy, TEM and X-ray obs. (*Chinese*) 0-24401  
 Ni-Fe-Nb-Al-Mo, wear resisting mag. head material, mag. props. and struct. 0-35350  
 Ni-Mo, sputtering rate, radiation-induced segregation and preferential sputtering effects, kinetic model 0-40199  
 Ni-Mo (10.7 wt.%) alloy, ordering energy calc. 0-10522  
 Ni-Mo (20.8 wt.%), order, heat treatment effects 0-40406  
 Ni-Mo-C-(Cr)(W), Vickers hardness and crystallisation temp. 0-16361  
 Ni-Mo-MoS<sub>2</sub>-composite, Mo alloying effect on physicochem. interactions 0-7692  
 Ni<sub>3</sub>Al-Mo, powder, X-ray spectral analysis exam. 0-16239  
 Ni<sub>3</sub>(Fe,W), elec. resist., temp. depend. anomalies, Hall and Nernst-Ettinghausen effects (*Russian*) 0-10942  
 Ni<sub>4</sub>Mo, coherent phase form. at stress concentrators (*Russian*) 0-49356  
 Ni<sub>6</sub>Mo<sub>4</sub>Fe, O<sub>2</sub> effect on secondary recrystallisation and mag. props. 0-35201  
 SiC fibre reinforced Ti, effect of Al, Zr and Mo alloying additions on reaction rate of Ti with fibres 0-16249  
 TZM, fatigue and threshold behaviour under high cycle fatigue 0-40487  
 TZM, irradi. between 425 and 1000°C ductility in bending 0-39164  
 Ti-Al-Cr-Mo alloy VT3-1, reactions with some refractory compounds 0-16585  
 Ti-Al-Cr-Mo system, VTZ-1 alloy, microstruct. influence on fatigue characts. 0-3195  
 Ti-Al-Mo, impact strength anisotropy, influence of texture (*Russian*) 0-20952  
 Ti-Al-Mo, thermomechanical treatment effect on mech. props., strengthening mechanisms 0-55441  
 Ti-Al-Mo, type Ti-6242S, irradi. induced creep 0-39163  
 Ti-Al-Mo alloy VT-14, spherical pressure vessel, correlation between fracture stresses and mech. laboratory characts. 0-25838  
 Ti-Al-Mo-Cr-Fe, distrib. of Sn, Zr between phases, temp. effect. 0-55357  
 ( $\alpha+\beta$ )-Ti-Al-Mo-Fe alloy VT-22, behaviour during creep testing, solid soln. disloc. (*Russian*) 0-40346  
 Ti-Al-Mo-Sn alloy, elastically and plastically deformed, positron annihilation meas. of deformation 0-21038  
 Ti-Al-Mo-Sn-Si, type IMI 680 and 551, internal friction study of martensitic transformations 0-7573  
 Ti-Al-Mo-Sn-Si, type IMI 680 and 551, stability of martensitic phases 0-7574

**molybdenum alloys continued**

- Ti-Al-Mo-V, crack resistance in chloride soln., electrochem. protection, polarization effect 0-55589  
 Ti-Al-Mo-Zr SiC fibre reinforced composites, matrix selection (*Russian*) 0-35192  
 Ti-Al-Mo-Zr-Si (6.6, 3.3, 1.8, 0.3 wt.%) SiC fibrous composite, component interaction kinetics (*Russian*) 0-55364  
 Ti-Al-Nb-Ta-Mo (6, 2, 1, 0.8 wt.%), elevated temp. flow strength, creep resist., diffusion welding characts. 0-30033  
 Ti-Al-Sn-Zr-Mo (6, 2, 4, 6 wt.%),  $\alpha$ - $\beta$  type 6246, fusion zone fracture behaviour in weldments 0-30093  
 Ti-Al-Sn-Zr-Mo alloy, Ti-6242,  $\alpha+\beta$ , creep property improvement by Pt ion plating 0-16408  
 Ti-Al-Sn-Zr-Mo-Si (6, 2, 4, 2, 0.1 wt.%), effect of elevated temperature and environment on fatigue crack growth 0-40486  
 Ti-Al-Zr-Mo alloy 685, phase at  $\alpha/\beta$  interface (*French*) 0-25661  
 Ti-CrB<sub>2</sub>-Ni-Mo, interphase reactions, electron probe anal., metallography and hardness exam. 0-2990  
 Ti-Mo (15.2 at.%), swaged and recrystallized, grain growth 0-3092  
 Ti-Mo-Fe (3, 0.13 at.%), metastable phases, Mossbauer study 0-7243  
 Ti-Mo-Zr-Sn (11.5, 6, 4.5 wt.%), metastable beta III phase, recrystallization and grain growth 0-3091  
 Ti-V-Mo-Cr system,  $\beta$ -phase stability 0-55353  
 TiC-Ni-Mo sintered hard alloy TN-20, fracture surfaces 0-7684  
 $\alpha$ -U-Mo, dil., electronic properties depend. on 2 $^{1/2}$ -th order phase transition under high press. (*Russian*) 0-11128  
 V-Ni-Mo, structure in alloy crystallisation region, peritectic equilibria (*Russian*) 0-50622  
 W-Mo, vapour deposited, long-term strength and thermocyclic creep 0-16405  
 Zr-Mo-H, catalytic props. 0-30274

**molybdenum compounds**

- see also molybdenum alloys  
 molybdenum formate, mol., Hartree-Fock instability of SCF wavefunctions 0-9492  
 rare earth compounds, RMo<sub>6</sub>X<sub>8</sub>, (X=S, Se), supercond. and long range mag. order coexistence 0-15642  
 refractory carbides, borides and nitrides, wetting by and interactions with liq. metals 0-54473  
 ternary sulphides, Chevrel phase, synthesis and superconductivity (*German*) 0-25038  
 BaO-MoO<sub>3</sub>, solid phase reaction, thermal analysis 0-55639  
 Cr-Mo-N system, at high-pressure, temp., X-ray anal., phase diagram 0-50607  
 Cu<sub>1.8</sub>Mo<sub>6</sub>S<sub>8</sub>, superconducting state, triclinic struct., X-ray powder diffr. anal. 0-6388  
 Cu<sub>4</sub>Mo<sub>6</sub>S<sub>8</sub>, supercond., two-phase, upper crit. field meas. 0-29509  
 Cu<sub>4</sub>Mo<sub>6</sub>S<sub>8</sub> system, low temp. modifications (*French*) 0-50606  
 Cu<sub>2</sub>O-CuO-MoO<sub>3</sub>, subsolidus phase diagram, mag. props. 0-50615  
 EuMo<sub>6</sub>S<sub>8</sub>, Chevrel phase, RE mag. isolation and supercond. 0-44470  
 GdMo<sub>6</sub>S<sub>8</sub>, Chevrel phase, RE mag. isolation and supercond. 0-44470  
 H<sub>1.6</sub>Mo<sub>6</sub> bronze, form., kinetic, thermodynamic investig. (*French*) 0-45247  
 H<sub>3</sub>PO<sub>4</sub>(MoO<sub>3</sub>)<sub>12</sub>.29H<sub>2</sub>O, electrochromic solid-state cells 0-2724  
 LaMo<sub>6</sub>S<sub>8</sub> thin films, crit. currents and pinning forces 0-34575  
 Mn<sub>0.394</sub>Ti<sub>0.606</sub>-O-S system, 1380 and 1485K, phase equilib. study 0-50616  
 Mo complex, redox enzyme, electron transfer peculiarities 0-16896  
 Mo-O crystals, electron microscopy study 0-28889  
 Mo<sub>2</sub>B<sub>5</sub> and MoB<sub>4</sub>, thermal, elec., and mag. props. 0-20187  
 Mo<sub>2</sub>B<sub>5</sub>, monocryst., grain size, abrasive and strength props. 0-11787  
 Mo<sub>2</sub>C, corrosion and electrochem. props. in aq. H<sub>2</sub>SO<sub>4</sub>, HCl, HNO<sub>3</sub> and KOH solns. 0-11813  
 Mo<sub>2</sub>C, free energy of form. and thermodynamic props. of C in solid Mo 0-15266  
 Mo(CO)<sub>6</sub>, multiphoton ionisation, mol. cooling in pulsed supersonic beam 0-28070  
 Mo<sub>2</sub>Cl<sub>8</sub><sup>4-</sup>,  $\delta$ - $\delta^*$  bond,  $\delta$ - $\delta^*$  excitation, CI, CC, and MBPT approaches to UHF model 0-32585  
 MoF<sub>3</sub>, gas, thermodynamic stability 0-26041  
 MoF<sub>3</sub>, mol. and electronic struct., vitreous, liq., and tetrameric states, <sup>19</sup>F NMR obs., mol. mobility 0-34787  
 MoF<sub>6</sub> reduction by H<sub>2</sub>, chemical kinetics eqn., adsorbed component interactions (*Russian*) 0-35569  
 MoF<sub>6</sub>, reduction by H<sub>2</sub> at 500-1200°C to Mo, exam. of Mo props. and MoF<sub>6</sub> props. (*Russian*) 0-7516  
 MoN, interatomic interactions from XPS 0-49171  
 MoN, matrix isolated visible absorpt. spectra, electronic, vibronic and vibr. states 0-28027  
 MoO, matrix isolated visible absorpt. spectra, electronic, vibronic and vibr. states 0-28027  
 MoO<sub>2</sub>, powder bed, H<sub>2</sub> reduction kinetics 0-16230  
 MoO<sub>3</sub> amorphous films, EPR of Mo<sup>5+</sup> centres 0-34771  
 MoO<sub>3</sub>-Si photodiode, fabrication as function of O<sub>2</sub> partial press. 0-29464  
 MoO<sub>6</sub><sup>4-</sup>, electronic struct., discrete variation and scatt. wave X<sub>n</sub> methods 0-917  
 MoO<sub>4</sub><sup>2-</sup>-Sn<sup>2+</sup>, (n=0-4), <sup>17</sup>O(<sup>33</sup>S)(<sup>95</sup>Mo)(<sup>97</sup>Mo) NMR investig. 0-53022  
 MoS<sub>2</sub>, additive to lubricant, friction and frictional temp. reduction 0-21125  
 MoS<sub>2</sub>, amorphous, cathode, electrochem. props. rel. to secondary Li battery 0-40851  
 MoS<sub>2</sub>, clean surface, AES and LEED exam. 0-10762  
 MoS<sub>2</sub>, containing sintered Mo composite, friction and wear props. 0-11786  
 MoS<sub>2</sub>, enthalpy and specific heat, temp. depend. 0-54406  
 MoS<sub>2</sub>, entropy, enthalpy and specific heat, temp. depend. 500 to 1700K 0-15260  
 MoS<sub>2</sub>, KKR calc. of energy bands 0-34355  
 MoS<sub>2</sub>, poorly crystalline 'rag' struct. 0-6391  
 MoS<sub>2</sub>, RF sputtered layers with variable stoichiometry, lubrication props. 0-40557  
 MoS<sub>2</sub>, RF sputtered lubricant, wear life, sputtering parameter effects 0-40558  
 MoS<sub>2</sub>, self-propag. high-temp. synthesis, wear props. 0-2975  
 MoS<sub>2</sub>, struct., XES and XPS obs. 0-43105  
 MoS<sub>2</sub>, surface electronic struct., slow electron reflection, total current spectroscopy (*Russian*) 0-54759  
 MoS<sub>2</sub>, synthetic molybdenite single crystals, growth from vapour, elec. props. 0-34446  
 MoS<sub>3</sub>, amorphous struct., X-ray radial distrib. anal. and XPS 0-49115



**molybdenum compounds continued**

- MoS<sub>3</sub>, prep., use as Li battery cathode 0-29892  
 Mo<sub>6</sub>S<sub>8</sub> and halogen substituted cpds., sp. ht. capacity 0-49986  
 Mo<sub>6</sub>S<sub>8</sub>Br<sub>2</sub>, X-ray cryst. struct. anal. (*French*) 0-33965  
 MoS<sub>2</sub>(2H), lattice dynamics, Coulomb and quasi-harmonic effects 0-39245  
 MoS<sub>2</sub>(2H), Raman spectra, phonon modes, high press. effects 0-40111  
 MoSe<sub>2</sub> coating, on Mo, support annealing influence on orientation, texture and hardness (*Russian*) 0-20961  
 MoSe<sub>2</sub>, IR and Raman spectra, lattice vibr. interlayer bonding 0-40110  
 MoSe<sub>2</sub>-I<sup>-</sup>, photoelectrode, time resolved photocurrent, nanosecond excitation 0-45708  
 Mo<sub>6</sub>Se<sub>8</sub> and halogen substituted cpds., sp. ht. capacity 0-49986  
 Mo<sub>6</sub>Se<sub>8</sub>, Chevrel phase, supercond. isotope effect meas. (*German*) 0-25038  
 MoSi<sub>2</sub>, ceramic additives effect on sintering, recrystallisation 0-40306  
 MoSi<sub>2</sub> coating for Nb alloy, oxidation protection, diffusion-slip casting appl. method 0-21187  
 MoSi<sub>2</sub> coating for SiC heating elements 0-21137  
 MoSi<sub>2</sub>, reactions with Ti-Al-Cr-Mo alloy VT3-1 0-16585  
 MoSi<sub>2</sub>, self-propag. high-temp. synthesis 0-2988  
 MoSi<sub>2</sub>, self-propag. high-temp. synthesised, sintering and props. 0-11616  
 MoSi<sub>2</sub>-CrSi<sub>2</sub>, phase equilib., struct. and props. 0-50608  
 Mo<sub>3</sub>Si, self-propag. high-temp. synthesis 0-2988  
 Mo<sub>3</sub>Si<sub>3</sub> based coating, interaction with Mo alloy substrate (*Russian*) 0-21167  
 MoTe<sub>2</sub>, IR and Raman spectra, lattice vibr. interlayer bonding 0-40110  
 $\alpha$ -MoTe<sub>2</sub>, KKR calc. of energy bands 0-34355  
 $\beta$ -MoTe<sub>2</sub>, layer cryst., dislocations and domain struct. 0-39102  
 Mo<sub>6</sub>Te<sub>8</sub> and halogen substituted cpds., sp. ht. capacity 0-49986  
 (Mo<sub>6</sub>V<sub>1-x</sub>)<sub>2</sub>O<sub>5</sub>, mag. and spectroscopic investigation 0-25206  
 Mo(ZrO<sub>2</sub>-La<sub>2</sub>O<sub>3</sub>) structural changes during reduction and sintering 0-25636  
 Mo<sub>2</sub>[(CH<sub>3</sub>)<sub>2</sub>P(CH<sub>3</sub>)<sub>2</sub>]<sub>2</sub>,  $\delta$ - $\delta^*$ (<sup>1</sup>A<sub>2u</sub>-<sup>1</sup>A<sub>1g</sub>) transition, vibr. struct. anal. 0-53006  
 Na<sub>2</sub>MoO<sub>4</sub>(S<sub>2</sub>)(Se<sub>4</sub>) crystals, charge transfer spectra of MoX<sub>4</sub><sup>2-</sup> complexes 0-54658  
 Na<sub>2</sub>O-B<sub>2</sub>O<sub>3</sub>-SiO<sub>2</sub>-MoO<sub>3</sub> glass containing high level radioactive waste, phase separation 0-25683  
 Na<sub>2</sub>O-MoO<sub>3</sub>, melt, EMF meas., rel. partial molar thermodynamic props. 0-6526  
 PbMo<sub>6</sub>S<sub>8</sub>Gd, EPR meas. (*French*) 0-54947  
 PbMo<sub>6</sub>S<sub>8</sub>Gd<sup>3+</sup>, powder EPR spectra, cryst. field, supercond. energy gap 0-34769  
 Pb<sub>1.125</sub>Mo<sub>6</sub>Se<sub>7.5</sub>, Chevrel phase supercond., NMR study 0-49989  
 Sn<sub>1-x</sub>Ga<sub>x</sub>Mo<sub>6</sub>S<sub>8</sub>, heat capacity meas., singularities at low temp. 0-49985  
 SnMo<sub>6</sub>S<sub>8</sub>, Chevrel phase, RE mag. isolation and supercond. 0-44470  
 SnMo<sub>6</sub>S<sub>8</sub>, isotope effect props. (*Russian*) 0-37751  
 SnMo<sub>6</sub>S<sub>8</sub>Gd, EPR meas. (*French*) 0-54947  
 SnMo<sub>6</sub>S<sub>8</sub>Gd<sup>3+</sup>, powder EPR spectra, cryst. field, supercond. energy gap 0-34769  
 SnMo<sub>6</sub>Se<sub>8</sub>, Chevrel phase, RE mag. isolation and supercond. 0-44470  
 V<sub>2</sub>O<sub>5</sub>-MoO<sub>3</sub> solid solns., small polaron cond., elec. resist. and thermoelec. power meas. 0-34447  
 WO<sub>3</sub>-MoO<sub>3</sub> system, on glass substrate, electrochromism of glass film compositions 0-29720

**moments (electric)** see *electric moments*

**moments (magnetic)** see *magnetic moments*

**moments (molecules)** see *molecular moments*

**momentum**

see also *angular momentum*

transfer from waves to particles 0-18977

**monitoring**

see also *patient monitoring; radiation monitoring*

acoustic emission activities in deep-level coal seams, bed rocks instability obs. (*Japanese*) 0-10071

airborne contaminants monitoring in chem. labs., USA regulations 0-12869

aircraft noise, concepts of instrumentation 0-33397

aircraft noise monitoring systems, requirements 0-23849

atmosphere SO<sub>2</sub>, long-term monitoring method using permeation sampling, development 0-26189

environmental noise monitoring installation 0-33396

fast aspheric mirror figure control by profile monitor, wire tester and null lens 0-14419

fission reactor pressure vessel and circuit development, conf. report 0-47541

heart electrical and mechanical monitoring on extensometer 0-45944

lake quality monitoring, multirate Landsat data extraction progrm 0-17299

laser beam indicator/visualiser made from new thermochromic material 0-9976

oxygen monitoring in process gas streams, sensor 0-52181

point defect concentrations during low-temp. irradiations and anneals using integrated system 0-7741

radioactive contamination, use of Xe probe 0-27826

solar heating systems, instrumentation principles for performance meas. 0-35743

temperature, using low-temperature radiometer, with conical light pipe, IC manufacture appl. 0-47105

thin film growth measurement using galvanically separated quartz monitor probe (*German*) 0-11576

water quality monitoring, modular system (*German*) 0-26186

welds, in-process, with acoustic emission 0-16620

O<sub>2</sub> analyser, OTOX 90, operation, and multipoint monitoring 0-55736

**monitoring, computerised** see *computerised monitoring*

**monitors** see *monitoring*

**monochromators**

see also *X-ray monochromators*

aberrations in spectra recorded with Seya-Namioka monochromator, correction using inverse convolution 0-23629

concave grating efficiency in VUV region, diffusion pump oil contamination effect 0-14429

construction, spectrosc. appl. (*Hungarian*) 0-43478

double monochromator with nonclassical concave diffraction gratings 0-38110

double-scanning, noncoherent optical signals coding method appl. (*Russian*) 0-5697

**monochromators continued**

Fresnel zone plate support UV window as lens and monochromator 0-1326

glancing incidence, with corrections for astigmatism and spectral-line curvature 0-43466

grating monochromator, real instrumental function 0-43452

grazing incidence and normal incidence, intensity calibration in VUV for plasma diagnostics 0-48995

grille filtering method and associated spectrometers, capability study, double grille monochromator 0-48427

heated vacuum monochromator for 40-280 nm spectroscopy 0-33176

IR and MM wavelengths, very rapidly scanning instrument 0-5829

laser monochromator-interferometer, probable high-resolution, with multi-channel electronic readout 0-33153

neutron reflectivities, Ni-Mn and Ni-Ti multilayers for monochromators and supermirrors 0-22880

photodetector spectral sensitivity meas. using two tandem monochromators (*Japanese*) 0-47107

prismatic double monochromator 0-23796

scanning rate restrictions in monochromators 0-48430

spectral instrument choice in plasma and flame emission spectrometry of traces 0-35613

spectral line profile recording, high resolution, using Fabry-Perot interferometer and monochromator 0-42268

spread function, graphical representation, stray light concept 0-33198

total spread function description of props. 0-19100

tunable radiation sources in interferometry 0-23787

vacuum monochromator low-temp. attachment construction and optics 0-31764

**monolayers**

see also *adsorbed layers*

adsorbed layers, two dimensional incommensurate crystal theory, thermodynamics (*Russian*) 0-49524

adsorbed monolayer, classification of continuous order-disorder transitions 0-19910

adsorbed monolayer of orientable molecules, lattice fluid model, real-space renormalisation group method 0-17882

adsorbed monolayers, order-disorder transitions, classification and characterisation, review 0-52149

anomalous thermal effects, statistical mechanics 0-15367

chemisorbed on W, anomalous Auger shifts 0-20738

cobalt stearate, monomolecular layer, electron escape depth, XPS (*Japanese*) 0-11532

desorption, Brownian motion of particles near free surface 0-54503

elastic and viscoelastic monolayers, dynamic surface potentials 0-3603

electron transfer in monolayer assemblies 0-3383

epitaxial, 2-D, and 1-D electron gas and 2-D Coulomb gas, family of mappings 0-34346

ethane, on graphite, struct. and melting, elastic neutron scatt. 0-29266

fatty alcohol solid monolayers in H<sub>2</sub>O, interface struct., model 0-54505

fluid monolayer at solid surface, density distrib. calcs. 0-49492

fluid-fluid interfaces, hydrodynamic stability, dipole interactions 0-6599

fluid-fluid interfaces, hydrodynamic stability, ion interactions 0-6598

graphite, dissolution into (110) face of Ni, 600-913K 0-49504

interfacial, thermodynamic treatment, excess quantities, adsorbed and spread layers 0-40732

Ising model for monolayers of coadsorbed atoms, phase transitions 0-19909

Langmuir monolayer, phase separation without gravity effects (*French*) 0-54534

methane, adsorbed on graphite, substrate deform. meas. 0-54520

mixed protein phospholipid films, viscoelastic behaviour and Marangoni effect 0-3602

nonregistered monolayers, lateral compression effects calc. 0-6641

organic dye on Ag, excited mol. decay near metal surface, energy transfer to plasmon surface polaritons 0-50440

phase transitions, review 0-44433

poly- $\gamma$ -benzyl-L-glutamate, monolayers, struct. studies, IR, ATR, and TEM obs. 0-44396

rare earth element submonolayer films, electronic phase transitions, heat of absorption 0-24736

rigid rodlike molecules adsorption onto planar surface, dispersion interactions, statistical mech. anal. 0-29265

stimulated Raman gain spectroscopy, ultrahigh sensitivity 0-48337

tetradecanoic acid, liq.-expanded/liq.-condensed phase changes press., effect of temp. diff. between liq. substrate and air 0-54476

Ag film, on Au substrate, monolayer overgrowth, quantitative AES method 0-10813

Ag/CN, coverage meas. using surface enhanced Raman scatt. and radioisotope meas., electrochemical treatments 0-29260

Al, effect on atomic modulation of interdiffusion at Au-GaAs interface 0-49432

Al<sub>2</sub>O<sub>3</sub>, core excitons and inner well resonances in surface soft X-ray absorpt. spectra 0-40187

Ar adsorbed on graphite, nonregistered-registered phase transition 0-39414

Ar monolayer adsorbed on graphite basal planes, heat capacity 0-6636

Ar, on graphite, equil. config. and lattice consts. 0-54524

Ar, on graphite, lattice spacing and isosteric heat below 50K, LEED obs. 0-34303

Ar-graphite system, effects of dynamic coupling 0-10771

Be film, on Cu substrate, monolayer overgrowth, quantitative AES method 0-10813

CN on Ag, picosecond Raman gain spectroscopy 0-25351

CO, on Pd (100), electronic states, tight-binding method appl. 0-49564

Cu (100), self consistent electronic struct. 0-6926

Cu, deposition on Au electrode in underpotential region, RHEED investig. 0-54539

H (1 $\times$ 1), adsorbed on Ti (0001) film, electronic struct., surface geometry 0-54750

H, on W (001), surface phonons, lattice dynamical model 0-39405

<sup>3</sup>He, adsorbed, on MgO, nucl. mag. relax. props. 0-49457

<sup>3</sup>He film, submonolayer and multilayer, adsorbed on Grafoil, pulsed NMR study 0-49456

<sup>3</sup>He film, theory of motional inhibition of interlayer quantum tunnelling 0-54466

<sup>3</sup>He, on solid Ar, desorption heat capacity 0-10735

<sup>3</sup>He, two-dimens. solid, melting mechanism 0-10643

<sup>4</sup>He, monolayer adsorbed on Kr-plated graphite, possible Ising transition 0-34298



**monolayers continued**

- <sup>4</sup>He, on solid Ne, desorption heat capacity 0-10736
- <sup>4</sup>He superlattices on graphite, ground-state energy, variational calc. 0-24710
- Ir (111), ( $\sqrt{3} \times \sqrt{3}$ )30° S overlayer struct., LEED obs. 0-15365
- Kr adsorption on graphite, monolayer regime phase diagram 0-49507
- Kr adsorbed on graphite, nonregistered-registered phase transition 0-39414
- Kr, adsorbed on graphite, substrate deform. meas. 0-54520
- Kr, on graphite basal face, fluid-registered solid transition 0-49491
- Ni (111) surface, C interaction, monolayer form. and struct. stability 0-10756
- SiO<sub>2</sub>, core excitons and inner well resonances in surface soft X-ray absorpt. spectra 0-40187
- Xe, adsorbed on graphite, substrate deform. meas. 0-54520
- Xe, adsorption on Ag (111), statistical mech. 0-34306
- Xe, physisorbed monolayer on graphite, dynamical and thermal props. 0-34292

**monolithic integrated circuits**

- see also bipolar integrated circuits; field effect integrated circuits; large scale integration
- plasma-removal of polymeric layers 0-1851
- social effects of microelectronics (Dutch) 0-20
- GaAs, ion implantation, trends 0-39132

**monomers see molecules****monomolecular films see monolayers****monomolecular layers see monolayers****Monte Carlo methods**

- Abelian lattice gauge theories, Monte Carlo anal. 0-18079
- adsorbed layer, classical octupoles on triangular lattice, orientational phases 0-2263
- adsorbing walls separated by Lennard-Jones liq., Monte Carlo calc. of force 0-15363
- AES, backscattering factor, Monte Carlo method calc. 0-7449
- air electron backscattering coeffs., 100 eV to 5 keV 0-9750
- alloy, binary, crystallisation kinetics, Monte Carlo computer simulation 0-16294
- amorphous solid, supercooled liquid-glass transition region, short-range order, simulation 0-44127
- analysis of backscattering and sputtering in vacuum systems 0-235
- aperture-type light conductor, photometric charact., computerised calc. by Monte Carlo method (Russian) 0-1339
- atmosphere proton and H atom precipitation in equatorial region 0-51596
- atom, highly excited, linearly polarised elec. field ionisation, freq. (amplitude) depend. 0-32630
- BCC Ising model with competing interactions, fluctuation-induced first-order transition 0-20424
- Brusselator, dynamic correl. functions, Mori-Zwanzig formalism 0-25988
- BWR/6 axial reflectors, Monte Carlo modelling 0-22939
- capture gamma-ray detector, neutron sensitivity 0-18767
- chemical system far from equilibrium, stochastic simulation 0-3339
- classical planar spin model, two-dimens., Monte Carlo study 0-25147
- classical quadrupoles on triangular net, orientational ordering calcs. 0-2262
- classical stretching dynamics of methylene 0-23400
- colloids, phase transition, statistical mechanics approach 0-40749
- colloids, solvation force between particles, Monte Carlo calc. 0-21328
- Comptonization of X-rays by low-temp. electrons, Monte Carlo calc. 0-12653
- computer modelling of matter, conf., Anaheim, USA (March 1978) 0-51954
- contribution Monte Carlo methods, appls. to neutron deep-penetration transport problems 0-47530
- cosmic ray propagation in interplanetary space 0-12623
- cosmic ray-nucleus reacts., 20 TeV, balloon-borne chamber, Monte Carlo simulation 0-9309
- covalent semiconductor, heating of charge carriers, energy dissipation 0-49755
- dendrites, Monte Carlo simulation of growth from melt 0-15427
- dense Lennard-Jones fluids, solvent struct. and solvation forces between rigid particles 0-30287
- dense simple fluid near wall, density profile calc., integral eqn.-Monte Carlo comparison 0-54083
- depth-dose relationships near the skin resulting from parallel beams of fast neutrons 0-30902
- diamond, natural, anisotropy and saturation of hot carrier drift velocity 0-6867
- diamond, natural, electron effective mass and lattice scatt., Monte Carlo anal. 0-44484
- dilute aqueous solutions, Monte Carlo studies of struct., review 0-54101
- dilute frustrated lattice, spin-glass ordering, triangle and FCC lattices, Monte Carlo simulation 0-15746
- diluted Ising and Heisenberg magnets with competing interactions, phase diagrams and mag. props. 0-34672
- disordered systems, dispersive hopping transport, Monte Carlo calcs., variable range percolation 0-44587
- disordered systems, time dependent spectral transfer, Monte Carlo calc. 0-11464
- dynamic fatigue tests, statistical reproducibility of crack propag. parameter 0-25842
- electrolyte soln. grand canonical ensemble Monte Carlo 0-54092
- electron avalanche simulation in hydrogen 0-38521
- electron diffusion to absorbing electrodes, Monte Carlo and Boltzmann calc. comparison 0-6204
- electron diffusion to anode, Monte Carlo and Boltzmann calcs. comparison 0-38519
- electron drift velocities simulation in inert gas mixtures, rel. to neutron counters 0-48843
- electron slowing down in water, spatial correlation of energy deposition events 0-9473
- electron transport, continuous-slowing-down approx., adjoint Monte Carlo model 0-49269
- electron transport, diffusion theory and Monte Carlo calcs., depend. on initial ang. distrib. of injected electrons 0-53136
- electron transport simulation in liq. water, appl. to microdosimetry and radiobiology (French) 0-12202
- ENDF/B-V cross section data for shielding appls., Monte Carlo MCNP integral calcs. 0-47744
- ethyl radical decomposition, mol. dynamics, trajectory studies 0-7780

**Monte Carlo methods continued**

- eutectic crystal-melt system, interphase boundary struct., Monte Carlo method study 0-1950
- fast ions, behaviour during H-neutral-beam-injection in large Tokamak plasma 0-28713
- fast liner reactor conceptual design, nucleonics 0-13790
- fast proton track energy deposition and ionisation calc. and obs. 0-12196
- fibre reinforced composites, Monte Carlo study of strength 0-25844
- fibrous material failure kinetics, internal stresses, computer simulation (Russian) 0-40479
- fission reactor reactivity perturbation calc. by difference iterations in the Monte Carlo method 0-5210
- fission reactors, integral experiments for testing Th and <sup>233</sup>U data 0-27707
- fluid, hard dumbbell mols., reference pot., perturbation theories, spherical reference systems 0-28898
- fluid, of hard prolate spherocylinders, pair distrib. function expansion validity 0-24336
- fluid, optimisation of sampling algorithms 0-54099
- Frenkel pair formation in solids, due to passage of relativistic electrons, computer simulation (Russian) 0-6402
- fused hard sphere fluids, equations of state, virial coeffs., Monte Carlo simulation 0-54095
- fusion reactor blanket thickness, improvements to cellular design 0-18630
- fusion reactor blanket thickness, minimization calcs., implication of cellular struct. 0-18629
- galaxy groups, ellipticity index Monte Carlo determ. rel. to average ellipticities 0-12820
- gamma Compton experiment, with annular <sup>241</sup>Am source, momentum resolution and reliability meas. 0-312
- gas dynamics, compressible inviscid ideal gas flow, direct simulation methods 0-48733
- graphite, neutron penetration, Monte Carlo calculations for 30, 45 MeV (Japanese) 0-18677
- hard sphere fluid, dielectric const., Monte Carlo simulations, mol. dynamics calcs. 0-28897
- hard sphere-spherocylinder equimolecular mixture, Monte Carlo simulation of fluids 0-44088
- hard spherocylinders and spheres mixtures, Monte Carlo study 0-49073
- heavy ions in low energy region, expt. and theoretical range comparison 0-32257
- Heisenberg model, two-dimensional classical, Monte Carlo evidence for inhomogeneous states 0-44790
- hole burning into molecular velocity distribution due to monochromatic radiation and molecular elastic collision 0-43116
- hydration, hydrophobic, of nonpolar mols. in dilute aq. soln., Monte Carlo simulation 0-3314
- ice, two-dimens. square, correl. function calcs., approx. methods, Bjerrum fault conc. effects 0-10513
- importance sampling with parametric depend. 0-13013
- inert gas crystals, Monte Carlo calc. of conc. of lattice vacancies, method of overlapping distrib. 0-39077
- interstellar gas heating and ionization by X-ray photoelectrons 0-46383
- ion reflection from metal surfaces 0-40197
- ion-Rydberg atom collision cross sections, classical trajectory Monte Carlo calcs. 0-43174
- ionosphere positive ion detection, with rocket-borne mass spectrometer 0-8459
- Ising ferromagnet, 4-D, correction to leading singularity of order parameter 0-25061
- Ising model, kinetic with triplet interactions 0-7061
- Ising model for monolayers of coadsorbed atoms, phase transitions 0-19909
- Ising square lattice, phase transitions, next nearest neighbour interactions 0-50128
- Ising two-dimens. random bond model, evidence against spin-glass order 0-15747
- large cell renormalisation groups for percolation 0-46994
- largest cluster at two dimensional percolation threshold, Hausdorff dimens. and fluctuations 0-46982
- laser, electron beam controlled, electron beam parameter optimization and choice of foil 0-48269
- lattices, finite, with traps, random walks, Monte Carlo simulations 0-52131
- linear chain, two-sublattice, hopping particle occupancy correlation function normal modes 0-49402
- linear radiation-flux functionals, estimation of local perturbations using Monte Carlo method 0-5457
- liquid, associated, radial correlations, comparison of Monte Carlo and Ewald mol. dynamics calc. methods 0-14984
- liquid-vapour interface, fluid phase coexistence, Monte Carlo computer simulation 0-49349
- liquid-vapour interface, pair correl. function at triple pt., Monte Carlo method 0-10753
- liquid-vapour interface, struct. at 110K 0-54477
- liquid-vapour interface structure near hard wall 0-14983
- long chain paraffins, thermodynamic functions, Monte Carlo method appl. (German) 0-19962
- LWR fuel assembly, lattice calculation by double sampling Monte Carlo approach 0-606
- LWR lattices, Monte Carlo radiation transport program for reactor bundle gamma transport and energy deposition analysis 0-22915
- Lyapunov characteristic numbers and Kolmogorov entropy of a four-dimensional mapping 0-46978
- melting, Lennard-Jones two-dimensional systems, Monte Carlo study 0-49338
- melting and freezing, computer simulation of simple systems using array processor 0-54353
- MIM system, electron emission modelling (Czech) 0-2479
- minimizing splitting costs in Monte Carlo particle transport 0-47532
- molecular fluid, hard-core triatomic, Monte Carlo simulations 0-38880
- monatomic gas, rarefied flows in two-dimens. expansion nozzle 0-28547
- multichain polymer system, simulating dynamic and equil. props. 0-53179
- NE213 liquid cylindrical neutron spectrom., anisotropy of response 0-5434
- NE 213 scintillator, neutron response functions, energy range to 40 MeV (Japanese) 0-18756
- neutral beam injector, simulation of neutral particle transport 0-37600
- neutron activation analysis for coal ash content measurement in moving wagons 0-3431



**Monte Carlo methods continued**

- neutron coincidence counting, removal of multiplication effects 0-37715  
 neutron polarisation meas. with high press. He scintillation counter 0-14061  
 neutron reflection, plane-parallel concrete interfaces, Monte Carlo calc. 0-27686  
 neutron response functions of organic scintillators 0-14047  
 neutron transport, contribution Monte Carlo, exponential biasing model 0-5195  
 neutron transport, contribution Monte Carlo technique, variational derivation 0-5194  
 neutron transport, multigroup, Monte Carlo game, moments method 0-52720  
 neutron transport in upper atmosphere, Monte Carlo calcs. 0-8468  
 neutronic analysis of the NBS intermediate-energy standard neutron field (ISNF) 0-27692  
 nongrey, nondiffuse surfaces, 3-dimens. radiative exchange factors, Monte Carlo method 0-10128  
 nucleation and crystal growth, two-dimensional, simulation using kinetic Ising model 0-54156  
 organic scintillator efficiency using Monte Carlo code 0-889  
 particle generation, Monte Carlo model of proton high energy collisions (Hungarian) 0-13336  
 photon, electron and positron prod. from primary proton beams 0-32555  
 photon beam dose calcs., power law tissue-air ratio algorithm for inhomogeneity corrects., verification 0-56222  
 photon source in lungs of phantom, external detector response calcs. 0-8132  
 plasma, laser-target interaction, Monte Carlo (hybrid) suprathermal electron transport 0-24200  
 point defects short term annealing, in  $\alpha$ -Fe, computer simulation 0-54282  
 polyethylene, neutron penetration, Monte Carlo calculations for 30, 45 MeV (Japanese) 0-18677  
 polymer, freely jointed chain, with excluded vol. interaction, Monte Carlo studies 0-10475  
 polymer network formation, struct. and mech. props., computer simulation 0-38965  
 polymer off-lattice chains, Monte Carlo anal. of excluded vol. problem 0-5647  
 polymers, Monte Carlo renormalisation group 0-42148  
 polymethylene coils in solution, dimension and shape, computer simulation (Russian) 0-54111  
 Potts model, first order phase transitions, Monte Carlo renormalisation group method 0-34645  
 Potts model, Monte Carlo simulation in three dims. 0-163  
 Potts model, three-state, phase transition continuity 0-22302  
 PWR core, thermal analysis, Monte Carlo method 0-47603  
 quantum liquids and crystals, computer modelling 0-54472  
 quantum many-body problems, nuclear physics 0-22727  
 quantum mechanical corrections to classical equilibrium statistical-mechanical results 0-135  
 radiation detector efficiency calc. for extended flat sources 0-9469  
 radiation dose from syringes, computer code for calc. 0-41246  
 radiation therapy, computer program for negative pion beam calcs. 0-46061  
 radiation transport theory, tracklength biasing in Monte Carlo methods 0-5335  
 radiative heat transfer between isothermal parallel plates, flow models, numerical analysis 0-14547  
 radiative transfer, resonance scattering with absorpt. or differential expansion, Monte Carlo calcs. 0-21901  
 radiometer, absolute, with uniform response, fabrication, characts. and anal. 0-268  
 recursive, optimal strategies for appl. 0-13014  
 Reggeon field theory on a lattice, critical behaviour, Monte Carlo calc. 0-18126  
 response functions of spherically moderated neutron detectors 0-37687  
 Rutherford 180° backscatt. anomaly in solid, Monte Carlo simulation 0-45189  
 schlieren instrument, amplitude transfer charact., Monte Carlo method 0-28336  
 scintillation counter, energy resolution optimisation at high energies 0-37697  
 SEM, signal treatment, backscattered electron spectral distrib. (French) 0-42305  
 shielding of structures against initial nuclear radiation: Monte Carlo methodology 0-47741  
 simple cubic lattice, orientational ordering of quadrupoles 0-44157  
 simulation of photon transport in a heterogeneous phantom 0-26257  
 Singer polymer tempering methods 0-52845  
 site-bond problems in percolation and cluster distributions, Monte Carlo calcs. 0-42160  
 soil infiltration, spatial var. of hydrological effects, Monte Carlo anal. 0-8363  
 solar radiation transfer under cumulus cloud conditions application (Russian) 0-21793  
 SOLASE laser fusion reactor, Monte Carlo shielding calc. for mirror-laser beam duct system 0-23174  
 solid angle integrals for rad. detectors, Monte Carlo solns. 0-9468  
 solid layers, conversion electron scatt. processes anal. 0-45181  
 solid-state diffusion in elec. field, Monte Carlo demonstration 0-27072  
 solution, aq., hydrophobic apolar spheres interaction, Monte Carlo simulation 0-6335  
 solution, aq., hydrophobic hydration around apolar species pair, Monte Carlo simulation 0-6336  
 spin system, cubic model, Monte Carlo simulation, phase transitions 0-34646  
 spin systems, model, Monte Carlo simulation appl. 0-20421  
 spinels, percolative phenomena in cationic B-sublattice 0-17893  
 SPODE radiation transport code, comparison of electron transport models 0-23030  
 spontaneously fissioning material, Monte Carlo neutronic and electronic model for thermal-neutron coincidence counting 0-23165  
 star clusters containing massive central black holes, dynamical simulations with self-consistent potentials 0-26915  
 succinonitrile, plastic phase, mol. motions correlation times, incoherent neutron scatt. 0-49138  
 surface flow of dilute gas in model pores, free mol. flow calc. in adsorbent force field 0-6100  
 teaching, two-dimens. Brownian motion simulation on micro-computer (Japanese) 0-31461

**Monte Carlo methods continued**

- thermonuclear reactions, rate enhancement due to strong screening, ionic mixtures case 0-36613  
 thermonuclear reactions in laser fusion, emitted particle spectra, Monte Carlo calcs. (Russian) 0-52780  
 three body phase space distrib. 0-37393  
 three-dimensional Ising model, crit. behaviour 0-4672  
 Tokamak, neutral beam injection, low density ignition scenarios 0-48937  
 Tokamak fusion test reactor, dose rates from induced activity in test cell 0-23144  
 Tokamak scrape-off plasma, metal impurity recycling effect 0-10421  
 toroidal plasma, Monte Carlo treatment for neutral particle transport 0-33750  
 Townsend discharge, macroscopic quantities, Boltzmann eqn. and Monte Carlo calcs. 0-38848  
 transition probabilities, functional form 0-27234  
 transport calcs., second moment functionals for last event and collision estimators 0-13012  
 transport equations, Monte Carlo game, variance versus efficiency 0-27238  
 TSEE from insulating layers, Monte Carlo method simulation (German) 0-2932  
 two-dimensional Ising model, Monte Carlo renormalisation-group method 0-4673  
 two-layer plate, random temp. fields and heat conduction, Monte Carlo method 0-33417  
 velocity filter SHIP, efficiency for unsolved evaporation residues 0-23244  
 water, liq., H bond distrib., Monte Carlo simulation calcs. 0-54106  
 water, liq., Monte Carlo studies of struct., review 0-54101  
 water, liq., Monte Carlo-Metropolis computer simulation, convergence characts. 0-10485  
 water, liq., structure and props., minimal basis set description 0-6347  
 water, Monte Carlo simulation 0-54113  
 water, X- and  $\gamma$ -irrad., electron slowing-down spectra and photon RBE 0-12197  
 water quality models 0-8367  
 Wiener path integrals, approx. evaluation 0-8829  
 X-ray fluorescence, Monte Carlo simulation, inter-element effects determ. 0-26080  
 X-ray fluorescence anal., matrix effects, reduction by Monte Carlo, fundamental parameters method 0-3460  
 X-ray photoelectron spectra relative intensities, elastic scatt. in solid effect on free path and ang. distrib. 0-11531  
 xeromammography, calc. of integral radiation dose 0-41248  
 Yukawa fluid, fluid-solid interface 0-38883  
 zero-variance multigroup Monte Carlo quadratures 0-5196  
 $e^+e^-$  hadron jets, QCD, Monte Carlo model 0-27514  
 AgBr, streaming cyclotron motion of hot electrons, at intense microwave fields 0-6703  
 $\alpha$ -AgI, superionic conductor, soft-core model, Monte Carlo study 0-54430  
 Al and Al-alloy films, struct. induced electromigration failure, Monte Carlo calcs. 0-49405  
 Al, vacancy distribution, interbonding atoms, heat peaks in scattered cascades (Russian) 0-39169  
 Ar, aqueous soln., dil., energy and struct., pair pot. energy function, Monte Carlo calc. 0-54107  
 Ar+H<sub>2</sub>, vibr. transition rates, thermally averaged, Monte Carlo trajectory calcs. 0-23519  
 Au condensed films on NaCl, ion bombarded, film growth, thermally stimulated exoelectron emission 0-50537  
 CO<sub>2</sub>, electron swarm parameters for high E/N, Monte Carlo simulation 0-19548  
 CS<sub>2</sub>, liq., struct. and equil. optical props. 0-45026  
<sup>60</sup>Co source irradiation of 2 media, absorbed dose in vicinity of an interface 0-30894  
 Cu, EXAFS Debye-Waller factors 0-45168  
 Cu, liquid, struct. factor, neutron diff. meas. and Monte Carlo calc. 0-38903  
 Fe, EXAFS Debye-Waller factors 0-45168  
 Fe slab (Japanese) 0-18595  
 Fe-Al, spin glass transition, Monte Carlo study 0-39801  
<sup>57</sup>Fe backscatt. electron Mossbauer spectroscopy 0-29661  
 GaAs, hot electron distrib. function, inter-carrier scatt. effect 0-2395  
 n-GaAs, limiting freq. of Gunn effect in polyharmonic LSA mode 0-6856  
 p-Ge, noise calc. in strong elec. field using Monte Carlo method 0-15578  
 H atom in mag. field, Schrodinger eqn., Monte Carlo soln. 0-31545  
 p-H<sub>2</sub>, solid, rotation-libration transition under press., Monte Carlo study 0-49460  
<sup>4</sup>He, HCP, ground-state props. 0-44389  
 InP, transferred electron effects under high press. 0-34453  
 InSb, electron mobility, low-field, Monte Carlo calc. 0-10973  
 InSb, HF props. of hot electrons at 77K, calc. using Monte Carlo method 0-15553  
 InSb, hot electrons, Monte Carlo calc. of transport characts. and distrib. functions of hot electrons 0-6853  
 Mg+H<sup>+</sup>, electron capture and impact ionisation cross sections, CI calc. 0-23343  
 N<sub>2</sub>, electron backscattering coeffs., 100 eV to 5 keV 0-9750  
 N<sub>2</sub>, electron swarm parameters for high E/N, Monte Carlo simulation 0-19548  
 Na, ions in liquid, Born-Oppenheimer pot. derivative, Monte Carlo calcs. 0-54117  
 Ne<sup>+</sup>+CO<sub>2</sub>, three dims. quadrupole ion storage, ion mobility, effect of charge exchange reactions, Monte Carlo calcs. 0-55738  
 O<sub>2</sub>, electron backscattering coeffs., 100 eV to 5 keV 0-9750  
 O<sub>2</sub>, thermal decomposition, vibr.-rot. state depletion, Monte Carlo calc. 0-35506  
 O<sub>2</sub>(b<sup>4</sup> $\Sigma_g^-$ , v'=4, N', F') predissociation fragments, ang. distrib., separation energies 0-5588  
 Pd, H(D) interstitial interactions rel. to diffusion and ordering transition 0-34249  
 PdH<sub>x</sub>, incoherent phase transition, lattice gas model 0-29171  
 Pt, EXAFS Debye-Waller factors 0-45168  
 Pu in situ array for electropolishing bath, Monte Carlo calcs. 0-37524  
 Rb, specific heat at high temp., Monte Carlo calc. 0-29182  
 Si amorphous film, hole carrier transport 0-2500



**Monte Carlo methods continued**

- Si:B sputtering by  $\text{Ar}^+$ , computer simulation of sputter broadening in impurity depth profiling 0-2908  
 Si:O, ion-implanted between 2 and 20 MeV, range and range straggling 0-44241

**Moon**

- see also lunar seismology; lunar structure*  
 brightness distribution over lunar and planetary discs, determ. from light refl. meas. 0-17512  
 Brown-Eckert Improved Lunar Ephemeris, Fourier series fast-evaluation 0-56711  
 capture by Earth rel. to solar mass var. in 3-body problem 0-56728  
 cartography of limb regions (*French*) 0-12696  
 charged particle albedo, Luna 22 data 0-56729  
 cometary collision, origin of swirl patterns on surface 0-51675  
 core formation in terrestrial planet, appl. to Moon 0-17514  
 crustal magnetic anomalies, sources 0-8566  
 density, vol. distrib., theoretical anal. 0-8567  
 distance and shape, laser ranging results 0-21933  
 early collisional heating 0-8563  
 Earth-Moon system, Moon position change, evidence from geological time considerations 0-3916  
 Earth-Moon system, palaeodynamics from nautiloid growth 0-41713  
 Earth-Moon system history, palaeontological data 0-17224  
 EM heating, EM heating in early solar system 0-36555  
 ephemeris correction for solar terms 0-12684  
 evolution and structure, review 0-4278  
 Fahrenheit crater ejecta, emplacement at Luna-24 site 0-8564  
 far-side magnetised regions, correl. with ringed impact basins 0-36521  
 fossil bulge to explain gravity field anomaly 0-56733  
 halo orbits in Earth-Moon restricted three body problem 0-36483  
 ice and trapped volatiles in lunar polar regions 0-26759  
 limb automatic meas. with Nice Obs. microdensitometer (*French*) 0-12692  
 lunar and planetary science, ninth conference, Houston, Texas, (1978 March 13 to 17) 0-17711  
 lunar theory of Hill and Brown 0-46370  
 $M_2$  ocean tide parameters and Moon's meas. longit. decel. from artificial satellite orbit data 0-31048  
 magnetic anomalies detected by Apollo subsatellite 0-36525  
 magnetic field determination from lunar fines 0-36526  
 magnetic field origin, conf., Nov. 1978, Texas USA 0-36234  
 magnetic field origin, constraints set by Apollo 15 and 16 subsatellite obs. 0-36523  
 magnetic field origin theories 0-36522  
 map of J.D. Cassini 0-8769  
 mapping, conf., Lagonissi, Greece (May 1978) 0-12688  
 mapping, from Schmidt's 1878 map to Apollo photography 0-12689  
 mapping program of United States and Apollo project 0-12690  
 Mare Crisium, view from Luna 24, conference, Houston, Texas (1977, December 1 to 3) 0-17710  
 mare grounds relative spectral reflectivity 0-12695  
 Mare Serenitatis, elec. cond. anomaly detect. by Lunokhod 2 and Apollo 16 magnetometers 0-56730  
 motion, literal soln., formal convergence (*French*) 0-36482  
 motion and Earth shrinking effects 0-46182  
 orbit computation, appl. of Urabe's method to Moon and artificial satellite cases 0-17477  
 orbital evolution, anal. 0-8565  
 origin from solar nebula, book 0-17266  
 periodic motion rel. to centre of mass in evolutionary circular orbit 0-21899  
 phase relation rel. to asteroidal regolith props. 0-36551  
 photometric and polarimetric obs., 1976 April to 1977 December 0-51677  
 plasma near surface, radiosource occultation obs. 0-8559  
 radar mapping, Earth-based, review 0-12694  
 reflectance meas. in thermal emission region, thermal component removal 0-17497  
 regolith mixing extent 0-8561  
 Rima Sirsalis magnetic anomaly 0-36524  
 rock magnetism, palaeointensity method and lunar sample 10017135 application 0-36527  
 selenodesic work in France 0-12693  
 selenodetic coord. system based on Kazan heliometric obs. (*Russian, English*) 0-41738  
 supernova  $\gamma$ -ray ablation, debris deposited on Earth 0-56731  
 surface features mapping at Kottamia obs. 0-12691  
 surface radio reflection, Luna 23 meas. at 3.1 cm wavelength 0-8560  
 swirl patterns produced by comet collision 0-51675  
 temperature inferred from gravity, stress state and tectonics 0-56732  
 temperature profile, rel. to lab. meas. of elec. cond. of pyroxene containing trivalent cations 0-31033  
 thermal images obs. Meteosat in-orbit calibration appl. 0-17511  
 total eclipse, 1978 March 24, 3.4 mm obs. 0-31220

**Moon structure** *see lunar structure***moonquakes** *see lunar seismology***Morin temperature**

- see also weak ferromagnetism*  
 $\alpha\text{-Fe}_2\text{O}_3$ , haematite, substituted, Morin transition, neutron diff. study 0-54897  
 $\alpha\text{-Fe}_2\text{O}_3\cdot\text{Al}^{3+}(\text{Ga}^{3+})(\text{Cr}^{3+})(\text{In}^{3+})$ , substitution effect on Morin transition, neutron diff. study 0-44827  
 $\text{Ho}_{0.5}\text{Dy}_{0.5}\text{FeO}_3$  orthoferrite, domain wall struct., stability conditions, Morin transition, anisotropy const. 0-34684

**Morse potential**

- see also intermolecular mechanics; kinetic theory*  
 collinear collisions of Morse oscillators, dissoc. vibr. enhancement, quasi-classical trajectory study 0-28089  
 diatomic molecule, vibr. Green's function and two-photon dissociation, appl. to  $\text{H}_2^+$  0-28075  
 inert gas atoms, pot. energy curves analysis 0-53083  
 nonequilibrium dissoc., Morse oscill. rigid rotator system, master eqn. soln. 0-40682  
 one-dimensional quiescent lattices, shock profiles, end condition effects 0-34138  
 position-momentum uncertainty products for exactly solvable potentials 0-12939  
 transition metals, amorphous, density of electronic states, effect of struct. variation due to interatomic pot. softness 0-54597

**Morse potential continued**

- triatomic nonlinear mol., stretching vibr., partial Morse oscills. 0-967  
 $\text{BiBr}$ ,  $\text{A}^2(0^+)$  and  $\text{X}^2\Sigma^+(0^+)$  states, pot. energy functions comparison 0-43133  
 $\text{CrO}$  molecule,  $\text{B}^2\pi$  and  $\text{X}^2\pi$  states, potential energy curves 0-42962  
 $\text{GeS}$ , band system vibr. anal. 0-48009  
**m.o.s. devices** *see metal-insulator-semiconductor devices*  
**m.o.s. integrated circuits** *see field effect integrated circuits*  
**m.o.s. structures** *see metal-insulator-semiconductor structures*  
**mosaic structure (microstructure)**  
 copper phthalocyanine, thermal behaviour (*Japanese*) 0-24753  
**m.o.s.f.e.t** *see insulated gate field effect transistors*  
**m.o.s.i.c.** *see field effect integrated circuits*  
**Mossbauer effect**  
 , 0-40010  
 , 0-44967  
 absolute Mossbauer fraction, determ. and transmission integral 0-37143  
 active data acquisition 0-9079  
 alkali halides, implantation of  $^{57}\text{Fe}$ , conversion electron Mossbauer spectroscopy technique 0-40012  
 allophane, synthetic, amorphous mineral struct. obs. using  $^{57}\text{Fe}$  Mossbauer effect 0-34836  
 alloy, many-body atomic correlations, Mossbauer spectroscopy study 0-15934  
 alloys, phase analysis by Mossbauer spectra 0-15922  
 Alnico 5, two-phase separation during ageing, Mossbauer study 0-7533  
 amorphous magnet, magnetisation, mag. moment temp. distrib. 0-15848  
 bacteria, freshwater magnetotactic, identification of magnetite, Mossbauer obs. 0-3657  
 bacteria magnetotaxis, Mossbauer study 0-41056  
 bacterial catalase,  $^{57}\text{Fe}$  enriched, active centre, Mossbauer spectra meas. 0-8024  
 BBOA, smectic liq. cryst. glass-supercooled transition and Debye temp.,  $^{57}\text{Fe}$  Mossbauer effect 0-54999  
 biomolecules, determ. of static and dynamic struct. 0-40952  
 blackbody absorber in Mossbauer spectroscopy using  $\text{SnO}_2$  with isotope  $^{119}\text{Sn}$  0-2669  
 carbonaceous chondrites, reduction kinetics, Mossbauer obs. 0-41777  
 carbonmonoxymyoglobin, frozen soln., recoilless fraction, Mossbauer spectra meas. 0-8025  
 chalcogenide glass, Fe, doped in equil. conditions, impurity cond. and Mossbauer effect 0-49726  
 chemical relaxation, tunnelling, Mossbauer emission spectroscopy studies 0-40683  
 chlorite,  $^{57}\text{Fe}$  Mossbauer analysis 0-40006  
 Clauser-Blume model for Mossbauer line shape with non-stationary relax. effects 0-34827  
 combination type maxima, hyperfine interactions on nuclei 0-25263  
 conference, Kyoto, Japan (Aug.-Sept. 78) 0-7199  
 conference, Portorez, Yugoslavia, (Sept. 1979) 0-36768  
 conversion electron Mossbauer spectra, electrons below 10 eV 0-37145  
 conversion electron Mossbauer spectrometry, back-scatter-type gas flow detector 0-37680  
 conversion electron spectroscopy at high temp., proportional counter 0-27886  
 cooling unit, continuous flow, for Mossbauer experiments, 4.2 to 300K 0-31954  
 correlation counting in time-domain Mossbauer spectroscopy 0-47161  
 corrosion processes and products Mossbauer study 0-40572  
 critical fluctuations obs. using Mossbauer spectroscopy 0-39955  
 cubic alloys, anisotropic hyperfine interactions, Mossbauer spectra 0-15854  
 data acquisition and processing system 0-18061  
 data centre 0-37148  
 deformation induced texture in absorbers 0-7214  
 deoxyhaemoglobin, high mag. field Mossbauer spectra, electronic states 0-35845  
 deoxymyoglobin, frozen soln., recoilless fraction, Mossbauer spectra meas. 0-8025  
 deoxymyoglobin, high mag. field Mossbauer spectra, electronic states 0-35845  
 deoxymyoglobin single crystals, Mossbauer study with polarised  $\gamma$ -rays 0-40962  
 depth selective, influence of atomic number of inert component in surface layer 0-15931  
 depth selective, low energy electrons in matter 0-15930  
 dichelated protohaeme, model haemoglobin cpd., Mossbauer spectra 0-16904  
 dichroism of polarised Mossbauer rays 0-7201  
 dielectric permittivity in X- and  $\gamma$ -ray regions, review 0-44998  
 diffractometer using microcomputer 0-7210  
 dimethyl stannous chloride di(pyridine 1-oxide),  $^{119}\text{Sn}$  Mossbauer spectra, elec. field gradient 0-15909  
 dimethyl tin diisothiocyanate,  $^{119}\text{Sn}$  Mossbauer spectra, elec. field gradient 0-15909  
 dimethylammonium iron tetrachloride, Mossbauer study of struct. phase transition 0-39278  
 E. coli cells, iron-storage protein, Mossbauer spectra obs. 0-8022  
 elbaite, Zn-Fe,  $\gamma$ -irradiated, Mossbauer study 0-44990  
 electric field gradients, shielding for various elements and electronic configurations 0-39535  
 electron spectrometer, internal conversion electrons detect. 0-7202  
 Faraday effect for Mossbauer radiation at oblique incidence 0-50236  
 Fe particles in glass-like C matrix, identification and props. 0-11229  
 ferredoxin, from *Clostridium pasteurianum*, Mossbauer effect, ESR, and mag. susceptibility meas. 0-40961  
 ferredoxin synthetic analogues,  $[\text{Fe}_4\text{S}_4(\text{SR})_4]^{3-}$  clusters, Mossbauer effect, EPR, and mag. props. 0-41057  
 ferredoxin-like centres, membrane bound, in photosystem I of blue-green algae, Mossbauer and EPR study 0-40974  
 ferric haeme complex of low spin, Mossbauer spectra, crystal field parameters 0-26203  
 ferric myoglobin cpds., single cryst., Mossbauer studies 0-8016  
 ferrichrome A, selective excitation double Mossbauer meas. 0-8015  
 ferrocene, dynamics in liquid and glassy o-terphenyl, Mossbauer obs. 0-55000  
 ferrocene derivatives, mixed and averaged valence types, Mossbauer spectra 0-15906  
 ferrocene related compounds,  $\text{C}_5\text{R}_5\text{Fe(I)}\text{-C}_6\text{R}'_6$  paramag. sandwiches, Mossbauer study 0-39982



**Mossbauer effect continued**

- ferroelectric transitions, Mossbauer spectroscopy study 0-39911  
ferromagnets, domain struct. effects on dynamic props., review 0-34678  
friction, lubrication and wear studies, Mossbauer spectroscopy appl. 0-40547  
G 0-40009  
gamma-ray lasers, direct pumping by resonance capture of neutrons 0-14310  
gamma-rays guides by total external refl. appl. 0-7200  
gamma-X ray coincidence Mossbauer measurements 0-14041  
garnets,  $^{57}\text{Fe}$  and  $^{119}\text{Sn}$  spectra 0-20568  
geochronology, possible appl. of  $^{57}\text{Fe}$  Mossbauer spectroscopy 0-41416  
glass,  $\text{Fe}^{2+}$  impurity ions struct.-chem. state, Mossbauer data 0-40028  
glaucinite group minerals, Norwegian-Greenland basin, age determ. by EPR and Mossbauer spectra 0-26467  
glaucinites, Mossbauer anal.,  $\text{Fe}^{3+}/\text{Fe}^{2+}$  ratio 0-17252  
glycerol, Mossbauer and neutron scatt. 0-20559  
graphite, pyrolytic, thermal diffuse scatt., Mossbauer  $\gamma$ -ray diffr. 0-40026  
graphite- $\text{FeCl}_2(\text{FeCl}_3)$  intercalation cpds., lattice dynamics, Mossbauer spectra 0-15925  
graphite- $\text{FeCl}_3$  intercalation compounds, Mossbauer spectra 0-20538  
haemoproteins, Fe-ligand binding and electronic struct., Mossbauer studies 0-8021  
HBPA, smectic liq. cryst. glass-supercooled transition and Debye temp.,  $^{57}\text{Fe}$  Mossbauer effect 0-54999  
hexadecapole spin resonance in cubic symm. cryst. by NQR, NMR, nuclear gamma reson. 0-20500  
horseradish peroxidase cpd. II, high-field Mossbauer spectra, 4.2 to 120K 0-8026  
Icelandic igneous rocks, Mossbauer anal. 0-17253  
ilvaits, Mossbauer spectra and mag. features 0-7248  
implanted atoms, Mossbauer studies 0-39913  
in-beam time-gated Mossbauer expt. 0-40021  
intermediate valence, phase diagram and Kondo behaviour 0-29366  
Invar, Fe-Ni-C, spin pinning effect in RF collapse studies, Mossbauer spectroscopy 0-44971  
Invar, magnetic structure, absorbed  $\text{H}_2$  effect 0-20534  
Invar, Mossbauer effect at high press. 0-15858  
Invar, RF collapse studies, skin depth effect, Mossbauer spectroscopy 0-39953  
iron (III) salicylates, Mossbauer and IR spectra, mag. susceptibility 0-50242  
isomer shift, rel. to orbital occupation numbers 0-39983  
isomer shift reference scales, Mossbauer Effect Data Centre 0-37147  
K-22 solid catalyst,  $\text{H}_2\text{O}_2$  decomp. rel. to Mossbauer spectra 0-34826  
liberation from electrolytic Ni during vacuum heating, Mossbauer spectra (Russian) 0-35594  
metal hydrides, rare earth and intermetallic, electronic and mag. props., Mossbauer study 0-34830  
metal/solution reactions, possible Mossbauer studies 0-39988  
metallic glass, short-range order, hyperfine field distrib. determ. by Mossbauer spectroscopy 0-39962  
metallic glasses, Mossbauer spectra, hyperfine field distrib. determ. 0-39965  
metallic glasses, Mossbauer studies 0-39917  
metalloenzymes and carriers, hydration effect on mobility of Mossbauer atoms 0-35819  
metals, phase analysis by Mossbauer spectra 0-15922  
meteorite, Toluca octahedrite, Mossbauer spectra petrological study 0-36589  
metmyoglobin, dynamics study using Rayleigh scatt. of Mossbauer radiation 0-40963  
molecular motion in solids, Mossbauer spectroscopic studies 0-39915  
molecules or clusters, interpretation of data from Mossbauer, ESR, susceptibility, optical and XPS meas. 0-37825  
montmorillonite group minerals, Norwegian-Greenland basin, age determ. by EPR and Mossbauer spectra 0-26467  
myoglobin- $\text{H}_2\text{O}_2$ , high-field Mossbauer spectra, 4.2 to 120K 0-8026  
myoglobin- $\text{O}(\text{CO})$ , elec. field gradient tensor, Mossbauer meas. 0-8017  
nitrogenase, cofactor centres, Mossbauer spectra obs. 0-8023  
nitrogenase active site, Mossbauer spectra of Mo-Fe-S clusters 0-45852  
noncubic metals,  $^{171}\text{Hf}$  Mossbauer transition, electric quadrupole interaction 0-39928  
nuclear reactor corrosion products phase composition determ. 0-5237  
obsidian, Lipari and Teotihuacan origin, Mossbauer, magnetisation, X-ray diffr. and fluoresc. study 0-46173  
organometallics, intermolecular interaction, Mossbauer spectra 0-15899  
organometallics, Mossbauer spectra of spin crossover 0-15903  
oxymyoglobin, frozen soln., recoilless fraction, Mossbauer spectra meas. 0-8025  
Permalloy, proton radiation effects, Mossbauer obs. 0-40008  
phase coherence of freq. modulated Mossbauer  $\gamma$ -rays 0-7211  
plasma, magnetised, applic. to gamma-ray lasers 0-28186  
PMMA, amorphous polymer, Rayleigh scattering of Mossbauer  $\gamma$ -rays 0-39926  
polycrystalline cubic BN plunger chamber for high-pressure Mossbauer meas. 0-31786  
Prussian blue analogues, Mossbauer spectra 0-15898  
pyrite structured 3d-transition metal chalcogenide mag. props. from Mossbauer effect obs. (Japanese) 0-15933  
pyrite type dichalcogenides,  $^{57}\text{Fe}$  isomer shift, quadrupole splitting, Mossbauer study 0-15832  
quantum beats, recoil-free  $\gamma$ -radiation 0-22498  
quantum beats of recoil-free  $\gamma$ -radiation 0-37142  
rare earth, heavy calibration of isomer shifts by conversion electron spectroscopy 0-39918  
rare earth alloys,  $\text{R}(\text{Fe}_2\text{Rh}_{1-x})_2$ , mag. props., Mossbauer spectra 0-25108  
rare earth amorphous alloys, mag. props., Mossbauer spectra 0-7225  
rare earth bone uptake, Mossbauer study 0-8019  
rare earth complexes, formation and props., book contrib. 0-43204  
rare earth dihydrides and dideuterides, electronic and mag. props. 0-25260  
rare earth metals, alloys, and cpds., book 0-36785  
rare earth mixed valence compounds, spin dynamics, mag. neutron scatt., Mossbauer effect, XPS studies 0-39786  
rare earth systems, NMR, EPR, and Mossbauer effect, book contribs. 0-39883  
rare earth-transition metal alloys, amorphous, struct. and mag. props., book contrib. 0-39818

**Mossbauer effect continued**

- rare earth-transition metal intermetallics, H absorpt., Mossbauer studies 0-39987  
Rayleigh and Compton contribs. to nuclear resonance scattering of gamma rays, line inversion 0-39919  
red blood cells of thalassemia, sickle-cell anaemia, and haemoglobin Hamersmith, ferritin-like Fe, Mossbauer study 0-8018  
relaxation theory 0-39954  
resonance energy shift for Mossbauer impurity atoms trapped by vacancies 0-25265  
review, and complementary techniques, muon spin rotation and Mossbauer effect 0-39912  
rubredoxin, frozen soln., recoilless fraction, Mossbauer spectra meas. 0-8025  
semiconductors and metals, spectra of implanted  $^{83}\text{Kr}$ , line widths, isomer shifts 0-39899  
shutter model, ultrafast, for resonant gamma rays 0-31955  
silicate minerals, Mossbauer anal. of Fe chem. state 0-20547  
silicates, elec. field gradient at  $\text{Fe}^{2+}$  sites, Mossbauer spectra 0-15484  
small metal clusters, isomer shift of  $^{57}\text{Fe}$ , nearest neighbour effect 0-44988  
sodium iron fluorophosphate glasses, EPR and Mossbauer resonance study 0-39968  
solid state properties of target 0-18060  
spectra fitting, influence of errors of vel. meas. on results 0-37144  
spectrometer, constant acceleration, with spring reaction compensation, circuit and construction 0-47158  
spectrometry (Japanese) 0-29660  
spectrum of Mossbauer radiation passed through vibr. resonant medium 0-40022  
spherical nuclei, isomer and isotope shifts, theory of finite Fermi systems 0-39929  
spinel containing  $\text{Fe}^{3+}$  and  $\text{Sb}^{5+}$ ,  $\text{M}_4^{2+}\text{Fe}^{3+}\text{Sb}^{5+}\text{O}_8$ , Mossbauer spectra 0-15892  
steel, austenitic, Al-C, microstruct., Mossbauer obs. (Russian) 0-29655  
steel, bainite and martensite,  $^{57}\text{Fe}$  Mossbauer spectra 0-15051  
steel, C, corrosion products, chem. state anal. by conversion electron Mossbauer spectroscopy 0-40595  
steel, Co-Cr-Mo, maraging, age hardening, Mossbauer study 0-40002  
steel, corrosion and organic coatings, possible Mossbauer studies 0-39988  
steel, Cr-Ni-Mo-V, magnetic induction, struct. dependence (Czech) 0-50141  
steel, Cr-Ni-Mo-V, Mossbauer austenitometry and mag. props. 0-40003  
steel, galvanized, Fe-Zn phases, Mossbauer study 0-50233  
steel, scoring and scuffing on lubricated sliding surfaces, Mossbauer study 0-7690  
steel, Si, commercial, ordering after heat treatment, Mossbauer meas. 0-7556  
steel, stainless, Mossbauer effect at high press. 0-15858  
steel alloyed with carbide formers, retained austenite determ. 0-20551  
steel fibres, polycrystalline, Mossbauer spectroscopy 0-44959  
steel surface, nitrided, chem. state anal. by conversion electron Mossbauer spectrometry 0-7718  
steel surfaces, corrosive reactions obs. by polarimetric Mossbauer spectroscopy 0-40594  
steel transformer, Mossbauer atomic struct. anal., decarburising annealing, cold rolling (Russian) 0-11294  
steels, high Cr, type 304, high C, low C, backscatter Mossbauer spectroscopy 0-40001  
superparamagnetic particles, Mossbauer spectra, magnetisation vector precession 0-15872  
surface and interface magnetism by Mossbauer spectroscopy 0-7218  
surface electronic structure, surface magnetism and surface phase transitions 0-39916  
talca,  $^{57}\text{Fe}$  Mossbauer analysis 0-40006  
tektites and natural glasses, Mossbauer anal. 0-21952  
texture problem and Goldanskii-Karagin effect, intensity matrix method 0-7215  
thermometer, high temp., based on line broadening 0-52202  
tourmaline, Mossbauer spectra, struct. 0-20566  
tourmaline, proton jumps, NGR obs. 0-15921  
tourmalines of dravite-schorl series, Mossbauer anal. 0-15920  
transition metal dichalcogenides:  $^{57}\text{Fe}$ , Mossbauer spectra, isomer shift 0-15885  
3d-transition metal-metalloid cryst. and glassy alloys, electronic struct. from magnetisation and Mossbauer meas. 0-29363  
tri-t-butylstannyl hydroxide, Mossbauer spectrum, tin coordination (German) 0-32716  
tri-t-butylstannylamine, and isotopomers, IR and Raman spectra, normal coord. anal., Mossbauer spectrum (German) 0-32716  
trimethyl tin cyanide,  $^{119}\text{Sn}$  Mossbauer spectra, elec. field gradient 0-15909  
ultrasonic excitation, phase effect on Mossbauer resonance 0-55004  
vermiculite, firing temp. depend. of Mossbauer parameters 0-15837  
( $2\text{CdTe}$ )-(In $_x\text{SnTe}$ ),  $x=0.25, 0.5, 0.75$ , tetrahedral semiconductor, chem. interaction of Sn atoms, Mossbauer study 0-39977  
Ag foils, polycryst. and bicrystals, grain boundaries,  $^{119}\text{Sn}$  Mossbauer anal. 0-7229  
Ag-Fe, dil., ion implanted, phase comp., Mossbauer study 0-7244  
 $\text{Ag}_{0.25}\text{Cu}_{0.25}\text{In}_{0.50}\text{Sn}_{0.50}\text{S}_3$ , Mossbauer spectra (French) 0-44326  
Ag $^{57}\text{Fe}$ , Mossbauer parameters in phase-transition region 0-11308  
 $^{109}\text{Ag}$ , Mossbauer resonance at 88 keV, temp. depend. 0-7213  
Al, interaction between  $^{57}\text{Co}$  atoms and quenched-in vacancies, Mossbauer meas. 0-7234  
Al- $^{57}\text{Co}$ , implanted, Mossbauer effect obs. of annealing 0-39126  
Al-Co, defect structs. introduced by electron irradi., Mossbauer study 0-7239  
Al-Cu-Sn, ageing process, effect of Sn atoms,  $^{119}\text{Sn}$  Mossbauer spectra obs. 0-7598  
Al-Dy, dil., ion implanted, crystal hyperfine field interaction, Mossbauer spectroscopy study 0-44968  
Al-Fe, dil., annealing after cold working, impurity-vacancy interactions, Mossbauer meas. 0-7236  
Al-Fe, dil., defects and phases, Mossbauer studies 0-40004  
Al-Fe, dil., Mossbauer spectra of implanted  $^{57}\text{Fe}$ , ageing behaviour 0-7233  
Al-Sn alloys, heat treatment effect on  $^{119}\text{Sn}$  Mossbauer spectrum 0-7228  
( $\text{Al}_2\text{O}_3\text{-Fe}_2\text{O}_3$ )- $\text{Cr}^{3+}$ , (0.04 mol.%  $\text{Fe}_2\text{O}_3$ ), paramag., cross relax., annealing temp. effect from Mossbauer meas. 0-44983  
 $^{241}\text{Am}$ ,  $\alpha$ -radiation self-damage effect on hyperfine interaction and Debye-Waller factor, Mossbauer meas. 0-7230



## Mossbauer effect continued

- Au, electrodeposit, Co-hardened, state of Co in as-deposited material, Mossbauer obs. 0-15397
- Au-Co, electrodeposit, characterisation by  $^{57}\text{Co}$ - $^{57}\text{Fe}$  Mossbauer spectroscopy 0-39989
- Au-Co, electrodeposit, Mossbauer meas. of Co chem. state 0-39990
- Au-Cs(Mg)(Rb)(Zn), charge transfer, Mossbauer effect  $^{197}\text{Au}$  isomer shifts, XPS valence-band spectra 0-2676
- Au-Fe, dil., ion implanted, phase comp., Mossbauer study 0-7244
- Au-Te, elec. field gradients and charge transfer, Mossbauer spectra 0-25268
- $\text{AuAl}_2(\text{Ga}_2)(\text{In}_2)(\text{Sn}_2)(\text{Sb}_2)(\text{Te}_2)$ , core-level binding energy shifts and charge transfer 0-25268
- $\text{BaO-Fe}_2\text{O}_3\text{-B}_2\text{O}_3$  glass, struct. and mag. props., Mossbauer spectra 0-7226
- $\text{BaO-Fe}_2\text{O}_3\text{-B}_2\text{O}_3$  glass, sput cooled, low temp. micromagnetism 0-34660
- $\text{Ba}_2\text{Ru}_2\text{MO}_{12}$ , ( $\text{M}=\text{Ta}, \text{Nb}$ ), Ru oxidation state, Mossbauer study 0-44965
- $\text{Ba}_{0.54}\text{Sr}_{0.46}\text{Nb}_2\text{O}_6$ , line broadening effect in Rayleigh scatt. of Mossbauer radiation 0-50238
- $\text{BaTiO}_3$ , line broadening effect in Rayleigh scatt. of Mossbauer radiation 0-50238
- $\text{BaTiO}_3$ -based ceramics, impurity atoms chem. state, Mossbauer spectra 0-15902
- $\text{Ba}_2\text{XRuO}_6$  ( $\text{X}=\text{La}, \text{Eu}$ ),  $^{99}\text{Ru}$  Mossbauer spectra and other techniques 0-29659
- $(\text{Ca}, \text{Fe})\text{SiO}_3$ , intracryst.  $\text{Fe}^{2+}\text{-Ca}^{2+}$  exchange, Mossbauer spectra 0-20548
- $\text{CaBaFe}_2\text{O}_8$ , overlap contribution to  $^{57}\text{Fe}^{3+}$  isomer shifts, nuclear size change 0-39903
- $\text{CaF}_2\text{-Fe}^{2+}$ , relax. meas., Mossbauer spectroscopy, 10-30K 0-44977
- $\text{Ca}_2\text{Fe}_2\text{Cr}_{2-x}\text{Ge}_x\text{O}_{12}$ , antiferromagnetic order below 12K, Mossbauer study 0-39945
- $\text{CaFe}^{2+}\text{Fe}^{3+}\text{Si}_2\text{O}_7(\text{OH})$ , Mossbauer spectra, temp. depend. electron delocalisation 0-20567
- $\text{CaFe}_2\text{O}_4$ , overlap contribution to  $^{57}\text{Fe}^{3+}$  isomer shifts, nuclear size change 0-39903
- $\text{CaO-SiO}_2\text{-Fe}_2\text{O}_3$  glass, Mossbauer spectra 0-15850
- $\text{Ca}_{1-x}\text{Sr}_x\text{FeO}_3$ , Mossbauer spectra, charge disproportionation 0-15891
- $\text{Ca}_{1-x}\text{Sr}_x\text{FeO}_3$ , Mossbauer spectra, charge disproportionation 0-20542
- $\text{Ca}_2\text{XRuO}_6$  ( $\text{X}=\text{Y}, \text{La}, \text{Eu}$ ),  $^{99}\text{Ru}$  Mossbauer spectra and other techniques 0-29659
- $\text{Cd}_{1-x}\text{Fe}_x\text{Cr}_2\text{S}_4$ , Fe II electronic struct., Mossbauer spectra 0-15876
- $\text{Cd}_{0.8}\text{Ni}_{0.2}\text{Fe}_2\text{O}_4$  ferrite, Fe spin relaxation Mossbauer study, mag. hyperfine struct. (Russian) 0-15932
- $(\text{CdTe})_x(\text{CdSe})_{1-x}$ , diamond-type semiconductor, Mossbauer spectra, quadrupole interaction of  $^{125}\text{Te}$  0-44992
- $\text{Ce}_{0.7}\text{Ho}_{0.3}\text{Ru}_2\text{Co}$ , spontaneous mag. order below superconducting transition temp., Mossbauer study 0-39701
- Co complex, bis-( $\beta$ -diketonato)  $\text{Co(II)}$  dihydrate, Fe chem. states, Mossbauer emission 0-15917
- Co complex, Werner complexes,  $^{57}\text{Fe}$  partial quadrupole splitting, emission Mossbauer spectra 0-15919
- Co complexes, acetylacetonates,  $^{57}\text{Fe}$  absorption and emission spectroscopy 0-40018
- Co complexes, tris(oxinato)  $\text{Co(III)}$  and tris( $\beta$ -diketonato)  $\text{Co(III)}$ , after effects of EC decay 0-15915
- $\text{Co}^{2+}[\text{Fe}(\text{CN})_6]^{3-}$ , time depend. phenomena caused by EC decay, Mossbauer study 0-44978
- Co-Mo catalyst, Mossbauer spectra 0-7222
- $\text{CoCl}_2\cdot 2\text{H}_2\text{O}$ , gamma-X-ray coincidence Mossbauer spectra 0-15913
- $\text{CoFeCN}\cdot x\text{H}_2\text{O}$ , electron irradi., Mossbauer spectra 0-29652
- $\text{Co}_2\text{Ga}_{1.9}\text{Fe}_{0.05}$ , mag. behaviour, Mossbauer effect and DC magnetisation meas. 0-50244
- $\text{Co(II)-octaethylporphyrin}$ , Mossbauer emission spectra 0-8020
- $\text{CoM}_2\text{O}_4\cdot x$  ( $\text{M}=\text{Rh}, \text{Mn}$ ), anomalous  $^{57}\text{Fe}^m$  charge states, Mossbauer study 0-40017
- CoO, Mossbauer lines, quadrupole splitting due to defects 0-2670
- $\text{CoSO}_4\cdot 7\text{H}_2\text{O}$ , time differential Mossbauer coincidence technique, time depend. of electron capture aftereffects 0-39927
- $\text{CoSeO}_4$ , electron capture and  $\gamma$ -radiolysis, radn. damage 0-16705
- $\text{Co}^{2+}[\text{Fe}(\text{CN})_6]^{3-}$ , struct. determ. 0-15901
- $\text{Co}^{2+}[\text{Fe}^{\text{III}}(\text{CN})_6]^{3-}$ , time depend. linewidth of Mossbauer spectrum 0-15911
- Cr chalcogenide spinels,  $\text{ACr}_{1.9}\text{Sn}_{0.1}\text{X}_4$ , Sn hyperfine interactions 0-15485
- Cr-Fe, antiferromagnetic, effect of press. on hyperfine mag. fields at Fe nuclei (Russian) 0-15936
- Cr-Fe, ( $x=0.5, 1.5$  and  $3.5$  at.%), antiferromag., Kondo anomaly 0-11163
- $\text{Cr}_{1-x}\text{Fe}_x$ , Mossbauer spectra, mag. behaviour 0-20532
- $\text{Cr}_2\text{Fe}_{1-x}\text{O}_4$ , spin and charge density oscillations due to impurities (Korean) 0-20565
- $\text{CrO}_2$ , amorphous thin films, Mossbauer and magnetisation data 0-34712
- $\text{CsCl:Fe}$ , defect struct., Mossbauer spectra and X-ray diff. obs. 0-7237
- $\text{CsM}_{13}$ , ( $\text{M}=\text{V}, \text{Cr}, \text{Mn}$ ), Mossbauer spectra, struct., electronic and mag. props. 0-15908
- Cu-Fe, dil., diffusion and ageing processes, Mossbauer study 0-7245
- Cu-Fe, dil., ion implanted, phase comp., Mossbauer study 0-7244
- Cu-Fe, force constant change with pressure, relative Mossbauer fraction 0-34163
- Cu-Fe (0.2 at.%), clustering, precipitation, and oxidation, 298 to 919K, Mossbauer study 0-7242
- Cu-Fe (0.2 at.%), quenched, Fe dimers and defects 0-40007
- Cu-Fe (0.2 at.%), surface oxidation, Mossbauer obs. 0-55564
- $\text{CuCr}_2\text{-Fe}_2\text{O}_3$ , charge transfer, Mossbauer spectroscopy 0-15836
- $\text{Cu}_2\text{SnS}_3\text{-CdSe}$ , diamond-type semiconductor, Mossbauer spectrum of  $^{119}\text{Sn}$  0-44991
- $(\text{Cu}_2\text{SnS}_3)_{1-x}(\text{3CdS})_x$ , diamond-type semiconductor, Mossbauer spectrum of  $^{119}\text{Sn}$  0-44991
- $(\text{Cu}_2\text{SnS}_3)_{1-x}(\text{3ZnS})_x$ , diamond-type semiconductor, Mossbauer spectrum of  $^{119}\text{Sn}$  0-44991
- $\text{Cu}_2\text{SnS}_3\text{-CdS}$ , diamond-type semiconductor, Mossbauer spectrum of  $^{119}\text{Sn}$  0-44991
- $(\text{Cu}_2\text{SnSe}_3)_{1-x}(\text{Cu}_2\text{SnS}_3)_x$ , diamond-type semiconductor, Mossbauer spectrum of  $^{119}\text{Sn}$  0-44991
- D NaCl:Fe, defect struct., Mossbauer spectra and X-ray diff. obs. 0-7237
- Dy, and  $\text{DyMn}(\text{Fe}_2)(\text{Co}_2)(\text{Ni}_2)$ , H<sub>2</sub> absorpt., Mossbauer study 0-44987
- $\text{DyAlO}_3\text{:Yb}^{3+}$ , Mossbauer relax. 0-15875

## Mossbauer effect continued

- $\text{Dy}_2\text{Co}_{17}$ , hyperfine interactions and cryst. field effects, Mossbauer spectra 0-2369
- $\text{DyCoO}_3$ , anomalous  $^{57}\text{Fe}^m$  charge states, Mossbauer study 0-40017
- DyFe amorphous film, Mossbauer and mag. meas. 0-15844
- $\text{DyFe}_3$ , Mossbauer spectra, easy magnetisation axis temp. rot. 0-15859
- $\text{Dy}_2\text{Fe}_{17}$ , hyperfine interactions and cryst. field effects, Mossbauer spectra 0-2369
- DyIG, non-cryst., Mossbauer and magnetisation studies 0-44979
- DyFe, noncrystalline, Mossbauer and magnetisation data 0-34828
- $\text{DyM}_2\text{Si}_2$ , ( $\text{M}=\text{Mn}, \text{Fe}, \text{Co}, \text{Ni}, \text{Cu}$ ), Mossbauer spectra 0-20558
- $\text{Dy}_2\text{Ni}_{17}$ , hyperfine interactions and cryst. field effects, Mossbauer spectra 0-2369
- $\text{Dy(OH)}_3$ , Mossbauer spectra, cryst. field and mag. props. 0-15873
- $\text{ErFe}_2$ , lattice dynamics, Mossbauer spectra 0-19888
- $\text{ErFe}_3$ , H<sub>2</sub> sorption, mag. and struct. props. of hydrides 0-34831
- $\text{Er(Fe}_{1-x}\text{Co}_x)_3$ , spin reorientation, easy axis of magnetisation 0-25144
- $\text{ErFe}_2\text{H}_{3.65}$ ,  $\text{ErFe}_2\text{H}_{4.12}$ , Mossbauer spectra, electronic and structural studies 0-15860
- $\text{Er(OH)}_3$ , Mossbauer spectra, cryst. field and mag. props. 0-15873
- $\text{ErRh}_4\text{B}_4$ , Mossbauer spectra 0-15926
- $\text{EuB}_6$ , pure single crystals, magnetic and electric props. 0-11260
- $\text{EuB}_{6-x}\text{C}_x$ , Mossbauer spectra, cond. electrons effect 0-20545
- $\text{Eu}_{0.95}\text{Ba}_{0.05}\text{Pt}_2$ , Mossbauer studies on  $^{151}\text{Eu}$  at high press. 0-39923
- $\text{EuCoO}_3$ , anomalous  $^{57}\text{Fe}^m$  charge states, Mossbauer study 0-40017
- EuIG, non-cryst., Mossbauer and magnetisation studies 0-44979
- EuIG, noncrystalline, Mossbauer and magnetisation data 0-34828
- $\text{EuMg}_5$ , Mossbauer effect, effective moments, mag. ordering temp. and isomer shifts 0-34833
- $\text{Eu}_2\text{Mg}_{17}$ , Mossbauer effect, effective moments, mag. ordering temp. and isomer shifts 0-34833
- $\text{EuO}_{1-x}\text{N}_x$ , blocking of valence fluctuations,  $^{151}\text{Eu}$  Mossbauer spectra 0-2678
- $\text{EuPt}_2$ ,  $^{151}\text{Eu}$  Mossbauer studies at high press. 0-39923
- $\text{Eu}_2\text{Sn}^{2+}$ , Mossbauer spectra,  $\text{Sn}^{2+}$  transferred hyperfine fields 0-15887
- $\text{EuTe:Sn}^{2+}$ , Mossbauer spectra,  $\text{Sn}^{2+}$  transferred hyperfine fields 0-15887
- $\alpha\text{-Fe}_2\text{O}_3$ , alkali metal hydroxides, reduction, Mossbauer spectra 0-16672
- (Fe, Ti) silicate glasses, optical absorption and Mossbauer spectra 0-55136
- Fe,  $^{155}\text{Tb}$  sources produced by recoil implantation,  $^{155}\text{Gd}$  Mossbauer transition 0-40009
- $\text{Fe}(\text{H}_2\text{O})_6^{2+}$ , in crystals and aqueous soln., asymmetrical quadrupole spectra 0-44974
- Fe aerosol fine particles, Mossbauer spectra 0-7223
- Fe alloys, BCC, Mossbauer spectra, local mag. moments 0-15861
- Fe, Armo, borided surface layers, Mossbauer and metallographic anal. 0-50769
- $\alpha\text{-Fe}$ , chem. interaction with aluminophosphate and aluminochromophosphate adhesives, Mossbauer obs. 0-40596
- Fe clusters, supported, Mossbauer spectra 0-7220
- Fe complex,  $^{57}\text{Fe}$ (2-aminomethylpyridine)<sub>3</sub>Cl<sub>2</sub>C<sub>2</sub>H<sub>5</sub>OH, temp. depend. spin state,  $^{57}\text{Fe}$  Mossbauer emission spectroscopy 0-39980
- Fe complex, Fe (alkylthiocarbamate)<sub>3</sub>X, X=Cl, I, mol. orbital calc., hyperfine fields, elec. field gradient 0-39981
- Fe complex,  $\text{Fe}, \text{M}_{1-x}(\text{1,10-phenanthroline})_2(\text{NCS})_2$ , M=Mn, Co, Ni, spin crossover, Mossbauer and magnetism study 0-44980
- Fe complex, Fe(III) Schiff-base complexes, mag. relax., Mossbauer spectra 0-15897
- Fe complex, Fe(II) oxalato-bridged chain compounds, Mossbauer spectra 0-15890
- Fe complex, ferrous pseudo-tetrahedral compounds, paramag. relax., Mossbauer spectra 0-15869
- Fe complex, iron 4,7-(CH<sub>3</sub>)<sub>2</sub>(1,10-phenanthroline)<sub>2</sub>(NCS)<sub>2</sub>, spin state transition, X-ray and Mossbauer obs. 0-7195
- Fe complex, pyridine-n-oxide perchlorate, Mossbauer spectra, site distortions enhanced by grinding 0-15883
- Fe complex, tris(monothio- $\beta$ -diketonato) Fe (III), spin equilib., Mossbauer spectra 0-15910
- Fe complexes, 1-(2-pyridylazo)-2-naphthol and 1-(2-pyridylazo)-2-phenanthroline, back co-ordination, Mossbauer study 0-20572
- Fe complexes, 2- or 3-pyridyl imine complexes of  $\text{FeCl}_2$ , Mossbauer and mag. props. 0-15896
- Fe complexes,  $\text{FeOCl}[\text{Co}(\text{cyclopentadienyl})_{10.16}]$  and  $\text{FeOCl}[\text{Fe}(\text{cyclopentadienyl})_{10.16}]$ , Mossbauer and mag. susceptibility meas. 0-44176
- Fe complexes,  $\text{M}[\text{Fe}(\text{C}_2\text{O}_4)_3]\cdot x\text{H}_2\text{O}$ , M=Li, Na, K, Rb, Cs, NH<sub>4</sub>, Mossbauer studies of electronic relax. phenomena 0-44973
- Fe complexes, tetraphenylporphyrins, mag. susceptibility, hyperfine mag. field value Mossbauer spectra 0-37824
- Fe complexes with dimethylformamide, dimethylthioformamide, Mossbauer and mag. props. 0-39974
- Fe containing minerals, basalt rocks, Mossbauer spectroscopy identification 0-8302
- Fe, conversion electron meas. of core polarisations 0-20530
- Fe, conversion spectrum anal., outer-shell s-electron density, ACSEMP program 0-7208
- Fe crystalline systems and metallic glasses, Mossbauer spectroscopy, effect of neighbours on hyperfine field 0-39931
- Fe, deoxidation of liq. by Al, Mossbauer meas. 0-20553
- Fe epitaxial film, Mossbauer effect, depth profiling of mag. hyperfine field 0-11295
- Fe epitaxial film, Mossbauer effect, interface magnetism 0-11297
- Fe film, on Cu and Ag substrates, mag. props., Mossbauer spectra meas. 0-11233
- Fe film, ultra-thin Mossbauer spectroscopic studies of mag. props. 0-44970
- Fe film coated by MgO, MgF<sub>2</sub> and Sb, surface mag. 0-7196
- Fe film coated by MgO, Mossbauer spectra, mag. hyperfine field 0-7221
- Fe, fine particles, chemisorption of CO, H<sub>2</sub>, Mossbauer study 0-39415
- Fe fine particles in matrices, lattice vibr., Mossbauer effect 0-15924
- Fe foil, Lamb-Mossbauer factor at 4.2K 0-20561
- Fe hexacyanoferrates,  $\text{M}_4\text{Fe}(\text{CN})_6\cdot n\text{H}_2\text{O}$ , Mossbauer and IR spectra 0-2739
- $\gamma\text{-Fe}$ , mag. struct., Mossbauer studies. 0-39917
- Fe, Mossbauer effect at high press. in  $\alpha$ -,  $\epsilon$ - and  $\gamma$ -phases 0-15858
- Fe, Mossbauer spectra, demagnetising field effect on magnetic splitting 0-39932
- Fe multilayer films stability, Mossbauer spectra 0-29651
- Fe organometallics, interaction of naked Fe atoms with small mols., Mossbauer study of bonding in products 0-43080



## Mossbauer effect continued

- Fe, oxidised aerosoled ultrafine particles, X-ray and Mossbauer examination 0-21183  
 Fe, small particles, Mossbauer effect study of lattice vibr. 0-44963  
 Fe, sponge, oxidation kinetics by nuclear  $\gamma$ -resonance method (Russian) 0-40681  
 Fe, surface, contamination in vac. depth selective conversion electron Mossbauer spectroscopy 0-2671  
 Fe, whiskers, polycrystn., Mossbauer study 0-20571  
 Fe<sup>2+</sup> compounds, Mossbauer spectra, spin-lattice relax. effects 0-50239  
 Fe<sup>3+</sup>/Fe<sup>2+</sup> ratio, quantitative Mossbauer spectra 0-7209  
 Fe-Al, Mossbauer spectra, local mag. moments 0-15861  
 Fe-Al alloys, cold-worked, Mossbauer study of recovery 0-7593  
 Fe-Al<sub>2</sub>O<sub>3</sub> granular film, interface props., Mossbauer spectroscopy 0-34336  
 Fe-B, amorphous, short-range order, Mossbauer meas. 0-44986  
 Fe-B, amorphous paramag. alloys, hyperfine field distrib., Mossbauer study 0-39958  
 Fe-B amorphous alloy, mag. anisotropy temp. depend. 0-15846  
 Fe-B amorphous alloys, Mossbauer spectra, soft ferromag. props. 0-11302  
 Fe-B amorphous alloys, Mossbauer spectra, mag. moment conc. depend. 0-15847  
 Fe-B-Si, amorphous ferromag. alloys, mag. struct., Mossbauer study 0-39746  
 Fe-B(Si) amorphous alloys, Mossbauer spectra, struct. 0-15840  
 Fe-C, martensite, struct., Mossbauer meas. 0-40000  
 Fe-C (1.2 wt.%), Mossbauer study of early stages of tempering 0-16342  
 Fe-Co-Si solid solutions, BCC, atomic configs., Mossbauer study 0-39006  
 Fe-Cr, disordered, mag. order, Mossbauer study 0-39992  
 Fe-implanted alloys, residence sites of Fe, Mossbauer data 0-39299  
 Fe-M-SiO<sub>2</sub> (M=Ru,Pt), supported catalysts, Mossbauer spectra 0-11296  
 Fe-Mn, Mossbauer spectroscopy of temp. hysteresis of phase transformations (Czech) 0-29949  
 Fe-Mn (9 to 20 wt.%), <sup>57</sup>Fe Mossbauer spectroscopy in phase transformations 0-29948  
 Fe-Mo catalyst, Mossbauer spectra 0-7222  
 Fe-Ni, ordered phase, L10 superstruct., Mossbauer spectrum, Debye-Scherrer pattern from LL-chondrite 0-50241  
 Fe-Ni alloy, anisotropic hyperfine interactions, Mossbauer spectra 0-15854  
 Fe-Ni alloy near crit. conc., Mossbauer  $\gamma$ -rays small angle scatt. 0-7217  
 Fe-Ni alloys, cold rolled, exam. of phase composition using Mossbauer spectroscopy 0-21204  
 Fe-Ni Invar alloys, Mossbauer spectra, heat treatment effect 0-15855  
 Fe-Ni ordered phase in meteorites, Mossbauer studies 0-41776  
 Fe-Ni superstructure in metal particles in chondrites 0-12713  
 Fe-Ni-Al, magnetic anisotropy form. and struct. changes by annealing, Mossbauer obs. 0-39994  
 Fe-Ni-Al-Co-Ti base alloys, highly coercive, phase comp., Mossbauer meas. 0-39996  
 Fe-Ni-P-B, amorphous ferromag. alloys, mag. struct., Mossbauer study 0-39746  
 Fe-Ni-P-B, amorphous paramag. alloys, hyperfine field distrib., Mossbauer study 0-39958  
 Fe-Ni-Si-B, amorphous paramag. alloys, hyperfine field distrib., Mossbauer study 0-39958  
 Fe-P-B, amorphous alloy, Mossbauer effect and short-range order 0-2675  
 Fe-P-C, amorphous alloy, Mossbauer effect and short-range order 0-2675  
 Fe-P-C amorphous alloys, Mossbauer spectra, struct. 0-15840  
 Fe-Ru(Os) alloys, antiferromag. ordering, hyperfine fields 0-15867  
 Fe-Sb-Ti(V)(Cr)(Mn)(Co)(Ni), dil., interactions and precip., Mossbauer study 0-39997  
 Fe-Si, hyperfine fields, Mossbauer meas. 0-40024  
 Fe-Si amorphous film, crystallisation, Mossbauer studies 0-33900  
 Fe-Si amorphous film, struct. and crystallisation, Mossbauer study 0-11300  
 Fe-SiO<sub>2</sub> granular film, interface props., Mossbauer spectroscopy 0-34336  
 Fe-SiO<sub>2</sub> supported catalysts, Mossbauer spectra 0-11296  
 Fe-SiO<sub>2</sub>(Al<sub>2</sub>O<sub>3</sub>)(ZrO<sub>2</sub>) granular films, superparamag., Mossbauer effect 0-7131  
 Fe-Sn, grain boundary embrittlement by Sn segregation, Mossbauer study 0-7239  
 Fe-Sn system, Sn binding state, using segregated <sup>119m</sup>Sn, Mossbauer anal. (Japanese) 0-20525  
 Fe-X-Sn dilute alloy, Mossbauer meas. of Sn interaction with solute atoms 0-15856  
 Fe-ZrO<sub>2</sub> granular film, interface props., Mossbauer spectroscopy 0-34336  
 Fe+<sub>2</sub>(NH<sub>3</sub>)<sub>2</sub> interaction, chemical species formed studied by Mossbauer effect 0-43080  
 Fe<sub>1-x</sub>Al<sub>x</sub>OOH, Mossbauer study, determ. of Al content and mag. props. 0-39938  
 FeAs, Mossbauer spectra of paramag. and ferromag. states, helimagnetic spin ordering 0-7197  
 Fe<sub>80</sub>B<sub>20</sub>, amorphous, elec. and mag. hyperfine field distrib., Mossbauer study 0-39964  
 Fe<sub>80</sub>B<sub>20</sub>, amorphous ferromag. metallic glass, stress-induced rot. of magnetisation, Mossbauer study 0-20445  
 Fe<sub>80</sub>B<sub>20</sub>, amorphous to cryst. transorm. 0-34188  
 Fe<sub>80</sub>B<sub>20</sub> metallic glass, spin texture determ. 0-15842  
 Fe<sub>84</sub>B<sub>16-x</sub>C<sub>x</sub>, amorphous alloys, short range order, Mossbauer and DSC study 0-39960  
 FeBO<sub>3</sub>, Laue refl. of Mossbauer radiation, depend. on mag. field direction 0-40020  
 Fe<sub>78</sub>B<sub>12</sub>Si<sub>10</sub>, amorphous, Mossbauer study of hyperfine interaction and mag. anisotropy 0-40027  
 Fe<sub>2</sub>C, alpha-particle irradi., Mossbauer study of nucl. reaction aftereffects 0-40015  
 Fe(ClO<sub>4</sub>)<sub>2</sub>, frozen aq. soln., Mossbauer spectra, ligand field calc. for Fe(H<sub>2</sub>O)<sub>6</sub><sup>2+</sup> complex 0-39971  
 FeCl<sub>3</sub>·4H<sub>2</sub>O, frozen solns., isotope effect of Mossbauer parameters 0-34835  
 FeCo disordered alloys, Mossbauer spectra, hyperfine mag. field distrib., Curie temp. 0-7198  
 FeCo molecules, matrix-isolation Mossbauer spectra 0-23448  
 FeCoCrO<sub>4</sub>, <sup>57</sup>Fe Mossbauer spectra, cation distrib. 0-15879  
 (Fe<sub>0.5</sub>Co<sub>0.8</sub>)<sub>80</sub>P<sub>17</sub>Al<sub>3</sub>, Mossbauer spectra, isomer shift, mag. hyperfine field 0-11301  
 Fe<sub>0.5</sub>Co<sub>0.5</sub>TiH<sub>x</sub>, transmission Mossbauer spectra 0-44964  
 FeCr<sub>2</sub>Se<sub>4</sub>, Mossbauer spectra, second order phase transition 0-20539  
 Fe<sub>2</sub>Cu<sub>1-x</sub>Cr<sub>2</sub>Se<sub>4</sub>, crystallographic and image props. 0-39049

## Mossbauer effect continued

- FeF<sub>2</sub>, Mossbauer effect at high press. 0-15858  
 FeF<sub>3</sub>, overlap contribution to <sup>57</sup>Fe<sup>3+</sup> isomer shifts, nuclear size change 0-39903  
 FeF<sub>3</sub>·3H<sub>2</sub>O,  $\alpha$  and  $\beta$  phase, <sup>57</sup>Fe Mossbauer study of local struct. 0-39973  
 FeF<sub>3</sub>·7H<sub>2</sub>O and oxidation products, <sup>57</sup>Fe Mossbauer study of local struct. 0-39973  
 FeGe, hyperfine interactions of <sup>119</sup>Sn atoms, Mossbauer spectra (Russian) 0-29665  
 FeGe<sub>2</sub>, antiferromag., biquadratic exchange 0-2371  
 Fe<sub>2</sub>Ge<sub>1-x</sub>, amorphous, conversion electron Mossbauer spectra down to 4.2K 0-7205  
 Fe(H<sub>2</sub>O)<sub>6</sub>·SiF<sub>6</sub>, pressure-induced orbital ground state inversion, Mossbauer study 0-39979  
 Fe(H<sub>2</sub>PO<sub>4</sub>)<sub>2</sub>,  $\gamma$ -ray and electron radiolysis, Mossbauer study 0-7816  
 FeI<sub>2</sub>, magnetic phase transitions, Mossbauer spectra in high mag. fields 0-39936  
 Fe(III) salt soln., hydrolysis products, Mossbauer spectra 0-16671  
 Fe<sub>3-x</sub>Mg<sub>x</sub>O<sub>4</sub>, Verwey transition, Mossbauer study 0-39942  
 Fe<sub>0.55</sub>Mg<sub>0.47</sub>SiO<sub>3</sub>, orthopyroxene, electron irradi. effects, Mossbauer study 0-40016  
 Fe<sub>2(1-y)</sub>Mg<sub>(1+y)</sub>Ti<sub>2</sub>O<sub>4</sub>, Mossbauer spectra anal., model 0-20560  
 (Fe<sub>2</sub>Mn<sub>1-x</sub>)<sub>75</sub>P<sub>16</sub>B<sub>6</sub>Al<sub>3</sub>, amorphous, mag. ordering temp., hyperfine field distrib., elec. resist. 0-34633  
 (Fe<sub>1-x</sub>Mn<sub>x</sub>)<sub>75</sub>P<sub>15</sub>C<sub>10</sub>, amorphous, mag. ordering, Mossbauer study 0-39747  
 Fe<sub>2</sub>MoO<sub>4</sub>, <sup>57</sup>Fe Mossbauer spectra, cation distrib. 0-15879  
 Fe<sub>2</sub>(N<sub>3</sub>)<sub>2</sub>, paramag. relax. in trigonal bipyramidal environment, Mossbauer spectra 0-15871  
 Fe(NH<sub>4</sub>)<sub>2</sub>(SO<sub>4</sub>)<sub>2</sub>·6H<sub>2</sub>O, Mohr salt, elec. field gradient determ., appl. of intensity tensor to thick single cryst. 0-44966  
 (Fe<sub>1-x</sub>Ni<sub>x</sub>)<sub>75</sub>B<sub>25</sub>, amorphous and cryst., short range order, Mossbauer study 0-39961  
 (Fe<sub>1-x</sub>Ni<sub>x</sub>)<sub>80</sub>B<sub>20</sub>, amorphous, Mossbauer spectra, mag. props. 0-15843  
 FeNiBO<sub>4</sub>, FeNi<sub>2</sub>BO<sub>4</sub>, Mossbauer spectra, mag. relax. 0-15889  
 Fe<sub>0.65</sub>(Ni<sub>1-x</sub>Co<sub>x</sub>)<sub>0.35</sub>, Mossbauer spectra, <sup>57</sup>Fe hyperfine field distrib. 0-20533  
 Fe<sub>0.65</sub>(Ni<sub>1-x</sub>Mn<sub>x</sub>)<sub>0.35</sub>, Mossbauer spectra, <sup>57</sup>Fe hyperfine field distrib. 0-20533  
 Fe<sub>2</sub>O<sub>3</sub> amorphous film, Mossbauer spectra, mag. props. 0-15851  
 Fe<sub>2</sub>O<sub>3</sub> amorphous RF sputtered thin films, Mossbauer and mag. study 0-34711  
 Fe<sub>2</sub>O<sub>3</sub> amorphous thin films, Mossbauer and magnetisation data 0-34712  
 $\alpha$ -Fe<sub>2</sub>O<sub>3</sub>, hematite, Morin transition, Mossbauer mag. diffr. spectra 0-20562  
 $\gamma$ -Fe<sub>2</sub>O<sub>3</sub>, hyperfine mag. field at <sup>119</sup>Sn, Mossbauer expt. 0-50232  
 $\gamma$ -Fe<sub>2</sub>O<sub>3</sub>, small particles, noncollinearity as crystallite-size effect, Mossbauer study 0-39939  
 Fe<sub>2</sub>O<sub>3</sub>-BaO-B<sub>2</sub>O<sub>3</sub> glass, Mossbauer spectra, <sup>57</sup>Fe hyperfine interactions 0-39969  
 $\alpha$ -Fe<sub>2</sub>O<sub>3</sub>-Li<sub>2</sub>O, structural and thermal phase behaviour from mag., spectral and thermal studies 0-2673  
 $\gamma$ -Fe<sub>2</sub>O<sub>3</sub>-organic interfaces, mag. struct., Mossbauer effect, IR absorpt., and magnetisation meas. 0-44869  
 Fe<sub>2</sub>O<sub>3</sub>-PbO-B<sub>2</sub>O<sub>3</sub> glass, X-ray and electron microscope studies, mag. and Mossbauer effect meas. 0-28919  
 Fe<sub>2</sub>O<sub>4</sub>, hyperfine mag. field at <sup>119</sup>Sn, Mossbauer expt. 0-50232  
 Fe<sub>2</sub>O<sub>4</sub>, magnetite, Mossbauer spectra of low temp. phase 0-20541  
 Fe<sub>2</sub>O<sub>4</sub>, magnetite, valence instabilities, Mossbauer effect 0-20543  
 Fe<sub>2</sub>O<sub>4</sub>, magnetite Mossbauer spectra, mag. dipolar and elec. quadrupole effects 0-20544  
 Fe<sub>2</sub>O<sub>4</sub> particles, nonstoichiometric, morphology and enhanced coercivity, Mossbauer meas. 0-7132  
 FeOCl, Mossbauer spectra, lattice dynamics, hyperfine interactions 0-44985  
 FeOOH gels, Mossbauer spectra, mag. props. 0-11303  
 $\delta$ -FeOOH, structure and phase transform., Mossbauer, X-ray, DTA study (Chinese) 0-54368  
 $\alpha$ -FeOOH ultrafine particle NGR spectra, size distrib. and surface effects 0-11299  
 FeOOH:Cl(F), quadrupole interaction, Mossbauer spectra 0-15895  
 20Fe<sub>2</sub>O<sub>3</sub>·80[3B<sub>2</sub>O<sub>3</sub>·(1-x)PbO·xGeO<sub>2</sub>] glass, phys. props. 0-49119  
 $\alpha$ -FeP<sub>2</sub>, diamag., semicond., Mossbauer study 0-50243  
 Fe<sub>2</sub>P:Cu, Mossbauer spectra, mag. transition 0-50240  
 Fe<sub>80</sub>P<sub>20</sub>, binary amorphous ferromagnet, Mossbauer study 0-34829  
 Fe<sub>2</sub>(PO<sub>4</sub>)Cl, Mossbauer study of mag. ordering and local co-ordination 0-39972  
 Fe<sub>3</sub>(PO<sub>4</sub>)<sub>2</sub>(OH)<sub>2</sub>, synthetic barbosolite, temp. depend. quadrupolar and mag. hyperfine interactions 0-25255  
 Fe<sub>2</sub>Pt, non-linear local environment effect, Mossbauer effect of <sup>57</sup>Fe and <sup>195</sup>Pt 0-39910  
 Fe<sub>2</sub>Pu(Np)(U)(Zr)(Tm), Mossbauer diffr., combination type maxima, hyperfine interactions on nuclei 0-25263  
 FeRO<sub>3</sub>, enhanced nuclear resonance scattering in dynamical diffraction of gamma-rays 0-44982  
 FeS, quadrupole splitting and ground state, Mossbauer spectra 0-29657  
 FeS<sub>2</sub>, (pyrite), angle-independent Mossbauer effect 0-20570  
 FeS<sub>2</sub>, Mossbauer elec. field gradient and mean square displacement 0-39991  
 FeS<sub>2</sub>, oxidation, Mossbauer spectroscopic and magnetokinetic studies, 400-500°C 0-44880  
 FeS<sub>2</sub>, pyrite, elec. field gradient, Mossbauer spectrum 0-15493  
 FeS<sub>2</sub>, pyrite, semiconducting props., energy gap press. and lattice parameter depend., Mossbauer obs. 0-44494  
 FeSO<sub>4</sub>·7H<sub>2</sub>O and FeSO<sub>4</sub>·7D<sub>2</sub>O, frozen solns., isotope effect of Mossbauer parameters 0-34835  
 FeSb alloy films, vapour-deposited, formation of metastable phase 0-44437  
 FeSb solid solution, supersaturated, mag. hyperfine field, Mossbauer study 0-44961  
 Fe<sub>2</sub>Se<sub>4</sub>, Fe<sub>2</sub>Se<sub>8</sub>, phase gap, Mossbauer spectra 0-20552  
 FeSeO<sub>4</sub>, electron capture and  $\gamma$ -radiolysis, radn. damage 0-16705  
 $\alpha$ -Fe<sub>1-x</sub>Si<sub>x</sub>, many-body atomic correlations, Mossbauer spectroscopy study 0-15934  
 Fe<sub>2</sub>Si<sub>2</sub>Al<sub>1-x</sub>Co<sub>x</sub>, dil., site preference of <sup>57</sup>Co impurities, Mossbauer study 0-39999  
 FeSiF<sub>6</sub>·6H<sub>2</sub>O, Lamb-Mossbauer factor isotropy in the Debye model (French) 0-44962  
 Fe<sub>2</sub>Sn<sub>1-x</sub>, amorphous alloy, Mossbauer spectra, charge transfer and atomic vol. effects 0-39959



## Mossbauer effect continued

- $\text{Fe}_{3-x}\text{Sn}_x\text{O}_4$ , mag. hyperfine fields,  $^{57}\text{Fe}$  and  $^{119}\text{Sn}$  Mossbauer spectra 0-39944  
 $\text{Fe}_{1+x}\text{Te}$ ,  $^{129}\text{I}$  transferred hyperfine field, Mossbauer spectroscopy study 0-44972  
 $\text{Fe}_{3-x}\text{Ti}_x\text{O}_4$ , Mossbauer spectra in paramag. phase 0-39943  
 $\text{Fe}_{(1+x)}\text{Ti}_{(1+x)}\text{S}_2$  non-stoichiometric cpds., vacancy-cation distrib., Mossbauer spectra 0-15900  
 $^{57}\text{Fe}$  backscatt. electron Mossbauer spectroscopy 0-29661  
 $^{57}\text{Fe}$  implantation in metals, electric hyperfine interactions, conversion electron Mossbauer meas. 0-7241  
 $^{57}\text{Fe}$  interstitial cpds. and solid solns., Mossbauer spectra 0-20557  
 $^{57}\text{Fe}$  isomer shift calibration const. rel. to biological cpds. 0-7227  
 $^{57}\text{Fe}$  Mossbauer isomer shift from electron capture rate of  $^{52}\text{Fe}$  0-7203  
 $^{57}\text{Fe}$  Mossbauer level excitation using synchrotron radiation 0-7204  
 $\text{FeCr}_2\text{S}_4$ , second-order phase transition, Mossbauer spectra 0-20569  
 $\text{GaAs}_{1-x}\text{Sn}_x$ , Mossbauer spectra 0-29667  
 $\text{GaAs:Sn}$ , implantation, annealing, impurity-defect struct., Mossbauer study 0-54269  
 $\text{GaP(As)(Sb)}$ , site selective doping by ion implantation of radioactive nuclei 0-34023  
 $\text{Gd-Ni}$ , amorphous, Mossbauer spectra 0-25262  
 $\text{GdCo}$  amorphous sputtered film mag. props. from Mossbauer effect obs. (Japanese) 0-15933  
 $\text{Gd}(\text{Co}_x\text{Ni}_{1-x})_2$ , Mossbauer spectra, mag. props. 0-20563  
 $\text{GdFe}$  amorphous film, Mossbauer and mag. meas. 0-15844  
 $\text{GdFe}_2$ , easy direction of magnetisation 0-20535  
 $\text{Gd}(\text{Fe}, \text{Co}_{1-x})_2$ , Mossbauer effect at 78 and 300K,  $^{57}\text{Fe}$  hyperfine fields 0-2677  
 $\text{Gd}(\text{Fe}, \text{Ti}_{1-x})_2$ , Mossbauer spectra, mag. props. 0-20563  
 $\text{GdIG}$ , amorphous, Mossbauer spectra, mag. props. 0-15849  
 $\text{Gd}_{1-x}\text{Sc}_x$ , Mossbauer spectra, hyperfine interactions 0-15923  
 $\text{Gd}_{1-x}\text{Y}_x$ , Mossbauer spectra, hyperfine interactions 0-15923  
 $\text{Ge}_{1-x}\text{Sn}_x$ , ion-implanted, Mossbauer study, annealing effects 0-7231  
 $\text{Ge:Fe}$ , implanted, Mossbauer spectra, conversion electron, temp. dependence 0-40025  
 $\text{Ge:Fe}$ , recoil implantation Mossbauer expt. in presence of external mag. field 0-44981  
 $\text{Ge:Sn}$ , Mossbauer spectra of  $^{119}\text{Sn}$  impurity atoms 0-15935  
 $\text{Ge-Fe}$ , laser annealing of implanted  $^{57}\text{Co}$  sources, Mossbauer obs. 0-39139  
 $\text{He}$  refrigerator for temp. varying Mossbauer meas., 20-300K 0-4726  
 $\text{Hf}(\text{Fe}_{1-x}\text{Co}_x)_2$ , mag. props., Mossbauer spectra and magnetisation meas. 0-39948  
 $\text{HfFe}_{2-x}\text{Si}_x$ , Mossbauer spectra, hyperfine interactions 0-15862  
 $(\text{HgTe})_x(\text{CdTe})_{1-x}$ , diamond-type semiconductor, Mossbauer spectra, quadrupole interaction of  $^{125}\text{Te}$  0-44992  
 $\text{HoAlO}_3:\text{Yb}^{3+}$ , Mossbauer relax. 0-15875  
 $\text{Ho}(\text{OH})_3$ , Mossbauer spectra, cryst. field and mag. props. 0-15873  
 $\text{Ho}_x\text{Y}_{1-x}(\text{Fe}_{0.9}\text{Co}_{0.1})_2$ ,  $^{57}\text{Fe}$  hyperfine interaction, mag. props., Mossbauer study 0-39951  
 $\text{I}$  complexes, charge transfer states, Mossbauer spectra 0-15907  
 $^{127}\text{I}$ , isomer shift calibration, using lifetime variations in electron capture decay of  $^{123}\text{I}$  0-39925  
 $^{127}\text{I}$ , Mossbauer isomer shift 0-39922  
 $^{129}\text{I}$  impurities implanted in semiconductors, isomer shift 0-20522  
 $^{129}\text{I}$  in transition metals, calibration of Mossbauer isomer shift 0-20520  
 $^{129}\text{I}$ , internal conversion electron and Mossbauer spectra, calibration of isomer shift 0-39921  
 $^{129}\text{I}$ , isomer shift calibration, using lifetime variations in electron capture decay of  $^{123}\text{I}$  0-39925  
 $^{129}\text{I}$ , Mossbauer isomer shift 0-39922  
 $\text{InP(Sb)(As)}$ , site selective doping by ion implantation of radioactive nuclei 0-34023  
 $\text{KAl[Fe(CN)}_6]$ , isomer shift of Mossbauer spectra 0-29662  
 $\text{KCl:Fe(CN)}_6$ , electron irradi., Mossbauer and ESR study 0-7238  
 $(\text{KF})_n\text{-FeF}_3$ , antiferromagnetic systems, dimensionality and spin reduction effects, Mossbauer study 0-39947  
 $\text{K}_3\text{Fe(CN)}_6$ , electronic struct., elec. field gradient tensor 0-15483  
 $\text{KFeF}_4$ , amorphous, Mossbauer study 0-39970  
 $\text{K}_2\text{FeF}_5$ , Mossbauer spectra, 1D antiferromag. 0-15886  
 $\text{K}_{1+x}\text{Fe}_x\text{Ga}_{11-x}\text{O}_{17}$ , electron hopping and excitation at room temp.,  $^{51}\text{Fe}$  Mossbauer spectra 0-25257  
 $\text{KFeO}_2$ , overlap contribution to  $^{57}\text{Fe}^{3+}$  isomer shifts, nuclear size change 0-39903  
 $\text{KFe}_2\text{O}_3$ ,  $\beta''$  phase, mag. props., hyperfine interactions, Mossbauer study 0-20524  
 $\text{K}_2\text{FeO}_4$ , antiferromag., critical fluctuations obs. using Mossbauer spectroscopy 0-39955  
 $\text{K}_2\text{O-B}_2\text{O}_3\text{-Fe}_2\text{O}_3$  glasses, nonbridging O formation, Mossbauer spectroscopy 0-55001  
 $\text{KTI[Fe(CN)}_6]$ , isomer shift of Mossbauer spectra 0-29662  
 $\text{La-Au}$  liq.-quenched alloys, Mossbauer spectra, struct. 0-15841  
 $\text{La-Fe}$ , FCC, Mossbauer spectra, Fe atom position 0-20549  
 $\text{LaCo}_2\text{Ca(Sr)}$ , anomalous  $^{57}\text{Fe}^m$  charge states, Mossbauer study 0-40017  
 $\text{LaNi}_{1-x}\text{Fe}_x\text{O}_3$ , Mossbauer spectra, mag. hyperfine field 0-20537  
 $\text{La}_{0.99}\text{Sn}_{0.01}\text{Mo}_2\text{Se}_8$ , Mossbauer spectra 0-15926  
 $\text{LiCl:Fe}$ , defect struct., Mossbauer spectra and X-ray diffr. obs. 0-7237  
 $\text{LiFeS}_2$ , magnetic hyperfine interactions, Mossbauer spectra and mag. susceptibility meas. 0-29658  
 $\text{LiNbO}_3\text{:Fe}$ , electron spin relaxation study, Mossbauer effect, mag. and crystal field effects 0-39902  
 $\text{LiNbO}_3\text{:Fe}$ , impurity valence state charge on X-ray irradi., Mossbauer meas. 0-7235  
 $\text{LiNbO}_3\text{:Fe}$ , Mossbauer spectra quadrupole doublet asymmetry 0-44960  
 $\text{LiNbO}_3\text{:Fe}$ , state of impurity Fe cation, nucl. gamma reson. study 0-40014  
 $\text{LiNbO}_3\text{:Fe}$ , X-ray and  $\gamma$ -ray irradiation effects on Fe charge state, Mossbauer study 0-40013  
 $\text{LiTi}$  ferrite, Mossbauer study, relax. and supertransferred hyperfine fields 0-39941  
 $\text{LiTi}$ , substituted ferrite, cation distribution, Mossbauer, X-ray, neutron diffr. study 0-28975  
 $\text{Li}_2\text{V}_{1-x}\text{Fe}_x\text{S}_2$ , intercalated battery cathode material, Mossbauer studies 0-44984  
 $\text{LiZn}$  ferrite, Mossbauer study, relax. and supertransferred hyperfine fields 0-39941  
 $\text{LiZn}$ , substituted ferrite, cation distribution, Mossbauer, X-ray, neutron diffr. study 0-28975

## Mossbauer effect continued

- $(\text{Mg, Fe})\text{SiO}_3$ , orthopyroxenes, cation distrib., electronic and Mossbauer spectra 0-7370  
 $\beta\text{-Mn-}^{57}\text{Fe-}^{119}\text{Sn}$  alloy mag. props. from Mossbauer effect obs. (Japanese) 0-15933  
 $\text{Mn}_3\text{Al}_2(\text{SiO}_4)_3$ , Mossbauer spectra and absorpt. bands 0-55144  
 $\text{Mn}_{1-x}\text{Fe}_x\text{Cr}_2\text{S}_4$ , Fe II electronic struct., Mossbauer spectra 0-15876  
 $\text{MnFeO}_4\text{:}^{57}\text{Fe}$ , Mossbauer spectrum, 4s covalent bonding 0-20540  
 $\text{MnFe}_2(\text{PO}_4)_2(\text{OH})_2 \cdot 6\text{H}_2\text{O}$ , strunzite, cryst. chem., Mossbauer study 0-39975  
 $\text{MnO}$ , alpha-particle irradi., Mossbauer study of nucl. reaction aftereffects 0-40015  
 $\text{MnTe}_2$ , Mossbauer spectra, hyperfine field 0-15866  
 $\text{Mo}$ , oxidation kinetics, Mossbauer study 0-40005  
 $\text{NH}_3\text{-}^{57}\text{Fe}$ , solid, Mossbauer study of iron bonding to solid ammonia and its photofragments 0-15833  
 $(\text{NH}_3)_2\text{FeF}_5$ , quasi two-dimens. antiferromagnet, Mossbauer study 0-39947  
 $\text{N}_2\text{H}_4\text{FeF}_5$ , Mossbauer spectra, 1D antiferromag. 0-15886  
 $\text{Na-Fe}$  fluorophosphate glass, EPR and Mossbauer resonance study 0-15838  
 $\text{NaFeF}_4$ , amorphous, Mossbauer study 0-39970  
 $\text{NaI}$ , temp. varying Mossbauer spectra, isomer shift 0-4726  
 $\text{Na}_2\text{RuO}_4$ ,  $^{99}\text{Ru}$  Mossbauer spectra, antiferromag. order, mag. relax. 0-50234  
 $\text{Na}_2\text{O} \cdot 3\text{B}_2\text{O}_3 \cdot x\text{Fe}_2\text{O}_3$ , borate glass,  $\text{Fe}^{3+}$  spin state and distrib. meas. 0-39966  
 $\text{Nb}_2\text{Sn}$ ,  $\text{O}^{4+}$  bombarded, Mossbauer studies 0-2672  
 $\text{NdFe}_2$ , Curie temp., elec. quadrupole couplings, Mossbauer study 0-39949  
 $\text{NdFe}_2$ , preparation and mag. props. 0-25259  
 $\text{Ni}$ , alpha-particle irradi., Mossbauer study of nucl. reaction aftereffects 0-40015  
 $\text{Ni-Al}$  system, Mossbauer spectroscopy investigation (Russian) 0-20523  
 $\text{Ni-Fe}$ , dil., temp. depend. of Mossbauer absorpt. near Curie point (French) 0-11305  
 $\text{Ni-Fe-Mo}$ , K-effect, Mossbauer study 0-39998  
 $\text{Ni-SiO}_2$  supported catalysts, particle size,  $\text{H}_2$  chemisorption, Mossbauer study 0-7219  
 $\text{Ni}_{1-x}\text{Au}_x\text{-Co}$ , dil., hyperfine field and isomer shift, precip. process, Mossbauer expts. 0-25267  
 $\text{Ni}_{1-x}\text{Au}_x\text{-Co}$ , dil., Mossbauer effect, mag. hyperfine field 0-20528  
 $\text{NiCr}_2\text{O}_4$ , sign of net mag. hyperfine field,  $^{61}\text{Ni}$  Mossbauer study 0-39946  
 $\text{NiCr}_2\text{O}_4\text{:Fe}$ , Mossbauer effect 0-15874  
 $\text{NiFe}$  disordered alloys, Mossbauer spectra, hyperfine mag. field distrib., Curie temp. 0-7198  
 $\text{Ni}_3\text{Fe}$  disordered alloys, Mossbauer spectra, hyperfine mag. field distrib., Curie temp. 0-7198  
 $\text{Ni}_3\text{Fe}$ , non-linear local environment effect, Mossbauer effect of  $^{57}\text{Fe}$  0-39909  
 $\text{Ni}_3\text{Fe}$ , order-disorder transition phase diagram, Mossbauer meas. 0-39995  
 $\text{Ni}_3\text{Fe-Sn}$ , dil., atomic order detection by  $^{119}\text{Sn}$  spectroscopy 0-39993  
 $\text{NiFe}_{2-x}\text{Al}_x\text{O}_4$ ,  $^{57}\text{Fe}$  and  $^{61}\text{Ni}$  Mossbauer spectra 0-39940  
 $\text{Ni}_6\text{Fe}_2\text{B}_{10}\text{I}_3$ , boracite, mag. hyperfine interactions, Mossbauer study 0-39935  
 $\text{NiFe}_2\text{O}_4$  precipitation from silicate glass, Mossbauer study 0-54998  
 $\text{Ni}_{0.98}\text{Fe}_{0.02}\text{S}_{10}$ , quadrupole splitting and ground state, Mossbauer spectra 0-29657  
 $\text{Ni}_2\text{Mn}_2\text{M}_{1-x}\text{Sn}$  ( $\text{M}=\text{Ti, V}$ ) mag. hyperfine fields,  $^{119}\text{Sn}$  Mossbauer spectra study 0-55003  
 $\text{Ni}_2\text{Mn}_2\text{Ti}_{1-x}\text{Sn}$ , Mossbauer spectra, mag. hyperfine field 0-15857  
 $\text{Ni}_{1-x}\text{S}$ , metal-semimetal transition, lattice dynamics and thermodynamic props. 0-29324  
 $\text{Ni}_{0.38}\text{Zn}_{0.62}\text{Fe}_2\text{O}_4$ , preparation, Mossbauer study 0-50231  
 $\text{NpAs}_2$ , magnetic props., 4.2 to 77K, Mossbauer study 0-39937  
 $\text{NpBa}_6\text{Zr}_{12}\text{F}_x$  glass, Mossbauer spectrum 0-11304  
 $\text{NpCo}_2\text{Si}_2$ , mag. props., high press. studies with  $^{237}\text{Np}(60)$ -resonance 0-39924  
 $\text{NpFe}_{2-x}\text{Co}_x\text{Si}_2$ , mag. and hyperfine props. 0-7247  
 $(\text{Np}_{1-x}\text{U}_x)\text{Fe}$ , Mossbauer spectra, magnetism and hyperfine interactions 0-20529  
 $^{231}\text{Pa}$  Mossbauer resonance, elec. field grad. 0-7207  
 $^{231}\text{Pa}$  Mossbauer resonance, elec. field gradient 0-15927  
 $\text{Pb-Sn}_{1-x}\text{Te}$ , thin film, oxidation, appl. of Mossbauer method 0-45410  
 $\text{Pd-Co}$ , very dil., Mossbauer emission spectra of  $^{57}\text{Co}$ , relax. effects 0-29656  
 $\text{Pd-Fe}$ , scatt. and transmission Mossbauer spectra near Curie temp. 0-15864  
 $\text{Pd-Si-Fe}$  amorphous alloy, Mossbauer spectra, struct. and bonding 0-7224  
 $\text{PdH}_x\text{:Co(Fe)}$ , diffusion and interstitial site occupancy, Mossbauer spectra 0-20555  
 $\text{PdH}_x\text{-Fe}$ , dil., Kondo system, local moment hyperfine studies, Mossbauer expt. 0-39908  
 $\text{Pd(MnCo)}$ , giant moments, Mossbauer study of  $^{57}\text{Fe}$  0-44969  
 $\text{Pd}_2\text{Mn}_{0.95}\text{Sn}_{1.05}$ , hyperfine mag. fields, Mossbauer spectra 0-15870  
 $\text{Pd}_2\text{MnSn}_{1-x}\text{Sb}_x$ , Mossbauer spectra, mag. hyperfine field 0-15868  
 $\text{Pr-Eu}$ , dil., magnetisation, Mossbauer spectra 0-15928  
 $\text{PrEu(Gd)}$ , magnetic interactions, Mossbauer spectra quadrupole splitting, crystal field parameters 0-39907  
 $\text{PrFe}_2$ , Curie temp., elec. quadrupole couplings, Mossbauer study 0-39949  
 $\text{PrFe}_2$ , preparation and mag. props. 0-25259  
 $\text{Pt-Sn/Al}_2\text{O}_3$  catalyst, Mossbauer effect, reactivity 0-11298  
 $\text{PuO}_2$ , Mossbauer resonance 0-20554  
 $\text{PuO}_2\text{C}_2\text{O}_4$ , Mossbauer resonance 0-20554  
 $\text{RM}_4\text{Al}_6$  ( $\text{M}=\text{Cr, Mn, Fe, Cu}$ ), magnetism and hyperfine interactions 0-25256  
 $\text{RbCaF}_3$ , critical scatt. at struct. phase transition, Mossbauer diffr. 0-20546  
 $\text{RbCaF}_3$ , cubic to tetragonal phase transform., X-ray, neutron, Mossbauer diffr. study 0-49360  
 $\text{Rb}_2\text{CoF}_4\text{:}^{57}\text{Fe}$ , Ising antiferromag., Mossbauer spectra, critical dynamics 0-15884  
 $\text{Rb}_2\text{CoF}_4\text{:}^{57}\text{Fe}$ , Mossbauer spectra, critical region anal. 0-15888  
 $\text{Rb}_2\text{Co}_{0.95}\text{Mg}_{0.05}\text{F}_4\text{:}^{57}\text{Fe}$ , Mossbauer spectra, critical region anal. 0-15888  
 $(\text{RbF})_n\text{-FeF}_3$ , antiferromagnetic systems, dimensionality and spin reduction effects, Mossbauer study 0-39947



**Mossbauer effect continued**

- RbFeCl<sub>2</sub>·2H<sub>2</sub>O, 2D Ising system, crit. fluctuations, Mossbauer spectra study 0-44842
- RbFeF<sub>3</sub>, Mossbauer spectra, mag. phases 0-15878
- Rb<sub>2</sub>FeF<sub>6</sub>, Mossbauer spectra, 1D antiferromag. 0-15886
- Ru<sub>2</sub>FeSn, hyperfine mag. field, Mossbauer spectra 0-15865
- Sb (III) compounds, Mossbauer spectra, direct population of solid-state bands 0-15905
- Sb complexes, dithiocarbamates, lone pair electrons, <sup>121</sup>Sb Mossbauer spectroscopy study 0-39984
- Sb, Mossbauer radiation, Rayleigh scatt., Debye-Waller factor determ., annealing effect 0-39963
- Sb<sub>2</sub>Te<sub>3</sub>, Mossbauer radiation, Rayleigh scatt., Debye-Waller factor determ., annealing effect 0-39963
- Si:<sup>57</sup>Co, ion-implanted, Mossbauer study, annealing effects 0-7231
- Si:<sup>57</sup>Co/<sup>57</sup>Fe, Mossbauer spectra, deep level Co impurity study 0-29666
- Si:Co, implanted or diffused, and annealed, localisation of Co atoms, Mossbauer obs. 0-39140
- Si:Fe, implanted, annealing and stripping, Mossbauer expts. 0-39141
- Si:Fe, implanted, Mossbauer spectra, conversion electron, temp. dependence 0-40025
- Si:Fe, laser annealing of implanted <sup>57</sup>Co sources, Mossbauer obs. 0-39139
- Si:Fe, laser implantation, Mossbauer obs. 0-39125
- Si:Sn, Mossbauer spectra of <sup>119</sup>Sn impurity atoms 0-15935
- Si:Te(Sm), implanted impurity location, Mossbauer and channelling expts. 0-39128
- n-Si:<sup>119</sup>Sn resonant detector for Mossbauer spectroscopy 0-883
- SiO<sub>2</sub>-Al<sub>2</sub>O<sub>3</sub>-Fe<sub>2</sub>O<sub>3</sub>-CaO, basalt glass ceramics, crystallite form. due to heat treatment 0-38917
- SiO<sub>2</sub>-Al<sub>2</sub>O<sub>3</sub>-Fe<sub>2</sub>O<sub>3</sub>-Na<sub>2</sub>O-K<sub>2</sub>O-CaO-MgO glasses, Mossbauer spectra study 0-39967
- Sn (II) compounds, Mossbauer spectra, direct population of solid-state bands 0-15905
- Sn (IV) in glassy aq. soln., Mossbauer spectra 0-15894
- Sn, anodically treated in borate buffer, passive film form., Mossbauer meas. 0-39990
- Sn, binding state of atoms segregated at boundary of Fe and Fe alloys, Mossbauer study 0-7232
- Sn, electric field gradient, Debye model calc. 0-49682
- Sn, filtered reson. radiation, time depend. 0-7216
- α-Sn, implanted with Sn, Sb or Te, impurity-defect structs., Mossbauer expts. 0-39129
- Sn, X-ray diffraction study of thermal motion of atoms in β-Sn 0-39243
- Sn-Ni, electrodeposit, Mossbauer meas. 0-39990
- <sup>119m</sup>SnCl<sub>2</sub> adducts with O and N containing cpds., Mossbauer emission 0-15918
- Sn<sub>0.75</sub>Eu<sub>0.25</sub>MoS<sub>8</sub>, Chevrel phase supercond., spin-depairing interaction, Mossbauer obs. 0-25258
- Sn<sub>0.9</sub>Ge<sub>0.1</sub>Te, Mossbauer spectra, soft modes 0-20550
- Sn<sub>1-x</sub>Ge<sub>x</sub>Te, solid soln. series, Mossbauer study 0-39985
- Sn(HPO<sub>3</sub>)<sub>2</sub>·H<sub>2</sub>O and its alkali metal salts, struct. and vibr. spectra 0-39030
- SnMo<sub>4</sub>S<sub>8</sub>(Se<sub>8</sub>), Mossbauer spectra 0-15926
- SnO chlorination, Mossbauer and X-ray phase anal. 0-21266
- SnO<sub>2</sub>, finely dispersed, Lamb-Mossbauer factor 0-39930
- SnO<sub>x</sub> films, phase composition, Mossbauer spectra 0-20051
- Sn<sub>1-x</sub>Pb<sub>x</sub>Se(Te) thin films, resistance to oxidation, Mossbauer study 0-39986
- SnS<sub>2</sub>, Mossbauer spectra, vibr. amplitudes anisotropy 0-15904
- SnSe<sub>2</sub>, Mossbauer spectra, vibr. amplitudes anisotropy 0-15904
- SnTe, displacive phase transition at 22K, Mossbauer spectra and elec. resist. meas. 0-6514
- SrCoO<sub>3</sub>:Fe<sup>3+</sup>, ferromag., sign of Fe<sup>4+</sup> hyperfine field, spin struct., Mossbauer study 0-39933
- SrEuFeO<sub>4</sub>, Neel temp. and spin reorientation, Mossbauer study 0-39934
- SrFe<sub>12-2x</sub>Cr<sub>x</sub>O<sub>19</sub>, effects of substitution of Fe by Cr, Mossbauer spectra 0-2674
- Sr<sub>2</sub>FeEuO<sub>5</sub>, <sup>57</sup>Fe Mossbauer study 0-39976
- SrFe<sub>12</sub>O<sub>19</sub> and Sr<sub>4</sub>Fe<sub>6</sub>O<sub>13</sub>, Mossbauer spectra 0-15882
- Sr<sub>2</sub>Fe<sub>3</sub>Ru<sub>1-x</sub>O<sub>4</sub> solid soln., Mossbauer spectrosc. study 0-50235
- SrGdFeO<sub>4</sub>, Neel temp. and spin reorientation, Mossbauer study 0-39934
- Sr<sub>1-x</sub>La<sub>x</sub>FeO<sub>3</sub>, Mossbauer spectra, charge disproportionation 0-20542
- SrO-Fe<sub>2</sub>O<sub>3</sub> system, non-existence of single phase SrFe<sub>2</sub>O<sub>4</sub>, Mossbauer expts. 0-29178
- SrFe<sub>2</sub>O<sub>4</sub> (R=La,Pr,Nd), Mossbauer spectra, spin reorientation 0-15880
- Sr<sub>2</sub>YRuO<sub>6</sub>, <sup>99</sup>Ru Mossbauer spectra and other techniques 0-29659
- Ta, Mossbauer states at 6.2 keV, freq. modulation 0-7212
- Ta, NMR-Mossbauer double reson. 0-40019
- Ta, NMR-γ double resonance, Mossbauer absorpt. spectra (Russian) 0-34824
- Ta, static and dynamic props. of O and H impurities, Mossbauer meas. 0-7246
- TbAlO<sub>3</sub>:Yb<sup>3+</sup>, Mossbauer relax. 0-15875
- TbFe<sub>2</sub>, amorphous, Mossbauer spectra (French) 0-25261
- Tb<sup>57</sup>Fe<sub>1-x</sub>Cr<sub>x</sub>O<sub>3</sub> mag. props. from Mossbauer effect obs. (Japanese) 0-15933
- Tc-Fe alloy, Mossbauer spectra, hyperfine field 0-20526
- Tc-Fe dilute alloys, supercond. and mag. props. 0-29494
- Te (IV) compounds, Mossbauer spectra, direct population of solid-state bands 0-15905
- Te, amorphous, Rayleigh scatt. of Mossbauer radn., lattice dynamics 0-15845
- Te complexes of thiourea, Mossbauer spectra 0-15914
- Te, trigonal, of <sup>129</sup>I, high press. expts., phase transition and electronic changes 0-55005
- Th-Dy, dil., supercond. Th, paramag. relax. of Dy moments, Mossbauer study 0-39957
- Th<sub>2</sub>Fe<sub>3</sub>, Mossbauer spectra, mag. props. 0-15852
- Th<sub>2</sub>Fe<sub>3</sub>H<sub>14.2</sub>, Mossbauer spectra, mag. props. 0-15852
- Ti-Fe, diffusion of stored H, Mossbauer study 0-34838
- Ti-Fe, force constant change with pressure, relative Mossbauer fraction 0-34163
- Ti-H, deposited on carriers, synthesis, structure and catalytic props. 0-29890
- Ti-Mo-Fe (3, 0.13 at.%), metastable phases, Mossbauer study 0-7243
- α-Ti-V(Al)(Sn), Mossbauer spectra, metastable β- and ω-phases 0-20556
- TiFeD, cryst. struct., Mossbauer and neutron diff. obs. 0-34839
- TiO<sub>2</sub>-based ceramics, impurity atoms chem. state, Mossbauer spectra 0-15902
- Tm and Tm compounds, electronic relaxation 0-39914

**Mossbauer effect continued**

- TmH<sub>2</sub>+<sup>169</sup>Tm Mossbauer studies 0-44975
- TmH<sub>3</sub>+<sup>169</sup>Tm Mossbauer study 0-44976
- V-Fe, <sup>57</sup>Co Mossbauer spectra, diffusion mechanism of Fe 0-15292
- V-Fe, force constant change with pressure, relative Mossbauer fraction 0-34163
- V<sub>1-x</sub>Fe<sub>2</sub>O<sub>2-x</sub>F<sub>x</sub>, 0<x<0.2, phase diagrams, <sup>57</sup>Fe-Mossbauer spectra, X-ray diff. studies (German) 0-29663
- V<sub>2</sub>O<sub>3+x</sub>, 0≤x≤0.08, mag. and elec. props. 0-49833
- (V<sub>1-x</sub>Ti<sub>x</sub>)<sub>2</sub>O<sub>3</sub>:Fe, metallic antiferromagnetism, Mossbauer spectra 0-15881
- W, implantation effects of <sup>133</sup>Xe, annealing behaviour, Mossbauer study 0-40011
- Xe compounds, Xe chemical and isomer shifts, electron valence struct. (Russian) 0-53056
- Xe: <sup>57</sup>Co, solid, ion implantation for rare gas matrix isolation, Mossbauer spectroscopy study 0-54271
- <sup>133</sup>Xe/<sup>133</sup>Cs, implanted in various hosts, isomer shift values, Mossbauer spectra 0-7240
- (Y,Sm,Lu,Cu)<sub>3</sub>(Fe,Ge)<sub>2</sub>O<sub>12</sub>, ion implanted, hard bubble suppression 0-11238
- Y<sub>1-x</sub>Ca<sub>x</sub>[Fe<sub>2-x</sub>Sn<sub>x</sub>]Fe<sub>2</sub>O<sub>12</sub>, Mossbauer spectra, Sn hyperfine mag. field 0-15893
- YCoO<sub>3</sub>, anomalous <sup>57</sup>Fe<sup>m</sup> charge states, Mossbauer study 0-40017
- YFe<sub>2</sub>, amorphous concentrated spin glass, susceptibility, Mossbauer and neutron scatt. meas. 0-39783
- Y(Fe<sub>0.9</sub>Al<sub>0.1</sub>)<sub>2</sub>, Mossbauer spectra and mag. props. 0-39950
- Y(Fe<sub>0.92</sub>Co<sub>0.08</sub>)<sub>2</sub>, ferromag. relax. model, Mossbauer spectra 0-15853
- Y(Fe<sub>0.9</sub>Co<sub>0.1</sub>)<sub>2</sub>, Mossbauer effect at 78 and 300K, <sup>57</sup>Fe hyperfine fields 0-2677
- Y<sub>3</sub>Fe<sub>5-x</sub>Ga<sub>x</sub>O<sub>12</sub>, garnet, magnetically inequivalent positions of cations in external mag. field 0-11307
- Y(Fe<sub>1-x</sub>Ir<sub>x</sub>)<sub>2</sub>, magnetisation, mag. hyperfine field 0-20531
- Y(Fe<sub>1-x</sub>Mn<sub>x</sub>)<sub>2</sub>, Mossbauer spectra and mag. props. 0-39952
- YFe<sub>2</sub>O<sub>4</sub>, Mossbauer spectra of <sup>57</sup>Fe in antiferromag. and paramag. states 0-15834
- Y(Fe<sub>x</sub>Ti<sub>1-x</sub>)<sub>2</sub>, Mossbauer spectra, mag. props. 0-20563
- YIG, Si substituted, spin reorientation, Mossbauer spectroscopy obs. 0-44989
- YM<sub>2</sub>Al<sub>8</sub> (M=Cr, Mn, Fe, Cu), magnetism and hyperfine interactions 0-25256
- YbCl<sub>3</sub>·6H<sub>2</sub>O, paramag. relax., Mossbauer spectra 0-20536
- YbFe<sub>2</sub>, Curie temp., elec. quadrupole couplings, Mossbauer study 0-39949
- YbFe<sub>2</sub>, preparation and mag. props. 0-25259
- Zn, Mossbauer spectra, quadrupole interaction 0-7206
- ZnCrFeO<sub>4</sub>, ferrite spinel, unsupported and SiO<sub>2</sub> supported, structural and catalytic studies 0-44191
- ZnF<sub>2</sub>, 93.3 keV Mossbauer transition in <sup>67</sup>Zn, isomer shifts 0-39978
- ZnFeO<sub>4</sub>, ferrite spinel, structural and catalytic studies 0-44191
- ZnMn<sub>1-x</sub>Cr<sub>x</sub>FeO<sub>4</sub>, Mossbauer effect, quadrupole splitting 0-29664
- Zn<sub>0.9</sub>Ni<sub>0.1</sub>Fe<sub>2</sub>O<sub>4</sub>, Mossbauer spectra, mag. hyperfine struct. 0-15877
- ZnO absorbers, <sup>67</sup>Zn isomer shift 0-39920
- ZnO(S)(Se)(Te), 93.3 keV Mossbauer transition in <sup>67</sup>Zn, isomer shifts 0-39978
- ZnS, <sup>57</sup>Co gamma source, time depend. Mossbauer spectra 0-50245
- ZnS, time differentiated Mossbauer spectra from <sup>57</sup>Co impurities, relaxation processes (Russian) 0-34834
- ZnS:Co Mossbauer source, Fe<sup>2+</sup> abnormal populations and vibronic props. 0-15912
- (ZnTe)<sub>1-x</sub>(ZnSe)<sub>x</sub>, diamond-type semiconductor, Mossbauer spectra, quadrupole interaction of <sup>125</sup>Te 0-44992
- <sup>67</sup>Zn spectrometer, double freq. interferometer for absolute velocity calibration of piezoelectric transducer 0-37146
- Zr-Fe alloy, Mossbauer spectra parameters of Zr<sub>2</sub>Fe particles (Russian) 0-29654
- Zr-Fe-Cu-W alloy, Mossbauer spectra parameters of Zr<sub>2</sub>Fe particles (Russian) 0-29654
- Zr-H, deposited on carriers, synthesis, structure and catalytic props. 0-29890
- Zr-Nb (20 wt.%), ω-phase form., diffuse Mossbauer scatt. 0-25324
- ZrFe<sub>2</sub>, lattice dynamics, Mossbauer spectra 0-19888
- Zr(Fe<sub>1-x</sub>Al<sub>x</sub>)<sub>2</sub>, transition region, spin glass or long range mag. order 0-44841
- Zr(Fe<sub>1-x</sub>Co<sub>x</sub>)<sub>2</sub>, mictomagnetism 0-15863
- Zr(Fe<sub>1-x</sub>Co<sub>x</sub>)<sub>2</sub>, transition region, spin glass or long range mag. order 0-44841
- ZrH<sub>2</sub>:Er (x=1.5 and 1.85), Mossbauer spectra 0-20527
- ZrN:<sup>57</sup>Fe mag. props. from Mossbauer effect obs. (Japanese) 0-15933
- Mossbauer spectra** see Mossbauer effect
- motion picture photography** see cinematography
- motorcoaches**  
acoustic noise propagation models, railway track 0-48500  
noise generation, static and moving tests 0-48498
- Mott insulator** see localised electron states
- movements, atmospheric** see atmospheric movements
- moving-coil instruments**  
microelectrode puller, biological appls. 0-30964
- moving coil microphones** see microphones
- MS SCF calculations** see Xalpha calculations
- MS Xalpha calculations** see Xalpha calculations
- μ-mesons** see muons
- mud** see sediments
- muffin-tin potential**  
actinide compounds, band structure and bonding calcs. 0-10871  
actinide dioxides, electronic struct. and ionicity 0-10872  
actinides, band structure and bonding calcs. 0-10871  
alloys, disordered, muffin-tin model, electronic struct. and density of states, theory 0-29301  
atomic cluster on metallic surface, density functional calculations 0-44699  
cyclobutane, MS-Xα-MT study 0-52906  
HEED, cross-grating, atomic string approx., dispersion surface and Bloch waves 0-49056  
metal, physisorbed inert atoms, polarisation due to short range interaction with substrate 0-39428  
metals and alloys, APS, multiple scatt. approach using muffin-tin pot. 0-25490



**muffin-tin potential continued**

- methane, electronic density, multiple scatt. method, muffin-tin approx. 0-27924
- noble metal alloys, disordered, bulk electronic structure 0-44467
- polyacetylene:  $\text{ASF}_6(\text{AsF}_6)(\text{SbF}_6)(\text{PF}_6)$ , metallic, band theory 0-49570
- transition metal alloys, disordered, bulk electronic structure 0-44467
- transition metals, liq., electronic struct. and transport props. 0-29314
- uranium mononitrides, NaCl struct., band struct. 0-6714
- $\text{CaB}_6$ , electronic struct. APW and muffin-tin calcs. 0-29320
- Ce, density functional theory 0-15442
- Cs, isostructural transition and lattice vibrs., relativistic LMTO calc. 0-20074
- Cu, Fermi surface orbit integrals, tetrahedron method, Dingle temps. for 3d transition metal impurities 0-44477
- $\text{Cu}_x\text{Ni}_{1-x}$ , bulk electronic structure, comparison of CPA and ATA techniques 0-44467
- $\text{Cu}_x\text{Ni}_{1-x}$ , disordered alloy, muffin-tin model, electronic struct. and density of states calc. 0-29302
- $\text{Cu}_x\text{Zn}_{1-x}$ , disordered alloy, muffin-tin model, electronic struct. and density of states calc. 0-29302
- $\text{EuMo}_2\text{S}_8$ , Chevrel phase, RE mag. isolation and supercond. 0-44470
- GaAs, electronic density, multiple scatt. method, muffin-tin approx. 0-27924
- GaAs, LMTO self consistent band struct. calc. 0-20078
- $\text{GdMo}_6\text{S}_8$ , Chevrel phase, RE mag. isolation and supercond. 0-44470
- $\text{H}_2$ , ground state, pot. curves,  $\text{MTX}\alpha_R$  method 0-5482
- La, density functional theory 0-15442
- LiH, ground state, pot. curves,  $\text{MTX}\alpha_R$  method 0-5482
- $\text{N}_2$ , electronic density, multiple scatt. method, muffin-tin approx. 0-27924
- NaH, ground state, pot. curves,  $\text{MTX}\alpha_R$  method 0-5482
- Ni, chemisorption of H, embedded cluster model 0-39427
- Ni, liquid, electronic struct. and transport props. 0-29314
- Pb, Fermi surface and non-muffin-tin energy bands, calc. 0-20072
- Pd, chemisorption of H, embedded cluster model 0-39427
- Pd, electron-phonon parameters and supercond. p-state pairing 0-25041
- $\alpha\text{-PdH}_x$ , electronic states and Fermi surface props. 0-29310
- Pl, chemisorption of H, embedded cluster model 0-39427
- PtTe, electronic struct., self-consistent and non-self-consistent band calcs. 0-44499
- ScCl, electronic struct., self-consistent and non-self-consistent band calcs. 0-44499
- $\text{ScH}_2$ , self-consistent bond struct., charge transfer 0-49590
- $\text{ScH}_2$ , self-consistent energy bands, KKR method with Hedin-Lundqvist approx. 0-49593
- $\text{SnMo}_6\text{S}_8$ , Chevrel phase, RE mag. isolation and supercond. 0-44470
- $\text{SnMo}_6\text{Se}_8$ , Chevrel phase, RE mag. isolation and supercond. 0-44470
- Th, density functional theory 0-15442
- Th, electronic states under press. 0-54600
- US, NaCl struct., band struct. 0-6714
- $\text{YH}_2$ , self-consistent energy bands, KKR method with Hedin-Lundqvist approx. 0-49593
- ZrBr(Cl), electronic struct., self-consistent and non-self-consistent band calcs. 0-44499

**multichannel analysers** *see pulse height analysers***multidimensional systems**

- Schlesinger systems, isomonodromy deformation, integrable Hamiltonian systems 0-22229

**multigroup diffusion** *see neutron diffusion***multimeters**

- automatic digital multimeter, PM 2517 0-22347
- digital, D 3012 high accuracy multimeter (German) 0-22343
- digital, design based on Intersil ICL IC series 0-206
- digital, matching true RMS or average-sensing RMS meters to applications 0-47072
- digital, Matsushita VP-2500 A 0-212

**multiperipheral models**

- jet analysis, QCD calcs. and phenomenological models 0-52523
- KNO scaling and scaling in the mean for semi-inclusive processes (Chinese) 0-22538

**multiphase flow**

- see also two-phase flow*
- conference, cavitation and polyphase flow, Niagara Falls, New York, USA (Jun. 1979) 0-4475
- density-wave oscillations, linear stability anal. 0-48775
- differential transfer equations for multiphase, multicomponent media 0-14794
- dispersed and heterogeneous systems, mechanics, spatial averaging, cellular scheme 0-48788
- dust entrainment in shock-induced turbulent air flow, dust entrainment 0-43763
- ferrofluid flow in circular pipe, uniform mag. field effects 0-43782
- fission reactor multiphase systems, expt. and theoretical review of density-wave oscillations 0-18369
- fluid force on oscillating disc in a still fluid 0-14724
- fluid-structural interactions, one-dimensional networks, MULTIFLEX code 0-13535
- fluidised, open channel flow 0-14826
- fluidised bed, fluidisation uniformity, disturbance criterion with uniform coding medium flow distrib. 0-43772
- fluidised bed, heat transfer from transverse streamlined cylinder during surface boiling 0-43708
- fluidised solids, open channel flow 0-14826
- gas-liquid fluidised beds, axial and radial dispersion in dispersed plug flow model 0-10290
- gas-liquid fluidised beds, axial liq. dispersion in plug flow model 0-10289
- gas-radiating particle mixture, shock wave struct. numerical investigation 0-10298
- granular particles, dynamic flow rates, meas. apparatus 0-14860
- microfluids, linear theory of chemically reacting mixtures 0-14777
- moisture transfer, multiphase, in porous media with temp. gradient 0-19497
- multicomponent flow through porous media from underground nuclear explosion, flow stability 0-53857
- multiphase mixture, two-dimens. nozzle and jet supersonic flows 0-48780
- non-Newtonian systems, rheological props. variation in barotreatment 0-19304
- particle flow, gravity-induced, stochastic theories 0-14798
- pipeline flows, measurement of component ratios using  $\gamma$ -ray attenuation 0-38513

**multiphase flow continued**

- radiational flame propagation over gas suspension of solid combustible particles 0-53880
- steel, liquid, Stokes coagulation model, particle motion according to Boltzmann eqn. (German) 0-40357
- suspension concentrates, physical stability criteria, review 0-45562

**multiphonons** *see phonons***multiphoton spectra**

- see also two-photon spectra*
- atomic transition in stochastic field, saturation and Stark splitting 0-9546
- coherent multiphoton intense interactions, convergent perturbation anal. 0-1037
- cyanogen fluoride, fund., hot bands, laser microwave two photon and double reson. spectroscopy 0-32752
- diatomic molecule, two identical 3-level atoms, excitation spectrum 0-23476
- diatomic molecules, rot. line strengths in multiphoton transitions 0-48051
- DNMR, multiple-quantum, tickling 0-23446
- dressed molecule, RF field, saturated absorpt. obs. 0-9648
- ethylene, IR multiphoton excitation, optoacoustic meas. 0-1038
- fifth order atomic optical nonlinearities in multiphoton resonances 0-28275
- fluoroacetylene, fund. and hot bands, laser microwave two-photon and double reson. spectroscopy 0-32752
- free-free transitions, multiphoton, energy absorption laser pulse shape-independ. 0-43184
- free-free transitions in quantum electronics 0-28183
- inert gas halide lasers, operation and use in photochem. 0-9860
- iodomethane, RF field dressed mol. saturated absorpt. obs. 0-9648
- IR laser chemistry research using mol. beam (German) 0-55683
- large molecules, multiphoton excitation models, numerical simulation 0-53078
- laser radiation, selective action on matter, review 0-7832
- methanol, multiphoton absorpt. of intense HF laser radiation 0-23475
- modelling of multiphoton absorption using  $\text{SF}_6$  energy-dependent absorption cross sections 0-32789
- multifrequency resonance transitions between quasi-energy states 0-43019
- multilevel molecular system, coherent pulse propag. effects 0-9968
- NMR, multiple-quantum coherence, selective excitation, appl. to benzene 0-23439
- nonmonochromatic chaotic field, double optical reson. and reson. fluoresc., AC Stark splitting 0-9547
- nonresonant excitation, ensemble of two-level systems, rel. to multiphoton spectra, polyatomic mols. 0-5585
- photoionisation, quantum beats, origin 0-52954
- polyatomic molecule, anharmonic model for mol. photoexcitation 0-9669
- polyatomic molecule, collisionless multiphoton dissociation, threshold behaviour, nonthermal theory 0-11905
- polyatomic molecule, multiphoton dissociation dynamics, classical model 0-11904
- polyatomic molecule, multiple-photon IR laser pumping, collisional effects 0-9668
- polyatomic molecules, forbidden rotation-vibration transitions (Russian) 0-5593
- polyatomic molecules, high intensity IR absorpt. 0-14183
- polyatomic molecules, laser-induced energy distrib. 0-5591
- polyatomic molecules, multiple-photon absorption, quantitative comparison 0-32790
- polyatomic mols., multiple photon IR processes, reviews 0-43125
- rotational heating during IR multiphoton excitation, dynamical effects on dissociation products 0-18892
- trifluoriodomethane, multiphoton IR excitation and dissociation (Russian) 0-35562
- unimolecular reactions, laser-induced, by multiphoton IR excitation, theory 0-9664
- unimolecular reactions induced by monochromatic IR radiation, intensity and laser energy fluence influence 0-11903
- Ba, laser spectroscopic anal. of Rydberg series, multichannel quantum defect theory 0-18815
- Ba + Ba(Tl), laser induced collisional and radiative energy transfer 0-53108
- CO, hole burning in single quantum power spectrum due to Autler-Townes splitting 0-9671
- CO, rot. line strengths in multiphoton transitions 0-48051
- CO, rovibr. multiphoton spectra comput., hole burning effect 0-9672
- Ca, laser spectroscopic anal. of Rydberg series, multichannel quantum defect theory 0-18815
- Ca + Sr, laser induced collisional and radiative energy transfer 0-53108
- $\text{CrO}_2\text{Cl}_2$ , electronically induced IR multiphoton absorpt., quasicontinuum states, excited singlet radiationless decay 0-48049
- Cs,  $7^2\text{P}_{3/2}$  sublevels, hyperfine struct., multiphoton elec. dipole transitions anal. 0-32692
- H, Rydberg levels, selective excitation by three-photon absorpt. 0-5518
- $\text{HN}_3$  IR multiphoton dissociation with electronic excitation 0-11934
- $2\text{HN}_3$  IR multiphoton dissociation with electronic excitation 0-11934
- $\text{I}_2$ , 2- and 3-photon absorpt. obs. 0-18864
- $\text{N}_2$ , rot. line strengths in multiphoton transitions 0-48051
- $\text{NO}$ , rot. line strengths in multiphoton transitions 0-48051
- $\text{NO}_2$ , excited, fluoresc. spectrum, IR multiphoton vibr. pumping, photon absorpt. probability distrib. study 0-18854
- $\text{O}_3$ , multiphoton dissociation dynamics, classical model 0-11904
- $\text{SF}_6$  and  $\text{S}_2\text{F}_{10}$ , absorpt. of intense laser radiation, vibr. excitation 0-9667
- $\text{SF}_6$  and  $\text{S}_2\text{F}_{10}$ , multiple-photon IR laser pumping, collisional effects 0-9668
- $\text{SF}_6$ , highly excited, time-resolved IR absorpt. obs. 0-9666
- $\text{SF}_6$ , laser-irrad., high-resolution double-reson. spectroscopy, collisionless multiphoton dissociation 0-9623
- $\text{SF}_6$ , model system, coherent pulse propag. effects 0-9968
- $\text{SF}_6$ , multiphoton absorpt., pulsed  $\text{CO}_2$  laser radiation absorpt., press., freq., fluence depend. 0-28080
- $\text{SF}_6$  multiphoton absorpt. meas. by third harmonic generation 0-1036
- $\text{SF}_6$ , multiphoton absorpt., energy transfer, dissociation probability, laser field interaction, classical trajectory approx. 0-37730
- $\text{SF}_6$ , time-resolved IR absorpt. meas. using injection-locked single mode TEA  $\text{CO}_2$  laser 0-9665
- Sr, laser spectroscopic anal. of Rydberg series, multichannel quantum defect theory 0-18815



multiple scattering SCF-X-alpha calculations *see* Xalpha calculations

## multiple stars

*see also* binary stars

- IU Aurigae, eclipsing binary, two-colour photometry rel. to presence of third body 0-36669  
 $\alpha$  and Proxima Centauri, radial vels. and bound state 0-41859  
 $\alpha$  Centauri C (Proxima Centauri), dMe flare star, quiescent corona, transition region, and chromosphere obs. 0-56850  
 $\beta$  Cygni, visual obs. of brighter component close companion 0-8663  
formation, role of ring form. in rotating protostellar clouds 0-56820  
DQ Herculis (Nova 1934), high time resolution spectrophotometry 0-22017  
nearby stars of Gliese catalogue, additional faint companions data (1969-1978) 0-36513  
 $\beta$  Persei (Algol), orbital inclination and masses determ. from speckle interferometry 0-36668  
planetary systems, cold satellites searching via speckle interferometry using coherent optical system (Russian) 0-12672  
planetary systems, post supernova survival 0-56860  
planetary systems, search strategies 0-46615  
Trapezium member stars, space motions (Chinese) 0-8654  
triple close approaches effect on stellar system evolution, one-parameter family appl. 0-17618  
 $\mu$  Draconis (ADS 10345), radial vel. var. from spectra in visible 0-17612

multiplex transmission *see* multiplexing

multiplexers *see* multiplexing equipment

## multiplexing

*see also* frequency division multiplexing; time division multiplexing

- anthraquinone, electrochromism, display devices, multiplexing 0-45037  
holographic representations of space-variant optical processors 0-48192  
nuclear power plant, instrumentation and control, remote multiplexing appl. 0-52752  
sound, graphical picture transmission, distrib. via domestic satellite, education appl. 0-31463

## multiplexing equipment

- biomedical recording system, TDM multiplexing system for multichannel signal averaging of visually evoked responses 0-36165  
electrooptical processor, iterative colour-multiplexed 0-23792  
fibre-optic communication applications, microoptic grating multiplexers, optical isolators 0-48408  
optical channel waveguide arrays coupled to integrated CCD 0-33244  
optical demultiplexer, using diffraction grating, for FDM fibre transmission system 0-5845  
optical demultiplexer using concave grating, 0.7 to 0.9  $\mu$ m, expt. results 0-38099  
optical demultiplexer using Si echelette grating 0-53422  
optical multiplexer using blazed grating, 1.1 to 1.5  $\mu$ m, for WDM transmission system 0-38100  
optical multiplexers/demultiplexers for single-fibre WDM transmission 0-43475  
optical wavelength-division multiplexing transmission via single fibre, multiplexer design 0-33222  
paper tape data transmission, optical fibres 0-43454  
physiological response measurement, multiplexing system 0-56292

multiplier phototubes *see* photomultipliers

multipliers, electron *see* electron multipliers

multivalley semiconductors *see* many-valley semiconductors

## multivibrators

*see also* flip-flops

- Mach-Zehnder interferometric switch for integrated optical multivibrators 0-53479

## muon absorption

No entries

## muon capture

*see also* muonic atoms; muonic molecules; radioactivity

- nuclear form factors of  $0^+ \rightarrow 0^-$  transition in A=16 system, nuclear struct. effects 0-18246  
 $\mu^+$  localisation in Cu, Al and Al-Mn, temp. depend. 0-44993  
 $\mu^- + (A,Z) \rightarrow e^- + (A,Z)$ , Z-dependence of coherent  $\mu e$  conversion rate in anomalous neutrinoless muon capture 0-13419  
Ag-Zn, negative muon capture ratios 0-55007  
 $^{12}\text{C}(\mu, \nu_e)^{12}\text{B}$ , Hartree Fock wavefunction, correlations, pseudoscalar coupling constant, capture rates, recoil nuclear polarisation 0-22774  
Cu-Al, negative muon capture ratios 0-55007  
 $^2\text{H}^+\text{H}\mu \rightarrow \text{He}^+ + n + \mu^- + 17.6$  MeV, muonic catalysis in synthesis reactions (Russian) 0-52706  
 $^3\text{H}(\mu, \nu)^3\text{He}$ , transitions from bound to continuum three nucleon states 0-5128  
KCl-KBr, solid soln., negative muon capture ratios 0-55007  
NaCl-NaBr, solid soln., negative muon capture ratios 0-55007  
 $^{16}\text{O}(e, \mu)$ , T=1 level form factors, Helm model, pion photoprod. and muon capture appls. 0-52553  
 $^{16}\text{O}(\mu, \nu)$ , recoil nucleus odd and even tensor orientations, general expressions 0-13451

## muon decay

- bound muons, decay characts. 0-42512  
inner bremsstrahlung effects and radiative corrections at start of electronic spectrum (Russian) 0-37273  
 $\mu^+ \rightarrow e^+ \bar{\nu}_e \nu_\mu$ ,  $\bar{\nu}_l$  search for muon number conservation test, neutrino expt. 0-47270  
 $\mu^+ \rightarrow e^+ \bar{\nu}_e \nu_\mu$ ,  $e^+$  polarisation, weak interactions and lepton number conservation 0-42444  
 $\mu^+ \rightarrow e^+ \bar{\nu}_e \nu_\mu$ ,  $\mu e$  universality and  $\mu$  number nonconservation in rare decays 0-42445

## muon detection and measurement

- absolute intensities of medium-energy muons in the vertical and at zenith angles 55°-85° 0-17460  
calorimeter to study cosmic ray muon interactions 0-37686  
cosmic ray muons, multiple scattering in mag. spectrometers 0-4215

muon interactions *see* lepton-hadron interactions; lepton-lepton interactions;

muon-nucleon interactions; muon-nucleus reactions; photon-lepton interactions

## muon-nucleon interactions

*see also* muon-nucleon scattering

- EM production of trimuons in deep inelastic muon scatt. 0-22619  
jet analysis, QCD calcs. and phenomenological models 0-52523  
nucleon Fermi motion in deuteron, smearing effects, (West  $\beta$  correction), on expt. results, 0-32107  
 $\mu$ N, deep inelastic scattering and asymptotic freedom 0-27511

## muon-nucleon interactions continued

- $\mu$ N, inclusive scatt. 96, 147, 219 GeV, nucleon struct. function determ. 0-42472  
 $\mu$ N deep inelastic reactions, trimuon EM prod., cross sections at 250 GeV (Russian) 0-37278  
 $\mu$ N  $\rightarrow \mu$ X, broken colour gauge theory of integer charge quarks 0-13313  
 $\mu$ N  $\rightarrow \mu$ X, diffractive and non-diffractive  $\psi$  leptoprod. in QCD 0-424  
 $\mu$ N  $\rightarrow \mu$ X,  $x=2$  or 3, charm muoprod. with small angle veto 0-47306  
 $\mu$ N  $\rightarrow \mu^+ \mu^- \mu^-$  N in Pb, 10.5 GeV/c, short lived particle search, QED trident 0-37275  
 $\mu^+$ N, 280 GeV/c in Fe,  $\Psi$  virtual photoprod. 0-37279  
 $\mu p$ , structure functions in deep inelastic scatt., second-order contributions, QCD predictions 0-13314  
N\*(1236) propagator, momentum depend. in N\*-excitation current 0-27559

## muon-nucleon scattering

*see also* muon-nucleon interactions

- muon scattering at Fermilab, inclusive scatt., quark models, scaling violation 0-5001  
S,P,T-type neutral weak current meas. in  $\mu$ N scatt. 0-32064  
 $\mu$ N, 270 GeV, multimoon final states, total cross section, associated charm prod. 0-13315

## muon-nucleus reactions

*for inelastic muon-nucleus scattering, see "muon-nucleus scattering"*

*see also* muon capture; muon-nucleon interactions

- charmed particle pair prod. in muon deep inelastic scatt., event location in nucl. emulsion target 0-27906  
muon capture progress, weak interaction form factors 0-42643  
nuclear muon capture, developments in theory and expts. 0-42642  
nucleon Fermi motion in deuteron, smearing effects, (West  $\beta$  correction), on expt. results, 0-32107  
stopped muons, macroscopic polarisation (Hanle) signals 0-5130  
 $(\mu, \nu)$ , 1p nuclei M2 giant resonance calcs. 0-22784  
 $\mu^-$  to  $e^+$  conversion in nuclei, mediation by Majorana lepton 0-22547  
 $\mu^\pm$  spin rotation,  $\mu$  relaxation and repolarisation, muonic X-rays 0-42644  
Al( $\mu^-, X$ ) energetic charged particle spectrum, integrated yield 0-18293  
Cu( $\mu^-, X$ ) energetic charged particle spectrum, integrated yield 0-18293  
 $^{16}\text{O}(0^+) \rightarrow ^{16}\text{N}(0^-)$ , beta decay and muon capture rate ratio, mesonic exchange currents 0-42594  
Pb( $\mu^-, X$ ) energetic charged particle spectrum, integrated yield 0-18293  
U (M,f), muon excitation probabilities, muonic atoms, Schrodinger eqn. 0-47515

## muon-nucleus scattering

*see also* muon-nucleon scattering

- cosmic ray muons, multiple scattering in mag. spectrometers 0-4215

## muon probes

- ferromagnetic metals, muon spin rotation; freqs., and relax. rates 0-55006  
ferromagnets, hyperfine field at positive muon 0-40029  
metal,  $\mu^+$  SR, localisation and diffusion, rel. to H 0-50248  
metals, muon trapping by defects and impurities 0-20573  
quartz, muonium EPR transitions by muon-spin rot. 0-29668  
quartz, muonium hyperfine splitting meas., muon spin rot. technique 0-50246  
spin relaxation, zero- and low-field, appl. 0-2680  
spin rotation and complementary techniques, EXAFS and Mossbauer effect 0-39912  
type II superconductor, positive muon diffusion coeff., determ. from transverse depolarisation 0-25269  
 $\mu^-$  depolarisation, exotic at. orbital ang. momentum alignment effect 0-18946  
Ag-Zn, negative muon capture ratios 0-55007  
Al,  $\mu^+$  localisation temp. depend. 0-44993  
Al, quenched, muon $^+$  trapping at vacancies, compared with positron annihilation 0-15937  
Al-Mn,  $\mu^+$  localisation temp. depend. 0-44993  
Bi, zero field spin relaxation studies as a probe of positive muon diffusion mechanisms 0-34840  
Cr<sub>2</sub>O<sub>3</sub>, antiferromag., muon spin rotation (German) 0-54877  
Cu, muon trapping, Knight shift, rel. to H interstitials 0-50247  
Cu,  $\mu^+$  localisation temp. depend. 0-44993  
Cu-Al, negative muon capture ratios 0-55007  
Fe, muon $^+$  diffusion, spin rotation, effect of impurities 0-7249  
Fe, positive muon spin precession, effect of press. 0-40030  
Fe-Al, hyperfine field meas. using muon-spin-rotation method 0-10933  
 $\alpha$ -Fe<sub>2</sub>O<sub>3</sub>, antiferromag., muon spin rotation (German) 0-54877  
Ge, deep donor character of muons and protons 0-10911  
KCl-KBr, solid soln., negative muon capture ratios 0-55007  
NaCl-NaBr, solid soln., negative muon capture ratios 0-55007  
Nb, critical field, muon spin relaxation (German) 0-50015  
Nb, muon trapping, Knight shift, rel. to H interstitials 0-50247  
Nb, zero field spin relaxation studies as a probe of positive muon diffusion mechanisms 0-34840  
Ni, ferromagnetic zero point motion effect on hyperfine field at interstitial positive muon site 0-2681  
Ni, positive muon spin precession, effect of press. 0-40030  
Si, deep donor character of muons and protons 0-10911  
Ta, critical field, muon spin relaxation (German) 0-50015  
Ta, muon trapping, Knight shift, rel. to H interstitials 0-50247  
V, muon trapping, Knight shift, rel. to H interstitials 0-50247  
ZrH<sub>3</sub>, non-secular part of nucl. dipolar broadening detected by  $\mu^+$  zero-field spin relaxation 0-7250

## muon production

- cosmic ray proton atmospheric interactions, direct leptons prod. (Russian) 0-12627  
hadronic muon pair prod. QCD radiation and mean scaling, longitudinal and transverse momentum 0-42405  
QCD,  $\mu^+ \mu^-$  prod. total cross section from Drell-Yan process, large perturbative corrections 0-385  
 $ee \rightarrow ee \mu^+ \mu^-$ , virtual photon-photon collisions, equivalent photon approx. validity 0-5033  
 $e^+ e^-$ , 27.4, 27.7 GeV/c, hadron prod./muon prod. cross section ratio, thrust distrib., average sphericity 0-426  
 $e^+ e^-$  annihilation, spin-0 electron or muon pair prod., cross section supersymmetry predictions 0-32092  
 $e^+ e^- \rightarrow l^+ l^- \gamma$ ,  $l = 3, \mu, \tau$ , charged lepton universality test 0-32091  
 $e^+ e^- \rightarrow \mu^+ \mu^-$ , 40-200 GeV, cross section, one loop corrections in Weinberg model 0-18139  
 $e^+ e^- \rightarrow \mu^+ \mu^-$ , early weak gauge boson restrictions from PETRA QED cut-off 0-52487



**muon production continued**

- $e^+e^- \rightarrow \mu^+\mu^-X$ , possible Higgs boson detection in missing mass plot 0-4977  
 $e^+e^- \rightarrow \mu^+\mu^- \gamma$ , virtual electrons bremsstrahlung photon, Feynman diagrams, Weizsacker-Williams approx. 0-52484  
 $\eta \rightarrow \mu^+\mu^- \gamma$ , in  $\pi^-p$  interactions at 25 and 33 GeV/c, form factors (*Russian*) 0-4984  
 $\gamma p \rightarrow \mu^+\mu^-$ , cross sections,  $\gamma$  struct. function determ. 0-42473  
 $\mu$  prod. in Fe+p reacts. at 400 GeV, missing energy obs. 0-22833  
 $\mu N$ , 270 GeV, multimuo final states, total cross section, associated charm prod. 0-13315  
 $\mu N$  deep inelastic reactions, trimuon EM prod., cross sections at 250 GeV (*Russian*) 0-37278  
 $\mu N$  scatt., deep-inelastic, EM production of trimuons 0-22619  
 $\mu N \rightarrow \mu X$ ,  $x=2$  or 3, charm muoprod. with small angle veto 0-47306  
 $\mu N \rightarrow \mu^+\mu^- \mu^+ N$  in Pb, 10.5 GeV/c, short lived particle search, QED tridents 0-37275  
 $\bar{\nu}_\mu + N \rightarrow \mu^+ + X$  deep inelastic interaction at 2 to 25 GeV (*Russian*) 0-13298  
 $\nu N \rightarrow \mu^- \mu^+ X$ , charm-pair production 0-22643  
 $\nu n \rightarrow \mu^- p$ , total cross-section and differential cross-section, estimation of nucleon mass 0-18128  
 $\bar{\nu} p \rightarrow \mu^+ X$ , deep inelastic scatt., MQM description 0-47305  
 $\bar{\nu} p \rightarrow \mu^+ + X$ , 4.5 GeV<sup>2</sup>, p struct. functions  $x$  depend., quark distrib. 0-32097  
pN, pN, 200 GeV/c, dimuon prod. cross section, Drell-Yan predictions, struct. functions 0-37300  
pN in Fe, 400 GeV/c, bottom meson prod. search in multimuo final states 0-47334  
pN  $\rightarrow \mu X$ , 350 GeV p-Fe collisions, prompt muon prod. rate 0-37311  
 $\pi N \rightarrow \mu^+ \mu^- X$ , longitudinal photon polarisation from helicity ang. distrib. 0-5025  
 $\pi^- N$  in Be, 150, 175 GeV/c, high mass muon pair prod., Drell-Yan QCD corrections 0-13343  
 $\pi^\pm N$ , 200 GeV/c, dimuon prod. cross section, Drell-Yan predictions, struct. functions 0-37300  
 $\pi^+ p$ , 11.46 GeV/c, search for new meson resonance prod. in  $\mu$  channel 0-22641

**muon scattering** see *lepton-hadron scattering; lepton-lepton scattering; muon-nucleon scattering; muon-nucleus scattering; photon-lepton scattering*

**muonic atoms**

- conference on high energy physics and nuclear struct. Vancouver, Canada (Aug. 1979) 0-41936  
configurational mixing in shell and neutral weak muon-nucl. interaction effects obs. feasibility (*Russian*) 0-32859  
light muonic atoms, nuclear size effects, energy levels, Lamb shift 0-14254  
long range parity violating interaction from  $\gamma Z^0$  conversion 0-48108  
low-Z elements and their hydrides, muonic X-ray intensities 0-9761  
muonic X-rays, formation and expts. 0-43215  
nuclear and atomic research review 0-43216  
orbital angular momentum, effect of alignment on depolarisation of  $\mu^-$  0-18946  
prompt fission, muon entrainment by fission fragment, probability (*Russian*) 0-37911  
valence nucleons, muonic atom analysis 0-27530  
X-ray vacuum corrections, nuclear moments, transitions and deformation parameters 0-37912  
(e,e), A=60 region, nuclear radius, core polarisation and isotone shifts, muonic X-rays 0-22685  
 $\mu^\pm$  spin rotation,  $\mu$  relaxation and repolarisation, muonic X-rays 0-42644  
( $\mu p$ )<sub>S</sub> muonic atoms in gaseous H, triplet state lifetime 0-23579  
 $\mu Xe$  muonic atoms, vanishing muon transfer effect 0-9765  
He, hyperfine struct., relativistic, radiative and recoil corrections, QED test 0-14256  
 $^A Mo$ , A=92, 94-98, 100, muonic atom X-ray transitions, nuclear charge radii 0-27545  
Mu+H, electron spin exchange cross-sections 0-9685  
Na compounds, muonic X-ray intensities, Lyman series 0-23578  
Nb-V, negative muon Coulomb capture ratio and Lyman series intensities 0-14255  
<sup>188</sup>Os, muonic resonance spectra, deduced isomer shifts and electric moments 0-18948  
P allotropic modifications, muonic X-ray intensities, computer analysis 0-23577  
P, muonic allotropes muonic Roentgen intensities (*German*) 0-53168  
<sup>31</sup>P, muonic, 3d-2p X-ray transition 0-9764  
Se allotropic modifications, muonic X-ray intensities, computer analysis 0-23577  
Se, muonic allotropes, muonic Roentgen intensities (*German*) 0-53168  
U (M,f), muon excitation probabilities, muonic atoms, Schrodinger eqn. 0-47515  
<sup>235</sup>U, fission studies, target preparation 0-23217  
<sup>238</sup>U, fission studies, target preparation 0-23217  
<sup>172</sup>Yb, muonic resonance spectra, deduced isomer shifts and electric moments 0-18948

**muonic molecules**

- muon spin resonance frequency spectra, theory 0-1088  
 $\mu H + He$ , interaction pots. and rot. scatt. calcs. 0-43158

**muonium**

- hyperfine splitting in quartz, precision determ. using muon spin rot. technique 0-50246  
quartz, muonium EPR transitions by muon-spin rot. 0-29668  
Ge, anomalous muonium states 0-34841

**muons**

- see also *cosmic ray muons; muon probes*  
anomalous mag. moment, finite QED 0-47222  
dimensions, mass, elec. and mag. moments (*French*) 0-13305  
gyromagnetic ratio, QED consequence 0-22548  
magnetic moment, weak coupling contribution, Weinberg-Salam model 0-22607  
magnetic moment form factor 0-18138  
mass formula, chronon in electron theory 0-47224  
mass formula of charged leptons 0-13244  
momentum measurements from  $\pi^+ \rightarrow \mu^+ \nu_\mu$  0-37253  
QED with internal fermion excitations,  $c_\mu$  system 0-9130  
velocity in comparison to neutrinos and antineutrinos 0-9190

**muscle**

- afterpotentials influence on shape and magnitude of extracellular pots. 0-3625

**muscle continued**

- amplifier-electrode hybrid module for surface EMG pots. meas. 0-41294  
antagonistic muscles, temporal firing sequences, EMG obs. 0-40984  
cardiac chemical power, derivation of chem. power eqn. and determ. of eqn. consts. 0-16911  
cardiac contractile filament and series elastic work and power, mathematical model 0-16981  
cardiac contractile filament and series elastic work and power, clinical corrls. 0-16982  
cardiac left ventricle, contractile filament stress rel. to wall stress 0-56096  
cardiac muscle force-velocity relation, anal. in time domain 0-35943  
cell osmotic state and membrane permselectivity repeated microwave irradi. effects quantitation 0-56131  
cell surface, heterogeneity of acetylcholine receptor molecules 0-16910  
chemical power, appl. of power, work and efficiency eqns. to left ventricular energetics in man 0-16912  
contractile element behaviour as force and shortening generator, Hill's model 0-3681  
contractile force in unskinned rat heart fibre 0-30955  
contraction, time-resolved X-ray diff., data-collection system (*Japanese*) 0-46108  
contraction kinetics obs., time-resolved X-ray diff. appl. (*Japanese*) 0-56291  
current noise parameters in embryonic heart cell aggregates 0-21459  
elbow joint, moments transmission, isometric tests 0-41083  
electrical depolarisation and repolarisation obs. 0-3624  
EM fields, direct influence on nerve and muscle cells of man in 1 Hz-30 MHz range 0-51160  
EM method for stretching muscles of chronically implanted animals 0-56308  
EMG, analysis of signals, myogram integration, amplitude value determ. 0-40997  
EMG, cutaneous trunci muscle in spinal reflexes 0-3635  
EMG, dynamic arm movements data, acquisition and anal. 0-36179  
EMG, EEG and unit activity in lateral geniculate, arousal and sleep effect in cats 0-40991  
EMG, evoked, evaluation of Wiener filter 0-3747  
EMG, freq. response of biceps brachii in isometric contraction to fatigue 0-3621  
EMG, instrumentation requirements 0-41301  
EMG, integrated, rel. to angular vel. in horizontal elbow flexion 0-3620  
EMG, myographs design and technical requirements 0-40996  
EMG, quantitative, value of automatic anal. 0-8203  
EMG, single fibre, microcomputer-based jittermeter 0-46078  
EMG analysis, normal values obtained by automated system 0-3845  
eMG comparison of quadriceps femoris activity during knee extension and straight leg raises 0-8038  
EMG F response, radicular injury evaluation 0-3852  
EMG feedback therapy after stroke, efficacy obs. 0-30927  
EMG in alcoholism, nerve conduct. vel. and sensory pot. studies 0-3617  
EMG in alcoholism, terminal latencies in superior gluteal, distal peroneal and tibial nerves 0-3618  
EMG in quadriparetics and quadriplegics, evoked giant sensory nerve pots. 0-3653  
EMG investigations of gait 0-8198  
EMG low freq. power spectra, motor units characs. determ. 0-3626  
EMG of Vastus medialis, power spectral changes for graded isometric torques 0-3622  
EMG power spectra linking to recruitment and rate coding 0-3616  
EMG recordings of muscular contract., estimations of active-state, linear systems muscle model 0-3623  
EMG studies of low back mobility and activity levels 0-41059  
EMG technique for percutaneous lateral pterygoid muscle 0-3841  
excitation spread in smooth muscle and myocardial tissues, fibre interaction 0-51068  
extraocular eye muscle force duction tests after administration of succinylcholine or pancuronium 0-26255  
fibres, elec. interaction 0-51063  
fibres, relaxed, skinned, stretch and radial compression obs., frog 0-30736  
flexibility of thin filaments, dynamic light-scatt. evidence 0-41064  
gastro-intestinal tract, physiological signals, spectral analysis, autoregressive technique appl. 0-41269  
insect fibrillar muscle fibres, stiffness and tension obs. during and after sudden length changes 0-56078  
intercellular junctions in FANFT-induced carcinomas of rat urinary bladder in tissue culture 0-8230  
intramuscular nerve action pot. derived from sensory fibres 0-56071  
isometric sustained voluntary contracts., changes in EMG and heart rate 0-3629  
isometric voluntary contracts., changes in mech. and bioelec. muscular activity and heart rate 0-3628  
locomotion, human, dynamic modelling 0-8095  
long-latency reflex pathway dynamics, monkey 0-30706  
lumbar spine, moments transmission, isometric tests 0-41083  
m. biceps brachii, human, extraterritorial pots. of high-threshold motor units 0-56005  
mechanical efficiency of fast- and slow-twitch muscle fibres during cycling 0-41074  
membrane potential and active transport, information theory approach 0-35855  
microwave dielectric relaxation in muscle 0-51146  
motor reactivity, isolated heart of grass snake, pH and temp. effects 0-26219  
motor unit surface pots. spectrum and muscle geometry 0-30704  
myocardial excitability evaluation, strength-interval curves generation under computer control 0-41336  
myoelectric control of an artificial hand, sequential movement, tropical climate 0-41323  
nervous system commands in normal walking, mathematical model of striated muscle (*French*) 0-51071  
neuromuscular information transmission, distortion suppression 0-35871  
neuromuscular junction, membrane surface pot. changes effect on drug interactions 0-3631  
NMR multiwindow anal. and proton local fields and magnetisation distrib., mouse 0-21444  
peristaltic reflex dynamics model 0-56080  
physical and biological science conf., Japan (Feb. 1979) 0-12846  
Purkinje fibers, delay, block, oneway conduction model 0-21462



**muscle** continued

- radioactivity of bone and muscle, separation by dermestid ingestion 0-30949
- receptors sensitive to muscle length in the horseshoe crab 0-12167
- regeneration of fibres after transplantation, by electromyographic activity 0-30701
- rhythmic heart-cell clusters, fluctuations in interbeat interval, membrane voltage noise role 0-30705
- sarcoplasmic reticulum of skinned cardiac cells,  $\text{Ca}^{2+}$ -induced release of  $\text{Ca}^{2+}$  0-3612
- segmental muscle stretch reflex, partitioning into completely decoupled parallel loops 0-41000
- shoulder movements, EMG analysis of levator scapulae and rhomboideus major muscles 0-3627
- single ionic channels obs. in tissue cultures 0-30699
- single postsynaptic channel currents in tissue cultures 0-30700
- skeletal, human, conduction vel. estimation in situ by surface electrodes 0-8196
- skeletal, red and pale, human, force rel. to fatigability, EMG obs. 0-8076
- skeletal, single fibres, laser light diff. theory 0-56110
- skeletal fibres, light diff. study 0-8096
- skeletal muscle, canine, blood flow and  $\text{O}_2$  uptake obs. in acute anaemia 0-45930
- skeletal muscle atrophy, influence on needle EMG 0-3853
- skeletal muscle const.-vel. contractions by sequential stimulation of muscle efferents 0-41309
- skeletal muscle fibre orientation, US attenuation meas. 0-30763
- skeletal muscle mech. props. from in vitro studies of biopsies 0-41098
- skeletal muscle motor unit contractile characts. determ. through twitch characts. 0-17159
- skeletal muscle motor units, system for rapid acquisition of surface pot. maps 0-46077
- skeletal muscles, attachment and composition rel. to function 0-41092
- smooth, contraction in a microwave field, rat obs. 0-56134
- soleus muscle, rat, electrogenic  $\text{Na}^+$ - $\text{K}^+$  transport obs. 0-21456
- soreness, artificially induced, effect of EMG feedback and static stretching 0-12069
- strength and movement speed rel. to age and morphology 0-3672
- strength gain, neural factors rel. to hypertrophy 0-12168
- stretched muscle fibres, mechanical activation and voltage-depend. charge movement 0-3630
- tension fluctuations in contracting myofibrils and their interpretation 0-41065
- tenuissimus muscle, cat dynamic properties 0-8041
- torque-velocity relationships and muscle fibre composition, elite female athletes 0-41080
- water, frog, varied mag. field, multiple-pulse and magic-angle spinning  $^1\text{H}$  NMR obs. 0-51135
- water, mouse,  $^1\text{H}$  NMR anal. above and below freezing 0-56073
- water, self diffusion in frog muscle 0-8037
- water, study of spin-lattice and spin-spin relax. times of  $^1\text{H}$ ,  $^2\text{H}$ , and  $^{17}\text{O}$  0-21443
- $\text{O}_2$ , facilitated diffusion in muscle tissues 0-56327

**muscovite** see mica**music**

- digital coding of high-quality musical sound 0-5883
- digital phase shifter using Bell Labs digital filter module 0-5884
- digital storage, synthesizing musical tones from stored impulse response 0-48525
- frequency perception, colour as a pervading principle over pitch, rhythm, and form 0-56059
- high fidelity sound, perception of sound and music 0-42014
- microphone techniques for recording and broadcasting symphonic music, comments and reply 0-53595
- microphone techniques for recording or broadcasting symphonic music 0-5885
- timbre differences between lowpass-filtered harmonic complex tones (*German*) 0-53571

**music, electronic** see electronic music**musical acoustics**

- air flow and sound generation in musical wind instruments, book contrib., review 0-19174
- non-linear regeneration mechanisms in wind instruments 0-33376
- pianos, review of acoustical research (*Japanese*) 0-33375
- psychoacoustic detection threshold of transient intermodulation distortion in recorded music 0-56060
- review 0-10096
- room reverberation time meas. in musical acoustics course 0-42000
- timbre recognition, perceptive effects of data reduction (*French*) 0-28387
- trombones, objective and subjective assessment of quality 0-23847
- wave motion experiment, phase vel. meas. using spring 0-8762
- woodwind tone production, effect of reed resonance 0-19172

**musical instruments**

- flue organ pipes, voicing adjustments 0-33374
- flue-pipes, tone generation and characteristics (*German*) 0-5882
- guitar strings, correl. of acoustic and subjective quality characts. 0-19173
- pianos, review of acoustical research (*Japanese*) 0-33375
- trombones, objective and subjective assessment of quality 0-23847
- violin G-string, resonant response and excitation of wolf-note 0-53540
- wind instruments, nonlinear regeneration mechanisms 0-33376
- wolf-tone occurrence criteria in cells (*German*) 0-53570
- woodwinds, effect of reed resonance on tone production 0-19172

**N-body problems**

- see also celestial mechanics; many-body problems
- billiard ball collisions, max. number of elastic collisions possible 0-12897
- central configurations 0-41702
- central configurations and relative equil. in Euclidean  $E^4$  space 0-41703
- clusters of galaxies, velocity dispersion profiles of N-body simulations 0-21908
- clusters of galaxies compared with N-body simulations, masses and mass segregation 0-22091
- curvature statistics of some few-body Debye-Huckel and Lennard-Jones systems 0-42051
- double encounter regularization (*Russian*) 0-46367
- elliptical galaxies, anisotropic vel. distrib. generation 0-36715
- four body Newtonian problem reduction to 14th order (*French*) 0-21894
- four-body problem, restricted planetary case 0-41742
- galaxies, rotation and clustering, N-body simulation 0-17670

**N-body problems** continued

- galaxy clustering N-point simulations, covariance function 0-31373
- galaxy clusters, missing mass, N-body expts. 0-41904
- galaxy clusters multiplicity function, self-similar gravitational clustering theory 0-4447
- galaxy merging, cosmological N-body simulations 0-56922
- galaxy merging, N-body simulations rel. to galaxies rot. 0-4439
- interacting particle systems, configuration with min. pot. energy per particle 0-4517
- invariant sets and polhodes in the rigid body problem 0-41706
- Jacobi's virial equation soln. for nonconservative systems, anal. of depend. on parameters 0-4243
- many-body problem solutions, symmetry conservation in moving coordinate system 0-17480
- masses for which triple collision is regularizable 0-41704
- merging galaxies, numerical simulations 0-36716
- moving electron in field of two Coulombic ions fixed in space, rel. to  $\text{H}_2^+$  line spectrum 0-42083
- Newtonian stellar dynamics, maximizing functionals, rel. to thermodynamic and dynamical stability 0-12782
- numerical solution accuracy 0-21896
- osculating elements reduction to proper elements for entire solar system 0-21897
- periodic systems dynamical coupling, particular case of homographic soln. 0-36480
- planar three body problem, eqn. system adoption for triple collision (*French*) 0-21895
- plane planetary three body problem, quasi-isosceles movement characterisation (*French*) 0-21893
- Poincare cycles of the linear chain of oscillators 0-4662
- quantum dynamics semiclassical approximation 0-12927
- rectilinear isosceles restricted problem, numerical study 0-4242
- relativistic two body problem, appl. of dynamic confinement from vel. depend. interactions 0-46800
- restricted problem, effect of perturbed potentials on libration points stability 0-4241
- rotating systems, steady motions, computational anal. 0-53618
- sine-Gordon equation solutions, interaction potential between soliton and antisoliton 0-12945
- star clusters containing massive central black holes, dynamical simulations with self-consistent potentials 0-26915
- three body, generalised twice restricted, appl. to galactic dynamics (*Russian*) 0-51643
- three body problems with Coulomb interaction, adiabatic representation, two-level approx. 0-47861
- three-body, doubly averaged elliptical restricted problem 0-17479
- three-body, limited circular, Delaunay-Hill method averaging error estimation (*Russian*) 0-8530
- three-body, restricted, attitude stability of spinning symmetric satellite in planar periodic orbit 0-4220
- three-body, unrestricted, Lagrangian solns. stability problem (*Russian*) 0-4245
- three-body, unrestricted, Laplace solns. stability (*Russian*) 0-8529
- three-body planar elliptic, appl. to long-period effects in Trojan asteroids motion 0-41755
- three-body problem, doubly-averaged elliptical restricted, trajectories 0-46376
- three-body problem, families of 3-dimens. periodic orbits 0-41698
- three-body problem, general, families of three-dimens. periodic orbits 0-26721
- three-body problem, general case, families of 3-dimens. periodic orbits 0-41700
- three-body problem, general case, topology of  $M_N$  manifold 0-8528
- three-body problem, general planar case, families of vertical periodic orbits 0-41699
- three-body problem, general planar case, periodic solns. of Poincare's second sort 0-41707
- three-body problem, photogravitational restricted core, Lagrangian points 0-26725
- three-body problem, planar case, reduction of eqns., of motion 0-41711
- three-body problem, planar case, variational eqn. 0-46371
- three-body problem, planar hyperbolic-elliptic motion, central configurations 0-41705
- three-body problem, planar restricted case, lunar capture with variable solar mass 0-56728
- three-body problem, rectilinear case 0-41708
- three-body problem, restricted, families of three-dimens. double-symm. periodic orbits, Sun-Jupiter case 0-26722
- three-body problem, restricted, halo orbits in Earth-Moon system 0-36483
- three-body problem, restricted case, Poincare's second species solutions 0-41709
- three-body problem, restricted planar elliptic case, stationary solns. 0-46369
- three-body problem, three-dimens. general case, periodic orbits determ. 0-56696
- three-body problem, three-dimens. periodic orbit families, Hill's problem 0-56695
- triple close approaches effect on stellar system evolution, one-parameter family appl. 0-17618
- triple collisions 0-56697
- two gravitating particles system, Lorentz-covariant model 0-8865
- two point-masses bound system, influence of weak gravit. wave 0-21903
- two solid body problem, force function 0-41701
- two-body problem, first and second isochronous derivatives 0-8527
- two-body problem, general case, translating-rotating motion, force function determ. 0-17478

**N/D method**

- $e^+e^- \rightarrow \pi^+\pi^-(\pi^0\omega)$ ,  $\rho'(1250)$  description, EM form factors, bound states, N/D method (*Russian*) 0-42465
- hyperon-nucleon low energy interaction, two-channel separable pot. model, hypernuclei 0-47325
- inelastic systems and CDD ambiguity, gap-matching N/D method 0-13234
- three particle level spectrum, Thomas theorem and Efimov effect, N/D eqns. 0-42562
- NN cross-sections and resonances in nonstatic OBEP 0-13386
- $\pi\omega \rightarrow \pi\omega$ ,  $\rho'(1250)$  meson and two channel  $\pi\pi$ ,  $\pi\omega$  problem, N/D method (*Russian*) 0-37297



## N/D method continued

- $\pi\pi \rightarrow \pi\omega$ ,  $\rho(1250)$  meson and two channel  $\pi\pi$ ,  $\pi\omega$  problem, N/D method (Russian) 0-37297  
 $\pi\pi \rightarrow \pi\pi$ ,  $\rho(1250)$  meson and two channel  $\pi\pi$ ,  $\pi\omega$  problem, N/D method (Russian) 0-37297  
<sup>3</sup>H doublet scatt. length, Phillips plot, N/D input parametrisation 0-42672

## narrow band gap semiconductor materials see narrow band gap semiconductors

## narrow band gap semiconductors

- band theory, effect of lattice constant variation 0-49596  
 chemiluminescence, heterogeneous, ionisation mechanism of excitation 0-50438  
 conference, Warsaw, Poland (Sept. 1977) 0-49703  
 electrophotographic processes 0-13169  
 gapless, theory of resonance states in mag. field 0-6773  
 gapless semiconductor valence band in mag. field 0-49600  
 gapless semiconductors, screening effects on electron-electron interaction 0-49647  
 Ge electrode, electron injection in liq.  $\text{NH}_3$  0-6977  
 heterojunction, band-edge discontinuities and interface pot. step, two-band narrow-gap approach 0-39665  
 high electric field conduction in space and time superlattices 0-49756  
 hot electron phenomena, I-V curve calc. 0-34457  
 IR devices appls. 0-48464  
 IV-VI small gap semiconductor alloys, band edge parameters 0-49594  
 Kane semiconductor, many photon electron spin orientation, EM wave absorption 0-44506  
 Nerst-Ettingshausen and Hall effects in type I zero-gap state 0-44622  
 recombination instability of electron-hole plasma in narrow-gap semiconductor 0-39621  
 resonant scattering, Green's function method and CPA 0-6827  
 Schottky barrier photovoltaic IR detector using narrow bandgap semiconductor 0-9040  
 superlattices, acoustic wave absorpt. and amplification 0-29445  
 transition metal borides, electronic density of states, many-electron Hubbard model calcs. 0-20064  
 two-dimensional electron spectrum, spin splitting 0-24861  
 zero gap semiconductor, magneto-optical and impurity effects 0-6721  
 zero-gap, indirect-exchange interactions 0-29370  
 zero-gap props. correlated to  $\Gamma_8$  symmetry, review 0-6717  
 zero-gap semicond., IR absorption coeff., theoretical anal. 0-20641  
 As, black phosphorous struct., Raman vibr. spectra and bonding 0-11411  
 Bi, magneto-thermopower, weak-field, implication for scatt. mech. 0-49790  
 $\text{Bi}_{1-x}\text{Sb}_x$ , far IR magnetoabsorption, band struct. study 0-50351  
 $\text{Bi}_{1-x}\text{Sb}_x$ , galvanomagnetic, optical and photoelectric props. galvanomagnetic, optical and photoelectric props. 0-15544  
 n- $\text{Bi}_2\text{Se}_3$ , single cryst., new aspect of carrier scatt. 0-49707  
 $\text{Bi}_2\text{Se}_3$ :Hg point defects in crystal lattice, Hall coefficient and IR spectra determ. 0-55129  
 $\text{Cd}_3\text{As}_2$ , band struct. and g-factor, Shubnikov-de Haas oscills. meas. 0-49598  
 $\text{Cd}_3\text{As}_2$ , band struct. from Shubnikov-de Haas and de Haas-van Alphen effects 0-49597  
 $\text{Cd}_3\text{As}_2$ , band structure, pressure dependence of galvano- and thermomagnetic effects 0-6722  
 $\text{Cd}_3\text{As}_2$ , effect of annealing on elec. transport props. 0-49739  
 $\text{Cd}_3\text{As}_2$  film, optical absorption edge 0-50450  
 $\text{Cd}_x\text{Hg}_{1-x}\text{Se}$ , narrow band gap semicond., electron scatt., and transport phenomena 0-49706  
 $\text{Cd}_x\text{Hg}_{1-x}\text{Te}$ , effects of electron heating at low temps. 0-49823  
 $\text{Cd}_x\text{Hg}_{1-x}\text{Te}$ , influence of nonparabolicity on transverse magnetoresist. near transition to zero gap 0-20228  
 $\text{Cd}_x\text{Hg}_{1-x}\text{Te}$ , zero gap semiconductor, interband optical-phonon scattering 0-6846  
 CeSb, forbidden band gap and electrotransfer parameters 0-39497  
 $\text{Co}_{1-x}\text{Fe}_x\text{Si}$ , elec. and optical props. 0-49740  
 $\text{EuB}_6$ , mag. and transport props. 0-54689  
 GaAs electrode, electron injection in liq.  $\text{NH}_3$  0-6977  
 GeSe, galvanomag. meas., anisotropy, metal to semiconductor transition 0-6847  
 GeTe, concentration of carriers, rel. to stoichiometry 0-6847  
 $\text{Hg}_{1-x}\text{Cd}_x\text{Se}$ , zinc blende structure, optical and electronic properties 0-6723  
 $\text{HgCdTe}$ , Magneto transport anomalies at low carrier densities, Wigner crystallisation 0-20222  
 $\text{HgCdTe}$ , narrow band gap semiconductor IR devices, advances 0-48464  
 $\text{Hg}_{1-x}\text{Cd}_x\text{Te}$ , acceptor impurity band form. 0-20119  
 $\text{Hg}_{1-x}\text{Cd}_x\text{Te}$ , high intensity IR transmission limit 0-7361  
 $\text{Hg}_{1-x}\text{Cd}_x\text{Te}$ , magneto-optical and impurity effects 0-6721  
 $\text{Hg}_{1-x}\text{Cd}_x\text{Te}$ , photolum. and optical pumping 0-50424  
 $\text{Hg}_{1-x}\text{Cd}_x\text{Te}$ , semiconducting phase, acceptor states and galvanomagnetic effects 0-11017  
 $\text{Hg}_{1-x}\text{Fe}_x\text{Te}$  mixed crystals, zero gap, magneto-optical evidence of exchange interactions 0-45045  
 $\text{Hg}_{1-x}\text{Mn}_x\text{Te}$ , acceptor reson., states in high mag. field 0-49668  
 $\text{Hg}_{1-x}\text{Mn}_x\text{Te}$ , mag. field induced microwave transparency 0-49797  
 $\text{Hg}_{1-x}\text{Mn}_x\text{Te}$ , mag. props., self-consistent two spin cluster model 0-54874  
 $\text{Hg}_{1-x}\text{Mn}_x\text{Te}$ , magneto-optical and impurity effects 0-6721  
 $\text{Hg}_{1-x}\text{Mn}_x\text{Te}$ , Shubnikov de Haas effect and quantum oscills. of thermoelec. power 0-49781  
 $\text{Hg}_{1-x}\text{Mn}_x\text{Te}$ , zero-gap semicond., indirect-exchange interactions 0-29370  
 $\text{Hg}_{1-x}\text{Mn}_x\text{Te(S)(Se)}$ , EPR of  $\text{Mn}^{2+}$ , order-disorder transitions 0-50176  
 $\text{HgSe}$ , magneto-optical and impurity effects 0-6721  
 $\text{HgSe(Te)}$ , narrow band gap semicond., electron scatt., and transport phenomena 0-49706  
 $\text{HgTe}$ , acceptor reson., states in high mag. field 0-49668  
 $\text{HgTe}$ , and ternary compounds, mag. field induced microwave transparency 0-49797  
 $\text{HgTe}$ , magnetophonon oscills. of thermoelec. power 0-49789  
 $\text{HgTe}$ , quantum galvanomag. effects 0-49782  
 $\text{HgTe}$  type semiconductors, spin-flip transitions in magneto-optics and magneto-transport 0-50306  
 $\text{HgTe}$ , VPE growth control by EM irradi. (Russian) 0-34338  
 $\text{HgTe}$ , zero gap semiconductor, resonant acceptor states 0-6772  
 $\text{HgTe}$ , zero-gap semicond., absorpt. spectrum in mag. field 0-11370  
 InAs, high intensity IR transmission limit 0-7361  
 InAs surface accumulation layers, magneto-transconductance study 0-49948

## narrow band gap semiconductors continued

- InSb, electron spin relaxation 0-25187  
 InSb, high intensity IR transmission limit 0-7361  
 InSb MOS structure, props. 0-49947  
 p-InSb, magnetoconductivity and cyclotron reson. in inversion layers 0-49946  
 n-InSb, narrow gap, appl. of effect of pot. fluctuations induced by cryst. inhomogeneities 0-49780  
 p-InSb, stress induced k-linear terms in band struct. 0-49595  
 InSb, surface, reson. excitation of electron subbands 0-49865  
 InSb type semiconductor, spin-flip transitions in magneto-optics and magneto-transport 0-50306  
 InSb:S(Se)(Te), reson. states and reson. scatt., elec. props. 0-49738  
 NdSb, forbidden band gap and electrotransfer parameters 0-39497  
 P, black phosphorous struct., Raman vibr. spectra and bonding 0-11411  
 (Pb, Sn)Te-type semiconductors, displacive ferroelec. phase transitions, vibronic theory 0-11354  
 Pb salts, advances in IR device appl. 0-48464  
 $\text{Pb}_{1-x}\text{Ge}_x\text{Te}$ , degenerate semiconducting ferroelectric, structural phase transition temp., mag. field effects 0-45017  
 PbS, first-principles calc. of eqn. of states 0-49649  
 n- $\text{Pb}_{0.94}\text{Sn}_{0.06}\text{Se}$  solid solns., Burstein-Moss effect and energy band struct. 0-40118  
 $\text{Pb}_{1-x}\text{Sn}_x\text{Se}$ , band struct. and transport props., hydrostatic press. effects 0-15452  
 $\text{Pb}_{1-x}\text{Sn}_x\text{Se}$ , n- and p-type, with band inversion, study of transport phenomena 0-49741  
 PbSnTe, Magneto transport anomalies at low carrier densities, Wigner crystallisation 0-20222  
 $\text{Pb}_{1-x}\text{Sn}_x\text{Te}$ , ( $x < 0.35$ ), permittivity and soft modes, carrier density and comp. effects 0-7256  
 $\text{Pb}_{1-x}\text{Sn}_x\text{Te}$ , mag. and kinetic props. near ferroelec. transition 0-11160  
 $\text{Pb}_{1-x}\text{Sn}_x\text{Te}$ , narrow gap, many-body interaction effects, Bloch electron scatt. lifetimes, energy renormalisation 0-49637  
 $\text{Pb}_{1-x}\text{Sn}_x\text{Te}$ , photoelec. props. 30 to 4.2K, temp. depend. of electron density 0-20246  
 $\text{Pb}_{1-x}\text{Sn}_x\text{Te}$ :Mn, Mn mag. and elec. active states, mag. impurity behaviour 0-44627  
 $\text{Pb}_{1-x}\text{Sn}_x\text{Te:In}$ , with low carrier conc., transport phenomena 0-49783  
 $\text{PbTe}$ , and  $\text{Pb}_{1-x}\text{Sn}_x\text{Te}$ , VPE growth control by EM irradi. (Russian) 0-34338  
 PbTe, ion implantation induced damage and reson. levels 0-49255  
 p-PbTe, MIS struct. inversion layer sub-bands, IR magnetoreflectance obs. 0-44731  
 PbTe, Magneto transport anomalies at low carrier densities, Wigner crystallisation 0-20222  
 PbTe surfaces, tunnelling spectroscopy in MOS and Schottky barrier junctions 0-49945  
 PrSb, forbidden band gap and electrotransfer parameters 0-39497  
 SmSb, forbidden band gap and electrotransfer parameters 0-39497  
 SnTe:Mn, EPR as probe of phase transitions 0-15790  
 YbB<sub>6</sub>, mag. and transport props. 0-54689  
 YbSb, forbidden band gap and electrotransfer parameters 0-39497  
 $\text{Zn}_x\text{Hg}_{1-x}\text{Se}$ , band struct. from Shubnikov de Haas effect and hydrostatic press. meas. 0-49599
- natural gas technology**  
 coal gas production using HTR 0-11996  
 formation compressibility and edge water encroachment on gas field performance 0-30355  
 French natural gas industry developments and prospects (French, English) 0-21364  
 gas turbine power stations, off shore, electricity generation, off shore gas utilisation 0-21360  
 LNG, transport and storage hazards 0-45620  
 H industrial scale production from natural gas 0-35791  
 H<sub>2</sub>-methane mixture properties for hydrogen supplementation of natural gas 0-45781
- natural resources**  
 see also agriculture; dams; energy resources; mining; water supply  
 Athabasca oil sands, electrical props. 0-31030  
 Diyala catchment, Iraq, water balance between Derbendikhan and Himrin dams 0-12462  
 gas-oil-source rock masses, lithogenesis (Russian) 0-4006  
 geothermal energy, technological aspects of exploitation 0-55799  
 geothermal energy in Holland, prospects (Dutch) 0-35634  
 geothermal resources in Nevada, gravity surveys interpretation 0-41365  
 hydrocarbon potential of Palaeozoic onshore Canning Basin, W.Australia 0-46176  
 Maui offshore gas field, in New Zealand 0-26103  
 sea use plan concepts and criteria 0-46203  
 strategy for integration of groundwater resources in regional planning 0-41472  
 undersea, world-wide survey 0-35622  
 USA developments, by means of technological innovations, federal regulations influence 0-16763  
 visible range spectrometric investigation from Salyut 4, radiation characteristics of environment 0-51638  
 Ge demand evaluation and supply comparison 0-33106  
 Li, estimates of economically recoverable resources for nuclear fusion appls. 0-52788  
 U, world resources, effect on development of nuclear power 0-55826
- natural rubber** see rubber
- natural sciences**  
 see also astronomy and astrophysics; biology; biophysics; chemistry; geology; geophysics; mathematics; physics  
 mathematical models, role (Afrikaans) 0-8771  
 popularisation of science problems 0-21
- natural sciences applications of computing** see natural sciences computing
- natural sciences computing**  
 see also astronomy computing; astrophysics computing; biology computing; chemistry computing; geophysics computing; medical computing; physics computing  
 power plant site zone evaluation using computer-aided methods 0-861  
 viscosity of fluids at evaluated pressures 0-2191
- Navier-Stokes equations**  
 aerodynamics, high Reynolds number, global approach and approach 0-48742  
 aerofoil, oscillating, viscous incompressible flow, finite 0-38427  
 airflow above waves, numerical simulation (Russian) 0-4



**Navier-Stokes equations continued**

- axisymmetric jet, interaction with plane obstacle, Navier-Stokes eqn. solns. (Russian) 0-1659  
 bistable wall attachment fluid amplifier, flow field anal. (Japanese) 0-53743  
 blunt body, boundary and wake, supersonic viscous gas flow, numerical soln. 0-38441  
 blunt body in supersonic flow, Navier-Stokes eqns. numerical computation 0-10263  
 Boltzmann eqn., fluid dynamical approx. at level of Navier-Stokes eqn. 0-22308  
 boundary problem, soln. via successive approximations 0-36865  
 compressible gas, heat exchange in free convection condition (Russian) 0-28502  
 cones at incidence, supersonic viscous flow 0-38439  
 confined flow, numerical simulation, anal. of higher order methods 0-19316  
 convection, turbulent, numerical models based on unsteady Navier-Stokes eqns. 0-38415  
 convective diffusion problems, finite element solns., Navier-Stokes eqns. 0-1583  
 curvature and displacement effects on separation of accelerated flow past cylinder 0-10272  
 curved semicircular sectors, fully developed viscous flow and heat transfer, Navier-Stokes soln. 0-14814  
 Czochralski bulk flow in the growth of garnet crystals 0-38979  
 discontinuities, appl. of distributions (French) 0-6022  
 Eulerian and Lagrangian computer codes, pressure iteration, multigrid method 0-53738  
 external disturbance transformation into boundary layer waves 0-28523  
 finite difference soln. errors 0-17807  
 finite element approximation, Stokes problem 0-27138  
 finite element methods for viscous and inviscid incompressible flow 0-17806  
 finite-element soln. procedures, for incompressible eqns., using equal order variable interpolation 0-10226  
 flow field, multiply connected, curvilinear coords. and macro-elements 0-19318  
 flow fields in plate and cone viscometers with small gap angles 0-19516  
 fluid mechanics, mathematical introduction, book 0-66  
 forward facing step, neutrally stable atmospheric flow, shear layer, separation, vortices 0-48685  
 furrowed channels with pulsatile flow, Navier-Stokes soln. flow patterns, separation 0-33672  
 gas suspension, closed dynamic eqn. system using kinetic theory 0-6190  
 group analysis in presence of rot. symmetry and exact solns. 0-8799  
 heart valves, blood flow, vortex-grid method 0-41105  
 homogeneous turbulence decay from given state at higher Reynolds number 0-1534  
 horizontal parallel plates, unsteady laminar flow of viscous fluid, Navier-Stokes eqn. solns. 0-1683  
 incompressible, soln. using primitive variables 0-6017  
 laminar vapor flow calculations in a flat-plate heat pipe 0-23869  
 laminar viscous incompressible liquid flow in plane channel 0-23985  
 low Reynolds-number flow in the vicinity of axisymmetric constrictions 0-6147  
 magnetohydrodynamic flow between rotating and stationary porous coaxial discs 0-43799  
 nonequilibrium thermally-induced flow fluctuations 0-14661  
 nonstationary viscous flow of thermally conductive gas around semi-infinite plate, numerical anal. 0-6104  
 operator version, convection propagation and convected curl operators, Lie algebra 0-46812  
 penalty function solution of steady-state Navier-Stokes equations 0-14648  
 photoabsorption convection in horizontal tube, unsteady-state convection, num. investig. 0-33594  
 plane Couette flow, transition to turbulence and finite amplitude disturbances 0-33558  
 plane Poiseuille flow, transition to turbulence and finite amplitude disturbances 0-33558  
 pseudo-spectral soln. method for incompressible flow (French) 0-52032  
 rotating disc in viscous fluid, deceleration 0-28515  
 second-order boundary-layer effects for large injection or suction, book contrib. 0-1531  
 separating flow, fluid-surface interface, static contact line, slip at wall and shape of free surface 0-53737  
 shock separated boundary layer, suction effects, compressible Navier-Stokes eqn. solns. 0-24050  
 smoothing techniques for finite element anal. solns. 0-17804  
 stability problems with time-depend. boundary conditions, numerical simulation methods, review 0-19411  
 steady incompressible flows in three dimensions, finite-difference methods 0-33554  
 steady streaming induced between oscillating circular cylinders 0-1602  
 stenosed tube, numerical solns. 0-16975  
 supersonic blunt body flow of viscous perfect gas and nonequilib. gas mixture 0-28578  
 swirling jet from vortex filament, Navier-Stokes eqn. soln. 0-38470  
 thermoplastic recording material, latent image and surface deformation (German) 0-42284  
 thermosphere, dynamics calcs., Navier-Stokes eqns. validity 0-26659  
 thin films with nondeformable surfaces, generalized equations of hydrodynamics 0-10224  
 three dimensional separated turbulent flows at supersonic speeds 0-19435  
 turbulence, decay of grid produced turbulence, velocity correlation equations, two- and three-point 0-53741  
 turbulence, observable motions, Navier-Stokes eqns. 0-10230  
 turbulence, two-dimens., ergodic behaviour 0-28494  
 turbulence and infinite bifurcations, five-mode truncation 0-52031  
 turbulence problem, physical and spectral space methods (French) 0-28493  
 two-dimensional space isothermal and nonisothermal turbulent flow (German) 0-28505  
 two-dimensional viscous flow accompanied by stagnation point on plane wall 0-6021  
 U-tube manometers, Navier-Stokes equations solution and expt. verification (Japanese) 0-6142  
 unsteady stagnation-point flow impinging obliquely on oscillating flat plate 0-6020

**Navier-Stokes equations continued**

- vertical layers, struct. of laminar-turbulence transition and turbulent convection conditions 0-6040  
 viscous flow, non-Navier Stokes computations, parabolic and thin layer approx. 0-48666  
 viscous gas flow, similarity of flows in strongly underexpanded jets 0-6111  
 viscous gas flow, subsonic and supersonic, simplified Navier-Stokes eqns. 0-31520  
 weather, severe convective event numerical simulation and prediction, Navier-Stokes eqns. initialisation 0-31111  
 AL, shock wave structure, at re-entry speeds 0-43927  
 CO<sub>2</sub>-N<sub>2</sub> downstream mixing gasdynamic laser, Navier Stokes eqns., laminar mixing flows 0-23662  
 \*He, superfluid, normal fluid heat-exchange drag 0-49441

**navigation**

- see also computerised navigation; inertial navigation; radar applications; radionavigation; sonar; tracking  
 oceanographic microwave remote sensing 0-56612  
 radar determination of winds at sea 0-26644  
 sea floor relief mapping considerations 0-46169

**NDO calculations**

- see also CNDO calculations; INDO calculations; MINDO calculations  
 acetic acid-pyridine, H-bonding, proton transfer, isolated system, solvent effect, MO calc. 0-55629  
 hydrocarbons, dipole moments, NDDO calcs. 0-47894  
 hyperfine coupling, constants, nucl. spin spin coupling const., NDDO MO calcs. 0-23310  
 lactam-lactim tautomeric equilibria, quantum chem. calcs. 0-50833  
 methyl formate(d<sub>1</sub>,d<sub>2</sub>,d<sub>3</sub>), mol. vibr. spectrum, struct., beginning with PCICO calc. (French) 0-23401  
 MNDO semiempirical calcs. accuracy rel. to current MO methods 0-47893  
 NDDO approximate MO theory, mols. containing first-row atoms 0-32612  
 semiempirical MO theory, modified NDO model 0-52887  
 third row element mols., general harmonic force field, SCF-MO-MNDO and freq. calc., MOCIC pot. 0-27948  
 O-containing compounds, dipole moments, NDDO calcs. 0-47894

**nearly-free-electron approximation**

- Br-graphite, intercalation cpd., magnetothermal oscill. and charge-density waves 0-11199

**nebulae**

- see also galaxies; planetary nebulae; supernova remnants  
 R Aquarii, UV obs. of hot component 0-56854  
 bright nebulosities in dust clouds, study of stars in R associations 0-56893  
 η Carinae, high-resolution IR radiation maps of homunculus, spectral and spatial distrib. 0-12767  
 η Carinae, silicate grains size distrib. in Homunculus Nebula 0-4382  
 η Carinae nebula, X-ray emission obs., sources identification 0-26876  
 Cassiopeia A, <sup>14</sup>N radioemission at 26 MHz 0-41886  
 ω Centauri region, faint filamentary nebulosity obs. near globular cluster 0-56914  
 S.Coalsack, obs. of IR sources 0-46652  
 Cone nebula, formaldehyde kinematics and distrib. 0-4418  
 Crab, lunar occultation obs. at 114 and 26.3 MHz, small-scale struct. 0-46627  
 Crab, radio emission from compact source, HF meas. with URAN-1 interferometer 0-31343  
 Crab Nebula, radiation origin through pulsar magnetosphere cyclotron instability (Russian) 0-8645  
 dark clouds, red and nebulous objects, survey, catalogue of 150 objects 0-56904  
 dense clouds, ion chemistry and molecular evolution 0-31346  
 dielectronic recombination through the forbidden levels, in low density and T<sub>e</sub> highly ionised plasma 0-43850  
 30 Doradus, interstellar and nebular lines towards central object (HD 38268) 0-51839  
 30 Doradus direction, unique interstellar Ca II K-line profile obs. 0-51850  
 30 Doradus nebula, in LMC, interstellar Ca II and Na I obs. 0-46643  
 dust cloud with embedded stars, heating and model 0-26952  
 emission nebulae, astronomical obs. using optical multichannel analysis of Sao Paulo Univ. 0-26743  
 Galaxy high latitude nebulosity, as source of enigmatic dark lines crossing (M81) 0-56947  
 gaseous nebulae, photoionisation models for third period elements 0-46640  
 gaseous nebulae, riddle of spectra, history 0-8676  
 giant molecular clouds, H<sub>2</sub> densities and <sup>12</sup>C/<sup>13</sup>C ratio from formaldehyde obs. 0-51837  
 giant molecular clouds, turbulent cores, CS obs. 0-51822  
 Gum Nebula, temp. and density vars. (French) 0-26951  
 Herbig-Haro object 1, exciting star identified as T Tauri star 0-17633  
 RW Hydrae, UV obs. of hot component 0-56854  
 IC 1318 nebular complex in Cygnus X region, light extinction 0-51835  
 ionisation-shock fronts hydrodynamic linear theory 0-17625  
 ionization front propag. in inhomogeneous medium 0-46379  
 Lynds 134, OH emission obs. in dark nebula 0-22062  
 Lynds 134, optical extinction and surface brightness obs. of dark nebula 0-17627  
 Lynds 1778/1780, H I and OH emission obs. in dark nebula 0-17628  
 Lynds 1778/1780, optical extinction and surface brightness obs. of dark nebula 0-17627  
 M17, far IR obs. rel. to H II region interaction with mol. cloud 0-22053  
 M43, small diffuse nebulae in Orion complex, optical linear polarization map 0-46644  
 M8 (Lagoon Nebula), far IR obs. 0-4413  
 Monoceros R1 molecular clouds ring struct., CO obs. 0-12784  
 NGC 1333, colliding molecular clouds, star formation, early evolution 0-12757  
 NGC 1999, electronographic imaging polarimetry obs. of reflection nebula 0-26964  
 NGC 2023, reflection nebula, far IR study 0-51831  
 NGC 2024 (Orion B) nebula, CO J=2 to 1 line obs. 0-8673  
 NGC 6334, variable far IR source detect. in group of nebulae 0-8671  
 NGC 6888, circumstellar nebula, violet displaced Na I and Ca II lines in Wolf-Rayet star (HD 192163) 0-17640



## nebulae continued

- NGC 7023, refl. nebula, far UV brightness rel. to HD 200775 reddening and dust albedo and scatt. 0-51832  
 NGC 7023, refl. nebula, surface brightness study 0-56903  
 North America and Pelican Nebula Complex, struct., visual extinction map 0-22063  
 OH 739-14, M-type giant in reflection nebula, IR obs. 0-46692  
 $\rho$  Ophiuchus dark cloud region, soft X-ray obs. 0-26947  
 Orion, H<sub>2</sub> 2.12  $\mu$ m emission, temporal vars. possibility 0-17631  
 Orion, low-luminosity X-ray sources obs., assoc. with star form. 0-26959  
 Orion, polarisation at 11.1 and 19.6  $\mu$ m meas., aligned absorbing grains 0-36690  
 Orion nebula, Becklin-Neugebauer source 3.3 to 5.5 microns spectrum 0-12796  
 Orion nebula, C and Mg abundances from UV spectrum 0-41882  
 Orion Nebula, fine-struct. lines obs. and elemental abundances 0-4410  
 Orion Nebula, H<sub>2</sub>O 183 GHz line emission obs. 0-41869  
 Orion Nebula, submillimetre emission obs. 0-36685  
 Orion Nebula peripheral regions, spectrum obs. rel. to element depletion and ionisation 0-36686  
 photoionisation models for gaseous nebulae with optically thin condensations 0-36693  
 protostellar rotating cloud, two-stage fragmentation 0-22061  
 R-associations, obs. of free-free emission from embedded B-type stars 0-26851  
 Red Rectangle (HD 44179), precessing jets model 0-4422  
 reflection nebulae, interstellar grains UV scatt. props. and size distrib. 0-26932  
 reflection nebulosities, high latitude, as false companions of galaxy (NGC 772) (*Russian*) 0-36723  
 Rosette Nebula (NGC 2237/2246), new physical parameters from 6.5 GHz obs. 0-4414  
 S252 (NGC 2175), mol. line obs. of star-forming complex 0-4411  
 Sharpless 235A, optical, radio and IR obs. of H II region 0-4415  
 solar nebulae, mass transport processes in rotating dust cloud 0-8556  
 stability of polytropic gas body, Lane-Emden eqn. 0-12802  
 symmetric nebulae surrounding four luminous stars, IUE low-dispersion spectra 0-46560  
 Taurus-Auriga dark clouds, proper motions of T Tauri variables and other stars 0-41821  
 W50, supernova remnant, optical filaments spectra rel. to SS 433 mass loss rates and lifetime 0-12804  
 W50, supernova remnant, spectrum of optical nebulosity 0-51851  
 W50 (SS 433), supernova remnant, optical filamentary nebulosity discovery 0-56916  
 Webb Society handbook 0-8743  
 William Herschel's early investigations of nebulae 0-12876  
 high-velocity clouds, dynamic coronal gas flows 0-56928  
 N<sup>+</sup> + H, charge transfer reaction in nebulae rel. to ionization struct. 0-46384  
 Ne II, III, IV, photoionisation cross sections calc. 0-43014  
 rho Ophiuchi dark cloud, o-formaldehyde excitation temp. and optical depths 0-51846  
 rho Ophiuchi dark cloud complex, gamma-ray sources and particle acceleration 0-31345  
 SO in dark and molecular clouds, 30 GHz obs. 0-46639

## necking

- dynamic analysis based on stress wave propagation 0-1440  
 loading history depend. 0-5957  
 polycarbonate of bisphenol A, neck form. and propag., strain anal. 0-16376  
 polyethylene, environmental stress cracking, liq. efficiency criteria 0-21134  
 polypropylene, oriented, compressive elastic modulus and yield strength 0-16385  
 snow, volumetric constitutive law based on neck growth model 0-48595  
 (*Russian*) 0-30017  
 steel, deformation and stresses during elongation, application of Ludwig eqn. (*German*) 0-40475  
 steel, stainless, clad Al, sandwich sheet material, forming limits 0-3131  
 Al, circular tube, forming limit of free bulge-forming (*Japanese*) 0-55477  
 Ni<sub>40</sub>Fe<sub>20</sub>P<sub>14</sub>B<sub>6</sub>Si<sub>2</sub>, glass, flow and failure 0-40438  
 Zn-Al (22 wt.%) superplastic alloy, cavitation and neck form. 0-30022

## Neel temperature

- antiferromagnet, cluster approximation, Neel temp. and specific heat calc. 0-54901  
 copper formate urea hydrate, two dims. antiferromagnet, EPR, temp. depend. 0-54937  
 graphite-FeCl<sub>3-x</sub> intercalation compounds, Mossbauer spectra 0-20538  
 Heisenberg antiferromagnet, AFMR freq. temp. depend., integral peak intensities (*Russian*) 0-54951  
 Heisenberg-Ising magnets, random, critical temps., binary mixture, amorphous magnet and spin glasses 0-54911  
 many-valley semiconductors, antiferromagnetic or atomic ordering effects on conduction electrons 0-2329  
 rare earth hydrides, props., book contrib. 0-45291  
 rare earth intermetallics, RGa<sub>2</sub>, ordering and exchange interactions 0-39779  
 rare earth perovskites, prep. and props. book contrib. 0-44193  
 rare earth tetraborides, mag. and elec. props., metallic character 0-20386  
 semiconductors, magnetic, static magnetic properties, mean field approach 0-7090  
 TMMC, quasi-1D antiferromag., mag. phase diagram 0-2573  
 Ba<sub>2</sub>XRuO<sub>6</sub> (X=La,Eu), <sup>99</sup>Ru Mossbauer spectra and other techniques 0-29659  
 Ca<sub>2</sub>XRuO<sub>6</sub> (X=Y,La,Eu), <sup>99</sup>Ru Mossbauer spectra and other techniques 0-29659  
 CeAl<sub>3</sub>, Anderson lattice system, mag. moment reduction, press. effects 0-7093  
 CeIn<sub>3</sub>, Neel temp., hydrostatic press. depend. 0-29549  
 Ce<sub>1-x</sub>La<sub>x</sub>, thermoelectric power, mag. transition temps. 0-20154  
 Cr, electronic structure model, Invar effect, antiferromagnetic-non mag. transitions 0-20370  
 Cr, magnetic phase diagram in external mag. field, spin reorientation curve, critical point coordinates (*Russian*) 0-29548  
 Cr-Co (4.0 at.%) alloy, antiferromag., disappearance of resist. min. under press., and press. coeff. of T<sub>N</sub> 0-10960  
 Cr<sub>2</sub>Fe<sub>3-x</sub>O<sub>8</sub>, spin and charge density oscillations due to impurities (*Korean*) 0-20565

## Neel temperature continued

- CrVO<sub>4</sub>, Neel temp., mag. susceptibility meas. 0-29550  
 CsMnF<sub>3</sub>, mag. phase boundaries, XY to Ising crossover, virtual bicritical point 0-50095  
 CsNiF<sub>3</sub>, demagnetising effects on antiferromag. reson. 0-15803  
 CuCl<sub>2</sub>·2H<sub>2</sub>O, magnetoelastic props. under press., antiferromagnetic resonance, lattice parameters 0-29598  
 CuCr<sub>2-x</sub>Fe<sub>x</sub>O<sub>4</sub>, charge transfer, Mossbauer spectroscopy 0-15836  
 Dy, critical exponents and amplitude ratios from elec. cond. data, theoretical model 0-50126  
 Dy, film, thermorefectance dispersion curves at 315K and 97K 0-7332  
 Dy-Th, single cryst., mag. susceptibility, transitions, anisotropy 0-54873  
 EuS<sub>1-x</sub>Se<sub>x</sub>, mag. phase diagram, from temp. depend. of magnetisation 0-7105  
 Fe-Mn mag. contributions to  $\gamma$ - $\epsilon$  phase transformations 0-25694  
 Fe-Ni(Cr), Invar, exchange interactions between ferromag. and antiferromag. components 0-29545  
 Fe-Ru(Os) alloys, antiferromag. ordering, hyperfine fields 0-15867  
 FeO<sub>3</sub>, metamagnetic insulator Neel temp. anal. by model including spin fluctuations (*Russian*) 0-15715  
 FeCO<sub>3</sub>, vibronic coupling at Neel temp. 0-15491  
 FeGe<sub>2</sub>, antiferromag., biquadratic exchange 0-2371  
 Fe<sub>2</sub>O<sub>3</sub> amorphous film, Mossbauer spectra, mag. props. 0-15851  
 Fe<sub>2</sub>O<sub>3</sub> amorphous RF sputtered thin films, Mossbauer and mag. study 0-34711  
 FeVO<sub>4</sub>, Neel temp., mag. susceptibility meas. 0-29550  
 GdSn<sub>3</sub>, Neel temp., hydrostatic press. depend. 0-29549  
 Ho<sub>2</sub>Y<sub>1-x</sub>Sb<sub>x</sub>, mag. props. 0-34634  
 KCrO<sub>2</sub>, two-dims. mag. order, neutron powder diff. obs. 0-44805  
 K<sub>2</sub>FeF<sub>6</sub>, Mossbauer spectra, 1D antiferromag. 0-15886  
 K<sub>1+x</sub>Fe<sub>2</sub>Ga<sub>11-x</sub>O<sub>17</sub>, electron hopping and excitation at room temp., <sup>51</sup>Fe Mossbauer spectra 0-25257  
 K<sub>2</sub>IrCl<sub>6</sub>, sp. ht. meas. at low temp. 0-7119  
 KMnCl<sub>3</sub>, magnetic spiral struct., neutron diff. study 0-39748  
 K<sub>2</sub>ReCl<sub>6</sub>, sp. ht. meas. at low temp. 0-7119  
 LiCrO<sub>2</sub>, two-dims. mag. order, neutron powder diff. obs. 0-44805  
 Mg<sub>1-x</sub>Mn<sub>x</sub>Te<sub>2</sub>, random dil. antiferromagnet, mag. props. 0-54870  
 $\alpha$ -Mn, electronic structure model, Invar effect, antiferromagnetic-non mag. transitions 0-20370  
 Mn-Cu (9.3 wt.%), cryst. struct. at FCC to FCT transform. (*Russian*) 0-11643  
 Mn-Cu alloy, volume effect, paramagnetic-antiferromagnetic and structural transition, lattice consts. 0-39007  
 Mn<sub>1-x</sub>Fe<sub>x</sub>As, magnetic transition under high press., exchange striction model calcs. (*Russian*) 0-50096  
 Mn<sub>2</sub>Fe<sub>1-x</sub>O<sub>4</sub>, ferrite film, exchange interaction depend. on conduction electrons (*Russian*) 0-34621  
 Mn<sub>2</sub>Ge<sub>2</sub>Mn<sub>2</sub>Si<sub>2</sub>, electrical resistivity meas., order-disorder transition 0-10945  
 N<sub>2</sub>H<sub>4</sub>FeF<sub>6</sub>, Mossbauer spectra, 1D antiferromag. 0-15886  
 NaCrO<sub>2</sub>, two-dims. mag. order, neutron powder diff. obs. 0-44805  
 Na<sub>3</sub>RuO<sub>4</sub>, <sup>99</sup>Ru Mossbauer spectra, antiferromag. order, mag. relax. 0-50234  
 Nd<sub>1-x</sub>La<sub>x</sub>, thermoelectric power, mag. transition temps. 0-20154  
 NdSn<sub>3</sub>, Neel temp., hydrostatic press. depend. 0-29549  
 NiO (111) platelets, magnetic anisotropy investigation by torque and mag. susceptibility meas. 0-54885  
 NiO:Cr, effect of Cr additives on structure parameters (*Bulgarian*) 0-44319  
 NpCo<sub>2</sub>Si<sub>2</sub>, mag. props., high press. studies with <sup>237</sup>Np(60)-resonance 0-39924  
 NpFe<sub>2-x</sub>Co<sub>x</sub>Si<sub>2</sub>, mag. and hyperfine props. 0-7247  
 PrSn<sub>3</sub>, Neel temp., hydrostatic press. depend. 0-29549  
 PuC<sub>2</sub> (x=0.8, 1.44, 1.67), low temp. sp. ht., mag. ordering obs. 0-49372  
 Rb<sub>2</sub>FeF<sub>6</sub>, Mossbauer spectra, 1D antiferromag. 0-15886  
 Sm, electrical resistivity, Neel temp., 15 to 300K 0-54672  
 Sm-Dy (3 wt.%), electrical resistivity, Neel temp., 15 to 300K 0-54672  
 SrEuFeO<sub>4</sub>, Neel temp. and spin reorientation, Mossbauer study 0-39934  
 SrGdFeO<sub>4</sub>, Neel temp. and spin reorientation, Mossbauer study 0-39934  
 Sr<sub>2</sub>RuO<sub>6</sub>, <sup>99</sup>Ru Mossbauer spectra and other techniques 0-29659  
 Tb, film, thermorefectance dispersion curves at 315K and 97K 0-7332  
 Tb-Sc(Y)(La)(Lu)(Yb)(Mg)(Th), mag. ordering temps., susceptibility meas. 0-25136  
 TbP, singlet-groundstate magnetism, static mag. props. 0-7109  
 UN, mag. susceptibility under press. 0-7086  
 UO<sub>2</sub>, crystalline elec. field studies using neutron inelastic scatt. at NRCN 0-10931  
 V<sub>2</sub>O<sub>5</sub>, spin order, one-dimensional, Neel transition 0-39799  
 V<sub>2</sub>O<sub>2n-1</sub> (3 $\leq$ 3 $\leq$ 9), Magneli phases, mag. susceptibilities at low temp. 0-20389  
 V<sub>2</sub>O<sub>2n-1</sub>, insulating Magneli phases, mag. susceptibility and sp. ht. meas. 0-34604

## negative feedback see feedback

## negative feedback control systems see closed loop systems

## negative ions

- acetophenone enolate anion radicals, substituted, electron photodetachment cross sections, reson. states 0-1030  
 air, negative corona low energy humid air ions, etching effect on Al foil 0-40593  
 anthracene dimer anion, charge reson. transition anal. 0-42931  
 autodetachment, spectroscopy 0-23385  
 DNA-Au (III) interaction, rate consts., activation energies, pH, spectro-photometric obs. 0-30228  
 electronegative gas plasma, negative ion ambipolar diffusion coeffs. 0-44046  
 formation in high elec. fields 0-2927  
 formation processes and props., review (*Japanese*) 0-53127  
 ground state Zeeman splittings, reson. Raman spectra and mag.-optical activity 0-5579  
 ionosphere, EM wave propag. 0-4164  
 laser induced one-photon transitions between two short-lived negative ion states 0-9731  
 lifetimes, review, book contrib. 0-9529  
 mass spectrometry 0-43211  
 molecule+negative ion, thermochemical data, gas phase acidity scale, mass spectroscopic techniques 0-30234  
 multicomponent polyanions, PMO<sub>3</sub>O<sub>14</sub> model vibr. freqs. 0-23408  
 naphthalene anions, electron affinities, transition energy, comparison for gaseous liquid and solid 0-29731



## negative ions continued

- plasma negative ions, broadening of free-bound radiation threshold, quasistatic theory 0-53941  
 positive corona electrode, negative ion counterflow, elec. field strength meas. 0-38817  
 production, in surface plasma source with unclosed electron drift discharge 0-38846  
 singly-charged, Thomas-Fermi-Amaldi eqn., approx. variational soln. 0-52870  
 styrene anions, electron affinities, transition energy, comparison for gaseous liquid and solid 0-29731  
 thiomethoxyl anion, and deuterate, electron photodetachment, affinities, vibr. freq. and spin-orbit splitting 0-53063  
 $[Re_2Cl_8]^{2-}$ , spectral assignment, metal-metal bonds, SCF X $\alpha$  SW calcs., relativistic corrections 0-53006  
 $^{26}Al/^{26}Mg$  isobars, separation via negative ion mass spectroscopy 0-31146  
 $Br^-$ , plasma, broadening of free-bound radiation thresholds 0-53940  
 $Br^-$  + He, electron detachment, SCF calcs.,  $BrHe^-$  and  $BrHe$  pots. 0-23503  
 $Br^-(H_2O)_n$ , hydration energies, orientation, ab initio-LCAO SCF MO calcs. 0-27944  
 $CO_2^-$ , dissociation,  $2\Sigma^+$  state, Wall Porter pot. surface, autodetachment and vibr. level population inversion 0-21275  
 $CO_2-N_2$ -He, vol. discharge, negative ions effect 0-14956  
 $CO_2-O_2-H_2O$ , photodissoc. and photodetachment of negative ions 0-14182  
 $Cl^-$ , plasma, broadening of free-bound radiation thresholds 0-53940  
 $CuBr_4^{2-}$ , ground state Zeeman splittings, reson. Raman spectra and mag.-optical activity 0-5579  
 $CuCl_4^{2-}$ , core ionisation in 3d, 4f and 5f series, rearrangement effects 0-53065  
 $F^-$ , mobility in He, flow-drift tube meas. 0-43831  
 $F^-$  + atom ( $Z=10-57$ ), K-shell ionisation, X-ray prod. in transition region, collision symmetry effects 0-43163  
 $FHF_2$ , H bonds, vibr. dynamics calcs. 0-23397  
 $FeBr_4^-$ , in various solvents,  $^4A_1$   $E$ -d-d band reson. Raman spectra, solvent depend. 0-55085  
 $H^-$  affinity radiation, theoretical study of negative absorption 0-38001  
 $H^-$ , density meas. by photodetachment 0-48976  
 $H^-$ , from  $H_2^+$  ion beam surface interaction,  $H^-$  formation by reson. electron capture 0-40691  
 $H^-$ , generalised quantum defect, energy and radius depend. 0-14067  
 $H^-$ , Hartree-Fock energies, scaled  $1/Z$  expansion, integral eqns. 0-47886  
 $H^-$  photodetachment cross section, narrow resonances near  $n=3$  threshold 0-27988  
 $H^-$  production cross section in  $e^-H_2^+$  collision 0-5628  
 $H^-$  production in laser-initiated alkali hydride arc 0-32550  
 $H^-$ , S autoionising states, appl. of at. reson. theory 0-23329  
 $H^-$ , S reson. state, appl. of improved line width expression 0-5505  
 $H_2^-$ ,  $Z-Z$  0-28104  
 $H^-+H_2^+ \rightarrow H_2^*+H$  recombination react., calcs. (Russian) 0-55659  
 $H^-+H_2^+$  charge exchange, quantum transition probabilities calc. 0-9557  
 $H_2^-$ , autoionising states, complex scaling method calcs. 0-9527  
 $H^-(D^-)+He$ , collisionally induced electron detachment, 0.5 MeV, target effect 0-37858  
 $HF_2^-$ , four electron three centre bonding units, ab initio valence bond calcs. 0-27949  
 $H_2O^-$  in flames, electron attachment kinetics 0-3349  
 $He^-$ , binding energy of metastable  $1s2s2p^4P^o$  state 0-9524  
 $He^-$ , isoelectronic sequence, triply excited bound state, variational calc. 0-9526  
 $He^-$  resons. in 56 to 64 eV electron collisions, autoionising states and spectral line polarisation 0-53145  
 $H^-$  source for hollow beams using  $H_2$ -Cs 0-23228  
 $I^-$ , plasma, broadening of free-bound radiation thresholds 0-53940  
 $IrCl_6^{2-}$ , ground state Zeeman splittings, reson. Raman spectra and mag.-optical activity 0-5579  
 $Kr-Cl_2$  mixture, glow discharge positive column, electron energy distrib. and rates of inelastic processes, negative Cl ions form. 0-19632  
 $LiF^-$ , ground and excited states, ab initio calcs. single config. and multi-config. SCF calcs. 0-52873  
 $MoO_4^{2-}Sn^{2-}$ , ( $n=0-4$ ),  $^{17}O(^{33}S)(^{95}Mo)^{(97}Mo)$  NMR investig. 0-53022  
 $MoSe_2-I^-$ , photoelectrode, time resolved photocurrent, nanosecond excitation 0-45708  
 $N^-$ , Sternheimer valence shielding and antishielding factors 0-18807  
 $N_2$  laser discharge,  $SF_6$  addition, negative ion prod., altered discharge parameters 0-38818  
 $NO^-$  destruction in collisions with excited molecules 0-14189  
 $NO_2^-$ , direct CI calcs. 0-52889  
 $NO_2^-$ ,  $NO_2^-H_2O$ , and peroxy isomers, photodissoc. and photodetachment 3500-8250 Å, rel. to ionosphere 0-35554  
 $NO_2^-$ , aq. soln., vibr. width and dephasing, conc. depend. 0-43029  
 $NO_2^-$ ,  $NO_2^-H_2O$ , and peroxy isomers, photodissoc. and photodetachment 3500-8250 Å, rel. to ionosphere 0-35554  
 $O^-+Ne(Ar)(Kr)$ , 0.2-1 keV, elastic and inelastic reduced differential cross-sections 0-32829  
 $O_2^-$  in flames, electron attachment kinetics 0-3349  
 $O_2^+AsF_6^-$ , thermal decomposition, Raman spectra study, free radical mechanism 0-55652  
 $PMo_3O_{14}$  model vibr. freqs. 0-23408  
 $(SCN)_2^-$  and  $(SCN)_2$ , vibr. anal., bond strengths 0-9582

## negative resistance

- polyacetonitrile film, in Pt/polymer/metal capacitors, electroforming and elec. cond. 0-54800  
 polytetrahydrofuran film, in Pt/polymer/metal capacitors, electroforming and elec. cond. 0-54800  
 semiconductors, differential conductivity with inelastic electron scatt. (Russian) 0-2399  
 unijunction transistor, negative resistance as phase transition, critical exponents (French) 0-49746  
 $Bi_2O_3$  film, thermally grown, I-V characts., current controlled neg. resist. 0-15637  
 $WO_3$  powders, hopping mechanism and Poole-Frenkel effect, elec. props. determ. 0-49734  
 $n-ZnSe$ , long persistent cond. relax. and frozen cond. 0-54735

## negative resistance effects

- see also Gunn effect  
 alkali fluoantimonates, dielectric props. and structural phase transitions (German) 0-25274

## negative resistance effects continued

- charge carrier with anisotropic energy spectrum, cond. oscills. in quantised mag. field (Russian) 0-6886  
 dielectric diode, Joule instability under space-charge-limited current conditions 0-15618  
 ferrite-semiconductor layer struct., with negative differential cond., spin wave instability 0-25118  
 graphite, with small-sized blocks, negative magnetoresist. (Russian) 0-49779  
 MIM diodes, negative differential resistance, stimulated inelastic tunnelling theory 0-49951  
 MOST-transistor struct., breakdown-initiated negative resist. device 0-20314  
 unijunction transistor transition critical exponents, negative resistance phenomena 0-44713  
 $Al-Sb_2O_3$ -In films, negative resistance characts. 0-11103  
 C, glassy and fibrous, density of states, magnetoresistance theory appl. 0-44620  
 $CdSe:Au$  impurity light absorpt. for current control in negative resistance region 0-11052  
 GaAs, influence of strong transverse mag. field on Gunn effect 0-6854  
 n-GaAs:Ni, negative photocond. at low temps., impurity levels 0-6900  
 GaAs- $Al_xGa_{1-x}As$ , negative differential resist., real-space electron transfer 0-6958  
 GaAs-GaAlAs, superlattice, subband related anisotropy in negative magnetoresistivity 0-11082  
 $Hg_{1-x}Cd_xGe$ , quantum oscillations of magnetoresistivity (Russian) 0-11007  
 InAs, longitudinal magnetoresistance in extreme quantum limit (Russian) 0-11008  
 n-InSb, longitudinal magnetoresistance in extreme quantum limit (Russian) 0-11008  
 p-InSb, negative magnetoresist. under press. 0-20224  
 p-InSb:In, two-phase polycryst. films, negative magnetoresist. 0-11011  
 $NH_4SbF_6$ , dielectric props. and structural phase transitions (German) 0-25274  
 Se- $Ag_2Se$ , heterojunction, electrically controlled negative differential conductance, mechanism 0-44720  
 n-Si, field and current domains, at low temp. 0-6868  
 Si MOS inversion layers, negative magnetoresist. 0-49922  
 n-Si-SiC film junction device, elec. props. 0-15591  
 $ZnIn_2S_4$  switching investigation, negative resistance state instability, resistivity transitions 0-6920

## negative temperature coefficient thermistors see thermistors

## nematic liquid crystals

- 4-octyl-4-cyano-biphenyl, nematic to smectic A phase transition texture changes, thermoelectrooptic effect 0-49098  
 adjustable access couplers for fibre-optic switching 0-33217  
 aliphatic compounds, trans, trans-cyclohexyl cyclohexanoates, synthesis, mesomorphic phases 0-44121  
 trans-p-n-alkoxy- $\alpha$ -methyl cyanophenyl cinnamates, elastic consts. and orientational order parameters 0-44244  
 p-n-alkoxybenzoic acid, elec. cond. anisotropy of nematic structs. 0-1928  
 alkyl cyanobiphenyls, pretransitional behaviour, alkyl chain length depend., light scatt. in isotropic phase 0-44301  
 alkylcyano-cyclohexyl-cyclohexanoates, nematic and smectic mesophases 0-19692  
 alkylcyanobiphenyls, far IR absorpt. in nematic and isotropic phases, order parameter determ. (French) 0-50330  
 trans-4-alkylcyclohexane carboxylic acids, visible and UV spectroscopy transparent matrix 0-45102  
 alkylcyclohexyl-cyclohexyl-cyclohexanoates, nematic and smectic mesophases 0-19692  
 trans-4-n-alkylcyclohexylbenzylamines, synthesis and mesomorphic props. 0-44116  
 BBOA, polymorphism, radiothermoluminescence and differential scanning calorimetric study 0-24570  
 biopolymers, conditions of liquid crystal formation 0-30642  
 biphenylbenzoates, synthesis, mesomorphic, and thermodynamic props. 0-44117  
 N-n-butoxybenzylidene-n-butylaniline, US propag. near nematic-smectic A transition, mag. field effect 0-39266  
 p-n-butyl-p-methylhydroxyazobenzene/p-n-butylheptanoylazobenzene mixture, temp. depend. of elec. cond. 0-1925  
 CBOOA, isotropic, nematic, smectic-A phases, Brillouin scatt. 0-11421  
 p-chlorobenzylidene-p-n-pentylaniline, metastable phases formed by rapid cooling of mesophase, IR and Raman spectra and DSC obs. 0-34919  
 cholesteric-nematic mixtures, helix inversion 0-24358  
 colour effects using birefringent films and pleochroic dyes 0-24353  
 colour generation, arbitrary, in display device 0-5815  
 continuum theory of crystals subject to EM fields 0-33876  
 critical dynamics near nematic-smectic A phase transition, renormalisation group approach 0-10646  
 4-cyano-4'(n-amy)-diphenyl, isotropic phase, induced molecular orientation relaxation time, Kerr effect (Russian) 0-19699  
 p-cyano-p'-pentylbiphenyl/p-pentylbenzoic acid, mixture, induced smectic phase, dielec. props. 0-6498  
 cyanobiphenyls, nematic, dielec. consots. and diamag. anisotropies 0-7253  
 cyanocyclohexylcyclohexanes, nematic, dielec. consots. and diamag. anisotropies 0-7253  
 4-cyanophenyl 4-n-pentyloxybenzoate, electrical Kerr effect studies 0-25339  
 p-cyanophenyl-p'-caproyloxybenzoate, charge carrier behaviour, thermal depolarisation current study 0-7283  
 cyanophenylcyclohexanes, nematic, dielec. consots. and diamag. anisotropies 0-7253  
 diacyl-cyclohexyl-cyclohexanoates, nematic and smectic mesophases 0-19692  
 p-p'-dibutyl-azobenzene, DIBAB, light scatt. studies (Dutch) 0-33885  
 dibutyl-phenyl-benzoyloxy-benzoate, nematic liq. cryst., rot. barrier, PCIL0 and CND0/2 calcs. 0-33874  
 dielectric polarisation, and relaxation, molecular mechanisms 0-34846  
 dielectric polarisation and relax., mol. mechanisms 0-29673  
 dielectric properties, of multicomponent mixtures 0-38909  
 4,4-dihexyloxybenzene, nematic liq. cryst., alignment on surfactant treated obliquely evaporated surfaces 0-49092  
 disorder, continuum theory, comparison with lattice-models 0-54126  
 display devices with twisted and tilted arrangements, guest-host interactions 0-34891



## nematic liquid crystals continued

dyes, field-induced colour changes 0-25340  
 dynamic light scatt., model 0-2730  
 EBBA, binary systems with non-nematic solutes, phase transition behaviour and <sup>1</sup>H NMR anal. 0-34174  
 EBBA, metastable phases formed by rapid cooling of mesophase, IR and Raman spectra and DSC obs. 0-34919  
 EBBA, polymorphism, radiothermoluminescence and differential scanning calorimetric study 0-24570  
 EBBA, temp. depend. of absorption and fluoresc. of tetracene and perylene-tetracene in liq. cryst. (*German*) 0-18887  
 electro-optic valve testing using laser light (*French*) 0-28311  
 electrode reactions control using dopants, Kerr meas. (*French*) 0-11898  
 electrooptical effects in inhomogeneous fields 0-44118  
 EM wave nonlinear interaction 0-19698  
 N-p-ethoxybenzylidene-p'-cyanoaniline, nematic, mol. reorientation in DC elec. field, IR ATR spectra study 0-45064  
 ethoxyhexyltolan, Raman spectra, molecular conformational instability, internal field effects 0-54127  
 ethoxyoctyltolan, Raman spectra, molecular conformational instability, internal field effects 0-54127  
 p-p-ethoxyphenylazophenyl hexanoate, dielec. relax. in stable and metastable solid phases 0-34851  
 flexural elasticity meas. (*Dutch*) 0-34112  
 Frank elastic constants, statistical mech. theory 0-29104  
 Fredericksz transition and anchoring effects for general config. 0-33875  
 Fredericksz transition in mag. field, domain struct. 0-33880  
 hard rod system, improved lattice model, nematic and isotropic phases 0-33882  
 4-n-heptyl-4'-β-cyanovinylbiphenyl, isotropic mechanism of mol. rot., dielec. permitt. meas. 0-10491  
 4-n-heptyl-4'-cyanobiphenyl, linear dichroism spectra in nematic and isotropic phases 0-25336  
 4-heptyl-4'-cyanobiphenyl, nematic liq. cryst., alignment on surfactant treated obliquely evaporated surfaces 0-49092  
 4-n-heptyloxyphenyl 4-n-hexydeoxybenzoate, freezing polarisation, electret effect (*Polish*) 0-10496  
 4-n-hexyl-4-cyanobiphenyl, isotropic mechanism of mol. rot., dielec. permitt. meas. 0-10491  
 4-n-hexyloxybenzylidene-4'-n-hexylaniline, liquid crystal, exam. of orientation order of dissolved molecules 0-44112  
 p-hexyloxyphenyl-p-pentoxybenzoate, nematic liq. cryst., elec. discharge meas. of persistent internal polarisation 0-10488  
 high frequency electrohydrodynamic instability, permittivity, elec. cond. (*Russian*) 0-49099  
 HOAB, chain ordering model 0-24357  
 HOAB, thermotropic mesophase, DMR chain segments assignment 0-24356  
 HOBHA, thermotropic mesophase, DMR chain segments assignment 0-24356  
 ionic conduction-induced flow alignment angle, NMR evidence 0-44125  
 layers, optical phase difference and capacitance, elec. and mag. field depend. 0-28911  
 light modulator, scanning mode of operation 0-33200  
 lyotropic, mag. susceptibility, mol. aggregation meas. 0-19690  
 macromolecule introduction, interactions 0-30639  
 magnetic susceptibility temp. depend. 0-25103  
 Maier Saupe model, soln. in mean field approx., Meyer-Lubensky transition model 0-19694  
 MBAB, liq. cryst., Brillouin-Mandelstam light scatt. and refr. index 0-55119  
 MBBA, dielectric permitt. rel. to molecular props., effect of anisotropy of medium and local field 0-25270  
 MBBA, dynamic critical behaviour in NLC above nematic-isotropic transition 0-49096  
 MBBA, EHD transitions, white noise effects 0-6159  
 MBBA, HF electrohydrodynamic instability in NLC (*Russian*) 0-54130  
 MBBA, isotropic phase, phase-conjugate refl. by degenerate four-wave mixing 0-43389  
 MBBA, metastable phases formed by rapid cooling of mesophase, IR and Raman spectra and DSC obs. 0-34919  
 MBBA, nematic liq. cryst., nonlinear optical suscept. using light combination scatt. (*Russian*) 0-38064  
 MBBA, nematic liquid crystals, wave number spectrum of dissipative structures 0-38904  
 MBBA, nematic-isotropic transition, intermolecular forces, IR N<sub>2</sub>O mol. probe obs. 0-29155  
 MBBA, omeotropically aligned thin slice, dielectric permeability (*Italian*) 0-6354  
 MBBA, pure and mixed with bezene (chlorobenzene), nematic-isotropic transition, US absorpt., visual hysteresis 0-54355  
 MBBA, refractive index distrib. and mol. alignment in electro-optical effect (*Japanese*) 0-20613  
 MBBA, temp. depend. of absorption and fluoresc. of tetracene and perylene-tetracene in liq. cryst. (*German*) 0-18887  
 MBBA liquid crystal wedge as a polarizing element and its use in shear-interferometry 0-53444  
 MBBA-BBCA-cholesteryl chloride, field induced nematic-cholesteric relax. processes, transient helical pitch 0-38906  
 MBBA-n-heptane system, thermodynamic functions in lattice model (*Russian*) 0-33887  
 MBBA/EBBA, mol. interaction energy 0-33881  
 MBBA/EBBA binary liquid crystal mixture, US absorpt. and vel. dispersion, phase transition and alignment effects (*Korean*) 0-29121  
 Merck 389, polymorphism, radiothermoluminescence and differential scanning calorimetric study 0-24570  
 microdynamics, computer study and models (*Hungarian*) 0-33878  
 mixture of hard rigid/flexible mols., unathermal, lattice model (*Russian*) 0-54129  
 multiple quantum spin-echo spectroscopy in one-deuteron system 0-31832  
 nematic bend-splay elasticity near the nematic-smectic-A transition 0-24360  
 nematic liquid cryst., forced light scatt. in interphase (*Russian*) 0-16051  
 nematic liquid cryst., tricritical behaviour near transition to isotropic fluid (*Russian*) 0-15001  
 nematic-cholesteric mixtures, spiral pitch temp. depend. (*Russian*) 0-19700  
 nematic-isotropic transition, correlation functions, Cotton-Mouton coeffs. 0-15228  
 nematic-isotropic transition in mixtures, phase separation and diffusive instabilities 0-29156

## nematic liquid crystals continued

4-nitrophenyl 4-n-octyloxybenzoate, electrical Kerr effect studies 0-25339  
 4-nitrophenyl 4-n-pentylloxybenzoate, electrical Kerr effect studies 0-25339  
 nonlinear instability in mag. field., Frederiks transition (*French*) 0-49095  
 4-n-octyl-4'-cyano-diphenyl, appl. in detection of graphite powder particles by optical microscopy 0-9034  
 4'-n-octyl-4-cyanobiphenyl, chain ordering model 0-24357  
 4'-n-octyl-4-cyanobiphenyl, thermotropic mesophase, DMR chain segments assignment 0-24356  
 4-n-octyloxybenzoyloxy-4'-cyanostilbene, re-entrant polymorphism, nematic-smectic A-nematic-smectic A, X-ray study 0-34172  
 n-p-octyloxybenzylidene-p-toluidine, dielectric behaviour in nematic mesophase at RF 0-34842  
 p-octyloxyphenyl-p'-pentylloxybenzoate, charge carrier mobility and cond. in nematic and isotropic phases 0-44347  
 p-octyloxyphenyl-p-pentoxybenzoate, nematic liq. cryst., elec. discharge meas. of persistent internal polarisation 0-10488  
 order parameter fluctuations and anomalous sound propag. just above clearing point, critical dynamics 0-15224  
 orientational acoustic nonlinearity 0-34143  
 orientationally ordered liquids, Helmholtz free energy, generalised van der Waals theory 0-44119  
 oscillatory instabilities in elec. and mag. fields 0-24361  
 octyloxycyanobiphenyl, nematic-smectic-A transition, high-resolution 0-10649  
 PAA, adjustable domain struct. in inhomogeneous elec. field, electro-optic props. obs. 0-10494  
 PAA, cryst. phase transitions, intermolecular motion, Raman and inelastic neutron scatt. spectra 0-2164  
 PAA, electric field effects, neutron diffr. study 0-28912  
 PAA, homologous series, isotropic phase, mol. self diffusion by spin echo method 0-44109  
 PAA, light scatt. near cryst. to nematic transition 0-16046  
 PAA, nematic liq. cryst., rot. barrier, PCILO and CNDO/2 calcs. 0-33874  
 PAP, cryst. phase transitions, intermolecular motion, Raman and inelastic neutron scatt. spectra 0-2164  
 4-n-pentyl-phenylthiol-4'-alkoxybenzoate, homologous series, specific heat meas., nematic-smectic-A tricritical point 0-15227  
 phase transition to smectic C phase, renormalisation group anal. 0-34173  
 phase transitions in Landau's theory 0-29158  
 Phase V, transient response to redirected mag. field, EPR study 0-33879  
 phenylcyclohexanes, alkylamino substituted, synthesis and mesomorphic props. 0-44120  
 photosensitive MIS structure in contact with nematic liq. cryst., light spatial modulation 0-48436  
 pleochroic dye solns., guest-host interactions, appl. to electrooptic displays 0-44113  
 Poisson brackets, nonlinear hydrodynamics eqns. in condensed matter physics 0-54296  
 polyazomethines in H<sub>2</sub>SO<sub>4</sub>, lyotropic nematic phase, threaded textures (*French*) 0-19691  
 polymer solutions in nematic liquids, dilute, viscosity 0-29199  
 polypeptides, electric field-induced phase transition 0-24571  
 N-p-propoxybenzylidene-p-pentylaniline, Williams domains, interference study 0-44114  
 reentrant nematic, oriented, capillary shear flow 0-49344  
 refractive index meas. by cylindrical cell method 0-11358  
 refractive index near smectic-A/smectic-C transition, orientational order 0-24572  
 self diffraction of laser beam by liquid crystal struct. 0-5803  
 shearing flow solns., stability and dissipation 0-49288  
 sodium decyl sulphate/water/decanol/Na<sub>2</sub>SO<sub>4</sub>, lyotropic mesophase, mag.-oriented, X-ray diffr. obs. 0-1921  
 solvents for polymer gels, theory 0-11963  
 space-time correlation function for scattered light fluctuation 0-19697  
 statistical model, orientational order parameters 0-28910  
 structural parameters and nematic-isotropic transition (*German*) 0-15003  
 TBBA, self diffusion coeffs., neutron diffr. and NMR study 0-19689  
 thermal instabilities in layer with oblique orientation at boundaries 0-44110  
 thermotropic, anomalous rheological responses, spectrometer study 0-6358  
 thermotropic liquid cryst., diffusion and nucl. mag. relax. 0-24362  
 thermotropic systems of rodlike molecules with orientation-depend. interactions 0-33883  
 transition to smectic A phase, system of hard rod molecules, effect of orientational fluctuation 0-6496  
 TTF derivatives, smectic and nematic, for liq. cryst. device appl. 0-54124  
 xylieneaniline-p'-benzonitri 0-44328  
 Ni complex, bis-[4-(n-butyl)-styryl-dithiolato] Ni nematic complex, IR absorption 0-49342  
 SiO<sub>2</sub> glasses surface textures and defects, exam. using liq. crystals. 0-6364

## neodymium

see also nuclei with .....  
 atom, new lines, 3930-6450 Å, isotope shifts 0-47929  
 basalt isotopic and element composition, Reykjanes Peninsula, Iceland 0-21725  
 carbon tetrachloride-GaCl<sub>3</sub>-Nd<sup>3+</sup> nontoxic liquid phosphor system, synthesis 0-55157  
 doped (fluoro) phosphate laser glass piezo-optic coeffs. meas. at 0.6328 and 1.15 μm 0-34888  
 electron and positron multiple scatt. 0-15171  
 energy transfer between 5d electronic states 0-2808  
 high-power lasers, review 0-32950  
 laser, emission freq. conversion by method of reson. pumping of active media 0-1206  
 laser, with mirror plasma-optical Q-switch (*Russian*) 0-33028  
 laser plasma diagnostics, probing radiation Raman scatt. (*Russian*) 0-19618  
 magnetic form factors, polarised neutron diffr. meas. 0-50057  
 magnetic structure, 2D modulated 0-15697  
 magnetoresistance, mag. struct., elec. resistance at low temps. (*Russian*) 0-54936  
 nuclear fuel, burn-up, chemical separation, ion exchange 0-42746  
 Oklo natural fission reactors, migration in core sample, appl. to dating of reactions (*French*) 0-21760  
 phosphate glass:Nd<sup>3+</sup>, highly conc., electron energy deactivation and transfer (*Russian*) 0-29802



## neodymium continued

- sediments of ocean bed, isotopic composition 0-21704  
 volcanic rock isotopic composition, Grenada, Lesser Antilles 0-21724  
 $\text{BaY}_2\text{F}_3\text{Nd}^{3+}$  ESR spectra and spin-lattice relax. 0-11263  
 $\text{Bi}_2\text{Ge}_2\text{O}_7\text{Nd}^{3+}$  and  $\text{Bi}_2\text{Si}_2\text{O}_7\text{Nd}^{3+}$  crystals, absorpt. and luminesc. spectra, 4.2-300K 0-34957  
 $\text{CaF}_2\text{Nd}^{3+}$ , Slater, Racah and Lande parameters, crystal bonding 0-16062  
 $\text{CaF}_2\text{Nd}^{3+}$ , crystal field study, absorption spectra 0-20668  
 $\text{CaWO}_4\text{Nd}^{3+}$ , phase relaxation, electron spin echo spectra 0-29613  
 $\text{CaWO}_4\text{Nd}^{3+}$ , phase relax. time rel. to g-factor anisotropy, electron spin echo obs. 0-29615  
 $\text{CaWO}_4\text{Nd}^{3+}$ , Slater, Racah and Lande parameters, crystal bonding 0-16062  
 $\text{CaY}_2\text{Mg}_2\text{Ge}_2\text{O}_{12}\text{Nd}^{3+}$ , optical absorpt. and fluoresc. intensities 0-29793  
 $\text{Gd}_2\text{Ga}_2\text{O}_7\text{Nd}^{3+}$ , optical absorpt. and fluoresc. intensities 0-29793  
 $\beta\text{-Gd}_2\text{S}_3\text{Nd}^{3+}$ , spectroscopic props. from absorpt., photoluminesc. and excitation spectra 0-34968  
 $\text{La}_2\text{Be}_2\text{O}_7\text{Nd}^{3+}$ , optical absorpt. and fluoresc. intensities 0-29793  
 $\text{LaF}_3\text{Nd}^{3+}$ , cryst. field anal. of triply ionised ion spectra 0-2796  
 $\text{LaF}_3\text{Nd}^{3+}$ , luminesc. decay times 0-2811  
 $\text{LaF}_3\text{Nd}^{3+}$ , thermal cond., 300-1450K 0-24686  
 $\text{La}_2\text{Mg}_2(\text{NO}_3)_{12}\cdot 24\text{H}_2\text{O}\cdot \text{Nd}^{3+}$ , polarised neutron diffr. from dynamically and statically polarised protons 0-44078  
 $\text{Nd}^{3+}\text{Cr}^{3+}$  glass, nonradiative energy transfer from Cr. to Nd, optical pumping efficiency improvement 0-33001  
Nd, lasers, efficiency enhancement by pump radiation conversion in luminesc. liq. 0-48293  
Nd pulsed garnet lasers, pulse repetition frequency, optimal operating regime 0-53303  
 $\text{Nd}^{3+}$  ion miniature phosphate glass lasers with high ion concentration 0-19038  
 $\text{Nd}^{3+}$  miniature laser principles, materials and integrated optical design 0-33004  
Nd:glass, silicate and phosphate glass, comparison of gains 0-19039  
Nd:glass 2 TW laser for fusion expts. 0-33035  
Nd:glass disc amplifiers, possibility for efficiency improvement 0-33000  
Nd:glass laser, generation of picosecond light continua depending on various nonlinear processes 0-33095  
Nd:glass laser, luminesc. filters efficiency 0-1213  
Nd:glass laser, optical inhomogeneity cancellation using  $\text{LiO}_3$  parametric convertor 0-33049  
Nd:glass laser amplifiers, self-focusing and suppression by spatial filtering 0-14406  
Nd:glass laser cooling and index-matching liquid props. 0-33015  
Nd:glass laser system with parametric freq. conversion 0-1277  
Nd:glass laser with periodic Q-switching, mathematical model 0-33043  
Nd:glass laser with US modulated emission 0-48309  
Nd:glass laser with unstable resonator and additional feedback, angular divergence 0-48307  
Nd:glass passively mode-locked laser, obs. of external feedback influence 0-23729  
Nd:glass rods in Mikron high-power multichannel laser pulse system 0-28249  
Nd:phosphate glass, high-power laser, design and performance 0-48270  
Nd:YAG, grown from melt, in Mo crucibles, laser props. 0-48261  
Nd:YAG, mode locked oscillator, operation at 1.052  $\mu\text{m}$  0-33017  
Nd:YAG, solid-state formation 0-35121  
Nd:YAG CW laser, active stabilisation, laser noise 0-48295  
Nd:YAG laser, CW, with high output coupling modulation 0-9917  
Nd:YAG laser, coherence time meas. of picosecond pulser by light-induced grating method 0-53347  
Nd:YAG laser, thermal lens effect on emission stability 0-19064  
Nd:YAG laser multipass cell for Raman scatt. diagnostics 0-1231  
Nd:YAG mode-locked laser pulse, quadratic phase evolution direct meas., time resolved interferometry 0-48318  
Nd:YAG oscillator, Q-switched, generation of high-power ns pulses 0-23730  
Nd:YAG unstable-resonator oscillator, stable single-axial-mode operation by injection locking 0-53331  
 $\text{Nd}^{3+}$ :Ba phosphate and silicate glasses, luminesc. quenching by transition metal and rare earth ions 0-25449  
 $\text{Nd}^{3+}$ : $\text{Ca}_2\text{Ga}_2\text{Ge}_2\text{O}_{12}$ , stimulated emission at 300K 0-38019  
 $\text{Nd}^{3+}$ :glass, nonlinear refractive index, two-photon resonant absorption by  $\text{Nd}^{3+}$  (Chinese) 0-43387  
 $\text{Nd}^{3+}$ :phosphate glass laser, brightness enhancement by spatial filtering in amplifying channel 0-48321  
 $\text{Nd}^{3+}$ :YAG, laser characts., comparison with Li-Nd-La phosphate glass active elements 0-33002  
 $\text{Nd}^{3+}$ :YAG CW ring laser, fluctuation spectrum 0-9914  
 $\text{Nd}^{3+}$ :YAG continuously pumped pulse-periodic laser, stability 0-28241  
 $\text{Nd}^{3+}$ :YAG laser, conc. determ. of  $^{137}\text{Cs}$  fission product in coated-particle fuel 0-18416  
 $\text{Nd}^{3+}$ :YAG laser, contrast and configs. of  $\text{LiNbO}_3$  electrooptic switches 0-33012  
Nd:YAG laser, Q-switched, freq. doubled, 200 kW output 0-33026  
 $^{143}\text{Nd}/^{144}\text{Nd}$ , geochemistry in hydrous mantle nodules and host alkali basalts 0-56420  
 $^{143}\text{Nd}/^{144}\text{Nd}$  in flood basalts from Siberian Platform 0-56435  
 $\text{SiO}_2\text{Nd}^{3+}$  films, cathodoluminesc. 0-20717  
YAG:Nd garnet, heat capacity and thermal diffusivity meas. 0-19956  
 $\text{Y}_3(\text{Al}_{1-x}\text{Ga}_x)_2\text{O}_{12}\text{Nd}^{3+}$ , time-resolved site-selection spectroscopy, energy transfer 0-2814  
 $\text{YF}_3\text{Nd}$ , Ce, energy transfer between 5d electronic states 0-2808  
 $\text{YF}_3\text{Nd}$ , energy transfer between 5d electronic states 0-2808  
 $\delta\text{-Y}_2\text{S}_3\text{Nd}^{3+}$ , spectroscopic props. from absorpt., photoluminesc. and excitation spectra 0-34968

## neodymium alloys

- misch metal, improvement of Al alloy 51S, for space appl. 0-55466  
 rare earth intermetallics,  $\text{Ra}_2\text{-Nd}$ , dil., (R=La, Yb, Lu), EPR and mag. susceptibility 0-15797  
 steel, austenitic, Cr-Ni-Na(Pr,Ce,La), nonmetallic inclusions modification using rare earth metals (Russian) 0-40369  
 Al-Sr-Nd phase diagram (Russian) 0-20893  
 $(\text{LaNd})\text{Sn}_3$ , containing Nd impurities, supercond. and normal state props. 0-49967  
 Mg-Y-Zn-Nd-Cd alloys, influence of Zr addition on struct. and mech. props. (Russian) 0-40370  
 Nd-Fe-B ternary systems, phase equilibria and cryst. struct. (Ukrainian) 0-11626

## neodymium alloys continued

- Nd-Ni-Al, isothermal section, 600°C, X-ray struct. anal. (Ukrainian) 0-33929  
 Nd-Pr, Kaufman approach to calc. of intra-rare earth phase diagrams 0-25657  
 NdAl, ferromagnetic, extraordinary Hall effect 0-39560  
 $\text{NdCo}_2$ , elec. resistivity, thermopower, X-ray struct. meas. 0-24874  
 $\text{Nd}_{0.35}\text{Co}_{0.65}$  film, vac. evaporated, magnetisation ripple struct., TEM and defocused Lorentz microscopy 0-7136  
 $\text{NdFe}_2$ , Curie temp., elec. quadrupole couplings, Mossbauer study 0-39949  
 $\text{NdFe}_2$ , preparation and mag. props. 0-25259  
 $\text{NdIn}_3$ , magnetisation 0-25106  
 $\text{Nd}_{1-x}\text{La}_x$ , thermoelectric power, mag. transition temps. 0-20154  
 $\text{Nd}_2\text{Pr}_2\text{Sm}_2\text{Co}_8$ , permanent magnets, coercive force, low-temp. annealing influence (Russian) 0-39812  
 $(\text{Nd},\text{Sm}_{1-x})_2(\text{Co},\text{Fe}_{0.3})_{17}$ , mag. anisotropy 0-34622  
 $\text{NdSn}_3$ , magnetoresistance 0-24877  
 $\text{NdSn}_3$ , Neel temp., hydrostatic press. depend. 0-29549  
 Pr-Nd (5 at.%), paramag. excitation spectrum, CPA calc. 0-50043  
 $\text{Sm}_{0.8}\text{R}_{0.4-x}\text{M}_x\text{Co}_5$  (R=Gd, Dy, M=Pr, Nd), temp. coeff. of magnetisation 0-34688  
 $\text{Y}_{1-x}\text{Nd}_x\text{Co}_5$ , exchange interactions and magnetocrystalline anisotropy 0-34618

## neodymium compounds

- see also neodymium alloys  
 glasses, GLS-1 and GLS-22, luminesc. band, forced transition cross sections, laser meas. 0-40152  
 laser emission cross sections and fluoresc. quantum efficiency meas. 0-48264  
 phosphors, liq., using aprotic solvents 0-20686  
 $\text{CaO-Nd}_2\text{O}_3\text{-Fe}_2\text{O}_3\text{-Al}_2\text{O}_3$  system, solid-state reactions 0-35173  
 $\text{Cr-NdAlO}_3$ , dielectric films, phase composition and structure 0-39464  
 $\text{K}_2\text{NdLi}_2\text{F}_{10}$  (KNLF), spectroscopy and lasing 0-5737  
 $\text{KNDP}_2\text{O}_{12}$ , determ. of fluoresc. quantum efficiency and laser emission cross sections 0-48264  
 $\text{KNDP}_2\text{O}_{12}$ , laser emission cross sections, fluorescence spectra, radiative lifetimes, quantum efficiency 0-23694  
 $\text{K}_3\text{Nd}(\text{PO}_4)_2$ , synthesis and IR spectra 0-16019  
 Li-Nd-La phosphate glass active elements, laser characts., comparison with Nd:YAG 0-33002  
 $\text{LiBi}_2\text{Nd}_{1-x}\text{P}_4\text{O}_{12}$  waveguide laser layer epitaxially grown on  $\text{LiNdP}_4\text{O}_{12}$  substrate 0-23709  
 $\text{LiNd}(\text{PO}_3)_4$  laser with external and Fabry-Perot resonators, 1.05, 1.32  $\mu\text{m}$  CW oscill. 0-23693  
 $\text{LiNdP}_4\text{O}_{12}$  efficient miniature laser pumped with GaAlAs laser diode 0-32994  
 $\text{LiNdP}_4\text{O}_{12}$  glass-clad rectangular waveguide, laser performance 0-32996  
 $\text{LiNdP}_4\text{O}_{12}$ , grown by top seeded pulling technique, possible laser material 0-25542  
 $\text{LiNdP}_4\text{O}_{12}$ , laser emission cross sections, fluorescence spectra, radiative lifetimes, quantum efficiency 0-23694  
 $\text{LiNdP}_4\text{O}_{12}$  substrate, growth of  $\text{LiBi}_2\text{Nd}_{1-x}\text{P}_4\text{O}_{12}$  waveguide laser layer 0-23709  
 $\text{Li}_2\text{O-Nd}_2\text{O}_3\text{-P}_2\text{O}_5$  phase diagram,  $\text{LiNdP}_4\text{O}_{12}$  single crystal growth 0-25668  
 $\text{NaNdP}_4\text{O}_{12}$ , laser emission cross sections, fluorescence spectra, radiative lifetimes, quantum efficiency 0-23694  
 $\text{Na}_3\text{Nd}(\text{PO}_4)_2$ , synthesis and IR spectra 0-16019  
 Nd-Hf, inelastic neutron scatt. exam. of lattice dynamics 0-29128  
 $\text{NdAlO}_3$ , dielectric films, phase composition and structure 0-39464  
 $\text{NdAl}_3(\text{BO}_3)_4$ , single phase crystallisation region from solvent melt 0-38977  
 $\text{Nd}(\text{BO}_3)_3$ , single cryst., IR absorpt. spectra 0-34903  
 $\text{Nd}(\text{ClO}_4)_3$ , osmotic coeffs. 0-45556  
 $\text{NdCl}_3\cdot 6\text{H}_2\text{O}\cdot \text{Gd}^{3+}$ , EPR spectra, angular var. calc. 0-54940  
 $\text{NdCl}_3\cdot 6\text{H}_2\text{O}\cdot \text{EuCl}_3\cdot 6\text{H}_2\text{O}$ , in DMSO soln.,  $\text{Eu}^{3+}\rightarrow\text{Nd}^{3+}$  radiationless energy transfer 0-5499  
 $\text{Nd}\cdot\text{Eu}_{1-x}\text{B}_6$  solid solution, mag. susceptibility, lattice parameters, Weiss temp. 0-29535  
 $\text{NdF}_3$ , bomb calorimetric determ. of enthalpy of formation 0-50879  
 $\text{NdF}_3$ , crystals, shift tensors and F-diffusion, ion interactions,  $\text{F}^-$  NMR study 0-20471  
 $\text{NdF}_3$ , enthalpy, entropy, heat capacity and Planck function from 5 to 350K 0-15257  
 $\text{NdF}_3$ , mol. consts., kinetic consts. and L-approx. methods 0-18839  
 $\text{NdFe}_2(\text{BO}_3)_4$ , solubility in  $\text{Bi}_2\text{O}_3\text{-B}_2\text{O}_3$  melt and crystallisation 0-19736  
 $\text{Nd}(\text{Ga},\text{Cr})_3(\text{BO}_3)_4$ , cryst. growth by LPE,  $\text{Nd}^{3+}$  fluorescence, lattice constants 0-29883  
 $\text{NdH}_{2.2-7}$ , low-temp. sp. ht., mag., elec., and cryst. field splitting effects 0-49379  
 $\text{NdIn}_2\text{S}_3$ , chalcogenide cryst. struct., diffr. and Patterson function anal. 0-39056  
 $\text{Nd}_2\text{La}_{1-x}\text{P}_5\text{O}_{14}$ , crystal growth, laser generation characts. 0-38020  
 $\text{Nd}_2(\text{MoO}_4)_3$ , thermo-optical spectroscopy, detection by mirage effect 0-47116  
 $\text{Nd}_2(\text{MoO}_4)_3\text{-Nd}_2(\text{SO}_4)_3$  system, sulphatomolybdates and isomorphous substitution 0-19763  
 $\text{Nd}_2\text{MoO}_5$ , cryst. struct., IR spectra, elec. and mag. props. 0-33954  
 $\text{Nd}(\text{NO}_3)_3$ , osmotic coeffs. 0-45556  
 $\text{NdNbO}_4\text{-CaWO}_4$ , phase transitions of fergusonite-scheelite (French) 0-19942  
 $\text{NdO}$ , mag. props., lattice consts., and X-ray absorpt. spectra 0-44798  
 $\text{Nd}_2\text{O}_3$ , isotopically enriched target preparation using electron gun 0-23226  
 $\text{Nd}_2\text{O}_3\text{-HfO}_2$  system, phase relationships 0-35169  
 $\text{NdP-UP}$  solid soln., cryst. field parameters 0-10927  
 $\text{Nd}(\text{PO}_3)_2$ , vitreous, microhardness 0-25864  
 $\text{NdP}_2\text{O}_4$  single crystals, fluoresc. decay times, excitation density effect 0-7390  
 $\text{NdP}_2\text{O}_4$  single crystals grown from polyphosphoric acids, morphology control 0-15395  
 $\text{Nd}_3\text{PO}_7$ , prep. and luminesc. props. 0-34964  
 $\text{Nd}_2\text{P}_2\text{O}_{11}$ , luminesc. props. 0-34964  
 $\text{NdPb}_{1-x}\text{Mo}_x\text{S}_8$ , sputtered supercond. props. 0-50019  
 NdSb, forbidden band gap and electrotransfer parameters 0-39497  
 $\text{Nd}_2\text{Ti}_2\text{O}_7$ , crystal struct. and phase transitions, rel. to isomorphous crystals (Japanese) 0-49208  
 $\text{NdTiO}_3$ , physicochem. props. 0-25625  
 $\text{Nd}_2\text{Y}_{10}\text{O}_{28}\cdot 28\text{H}_2\text{O}$ , X-ray cryst. struct. anal. 0-39060



## neodymium compounds continued

- Nd<sub>2</sub>Zr<sub>2</sub>O<sub>7</sub>-Nd<sub>2</sub>Hf<sub>2</sub>O<sub>7</sub>, struct., elec. cond. and melting point 0-54197  
 Rb<sub>3</sub>Nd(PO<sub>4</sub>)<sub>3</sub>, synthesis and IR spectra 0-16019  
 SrNdFeO<sub>4</sub>, Mossbauer spectra 0-15880  
 UO<sub>2</sub>+Nd<sub>2</sub>O<sub>3</sub>, sintering, initial stage kinetics, diffusion coeff. 0-2987  
 YAl<sub>3</sub>(BO<sub>3</sub>)<sub>4</sub>-NdAl<sub>3</sub>(BO<sub>3</sub>)<sub>4</sub>, substitution of Nd for Y in YAl<sub>3</sub>(BO<sub>3</sub>)<sub>4</sub>, exam. 0-11551  
 ZnS:Tb<sup>3+</sup>, NdF<sub>3</sub> film, vac. deposited, electrolum. energy transfer 0-2861  
 ZrO<sub>2</sub>-Nd<sub>2</sub>O<sub>3</sub> eutectic, unidirectional solidification, microstruct. and crystallographic characterization 0-35176

## neon

see also nuclei with .....

- <sup>3</sup>He-<sup>20</sup>Ne stabilised transverse Zeeman laser, tuning characts., freq. fluctuation 0-48273  
 aerodynamic isotope separation technique based on vel. slip in freejet expansions 0-19441  
 atom, 1s and 2s photoionis. cross sections, L<sup>2</sup> calc. 0-951  
 atom, 2p<sup>3</sup>3p-2p<sup>5</sup>5s emission lines, press. broadening, with Ne(He), rel. to repulsive forces 0-9692  
 atom, 2p<sup>3</sup>3s<sup>2</sup>P<sub>0</sub> state, optical pumping, g-factor, metastability exchange cross section 0-947  
 atom, 2p<sup>3</sup>3s and 2p<sup>3</sup>3p states excitation by slow electrons, H<sup>+</sup>, H<sub>2</sub><sup>+</sup>, and He<sup>+</sup> 0-43185  
 atom, 2p<sup>6</sup>(<sup>1</sup>S<sub>0</sub>) ground state electron impact excitation cross sections 0-23558  
 atom, 2p levels prod. by disoc. recomb. in afterglow, recomb. coeffs., level population 0-43855  
 atom, atomic struct. calc., symmetry adapted pair functions, Rayleigh Schrodinger HF variational perturbation theory 0-42944  
 atom, Auger spectra, correl. effects, energies and wavefunctions, ab initio CI calc. 0-14125  
 atom, autoionising resons. near 575 Å, ab initio relativistic RPA calc. 0-32681  
 atom, beam-foil excited <sup>4</sup>P state, delayed coincidence Auger electron lifetime meas. 0-14117  
 atom, below ionisation threshold (French) 0-43187  
 atom, collisional transfer coeffs. between 2p levels, in afterglow, laser excitation obs. 0-43856  
 atom, Compton profiles using Gaussian expansion of at. orbitals 0-945  
 atom, elastic electron scattering, crit. point 0-5622  
 atom, electron impact ionisation, eikonal approx., shell-averaged, distorted-wave impulse approx. 0-37888  
 atom, excited, reactions in pure afterglow, plasmas using resonance absorpt. spectrometry 0-33835  
 atom, few-electron states prod. K X-rays obs. 0-9718  
 atom, fine struct. obs. by beam-gas spectroscopy, level crossing resonances 0-9719  
 atom, highly-ionised, heavy ion impact, selective electron capture effects 0-14202  
 atom, independent particle pots. comparison 0-52846  
 atom, isoelectronic sequence, excitation energy and oscillator strength, level crossing anomaly, relativistic RPA calc. 0-14077  
 atom, isoelectronic series, ionisation pots., Ritz law and Edlen formula 0-32854  
 atom, isotopic shift and fine struct. for 2p<sup>5</sup>4d and 2p<sup>5</sup>5s config., Doppler-free two-photon spectroscopy 0-23387  
 atom, K-absorption spectrum, core electron rearrangement effect 0-47880  
 atom, optical transitions, Doppler broadening, compensation by vel. depend. light shifts 0-52930  
 atom, outer shell photoionisation, relativistic RPA calcs. 0-9571  
 atom, pair excitation correl. numerical coupled cluster method 0-47906  
 atom, reson. transition oscill. strengths, rel. to electron impact 0-27985  
 atom, SCF electron-gas local-spin-density model including correlation 0-9488  
 atom, transition probabilities in const. elec. field 0-37785  
 atom, zero-order Hamiltonian, for many-body perturbation theory 0-9483  
 atom broadening of 632.8 nm lasing level line width and shift meas. method 0-37066  
 atom doubly excited energy levels, subshell ang. momenta coupling, frozen core superposition of config. method 0-52874  
 buffer gas line broadening in Cu vapour laser, gas temp. meas. 0-19020  
 crystal, vacancy, electronic structure, Green's function theory 0-39525  
 crystalline, self-localized exciton, cavity radius, wave function and energy 0-6737  
 dielectric constant near liquid-vapour critical point 0-50252  
 diffusion and solubility in PTFE 0-6561  
 discharge, excitation mechanisms investig. using radial distrib. of excited atoms 0-38744  
 discharge, low-press., atom densities of first excited state 0-38750  
 discharge plasma, Faraday rot. anomalies in a weak mag. field 0-38659  
 dye laser with modes locked to atomic absorption lines, spectral characts. 0-9881  
 electron energy distrib. functions in weakly ionised gas under high E/N 0-53916  
 electron impact excitation, total cross section below ionisation threshold (French) 0-43187  
 electron swarm with anisotropic vel. distrib. function 0-38520  
 electronic Compton profile beyond impulse approx. (French) 0-53057  
 galactic cosmic rays, Ne, Mg and Si isotopes high resolution meas. 0-51631  
 gas, thermal cond., 90-273K 0-48836  
 gas discharge plasma, electron impact depolarization 0-43847  
 glow discharge, investigation with cylindrical hollow cathode in Ne and He (Russian) 0-28856  
 hot cathode discharge plasma, second order harmonic surface wave generation 0-38849  
 isoelectronic series, dielectronic recombination rate, scaling props. 0-32668  
 isotope separation, HF stationary discharge, travelling mag. field, barodiffusion separation 0-44049  
 laser line, 260 THz, direct freq. meas. 0-53266  
 lattice heat capacity, thermal vibrations, Lindeman parameter, lattice dynamic model (Russian) 0-29141  
 liquid, neutron scatt. determ. of dynamic struct. factor, generalised hydrodynamic anal. 0-54103  
 liquids, optimised cluster expansion, struct. function evaluation 0-49085  
 lunar dust, inert gas conc., separation methods and methods of treatment (French) 0-51674  
 Orion Nebula, Ne, S and O abundances from fine-struct. lines obs. 0-4410

## neon continued

- physisorbed on metal, polarisation due to short range interaction with substrate 0-39428  
 plasma, 60 MeV ion beam-created, electron props. diagnostics (French) 0-10407  
 plasma, low ionised anisothermal plasma, ionising electron collision kinetics (German) 0-33731  
 plasma, weakly ionised, photon echo relax. obs. in RF discharge 0-43986  
 population inversion mechanism between 4p-3d, laser generation conditions 0-1185  
 population of 5s'[1/2]<sub>1</sub><sup>0</sup>, 4p'[3/2]<sub>2</sub> levels interacting with laser radiation 0-23670  
 positive column contraction under diffusion-recombination conditions 0-24293  
 solar wind, inert gas abundance, 500 Myr ago from lunar dust anal. (German) 0-51637  
 solid, desorption heat capacity of adsorbed <sup>4</sup>He 0-10736  
 solid, lattice dynamics calc. using energy band theory 0-49320  
 solid, NMR study of dilute o-H<sub>2</sub> impurity 0-25228  
 solid, solubility in high press. He 0-10674  
 solid adsorbed layer, porosity of solid gas layers, appl. to cryosorption pump (Japanese) 0-20031  
 spectral line relative intensity, radial depend. in low press. discharge 0-37764  
 thermal conductivity, Lennard-Jones (12-6) pot. parameters calcs. 0-28591  
 Ar-Ne mixtures, thermal diffusion 0-1726  
 Cu-Ne CW mW-level laser source at 250 nm 0-43352  
 He-Ne, gas discharge laser, stimulated emission, vel. to striation 0-37994  
 He-Ne, laser wavelength measurement using digital interferometer 0-37079  
 He-Ne, single mode laser, emission zone nonlinear active lens effect 0-32960  
 He-Ne commercial multimode low power laser, conversion to single mode laser 0-53325  
 He-Ne discharges, striations in narrow discharges 0-38736  
 He-Ne gas laser, modulation method, for relative excitation level, cavity bandwidth and at. temp 0-5771  
 He-Ne gas mixture plasma, role of charge exchange in form. of optical props. 0-28600  
 He-Ne I<sub>2</sub> stabilised laser, practical approach to design and construction 0-19051  
 He-Ne laser, 0.633μm line freq. stabilisation with 3.39μm line locked to CH<sub>4</sub> 0-28258  
 He-Ne laser, beat freq. generation between CW dye laser with 80-GHz freq. offset 0-1253  
 He-Ne laser, doubly resonant intracavity SHG of 1153 nm radiation with stabilization on HFS components of <sup>127</sup>I<sub>2</sub> 0-33077  
 He-Ne laser, freq. characts. under two-mode generation 0-53264  
 He-Ne laser, Ne 3s<sub>2</sub>-2p<sub>4</sub> transition, relaxation characts. of degenerate states obs. using polarisation spectroscopy (Russian) 0-27348  
 He-Ne laser, optimal conditions for microwave pumping 0-32961  
 He-Ne laser, simultaneous oscillation at 0.63 and 3.39 μm, output power depend. on loss in mag. fields (Japanese) 0-32959  
 He-Ne laser, two-photon amplification on cascade-transitions, power tuning curve meas. 0-48219  
 He-Ne laser, type 300.1 TEM<sub>00</sub> (Rumanian) 0-9898  
 He-Ne laser photon statistics variation with cavity length 0-53265  
 He-Ne laser stabilisation and performance for dimensional meas. 0-19049  
 He-Ne laser stabilised by methane E-component saturated absorpt., quantum freq. standard 0-9901  
 He-Ne laser tube, laser module LGK 7621, construction 0-53314  
 He-Ne laser wavelength stability, calibration and traceability 0-19050  
 He-Ne laser with internal mirrors, mode polarisation props. 0-23672  
 He-Ne laser with transverse microwave discharge, use of secondary electrons 0-9899  
 He-Ne mixtures, disparate mass, double sound propag., theory 0-33724  
 He-Ne mixtures, thermal diffusion 0-1726  
 He-Ne nuclear-pumped CW lasing 0-48216  
 He-Ne optical waveguide amplifier, operation 0-43363  
 He-Ne ring laser, absorbing medium press. influence on power resonance characts. (Russian) 0-23725  
 He-Ne ring laser, influence of pressure on Zeeman effect 0-19056  
 He-Ne ring laser, operating well above lasing threshold Zeeman effect 0-33039  
 He-Ne ring laser, opposing waves competition at lasing line centre of Ne isotope 0-1187  
 He-Ne ring laser placed in longit. mag. field, nonlinear nonreciprocity effects 0-43377  
 He-Ne ring laser with methane absorpt. cell, power reson. characts. 0-28255  
 He-Ne single mode lasers, meas. of intensity of sources of inherent fluctuations 0-32958  
 He-Ne stabilised transverse Zeeman laser, light source for optical meas. 0-48272  
 He-Ne stable gas laser with 0.4 Hz line width 0-48294  
 He-Ne travelling wave laser, spontaneous emission spectra, 3.39 μm region 0-37995  
 He-Ne/CH<sub>4</sub> laser, IR freq. absolute meas. (Russian) 0-9851  
 He-Ne-Xe, ion laser transitions, hollow cathode excitation 0-1184  
 He-Ne-methane ring laser, frequency stabilized, operating charact. 0-14366  
 He+Ne, afterglow, metastable state energy transfer, spectra 0-43167  
<sup>3</sup>He-<sup>22</sup>Ne 0.63 μm laser stabilised with <sup>129</sup>I<sub>2</sub> nonlinear absorpt. cell, freq. characts. 0-53333  
 He\*+Ne, (3<sup>1</sup>S, 3<sup>3</sup>S, 3<sup>1</sup>P, 3<sup>3</sup>P) de-excitation cross section temp. depend., time resolved spectra 0-28100  
 Ne I, beam-foil excitation, Rydberg states, relative populations 0-14208  
 Ne I to Ne IV, excitation in ion-atom collisions, 100 keV region, emission spectra obs. 0-14205  
 Ne II, III, and IV ground state, photoionis. cross sections, close coupling calcs. 0-5513  
 Ne II, III, IV, photoionisation cross sections calc. 0-43014  
 Ne VII solar emission line ratios, electron density and temp. determ. 0-17559  
 Ne VIII, in plasma, ion electron collisional radiative recomb. coeffs., bottleneck calc. 0-53942  
 Ne VIII, X, electron ionisation cross sections of excited atoms and ions 0-43186  
 Ne<sup>+</sup>, reson. line regularities in plasma Stark widths and shifts 0-43881



## neon continued

- Ne<sup>3+</sup>, CI calc. of at. energy levels 0-5624  
 Ne<sup>4+</sup>, electron impact excitation, collision strength calc. 0-5624  
 Ne-Ar, thermal cond., 90-273 K 0-48836  
 Ne-Ar discharge, transient cathodoluminescence, time depend. 0-38753  
 Ne-Ar(Kr), gas mixtures, thermal cond. meas. in the range 0.5-15 MPa 0-14874  
 Ne-H<sub>2</sub> mixture, liquid vapour phase equilib., sound vel., compressibility, thermodynamic perturbation theory obs. (*Russian*) 0-39306  
 Ne-H-H<sub>2</sub> mixture, positive column characts. and comparison with approx. diffusion theory 0-44025  
 Ne-Kr, gas, diffusion coeffs. meas., 350-1200 K 0-14869  
 Ne-Kr, time-dependent props. near crit. mixing point, 2000 bar, mol. dynamics calcs. 0-24580  
 Ne-Kr Penning mixtures, Townsend ionisation coeffs. and breakdown pot. meas. 0-19641  
 Ne-N<sub>2</sub>, energy transfer, H<sup>+</sup> ion beam produced plasma, ion density and temp. 0-38539  
 Ne-Ne, correl. diagrams, Thomas-Fermi calcs. 0-23294  
 Ne-Ne, Thomas-Fermi-Dirac model, inhomogeneity corrections 0-23308  
 Ne-TiCl hollow-cathode discharge, CW laser oscill. on 594.9, 695.1 nm Ti<sup>+</sup> transitions 0-23674  
 Ne-Xe glow discharge, negative flow charge exchange excitation of Xe<sup>+</sup> levels 0-38857  
 Ne+Al, recoil effects on molecular-orbital X-ray spectra in solid targets 0-25510  
 Ne+Ar<sup>2+</sup>, charge transfer, energy defect and sealing laws 0-48083  
 Ne+Ar(Xr)(Xe), total cross section, glory struct. 0-23494  
 Ne+CO<sub>2</sub>, energy transfer, anharmonic coupling terms, semiclassical calcs. 0-37861  
 Ne+Cl<sup>+</sup>, highly charged low vel. recoil ion time of flight spectra, cross section energy depend. 0-14222  
 Ne+e<sup>-</sup>(H<sup>+</sup>)(pion), specific primary excitation by fast accelerator particles 0-23559  
 Ne+H<sub>2</sub>, gas discharge plasma, H<sub>2</sub> dissoc. excitation, cross section anal. 0-33735  
 Ne+H<sup>+</sup>, electron capture, charge-state distrib. 0-32814  
 Ne+H<sup>+</sup> 0-18916  
 Ne+H<sup>+</sup>(He<sup>+</sup>)(Ne<sup>+</sup>), multiple ionisation of Ne 2s and 2p electrons 0-18918  
 Ne+H<sup>+</sup>(He<sup>2+</sup>)(N<sup>x+</sup>), multiply ionised ats. prod. 0-28098  
 Ne+HD, j=0 to 1 rot. excitation, differential cross sections, time of flight obs. 0-48104  
 Ne+H(2s), 5-25 keV, H(n=3) excitation, Balmer  $\alpha$  emission obs. 0-53113  
 Ne+He, 2p-levels, excitation obs. 0-9712  
 Ne+He(2<sup>2</sup>S,2<sup>2</sup>S), Van der Waals forces, one-electron model pot. calcs. 0-14094  
 Ne+K, K 5<sup>2</sup>P level broadening and collisional relax., quantal, semiclassical and expt. comparison 0-18903  
 Ne+K, photon emission polarisation anal., coincidence studies 0-5614  
 Ne+K(Zn<sup>+</sup>), 0.7-500 keV, K(Zn<sup>+</sup>) excitation, reson.-line emission and polaris. 0-18911  
 Ne+Kr, K-L vacancy sharing process, Nikitin two-state model 0-9684  
 Ne+Li(Be<sup>+</sup>)(Na)(Mg<sup>+</sup>)(K)(Zn<sup>+</sup>), collision-induced alignment, reson.-line emission polaris. obs. 0-18912  
 Ne+NO, angle depend. intermolecular pot., crossed beams study 0-9682  
 Ne+Na, differential cross section at thermal energy, expt. and theoretical results comparison 0-37851  
 Ne+Na, Na(3p) excitation 0-1056  
 Ne+Ne, exchange-repulsion energy, many-orbital cluster expansion 0-18896  
 Ne+Ne, pot. curve derived from gas and solid scatt. data, EMSV pot. 0-1040  
 Ne+O<sup>-</sup>, 0.2-1 keV, elastic and inelastic reduced differential cross-sections 0-32829  
 Ne+O<sup>+</sup>, pot. energy curves, nonadiabatic coupling matrix elements 0-53110  
 Ne+OCS, gas, EPR of rot. transitions, T<sub>1</sub> press. depend. 0-9621  
 Ne+SF<sub>6</sub>(N<sub>2</sub>), metastable state de-excitation, rate consts., radiolysis obs. 0-40709  
 Ne<sup>+</sup>+Co<sub>2</sub>, three dims. quadrupole ion storage, ion mobility, effect of charge exchange reactions, Monte Carlo calcs. 0-55738  
 Ne<sup>+</sup>+He, impact excitation, cascade-fluorescence spectroscopy, level-crossing techniques 0-23357  
 Ne<sup>+</sup>+He, multiple ionisation of Ne 2s and 2p electrons 0-18918  
 Ne<sup>+</sup>+Ne, (He<sup>+</sup>), gas-phase collisions, intermediate and high velocities, excitation 0-32822  
 Ne<sup>+</sup>+Ne, multiple ionisation of Ne 2s and 2p electrons 0-18918  
 Ne<sup>+</sup>+Ne, quasi-resonant charge transfer at thermal energies 0-48082  
 Ne<sup>10+</sup>+H, charge transfer, total and partial cross-sections calcs. 0-23542  
 Ne<sup>2+</sup>+He, charge transfer rate coeff. and astrophysical appls. 0-56701  
 Ne<sup>4+</sup>+H<sup>+</sup>, <sup>3</sup>P<sub>1</sub> fine structure transitions 0-37864  
 Ne<sup>4+</sup>+Ne, collision, correl. diagram calcs. 0-23504  
 Ne<sub>2</sub>, excited state pots., fast calc. 0-9490  
 Ne<sub>2</sub>, vibr. spectra, calc. from pot. curve 0-1040  
 Ne<sub>2</sub><sup>+</sup>, A<sup>2</sup> $\Sigma_{1/2u}^+$ →D<sup>2</sup> $\Sigma_{1/2g}^+$  system, theoretical absorption spectrum 0-32734  
 Ne<sub>2</sub><sup>+</sup>, formation and destruction in Townsend discharges 0-38747  
 Ne<sub>2</sub>+Ar, total integral cross sections for excitation, exchange and dissoc. 0-1044  
 Ne<sub>2</sub>+Kr total integral cross sections for excitation, exchange and dissoc. 0-1044  
 Ne<sub>2</sub><sup>+</sup>+He, pot. energy surface, reaction cross sections, ab initio calcs. 0-11881  
 NeV, solar emission lines, density dependence 0-21963  
<sup>21</sup>Ne, hyperfine interaction in 4d subconfiguration, Doppler-free two-photon spectroscopy meas. 0-18944  
<sup>22</sup>Ne anomalous abundance in Orgueil meteorite, evidence for presolar grains 0-41773  
 Si:Ne, amorphous, implanted and sputtered, epitaxial regrowth, influence of noble gas atoms 0-2289  
 Xe-He(Ne), gas mixture, element and isotope separation in impulse plasma centrifuge (*Russian*) 0-38725  
 ZnS:Ne, implanted single crystals, photolum. and bombardment effect, thermolum. curve obs. 0-55166

## neon compounds

- NeCO<sub>2</sub>, energy transfer, anharmonic coupling terms, semiclassical calcs. 0-37861  
 Ne.H<sub>2</sub>O, excited dimer, first order interaction energy, ab initio calc. 0-32598  
**nephelometry** see turbidimetry  
**Neptune**  
 atmosphere, IR radiation, review 0-8568  
 IR spectrum from 0.8 to 2.5 microns, obs. 0-21946  
 magnetic field origin 0-36564  
 Nereid (Neptune II), ephemeris (1980 March 2 to September 8) 0-46481  
 occultation on 1980 February 10, no event, revised calcs. 0-26805  
 orbital perturbations by Pluto, representation (*French*) 0-26724  
 rotation period, effects of seeing on reflected spectrum 0-46479  
 stratosphere, mixing ratios of methane, ethane and acetylene 0-51692  
 Triton, diameter and reflectance, spectral and radiometric obs. 0-17546  
 Triton, satellite with atmosphere, IR spectrum obs. 0-21945  
**neptunium**  
 see also nuclei with .....  
<sup>241</sup>Am(n,X), Japan Material Testing Reactor, separation of transuranium elements (*Japanese*) 0-52731  
 Cs<sub>2</sub>ZrCl<sub>6</sub>:Np<sup>4+</sup>, EPR data interpretation for octahedral  $\Gamma_8$  state in cubic cryst. field 0-2634  
 Cs<sub>2</sub>ZrCl<sub>6</sub>:Np<sup>4+</sup>, EPR of np<sup>4+</sup> ground state 0-44903  
<sup>237</sup>Np migration potential in radioactive waste 0-3537  
**neptunium compounds**  
 cyclopentadienyl compounds, (C<sub>5</sub>H<sub>5</sub>)<sub>3</sub>NpX, (X=F, Cl, Br, I, (SO<sub>4</sub>)<sub>1/2</sub>), mag. susceptibility 0-11152  
 NpAs<sub>2</sub>, magnetic props., 4.2 to 77K, Mossbauer study 0-39937  
 NpBa<sub>4</sub>Zr<sub>12</sub>F<sub>12</sub> glass, Mossbauer spectrum 0-11304  
 NpO<sub>2</sub>, cryst. growth by chem. transport 0-16166  
**Nernst effect** see thermomagnetic effects  
**Nernst-Ettingshausen effect** see thermomagnetic effects  
**network analysers**  
 dual six-port automatic network analyser, performance 0-47074  
 microwave reflectometers, thru reflect line, improved technique for calibrating dual six-port automatic network analyser 0-47073  
**network analysis**  
 see also circuit analysis computing; linear network analysis; nonlinear network analysis  
 reciprocity theorem, calibration of acoustic emission transducers 0-28401  
**network equalisers** see equalisers  
**network theory** see circuit theory  
**network topology**  
 rivers, tributary diameter, topologically random channel networks anal. 0-8372  
**networks** see networks (circuits)  
**networks (circuits)**  
 see also specific network and circuit headings e.g. communication networks, pulse circuits, oscillators  
 energy fluctuations power conversion, in diode circuit, thermodynamics 0-17911  
**Neumann algebra** see algebra  
**neural nets**  
 see also brain models  
 analytic solution based on Ising spin system analogy 0-12074  
 automaton model I/O characteristic for semi-Markov impulse sequences (*Japanese*) 0-16917  
 colour sensing optoelectronic device, neural mechanism modelling 0-12128  
 dynamical response, effect of boundaries, Limulus retina 0-30717  
 excitation of neurons by electrical synapse, in-phase and antiphase, nonlinear oscillators interaction 0-16918  
 finger tapping, human, neural networks studies by phase transition curves 0-8042  
 homogeneous neural fields, existence and stability of local excitation 0-26220  
 image processing algorithm based on neural net props. 0-40993  
 information processing in neuronal synapses, electrical neuronal model design (*Korean*) 0-35865  
 IPFM neural model, input-output anal., spike regularity and record length effects 0-56016  
 Morishita neurons, modelling networks, cerebellum appl. 0-30703  
 observation methods, US and optical data processing 0-8234  
 pattern generation in lobster stomatogastric ganglion, pyloric network simulation 0-12076  
 random, experimental studies 0-12077  
 random topology networks, randomness of generated eigenvalues 0-22291  
 signal focusing in segmented stretch reflex system, auxiliary spinal networks 0-40999  
 synaptic transmission, nonimpulse-mediated, during cyclic motor program generation 0-51072  
 temporal oscillations, cortical neurons interactions model 0-3636  
 visual hallucination patterns, mathematical theory of neuronal activity 0-35892  
 visual information processing, primate visual system appl. 0-30722  
 visual system, human, transient characteristic using masking experiments 0-41009  
 Ba-treated nerve cells, reduced systems, qualitative anal. of model generating long potential waves 0-26213  
**neuristor networks** see neural nets  
**neuron models** see neural nets  
**neurophysiology**  
 see also brain; neural nets  
 accessory optic projections upon oculomotor nuclei and vestibulocerebellum 0-3643  
 acoustic biotope, neural representation 0-51116  
 action potential changes associated with proved lumbosacral root compression 0-56006  
 action potentials in single axons, effects of hyperbaric air and hydrostatic press. 0-56007  
 afterpotentials influence on shape and magnitude of extracellular pots. 0-3625  
 Aplysia, restoration of transmission in synapses inactivated by habituation 0-56009  
 auditory interneurons, locust, time-intensity trading obs. 0-26238  
 auditory nerve response and brain stem transmission time 0-45917



## neurophysiology continued

- axon adsorption model, action pot. and excitation currents, volt. clamp test 0-56018  
 axon membrane, squid, freq. domain anal. of asymmetry current 0-51064  
 axon-bearing horizontal cells, teleost retina, functionality obs. 0-51084  
 axonal transport of vasoactive intestinal peptide in sciatic nerve 0-21463  
 axoplasmic transport along nerve fibres (*German*) 0-45878  
 axoplasmic transport of proteins, review 0-21464  
 blink reflex, peripheral electrical stimulation inhibitory effect, abolition by naloxone (*French*) 0-35880  
 brain, elec. response rel. to brain functioning in health and neurological disease 0-40998  
 brain, planning and problem solving mechanisms 0-45877  
 brainstem potentials, microwave-evoked, auditory responses, in cats 0-56061  
 center-surround retinal ganglion cells: receptive field organization with special reference to light-dark adaptation 0-12104  
 cerebellar stimulation and eye movement in cats 0-30719  
 cerebral potential sources location for visual field impairment assessment in humans 0-30922  
 cerebral potentials preceding unilateral and simultaneous bilateral finger movements 0-26217  
 colour sensing optoelectronic device, neural mechanism modelling 0-12128  
 compound eye, Dipteran, small signal phototransduction 0-35882  
 cone activity, correl. with horizontal cell morphology, goldfish retina 0-45900  
 cones, evidence for equivalent-background hypothesis 0-16931  
 contingent negative variation and accuracy of time estimation. A study on cats 0-26216  
 cornea sensitivity in normal human eyes 0-12093  
 cortical cells as bar and edge detectors or spatial freq. filters 0-12109  
 cortical electrical phosphene props. 0-12112  
 cortical orientation selectivity, of partially visually deprived cats 0-26230  
 coupled solitary waves in neurophysics 0-51067  
 cryoprobe, for medical surgery 0-56274  
 cyprinid retina, model of function at outer plexiform layer 0-12103  
 digit-wrist sensory compound nerve action pot. obs. in patients with focal nerve injuries 0-3655  
 EEG, pattern-evoked potentials and nerve conduction vel. in family with adrenoleucodystrophy 0-45875  
 electrode pair, implantable, for recording from intact small nerves 0-36204  
 electronic neuron model incorporating both active and passive responses 0-8040  
 EM fields, direct influence on nerve and muscle cells of man in 1 Hz-30 MHz range 0-51160  
 EM radiation effects on neuroelec. transmembrane potentials, possible model of mechanisms 0-26259  
 EMG, cutaneous trunci muscle in spinal reflexes 0-3635  
 EMG in alcoholism, nerve conduct. vel. and sensory pot. studies 0-3617  
 EMG in alcoholism, terminal latencies in superior gluteal, distal peroneal and tibial nerves 0-3618  
 EMG in quadriparetics and quadriplegics, evoked giant sensory nerve pots. 0-3653  
 epiphysis, frog, characts. of slow pots. 0-56029  
 equilibrium reception in an insect, mediation by giant interneurons 0-45925  
 excitable membrane analysis, computer calcs. 0-56004  
 excitation of neurons by electrical synapse, in-phase and antiphase, non-linear oscillators interaction 0-16918  
 experience neural correlates in single units of cat visual and somatosensory cortex 0-12120  
 external geniculate body, metric of space of description of images 0-30716  
 eye and retina development in kittens 0-12113  
 eye movement amplitudes, information used by the perceptual and oculomotor systems 0-35885  
 F-wave and M-response conduction velocity in diabetes mellitus 0-56015  
 finger tapping, human, neural networks studies by phase transition curves 0-8042  
 finger tapping phase transition curves, human (*Japanese*) 0-56333  
 foveal vision central mechanisms, monkey 0-12108  
 giant axon of the squid, gating current and K channels obs. 0-56012  
 hair cell receptor pot., ionic basis in vertebrates, bullfrog obs. 0-26239  
 hearing nonlinearities model described by active processes with saturation at 40 dB 0-56058  
 hippocampal afterdischarges in rats, activity spread by  $^{14}\text{C}$  method 0-26221  
 histological section, computer-assisted mapping with the light microscope 0-30963  
 homogeneous neural fields, existence and stability of local excitation 0-26220  
 impulses in 2 parallel unmyelinated fibres, induced excitation and synchronisation calcs. 0-56017  
 information processing in neuronal synapses, electrical neuronal model design (*Korean*) 0-35865  
 intracerebral implants of embryonic neural tissue in rats, neuronal interactions study technique 0-30702  
 intraspinal nerve fibres, cat, electrical threshold continuous monitoring method 0-46104  
 IPFM neural model, input-output anal., spike regularity and record length effects 0-56016  
 lateral geniculate nucleus in cat, struct. of identified X and Y cells 0-26231  
 lateral geniculate nucleus of cat, periodic stimulation, neural activity transient persistence 0-56021  
 lateral geniculate nucleus postnatal development in humans 0-12114  
 lateral line, onset of neural function in South African clawed frog 0-21480  
 lens accommodation, interpositus neuron control obs. 0-21469  
 luminosity-type cells in the turtle retina, short-wavelength input 0-41012  
 median nerve lesion localisation, usefulness of F-wave conduction time, post mastectomy patient 0-56267  
 membrane excitability mechanisms, book contrib. 0-12062  
 microcomputer-based neurophysiological stimulator, design of and impact on clinical procedures 0-26393  
 microprocessor-based unit data acquisition and reducing system 0-21598  
 microwave biological effects, overview 0-35964  
 modular gating channel and the Cole-Moore effect 0-30708

## neurophysiology continued

- monitoring system for stroke patients 0-26394  
 Morishita neurons, modelling networks, cerebellum appl. 0-30703  
 motion and vision, stabilised spatio-temporal threshold surface 0-16926  
 motoneurone model with early inactivation, after hyperpolarisation conductance time-course and repetitive firing 0-40987  
 motor systems, eye and hand, optimal response in pointing at visual target 0-56079  
 multiunit signals, educable waveform recognition system for sorting unit discharges 0-51312  
 muscarinic suppression of voltage-sensitive  $\text{K}^+$  current 0-51070  
 muscle strength gain, neural factors rel. to hypertrophy 0-12168  
 myelin lattice swelling kinetics study X-ray diffr. obs. 0-21436  
 nerve action potential model 0-30697  
 nerve fibre conduction vel. distrib., estimation from action pots. 0-3633  
 nerve fibre conduction vel. distrib., estimation from two compound action pots. 0-8044  
 nerve fields, topographic maps and columnar microstructure formation 0-56013  
 nerve spike trains, Fourier anal. 0-12070  
 nervous activity monitoring in *Drosophila* by  $[^3\text{H}]$ deoxyglucose 0-56024  
 network dynamical response, effect of boundaries, Limulus retina 0-30717  
 neural coding schemes, integrate-to-threshold anal. 0-35868  
 neural network theory, analytic soln. based on Ising spin system analogy 0-12074  
 neuroendocrine effects, microwave-induced, nonspecific stress reaction 0-35969  
 neuromuscular information transmission, distortion suppression 0-35871  
 neuromuscular junction, membrane surface pot. changes effect on drug interactions 0-3631  
 neuron mathematical model, freq. characts. (*Japanese*) 0-35866  
 neuron single-unit pots. recording, multi-microelectrode system characts. (*Japanese*) 0-21581  
 neuronal activity and focal blood flow coupling in experimental seizures 0-40989  
 neuronal activity model, Ornstein-Uhlenbeck process 0-51030  
 neuronal impulse generation, modulation of point processes 0-30698  
 neuronal waveforms, optimal recognition 0-56003  
 neurosecretory cell IR photomicrography 0-30959  
 noradrenaline-induced hyperpolarisation of spinal motoneurons 0-56010  
 nuclei of raphe system, electric stimulation and cooling effects on alertness in cat (*French*) 0-35864  
 olfactometry, smell intensity meas. (*French*) 0-8073  
 olfactory bulb, gain mediating cortical stimulus-response relations, non-linear 0-12165  
 olfactory receptor sites location, inferences from latency meas. 0-56068  
 olfactory tubercle, unilateral lesions, modification of general arousal effects, rat 0-3652  
 optic nerve fibre arrangement in cat, non-retinotopic 0-30720  
 optic tectum, pigeon, single cell spatial- and temporal-freq. selectivity 0-41016  
 optic tectum, pigeon, single-neuron responses to moving sine-wave gratings 0-41015  
 optic tract fibers, cat, Markov properties of nonstationary spike trains 0-51077  
 oscillators, phase locking model 0-21460  
 pacemaker neurons, Aplysia, effects of irradiation with 20 MeV electrons 0-17013  
 pacemaker synaptic interactions: modelled locking and paradoxical features 0-51069  
 palmar conduction time of median and ulnar nerves in carpal tunnel syndrome 0-12075  
 Parkinson tremor generation, linear modelling of possible mechanisms 0-3615  
 pattern generation in lobster stomatogastric ganglion, pyloric neuron kinetics and synaptic interactions 0-8043  
 pattern-evoked potential, modifications rel. to stimulated part of visual field 0-26225  
 peripheral motor nerve conduct. studies in lethargic mice 0-3634  
 peripheral nervous system multichannel data anal., frog sartorius muscle mechanoreceptor transducer characts. (*Japanese*) 0-3656  
 phasic pupillary light reflex and visual evokes potentials, simultaneous anal. 0-26226  
 photic sensitivity of macaque monkey and pulvinar neurons 0-12106  
 photoreceptor, barnacle, conditioning light effect modification by metarhodopsin absorpt. of light 0-8064  
 photoreceptor, barnacle, effects on prolonged depolarising afterpot. of  $\text{Mn}^{2+}$ ,  $\text{Ca}^{2+}$  0-8051  
 photoreceptor, barnacle, props. of on-transient of intracellular response 0-8052  
 photoreceptor, barnacle, upper limit on translational diffusion of visual pigment 0-8053  
 photoreceptor transduction, determ. of pigment transition or state coupled to excitation 0-8054  
 pretectum organisation, cat 0-12107  
 primary auditory neurons, preferred intervals in spontaneous activity 0-45921  
 primary visual cortex, orientation selectivity development models, normally and dark reared kittens 0-41007  
 primary visual cortex orientation selectivity development kinetics, normally and dark reared kittens 0-41006  
 proprioceptors with central cell bodies, in locust 0-51132  
 prosthetic sensory feedback, human tracking performance with afferent elec. nerve stimulation 0-17195  
 psychophysiological techniques applied to aircraft design and other operational problems 0-26384  
 random neural nets, experimental studies 0-12077  
 receptive field props. of neurones in visual cortex of cat 0-26227  
 repetitive firing mechanism excitation parameters, nerve impulse trains statistical evaluation 0-40986  
 respiratory rhythm generation, mathematical model, respiratory neuron classification 0-35873  
 retina, significance of antidromic potentiation and induced activity 0-12092  
 retina chromaticity horizontal cells of turtle, synapse mechanisms 0-51079  
 retinal chromophore transition dipole moment, orientational changes obs. 0-41023  
 retinal degeneration, hereditary, cone inputs to ganglion cells 0-8056



## neurophysiology continued

- retinal ganglion cell activity induced by ELF mag. fields, method for study 0-56321  
 retinal ganglion cell response props. in Siamese cat 0-12115  
 retinal ganglion cell types, of cat, visual resolution and receptive field size 0-56037  
 retinal ganglion cells, responses to stationary and moving stimuli 0-51080  
 retinal ganglion cells of a tree shrew, definition of neural response and incremental sensitivity 0-41011  
 retinal horizontal cells, nonlinear characts. of spatial summation in receptive field, model 0-26232  
 retinal L-type horizontal cells, dynamic interaction in receptive field 0-26233  
 retinal model, layered visual processing 0-16925  
 retinal neurons, catfish, spatiotemporal testing and modelling 0-41005  
 retinal receptor directional sensitivity, flicker effects 0-8057  
 retinotectal pathway, uncrossed, development rel. to plasticity studies, rat 0-56025  
 retinotectal projection development, Gierer-Meinhardt eqns. appl. 0-56022  
 rod outer segments, spread of activation and desensitisation 0-35881  
 rod-cone interaction, spatial patterns 0-16930  
 saccade-related unit activity in monkey superior colliculus 0-12101  
 saccadic eye movement, accompanying pots. 0-12102  
 saccadic eye-movement system, processing of direction and magnitude obs. 0-56035  
 Schwann cell layer of squid axon, diffusion models 0-40985  
 sensory nerve conduct. vel. of medial antebrachial cutaneous nerve 0-3654  
 signal focusing in segmented stretch reflex system, auxiliary spinal networks 0-40999  
 somatosensory evoked potentials, short latency, stimulus intensity effect 0-35924  
 spectrally-opponent responses in ground squirrel optic nerve 0-35883  
 spike separation in multiunit records, multivariate anal. 0-26215  
 spinal cord seizures elicited by high pressures of He 0-12071  
 stereology conference, Salzburg, Austria (Sep. 1979) 0-22134  
 stereoscopic depth channels for position and for motion 0-12146  
 stochastic neuron models, multi-input-output information transmission 0-30707  
 striate neurons in area 17 of Siamese cats, response props. 0-12116  
 superior colliculus and its sensory inputs, primate 0-12100  
 swimming control in a cubomedusan jellyfish 0-3637  
 sympathetic ganglion cell in bullfrog, oscill. of  $[Ca^{2+}]_i$ -linked  $K^+$  conductance 0-35867  
 synaptic cause of neural synergism and antagonism 0-30696  
 synaptic facilitation and bursting patterns, modification by hyperbaric air, *Aplysia californica* 0-56008  
 synaptic potential, release of transmitter from locust nonspiking interneurons 0-3632  
 synaptic proteins after electroconvulsive stimulation 0-56011  
 synaptic transmission, nonimpulse-mediated, during cyclic motor program generation 0-51072  
 tactile sensation, mechanoreception physiology and psychophysics (*Japanese*) 0-16962  
 template-matching mechanism for sensory search with olfactory bulb, anal. 0-56069  
 temporal oscillations in neural nets, cortical neurons interactions model 0-3636  
 thalamus, cat, stimulus induced and seizure related changes in extracellular K conc. 0-35870  
 threshold model of neuron firing, empirical examination 0-56014  
 transmitter-specific retrograde labelling in the striato- and raphe-nigral pathways 0-51309  
 ventral photoreceptors, *Limulus*, excitation by photons and fluoride ions 0-8065  
 vision, IR nonlinear perception in 800-1355 nm range 0-12123  
 vision, masking-induced sensitivity changes in *Limulus* photoreceptors 0-41024  
 vision, photoconvertible pigment states and excitation, prolonged depolarising afterpot., blowfly 0-8060  
 vision, photopigment and receptor props. in *Drosophila* compound eye and ocellar receptors 0-8063  
 vision, photopigment rapid conversions in blowfly visual sense cells, effect on receptor pot., pupillary response 0-8062  
 vision, preferred orientation, variability due to methodology 0-56032  
 vision, prolonged depolarising afterpot., transduction in photoreceptors with bistable pigments 0-8050  
 vision, psychophysical functions in fish with respecified retinotectal connections 0-12152  
 vision, red-green opponent channel, short-wave cone input obs. 0-41028  
 vision short-wavelength cone pathways, response saturation, colour opponent mechanisms control 0-41017  
 visual cortex, altered connections in Siamese cat 0-12091  
 visual cortex cat, effects of alternating monocular occlusion 0-16932  
 visual cortex of cat, neural mechanisms underlying stereoscopic depth perception 0-12147  
 visual cortical effects of early visual experience 0-12119  
 visual development in humans, animal models 0-12118  
 visual evoked potentials, n-hexane induced changes, ERG of industrial workers 0-45886  
 visual evoked potentials in monkeys 0-45885  
 visual information processing, primate visual system appl. 0-30722  
 visual monocular space perception, math. model rel. to retinal neurophysiology 0-45910  
 visual neuron-discharges in eye movements 0-12099  
 visual neurones in dipterous insects, sexual differences 0-41010  
 visual pigment processes and prolonged pupillary responses in insect photoreceptor cells 0-8061  
 visual stimulus onsets and offsets, response of visual mechanisms 0-16937  
 visual system, crayfish, coding and decoding of steady state information by patterned pulse trains 0-12105  
 visual system, primate, subdivisions and interconnections 0-12110  
 visual system development in cat, role of binocular interactions 0-12117  
 visual tracking, target vel. signals in vermal Purkinje cells, monkey obs. 0-56026  
 visual Wulst retinotopic organisation in nocturnal and diurnal raptors 0-12098  
 walking, mathematical model of muscle commands from nervous system (*French*) 0-51071  
 Ba treated nerve cells, generation of long potential waves 0-56002

## neurophysiology continued

- $Ca^{2+}$  intracerebral transients, photoelectrode for recording 0-30961  
 Na channel fluctuations, phys. nature, microscopic model 0-35869
- neutral currents**  
 atom, metastable, sensitivity and level crossing role in parity nonconservation meas. 0-43005  
 b-quark, horizontal gauge symmetry, Cabibbo universality and fermion masses 0-22583  
 conference on hadron struct. and lepton-hadron interactions, Cargèse, France (July 1977) 0-4473  
 $E_7$  grand unification using  $SU(3) \times U(1)^3$  gauge group, neutral currents 0-27444  
 elastic electron scatt. and atom parity nonconservation caused by nuclear parity violation 0-27427  
 factorisation and coupling constant determ. for  $\nu e$ ,  $e d$ , and  $\nu +$  hadron 0-27451  
 flavour-changing neutral currents 0-22553  
 grand unified field theories, two-loop corrections to mixing angle and lifetime of proton 0-13249  
 Higgs bosons, effects on experimental observables, and fermion mass scale 0-32061  
 Higgs induced neutral currents, natural flavour conservation and quark mixing angles 0-42392  
 high energy neutrino physics, recent expt. results 0-4982  
 hyperon semileptonic decay,  $SU(3)$  spectrum generation, Cabibbo angle 0-9119  
 isoscalar neutral current axial vector couplings and nucleon anomalous moments 0-27452  
 L-amino acids, weak neutral currents and biological stereoselection 0-26196  
 lepton-nucleus scattering, bremsstrahlung and neutral currents 0-32268  
 leptonproduction,  $\mu N \rightarrow \mu X$ , broken colour gauge theory of integer charge quarks 0-13313  
 molecules, parity-violating effects of weak interactions 0-52455  
 muonic atom, configurational mixing in shell and neutral weak muon-nucl. interaction effects obs. feasibility (*Russian*) 0-32859  
 muonic atoms, long range parity violating interaction from  $\gamma-Z^0$  conversion 0-48108  
 nuclear matter, high-temperature, neutral currents and neutrino Comptonisation 0-21905  
 nucleon weak interaction pots. in the Weinberg-Salam model (*Russian*) 0-13258  
 parity violating neutral currents, radiative corrections, Weinberg-Salam and left-right symmetric models 0-52451  
 parity violating neutral currents in two-photon and autoionisation atomic transitions 0-32034  
 quark-lepton correspondence in neutral current interactions 0-27450  
 reactor neutrino expts., fission fragment  $\nu$  radiation, neutral currents, inverse  $\beta$ -decay,  $\bar{\nu}$  scatt. (*Russian*) 0-42736  
 S,P,T-type neutral weak current meas. in  $\mu N$  scatt. 0-32064  
 simultaneous constraints and s $\bar{s}$  effects in neutral-current-coupling determinations 0-37205  
 $SU(2)_L \times (T_3)_R \times U_V(1)$  gauge unified model, neutral current interactions,  $e d$  and  $\nu$  scatt. 0-18107  
 $SU(2) \times U(1)$  unified theory, symmetry and renormalisation 0-22551  
 $SU(2) \times U(1) \times G$  expanded gauge models of neutral currents, propagator momentum transfer 0-47237  
 $SU(6)$  grand unification model, hierarchy of symmetry breakings and neutral currents 0-52446  
 unified model for atomic parity violation and neutral currents in gauge theories 0-4912  
 weak quark and lepton chiral symmetries, dynamical breaking gauge interaction 0-47215  
 Z-boson and two-boson models 0-18109  
 $D^0$ ,  $D^0$ , decays, charm changing neutral current limits, QCD depend., mass differences 0-32062  
 $e d$  elastic scatt., P-odd effects due to neutral weak currents, cross sections (*Russian*) 0-13312  
 $e d$  scatt., P-violation calc. in weak interaction theory 0-42469  
 $e^+ e^- \rightarrow N^* \bar{N}^*$ , weak neutral current effects for polarised  $e^+ e^-$  pair 0-37287  
 $e^+ e^-$ , weak corrections to three-jet angular distributions 0-22629  
 $e^+ e^- \rightarrow \gamma +$  hadrons, high energy, lepton radiation and  $\gamma$  struct. functions, quark parton model 0-32113  
 $e^+ e^- \rightarrow$  hadron jets, quark helicities, neutral current vector and axial couplings 0-32114  
 $e^+ e^- \rightarrow \mu^+ (\tau^+) \mu^- (\tau^-)$ , neutral current couplings, lepton polarisation, p violation in  $SU(2) \times U(1)$  model 0-4975  
 $e^+ e^- \rightarrow q \bar{q} \rightarrow B X$ , weak-neutral current effects 0-42480  
 ep, high  $Q^2$ , QCD corrections to parity-violating asymmetries 0-22618  
 ep deep inelastic scatt., parity violation and neutral currents 0-22559  
 $\gamma N \rightarrow l^+ l^- X$ , pol.  $\gamma$ , neutral current effect, Weinberg Salam model calcs., p violation 0-5000  
 $\gamma N \rightarrow l^+ l^- X$ , polarisation effects on P-violating asymmetry in Weinberg-Salam model 0-32055  
 $K \rightarrow 2\pi$ , decay amplitudes in  $SU(2) \times U(1) \times U(1)$  model with new neutral current 0-4986  
 $\mu$  magnetic moment, weak coupling contribution, Weinberg-Salam model 0-22607  
 $\nu$  neutral current couplings and  $\nu e^-$  weak neutral current coupling constraint, fermionic assignments 0-4915  
 $\nu(p)d$ , scatt., weak hadronic neutral current struct. investig. 0-42438  
 $\nu_e(\bar{\nu}_e)e$ , charged and neutral current interference, test of Weinberg-Salam model 0-42385  
 $\bar{\nu} N$ , neutral current charm particle prod. search 0-22600  
 $\nu N \rightarrow \nu n \pi^0$ , neutral current induced one-pion production, Weinberg-Salam structure 0-52454  
 $\nu N \rightarrow \nu p \pi^+$ , neutral current induced one-pion production, Weinberg-Salam structure 0-52454  
 $\nu P$ , neutral to charged current cross section ratio, coupling constant 0-27497  
 $\nu p \rightarrow \nu n \pi^+$ , neutral current induced one-pion production, Weinberg-Salam structure 0-52454  
 $\nu p \rightarrow \nu p \pi^0$ , neutral current induced one-pion production, Weinberg-Salam structure 0-52454  
 $W^0$  effects in  $e^+ e^-$  interactions on  $a^-$  resonances 0-42386  
 Z-mass prediction as test of standard model 0-47239  
 Bi, neutral current-induced parity nonconserving optical rot., Dirac-HF calcs. 0-47948  
 Bi, vapour, optical rot., parity nonconservation expts. 0-23354



**neutral currents continued**

$^2\text{H}(\bar{\nu}_e, \bar{\nu}_e)n$ , neutral current cross section for reactor  $\bar{\nu}$  0-5129  
 TIF, P- and T-violating interactions in hyperfine struct., mol. beam reson. expt. 0-53019

**neutrino detection and measurement**

high-energy neutrino astronomy, as probe of galactic nuclei 0-4432  
 solar neutrino detectors, absorpt. cross section rel. to neutrino problem 0-17566  
 $\nu_\tau$ , beam-dump experiment, observation of  $\nu_\tau$  interactions 0-22601

**neutrino-electron interactions**

see also *neutrino-electron scattering*  
 neutral current processes, factorisation and coupling constant determ. for  $\nu_e$ , ed, and  $\nu$ +hadron 0-27451  
 $\nu$  interaction, local conservation law from neutrino massless, gauge invariance 0-42355  
 $\nu e \rightarrow W^\pm Z^0(\gamma)X$ , high energy behaviour and hard photon prod., cosmic rays 0-5028  
 $\bar{\nu}_e e \rightarrow W^- \rightarrow X$ , obs. in direct lepton prod. from cosmic ray protons (*Russian*) 0-12627

**neutrino-electron scattering**

see also *neutrino-electron interactions*  
 reactor neutrino expts., fission fragment  $\nu$  radiation, neutral currents, inverse  $\beta$ -decay,  $\bar{\nu}$  scatt. (*Russian*) 0-42736  
 $\nu_e(\bar{\nu}_e)e$ , charged and neutral current interference, test of Weinberg-Salam model 0-42385  
 $\nu_e e$ , scatt. meas., interaction gauge models (*German*) 0-37251  
 $\nu_e e \rightarrow \nu_e e$ , cross section meas. 0-47273

**neutrino interactions**

see also *neutrino-electron interactions*; *neutrino-neutrino interactions*; *neutrino-nucleon interactions*; *neutrino scattering*  
 asymptotic freedom and parton model appl. to leptonic processes 0-4959  
 charged current induced weak one pion prod., form factors from PCAC 0-18129  
 Comptonisation in high-temp. nuclear matter, neutral current theory 0-21905  
 conference on hadron struct. and lepton-hadron interactions, Cargèse, France (July 1977) 0-4473  
 dilepton production in  $\nu(\bar{\nu})$  reactions, bottom quark excitation contrib. 0-42439  
 high energy neutrino physics, recent expt. results 0-4982  
 magnetic field interactions, synchrotron neutrino emission, charge collision emission, star neutrino luminosity 0-41719  
 neutral charmed particle decay, direct observation in  $\nu$ -emulsion interactions 0-9165  
 QCD structure function relation between deep inelastic  $\nu$  reactions and polarised electroprod. 0-37221  
 reactor neutrino expts., fission fragment  $\nu$  radiation, neutral currents, inverse  $\beta$ -decay,  $\bar{\nu}$  scatt. (*Russian*) 0-42736  
 trimuon events, spin-parity selection rules 0-22603  
 unified model for atomic parity violation and neutral currents in gauge theories 0-4912  
 Z-boson and two-boson models, neutral current phenomena,  $\mu$ -e universality 0-18109  
 $e^+e^- \rightarrow \gamma V \rightarrow \gamma \nu \bar{\nu}$ , neutral vector meson radiative prod. and decay (*Russian*) 0-52492  
 $\nu$ ,  $\bar{\nu}$  charged current induced one pion weak prod.,  $I=1/2$  resonant contrib. 0-47274  
 $\nu(\bar{\nu})$  charged current induced one  $\pi$  prod., model total cross sections 0-4979  
 $\bar{\nu}_e d \rightarrow n \bar{\nu}_e$ , cross-section calcs. 0-42440

**neutrino-neutrino interactions**

see also *neutrino-neutrino scattering*

No entries

**neutrino-neutrino scattering**

see also *neutrino-neutrino interactions*

No entries

**neutrino-nucleon interactions**

see also *neutrino-nucleon scattering*  
 Bjorken scaling law violation, mass dependent, quark-quark interactions 0-9160  
 cumulative proton production in neutrino and antineutrino interactions with freeon, 2 to 30 GeV (*Russian*) 0-4980  
 electromagnetic radiative corrections to deep-inelastic neutrino interactions 0-22602  
 jet analysis, QCD calcs. and phenomenological models 0-52523  
 quark properties and existence studies, book contrib. 0-42441  
 $\gamma N$ , deep inelastic scatt., QCD phenomenology 0-42443  
 $\mu^+ \rightarrow e^+ \bar{\nu}_e \nu_\mu$ ,  $\bar{\nu}$  search for muon number conservation test, neutrino expt. 0-47270  
 $\mu N$ , deep inelastic struct. function, Nachtmann moments in QCD 0-27510  
 $\mu^- N \rightarrow \nu X$ , six-quarks model, upper bounds for t-quark production 0-13297  
 $\nu(\bar{\nu})N$ , 5-35 GeV, total cross sections via charged current channel, energy depend. (*Russian*) 0-4981  
 $\nu(\bar{\nu})N \rightarrow \mu^- \mu^+ e^+ e^- X$ , trilepton event EM and hadronic contrib. 0-409  
 $\nu(\bar{\nu})N \rightarrow \nu(\bar{\nu})X$ , zero muon channel visible energy distrib.,  $\nu_\tau$  test eval. 0-52489  
 $\nu_\mu(\bar{\nu}_\mu)N$ , charm meson prod. and decay, lepton inclusive distrib., c-quark fragmentation function (*Russian*) 0-52493  
 $\nu_\mu(\bar{\nu}_\mu)N \rightarrow \tau^\pm X$ , beam-dump experiment, observation of  $\nu_\tau$  interactions 0-22601  
 $\bar{\nu}_\mu + N \rightarrow \mu^+ + X$  deep inelastic interaction at 2 to 25 GeV (*Russian*) 0-13298  
 $\nu N$ , deep inelastic scattering and asymptotic freedom 0-27511  
 $\nu N$ , high energy, dilepton events, D meson semileptonic decay 0-42446  
 $\bar{\nu} N$ , neutral current charm particle prod. search 0-22600  
 $\nu N \rightarrow \mu^- \mu^+ X$ , charm-pair production 0-22643  
 $\nu n \rightarrow \mu^- p$ , total cross-section and differential cross-section, estimation of nucleon mass 0-18128  
 $\nu N \rightarrow \nu X$ , broken colour gauge theory of integer charge quarks 0-13313  
 $\nu n \rightarrow \nu n \pi^0$ , neutral current induced one-pion production, Weinberg-Salam structure 0-52454  
 $\nu n \rightarrow \nu p \pi^+$ , neutral current induced one-pion production, Weinberg-Salam structure 0-52454  
 $\bar{\nu}_\mu N$ ,  $K^0$  and  $\Lambda$  inclusive prod., fragmentation function and transverse momentum squared 0-32093  
 $\nu P$ , neutral to charged current cross section ratio, coupling constant 0-27497  
 $\bar{\nu} p$  charged current jet size, comparison with  $e^+e^-$  jets 0-22599

**neutrino-nucleon interactions continued**

$\nu p$  inelastic interactions, scaling deviations in secondary hadron energy distrib. 0-9161  
 $\nu p \rightarrow \Lambda^+ X$ , evidence for  $\Lambda_c^+$  (2260) prod. 0-42442  
 $\bar{\nu} p \rightarrow \mu^+ X$ , deep inelastic scatt., MQM description 0-47305  
 $\bar{\nu} p \rightarrow \mu^+ + X$ , 4.5 GeV<sup>2</sup>, p struct. functions x depend., quark distrib. 0-32097  
 $\nu p \rightarrow \nu n \pi^+$ , neutral current induced one-pion production, Weinberg-Salam structure 0-52454  
 $\nu p \rightarrow \nu p \pi^0$ , neutral current induced one-pion production, Weinberg-Salam structure 0-52454  
 $\nu p \rightarrow \Sigma_c^{++} X$ , evidence for  $\Sigma_c^{++}$  (2424) prod. 0-42442  
**neutrino-nucleon scattering**  
 see also *neutrino-nucleon interactions*  
 No entries  
**neutrino-nucleus reactions**  
 for inelastic neutrino-nucleus scattering, see "neutrino-nucleus scattering"  
 see also *neutrino-nucleon interactions*  
 stellar collapsing cores, neutrino prod. and inelastic scatt. by nuclei at extreme temps. 0-36488  
 $^{37}\text{Cl}(\nu, e^-)^{37}\text{Ar}$ , shell model cross section calc., appl. to cosmic ray and background elimination (*Russian*) 0-5131  
 $^{71}\text{Ga}(\nu, e^-)^{71}\text{Ge}$ , shell model cross section calc., appl. to cosmic ray and background elimination (*Russian*) 0-5131  
 $\text{Ne}(\bar{\nu}, p)$ , 0.6-25 GeV, backward emitted proton inclusive spectra, short range correlation 0-32281

**neutrino-nucleus scattering**

see also *neutrino-nucleon scattering*  
 interactions in vertical emulsion target of hybrid apparatus 0-5126  
 $^{12}\text{C}(\nu, \nu')$ , ( $\bar{\nu}, \bar{\nu}'$ ), 15.11 MeV state excitation, cross sections, level decay 0-9258

**neutrino production**

cosmic ray proton atmospheric interactions, direct leptons prod. (*Russian*) 0-12627  
 deep inelastic  $\nu$  prod., QCD and hadronic energy ang. distrib. 0-390  
 galaxies active nuclei, high-energy neutrino luminosity and detectability 0-4432  
 Higgs bosons, effects on experimental observables, and fermion mass scale 0-32061  
 review, of neutrino-generating reactions (*Russian*) 0-13344  
 stellar collapsing cores, neutrino prod. and inelastic scatt. by nuclei at extreme temps. 0-36488  
 synchrotron neutrino emission, charge collision emission, star neutrino luminosity 0-41719  
 target complex at Fermilab, operating experience 0-23230  
 $F^\pm \rightarrow \tau^\pm \nu_\tau(\bar{\nu}_\tau)$ , beam-dump experiment, observation of  $\nu_\tau$  interactions 0-22601  
 $pN$ , 28 GeV in Cu, prompt neutrinos and penetrating particles 0-47336  
 $^{12}\text{C}(\mu^- \nu_\mu)^{12}\text{B}$ , Hartree Fock wavefunction, correlations, pseudoscalar coupling constant, capture rates, recoil nuclear polarisation 0-22774

**neutrino scattering**

see also *neutrino-electron scattering*; *neutrino interactions*; *neutrino-neutrino scattering*; *neutrino-nucleon scattering*  
 deep inelastic structure functions and the quark parton model 0-4992  
 $\text{SU}(2)_L \times (\text{U}_3)_R \times \text{U}_V(1)$  gauge unified model, neutral current interactions, ed and  $\nu$  scatt. 0-18107

**neutrinos**

see also *cosmic ray neutrinos*

Bianchi IX model, spectral asymmetry and QFT in curved spacetime 0-56982  
 black holes, rotating, neutrino fluxes resulting from macroscopic parity violation 0-22034  
 elementary particle physics, information from astronomical observations 0-51935  
 flux from quark matter at core of collapsed stars 0-22028  
 form factors in 2-D approx. of QED 0-9132  
 ghost neutrinos in Einstein Cartan theory 0-52108  
 identification and research at Laue Langevin Institute, Grenoble (*French*) 0-21883  
 masses,  $\text{SO}_{10}$  hierarchical breaking 0-22550  
 massless  $\nu_\tau$ , left-right symmetric gauge models,  $\text{SU}_{2,L} \times \text{SU}_{2,R} \times \text{U}_1$  0-27461  
 neutral current couplings and  $\nu e^-$  weak neutral current coupling constraint, fermionic assignments 0-4915  
 quark-lepton correspondence, multigeneration  $\text{SU}(2)_L \times \text{U}(2)$ -based model, neutrino flavours and masslessness property 0-22584  
 review, of discovery, production, meas. and appls. (*Russian*) 0-13344  
 $\text{SO}(10)$  grand unified theory, breaking scheme and neutrino mass 0-47230  
 solar, capture rate problem, role of pion in composite neutron mode 0-41808  
 solar neutrino problem, theory versus obs. 0-17566  
 species number, rel. to universe lepton number 0-8730  
 $\text{SU}(s)$  grand unification, neutrino mass and oscillations, B-L nonconservation 0-52449  
 Sun, exchange current corrections to proton-proton reaction 0-26733  
 vacuum neutrino oscills. inhibition by high matter density in stellar core collapse 0-36496  
 velocity in comparison to muons 0-9190  
 $\nu_\mu$ , rest mass measurements from  $\pi^+ \rightarrow \mu^+ \nu_\mu$  0-37253  
 $\nu_\tau$ , mass, lifetime, decay modes and mixing angles 0-445  
 $\nu_\tau$  test eval. in zero muon channel visible energy distrib. 0-52489

**neutron absorption**

CANDU reactor, Th-fuelled, importance of  $^{233}\text{Pa}$  in neutron economy 0-22980  
 FFTF, critical expts., with solid neutron absorbers 0-52727  
 FTR fuel pins with solid neutron absorbers, criticality expts. 0-18476  
 graphite rods, damage by high energy neutrons 0-29070  
 HTGCR, fuel with double heterogeneity, resonance absorpt. 0-32321  
 multizonal absorbing rod, effectiveness in albedo and diffusion studies (*Russian*) 0-556  
 nuclear reactor criticality safety anal., determ. of Dancoff factor for cubic arrays of spherical fuel particles 0-13725  
 regulation, dynamic simulation of two-phase control absorber in nuclear reactor 0-13731  
 solid neutron shield development, materials eval. for spent fuel shipping cask 0-13939  
 solid neutron shield material tests 0-37543  
 transfer matrix calcs. for thermal neutrons 0-27687



**neutron absorption continued**

- two-phase control absorber, horizontal absorber elements, expt. study 0-42841  
 two-phase control absorber development program for CANDU reactors 0-42839  
 vitreous silica blocks, damage by high energy neutrons 0-29070  
 Ag-Cu-Pb coin chem. anal. by low energy  $\gamma$ -rays and neutron transmission meas. 0-35591  
 $B_2C$ , neutron absorber material for FBR, in-reactor performance meas. 0-18429  
 $UO_2(NO_3)_2$  highly enriched soln. with  $Cd(NO_3)_4 \cdot 4H_2O$  neutron poison, criticality expts. 0-13724

**neutron activation analysis**

- activation cross section, integral tests in  $^9Be(d,n)$  field 0-851  
 air, trace amounts of In, extraction and neutron activation determ. 0-12045  
 air dust, environmental data evaluation problems 0-21425  
 air particulates in Hong Kong, nondestructive multielement determ. 0-12040  
 air pollution, emissions from nonferrous plants, neutron-activation anal. 0-21343  
 air pollution control, activation analysis for 14 volatile heavy metals as constituents of aerosol particles 0-16891  
 $Al_2O_3$ - $SiO_2$  refractories, using neutron-2 equipment 0-45612  
 biological material analysis, As and Hg determ. 0-36216  
 biological samples, pseudo-cyclic instrumental neutron activation anal. of trace multielement conc. 0-17214  
 bone, short-lived radionuclides, gamma-ray spectrometry, correction for dead-time losses 0-42312  
 breast tissue exam. using neutron activation and electron microscopy 0-21536  
 capture cross section meas. using neutron activation anal. 0-32282  
 coal ash content measurement in moving wagons 0-3431  
 diamond, natural, trace element anal., genetic significance 0-55759  
 element analysis, role of neutron capture  $\gamma$ -rays 0-50926  
 elemental analysis by neutron inelastic scatter gamma rays with a radioisotope neutron source 0-30311  
 epidemiologic monitoring, neutron activation analysis of blood and blood components 0-17099  
 epidemiologic monitoring, trace elements in human skin lesions 0-17100  
 epidemiological monitoring of human hair, neutron activation trace element anal. 0-17212  
 epidemiology, determ. of organically-bound chlorine and bromine in biological samples 0-21593  
 gamma-ray spectroscopy, instrumental NAA, improvements to basic advance prediction program 0-14042  
 geochemical indicators for genesis of ore deposits (*German*) 0-30301  
 geological materials, multielement anal. 0-16747  
 granulitic rock outcropping, trace elements determination (*Portuguese*) 0-7874  
 hair, human, multielement neutron activation anal. of trace element concs., Tokyo area 0-45602  
 HTGR fuel refabrication plant, nondestructive fissile assay technique 0-37562  
 human body N meas. by anal. of prompt  $\gamma$ s from neutron capture 0-51220  
 human brain, instrumental NAA of trace element distrib., rel to blood serum conc. 0-17215  
 in-vivo activation analysis, diagnostic technique 0-56210  
 inertial confinement fusion target, density in fuel region by activation anal. 0-33807  
 instrumental neutron activation analysis studies of tissues from patients with pulmonary diseases 0-21535  
 kidney, human, PIXE and neutron activation anal., appl. to cancer tissues 0-56199  
 liver, bovine, PIXE and neutron activation anal. 0-56199  
 LMFBR fuel pins, assay with Pb spectrom. 0-37461  
 neutron activation analysis meas. of O and N 0-46032  
 neutron capture  $\gamma$ -rays, practical appls., analytical techniques, PNAAL facilities 0-40794  
 neutron capture cross sections at 14.6 MeV, activation anal. 0-52665  
 neutron-capture prompt gamma-ray activation analysis: multi-element measurements on various materials 0-40796  
 nuclear spent fuel, neutron interrogation 0-5307  
 passive activation for environmental transuranic and moisture assay 0-21431  
 photon activation anal. for high energy radiation therapy 0-21534  
 quartz, high purity, impurity distrib., neutron activation anal. 0-24485  
 radioactive waste from leach rate determ. 0-37523  
 radiochemical neutron activation anal. of environmental matrices for Hg and noble metals 0-16889  
 sample posture converter for nondestructive activation analysis with neutron generator 0-35497  
 sediment pollution by Hg and As, instrumental neutron activation and atomic abs. spectrometric anal. 0-16890  
 serum, human, PIXE and neutron activation anal. 0-56199  
 skin lesion Mn, Cu and Zn conc. meas. by neutron activation 0-17063  
 solutes in liquids, conc. determ. by  $(n,\alpha)$  and  $(n,\gamma)$  reacts., scintillation counting 0-35602  
 steel, neutron activation anal. in VVER reactor (*Czech*) 0-5234  
 steel, stainless, fusion blanket structures, NAA 0-23145  
 thermal  $(n,\gamma)$  reaction, elemental anal. appl. 0-40795  
 trace element anal. of medical samples, using neutron activation, clinical appl. 0-17101  
 trace element determ. in dry biological samples by neutron activation anal. and collection of active C 0-17213  
 two-phase flow characterisation using neutron techniques, review (*Italian*) 0-19479  
 urine U analysis by delayed neutrons 0-26331  
 water, multielement instrument neutron-activation analysis, ecology appl. 0-40946  
 X-ray registration, reduction of background using mag. field 0-16738  
 $^{197}Au$  isotopic neutron source, form. cross sections for 3 and 14.1 MeV neutrons 0-32283  
 BN, O content depend. on heat treatment temp., neutron activation analysis 0-16356  
 Ca, whole-body, determ. method for rats 0-51302  
 Cr, floating zone-refining, activation anal. 0-29875  
 Hg, volatilisation losses during neutron irradiation in a reactor 0-13596

**neutron activation analysis continued**

- Na estimation in cotton clothing for use in neutron activation dosimetry 0-47729  
 Pu borehole assay using delayed-neutron activation anal. 0-21419  
 Pu, neutron analysis in solid waste 0-42840  
 Se, determ. of quantity in human urine 0-36079  
 Si wafers, Au contamination during plasma etching 0-19831  
 Si:P, determ. of P content in high-purity Si using meas. of Mo in 12-molybdophosphoric acid by NAA and AAS 0-15148  
 Si:Sb, epitaxial film, growth by mol. beam technique 0-2292  
 Si:Sb, ion implanted doping, isotopic composition shifts on neutron activation determination 0-24487  
 $SiO_2$  wafers, Au contamination during plasma etching 0-19831  
 $SiO_2$ :Ga film, impurity distrib. after annealing, neutron activation anal. 0-24484  
 $(U,Pu)O_2$ , determ. of O<sub>2</sub> coeff. 0-37457  
 U, nondestructive assay of mixed samples 0-18423  
 Zn dust, for O<sub>2</sub> determ. (*Japanese*) 0-11977  
 ZnS single crystals, O content determ. by fast neutron activation anal. 0-15142

**neutron angular distribution**

- see also neutron spectra*  
 accelerator facility, Van de Graaff generator and cyclotron for fast neutron detection and neutron reaction cross-sections 0-47805  
 Boltzmann equation, eigenvalue precision, influence of boundary conditions 0-27689  
 Boltzmann equation, eigenvalue precision, influence of boundary conditions 0-27690  
 heavy ion reactors, neutron ang. distrib., compound nucleus decay, fission fragment anisotropy (*Russian*) 0-5160  
 LWR, outgoing neutron spectrum from  $H_2O$  in  $H_2O/V$  interface 0-27697  
 organic, neutron response functions, Monte Carlo program 0-14047  
 $^{13}C(\gamma,n)$ , 7.6-24 MeV, photoneutron ang. distrib., level scheme and  $J^\pi$  assignments 0-466  
 $^{94}Nb$  level density, neutron spectra and ang. distrib. nonequilib. processes from  $^{94}Zr(p,n)$  (*Russian*) 0-37376  
 $^{ASb}$ , A=119,122, level density, neutron spectra and ang. distrib. nonequilib. processes from  $Sn(p,n)$  (*Russian*) 0-37376

**neutron beam effects *see neutron effects*****neutron detection and measurement**

- see also neutron spectrometers*  
 accelerator facility, fast neutron research, data acquisition and anal. 0-47806  
 accelerator facility, Van de Graaff generator and cyclotron for fast neutron detection and neutron reaction cross-sections 0-47805  
 BWR, method for detecting bypass coolant boiling 0-571  
 BWR noise, response of neutron detector to local coolant void distrib. 0-683  
 BWR power reactor, in-core startup system with neutron flux monitor 0-32405  
 CANDU self-powered flux detectors, response characts. 0-32404  
 cellulose nitrate,  $^6Li$  enriched, neutron detection props. 0-52828  
 coincidence counting, removal of multiplication effects by Monte Carlo method 0-37715  
 coincidence counting of thermal neutrons, detector and calcs. 0-37716  
 coumarin in water and heavy water, fast neutron response 0-845  
 counter development, electron drift vel. in inert gas mixtures 0-48843  
 critical assembly, neutron spectra meas. by activation method 0-32390  
 delayed neutron meas. in PWR primary circuit, influence of photoneutrons (*Czech*) 0-5205  
 DePangher precision long counter and neutron dose-rate meters, calibration 0-47822  
 dosimeter and monitoring instrumentation calibration using  $^{252}Cf$  and  $^{238}PuBe$  sources 0-13946  
 dosimeters, integral, calibration for personal dosimetry (*Czech*) 0-27825  
 electret pulse-detector for fast neutrons 0-23260  
 equivalent-dose measurement with Rossi counter 0-18678  
 fast neutron detection system, response function and efficiency calcs. 0-14056  
 fast neutron induced tracks in plastics, comparison using electrochem. etching 0-23154  
 fast neutron time of flight spectroscopy, multi-angle detector system 0-52810  
 fission counter, absolute neutron flux meas. and  $^{239}Pu(n,f)$  resonance integral 0-5453  
 fission reactor core, neutron detector telecontrol device with direct loading (*Russian*) 0-52770  
 fuel elements during irradiation, thermal state study using contactless method 0-32392  
 gas proportional  $\alpha$ -recoil spectrum 0-5433  
 gas scintillation counter with selective level population for high-intensity neutron fluxes detection 0-23253  
 high LET radiation therapy beams, expt. microdosimetry 0-12280  
 HTGR fuel refabrication plant, nondestructive fissile assay technique 0-37562  
 Inconel-Inconel coaxial cable self-powered flux detector 0-42842  
 ionisation chamber mean energy deposition calc., 0.1 to 20 MeV 0-9467  
 IVV-2 research reactor, thermal neutron flux distrib. using neutron probes 0-32391  
 laser detection of scattered neutrons from luminesc. line freq. change 0-23272  
 linear radiation-flux functionals, estimation of local perturbations using Monte Carlo method 0-5457  
 LMFBR fuel pins, assay with Pb spectrom. 0-37461  
 LR115 red cellulose nitrate personnel neutron rem dosimeter, design 0-52826  
 LWR, fuel reprocessing plant, NDT control methods 0-5314  
 mixed  $n$ - $\gamma$  field microdosimetry and neutron/gamma discrimination (*French*) 0-12279  
 NE213 liquid scintillator, light output for electrons and protons 0-32564  
 NE213 neutron counter, efficiency calibration 0-27877  
 NE 213 scintillator, neutron response functions, energy range to 40 MeV (*Japanese*) 0-18756  
 neutral beam test facility, D-D neutron meas. 0-37710  
 neutron collimated fast beam, radiation quality local distrib. 0-12247  
 neutron counting statistics in subcritical cyclo stationary multiplying system 0-32323  
 neutron dosimetry, meas. standardisation for biological and biomedical appl. 0-12271



**neutron detection and measurement continued**

- neutron flux distrib. in nonhomogeneous samples, computational model for prompt gamma-ray analysis 0-14060  
 neutron multiplicity for gamma rays from (particle, x $\gamma$ ) reacts. 0-37689  
 nuclear fuel reprocessing plant, neutron monitors for process and safety control 0-5458  
 nuclear track detector, appl. as neutron dosimeter, response to standard neutron sources 0-5342  
 personnel dosimeter calibration, US NBS standard reference neutron fields 0-9417  
 Pilot U scintillator for 55-225 MeV neutrons 0-18762  
 polarimeter, 3-D calibration procedure 0-18770  
 polarisation meas. with high press. He scintillation counter, Monte Carlo convections 0-14061  
 polariser-analyser efficiency meas. by spin flip meas. 0-27911  
 polycarbonate track detector, electrochemically etched, meas. of low neutron fluences 0-32577  
 polyester foil neutron track detection, dosimeter appl. 0-5439  
 polyethylene-terephthalate track detector, electrochemically etched, meas. of low neutron fluences 0-32577  
 proportional, methane filled telescopes for fast neutron spectrometry 0-37683  
 proportional counters, geom. effects on proton recoil spectra 0-14050  
 proton-recoil counter technique for measurement of fast neutron spectrum 0-9447  
 PWR, fuel monitoring, by delayed-neutron detectors 0-737  
 PWR, r.m.s. ex-core detector signal to core barrel amplitude scale factor 0-52767  
 PWR neutron flux detectors, reliability tests (*French*) 0-32403  
 quartz resonators appl. for recording intense fluxes 0-23254  
 radiotherapy, high-energy accelerators, mixed photon-neutron field meas. 0-51267  
 random search algorithm for 2-D data fitting 0-27915  
 reactor in-core flux monitoring 0-5297  
 rem-dose measurement of mixed p-n radiation using solid state detectors of fission fragments 0-36137  
 response functions of spherically moderated neutron detectors 0-37687  
 scintillation counter, calibration of threshold 0-23258  
 scintillation counter, NE213, detection efficiency meas. for 130 MeV neutrons 0-27888  
 scintillation counter, test of Monte Carlo calcs. by  $^{12}\text{C}(\text{p},\text{n})$  and  $^{12}\text{C}(\text{p},\text{p}')$  cross section meas. 0-37713  
 scintillation counters, organic, neutron response functions, Monte Carlo program 0-14047  
 scintillation detectors for neutrons from short-lived plasma 0-23263  
 scintillation pickups with plateau in counting characteristic, review 0-47811  
 scintillation spectroscopy, organic, use of logarithmic pulse height and energy scales 0-37690  
 self-powered detectors, beta particle escape efficiency determ. 0-47816  
 self-powered detectors for in-core reactor neutron flux meas., detector signal composition 0-32402  
 solid state nuclear track detector 0-27876  
 solutes in liquids, conc. determ. by (n, $\alpha$ ) and (n, $\gamma$ ) reacts., scintillation counting 0-35602  
 spherical survey meter response 0-18679  
 spontaneously fissioning material, Monte Carlo neutronic and electronic model for thermal-neutron coincidence counting 0-23165  
 Stern-Gerlach polarimeter for measuring polarisation of cold neutron beams 0-37679  
 thermometer, lack of accuracy considerations 0-42869  
 thermal and epithermal neutron flux densities, self-powered neutron detector sensitivity 0-52817  
 thermal neutron detection by activation of  $\text{CaSO}_4\text{:Dy-KBr}$  0-32581  
 thermal neutron spectra parameter meas. in reactor core 0-9348  
 thin monitors for reactor dosimetry 0-32522  
 thin-film fission thermocouple detectors for reactors safety expts. 0-22987  
 TOF meas., rate depend. of counting losses 0-37692  
 TOF neutron detector for meas. with very fast burst source (*French*) 0-14040  
 UCN, detection systems, sources, transport, book contrib. 0-22882  
 VVR-SM reactor, neutron flux and dose meas. and evaluation (*Czech*) 0-5252  
 water moderated reactor, influence of air bubbles on neutron detector response 0-18442  
 Ar, liquid, scintillating target, fast neutron polarisation analyser 0-47833  
 $\text{CaF}_2 + \text{Dy}_2\text{O}_3 + \text{KCl}$ , intermediate neutron detection by thermoluminescence 0-5444  
 $\text{CaSO}_4\text{:Dy} + \text{Dy}_2\text{O}_3 + \text{KCl}$ , intermediate neutron detection by thermoluminescence 0-5444  
 $\text{CaSO}_4\text{:Tm}$ /polythene mixture, thermoluminesc. response to fast neutrons 0-5340  
 Cu as activation detector for thermal neutron meas. 0-52814  
 $\text{Dy}_2\text{O}_3$ , activation detectors for thermal and fast neutron detection 0-887  
 Ge(Li) detectors, fast neutron leakage spectrum determ. 0-32565  
 $^3\text{H}(\text{d},\text{n})^4\text{He}$ , neutron energy meas. with Si detector 0-32566  
 Li glass NE-912, neutron detection efficiency (*Russian*) 0-27901  
 $^6\text{Li}$  sandwich counter, meas. of neutron spectra in fast neutron systems 0-27884  
 Pu in waste, anal. of enhanced variance and twin gate methods 0-5454  
 $^{235}\text{U}$ - $^{238}\text{U}$  fuel, nondestructive isotopic meas. using fission neutron counting 0-32385  
 W, radiation shielding material, integral tests of ENDF/B-IV high-energy neutron cross-section data 0-23162

**neutron diffraction**

- see also *neutron diffraction crystallography; neutron diffraction examination of materials*  
 high pressure sample container for thermal neutron inelastic scattering on fluids 0-37681  
 small angle neutron scattering on the Harwell linac 0-19675

**neutron diffraction crystallography**

- see also *crystal atomic structure*  
 amorphous substances, neutron diffraction. struct. investigations (*German*) 0-44108  
 bent mosaic crystals, preliminary theoretical approach 0-1901  
 Bragg reflections, ang. positions calcs. by computer program 0-38863  
 elastic neutron scattering, automatic processing of data obtained with DN-520 neutron diffractometer (*Russian*) 0-54079

**neutron diffraction crystallography continued**

- FORTAN software, for mini-computers to control four-circle neutron diffractometer 0-38876  
 furnace, high temp., for neutron diffraction studies 0-19673  
 Grenoble high flux reactor, neutron physics expts., methodical aspects (*German*) 0-554  
 magnetic materials, neutron studies, book contrib. 0-11169  
 magnetic structure elastic polarised neutron scattering. atomic mag. moments 0-29531  
 magnetic structures, neutron diffraction, symmetry anal., group theoretical group anal. of exchange Hamiltonian 0-29527  
 melts, neutron diffraction. struct. investigations (*German*) 0-44108  
 Michelson interferometer for ultracold neutrons 0-33858  
 orientationally disordered structures, orientation and position correlations of a mol. 0-14966  
 orientationally disordered structures, positive definiteness of orientational distribution functions 0-14958  
 particle-size distribution functions, determ. from SAS data by indirect transformation method 0-38860  
 perfect and regularly imperfect crystal, diffraction props. and neutron optics appl. 0-24323  
 polarised neutron diffraction, determ. of magnetic form factors, pioneering work 0-24321  
 polarised neutron diffractometry, method of secondary extinction correction 0-28882  
 polarised neutron expts., extinction models 0-24322  
 powder least-squares program, POWLS 0-1892  
 radial distribution anal., computer program 0-28875  
 Rietveld neutron profile refinement, interactive computer system, POWDER 0-1900  
 Rietveld profile refinement algorithm, modification for powder data 0-24320  
 Rietveld profile refinement method, anal. 0-24315  
 rotating single-crystal slab, secondary extinction 0-14965  
 secondary extinction correction, method in polarised neutron diffractometry 0-28882  
 slow neutron scattering by rotating systems of identical nuclei (*Russian*) 0-14968  
 small angle scattering. depend. on divergence (*French*) 0-49045  
 spectroscopy techniques and examples (*Dutch*) 0-28884  
 spin-echo spectrometry and neutron optical polarisers 0-49051  
 vibrating single crystal, Umweganregung peaks 0-10461  
 $\text{Fe}_3\text{Mn-Fe}_2\text{Si}$ , slow neutron polariser, by single crystal. (111) refl. 0-49052

**neutron diffraction examination of materials**

- see also *neutron diffraction crystallography*  
 acetylcholine receptor from Torpedo Californica, struct. anal., low-angle neutron scattering. obs. 0-30651  
 actinide compounds, structure, mag. and related props., review 0-6389  
 adamantane, Ising, diffuse scattering, hard-core correl., weak-graph method 0-49137  
 alkali metal dicarboxylates, H bonding and motion, incoherent inelastic neutron scattering. spectroscopy 0-48095  
 alloys, concentrated, local atomic arrangements, associated with ordering, review 0-50632  
 amorphous ferromagnets, neutron scattering. rel. to elementary excitations, amorphous 0-39494  
 amorphous solids, inorganic, struct., review 0-15004  
 benzenetricarbonylchromium, neutron inelastic scattering. spectrum and valence force field 0-48096  
 biphenyl, incommensurate phases, obs. of excitations, inelastic neutron scattering. 0-49334  
 ceramics, local atomic arrangements, associated with ordering, review 0-50632  
 colloids, structure determ. by neutron diffraction and small angle scattering. 0-40748  
 condensed H-containing media, cold neutron total section data interpretation 0-33857  
 critical molecules, neutron scattering, 'optical activity' 0-23567  
 cytosine monohydrate, deuterated, neutron diffraction. crystal. struct. determ. 0-54215  
 di-(2,2,6,6-tetramethyl-4-piperidiny-1-oxyl)-suberate, spin densities, polarised neutron diffraction. meas. 0-50037  
 dilute ferromagnet, slow neutron inelastic scattering by spin excitations, cluster approx. 0-11168  
 dimethyl tin difluoride, solid, methyl group motion, neutron scattering. study 0-10607  
 dimethylammonium manganese tetrachloride, phonon density of states, expt. and calc. 0-54323  
 dimethylammonium manganese tetrachloride-d<sub>2</sub>, structural and mag. phase transitions, neutron scattering and AC susceptibility meas. 0-44825  
 diphenylsilanediol, randomised X-ray powder diffraction patterns, adjustable sample holder 0-6317  
 Elinvär,  $\gamma$  to  $\gamma'$  transformation and  $\gamma'$  phase form. kinetics, lattice consts. 0-35191  
 ethane submonolayer on graphite, struct. and melting, elastic neutron scattering. 0-29266  
 exciton scattering of neutrons, theory 0-29330  
 1,1'-ferrocenedicarboxylic acid, triclinic, X-ray and neutron crystal. and mol. struct. determ. at 78 and 298K 0-29008  
 ferroelectrics, inelastic neutron scattering, one-phonon differential cross section 0-28883  
 ferromagnet, domain struct. study by time depend. neutron depolarisation 0-50138  
 ferromagnet, Heisenberg, Bose-representation correctness of spin operators, anal. 0-15700  
 2-fluoronaphthalene, disordered form, thermal expansion, neutron and X-ray diffraction. study 0-24621  
 glycerol, Mossbauer and neutron scattering. 0-20559  
 $\gamma$ -glycine, crystal. struct. by neutron diffraction at 83K and 298K 0-35825  
 $\alpha$ -glycine, deuterated, low freq. intermol. modes, neutron diffraction. obs. 0-15086  
 Heisenberg, impure classical chain, dynamic props. using local-moment pair correl. functions 0-15728  
 hexachloroethane, orthorhombic, neutron struct. refinement 0-29009  
 hydration, anionic, press. effect, neutron diffraction. obs. of  $\text{NiCl}_2(\cdot\text{LiCl})$  heavy water solns. 0-30212  
 Inconel X750, positron annihilation study of ageing and creep 0-29824  
 ion-water interactions, survey of diffraction studies 0-24347  
 ionic liquids, struct. determ., summer school lecture series 0-6349  
 itinerant electron system, mag. excitations, neutron scattering. studies 0-44838



## neutron diffraction examination of materials continued

- IV-VI compounds, phase transitions induced by electron-phonon interaction 0-10656  
 $^6\text{LiH}_3(\text{SeO}_3)_2$ , absolute atomic arrangement rel. to spontaneous polarisation, neutron diffr. study 0-15067  
 liquid crystals, struct. and optical props., neutron and X-ray diffr. obs. 0-24323  
 low-dimensional mag. systems, neutron scatt., review 0-50103  
 macroparticle diffusion, role of inertial effects 0-29196  
 magnetic crystal, perfect, spin rot. of forward transmitted beam in neutron diffr. 0-50113  
 magnetic crystal neutron diffr., integrated intensity heats, crystal and mag. struct. determ. 0-44079  
 magnetic densities and magnetic excitations, neutron studies, book contrib. 0-11170  
 magnetic system, solitons near critical point, neutron scattering observation 0-34650  
 magnetic systems, conference, Julich, Germany (Aug. 79) 0-41934  
 magnetic systems, polarisation analysis of diffuse neutron scattering 0-25098  
 manganese zinc formate dihydrate, two-dimens. antiferromag., anomalous crit. phenomena, neutron scatt. and PMR obs. 0-50104  
 materials science, phys. and mech. props. 0-25538  
 metal, diffusion of H(D), slow neutron scatt. obs., review 0-34248  
 metal-H system study by neutron scattering, review (*French*) 0-34226  
 metals, diffusion of H, complex jump diffusion model rel. to quasi-elastic neutron scatt. by H 0-24638  
 N-methylacetamide, structure, Raman spectroscopy and neutron diffr. obs. (*French*) 0-7343  
 molecular and molecular group rotational motion in solid state, neutron scatt. studies 0-24384  
 molecular crystals, spectroscopy, bibliography (1977) 0-7317  
 molten salt, possibility of plasmon mode obs., struct. dynamics 0-10477  
 naphthalene, phonon eigenvectors, neutron scatt. intensities determ. 0-44271  
 nematic liquid crystals, microdynamics, computer study and models (*Hungarian*) 0-33878  
 neutron induced X-ray atomic excitation 0-23510  
 one-dimensional magnetic systems, obs. of mag. solitons (*Japanese*) 0-2555  
 organic liquid, simple, struct. exam. and scatt. data interpret. 0-54096  
 orientationally disordered cryst., diffuse scatt., hard-core correl., weak-graph method 0-49137  
 PAA, cryst. phase transitions, intermolecular motion, Raman and inelastic neutron scatt. spectra 0-2164  
 PAA, nematic liq. cryst., elec. field effects, neutron diffr. study 0-28912  
 PAP, cryst. phase transitions, intermolecular motion, Raman and inelastic neutron scatt. spectra 0-2164  
 paramagnetic metal, polarised neutron inelastic and quasi-elastic scattering 0-50045  
 paramagnetic metals, polarised neutron studies of field induced magnetisation 0-25084  
 polarised neutrons in condensed matter [conference, Zaborow, Poland (Sept. 1979)] 0-22136  
 polyatomic fluid, local dynamics, spectroscopic studies, summer school lecture series 0-6343  
 polyelectrolyte in solution, variation of contrast, neutron forward scatt. calc. (*French*) 0-54104  
 polyethylene, semi-crystn., neutron scattering study 0-38936  
 polymer, amorphous, chain conform., small-angle neutron scatt. obs. (*Polish*) 0-10511  
 polymer network, small-angle neutron scatt. obs. of mol. behaviour 0-37918  
 polymer semicrystallised chains, small-angle neutron scatt., mean dimension evaluation 0-43220  
 polymer solution, dynamical scaling, neutron spin echo obs. 0-14990  
 polymer solution and bulk state, partially labelled chains, neutron scatt. obs. 0-38899  
 polyolefins, semi-crystn., neutron scattering study 0-38936  
 polypropylene, semi-crystn., neutron scattering study 0-38936  
 polystyrene, isotactic, conformation in bulk crystallised state 0-43221  
 polystyrene-polyisoprene two-block copolymer soln., conformation, small angle neutron scattering, X-ray diffraction, review (*Rumanian*) 0-6348  
 polysulphur nitride, Kohn anomalies in phonon dispersion 0-24555  
 quasi-localised spin system, mag. excitations, neutron scatt. studies 0-44838  
 rare earth alloys,  $\text{RZn}_{12}$  and  $\text{RCu}_4\text{Al}_8$ , mag. struct. and interactions 0-25092  
 rare earth cpds.,  $\text{RRh}_4\text{B}_4$  and  $\text{RMo}_6\text{X}_8$  (X=S, Se), mag. order and supercond., neutron scatt. studies 0-44807  
 rare earth intermediate valence systems, neutron scatt., review 0-49674  
 rare earth intermetallic compounds with  $\text{Cu}_3\text{Au}$  structure, crystal field splitting 0-54663  
 rare earth intermetallics, mag. struct. 0-15698  
 rare earth intermetallics, neutron scatt., induced moment magnetism, high press. 0-15699  
 rare earth intermetallics, RPt, (R=Gd, Tb, Dy, Ho, Er, Tm), structs. and mag. props. 0-50069  
 rare earth mixed valence compounds, spin dynamics, mag. neutron scatt., Mossbauer effect, XPS studies 0-39786  
 rubber, materials props. prediction, elasticity model 0-3113  
 slow neutron scatt. by rotating systems of identical nuclei (*Russian*) 0-14968  
 sodium acetate trihydrate, press. depend. of methyl tunnelling motion 0-10603  
 spin glass, relaxation times, influence of spectral distrib. on freq. depend. of freezing temp. 0-44848  
 spin system, mag. excitations, polarised neutron inelastic and quasi-elastic scattering 0-50045  
 spinels, mag. struct., symmetry anal. in neutron diffr. studies 0-25091  
 steel, Cr-Mn, metastable constitution diagram and phase transforms. (*Russian*) 0-50590  
 steel, stainless, polycrystalline, elastic constns., inelastic coherent neutron scatt. meas. 0-34122  
 steel with micro-duplex structure, analysis of rolling texture and its development 0-16327  
 succinonitrile, plastic, diffuse scatt., hard-core correl., weak-graph method 0-49137  
 succinonitrile, plastic phase, mol. motions correlation times, incoherent neutron scatt. 0-49138

## neutron diffraction examination of materials continued

- superionic conductors, struct. and dynamical props., X-ray and neutron scatt. studies, book contrib. 0-24433  
 TBBA liquid crystal, self diffusion coeffs., neutron diffr. and NMR study 0-19689  
 tetramethylammonium tetrachlorozincate, ferroelec., incommensurate-commensurate transition, neutron scatt. study 0-40073  
 TGS, ferroelectric transition, neutron diffr. obs. 0-25324  
 thiourea, lock-in phase transform. 0-29698  
 TMMC, one-dimensional antiferromag., solitons, neutron inelastic-scatt. meas. 0-44810  
 TMMC, XY-Ising crossover transition, quasi-elastic neutron scatt. obs. 0-44826  
 tooth enamel, human cryst. struct. refinement, Rietveld method 0-51040  
 transition metal elements and alloys, spin distribution, neutron diffraction expts. 0-25097  
 transition metal magnetic clusters, neutron inelastic scatt., review 0-50083  
 transition metal-H system, exam. of excitation spectra and diffusion mobility of H using neutrons 0-29203  
 (TTF) $\text{CuS}_2\text{C}_4(\text{CF}_3)_4$ , spin Peierls system, mag. field effects 0-7123  
 TTF-TCNQ, elastic neutron scatt. evidence for charge transfer change at high power 0-2163  
 tungsten bronzes, hexagonal, supercond. and special phonons, neutron scatt. obs. 0-15643  
 velocity selector for neutrons, high resolution, applic. to materials research (*German*) 0-47803  
 $\text{Al}_2\text{O}_3\text{-CoO-SiO}_2$  glasses, spin correls., neutron diffr. meas. 0-15694  
 Ag-Te, liq., struct. and elec. props. 0-49083  
 $\text{AgBi}(\text{CrO}_4)$ , cryst. struct., neutron diffr. time-of-flight study (*French*) 0-15057  
 $\alpha\text{-AgI}$ , neutron powder diffr. meas. interpretation 0-10533  
 $\alpha\text{-AgI}$ , neutron scatt. expts.,  $\text{Ag}^+$  ion motion 0-6552  
 $\beta\text{-Ag}_2\text{S}$ , fast-ion conductor, Ag ion density, neutron diffr. study 0-34234  
 $\text{Ag}_3\text{SI}$ , superionic cond., phase transition and cryst. structs., sp. ht., neutron and X-ray diffr. obs. 0-10662  
 Al melt, struct. factors, at. distrib. curves, thermodynamic and neutron diffr. study (*German*) 0-19687  
 Al, phonon anharmonic response, neutron-scatt. test of computer calcs. 0-44281  
 Al, phonon density of states by neutron scatt., sp. ht. and Debye temp. 0-2132  
 Al, polycrystalline, elastic constns., inelastic coherent neutron scatt. meas. 0-34122  
 Al, single crystals, total thermal neutron cross sections 0-19672  
 Al-Mg, determ. of distortion field, induced by substitutional defect 0-44536  
 Al-Mg (13 wt.%), aged single crystals, small angle neutron scattering 0-1961  
 Al-Si melts, struct. factors, at. distrib. curves, thermodynamic and neutron diffr. study (*German*) 0-19687  
 Al-Zn, comparison between very-slow-neutron transmission and small-angle neutron scatt. expts. 0-19677  
 $\text{Al}_3\text{Ce}$  and  $\text{Al}_3\text{Ce}_2$ , Kondo cpds., mag. behaviour obs. by neutron diffr. 0-50049  
 $\text{Al}_2\text{Mn}_2\text{Si}_2\text{O}_{12}$  amorphous spin glass, spin dynamics, neutron scatt. meas. 0-15741  
 $\text{Al}_2\text{O}_3\text{-MnO-SiO}_2$  glasses, spin correls., neutron diffr. meas. 0-15694  
 Au-Fe (16.2 at.%), cluster glass, mag. small angle neutron scatt. 0-50111  
 $\text{BaCl}_2\cdot 2\text{H}_2\text{O}$ , polycryst. hydrates, librational motion of  $\text{H}_2\text{O}$  mols., neutron diffr. exam. 0-10604  
 $\text{BaCo}_2(\text{AsO}_4)_2$ , magnetic field effect on mag. ordering neutron diffr. obs. 0-50053  
 $\text{BaF}_{2-x}\text{H}_x$ , synthesis and struct. determ. using neutron diffr. (*French*) 0-24425  
 $\text{BaVS}_3$ , annealing influence on lattice constants, neutron diffr. profile anal. 0-1976  
 Be, phonon spectrum from inelastic coherent scatt. of cold neutrons 0-10617  
 Be, single cryst., mean square atomic displacement and antisymmetric atom vibrations, neutron data 0-49180  
 Bi, phonon density of states by neutron scatt., sp. ht. and Debye temp. 0-2132  
 Bi, single crystals, total thermal neutron cross sections 0-19672  
 $\text{BiVO}_4$ , cryst. growth and struct. 0-35078  
 $\text{CaCl}_2$ , aqueous soln., ion hydration 0-35518  
 $\text{CaHPO}_4$ , monetite, low-temp. ordering of H atoms, X-ray and neutron diffr. study at 145K 0-39022  
 $\text{Ca}_3\text{Mn}_2\text{Ge}_2\text{O}_{12}$ , antiferromagnetic garnet, neutron diffr. study in mag. field 0-50060  
 $\text{Ca}_3\text{Mn}_2\text{Ge}_2\text{O}_{12}$ , mag. struct. study 0-2554  
 Ce, liq., 4f electron susceptibility temp. depend. 0-20378  
 Ce-H(D), inelastic neutron scattering exam. of lattice dynamics 0-29128  
 $\text{CeAl}_2$ , multiple-q mag. struct. 0-25100  
 $\text{CeAl}_2$ , neutron diffr. at low temp., magnetism 0-20383  
 CeBi, phase diagram in mag. field, hydrostatic press. effect 0-25132  
 $\text{CeD}_{2.12}$ , neutron cryst.-field spectroscopy 0-14967  
 $\text{Ce}_{0.73}\text{Ho}_{0.27}\text{Ru}_2$ , superconductors, mag. correlations and crystal-field levels 0-34547  
 $(\text{Ce}_{1-x}\text{Ho}_x)\text{Ru}_2$ , superconducting, mag. props., neutron scatt. study 0-44808  
 $\text{Ce}_{1-x}\text{La}_x\text{Sn}_2$  (x=0 to 1), mag. susceptibility and magnetisation, lattice parameters, X-ray and neutron diffr. meas. 0-49675  
 $\text{Ce}_{1-x}\text{Pr}_x\text{Al}_2$ , mag. struct., comp. depend., neutron diffr. and mag. susceptibility meas. 0-50054  
 CeSb, mag. excitations dispersion 0-25121  
 $\text{CeSn}_3$ , induced magnetic form factor, polarised neutron studies 0-25078  
 $\text{CeSn}_3$ , polarised neutron study of induced magnetisation 0-34594  
 $\text{Ce}_{0.74}\text{Th}_{0.26}$ , induced magnetic form factor, polarised neutron studies 0-25078  
 CeX (X=P, As, Sb, Bi), neutron inelastic scatt. expts. 0-19674  
 $\text{CeZn}$ , cryst. field and exchange effects, inelastic neutron scatt. study 0-24855  
 Co, itinerant ferromag., Fermi surface and single particle excitations 0-34350  
 Co, spin fluctuations above Curie temp., diffuse mag. neutron scatt. obs. 0-50102  
 $\text{CoBr}_2$ , magnetic excitations, neutron scatt. investigation 0-39761  
 $\text{CoCl}_2\cdot 2\text{H}_2\text{O-FeCl}_2\cdot 2\text{H}_2\text{O}$ , random mixture with competing spin anisotropies, tetracrit. transition, neutron diffr. obs. 0-2575



## neutron diffraction examination of materials continued

- CoMnP, ferromagnetism and metamagnetism, polarized neutron diff. study 0-44809  
 CoNb<sub>2</sub>O<sub>6</sub>, magnetic struct., neutron diff. and mag. susceptibility meas. 0-15693  
 Co<sub>2</sub>Ni<sub>1-x</sub>O, antiferromagnet, neutron diff. study of mag. struct. 0-34595  
 CoS<sub>2-x</sub>Se, magnetism and metamagnetic transition, neutron diff. and NMR meas. 0-15717  
 Cr, incommensurate antiferromag., inelastic neutron scatt. meas. 0-25088  
 Cr, inelastic neutron scatt. expts., spin density waves 0-44818  
 Cr, magnetic excitations of incommensurate spin density wave 0-11183  
 Cr-Fe, disordered, polarised neutron diffuse scatt. meas., 4.6-110K 0-34592  
 Cr-Re, mag. excitations in commensurate antiferromag. phase 0-50079  
 CrFe, mag. cor. rels. and onset of ferromag., neutron scatt. study 0-50105  
 Cr<sub>2</sub>Te<sub>1-x</sub> (x=0 to 0.2), magnetic props. study 0-11194  
 Cr<sub>1-x</sub>Ti<sub>x</sub>N, cryst. and mag. struct., at low temps. (French) 0-29005  
 Cs, liquid, neutron diff. struct. anal., density and viscosity temp. depend. 0-6352  
 CsCoCl<sub>3</sub>, mag. excitation spectrum, spin-wave response, neutron scatt. study 0-50080  
 Cs<sub>2</sub>CoCl<sub>3</sub>, neutron diff. struct. at 4.2K 0-54176  
 CsCrCl<sub>3</sub>, mag. structure and excitations, neutron diff. and susceptibility meas. 0-44806  
 Cd<sub>2</sub>PO<sub>4</sub>, one dimens. ordering, ferroelec. transitions, neutron scatt. study 0-25316  
 CsH<sub>2</sub>PO<sub>4</sub>, one dimens. ordering, ferroelec. transitions, neutron scatt. study 0-25316  
 Cs<sub>2</sub>KFe(CN)<sub>6</sub>, single cryst. neutron diff. struct. determ. 0-28972  
 CsPbCl<sub>3</sub>, high-resolution elastic neutron diff. study 0-28984  
 CsPbX<sub>3</sub>, (X=Cl,Br), anharmonic thermal vibrs., neutron diff. study 0-29125  
 Cu, defect-phonon perturbations after neutron irradi., neutron scatt. study 0-44278  
 Cu, liquid, struct. factor, neutron diff. meas. and Monte Carlo calc. 0-38903  
 Cu, polycrystalline, elastic consts., inelastic coherent neutron scatt. meas. 0-34122  
 Cu, single crystals, total thermal neutron cross sections 0-19672  
 Cu-Co, superparamagnetic, mag. aftereffects, dynamic neutron depolarisation study 0-50147  
 Cu-Mn (15 at.%), micromagnetic, short-range ordering, neutron scatt. polarisation anal. 0-50110  
 Cu-Mn spin glass alloy, spin correl. function, combined neutron spin echo and polarisation anal. 0-50107  
 Cu-Te, liq., struct. and elec. props. 0-49083  
 Cu<sub>2</sub>FeGeS<sub>4</sub>, crystallographic and magnetic structure (French) 0-28998  
 CuMn, spin glass, mag. cor. rels., neutron scatt. study 0-50105  
 Cu<sub>0.95</sub>Mn<sub>0.05</sub>, spin glass, inelastic neutron scatt., time-of-flight and three-axis techniques 0-50108  
 Cu<sub>0.95</sub>Mn<sub>0.05</sub>, spin glass, low temp. mag. excitation spectrum, inelastic neutron scatt. obs. 0-50109  
 γ-Cu<sub>15</sub>Mn<sub>85</sub>, antiferromag., neutron diff. 0-2550  
 γ-(NO<sub>2</sub>)<sub>2.5</sub> D<sub>2</sub>O, magnetic ordering, neutron diff. meas., 0.08-0.25K 0-39749  
 Cu<sub>66</sub>Ti<sub>34</sub>, metallic glass, neutron diff. meas. of struct. factor 0-24367  
 Cu<sub>46</sub>Zr<sub>54</sub>, metallic glass, dynamical struct. factor and freq. distrib. meas. 0-54136  
 DAl<sub>11</sub>O<sub>17</sub>, anhydrous, cryst. struct. from powder neutron diff. 0-1983  
 dimethylammonium manganese tetrachloride, 2D Heisenberg antiferromag., spin wave anal. 0-54879  
 DyB<sub>4</sub>, cryst. and mag. struct., neutron diff. meas. 0-15692  
 ErB<sub>4</sub>, cryst. and mag. struct., neutron diff. meas. 0-15692  
 ErB<sub>4</sub>, mag. phase diagram, neutron diff. study 0-50091  
 Er<sub>2</sub>Ce<sub>1-x</sub>Pd<sub>x</sub>, cryst. field spectra, neutron scatt. study 0-50047  
 (Er<sub>1-x</sub>Al<sub>x</sub>)<sub>2</sub>, cryst. field splitting, inelastic neutron scatt. data 0-44551  
 Er<sub>2</sub>Y<sub>1-x</sub>Al<sub>x</sub>, mag. props. meas. and neutron diff. data 0-7126  
 EuSr<sub>1-x</sub>S, ferromagnet-spin glass transition, mag. ordering, mag. susceptibility and neutron scatt. meas. 0-50135  
 EuSr<sub>1-x</sub>S, insulating spin glass, mag. props. 0-2589  
 Fe, band theoretic interpretation of neutron scatt. expts., spin wave modes 0-44791  
 Fe, itinerant ferromag., Fermi surface and single particle excitations 0-34350  
 Fe, spin fluctuations above Curie temp., diffuse mag. neutron scatt. obs. 0-50102  
 Fe-Co-Si, BCC solid soln. interchange energies, high temp. neutron diff. 0-29166  
 Fe-Cr, spin waves by neutron spectrometry 0-44819  
 Fe-Ni-(Mn)(Cr)(V), concentration ferromag. antiferromag. phase transition and mag. state diagram. (Russian) 0-20401  
 Fe-Si (4 at.%), Bloch wall thickness determ. by neutron small-angle scatt. 0-15754  
 Fe-SiO multilayer film, interface magnetisation 0-7135  
 Fe-Ti, mag. moment distrib. and environmental effects around Ti impurity 0-7092  
 Fe-V(Cr)(Mn), dil., local mag. moments, polarised neutron elastic diffuse scatt. 0-50088  
 Fe<sub>64</sub>B<sub>17</sub>, metallic glass, struct. from neutron diff. study 0-6363  
 Fe<sub>2</sub>, neutron inelastic scatt. from mag. excitations 0-50078  
 (Fe<sub>1-x</sub>Mn<sub>x</sub>)<sub>2</sub>P<sub>2</sub>C<sub>10</sub>, amorphous pair radial distrib. functions, neutron scatt. study 0-49128  
 Fe<sub>1-x</sub>O, wustite, struct. at high temp., neutron diff. (French) 0-1982  
 α-Fe<sub>2</sub>O<sub>3</sub>, haematite, substituted, Morin transition, neutron diff. study 0-54897  
 α-Fe<sub>2</sub>O<sub>3</sub>:Al<sup>3+</sup>(Ga<sup>3+</sup>)(Cr<sup>3+</sup>)(In<sup>3+</sup>), substitution effect on Morin transition, neutron diff. study 0-44827  
 Fe<sub>3</sub>O<sub>4</sub>, crit. exponents meas. by polarized neutron scatt. 0-44828  
 Fe<sub>2</sub>O<sub>3</sub>, neutron diffuse scatt. due to mol. polarons 0-15460  
 FeP(Ga)(As)(Sb), dil., short-range order, neutron diffuse scatt. and spin echo NMR 0-50106  
 FeSi, domain struct. and magnetisation reversal, time depend. neutron depolarisation 0-50138  
 α-FeTiD<sub>0.057</sub>, solid soln., interstitial D, neutron diff. study 0-39071  
 Fe<sub>2</sub>TiO<sub>4</sub>, cooperative Jahn-Teller effect, neutron scatt. study 0-49678  
 Ga<sub>0.67</sub>Cr<sub>2</sub>S<sub>4</sub>, semiconducting thiospinelide, spin glass type mag. ordering (Russian) 0-50123  
 Ge melt, tetrahedral concs., neutron diff. study (German) 0-19688  
 Ge, single crystals, total thermal neutron cross sections 0-19672  
 Ge<sub>2</sub>N<sub>2</sub>O, pressure induced tetrahedral tilting and deform. 0-24415

## neutron diffraction examination of materials continued

- Ge<sub>0.5</sub>Te<sub>0.5</sub>, structural anal. by neutron diff., radial distribution functions 0-15010  
 H storage materials, H diffusion in Ti<sub>2</sub>NiH<sub>2</sub>(FeTiH)(LaNi<sub>5</sub>H<sub>6</sub>), neutron diff. obs. 0-51013  
 HCl, intermol. partial struct. factors, isotopic substitution and neutron diff. obs. 0-53157  
 H<sub>2</sub>Co(CN)<sub>6</sub>, strong NHN hydrogen bond, vibr. lattice and mol., incoherent inelastic neutron scatt. 0-39232  
 H<sub>2</sub>O-organic aerosol-n-heptane reverse-type micellar soln., neutron small-angle scatt. (French) 0-26059  
 He, condensed phases, neutron scatt. techniques and results, book contrib. 0-2230  
 He II, superfluid, single atom neutron scatt. and two roton connected state branches (Russian) 0-44381  
<sup>3</sup>He, liq., spin fluctuation peak obs. by inelastic neutron scatt. 0-49447  
<sup>3</sup>He, liquid, low-energy spin fluctuation peak, theoretical anal. of neutron obs. 0-6584  
<sup>4</sup>He film, adsorbed, few atomic layers, excitations, two-dimensional roton. 0-39381  
<sup>4</sup>He, superfluid, condensate fractions and pair correlations 0-39375  
<sup>4</sup>He, superfluid, phonon dispersion 0-10722  
<sup>4</sup>He, superfluid, singular f-sum rule, applicability to inelastic neutron scatt. 0-6577  
 Hg<sub>3-δ</sub>AsF<sub>6</sub>, one dimensional phonons and chain ordering 0-24544  
 HgCr<sub>2</sub>S<sub>4</sub>, spinel, mag. struct., symmetry anal. in neutron diff. studies 0-25091  
 HgSO<sub>4</sub>·H<sub>2</sub>O, X-ray and neutron diff. study of struct. 0-33936  
 HoCo<sub>2</sub>, ground state spin excitations, inelastic neutron scatt. study 0-50077  
 HoF<sub>3</sub>, crystal structure by powder neutron diff. study 0-15077  
 Ho<sub>2</sub>Ge<sub>4</sub>, mag. struct., neutron diff. study 0-25093  
 HoP, flopside mag. struct. to ferromag. transition, elastic neutron scatt. obs. 0-50058  
 K, CDW, detection attempt by neutron diff. 0-49634  
 KBr:CN<sup>-</sup> 0-49316  
 (KCN)<sub>0.5</sub>(KBr)<sub>0.5</sub>, lattice dynamics neutron scatt. obs., glass phase formation 0-15207  
 KCl:CN<sup>-</sup>, coherent admixtures of phonons with impurity librionic excitations, neutron scatt. study 0-49316  
 KCrO<sub>2</sub>, two-dimens. mag. order, neutron powder diff. obs. 0-44805  
 KCoF<sub>3</sub>, nearly 1-D spin-1/2 antiferromagnet, spin wave energy dispersion 0-2551  
 K<sub>2</sub>CuF<sub>4</sub>, two-dimensional planar ferromagnet, giant fluctuation of spins (Japanese) 0-54894  
 K<sub>2</sub>Cu<sub>2</sub>Zn<sub>1-x</sub>F<sub>4</sub>, two-dimens. ferromag., spin cor. rels. near percolation limit 0-44840  
 KD<sub>3</sub>(SeO<sub>3</sub>)<sub>2</sub>, phase transition, neutron diff. 0-2158  
 KFeS<sub>2</sub>, cryst. struct. and mag. ordering, neutron diff. and mag. susceptibility meas. 0-54867  
 KH<sub>2</sub>PO<sub>4</sub>, ferroelectric transition, neutron diff. obs. 0-25324  
 KMnCl<sub>3</sub>, magnetic spiral struct., neutron diff. study 0-39748  
 KNO<sub>3</sub>, tetragonal phase, inelastic neutron scatt. 0-19676  
 K<sub>2</sub>Pt(CN)<sub>4</sub>, quasi-one-dimens. Peierls system, phonon dispersion and neutron scatt., calc. 0-24550  
 Kr gas structure, three-body-contrib., neutron diff. obs 0-43820  
 La-H(D), inelastic neutron scattering exam. of lattice dynamics 0-29128  
 LaAg, Tb and Pr substituted, superconductors, cryst. field transitions line-widths 0-24854  
 LaAg, In<sub>1-x</sub>, crystal struct., neutron diff. obs. 0-49187  
 LaAl<sub>2</sub>, inelastic neutron scatt. 0-11165  
 LaAl<sub>3</sub>, Tb and Pr substituted, superconductors, cryst. field transitions line-widths 0-24854  
 La<sub>2</sub>Mg<sub>3</sub>(NO<sub>3</sub>)<sub>12</sub>·24H<sub>2</sub>O:Nd<sup>3+</sup>, polarised neutron diff. from dynamically and statically polarised protons 0-44078  
 La<sub>2</sub>MnZnS<sub>5</sub>, antiferromag., neutron diff. study 0-25099  
 LaNi<sub>3</sub>, crystal field investigation from inelastic slow neutron scatt. expts. 0-39538  
 LaNi<sub>5</sub>H<sub>6</sub> sponges, Al or Mn substitution, neutron diff. 0-24427  
 LaNi<sub>5</sub>H<sub>3.0</sub>, H diffusion coeff., neutron scatt. obs. 0-24643  
 LaPb<sub>3</sub>, Tb and Pr substituted, superconductors, cryst. field transitions line-widths 0-24854  
 La<sub>1-x</sub>Pr<sub>x</sub>(Sn<sub>3</sub>), superconducting, cryst. field excitations, inelastic neutron scatt. obs. 0-15653  
 LaSn<sub>3</sub>, inelastic neutron scatt. 0-11165  
 LaSn<sub>3</sub>, Tb and Pr substituted, superconductors, cryst. field transitions line-widths 0-24854  
 β-LiAlSiO<sub>4</sub>, eucryptite, one-dimensional ionic conductor, neutron scatt. study 0-49361  
 LiCrO<sub>2</sub>, two-dimens. mag. order, neutron powder diff. obs. 0-44805  
 LiF, γ-irradiated, Huang diffuse scattering of neutrons 0-10544  
 LiH, mag. domains and nucl. mag. ordered phases, antiferromag. and ferromag. neutron diff. obs. 0-50051  
 LiH, nuclear ordered ferromag. and antiferromag. phases, neutron diff. study 0-50052  
 α-LiIO<sub>3</sub>, neutron diff. intensity enhancement under DC field, investig. 0-10462  
 LiIO<sub>3</sub> single crystal, DC field effect, neutron diff. enhancement (Chinese) 0-44077  
 LiTi, substituted ferrite, cation distribution, Mossbauer, X-ray, neutron diff. study 0-28975  
 Li<sub>2</sub>TiS<sub>2</sub>, struct. determ. by neutron diffraction 0-54196  
 LiZn, substituted ferrite, cation distribution, Mossbauer, X-ray, neutron diff. study 0-28975  
 Mg-Bi melt; X-ray and neutron diff., conc. depend., correl. number and nearest neighbours 0-49091  
 MgCu<sub>2-x</sub>Zn<sub>x</sub>, X-ray and neutron diff. investigation of Laves phases of MgCu<sub>2</sub>-type (German) 0-15050  
 MgCu<sub>2-x</sub>Zn<sub>x</sub>, X-ray and neutron diff. investigation of Laves phases of MgCu<sub>2</sub>-type (German) 0-15050  
 Mg<sub>1-x</sub>Er<sub>x</sub>, dil., cryst. field interactions, neutron scatt. spectra 0-50048  
 MgNi<sub>2-x</sub>Zn<sub>x</sub>, X-ray and neutron diff. investigation of Laves phases of MgCu<sub>2</sub>-type (German) 0-15050  
 MgO, neutron irradiated, Huang diffuse scattering of neutrons 0-10544  
 MgV<sub>2</sub>O<sub>9</sub>, spinel, mag. struct., symmetry anal. in neutron diff. studies 0-25091  
 γ-Mn-Ni (15 at.%), antiferromag. defect scatt., neutron polarisation anal. 0-50056  
 γ-MnCu, antiferromag., stressed, mag. defects meas. by neutron polarisation anal. 0-50076



## neutron diffraction examination of materials continued

- MnD<sub>2</sub>, synthesized at high pressures, neutron diff. anal. of struct. 0-28977
- Mn<sub>2</sub>F, non-collinear component in mag. struct. 0-25089
- Mn<sub>1-x</sub>Fe<sub>x</sub>Pt<sub>3</sub>, noncollinear mag. structs., neutron diff. anal. (Russian) 0-25087
- MnO, antiferromagnetic-paramagnetic phase transition at high press. 0-39778
- Mn<sub>1-x</sub>Sb<sub>x</sub>, ferromag., mag. disturbance around Mn interstitials 0-54868
- Mn<sub>2</sub>TeO<sub>6</sub>, magnetic structure, stability of mag. modes, neutron diffraction study (French) 0-39744
- N<sub>2</sub>, liq., struct. factor, short-wavelength neutron scatt. obs. 0-44105
- N<sub>2</sub> overlayer on graphite, orientational ordering, neutron scatt. meas. 0-10783
- (NH<sub>4</sub>)<sub>2</sub>PbCl<sub>6</sub>, inelastic neutron scatt. and pot. shape 0-1946
- (NH<sub>4</sub>)<sub>2</sub>PdCl<sub>6</sub>, inelastic neutron scatt. and pot. shape 0-1946
- (NH<sub>4</sub>)<sub>2</sub>PtCl<sub>6</sub>, inelastic neutron scatt. and pot. shape 0-1946
- (NH<sub>4</sub>)<sub>2</sub>SnCl<sub>6</sub>, inelastic neutron scatt. and pot. shape 0-1946
- (NH<sub>4</sub>)<sub>2</sub>TeCl<sub>6</sub>, inelastic neutron scatt. and pot. shape 0-1946
- NaBr.2H<sub>2</sub>O, polycryst. hydrates, librational motion of H<sub>2</sub>O mols., neutron diff. exam. 0-10604
- NaCN, diffuse scatt., hard-core correl., weak-graph method 0-49137
- NaCrO<sub>2</sub>, two-dimens. mag. order, neutron powder diff. obs. 0-44805
- NaNO<sub>2</sub>, antiferroelec. phase, struct. anal. by neutron diffraction 0-24410
- NaNO<sub>2</sub>, ferroelec., electron distrib., X-ray and neutron diffraction study 0-24411
- Na<sub>2</sub>O-GeO<sub>2</sub> glasses, neutronographic study of Ge<sup>4+</sup> struct. state 0-19711
- Nb, fluxoid lattice, eqn. props., small-angle neutron diffraction measurements 0-34573
- Nb-B, atomic order, stability, supercond. (French) 0-50021
- Nb-D, Huang diffuse scattering of neutrons 0-10544
- Nb-Zr, acoustic phonon anomalies and superstructure, neutron inelastic scatt. meas. 0-19892
- NbH<sub>0.73</sub>, multiple wavelength neutron powder diff. data, Rietveld profile refinement algorithm 0-24320
- NbH<sub>x</sub>, HF phonons, neutron spectral obs. 0-49317
- Nd, magnetic form factors, polarised neutron diff. meas. 0-50057
- Nd-H, inelastic neutron scatt. exam. of lattice dynamics 0-29128
- NdP-UP solid soln., cryst. field parameters 0-10927
- Ne, liq., neutron scatt. determ. of dynamic struct. factor\*, generalised hydrodynamic anal. 0-54103
- Ni (100), Bloch wall meas. by neutron small-angle meas. 0-15753
- Ni, band theoretic interpretation of neutron scatt. expts., spin wave modes 0-44791
- Ni, itinerant ferromag., Fermi surface and single particle excitations 0-34350
- Ni, magnetic susceptibility, generalised, neutron scatt. meas. 0-34606
- Ni, multiple wavelength neutron powder diff. data, Rietveld profile refinement algorithm 0-24320
- Ni powder, neutron diff. study of Debye-Waller factor using reverse Fourier time-of-flight method 0-49050
- Ni-Fe-Cu, Mu-metal, mag. aftereffects, dynamic neutron depolarisation study 0-50147
- Ni-Mn, mag. moment and asphericity of spin density distrib., polarised neutron scatt. obs. 0-44813
- Ni-Pd, mag. form. factor, polarised neutron diff. meas. 0-29525
- Ni-Pt, magnetic moment distrib., diffuse neutron scatt. meas. 0-34593
- Ni-SiO multilayer film, interface magnetisation 0-7135
- Ni-Te, liq., struct. and elec. props. 0-49083
- Ni-Ti, mag. moment distrib. and environmental effects around Ti impurity 0-7092
- Ni<sub>3</sub>Al, itinerant ferromag., Fermi surface and single particle excitations 0-34350
- NiD<sub>2</sub>, synthesized at high pressures, neutron diffraction anal. of struct. 0-28977
- Ni<sub>2</sub>Fe, short-range order, diffusive elastic neutron scattering 0-24400
- Ni<sub>2</sub>Mn, partially ordered, spin-wave dispersion relation, inelastic neutron scatt. meas. 0-20394
- Ni<sub>62</sub>Nb<sub>38</sub>, metallic glass, struct., neutron diff. study 0-54148
- Ni<sub>1-x</sub>S, metal-semimetal transition, lattice dynamics and thermodynamic props. 0-29324
- NpFe<sub>2-x</sub>Co<sub>x</sub>Si<sub>2</sub>, mag. and hyperfine props. 0-7247
- Pb, liq., dynamic struct. factor, slow neutron scatt. obs. 0-28908
- Pb melt, struct. factors, tetrahedral concs., neutron diff. study (German) 0-19688
- Pb, single crystals., total thermal neutron cross sections 0-19672
- Pb<sub>3</sub>(PO<sub>4</sub>)<sub>2</sub>, ferroelastic phase transition, inelastic neutron scatt. (French) 0-24584
- Pb<sub>3</sub>Se<sub>2-x</sub> melts, viscosity and radial distrib. function for stoichiometric and peritectic comp. 0-1916
- Pd-Mn(Fe), mag. ordering phenomena, neutron scatt. obs. 0-44812
- Pd<sub>0.96</sub>Ag<sub>0.04</sub>, phonon dispersion curves at 296K 0-24546
- Pd<sub>0.98</sub>Fe<sub>0.01</sub>Gd<sub>0.01</sub>, ferromag., Pd-Gd exchange const. and Pd polarisation, neutron scatt. meas. 0-25122
- α-PdH<sub>x</sub>, impurity motion, neutron scatt. obs. 0-24682
- Pd<sub>3</sub>Mn, disordered, mag. corrs., neutron scatt. study 0-50105
- Pd<sub>2</sub>MnIn<sub>1-y</sub>Sb<sub>y</sub>, Heusler alloy, mag. order obs. 0-29528
- Pd<sub>0.9</sub>Rh<sub>0.1</sub>, lattice dynamics, inelastic neutron scatt. meas. at 296K 0-29135
- Pr, magnetic excitations, exchange, crystal field and magnetoelastic interactions 0-2563
- Pr, magnetic form factors, polarised neutron diff. meas. 0-50057
- Pr-H, inelastic neutron scatt. exam. of lattice dynamics 0-29128
- Pr<sub>2</sub>La<sub>1-x</sub>Al<sub>3</sub>, cryst. elec. field 0-24856
- PrNi<sub>5</sub>, crystal field investigation from inelastic slow neutron scatt. expts. 0-39538
- PrSb, neutron scatt., press. induced antiferromag. 0-15699
- PrSb, pressure-induced antiferromag., neutron scatt. study 0-39750
- Pr<sub>2</sub>Ti, critical fluctuations temp. depend. 0-25160
- Pt<sub>2</sub>Mn, mag. excitation dispersion relation 0-25090
- RbCaF<sub>3</sub>, cubic to tetragonal phase transform., X-ray, neutron, Mossbauer diff. study 0-49360
- RbCaF<sub>3</sub>, struct., phase transitions, neutron diff. study 0-33918
- RbCaF<sub>3</sub>, structural phase transition, superlattice points, neutron diff. obs. 0-19944
- RbCoCl<sub>2</sub>.2D<sub>2</sub>O, metamagnetic phase transition, crystallographic and mag. struct., neutron diff. meas. 0-44174
- Rb<sub>3</sub>CoMg<sub>1-x</sub>F<sub>x</sub>, random two-dimens. Ising antiferromag., unstable mag. long-range order, neutron scatt. obs. 0-44839
- RbD<sub>3</sub>(SeO<sub>3</sub>)<sub>2</sub>, incommensurate nature of intermediate phase, neutron diff. obs. 0-50276

## neutron diffraction examination of materials continued

- RbI, NaCl to CsCl phase transition by elastic diffuse and inelastic neutron scatt. 0-2162
- Rb<sub>2</sub>MnCl<sub>4</sub>, 2D Heisenberg antiferromag. spin wave analysis 0-54879
- Rb<sub>2</sub>MnMg<sub>1-x</sub>F<sub>x</sub>, two-dimens. antiferromag., spin fluctuations, neutron diff. study 0-44846
- RbNiF<sub>3</sub>, neutron scatt., automatic data processing (Russian) 0-54079
- RuF<sub>5</sub>, mag. props. 0-15707
- SbCl<sub>3</sub>, liquid, neutron X-ray diffraction pattern and models 0-38893
- Se, trigonal, vitreous and red amorphous, phonon density of states comparison 0-54329
- Se<sub>1-x</sub>Te<sub>x</sub> systems, amorphous and liq. states, short range order, neutron scatt. study 0-49124
- Si melt, struct. factors, at. distrib. curves, thermodynamics, neutron diff. study (German) 0-19687
- Si melt, struct. factors, tetrahedral concs., neutron diff. study (German) 0-19688
- Si, neutron irradi., small angle neutron scatt. meas. 0-29073
- Si, single crystals., total thermal neutron cross sections 0-19672
- Si, vibrating single crystal, Umweganregung peaks 0-10461
- Si-Ge solid solution, thermal neutron monochromators 0-49053
- Si<sub>3</sub>N<sub>4</sub>, amorphous, CVD prep., struct. characts. by pulsed neutron diff. 0-33891
- SmAl<sub>3</sub>, exchange and cryst. field effects 0-24857
- SmCo<sub>5</sub>, exchange and cryst. field effects 0-24857
- SmN, magnetic props., neutron diff. and mag. susceptibility meas. 0-50036
- SmS, induced magnetic form factor, polarised neutron studies 0-25078
- Sm<sub>0.75</sub>Y<sub>0.25</sub>Fe<sub>2</sub>, intermediate valence compound, phonon investigation by neutron scatt. 0-6476
- Sn melt, struct. factors, tetrahedral concs., neutron diff. study (German) 0-19688
- SnCl<sub>2</sub>.2D<sub>2</sub>O, order-disorder transition, neutron diff. study, lattice statistical model 0-24558
- SrF<sub>2</sub>·H<sub>2</sub>O, synthesis and struct. determ. using neutron diff. (French) 0-24425
- SrLaFeO<sub>4</sub>, mag. and cryst. struct. determ. (French) 0-54866
- Ta<sub>2</sub>D, neutron diff. meas. of disorder-order phase transitions 0-29947
- Tb, magnon lifetimes at 4.2K 0-15710
- TbAl<sub>2</sub>Ga<sub>2-x</sub>, mag. props. and phase transitions 0-25133
- TbB<sub>2</sub>, mag. struct., ferromag. ordering, neutron diff. study 0-15692
- TbBe<sub>3</sub>, magnetic structure at low temps., antiferromagnetic, neutron diffraction study (French) 0-39743
- TbD<sub>2</sub>, non-stoichiometric, complex antiferromag. struct., neutron diff. study 0-50061
- TbF<sub>3</sub>, crystal structure by powder neutron diff. study 0-15077
- TbP, mag. excitations above antiferromag. ordering temp., inelastic neutron scatt. obs. 0-50112
- TbP, magnetic  $\Gamma_1-\Gamma_4$  exciton, inelastic neutron scatt. study 0-11159
- TbP, singlet-groundstate magnetism, static mag. props. 0-7109
- Tc, paramagnetic form factor, polarised neutron diff. study 0-39745
- TeO<sub>2</sub>-Li<sub>2</sub>O glassy system, struct. recomb. model 0-19707
- ThCo<sub>5</sub>, itinerant electron metamagnetism, polarised neutron study 0-39742
- ThSn<sub>3</sub>, inelastic neutron scatt. 0-11165
- α-Ti, solubility of H, neutron diff. study 0-15254
- TiBe<sub>2</sub>, neutron diff. study of mag. ordering 0-44811
- TiCl<sub>4</sub>-SiCl<sub>4</sub>(SnCl<sub>4</sub>), liq., beat effects, neutron diff. studies 0-38897
- TiFeD, cryst. struct., Mossbauer and neutron diff. obs. 0-34839
- TiSe<sub>2</sub>(S<sub>2</sub>) (1T), electronic and vibronic struct. 0-44500
- TiCl, Debye-Waller parameter by powder elastic neutron diff. 0-29140
- (Tm<sub>2</sub>La)<sub>2</sub>Al<sub>2</sub>, disordered alloys, cryst. field transitions, inelastic neutron scatt. obs. 0-50055
- TmAl<sub>2</sub>, ferromagnetic structs., elastic neutron scatt. obs. 0-50055
- TmSe, mag. neutron scatt. 0-25096
- TmSe, mag. props. and struct. 0-25109
- α-U, charge density wave, first order transition 0-10664
- UAl<sub>2</sub>, elastic consts., temp. and mag. field depend. 0-55450
- UAl<sub>2</sub>, inelastic neutron scatt. 0-11165
- UAs, magnetic struct. in high mag. fields, neutron diff. study 0-34597
- UD<sub>3</sub>, crystalline elec. field studies using neutron inelastic scatt. at NRCN 0-10931
- UF<sub>4</sub>, crystalline elec. field studies using neutron inelastic scatt. at NRCN 0-10931
- UGe<sub>3</sub>, induced magnetisation density and f-d bonding, polarised neutron diff. study 0-50063
- UGe<sub>3</sub>, magnetisation density, neutron scatt. meas. 0-50038
- UN, mag. inelastic scatt. 0-7079
- UO<sub>2</sub>, crystalline elec. field studies using neutron inelastic scatt. at NRCN 0-10931
- UO<sub>2</sub> powder, temp. depend. of atomic thermal displacements, Rietveld profile-refinement procedure 0-49190
- UO<sub>2</sub>, reanal. of neutron diff. data 0-15084
- UPb<sub>3</sub>, crystal field energy levels, magnetisation and susceptibility, neutron spectra obs. 0-50064
- UPd<sub>3</sub>, crystalline elec. field studies using neutron inelastic scatt. at NRCN 0-10931
- USb, neutron inelastic scatt. from collective excitation 0-7080
- USb, neutron inelastic scatt. meas., phonon spectra, mag. response, anisotropy 0-50065
- USb<sub>0.8</sub>Te<sub>0.2</sub>, magnetisation and neutron meas., mag. moments 0-15703
- USb<sub>0.9</sub>Te<sub>0.1</sub>, multiaxial mag. structure 0-15696
- USb<sub>1-x</sub>Te<sub>x</sub>, mag. struct. and mag. phase diagram, neutron diff. study 0-50059
- U<sub>3</sub>Si, crystalline elec. field studies using neutron inelastic scatt. at NRCN 0-10931
- USn<sub>3</sub>, crystalline elec. field studies using neutron inelastic scatt. at NRCN 0-10931
- USn<sub>3</sub>, inelastic neutron scatt. 0-11165
- UTe, critical mag. fluctuations near T<sub>c</sub> 0-7122
- UTE, magnetisation and neutron meas., mag. moments 0-15703
- VC<sub>2</sub>N<sub>x</sub>, superstructure induced by ageing, neutron diff. obs. (Russian) 0-49195
- V<sub>1-x</sub>Cr<sub>x</sub>Si, x=0 to 3, struct., supercond. and mag. props. 0-1962
- VH<sub>0.51</sub>, optic modes study by neutron spectroscopy 0-19891
- β-V<sub>2</sub>N, neutron powder profile-refinement cryst. struct. determ. 0-15060
- V<sub>2</sub>Si, d-spacing fluctuations above Martensitic phase transition 0-7570
- V<sub>2</sub>WO<sub>6</sub>, magnetic structure, stability of mag. modes, neutron diffraction study (French) 0-39744
- Va<sub>2</sub>D, neutron diff. meas. of disorder-order phase transitions 0-29947
- Y(Co<sub>1-x</sub>Cu<sub>x</sub>)<sub>2</sub>, neutron diff., thermal expts. (French) 0-19749



**neutron diffraction examination of materials continued**

- Y(Co<sub>1-x</sub>,Cu<sub>x</sub>)<sub>2</sub>, neutron diffraction study (*Chinese*) 0-39000  
 Y(Co<sub>1-x</sub>,Ni<sub>x</sub>)<sub>2</sub>, mag. heterogeneities and coercive force, neutron scatt. study 0-2553  
 Y<sub>1-x</sub>Er<sub>x</sub>, dil., cryst. field interactions, neutron scatt. spectra 0-50048  
 YFe<sub>2</sub>, amorphous concentrated spin glass, susceptibility, Mossbauer and neutron scatt. meas. 0-39783  
 YFe<sub>2</sub>O<sub>4</sub>, two-dimensional spin ordering, neutron diff. study 0-29530  
 YIG, polarised neutron expts., extinction models 0-24322  
 YIG, polariser neutron study of covalency effects 0-2552  
 YNi<sub>2</sub>, amorphous alloy, at. struct. 0-19704  
 Zn, single crystals, total thermal neutron cross sections 0-19672  
 Zn(HSeO<sub>3</sub>)<sub>2</sub>·2H<sub>2</sub>O, neutron diff. cryst. struct. determ. 0-33983  
 Zr, magnetic form factor, field-induced, polarised neutron scatt. meas. 0-50044  
 ZrV<sub>2</sub>D<sub>4</sub>, deuterated cubic Laves phase, D atom distrib., neutron diff. anal. 0-29006

**neutron diffusion**

- see also *neutron flux*; *neutron transport theory*  
 breeder reactor piles, instantaneous neutron kinetics in cavities 0-32393  
 buckling approximation, assessment of DB<sup>2</sup> transverse leakage predictions in neutron transport computations 0-13529  
 BWR, neutron noise field, two-group diffusion theory 0-18461  
 cold neutrons and applications of quasielastic scattering (*Japanese*) 0-27685  
 collision probability method, development and applications 0-27706  
 criticality safety anal. at Oak Ridge 0-37431  
 discrete-ordinates neutron transport equations in slab geometry, convergence rates of spatial difference equations 0-27688  
 energy dependent transport theory, exact solns. 0-32319  
 fast neutron transport through laminated Fe-H<sub>2</sub>O shield 0-13931  
 fission reactors, homogeneous reactor cells, few-group cell parameters 0-27696  
 flux synthesis, single channel, finite element trial functions for 3-D reactor calcs. 0-42734  
 Fourier expansion for xyz-geometry 0-9326  
 fusion reactor radiation protection, shield integral expts. at ORNL 0-47709  
 Grenoble high flux reactor, neutron physics expts., methodical aspects (*German*) 0-554  
 HWR, multidimensional space time kinetics, TRIMHX code 0-47538  
 LMFBFR, neutron streaming through control rod followers, diffusion coeff. by numerical integration 0-13636  
 LMFBFR simulated meltdown configs., integral physics parameter meas. 0-13698  
 multichannel synthesis approximation, basis functions for finite element formulation 0-47528  
 multidimensional calculations using a nodal Green's function method 0-47547  
 multigroup diffusion equation, synthesis-finite element method 0-27699  
 multigroup diffusion theory, current weighted total cross section determ. in unresolved energy region 0-18365  
 multigroup neutron diffusion equation, time-integrated method of soln. 0-27695  
 multigroup theory, functional analysis 0-13525  
 multigroup transfer coeffs., efficient eval. for shielding appls. 0-47747  
 multizonal absorbing rod, effectiveness in albedo and diffusion studies (*Russian*) 0-556  
 nuclear reactor cylindrical models, diffusional approx., finite element anal. (*Russian*) 0-18414  
 nucleate pool boiling, meas. of void frequency distrib. and profiles using neutron beams 0-27691  
 power reactor parameter identification in Xe oscillation model using maximum likelihood method 0-18466  
 pulsed neutron die-away in fast multiplying assemblies 0-18366  
 quantum neutron diffusion eqn., Boltzmann eqn. classical limit 0-13524  
 radiation protection, benchmark shielding problems obtained from integral tests of neutron cross sections 0-47740  
 reactor physics, grid-coupling methods for the multigrid solution of the neutron diffusion equation 0-47555  
 S<sub>N</sub> calculations, modified transport formulation compatible with anisotropic diffusion theory using ANL DIF3D diffusion code 0-47526  
 thermal neutron diffusion eqn. in medium with cylindrical hole, soln. 0-51548  
 transfer matrix calcs. for thermal neutrons 0-27687

**neutron economy** see *neutron flux***neutron effects**

- see also *irradiation induced creep*  
 BWR, control blade worth depletion meas. 0-719  
 cardiac ultrastructural effects, aged mouse, fission spectrum neutrons rel. to γ-rays 0-41138  
 cell nucleoside effect, dependence on LET 0-35980  
 cells, repair of radiation damage due to cyclotron-produced neutrons 0-3740  
 ceramics, applications in fusion systems, neutron effects 0-32473  
 ceramics, ion beam irradiation techniques for simulation of 14 MeV neutron irradiation 0-10584  
 Chinese hamster ovary cells, response to fast neutron radiotherapy beams 0-21497  
 cyclohexane, neutron irradiation, radical distribution, ESR study (*Japanese*) 0-44920  
 dilute alloys, defect trapping and solute segregation in irradiated alloys 0-13603  
 doped-silica optical fibres, nuclear radiation effects 0-33172  
 dose-response relationship of neutrons and γ-rays to leukemia incidence, atomic bomb survivors 0-36148  
 Fabry-Perot interference filters, neutron irradi. effects 0-14437  
 fast neutron exposure, risk of leukemia 0-30782  
 fast neutron therapy, radiobiological bases 0-35995  
 fast reactor steels and alloys, neutron damage development, irradiation conditions, chemical composition 0-34082  
 fusion materials, damage parameters spatial variations, implications 0-34065  
 fusion reactor first wall material, mobile He inclusion in void swelling rate theory model 0-34069  
 fusion reactor first wall materials development evaluations, fatigue crack growth testing optimisation 0-35444  
 fusion reactor insulators, radiation damage calcs. using MORSE code 0-34061

**neutron effects continued**

- fusion reactor materials, microstruct. development in simulated irradiation 0-34072  
 fusion reactor materials, primary damage, energy depend. 0-34064  
 fusion reactor materials, range calculations using multigroup transport methods 0-34070  
 fusion reactor metals, He embrittlement, grain boundary cavity model 0-34075  
 fusion reactor metals and alloys, microvoid form., gaseous impurity atom effects, positron annihilation study 0-49275  
 gas bubbles growth, during irradiation, stress effect 0-49277  
 GCFR claddings, neutron-induced He implantation, calc. of total flux 0-42773  
 graphite, development and irradiation program for PBHTR appls. 0-5245  
 graphite, EPR, effect of motional averaging, anisotropy, skin effect rel. to heat treatment and neutron irradiation (*French*) 0-34752  
 graphite, irradiated, stored at room temp., neutron damage annealing and C<sub>44</sub> shear modulus 0-2080  
 graphite, irradiation-induced temp.-change effects, semiempirical model calc. 0-42775  
 graphite, neutron effects on shrinkage 0-37456  
 graphite, neutron irradiation, electron transport, annealing study 0-39165  
 graphite, pyrolytic, galvanomag. effects, effect of fast neutron irradiation 0-34465  
 graphite, radiation alteration over wide range of neutron flux and irradiation temp. 0-29072  
 graphite damage function in neutron irradi. up to 15 MeV 0-34059  
 graphite rods, damage by high energy neutrons 0-29070  
 gustatory function, radiation-induced changes, neutrons rel. to photons 0-12184  
 haematopoietic microenvironment, progenitor cells radiosensitivity, mouse expts. 0-45983  
 heavy ion simulation of neutron radiation damage 0-29071  
 ion accelerators for fusion ignition, neutron resistant ceramic insulator development 0-37639  
 Kapton (polyimide), insulators for superconducting magnets, effect of low temp. irradiation 0-25817  
 life shortening in RFM and BALB/c mice as function of radiation quality, dose and dose rate 0-41134  
 low and intermediate energy radiation physics 0-19845  
 lung, canine, relative effectiveness of fast neutron and <sup>60</sup>Co γ-ray irradiation 0-3737  
 LWR, fission product activities, fuel survey 0-736  
 mammalian cells, influence of radiation quality on effectiveness of small doses 0-30785  
 metallic mirrors for laser fusion reactors, neutron and gamma irradi. response calc. 0-23121  
 metals, radiation effects on elasticity and elastic moduli, yield stress 0-2078  
 Mylar (polyester), insulators for superconducting magnets, effect of low temp. irradiation 0-25817  
 Nomex (nylon paper), insulators for superconducting magnets, effect of low temp. irradiation 0-25817  
 nonmetallic crystals, collapse of tracks formed by fission fragments 0-24510  
 nuclear fuel, transport phenomena under severe temp. gradient 0-615  
 nuclear reactor pressure vessel material surveillance capsule, neutron radiation, limiting condition 0-47572  
 oil, lubricating, radn. effects and radn. dosimetry appl. 0-2069  
 PAN fibres, neutron irradiated, struct. and props. (*Russian*) 0-25763  
 pathologic effects of neutron and photon exposures of lung and spinal cord, rabbit expts. 0-41126  
 PMMA, neutron irradiation, radical distribution, ESR study (*Japanese*) 0-44920  
 point defect nucleation and growth, rate theory model for simultaneous clustering 0-13604  
 polycarbonate, insulators for superconducting magnets, effect of low temp. irradiation 0-25817  
 polyethylene, neutron irradiation, radical distribution, ESR study (*Japanese*) 0-44920  
 polypropylene, insulators for superconducting magnets, effect of low temp. irradiation 0-25817  
 pyrocarbon coatings, deposition in fluidized bed, TEM, changes by irradiation 0-34084  
 pyrocarbons, EPR, effect of motional averaging, anisotropy, skin effect rel. to heat treatment and neutron irradiation (*French*) 0-34752  
 quartz, TFTR diagnostic windows, radiation damage 0-34063  
 radiotherapy planning and radiation quality definition 0-12246  
 rate equations, irradi. induced voids, swelling, creep 0-49274  
 reactor irradiations facility, 70-400°C 0-6439  
 refractory fusion reactor materials, neutron irradi., microstruct., voids, nucleation TEM study 0-29065  
 root meristem cells, Vicia faba, subnuclear chromosome aberrations rel. to neutron energy deposition 0-26280  
 sapphire, 14.8 MeV neutron damaged, optical vibronic absorption spectra 0-50384  
 semiconductor, neutron transmutation doping, damage-energy distrib. 0-15137  
 semiconductor, neutron transmutation doping 0-15133  
 semiconductor doping, computer controlled neutron irradi. system 0-19851  
 semiconductors transmutation doping, conf., Columbia, USA (April 1978) 0-12849  
 silicate glasses, effect of high dose X-rays and reactor radiation 0-19838  
 skin, X-ray and fast neutron damage, relationship between OER, RBE and no. of fractions 0-35978  
 stainless steel, type 316, irradi. in simulated environment, tensile props. 0-34076  
 stainless steel, ferritic SUS 410 type, coated with organometallic complexes and Ti alkoxides 0-34078  
 stainless steel, type 316, neutron irradi., microstruct. and tensile props. 0-34077  
 steel, austenitic stainless, fusion reactor first-wall and blanket material, mech. props. 0-34074  
 steel, austenitic stainless, He role in neutron induced microstruct. evolution 0-29064  
 steel, austenitic stainless, mech. props. correl. methodology development for fusion environments 0-29068  
 steel, austenitic stainless, neutron irradi., mag. props. 0-29067  
 steel, austenitic stainless, neutron irradi. effects on fatigue crack propag. 0-29069



## neutron effects continued

- steel, austenitic stainless FV548, neutron irradiated, Si-rich phase occurrence of  $M_{23}C_6$  phase 0-15156
- steel, austenitic type 316, continuous gas generation effects in neutron and simulation environments 0-34068
- steel, ferritic alloy and martensitic stainless, void swelling response after fast reactor irradiation 0-6437
- steel, mild, yield point, effect of neutron irradiation and  $N_2$  conc. 0-45365
- steel, reactivity meas., determination method (Russian) 0-664
- steel, reactor pressure vessel failure and radiation damage (Czech) 0-619
- steel, stainless, 316, neutron irradiation embrittlement, pre-irradiation treatment and composition modification 0-3171
- steel, stainless, effect of He preinjection on swelling during neutron radiation damage simulation 0-44236
- steel, stainless, FBR cladding stress distrib., effect of irradiation-induced swelling 0-19850
- steel, stainless, in-reactor deformation and fracture behaviour of EBR-II driver fuel cladding 0-42769
- steel, stainless, neutron irradiation and  $N_2O_4$  corrosion effects (Russian) 0-52741
- steel, stainless, neutron irradiation effect on low cycle fatigue and tensile props. at 298K 0-30059
- steel, stainless, type 316, cold worked, precipitation response to neutron irradiation 0-34073
- steel, stainless AISI 316, neutron irradiated, rel. between irradiation induced swelling and shear modulus 0-15157
- steel, tubular, type OKH16N15M3B, reactor irradiated, creep resist. (Russian) 0-25762
- steel, type 1Kh18N9T, neutron irradiated, microstruct. and mech. props. (Russian) 0-24503
- stopping power data, air/nitrogen gaps, graphite-tissue and polythene tissue interfaces 0-26353
- TCNQ salt, N-propyl-quinolinium(TCNQ)<sub>2</sub>, defect conc. depend. phase transition 0-44577
- TCNQ salt, NPQn (TCNQ)<sub>2</sub>, neutron irradiation induced defect concentration depend. phase transition 0-29449
- TCNQ salt, Qn (TCNQ)<sub>2</sub>, configurational entropy, thermoelec. power meas. 0-34432
- testis weight loss following high energy neutron or  $\gamma$  irradiation, mouse expts. 0-35985
- TFTR coil materials, neutron irradiation effects 0-34060
- therapy beams, radiobiological intercomparisons 0-3739
- tissue and equivalent material recoil spectra 0-17022
- tissue neutron and gamma-ray response function, mid-head, military appl. 0-8185
- transition metals, implantation of  $He^+$ , range profiles and thermal release 0-39138
- TTF-TCNQ, and related compounds, low temp. irradiation effects 0-24906
- $TTT_{I,5-7}Br_3$ , chem. impurities and neutron irradiation induced defects, effects on DC cond. 0-49699
- $TTT_{I,3}$ , chem. impurities and neutron irradiation induced defects, effects on DC cond. 0-49699
- vitreous silica blocks, damage by high energy neutrons 0-29070
- Zircaloy-2, cold worked, temp. cycling effects on irradiation growth 0-2079
- Zircaloy-2, neutron irradiated, inhomogeneous deformation behaviour 0-50679
- Ag-Zn, vacancy prod. rate by displacement cascades, anelastic meas. during neutron irradiation 0-19794
- Al, fast neutron irradiated, struct. of defect cascades, diffuse X-ray scatt. study 0-39167
- Al, high purity, neutron irradiated, void annealing kinetics 0-44234
- Al, neutron irradiation, mobile interstitials production 0-34080
- Al, positron annihilation, effects of quenching, annealing and neutron irradiation 0-20732
- Al, quenched, irradiated, and quenched plus irradiated, grain boundary hardening 0-3162
- Al, stabiliser for fusion reactor supercond. mag., neutron irradiation effects on magnetoresistance 0-34062
- Al, vacancy distribution, interbonding atoms, heat peaks in scattered cascades (Russian) 0-39169
- Al-Cr, neutron irradiation, Cr atom distribution NMR study 0-54957
- Al-Si-Al contact current response to 100 keV neutron irradiation (Russian) 0-49956
- $\alpha-Al_2O_3$ , neutron damage, fusion/fission ratio 0-34066
- Au, neutron damage, defect clusters 0-34067
- $B_2C$ , FBR control rod elements, neutron damage and post-irradiation annealing 0-13581
- $B_2C-Al(silicone)(graphite)$ , neutron shielding materials, long term radiation effects 0-9413
- $BaF_2$ , thermoluminesc. and F-centre annealing, after neutron irradiation 0-7422
- $BaF_2$ , undoped and U-doped, neutron irradiation, absorpt. band attributed to  $F_2^-$  centres 0-7380
- $BaF_2:U$ , absorption band spectra following neutron irradiation 0-29763
- $CaF_2$ , thermoluminesc. and F-centre annealing, after neutron irradiation 0-7422
- $Cr_2O_3$ -stainless steel system under fusion reactor first wall condition, oxide dispersoid stability 0-40374
- Cu, defect-phonon perturbations after neutron irradiation, neutron scatt. study 0-44278
- Cu, inhomogeneous clustering of radiation damage after neutron irradiation between 200 and 400°C 0-15161
- Cu, neutron damage, defect clusters 0-34067
- Cu, neutron irradiation, mobile interstitials production 0-34080
- Cu neutron production of free interstitials 0-34071
- Cu, stabiliser for fusion reactor supercond. mag., neutron irradiation effects on magnetoresistance 0-34062
- Cu-Ni, neutron irradiation, enhanced diffusion, elec. resist. meas. 0-6440
- $\alpha-Fe$ , irradiation induced void swelling, Cr additions effect 0-55408
- $\alpha-Fe$ , magnetic aftereffect disaccommodation between 30 and 300K after low-temp. neutron irradiation 0-29585
- $\alpha-Fe$ , void swelling response after fast reactor irradiation 0-6437
- Fe-C, neutron irradiation at low temp., mag. disaccommodation 0-44881
- Fe-Cr, irradiation induced void swelling, Cr additions effect 0-55408
- Fe-Cr-Ni, neutron irradiation, rel. between irradiation induced swelling and shear modulus 0-15157
- $Fe_{80}B_{20}$ , amorphous, fast neutron and fission fragment irradiation, effect on elec. resist. 0-19846
- $Fe_{50}Co_{50}$ , neutron irradiation, close pair recombination (French) 0-39162

## neutron effects continued

- $Fe_{49}Co_{51}V_2$ , neutron irradiation, close pair recombination (French) 0-39162
- $Fe_{73}Mo_{27}B_{20}$ , amorphous, fast neutron and fission fragment irradiation, effect on elec. resist. 0-19846
- GaAs, defect clusters induced by  $\gamma$ -rays and neutrons, effect on elec. props. 0-29408
- GaAs, electron and neutron irradiation, defect clusters 0-2077
- GaAs, neutron transmutation doping, shallow donors magneto-optical effects 0-20255
- GaAs, transmutation doping by thermal neutrons 0-10581
- Ge, As impurity precipitation from solid soln., neutron irradiation effect 0-29177
- Ge, defects, radiation effects 0-29016
- Ge, dislocation ensembles motion in neutron irradiated covalent crystals (Ukrainian) 0-10579
- n-Ge, lightly doped, compensated by disordered regions, conductivity and Hall mobility 0-11016
- Ge, neutron irradiation, Hall effect and magnetoresist. meas. 0-6883
- Ge, neutron irradiation, substitution of impurity atoms by self-interstitials,  $Ge(n,\gamma)$  reaction 0-39166
- Ge, neutron irradiation, positron annihilation, ESR and resist. meas. 0-15160
- $GeS_{1.35}$  glass, neutron irradiation, AC elec. cond. 0-24924
- He accumulation fluence dosimetry for fusion materials neutron irradiation testing 0-32479
- Hg, volatility in NAA from samples and standards (Russian) 0-41128
- n-InSb, high-resist., prep. using radiation compensation 0-34016
- LiF, radiation induced voids, formation on dislocations 0-1519
- LiF, single crystal, neutron and gamma irradiation, SEM and Bragg profile anal. 0-15158
- LiI crystal, irradiated at low temps., optical absorption spectra 0-45123
- MgO, neutron irradiation, Huang diffuse scattering of neutrons 0-10544
- Mo alloys, fusion reactor first wall and blanket material, props. for struct. appl. 0-30071
- Mo alloys, fusion reactor first-wall and blanket material, mech. props. 0-34074
- Mo, irradiation between 425 and 1000°C, ductility in bending 0-39164
- Mo, neutron bombardment, radiation damage, electron microscopy obs. (Russian) 0-44235
- Mo, neutron irradiation, radiation softening and hardening 0-34083
- Mo, neutron irradiation, void swelling and shrinkage, TEM study 0-34079
- Mo, neutron low energy interaction cross sections, gravitational spectrometer meas. 0-24521
- Mo-Ti, irradiation between 425 and 1000°C, ductility in bending 0-39164
- Mo-Zr-B, porosity and mech. props. after neutron bombardment, 780-1080°C (Russian) 0-24502
- Mo-Zr-B alloy, neutron irradiation at 780-1080°C, porosity, hardening and embrittlement (Russian) 0-29062
- $(Mo_{0.8}Ru_{0.4})_{82}B_{18}$ , supercond. metallic glass, neutron irradiation effects 0-29060
- NaCl, effect of annealing and neutron irradiation on block struct. 0-29061
- Nb alloys, fusion reactor first wall and blanket material, props. for struct. appl. 0-30071
- Nb alloys, fusion reactor first-wall and blanket material, mech. props. 0-34074
- Nb based alloys, He and simultaneous damage production simulation 0-32480
- Nb, neutron bombardment, defect size distrib. influence on hardening (Russian) 0-10580
- Nb, neutron irradiation, microstruct. and tensile props. 0-34077
- Nb, radiation damage in fusion reactors, computer expts. 0-13839
- $Nb_3Sn$ , A-15 struct. Nb based superconductors, irradiation type influence on radiation defects 0-15093
- Ni, neutron irradiation, microstruct. and tensile props. 0-34077
- Ni-Al, neutron irradiation, rel. between irradiation induced swelling and shear modulus 0-15157
- Ni-base alloys, Nimonic PE-16, type 718 and type 625, neutron irradiation effects on fatigue crack propag. 0-29069
- Ni-Cr (0-35 at.%), neutron irradiation at 25K, damage, elec. resist. obs. (French) 0-54286
- Ni-Fe, 79 NM alloy, gamma and neutron influence on mag. susceptibility comparative study (Russian) 0-39751
- Ni-Ti(Fe), neutron irradiation, thermally activated deform. 0-6438
- Ni-Zn ferrites 600 NN and M450 NN1, Curie point radiative shift due to neutron irradiation (Russian) 0-39775
- $Pd_{80}Si_{20}$ , amorphous, structural changes with neutron irradiation, X-ray scatt. obs. 0-33898
- Pt, crowdion conversion to dumbbell, two-interstitial model, thermal neutron irradiation 0-33992
- sapphire, TFTR diagnostic windows, radiation damage 0-34063
- Si, defect storage kinetics during neutron irradiation 0-24505
- Si depletion regions, radiation damage coeffs. for fission neutron and gamma-ray irradiation 0-34058
- Si, dislocation ensembles motion in neutron irradiated covalent crystals (Ukrainian) 0-10579
- Si doping by thermal neutron irradiation, annealing characts. of bulk electron traps obs. 0-49244
- Si, ESR in neutron transmutation doped samples 0-20462
- Si, homogeneous n-type doping by thermal neutrons 0-2051
- n-Si, irradiated with large neutron doses, defect annealing 0-19849
- Si, minority carrier lifetime in neutron doped samples 0-20218
- n-Si neutron and electron irradiation, isochronous annealing influence on edge absorpt. 0-11449
- Si, neutron doped,  $\gamma$ -irradiation, influence on elec. props. 0-6845
- Si, neutron irradiation, Hall effect and magnetoresist. meas. 0-6883
- Si, neutron irradiation, point defects photopopulation and photoionisation, IR spectra meas. 0-25423
- Si, neutron irradiation, residual radioactivity meas. 0-19829
- Si, neutron irradiation, small angle neutron scatt. meas. 0-29073
- n-Si, neutron irradiation, annealing behaviour characterisation by electrochem. meas. 0-19847
- Si, neutron transmutation doping, photoluminesc. characterisation 0-11453
- Si, neutron transmutation doping, impurities 0-15134
- Si, neutron transmutation doping, radioactivity form. 0-15135
- Si, neutron transmutation doping for IR detector material 0-15136
- Si, neutron transmutation doping in Harwell reactors 0-15138
- Si, neutron transmutation doping, irradiation facilities 0-15139
- Si, neutron transmutation doping, General Electric test reactor 0-15140
- Si, neutron transmutation doping, automated irradiation facility 0-15141



**neutron effects continued**

- Si, neutron transmutation doping, annealing, lattice damage 0-15163  
 Si, neutron transmutation doped, highly compensated, resistivity fluctuations 0-15531  
 Si, neutron transmutation doped, elec. props. 0-15532  
 Si, neutron transmutation doping, irradiation techniques 0-19827  
 Si, neutron transmutation doped, isochronal annealing of resistivity 0-19828  
 Si, neutron transmutation doping,  $^{31}\text{P}$  concn. meas. 0-19833  
 Si, neutron transmutation doping, at. displacement effects 0-19852  
 Si, neutron transmutation doping, annealing, deep defect levels 0-20123  
 Si, neutron transmutation doping using nuclear reactor thermal neutron irradiation, review 0-39161  
 Si, O impurity precipitation from solid soln., neutron irradiation effect 0-29177  
 Si, p-n junctions, neutron transmutation doping, breakdown process 0-15600  
 Si, piezospectroscopic effect on zero phonon luminescence lines 0-50406  
 Si:Ga, neutron irradiation, Hall effect meas. of shallow donor levels 0-20124  
 Si:P, doped by neutron transmutation, lattice defects 0-34018  
 Si:P, neutron irradiation, crystals, qualitative distrib. of P using autoradiography 0-24486  
 $\text{Si}_3\text{N}_2\text{O}$ , fast neutron irradiation, variation of lattice parameters 0-24504  
 $\text{SiO}_2$ , amorphous and crystal, neutron irradiation, and unirradiated, intrinsic defect photolum. 0-50401  
 SmS:P, neutron irradiation, semiconductor-metal transition 0-24975  
 $\text{SrF}_2$ , thermoluminescence and F-centre annealing, after neutron irradiation 0-7422  
 $\text{SrO}$ , neutron- or proton-irradiation,  $\text{F}^+$  centre fluorescence yield and lifetime, 5 to 140K 0-55181  
 $\text{SrO}$ , neutron-irradiated single crystal,  $\text{F}^+$  centres, ENDOR obs. 0-15824  
 $\text{TTT}_{13}$ , neutron irradiation, induced defects and chemical impurity effects on DC cond. 0-39565  
 TZM, irradiation between 425 and 1000°C ductility in bending 0-39164  
 Ti alloys, fusion reactor first-wall and blanket material, mech. props. 0-34074  
 Ti based alloys, He and simultaneous damage production simulation 0-32480  
 Ti, neutron low energy interaction cross sections, gravitational spectrometer meas. 0-24521  
 Ti-Al-Mo, type Ti-6242S, irradiation, induced creep 0-39163  
 Ti-Al-Sn, type Ti-5621S, irradiation, induced creep 0-39163  
 Ti-Al-V, irradiation, induced creep 0-39163  
 Ti-V-Cr, type Ti-15-333, irradiation, induced creep 0-39163  
 U concn. in blood meas. by thermal neutron induced fission, chem. etching, concn. rel. to leukaemia 0-21532  
 U, reactivity meas., determination method (Russian) 0-664  
 UC, low temp. reactor irradiation 0-39168  
 $\text{UO}_2$ , equiaxed grain growth modelling 0-13589  
 $\text{UO}_2$ , pressurised rods, He fill-gas absorpt. during irradiation 0-37454  
 $\text{UO}_2$ , pyrocarbon-coated HTR fuel particles, fast neutron influence on fission product transport 0-42777  
 $\text{UO}_2\text{:Cr}_2\text{O}_3$ , fission gas release and swelling 0-47567  
 V alloys, fusion reactor first wall and blanket material, props. for struct. appl. 0-30071  
 V alloys, fusion reactor first-wall and blanket material, mech. props. 0-34074  
 V based alloys, He and simultaneous damage production simulation 0-32480  
 V, neutron low energy interaction cross sections, gravitational spectrometer meas. 0-24521  
 V, purification and plastic props. 0-25810  
 V surface, particle release by neutrons 0-25493  
 V $_2\text{O}_5$ , neutron irradiation, void form., 673-1073K 0-29066  
 V-H, effect of neutron irradiation on electrical resistance, magnetic susceptibility 0-29063  
 W, neutron low energy interaction cross sections, gravitational spectrometer meas. 0-24521  
 W, thermal neutron irradiation, recovery processes 0-19848  
 Zn, neutron irradiation, recovery of c-axis spacing and elec. resist. 0-34081  
 Zr-Al (8.0 wt.%), tensile props. and fracture toughness after fast neutron irradiation 0-3198  
 Zr-Al (8.6 wt.%), neutron irradiation, irradiation growth and recovery, annealing 0-15162  
 Zr-base alloys, annealed specimens, irradiation growth 0-49276  
 Zr-H, effect of neutron irradiation on electrical resistance, magnetic susceptibility 0-29063  
 $\text{Zr}_3\text{Al}$ , neutron irradiation, effect on tensile props. 0-3156

**neutron flux**

- accelerator facility, fast neutron research, data acquisition and anal. 0-47806  
 anisotropic scattering treatment using improved comput. code (Japanese) 0-13526  
 Argonaut reactors, coupled core, neutron wave propagation, Be, graphite and  $\text{D}_2\text{O}$  as internal reflectors 0-27752  
 beam experiments (Japanese) 0-27684  
 BWR, effect of multiple boiling channels on void fluctuation spectra 0-18464  
 BWR, neutron noise field, two-group diffusion theory 0-18461  
 BWR, shield design against neutron streaming in pressure vessel vicinity 0-13678  
 BWR fluctuations, in neutron flux, due to steam bubbles 0-47534  
 BWR noise, response of neutron detector to local coolant void distrib. 0-683  
 BWR parameter estimation, multivariate anal. of neutron noise signals 0-18465  
 BWR power reactor, in-core startup system with neutron flux monitor 0-32405  
 BWR stability monitoring using time series anal. of neutron noise 0-47625  
 CANDU reactor, Th-fuelled, importance of  $^{233}\text{Pa}$  in neutron economy 0-22980  
 CANDU self-powered flux detectors, response characts. 0-32404  
 CANDU-PHW, thermal neutron flux-mapping system 0-792  
 collision probability integrals, annular geometry, evaluation using analytic expansions 0-32317  
 counting-Campbell channel for in-core and out of core meas. 0-32406  
 critical assembly, Big Ten,  $^{235}\text{U}$  enriched U (10%) 0-823

**neutron flux continued**

- critical slab, isotropic and anisotropic scattering, asymptotic solution, strained coords. method 0-42733  
 cross-section adjustments, sensitivity to uncertainties 0-47531  
 detection using self-powered Inconel-Inconel coaxial cable 0-42842  
 diffusion equation, Fourier expansion for xyz-geometry 0-9326  
 fission counter, absolute neutron flux meas. and  $^{239}\text{Pu}(n,f)$  resonance integral 0-5453  
 fission reactors, homogeneous reactor cells, few-group cell parameters 0-27696  
 fuel element rod bundle, neutron field calc., surface pseudosource method 0-27772  
 full flux covariance matrix calc. for NBS intermediate-energy standard neutron field 0-5348  
 gamma-ray laser pumping, Mossbauer effect in magnetised plasma 0-28186  
 Grenoble high flux reactor, neutron physics expts., methodical aspects (German) 0-554  
 heterogeneous critical assemblies with strongly blocked absorber, reactivity temp. effects 0-32395  
 HTGR, large pebble bed, Xe oscillations detection 0-22988  
 HTPBR, neutron and physical aspect calcs. (German) 0-22941  
 hybrid reactor, reaction rate sensitivity to fission spectrum changes 0-47712  
 IVV-2 research reactor, thermal neutron flux distrib. using neutron probes 0-32391  
 laser detection of scattered neutrons from luminescence line freq. change 0-23272  
 linear radiation-flux functionals, estimation of local perturbations using Monte Carlo method 0-5457  
 LMFBR, neutron streaming through control rod followers, diffusion coeff. by numerical integration 0-13636  
 LMFBR meltdown cores, exptl. study of integral physics parameters 0-13664  
 microexplosion reactor neutronics, adjoint transport eqn. technique 0-47713  
 monitoring by in-core detectors 0-5297  
 monitoring during reactor refuelling and start-up, instrum. (Polish) 0-42792  
 multigroup diffusion equation, synthesis-finite element method 0-27699  
 neutron analysis of the NBS intermediate-energy standard neutron field (ISNF) 0-27692  
 noise studies in BWR and PWR 0-557  
 nuclear reactor pressure vessel material surveillance capsule, neutron radiation, limiting condition 0-47572  
 Oklo natural fission reactor, computer calc. of neutron balance and flux distrib. (French) 0-21767  
 prompt gamma-ray anal. of neutron flux distrib. in nonhomogeneous samples, computational model 0-14060  
 proton-recoil counter technique for measurement of fast neutron spectrum 0-9447  
 pulsed neutron research, book 0-22146  
 pulsed source, maximum density and capture rate of neutrons moderated 0-13522  
 PWR, calcs. of neutron environment inside containment 0-13676  
 PWR, fast-neutron dose rate meas. inside containment shell 0-13674  
 PWR, fixed in-core gamma thermometer for neutron flux meas. 0-717  
 PWR neutron flux detectors, reliability tests (French) 0-32403  
 PWR noise analysis using multivariate autoregressive time series modelling 0-23028  
 rare earths, isotopic analysis, Oklo natural fission reactor fluence distrib. meas. (French) 0-21759  
 reactivity effect of cross-section processing for moist bulk-oxide criticals 0-37493  
 reactor neutron field fluctuations, energy distrib. and reactor power 0-32396  
 reactors, ex-core detector neutron noise to core barrel amplitude scale factor 0-27779  
 self-powered detectors for in-core reactor neutron flux meas., detector signal composition 0-32402  
 single channel flux synthesis, finite element trial functions for 3-D reactor calcs. 0-42734  
 thermal and epithermal neutron flux densities, self-powered neutron detector sensitivity 0-52817  
 thin monitors for reactor dosimetry 0-32522  
 Twin Beam Mirror, effect of hot beam injection angle 0-48939  
 two-phase control absorber, horizontal absorber elements, expt. study 0-42841  
 two-phase control absorber development program for CANDU reactors 0-42839  
 VVR-SM reactor, neutron flux and dose meas. and evaluation (Czech) 0-5252  
 ZPPR, loading error simulations and control worth meas. 0-27777  
 $\text{D}_2\text{O}$  thermal column irradiation facility Penn State Breazeale Reactor 0-9339  
 $\text{Li}_2\text{O}$  pellets, thermal neutron flux distrib. inside and outside 0-47700  
 $^{159}\text{Tb}$ , neutron resonances, time-of-flight spectra 0-27633

**neutron flux density see neutron flux**

**neutron interactions** see kaon-nucleon interactions; lepton-nucleon interactions; neutron-nucleus reactions; nucleon-nucleon interactions; photon-nucleon interactions; pion-nucleon interactions

**neutron moderation**

see also neutron transport theory

- albedo cell calculations in the thermal region taking into account thermalisation (Russian) 0-52710  
 anisotropy effects on differential cross sections in CM frame (Portuguese) 0-18364  
 energy dependent transport theory, exact solns. 0-32319  
 fission reactors, integral experiments for testing Th and  $^{233}\text{U}$  data 0-27707  
 fusion reactor, pellet neutron moderation on blanket neutronics 0-836  
 graphite moderator structure design and manufacturing specification 0-23110  
 HFBR, safety features of cold neutron moderator 0-23114  
 inertial confinement fusion pellets, neutron moderation, effects on damage and radioactive inventory 0-47704  
 pulsed source, maximum density and capture rate of neutrons moderated 0-13522  
 resonance capture of neutrons, light or heavy atom moderators 0-14310  
 response functions of spherically moderated neutron detectors 0-37687



## neutron moderation continued

- space craft thermionic reactors, reflector drums as control mechanism 0-42784  
 transfer matrix calcs. for thermal neutrons 0-27687  
 Be, anisotropy in thermal neutron scatt., anal. 0-552  
 ZrH rethermaliser for IVV-2 reactor hot neutron flux increase 0-37676

## neutron-nucleus reactions

- for inelastic neutron-nucleus scattering, see "neutron-nucleus scattering"  
 see also neutron radiative capture; nucleon-nucleon interactions  
 capture cross sections at 14.6 MeV, activation anal. 0-52665  
 fast neutron dose to the human body, contrib. for  $^{39}\text{K}$ ,  $^{35}\text{Cl}$  and  $^{32}\text{S}$  0-51263  
 fast reactor physics, assessment of JAERI fast group constants set version 2 0-602  
 fission cross sections, parameter testing in statistical model (Russian) 0-52653  
 fission reactor, nuclear yields, production of transuranium elements by multi-step neutron irradiation (Japanese) 0-52729  
 reactor structural material transmission meas. using TOF spectrometer 0-18440  
 resonance analysis of neutron transmission data, least square fitting program REFIT 0-22840  
 thermonuclear reaction rate data for intermediate mass nuclei 0-31427  
 Voigt functions analysis, appl. to neutron cross sections 0-22879  
 yeast isomer prod., pulsed beam meas. using plastic scintillation spectrum 0-27871  
 (n, $\alpha$ ), fast n,  $^3\text{He}$  emission cross sections for A=27-115 0-13475  
 (n,e $^-$ ) high precision spectroscopy, internal conversion coeffs. for nuclear struct. 0-37353  
 (n,f), parity violation in compound nuclei 0-47368  
 (n,f) simulated cross sections for exotic actinide nuclei 0-544  
 (n, $^3\text{He}$ ), fast n,  $^3\text{He}$  emission cross sections for A=27-115 0-13475  
 (n,n $\alpha$ ), fast n,  $^3\text{He}$  emission cross sections for A=27-115 0-13475  
 (n,Z $\alpha$ ), fast n,  $^3\text{He}$  emission cross sections for A=27-115 0-13475  
 $^{107}\text{Ag}$ (n,e $^-$ ),  $^{108}\text{Ag}$  transition multipolarity and conversion electrons 0-52627  
 $^{\text{A}}\text{Am}$ (n,f), thermal, sub-barrier fission fragment energy correlations for A=241, 243 0-42715  
 $^{241}\text{Am}$ -Be neutron spectrum, (n,p) reaction average cross-sections 0-22827  
 $^{241}\text{Am}$ (n,X)Cm, Japan Material Testing Reactor, separation of transuranium elements from fission products and cladding (Japanese) 0-52731  
 $^{241}\text{Am}$ (n,f), 14.8 MeV, mass yield distrib., and absolute fission yield, isomer ratios 0-18352  
 $^{241}\text{Am}$ (n,f), thermal neutron induced fission cross section 0-37403  
 $^{40}\text{Ar}$ (n,d) $^{39}\text{Cl}$ , 14.5 MeV, charge state study in liquid Ar ionization chamber (Russian) 0-9298  
 $^{40}\text{Ar}$ (n,p) $^{40}\text{Cl}$ , 14.5 MeV, charge state study in liquid Ar ionization chamber (Russian) 0-9298  
 $^{197}\text{Au}$ , 14.7 MeV neutron capture cross-section measurements with activation technique 0-32282  
 $^{10}\text{B}$ (n, $\alpha$ ) $^7\text{Li}$ , thermal polarised n capture, P-odd asymmetry meas. (Russian) 0-13452  
 $^{138}\text{Ba}$ , 14.7 MeV neutron capture cross-section measurements with activation technique 0-32282  
 $^{80}\text{Br}$ (n,X), annihilation, 1.4 GeV/c,  $\pi^\pm$ , p emission angles, momentum and multiplicity distrib. 0-532  
 $^{12}\text{C}$ (n,X), compound resonance decay based on bound and metastable single nucleon states (Russian) 0-5107  
 $^{12}\text{C}$ ( $\bar{n}$ ,X), annihilation, 1.4 GeV/c,  $\pi^\pm$ , p emission angles, momentum and multiplicity distrib. 0-532  
 $^{12}\text{C}$ (n,2 $\alpha$ ), 60 kev-20 MeV, average energy per ion pair, calc. 0-22841  
 $^{12}\text{C}$ (n,2n), 60 kev-20 MeV, average energy per ion pair, calc. 0-22841  
 $^{12}\text{C}$ (n,n) $^{13}\text{C}$ , 60 kev-20 MeV, average energy per ion pair, calc. 0-22841  
 $^{12}\text{C}$ (n,n $\alpha$ ), 60 kev-20 MeV, average energy per ion pair, calc. 0-22841  
 $^{12}\text{C}$ (n,p), 60 kev-20 MeV, average energy per ion pair, calc. 0-22841  
 $^{\text{A}}\text{Cd}$ (n, $\gamma$ ) A=114,116, energy levels, spins, and gamma-ray multipole mixing ratios investig. 0-52580  
 $^{\text{A}}\text{Cm}$ (n,f), A=224,246, 0.3-45 MeV, near threshold fission cross section, energy depend. (Russian) 0-37406  
 $^{245}\text{Cm}$ (n,f), thermal neutron induced fission, mass yield obs. 0-32309  
 C(n, $\alpha$ ), thick target corrections for charged particle spectra 0-37714  
 Co isotopes,  $E_n=14$  MeV, cross sections for charged particle prod., data compilation 0-9289  
 $^{59}\text{Co}$ (n,2n), isomeric cross-section ratio and excitation function, mixed-powder method and gamma-ray spect. 0-47472  
 $^{59}\text{Co}$ (n, $\alpha$ ), excitation function, mixed-powder method and gamma-ray spect. 0-47472  
 $^{59}\text{Co}$ (n, $\gamma$ ), level transitions, deexcitations and lifetimes 0-18222  
 $^{\text{A}}\text{Cr}$ (n,X), A=50, 52-54, 14 MeV, X=p,n,p $\alpha$ ,n $\alpha$ , $^3\text{He}$ , production cross-sections 0-42648  
 $^{164}\text{Dy}+n$ , capture cross section meas. in Triton reactor (French) 0-18308  
 $^{\text{A}}\text{Eu}$ (n,X), A=153, 154, 155, total neutron cross sections, effect on reactor characts. 0-32284  
 $^{157}\text{Eu}+n$ , capture cross section meas. in Triton reactor (French) 0-18308  
 $^{19}\text{F}$ (n, $\alpha$ ) $^{16}\text{O}$ , average cross sections in  $^{235}\text{U}$  fission neutron spectrum 0-22828  
 $^{19}\text{F}$ (n,p) $^{19}\text{O}$ , average cross sections in  $^{235}\text{U}$  fission neutron spectrum 0-22828  
 $^{19}\text{F}$ (n,X), annihilation, 1.4 GeV/c,  $\pi^\pm$ , p emission angles, momentum and multiplicity distrib. 0-532  
 Fe isotopes,  $E_n=14$  MeV, cross sections for charged particle prod., data compilation 0-9289  
 $^{\text{A}}\text{Fe}$ (n,X) A=54, 56, 57, transmission and capture meas. 0-18313  
 $^{57}\text{Fe}$ (n,X) transmission data up to 400 keV, J $^\pi$  value for resonances 0-18311  
 $^{\text{A}}\text{Fe}$ (n,X), 3 eV-1 MeV transmission meas., resonance anal. 0-18316  
 $^{\text{A}}\text{Fm}$ (n,f), A=253, 255, 257, 259, fission mass distrib. transition, liquid drop and shell model calcs. 0-32310  
 $^{69}\text{Ga}$ (n, $\gamma$ ), fast n, levels, J $^\pi$ , transitions and mixing ratios, statistical anal. (Russian) 0-13382  
 $^{158}\text{Gd}+n$ , capture cross section meas. in Triton reactor (French) 0-18308  
 $^{\text{A}}\text{H}$ (n,X), annihilation, 1.4 GeV/c,  $\pi^\pm$ , p emission angles, momentum and multiplicity distrib. 0-532  
 $^{\text{A}}\text{H}$ (n,d) $^{\text{A}}\text{He}$ , 459, 648, 802 MeV, relative diff. cross section and ang. distrib. 0-52671  
 $^{\text{A}}\text{H}$ (n, $\pi^0$ ) $^{\text{A}}\text{H}$ , nuclear forces charge symmetry test 0-5071  
 $^{\text{A}}\text{H}$ ( $\bar{\nu}$ ,e $^-$ )n, neutral current cross section for reactor  $\bar{\nu}$  0-5129  
 $^{127}\text{I}$ , 14.7 MeV neutron capture cross-section measurements with activation technique 0-32282

## neutron-nucleus reactions continued

- $^{127}\text{I}$ (n,n $\gamma$ ), fast n,  $\gamma$ -ang. distrib., level ang. momenta 0-18224  
 $^{84}\text{Kr}+n$ , capture cross section meas. in Triton reactor (French) 0-18308  
 $^6\text{Li}$ (n, $\alpha$ ), 2-10 MeV, total cross section,  $^7\text{Li}$  3/2 $^-$  state 0-18297  
 $^6\text{Li}$ (n, $\alpha$ ) $^3\text{H}$ , 23 keV cross section, absolute meas., ang. distrib. 0-18305  
 $^6\text{Li}$ (n, $\alpha$ ) $^3\text{H}$ , use in quantitative microlocation of Li in the brain 0-41353  
 $^6\text{Li}$ (n,t) $^4\text{He}$ , thermal polarised n capture, P-odd asymmetry meas. (Russian) 0-13452  
 $^7\text{Li}$ (n,n $\alpha$ )t, three body sequential reactions, kinetics modelling 0-37371  
 $^7\text{Li}$ (n,X), A=6, 7, 14.6 MeV, ang. distrib. and cross sections for  $^6,7\text{Li}$ ,  $^6\text{He}$  products 0-42650  
 $^{55}\text{Mn}$ , 14.7 MeV neutron capture cross-section measurements with activation technique 0-32282  
 $^{55}\text{Mn}$ (n,X), 14 MeV, X=p,n,p $\alpha$ ,n $\alpha$ , $^3\text{He}$ , production cross-sections 0-42648  
 Mo stable isotope eval., 5 keV-5 MeV neutrons, rel. to reactor structural steel 0-13620  
 $^{14}\text{N}$ (n, $\alpha$ ) $^{11}\text{B}$ , 12-18 MeV, pickup of three nucleons, distorted wave approx. 0-22793  
 $^{23}\text{Na}$ , 14.7 MeV neutron capture cross-section measurements with activation technique 0-32282  
 $^{23}\text{Na}$ (n, $\alpha$ ) $^{20}\text{F}$ , average cross sections in  $^{235}\text{U}$  fission neutron spectrum 0-22828  
 $^{23}\text{Na}$ (n,p) $^{23}\text{Ne}$ , average cross sections in  $^{235}\text{U}$  fission neutron spectrum 0-22828  
 $^{\text{A}}\text{Nd}+n$ , A=143,145, capture cross section meas. in Triton reactor (French) 0-18308  
 Ni isotopes,  $E_n=14$  MeV, cross sections for charged particle prod., data compilation 0-9289  
 $^{\text{A}}\text{Ni}$ (n,X) A=58, 60, transmission data, resonance anal. 0-18317  
 $^{\text{A}}\text{Ni}$ (n,X), transmission and capture data up to 120 keV 0-18311  
 $^{60}\text{Ni}+n$ , total and differential cross-sections, optical-statistical and coupled-channel models 0-13472  
 $^{237}\text{Np}$  fission and capture cross sections in GCFR neutron spectra 0-37404  
 $^{233}\text{Pa}$ (n,f), cross sections, semi-empirical formula 0-22864  
 $\text{Pb}$ (n,n), 13.7-15 MeV, differential cross section energy depend., meas. and optical model 0-18304  
 $^{\text{A}}\text{Pu}$ / $^{235}\text{U}$ , A=240, 242, fission cross section ratio meas. 0.127 to 7.4 MeV 0-5180  
 $^{239}\text{Pu}$ (n,f), 10 eV-100 keV, fission cross section 0-27681  
 $^{239}\text{Pu}$ (n,f), undisturbed resonance integral determ., and neutron flux meas. 0-5453  
 $^{239}\text{Pu}$ (n,X), nuclear reaction statistical model parameters (Russian) 0-18280  
 $^{239}\text{Pu}$ (n,X), thermal n, gamma spectra from capture, fission and fission products 0-37352  
 $^{239}\text{Pu}$ (n,f), 0.005-0.4 eV, fission fragment average kinetic energies in resonance region 0-18358  
 $^{239}\text{Pu}$ (n,f), cross section, parameter testing in statistical model (Russian) 0-52653  
 $^{239}\text{Pu}$ (n,f) 0-37405  
 $^{239}\text{Pu}$ (n,f) 0.009-0.6 eV cross-section, Westcott factor 0-546  
 $^{242}\text{Pu}+n$ , 10 keV-20 MeV, ENDF/B-V cross sections 0-22837  
 $\text{Pu}$ (n,f), 0-18 MeV, prompt neutron spectrum, evaporation model (Chinese) 0-42721  
 $^{\text{A}}\text{Sb}$ (n,2n), A=121,123, 12.8-18.1 MeV, activation cross sections 0-47477  
 $^{28}\text{Si}$ (n,n $\gamma$ ), 13.9 MeV, spin flip probability from 1.78 MeV state, direct theory 0-9234  
 $^{147}\text{Sm}+n$ , capture cross section meas. in Triton reactor (French) 0-18308  
 $^{147}\text{Sm}$ (n, $\alpha$ ) $^{144}\text{Nd}$ , 12 to 18 MeV, energy and angular distribution of  $\alpha$ -particles, statistical, pre-equilibrium and knock-on models 0-13477  
 $^{147}\text{Sm}$ (n, $\alpha$ ), 2 keV,  $^{148}\text{Sm}$  compound states partial  $\alpha$ -widths,  $\alpha$ -spectra 0-47392  
 Sn, solid and liquid, neutron cross sections, Doppler effect meas. 0-22933  
 $^{181}\text{Ta}$ (n, $\alpha$ ), 270-875 keV,  $^{178}\text{Lu}$  isomeric states and spins, transition probability 0-52582  
 $^{99}\text{Tc}+n$ , capture cross section meas. in Triton reactor (French) 0-18308  
 $^{230}\text{Th}$ (n, $\gamma$ ), 680-1050 keV, fission barriers and cross sections, fragment ang. distrib. 0-18357  
 $^{232}\text{Th}$ , neutron cross section meas. 0-526  
 $^{232}\text{Th}+n$ , 0.1-18 eV, neutron total cross section determ. 0-22838  
 $^{232}\text{Th}$ (n,f), cross sections, semi-empirical formula 0-22864  
 $^{\text{A}}\text{Ti}$ (n,X), A=46-50, 14 MeV, X=p,n,p $\alpha$ ,n $\alpha$ , $^3\text{He}$ , production cross-sections 0-42648  
 $^{\text{A}}\text{U}$ (n,X), A=233, 235, thermal n, gamma spectra from capture, fission and fission products 0-37352  
 $^{235}\text{U}$  fission by polarised neutrons, P odd asymmetry of emitted fragments (Russian) 0-18354  
 $^{235}\text{U}$ (n,2n), threshold to 13 MeV, cross section meas. by Gd loaded liquid scintillator 0-52669  
 $^{235}\text{U}$ (n, $\alpha$ ), thermal fission neutron spectrum 0-42712  
 $^{235}\text{U}$ (n,e $^-$ ),  $^{236}\text{U}$  low lying levels from 4 $^-$  isomer decay 0-47396  
 $^{235}\text{U}$ (n,f), fission fragment average kinetic energies in resonance region 0-18358  
 $^{235}\text{U}$ (n,f), thermal, appl. of  $\bar{\nu}$  constraint to fission product yields 0-22874  
 $^{235}\text{U}$ (n,f), thermal, Rb and Cs relative and independ. fission yields 0-27679  
 $^{235}\text{U}$ (n,f), thermal polarised n capture, P-odd asymmetry meas. (Russian) 0-13452  
 $^{235}\text{U}$ (n,f), fast n, fragment mass and kinetic energy distrib. (Russian) 0-5181  
 $^{238}\text{U}$  neutron cross sections evaluation for incident neutron energies up to 4 keV 0-5146  
 $^{238}\text{U}$ , neutron resonance parameters, time-of-flight spectroscopy 0-47375  
 $^{238}\text{U}$ (n,f), 14.5 MeV, neutron emission, mass distrib. and energetics 0-47512  
 $\text{U}$ (n,X), Japan Material Testing Reactor, U and Pu isolation and isotopic ratios (Japanese) 0-52730  
 $\text{U}$ (n,f), 0-18 MeV, prompt neutron spectrum, evaporation model (Chinese) 0-42721  
 $^{238}\text{U}$ (n,X), 14 MeV, X=p,n,p $\alpha$ ,n $\alpha$ , $^3\text{He}$ , production cross-sections 0-42648  
 $^{186}\text{W}$ , 14.7 MeV neutron capture cross-section measurements with activation technique 0-32282  
 $^{137}\text{Xe}+n$ , capture cross section meas. in Triton reactor (French) 0-18308  
 Y isotopes, Hauser Feshbach calcs., of neutron cross sections 0-22839  
 $^{89}\text{Y}$ , 14.7 MeV neutron capture cross-section measurements with activation technique 0-32282



**neutron-nucleus reactions continued**

- Zr isotopes, Hauser Feshbach calcs., of neutron cross sections 0-22839  
<sup>90</sup>Zr neutron absorption, multipole giant resonance contrib. to optical pot. imaginary part 0-18263

**neutron-nucleus scattering**

see also nucleon-nucleon scattering

- anisotropy effects on differential cross sections in CM frame (*Portuguese*) 0-18364  
 elastic neutron scattering, probability density function approach 0-13480  
 (n,n), pol. n, 16.1 MeV, differential cross section, optical model fit 0-32259  
 (n,n), single particle bound state, energy independ. optical model, asymmetry term 0-37316  
 (n,n') cross sections meas. from 160-375 GeV/c 0-13474  
<sup>107</sup>Ag(n,n), 0.25-4.5 MeV, total, elastic and inelastic cross sections, optical-statistical anal. 0-27639  
<sup>197</sup>Au(n,n')<sup>197m</sup>Au, E<sub>n</sub>=3 and 14.1 MeV, form. cross sections of short-lived isomer, cyclic activation technique 0-32283  
<sup>9</sup>Be(n,2n) pseudolevel eval. validation 0-22697  
<sup>209</sup>Bi(n,n), 50, 100, 200 MeV, eikonal scatt. by complex pots., cross sections 0-27643  
<sup>12</sup>C(n,n), <17 MeV, resonating group calcs., phase shifts and differential cross sections 0-32275  
<sup>40</sup>Ca(n,n), 11-26 MeV, differential cross sections, global optical model anal. 0-18298  
<sup>40</sup>Ca(n,n) 2-3 MeV neutrons studied using assoc. particle TOF spectrometer 0-13468  
 C(n,n), total cross sections below 2 MeV, R-matrix fits to data 0-13466  
<sup>60</sup>Co, neutron scatt. cross section meas., parameters of neutron levels 0-5147  
<sup>69</sup>Co(n,n), deformation effect in aligned target 0-47364  
<sup>52</sup>Cr(n,n), 1.77 to 3 MeV, validity of Wick's inequality in the calculation of the lower limits of the differential elastic cross sections 0-5137  
 Cu(n,n), 14.2 MeV, polarisation in forward angle scatt. 0-18282  
<sup>152</sup>Eu<sup>m</sup>(n,n'), thermal neutron acceleration by isomeric nuclei (*Russian*) 0-52680  
<sup>56</sup>Fe(n,n), 1.77 to 3.0 MeV, validity of Wick's inequality in the calculation of the lower limits of the differential elastic cross sections 0-5137  
<sup>57</sup>Fe(n,n), high resoln. scatt. meas. 0-18311  
 Fe(n,n), MeV elastic and inelastic cross sections meas. 0-32277  
 H(n,n)p, 210-495 MeV, free elastic scatt., phase shift anal. 0-52676  
 H(n,p), pol. n and p, 220-495 MeV, free elastic scatt., D<sub>i</sub> and P parameters 0-52674  
 H(n,p), pol. n and p, 220-495 MeV, free elastic scatt., Wolfenstein parameters R<sub>i</sub>, A, 0-52675  
 H(n, np)n, 17 to 27 MeV, neutron-neutron scattering length determination, Monte Carlo analysis 0-13476  
<sup>A</sup>Li(n,x), A=6, 7, 14.6 MeV, ang. distrib. and cross sections for <sup>6,7</sup>Li, <sup>9</sup>He products 0-42650  
<sup>92</sup>Mo(n,n), 7-26 MeV, differential cross sections, global optical model anal. 0-18298  
 Mo(n,X), 2 keV-20 MeV cross sections, coherent optical and statistical model calcs. 0-18318  
<sup>15</sup>N(n',n)<sup>15</sup>N, continuum random phase approx. 0-27635  
<sup>A</sup>Ni(n,n'), A=58-64, <4 MeV, gamma prod. and inferred cross sections 0-525  
<sup>A</sup>Ni(n,n), A=58,60,62,64, 5 MeV, differential cross sections, optical, statistical and coupled channel anal. (*Russian*) 0-37377  
<sup>58</sup>Ni(n,n), 1.77 to 3.0 MeV, validity of Wick's inequality in the calculation of the lower limits of the differential elastic cross sections 0-5137  
<sup>60</sup>Ni+n, total and differential cross-sections, optical-statistical and coupled-channel models 0-13472  
<sup>16</sup>O(n,n), elastic cross section, microscopic calc. 0-531  
<sup>208</sup>Pb(n,n) 25-700 keV, <sup>209</sup>Pb parity assignments and M1 radiative strength 0-52614  
<sup>208</sup>Pb, fast neutron scatt. and capture, microscopic isovector optical pot. test 0-52682  
<sup>208</sup>Pb(n,n), <sup>209</sup>Pb excited states and 3/2<sup>-</sup> resonances, shell model, calcs. 0-18262  
<sup>208</sup>Pb(n,n), 7-26 MeV, differential cross sections, global optical model anal. 0-18298  
 Pb(n,n), 14.0-17.4 MeV, neutron polarisation, ang. depend. diffraction struct. 0-18283  
 Pb(n,n), 14.2 MeV, polarisation in forward angle scatt. 0-18282  
<sup>32</sup>Si(n,X), 2.5-1100 keV, resonance struct. from total and capture cross sections 0-42620  
<sup>32</sup>Si(n,n), 2-3 MeV neutrons studied using assoc. particle TOF spectrometer 0-13468  
<sup>32</sup>Si(n,n), 5 MeV, elastic and inelastic scatt., differential cross-sections, model anal. (*Russian*) 0-42668  
 Sb(n,n'), 1.5-2.7 MeV, <sup>A</sup>Sb, A=121,123, levels below 2 MeV, spins, transitions and mixing ratio 0-32191  
<sup>28</sup>Si(n,n), 5 MeV, elastic and inelastic scatt., differential cross-sections, model anal. (*Russian*) 0-42668  
<sup>152</sup>Sm(n,n), 2.4-7.2 MeV, inelastic and elastic optical model and deformation parameter depend. (*Russian*) 0-13481  
 Sn, neutron cross section, filtered neutron beam technique, Doppler effect 0-52670  
<sup>A</sup>Sn(n,n) A=116, 124, 11, 24 KeV, differential cross sections, global optical model anal. 0-18298  
<sup>124</sup>Sn(p,p), threshold enhancement of parity violation, Born approx. 0-18191  
<sup>232</sup>Th, neutron cross section meas. 0-526  
<sup>90</sup>Zr(n,n), 11 MeV, differential cross sections, global optical model anal. 0-18298

**neutron polarisation**

- depolarisation meas., exptl. set up and process program 0-18771  
 electric and magnetic dipole moments 0-4993  
 ferromagnetic domain structures, neutron depolarisation studies 0-25155  
 multilayer monochromator-polariser (*Russian*) 0-27854  
 neutron stars, spin alignment, spin-torsion forces and strong-gravity interactions 0-56870  
 nuclear and neutron polarisation expts., spin depend. of neutron cross-sections, mag. moments, radiation capture of neutrons (*Russian*) 0-52654  
 polarimeter, 3-D calibration procedure 0-18770  
 polarisation meas. with high press. He scintillation counter, Monte Carlo convections 0-14061  
 polarised neutron diffraction, determ. of magnetic form factors, pioneering work 0-24321

**neutron polarisation continued**

- polarised neutrons in condensed matter [conference, Zaborow, Poland (Sept. 1979)] 0-22136  
 polariser-analyser efficiency meas. by spin flip meas. 0-27911  
 secondary neutron polarization via penetration through a ferromagnetic shielding wall 0-47742  
 Stern-Gerlach polarimeter for measuring polarisation of cold neutron beams 0-37679  
 tuneable polarisers for neutrons 0-315  
 Fe<sub>2.45</sub>Mn<sub>0.05</sub>Si, slow neutron polariser, by single cryst. (111) refl. 0-49052  
 Li<sub>0.5</sub>Fe<sub>2.5</sub>O<sub>4</sub>, slow neutron polariser, by single cryst. (222) refl. 0-49052
- neutron production**
- linear acceleration reactors, anal. of neutron yield produced by high-energy protons 0-22895  
 Maxwellian D ion plasma, ion temp. diagnostics appls. 0-49005  
 (α,n), mixture and compound neutron yield from separate component thick target yields 0-37414  
 DD reaction for neutron generation in thermonuclear reaction initiation (*Russian*) 0-42848  
 γp→nπ<sup>+</sup> section asymmetry, pion-proton twin birth contribution (*Russian*) 0-47308  
 pd, 350-1000 MeV, neutron prod. double differential cross section in meson generation reactions (*Russian*) 0-42490  
 pp, 350-1000 MeV, neutron prod. double differential cross section in meson generation reactions (*Russian*) 0-42490  
 π<sup>+</sup>d→π<sup>+</sup>pn final state interactions and d breakup for 438 MeV/c π<sup>+</sup> impulse (*Russian*) 0-18145  
<sup>197</sup>Au(<sup>63</sup>Cu,X), 400 MeV, neutron multiplicity in deep inelastic collisions 0-18324  
<sup>A</sup>Cf, A=250, 252, 254, spontaneous fission fragment kinetic energy and neutron multiplicity meas. 0-42717  
 C(π<sup>+</sup>,X), 3 GeV/c, n inclusive spectra, neutron yield (*Russian*) 0-13510  
 Cu(π<sup>+</sup>,X), 3 GeV/c, n inclusive spectra, neutron yield (*Russian*) 0-13510  
 D, shell target compression on laser heating (*Russian*) 0-47718  
 D<sub>2</sub> plasma, compression by microfusion explosion, expt. biconical system 0-13783  
<sup>257</sup>Fm, spontaneous fission fragment kinetic energy and neutron multiplicity meas. 0-42717  
 Pb(π<sup>+</sup>,X), 3 GeV/c, n inclusive spectra, neutron yield (*Russian*) 0-13510  
 U(Ne,n)X, 337 MeV/N inclusive double differential neutron prod. cross sections 0-32294  
<sup>238</sup>U(p,f) 12 MeV, estimation of neutron yield from individual fragment in medium-excitation fission 0-542  
 U(π<sup>+</sup>,X), 3 GeV/c, n inclusive spectra, neutron yield (*Russian*) 0-13510
- neutron-proton interactions**
- see also neutron-proton scattering
- charged-particle multiplicity distrib. at 400 GeV/c 0-13337  
 np→dγ radiative capture, relativistic effects, parity violation, Weinberg-Salam model (*Russian*) 0-32120  
 np→dα<sup>0</sup>, nuclear forces charge symmetry test 0-5071  
 np→pn, 5-25 GeV/c, charge exchange scatt., πNN vertex function, one pion exchange 0-37291  
 pN, charm-pair production 0-22643  
 pN collision, 200 GeV/c, production of long-lived hadrons and leptons, antinuclei production 0-13342  
 pn→np, charge exchange processes, baryonium trajectories, Regge pole description 0-9180  
 pn→pX, 100 to 400 GeV/c, slow-proton prod., Regge trajectory 0-22646  
 pn→ppr<sup>+</sup>, 2.98 GeV/c, Δ<sup>++</sup> prod. in additive quark model framework 0-52529
- neutron-proton scattering**
- see also neutron-proton interactions
- polarized proton-neutron total cross sections from proton-deuteron data 0-22633  
 spin-spin forces in 6 GeV polarised elastic scatt. 0-433
- neutron radiative capture**
- A=10-58, neutron separation energies, self consistent set from (n,γ) reaction 0-52563  
 average resonance parameter eval. and calcs., statistical model for capture process 0-18271  
 chondrite Yamato-74191, inert gas composition and neutron capture effects 0-46504  
 conference on neutron capture gamma ray spectroscopy, Upton, USA. (Sep. '78) 0-36780  
 cross sections for fission product nuclides in fast reactors (*Japanese*) 0-521  
 direct and resonance capture, giant dipole and quadrupole resonances 0-37385  
 element analysis, role of neutron capture γ-rays 0-50926  
 gamma-ray lasers, direct pumping by resonance capture of neutrons 0-14310  
 high spin state studies, heavy ion reaction complementarity 0-37381  
 induced capture by nuclei in laser radiation field (*Russian*) 0-13479  
 isotopic anomalies from neutron reactions during stellar explosive C burning 0-12651  
 neutron capture γ-rays, practical appls., analytical techniques, PNAAL facilities 0-40794  
 neutron capture gamma and electron spectroscopy, instruments and techniques 0-37695  
 neutron-capture prompt gamma-ray activation analysis: multi-element measurements on various materials 0-40796  
 nonfissile nuclei, inherent inaccuracy in capture cross section calc. reactor appl. 0-22836  
 parity violation in nuclear forces, neutron capture γ-ray expts. 0-37322  
 polarised neutron expts., spin depend. of neutron cross-sections, mag. moments, radiation capture of neutrons (*Russian*) 0-52654  
 pulsed source, maximum density and capture rate of neutrons moderated 0-13522  
 reactor decay spectra, absorption effects on decay heat and spectral pulse kernels 0-22931  
 resonance capture reactions with a total energy detector 0-37694  
 spin assignments using polarised beams and gamma spectroscopy 0-37323  
 thermal (n,γ) reaction, elemental anal. appl. 0-40795  
 γ source generation and properties, review 0-14029  
 γ-ray resonant scattering, solid state properties of target 0-18060  
 (n,e<sup>-</sup>) high precision spectroscopy, internal conversion coeffs. for nuclear struct. 0-37353



## neutron radiative capture continued

- (n,γ), (n,γγ), recent experiment review, future experiment suggestions 0-37382
- (n,γ), A=20 to 240, E1 and M1 strength functions 0-52625
- (n,γ), A=75 to 103, γ-strength functions and stat. model cross section calcs. 0-52612
- (n,γ), A=94-190, resonance capture, low lying level population fluctuations, γ-rays 0-52619
- (n,γ), E1 and M1 strength functions, A- and energy-depend., giant dipole resonances 0-37348
- (n,γ), Fast n, gamma rays in giant dipole region, review 0-37351
- (n,γ), γ-rays, QED test review 0-37199
- (n,γ), interacting boson and Nilsson model tests, Pt-Os transition region 0-37380
- (n,γ), mechanism in 3s size resonance, s-wave radiative width partition 0-37387
- (n,γ), mechanism in 3s size resonance, radiative width statistical and valence effects 0-37388
- (n,γ), non-spherical even-even nuclei, energy gap from γ-transitions 0-47395
- (n,γ), on-line gamma anal. using Ge detector 0-52624
- (n,γ), parity violation in compound nuclei 0-47368
- (n,γ) gamma ray spectra calc. 0-52620
- (n,γ) spectroscopy, nuclear struct. investigation, review 0-37379
- (n,γ), thermal n, systematic search, γ-spectra and selective state population 0-37390
- (n,γ), thermal n, systematic search, γ-spectra and selective state population 0-37390
- (n,γ), pol. N, anal. power and giant multipole resonances, direct-semidirect model 0-18265
- (n,γ), thermal, <sup>53</sup>Cr levels, J<sup>π</sup>, γ-transitions and 1626 eV resonance 0-42610
- <sup>107</sup>Ag(n,γ)<sup>108</sup>Ag<sup>m</sup>, in stainless-steel structure of high-power nuclear reactors 0-42747
- <sup>107</sup>Ag(n,γ), <sup>110</sup>Ag low lying states, decay scheme and T<sub>1/2</sub> 0-47393
- <sup>107</sup>Ag(n,γ), <sup>110</sup>Ag low-lying levels obs. 0-47422
- <sup>27</sup>Al(n,γ), pol. thermal, <sup>28</sup>Al levels, spins and γ-rays, multipole mixing 0-47398
- <sup>27</sup>Al(n,γ), resonance capture, <sup>28</sup>Al E1 transitions and partial radiative widths 0-52618
- <sup>197</sup>Au, effective cross section dependence on thermal neutron temp. 0-547
- <sup>197</sup>Au(n,γ), <sup>198</sup>Au level spin assignments from γ ang. distrib. and circular polarisation 0-52570
- <sup>197</sup>Au(n,γ), 0.5-3.0 MeV, <sup>198</sup>Au gamma-ray strength functions from spectrum fitting method 0-52616
- <sup>197</sup>Au(n,γ) <sup>198</sup>(n,γ)<sup>199</sup>Au, high energy transitions 0-22878
- <sup>198</sup>Au(n,γ), 0.5-3.0 MeV, γ-spectra strength functions 0-32240
- <sup>138</sup>Ba(n,γ), 30 keV, capture cross sections, stellar nucleosynthesis 0-42663
- <sup>12</sup>C+n, TOF transmission meas. of neutron resonances 0-37374
- <sup>107</sup>Cd, production in nuclear reactors by neutron irradiation of <sup>107</sup>Ag 0-52798
- <sup>107</sup>Cd(n,γ), A=140, 142, 30 keV, capture cross sections, stellar nucleosynthesis 0-42663
- <sup>252</sup>Cf(n,γ), neutron capture gamma expt. equipment designs 0-52832
- <sup>248</sup>Cm(n,γ), <sup>248</sup>Cm excited and single particle states, γ-transitions 0-47399
- <sup>59</sup>Co, neutron capture cross section meas. 0-5147
- <sup>163</sup>Dy(n,γ), thermal, <sup>164</sup>Dy multipole mixing in γ to ground bands 0-52615
- <sup>167</sup>Er(n,γ), thermal, CC <sup>168</sup>Er high intrinsic excitation levels, γ-decay props. 0-52588
- <sup>151</sup>Eu(N, γ), A=151, 153, cross sections, time of flight spectra, scintillation detectors 0-27634
- <sup>54</sup>Fe(n,X) A=54, 56, 57, transmission and capture meas. 0-18313
- <sup>54</sup>Fe(n,γ), cross section, resonance and background interference 0-18310
- <sup>57</sup>Fe, (n,γ), cross section, 2.5-200 keV, s-wave resonances 0-18309
- <sup>58</sup>Fe(n,γ) capture and total cross section meas. below 325 keV, resonance parameters 0-18314
- <sup>58</sup>Fe(n,n), resonance capture cross section s- and p-wave radiative widths 0-47476
- Fe(n,γ), cross-section meas. principal resonance parameters 0-18312
- <sup>154</sup>Gd(n,γ), A=154, 156-8, 2, 24 keV, resonance averaged γ-spectra, level and J<sup>π</sup> appls. 0-37347
- <sup>1</sup>H(n,γ), <sup>2</sup>H γ-energy and binding energy 0-52564
- <sup>1</sup>H(n,γ), thermal, γ-ray energy, <sup>2</sup>H neutron binding energy and n mass excess 0-47362
- <sup>1</sup>H(n,γγ)<sup>2</sup>H, cross section upper limit 0-52683
- <sup>3</sup>He(n,γ), thermal, effective cross section (Russian) 0-37378
- <sup>115</sup>In, effective cross section dependence on thermal neutron temp. 0-547
- <sup>191</sup>Ir(n,γ), resonance, <sup>192</sup>Ir levels, resonances and low energy γ-rays 0-47397
- <sup>139</sup>La(n,γ), non-statistical capture, radiative widths, γ-ray doorway state model 0-37389
- <sup>175</sup>Lu(n,γ), A=175, 176, 30 keV, capture cross sections, stellar nucleosynthesis, <sup>176</sup>Lu cosmic clock 0-42663
- <sup>176</sup>Lu, effective cross section dependence on thermal neutron temp. 0-547
- Mo stable isotope eval., 5 keV-5 MeV neutrons, rel. to reactor structural steel 0-13620
- <sup>98</sup>Mo(n,γ) A=98, 100 resonance parameters, capture γ-rays and reaction mechanism 0-18272
- Mo(n,X), 2 keV-20 MeV cross sections, coherent optical and statistical model calcs. 0-18318
- <sup>14</sup>N(n,γ), γ-ray energies, calibration standards 0-52613
- <sup>144</sup>Nd(n,γ), <sup>144</sup>Nd capture states partial α-decay widths 0-37328
- <sup>143</sup>Nd(n,γ), thermal n, <sup>140</sup>Ce γ-spectra, E1 and M1 hindrance factors 0-37386
- <sup>148</sup>Nd(n,γ)<sup>149</sup>Nd-<sup>149</sup>Pm, energy levels 0-27592
- <sup>58</sup>Ni(n,X), transmission and capture data up to 120 keV 0-18311
- <sup>58</sup>Ni(n,γ), cross-section meas. principal resonance parameters 0-18312
- <sup>237</sup>Np fission and capture cross sections in GCFR neutron spectra 0-37404
- <sup>237</sup>Np(n,γ), thermal, <sup>238</sup>Np levels, resonances and transitions 0-52589
- <sup>16</sup>O+n, 3-30 MeV, TOF transmission meas. of neutron resonances 0-37374
- <sup>17</sup>O(γ,n), cross section, Lane-Lynn radiative capture mechanisms 0-52660
- <sup>17</sup>O(n,γ), thermal cross section, <sup>18</sup>O level gamma decay 0-52623
- <sup>18</sup>Os(n,γ), A=186-188, 2.6-800 keV, capture Maxwellian cross sections, galactic nucleosynthesis 0-42664
- <sup>141</sup>P(n,γ), resonance parameters, s-wave radiative and reduced neutron widths 0-47471

## neutron radiative capture continued

- <sup>207</sup>Pb(n,γ), <sup>208</sup>Pb M1, E1, M2, E2 localised γ-ray strengths 0-37350
- <sup>208</sup>Pb, fast neutron scatt. and capture, microscopic isovector optical pot. test 0-52682
- <sup>208</sup>Pb(n,γ), fast, direct-semidirect and pure resonance model calcs. 0-47486
- <sup>108</sup>Pd(n,γ), thermal and resonant, <sup>109</sup>Pd levels, J<sup>π</sup>, transitions, unique parity states, and spectroscopic factors 0-42547
- <sup>141</sup>Pr(n,γ), circular polarisation, ang. distrib. meas. 0-32285
- <sup>141</sup>Pr(n,γ), non-statistical capture, radiative widths, γ-ray doorway state model 0-37389
- <sup>191</sup>Pt(n,γ), <sup>192</sup>Pt negative parity states in partially decoupled bands, γ-transitions 0-47360
- <sup>239</sup>Pu(n,X), thermal n, gamma spectra from capture, fission and fission products 0-37352
- <sup>103</sup>Rh(n,γ), cross-sections above 2.6 keV 0-32276
- <sup>104</sup>Rh(n,γ), 0.5-3.0 MeV, γ-spectra strength functions 0-32240
- <sup>46</sup>Ru(n,γ), A=100-104, cross-sections above 2.6 keV 0-32276
- <sup>32</sup>Si(n,X), 2.5-1100 keV, resonance struct. from total and capture cross sections 0-42620
- <sup>32</sup>Si(n,γ), fast n, doorway structs. and single particle resonances, microscopic treatment 0-52646
- <sup>32</sup>Si(n,γ), non-statistical effects in shell model calcs. 0-32274
- <sup>32</sup>Si(n,γ), single particle resonances and doorway states, K matrix formalism 0-37384
- <sup>124</sup>Sb(n,γ)<sup>125</sup>Sb, reactor neutron capture cross section of 60.3-day <sup>124</sup>Sb 0-13469
- <sup>45</sup>Sc(n,γ), <sup>46</sup>Sc energy levels, resonances, spin and parity 0-52673
- <sup>45</sup>Sc(n,γ), <sup>46</sup>Sc level deexcitation, E1 and M1 absolute radiative widths 0-52622
- <sup>45</sup>Sc(n,γ), pol. n, <sup>46</sup>Sc transition polarisation, levels and spin assignments 0-52656
- <sup>28</sup>Si(n,γ), 565, 813 keV, <sup>29</sup>Si neutron resonance, γ-spectra, partial and total radiative widths 0-42578
- <sup>28</sup>Si(n,γ), fast n, doorway structs. and single particle resonances, microscopic treatment 0-52646
- <sup>28</sup>Si(n,γ), single particle resonances and doorway states, K matrix formalism 0-37384
- Si(n,γ), <sup>28</sup>Si p3/2 neutron resonance γ-decay, partial rad. widths 0-52617
- <sup>144</sup>Sm(n,γ), resonance and thermal n, γ-spectra, recent expt. review, non-statistical effects 0-37383
- <sup>145</sup>Sm(n,γ), 3-7.2 MeV, <sup>145</sup>Sm neutron separation and level exciton (n,γ) and (d,p) correlations 0-22756
- <sup>115</sup>Sn(n,γ), thermal, <sup>116</sup>Sn levels, J<sup>π</sup> and transitions 0-52587
- <sup>181</sup>Ta(n,γ), 30 keV, capture cross sections, stellar nucleosynthesis 0-42663
- <sup>159</sup>Tb, neutron resonances, time-of-flight spectra 0-27633
- <sup>124</sup>Te(n,γ), <sup>124</sup>Te capture states partial α-decay widths 0-37328
- <sup>124</sup>Te(n,γ), thermal n, <sup>120</sup>Sn γ-spectra, E1 and M1 hindrance factors 0-37386
- <sup>130</sup>Te(n,γ), resonance and thermal n, γ-spectra, recent expt. review, non-statistical effects 0-37383
- <sup>232</sup>Th, effective cross section dependence on thermal neutron temp. 0-547
- <sup>232</sup>Th, neutron cross section meas. 0-526
- <sup>46</sup>Ti(n,γ) A=46, 47, 49, 50, 45 MeV, cross section meas., resonance parameters 0-18315
- <sup>169</sup>Tm(n,γ), 0.5-3.0 MeV, <sup>170</sup>Tm, gamma-ray strength functions from spectrum fitting method 0-52616
- <sup>170</sup>Tm(n,γ), 0.5-3.0 MeV, γ-spectra strength functions 0-32240
- <sup>14</sup>U(n,X), A=233, 235, thermal n, gamma spectra from capture, fission and fission products 0-37352
- <sup>235</sup>U(n,γ), <sup>236</sup>U low lying levels from 4<sup>-</sup> isomer decay 0-47396
- <sup>236</sup>U(n,γ), 5-125 eV, <sup>237</sup>U levels, bands and J<sup>π</sup> assignments, n binding energy 0-5041
- <sup>238</sup>U, effective cross section dependence on thermal neutron temp. 0-547
- <sup>238</sup>U, neutron cross sections evaluation for incident neutron energies up to 4 keV 0-5146
- <sup>238</sup>U(n,γ), 2, 24 keV, resonance averaged γ-spectra, level and J<sup>π</sup> appls. 0-37347
- <sup>238</sup>U(n,γ), cross section and resonance shape, gas molecule vibr. effects 0-42661
- <sup>51</sup>V(n,γ), circular polarisation, ang. distrib. meas. 0-32285
- <sup>52</sup>V(n,γ), sputtering yields from V metal surface 0-25493
- <sup>136</sup>Xe(n,γ), resonance and thermal n, γ-spectra, recent expt. review, non-statistical effects 0-37383
- <sup>170</sup>Yb(n,γ), 10-70 keV capture cross-section 0-27631
- <sup>90</sup>Zr(n,γ), thermal cross section, <sup>91</sup>Ze primary γ-rays and binding energies 0-52566
- Zr(n,γ), 2-24 keV, <sup>91</sup>Zr, A=91, 92, 94, binding energy and primary γ-ray intensities 0-52565

## neutron radiography

- see also nondestructive testing
- albedo method, local nonuniformity monitoring obs. 0-35482
- cardiac pacemaker batteries, investigation of electrolyte, USA National Bureau of Standards 0-56179
- contrast enhancement using Gd<sub>2</sub>O<sub>3</sub> additive, ordnance appl. 0-30177
- painting and artist identity, autoradiography and gamma-ray spectroscopy appl. 0-26073
- reactor test facility, fast flux 0-18371
- resonance neutron radiography using a position-sensitive proportional counter, appl. to meas. of nuclear fuel 0-13597
- Texas A and M Nuclear Science Centre, neutron radiography facility, development and utilisation 0-9401
- Li-I<sub>2</sub> pacemaker battery electrolyte exam. 0-30940

## neutron reflection

- Argonaut reactors, coupled core, neutron wave propagation, Be, graphite and D<sub>2</sub>O as internal reflectors 0-27752
- BWR/6 axial reflectors, Monte Carlo modelling 0-22939
- concrete interfaces, Monte Carlo Spectra calc. 0-27686
- neutron charge, upper limit determination method using neutron reflection (Russian) 0-32316
- neutron generation time for reflected systems 0-563
- reactor control rods, influence of neutron trap on critical loading and efficiency (Russian) 0-37474
- space craft thermionic reactors, reflector drums as control mechanism 0-42784
- ultracold neutrons, neutron-optical image formation (Russian) 0-5193
- Fe<sub>2.45</sub>Mn<sub>0.05</sub>Si, slow neutron polariser, by single cryst. (111) refl. 0-49052



**neutron reflection continued**

- $\text{Li}_0.5\text{Fe}_{2.5}\text{O}_4$ , slow neutron polariser, by single cryst. (222) refl. 0-49052  
 Ni-Mn multilayer for monochromators and supermirrors, neutron reflectivities 0-22880  
 Ni-Ti multilayers for monochromators and supermirrors, neutron reflectivities 0-22880  
 $\text{UO}_2$  rods in water with U or Pb reflecting walls, critical expts. 0-32331

**neutron scattering** *see kaon-nucleon scattering; lepton-nucleon scattering; neutron-nucleus scattering; nucleon-nucleon scattering; photon-nucleon scattering; pion-nucleon scattering*

**neutron scattering (crystallography)** *see neutron diffraction; neutron diffraction crystallography; neutron diffraction examination of materials*

**neutron sources**

- 14 MeV neutron generators for radionuclide prod. 0-3811  
 accelerator-based pulsed cold neutron source (*Japanese*) 0-47796  
 beam experiments (*Japanese*) 0-27684  
 burst source, TOF meas. (*French*) 0-14040  
 cold neutrons and applications of quasielastic scattering (*Japanese*) 0-27685  
 conference on neutron capture gamma ray spectroscopy, Upton, USA. (Sep. '78) 0-36780  
 fast neutron fields produced by Kyoto University Cyclotron 0-27840  
 FMIT neutron source, energy spectra and yields, fusion reactor mat. development appl. 0-32552  
 Frascati Tokamak, 1MJ plasma focus dynamics, neutron production scaling 0-24220  
 fusion materials development studies, irradiation sources 0-32478  
 Fusion Materials Irradiation Test Facility, high flux neutron source for material development 0-32551  
 generator facility with alternative  $30^\circ$  target 0-9444  
 HFBR, safety features of cold neutron moderator 0-23114  
 high intensity neutron sources in thermal, resonance and fast ranges 0-37677  
 intense neutron source facility, skyshine anal. methods comparison 0-5349  
 intense pulsed spallation source, UCN production 0-14024  
 ion pulse stacking for prod. of intense current pulses 0-23209  
 neutronic analysis of the NBS intermediate-energy standard neutron field (ISNF) 0-27692  
 photoneutron target design for fast-neutron spectrum measurements 0-23232  
 plasma focus devices, neutron emission parameters 0-24221  
 polarised generator, intensity increase of polarized deuterium by using a short compressor magnet 0-18732  
 primary beam and shielding radiation quality and absorbed dose obs. 0-12281  
 pulsed, neutron guides, geometry optimisation and simulation 0-47802  
 pulsed neutron generator, ING-2 0-23204  
 pulsed neutron generator with laser deuteron source 0-27844  
 pulsed neutron research, book 0-22146  
 pulsed spallation neutron sources 0-27852  
 pulsed thermonuclear sources, book contrib. 0-23235  
 pulsed UCN source, meas., produced by Doppler-shifted Bragg refl. 0-32556  
 radiotherapy, linear accelerator neutron sources and characts. 0-51239  
 subsonic gas target neutron generator 0-5424  
 target design for intense pulsed neutron source 0-23233  
 TRIGA Mk.II reactor for  $\text{B}(\text{n},\alpha)$  therapy, remodelling and dosimetry 0-56200  
 UCN, detection systems, sources, transport, book contrib. 0-22882  
 UCN, gravitation influence on lifetimes on traps 0-18750  
 UCN, storage in pulsed aperiodic-action reactor 0-18749  
 UCN conservation in Al and Cu walled vessels (*Russian*) 0-14034  
 UCN container materials, reduction of surface H by ion bombardment 0-9446  
 UCN prod. using Doppler shifted Bragg scatt. and intense pulsed neutron spallation source 0-14024  
 ultra cold neutron source, expt. current status and results 0-37678  
 ultra cold neutrons, super thermal source 0-52807  
 ultrahigh flux reactor, Grenoble, neutron-physical expts. (*German*) 0-5209  
 very cold neutrons from linac-cold moderator system 0-27842  
 water-cooled target for the 14 MeV neutron source, design and experiment 0-47795  
<sup>241</sup>Am-Be neutron spectrum, (n,p) reaction average cross-sections 0-22827  
<sup>197m</sup>Au, for neutron activation analysis, form. cross sections for 3 and 14.1 MeV neutrons 0-32283  
 B<sub>K</sub> filtering of FBR spectra for generation of neutron reference source 0-42884  
 Be, neutron spectra from p,d, <sup>3</sup>He collisions 0-524  
 Be(d,n) neutron field, integral tests of activation cross sections 0-851  
 Be(d,n), activation cross-section, integral tests, dosimeter appl. 0-32553  
<sup>252</sup>Cf neutron sources, apps. of activation anal., review 0-18728  
<sup>252</sup>Cf, neutron sources for calibration of personnel dosimeters 0-13946  
<sup>252</sup>Cf source in tissue-equivalent phantom, neutron absorbed dose obs. 0-12278  
 D<sub>2</sub>O thermal column irradiation facility Penn State Breazeale Reactor 0-9339  
<sup>3</sup>H(d,n)<sup>3</sup>He, neutron energy meas. with Si detector 0-32566  
<sup>7</sup>Li(p,n)<sup>7</sup>Be as therapy neutron source especially for small cyclotrons 0-26335  
 O<sub>2</sub> filtered neutron beam of 2.35 MeV 0-27848  
<sup>239</sup>PuBe, neutron sources for calibration of personnel dosimeters 0-13946  
<sup>187</sup>Ta( $\gamma$ ,n) photoneutron absorpt. cross section meas. 20.9 to 837.8 keV (*German*) 0-5122  
 Ti, tritiated self supported target prep. 0-23211  
 ZrH rethermaliser for IVV-2 reactor hot neutron flux increase 0-37676

**neutron spectra**

- see also neutron spectrometers*  
 absorber rod vibr. induced neutron density fluctuations, QMC reactor expt. 0-37469  
 coupled core reactor, space depend. neutron fluctuation spectra, HF struct. 0-37468  
 critical assembly, neutron spectra meas. by activation method 0-32390  
 efficiencies and light curves for meas. using NE-213 0-878  
 fallout observation, Chinese A-tests 0-27820  
 fast neutron transport through laminated Fe-H<sub>2</sub>O shield 0-13931  
 full flux covariance matrix calc. for NBS intermediate-energy standard neutron field 0-5348

**neutron spectra continued**

- fusion reactor radiation protection, shield integral expts. at ORNL 0-47709  
 Hauser-Feshbach calculation of the fission neutron spectrum 0-22801  
 LMFBR core design, benchmark tests of JENDL-1 for structural materials 0-13616  
 LWR, fuel utilisation, spectral shift control methods 0-47586  
 LWR, outgoing neutron spectrum from H<sub>2</sub>O in H<sub>2</sub>O/V interface 0-27697  
 molecular spectroscopy book 0-27052  
 neutron collimated fast beam, radiation quality local distrib. 0-12247  
 overlapping, multigroup collision prob. method 0-52718  
 primary beam and shielding radiation quality and absorbed dose obs. 0-12281  
 prompt fission neutron spectra calc., nucl. evaporation theory 0-22870  
 prompt fission neutron spectra for ENDF/B-V 0-22869  
 prompt fission spectrum uncertainties, implications for integral data testing 0-22871  
 PWR, survey of neutrons inside containment 0-13675  
 radiation protection, benchmark shielding problems obtained from integral tests of neutron cross sections 0-47740  
 radiation shielding materials, benchmark radiation transport data, air-over-ground neutron and gamma spectroscopy 0-23161  
 reflection of neutrons between plane-parallel concrete interfaces, Monte Carlo calc. 0-27686  
 tissue neutron energy deposition spectra from improved cross-section values 0-26300  
 TOF meas., rate depend. of counting losses 0-37692  
 TR-O reactor, neutron spectrum meas., oscillation techniques (*Czech*) 0-52754  
 TRIGA Mk.II reactor core, thermal neutron spectra parameters meas. 0-9348  
 unfolding, optimised smoothing, FERDOR method 0-27860  
 (p, n), 22.2 MeV, A=27-197, neutron spectra, direct and equilb. processes (*Russian*) 0-52648  
<sup>12</sup>B\* neutron decay in <sup>12</sup>C( $\pi^-$ ,  $\gamma$ )<sup>12</sup>B\*, shell model 0-22652  
 Be, neutron spectra from p,d, <sup>3</sup>He collisions 0-524  
<sup>12</sup>C( $\pi^-$ , n), stopped pion, neutron energy spectra, mean energies and multiplicities 0-9311  
<sup>252</sup>Cf fission-neutron spectrum unfolding experiment 0-13514  
<sup>252</sup>Cf, measured neutron and  $\gamma$  spectra in a tissue equivalent medium 0-3805  
<sup>252</sup>Cf, neutron emission 0-37405  
<sup>252</sup>Cf spontaneous fission, meas. of fission neutron spectra 0-22873  
 Cu fusion + hybrid reactor materials, neutron spectra meas. and calcs. 0-23142  
 Fe shield, meas. of neutron and gamma ray penetration 0-47730  
 Ge(Li) detectors, fast neutron leakage spectrum determ. 0-32565  
<sup>6</sup>Li sandwich counter, meas. of neutron spectra in fast neutron systems 0-27884  
<sup>14</sup>N( $\pi^-$ , n), stopped pion, neutron energy spectra, mean energies and multiplicities 0-9311  
 Nb fusion + hybrid reactor materials, neutron spectra meas. and calcs. 0-23142  
<sup>16</sup>O( $\pi$ ,  $\gamma$ n), direct and resonance reaction unified shell model, n,  $\gamma$  spectra 0-52696  
<sup>16</sup>O( $\pi^-$ , n), stopped pion, neutron energy spectra, mean energies and multiplicities 0-9311  
<sup>239</sup>Pu(n,f) 0-37405  
 Pu(n,f), 0-18 MeV, prompt neutron spectrum, evaporation model (*Chinese*) 0-42721  
<sup>93</sup>Sr excited state depopulation  $\gamma$ -rays, n coincidence from <sup>94</sup>Rb  $\beta$ -delayed n decay 0-52631  
<sup>159</sup>Tb, neutron resonances, time-of-flight spectra 0-27633  
<sup>232</sup>Th, fusion + hybrid reactor materials, neutron spectra meas. and calcs. 0-23142  
<sup>235</sup>U(n, $\alpha$ ), thermal fission neutron spectrum 0-42712  
<sup>235</sup>U(n,f), 0.6, 7 MeV, fission neutron spectra meas. 0-22872  
<sup>238</sup>U, fusion + hybrid reactor materials, neutron spectra meas. and calcs. 0-23142  
<sup>238</sup>U, neutron resonance parameters, time-of-flight spectroscopy 0-47375  
<sup>238</sup>U(n,f), 7 MeV, fission neutron spectra meas. 0-22872  
 U(n,f), 0-18 MeV, prompt neutron spectrum, evaporation model (*Chinese*) 0-42721

**neutron spectrometers**

- accelerator facility, fast neutron research, data acquisition and anal. 0-47806  
 accelerator facility, Van de Graaff generator and cyclotron for fast neutron detection and neutron reaction cross-sections 0-47805  
 calibration and testing using moderator spheres (*Czech*) 0-47804  
 fast neutron time of flight spectroscopy, multi-angle detector system 0-52810  
 gas proportional  $\alpha$ -recoil spectrum 0-5433  
 NE213, detection efficiency meas. for 130 MeV neutrons 0-27888  
 NE213 liquid cylindrical neutron spectrom., anisotropy of response 0-5434  
 NE213 liquid scintillator, light output for electrons and protons 0-32564  
 NE 213, pulse shape discrimination 0-27862  
 organic, neutron response functions, Monte Carlo program 0-14047  
 PANSI, polarisation anal. neutron scattering instrument, description and apps. 0-23280  
 Pilot U scintillator for 55-225 MeV neutrons 0-18762  
 polarised neutron diffraction, determ. of magnetic form factors, pioneering work 0-24321  
 polarised neutrons in condensed matter [conference, Zaborow, Poland (Sept. 1979)] 0-22136  
 reactor structural material transmission meas. using TOF spectrometer 0-18440  
 scintillation spectrometers, with LED and PIN photodiode, stabilising system 0-47821  
 scintillation TOF meas. with very fast burst source (*French*) 0-14040  
 shielding of analyzer crystal of neutron spectrometer 0-42887  
 small angle neutron scattering on the Harwell linac 0-19675  
 spin-echo integral transform spectroscopy 0-4748  
 spin-echo spectrometry and neutron optical polarisers 0-49051  
 system for nuclear fuel rod inspection 0-47669  
 TOF meas. of direct react. spectra, resolution improvement 0-18753  
 triple axis spectrom., energy resolution function 0-9449  
 velocity selector for neutrons, high resolution, applic. to materials research (*German*) 0-47803



## neutron spectrometers continued

- Ge(Li) detectors, fast neutron leakage spectrum determ. 0-32565  
<sup>6</sup>Li sandwich counter, meas. of neutron spectra in fast neutron systems 0-27884

## neutron stars

see also pulsars

- accreting compact object in binary system, magnetosphere theory, X-ray sources 0-46394  
 accretion by rotating mag. neutron stars, torques rel. to pulsating X-ray sources period changes 0-31320  
 accretion onto magnetised neutron stars, fate of sinking filaments 0-51798  
 Centaurus X-3, stellar wind vel. change during transition 0-12829  
 Crab Nebula, central mag. dipole rot. neutron star theory for supernova remnant 0-51834  
 cyclotron line emissions meas. with Ge(Li) balloon borne spectrom. 0-41721  
 cyclotron self-absorption in accretion columns of magnetic degenerate stars, X-ray sources appl. 0-12760  
 Cygnus X-1, model of neutron star surrounded by massive disc 0-36736  
 disk accretion, transition zone radial and vertical structure 0-4393  
 $e^+e^-$  spontaneous creation in inhomogeneous magnetic fields 0-22540  
 HD 50896, WN5 star, emission-line spectrum vars. rel. to possible neutron star companion 0-51791  
 Hercules X-1, cyclotron line form. by reson. Compton cyclotron scatt. 0-8711  
 Hercules X-1, cyclotron self-absorpt. in accretion column of mag. degenerate star 0-12760  
 inner crust nuclear compositions 0-31322  
 interior plasma, mag. field rel. to pulsar periods long-term changes 0-22029  
 magnetised neutron stars, thermal radiation 0-56869  
 mass-radius relation, obs. constraints, dense matter eqn. of state 0-46597  
 mass-radius relations for cold spherical body, relativistic effects 0-26730  
 massive cold spherical stars, rest-mass density and redshift 0-56859  
 neutron <sup>3</sup>P<sub>2</sub> superfluidity under  $\pi^0$  condensation in neutron star matter 0-47417  
 nuclear matter equation of state, relativistic quantum field theory of neutron stars 0-5088  
 nuclei excitation energies in hot matter, limits 0-56703  
 outer crust, electron solid in superstrong mag. field, bifurcation theory approach 0-4640  
 $\phi$  Persei, binary Be star, HE II emission rel. to compact secondary component 0-12768  
 pion condensation in dense nuclear and neutron matter 0-37333  
 pulsar, quasar and X-ray source obs. 0-36657  
 pulsar electron cap, electrons accel. in internal zone 0-46592  
 pulsar magnetosphere, magnetoactive plasma equilb. in gravit. field (*Russian*) 0-26895  
 pulsar magnetosphere model, cylindrical, with particle inertia but no dissipative forces 0-51796  
 pulsar magnetosphere models, interior and exterior struct., pair prod. 0-46594  
 pulsar NP 0531, distrib. model of press., density, ang. vel., matter rot., grav. field (*Ukrainian*) 0-12775  
 pulsar polar caps as foil-less diodes, nonneutral relativistic beam accel. 0-17604  
 secular instabilities of rigidly rotating stars in general relativity, theoretical formalism 0-4341  
 secular instabilities of rigidly rotating stars in general relativity, numerical results 0-4342  
 secular instability in rotating stars, resulting from thermal cond. 0-21986  
 sources of gravitational radiation, conf. proceedings (Seattle, 24 July-4 Aug. 1978) 0-36778  
 spin alignment, spin-torsion forces and strong-gravity interactions 0-56870  
 SS 433, accreting mag. neutron star model (*Russian*) 0-36647  
 SS 433, early-type star plus neutron star model 0-56843  
 SS 433, Of star orbited by neutron star, model 0-22025  
 stellar collapse to neutron stars and black holes, computer generation of spherical spacetimes 0-46385  
 supercritical accretion discs winds struct. and appearance, numerical models 0-21984  
 superdense magnetised astrophysical objects, interiors physical conditions 0-17603  
 superdense quark core, spontaneous magnetisation possibilities 0-8646  
 thermal properties and detectability, cooling and heating processes 0-31323  
 thermal X-ray emission, review of theory 0-41849  
 thermonuclear flashes on accreting neutron stars 0-31321  
 thermonuclear runaways on neutron stars, theory 0-22032  
 triple close approaches effect on stellar system evolution, one-parameter family appl. 0-17618  
 4U 1626-67, 7.7-second X-ray pulsar, simultaneous X-ray and optical obs. 0-51914  
 Universe, high density matter, many body treatment, pulsars 0-26738  
 X-ray source, intensities from stellar wind flow past compact object 0-22116  
 X-ray sources, strongly magnetised plasma collisional relax. of ion beam 0-33785

## neutron transport theory

see also neutron diffusion; neutron moderation

- albedo cell calculations in the thermal region taking into account thermalisation (*Russian*) 0-52710  
 albedo method for single group calculations of multiband spherical cells (*Russian*) 0-52709  
 anisotropic scattering treatment using improved comput. code (*Japanese*) 0-13526  
 Argonaut research reactors, effect of atmos. press. variation on reactivity (*German*) 0-5199  
 benchmark testing of anisotropic diffusion coefficients, void-worth calcs. for finite lattices 0-47546  
 Boltzmann equation, eigenvalue precision, influence of boundary conditions 0-27689  
 Boltzmann equation, eigenvalue precision, influence of boundary conditions 0-27690  
 boral shielding material, neutron transmission calc. 0-854  
 CANDU, LOCA, space-time neutronic anal. 0-13663  
 CANDU-PHW, neutron group cross sections in resolved resonance region calcs. 0-13573

## neutron transport theory continued

- capture probability, linear Boltzmann eqn., Pade approximants, appl. to spherical geometry 0-52143  
 CHART program, eqn. soln. in cylindrical and spherical geometries 0-5197  
 coarse-mesh eqns. for the numerical soln. of 2nd-order transport eqn. 0-47527  
 collision probability integrals, annular geometry, evaluation using analytic expansions 0-32317  
 collision probability method, development and applications 0-27706  
 contribution Monte Carlo, exponential biasing model 0-5195  
 contribution Monte Carlo technique, variational derivation 0-5194  
 contribution transport, deterministic approaches 0-555  
 convolution integral calculations for neutron transport in reactors 0-47561  
 coupled neutron-nuclide problems, time depend. generalised perturbation theory 0-32322  
 critical slab, isotropic and anisotropic scatt., asymptotic solution, strained coords. method 0-42733  
 cyclotron radiation transport in plasmas by neutron transport techniques 0-38660  
 deep penetration problems, rebalance methods, effectiveness 0-47533  
 deep-penetration transport problems, appl. of contribution Monte Carlo methods 0-47530  
 diffusion acceleration, modified approach 0-13528  
 discrete eigenvalues of transport eqn. with anisotropic scatt. 0-553  
 discrete-ordinates neutron transport equations in slab geometry, convergence rates of spatial difference equations 0-27688  
 dispersion function, consequences in anisotropic scattering 0-27241  
 DWR core global power distrib. calcs. equivalent, Homogenized, and condensed nuclear parameters 0-655  
 earth, radiation transport for neutron and  $\gamma$ -ray point sources above air-ground interface 0-32526  
 eigendistributions in linear transport theory 0-13523  
 electron beam fusion of D-T pellets, neutronics and photonics 0-52781  
 electron-beam fusion coupled pellet-blanket neutronics 0-47717  
 ENDF/B-V cross section data for shielding appls., Monte Carlo MCNP integral calcs. 0-47744  
 ENDF/B-V nuclear data for shielding appls., energy balance anal. 0-47745  
 escape probability, Boltzmann linear eqn., Pade approximants 0-551  
 escape probability from absorbing body, polynomial expression 0-47523  
 fast liner reactor conceptual design, nucleonics 0-13790  
 fast reactor, effective cross section preparation from multigroup cross sections (*Rumanian*) 0-47543  
 fast reactor physics, assessment of JAERI fast group constants set version 2.0-602  
 finite element analysis, modified method for neutron transport eqn. 0-47529  
 finite element method, two-dimens., one-group test problems 0-37412  
 fission reactor reactivity perturbation calc. by difference iterations in the Monte Carlo method 0-5210  
 fission reactor theory, reduced three-dimensional transport equation with anisotropic scattering 0-18368  
 flux synthesis, single channel, finite element trial functions for 3-D reactor calcs. 0-42734  
 fuel enrichment and neutron density problems 0-27693  
 fusion reactor blanket with synthetic fuel prod., neutronics and heating analyses 0-13812  
 fusion reactor duct neutron streaming simulations, perturbation and variational corrections 0-23143  
 fusion reactor inertial confinement pellets, neutronics modelling 0-37593  
 fusion reactor materials, neutronics analysis using ENDF/B-V cross-section covariance data 0-47710  
 fusion reactor shielding experiment, cross-section sensitivity calcs., one- and two-dimensional models 0-27799  
 GCFR, design of deep penetration integral expt. for ThO<sub>2</sub> blanket and radial shield mockup 0-23167  
 heterogeneous lattices, unified theory 0-37428  
 homogenization methods to obtain group-diffusion parameters for reactor calculations 0-670  
 homogenized diffusion approximations to the neutron transport equation 0-47522  
 HTGCR, fuel with double heterogeneity, resonance absorpt. 0-32321  
 HTPBR, neutron and physical aspect calcs. (*German*) 0-22941  
 hybrid anal., separation technique and sensitivity theory 0-37632  
 hybrid fusion-fission blanket design, Th based, nucleonic performance aspects 0-47714  
 integral transport theory, 3-D appls., criticality calculations for a finite prism 0-18367  
 integro-differential coupled-core reactor models, asymptotic stability 0-13531  
 irreversible circulation of fluctuation 0-27700  
 laser-driven fission-fusion microexplosions, nuclear and thermohydrodynamic calcs. 0-47696  
 lattices, uniform, homogenisation, small buckling approx. 0-52721  
 LMFBR critical assembly, neutron diffusion calc., DB<sup>2</sup> transverse leaking predictions 0-13529  
 LWR cones, computation of cell group consts. 0-566  
 LWR core transient anal. using coupled neutronics and thermal hydraulic models 0-715  
 LWR kinetic anal. with feedback, hypothetical accident transients 0-13697  
 LWR shielding, neutron transport anal. comparison of several multigroup libraries 0-23168  
 microexplosion reactor neutronics, adjoint transport eqn. technique 0-47713  
 minimizing splitting costs in Monte Carlo particle transport 0-47532  
 Monte Carlo neutronic and electronic model for thermal-neutron coincidence counting 0-23165  
 multidimensional inverse problem in transport theory 0-174  
 multigroup, Chandrasekhar H-eqns., comparison of iterative methods 0-47521  
 multigroup collision prob. method, applied to overlapping neutron spectra theory 0-52718  
 multigroup diffusion theory, current weighted total cross section determ. in unresolved energy region 0-18365  
 multigroup theory, functional analysis 0-13525  
 multigroup transfer coeffs., efficient eval. for shielding appls. 0-47747  
 multigroup transfer cross-sections for elastic and discrete level inelastic neutron scatt. 0-42732



**neutron transport theory continued**

- multigroup transport problems, Monte Carlo game, moments method 0-52720
- noise studies in BWR and PWR 0-557
- nonstationary transport in systems with large spherical cavities book contrib. 0-22881
- Nordheim integral treatment for resonance processing, proper use 0-3427
- $P_n$  approx., modified form with exact asymptotic roots, change in Marshak free surface boundary conditions 0-52717
- PDX Tokamak, neutron skyshine Monte Carlo calcs. 0-47711
- prompt gamma-ray anal. of neutron flux distrib. in nonhomogeneous samples, computational model 0-14060
- pulsed neutron die-away in fast multiplying assemblies 0-18366
- pulsed neutron research, book 0-22146
- radiation dose deposition calcs. in human marrow 0-26365
- radiation protection studies expt. and theoretic results comparison 0-47750
- reactor lattices, functional estimation using first-order perturbation 0-27698
- reactor physics, grid-coupling methods for the multigrid solution of the neutron diffusion equation 0-47555
- reflected critical slab, asymptotic soln. using invariant embedding principle 0-27683
- response matrix finite element soln. 0-13527
- $S_N$  calculations, modified transport formulation compatible with anisotropic diffusion theory 0-47526
- second order transport eqn., variational formulation and projectional methods 0-164
- secondary neutron polarization via penetration through a ferromagnetic shielding wall 0-47742
- SOLASE-H hybrid reactor, blanket neutronics calc. for blanket design 0-13805
- space craft thermionic reactors, reflector drums as control mechanism 0-42784
- spatial approximation methods for the  $S_N$  equations in x, y geometry 0-47525
- spatial differencing schemes for slab transport eqns., linear characteristic and quadratic methods 0-47524
- stationary nonlinear transport problem 0-27242
- stochastic transport, functional theory 0-37413
- streaming ray technique for particle transport calculations 0-47716
- subcritical limits for special fissile actinides 0-52708
- temperature-dependent nonlinear neutron transport problem 0-47520
- TFTR neutral-beam injectors, shielding calcs. 0-23172
- thermal lattice leakage calcs. using modified  $B_1$  method 0-47545
- time-dependent neutron transport in spherical geometry 0-13530
- Tokamak reactor blankets, effects of neutral beam injection tubes, shielding calcs. 0-23173
- transfer matrix calcs. for thermal neutrons 0-27687
- transverse buckling effects in 2-D calcs. 0-32318
- two-dimensional, comparison of rebalance stabilization methods 0-5220
- UCN, detection systems, sources, transport, book contrib. 0-22882
- UCN, gravitation influence on lifetimes on traps 0-18750
- UCN, storage in pulsed aperiodic-action reactor 0-18749
- upper atmosphere, Monte Carlo calcs. 0-8468
- Voigt functions analysis, appl. to neutron cross sections 0-22879
- wave propagation in heavy  $H_2O$ , scattering kernel, molecular mode contrib. 0-52707
- zero-variance multigroup Monte Carlo quadratures 0-5196
- D-D fusion-fission hybrid blankets, neutronics anal. 0-13809
- Fe radiation shielding, computational benchmark for deep penetration 0-47738
- Fe-Ni-Co-V alloys, effects on fusion reactor neutronics performance 0-47705
- Li, T breeding performance eval., multigroup neutron and photon transport calc. 0-13831
- $LiO_2$ , T breeding performance eval., multigroup neutron and photon transport calc. 0-13831
- $Li_2Pb_3$ , T breeding performance eval., multigroup neutron and photon transport calc. 0-13831
- $Pu(NO_3)_4$ , slab tanks for criticality control, neutron multiplication calc. 0-13606
- $^{239}Pu$  direct enrichment of LWR assemblies in a fusion hybrid 0-37604
- $^{235}U$ ,  $^{238}U$ ,  $^{239}Pu$ , a=233, 235, slab tanks for criticality control, neutron multiplication calc. 0-13606
- $^{235}U + BeO$  nearly homogeneous multiplying systems, pulsed neutron study, age-diffusion model 0-37442
- W, radiation shielding material, integral tests of ENDF/B-IV high-energy neutron cross-section data 0-23162

**neutrons**

- see also cosmic ray neutrons; delayed neutrons
- anomalous magnetic moment in struct. model using pions 0-18134
- charge, upper limit determination method using neutron reflection (Russian) 0-32316
- charge form factor zeros 0-413
- electric and magnetic dipole moments 0-4993
- electric dipole moment, quark and gluon corrections 0-4994
- electric dipole moment search with ultra-cold neutrons, expt. set-up 0-37270
- electric dipole moment using ultra cold neutron source, expt. current status and results 0-37678
- EM structure functions from electron scatt. data 0-13306
- magnetic moment meas. separated oscillatory-field magnetic resonance technique 0-22613
- QCD, neutron electric dipole moment, chiral estimate, current algebra, CP violating reactions 0-27471
- spin rotation by precession during interferometry 0-32584
- ultracold, storage and investigation of fundamental props. 0-447
- ultracold, use for lifetime meas., collision loss calcs. (Russian) 0-52504

**Newtonian fluids see fluids****nickel**

- see also nuclei with .....
- acoustic hardening, influence of US treatment temps. and material purity (Russian) 0-11656
- adsorbed  $c(2 \times 2)$  Na overlayer, core level excitation effects, synchrotron radiation UPS study 0-40234
- adsorbed C on Ni (100), LEED struct. anal., substrate distortion 0-6637
- adsorbed CO, core level spectrum, satellite struct., ab initio HF-LCAO calc. 0-40233

**nickel continued**

- adsorbed CO  $c(2 \times 2)$  on (001) face, surface geometry determ. by deep-core-level XPS 0-40224
- adsorbed S and O on (110), surface struct. anal. using hybridisation model 0-44423
- adsorbed Se and Te on (001) surface, photoelectron diff. obs. 0-40223
- adsorption and decomp. of hydrocarbons on (111) surface, high resolution EELS study 0-40739
- adsorption of C on (100) surface, substrate reconstruction, LEED constant momentum transfer averaging study 0-39445
- adsorption of chalcogens on (111) surface, angle-resolved photoemission 0-40230
- adsorption of CO on (100) surface, EELS and concomitant surface anal. 0-7453
- adsorption of ethylene on (111) surface, dehydrogenation, thermal desorption and AES study 0-29274
- adsorption of H on (110) surface, substrate reconstruction, LEED constant momentum transfer averaging study 0-39445
- adsorption of Na, hybridisation between adatom s and p reson., jellium model 0-6932
- adsorption of O on {100} surface, low energy ion scatt. study 0-39420
- adsorption of S, Se, photoelectron diff. data 0-29851
- alpha particle energy loss straggling 0-42902
- alpha-particle impact, exfoliation depth and damage energy distrib., range 0-29075
- alpha-particle irradi., Mossbauer study of nucl. reaction aftereffects 0-40015
- annealing twins density, photoemission microscopy 0-35208
- atom, from  $Ni(CO)_4$ +inert gas, chemiluminesc. 0-55647
- atom, X $\alpha$  theory appls. approximations 0-9510
- atoms, Xe matrix isolation, photoemission 0-27987
- Auger effect, K-M $^2$  radiative, low energy satellites meas. 0-45174
- band structure, rel. to lattice const., spin polarised APW calc. 0-20073
- band theoretic interpretation of neutron scatt. expts., spin wave modes 0-44791
- blistering, He $^+$  ion energy and irradiation temp. effects 0-34103
- Bloch wall meas. by enutron small-angle meas. 0-15753
- borate glass: Ni, absorption spectra, mag. props., coordination behaviour (German) 0-40147
- bound hole pairs, XPS study, satellite peaks 0-40218
- cavity evolution in 500 keV  $^4He^+$  irradi. 0-29082
- chemisorption, of  $H_2$ , isothermal desorption near Curie temp., rate meas. 0-29268
- chemisorption geometry of H on (111) surface, LEED, thermal desorption, and work function meas. 0-39433
- chemisorption of benzene on (111) and (100) faces, vibr. EELS study 0-39436
- chemisorption of CO, Raman spectra 0-2755
- chemisorption of CO on (100) and polycrystalline surfaces, low energy SIMS and AES 0-34309
- chemisorption of H, bond nature 0-34297
- chemisorption of H, embedded cluster model 0-39427
- chemisorption of H on (111) surface, order-disorder transition, cluster-variation method 0-15372
- chemisorption of  $N_2$  on (110) surface, mol. and dissociative mechanisms 0-39431
- chemisorption of NO on (100), LEED, AES, UPS, and thermal desorption study 0-39449
- chemisorption of  $O_2$  on (110) surface and initial oxidation, AES, EELS, and work function meas. 0-54523
- chemisorption of O, S, Se, NO and  $O_2$ , cluster theory 0-29264
- chemisorptive binding of O, CNDO calc. of potential energy curves (German) 0-44431
- coating, heat treated, as plated, electrochemical study of corrosive wear 0-16536
- coating, self lubricating containing oxides, carbides and borides on steel 0-21189
- coating on Al alloy substrates, adhesion strength, meas. using microindentation method 0-40640
- compressive deformation, single crystals, strengthening, tested at 293 and 77K (German) 0-50689
- core level excitation effects, synchrotron radiation UPS study 0-40234
- corrosion of electrolytic coatings in 40% wt. KOH 0-30175
- creep, struct. and activation characts., effective stress, electron microscopy and resistometric obs. (Russian) 0-40427
- creep parameters, high temp. 0-50685
- crystals in strong magnetic field, EM excitation and vel. dispersion of sound (Russian) 0-39837
- cubic crystals, anisotropic, dislocation loops, electron microscope image contrast 0-39101
- cubic single crystal misorientation angle determ. by US speed meas. 0-54315
- Curie temperature, press. depend., using press. cell developed for meas. with cubic-anvil press 0-13109
- cyclic deformation, high temp. 0-16429
- Debye-Waller factor, using reverse Fourier time-of-flight method, neutron powder diff. study 0-49050
- decarburisation rate, resistivity relaxation measuring system, for surface reaction meas. 0-55718
- defect structure, formation kinetics, work hardening and resistivity study (Russian) 0-10557
- deformation, cyclic, at high temps. of alloy 200 0-21055
- deformation in const. mag. field, 4.2K (Russian) 0-29591
- deformed, struct. form. during annealing,  $Ni_3Al$  type ordered phase precipitation (Russian) 0-45325
- desorption, associative from mixed adlayers of O and N 0-54512
- desorption of CO, on (111) preexponential factor 0-49515
- determ. in vitreous silicates by ESCA (Japanese) 0-40787
- deuteron irradiation-induced creep mechanisms 0-39171
- diamond:Ni, synthetic, X-ray absorpt. fine structure study of impurities 0-55133
- diffusion into Cu and Cu-Ni, resistometric meas. 0-29222
- diffusion of  $H_2$  in single- and polycrystals at 60°C grain boundary effects (German) 0-2211
- diffusion of H, trapping and mobility near vacancies, dislocations and cracks 0-49426
- diffusion of H in imperfect lattices 0-49425
- dislocation intersection and solution strengthening, effect of solute on obstacle profiles 0-7590
- dislocation structure parameter determ. due to plastic deformation (Russian) 0-54242



## nickel continued

dispersion strengthened, high-temp. cyclic deformation 0-21056  
 dispersions, semi-amorphous, on  $\text{Al}_2\text{O}_3$ -graphite, mag. characterisation 0-44876  
 dissolution and passivation in acid environment, effect of P (French) 0-45440  
 electrical resistance in DC mag. field after ultrasonic deform. (Russian) 0-54671  
 electrodeposit on Cu, defects and their effect on props. 0-39474  
 electrodeposited film, appl. of stereomicroscopic method for obs. of organic molecule incorporation 0-2288  
 electrodeposited in sulphamate bath, cyclic stress, meas. appl. in high temp. range 0-19295  
 electrodeposition, chemical factors 0-16207  
 electrodeposits, struct., electrolyte anions influence 0-20056  
 electroless plating process and props. for diamond turning optical surfaces 0-1375  
 electrolytic, O, H, N liberation during vacuum heating, Mossbauer spectra (Russian) 0-35594  
 electron microscopic observation of {220} planes 0-18047  
 electronic structure and optical consts. by inelastic electron scatt. 0-7451  
 EM and acoustic energy attenuation in many-domain magnets 0-7140  
 energy band structure, investigating near-Fermi part from PES 0-2328  
 epitaxial electrodeposition, surface-stress phenomena at start 0-35542  
 epitaxial growth, on  $\text{NiO}(100)$ , by low pressure hydrogen reduction (French) 0-11578  
 EXAFS in photoelectron yield spectra 0-16123  
 fast reactor structural material, integral expts. 0-13612  
 fast reactor structural materials, activation, (n,p), (n, $\alpha$ ) cross sections 0-13624  
 fast reactor structural materials, nuclear data 0-13611  
 FCC, props. of vacancies and divacancies 0-10545  
 ferromagnetic, calc. hyperfine fields and their press. derivations 0-6796  
 ferromagnetic, chemisorption of H, spin-spin interactions, UPS spectra calc. 0-6630  
 ferromagnetic, electron spin polarised photoemission spectrum for (111) surface 0-25525  
 ferromagnetic, Hall effect, anomalous, rel. to scatt. processes 0-44572  
 ferromagnetic, itinerant, Fermi surface and single particle excitations 0-34350  
 ferromagnetic, temp. depend. of hyperfine fields for F 0-20141  
 ferromagnetic single cryst., transmission of 24 GHz radiation, effect of diffuse surface scatt. of carriers, calc. 0-34780  
 ferromagnetic zero point motion effect on hyperfine field at interstitial positive muon site 0-2681  
 ferromagnetism, itinerant electron model, spin quantization direction fluctuations, short range order. 0-34582  
 field-emitted electron spin polarisation by tunnelling through surface pot. 0-29861  
 film, damping and vel. of longit. elastic waves at 9.4 GHz 0-10596  
 film, ferromag., magnetoresistance parameter meas. (Spanish) 0-2485  
 film, few atomic layers thick, transition from Pauli paramag. to band ferromag. 0-44885  
 film, ion beam sputtering prep., struct. and mag. props. 0-35085  
 film, layer mode growth on Fe (001) surface, AES study 0-49540  
 film, multi- and single-layer, reson. curves subjected to tangential mag. reversals (Russian) 0-50195  
 film, phonon transport into  $\text{SrF}_2$  substrate, diffusive scatt. at impurities 0-49487  
 film, single cryst., domain width from ferromag. reson. 0-39879  
 film, solar collector coating, microstruct., FIM and SEM obs. 0-26166  
 film, sputter deposited on Cu, induced stresses 0-24774  
 film, ultrathin, field effect meas., influence of CO adsorption 0-11108  
 film, work function changes upon water contamination 0-44705  
 film coatings for Mo tips, film characterisation by atom probe FIM atomic clusters, voids 0-33863  
 films, Faraday rotation effect dispersion 0-40092  
 films, HCP and amorphous, RF sputtered,  $\text{O}_2$  incorporation, ESCA obs. 0-10832  
 fission reactor structural material, resonance data eval. below 300 keV, Doppler effect calc. 0-13618  
 fission reactor structural material data eval. for JENDL-1 0-13617  
 fluid bed electrolysis, deposition 0-55672  
 foil, crystal struct. as function of substrate temp. during deposition 0-18742  
 foil, electron bombard., impurity redistrib. during third stage of annealing, residual resist. meas. 0-6434  
 forced magnetostriction at 4.2K 0-50155  
 frictional behaviour, effect of mechanical properties 0-55548  
 grain boundary sliding and deformation mechanism maps 0-3128  
 heat capacity temp. depend. meas., internal energy and entropy, anharmonic theory calcs. (Russian) 0-54402  
 heat transfer during cooling with water (German) 0-23873  
 hydrogen, and liquid Hg-embrittlement 0-25862  
 hyperfine field and magnetisation, press. and temp. depend. 0-6795  
 hyperfine field at positive muon 0-40029  
 implanted,  $^{155}\text{Tb}$  sources produced by recoil implantation,  $^{155}\text{Gd}$  Mossbauer transition 0-40009  
 interatomic pair potential, phonon spectra 0-33927  
 interband optical conductivity, self energy correction 0-2792  
 interface with polymer, electronic struct., XPS study 0-45204  
 intergranular corrosion in dil.  $\text{H}_2\text{SO}_4$  solns., S segregation effects 0-30152  
 ion bombarded, He gas-bubble superlattice form. 0-2086  
 ion implantation produced crystalline phase transitions 0-7558  
 ions, beam-foil spectra from 20 to 238 MeV energy, 5 to 60 nm, lifetime meas. problems 0-9722  
 ions in Tokamak plasmas, spectroscopy and atomic physics 0-53938  
 isothermal desorption of CO, UPS study, time-resolved approach 0-39440  
 kinetic friction re-examination using modified pin and disc machine 0-55547  
 Landau-Lifshitz damping, wave no. and temp. depend. 0-34779  
 layers, thickness determ. by laser microprobe and flame atomic absorpt. 0-27355  
 light ion (H, D, He, Li) irradi., defect prod. and electronic stopping power 0-34088  
 light scattering from surface and bulk thermal magnons 0-45087  
 liquid, contact reaction with  $\text{B}_4\text{C-Ti(V)(Cr)}$  0-55707  
 liquid, coordination numbers, calc. in microinhomogeneous struct. model (Russian) 0-38902

## nickel continued

liquid, crystallographic orientation relationships in coalescing sintered W spheres 0-45249  
 liquid, electronic struct. and transport props. 0-29314  
 liquid, viscosity calc. using microinhomogeneous struct. model (Russian) 0-15284  
 magnetic hyperfine fields of Zr, DPAD meas. 0-39901  
 magnetic impurity in  $\beta$ -NiAl, self consistent embedded cluster model 0-2549  
 magnetic surface anisotropy of transition metals, model calc. 0-34625  
 magnetic surface states, photoelectron spectra, surface Brillouin zones 0-6928  
 magnetic susceptibility, generalised, neutron scatt. meas. 0-34606  
 magnetisation in high mag. field, Arrott-Noakes plot 0-54919  
 magnetostrictive vibration meas., appl. of laser interferometric technique 0-37059  
 magnon relaxation, spin-orbit interaction, itinerant electron ferromagnets 0-11179  
 mass transfer parameters, lattice defect effects under laser pulse action (Ukrainian) 0-6537  
 melt, struct. charact. time depend. in X-ray studies (Russian) 0-24350  
 microvoid form., gaseous impurity atom effects, positron annihilation study 0-49275  
 molten, contact reaction with graphite 0-15342  
 monolayer and submonolayer films, on ZnO, UPS study 0-7472  
 multiple wavelength neutron powder diff. data, Rietveld profile refinement algorithm 0-24320  
 muon spin rotation; freqs., and relax. rates 0-55006  
 neutron irradiated, microstruct. and tensile props. 0-34077  
 Ni powder 2JJ, porous, effect of sintering conditions in struct. and strength 0-20823  
 optical constants, influence of temp. and relation to bandstruct. 0-25403  
 optical spectrum, anomalous temp. depend. around  $T_c$ , band struct. 0-40128  
 oxidation in air, 50-150°C, film growth obs. using AES and contact resist. 0-3242  
 oxidation transport processes using tracers in growing NiO scales 0-25913  
 oxide scale, high temp., metallographic obs. of inner layer 0-3240  
 pair potentials calc., appl. to point defect props. 0-19798  
 phase transformations and vacancy form. by positron annihilation 0-2155  
 phonon generation and attenuation at FMR 0-39875  
 phosphate glass: Ni, absorption spectra, mag. props., coordination behaviour (German) 0-40147  
 photoelectron spectra, threshold Auger emission 0-29849  
 photoelectron spectroscopy, one-electron energy investig. 0-55263  
 photoemission, d-band, resonance enhancement by coupling to 3p excitation 0-20766  
 photoemission, exchange-split energy-band dispersions 0-35059  
 photoemission spectra, core-level satellite struct. 0-29855  
 photoneutron yields released by incident electrons, improved calc. 0-27630  
 pigmented anodic  $\text{Al}_2\text{O}_3$ , for selective absorpt. of solar energy, optical and struct. props. 0-55892  
 plasma, Tokamak-produced,  $2s^2 2p^k 2s 2p^{k+1}$  transitions in F I to Be I isoelectronic sequences 0-37765  
 plasma impurity, flux on wall of DITE Tokamak 0-28688  
 plasma sprayed coating, effect of Si substrate surface conditions and impact velocity of sprayed particles 0-21145  
 plastic deformation, effect on H transport rates 0-21044  
 plated aspheric metal mirror fabrication for IR optical systems 0-14497  
 plated Nb(Ta), H absorption rate, metallic film effect 0-49525  
 point defect estimation from specific heat and volume in plastically deformed pure metals (Russian) 0-54223  
 porosity depth distrib. of annealed samples following bombardment by 1 MeV  $\text{Ar}^+$  ions 0-5333  
 positive muon spin precession, effect of press. 0-40030  
 powder, hot pressing on steel substrate, densification kinetics 0-40290  
 powder, porous, relationships between mech., physical, and microstructural characts. 0-20846  
 powder, resist.-sintability (Japanese) 0-16228  
 powder, sintered, use of extruded porous materials as fuel cell electrodes 0-40853  
 powder, subjected to vibratory milling, exam. of plastic deformation, recrystallisation, sintering 0-16234  
 pure, anomalous grain growth 0-20984  
 radiation damage and diffusion 0-24645  
 reactor structural material transmission meas. using TOF spectrometer 0-18440  
 rectilinear screw dislocation, magnetisation distrib., mag. moment anal. 0-44897  
 secondary electron emission under  $\text{Ar}^+$  ion bombard. near Curie point 0-29838  
 shock hardening, anomalous residual, at short pulse duration 0-20942  
 single crystal, preferred growth direction in floating zone method 0-25555  
 single crystal, stretched, electron microscope exam. of deformation cell structure during polygonization (German) 0-7651  
 single phase FCC, cyclic deform. long range stress changes 0-54308  
 single-domain particles, LF mag. susceptibility, 2K up to Curie point 0-29582  
 softening of strained single crystals (Russian) 0-40499  
 solar selective black coatings, electrochem. deposition on Zn surfaces 0-29885  
 spontaneous magnetostriction determ. method, molecular field theory study (Russian) 0-50157  
 spreading kinetics of Al 0-24717  
 sputtered, ionisation probability, energy dependence 0-35041  
 sputtering by low energy  $\text{H}^+$ , Rutherford backscattering technique 0-40198  
 sputtering rate on Ar ion bombard. 0-55245  
 steel, maraging, 0Kh6N8M7S, effect of Cr, Ni and Mo on hardness 0-21093  
 substrate, kinetics,  $\text{Ni}_2\text{Al}_3$  layers growth by cementation (French) 0-35127  
 substrate for polystyrene film, electrode effect on carrier injection, TSC, I-V characts. 0-34463  
 supercooled, struct. refinement mech. (Russian) 0-20975  
 surface, (100), chalcogen adsorption, UPS study 0-6648  
 surface, (100), secondary electron spectra, adsorbed elements effects 0-50480



## nickel continued

- surface, (110), theory of ion scatt. 0-7458  
 surface, C interaction, monolayer form. and struct. stability 0-10756  
 surface, charged-particle emission caused by laser beam scanning 0-11518  
 surface, coadsorption of Pb or Sn with P or C, AES study 0-54521  
 surface, coverage and desorption of CO flash desorption spectrum 0-49493  
 surface, Cs and K coated, survival probabilities of emerging H<sup>-</sup> ions 0-45187  
 surface, d-band narrowing, obs. using angle-resolved XPS 0-11062  
 surface, H ion impact, elliptic polarisation in Balmer radiation 0-35039  
 surface, Ni (100)-c(2×2)CO, surface struct., LEED meas. 0-6647  
 surface, oxidation, structural changes, low energy ion scatt. study 0-35423  
 surface, polycryst. and single cryst., ang. distrib. of CsCl restituted to gas phase 0-6626  
 surface, Te c(2×2) overlayer, 4d levels, angle resolved photoemission cross section, atomic and solid-state effects 0-29853  
 surface (001), adsorbed N<sub>2</sub>, p(2×2) struct., LEED and AES study 0-54515  
 surface (001), barrier struct., LEED anal. 0-20023  
 surface (001), Ne<sup>+</sup> scattering and neutralisation on first and second layers 0-35045  
 surface (100), adsorbed CO vibr. EELS, large-ang defl. 0-44405  
 surface (100), clean and with chemisorbed O, rapid LEED intensity meas. 0-44420  
 surface (100), mag. props. 0-44861  
 surface (100), spin polarised photoemission 0-45221  
 surface (110), dissolution of C adlayer, 600-913K 0-49504  
 surface (111), photoyield near threshold negative-positive spin polaris. crossover 0-2922  
 surface (111), single crystal, spin polarisation of emitted photoelectrons 0-45215  
 surface (111), with submonolayer of O, H or C<sub>2</sub>H<sub>2</sub>, surface phonons obs. by EELS 0-39403  
 surface (111)(110)(100), H adsorption, model 0-50889  
 surface dopant in Mo, effect on fatigue (*Russian*) 0-7660  
 surface hyperchannelling, scatt. of low energy Ar ions, computer simulation 0-34110  
 surface reaction of H<sub>2</sub> and O<sub>2</sub>, SIMS and thermal desorption meas. 0-40742  
 surface self-diffusion in presence of adsorbed halogens (*French*) 0-24723  
 thermal desorption of <sup>3</sup>He, low temp. release 0-34294  
 thermotransmission spectrum, M<sub>2,3</sub> edge, temp. depend. 0-50463  
 thickness meas. of Au and Ni layers on Cu substrates simultaneously 0-13041  
 thin film (*French*) 0-44446  
 transient magnetic field discontinuity seen by O(F) ions 0-24515  
 UPS, two-electron reson. at 3p threshold, rel. to Cu (100) expt. 0-25522  
 valence-band photoemission spectra, self-energy corrections effect 0-11534  
 vapour deposition on O-treated polystyrene, microscopic interactions 0-3407  
 void swelling rates in self-ion irradiation sample 0-29081  
 wire plasma sputtering with W particles, coagulation, struct. and particle size (*Russian*) 0-40260  
 X-ray K-absorpt. edge shifts, plasmon energies correlation 0-20734  
 X-ray K-absorpt. spectra, depend. on composition and temp. changes (*Russian*) 0-55226  
 X-ray photoemission spectroscopy of 1S<sub>1/2</sub>O, 1S<sub>1/2</sub>C and 2P<sub>3/2</sub>Ni states, Ar ion implanted Ni 0-16149  
 yield point, effect of alloying elements (*Russian*) 0-50670  
 AgCl:Ni, double quantum EPR transition, superhyperfine struct. 0-7154  
 AgCl:Ni, optically detected double resonance, radiative recombination electron traps 0-20518  
 Al<sub>2</sub>O<sub>3</sub>:Ni anodised films, electrolytically coloured, spectrally selective surface 0-11490  
 Al<sub>2</sub>O<sub>3</sub>:Ni cermets, prep. and props. (*French*) 0-20877  
 As:Ni film, amorphous, chemical modification of props. 0-49250  
 BaTiO<sub>3</sub>:Ni, annealed in H<sub>2</sub> and O<sub>2</sub>, valence change in phase stability 0-20600  
 C content determ., isotope-spectral method (*Russian*) 0-55766  
 C precipitation 0-29958  
 Ca(OH)<sub>2</sub>:Ni<sup>2+</sup> single cryst., X-irrad., Ni<sup>+</sup> EPR, g-factors and point-charge model 0-2626  
 CdS:Ni, recomb. parameters, photocond. spectra meas. (*Russian*) 0-49820  
 CdTe:Ni, luminesc. and refl. spectra, high temp. annealing effects 0-24472  
 Cu:Ni, Dingle temps. calcs., tetrahedron method 0-6699  
 Cu/Ni multilayer films, electron beam induced diffusion during AES depth profiling 0-19993  
 diffusion of As, 970-1360°C (*Russian*) 0-29218  
 Fe-Cr-Mn-Ni, influence of Ni on defect conc. energy (*Russian*) 0-54241  
 n-GaAs:Ni, negative photocond. at low temps., impurity levels 0-6900  
 n-GaAs:Ni, VPE, deep-level transient spectroscopy 0-34383  
 GaP:Ni, deep traps, near IR luminesc., polarised spectra meas. 0-16077  
 GaP:Ni<sup>2+</sup>, d-d luminesc. spectra 0-7414  
 n-Ge:Ni, recombination of hot electrons on Ni impurity centres 0-44612  
 Ge-Ni contacts, surface electron state spectrum, surface treatment effects (*Russian*) 0-34497  
 H assisted cracking, mechanisms, review 0-50721  
 KMgF<sub>2</sub>:Ni, Ni-Ni pair optical spectra 0-45042  
 KZnF<sub>3</sub>:Ni<sup>2+</sup>, Mn<sup>2+</sup>, interference transition electric dipole mechanism 0-34896  
 LiCl(Br):Ni<sup>2+</sup>, optical absorpt., charge transfer spectra 0-2797  
 MnCO<sub>3</sub> crystals, gel. grown, Ca<sup>2+</sup>, Ni<sup>2+</sup> impurity influence, SEM study 0-20778  
 Ni:MgF<sub>2</sub>, laser, broadly tunable CW operation, output powers, optical pumping 0-32995  
 Ni (001)/CO(O) system, adsorbate geometries determ. from final state scattering in X-ray photoemission 0-54488  
 Ni, grain boundary cavities growth under applied stress and internal pressure 0-29032  
 Ni, magnetoelastic and magnetostrictive sensitivities, reversible and irreversible components (*Russian*) 0-25172  
 Ni powders, stereological appl. in study of compacting process, elec. and mech. props. (*French*) 0-40286  
 Ni XVII solar coronal EUV line intensities 0-51731

## nickel continued

- Ni XXI, XXIII, spectral energy levels, relativistic corrections, config. superposition method 0-32616  
 Ni<sup>+</sup>, generation by laser ionis. source for ICR spectroscopy, chem. appls. 0-45597  
 Ni<sup>2+</sup>, Rayleigh and Compton scatt., differential cross section determ. 0-52912  
 Ni:Kr gas trapping and release, thermal evolution mass spectrometric study 0-34026  
 Ni<sup>2+</sup>:MgO laser system, optical parameters 0-48260  
 Ni/Au-Ge/GaAs contact system, alloying behaviour, microprobe AES and X-ray diffr. 0-54548  
 Ni/SiO<sub>2</sub>, adsorption of CO, scavenging effect of H<sub>2</sub>, in situ Fourier transform IR spectra obs. 0-39410  
 Ni/ThO<sub>2</sub>, adhesive energy, meas. techniques 0-50803  
 Ni/ZrO<sub>2</sub>-Y<sub>2</sub>O<sub>3</sub>, sputtered multilayered ceramic/metal coatings, props. 0-40620  
 Ni-Cd, with plastic bonded Ni oxide electrodes, basic electrochemical parameters 0-50951  
 Ni-Cd accumulators, plastic bonded electrodes, active layer composition influence on galvanostatic and potentiostatic discharge curves 0-55834  
 Ni-Cd cell lifetime prediction, computerised pattern recognition 0-3504  
 Ni-Mn multilayer for monochromators and supermirrors, neutron reflectivities 0-22880  
 Ni-n-GaP:Si(Ge) contacts, doping effect in elec. props. 0-6983  
 Ni-sapphire interface, effect on shear strength of adsorbed species 0-49485  
 Ni-SiO multilayer film, interface magnetisation 0-7135  
 Ni-SiO<sub>2</sub> supported catalysts, particle size, H<sub>2</sub> chemisorption, Mossbauer study 0-7219  
 Ni-Ti multilayers for monochromators and supermirrors, neutron reflectivities 0-22880  
 Ni-V system, interdiffusion, kinetics of phase growth (*Russian*) 0-29230  
 Ni-W surfaces in contact, deform. and adhesion at very low loads 0-39457  
 Ni+H<sup>+</sup>, K-shell ionisation calcs. 0-23534  
 Ni+H<sup>+</sup>, K-shell ionisation cross-sections calcs. 0-43165  
 Ni+Ni, continuum X-ray radiation, collision broadening 0-9539  
 Ni+Ni, exchange interactions and exchange integrals 0-37849  
 Ni+Ni, recoil effects on molecular-orbital X-ray spectra in solid targets 0-25510  
 Ni+Ni<sup>+</sup>, with nuclear sticking, molecular orbital and compounds nucleus X-ray emission 0-1048  
 Ni<sub>2</sub>, A→X system, Ar matrix isolation fluoresc. spectrosc. obs. 0-9628  
 Ni(IX), resonance transitions, classification 0-42985  
<sup>59</sup>Ni, management of radioactive waste produced on dismantling PWRs 0-27756  
<sup>63</sup>Ni, applications in biological research 0-12321  
<sup>63</sup>Ni, management of radioactive waste produced on dismantling PWRs 0-27756  
 Pd/Ni/Cr layered catalyst for H<sub>2</sub>-O<sub>2</sub> recombination in BWR coolant 0-18504  
 plasticity, high temp., oxide inclusions effect 0-50681  
 Si:Ni, amorphous, vac. evaporated, doping, transport and optical props. 0-49715  
 Si:Ni, capture probabilities of two deep impurity levels by photocond. decay 0-49799  
 Si:Ni amorphous films, ESR and elec. cond. 0-50171  
 SiO:Ni, optical absorption spectra in visible and near IR region 0-45119  
 SrO:Ni<sup>+</sup>, noncentral Jahn-Teller ion, energy minimum localisation, ESR study 0-25198  
 TiCrB<sub>2</sub>-Ni, interphase reactions, electron probe anal., metallography and hardness exam. 0-2990  
 VC-Ni, fracture mode determination, using Auger electron spectroscopy 0-7680  
 ZnSe:Ni, evidence for exciton binding at Ni impurity sites, photolum. excitation spectrum 0-45135  
 ZnSiF<sub>6</sub>·6H<sub>2</sub>O, spin-phonon interaction between Ni<sup>2+</sup> ions, phonon bottleneck effects, splitting parameters (*Russian*) 0-15796
- nickel alloys**  
 see also *Elinvar*; *Invar*; *nickel compounds*; *Permalloy*  
 -Z 0-11646  
 Alnico, high-energy magnetic materials technology developments and props. (*Italian*) 0-54914  
 alumel thermocouples, decalibration, quantitative SIMS anal. 0-4705  
 amalgam, anodic polarisation in alkaline soln. 0-11823  
 amorphous metal-metalloid alloys production by ion implantation, TEM study 0-15128  
 binary alloy, irradi. with heavy ions, non-equilib. segregation phenomena 0-19950  
 binary substitutional solutions, thermodynamics 0-44336  
 Brightray S, lattice contraction during ageing 0-3030  
 chromel thermocouples, decalibration, quantitative SIMS anal. 0-4705  
 coated with Cr<sub>2</sub>C<sub>3</sub> (Cr<sub>2</sub>C<sub>3</sub>) based coatings, detonation deposited, wear resist., 20-1000°C 0-11843  
 Colmonoy, friction behavior in high temp. Na environment (*Japanese*) 0-40546  
 constitution changes due to radiation effects 0-34048  
 correl. between void swelling and thermodynamic stability 0-641  
 Cunial MNA13-3, Mn addition effect on props. 0-21035  
 dilute, hyperfine field at positive muon 0-40029  
 dilute metastable alloy formation by ion implantation 0-15130  
 eutectic alloys, unidirectionally solidified, solidification and morphology relationship 0-25684  
 glassy, continuous-biased sputter-deposited Kr entrapment 0-24603  
 Hastelloy C-276 and G, accelerated H<sub>2</sub> charging in aq. H<sub>2</sub>SO<sub>4</sub> at 0.2% yield stress 0-30144  
 Hastelloy C-4, loaded at high temp., useful life 0-40523  
 Hastelloy X, carburisation and dimens. stability in HTGR, He environment 0-45366  
 Hastelloy X, grain size effect. creep and creep-rupture (*Japanese*) 0-16382  
 Hastelloy X, thermal fatigue props. 0-21071  
 heat resistant alloy EhP539L, heat treatment effect on props. and hardening phase morphology 0-29995  
 high-temperature materials, technological requirements, R and D, report 0-45222  
 In 519 high temp. low-cycle fatigue behaviour for nuclear process heat appl. 0-628  
 IN-100, fatigue crack growth retardation at elevated temp. 0-3158



## nickel alloys continued

- Incoloy, alloy 800,  $M_{23}C_6$ /austenite phase boundary defect struct. resolution by weak beam microscopy 0-3046
- Incoloy 600,  $H_2SO_4$  vapour corrosion, in general atomic S-I thermochem. water-splitting cycle 0-45449
- Incoloy 600 and 800, surface film in hot conc. NaOH, XPS study 0-11824
- Incoloy 600 vacuum heat treatment for improved corrosion resistance of PWR steam generator tubing 0-5246
- Incoloy 800, stress corrosion cracking and anodisation during straining in boiling NaOH soln. 0-30140
- Incoloy 800 for HTR appls., correlation of carburization behavior, mechanical property degradation, and exposure conditions 0-5244
- Incoloy 800 H, 617, high temp. low-cycle fatigue behaviour for nuclear process heat appl. 0-628
- Incoloy 800 in 50% NaOH, stress corrosion cracking, slow strain rate method (*Japanese*) 0-55575
- Incoloy 800H, carburisation and dimens. stability in HTGR, He environment 0-45366
- Incoloy 800H,  $H_2SO_4$  vapour corrosion, in general atomic S-I thermochem. water-splitting cycle 0-45449
- Incoloy-800, annealed, mech. behaviour anal. for elevated-temp. LMFBR appl. 0-18428
- Inconel, D trapping in fusion reactor materials, temp. dependence 0-37577
- Inconel, fatigue crack growth rate in high temp., high purity oxygenated water 0-40622
- Inconel 600, corrosion fatigue crack propag. at 85°C in 50% NaOH, potential effect (*Japanese*) 0-11834
- Inconel 600, oxide layer, mechanical impedance meas. method 0-45444
- Inconel 600, PWR primary corrosion products 0-13578
- Inconel 600, stress corrosion cracking and anodisation during straining in boiling NaOH soln. 0-30140
- Inconel 600 and 601, films deposited by cylindrical magnetron sputtering, internal stresses 0-24773
- Inconel 600 and 718 in liquid Na environment, fatigue crack propag. 0-40624
- Inconel 600 in 50% NaOH, stress corrosion cracking, slow strain rate method (*Japanese*) 0-55575
- Inconel 625, accelerated  $H_2$  charging in aq.  $H_2SO_4$  at 0.2% yield stress 0-30144
- Inconel 625, creep rupture behaviour in Ag environment 0-25853
- Inconel 625, nitriding in  $N_2$ - $H_2$  glow discharge 0-16590
- Inconel 625, plasma nitriding, hardness meas., Rutherford backscatt. surface anal. 0-45442
- Inconel 718, environment effect on high temp. fatigue crack growth 0-30090
- Inconel 718, H plasma effects on fusion device vacuum vessel 0-21111
- Inconel 718, high temp. fretting fatigue, fatigue and fretting wear 0-3197
- Inconel X750, positron annihilation study of ageing and creep 0-29824
- interatomic interaction by XPS 0-7474
- intermetallic compounds, containing d-transition metal, hydrogenated, magnetism 0-34609
- low C 80 A, TEM obs. of cellular transformation products 0-3045
- mathematical-physical considerations rel. to metal powder prod. 0-11595
- Mischmetal-Ni,  $MMNi_3$  substituted hydrides for H storage appls. 0-45791
- Nichrome, alloyed with refractory metal borides, mech. props., rel. to appl. as electrodes in electrospray machining 0-21174
- Nichrome-silicate glass- $CaF_2$  multicomponent self-lubricating coating, prep. by plasma spraying, and props. 0-40604
- Nicalloy-coated 0-40611
- Nimonic, IN100,  $\gamma'$  precipitates, casting conditions effect on morphology 0-7548
- Nimonic 80 A, TEM obs. of cellular transformation products 0-3045
- Nimonic 80A, lattice contraction during ageing 0-3030
- Nimonic 80A, struct., fracture characts. 0-3071
- Nimonic 90, creep rate stress exponents and friction stress, comparison with Lagneborg particle by-passing model 0-55481
- Nimonic 90, dispersion hardened, friction stress rel. to initial and secondary creep 0-11711
- Nimonic PE16, He injected, bubble-void transitions in Ni ion bombard. 0-34095
- Nimonic PE-16, neutron irradiation effects on fatigue crack propag. 0-29069
- powder, crystallised by supercooling methods, struct. props. (*Russian*) 0-54483
- powder, hot hydrostatic pressing of disk, capsule design 0-20839
- precipitation hardening, effect on dynamic strain ageing and jerky flow 0-20945
- recrystallisation after hot deformation (*German*) 0-25716
- Rene 95, as hot isostatically pressed (HIP) and HIP+forged, low cycle fatigue 0-25854
- spin waves, mag. props. of alloys, review 0-44823
- sputter induced surface composition changes, in alloys 0-49470
- steel, alloy low, Ni-Cr, tempered martensite embrittlement 0-7669
- steel, austenitic, cold worked 10Kh11N23T3MR, structural transformations, aging effect, electron microscope obs. 0-40402
- steel, austenitic, Cr-Ni, anomalous stress-depend. of creep rate 0-11712
- steel, austenitic, Cr-Ni, nonmetallic inclusions modification using rare earth metals (*Russian*) 0-40369
- steel, austenitic, Ni alloy, stacking fault energy of austenite, high resolution electron microscopy (*Russian*) 0-44219
- steel, austenitic stainless, biphasic, ferritic, ageing and thermomech. treatment effects on struct. and props. 0-35226
- steel, austenitic stainless, Cr-Ni (18, 10 wt.%),  $^{59}Fe$  self-diffusion in ferrite/austenite interface (*French*) 0-19975
- steel, austenitic stainless 12Kh18N10T and 15Kh17N2, corrosion cracking in chloride and alkaline solutions 0-55576
- steel, austenitic stainless Cr-Ni,  $^{51}Cr$  tracer diffusion coeffs. 0-34225
- steel, Co-Cr-Ni-Mo-Mn (39.65, 20.25, 15.33, 7.08, 1.9 wt.%) carbide formation during tempering after plastic deformation 0-16330
- steel, Cr-Ni (18%, 12(8)%), martensite formation and reversion, effect on void swelling 0-11641
- steel, Cr-Ni-Mo, dynamic and static softening behaviour at hot forming temp. (*German*) 0-25728
- steel, Cr-Ni-Mo, for boiler tubes, austenisation conditions effect obs., on structure and mechanical props. 0-3151
- steel, Cr-Ni-Mo-V, magnetic induction, struct. dependence (*Czech*) 0-30141
- steel, Cr-Ni-Mo-V, Mossbauer austenitometry and mag. props. 0-40003

## nickel alloys continued

- steel, Cr-Ni-Ti-B, grain size effect on mech. and struct. props. (*French*) 0-45361
- steel, fatigue crack growth data, three component model anal. 0-3161
- steel, low-temperature behaviour, mechanical, electrical and magnetic props. (*German*) 0-3081
- steel, martensitic 07Kh16N4B, corrosion cracking in chloride and alkaline solutions 0-55576
- steel, Mn-Ni-Mo low alloy steels for nuclear appl., toughness and heat treatment 0-5239
- steel, Ni (21 wt.%), ageing, nitrated case struct. investigation 0-35416
- steel, Ni ion implanted, corrosion behaviour 0-11840
- steel, Ni-Cr, corrosion on  $N_2O_4$  flow 520-890K and 8-9 MPa (*Russian*) 0-3256
- steel, Ni-Cr, cyclic re-austenitizing 0-35222
- steel, Ni-Cr-Mo, cleavage fracture toughness, temperature and notch sharpness influence (*German*) 0-35291
- steel, Ni-Cr-Mo, fracture toughness determ. from yield strength and cleavage fracture strength (*German*) 0-35292
- steel, Ni-Cr-Mo, quenched and tempered, notched bar tensile tests (*German*) 0-35247
- steel, Ni-Cr-Mo (11, 5, 3 wt.%), maraging, corrosion cracking in chloride and alkaline solutions 0-55576
- steel, stainless, Cr-Ni (18, 10 wt.%), long-term strength in H at high pressure 0-55485
- steel, stainless, Cr-Ni-Mo-N, phase diagrams 0-35161
- steel, stainless, Ni-Cr-Mo-W (29, 13, 3, 2 wt.%), long-term strength in H at high pressure 0-55485
- steel, stainless, type 430, Ni<sup>+</sup>-implanted, struct., comp. and electrochem. anal. of surface alloy 0-16603
- steel, stainless complex alloy, hot ductility, B effect 0-30038
- steel, struct. change of hot-worked austenite during post-deform. holding 0-35228
- strength properties, dispersity of struct. effect, alloy KhN45Yu 0-55486
- superalloy,  $\gamma'$ -precipitation influence on recrystallisation 0-29955
- superalloy, directionally solidified, struct. and props. (*Chinese*) 0-20918
- superalloy, fatigue crack opening load variation with meas. location 0-16425
- superalloy, IN 718, acoustic emission interpretation of ductile fracture processes 0-35300
- superalloy, IN-100, aluminised, microstruct. degradation, influence of corrosion protective coating 0-40611
- superalloy, microscopic inhomogeneity of plastic strain influence on fatigue cracks (*German*) 0-40470
- superalloys, low temp. hot corrosion,  $Na_2SO_4$ -induced, mechanism, burner rig tests 0-40610
- superalloys, Si-based coatings for high temp. appl., process development and props. 0-40614
- superalloys, sigma phase prediction techniques 0-7567
- Ti-Ni, electron emission and shape memory effect 0-50687
- Ticonal, two- and one-dimens. modulated struct. after thermomag. treatment and water quenching (*Russian*) 0-29983
- type 625, neutron irradiation effects on fatigue crack propag. 0-29069
- type 718, neutron irradiation effects on fatigue crack propag. 0-29069
- Udimet 520, Nicalloy-coated, microstruct. degradation, influence of corrosion protective coating 0-40611
- Zircaloy, H absorption,  $Sn(Fe)(Cr)(Ni)$  effect 0-49527
- Zircaloy cladding, stress corrosion cracking due to I and Cs redistrib. in LWR fuel rods 0-32343
- Zircaloy-2, neutron irradiated, inhomogeneous deformation behaviour 0-50679
- Zircaloy-2, tritium diffusion 0-32341
- Zircaloy-4, anomalous oxide growth during transient temp. oxidation 0-50773
- Zircaloy-4, microstrain and particle size meas. by Warren-Averbach method 0-55420
- Zircaloy-4 tubes, texture influence on anal. of thermoelastic/plastic anisotropy and initial yielding 0-35260
- Al-Al<sub>3</sub>Ni, eutectic composite, abrasive fragmentation (*Czech*) 0-30110
- Al-Al<sub>3</sub>Ni directionally solidified eutectic alloy, struct. and mech. props. (*Korean*) 0-29944
- Al-Cu-Mg-Fe-Ni, Hyduminium RR58, crack propag. rates in air and salt soln. 0-21063
- Al-Cu-Ni, alloy RR 350,  $\theta'$ -hardened, deform. induced microstructural instability, high temps. 0-16321
- Al-Fe-Ni, influence of strain path on mech. props., orthogonal tensile paths 0-30035
- Al-Ni, liq., dissoln. and diffusion of alloying components, 700-1000°C (*Russian*) 0-15275
- Al-Ni, thermoelastic phase transform., acoustic emission 0-3039
- Al-Ni alloys, solid and liq. mag. susceptibility, 600-1650°C (*Russian*) 0-15685
- Al-Ni with multiple layer plasma coating, exam. of cohesion strength (*Russian*) 0-7714
- Al-Ni-Co(Si), directionally solidified eutectic, morphological and mech. props. (*Russian*) 0-30057
- Al-Pt-Ni<sub>1-x</sub>-Ni system, Schottky-barrier height 0-34520
- Al-Pt-Ni<sub>1-x</sub>-Si system, diffusion, compound form., and microstructure 0-34253
- Al-Si-Cu-Mg-Ni, piston, depend. between min. creep rate and time of beginning of secondary creep (*Czech*) 0-35267
- Au-Fe-Ni layer coating, Fe and Ni conc. meas. by X-ray diffr. (*German, English*) 0-34330
- Au-Ni-Cu-Zn, white gold, metallographic struct., heat treatment and plastic working effect 0-40403
- Ce-Ni-Si, thermoelectromotive force and electrocond. (*Ukrainian*) 0-54670
- (Co,Ni)-Cr<sub>23</sub>C<sub>6</sub> eutectic, microstruct. effect on fracture energy 0-7662
- Co-Ni, (10 at.%), magnetisation in high mag. field, Arrott-Noakes plot 0-54919
- Co-Ni, cryst. struct. and stacking fault influence on mag. props. (*Russian*) 0-25164
- Co-Ni, deformed and isochronally annealed, positron lifetimes, annihilation at dislocation trapped monovacancy 0-55221
- Co-Ni, magnetic anisotropy induced by mag. annealing and cold rolling, expt. 0-7695
- Co-Ni, magnetic anisotropy induced by mag. annealing and cold rolling, calc. 0-7696
- Co-Ni alloy, electrodeposition of cylindrical thin films 0-29886
- Co-Ni alloy, slip charact., and fatigue, FCC twinning and FCC to HCP martensite transform. effect 0-35182



## nickel alloys continued

- Co-Ni-Cr-Al-Ta, S-57 alloy hot corrosion, cyclic oxidation, depth of attack determinations 0-11837  
 Co-Ni-Cr-Nb, effect of Fe addition on precipitation behaviour 0-29962  
 Co-Ni-Cr-W-Fe, HA-188 alloy, hot corrosion, cyclic oxidation, depth of attack determinations 0-11837  
 Co-Ni-Fe-Si(B), amorphous ribbon, magnetostriction meas. 0-15778  
 Co-Ni-P, film, props. independent of mag. hysteretic and anhysteretic remanences (*French*) 0-2604  
 Co-Ni-P electrolytic layers, partial anhysteretic remanent magnetisation, additivity prop. (*French*) 0-44882  
 $(\text{Co}_{1-x}\text{Fe}_x\text{Ni}_{1-x})_{80}(\text{Si}_{1-x}\text{B}_x)_{20}$ , amorphous films, spin wave spectra 0-34777  
 $\text{Co}_{1-x}\text{M}_x\text{Si}$  (M=Fe, Ni), elec. field gradient, quadrupole splitting of  $^{59}\text{Co}$  0-29641  
 $\text{Co}_{20}\text{Ni}_{80}$ , oxidation study by Auger electron spectroscopy (*Ukrainian*) 0-7711  
 $\text{Co}_{1-x}\text{Ni}_x\text{Al}$ , Knight shift and mag. susceptibility study, electron struct. peculiarities (*Russian*) 0-15814  
 CoNiB, corrosion-resistant amorphous mag. thin films 0-54923  
 $\text{Co}_{50}\text{Ni}_{20}\text{Fe}_{10}\text{Si}_{12}\text{B}_{12}$ , amorphous, mag. props., effects mech. deform. 0-39840  
 $(\text{Co}_{1-x}\text{Ni}_x)_{75}(\text{PBAI})_{25}$ , amorphous, high-field magnetoresist. meas. 0-34423  
 Cr-Co-Ni hard film on Mo substrate for magnetic recording 0-2608  
 Cr-Ni, blistering after 40 keV He ion bombard. 0-39175  
 Cr-Ni, dil., mag. susceptibility, 77 to 400K (*Russian*) 0-50066  
 Cr-Ni, fusion reactor first wall materials, compatibility with impure He 0-32469  
 Cr-Ni, Inconel, first wall material thermal response 0-32456  
 Cr-Ni, Inconel 718, fusion reactor blanket materials for Argonne Experimental Power Reactor 0-32450  
 Cr-Ni alloy, 01Kh18N40M5, blistering under high  $\text{He}^+$  irradiation 0-29095  
 Cr-Ni steel, low-temperature behaviour, mechanical, electrical and magnetic props. (*German*) 0-3081  
 Cr-Ni VKh-4 alloy, deformation and fracture mechanism investigation (*Russian*) 0-11738  
 Cr-Ni-Fe, Inconel 625, plasma chamber material for power generating Tokamak, suitability tests 0-32449  
 Cr-Ni-Mo-Cr-C<sub>6</sub>, wear resistant coating prep. by laser beam melting, and props. 0-40607  
 CrC-Ni alloys, exam. of activated sintering 0-16241  
 $\text{Cr}_3\text{C}_2$ -Ni, friction and wear, 20-1000°C 0-30112  
 $\text{Cr}_3\text{C}_2$ -(Ni-Cr) sprayed coatings, for gas cooled reactor heat exchangers, factors affecting performance 0-40609  
 Cu-Al-Ni, duplex shape memory effect after nonuniform plastic deform. (*Russian*) 0-25759  
 Cu-Al-Ni, mixed powder compacts, Ni content influence in sintering behaviour (*Japanese*) 0-35130  
 Cu-Al-Ni, sintered, internal friction after heat treatment (*Japanese*) 0-11686  
 Cu-Al-Ni (13.8, 7.9 wt.%), cooling rates effect on internal friction (*Japanese*) 0-39217  
 Cu-Al-Ni (14, 8 wt.%),  $\gamma'$ -martensitic, sintered high damping 0-50577  
 Cu-Al-Ni (14.3, 4 wt.%),  $\omega$ -phase form. during quenching and ageing (*Russian*) 0-25686  
 Cu-Al-Ni-Fe system, corrosion behaviour in sea water 0-45421  
 Cu-Au, elastic modulus and internal friction during plastic deform., dislocation props. determ. 0-35244  
 Cu-Be-Ni-Ti-Mg bronze, alloying element influence on minimum thermo EMF, cold working (*Russian*) 0-34426  
 Cu-Ni, (10 at.%), magnetisation in high mag. field, Arrott-Noakes plot 0-54919  
 Cu-Ni, annealing effect on oxidation kinetics, reduction in vacancy level 0-50760  
 Cu-Ni, clean surface, surface segregation and growth process of altered layer (*Japanese*) 0-24720  
 Cu-Ni, cold worked solid solution, flow stress and activation volume 0-16393  
 Cu-Ni, diffusion of Ni, resistometric meas. 0-29222  
 Cu-Ni, elastic modulus and internal friction during plastic deform., dislocation props. determ. 0-35244  
 Cu-Ni, electrolytic plating 0-35425  
 Cu-Ni, microvoid form., gaseous impurity atom effects, positron annihilation study 0-49275  
 Cu-Ni, neutron irradiation, enhanced diffusion, elec. resist. meas. 0-6440  
 Cu-Ni, optical absorption and photoemission spectra 0-45216  
 Cu-Ni, parametric eval. of susceptibility to sulphide induced corrosion in sea water 0-16560  
 Cu-Ni, sintered, props. and degree of nonhomogeneity 0-20848  
 Cu-Ni, sputter-induced subsurface segregation, Auger electrons obs. 0-10757  
 Cu-Ni, sputtering yield, surface binding energies 0-50503  
 Cu-Ni, surface layer, effect of Ar<sup>+</sup> bombardment, AES and SIMS 0-25504  
 Cu-Ni (100), UPS spectra, direct transition and matrix element effects 0-55268  
 Cu-Ni (20 wt.%) contour plate, for relay appl. creep characts. obs., use of Larson-Miller method (*Japanese*) 0-55454  
 Cu-Ni (50 wt.%) alloys, estimation of sublimation energy of Cu atoms, evaporation rate and surface composition, AES meas. (*Japanese*) 0-49352  
 Cu-Ni alloys, artefacts in thin foil images 0-3056  
 Cu-Ni alloys 706 and 715, corrosion in flowing sea water, dissolved sulfide effect 0-35379  
 Cu-Ni sulphidised alloys, Ru and Os behaviour during carbonylation (*Russian*) 0-40584  
 Cu-Ni:polyethylene, surface, obs. at very low accel. voltage (200 V-1 kV) by SEM 0-10764  
 Cu-Ni-Al, review 0-7564  
 Cu-Ni-Be-(Al) (30,0.5,(0.2-2) wt.%), Al addition effect on grain boundary reaction (*Japanese*) 0-54254  
 Cu-Ni-Co, alloy pre-form prep. through reduction of sintered oxides 0-40284  
 Cu-Ni-Fe, alloy pre-form prep. through reduction of sintered oxides 0-40284  
 Cu-Ni-Fe, permanent magnet, temp. effect 0-34701  
 Cu-Ni-Fe, spinodally decomposable, densification using four different powder methods 0-40283  
 Cu-Ni-Nb-Al, correlation of  $\gamma'$  and  $\gamma''$  precipitates phase stability 0-25704

## nickel alloys continued

- Cu-Ni-Sn, liq. alloy, calc. and anal. of mixing enthalpies (*German*) 0-44325  
 Cu-Ni-Sn, liq. alloy, mixing enthalpies determ. using a SETARAM high temp. calorimeter (*German*) 0-44324  
 Cu-Ni-Sn (10, 6 wt.%), temp. depend of yield stress and work hardening 0-21026  
 Cu-Ni-Sn (4-15, 4-8 wt.%), strip strengthened by spinodal decomp., stress relax. in bending 0-7616  
 Cu-Ni-Sn (9, 6 wt.%), decomposition, initial stages, TEM study 0-2992  
 Cu-Ni-Sn spinodal substitute for Be-Cu alloy 0-35217  
 Cu-Ni-Zn, diffusion couples, zero-flux planes and flux reversals 0-15313  
 Cu-Ni-Zn system, tie lines in a two phase region 0-24404  
 Cu-Ni(10 (30) wt.%), seawater corrosion rate meas., electrochem. method validity 0-45426  
 $\text{Cu}_3\text{Ni}_{1-x}$ , bulk electronic structure, comparison of CPA and ATA techniques 0-44467  
 $\text{Cu}_3\text{Ni}_{1-x}$ , disordered alloy, muffin-tin model, electronic struct. and density of states calc. 0-29302  
 CuNiCr, IN838, heat treatment effect on fatigue and corrosion fatigue behaviour 0-20982  
 $\alpha$ -CuNiZn alloys, Zener-relaxation effect 0-3121  
 $\text{DyNi}_2$ , H<sub>2</sub> absorpt., Mossbauer study 0-44987  
 $\text{Dy}_2\text{Ni}_7$ , hyperfine interactions and cryst. field effects, Mossbauer spectra 0-2369  
 $\text{DyNi}_2\text{Si}_2$ , Mossbauer spectra 0-20558  
 $\text{Er}_6\text{Ga}_{15}\text{Ni}_{25}$ , struct. determ. by X-ray powder method (*Ukrainian*) 0-39001  
 (Fe, Co, Ni)<sub>3</sub>V, control of ordered struct. and ductility 0-21029  
 (Fe,Ni,Co)<sub>3</sub>V, long-range ordered alloy for fusion reactor appl. 0-32481  
 Fe-(Ni), cast, influence of Ni content on corrosion props. (*German*) 0-35370  
 Fe-Co-Ni-Al (35, 14.5, 7.2 wt.%), high-coercivity, substructure and texture change during bending and upsetting 0-21037  
 Fe-Cr-Ni, austenitic, self-diffusion and swelling under irradiation 0-39343  
 Fe-Cr-Ni, cold-rolled foils, dilatometric study 0-21033  
 Fe-Cr-Ni, corrosion by coal char at 871° and 982°C 0-3237  
 Fe-Cr-Ni, neutron irradiated, rel. between irradiation induced swelling and shear modulus 0-15157  
 Fe-Cr-Ni austenitic alloys, environment sensitive cracking, metallurgical variables effect 0-35391  
 Fe-Cr-Ni austenitic alloy, cold deformed,  $\alpha$ - $\gamma$  transition, calorimetric study (*Russian*) 0-55390  
 Fe-Cr-Ni melts, S solubility and solid soln. precipitation (*Russian*) 0-15251  
 Fe-Cu-Ni, austenite to ferrite+precipitate reaction, TEM/STEM study 0-3075  
 Fe-Cu-Ni, Ni effect on austenite decomposition 0-3048  
 Fe-Cu-Ni (2, 5 wt.%), interphase precipitation obs. in assoc. with Widmanstätten ferrite lateral growth 0-40365  
 Fe-Cu-Ni (2.2 wt.%), isothermally transformed, precipitate orientations 0-50640  
 Fe-Cu-Ni-Cr<sub>3</sub>C<sub>2</sub>-C based sintered friction material, wear, surface geometry and struct. effects 0-25875  
 Fe-Ni, (10 at.%), magnetisation in high mag. field, Arrott-Noakes plot 0-54919  
 Fe-Ni, BCC, cyclic cleavage crack growth model for fatigue 0-55519  
 Fe-Ni, electron state density and elec. resist. 0-39558  
 Fe-Ni, electronic struct., XPS study 0-29842  
 Fe-Ni, fatigue crack propag., low temp. 0-35311  
 Fe-Ni, ferromag., high-field susceptibility 0-7083  
 Fe-Ni, ion-implanted, depth profile and diffusion coeff. 0-54277  
 Fe-Ni, liq., thermodynamic characts. calc. (*Russian*) 0-15264  
 Fe-Ni, liq. alloy, electrochem. meas. of O, thermodynamic props. at 1873K 0-30244  
 Fe-Ni, ordered, tetragonal, identification with clear taenite in meteorites 0-8604  
 Fe-Ni, ordered phase, Llo superstruct., Mossbauer spectrum, Debye-Scherrer pattern from LL-chondrite 0-50241  
 Fe-Ni, solid and liq., paramag. susceptibility and electron struct., 800-1800°C (*Russian*) 0-25081  
 $\alpha$ -Fe-Ni, struct. after polymorphic transform. under press. (*Russian*) 0-29946  
 Fe-Ni, struct. defects effect on interdiffusion 0-15314  
 Fe-Ni, thermal expansion, ferromagnetic-paramagnetic transition (*Russian*) 0-54412  
 Fe-Ni, thermodynamic props., anomalous 0-39313  
 Fe-Ni, unlimited component solubility, intercrystallite internal adsorption (*Russian*) 0-39294  
 Fe-Ni (23 wt.%), struct., composition changes during  $\alpha$  to  $\gamma$  transform., martensite plastic deformation influence (*Russian*) 0-11642  
 Fe-Ni (24 wt.%), isothermal decomp., mag. determ. of austenite content 0-20886  
 Fe-Ni (29 wt.%), martensite nucleation at dislocations, elasticity model 0-55393  
 Fe-Ni (30 wt.%), Ni segregation singularities during dendrite-cellular solidification (*Russian*) 0-7542  
 Fe-Ni (31 wt.%), thermoelastic martensite obs. 0-3052  
 Fe-Ni alloy, anisotropic hyperfine interactions, Mossbauer spectra 0-15854  
 Fe-Ni alloy,  $\alpha$  to  $\gamma$  slow transformation mechanism, Ni content influence (*Russian*) 0-7569  
 Fe-Ni alloy, positron lifetime 0-2891  
 Fe-Ni alloy near crit. conc., Mossbauer  $\gamma$ -rays small angle scatt. 0-7217  
 Fe-Ni alloys, cold rolled, exam. of phase composition using Mossbauer spectroscopy 0-21204  
 Fe-Ni alloys, mag. state of austenite and  $\gamma$ - $\alpha$  transform. (*Russian*) 0-40350  
 Fe-Ni austenitic, effect of Al and Ti on relaxation resist. 0-20993  
 Fe-Ni base amorphous alloys, effect of annealing on Curie temp. 0-34632  
 Fe-Ni electrodeposit, sectional analyses and impurities (*Japanese*) 0-21350  
 Fe-Ni heterogeneous alloys, ferrite, martensite and austenite phase distrib., effect on mech. props. 0-45363  
 Fe-Ni ordered phase in meteorites, Mossbauer studies 0-41776  
 Fe-Ni ordering on annealing and electron irradi., mech. props. change (*Russian*) 0-29981  
 Fe-Ni single crystal, lattice strain induced by anisotropic distrib. of M<sub>2</sub> (*Japanese*) 0-35262



## nickel alloys continued

- Fe-Ni solid solution, deformation mechanism, softening phenomena, dislocation-solute atom interactions (*French*) 0-45344  
 Fe-Ni superstructure in metal particles in chondrites 0-12713  
 Fe-Ni-Al, liq. alloys, N solubility and AlN precipitation 0-11648  
 Fe-Ni-Al, magnetic anisotropy form. and struct. changes by annealing, Mossbauer obs. 0-39994  
 Fe-Ni-Al, type YuN14DK25BA, thermomag. treatment 0-16512  
 Fe-Ni-Al system, multiphase diffusion at 1000°C, diffusion structs. and props. 0-19995  
 Fe-Ni-Al system, multiphase diffusion at 1000°C, interdiffusion coeffs. for  $\beta$  and  $\gamma$  alloys 0-24684  
 Fe-Ni-Al-Co-Ti base alloys, highly coercive, phase comp., Mossbauer meas. 0-39996  
 Fe-Ni-Al-Cu (25, 14, 4 wt.%), alloy YuND4, effect of Ti addition on structure, mag. props. 0-15714  
 Fe-Ni-C, atomized, O/C ratio effect, particle size on annealing kinetics, physicochemical props. 0-20832  
 Fe-Ni-C, austenite cryst. volume effect on martensitic transformation temp. 0-40352  
 Fe-Ni-C, lattice parameters of cementite, annealing effect 0-29007  
 Fe-Ni-C, plastic deform. effect on austenite stabilisation (*Korean*) 0-21021  
 Fe-Ni-C (0.15, 0.05 wt.%) pore formation kinetics during crystallisation, FORTRAN study (*Russian*) 0-54158  
 Fe-Ni-C (23, 0.39 wt.%), austenitic or martensitic structs., corrosion faces anal. (*French*) 0-21181  
 Fe-Ni-C (25, 0.02 wt.%), thermal stabilisation role in martensitic transformations 0-25697  
 Fe-Ni-C (31, 0.1 wt.%), pre-deformation and temp. effect on transformation-deformation behaviour 0-3127  
 Fe-Ni-C (31, 0.28 wt.%), crossings of thin plate martensites, TEM obs. 0-25756  
 Fe-Ni-Co, texture form. after cold working and annealing (*German*) 0-3089  
 Fe-Ni-Co-C, substruct. effect in mech. props. 0-30086  
 Fe-Ni-Co-C (29.6, 10.7, 0.009 wt.%), thermal stabilisation role in martensitic transformations 0-25697  
 Fe-Ni-Co-Mo phase diagram and structure (*Russian*) 0-20899  
 Fe-Ni-Co-Mo-Ge alloy 40NKM, excess mag. noise after various thermomag. treatments (*Russian*) 0-29575  
 Fe-Ni-Co-Ti, shape memory effect after appl. of bending moment (*Russian*) 0-45305  
 Fe-Ni-Co-V, effects on fusion reactor neutronics performance 0-47705  
 Fe-Ni-Cr, austenitic with dispersed phases, oxidation 0-16540  
 Fe-Ni-Cr, high Ni content, intergranular corrosion, effect of Cr (*French*) 0-7708  
 Fe-Ni-Cr, pulsed HVEM irradiat., effect on microstruct. evolution 0-34053  
 Fe-Ni-Cr (20, 15 wt.%), single and dual ion irradiat., microstruct. studies 0-29077  
 Fe-Ni-Cr (25, 15 wt.%), mobile dislocation density in steady state creep, strain transient dip test, TEM exam. 0-7650  
 Fe-Ni-Cr (35, 15 wt.%), high temp. alloys, for HTR primary components, alloying additions for carburisation protection 0-5243  
 Fe-Ni-Cr base alloy, oxidation and hot corrosion (*Chinese*) 0-21149  
 Fe-Ni-Cr melts, O solubility (*Russian*) 0-15250  
 Fe-Ni-Cr system, absolute partial pressures and chem. activities of component metals 0-50600  
 Fe-Ni-Cr-Mo superalloy, mech. props.,  $\eta$ -phase form. effect (*Chinese*) 0-20925  
 Fe-Ni-Cr-P-B amorphous alloy, localized corrosion 0-16559  
 Fe-Ni-Cr-ZZ 0-5242  
 Fe-Ni-Cu-C-O powder, atomized, reduction and decarburizing annealing parameters 0-25603  
 Fe-Ni-Mn (20, 5 wt.%), surface martensite, crystallography and morphology 0-40354  
 Fe-Ni-Mn-C (5.9, 4.4, 0.48 wt.%) alloy, elastic moduli near martensitic transform. 0-7619  
 Fe-Ni-Mo (16.4, 8.1 wt.%), effect of substituting Mo by W during ageing 0-29991  
 Fe-Ni-P, segregation kinetics, theory, and temper brittleness 0-11649  
 Fe-Ni-P-B, amorphous ferromag. alloys, mag. struct., Mossbauer study 0-39746  
 Fe-Ni-P-B, amorphous paramag. alloys, hyperfine field distrib., Mossbauer study 0-39958  
 Fe-Ni-Sb-S, S/Sb surface site competition in segregation 0-40366  
 Fe-Ni-Si-B, amorphous paramag. alloys, hyperfine field distrib., Mossbauer study 0-39958  
 Fe-Ni-Si-Mn-Cr(Co-Mo), effect of prolonged aging on mag. props. 0-16513  
 Fe-Ni-Ta (-Co), alloys, Co effect on martensite ageing at 300-600°C (*Russian*) 0-20972  
 Fe-Ni-Ti-Al-Nb, struct. mechanism for inverse  $\alpha$ - $\gamma$  transform. (*Russian*) 0-40351  
 Fe-Ni(-Mn)(Cr)(V), concentration ferromag. antiferromag. phase transition and mag. state diagram. (*Russian*) 0-20401  
 Fe-Sb-Ni, dil., interactions and precip., Mossbauer study 0-39997  
 FeNi, itinerant electron model, spin wave stiffness calc. 0-34613  
 (Fe<sub>0.5</sub>Ni<sub>0.5</sub>)-Co, solid and liq., paramag. susceptibility and electron struct., 800-1800°C (*Russian*) 0-25081  
 Fe<sub>40</sub>Ni<sub>38</sub>Mo<sub>2</sub>B<sub>18</sub> amorphous alloys, compatibility of DC and AC mag. props. 0-34695  
 Fe<sub>x</sub>Ni<sub>1-x</sub> amorphous film, growth stress and structure factor, stabilisation by conduction electrons 0-38920  
 Fe<sub>x</sub>Ni<sub>1-x</sub> amorphous films, crystallisation, effect of codeposited O<sub>2</sub>, N<sub>2</sub> or Kr gases 0-10807  
 Fe<sub>1-x</sub>Ni<sub>x</sub>Al, Knight shift and mag. susceptibility study, electron struct. peculiarities (*Russian*) 0-15814  
 (Fe<sub>1-x</sub>Ni<sub>x</sub>)<sub>75</sub>B<sub>25</sub>, amorphous and cryst., short range order, Mossbauer study 0-39961  
 (Fe<sub>100-x</sub>Ni<sub>x</sub>)<sub>100-y</sub>B<sub>y</sub>, metallic glass, embrittlement and crystn. 0-7685  
 Fe<sub>40</sub>Ni<sub>28</sub>B<sub>20</sub>, metallic glassy ribbon, casting conditions (*Japanese*) 0-55386  
 Fe<sub>40</sub>Ni<sub>40</sub>B<sub>20</sub>, amorphous, high-field magnetisation curve, spin wave spectrum and microstructural inhomogeneities 0-15702  
 Fe<sub>40</sub>Ni<sub>40</sub>B<sub>20</sub>, amorphous, casting conditions effect on mag. props. (*Japanese*) 0-34698  
 Fe<sub>40</sub>Ni<sub>40</sub>B<sub>20</sub>, amorphous, mag. props., effects mech. deform. 0-39840  
 Fe<sub>40</sub>Ni<sub>40</sub>B<sub>20</sub> glass, <sup>10</sup>B self-diffusion, meas. by SIMS 0-49406  
 Fe<sub>40</sub>Ni<sub>40</sub>B<sub>20</sub>, metallic glass, low temp. specific heat, metalloid effects 0-34654

## nickel alloys continued

- Fe<sub>40</sub>Ni<sub>40</sub>B<sub>20</sub>, molten, jet streaming, planar and cylindrical, instabilities rel. to glassy alloy casting 0-35129  
 (Fe<sub>x</sub>Ni<sub>1-x</sub>)<sub>80</sub>B<sub>20</sub>, amorphous, Mossbauer spectra, mag. props. 0-15843  
 Fe<sub>x</sub>Ni<sub>100-x</sub>B<sub>20</sub>, quenched ferromag. ribbon, Brillouin spectra 0-2776  
 Fe<sub>32</sub>Ni<sub>36</sub>Cr<sub>14</sub>P<sub>12</sub>B<sub>6</sub> glass, thermal expansion, glass transform. and crystn. temps. 0-2183  
 Fe<sub>32</sub>Ni<sub>36</sub>Cr<sub>14</sub>P<sub>12</sub>B<sub>6</sub>, metallic glass, high-resolution XPS study, electronic state struct. 0-29846  
 Fe<sub>40</sub>Ni<sub>38</sub>Mo<sub>2</sub>B<sub>18</sub>, metallic glass, mag. and transport props. 0-39752  
 Fe<sub>40</sub>Ni<sub>38</sub>Mo<sub>2</sub>B<sub>18</sub> ribbon, magnetic characterisation 0-34680  
 (Fe<sub>0.04</sub>Ni<sub>0.96</sub>)<sub>80</sub>P<sub>10</sub>B<sub>10</sub>, amorphous magnetisation, field and temp. depend. 0-39755  
 Fe<sub>73</sub>Ni<sub>53</sub>P<sub>14</sub>B<sub>6</sub>, amorphous, Hall resist. and mag. props., short range order effects 0-34422  
 Fe<sub>40</sub>Ni<sub>40</sub>P<sub>14</sub>B<sub>6</sub>, amorphous, strip domains, anisotropy const. effects 0-29571  
 Fe<sub>40</sub>Ni<sub>40</sub>P<sub>14</sub>B<sub>6</sub>, amorphous ribbon, influence of torsion on mag. props. 0-7138  
 Fe<sub>40</sub>Ni<sub>40</sub>P<sub>14</sub>B<sub>6</sub>, amorphous, transverse magnetoresist., stress effect 0-15501  
 Fe<sub>40</sub>Ni<sub>40</sub>P<sub>14</sub>B<sub>6</sub>, amorphous, mag. props., effects mech. deform. 0-39840  
 Fe<sub>40</sub>Ni<sub>40</sub>P<sub>14</sub>B<sub>6</sub> glass, thermal expansion, glass transform. and crystn. temps. 0-2183  
 Fe<sub>40</sub>Ni<sub>40</sub>P<sub>14</sub>B<sub>6</sub>, metallic glass, cryst., isothermal annealing behaviour 0-6367  
 Fe<sub>40</sub>Ni<sub>40</sub>P<sub>14</sub>B<sub>6</sub> metallic glass, ferromag. reson., spin waves, thermal ageing and long-range order effects 0-25214  
 Fe<sub>40</sub>Ni<sub>40</sub>P<sub>14</sub>B<sub>6</sub>, metallic glass, high-resolution XPS study, electronic state struct. 0-29846  
 Fe<sub>40</sub>Ni<sub>40</sub>P<sub>14</sub>B<sub>6</sub> metallic glass, isothermal viscosity and crystn. 0-49395  
 Fe<sub>40</sub>Ni<sub>40</sub>P<sub>14</sub>B<sub>6</sub>, amorphous, kinetics of induced mag. directional order 0-44824  
 Fe<sub>44</sub>Ni<sub>40</sub>P<sub>14</sub>B<sub>6</sub>, homogeneous deformation effect on crystn. and Curie temp. 0-21045  
 Fe<sub>x</sub>Ni<sub>1-x</sub>P<sub>14</sub>B<sub>6</sub>, amorphous, spin-glass regime, magnetoresist. meas. 0-34418  
 (Fe<sub>0.100-x</sub>Ni<sub>x</sub>)<sub>80</sub>P<sub>10</sub>B<sub>10</sub>, amorphous, elec. resist., 2 to 300K, composition depend. 0-44562  
 Fe<sub>x</sub>Ni<sub>80-x</sub>P<sub>14</sub>B<sub>6</sub> (x=0, 20, 40, 60, 80), metallic glass, low temp. sp. ht. 0-2588  
 (Fe<sub>1-x</sub>Ni<sub>x</sub>)<sub>75</sub>(PBAI)<sub>25</sub>, amorphous, high-field magnetoresist. meas. 0-34423  
 (Fe<sub>x</sub>Ni<sub>1-x</sub>)<sub>75</sub>P<sub>14</sub>B<sub>6</sub>Al<sub>3</sub>, magnetisation temp. depend., spin wave theory 0-44927  
 (Fe<sub>1-x</sub>Ni<sub>x</sub>)<sub>77</sub>Si<sub>10</sub>B<sub>13</sub>, amorphous magnetic alloys, density meas. 0-1934  
 (Fe<sub>1-x</sub>Ni<sub>x</sub>)<sub>77</sub>Si<sub>10</sub>B<sub>13</sub> amorphous alloy system, saturation mag. moment, Curie temp., mag. susceptibility 0-39753  
 FeNiTe alloys, disordered, polycrystalline, elec. resist., temp. depend. 0-49692  
 GCFR fuel pin claddings, oxidation behaviour in He environment 0-16594  
 Ga-Ni-R, (R=Dy, Ho, Er, Tm, Lu), struct. determ. by X-ray powder method (*Ukrainian*) 0-39001  
 Gd-Ni, amorphous, Mossbauer spectra 0-25262  
 Gd(Co,Ni)<sub>1-x</sub>, Mossbauer spectra, mag. props. 0-20563  
 (Gd<sub>1-x</sub>R<sub>x</sub>)(Co<sub>1-x</sub>Ni<sub>x</sub>)<sub>5</sub>, origin of hyperfine fields acting on Gd, Mossbauer study 0-44967  
 Ge-Ni, amorphous, struct., EXAFS study 0-49110  
 Ge-Ni, liq., enthalpy of formation meas. 0-30267  
 GraNi-rare earth intermetallics, struct. by X-ray powder method (*Ukrainian*) 0-10529  
 H assisted cracking, mechanisms, review 0-50721  
 Hf-Ni, amorphous, formation, decomposition and elec. transport props. 0-20143  
 Hf-Ni-H, catalytic activity, exam. by conversion of toluene, and bicyclic aromatic hydrocarbons 0-30276  
 Hf-Ni-H, catalytic props. 0-30274  
 Hf-Ni;Ga, alloys, phase diagrams and cryst. struct. (*Russian*) 0-25658  
 Ho-Ga-Ni (60, 30 wt.%) cryst. struct., isostructural compound structural study 0-33930  
 HoNi<sub>5</sub>, ferromag., magnetisation and paramag. susceptibility 0-25082  
 In-Ni, liq., spreading kinetics on Cu surface 0-10742  
 La-Ni-H, catalytic props. in hydrogenation of propylene, dehydrogenation of propane 0-30277  
 La-Ni(-Ce)(-Co), H absorption for storage appls. 0-45790  
 LaNi<sub>5</sub>, crystal field investigation from inelastic slow neutron scatt. expts. 0-39538  
 LaNi<sub>5</sub>, H storage using metal hydrides, self restoring of active surface 0-45815  
 LaNi<sub>5</sub>, metal hydrides, numerical physical property data for H storage 0-40929  
 LaNi<sub>5</sub>, surface segregation, influence of O<sub>2</sub>, H<sub>2</sub>, H<sub>2</sub>O, SO<sub>2</sub> (*German*) 0-51008  
 LaNi<sub>5</sub> type ternary alloys, H<sub>2</sub> sorption/desorption reaction kinetics 0-45813  
 LaNi<sub>5</sub>/Ti-Zr-Cr-Mn hydriding alloy mixtures for H storage 0-45788  
 LaNi<sub>5</sub>-Gd, dil., ESR spectra, fine struct. and random stresses 0-25203  
 LaNi<sub>5</sub>-H, with small Cr additions, NMR parameters (*Russian*) 0-29637  
 LaNi<sub>5</sub>-H system, rel. partial absorption (desorption) enthalpies 0-50881  
 LaNi<sub>5</sub>-type ternary alloys, H<sub>2</sub> absorption and desorption kinetics 0-55932  
 LaNi<sub>5-y</sub>Al<sub>y</sub> alloys and related hydrides, thermodynamic and struct. props. for H<sub>2</sub> storage appl. 0-16847  
 LaNi<sub>5-y</sub>Al<sub>y</sub> alloys and their hydrides, for H storage appls. 0-45816  
 $\beta$ -LaNi<sub>5-y</sub>Al<sub>y</sub> hydrides, H diffusion, NMR studies 0-15298  
 LaNi<sub>5</sub>H<sub>6</sub>, effect of synthesis, heat treatment, on comp. stability, chemical props. 0-29985  
 LaNi<sub>5</sub>H<sub>6</sub>, H storage material, H diffusion, neutron diffr. obs. 0-51013  
 LaNi<sub>5</sub>H<sub>2-3.0</sub>, H diffusion coeff., neutron scatt. obs. 0-24643  
 La<sub>2</sub>Ni<sub>2</sub>H<sub>7</sub>, thermokinetics of H evolution 0-30593  
 Mg-Mg<sub>2</sub>Ni eutectic alloy and Mg<sub>2</sub>Ni, catalytic effect in hydrogenation, surface analysis 0-30283  
 Mg-Ni-S, electroforming, mech. props. rel. to heat treatment 0-35133  
 Mg-Ni-W-Co-Al-Cr alloy KhN56VMKYu, Al effect on excess Mg phase 0-29926  
 Mg<sub>2</sub> Ni metal hydrides, numerical physical property data for H storage 0-40929  
 MgCu<sub>2-x</sub>Zn<sub>x</sub>, X-ray and neutron diffr. investigation of Laves phases of MgCu<sub>2</sub>-type (*German*) 0-15050  
 MgNi<sub>2-x</sub>Zn<sub>x</sub>, X-ray and neutron diffr. investigation of Laves phases of MgCu<sub>2</sub>-type (*German*) 0-15050



## nickel alloys continued

- MgO/Ni-Cr (80, 20 wt.%) cermets, sintered, elec. resist. temp. effect 0-3206
- $\gamma$ -Mn-Ni (15 at.%), antiferromag. defect scatt., neutron polarisation anal. 0-50056
- Mo-B-Ni, microalloying influence on mechanical props., cold rolling, plasticity (*Russian*) 0-40502
- Mo-Hf-C-Ni, electrochemical phase composition anal., precip. of HfC phase (*Russian*) 0-20901
- Mo-Ti-C-Ni phase equilibria, subsolidus temp., metallographic and X-ray anal. 0-16278
- Monel, Norton-Bailey parameters, from creep rupture data 0-30098
- Nb-Ge-Ni, phase composition and superconducting props., influence of Ni (*Russian*) 0-20898
- Nb-Ni, cathodic polarization in conc. KOH soln. 0-16591
- Nb-Ni glasses, struct. factor temp. depend. 0-28920
- Nb<sub>0.4</sub>Ni<sub>0.6</sub>, amorphous, pair distrib. function, temp. depend., rel. to glass transition 0-24368
- Nd-Ni-Al, isothermal section, 600°C, X-ray struct. anal. (*Ukrainian*) 0-33929
- Ni alloy Ehl698, new etchant for revealing microstructure 0-25934
- Ni/Cr-Fe-C, Inconel, dislocation intersection and solution strengthening, effect of solute on obstacle profiles 0-7590
- Ni-Ag alloy, metallographic struct. and formability (*German, English*) 0-30201
- Ni-Al, band struct. and density of states, KKR method and X-ray meas. 0-10863
- $\beta_2$ -Ni-Al, elastic consts., supersaturated thermal vacancy effects 0-54298
- Ni-Al, electronic, mag., and cohesive props. 0-44491
- Ni-Al, liquid, diffusion coeff. differences, rotating-disc determ. 0-39330
- Ni-Al, neutron irradiated, rel. between irradiation induced swelling and shear modulus 0-15157
- $\beta'$ -Ni-Al, precipitation studies 0-3067
- Ni-Al, spinodal decomposition, atom probe field ion microscopy study 0-3028
- Ni-Al, transition metal group VIII aluminide, NMR near equiatomic composition (*Russian*) 0-20479
- $\beta$ -Ni-Al, X-ray absorpt. spectra meas., Fermi level location 0-35005
- Ni-Al alloy, solid phase reaction kinetic parameter calcs., defect formation (*Russian*) 0-54399
- Ni-Al coating, low temp. hot corrosion, Na<sub>2</sub>SO<sub>4</sub>-induced, mechanism, burner rig tests 0-40610
- Ni-Al films, evaporated, grain size and microstruct. 0-15423
- Ni-Al spraying powders, alumina and aluminide formation 0-25920
- Ni-Al system, Mossbauer spectroscopy investigation (*Russian*) 0-20523
- Ni-Al system, ordering and instability of  $\beta$  phase near martensitic transform. (*Russian*) 0-45304
- Ni-Al thermally reactive powder, particle heating dynamics during plasma deposition 0-16179
- Ni-Al<sub>2</sub>O<sub>3</sub>, dispersion strengthened, thick vacuum condensate, control of struct. and mech. props. 0-16324
- Ni-Al-Cr<sub>3</sub>C<sub>2</sub>, eutectic, directionally solidified, high-temp. oxidation 0-50775
- Ni-Al-Cr<sub>3</sub>C<sub>2</sub>, eutectic, Al<sub>2</sub>O<sub>3</sub> coatings for oxidation resist. 0-50776
- Ni-Al-Ti ferromagnetic non-homogeneous alloy, composition determination by Curie temp. meas. 0-11196
- Ni-Al-Ti-(W) (Cr) (Co) (Mo) (Ta) (Nb), heat resist., solidification range 0-35177
- Ni-Al-Ti(Nb), heat-resisting dispersion-hardening alloys, props. and struct.,  $\gamma$ -phase comp. influence (*Russian*) 0-20943
- Ni-Au, oxidation in air, 50-150°C, film growth obs. using AES and contact resist. 0-3242
- Ni-b, hyperfine interactions from 6 to 730K, <sup>12</sup>B NMR 0-29372
- Ni-B amorphous films, electronic transport and crystn. activation energies (*French*) 0-6807
- Ni-base superalloy, effects of grain boundary carbides on creep and back stress 0-3130
- Ni-C, graphite nucleation on surface (*Russian*) 0-40360
- Ni-C-Ce, overmodification (*Russian*) 0-40432
- Ni-C-W-Cr-(Mo), Vickers hardness and crystallisation temp. 0-16361
- Ni-Ce-Fe-Ti (77, 20, 4, 2.5 wt.%), long-term strength in H at high pressure 0-55485
- Ni-Co, dislocation intersection and solution strengthening, effect of solute on obstacle profiles 0-7590
- Ni-Co, solid and liq., paramag. susceptibility and electron struct., 800-1800°C (*Russian*) 0-25081
- Ni-Co (25 wt.%), single crystals, mag. annealing effect on magnetostriction and magnetisation (*Japanese*) 0-34744
- Ni-Co (566 wt.%), internal stresses during creep 0-3142
- Ni-Co amorphous alloys, magnetostriction 0-34738
- Ni-Co films, electron-beam evaporated, magnetoresist. anisotropy, deposition temp. effect 0-34528
- Ni-Co thin films, spin-wave reson. obs., exchange stiffness const. 0-44924
- Ni-Co-Cr superalloy, powder produced, necklace struct. development 0-40395
- Ni-Co-Cr system, heats of formation and of transformation 0-50599
- Ni-Co-Cr-Al-Ti-Mo superalloy IN738, caskings porosity removal using hydrostatic press. sintering 0-55322
- Ni-Co-Cr-Al-Y, plasma-arc-sprayed, metallurgical characts. and oxidation behaviour 0-40618
- Ni-Co-Cr-Al-Y protective coating for combustion turbines, hot corrosion evaluation 0-40608
- Ni-Co-H, solid soln., Curie points and spontaneous magnetisation behaviour 0-50093
- Ni-Co-Mo-Ti, maraging, electron diffr. obs. of second phase (*Chinese*) 0-11655
- Ni-Cr, creep-fatigue failures, damage concept appl. 0-40535
- Ni-Cr, deformed, struct. form. during annealing, Ni<sub>3</sub>Al type ordered phase precipitation (*Russian*) 0-45325
- Ni-Cr, phosphidation in P vapour, 700°C, phosphide layer struct. and kinetics 0-25906
- Ni-Cr, solid soln., lattice parameter meas. rel. to conc. and temp. depend. (*Czech*) 0-28949
- Ni-Cr, surface oxide characterisation by Raman spectroscopy 0-50308
- Ni-Cr (0-35 at.%), neutron irradi. at 25K, damage, elec. resist. obs. (*French*) 0-54286
- Ni-Cr (20 wt.%), high temp. frictional characts. 0-21118
- Ni-Cr (20 wt.%), Norton-Bailey parameters, from creep rupture data 0-30098
- Ni-Cr (20 wt.%) alloy LNKH, room-temp. friction characts. 0-25874

## nickel alloys continued

- Ni-Cr alloy, Kh20N80, inclusions and plasticity, crystn. conditions influence (*Russian*) 0-20923
- Ni-Cr type alloys, Co surface pretreatment to attain pore-free aluminised coatings 0-40612
- Ni-Cr/ThO<sub>2</sub>, adhesive energy, meas. techniques 0-50803
- Ni-Cr/ZrO<sub>2</sub>-Y<sub>2</sub>O<sub>3</sub> sputtered multilayered ceramic/metal coatings, props. 0-40620
- Ni-Cr-Al-ThO<sub>2</sub>, hot corrosion, cyclic oxidation depth of attack determinations 0-11837
- Ni-Cr-Al-Y/ZrO<sub>2</sub>-Y<sub>2</sub>O<sub>3</sub>, NASA two-layer thermal barrier coating, for gas turbine engines, test results 0-40617
- Ni-Cr-Al-Y<sub>2</sub>O<sub>3</sub> superalloy, recrystn. and texture development 0-16328
- Ni-Cr-Co, Mo, Ti, Y and R alloying additions influence on oxidation (*Russian*) 0-40587
- Ni-Cr-Co-Mo alloy MP35N, accelerated H<sub>2</sub> charging in aq. H<sub>2</sub>SO<sub>4</sub> at 0.2% yield stress 0-30144
- Ni-Cr-Co-Mo-Al, IN-67 alloy, hot corrosion, cyclic oxidation, depth of attack determinations 0-11837
- Ni-Cr-Co-Ti, superalloy sintering thermochemical surface treatment 0-25617
- Ni-Cr-Fe, Inconel, effects of heat treatment on surface segregation, Auger spectroscopic exam. 0-7602
- Ni-Cr-Fe-Si-B wear-resist. and corrosion-resist. coatings by furnace melting 0-35428
- Ni-Cr-Fe-W, type EHI868, loading history effect on resist. to cyclic elastoplastic strain 0-16398
- Ni-Cr-Mn-Fe-Nb (20,3,3,2.5 wt.%), short-range order effects on tensile behaviour 0-25793
- Ni-Cr-Mo (74, 20, 4 wt.%), long-term strength in H at high pressure 0-55485
- Ni-Cr-Mo-Mn alloy 02KhN40MB, corrosion-resist, heat-resist., phys. and mech. props. 0-35411
- Ni-Cr-Mo-Ti (19,11,3 wt.%) for TiC reactively sputtered coatings, adherence, XPES and wear study 0-25565
- Ni-Cr-Ti, type EHI698, loading history effect on resist. to cyclic elastoplastic strain 0-16398
- Ni-Cr-Ti(Al), effect of ultrasound on crystallisation, dendritic structure, and plasticity (*Russian*) 0-11637
- Ni-Cr-W (20, 10 to 40 wt.%), phase composition, struct. and props. 0-21034
- Ni-Cr-W-Mo-Al-Ti (15,6,3,2,2, wt.%), wrought, Si effect on transition brittleness (*Chinese*) 0-55491
- Ni-Cr-ZZ 0-5242
- Ni-Cr-(Mo), creep parameters, high temp. 0-50685
- Ni-Cu, ferromagnetic, Hall effect, anomalous, rel. to scatt. processes 0-44572
- Ni-Cu, liq., activity meas. of O<sub>2</sub> by EMF method (*Japanese*) 0-54408
- Ni-Cu, Ni-rich, temp. depend. resist. 0-10943
- Ni-Cu, short-range atomic clustering, residual resist. meas. 0-29386
- Ni-Cu, sputtering rate, radiation-induced segregation and preferential sputtering effects, kinetic model 0-40199
- Ni-Cu alloy, surface comp. and catalysis 0-54489
- Ni-Cu film, deposited by cylindrical magnetron sputtering, internal stresses 0-24773
- Ni-Fe, 79 NM alloy, gamma and neutron influence on mag. susceptibility comparative study (*Russian*) 0-39751
- Ni-Fe, alloy pre-form prep. through reduction of sintered oxides 0-40284
- Ni-Fe, dil., temp. depend. of Mossbauer absorpt. near Curie point (*French*) 0-11305
- Ni-Fe, magnetostrictive vibr. meas., appl. of laser interferometric technique 0-37059
- Ni-Fe alloy, continuous electrodeposition 0-16208
- Ni-Fe alloy, Ni base cathodes, powder metallurgy technique 0-29903
- Ni-Fe alloy film electrodeposition, modification of soln. composition 0-16209
- Ni-Fe conductor, EM pulse shielding, magnetisation curves 0-28143
- Ni-Fe film, electrodeposition, role of buffers and anions 0-25583
- Ni-Fe film, low field domain wall mobility 0-25167
- Ni-Fe films, magnetisation reversal in narrow strips, TEM study 0-34720
- Ni-Fe polycrystalline film cross-tie memory for shipborne radar/sonar 0-42204
- Ni-Fe-Cr, extraordinary Hall effect, elec. and mag. meas. at 77 and 300K 0-34421
- Ni-Fe-Cr base superalloy, addition effect on mech. props. (*Chinese*) 0-20998
- Ni-Fe-Cr-Nb-Ta-Mo alloy, fatigue crack growth, stress ratio and hold-time effects 0-40531
- Ni-Fe-Cu, Mu-metal, mag. aftereffects, dynamic neutron depolarisation study 0-50147
- Ni-Fe-Mo, K-effect, Mossbauer study 0-39998
- Ni-Fe-Nb (Mo), magnetic alloy, TEM and X-ray obs. (*Chinese*) 0-24401
- Ni-Fe-Nb-Al-(Mo), wear resisting mag. head material, mag. props. and struct. 0-35350
- Ni-Fe-Pd thin films, mag., surface and corrosion props. 0-34707
- Ni-Fe-Rh films, mag. and corrosion props. 0-34702
- Ni-Ge, defect-solute interactions and radiation-induced segregation 0-25705
- Ni-HfO<sub>2</sub> (2.14 wt.%), dispersion hardened, HfO<sub>2</sub> particle size effect on struct. and mech. props. (*Russian*) 0-20944
- Ni-In, ion-implanted, impurity defect interaction and diffusion, Rutherford backscatter and TDPAC expts. 0-34039
- Ni-In, protective coating on Kovar, vacuum seal for borosilicate glass appl. (*Italian*) 0-40621
- Ni-Mn, hydrogenation kinetics, magnetisation, interstitial H influence 0-35528
- Ni-Mn, mag. moment and asphericity of spin density distrib., polarised neutron scatt. obs. 0-44813
- Ni-Mn (up to 32 at.%), Curie temp., press. depend., using press. cell developed for meas. with cubic-anvil press 0-13109
- Ni-Mn-Al-Si-Co, AluMel, Etingshausen-Nernst coeff. and transport props. from 200 to 473K 0-44573
- Ni-Mo, sputtering rate, radiation-induced segregation and preferential sputtering effects, kinetic model 0-40199
- Ni-Mo (10.7 wt.%) alloy, ordering energy calc. 0-10522
- Ni-Mo (20.8 wt.%), order, heat treatment effects 0-40406
- Ni-Mo-Cr-(Cr)(W), Vickers hardness and crystallisation temp. 0-16361
- Ni-Mo-MoS<sub>2</sub> composite, Mo alloying effect on physicochem. interactions 0-7692
- Ni-Nb alloys, oxidation at high temp., high energy ion backscattering anal. (*Japanese*) 0-35405



## nickel alloys continued

- Ni-Nb-Al (25, 2.5 wt.%), directionally solidified  $\gamma/\gamma'$ - $\delta$  eutectic, growth conditions on struct. 0-11639
- Ni-Nichrome, MOM diode, breakdown effect in visible and near-IR regions 0-6999
- Ni-P, amorphous electrodeposited alloys, phase-separation (*Japanese*) 0-54140
- Ni-P, coating onto  $\text{BeFe}_{12}\text{O}_{19}$  and  $\text{SrFe}_{12}\text{O}_{19}$  0-25593
- Ni-Pb, conc. profiles across solid-liq. interfaces 0-55382
- Ni-Pd, anodic behaviour, potentiodynamic current density and impedance potential meas. (*German*) 0-25925
- Ni-Pd, mag. form. factor, polarised neutron diffr. meas. 0-29525
- Ni-Pd surfaces, electrochem. passive film form. and comp. determ. by SEM, SIMS, XPS 0-39401
- Ni-Pd-H, film, struct. and phases formed, when Ni, Pd are sputtered in H 0-29289
- Ni-Pt, magnetic moment distrib., diffuse neutron scatt. meas. 0-34593
- Ni-Pt, short-range order parameter calc. in pseudopot. approx. (*Russian*) 0-49183
- Ni-Pt disordered alloy, off-diagonal, T-matrix itinerant electron ferromagnetism calcs. 0-25067
- Ni-Ru peritectic alloys, rapidly cooled, crystn. peculiarities (*Russian*) 0-20922
- Ni-S, dil. alloy, AES of grain boundaries (*French*) 0-50477
- Ni-Si, defect-solute interactions and radiation-induced segregation 0-25705
- Ni-Si, proton irradi.,  $\gamma'$  precipitation, early stages 0-34096
- Ni-Si (up to 3.7 wt.%), supercooled, struct. refinement mech. (*Russian*) 0-20975
- Ni-Si liquid alloys, thermodynamic props., enthalpy of mixing (*Russian*) 0-34207
- Ni-Si-B powder, oxidation at 850°C, SEM, ESCA, and elec. cond. meas. 0-7717
- Ni-SiC coating, heat treated, as plated, electrochemical study of corrosive wear 0-16536
- Ni-Ta-Al system, phase equilibria and diagram, electron probe, X-ray diffr. anal. 0-29927
- Ni-Te, liq., struct. and elec. props. 0-49083
- Ni-ThO<sub>2</sub>, dispersion strengthened, high temperature cyclic deformation 0-16430
- Ni-Ti, mag. moment distrib. and environmental effects around Ti impurity 0-7092
- Ni-Ti, martensitic phase transformation effect on low cycle fatigue behaviour 0-7666
- Ni-Ti, Ni-rich, temp. depend. resist. 0-10943
- Ni-Ti, Nitinol memory material heat engine, comment on efficiency 0-3529
- Ni-Ti, Nitinol memory material heat engine, reply to comments on efficiency 0-3530
- Ni-Ti, shape memory effect, criteria for efficiency assessment (*Russian*) 0-21015
- Ni-Ti, structural instability, deform. effects on electron energy spectrum 0-39284
- Ni-Ti (1.6, 7.64 wt.%), monophasic high temp. scaling, metallography study 0-21159
- Ni-Ti (3 wt.%), C precipitation 0-29958
- Ni-Ti (9.6 wt.%), mag. study on phase decomposition (*Japanese*) 0-15758
- Ni-Ti shape memory alloy processing and medical applications (*German*) 0-17203
- Ni-Ti shape memory alloy trigger for space satellite boom latch and release mechanism 0-7575
- Ni-Ti(Fe), neutron irradiated, thermally activated deform. 0-6438
- Ni-V, solid and liq., mag. susceptibility and electronic struct. 0-39738
- Ni-V system, interdiffusion, kinetics of phase growth (*Russian*) 0-29230
- Ni-W sintered powder pressings, intermetallic phases (*Russian*) 0-55349
- Ni-W-C(Nb) system,  $\gamma$  to ( $\gamma$ +W) phase boundary calcs. using Wigner method (*Russian*) 0-54346
- $\alpha$ -Ni-Zn, solid soln. diffusion annealing effect (*Japanese*) 0-34255
- Ni-Zn-Mn-Fe spinel, crystn. from soln. in melt 0-2945
- Ni-ZrO<sub>2</sub>, dispersion strengthened, thick vacuum condensate, control of struct. and mech. props. 0-16324
- Ni-ZrO<sub>2</sub>, electron-beam-evaporated condensate, cold deform. and annealing effects on microstruct. 0-16331
- Ni<sub>0.95</sub>S Fe, spin glass, spin flop in exchange field 0-34640
- Ni<sub>2</sub> (Al, Nb) single crystals, orientation and temp. depend. of yield stress 0-25791
- $\beta$ -NiAl B2 phase, mag. aftereffect 0-34700
- NiAl, kinetics, Ni<sub>2</sub>Al<sub>3</sub> layers growth by cementation (*French*) 0-35127
- $\beta$ -NiAl, self consistent embedded cluster model for Fe, Co, Ni mag. impurities 0-2549
- NiAl, thermal defects, dilatometric study (*Japanese*) 0-15092
- Ni<sub>2</sub>Al<sub>3</sub> layers, growth on Ni, NiAl substrates by cementation, kinetics, interdiffusion (*French*) 0-35127
- Ni<sub>3</sub>Al, itinerant ferromag., Fermi surface and single particle excitations 0-34350
- Ni<sub>3</sub>Al-B, L1<sub>2</sub> type intermetallic cpd. room temp. ductility improvement by B addition (*Japanese*) 0-35263
- Ni<sub>3</sub>Al-Ni<sub>3</sub>Nb, eutectic, temp. and thermal cycling influence on oxidation 0-45417
- Ni<sub>3</sub>Al-Ni<sub>3</sub>Nb, eutectic alloy, crack development, failure energy capacity (*Russian*) 0-40480
- Ni<sub>3</sub>Al-Ni<sub>3</sub>Nb eutectic, directionally solidified, high-temp. oxidation mechanism 0-16544
- Ni<sub>3</sub>Al-Ti(Cr)(Fe)(Zr)(Mo)(W), powder, X-ray spectral analysis exam. 0-16239
- Ni<sub>1-x</sub>Au<sub>x</sub>-Co, dil., hyperfine field and isomer shift, precip. process, Mossbauer expts. 0-25267
- Ni<sub>1-x</sub>Au<sub>x</sub>-Co, dil., Mossbauer effect, mag. hyperfine field 0-20528
- Ni<sub>6</sub>B<sub>34</sub>, morphological, structural and phys. props. (*French*) 0-44444
- Ni<sub>3</sub>C films, form. by carburisation, characterisation 0-34337
- NiCo, itinerant electron model, spin wave stiffness const. calc. 0-34613
- (NiCo)-Cr-Al-Y/ZrO<sub>2</sub>-Y<sub>2</sub>O<sub>3</sub> plasma sprayed ceramic coating for turbine engine components 0-40616
- (Ni<sub>3</sub>Co<sub>1-x</sub>)<sub>2</sub>Ge single crystals, L1<sub>2</sub> struct., cross-slip 0-40459
- NiCoPd, anodic dissolution, SFE effect (*German*) 0-25924
- NiCr, sputtered, detection by electron probe microanal., substrate depend. 0-35607
- NiCr-Ge, amorphous, junction, current-voltage charact. 0-44725
- Ni<sub>1-x</sub>Cu<sub>x</sub>+CO, Ni(CO)<sub>4</sub> form. activation energy, mag. phase depend. 0-3409

## nickel alloys continued

- (Ni<sub>1-x</sub>Cu<sub>x</sub>)Ti, martensitic, shape memory effect kinetics and thermodynamics 0-3021
- Ni<sub>3</sub>(Fe,M), M=Cr,Mo,W, elec. resist., temp. depend. anomalies, Hall and Nernst-Ettinghausen effects (*Russian*) 0-10942
- NiFe disordered alloys, Mossbauer spectra, hyperfine mag. field distrib., Curie temp. 0-7198
- NiFe, itinerant electron model, spin wave stiffness const. calc. 0-34613
- NiFe, magnetic surface anisotropy of transition metals, model calc. 0-34625
- NiFe stripes, mag. props. and domain struct. 0-44886
- Ni<sub>0.83</sub>Fe<sub>0.17</sub> films, reson. oscills. of mag. domain walls and Bloch lines, stroboscopic electron microscopy 0-54931
- Ni<sub>3</sub>Fe disordered alloys, Mossbauer spectra, hyperfine mag. field distrib., Curie temp. 0-7198
- Ni<sub>3</sub>Fe, non-linear local environment effect, Mossbauer effect of <sup>57</sup>Fe 0-39909
- Ni<sub>3</sub>Fe, nondislocation origin friction stress in alloys, deformation hardening 0-21050
- Ni<sub>3</sub>Fe, order-disorder transition phase diagram, Mossbauer meas. 0-39995
- Ni<sub>3</sub>Fe, ordered, monocrystals, thermally activated deform. processes 0-50684
- Ni<sub>3</sub>Fe, short-range order, diffusive elastic neutron scattering 0-24400
- Ni<sub>3</sub>Fe, short-range order parameter calc. in pseudopot. approx. (*Russian*) 0-49183
- Ni<sub>3</sub>Fe, single crystals, long range order degree influence on strain hardening (*Russian*) 0-11660
- Ni<sub>3</sub>Fe:C, mag. anisotropy depend. on C content, magnetometric study (*Russian*) 0-54887
- Ni<sub>3</sub>Fe-Sn, dil., atomic order detection by <sup>119</sup>Sn spectroscopy 0-39993
- Ni<sub>3</sub>Fe<sub>2</sub>Cr<sub>1-x</sub> films, struct., mag. props., and corrosion resist. 0-34706
- Ni<sub>36</sub>Fe<sub>23</sub>Cr<sub>14</sub>P<sub>12</sub>B<sub>6</sub>, amorphous, electrochem. corrosion in chloride solns. 0-50763
- (Ni<sub>1-x</sub>Fe<sub>x</sub>)<sub>99</sub>Mn, ferromagnetic, NMR study of local environment effect, relaxation mechanism 0-7193
- Ni<sub>49</sub>Fe<sub>29</sub>P<sub>14</sub>B<sub>6</sub>Si<sub>2</sub> glass, flow and failure 0-40438
- Ni<sub>3</sub>Ge<sub>3</sub>, solid and liquid, physicochemical props. and structure 0-39548
- NiMn, high field magnetisation 0-2557
- Ni<sub>1-x</sub>Mn<sub>x</sub>, ferromagnetic, NMR study of local environment effect, relaxation mechanism 0-7193
- Ni<sub>3</sub>Mn, partially ordered, spin-wave dispersion relation, inelastic neutron scatt. meas. 0-20394
- Ni<sub>3</sub>Mn, thermoremanent magnetisation and blocking temp. 0-34601
- Ni<sub>2</sub>Mn<sub>2</sub>M<sub>1-x</sub>Sn (M=Ti,V) mag. hyperfine fields, <sup>119</sup>Sn Mossbauer spectra study 0-55003
- NiMnSb, hyperfine mag. field at Cd impurity, TDPAC study 0-39906
- (Ni<sub>0.75</sub>Mn<sub>0.25</sub>)<sub>8</sub>Si<sub>10</sub>B<sub>8</sub>, amorphous, exchange anisotropy, mag. susceptibility meas., 4.2K to room temp. 0-11186
- Ni<sub>2</sub>MnSn, ferromag. Heusler alloy, electronic struct., spin polarisations, theory 0-54598
- Ni<sub>2</sub>Mn<sub>2</sub>Ti<sub>1-x</sub>Sn, Mossbauer spectra, mag. hyperfine field 0-15857
- Ni<sub>3</sub>Mo, coherent phase form. at stress concentrators (*Russian*) 0-49356
- Ni<sub>65</sub>Mo<sub>35</sub>Fe, O<sub>2</sub> effect on secondary recrystallisation and mag. props. 0-35201
- Ni<sub>62</sub>Nb<sub>38</sub>, metallic glass, struct., neutron diffr. study 0-54148
- Ni<sub>76</sub>P<sub>24</sub>, cryst. and amorphous, thermopower and resist. meas. 0-20145
- NiPt, short-range order, effect of plastic deform., electron diffr. anal. (*Russian*) 0-24403
- NiPt<sub>2</sub>GeN<sub>2</sub>, crystal struct. (*German*) 0-44171
- (Ni<sub>1-x</sub>Rh<sub>x</sub>)<sub>99</sub>Mn, ferromagnetic, NMR study of local environment effect 0-7192
- (Ni<sub>1-x</sub>Rh<sub>x</sub>)<sub>99</sub>Mn, ferromagnetic, NMR study of local environment effect, relaxation mechanism 0-7193
- (Ni<sub>1-x</sub>Ru<sub>x</sub>)<sub>99</sub>Mn, ferromagnetic, NMR study of local environment effect 0-7192
- NiSi<sub>2</sub>, epitaxial film on Si, <sup>4</sup>He ion channelling meas. and RHEED anal. 0-10834
- Ni<sub>1-x</sub>Si<sub>x</sub>, electronic states of Si NMR study 0-50216
- Ni<sub>3</sub>Si coatings, form. and stability during high temp. irradi. 0-35088
- NiTaC eutectics, high cycle fatigue at room temp. 0-16459
- NiTi, martensitic, shape memory effect kinetics and thermodynamics 0-3021
- Ni<sub>1-x</sub>Ti<sub>x</sub>, ferromag. props., Ti conc. effect 0-54872
- Ni<sub>3</sub>Ti, electronic struct., Xa calc., photoelectron and AES spectra 0-20769
- Ni<sub>2</sub>Ti<sub>29</sub>Zr<sub>9</sub>, amorphous, H-sorption, X-ray and DSC obs. 0-49526
- Ni<sub>100-x</sub>Zr<sub>x</sub> (x=34-40) metallic glass, cryst., isothermal annealing behaviour 0-6367
- Ni<sub>64</sub>Zr<sub>36</sub>, amorphous and cryst., H-sorption, X-ray and DSC obs. 0-49526
- Nichrome, plasma spray coatings, relaxation phenomena 0-19876
- NpNi<sub>2</sub>, lattice distortions in ferromag. phase, X-ray obs. 0-15774
- Pd Ni, effect of hydrogenation on thermopower 0-39562
- Pd-Ni, dil., resist. min. 0-11050
- PdAl-Ni, phase diagrams, eutectic points and solubility (*Russian*) 0-40333
- Pd<sub>60</sub>Ni<sub>20</sub>Si<sub>20</sub>, amorphous, struct., high resolution electron microscopy 0-1969
- PrNi<sub>5</sub>, crystal field investigation from inelastic slow neutron scatt. expts. 0-39538
- PrNi<sub>5</sub>, hexagonal, cryst. field effect in thermal expansion 0-49390
- PrNi<sub>5</sub>, metallic Van Vleck paramag., nucl. interactions, NMR meas. 0-44953
- PrNi<sub>5</sub>, nucl. cooling agent, relax. and exchange, EPR and NMR study 0-25237
- Sc-Ni-Ga, phase equilibria, diagrams of state, X-ray, microstructural study (*Russian*) 0-55356
- SiC-Ni based superalloy reaction, at elevated temps. 0-3287
- Sn-Ni, electrodeposit, Mossbauer meas. 0-39990
- TbNi<sub>3</sub>, ferromag., magnetisation and paramag. susceptibility 0-25082
- Ti-CrB<sub>2</sub>-Ni-Mo, interphase reactions, electron probe anal., metallography and hardness exam. 0-2990
- Ti-Ni, effect of alloying on crit. points and martensitic transform. hysteresis 0-20935
- Ti-Ni, electron phase transition XPS, optical spectra and mag. susceptibility meas. 0-19943
- Ti-Ni, H<sub>2</sub> diffusion at room temp. (*Japanese*) 0-19987
- Ti-Ni, laser melting and splat quenching to form foils for TEM obs. 0-29986



## nickel alloys continued

- Ti-Ni, martensite transform. B2-B19', optical props. and electron struct. (Russian) 0-34878  
Ti-Ni, thermoelastic phase transform., acoustic emission 0-3039  
Ti-Ni, vacuum pressure seal with thermomechanical drive 0-31773  
Ti-Ni alloys, absorpt. of H<sub>2</sub>, press.-composition-temp. relationships, enthalpy, entropy 0-2267  
Ti-Ni alloys, absorpt. of H<sub>2</sub>, thermodynamic parameters calc. 0-2268  
Ti-Ni-H, catalytic props. 0-30274  
Ti-C-Ni powder compact, wetting problems in sintering 0-11596  
Ti-Ni-Mo sintered hard alloy TN-20, fracture surfaces 0-7684  
TiNiH system, thermodynamic rels. and struct. transformations 0-49385  
Ti<sub>0.60</sub>Ni<sub>0.40</sub> metallic glass, Young's modulus meas. by impulse induced resonance technique 0-40411  
Ti<sub>1-x</sub>Ni<sub>x</sub>, electronic struct. and anomalies of elec. and mag. props. 0-6710  
Ti<sub>2</sub>NiH<sub>2</sub>, H storage material, H diffusion, neutron diff. obs. 0-51013  
U(Co<sub>1-x</sub>Ni<sub>x</sub>)<sub>2</sub>, cryst. struct. and mag. props. at 4.2K 0-54175  
UNi<sub>5</sub>, core and valence band spectra, XPS obs. 0-50530  
UNi<sub>5</sub>Cu<sub>4</sub>, core and valence band spectra, XPS obs. 0-50530  
UNi<sub>5-x</sub>Cu<sub>x</sub>, NMR and press. effects 0-25230  
U<sub>3</sub>Ni<sub>4</sub>Si<sub>4</sub>, X-ray cryst. struct. determ. 0-33931  
UO<sub>2</sub> pellets-graphite-Zircaloy cladding, evaluation of graphite lubrication 0-32342  
V-Ni, ion bombard., void form. 0-34097  
V-Ni-Mo, structure in alloy crystallisation region, peritectic equilibria (Russian) 0-50622  
W-Ni, liquid phase sintering 0-16232  
W-Ni, liquid phase sintering 0-25613  
W-Ni, MBM diode, resist. depend. of detected signals 0-2482  
W-Ni, MOM diode, breakdown effect in visible and near-IR regions 0-6999  
W-Ni, surface barrier influence on C diffusion in stainless steel type 1Kh18N9T (Russian) 0-54434  
W-Ni compact, sintering behaviour and workability (Japanese) 0-20822  
W-Ni-Fe, W-Ni-Fe-Mo (Mn), sintering and mechanical props. (Japanese) 0-21086  
W-Ni-Fe (5(2), 5(2) wt.%) pore formation, effect on mech. props. 0-45396  
Y(Co<sub>1-x</sub>Ni<sub>x</sub>)<sub>5</sub>, mag. heterogeneities and coercive force, neutron scatt. study 0-2553  
Y(Co<sub>1-x</sub>Ni<sub>x</sub>)<sub>5</sub>, spontaneous magnetisation mag. anisotropy, spin reorientation transformation (Russian) 0-7082  
YNi<sub>2</sub>, amorphous alloy, at. struct. 0-19704  
YNi<sub>3</sub>, loss of ferromagnetism after H<sub>2</sub> absorpt., Pauli paramag. props. 0-34588  
Y<sub>2</sub>Ni<sub>1-x</sub>, amorphous, high press. magnetisation and Curie temp. 0-20442  
YbNi<sub>2</sub>-YbCu<sub>2</sub>, system, valency state, Yb behaviour (French) 0-45277  
Zircaloy 4, vapour transport of Zr and Si 0-55437  
Zn-Cd liquid/Fe-Ni-Al mag. powder, effective viscosity of composites (Russian) 0-54424  
Zr-Nb (2.25 wt.%), oxidation kinetics in flowing CO<sub>2</sub>, 873 to 1173K 0-16596  
Zr-Nb-Sn (3.0, 1.0 wt.%), oxidation kinetics in flowing CO<sub>2</sub>, 873 to 1173K 0-16596  
Zr-Ni, diffusion of H<sub>2</sub>, 900 to 1080°C (Korean) 0-19988  
Zr-Ni, surface layer, segregation of ferromag. Ni, magneto-optic investigation 0-22256  
Zr-Ni-Cu-H, catalytic activity, exam. by conversion of toluene, and bicyclic aromatic hydrocarbons 0-30276  
Zr-Ni-Cu-H, catalytic props. 0-30274  
Zr-Ni-H, catalytic activity, exam. by conversion of toluene, and bicyclic aromatic hydrocarbons 0-30276  
Zr-Ni-H, synthesis at high H pressure exam. of props. 0-29924  
Zr-Ni-H<sub>2</sub> (x=2.8 to 3), surface layer, segregation of ferromag. Ni, magneto-optic investigation 0-2256  
ZrNi, surface segregation of Ni, influence on catalytic activity 0-30275

## nickel compounds

see also nickel alloys

- nickel acetate tetrahydrate: Mn<sup>2+</sup>, EPR spectra, angular var. calc. 0-54940  
oxide, interatomic interaction by XPS 0-7474  
systems Ni ions anal. by ESCA (Japanese) 0-40787  
C<sub>11.3</sub>NiCl<sub>2.13</sub> intercalation compounds, cryst. struct. (French) 0-33947  
Ca<sub>2</sub>Ni<sub>1-x</sub>Fe<sub>x</sub>O<sub>4</sub>, initial permeability and Curie temp. 0-25130  
CaO-SiO<sub>2</sub>-NiO-MgO glass melt, interaction of NiO and MgO, elec. cond. and IR spectra obs. (Japanese) 0-24632  
Cd<sub>0.8</sub>Ni<sub>0.2</sub>Fe<sub>2</sub>O<sub>4</sub> ferrite, Fe spin relaxation Mossbauer study, mag. hyperfine struct. (Russian) 0-15932  
CeNiC<sub>2</sub>, struct. determ. using X-ray diffraction (Ukrainian) 0-33949  
Co<sub>2</sub>Ni<sub>1-x</sub>Cl<sub>2</sub>·6H<sub>2</sub>O, solid solution, mag. props. and phase diagram, calc. 0-7104  
Co<sub>2</sub>Ni<sub>1-x</sub>O, antiferromagnet, neutron diff. study of mag. struct. 0-34595  
Cr-Ni-O, computer-assisted anal. and calcs. of phase diagrams 0-25667  
Cr<sub>1-x</sub>Ni<sub>x</sub>Si<sub>2</sub>, prep., elec. cond. and thermoelec. props. 0-49697  
CsNiF<sub>3</sub>, one-dimens. ferromag., collective excitations in mag. field 0-44822  
Dy<sub>2</sub>Ni<sub>2</sub>B<sub>2</sub>, struct., space groups, X-ray study (Ukrainian) 0-39029  
(Fe,Ni)O<sub>4</sub>, magnetostriction calcs. (Dutch) 0-2619  
Fe-Ni-O, computer-assisted anal. and calcs. of phase diagrams 0-25667  
FeNiBO<sub>4</sub>, FeNi<sub>2</sub>BO<sub>4</sub>, Mossbauer spectra, mag. relax. 0-15889  
Fe<sub>2</sub>Ni<sub>1-x</sub>(1,10-phenanthroline)<sub>2</sub>(NCS)<sub>2</sub>, spin crossover, Mossbauer and magnetism study 0-44980  
Fe<sub>2</sub>O<sub>3</sub>-NiFe<sub>2</sub>O<sub>4</sub>, solid soln., activities determ. from EMF of galvanic cell 0-16290  
(Ge<sub>1/3</sub>Se<sub>2/3</sub>)<sub>100-x</sub>Ni<sub>x</sub>, ESR, rel. to elec. cond. 0-7155  
(Ge<sub>0.32</sub>Se<sub>0.32</sub>Te<sub>0.32</sub>As<sub>0.4</sub>)<sub>100-x</sub>Ni<sub>x</sub>, ESR, rel. to elec. cond. 0-7155  
InSb-NiSb eutectic, struct. and optical props., IR polariser appl. 0-45078  
KNiMn<sub>1-x</sub>F<sub>3</sub>, mixed antiferromagnet, light scatt. meas. 0-16025  
K<sub>2</sub>Ni(MoO<sub>4</sub>)<sub>2</sub>, paramag. props., 90-800K (French) 0-39734  
LaNiC<sub>2</sub>, struct. determ. using X-ray diffraction (Ukrainian) 0-33949  
LaNi<sub>2</sub>H<sub>6</sub> sponges, Al or Mn substitution, neutron diff. 0-24427  
LaNi<sub>1-x</sub>Mn<sub>x</sub>O<sub>3</sub>, <sup>55</sup>Mn NMR study, magnetisation meas., ferromag. and Pauli paramag. components 0-7191  
Li<sub>2</sub>Ni<sub>2</sub>(MoO<sub>4</sub>)<sub>3</sub>, paramag. props., 90-800K (French) 0-39734  
Li<sub>2</sub>Ni<sub>1-x</sub>O (x=0 to 0.03), solid soln. effect of Li on densification during sintering 0-25638  
Mg<sub>2</sub>Ni<sub>1-x</sub>(NO<sub>3</sub>)<sub>3</sub>·6H<sub>2</sub>O, crystal structure changes due to substitution of Mg<sup>2+</sup> (German) 0-24428

## nickel compounds continued

- Na<sub>2</sub>Ni<sub>8</sub>(MoO<sub>4</sub>)<sub>2</sub>, paramag. props., 90-800K (French) 0-39734  
Na<sub>2</sub>Ni<sub>2</sub>Ti<sub>6</sub>O<sub>4</sub>F<sub>2</sub>, characterisation and mag. props., 90-800K, Na<sub>2</sub>Ti<sub>6</sub>O<sub>8</sub> bronze isotypes (French) 0-39735  
Na<sub>2</sub>O-BaO-NiO<sub>2</sub>-SiO<sub>2</sub> glass, ion-bombarded, optical time intensities 0-35037  
Na<sub>2</sub>O-SiO<sub>2</sub>-NiO systems Ni ions anal. by ESCA (Japanese) 0-40787  
Ni bi-univalent cpds., soln., activity coeffs., osmotic coeffs., water activity, Gibbs energy, molality depend. 0-51963  
Ni cermet selective absorbers, photothermal conversion appls. 0-21413  
Ni complex, (1,4,5,8,9,12,13,16-octamethyltetradibenzporphinato nickel)<sup>2+</sup> (I<sub>3</sub>)<sub>2</sub>, atomic limit of Hubbard model and polarons 0-39860  
Ni complex, BDN II in tetrahydrothiophene-1,1-dioxide, saturation behaviour, Q-switching appl. 0-48354  
Ni complex, bis-4-dimethylaminodithiobenzyl nickel, tetrachlorethane soln., photochem. and thermal stability 0-16708  
Ni complex, bis-[4-(n-butyl)-styryl-dithiolato] Ni nematic complex, IR absorption 0-49342  
Ni complex, cis-dichloro-bis(1,2-cyclohexanedioxime) cryst. and mol. struct. 0-44198  
Ni complex, hexa(pyridine 1-oxide) di-perchlorate, S=1 ground state, mag. props. in external field 0-11157  
Ni complex, Ni(C<sub>2</sub>H<sub>3</sub>NO)<sub>6</sub>(ClO<sub>4</sub>)<sub>2</sub>, field induced antiferromag., magneto-caloric effect 0-29551  
Ni complex, Ni(l-sparteine)Cl<sub>2</sub>, IR circular dichroism spectra, vibr.-electronic interaction 0-55074  
Ni complexes, Ni(II) porphyrins, picosec. flash photolysis, transient absorpt. 0-52976  
Ni-Fe-O ferrite system, thermodynamic stability, dissociation and phase relations (Japanese) 0-55378  
Ni-ferrite, ultrafine powder, prod. by cryochemical, freeze drying, spray drying or soln. techniques 0-55336  
Ni-Pd-H, film, struct. and phases formed, when Ni, Pd are sputtered in H 0-29289  
Ni-S melt, thermodynamic props. 0-19957  
Ni-Zn ferrite, grain size depend. of grain boundary sliding (Japanese) 0-15120  
Ni-Zn ferrites 600 NN and M450 NNI, Curie point radiative shift due to neutron irradi. (Russian) 0-39775  
Ni<sub>2</sub>B<sub>2</sub>O<sub>7</sub>, unit cell parameters and struct. transitions, 20 to 293K, X-ray diff. study 0-24431  
NiBr, band system in near UV, vibr. analysis 0-32733  
NiBr<sub>2</sub>, two-phonon vibronic progressions, Raman obs. 0-29742  
Ni(CN)<sub>4</sub>-dodecylamine, lamellar paraffinic system, phase transitions, wide-line NMR obs. (French) 0-44929  
Ni(CO)<sub>4</sub>, bonding, shakeup energies, and shakeup intensities for photoelectron spectra 0-50528  
Ni(CO)<sub>4</sub>, ppb in air meas. by chemiluminesc. detector 0-40692  
NiCl<sub>2</sub>, aq. soln., Ni<sup>2+</sup> coordination from extended X-ray absorption fine struct. 0-1913  
NiCl<sub>2</sub>, heavy water soln., anionic hydration, 1 bar and 1 kbar, neutron diff. obs. 0-30212  
NiCl<sub>2</sub>, soln., activity coeffs., osmotic coeffs., water activity, Gibbs energy, molality depend. 0-51963  
NiCl<sub>2</sub>, two-phonon vibronic progressions, Raman obs. 0-29742  
NiCl<sub>2</sub>-CdS interface, transverse acoustoelec. voltage spectroscopy 0-49828  
Ni(ClO<sub>4</sub>)<sub>2</sub>, soln., activity coeffs., osmotic coeffs., water activity, Gibbs energy, molality depend. 0-51963  
NiCl<sub>2</sub>·nH<sub>2</sub>O, cryst. struct. (German) 0-1987  
Ni(Co)<sub>4</sub>+inert gas, dissc. energy transfer, chemiluminesc. 0-55647  
Ni<sub>50</sub>Co<sub>40</sub>P<sub>10</sub> amorphous film, spin wave excitation, ferromagnetic resonance study 0-50198  
Ni<sub>1-x</sub>Co<sub>x</sub>S<sub>2</sub>, elec. transport and semicond.-metal transition 0-10985  
Ni<sub>1-x</sub>Co<sub>x</sub>S<sub>2</sub>, Mott transitions, temperature induced, Hubbard model theory 0-29326  
Ni<sub>0.5-x</sub>Co<sub>x</sub>Zn<sub>0.5</sub>Fe<sub>2</sub>O<sub>4</sub> ferrosilical solid solutions, cryst. lattice defects and props. 0-19796  
NiCr<sub>2</sub>O<sub>4</sub>, acoustic props. rel. to cooperative Jahn Teller effect and structural phase transform 0-24538  
NiCr<sub>2</sub>O<sub>4</sub>, sign of net mag. hyperfine field, <sup>61</sup>Ni Mossbauer study 0-39946  
NiCr<sub>2</sub>O<sub>4</sub>:Fe, Mossbauer effect 0-15874  
NiD<sub>2</sub>, synthesized at high pressures, neutron diffraction anal. of struct. 0-28977  
NiF<sub>2</sub>, magnetisation and antiferromagnetic resonance freq. in mag. field (Russian) 0-34781  
NiF<sub>2</sub> powder, preferred orientation, X-ray intensity corrections 0-1880  
(NiF<sub>2</sub>)<sub>4</sub><sup>4-</sup> complex, open-shell cluster calcs., semiempirical LCAO-MO method 0-54583  
NiF<sub>6</sub><sup>4-</sup> spectra, cryst. field least squares fitting interpretation 0-44548  
Ni<sub>1-3x</sub><sup>2+</sup>Fe<sub>2+2x</sub><sup>3+</sup>Vac<sub>0.4</sub><sup>2-</sup> (Vac=cation vacancy), solid solns., cryst. lattice imperfections 0-39069  
NiFe<sub>2-x</sub>Al<sub>x</sub>O<sub>4</sub>, <sup>57</sup>Fe and <sup>61</sup>Ni Mossbauer spectra 0-39940  
Ni<sub>0.8</sub>Fe<sub>0.2</sub>B<sub>2</sub>O<sub>7</sub>, boracite, mag. hyperfine interactions, Mossbauer study 0-39935  
NiFe<sub>2</sub>O<sub>4</sub> precipitation process from silicate glass, ESR study, effective g value, transition temp. 0-25194  
NiFe<sub>2</sub>O<sub>4</sub> precipitation from silicate glass, Mossbauer study 0-54998  
Ni<sub>2</sub>Fe<sub>2</sub>/O<sub>4</sub>, precipitation of α-Fe<sub>2</sub>O<sub>3</sub>, optical microscopy, SEM and TEM studies (French) 0-11650  
Ni<sub>0.98</sub><sup>2+</sup>Fe<sub>0.02</sub>S<sub>1.0</sub>, quadrupole splitting and ground state, Mossbauer spectra 0-29657  
(Ni<sub>1-x</sub>Fe<sub>x</sub>)<sub>1-8</sub>, anisotropic spin glass, mag. props. 0-39793  
(Ni<sub>1-x</sub>Fe<sub>x</sub>)<sub>1-8</sub>, anomalous thermal hysteresis in metal-semicond. transition 0-39640  
Ni<sup>2+</sup>Fe<sub>0.75</sub><sup>3+</sup>V<sub>0.25</sub><sup>3+</sup>O<sub>4</sub>, acoustic props. rel. to cooperative Jahn Teller effect and structural phase transform 0-24538  
NiGeO<sub>3</sub>, HP phase transform. 0-19941  
Ni(H<sub>2</sub>V)<sub>2</sub>(H<sub>2</sub>O)<sub>2</sub>, synthesis and characterisation (French) 0-45225  
Ni<sub>2</sub>La, connected storage of H (Russian) 0-55937  
NiLa<sub>2</sub>O<sub>4</sub> electrochemical electrodes, kinetics of O<sub>2</sub> evolution, appl. to electrolytic H energy prod. 0-30430  
Ni<sub>2</sub>Mg<sub>1-x</sub>O, EPR in magnetoconcentrated solid solution (Russian) 0-39856  
Ni(Mo<sub>2</sub>Re<sub>2</sub>)S<sub>8</sub>, synthesis and electrical props. of mixed tetrahedral cluster phases 0-2971  
Ni(NH<sub>3</sub>)<sub>6</sub>Cl<sub>2</sub>, EPR of Ni<sup>2+</sup> ion near structural phase transformation 0-11248  
Ni(NH<sub>4</sub>)<sub>2</sub>(SO<sub>4</sub>)<sub>2</sub>·6H<sub>2</sub>O, precipitation from equimolar aqueous solns., kinetics study 0-7848



## nickel compounds continued

- Ni(NH<sub>4</sub>)<sub>2</sub>(SO<sub>4</sub>)<sub>2</sub>·6H<sub>2</sub>O, Mn<sup>2+</sup> doped, EPR study 0-34763  
 NiNO, ground and core hole states, config. depend. HF LCAO SCF calc., relax. and binding energy 0-29453  
 Ni(NO<sub>3</sub>)<sub>2</sub>, soln., activity coeffs., osmotic coeffs., water activity, Gibbs energy, molality depend. 0-51963  
 β-Ni(NO<sub>3</sub>)<sub>2</sub>·4H<sub>2</sub>O, X-ray cryst. struct. determ. 0-28958  
 Ni(NO<sub>3</sub>)<sub>2</sub>·6H<sub>2</sub>O, susceptibility and specific heat meas., spin ordering, antiferromag. spin pair coupling 0-7084  
 NiO (100), surface struct., LEED study 0-39396  
 NiO (111) platelets, antiferromag. S domains, optical obs., spin flop 0-54915  
 NiO (111) platelets, magnetic anisotropy investigation by torque and mag. susceptibility meas. 0-54885  
 NiO (111) surfaces, antiferromag., mag. scattering by polarised LEED, spin polarisation effect in theory 0-29529  
 NiO, (001) tilt boundary relative energy 0-29033  
 NiO and lithiated NiO, thermally grown, electrochemical capacitance variations 0-29475  
 NiO based pigments, willemite struct., synthesis 0-20855  
 NiO, cubic NaCl-type cryst., Debye temp. 0-54333  
 NiO, dielec. behaviour, Dick and Overhauser shell model calcs. 0-45001  
 NiO electrode for photolysis 0-40696  
 NiO electrodes, effect of Co(OH)<sub>2</sub> on self-discharge, IR spectra obs. 0-21295  
 NiO, grain boundary thermal grooving, mass transport, self-diffusion coeffs. 0-44217  
 NiO, lattice parameters, microstrains, non-stoichiometry, comparison between mosaic microcrystals and quasi-perfect single microcrystals. 0-24414  
 NiO, matrix isolated IR spectra, ground state vibr. freqs. 0-28015  
 NiO, physicochem. props. at high temps. (French) 0-39582  
 NiO, plasmachemical synthesis, oxidised from metals, exam. of props. 0-2984  
 NiO, thin films with spinel-type defect structure, FMR study 0-39877  
 NiO, transport number and cationic cond. (French) 0-15297  
 NiO, X-ray determ. of electron density distrib., atomic scatt. factors 0-15078  
 NiO:Cr, surface charge, O(1s), C(1s) and Ni(2p) XPS 0-45196  
 NiO:Cr, effect of Cr additives on structure parameters (Bulgarian) 0-44319  
 NiO:Li<sub>2</sub>O-ZnO p-n heterojunction, contact resist., effects of water vapour 0-34506  
 NiO-CuO, equilibrium relations 0-55375  
 NiO-H<sub>2</sub>, interaction with surface, quantum chemical study 0-45549  
 NiO-ZnO, solid solution, exam. of mechanism and kinetics of reaction with Fe<sub>2</sub>O<sub>3</sub> ferrite formation 0-3309  
 Ni(OH)<sub>2</sub> electrodes, charged, reversible potentials meas. 0-55669  
 NiOOH, sintered plate electrodes, residual capacity cause expts. 0-55745  
 Ni<sub>2</sub>P<sub>2</sub>O<sub>7</sub>·K<sub>2</sub>P<sub>2</sub>O<sub>7</sub>·H<sub>2</sub>O solubility at 25 degrees C, double phosphates formation 0-54381  
 Ni<sub>2</sub>Cl<sub>2</sub>·6H<sub>2</sub>O, S=1 ground state, mag. props. in external field 0-11157  
 NiS film, electrolytically deposited, mag. props., S content influence 0-44884  
 NiS<sub>2</sub> 0-15832  
 NiS<sub>2</sub>-NiSe<sub>2</sub>(CoS<sub>2</sub>)(FeS<sub>2</sub>), <sup>57</sup>Fe isomer shift, quadrupole splitting, Mossbauer study 0-15832  
 Ni<sub>1-x</sub>S, metal-semimetal transition, lattice dynamics and thermodynamic props. 0-29324  
 NiSO<sub>4</sub>, spirals, growth and dissolution from liq. state 0-15027  
 NiSO<sub>4</sub>·6H<sub>2</sub>O, uniaxial crystals, circular dichroism and optical activity 0-45029  
 NiSO<sub>4</sub>·7H<sub>2</sub>O, Mn<sup>2+</sup> doped, EPR study 0-34763  
 NiSe film, vac. deposited, phase transformation, electron microscope studies 0-2302  
 NiSe<sub>2</sub> 0-15832  
 Ni<sub>2</sub>Si, chemical composition of Earth's inner core 0-8266  
 NiSiF<sub>6</sub>·6H<sub>2</sub>O, EPR line shape, Tanaka-Kondo method 0-29602  
 Ni<sub>2</sub>SiO<sub>3</sub>, elec. cond. under defined thermodynamics activities, up to 20 kbar, 340-1100°C 0-6832  
 Ni<sub>1/3</sub>Ta<sub>2</sub>S<sub>2</sub>, Hall coefficient and resistivity 0-39610  
 Ni<sub>1/3</sub>Ta<sub>2</sub>S<sub>2</sub>, magnetic susceptibility, function of temp. 0-39756  
 NiTiO<sub>3</sub>, HP phase transform. 0-19941  
 Ni<sub>2</sub>(VO<sub>4</sub>)<sub>2</sub>, Neel temp., mag. susceptibility meas. 0-29550  
 NiWO<sub>4</sub>, monoclinic antiferromagnet, orientational phase transition and intermediate state (Russian) 0-15725  
 NiWO<sub>4</sub>, monoclinic antiferromag., domain struct. induced by strong mag. field 0-44856  
 Ni<sub>2</sub>Zn ferrite, wall topography change induced by external press. 0-34734  
 Ni<sub>0.38</sub>Zn<sub>0.62</sub>Fe<sub>2</sub>O<sub>4</sub>, preparation, Mossbauer study 0-50231  
 Ni<sub>2</sub>Zn<sub>1-x</sub>Fe<sub>2</sub>O<sub>4</sub>, catalytic oxidation of CO, mag. props., kinetic parameters and composition depend. 0-16723  
 Ni<sub>x</sub>Zn<sub>1-x</sub>Fe<sub>2</sub>O<sub>4</sub>, crystal growth from BaO-B<sub>2</sub>O<sub>3</sub>-ZnO-NiO-Fe<sub>2</sub>O<sub>3</sub> melt, exam. of crystal props. 0-40249  
 Ni<sub>2</sub>ZrS<sub>2</sub>, (0<x≤0.50), intercalation compounds, ordered phases obs. 0-33962  
 PbO-SiO<sub>2</sub>-NiO-MgO glass melt, interaction of NiO and MgO, elec. cond. and IR spectra obs. (Japanese) 0-24632  
 Pb<sub>0.94</sub>Sr<sub>0.06</sub>(Ti<sub>0.47</sub>Zr<sub>0.53</sub>)O<sub>3</sub>-NiO, modified, dielec. and piezoelec. props. 0-11342  
 PrNiC<sub>2</sub>, struct. determ. using X-ray diffraction (Ukrainian) 0-33949  
 Rb<sub>2</sub>NiF<sub>4</sub>, planar antiferromagnet, cluster-Bethe-lattice method 0-22306  
 RbNi<sub>2</sub>Mn<sub>1-x</sub>F<sub>3</sub>, powder, mag. props. 0-2560  
 Zn<sub>1-x</sub>Ni<sub>x</sub>Fe<sub>2</sub>O<sub>4</sub>, heat treatment and sintering effect on porosity 0-25610  
 Zn<sub>2</sub>Ni<sub>1-x</sub>Fe<sub>2</sub>O<sub>4</sub>, Mossbauer spectra, mag. hyperfine struct. 0-15877  
 Zr-Ni-H, surface segregation of Ni, influence on catalytic activity 0-30275

## night airglow see nightglow

## night sky

- see also nightglow; twilight  
 galactic Ha background emission, high spatial and spectral resolution pictures 0-56897  
 heat engine using clear night sky as heat sink for teaching 0-27082  
 light pollution over Jena, night sky brightening at Karl-Schwarzschild Observatory 0-51533  
 Sacramento Peak Observatory, night sky brightness conditions 0-12545  
 Sacramento Peak Observatory night sky conditions, cloud cover, seeing and precipitable water 0-51653  
 starlight, integrated, synthetic spectrum between 3000 and 10000 Å, calc. method and results 0-46536

## nightglow

- intensity fluctuations during stratospheric warmings 0-4162  
 IR emission meas. (0.9-2.3 μm) using interferometer-spectrometer 0-12583  
 O I nocturnal 6300 Å luminesc., profiles from incoherent scatt. radar and photometry (Portuguese) 0-41591  
 visible spectra using field compensated interference spectrometer 0-36424  
 Na density correl. to Na I, OH and O I emissions 0-41585  
 O I, 6300 Å nightglow enhancements by high powered HF radiowaves (Portuguese) 0-41592  
 O I 5577 Å line, intensity var., related to solar tides (Russian) 0-12585  
 O I 6300 Å forbidden emission at mag. equator, rel. to vertical E×B plasma drift vel. 0-36435  
 O I 6300 Å nightglow, obs. rel. to neutral comp. vars. at F-region heights (Portuguese) 0-41584  
 O<sub>2</sub>, UV nightglow emission meas. 0-41590  
 OI, F-region neutral temp. by 630 nm spectra, during spread-F activity 0-41587

## Nilsson's model see nuclear shell model

## niobium

- see also nuclei with .....  
 absorption rate of H, metallic film effect 0-49525  
 alloy addition to hot rolled medium C steel, effect on transformation and strength 0-7607  
 anodic oxidation, open circuit transient anal., dielec. and elec. props. of oxide film 0-3245  
 band effective mass, Animalu TMMP theory 0-29312  
 BCC, void nucleation following electron irradi. 0-29054  
 BCC crystal, elastic constants, thermal expansion and bulk modulus 0-6452  
 bicrystals, impact strength at 20° and -190°C (Russian) 0-45379  
 blistering by He<sup>+</sup> bombardment at thermonuclear reactor energies 0-34104  
 chemical vapour deposited, kinetics and microstruct., pressure and temp. depend. 0-11569  
 chemisorption of O<sub>2</sub> and initial oxidation on (110) and (750), LEED, AES, SIMS, and EELS obs. 0-44408  
 corrosion kinetics in sulphidizing atm. 0-35396  
 cubic crystals, anisotropic, dislocation loops, electron microscope image contrast 0-39101  
 CVD coatings on graphite, grain struct. depend. on temp. 0-25574  
 defect annealing in 7 MeV-irrad. samples, positron annihilation obs. 0-24497  
 deformed, α'-peak in internal friction spectra 0-16368  
 desorption kinetics of halogens, pulsed ion beam method 0-34300  
 desorption of O<sub>2</sub> in a vacuum, thermodynamic props. calcs. (Russian) 0-54501  
 diffusion of H and D in Nb, low temp., from quenching and annealing study 0-6555  
 dislocation struct. after tensile creep test under reactor radiation conditions (Russian) 0-45348  
 elastic properties, at high temp. 0-30007  
 electrotransport of H(D) at high H concs. 0-34246  
 film, critical currents due to microwave field 0-25058  
 film, electron beam evaporator for in situ deposition studies in UHV electron microscope 0-40264  
 film, evaporated, optical props., rel. to struct. 0-55211  
 film, magnetron-sputtered, intrinsic stresses and supercond. props. 0-24772  
 film on Si, Ar ion bombard., NbSi<sub>2</sub> form. 0-10709  
 film on Si substrate, intermixing, ion induced silicide formation 0-34101  
 flaking and blistering due to He and Ne ion bombardment 0-29092  
 fluxoid lattice, eqn. props., magnetisation measurements 0-39725  
 foil, electron energy loss spectra 0-7452  
 fusion reactor blanket struct. material, low cycle fatigue behaviour 0-30073  
 fusion reactor first wall material, cyclic deform. tests 0-30074  
 heteroepitaxial layers on sapphire, residual mechanical stress and strain influence on superconductivity 0-15644  
 interatomic pair potential, phonon spectra 0-33927  
 ion bombardment, sputtering, re-emitted kinetic energy ang. distrib. 0-2910  
 local heating during abrupt strain, catastrophic slip band formation 0-7652  
 mechanical props. and dislocation struct., mag. field effect 0-54935  
 muon trapping, Knight shift, rel. to H interstitials 0-50247  
 nanobridge, Josephson effect, quasiparticle diffusion time, inelastic scatt. time 0-34556  
 neutron irradiated, microstruct. and tensile props. 0-34077  
 neutron spectra for fusion + hybrid reactor materials 0-23142  
 nitriding, kinetics 0-35415  
 NMR study up to 1700K, Knight shift and spin-lattice relax. time 0-2653  
 oxide growth and oxide coatings, XPS and AES studies 0-50765  
 phonon spectra, self-consistency condition for force const. models 0-44264  
 plastic deformation effects on superconducting specific heat transition 0-20352  
 plastically deformed single crystal, foil, damage free prep. for TEM and X-ray topography (German, English) 0-30200  
 positive muon diffusion mechanisms, zero field spin relax. studies as probe 0-34840  
 positron annihilation and vacancy formation 0-16119  
 positron trapping and annihilation at vacancies 0-29823  
 preparation by electromagnetic levitation in ultrahigh vac. 0-29899  
 proton diffusion, NMR obs., 120-480K 0-34812  
 pure, reaction with gas residual in vacuum, physicochem. props. effect 0-16587  
 radiation damage in fusion reactors, computer expts. 0-13839  
 SQUID using thin film microbridge (Japanese) 0-31816  
 steel, martensitic, age hardening with Cu, Nb additions, exam. of hardness 0-7681  
 superconducting, amorphous film, conductivity and transition temp., ion bombardment effects (Russian) 0-49969  
 superconducting, muon spin relaxation (German) 0-50015  
 superconducting, optical props. and electron-phonon interactions 0-2510  
 superconducting, spin fluctuations effect on T<sub>c</sub>, from sp. ht. and mag. suscept. 0-7030  
 superconducting bridges by electron beam lithography and ion implantation Josephson effect 0-20355



**niobium continued**

- superconducting film, vac. deposited, deposition parameter effects on crit. temp. 0-2514
- superconducting films, crit. depairing currents, temp. and mag. field depend. 0-7058
- superconducting point contact, high freq. props. in far IR 0-54840
- superconducting transition temperature, ab initio calc. 0-25036
- surface, (001), low energy  $H^+$  and  $He^{++}$  ion refl., computer simulation 0-11524
- surface damage caused by  $He^+$  ion bombard. 0-39177
- surface topography formation due to elec. transfer processes (*Russian*) 0-54482
- vacuum technology appl., melt processing and appl. (*Hungarian*) 0-55318
- X-ray  $M\beta$  energy, revised values 0-14102
- $Al_2O_3/Nb$  laminates, metal to ceramic joints, adherence props. 0-45386
- $Al_2O_3-Nb$  composites, influence of gas impurities on solid-state bonding on annealing 0-11739
- $H_2$  isotope release 0-37580
- $La_2Mg_3(NO_3)_{12} \cdot 24H_2O \cdot Nd^{3+}$ , proton raser, self-radiating nuclear spin system (*German*) 0-53298
- Nb, fluxoid lattice, eqn. props., small-angle neutron diffraction measurements 0-34573
- Nb, neutron bombarded, defect size distrib. influence on hardening (*Russian*) 0-10580
- Nb thin foils, surface segregation during sputtering at elevated temps., Auger study 0-54386
- Nb XXXII, XXXIII, XXXIV, transition identification X-ray spectra 0-32648
- Nb XXXIX and XL, X-ray spectrum weak line detection 0-5497
- $Nb^{39+}$ ,  $^1P$  and  $^3P$  energy levels, relativistic RPA calc. 0-47913
- Nb-Al proximity sandwiches, supercond. transition temp. and tunnelling meas. 0-7045
- Nb-D, Huang diffuse scattering of neutrons 0-10544
- Nb-H system, temp.-stimulated acoustic emission, hydride precip. 0-3044
- Nb-Nb $_2O_5$ -Pb, two-dimens. Josephson junction, supercurrent vs. mag. field characts. 0-34562
- Nb-Nb $_2O_5$ -Pb Josephson tunnel junctions, fabrication using FR glow discharge oxidation 0-34559
- Nb-Nb $_2O_5$ -Pb tunnel junctions at 4.2K, conductance of oxide barrier 0-7046
- Nb-Nb $_2O_5$ -Pb tunnel junctions, current density distrib. 0-39717
- Nb-Si, bridge, crit. current 0-20359
- Nb+Mo, K-shell vacancy prod., impact parameter depend. 0-14225
- Nb+Nb, selected MO X-ray coincidence with separated at. K X-rays 0-43148
- YAG:Nd laser pulses, mutual exchanges with plasma (*German*) 0-48918
- ZrB $_2$ -SiC-C-Nb, refractory cermets hot pressing and oxidation resist. 0-3231

**niobium alloys**

see also niobium compounds

- ageing, high-temp., ageing struct. and morphology of hardening phases (*Russian*) 0-40390
- ageing, high-temp., struct. and morphology of hardening phases (*Russian*) 0-40390
- BCC, solid solution hardening, crystal resolved shear stress depend. on dislocations 0-40373
- cold worked, chemothermal strengthening, internal oxidation 0-35229
- fusion reactor first wall and blanket material, props. for struct. appl. 0-30071
- fusion reactor first-wall and blanket material, mech. props. 0-34074
- fusion reactor materials, He and simultaneous damage production simulation 0-32480
- low-alloy, strength and ductility at high temp. and different strain rates 0-16401
- oxidation protection from MoSi $_2$  coating, diffusion-slip casting appl. method 0-21187
- steel, Cr-Mo-Ni-Nb, Nb effect on mech. props. (*German*) 0-30012
- steel, high Nb, HSLA, low temp. fatigue props. 0-40490
- steel, Mo-Nb (2.5, 0.035 wt.%) Mo content effect on sulphide stress cracking resistance 0-21157
- steel, Nb-Va microalloyed, mech. props. (*French*) 0-35252
- steel, stainless, oxidation effect of Nb 0-35394
- Al-Nb, struct. and props. of alloys obtained from granules 0-50717
- Au-Nb, dil., Friedel d-reson. scatt. and elec. resists. 0-44566
- Co-Ni-Cr-Nb, effect of Fe addition on precipitation behaviour 0-29962
- Cu-Nb alloys for superconducting wire, casting of dendritic structure 0-2976
- Cu-Nb $_2$ Sn superconducting composite, crit. props., AC hysteretic losses 0-50014
- Cu-Nb-Sn, multifilamentary supercond. composite wires, fabrication on laboratory scale and mech. props. 0-29897
- Cu-Nb-Sn system, phase equilibria and supercond. props. (*Russian*) 0-50589
- Cu-Ni-Nb-Al, correlation of  $\gamma'$  and  $\gamma''$  precipitates phase stability 0-25704
- Fe-Nb creep resistant alloy, precipitate free zones elimination 0-16312
- Fe-Ni-Ti-Al-Nb, struct. mechanism for inverse  $\alpha \rightarrow \gamma$  transform. (*Russian*) 0-40351
- Fe-Fe-Nb, cold-worked and aged, mag. props. and microstruct. 0-34690
- Mo-Nb, impurity diffusion and vacancy-impurity binding energy 0-15307
- Mo-Nb solid solutions, enthalpy of soln. of H meas. 0-2166
- Nb/Cu-Sn-Mg, superconductor, effect of Mg addition to Cu-Sn matrix 0-25028
- Nb/H, heat capacity and supercond. between 1.5 and 16K 0-2521
- Nb-B, atomic order, stability, supercond. (*French*) 0-50021
- Nb-Ga-Fe ternary system, phase equilib. at 1000°C, supercond. transition temp. 0-35158
- Nb-Ge, A15 struct. superconductor, high field transport props. TEM study 0-34574
- Nb-Ge, supercond. A-15 phase, supercond. transition temp. after ion implantation 0-49972
- Nb-Ge film, phase transformations due to annealing, electron diff. study 0-54551
- Nb-Ge-Cu, phase equilib. and supercond. props. (*Russian*) 0-40332
- Nb-Ge-Ni, phase composition and superconducting props., influence of Ni (*Russian*) 0-20898
- Nb-Ge-Si, A15 struct. superconductor, high field transport props. TEM study 0-34574
- Nb-Ge-Si film, CVD, struct., comp., stability and homogeneity 0-15421
- Nb-H, BCC, quasimolecular Jahn-Teller reson. states 0-44550

**niobium alloys continued**

- Nb-H, electron work function, 300 to 600 degrees C, contact potential difference meas. 0-29462
- Nb-H, fusion reactor first wall material, cyclic deform. tests 0-30074
- Nb-H(D) system, anelastic behaviour, 0.5-15K 0-49300
- Nb-Hf (38 at.%) superconductor, peak effect, summation problem, mag. history flux pinning force 0-20362
- Nb-Mo, electronic struct., thermoreflectance meas. 0.5-5.0 eV 0-45050
- Nb-Mo, prod. by simultaneous carbothermic reduction of oxides/electron beam melting method (*Japanese*) 0-11590
- Nb-Mo steel, HSLA, low temp. fatigue props. 0-40490
- Nb-Mo system, electron-phonon coupling const. and supercond. transition temp., average T-matrix approx. 0-39707
- Nb-Mo-Al-(Cr) eutectic directionally crystallised alloy, heat resistance, alloy struct. (*Russian*) 0-40481
- Nb-Mo-Ti-Zr-C, work function temp. and phase depend. (*Russian*) 0-2449
- Nb-Mo(Ti)(Zr), nitriding, diffusive saturation, lattice spacing and activation coeffs. (*Russian*) 0-21168
- Nb-Ni, cathodic polarization in conc. KOH soln. 0-16591
- Nb-Ni glasses, struct. factor temp. depend. 0-28920
- Nb-Pt-O system, phase equilibria, diagram, unit cell parameters, supercond. 0-55352
- Nb-Rh, radiation disorder model of phase stability 0-16297
- Nb-Ru(Pd), dil., impurity diffusion and vacancy-impurity binding energy 0-15307
- Nb-Si diagram of state, melting temp., polymorphic transform. temp. (*Russian*) 0-50594
- Nb-Si liquid quenched alloy, metastable A-15 and amorphous phases, interstitials 0-54394
- Nb-Si-Cu, struct. and supercond., Cu influence 0-50592
- Nb-Sn(Al)(Ga)(Ge)(Si)-C, phase equilib. and supercond. 0-50593
- Nb-Ti, multifilament wire, superconducting magnet system, development for physical experiments 0-9008
- Nb-Ti, sheet, flux trapping, appl. to mag. shielding and levitation 0-31806
- Nb-Ti, single core conductor, carrying DC transport current, alternating field losses 0-34550
- Nb-Ti superconducting magnet system, for short sample test on Tokamak superconductor 0-9010
- Nb-Ti/Cu sheet composite, flux trapping and shielding capabilities in transverse fields 0-15667
- Nb-Ti-Zr, superconducting wire, coil simulation meas. of losses and instabilities 0-37050
- Nb-V, negative muon Coulomb capture ratio and Lyman series intensities 0-14255
- Nb-V oxidation in air, rate determining process (*Russian*) 0-21170
- Nb-V-Cr, Nb-V, and Nb-Cr, oxidation resist., Cr and V effects (*Russian*) 0-40585
- Nb-W-Mo-Zr, 5MVTs, reaction with gas residual in vacuum, physicochem. props. effect 0-16587
- Nb-W-Mo-Zr, long-term strength props., vac. level effect 0-55484
- Nb-W-Mo-Zr-C, strength and ductility, prolonged high-temp. soaking effect 0-55483
- Nb-W-Ta-Zr, 5VTT, reaction with gas residual in vacuum, physicochem. props. effect 0-16587
- Nb-W-Zr-Ta, long-term strength props., vac. level effect 0-55484
- Nb-Zn-N alloys, Zr-N complex formation, internal friction temp. depend. (*Russian*) 0-54311
- Nb-Zr, acoustic phonon anomalies and superstructure, neutron inelastic scatt. meas. 0-19892
- Nb-Zr, fusion reactor first wall materials, compatibility with impure He 0-32469
- Nb-Zr (1 at.%), annealed, TEM study of ion implanted irregular He bubbles 0-15164
- Nb-Zr (1 wt.%), fusion reactor blanket struct. material, low cycle fatigue behaviour 0-30073
- Nb-Zr (1.5 wt.%) alloy, field ion microscopy investigation, surface struct. 0-45220
- Nb-Zr-C, plastic deform. and annealing, dislocation struct. (*Russian*) 0-20951
- Nb-Zr-C (0.1, 0.01 wt.%) plastic deform. influence on electronic state of Nb atoms 0-40463
- Nb $_3$ Al core wires and pressed powder compacts, supercond. transition 0-34541
- Nb $_3$ As, structural and supercond. props. press. effects 0-39700
- NbFe $_{2-x}$ Si $_x$ , crystalline struct., electron microscopy determ. 0-54174
- Nb $_{78}$ Fe $_{40}$ Si $_{80}$ , X-ray cryst. struct. determ. (*French*) 0-15048
- Nb $_{78}$ Ga $_{22-x}$ Mn $_x$ , supercond. props., influence of Mn mag. impurities 0-54825
- Nb $_{80}$ Ga $_{20-x}$ Mn $_x$ , supercond. props., influence of Mn mag. impurities 0-54825
- Nb $_3$ Ga(So)(Ir)(Pt)(Au), X-ray  $M_{IV,V}$  emission bands (*Russian*) 0-45170
- NbGe $_2$ , superconducting transition temp. meas. of sputtered films and bulk 0-7019
- Nb $_{0.82}$ Ge $_{0.18}$ , structural and supercond. props. press. effects 0-39700
- Nb $_{1-x}$ Ge $_x$ , supercond., mag. field props. 0-54822
- Nb $_3$ Ge, A-15 diffusion layers, influence of additions of growth and supercond. props. (*German*) 0-11130
- Nb $_3$ Ge A15 cpd., bulk modulus 0-7611
- Nb $_3$ Ge, amorphous nongranular thin superconducting film, thermodynamic and resistive transitions 0-34571
- Nb $_3$ Ge, disordered superconductor,  $T_c$  depression by acoustic plasmon overdamping 0-7020
- Nb $_3$ Ge, electron-lifetime effects on props. 0-10951
- Nb $_3$ Ge, structural and supercond. props. press. effects 0-39700
- Nb $_3$ Ge supercond. film, of high transition temp., US attenuation 0-49991
- Nb $_3$ Ge supercond. thin films, He- and Ar-irradiated, X-ray diff. studies 0-29503
- Nb $_3$ Ge, superconducting A-15 type compounds, transition temp., radii ratio and structure (*Chinese*) 0-44752
- Nb $_3$ Ge superconducting film, crit. temp. correl. with resist. relations and film struct. (*Russian*) 0-15646
- Nb $_3$ Ge superconducting films, high critical temp., optimum sputtering conditions 0-15647
- Nb $_3$ Ge superconducting films, quantitative Auger anal. 0-55740
- Nb $_3$ Ge, superconducting thin films, energy gaps from tunnelling meas. 0-25050



**niobium alloys continued**

- Nb<sub>3</sub>Ge superconductivity film, Nb<sub>3</sub>Ge<sub>3</sub> and NbO content, X-ray diffr. obs. 0-2515
- Nb<sub>3</sub>Ge(Sn), superconducting, optical props. and electron-phonon interactions 0-2510
- NbH<sub>3</sub>, harmonic and anharmonic elastic props. 0-10589
- $\alpha$ -NbH<sub>3</sub>D<sub>2</sub>, H diffusion, NMR spin echo obs. 0-34228
- Nb<sub>0.55</sub>Ir<sub>0.45</sub> metallic glass, Young's modulus meas. by impulse induced resonance technique 0-40411
- Nb<sub>3</sub>Ir, A-15 struct. <sup>93</sup>Nb NQR spectra 0-20496
- Nb<sub>0.5</sub>Mo<sub>0.5</sub>, soft X-ray spectra, theoretical considerations 0-11511
- Nb<sub>0.4</sub>Ni<sub>0.6</sub>, amorphous, pair distrib. function, temp. depend., rel. to glass transition 0-24368
- Nb<sub>3</sub>Os, A-15 struct. <sup>93</sup>Nb NQR spectra 0-20496
- Nb<sub>3</sub>Pt, A-15 struct. <sup>93</sup>Nb NQR spectra 0-20496
- NbSi<sub>2</sub>, superconducting transition temp. meas. of sputtered films and bulk 0-7019
- Nb<sub>3</sub>Si, A-15 diffusion layers, influence of additions of growth and supercond. props. (German) 0-11130
- Nb<sub>3</sub>Si, high T<sub>c</sub>, supercond. props. from extrapolation of sp. ht. meas. on A-15 Nb-Si 0-25045
- Nb<sub>3</sub>Si, metastable A-15 struct. synthesis by ion implantation, supercond. transition temp. 0-55319
- Nb<sub>3</sub>Si, structural and supercond. props. press. effects 0-39700
- Nb<sub>3</sub>Si, supercond., A15 film, electron beam evaporation 0-29284
- Nb<sub>3</sub>Si, superconducting A-15 type compounds, transition temp., radii ratio and structure (Chinese) 0-44752
- Nb<sub>3</sub>Sn, A-15 struct. Nb based superconductors, irradi. type influence on radiation defects 0-15093
- Nb<sub>3</sub>Sn, alloying agent influence on struct. and supercond. props. (Russian) 0-39698
- Nb<sub>3</sub>Sn, atomic displacements induced by radiation damage, X-ray study 0-2085
- Nb<sub>3</sub>Sn, composite supercond., powder metallurgical prep. 0-2981
- Nb<sub>3</sub>Sn cryotron, thermally controlled, used in transformer-rectifier flux pump for superconducting magnet 0-4727
- Nb<sub>3</sub>Sn, Cu admixture in Sn bath effect on critical current and stability temp. 0-7059
- Nb<sub>3</sub>Sn, current carrying capacity increase by Hf addition 0-7056
- Nb<sub>3</sub>Sn, electron-lifetime effects on props. 0-10951
- Nb<sub>3</sub>Sn fatigue effects in unidirectional composites, computer simulated model 0-35289
- Nb<sub>3</sub>Sn films, deposition by quasi-closed vol. method, supercond. crit. temp. 0-15645
- Nb<sub>3</sub>Sn, flux trapping and shielding capabilities in transverse fields 0-15667
- Nb<sub>3</sub>Sn, high-current A-15 microcomposite material 0-44781
- Nb<sub>3</sub>Sn, high-rate sputter-deposited, effect of oxygen on microstruct. 0-20343
- Nb<sub>3</sub>Sn monofilamentary wires, supercond. crit. current density, bending effects 0-50018
- Nb<sub>3</sub>Sn, multifilament conductors appl., production and props. (German) 0-3081
- Nb<sub>3</sub>Sn, multifilament superconductor, pulsed mag. field losses and critical current densities 0-54853
- Nb<sub>3</sub>Sn, O<sup>4+</sup> bombarded, Mossbauer studies 0-2672
- Nb<sub>3</sub>Sn, supercond., thin film, US attenuation of SAWs 0-49988
- Nb<sub>3</sub>Sn superconducting composite, bronze process, metallurgy 0-3004
- Nb<sub>3</sub>Sn, superconducting thin films, energy gaps from tunnelling meas. 0-25050
- Nb<sub>3</sub>Sn superconducting wire, fabrication from Cu-Nb-Sn alloy using controlled high temp. gradient 0-25056
- Nb<sub>3</sub>Sn-Cu, high-current A-15 microcomposite material 0-44781
- Nb<sub>3</sub>Sn<sub>4</sub> film, critical currents due to microwave field 0-25058
- Nb<sub>3</sub>(Sn-Al) system, X-ray spectroscopic studies of electronic struct. of A15 cps. 0-2900
- Nb<sub>3</sub>Su-Cu supercond. composites, fabrication, magnet appl. 0-11602
- Nb<sub>3</sub>Ta<sub>47</sub>, pure and hydrogenated crystals, effect of pressure on elastic consts. 0-7614
- NbTi, superconducting multifilamentary conductors, crit. current density, bending effects (German) 0-39727
- NbTi, superconductor, acoustic emission during flux jump 0-39724
- NbTi/In granular composite, resistivity mag. field depend. 0-15654 (Nb<sub>0.99</sub>Ti<sub>0.01</sub>)<sub>1-x</sub>Ge<sub>x</sub>, supercond., mag. field props. 0-54822
- Nb<sub>0.75</sub>Zr<sub>0.25</sub>, effect of force constant, disorder on Eliashberg function 0-29504
- Nb<sub>20</sub>Zr<sub>80</sub>, supercond., US attenuation 0-44766
- (Nb<sub>0.99</sub>Zr<sub>0.01</sub>)<sub>1-x</sub>Ge<sub>x</sub>, supercond., mag. field props. 0-54822
- Ni-Al-Nb, heat resist., solidification range 0-35177
- Ni-Al-Nb, heat-resisting dispersion-hardening alloys, props. and struct.,  $\gamma'$ -phase comp. influence (Russian) 0-20943
- Ni-Cr-Mn-Fe-Nb (20,3,3,2.5 wt.%), short-range order effects on tensile behaviour 0-25793
- Ni-Fe-Cr-Nb-Ta-Mo alloy, fatigue crack growth, stress ratio and hold-time effects 0-40531
- Ni-Fe-Nb, magnetic alloy, TEM and X-ray obs. (Chinese) 0-24401
- Ni-Fe-Nb-Al-(Mo), wear resisting mag. head material, mag. props. and struct. 0-35350
- Ni-Nb alloys, oxidation at high temp., high energy ion backscattering anal. (Japanese) 0-35405
- Ni-Nb-Al (25, 2.5 wt.%), directionally solidified  $\gamma/\gamma'$ - $\delta$  eutectic, growth conditions on struct. 0-11639
- Ni-W-Nb system,  $\gamma$  to ( $\gamma$ +W) phase boundary calcs. using Wigner method (Russian) 0-54346
- Ni-ZrB<sub>3</sub> powders, densification by hot pressing 0-25604
- Ni<sub>2</sub> (Al, Nb) single crystals, orientation and temp. depend. of yield stress 0-25791
- Ni<sub>3</sub>Al-Ni<sub>3</sub>Nb, eutectic, temp. and thermal cycling influence on oxidation 0-45417
- Ni<sub>3</sub>Al-Ni<sub>3</sub>Nb, eutectic alloy, crack development, failure energy capacity (Russian) 0-40480
- Ni<sub>3</sub>Al-Ni<sub>3</sub>Nb eutectic, directionally solidified, high-temp. oxidation mechanism 0-16544
- Ni<sub>62</sub>Nb<sub>38</sub>, metallic glass, struct., neutron diffr. study 0-54148
- Ti-Al-Nb-Ta-Mo (6, 2, 1, 0.8 wt.%), elevated temp. flow strength, creep resist., diffusion welding characts. 0-30033
- Ti-Nb-Al, decomposition during isothermal annealing 0-25653
- Ti-Nb-Zr (35, 3 wt.%), martensitic  $\tau$  phase, X-ray diffr. obs. 0-16300
- Ti<sub>1-x</sub>Nb<sub>x</sub>H<sub>1.94</sub>, electronic struct. MNR meas. 0-15439
- Ti<sub>1-x</sub>Nb<sub>x</sub>H<sub>1.94</sub>, x=0.25, 0.50, low temp. specific heat meas. 0-2179

**niobium alloys continued**

- WC-Co-TaC-TiC-NbC cemented carbide, microstructure, high temp. deformation, uniaxial plastic compression 0-40451
- Zr-Nb (20 wt.%),  $\omega$ -phase form., diffuse Mossbauer scatt. 0-25324
- Zr-Nb (2.5 wt.%), crack resistance, influence of ZrH<sub>3</sub> fracture toughness 0-16444
- Zr-Nb (2.5 wt.%), hydride induced crack growth, effect of stress, temp. and H<sub>2</sub> content 0-3178
- Zr-Nb (2.5 wt.%), superplastic and strain rate depend. plastic flow, 873 to 1373K 0-30052
- Zr-Nb (2.5 wt.%), transforms. during annealing of welded joint, after thermal cycling (Russian) 0-29984
- Zr-Nb-Ga, phase equilibria 800°C (Ukrainian) 0-35157
- Zr-Nb-Sn (3,1 wt.%), corrosion resist. depend. on mech. and heat treatments 0-653
- Zr-Nb-Sn(3 wt.%, 1 wt.%), oxidation kinetics in flowing CO<sub>2</sub> at high temp. 0-47575
- Zr-Nb(2.5 wt.%), oxidation kinetics in flowing CO<sub>2</sub> at high temp. 0-47575
- (Zr<sub>1-x</sub>Nb<sub>x</sub>)Fe<sub>2</sub>, magnetovolume effects and Invar characters 0-15773
- Zr<sub>1-x</sub>Nb<sub>x</sub>Zn<sub>2</sub>, microscopic mag. props., NMR investigation 0-15807

**niobium compounds***see also niobium alloys*

- KKR calc. of energy bands 0-34355
- niobate based ceramics, synthesis, struct., elec. cond., mag. props. (Czech) 0-45259
- refractory carbides, borides and nitrides, wetting by and interactions with liq. metals 0-54473
- strength of nonlinear interaction between collinear surface acoustic waves 0-33295
- Bi-NbO<sub>2</sub>-Bi system, Schottky barrier effects in transport and dielec. props. 0-29486
- CoNb<sub>2</sub>O<sub>6</sub>, magnetic struct., neutron diffr. and mag. susceptibility meas. 0-15693
- Cr-Ti/MgO-NbC dispersion-strengthened, high temp. wear and oxidation resist. 0-25877
- Cr-Ti/NbC dispersion-strengthened, high temp. wear and oxidation resist. 0-25877
- Fe-NbC, dispersion strengthened, thick vacuum condensate, control of struct. and mech. props. 0-16324
- FeNbSe<sub>2</sub> (2H), mag. susceptibility meas., 1.3-300K 0-39740
- Y-Zr LiNbO<sub>3</sub>, radiation patterns of bulk acoustic modes from finite interdigital transducer 0-43491
- LiNbO<sub>3</sub>, SAW reflection from conducting strips 0-5853
- NaYb(WO<sub>4</sub>)<sub>2</sub>, thermal expansion, X-ray determ. 0-39323
- Nb-C-N-O-H, solid solns. of H, exam. of props. 0-29172
- Nb-H, electron work function, 300 to 600 degrees C, contact potential difference meas. 0-29462
- Nb-H, exam. of electron structure 0-29306
- Nb-H system, temp.-stimulated acoustic emission, hydride precip. 0-3044
- Nb-Nb<sub>2</sub>O<sub>7</sub>-Pb, two-dimens. Josephson junction, supercurrent vs. mag. field characts. 0-34562
- Nb-NbO<sub>2</sub>-Pb Josephson tunnel junctions, fabrication using FR glow discharge oxidation 0-34559
- Nb-NbO<sub>2</sub>-Pb tunnel junctions, current density distrib. 0-39717
- Nb-S system, phase relations at high temp., elec. and mag. props. 0-29932
- Nb-Ta-N sputtered films and their anodic oxides, elec. props. of resist. and dielec. films 0-11126
- NbB<sub>2</sub>, hot pressing 0-25635
- NbB<sub>2</sub>, single crystals, hardness anisotropy and slip 0-21085
- NbB<sub>2</sub>, superconductivity below 1K 0-20342
- NbC crystals, electron energy spectra 0-49568
- NbC, deformation behaviour during rubbing in wide temp. range 0-16486
- NbC, electronic struct. of vacancies, effect on supercond. transition temp. 0-29347
- NbC micro powder surface finishing of metals, surface struct. 0-11842
- NbC single crystals, synthesis and impurities 0-55329
- NbC, true heat capacity meas. by pulse method 0-19953
- NbC, valence band XPS meas., comparison with X-ray emission spectra and band struct. spectral calcs. 0-50535
- NbC<sub>x</sub> (x=0.868, 0.834, 0.766), single crystals, thermomech. behaviour during annealing 0-3104
- NbC<sub>x</sub>, x=0.868, 0.834, 0.766, self-diffusion of <sup>14</sup>C 0-29206
- NbC(N), critical temp. enhancement, surface effect on phonon spectrum and electronic state density (Chinese) 0-2507
- Nb<sub>2</sub>C<sub>2</sub>O<sub>7</sub>, H solubility 0-34191
- NbCl<sub>4</sub>, high press. elec. resistivity 0-29404
- NbCl<sub>5</sub> in chloroaluminate melts, Raman spectral study 0-34915
- (NbCl<sub>4</sub>Br<sub>6-n</sub>)<sup>-</sup> complexes in acetonitrile soln., <sup>93</sup>Nb spin relax. and mag. shielding 0-44944
- NbD, structs. phase diagrams, morphologies, prep. methods, book contrib. 0-25675
- NbH, structs. phase diagrams, morphologies, prep. methods, book contrib. 0-25675
- NbH<sub>0.73</sub>, multiple wavelength neutron powder diffr. data, Rietveld profile refinement algorithm 0-24320
- NbH<sub>x</sub>, HF phonons, neutron spectral obs. 0-49317
- NbN granular films, crit. current behaviour 0-15672
- NbN, interatomic interactions from XPS 0-49171
- NbN preparation, by precip. from gaseous NgF<sub>3</sub>-N<sub>2</sub>-H<sub>2</sub> mixture 0-20857
- NbO and NbO<sub>2</sub>, H solubility 0-34191
- NbO, high press. elec. resistivity, semiconductor to semiconductor transition 0-29404
- NbO<sub>2</sub>, high press. elec. resistivity, phase transition 0-29404
- NbO<sub>2</sub>, rutile phase, energy levels, momentum density, and Compton profile, embedded cluster model 0-50453
- NbO<sub>2</sub>, semicond., thermal expansivity 0-34213
- NbO<sub>2</sub>, threshold switching recovery curve, distribution trapped carrier lifetime 0-20258
- NbO<sub>2.417</sub> to NbO<sub>2.5</sub>, equilib., chem. transport with TeCl<sub>4</sub> 0-2934
- NbO<sub>2</sub>, phase comp. on heating 2000-4000K 0-21267
- Nb<sub>2</sub>O<sub>5</sub>, B-form single crystals, ESR of Mo<sup>5+</sup> and W<sup>5+</sup>, site symmetry 0-54946
- Nb<sub>2</sub>O<sub>5</sub>, chemical effect, influence on stopping power 0-47830
- Nb<sub>2</sub>O<sub>5</sub> electrodes, in aq. and acetonitrile solns., electrochromism 0-50298
- Nb<sub>2</sub>O<sub>5</sub> waveguide, in-plane scatt. and loss mechanisms 0-33216
- NbOAsO<sub>4</sub> and NbOAsO<sub>4</sub> 4H<sub>2</sub>O, crystal growth, composition, struct. and crystallographic characts. 0-54198



**niobium compounds continued**

- NbS<sub>2</sub>, enthalpy and specific heat, temp. depend. 0-54406  
 NbS<sub>2</sub>, intercalation complexes with 3d transition metals, mag. and metallic transport props. 0-44814  
 NbS<sub>2</sub>, intercalation cpd. with pyridine, nucl. spin-lattice relax. meas. 0-54962  
 NbS<sub>2</sub>, nucl. spin-lattice relax. meas. 0-54962  
 NbS<sub>3</sub>, Peierls distortion, electron diffr. obs. 0-39503  
 NbS<sub>3</sub>, phase transitions and elec. props. 0-20178  
 NbS<sub>3</sub>, transport props. 0-20175  
 Nb<sub>3</sub>S<sub>4</sub>, anisotropic superconductor, critical field and specific heat meas. 0-44779  
 NbS<sub>2</sub>Cl<sub>2</sub>(Br<sub>2</sub>)(I<sub>2</sub>), prep., struct. and props. 0-28994  
 NbSe<sub>2</sub> (2H), intercalated with TCNQ, elec. resistivity temp. behaviour anomaly (*Russian*) 0-10953  
 NbSe<sub>2</sub>, intercalated with Rb, EXAFS 0-2897  
 NbSe<sub>2</sub>, intercalated with Rb, EXAFS meas. 0-40185  
 NbSe<sub>2</sub>, intercalation complexes with 3d transition metals, mag. and metallic transport props. 0-44814  
 NbSe<sub>2</sub>:Fe (2H), pure and doped, magnetoresist. and elec. resist. temp. depend. rel. to CDW form. 0-44574  
 NbSe<sub>2</sub> and Nb<sub>1-x</sub>Ta<sub>x</sub>Se<sub>2</sub>, thermoelec. power meas., 10-300K 0-20177  
 NbSe<sub>2</sub>, CDW form., non-linear props., temp. and press. depend. 0-49753  
 NbSe<sub>2</sub>, Fermi surface, press. effects, Shubnikov-de Haas effect meas. at 1.5K 0-20068  
 NbSe<sub>3</sub>, mag. anomalies at CDW transitions 0-11158  
 NbSe<sub>3</sub>, metallic, non-ohmic cond., CDW pinning 0-39563  
 NbSe<sub>3</sub>, Peierls distortion, electron diffr. obs. 0-39503  
 NbSe<sub>3</sub>, phase transitions and elec. props. 0-20178  
 NbSe<sub>3</sub>, phonon study of chemical bonding 0-20645  
 NbSe<sub>3</sub>, quasi one-dimens. conductor, CDW phase transform., X-ray scatt. study 0-24594  
 NbSe<sub>3</sub>, transport props. 0-20175  
 NbSe<sub>3</sub>, two band model and galvanomagnetic study 0-20176  
 NbSe<sub>2</sub>:Zr, dopant effect on supercond. transition temp. rel. to CDW 0-39699  
 NbSe<sub>2</sub>Cl<sub>2</sub>(Br<sub>2</sub>)(I<sub>2</sub>), prep., struct. and props. 0-28994  
 NbSe<sub>2</sub>Cu<sub>x</sub>, ordering study using electron diffr. and microscopy 0-39043  
 NbSi<sub>2</sub>, formation by Ar ion bombard. of Nb-on-Si system 0-10709  
 NbSi<sub>2</sub>, self-propag. high-temp. synthesis 0-2988  
 Nb<sub>3</sub>Si, A-15 struct. stability, atomic radii ratio (*Chinese*) 0-54393  
 Nb<sub>1-x</sub>Ta<sub>x</sub>Sn<sub>2</sub>, supercond. transition temp. and upper crit. field 0-39723  
 NbTe<sub>2</sub>, layer cryst., dislocations and domain struct. 0-39102  
 Nb<sub>1-x</sub>Ti<sub>x</sub>O<sub>2</sub>, X-ray struct. anal. 0-28954  
 Nb<sub>0.87</sub>V<sub>0.13</sub>Se<sub>2</sub>(4Hb), stacking layer study, appl. of convergent beam electron diffr. 0-39116  
 NiO, stress appl. high temp. creep and point defects, creep rate obs. 0-49297  
 Pb<sub>0.99</sub>Nb<sub>0.02</sub>(Zr<sub>0.95</sub>Ti<sub>0.05</sub>)<sub>0.98</sub>O<sub>3</sub>, ferroelec. ceramic, stress effects 0-2119  
 Ti<sub>1-x</sub>Nb<sub>x</sub>H<sub>1.94</sub>, x=0.25, 0.50, low temp. specific heat meas. 0-2179  
 TiO<sub>2</sub>:Ta<sub>2</sub>O<sub>3</sub>(Nb<sub>2</sub>O<sub>3</sub>), rutile, defect struct. and elec. cond. at 1273K 0-44604  
 (V<sub>1-x</sub>Ta<sub>x</sub>)<sub>2</sub>C, C ordering formation of varieties 0-38968

**nitrogen**

see also nuclei with .....

- absorption by LaCo<sub>5</sub> at low temps. 0-24599  
 abundance in H II regions 0-46680  
 active, heterogeneous atom recomb. on glass Langmuir-Rideal mechanism 0-7853  
 active condensed, thermolum. meas. (*French*) 0-11484  
 adsorbed layer (1×1), on Ti (0001), underlayer geometry, electronic struct. calcs. and UPS meas. 0-54751  
 adsorbed layer on W (001) clean surface, long-range inhibition of displacive phase 0-2266  
 adsorbed on graphite, Mossbauer obs. 0-18060  
 adsorbed on metal-sapphire interface, effect on shear strength 0-49485  
 adsorbed on Ni (001) surface, p(2×2) struct., LEED and AES study 0-54515  
 adsorbed on W, effect of SIMS sputtering induced recomb. anal. 0-55243  
 adsorption on GaAs (110), UPS and EELS study, tight-binding calcs. 0-49496  
 adsorption on Sc and Lu surfaces, effect on reflection EELS 0-20742  
 adsorption on W, thermal desorption and pulsed time of flight mass spectrometry anal. 0-30285  
 adsorption on W(110) vicinals, step sites as dissociation centres 0-6642  
 arc, laminar flow, equilib. composition deviation 0-24274  
 arc plasma, stabilised by gas injection, thermochem. nonequilibrium, particle excitation, vibr. temps. 0-19634  
 atom, 3p<sup>4</sup>S<sup>0</sup>-state quenching in low-pressure glow discharge 0-23355  
 atom, dipole properties and dispersion energies additivity, using atoms and small mol. models 0-53091  
 atom, many electron autoionisation states, perturbation theory Z-expansion, numerical results 0-52863  
 atom, np<sup>2</sup>(n+1)s excited-state config. quadrupole moments, Sternheimer shielding factor 0-37755  
 atom, SCF electron-gas local-spin-density model including correlation 0-9488  
 atom, spherical ground state nuclear quadrupole interaction, Breit interaction, relativistic perturbation theory 0-42939  
 atom-atom pot. parameter in azabenzene, dispersion energy calcs. 0-23489  
 boiling 0-53770  
 boiling heat transfer from stainless steel surface, surface roughness effect 0-48705  
 breakdown in crossed elec. and mag. fields, modified Paschen's law 0-24121  
 capillary condensation and evap., apparatus and calc. method 0-2150  
 capillary condensation and evap., scanning curves within B-type hysteresis loops 0-2151  
 chemisorbed on Ag film, reflectance and elec. resist. changes 0-11495  
 chemisorption on LaB<sub>6</sub>, time of flight atom-probe FIM study 0-6652  
 chemisorption on Ni (110), mol. and dissociative mechanisms 0-39431  
 chemisorption on Ti (0001), valence band struct., XPS and UPS study 0-35062  
 chemisorption on W {110}, underlayer mechanism 0-39432  
 chloroform-N<sub>2</sub>, gaseous compressed mixture, mol. reorientation, Raman spectra 0-23422  
 CO<sub>2</sub>-N<sub>2</sub>, highly efficient gas for nanosecond pulse CO<sub>2</sub> laser system (*Japanese*) 0-48214

**nitrogen continued**

- coating, on Al thin film, effect on supercond. 0-7026  
 concentration meas. by <sup>14</sup>N(d, p)<sup>15</sup>N 0-42671  
 determination, combustion-gas chromatographic method, data processing 0-40762  
 diamond:N, paramagnetic centres, exchange interaction, spin density delocalisation 0-39847  
 diamond:N, synthetic, impurity effect on strength characts. and thermal stability 0-11726  
 diatomic mols., internal partition functions for O<sub>2</sub>, N<sub>2</sub>, NO and their ions, max. summation indices 0-27995  
 diffusion in Ti and Zr fibres, high-temp. nitriding kinetics (*Russian*) 0-21166  
 discharge, anomalous heating (*Russian*) 0-1866  
 discharge, combined, in average press. gas using two HV pulse sources, gas laser development 0-44027  
 discharge, electron beam sustained high press., time behaviour of recomb. coeff. 0-10447  
 discharge, excitation efficiency of rot. and vibr. levels, heating due to collisions and relax. 0-38751  
 discharge, externally maintained, instability growth time, associative ionisation 0-6254  
 discharge, high-current, with inductive storage bank, exploding wire-initiated 0-10450  
 discharge, ionisation current increase, metastable mol. induced cathode secondary electron emission 0-38830  
 electric breakdown, vol. discharge with external photoionisation, plasma focus spark channel (*Russian*) 0-38738  
 electric breakdown gas discharge, Paschen curve double minima 0-44036  
 electric breakdown in filled diodes, electrode temp. depend. 0-1735  
 electrical and optical discharge parameters at moderate press. 0-6300  
 electrical current, bipolar, in dense gas without volume ions. 0-6208  
 electron backscattering coeffs., 100 eV to 5 keV 0-9750  
 electron drift vels., time-of-flight meas. 0-28855  
 electron swarm development, Boltzmann eqn. method 0-43832  
 electron swarm parameters for high E/N, Monte Carlo simulation 0-19548  
 electron transmission function and mean energy per ion pair, obs. 0-23566  
 electrotransport in La 0-24674  
 fixation, semiempirical INDO study 0-16898  
 fixation using fusion energy heat source 0-32510  
 fluid, structure and dynamics 0-38889  
 gas discharge, low press., emitted photon probe for electron swarm parameters 0-43839  
 gas filled chamber, passage of low current electron beam 0-38523  
 glow discharge, DC, metastable atoms prod. 0-38758  
 glow discharge, neutral components comp., mass spectroscopy study (*Russian*) 0-10439  
 glow discharge instability in afterglow 0-6313  
 heat transfer in boiling on surface of vertical cylindrical rod 0-48706  
 human body N meas. by anal. of prompt γs from neutron capture 0-51220  
 interstellar neutral <sup>14</sup>N, search for radioemission 0-41886  
 ion+Ar, Kα X-ray satellites prod. 0-9541  
 ion implantation in GaAs<sub>1-x</sub>P<sub>x</sub>, characterisation by photolum. and channelling 0-54262  
 ion stimulated sorption onto Ti film, TiN<sub>x</sub> form., sorption ratio, capture coeff. anal. 0-39411  
 ions, beam-foil excitation, relative initial populations, lifetime curves 0-14210  
 ions, collective acceleration 0-5406  
 ions and neutral atoms in Venus daytime thermosphere 0-17517  
 isotope fractionations in Fischer-Tropsch and Miller-Urey reactions, appl. to carbonaceous chondrites 0-46496  
 jets, single and multiple free, CW laser Raman spectroscopy 0-32727  
 K-shell, excitation and ionisation, vibr. struct., electron energy loss spectra obs. 0-18943  
 laser, double-channel 0-19046  
 laser, helical TE, with circular beam cross section 0-33023  
 laser, high power tunable liq. Raman type, for spectroscopy 0-48277  
 laser, oscillator-amplifier system using press.-depend formative time lag of discharge 0-14354  
 laser, TEA high-power, using modified Marx generator 0-1229  
 laser, travelling wave, pump for short resonator tunable dye laser 0-48291  
 laser induced gas breakdown threshold at 1.06 micron 0-28594  
 laser near-threshold IR enhancement by He additive (*Japanese*) 0-14324  
 laser spark in dense gas near metallic target (*Russian*) 0-38682  
 laser UV-IR pulse time lag theory (*Japanese*) 0-14325  
 liberation from electrolytic Ni during vacuum heating, Mossbauer spectra (*Russian*) 0-35594  
 liquid, Brillouin scatt. obs., US vel. and absorpt. 0-45085  
 liquid, cryogenic, elec. breakdown, time lag 0-29684  
 liquid, dielectric breakdown, using discharge figures 0-11338  
 liquid, film boiling heat transfer, orientation effect 0-48554  
 liquid, film boiling heat transfer coeff. for vertical surfaces 0-48556  
 liquid, high-field carrier transport at pre-breakdown and breakdown regions 0-25305  
 liquid, mol. correl. functions, effective pair pot. evaluation 0-10476  
 liquid, nucleate boiling heat transfer at reduced pressures 0-48557  
 liquid, possible active media in high-power Raman lasers 0-19028  
 liquid, powerful tunable IR and far IR Raman sources 0-5787  
 liquid, PTC thermistor P310-C11 level sensor 0-52247  
 liquid, Raman lineshape 0-11384  
 liquid, shock compression temp., detonation front glow 0-43737  
 liquid, solubility of light olefins 0-39286  
 liquid, struct. factor, short-wavelength neutron scatt. obs. 0-44105  
 liquid, supply to vacuum installations 0-31762  
 liquid, thermodynamic props., perturbation theory with hard dumbbell reference system 0-14991  
 liquid, two level controller 0-52241  
 liquid-vapour surface, computer simulation 0-54478  
 molecular cluster formation, in rarefied nozzle flowfield 0-5639  
 molecular electron scattering, local-exchange approx. for intermediate-energy-differential cross sections 0-48094  
 molecular liquid, mean squared torque and mean squared force, interaction energy spherical harmonic expansion 0-54093  
 molecular overlayer on graphite, orientational ordering, neutron scatt. meas. 0-10783



## nitrogen continued

molecular photoionisation cross sections, at. extrapolation, ground state inversion method appl. 0-18787  
 molecule,  $3\sigma_g$  photoionis., shape-reson.-induced non-Franck-Condon vibr. intensities 0-43120  
 molecule, adsorption on graphite, orientational ordering, theory 0-2262  
 molecule,  $C^1\Pi_u$ -state, electron impact excitation, low energy 0-9746  
 molecule, correlated electron density using AHF GTO wavefunctions 0-23313  
 molecule, dipole properties and dispersion energies additivity, using atoms and small mol. models 0-53091  
 molecule, elastic and inelastic electron scatt. differential cross section, obs. and calc., struct., binding energy 0-28109  
 molecule, elastic electron scatt., 50 eV, centrifugal-dominant channel decoupling, INDOX polarised SCF model 0-32831  
 molecule, elastic electron scatt. from 0 to 1000 eV, energy dependent exchange pots., continuum multiple scatt. method 0-43182  
 molecule, electrical discharge excitation, vibr. level population distrib., electron beam fluoresc. obs. 0-48031  
 molecule, electron elastic scatt. cross-sections calcs. 0-48088  
 molecule, electron impact, electron distrib. function in laser radiation field, vibr. excitation influence 0-28112  
 molecule, electron impact, reson. vibr. excitation, ab initio R matrix calc. 0-32842  
 molecule, electron impact enhanced vibr. excitation, continuum multiple scatt. model with Hara exchange approx. 0-43196  
 molecule, electron impact excitation cross-sections for  $B^3\Pi_g$ ,  $C^3\Pi_u$  and  $E^2\Sigma_g^+$  states 0-1073  
 molecule, electron impact rot. and vibr. excitation, elastic scatt., close coupling and Born approx. 0-28108  
 molecule, electron scatt., effective pot. calcs. 0-53131  
 molecule, electron scatt., Glauber eikonal approx. calcs. 0-53130  
 molecule, electron scattering, iterative static exchange method 0-53155  
 molecule, electron scattering, total cross section 0-37881  
 molecule, electron-mol. adiabatic polarisation pots. and ab initio SCF polarisabilities 0-9499  
 molecule, electronic density, multiple scatt. method, muffin-tin approx. 0-27924  
 molecule, electronic struct., binding energy and interatomic distance, SCF variational cellular calc. 0-9498  
 molecule, flame temp., CARS spectra diagnostic investigation 0-43404  
 molecule, ground state ionis. pots., generalized Mo theory 0-52907  
 molecule, ground state props., coupled cluster and MBPT methods appl. 0-47881  
 molecule, large angle elastic and inelastic electron scatt. differential cross section, exchange corrections 0-28111  
 molecule, light polarisability parameters, Raman scatt. ang. meas. 0-37814  
 molecule, low energy electron (positron) collisions, ab initio adiabatic polarisation pots. 0-14240  
 molecule, low energy electron impact dissociative ionis.,  $N_2^{2+}$  form. and energy distrib. 0-5626  
 molecule, matrix isolated, fundamental vibr. Raman spectra 0-272  
 molecule, metastable level electron impact excitation, resonances (Russian) 0-43198  
 molecule, MSX $\alpha$  calc., partial wave expansion, binding energy and orbital energy 0-37738  
 molecule, multiple moments, polarisabilities and anisotropic long range interaction coeffs. 0-43206  
 molecule, N K-shell excitation, high-resolution electron energy loss spectra 0-53152  
 molecule, one-electron props., polarisabilities and polarisability derivatives, SCF and CI calcs. 0-37746  
 molecule, PE curve, spectroscopic consts., perturbation theory appl. 0-23341  
 molecule, photoelectron ang. distrib., photon energy depend., 16-25 eV 0-53046  
 molecule, photoionis. and photoabsorpt. cross sections for aeronomic calcs., data tables 0-41599  
 molecule, polarisability tensor anisotropy, Raman spectra differential scatt. cross section 0-18860  
 molecule, pot. curves, binding and ionisation energies and config. variational cellular method 0-32597  
 molecule, quadrupole moments calcs. from line broadening collision with acetaldehyde 0-28065  
 molecule, Raman intensities calcs., ab initio method 0-52993  
 molecule, Raman intensity, ab initio calc. 0-1028  
 molecule, Raman spectra, intermol. torques and orientational correlation times 0-48006  
 molecule, rot. line strengths in multiphoton transitions 0-48051  
 molecule, rotational Raman calibration of Thomson scatt. 0-1844  
 molecule, supersonic mol. beam, CARS rot. temp. meas. 0-23423  
 molecule, three-body electron attachment 0-24245  
 molecule, total  $X\alpha$  energy, LCAO calc., rel. to local density models 0-32607  
 molecule, triplet-triplet transitions, Einstein-A coeffs., oscill. strengths, lifetimes, theory and experiment comparison 0-47876  
 molecule, V-V and V-T/R energy transfer rate coeffs. by semiclassical collision model 0-9694  
 molecule, vibr. struct., core and valence ESCA spectra, Franck-Condon and HF anal. 0-32602  
 molecule, vibr. temp. meas. in  $CO_2$  fast flow laser 0-32955  
 molecule,  $X\alpha$  theory appls. approximations 0-9510  
 molecule, X-ray K-absorpt. spectra, reson. obs., near fine struct. 0-37817  
 molecule, electron impact dissociation rel. to  $O_3$  generation in air-fed ozonisers 0-3323  
 molecules, collisional destruction of singlet He I states in low press. glow discharge 0-49030  
 molecules, gaseous, density behaviour of rototranslational spectrum, IR spectra obs. 0-28002  
 molecules, structure factor 0-43137  
 $\beta$ - $N_2$ , cryst. struct. at 25 kbar and 296K 0-10528  
 neutron activation analysis meas. of O and N 0-46032  
 nitridation of Mg in HF discharge, temp. effect 0-3399  
 nitriding of steel through ionic bombardment 0-45414  
 permeability in hard elastic polypropylene films, extension effects 0-40412  
 in planetary nebula in irregular galaxy NGC 6822, abundance and nucleosynthesis 0-41867  
 plasma, beam and glow discharge type, macroscopic props., kinetic eqns. 0-43864

## nitrogen continued

plasma, dense molecular gas, breakdown due to laser radiation, numerical simulation 0-38686  
 plasma, diffuse, population densities of triplet states, correl. with electron impact processes 0-43966  
 plasma, electronic excitation levels in gas-discharge 0-24280  
 plasma, non-equilib., excited species, vibr.-rot. anal. fluoresc. obs. 0-54034  
 plasma, non-self sustained discharge current, gas purity effects 0-38845  
 plasma, of theta pinch,  $N^{+2+3+}$  lines Stark broadening, He(II) line diagnostics 0-24249  
 plasma, spatial distrib. in transverse-discharge supersonic stream, continuum theory and probe meas. 0-48866  
 plasma jet, heat transfer to rotating water-cooled cylindrical wall (French) 0-28850  
 positive column, flowing, visible spectrum obs. 0-49026  
 positive column, superelastic collisions and electron distrib. function 0-1858  
 premixed  $H_2-O_2-N_2$  laminar flames, temp. profile, comparison of spectroscopic meas. 0-42227  
 premixed  $H_2-O_2-N_2$  laminar flames, temp. profiles, Raman, absorpt. and line reversal obs. 0-42227  
 primary origin and N/O abundance ratio in galaxies 0-8686  
 pulsed laser stroboscopic fluorimeter 0-35593  
 PWR,  $N_2$  bubble appl. to eliminate solid water plant evolutions 0-18557  
 rare earth-transition metal alloy thin films vapour deposition, influence of gaseous phase on mag. props. (Polish) 0-39820  
 rarefied fluid dynamics, flow meas. by electron beam-body interactions 0-6186  
 reaction with Al powder, in low-temp. plasma 0-16257  
 recombining atomic plasmas, population inversion 0-32679  
 rotational collision number from thermal cond., 700-2500K 0-23526  
 solid,  $\alpha$ - and  $\gamma$ -forms, Raman spectra, vibron and lattice freq. shifts, libration 0-16020  
 solid,  $\beta$ -phase, for IR absorption spectra 0-11385  
 solid, mol. libration and  $\alpha$ - $\gamma$  phase transition, Kihara pot. calcs. 0-44312  
 solid, Raman spectroscopy up to 374 kbar 0-7353  
 solid and matrix isolated mol., triplet state spectra (Russian) 0-5574  
 solid-state  $\alpha$ - $\beta$  transition obs., thermometric fixed point applicability 0-13076  
 sorption by Ti, gas-discharge device appl. 0-10796  
 stationary beam discharge plasma, electron kinetics 0-38775  
 steel, ferritic, with interstitial N, continuous precipitation and clustering 0-7585  
 steel, unskilled deep drawing sheets, influence of N content on recrystn. (German) 0-40376  
 steels, ferritic and martensitic, C and N migration at low temps., monograph 0-22149  
 sticking probability and coverage determ. on W{411} and W{320} 0-54528  
 tektites and natural glasses, N concs. 0-41446  
 thermodynamic perturbation theory 0-14985  
 vibration stimulated Raman scatt., four photon parametric effects 0-33087  
 $^{15}N_2$  monolayer, adsorbed on Grafoil, reson. photon scatt. 0-34832  
 Al-C-siliceous sand mixture in  $N_2$  atmos., weight loss during heating, compaction (Japanese) 0-35151  
 $Al_3Ga_{1-x}As_N$ , ion implantation, in situ annealing photoluminesc. obs. 0-10567  
 $Al_3Ga_{1-x}As_N$ , laser annealing of optically active impurities, photolum. charact. 0-20682  
 Ar- $N_2$ , proton beam pumped, laser actn at 3577 Å 0-9861  
 Ar- $N_2$  laser, electron beam excited, gain measurements using amplified spontaneous emission 0-37986  
 Ar- $N_2$  mixture, electrodeless RF discharge, discharge current harmonics obs., conc. depend. 0-44029  
 Ar- $N_2(CO)$ , non-self-sustained discharge instability, negative differentiated cond. (Russian) 0-38740  
 $Ar^{*+}N_2$ , Ar+ $N_2^+$ , electronic to vibr. energy transfer, time depend. theory 0-23514  
 $CO_2-N_2$  and CO lasers, energy and spectral characteristics 0-14327  
 $CO_2-CO-N_2-He$  in  $CO_2$  lasers, ionisation wave, slow changes, dispersion curves 0-38822  
 $CO_2-He-N_2$ , gas dynamic laser, gain coeff. numerical estimates, book contrib. 0-1183  
 $CO_2-N_2$ , glow discharge instability, non self sustained ionisation source, mechanism 0-38819  
 $CO_2-N_2$ , kinetic cooling effect by  $CO_2$  laser radiation, temp. dependence 0-10347  
 $CO_2-N_2$ , non self sustained repetitively pulsed discharge instability obs. 0-38820  
 $CO_2-N_2$  gasdynamic laser, thermal nonequilibrium heating of active medium by elec. arc 0-53258  
 $CO_2-N_2-He$ , vol. discharge, negative ions effect 0-14956  
 $CO_2-N_2-He$  CW gasdynamic laser, closed-cycle, construction and operating parameters 0-23717  
 $CO_2-N_2-He$  discharge, electron distrib. relax., numerical study 0-54070  
 $CO_2-N_2-He$  gasdynamic laser, effect of weak flow perturbations on gain 0-14316  
 $CO_2-N_2-He$  laser mixture in nonself-sustained discharge, direct heating mechanism 0-28195  
 $CO_2-N_2-He$  mixture supersonic adiabatic expansion, population inversion and gain 0-19017  
 $CO_2-N_2-He$  nozzle flows with boundary layer, gain coefficients 0-14312  
 $CO_2-N_2-He$  pulsed transverse discharge, investigation of gain 0-9855  
 CdSe:N, implanted, electroreflection obs. 0-40089  
 $Co_2:He:N$ , glow discharge instability in afterglow 0-6313  
 Fe:C(N), small concs. determ., mag. and mech. relax. methods 0-7879  
 Fe-CR (26 wt.%), role of C and N in brittle fracture 0-16456  
 Fe-Cr-Mn-N, influence of N on defect conc. energy (Russian) 0-54241  
 GaAs $_{0.6}P_{0.4}$ :N, photoconductive tape by ion implantation and  $CO_2$  laser annealing 0-24464  
 GaP:N, electron-hole liq., luminesc. obs. 0-25438  
 GaP:N, epitaxial layers, N concentration determination by two independent methods 0-39142  
 GaP:N LED, deep level studies, growth by time difference method at controlled vapour pressure 0-39522  
 GaP:N(N,O) epitaxial struct., luminesc. study of degradation during heat treatment 0-45139  
 He- $N_2$ , de excitation rate consts., energy transfer, pulse radiolysis obs. 0-30303



## nitrogen continued

- He-N<sub>2</sub> mixtures, thermal diffusion 0-1726  
 He-N<sub>2</sub> plasma, N<sub>2</sub> B<sup>2</sup>Π<sub>g</sub> state excitation, role of long lived states, luminesc. 0-37829  
 N and N<sub>2</sub> in thermosphere, annual var. from Aeros Nims data 0-12578  
 N I, weighted oscillator strengths for elec. dipole and forbidden transitions, data tables 0-37779  
 N I interstellar absorption in γ Cassiopeiae direction, UV obs. 0-51823  
 N I plasma jet, spectroscopic diagnostics, Stark broadening and shift, study 0-38727  
 N III, electron impact excitation cross sections, generalised oscillator strengths, Born approx. 0-18928  
 N III, electron impact width of plasma lines, approximative semiclassical formula 0-43972  
 N III, VUV spectrum (*Chinese*) 0-42974  
 N III intersystem multiplet as density indicator for solar plasmas 0-31264  
 N IV, 2s3p <sup>3</sup>P<sub>1</sub>-2s<sup>2</sup> <sup>1</sup>S<sub>0</sub> intercombination line transition probabilities 0-18823  
 N IV solar emission line ratios, electron density and temp. determ. 0-17559  
 α-N, low freq. absorpt. spectra, libration modes (*Russian*) 0-55078  
 N V, beam-foil decay curves, mean lives determ. 0-9553  
 N V, electron ionisation cross sections of excited atoms and ions 0-43186  
 N V, optical oscillator strength 0-47941  
 N VII, and isoelectronic series, in laser-produced plasma, Balmer fine struct. (broadening) 0-48860  
 N<sup>-</sup>, Sternheimer valence shielding and antishielding factors 0-18807  
 N<sup>+</sup> and N<sub>2</sub><sup>+</sup>, beam-foil and beam-gas excitation, Coulomb explosion effects, Auger spectra obs. 0-14220  
 N<sup>+</sup>, beam-foil excitation, absolute Auger yield meas. 0-14203  
 N<sup>+</sup>, from exploding fast mol. ions, Auger spectra 0-32781  
 N<sup>+</sup>, reson. line regularities in plasma Stark widths and shifts 0-43881  
 N<sub>2</sub><sup>+</sup>, spectral line breadth in molecular nonequilibrium plasma (*Russian*) 0-48044  
 N<sup>n+</sup>, n≤5, extracted from ECR plasma ion source, charge state distrib. 0-24268  
 N/C ratio determination in atmospheres of C stars, peculiar red giants 0-17580  
 N/S gradient in M33 galaxy, supernova remnant evidence 0-56929  
 N-N, correl. diagrams, Thomas-Fermi calcs. 0-23294  
 N+alkene (1,3-butadiene)(acetylene), reaction rate const., pulse radiolysis obs. 0-35508  
 N+Bi, BiN form., IR matrix spectra, comparison with group V nitrenes 0-18853  
 N+H<sub>2</sub>, NH+H, pot. surface, HF calc. 0-16669  
 N+N, K-shell excitation, Auger electron spectrosc. obs. 0-9714  
 N+OH, direct rate meas. 0-30217  
 N+O(C), K-shell excitation, Auger electron spectrosc. obs. 0-9715  
 N<sup>+</sup>+H, charge transfer reaction in astrophys. nebulae rel. to ionization struct. 0-46384  
 N<sup>+</sup>+H<sup>+</sup>, <sup>3</sup>P<sub>1</sub> fine structure transitions 0-37864  
 N<sup>+</sup>+O<sub>2</sub>, NO<sup>+</sup>(a<sup>2</sup>Σ<sup>+</sup>) ion prod. 0-7784  
 N<sub>2</sub><sup>+</sup>+inert gas target, 60-200 keV single electron capture 0-43172  
 N<sub>2</sub><sup>+</sup>+O, collision, correl. diagram calcs. 0-23504  
 N<sub>2</sub><sup>+</sup>+H, charge exchange, assoc. reaction, rel. to interstellar gas 0-7763  
 N<sub>2</sub><sup>+</sup>+Ti, ratio of single K-shell ionisation cross section to double K-shell ionisation cross section 0-53119  
 N<sub>2</sub><sup>+</sup>+Ti, ratio of single K-shell ionisation cross section to double K-shell ionisation cross section 0-53119  
 N<sub>2</sub><sup>+</sup>+He(Ne), multiply ionised ats. prod. 0-28098  
 N<sub>2</sub> afterglow, chem. reactions rel. to plasma props, appl. to toluene polymerisation 0-3346  
 N<sub>2</sub> arc, magnetically stabilised cross-flow, temp. and flow fields meas. 0-54054  
 N<sub>2</sub>, bond order values, ab initio calcs. and basis set depend. 0-32605  
 N<sub>2</sub> dayglow intensity from photoelectron impact 0-46331  
 N<sub>2</sub> discharge, electron shock wave formation, numerical simulation 0-38777  
 N<sub>2</sub> dissolved in Ar, mol. orientation, Raman spectrosc. obs. 0-52994  
 N<sub>2</sub>, gas-liquid surface of mol. fluids, mol. dynamics computer simulations 0-39387  
 N<sub>2</sub> glow discharge, non-self-sustained, cathode spots annular structure investig. 0-24281  
 N<sub>2</sub> in upper atmos., vibr. level distrib., theory 0-41576  
 N<sub>2</sub> laser discharge, SF<sub>6</sub> addition, negative ion prod., altered discharge parameters 0-38818  
 α-N<sub>2</sub>, lattice energies, non-additive three body contributions, triple-dipole term 0-54168  
 N<sub>2</sub>, non self sustained repetitively pulsed discharge instability obs. 0-38820  
 N<sub>2</sub>, photoionis., shape-reson. enhanced nucl. motion effects 0-1031  
 N<sub>2</sub> positive corona into spark, prebreakdown phase, spectroscopic anal. 0-38790  
 N<sub>2</sub>, thermosphere composition, temp. and turbulence, 1967-75 obs. 0-51588  
 N<sub>2</sub>, vibr. excitation using steady state chemical reaction between CO and N<sub>2</sub>O 0-50851  
 N<sub>2</sub><sup>+</sup> 4278 Å auroral intensity in DMSP data calibration 0-8443  
 N<sub>2</sub><sup>+</sup>, A- and B-states interactions, time-resolved obs. 0-18862  
 N<sub>2</sub><sup>+</sup>, dissociative recombination in ionosphere, rate cont. 0-17435  
 N<sub>2</sub><sup>+</sup>, exploding fast mol. ions, Auger spectra 0-32781  
 N<sub>2</sub><sup>+</sup> in rarefied plasma stream, energy accommodation coeffs. meas. by thermoanemometric sounding 0-16722  
 N<sub>2</sub><sup>+</sup> UV spectral line width in rarefied free jet, for rot. temp. 0-6184  
 N<sub>2</sub><sup>+</sup>, auroral ionosphere spectral emission process 0-41577  
 N<sub>2</sub>/SF<sub>6</sub> positive-point corona phenomena, breakdown voltage/press. characts. 0-38859  
 N<sub>2</sub>-Ar, thermal diffusion factors meas. 0-10344  
 N<sub>2</sub>-Ar corona discharge, convection and mixing, atm. press., mass spectra obs. 0-1853  
 N<sub>2</sub>-Ar equimolar mixture, transverse Dufour effect 0-6194  
 N<sub>2</sub>-Ar-O<sub>2</sub> system, vapour-liq. equil. 0-54358  
 N<sub>2</sub>-Ar(methane)(ethane) binary and ternary mixtures, dielec. const., excess vol. 0-7254  
 N<sub>2</sub>-CO, angularly resolved CARS 0-22453  
 N<sub>2</sub>-CO, electrical discharge excitation, vibr. level population distrib., electron beam fluoresc. obs. 0-48031  
 N<sub>2</sub>-CO pulsed non self sustained discharges, peculiarities 0-38811  
 N<sub>2</sub>-CO<sub>2</sub> laser mixture, electron drift vels., time-of-flight meas. 0-28855

## nitrogen continued

- N<sub>2</sub>-CO<sub>2</sub>-He, vol. discharge with UV preionisation by capillary discharge, ionis. pots. depend. 0-44065  
 N<sub>2</sub>-CO<sub>2</sub>-(He) volume discharge, N<sub>2</sub> vibr. levels, stepwise excitation, effect on electron energy balance 0-54071  
 N<sub>2</sub>-CO<sub>2</sub>-He, nucl. reactor active zone, plasma and sustained discharge props. 0-5729  
 N<sub>2</sub>-CO-Ar, C<sub>2</sub> and CN form. by optical pumping, room temp. 0-16701  
 N<sub>2</sub>-ethane(propane)(n-butane) mixtures, viscosity, diffusion coeffs. 0-1722  
 N<sub>2</sub>-He, binary diffusion coeffs., press. depend., 300 and 323K, Thorne's eqn. 0-1724  
 N<sub>2</sub>-Kr-Xe, liquefaction, retention of <sup>85</sup>Kr from fission exhaust gases, separation technique (*German*) 0-27753  
 N<sub>2</sub>-NF<sub>3</sub>, electron attachment coeffs. using swarm techniques 0-53915  
 N<sub>2</sub>-O<sub>2</sub> mixture, impulse breakdown processes at low press. 0-44021  
 N<sub>2</sub>-SF<sub>6</sub> mixtures, effective ionisation coeff. and static breakdown voltage meas. 0-19549  
 N<sub>2</sub>+Ar, binary diffusion coeff. pressure depend. meas. 0-43826  
 N<sub>2</sub>+Ar, form-factors, l-dominant, analytical formulae 0-1052  
 N<sub>2</sub>+Ar rotational excitation, differential cross sections and orientation effects, classical trajectory method 0-23523  
 N<sub>2</sub>+Ar+POPOP, electron beam excited, energy transfer mechanisms 0-23497  
 N<sub>2</sub>+C<sup>+</sup> collisions, luminesc. 0-1055  
 N<sub>2</sub>+CO, electronically inelastic collision, distorted wave calc. and pot. energy curve 0-9709  
 N<sub>2</sub>+CO<sub>2</sub>(O<sub>2</sub>)(N<sub>2</sub>), IR spectral absorpt. induced by press. in atmos. (*Russian*) 0-56600  
 N<sub>2</sub>+Cd(Zn)(Sr), A<sup>3</sup>Σ<sub>u</sub><sup>+</sup> state, vibr. excitation 0-1054  
 N<sub>2</sub>+Cd(<sup>5</sup>P<sub>0,1</sub>), absolute quenching cross sections 0-5604  
 N<sub>2</sub>+CsF, rot. inelastic collisions, mol. beam meas. 0-1049  
 N<sub>2</sub>+Cu, preferential energy transfer from N<sub>2</sub> to specific Cu energy levels 0-43152  
 N<sub>2</sub>+Fe interaction, chemical species formed studied by Mossbauer effect 0-43080  
 N<sub>2</sub>+H<sup>+</sup>, 5-100 keV, secondary electron energy and ang. distrib. 0-14223  
 N<sub>2</sub>+H<sup>+</sup>(e), vibrational N<sub>2</sub><sup>+</sup> excitation (*Russian*) 0-53156  
 N<sub>2</sub>+HCN (001), relax. rate const., using Cs vap. IR source 0-9696  
 N<sub>2</sub>+H(2s), 5-25 keV, H(n=3) excitation, Balmer α emission obs. 0-53113  
 N<sub>2</sub>+He\*, Penning ionisation, ejected electron spectra obs. 0-48074  
 N<sub>2</sub>+K, rot. inelastic scatt., quantum effects, simple model surfaces 0-48064  
 N<sub>2</sub>+K (Na), atom electronic excitation, vibr. to electronic energy transfer, seeded mol. beam studies 0-47919  
 N<sub>2</sub>+K collision, electronic excitation and energy transfer, time of flight spectra 0-43151  
 N<sub>2</sub>+K+Cd, optical excitation, rate const., collisional energy transfer kinetics 0-32801  
 N<sub>2</sub>+K<sup>2+</sup>(Xe<sup>2+</sup>)(C<sup>2+</sup>), charge transfer reaction rate const. 0-7779  
 N<sub>2</sub>+Li<sup>+</sup>, comparison with classical small-ang. pot. scatt. theory 0-1043  
 N<sub>2</sub>+N<sub>2</sub>, dispersion forces calcs. 0-9675  
 N<sub>2</sub>+NO<sup>+</sup>, reaction rate const. meas. 0-7782  
 N<sub>2</sub>+Na(3p<sup>2</sup>P<sub>3/2</sub>), electronic energy quenching dynamics, crossed beam expt. 0-9683  
 N<sub>2</sub>+negative ion, electron-loss cross sections 0-37877  
 N<sub>2</sub>+O, excitation and deactivation at above-thermal energies 0-43171  
 N<sub>2</sub>+O<sub>2</sub>, binary diffusion coeff. pressure depend. meas. 0-43826  
 N<sub>2</sub>+O<sub>2</sub> plasma jet, NO synthesis, chem. kinetics anal., model 0-38728  
 N<sub>2</sub>+OCS, gas, EPR of rot. transitions, T<sub>1</sub> press. depend. 0-9621  
 N<sub>2</sub>+OH, mean collision cross sections from microwave spectroscopy 0-1046  
 N<sub>2</sub>+OH(A<sup>2</sup>Σ<sup>+</sup>), quenching rates and fluoresc. efficiency, rel. to atmosphere 0-14199  
 N<sub>2</sub>+O(2<sup>1</sup>D<sub>2</sub>), collisional deactivation meas., 295K, rel. to atmospheric processes 0-16663  
 N<sub>2</sub><sup>+</sup>+He collisions, vibronic excitation, curve-crossing trajectories 0-23520  
 N<sub>2</sub><sup>+</sup>+Li(Na)(K), 50-1000 eV, crossed beams, electron transfer and excitation 0-14226  
 N<sub>3</sub>, polarisability correl. with mol. dims. 0-23288  
 N(D<sup>2</sup>P) metastable ats. prod. in N<sub>2</sub> DC glow discharge 0-38758  
 N(D<sup>2</sup>D)+O, associative ionisation 0-4161  
 NO<sup>+</sup>, (a<sup>2</sup>Σ<sup>+</sup>), prod. from N<sup>+</sup>+O<sub>2</sub> reaction 0-7784  
 NO<sub>3</sub> in nighttime stratosphere, composition change following sunset 0-31097  
 N<sub>2</sub>O-N<sub>2</sub>-He, gasdynamic laser, effect of weak flow perturbations on gain 0-14316  
 N<sub>2</sub><sup>+</sup>(<sup>2</sup>P<sub>0</sub>)+H, charge transfer, ab initio CI pot. curves and coupling-matrix elements 0-37878  
 N<sub>3</sub><sup>+</sup>(<sup>1</sup>S)+H, charge transfer, ab initio CI pot. curves and coupling-matrix elements 0-37878  
 N<sub>2</sub><sup>+</sup>(<sup>2</sup>Σ<sub>g</sub><sup>+</sup>), B and C states, unimolecular decay, nonadiabatic interactions, transition probability as function of Massey parameter 0-35503  
<sup>13</sup>N production for nuclear medicine use 0-30889  
<sup>13</sup>N production in cyclotron by <sup>16</sup>O(p,α)<sup>13</sup>N, water loop target 0-23201  
<sup>13</sup>N species formed by proton irradiation of water 0-45532  
<sup>13</sup>N pulsed NQR-FFT radiofrequency spectrometer description and operation 0-17982  
<sup>14</sup>N+CO, vibr. energy transfer, laser fluoresc. obs. 0-28050  
<sup>14</sup>N<sup>15</sup>N+CO, vibr. energy transfer, laser fluoresc. obs. 0-28050  
<sup>15</sup>N, beam foil and quantum beat spectra (*Chinese*) 0-32638  
<sup>15</sup>N, highly ionized, atomic transition polarisation by beam-foil interaction, 3-8 MeV 0-18908  
<sup>15</sup>N NMR heteronuclear spectroscopy, two dimensional Fourier transform technique 0-31818  
<sup>15</sup>N/<sup>14</sup>N ratio and solar nebula differentiation 0-36519  
<sup>15</sup>N-<sup>13</sup>C spin-spin coupling constants calc. using SCF and INDO method 0-32609  
<sup>15</sup>N-NH<sub>4</sub><sup>+</sup>, absorpt. and transfer to amino-N, rat small intestinal sac 0-16909  
<sup>15</sup>N+CO, vibr. energy transfer, laser fluoresc. obs. 0-28050  
 N<sub>2</sub>\*+OCS 0-48063  
 Na-CO<sub>2</sub> mixing-type gasdynamic laser, experimental and theoretical studies (*Japanese*) 0-23666  
 Ne-N<sub>2</sub>, energy transfer, H<sup>+</sup> ion beam produced plasma, ion density and temp. 0-38539  
 Ns+Ne, metastable state de-excitation, rate const., radiolysis obs. 0-40709



## nitrogen continued

- SF<sub>6</sub>-N<sub>2</sub>, dielec. props., ionisation and attachment coeffs. 0-33726  
 Si<sub>3</sub>N<sub>4</sub>, amorphous, prep. by RF sputtering and props. 0-44229  
 Si<sub>3</sub>N<sub>4</sub>, ion implantation, refractive index, IR spectra, ion range and straggling meas. 0-34020  
 SiC, exam. of N solubility, in epitaxial layers 0-6520  
 Ta<sub>3</sub>N<sub>5</sub>, superconductive to normal transition anisotropy 0-25031  
 V<sub>2</sub>N, ion bombard., void form. 0-34097

## nitrogen compounds

- see also ammonia; ammonium compounds  
 alkali halide:NO<sub>2</sub><sup>-</sup>, EPR isotropic hyperfine triplets 0-2636  
 atmospheric NO<sub>2</sub> total content meas. by absorption spectroscopy (Japanese) 0-12469  
 bridged complexes, vibr. and electronic props., reson. Raman spectra appl. 0-52996  
 nitrates, distrib. in Pacific ocean waters 0-31065  
 nitrates in Bering Sea shelf sediments, denitrification estimates 0-12433  
 nitrides, struct. and cryst. growth 0-29865  
 nitrides, XPS (Japanese) 0-16154  
 oxides, rain and snow acidity, release by burning of fossil fuels 0-26590  
 oxides in atmospheric samples, meas. using luminescence (Dutch) 0-3565  
 thionitrates, mol. struct., S-substitution effect (French) 0-23335  
 Ar-Xe-NF<sub>3</sub>, mixture in XeF laser, discharge stabilised by short-pulse electron beam 0-14358  
 Br+O<sub>2</sub>(NO), quencher paramagnetism, deactivation rate const., spin-orbit relax. study 0-21263  
 CO-NO mixtures, Ar matrix isolation, laser-included vibr. fluoresc. 0-9707  
 HN<sub>3</sub>, ground 'A' state, SCF and CI calcs., conform., geom., vibr. freqs. and dissoci. 0-18806  
 NBr, in solid Ar, b'<sup>2</sup>Σ<sup>+</sup> ↔ X<sup>3</sup>Σ<sup>-</sup> transitions 0-32702  
 N(CH<sub>3</sub>)<sub>4</sub>GeCl, cryst. and powder diff. data 0-24422  
 NCl, in solid Ar, b'<sup>2</sup>Σ<sup>+</sup> ↔ X<sup>3</sup>Σ<sup>-</sup> transitions 0-32702  
 ND c 'II-a' Δ system, new bands, spectroscopic consts. 0-9612  
 ND<sub>3</sub>, vibr. levels inversion splitting, generalised WKB method 0-9585  
 ND<sub>3</sub>(NH<sub>2</sub>), ν<sub>2</sub> band, laser mag. reson., 9-10 micron 0-9601  
 NF, pot. energy curves and dissoci. energy, Hulbert-Hirschfelder calc. 0-30210  
 NF<sub>2</sub>, IR spectra, ν<sub>1</sub> and ν<sub>2</sub> bands, vibr. excitation and spin-rot. interaction, doublet splitting 0-28011  
 NF<sub>3</sub>, dissoci. electron attachment, negative ion prod. rates 0-18938  
 NF<sub>3</sub>, electron dissociative attachment rate consts. at 300 and 500K, in discharge plasma 0-43849  
 NF<sub>3</sub>, mol. orbital calcs., core-valence approx. scheme 0-42927  
 NF<sub>3</sub>, NF<sub>3</sub><sup>+</sup>, and NF<sub>3</sub><sup>+</sup>, optimised struct. and bonding, ab initio SCF MO calc. 0-23334  
 NF<sub>3</sub>-He hollow-cathode laser using F transitions 0-48289  
 NF<sub>3</sub>-N<sub>2</sub>(Ar)(He), electron attachment coeffs. using swarm techniques 0-53915  
 NF<sub>3</sub>+Kr(P<sub>2</sub>), KrF\* bound-free oscill. emission spectra calc. 0-7799  
 NH, lower valence states, predissociations, Franck-Condon anal. 0-5590  
 NH<sup>+</sup>, interstellar, Δ-doublet population inversion by collisions 0-22065  
 NH<sub>2</sub> (A<sup>2</sup>A<sub>1</sub>), excited state dynamics and bimol. quenching processes 0-9681  
 NH<sub>2</sub> fragments, multiple photon dissoci. of CH<sub>3</sub>NH<sub>2</sub> and NH<sub>3</sub>, laser-excited fluoresc. obs. 0-11938  
 NH<sub>2</sub>, ground state mol. consts., absorption spectra 0-28030  
 NH<sub>2</sub>+H rot. energy transfer in vibronic levels, absolute transfer rates 0-9701  
 NH<sub>2</sub>+NO<sub>2</sub>, reaction rate const. meas. 0-7772  
 NH<sub>3</sub> photodissociation, appl. to solar energy conversion 0-30513  
 NH<sub>3</sub> small scale prod. for H storage 0-45782  
 NH<sub>3</sub><sup>+</sup>+molecule (n=0 to 4), reactions, selected ion flow tube obs. 0-45489  
 N<sub>2</sub>H<sub>2</sub>, model rearrangement system, electron correlation and basis set effects 0-3317  
 N<sub>2</sub>H<sub>4</sub> production from NH<sub>3</sub> in atmospheric press. electron-beam controlled discharge 0-38799  
 N<sub>2</sub>H<sub>3</sub> radical, lowest two electronic states 0-925  
 NH<sub>2</sub>(A<sup>2</sup>A<sub>1</sub>, X<sup>2</sup>B<sub>1</sub>), obs. in UV laser photodissoc. of NH<sub>3</sub> 0-11901  
 NH(A<sup>2</sup>Π, b'<sup>2</sup>Σ), two-photon generation in NH<sub>3</sub> UV laser photodissoc. 0-11901  
 (N<sub>2</sub>H<sub>2</sub>)<sub>2</sub>F<sub>2</sub>[TiF<sub>6</sub>], X-ray cryst. struct. determ. 0-54182  
 N<sub>2</sub>H<sub>2</sub>FeF<sub>6</sub>, Mossbauer spectra, 1D antiferromag. 0-15886  
 NH<sub>2</sub>(X<sup>2</sup>B<sub>1</sub>) radical, and ND<sub>2</sub>, ionisation pot., vibr. anal., ab initio calcs. and vacuum UPS obs. 0-53047  
 NH<sub>2</sub>HF, H-bonded complex, ab initio calcs. (French) 0-52866  
 NI, in solid Ar, b'<sup>2</sup>Σ<sup>+</sup> ↔ X<sup>3</sup>Σ<sup>-</sup> transitions 0-32702  
 NO admixture effect on electron beam controlled CO laser energy and spectral characts. 0-9867  
 NO adsorption, reactions, catalysis by ferroelectric KNbO<sub>3</sub> 0-30282  
 NO, adsorption on Ni, ground and core hole states, config. depend. HF LCAO SCF calc., relax. and binding energy 0-29453  
 NO, adsorption on Ru (001), KPS, UPS, and X-ray AES meas. 0-6655  
 NO, adsorption on Ru (001) surface, EELS obs. 0-20741  
 NO, adsorption on W (110) surface, chemical changes detected by AES 0-10787  
 NO, and isotopic forms, ν=0 electronic states, spin-rot. doubling 0-5540  
 NO chemiluminescent emission at 2.9 μm wavelength, auroral enhancement 0-12586  
 NO, chemisorption on Cu, cluster theory 0-29264  
 NO, chemisorption on goethite, IR spectra 0-7855  
 NO, chemisorption on Ni, cluster theory 0-29264  
 NO, chemisorption on Ni (100), LEED, AES, UPS, and thermal desorption study 0-39449  
 NO densities, horizontal winds effects in aurora 0-26656  
 NO, desorption, associative, from Pt, Ni, Ru 0-54512  
 NO, diatomic mols., internal partition functions for O<sub>2</sub>, N<sub>2</sub>, NO and their ions, max. summation indices 0-27995  
 NO, dipole properties and dispersion energies additivity, using atoms and small mol. models 0-53091  
 NO, gas complex analysis method, resonance absorption with pulsed laser light (Japanese) 0-36421  
 NO in lower ionosphere, height profile during auroral absorpt. event 0-36443  
 NO, intracavity Zeeman modulation detect., passive Q-switching, CO IR laser obs. 0-9597  
 NO, NO<sup>+</sup>, in winter anomalous D-region over Sardinia (40°N), densities 0-21871  
 NO, photodissoc. in mesosphere and stratosphere, theory 0-41580

## nitrogen compounds continued

- NO, photofragment of NO<sub>2</sub>, Doppler spectroscopy 0-53124  
 NO predissociation in mesosphere and stratosphere, photochemistry 0-21802  
 NO, press. broadening coeffs., spin-flip Raman laser spectrosc. 0-43147  
 NO production by lightning in clouds, odd N chem. reactions on Venus 0-26768  
 NO, Q-branch spectra, external-resonator controlled Raman laser pumped by CW CO laser 0-9624  
 NO, rot. line strengths in multiphoton transitions 0-48051  
 NO, Rydberg states quenching rate consts., two photon excitation method 0-5581  
 NO, state selective step-wise photoionis. with mass spectroscopic ion detect. 0-43119  
 NO, stratospheric and mesospheric photodissoc. rate, calc. 0-51498  
 NO synthesis in N<sub>2</sub>+O<sub>2</sub> plasma jet, chem. kinetics anal., model 0-38728  
 NO, troposphere content, 0-7 km altitude over clean and polluted areas 0-51478  
 NO, UV fluorescence, IR laser induced 0-53032  
 NO X<sup>2</sup>Π(ν=0), ionis. energies to NO<sup>+</sup> X<sup>1</sup>Σ<sup>+</sup>(ν=0-34), NO<sup>+</sup> mol. consts., UPS obs. 0-14177  
 NO<sup>+</sup> destruction in collisions with excited molecules 0-14189  
 NO<sup>+</sup>+molecule, reaction rate consts. meas. 0-7782  
 NO<sup>+</sup> in ionosphere, form. by N<sup>(2)D</sup>+O associative ionisation 0-4161  
 NO<sup>+</sup>, interstellar transitions in mm and IR wavelengths 0-56906  
 NO<sup>+</sup>, mobility in CO<sub>2</sub> 0-43834  
 NO<sup>+</sup>, pot. energy curves calcs. 0-5602  
 NO<sup>+</sup> recombination in mid-latitude trough and polar ionization hole 0-12575  
 NO<sup>+</sup> X<sup>1</sup>Σ<sup>+</sup>(ν=0-34)←NO X<sup>2</sup>Π(ν=0) ionis. energies, NO<sup>+</sup> mol. consts., UPS obs. 0-14177  
 NO<sub>2</sub> flame, OH form., collisional broadening parameter, curve of growth method 0-53052  
 NO+Ar<sup>+</sup>, reaction product ratios, 300K 0-7783  
 NO+BrO, temp. depend. kinetic study, stratospheric Br photochemistry implication 0-50866  
 NO+CO<sub>2</sub>, Senftleben-Beenakker effect, saturation field, Kohler-Raum theory and obs. 0-28596  
 NO+ClO<sub>2</sub>, reaction initiating HCl chemical laser 0-14333  
 NO+dimethylamino radical, reaction rate constants, FTIR obs. 0-16652  
 NO+HO<sub>2</sub>(DO<sub>2</sub>), reaction kinetics, near IR chemiluminesc. determ. 0-21261  
 NO+HO<sub>2</sub>←OH+NO<sub>2</sub>, kinetics temp. depend. 0-3313  
 NO+Na(3p<sup>2</sup>P<sub>3/2</sub>), electronic energy quenching dynamics, crossed beam expt. 0-9683  
 NO+Ne(Ar)(Kr)(Xe), angle depend. intermolecular pot., crossed beams study 0-9682  
 NO+O, chemiluminesc., absolute rate consts., O<sub>3</sub> effect 0-45507  
 NO+O, vibr. relaxation of NO, laser induced IR fluoresc. study 0-9626  
 NO+O<sub>3</sub>←NO<sub>2</sub><sup>+</sup>+O<sub>2</sub>←NO<sub>2</sub>+hv+O<sub>2</sub>, chemiluminesc., translational and rot. energy effects 0-30218  
 NO+OH radical-molecule reactions, relax. and rate consts. 0-11918  
 NO+S<sup>+</sup>←NO<sup>+</sup>+S+1.1 eV, rate consts. kinetic energy depend., drift tube meas. 0-7778  
 NO<sup>+</sup>+Ar, reaction product ratios, 300K 0-7783  
 NO<sub>2</sub> (101) band, line strengths, spin-splittings and forbidden transitions 0-47987  
 NO<sub>2</sub>, air over N.Germany coast, obs. 0-26584  
 NO<sub>2</sub>, complete quartic force field calc., algorithm 0-37736  
 NO<sub>2</sub>, detailed spectroscopic study, sub-Doppler spectroscopic techniques 0-52339  
 NO<sub>2</sub>, direct CI calcs. 0-52889  
 NO<sub>2</sub>, dissociative limit, mol. beam characts. determ. by fluoresc. excitation spectra 0-53074  
 NO<sub>2</sub>, excited, fluoresc. spectrum, IR multiphoton vibr. pumping, photon absorpt. probability distrib. study 0-18854  
 NO<sub>2</sub>, Hanle effect, nonstationary states in molecular spectroscopy, level splitting 0-23465  
 NO<sub>2</sub>, in stratosphere, global behaviour 0-17334  
 NO<sub>2</sub>, in stratosphere, meas. method and behaviour at mid-latit. 0-17414  
 NO<sub>2</sub>, inter and intramolecular radiationless transitions, relax., time resolved excitation and fluoresc. spectra 0-27966  
 NO<sub>2</sub>, laser and flash lamp fluoresc. monitors, comparison 0-17367  
 NO<sub>2</sub>, laser-induced fluoresc. quenching rate const. and lifetimes 0-11930  
 NO<sub>2</sub>, minor atm. components, visible absorpt. spectra, temp. depend. (French) 0-36355  
 NO<sub>2</sub>, one-photon dissoci. to NO+O, Doppler spectroscopy 0-53124  
 NO<sub>2</sub>, species in an irradi. single crystal of uridine 5'-phosphate (Na salt), EPR obs. 0-40719  
 NO<sub>2</sub>, stratospheric composition during major warming, 1979 obs. 0-51476  
 NO<sub>2</sub>, sub-Doppler laser spectrosc., high resolution 0-52320  
 NO<sub>2</sub>, teledetection of gaseous atmos. pollutants, data acquisition and anal., pollution mapping (French) 0-7989  
 NO<sub>2</sub>, thermal decomposition kinetics (Russian) 0-3329  
 NO<sub>2</sub>, transport into stratosphere, prod. in thunderstorms 0-8376  
 NO<sub>2</sub>, vertical profile, balloon obs. in stratosphere (Japanese) 0-31086  
 NO<sub>2</sub>, visible spectrum simplification, rot.-vibr. levels, excitation, polarisation labelling spectroscopy 0-32730  
 NO<sub>2</sub>, direct CI calcs. 0-52889  
 NO<sub>2</sub>, impurity in alkali halides, reorientation, linear dichroism (Russian) 0-45127  
 NO<sub>2</sub><sup>-</sup>, NO<sub>2</sub><sup>-</sup>.H<sub>2</sub>O, and peroxy isomers, photodissoc. and photodetachment 3500-8250 Å, rel. to ionosphere 0-35554  
<sup>15</sup>NO<sub>2</sub>, and <sup>18</sup>NO<sub>2</sub>, inertia defects and dipole moments by kinetic consts. method 0-928  
 NO<sub>2</sub>+B, chemiluminesc. metal oxide formation 0-35509  
 NO<sub>2</sub>+dimethylamino radical, reaction rate constants, FTIR obs. 0-16652  
 NO<sub>2</sub>+ethylperoxy radical, reaction rate const. meas. 0-21262  
 NO<sub>2</sub>+H, population inversion of A doublets in microwave spectrum of OH(<sup>2</sup>Π<sub>3/2</sub>, v=1) 0-974  
 NO<sub>2</sub>+K, charge transfer reactions, energy and ang. differential cross-sections meas. 0-53125  
 NO<sub>2</sub>+NH<sub>2</sub>, reaction rate const. meas. 0-7772  
 NO<sub>2</sub>+OH, mean collision cross sections from microwave spectroscopy 0-1046  
 NO<sub>2</sub>+OH+M→HNO<sub>3</sub>+M, rate constant under simulated atmospheric conditions 0-50846  
 NO<sub>2</sub><sup>-</sup>, aq. soln., vibr. width and dephasing, conc. depend. 0-43029  
 NO<sub>3</sub> in Antarctic ice, γ- and X-irrad. due to supernovae 0-31314



**nitrogen compounds continued**

- $\text{NO}_2^-$ , level in reacting atmospheric aerosol, calcs. 0-26056  
 $\text{NO}_3^-$ ,  $\text{NO}_3$ ,  $\text{H}_2\text{O}$ , and peroxy isomers, photodissoc. and photodetachment 3500-8250 Å, rel. to ionosphere 0-35554  
 $\text{NO}_3^-$ ,  $\text{PO}_4^{3-}$ ,  $\text{Si}(\text{OH})_4$ , ratios in Moroccan upwelling region 0-4045  
 $\text{NO}_3^-$ , positronium formation, Doppler broadened positron annihilation line shapes 0-45164  
 $\text{NO}_x$ , air pollution in Sheffield, conc. var. 0-16863  
 $\text{NO}_x$ , formation by heated corona wires of electrostatic precipitator 0-47081  
 $\text{NO}_x$  removal rate in urban atmosphere 0-56524  
 $\text{NO}_x$ - $\text{HNO}_3$ - $\text{H}_2\text{O}$  clusters, gas phase, thermodynamic quantities, mass spectra obs. 0-50875  
 $\text{N}_2\text{O}$ , 40°00'-00°00' band, IR high press. absorpt. spectra profiles 0-52988  
 $\text{N}_2\text{O}$  and NO in atmosphere, biomass burning as source 0-26586  
 $\text{N}_2\text{O}$ , as mol. probe in MBBA, solute solvent interaction, IR spectra vibr.-rot. fundamental 0-29155  
 $\text{N}_2\text{O}$ , atmospheric, instantaneous global photochemical reaction rates 0-17335  
 $\text{N}_2\text{O}$ , dipole properties and dispersion energies additivity, using atoms and small mol. models 0-53091  
 $\text{N}_2\text{O}$  dissolved in liq. cryst., NMR, relax. times 0-25233  
 $\text{N}_2\text{O}$ , global atmos. and Pacific Ocean composition 0-51519  
 $\text{N}_2\text{O}$  interaction with Cu (110) surface, ellipsometry, AES, LEED study 0-6635  
 $\text{N}_2\text{O}$ , interactions with Ru (10 $\bar{1}$ 0) surface 0-55713  
 $\text{N}_2\text{O}$ , K-shell photoabsorption coeffs., 500-600 eV 0-9617  
 $\text{N}_2\text{O}$ , N 1s $^2$ ,  $\pi^*$ -state decay, fragment ion relative abundance by electron-ion coincidence technique 0-9743  
 $\text{N}_2\text{O}$  photodissociation, CC O(1S), prod. and props. in liq. Ar and  $\text{N}_2$  0-43063  
 $\text{N}_2\text{O}$ , photolysis, O(1S) absolute quantum yield spectral depend. meas. using XeO luminesc. 0-35561  
 $\text{N}_2\text{O}$ , pulsed photoacoustic Raman spectrosc., gaseous trace anal. 0-40769  
 $\text{N}_2\text{O}$ , pure and in mixtures, electron attachment near 1 atm., microwave cond. meas. 0-1063  
 $\text{N}_2\text{O}$ , pure liq., mol. motion, anisotropic interaction 0-24345  
 $\text{N}_2\text{O}$ , pure rotational stimulated Raman photoacoustic spectroscopy 0-32724  
 $\text{N}_2\text{O}$  quadrupole hyperfine struct., vibr. depend. obs. using twin-laser spectrometer 0-43097  
 $\text{N}_2\text{O}$  solutions and aq. thymine, radiolysis products anal. 0-30257  
 $\text{N}_2\text{O}$ , spin polarised photoelectrons, synchrotron excited 0-43101  
 $\text{N}_2\text{O}$ , submillimetre rot. lines, press. shifts 0-23463  
 $\text{N}_2\text{O}$ , valence and core photoionisation, spectral lines, many body effects 0-47853  
 $\text{N}_2\text{O}$ , valence shell ionic photofragmentation, oscill. strengths, EELS and electron-ion coincidence meas. 0-37879  
 $\text{N}_2\text{O}$ -He(Kr), thermal diffusion factors meas. 0-10344  
 $\text{N}_2\text{O}$ - $\text{N}_2$ -He, gasdynamic laser, effect of weak flow perturbations on gain 0-14316  
 $\text{N}_2\text{O}+\text{B}$ , chemiluminesc. metal oxide formation 0-35509  
 $\text{N}_2\text{O}+\text{CO}$ ,  $\text{CO}_2$  vibr. temps. under gasdynamic laser conditions 0-21276  
 $\text{N}_2\text{O}+\text{CO}$ , use of steady state chemical reaction for vibr. excitation of  $\text{CO}_2$  and  $\text{N}_2$  0-50851  
 $\text{N}_2\text{O}+\text{CsF}$ , rot. inelastic collisions, mol. beam meas. 0-1049  
 $\text{N}_2\text{O}+\text{inert gas}$ , reactant decomp., rot.-vibr. energy transfer, relax. anal. soln. 0-55650  
 $\text{N}_2\text{O}+\text{O}(2\text{D}_2)$ , collisional deactivation meas., 295K, rel. to atmospheric processes 0-16663  
 $\text{N}_2\text{O}+\text{Sn}=\text{SnO}(a^3\Sigma)+\text{N}_2$ , chemiluminesc. high temp. fast flow reactor obs. 0-45493  
 $(\text{N}_2\text{O})_2$ , IR continuum spectrum at low temps. 0-980  
 $\text{N}_2\text{O}_4$  corroded annular channels, heat transfer and pressure drop 0-1569  
 $\text{N}_2\text{O}_4$ , dissociating in vertical tube, boiling heat transfer 0-1568  
 $\text{N}_2\text{O}_4$ , dissociating turbulent convection on horizontal plate (Russian) 0-1587  
 $\text{N}_2\text{O}_4$  flowing in axisymmetric channels, mass and heat transfer calcs. 0-1570  
 $\text{N}_2\text{O}_4$ , reactor coolant, stability in two-phase flow (Russian) 0-609  
 $\text{N}_2\text{O}_4$ , sound dispersion and velocity mol. dissoc. effects (Russian) 0-1730  
 $\text{N}_2\text{O}_4$ -NO- $\text{H}_2\text{O}$ , distrib. coeff. for  $\text{N}_2\text{O}_4$  on liquid-vapour equilib. (Russian) 0-55699  
 $\text{N}_2\text{O}_5$ , from smouldering discharge at  $\text{O}_3$  liq. surface in  $\text{N}_2$ , thin solid pellicle formation 0-38827  
 $\text{NOBr}+\text{Br}$ , primary and secondary photochemistry, vibrationally excited NO, IR fluoresc. obs. 0-48030  
 $\text{NOCl}+\text{Cl}$ , primary and secondary photochemistry, vibrationally excited NO, IR fluoresc. obs. 0-48030  
 $\text{NOH}$ , groundstate electronic struct., MRD CI calc., dissoc. energy, isomerisation energy 0-14088  
 $\text{NOH}$  polycryst. radicals, low temp. PMR 0-25220  
 $\text{NO}_2^*$ , multiple IR photon fluoresc. excitation and dissoc., electronically excited 0-48050  
 $\text{N}_2\text{O}_4=2\text{NO}_2=2\text{NO}+\text{O}_2$ , precipitation of corrosion products in a fractionating column (Russian) 0-25707  
 $\text{N}_2\text{O}_4=2\text{NO}_2=2\text{NO}+\text{O}_2$ , working fluid for power-producing thermodynamic cycles 0-13536  
 $\text{NO}(a^1\Pi)$ , in Ar(Kr)(ArKr), matrices, multiphonon vibr. relax., time-resolved emission obs. 0-18861  
 $\text{N}_2\text{O}$ , viscosity meas. at low temps. 0-6193  
 $^{14}\text{N}$ , isotropic hyperfine coupling consts. in small radicals 0-52894  
 $\text{NO}_3^-$ - $\text{Cl}^-$  soln., inhibition of o-Ps formation 0-1089

**NMR line breadth**

- acetic acid-methanol-tetrahydrofuran- $d_3$ , superimposed intermolecular spin exchange reactions, NMR lineshape theory 0-32740  
 coupled systems, A-line intensity, phase, oscill. with time, heteronuclear double reson. spectra 0-34823  
 p-dihalobenzenes, apparent NQR spin-spin relax. times obs. 0-54991  
 dimethylammonium copper chloride bromide, mag. props., pulsed NMR expts. 0-11292  
 2,6-dimethylbenzoic acid,  $^1\text{H}$  chem. shift recovery from combined multiple pulse NMR and sample spinning 0-32738  
 dispersion vs. absorption curve method for distinguishing peak position distrib. from linewidth distrib. 0-4775  
 graphite-SbF $_5$  intercalation cpd., carrier density from  $^{19}\text{F}$  NMR line shapes 0-25224  
 lecithin-deoxycholate mixed micelles, surface curvature and mobility, PMR study 0-21452

**NMR line breadth continued**

- line narrowing, selective population transfer induced 0-31827  
 line narrowing with large reson. offset, appls. to solids (German) 0-7176  
 liquid, undergoing inhomogeneous Poiseuille flow, spin echo signal shape (Russian) 0-50225  
 lithium perfluoro-octanoate-water, liquid crystal,  $^{19}\text{F}$  multipulse NMR obs. 0-34795  
 macromolecule, NMR estimation of equilib. consts., intermediate exchange processes effect 0-1094  
 monovalent ions in aq. metal ion solns.,  $^{14}\text{N}$  NMR relax. 0-20481  
 multiple pulse NMR of solids, accurate phase adjustment 0-22404  
 multipulse NMR, relax. processes anal. 0-34798  
 paramagnetic ion nuclei in magnetically conc. solid, theory 0-25238  
 phospholipids,  $^{31}\text{P}$  NMR, slow-motional lineshapes for very anisotropic rot. diffusion 0-5644  
 polymer, cryst., broadline PMR spectra, math. separation procedure 0-2647  
 powders with spin 1/2 nuclei arranged in isosceles triangular mag. config., shape function 0-2648  
 proton chemical shifts, combined pulse NMR and magic-angle spinning 0-44934  
 rare earth rhodium borides,  $\text{RRh}_2\text{B}_4$ , NMR and sp. ht. in supercond. and mag. ordered phases 0-7037  
 ruby, ESR and NMR correl. line broadening effect assoc. with external mag. field inhomogeneities 0-50227  
 solids, selective spin imaging 0-29629  
 solution,  $^{89}\text{Y}$  spin-spin relax. times, no pH depend. 0-2657  
 spin echo, phase-modulated, derivation of pure absorpt. spectra 0-22410  
 spin systems under multiple pulse NMR conditions, chem. shift relax. 0-34808  
 surfaces line broadening, quantum mechanical calc. 0-29639  
 tetrafluoromethane, bond length and chemical shielding, NMR lineshape anal. of multispin system 0-32741  
 TGS, proton and deuteron NMR anal. of temp. depend. 0-33919  
 trichlorofluoromethane,  $^{19}\text{F}$  spin-rot. tensors, appl. to liq.-phase rot. diffusion 0-43068  
 trichlorophosphazoperfluoro-1,1-dimethylethane, cryst.,  $^{19}\text{F}$  NMR and mol. mobility, fluorination influence 0-34809  
 two-dimensional NMR spectra, elimination of dispersion-mode contribs. 0-20508  
 two-dimensional NMR spectra in phase-sensitive mode 0-20470  
 Al wires, eddy current effects on NMR 0-2645  
 $\text{ClO}_3\text{F}$ ,  $^{19}\text{F}$  spin-rot. tensors, appl. to liq.-phase rot. diffusion 0-43068  
 Cu complexes, Cu(II)-P tetrahedral,  $^{63}\text{Cu}$  FT-NMR 0-53021  
 $\text{CuBr}_2$ ,  $^{63}\text{Cu}$  and  $^{61}\text{Br}$  NQR line width obs. 0-50219  
 $\text{CuF}_2$ ,  $^{63}\text{Cu}$  NQR meas. 0-50219  
 $\text{D}_2$ , solid, quadrupolar glass ordering NMR adsorption line shapes 0-7178  
 $^3\text{He}$ , superfluid A-phase, have persistent currents been obs.? 0-10731  
 $\text{K}_2\text{Pt}(\text{CN})_4\text{Br}_{0.3}\cdot 3.2\text{H}_2\text{O}$ , linear cond.,  $^{195}\text{Pt}$  NMR evidence of low lying non-linear excitation 0-44933  
 $\text{K}_2\text{Pt}(\text{CN})_4\text{Br}_{0.3}\cdot 3\text{H}_2\text{O}$ , dynamic  $^{195}\text{Pt}$  NMR meas. below metal-insulator transition 0-34810  
 $\text{La}_{1-x}\text{Gd}_x\text{Ag}$ , antiferromagnet, spin echo NMR anal. 0-15821  
 $\text{LaNi}_2\text{H}_7$ , with small Cr additions, NMR parameters (Russian) 0-29637  
 Li wire, NMR line shape, eddy current effect in presence of self-diffusion 0-54955  
 LiH, solid, anion and cation diffusion, NMR relax. and linewidth obs., Schottky disorder 0-15815  
 $\text{LiTmF}_4$ , strongly isotropic Van Vleck paramag., nucl. spin interaction (Russian) 0-34792  
 $\text{MoO}_{4-n}\text{Sn}^{2-}$ , ( $n=0-4$ ),  $^{17}\text{O}(^{33}\text{S})(^{95}\text{Mo})(^{97}\text{Mo})$  NMR investig. 0-53022  
 $\text{NH}_4\text{Br}$  single cryst., low temp. PMR lineshapes of tunnelling  $\text{NH}_4^+$  ions 0-25223  
 $\text{NH}_4\text{HF}_2$ , powder, proton and fluorine 2nd moments meas., 77-395K 0-34803  
 $\text{Ni}(\text{CN})_2$ -dodecylamine, lamellar paraffinic system, phase transitions, wide-line NMR obs. (French) 0-44929  
 $\text{O}$ , metastable  $^3\text{S}$ -state, optical pumping 0-32678  
 $^{17}\text{O}$  nuclear quadrupole double resonance spectroscopy, line shapes and examples 0-31820  
 $\text{PF}_3\text{Br}_2$ , spin systems under multiple pulse NMR conditions, chem. shift relax. 0-34808  
 $\text{Pb}(\text{NO}_3)_2$ ,  $^{207}\text{Pb}$  NMR linewidth, angular depend. due to  $^{14}\text{N}$ - $^{207}\text{Pb}$  direct dipole-dipole interaction 0-11280  
 $\text{Pb}(\text{NO}_3)_2$ , nucl. mag. shielding tensors of  $^{207}\text{Pb}^{2+}$ , NMR obs. 0-44939  
 $\text{PrNi}_3$ , metallic Van Vleck paramag., nucl. interactions, NMR meas. 0-44953  
 $\text{PrNi}_3$ , nucl. cooling agent, relax. and exchange, EPR and NMR study 0-25237  
 $\text{Rb}_2\text{ZnCl}_4$ , spin-lattice relax. in incommensurate phase, phason and amplitudon excitations 0-50213  
 $\text{SiO}_2\cdot\text{Co}(\text{II})$ , adsorption of  $\text{H}_2\text{O}$ , coord. lifetime, surface effect, NMR obs. 0-34299  
 $\text{SnBr}_2$ ,  $^{81}\text{Br}$  NQR line width obs. 0-50219  
 $\text{UNi}_{1-x}\text{Cu}_x$ , NMR and press. effects 0-25230  
 $\text{V}_2\text{O}_5$ , quadrupole broadening in  $^{51}\text{V}$  NMR spectrum 0-20469  
 $\text{ZnBr}_2$ ,  $^{81}\text{Br}$  NQR line width obs. 0-50219  
 $\text{ZnO}$ , accumulation layer, ESR and NMR studies of adsorbed  $\text{H}_2$  (Japanese) 0-50186

**nobelium**

No entries

**nobelium compounds**

$\text{NoH}^+$ ,  $\text{YbH}_2$ , relativistic (non-relativistic) HF one-centre expansion calcs. 0-52908

**noble gases see inert gases****noctilucent clouds see clouds****noise**

- see also acoustic noise; atmospheric; electron device noise; random noise; white noise  
 bidirectional laser amplifiers, amplified spontaneous emission intensity fluctuations 0-37988  
 biomedical metal microelectrodes, noise characts. (Japanese) 0-3846  
 BWR, neutron noise field, two-group diffusion theory 0-18461  
 chromatography, correlation type, noise sources eval. and practical considerations 0-40771  
 colorimetric system chromatatic fluctuations anal. (Russian) 0-42249  
 computed tomographic reconstruction, detective quantum efficiency in detection of small objects 0-46046



## noise continued

- computed tomography image second-order statistics, information and artifacts 0-46040
- computerised tomography, detectability in CT images 0-3806
- computerised tomography, dual energy scanning, noise considerations 0-3804
- current noise parameters in embryonic heart cell aggregates 0-21459
- discontinuous metal films, electrical noise, high temp. behaviour 0-54807
- ECG, QRS detection accuracy rel. to anal. of HF components 0-17158
- emission CT system, expt. meas. of impulse response and noise 0-56182
- Helmholtz resonator as optoacoustic detector 0-31896
- holograms recorded using time-dependent reference wave, S/N ratio, energy chars. 0-32935
- lipid bilayer, hydrophobic ion current noise, autocorrel. anal. 0-30676
- mammography, detective quantum efficiency anal. of electrostatic imaging and screen-film imaging 0-41232
- microcalorimeters, conductive, limiting potentialities, anal. 0-17942
- multilayer semiconductor structure, current noise 0-20302
- nuclear reactor noise analysis, time series modelling methods, comparative eval. (*Japanese*) 0-13552
- nuclear reactors, coupled-core, irreversible circulation of fluctuation 0-27700
- optomechanical scanner, noise analysis 0-47090
- photoelectron statistics, joint moment method, phase radiation 0-23647
- photographic film, noise diffraction spectra 0-27368
- quantum statistics of photocurrent in optimal light detector, atm. 'seeing' conditions 0-53244
- radiography, detection of bars and discs in quantum noise [radiography] 0-41042
- radionuclide imaging, fundamental limitations 0-30882
- ring laser, two-mode, intensity fluctuations 0-33038
- scanning background-limited IR sensor with adaptive threshold signal processing logic, performance 0-37082
- semiconductor-liquid electrolyte interface, conduction noise (*French*) 0-20306
- spectrometer efficiency, S/N ratio formula 0-31881
- stellar interferometry, long baseline, S/N ratio 0-26749
- Al films, plastic deformation, appl. of current noise technique for dislocation processes 0-35442
- Au discontinuous films, on sapphire substrates, electrical noise, high temp. behaviour 0-54807
- CdS crystal, SAW amplification, bulk and acoustic noise 0-39637
- Fe-Ni-Co-Mo-Ge alloy 40NM, excess mag. noise after various thermomag. treatments (*Russian*) 0-29575
- GaAs DH laser, self-induced modulation, noise, instability 0-48250
- GaP Schottky barriers, voltage fluctuations, meas. 0-15604
- p-Ge, diffusion coeff. for hot holes in mag. field 0-39614
- p-Ge, noise calc. in strong elec. field using Monte Carlo method 0-15578
- Se, amorphous, monostable switching, current noise 0-44682
- Se, amorphous thin film, elec. noise, monostable switching 0-44684

## noise abatement

- see also *acoustic wave absorption*
- absorption mechanism of porous material of sound pulse 0-38170
- acoustic intensity measurement during noise abatement exercises (*German*) 0-1389
- acoustic paths between two rooms connected by ventilation duct, anal. 0-10074
- acoustic planning of plants, technical and economic advantages 0-3561
- agricultural tractor operator noise, investigations on cab 0-43529
- air compressor used in system for treatment of decubitus ulcers 0-48513
- airborne noise level criteria for buildings 0-10075
- aircraft landing trajectories of minimum noise (*Spanish*) 0-53546
- aircraft takeoff procedures, effectiveness 0-16880
- apartment blocks, noise transmission through wood joist floors, sound insulation methods 0-38178
- arbitrary random noise and vibration waves, statistical consideration of peak distribution 0-23836
- architectural acoustics, sound transmission between absorbing parallel planes 0-33344
- barriers on finite impedance ground for noise reduction 0-33301
- bulldozers, use of retrofit noise control treatments 0-43532
- centrifugal blower noise, exptl. studies 0-14518
- circular saws in S.Australia's woodworking and metal industries 0-48517
- cold heading equipment noise and control 0-43538
- combustion noise, flow induced, suppression using appl. of DC elec. field 0-38176
- community, estimation of  $L_{eq}$  using Weibull distribution (*Japanese*) 0-55964
- computerised noise environment modelling at General Motors Corporation 0-43542
- control, engineering approach 0-16879
- covered panels, sound insulation characteristics of panels having porous material coverings (*Japanese*) 0-33334
- dairy packaging industry, survey procedures 0-53551
- diesel machine, 300 ton, acoustic and vibratory chars. 0-43541
- diesel-powered underground mining equipment 0-53557
- domestic acoustic noise control and measurement (*Spanish*) 0-1380
- ELMO-G quiet running vacuum pumps and compressors for plant noise reduction 0-5872
- engine components and vibration isolation 0-53552
- engine structure vibrations, transmission path and dynamic behavior, background and static tests 0-43520
- engine structure vibrations, transmission path and dynamic behavior, motoring tests 0-48487
- England and Wales, noise abatement zones 0-16881
- environmental noise, absorption by walls, statistical evaluation of noise control mechanisms (*Japanese*) 0-33336
- environmental noise, annoyance due to different sources 0-48504
- environmental railway noise impact assessment, high speed trains in AMTRAK Northeast corridor 0-48507
- exhaust noise and its control for construction equipment 0-43531
- exhaust systems, appl. of transmission matrices 0-53554
- factory spaces, performance of absorptive treatments 0-48514
- fan drives on construction equipment 0-43530
- fibrous glass and mineral fibre acoustical materials, development 0-33341
- foliage as low-pass filter, expts. with model forests in anechoic chamber 0-33303
- forge hammers, control of impact noise 0-43539
- foundry industry, investigation of acoustical barriers 0-48515
- high speed trains, aerodynamic noise study 0-48512

## noise abatement continued

- hydraulic equipment 0-53561
- impact noise level criteria for buildings 0-10075
- impact noise reduction by floor coverings (*Japanese*) 0-33331
- impulse method of measuring acoustic normal impedance at oblique incidence 0-53582
- indoor machinery, sound transmission loss for various ventilation louvre geometries 0-45839
- induced draft cooling towers, noise prediction and control 0-16878
- industrial, protecting workers on an individual basis, Occupational Safety and Health Act 0-45841
- industrial, sound attenuation by multiple barriers 0-43524
- infrasound, problems on environmental pollution (*Japanese*) 0-35805
- job shop environment, analysis for noise regulations 0-45840
- lathes, stock feed tubes silencing with ultrahigh molecular weight polyolefin 0-10085
- legal remedies for noise and vibration problems 0-10084
- legislation and the noise consultant 0-10083
- LF industrial noise problem 0-33339
- long-hole drilling machine 0-53559
- machine tools, vibration-damping plug 0-43525
- machinery, activities of EPA Office of Noise Abatement and Control 0-43527
- machinery, conf., W.Lafayette, IN, USA (Apr/May 1979) 0-43526
- machines employing circular saw blades 0-43533
- mechanical input power meas. method for wall structures 0-19176
- metal cutting methods and machinery 0-53548
- mining industry 0-53556
- mobile equipment noise control in surface mining 0-53558
- newspaper pressroom, noise level reduction by screens and insulation 0-14517
- noise control in industry, costs 0-16877
- noise generation by railroad coaches 0-48498
- nuclear power stations, environmental acoustic protection (*French*) 0-19155
- occupational noise standard, 29 CFR 1910.95, problems in enforcement 0-43528
- optimised multisectioned acoustic liners 0-19145
- outdoor noise control barriers, practical appls. and attenuation estimation procedures 0-33340
- paging systems, noise reduction using selective methods 0-40944
- petro-chemical industrial plants, piping networks, noise abatement 0-28381
- piezoelectric transducer systems, noise suppression and prevention for shock and vibration meas. 0-22353
- pile driving devices 0-23832
- power plant effects on environment, protection measures (*German*) 0-26574
- punch presses, noise reduction by means of shock absorbers 0-43540
- rail traffic noise, attenuation by tree belts, pilot study 0-48501
- railway, effect of train noise on sleeping subjects 0-48509
- railway, environmental controls for new housing sites 0-48505
- railway, environmental impact in Britain 0-48508
- railway traffic, Dutch study 0-48511
- railway wayside noise, high-speed trains 0-48497
- rectangular wide barriers for sound reduction, approx. formula for calculation 0-38175
- residences, energy conservation and noise control measures comparison 0-35807
- road traffic, improvements to the equally-spaced vehicles model, grouping effect (*Japanese*) 0-55963
- road traffic, prediction of time pattern of fluctuating sound levels (*Japanese*) 0-55965
- road traffic noise, analysis of sequence of sound level readings (*Japanese*) 0-35806
- road traffic noise, effect of structure-borne tunnel vibrations on buildings 0-48492
- road traffic noise, human response in residential areas, possibility of reduction for the future 0-55962
- road traffic noise, its relation to traffic volume (*Japanese*) 0-33335
- road traffic noise, new theoretical model (*Japanese*) 0-35804
- road traffic noise, prediction using a scale model 0-45838
- road vehicle vibration analysis, digital modal analysis system 0-38173
- rolling-contact noise generation in wire stranding machines, use of elastomers 0-43534
- room noise reduction, use of window cills and reveals 0-33343
- rotary scrap chopper noise 0-53549
- saws, control of vibrations through thermal tensioning 0-48516
- self-protecting buildings, acoustical performance 0-23839
- service evaluation tests on locomotives, AMTRAK Northeast corridor 0-48506
- silencers, optimisation of silencing characteristics and positioning of expansion chamber mufflers (*Japanese*) 0-33333
- silencing systems, acoustic charact. anal., 4-terminal matrices of tube system (*Japanese*) 0-10082
- silencing systems, acoustic charact. anal., attenuation const. of plane wave in tube (*Japanese*) 0-10081
- sound propagation in urban and forest areas, prediction of noise appl. (*German*) 0-38142
- standardisation, activities of ISO (*Japanese*) 0-19154
- STOL aircraft and helicopters, interior noise control 0-14519
- stopper drills for coal mines 0-53560
- structure damping, evaluation of viscoelastic props. 0-43632
- structures under impact loading, finite element modelling as tool for noise analysis and control 0-43535
- subjective annoyance by low level sound, sound character as a physical attribute 0-35902
- supersonic transport planes, reduction of local ground noise 0-38174
- telephone exchanges, PTT premises (*French*) 0-10079
- telephone operator's office 0-10086
- traffic noise, model investigation on acoustical performance of courtyard houses 0-10077
- traffic noise reduction by multiple finite barriers, prediction method 0-38171
- traffic noise screening effect by buildings (*German*) 0-10076
- trains, annoyance in residential areas from noise and vibration 0-48503
- transportation systems, importance in France 0-48510
- trucks and portable compressors, enforcement of EPA regulations 0-53550
- urban, noise mapping using grid method with Rohde and Schwarz integrating sound level meter ELDO 4 0-48533



**noise abatement** continued

urban noise level variation and attenuation with height 0-10078  
vibration isolation, survey of use and characterization 0-19144  
vibration-stimulated material handling equipment 0-43537

**noise control (acoustic)** *see* **noise abatement****noise control (interference)** *see* **interference suppression****noise elimination** *see* **interference suppression****noise generators**

analytical method to predict noise radiation from vibrating machine systems 0-43521

**noise levels, acoustic** *see* **acoustic noise****noise measurement**

*see also* **acoustic noise measurement**; **electric noise measurement**; **optical noise measurement**

antenna in plasma, detect. of natural noises 0-24181  
X-ray image intensifiers, quantum noise meas. 0-46033

**nomenclature and symbols**

*see also* **units (measurement)**

asteroids, Minor planet circulars 5017-5066, new names for seven objects 0-17533  
asteroids, new names for 35 objects 0-46459  
colloids, rheological props., terminology and symbols 0-26065  
comets, perihelion passage designations for 1978 period 0-31241  
crystal-chemical formulae, for simple inorganic cryst. structs. 0-33910  
electroanalytical chemistry, terms, symbols and definitions 0-21348  
elements of atomic numbers >100, nomenclature 0-3295  
graphite intercalation compounds, nomenclature 0-1948  
magnetism teaching w.r.t. chemistry, guide to units 0-12871  
measurement technical term translation problems (*German*) 0-36965  
organic chemistry, isotopically modified compounds, nomenclature 0-3294  
physicochemical quantities, symbols and terminology 0-3296  
polymers, stereochemical definitions, IUPAC nomenclature 0-23593  
SI units, conventions and practices, physics teacher's viewpoint 0-36968  
SI units, rationalisation and need for approximation to SI 0-36969  
surface chemistry, rheological props., terminology and symbols 0-26065  
weather and climate, definitions 0-41540

**nomograms**

*see also* **graphs**

antireflection coating, three-layer, refractive index optimum combination 0-28306  
fibre, self-focusing, matching elements calc. 0-28339  
paraxial optical systems, nomographic diagrams for design and anal. 0-48377  
pressure inside hollow organs, recording through tubes, nomograms for calc. of system parameters 0-3836  
rainfall frequency relationships study for Karnataka region, India 0-31094  
Schottky barrier IR detector, nomographs for parameter evaluation, 77K 0-31870  
US propag. calcs., multiple nomogram 0-28371  
Voigt contour of spectral line, nomogram for parameters determ. 0-52321

**nomographs** *see* **nomograms****non-Newtonian flow**

*see also* **non-Newtonian fluids**

annular two-phase flow of non-Newtonian liqs. and gases, press. drop and gas vol. fraction 0-10286  
annulus with non-Newtonian fluids, mass transfer to inner wall, Leveque soln. adaptation 0-10267  
asymmetrical fluid, thermoconvection wave propagation, microinertial and couple stress effect 0-19446  
Bingham fluid, entrance flow through noncircular ducts, finite difference anal. 0-1684  
capillary and slit methods of normal stress measurements 0-43807  
circular cylinder, non-Newtonian fluid flow boundary layer eqn. approx. soln. 0-14752  
clay aqueous suspension turbulent flow, average velocity profile and functional loss in pipe 0-48778  
convective stability, energy method 0-38455  
creeping flow round sphere, fluid elasticity effect on drag coefficient 0-43742  
creeping motion of fluid past sphere 0-24057  
critical fluids, non-Newtonian effect and normal stress effect 0-49396  
die swell problems, viscoelastic fluid flow, collocation and Galerkin finite element anal. 0-14751  
droplet deformation in extensional flow 0-19449  
electrohydrodynamic instability 0-14832  
emulsion, concentrated unstable, turbulent flow in pipes 0-28537  
entangled monodisperse polymers kinetic network model for nonlinear viscoelastic flow props. 0-28538  
fibre suspension, dil., mechanistic aspects of drag reduction in turbulent pipe flow 0-6102  
flat plate, MHD unsteady flow of Maxwell fluid, relaxation parameter 0-24101  
flow regulating system operating with Newtonian and non-Newtonian fluids (*German*) 0-1535  
fluid-film flows, of differential fluids of complexity  $n$  dimensional approach, lubrication theory appl. 0-16492  
fluid-particle dynamic interactions (*Portuguese*) 0-19452  
glass-forming liquids, viscous flow and valence config. theory 0-14756  
Hele-Shaw unsteady flow 0-14754  
hydraulic resistance of channels calc. (*Russian*) 0-38451  
incompressible fluid with pressure gradient and fluid injection, MHD flow 0-33686  
incompressible liquid film, surface waves 0-43748  
incompressible simple fluid with fading memory, stability 0-43741  
infinite vertical porous plate, unsteady free convective elastica-viscous flow, viscous dissipation heat 0-24012  
injection effects of viscoelastic liquid flowing into channel 0-53823  
jets, micropolar fluid, impinging normally on flat plate, thermal boundary layer 0-28536  
laminar boundary-layer flow of non-Newtonian fluid, surface heat transfer rate 0-24055  
laminar far wake flow of non-Newtonian power law fluid 0-53824  
laminar jet flow 0-1662  
low Reynolds-number flow in the vicinity of axisymmetric constrictions 0-6147

**non-Newtonian flow** continued

MHD viscoelastic free convection boundary layer flow past porous plate 0-10317  
micropolar fluid, laminar boundary layer, longitudinal surface curvature effects 0-48669  
micropolar fluid, laminar flow through slot 0-10313  
micropolar fluid, thermal boundary layer at stagnation point 0-53820  
micropolar fluid drop in viscous fluid, flow, stream functions, velocities, spins, drag 0-53821  
micropolar liquid between two infinite slowly rotating discs 0-53796  
nearly extensional flow, consistency relations 0-53822  
nonisothermal flow of anomalous systems in pipes, rheological aspects (*Russian*) 0-43775  
nonisothermal flow of anomalously viscous liquids in channels of screw extruders 0-19305  
nonstationary viscous flow of thermally conductive gas, around semi-infinite plate, numerical anal. 0-6104  
orthogonal stagnation flow, a framework for steady extensional flow experiments 0-1653  
particle distribution in Poiseuille flow of suspension in micropolar fluid model 0-10314  
Poiseuille flow of viscoelastic fluid between eccentric cylinders 0-1652  
polyacrylamides-water-glycerol, streaming birefringence in extensional flow 0-6013  
polymer flow on inclined plane, edge effects 0-19451  
polymer melts, blended resins, flow charact. (*Japanese*) 0-24059  
polymer melts, elongational behaviour in const. elongation rate, tensile stress and tensile force expts. 0-38372  
polymer solns., hydraulic resistance of channels calc. (*Russian*) 0-38451  
polymer solution, dil., turbulent flow behaviour in annulus 0-33633  
polymer solution, flow in exit region of tube, jet swell problem 0-38452  
polymer solutions, weak, flow anomalies (*Russian*) 0-19454  
polymeric, liq., spike-strain test relevance for network connectivity destruction by deformation 0-6001  
polymeric systems, fluid, rheology, characterised by mol. int. distrib., review 0-1504  
polystyrene-Aroclor 1254, streaming birefringence in extensional flow 0-6013  
polytropic plastic gas, nonstationary shock wave propag., closed form soln., thermonuclear microfusion 0-28534  
pore geometry effects on pressure loss, model channels with varying diameter (*German*) 0-1677  
power law fluids, laminar flow through granular beds 0-38488  
power-law fluid, two-stream mixing along flat plate, variational solns. 0-53817  
power-law non-Newtonian conducting fluid, laminar boundary layer in transverse mag. field 0-33694  
pseudoplastic fluid crossflow around circular cylinder, heat and mass transfer 0-19370  
rectilinear flow, pressure error upper and lower bounds with pressure gradient 0-6010  
rheological electrokinetic phenomena in rectangular capillary, numerical simulation 0-26023  
solid-fluid interaction in flow through porous media, fluidised beds (*Portuguese*) 0-38454  
solid-liquid mixtures, rheological characts., shear stress/strain rate relationships 0-10287  
solute dispersion in non-Newtonian fluids, chemical reaction effects 0-38503  
square duct entrance region, Laminar flow and heat transfer to non-Newtonian fluid 0-10243  
structural relaxing fluids, hydrodynamics theory (*Russian*) 0-19453  
suspension, dil., of spherical particles in non-Newtonian liq., rheological behaviour 0-24058  
thermoviscous fluid, steady flow through straight tubes 0-33636  
thixotropic fluids, rheological characterisation 0-38373  
transient viscosity determination method 0-43746  
unsteady laminar flow of elastic viscous fluid through porous channel, applied mag. field effects 0-38499  
viscoelastic flow, finite element simulation 0-43745  
viscoelastic flow past stationary and rotating cylinders 0-43744  
viscoelastic fluid, flow stability in converging channel against perturbations (*German*) 0-1654  
viscoelastic fluid, free convection flow past a vertical wall 0-10239  
viscoelastic fluid, steady flow and heat transfer between two coaxial rot. discs 0-14755  
viscoelastic fluid flow in fixed geometry, collocation and Galerkin finite element methods 0-14750  
viscoelastic fluid layer heated from below, vertical periodic oscillations, convection, overstability 0-48755  
viscoelastic fluids, heat transfer at low Deborah numbers, rheological effects 0-19445  
viscoelastic liq., motion of slender rod falling near vertical wall 0-43743  
viscoelastic liquid, flow through porous channel, free and forced convection effects 0-53861  
viscoelastic medium, transitional flow, lag time eval. 0-38371  
viscoelastic unsteady flow through tubes 0-14753  
viscoplastoplastic laminar tube flow, heat transfer 0-10269  
viscoplastic fluid Couette flow, heat transfer 0-10270  
wall region heat and mass transfer in turbulent Newtonian and viscoelastic flow 0-14680

**non-Newtonian fluids**

*see also* **colloids**; **polymer melts**; **polymer solutions**; **rheology**

annulus with non-Newtonian fluids, mass transfer to inner wall, Leveque soln. adaptation 0-10267  
bituminous pitch oils, flow curves, mag. field effect 0-33553  
couple stress theory, integral representation 0-33639  
crosslinked polymer systems, probabilistic theory 0-19314  
dilatant liquids, propag. of shear perturbations 0-6103  
drag for fluids of grade three 0-33635  
elastico-viscous fluid, compressible, nonperiodic wave propag. 0-43724  
elastohydrodynamic problems for rough bodies with non-Newtonian lubrications (*Ukrainian*) 0-24054  
extrudate swell, inelastic theory 0-43684  
fluid-film flows, of differential fluids of complexity  $n$  dimensional approach, lubrication theory appl. 0-16492  
gas and non-Newtonian liquid, stratified flow in horizontal pipes 0-48787  
macromolecular solutions, laminar filtration under low polarization conditions 0-24056  
Maxwell fluid, Rayleigh-Taylor instability 0-33631



**non-Newtonian fluids continued**

- multiphase non-Newtonian systems, rheological props. variation in barotreatment 0-19304
- primary macromolecules, mol. wt. distrib. influence on crosslinked polymer systems 0-19313
- Rayleigh classical equation generalisation to several non-Newtonian liquids 0-19444
- Reiner-Rivlin fluids, rheological props. 0-14646
- review, description and behaviour 0-33637
- rheological props., pressure induced change of yield stress 0-53736
- second order fluids, model, anomalous features 0-33632
- third grade fluids, thermodynamics and stability 0-33638
- thixotropic fluids, coagulation kinetics, diffusion effects and rheological models 0-43740
- thixotropic fluids, rheological characterisation 0-38373
- viscoelastic, resist. to tensile stress 0-1505
- viscoelastic flow, heat transfer at low Deborah numbers, rheological effects 0-19445
- viscoelastic fluid, flow anal. between 2-D surfaces subject to normal high freq. oscillations 0-16493
- viscoelastic theories based on left Cauchy-Green tensor history 0-4534
- viscosity measurement in rotational viscometer 0-19529
- C black conc. suspensions in low mol. wt. vehicles, rheology anal. 0-19312

**noncrystalline state structure**

see also *amorphous state*; *vitreous state*

- alkali germanate glasses, struct., Raman scatt. obs. 0-1936
- alkaline earth phosphate ( $\text{MO} \cdot \text{Al}_2\text{O}_3 \cdot \text{P}_2\text{O}_5$ ) irradiated electret glasses, relax. of external field intensity on heating 0-25282
- alkaline earth silicate glasses, morphology effects on props. 0-49118
- allophane, synthetic, amorphous mineral struct. obs. using  $^{57}\text{Fe}$  Mossbauer effect 0-34836
- amorphous and liquid semiconductors, conference, Cambridge, MA, USA (Aug. 1979) 0-41933
- amorphous materials, small area struct. studies 0-44087
- amorphous semiconductors, fluctuations and non-randomness in continuous network models 0-49112
- amorphous solid, supercooled liquid-glass transition region, short-range order, simulation 0-44127
- amorphous solids, low-energy excitations of phonons, magnons, electrons rel. to struct. factor 0-44488
- amorphous tetrahedrally coord. solids, bond charge model 0-49108
- Bernal holes, size statistics 0-33892
- borate glass: Ni, absorption spectra, mag. props., coordination behaviour (German) 0-40147
- borosilicate glass sputtered film, phys. and chem. props., B diffusion into Si,  $\text{SiO}_2$  0-29040
- butadiene-acrylonitrile elastomer, supramol. formations (French) 0-1941
- chalcogenide glass films, photostructural changes, photodarkening 0-49121
- chalcogenide glasses, heteropolar, coordinations of ground state and of negative U defects 0-54137
- chalcogenide glasses, struct. and growth kinetics, topological principles 0-49123
- cholesteryl methyl carbonate, liq. cryst., low-ang. X-ray diffr. obs., solid and liq. 0-49093
- covalent alloys, amorphous, dimensionality of subnetworks 0-28916
- crystallography of amorphous solids, tentative description 0-6360
- electropolymerisation, on electrodes, book contribs. 0-50854
- epoxy resin cross linked with aliphatic polyamines, struct. and dynamic mech. props. (Japanese) 0-38956
- epoxy resins, struct. changes under mag. field action 0-40516
- ethylene copolymers, partially cryst. pseudoeutectoid, swelling, thermodynamics 0-39311
- ethylene copolymers with acrylic monomers, NMR investig (Russian) 0-54959
- fluoride systems, fundamental condition for glass formation 0-44135
- GdCo films, deposited on glass substrates (Russian) 0-24747
- glass, coloured, toughening process, spectral characts. 0-43416
- glass, disclination lines, topological stability 0-33902
- glass, insulating, thermal, acoustic props., low temp. anomaly microscopic model 0-28921
- glass, rupture behaviour, long-term strength, thermofluctuation theory (Russian) 0-40536
- glass, silicate, ultimate strength, and max. breaking rate 0-25863
- glass, struct. determ. using EXAFS 0-45169
- glass, structure, influence of thermal history (German) 0-38930
- glass fibre, elastic moduli, thermal history depend. (Japanese) 0-45333
- glass state, microscopic theory 0-44137
- glass transition temperature, determ. from expansion and elec. cond. temp. depend. 0-19967
- glass workability rel. to melting history, microstruct., apparent liquidus temp., mechanical props. 0-11633
- glass-ceramics and photosensitive glass, microstructure rel. to properties (German) 0-38926
- glass-forming systems, structure (Russian) 0-38925
- glass-forming systems, structure and thermodynamics (German) 0-38924
- hole structure of computer models 0-49109
- inorganic amorphous solids, struct., review 0-15004
- inorganic glasses, thermal expansion coeff. rel. to phys. props. 0-49389
- Kevlar 29 and 49, aramid fibres, microvoid obs. 0-38960
- Lennard-Jones amorphous solid, edge and screw dislocation, stability, elasticity, simulation 0-15099
- metallic glass, bulk and surface properties, review 0-44147
- metallic glass, composition, mech. props., simulation 0-49117
- metallic glasses, structure direct obs. by bright field TEM 0-10502
- metallic glasses props., developments and appl. 0-19710
- $\alpha,\omega$ -methoxy-poly(ethylene oxide) effect of swelling on longitudinal acoustic mode 0-29739
- nitrate glass:  $\text{Eu}^{3+}$  struct. reorganisation in glass transition interval, polarised luminesc. obs. 0-45141
- nonvinyl polymers, diffusion of simple penetrants, statistical mechanical model 0-6556
- nylon 6,  $\alpha$ -form, crystal struct. and molecular packing 0-33905
- nylon 6-LiCl mixtures, DC cond. and struct., Lill effects 0-44149
- Nylon-6, injection moulded, struct. and morphology 0-38949
- Nylon-6 fibre, crystal struct., WAXS obs. 0-15015
- PET, glassy polymer, local struct. determ. 0-33904
- PET fibre, rel. to anisotropy of dielec. relax. 0-25297
- PET fibres, amorphous, exam. of birefringence 0-11360

**noncrystalline state structure continued**

- phosphate glass: Ni, absorption spectra, mag. props., coordination behaviour (German) 0-40147
- photoemulsions, gels, coloured component addition, struct. form., dynamic shear modulus, viscosity meas. (Russian) 0-7871
- poly( $\gamma$ -n-amyI L-glutamate), crystal transition, X-ray diffr. exam. of structure 0-24374
- poly( $\gamma$ -n-butyl L-glutamate), crystal transition, X-ray diffr. exam. of structure 0-24374
- poly( $\gamma$ -n-ethyl L-glutamata), crystal transition, X-ray diffr. exam. of structure 0-24374
- poly( $\gamma$ -n-propyl L-glutamate), crystal transition, X-ray diffr. exam. of structure 0-24374
- poly(N-vinylcarbazole) layers, supermol. struct. effect on elec. props. 0-44606
- poly(tetramethylene terephthalate), IR obs. of reversible stress induced crystal-crystal phase transition 0-20627
- poly(tetramethylene terephthalate), struct., X-ray obs. 0-19725
- poly (N,N-dipropylacrylamide), 'feathered' polymer resin, prep. from suspension 0-35533
- polyacetylene, nascent morphology obs. 0-24379
- polyacetylene film, (CH), synthesis, struct. and elec. props., doped materials, review 0-15623
- polyalkenamers, longitudinal accordion mode, low frequency Raman spectroscopy 0-25369
- polyamide blends, formation by injection moulding, structs. (Russian) 0-44155
- polyamide-polyoxirane copolymers, mechanical properties evaluated 0-11700
- polybutene-1 film, tubular-extended, anal. of orientational and form birefringence 0-29712
- polycarbonates unstretched and stretched, orientation relationships,  $^{13}\text{C}$  NMR meas. (German) 0-20474
- polyester-polyurethane semi-interpenetrating networks, mech. props., morphology 0-45362
- polyesteramide 6NT6 crystals, lamellar thickness invariance with crystallisation temp. 0-24380
- polyesters from bridged bicyclic lactones, struct. characterisation by NMR 0-20476
- polyether sulphone, evidence for crystallinity 0-28928
- polyethylene, amorphous, struct. from NMR line shape analysis and MAR-NMR 0-28931
- polyethylene, high density, oriented extended chain crystals, transparency (Japanese) 0-38955
- polyethylene, high- and low-density, crystallinity degree, comparative obs. (Polish) 0-1943
- polyethylene, lightly crosslinked, processed under mol. orient., struct., props., review 0-38957
- polyethylene, linear,  $^{13}\text{C}$  spin-lattice relaxation 0-25235
- polyethylene, linear, quenching of thin films to amorphous state 0-28929
- polyethylene, rapid crystn. from melt rel. to struct. 0-44152
- polyethylene, single crystal, estimation of fold surface densities using space filling models 0-10507
- polyethylene, single crystal, structural changes due to electron irradi. 0-29053
- polyethylene crystal, longitudinal growth in flowing soln., melting of continuous fibrillar crystal 0-19917
- polyethylene fibres, electron microscope investig. of internal struct. 0-28926
- polyethylene fibril, high mol. wt., high melting point crystal (Japanese) 0-38954
- polyethylene oxide, peculiarities of struct. form. near below the melting point 0-54150
- polyethylene-polyoxymethylene mixtures connection of melt thermodynamic props. with solid state struct. (Russian) 0-54152
- polyethyleneterephthalate, crystallised from thin layer melts, temp. depend. of morphology 0-54149
- polymer, amorphous, chain conform., small-angle neutron scatt. obs. (Polish) 0-10511
- polymer, diffusion of simple penetrants, statistical mechanical model 0-10704
- polymer, molecular dynamics simulation of struct. 0-28923
- polymer, multicomponent, homopolymer blends, macroscopic phase separation 0-45289
- polymer, oriented crystalline, anisotropic thermal expansion 0-39324
- polymer, packing coefficient determ. from acoustical meas. data 0-38959
- polymer crystal, hydrostatic compressibility,  $\text{H}_2$  bonding effect on anisotropy 0-25782
- polymer fibrils, formation by flow-induced crystallisation 0-33908
- polymer network, crosslinks and trapped entanglements, two-network model 0-38962
- polymer network, crystn. and form. through crystn., crystallinity influence on radiation induced form. 0-38964
- polymer network, permanently crosslinked, topological struct. and macroscopic behaviour 0-37919
- polymer network, Riemann's metric degeneration to graph metric demonstration, chain entanglement problems 0-38963
- polymer network, small-angle neutron scatt. obs. of mol. behaviour 0-37918
- polymer network formation, pre-gel intramol. reaction and gelation, shear moduli and glass transition 0-45501
- polymer network formation, relaxational props. variation 0-38961
- polymer network formation, struct. and mech. props., computer simulation 0-38965
- polymer networks and semi-crystalline polymers, diffusion mechanism and model, local conform. change 0-15288
- polymeric chain orientation evaluation, with polarised fluorescence method (Japanese) 0-6368
- polymers, crystallinity, kinetic and morphological aspects (French) 0-1942
- polymers, crystallinity determ. by thermal method (Russian) 0-38966
- polymers, defocus transmission electron microscopy 0-28927
- polymers, Fourier anal. of X-ray diffr. patterns 0-15016
- polymers, oriented, partly cryst., macromols. in amorphous regions, length, mobility 0-49132
- polymers, short range order, amorphous and liquid, ideal peak method calcs. 0-28900
- polyoxymethylene, drawn, extra meridional reflections 0-24376
- polyoxymethylene, rapid crystn. from melt rel. to struct. 0-44153
- polyoxymethylene-copolyamide mixtures, melt rheological props., extrudate microstruct. (Russian) 0-7530



## noncrystalline state structure continued

- polyphenylacetylene films, phys. struct., AC and DC cond. 0-44750  
 polypropylene fibres,  $\gamma$ -irrad., microstruct. changes in glassy-high elastic state transition (*Rumanian*) 0-49347  
 polypropylene fibres, high strength, elastic 0-20992  
 polypropylene spherulites, refl. acoustic microscopy obs. 0-28922  
 polysiloxane dizwitterionomers, mech. props., microstruct. 0-49131  
 polysiloxane dizwitterionomers, morphology, ionic aggregation 0-49130  
 polysiloxane dizwitterionomers, sorption of  $H_2O$ , mechanism 0-49506  
 polystyrene, end group modified, chain dynamics studied by fluorescence depolarization 0-19724  
 polystyrene, isotactic and static cold-crystallised blends, thermal transitions 0-24381  
 polystyrene amorphous film, cyclically fatigued, molecular behaviour 0-35310  
 polystyrene sphere crystals, in aqueous suspensions, solid-like phase transition 0-50893  
 polystyrene-polyisoprene copolymers, macromol. chain conform. in lamellar phase (*French*) 0-2720  
 polytetramethylene glycol, short range order, amorphous and liquid, ideal peak method calcs. 0-28900  
 polytrimethylene terephthalate, struct. determ. 0-19727  
 polyvinylidene fluoride, dielec. props. and phase transitions (*French*) 0-55008  
 polyvinylidene fluoride, struct. study, piezoelec. and pyroelec. props. 0-7300  
 polyvinylidene fluoride, TSC and thermoluminescence, reln. to molecular motion (*Japanese*) 0-55200  
 polyvinylidene fluoride, X-ray high press. study 0-6369  
 polyvinylidene fluoride film, uniaxially stretched and corona poled, piezoelec. meas. 0-25311  
 polyvinylidene fluoride films, stretched and rolled, electrostriction and piezoelectric effects (*Japanese*) 0-55041  
 PVA, swollen crystallinity determ. by laser Raman spectroscopy 0-38953  
 PVC, crystalline syndiotactic, exam. of chain folding, lattice energy 0-24373  
 PVC, rigid, microdomains, small angle X-ray scattering study 0-28930  
 quartz, amorphous layer on mech. treated single crystals, electron microscope and RHEED obs. 0-24721  
 rare earth-transition metal alloys, amorphous, struct. and mag. props., book contrib. 0-39818  
 rubber, network, highly swollen, long time dynamics 0-38291  
 rubber, network entanglement contrib. to elasticity 0-39203  
 rubber, nitrite, heat ageing, light scatt. method study (*Russian*) 0-40407  
 rubber network elasticity, mol. theory 0-38290  
 semiconductors, amorphous, elementary excitations, struct. 0-49577  
 silicate glass, thermodynamic theory of structural relaxation (*German*) 0-38929  
 silk fibroin films, conformational changes induced by water immersion 0-10498  
 sodium iron fluorophosphate glasses, EPR and Mossbauer resonance study 0-39968  
 sodium tetraborate glass, melt, temp. depend. of high viscosity property (*Russian*) 0-39336  
 steel, stainless, alloyed with C, magnetron-sputtered, microstruct., and cryst.-amorphous transition 0-19719  
 structural relaxation, order parameter model (*German*) 0-44146  
 thermoplastic elastomers, crosslinked by secondary valence interactions, elasticity and processing, crosslinking behaviour 0-40320  
 vinyl and related polymers, diffusion of simple penetrants, statistical mechanical model 0-10705  
 Vycor glass, manufacture, struct., physical and chem. props. 0-7527  
 X-ray Raman edge extended modulation for struct. study of low atomic number materials 0-49111  
 Ag-Ge-S glasses, X-ray determ. of struct. (*Japanese*) 0-10501  
 $(Ag)_x(O,B,O)_y$  glass, ionic cond. and disorder modes 0-39344  
 Al, and Al-Cu(Pb) dil. alloys, pulsed ruby laser irrad., noncryst. phase form 0-35012  
 $Al_{20}As_{40}Te_{40}$  amorphous alloy, radial distribution function anal., X-ray diffr. (*Spanish*) 0-28915  
 $Al_2O_3$  amorphous films, struct., electron diffr. investigation 0-20046  
 $Al(PO_3)_3$ -NaF-LiF glasses, mixed-alkali effect 0-19715  
 As, amorphous, intermediate range order from polarised features of Raman spectrum 0-49113  
 As, amorphous, low-temp., elementary excitations, struct. 0-49577  
 As, amorphous, vibr. excitations at defect sites, IR and Raman spectra calc. 0-49329  
 As amorphous films, interference enhanced Raman scatt. 0-50326  
 As, pulsed NQR, bonding, bond angle distrib. obs. in different phases 0-54984  
 As-S, amorphous, glass transition and specific heat, intermolecular bond saturation 0-15011  
 As-S glasses, acousto-induced structural changes, optical props. 0-49122  
 As-S glasses, resonance Raman scatt. 0-50325  
 As-Se, amorphous, glass transition and specific heat, intermolecular bond saturation 0-15011  
 $As_2O_3$  crystalline and amorphous, EXAFS study of struct. 0-19776  
 $As_2O_3$  glasses, intermediate range order from polarised features of Raman spectrum 0-49113  
 $As_2(S_2)_{1-x}$  chalcogenide, covalent non crystalline topology, short range order 0-15009  
 $As_{1-x}S_x$  glasses, building blocks and bonds 0-54141  
 $As_2S_3$  ( $Se_2$ ), electron irradiated, effects on elec., photoelec. and optical props. 0-49806  
 $As_2S_3$  amorphous, luminesc. and optically detected ESR, photoinduced struct. change 0-50399  
 $As_2S_3$  structure simulation of some tellurite and chalcogenide glasses quasi-crystalline structural diffusion method (*Russian*) 0-54147  
 $As_2S_3$ -Ga system chalcogenide glasses, thermophysical and struct. props. 0-15007  
 AsSe-GeSe $_2$ -PbSe, glass form., struct. defects, elec. cond., assoc. (*Russian*) 0-54144  
 $As_2Se_3$  glass, microwave elec. cond. and struct. 0-49793  
 $As_2Se_3$ , electron irradiated, effects on elec., photoelec. and optical props. 0-49806  
 $As_2Se_3(S_2)$ , glassy film, photostructural effects, NQR study 0-49549  
 B, amorphous, X-ray Raman edge extended modulation for struct. study 0-49111  
 B amorphous film, interference enhanced Raman scatt. 0-50326  
 B dispersed fractionated powder, struct. obs. 0-19703  
 $B_2O_3$  glass, struct. and phonon spectra 0-50324

## noncrystalline state structure continued

- $B_2O_3$ , vitreous,  $BO_3$  triangles in boroxyl rings and random networks, Raman intensity investig. 0-45058  
 $B_2O_3$ - $K_2O$ - $Na_2O$ - $Rb_2O$ - $Cs_2O$  glass, small angle X-ray scatt. exam. of struct. 0-38922  
 $B_2O_3$ - $SiO_2$  glass film, CVD, differential IR studies 0-55213  
 $BaCl_2$  film, very-low-freq. inelastic light scatt. 0-25367  
 $BaFCl$  film, very-low-freq. inelastic light scatt. 0-25367  
 $BaO-Al_2O_3-SiO_2-Ta_2O_5-Mo$  glass ceramic metal composites, cermet prep. 0-11618  
 $BaO-Al_2O_3-TiO_2-SiO_2$ , glass formation, structure of cations (*Russian*) 0-38933  
 $BaO-Fe_2O_3-B_2O_3$  glass, struct. and mag. props., Mossbauer spectra 0-7226  
 C, amorphous, diamond-like 3-fold coord. 0-50323  
 C, amorphous film, struct. props., Raman scatt. study 0-11417  
 C film, amorphous, struct. and semicond. props. and heterojunction form. with single cryst. Si 0-25002  
 C, structure change, during thermal ordering, radiation disordering 0-54283  
 $CaO-Al_2O_3-TiO_2-SiO_2$ , glass formation, structure of cations (*Russian*) 0-38933  
 $CaO-SiO_2$  system glasses, IR absorpt. struct. obs. of phases and struct. 0-34918  
 $CdO-Bi_2O_3-Al_2O_3$ , glass formation and IR transmission (*Japanese*) 0-54146  
 Cr-Ge amorphous films, annealing effect on elec. resistance and struct. 0-54667  
 $Cu_{46}Zr_{54}$ , metallic glass, dynamical struct. factor and freq. distrib. meas. 0-54136  
 $Cu_{60}Zr_{40}$ , metallic glass, composition, mech. props., simulation 0-49117  
 DylG, non-cryst., Mossbauer and magnetisation studies 0-44979  
 EuIG, non-cryst., Mossbauer and magnetisation studies 0-44979  
 Fe-B, amorphous, short-range order, Mossbauer meas. 0-44986  
 Fe-B(Si) amorphous alloys, Mossbauer spectra, struct. 0-15840  
 Fe-P-C amorphous alloys, Mossbauer spectra, struct. 0-15840  
 $Fe_{80}B_{20}$ , metallic glass, triplet correlation, field-ion microscopy study 0-38921  
 $Fe_{83}B_{17}$  metallic glass, struct. from neutron diffr. study 0-6363  
 $Fe_{100-x}$ , rel. to stress relax. after annealing 0-55447  
 $(Fe_{1-x}Mn_x)_{75}P_{15}C_{10}$ , amorphous pair radial distrib. functions, neutron scatt. study 0-49128  
 $Fe_{78}Mo_{22}B_{20}$ , metallic glass, triplet correlation, field-ion microscopy study 0-38921  
 $Fe_2Ni_{1-x}$  amorphous film, growth stress and structure factor, stabilisation by conduction electrons 0-38920  
 $Fe_2O_3$ -PbO- $B_2O_3$  glass, X-ray and electron microscope studies, mag. and Mossbauer effect meas. 0-28919  
 FeSb alloy films, vapour-deposited, formation of metastable phase 0-44437  
 Gd-Co amorphous films, correlation between struct. and mag. props. (*Chinese*) 0-54532  
 GdFe films, deposited on glass substrates (*Russian*) 0-24747  
 Ge, amorphous, dislocation model 0-1929  
 Ge, amorphous, dislocation model 0-1930  
 Ge, amorphous, growth rate of crystallisation, Raman spectroscopy study 0-44227  
 Ge, amorphous, molecular liquid model and electronic structure 0-54133  
 Ge, amorphous, struct. and growth kinetics, topological principles 0-49123  
 Ge-Ni, amorphous, struct., EXAFS study 0-49110  
 Ge-S-Ga(In) system glasses, photoinduced changes 0-24365  
 Ge-S-Se system, glass-forming, struct. and props. 0-19713  
 $Ge_{1-x}H_x$ , amorphous, atomic struct., X-ray study 0-49106  
 $GeO_2-K_2O$  glass composition effect on solubility in  $H_2O$  0-39303  
 $GeO_2-Na_2O$  glass composition effect on solubility in  $H_2O$  0-39303  
 $Ge(S_2Se_2)$  glasses, comparison  $A_1$  Raman line, microscopic origin 0-29740  
 $Ge_2(S_2Se_2)_{1-x}$  chalcogenide covalent non crystalline topology, short range order 0-15009  
 $GeS_2$ , chalcogenide glass, hollow cluster model of atomic structure 0-6366  
 $Ge_{1-x}S_x$  glasses, building blocks and bonds 0-54141  
 $Ge_2S_3$ , electron irradiated, effects on elec., photoelec. and optical props. 0-49806  
 $GeS(S_2)$  amorphous films, photostructural changes, UPS study 0-49550  
 GeSe, amorphous, pair distrib. function, anomalous X-ray scatt. 0-49126  
 $GeSe_2$ , chalcogenide glass, hollow cluster model of atomic structure 0-6366  
 $Ge_2Se_{1-x}$  amorphous, X-ray diffr. and local order modelling 0-49125  
 $GeSe(Se_2)$  amorphous films, photostructural changes, UPS study 0-49550  
 $K_2O-B_2O_3-SiO_2$  glass, crystallisation range (*German*) 0-38934  
 $K_2O-SiO_2$  glass, X-ray diffr. (*Japanese*) 0-19720  
 La-Au liq.-quenched alloys, Mossbauer spectra, struct. 0-15841  
 $LiF-NaPO_3-MeF_x$  ( $Me=Mg, Ca, Al$ ) glasses, IR spectroscopy study 0-16042  
 $Li_2Si_2O_5-TiO_2$  glasses, struct. and crystn. investigation using Raman spectra 0-38918  
 $MgO-Al_2O_3-TiO_2-SiO_2$ , glass formation, structure of cations (*Russian*) 0-38933  
 Mn-Ge amorphous films, short-range order, electron diffr. obs. 0-39473  
 MnSi, amorphous, sputtered, mag., elec., struct. and thermal props., spin glass behaviour 0-50124  
 $MoF_3$ , mol. and electronic struct., vitreous, liq., and tetrameric states,  $^{19}F$  NMR obs., mol. mobility 0-34787  
 $MoS_3$  amorphous struct., X-ray radial distrib. anal. and XPS 0-49115  
 Na-Fe fluorophosphate glass, EPR and Mossbauer resonance study 0-15838  
 $Na_2S-GeS_2$  system, glass formation, struct. and ionic conduction 0-54138  
 $Na_2O-B_2O_3-SiO_2-Yb(Tb)$ , luminesc. cooperative processes, glass struct. and comp. effect 0-16101  
 $Na_2O-CaO-SiO_2$  glass, effect of phase on liquids and gas diffusion (*German*) 0-38931  
 $Na_2O-GeO_2$  glass, X-ray diffr. study of Ge coordination number 0-10503  
 $Na_2O-GeO_2$  glasses, neutronographic study of  $Ge^{4+}$  struct. state 0-19711  
 $Na_2O-P_2O_5$  glass, XPS quantitative struct. anal. 0-2917  
 $Na_2O-SiO_2$  glasses, struct., mol. dynamic calcs. 0-24366  
 Nb-Ni glasses, struct. factor temp. depend. 0-28920



**noncrystalline state structure continued**

- Nb-Si liquid quenched alloy, metastable A-15 and amorphous phases, interstitials 0-54394  
 Nb<sub>0.4</sub>Ni<sub>0.6</sub>, amorphous, pair distrib. function, temp. depend., rel. to glass transition 0-24368  
 Ni<sub>42</sub>Nb<sub>38</sub>, metallic glass, struct., neutron diffr. study 0-54148  
 P-S, amorphous, glass transition and specific heat, intermolecular bond saturation 0-15011  
 P-Se, amorphous, glass transition and specific heat, intermolecular bond saturation 0-15011  
 P-Se-Tl glasses, NMR of <sup>31</sup>P and <sup>205</sup>Tl 0-15812  
 PbO-Bi<sub>2</sub>O<sub>3</sub>-Al<sub>2</sub>O<sub>3</sub>, glass formation and IR transmission (*Japanese*) 0-54146  
 PbSe-GeSe-AsSe, glass form., elec. cond., struct. defects, assoc. (*Russian*) 0-54145  
 Pd-Si-Fe amorphous alloy, Mossbauer spectra, struct. and bonding 0-7224  
 Pd<sub>80</sub>Si<sub>20</sub>, amorphous, structural changes with neutron irradiat., X-ray scatt. obs. 0-33898  
 Pd<sub>80</sub>Si<sub>20</sub>, metallic glass, composition, mech. props., simulation 0-49117  
 Se amorphous film, interference enhanced Raman scatt. 0-50326  
 Se film, noncryst., ageing and crystn. obs., tentative struct. model 0-2295  
 Se-Ge, amorphous, Raman spectra and average band gap 0-50327  
 Se-Si system glasses, vibr. IR spectra 0-20643  
 Se-Te crystallised glasses, struct. transforms. and IR spectra 0-19712  
 Se<sub>1-x</sub>Te<sub>x</sub> systems, amorphous and liq. states, short range order, neutron scatt. study 0-49124  
 Si, amorphous, molecular liquid model and electronic struct. 0-54133  
 Si, amorphous, photostructural changes, photodarkening 0-49121  
 Si, amorphous, struct. and growth kinetics, topological principles 0-49123  
 Si amorphous film, vacuum deposited, microscopic voids, gas absorpt., crystn. study 0-49534  
 Si-F, amorphous, pure and doped, vibr. excitations at defect sites, IR and Raman spectra calc. 0-49329  
 Si:H, amorphous, defect creation and H evolution 0-50392  
 Si:H, amorphous, glow discharge deposited, laser annealing 0-49104  
 Si:H, amorphous, structural model 0-49105  
 Si:H amorphous film, plasma-deposited, growth morphology and defects 0-44128  
 Si:H amorphous films, interference enhanced Raman scatt. 0-50326  
 Si:P, heavily doped, glow-discharge-produced, elec. and optical props 0-2497  
 Si-H, amorphous, H three-dimens. distrib., ion-induced AES and Rutherford backscattering 0-44132  
 Si-H, amorphous, random network model 0-1932  
 Si-H, amorphous, struct. and press. induced transition 0-44131  
 Si-H, amorphous, thermal stability and decomp. kinetics 0-24758  
 Si<sub>x</sub>As<sub>1-x</sub>-H, amorphous system, struct. and defects, Raman and EPR meas. 0-49103  
 Si<sub>1-x</sub>H<sub>x</sub>, amorphous, atomic struct., X-ray study 0-49106  
 Si<sub>3</sub>N<sub>4</sub>, amorphous, CVD prep., struct. characts. by pulsed neutron diffr. 0-33891  
 Si<sub>3</sub>N<sub>4</sub>, CVD, chem. bond nature, Compton scatt. expts. 0-49539  
 Si<sub>3</sub>N<sub>4</sub> films, struct. 0-54545  
 SiO<sub>2</sub>, amorphous, local at. struct., XPS obs. 0-20042  
 SiO<sub>2</sub>, amorphous and cryst., neutron irradiat. and unirradiat., intrinsic defect photolum. 0-50401  
 SiO<sub>2</sub> and SiO<sub>2</sub>-B<sub>2</sub>O<sub>3</sub> glasses, struct. and phonon spectra 0-50324  
 SiO<sub>2</sub>, vitreous, heat treatment effect on viscosity and struct. 0-19714  
 SiO<sub>2</sub>, vitreous, intrinsic radiation defects, nonbridging O 0-19837  
 SiO<sub>2</sub>, vitreous film on Si, defect struct. comparison with crystalline SiO<sub>2</sub> and Si-O bond nature 0-54557  
 SiO<sub>2</sub>:Fe<sup>3+</sup>, vitreous silica, absorpt. spectra and structural state 0-16071  
 SiO<sub>2</sub>-Al<sub>2</sub>O<sub>3</sub>-Fe<sub>2</sub>O<sub>3</sub>-Na<sub>2</sub>O-K<sub>2</sub>O-CaO-MgO glasses, Mossbauer spectra study 0-39967  
 SiO<sub>2</sub>-glasses, radial distrib. functions 0-44136  
 SiO<sub>2</sub>-ZrO<sub>2</sub>-Li<sub>2</sub>O-Na<sub>2</sub>O based crystallisable glasses composition and properties 0-50731  
 SiO<sub>x</sub> amorphous films, high energy electron diffr. study 0-38911  
 SiO<sub>x</sub>, powder and vac. deposited, amorphous struct., X-ray diffr. meas. 0-1931  
 SrCl<sub>2</sub> film, very-low-freq. inelastic light scatt. 0-25367  
 SrO-Al<sub>2</sub>O<sub>3</sub>-TiO<sub>2</sub>-SiO<sub>2</sub>, glass formation, structure of cations (*Russian*) 0-38933  
 TeO<sub>2</sub>, structure simulation of some tellurite and chalcogenide glasses quasi-crystalline structural diffusion method (*Russian*) 0-54147  
 TeO<sub>2</sub>-Li<sub>2</sub>O glassy system, struct. recomb. model 0-19707  
 Te<sub>2</sub>Si<sub>3</sub>, (x=78.87, y=22.13), amorphous, struct., X-ray diffr. study 0-6362  
 TiO<sub>2</sub>, amorphous film, vac. deposited, struct. and crystn., TEM obs. 0-2291  
 TiO<sub>2</sub>-Ti<sub>2</sub>O<sub>3</sub>-P<sub>2</sub>O<sub>5</sub>, glass form., struct. and elec. props. 0-44592  
 TiSe, amorphous phase struct., rapid electron density distrib. curves 0-33896  
 V<sub>2</sub>O<sub>5</sub> amorphous films, CVD prep., structural characts. 0-49114  
 V<sub>2</sub>O<sub>5</sub>-BaO-K<sub>2</sub>O-ZnO glasses, elect. props. and struct. 0-15547  
 W-Ru based refractory transition metal-metalloid glass, X-ray determ. 0-1938  
 WO<sub>3</sub>, amorphous film, vac. deposited, struct. and crystn., TEM obs. 0-2291  
 WS<sub>2</sub>, amorphous struct., X-ray radial distrib. anal. and XPS 0-49115  
 Y-Si-Al-O-N glass, prep. and props. 0-25647  
 YIG, amorphous, ionic glass, hard-sphere random-packing model 0-24369  
 YNi<sub>2</sub> amorphous alloy, at. struct. 0-19704

**nondestructive testing**

- see also crack detection; ultrasonic materials testing; X-ray fluorescence analysis*  
 accelerated electrons, use in NDT, review 0-35480  
 acoustic emission, principles of technique and measuring instrums. 0-28375  
 acoustic emission analysis for vibration and shock testing of industrially produced substances (*German*) 0-3279  
 acoustic waves generation, by pulsed electron flux, for nondestructive inspection 0-5905  
 adhesive bondline interrogation, using Stoneley wave methods 0-49530  
 adhesive joints, thin films, thick films and bulk coatings, conf. Philadelphia, USA (Nov. 1976) 0-46729  
 anisotropic specimen, dielectric const., NDT 0-35475

**nondestructive testing continued**

- astigmatic X-rays, diaphragm for investigating materials by this method 0-25935  
 autoradiography of thin laminars, resolution improvement (*French*) 0-35438  
 bar insulation in stator winding of large turbogenerator, inspection using microwave defectoscope 0-35474  
 blind hole drilling technique for residual stress measurement: application in NDT 0-40660  
 brittle coatings 0-11851  
 CANDU fuel, post-irradiation test facilities at Chalk River 0-30206  
 chromorheology, expl. verification of numerical solns. of elastic-plastic problems 0-48659  
 chromorheology, new expl. method 0-48658  
 circular ring, inner boundary shapes, optimised, diametral compression 0-38369  
 composite materials damageability, NDT methods 0-11867  
 composites, appl. of expl. methods to fracture 0-11869  
 concrete (*Japanese*) 0-30188  
 CRISP-E, use in a phase-in mode 0-40654  
 cylindrical part edge quality determ., acoustic method and equipment 0-35491  
 data processing and acquisition 0-11862  
 dielectrics, potential distrib. determ., non-destructive method (*French*) 0-40060  
 diesel nozzle sprayer castings, heat treatment quality inspection 0-35471  
 digital filtering of speckle-photography data 0-27338  
 economic significance, of non-destructive testing (*German*) 0-7735  
 eddy current fastener hole tester, improved design 0-30194  
 eddy current nondestructive evaluation, finite element analysis appl. 0-35439  
 eddy current probe, high saturation with internal reference, design and specifications 0-40658  
 eddy current testing of tubes, rods and wires (*German*) 0-25971  
 elastic waves, attenuation and propag. speed in materials under uniaxial static compression, installation for determ. 0-21233  
 electromagnetic inspection review 0-35468  
 electron diffraction pattern analysis, design and development of projection system, for a negative viewer 0-22476  
 EM NDT phenomena, fissile element modelling 0-40633  
 EM transient response of solenoid driver conducting cylinder 0-23599  
 fast reactor burnup, correlation of <sup>134</sup>Cs/<sup>137</sup>Cs 0-677  
 fatigue life prediction, acoustic emission signals distrib. anal. 0-25852  
 ferromagnetic object inspection, investigation of the through-transducer signal spectrum 0-35487  
 ferromagnetic probe corcimeter for inspecting the quality of parts with variable geometric dimensions 0-35488  
 ferrous metallurgy, nondestructive inspection and quality control review 0-21201  
 fibre texture, quantitative determ. of volume fraction, analytical method by pole figures 0-11863  
 fibrous materials, NDT determ. of mech. strength anisotropy using radio-wave method 0-25969  
 fission reactor fuel, irradiated, nondestructive assay methods (*Slovenian*) 0-27744  
 fluorescent penetrant inspection, heat assisted 0-45466  
 fractography, applications (*Japanese*) 0-16446  
 fusion reactor JT-60 toroidal field coil, brazed connection, nondestructive test methods 0-13930  
 glass, medieval, simulated, durability anal. using IR reflection spectroscopy 0-40777  
 glass fibre reinforced plastic, failure due to deform., optical investigation method (*Russian*) 0-35437  
 holographic, method for fringe control 0-31851  
 holographic interferograms, computer anal. for nondestructive testing 0-9836  
 holographic NDT fringe control techniques 0-45450  
 industrial optical microscopy, qualitative and quantitative surface testing 0-9033  
 insulators, nondestructive acoustic elec. field probe 0-47076  
 inverse signal filtering, method in nondestructive testing 0-7749  
 laser microprobe mass analyser (LAMMA) appl. 0-18041  
 luster quality, meas. method, texture and microreflection characteristics (*Japanese*) 0-35466  
 medical implant device evaluation by holographic interferometry and optical correl. 0-40659  
 metal fatigue, eddy current sensors, tuning method 0-21231  
 metal wire and bar NDT, electrical and EM methods 0-11865  
 metals, positron annihilation, localised probe of lattice defects 0-55224  
 microwave detection of third-order nonlinearities 0-55594  
 moving material fault test rig (*German*) 0-11855  
 multicomponent assemblies, moire inspection 0-35434  
 neutron activation analysis, sample posture converter 0-35497  
 neutron dosimetry characterization of spent thermal reactor fuel assemblies 0-23164  
 nuclear fuel and materials, nondestructive surface exam. 0-21246  
 nuclear fuel cycle materials, neutron and photon assay techniques and instrumentation 0-18426  
 nuclear power plant system, optimisation with regard to design, materials and testing (*German*) 0-42739  
 optical fibre preform, simultaneous determ. of refractive-index profile and cross-sectional geometry 0-1312  
 optical fibres, measurement of refractive-index profiles in optical-fibre preforms by spatial-filtering technique 0-48403  
 optical reflectance method, for anal. of anodic films on Al 0-37073  
 optical spatial filtering, of visualised results of flaw detection monitoring, rational regions of appl. 0-7751  
 optically isotropic mats., stress intensity factor determ. by dynamic method of caustics 0-33546  
 penetrants, high temp., precautions in use 0-30192  
 photographic pulp quality control using He-Ne laser scanning system (*German*) 0-3272  
 polymers, stress-state meas. using chemiluminesc. system 0-40628  
 positron measurements, for NDT of metals and alloys 0-55222  
 pressure vessels, heat treated, fracture modelling, acoustic emission 0-35303  
 PWR, primary circuits in-service inspection 0-5268  
 radio detection of local defects, strongly absorbing dielec. medium 0-35481  
 refractory products, apparent density determination, using surface  $\gamma$  densimeter 0-35464



**nondestructive testing continued**

- refractory slabs, radio wave phase method for quality control 0-40667  
 resonance neutron radiography using a position-sensitive proportional counter, appl. to meas. of nuclear fuel 0-13597  
 semiconductor materials and devices, SEM characterisation methods 0-49064  
 semiconductor resistivity and Hall effect meas., nondestructive four-electrode characterization 0-49743  
 semiconductor resistivity profile meas. using two-probe spreading resistance techniques 0-49742  
 semiconductor surface characterisation using SAW 0-11069  
 signal processing in ultrasonics, conf., London, England, Jan. 1980 0-33351  
 skull, holographic interferometric NDT 0-41162  
 steel, austenitic, thermonuclear reactor walls, ferromagnetic layer form. magneto-optical testing method 0-35465  
 steel, C, ferromagnetic parts, mech. property meas., method and instrument 0-35469  
 steel, electric generator, anisotropic mag. props. obs. using NDT 0-21212  
 steel, KhVG, annealed, mag. inspection of hardness and struct. 0-7750  
 steel, Mn-Si, mag. method of NDT of mech. props. 0-21211  
 steel, Si, highly-oriented domain and grain obs. methods, using ferromagnetic colloid technique 0-11856  
 steel, stainless, pipes, electro-thermal method for NDT of welds 0-35447  
 steel, thread rolled, Moire fringe method for examining local deform. zones 0-21220  
 steel fibre reinforced Al alloy, stressed state nondestructive testing method (Russian) 0-40631  
 stress measurement by sandwich speckle photography (German) 0-10216  
 stress pattern analysis by thermal emission 0-33552  
 surface defect parameter determ. of a thin wire, capacitance method 0-35489  
 surface stress meas. by optical waveguide effect 0-43681  
 thermal vision systems, theoretical basis of use to monitor boundary stratification in hot metals 0-7748  
 thermography, NDI method for damage detection 0-35445  
 thick film, adhesion to ceramic, destructive and nondestructive meas. 0-50809  
 thin rolled sheet, IMA-4 impulse magnetic analyser 0-35470  
 TLD, aluminophosphate glass, improvement of fast neutron response 0-13932  
 transition elements, 3d, ESR for valency assessment, appl. to ceramics and glass industries (German) 0-34757  
 ultrasonic concrete analyser, pulse velocity method 0-45472  
 US probe array using 4 transducers 0-35499  
 US visualisation for NDT of solids 0-22424  
 weld flaws, acoustic emission monitoring, with aid of microcomputer 0-11866  
 X-ray photographs, determ. of structural and quantum granularity 0-35477  
 X-ray portable stress analyser using position-sensitive scintillation detector 0-13190  
 X-ray stress measurement method, appl. to practical materials (Japanese) 0-52379  
 X-ray structural anal., high temp. system, for examining liquid metals 0-25950  
 Zircaloy-UO<sub>2</sub> fuel rods, eddy-current testing of claddings using encircling and probe coils 0-21245  
 Ag-Cu-Pb coin chem. anal. by low energy  $\gamma$ -rays and neutron transmission meas. 0-35591  
 Al alloys, contamination, automated nondestructive inspection 0-16629  
 Al alloys, crack opening stress level in fatigue, determ. by eddy current technique 0-16617  
 Al, appl. of current noise technique for dislocation processes during plastic deform. 0-35442  
 Al coated steel, porosity evaluation, micro X-ray spectral anal. (Russian) 0-35389  
 Al-Zn-Mg, acoustic emission meas. during tensile testing, reproducibility of results 0-50782  
 B fibre reinforced Al, stressed state nondestructive testing method (Russian) 0-40631  
 Fe, cast, grey, eddy current test for hardness certification 0-7733  
 Fe, high dispersion ferromagnet, magnetic powder defectoscopy material 0-35137  
 Fe-Ni alloys, cold rolled, exam. of phase composition using Mossbauer spectroscopy 0-1204  
 Ge amorphous film, evaporated, non-destructive density meas. 0-6680  
 He-Ne lasers, sealed, using spectral emission methods 0-1210  
 Li-I<sub>2</sub> pacemaker battery electrolyte exam. by neutron radiography 0-30940  
 Pb, SO type, commercial purity, local deform. meas., using Moire method 0-21219  
 Si:B, inhomogeneous surface layer, diffusion and implanted, X-ray rocking curves 0-6603  
 SiO<sub>2</sub>, glasses surface textures and defects, exam. using liq. crystals 0-6364  
 Sn-Pb composition anal. of PCBs using beta-backscatter gauge 0-16631  
 Ti, pure (0.9998), positron annihilation study of defects 0-3281  
 Ti-Al-Mo-Sn alloy, elastically and plastically deformed, positron annihilation meas. of deformation 0-21038  
 TiC coating thickness meas. using X-ray diffr. 0-21243  
 U, nondestructive assay of mixed samples using neutron activation anal. 0-18423  
<sup>235</sup>U, nondestructive determ. of content in fuel elements using passive gamma ray spectrometry 0-18418

**nonelectric sensing devices**

- acousto-optic sensor development 0-14542  
 magnetic suspension densimeter, differential capacitance sensor as position detector 0-196

**noneleptonic decays**

- see also *baryon hadronic decay; meson hadronic decay*  
 QCD, six-quark model,  $\Delta S=1$  weak noneleptonic decays 0-22582  
 $\eta^0$ - $\pi^0$  mixing effects and  $\Delta S=1$  noneleptonic weak decays 0-4991  
 $\Omega^-$  noneleptonic decay branching ratios from Weinberg-Salam and MIT bag models 0-37261  
 $Z^0 \rightarrow \Lambda\pi^+$ , asymmetry parameter 0-42457

**nonlinear acoustics**

- 2D finite amplitude acoustic waves radiating from flat plate in arbitrary periodic vibrations 0-33283  
 absorbent materials, models for propag. 0-53524

**nonlinear acoustics continued**

- acoustic wave evolution in incompressible flow with density as function of time (French) 0-53517  
 acoustoelasticity of isotropic elastic materials, thermal effect 0-33276  
 aeroacoustics and aircraft 0-53532  
 asymmetric double exponential waveform, weak-shock soln. for nonlinear propag. 0-10061  
 axial field of parametric acoustic radiator 0-33290  
 Burgers eqn., finite-amplitude propagation through gas droplet mixture 0-33282  
 combustion zones, nonlinear feature of coherent acoustic amplification 0-38156  
 comparison with nonlinear optics (French) 0-33293  
 contactless semiconductor surface charact. using nonlinear SAW interaction 0-11069  
 coupled system for subharmonics of any order 0-43504  
 dielectric crystals, nonlinear electroacoustic, fundamentals and appl. 0-34489  
 diffusivity of nonlinear wave propagation in pipes 0-33286  
 elastic solids, homogeneous and heterogeneous, nonlinear waves 0-34134  
 energy eqns. for acoustic fields in stationary and moving fluids 0-53525  
 explosive wave profile transformation, time constant derivation 0-48485  
 finite amplitude distortion of intense sinusoidal pressure waves in air 0-33273  
 finite-amplitude wave propag. in media of various degrees of nonlinearity 0-53528  
 flint glass, dense, nonlinear elastic props. (French) 0-34132  
 fluid-loaded cylindrical shell, resonant component isolation in acoustic scatt. 0-5864  
 focused acoustic beam in nonlinear medium 0-33287  
 Gaussian noise and its transformation by moving boundary condition effect 0-33281  
 harmonic generation in sound beams 0-5862  
 harmonic oscillator, perturbation theory 0-19272  
 interaction of two collinear, spherically spreading beams, appl. to parametric acoustic arrays 0-48484  
 Isom's thickness noise formula, extension to near field 0-53520  
 Lagrangian and Eulerian representations (French) 0-33285  
 Lamb wave propag. on isotropic plates, second harmonic acousto-optic interaction 0-34886  
 Landau damping in regular wave interaction with noise 0-33284  
 liquid, weakly assoc., US wave reson. absorpt. 0-34141  
 liquid crystal, nematic, orientational acoustic nonlinearity 0-34143  
 liquid with gas bubbles, acoustic wave self-transparency effect (Russian) 0-14509  
 liquid-solid interface, plane sound wave reflection and refraction in mag. field 0-38150  
 marine sediments, saturated, nonlinear parameter 0-19132  
 model equations, book contrib., review 0-19126  
 moving fluids, transport eqns. and acoustic motion 0-53523  
 moving sources in flow, acoustic radiation, appl. to aircraft noise 0-53526  
 near field parametric emission study by Fourier anal., appl. to focal emitter (French) 0-33291  
 neutrino detection in ocean by nonlinear sound generation by hadron showers 0-36465  
 nonlinear acoustics 8th symposium, conf., Paris, France, July 1978 0-33277  
 optoacoustic exciter, nonlinear limit on efficiency 0-28406  
 parametric acoustic arrays, nonlinear interaction of finite-amplitude sound waves 0-53529  
 parametric acoustic arrays, theory 0-33289  
 parametric interaction of two HF collinear beams 0-43507  
 parametric sound reception in freq. range 10 to 20000 cps, expt. research 0-33391  
 passive range estimation from array of sensors 0-53583  
 piezoelectric crystal, acoustic transverse wave polarisation and energy flow in external static fields 0-19123  
 piezoelectric film, third-order piezoelec. and dielec. const. meas. using surface acoustic waves (Japanese) 0-55042  
 piezoelectric semiconductor, US parametric amplification effects, contributions to nonlinear material coefficients 0-34144  
 polarisation effects in crystal acoustics, linear and nonlinear 0-5855  
 propagation in absorbant fluid, Fourier propag. theory (French) 0-33288  
 quadrupole resonance of drops driven by modulated acoustic radiation pressure, experimental props. 0-33275  
 radiation of plane circular source, nonlinear solutions (French) 0-33280  
 random, methods of analysis 0-53527  
 resonator, nonlinear thermoelastic couplings (French) 0-34118  
 second harmonic generation in finite amplitude SAW, anisotropic media (French) 0-34285  
 shape oscillation and static deformation of drops and bubbles driven by modulated acoustic radiation stresses 0-33274  
 strength of nonlinear interaction between collinear surface acoustic waves 0-33295  
 structure of sound field in arbitrary smoothly inhomogeneous medium 0-38155  
 surface wave memory correlator using nonlinear interactions (French) 0-33294  
 third and fourth order elastic const. (French) 0-34116  
 transient parametric acoustic sources 0-10060  
 transonic flow, excitation on nonlinear plane waves by volume sources 0-38154  
 underwater explosion generation of sound pulse, nonlinear region 0-56493  
 US fields in air, numerical representation, microphone signal example (French) 0-53521  
 US SAW, nonlinear interaction in 2-6 MHz range (French) 0-33296  
 water-ethanol(methanol) mixtures, nonlinear acoustic coeff. meas., 0-50°C (French) 0-34142  
 wave propagation as guided modes, parabolic approx. 0-43506  
 Al alloys, fatigue, microcrack development, acoustic SHG study 0-35440  
 Bi<sub>12</sub>GeO<sub>20</sub>, finite amplitude SAW distorted rippling profiles, optical probing obs. 0-34287  
 Cu, nonlinear acoustics, third-order elastic const. meas. 0-33292  
 CuCl<sub>2</sub>, aqueous soln., nonlinear conversion of acoustic pulses with thermooptic excitation 0-14510  
 Cu<sub>2</sub>-O, nonlinear elastic props., nonstoichiometry effects (French) 0-34133  
 Ge, nonlinear acoustics, third-order elastic const. meas. 0-33292  
<sup>3</sup>He-<sup>4</sup>He, superfluid solns., nonlinear sound interaction 0-34267



**nonlinear acoustics continued**

- LiNbO<sub>3</sub>, and LiTaO<sub>3</sub>, finite amplitude SAW distorted rippling profiles, optical probing obs. 0-34287  
 SiO<sub>2</sub>, finite amplitude SAW distorted rippling profiles, optical probing obs. 0-34287  
 TeO<sub>2</sub> paratellurite crystals, parametric excitation of sound, calc. 0-24537  
 TiCdF<sub>3</sub>, third and fourth order elastic consts., press. depend. near phase transition (*French*) 0-34116  
 (YGd)(GaFe)<sub>5</sub>O<sub>12</sub> epitaxial film, nonlinear magnetoelastic effects (*French*) 0-34745

**nonlinear differential equations**

- Alfvén waves, circularly polarised, spiky soliton soln. to nonlinear evolution eqn. 0-38590  
 Backlund transformations and solns. for nonlinear field eqns. in 4-dimens. spacetime 0-338  
 Benjamin-Ono equation, internal wave solitons, linear stability 0-53802  
 Benjamin-Ono equation, meromorphic solutions 0-31980  
 bound state energy levels, quantum mechanical formalism, convergent perturbation theory (*Russian*) 0-4573  
 bubbles motion dynamics in oscillating fluids 0-38483  
 buckling, tall vertical column, optical load, optimal shape, nonlinear differential-integral equation 0-53663  
 catastrophe theory, bifurcation properties of solutions of nonlinear operator equations 0-8789  
 classical nonconservative systems, appl. of time depend. canonical transforms 0-17792  
 complex potential eqns., all solns. to nonlinear system 0-46795  
 composite layered slab, solute diffusion, conc. depend., with/without chem. reactions 0-54427  
 conference, nonlinear problems in theoretical physics, Jaca, Gain 1978 0-4478  
 continuum Heisenberg spin system, stationary spherically and axially symm. spin waves 0-34615  
 deep water gravity waves, two-dimens. nonlinear wave eqn., exact envelope soliton solns. 0-43725  
 diffusion equation, similarity solutions 0-27239  
 E×B effects on nonlinear mode-converted lower-hybrid waves 0-1785  
 education, soliton solns. to nonlinear wave eqns. 0-17737  
 elliptic problems involving a free boundary 0-24130  
 evolution eqn., family of H-theorems 0-31685  
 evolution equations, completely integrable, natural generalisation (*French*) 0-27152  
 evolution equations, integrable, inverse scatt. method 0-12913  
 evolution equations, inverse scattering method 0-12919  
 fluids of finite depth, exact one- and two-periodic wave solns. 0-53797  
 fluids of finite depth, N-soliton soln. of higher order wave eqn. 0-48724  
 Fokker Planck eqn., non-linear, with nonconstant diffusion, non-Gaussian time dependent 0-31686  
 friction, stochastic quantisation, nonlinear Schrödinger equation 0-27164  
 gauge generators, Cawley's counter example to Dirac conjecture 0-13225  
 generalized symmetries of nonlinear partial differential equations, Lie derivatives 0-4886  
 glass cylinder refractive index variation by field-assisted ion exchange 0-14500  
 gradually varying channel, solitary wave evolution, KdV eqn. soln. 0-24040  
 gravitating disc, rotating, nonlinear stability theory 0-17488  
 heat conduction, quasilinear equations, approx. Galerkin method 0-33416  
 hyperbolic balance laws in continuum physics 0-4525  
 invariant group of KdV, MKdV or Burgers eqn., commutative Lie algebra 0-365  
 Jaulent-Miodek family of nonlinear evolution eqns., Hamiltonian formulation 0-31511  
 Kadomtsev-Pyatvashvili eqn., asymptotic behaviour of solns. (two-dimensional Korteweg-de Vries eqn.) 0-52036  
 Kolmogorov direct equation, solution, Galerkin measures (*Russian*) 0-46981  
 Korteweg-de Vries equation, Padé approximants, soliton solns. 0-42071  
 Korteweg-de Vries, cylindrical eqn., soln. asymptotic behaviour 0-31526  
 Korteweg-de Vries eqn., Lie-Backlund transformation group study 0-9114  
 Korteweg-de Vries eqn., slowly varying solitary wave solns. 0-72  
 Korteweg-de Vries eqns., perturbed solns. and soliton production 0-42074  
 Korteweg-de Vries equation, numerical methods of solution, difference and transform schemes, accuracy 0-46833  
 Korteweg-de Vries equation, solns. for slowly decreasing boundary conditions 0-36872  
 Korteweg-de Vries equations, N-soliton soln., functional integral representation 0-4542  
 laser, free electron type, nonlinear theory, efficiency enhancement 0-43317  
 liquid-solid phase transition, dynamic Ginzburg-Landau theory 0-44292  
 mechanical system, periodic vibr. 0-33513  
 mechanical systems with time optimal condition 0-31492  
 meromorphic solutions of nonlinear partial differential equations and many-particle completely integrable systems 0-31523  
 modified Korteweg-de Vries eqn., N-soliton solns. 0-36876  
 modified Korteweg-de Vries solitary wave in a slowly varying medium 0-36873  
 nonlinear hydrodynamical eqn. of Kaup, periodic and N-soliton solns. (*French*) 0-31521  
 nonlinear Schrödinger equation solns., recurrent motion in continuum dynamical systems 0-22235  
 nonrelativistic limits for Klein-Gordon and Dirac eqn. 0-330  
 nuclear reactor kinetics, quasistatic solutions, nonlinear system, iterative procedure 0-52711  
 oscillators, coupled, with slow, nonexplicitly time-depend. evolution 0-52009  
 oscillators, nonlinear stochastic, triangular wave, optimally controlled, Weiner process and Poisson process, numerical studies 0-52128  
 partial appls. 0-4510  
 piezoelectric semiconductors, growth of wave discontinuities 0-34488  
 plasma sheath, integro-differential eqns., nonlinear, nonlocal, soln. formalism 0-43936  
 point charge as electrically invisible object, nonlinear Poisson-Boltzmann theory Coulomb singularity 0-43228  
 Poisson's equation, linear and nonlinear numerical solution including spatially variable dielectric const. 0-6825  
 Poisson-Boltzmann eqn., spherical, Debye-Hückel linearisation 0-35538  
 quantum dissipative systems, finite-difference retarded equation 0-12935

**nonlinear differential equations continued**

- quantum electrodynamics, nonlinear problems 0-4901  
 Schrödinger eqn., slowly varying solitary wave solns. 0-73  
 Schrödinger eqn., soliton solns. 0-27173  
 Schrödinger equation, relativistic wave equations, scattering theory 0-4882  
 Schrödinger equation with variable coefficients, differential-difference analogue, single-soliton solution behaviour 0-8819  
 sine-Gordon equation, approx. rotationally symmetric solns. 0-8807  
 sine-Gordon equation, in one and more dimensions, break-up of quasi-soliton solns. 0-8806  
 sine-Gordon equation, two soliton solutions, breather solution 0-12945  
 sine-Gordon perturbed equation, soliton mass formulae 0-22200  
 solitary wave solns. of classical nonlinear field eqns., for teaching 0-17756  
 soliton collisions, structural stability 0-10382  
 soliton generation, nonlinear differential evolution eqns., 3+1 dimens. 0-46828  
 soliton instability in one-dimensional nonlinear systems (*Russian*) 0-52039  
 soliton solution to Korteweg-de Vries equation using matrix trace 0-36870  
 soliton solution to modified Korteweg-de Vries equation, matrix trace method 0-36871  
 soliton solutions and their applications 0-8813  
 spectral transform, nonlinear discrete evolution equations 0-4553  
 spectral transform and nonlinear evolution equations 0-4551  
 spectral transforms, nonlinear evolution equations 0-4552  
 superposition of solitons from same nonlinear differential eqns. 0-67  
 transformations for partial differential eqns. 0-42043  
 transport equations, use of transformation groups to deduce properties 0-4680  
 two-dimensional space isothermal and nonisothermal turbulent flow (*German*) 0-28505  
 vascular bed modelling, optimal dialysis appl. 0-30758  
 vibrating system defined by characteristic quantities bounded by nonlinear equation (*French*) 0-33278  
 viscous liquid emerging from slot, nonlinear differential equation, Runge-Kutta numerical integration 0-52030  
 He, superfluid B phase, spin wave breathers, double sine-Gordon equations 0-15329

**nonlinear equations**

- see also nonlinear differential equations  
 analytical approximate solutions of the nonlinear basic equations in classical physics 0-52001  
 Ball-Zachariassen model of diffractive scattering, numerical soln. near singularity of Frechet derivative 0-9158  
 Bessel functions, infinite systems of nonlinear equations containing zeros 0-46786  
 Born-Infeld equation, two-dimensional system of conservation laws (*Russian*) 0-42365  
 classical hard sphere system, statistical theory of freezing 0-33868  
 elastic shells, stable solutions, finite element and Newton-Raphson methods 0-14593  
 evolution equation, exact two-periodic wave soln. 0-12914  
 explosion, thermal, crit. parameters analysis 0-11891  
 heat conduction with absorpt., similarity of nets method (*Russian*) 0-53603  
 higher order Benjamin-Ono equation, N-soliton and N-periodic wave solns. 0-12915  
 3×3 inverse scattering transform, soliton perturb. scheme 0-27151  
 Korteweg-de Vries eqn., soliton soln., Hugoniot conditions for gas dynamics 0-42069  
 nonlinear reaction-diffusion equations, pattern selection at the bifurcation point 0-50827  
 orthogonal polynomials, nonlinear eqns. for zeros 0-12888  
 Percus-Yevick eqn., existence and local uniqueness of solutions 0-36936  
 plasma, collisionless drift modes, graphical method for finding complex roots of nonlinear eqn. 0-33762  
 plasma transverse Cherenkov mode nonlinear stabilisation by external mag. field 0-38642  
 Schrödinger equation, appl. to deep water waves, O(ε<sup>4</sup>) perturb. anal. 0-4569  
 semiconductor, nonlinear equation, asymptotics of spectral boundary-value problem 0-6851  
 transport processes, nonlinear, hydrodynamics 0-22310  
 waves in nonlinear media, Poincaré normal form method 0-36875  
 weakly dissipative system, higher order approx. in reductive perturbation method, shock wave appl. 0-14743

**nonlinear field theory**

- (1+1) dimensional model field, fermion-boson correspondence, Klein transformation 0-42379  
 σ model, instantons and 1/N expansion 0-42339  
 σ model, SU<sub>2</sub>×SU<sub>2</sub>, modified Goldberger-Treiman relation, pseudoscalar form factor 0-27421  
 σ model, supersymmetric nonlocal conservation laws 0-46938  
 σ model in symmetric spaces 0-42341  
 σ model representation of Yang-Mills theory as a spontaneous violation (*Russian*) 0-13220  
 σ models, nonlinear, perturbative approach to symmetry restoration 0-37163  
 σ models, nonlinear, soft mass renormalisation of 1/N expansion 0-47164  
 σ SU(N) model, spontaneous symmetry breaking, renormalisation 0-42340  
 σ-model, nonlinear, superconformal invariance in 4-dimens. space-time 0-37154  
 σ-model, O(2k+1), Euclidean, nonlinear, local theory of solutions, Euler-Lagrange eqns. 0-52387  
 σ-model, similar to anti-self-dual field in 4-D Euclidean space 0-52386  
 σ-models, nonlinear, with N=Z extended supersymmetry in 4-dimens. 0-47174  
 σ-models, two-dimens. nonlinear, on Riemannian and Hermitian symmetric spaces 0-52404  
 φ<sup>4</sup>, massive and massless, elliptic function methods 0-4829  
 φ<sup>4</sup> soliton behaviour in presence of an impurity potential, collective coordinate method 0-31528  
 φ<sup>4</sup> theory, renormalisation groups transformation explicit construction 0-4832  
 φ<sup>4</sup>-model, dimensional regularisation and instantons, scalar field theory model 0-4830



**nonlinear field theory continued**

- ( $\psi\psi$ )<sup>2</sup> model, spontaneous symmetry breaking, renormalisation 0-42340  
 AKNS-ZS inverse method, canonical struct. and generalised Marchenko eqn. calcs. 0-47192  
 axially symmetric multi-instanton solutions generated by conformal mappings in SU(2) Yang-Mills field 0-42337  
 Backlund transform. derivation in inverse scatt. formalism 0-8810  
 Backlund transformation, dynamical systems, field theories calcs. 0-27386  
 Backlund transformations, group struct. 0-13219  
 Backlund transformations and solns. for nonlinear field eqns. in 4-dimens. spacetime 0-338  
 Backlund transforms and symmetries of Yang eqns. 0-52393  
 Bethe-Salpeter model, scaling reconstruction using renormalisation group, Callan-Symanzik eqn.,  $\phi_3^2$  theory (*Russian*) 0-42351  
 binding energy in model classical field theories 0-4927  
 boson-fermion system, semiclassical anal. approach 0-27401  
 boson-soliton scatt., sine-Gordon model 0-9109  
 chiral invariant Gross-Neveu model, Hamiltonian diagonalization 0-22516  
 chiral model analog 0-52415  
 chiral SU(N) Thirring model, S-matrix bound state poles fixing 0-360  
 classical field eqns., mathematical aspects 0-4882  
 classical solutions of a nonlinear field equation 0-4841  
 classical theory with positive mass square, static finite energy solns. 0-31984  
 collapsons, new form of nonlinear excitations 0-4876  
 complex scalar field with nontrivial asymptotic behaviour of soliton solns. 0-4867  
 conference, nonlinear problems in theoretical physics, Jaca, Gain 1978 0-4478  
 covariant  $\sigma$  models, first order system of differential eqns. 0-31978  
 CP<sub>N-1</sub> models and non-Abelian HP<sub>N-1</sub>, quantum props.,  $\sigma$  relation, renormalisation 0-13210  
 CP<sup>N-1</sup> model, QCD toy model, instantons  $\theta$  vacua and confinement 0-9138  
 CP<sup>N-1</sup> model (D=2,3), UV renormalisation and phase transition 0-31989  
 CP<sup>N-1</sup> multi-instanton fields, quantum fluctuation 0-329  
 CP<sup>N-1</sup> two-dimens. model, infinitely many conserved local charges 0-47179  
 critical exponents, three dimensional system with short-range interaction, calc. 0-42348  
 dense and dilute instanton-anti-instanton pair configurations 0-52424  
 Dirac's monopole and the Hopf map 0-27402  
 double quadratic chain, statistical mech., nonreflectionless solitary wave 0-22518  
 dynamical groups of completely integrable eqns., nonlinear realisations 0-4885  
 Euclidean approach in curved spacetime, functional anal. 0-27181  
 Euclidean manifolds, N-dimensional instantons and monopoles 0-42321  
 Euclidean P(0)<sub>2</sub> model, quasiclassical expansions 0-47200  
 exterior calculus and two-dimensional supersymmetric models, super sine-Gordon model 0-47214  
 finite element method, with variable basis functions (*Russian*) 0-37160  
 four-dimensional  $\sigma$ -model on quaternionic projective space 0-9092  
 free Klein Gordon fields, conservation laws 0-340  
 frequency decompositions in curved space-time 0-31973  
 gauge equivalent fields, existence near instantons (*Russian*) 0-27414  
 generalised sine-Gordon eqn., Backlund transformation, nonlinear  $\sigma$  model 0-4844  
 gravitational duality and Backlund transformations 0-12971  
 Gross-Neveu chiral model, scatt. theory, 1/N expansion 0-348  
 Gross-Neveu model, mass generation, renormalisation 0-27393  
 H-spaces, gravitational instantons, spin coeff. method 0-31654  
 Heisenberg-Klein-Gordon equation, localised solns. in flat Schwarzschild space-time 0-4620  
 Higgs model, 1+1 dimensional, charge confinement and vacuum struct., instantons 0-341  
 instanton correction to vac. energy densities and bag const. 0-37211  
 instanton density in a theory with massless quarks 0-37210  
 instanton distribution, external field effects in SU(2) gauge field 0-4849  
 instanton quantum fluctuations, in 2-D nonlinear theories (*Russian*) 0-4868  
 instantons and embeddings in gauge field configurations, group theoretic study 0-4878  
 instantons and the 1/N expansion 0-400  
 instantons as link between weak and strong coupling in QCD 0-42403  
 inverse scattering problem and instanton construction by algebraic geometry, review 0-47203  
 k-instantons in Sp(1) Yang-Mills theory, calculation method 0-13223  
 Kadomtsev-Petviashvili eqn., appl of variation of action method of one field solitons 0-331  
 Lie-Backlund operators props. from variational derivatives 0-37159  
 mass generation for fermion field in absence of chiral symmetry breaking 0-347  
 massive Thirring model, multisoliton solns. in Pohlmeyer-Lund-Regge system 0-47195  
 massive Thirring model, S-matrix calcs., required number of conserved currents 0-42329  
 massless boson, unified nonlinear theory 0-376  
 multidimensional stable relativistic solitons (*Russian*) 0-13224  
 nonAbelian, nonlinear Yang-Mills field eqns., self-duality, helicity, coherent states 0-31988  
 nonlinear super-Poincare fermion, quantisation in bag like formulation 0-4923  
 nonlinear superfields and quark confinement (*Chinese*) 0-42346  
 nonlinear Schrodinger eqn., appl of variation of action method of one field solitons Kadomtsev-Petviashvili eqn., appl of variation of action method of one field solitons 0-331  
 nonlocal currents for supersymmetric nonlinear models 0-52414  
 nonrelativistic effective  $\pi$ N vertex, PCAC and  $\sigma$ -model 0-52591  
 nontopological solitons, hadron appl. 0-47191  
 O(3) nonlinear  $\delta$ -model, instanton-anti-instanton interactions, fermion theory (*Russian*) 0-47193  
 O(n)  $\sigma$  model, nonlocal charges in two dimensions 0-18075  
 O(N)  $\sigma$ -model, two-dimens., mag. susceptibility, phase transitions and high temp. expansion 0-47177  
 O(N) nonlinear  $\sigma$ -model, analyticity of solns. 0-52384  
 O(n) nonlinear  $\sigma$ -model, field eqn. reduction 0-31979

**nonlinear field theory continued**

- O(N) nonlinear  $\sigma$ -model, two-dimens., fifth Painleve transcendent 0-32002  
 on-shell counterterms and nonlinear invariances 0-22522  
 one-dimensional  $\phi^4$  and double quadratic systems, kinks, quantum statistical mechanics 0-47197  
 one-dimensional complex scalar fields with phase anisotropy, statistical mech. 0-22517  
 P( $\phi$ )<sub>2</sub> models, soliton solns. 0-42333  
 phase transition in 2D Coulomb gas, sine-Gordon theory and XY model, renormalisation group anal. 0-36950  
 Poincare self-stresses, model and field Lagrangian densities 0-52438  
 Prasad-Sommerfield soliton, excited states, SU(3) generalisation 0-4877  
 quantum chiral model, local polynomial current conservation in renormalised 1/N perturbation theory 0-13232  
 quantum soliton and classical soliton 0-12986  
 quark field quantum fluctuation computation in arbitrary Yang-Mills instanton background 0-13268  
 quartz resonator, large mag. field effect on rate of time 0-27195  
 quaternionic multi S<sup>4</sup>  $\approx$  HP(1) gravitational and chiral instantons 0-31656  
 scale-invariant gauge theories, instanton role in QCD, QED and CP<sup>(N-1)</sup> 0-27400  
 semiclassical soliton solns. in quantised field theories 0-4874  
 sigma model, nonlinear, soliton stability in S<sup>2</sup> 0-37165  
 sine-Gordon eqn. generalisation for any symmetric space, eqns. of motion 0-32001  
 sine-Gordon eqns., Lax pairs for certain generalisations 0-31997  
 sine-Gordon field theory Coulomb gas equivalence, classical gas with logarithmic pot. 0-4850  
 sine-Gordon model, supersymmetric solitons and monopoles 0-31991  
 sine-Gordon model for large coupling consts., soliton scatt. matrix (*Russian*) 0-13221  
 sine-Gordon supersymmetric model, higher local quantum conserved currents 0-52435  
 sine-Gordon system, bion dissoc. 0-13201  
 sine-Gordon system, breathers, extended object QSM 0-42347  
 Skyrme gauge model, topological solitons 0-9086  
 soliton, non-topological, non-Abelian internal symmetry in 3+1 dimensional space-time, quantisation, collective coord. and Lorentz covariant methods 0-47199  
 soliton free energies calcs., WKB approx. failure 0-42073  
 soliton quantum mechanical mass in supersymmetric theories 0-22536  
 soliton theory, review 0-47204  
 solitonlike fields, gauge phase factor operators, extended Higgs models and 't Hooft algebra 0-42324  
 solitons, static form factor, quantum correction in 2-D field theory with classical lump, asymptotic behaviour 0-52395  
 solitons in some geometrical field theories 0-27390  
 stationary multisolitons, existence 0-13218  
 SU<sub>2</sub> nonlocal conserved currents for two-dimensional chiral theories 0-52413  
 SU(2) theory with four fermion interaction and asymptotic freedom, exact soln. 0-4858  
 SU(3) quark-meson  $\sigma$ -model, quark masses 0-47178  
 SU(N)  $\times$  SU(N) chiral symmetry, spontaneous breaking, instanton role 0-47219  
 SU(N) chiral Gross-Neveu spectrum derivation 0-47176  
 superconformal group and quark-like fermionic coordinates 0-9145  
 supersymmetric  $\sigma$  model, nonlocal charges from zero curvature 0-31995  
 supersymmetric extension, Kahler manifolds, Grassmann manifolds and CP<sup>n-1</sup> models 0-9113  
 supersymmetric nonlinear  $\sigma$  model, nonlocal charges and currents 0-27410  
 supersymmetric sine-Gordon eqn., polongation struct. and inverse scatt. formalism 0-47173  
 Thirring model coupled to gravity, classical solns. in generally covariant model with fermions 0-9091  
 Thirring model massive phase, dynamic mass generation 0-4851  
 two dimensional field theories with infinite number of conservation laws and Backlund transformations 0-9095  
 unitary quantum mechanics, nonlinear and relativistic invariant fields 0-4567  
 weak interactions, CP violation and instantons 0-354  
 K  $\rightarrow \pi e(\mu)\nu$ , form factors, SU(3)  $\sigma$ -model one loop calc., chiral symmetry breaking 0-52506
- nonlinear network analysis**  
 JET, synchronous-generator/bridge-converter/ohmic heating circuit anal. 0-13893
- nonlinear optical susceptibility**  
 aerosol of glass spheres, broadband degenerate four-wave mixing medium 0-43390  
 CARS in condensed phases, perturbation theory of third-order nonlinear susceptibility 0-14393  
 degenerate 4-wave mixing in plasmas 0-24179  
 diamond, nonlinear optical susceptibility, tight binding bonding orbital model 0-5784  
 fifth order atomic optical nonlinearities in multiphoton resonances 0-28275  
 MBBA, nematic liq. cryst., nonlinear optical suscept. using light combination scatt. (*Russian*) 0-38064  
 organic system, nonlinear second-order optical susceptibility 0-9947  
 resonator, containing medium with quadratic susceptibility, props. 0-33074  
 semiconductor, degenerate four-wave mixing near band gap 0-5782  
 stimulated Raman scattering frequency shifts, nonreson. contribs. to nonlinear susceptibility 0-53373  
 two-photon resonant four-wave mixing with non-monochromatic waves 0-38066  
 CdS, biexciton, low intensity nonlinear coherent mixing study 0-49619  
 CdTe, backward degenerate four-wave mixing obs. 0-53361  
 GaAs, nonlinear electro-optical susceptibility, coupled anharmonic oscill. model 0-2723  
 Ge, four-wave mixing at room temp. for tunable IR generation 0-9940  
 Ge, nonlinear optical susceptibility, tight binding bonding orbital model 0-5784  
 n-InSb, spin resonant four-wave mixing, CW meas. and transient effects 0-48344  
 KH<sub>2</sub>PPO<sub>4</sub>, KD<sub>2</sub>PO<sub>4</sub>, nonlinear electrooptic effects 0-29721  
 La<sub>2</sub>Ti<sub>2</sub>O<sub>7</sub>, ferroelects., nonlinear optical props. 0-33086



**nonlinear optical susceptibility continued**

- (NH<sub>4</sub>)<sub>2</sub>BeF<sub>4</sub>, incommensurate phase superstructure, linear and nonlinear  
cryst. optics (*Russian*) 0-14387  
Na vapour, effective freq. conversion of radiation 0-28278  
SF<sub>6</sub> multiphoton absorpt. meas. by third harmonic generation 0-1036  
Si, nonlinear optical susceptibility, tight binding bonding orbital model  
0-5784  
Sr<sub>2</sub>Nb<sub>2</sub>O<sub>7</sub>, ferroelects., nonlinear optical props. 0-33086

**nonlinear optics**

- see also *nonlinear optical susceptibility; optical coherent transients; optical frequency conversion; optical parametric devices; optical phase conjugation; optical saturation; optical self-focusing; self-induced transparency; stimulated scattering*  
absorbing liquid, coherent light transient self-diffr., simulated thermal  
scatt. laser expt. 0-48361  
adaptive system, characteristic purposes 0-28273  
aerosol of glass spheres, broadband degenerate four-wave mixing medium  
0-43390  
alkali halides, pulsed-laser-induced damage, role of avalanche multiplication and multiphoton absorpt. 0-48316  
alkali halides, two-photon absorpt. 0-50292  
anthracene vapour, optically induced dynamic gratings 0-28289  
antiferromagnets, magnon parametric generation with impulses at Brillouin zone boundary (*Russian*) 0-29540  
atomic RF spectroscopy, nonlinear and parametric effects, review  
0-18816  
bistability equations for standing wave cavity, analytic solns. 0-48328  
bistability in nonlinear distributed feedback structs. 0-5780  
bistable optical device, transient response and applications 0-33214  
bistable steady states in optical subharmonic generation, Wigner distrib.  
0-53370  
bistable TV-optical feedback system using optical flip-flops 0-53354  
bounded medium, nonlinear parametric reson., limit cycle solns. 0-19071  
carrier scattering by lattice defects, nonlinear optical props. 0-29399  
coherent and nonlinear optics, Conf., Leningrad, USSR (June 1978)  
0-27027  
coherent multiphoton intense interactions, convergent perturbation anal.  
0-1037  
coherent pulse propagation,  $\pi$  pulse generation from zero-area pulse  
0-48352  
coherent waves in nonlinear medium, nonresonant interaction, eqns. system  
development and examples (*Czech*) 0-24149  
collision effects on nonreson. interactions, nonlinear spectrosc. obs.  
0-23496  
combustion, coherent Raman spectrosc. obs. 0-16691  
comparison with nonlinear acoustics (*French*) 0-33293  
cooperative multiphoton ionisation, bistability effects, Bonifacio-Lugiato  
model 0-19010  
cryogenic liquids, vibr. kinetics, nonlinear optics appls. 0-13082  
crystal accelerator, radiative energy loss 0-23611  
dielectric liquid nonlinear third-order polarisation, transient effects elucidating molecular props. 0-15955  
 $\beta$ -dinaphthylene oxide vapour, optically induced dynamic gratings  
0-28289  
disorienting collisions, nonlinear resonance induction 0-37900  
dispersive media, interaction between weak pulses and high intensity low  
freq. wave (*Russian*) 0-48332  
dispersive optical bistability, anomalous switching 0-23740  
dispersive optical bistability with inhomogeneous broadening, exact soln.  
0-53360  
distortions, nonlinear, of scanning light beams 0-14407  
DODCI dye dissolved in glycerine, time delayed picosecond pulse transmission obs. 0-48355  
dye laser, narrow band CW oscillator/pulsed amplifier system for precision nonlinear spectrosc. 0-53318  
dynamic behaviour of optical bistability, time depend. Fokker-Planck eqn.  
soln. 0-37980  
elliptically polarized Gaussian beams, nonlinear precession 0-28269  
EM wave reflection coeff. of nonlinear medium, discontinuity 0-28151  
Fabry-Perot cavity, instabilities for coherently driven absorber 0-53387  
Fabry-Perot cavity, optical pulse tailoring and termination by self-sweeping 0-23760  
fast transform calcs., appl. to SHG with depletion and diffraction  
0-53376  
ferroelectric theory and dynamics, optical, acoustic electro-optical props., Brillouin zone struct. 0-11347  
ferromagnetic semiconductor, refr. index variation in strong alternating mag. field 0-23741  
flame diagnosis, CARS appls. 0-16689  
fog, laser light nonlinear transmission 0-1256  
four-wave mixing spectroscopy, recent developments 0-53383  
g-factor difference between atomic transition levels, nonlinear spectroscopic determ. 0-23346  
gas, Stark tunable, mirrorless optical bistability and optical limiting, obs. 0-38056  
gas flow through optical train, thermal blooming control, optical degradation 0-33045  
highly directional light beams by wave front convolution (*Russian*) 0-14385  
hole burning into molecular velocity distribution due to monochromatic radiation and molecular elastic collision 0-43116  
inhomogeneous nonlinear medium and time-varying medium, decay interaction of wave packets 0-14386  
initial-value problem for zero-area pulses, anal. props. 0-23756  
invariant molecular tensors, definition in origin change, refraction and Faraday, effect 0-53363  
invariant molecular tensors, definition in origin change 0-53362  
isotropic medium with two-photon absorpt., propag. of polarised radiation 0-28290  
laser, nonlinear stratified system, plane wave propagation 0-43343  
laser amplifier with spatial filters, graphoanalytic determ. of energy parameters 0-48322  
laser beam spatial coherence in a randomly inhomogeneous medium, effect of thermal nonlinearity 0-9926  
laser beam transient self-diffraction in absorbing liquid 0-9927  
laser engineering and appls., conf., Washington, USA (May-June 1979) 0-1216  
laser radiation wavefront instability and optical inhomogeneity evolution dynamics 0-9876

**nonlinear optics continued**

- light-induced grating, possible energy transfer control by acoustic vibrs. 0-28267  
linear dynamic mol. system, correlated radiation impulse sequence interaction 0-38058  
liquid crystals, four wave mixing and relaxation effects (*Chinese*) 0-53351  
longitudinally inhomogeneous running waves and their role in the nonlinear reflection and refraction of light 0-38059  
lower hybrid waves, quasi-optical beam self-action in magnetoplasma 0-38657  
mirror coatings, selective reflectors, and antireflection coatings for nonlinear optics, chemical method 0-28300  
multi-level atom with Raman reson., time-delayed laser scatt. 0-48343  
multifrequency laser radiation, nonlinear power type interaction with matter 0-53356  
N two-level atoms, quantum theory of nonlinear optical phenomena 0-5790  
nematic liq. crystal, EM wave nonlinear interaction 0-19698  
nonlinear Schrödinger equation, exact solution, localised wavefield evolution 0-53191  
optical bistability, nonlinear polarisability model 0-37976  
optical echo spectroscopy 0-48357  
optical fibre, high power narrow band laser radiation transmission, nonlinear optical processes 0-53443  
optical glass, Raman scatt. and nonlinear refr. index 0-2749  
parametric wave excitation in bounded systems 0-6252  
particle acceleration in nonlinear crystal by 'rectified' light 0-23610  
photon stationary distribution in optical bistability 0-48197  
photon statistics after destructive interf. of two-photon absorbed light 0-48199  
picosecond light continua generation depending on various nonlinear processes 0-33095  
picosecond light pulse, meas. techniques (*Japanese*) 0-52291  
polarisation resonance in a continuum, optical activity, spin-orbit interactions (*Russian*) 0-53391  
polarisation-sensitive nonlinear spectroscopy, improved geometry 0-1285  
POPOP vapour, optically induced dynamic gratings 0-28289  
processing with Fabry-Perot interferometers containing phase recording media 0-48158  
quantum systems, wave packet behaviour in pseudo-coherent state method (*Russian*) 0-1175  
quartz, nonlinear polarisation plane rotation due to ruby laser irradi. (*Russian*) 0-53390  
rare earth titanates, pseudoperovskite struct., nonlinear spectral and luminesc. characts. 0-29771  
recent advances, review 0-33075  
refraction into a nonlinear medium: wave profiles and hysteresis 0-43395  
refractive index changes on degenerate four-wave mixing 0-9936  
resonance medium, induced dichroism and gyrotropy 0-9971  
resonance two-photon absorption, theory 0-28268  
resonant media, transverse relax. effect and spatial optical parametric coupling of picosecond light pulses 0-19070  
resonant propagation of two concomitant optical pulses interacting with three-level atomic system, num. modelling 0-9942  
resonant Raman scattering in laser fields of arbitrary strength, antibunching effects 0-23653  
ring cavity, dressed mode dynamics of optical bistability 0-19013  
ring laser, nonlinear polarisability of two-isotope active medium 0-14369  
ring laser, nonreciprocal effects on appl. of transverse mag. field to active medium 0-53341  
ruby, phonons, at 29 cm<sup>-1</sup>, stimulated emission 0-45114  
scattering of two light beams, ultrastrong fields, differential scatt. power 0-43388  
self diffraction of laser beam by liquid crystal struct. 0-5803  
self-action problems, finite element method appl. 0-9941  
self-diffraction of light by excitons 0-53389  
self-diffraction of polarised light waves in two photon absorpt. in isotropic media 0-38077  
semiconductor, degenerate four-wave mixing near band gap 0-5782  
semiconductor, nonlinear optical props. 0-25333  
semiconductors, direct-gap, two-photon absorpt. 0-50292  
semiconductors, II-VI and III-VI types, competition between two-photon absorption and two-stage absorption via deep traps 0-29764  
soliton solutions, light beam self-action in nonlinear media 0-14404  
sooty diffusion flame, CARS obs. 0-16690  
spatial filtering, nonlinear medium, loss formation 0-53357  
stochastic multiphoton resonance interaction with matter 0-33073  
surface polaritons, linear photon and two photon absorpt. 0-49863  
surface waves at absorbing/amplifying media interface 0-43239  
synchronous nonlinear interaction between waves on Bragg diff. in media with periodic struct. (*Russian*) 0-14399  
thermal blooming: round beam vs square beam, computer study 0-38076  
thermal blooming cell design for adaptive optics evaluation 0-33096  
three-wave interactions in randomly inhomogeneous dispersive media (*Russian*) 0-53364  
transport equation for electrons in nonmonochromatic EM field 0-10937  
two photon coherent states in degenerate four wave mixing 0-5717  
two-photon field nonlinear optical efficiency 0-9949  
urea, electro-optical coeffs. meas., rel. to nonlinear optics calcs. 0-34889  
UV nonlinear optical processes using excimer lasers 0-38060  
vector matching ang. width, for optical harmonics 0-9946  
wave beam distortion by thermal self-interaction in droplet medium 0-19082  
wavefront registration and volume object image reconstruction by stimulated Raman scatt. (*German*) 0-53367  
Zeeman laser or amplifier, bistability and intensity fluctuations 0-53254  
AlN, epitaxial film growth by MBE, physical and optical props. 0-2293  
As<sub>2</sub>S<sub>3</sub>-Se<sub>2</sub>, amorphous, ps. relax., optically induced absorpt. 0-48325  
Ba atomic beam, light-shift induced zero-field level crossing, optical Hanle effect 0-52947  
Ba, vapour, laser excited, anomalous conical emission and self focusing 0-43411  
CO, hole burning in single quantum power spectrum due to Autler-Townes splitting 0-9671  
CO<sub>2</sub> laser radiation, single pulse, thermal blooming 0-19080  
CS<sub>2</sub>-glass boundary, optical bistability at nonlinear interface 0-33094  
CdCr<sub>2</sub>Se<sub>4</sub>, refr. index variation in strong alternating mag. field 0-23741  
CdS, three-photon absorpt. coeff. determ. by nonlinear luminesc. expt. 0-14384



**nonlinear optics continued**

- CdS,  $\text{Se}_{1-x}$ , photoconductor, optically controlled deflector based on thin-film waveguide 0-33206  
 GaAlAs-GaAs-GaAlAs etalon, optical bistability 0-5781  
 GaAs, amorphous sputtered films, hydrogenated, photoinduced optical absorpt. 0-50362  
 GaP, surface polariton linear photon and two photon absorpt. 0-49863  
 Ge, amorphous sputtered films, hydrogenated, photoinduced optical absorpt. 0-50362  
 Ge, picosecond optical response, effects of parametric scatt., energy-gap narrowing and state filling 0-11424  
 He,  $2^3\text{S}$  and  $2^1\text{S}$  states, two-photon ionization 0-37791  
 He-Ne, single mode laser, emission zone nonlinear active lens effect 0-32960  
 InSb, degenerate four-wave mixing obs. at 5K 0-53355  
 InSb, nonlinear refraction and absorpt. 0-9939  
 InSb, optical bistability, signal amplification, low power nonlinear effect applications 0-19066  
 InSb optical signal amplification and bistability 0-9937  
 $\text{KD}_2\text{PO}_4$ , nonlinear electrooptic coeffs. near Curie temp. 0-11366  
 $\text{LiH}_2\text{PO}_4$ , nonlinear and linear optical props. 0-48330  
 $\text{LiNbO}_3$ :Fe, nonlinear image processing in 3-dimens. hologram 0-14303  
 $\text{LiO}_3$ , up-conversion of signal from thermal source 0-9938  
 $\text{N}_2$ , vibration stimulated Raman scatt., four photon parametric effects 0-33087  
 Na atomic vapour, Doppler-broadened system, degenerate four-wave mixing, line shape and strength angular depend. 0-43391  
 $\text{Na}_2\text{W}_2\text{O}_7\text{F}_5$ , single cryst., prep., optical and dielec. studies (French) 0-15994  
 $\text{Nd}^{3+}$ , glass, nonlinear refractive index, two-photon resonant absorption by  $\text{Nd}^{3+}$  (Chinese) 0-43387  
 Ni complex, BDN, saturable absorber, degenerate four-wave mixing, amplification and phase conjugation 0-43394  
 $\text{PbI}_2$ , three-photon absorpt. coeff. determ. by nonlinear luminesc. expt. 0-14384  
 $\text{SF}_6$ , polarization-rotation and thermal-motion studies via resonant degenerate four-wave mixing 0-5779  
 Si, amorphous sputtered films, hydrogenated, photoinduced optical absorpt. 0-50362  
 Si, and Si:H, amorphous, ps. relax., optically induced absorpt. 0-48325  
 Si, degenerate four wave mixing of 1.06  $\mu\text{m}$  laser radiation 0-5794  
 Si:H amorphous films, photoinduced optical absorpt. and photocond. 0-50361  
 $\alpha\text{-SiC(6H)}$ , two stage transitions, nonlinear absorpt., thermoluminesc. method 0-7425

**nonlinear programming**

- optimal nodal point distribution for improved accuracy in computational fluid dynamics 0-48670  
 optimum laminate design, natural frequency restraints 0-53688  
 PHWR-1000, uniformity factor maximisation, nonlinear programming 0-739

**nonlinear symmetries**

- affine gravity and strong interactions in SL(4,R) nonlinear representations 0-18108  
 chiral symmetry, nonlinear realisations and local invariance 0-361

**nonlinear systems**

- see also bang-bang control  
 crystallographic structures, non-linear physics anal. 0-10631  
 nuclear industry, nonlinear systems, nonparametric system identification 0-32325

**nonparametric statistics**

- No entries

**nonradiative transitions**

- alkali halides, luminescence quenching of F-centres 0-50417  
 antiresonance line shapes and radiationless decay, compatibility restrictions 0-48040  
 aromatic hydrocarbon, centrosymmetric, two photon excited upper state fluoresc. spectra, reson. fluoresc. and vibr. mode selectivity 0-18878  
 aromatic hydrocarbons, singlet-triplet conversion at low temp. 0-43094  
 aromatic isolated mol. nonradiative conversion, internal and S-T conversion, vibr. excitation and fluoresc. quantum yield 0-43095  
 atoms, autoionising and inner shell vacancy states, decay, time independent multichannel scatt. theory 0-47854  
 aza-aromatic molecules, intersystem crossing, quantum interference effects 0-53037  
 benzene,  $T_1$ - $S_0$  intersystem crossing vibronic interactions IR absorpt. spectrum obs. 0-28042  
 complex potential energy surface systems, nonradiative processes, WKB calcs. 0-45133  
 dialkylaniline derivatives, twisted intramol. charge transfer states, dual fluoresc. obs. and form., dipole moments 0-18881  
 diatomic molecules, matrix isolated, vibr. relax., rot.-translational coupling 0-53102  
 dihydrophenazine derivatives, in 3-methylpentane (ethanol) (PMMA), radiationless processes, temp. depend. 0-43087  
 1,8-diphenyl-1,3,5,7-octatetraene, high press. fluoresc. studies of radiative and nonradiative processes 0-1011  
 1,6-diphenyl-1,3,5-hexatriene, high press. fluoresc. studies of radiative and nonradiative processes 0-1011  
 dyes, rot. diffusion of prolate, oblate mols. from absorpt. relax. 0-1008  
 dynamic multiphoton processes as criteria for luminesc. of electronically excited centres 0-11463  
 excitation energy transfer and migration, spectral line broadening 0-2841  
 fluorobenzene cations, fluoresc. quantum yields and lifetimes, electronic state relax. processes 0-48027  
 glyoxal, internal conversion, energy redistrib. 0-53036  
 glyoxal, vibr. energy redistrib. following internal conversion 0-23452  
 glyoxal ( $A_2$ ), fluoresc. quantum yields, radiative and nonradiative lifetimes 0-32759  
 halides, aryl and aryl-alkyl 193 nm photodissoc., fragment translational energy distrib. 0-48048  
 halonaphthalenes, intersystem crossing-singlet excited state to triplet state spin sublevel 0-53035  
 heterocyclic N compounds, radiationless transitions, isotope effects 0-48033  
 hot luminescence in F centres, nonradiative quenching 0-11467  
 ortho-hydroxybenzophenone, soln., intramol. proton transfer and energy relax. photostability, transient absorption obs. 0-28032  
 impurity centre, nonradiative transitions, with participation of short-wavelength phonons 0-16099

**nonradiative transitions continued**

- impurity ions and molecules in solids, non-radiative decay, book 0-2858  
 indigo dyes, triplet state config., laser flash absorpt. spectrosc. obs. 0-5557  
 intramolecular energy transfer, quantum effects 0-42964  
 9-iodoanthracene, picosecond fluoresc. lifetimes, thermally activated  $S_1 \rightarrow T_1$  intersystem crossing 0-28045  
 ion fragmentation mechanisms and photoelectron spectroscopy, book contrib. 0-14179  
 ionic crystals, nonradiative multiphonon transitions in impurity centres with extremely weak electron-phonon coupling 0-25436  
 lanthanides complexes with L-histidine, intermolecular energy transfer, influence of metal-to-ligand ratio 0-32763  
 luminescence decay, exchange mechanism, parameters 0-28051  
 M-shell radiationless transitions, subshell fluoresc., Coster Kronig yields and X-ray linewidths, relativistic Dirac Hartree Slater calcs. 0-52959  
 methylated benzene+tetracyanobenzene, fluorescent exciplex form., electronic relax. 0-5573  
 microemulsions, aerosol OT, inhomogeneous interior, fluoresc. and polarisation decay probes 0-50891  
 molecular crystal, multicomponent, energy migration master eqn. 0-16075  
 molecular electron-vibration system, nonequilib. first-order type phase transition 0-9633  
 molecular excited state relaxation processes, oscillatory versus dissipative limits, education appl. 0-31468  
 molecular multiphoton ionisation dynamics, rate eqn. modelling 0-48046  
 molecular relax. phenomena, quantum statistical mechanical approach, irreversible thermodynamic theory 0-48028  
 molecular vibrational promoting modes, geometry, effect on radiationless transition rate consts. 0-5569  
 naphthalene, triplet state time evolution after radiationless transition, initial vibronic distrib. effects 0-23450  
 organic dye, excited mol. decay near metal surface, energy transfer to plasmon surface polaritons 0-50440  
 orientation factor in conc. effects due to nonradiative energy transfer in luminescent system 0-25425  
 pentacene in naphthalene, intersystem crossing rates following single-mode laser excitation 0-43085  
 photoacoustic spectroscopy, time-domain, nonradiative lifetime meas. of condensed phases 0-55232  
 photoacoustic spectroscopy in solids, phase measurement, appl. to nonradiative transitions, optical absorpt. 0-31885  
 photochemical reactions, isomerisation, complexing, proton transfer, initiation of internal conversion processes 0-40713  
 pigment associations, conc. effects, luminesc., absorpt. spectra and dichroism obs. 0-1007  
 poly-2-vinylanthracene, soln., lowest triplet props., flash photolysis and radiolysis obs. 0-32861  
 polyatomic molecules, radiationless conversion processes, regularities 0-14171  
 polyatomic mols., quantum beats 0-37826  
 pyrazine, excited and  $N_2$  ionised states, ab initio calcs. broken orbital symm. 0-27931  
 rare earth activated phosphors, chemistry and physics, book contrib. 0-55187  
 rare earth doped crystals, intra- and inter-ionic multiphonon transitions 0-34973  
 rare earth ions in crystals, nonradiative processes, book contrib. 0-55188  
 redox enzyme, Fe-, Cu-, or Mo-containing, electron transfer peculiarities 0-16896  
 retinyl acetate, high press. fluoresc. studies of radiative and nonradiative processes 0-1011  
 semiconductor, acoustic studies progress (Japanese) 0-49310  
 semiconductor, strong electron-lattice interaction, review (Japanese) 0-49664  
 solution, rigid, luminesc. exchange promotion kinetics 0-50387  
 solvent effects, dynamic coupling model, quantum mechanical theory 0-29787  
 symmetric top molecule, radiationless processes, angular momentum constraints 0-28052  
 tetracene-Kr(Xe), intramol. intersystem crossing in supersonic beam, external heavy atom effect 0-14167  
 tetraphenylchlorin- $d_0$ , - $d_1$ , lowest triplet state, intersystem crossing rates, temp. and isotope effects 0-48026  
 thioindigo dyes, triplet state config., laser flash absorpt. spectrosc. obs. 0-5557  
 vibrationally coupled electronic states, radiationless decay, non-Condon effects 0-52966  
 xanthene dyes, internal heavy atom effect on radiative and non-radiative rate consts. 0-32765  
 AlGaAs-GaAs heterostructures, luminescent characts., efficiency and radiative lifetime conc. depend. 0-55151  
 $\text{As}_2\text{S}_3$ :Fe glass, photolum. and ESR, Fe impurities as non-radiative recomb. centres 0-29788  
 $\text{As}_2\text{Se}_3$ , amorphous, nonradiative recombination of photocarriers 0-11046  
 CO,  $A^1\Pi(\nu=1)$ , vibr. relax. by reversible intersystem crossing, fluoresc. obs. 0-14170  
 CIFS, second excited singlet state photophysics, laser excitation obs. 0-32758  
 $\text{CrO}_2\text{Cl}_2$ , electronically induced IR multiphoton absorpt., quasicontinuum states, excited singlet radiationless decay 0-48049  
 $\text{Dy}^{3+}$ , in soln., non-radiative transitions as Forster's energy transfer to solvent vibrations 0-1014  
 $\text{Eu}^{3+}$ , in soln., non-radiative transitions as Forster's energy transfer to solvent vibrations 0-1014  
 Fe-Al, X-ray emission spectra 0-25489  
 GaAs, deep radiation centres from heat treatment,  $\gamma$ -irrad., deform., probability of nonradiative electronic transitions 0-50408  
 Ge, nonradiative transitions at impurity centre with participation of short-wavelength phonons 0-16099  
 $I_2$ ,  $^2\Pi_{3/2}$  state, relax. between hyperfine levels 0-18880  
 $I_2$ ,  $\text{Ne}$ ,  $\text{He}$ , van der Waals complexes photodissoc. 0-50864  
 $\text{KI:Tl}^+$ ,  $A_T$  emission, mag. circular polarisation, WKB approx. for non-radiative transition rate 0-55180  
 $\text{KI:Tl}$ ,  $A_T$  emission, linear polarisation, appl. of semi-classical WKB formalism 0-45134  
 $\text{Mn}^{2+}$ , in soln., non-radiative transitions as Forster's energy transfer to solvent vibrations 0-1014  
 $\text{NO}_2$ , inter and intramolecular radiationless transitions, relax., time resolved excitation and fluoresc. spectra 0-27966



**nonradiative transitions continued**

- Na-fluorescein, glycerol-alcohol soln., luminesc. decay time, conc. depend. 0-34960  
 $O_2(c\Sigma_u^-)$ , in Ar(Kr)(Ar-Kr) matrices, multiphonon vibr. relax. time-resolved emission obs. 0-18861  
 $P_2$ , intersystem transition obs. in absorpt. spectrum 0-48008  
 Ru complexes, Ru(bipy)<sub>3</sub>Cl<sub>2</sub>·6H<sub>2</sub>O and Ru(bipy-d<sub>4</sub>)<sub>3</sub>Cl<sub>2</sub>·6H<sub>2</sub>O, soln. electronic excitation energy, deactivation determ. 0-55173  
 SF<sub>6</sub>, nonradiative collisionless dephasing rate, two-photon coherent transient meas. 0-14176  
 SO<sub>2</sub>, nonradiative transitions and intersystem crossing rates in gas phase, theory 0-23451  
 Si, amorphous, spin depend. recomb., luminesc. and light induced ESR 0-50393  
 Si:H sputtered amorphous film, luminesc. and non-radiative decay 0-50395  
 SrO, neutron- or proton-irrad., F<sup>+</sup> centre fluoresc. yield and lifetime, 5 to 140K 0-55181  
 TR<sup>3+</sup> ion excited state population depend. on lattice on IR excitation. (Russian) 0-50425  
 Yb<sup>3+</sup>, in soln., non-radiative transitions as Forster's energy transfer to solvent vibrations 0-1014

**normalising**

- steel, cast, high tensile strength, heat treatment 0-16358

**notch brittleness**

- fracture, notch angle effects obs. (Japanese) 0-6459  
 steel, low alloy, blunt-notched, fracture mechanism and failure assessment 0-16450

**notch ductility**

- geometry of notch-tip, influence on stress and strain distrib. 0-33535  
 glass fibre reinforced plastic, load-time history anal. in instrumented Charpy test (Japanese) 0-55511  
 metal ductile fracture, void growth stress/strain relations (French) 0-19280  
 polycarbonate, brittle fracture of notched ductile polymers (Japanese) 0-16448  
 polyethylene, brittle fracture of notched ductile polymers (Japanese) 0-16448  
 PVC, brittle fracture of notched ductile polymers (Japanese) 0-16448  
 steel, C, inclusions, influence on toughness and fatigue props. 0-40533  
 steel, nonmetallic inclusions effect on ductility 0-30042

**notch sensitivity** *see* notch strength**notch strength**

- see also* fracture toughness  
 acetal copolymer, notches effect on fatigue strength 0-25857  
 glass fibre reinforced epoxy, fracture mechanics 0-35294  
 graphite fibre reinforced epoxy, fracture mechanics 0-35294  
 metal, notched, fatigue under alternately over- and under-stresses (Japanese) 0-35307  
 PMMA notched beam, fracture due to central impact 0-16426  
 polycarbonate notched beam, fracture due to central impact 0-16426  
 polyisocyanurate foams, strength, cellular struct. effect 0-40518  
 polyurethane foams, strength, cellular struct. effect 0-40518  
 steel, Cr, hypereutectic, structural, critical rates of impact, kinetics of failure 0-35325  
 steel, Cr-Mo-V, notch geometry influence on creep rupture props. (German) 0-30055  
 steel, Cr-Mo-V, stress rupture strength at high temps. (German) 0-40474  
 steel, ferritic, impurity defect interaction influence on radiation hardening and embrittlement 0-35199  
 steel, high purity, low S content, for tough semi-finished products in nuclear power plant (German) 0-45393  
 steel, inclusion effect on cold formability 0-29975  
 steel, low C, dual phase, impact props., microstruct. element influence 0-40525  
 steel, mild, fatigue crack growth in compression, notch effect 0-30065  
 steel, mild, subject to three point bending and tensile load, acoustic emission 0-3154  
 steel, Ni-Cr-Mo, quenched and tempered, notched bar tensile tests (German) 0-35247  
 steel, Ni-Si-Nb (1.5,0.02,0.03 wt.%), fatigue crack growth under bending (French) 0-21089  
 steel, SHE 4340, tempered martensite embrittlement 0-30084  
 steels, cleavage fracture model at low temperatures (German) 0-35293  
 stress intensity factors, mixed mode, photoelastic determ., notch effects 0-14632  
 Al-Zn-Mg-Cu (6.76, 2.37, 1.80 wt.%), cyclic SCC in salt water (Japanese) 0-45435  
 Al<sub>2</sub>O<sub>3</sub>-Ca (0.6 to 1.6 at.%), fracture behaviour, Ca segregation effect 0-40504  
 B fibre reinforced epoxy, fracture mechanics 0-35294  
 Fe, cast, spheroidal graphite pipe, fatigue strength 0-16419  
 Fe, nitrogen, impurity defect interaction influence on radiation hardening and embrittlement 0-35199  
 V, oxygen impurity defect interaction influence on radiation hardening and embrittlement 0-35199

**notch testing**

- see also* fracture toughness testing  
 cylindrical notched specimen, four-point bending, crack resist. tests 0-53735  
 glass fibre reinforced plastic, load-time history anal. in instrumented Charpy test (Japanese) 0-55511  
 steels, structural St 37-2, cleavage fracture, report 0-25868  
 Al alloy, 7175 T 651, crack tip opening under cyclic loading, effect of environmental and R-ratio 0-45377  
 Fe, slip-initiation phenomenon by fatigue, appl. to stress meas. 0-45342

**novae**

- see also* supernovae  
 AE Aquarii, rapid light oscills. rel. to white dwarf oblique rotator model 0-36634  
 UZ Boötis, cataclysmic variable similar to WZ Sagittae, outburst characts. 0-17596  
 Z Camelopardalis, dwarf nova, photometric obs. and light curve (1973-77) 0-56853  
 AM Canum Venaticorum, orbital period increase 0-12765  
 cataclysmic binaries, evolution and origin 0-56885  
 cataclysmic variables, role of accretion disks (Polish) 0-26739  
 cataclysmic variables, visual continuum flux distrib. 0-36636  
 BV Centauri, dwarf nova, identification as spectroscopic binary 0-51775

**novae continued**

- V436 Centauri, dwarf nova, photometry during superoutburst (May 1978) 0-46570  
 WX Ceti, cataclysmic variable similar to WZ Sagittae, outburst characts. 0-17596  
 Z Chamaeleontis, cataclysmic binary, possible gravit. radiation emission 0-4386  
 SS Cygni, colour variations during dwarf nova outbursts 0-46576  
 SS Cygni, dwarf nova, soft X-ray pulsation obs. 0-46563  
 SS Cygni, dwarf nova, spectrophotometry rel. to accretion disc models in eruption and at min. light 0-36635  
 Cygni 1975 (V1500 Cygni), H $\alpha$  and H $\beta$  emission line vars. 0-4389  
 Cygni 1975 (V1500 Cygni), light curve for 1975 Aug.-1977 July period 0-4372  
 Cygni 1975 (V1500 Cygni), radio emission from expanding shell 0-26868  
 Cygni 1975 (V1500 Cygni), review of development (French) 0-17598  
 Cygni 1975 (V1500 Cygni), visible and UV spectra and light curve 0-12771  
 Cygni 1978 (V1668 Cygni), linear polarisation obs. 0-26875  
 Cygni 1978 (V1668 Cygni), photoelec. photometry, rapid flickering 0-36640  
 Cygni 1978 (V1668 Cygni), UVB light curve 0-46565  
 Cygni 1978 (V1668 Cygni), spectral development 0-51789  
 Delphini 1967 (HR Delphini), cataclysmic binary spectrum 0-4359  
 Delphini 1967 (HR Delphini), emission lines at nebular stage (Russian) 0-17597  
 Delphini 1967 (HR Delphini), photoionisation models, binary system evolution 0-17590  
 Delphini 1967 (HR Delphini), physical conditions of different regions of envelope 0-4369  
 Delphini 1967 (HR Delphini), radio emission from expanding shell 0-26868  
 Delphini 1967 (HR Delphini), spectra, line ident., radial vels. 0-17594  
 Delphini 1967 (HR Delphini), UV spectrum, stellar wind 0-26880  
 dust grains, IR spectra and props 0-26943  
 dwarf nova outbursts, colour vars. 0-46576  
 dwarf novae, HEAO-A2 soft X-ray survey during optical outburst 0-46574  
 dwarf novae, quasi-periodic oscills. and nonradial pulsations of accretion disks 0-46568  
 dwarf novae, spectra (Russian) 0-8638  
 dwarf novae, spectrophotometry, 1250-7500 Å region 0-46577  
 ejecta, dust grains sudden nucleation and growth 0-26941  
 Herculis 1934 (DQ Herculis), high time resolution spectrophotometry 0-22017  
 Herculis 1934 (DQ Herculis), short-period oscills. modulation and pulsed emission lines asymmetry interpretation 0-22044  
 Herculis 1934 (DQ Herculis), UVB photometry of visual binary 0-8661  
 Herculis 1963 (V533 Herculis), 63 sec. oscill., UVB photometry 0-17592  
 EX Hydrae, 2:3 period ratio in light curve 0-46580  
 EX Hydrae, dwarf nova, identification with high galactic latit. X-ray source (4U 1249-28) 0-22118  
 VW Hydri, colour variations during dwarf nova outbursts 0-46576  
 VW Hydri, dwarf nova, light curve superhumps model 0-4381  
 magnetic field generation by close binary interaction 0-26903  
 maximum of outburst as opportunity for mutual CETI search strategy 0-56723  
 Monocerotis 1975 (V616 Monocerotis=A 0620-00), UVB photometry 0-56846  
 optically thin winds struct. in classical novae 0-36643  
 BX Puppis, cataclysmic variable, possible member of Hyades-like cluster (NGC 2482) 0-31289  
 radio emission from nova shells, review of obs. 0-26868  
 recurrent novae and symbiotic stars, survey at 1612 MHz 0-12774  
 WZ Sagittae, recurrent nova, light curve superhumps model 0-4381  
 WZ Sagittae, recurrent nova, spectroscopic obs. during 1978 outburst 0-26862  
 WZ Sagittae, recurrent nova, spectroscopic study during 1978 outburst 0-56849  
 Sagittarius, discovery of probable declining nova (1978 March) 0-4376  
 Serpenteis 1909 (RT Serpenteis), spectrum in 1964, 1975 and (1978) 0-46566  
 Serpenteis 1970 (FH Serpenteis), radio emission from expanding shell 0-26868  
 Serpenteis 1978, IR photometry 0-4365  
 Star of Bethlehem, Far East record searches 0-17507  
 supercritical accretion discs winds struct. and appearance, numerical models 0-21984  
 symbiotic stars, obs. of unidentified bands at 6830 and 7088 Å 0-46573  
 SU Ursae Majoris, probable 1980 March super outburst 0-51785  
 Vulpeculae 1976 (NQ Vulpeculae), UV and visible spectra anal. (Chinese) 0-12770  
 Vulpeculae 1979, slow nova, pre-maximum light curve 0-4364  
 SS Cygni, soft X-ray emission detect. during optical outburst 0-46574  
 U Geminorum, soft X-ray emission detect. during optical outburst 0-46574

**novoids** *see* novae**nozzles**

- airdroplet flight in air, drift loss from spray cooling pond, numerical estimation 0-19471  
 arc nozzle clogging theory 0-38791  
 atomic beam, produced from He nozzle flow, high speed ratio 0-5636  
 atomic beam production, He skimmed from freejet zone of silence 0-5635  
 axisymmetric hypersonic nozzle, viscous gas flow calc. with departure from vibr. equilib. 0-33649  
 circuit breaking arcs, current zero arc model based on forced convection 0-33831  
 cluster beam, nozzle flow formation and detection, high energy beam 0-5638  
 cluster formation, in rarefied nozzle flowfield 0-5639  
 compressible and incompressible flows, recent theoretical and expt. developments, book 0-1620  
 conical, flow characts., obs. (Russian) 0-33650  
 conical nozzle and diffuser, laminar compressible boundary layer swirling flow 0-48768  
 control jets, gasdynamic features, 3-D subsonic and supersonic flows 0-6112  
 convergent nozzles incorporated into gas flowmeter, comparison with standard 0-6126



**nozzles continued**

- critical flow venturi nozzles, primary calibration in high pressure gas 0-53832  
cylindrical nozzles with sharp upstream edges, critical flowmetering appl. 0-28546  
DC arc in blocked nozzle, boundary layer integral method anal. 0-6295  
flow visualization using two-phase flow 0-33714  
free surface flows from nozzle at low Reynolds number 0-43758  
gas flow into duct, self-excited oscillations 0-33647  
gas flow parameters in Laval nozzles and curvilinear channels, 1-D theory 0-6124  
gas jet-liquid bath interaction for different degrees of assimilation during blowing 0-43754  
gasdynamic laser nozzle wake, flowfield props. boundary layers 0-24027  
gasdynamic laser resonator cavity, flow fields and amplification coeffs., 2-D calc. 0-5722  
Hartmann-Sprenger tube, air jet from convergent nozzle, air column oscillations generative mech. 0-14828  
heat transfer in aerodynamic-tube nozzles 0-24068  
high subsonic nozzle flows, pressure waves from convection of temp. disturbances 0-6125  
hyperbolic Laval nozzles, transonic flow in throat region (*Chinese*) 0-6122  
hypersonic conical nozzle, boundary layer separation from compression shock 0-48766  
hypersonic wind tunnel, flow core relative area, nozzle similitude ratios 0-48747  
ideal gas flow, choked and supercritical, through orifices and convergent conical nozzles, numerical soln. 0-38474  
ideal gas in ejector nozzles, theory of combined flow of high/low pressure streams 0-6123  
ideal radial free jet, nozzle length effects 0-14768  
isotope separation by laser photochemistry in nozzle flows with heterogeneous condensation 0-50862  
laminar compressible boundary layers for laser heated swirling nozzle and diffuser flow 0-53831  
laser heated nozzle flow with swirl, axisymmetric comp. boundary layer 0-14775  
laser-heated H<sub>2</sub> rocket, analysis of nozzle flow 0-10283  
Laval, boiling water discharge and dynamic characteristics 0-19470  
Laval nozzle, supercritical steam supersonic discharge 0-48765  
Laval nozzle with gasdynamic regulation, characts. 0-33651  
Laval nozzles, flows with heat addition, book contrib. 0-1671  
liquid ejector with perforated nozzle 0-24069  
medium speed turbulent, two-dimens. meas. near nozzle outlet using laser Doppler anemometer 0-28582  
MHD, gas boundary layer swirling nozzle and diffuser flows with mag. field 0-1693  
microwave discharge, supersonic flow in waveguide, electron densities, possible laser 0-38842  
monatomic gas, rarefied flows in two-dimens. expansion nozzle 0-28547  
multiphase mixture, two-dimens. nozzle and jet supersonic flows 0-48780  
nozzle expansion in turbulent flow, downstream heat and mass transfer 0-1669  
nozzle fluid concentrations, probability density functions in free-diffusion flames, laser-light technique 0-10235  
nuclear reactor, control rod drive hydraulic return nozzle repair 0-23043  
orifice plate calibrations, extrapolation to high Reynolds no. 0-53833  
Prandtl supersonic jet problem, linear aerodynamic theory formulae, validity, book contrib. 0-6090  
pulsed nozzle jet struct., direct shadow method and streak photography 0-10323  
PWR components subject to thermal shock, heat transfer coeffs. 0-32332  
reattachment flow issuing from finite width nozzle, bubble press. parameter 0-10275  
resonance tube, jet flow and heating, unsteady complex shock struct. 0-6115  
rotating propulsive nozzle flowfields for nonequilibrium chemically reacting supersonic flow 0-48764  
sampling probe, molecular beam mass spectrometry, in situ anal. in crystal growth ambients 0-52357  
slit nozzle, for cluster beam generation with strong flux intensity (*Japanese*) 0-52361  
sonic nozzle expansions, rot. relax. theory 0-43827  
steady transonic Euler eqns., Newton's method soln., nozzle appl. 0-38437  
steam turbine nozzle cascades, local heat transfer, approach flow turbulence effects 0-38381  
submerged jets in water with slit nozzles, interaction between two opposed jets 0-6113  
supersonic axisymmetric, film cooling efficiency 0-48710  
supersonic flow, amplification coefficient, effect of mixing conditions in a laval nozzle 0-6085  
supersonic nozzle beam, high temp. and press. device 0-37907  
supersonic nozzle flowfields, fully viscous and Navier-Stokes solns., comparison, book contrib. 0-1641  
throttling liquids, temp. field near boundary 0-43757  
transonic potential flows past cascades, in nozzles and channels, pseudo-unsteady method 0-14727  
two-dimensional Laval micronozzles, laminar boundary layer approx. calcs. 0-24070  
two phase, efficiency at high rates of heat and mass transfer 0-48767  
two-dimensional long slots, rarefied gas transition flow 0-43738  
two-phase flow, critical, nonequilibrium vapour production model 0-52719  
vibration relaxation time in nozzle and shocktube expansion flows, physical model 0-24067  
water jet appearance, nozzle shape and polymer additive effects, boundary layers 0-53828  
Ar, gas in planar nozzle, shock-wave propag., effect of transverse mag. field 0-6094  
CO<sub>2</sub> aerosol/hypersonic air stream interaction, gasdynamic CO<sub>2</sub> laser energy characts. 0-48211  
CO<sub>2</sub>-He-N<sub>2</sub> gas dynamic laser, gain coeff. numerical estimates, book contrib. 0-1183  
CO<sub>2</sub>-N<sub>2</sub>-He nozzle flows with boundary layer, gain coefficients 0-14312  
H<sub>2</sub>, cluster beam formed from nozzle flow, isotope effect 0-6127  
SF<sub>6</sub>-Ar, condensing flow, gasdynamic and IR meas. 0-6501

NTC thermistors *see thermistors*

$\nu$  (neutrino) *see neutrinos*

nuclear acoustic resonance *see acoustic nuclear magnetic resonance*

nuclear alignment *see nuclear polarisation*

**nuclear binding energy**

*see also nuclear forces*

- <sup>145</sup>Sm neutron separation and level exciton (n, $\gamma$ ) and (d,p) correlations 0-22756  
A=10-58, neutron separation energies, self consistent set from (n, $\gamma$ ) reaction 0-52563  
A=3-4 hypernuclei, binding energy anal.,  $\Lambda$ -N pot., scatt. length and effective range 0-9256  
abnormally large density and binding energy states, book contrib. 0-489  
conference on many-body theories, Trieste, Italy (Oct. 1978) 0-22135  
even-even nuclei, phenomenological calcs. in n-p interacting boson approx. 0-27597  
even-odd mass difference ratio, mass and binding energy formula 0-47361  
Fermi systems, semi-infinite, surface props., thickness and energy 0-52600  
impure nuclear matter with  $\Lambda$ , binding energy, functional variational approach 0-22744  
isobar degrees of freedom, binding energy from BHF approx. 0-22734  
isobar degrees of freedom in nuclear matter, binding, NN interactions and  $2\pi$  exchange 0-22735  
light nuclei, alpha cluster model, 3-body problem 0-32217  
light nuclei, hyperspherical functions for size, excited states, compressibility, binding energy 0-22679  
neutron-rich nuclear potential energy surfaces 0-18183  
nuclear, matter, V<sup>8</sup> models, variational calcs. for binding energy and density 0-42571  
nuclear bound states of  $k$ -,  $p$  and  $\Sigma$  0-13399  
nuclear matter BBG theory, auxiliary single particle field for binding energy 0-22723  
nuclear matter binding energy expansion convergence in Brueckner-Bethe-Goldstone theory 0-488  
nuclear matter binding energy from low density expansions, Brueckner-Hartree-Fock approx. 0-22720  
p-f shell nuclei, HF calcs., vel. depend. effective pot., binding energy, quadrupole moment 0-461  
Paris NN pot. parametrisation, phase shifts, nuclear matter binding energy 0-47405  
s-d shell nuclei, HF calcs., vel. depend. effective pot., binding energy, quadrupole moment 0-461  
single-particle motion in nucleus, forces between constituent nucleons, shell model 0-47408  
strongly bound  $\pi^-$  nuclear states, vel. depend. pot. binding, pionic atoms 0-37331  
superheavy nuclei and multineutron systems, possibility of existence (*Russian*) 0-462  
three particles with Coulomb interaction, binding energy and scatt. states (*Russian*) 0-5051  
 $\Lambda$  binding energy in nuclear matter with Nijmegen baryon-baryon interaction 0-13400  
<sup>28</sup>Al, neutron binding energy precision meas. 0-18182  
<sup>4</sup>C, A=13,14, neutron binding energy from <sup>1</sup>H(n, $\gamma$ ) 0-52564  
<sup>4</sup>C, A=13,14, neutron binding energy 0-47362  
<sup>114</sup>Cd, neutron binding energy precision meas. 0-18182  
<sup>165</sup>Dy, neutron binding energy precision meas. 0-18182  
<sup>168</sup>Er, neutron binding energy precision meas. 0-18182  
<sup>2</sup>H  $\gamma$ -energy and binding energy from <sup>1</sup>H(n, $\gamma$ ) 0-52564  
<sup>2</sup>H neutron binding energy and n mass excess from <sup>1</sup>H(n, $\gamma$ ) 0-47362  
<sup>3</sup>H binding energy, 3N bound state with separable interactions, Faddeev theory corrections 0-13388  
<sup>3</sup>H neutron binding energy 0-47362  
<sup>3</sup>H neutron binding energy from <sup>1</sup>H(n, $\gamma$ ) 0-52564  
<sup>3</sup>H, three-particle bound states for partly nonlocal interactions with continuum bound states 0-32206  
<sup>3</sup>H-n+d, s-wave asymptotic normalisation consts. in one-boson exchange model 0-37334  
<sup>3</sup>H binding energy using phenomenological  $\Lambda$ N pots. 0-9254  
<sup>3</sup>He, Coulomb energy, charge symmetry breaking 0-27564  
<sup>3</sup>He, trinucleon bound state problem, binding energy, form factors and mag. moment 0-22710  
<sup>4</sup>He binding energy,  $\Delta(3-3)$  effects, reaction matrix calc.,  $\Delta$  degrees of freedom 0-9218  
<sup>4</sup>He, shell model calcs. 0-13393  
<sup>4</sup>He-<sup>4</sup>He binding energy difference, bound states, exact four body calc. 0-9255  
<sup>200</sup>Hg, neutron binding energy precision meas. 0-18182  
<sup>15</sup>N, neutron binding energy 0-47362  
<sup>15</sup>N, neutron binding energy from <sup>1</sup>H(n, $\gamma$ ) 0-52564  
<sup>16</sup>O and <sup>16</sup>S shell nuclei, binding energy from realistic Hamiltonians and spectral distrib. theory 0-22678  
<sup>16</sup>O, energy calcs., Jastrow variational method extension, FAHT cluster expansion 0-22677  
<sup>16</sup>O ground state and binding energy, microscopic calc. with realistic NW interaction (*Russian*) 0-5052  
<sup>45</sup>Sc-<sup>41</sup>Ca Coulomb displacement energy, HF calcs. 0-42527  
<sup>237</sup>U levels, bands and J<sup>+</sup> assignments, n binding energy from <sup>236</sup>U(n, $\gamma$ ) 0-5041  
<sup>239</sup>U, neutron binding energy precision meas. 0-18182  
<sup>91</sup>Zr primary  $\gamma$ -rays and binding energies from <sup>90</sup>Zr(n, $\gamma$ ) 0-52566  
<sup>91</sup>Zr neutron separation energies from (d,t) and (d,p) reactions 0-47489  
<sup>94</sup>Zr, A=90, 92 and 94, charge densities and single-particle structure 0-9224  
<sup>94</sup>Zr, A=91, 92, 94, binding energy and primary  $\gamma$ -ray intensities from <sup>92</sup>Zr(n, $\gamma$ ) 0-52565  
<sup>92</sup>Zr, neutron binding energy precision meas. 0-18182

**nuclear bombardment targets**

*see also nuclear reactions and scattering*

- actinide target prep. for synthesis of transactinide elements 0-23206  
actinide target preparation by focused ion beam sputtering 0-23219  
biomedical target, water-cooled pion-production, remote exam. and disassembly 0-25975  
diamond target preparation for tandem expts. 0-23222  
EM isotope separation and in-beam electron spectroscopy, Pt target preparation 0-52812  
enriched isotope target preparation, design of quasi-hyperbolic electrostatic fields 0-23597  
explosively clad uranium targets 0-18737  
gaseous windowless high density target for scatt. expts. 0-23210



**nuclear bombardment targets continued**

- heavy ion facility, target production 0-23213  
 high pressure sample container for thermal neutron inelastic scattering on fluids 0-37681  
 isomeric state g-factor meas., target preparation 0-23217  
 isotope, quartz crystal thickness sensor 0-17923  
 isotope compounds, conversion to metals by reduction-distillation methods 0-23223  
 isotope induction at LAMPF, fabrication, cladding, handling of irradiated targets 0-23231  
 isotope target preparation by laser beam evaporation techniques 0-18735  
 isotopic target preparation by ion beam sputtering 0-23220  
 neutrino target complex at Fermilab, operating experience 0-23230  
 neutron generator facility with alternative  $30^\circ$  target 0-9444  
 NIM-controlled rabbit system 0-18731  
 optically pumped electron spin polarised targets, polarised ion beam prod. 0-27851  
 ORNL EM isotope separation program 0-18673  
 polarised, proton and deuteron, for precise polarisation meas. at KEK 0-37670  
 polarised  $^3\text{He}$  continuous flow cryostat 0-52240  
 polyimide substrate foils for nuclear targets 0-18739  
 powdered isotopic material prod. by centrifugal method 0-18738  
 radioactive target preparation and characterisation 0-18734  
 reference fission foils preparation by fluoride deposition, characterisation 0-23218  
 solid target preparation by reactions with gases 0-18733  
 solid targets from gaseous elements, prod. and use 0-23212  
 thickness determination method using series integration 0-18748  
 vacuum evaporation, substrate temp. meas. by laser beam 0-20794  
 water-cooled target for the 14 MeV neutron source, design and experiment 0-47795  
 X-ray fluorescence thin film calibration standards 0-22496  
 13 self supporting film production 0-18747  
 241Am, target prep. for synthesis of transactinide elements 0-23206  
 Ar isotopically enriched solid target prod. and use 0-23212  
 10B self supporting target preparation up to  $500 \mu\text{g}/\text{cm}^2$  0-18745  
 11B self supporting target preparation up to  $500 \mu\text{g}/\text{cm}^2$  0-18745  
 Be foil, rolling procedures 0-23225  
 249Bk, target prep. for synthesis of transactinide elements 0-23206  
 C deposition on targets during beam bombardment 0-18741  
 C evaporated thin films, yield tensile strength meas. 0-23214  
 C foil, ion irradiation, correlation of energy loss and crystallographic transform. 0-23215  
 C foils, impurity anal. by PIXE 0-18740  
 C stripper foil, lifetime meas. 0-23216  
 C stripper foil preparation, under heavy ion bombardment 0-18717  
 C stripper foils, ethylene cracking in glow discharge, irradiation lifetimes 0-23207  
 C stripper foils, lifetime enhancement by slackening technique 0-23186  
 Ca, evaporation preparation 0-23224  
 CaO, isotopically enriched target preparation using electron gun 0-23226  
 241Cf, target prep. for synthesis of transactinide elements 0-23206  
 Cl target prod. 0-9441  
 248Cm, target prep. for synthesis of transactinide elements 0-23206  
 Cu+Fe+Cd, nuclear target preparation by evaporation and rolling 0-23224  
 Cu+Fe+Sn, nuclear target preparation by evaporation and rolling 0-23224  
 Gd<sub>2</sub>O<sub>3</sub>, isotopically enriched target preparation using electron gun 0-23226  
 H scintillating gaseous drift chamber for use as positron sensitive target 0-9457  
 Hf, preparation from HfO<sub>2</sub> reduction by Ca 0-18746  
 Li, evaporation preparation 0-23224  
 Me, isotopically enriched target preparation using electron gun 0-23226  
 Na-vapour jet charge-exchange continuous-action target 0-23205  
 Nd<sub>2</sub>O<sub>3</sub>, isotopically enriched target preparation using electron gun 0-23226  
 Ni foil, crystal struct. as function of substrate temp. during deposition 0-18742  
 16O(p, $\alpha$ )<sup>13</sup>N, in-cyclotron <sup>13</sup>N prod., water loop target 0-23201  
 Pb isotopically enriched rotating sandwich targets for high intensity heavy ion beams 0-18743  
 Pt foil, crystal struct. as function of substrate temp. during deposition 0-18742  
 SiO<sub>2</sub>, isotopically enriched target preparation using electron gun 0-23226  
 Sm<sub>2</sub>O<sub>3</sub>, isotopically enriched target preparation using electron gun 0-23226  
 144Sm, enriched isotope target preparation, design of quasi-hyperbolic electrostatic field 0-23597  
 sputter, isotopically enriched targets for <sup>148</sup>Ca and <sup>14</sup>C prod. 0-23221  
 Ti rolled foil preparation 0-18744  
 Ti, tritiated self supported target prep. 0-23211  
 U deposit spray painting on metallic backing 0-18736  
 235U, muonic, fission studies, target preparation 0-23217  
 238U, muonic, fission studies, target preparation 0-23217  
 238U thin self supporting foils 0-9440  
 V foil, rolling procedures 0-23225  
 W foil, rolling procedures 0-23225  
 W, isotopically enriched target preparation using electron gun 0-23226

**nuclear branching and mixing ratios**

- A $\leq$ 57 nuclei, E2, M1 multipole mixing ratios 0-22751  
 E2:M1 multipole mixing ratio, sign change in A=150 region 0-493  
 particle rotor model study of transitional N=89 and N=91-95 nuclei 0-42529  
<sup>Ag</sup>, A=105,107, positive parity band, mixing and branching ratios lifetimes from (<sup>16</sup>O,2np)(<sup>14</sup>N,3n) 0-9197  
 26Al low energy resonances, decay and J<sup>π</sup> assignments, branching ratios from <sup>25</sup>Mg(p, $\gamma$ ) 0-42624  
 27Al levels, spins and  $\gamma$ -rays, multipole mixing from <sup>27</sup>Al(n, $\gamma$ ), pol. thermal 0-47398  
 10B T=1 states,  $\gamma$ -transition strengths, lifetimes, branching and mixing ratios from <sup>9</sup>Li( $\alpha$ , $\alpha$ ) 0-27594  
 12C( $\pi^-$ ,  $2\gamma$ ), doubly radiative capture theory, branching ratio and ang. correlations 0-9314  
<sup>Ac</sup>(n, $\gamma$ ) A=114,116, energy levels, spins, and gamma-ray multipole mixing ratios investig. 0-52580  
 54Co, resonance decays, branching ratios and analogue resonances from <sup>54</sup>Fe(p, $\gamma$ ) 0-52643

**nuclear branching and mixing ratios continued**

- <sup>51</sup>Cr, bands, levels, EM transitions, J<sup>π</sup>, branching and mixing ratios from <sup>48</sup>Ti( $\gamma$ ,n)<sup>51</sup>Cr and <sup>51</sup>V(p,n)<sup>51</sup>Cr 0-52606  
 114Cs  $\beta$ -decay, half life and branching ratio, <sup>114</sup>Xe excited states and  $\gamma$ -rays 0-47436  
 163Dy multipole mixing in  $\gamma$  to ground bands from <sup>163</sup>Dy(n, $\gamma$ ) 0-52615  
 69Ga(n, $\gamma$ ), fast n, levels, J<sup>π</sup>, transitions and mixing ratios, statistical anal. (Russian) 0-13382  
<sup>Gd</sup>, A=150-156, E2:M1 multipole mixing ratio, sign change in A=150 region 0-493  
 145Gd EC/ $\beta^+$ -decay branching ratio anomalies, <sup>145</sup>Eu level and transition effects 0-32244  
 66Ge levels, lifetimes and mixing ratio, in-beam  $\gamma$ -spectroscopy from <sup>54</sup>Fe(<sup>14</sup>N,np $\gamma$ ) 0-42541  
 69Ge high spin states, EM props., branching and mixing ratios from <sup>55</sup>Mn(<sup>16</sup>O,pn) 0-13347  
 201Hg missing  $f_{5/2}$  state Coulomb excitation, level scheme, J<sup>π</sup>, transitions using ( $\alpha$ , $\alpha'$ ), (<sup>1</sup>O, <sup>16</sup>O) 0-47386  
 157Lu, short lived  $\alpha$  emitter,  $\alpha$  energy, T<sub>1/2</sub> and branching ratio 0-501  
 24Mg continuum states, branching ratios from <sup>12</sup>C(<sup>16</sup>O,  $\alpha$ ) 0-22661  
 20Ne continuum states, J<sup>π</sup> and branching from <sup>12</sup>C(<sup>12</sup>C,  $\alpha$ ) 0-22660  
 20Ne high spin states, J<sup>π</sup> and  $\alpha$ -decay branching ratios from <sup>16</sup>O(<sup>12</sup>C, <sup>8</sup>Be) 0-18166  
 20Ne levels, J<sup>π</sup>, branching ratio and EM transition rates from <sup>16</sup>O+ $\alpha$  0-42540  
 20Ne levels and branching ratio from <sup>12</sup>C(<sup>16</sup>O,  $\alpha$ ) 0-22661  
 20Ne resonances, J<sup>π</sup>, excitation functions and branching ratio from <sup>19</sup>F(p, $\gamma$ ) 0-22787  
 60Ni, 1173 keV transition M3/M2 mixing ratio meas. 0-52608  
 16O high spin states, J<sup>π</sup> and  $\alpha$ -decay branching ratios from <sup>12</sup>C(<sup>12</sup>C, <sup>8</sup>Be) 0-18166  
 147Pm,  $\beta$ -decay, branching ratio and K-shell autoionisation 0-42598  
 196Pt (<sup>20</sup>Ne, <sup>20</sup>Ne'), excited states, lifetime meas. using recoil-distance method 0-13413  
 196Pt (<sup>58</sup>Ni, <sup>58</sup>Ni'), excited states, lifetime meas. using recoil-distance method 0-13413  
 187Re low lying level struct. and transitions, E2/E1 mixing ratios from <sup>187</sup>W decay 0-27557  
<sup>A</sup>Ru(p, $\gamma$ ), A=96, 98, 5-8 MeV, level schemes, transitions, vibr. state, mixing ratios 0-18199  
 97Ru populated in <sup>88</sup>Sr(<sup>13</sup>C, 3n $\gamma$ ), band-like structures 0-32146  
<sup>Sb</sup>, A=121,123, levels below 2 MeV, spins, transitions and mixing ratio from (p, $\gamma$ ), (n,n' $\gamma$ ) 0-32191  
<sup>Sm</sup>, A=150, 152, E2:M1 multipole mixing ratio, sign change in A=150 region 0-493  
 151Sm,  $\beta$ -decay, branching ratio and K-shell autoionisation 0-42598  
 116Sn(<sup>16</sup>O, <sup>16</sup>O) 48 MeV, collective states, E2, E0 transition probabilities, half-life, branching ratios 0-18172  
 160Tb  $\beta$ -decay, oriented nuclei,  $\gamma$  transitions multipole mixing parameters 0-18240  
 95Tc, energy levels from <sup>95</sup>Mo(p, n $\gamma$ )<sup>95</sup>Tc 0-37372  
 99Tc,  $\beta$ -decay, branching ratio and K-shell autoionisation 0-42598  
 99Tcm  $\beta$ -decay,  $\beta$ -branching, <sup>99</sup>Ru decay scheme 0-42596  
 204Tl,  $\beta$ -decay, branching ratio and K-shell autoionisation 0-42598  
 153Tm, short lived  $\alpha$  emitter,  $\alpha$  energy, T<sub>1/2</sub> and branching ratio 0-501  
 182W high spin states, J assignments and mixing ratios from <sup>182</sup>Re isomer decay 0-42593  
<sup>Xe</sup>, A=129, 131, populated in ( $\alpha$ ,n $\gamma$ ), props. of low-lying levels 0-464

**nuclear charge**

- see also form factors (nuclear)  
 A=16-58, charge, proton and neutron density distrib. calc. 0-22680  
 A=42 isotopic spin triplet, Coulomb energies and shifts, microscopic calcs. 0-9200  
 A=76-79 charge dispersion curve from <sup>232</sup>Th(p, f) 0-18349  
 deep inelastic heavy ion collisions, mass and charge distrib., statistical model 0-18332  
 deeply inelastic heavy ion collisions, charge transfer ang. momentum depend., fragment kinetic energies 0-47505  
 fission, isobaric widths, frozen quantal fluctuations, charge equilibration 0-37365  
 fission, spontaneous, mass and charge division, asymmetry, order-disorder model 0-22866  
 heavy ion collisions, charge equilibrium model using collective high freq. mode and quantal master eqn. 0-27667  
 isoscalar effective charge in large A limit Tamm-Dancoff and RPA calcs. 0-42534  
 nuclear forces, charge dependence and nuclear struct. effects, nuclear charge distrib. 0-32197  
 quadrupole moments and rms charge radii, shell model calcs. 0-47369  
 transitional nuclei, particle-rotor recoil term and pairing interaction, Fermi surface 0-32174  
 197Au(<sup>4</sup>Xe,X), A=129, 132, 136, <787 MeV, light and heavy fragment N/Z ratios 0-32292  
 197Au(<sup>13</sup>Xe,X), damped collisions, charge distrib. second moments and giant E1 quantal fluctuations 0-27547  
 40Ca(e,e), cross sections, model independ. charge density 0-27548  
 45Ca, nuclear charge radius, spin, moments, by laserspectroscopy 0-18187  
 1H(n, $\pi^0$ )<sup>2</sup>H, nuclear forces charge symmetry test 0-5071  
 2H(d,n)<sup>3</sup>He, 1.5-15.5 MeV, tensor anal. power, charge symmetry violation in mirror reaction 0-13368  
 2H(d,p)<sup>3</sup>H, 1.5-15.5 MeV, tensor anal. power, charge symmetry violation in mirror reaction 0-13368  
 3He, rigorous bounds for charge densities from form factor data 0-5055  
 4He, soft-core radial wave function, photo-disintegration calculation 0-18209  
 40Mo, A=92, 94-98, 100, muonic atom X-ray transitions, nuclear charge radii 0-27545  
 14N(e,e) in storage ring, elastic form factor, charge distributions 0-22819  
 110Pd(<sup>208</sup>Pb, X), 1.18-1.28 GeV, charge equil. time scale, relaxation time 0-18188  
 238U( $\gamma$ ,f), 20 MeV, fission product yields, charge distrib. 0-42533  
 4Zr, A=90, 92 and 94, charge densities and single-particle structure 0-9224

**nuclear chemistry**

- see also chemical effects of nuclear reactions and scattering; radiation chemistry; radiochemistry  
 acetic acid-formic acid, 'dimer', tritium  $\beta^-$ -decay causing H<sup>+</sup> transfer, ab initio MO calc. 0-3391



**nuclear chemistry continued**

- formamide dimer, tritium  $\beta^-$ -decay causing  $H^+$  transfer, ab initio MO calc. 0-3391  
formic acid dimer, tritium  $\beta^-$ -decay causing  $H^+$  transfer, ab initio MO calc. 0-3391

**nuclear cluster model**

- A=15-18, effective interaction from coupled cluster many-body method extension 0-22701  
A $\leq$ 44, fp-shell nuclei struct., effect of core-excitation and  $\alpha$ -clustering correl. 0-9245  
alpha cluster reactions, effective single particle operator 0-32218  
BBG theory developments, hole and particle lines, dispersion effects and healings 0-22719  
bound state poles, effect on N-body scatt. amplitudes (*Chinese*) 0-5111  
composite particles, N-cluster dynamics and effective interaction, dynamical eqn. 0-42560  
conference on many-body theories, Trieste, Italy (Oct. 1978) 0-22135  
coupling effects of two-particle and alpha two-hole states in A=18 nuclei 0-5081  
double folding pot. for inelastic scatt. between nuclei 0-13425  
double well cluster shell model folding potential (*Chinese*) 0-52596  
hadron+nucleus, high energy, cluster cascade model 0-18300  
hadron-nucleus interaction, cluster prod., at cosmic ray energies 0-13467  
heavy ion reactions, cluster correlation, review, book contrib. 0-27670  
heavy ion resonance reactions as orbiting cluster phenomena 0-47446  
light nuclei, alpha cluster model, 3-body problem 0-32217  
light nuclei, hyperspherical functions for size, excited states, compressibility, binding energy 0-22679  
light nuclei, props. from double well cluster shell model 0-27572  
microscopic description, review 0-487  
neutron matter, spin and tensor correlations, cluster expansion hypernetted chain eqns. 0-22728  
neutron or nuclear matter, spin depend. correlations, variational method 0-22726  
nuclear matter, Brueckner Bethe and variational calcs. review, nuclear saturation problem 0-22745  
nuclear matter, constrained variational calcs., three body and N\* (1234) contribs., cluster energy 0-22743  
nuclear matter BBG theory, auxiliary single particle field for binding energy 0-22723  
reaction matrix approach to the cluster state, Brueckner generator coordinate method, appl. to  $\alpha$ - $\alpha$  scatt. 0-9250  
Su(3) symmetry and integral kernels in cluster problems 0-9251  
three-body scatt. problem, cluster expansions, effective intercluster pots. 0-5082  
wavefunctions, correlation operators, variational techniques, review 0-22748  
( $\alpha$ ,  $^{12}C$ ), 90.3 MeV, cross sections and systematics multi- $\alpha$ -cluster transfer implications 0-42675  
(d,  $^6Li$ ), 54.25 MeV,  $\alpha$ -cluster spectroscopic factors, DWBA anal. 0-52571  
(p,  $\alpha$ ) microscopic form factors, DWBA cluster form factor replacement 0-47478  
(p,X) in emulsion 24 GeV, clusters in rapidity interval method, multiperipheral model 0-5135  
 $^{27}Al(p,\alpha)^{24}Mg$ , finite-range cluster-model description, DWBA approach 0-52667  
 $^{11}B$ , struct. study of  $2\alpha+t$  system in orthogonality condition model, level energies and parity 0-5080  
 $^8Be$  lowest negative parity state, shell and cluster model calcs. from  $^7Li(p,p)$ ,  $^8Be$  lowest negative parity state, shell and cluster model calcs. 0-18205  
 $^8Be$  spontaneous fission pot. energy curve, cluster shell model (*Chinese*) 0-22867  
 $^{12}C$ , excited state struct.,  $\alpha$ -particle model 0-47385  
 $^{12}C$ ,  $3\alpha$  model, composite particle interactions, Pauli principle (*Russian*) 0-18214  
 $^{12}C+^{12}C$  system, nuclear molecule microscopic description, HF and coupled channel calcs. 0-13493  
 $^{12}C(^{12}C,\alpha)$ , 12-31.5 MeV, inclusive  $\alpha$ -particle yield, resonant like structs. 0-42691  
 $^{12}C(^9Be,\alpha)^{17}O$ , ang. distrib. from pick-up model anal. of cluster transfer (*Russian*) 0-37396  
 $^{14}Ce$  quasi-f $_{7/2}$  low lying states spectroscopic factors, cluster-vibr. model from  $^{142}Ce(d,p)$  0-47391  
 $^{18}F$ , semi-microscopic calc. of  $\alpha$ -cluster states, shell model approx. 0-465  
 $^{18}F$ , coupled channel orthogonality condition model 0-47384  
 $^{19}F$ , energy levels from  $\alpha$ - $^{15}N$  and  $t$ - $^{16}O$  coupled channel orthogonality condition model 0-37326  
 $^{19}F$  final state selective population, triton clustering from band anal. from ( $^7Li,t$ ), ( $^6Li$ , $^3He$ ) 0-9306  
 $^{19}F$  levels, resonances and phase shifts, resonating group calcs. from  $^{15}N(\alpha,\alpha)$  0-32189  
 $^{19}F+^{28}Si$  spin orbit pot., single folding model and cluster model 0-9196  
 $^{19}F(d,X)$ ,  $X=^7Li$ ,  $^8Be$ , 13.6 MeV, diff. cross sections,  $^5He$  cluster direct transfer (*Russian*) 0-52650  
 $^4He$  binding energy,  $\Delta(3-3)$  effects, reaction matrix calc.,  $\Delta$  degrees of freedom 0-9218  
 $^5He$ , 16.7 MeV states energy calc. using mixed cluster representation 0-27555  
 $^4Li$ , cluster model study using generator coord. method on  $^3He+p$  scatt. 0-27581  
 $^6Li$ , EM form factors and spectroscopic factors in phenomenological cluster models 0-496  
 $^6Li(^3He,p\alpha)$ , 2.9 MeV, quasifree reaction,  $^2H(^3He,p\alpha)$  contrib., cluster motion 0-13485  
 $^6Li(p,pd)$ , 590 MeV,  $\alpha$ -d motion, impulse distrib., cluster momentum distrib. 0-52679  
 $^7Li$ ,  $d\sigma(p,p'd)/d\sigma(p,nd)$ , 670 MeV, cross section ratio, cluster model estimate 0-22829  
 $^7Li(\gamma,t)$ ,  $<50$  MeV, total and differential cross sections, levels, cluster model calcs. 0-32265  
 $^{24}Mg$ ,  $^{16}O+\alpha$  cluster model, energy level structure 0-18215  
 $^{23}Na$  level  $\alpha$ -spectroscopic strengths assuming direct cluster transfer from  $^{19}F(^6Li,d)$  0-27552  
 $^{19}Ne$ , final state selective population, triton clustering from band anal. from  $^{16}Li(^6Li,t)$  0-9306  
 $^{16}O$ , energy calcs., Jastrow variational method extension, FAHT cluster expansion 0-22677  
 $^{16}O+^4He$ , group theory appl. to reaction studies 0-9276

**nuclear cluster model continued**

- $^{16}O(^6Be,^3He)^{20}Ne$ , sub-Coulomb alpha transfer cross sections 0-37394  
 $^{92}Zr(p,\alpha)^{89}Y$ , finite-range cluster-model description, DWBA approach 0-52667

**nuclear collective model**

- see also *nuclear cranking model*; *nuclear liquid drop model*  
A $\sim$ 150 transitional region, collective props., interacting boson model 0-27538  
adiabatic collective motion, quantum Hamiltonian microscopic derivation 0-47345  
collective mass parameter, super-normal phase transition effect 0-5046  
collective path curvature as collectivity meas., quasi-boson approx. validity 0-22658  
conference on interacting bosons in nuclear physics, Erice, Italy (June '78) 0-27042  
even-even nuclei, low lying collective states from p-n interacting boson model 0-32158  
even-even nuclei, phenomenological calcs. in n-p interacting boson approx. 0-27597  
even-even nuclei with A $\approx$ 150, excited states calculation, phenomenological models: band-mixing, vibrational-rotational and interacting-boson model 0-22653  
generator coordinate method with conjugate parameters 0-47413  
giant multiple resonances, excitation strength functions 0-5037  
giant multipole resonances, Regge poles and collective model 0-13436  
group theoretical advances in collective motion anal. 0-9201  
Hamiltonian decompositions, restricted dynamics, microscopic nuclear theory (*Russian*) 0-52594  
 $i_{13/2}$  shell, particle-rotor model soln., backbending, transition rates, ang. momentum spread 0-47344  
interacting boron model of collective state, O(6) limit 0-32214  
interacting boson and triaxial rotor models, O(6) limit 0-27579  
interacting boson model, collective motion descript., shell model test 0-27542  
interacting boson model, collective state description, shell model connection 0-37341  
interacting boson model, relation to expanding boson and truncated quadrupole phonon models 0-27580  
interacting boson model, shell model and microscopic nuclear struct. 0-27575  
interacting boson model, shell model description 0-27574  
interacting boson model, shell model fermion Hamiltonians with monopole and quadrupole pairing 0-27576  
interacting boson model, shell model foundation 0-37340  
interacting boson model 0-52595  
interacting boson model for collective states, present status 0-27573  
isobaric distributions in deep inelastic reactions 0-18270  
Kostant-Souriau geometric quantization of nuclear collective models 0-9247  
large amplitude collective motion, collective subspaces and generator coordinate method 0-9199  
many-phonon monopole pairing vibr. interaction in nuclear field theory, IBM 0-27578  
mass quadrupole model, algebraic formulation 0-18211  
neutron pickup reactions to  $(i_{13/2})^2$  bands, theoretical rot. signatures, backbending 0-52558  
nuclear field theory treatment of the interacting boson model 0-27577  
particle rotor model study of transitional N=89 and N=91-95 nuclei 0-42529  
particle-rotor model, two-body nature of recoil term 0-22713  
particle-rotor model Hamiltonian, Coriolis interaction and recoil term attenuations, possible connection 0-32215  
pseudomagic nuclei, yrast bands, variable moment of inertia model 0-449  
quadrupole phonon states, fifth label values, exact derivation 0-31664  
quadrupole transition densities and electron scatt. in the interacting boson model 0-27598  
rapidly rotating nuclei, semiclassical HF description, smooth quantal corrections, density and total energy 0-32171  
rotational band approach, pure zero-rank operators 0-47341  
Schwinger boson representation, quantised rotator 0-18164  
transitional nuclei, particle-rotor recoil term and pairing interaction, Fermi surface 0-32174  
wobbling motion at high spin, microscopic model in small oscillation approx. 0-22666  
yrast-band of odd nuclei 0-22651  
(n, $\gamma$ ), interacting boson and Nilsson model tests, Pt-Os transition region 0-37380  
 $^{232}Th(\alpha,\alpha')$ , coupled channel Born anal. of deformation correl 0-5149  
 $^A$ , A=105,107, positive parity band, mixing and branching ratios lifetimes from ( $^{16}O,2np$ )( $^{14}N,3n$ ) 0-9197  
 $^{197}Au(p,X)^{149}Tb$ , target fragmentation momentum transfer, collective tube model, collectivity effects 0-37359  
 $^{76}Br$ , Coriolis distorted bands, common  $g_{9/2}$  parentage in N=41 nuclei 0-13349  
CC  $^{158}Dy$  high spin states B(E2) values, IBA model test from  $^{26}Ng(^{136}Xe,4n)$  CC  $^{158}Dy$  high spin states B(E2) values, IBA model test 0-27541  
 $^{110}Cd$ , A=113, 115 from  $^{113,115}Ag$   $\beta$ -decay 0-47432  
 $^{110}Cd$ , collective excitations in the interacting boson model (*Russian*) 0-5044  
 $^A$ , A=151, 152, 153, 154, 155, excited states of transitional region nuclei, rot. bands (*Russian*) 0-52556  
 $^A$ , A=152, 154, 156, 158, excited states of transitional region nuclei, rot. bands (*Russian*) 0-52556  
 $^A$ , A=198, 200, rigid asymmetric rotor model descript., E2 and E4 props. 0-13403  
Kr even isotopes, collective levels and B(E2) values, IBA calcs. 0-27539  
 $^A$ , A=74-82, even-even isotopes, B(E2) values and collectivity, interacting boson approx. 0-27537  
 $^A$ , A=186, 188, 190, 192, rigid asymmetric rotor model descript., E2 and E4 props. 0-13403  
 $^{190}Os$ , collective states and static quadrupole moment, boson expansion theory 0-47346  
Os(t,p), 17 MeV, two neutron transfer strength, O(6) limiting symmetry in IBA, Pt comparison 0-32287  
Pd, even isotopes, low lying collective states, IBA 0-27540  
 $^A$ , A=106, 108, collective excitations in the interacting boson model (*Russian*) 0-5044  
 $^{149}Pm$  high spin states and bands, rot. description and in-beam study from  $^{150}Nd(p,2n\gamma)$  0-32153



**nuclear collective model continued**

- Pt, even mass, ground and gamma band EM transition rates, asymmetric rotor model 0-32231  
<sup>196</sup>Pt, A=192, 194, 196, rigid asymmetric rotor model descript., E2 and E4 props. 0-13403  
<sup>190</sup>Pt, collective excitations in the interacting boson model (*Russian*) 0-5044  
<sup>196</sup>Pt, collective states and static quadrupole moment, boson expansion theory 0-47346  
<sup>196</sup>Pt, O(6) symmetry of interacting boson approx. model in shape transition 0-27550  
Pt(t,p), 17 MeV, two neutron transfer strength, O(6) limiting symmetry in IBA, Os comparison 0-32287  
<sup>186</sup>Re, A=181, 182, 187, spin polarisation, state struct. and mag. moments in rot. model 0-18194  
Ru, even isotopes, low lying collective states, IBA 0-27540  
<sup>78</sup>Se, collective excitations in the interacting boson model (*Russian*) 0-5044  
Sm isotopes, shape transition, s-d IBA model Hamiltonian struct. 0-32173  
<sup>148</sup>Sm, A=148, 150, 152, 154, 156, excited states of transitional region nuclei, rot. bands (*Russian*) 0-52556  
Sn isotopes, relation between interacting boson approx. and quasiparticle formalism 0-32216  
<sup>177</sup>Ta spin polarisation, state struct. and mag. moments in rot. model 0-18194  
<sup>180</sup>U( $\alpha$ ,  $\alpha'$ ), A=234, 236, 238, coupled channel Born anal. of deformation correl 0-5149  
<sup>180</sup>W, A=184, 186, rigid asymmetric rotor model descript., E2 and E4 props. 0-13403  
<sup>167</sup>Yb  $i_{13/2}$  band, spin alignment in the particle-rotor and cranking models 0-42536

**nuclear collective motion see nuclear collective model****nuclear collective states and giant resonances**

see also isobaric analogue resonances

- 1p nuclei, M2 giant resonance calcs. from (e,e'), ( $\pi^-$ ,  $\gamma$ ), ( $\mu^-$ ,  $\nu$ ) 0-22784  
A=19-31 odd nuclei,  $K^\pi=1/2^-$  bands, spectroscopic factors and transitions 0-32151  
A=24-60, yrast lines using Strutinsky method, empirical fusion bands 0-42514  
A=40-56, spectroscopy props. using pure configuration shell model (*Chinese*) 0-42584  
A=40-80, yrast props. and high spin isomers, cranking plus Strutinsky formalism 0-32152  
A=4-16, monopole giant resonances, state density radii and compressibility using hyperspherical functions (*Russian*) 0-27615  
A=60-80 even-even nuclei, collective motions and band structs. 0-9202  
A $\leq$ 28, giant quadrupole resonance, E2 intensity distrib., from ( $\alpha$ ,  $\alpha'$ ), DWBA anal. (*Hungarian*) 0-52642  
A $\sim$ 150 transitional region, collective props., interacting boson model 0-27538  
actinide nuclei, photo- and electro-fission cross sections and yields, giant resonances 0-5187  
adiabatic collective motion, quantum Hamiltonian microscopic derivation 0-47345  
angular momentum depend. cranked HFB inertia parameter, high spin states 0-42524  
asymmetric rotator, yrast states, wobbling freq., boson representation 0-32167  
atomic negative meson capture, nuclear giant resonance excitation (*Russian*) 0-42623  
backbenders, rot. energy expressions and least squares fitting 0-27531  
band level staggering in doubly-odd nuclei, evidence for predicted phase change 0-32144  
band structures, generalised HFB approach in intrinsic frame of reference, equilib. deformation 0-22664  
band structures, generalised HFB approach in SU(3) framework 0-22663  
coherent rot. states, quantum flow pattern and vortex struct. 0-22656  
coherent rotational states formed in heavy ion collisions,  $\gamma$ -decay 0-27657  
collective angular momentum in classical mechanics 0-4516  
collective excitations from high-q electron scatt., RPA AND ATDMF calcs. 0-22673  
collective mass parameter, super-normal phase transition effect 0-5046  
collective modes in fission and deep inelastic scatt., ang. momenta equilib. statistical treatment 0-42688  
collective motion, gauge invariant periodic TDHF eigenstates 0-27532  
collective path curvature as collectivity meas., quasi-boson approx. validity 0-22658  
collective rotation, quantisation, Schwinger boson representation 0-18164  
collective structure inferred from heavy ion Coulomb excitation 0-5167  
complex cascade processes decay law, high spin state mean lifetime corrections (*Chinese*) 0-22761  
conference on interacting bosons in nuclear physics, Erice, Italy (June '78) 0-27042  
conference on neutron capture gamma ray spectroscopy, Upton, USA. (Sep. '78) 0-36780  
conference on nuclear interactions, Canberra, Australia (Aug.-Sep. 1978) 0-4476  
conference on nuclear physics with EM interactions, Mainz, Germany (June 1979) 0-22145  
Coulomb effect in rotating nuclei in the Thomas-Fermi approach 0-47355  
coupled rotational bands in even-even nuclei, model 0-27529  
deep inelastic processes, large scale collective motion in nuclear matter 0-5087  
deformed nuclei, bandcrossing in  $K \neq 0$  bands, odd-A rare earths 0-5045  
deformed rare earth nuclei, bandcrossing in  $K \neq 0$  bands, backbending 0-9204  
dipole resonance, even-even deformed nuclei, quasiparticle-phonon nuclear model (*Russian*) 0-52641  
dipole sum rule schematical eval., collective isovector quadrupole strength 0-47428  
E1-giant dipole resonance, strength function pygmy anomaly, nonstatistical background coupling 0-37358  
EM sum rules for ( $\gamma$ ,  $\gamma$ ), (e,e), transitions and giant resonances 0-5090  
even actinides, lowest  $0^+$  state excitation, collective phonon state, spectroscopic factors from (p,t), (t,p) 0-13410  
even actinides, two-nucleon transfer, first  $0^+$  collective state excitation, spectroscopic factor (*Russian*) 0-42530

**nuclear collective states and giant resonances continued**

- even-even deformed nuclei, collective  $K^\pi=0^+$  states, realistic boson expansion comparison 0-5043  
even-even nuclei, low lying collective states from p-n interacting boson model 0-32158  
even-even nuclei,  $z=6$  to 100, probable members of quasi-bands in spherical and deformed regions 0-13357  
even-even nuclei with A $\approx$ 150, excited states calculation, phenomenological models: band-mixing, vibrational-rotational and interacting-boson model 0-22653  
excited nuclei, self-consistent theory of giant dipole resonance, thermodynamic RPA (*Russian*) 0-5106  
excited simple and yrast states, mag. moments, transient mag. fields 0-5064  
fission, isobaric widths, frozen quantal fluctuations, charge equilibration 0-37365  
giant dipole resonance, particle-hole calcs., M1 strength 0-22785  
giant isovector monopole states, isospin splitting and mixing 0-27609  
giant multiple resonances, excitation strength functions 0-5037  
giant multipole resonances, Regge poles and collective model 0-13436  
giant resonances, electric monopole and dipole vibrations, TDHF equations, fluid dynamical Lagrangian 0-47447  
Griffin-Hill-Wheeler spaces, 1- and 2-conjugate parameter generator states, giant resonances and scatt. 0-42618  
ground state deformation energy, rot. band inertial parameter depend. 0-18185  
group theoretical advances in collective motion anal. 0-9201  
heavy ion collisions, charge equilibrium model using collective high freq. mode and quantal master eqn. 0-27667  
heavy ion collisions, collective effects rel. to pion prod. 0-37392  
heavy ion large-angle scatt., inelastic cross-section and collective state excitation 0-52690  
heavy ion scattering, angle depend. phase shifts, coupled channel formalism 0-18253  
high angular momentum fusion compound nucleus deexcitation, high spin states, rare earths 0-9259  
high spin state studies, (n, $\gamma$ ) and heavy ion reaction complementarity 0-37381  
high spin states and band coupling, theory and heavy ion expts. (*Russian*) 0-18160  
high-spin selectivity of heavy-ion compound reactions 0-5048  
high-spin states and shell struct. in N=Z nuclei, <sup>20</sup>Ne appl. 0-47342  
 $i_{13/2}$  shell, particle-rotor model soln., backbending, transition rates, ang. momentum spread 0-47344  
interacting boson model of collective state, O(6) limit 0-32214  
interacting boson model, collective motion descript., shell model test 0-27542  
interacting boson model, collective state description, shell model connection 0-37341  
interacting boson model for collective states, present status 0-27573  
interacting boson model for collective states in even even nuclei 0-22715  
isobar propagation and collective effects, pion-nucleus and photonuclear investigation 0-22676  
isobaric distributions in deep inelastic reactions, collective model and independent particle model 0-18270  
isoscalar dipole strength excitation in GQR region by inelastic electron and hadron scatt. 0-47448  
isoscalar giant electric resonances, excitation and decay 0-5108  
isovector pairing collective motions and transition rates, projected BCS solns., generator coordinate simplification 0-22654  
large amplitude collective motion, collective subspaces and generator coordinate method 0-9199  
large amplitude collective motion, semiclassical approach, degenerate shell model appl. 0-27535  
large deformations and dissipation in a random-matrix model approach for fission or colliding nuclei 0-18162  
large amplitude collective motion, field theory, excitation energies 0-22665  
large scale collective motion in very heavy ion reactions, macroscopic description 0-5049  
large-amplitude collective nuclear motion in fission and heavy ion reactions 0-22675  
light heavy ion induced fusion, cross sections and yrast line limitations 0-5192  
liquid drop model description (*French*) 0-22669  
many body effective interaction theory problem, comparison with atoms 0-47406  
medium nuclei, photoproton spectra and preequilib. decay, microscopic theory 0-47464  
N=82-86, high spin isomers, gamma spectroscopy 0-47358  
neutron induced yrast isomer prod., pulsed beam meas. using plastic scintillation spectrum 0-27871  
neutron pickup reactions to ( $i_{13/2}$ )<sup>2</sup> bands, theoretical rot. signatures, backbending 0-52558  
nuclear field theory treatment of the interacting boson model 0-27577  
nuclear inertia for excited states, adiabatic cranking model calcs. 0-9216  
octupole resonance, even-even deformed nuclei, quasiparticle-phonon nuclear model (*Russian*) 0-52641  
particle rotor model study of transitional N=89 and N=91-95 nuclei 0-42529  
photonuclear reactions review, giant dipole resonances and cross sections 0-5125  
polarised nucleus fission, parity nonconservation mechanism, rot. state mixing (*Russian*) 0-37408  
potential model, energy dissipation heavy ions reactions 0-22849  
pre-actinide nuclei, level density and fission probability collective effects (*Russian*) 0-13455  
pseudomagic nuclei, yrast bands, variable moment of inertia model 0-449  
quadrupole resonance, even-even deformed nuclei, quasiparticle-phonon nuclear model (*Russian*) 0-52641  
quadrupole strength, giant quadrupole resonance 0-52575  
quasiparticle spectra near the yrast line 0-453  
radiative strength distrib. with energy, E1, M1 giant resonances, particle-hole calcs. 0-37349  
rapidly rotating nuclei, high spin rot. including shell fluctuations, semiclassical description 0-47348  
rapidly rotating nuclei, semiclassical HF description, smooth quantal corrections, density and total energy 0-32171  
rare earth nuclei, high spin states from (HI, xn) reactions, discrete  $\gamma$ -transitions 0-5050



**nuclear collective states and giant resonances continued**

- rotating nuclei, critical ang. momentum and equilibrium figures from ellipsoid, liquid drop model (*Russian*) 0-37339
- rotating nuclei, M1 and E1 transitions within and between bands, cranking model 0-494
- rotational band approach, pure zero-rank operators 0-47341
- rotational band termination, shell model calcs. in sd shell 0-32145
- RPA, for open shell nuclei by seniority and reduced isospin projections 0-47415
- semi-infinite nuclear medium, kinetic energy density, simple approx., giant monopole resonance 0-32222
- spherical nuclei, dipole states, transition densities and electroexcitation, GDR form factors (*Russian*) 0-52611
- spherical nuclei, giant monopole resonance transition densities, dynamical Thomas-Fermi theory 0-9278
- spin giant resonance and core polarization effects, coupling term effects (*Chinese*) 0-47450
- strongly deformed nuclei, shortlived states, g-factor meas. method 0-52577
- superheavy elements, collective motion, stability and prod. in heavy ion collisions 0-18169
- three parameter rotational formula, physical meaning, rot. and vibr. limits 0-18157
- transitional nuclei, pairing rotations and quadrupole modes, dynamical interplay 0-18165
- transitional nuclei, rotation along axis of symmetry 0-448
- transitional nuclei, single particle and collective degrees of freedom coupling (*Russian*) 0-13345
- two rotation regimes, cranked harmonic oscillator soln. 0-22657
- very high spin states from liquid drop model 0-5047
- volume and surface vibr. relations, quantum hydrodynamics 0-9227
- wobbling motion at high spin, microscopic model in small oscillation approx. 0-22666
- yrast and statistical cascades, M1 radiation after (MI, XN) reactions 0-42583
- yrast band, backbending, canonical formalism (*French*) 0-52555
- yrast traps, obs. in heavy ion collisions 0-37319
- yrast-band of odd nuclei 0-22651
- ( $\alpha, X$ ), isoscalar giant quadrupole resonance decay props. 0-22792
- ( $\alpha, \gamma$ ), direct and resonance capture, giant dipole and quadrupole resonances 0-37385
- (e,e), low-q, A=14 nuclei, isospin T=2, 1 and 0 collective resonances, shell model 0-510
- ( $\gamma, X$ ), A=14 nuclei, isospin T=2, 1 and 0 collective resonances, shell model 0-510
- (n, $\gamma$ ), direct and resonance capture, giant dipole and quadrupole resonances 0-37385
- (n, $\gamma$ ), E1 and M1 strength functions, A- and energy-depend., giant dipole resonances 0-37348
- (n, $\gamma$ ), Fast n, gamma rays in giant dipole region, review 0-37351
- (p,d), 52 MeV, deeply bound hole state transition strength giant resonance, DWBA anal. 0-47426
- (p, $\gamma$ ), direct and resonance capture, giant dipole and quadrupole resonances 0-37385
- pp scattering, dibaryon resonance behaviour, nonadiabatic rotational bands in light nuclei 0-13353
- ( $\pi, \gamma$ ), A=14 nuclei, isospin T=2, 1 and 0 collective resonances, shell model 0-510
- ( $\pi, \pi$ ), collective transitions, giant resonances, isospin content and spin transfer 0-42580
- ( $\pi, X$ ) slow pion capture in deformed nuclei, effects on high spin state excitation 0-18345
- <sup>208</sup>(N, $\gamma$ ), pol. N, anal. power and giant multipole resonances, direct-semidirect model 0-18265
- <sup>A</sup>Ag, A=105,107, positive parity band, mixing and branching ratios lifetimes from (<sup>16</sup>O,2np)(<sup>14</sup>N,3n) 0-9197
- <sup>107</sup>Ag high spin states, J<sup>\*</sup> assignments, polarisations and transitions from (<sup>7</sup>Li,4n $\gamma$ ), (<sup>6</sup>Li,3n $\gamma$ ) 0-27536
- <sup>38</sup>Ar high spin state density,  $\gamma$ -decay mode, deformed states from <sup>35</sup>Cl( $\alpha, \pi \gamma$ ) 0-32168
- <sup>40</sup>Ar( $\gamma$ , xp yn), 9-29 MeV, cross sections in giant resonance region, particle decay modes 0-13462
- <sup>212</sup>At high spin states, decay, g factor, J<sup>\*</sup> assignments, level energies from <sup>208</sup>Pb(<sup>7</sup>Li,3n) 0-5042
- <sup>A</sup>Au, A=189, 191, 193, high spin states and transitions, isomeric states from Ir( $\alpha, n \gamma$ ) 0-5038
- <sup>A</sup>Au A=190, 192, 194, levels, J<sup>\*</sup>, isomers and rot, aligned bands from Ir( $\alpha, n$ ) 0-9215
- <sup>197</sup>Au(<sup>13</sup>Xe,X), damped collisions, charge distrib. second moments and giant E1 quantal fluctuations 0-27547
- <sup>1</sup>B( $\gamma, n \gamma$ ) 30 MeV giant dipole resonance decay, <sup>10</sup>B transitions (*Russian*) 0-13433
- <sup>126</sup>Ba backbending, shell model calc., pair realignment and Coriolis antipairing 0-32164
- <sup>9</sup>Be deformed nucleus, continuum states in strong coupling model 0-22682
- <sup>76</sup>Br, Coriolis distorted bands, common g<sub>9/2</sub> parentage in N=41 nuclei 0-13349
- <sup>77</sup>Br collective bands, lifetimes, spins and E2 transition probabilities from <sup>64</sup>Ni(<sup>16</sup>O, 2n $\gamma$ ) 0-13415
- CC <sup>158</sup>Dy high spin states B(E2) values, IBA model test from <sup>26</sup>Ng(<sup>136</sup>Xe, 4n) CC <sup>158</sup>Dy high spin states B(E2) values, IBA model test 0-27541
- <sup>12</sup>C, isoscalar giant quadrupole resonances, RPA calcs., E2 strength fragmentation, spectroscopic factors 0-13437
- <sup>12</sup>C p<sub>0</sub> channel E2 strength from <sup>11</sup>B(p, $\gamma$ ) pol p. 0-22790
- <sup>12</sup>C(<sup>6</sup>Li,<sup>3</sup>Li), 153 MeV, isoscalar giant quadrupole resonances 0-13440
- <sup>12</sup>C(e,e), 180° scatt., transverse inelastic form factors and spectra, collective 2<sup>+</sup> state 0-9261
- <sup>12</sup>C(p,p')<sup>12</sup>C\*, pol. p., 19-23 MeV, giant resonances as doorway states, virtual excitation 0-5102
- <sup>12</sup>C( $\pi^-$ ,  $\gamma$ )<sup>12</sup>B\*, excitation of collective states, shell model 0-22652
- <sup>13</sup>C, giant quadrupole resonance blocking mechanism 0-13437
- <sup>13</sup>C, photoexcited giant dipole resonance, continuum shell model anal. 0-18266
- <sup>13</sup>C( $\pi^+$ ,  $\pi^-$ ), near  $\pi$ N (3,3) resonance, 180 MeV, collective states and cross sections 0-13507
- <sup>A</sup>Ca(<sup>6</sup>Li,<sup>6</sup>Li), A=40, 44, 48, 153 MeV, isoscalar giant quadrupole resonances 0-13440
- <sup>40</sup>Ca ( $\alpha, \alpha'$ ), 104 MeV, giant resonance ang. distrib., L-transfer contribs. 0-27610

**nuclear collective states and giant resonances continued**

- <sup>40</sup>Ca, giant isoscalar monopole state energies in generator coordinate method 0-37317
- <sup>40</sup>Ca, monopole vibration damping, TDHF calcs. 0-22667
- <sup>40</sup>Ca(<sup>16</sup>O,<sup>16</sup>O), rot. band of molecular resonances, generator coordinate model 0-13428
- <sup>40</sup>Ca(<sup>40</sup>Ca,X), 400 MeV, fragment energy spectra struct., giant resonances, direct process 0-47452
- <sup>40</sup>Ca( $\alpha, \alpha'$ ), 6-18 MeV, resonances, anomalous large angle scatt. and quasi-molecular states 0-27613
- <sup>40</sup>Ca( $\alpha, \alpha'$ ), giant isoscalar quadrupole resonance,  $\alpha$ -over p-decay ratio, SU(3) and shell model 0-27608
- <sup>41</sup>Ca giant dipole resonance, isospin struct., direct-semidirect anal. from <sup>40</sup>K(p, $\gamma$ ) 0-47449
- <sup>42</sup>Ca high spin state density,  $\gamma$ -decay mode, deformed states from <sup>39</sup>K( $\alpha, \pi \gamma$ ) 0-32168
- <sup>A</sup>Cd, A=107, 109, 111, from Pd( $\alpha, 3n \gamma$ )Cd, high spin states obs. 0-450
- <sup>110</sup>Cd, collective excitations in the interacting boson model (*Russian*) 0-5044
- <sup>135</sup>Ce, yrast cascade dipole component from <sup>122</sup>Sn(<sup>16</sup>O,4n) 0-9266
- <sup>250</sup>Cf(d,d'), 15 MeV, vibr. states, J<sup>\*</sup> and reduced transition probabilities 0-47351
- <sup>A</sup>Cm, A=246,248, fission isomer rot. spectra I<sup>2</sup>(I+1)<sup>2</sup> correction 0-18229
- <sup>48</sup>Cr high spin states, yrast levels and 6<sup>+</sup> isomeric state from <sup>40</sup>Ca(<sup>10</sup>B,np) 0-454
- <sup>51</sup>Cr, bands, levels, EM transitions, J<sup>\*</sup>, branching and mixing ratios from <sup>48</sup>Ti( $\gamma, n \gamma$ )<sup>51</sup>Cr and <sup>51</sup>V(p, $\pi \gamma$ )<sup>51</sup>Cr 0-52606
- <sup>52</sup>Cr high spin states, transitions and J<sup>\*</sup> values from <sup>50</sup>Ti( $\alpha, 2n \gamma$ ) 0-455
- <sup>52</sup>Cr( $\alpha, \alpha'$ ), 8-18 MeV, cross sections, search for giant dipole resonance 0-9281
- Dy even isotopes, aligned Stockholm band intrinsic spin I<sub>0</sub><sup>eff</sup> 0-13363
- <sup>A</sup>Dy, (A=151,152), high spin yrast states,  $\gamma$ -ray polarisation in (<sup>32</sup>S,n) reactions 0-497
- <sup>148</sup>Dy, p single particle states and pairing force calcs., high spin states 0-42522
- <sup>151</sup>Dy levels, bands and transitions, in-beam  $\gamma$ -rays from <sup>142</sup>Nd(<sup>12</sup>C,3n $\gamma$ ) 0-458
- <sup>152</sup>Dy, collective bands and absence of yrast traps 0-9207
- <sup>152</sup>Dy high spin isomeric states, g-factors from <sup>140</sup>Ce(<sup>16</sup>O, 4n) 0-13377
- <sup>152</sup>Dy high spin isomers, yrast states and level lifetimes from (<sup>15</sup>N, 4n), (<sup>16</sup>O, 4n) 0-13361
- <sup>152</sup>Dy high spin struct., in beam  $\gamma$  meas. from (<sup>15</sup>N, 4n), (<sup>16</sup>O, 4n) 0-18179
- <sup>152</sup>Dy, rotation along axis of symmetry 0-448
- <sup>152</sup>Dy yrast continuum  $\gamma$ -ray multipolarity via polarisation meas. from <sup>140</sup>Ce(<sup>16</sup>O,4n) 0-9264
- <sup>152</sup>Dy yrast traps, isomers and oblate deformations from <sup>124</sup>Te(<sup>32</sup>S, 4n) 0-13362
- <sup>153</sup>Dy, populated in <sup>153</sup>Ho  $\beta$ -decay, lower excited states 0-22765
- <sup>156</sup>Dy high spin states,  $\gamma$ -ang. distrib., lifetimes and feeding times from <sup>148</sup>Nd(<sup>13</sup>C, 5n) 0-13364
- <sup>156</sup>Dy high spin states lifetimes and feeding times, quadrupole moments from <sup>24</sup>Mg(<sup>136</sup>Xe,4n) 0-32239
- <sup>162</sup>Dy(<sup>136</sup>Xe,<sup>136</sup>Xe'), 547, 612 MeV, high spin state energies and reduced transition probabilities 0-18232
- <sup>164</sup>Dy multipole mixing in  $\gamma$  to ground bands from <sup>163</sup>Dy(n, $\gamma$ ) 0-52615
- Er even isotopes, aligned Stockholm band intrinsic spin I<sub>0</sub><sup>eff</sup> 0-13363
- Er yrast levels, spin alignment, populated by preequilibrium ( $\alpha, n \gamma$ ) reactions 0-52557
- <sup>A</sup>Er, (A=154,155), rotational struct. at high spins 0-457
- <sup>A</sup>Er (A=156,157,158), high spin yrast states,  $\gamma$ -ray polarisation in (<sup>32</sup>S,n) reactions 0-497
- <sup>A</sup>Er, A=156, 164, aligned positive parity bands from rot. aligned model 0-9209
- <sup>153</sup>Er 360 ns yrast trap,  $\gamma$  transitions and lifetimes from <sup>144</sup>Sm(<sup>12</sup>C,3n) 0-9205
- <sup>154</sup>Er, collective bands and absence of yrast traps 0-9207
- <sup>154</sup>Er yrast trap and transitions, decay scheme from (<sup>64</sup>Ni,4n), (<sup>16</sup>O,4n) 0-9206
- <sup>160</sup>Er high spin yrast states and transitions from <sup>152</sup>Sm(<sup>13</sup>C,5n) 0-9208
- <sup>Er</sup> deformed nucleus, excited rot. bands, selfconsistent HFB treatment 0-42515
- <sup>164</sup>Er rot. states, HF and HFB self consistent calc. with Skyrme interaction 0-22662
- <sup>A</sup>Eu, A=151, 152, 153, 154, 155, excited states of transitional region nuclei, rot. bands (*Russian*) 0-52556
- <sup>145</sup>Eu high spin and isomeric states, transitions, weak coupling from <sup>144</sup>Sm( $\alpha, 2n \gamma$ ) 0-13348
- <sup>145</sup>Eu high spin core coupled states and transitions from <sup>142</sup>Nd(<sup>6</sup>Li, 3n $\gamma$ ) 0-42520
- <sup>145</sup>Eu high spin states, J<sup>\*</sup> and transitions from (<sup>7</sup>Li,4n $\gamma$ ) and (<sup>6</sup>Li,3n $\gamma$ ) 0-47350
- <sup>154</sup>Eu(p,p'), 12 MeV, ground band rot. states, deformation parameters, coupled channels anal. 0-9195
- <sup>19</sup>F final state selective population, triton clustering from band anal. from (<sup>7</sup>Li,t), (<sup>6</sup>Li,<sup>3</sup>He) 0-9306
- <sup>19</sup>F low lying band state lifetimes, stopping power, transition strengths from <sup>15</sup>N( $\alpha, \gamma$ ) 0-42585
- <sup>A</sup>Fe, A=54-56, high spin states, energy levels, spectroscopic factors, EM props., shell model 0-47359
- <sup>A</sup>Fe( $\alpha, \alpha'$ ), A=54,58, 8-18 MeV, cross sections, search for giant dipole resonance 0-9281
- <sup>54</sup>Fe high spin states, transitions and J<sup>\*</sup> values from <sup>52</sup>Cr( $\alpha, 2n \gamma$ ) 0-455
- <sup>54</sup>Fe( $\alpha, \alpha'$ ), coupled channels calc., capture cross section, GQR decay modes 0-27654
- <sup>54</sup>Fe(p,p'), 39, 62 MeV, DWBA anal., collective spectra, direct process contrib. (*Russian*) 0-13408
- <sup>A</sup>Gd, A=152, 154, 156, 158, excited states of transitional region nuclei, rot. bands (*Russian*) 0-52556
- <sup>146</sup>Gd, p single particle states and pairing force calcs., high spin states 0-42522
- <sup>147</sup>Gd<sup>m</sup> high spin yrast trap, oblate deformation and quadrupole moment 0-32157
- <sup>150</sup>Gd, collective bands and absence of yrast traps 0-9207
- <sup>150</sup>Gd, high spin states, pairing correlations and nuclear shape, HFB approach 0-42517
- <sup>154</sup>Gd multiphonon vibr. bands, dynamic deformation theory 0-5035
- <sup>68</sup>Ge multiple band struct., g<sub>9/2</sub> orbital, level lifetimes from <sup>58</sup>Ni(<sup>12</sup>C, 2p) 0-13358



## nuclear collective states and giant resonances continued

- <sup>69</sup>Ge high spin states, EM props., branching and mixing ratios from <sup>55</sup>Mn(<sup>16</sup>O,pn) 0-13347
- <sup>72</sup>Ge levels pop. in <sup>72</sup>Zn(<sup>6</sup>Li,pn), in beam gamma-ray spectroscopy 0-47343
- <sup>74</sup>Hf, A=166, 168, 170, 172, yrast states, quadrupole moments and B(E2) values, microscopic calcs. 0-32147
- <sup>74</sup>Hf(HI,xn), A=170-173, two and three quasiparticle isomers, rot. bands, decays and lifetimes 0-9211
- <sup>171</sup>Hf one- and three-quasiparticle states, high spin rot. bands from (<sup>16</sup>O,5n), (<sup>13</sup>C,4n) 0-18163
- <sup>172</sup>Hf yrast band and high spin states, 22<sup>+</sup>→20<sup>+</sup> transition, band crossing from <sup>160</sup>Gd(<sup>16</sup>O,4n) 0-42523
- <sup>173</sup>Hf multi-quasiparticle states and bands, isomeric states, lifetimes from <sup>170</sup>Er(<sup>6</sup>Be,4n) 0-9213
- <sup>180</sup>Hf band crossing and giant backbending 0-32156
- <sup>180</sup>Hg( $\alpha,\alpha'$ ), A=198, 200, 204, 16-27 MeV backward scatt., collective states 0-13365
- <sup>188</sup>Hg, HF calc., shape and lowest band struct., B(E2) values 0-32148
- <sup>123</sup>I, bands and decay props., core-particle coupling and polarisation effects 0-13354
- <sup>109</sup>In high spin states, transitions, isomeric state, negative parity bands from <sup>107</sup>Ag( $\alpha$ , 2n $\gamma$ ) 0-451
- <sup>185</sup>Ir levels excited in ( $\alpha$ ,xn) reactions, positive parity band 0-9231
- <sup>185</sup>Ir levels populated in <sup>185</sup>Pt<sup>m+g</sup> decay 0-9269
- Kr even isotopes, collective levels and B(E2) values, IBA calcs. 0-27539
- <sup>84</sup>Kr, A=74,76, rot. bands, band crossing and backbending 0-18176
- <sup>84</sup>Kr, A=74-82, even-even isotopes, B(E2) values and collectivity, interacting boson approx. 0-27537
- <sup>84</sup>Kr, A=76,78,80, yrast states and band struct., backbending from Zn(<sup>12</sup>C, 2n) 0-13359
- <sup>84</sup>Kr, A=78, 80, quasi- $\gamma$  bands and negative parity levels from Br(p,2n $\gamma$ ) 0-456
- <sup>78</sup>Kr band struct., level scheme, from  $\gamma\gamma$ -coincidence from <sup>65</sup>Cu(<sup>16</sup>O, 2np) 0-18177
- <sup>78</sup>Kr band structs., in-beam  $\gamma$ -rays from <sup>68</sup>Zn(<sup>12</sup>C, 2n) 0-22672
- <sup>78</sup>Kr high spin levels, bands and transitions, level lifetimes from <sup>68</sup>Zn(<sup>12</sup>C,2n) 0-42525
- <sup>78</sup>Kr high spin states, transitions and lifetimes from (<sup>16</sup>O,2np), (<sup>19</sup>F,2n $\alpha$ ), (<sup>16</sup>O,2n), (<sup>12</sup>C,2n) 0-27534
- <sup>24</sup>Mg, <sup>16</sup>O+ $\alpha$ + $\alpha$  cluster model, energy level structure 0-18215
- <sup>24</sup>Mg ( $\gamma$ ,p), 17-30 MeV, giant dipole resonances and transitions, shell effects (*Russian*) 0-13344
- <sup>24</sup>Mg continuum states, branching ratios from <sup>12</sup>C(<sup>16</sup>O,  $\alpha\alpha$ ) 0-22661
- <sup>24</sup>Mg giant isoscalar quadrupole fission/fusion doorway states from <sup>12</sup>C(<sup>12</sup>C, <sup>12</sup>C) 0-37410
- <sup>24</sup>Mg ground state band from <sup>12</sup>C(<sup>12</sup>C,X) 0-42727
- <sup>24</sup>Mg high spin selectivity, critical ang. momentum effects from <sup>10</sup>B(<sup>16</sup>O,d) 0-13366
- <sup>24</sup>Mg high spin states from selective compound reactions, stat. anal. from <sup>10</sup>B(<sup>16</sup>O,d) 0-18180
- <sup>24</sup>Mg, K<sup>+</sup>=0, K<sup>-</sup>=3<sup>-</sup> bands, radiative and  $\alpha$ -widths from ( $\alpha,\gamma$ ), (<sup>16</sup>O, $\alpha\gamma$ ) 0-18173
- <sup>24</sup>Mg low lying K-band from <sup>28</sup>Si  $\alpha$ -decay 0-47438
- <sup>24</sup>Mg rot. band termination, level lifetimes from <sup>12</sup>C(<sup>16</sup>O,  $\alpha$ ) 0-18174
- <sup>24</sup>Mg yrast and high spin states up to 24 MeV, ang. distrib. from <sup>10</sup>B(<sup>16</sup>O, d) 0-18175
- <sup>24</sup>Mg yrast line, Strutinsky type cranking calc., pairing correlation inclusion 0-13355
- <sup>24</sup>Mg(p,p'), 0.8 GeV, rot.,  $\gamma$  and  $\beta$  bands, ground state deformation, DWBA, coupled channels anal. 0-9198
- <sup>24</sup>Mg(p,p'), 20, 40, 800 MeV,  $\gamma$ -vibr. band, coupled channels anal. 0-9194
- <sup>24</sup>Mg(p,p'), 15 MeV, excitation functions 0-22825
- <sup>84</sup>Mo(<sup>He</sup>,He), A=92,94,96,98,100, 110 MeV, giant quadrupole resonance isotopic depend. 0-9282
- <sup>14</sup>N(<sup>6</sup>Li,<sup>6</sup>Li'), 153 MeV, isoscalar giant quadrupole resonances 0-13440
- <sup>14</sup>N( $\gamma$ ,n<sub>0</sub>) <sup>13</sup>N, 17 to 26 MeV, angular distrib., giant dipole resonance, single-particle nuclear model 0-52659
- <sup>145</sup>Nd from <sup>145</sup>Pr  $\beta$ -decay, low lying energy levels, quasi band description 0-5096
- <sup>150</sup>Nd(<sup>20</sup>Ne,X), 115, 130 MeV,  $\gamma$ -continuum multiplicity distrib., yrast bump 0-9265
- <sup>19</sup>Ne, final state selective population, triton clustering from band anal. from <sup>16</sup>Li(<sup>6</sup>Li,t) 0-9306
- <sup>20</sup>Ne continuum states, J<sup>+</sup> and branching from <sup>12</sup>C(<sup>12</sup>C,  $\alpha\alpha$ ) 0-22660
- <sup>20</sup>Ne E1 resonance from <sup>19</sup>F(p, $\gamma$ ) pol. p 0-22790
- <sup>20</sup>Ne high spin states, J<sup>+</sup> and  $\alpha$ -decay branching ratios from <sup>16</sup>O(<sup>12</sup>C,<sup>8</sup>Be) 0-18166
- <sup>20</sup>Ne high spin states, J<sup>+</sup> assignments from <sup>16</sup>O(<sup>6</sup>Li,d) 0-18167
- <sup>20</sup>Ne( $\gamma$ ,n) cross sections and giant resonance struct. 0-13441
- Ni giant resonances using virtual and real photons 0-22791
- <sup>8</sup>Ni(e,e'), 102 MeV, A=58,60, E1-E4 giant multipole resonance comparison, shell model anal. 0-42614
- <sup>58</sup>Ni, HFB and dynamic anal., collective motion, zero point energy correction 0-18161
- <sup>58</sup>Ni( $\alpha,\alpha'$ ), 150 MeV, c=charged particle, particle decay from isoscalar giant resonance region 0-13439
- <sup>60</sup>Ni( $\alpha,\alpha'$ ), 8-18 MeV, cross sections, search for giant dipole resonance 0-9281
- <sup>62</sup>Ni( $\gamma$ ,X), 19.2-26.2 MeV, photoneutron and photoproton spectra, giant dipole resonance-decay, isospin conservation 0-13443
- <sup>16</sup>O collective and giant multipole states, Brueckner RPA particle-hole state description 0-32169
- <sup>16</sup>O E1 and p<sub>1</sub> channel E2 strength from <sup>15</sup>N(p, $\gamma$ ) 0-22790
- <sup>16</sup>O, giant isoscalar monopole state energies in generator coordinate method 0-37317
- <sup>16</sup>O high spin states, J<sup>+</sup> and  $\alpha$ -decay branching ratios from <sup>12</sup>C(<sup>12</sup>C,<sup>8</sup>Be) 0-18166
- <sup>16</sup>O, isoscalar giant quadrupole resonances, RPA calcs., E2 strength fragmentation, spectroscopic factors 0-13437
- <sup>16</sup>O, monopole vibration damping, TDHF calcs. 0-22667
- <sup>16</sup>O(<sup>6</sup>Li,<sup>6</sup>Li'), 153 MeV, isoscalar giant quadrupole resonances 0-13440
- <sup>16</sup>O( $\alpha,\alpha'$ ), giant isoscalar quadrupole resonance,  $\alpha$ -over p-decay ratio, SU(3) and shell model 0-27608
- <sup>16</sup>O( $\gamma$ ,n), 25-45 MeV, isovector giant quadrupole resonance evidence, E2 cross section 0-18268
- <sup>10</sup>O(p,p'), 135 MeV, high spin particle-hole states, 4<sup>-</sup> states 0-9217
- <sup>10</sup>O( $\gamma$ ,n), 8.5-39.7 MeV, cross section, giant dipole and pygmy resonance decays 0-42619

## nuclear collective states and giant resonances continued

- <sup>18</sup>O( $\pi,\pi'$ ), 164 MeV, yrast state and level excitation, DWIA calcs., shell model context 0-42526
- <sup>190</sup>Os, collective states and static quadrupole moment, boson expansion theory 0-47346
- <sup>30</sup>P high spin two nucleon states decay props. from <sup>28</sup>Si( $\alpha$ , d $\gamma$ ) 0-13402
- <sup>208</sup>Pb( $\alpha,\alpha'$ ), A=204, 206, 208, 16-27 MeV backward scatt., collective states 0-13365
- <sup>205</sup>Pb multipole resonance E1-E2 and E1-M1 interference from <sup>206</sup>Pb( $\gamma$ ,n) 0-32251
- <sup>208</sup>Pb ( $\alpha,\alpha'$ ), 100-172 MeV, giant monopole resonance evidence from strong energy depend. 0-13432
- <sup>208</sup>Pb core with valence nucleon or hole, mag. props., exchange currents, electron scatt. 0-22689
- <sup>208</sup>Pb, isoscalar giant multipole resonances, simple macroscopic model, damping mechanisms 0-42617
- <sup>208</sup>Pb isoscalar giant reson., decay scheme 0-9277
- <sup>208</sup>Pb(<sup>16</sup>O,<sup>16</sup>O'), 315 MeV, continuous spectrum and giant resonance excitation, coherent state model test 0-32252
- <sup>208</sup>Pb( $\alpha,\alpha'$ ), 65 MeV, inclusive reaction, giant resonance background, heavy ion model anal. 0-5150
- <sup>208</sup>Pb( $\alpha,\alpha'$ ), 172 MeV, strongly excited giant monopole resonance 0-18273
- <sup>208</sup>Pb(e,e'), E2 transitions of fragmented isoscalar quadrupole giant resonance 0-22758
- <sup>208</sup>Pb(e,e'), giant multipole resonance excitation, particle-hole interaction 0-22789
- <sup>208</sup>Pb(p,p'), 39, 62 MeV, DWBA anal., collective spectra, direct process contrib. (*Russian*) 0-13408
- Pd, even isotopes, low lying collective states, IBA 0-27540
- <sup>140</sup>Pd, A=106, 108, collective excitations in the interacting boson model (*Russian*) 0-5044
- <sup>143</sup>Pm high spin states, J<sup>+</sup>, transitions, isomer g-factors from (d,2N), ( $\alpha$ ,2N) 0-32154
- <sup>149</sup>Pm high spin states and bands, rot. description and in-beam study from <sup>150</sup>Nd(p,2n $\gamma$ ) 0-32153
- Pt, even mass, ground and gamma band EM transition rates, asymmetric rotor model 0-32231
- <sup>190</sup>Pt, collective excitations in the interacting boson model (*Russian*) 0-5044
- <sup>196</sup>Pt, collective states and static quadrupole moment, boson expansion theory 0-47346
- <sup>196</sup>Pt negative parity states in partially decoupled bands,  $\gamma$ -transitions from <sup>195</sup>Pt(n, $\gamma$ ) 0-47360
- <sup>238</sup>Pu, A=238,240, fission isomer rot. spectra I<sup>2</sup>(1+1)<sup>2</sup> correction 0-18229
- <sup>223</sup>Ra rotational band level diagram from  $\alpha$ -decay and conversion electrons 0-18156
- <sup>83</sup>Rb high spin states, positive and negative parity bands from (<sup>6</sup>Li, 3n), ( $\alpha$ , 2n) 0-18178
- <sup>210</sup>Rn high spin states, decay and lifetimes, spin assignments from <sup>204</sup>Pb(<sup>6</sup>Be,3n) 0-18168
- Ru, even isotopes, low lying collective states, IBA 0-27540
- <sup>84</sup>Ru(p,p'), A=96, 98, 5-8 MeV, level schemes, transitions, vibr. state, mixing ratios 0-18199
- <sup>97</sup>Ru populated in <sup>88</sup>Sr(<sup>13</sup>C, 3n $\gamma$ ), band-like structures 0-32146
- Sb isomer ratio, high spin trapping from ( $\alpha$ ,xn)( $\alpha$ , pn) 0-22655
- <sup>74</sup>Se, collective excitations in the interacting boson model (*Russian*) 0-5044
- <sup>74</sup>Se quasi- $\gamma$  bands and negative parity levels from <sup>75</sup>As(p,2n $\gamma$ ) 0-456
- <sup>79</sup>Se high spin levels, transitions, J<sup>+</sup> assignments from <sup>76</sup>Ge( $\alpha$ ,n $\gamma$ ) 0-459
- <sup>28</sup>Si 8<sup>+</sup> state, level systematics and energy spectra from <sup>25</sup>Mg(<sup>12</sup>C,<sup>9</sup>Be) 0-42528
- <sup>28</sup>Si, isoscalar giant quadrupole resonances, RPA calcs., E2 strength fragmentation, spectroscopic factors 0-13437
- <sup>28</sup>Si( $\alpha,\alpha'$ ), c=charged particle, 150 MeV, isoscalar giant quadrupole resonance struct. 0-13438
- <sup>28</sup>Si( $\gamma$ , p), 18.1-29 MeV, giant dipole resonance, contrib. from various configs. 0-18264
- <sup>8</sup>Sm, A=148, 150, 152, 154, 156, excited states of transitional region nuclei, rot. bands (*Russian*) 0-52556
- <sup>144</sup>Sm, p single particle states and pairing force calcs., high spin states 0-42522
- <sup>154</sup>Sm giant multipole resonance fragmentation among two-phonon states 0-18260
- <sup>154</sup>Sm(p,p'), 35 MeV, ground state rot. band and multipole moment 0-32178
- Sn, deep h-l state fragmentation, strength functions, giant resonances, quasiparticle phonon model 0-37320
- <sup>8</sup>Sn(p,p'), A=115, 117, 119, 18 MeV, state spin assignment, particle-vibr. coupling 0-32160
- <sup>116</sup>Sn(<sup>16</sup>O,<sup>16</sup>O), 48 MeV, collective states, E2, E0 transition probabilities, half-life, branching ratios 0-18172
- <sup>118</sup>Sn(<sup>6</sup>Li,<sup>6</sup>Li'), 153 MeV, isoscalar giant quadrupole resonances 0-13440
- <sup>119</sup>Sn( $\gamma$ ,n), giant mag. dipole resonance location, photoneutron polarisation method 0-37357
- Sn( $\alpha$ ,3n), 16-38 MeV, Te isomer ratio, high spin trapping 0-22655
- <sup>83</sup>Sr high spin states, J<sup>+</sup> and de-excitation from Kr( $\alpha$ ,xn) 0-42516
- <sup>84</sup>Sr quasi- $\gamma$  bands and negative parity levels from <sup>85</sup>Rb(p,2n $\gamma$ ) 0-456
- <sup>4</sup>Ta, A=147, 148, high spin particle-hole states, octupole M2/E3 isomers from <sup>151</sup>Eu( $\alpha$ ,xn) 0-18171
- <sup>149</sup>Tb, high spin states obs. 0-18158
- <sup>95</sup>Tc, energy levels from <sup>95</sup>Mo(p, n $\gamma$ )<sup>95</sup>Tc 0-37372
- <sup>96</sup>Tc, high spin states,  $\gamma$ -energy, intensity, coincidence, ang. distrib. and electron conversion from <sup>93</sup>Nb( $\alpha$ ,n) 0-52554
- Te isomer ratio, high spin trapping from Sn( $\alpha$ ,3n) 0-22655
- <sup>4</sup>Te, A=117, 119, 121, collective excitations, high spin states and transitions from ( $\alpha$ , Zn)(d, Zn)(<sup>3</sup>He, 3n) 0-13346
- <sup>132</sup>Te from fission, 10<sup>+</sup> isomeric state, J<sup>+</sup> from deexcitation pattern, half life 0-460
- <sup>231</sup>Th, rotational band level diagram from  $\alpha$ -decay and  $\gamma$ -transitions 0-18156
- <sup>232</sup>Th( $\alpha,\alpha'$ ), 120 MeV, isoscalar giant resonances, DWBA anal. 0-42621
- <sup>232</sup>Th(p,p'), 35 MeV, ground state rot. band and multipole moment 0-32178
- <sup>48</sup>Ti high spin states,  $\gamma$ -decay, J<sup>+</sup> assignments, lifetimes from <sup>45</sup>Sc( $\alpha$ ,p $\gamma$ ) 0-13356
- <sup>50</sup>Ti high spin states, transitions and J<sup>+</sup> values from <sup>48</sup>Ca( $\alpha$ ,Zn $\gamma$ ) 0-455
- <sup>50</sup>Ti( $\gamma$ ,X), photoneutron and photoproton cross sections, giant dipole resonance isospin splitting 0-13442
- <sup>192</sup>Tl high spin band struct. and transitions, isomeric state from <sup>181</sup>Ta(<sup>16</sup>O,xn $\gamma$ ) 0-47353



**nuclear collective states and giant resonances continued**

- <sup>194</sup>Tl high spin states, excitation functions,  $I^\pi = 8^-$  isomeric state from <sup>184</sup>Ta(<sup>16</sup>O,5n) 0-32163
- <sup>175</sup>Tm single proton states, rot. bands,  $J^\pi$  assignments from <sup>176</sup>Yb(t, $\alpha$ ), pol. t 0-452
- <sup>14</sup>U, A=236, 238, strength function of  $\beta$ -transitions, probability of delayed fission 0-22764
- <sup>14</sup>U, A=236,238, fission isomer rot. spectra  $I^2(I+1)^2$  correction 0-18229
- <sup>232</sup>U high spin states and ground state rot. band from <sup>232</sup>Th( $\alpha$ ,4n $\gamma$ ) 0-47349
- <sup>236</sup>U, giant E2 isoscalar resonance determ. 0-27607
- <sup>237</sup>U levels, bands and  $J^\pi$  assignments, n binding energy from <sup>236</sup>U(n, $\gamma$ ) 0-5041
- <sup>238</sup>U(e,e'), 87.5 MeV, deformed fissionable nucleus, giant multipole resonances and isovector states 0-42612
- <sup>238</sup>U(p,p'), 22 MeV, rot. band, multipole deformation parameters from coupled channel anal. 0-13369
- <sup>238</sup>U(p,p'), 35 MeV, ground state rot. band and multipole moment 0-32178
- <sup>14</sup>W, A=172-175, bands and backbending,  $i_{1/2}$  neutron decoupling from Dy(<sup>16</sup>O,xn) 0-9212
- <sup>14</sup>W, A=174, 175 quasicontinuum  $\gamma$ -rays yrast cascade dipole component, moment of inertia from Dy(<sup>16</sup>O, xn $\gamma$ ) 0-47424
- <sup>178</sup>W high spin states, yrast bands and backbending from <sup>170</sup>Er(<sup>12</sup>C,4n) 0-13352
- <sup>180</sup>W ground and K=2<sup>-</sup> octupole band ang. momenta coupling, lifetimes from <sup>181</sup>Ta(p,2n $\gamma$ ) 0-9214
- <sup>182</sup>W high spin states, J assignments and mixing ratios from <sup>182</sup>Re isomer decay 0-42593
- <sup>183</sup>W( $\alpha$ , $\alpha'$ ), 15 MeV, level and band Coulomb excitation, B(E2) values 0-32233
- <sup>116</sup>Xe level scheme and yrast band, in-beam  $\gamma$ -study from <sup>106</sup>Cd(<sup>12</sup>C, 2n) 0-13360
- <sup>125</sup>Xe 11/2<sup>-</sup>  $\rightarrow$  9/2<sup>-</sup> transition in odd parity band from <sup>124</sup>Te( $\alpha$ , 3n) 0-9203
- <sup>125</sup>Xe odd and even parity band structs., level lifetimes from <sup>125</sup>Ce(<sup>4</sup>He,3n $\gamma$ ) 0-27533
- <sup>89</sup>Y high spin states and decay scheme from <sup>87</sup>Rb( $\alpha$ ,2n $\gamma$ ) 0-32166
- <sup>89</sup>Y( $\pi$ ,  $\pi'$ ), 163, 240 MeV, giant resonance pionic excitation 0-52561
- <sup>14</sup>Yb, A=160, 161, backbending, multiple band crossing freq. and alignment from Sm(<sup>16</sup>O,3n) 0-47347
- <sup>14</sup>Yb, A=161, 162, 166, yrast cascade dipole component from Sm(<sup>16</sup>O,4n) 0-9266
- <sup>14</sup>Yb, A=164, 166, high spin yrast states and transitions from Gd(<sup>13</sup>C,5n) 0-9208
- <sup>14</sup>Yb, A=166, 168, 170, backbending and moment of inertia in HFB cranking method 0-42521
- <sup>14</sup>Yb(<sup>16</sup>O,<sup>16</sup>O' $\gamma$ ), A=168-176, even nuclei, 58-62 MeV, Coulomb excitation, vibr. and rot. states 0-32162
- <sup>14</sup>Yb(<sup>40</sup>Ca,<sup>40</sup>Ca'), A=170,172,174, 168 MeV, rotational g-factor meas. using transient field interactions 0-18193
- <sup>160</sup>Yb double backbending and rot. states, HFB cranking model anal. 0-32155
- <sup>161</sup>Yb quasicontinuum  $\gamma$ -rays yrast cascade dipole component, moment of inertia from Sm(<sup>16</sup>O, xn $\gamma$ ) 0-47424
- <sup>162</sup>Yb high spin states, HF self consistent calc. with Skyrme interaction, cranking approach 0-9210
- <sup>162</sup>Yb rot. states, HF and HFB self consistent calc. with Skyrme interaction 0-22662
- <sup>161</sup>Yb  $i_{1/2}$  band, spin alignment in the particle-rotor and cranking models 0-42536
- <sup>172</sup>Yb octupole band, particle vibrational alignment from <sup>170</sup>Er( $\alpha$ ,2n) 0-13351
- <sup>176</sup>Yb(p,p'), 35 MeV, ground state rot. band and multipole moment 0-32178
- <sup>90</sup>Zr neutron absorption, multipole giant resonance contrib. to optical pot. imaginary part 0-18263
- <sup>90</sup>Zr(<sup>6</sup>Li,<sup>6</sup>Li'), 153 MeV, isoscalar giant quadrupole resonances 0-13440

**nuclear coupling, molecular** *see molecular nuclear coupling***nuclear cranking model**

- A=40-80, yrast props. and high spin isomers, cranking plus Strutinsky formalism 0-32152
- angular momentum depend. cranked HFB inertia parameter, high spin states 0-42524
- coupled bands in even-even nuclei in RPA approach 0-32143
- high spin states and band coupling, theory and heavy ion expts. (*Russian*) 0-18160
- Inglis cranking formula, temp. dependent mass. parameter behaviour 0-22714
- nuclear inertia for excited states, adiabatic cranking model calcs. 0-9216
- rotating nuclei, M1 and E1 transitions within and between bands, cranking model 0-494
- spontaneous fission mass parameters, cranking and hydrodynamic models, deformation depend. (*Russian*) 0-13511
- two rotation regimes, cranked harmonic oscillator soln. 0-22657
- <sup>24</sup>Mg yrast line, Strutinsky type cranking calc., pairing correlation inclusion 0-13355
- <sup>14</sup>Yb, A=166, 168, 170, backbending and moment of inertia in HFB cranking method 0-42521
- <sup>160</sup>Yb double backbending and rot. states, HFB cranking model anal. 0-32155
- <sup>162</sup>Yb high spin states, HF self consistent calc. with Skyrme interaction, cranking approach 0-9210
- <sup>162</sup>Yb  $i_{1/2}$  band, spin alignment in the particle-rotor and cranking models 0-42536

**nuclear decay schemes** *see radioactive decay schemes***nuclear decay theory**

- see also alpha decay theory; beta decay theory*
- Fermi model for high multiplicity compound nucleus decay 0-22799
- Gamow state vectors as functionals over subspaces of the nuclear space 0-32227
- preequilibrium decay models (*Rumanian*) 0-47457
- two peaked pot. barrier, quasi-stationary state decay, semiclassical approx. (*Russian*) 0-37366
- two photon decay, time correlation 0-27506
- <sup>12</sup>C, excited state decay, axion emission search 0-32235

**nuclear deformation** *see nuclear shape***nuclear density**

- $\beta$ -active superdense nuclei search in (p,X), (d,X) reactions (*Russian*) 0-42535

**nuclear density continued**

- A=16-58, charge, proton and neutron density distrib. calc. 0-22680
- A=4n, densities, form factors, transitions, multipole moments in s-d shell, HFC 0-37321
- abnormally large density and binding energy states, book contrib. 0-489
- direct energy minimisation methods in self-consistent nuclear fields, ground state props. 0-22702
- Hamiltonians, semiclassical approx., spin-independ. pots. 0-32208
- heavy ion collisions, fluid dynamical and TDHF models, abnormal nuclear matter, density isomers 0-47502
- heavy ion deep inelastic collisions, kinetic energy dissipation, nuclear matter density oscillations (*Russian*) 0-37397
- heavy ion fusion cross section, energy depend., nuclear matter density distrib., depend. 0-47519
- neutron distribution in nuclei, elastic and inelastic proton scattering, review 0-22649
- neutron skin, compared with droplet model theory 0-52599
- nuclear, matter, V<sup>8</sup> models, variational calcs. for binding energy and density 0-42571
- nuclear matter, pion condensation and density isomerism 0-5085
- rapidly rotating nuclei, semiclassical HF description, smooth quantal corrections, density and total energy 0-32171
- semi-infinite nuclear matter calc., nuclear density oscillations 0-22681
- (e,e), proton and neutron densities 0-22684
- $\pi$ N scattering amplitude in nuclear matter, quantum field theory approach 0-42570
- <sup>12</sup>C( $\pi$ , $\pi'$ ), total cross section, density distrib. and ray bending effects 0-47509
- <sup>4</sup>Ca, A=40, 48, neutron densities and single particle struct. 0-32165
- <sup>40</sup>Ca, finite nuclear props. in relativistic quantum field theory, mass and p densities 0-9219
- <sup>6</sup>He, density distribution function of nucleons 0-22650
- <sup>4</sup>Ni, A=58, 64, neutron densities and single particle struct. 0-32165
- <sup>208</sup>Pb, finite nuclear props. in relativistic quantum field theory, mass and p densities 0-9219
- <sup>208</sup>Pb, neutron densities and single particle struct. 0-32165
- <sup>208</sup>Pb(<sup>16</sup>O,X), 80-313 MeV, optical model anal., dynamic shape or density changes 0-18186
- <sup>208</sup>Pb( $\pi$ , $\pi'$ ), total cross section, density distrib. and ray bending effects 0-47509
- <sup>32</sup>S( $\pi$ , $\pi'$ ), total cross section, density distrib. and ray bending effects 0-47509
- <sup>4</sup>Sn, A=116, 124, neutron densities and single particle struct. 0-32165
- <sup>120</sup>Sn( $\pi$ , $\pi'$ ), total cross section, density distrib. and ray bending effects 0-47509
- <sup>236</sup>U, nuclear matter density distrib., in asymmetric two centre shell model 0-32209

**nuclear electric moment***see also molecular nuclear coupling*

- E0 conversion, reduced probability, quadrupole moment effects 0-18235
- even nuclei, 2<sup>+</sup> excited states quadrupole moments, energy weighted sum rule appl. 0-9229
- even-even rare earths, microscopic quadrupole and hexadecapole moments 0-13376
- excited state quadrupole moments meas. using Coulomb excitation 0-5065
- Muonic atoms, X-ray vacuum corrections, nuclear moments, transitions and deformation parameters 0-37912
- nuclei, transitional, pairing rotations and quadrupole modes 0-18165
- p-f shell nuclei, HF calcs., vel. depend. effective pot., binding energy, quadrupole moment 0-461
- quadrupole moments and rms charge radii, shell model calcs. 0-47369
- quadrupole strength, giant quadrupole resonance 0-52575
- s-d shell nuclei, HF calcs., vel. depend. effective pot., binding energy, quadrupole moment 0-461
- in (p,n) reactions quadrupole moment, isovector component, nuclear spin re-orientation effect 0-52573
- <sup>4</sup>Ba, A=130, 132, 134, 136, levels and EM props., ang. momentum projected quasiboson model 0-5067
- <sup>4</sup>Ca, nuclear charge radius, spin, moments, by laserspectroscopy 0-18187
- <sup>111</sup>Cd, elec. quadrupole moment from elec. field gradients of trans-dimethyl organometallic moieties 0-29371
- <sup>111</sup>Cd<sup>m</sup>, nuclear orientation in Zn and Be, 245 keV state quadrupole moment, half-life 0-37324
- <sup>131</sup>Cs, 133.5 keV state, electric quadrupole interaction 0-32228
- Dy, deformed nuclei, quasicontinuum  $\gamma$ -spectrum, M1, E1, E2 components 0-498
- Dy, quadrupole moment calc. using HF method (*Russian*) 0-13375
- <sup>156</sup>Dy high spin states lifetimes and feeding times, quadrupole moments from <sup>24</sup>Mg(<sup>136</sup>Xe,4n) 0-32239
- Er (*Russian*) 0-13375
- Gd, quadrupole moment calc. using HF method (*Russian*) 0-13375
- <sup>147</sup>Gd<sup>m</sup> high spin yrast trap, oblate deformation and quadrupole moment 0-32157
- H<sup>+</sup>, upper limit from P- and T-violating interactions in hyperfine struct., mol. beam reson. expt. on TIF 0-53019
- H<sup>+</sup>, value from electric dipole hyperfine struct. calc. of TIF 0-53162
- Hf, quadrupole moment calc. using HF method (*Russian*) 0-13375
- <sup>4</sup>He, A=166, 168, 170, 172, yrast states, quadrupole moments and B(E2) values, microscopic calcs. 0-32147
- <sup>4</sup>Hg, quadrupole moment, change between first 5/2<sup>-</sup> states for A=197,199, shell model anal. 0-52576
- <sup>166</sup>Ho, internal hyperfine field obs. using  $\beta$ - $\gamma$  directional correl. 0-32229
- <sup>115</sup>In, elec. quadrupole moment from elec. field gradients of trans-dimethyl organometallic moieties 0-29371
- <sup>138</sup>La/<sup>139</sup>La nuclear electric quadrupole moment ratio, laser RF double reson. obs. 0-23447
- <sup>24</sup>Mg 2<sup>+</sup> state quadrupole moment from <sup>208</sup>Pb(<sup>24</sup>Mg,<sup>24</sup>Mg) 0-9230
- <sup>26</sup>Mg, 2<sup>+</sup> state quadrupole moment in band mixed HF model 0-52578
- <sup>4</sup>Mo, A=94, 96, 98, multiparticle states, method of generalised seniority 0-22759
- <sup>98</sup>Mo static quadrupole moment of first 2<sup>+</sup> state from ( $\alpha$ , $\alpha'$ ), (<sup>16</sup>O,<sup>16</sup>O') 0-5061
- <sup>12</sup>N ground state electric quadrupole moment from <sup>12</sup>C( $\gamma$ ,  $\pi$ ), <sup>12</sup>N ground state electric quadrupole moment (*Russian*) 0-42538
- <sup>13</sup>N, quadrupole strength, from <sup>12</sup>C(p, $\gamma$ )<sup>13</sup>N, semi-direct capture model calcs. 0-47370
- Nd(<sup>16</sup>O,<sup>16</sup>O), 40-48 MeV, even nuclei, 2<sup>+</sup> state E2 transition probabilities and quadrupole moments 0-18234



**nuclear electric moment continued**

- <sup>16</sup>O(<sup>10,11</sup>B, <sup>10,11</sup>B), 33.7-49.5 MeV, mag. distrib., ground state quadrupole moment contrib. 0-42689  
<sup>18</sup>O 1.98 MeV 2<sup>+</sup> state static quadrupole moment, from nuclear sum rules 0-13374  
 Os even nuclei, spin expan. Hamiltonian, quadrupole moments 0-5058  
<sup>A</sup>Os, A=191,193, ground state spectroscopic quadrupole moment meas. 0-27553  
<sup>188</sup>Os, muonic resonance spectra, deduced isomer shifts and electric moments 0-18948  
<sup>190</sup>Os, collective states and static quadrupole moment, boson expansion theory 0-47346  
<sup>A</sup>Pb, A=200,206, 12<sup>+</sup> isomer states, quadrupole moments 0-27554  
<sup>190</sup>Pt, collective states and static quadrupole moment, boson expansion theory 0-47346  
<sup>A</sup>Ru, A=96, 98, 100, multiparticle states, method of generalised seniority 0-22759  
<sup>A</sup>Ru(<sup>16</sup>O, <sup>16</sup>O), 36-45 MeV, A=96, 98, 100, 102, 104, first 2<sup>+</sup> excited state quadrupole moment 0-47374  
<sup>A</sup>Ru( $\alpha$ ,  $\alpha'$ ), 8.5-9.5 MeV, A=96, 98, 100, 102, 104, first 2<sup>+</sup> excited state quadrupole moment 0-47374  
<sup>102</sup>Ru 2<sup>+</sup> state quadrupole moment, reorientation effects and multiple Coulomb excitation from ( $\alpha$ ,  $\alpha'$ ), (<sup>16</sup>O, <sup>16</sup>O) 0-5063  
<sup>121</sup>Sb, elec. quadrupole moment from elec. field gradients of trans-dimethyl organometallic moieties 0-29371  
<sup>30</sup>Si, 2<sub>1</sub><sup>+</sup> state quadrupole moment in band mixed HF model 0-52578  
<sup>30</sup>Si first excited state, static quadrupole moment from <sup>208</sup>Pb(<sup>30</sup>Si, <sup>30</sup>Si) 0-13373  
<sup>154</sup>Sm(p, p'), 35 MeV, ground state rot. band and multipole moment 0-32178  
<sup>119</sup>Sn elec. quadrupole moment from elec. field gradients of trans-dimethyl organometallic moieties 0-29371  
 TaS<sub>3</sub>(1T), inequivalent lattice sites in charge density distorted phases 0-15835  
<sup>232</sup>Th(p, p'), 35 MeV, ground state rot. band and multipole moment 0-32178  
<sup>202</sup>Tl, electric dipole interaction energy from electric dipole hyperfine struct. calc. of TlF 0-53162  
<sup>238</sup>U(p, p'), 35 MeV, ground state rot. band and multipole moment 0-32178  
 W, quadrupole moment calc. using HF method (*Russian*) 0-13375  
 Yb, quadrupole moment calc. using HF method (*Russian*) 0-13375  
<sup>172</sup>Yb, muonic resonance spectra, deduced isomer shifts and electric moments 0-18948  
<sup>176</sup>Yb(p, p'), 35 MeV, ground state rot. band and multipole moment 0-32178  
 Zr even isotopes, quadrupole moments and E2 transition rates, broken pair approx. 0-52579  
<sup>A</sup>Zr, A=92, 94, 96, multiparticle states, method of generalised seniority 0-22759

**nuclear electric shielding** *see nuclear screening***nuclear electromagnetic transitions** *see nuclear energy level transitions***nuclear electron capture**

- see also beta-decay*  
 radioactive decay constant, effect of chem. surroundings, electron capture 0-42601  
 radioactive decay constants constancy limits 0-18245  
<sup>106</sup>Ag<sup>m</sup> decay, IC and  $\gamma$ -rays, <sup>106</sup>Pd energy states and J <sup>$\pi$</sup>  0-18197  
<sup>187</sup>Au decay, <sup>187</sup>Pt, levels, J <sup>$\pi$</sup> , T<sub>1/2</sub>, possible E0 transitions (*French*) 0-32230  
<sup>A</sup>Bk, A=240, 242, electron capture, delayed fission prob. and fission barrier height (*Russian*) 0-42722  
 Cd decay and half life, <sup>A</sup>Ag A=99, 101, 103, levels, transitions and J <sup>$\pi$</sup>  0-47383  
<sup>104</sup>Cd,  $\beta^+$ /(EC+ $\beta^+$ ) probability ratio, EC decay energies, mass excesses 0-27543  
<sup>109</sup>Cd EC decay data revision 0-5095  
 Co complex, bis-( $\beta$ -diketonato) Co(II) dihydrate, Fe chem. states, Mossbauer emission 0-15917  
 Co complex, Werner complexes, <sup>57</sup>Fe partial quadrupole splitting, emission Mossbauer spectra 0-15919  
 CoSO<sub>4</sub>·7H<sub>2</sub>O, electron capture aftereffects, time differential Mossbauer coincidence technique 0-39927  
<sup>57</sup>Co, Mossbauer gamma-X-ray coincidence meas. 0-14041  
<sup>58</sup>Co, student expt. 0-12875  
 Co<sup>2+</sup>[Fe<sup>III</sup>(CN)<sub>6</sub>]<sup>3-</sup>, time depend. linewidth of Mossbauer spectrum 0-15911  
<sup>A</sup>Es, A=244, 246, 248, electron capture, delayed fission prob. and fission barrier height (*Russian*) 0-42722  
<sup>152</sup>Eu, X-ray emission probabilities per decay 0-14027  
<sup>67</sup>Ga  $\gamma$ - and X-ray emission probabilities and half-life obs. 0-32242  
<sup>145</sup>Gd EC/ $\beta^+$ -decay branching ratio anomalies, <sup>145</sup>Eu level and transition effects 0-32244  
<sup>172</sup>Hf EC decay, <sup>172</sup>Lu levels, transitions and J <sup>$\pi$</sup>  values 0-18249  
<sup>123</sup>I, isomer shift calibration of <sup>29</sup>I and <sup>127</sup>I, lifetime variations in electron capture decay 0-39925  
<sup>125</sup>I, electron capture decay lifetime, calibration of Mossbauer isomer shift of <sup>127</sup>I and <sup>129</sup>I 0-39922  
<sup>40</sup>K, pressure-induced changes in electron-capture decay const., theory 0-22771  
<sup>138</sup>La, radioactive decay meas., half life,  $\gamma$  energies 0-13418  
<sup>A</sup>Md, A=248, 250, electron capture, delayed fission prob. and fission barrier height (*Russian*) 0-42722  
<sup>258</sup>Md isomer, EC decay, <sup>258</sup>Fm spontaneous fission, mass and kinetic energy distrib. 0-47518  
<sup>201</sup>Pb decay, <sup>201</sup>Tl levels, transitions and J <sup>$\pi$</sup>  assignments 0-5099  
<sup>101</sup>Pd, K-electron capture decay, double K-shell vacancy creation 0-22773  
<sup>204</sup>Po, EC, <sup>204</sup>Bi excited states,  $\gamma$  rays, conversion electrons and  $\gamma\gamma$  coincidences 0-18241  
<sup>94</sup>Rh decay, T<sub>1/2</sub>, <sup>94</sup>Ru levels and  $\gamma$ -transitions 0-18244  
<sup>208</sup>Rn decay, <sup>208</sup>At energy levels and transitions, IC electrons 0-18242  
<sup>A</sup>Sn, A=106,108,  $\beta^+$ /(EC+ $\beta^+$ ) probability ratio, EC decay energies, mass excesses 0-27543  
<sup>201</sup>Tl  $\gamma$ - and X-ray emission probabilities and half-life obs. 0-32242  
<sup>169</sup>Tm, high resolution meas. of anisotropic directional correl. between  $\gamma$ -rays and KX rays 0-32243

**nuclear emulsions** *see nuclear track emulsions***nuclear energy** *see nuclear power***nuclear energy level lifetimes**

- complex cascade processes decay law, high spin state mean lifetime corrections (*Chinese*) 0-22761  
 conference on nuclear interactions, Canberra, Australia (Aug.-Sep. 1978) 0-4476  
 DSAM, nuclear spectroscopy techniques (*Hungarian*) 0-14036  
 excited nuclear states, lifetime meas. 0-5093  
 gamma ray ang. distrib., Doppler effect appl. in nucl. spectroscopy (*Hungarian*) 0-14036  
 interacting boron model of collective state, O(6) limit 0-32214  
 laser radiation effects on nuclear transition lifetime 0-22760  
 N=82-86, high spin isomers, gamma spectroscopy 0-47358  
 Poisson and Brockwell-Moyal freq. distrib.,  $\chi$ -square test 0-5430  
 recoil distance method, Doppler effect appl. in nucl. spectroscopy (*Hungarian*) 0-14036  
 yrast isomer prod., pulsed beam meas. using plastic scintillation spectrum 0-27871  
<sup>A</sup>Ag, A=105,107, positive parity band, mixing and branching ratios lifetimes from (<sup>16</sup>O, 2np)(<sup>14</sup>N, 3n) 0-9197  
<sup>110</sup>Ag low lying states, decay scheme and T<sub>1/2</sub> from <sup>109</sup>Ag(n,  $\gamma$ ) 0-47393  
<sup>A</sup>As, A=70, 72, level scheme, transitions, J <sup>$\pi$</sup>  and lifetimes from Ge(p, n $\gamma$ ) 0-22695  
<sup>10</sup>B T=1 states,  $\gamma$ -transition strengths, lifetimes, branching and mixing ratios from <sup>6</sup>Li( $\alpha$ ,  $\alpha'$ ) 0-27594  
<sup>11</sup>B analogue of <sup>11</sup>C 6478 keV state, lifetime from <sup>7</sup>Li( $\alpha$ ,  $\gamma$ ) 0-5092  
<sup>77</sup>Br collective bands, lifetimes, spins and E2 transition probabilities from <sup>64</sup>Ni(<sup>16</sup>O, 2np) 0-13415  
<sup>77</sup>Br E2 transition probabilities and mean lives from <sup>64</sup>Ni(<sup>16</sup>O, 2np $\gamma$ ) 0-13414  
<sup>11</sup>C negative parity states lifetime limits and transition strengths from <sup>10</sup>B(p,  $\gamma$ ) 0-5092  
<sup>1</sup>Cd, A=113, 115 from <sup>113</sup>, <sup>115</sup>Ag  $\beta$ -decay 0-47432  
<sup>111</sup>Cd<sup>m</sup>, nuclear orientation in Zn and Be, 245 keV state quadrupole moment, half-life 0-37324  
<sup>59</sup>Co(n, n' $\gamma$ ), level transitions, deexcitations and lifetimes 0-18222  
<sup>54</sup>Cr levels, transitions, T<sub>1/2</sub>, J <sup>$\pi$</sup> , shell model anal. from <sup>51</sup>V( $\alpha$ , p $\gamma$ ) 0-47381  
<sup>152</sup>Dy high spin isomers, yrast states and level lifetimes from (<sup>15</sup>N, 4n), (<sup>16</sup>O, 4n) 0-13361  
<sup>158</sup>Dy high spin states,  $\gamma$ -ang. distrib., lifetimes and feeding times from <sup>148</sup>Nd(<sup>13</sup>C, 5n) 0-13364  
<sup>156</sup>Dy high spin states lifetimes and feeding times, quadrupole moments from <sup>24</sup>Mg(<sup>136</sup>Xe, 4n) 0-32239  
<sup>162</sup>Dy(<sup>136</sup>Xe, <sup>136</sup>Xe'), 547, 612 MeV, high spin state energies and reduced transition probabilities 0-18232  
<sup>153</sup>Er 360 ns yrast trap,  $\gamma$  transitions and lifetimes from <sup>144</sup>Sm(<sup>12</sup>C, 3n) 0-9205  
<sup>19</sup>F low lying band state lifetimes, stopping power, transition strengths from <sup>15</sup>N( $\alpha$ ,  $\gamma$ ) 0-42585  
<sup>66</sup>Ge levels, lifetimes and mixing ratio, in-beam  $\gamma$ -spectroscopy from <sup>58</sup>Fe(<sup>14</sup>N, np $\gamma$ ) 0-42541  
<sup>66</sup>Ge states and decay scheme, polarisations J <sup>$\pi$</sup>  and ang. distrib. from <sup>58</sup>Ni(<sup>10</sup>B, pn $\gamma$ ) 0-22692  
<sup>68</sup>Ge multiple band struct., g<sub>9/2</sub> orbital, level lifetimes from <sup>58</sup>Ni(<sup>12</sup>C, 2p) 0-13358  
<sup>A</sup>Hf(HI, xn), A=170-173, two and three quasiparticle isomers, rot. bands, decays and lifetimes 0-9211  
<sup>171</sup>Hf, hindered electric dipole transitions and lifetimes from (HI, xn) reactions 0-9263  
<sup>171</sup>Hf one- and three-quasiparticle states, high spin rot. bands from (<sup>16</sup>O, 5n), (<sup>13</sup>C, 4n) 0-18163  
<sup>170</sup>Hf multi-quasiparticle states and bands, isomeric states, lifetimes from <sup>170</sup>Er(<sup>9</sup>Be, 4n) 0-9213  
<sup>A</sup>K, A=45,46, levels, lifetimes and transitions from Ar  $\beta$ -decay 0-42597  
<sup>78</sup>Kr high spin levels, bands and transitions, level lifetimes from <sup>68</sup>Zn(<sup>13</sup>C, Zn) 0-42525  
<sup>78</sup>Kr high spin states, transitions and lifetimes from (<sup>16</sup>O, 2np), (<sup>19</sup>F, 2n $\alpha$ ), (<sup>16</sup>O, 2n), (<sup>13</sup>C, 2n) 0-27534  
<sup>171</sup>Lu, excited state lifetimes by delayed coincidence method 0-18231  
<sup>24</sup>Mg rot. band termination, level lifetimes from <sup>12</sup>C(<sup>16</sup>O,  $\alpha$ ) 0-18174  
<sup>55</sup>Mn, energy levels, bound state mean lifetimes and spins from <sup>54</sup>Cr(p,  $\gamma$ ) 0-42586  
<sup>15</sup>N states, cross sections and lifetimes, EM decay strengths from 3 and 4 particle transfers 0-9237  
<sup>A</sup>Pb, A=197, 198, low energy  $\gamma$ -transitions and level lifetimes from <sup>186</sup>W(<sup>16</sup>O, xn) 0-18221  
<sup>102</sup>Pd, 1592 keV E0 transition T<sub>1/2</sub> meas. using e- $\gamma$  coincidence 0-22762  
<sup>187</sup>Pt, levels, J <sup>$\pi$</sup> , T<sub>1/2</sub>, possible E0 transitions from <sup>187</sup>Au decay (*French*) 0-32230  
<sup>196</sup>Pt (<sup>20</sup>Ne, <sup>20</sup>Ne'), excited states, lifetime meas. using recoil-distance method 0-13413  
<sup>196</sup>Pt (<sup>38</sup>Ni, <sup>58</sup>Ni'), excited states, lifetime meas. using recoil-distance method 0-13413  
<sup>237</sup>Pu fission single particle isomers, half lives and isomeric ratio from <sup>239</sup>Pu( $\gamma$ , 2n) 0-18181  
<sup>82</sup>Rb, level structure, gamma angular and time distrib. from <sup>81</sup>Br( $\alpha$ , 3n) 0-52583  
<sup>210</sup>Rn high spin states, decay and lifetimes, spin assignments from <sup>204</sup>Pb(<sup>9</sup>Be, 3n) 0-18168  
<sup>113</sup>Sb, 15 MeV excitation, average nucl. lifetime determ. 0-43164  
<sup>112</sup>Sb mean nuclear lifetime from X-ray spectrum in <sup>112</sup>Sn(p, p') 0-9267  
<sup>116</sup>Sn(<sup>16</sup>O, <sup>16</sup>O) 48 MeV, collective states, E2, E0 transition probabilities, half-life, branching ratios 0-18172  
<sup>119</sup>Sn, 23.87 keV level half-life 0-47433  
<sup>135</sup>Sn level struct., lifetimes,  $\gamma$ - $\gamma$  coincidences, internal conversion from <sup>235</sup>U fission 0-52584  
<sup>100</sup>Tc low lying and isomeric levels, transitions and mean lines from <sup>100</sup>Mo(p, n $\gamma$ ) 0-42548  
<sup>121</sup>Tc isomeric state, spin, lifetime and mag. moment from ( $\alpha$ , n), (d, Zn) 0-47387  
<sup>133</sup>Te from fission, 10<sup>+</sup> isomeric state, J <sup>$\pi$</sup>  from deexcitation pattern, half life 0-460  
<sup>48</sup>Ti high spin states,  $\gamma$ -decay, J <sup>$\pi$</sup>  assignments, lifetimes from <sup>45</sup>Sc( $\alpha$ , p $\gamma$ ) 0-13356  
<sup>1</sup>u2C mean life, Pauli exclusion principle validity for nucleons 0-18233  
<sup>A</sup>W, A=173, 175, hindered electric dipole transitions and lifetimes from (<sup>1</sup>H, xn) reactions 0-9263



**nuclear energy level lifetimes continued**

- <sup>180</sup>W ground and K=2<sup>+</sup> octupole band ang. momenta coupling, lifetimes from <sup>181</sup>Ta(p,2n $\gamma$ ) 0-9214  
<sup>125</sup>Xe odd and even parity band structs., level lifetimes from <sup>125</sup>Te(<sup>4</sup>He,3n $\gamma$ ) 0-27533  
<sup>129</sup>Xe, excited state lifetimes by delayed coincidence method 0-18231  
<sup>64</sup>Zn,  $\gamma$ -ray studies of levels above 3.1 MeV 0-32238

**nuclear energy level transitions**

see also internal conversion; Mossbauer effect; nuclear branching and mixing ratios; nuclear energy level lifetimes

- <sup>147</sup>Sm neutron separation and level excitation (n, $\gamma$ ) and (d,p) correlations 0-22756  
 A=11, 12, energy levels, transitions and resonances, compilation 0-46743  
 A=140, nuclear data sheets, levels and transitions 0-31435  
 A=19-31 odd nuclei, K $\pi$ =1/2<sup>+</sup> bands, spectroscopic factors and transitions 0-32151  
 A=204, nuclear data sheets, levels, J $\pi$  and transitions 0-31429  
 A=212, nuclear data sheets, levels, J $\pi$ , transitions 0-31430  
 A=221, nuclear data sheets, levels, J $\pi$ , transitions 0-31431  
 A=225, nuclear data sheets, levels, J $\pi$ , transitions 0-31432  
 A=40-56, spectroscopy props. using pure configuration shell model (Chinese) 0-42584  
 A=4n, densities, form factors, transitions, multipole moments in s-d shell, HFC 0-37321  
 A=60, nuclear data sheets, levels and transitions 0-31433  
 A=64, nuclear data sheets, levels and transitions 0-31434  
 A=6-44, gamma-ray transition strengths, data tables 0-37345  
 A=71 nuclear data sheets, levels, J $\pi$  and transitions 0-31428  
 A<100, average E1/M1 strength ratio 0-52621  
 A=28, giant quadrupole resonance, E2 intensity distrib., from ( $\alpha$ ,  $\alpha'$ ), DWBA anal. (Hungarian) 0-52642  
 analog-antianalog gamma transition strength 0-13429  
 atomic negative meson capture, nuclear giant resonance excitation (Russian) 0-42623  
 coherent rotational states formed in heavy ion collisions,  $\gamma$ -decay 0-27657  
 collective structure inferred from heavy ion Coulomb excitation 0-5167  
 complex cascade processes decay law, high spin state mean lifetime corrections (Chinese) 0-22761  
 conference on neutron capture gamma ray spectroscopy, Upton, USA. (Sep. '78) 0-36780  
 deformed nuclei, single particle matrix elements of radiative M2-transitions, Nilsson model 0-22753  
 dipole sum rule schematical eval., collective isovector quadrupole strength 0-47428  
 electron scatt. theory, EM struct. from DWBA and other models 0-5133  
 EM sum rules for ( $\gamma$ , $\gamma$ ), (e,e), transitions and giant resonances 0-5090  
 energy standard value and accurate determ. (Czech) 0-22755  
 energy weighted electronuclear sum rules, centre-of-mass corrections 0-5091  
 even actinides, lowest 0<sup>+</sup> state excitation, collective phonon state, spectroscopic factors from (p,t), (t,p) 0-13410  
 even actinides, two-nucleon transfer, first 0<sup>+</sup> collective state excitation, spectroscopic factor (Russian) 0-42530  
 even-even nuclei, 1<sup>+</sup> excitations, self consistent shell model description (Russian) 0-13407  
 even-even nuclei, phenomenological calcs. in n-p interacting boson approx. 0-27597  
 even-even spherical nuclei, 2<sub>1</sub><sup>+</sup> state deformation parameter from (p,p) and EM excitation 0-27549  
 excitation energies, calc. by energy density method 0-47425  
 excitation energies in hot matter, limits 0-56703  
 form factors of 0<sup>+</sup>-0<sup>+</sup> transition in A=16 system, nuclear struct. effects 0-18246  
 giant dipole resonance, particle-hole calcs., M1 strength 0-22785  
 giant multiple resonances, excitation strength functions 0-5037  
 heavy ion deep inelastic reactions,  $\gamma$ -ray multiplicity, partial ang. momenta (Russian) 0-37346  
 heavy ion inner shell excitations, multistep processes, quasimolecular model, coupled channels calc. 0-9303  
 heavy ion large-angle scatt., elastic cross-section, excitation functions 0-52689  
 heavy ion large-angle scatt., inelastic cross-section and collective state excitation 0-52690  
 heavy ion reactions, phenomenological nuclear friction mechanism, particle-hole excitation, nucleon exchange (Chinese) 0-42694  
 high angular momentum fusion compound nucleus deexcitation, high spin states, rare earths 0-9259  
 1<sub>1/2</sub> shell, particle-rotor model soln., backbending, transition rates, ang. momentum spread 0-47344  
 irreducible spin precession theory applied to atomic and nuclear RF spectroscopy 0-27969  
 isoscalar dipole strength excitation in GQR region by inelastic electron and hadron scatt. 0-47448  
 isoscalar giant electric resonances, excitation and decay 0-5108  
 isovector pairing collective motions and transition rates, projected BCS solns., generator coordinate simplification 0-22654  
 large amplitude collective motion, field theory, excitation energies 0-22665  
 laser radiation effects on nuclear transition lifetime 0-22760  
 laser-induced resonant absorption of  $\gamma$  radiation 0-18290  
 mathematical modelling for radionuclide gamma emission 0-32236  
 Muonic atoms, X-ray vacuum corrections, nuclear moments, transitions and deformation parameters 0-37912  
 N=50 isotones, transition probabilities, 1p<sub>3/2</sub> and 0f<sub>7/2</sub> hole excitation effects 0-47431  
 N=82-86, high spin isomers, gamma spectroscopy 0-47358  
 pairing rotations and quadrupole modes, dynamical interplay 0-18165  
 parity violation in nuclear forces, neutron capture  $\gamma$ -ray expts. 0-37322  
 preactinide nuclei, fission excitation functions and fission barrier height, liquid drop model 0-47513  
 quadrupole transition densities and electron scatt. in the interacting boson model 0-27598  
 quasiparticle spectra near the yrast line 0-453  
 radiative strength distrib. with energy, E1, M1 giant resonances, particle-hole calcs. 0-37349  
 radioactive decay constant, effect of chem. surroundings, electron capture 0-42601  
 rare earth nuclei, high spin states from (HI, xn) reactions, discrete  $\gamma$ -transitions 0-5050

**nuclear energy level transitions continued**

- rotating nuclei, M1 and E1 transitions within and between bands, cranking model 0-494  
 Sn Z=50 region isotopes, system struct calcs. 0-18192  
 spectroscopy using ( $\gamma$ , $\gamma$ ) and (n, $\gamma$ ) scatt. 0-18287  
 spherical nuclei, dipole states, transition densities and electroexcitation, GDR form factors (Russian) 0-52611  
 spherical nuclei, giant monopole resonance transition densities, dynamical Thomas-Fermi theory 0-9278  
 yrast and statistical cascades, M1 radiation after (MI, XN) reactions 0-42583  
 ( $\alpha$ , $\alpha'$ ), isoscalar giant quadrupole resonance decay props. 0-22792  
 ( $\alpha$ ,xn $\gamma$ ), rare earth nuclei, complete fusion process n and  $\gamma$  multiplicity 0-18363  
 $\beta^+$ -decay, e<sup>+</sup> annihilation in atomic K-shell, nuclear excitations (Russian) 0-42602  
 (dx) breakup on nucleus, adiabatic treatment stripping and forbidden transition cross section 0-9299  
 (e,e) elastic scatt., spectroscopic information and form factors 0-9260  
 $\Lambda$ - and  $\Sigma$ -hypernuclei,  $\gamma$ -transitions, spin-orbit components of single particle pots. 0-42574  
 (n, $\gamma$ ), A=20 to 240, E1 and M1 strength functions 0-52625  
 (n, $\gamma$ ), A=75 to 103,  $\gamma$ -strength functions and stat. model cross section calcs. 0-52612  
 (n, $\gamma$ ), A=94-190, resonance capture, low lying level population fluctuations,  $\gamma$ -rays 0-52619  
 (n, $\gamma$ ), E1 and M1 strength functions,  $\Lambda$ - and energy-depend., giant dipole resonances 0-37348  
 (n, $\gamma$ ), Fast n, gamma rays in giant dipole region, review 0-37351  
 (n, $\gamma$ ),  $\gamma$ -rays, QED test review 0-37199  
 (n, $\gamma$ ), mechanism in 3s size resonance, s-wave radiative width partition 0-37387  
 (n, $\gamma$ ), mechanism in 3s size resonance, radiative width statistical and valence effects 0-37388  
 (n, $\gamma$ ), non-spherical even-even nuclei, energy gap from  $\gamma$ -transitions 0-47395  
 (n, $\gamma$ ), on-line gamma anal. using Ge detector 0-52624  
 (n, $\gamma$ ), spin assignments using polarised beams and gamma spectroscopy 0-37323  
 (n, $\gamma$ ) gamma ray spectra calc. 0-52620  
 (n, $\gamma$ ) spectroscopy, nuclear struct. investigation, review 0-37379  
 (n, $\gamma$ ), thermal n, systematic search,  $\gamma$ -spectra and selective state population 0-37390  
 (n, $\gamma$ ), thermal n, systematic search,  $\gamma$ -spectra and selective state population 0-37390  
 (p,d), 52 MeV, deeply bound hole state transition strength giant resonance, DWBA anal. 0-47426  
 (p, $\gamma$ ), isobaric analogue doorway states, excitation functions 0-47388  
 (p,xn $\gamma$ ), rare earth nuclei, complete fusion process n and  $\gamma$  multiplicity 0-18363  
 ( $\pi$ , $\gamma$ ),  $\gamma$ -transitions on and off line 0-37912  
 ( $\pi$ , $\pi'$ ), 1p shell targets, DWIA calcs., strong transitions, isospin effects 0-42708  
 ( $\pi$ , $\pi'$ ), collective transitions, giant resonances, isospin content and spin transfer 0-42580  
 ( $\pi$ , $\pi'$ ), particle-hole state excitation, field theory calcs. (Russian) 0-37318  
 ( $\pi$ , X) slow pion capture in deformed nuclei, effects on high spin state excitation 0-18345  
<sup>208</sup>(N, $\gamma$ ), pol. N, anal. power and giant multipole resonances, direct-semidirect model 0-18265  
<sup>227</sup>Ac, high pressure meas. of gamma transitions 0-18225  
<sup>210</sup>Ag, A=104, 106, levels, J $\pi$ , and isobaric analogue resonances from Pd(p,n) 0-32180  
<sup>210</sup>Ag, A=99, 101, 103, levels, transitions and J $\pi$  from Cd decay, Pd(p,2n $\gamma$ ) 0-47383  
<sup>210</sup>Ag(<sup>86</sup>Kr,X), A=107,109, 620 MeV, deep inelastic scatt., ang. momentum transfer,  $\gamma$ -ray multiplicities 0-27665  
<sup>107</sup>Ag high spin states, J $\pi$  assignments, polarisations and transitions from (<sup>7</sup>Li,4n $\gamma$ ), (<sup>6</sup>Li,3n $\gamma$ ) 0-27536  
<sup>108</sup>Ag transition multipolarity and conversion electrons from <sup>107</sup>Ag(n,e<sup>-</sup>) 0-52627  
<sup>110</sup>Ag low lying states, decay scheme and T<sub>1/2</sub> from <sup>109</sup>Ag(n, $\gamma$ ) 0-47393  
<sup>26</sup>Al low energy resonances, decay and J $\pi$  assignments, branching ratios from <sup>25</sup>Mg(p, $\gamma$ ) 0-42624  
<sup>27</sup>Al(<sup>12</sup>C,<sup>12</sup>C), 14-25 MeV, 180° scatt. excitation function and ang. distrib. struct. 0-32253  
<sup>28</sup>Al E1 transitions and partial radiative widths from <sup>27</sup>Al(n, $\gamma$ ) 0-52618  
<sup>28</sup>Al levels, spins and  $\gamma$ -rays, multipole mixing from <sup>27</sup>Al(n, $\gamma$ ), pol. thermal 0-47398  
<sup>243</sup>Am, absolute yields of 43.5, 74.7 and 117.8 keV photons 0-32568  
<sup>245</sup>Am, high pressure meas. of gamma transitions 0-18225  
<sup>36</sup>Ar, delayed proton and alpha emission, transition energies, levels, J $\pi$ , from <sup>36</sup>K decay 0-52629  
<sup>38</sup>Ar high spin state density,  $\gamma$ -decay mode, deformed states from <sup>35</sup>Cl( $\alpha$ ,p $\gamma$ ) 0-32168  
<sup>38</sup>Ar levels, J $\pi$  and transition strengths, DWBA anal. of <sup>40</sup>Ar(p,t) 0-47378  
<sup>41</sup>As, A=70, 72, level scheme, transitions, J $\pi$  and lifetimes from Ge(p, $\gamma$ ) 0-22695  
<sup>75</sup>As populated in <sup>75</sup>Se decay, E0 transitions 0-22752  
<sup>76</sup>As, level structure, transitions and J $\pi$ , from <sup>76</sup>Ge(p, $\gamma$ ) 0-47379  
<sup>208</sup>At energy levels and transitions, IC electrons from <sup>208</sup>Rn decay 0-18242  
<sup>212</sup>At high spin states, decay, g factor, J $\pi$  assignments, level energies from <sup>208</sup>Pb(<sup>7</sup>Li,3n) 0-5042  
<sup>197</sup>Au, A=189, 191, 193, high spin states and transitions, isomeric states from Ir( $\alpha$ ,xn $\gamma$ ) 0-5038  
<sup>197</sup>Au + <sup>136</sup>Xe, 1064 MeV, fragment spin orientation from continuum  $\gamma$ -ray anisotropy meas. 0-22853  
<sup>197</sup>Au(<sup>86</sup>Kr,X), 620 MeV, deep inelastic scatt., ang. momentum transfer,  $\gamma$ -ray multiplicities 0-27665  
<sup>197</sup>Au(<sup>86</sup>Kr,X) 612 MeV,  $\gamma$ -ray circular polarisation 0-13453  
<sup>197</sup>Au( $\alpha$ , $\alpha'$ ), 120 MeV, isoscalar resonance excitation, low lying transitions, DWBA calc. 0-512  
<sup>198</sup>Au, 411 keV transition energy, absolute meas. rel. to He-Ne laser freq. (Czech) 0-22755  
<sup>198</sup>Au gamma-ray strength functions from spectrum fitting method from <sup>197</sup>Au(n, $\gamma$ ) 0-52616  
<sup>198</sup>Au level spin assignments from  $\gamma$  ang. distrib. and circular polarisation from <sup>197</sup>Au(n, $\gamma$ ) 0-52570  
<sup>198</sup>Au, populated in <sup>198</sup>Au(n, $\gamma$ ), high energy transitions 0-22878



## nuclear energy level transitions continued

- <sup>198</sup>Au(n,γ), 0.5-3.0 MeV, γ-spectra strength functions 0-32240  
<sup>198</sup>Au, populated in <sup>198</sup>Au(n,γ), high energy transitions 0-22878  
 (α,γ), excitation function competition cusps, Mauser-Feshbach calcs. 0-13404  
<sup>10</sup>B T=1 states, γ-transition strengths, lifetimes, branching and mixing ratios from <sup>6</sup>Li(α,α) 0-27594  
<sup>10</sup>B transitions and levels from <sup>11</sup>B(γ,nγ<sup>1</sup>) (*Russian*) 0-13433  
<sup>11</sup>B(e,e<sup>+</sup>), E1 transitions to unnatural parity states 0-22758  
<sup>11</sup>B(γ,nγ) 30 MeV giant dipole resonance decay, <sup>10</sup>B transitions (*Russian*) 0-13433  
<sup>A</sup>Ba, A=130, 132, 134, 136, levels and EM props., ang. momentum projected quasiboson model 0-5067  
<sup>13</sup>Ba level scheme, J<sup>π</sup> and γ-transitions from <sup>139</sup>Cs β-decay 0-42590  
<sup>7</sup>Be excitation functions from <sup>6</sup>Li(<sup>3</sup>He, d) 0-18223  
<sup>204</sup>Bi excited states, γ rays, conversion electrons and γγ coincidences from <sup>204</sup>Po, EC 0-18241  
<sup>208</sup>Bi two-particle, two-hole configuration, levels, J<sup>π</sup> and excitation energies from <sup>210</sup>Bi(m,p,t) 0-32190  
<sup>207</sup>Bi(α,α'), 120 MeV, isoscalar resonance excitation, low lying transitions, DWBA calc. 0-512  
<sup>78</sup>Br, high-spin states, from <sup>77</sup>Se(α,2np), decay into isomers 0-52569  
<sup>CC</sup><sup>158</sup>Dy high spin states B(E2) values, IBA model test from <sup>26</sup>Ne(<sup>136</sup>Xe, 4n) CC <sup>158</sup>Dy high spin states B(E2) values, IBA model test 0-27541  
<sup>CC</sup><sup>168</sup>Er high intrinsic excitation levels, γ-decay props. from <sup>167</sup>Er(n,γ) 0-52588  
<sup>A</sup>C(π,π'), A=12, 13, ~180 MeV, isospin mixing, levels, excitation functions and ang. distrib. 0-42543  
<sup>11</sup>C levels and resonance, γ-ray excitation curves from (p,αγ), (p,py) 0-9280  
<sup>12</sup>C, α-transfer spectroscopic factors for O<sup>+</sup>, 2<sup>+</sup> and 4<sup>+</sup> states, transitions from (d, <sup>6</sup>Li) 0-13370  
<sup>12</sup>C, excited state decay, axion emission search 0-32235  
<sup>12</sup>C, excited state struct., α-particle model 0-47385  
<sup>12</sup>C M1 (15.11 MeV) form factor, evidence for nuclear pion field critical opalescence 0-32232  
<sup>12</sup>C(<sup>12</sup>C, <sup>12</sup>C)<sup>12</sup>C\*, 0<sub>2</sub><sup>+</sup>, 3<sub>1</sub><sup>-</sup>, 4<sub>1</sub><sup>+</sup> state excitation functions, resonance structures 0-42616  
<sup>12</sup>C(<sup>16</sup>O, <sup>12</sup>C\*), 45-53 MeV, <sup>12</sup>C\* m-substate population, spin alignment and excitation functions 0-42615  
<sup>12</sup>C(<sup>16</sup>O, <sup>16</sup>O), 35 to 50 MeV, backscatt., dynamic deformation and excitation functions, optical anal. 0-18227  
<sup>12</sup>C(<sup>20</sup>Ne, <sup>20</sup>Ne), back angle scatt. systematics, structured excitation functions and oscillatory ang. distrib. 0-32295  
<sup>12</sup>C(<sup>24</sup>Mg, <sup>24</sup>Mg), back angle scatt. systematics, structured excitation functions and oscillatory ang. distrib. 0-32295  
<sup>12</sup>C(<sup>40</sup>Ca, <sup>40</sup>Ca), 90° and 180° excitation functions energy depend., DWBA anal. 0-42582  
<sup>12</sup>C(e,e), 180° scatt., transverse inelastic form factors and spectra, collective 2<sup>+</sup> state 0-9261  
<sup>12</sup>C(n, X), compound resonance decay based on bound and metastable single nucleon states (*Russian*) 0-5107  
<sup>12</sup>C(ν,ν'), (ν̄,ν̄'), 15.11 MeV state excitation, cross sections, level decay 0-9258  
<sup>12</sup>C(p,p'), 1 GeV, proton polarisation in natural parity level excitation (*Russian*) 0-42634  
<sup>12</sup>C(π<sup>+</sup>, 2γ), doubly radiative capture theory, branching ratio and ang. correlations 0-9314  
<sup>12</sup>C(π<sup>±</sup>, πN), 40-600 MeV, excitation functions and absolute cross sections 0-18226  
<sup>13</sup>C(p,γ), pol. p, 6.25-17.0 MeV, anal. power and cross section ang. distrib., E1, E2 amplitudes 0-47461  
<sup>14</sup>C(<sup>12</sup>C,X), 40-57 MeV, strong resonant behaviour in inelastic and transfer channels, γ-yields 0-52644  
<sup>40</sup>Ca, weak s resonance γ-ray decay in negative parity low lying levels 0-27591  
<sup>42</sup>Ca high spin state density, γ-decay mode, deformed states from <sup>39</sup>K(α,py) 0-32168  
<sup>A</sup>Cd(n,nγ) A=114,116, energy levels, spins, and gamma-ray multipole mixing ratios investig. 0-52580  
<sup>111</sup>Cd, excitation by photon less positron annihilation, isomeric γ-transitions (*Russian*) 0-5089  
<sup>135</sup>Ce, yrast cascade dipole component from <sup>122</sup>Sn(<sup>16</sup>O,4n) 0-9266  
<sup>140</sup>Ce γ-spectra, E1 and M1 hindrance factors from <sup>143</sup>Nd(n,γα) 0-37386  
<sup>144</sup>Ce, e-γ and e-e coincidences, improved detection system 0-52605  
<sup>258</sup>Cf(d,d'), 15 MeV, vibr. states, J<sup>π</sup> and reduced transition probabilities 0-47351  
<sup>39</sup>Cl excited states and transitions from <sup>39</sup>S decay 0-42595  
<sup>A</sup>Cm, A=246,248, fission isomer rot. spectra I<sup>2</sup>(1+1)<sup>2</sup> correction 0-18229  
<sup>249</sup>Cm excited and single particle states, γ-transitions from <sup>248</sup>Cm(n,γ) 0-47399  
<sup>55</sup>Co, resonance decays, branching ratios and analogue resonances from <sup>54</sup>Fe(p,γ) 0-52643  
<sup>59</sup>Co(n,2n), isomeric cross-section ratio and excitation function, mixed-powder method and gamma-ray spect. 0-47472  
<sup>59</sup>Co(n,α), excitation function, mixed-powder method and gamma-ray spect. 0-47472  
<sup>59</sup>Co(n,nγ), level transitions, deexcitations and lifetimes 0-18222  
<sup>51</sup>Cr, bands, levels, EM transitions, J<sup>π</sup>, branching and mixing ratios from <sup>48</sup>Ti(γ,nγ)<sup>51</sup>Cr and <sup>51</sup>V(p,nγ)<sup>51</sup>Cr 0-52606  
<sup>52</sup>Cr high spin states, transitions and J<sup>π</sup> values from <sup>50</sup>Ti(α,Znγ) 0-455  
<sup>52</sup>Cr(γ,γ<sup>1</sup>), 35 MeV, 2<sup>+</sup> state deexcitation γ-rays, differential cross sections, deformation (*Russian*) 0-13406  
<sup>52</sup>Cr(γ,γ), up to 12 MeV, highly excited spin-1 resonances, γ-transitions 0-13427  
<sup>53</sup>Cr levels, J<sup>π</sup>, γ-transitions and 1626 eV resonance from <sup>52</sup>Cr(n,γ) 0-42610  
<sup>54</sup>Cr levels, transitions, T<sub>1/2</sub>, J<sup>π</sup>, shell model anal. from <sup>51</sup>V(α,py) 0-47381  
<sup>131</sup>Cs, 133.5 keV state, electric quadrupole interaction 0-32228  
<sup>131</sup>Cs populated in <sup>131</sup>Ba decay, E0 transitions 0-22752  
<sup>139</sup>Cs level scheme, J<sup>π</sup> and γ-transitions from <sup>139</sup>Xe β-decay 0-42590  
<sup>63</sup>Cu levels and transition j-depend., DWBA anal. of <sup>60</sup>Ni(<sup>19</sup>F, <sup>16</sup>O) 0-42542  
<sup>64</sup>Cu levels and transitions, stat. anal. of <sup>64</sup>Ni(p, nγ) (*Russian*) 0-5104  
<sup>65</sup>Cu levels and transitions, γ-strength function using average resonance capture from <sup>64</sup>Ni(p,γ) 0-13411  
 (d,p), A=88-106, pol. d, excitation curve isospin anomaly, neutron single particle resonances 0-27595

## nuclear energy level transitions continued

- <sup>151</sup>Dy levels, bands and transitions, in-beam γ-rays from <sup>142</sup>Nd(<sup>12</sup>C,3nγ) 0-458  
<sup>152</sup>Dy high spin struct., in beam γ meas. from (<sup>15</sup>N, 4n), (<sup>16</sup>O, 4n) 0-18179  
<sup>152</sup>Dy yrast continuum γ-ray multipolarity via polarisation meas. from <sup>140</sup>Ce(<sup>16</sup>O,4n) 0-9264  
<sup>156</sup>Dy high spin states lifetimes and feeding times, quadrupole moments from <sup>24</sup>Mg(<sup>136</sup>Xe,4n) 0-32239  
<sup>160</sup>Dy anomalous γ-L X-ray directional correlations from <sup>160</sup>Tb decay 0-52610  
<sup>163</sup>Dy multipole mixing in γ to ground bands from <sup>163</sup>Dy(n,γ) 0-52615  
<sup>153</sup>Er 360 ns yrast trap, γ transitions and lifetimes from <sup>144</sup>Sm(<sup>12</sup>C,3n) 0-9205  
<sup>154</sup>Er yrast trap and transitions, decay scheme from (<sup>64</sup>Ni,4n), (<sup>16</sup>O,4n) 0-9206  
<sup>166</sup>Er high spin yrast states and transitions from <sup>152</sup>Sm(<sup>13</sup>C,5n) 0-9208  
<sup>166</sup>Er(<sup>86</sup>Kr, X), 600 MeV, deeply inelastic, alignment of transferred ang. momentum, discrete γ-ray ang. correlations 0-47498  
<sup>145</sup>Eu high spin and isomeric states, transitions, weak coupling from <sup>144</sup>Sm(α,2npγ) 0-13348  
<sup>145</sup>Eu high spin core coupled states and transitions from <sup>142</sup>Nd(<sup>6</sup>Li, 3nγ) 0-42520  
<sup>145</sup>Eu high spin states, J<sup>π</sup> and transitions from (<sup>7</sup>Li,4nγ) and (<sup>6</sup>Li,3nγ) 0-47350  
<sup>145</sup>Eu level and transition effects on <sup>145</sup>Gd decay anomalies 0-32244  
<sup>152</sup>Eu, isomeric levels and transitions, Nilsson model 0-18195  
<sup>A</sup>F, A=18, 19, E2 transition rates calc., shell model with effective interaction and charges 0-47423  
<sup>19</sup>F, coupled channel orthogonality condition model 0-47384  
<sup>19</sup>F low lying band state lifetimes, stopping power, transition strengths from <sup>15</sup>N(α,γ) 0-42585  
<sup>20</sup>F cross sections and anal. power, compound nucleus contrib. Ericson fluctuations from <sup>18</sup>O(d,p), pol. d 0-22803  
<sup>A</sup>Fe, A=54-56, high spin states, energy levels, spectroscopic factors, EM props., shell model 0-47359  
<sup>54</sup>Fe high spin states, transitions and J<sup>π</sup> values from <sup>52</sup>Cr(α,Znγ) 0-455  
<sup>54</sup>Fe(α,α'), coupled channels calc., capture cross section, GQR decay modes 0-27654  
<sup>54</sup>Fe(p,p'), 39, 62 MeV, DWBA anal., collective spectra, direct process contrib. (*Russian*) 0-13408  
<sup>56</sup>Fe(γ,γ), up to 12 MeV, highly excited spin-1 resonances, γ-transitions 0-13427  
<sup>67</sup>Ga γ- and X-ray emission probabilities and half-life obs. 0-32242  
<sup>69</sup>Ga(n,n'γ), fast n, levels, J<sup>π</sup>, transitions and mixing ratios, statistical anal. (*Russian*) 0-13382  
<sup>72</sup>Ga, 3-2<sup>+</sup> first forbidden beta transitions, β-γ ang. correlation, nuclear matrix elements 0-42599  
<sup>A</sup>Gd(n,γ), A=154,156-8, 2, 24 keV, resonance averaged γ-spectra, level and J<sup>π</sup> appls. 0-37347  
<sup>153</sup>Gd, populated in <sup>152</sup>Eu decay 0-22768  
<sup>154</sup>Gd multiphonon vibr. bands, dynamic deformation theory 0-5035  
<sup>66</sup>Ge levels, lifetimes and mixing ratio, in-beam γ-spectroscopy from <sup>54</sup>Fe(<sup>14</sup>N,npγ) 0-42541  
<sup>66</sup>Ge states and decay scheme, polarisations J<sup>π</sup> and ang. distrib. from <sup>58</sup>Ni(<sup>10</sup>B,pnγ) 0-22692  
<sup>69</sup>Ge high spin states, EM props., branching and mixing ratios from <sup>53</sup>Mn(<sup>16</sup>O,pn) 0-13347  
<sup>2</sup>H γ-energy and binding energy from <sup>1</sup>H(n,γ) 0-52564  
<sup>2</sup>H(γ,pr) photoexcitation in Δ(1236) region 0-22813  
<sup>3</sup>He(<sup>3</sup>He,d<sup>3</sup>He), three body break up reaction energy spectra, computer program 0-27593  
<sup>3</sup>He(<sup>3</sup>He,p<sup>3</sup>He), three body break up reaction energy spectra, computer program 0-27593  
<sup>4</sup>He, parity mixing below 30 MeV excitation energy for ΔT=0,1 transitions 0-52604  
<sup>He</sup>(γ,pr), photoexcitation in Δ(1236) region 0-22813  
<sup>A</sup>Hi, A=166, 168, 170, 172, yrast states, quadrupole moments and B(E2) values, microscopic calcs. 0-32147  
<sup>171</sup>Hf, hindered electric dipole transitions and lifetimes from (HI,xn) reactions 0-9263  
<sup>172</sup>Hf yrast band and high spin states, 22<sup>+</sup>→20<sup>+</sup> transition, band crossing from <sup>160</sup>Gd(<sup>16</sup>O,4n) 0-42523  
<sup>A</sup>Hg, A=198, 200, rigid asymmetric rotor model descript., E2 and E4 props. 0-13403  
<sup>201</sup>Hg, HF calc., shape and lowest band struct., B(E2) values 0-32148  
<sup>201</sup>Hg missing  $\epsilon_{1/2}$  state Coulomb excitation, level scheme, J<sup>π</sup>, transitions using (α,α), (<sup>16</sup>O, <sup>16</sup>O) 0-47386  
<sup>A</sup>Ho, A=153, 160, isomeric levels and transitions, Nilsson model 0-18195  
<sup>163</sup>Ho(<sup>86</sup>Kr,X), 620 MeV, deep inelastic scatt., ang. momentum transfer, γ-ray multiplicities 0-27665  
<sup>166</sup>Ho, internal hyperfine field obs. using β-γ directional correl. 0-32229  
<sup>166</sup>Ho low lying levels and transitions, 54.24 keV level mag. moment from <sup>166</sup>Dy decay 0-13380  
<sup>123</sup>I, bands and decay props., core-particle coupling and polarisation effects 0-13354  
<sup>121</sup>In(n,nγ), fast n, γ-ang. distrib., level ang. momenta 0-18224  
<sup>121</sup>In, A=113, 115, excitation by photon less positron annihilation, isomeric γ-transitions (*Russian*) 0-5089  
<sup>109</sup>In high spin states, transitions, isomeric state, negative parity bands from <sup>107</sup>Ag(α, 2nγ) 0-451  
<sup>114</sup>In, internal conversion on outer electron shells, 191 keV E4 transition 0-42587  
<sup>117</sup>In level scheme, J<sup>π</sup> and transitions from <sup>117</sup>Cd isomer decay, unified model anal. 0-32193  
<sup>192</sup>Ir levels, resonances and low energy γ-rays from <sup>191</sup>Ir(n,γ) 0-47397  
<sup>A</sup>K, A=37,39, levels, excitation and microscopic form factors, DWBA calcs. from Ca(p,α) 0-32185  
<sup>A</sup>K, A=45,46, levels, lifetimes and transitions from Ar β-decay 0-42597  
<sup>Kr</sup> even isotopes, collective levels and B(E2) values, IBA calcs. 0-27539  
<sup>A</sup>Kr, A=74-82, even-even isotopes, B(E2) values and collectivity, interacting boson approx. 0-27537  
<sup>78</sup>Kr band struct., level scheme, from γγ-coincidence from <sup>65</sup>Cu(<sup>16</sup>O, 2np) 0-18177  
<sup>78</sup>Kr band structs., in-beam γ-rays from <sup>68</sup>Zn(<sup>12</sup>C, 2n) 0-22672  
<sup>78</sup>Kr high spin levels, bands and transitions, level lifetimes from <sup>68</sup>Zn(<sup>12</sup>C,Zn) 0-42525  
<sup>78</sup>Kr high spin states, transitions and lifetimes from (<sup>16</sup>O,2np), (<sup>19</sup>F,2nα), (<sup>16</sup>O,2n), (<sup>12</sup>C,2n) 0-27534



## nuclear energy level transitions continued

- <sup>85</sup>Kr level scheme and transitions, delayed neutrons from <sup>85</sup>Br  $\beta$ -decay 0-42600
- <sup>131</sup>La—<sup>131</sup>La decay scheme,  $\gamma$ , X-ray and conversion electron spectra (*Russian*) 0-32241
- <sup>138</sup>La, radioactive decay meas., half life,  $\gamma$  energies 0-13418
- <sup>139</sup>La(n, $\gamma$ ), non-statistical capture, radiative widths,  $\gamma$ -ray doorway state model 0-37389
- <sup>6</sup>Li(<sup>3</sup>He, <sup>3</sup>He), excitation functions 0-18223
- <sup>171</sup>Lu levels, transitions and  $J^\pi$  values from <sup>172</sup>Hf EC decay 0-18249
- <sup>171</sup>Lu isomeric states and spins, transition probability from <sup>181</sup>Ta(n, $\alpha$ ) 0-52582
- <sup>2</sup>Mg hole states, transitions and spectroscopic factors, DWBA anal. of <sup>24</sup>Mg(p,d) 0-32161
- <sup>24</sup>Mg, <sup>16</sup>O+ $\alpha$ + $\alpha$  cluster model, energy level structure 0-18215
- <sup>24</sup>Mg ( $\gamma$ ,p), 17-30 MeV, giant dipole resonances and transitions, shell effects (*Russian*) 0-13434
- <sup>24</sup>Mg continuum states, branching ratios from <sup>12</sup>C(<sup>16</sup>O,  $\alpha\alpha$ ) 0-22661
- <sup>24</sup>Mg,  $K^\pi=0^-$ ,  $K^\pi=3^-$  bands, radiative and  $\alpha$ -widths from ( $\alpha$ , $\gamma$ ), (<sup>16</sup>O, $\alpha$ ) 0-18173
- <sup>24</sup>Mg yrast and high spin states up to 24 MeV, ang. distrib. from <sup>10</sup>B(<sup>16</sup>O, d) 0-18175
- <sup>24</sup>Mg(<sup>13</sup>C, <sup>13</sup>C'), 35 MeV,  $\gamma$ -rays and spin flip 0-18189
- <sup>Mo</sup>, A=94, 96, 98, multiparticle states, method of generalised seniority 0-22759
- <sup>Mo</sup>(n, $\gamma$ ) A=98, 100 resonance parameters, capture  $\Gamma$ -rays and reaction mechanism 0-18272
- <sup>Mo</sup> static quadrupole moment of first  $2^+$  state from ( $\alpha$ , $\alpha'$ ), (<sup>16</sup>O, <sup>16</sup>O') 0-5061
- <sup>14</sup>N( $\alpha$ ,n $\gamma$ ), rare earth nuclei, complete fusion process n and  $\gamma$  multiplicity 0-18363
- <sup>14</sup>N, energy levels up to 11.05 MeV, transitions and resonance decay from <sup>13</sup>C(p, $\gamma$ ) 0-47376
- <sup>14</sup>N( $\gamma$ , $\pi^-$ ) <sup>14</sup>O, 145-325 MeV, Gamow-Teller suppression and M1 radiative widths 0-52609
- <sup>14</sup>N(n, $\gamma$ ),  $\gamma$ -ray energies, calibration standards 0-52613
- <sup>15</sup>N excited states and transitions from <sup>15</sup>C beta decay 0-18248
- <sup>15</sup>N low lying states, cross sections and anal. power, transitions, spectroscopic factors from <sup>14</sup>N(d,p), pol. d 0-32183
- <sup>91</sup>Nb, energy spectra and EM props. using broken pair model 0-499
- <sup>91</sup>Nb B(E $\lambda$ ) transitions, quasiparticle-phonon multiplet, nuclear field theory for superfluid nuclei 0-47427
- <sup>93</sup>Nb( $\alpha$ , X), 15-72 MeV, excitation functions and spallation cross-sections 0-18274
- Nd(<sup>16</sup>O, <sup>16</sup>O), 40-48 MeV, even nuclei,  $2^+$  state E2 transition probabilities and quadrupole moments 0-18234
- <sup>144</sup>Nd levels and transitions,  $\gamma$ -ray spectra from <sup>144</sup>Pr $\beta$ -decay (*French*) 0-18250
- <sup>147</sup>Nd, beta spectrum, hard component 0-22769
- <sup>150</sup>Nd(<sup>20</sup>Ne,X), 115, 130 MeV,  $\gamma$ -continuum multiplicity distrib., yrast bump 0-9265
- <sup>18</sup>Ne cross section, excitation function and double isobaric analogue state from <sup>18</sup>O( $\pi^+$ ,  $\pi^-$ ) 0-27596
- <sup>20</sup>Ne continuum states,  $J^\pi$  and branching from <sup>12</sup>C(<sup>12</sup>C,  $\alpha\alpha$ ) 0-22660
- <sup>20</sup>Ne excitation functions, resonance search from <sup>10</sup>B(<sup>14</sup>N,  $\alpha$ ) 0-27614
- <sup>20</sup>Ne high spin states,  $J^\pi$  and  $\alpha$ -decay branching ratios from <sup>16</sup>O(<sup>12</sup>C, <sup>8</sup>Be) 0-18166
- <sup>20</sup>Ne levels,  $J^\pi$ , branching ratio and EM transition rates from <sup>16</sup>O+ $\alpha$  0-42540
- <sup>20</sup>Ne non-isolated resonances, excitation functions and ang. distrib. from <sup>20</sup>Na(p, $\alpha$ ) (*Chinese*) 0-22788
- <sup>20</sup>Ne resonances,  $J^\pi$ , excitation functions and branching ratio from <sup>19</sup>F(p, $\gamma$ ) 0-22787
- <sup>20</sup>Ne+<sup>12</sup>C, 6.3-13.8 MeV, total fusion cross section, S-factor,  $\gamma$ -yields 0-22877
- <sup>4</sup>Ni, A=57, 59, 61, 63, variation of spectra, isospin mixing 0-13401
- <sup>4</sup>Ni(<sup>40</sup>Ca, fusion), A=58, 60, 62, 113-170 MeV, fusion cross sections and excitation functions 0-32315
- <sup>56</sup>Ni excitation functions from <sup>40</sup>Ca(<sup>16</sup>O, X) fusion 0-18362
- <sup>58</sup>Ni(<sup>16</sup>O, X), 100 MeV, deep inelastic, fragment spin polarisation and alignment,  $\gamma$ -rays 0-18284
- <sup>58</sup>Ni(e,e'), 120-264 MeV,  $J^\pi=6^+$ , 5.125 MeV state isoscalar character, form factors, transition strengths 0-9262
- <sup>58</sup>Ni( $\gamma$ , $\gamma$ ), M1 strength isospin splitting for dipole ang. distrib. states 0-13412
- <sup>60</sup>Ni, 1173 keV transition M3/M2 mixing ratio meas. 0-52608
- <sup>62</sup>Ni( $\gamma$ ,X), 19.2-26.2 MeV, photoneutron and photoproton spectra, giant dipole resonance-decay, isospin conservation 0-13443
- <sup>238</sup>Np levels, resonances and transitions from <sup>237</sup>Np(n, $\gamma$ ) 0-52589
- <sup>239</sup>Np, high pressure meas. of gamma transitions 0-18225
- <sup>40</sup>O, A=18, 19, E2 transition rates calc., shell model with effective interaction and charges 0-47423
- <sup>16</sup>O high spin states,  $J^\pi$  and  $\alpha$ -decay branching ratios from <sup>12</sup>C(<sup>12</sup>C, <sup>8</sup>Be) 0-18166
- <sup>16</sup>O magnetic dipole strength 0-37385
- <sup>16</sup>O+<sup>16</sup>O, fusion cross section gross struct., excitation functions, coupled channel method 0-52705
- <sup>16</sup>O( $\alpha$ , $\alpha'$ ) 17 to 27 MeV, backscatt., dynamic deformation and excitation functions, optical anal. 0-18227
- <sup>16</sup>O(e,e), T=1 level form factors, Helm model, pion photoprod. and muon capture appls. 0-52553
- <sup>16</sup>O( $\gamma$ ,n), 25-45 MeV, isovector giant quadrupole resonance evidence, E2 cross section 0-18268
- <sup>16</sup>O(p,p'), 1 GeV, proton polarisation in natural parity level excitation (*Russian*) 0-42634
- <sup>16</sup>O( $\pi$ , $\pi'$ ), ~180 MeV, isospin mixing, levels, excitation functions and ang. distrib. 0-42543
- <sup>17</sup>O levels, resonances,  $J^\pi$  and radiative width from <sup>14</sup>N(t, $\gamma$ ) 0-47389
- <sup>17</sup>O( $\gamma$ ,n), 8.5-39.7 MeV, cross section, giant dipole and pygmy resonance decays 0-42619
- <sup>18</sup>O level gamma decay from <sup>17</sup>O(n, $\gamma$ ) 0-52623
- <sup>18</sup>O( $\pi$ , $\pi'$ ), 164 MeV, yrast state and level excitation, DWIA calcs., shell model context 0-42526
- <sup>Os</sup>, A=186, 188, 190, 192, rigid asymmetric rotor model descript., E2 and E4 props. 0-13403
- <sup>P</sup>, A=31, 33, levels and transition j-depend., DWBA anal. for Si(<sup>19</sup>F, <sup>16</sup>O) 0-42542
- <sup>30</sup>P high spin two nucleon states decay props. from <sup>28</sup>Si( $\alpha$ , d $\gamma$ ) 0-13402
- <sup>141</sup>P(n, $\gamma$ ), resonance parameters, s-wave radiative and reduced neutron widths 0-47471
- <sup>231</sup>Pa, high pressure meas. of gamma transitions 0-18225

## nuclear energy level transitions continued

- <sup>233</sup>Pa, high pressure meas. of gamma transitions 0-18225
- Pb region, mag. moments and M1, M2 and M4 values, self consistent calcs. 0-47371
- <sup>208</sup>Pb, A=197, 198, low energy  $\gamma$ -transitions and level lifetimes from <sup>186</sup>W(<sup>16</sup>O, xn) 0-18221
- <sup>208</sup>Pb( $\alpha$ , $\alpha$ ), A=206, 208, 120 MeV, isoscalar resonance excitation, low lying transitions, DWBA calc. 0-512
- <sup>210</sup>Pb, population of  $0^+$ , alpha-decay of <sup>210</sup>Po 0-22775
- <sup>207</sup>Pb parity assignments and M1 radiative strength from <sup>206</sup>Pb(n,n) 0-52614
- <sup>208</sup>Pb M1, E1, M2, E2 localised  $\gamma$ -ray strengths from <sup>207</sup>Pb(n, $\gamma$ ) 0-37350
- <sup>208</sup>Pb(<sup>16</sup>O, <sup>16</sup>O'), 315 MeV, continuous spectrum and giant resonance excitation, coherent state model test 0-32252
- <sup>208</sup>Pb(e,e'), E2 transitions of fragmented isoscalar quadrupole giant resonance 0-22758
- <sup>208</sup>Pb(e,e'), 60 MeV, backward scatt.,  $2\hbar\omega$  M1 excitation search 0-32234
- <sup>208</sup>Pb(p,p'), 39, 62 MeV, DWBA anal., collective spectra, direct process contrib. (*Russian*) 0-13408
- <sup>210</sup>Pb ground state decay 0-47429
- <sup>109</sup>Pd levels,  $J^\pi$ , transitions, unique parity states, and spectroscopic factors from <sup>108</sup>Pd(n, $\gamma$ ) 0-42547
- <sup>143</sup>Pm high spin states,  $J^\pi$ , transitions, isomer g-factors from (d,2N), ( $\alpha$ ,2N) 0-32154
- <sup>147</sup>Pm levels, transitions,  $\gamma\gamma$ -coincidences and IC electrons from <sup>147</sup>Nd decay 0-18243
- <sup>149</sup>Pm,  $\beta^-$  decay, <sup>149</sup>Sm level scheme 0-22750
- <sup>149</sup>Pm,  $\beta$ -decay, nucl. matrix elements, calc.,  $\gamma$ -transitions 0-52628
- <sup>149</sup>Pm high spin states and bands, rot. description and in-beam study from <sup>150</sup>Nd(p,2n $\gamma$ ) 0-32153
- <sup>210</sup>Po, alpha-decay, population of  $0^+$  of <sup>206</sup>Pb 0-22775
- <sup>Pr</sup> atom, nucl. level shift and radiative transitions (*Russian*) 0-28121
- <sup>147</sup>Pr(n, $\gamma$ ), non-statistical capture, radiative widths,  $\gamma$ -ray doorway state model 0-37389
- Pt, even mass, ground and gamma band EM transition rates, asymmetric rotor model 0-32231
- <sup>195</sup>Pt, A=190, 192, 194, levels and  $\gamma$ -transition reduced probab., interacting boson model 0-18196
- <sup>195</sup>Pt, A=192, 194, 196, rigid asymmetric rotor model descript., E2 and E4 props. 0-13403
- <sup>195</sup>Pt, A=192, 194, 196, states,  $J^\pi$ , ang. distrib. and transitions, DWBA anal. of Pt(p,t) 0-468
- <sup>187</sup>Pt, levels,  $J^\pi$ ,  $T_{1/2}$ , possible E0 transitions from <sup>187</sup>Au decay (*French*) 0-32230
- <sup>196</sup>Pt (<sup>20</sup>Ne, <sup>20</sup>Ne'), excited states, lifetime meas. using recoil-distance method 0-13413
- <sup>196</sup>Pt (<sup>58</sup>Ni, <sup>58</sup>Ni'), excited states, lifetime meas. using recoil-distance method 0-13413
- <sup>196</sup>Pt negative parity states in partially decoupled bands,  $\gamma$ -transitions from <sup>195</sup>Pt(n, $\gamma$ ) 0-47360
- <sup>239</sup>Pu, A=238, 240, fission isomer rot. spectra  $I^2(1+1)^2$  correction 0-18229
- <sup>239</sup>Pu, high pressure meas. of gamma transitions 0-18225
- <sup>239</sup>Pu(n,X), thermal n, gamma spectra from capture, fission and fission products 0-37352
- <sup>244</sup>Pu excited states, mass excess and shell gap, L=0 transition from <sup>244</sup>Pu(t,p) 0-9236
- <sup>83</sup>Rb, A=96, 98,  $\beta$ -decay schemes and total energies, mass excess and separation energies 0-27601
- <sup>83</sup>Rb high spin states, positive and negative parity bands from (<sup>6</sup>Li, 3n), ( $\alpha$ , 2n) 0-18178
- <sup>Re</sup>, A=181, 182, 187, magnetic moments meas. by PAC 0-22688
- <sup>Re</sup>, A=183, 184, nuclear K-X-ray satellites, Z=50-83, decay scheme 0-42984
- <sup>187</sup>Re low lying level struct. and transitions, E2/E1 mixing ratios from <sup>187</sup>W decay 0-27557
- <sup>104</sup>Rh(n, $\gamma$ ), 0.5-3.0 MeV,  $\gamma$ -spectra strength functions 0-32240
- <sup>223</sup>Rn—<sup>223</sup>Fr—<sup>224</sup>Ra decay,  $\gamma$ -rays IC electrons and  $e\gamma$  coincidences 0-18239
- <sup>96</sup>Ru, A=96, 98, 100, multiparticle states, method of generalised seniority 0-22759
- <sup>96</sup>Ru(p,p' $\gamma$ ), A=96, 98, 5-8 MeV, level schemes, transitions, vibr. state, mixing ratios 0-18199
- <sup>94</sup>Ru levels and  $\gamma$ -transitions from <sup>94</sup>Rh decay 0-18244
- <sup>97</sup>Ru populated in <sup>88</sup>Sr(<sup>13</sup>C, 3n $\gamma$ ), band-like structures 0-32146
- <sup>97</sup>Ru decay scheme from <sup>99</sup>Tc $\beta$ -decay 0-42596
- <sup>102</sup>Ru  $2^+$  state quadrupole moment, reorientation effects and multiple Coulomb excitation from ( $\alpha$ , $\alpha'$ ), (<sup>16</sup>O, <sup>16</sup>O) 0-5063
- <sup>32</sup>S levels and  $J^\pi$  from <sup>32</sup>Cl  $\beta^-$  decay 0-22772
- <sup>113</sup>Sb, A=121, 123, levels below 2 MeV, spins, transitions and mixing ratio from (p, $\gamma$ ), (n,n' $\gamma$ ) 0-32191
- <sup>113</sup>Sb, 15 MeV excitation, average nucl. lifetime determ. 0-43164
- <sup>45</sup>Sc energy levels, resonances, spin and parity from <sup>45</sup>Sc(n, $\gamma$ ) 0-52673
- <sup>46</sup>Sc level deexcitation, E1 and M1 absolute radiative widths from <sup>45</sup>Sc(n, $\gamma$ ) 0-52622
- <sup>46</sup>Sc transition polarisation, levels and spin assignments from <sup>45</sup>Sc(n, $\gamma$ ), pol. n 0-52656
- <sup>76</sup>Se, level scheme from  $\gamma\gamma$  coincidence meas. of <sup>76</sup>As decay 0-22754
- <sup>76</sup>Se high spin levels, transitions,  $J^\pi$  assignments from <sup>76</sup>Ge( $\alpha$ ,n $\gamma$ ) 0-459
- <sup>28</sup>Si  $8^+$  state, level systematics and energy spectra from <sup>25</sup>Mg(<sup>12</sup>C, <sup>8</sup>Be) 0-42528
- <sup>28</sup>Si levels and  $J^\pi$  from <sup>28</sup>P  $\beta^+$  decay 0-22772
- <sup>28</sup>Si p3/2 neutron resonance  $\gamma$ -decay, partial rad. widths from Si(n, $\gamma$ ) 0-52617
- <sup>28</sup>Si(<sup>12</sup>C, <sup>12</sup>C), 27.8-31.5 MeV, elastic and inelastic excitation functions, fine struct., statistical anal. 0-18269
- <sup>28</sup>Si(<sup>16</sup>O, <sup>16</sup>O), 30-32.7 MeV, elastic and inelastic excitation functions, fine struct., statistical anal. 0-18269
- <sup>28</sup>Si(n,n' $\gamma$ ), 13.9 MeV, spin flip probability from 1.78 MeV state, direct theory 0-9234
- <sup>27</sup>Al excitation functions from <sup>27</sup>Al(<sup>3</sup>He, p) 0-47493
- <sup>29</sup>Si neutron resonance,  $\gamma$ -spectra, partial and total radiative widths from <sup>28</sup>Si(n, $\gamma$ ) 0-42578
- <sup>150</sup>Sm(<sup>10</sup>Kr,X), A=144, 154, 490 MeV, transfer reactions and associated  $\gamma$ -multiplicity moments 0-18342
- <sup>150</sup>Sm(n, $\gamma$ ), resonance and thermal n,  $\gamma$ -spectra, recent expt. review, non-statistical effects 0-37383
- <sup>151</sup>Sm, gamma spectra, energy levels (*Dutch*) 0-47430
- <sup>152</sup>Sm, populated in <sup>152</sup>Eu decay 0-22768
- Sn, deep h-le state fragmentation, strength functions, giant resonances, quasiparticle phonon model 0-37320



## nuclear energy level transitions continued

- <sup>54</sup>Sn odd-mass isotopes, hole-state analogues, line broadening and Coulomb displacement energies 0-52560
- <sup>106</sup>Sn excited states from <sup>106</sup>Co (<sup>3</sup>He,3n), coincidence experiments 0-52607
- <sup>112</sup>Sn(p,p'), 20.51, 25.0 MeV, energy levels, excitation functions and ang. distrib. 0-32184
- <sup>116</sup>Sn levels, J<sup>π</sup> and transitions from <sup>115</sup>Sn(n,γ) 0-52587
- <sup>120</sup>Sn γ-spectra, E1 and M1 hindrance factors from <sup>123</sup>Te(n,γ,α) 0-37386
- <sup>132</sup>Sn, energy levels, gamma transitions, spin and parity 0-9239
- <sup>132</sup>Sn level struct., lifetimes, γ-γ coincidences, internal conversion from <sup>235</sup>U fission 0-52584
- <sup>84</sup>Sr, A=80,82,84-86, levels and transitions from Kr(<sup>3</sup>He,n) 0-18201
- <sup>84</sup>Sr, A=96,98, β-decay schemes and total energies, mass excess and separation energies 0-27601
- <sup>85</sup>Sr high spin states, J<sup>π</sup> and de-excitation from Kr(α,xn) 0-42516
- <sup>93</sup>Sr excited state depopulation γ-rays, n coincidence from <sup>94</sup>Rb β-delayed n decay 0-52631
- <sup>177</sup>Ta, magnetic moments meas. by PAC 0-22688
- <sup>147</sup>Tb, A=147, 148, high spin particle-hole states, octupole M2/E3 isomers from <sup>151</sup>Eu(α,xn) 0-18171
- <sup>160</sup>Tb β-decay, oriented nuclei, γ transitions multipole mixing parameters 0-18240
- <sup>14</sup>Tc, A=93-96, excitation functions and isomer ratios from <sup>93</sup>Nb(α,xn) (x=1 to 4) 0-492
- <sup>95</sup>Tc, energy levels from <sup>95</sup>Mo(p, nγ) <sup>95</sup>Tc 0-37372
- <sup>96</sup>Tc, high spin states, γ-energy, intensity, coincidence, ang. distrib. and electron conversion from <sup>93</sup>Nb(α,n) 0-52554
- <sup>100</sup>Tc low lying and isomeric levels, transitions and mean lines from <sup>100</sup>Mo(p,n,γ) 0-42548
- <sup>102</sup>Tc deduced levels, tentative J<sup>π</sup> and transitions from <sup>102</sup>Mo decay 0-52630
- <sup>117</sup>Te, A=117, 119, 121, collective excitations, high spin states and transitions from (α, Zn)(d, Zn)(<sup>3</sup>He, 3n) 0-13346
- <sup>130</sup>Te(n,γ), resonance and thermal n, γ-spectra, recent expt. review, non-statistical effects 0-37383
- <sup>132</sup>Te low lying levels and EM props., shell model description 0-42549
- <sup>228</sup>Th, high pressure meas. of gamma transitions 0-18225
- <sup>231</sup>Th, rotational band level diagram from α-decay and γ-transitions 0-18156
- <sup>232</sup>Th(<sup>16</sup>O,γ), transfer induced fission, excitation functions and cross sections 0-13515
- <sup>232</sup>Th(<sup>19</sup>F,γ), transfer induced fission, excitation functions and cross sections 0-13515
- <sup>232</sup>Th(p,X), 10-100 MeV, spallation residue excitation functions, fissionability 0-18353
- <sup>50</sup>Ti high spin states, transitions and J<sup>π</sup> values from <sup>48</sup>Ca(α,Zn,γ) 0-455
- <sup>117</sup>Ti, A=199, 200 cross section and excitation function statistical anal. from <sup>197</sup>Au(α,xn) (Rumanian) 0-22846
- <sup>192</sup>Ti high spin band struct. and transitions, isomeric state from <sup>181</sup>Ta(<sup>16</sup>O,xn,γ) 0-47353
- <sup>194</sup>Ti high spin states, excitation functions, I<sup>π</sup>=8<sup>-</sup> isomeric state from <sup>181</sup>Ta(<sup>16</sup>O,5n) 0-32163
- <sup>201</sup>Ti γ- and X-ray emission probabilities and half-life obs. 0-32242
- <sup>201</sup>Ti levels, transitions and J<sup>π</sup> assignments from <sup>201</sup>Pb decay 0-5099
- <sup>169</sup>Tm, excited state lifetime meas. 0-32237
- <sup>170</sup>Tm gamma-ray strength functions from spectrum fitting method from <sup>169</sup>Tm(n,γ) 0-52616
- <sup>170</sup>Tm(n,γ), 0.5-3.0 MeV, γ-spectra strength functions 0-32240
- U (M.f), muon excitation probabilities, muonic atoms, Schrodinger eqn. 0-47515
- <sup>184</sup>U, A=236,238, fission isomer rot. spectra I<sup>2</sup>(I+1)<sup>2</sup> correction 0-18229
- <sup>184</sup>U(n,X), A=233, 235, thermal n, gamma spectra from capture, fission and fission products 0-37352
- <sup>232</sup>U, high pressure meas. of gamma transitions 0-18225
- <sup>235</sup>U<sup>M</sup> prod. by nuclear excitation by electron transition in plasma 0-22668
- <sup>236</sup>U fission shape isomer, γ-decay from <sup>238</sup>U(γ,2n) 0-18230
- <sup>236</sup>U low lying levels from 4<sup>-</sup> isomer decay in (n,e), (n,γ) 0-47396
- <sup>237</sup>U virtual photon excited state decay and total cross section of <sup>238</sup>U(e,n) 0-22757
- <sup>238</sup>U(n,γ), 2, 24 keV, resonance averaged γ-spectra, level and J<sup>π</sup> appls. 0-37347
- <sup>51</sup>V, γ-strength function, γ-ray spectra, average resonance method from <sup>50</sup>Ti(p,γ) 0-9257
- <sup>171</sup>W, A=173, 175, hindered electric dipole transitions and lifetimes from (H<sup>1</sup>,xn) reactions 0-9263
- <sup>171</sup>W, A=174, 175 quasicontinuum γ-rays yrast cascade dipole component, moment of inertia from Dy(<sup>16</sup>O, xn,γ) 0-47424
- <sup>171</sup>W, A=184, 186, rigid asymmetric rotor model descript., E2 and E4 props. 0-13403
- <sup>183</sup>W(α,α'), 15 MeV, level and band Coulomb excitation, B(E2) values 0-32233
- <sup>114</sup>Xe excited states and γ-rays from <sup>114</sup>Cs β-decay 0-47436
- <sup>116</sup>Xe level scheme and yrast band, in-beam γ-study from <sup>106</sup>Cd(<sup>12</sup>C, 2n) 0-13360
- <sup>125</sup>Xe 11/2<sup>-</sup>→9/2<sup>-</sup> transition in odd parity band from <sup>124</sup>Te(α, 3n) 0-9203
- <sup>136</sup>Xe(n,γ), resonance and thermal n, γ-spectra, recent expt. review, non-statistical effects 0-37383
- <sup>89</sup>Y, energy spectra and EM props. using broken pair model 0-499
- <sup>89</sup>Y high spin states and decay scheme from <sup>87</sup>Rb(α,2n,γ) 0-32166
- <sup>89</sup>Y(π, π'), 163, 240 MeV, giant resonance pionic excitation 0-52561
- <sup>98</sup>Y<sup>β</sup>, β-decay schemes and total energies, mass excess and separation energies 0-27601
- <sup>146</sup>Yb, A=161, 162, 166, yrast cascade dipole component from Sm(<sup>16</sup>O,4n) 0-9266
- <sup>146</sup>Yb, A=164, 166, high spin yrast states and transitions from Gd(<sup>13</sup>C,5n) 0-9208
- <sup>146</sup>Yb, A=169-x, γ de-excitation and ang. momentum distrib. after fast α-emission from <sup>159</sup>Tb(<sup>14</sup>N,αxn) 0-18228
- <sup>146</sup>Yb(<sup>16</sup>O,γ), A=168-176, even nuclei, 58-62 MeV, Coulomb excitation, vibr. and rot. states 0-32162
- <sup>161</sup>Yb quasicontinuum γ-rays yrast cascade dipole component, moment of inertia from Sm(<sup>16</sup>O, xn,γ) 0-47424
- <sup>169</sup>Yb, populated in <sup>169</sup>Lu decay, meas. of γ-ray and conversion electron spectra 0-22766
- <sup>169</sup>Yb populated in <sup>169</sup>Lu decay, γ-ray and conversion electron spectra 0-22767
- <sup>173</sup>Yb M1 transitions from 636 keV level, multipole mixture parameters, penetration effect 0-18220

## nuclear energy level transitions continued

- <sup>91</sup>Zr primary γ-rays and binding energies from <sup>90</sup>Zr(n,γ) 0-52566
- <sup>64</sup>Zn, γ-ray studies of levels above 3.1 MeV 0-32238
- Zr even isotopes, quadrupole moments and E2 transition rates, broken pair approx. 0-52579
- <sup>42</sup>Zr, A=91, 92, 94, binding energy and primary γ-ray intensities from Zr(n,γ) 0-52565
- <sup>42</sup>Zr, A=92, 94, 96, multiparticle states, method of generalised seniority 0-22759
- <sup>42</sup>Zr(p,p'), A=94,96, 11.2-13.4 MeV, anal. power and excitation function T<sup>+</sup> fluctuations 0-42626
- <sup>90</sup>Zr, proton orbit sizes and E0 matrix element for 2 lowest 0<sup>+</sup> states 0-27546

## nuclear energy levels

- see also isobaric analogue states; nuclear collective states and giant resonances; nuclear resonances; nuclear spectroscopic factors
- <sup>19</sup>F levels, J<sup>π</sup> and ang. distrib. DWBA anal. of <sup>19</sup>F(p,d) 0-42545
- <sup>5</sup>Li states, phase shift anal. of <sup>3</sup>He(d,d) 0-47382
- A=11, 12, energy levels, transitions and resonances, compilation 0-46743
- A=140, nuclear data sheets, levels and transitions 0-31435
- A=190, Nilsson strength fragmentation, quadrupole and hexadecapole deformations 0-47394
- A=204, nuclear data sheets, levels, J<sup>π</sup> and transitions 0-31429
- A=212, nuclear data sheets, levels, J<sup>π</sup>, transitions 0-31430
- A=221, nuclear data sheets, levels, J<sup>π</sup>, transitions 0-31431
- A=225, nuclear data sheets, levels, J<sup>π</sup>, transitions 0-31432
- A=40-56, spectroscopy props. using pure configuration shell model (Chinese) 0-42584
- A=4-16, monopole giant resonances, state density radii and compressibility using hyperspherical functions (Russian) 0-27615
- A=60, nuclear data sheets, levels and transitions 0-31433
- A=64, nuclear data sheets, levels and transitions 0-31434
- A=71 nuclear data sheets, levels, J<sup>π</sup> and transitions 0-31428
- average resonance parameter eval. and calcs., statistical model for capture process 0-18271
- baryon-antibaryon nuclei, energy spectra and properties 0-22709
- boson model, interacting, shell-model basis, correspondence between fermion and boson states and operators 0-52593
- classification of states, unitary scheme 0-42550
- conference on neutron capture gamma ray spectroscopy, Upton, USA. (Sep. '78) 0-36780
- conference on nuclear physics with EM interactions, Mainz, Germany (June 1979) 0-22145
- coupled bands in even-even nuclei in RPA approach 0-32143
- dense Fermi systems, generalised perturbation theory, ground and low excited states 0-22741
- electron prod., deep inelastic scatt. and struct. from electron coincidence expts. at Stanford 0-22821
- even actinides, lowest 0<sup>+</sup> state excitation, collective phonon state, spectroscopic factors from (p,t), (t,p) 0-13410
- even nuclei, 2<sup>+</sup> excited states quadrupole moments, energy weighted sum rule appl. 0-9229
- even-even spherical nuclei, 2<sub>1</sub><sup>+</sup> state deformation parameter from (p,p) and EM excitation 0-27549
- excited nuclear states, lifetime meas. 0-5093
- excited simple and yrast states, mag. moments, transient mag. fields 0-5064
- excited state quadrupole moments meas. using Coulomb excitation 0-5065
- excited states, Young's diagram 0-42566
- finite nuclei and inhomogeneous infinite systems, ground states, FHNC method extension 0-22736
- fixed angular momentum moments and level densities, statistical spectroscopic methods 0-467
- ground state deformation energy, rot. band inertial parameter depend. 0-18185
- ground-state proton-neutron occupancies in the f-p shell 0-13381
- heavy ion collisions, nuclear level shifts, generalised relativistic Coulomb problem (Russian) 0-52586
- isobar propagation and collective effects, pion-nucleus and photoneuclear investigation 0-22676
- level density of nuclei and the superconductive-type pair interaction (Russian) 0-13383
- light muonic atoms, nuclear size effects, energy levels, Lamb shift 0-14254
- light nuclei, hyperspherical functions for size, excited states, compressibility, binding energy 0-22679
- N=50 isotones, transition probabilities, 1p<sub>3/2</sub> and 0f<sub>5/2</sub> hole excitation effects 0-47431
- neutron, alpha and nuclear matter, ground vacuum states 0-22738
- odd mass nuclei in 1f<sub>7/2</sub>, level density and spacings from resonance data anal. 0-18206
- odd-odd nuclei, pn multiplets x=I(I+1) energy depend., parabolic rule, nuclear states 0-13379
- pairing properties and superconductivity, semiclassical treatment, local density approx. of nuclear gap 0-32188
- pre-actinide nuclei, level density and fission probability collective effects (Russian) 0-13455
- proton-neutron basis, decomposition matrix rel. to basis of specified isospin T 0-37337
- quasi-elastic direct transfer reaction to continuum states, DWBA and diffraction model 0-18277
- radiative strength distrib. with energy, E1, M1 giant resonances, particle-hole calcs. 0-37349
- self-consistent field rearrangement in large nuclear deformations, HF calcs. 0-18184
- single particle orbitals, Coriolis attenuation problem, pairing plus recoil model 0-32159
- single-particle level density, excitation dependence of nuclear level density parameter 0-32149
- Skyrme-type interactions, spectroscopy of light nuclei, density dependent Hartree-Fock 0-22717
- Sn Z=50 region isotopes, system struct calcs. 0-18192
- strength functions, shell model calc. 0-32187
- SU<sub>3</sub> representation 0-42552
- superfluid model, isotopic invariance and pairing energies 0-22687
- three particle level spectrum, Thomas theorem and Efimov effect, N/D eqns. 0-42562
- total single particle energies, energy and N-averagings in shell correction method 0-22671



## nuclear energy levels continued

- warm nuclei, Thomas-Fermi model rel. to stellar collapse 0-51648  
 $Z=55-63$ , odd proton nuclei, low lying even parity states 0-27551  
 $(\gamma, p)$ ,  $>100$  MeV, using monochromatic photons, leading to final nuclear states 0-22814  
 $(n, e^-)$  high precision spectroscopy, internal conversion coeffs. for nuclear struct. 0-37353  
 $(n, \gamma)$ ,  $A=94-190$ , resonance capture, low lying level population fluctuations,  $\gamma$ -rays 0-52619  
 $(n, \gamma)$ , non-spherical even-even nuclei, energy gap from  $\gamma$ -transitions 0-47395  
 $(n, \gamma)$  spectroscopy, nuclear struct. investigation, review 0-37379  
 $(n, n)$ , single particle bound state, energy independ. optical model, asymmetry term 0-37316  
 $(N, X)$ , complex shell model, narrow resonances and bound states (Chinese) 0-42622  
 $(p, d)$ , 52 MeV, deeply bound hole state transition strength giant resonance, DWBA anal. 0-47426  
 $(p, p)$ , single particle bound state, energy independ. optical model, asymmetry term 0-37316  
 $(\pi, \gamma)$ , inverse pion photoprod., level struct. determ. 0-22863  
 $(\pi, \pi)$ , particle-hole state excitation, field theory calcs. (Russian) 0-37318  
 $(t, p)$  ground state cross section systematics in 2s-1d shell 0-5148  
 $^A\text{Ag}$ ,  $A=104, 106$ , levels,  $J^\pi$ , and isobaric analogue resonances from  $^{\text{Pd}}(n, n)$  0-32180  
 $^A\text{Ag}$ ,  $A=99, 101, 103$ , levels, transitions and  $J^\pi$  from Cd decay,  $^{\text{Pd}}(p, 2n\gamma)$  0-47383  
 $^{110}\text{Ag}$  low lying states, decay scheme and  $T_{1/2}$  from  $^{109}\text{Ag}(n, \gamma)$  0-47393  
 $^{110}\text{Ag}$  low-lying levels, from  $^{109}\text{Ag}(n, \gamma)$  obs. 0-47422  
 $\text{Ag}(p, f)$ , 600 MeV, fragment energies, cross sections level density and barrier heights 0-42723  
 $^{27}\text{Al}$ ,  $J^\pi=5/2$  state, cross section and analysing power ang. distrib. 0-18296  
 $^{28}\text{Al}$  ground state doublet ang. distrib., direct charge exchange model anal. from  $^{28}\text{Si}(^{18}\text{O}, ^{18}\text{F})$  0-9307  
 $^{28}\text{Al}$  levels, spins and  $\gamma$ -rays, multipole mixing from  $^{27}\text{Al}(n, \gamma)$ , pol. thermal 0-47398  
 $^{36}\text{Ar}$ , delayed proton and alpha emission, transition energies, levels,  $J^\pi$ , from  $^{36}\text{K}$  decay 0-52629  
 $^{38}\text{Ar}$  levels,  $J^\pi$  and transition strengths, DWBA anal. of  $^{40}\text{Ar}(p, t)$  0-47378  
 $^A\text{As}$ ,  $A=70, 72$ , level scheme, transitions,  $J^\pi$  and lifetimes from  $^{\text{Ge}}(p, n\gamma)$  0-2695  
 $^A\text{As}$  populated in  $^{75}\text{Se}$  decay, E0 transitions 0-22752  
 $^A\text{As}$ , level structure, transitions and  $J^\pi$ , from  $^{76}\text{Ge}(p, n\gamma)$  0-47379  
 $^{208}\text{At}$  energy levels and transitions, IC electrons from  $^{208}\text{Rn}$  decay 0-18242  
 $^{212}\text{At}$ , relative  $\alpha$ -decay width and excited levels, nuclear field theory 0-47437  
 $^{196}\text{Au}$  energy levels and Q-value from  $^{197}\text{Au}(\gamma, n)$  0-37329  
 $^{196}\text{Au}$  level spin assignments from  $\gamma$  ang. distrib. and circular polarisation from  $^{197}\text{Au}(n, \gamma)$  0-52570  
 $^{10}\text{B}$  levels,  $J^\pi$  and ang. distrib. from  $^9\text{Be}(^3\text{He}, d)$  0-42546  
 $^{10}\text{B}$   $T=1$  states,  $\gamma$ -transition strengths, lifetimes, branching and mixing ratios from  $^6\text{Li}(\alpha, \alpha)$  0-27594  
 $^{10}\text{B}$  transitions and levels from  $^{11}\text{B}(\gamma, n\gamma)$  (Russian) 0-13433  
 $^{11}\text{B}$  states, spectroscopic factors from DWBA anal. of  $^{12}\text{C}(p, 2p)$  0-5057  
 $^{11}\text{B}$ , struct. study of  $2\alpha+t$  system in orthogonality condition model, level energies and parity 0-5080  
 $^{11}\text{B}(e, e')$ , E1 transitions to unnatural parity states 0-22758  
 $^{14}\text{B}$ , mass excess and excited states from  $^{14}\text{C}(^{14}\text{C}, ^{14}\text{B})$  0-42676  
 $^A\text{B}$ ,  $A=130, 132, 134, 136$ , levels and EM props., ang. momentum projected quasiboson model 0-5067  
 $^A\text{Ba}(^3\text{S}, ^3\text{S})$ ,  $A=130, 132, 134, 136, 72-80$  MeV,  $2_1^+$  state mag. moments 0-47373  
 $^{139}\text{Ba}$  level scheme,  $J^\pi$  and  $\gamma$ -transitions from  $^{139}\text{Cs}$   $\beta$ -decay 0-42590  
 $^8\text{Be}$  isospin mixed  $2_1^+$  doublet, level parameters from  $^4\text{He}(\alpha, \alpha)$  0-27556  
 $^8\text{Be}$  lowest negative parity state, shell and cluster model calcs. from  $^7\text{Li}(p, p)$ ,  $^8\text{Be}$  lowest negative parity state, shell and cluster model calcs. 0-18205  
 $^9\text{Be}$ ,  $2s_{1/2}$  state obs. in  $^{10}\text{B}(t, \alpha)$  0-22691  
 $^9\text{Be}(e, e'p)$ , single hole state momentum and energy distrib. 0-22674  
 $^9\text{Be}(\gamma, \pi)$ , photoabsorption and sum rules, structure, RMS radius, polarizability and exchange parameters 0-22686  
 $^9\text{Be}(n, 2n)$  pseudolevel eval. validation 0-22697  
 $^{10}\text{Be}$  near threshold state from  $^7\text{Li}(t, ^7\text{Li})$  (Russian) 0-13484  
 $^{204}\text{Bi}$  excited states,  $\gamma$  rays, conversion electrons and  $\gamma\gamma$  coincidences from  $^{204}\text{Po}$ , EC 0-18241  
 $^{208}\text{Bi}$  two-particle, two-hole configuration, levels,  $J^\pi$  and excitation energies from  $^{210}\text{Bi}^m(p, t)$  0-32190  
 $^{208}\text{Bi}$  low lying levels and spectroscopic factors, EFR-DWBA anal. of  $^{208}\text{Pb}(^7\text{Li}, ^6\text{He})$  0-32182  
 $^{167}\text{Er}$  high intrinsic excitation levels,  $\gamma$ -decay props. from  $^{167}\text{Er}(n, \gamma)$  0-52588  
 $^{16,17}\text{O}$ , two centre shell model, molecular single particle states at level crossings 0-47354  
 $^A\text{C}(\pi, \pi)$ ,  $A=12, 13$ ,  $\sim 180$  MeV, isospin mixing, levels, excitation functions and ang. distrib. 0-42543  
 $^{12}\text{C}$  levels and resonance,  $\gamma$ -ray excitation curves from  $(p, \alpha\gamma)$ ,  $(p, p\gamma)$  0-9280  
 $^{12}\text{C}$  negative parity states lifetime limits and transition strengths from  $^{10}\text{B}(p, \gamma)$  0-5092  
 $^{12}\text{C}$  energy levels from  $(p, d)$  0-42667  
 $^{12}\text{C}$ , excited state struct.,  $\alpha$ -particle model 0-47385  
 $^{12}\text{C}(^{12}\text{C}, ^{12}\text{C})^*$ ,  $0_2^+$ ,  $3_1^-$ ,  $4_1^+$  state excitation functions, resonance structures 0-42616  
 $^{12}\text{C}(e, e')$ , 12.71 and 15.11 MeV level struct. and isospin mixing from form factors 0-32186  
 $^{12}\text{C}(n, X)$ , compound resonance decay based on bound and metastable single nucleon states (Russian) 0-5107  
 $^{12}\text{C}(\nu, \nu)$ ,  $(\bar{\nu}, \bar{\nu})$ , 15.11 MeV state excitation, cross sections, level decay 0-9258  
 $^{12}\text{C}(p, p)$ , 1 GeV, proton polarisation in natural parity level excitation (Russian) 0-42634  
 $^{13}\text{C}(\gamma, n)$ , 7.6-24 MeV, photoneutron ang. distrib., level scheme and  $J^\pi$  assignments 0-466  
 $^{13}\text{C}(\pi, \pi)$ , 162 MeV, pure n and p transitions, differential cross sections 0-5040  
 $^{15}\text{C}$  0.74 MeV  $5/2^+$  state g-factor, shell model interpretation from  $^3\text{H}(^{13}\text{C}, p)$  0-32176  
 $^A\text{Ca}$ ,  $A=40, 48$ , neutron densities and single particle struct. 0-32165

## nuclear energy levels continued

- $^{41}\text{Ca}$   $1f_{7/2}$  neutron radial distrib., single particle, orbits, RMS radii from  $^{40}\text{Ca}(^{13}\text{C}, ^{12}\text{C})$  0-42532  
 $^{48}\text{Ca}$  ( $^{12,13}\text{C}, X$ ), elastic, inelastic and single nucleon transfer excitation functions,  $^{48}\text{Ca}$  levels 0-13492  
 $^{111}\text{Cd}$ ,  $A=113, 115$  from  $^{113,115}\text{Ag}$   $\beta$ -decay 0-47432  
 $^{106}\text{Cd}(^{32}\text{S}, ^{32}\text{S})$ ,  $A=106, 108, 110, 112, 114, 116, 72-80$  MeV,  $2_1^+$  state mag. moments 0-47373  
 $^{140}\text{Cd}(n, n\gamma)$ ,  $A=114, 116$ , energy levels, spins, and gamma-ray multipole mixing ratios investig. 0-52580  
 $^{111}\text{Cd}^m$ , nuclear orientation in Zn and Be, 245 keV state quadrupole moment, half-life 0-37324  
 $^{143}\text{Ce}$  quasi- $1f_{7/2}$  low lying states spectroscopic factors, cluster-vibr. model from  $^{142}\text{Ce}(d, p)$  0-47391  
 $^{144}\text{Ce}$  levels from  $^{144}\text{La}$  decay 0-13417  
 $^{39}\text{Cl}$  excited states and transitions from  $^{39}\text{S}$  decay 0-42595  
 $^{12}\text{C}$  low lying excited states, ang. distrib. from  $^{12}\text{C}(K^-, \pi^-)$  0-32226  
 $^{249}\text{Cm}$  excited and single particle states,  $\gamma$ -transitions from  $^{248}\text{Cm}(n, \gamma)$  0-47399  
 $^{51}\text{Cr}$ , bands, levels, EM transitions,  $J^\pi$ , branching and mixing ratios from  $^{48}\text{Ti}(\gamma, n\gamma)$ ,  $^{51}\text{Cr}$  and  $^{51}\text{V}(p, n\gamma)$   $^{51}\text{Cr}$  0-52606  
 $^{52}\text{Cr}(^{12,13}\text{C}, X)$ , elastic, inelastic and single nucleon transfer excitation functions,  $^{52}\text{Cr}$  levels 0-13492  
 $^{52}\text{Cr}(\gamma, \gamma)$ , 35 MeV,  $2^+$  state deexcitation  $\gamma$ -rays, differential cross sections, deformation (Russian) 0-13406  
 $^{52}\text{Cr}$  levels,  $J^\pi$ ,  $\gamma$ -transitions and 1626 eV resonance from  $^{52}\text{Cr}(n, \gamma)$  0-42610  
 $^{54}\text{Cr}$  levels, transitions,  $T_{1/2}$ ,  $J^\pi$ , shell model anal. from  $^{51}\text{V}(\alpha, p\gamma)$  0-47381  
 $^{52}\text{Cr}$  deduced levels and spins, from  $^{54}\text{Cr}(d_{\text{pol}}, p)$ , cross section and vector analysing power 0-52684  
 $^{131}\text{Cs}$  populated in  $^{131}\text{Ba}$  decay, E0 transitions 0-22752  
 $^{139}\text{Cs}$  level scheme,  $J^\pi$  and  $\gamma$ -transitions from  $^{139}\text{Xe}$   $\beta$ -decay 0-42590  
 $^A\text{Cu}$ ,  $A=65, 67, 68$ , energy levels, core coupling model calcs. 0-9238  
 $^{63}\text{Cu}$  levels and transition j-depend., DWBA anal. of  $^{60}\text{Ni}(^{19}\text{F}, ^{16}\text{O})$  0-42542  
 $^{64}\text{Cu}$  levels and transitions, stat. anal. of  $^{64}\text{Ni}(p, n\gamma)$  (Russian) 0-5104  
 $^{63}\text{Cu}$  levels and transitions,  $J^\pi$  and  $\gamma$ -strength function using average resonance capture from  $^{64}\text{Ni}(p, \gamma)$  0-13411  
 $^{148}\text{Dy}$ , p single particle states and pairing force calcs., high spin states 0-42522  
 $^{151}\text{Dy}$  levels, bands and transitions, in-beam  $\gamma$ -rays from  $^{142}\text{Nd}(^{12}\text{C}, 3n\gamma)$  0-458  
 $^{153}\text{Dy}$ , populated in  $^{153}\text{Ho}$   $\beta$ -decay, lower excited states 0-22765  
 $^{166}\text{Er}$ , 2-quasiparticle states obs. 0-18198  
 $^{145}\text{Eu}$  level and transition effects on  $^{145}\text{Gd}$  decay anomalies 0-32244  
 $^{18}\text{F}$  integrated cross sections to excited residual states from  $^{19}\text{F}(\gamma, n)$  0-18200  
 $^{18}\text{F}$  levels and resonances, cross sections in R-matrix formalism from  $^{17}\text{O}(p, \alpha)$  0-18267  
 $^{18}\text{F}$ , semi-microscopic calc. of  $\alpha$ -cluster states, shell model approx. 0-465  
 $^{19}\text{F}$ , energy levels from  $\alpha$ - $^{15}\text{N}$  and  $t$ - $^{16}\text{O}$  coupled channel orthogonality condition model 0-37326  
 $^{19}\text{F}$  final state selective population, triton clustering from band anal. from  $^{7}\text{Li}(t)$ ,  $(^7\text{Li}, ^4\text{He})$  0-9306  
 $^{19}\text{F}$  level struct., ang. distrib. anal. using DWBA of  $^{17}\text{O}(^3\text{He}, p)$  0-9232  
 $^{19}\text{F}$  levels, resonances and phase shifts, resonating group calcs. from  $^{15}\text{N}(\alpha, \alpha)$  0-32189  
 $^{19}\text{F}(p, p)$ , 17.5 and 30 MeV, low lying level cross-sections, coupled-channel method 0-42649  
 $^A\text{Fe}$ ,  $A=54-56$ , high spin states, energy levels, spectroscopic factors, EM props., shell model 0-47359  
 $^{56}\text{Fe}(^{12,13}\text{C}, X)$ , elastic, inelastic and single nucleon transfer excitation functions,  $^{56}\text{Fe}$  levels 0-13492  
 $^{56}\text{Fe}$  deduced levels, from  $^{54}\text{Fe}(d_{\text{pol}}, p)$ , cross section and vector analysing power 0-52684  
 $^{56}\text{Fe}$  deduced levels and spins, from  $^{58}\text{Fe}(d_{\text{pol}}, p)$ , cross section and vector analysing power 0-52684  
 $^{60}\text{Ga}(n, \gamma)$ , fast n, levels,  $J^\pi$ , transitions and mixing ratios, statistical anal. (Russian) 0-13382  
 $^{14}\text{Gd}(n, \gamma)$ ,  $A=154, 156-8, 2, 24$  keV, resonance averaged  $\gamma$ -spectra, level and  $J^\pi$  apps. 0-37347  
 $^{146}\text{Gd}$ , p single particle states and pairing force calcs., high spin states 0-42522  
 $^{66}\text{Ge}$  levels, lifetimes and mixing ratio, in-beam  $\gamma$ -spectroscopy from  $^{54}\text{Fe}(^{44}\text{Ni}, n\gamma)$  0-42541  
 $^{66}\text{Ge}$  states and decay scheme, polarisations  $J^\pi$  and ang. distrib. from  $^{58}\text{Ni}(^{10}\text{B}, p\gamma)$  0-22692  
 $^2\text{H}(e, e'p)$ , single hole state momentum distrib. 0-22674  
 $^3\text{H}$ , energy levels using ATMS method and realistic nuclear forces 0-22707  
 $^4\text{He}$ , energy levels using ATMS method and realistic nuclear forces 0-22707  
 $^4\text{He}$ , shell model calcs. 0-13393  
 $^4\text{He}$  system,  $O^+$  states, microscopic wave function 0-463  
 $^4\text{He}(\gamma, 2d)$ , 30-35 MeV,  $2^+$  state search (Russian) 0-42553  
 $^4\text{He}(n, n)$ , 30-35 MeV,  $2^+$  state search (Russian) 0-42553  
 $^4\text{He}$ , 16.7 MeV states energy calc. using mixed cluster representation 0-27555  
 $^5\text{He}$  energy levels deduced from  $d(t, t)d$  0-47488  
 $^4\text{He}$ ,  $^4\text{H}$  binding energy difference, bound states, exact four body calc. 0-9255  
 $^{\text{Hf-Os}}$  region, high lying states, Nilsson strength fragmentation 0-42539  
 $^{201}\text{Hg}$  missing  $f_{5/2}$  state Coulomb excitation, level scheme,  $J^\pi$ , transitions using  $(\alpha, \alpha)$ ,  $(^{16}\text{O}, ^{16}\text{O})$  0-47386  
 $^{166}\text{Ho}$  low lying levels and transitions, 54.24 keV level mag. moment from  $^{166}\text{Dy}$  decay 0-13380  
 $^{121}\text{I}$  mass excess, energy levels and single particle strength distrib. from  $^{120}\text{Te}(^3\text{He}, d)$  0-5053  
 $^{127}\text{I}(n, n\gamma)$ , fast n,  $\gamma$ -ang. distrib., level ang. momenta 0-18224  
 $^{117}\text{In}$  level scheme,  $J^\pi$  and transitions from  $^{117}\text{Cd}$  isomer decay, unified model anal. 0-32193  
 $^{185}\text{Ir}$  levels excited in  $(\alpha, xn)$  reactions 0-9231  
 $^{185}\text{Ir}$  levels populated in  $^{185}\text{Pt}^m + \beta$  decay 0-9269  
 $^{192}\text{Ir}$  levels, resonances and low energy  $\gamma$ -rays from  $^{191}\text{Ir}(n, \gamma)$  0-47397  
 $^A\text{K}$ ,  $A=37, 39$ , levels, excitation and microscopic form factors, DWBA calcs. from  $\text{Ca}(p, \alpha)$  0-32185  
 $^A\text{K}$ ,  $A=45, 46$ , levels, lifetimes and transitions from Ar  $\beta$ -decay 0-42597  
 $^{38}\text{K}$  low lying  $1^+$ ,  $T=0$  states, DWBA anal. of  $^{40}\text{Ca}(p, ^6\text{He})$  0-470  
 $^{39}\text{K}$  states and spectroscopic strengths DWBA anal. of  $^{40}\text{Ca}(\text{Li}, ^8\text{Be})$  0-5069



## nuclear energy levels continued

- <sup>48</sup>K mass excess and states from <sup>48</sup>Cu(<sup>7</sup>Li,<sup>6</sup>Be) 0-9221  
<sup>4</sup>Kr, A=78, 80, quasi- $\gamma$  bands and negative parity levels from Br(p,2n $\gamma$ ) 0-456  
<sup>88</sup>Kr level scheme and transitions, delayed neutrons from <sup>88</sup>Br  $\beta$ -decay 0-42600  
<sup>139</sup>La, level props., Coulomb excitation obs. 0-13378  
<sup>139</sup>La(p,f), 600 MeV, fragment energies, cross sections level density and barrier heights 0-42723  
<sup>6</sup>Li energy levels from (p,d) 0-42667  
<sup>6</sup>Li excited states, D( $\alpha,\alpha$ )D cross-sections,  $\alpha$ -d systems 0-47491  
<sup>7</sup>Li 3/2<sup>-</sup> state from <sup>6</sup>Li(n, $\alpha$ ) 0-18297  
<sup>7</sup>Li( $\gamma$ ,t), <50 MeV, total and differential cross sections, levels, cluster model calcs. 0-32265  
<sup>6</sup>Li( $\gamma$ , $\pi$ ), A=6, 7 0-22686  
<sup>172</sup>Lu levels, transitions and J <sup>$\pi$</sup>  values from <sup>172</sup>Hf EC decay 0-18249  
<sup>23</sup>Mg hole states, transitions and spectroscopic factors, DWBA anal. of <sup>24</sup>Mg(p,d) 0-32161  
<sup>24</sup>Mg 2<sup>+</sup> state quadrupole moment from <sup>208</sup>Pb(<sup>24</sup>Mg,<sup>24</sup>Mg) 0-9230  
<sup>24</sup>Mg(p,p'), 40 MeV, two step pickup-stripping process, negative parity states 0-32256  
<sup>27</sup>Mg energy levels, spectroscopic factors, DWBA, Hauser-Feshbach anal. from <sup>26</sup>Mg(d,p) 0-52581  
<sup>51</sup>Mn, 21 MeV analogue state, excitation 0-13471  
<sup>51</sup>Mn low lying states, DWBA anal., shell model wave functions from <sup>56</sup>Fe(p, $\alpha$ ) 0-32211  
<sup>55</sup>Mn, energy levels, bound state mean lifetimes and spins from <sup>54</sup>Cr(p, $\gamma$ ) 0-42586  
<sup>89</sup>Mo mass excess and excited states from <sup>92</sup>Mo(<sup>3</sup>He,<sup>6</sup>He) 0-42531  
<sup>90</sup>Mo static quadrupole moment of first 2<sup>+</sup> state from ( $\alpha,\alpha'$ ), (<sup>16</sup>O,<sup>16</sup>O') 0-5061  
<sup>12</sup>N ground state electric quadrupole moment from <sup>12</sup>C( $\gamma$ , $\pi$ ), <sup>12</sup>N ground state electric quadrupole moment (Russian) 0-42538  
<sup>12</sup>N 1<sup>+</sup> state cross sections, effective two nucleon interaction, isovector tensor component from <sup>14</sup>C(p,n) 0-18208  
<sup>12</sup>N, energy levels up to 11.05 MeV, transitions and resonance decay from <sup>13</sup>C(p, $\gamma$ ) 0-47376  
<sup>15</sup>N 3/2<sup>-</sup> state spin alignment and polarisation, 1/2-spin orbit interaction from <sup>27</sup>Al, <sup>88</sup>Sr(<sup>16</sup>O,<sup>15</sup>N) 0-27622  
<sup>15</sup>N excited states and transitions from <sup>15</sup>C beta decay 0-18248  
<sup>15</sup>N integrated cross sections to excited residual states from <sup>19</sup>F( $\gamma$ , $\alpha$ ) 0-18200  
<sup>15</sup>N low lying states, cross sections and anal. power, transitions, spectroscopic factors from <sup>14</sup>N(d,p), pol. d 0-32183  
<sup>15</sup>N states, cross sections and lifetimes, EM decay strengths from 3 and 4 particle transfers 0-9237  
<sup>15</sup>N levels and ang. distrib. meas., shell model calcs. from <sup>15</sup>N(t,p) 0-9233  
<sup>18</sup>N, mass excess and excited states from <sup>14</sup>C(<sup>18</sup>O,<sup>18</sup>N) 0-42676  
<sup>21</sup>Na deduced levels and cross sections from <sup>12</sup>C(<sup>12</sup>C,t) 0-469  
<sup>91</sup>Nb, 17/2<sup>-</sup> state, g-factor meas. 0-32179  
<sup>91</sup>Nb level density, neutron spectra and ang. distrib. nonequib. processes from <sup>94</sup>Zr(p,n) (Russian) 0-37376  
<sup>94</sup>Nd(<sup>16</sup>O,<sup>16</sup>O'), 40-48 MeV, even nuclei, 2<sup>+</sup> state E2 transition probabilities and quadrupole moments 0-18234  
<sup>144</sup>Nd capture states partial  $\alpha$ -decay widths from <sup>143</sup>Nd(n, $\gamma$ ) 0-37328  
<sup>144</sup>Nd levels and transitions,  $\gamma$ -ray spectra from <sup>144</sup>Pr<sup>m</sup> $\beta$ -decay (French) 0-18250  
<sup>148</sup>Nd from <sup>148</sup>Pr  $\beta$ -decay, low lying energy levels, quasi band description 0-5096  
<sup>18</sup>Ne analogue and nonanalogue states,  $\pi$  double charge exchange form factors from <sup>18</sup>O( $\pi^+$ , $\pi^-$ ) 0-13405  
<sup>19</sup>Ne, final state selective population, triton clustering from band anal. from <sup>16</sup>Li(<sup>4</sup>Li,t) 0-9306  
<sup>20</sup>Ne levels, J <sup>$\pi$</sup> , branching ratio and EM transition rates from <sup>16</sup>O+ $\alpha$  0-42540  
<sup>20</sup>Ne, levels, J <sup>$\pi$</sup>  and ang. distrib. from <sup>18</sup>O(t,p) 0-18204  
<sup>20</sup>Ne levels and branching ratio from <sup>12</sup>C(<sup>16</sup>O, $\alpha$ ) 0-22661  
<sup>20</sup>Ne low lying states, configuration mixing calcs. with basis states from variational method 0-22693  
<sup>20</sup>Ne states, J <sup>$\pi$</sup> , differential cross sections and ang. distrib. from <sup>16</sup>O( $\alpha,\alpha'$ ) 0-18203  
<sup>20</sup>Ne(<sup>12</sup>C,<sup>12</sup>C), symmetry and shell struct. effects on absorption, precompound states 0-27666  
<sup>21</sup>Ne states cross section, coupled channel and fluctuations anal. from <sup>20</sup>Ne(d,p) 0-27617  
<sup>23</sup>Ne structure, differential cross sections from <sup>27</sup>Al( $\alpha$ ,<sup>8</sup>B) 0-5153  
Ni doubly even nuclei, eqns. of motion method, pairing correlations, ground state energies 0-52585  
<sup>61</sup>Ni A=57-59, f<sub>7/2</sub> hole configuration effects, shell model calcs. 0-22670  
<sup>61</sup>Ni, A=58, 64, neutron densities and single particle struct. 0-32165  
<sup>58</sup>Ni(<sup>7</sup>Li,<sup>7</sup>Li'), 19 MeV, first 2<sup>+</sup> states Coulomb-nuclear interference, optical and DWBA anal. 0-22852  
<sup>58</sup>Ni(e,e'), 120-264 MeV, J <sup>$\pi$</sup> =6<sup>+</sup>, 5.125 MeV state isoscalar character, form factors, transition strengths 0-9262  
<sup>58</sup>Ni( $\gamma$ , $\gamma$ ), M1 strength isospin splitting for dipole ang. distrib. states 0-13412  
<sup>59</sup>Ni deduced levels, from <sup>58</sup>Ni(d,pol,p), cross section and vector analysing power 0-52684  
<sup>60</sup>Ni deduced levels from <sup>58</sup>Fe(<sup>16</sup>O,<sup>14</sup>C)<sup>60</sup>Ni, DWBA anal., spectroscopic strengths 0-47380  
<sup>237</sup>Np, quasi-stationary state decay through two bump barrier (Russian) 0-13420  
<sup>238</sup>Np levels, resonances and transitions from <sup>237</sup>Np(n, $\gamma$ ) 0-52589  
<sup>17</sup>O, A=17, 19, level scheme, two-step transfer contribs., coupled channel anal. from O(<sup>13</sup>C,X) 0-32181  
<sup>17</sup>O, normal parity levels from P-model calcs. with realistic NN interaction (Russian) 0-32194  
<sup>16</sup>O, bound isobars  $\Delta$ (1236), single particle energies, wave functions (Chinese) 0-52562  
<sup>16</sup>O, Brueckner-Hartree-Fock approach, variational definition of single particle pot. 0-32170  
<sup>16</sup>O collective and giant multipole states, Brueckner RPA particle-hole state description 0-32169  
<sup>16</sup>O excited 0<sup>+</sup> levels 0-42551  
<sup>16</sup>O ground state and binding energy, microscopic calc. with realistic NW interaction (Russian) 0-5052  
<sup>16</sup>O levels and ang. distrib., <sup>3</sup>He spectroscopic strengths, Hauser-Feshbach/DWBA anal. of <sup>13</sup>C(<sup>6</sup>Li,t) 0-47390  
<sup>16</sup>O, odd parity levels, correlated basis functions method 0-22721  
<sup>16</sup>O states, J <sup>$\pi$</sup>  from <sup>12</sup>C(<sup>12</sup>C, $\alpha$ ) 0-22660

## nuclear energy levels continued

- <sup>16</sup>O(<sup>16</sup>O,<sup>16</sup>O), symmetry and shell struct. effects on absorption, precompound states 0-27666  
<sup>16</sup>O(e,e'p), single hole state momentum and energy distrib. 0-22674  
<sup>16</sup>O(e,e), T=1 level form factors, Helm model, pion photoprod. and muon capture appls. 0-52553  
<sup>16</sup>O( $\gamma$ ,p)<sup>15</sup>N up to 120 MeV, cross-sections, energy levels (Russian) 0-47465  
<sup>16</sup>O(p,p'), 1 GeV, proton polarisation in natural parity level excitation (Russian) 0-42634  
<sup>16</sup>O(p,p'), 135 MeV, 4<sup>-</sup> particle-hole states, J <sup>$\pi$</sup>  ambiguity removal 0-5036  
<sup>16</sup>O( $\pi$ , $\pi'$ ), ~180 MeV, isospin mixing, levels, excitation functions and ang. distrib. 0-42543  
<sup>17</sup>O, cross sections to ground, 0.87 and 5.09 MeV states, neutron strength from <sup>16</sup>O(d,p) 0-5066  
<sup>17</sup>O levels, resonances, J <sup>$\pi$</sup>  and radiative width from <sup>14</sup>N(t, $\gamma$ ) 0-47389  
<sup>18</sup>O integrated cross sections to excited residual states from <sup>19</sup>F( $\gamma$ ,p) 0-18200  
<sup>18</sup>O level gamma decay from <sup>17</sup>O(n, $\gamma$ ) 0-52623  
<sup>18</sup>O(<sup>18</sup>O,<sup>18</sup>O), symmetry and shell struct. effects on absorption, precompound states 0-27666  
<sup>18</sup>O<sub>2</sub>, pairing correlation effects (Chinese) 0-47420  
<sup>31</sup>P, A=31, 33, levels and transition j-depend., DWBA anal. for Si(<sup>19</sup>F,<sup>16</sup>O) 0-42542  
<sup>208</sup>Pb, A=200,206, 12<sup>+</sup> isomer states, quadrupole moments 0-27554  
<sup>208</sup>Pb, A=205-207, neutron hole states, spectroscopic factors, DWBA anal. of Pb(<sup>3</sup>He, $\alpha$ ) 0-47352  
<sup>208</sup>Pb(e,e'), A=204, 206-208, levels and inelastic cross sections 0-22698  
<sup>208</sup>Pb( $\gamma$ ,n), A=206, 208, levels using tagged photons 0-23245  
<sup>207</sup>Pb parity assignments and M1 radiative strength from <sup>206</sup>Pb(n,n) 0-52614  
<sup>207</sup>Pb( $\gamma$ ,n), 7632 keV level photoexcitation, cross section and J <sup>$\pi$</sup>  0-37330  
<sup>208</sup>Pb core with valence nucleon or hole, mag. props., exchange currents, electron scatt. 0-22689  
<sup>208</sup>Pb, neutron densities and single particle struct. 0-32165  
<sup>209</sup>Pb excited states and 3/2<sup>-</sup> resonances, shell model, calcs. from <sup>208</sup>Pb(n,n) 0-18262  
<sup>102</sup>Pd(<sup>32</sup>S,<sup>32</sup>S'), A=102, 104, 106, 108, 110, 72-80 MeV, 2<sup>+</sup> state mag. moments 0-47373  
<sup>106</sup>Pd energy states and J <sup>$\pi$</sup>  from <sup>106</sup>Ag<sup>m</sup> decay 0-18197  
<sup>109</sup>Pd levels, J <sup>$\pi$</sup> , transitions, unique parity states, and spectroscopic factors from <sup>108</sup>Pd(n, $\gamma$ ) 0-42547  
<sup>143</sup>Pm, p single particle states and pairing force calcs., low lying levels 0-42522  
<sup>147</sup>Pm levels, transitions,  $\gamma\gamma$ -coincidences and IC electrons from <sup>147</sup>Nd decay 0-18243  
<sup>149</sup>Pm, energy levels from <sup>149</sup>Nd beta decay 0-27592  
<sup>149</sup>Pm single proton states, spin assignments, spectroscopic factors from <sup>150</sup>Sm(t, $\alpha$ ), pol.t 0-18170  
<sup>212</sup>Po levels and J <sup>$\pi$</sup> , weak coupling calc. using realistic matrix elements 0-5068  
<sup>191</sup>Pt, A=190, 192, 194, levels and  $\gamma$ -transition reduced probab., interacting boson model 0-18196  
<sup>191</sup>Pt, A=192, 194, 196, states, J <sup>$\pi$</sup> , ang. distrib. and transitions, DWBA anal. of Pt(p,t) 0-468  
<sup>187</sup>Pt, levels, J <sup>$\pi$</sup> , T<sub>1/2</sub>, possible E0 transitions from <sup>187</sup>Au decay (French) 0-32230  
<sup>196</sup>Pt (<sup>20</sup>Ne, <sup>20</sup>Ne'), excited states, lifetime meas. using recoil-distance method 0-13413  
<sup>196</sup>Pt (<sup>58</sup>Ni, <sup>58</sup>Ni'), excited states, lifetime meas. using recoil-distance method 0-13413  
<sup>246</sup>Pu excited states, mass excess and shell gap, L=0 transition from <sup>24</sup>Pu(t,p) 0-9236  
<sup>81</sup>Rb, level structure, gamma angular and time distrib. from <sup>81</sup>Br( $\alpha$ ,3n) 0-52583  
<sup>181</sup>Re, A=181, 182, 187, magnetic moments meas. by PAC 0-22688  
<sup>181</sup>Re, A=181, 182, 187, spin polarisation, state struct. and mag. moments in rot. model 0-18194  
<sup>187</sup>Re low lying level struct. and transitions, E2/E1 mixing ratios from <sup>187</sup>W decay 0-27557  
<sup>188</sup>Re, energy levels obs., form. by <sup>189</sup>Os(t, $\alpha$ )<sup>188</sup>Re 0-47487  
<sup>96</sup>Ru(<sup>16</sup>O,<sup>16</sup>O'), 36-45 MeV, A=96, 98, 100, 102, 104, first 2<sup>+</sup> excited state quadrupole moment 0-47374  
<sup>96</sup>Ru( $\alpha,\alpha'$ ), 8.5-9.5 MeV, A=96, 98, 100, 102, 104, first 2<sup>+</sup> excited state quadrupole moment 0-47374  
<sup>96</sup>Ru(p,p'), A=96, 98, 5-8 MeV, level schemes, transitions, vibr. state, mixing ratios 0-18199  
<sup>94</sup>Rh levels and  $\gamma$ -transitions from <sup>94</sup>Rh decay 0-18244  
<sup>32</sup>S levels and J <sup>$\pi$</sup>  from <sup>32</sup>Cl  $\beta^+$  decay 0-22772  
<sup>32</sup>S levels and spectroscopic factors from pickup DWBA anal. of <sup>33</sup>S(<sup>3</sup>He, $\alpha$ ) 0-9235  
<sup>32</sup>S(n, $\gamma$ ), single particle resonances and doorway states, K matrix formalism 0-37384  
<sup>119</sup>Sb, A=119,122, level density, neutron spectra and ang. distrib. nonequib. processes from Sn(p,n) (Russian) 0-37376  
<sup>121</sup>Sb, A=121,123, levels below 2 MeV, spins, transitions and mixing ratio from (p, $\gamma$ ), (n,n' $\gamma$ ) 0-32191  
<sup>123</sup>Sb, A=123,125,127,129, cross-sections, ang. distrib., spectroscopic factors, DWBA anal. of Te(t, $\alpha$ ) 0-52572  
<sup>45</sup>Sc energy levels, resonances, spin and parity from <sup>45</sup>Sc(n, $\gamma$ ) 0-52673  
<sup>45</sup>Sc level deexcitation, E1 and M1 absolute radiative widths from <sup>45</sup>Sc(n, $\gamma$ ) 0-52622  
<sup>45</sup>Sc transition polarisation, levels and spin assignments from <sup>45</sup>Sc(n, $\gamma$ ), pol. n 0-52656  
<sup>75</sup>Se, A=75, 77, 79, 81, levels and ang. distrib., spectroscopic factors from Se(p,d) 0-22696  
<sup>75</sup>Se quasi- $\gamma$  bands and negative parity levels from <sup>75</sup>As(p,2n $\gamma$ ) 0-456  
<sup>76</sup>Se, level scheme from  $\gamma\gamma$  coincidence meas. of <sup>76</sup>As decay 0-22754  
<sup>28</sup>Si (e,f), K=2 symmetry intermediate state 0-47514  
<sup>28</sup>Si  $\alpha$ -doorway states in  $\alpha$ -decay to <sup>24</sup>Mg low lying K-band 0-47438  
<sup>28</sup>Si levels and J <sup>$\pi$</sup>  from <sup>28</sup>P  $\beta^+$  decay 0-22772  
<sup>28</sup>Si(n, $\gamma$ ), single particle resonances and doorway states, K matrix formalism 0-37384  
<sup>28</sup>Si(n,n'), 13.9 MeV, spin flip probability from 1.78 MeV state, direct theory 0-9234  
<sup>29</sup>Si(p,p), pol. p, 12-18 MeV, cross section, anal. power and states, <sup>29</sup>P resonance coherence widths 0-32258  
<sup>208</sup>Pb(<sup>30</sup>Si,<sup>30</sup>Si) 0-13373



**nuclear energy levels continued**

- <sup>144</sup>Sm, p single particle states and pairing force calcs., high spin states 0-42522
- <sup>148</sup>Sm compound states partial  $\alpha$ -widths,  $\alpha$ -spectra of <sup>147</sup>Sm(n, $\alpha$ ) 0-47392
- <sup>149</sup>Sm, level scheme following <sup>149</sup>Pm  $\beta^-$  decay 0-22750
- <sup>151</sup>Sm, gamma spectra, energy levels (*Dutch*) 0-47430
- Sn, deep h-lc state fragmentation, strength functions, giant resonances, quasiparticle phonon model 0-37320
- Sn, odd mass isotopes, low lying negative parity states, energy levels, shell model calc. 0-5076
- <sup>116</sup>Sn ( $\alpha$ ), 4.75-5.25 MeV, A=112, 116, 118, 120, 124, single proton states RMS radius 0-13350
- <sup>116</sup>Sn, A=111,115,119, neutron hole distrib., IAS and spectroscopic factors from Sn(<sup>3</sup>He, $\gamma$ ) 0-42519
- <sup>116</sup>Sn, A=116, 118, 120, 122, 124, 0<sup>+</sup>, 2<sup>+</sup> and 4<sup>+</sup> states 1 number conserving approach 0-22694
- <sup>116</sup>Sn, A=116, 124, neutron densities and single particle struct. 0-32165
- <sup>116</sup>Sn(p,p'), A=115, 117, 119, 18 MeV, state spin assignment, particle-vibr. coupling 0-32160
- <sup>112</sup>Sn(p,p'), 20.51, 25.0 MeV, energy levels, excitation functions and ang. distrib. 0-32184
- <sup>116</sup>Sn levels, J<sup>\*</sup> and transitions from <sup>115</sup>Sn(n, $\gamma$ ) 0-52587
- <sup>119</sup>Sn, 23.87 keV level half-life 0-47433
- <sup>132</sup>Sn level struct., lifetimes,  $\gamma$ - $\gamma$  coincidences, internal conversion from <sup>235</sup>U fission 0-52584
- <sup>84</sup>Sr, A=80,82,84-86, levels and transitions from Kr(<sup>3</sup>He,n) 0-18201
- <sup>84</sup>Sr quasi- $\gamma$  bands and negative parity levels from <sup>85</sup>Rb(p,2n $\gamma$ ) 0-456
- <sup>91</sup>Sr excited state depopulation  $\gamma$ -rays, n coincidence from <sup>94</sup>Rb  $\beta$ -delayed n decay 0-52631
- <sup>177</sup>Ta, magnetic moments meas. by PAC 0-22688
- <sup>177</sup>Ta spin polarisation, state struct. and mag. moments in rot. model 0-18194
- <sup>147</sup>Tb, p single particle states and pairing force calcs., low lying levels 0-42522
- <sup>159</sup>Tb(p,f), 600 MeV, fragment energies, cross sections level density and barrier heights 0-42723
- <sup>95</sup>Tc, energy levels from <sup>95</sup>Mo(p, n $\gamma$ ) <sup>95</sup>Tc 0-37372
- <sup>100</sup>Tc low lying and isomeric levels, transitions and mean lines from <sup>100</sup>Mo(p,n $\gamma$ ) 0-42548
- <sup>102</sup>Tc deduced levels, tentative J<sup>\*</sup> and transitions from <sup>102</sup>Mo decay 0-52630
- <sup>121</sup>Te isomeric state, spin, lifetime and mag. moment from ( $\alpha$ ,n),(d,Zn) 0-47387
- <sup>124</sup>Te capture states partial  $\alpha$ -decay widths from <sup>123</sup>Te(n, $\gamma$  $\alpha$ ) 0-37328
- <sup>132</sup>Te 2<sup>+</sup> level, shell model calc., Lanczos and Householder method comparison 0-22711
- <sup>132</sup>Te low lying levels and EM props., shell model description 0-42549
- <sup>41</sup>Ti (<sup>3</sup>Li,<sup>3</sup>Li'), A=46,48, 17 MeV, first 2<sup>+</sup> states Coulomb-nuclear interference, optical and DWBA anal. 0-22852
- <sup>47</sup>Ti levels, DWBA and Hauser Feshbach anal., compound nucleus cross sections from <sup>46</sup>Ti(d,p) 0-47377
- <sup>49</sup>Ti nuclear levels from n-capture  $\gamma$ -rays in <sup>50</sup>Ti( $\gamma$ ,n) 0-37327
- <sup>49</sup>Ti( $\gamma$ , $\gamma$ ), nuclear levels from n-capture  $\gamma$ -rays 0-37327
- <sup>50</sup>Ti (<sup>12</sup>C,X), elastic, inelastic and single nucleon transfer excitation functions, <sup>49</sup>Ti levels 0-13492
- <sup>201</sup>Tl levels, transitions and J<sup>\*</sup> assignments from <sup>201</sup>Pb decay 0-5099
- <sup>175</sup>Tm single proton states, rot. bands, J<sup>\*</sup> assignments from <sup>176</sup>Yb(t, $\alpha$ ), pol. 0-452
- <sup>236</sup>U low lying levels from 4<sup>-</sup> isomer decay in (n,e), (n, $\gamma$ ) 0-47396
- <sup>237</sup>U levels, bands and J<sup>\*</sup> assignments, n binding energy from <sup>238</sup>U(n, $\gamma$ ) 0-5041
- <sup>237</sup>U virtual photon excited state decay and total cross section of <sup>238</sup>U(e,n) 0-22757
- <sup>238</sup>U(e,e'), 87.5 MeV, deformed fissionable nucleus, giant multipole resonances and isovector states 0-42612
- <sup>238</sup>U(e,e'), 5.5-9 MeV, fission fragment ang. distrib. DWBA anal., low lying fissioning levels 0-42713
- <sup>238</sup>U(n, $\gamma$ ), 2, 24 keV, resonance averaged  $\gamma$ -spectra, level and J<sup>\*</sup> appls. 0-37347
- U(p,f), 600 MeV, fragment energies, cross sections level density and barrier heights 0-42723
- <sup>138</sup>Xe, A=129, 131, populated in ( $\alpha$ ,n $\gamma$ ) props. of low-lying levels 0-464
- <sup>138</sup>Xe excited states and  $\gamma$ -rays from <sup>138</sup>Cs  $\beta$ -decay 0-47436
- <sup>116</sup>Xe level scheme and yrast band, in-beam  $\gamma$ -study from <sup>106</sup>Cd(<sup>12</sup>C, 2n) 0-13360
- <sup>137</sup>Xe, populated in <sup>138</sup>I  $\beta$ -decay, delayed neutrons feeding excited states obs. 0-27600
- <sup>139</sup>Xe, populated in <sup>138</sup>I  $\beta$ -decay, level scheme 0-27600
- <sup>169</sup>Yb populated in <sup>169</sup>Lu decay,  $\gamma$ -ray and conversion electron spectra 0-22767
- <sup>173</sup>Yb M1 transitions from 636 keV level, multipole mixture parameters, penetration effect 0-18220
- <sup>69</sup>Zn, energy levels, core coupling model calcs. 0-9238
- <sup>90</sup>Zr, proton orbit sizes and E0 matrix element for 2 lowest 0<sup>+</sup> states 0-27546
- <sup>92</sup>Zr level struct. and reduced spectroscopic factors from <sup>91</sup>Zr(d,p) 0-32192

**nuclear engineering**

- see also fission reactors*
- air-core Tokamak, optimisation of ohmic heating coil configurations 0-14914
- dynamic isotope power system, PuO<sub>2</sub> fuelled, organic Rankine cycle turbine power system for space appls. 0-18692
- education, energy option for undergraduates 0-31447
- education in Japan (*Japanese*) 0-27067
- energy conversion engineering, alternative energy sources (*Japanese*) 0-26105
- fusion experiments, microprocessor applications in data acquisition and control 0-13918
- fusion-fission concepts, nuclear energy systems synthesis 0-13838
- hockey stick heat exchanger, elbow centroid 0-9329
- HTR, coal gasification appl. 0-11996
- JAERI program, probabilistic risk assessment techniques in Japan 0-18515
- LMFBR, 1000 MW(e) pool plant, fabrication and construction 0-5213
- LMFBR, pool-type, engineering design and construction 0-5212
- medical radiological physics education based on nucl. engineering 0-31448
- nondestructive analysis applications in the nuclear industry 0-13706
- NRC standardisation in licensing, B and W viewpoint 0-23023

**nuclear engineering continued**

- nuclear reactor redundancy systems, common mode failures 0-13641
- PWR, control of fission products activity in primary coolant, computer code 0-32537
- risk estimates, communication techniques 0-18514
- Stirling isotope power system for space appls., development and test results 0-18693
- technology transfer to developing countries, IAEA's contribution 0-13952
- U isotope separation appl. to nucl. fuel cycle, teaching module 0-36805

**nuclear engineering computing**

- see also computerised control; computerised instrumentation*
- accident risk calcs., models and data, CRAC 0-47613
- AGR, helical monotube vapour generator, density wave instability, experimental-stochastic and theoretical anal. 0-47539
- AGR fuel pins, pellet-clad interactions, comparison of expts. and SLEUTH-SEER code results 0-42755
- air cool transformers for fusion reactors, computer aided design 0-18662
- Arkansas Nuclear One, refueling shuffle movement sequencing program 0-9357
- BACO code, simulation of fuel rod performance 0-37450
- benchmark rod-bundle thermal-hydraulic analysis using boundary-fitted coordinates 0-47548
- BERTA, laser-driven fission-fusion microexplosions, nuclear and thermohydrodynamic calcs. 0-47696
- BNL-TWIGL, anal. of BWR rod drop accident, effect of thermal-hydraulic feedback 0-42815
- BNL-TWIGL anal. of BWR turbine trip without bypass transient 0-42814
- BRINE, cross-section self shielding factors, analytic bounds 0-37426
- BWR, benchmarking ARMP system against Quad Cities Unit 1 Cycle 1 meas. 0-27712
- BWR, condensate feedwater system dynamics anal. 0-23025
- BWR, control rod programming using heuristic and mathematical methods 0-52766
- BWR, fuel element positioning and control patterns, optimisation system 0-733
- BWR, improved fuel utilisation 0-732
- BWR, KKM turbine trip simulation with a one-dimensional transient model 0-18510
- BWR, min. critical power ratio thermal limit 0-18398
- BWR, ONDA-3 system for in-reactor fuel management 0-735
- BWR, optimum fuel loading and operation planning, FAPMAN model 0-47606
- BWR, process monitoring and parameter estimation, multivariate signal analysis algorithms 0-47585
- BWR, safety evaluation, experiments and analytical analysis, NRC codes 0-13703
- BWR, startup control rod programming code system 0-13688
- BWR dynamics, imbedded flux calc. 0-714
- BWR fuel management anal., consistent modelling procedure 0-23052
- BWR licensing basis transients, computer anal. of turbine trip without bypass transient 0-42814
- BWR LOCA, computer prediction of loading conditions on pressure suppression system 0-764
- BWR LOCA analysis, RELAP4/MOD7 calc. of level swell test data 0-23003
- BWR power distrib. prediction system, on-line performance test 0-13689
- BWR power plant, computerised core component accounting system shortens shuffling time 0-699
- BWR pressurisation transient anal. using MEKIN neutronics/thermal-hydraulic code 0-47626
- BWR reactivity feedback modelling effects 0-22927
- BWR rod drop accident, effect of thermal-hydraulic feedback, BNL-TWIGL code anal. 0-42815
- bWR servicing and refueling improvement program 0-9390
- BWR shutdown dose rate prediction, calc. code 0-23061
- BWR suppression pool temperature transients following LOCA, computer anal. 0-762
- BWR transient anal., iterative procedure for predicting critical power ratio 0-42816
- BWR transient anal. model for pressurisation transients 0-18509
- BWR turbine trip test, computer anal. 0-692
- BWR turbine trip transients, additional separator modelling considerations 0-18511
- BWR vent clearing hydrodynamics, SOLA VOF simulation 0-32356
- BWR/6 axial reflectors, Monte Carlo modelling 0-22939
- CACECO, FFTF containment response to postulated core meltdown accidents 0-32381
- CANDU, feedback coeff. anal. 0-27716
- CANDU, LOCA, space-time neutronic anal. 0-13663
- CANDU fuel pellet stacking, mathematical model of automatic assembler 0-37464
- capacitor fed fusion expts., computer based control system 0-13912
- CATFISH for LMFBR core flow distrib. anal. 0-23018
- COBRA code for LMFBR fuel assemblies, thermal-hydraulic anal. wire-wrap modelling 0-47549
- COBRA III/MELT code, anal. of FFTF transient overpower accidents 0-32373
- COBRA subchannel anal. code, LMFBR whole core transient anal. 0-18388
- COBRA-IV comparison with the W-ARD 11:1 LMFBR air flow tests 0-27734
- CODA 1-D coolant dynamics code for PWR flow transients, critical heat flux predictions 0-42817
- COMETHE code, benchmarking results 0-37452
- COMETHE code with transient capability 0-42761
- COMETHE III-J code, fuel behaviour models 0-42752
- COMETHE III-J code improvements for fuel rod modelling 0-42754
- COMETHE III-J programme, anal. of integral fuel rods 0-37448
- containment structures pressure tightness verification, pressurisation plant, data acquisition and processing (*Spanish*) 0-13775
- CORA transient anal. code for cluster of reactor core assemblies 0-18389
- COROPT code, anal. of LMFBR design 0-27714
- CORTAC 3-D thermal hydraulic model of LMFBR core restraint transient responses 0-18390
- CORTAN code, LMFBR whole core transient thermal hydraulic anal. with CORTAN code 0-18392
- CRAC, accident risk calcs., models and data 0-47613



**nuclear engineering computing continued**

CRATER code calc. of LWR fuel rod under power transients (*French*) 0-42789  
 CRBR mild transient overpower accidents with advanced fuels 0-18539  
 criticality control of intermediate U enrichments, computer calcs. 0-37435  
 criticality safety anal. at Oak Ridge 0-37431  
 criticality search techniques for low and high switched systems 0-37494  
 CRONOS code development, PWR fast transients anal. 0-23055  
 cross-section self shielding factors, analytic bounds 0-37426  
 Culham fusion expts., distributed control systems using microcomputers 0-13909  
 Culham fusion expts., integrated data network for microcomputer based diagnostics 0-13910  
 Culham fusion studies, appl. of microcomputer to data acquisition and control 0-13908  
 CUPIDON code anal. of PWR fuel rod during depressurisation accident (*French*) 0-42791  
 defense waste processing facility, anal. of radionuclides 0-37518  
 DIGRAS, dynamic intragranular fission gas release and swelling 0-32345  
 DNB open core algorithm for on-line thermal margin evaluation 0-27782  
 DOT-IV neutron transport theory code, use on vector processing computer 0-47836  
 EBR-II delayed neutron concentrations, computer modelling 0-27717  
 educational module, in-core fuel management computer system 0-36826  
 ENDF/B-IV, absorption effects on decay heat and spectral pulse kernels 0-22931  
 ENDF/B-V, prompt fission neutron spectra 0-22869  
 ENDF/B-V cross section data for shielding appls., Monte Carlo MCNP integral calcs. 0-47744  
 ENDF/B-V cross-section covariance data for neutronics anal. of fusion reactor materials 0-47710  
 ENDF/B-V nuclear data for shielding appls., energy balance anal. 0-47745  
 ETA-BETA fusion expt., data acquisition and anal. programs 0-13914  
 Euratom Data Acquisition Co-ordinating Committee activities 0-13904  
 EURDYN-1M, containment and fuel subassembly analyses for fast reactor safety studies 0-52772  
 FACSIMILE VSI code for void swelling calcs. 0-42782  
 FAPMAN8, LWR, operation planning, optimum fuel loading and generation planning 0-47673  
 fast reactor parameters, influence of fission spectra uncertainties 0-22928  
 fast reactor physics, assessment of JAERI fast group constants set version 2 0-602  
 FAXMOD anal. of creep and sheath ballooning 0-42759  
 FBR carbide fuel, Sphere-Pac form, performance evaluation using computer code SPECKLE-I 0-637  
 FBR containment response to HCDA, effect of struct. components, Eulerian hydrodynamic anal. 0-23014  
 FBR core disruptive accident, response of upper internal structures, finite element computer anal. 0-47645  
 FBR HCDA, fluid-struct. interaction anal., evaluation of computer code 0-23015  
 FBR HCDA, structural response of the upper internals, finite element anal. 0-18537  
 FBR safety anal. modelling of fission gas behaviour 0-748  
 FEMAXI-II, fuel rod deform. code, appl. 0-37446  
 FFTF, containment response to postulated core meltdown accidents 0-32381  
 FFTF, transient overpower accidents, effect of intrasubassembly incoherencies 0-32373  
 FFTF fuel, neutron source strength as function of irradiation 0-22929  
 FFTF loss-of-electric-power transient response, natural circulation tests, pre-test simulation using SSC-L code 0-42836  
 FIPMIGR program, fission product migration, anal. 0-37453  
 FISPIN, nuclide inventory calculation code 0-42781  
 fission product migration in fuel pin, FIPMIGR program 0-37453  
 fission-fusion systems, laser-driven, nuclear and thermohydrodynamic calcs. 0-47696  
 FRAP-S3, steady state fuel rod anal. program, calc. of stored energy for PWR-type fuels 0-9349  
 fuel behaviour models incorporated in COMETHE III-J 0-42752  
 fuel cycle strategies, simulation using FISS computer program 0-5317  
 fuel element modelling at CNEA 0-37449  
 fuel element performance modelling, IAEA specialists meeting, 1978 0-36769  
 fuel fabrication control system for remote operation 0-18571  
 fuel failure, relating uncertainty allowance in operating limits 0-13721  
 fuel performance anal. by finite element method, MIPAC code 0-42750  
 fuel pins, computer controlled meas. 0-5300  
 fuel rod, simulation of performance with BACO computer code 0-37450  
 fuel rod anal., statistical version of URANUS programme 0-42749  
 fuel rod deformation code FEMAXI-II and its application 0-37446  
 fuel rod mechanical design, DIMCO system 0-37418  
 fuel rod simulation in COMETHE III-J code improvements 0-42754  
 fuel rod thermal stored energy, calculational uncertainty anal. 0-47609  
 fusion experimental facilities, computerised control and data acquisition 0-13890  
 fusion experiments, 10 bit transient data recorded 0-13917  
 fusion experiments, fibre optic signalling in control 0-13919  
 fusion mirror reactors, finite orbit treatment of plasma buildup 0-37631  
 fusion reactor, stainless steel first wall, swelling and irradiation creep, FWLTB computer code 0-32446  
 fusion reactor cavity gas response to particle beam target explosions 0-37602  
 fusion reactor first wall, lifetime calc. in FWLTB program 0-18646  
 fusion reactor inertial confinement pellets, neutronics modelling 0-37593  
 fusion reactor Ingra injector, control and data acquisition system 0-13913  
 fusion reactor insulators, radiation damage calcs. using MORSE code 0-34061  
 fusion reactor materials, neutronics analysis using ENDF/B-V cross-section covariance data 0-47710  
 FWLTB computer code, stainless steel first wall, swelling and irradiation creep 0-32446  
 gamma photons penetration, 6 MeV, through Al, concrete and graphite, expt. and computed results comparison 0-5256  
 GCFR fuel assembly thermal-hydraulic anal., modification of COBRA code 0-588

**nuclear engineering computing continued**

GCFR proliferation-resistant heterogeneous fuel cycles, computer neutronic anal. 0-18435  
 GRASS-SST code, LWR fuel, mechanistic prediction of transient fission gas release 0-47571  
 heat transfer simulation using analogue computer elements (*Russian*) 0-52733  
 heterogeneous lattices, unified theory 0-37428  
 HOTRAN-3, LWR core, thermal and hydraulic behaviour code (*Hungarian*) 0-32401  
 HOTROD code, fuel performance during LOCA 0-42790  
 HTGR primary coolant system depressurisation accident, expt. and numerical anal. 0-775  
 HWR, multidimensional space time kinetics, TRIMHX code 0-47538  
 hydrid reactor, reaction rate calcs. in  $^{238}\text{U}$  and  $^{232}\text{Th}$  blankets around D-T neutron source 0-52782  
 ICECO code, anal. of LMFBR Na spillage 0-32364  
 ICF, parametric studies 0-32507  
 inertial confinement fusion pellets, neutron moderation, effects on damage and radioactive inventory 0-47704  
 integral rods, anal. with COMETHE III-J programme 0-37448  
 integrated PWR, anticipated transients without scram, calc. of dynamical behaviour 0-5250  
 IRT code for PWR non-LOCA transient anal. 0-42819  
 JET, control and data acquisition system 0-13905  
 JT-60, control system 0-13906  
 laboratory instructional programs in computer instrumentation at RPI 0-31472  
 laser fusion power plant, capital cost data base 0-32504  
 laser fusion system studies model, TROFAN 0-32505  
 LEVITATE code anal. of steel ablation and fuel-steel mixing phenomena following LMFBR accident 0-47649  
 Levitron experiment, Culham, plasma fluctuation and by microcomputer system 0-13911  
 linear acceleration reactors, anal. of neutron yield produced by high-energy protons 0-22895  
 LMFBR, accident progression within secondary containment boundary 0-32368  
 LMFBR, breeding ratio and fissile inventory for homogeneous and heterogeneous cover 0-32374  
 LMFBR, containment pressurisation by Na spray fires 0-32365  
 LMFBR, coolant cavitation in dynamic containment loading 0-32326  
 LMFBR, core flow distrib., analytical prediction, using CATFISH hydraulic code 0-23018  
 LMFBR, core restraint systems, interassembly heat transfer model 0-567  
 LMFBR, development and Pu allocation, optimal policies 0-725  
 LMFBR, LOFA, fuel assembly boiling and voiding, THARC-S code 0-13646  
 LMFBR, loop-type, effect of pumped stored kinetic energy on natural circulation decay heat removal 0-23010  
 LMFBR, loop-type, transition to natural convection from low temp., low flow conditions 0-18533  
 LMFBR, Na spillage due to slug impact on reactor cover 0-32364  
 LMFBR, post HCDA aerosols, gravitational collision efficiency 0-32375  
 LMFBR, primary containment response with upper internal struct. 0-32361  
 LMFBR, U-Pu-Zr fuelled, study of core disruptive accidents 0-18540  
 LMFBR, W-ARD air flow tests, COBRA-IV comparison 0-27734  
 LMFBR, whole core thermal hydraulic transient code 0-18387  
 LMFBR accidents, steel ablation and fuel-steel mixing phenomena, LEVITATE code anal. 0-47649  
 LMFBR design codes, multigroup diffusion, current weighted total cross section determ. in unresolved energy region 0-18365  
 LMFBR finite hexagonal bundles, three-dimensional coupled coolant cell heat transfer anal. 0-586  
 LMFBR fuel assembly, 19 pin, simulation of flow blockage 0-582  
 LMFBR fuel assembly, anal. of loss of piping integrity accident 0-27783  
 LMFBR fuel assembly, thermal consequences of plenum fission gas release, TRUMP thermal anal. 0-47646  
 LMFBR HCDA,  $\text{Na}_2\text{O}$  aerosol gravitational fallout rate, validation of computer code 0-18535  
 LMFBR HCDA containment response productions, validation of computer code 0-18538  
 LMFBR LOF-TOP, axial propagation of fuel failure, SAS3D-EPIC anal. 0-47650  
 LMFBR outlet plenums, transient anal. with PLENUM-2A program 0-32378  
 LMFBR safety, collocation method soln. of radiation-conduction problems 0-13720  
 LMFBR subassembly, multichannel model for fuel coolant interaction 0-13653  
 LMFBR thermohydraulic transient simulation, appl. of multiple time-step integration in Super System Code 0-47552  
 LMFBR TOP accident, effect of transient power histories on intrasubassembly failure incoherencies 0-47647  
 LOCA, experimental and theoretical study of the blowdown of the secondary side of a steam generator 0-761  
 LOCA, straight pipe blowdown tests and code verification [of reactor LOCA] 0-759  
 LOCA quench front model for Transient Analysis Reactor Code 0-47550  
 LOCA reflood phase, thermo-hydrodynamic behaviour, REFLA-1D code 0-47592  
 LOFT, zero power physics testing, meas. vs. calcs. 0-27713  
 LOFT non nucl. test L1-4, TRAC anal. 0-13655  
 loss of coolant effect on resonance escape probability, COCAP and WIMS codes 0-22963  
 LWR, 3D flux distrib. calc., axial continuous synthesis model with finite element trial functions 0-713  
 LWR, actinide decay power 0-22930  
 LWR, B and W cross-flow anal. by LYNX codes 0-22906  
 LWR, calc. of optimum power profiles using pattern search techniques, PROFILE code 0-47557  
 LWR, first order perturbation methods in sensitivity anal. 0-37425  
 LWR, interpretation of in-core measurements by semianalytical approach 0-712  
 LWR, NEPTUNE reactor calc. system, development and assessment 0-600  
 LWR, NRC safety research programs, fuel behaviour, operational safety, metallurgy and materials 0-13705  
 LWR, operation planning, optimum fuel loading and generation planning, comp. code FAPMAN8 0-47673



**nuclear engineering computing continued**

- LWR, optimum fuel loading and operation planning, FAPMAN model 0-47607
- LWR, outgoing neutron spectrum from H<sub>2</sub>O in H<sub>2</sub>O/V interface 0-27697
- LWR, pellet-clad interaction modelling 0-37445
- LWR, PROFIP 3, fission product activities, fuel survey 0-736
- LWR, Pu recycling, CEA-EdF studies 0-722
- LWR, Pu recycling, technical and economic study 0-720
- LWR, Scale system cross-section validation with shipping-cask critical experiments 0-37559
- LWR, sensitivity of fuel cycle cost to uncertainties in nucl. data 0-680
- LWR, spray droplet heat transfer in LOCA 0-32380
- LWR, thermal-margin methodology improvements 0-23022
- LWR cones, computation of cell group consts. 0-566
- LWR containment vessel, I removal by spray after LOCA, MIRA-PB code 0-47593
- LWR core, thermal and hydraulic behaviour, modelling in HOTRAN-3 (Hungarian) 0-32401
- LWR core blowdown, dynamic behavior of valves, computer simulation 0-5288
- LWR core flux distrib. using CETRA core simulator 0-716
- LWR core following and in-core fuel management code package, benchmarking and operating experience 0-704
- LWR core meltdown, accident anal. using computer system KESS 0-752
- LWR core meltdown and containment anal., computer code solns. 0-753
- LWR core performance studies in the UK, review of computer codes for static reactor physics anal. and kinetic anal. 0-703
- LWR core transient anal. using coupled neutronics and thermal hydraulic models 0-715
- LWR cores, single-fluid thermal hydraulic anal. 0-18410
- LWR fuel, mechanistic prediction of transient fission gas release 0-47571
- LWR fuel cycle resource requirements, implications of data uncertainties 0-18437
- LWR fuel management, power distrib. calcs. by nodal one-group simulators 0-706
- LWR fuel performance anal., WAFER-2 code 0-37447
- LWR fuel rod failure probability, comparison of FRAP T4 and meas. 0-13644
- LWR fuel rod under power transients, CRATER code calc. (French) 0-42789
- LWR LOCA, analysis, role of LOFT program 0-18531
- LWR LOCA, assessment of the RELAP4/MOD6 reactor transient thermal-hydraulic code 0-42826
- LWR LOCA, two-dimensional temperature distributions in fuel rods under blowdown conditions 0-774
- LWR LOCA, utilisation of LOFT information for licensing 0-18532
- LWR NRC safety research programs, thermo-hydraulics and computer code development 0-13704
- MAC code, fuel rod behaviour in PWR assemblies (French) 0-37451
- MAKOKOT code, equilibrium of plasma without shell, impurities outside coronal equilibrium and hollow profiles 0-28774
- MARIA research reactor, dynamics model for fast transients anal., code TOTEM 0-37419
- MEKIN, BWR benchmark calcs. 0-18385
- MEKIN code, experience in LWR core anal. 0-23054
- MEKIN neutronics/thermal-hydraulic code for BWR pressurisation transient anal. 0-47626
- MELSIM-1 code, LWR core meltdown accident simulation 0-18507
- MIPAC, fuel performance anal. by finite element method 0-42750
- Monte Carlo infinite cell calculations for TRX-1 and TRX-2 benchmarks 0-27711
- MORSE transport code, fusion reactor insulator, radiation damage calcs. 0-34061
- Muehleberg BWR, core simulation by fuel Management System, expt. verification 0-705
- MULTIFLEX, fluid-structural interactions, one-dimensional networks 0-13535
- multigroup collision prob. method, applied to overlapping neutron spectra theory, THERMAL 0-52718
- multigroup transfer coeffs., efficient eval. for shielding appls. 0-47747
- MWR feedwater and recirculation flow, minicomputer-based digital control 0-23027
- Netherlands fusion expts., data acquisition and anal. systems 0-13915
- neutron diffusion, multigroup equation, synthesis-finite element method 0-27699
- neutron diffusion equation, multigroup theory 0-27695
- neutron flux regulation, dynamic simulation of two-phase control absorber 0-13731
- neutron reflection, plane-parallel concrete interfaces, Monte Carlo calc. 0-27686
- neutron transport, anisotropic scattering treatment using improved comput. code (Japanese) 0-13526
- neutron transport, transverse buckling effects in 2-D calcs. 0-32318
- neutron transport eqn., response matrix finite element soln. 0-13527
- neutron transport theory, S<sub>N</sub> calcs. using ANL DIF3D diffusion code 0-47526
- neutronic analysis of the NBS intermediate-energy standard neutron field (ISNF) 0-27692
- Nordheim integral treatment for resonance processing, proper use 0-37427
- NORMA-CLARA, laser-driven fission-fusion microexplosions, nuclear and thermohydrodynamic calcs. 0-47696
- NORMA-LIBERTAS, laser-driven fission-fusion microexplosions, nuclear and thermohydrodynamic calcs. 0-47696
- NSSS, computerised simulator 0-22914
- nuclear criticality data, computerised bibliographic data base 0-13568
- nuclear laboratory instruction with multichannel analyser/microcomputer system 0-31471
- nuclear materials transportation, SABRE II combat simulation model 0-37542
- nuclear pumped laser fusion blanket optimisation in space and time 0-37616
- nuclear reactor pressure vessels, stress analysis program, STANSAS (Japanese) 0-22969
- nuclide inventory calculation code, FISPIN 0-42781
- operating reactor data retrieval and evaluation system RECORDS 0-13690
- ORNL interface and logistics studies 0-37540
- ORNL Nuclear Legislative Data Base program 0-37539
- PDQ program, diffusion theory calcs., fuel swelling and cladding shrinkage effects 0-22926

**nuclear engineering computing continued**

- PECITIS-II program, anal. of UO<sub>2</sub> collapsible clad elements 0-42751
- PEST code, MHD stability limits of high- $\beta$  Tokamaks 0-28643
- PHWR-1000, uniformity factor maximisation, nonlinear programming 0-739
- plasma simulation, heat transport 0-28817
- PLENUM-2A, transient anal. of LMFBR outlet plenums 0-32378
- PREP-KITT, HTGR core auxiliary cooling system, failure analysis 0-22964
- PROFILE, calc. of optimum power profiles using pattern search techniques for LWR 0-47557
- PWR, computer code for the study of migration and deposition of corrosion products 0-13700
- PWR, critical B concs. and cycle lifetime predictions 0-9365
- PWR, depressurisation accident, CUPIDON anal. of fuel rod behaviour (French) 0-42791
- PWR, development and Pu allocation, optimal policies 0-725
- PWR, HERMITE coupled neutronic thermal hydraulic code 0-23051
- PWR, LOCA, steam-water mixing 0-13651
- PWR, Markov model for quantitative systems interactions anal. of system unavailability 0-22898
- PWR, operational dynamics, digital simulation model 0-27751
- PWR, physics design of reload with nodal code system 0-723
- PWR, process monitoring and parameter estimation, multivariate signal analysis algorithms 0-47585
- PWR, Pu recycling, CEA-EdF studies 0-722
- PWR, Tihange-type, Pu recycling, physics and safety anal. 0-724
- PWR, two-phase critical flow in long nozzles 0-13550
- PWR assembly, MAC code model of fuel rod behaviour (French) 0-37451
- PWR blowdown, pressure field and core barrel loadings, computer codes 0-13665
- PWR core meltdown accident, computer simulation of second phase 0-754
- PWR core thermal-hydraulic response during steam line break accident 0-18384
- PWR dynamics, lumped parameter model, eval. of assumptions 0-585
- PWR flow transients, critical heat flux predictions using CODA 1-D coolant dynamics code 0-42817
- PWR fuel management program 0-18434
- PWR LOCA, effect of steam generator tube rupture, computer simulation 0-23006
- PWR LOCA, licensing evaluation calcs. at LOFT 0-23008
- PWR LOCA, LOFT post-test anal. using RELAP4/MOD5 blowdown model 0-42825
- PWR LOCA, LOFT tests, TRAC-P1A pre-test calculations 0-42824
- PWR LOCA Standard Problem 5, TRAC-P1A anal. 0-42823
- PWR neutronic calcs., subcooled boiling and open channel effects 0-23053
- PWR non-LOCA transient anal. using IRT code 0-42819
- PWR steam generator force anal. during LOCA 0-13666
- PWR thermodynamic design calcs., using iteration system based on secondary circuit system model (German) 0-13571
- PWR transient anal. methods, qualification with plant startup meas. 0-18508
- radioactive high-level waste disposal in salt formations, far-field temp. calcs. 0-5277
- reactimeter, microprocessor based, nucl. engineering lab. class enhancement 0-36825
- reactivity effect of cross-section processing for moist bulk-oxide criticals 0-37493
- reactor coolant activity monitoring, automatic on-line system 0-684
- reactor core system, bowed, NUBOW-3D program for static anal. including irradiation creep and swelling 0-5215
- reactor neutron flux regulation dynamic simulation algorithm 0-27738
- reactor noise analysis, time series modelling methods, comparative eval. (Japanese) 0-13552
- reflecting boundary conditions for diffusion coefficient calculations in Wigner-Seitz cells 0-27710
- RELAP4 BWR jet pump model, improved version 0-18380
- RELAP4/MOD5 blowdown model of PWR LOCA LOFT experiment 0-42825
- RELAP4/MOD6 LWR LOCA thermal-hydraulic anal. code 0-42826
- RELAP4/MOD6 program, test prediction for German PKL test K5A 0-13642
- RELAP 4/REIPE, subcooled blowdown thrust force calc. 0-18382
- RELAP-3B anal. of BWR turbine trip without bypass transient 0-42814
- research reactor, core and console, long term service and reliability investigation 0-9359
- research reactor, DIDO, three-dimensional SNAP diffusion theory calc., including up-scattering 0-5208
- RETRAN, LOFT test L2-2 pre-test calc. 0-18518
- RETRAN, macroscopic balance equations for two-phase flow models 0-9332
- RETRAN code, non-LOCA transient safety anal. 0-18506
- RETRAN simulation of the Three Mile Island Unit 1 turbine trip test 0-18512
- RETRAN two-phase flow model, comparison with expt. 0-32330
- risk studies, data specialisation, Bayes' theorem 0-47601
- rocket propulsion using nuclear reactor, optimisation problem, calculus of variation 0-27694
- rod bundle thermal-hydraulic anal., commix-1 program 0-13645
- rod swap test results, VEPCO analytical methods for Surry 1, cycle 5 0-9338
- SABRE II, nucl. materials transportation model 0-37542
- SAND-II, neutron spectrum unfolding, <sup>252</sup>Cf 0-13514
- SAS3D-EPIC, anal. of axial propagation of fuel failure in LMFBR LOFTOP 0-47650
- Scale system cross-section validation with shipping-cask critical experiments 0-37559
- SGHWR fuel pins, pellet-cladding interactions and length changes 0-42763
- SHIELD system, nucl. fuel cycle appl. 0-37517
- SIMON cavitation model, anal. of LMFBR coolant cavitation in dynamic containment loading 0-32326
- SIMULATE code for startup test predictions 0-18558
- SIMULATE models, BWR split void assembly benchmark verification 0-22938
- SLEUTH-SEER code predictions of pellet-clad interactions in AGR fuel pins 0-42755



**nuclear engineering computing continued**

- SLIM, SGHWR fuel pins, pellet-cladding interactions and length changes 0-42763  
 SNR-300 LMFBR steam generator transients, computer simulation 0-23012  
 SOMIX-1 Na spray fire code, containment pressurisation 0-32365  
 spin lattice relaxation time meas. simulation, systematic and random error effects 0-37062  
 SSC-L simulation, FFTF loss-of-electric-power transient response, natural circulation tests 0-42836  
 statistical fuel model, FRP 0-42748  
 steam generators, linearised transient anal. 0-18378  
 steel, austenitic stainless type 316, corrosion mechanism in hot flowing Na, computer simulation 0-3251  
 Super System Code for LMFBR thermohydraulic transient simulation, appl. of multiple time-step integration 0-47552  
 synthesis finite element method for three-dimensional reactor calculations 0-13566  
 tandem mirror fusion-fission system studies 0-37607  
 tandem mirror hybrid reactor, nucl. performance sensitivity of Be/molten salt blanket 0-37606  
 TCLUD1 transient code, anal. of LMFBR subassemblies 0-18391  
 TEXTOR, computerised control system design 0-13907  
 TFR Tokamak, microcomputer data acquisition system 0-13916  
 TFR breeding modules, neutronics 0-37611  
 THERMAL, multigroup collision prob. method, applied to overlapping neutron spectra theory 0-52718  
 thermal hydraulics anal., teaching appl. of computer graphics 0-36824  
 thermal lattice leakage calcs. using modified B<sub>1</sub> method 0-47545  
 thermonuclear fusion research, user-engineered command language 0-27819  
 Tokamak, physics of burn control 0-37599  
 Tokamaks, large, impurity effects and control, neutral beam injection, computational models 0-28773  
 Tokamaks, transport losses, computer modelling and scaling 0-28612  
 TRAC anal. of LOCA in PWR with combined ECC injection 0-18522  
 TRAC anal. of PWR LOCA 0-18521  
 TRAC pre-test and post test calcs. of LOFT nucl. test L2-2 0-18519  
 TRAC-PIA anal. of PWR LOCA Standard Problem 5 0-42823  
 TRAC-PIA calcs. of blowdown expt. 0-18383  
 TRAC-PIA pre-test calculations of LOFT PWR LOCA tests 0-42824  
 TRANSENERGY, transient thermal hydraulic anal. in forced convection regime 0-18393  
 Transient Analysis Reactor Code LOCA quench front model 0-47550  
 transient heat transfer, COMETHE code 0-42761  
 transient two-phase flow system, three-dimensional numerical simulation 0-687  
 transverse momentum eqn. for COBRA-IV-I, improved version 0-578  
 TROFAN, laser fusion system studies model 0-32505  
 TRUMP thermal anal. of plenum fission gas release in LMFBR fuel assembly 0-47646  
 turbulent diffusion, connected flow passages, computer prediction using k-ε turbulence model 0-9331  
 TWOTRAN-DA, diffusion synthetic acceleration module, grid-coupling methods for the multigrid solution of the neutron diffusion equation 0-47555  
 URANUS and EPRI code evaluation 0-42756  
 URANUS programme, statistical version 0-42749  
 vent clearing analysis of a mark III pressure suppression containment 0-32371  
 void swelling calculations using FACSIMILE VSI 0-42782  
 WAFER-2, simulation fission gas release in UO<sub>2</sub>-Zr BWR type fuel rods 0-42758  
 WAFER-2 code, LWR fuel performance anal. 0-37447  
 Westinghouse nuclear training reactor fuel inventory reduction plan 0-23115  
 Westinghouse plant, hardware considerations for new DNB design procedure 0-18396  
 Westinghouse plant availability anal. with operating data base 0-23050  
 WRAP-EM system, complete BWR-EM LOCA anal. 0-18523  
 ZED II reactor lattice parameter calcs. using LATREP CYCLE 4 0-27787  
 Zircaloy cladding, stresses due to pellet cladding interaction 0-42762  
<sup>137</sup>Cs, 10 GeV proton spallation for transmutation of radioactive waste, calc. of transmutation number 0-13470  
 O<sub>2</sub> deposition in a mesh-packed cold trap 0-22905  
 Pu-island element, B304, gamma scanning of power and burnup distrib. 0-721  
<sup>239</sup>Pu direct enrichment of LWR assemblies in a fusion hybrid 0-37604  
 UO<sub>2</sub> collapsible clad elements, PECITIS-II program 0-42751  
 UO<sub>2</sub>-Zr BWR type fuel rods, fission gas release 0-42758  
 Xe spatial oscillations, time optimal control 0-32320  
 Xe-I induced spatial power oscillations, integration method 0-13567

**nuclear explosions**

- Baneberry event, numerical simulation 0-841  
 fallout observation, Chinese A-tests 0-27820  
 fission products, removal rate seasonal vars. in lower stratosphere 0-55957  
 neutron bomb radiation protection, calc. of rad. penetration in air and shielded human tissue dose equiv. 0-47743  
 Nevada test site, nuclear testing fallout possible association with childhood leukaemia 0-12186  
 P-wave codas, spectral composition of earthquakes and explosions 0-21640  
 P-waves records complexity appl. for discrimination of artificial and natural seismic sources 0-12340  
 pollution, radioactive dust captured by wind from Earth's surface (*Russian*) 0-16869  
 radiation transport in Earth for neutron and gamma-ray point sources above an air-ground interface 0-32526  
 radioactive contamination of biosphere, explosion and power plant influence (*Hungarian*) 0-21548  
 Soviet disaster 1957-8, explosion of stored nucl. waste, causes 0-22974  
 space vehicle nuclear propulsion, historical review of advanced consent 0-36475  
 structural integrity in postulated accidents, scaling laws for contained explosions 0-47604  
 tissue neutron and gamma-ray response function, mid-head, military appl. 0-8185

**nuclear fission see fission****nuclear fission of plutonium see fission of plutonium****nuclear fission of uranium see fission of uranium****nuclear fission piles see fission reactors****nuclear fission products see fission products****nuclear forces**

- see also binding energy; meson field theory; nuclear binding energy  
 Of<sub>1/2</sub> and Og<sub>9/2</sub> nuclei, mag. form factors, core polarisation and exchange current effects 0-13409  
 0p shell nuclei, effective interaction spin-tensor decomposition 0-32198  
 (π,π'), inelastic scatt. in Fermi liquid, nucleon-nucleon interaction effects 0-22862  
 A=15-18, effective interaction from coupled cluster many-body method extension 0-22701  
 A=16 to 40, mag. moments, shell model calcs, mesonic exchange current effects, book contrib. 0-479  
 A=18, multiple scattering, three-particle one-hole nuclear effective interaction 0-13384  
 A=3 systems, charge form factor and bound nucleon polarisation 0-22708  
 A=3-4 hypernuclei, binding energy anal., A-N pot., scatt. length and effective range 0-9256  
 A≤44, fp-shell nuclei struct., effect of core-excitation and α-clustering correl. 0-9245  
 abnormally large density and binding energy states, book contrib. 0-489  
 alpha cluster reactions, effective single particle operator 0-32218  
 baryon-antibaryon nuclei, energy spectra and properties 0-22709  
 BBG theory developments, hole and particle lines, dispersion effects and healings 0-22719  
 boson model, interacting, shell-model basis, correspondence between fermion and boson states and operators 0-52593  
 charge dependence and nuclear struct. effects, nuclear charge distrib. 0-32197  
 chiral symmetry and pion condensation, review book contrib. 0-437  
 cluster model, coupling effects of two-particle and alpha two-hole states in A=18 nuclei 0-5081  
 composite particles, N-cluster dynamics and effective interaction, dynamical eqn. 0-42560  
 conference on high energy physics and nuclear struct. Vancouver, Canada (Aug. 1979) 0-41936  
 conference on many-body theories, Trieste, Italy (Oct. 1978) 0-22135  
 dense nuclear matter, construction in lab., book contrib. 0-490  
 deuteron wave functions, relativistic, π-NN coupling 0-22595  
 direct energy minimisation methods in self-consistent nuclear fields, ground state props. 0-22702  
 double folding pot. for inelastic scatt. between nuclei 0-13425  
 droplet-model theory of the neutron skin 0-47416  
 effective form factor pot. due to unbound core after direct process, asymptotic behaviour 0-27560  
 effective interaction with three-body effects 0-27562  
 even-even spherical nuclei, neutron strength function, spin depend., quasi-particle-phonon model (*Russian*) 0-42561  
 exchange mag. moments, meson exchange currents, field theoretical approach 0-52574  
 Green's function method for many-body problem for relativistic meson field theory, book contrib. 0-357  
 Hamiltonians, semiclassical approx., spin-independ. pots. 0-32208  
 Hartree-Fock and linear response, coordinate space representation and gradient iteration 0-18216  
 Hartree-Fock calcs., fast iterative procedure 0-47414  
 heavy ion collisions, collective effects rel. to pion prod. 0-37392  
 heavy ion reactions, phenomenological nuclear friction mechanism, particle-hole excitation, nucleon exchange (*Chinese*) 0-42694  
 heavy ion-nucleus reactions, Pauli blocking on exchange and dissipation mechanism 0-42684  
 impulse approx. with nuclear current conservation, off-shell form factors 0-52632  
 isobar degrees of freedom, binding energy from BHF approx. 0-22734  
 isobar degrees of freedom in nuclear matter, binding, NN interactions and 2π exchange 0-22735  
 isoscalar effective charge in large A limit Tamm-Dancoff and RPA calcs. 0-42534  
 light nuclei, alpha cluster model, 3-body problem 0-32217  
 light nuclei, isospin mixing, charge depend. nuclear forces and Coulomb interactions 0-5056  
 many body effective interaction theory problem, comparison with atoms 0-47406  
 meson exchange, relativistic corrections, book contrib. 0-475  
 meson exchange 0-32195  
 meson exchange currents, configuration mixing, role in nucl. mag. moment, beta decay, review, book contrib. 0-478  
 meson exchange currents, conservation principles, symmetries, book contrib. 0-473  
 meson exchange currents, effect in electron inelastic scatt., book contrib. 0-480  
 meson presence in nuclei, nuclear g-factor exchange current controls., EM interaction role 0-22706  
 meson theory of nuclear vector and axial vector exchange currents, review, book contrib. 0-474  
 mesonic and relativistic effects in the nuclear electromagnetic interaction 0-22818  
 mesonic effects in photonuclear sum rules, book contrib. 0-476  
 mesonic exchange effect on nuclear mag. moment, expt. study, book contrib. 0-477  
 mesons in nuclei, exchange current effects on nuclear mag. moments, book 0-471  
 mesons in nuclei, field theoretical aspects, book 0-481  
 microscopic versus empirical effective interactions in a single j shell 0-18210  
 neutron distribution in nuclei, elastic and inelastic proton scattering, review 0-22649  
 nonrelativistic effective πN vertex, PCAC and σ-model 0-52591  
 nonrelativistic quark model study, resonating group method 0-47403  
 nuclear critical opalescence, pion field and condensation 0-42559  
 nuclear Dirac phenomenology, consistency with meson-nucleon interactions 0-9272  
 nuclear field theory, Dyson boson expansion and Faddeev-Watson resummation technique 0-13385  
 nuclear matter, Hugenholtz Van Hove theorem and density depend. effective interactions 0-32219



**nuclear forces continued**

- nuclear pion field struct., book contrib. 0-482  
 nuclei, description in relativistic field theory, book contrib. 0-358  
 nucleon-nucleus optical pot. from nuclear matter t-matrix, effective force. 0-22783  
 nucleon-nucleus potential at low and intermediate energy in a Dirac-Hartree model 0-5070  
 nucleonic form factor, pion exchange, model 0-22608  
 odd-odd nuclei, role of tensor force as an effective interaction 0-37332  
 Paris NN pot. parametrisation, phase shifts, nuclear matter binding energy 0-47405  
 parity violating nucl. force, unified treatment 0-47400  
 parity violation in nuclear forces, neutron capture  $\gamma$ -ray expts. 0-37322  
 parity-non-conserving nuclear forces, theoretical and phenomenological approach review 0-42556  
 photonuclear sum rules from continuum calcs., dependence on residual interactions 0-22807  
 pion Bose-Einstein condensation in energetic heavy ion collisions 0-22705  
 pion condensate, superconductivity in mag. field, critical field (*Russian*) 0-13387  
 pion condensation, field theoretic many-body system 0-22703  
 pion condensation and the pion-nuclear interaction, book contrib. 0-485  
 pion condensation in dense nuclear and neutron matter 0-37333  
 pion condensation in nuclear matter, book contrib. 0-484  
 pion condensation threshold in finite nuclei 0-18218  
 pion excitations and phase transitions in nuclear matter, review, book contrib. 0-483  
 proton-neutron multiplets, odd-odd nuclei, parabolic Regge trajectories, exchange of quadrupole phonon 0-52590  
 proton-proton potential models obtained from the Virginia phase-shift analysis 0-47401  
 reaction matrix approach to the cluster state, Brueckner generator coordinate method, appl. to  $\alpha$ - $\alpha$  scatt. 0-9250  
 realistic NN pot. construction for three body systems and nuclear matter 0-22699  
 Reid soft core potential, low-rank separable matrix formalism 0-22704  
 relativistic mean field theories, correlation effects estimate 0-5073  
 relativistic two-body forces in many-body systems, Weinberg and Yukawa interactions 0-32203  
 resonance degrees of freedom in the two-nucleon system 0-5072  
 ring diagrams in nuclear matter, many-body forces contrib.,  $\rho$  and  $\pi$  exchange 0-22740  
 Saito potential, off-energy-shell unitarity 0-18207  
 scalar meson field and many-body forces, book contrib. 0-359  
 second class current upper limit from  $\beta$ -decay data 0-47404  
 short range NN interaction from nonrelativistic QCD 0-32200  
 single-particle motion in nucleus, forces between constituent nucleons, shell model 0-47408  
 Skyrme-type interactions, spectroscopy of light nuclei, density dependent Hartree-Fock 0-22717  
 solid like aspect with alternating layer spin and  $\pi$  condensation 0-22733  
 spherical nuclei, isomer and isotope shifts, theory of finite Fermi systems 0-39929  
 spin-isospin density phase in finite nuclei, strongly oblate shape 0-22746  
 strongly bound  $\pi^-$  nuclear states, vel. depend. pot. binding, pionic atoms 0-37331  
 structure theory, nuclear reaction matrix and nuclear forces 0-9242  
 superfluid model, isotopic invariance and pairing energies 0-22687  
 superheavy nuclei and multineutron systems, possibility of existence (*Russian*) 0-462  
 surface properties from Thomas-Fermi calc. 0-13394  
 three-body scatt. problem, cluster expansions, effective intercluster pots. 0-5082  
 Universe and microcosm, gravitational-inertial field theory 0-8721  
 valence nucleon effective interactions 0-9244  
 variational techniques, wave functions correlation operators, review 0-22748  
 virtual mesons effect on hadron-nucleus reactions, book contrib. 0-472  
 weak, EM and strong interactions in the nucleus 0-4978  
 Yukawa quantum field theory, Matthews-Salam integral representations 0-327  
 Yukawa quantum field theory in 2D space-time, linear  $N_c$  bound, locally Fock property 0-326  
 Z-boson and two-boson models, neutral current phenomena,  $\mu$ -e universality 0-18109  
 $\Delta(33)$  interaction with nucleus, effective shell model pot., pion scatt. test 0-32202  
 $(\gamma, N)$ , intermediate energies, nucleon current interactions, direct knock out mechanism 0-27624  
 $^3H(\pi^+, pp)$ , pion absorpt., effect of  $\rho\pi$  exchange currents (*Korean*) 0-47402  
 NN cross-sections and resonances in nonstatic OBEP 0-13386  
 NN interaction in pion exchange, nuclear matter and pion condensation, review 0-42557  
 NN potential short range behaviour with the quark model 0-47409  
 NN resonances and total cross sections, expt. evidence review 0-42558  
 $(p, p)$ , pol. p, sd, fp shell nuclei, 65 MeV, effective two-body interaction range 0-32201  
 pp reaction, exchange current corrections  $\pi$  and  $\rho$  exchange 0-26733  
 $\pi$  electromag. processes, theoretical aspects 0-22822  
 $^3He$ - $^4He$  coupling on basis of PCAC 0-32196  
 $\pi N$  coupling in  $\Delta(1231)$  isobar region, pion index of refraction, self-energy in low density limit 0-42554  
 $\pi N$  low energy partial wave anal., cross sections,  $\Delta^0$  and  $\Delta^{++}$  0-52531  
 $\pi N$  P11 ground state potential, meson probability density 0-27558  
 $\pi N$  scattering amplitude in nuclear matter, quantum field theory approach 0-42570  
 $\pi NN$  form factor; relativistic calc. of  $\Delta(1232)$  contribution to imaginary part (*Korean*) 0-47292  
 $\pi N$  vertex, virtual nucleon propagator, and pionic vertex, form factor enhancement 0-22700  
 $^6Li(p, n)$ , 144 MeV, one pion exchange and PCAC expt. test 0-528  
 $^{27}Al(^4He, p)$  9-14 MeV, stat. multistep compound emission, residual two-body interaction 0-47493  
 $^{10}B$ , triaxial deformation in shell model non-central forces, projected HF calc. 0-13367  
 $^{12}Be$ , Hartree-Fock calculations of nuclear bulk properties with density- and starting-energy dependent effective interaction 0-9246  
 $^{12}C(^{12}C, p)X$ , 800 MeV/N, fireball and preequilibrium cross sections,  $\pi$  condensation proximity influence 0-27659

**nuclear forces continued**

- $^{12}C(\mu^-, \nu_e)^{12}B$ , Hartree Fock wavefunction, correlations, pseudoscalar coupling constant, capture rates, recoil nuclear polarisation 0-22774  
 $^{12}C(p, n)$ , 144 MeV, one pion exchange and PCAC expt. test 0-528  
 $^A Ca$ , ( $A=43-46$ ), pairing force, seniority number 0-27563  
 $^A Ca = A=40, 48$ , Hartree-Fock calculations of nuclear bulk properties with density- and starting-energy dependent effective interaction 0-9246  
 $^{40}Ca$ , giant isoscalar monopole state energies in generator coordinate method 0-37317  
 $H+H^+$ , nuclear repulsion, contrib. to charge transfer 0-18922  
 $^1H(n, \pi^0)^1H$ , nuclear forces charge symmetry test 0-5071  
 $^2H(\pi, \pi)$ , relativistic description,  $\pi N$  waves, NN rescatt.,  $\rho$ -exchange,  $\pi$  absorption and emission 0-9310  
 $^3H$ , energy levels using ATMS method and realistic nuclear forces 0-22707  
 $^3H \rightarrow n+d$ , s-wave asymptotic normalisation consts. in one-boson exchange model 0-37334  
 $^3He$ , Coulomb energy, charge symmetry breaking 0-27564  
 $^3He$ , trinucleon bound state problem, binding energy, form factors and mag. moment 0-22710  
 $^4He$ , energy levels using ATMS method and realistic nuclear forces 0-22707  
 $^4He$ , soft-core radial wave function, photo-disintegration calculation 0-18209  
 $^4He(p, d)$ , intermediate energies, pion exchange currents in DWBA anal. 0-32199  
 $^4He(p, d)$  pickup reaction, isobar configurations and short range correlations 0-22798  
 $^4He(\pi, \pi)$ , low energy, first order optical pot., Pauli principle corrections, nuclear binding 0-27675  
 $^{1231}$ , bands and decay props., core-particle coupling and polarisation effects 0-13354  
 $^6Li + \alpha$  system, exchange effects, resonating-group study 0-9240  
 $^{18}N$   $1^+$  state cross sections, effective two nucleon interaction, isovector tensor component from  $^{14}C(p, n)$  0-18208  
 $^{14}N(p, n)$ , 144 MeV, one pion exchange and PCAC expt. test 0-528  
 $N^*(1236)$  propagator, momentum depend. in  $N^*$ -excitation current 0-27559  
 $^{22}Na$ , effective interactions for dominant shell-model configurations: ds-shell example 0-32204  
 $^{20}Ne$ , nuclear current from cranked HF solns. 0-9241  
 $^{21}Ne$ , energy moments, sd shell realistic effective interactions, shell model spectra 0-18190  
 $^{16}O$ , bound isobars  $\Delta(1236)$ , single particle energies, wave functions (*Chinese*) 0-52562  
 $^{16}O$ ,  $\Delta(3,3)$  excitations and effective 3-nucleon forces 0-27561  
 $^{16}O$ , giant isoscalar monopole state energies in generator coordinate method 0-37317  
 $^{16}O$ , Hartree-Fock calculations of nuclear bulk properties with density- and starting-energy dependent effective interaction 0-9246  
 $^{16}O$ , pion condensation effects, RPA calcs. (*Chinese*) 0-47407  
 $^{16}O$  region, effect operators, number conserving set generalisation 0-42555  
 $^{16}O(0^+) \rightleftharpoons ^{16}N(0^-)$ , beta decay and muon capture rate ratio, mesonic exchange currents 0-42594  
 $^{22}O$ , Hartree-Fock calculations of nuclear bulk properties with density- and starting-energy dependent effective interaction 0-9246  
 $^{207}Pb(e, e)$ , magnetisation distrib. from elastic mag. form factors, core polarisation, exchange currents 0-47372  
 $^{208}Pb$  core with valence nucleon or hole, mag. props., exchange currents, electron scatt. 0-22689  
 $^{28}Si$ , spin cutoff factors, sd shell realistic effective interactions, shell model spectra 0-18190
- nuclear fusion**  
 see also nuclear explosions; nuclear reactions involving few nucleon systems  
 complete fusion in heavy-ion collisions 0-37400  
 complete fusion systems, barrier penetration, enhanced fusion-fission yields 0-13520  
 conference on heavy ion reaction dynamical props., Johannesburg, S.Africa (Aug. 78) 0-17715  
 conference on nuclear interactions, Canberra, Australia (Aug.-Sep. 1978) 0-4476  
 controlled fusion research and the Joint European Torus project 0-18593  
 heavy ion fusion, expt. data comparison with classical trajectory models, review 0-9324  
 heavy ion fusion and deep inelastic scatt., shape degrees of freedom, classical dynamic model 0-22876  
 heavy ion fusion and transfer reactions, resonance effects 0-9283  
 heavy ion fusion cross section, energy depend., nuclear matter density distrib., depend. 0-47519  
 heavy ion fusion reaction excitation function anal., nucleus-nucleus pots. 0-42728  
 heavy ion fusion reactions, statistical model calcs. 0-42726  
 high angular momentum fusion compound nucleus deexcitation, high spin states, rare earths 0-9259  
 ion+electron, energy transfer term in rate eqn., fusion targets 0-5331  
 ion-ion proximity pot. radial depend. test using fusion excitation functions 0-22859  
 laser fusion prod. of  $H$  by radiolytic-thermochem. cycles 0-45811  
 light heavy ion induced fusion, cross sections and yrast line limitations 0-5192  
 magnetic mirror experiments, measuring MeV ions from fusion reactions 0-6281  
 microwaves appl., economic and safety aspects 0-3754  
 power, state-of-the-art and problems to be overcome (*Dutch*) 0-37574  
 promptly emitted particles in nuclear collisions, fusion nucleon spectra 0-42678  
 resonant thermonuclear reaction rate integrals, closed-form evaluation and approximation considerations 0-8535  
 stellar interiors, thermonuclear reaction rate enhancement due to strong screening, ionic mixtures case 0-36613  
 thermonuclear fusion plasmas, elem. processes and role of atomic, ionic and mol. data 0-14916  
 thermonuclear reaction rate data for intermediate mass nuclei 0-31427  
 unified nuclear pot. for heavy ion elastic scatt., fission, fusion, masses and deformations 0-5189  
 $Z=103, 105, 107$  element prod. from heavy ion fusion, cross sections from statistical model 0-32313



**nuclear fusion continued**

- ( $\alpha, n\gamma$ ), rare earth nuclei, complete fusion process  $n$  and  $\gamma$  multiplicity 0-18363  
 ( $p, n\gamma$ ), rare earth nuclei, complete fusion process  $n$  and  $\gamma$  multiplicity 0-18363  
 $\rho$  reaction, exchange current corrections  $\pi$  and  $\rho$  exchange 0-26733  
 $^{27}\text{Al} + ^{16}\text{O}$ , 34-81 MeV, total fusion-evaporation cross sections, fusion barrier 0-5190  
 $^{27}\text{Al} (^{16}\text{O}, X)$ , 88 MeV, inelastic scatt. and multinucleon transfer,  $Q$ -value depend. 0-42690  
 $^{197}\text{Au} (^{40}\text{Ar}, X)$ , 222, 340 MeV, fusion cross sections, direct and evaporative  $p$  and  $\alpha$  prod., evaporation, fission 0-13518  
 $^{197}\text{Au} (\text{HI}, X)$ , 60-120 MeV complete fusion cross sections from fission fragment ang. distrib. 0-13516  
 $^{10}\text{B} + ^{10}\text{B}$ , fusion below Coulomb barrier, quantum mechanical barrier penetration model anal. 0-18361  
 $^{11}\text{B} + ^{10,11}\text{B}$ , fusion below Coulomb barrier, quantum mechanical barrier penetration model anal. 0-18361  
 $^{209}\text{Bi} (^{84}\text{Kr}, X)$ , TDHF fusion calcs., fusion cross sections 0-37409  
 $^{209}\text{Bi} (\text{HI}, X)$ , 60-120 MeV complete fusion cross sections from fission fragment ang. distrib. 0-13516  
 $^{12}\text{C} (X)$ ,  $A=12$ -19, total fusion cross sections and fusion barrier parameters 0-9322  
 $^{12}\text{C} + ^{10,11}\text{B}$ , fusion below Coulomb barrier, quantum mechanical barrier penetration model anal. 0-18361  
 $^{12}\text{C} + ^9\text{Be}$ , 11.4 MeV cm energy,  $p$ ,  $d$ ,  $t$ ,  $\alpha$  production 0-9302  
 $^{12}\text{C} (^{12}\text{C}, X)$ , 14-31 MeV, total and fusion cross sections,  $^{24}\text{Mg}$  ground state band 0-42727  
 $^{12}\text{C} (^{12}\text{C}, X)$  fusion cross section oscillations, overlapping compound states availability 0-9321  
 $^{13}\text{C} (^{13}\text{C}, ^{24}\text{Mg})$ , 3.05-6.88 MeV, fusion cross section energy depend., optical anal. 0-42724  
 $^{40}\text{Ca} (^{16}\text{O}, X)$ , 36-75 MeV, absolute and fusion total cross sections,  $^{56}\text{Ni}$  excitation functions 0-18362  
 $^{40}\text{Ca} (^{16}\text{O}, X)$ , 40-214 MeV, fusion and elastic scatt. cross sections, optical anal. 0-32314  
 $^{40}\text{Ca} (^{20}\text{Ne}, X)$ , 44.1-70.4 MeV, fusion and elastic scatt. cross sections, evaporation residues 0-550  
 $\text{D}(\text{d}, n)^3\text{He}$ , fusion cross sections and thermonuclear reaction rates 0-533  
 $\text{D}(\text{d}, p)^3\text{He}$ , fusion cross sections and thermonuclear reaction rates 0-533  
 $^{164}\text{Dy} (^{40}\text{Ar}, X)$ , 222, 340 MeV, fusion cross sections, direct and evaporative  $p$  and  $\alpha$  prod., evaporation, fission 0-13518  
 $^{160}\text{Gd} (^{12}\text{C}, \alpha x)$ , 120, 200 MeV, average  $\alpha$ -multiplicities, incomplete fusion and breakup 0-27661  
 $^{160}\text{Gd} (^{12}\text{C}, \alpha n\gamma)$ , 90-200 MeV, incomplete fusion, fast  $\alpha$  prod. absolute cross sections 0-18359  
 $^2\text{H}^3\text{H} \mu \rightarrow ^4\text{He} + n + \mu^- + 17.6$  MeV, muonic catalysis in synthesis reactions (Russian) 0-52706  
 $^3\text{He} (\text{H}, n)^4\text{He}$ , fusion through metallic D 0-13517  
 $^3\text{He} (\text{d}, p)^4\text{He}$ , fusion cross sections and thermonuclear reaction rates 0-533  
 $^{139}\text{La} (^{86}\text{Kr}, X)$ , TDHF fusion calcs., fusion cross sections 0-37409  
 $^{139}\text{La} (^{86}\text{Kr}, X)$ , 505, 610, 710 MeV, TDHF calcs., fusion behaviour 0-9323  
 $^6\text{Li} + p$  propagating fusion fuel cycle 0-37629  
 $^{24}\text{Mg}$  giant isoscalar quadrupole fission/fusion doorway states from  $^{12}\text{C} (^{12}\text{C}, ^{12}\text{C})$  0-37410  
 $^{14}\text{N} (n, \gamma)$ , rare earth nuclei, complete fusion process  $n$  and  $\gamma$  multiplicity 0-18363  
 $^{20}\text{Ne} + ^{12}\text{C}$ , 6.3-13.8 MeV, total fusion cross section,  $S$ -factor,  $\gamma$ -yields 0-22877  
 $^{20}\text{Ne} (^{20}\text{Ne}, X)$ , 132 MeV, TDHF calc. for total fusion cross section 0-13521  
 $^{40}\text{Ni} (^{40}\text{Ca}, \text{fusion})$ ,  $A=58, 60, 62, 113$ -170 MeV, fusion cross sections and excitation functions 0-32315  
 $^{16}\text{O} + ^{16}\text{O}$ , fusion cross section gross struct., excitation functions, coupled channel method 0-52705  
 $^{16}\text{O} (^{12}\text{C}, X)$ , sub-barrier energies, fusion cross section, static and dynamic deformation effects 0-42729  
 $^{16}\text{O} (^{16}\text{O}, X)$ , total fusion cross sections and fusion barrier parameters 0-9322  
 $^{208}\text{Pb} (^{16}\text{O}, X)$ , 80-313 MeV, optical model anal., dynamic shape or density changes 0-18186  
 $^{32}\text{S}$  compound nucleus formation and deexcitation entrance channel effects from  $^{16}\text{O} + ^{16}\text{O}$ ,  $^{12}\text{C} + ^{20}\text{Ne}$  0-549  
 $\text{Si} + ^{16,18}\text{O}$ , 34-81 MeV, total fusion-evaporation cross sections, fusion barrier 0-5190  
 $^{28}\text{Si} (^{12}\text{C}, X)$ , 20-49 MeV,  $A=28$ -30, complete fusion cross sections, excitation function weak struct. 0-5188  
 $^{28}\text{Si} (^{16}\text{O}, X)$ , 21-61 MeV,  $A=28$ -30, complete fusion cross sections, excitation function weak struct. 0-5188  
 $^{28}\text{Si} + ^{16}\text{O}$ , fusion oscillations, evaporation residue gamma yields, cross section 0-42725  
 $^{48}\text{Sm} (^{16}\text{O}, X)$ , 60-75 MeV,  $A=148, 150, 152, 154$  deformation effects on fusion 0-18360  
 $^{154}\text{Sm} (^{16}\text{O}, X)$ , 153 MeV, angular momentum transfer in incomplete-fusion reactions 0-9320  
 $^{154}\text{Sm} (^{40}\text{Ar}, X)$ , 222, 340 MeV, fusion cross sections, direct and evaporative  $p$  and  $\alpha$  prod., evaporation, fission 0-13518  
 $^{116}\text{Sn} (^{40}\text{Ar}, X)$ , 187, 222, 340 MeV, fusion cross sections, direct and evaporative  $p$  and  $\alpha$  prod., evaporation, fission 0-13518  
 $\text{T}(\text{d}, n)^4\text{He}$ , fusion cross sections and thermonuclear reaction rates 0-533  
 $\text{T}(\text{t}, 2n)^4\text{He}$ , fusion cross sections and thermonuclear reaction rates 0-533  
 $^{238}\text{U} (^{56}\text{Fe}, X)$ , 538 MeV, binary coincident fragments, fragment mass and energy, fission following fusion 0-548  
 $^{182}\text{W} (^{12}\text{C}, X)$ , 77-167 MeV, fusion cross sections, direct and evaporative  $p$  and  $\alpha$  prod., evaporation, fission 0-13518

**nuclear fusion reactors** *see fusion reactors***nuclear giant resonances** *see nuclear collective states and giant resonances***nuclear induction** *see nuclear magnetic resonance***nuclear instrumentation**

- see also angular correlation techniques; beam handling equipment; counters; counting circuits; nuclear reactor instrumentation; particle accelerators; particle detectors; particle track visualisation*  
 activation meas. using Nairi-K multichannel installation 0-23271  
 amplifier, linear, solid-state, for photomultiplier pulses 0-5451  
 AZ MS IV scanning measuring projector system, calibration methods 0-5449  
 BASIC overlay for CAMAC data and command handling 0-18772

**nuclear instrumentation continued**

- CAMAC diagnostic module for on-line monitoring of CAMAC integrity 0-5459  
 CAMAC high rate data acquisition system 0-23281  
 colloquium on nucl. instrumentation, London, England 1979 0-4480  
 computer-controlled pulser system 0-52841  
 data acquisition system on-line, for particle physics expts. using PDP-11 computers 0-27913  
 electronics in nuclear science and technology 0-9347  
 FASTBUS, medium energy physics appls. 0-42912  
 FASTBUS, molecular data bus system for high energy physics 0-42911  
 laboratory course, computer based data acquisition and anal. 0-36820  
 level and density measurement using nuclear gauges 0-843  
 magnetic spectrograph, multi-ang., for charged particles emitted in nucl. reactions 0-5429  
 magnetic tape interfaces for a dual-parameter coincidence experiment 0-14055  
 particle-particle correlation experiment, on-line four parameter anal. system (Chinese) 0-42910  
 programmable fast logic unit 0-52842  
 pulse height store for A/D conversion 0-14054  
 teaching, undergraduate, courses, facilities 0-27086  
 time to amplitude converters, precision 1 GHz time calibration 0-27903  
 $^{12}\text{I}$ , counting device with automatic efficiency correction 0-42897
- nuclear interactions** *see nuclear reactions and scattering*
- nuclear internal conversion** *see internal conversion*
- nuclear isobaric analogue resonances** *see isobaric analogue resonances*
- nuclear isobaric analogue states** *see isobaric analogue states*
- nuclear isomerism**  
*see also nuclear energy levels*  
 $A=40$ -80, yrast props. and high spin isomers, cranking plus Strutinsky formalism 0-32152  
 heavy ion collisions, fluid dynamical and TDHF models, abnormal nuclear matter, density isomers 0-47502  
 high-spin states and shell struct. in  $N=Z$  nuclei,  $^{20}\text{Ne}$  appl. 0-47342  
 $N=82$ -86, high spin isomers, gamma spectroscopy 0-47358  
 $N \approx 50$  nuclei, unsuccessful search with 42 MeV  $^{16}\text{O}$  projectile 0-9223  
 neutron induced yrast isomer prod., pulsed beam meas. using plastic scintillation spectrum 0-27871  
 nuclear matter, pion condensation and density isomerism 0-5085  
 spherical nuclei, isomer and isotope shifts, theory of finite Fermi systems 0-39929  
 yrast traps, obs. in heavy ion collisions 0-37319  
 $^{110}\text{Ag}$  low-lying levels, from  $^{109}\text{Ag}(n, \gamma)$  obs. 0-47422  
 $^{241}\text{Am}(n, f)$ , 14.8 MeV, mass yield distrib., and absolute fission yield, isomer ratios 0-18352  
 $^{197}\text{Au}$ ,  $A=189, 191, 193$ , high spin states and transitions, isomeric states from  $\text{Ir}(\alpha, n\gamma)$  0-5038  
 $^{197}\text{Au}$ ,  $A=190, 192, 194$ , levels,  $J^\pi$ , isomers and rot. aligned bands from  $\text{Ir}(\alpha, n)$  0-9215  
 $^{197}\text{Au}(n, n')^{197m}\text{Au}$ ,  $E_n=3$  and 14.1 MeV, form. cross sections of short-lived isomer, cyclic activation technique 0-32283  
 Br, isomer ratios in fission fragments at high excitation 0-32261  
 $^{76}\text{Br}$ , Coriolis distorted bands, common  $g_{9/2}$  parentage in  $N=41$  nuclei 0-13349  
 $^{78}\text{Br}$ , high-spin states, from  $^{77}\text{Se}(\alpha, 2np)$ , decay into isomers 0-52569  
 $^{111}\text{Cd}$ , excitation by photon less positron annihilation, isomeric  $\gamma$ -transitions (Russian) 0-5089  
 $^{111}\text{Cd}^m$ , nuclear orientation in Zn and Be, 245 keV state quadrupole moment, half-life 0-37324  
 $^{111}\text{Cd}(\gamma, \gamma)$ , isomeric states excitation, integral cross sections 0-27528  
 $^{137}\text{Cs}$ ,  $A=246, 248$ , fission isomer rot. spectra  $I^2(I+1)^2$  correction 0-18229  
 $^{48}\text{Cr}$  high spin states, yrast levels and  $6^-$  isomeric state from  $^{40}\text{Ca} (^{10}\text{B}, np)$  0-454  
 $^{152}\text{Dy}$ , collective bands and absence of yrast traps 0-9207  
 $^{152}\text{Dy}$  high spin isomeric states,  $g$ -factors from  $^{140}\text{Ce} (^{16}\text{O}, 4n)$  0-13377  
 $^{152}\text{Dy}$  high spin isomers, yrast states and level lifetimes from  $^{15}\text{N}, 4n)$ ,  $(^{16}\text{O}, 4n)$  0-13361  
 $^{152}\text{Dy}$  yrast traps, isomers and oblate deformations from  $^{124}\text{Te} (^{32}\text{S}, 4n)$  0-13362  
 $^{153}\text{Er}$  360 ns yrast trap,  $\gamma$  transitions and lifetimes from  $^{144}\text{Sm} (^{12}\text{C}, 3n)$  0-9205  
 $^{154}\text{Er}$ , collective bands and absence of yrast traps 0-9207  
 $^{154}\text{Er}$  yrast trap and transitions, decay scheme from  $(^{64}\text{Ni}, 4n)$ ,  $(^{16}\text{O}, 4n)$  0-9206  
 $^{145}\text{Eu}$  high spin and isomeric states, transitions, weak coupling from  $^{144}\text{Sm}(\alpha, 2np\gamma)$  0-13348  
 $^{152}\text{Eu}$ , isomeric levels and transitions, Nilsson model 0-18195  
 $^{152}\text{Eu}^m$  ( $n, n'$ ), thermal neutron acceleration by isomeric nuclei (Russian) 0-52680  
 $^{147}\text{Gd}^m$  high spin yrast trap, oblate deformation and quadrupole moment 0-32157  
 $^{150}\text{Gd}$ , collective bands and absence of yrast traps 0-9207  
 $^{171}\text{Hf}(\text{HI}, xn)$ ,  $A=170$ -173, two and three quasiparticle isomers, rot. bands, decays and lifetimes 0-9211  
 $^{171}\text{Hf}$  one- and three-quasiparticle states, high spin rot. bands from  $(^{16}\text{O}, 5n)$ ,  $(^{13}\text{C}, 4n)$  0-18163  
 $^{173}\text{Hf}$  multi-quasiparticle states and bands, isomeric states, lifetimes from  $^{170}\text{Er} (^{6}\text{Be}, 4n)$  0-9213  
 $^{191}\text{Hg}$ , and  $^{190m-185m}\text{Hg}$ , nucl. spins, on-line quantum beat spectrosc. determ. 0-9562  
 $^{187}\text{Ho}$ ,  $A=153, 160$ , isomeric levels and transitions, Nilsson model 0-18195  
 $^{187}\text{In}$ ,  $A=113, 115$ , excitation by photon less positron annihilation, isomeric  $\gamma$ -transitions (Russian) 0-5089  
 $^{109}\text{In}$  high spin states, transitions, isomeric state, negative parity bands from  $^{107}\text{Ag}(\alpha, 2n\gamma)$  0-451  
 $^{115}\text{In}(\gamma, \gamma)$ , isomeric states excitation, integral cross sections 0-27528  
 $^{114m}\text{In}$ , prod. in  $\text{Cd}(\text{d}, xn)$  reactions,  $E_d \leq 27.5$  MeV, cross sections 0-13482  
 $^{116m}\text{In}$ , prod. in  $\text{Cd}(\text{d}, xn)$  reactions,  $E_d \leq 27.5$  MeV, cross sections 0-13482  
 $^{178}\text{Lu}$  isomeric states and spins, transition probability from  $^{181}\text{Ta}(n, \alpha)$  0-52582  
 $^{258}\text{Md}$  isomer, EC decay,  $^{258}\text{Fm}$  spontaneous fission, mass and kinetic energy distrib. 0-47518  
 $^{24}\text{Na}^m$ ,  $1^-$  isomer, mag. moment 0-32177  
 $^{91}\text{Nb}$ ,  $17^-/2$  state,  $g$ -factor meas. 0-32179



**nuclear isomerism continued**

- <sup>188</sup>Os, muonic resonance spectra, deduced isomer shifts and electric moments 0-18948  
<sup>208</sup>Pb, A=200,206, 12<sup>+</sup> isomer states, quadrupole moments 0-27554  
<sup>143</sup>Pm high spin states, J<sup>π</sup>, transitions, isomer g-factors from (d,2N), (α,2N) 0-32154  
<sup>143</sup>Pm β-decay, <sup>144</sup>Nd levels and transitions, γ-ray spectra (French) 0-18250  
<sup>148</sup>Pr isomerism study from β and γ decay meas. 0-5096  
<sup>183</sup>Pt<sup>m</sup> decay, population of <sup>183</sup>Ir levels 0-9269  
<sup>238</sup>Pu, A=238,240, fission isomer rot. spectra I<sup>2</sup>(1+1)<sup>2</sup> correction 0-18229  
<sup>238</sup>Pu fission single particle isomers, half lives and isomeric ratio from (γ,2n) 0-18181  
<sup>240</sup>Pu, hexadecapole shape isomeric state, shell correction method fission barrier calcs. 0-545  
<sup>78</sup>Rb β-decay half-lives of isomeric and ground state from (<sup>16</sup>O,3n) 0-27534  
<sup>182</sup>Re isomer decay mag. moment, <sup>182</sup>W high spin states, J assignments and mixing ratios 0-42593  
<sup>103</sup>Rh(e,e'), 350-800 keV, isomer Coulomb excitation cross sections 0-22659  
<sup>90</sup>Sr isomer ratios in fission fragments at high excitation 0-32261  
<sup>90</sup>Sr isomer ratio, high spin trapping from (α,xn)(α, pn) 0-22655  
<sup>132</sup>Sn, energy levels, gamma transitions, spin and parity 0-9239  
<sup>14</sup>Tb, A=147, 148, high spin particle-hole states, octupole M2/E3 isomers from <sup>151</sup>Eu(α,xn) 0-18171  
<sup>14</sup>Tb, A=93-96, excitation functions and isomer ratios from <sup>93</sup>Nb(α,xn) (x=1 to 4) 0-492  
<sup>99</sup>Tc<sup>m</sup> β-decay, β-branching, <sup>99</sup>Ru decay scheme 0-42596  
<sup>99</sup>Tc<sup>m</sup> decay constant, chemical state effect 0-42591  
<sup>100</sup>Tc low lying and isomeric levels, transitions and mean lines from <sup>100</sup>Mo(p,nγ) 0-42548  
<sup>100</sup>Tc isomer ratio, high spin trapping from Sn(α,3n) 0-22655  
<sup>14</sup>Tc<sup>m</sup>, A=125, 127, 129, 11/2<sup>-</sup> isomeric state magnetic moments 0-42537  
<sup>121</sup>Te isomeric state, spin, lifetime and mag. moment from (α,n)(d,Zn) 0-47387  
<sup>132</sup>Te from fission, 10<sup>+</sup> isomeric state, J<sup>π</sup> from deexcitation pattern, half life 0-460  
<sup>232</sup>Th(γ,f), deep subthreshold photofission, double humped fission barrier anal., shape isomer 0-5179  
<sup>192</sup>Tl high spin band struct. and transitions, isomeric state from <sup>181</sup>Ta(<sup>16</sup>O,xnγ) 0-47353  
<sup>194</sup>Tl high spin states, excitation functions, I<sup>π</sup>=8<sup>-</sup> isomeric state from <sup>181</sup>Ta(<sup>16</sup>O,5n) 0-32163  
<sup>14</sup>U, A=236,238, fission isomer rot. spectra I<sup>2</sup>(1+1)<sup>2</sup> correction 0-18229  
<sup>14</sup>U(γ,f), A=235, 236, 238, deep subthreshold photofission, double humped fission barrier anal., shape isomer 0-5179  
<sup>235</sup>U<sup>m</sup> prod. by nuclear excitation by electron transition in plasma 0-22668  
<sup>236</sup>U fission shape isomer, γ-decay from <sup>238</sup>U(γ,2n) 0-18230  
<sup>236</sup>U low lying levels from 4<sup>-</sup> isomer decay in (n,e), (n,γ) 0-47396  
<sup>125</sup>Xe odd and even parity band structs., level lifetimes from <sup>125</sup>Te(<sup>3</sup>He,3nγ) 0-27533  
<sup>172</sup>Yb, muonic resonance spectra, deduced isomer shifts and electric moments 0-18948

**nuclear isospin**

- A=42 isotopic spin triplet, Coulomb energies and shifts, microscopic calcs. 0-9200  
 dense neutron and nuclear matter, spin and isospin stability 0-22737  
 double folding pot. for inelastic scatt. between nuclei 0-13425  
 giant isovector monopole states, isospin splitting and mixing 0-27609  
 light nuclei, isospin mixing, charge depend. nuclear forces and Coulomb interactions 0-5056  
 medium nuclei, photoproton spectra and preequil. decay, microscopic theory 0-47464  
 open shell nuclei by seniority and reduced isospin projections 0-47415  
 photoneutron reactions review, giant dipole resonances and cross sections 0-5125  
 proton-neutron basis, decomposition matrix rel. to basis of specified isospin T 0-37337  
 quadrupole moments and rms charge radii, shell model calcs. 0-47369  
 spin-isospin density phase in finite nuclei, strongly oblate shape 0-22746  
 superfluid model, isotopic invariance and pairing energies 0-22687  
 Z=73-85, preactinide nuclei, fission barriers in droplet model, isospin depend. (Russian) 0-5120  
 (π,π<sup>+</sup>), 1p shell targets, DWIA calcs., strong transitions, isospin effects 0-42708  
 (π,π<sup>+</sup>), collective transitions, giant resonances, isospin content and spin transfer 0-42580  
<sup>8</sup>Be isospin mixed 2<sup>+</sup> doublet, level parameters from <sup>4</sup>He(α,α) 0-27556  
<sup>1</sup>C(π,π<sup>+</sup>), A=12, 13, ~180 MeV, isospin mixing, levels, excitation functions and ang. distrib. 0-42543  
<sup>12</sup>C(e,e), 12.71 and 15.11 MeV level struct. and isospin mixing from form factors 0-32186  
<sup>12</sup>C(π<sup>+</sup>,π<sup>+</sup>), 100-291 MeV, cross sections and ang. distrib., spin and isospin transfer 0-52697  
<sup>4</sup>Ca giant dipole resonance, isospin struct., direct-semidirect anal. from <sup>40</sup>K(p,γ) 0-47449  
<sup>53</sup>Cr(γ,p)<sup>52</sup>V, cross-section, 14.4-27 MeV, isospin splitting 0-520  
 (d,p), A=88-106, pol. d. excitation curve isospin anomaly, neutron single particle resonances 0-27595  
<sup>18</sup>F J<sup>π</sup>=3<sup>-</sup> doublet at 6241 keV, isospin mixing from (p,γ), (p,α), (α,γ) (<sup>14</sup>N,α) 0-511  
<sup>2</sup>H(d,n)<sup>3</sup>He, 15.5, 17 MeV, pol. d. anal. power direct reaction and isospin symmetries 0-515  
<sup>2</sup>H(π<sup>+</sup>,π<sup>+</sup>), 340 MeV/c, reaction mechanisms and isospin effects 0-32306  
<sup>14</sup>N(γ,n)<sup>13</sup>N, 17 to 26 MeV, angular distrib., giant dipole resonance, single-particle nuclear model 0-52659  
<sup>6</sup>Ni, A=57, 59, 61, 63, variation of spectra, isospin mixing 0-13401  
<sup>58</sup>Ni(γ,γ), M1 strength isospin splitting for dipole ang. distrib. states 0-13412  
<sup>62</sup>Ni(γ,X), 19.2-26.2 MeV, photoneutron and photoproton spectra, giant dipole resonance-decay, isospin conservation 0-13443  
<sup>16</sup>O(π,π<sup>+</sup>), ~180 MeV, isospin mixing, levels, excitation functions and ang. distrib. 0-42543  
<sup>56</sup>Ti(γ,X), photoneutron and photoproton cross sections, giant dipole resonance isospin splitting 0-13442

**nuclear liquid drop model**

- alpha-decay, decay periods in liq. drop model (Russian) 0-32246  
 CM(3) collective model, geometric quantisation 0-5078  
 even-even rare earths, microscopic quadrupole and hexadecapole moments 0-13376  
 giant resonances, stability and polarisation (French) 0-22669  
 neutron skin, compared with droplet model theory 0-52599  
 neutron-rich nuclear potential energy surfaces 0-18183  
 preactinide nuclei, fission excitation functions and fission barrier height, liquid drop model 0-47513  
 rotating nuclei, critical ang. momentum and equilibrium figures from ellipsoid, liquid drop model (Russian) 0-37339  
 unified nuclear pot. for heavy ion elastic scatt., fission, fusion, masses and deformations 0-5189  
 very high spin states from liquid drop model 0-5047  
 Z=73-85, preactinide nuclei, fission barriers in droplet model, isospin depend. (Russian) 0-5120  
<sup>15</sup>Fm(n,f), A=253, 255, 257, 259, fission mass distrib. transition, liquid drop and shell model calcs. 0-32310  
<sup>15</sup>Fm(sf), A=254, 256, 258, 260, fission mass distrib. transition, liquid drop and shell model calcs. 0-32310  
<sup>240</sup>Pu, hexadecapole shape isomeric state, shell correction method fission barrier calcs. 0-545  
<sup>236</sup>U fission fragment kinetic energies, wall and window one body dissipation model 0-52703

**nuclear magnetic acoustic resonance** see *acoustic nuclear magnetic resonance***nuclear magnetic moment**

- see also *gyromagnetic ratio; molecular nuclear coupling; nuclear magnetic resonance*  
 A=15 mag. moments, nuclear Dirac wave function test 0-5060  
 A=16 to 40, mag. moments, shell model calcs, mesonic exchange current effects, book contrib. 0-479  
 exchange mag. moments, meson exchange currents, field theoretical approach 0-52574  
 excited nuclei moving through ferromag. media, transient mag. field effect, mag. moment meas. 0-37325  
 excited simple and yrast states, mag. moments, transient mag. fields 0-5064  
 isomeric state g-factor meas., target preparation 0-23217  
 magnetic order determ. using low-temperature techniques (French) 0-5062  
 meson exchange currents, configuration mixing, role in nucl. mag. moment, beta decay, review, book contrib. 0-478  
 meson presence in nuclei, nuclear g-factor exchange current controls, EM interaction role 0-22706  
 mesonic exchange effect on nuclear mag. moment, expt. study, book contrib. 0-477  
 mesons in nuclei, exchange current effects on nuclear mag. moments, book 0-471  
<sup>13</sup>C-methane-d<sub>3</sub>O, annealed, spin conversion and proton 2nd moment time-depend. 0-11283  
 nuclear Dirac phenomenology and the A-nucleus potential, anomalous mag. moment 0-37344  
 (e,e), form factors, magnetisation density, mag. moments and valence nucleon orbits 0-22690  
<sup>242</sup>Am, mag. dipole moment-atomic electron satellite states, influence on E0 conversion 0-18236  
<sup>212</sup>At high spin states, decay, g factor, J<sup>π</sup> assignments, level energies from <sup>208</sup>Pb(Li,3n) 0-5042  
<sup>138</sup>Ba(<sup>32</sup>S,<sup>32</sup>S), A=130, 132, 134, 136, 72-80 MeV, 2<sub>1</sub><sup>+</sup> state mag. moments 0-47373  
<sup>15</sup>C 0.74 MeV 5/2<sup>+</sup> state g-factor, shell model interpretation from <sup>3</sup>H(<sup>13</sup>C,p) 0-32176  
<sup>45</sup>Ca, nuclear charge radius, spin, moments, by laserspectroscopy 0-18187  
<sup>138</sup>Cd(<sup>32</sup>S,<sup>32</sup>S), A=106, 108, 110, 112, 114, 116, 72-80 MeV, 2<sub>1</sub><sup>+</sup> state mag. moments 0-47373  
 Cs neutron rich isotopes, nucl. spins and mag. moments 0-47367  
 Dy, deformed nuclei, quasicontinuum γ-spectrum, M1, E1, E2 components 0-498  
<sup>157</sup>Dy high spin isomeric states, g-factors from <sup>140</sup>Ce(<sup>16</sup>O, 4n) 0-13377  
<sup>13</sup>He, trinucleon bound state problem, binding energy, form factors and mag. moment 0-22710  
<sup>16</sup>Ho in HoVO<sub>4</sub>, NMR predictions of properties, dipolar interactions and antiferromagnetic exchange 0-50203  
<sup>166</sup>Ho, internal hyperfine field obs. using β-γ directional correl. 0-32229  
<sup>166</sup>Ho low lying levels and transitions, 54.24 keV level mag. moment from <sup>166</sup>Dy decay 0-13380  
<sup>25</sup>Mg(e,e), 180° scatt., magnetisation distrib., mag. multipole moments 0-9228  
<sup>1</sup>Mo, A=94, 96, 98, multiparticle states, method of generalised seniority 0-22759  
<sup>24</sup>Na<sup>m</sup>, 1<sup>+</sup> isomer mag. moment 0-32177  
<sup>91</sup>Nb, 17<sup>-</sup>/2 state, g-factor meas. 0-32179  
<sup>93</sup>Nb(e,e), 180° scatt., magnetisation distrib., mag. multipole moments 0-9228  
 Pb region, mag. moments and M1, M2 and M4 values, self consistent calcs. 0-47371  
<sup>207</sup>Pb(e,e), magnetisation distrib. from elastic mag. form factors, core polarisation, exchange currents 0-47372  
<sup>208</sup>Pb core with valence nucleon or hole, mag. props., exchange currents, electron scatt. 0-22689  
<sup>146</sup>Pd(<sup>32</sup>S,<sup>32</sup>S), A=102, 104, 106, 108, 110, 72-80 MeV, 2<sub>1</sub><sup>+</sup> state mag. moments 0-47373  
 Rb neutron rich isotopes, nucl. spins and mag. moments 0-47367  
<sup>18</sup>Re, A=181, 182, 187, magnetic moments meas. by PAC 0-22688  
<sup>18</sup>Re, A=181, 182, 187, spin polarisation, state struct. and mag. moments in rot. model 0-18194  
<sup>182</sup>Re isomer decay mag. moment, <sup>182</sup>W high spin states, J assignments and mixing ratios 0-42593  
<sup>14</sup>Ru, A=96, 98, 100, multiparticle states, method of generalised seniority 0-22759  
<sup>177</sup>Ta, magnetic moments meas. by PAC 0-22688  
<sup>177</sup>Ta spin polarisation, state struct. and mag. moments in rot. model 0-18194  
<sup>14</sup>Tc, A=127, 129, 131, ground state mag. moments 0-5059  
<sup>14</sup>Tc<sup>m</sup>, A=125, 127, 129, 11/2<sup>-</sup> isomeric state magnetic moments 0-42537  
<sup>121</sup>Te isomeric state, spin, lifetime and mag. moment from (α,n)(d,Zn) 0-47387



**nuclear magnetic moment continued**

- $^{40}\text{Ca}$ ,  $^{40}\text{Ca}$ ,  $A=170,172,174$ , 168 MeV, rotational g-factor meas. using transient field interactions 0-18193  
 $^{92}\text{Zr}$ ,  $A=92, 94, 96$ , multiparticle states, method of generalised seniority 0-22759

**nuclear magnetic resonance**

see also acoustic nuclear magnetic resonance; chemical shift; double nuclear magnetic resonance; ENDOR; Knight shift; molecular nuclear coupling; NMR line breadth; nuclear quadrupole resonance; nuclear spin-lattice relaxation; proton magnetic resonance; spin echo (NMR); spin-spin relaxation  
 Z 0-50222

- N-acetyl-L-phenylalanine methyl ester, model for amino acid side chains internal motions in peptides and proteins 0-48017  
 adenosine 5'-diphosphate, interactions with myosin, intermolecular spin diffusion study 0-18951  
 agriculture appls. of pulsed NMR 0-56297  
 alkali iodates, chem. shift, NMR obs. 0-48015  
 alkali metanepodates, chem. shift, NMR obs. 0-48015  
 alkali silicate glass,  $\text{Li}^+$  motion,  $^7\text{Li}$  NMR spectra, nucl. relax. 0-34804  
 4-alkyl-3-phenyl-3,4-dihydrocoumarins cis- and trans-,  $^{13}\text{C}$  NMR spectra 0-43067  
 amino acid side chains, internal motions in peptides and proteins, N-acetyl-L-phenylalanine methyl ester model 0-48017  
 analogue Fourier transforms, pulsed NMR spectroscopy methods 0-47085  
 anthracene, mag. susceptibility anisotropies, high field  $^2\text{H}$  NMR quadrupolar effects obs. 0-25225  
 antiferromagnets, low anisotropy, nuclear spin waves spectra, relaxation, parametric excitation, NMR dynamic shift (Russian) 0-11180  
 aryl ammonium hydrogen difluorides, IR vibr. spectra and NMR reson. obs. 0-34788  
 automatic system, for recording, processing and summation 0-27327  
 benzene, chem. shielding tensor obs. using proton-enhanced  $^{13}\text{C}$  reson. in He-cooled probe 0-17978  
 benzyl fluoride, mol. struct., NMR and gas electron diffraction obs., ab initio and mol. mechanics calcs. 0-23574  
 bilayer membrane head group, orientational order and rotational diffusion 0-21451  
 biological and medical imaging by NMR 0-26319  
 biological systems, simultaneous multinucl. NMR by alternate scan recording of  $^{31}\text{P}$  and  $^{13}\text{C}$  spectra 0-26426  
 biotin, of  $^{13}\text{C}$ , spectrum assignment 0-26204  
 Bloch equations solution in presence of varying  $B_1$  field, selective pulse analysis 0-25222  
 blood flow evaluation in peripheral circulation, noninvasive techniques 0-56163  
 blood flowmeter, noninvasive clinical diagnosis appls. 0-17178  
 borate glass,  $\text{Li}^+$  motion,  $^7\text{Li}$  NMR spectra, nucl. relax. 0-34804  
 bromoform liquid, NMR spin-lattice relax. time 0-25232  
 capsular polysaccharide antigen, structure investig. by  $^{13}\text{C}$  NMR 0-35828  
 cellular applications of  $^{31}\text{P}$  and  $^{13}\text{C}$  NMR 0-46110  
 chemical fast kinetics studied by NMR, review 0-55662  
 chrysene, mag. susceptibility anisotropies, high field  $^2\text{H}$  NMR quadrupolar effects obs. 0-25225  
 computer applications to NMR 0-54958  
 copper chalcogen compounds, NMR chemical shifts 0-29636  
 coronene, mag. susceptibility anisotropies, high field  $^2\text{H}$  NMR quadrupolar effects obs. 0-25225  
 coupled spin systems, multiple quantum transitions, excitation, detection, Fourier transform multiple quantum NMR 0-31819  
 cross-peptide bond  $^{13}\text{C}$ - $^{15}\text{N}$  coupling constant, NMR obs. 0-55980  
 Cu, from below 1 kHz to 100 kHz, use of transverse SQUID 0-37064  
 data bank,  $^{13}\text{C}$ , DARC PLURIDATA system 0-30298  
 dicarbacosododecaboranes, icosahedral, electron transfer phenomena in isolated borane units 0-18871  
 1,1-dichloroethane, tilt-effect and interference with rel. sign determination in weak irradi. expts. 0-32742  
 diethylammonium copper tetrachloride,  $^{63}\text{Cu}$  NMR, hyperfine interactions 0-54956  
 digital phase-shifter for multiple quantum NMR 0-17974  
 dipolar spin fluctuations in rot. frame 0-20465  
 dynamic magnetoresonance effects in solids 0-20447  
 epoxy polymers, cured spin-spin and lattice relax., proton coupling,  $^{13}\text{C}$  NMR obs. 0-34799  
 ethyl-trimethyl phosphines,  $(\text{C}_2\text{H}_5)_3\text{P}\{\text{E}^{1\text{VB}}(\text{CH}_3)_3\}_n$  ( $\text{E}^{1\text{VB}}=\text{C}, \text{Si}, \text{Sn}$ ;  $n=0,1,2,3$ ), ( $^1\text{H}$ ,  $^{13}\text{C}$ ,  $^{29}\text{Si}$ ,  $^{31}\text{P}$ ,  $^{119}\text{Sn}$ ) NMR 0-32744  
 ethylene, solid, phase diagram and NMR at high press. 0-11279  
 ethylene copolymers with acrylic monomers, NMR investig. (Russian) 0-54959  
 (ethylene-co-vinyl alcohol)-g-ethylene oxide graft copolymers, sol. behavior 0-19682  
 exchange processes, two-dimensional NMR spectrosc. investig. 0-25218  
 Fischer-Tropsch wax, NMR investigation 0-7186  
 flow meas., CW NMR to determine volume fractions and flow rates of component mixtures 0-33710  
 flowmeter for automatic liquid dosage system 0-43815  
 p-fluoranol,  $^{19}\text{F}$  NMR and spin-lattice relax. meas., pot. profile calc., mole. reorientation 0-29634  
 fluoroite lattices,  $^{19}\text{F}$ , self-diffusion, spin lattice relax., NMR techniques 0-34801  
 Fourier transform, pulse system, commercial waveform analyser use 0-17977  
 Fourier transform spectrometry, error estimates 0-37061  
 Fourier transform spectroscopy, flip angle depend., pulse cascade description 0-28036  
 from velocity measurement, repetitive pulse NMR technique 0-31829  
 glycerol- $\text{d}_3$ (- $\text{d}_4$ ), compressed viscous liq., reorientational motion, NMR obs. 0-7183  
 1-glyceryl 1-octanoate-water- $\text{CsCl}$ ,  $\text{Cs}^+\text{H}_2\text{O}$  interaction in lamellar phase, NMR quadrupole splitting and chemical shift 0-50209  
 graphite intercalation cpds. with  $\text{Li}$ , nucl. relax. times 0-44947  
 group theory, independent-particle Hamiltonian 0-43074  
 gutta percha, partially hydrogenated,  $^{13}\text{C}$  NMR 0-20472  
 $\text{O}_2$  dilute impurity in rare gas solids and  $\text{p-H}_2$ , NMR study 0-25228  
 hexadecapole spin resonance in cubic symm. cryst. by NQR, NMR, nuclear gamma reson. 0-20500  
 hexafluorobutene, vibrational broadening, dense fluid region, Raman and NMR study 0-43056

**nuclear magnetic resonance continued**

- high-resolution, broadband decoupling and scaling of heteronucl. spin-spin interactions 0-17980  
 homonuclear coupled NMR spectra, pulses applied to multiplets, mutual coupling determ. 0-18873  
 human samples, elec. conducting, RF losses 0-21580  
 human samples, zeugmatographic expt. sensitivity 0-21579  
 imaging, and biomedical appls. 0-46006  
 ionic solvation, spectroscopic data comparison for methanolic and aqueous solns. 0-26099  
 irreducible spin precession theory applied to atomic and nuclear RF spectroscopy 0-27969  
 J-resolved two-dimensional NMR, spin decoupling, appl. to 2,3,4-trichlorophenol 0-31823  
 lamellar intercalation compounds, NMR studies 0-39882  
 lanthanide complexes, paramag., and shift reagents, NMR, book contrib. 0-53023  
 lipid bilayer, paraffin chain dynamics, ang. correl. function decay by multiple rot. pot. diffusion 0-3569  
 liquid, J cross-polarisation, refocusing method 0-22406  
 liquid crystal, thermotropic mesophase, DMR chain segments assignment 0-24356  
 liquid crystals, deuterated, duetron mag. resonance mol. ordering, conformational changes 0-34789  
 liquid crystals, lyotropic, counterion binding, NMR, ion condensation model 0-1922  
 liquid system, Earth field range, review 0-50206  
 lithium acetate dihydrate, nearly free methyl rotors, rot. energy states, nucl. reson. props. 0-34784  
 lithium perfluoro-octanoate-water, liquid crystal,  $^{19}\text{F}$  multipulse NMR obs. 0-34795  
 lyotropic nematic liquid crystals, mag. susceptibility, mol. aggregation meas. 0-19690  
 'magic angle' spinning apparatus in solid NMR spectroscopy 0-17983  
 magic-angle rotor, using forced air bearing for NMR of solids 0-47083  
 magnetic field distributions rapid meas. method 0-27322  
 magnetic props. of materials, appl. of nucl. orientation, review 0-44928  
 magnetic relaxation depend. on internal motion in solid, correlations 0-25239  
 magnetic shielding constants calc. by GIAO method using Gaussian functions 0-1001  
 magnetically ordered crystal, dynamic shift of NMR freq. of nuclei located in domain walls 0-15823  
 many-spin system dynamics, group approach (Russian) 0-50221  
 medical imaging by NMR, book 0-31426  
 medical imaging by NMR, book contrib. 0-36064  
 medical technology, appl. (Japanese) 0-51202  
 metabolite mapping by  $^{31}\text{P}$  NMR in whole animals, diagnosis appl. 0-36211  
 methane, adsorbed on graphite, NMR pulsed field gradient method, diffusion coeff. meas. 0-15362  
 methane, solid, high press. NMR obs. 0-50214  
 methanol, mol., nucl. spin-spin coupling const., Hartree-Fock calc. 0-9618  
 methyl methacrylate-styrene copolymers,  $^{13}\text{C}$  NMR 0-20473  
 methylmercuric halides, partially oriented,  $^1\text{H}$  and  $^{13}\text{C}$  NMR obs. 0-23437  
 methylmercury nitrate, in nematic and lyotropic liq. crystals,  $r_{\text{H}}$ -struct. and anisotropy of Hg-C coupling const. 0-43071  
 micellar solutions, micellar aggregation number,  $^{13}\text{C}$  NMR chemical shift conc. depend. 0-48016  
 molecular crystals, chem. shielding, spin-lattice, quadrupole interactions,  $^2\text{D}$  NMR spin echo spectroscopy 0-34817  
 molecular motion dynamics in crystal influence on spectral parameters of NQR, NMR and EPR 0-20486  
 molecular spectroscopic laboratory strategies, queuing theory and digital simulation use 0-30299  
 multiple-quantum coherence, selective excitation, appl. to benzene 0-23439  
 myosin, interaction with adenosine 5'-diphosphate, intermolecular spin diffusion study 0-18951  
 myosin, interactions with HDO, intermolecular spin diffusion study 0-18951  
 nematic liquid crystal, ionic conduction-induced flow alignment angle, NMR evidence 0-44125  
 neopentane, adsorbed on graphite ( $\text{TiO}_2$ ), NMR pulsed field gradient method, diffusion coeff. meas. 0-15362  
 NMR under optical pumping conditions 0-25253  
 nucleic acid bases,  $^{14}\text{N}$  relax. and N-proton spin coupling, NH-proton spin-lattice relax. 0-26202  
 oil, lubricating, radn. effects and radn. dosimetry appl. 0-2069  
 oligoethylene glycol, crystallisation kinetics in presence of tetrachloromethane, NMR investig. (Russian) 0-54153  
 one-dimensional planar magnets, low temp. NMR 0-44943  
 organic molecules, polycryst., NMR, selection of nonprotonated C resonances 0-50201  
 organometallic, fluxional, solid state chem. exchange,  $^{13}\text{C}$  NMR magic angle spinning 0-7775  
 oriented molecules, NMR spectra, vibr. correction study 0-18840  
 paramagnetic polycryst. mols., NMR 0-23436  
 paramagnetic systems, NMR shifts calc. using nonmultipole expansion method 0-2651  
 phase device for low freq. NMR expts. 0-31837  
 phase transitions, high press., NQR and stationary NMR studies 0-19934  
 phenylene sulphides, NMR relaxation for mol. motions (German) 0-11288  
 phosphate glass,  $\text{Li}^+$  motion,  $^7\text{Li}$  NMR spectra, nucl. relax. 0-34804  
 phospholipid membrane, polar head motion, NMR and EPR linewidth study using TCNQ $^-$  ion-radical (French) 0-45865  
 piperylene-acrylonitrile copolymers, polymerisation, monomer composition rel. to copolymer struct. (Russian) 0-5651  
 pivalic acid, liq. and plastic crystals,  $^{13}\text{C}$  NMR chem. shift, temp. depend. 0-2652  
 poly(L-histidine), molecular motions in solid state, NMR and dielec. meas. 0-11332  
 poly- $\beta$ -substituted vinyl ethers, cationic polymeris., stereochem. 0-21284  
 poly-p-phenylene sulphide, NMR relaxation for mol. motions (German) 0-11288  
 poly-thio-1-N,N-diethylaminomethylethylene, optically active samples,  $^{13}\text{C}$  NMR spectra 0-28127



## nuclear magnetic resonance continued

- polyacetylene:1, NMR investigation of struct. 0-39011  
 polyacetylene and polyacetylene:  $\text{AsF}_6^-$ , one-dimens. spin diffusion, NMR  $T_1$  and dynamic nuclear polarisation meas. 0-44946  
 polyatomic fluid, local dynamics, spectroscopic studies, summer school lecture series 0-6343  
 polybutadiene, mol. motion in solid and soln.,  $^{13}\text{C}$  NMR relaxation meas. (Japanese) 0-2666  
 cis-1,4-polybutadiene, partially hydrogenated,  $^{13}\text{C}$  NMR 0-20472  
 polycarbonates unstretched and stretched, orientation relationships,  $^{13}\text{C}$  NMR meas. (German) 0-20474  
 polyesters from bridged bicyclic lactones, struct. characterisation by NMR 0-20476  
 polyethylene,  $^{13}\text{C}$  NMR rotating frame relaxation 0-7182  
 polyethylene, NMR, IR spectra and elemental anal. 0-29681  
 polyisobutylene soln., NMR, chain segment motions 0-20475  
 polyisocyanides, solns., struct. and acidification 0-19915  
 polymer, self-diffusion detection, NMR matrix technique 0-15806  
 polymer chain dynamics, ang. correl. function decay by multiple rot. pot. diffusion 0-3569  
 polymer glassy and crystalline, relax. process characterisation,  $^{13}\text{C}$  NMR obs. 0-34802  
 polymer solns., dynamical polymer coil overlap, NMR model 0-23583  
 polymers, oriented, partly cryst., macromols. in amorphous regions, length, mobility 0-49132  
 polymers, review 0-11277  
 polymethacrylic acid:  $^{23}\text{Na}$ , nuclear relax. correl. times and counterion behaviour 0-50212  
 probe assembly, He-cooled, for proton-enhanced  $^{13}\text{C}$  reson. 0-17978  
 probe for high-pressure and high-temp. expts. 0-22403  
 propylene/butene-1 copolymers, coisotactic shift contribs. in  $^{13}\text{C}$  NMR spectra 0-29635  
 proteins, solid, NMR, detection of individual C resonances, appls. 0-51042  
 pulse programmer, microprocessor-based 0-52289  
 pulse type, programmable pulse sequence generator 0-17979  
 pulsed, automatic trigger pulse logic for pulse programmer 0-47084  
 pulsed gradient diffusion meas. with microcomputer 0-17973  
 pulsed NMR data acquisition system, devel., appl. to polyisobutylene 0-34807  
 pulsed NMR in solids, survey 0-34782  
 PVC, reduced, NMR, IR spectra and elemental anal. 0-29681  
 di- $\alpha$ -pyridyl hydropchlorates, intramol. H bonds, steric conditions and polarisability obs. 0-53160  
 quick sample change probe for magic-angle-spinning NMR in a superconducting magnet 0-31834  
 rare earth complexes, formation and props., book contrib. 0-43204  
 rare earth nuclei in cubic cpds., self polarisation field calc. 0-15487  
 rare earth systems, NMR, EPR, and Mossbauer effect, book contribs. 0-39883  
 relaxation processes, macroscopic evolution eqns. and virtual spins importance (French) 0-32739  
 relaxation time relationship in rotating and laboratory coordinate systems 0-39887  
 rotating frame,  $^{13}\text{C}$  spin-lattice relax. using proton decoupled Fourier transform spectra, errors origin 0-18945  
 rubber, partially hydrogenated,  $^{13}\text{C}$  NMR 0-20472  
 ruby laser,  $^{27}\text{Al}$  nucl. spin system, collective ordering phenomena, instabilities 0-11278  
 ruby NMR laser, dynamic props. from point of view of synergetics 0-43341  
 second moment, lattice vibrs. effect 0-20467  
 selective excitation with single-freq. off-reson. decoupling 0-17981  
 semiempirical theory of NMR parameters, chem. shielding,  $^{13}\text{C}$  chem. shifts 0-23435  
 skin, rat,  $^1\text{H}$  and  $^{13}\text{C}$  NMR obs. 0-40965  
 smectic-C liquid crystals, biaxial mol. order, NMR meas. 0-25227  
 solid, double-cross-polarisation NMR 0-20468  
 solids, averaging method application to high resolution NMR, Magnus expansion (Russian) 0-34793  
 solids, pulsed NMR, conf., London, England (Dec. 1978) 0-31404  
 spectrometer, commercial, modification for rot. frame spin-lattice relax. meas. 0-22407  
 spectrometer for NMR in internal fields of ferromagnets for freq. range 10 to 230 MHz 0-27325  
 spectrometer-computer interface, demonstration expt., signal averaging influences on S/N ratio 0-36813  
 spectroscopy, computer appl. (Czech) 0-17984  
 spectroscopy, resolution enhancement, effective sample volume restriction effects 0-31836  
 spherical conductor, free induction decay and skin effect 0-2649  
 spin lattice relaxation time meas. simulation, systematic and random error effects 0-37062  
 spin system, ABC type, matrix elements of tensor operators calc., transition probability matrix 0-25182  
 spin-lattice relaxation times, measurement based on null method 0-22402  
 superconducting spectrometer, efficient decoupler coil design to reduce heating in conductive samples 0-31828  
 superionic conductor, paramag. impurity contrib. to NMR relax. in one-dimension 0-20477  
 superionic conductors, mag. reson., book contrib. 0-25240  
 symmetry groups of nonrigid molecules as generalized wreath products and their representations 0-48013  
 TBBA liquid crystal, self diffusion coeffs., neutron diffr. and NMR study 0-19689  
 tetraalkylammonium halides, mol. reorientation, spin lattice relax. time study 0-18875  
 tetramethylammonium zinc tetrachloride,  $^{13}\text{C}$  NMR and PMR study of incommensurate phase transition 0-34863  
 thermodynamics of nuclear spins 0-54964  
 transition metal complexes, vibronic coupling and spin relax. NMR decay rate study 0-18870  
 triethylacetic acid, high resolution  $^1\text{H}$  and  $^{13}\text{C}$  NMR spectra at liquid-solid phase transition 0-11281  
 trimethylacetic acid, high resolution  $^1\text{H}$  and  $^{13}\text{C}$  NMR spectra at liquid-solid phase transition 0-11281  
 2-tromopropane, tilt-effect and interference with rel. sign determination in weak irr. expts. 0-32742  
 TTF(MBDT) spin-Peierls transition, mag. exchange interactions, mag. props. 0-25138  
 two dimensional  $^{13}\text{C}$  NMR spectroscopy, high sensitivity 0-31826

## nuclear magnetic resonance continued

- undergraduate instruction, general purpose microcomputers use for hypothetical spectra synthesis 0-42009  
 water, studies in biological systems 0-3886  
 zeugmatographic imaging 0-51203  
 zeugmatographic imaging of heart and lungs 0-17053  
 $\text{AgIO}_4$ , chem. shift, NMR obs. 0-48015  
 Al-Cr, neutron irr., Cr atom distribution NMR study 0-54957  
 $\beta\text{-Al}_2\text{O}_3\text{-Na}_2\text{O}$   $^{23}\text{Na}$  asymmetry parameter, temp. variations 0-6540  
 $\text{AsF}_6^-$  intercalation with graphite and benzenoid systems, EPR, NMR and X-ray diffr. obs. 0-19775  
 $\text{As}_2\text{Se}_3\text{:X}$  (X=Cu, Ag, Ti, I, Ge), effect of doping, NMR meas. 0-11282  
 $\text{B}_2\text{O}_3\text{-Li}_2\text{O-LiCl}$  glasses, solid electrolyte, NMR meas. 0-29208  
 $(\text{CF}_3)_n$ , fluorinated graphite,  $^{13}\text{C}$  NMR and  $^{19}\text{F}$  NMR spectra 0-15808  
 CO chemisorbed on Rh dispersed on  $\text{Al}_2\text{O}_3$ ,  $^{13}\text{C}$  NMR obs. 0-1000  
 $^{13}\text{C}$  NMR in solids, high-resolution 0-34802  
 $^{13}\text{C}$  NMR spectra of natural rubber latex 0-15816  
 $^{13}\text{C}$ , shielding constns. and anisotropy of NMR shielding tensor, modified CNDO/S calcs. (French) 0-32610  
 $\text{CaF}_2\text{-H}_2$ , ionic conductivity study (French) 0-29210  
 $\text{CoS}_2\text{-Se}$ , magnetism and metamagnetic transition, neutron diffr. and NMR meas. 0-15717  
 $\text{CoSiF}_6\cdot 6\text{D}_2\text{O}$ , deuteron mag. reson. study 0-2646  
 $\text{Cr}_{1-x}\text{V}_x$ , nucl. spin relax., spin fluctuation effect 0-34811  
 $\text{CsCoCl}_3$ , Ising like antiferromag., mag. phase transition,  $^{133}\text{Cs}$  NMR 0-7184  
 $\text{Cs}_2\text{CuCl}_4\cdot 2\text{H}_2\text{O}$ , ferromag., hyperfine and exchange interactions, NMR study 0-50208  
 $\text{CsMnF}_3$ , NMR saturation, nuclear spin wave excitation, large freq. shifts (Russian) 0-50207  
 $\text{Cs}_2\text{NaCl}_6$  (R=Ce, Nd), tetragonal distortion from cubic symm., magnetisation and NMR meas. 0-34403  
 Cu, NMR at high polarisation and low field, nuclear spin exchange interaction 0-34790  
 Cu-Ga, high dislocation density alloys and oxide precipitated struct., NMR, spin echo 0-39892  
 Cu-Si, high dislocation density alloys and oxide precipitated struct., NMR, spin echo 0-39892  
 Cu-Ti, solubility of Ti, exam. using NMR of  $^{63}\text{Cu}$  (French) 0-7179  
 Cu-transition metal, alloys, satellite NMR study, lineshifts and splitting 0-34786  
 CuMn, spin glass, remanence, new approach from zero field NMR 0-34785  
 $\text{Dy}_{0.9}\text{M}_{0.1}\text{Al}_2$ , (M=Sc, Y, La, Lu), hyperfine field, NMR spectra 0-15811  
 $\text{ErCrO}_3$ , magnetisation, NMR freq. temps. depend. weak ferromagnetic-antiferromagnetic spin reorientation transition 0-29631  
 $^{57}\text{Fe}$  powder, NMR excitation function, drumhead model of Bloch walls 0-15810  
 $\text{GdAl}_2$ , hyperfine fields, ferromagnetic coupling between rare earth spins, NMR study 0-39880  
 $\text{H}^+$  chemical shifts, INDO calcs. 0-32743  
 $\text{p-H}_2$ , solid, cryst. field energy for o- $\text{H}_2$  impurities, NMR studies 0-15331  
 $\text{p-H}_2$ , solid, NMR spectrum of isolated o- $\text{H}_2$  pairs 0-15332  
 HDO, interactions with myosin, intermolecular spin diffusion study 0-18951  
 $\text{H}(\text{UO}_2\text{PO}_4)_4\text{H}_2\text{O}$ , solid, fast hydrogen ion diffusion, NMR relax. time meas. 0-2205  
 He beam, magnetic spectrom. meas. using automatic tracking NMR system 0-27869  
 $^3\text{He}$ , adsorbed on Vycor glass under press., nature of phases, entropy and magnetisation expts. 0-49458  
 $^3\text{He}$  film, submonolayer and multilayer, adsorbed on Grafoil, pulsed NMR study 0-49456  
 $^3\text{He}$  film, theory of motional inhibition of interlayer quantum tunnelling 0-54466  
 $^3\text{He}$ , solid, mag. ordering, NMR study 0-54470  
 $^3\text{He}$ , solid, nuclear antiferromag. reson. 0-54471  
 $^3\text{He}$ , superfluid, B-phase, low temp. spin relax. 0-15323  
 $^3\text{He}$ , superfluid A-phase, composite solitons in presence of superflow, satellite freq. 0-2233  
 $^3\text{He}$ , superfluid A-phase, composite soliton in narrow circ. cylinder, satellite freq., thermal fluctuations 0-34266  
 $^3\text{He}$ , superfluid A-phase, phase diagram for helical texture 0-24704  
 $^3\text{He}$ , superfluid A-phase, soliton lattice for NMR behaviour 0-2234  
 $^3\text{He}$ , superfluid A-phase, textures in narrow cylinders 0-24703  
 $^3\text{He}$ , superfluid B phase, soliton-like spin waves 0-44385  
 $^3\text{He}$ , two-dimens. solid, melting mechanism 0-10643  
 $^3\text{He-A}$ , superfluid, spin dynamics, spin-orbit configurations, spin waves (Russian) 0-54462  
 $\text{HoVO}_4$ , NMR predictions of properties, dipolar interactions and antiferromagnetic exchange 0-50203  
 $\text{K}_3\text{Co}(\text{CN})_6$ , NMR spin lattice relax. of  $^{59}\text{Co}$  rel. to  $\text{Co}(\text{CN})_6$  octahedra vibr. modes 0-39885  
 $\text{K}_2\text{CuCl}_4\cdot 2\text{H}_2\text{O}$ , ferromag., hyperfine and exchange interactions, NMR study 0-50208  
 $\text{K}_2\text{MnF}_4$ , nucl. spin-magnon relax. time, temp. depend., NMR study 0-25117  
 $\text{KNbF}_6$ , NMR, quadrupole effects and struct. distortion 0-15809  
 $\text{K}_2\text{NiF}_4$ , nucl. spin-magnon relax. time, temp. depend., NMR study 0-25117  
 $\text{K}_2\text{PtCl}_6$ ,  $\text{K}_2\text{ReCl}_6$ ,  $\text{K}_2\text{SnCl}_6$ , solid state phase transitions, lattice vibr., NMR and NQR obs. 0-34814  
 $^{39}\text{K}$  pulsed NMR obs. of whole body live and dead newborn mice 0-40964  
 $^{83}\text{Kr}$ , NMR gaseous study (German) 0-52917  
 $^{83}\text{Kr}$ , nucl. mag. relax. meas. in gas 0-43072  
 $\text{LaB}_6$ , synthesis and props., review (Japanese) 0-40255  
 $\beta\text{-LaNi}_{1-x}\text{Al}_x$  hydrides, H diffusion, NMR studies 0-15298  
 $\text{Li}_{4-x}\text{B}_2\text{O}_{12+x/2}\text{Cl}$ , solid electrolyte, NMR meas. 0-29208  
 $\text{Li}_2\text{In}_2\text{O}_6$ , pseudo-two-dimens. electrolytic solid, Li ion mobility, NMR study (French) 0-34235  
 $\text{Li}_2\text{NbO}_6$ , pseudo-two-dimens. electrolytic solid, Li ion mobility, NMR study (French) 0-34235  
 $\text{Li}_2\text{SnO}_6$ , pseudo-two-dimens. electrolytic solid, Li ion mobility, NMR study (French) 0-34235  
 $\text{MnCO}_3$ , NMR saturation, nuclear spin wave excitation, large freq. shifts (Russian) 0-50207  
 $\text{Mn}_2\text{Sb}$ , domain and domain wall resons. in  $^{55}\text{Mn}$  NMR spectrum 0-25219



**nuclear magnetic resonance continued**

- MoF<sub>3</sub>, mol. and electronic struct., vitreous, liq., and tetrameric states, <sup>19</sup>F NMR obs., mol. mobility 0-34787
- ND<sub>3</sub>, dissolved in poly-γ-benzyl-L-glutamate-chloroform, NMR study 0-34805
- NH<sub>3</sub>, adsorbed on graphite, NMR pulsed field gradient method, diffusion coeff. meas. 0-15362
- (NH<sub>4</sub>)<sub>2</sub>CuBr<sub>4</sub>·2H<sub>2</sub>O, ferromag., hyperfine and exchange interactions, NMR study 0-50208
- (NH<sub>4</sub>)<sub>2</sub>CuCl<sub>4</sub>·2H<sub>2</sub>O, ferromag., hyperfine and exchange interactions, NMR study 0-50208
- NH<sub>4</sub>IO<sub>4</sub>, chem. shift, NMR obs. 0-48015
- N<sub>2</sub>O dissolved in liq. cryst., NMR, relax. times 0-25233
- <sup>15</sup>N NMR, single cryst., separation of dipolar and quadrupolar splittings, new technique 0-25217
- <sup>15</sup>N NMR heteronuclear spectroscopy, two dimensional Fourier transform technique 0-31818
- Na, self-diffusion mech., NMR meas. 0-44356
- NaCN, struct. domains, NMR determ. 0-50204
- NaCl:Sr, dimer and trimer aggregate formation by NMR, ionic cond. and dielectric losses 0-15094
- NaHSeO<sub>3</sub>, and NaDSeO<sub>3</sub>, NMR of <sup>23</sup>Na and <sup>2</sup>D, hydrogen bonding 0-44190
- NaNbF<sub>6</sub>, NMR, quadrupole effects and struct. distortion 0-15809
- NaReO<sub>4</sub>, <sup>23</sup>Na and <sup>187</sup>Re NMR and NQR temp. depend. 0-54973
- Na<sub>2</sub>WO<sub>3</sub>, Knight shift, spin-lattice and spin-spin relax., high press. NMR obs. 0-50211
- NdF<sub>3</sub>, crystals, shift tensors and F-diffusion, ion interactions, F<sup>-</sup> NMR study 0-20471
- Ni-b, hyperfine interactions from 6 to 730K, <sup>12</sup>B NMR 0-29372
- Ni<sub>1-x</sub>Fe<sub>x</sub>, <sup>2</sup>Fe<sub>2+2x</sub><sup>3+</sup> Vac<sub>0.2-0.6</sub> (Vac=cation vacancy), solid solns., cryst. lattice imperfections 0-39069
- <sup>31</sup>P NMR analysis of intact tissue, review 0-26432
- P-Se-Tl glasses, NMR of <sup>31</sup>P and <sup>205</sup>Tl 0-15812
- <sup>31</sup>P, shielding const. and anisotropy of NMR shielding tensor, modified CNDO/S calcs. (French) 0-32610
- PbSnF<sub>4</sub>, fast ionic cond. of F<sup>-</sup> ions, NMR study (French) 0-39345
- Pr compounds, Van Vleck paramagnets, mag. props., anisotropy from NMR anal. 0-54862
- PrF<sub>3</sub> crystals, shift tensors and F-diffusion, ion interactions, F<sup>-</sup> NMR study 0-20471
- Pt cluster, conduction electron density oscil., NMR spin-echo meas., indirect exchange interaction 0-44954
- RbCoCl<sub>2</sub>·2D<sub>2</sub>O, metamagnetic phase transition, crystallographic and mag. struct., neutron diffr. meas. 0-44174
- Rb<sub>2</sub>CuBr<sub>4</sub>·2H<sub>2</sub>O, ferromag., hyperfine and exchange interactions, NMR study 0-50208
- Rb<sub>2</sub>CuCl<sub>4</sub>·2H<sub>2</sub>O, ferromag., hyperfine and exchange interactions, NMR study 0-50208
- RbMnF<sub>3</sub>, nuclear spin waves spectra, relaxation, parametric excitation, NMR dynamic shift (Russian) 0-11180
- SiO<sub>2</sub>-B<sub>2</sub>O<sub>3</sub>-Al<sub>2</sub>O<sub>3</sub>-Na<sub>2</sub>O(K<sub>2</sub>O) glasses, Ag interdiffusion, optical and NMR studies 0-24683
- SmAl<sub>3</sub>, hyperfine fields, ferromagnetic coupling between rare earth spins, NMR study 0-39880
- Sm<sub>1-x</sub>Gd<sub>x</sub>Al<sub>3</sub>, hyperfine fields, ferromagnetic coupling between rare earth spins, NMR study 0-39880
- SnTe:Mn, NMR study 4.2 to 300K (French) 0-54960
- Tb, ferromagnetic, mag. dipole and elec. quadrupole hyperfine fields, NMR obs. 0-34791
- β-TiFeH<sub>1.03</sub>, H diffusion, NMR meas. 0-10707
- TiCoF<sub>3</sub>, paramagnetic, nonmagnetic atomic nuclei spin density, NMR study 0-29633
- TiF, P- and T-violating interactions in hyperfine struct., mol. beam reson. expt. 0-53019
- TmVO<sub>3</sub>, Jahn-Teller distortion, RF susceptibility and NMR meas. 0-44930
- UNi<sub>5-5.5</sub>Cu<sub>5.5</sub>, NMR and press. effects 0-25230
- UO<sub>2</sub>(NO<sub>3</sub>)<sub>2</sub>, aq. soln., pulsed NMR relax. time, <sup>235</sup>U enrichment depend. 0-2658
- V<sub>2</sub>O<sub>3+x</sub>, 0≤x≤0.08, mag. and elec. props. 0-49833
- V<sub>2</sub>O<sub>3</sub>, microscopic mag. props., NMR 0-7177
- YCrO<sub>3</sub>, magnetisation, NMR freq. temps. depend. weak ferromagnetic-antiferromagnetic spin reorientation transition 0-29631
- YIG, domain boundary nuclear spin echo excitation, NMR domain freq. capture effect (Russian) 0-44955
- YRh<sub>2</sub>B<sub>4</sub>, supercond., anomalous cond.-electron polaris. 0-25047
- Zr<sub>1-x</sub>Nb<sub>x</sub>Zn<sub>2</sub>, microscopic mag. props., NMR investigation 0-15807

**nuclear magnetic shielding see nuclear screening****nuclear mass**

see also atomic mass

- A=60-260 nuclei, violated Wigner SU(4) symmetry reconstruction from mass data (Russian) 0-37336
- collective mass parameter, super-normal phase transition effect 0-5046
- deep inelastic heavy ion collisions, mass and charge distrib., statistical model 0-18332
- even-odd mass difference ratio, mass and binding energy formula 0-47361
- fission, spontaneous, mass and charge division, asymmetry, order-disorder model 0-22866
- hadron-nucleus inelastic interactions, high energy, mean normalised multiplicity target depend. 0-47454
- Inglis cranking formula, temp. dependent mass parameter behaviour 0-22714
- meson presence in nuclei, nuclear g-factor exchange current controls., EM interaction role 0-22706
- nuclear matter, finite temperature props., variational theory, effective mass 0-5084
- optimum atomic mass formula from nuclear mass shell and parity corrections (Russian) 0-37902
- particle-number-projected mass tensor 0-9220
- spontaneous fission mass parameters, cranking and hydrodynamic models, deformation depend. (Russian) 0-13511
- statistical theory of fission, nucleon tunnelling, mass distrib. widths (Russian) 0-5121
- unified nuclear pot. for heavy ion elastic scatt., fission, fusion, masses and deformations 0-5189
- <sup>As</sup>, A=79.81, Q-values and mass excess from Se(d,<sup>3</sup>He) 0-9222
- <sup>14</sup>B, mass excess and excited states from <sup>14</sup>C(<sup>14</sup>C,<sup>14</sup>B) 0-42676

**nuclear mass continued**

- <sup>40</sup>Ca, finite nuclear props. in relativistic quantum field theory, mass and p densities 0-9219
- <sup>104</sup>Cd, β<sup>+</sup>/(EC+β<sup>+</sup>) probability ratio, EC decay energies, mass excesses 0-27543
- <sup>69</sup>Cu Q-values and mass excess from <sup>70</sup>Zn(d,<sup>3</sup>He) 0-9222
- <sup>As</sup>, A=73.75, Q-values and mass excess from Ge(d,<sup>3</sup>He) 0-9222
- <sup>121</sup>I mass excess, energy levels and single particle strength distrib. from <sup>120</sup>Te (<sup>3</sup>He,d) 0-5053
- <sup>48</sup>K mass excess and states from <sup>48</sup>Cu(<sup>7</sup>Li,<sup>7</sup>Be) 0-9221
- <sup>89</sup>Mo mass excess and excited states from <sup>92</sup>Mo(<sup>3</sup>He,<sup>6</sup>He) 0-42531
- <sup>18</sup>N, mass excess and excited states from <sup>14</sup>C(<sup>18</sup>O,<sup>18</sup>N) 0-42676
- <sup>208</sup>Pb, finite nuclear props. in relativistic quantum field theory, mass and p densities 0-9219
- <sup>246</sup>Pu excited states, mass excess and shell gap, L=0 transition from <sup>244</sup>Pu(l,p) 0-9236
- <sup>As</sup>Rb, A=96.98, β-decay schemes and total energies, mass excess and separation energies 0-27601
- (<sup>32</sup>S,X), 153-184 MeV, fission like processes around A<sub>CN</sub>=100, mass distrib. strong change 0-9318
- <sup>As</sup>Sn, A=106.108, β<sup>+</sup>/(EC+β<sup>+</sup>) probability ratio, EC decay energies, mass excesses 0-27543
- <sup>As</sup>Sr, A=96.98, β-decay schemes and total energies, mass excess and separation energies 0-27601
- <sup>80</sup>Sr ground state mass from Kr(<sup>3</sup>He,n) 0-18201
- <sup>238</sup>U(n,f), 14.5 MeV, neutron emission, mass distrib. and energetics 0-47512
- <sup>238</sup>U(p,f), 9.5-17 MeV, symmetric to asymmetric mass ratios for fragments 0-5178
- <sup>98</sup>Yf, β-decay schemes and total energies, mass excess and separation energies 0-27601

**nuclear matter**

- A=16-58, charge, proton and neutron density distrib. calc. 0-22680
- A=4-16, monopole giant resonances, state density radii and compressibility using hyperspherical functions (Russian) 0-27615
- abnormally large density and binding energy states, book contrib. 0-489
- BBG theory, auxiliary single particle field for binding energy 0-22723
- BBG theory developments, hole and particle lines, dispersion effects and healings 0-22719
- binding energy expansion convergence in Brueckner-Bethe-Goldstone theory 0-488
- binding energy from low density expansions, Brueckner-Hartree-Fock approx. 0-22720
- Brueckner Bethe and variational calcs. review, nuclear saturation problem 0-22745
- Brueckner-Bethe calculations of nuclear matter 0-22718
- charge constrained coherent pion states from transversing fast nucleon 0-27585
- cold, stationary finite amplitude motions, quantum shock waves and solitons 0-42573
- compression and speed of sound, heavy-ion collisions 0-27584
- conference on many-body theories, Trieste, Italy (Oct. 1978) 0-22135
- constrained variational calcs., three body and N\* (1234) contribs., cluster energy 0-22743
- deep inelastic processes, large scale collective motion in nuclear matter 0-5087
- dense Fermi systems, generalised perturbation theory, ground and low excited states 0-22741
- dense neutron and nuclear matter, spin and isospin stability 0-22737
- dense nuclear matter, construction in lab., book contrib. 0-490
- droplet-model theory of the neutron skin 0-47416
- effective interaction with three-body effects 0-27562
- elongated soliton-type wave solutions, finite amplitude wave propagation (Russian) 0-13397
- equation of state, relativistic quantum field theory of neutron stars 0-5088
- explosive quark matter, hypothesis for Centauro event 0-22648
- Fermi systems, semi-infinite, surface props., thickness and energy 0-52600
- fermion hypernetted chain variational calc. 0-22725
- finite Fermi system correlation energy, fast configuration interaction approach 0-22739
- finite nuclei, low energy optical pot. from Reid hard core interaction 0-52640
- finite nuclei and inhomogeneous infinite systems, ground states, FHNC method extension 0-22736
- finite temperature props., variational theory, effective mass 0-5084
- Green's function method for many-body problem for relativistic meson field theory, book contrib. 0-357
- heavy ion collisions, fluid dynamical and TDHF models, abnormal nuclear matter, density isomers 0-47502
- heavy ion deep inelastic collisions, kinetic energy dissipation, nuclear matter density oscillations (Russian) 0-37397
- heavy ion fusion cross section, energy depend., nuclear matter density distrib., depend. 0-47519
- high-temperature nuclear matter, neutral currents and neutrino Comptonisation 0-21905
- hole states in nuclear matter, single-particle potential 0-32150
- Hugenholtz Van Hove theorem and density depend. effective interactions 0-32219
- impure nuclear matter with Λ, binding energy, functional variational approach 0-22744
- infinite, correlated basis functions method 0-22721
- infinite nuclear matter, PCAC relations, πN vertices, π condensate instability (Russian) 0-13398
- infinite nuclear matter ambiguities, harmonic oscillator and infinite well solns. 0-22742
- inhomogeneous many-body system integral equations 0-22732
- isobar degrees of freedom, binding energy from BHF approx. 0-22734
- isobar degrees of freedom in nuclear matter, binding, NN interactions and 2π exchange 0-22735
- isospin symmetric nuclear matter, pion condensation, heavy ion collision appl. 0-9252
- light nuclei, hyperspherical functions for size, excited states, compressibility, binding energy 0-22679
- many body theory, appls. review of development 0-46968
- meson condensation, quasiclassical model (Russian) 0-5086
- mesons in nuclei, field theoretical aspects, book 0-481
- model energy including δ-function contribs. Jastrow correlation factor 0-13396



**nuclear matter continued**

- Monte Carlo methods in quantum many-body problems 0-22727  
 neutron, alpha and nuclear matter, ground vacuum states 0-22738  
 neutron  $^3\text{P}_2$  superfluidity under  $\pi^0$  condensation in neutron star matter 0-47417  
 neutron and nuclear matter, non-plane wave HF states, nuclear homework pot. 0-32224  
 neutron and nuclear matter, variational calc. models 0-22724  
 neutron distribution in nuclei, elastic and inelastic proton scattering, review 0-22649  
 neutron matter, energy density in relativistic harmonic approx. 0-18217  
 neutron matter, long range order, extended boson matter density matrices 0-22731  
 neutron matter, pair condensation, variational theory using correlated basis functions 0-32220  
 neutron matter, spin and tensor correlations, cluster expansion hypernetted chain eqns. 0-22728  
 neutron or nuclear matter, spin depend. correlations, variational method 0-22726  
 neutron skin, compared with droplet model theory 0-52599  
 neutron stars, inner crust nuclear compositions 0-31322  
 neutron stars, mass-radius relation, obs. constraints, dense matter eqn. of state 0-46597  
 neutron stars, superdense quark core, spontaneous magnetisation possibilities 0-8646  
 neutron stars, surface temp., density and mag. field determ. from thermal radiation 0-56869  
 neutron stars thermal properties and detectability, cooling and heating processes 0-31323  
 nuclei excitation energies in hot matter, limits 0-56703  
 nucleon-nucleus optical pot. from nuclear matter t-matrix, effective force. 0-22783  
 optimal plane-wave Hartree-Fock states for many-fermion systems 0-27587  
 optimised Jastrow correlations for Fermi liquids 0-32223  
 Paris NN pot. parametrisation, phase shifts, nuclear matter binding energy 0-47405  
 pion condensation and density isomerism 0-5085  
 pion condensation in dense nuclear and neutron matter 0-37333  
 pion condensation in nuclear matter, book contrib. 0-484  
 pion condensation threshold in finite nuclei 0-18218  
 pion dispersion relation in nuclear matter 0-42572  
 pion excitations and phase transitions in nuclear matter, review, book contrib. 0-483  
 quark attenuation and recombination in nuclear matter, hadron-nucleus reactions 0-52601  
 realistic NN pot. construction for three body systems and nuclear matter 0-22699  
 relativistic heavy ion collisions, charged particle emission multiplicities and ang. correlations, firestreak models 0-18328  
 relativistic nuclear matter, shock waves, heavy ion collision hydrodynamics 0-52602  
 ring diagrams in nuclear matter, many-body forces contrib.,  $\rho$  and  $\pi$  exchange 0-22740  
 self-consistent pseudopots. in thermodynamic limit, correlation field, nuclear matter single particle orbitals 0-9253  
 semi-infinite nuclear matter calc., nuclear density oscillations 0-22681  
 semi-infinite nuclear medium, kinetic energy density, simple approx., giant monopole resonance 0-32222  
 simple quantum liquids, Jastrow variational wave functions, for nuclear matter, liquid  $^3\text{He}$  and  $^4\text{He}$  0-22729  
 soft nuclear matter eqn. of state, from heavy nuclei central collision fireballs 0-13395  
 solid like aspect with alternating layer spin and  $\pi$  condensation 0-22733  
 spatial correlations and elementary excitations in many-body systems 0-22730  
 spin-isospin density phase in finite nuclei, strongly oblate shape 0-22746  
 spin-orbit correlations in nuclear matter from correlated basis functions 0-37343  
 stellar collapsing core, Thomas-Fermi model of warm nuclei 0-51648  
 strong compression effects in high energy heavy ion reactions, nuclear fluid dynamics anal. 0-18341  
 superdense magnetised astrophysical objects, interiors physical conditions 0-17603  
 surface properties from Thomas-Fermi calc. 0-13394  
 three-body problem, variational and Bethe-Faddeev methods 0-27586  
 uniform extended Fermi medium, correlated basis functions, graphical anal., integral eqn. methods 0-22722  
 Universe, high density matter, many body treatment, pulsars 0-26738  
 $V^8$  models, variational calcs. for binding energy and density 0-42571  
 variational techniques, wave functions correlation operators, review 0-22748  
 $\Delta$ -propagation in nuclear matter, Pauli principle effects 0-32221  
 $\Delta$  binding energy in nuclear matter with Nijmegen baryon-baryon interaction 0-13400  
 NN interaction in pion exchange, nuclear matter and pion condensation, review 0-42557  
 (p, p), 1 GeV, polarisation data, Glauber anal. spin-orbit parameters, matter distrib. 0-52655  
 $\pi$ N coupling in  $\Delta(1231)$  isobar region, pion index of refraction, self-energy in low density limit 0-42554  
 $\pi$ N scattering amplitude in nuclear matter, quantum field theory approach 0-42570  
 Ag ( $\alpha, x$ ), 0.2-4.2 GeV/N, compression phenomena and Mach shock waves 0-22851  
 Ag+C(O), 0.2-4.2 GeV/N, compression phenomena and Mach shock waves 0-22851  
 (Ar,X), in emulsion, nuclear shock wave search 0-22747  
 Ar(HI,X) 0.2-4.2 GeV/N, nonperipheral collisions, forward-backward asymmetry, compression phenomena 0-18329  
 Br+C(O), 0.2-4.2 GeV/N, compression phenomena and Mach shock waves 0-22851  
 Br(HI,X), 0.2-4.2 GeV/N, nonperipheral collisions, forward-backward asymmetry, compression phenomena 0-18329  
 Br( $\alpha, X$ ) 0-22851  
 (Fe,X), in emulsion, nuclear shock wave search 0-22747  
 $^3\text{He}(\gamma, \pi^+)^3\text{H}$ , Fermi motion and off-shell effects, impulse approx. 0-27626

**nuclear matter continued**

- $^{110}\text{Pd}(^{208}\text{Pb}, X)$ , 1.2 GeV, central collisions, neutron rich nucleon flow, mass, charge and energy 0-18337  
 $^{236}\text{U}$ , nuclear matter density distrib., in asymmetric two centre shell model 0-32209  
**nuclear models**  
*see also nuclear cluster model; nuclear collective model; nuclear reaction and scattering models; nuclear shell model*  
 classification of states, unitary scheme 0-42550  
 form factors of  $0^+-0^-$  transition in  $A=16$  system, nuclear struct. effects 0-18246  
 hyperspherical harmonic expansion method, first order  $L_m$ -approx. 0-18212  
 mode coupling method, a reformulation 0-37335  
 neutron distribution in nuclei, elastic and inelastic proton scattering, review 0-22649  
 quasiclassical model, meson condensation in nuclear matter (*Russian*) 0-5086  
 single-particle models, relation between average kinetic energy and mean-square radius 0-52567  
 superfluid model, isotopic invariance and pairing energies 0-22687  
 Thomas-Fermi model of warm nuclei 0-51648  
 $^{191}\text{Hg}^m$ , and  $^{190m-185m}\text{Hg}$ , nucl. spins, on-line quantum beat spectrosc. determ. 0-9562  
 $^{14}\text{N}(\gamma, n)^{13}\text{N}$ , 17 to 26 MeV, angular distrib., giant dipole resonance, single-particle nuclear model 0-52659  
**nuclear moment of inertia**  
 angular momentum depend. cranked HFB inertia parameter, high spin states 0-42524  
 coupled bands in even-even nuclei in RPA approach 0-32143  
 even-even and odd A nuclei, nuclear shapes and motions, review 0-5054  
 pseudomagic nuclei, yrast bands, variable moment of inertia model 0-449  
 $^{158}\text{Er}$ , back-bending phenomenal, rotating potential (*Chinese*) 0-47357  
 $^{72}\text{Ge}$  levels pop. in  $^{82}\text{Zn}(\text{Li}, p, n)$ , in beam gamma-ray spectroscopy 0-47343  
 $^6\text{He}$ , density distribution function of nucleons 0-22650  
 $^{171}\text{Hf}$  one- and three-quasiparticle states, high spin rot. bands from ( $^{16}\text{O}, 5n$ ), ( $^{13}\text{C}, 4n$ ) 0-18163  
 $^A\text{W}$ ,  $A=174$ , 175 quasicontinuum  $\gamma$ -rays yrast cascade dipole component, moment of inertia from  $\text{Dy}(^{16}\text{O}, xn\gamma)$  0-47424  
 $^{178}\text{W}$  high spin states, yrast bands and backbending from  $^{170}\text{Er}(^{12}\text{C}, 4n)$  0-13352  
 $^A\text{Yb}$ ,  $A=166, 168, 170$ , backbending and moment of inertia in HFB cranking method 0-42521  
 $^{161}\text{Yb}$  quasicontinuum  $\gamma$ -rays yrast cascade dipole component, moment of inertia from  $\text{Sm}(^{16}\text{O}, xn\gamma)$  0-47424  
**nuclear moments**  
*see also nuclear electric moment; nuclear magnetic moment; nuclear moment of inertia*  
 $A=4n$ , densities, form factors, transitions, multipole moments in s-d shell, HFC 0-37321  
 conference on nuclear interactions, Canberra, Australia (Aug.-Sep. 1978) 0-4476  
 fixed angular momentum moments and level densities, statistical spectroscopic methods 0-467  
 ion implantation in samples colder than 0.5K, low temp. nuclear orientation studies 0-34033  
 mesoatoms in static electromagnetic fields, excited state lifetimes and population, nuclear moments (*Russian*) 0-53170  
 $^A\text{As}$ ,  $A=69-72$ ,  $^{45}\text{S}_{3/2}$  ground state hyperfine struct. and nuclear moments 0-32853  
 $^{154}\text{Gd}$  multiphonon vibr. bands, dynamic deformation theory 0-5035  
 $^{21}\text{Ne}$ , energy moments, sd shell realistic effective interactions, shell model spectra 0-18190  
**nuclear muon capture** *see muon capture*  
**nuclear optical model**  
 $A=40$  to 56, two-nucleon transfer reactions, coupled channel formalism for isospin depend. optical pot. 0-42609  
 double folding pot. for inelastic scatt. between nuclei 0-13425  
 elastic scatt. with optical potential, complex angular momentum methods, poles and zeros of S-matrix, REGGE 0-47445  
 elastic scattering, empirical optical model 0-509  
 finite nuclei, low energy optical pot. from Reid hard core interaction 0-52640  
 folding model, elastic scatt. of light heavy ions 0-13424  
 four-body problem, generalised optical potentials 0-22781  
 heavy ion elastic and inelastic scatt., optical pots. and folding model 0-5169  
 heavy ion elastic and inelastic scatt., review, book contrib. 0-27668  
 heavy ion elastic scattering, folding model pots. from realistic NN interactions 0-5159  
 heavy ion inelastic scattering, optical pot. deformation 0-13505  
 heavy ion scattering cross-sections, WKB calcs., unphysical reflection phenomena 0-27656  
 Hilbert space theory of nonunitary scatt. and capture 0-52639  
 nuclear bound states of  $k^-$ ,  $\bar{p}$  and  $\Sigma$  0-13399  
 nucleon optical pot., spin-orbit term 0-27606  
 nucleon-nucleus optical pot. from nuclear matter t-matrix, effective force. 0-22783  
 parabolic repulsion potential for scattering of  $^6\text{Li}$  and  $^9\text{Be}$  ions by light and medium nuclei 0-22782  
 spin-unsaturated subshells and the nucleon-nucleus optical-model spin-orbit potential 0-18259  
 spline interpolation method appl. to optical potential 0-32272  
 strongly interacting particles, optical pot. theory 0-32250  
 (d,d), pol. d, 12 MeV,  $A=46-82$ , cross sections, anal. powers, global optical model anal. 0-47459  
 d breakup effect on spin orbit and tensor pots. 0-32286  
 (n,n), pol. n, 16.1 MeV, differential cross section, optical model fit 0-32259  
 (n,n), single particle bound state, energy independ. optical model, asymmetry term 0-37316  
 (p,n), 2.5-5.8 MeV,  $A=89-130$ , cross sections, sub-Coulomb proton anomalous optical pot. 0-32278  
 (p,n) excitation functions for  $A=45$  to 80, proton optical pot. at sub-Coulomb energies 0-9292  
 (p,p), 100-2200 MeV, total and reaction cross sections from optical pot. 0-18303  
 (p,p),  $A=9$  to 70, differential cross sections, struct. effects, optical and coupled channel anal. 0-47482



## nuclear optical model continued

- (p,p), pol. p, sd, fp shell nuclei, 65 MeV, effective two-body interaction range 0-32201  
 (p,p), single particle bound state, energy independ. optical model, asymmetry term 0-37316  
 (p, t) ang. distrib., zero-range DWBA calc., volume absorptive optical pot. singular prop. 0-523  
 ( $\pi$ , nn), S-wave and p-wave absorptive pion-nucleus optical pot. 0-27677  
 ( $\pi$ ,  $\pi$ ), relativistic Schrödinger and Klein-Gordon optical models, off-shell sensitivity 0-5175  
 ( $\pi^+$ ,  $\pi^0$ ), isobar-doorway model optical pot. appl. to isospin nonzero nuclei 0-52699  
 (t, t), A=40-208, 17 MeV, pol. t, cross sections and anal. powers, optical anal. 0-47462  
<sup>1</sup>Ag(p,p), A=107,109, 2.0-6.7 MeV, cross sections, Hauser-Feshbach optical calcs. for p absorption systematics 0-47483  
<sup>107</sup>Ag(n,n), 0.25-4.5 MeV, total, elastic and inelastic cross sections, optical-statistical anal. 0-27639  
<sup>12</sup>C(<sup>16</sup>O, <sup>16</sup>O), 35 to 50 MeV, backscatt., dynamic deformation and excitation functions, optical anal. 0-18227  
<sup>12</sup>C(e, e'p), quasifree scatt., spin-orbit distortion of emerging nucleon 0-52664  
<sup>12</sup>C(e, e'p), cross sections from DWIA, optical, and shell model calcs. (Russian) 0-32270  
<sup>12</sup>C( $\gamma$ ,  $\pi^-$ ), ( $\gamma$ ,  $\pi^-$ ), knockout p interaction, optical model and quasifree  $\pi$  photoprod. mechanism (Russian) 0-42638  
<sup>12</sup>C(p,p), 144 MeV, elastic scatt. cross sections, optical pot. 0-42660  
<sup>12</sup>C(p,p), 50-160 MeV, energy depend. optical pot. 0-22830  
<sup>12</sup>C(p,p), optical potential, spin-orbit term 0-52668  
<sup>12</sup>C( $\pi$ , X), deep inelastic,  $\pi$  and  $\Delta$  optical pot. effects, semiclassical transport model 0-52698  
<sup>12</sup>C( $\pi^+$ ,  $\pi^+$ ), 40 MeV, differential cross sections and strength parameters, optical model fit 0-18347  
<sup>13</sup>C( $\pi^+$ ,  $\pi^+$ ), angle integrated cross section, optical pot., n and p radius differences 0-32307  
<sup>13</sup>C spectroscopic factors, cross sections DWBA anal. optical model parameters from <sup>12</sup>C(<sup>16</sup>O, X) 0-13371  
<sup>13</sup>C(<sup>13</sup>C, <sup>24</sup>Mg), 3.05-6.88 MeV, fusion cross section energy depend., optical anal. 0-42724  
<sup>14</sup>C spectroscopic factors, cross sections DWBA anal. optical model parameters from <sup>12</sup>C(<sup>16</sup>O, X) 0-13371  
 (<sup>12,13</sup>C, X) elastic, inelastic and single nucleon transfer excitation functions optical and DWBA anal. 0-13492  
<sup>14</sup>Ca, A=40, 42-44, 48, pionic X-rays, strong interaction and isotope shifts,  $\pi$ -nuclear optical pot. 0-53169  
<sup>14</sup>Ca(<sup>7</sup>Li, <sup>7</sup>Li), A=40, 48, 88 MeV, optical potentials, phenomenological and microscopic 0-52687  
<sup>40</sup>Ca(<sup>4</sup>B, <sup>4</sup>B), A=10,11, angular distrib., Woods-Saxon and double-folding optical models 0-52691  
<sup>40</sup>Ca(<sup>16</sup>O, <sup>16</sup>O), 60 MeV, long range absorption and optical model effects from strong inelastic coupling 0-535  
<sup>40</sup>Ca(<sup>16</sup>O, X), 40-214 MeV, fusion and elastic scatt. cross sections, optical anal. 0-32314  
<sup>40</sup>Ca(<sup>17</sup>O, <sup>17</sup>O), 61 MeV, elastic and inelastic, microscopic single folding model anal. 0-52692  
<sup>40</sup>Ca(<sup>3</sup>He, <sup>3</sup>He), pol. <sup>3</sup>He, 33.3 MeV, differential cross section and anal. power, optical pots. 0-42627  
<sup>40</sup>Ca(<sup>40</sup>Ar, <sup>40</sup>Ar), 191, 236, 272 MeV, elastic cross sections, optical and Fresnel model anal. 0-22858  
<sup>40</sup>Ca(<sup>9</sup>Be, <sup>9</sup>Be), 45, 60 MeV cross sections, ang. distrib., Wegner plot, optical and double folding anal. 0-47497  
<sup>40</sup>Ca( $\alpha$ ,  $\alpha$ ), (<sup>6</sup>Li, <sup>6</sup>Li), velocity of refined folding model approaches 0-541  
<sup>40</sup>Ca(n,n), 11-26 MeV, differential cross sections, global optical model anal. 0-18298  
<sup>40</sup>Ca(p,p), 20-50 MeV differential cross section, polarisation ang. distrib., optical model exchange terms 0-27638  
<sup>40</sup>Ca(p,p), spline interpolation method appl. to optical potential 0-32272  
<sup>40</sup>Ca( $\pi$ ,  $\pi^+$ ), 40 MeV, differential cross sections and strength parameters, optical model fit 0-18347  
<sup>48</sup>Ca(<sup>7</sup>Li, <sup>7</sup>Li), ( $\alpha$ ,  $\alpha$ ), velocity of refined folding model approaches 0-541  
<sup>52</sup>Cr(d,p)<sup>53</sup>Cr, deuteron break-up model anal. of cross-section, vector analysing power and angular correlation 0-27648  
Cu(n,n), 14.2 MeV, polarisation in forward angle scatt. 0-18282  
<sup>19</sup>F+<sup>28</sup>Si spin orbit pot., single folding model and cluster model 0-9196  
<sup>2</sup>H( $\pi$ , p), reactive two body contrib. to pion-nucleus optical pot. 0-9313  
(<sup>3</sup>He, <sup>3</sup>He), 119 MeV, optical pot. parameters energy and mass depend. 0-32289  
<sup>3</sup>He elastic scatt. angular distrib., optical potentials and volume integrals for targets with A=10 to 58 0-52686  
<sup>4</sup>He(d,d), pol. d, 20 MeV, optical pot. strong tensor term, anal. powers 0-37364  
<sup>4</sup>He(<sup>3</sup>He, <sup>3</sup>He), 60.2, 113.1 MeV, ang. distrib., optical and coupled channel anal., cross sections 0-47492  
<sup>4</sup>He( $\pi$ ,  $\pi$ ), (3,3) region, multiple scatt. theory study by optical pot. method (Russian) 0-13509  
<sup>4</sup>He( $\pi$ ,  $\pi$ ), low energy, first order optical pot., Pauli principle corrections, nuclear binding 0-27675  
<sup>115</sup>In(p,p), 2.0-6.7 MeV, cross sections, Hauser-Feshbach optical calcs. for p absorption systematics 0-47483  
<sup>39</sup>K(<sup>12</sup>C, <sup>12</sup>C), 54, 63 MeV, angular distrib., Woods-Saxon and double-folding optical models 0-52691  
<sup>6</sup>Li(p,p), 144 MeV, elastic scatt. cross sections, optical pot. 0-42660  
<sup>6</sup>Mg(<sup>7</sup>Li, <sup>7</sup>Li), A=24, 26, 88 MeV, optical potentials, phenomenological and microscopic 0-52687  
Mo stable isotope eval., 5 keV-5 MeV neutrons, rel. to reactor structural steel 0-13620  
<sup>1</sup>Mo(p,n), A=94-96, 98, 1.7-6.7 MeV, total cross sections, p strength functions, optical model anal. 0-18301  
<sup>92</sup>Mo(N,N)<sup>92</sup>Mo, optical model anal. 0-47473  
<sup>92</sup>Mo(n,n), 7-26 MeV, differential cross sections, global optical model anal. 0-18298  
Mo(n,X), 2 keV-20 MeV cross sections, coherent optical and statistical model calcs. 0-18318  
<sup>14</sup>N spectroscopic factors, cross sections DWBA anal. optical model parameters from <sup>12</sup>C(<sup>16</sup>O, X) 0-13371  
<sup>14</sup>N(p,p), 144 MeV, elastic scatt. cross sections, optical pot. 0-42660  
<sup>58</sup>Ni(n,n), A=58,60,62,64, 5 MeV, differential cross sections, optical, statistical and coupled channel anal. (Russian) 0-37377  
<sup>58</sup>Ni(<sup>7</sup>Li, <sup>7</sup>Li), 19 MeV, first 2<sup>+</sup> states Coulomb-nuclear interference, optical and DWBA anal. 0-22852

## nuclear optical model continued

- <sup>58</sup>Ni(d,p)<sup>59</sup>Ni, deuteron break-up model anal. of cross-section, vector analysing power and angular correlation 0-27648  
<sup>58</sup>Ni( $\pi$ ,  $\pi$ ), 162 MeV, elastic and inelastic ang. distrib., optical and PWIA anal. 0-42706  
<sup>60</sup>Ni+n, total and differential cross-sections, optical-statistical and coupled-channel models 0-13472  
<sup>16</sup>O(<sup>3</sup>He, <sup>3</sup>He), pol. <sup>3</sup>He, 33.3 MeV, differential cross section and anal. power, optical pots. 0-42627  
<sup>16</sup>O( $\alpha$ ,  $\alpha$ ) 17 to 27 MeV, backscatt., dynamic deformation and excitation functions, optical anal. 0-18227  
<sup>16</sup>O(p,p), 20-50 MeV differential cross section, polarisation ang. distrib., optical model exchange terms 0-27638  
<sup>16</sup>O(p,p), 50-160 MeV, energy depend. optical pot. 0-22830  
<sup>16</sup>O(p,p), spline interpolation method appl. to optical potential 0-32272  
<sup>16</sup>O( $\pi$ ,  $\pi$ ), T-matrix from isobar-hole model, many-body corrections, optical pot. parameter 0-9312  
<sup>16</sup>O( $\pi^+$ ,  $\pi^+$ ), 40 MeV, differential cross sections and strength parameters optical model fit 0-18347  
<sup>208</sup>Pb, fast neutron scatt. and capture, microscopic isovector optical pot. test 0-52682  
<sup>208</sup>Pb(<sup>16</sup>O, <sup>16</sup>O), elastic scatt., exponential optical pots. 0-42681  
<sup>208</sup>Pb(<sup>16</sup>O, X), 80-313 MeV, optical model anal., dynamic shape or density changes 0-18186  
<sup>208</sup>Pb(N,N), <30 MeV, microscopic optical pot. in nuclear struct. approach, HF field 0-527  
<sup>208</sup>Pb(n,n), 7-26 MeV, differential cross sections, global optical model anal. 0-18298  
<sup>208</sup>Pb(p,p), pol. p, 9, 10 MeV, vol. integrals for optical pots., real symmetry pot. 0-42659  
<sup>208</sup>Pb(p,p), 20-50 MeV differential cross section, polarisation ang. distrib., optical model exchange terms 0-27638  
<sup>208</sup>Pb( $\pi$ ,  $\pi$ ), 162 MeV, elastic and inelastic ang. distrib., optical and PWIA anal. 0-42706  
<sup>208</sup>Pb( $\pi^+$ ,  $\pi^+$ ), 40 MeV, differential cross sections and strength parameters, optical model fit 0-18347  
Pb(n,n), 13.7-15 MeV, differential cross section energy depend., meas. and optical model 0-18304  
Pb(n,n), 14.2 MeV, polarisation in forward angle scatt. 0-18282  
<sup>28</sup>Si(<sup>12</sup>C, <sup>12</sup>C), 19-48 MeV, ang. distrib., cross sections and optical parameters 0-5157  
<sup>28</sup>Si(<sup>15</sup>N, <sup>14</sup>N), 44 MeV, modified optical pot. from backward elastic scatt. 0-32255  
<sup>28</sup>Si(<sup>15</sup>N, <sup>16</sup>O), 44 MeV, modified optical pot. from backward elastic scatt. 0-32255  
<sup>28</sup>Si(<sup>9</sup>Be, <sup>9</sup>Be), 45, 60 MeV cross sections, ang. distrib., Wegner plot, optical and double folding anal. 0-47497  
<sup>28</sup>Si( $\pi$ ,  $\pi$ ), 162 MeV, elastic and inelastic ang. distrib., optical and PWIA anal. 0-42706  
<sup>152</sup>Sm(n,n), 2.4-7.2 MeV, inelastic and elastic optical model and deformation parameter depend. (Russian) 0-13481  
<sup>152</sup>Sm( $\alpha$ ,  $\alpha$ ), 50 MeV, long range absorption and optical model effects from strong inelastic coupling 0-535  
<sup>152</sup>Sn(n,n) A=116, 124, 11, 24 MeV, differential cross sections, global optical model anal. 0-18298  
<sup>152</sup>Ti, A=46, 48, 50, pionic X-rays, strong interaction and isotope shifts,  $\pi$ -nuclear optical pot. 0-53169  
<sup>152</sup>Ti(<sup>7</sup>Li, <sup>7</sup>Li), A=46,48, 17 MeV, first 2<sup>+</sup> states Coulomb-nuclear interference, optical and DWBA anal. 0-22852  
<sup>90</sup>Zn(p,p), A=66,68, 20-50 MeV differential cross section, polarisation ang. distrib., optical model exchange terms 0-27638  
<sup>90</sup>Zr(p,p), A=92, 94, 2-6.5 MeV, optical and Lane model anal. comparison 0-18302  
<sup>90</sup>Zr(p,n), A=92, 94, 1.7-6.7 MeV, total cross sections, p strength functions, optical model anal. 0-18301  
<sup>90</sup>Zr neutron absorption, multipole giant resonance contrib. to optical pot. imaginary part 0-18263  
<sup>90</sup>Zr(n,n), 11 MeV, differential cross sections, global optical model anal. 0-18298  
<sup>90</sup>Zr( $\pi^+$ ,  $\pi^+$ ), 40 MeV, differential cross sections and strength parameters, optical model fit 0-18347  
<sup>92</sup>Zr(N,N)<sup>92</sup>Zr, optical model anal. 0-47473
- nuclear orientation** see **nuclear polarisation**
- nuclear Overhauser effect**  
 biological macromolecule, truncated driven nucl. Overhauser effect in presence of spin diffusion 0-1095  
 bromobenzenes <sup>13</sup>CBr bond, spin-spin coupling const., correl. with C hybridisation s-character 0-34806  
 coupled spin systems, selective nucl. Overhauser effects calc., use in struct. chem. 0-23588  
 formic acid, <sup>13</sup>C NMR spectra and relax. under intermediate decoupling power conditions 0-20515  
 lysozyme, tryptophan residues, H exchange for D, relax., proton NMR spectra 0-35846  
 multispin system, time development of nuclear Overhauser effects 0-34822  
 nonstationary nutations in heteronuclear double resonance 0-20516  
 polybutadiene, mol. motion in solid and soln., <sup>13</sup>C NMR relaxation meas. (Japanese) 0-2666  
 polystyrene, dilute soln., <sup>1</sup>H mag. relax., selective inversion technique appl. 0-44957  
 thermodynamics of nuclear spins 0-54964  
 vinyl bromide-d<sub>3</sub>, <sup>13</sup>CBr bond, coupling const., correl. with C hybridisation s-character 0-34806
- nuclear particle track visualisation** see **particle track visualisation**
- nuclear photoeffect** see **photon-nucleus reactions**
- nuclear physics**  
 see also **fission**; **fission reactors**; **nuclear bombardment targets**; **nuclear decay theory**; **nuclear explosions**; **nuclear reactions and scattering**; **nuclear structure**; **radioactivity**  
 computer simulation techniques for an undergraduate nuclear physics course 0-36823  
 Ernest Rutherford, biography 0-8768  
 teaching, undergraduate, courses, facilities 0-27086
- nuclear polarisation**  
 see also **dynamic nuclear polarisation**; **magnetic double resonance**; **nuclear polarisation in liquids and solids**  
 Of<sub>7/2</sub> and Og<sub>9/2</sub> nuclei, mag. form factors, core polarisation and exchange current effects 0-13409



**nuclear polarisation continued**

- A=3 systems, charge form factor and bound nucleon polarisation 0-22708  
 deformed nuclei, static isoscalar and isovector polarisability, isovector  $K = \pm 1^+$  modes 0-32260  
 ion implantation in samples colder than 0.5K, low temp. nuclear orientation studies 0-34033  
 neutron and nuclear polarisation expts., spin depend. of neutron cross-sections, mag. moments, radiation capture of neutrons (*Russian*) 0-52654  
 orbital angular momentum transfer to nucl. spin polarisation in external mag. fields 0-14217  
 spin giant resonance and core polarization effects, coupling term effects (*Chinese*) 0-47450  
 target  $^3\text{He}$  continuous flow cryostat 0-52240  
 valence nucleons, muonic atom analysis 0-27530  
 (e,e), A=60 region, nuclear radius, core polarisation and isotone shifts, muonic X-rays 0-22685  
 $^{240}\text{Am}^m$ , spontaneously fissioning isomer optical shift in pumped  $^{87}\text{Sr}_{7/2} \rightarrow ^{107}\text{Pb}_{7/2}$  transition, nuclear deformation 0-27971  
 $^{15}\text{B}(1^-, \text{g.s.})$ , polarisation in  $^{12}\text{C}(\mu^-, \nu_n)$ , effect of correlations 0-22774  
 $^{111}\text{Cd}^m$ , nuclear orientation in Zn and Be, 245 keV state quadrupole moment, half-life 0-37324  
 $^{123}\text{I}$ , bands and decay props., core-particle coupling and polarisation effects 0-13354  
 $^{20}\text{Ne}$  from  $^{16}\text{O}(^{16}\text{O}, ^{12}\text{C})^{20}\text{Ne}$ , polarisation measurements 0-9301  
 $^{208}\text{Pb}$  core with valence nucleon or hole, mag. props., exchange currents, electron scatt. 0-22689  
 $^A\text{Re}$ , A=181, 182, 187, spin polarisation, state struct. and mag. moments in rot. model 0-18194  
 $^{177}\text{Ta}$  spin polarisation, state struct. and mag. moments in rot. model 0-18194  
 $^{160}\text{Tb}$   $\beta$ -decay, oriented nuclei,  $\gamma$  transitions multipole mixing parameters 0-18240

**nuclear polarisation in liquids and solids**

- see also *dynamic nuclear polarisation*  
 cross polarisation in solids with flip-back of I-spin magnetisation 0-39894  
 p-dibromobenzene, crystal nucl. spin polarisation cross relax. study 0-29647  
 dilute alloy, appl. of low temp. nucl. orientation 0-15825  
 double-cross-polarisation NMR of solids 0-20468  
 fluorene: acridene, radical pair form. from excited states, optical nucl. polarisation obs. 0-14155  
 graphite intercalation cpds. with Li, nucl. relax. times 0-44947  
 magnetic props. of materials, appl. of nucl. orientation, review 0-44928  
 NMR J cross-polarisation in liquids, refocusing method 0-22406  
 spin polarisation torsional spectroscopy, four time domains 0-20510  
 $\text{Al}_x\text{Ga}_{1-x}\text{As}$ , optically magnetised, luminescence polarisation anisotropy, hysteresis effect symmetry props. 0-34982  
 Cu-Cs diluted deuterated Tutton salts, electron non-Zeeman system, nuclear relaxation study 0-44951  
 Mn-Tb, dil., hyperfine interactions, nuclear orientation 0-15929

**nuclear power**

- accident prevention and control (*French*) 0-52747  
 AGR design for Heysham II and Torness 0-23108  
 AGR development and exploitation prospects 0-23109  
 AGR fuel element design improvement 0-23112  
 American Nuclear Society 25th Annual Meeting (Atlanta, GA, USA (June 1979)) 0-12847  
 book 0-46750  
 breeder reactors introduction, essential conditions 0-829  
 centralised heat supply from nuclear boiler units, technoeconomic assessment 0-7899  
 civil AGR multistart helically ribbed fuel pin development 0-23111  
 coal gasification by nuclear steam reforming of methane 0-55775  
 commercial nuclear capacity and spent-fuel accumulation, US projection 0-18574  
 conf., American Nuclear Society San Francisco, Calif., USA (Nov. 1979) 0-31414  
 developing countries, regulatory capability transfer 0-13634  
 development utilising FBRs, ACRs and alternative fuel cycles 0-47565  
 dual purpose nuclear power station and integrated agro-industrial complex in E. India 0-7904  
 economic competitiveness, w.r.t. West German Government expenditure (*German*) 0-23180  
 education, nuclear nonproliferation, fuel cycle economics, numerical estimates 0-51982  
 electric generating capacity for US by 2000 0-40846  
 energy conversion engineering, alternative energy sources (*Japanese*) 0-26105  
 energy self-sufficiency by 1990, use of Nuclear forms - complex of reactors 0-18456  
 environmental analysis, bi-Gaussian atmos. diffusion model, influence of turbulence typing scheme 0-3554  
 environmental radiation dose assessment of a growing nuclear industry 0-3553  
 FBR solution to world energy problem (*French, English*) 0-18591  
 FBR technology and strategies, role of nuclear power in world energy supply 0-50948  
 fission and fusion reactors, research and development in Japan 0-47701  
 fission electric cells, synergetics using catastrophe theory 0-45761  
 from fusion, state-of-the-art and problems to be overcome (*Dutch*) 0-37574  
 fusion energy heat source for  $\text{N}_2$  fixation 0-32510  
 fusion first-wall/blanket and associated structural mats., performance, safety and economics 0-32432  
 fusion reactors for synthetic fuels 0-13793  
 fusion research, philosophy 0-42854  
 fusion-supported decentralized nuclear energy system with 10 to 300 MW PWR 0-32515  
 global nuclear power is alternate source of energy, prospects and issues 0-7897  
 growth rates, influence on introduction dates for ACR and FBR 0-18379  
 H, thermochemical production by  $\text{H}_2\text{O}$  decomp., optimum temp. conditions utilizing HTGR nuclear heat 0-35781  
 Hinkley Point B AGR commissioning and three years' operational experience 0-23107  
 HTR nuclear long distance energy system, heat transport by chemical circuit 0-7905

**nuclear power continued**

- HTR plant with methane reformers for long distance energy system 0-7906  
 hydrogen power system, global energetic system, mathematical model (*Rumanian*) 0-35623  
 International Nuclear Fuel Cycle Evaluation Association structure (*Dutch*) 0-7896  
 low temperature nuclear heat utilisation 0-7903  
 low temperature nuclear heat utilization in Italy 0-7902  
 mathematical modelling of nuclear power engineering development 0-7901  
 methane reforming by nuclear steam for coal hydrogasification 0-30325  
 multicriterial optimization of the development of nuclear power in the framework of the perspectives of COMECON 0-7900  
 nuclear power stations, long term radioactivity values, meas. in marine life (*Spanish*) 0-7962  
 optimal development strategies for a whole energy system based on hydrogen 0-45795  
 PNP project, prototype HTR and coal gasification plant review 0-5393  
 progress review (1939-79) (*French, English*) 0-18590  
 public opposition, legislative aspects and effects (*German*) 0-23181  
 radioactive impact of nuclear facilities, preoperational evaluation 0-3534  
 radiological impact of the Rhein-Maas region from nuclear facilities under normal operation 0-3535  
 reactors, factors affecting choice of type and power (*French*) 0-52712  
 research programmes of Swiss Federal Institute for Reactor Research 0-52722  
 seawater desalination, evaluation of single purpose fission reactor 0-5319  
 ship propulsion, technical and economic aspects of a nuclear-powered containership 0-5392  
 solar assisted LWR nuclear reactors, SOAR power system concept 0-55820  
 space vehicle appls., missions and planning, elect. and propulsion power requirements 0-30428  
 space vehicle nuclear propulsion, historical review of advanced consent 0-36475  
 spacecraft, nuclear integrated multimission spacecraft, definition and evaluation 0-18715  
 synergetic aspects of solar energy and the fast breeder reactor 0-7907  
 synthetic fuel production in a particle-beam driven fusion reactor 0-55780  
 Turkey, nuclear power prod., utilisation and safety 0-3481  
 United States policy towards nuclear power and nuclear weapon nonproliferation, overview 0-3484  
 urban district heating, review 0-26118  
 H production using fusion reactor heat and gas dynamic compression heating 0-35793  
 H production using nuclear process heat from HTRs 0-30595  
 H synfuel prod. by high temp. electrolysis using fusion energy 0-35792  
 H synfuel prod. from fusion power using hybrid thermochem.  $\text{Bi}_2\text{O}_3\text{SO}_3$  cycle 0-40931  
 U exploration in developing countries, facts and trends 0-16764  
 U utilisation, improved fuel cycles 0-787

**nuclear power stations**

- see also *power station control*  
 1980s world's trends and Czechoslovak nuclear power program (*Czech*) 0-47784  
 4150 MW nuclear power station with PWRs, at Bugey, in France, commissioning report, (*French*) 0-37571  
 abandonment at end of working life, problems (*French*) 0-18588  
 accident prevention, 1300 MW nuclear reactor steam isolating valve blow-down tests (*German*) 0-22967  
 aseismic design and testing of equipment and components, Japan 0-52763  
 atmospheric radioactivity, radiological impact from model coal-fired power plants and from nuclear systems 0-3557  
 axisymmetric seismic response of thick circular plate supporting many rods, nuclear power plant appl. 0-1458  
 battered piles for nuclear power plant support, dynamic stiffness and seismic input motion 0-13954  
 breakdown in Three Mile Island plant (*Hungarian*) 0-18454  
 breakdown in TMI-2 power plant, consequences (*Hungarian*) 0-18455  
 breeder reactors, current status in Europe 0-27796  
 Brunswick plant post-startup optimization 0-23048  
 BWR, ASEA-ATOM supplied, operating experience 0-9375  
 BWR, Millstone Unit No. 1, augmented off gas system experience 0-22919  
 BWR, off-gas recombiner operating experience at Chin-Shan 0-22920  
 BWR, revised Inservice Inspection program, implementation at Millstone Unit 1 0-23020  
 BWR, sustaining improved plant operation 0-9374  
 BWR, TVO 1, startup principles 0-9372  
 BWR, Wm. H. Zimmer station, startup and testing 0-9373  
 BWR power plant, computerised core component accounting system shortens shuffling time 0-699  
 BWR power plant shielding concept 0-18712  
 BWR steam turbine, blast cleaning to remove radioactive deposits 0-18554  
 cables, damage mechanisms in LOCA environment 0-13658  
 California underground siting study, anal. 0-18400  
 California underground siting study, effectiveness in mitigating health consequences 0-18402  
 California underground siting study, selection and analysis of accident sequences 0-18401  
 CANDU power plants, automated anal. system for control of secondary coolant chemistry 0-18446  
 CANDU power stations, reduction, control and prediction of radioactivity transport 0-18448  
 CANDU-PHW decommissioning, costs, environmental impact, radioactive waste management 0-13964  
 Clinch River Breeder Reactor Plant, role and progress in LMFBR development 0-13781  
 Commonwealth Edison's Zion Generating station, decontamination of rad-waste evaporation 0-9376  
 containment structures pressure tightness verification, pressurisation plant, data acquisition and processing (*Spanish*) 0-13775  
 Creys-Malville plant, installation, design and construction planning (*French*) 0-47691  
 Creys-Malville plant worksite and progress (*French*) 0-47692  
 decommissioning, conf., Vienna, Austria (Nov. 1978) 0-12855



**nuclear power stations continued**

decommissioning, criteria for the management of redundant nuclear facilities 0-13975  
 decommissioning, deform. of acceptable residual radioactive contamination levels 0-13973  
 decommissioning, dismantling of French-type fast-neutron power reactors (French) 0-13968  
 decommissioning, disposition planning system for engineered approach 0-13963  
 decommissioning, establishment of activity limits for items to be released for unrestricted use 0-13972  
 decommissioning, experience gained with the decontamination of a shut-down reprocessing plant 0-13981  
 decommissioning, French experience rel. to safety (French) 0-13965  
 decommissioning, Italian experience 0-13967  
 decommissioning, industrial experience gained in the decontamination and partial dismantling of a shut-down reprocessing plant 0-13985  
 decommissioning, legal aspects 0-13961  
 decommissioning, main problems 0-676  
 decommissioning, national policies and international aspects 0-13959  
 decommissioning, partial dismantling of the Avogadro RS-1 materials testing reactor (French) 0-13980  
 decommissioning, progress report on dismantling of the Sodium Reactor Experiment 0-13978  
 decommissioning, radioactive waste disposal (French) 0-13736  
 decommissioning, radioactivity limits for release of liquid radwaste, math. model 0-13737  
 decommissioning, residual activity levels allowing radioactive waste to be considered inactive 0-13735  
 decommissioning, state-of-the-art handbook 0-824  
 decommissioning, summary of US DOE handbook 0-13969  
 decommissioning, treatment of contaminated metallic wastes by smelting 0-13741  
 decommissioning, US policy and standards 0-13960  
 decommissioning and dismantling projects at Idaho National Engineering laboratory 0-13984  
 decommissioning and reconstruction of the fast reactor fuel reprocessing plant, Dounreay 0-13983  
 decommissioning and total dismantling of PWR power plant 0-13982  
 decommissioning aspects of a nuclear chemical plant 0-13986  
 decommissioning of a  $^{239}\text{Pu}$  contaminated incinerator facility 0-13987  
 decommissioning of LWR power plants by German utilities 0-13962  
 decommissioning of LWR power station, radioactive waste decay behaviour 0-13738  
 decommissioning of nuclear installations in the preliminary safety report (French) 0-13966  
 decommissioning of PWR and fuel reprocessing plant 0-13970  
 decommissioning of the Lucens experimental nuclear power plant (French) 0-13979  
 decommissioning quantitative anal. of radioactive waste development 0-13974  
 design standardisation, scoping anal., and early site review for 1980's generation 0-22912  
 development of techniques for radwaste systems in CANDU power stations 0-37547  
 district heating plant, safety 0-767  
 dual purpose nuclear power station and integrated agro-industrial complex in E. India 0-7904  
 dual-purpose nuclear-electric reverse osmosis seawater conversion plant design and cost study 0-47683  
 Dungeness A, radiation and contamination control 0-5386  
 electrical power supply, safety requirements, emergency supplies 0-52762  
 electrical supply system performance, reliability of protection and control systems 0-52761  
 electricity supplies for safety system, German Regulation KTA 3701.1 (German) 0-37466  
 energy self-sufficiency by 1990, use of Nuclear forms - complex of reactors 0-18456  
 environmental acoustic protection (French) 0-19155  
 environmental radioactivity and dosage models (Spanish) 0-32518  
 fast breeder reactor boiler tubes, eddy current probe insertion for in-service inspection, method development (Japanese) 0-822  
 fast reactor electricity generation, experience and future development 0-18587  
 Fessenheim, France, PWR core physics meas. c.f. design values 0-718  
 fire barriers, analytical hazards analysis 0-18534  
 fire occurrences, Bayesian prediction model 0-18527  
 fire risk assessment 0-23002  
 fission reactors testing using ultrasonic test apparatus (German) 0-13730  
 fluid systems, program for initial cleaning 0-23047  
 forced outages, statistical data anal. 0-13776  
 Forsmark 3 plant, reactor safety study 0-18516  
 fuel circuit review, radioactive conditioned waste final storage (German) 0-799  
 fuel damage impact on plant operations 0-686  
 fusion plant layout,  $\text{CO}_2$  driven 0-32503  
 fusion plants,  $\text{D}^3\text{He}$  field-reversed mirror concept appl. 0-23126  
 fusion reactor, inertial confinement, parametric studies 0-32507  
 fusion reactor, inertial confinement economics 0-32506  
 fusion reactor, laser systems, plant development problems in Yugoslavia (Croatian) 0-833  
 fusion Tokamak, development problems, Yugoslavia (Croatian) 0-832  
 gaseous effluent standards comparison for nuclear and fossil fuel power prod. facilities 0-32536  
 German, assessment of accident risks 0-18517  
 Harrisburg (TMI-2), fuel element defects quantitative calc. (German) 0-23105  
 Hinkley Point B, AGR radiation protection, design criteria and operating experience 0-27832  
 HTGR, 330 MWe nuclear power station, start-up and operating experience since 1975 0-830  
 HTGR plant, reoptimisation using nonproliferation fuel cycle 0-13576  
 HTR nuclear long distance energy system, heat transport by chemical circuit 0-7905  
 HTR plant with methane reformers for long distance energy system 0-7906  
 impact of new security regulations on nuclear plant design and operations 0-796  
 Indian Point Unit No.2 reactor vessel, detection and identification of loose object 0-18553  
 instrumentation and control, remote multiplexing appl. 0-52752

**\* nuclear power stations continued**

integrated nuclear energy complex system of CMEA member countries (Czech) 0-52715  
 Krsko, construction, architecture and reactor system cooling (Croatian) 0-37416  
 laser fusion power plant, capital cost data base 0-32504  
 laser fusion system studies model, TROFAN 0-32505  
 leakage tests, Spanish safety policies (Spanish) 0-5247  
 licensing procedures in the UK 0-27708  
 LMFBFR, selection of steam conditions 0-18404  
 LMFBFR critical technical issues 0-13779  
 LMFBFR steam cycle conditions, comparison 0-18406  
 LMFBFR steam cycle selection 0-18403  
 LMFBFR steam cycles comparison, PLBR design 0-18405  
 locations around world, part in electrical energy production 0-18589  
 low temperature nuclear heat utilization in Italy 0-7902  
 LWR, deterministic criteria vs. probabilistic analyses 0-32377  
 LWR, Dutch nuclear safety requirements 0-768  
 LWR, liquid effluent treatment 0-18444  
 LWR, multigoal fuel cycle optimization including nonproliferation objectives 0-52764  
 LWR nuclear power plant with passive containment system, surveillance system importance 0-795  
 LWR power plant, radioisotope activity meas. in secondary loop coolant 0-5345  
 LWRs at Harrisburg and Mulheim-Karlich, safety systems comparison (German) 0-22966  
 Magnox power station, decommissioned, rad. levels, neutron activation, waste disposal 0-13976  
 maintainability, human factors engineering review of design, c.f. fossil plant 0-22913  
 maintenance optimization through trend monitoring 0-18552  
 Millstone power plant, Unit 3 design 0-22922  
 noise analysis, time series modelling methods, comparative eval. (Japanese) 0-13552  
 NRC standardisation in licensing, B and W viewpoint 0-23023  
 nuclear materials, safeguarding experiences (German) 0-611  
 occupational radiation exposure, evaluation and control, US research program 0-5370  
 operating experience, conf., Arlington, Texas, USA (Aug. 1979) 0-8735  
 Peach Bottom power station radwaste system backfit considerations 0-9351  
 Phenix and Super Phenix breeder reactor plants, status report 0-13780  
 Phenix plant operations and modifications (French) 0-47615  
 PNP project, prototype HTR and coal gasification plant review 0-5393  
 power conf., Chicago, United States, July 1979 0-794  
 power reactors, min. unit generation cost 0-734  
 pressurised heavy water Candu nuclear power plants, cost and safety aspects (French) 0-18463  
 prospects w.r.t. environmental problems (Hungarian) 0-13742  
 protection of nuclear power plant against seismic-aseismic bearings 0-857  
 PWR, 836 MWe nuclear power station, operating experience since 1974 0-831  
 PWR, Oconee station, steam generator availability 0-22921  
 PWR balance-of-plant design standardisation 0-22911  
 PWR containment building, design and anal. of cavity shield system 0-18713  
 PWR power plant flow pressure fluctuations as vibration source, relationships (Hungarian) 0-47685  
 PWR power plants, design concepts to facilitate dismantling 0-13577  
 PWR radiation shielding design 0-5372  
 PWR reactor dismantling, model scheme to meet West German regulations 0-825  
 PWR steam generator repair options 0-22923  
 quality assurance criteria, international standardisation 0-780  
 quality assurance program for nuclear plant operations 0-783  
 quality assurance standards in USA, present status and appl. 0-781  
 radiation dosage determination, monitoring and control for personnel safety (German) 0-842  
 radiation exposure ALARA concept 0-32388  
 radiation monitoring, decentralised system using microprocessors (Spanish) 0-47727  
 radiation monitoring, on-line computer appl. 0-5391  
 radiation protection, regulatory control, implications of ICRP publication 26 0-18706  
 radiative waste water treatment methods (Hungarian) 0-18450  
 radioactive contamination of biosphere, explosion and power plant influence (Hungarian) 0-21548  
 radwaste disposal operations Peach Bottom power station system backfit considerations 0-5261  
 reactor containment structures, design and construction, ACI-ASME code of practice impact 0-798  
 reactor diagnostic system tasks and installation (Hungarian) 0-18452  
 reactor parameter monitoring system, microcomputer-based (Hungarian) 0-18451  
 reactor protection computer systems, statistical verification of reliability 0-32417  
 reactor safety, probable risk assessment 0-797  
 safeguarding of nuclear facilities, methodology to aid decision-making 0-18477  
 safeguards systems, directed graph and fault tree anal. of material theft detection 0-13728  
 safety, aircraft crash probabilities for selected parts of a nuclear plant 0-859  
 safety, Czechoslovak legislation and practices (Slovak) 0-13632  
 safety, regulatory control of nuclear power stations in the United Kingdom 0-18707  
 safety, risk assessment of necessary functions for protection against external accidents 0-743  
 safety, seismotectonic map of France for appl. to antiseismic design of nuclear installations 0-860  
 safety analysis capability at nuclear utilities 0-23013  
 safety aspects, Japanese regulations 0-47599  
 secondary system radioactivity monitoring 0-18445  
 security, sabotage and terrorist attack, statistical anal. of threat reality and consequences 0-13727  
 seismic category I building design, structural anal. 0-858  
 siting policy in the USA 0-27835  
 Sizewell power station, radiation and contamination control 0-5387  
 standardisation, of plant design, General Electric standard safety anal. report for licensing 0-22908



**nuclear power stations continued**

- standardisation, rel. to w.r.t. plant rating, plant engineering and system engineering 0-594  
 standardisation of balance-of-plant design and final design evolution 0-22909  
 standardisation of design, licensing experience at Palo Verde 0-22910  
 startup, benefits of standardisation 0-13686  
 startup planning, comparison of domestic Westinghouse plant and PWR 0-9371  
 steam generator leakage in the AVR nuclear power station 0-596  
 surface protection materials, tests on 900 commercial products (German) 0-35356  
 surveillance testing feedback to improve plant availability 0-9384  
 surveillance testing safety system unavailability 0-9385  
 TFTR electric power module, conceptual design 0-32508  
 Three Mile Island accident, commission report 0-32372  
 three-loop, intermediate heat exchangers effectiveness determ. 0-608  
 tritium distribution in technological systems of Novovoronezh nuclear power station 0-32533  
 turbo-alternator driven by heat stored by NaOH fusion (French) 0-40915  
 IVA pipe rupture evaluation and typical mitigation fixes 0-18549  
 underground nuclear power plant, accidents, containment of fission products, finite element anal. 0-27768  
 underground siting, conceptual design and estimated cost of nuclear power plants in mined caverns 0-688  
 vibrations caused by flow, indirect meas. methods (Hungarian) 0-18453  
 volume reduction and solidification of low level radioactive wastes 0-42794  
 water cooled channel reactor, electrical energy cost of change in fuel component 0-37480  
 Westinghouse plant availability anal. with operating data base 0-23050  
<sup>60</sup>Co long-lived  $\gamma$ -emitting aerosols, max. allowable emission rate from nuclear power station 0-32532  
 T monitoring at Oconee 1 in-core sources and diffusion rates 0-18691  
 Zr nuclear steam superheating channels, design testing 0-5211

**nuclear pumped lasers**

- fission pumped gas lasers for H prod. by H<sub>2</sub>O photolysis 0-45810  
 fusion blanket optimisation in space and time 0-37616  
 gamma-ray laser pumping by neutron flux from thermonuclear microexplosion 0-28186  
 gamma-ray lasers, direct pumping by resonance capture of neutrons 0-14310  
 gas core reactor utilising UF<sub>6</sub> and CO<sub>2</sub> laser 0-23117  
 inert gas IR lasers pumped by U fission fragments 0-28198  
 reactor-laser for disintegrating thermonuclear plasma 0-19598  
 Ar-Xe, low-threshold nuclear pumped laser, generation characts. 0-19018  
 CO-N<sub>2</sub>-<sup>3</sup>He, laser mixture, excitation in externally maintained discharge in reactor core 0-28193  
 CO-N<sub>2</sub>-<sup>3</sup>He, nucl. reactor active zone, plasma and sustained discharge props. 0-5729  
 CO<sub>2</sub>-N<sub>2</sub>-<sup>3</sup>He laser mixture, excitation in externally maintained discharge in reactor core 0-28193  
 He-CO<sub>2</sub> atomic C nuclear pumped laser collision processes, output delay 0-38002  
 He-Ne nuclear-pumped CW lasing 0-48216  
 He-Xe, low-threshold nuclear pumped laser, generation characts. 0-19018  
 XeF\*(B), buffer effects 0-37617

**nuclear quadrupole moments** *see nuclear electric moment***nuclear quadrupole resonance**

- 3d-acetonitrile, cryst. struct., <sup>14</sup>N NQR free induction decay times meas. 0-54985  
 alkali metal bromates and chlorates, alkali and <sup>17</sup>O NQR, spin echo double reson. method, electronegativity 0-54970  
 apparent spin-spin relaxation time, super-regenerative NQR spectrometric obs. 0-54963  
 autotype detector, spin resonance detection 0-22397  
 bridge RF spectrometer, high freq. preamplifier 0-22380  
 caesium trichloroacetate, temp. depend. of <sup>31</sup>Cl NQR spectra 0-20495  
 chloral hydrate, phase transform. rate, <sup>35</sup>Cl NQR rate 0-54983  
 6-chloro 2,4-dimethoxypyrimidine, <sup>35</sup>Cl NQR, Zeeman effect 0-18874  
 2-chloro-1,3,2-dioxo-arsolane, temp. depend. of NQR spectra parameters of <sup>75</sup>As and <sup>35</sup>Cl 0-20494  
 2-chloro-1,3,2-X, Y-arsolanes, temp. depend. of NQR spectra parameters of <sup>75</sup>As and <sup>35</sup>Cl 0-20494  
 chlorobenzenes, substituted, NQR freqs. 0-20504  
 N-5'-chlorosalicylideneaniline, photochromism and thermochromism, NQR spectra, temp. and UV irradiat. depend. 0-54968  
 coherent NQR relaxometer, two freq. processes by multichannel analyser 0-20498  
 conference, 5th International Symposium on NQR spectroscopy, Toulouse, France (Sept. 79) 0-51947  
 3-cyanopyridine, NQR Zeeman obs., crystal packing 0-54978  
 deep struct. changes, NQR obs., high-pressure, and temp. effects 0-54139  
 p-dibromobenzene crystal nucl. spin polarisation cross. relax. study 0-29647  
 p-dichlorobenzene, <sup>35</sup>Cl powder Zeeman NQR, injection and phase locked NQR spectrometer 0-54979  
 p-dichlorobenzene, in p-dibromobenzene, optical detection of Cl NQR in mag. field 0-50228  
 3,5-dichloronitrobenzene, NQR line, Zeeman effect 0-28034  
 4,6-dichloropyrimidine, <sup>35</sup>Cl NQR, Zeeman effect 0-18874  
 p-dihalobenzenes, apparent NQR spin-spin relax. times obs. 0-54991  
 dipole width suppression by strong elec. field 0-20493  
 double quadrupole spin echo reson. 0-20513  
 echo in quadrupole spin-system, and energy levels in interaction representation 0-20492  
 exchange clusters, hybrid electronic-nuclear states, quadrupole moments (Russian) 0-34816  
 gas phase quadrupole coupling const. anomalous positive temp. coeff., vibr. depend. 0-53016  
 glasses, nuclear quadrupole spin-lattice relax., soliton-nucl. quadrupole moment interaction, temp. depend. 0-50220  
 hexadecapole spin resonance in cubic symm. cryst. by NQR, NMR, nuclear gamma reson. 0-20500  
 hydrazide derivatives, symm., <sup>14</sup>N NQR echo envelope slow beats 0-29643  
 hydrazine monohydrate, <sup>14</sup>N NQR, echo envelope modulation obs. 0-50218  
 I=1 NQR data from single crystal ENDOR expts. 0-54994  
 nuclear quadrupole resonance continued  
 ice, <sup>17</sup>O, NQR spectrum by double reson. with coupled multiplets, fine struct. 0-54969  
 ionic lattice ABCL<sub>3</sub> systems, covalency parameters estimation from nucl. quadrupole coupling 0-25246  
 layered compounds and intercalates, TDPAC studies 0-39890  
 many-spin system dynamics, group approach (Russian) 0-50221  
 metal complexes, NQR spectrosc. appls. 0-54986  
 molecular crystals NQR freq. press. depend. 0-54971  
 molecular motion dynamics in crystal influence on spectral parameters of NQR, NMR and EPR 0-20486  
 molecular reorientations between unequal potential wells 0-54989  
 molecular torsional oscills., NQR freq. temp. depend. electric field gradient asymmetry 0-18868  
 molecules, wavefunction shape, field gradient and density distrib. calcs. 0-53017  
 multiple and combinational freq. NQR, dipole-dipole, spin-spin interactions 0-20499  
 NMR-NQR double resonance, two-freq. methods, resonance spectrometers 0-20512  
 NQR-NMR double resonance line intensities, level crossing method, two freq. saturation 0-20514  
 paradibromobenzene-paradichlorobenzene solid solutions, mol. cryst., NQR study 0-25242  
 perchloro-3-cyclopentenone, <sup>35</sup>Cl NQR Zeeman obs. 0-54981  
 phase transitions, high press., NQR and stationary NMR studies 0-19934  
 phase transitions, nuclear quadrupole splittings 0-20489  
 phosphamides, carcinostatic, <sup>14</sup>N NQR, electron distrib. and bonding configs. 0-48018  
 poly- $\gamma$ -benzyl-L-glutamate, sidechain order parameters, <sup>2</sup>H NMR meas. 0-1923  
 polycrystalline samples, <sup>14</sup>N NQR, Zeeman effect, second-order theory 0-20503  
 polyelectrolyte solutions, counterion nucl. mag. relax., quadrupolar mechanism 0-2659  
 precision thermometry, freq. meas. improvement 0-22356  
 pulse spectrometer modulator 0-17971  
 pulsed NQR-FFT radiofrequency spectrometer for <sup>14</sup>N, description and operation 0-17982  
 pyridine and salts, deuterium NQR, double reson. method, ring charge distrib. 0-53015  
 pyridine-H<sub>2</sub>O, bonding, double quadrupole reson. obs. 0-32749  
 quadrupole spin echo envelope EFG tensor axisymmetry in mag. field 0-20497  
 quantum kinetic theory 0-52288  
 rare earth Cu<sub>2</sub>Si<sub>2</sub>, interconfiguration fluctuation system, NMR meas. 0-15817  
 rotating co-ordinate system, direct obs. of NQR 0-7188  
 rotating coordinate system with quadrupole splitting, paramag. susceptibility 0-11178  
 ruby, ESR and NMR correl. line broadening effect assoc. with external mag. field inhomogeneities 0-50227  
 salicylidene-2-chloroaniline, photochromism and thermochromism, NQR spectra, temp. and UV irradiat. depend. 0-54968  
 saturation of NQR lines in presence of paramag. impurities 0-20491  
 short range remote spectrometer for anal. 0-55742  
 single channel two freq. <sup>14</sup>N NQR pulse spectrometer, multiplet spectra 0-17968  
 small sample enhanced coupling using ferrite coils 0-52287  
 solid, mol. and complex ion intramolecular configs., nucl. quadrupole double reson. obs. intramolecular configs., nucl. quadrupole double reson. obs. 0-34821  
 spectrometer, programming device for a spin-echo installation 0-17972  
 spectrometer, weak signal relax. meas. with Sigma type digital storage device, pulse-train program blocks 0-17970  
 spectrometers for precision measurement of temp., optimisation (Russian) 0-22412  
 spin 3/2 nuclei, Zeeman NQR powder spectra 0-20502  
 spin lattice relax. time meas., steady state pulse method, master eqn. 0-54975  
 spin-lattice relax. due to mol. fragments reorientation (Russian) 0-7189  
 stroboscopic integrator for studying NQR relax. processes 0-17969  
 structural phase transitions, elec. field effects in NQR 0-20488  
 temperature meas. methods (Russian) 0-223  
 thermometer, calibration in 203-398K range 0-42222  
 three-level system transition probabilities, molecular motion anisotropy 0-18867  
 3,4,5-trichloroaniline, polymorphism, <sup>35</sup>Cl NQR 0-54163  
 trichloromethane glass:O<sub>3</sub>, <sup>17</sup>O, NQR by proton double reson., broad reson. assignments 0-53014  
 two frequency spin echo spectroscopy, review 0-20506  
 Ag<sub>3</sub>As<sub>3</sub>, proustite, structural changes in low temp. phase transition, NQR study 0-19935  
 AgClO<sub>3</sub>, <sup>35</sup>Cl NQR spectrum under press. at 311K 0-11291  
 AgClO<sub>3</sub>, mol. torsional oscills., cooperative study by NQR 0-25244  
 AgClO<sub>3</sub>, structural phase transition, <sup>35</sup>Cl NQR meas. 0-15819  
 As, pulsed NQR, bonding, bond angle distrib. obs. in different phases 0-54984  
 As<sub>2</sub>S<sub>3</sub>, glassy, deep struct. changes, NQR obs., high-pressure and temp. effects 0-54139  
 As<sub>2</sub>Se<sub>3</sub>, photodarkening and photostructural effects, Raman, IR and NQR studies 0-16036  
 As<sub>2</sub>Se<sub>3</sub>(S<sub>2</sub>), glassy film, photostructural effects, NQR study 0-49549  
 CaB<sub>6</sub>, <sup>11</sup>B nucl. quadrupole interaction, NMR meas. 0-2660  
 Ca(ClO<sub>3</sub>)<sub>2</sub>, mol. torsional oscills., cooperative study by NQR 0-25244  
 CaSnCl<sub>6</sub>, Cl NQR anomalous temp. depend., crystal struct. and phase transitions 0-54977  
 Ce<sub>1-x</sub>Sc<sub>x</sub>Al<sub>2</sub>, fluctuating valence system, quadrupole interaction temp. depend. 0-54972  
 Cl NQR spectrometer with exact reading of resonant freq. 0-42247  
 Cl NQR spectroscopy, parametric superregenerator with phase quantisation application 0-22398  
 Cl<sub>2</sub>PNC(Cl<sub>2</sub>CF<sub>3</sub>)<sub>2</sub>, cryst., <sup>35</sup>Cl NQR obs. of molecular reorientations between unequal potential wells 0-54989  
 Co complex, tris(ethylenediamine)cobalt(III) ion in complex anion solns., <sup>59</sup>Co NMR relax. obs. 0-25234  
 Co<sub>1-x</sub>M<sub>x</sub>Si (M=Fe, Ni), elec. field gradient, quadrupole splitting of <sup>59</sup>Co 0-29641  
 CsCoCl<sub>3</sub>, covalency parameters estimation from nucl. quadrupole coupling 0-25246



**nuclear quadrupole resonance continued**

- CsCuBr<sub>3</sub>, quasi-1-dimens., NQR obs. 0-54987  
 CsCuCl<sub>3</sub>, quasi-1-dimens., NQR obs. 0-54987  
 Cs<sub>2</sub>HgBr<sub>4</sub>, phase transitions and singularities of cryst. struct., NQR study 0-19936  
 CsIO<sub>3</sub>, hexagonal modification, temp. depend. of NQR freq., interpretation of long-wave spectra 0-25243  
 Cu complex, (CH<sub>3</sub>NH<sub>2</sub>)<sub>2</sub>Cu(Cl<sub>1-x</sub>Br<sub>x</sub>)<sub>4</sub>, ferromag., Br NMR mas. 0-29642  
 Cu complex, dichloro(N-nitrosopiperidine) Cu II, <sup>14</sup>N NQR obs. 0-54988  
 Cu complex, dichloro(dimethylnitrosamine)copper(II), magnetic phase transition, <sup>14</sup>N NQR obs. 0-11289  
 Cu complex, dichloro(dimethylnitrosamine) Cu II, mag. props., <sup>14</sup>N NQR obs. 0-54988  
 Cu<sub>2</sub>BiS<sub>3</sub>, wittichenite, NQR of <sup>63,65</sup>Cu and <sup>209</sup>Pb 0-20490  
 CuBr<sub>2</sub>, <sup>63</sup>Cu and <sup>81</sup>Br NQR line width obs. 0-50219  
 CuBr<sub>2</sub>, quasi-1-dimens., NQR obs. 0-54987  
 CuCl<sub>2</sub>, quasi-1-dimens., NQR obs. 0-54987  
 Cu(ClO<sub>4</sub>)<sub>2</sub>, mol. torsional oscills., cooperative study by NQR 0-25244  
 CuF<sub>2</sub>, <sup>63</sup>Cu NQR meas. 0-50219  
 Cu(I) complexes, cuprous halide triphenylphosphines, NQR, Zeeman effect 0-54980  
 Cu<sub>2</sub>SbS<sub>3</sub>, skinnerite, polymorphism, X-ray diffr. and NQR meas. 0-49165  
 Er<sub>1-x</sub>Gd<sub>x</sub>Al<sub>2</sub>, nuclear hyperfine field, quadrupolar splitting, NMR study 0-39888  
 EuB<sub>6</sub>, <sup>11</sup>B nucl. quadrupole interaction, NMR meas. 0-2660  
 EuCu<sub>2</sub>Si<sub>2</sub>, fluctuating valence system, quadrupole interaction temp. depend. 0-54972  
 EuCu<sub>2</sub>Si<sub>2</sub>, valence fluctuation and temp. depend. of Cu nuclear quadrupole interaction 0-15818  
 GaAs, nucl. spin levels, elec. induced shifts 0-34408  
 GaCl<sub>3</sub>, cryst. struct., Zeeman split fine struct. lines, FT NQR obs. 0-54982  
 α-HIO<sub>3</sub>, HI<sub>2</sub>O<sub>8</sub>, I<sub>2</sub>O<sub>5</sub> and deuterated cpds., crystalline, <sup>127</sup>I NQR, bonding and mol. dynamics 0-39889  
 H<sub>2</sub>O<sub>2</sub>, <sup>17</sup>O pure NQR spectrum 0-9620  
 HgCl<sub>2</sub>, <sup>35</sup>Cl powder Zeeman NQR, injection and phase locked NQR spectrometer 0-54979  
 In<sub>1-x</sub>I<sub>x</sub>, molten mixture, NMR, reson. shifts, relax. rates, quadrupole relax. 0-2654  
 InP:Te, quadrupole struct. of NMR line 0-20505  
 KBrO<sub>3</sub>, hexagonal modification, temp. depend. of NQR freq., interpretation of long-wave spectra 0-25243  
 K<sub>2</sub>Co(CN)<sub>6</sub>, <sup>59</sup>Co quadrupole coupling const., temp. depend. 0-44557  
 K<sub>2</sub>CoF<sub>6</sub>, <sup>63</sup>Cu NQR meas. 0-50219  
 KIO<sub>3</sub>, HIO<sub>3</sub>, structural modifications, NQR study 0-20487  
 K<sub>2</sub>PtCl<sub>6</sub>, K<sub>2</sub>ReCl<sub>6</sub>, K<sub>2</sub>SnCl<sub>6</sub>, solid state phase transitions, lattice vibr., NMR and NQR obs. 0-34814  
 LaB<sub>6</sub>, <sup>11</sup>B nucl. quadrupole interaction, NMR meas. 0-2660  
 LiN<sub>3</sub>, ionic nature, quadrupole splitting, mag. field depend., N<sup>3-</sup> electron cloud deform., NMR 0-50210  
 LiReO<sub>4</sub>, <sup>187</sup>Re HQR freq. temp. depend. 0-25245  
 LiReO<sub>4</sub>·2H<sub>2</sub>O, <sup>187</sup>Re HQR freq. temp. depend. 0-25245  
 Mg<sub>2</sub>V<sub>2</sub>O<sub>7</sub>, quadrupole coupling tensor of <sup>51</sup>N nucleus 0-11290  
 ND<sub>3</sub> dissolved in poly-γ-benzyl-L-glutamate-chloroform, NMR study 0-34805  
 NG<sub>4</sub>HgCl<sub>3</sub>, NQR freq. anomalous temp. depend., reorientation 0-54976  
 NH<sub>4</sub>I<sub>3</sub>, NQR freq. anomalous temp. depend., reorientation 0-54976  
 NH<sub>4</sub>IO<sub>4</sub>, high order phase transition, quadrupole coupling temp. depend. 0-54371  
 ((NH<sub>4</sub>)<sub>2</sub>K<sub>1-x</sub>)<sub>2</sub>SnCl<sub>6</sub>, mixed cryst., NQR relax. and reson. 0-54990  
 (NH<sub>4</sub>)<sub>2</sub>PtCl<sub>6</sub>, crystal symm., struct. phase transition, <sup>127</sup>I NQR freq. 0-34815  
 NH<sub>4</sub>ReO<sub>4</sub>, <sup>187</sup>Re HQR freq. temp. depend. 0-25245  
 NH<sub>4</sub>ReO<sub>4</sub>, high order phase transition, quadrupole coupling temp. depend. 0-54371  
 NH<sub>4</sub>ReO<sub>4</sub>, NQR freq. anomalous temp. depend., reorientation 0-54976  
 (NH<sub>4</sub>)<sub>2</sub>SnCl<sub>6</sub>, <sup>35,37</sup>Cl NQR, Raman spectra and spin lattice relax., hindered rot. 0-54974  
<sup>14</sup>N, observation equipment and techniques 0-22399  
 NaClO<sub>3</sub>, mol. torsional oscills., cooperative study by NQR 0-25244  
 Na<sub>2</sub>In<sub>2</sub>Sn<sub>1-x</sub>S<sub>2</sub>, intercalation-substitution compounds, NMR study 0-44952  
 NaNO<sub>3</sub>, size effect and spin-lattice relax. of <sup>14</sup>N 0-20480  
 NaReO<sub>4</sub>, <sup>23</sup>Na and <sup>187</sup>Re NMR and NQR temp. depend. 0-54973  
<sup>23</sup>Na spin-<sup>1</sup>/<sub>2</sub> nuclei, double quadrupole resonance 0-32634  
 Nb<sub>3</sub>Ir, A-15 struct., <sup>93</sup>Nb NQR spectra 0-20496  
 Nb<sub>3</sub>Os, A-15 struct., <sup>93</sup>Nb NQR spectra 0-20496  
 Nb<sub>3</sub>Pt, A-15 struct., <sup>93</sup>Nb NQR spectra 0-20496  
<sup>17</sup>O, NQR at natural isotope abundance, double reson. new techniques, review 0-53013  
<sup>17</sup>O nuclear quadrupole double resonance spectroscopy, line shapes and examples 0-31820  
 Pd, nucl. acoustic reson from 4-200K 0-25247  
 PrNi<sub>5</sub>, metallic Van Vleck paramag., nucl. interactions, NMR meas. 0-44953  
 RbBrO<sub>3</sub>, hexagonal modification, temp. depend. of NQR freq., interpretation of long-wave spectra 0-25243  
 RbCaF<sub>3</sub>, cubic to tetragonal phase transition, <sup>87</sup>NMR meas. 0-7187  
 RbCuCl<sub>3</sub>, quasi-1-dimens., NQR obs. 0-54987  
 RbCuF<sub>3</sub>, <sup>63</sup>Cu NQR meas. 0-50219  
 RbD<sub>2</sub>(SeO<sub>3</sub>)<sub>2</sub>, <sup>2</sup>D NMR struct. anal. 0-2661  
 RbCl<sub>4</sub>, <sup>35</sup>Cl NQR spectra, press. cond. temp. depend 0-20501  
 RbCl<sub>4</sub>, NQR of <sup>35</sup>Cl, press. and temp. depend., phase transform. obs. 0-15820  
 RbIO<sub>3</sub>, hexagonal modification, temp. depend. of NQR freq., interpretation of long-wave spectra 0-25243  
 ReO<sub>3</sub>, compressibility collapse phase transition, NQR study 0-39282  
 Sb<sup>117</sup>Cd, In, elec. field gradient, TDPAC expts. 0-55002  
 SbCl<sub>3</sub>, cryst. struct., Zeeman split fine struct. lines, FT NQR obs. 0-54982  
 Sb<sub>2</sub>S<sub>3</sub>, deep struct. changes, NQR obs., high-press. and temp. effects 0-54139  
 SmB<sub>6</sub>, <sup>11</sup>B nucl. quadrupole interaction, NMR meas. 0-2660  
 SnBr<sub>2</sub>, <sup>81</sup>Br NQR line width obs. 0-50219  
 Sr(ClO<sub>4</sub>)<sub>2</sub>, mol. torsional oscills., cooperative study by NQR 0-25244  
 UNi<sub>1-x</sub>Co<sub>x</sub>, NMR and press. effects 0-25230  
 V<sub>2</sub>Si, NMR of <sup>51</sup>V above and below 21K struct. transition (Russian) 0-34796

**nuclear quadrupole resonance continued**

- Y(ReO<sub>4</sub>)<sub>3</sub>·4H<sub>2</sub>O, <sup>187</sup>Re HQR freq. temp. depend. 0-25245  
 YbB<sub>6</sub>, <sup>11</sup>B nucl. quadrupole interaction, NMR meas. 0-2660  
 YbCu<sub>2</sub>Si<sub>2</sub>, valence fluctuation and temp. depend. of Cu nuclear quadrupole interaction 0-15818  
 ZnBr<sub>2</sub>, <sup>81</sup>Br NQR line width obs. 0-50219

**nuclear radius see nuclear size****nuclear reaction and scattering models**

- see also nuclear optical model  
 collective tube model of high energy proton scatt. on polarised nuclei 0-32273  
 double folding pot. for inelastic scatt. between nuclei 0-13425  
 energetic heavy ion beam model for radiobiology 0-26293  
 exciton model, preequilibrium reactions, angular distrib. 0-52652  
 heavy ion elastic collisions and nuclear surface diffuseness, diffraction formulae 0-47494  
 hydrodynamical and phenomenological models for central asymmetric heavy-ion collisions, moderate energies 0-5164  
 inelastic collisions of light nuclei and nucleon-nucleus collisions, dynamical model (Russian) 0-37356  
 peripheral model, single-nucleon transfers due to multiply charged ions 0-22850  
 peripheral model for DD (e<sup>-</sup>,av) on heavy nuclei 0-37369  
 potential model, energy dissipation heavy ions reactions 0-22849  
 preequilibrium decay models (Rumanian) 0-47457  
 single-particle level density, excitation dependence of nuclear level density parameter 0-32149  
 (d,p) reacts. at intermediate energies, triangle graph model 0-27616  
<sup>12</sup>C(K<sup>±</sup>,K<sup>±</sup>), Glauber model anal. 0-42697  
<sup>40</sup>Ca(K<sup>±</sup>,K<sup>±</sup>), Glauber model anal. 0-42697  
<sup>15</sup>N(α,γ)<sup>19</sup>F, energy levels from α-<sup>15</sup>N and t-<sup>16</sup>O coupled channel orthogonality condition model 0-37326  
<sup>16</sup>O(t,γ)<sup>19</sup>F, energy levels from α-<sup>15</sup>N and t-<sup>16</sup>O coupled channel orthogonality condition model 0-37326  
 Sn(α,α'), even-even isotopes, nuclear struct. effects in microscopic theory 0-37391

**nuclear reaction and scattering theory**

- see also nuclear reaction and scattering models; statistical theory of nuclear reactions and scattering  
 3-body problem with one infinite mass particle, integral and Schrodinger eqn. equivalence 0-18255  
<sup>19</sup>F levels, J<sup>π</sup> and ang. distrib. DWBA anal. of <sup>19</sup>F(p,d) 0-42545  
 A=40 to 56, two-nucleon transfer reactions, coupled channel formalism for isospin depend. optical pot. 0-42609  
 alpha cluster reactions, effective single particle operator 0-32218  
 antisymmetrisation, redundant solns., scatt. solns., and nonsymmetric non-local pots. 0-27604  
 Baer-Kouri-Levin-Tobocman many body scatt. theory, Feshbach projection operator method 0-508  
 Born series rearrangement in model space, resolvent operator expansion 0-13422  
 charged particle elastic scatt., effect of Coulomb-nuclear interference on cross-section determ. 0-502  
 charged three body problems with Coulomb pots. 0-18256  
 complete fusion systems, barrier penetration, enhanced fusion-fission yields 0-13520  
 complex nuclear collisions, quantum description of friction, phenomenological ansatz 0-18340  
 composite particles, N-cluster dynamics and effective interaction, dynamical eqn. 0-42560  
 compound nucleus nonstatistical struct., runs tests as indicators 0-506  
 conference on heavy ion reaction dynamical props., Johannesburg, S.Africa (Aug. 78) 0-17715  
 conference on nuclear interactions, Canberra, Australia (Aug.-Sep. 1978) 0-4476  
 cosmic-ray events, energy estimates 0-22647  
 coupled reaction channel calculations, iterative solutions, method of moments 0-18251  
 cross sections for ion beam anal. 0-45606  
 deep inelastic collisions, parametrised S-matrix approach 0-32249  
 deep inelastic heavy ion collision, shape relaxation and fragment deformation 0-22683  
 deeply inelastic heavy ion collisions, charge transfer ang. momentum depend., fragment kinetic energies 0-47505  
 deeply inelastic heavy ion collisions, helicity representation, quantum mechanical cross section 0-47506  
 deeply inelastic heavy ion collisions, transport eqn. strong coupling effects 0-52693  
 dipole sum rule schematical eval., collective isovector quadrupole strength 0-47428  
 distorted waves method, finite radius of interaction, reaction mechanisms (Russian) 0-52647  
 dominant partition method 0-47455  
 eigenstates calc. for system of core and two valence nucleons 0-42606  
 elastic and quasi-elastic polarised heavy ion collision theory, semi-quantal description 0-18330  
 elastic projectile-nucleus scatt., optimal approx., multiple scatt. amplitudes 0-9275  
 elastic scattering, semiclassical time-independ. formulation in three-dimens with complex trajectories 0-27605  
 electro- and photonuclear EM sum rules 0-22810  
 electron pair production, cross section calc. on nuclei in range 1≤Z≤92 0-503  
 electron scatt. theory, EM struct. from DWBA and other models 0-5133  
 electroproduction above pion threshold, EM interactions and mag. sum rules 0-42639  
 exact finite range DWBA form factor for heavy-ion induced nuclear reactions, calc. program adaption 0-9271  
 exchange effects in direct reactions, antisymmetrisation and three body models 0-13446  
 fission, first order adiabatic approx., fission fragment excitation energy 0-32312  
 fission, slope constant of the exponential prompt-neutron yield formula 0-22806  
 Griffin-Hill-Wheeler spaces, 1- and 2-conjugate parameter generator states, giant resonances and scatt. 0-42618  
 hadron-nucleus collisions, high energy, simple space time description, zero parameter model 0-47479  
 hadron-nucleus elastic scatt., explicit formula in eikonal approx. 0-42665



**nuclear reaction and scattering theory continued**

- hadron-nucleus inclusive-inelastic scatt. in phase space, quantum theory 0-32247
- hadron-nucleus scatt., reggeon parton spacetime struct. Koplik-Mueller paradox (*Russian*) 0-42730
- heavy ion collision polarisation, damping mechanism approach via elementary excitation modes 0-18338
- heavy ion collisions, charge equilibrium model using collective high freq. mode and quantal master eqn. 0-27667
- heavy ion collisions, composite particle formation, direct, classical thermodynamic and quantum statistical theories 0-32297
- heavy ion collisions, nuclear level shifts, generalised relativistic Coulomb problem (*Russian*) 0-52586
- heavy ion collisions, pion spectra, Coulomb distortion in final state EM interaction 0-13497
- heavy ion deep inelastic collisions, interaction times and transport coeffs. (*Chinese*) 0-42693
- heavy ion deep inelastic collisions, kinetic energy dissipation, nuclear matter density oscillations (*Russian*) 0-37397
- heavy ion deep inelastic reactions,  $\gamma$ -ray multiplicity, partial ang. momenta (*Russian*) 0-37346
- heavy ion fusion and deep inelastic scatt., shape degrees of freedom, classical dynamic model 0-22876
- heavy ion fusion cross section, energy depend., nuclear matter density distrib., depend. 0-47519
- heavy ion fusion reaction excitation function anal., nucleus-nucleus pots. 0-42728
- heavy ion inner shell excitations, multistep processes, quasimolecular model, coupled channels calc. 0-9303
- heavy ion large-angle scatt., elastic cross-section, excitation functions 0-52689
- heavy ion large-angle scatt., inelastic cross-section and collective state excitation 0-52690
- heavy ion reactions, phenomenological nuclear friction mechanism, particle-hole excitation, nucleon exchange (*Chinese*) 0-42694
- heavy ion scattering, angle depend. phase shifts, coupled channel formalism 0-18253
- heavy ion transfer reactions 0-5165
- high energy inelastic scatt., non-eikonal effects 0-42608
- impulse approx. with nuclear current conservation, off-shell form factors 0-52632
- inelastic electron scatt., nuclear charge and current spatial struct. 0-5134
- interacting composite systems, generalised spectator expansion in multiple scatt. framework 0-27664
- ion-ion cross section, Pauli principle effects in impulse approx. 0-47500
- kinetic energy distrib. of fission fragments, thermal fluctuation influence 0-22865
- kinetics, quasiclassical method, and angular distribution of nucleons 0-22777
- large deformations and dissipation in a random-matrix model approach for fission or colliding nuclei 0-18162
- large scale collective motion in very heavy ion reactions, macroscopic description 0-5049
- light heavy ion total reaction cross sections in diffraction model, resonance oscillations 0-13503
- light nuclei,  $\alpha$ -transfer reactions, spectroscopic factors, exact finite range DWBA anal. 0-13372
- long-range heavy-ion potential induced by multiple Coulomb excitation 0-13496
- mesonic processes and quarks in nuclei 0-42564
- multi-particle rescatt. effects, cumulative  $\pi$ , p, K prod. (*Russian*) 0-52638
- multichannel scattering, exact and Glauber amplitudes 0-13421
- multidimensional barrier penetration and fission-widths, barrier resonance 0-13454
- multiple scattering and few-body Hamiltonian models of nuclear reactions 0-47443
- muonic atoms, prompt fission, muon entrainment by fission fragment, probability (*Russian*) 0-37911
- nearly head-on heavy ion collision, centrality parameter for intermediate energy 0-22856
- nonfissile nuclei, inherent inaccuracy in capture cross section calc. reactor appl. 0-22836
- nuclear Dirac phenomenology, consistency with meson-nucleon interactions 0-9272
- nucleon Fermi motion in deuteron, smearing effects, (West  $\beta$  correction), on expt. results. 0-32107
- nucleus-nucleus pot., static polarisation effects, nuclear shapes 0-5154
- off energy two body t-matrix in the R-matrix theory (*Russian*) 0-22780
- off-energy-shell generalisation 0-18257
- off-shell Coulomb T-matrix, three particle eqns. with Coulomb interaction, exact soln. 0-42605
- off-shell T-matrix in nuclear reactions 0-47441
- one-particle formalism in continuum approach for photonuclear cross-section calcs. 0-37355
- path integrals and time-dependent mean-field theories, many-body problem, Hartree-Fock eqns., Slater determinants 0-37342
- photonuclear sum rule, spin current contribs., strong violations 0-18291
- pion interferometry of relativistic nuclear collisions, theory 0-32301
- pion multiplicity and nonlinear effects in pion production, NN inelastic interactions (*Russian*) 0-52637
- promptly emitted particles in nuclear collisions, fusion nucleon spectra 0-42678
- quantal fluctuation squeezing, Schrodinger eqn., deep inelastic reactions 0-47444
- quantum three-body problem, distorted Faddeev eqns. with coupled channel approach 0-52635
- quark lattice and QCD in nuclei 0-5101
- quasi-elastic direct transfer reaction to continuum states, DWBA and diffraction model 0-18277
- quasi-elastic heavy ion scatt., multistep processes and interference phenomena 0-22857
- quasielastic heavy ion reaction, amplitude for transitions between molecular (two-center) channels 0-18322
- rearrangement reactions, coupled channel methods, non-orthogonality effects 0-42607
- rearrangement reactions, coupled reaction channels compared with coupled channels array 0-47442
- redundant states, reduced potentials, and extra nodes in the radial wave function 0-42603
- redundant states and Jost functions for nonlocal potentials 0-9274

**nuclear reaction and scattering theory continued**

- relativistic heavy ion collisions, charged particle emission multiplicities and ang. correlations, firestreak models 0-18328
- relativistic heavy ion collisions, effective nucleon numbers 0-13499
- relativistic heavy ion peripheral collisions, charge exchange (*Russian*) 0-37398
- relativistic heavy ion-nucleus reactions, review, book contrib. 0-27672
- relativistic nucleus-nucleus collisions, secondary particle multiplicity, multiple scatt. model 0-22847
- relativistic two-body forces in many-body systems, Weinberg and Yukawa interactions 0-32203
- Saito potential, off-energy-shell unitarity 0-18207
- scission region, nascent fragment bending and wriggling modes, quantum numbers 0-18285
- spectroscopic investigation of decaying states using continuum shell model 0-486
- spherical nuclei, dipole states, transition densities and electroexcitation, GDR form factors (*Russian*) 0-52611
- statistical significance of spreading widths for doorway states, comments 0-27611
- strongly damped collisions, nonequilibrium process 0-18258
- TDHF approximation and exact Schrodinger dynamics, Taylor series comparison 0-42568
- three body phase space distrib. 0-37393
- three body scatt., spline function moment methods 0-505
- three particle systems with Coulomb interaction, scatt. and breakup eqns. exact solns. 0-504
- three particles with Coulomb interaction, binding energy and scatt. states (*Russian*) 0-5051
- three-body Lippmann-Schwinger equations, asymptotic behaviour and soln. uniqueness 0-42604
- three-body scatt. problem, cluster expansions, effective intercluster pots. 0-5082
- three-particle relativistic kinematics 0-27602
- time delay of resonance wave packets, stat. model anal. 0-22802
- time dependent Schrodinger eqn., alternative approx. soln. for heavy ion reactions 0-32296
- transfer induced transport in nuclear collisions 0-507
- transparency in composite particle-nucleus reactions 0-9273
- triplet S channel, half shell function parametrisation in separable form 0-52636
- two nucleon distrib. function for two nucleon transfer, effective Hamiltonian approach 0-22778
- two-body interaction, shell model calc. matrix elements 0-42567
- unified nuclear pot. for heavy ion elastic scatt., fission, fusion, masses and deformations 0-5189
- variational principles for true three- and four-particle scatterings 0-18254
- very heavy ions with complex trajectories, elastic scatt., semiclassical anal. 0-18331
- wave-spreading effects in nuclear scattering at intermediate energies 0-18252
- Weinberg functions, Born approx. in scattering problems, phase shift 0-32248
- Wigner transform and the eikonal approximation for nonlocal potentials, inclusive scatt. 0-13423
- ( $\alpha,\alpha$ ), 1.37-2.55 GeV, microscopic anal. 0-47490
- ( $\alpha,\alpha$ ), elastic scatt. critical radius, single particle anal. 0-13490
- ( $\alpha,\alpha$ ), 1 GeV/N, inclusive hadron-nucleus cross-sections, multiple scatt. series 0-13519
- ( $\alpha,X$ ), 140 MeV, inclusive spectra, 'quasi-two-body scaling' and 'hot spots' 0-5142
- $\alpha$ -decay spectroscopic factors, coupled channel problem, local pots. justification 0-47439
- (d,  $^6\text{Li}$ ), 54.25 MeV,  $\alpha$ -cluster spectroscopic factors, DWBA anal. 0-52571
- (d,t), DWBA anal., form factors and d-t overlap integral S- and D-state components 0-18320
- d breakup effect on spin orbit and tensor pots. 0-32286
- (dx) breakup on nucleus, adiabatic treatment stripping and forbidden transition cross section 0-9299
- (e,e),  $A=2, 3, 4$ , scaling laws in relativistic impulse approx. model, spin effects 0-52662
- (e,e), relativistic e, helicity representation 0-5132
- (e, e'), eN interaction in quasifree scatt., nonrelativistic Hamiltonian through 2nd order 0-52663
- (e,e') quasi-free scatt., spectral function, sum rule discrepancy, shell model deviation 0-42641
- ( $e,e'\pi$ ),  $\pi$  electromag. processes, theoretical aspects 0-22822
- ( $\gamma,\pi$ ), few body pion photoprod. in  $\Delta$ -resonance, region 0-42636
- ( $\gamma,\pi$ ), light nuclei near threshold,  $\pi$  mass difference effects, nuclear K-matrix 0-27674
- ( $\gamma,\pi$ ),  $\pi$  electromag. processes, theoretical aspects 0-22822
- (n, $\gamma$ ), mechanism in 3s size resonance, s-wave radiative width partition 0-37387
- (n, $\gamma$ ), mechanism in 3s size resonance, radiative width statistical and valence effects 0-37388
- (n, $\gamma$ ) gamma ray spectra calc. 0-52620
- (p,  $\alpha$ ) microscopic form factors, DWBA cluster form factor replacement 0-47478
- (p,d), 52 MeV, deeply bound hole state transition strength giant resonance, DWBA anal. 0-47426
- (p, n), 22.2 MeV,  $A=27$ -197, neutron spectra, direct and equilb. processes (*Russian*) 0-52648
- (p, p), 1 GeV, polarisation data, Glauber anal. spin-orbit parameters, matter distrib. 0-52655
- (p,p), 600, 750 MeV, polarisation and cross section, Glauber model calc., NN matrix test 0-47485
- (p,p),  $A=9$  to 70, differential cross sections, struct. effects, optical and coupled channel anal. 0-47482
- (p,p), elastic scattering theory, multiple scatt. test review 0-42654
- (p,p'),  $A=6$  to 208, 800 MeV, proton spectra, quasifree scatt., DWIA anal. 0-52677
- ( $p,\pi$ ), exclusive single nucleon transfer, theoretical status 0-42652
- (p, t) ang. distrib., zero-range DWBA calc., volume absorptive optical pot. singular prop. 0-523
- (p, t) ang. distrib. with deep minima, DWBA calcs. geometrical aspects 0-522
- (p,X), 24 and 70 GeV/c, pseudorapidity distribution, energy and target depends. 0-5138
- (p,X) 90 MeV, inclusive spectra, 'quasi-two-body scaling' and 'hot spots' 0-5142



## nuclear reaction and scattering theory continued

- (p,X) in emulsion 24 GeV, clusters in rapidity interval method, multiperipheral model 0-5135
- ( $\pi,\gamma$ ),  $\pi$  electromag. processes, theoretical aspects 0-22822
- ( $\pi,\pi$ ),  $A>2$  nuclei, three rung ladder graph, singularity curves 0-32303
- ( $\pi,\pi$ ), light nuclei near threshold,  $\pi$  mass difference effects, nuclear K-matrix 0-27674
- ( $\pi,\pi$ ) elastic scatt., reaction mechanisms, structure information and neutron radii 0-42702
- ( $\pi,\pi'$ ), 1p shell targets, DWIA calcs., strong transitions, isospin effects 0-42708
- ( $\pi,\pi'$ ), particle-hole state excitation, field theory calcs. (Russian) 0-37318
- ( $\pi,\pi'$ ) many body QFT framework anal., final state particle-hole correlations 0-13508
- ( $\pi,X$ ), reaction mechanisms, nuclear environment and models 0-42700
- ( $\pi,X$ ), total cross section treatment for (3,3) resonance region 0-42703
- Al(Ne,X), 400 MeV/N, direct vs. thermal particle emission, inclusive cross sections 0-52688
- <sup>27</sup>Al(<sup>14</sup>N,X), 70, 100 MeV, deep inelastic, charged reaction products ang. correlations, 3-body kinematics 0-5162
- <sup>27</sup>Al(p, $\alpha$ )<sup>24</sup>Mg, finite-range cluster-model description, DWBA approach 0-52667
- Al(d,d), 4.3, 6.3, 8.9 GeV/c, secondary momentum spectra, multiple scatt. model anal. (Russian) 0-27650
- (Ar,  $\pi$  X), 800 MeV/A,  $\pi^-$  energy and ang. distrib., firebreak and hard scatt. model anal. 0-13498
- <sup>38</sup>Ar levels, J $\pi$  and transition strengths, DWBA anal. of <sup>40</sup>Ar(p,t) 0-47378
- <sup>40</sup>Ar + <sup>40</sup>Ar, 250-1000 MeV/N, intranuclear cascade calcs. for multiplicity and cross sections 0-32300
- <sup>40</sup>Ar(p,p), 18-44 MeV, differential cross sections, phase shift anal., energy depend. 0-47481
- <sup>197</sup>Au(<sup>6</sup>Li,X), 75 MeV, Z=1 or 2 fast particle prod. mechanism above Coulomb barrier 0-42687
- <sup>197</sup>Au( $\alpha,\alpha'$ ), 120 MeV, isoscalar resonance excitation, low lying transitions, DWBA calc. 0-512
- <sup>10</sup>B + <sup>10</sup>B, fusion below Coulomb barrier, quantum mechanical barrier penetration model anal. 0-18361
- <sup>10</sup>B(p, $\pi^+$ ), 320-605 MeV, cross sections, pion exchange model anal. 0-27676
- <sup>11</sup>B states, spectroscopic factors from DWBA anal. of <sup>12</sup>C(p,2p) 0-5057
- <sup>11</sup>B + <sup>10,11</sup>B, fusion below Coulomb barrier, quantum mechanical barrier penetration model anal. 0-18361
- <sup>138</sup>Ba( $\gamma,\pi^-$  xn)La, 150-300 MeV, pion production cross sections calc. 0-9287
- <sup>9</sup>Be( $\gamma,\pi^+$ ), 100-800 MeV, cross section, surface prod. model anal. 0-47466
- <sup>9</sup>Be( $\gamma,\pi^+$ ), threshold to 175 MeV, total cross sections, DWIA anal. 0-13459
- <sup>9</sup>Be(p, $\pi^+$ ), 320-605 MeV, cross sections, pion exchange model anal. 0-27676
- Bi+Xe, 1.13 GeV, deep inelastic nuclear reaction, electronic 1s $\sigma$  vacancy prod., compound nucleus 0-27662
- Bi(Kr,X), strongly damped collisions, classical dynamical model with shape deformation 0-27658
- Bi(Xe,X), strongly damped collisions, classical dynamical model with shape deformation 0-27658
- <sup>208</sup>Bi low lying levels and spectroscopic factors, EFR-DWBA anal. of <sup>208</sup>Pb(Li, <sup>6</sup>He) 0-32182
- <sup>209</sup>Bi( $\alpha,X$ ), 69.2, 140 MeV, scatt. and fission reaction mechanisms, cross sections 0-18350
- <sup>209</sup>Bi( $\alpha,\alpha'$ ), 120 MeV, isoscalar resonance excitation, low lying transitions, DWBA calc. 0-512
- <sup>209</sup>Bi(n,n), 50, 100, 200 MeV, eikonal scatt. by complex pots., cross sections 0-27643
- Bi(d,d), 4.3, 6.3, 8.9 GeV/c, secondary momentum spectra, multiple scatt. model anal. (Russian) 0-27650
- (C,  $\pi$  X), 800 MeV/A,  $\pi^-$  energy and ang. distrib., firebreak and hard scatt. model anal. 0-13498
- <sup>12</sup>C,  $\alpha$ -transfer spectroscopic factors for O<sup>+</sup>, 2<sup>+</sup> and 4<sup>+</sup> states, transitions from (<sup>10</sup>,<sup>6</sup>Li) 0-13370
- <sup>12</sup>C + <sup>10,11</sup>B, fusion below Coulomb barrier, quantum mechanical barrier penetration model anal. 0-18361
- <sup>12</sup>C + <sup>12</sup>C, 250-1000 MeV/N, intranuclear cascade calcs. for multiplicity and cross sections 0-32300
- <sup>12</sup>C + <sup>12</sup>C system, nuclear molecule microscopic description, HF and coupled channel calcs. 0-13493
- <sup>12</sup>C + <sup>6</sup>Li  $\rightarrow$  <sup>8</sup>He + <sup>2</sup>H + <sup>12</sup>C, three body phase space distrib. 0-37393
- <sup>12</sup>C(<sup>12</sup>C,<sup>12</sup>C), gross struct., barrier top resonance model calc. 0-9279
- <sup>12</sup>C(<sup>12</sup>C,<sup>12</sup>C), intermediate resonance, coupled channels calcs. 0-42611
- <sup>12</sup>C(<sup>12</sup>C,<sup>12</sup>C), elastic scatt., incoming wave boundary condition model calcs. 0-47504
- <sup>12</sup>C(<sup>12</sup>C,X) fusion cross section oscillations, overlapping compound states availability 0-9321
- <sup>12</sup>C(<sup>12</sup>C,p)X, 800 MeV/N, fireball and preequilibrium cross sections,  $\pi$  condensation proximity influence 0-27659
- <sup>12</sup>C(<sup>40</sup>Ar,X), 213 MeV/N, relativistic fragmentation, microscope and macroscopic calcs., np correlation 0-13495
- <sup>12</sup>C(<sup>40</sup>Ca,<sup>40</sup>Ca), 90° and 180° excitation functions energy depend., DWBA anal. 0-42582
- <sup>12</sup>C(<sup>6</sup>Li,d)<sup>16</sup>O\*, 18-28 MeV, configuration mixing effect and cross sections, zero range DWBA 0-42692
- <sup>12</sup>C(K $\pi^-$ ,  $\pi^-$ )<sup>12</sup>C\*, 800 MeV/c, ang. distrib. from DWIA calcs. 0-32225
- <sup>12</sup>C(e,  $\nu$ )<sub>e</sub> n interaction in quasifree scatt., nonrelativistic Hamiltonian through 4th order 0-47469
- <sup>12</sup>C(e,e

), cross sections from DWIA, optical, and shell model calcs. (Russian) 0-32270

<sup>12</sup>C(e,e), electroexcitation cross sections, incoherent superposition of single nucleon processes 0-32269

<sup>12</sup>C(e, $\pi$ ), total cross section from square reaction matrix element (Russian) 0-32271

<sup>12</sup>C( $\gamma,\pi^-$ ), 160-250 MeV, total cross section from elementary Hamiltonian model 0-18292

<sup>12</sup>C( $\gamma,\pi^-$ ), total cross section calc. in impulse approx. 0-13458

<sup>12</sup>C(p,p'), 800 MeV, multistep processes, ang. distrib., Glauber model anal. 0-47475

<sup>12</sup>C(p,p'), non-eikonal effects in high energy inelastic scatt. 0-42608

<sup>12</sup>C(p,p), pol. p, 450-600 keV, Mott-Schwinger interaction existence, anal. power 0-22805

<sup>12</sup>C(p,p) spin 0-spin 1/2 phase shift anal. discrete ambiguities 0-18307

## nuclear reaction and scattering theory continued

- <sup>12</sup>C(p,py), bremsstrahlung cross section near 1.7 MeV resonance, Feshbach-Yennie approx. 0-42662
- <sup>12</sup>C(p,pn), pol. nucleon quasi-elastic scatt., nuclear wave function and model tests 0-42656
- <sup>12</sup>C( $\pi^-$ , 2 $\gamma$ ), doubly radiative capture theory, branching ratio and ang. correlations 0-9314
- <sup>12</sup>C( $\pi^+$ d), DWBA cross section formula, PWBA differential cross section (Chinese) 0-22861
- <sup>12</sup>C( $\pi^+$ ,  $\pi^+$ ), model Coulomb corrections in eikonal 0-5171
- <sup>13</sup>C spectroscopic factors, cross sections DWBA anal. optical model parameters from <sup>12</sup>C(<sup>16</sup>O,X) 0-13371
- <sup>13</sup>C(<sup>12</sup>C,<sup>12</sup>C), mixed parity neutron orbits, coupled channel theory with adiabatic assumption 0-9304
- <sup>13</sup>C(<sup>12</sup>C,<sup>12</sup>C) 15, 87 MeV, elastic transfer exchange amplitude, coupled reaction channel and DWBA calcs. 0-32298
- <sup>13</sup>C(p, $\alpha$ )<sup>10</sup>B<sub>g.s.</sub>, 65 MeV, pol. p, DWBA form factor 0-52559
- <sup>13</sup>C(d,p), 800 MeV, cross sections, DWBA anal. 0-42667
- <sup>14</sup>C spectroscopic factors, cross sections DWBA anal. optical model parameters from <sup>12</sup>C(<sup>16</sup>O,X) 0-13371
- (<sup>12,13</sup>C,X) elastic, inelastic and single nucleon transfer excitation functions optical and DWBA anal. 0-13492
- Ca+Ca, classical many-body model for heavy ion collisions 0-536
- Ca( $\pi^+$ ,  $\pi^+$ ), model Coulomb corrections in eikonal 0-5171
- Ca(<sup>40</sup>Ca, X), 10 MeV/N, charged particle emission Q-value depend. 0-47503
- Ca(t,p), centre of mass corrections to DWBA overlap factors 0-18319
- Ca(<sup>3</sup>He,t), 66, 70 MeV, reaction mech. and <sup>48</sup>Sc Gamow-Teller strength, ang. distrib. 0-42589
- Ca(p,p), 1 GeV, elastic scatt. differential cross section calc. 0-47480
- C(d,d), 4.3, 6.3, 8.9 GeV/c, secondary momentum spectra, multiple scatt. model anal. (Russian) 0-27650
- <sup>52</sup>Cr(d,p)<sup>53</sup>Cr, Coulomb stripping, 2.12-2.48 MeV, DWBA anal., spectroscopic strengths 0-516
- <sup>63</sup>Cu levels and transition j-depend., DWBA anal. of <sup>60</sup>Ni(<sup>19</sup>F, <sup>16</sup>O) 0-42542
- <sup>154</sup>Eu(p,p'), 12 MeV, ground band rot. states, deformation parameters, coupled channels anal. 0-9195
- <sup>18</sup>F levels and resonances, cross sections in R-matrix formalism from <sup>17</sup>O(p, $\alpha$ ) 0-18267
- <sup>19</sup>F level struct., ang. distrib. anal. using DWBA of <sup>17</sup>O(<sup>3</sup>He,p) 0-9232
- <sup>19</sup>F levels, resonances and phase shifts, resonating group calcs. from <sup>15</sup>N( $\alpha,\alpha$ ) 0-32189
- <sup>19</sup>F(d,X), X=<sup>7</sup>Li, <sup>9</sup>Be, 13.6 MeV, diff. cross sections, <sup>5</sup>He cluster direct transfer (Russian) 0-52650
- <sup>19</sup>F(p,p), 17.5 and 30 MeV, low lying level cross-sections, coupled-channel method 0-42649
- <sup>54</sup>Fe( $\alpha,\alpha'$ ), coupled channels calc., capture cross section, GQR decay modes 0-27654
- <sup>54</sup>Fe(p,p'), 39, 62 MeV, DWBA anal., collective spectra, direct process contrib. (Russian) 0-13408
- <sup>55</sup>Fe Zp<sub>3/2</sub> neutron orbit radius isotone shift from DWBA anal. of <sup>54</sup>Fe(t,d) 0-32172
- <sup>56</sup>Fe(<sup>6</sup>Li, X), 75 MeV, Z=1 or 2 fast particle prod. mechanism above Coulomb barrier 0-42687
- <sup>56</sup>Fe(e,e'), 0.1-14 GeV, deep inelastic inclusive scatt. response functions and momentum distrib. 0-42640
- <sup>1</sup>H(n,n

), 210-495 MeV, free elastic scatt., phase shift anal. 0-52676

<sup>2</sup>H( $\alpha,\alpha$ ), quasi-elastic scatt., direct reaction unitarised impulse approx. 0-42674

<sup>2</sup>H( $\alpha,\alpha$ )<sup>4</sup>He, differential cross section and polarisation, three body model 0-47460

<sup>2</sup>H(e,e), EM interactions and mag. sum rules 0-42639

<sup>2</sup>H(e,e), energy weighted sum rules, almost realistic NN pot. anal. (Russian) 0-13465

<sup>2</sup>H( $\gamma,\pi^0$ ), coherent photoprod., binding effects and threshold amplitude calc. 0-32264

<sup>2</sup>H( $\gamma,\pi^0$ ), cross section and threshold effects using dynamical  $\gamma$ N $\rightarrow$ N $\pi^0$  model 0-27627

<sup>2</sup>H(p, $\pi^+$ )<sup>3</sup>H, 400, 470, 600 MeV, differential cross section using isobar model 0-9291

<sup>2</sup>H( $\pi,\pi$ ), expt. and theoretical work, present status, model testing,  $\pi$ N interaction 0-42699

<sup>2</sup>H( $\pi,\pi$ ), high energy total cross section in Glauber model 0-18346

<sup>2</sup>H( $\pi,\pi$ ), medium energy elastic scatt. amplitudes, covariant multiple scatt. model convergence test 0-42710

<sup>2</sup>H( $\pi,\pi$ ), relativistic description,  $\pi$ N waves, NN rescatt.,  $\rho$ -exchange,  $\pi$  absorption and emission 0-9310

<sup>2</sup>H( $\pi^-$ ,  $\pi^-$ ), 552 MeV/c, elastic differential cross section Glauber theory anal. (Russian) 0-52700

<sup>2</sup>H( $\pi^-$ ,  $\pi^-$ )pn, 438 GeV/c, break up process, kinematic variables, np final state interaction (Russian) 0-52701

<sup>3</sup>H doublet scatt. length, Phillips plot, N/D input parametrisation 0-42672

<sup>3</sup>H(e,e

2n), realistic NN interactions, three body variational wave functions, spectral functions 0-47470

<sup>3</sup>H(p, $\gamma$ )<sup>3</sup>He, intermediate energy, ang. distrib., reaction amplitude and <sup>3</sup>He vertices 0-22835

H(e<sup>+</sup>,e<sup>+</sup>)H, s-wave scatt., effective range expansion 0-47467

(<sup>3</sup>He,<sup>3</sup>He), 12-51.3 MeV, ang. distrib., S-matrix formalism frame anal., fission ingoing channel (Russian) 0-5152

<sup>3</sup>He( $\pi$ ,  $\pi$ )  $\Delta$ (1236) resonance region, Watson multiple scatt. series. integral eqns. 0-37402

<sup>3</sup>He(<sup>3</sup>He,d)<sup>3</sup>He, three body break up reaction energy spectra, computer program 0-27593

<sup>3</sup>He(<sup>3</sup>He,p)<sup>3</sup>He, three body break up reaction energy spectra, computer program 0-27593

<sup>3</sup>He(d,d), 0.32-5.0 MeV, anal. power, scatt. amps., <sup>3</sup>Li states, phase shift anal. 0-47382

<sup>3</sup>He(e, e), charge formfactors, second Born approx. and pole model 0-18155

<sup>3</sup>He(e,e'), 0.1-14 GeV, deep inelastic inclusive scatt. response functions and momentum distrib. 0-42640

<sup>3</sup>He( $\gamma$ ,p)<sup>3</sup>H, intermediate energy, ang. distrib., reaction amplitude and <sup>3</sup>He vertices 0-22835

<sup>3</sup>He( $\gamma,\pi^0$ ), cross section and threshold effects using dynamical  $\gamma$ N $\rightarrow$ N $\pi^0$  model 0-27627

<sup>3</sup>He( $\gamma,\pi^+$ )<sup>3</sup>H, Fermi motion and off-shell effects, impulse approx. 0-27626

<sup>4</sup>He(<sup>3</sup>He,<sup>3</sup>He), 60.2, 113.1 MeV, ang. distrib., optical and coupled channel anal., cross sections 0-47492



## nuclear reaction and scattering theory continued

- <sup>4</sup>He( $\alpha,\alpha$ ), composite particle scatt., generator coordinate and natural boundary condition methods 0-13489
- <sup>4</sup>He(d,d), pol. d, 12-17 MeV, differential cross sections, anal. powers, phase shift anal. 0-13449
- <sup>4</sup>He(d,pn)<sup>4</sup>He, differential cross section and polarisation, three body model 0-47460
- <sup>4</sup>He( $\gamma,\pi^0$ ), differential cross section, complex momenta theory for nondiffractive processes (*Russian*) 0-32266
- <sup>4</sup>He(p,p), 250, 350, 500 MeV, cross section energy depend., DWIA calcs. 0-37375
- <sup>4</sup>He(p,p), pol. nucleon quasi-elastic scatt., nuclear wave function and model tests 0-42656
- <sup>4</sup>He(p,d), intermediate energies, pion exchange currents in DWBA anal. 0-32199
- <sup>4</sup>He(p,d) pickup reaction, isobar configurations and short range correlations 0-22798
- <sup>4</sup>He(p,d)<sup>3</sup>He, 770 MeV, multiple-scattering approach 0-27636
- <sup>4</sup>He(p, $\pi^+$ ), pion prod. operator non-relativistic approx. 0-27640
- <sup>4</sup>He(p,p), 45-65 MeV, phase shift anal. 0-22832
- <sup>4</sup>He( $\pi,\pi$ ), A=3, 4, low energy scatt. length and phase calcs. 0-47508
- He(e<sup>+</sup>,e<sup>-</sup>)He, s-wave scatt., effective range expansion 0-47467
- <sup>16</sup>O( $\pi,\pi$ ), aligned deformed nuclei, cross sections and diffractive minima from eikonal approx. 0-22860
- <sup>4</sup>K, A=37,39, levels, excitation and microscopic form factors, DWBA calcs. from Ca(p, $\alpha$ ) 0-32185
- <sup>38</sup>K low lying 1<sup>+</sup>, T=0 states, DWBA anal. of <sup>40</sup>Ca(p,<sup>3</sup>He) 0-470
- <sup>139</sup>La(n, $\gamma$ ), non-statistical capture, radiative widths,  $\gamma$ -ray doorway state model 0-37389
- <sup>6</sup>Li( $\alpha,\alpha$ ), 59 MeV, elastic and inelastic, differential cross section systematic anal. 0-22845
- <sup>6</sup>Li(e,e), charge formfactors, second Born approx. and pole model 0-18155
- <sup>6</sup>Li(e,e), electroexcitation cross sections, incoherent superposition of single nucleon processes 0-32269
- <sup>6</sup>Li(p,pd), 590 MeV,  $\alpha$ -d motion, impulse distrib., cluster momentum distrib. 0-52679
- <sup>7</sup>Li(d,t), 12 MeV, nuclear vertex constant in peripheral model for virtual decay <sup>7</sup>Li $\rightarrow\alpha+t$  0-18295
- <sup>7</sup>Li( $\gamma,\pi^-$ ), total cross section calc. in impulse approx. 0-13458
- <sup>7</sup>Li(n,n) $\alpha$ t, three body sequential reactions, kinetics modelling 0-37371
- <sup>7</sup>Li(p, $\alpha$ ), 45 MeV, nuclear vertex constant in peripheral model for virtual decay <sup>7</sup>Li $\rightarrow\alpha+t$  0-18295
- <sup>7</sup>Li(p,d), 800 MeV, cross sections, DWBA anal. 0-42667
- <sup>23</sup>Mg hole states, transitions and spectroscopic factors, DWBA anal. of <sup>24</sup>Mg(p,d) 0-32161
- <sup>24</sup>Mg(p,p), 0.8 GeV, rot.,  $\gamma$  and  $\beta$  bands, ground state deformation, DWBA, coupled channels anal. 0-9198
- <sup>24</sup>Mg(p,p'), 20, 40, 800 MeV,  $\gamma$ -vibr. band, coupled channels anal. 0-9194
- <sup>24</sup>Mg(p,p), 18-44 MeV, differential cross sections, phase shift anal., energy depend. 0-47481
- <sup>26</sup>Mg( $\alpha,\alpha$ ), 104 MeV, oblate-prolate effects in struct. and reactions 0-9225
- <sup>26</sup>Mg(p, $\pi^+$ ), isobar configuration effects, p $\rightarrow\Delta^0\pi$  model, ang. distrib. (*Chinese*) 0-47484
- <sup>27</sup>Mg energy levels, spectroscopic factors, DWBA, Hauser-Feshbach anal. from <sup>26</sup>Mg(d,p) 0-52581
- <sup>53</sup>Mn low lying states, DWBA anal., shell model wave functions from <sup>56</sup>Fe(p, $\alpha$ ) 0-32211
- <sup>14</sup>N 1<sup>+</sup> state cross sections, effective two nucleon interaction, isovector tensor component from <sup>14</sup>C(p,n) 0-18208
- <sup>14</sup>N spectroscopic factors, cross sections DWBA anal. optical model parameters from <sup>12</sup>C(<sup>16</sup>O,X) 0-13371
- <sup>15</sup>N(n',n)<sup>15</sup>N, continuum random phase approx. 0-27635
- <sup>15</sup>N(p,p), 18-44 MeV, differential cross sections, phase shift anal., energy depend. 0-47481
- Na(Ne,X), 800 MeV/N, direct vs. thermal particle emission, inclusive cross sections 0-52688
- <sup>197</sup>Au fragment ang. and energy distrib., two-step model anal. of <sup>197</sup>Au(p,X) 0-52678
- <sup>97</sup>Nb high spin analogue resonance near N=50 neutron shell, DWBA anal. of <sup>96</sup>Zr(<sup>3</sup>He,d) 0-42613
- (Ne,  $\pi^-$ X), 800 MeV/A,  $\pi^-$  energy and ang. distrib., firebreak and hard scatt. model anal. 0-13498
- Ne+Ne, classical many-body model for heavy ion collisions 0-536
- <sup>40</sup>Ne breakup cross section, direct mechanism, DWBA anal. of <sup>40</sup>Ca(<sup>20</sup>Ne,<sup>16</sup>O) 0-18276
- <sup>20</sup>Ne+<sup>20</sup>Ne, 250-1000 MeV/N, intranuclear cascade calcs. for multiplicity and cross sections 0-32300
- <sup>20</sup>Ne(d,d), pol. d, 10-12 MeV, cross section, coupled channel and fluctuations anal. 0-27617
- <sup>20</sup>Ne(e,e $\alpha$ ), EM induced  $\alpha$  emission,  $\alpha$  spectroscopic amplitudes, anal. solvable model 0-32267
- <sup>20</sup>Ne( $\gamma,\alpha$ ), EM induced  $\alpha$  emission,  $\alpha$  spectroscopic amplitudes, anal. solvable model 0-32267
- <sup>21</sup>Ne states cross section, coupled channel and fluctuations anal. from <sup>20</sup>Ne(d,p) 0-27617
- <sup>41</sup>Ni(n,n), A=58,60,62,64, 5 MeV, differential cross sections, optical, statistical and coupled channel anal. (*Russian*) 0-37377
- <sup>58</sup>Ni(<sup>7</sup>Li,<sup>7</sup>Li'), 19 MeV, first 2<sup>+</sup> states Coulomb-nuclear interference, optical and DWBA anal. 0-22852
- <sup>58</sup>Ni(p,p), pol. p, 40 MeV, elastic and inelastic, asymmetries and differential cross sections (*Russian*) 0-27623
- <sup>58</sup>Ni( $\pi,\pi$ ), 162 MeV, elastic and inelastic ang. distrib., optical and PWIA anal. 0-42706
- <sup>60</sup>Ni deduced levels from <sup>58</sup>Fe(<sup>16</sup>O,<sup>14</sup>C)<sup>60</sup>Ni, DWBA anal., spectroscopic strengths 0-47380
- <sup>4</sup>O, A=17, 19, level scheme, two-step transfer contribs., coupled channel anal. from O(<sup>13</sup>C,X) 0-32181
- <sup>16</sup>O form factor effects, zero range DWBA calcs. from <sup>18</sup>O(p,t) 0-491
- <sup>16</sup>O induced reactions in nuclear emulsions at 2.1 GeV/nucleon, multiplicity distrib. of white and grey tracks (*Spanish*) 0-47495
- <sup>16</sup>O levels and ang. distrib., <sup>3</sup>He spectroscopic strengths, Hauser-Feshbach/DWBA anal. of <sup>13</sup>C(<sup>4</sup>Li,t) 0-47390
- <sup>16</sup>O+<sup>16</sup>O, fusion cross section gross struct., excitation functions, coupled channel method 0-52705
- <sup>16</sup>O+<sup>4</sup>He, group theory appl. to reaction studies 0-9276
- <sup>16</sup>O(<sup>12</sup>C,X), sub-barrier energies, fusion cross section, static and dynamic deformation effects 0-42729
- <sup>16</sup>O(<sup>16</sup>O,<sup>16</sup>O'), gross struct., barrier top resonance model calc. 0-9279

## nuclear reaction and scattering theory continued

- <sup>16</sup>O(<sup>16</sup>O,<sup>16</sup>O), Coulomb field effects using generalised JWKB method 0-13504
- <sup>16</sup>O(<sup>16</sup>O,<sup>16</sup>O), elastic scatt., incoming wave boundary condition model calcs. 0-47504
- <sup>16</sup>O( $\alpha,\alpha$ ), 28-33.6 MeV, forward peaking variation, DWBA with optical pots., ang. distrib. 0-13488
- <sup>16</sup>O( $\alpha,d$ ), 1.12 MeV, forward peaking variation, DWBA with optical pots., ang. distrib. 0-13488
- <sup>16</sup>O(e,e), T=1 level form factors, Helm model, pion photoprod. and muon capture appls. 0-52553
- <sup>16</sup>O( $\gamma,\pi^+$ ), differential cross section from elementary Hamiltonian model 0-18292
- <sup>16</sup>O( $\gamma,\pi^+$ ), threshold to 175 MeV, total cross sections, DWIA anal. 0-13459
- <sup>16</sup>O( $\mu,\mu$ ), recoil nucleus odd and even tensor orientations, general expressions 0-13451
- <sup>16</sup>O(n,n), elastic cross section, microscopic calc. 0-531
- <sup>16</sup>O( $\pi,\pi$ ), T-matrix from isobar-hole model, many-body corrections, optical pot. parameter 0-9312
- <sup>16</sup>O( $\pi,\pi$ ), three-body model of  $\pi$ N interaction using finite-binding pots. 0-42707
- <sup>16</sup>O(t,p), centre of mass corrections to DWBA overlap factors 0-18319
- <sup>17</sup>O(<sup>16</sup>B,<sup>1</sup>Li), 115 MeV, shell and semiclassical reaction model anal. 0-13494
- <sup>17</sup>O(<sup>12</sup>C,<sup>9</sup>Be), 115 MeV, shell and semiclassical reaction model anal. 0-13494
- <sup>17</sup>O(<sup>13</sup>C,<sup>10</sup>B), 105 MeV, shell and semiclassical reaction model anal., <sup>20</sup>F spins 0-13494
- <sup>17</sup>O(e,e), mag scatt., form factors, HF calcs., core polarisation effects 0-42579
- <sup>17</sup>O( $\gamma,n$ ), cross section, Lane-Lynn radiative capture mechanisms 0-52660
- <sup>18</sup>O, heavy ion excitation, single particle and core polarisation amplitude interference 0-5117
- <sup>18</sup>O(p,p), 18-44 MeV, differential cross sections, phase shift anal., energy depend. 0-47481
- <sup>18</sup>O( $\pi,\pi$ ), 164 MeV, yrast state and level excitation, DWIA calcs., shell model context 0-42526
- <sup>19</sup>F, A=31, 33, levels and transition j-depend., DWBA anal. for Si(<sup>19</sup>F,<sup>16</sup>O) 0-42542
- <sup>30</sup>P high spin two nucleon states decay props. from <sup>28</sup>Si( $\alpha,\gamma$ ) 0-13402
- <sup>208</sup>Pb, A=205-207, neutron hole states, spectroscopic factors, DWBA anal. of Pb(<sup>3</sup>He, $\alpha$ ) 0-47352
- <sup>208</sup>Pb( $\alpha,\alpha$ ), A=206, 208, 120 MeV, isoscalar resonance excitation, low lying transitions, DWBA calc. 0-512
- <sup>208</sup>Pb+<sup>208</sup>Ne(<sup>40</sup>Ar), 250-1000 MeV/N, intranuclear cascade calcs. for multiplicity and cross sections 0-32300
- <sup>208</sup>Pb(<sup>16</sup>O,<sup>16</sup>O'), 315 MeV, continuous spectrum and giant resonance excitation, coherent state model test 0-32252
- <sup>208</sup>Pb(<sup>86</sup>Kr,X), 610 MeV, deep inelastic ang. momentum transfer from sequential fission fragments 0-18325
- <sup>208</sup>Pb( $\alpha,\alpha$ ), 65 MeV, inclusive reaction, giant resonance background, heavy ion model anal. 0-5150
- <sup>208</sup>Pb(n, $\gamma$ ), fast, direct-semidirect and pure resonance model calcs. 0-47486
- <sup>208</sup>Pb(p,p'), 39, 62 MeV, DWBA anal., collective spectra, direct process contrib. (*Russian*) 0-13408
- <sup>208</sup>Pb(p,t)<sup>208</sup>Pb(3<sup>+</sup>), pol. p, 22 MeV, anal. power and (p,d)(d,t) sequential transfer processes 0-5119
- <sup>208</sup>Pb( $\pi,\pi$ ), 162 MeV, elastic and inelastic ang. distrib., optical and PWIA anal. 0-42706
- <sup>208</sup>Pb(t,p), centre of mass corrections to DWBA overlap factors 0-18319
- Pb(n,n), 14.0-17.4 MeV, neutron polarisation, ang. depend. diffraction struct. 0-18283
- <sup>141</sup>Pr(n, $\gamma$ ), non-statistical capture, radiative widths,  $\gamma$ -ray doorway state model 0-37389
- <sup>191</sup>Pt, A=192, 194, 196, states, J<sup>+</sup>, ang. distrib. and transitions, DWBA anal. of Pt(p,t) 0-468
- <sup>244</sup>Pu fission total kinetic energy release, excitation energy depend., scission point anal. of <sup>244</sup>Pu(<sup>3</sup>He, $\alpha$ f) 0-18351
- Pu( $\gamma,\gamma$ ) 12.754 MeV, Delbruck scatt., Coulomb correction terms, differential cross sections 0-27629
- <sup>32</sup>S levels and spectroscopic factors from pickup DWBA anal. of <sup>33</sup>S(<sup>3</sup>He, $\alpha$ ) 0-9235
- <sup>32</sup>S(n, $\gamma$ ), fast n, doorway structs. and single particle resonances, microscopic treatment 0-52646
- <sup>32</sup>S(n,n), 5 MeV, elastic and inelastic scatt., differential cross-sections, model anal. (*Russian*) 0-42668
- <sup>153</sup>Sb, A=123,125,127,129, cross-sections, ang. distrib., spectroscopic factors, DWBA anal. of Te(t, $\alpha$ ) 0-52572
- Sc fragment differential ranges and energy spectra from <sup>238</sup>U(p,X), reaction mechanisms 0-42666
- <sup>28</sup>Si(<sup>18</sup>O,X), 56 MeV, multinucleon transfers, ang. distrib., distorted wave and shell model anal. 0-27663
- <sup>28</sup>Si(<sup>19</sup>F,<sup>16</sup>O), 60 MeV, exact finite range DWBA and CCBA calcs. 0-538
- <sup>28</sup>Si(<sup>20</sup>Ne,X), 120 MeV, linear response theory anal., frictional coeffs. and energy dissipation 0-13502
- <sup>28</sup>Si(n, $\gamma$ ), fast n, doorway structs. and single particle resonances, microscopic treatment 0-52646
- <sup>28</sup>Si(n,n), 5 MeV, elastic and inelastic scatt., differential cross-sections, model anal. (*Russian*) 0-42668
- <sup>28</sup>Si( $\pi,\pi$ ), 162 MeV, elastic and inelastic ang. distrib., optical and PWIA anal. 0-42706
- <sup>152</sup>Sm(<sup>20</sup>Ne,<sup>20</sup>Ne), 70 MeV, A=148, 150, 152, Coulomb polarisation pot., coupled channel calcs. 0-22855
- <sup>118</sup>Sn(p,t), ang. distrib. and cross sections full finite range CCBA anal. 0-5141
- <sup>124</sup>Sn(p,p), threshold enhancement of parity violation, Born approx. 0-18191
- <sup>93</sup>Tc high spin analogue resonance near N=50 neutron shell, DWBA anal. of <sup>92</sup>Mo(<sup>3</sup>He,d) 0-42613
- <sup>232</sup>Th( $\alpha,\alpha$ ), 120 MeV, isoscalar giant resonances, DWBA anal. 0-42621
- <sup>7</sup>Ti(<sup>7</sup>Li,<sup>7</sup>Li'), A=46,48, 17 MeV, first 2<sup>+</sup> states Coulomb-nuclear interference, optical and DWBA anal. 0-22852
- <sup>46</sup>Ti(d,d), 7,10 MeV, ang. distrib., DWBA and Hauser Feshbach anal. 0-47377
- <sup>47</sup>Ti levels, DWBA and Hauser Feshbach anal., compound nucleus cross sections from <sup>46</sup>Ti(d,p) 0-47377
- <sup>48</sup>Ti(p,p), 1 GeV, elastic scatt., differential cross section calc. 0-47480



**nuclear reaction and scattering theory continued**

- <sup>51</sup>Ti Zp<sub>3/2</sub> neutron orbit radius isotope shift from DWBA anal. of <sup>50</sup>Ti (t,d) 0-32172  
 U(Ne,X), 250, 400 MeV/N direct vs. thermal particle emission, inclusive cross sections 0-52688  
<sup>233</sup>U( $\alpha$ ,X), 28-140 MeV, scatt. and fission reaction mechanisms, cross sections 0-18350  
<sup>238</sup>U + <sup>20</sup>Ne(<sup>40</sup>Ar), 250-1000 MeV/N, intranuclear cascade calcs. for multiplicity and cross sections 0-32300  
<sup>238</sup>U(HI,f), Coulomb fission cross sections from coupled channel calcs. 0-9319  
<sup>238</sup>U(e,e'f), 5.5-9 MeV, fission fragment ang. distrib. DWBA anal., low lying fissioning levels 0-42713  
<sup>238</sup>U(n, $\gamma$ ), cross section and resonance shape, gas molecule vibr. effects 0-42661  
<sup>238</sup>U(p,p'), 22 MeV, rot. band, multipole deformation parameters from coupled channel anal. 0-13369  
<sup>51</sup>V( $\alpha$ ,t), absolute normalisation from spin depend. sum rule anal. 0-27652  
 Zr-region, two nucleon transfer reactions, spectroscopic amplitudes, form factors, ang. distrib. 0-22779  
<sup>92</sup>Zr (p,p), A=92, 94, 2-6.5 MeV, optical and Lane model anal. comparison 0-18302  
<sup>90</sup>Zr(t,p), centre of mass corrections to DWBA overlap factors 0-18319  
<sup>92</sup>Zr(<sup>30</sup>Si,<sup>30</sup>Y), finite-range cluster-model description, DWBA approach 0-52667

**nuclear reactions and scattering**

- see also alpha particle-nucleus reactions; alpha particle-nucleus scattering; chemical effects of nuclear reactions and scattering; cosmic ray-nucleus reactions; cosmic ray-nucleus scattering; deuteron-nucleus reactions; deuteron-nucleus scattering; direct nuclear reactions and scattering; electron-nucleus reactions; electron-nucleus scattering; fission; form factors (nuclear); hadron-nucleus reactions; hadron-nucleus scattering; heavy ion-nucleus reactions; heavy ion-nucleus scattering; helium 3-nucleus reactions; helium 3-nucleus scattering; muon-nucleus reactions; muon-nucleus scattering; neutrino-nucleus reactions; neutrino-nucleus scattering; nuclear fusion; nuclear reaction and scattering theory; nuclear reactions involving few nucleon systems; nuclear resonance reactions and scattering; nuclear scattering involving few nucleon systems; nuclear spallation; nuclear spectroscopic factors; nucleosynthesis; photon-nucleus reactions; photon-nucleus scattering; polarisation in nuclear reactions and scattering; triton-nucleus reactions; triton-nucleus scattering  
 modern atomic and nuclear physics (book) 0-11  
 optical model, parabolic repulsion potential for scattering of <sup>6</sup>Li and <sup>9</sup>Be by light and medium nuclei 0-22782  
 (particle, xny), neutron multiplicity for gamma rays 0-37689

**nuclear reactions involving few nucleon systems**

- for nuclear inelastic scattering involving few nucleon systems see "nuclear scattering involving few nucleon systems"  
 few body systems, anal. coupling constant continuation for resonance and stripping reactions (Russian) 0-13435  
 three particle systems with Coulomb interaction, scatt. and breakup eqns. exact solns. 0-504  
<sup>2</sup>H + p(n), differential cross sections, Coulomb penetration factor in DWBA calc. (Chinese) 0-27603  
<sup>2</sup>H(<sup>3</sup>He,n)<sup>3</sup>He, fusion through metallic D 0-13517  
<sup>2</sup>H(<sup>3</sup>He,p), cross section meas., appl. in ion beam anal. 0-42673  
<sup>2</sup>H( $\alpha$ , np), 28.3 MeV, <sup>3</sup>Li (3/2<sup>-</sup>) tensor polarisation 0-13450  
<sup>2</sup>H(d,n), 13.6, 24.3 MeV, 0<sup>+</sup> absolute differential cross section 0-27649  
<sup>2</sup>H(d,n), 290, 460 keV, neutron polarisation, ang. depend. 0-42632  
<sup>2</sup>H(d,n)<sup>3</sup>He, 1.5-15.5 MeV, tensor anal. power, charge symmetry violation in mirror reaction 0-13368  
<sup>2</sup>H(d,p)<sup>3</sup>H, 13.4, 17 MeV, pol. d, anal. power direct reaction and isospin symmetries 0-515  
<sup>2</sup>H(d,p)<sup>3</sup>H, 1.5-15.5 MeV, tensor anal. power, charge symmetry violation in mirror reaction 0-13368  
<sup>2</sup>H(n, np)n, 17 to 27 MeV, neutron-neutron scattering length determination, Monte Carlo analysis 0-13476  
<sup>2</sup>H(p,2p)n, 28.6 MeV, breakup cross sections in collinear geometry 0-9296  
<sup>2</sup>H(p,n)2p, pol. n and p, 10.6-15.1 MeV, transverse polarisation transfer at 0<sup>+</sup> 0-42630  
<sup>2</sup>H(p,pn)p, 1.67 GeV/c, secondary particle ang. distrib. and correlations (Russian) 0-27646  
<sup>3</sup>H(<sup>4</sup>He, X), 50, 65, 78 MeV, quasifree scattering and quasifree reaction processes 0-13486  
<sup>3</sup>H(d,n), pol. d, below 6.75 MeV, tensor anal. power 0-42633  
<sup>3</sup>H(d,n)<sup>3</sup>He, neutron energy meas. with Si detector 0-32566  
<sup>3</sup>He(<sup>3</sup>He,X) 50, 65, 78 MeV, quasifree scattering and quasifree reaction processes 0-13486  
<sup>3</sup>He(d,p), pol. d, below 6.75 MeV, tensor anal. power 0-42633  
<sup>4</sup>He(p,<sup>3</sup>He), <sup>2</sup>H, large momentum transfers,  $\pi$  exchange effects 0-5143  
<sup>4</sup>He(p,d), intermediate energies, pion exchange currents in DWBA anal. 0-32199  
<sup>4</sup>He(p,d)<sup>3</sup>He, large momentum transfers,  $\pi$  exchange effects 0-5143

**nuclear reactor fuel** see fission reactor fuel**nuclear reactor instrumentation**

- AGR, Central Inertial Collector for removal of spalled oxide particles from coolant 0-5231  
 BR3 reactor, instrumentation for continuous monitoring of primary water B content (French) 0-32408  
 BWR, H<sub>2</sub> and O<sub>2</sub> monitoring in containment and off-gas systems 0-32414  
 BWR, in-service inspection and external base-line tests, instrumentation 0-784  
 BWR, method for detecting bypass coolant boiling 0-571  
 BWR noise, response of neutron detector to local coolant void distrib. 0-683  
 BWR power reactor, in-core startup system with neutron flux monitor 0-32405  
 CANDU nuclear power reactors, automated chemistry control system development 0-42738  
 CANDU self-powered flux detectors, response characts. 0-32404  
 CANDU-PHW, thermal neutron flux-mapping system 0-792  
 Compton recoil gamma-ray spectroscopy, current status 0-47808  
 containment structures pressure tightness verification, pressurisation plant, data acquisition and processing (Spanish) 0-13775  
 control rod drop damping and velocity meas. instrumentation (German) 0-5248

**nuclear reactor instrumentation continued**

- counting-Campbell channel for in-core and out of core neutron flux meas. 0-32406  
 Dounreay Fast Reactor, instrumentation developments since 1972 0-23118  
 fast flux reactor tests, neutron radiography facility 0-18371  
 fission counters, performance optimisation algorithm 0-47828  
 flowmeters for two-phase mass flow rate meas. during LOCA blowdown phase 0-778  
 fuel pin simulators for thermodynamic expts. with nucl. fuel elements 0-37420  
 gamma densitometer meas., anal. of dynamic bias 0-27730  
 gamma densitometry, static error evaluation 0-27729  
 gamma-ray densitometer, dynamic bias 0-27728  
 gas tagging, analytical design for optimization of tag gas isotopic compositions 0-23026  
 GCR He primary coolant impurity monitor 0-32413  
 HTGR, He circulators for primary coolant cycle, developmental and performance tests 0-597  
 impurity monitoring in liquid Na, electrochemical meters 0-22886  
 irradiated fuel, nondestructive devices for on-site examination 0-13699  
 k( $\infty$ ) meter for LWR spent fuel storage pools 0-37560  
 laboratory instructional programs in computer instrumentation at RPI 0-31472  
 laser scanning camera 0-52748  
 LMFBR blanket assembly cooling, flow regulating device 0-23029  
 LMFBR coolant temp. meas. using high integrity coaxial thermocouples 0-32410  
 LMFBR cooling circuit, calibration of EM flowmeters by average frequency method 0-570  
 LMFBR safety testing, scram signal generator for fluid motion monitoring 0-18551  
 LOFT reactor advanced instrumented center fuel bundle, in-reactor meas. devices for LOCA expts. 0-23024  
 MWR feedwater and recirculation flow, minicomputer-based digital control 0-23027  
 neutron counters, development, electron drift vel. in inert gas mixtures 0-48843  
 neutron detector response in water moderated reactor, influence of air bubbles 0-18442  
 neutron flux density monitor of non-flux perturbing thin foil 0-32522  
 neutron flux detection using self-powered Inconel-Inconel coaxial cable 0-42842  
 neutron flux monitoring during reactor refuelling and start-up, instrum. (Polish) 0-42792  
 neutron instrumentation for protection and control of nuclear reactors (French) 0-32407  
 neutron radiography facility at Texas A and M Nuclear Science Centre 0-9401  
 neutron spectroscopy using miniature detectors and preamplifiers 0-47669  
 primary-circuit components, surveillance of vibr. behaviour 0-790  
 PWR, equipment for the limitation of power density 0-697  
 PWR, fixed in-core gamma thermometer for neutron flux meas. 0-717  
 PWR, on-line meas. of B concentration in water using neutron absorption method (French) 0-32409  
 PWR coolant two-phase flow, meas. instrumentation 0-37550  
 PWR fuel assembly test instrumentation at LOFT facility 0-37551  
 PWR LOCE at LOFT facility, instrument calibration for mass flow rate meas. in two-phase flow 0-37552  
 PWR neutron flux detectors, reliability tests (French) 0-32403  
 PWR primary circuit component exam., development of automatic equipment 0-13559  
 PWR steam generators, remote controlled TV for detection of leaking tubes (French) 0-791  
 reactimeter, microprocessor based, nucl. engineering lab. class enhancement 0-36825  
 reactivity meter for LMFBR 0-32415  
 reactor diagnosis by acoustic meas. methods, magnetostrictive and piezoelec. high-temp.-resistant sensors 0-32411  
 reactor protection computer systems, statistical verification of reliability 0-32417  
 refractory metals, work function, ionising radiation effects meas. method 0-6951  
 reliability improvements of nuclear reactor instrumentation 0-32416  
 remote multiplexing appl., functional and cost analyses review 0-52752  
 RF local probe development for void fraction meas. 0-568  
 rod bundle blowdown heat transfer instrumentation, transient two-phase flow meas. 0-685  
 safety equipment, reliability in design 0-37555  
 safety related instruments qualification, impact of IEEE Std. (323-1974) 0-52753  
 seismic qualification of safety-related instrumentation cabinets 0-23063  
 self-powered detectors for in-core reactor neutron flux meas., detector signal composition 0-32402  
 spent fuel bundle counter, performance study 0-23064  
 spool piece, improved, for LOCE blowdown flow meas. 0-27727  
 subchannel void fraction by gamma scattering 0-27726  
 thin film fission thermocouples for energy deposition meas. in FBR safety expts. 0-47658  
 thin-film fission thermocouple detectors for reactors safety expts. 0-22987  
 two-phase flow system, local density measurements, side-scatter gamma technique 0-569  
 US flowmeter for LMFBR Na flow meas. 0-32412  
 US temp. profiling system for critical heat flux meas. of nuclear reactor fuel assembly 0-37032  
<sup>7</sup>Be, impurity in Li liq. in fusion reactor, control system 0-32466  
 Bi<sub>2</sub>Ge<sub>2</sub>O<sub>12</sub> scintillators, appl. as high energy gamma detectors 0-47827  
 Li, liq., impurity monitoring and control system for fusion reactor 0-32465  
<sup>6</sup>Li sandwich counter, meas. of neutron spectra in fast neutron systems 0-27884  
 Na loop, plugging meter behaviour obs., hydride and oxide deposition analysis 0-5207  
 Na valves for advanced reactors, reliability data collection at CREDO 0-22897  
 O<sub>2</sub> activity meas. in liquid Na, development of electrolytic probes 0-18550



nuclear reactor materials *see fission reactor materials*

nuclear reactor operation *see fission reactor operation*

nuclear reactor theory and design *see fission reactor theory and design*

nuclear reactors *see fission reactors*

# nuclear resonance reactions and scattering

*see also nuclear resonances*

A $\leq$ 28, giant quadrupole resonance, E2 intensity distrib., from ( $\alpha$ ,  $\alpha'$ ), DWBA anal. (*Hungarian*) 0-52642

average resonance parameter eval. and calcs., statistical model for capture process 0-18271

direct reactions, semiclassical time-indep. formulation in three-dimens with complex trajectories 0-27605

Doppler effect calcs., resonance data set choice in unresolved resonance region, sensitivity study 0-52651

fast reactor physics, assessment of JAERI fast group constants set version 2 0-602

few body systems, anal. coupling constant continuation for resonance and stripping reactions (*Russian*) 0-13435

heavy ion resonance reactions as orbiting cluster phenomena 0-47446

Rayleigh and Compton contribs. to nuclear resonance scattering of gamma rays, line inversion 0-39919

resonance analysis of neutron transmission data, least square fitting program REFIT 0-22840

thermonuclear reaction rate integrals, closed-form evaluation and approximation considerations 0-8535

( $\gamma$ , $\gamma$ ) processes using (n, $\gamma$ ) photons 0-18288

( $\gamma$ , $\gamma'$ ), spin, parity and width of resonance level 0-18287

( $\gamma$ ,n), spin, parity and width of resonance level 0-18287

(n, $\gamma$ ), A=94-190, resonance capture, low lying level population fluctuations,  $\gamma$ -rays 0-52619

(n, $\gamma$ ), mechanism in 3s size resonance, s-wave radiative width partition 0-37387

(n, $\gamma$ ), mechanism in 3s size resonance, radiative width statistical and valence effects 0-37388

NN resonances and total cross sections, expt. evidence review 0-42558

A( $\alpha$ ,ax)B type resonance reactions, chain struct. states (*Chinese*) 0-52645

<sup>27</sup>Al(n, $\gamma$ ), resonance capture, <sup>28</sup>Al E1 transitions and partial radiative widths 0-52618

<sup>10</sup>B(t,  $\alpha'$ )<sup>9</sup>Be\*(2s<sub>1/2</sub>), resonant spectra 0-22691

<sup>12</sup>C+n, TOF transmission meas. of neutron resonances 0-37374

<sup>12</sup>C(<sup>16</sup>O, <sup>12</sup>C\*), 45-53 MeV, <sup>12</sup>C\* m-substate population, spin alignment and excitation functions 0-42615

<sup>12</sup>C( $\pi$ ,X), angular distrib. of inelastic diffusion of  $\pi^+$  (*French*) 0-47507

<sup>14</sup>C(<sup>12</sup>C,X), 40-57 MeV, strong resonant behaviour in inelastic and transfer channels,  $\gamma$ -yields 0-52644

<sup>40</sup>Ca(<sup>40</sup>Ca,X), 400 MeV, fragment energy spectra struct., giant resonances, direct process 0-47452

<sup>52</sup>Cr( $\pi$ ,X), angular distrib. of inelastic diffusion of  $\pi^+$  (*French*) 0-47507

<sup>54</sup>Fe(n, $\gamma$ ), cross section, resonance and background interference 0-18310

<sup>57</sup>Fe, (n, $\gamma$ ), cross section, 2.5-200 keV, s-wave resonances 0-18309

<sup>58</sup>Fe(n, $\gamma$ ), resonance capture cross section s- and p-wave radiative widths 0-47476

<sup>3</sup>He ( $\pi$ ,  $\pi'$ )  $\Delta$ (1236) resonance region, Watson multiple scatt. series. integral eqns. 0-37402

<sup>24</sup>Mg(p,p), 15 MeV, excitation functions 0-22825

<sup>16</sup>O+n, 3-30 MeV, TOF transmission meas. of neutron resonances 0-37374

<sup>16</sup>O( $\pi$ , $\gamma$ n), direct and resonance reaction unified shell model, n,  $\gamma$  spectra 0-52696

<sup>18</sup>O( $\pi$ ,X), angular distrib. of inelastic diffusion of  $\pi^+$  (*French*) 0-47507

<sup>208</sup>Pb(n, $\gamma$ ), fast, direct-semidirect and pure resonance model calcs. 0-47486

<sup>239</sup>Pu(n, f), undisturbed resonance integral determ., and neutron flux meas. 0-5453

<sup>46</sup>Sc energy levels, resonances, spin and parity from <sup>45</sup>Sc(n, $\gamma$ ) 0-52673

<sup>28</sup>Si  $\alpha$ -doorway states in  $\alpha$ -decay to <sup>24</sup>Mg low lying K-band 0-47438

<sup>28</sup>Si( $\pi$ ,X), angular distrib. of inelastic diffusion of  $\pi^+$  (*French*) 0-47507

<sup>238</sup>U, giant E2 isoscalar resonance determ. 0-27607

<sup>238</sup>U neutron cross sections evaluation for incident neutron energies up to 4 keV 0-5146

<sup>238</sup>U(n, $\gamma$ ), cross section and resonance shape, gas molecule vibr. effects 0-42661

## nuclear resonances

*see also isobaric analogue resonances; nuclear collective states and giant resonances*

A=11, 12, energy levels, transitions and resonances, compilation 0-46743

A=60-140, spherical nuclei, two phonon admixture effect on M1 resonance (*Russian*) 0-5105

average resonance parameter eval. and calcs., statistical model for capture process 0-18271

conference on heavy ion reaction dynamical props., Johannesburg, S.Africa (Aug. 78) 0-17715

heavy ion fusion and transfer reactions, resonance effects 0-9283

hypernuclei, interdisciplinary viewpoint of theories and developments (*Czech*) 0-22749

irreducible spin precession theory applied to atomic and nuclear RF spectroscopy 0-27969

light heavy ion total reaction cross sections in diffraction model, resonance oscillations 0-13503

multidimensional barrier penetration and fission-widths, barrier resonance 0-13454

Nordheim integral treatment for resonance processing, proper use 0-37427

sd shell nuclei, (p, $\gamma$ ) resonance strengths 0-22786

statistical significance of spreading widths for doorway states, comments 0-27611

time delay of resonance wave packets, stat. model anal. 0-22802

(e,e), low-q, A=14 nuclei, isospin T=2, 1 and 0 collective resonances, shell model 0-510

( $\gamma$ , $\gamma'$ ), spin, parity and width of resonance level 0-18287

( $\gamma$ ,n), spin, parity and width of resonance level 0-18287

( $\gamma$ ,X), A=14 nuclei, isospin T=2, 1 and 0 collective resonances, shell model 0-510

(n, $\gamma$ ), mechanism in 3s size resonance, s-wave radiative width partition 0-37387

(n, $\gamma$ ), mechanism in 3s size resonance, radiative width statistical and valence effects 0-37388

(N,X), complex shell model, narrow resonances and bound states (*Chinese*) 0-42622

## nuclear resonances continued

( $\pi$ , $\gamma$ ), A=14 nuclei, isospin T=2, 1 and 0 collective resonances, shell model 0-510

<sup>26</sup>Al low energy resonances, decay and J $\pi$  assignments, branching ratios from <sup>25</sup>Mg(p, $\gamma$ ) 0-42624

<sup>27</sup>Al(<sup>12</sup>C,<sup>12</sup>C), 14-25 MeV, 180 $^\circ$  scatt. excitation function and ang. distrib. struct. 0-32253

<sup>197</sup>Au( $\alpha$ , $\alpha'$ ), 120 MeV, isoscalar resonance excitation, low lying transitions, DWBA calc. 0-512

<sup>9</sup>Be(e,e), longitudinal form factor for 1/2 $^+$  resonance 0-22682

<sup>209</sup>Bi( $\alpha$ , $\alpha'$ ), 120 MeV, isoscalar resonance excitation, low lying transitions, DWBA calc. 0-512

<sup>11</sup>C levels and resonance,  $\gamma$ -ray excitation curves from (p, $\alpha$ ), (p, $\gamma$ ) 0-9280

<sup>12</sup>C (<sup>16</sup>O, <sup>16</sup>O'), 19-23 MeV, intermediate width structs., ang. correlations, spins 0-13431

<sup>12</sup>C(<sup>12</sup>C, <sup>12</sup>C) intermediate struct. resonances, <sup>24</sup>Mg giant isoscalar quadrupole fission/fusion doorway states 0-37410

<sup>12</sup>C(<sup>12</sup>C, <sup>12</sup>C)<sup>2</sup>C\*, O<sub>2</sub><sup>+</sup>, 3<sub>1</sub><sup>-</sup>, 4<sub>1</sub><sup>+</sup> state excitation functions, resonance structures 0-42616

<sup>12</sup>C(<sup>12</sup>C, <sup>12</sup>C'), gross struct., barrier top resonance model calc. 0-9279

<sup>12</sup>C(<sup>12</sup>C, <sup>12</sup>C'), intermediate resonance, coupled channels calcs. 0-42611

<sup>12</sup>C(<sup>12</sup>C, <sup>12</sup>C), 13-14.1 MeV, Coulomb barrier resonance parameter direct determ., J $\pi$  assignments 0-513

<sup>12</sup>C(<sup>12</sup>C,x $\alpha$ ), 12-31.5 MeV, inclusive  $\alpha$ -particle yield, resonant like structs. 0-42691

<sup>12</sup>C(n, X), compound resonance decay based on bound and metastable single nucleon states (*Russian*) 0-5107

<sup>13</sup>C, TOF transmission meas. of neutron resonances 0-37374

<sup>40</sup>Ca(<sup>16</sup>O, <sup>16</sup>O), rot. band of molecular resonances, generator coordinate model 0-13428

<sup>40</sup>Ca(<sup>40</sup>Ca,X), deep inelastic, doubly differential cross section, spectra struct. 0-5103

<sup>40</sup>Ca( $\alpha$ , $\alpha'$ ), 6-18 MeV, resonances, anomalous large angle scatt. and quasi-molecular states 0-27613

<sup>40</sup>Ca( $\alpha$ , $\alpha'$ ), entrance channel resonances, backward angle scatt., elastic scatt. enhancement 0-27612

<sup>50</sup>Co f-wave resonances, inelastic p amplitudes, analogue state spectroscopic factors from <sup>54</sup>Fe(p,p' $\gamma$ ) 0-47451

<sup>52</sup>Cr( $\gamma$ , $\gamma'$ ), up to 12 MeV, highly excited spin-1 resonances,  $\gamma$ -transitions 0-13427

<sup>53</sup>Cr levels, J $\pi$ ,  $\gamma$ -transitions and 1626 eV resonance from <sup>52</sup>Cr(n, $\gamma$ ) 0-42610

Cu( $\pi^+$ , spallation) 0.6, 0.9, 12 GeV, T=1/2 resonances, Na, Sc and Co rel. yields 0-5109

(d,p), A=88-106, pol. d, excitation curve isospin anomaly, neutron single particle resonances 0-27595

<sup>4</sup>Es, A=255,256, fission barrier first peak height, pot. energy surface struct. 0-42720

<sup>18</sup>F J $\pi$ =3 $^-$  doublet at 6241 keV, isospin mixing from (p, $\gamma$ ), (p, $\alpha$ ), ( $\alpha$ , $\gamma$ ) (<sup>14</sup>N, $\alpha$ ) 0-511

<sup>18</sup>F levels and resonances, cross sections in R-matrix formalism from <sup>17</sup>O(p, $\alpha$ ) 0-18267

<sup>19</sup>F levels, resonances and phase shifts, resonating group calcs. from <sup>15</sup>N( $\alpha$ , $\alpha'$ ) 0-32189

<sup>56</sup>Fe( $\gamma$ , $\gamma'$ ), up to 12 MeV, highly excited spin-1 resonances,  $\gamma$ -transitions 0-13427

<sup>57</sup>Fe(n,X) transmission data up to 400 keV, J $\pi$  value for resonances 0-18311

<sup>58</sup>Fe(n, $\gamma$ ) capture and total cross section meas. below 325 keV, resonance parameters 0-18314

Fe(n,X), 3 eV-1 MeV transmission meas., resonance anal. 0-18316

Fe(n, $\gamma$ ) cross-section meas. principal resonance parameters 0-18312

<sup>255</sup>Fm, fission barrier first peak height, pot. energy surface struct. 0-42720

<sup>192</sup>Ir levels, resonances and low energy  $\gamma$ -rays from <sup>191</sup>Ir(n, $\gamma$ ) 0-47397

<sup>24</sup>Mg ( $\alpha$ , $\alpha'$ ) <sup>12</sup>C), 120 MeV, symmetric fission, resonances and average partial widths 0-42714

<sup>24</sup>Mg nuclear molecular resonances in <sup>12</sup>C-<sup>12</sup>C system from <sup>12</sup>C(<sup>16</sup>O, $\alpha$ ) 0-13430

<sup>140</sup>Mo(n, $\gamma$ ) A=98, 100 resonance parameters, capture  $\Gamma$ -rays and reaction mechanism 0-18272

<sup>14</sup>N, energy levels up to 11.05 MeV, transitions and resonance decay from <sup>13</sup>C(p, $\gamma$ ) 0-47376

<sup>20</sup>Ne excitation functions, resonance search from <sup>10</sup>B(<sup>14</sup>N, $\alpha$ ) 0-27614

<sup>20</sup>Ne non-isolated resonances, excitation functions and ang. distrib. from <sup>20</sup>Na(p, $\alpha$ ) (*Chinese*) 0-22788

<sup>20</sup>Ne resonances, J $\pi$ , excitation functions and branching ratio from <sup>19</sup>F(p, $\gamma$ ) 0-22787

<sup>4</sup>Ni(n,X) A=58, 60, transmission data, resonance anal. 0-18317

Ni(n, $\gamma$ ) cross-section meas. principal resonance parameters 0-18312

<sup>238</sup>Np levels, resonances and transitions from <sup>237</sup>Np(n, $\gamma$ ) 0-52589

<sup>16</sup>O+<sup>16</sup>O, fusion cross section gross struct., excitation functions, coupled channel method 0-52705

<sup>16</sup>O(<sup>16</sup>O, <sup>16</sup>O'), gross struct., barrier top resonance model calc. 0-9279

<sup>17</sup>O levels, resonances, J $\pi$  and radiative width from <sup>14</sup>N(t, $\gamma$ ) 0-47389

<sup>17</sup>O, TOF transmission meas. of neutron resonances 0-37374

<sup>17</sup>O( $\gamma$ ,n), 8.5-39.7 MeV, cross section, giant dipole and pygmy resonance decays 0-42619

<sup>188</sup>Os, muonic resonance spectra, deduced isomer shifts and electric moments 0-18948

<sup>29</sup>P resonance coherence widths from <sup>28</sup>Si(p,p), pol. p 0-32258

<sup>141</sup>P(n, $\gamma$ ), resonance parameters, s-wave radiative and reduced neutron widths 0-47471

<sup>4</sup>Pb( $\alpha$ , $\alpha'$ ), A=206, 208, 120 MeV, isoscalar resonance excitation, low lying transitions, DWBA calc. 0-512

<sup>208</sup>Pb( $\gamma$ ,n), 9.5-12 MeV, photoneutron ang. distrib., struct. below giant resonance 0-13444

<sup>209</sup>Pb excited states and 3/2 $^-$  resonances, shell model, calcs. from <sup>208</sup>Pb(n, n) 0-18262

<sup>32</sup>S(n,X), 2.5-1100 keV, resonance struct. from total and capture cross sections 0-42620

<sup>32</sup>S(n, $\gamma$ ), fast n, doorway structs. and single particle resonances, microscopic treatment 0-52646

<sup>32</sup>S(n, $\gamma$ ), single particle resonances and doorway states, K matrix formalism 0-37384

<sup>48</sup>Sc Gamow-Teller strength, ang. distrib., from <sup>48</sup>Ca (<sup>3</sup>He,t) 0-42589

<sup>28</sup>Si p3/2 neutron resonance  $\gamma$ -decay, partial rad. widths from Si(n, $\gamma$ ) 0-52617

<sup>28</sup>Si resonance wave functions and differential cross sections from <sup>27</sup>Al(p, n), (p, p), (p,  $\alpha$ ) 0-18261



**nuclear resonances continued**

- <sup>28</sup>Si(<sup>12</sup>C,<sup>12</sup>C), 27.8-31.5 MeV, elastic and inelastic excitation functions, fine struct., statistical anal. 0-18269  
<sup>28</sup>Si(<sup>12</sup>C,<sup>12</sup>C), entrance channel resonances, backward angle scatt., elastic scatt. enhancement 0-27612  
<sup>28</sup>Si(<sup>16</sup>O,<sup>16</sup>O), 30-32.7 MeV, elastic and inelastic excitation functions, fine struct., statistical anal. 0-18269  
<sup>28</sup>Si(<sup>16</sup>O,<sup>16</sup>O), entrance channel resonances, backward angle scatt., elastic scatt. enhancement 0-27612  
<sup>28</sup>Si(n,γ), fast n, doorway structs. and single particle resonances, microscopic treatment 0-52646  
<sup>28</sup>Si(n,γ), single particle resonances and doorway states, K matrix formalism 0-37384  
<sup>29</sup>Si neutron resonance, γ-spectra, partial and total radiative widths from <sup>28</sup>Si(n,γ) 0-42578  
<sup>151</sup>Sm, solid and liquid, neutron cross sections, Doppler effect meas. 0-22933  
<sup>159</sup>Tb, neutron resonances, time-of-flight spectra 0-27633  
<sup>4</sup>Ti(n,γ) A=46, 47, 49, 50, 45 MeV, cross section meas., resonance parameters 0-18315  
<sup>238</sup>U virtual photon excited state decay and total cross section of <sup>238</sup>U(e,n) 0-22757  
<sup>238</sup>U, neutron resonance parameters, time-of-flight spectroscopy 0-47375  
<sup>172</sup>Yb, muonic resonance spectra, deduced isomer shifts and electric moments 0-18948

**nuclear scattering** *see nuclear reactions and scattering***nuclear scattering involving few nucleon systems**

- few body systems, anal. coupling constant continuation for resonance and stripping reactions (*Russian*) 0-13435  
 quantum three-body problem, distorted Faddeev eqns. with coupled channel approach 0-52635  
 three body scatt., spline function moment methods 0-505  
 three particle systems with Coulomb interaction, scatt. and breakup eqns. exact solns. 0-504  
 three particles with Coulomb interaction, binding energy and scatt. states (*Russian*) 0-5051  
 three-body scatt. problem, cluster expansions, effective intercluster pots. 0-5082  
<sup>1</sup>H(d,d), 2 GeV, polarised d, tensor and vector asymmetries 0-9285  
<sup>1</sup>H(n,n,p), 210-495 MeV, free elastic scatt., phase shift anal. 0-52676  
<sup>1</sup>H(n,p), pol. n and p, 220-495 MeV, free elastic scatt., D<sub>1</sub> and P parameters 0-52674  
<sup>1</sup>H(n,p), pol. n and p, 220-495 MeV, free elastic scatt., Wolfenstein parameters R<sub>1</sub>, A<sub>1</sub> 0-52675  
<sup>2</sup>H(α,α)<sup>2</sup>H, 6 to 14 MeV, cross section meas. 0-27655  
<sup>2</sup>H(p,p)n, 23, 39.5 MeV, noncoplanar reaction, breakup cross section 0-530  
<sup>2</sup>H(p,p'), 0.6-25 GeV, backward emitted proton inclusive spectra, short range correlation 0-32281  
<sup>2</sup>H(p,p), backscattering, large momentum transfers, π exchange effects 0-5143  
<sup>3</sup>He(p,p), generator coord. method study of <sup>4</sup>Li 0-27581  
<sup>3</sup>He(p,p), pol. p, 0.3-1.0 MeV, differential cross section, anal. power, and phase shifts 0-42629  
<sup>4</sup>He(d,d) pol. d, 17-43 MeV, vector anal. power, highly excited six nucleon system 0-47458  
<sup>4</sup>He(d,d), pol. d, 12-17 MeV, differential cross sections, anal. powers, phase shift anal. 0-13449  
<sup>4</sup>He(p,p), 45-65 MeV, phase shift anal. 0-22832  
<sup>4</sup>He(p,p), A=3,4, backscattering, large momentum transfers, π exchange effects 0-5143

**nuclear screening**

- atom, many-electron, using Slater's value of at. screening parameters 0-912  
 atomic electron screening and correlations, effects on internal conversion coeffs. 0-18237  
 atomic np<sup>2</sup>(n+1)s excited-state config. quadrupole moments, Sternheimer shielding factor, of N(P)(As)(Sb) 0-37755  
 diatomic molecule, nucl. spin-rot. interaction const., electron spin current contrib. 0-23441  
 first row elements, ground state, self-consistent orbitals with uniform long-range behaviour 0-9485  
 highly ionised atoms, dipole and quadrupole polarisabilities, extrapolation method calcs. 0-9534  
 induction energy between neutral spherical S-state atoms, nonexpanded multipoles 0-23485  
 ionic crystal, Sternheimer antishielding factors of F<sup>-</sup>, Cl<sup>-</sup>, Br<sup>-</sup> and I<sup>-</sup>, approx. free- and cryst.-ion pot. influence 0-39544  
 magnetic shielding constants calc. by GIAO method using Gaussian functions 0-1001  
 metal, single-particle density matrix, perturbation expansion 0-54635  
 paramagnetic systems, NMR shifts calc. using nonmultipole expansion method 0-2651  
 polystyrene, chem. shift, conformational struct. (*Russian*) 0-5652  
 polyvinylpyridines, atactic, chem. shift, conformational struct. (*Russian*) 0-5652  
 Sternheimer shielding parameters role in core electronic and nucl. splittings 0-43106  
 Sternheimer valence shielding and antishielding factors for 2p and 3p ats. and ions 0-18807  
 tetrafluoromethane, bond length and chemical shielding, NMR lineshape anal. of multiplet system 0-32741  
 CO, one-electron props., SCF and CI calcs. 0-27951  
<sup>13</sup>C, shielding consts. and anisotropy of NMR shielding tensor, modified CNDO/S calcs. (*French*) 0-32610  
 H halides, spin-orbit coupling effect on proton mag. shielding 0-23440  
 H<sup>+</sup> chemical shifts, INDO calcs. 0-32743  
 HF, NMR shielding consts. and mag. susceptibilities, coupled HF with extended GTO basis 0-5480  
 Li, dipole (quadrupole) polarisabilities, shielding factors, using hydrodynamic analogy 0-52905  
 LiH, NMR shielding consts. and mag. susceptibilities, coupled HF with extended GTO basis 0-5480  
 N<sub>2</sub>, one-electron props., polarisabilities and polarisability derivatives, SCF and CI calcs. 0-37746  
 (NbCl<sub>5</sub>Br<sub>5-n</sub>)<sup>-</sup> complexes in acetonitrile soln., <sup>93</sup>Nb spin relax. and mag. shielding 0-44944  
 PH<sub>3</sub>, NMR shielding consts. and mag. susceptibilities, coupled HF with extended GTO basis 0-5480

**nuclear screening continued**

- <sup>31</sup>P, shielding consts. and anisotropy of NMR shielding tensor, modified CNDO/S calcs. (*French*) 0-32610  
 Pb(NO<sub>3</sub>)<sub>2</sub>, nucl. mag. shielding tensors of <sup>207</sup>Pb<sup>2+</sup>, NMR obs. 0-44939

**nuclear shape**

- see also nuclear collective states and giant resonances; nuclear energy levels; nuclear resonances*  
 A=190, Nilsson strength fragmentation, quadrupole and hexadecapole deformations 0-47394  
 asymmetric rotator, yrast states, wobbling freq., boson representation 0-32167  
 band structures, generalised HFB approach in intrinsic frame of reference, equilib. deformation 0-22664  
 Coulomb effect in rotating nuclei in the Thomas-Fermi approach 0-47355  
 deep inelastic heavy ion collision, shape relaxation and fragment deformation 0-22683  
 deformed nuclei, bandcrossing in K≠0 bands, odd-A rare earths 0-5045  
 deformed nuclei, even-even, phonon space and giant resonances (*Russian*) 0-52641  
 deformed nuclei, single particle matrix elements of radiative M2-transitions, Nilsson model 0-22753  
 deformed nuclei, static isoscalar and isovector polarisability, isovector K=±1<sup>+</sup> modes 0-32260  
 deformed rare earth nuclei, bandcrossing in K≠0 bands, backbending 0-9204  
 even-even and odd A nuclei, nuclear shapes and motions, review 0-5054  
 even-even deformed nuclei, collective K<sup>π</sup>=0<sup>+</sup> states, realistic boson expansion comparison 0-5043  
 even-even nuclei, z=6 to 100, probable members of quasi-bands in spherical and deformed regions 0-13357  
 even-even nuclei with A≈150, excited states calculation, phenomenological models: band-mixing, vibrational-rotational and interacting-boson model 0-22653  
 even-even spherical nuclei, 2<sub>1</sub><sup>+</sup> state deformation parameter from (p,p) and EM excitation 0-27549  
 ground state deformation energy, rot. band inertial parameter depend. 0-18185  
 heavy ion fusion and deep inelastic scatt., shape degrees of freedom, classical dynamic model 0-22876  
 heavy ion induced deep inelastic transfer, decay of binary nuclear system 0-22848  
 large deformations and dissipation in a random-matrix model approach for fission or colliding nuclei 0-18162  
 light deformed nuclei, stability, shape, Hartree-Fock calcs. (*Russian*) 0-52568  
 Muonic atoms, X-ray vacuum corrections, nuclear moments, transitions and deformation parameters 0-37912  
 Nilsson states, asymptotic quantum numbers for prolate and oblate deformations 0-9226  
 nucleus-nucleus pot., static polarisation effects, nuclear shapes 0-5154  
 self-consistent field rearrangement in large nuclear deformations, HF calcs. 0-18184  
 spherical nuclei, isomer and isotope shifts, theory of finite Fermi systems 0-39929  
 spherical nuclei, odd, l-forbidden M1 conversion transitions, penetration matrix elements 0-22763  
 spin-isospin density phase in finite nuclei, strongly oblate shape 0-22746  
 spontaneous fission mass parameters, cranking and hydrodynamic models, deformation depend. (*Russian*) 0-13511  
 strongly deformed nuclei, shortlived states, g-factor meas. method 0-52577  
 transitional nuclei, single particle and collective degrees of freedom coupling (*Russian*) 0-13345  
 unified nuclear pot. for heavy ion elastic scatt., fission, fusion, masses and deformations 0-5189  
 volume and surface vibr. relations, quantum hydrodynamics 0-9227  
 (n,γ), interacting boson and Nilsson model tests, Pt-Os transition region 0-37380  
 (p,p), A=9 to 70, differential cross sections, struct. effects, optical and coupled channel anal. 0-47482  
 (π<sup>-</sup>, X) slow pion capture in deformed nuclei, effects on high spin state excitation 0-18345  
<sup>232</sup>Th(α, α'), coupled channel Born anal. of deformation correl 0-5149  
<sup>109</sup>Ag (<sup>40</sup>Ar, X), α-decay amplification in superdeformed nuclei, high ang. momentum deexcitation 0-22776  
<sup>240</sup>Am<sup>m</sup>, spontaneously fissioning isomer optical shift in pumped <sup>8</sup>S<sub>7/2</sub>-<sup>10</sup>P<sub>7/2</sub> transition, nuclear deformation 0-27971  
<sup>38</sup>Ar high spin state density, γ-decay mode, deformed states from <sup>35</sup>Cl(α,py) 0-32168  
<sup>197</sup>Au(<sup>40</sup>Ar,X), 240 MeV, fragment shape deformation in deep inelastic collisions 0-47365  
<sup>10</sup>B, triaxial deformation in shell model non-central forces, projected HF calc. 0-13367  
<sup>9</sup>Be deformed nucleus, continuum states in strong coupling model 0-22682  
 Bi(Kr,X), strongly damped collisions, classical dynamical model with shape deformation 0-27658  
 Bi(Xe,X), strongly damped collisions, classical dynamical model with shape deformation 0-27658  
<sup>12</sup>C(<sup>16</sup>O, <sup>16</sup>O), 35 to 50 MeV, backscatt., dynamic deformation and excitation functions, optical anal. 0-18227  
<sup>42</sup>Ca high spin state density, γ-decay mode, deformed states from <sup>39</sup>K(α,py) 0-32168  
<sup>59</sup>Co, deformation effect of aligned target, fast-neutron transmission 0-47364  
<sup>52</sup>Cr(γ,γ'), 35 MeV, 2<sup>+</sup> state deexcitation γ-rays, differential cross sections, deformation (*Russian*) 0-13406  
 Dy, deformed nuclei, quasicontinuum γ-spectrum, M1, E1, E2 components 0-498  
<sup>Δ</sup>Dy, (A=151,152), high spin yrast states, γ-ray polarisation in (<sup>32</sup>S,n) reactions 0-497  
<sup>152</sup>Dy yrast trps, isomers and oblate deformations from <sup>124</sup>Te(<sup>32</sup>S, 4n) 0-13362  
<sup>153</sup>Dy, populated in <sup>153</sup>Ho β-decay, lower excited states 0-22765  
<sup>Δ</sup>Er (A=156,157,158), high spin yrast states, γ-ray polarisation in (<sup>32</sup>S,xn) reactions 0-497  
<sup>164</sup>Er deformed nucleus, excited rot. bands, selfconsistent HFB treatment 0-42515



## nuclear shape continued

- <sup>154</sup>Eu(p,p'), 12 MeV, ground band rot. states, deformation parameters, coupled channels anal. 0-9195  
<sup>147</sup>Gd<sup>m</sup> high spin yrast trap, oblate deformation and quadrupole moment 0-32157  
<sup>150</sup>Gd, high spin states, pairing correlations and nuclear shape, HFB approach 0-42517  
<sup>154</sup>Gd multiphonon vibr. bands, dynamic deformation theory 0-5035  
<sup>6</sup>He, density distribution function of nucleons 0-22650  
<sup>188</sup>Hg, HF calc., shape and lowest band struct., B(E2) values 0-32148  
<sup>165</sup>Ho( $\pi,\pi$ ), aligned deformed nuclei, cross sections and diffractive minima from eikonal approx. 0-22860  
<sup>123</sup>I, bands and decay props., core-particle coupling and polarisation effects 0-13354  
<sup>183</sup>Ir levels excited in ( $\alpha,xn$ ) reactions rel. to shape of Ir nucleus 0-9231  
<sup>24</sup>Mg(p,p'), 0.8 GeV, rot.,  $\gamma$  and  $\beta$  bands, ground state deformation, DWBA, coupled channels anal. 0-9198  
<sup>26</sup>Mg ( $\alpha,\alpha$ ), 104 MeV, oblate-prolate effects in struct. and reactions 0-9225  
<sup>4</sup>Ni(<sup>40</sup>Ca, fusion), A=58, 60, 62, 113-170 MeV, fusion cross sections and excitation functions 0-32315  
<sup>16</sup>O(<sup>12</sup>C,X), sub-barrier energies, fusion cross section, static and dynamic deformation effects 0-42729  
<sup>16</sup>O( $\alpha,\alpha$ ) 17 to 27 MeV, backscatt., dynamic deformation and excitation functions, optical anal. 0-18227  
<sup>208</sup>Pb(<sup>16</sup>O,X), 80-313 MeV, optical model anal., dynamic shape or density changes 0-18186  
<sup>196</sup>Pt, O(6) symmetry of interacting boson approx. model in shape transition 0-27550  
<sup>240</sup>Pu, hexadecapole shape isomeric state, shell correction method fission barrier calcs. 0-545  
Sm isotopes, shape transition, s-d IBA model Hamiltonian struct. 0-32173  
<sup>4</sup>Sm(<sup>16</sup>O,X), 60-75 MeV, A=148, 150, 152, 154 deformation effects on fusion 0-18360  
<sup>151</sup>Sm, gamma spectra, energy levels (*Dutch*) 0-47430  
<sup>152</sup>Sm (n,n), 2.4-7.2 MeV, inelastic and elastic optical model and deformation parameter depend. (*Russian*) 0-13481  
<sup>235</sup>Th( $\gamma,f$ ), deep subthreshold photofission, double humped fission barrier anal., shape isomer 0-5179  
<sup>4</sup>U( $\alpha,\alpha'$ ), A=234, 236, 238, coupled channel Born anal. of deformation correl. 0-5149  
<sup>4</sup>U( $\gamma,f$ ), A=235, 236, 238, deep subthreshold photofission, double humped fission barrier anal., shape isomer 0-5179  
<sup>236</sup>U fission shape isomer,  $\gamma$ -decay from <sup>235</sup>U( $\gamma,2n$ ) 0-18230  
<sup>236</sup>U, nuclear matter density distrib., in asymmetric two centre shell model 0-32209  
<sup>238</sup>U(e,e'), 87.5 MeV, deformed fissionable nucleus, giant multipole resonances and isovector states 0-42612  
<sup>238</sup>U(p,p'), 22 MeV, rot. band, multipole deformation parameters from coupled channel anal. 0-13369

## nuclear shell model

- A=16 to 40, mag. moments, shell model calcs, mesonic exchange current effects, book contrib. 0-479  
A=190, Nilsson strength fragmentation, quadrupole and hexadecapole deformations 0-47394  
A=40-56, spectroscopy props. using pure configuration shell model (*Chinese*) 0-42584  
A $\leq$ 44, fp-shell nuclei struct., effect of core-excitation and  $\alpha$ -clustering correl. 0-9245  
boson model, interacting, shell-model basis, correspondence between fermion and boson states and operators 0-52593  
conference on interacting bosons in nuclear physics, Erice, Italy (June '78) 0-27042  
Davidson's algorithm with and without perturbation corrections 0-27570  
deformed nuclei, single particle matrix elements of radiative M2-transitions, Nilsson model 0-22753  
double folding pot. for inelastic scatt. between nuclei 0-13425  
double well cluster shell model folding potential (*Chinese*) 0-52596  
effective Hamiltonian, form throughout sd shell 0-27571  
eigenvector component nongaussian distrib., statistical study 0-5077  
even-even nuclei, 1<sup>+</sup> excitations, self consistent shell model description (*Russian*) 0-13407  
even-even rare earths, microscopic quadrupole and hexadecapole moments 0-13376  
Fano effect in photonuclear reactions? 0-519  
Hamiltonians, semiclassical approx., spin-independ. pots. 0-32208  
Hartree-Fock-Bogolubov eqns., exact soln. 0-27582  
heavy ion reactions, cluster correlation, review, book contrib. 0-27670  
high-spin states and shell struct. in N=Z nuclei, <sup>20</sup>Ne appl. 0-47342  
hypernuclei, interdisciplinary viewpoint of theories and developments (*Czech*) 0-22749  
interacting boson model, collective motion descript., shell model test 0-27542  
interacting boson model, collective state description, shell model connection 0-37341  
interacting boson model, shell model and microscopic nuclear struct. 0-27575  
interacting boson model, shell model description 0-27574  
interacting boson model, shell model fermion Hamiltonians with monopole and quadrupole pairing 0-27576  
interacting boson model, shell model foundation 0-37340  
isobaric distributions in deep inelastic reactions 0-18270  
large amplitude collective motion, semiclassical approach, degenerate shell model appl. 0-27535  
light nuclei, props. from double well cluster shell model 0-27572  
neutron skin, compared with droplet model theory 0-52599  
Nilsson states, asymptotic quantum numbers for prolate and oblate deformations 0-9226  
optimum atomic mass formula from nuclear mass shell and parity corrections (*Russian*) 0-37902  
photonuclear sum rules from continuum calcs., dependence on residual interactions 0-22807  
proton-neutron basis, decomposition matrix rel. to basis of specified isospin T 0-37337  
proton-neutron multiplets, odd-odd nuclei, parabolic Regge trajectories, exchange of quadrupole phonon 0-52590  
quadrupole moments and rms charge radii, shell model calcs. 0-47369  
rapidly rotating nuclei, high spin rot. including shell fluctuations, semiclassical description 0-47348

## nuclear shell model continued

- rotational band termination, shell model calcs. in sd shell 0-32145  
shell correction accuracy calc. (*Russian*) 0-37338  
single-particle level density, excitation dependence of nuclear level density parameter, shell effects 0-32149  
single-particle motion in nucleus, forces between constituent nucleons, shell model 0-47408  
spectroscopic investigation of decaying states using continuum shell model 0-486  
strength functions, shell model calc. 0-32187  
total single particle energies, energy and N-averagings in shell correction method 0-22671  
two-body interaction, shell model calc. matrix elements 0-42567  
two-body shell model matrix elements by Taylor-series method 0-32212  
two-body spin-orbit interaction matrix elements, shell model (*Chinese*) 0-47356  
two-nucleon reduced widths in symmetric two-centre shell model 0-32213  
valence nucleon effective interactions 0-9244  
valence nucleons, muonic atom analysis 0-27530  
 $\Delta(33)$  interaction with nucleus, effective shell model pot., pion scatt. test 0-32202  
(e,e), low-q, A=14 nuclei, isospin T=2, 1 and 0 collective resonances, shell model 0-510  
(e,e') quasi-free scatt., spectral function, sum rule discrepancy, shell model deviation 0-42641  
( $\gamma,X$ ), A=14 nuclei, isospin T=2, 1 and 0 collective resonances, shell model 0-510  
(n, $\gamma$ ), interacting boson and Nilsson model tests, Pt-Os transition region 0-37380  
(N,X), complex shell model, narrow resonances and bound states (*Chinese*) 0-42622  
( $\pi,\gamma$ ), A=14 nuclei, isospin T=2, 1 and 0 collective resonances, shell model 0-510  
<sup>27</sup>Al( $\gamma,p$ )<sup>26</sup>Mg, energy and angular distribution (*Korean*) 0-18289  
<sup>76</sup>As, level structure, transitions and J<sup>π</sup>, from <sup>76</sup>Ge(p, $\gamma$ ) 0-47379  
<sup>10</sup>B, triaxial deformation in shell model non-central forces, projected HF calc. 0-13367  
<sup>1</sup>B(p,n)<sup>11</sup>C, shell model anal. of polarisation-analysing power differences 0-22804  
<sup>126</sup>Ba backbending, shell model calc., pair realignment and Coriolis antipairing 0-32164  
<sup>8</sup>Be lowest negative parity state, shell and cluster model calcs. from <sup>7</sup>Li(p,p), <sup>8</sup>Be lowest negative parity state, shell and cluster model calcs. 0-18205  
<sup>8</sup>Be spontaneous fission pot. energy curve, cluster shell model (*Chinese*) 0-22867  
<sup>12</sup>Be, Hartree-Fock calculations of nuclear bulk properties with density- and starting-energy dependent effective interaction 0-9246  
C(<sup>16,17</sup>O,<sup>16,17</sup>O), two centre shell model, molecular single particle states at level crossings 0-47354  
<sup>12</sup>C, centre-of-mass spuriousity in continuum shell-model calculations 0-32210  
<sup>12</sup>C(e,e'), cross sections from DWIA, optical, and shell model calcs. (*Russian*) 0-32270  
<sup>12</sup>C( $\gamma,\pi$ ), 340-380 MeV, quasi-free photoprod., impulse and shell model anal. (*Russian*) 0-5124  
<sup>12</sup>C(n,n), <17 MeV, resonating group calcs., phase shifts and differential cross sections 0-32275  
<sup>12</sup>C( $\pi^-, \gamma$ )<sup>12</sup>B\*, excitation of collective states, shell model 0-22652  
<sup>13</sup>C, photoexcited giant dipole resonance, continuum shell model anal. 0-18266  
<sup>13</sup>C( $\pi,\pi'$ ), 162 MeV, pure n and p transitions, differential cross sections 0-5040  
<sup>13</sup>C 0.74 MeV 5/2<sup>+</sup> state g-factor, shell model interpretation from <sup>3</sup>H(<sup>13</sup>C,p) 0-32176  
<sup>4</sup>Ca, (A=43-46), pairing force, seniority number 0-27563  
<sup>4</sup>Ca= A=40, 48, Hartree-Fock calculations of nuclear bulk properties with density- and starting-energy dependent effective interaction 0-9246  
<sup>40</sup>Ca( $\alpha,\alpha$ ), giant isoscalar quadrupole resonance,  $\alpha$ -over p-decay ratio, SU(3) and shell model 0-27608  
<sup>37</sup>Cl(v,e)<sup>37</sup>Ar, shell model cross section calc., appl. to cosmic ray and background elimination (*Russian*) 0-5131  
<sup>54</sup>Cr levels, transitions, T<sub>1/2</sub>, J<sup>π</sup>, shell model anal. from <sup>51</sup>V( $\alpha,\gamma$ ) 0-47381  
<sup>152</sup>Eu, isomeric levels and transitions, Nilsson model 0-18195  
<sup>4</sup>F, A=18, 19, E2 transition rates calc., shell model with effective interaction and charges 0-47423  
<sup>18</sup>F, semi-microscopic calc. of  $\alpha$ -cluster states, shell model approx. 0-465  
<sup>4</sup>Fe, A=54-56, high spin states, energy levels, spectroscopic factors, EM props., shell model 0-47359  
<sup>56</sup>Fe, shell model wave functions from <sup>56</sup>Fe(p, $\alpha$ ) 0-32211  
<sup>4</sup>Fm(n,f), A=253, 255, 257, 259, fission mass distrib. transition, liquid drop and shell model calcs. 0-32310  
<sup>4</sup>Fm(sf), A=254, 256, 258, 260, fission mass distrib. transition, liquid drop and shell model calcs. 0-32310  
<sup>71</sup>Ga(v,e)<sup>71</sup>Ge, shell model cross section calc., appl. to cosmic ray and background elimination (*Russian*) 0-5131  
<sup>150</sup>Gd, high spin states, pairing correlations and nuclear shape, HFB approach 0-42517  
<sup>4</sup>He, shell model calcs. 0-13393  
<sup>4</sup>He, density distribution function of nucleons 0-22650  
Hf-Os region, high lying states, Nilsson strength fragmentation 0-42539  
<sup>4</sup>Hg, quadrupole moment, change between first 5/2<sup>-</sup> states for A=197,199, shell model anal. 0-52576  
<sup>4</sup>Ho, A=153, 160, isomeric levels and transitions, Nilsson model 0-18195  
<sup>6</sup>Li(e,e'), 140-330 MeV, 3.65 MeV 0<sup>+</sup> state form factor at high momentum transfer 0-495  
<sup>53</sup>Mn low lying states, DWBA anal., shell model wave functions from <sup>56</sup>Fe(p, $\alpha$ ) 0-32211  
<sup>4</sup>Mo, A=94, 96, 98, multiparticle states, method of generalised seniority 0-22759  
<sup>17</sup>N levels and ang. distrib. meas., shell model calcs. from <sup>15</sup>N(t,p) 0-9233  
<sup>22</sup>Na, effective interactions for dominant shell-model configurations: ds-shell example 0-32204  
<sup>21</sup>Ne, energy moments, sd shell realistic effective interactions, shell model spectra 0-18190  
<sup>4</sup>Ni A=57-59, f<sub>7/2</sub> hole configuration effects, shell model calcs. 0-22670  
<sup>4</sup>Ni(e,e'), 102 MeV, A=58,60, E1-E4 giant multipole resonance comparison, shell model anal. 0-42614



**nuclear shell model continued**

- <sup>62</sup>Ni( $\gamma, X$ ), 19.2-26.2 MeV, photoneutron and photoproton spectra, giant dipole resonance-decay, isospin conservation 0-13443  
<sup>A</sup>O, A=18, 19, E2 transition rates calc., shell model with effective interaction and charges 0-47423  
<sup>16</sup>O, centre-of-mass spuriousity in continuum shell-model calculations 0-32210  
<sup>16</sup>O, Hartree-Fock calculations of nuclear bulk properties with density- and starting-energy dependent effective interaction 0-9246  
<sup>16</sup>O+<sup>4</sup>He, group theory appl. to reaction studies 0-9276  
<sup>16</sup>O( $\alpha, \alpha$ ), giant isoscalar quadrupole resonance,  $\alpha$ -over p-decay ratio, SU(3) and shell model 0-27608  
<sup>16</sup>O( $\pi, \gamma$ ), direct and resonance reaction unified shell model, n,  $\gamma$  spectra 0-52696  
<sup>17</sup>O(<sup>1</sup>B,<sup>8</sup>Li), 115 MeV, shell and semiclassical reaction model anal. 0-13494  
<sup>17</sup>O(<sup>12</sup>C,<sup>9</sup>Be), 115 MeV, shell and semiclassical reaction model anal. 0-13494  
<sup>17</sup>O(<sup>12</sup>C,<sup>10</sup>B), 105 MeV, shell and semiclassical reaction model anal., <sup>20</sup>F spins 0-13494  
<sup>18</sup>O( $\pi, \pi'$ ), 164 MeV, yrast state and level excitation, DWIA calcs., shell model context 0-42526  
<sup>22</sup>O, Hartree-Fock calculations of nuclear bulk properties with density- and starting-energy dependent effective interaction 0-9246  
<sup>208</sup>Pb and neighbouring nuclei, shell model calcs. with correlated pairs basis 0-22712  
<sup>209</sup>Pb excited states and 3/2<sup>-</sup> resonances, shell model, calcs. from <sup>208</sup>Pb(n, n) 0-18262  
<sup>212</sup>Po, shell model  $\alpha$ -spectroscopic factors 0-32245  
<sup>A</sup>Ru, A=96, 98, 100, multiparticle states, method of generalised seniority 0-22759  
<sup>32</sup>S(n,  $\gamma$ ), non-statistical effects in shell model calcs. 0-32274  
<sup>32</sup>Si, spin cutoff factors, sd shell realistic effective interactions, shell model spectra 0-18190  
<sup>28</sup>Si(<sup>18</sup>O, X), 56 MeV, multinucleon transfers, ang. distrib., distorted wave and shell model anal. 0-27663  
 Sn, odd mass isotopes, low lying negative parity states, energy levels, shell model calc. 0-5076  
<sup>132</sup>Sn, energy levels, gamma transitions, spin and parity 0-9239  
<sup>132</sup>Te 2<sup>+</sup> level, shell model calc., Lanczos and Householder method comparison 0-22711  
<sup>132</sup>Te low lying levels and EM props., shell model description 0-42549  
<sup>236</sup>U, nuclear matter density distrib., in asymmetric two centre shell model 0-32209  
 Zr even isotopes, quadrupole moments and E2 transition rates, broken pair approx. 0-52579  
 Zr-region, two nucleon transfer reactions, spectroscopic amplitudes, form factors, ang. distrib. 0-22779  
<sup>A</sup>Zr, A=90, 92 and 94, charge densities and single-particle structure 0-9224  
<sup>A</sup>Zr, A=92, 94, 96, multiparticle states, method of generalised seniority 0-22759

**nuclear size**

- A=4-16, monopole giant resonances, state density radii and compressibility using hyperspherical functions (*Russian*) 0-27615  
 A=4n, densities, form factors, transitions, multipole moments in s-d shell, HFC 0-37321  
 light muonic atoms, nuclear size effects, energy levels, Lamb shift 0-14254  
 light nuclei, hyperspherical functions for size, excited states, compressibility, binding energy 0-22679  
 neutron distribution in nuclei, elastic and inelastic proton scattering, review 0-22649  
 quadrupole moments and rms charge radii, shell model calcs. 0-47369  
 single-particle models, relation between average kinetic energy and mean-square radius 0-52567  
 single-particle motion in nucleus, forces between constituent nucleons, shell model 0-47408  
 spherical nuclei, isomer and isotope shifts, theory of finite Fermi systems 0-39929  
 (e, e), A=60 region, nuclear radius, core polarisation and isotope shifts, muonic X-rays 0-22685  
 (p, t) ang. distrib. with deep minima, DWBA calcs. geometrical aspects 0-522  
 (p, X), 5-9 GeV/c, total inelastic and knock-out cross sections, nuclear RMS radius (*Russian*) 0-32175  
 (p, X), nuclear size dependence of particle prod., hydrodynamical model 0-22593  
 ( $\pi, \pi$ ) elastic scatt., reaction mechanisms, structure information and neutron radii 0-42702  
 ( $\pi, X$ ), 1.75-6.5 GeV/c, total inelastic and knock-out cross sections, nuclear RMS radius (*Russian*) 0-32175  
<sup>9</sup>Be( $\gamma, \pi$ ), photoabsorption and sum rules, structure, RMS radius, polarisability and exchange parameters 0-22686  
<sup>A</sup>Ca, A=40, 48, nuclear radii, energy density and HF-BCS methods 0-47363  
<sup>41</sup>Ca 1f<sub>7/2</sub> neutron radial distrib., single particle, orbits, RMS radii from <sup>40</sup>Ca(<sup>13</sup>C, <sup>12</sup>C) 0-42532  
<sup>42</sup>Ca, nuclear charge radius, spin, moments, by laserspectroscopy 0-18187  
<sup>52</sup>Cr, If nucleon orbit RMS radii from transfer data 0-27544  
<sup>55</sup>Fe Zp<sub>3/2</sub> neutron orbit radius isotope shift from DWBA anal. of <sup>54</sup>Fe(t, d) 0-32172  
<sup>A</sup>Li( $\gamma, \pi$ ), A=6, 7 0-22686  
<sup>A</sup>Mo, A=92, 94-98, 100, muonic atom X-ray transitions, nuclear charge radii 0-27545  
<sup>58</sup>Ni, nuclear radii, energy density and HF-BCS methods 0-47363  
<sup>208</sup>Pb, nuclear radii, energy density and HF-BCS methods 0-47363  
<sup>32</sup>S, nuclear radii, energy density and HF-BCS methods 0-47363  
<sup>A</sup>Sn (t,  $\alpha$ ), 4.75-5.25 MeV, A=112, 116, 118, 120, 124, single proton states RMS radius 0-13350  
<sup>51</sup>Ti Zp<sub>3/2</sub> neutron orbit radius isotope shift from DWBA anal. of <sup>50</sup>Ti(t, d) 0-32172  
<sup>51</sup>V, If nucleon orbit RMS radii from transfer data 0-27544  
<sup>90</sup>Zr, nuclear radii, energy density and HF-BCS methods 0-47363  
<sup>90</sup>Zr, proton orbit sizes and E0 matrix element for 2 lowest 0<sup>+</sup> states 0-27546

**nuclear spallation**

- pulsed spallation neutron sources 0-27852  
 (p, spallation), 0.08-24 GeV, Ar isotopes, spallation ratios and prod. cross sections 0-9284

**nuclear spallation continued**

- (p, X), 0.6-21 GeV, <sup>A</sup>Rb, A=83, 84, 86 prod. cross sections and recoil props. 0-9295  
<sup>197</sup>Au( $\pi^+$ , spallation), 100-300 MeV, cross sections for products A=167-196 0-27619  
<sup>137</sup>Cs, 10 GeV proton spallation for transmutation of radioactive waste, calc. of transmutation number 0-13470  
 Cu( $\pi^+$ , spallation) 0.6, 0.9, 12 GeV, T=1/2 resonances, Na, Sc and Co rel. yields 0-5109  
<sup>10</sup>He isotope search in <sup>232</sup>Th target nucleus spallation (*Russian*) 0-5110  
<sup>93</sup>Nb( $\alpha, X$ ), 15-72 MeV, excitation functions and spallation cross-sections 0-18274  
<sup>232</sup>Th( $\alpha, X$ ), 140 MeV, spallation and fission product yields 0-13512  
<sup>232</sup>Th(p, X), 10-100 MeV, spallation residue excitation functions, fissionability 0-18353  
<sup>238</sup>U(p, X), 0.8-11.5 GeV, formation of A=131 isobaric nuclides 0-9293  
<sup>238</sup>U(p, X), 400 GeV/c, unusual backward enhancement in product ang. distrib. 0-514  
<sup>A</sup>Zr(p, 4pxn)Rb, A=90, 91, 94, spallation reactions, nuclear structure influence on yields of product nuclei 0-22794  
<sup>A</sup>Zr(p, 6pxn)Br, A=90, 91, 94, spallation reactions, nuclear structure influence on yields of product nuclei 0-22794

**nuclear spectroscopic factors**

- A=19-31 odd nuclei, K $\pi$ =1/2<sup>-</sup> bands, spectroscopic factors and transitions 0-32151  
 continuum shell model of decaying states, spectroscopic amplitudes, decay widths and partial widths 0-486  
 even actinides, lowest 0<sup>+</sup> state excitation, collective phonon state, spectroscopic factors from (p, t), (t, p) 0-13410  
 even actinides, two-nucleon transfer, first 0<sup>+</sup> collective state excitation, spectroscopic factor (*Russian*) 0-42530  
 Skyrme-type interactions, spectroscopy of light nuclei, density dependent Hartree-Fock 0-22717  
 Sn Z=50 region isotopes, system struct calcs. 0-18192  
 $\alpha$ -decay spectroscopic factors, coupled channel problem, local pots. justification 0-47439  
 (d, <sup>6</sup>Li), 54.25 MeV,  $\alpha$ -cluster spectroscopic factors, DWBA anal. 0-52571  
<sup>10</sup>B,  $\alpha$ -transfer reactions, spectroscopic factors, exact finite range DWBA anal. 0-13372  
<sup>11</sup>B states, spectroscopic factors from DWBA anal. of <sup>12</sup>C(p, 2p) 0-5057  
<sup>209</sup>Bi low lying levels and spectroscopic factors, EFR-DWBA anal. of <sup>208</sup>Pb(<sup>7</sup>Li, <sup>6</sup>He) 0-32182  
<sup>12</sup>C,  $\alpha$ -transfer reactions, spectroscopic factors, exact finite range DWBA anal. 0-13372  
<sup>12</sup>C,  $\alpha$ -transfer spectroscopic factors for 0<sup>+</sup>, 2<sup>+</sup> and 4<sup>+</sup> states, transitions from (d, <sup>6</sup>Li) 0-13370  
<sup>12</sup>C, isoscalar giant quadrupole resonances, RPA calcs., E2 strength fragmentation, spectroscopic factors 0-13437  
<sup>13</sup>C spectroscopic factors, cross sections DWBA anal. optical model parameters from <sup>12</sup>C(<sup>16</sup>O, X) 0-13371  
<sup>14</sup>C spectroscopic factors, cross sections DWBA anal. optical model parameters from <sup>12</sup>C(<sup>16</sup>O, X) 0-13371  
<sup>40</sup>Ca, weak s resonance  $\gamma$ -ray decay in negative parity low lying levels 0-27591  
 Cd,  $\alpha$ -spectroscopic factors from (d, <sup>6</sup>Li) 0-534  
<sup>143</sup>Ce quasi-f<sub>7/2</sub> low lying states spectroscopic factors, cluster-vibr. model from <sup>142</sup>Ce(d, p) 0-47391  
<sup>55</sup>Co f-wave resonances, inelastic p amplitudes, analogue state spectroscopic factors from <sup>54</sup>Fe(p, p' $\gamma$ ) 0-47451  
<sup>52</sup>Cr(d, p) <sup>53</sup>Cr, Coulomb stripping, 2.12-2.48 MeV, DWBA anal., spectroscopic strengths 0-516  
<sup>19</sup>F, coupled channel orthogonality condition model 0-47384  
<sup>A</sup>Fe, A=54-56, high spin states, energy levels, spectroscopic factors, EM props., shell model 0-47359  
<sup>3</sup>He spectroscopic strengths from <sup>13</sup>C(<sup>6</sup>Li, t) 0-47390  
<sup>39</sup>K states and spectroscopic strengths DWBA anal. of <sup>40</sup>Ca(<sup>7</sup>Li, <sup>8</sup>Be) 0-5069  
<sup>6</sup>Li, EM form factors and spectroscopic factors in phenomenological cluster models 0-496  
<sup>23</sup>Mg hole states, transitions and spectroscopic factors, DWBA anal. of <sup>24</sup>Mg(p, d) 0-32161  
<sup>24</sup>Mg, <sup>16</sup>O+ $\alpha$ + $\alpha$  cluster model, energy level structure 0-18215  
<sup>24</sup>Mg, K $\pi$ =0<sup>-</sup>, K $\pi$ =3<sup>-</sup> bands, radiative and  $\alpha$ -widths from ( $\alpha, \gamma$ ), (<sup>16</sup>O,  $\alpha\gamma$ ) 0-18173  
<sup>27</sup>Mg energy levels, spectroscopic factors, DWBA, Hauser-Feshbach anal. from <sup>26</sup>Mg(d, p) 0-52581  
<sup>14</sup>N,  $\alpha$ -transfer reactions, spectroscopic factors, exact finite range DWBA anal. 0-13372  
<sup>14</sup>N spectroscopic factors, cross sections DWBA anal. optical model parameters from <sup>12</sup>C(<sup>16</sup>O, X) 0-13371  
<sup>15</sup>N low lying states, cross sections and anal. power, transitions, spectroscopic factors from <sup>14</sup>N(d, p), pol. d 0-32183  
<sup>23</sup>Na level  $\alpha$ -spectroscopic strengths assuming direct cluster transfer from <sup>19</sup>F(<sup>6</sup>Li, d) 0-27552  
<sup>20</sup>Ne,  $\alpha$ -transfer reactions, spectroscopic factors, exact finite range DWBA anal. 0-13372  
<sup>20</sup>Ne from <sup>16</sup>O(<sup>16</sup>O, <sup>12</sup>C)<sup>20</sup>Ne, polarisation measurements 0-9301  
<sup>20</sup>Ne(e, e' $\alpha$ ), EM induced  $\alpha$  emission,  $\alpha$  spectroscopic amplitudes, anal. solvable model 0-32267  
<sup>20</sup>Ne( $\gamma, \alpha$ ), EM induced  $\alpha$  emission,  $\alpha$  spectroscopic amplitudes, anal. solvable model 0-32267  
<sup>60</sup>Ni deduced levels from <sup>58</sup>Fe(<sup>16</sup>O, <sup>14</sup>C)<sup>60</sup>Ni, DWBA anal., spectroscopic strengths 0-47380  
<sup>16</sup>O,  $\alpha$ -transfer reactions, spectroscopic factors, exact finite range DWBA anal. 0-13372  
<sup>16</sup>O, isoscalar giant quadrupole resonances, RPA calcs., E2 strength fragmentation, spectroscopic factors 0-13437  
<sup>16</sup>O(e, e), spectroscopic amplitude determ. 0-5127  
<sup>A</sup>Pb, A=205-207, neutron hole states, spectroscopic factors, DWBA anal. of Pb(<sup>3</sup>He,  $\alpha$ ) 0-47352  
<sup>109</sup>Pd levels, J $\pi$ , transitions, unique parity states, and spectroscopic factors from <sup>108</sup>Pd(n,  $\gamma$ ) 0-42547  
<sup>149</sup>Pm single proton states, spin assignments, spectroscopic factors from <sup>150</sup>Sm(t,  $\alpha$ ), pol. t 0-18170  
<sup>212</sup>Po, shell model  $\alpha$ -spectroscopic factors 0-32245  
<sup>32</sup>S levels and spectroscopic factors from pickup DWBA anal. of <sup>33</sup>S(<sup>3</sup>He,  $\alpha$ ) 0-9235  
<sup>A</sup>Sb, A=123, 125, 127, 129, cross-sections, ang. distrib., spectroscopic factors, DWBA anal. of Te(t,  $\alpha$ ) 0-52572



**nuclear spectroscopic factors continued**

- <sup>54</sup>Se, A=75, 77, 79, 81, levels and ang. distrib., spectroscopic factors from Se(p, d) 0-22696  
<sup>28</sup>Si, isoscalar giant quadrupole resonances, RPA calcs., E2 strength fragmentation, spectroscopic factors 0-13437  
<sup>50</sup>Sn,  $\alpha$ -spectroscopic factors from (d, <sup>6</sup>Li) 0-534  
<sup>50</sup>Sn, A=111, 115, 119, neutron hole distrib., IAS and spectroscopic factors from Sn(<sup>3</sup>He,  $\gamma$ ) 0-42519  
<sup>92</sup>Zr level struct. and reduced spectroscopic factors from <sup>91</sup>Zr(d, p) 0-32192

**nuclear spin and parity**

see also nuclear isospin

- <sup>18</sup>F levels, J<sup>π</sup> and ang. distrib. DWBA anal. of <sup>19</sup>F(p, d) 0-42545  
 A=204, nuclear data sheets, levels, J<sup>π</sup> and transitions 0-31429  
 A=212, nuclear data sheets, levels, J<sup>π</sup>, transitions 0-31430  
 A=221, nuclear data sheets, levels, J<sup>π</sup>, transitions 0-31431  
 A=225, nuclear data sheets, levels, J<sup>π</sup>, transitions 0-31432  
 A=71 nuclear data sheets, levels, J<sup>π</sup> and transitions 0-31428  
 deformed rare earth nuclei, backcrossing in K $\neq$ 0 bands, backbending 0-9204  
 dense neutron and nuclear matter, spin and isospin stability 0-22737  
 elastic electron scatt. and atom parity nonconservation caused by nuclear parity violation 0-27427  
 even-even and odd A nuclei, nuclear shapes and motions, review 0-5054  
 even-even nuclei, z=6 to 100, probable members of quasi-bands in spherical and deformed regions 0-13357  
 even-even spherical nuclei, neutron strength function, spin depend., quasi-particle-phonon model (Russian) 0-42561  
 high-spin states and shell struct. in N=Z nuclei, <sup>20</sup>Ne appl. 0-47342  
 nuclear force, parity violating, unified treatment 0-47400  
 optimum atomic mass formula from nuclear mass shell and parity corrections (Russian) 0-37902  
 parity violation in nuclear forces, neutron capture  $\gamma$ -ray expts. 0-37322  
 parity-non-conserving nuclear forces, theoretical and phenomenological approach review 0-42556  
 photonuclear sum rule, spin current contribs., strong violations 0-18291  
 polarised nucleus fission, parity nonconservation mechanism, rot. state mixing (Russian) 0-37408  
 spectroscopy using ( $\gamma$ ,  $\gamma$ ) and (n,  $\gamma$ ) scatt. 0-18287  
 spin giant resonance and core polarization effects, coupling term effects (Chinese) 0-47450  
 spin-isospin density phase in finite nuclei, strongly oblate shape 0-22746  
 strongly deformed nuclei, shortlived states, g-factor meas. method 0-52577  
 SU<sub>3</sub> representation, maximal basis restriction 0-42552  
 yrast traps, obs. in heavy ion collisions 0-37319  
 Z=55-63, odd proton nuclei, low lying even parity states 0-27551  
 (c.e.), A=2, 3, 4, scaling laws in relativistic impulse approx. model, spin effects 0-52662  
 in (p, n) reactions quadrupole moment, isovector component, nuclear spin re-orientation effect 0-52573  
 $\Lambda$ - and  $\Sigma$ -hypernuclei,  $\gamma$ -transitions, spin-orbit components of single particle pots. 0-42574  
 (n, f), parity violation in compound nuclei 0-47368  
 (n,  $\gamma$ ), parity violation in compound nuclei 0-47368  
 (n,  $\gamma$ ), spin assignments using polarised beams and gamma spectroscopy 0-37323  
 ( $\pi$ ,  $\pi$ ), collective transitions, giant resonances, isospin content and spin transfer 0-42580  
<sup>107</sup>Ag, A=104, 106, levels, J<sup>π</sup>, and isobaric analogue resonances from Pd(p, n) 0-32180  
<sup>107</sup>Ag, A=99, 101, 103, levels, transitions and J<sup>π</sup> from Cd decay, Pd(p, 2n $\gamma$ ) 0-47383  
<sup>107</sup>Ag high spin states, J<sup>π</sup> assignments, polarisations and transitions from (<sup>7</sup>Li, 4n $\gamma$ ), (<sup>6</sup>Li, 3n $\gamma$ ) 0-27536  
<sup>26</sup>Al low energy resonances, decay and J<sup>π</sup> assignments, branching ratios from <sup>25</sup>Mg(p,  $\gamma$ ) 0-42624  
<sup>27</sup>Al, J<sup>π</sup>=5/2 state, cross section and analysing power ang. distrib. 0-18296  
<sup>27</sup>Al levels, spins and  $\gamma$ -rays, multipole mixing from <sup>27</sup>Al(n,  $\gamma$ ), pol. thermal 0-47398  
<sup>36</sup>Ar, delayed proton and alpha emission, transition energies, levels, J<sup>π</sup>, from <sup>36</sup>K decay 0-52629  
<sup>38</sup>Ar levels, J<sup>π</sup> and transition strengths, DWBA anal. of <sup>40</sup>Ar(p, t) 0-47378  
<sup>4</sup>As, A=70, 72, level scheme, transitions, J<sup>π</sup> and lifetimes from Ge(p, n $\gamma$ ) 0-22695  
<sup>75</sup>As populated in <sup>75</sup>Se decay, E0 transitions 0-22752  
<sup>76</sup>As, level structure, transitions and J<sup>π</sup>, from <sup>76</sup>Ge(p, n $\gamma$ ) 0-47379  
<sup>12</sup>At high spin states, decay, g factor, J<sup>π</sup> assignments, level energies from <sup>208</sup>Pb(<sup>7</sup>Li, 3n) 0-5042  
<sup>86</sup>Kr, A=724 MeV, deeply inelastic, <sup>4</sup>He, <sup>1</sup>H emission, fragment spin, semiempirical method 0-47366  
<sup>190</sup>Au, A=190, 192, 194, levels, J<sup>π</sup>, isomers and rot, aligned bands from Ir( $\alpha$ , xn) 0-9215  
<sup>198</sup>Au level spin assignments from  $\gamma$  ang. distrib. and circular polarisation from <sup>197</sup>Au(n,  $\gamma$ ) 0-52570  
<sup>10</sup>B levels, J<sup>π</sup> and ang. distrib. from <sup>9</sup>Be(<sup>3</sup>He, d) 0-42546  
<sup>10</sup>B(n,  $\alpha$ ) Li, thermal polarised n capture, P-odd asymmetry meas. (Russian) 0-13452  
<sup>11</sup>B, struct. study of 2 $\alpha$ +t system in orthogonality condition model, level energies and parity 0-5080  
<sup>4</sup>Ba, A=130, 132, 134, 136, levels and EM props., ang. momentum projected quasiboson model 0-5067  
<sup>135</sup>Ba level scheme, J<sup>π</sup> and  $\gamma$ -transitions from <sup>139</sup>Cs  $\beta$ -decay 0-42590  
<sup>208</sup>Bi two-particle, two-hole configuration, levels, J<sup>π</sup> and excitation energies from <sup>210</sup>Bi(m, p, t) 0-32190  
<sup>12</sup>B hypernucleus, spin determ. from <sup>12</sup>B $\rightarrow$ <sup>12</sup>C\*+ $\pi^-$  0-27589  
<sup>79</sup>Br collective bands, lifetimes, spins and E2 transition probabilities from <sup>64</sup>Ni(<sup>16</sup>O, 2n p) 0-13415  
<sup>79</sup>Br, high-spin states, from <sup>77</sup>Se( $\alpha$ , 2n p), decay into isomers 0-52569  
<sup>12</sup>C (<sup>16</sup>O, <sup>16</sup>O<sup>+</sup>), 19-23 MeV, intermediate width structs., ang. correlations, spins 0-13431  
<sup>12</sup>C (<sup>12</sup>C, <sup>12</sup>C), 13-14.1 MeV, Coulomb barrier resonance parameter direct determ., J<sup>π</sup> assignments 0-513  
<sup>12</sup>C (<sup>16</sup>O, <sup>12</sup>C\*), 45-53 MeV, <sup>12</sup>C\* m-substate population, spin alignment and excitation functions 0-42615  
<sup>12</sup>C(p, p') proton polarisation and natural parity level excitations (Russian) 0-5144

**nuclear spin and parity continued**

- <sup>12</sup>C( $\pi^+$ ,  $\pi^+$ ), 100-291 MeV, cross sections and ang. distrib., spin and isospin transfer 0-52697  
<sup>13</sup>C( $\gamma$ , n), 7.6-24 MeV, photoneutron ang. distrib., level scheme and J<sup>π</sup> assignments 0-466  
<sup>40</sup>Ca, weak s resonance  $\gamma$ -ray decay in negative parity low lying levels 0-27591  
<sup>45</sup>Ca, nuclear charge radius, spin, moments, by laserspectroscopy 0-18187  
<sup>45</sup>Ca,  $\alpha$ -spectroscopic factors from (d, <sup>6</sup>Li) 0-534  
<sup>110</sup>Cd, A=107, 109, 111, from Pd( $\alpha$ , 3n $\gamma$ )Cd, high spin states obs. 0-450  
<sup>110</sup>Cd(n, n $\gamma$ ) A=114, 116, energy levels, spins, and gamma-ray multipole mixing ratios investig. 0-52580  
<sup>250</sup>Cf(d, d'), 15 MeV, vibr. states, J<sup>π</sup> and reduced transition probabilities 0-47351  
<sup>55</sup>Co, resonance decays, branching ratios and analogue resonances from <sup>54</sup>Fe(p,  $\gamma$ ) 0-52643  
<sup>51</sup>Cr, bands, levels, EM transitions, J<sup>π</sup>, branching and mixing ratios from <sup>48</sup>Ti ( $\gamma$ , n $\gamma$ ), <sup>51</sup>Cr and <sup>51</sup>V(p, n $\gamma$ ) <sup>51</sup>Cr 0-52606  
<sup>52</sup>Cr high spin states, transitions and J<sup>π</sup> values from <sup>50</sup>Ti( $\alpha$ , 2n $\gamma$ ) 0-455  
<sup>53</sup>Cr levels, J<sup>π</sup>,  $\gamma$ -transitions and 1626 eV resonance from <sup>52</sup>Cr(n,  $\gamma$ ) 0-42610  
<sup>54</sup>Cr levels, transitions, T<sub>1/2</sub>, J<sup>π</sup>, shell model anal. from <sup>51</sup>V( $\alpha$ , p $\gamma$ ) 0-47381  
<sup>55</sup>Cr deduced levels and spins, from <sup>54</sup>Cr(d, p), cross section and vector analysing power 0-52684  
<sup>55</sup>Cr neutron rich isotopes, nucl. spins and mag. moments 0-47367  
<sup>131</sup>Cs populated in <sup>131</sup>Ba decay, E0 transitions 0-22752  
<sup>139</sup>Cs level scheme, J<sup>π</sup> and  $\gamma$ -transitions from <sup>139</sup>Xe  $\beta$ -decay 0-42590  
<sup>139</sup>Cs even isotopes, aligned Stockholm band intrinsic spin I<sub>0</sub><sup>eff</sup> 0-13363  
<sup>139</sup>Cs, (A=151, 152), high spin yrast states,  $\gamma$ -ray polarisation in (<sup>32</sup>S, n) reactions 0-497  
<sup>139</sup>Cs even isotopes, aligned Stockholm band intrinsic spin I<sub>0</sub><sup>eff</sup> 0-13363  
<sup>139</sup>Cs yrast levels, spin alignment, populated by preequilibrium ( $\alpha$ , xn $\gamma$ ) reactions 0-52557  
<sup>139</sup>Cs, (A=154, 155), rotational struct. at high spins 0-457  
<sup>139</sup>Cs, (A=156, 157, 158), high spin yrast states,  $\gamma$ -ray polarisation in (<sup>32</sup>S, xn) reactions 0-497  
<sup>143</sup>Eu high spin states, J<sup>π</sup> and transitions from (<sup>7</sup>Li, 4n $\gamma$ ) and (<sup>6</sup>Li, 3n $\gamma$ ) 0-47350  
<sup>18</sup>F J<sup>π</sup>=3<sup>-</sup> doublet at 6241 keV, isospin mixing from (p,  $\gamma$ ), (p,  $\alpha$ ), ( $\alpha$ ,  $\gamma$ ) (<sup>14</sup>N,  $\alpha$ ) 0-511  
<sup>19</sup>F, energy levels from  $\alpha$ -<sup>13</sup>N and t-<sup>16</sup>O coupled channel orthogonality condition model 0-37326  
<sup>20</sup>F spins from <sup>17</sup>O(<sup>13</sup>C, <sup>10</sup>B) 0-13494  
<sup>54</sup>Fe high spin states, transitions and J<sup>π</sup> values from <sup>52</sup>Cr( $\alpha$ , Zn $\gamma$ ) 0-455  
<sup>54</sup>Fe(p,  $\alpha$ ) <sup>51</sup>Mn, 21 MeV analogue state, excitation 0-13471  
<sup>57</sup>Fe(n, X) transmission data up to 400 keV, J<sup>π</sup> value for resonances 0-18311  
<sup>59</sup>Fe deduced levels and spins, from <sup>58</sup>Fe(d, p), cross section and vector analysing power 0-52684  
<sup>69</sup>Ga(n, n $\gamma$ ), fast n, levels, J<sup>π</sup>, transitions and mixing ratios, statistical anal. (Russian) 0-13382  
<sup>147</sup>Gd(n,  $\gamma$ ), A=154, 156-8, 2, 24 keV, resonance averaged  $\gamma$ -spectra, level and J<sup>π</sup> appls. 0-37347  
<sup>66</sup>Ge states and decay scheme, polarisations J<sup>π</sup> and ang. distrib. from <sup>58</sup>Ni(<sup>10</sup>B, p n $\gamma$ ) 0-22692  
<sup>72</sup>Ge levels pop. in <sup>8</sup>Zn(<sup>6</sup>Li, p n), in beam gamma-ray spectroscopy 0-47343  
<sup>4</sup>He, parity mixing below 30 MeV excitation energy for  $\Delta T=0, 1$  transitions 0-52604  
<sup>191</sup>Hg<sup>m</sup> and <sup>190m-185m</sup>Hg, nucl. spins, on-line quantum beat spectrosc. determ. 0-9562  
<sup>201</sup>Hg missing f<sub>5/2</sub> state Coulomb excitation, level scheme, J<sup>π</sup>, transitions using ( $\alpha$ ,  $\alpha$ ), (<sup>16</sup>O, <sup>16</sup>O) 0-47386  
<sup>117</sup>In level scheme, J<sup>π</sup> and transitions from <sup>117</sup>Cd isomer decay, unified model anal. 0-32193  
<sup>185</sup>Ir levels excited in ( $\alpha$ , xn) reactions, positive parity band 0-9231  
<sup>185</sup>Ir levels populated in <sup>185</sup>Pt<sup>m</sup>+ $\beta$  decay 0-9269  
<sup>4</sup>Kr, A=74, 76, rot. bands, band crossing and backbending 0-18176  
<sup>4</sup>Kr, A=76, 78, 80, yrast states and band struct., backbending from Zn(<sup>12</sup>C, 2n) 0-13359  
<sup>6</sup>Li(n, t) He, thermal polarised n capture, P-odd asymmetry meas. (Russian) 0-13452  
<sup>178</sup>Lu isomeric states and spins, transition probability from <sup>181</sup>Ta(n,  $\alpha$ ) 0-52582  
<sup>24</sup>Mg, <sup>16</sup>O+ $\alpha$ + $\alpha$  cluster model, energy level structure 0-18215  
<sup>24</sup>Mg(<sup>13</sup>C, <sup>13</sup>C), 35 MeV,  $\gamma$ -rays and spin flip 0-18189  
<sup>55</sup>Mn, energy levels, bound state mean lifetimes and spins from <sup>54</sup>Cr(p,  $\gamma$ ) 0-42586  
<sup>15</sup>N 3/2- state spin alignment and polarisation, 1/2-spin orbit interaction from <sup>27</sup>Al, <sup>88</sup>Sr(<sup>16</sup>O, <sup>15</sup>N) 0-27622  
<sup>20</sup>Ne continuum states, J<sup>π</sup> and branching from <sup>12</sup>C(<sup>12</sup>C,  $\alpha$ ) 0-22660  
<sup>20</sup>Ne high spin states, J<sup>π</sup> and  $\alpha$ -decay branching ratios from <sup>16</sup>O(<sup>12</sup>C, <sup>8</sup>Be) 0-18166  
<sup>20</sup>Ne high spin states, J<sup>π</sup> assignments from <sup>16</sup>O(<sup>6</sup>Li, d) 0-18167  
<sup>20</sup>Ne levels, J<sup>π</sup>, branching ratio and EM transition rates from <sup>16</sup>O+ $\alpha$  0-42540  
<sup>20</sup>Ne, levels, J<sup>π</sup> and ang. distrib. from <sup>18</sup>O(t, p) 0-18204  
<sup>20</sup>Ne resonances, J<sup>π</sup>, excitation functions and branching ratio from <sup>19</sup>F(p,  $\gamma$ ) 0-22787  
<sup>20</sup>Ne states, J<sup>π</sup>, differential cross sections and ang. distrib. from <sup>16</sup>O( $\alpha$ ,  $\alpha'$ ) 0-18203  
<sup>58</sup>Ni(<sup>16</sup>O, X), 100 MeV, deep inelastic, fragment spin polarisation and alignment,  $\gamma$ -rays 0-18284  
<sup>16</sup>O high spin states, J<sup>π</sup> and  $\alpha$ -decay branching ratios from <sup>12</sup>C(<sup>12</sup>C, <sup>8</sup>Be) 0-18166  
<sup>16</sup>O states, J<sup>π</sup> from <sup>12</sup>C(<sup>12</sup>C,  $\alpha$ ) 0-22660  
<sup>16</sup>O(p, p'), proton polarisation and natural parity level excitations (Russian) 0-5144  
<sup>16</sup>O(p, p'), 135 MeV, 4<sup>-</sup> particle-hole states, J<sup>π</sup> ambiguity removal 0-5036  
<sup>17</sup>O levels, resonances, J<sup>π</sup> and radiative width from <sup>14</sup>N(t,  $\gamma$ ) 0-47389  
<sup>17</sup>O even nuclei, spin expt. Hamiltonian, quadrupole moments 0-5058  
<sup>20</sup>Pb high spin two nucleon states decay props. from <sup>28</sup>Si( $\alpha$ , d $\gamma$ ) 0-13402  
<sup>207</sup>Pb parity assignments and M1 radiative strength from <sup>206</sup>Pb(n, n) 0-52614  
<sup>207</sup>Pb( $\gamma$ , n), 7632 keV level photoexcitation, cross section and J<sup>π</sup> 0-37330  
<sup>106</sup>Pd energy states and J<sup>π</sup> from <sup>106</sup>Ag<sup>m</sup> decay 0-18197  
<sup>106</sup>Pd levels, J<sup>π</sup>, transitions, unique parity states, and spectroscopic factors from <sup>108</sup>Pd(n,  $\gamma$ ) 0-42547



**nuclear spin and parity continued**

- <sup>149</sup>Pm single proton states, spin assignments, spectroscopic factors from <sup>150</sup>Sm( $\alpha$ , $\alpha$ ), pol. t 0-18170  
<sup>212</sup>Po levels and  $J^\pi$ , weak coupling calc. using realistic matrix elements 0-5068  
<sup>A</sup>Pt, A=192, 194, 196, states,  $J^\pi$ , ang. distrib. and transitions, DWBA anal. of Pt(p,t) 0-468  
<sup>187</sup>Pt, levels,  $J^\pi$ ,  $T_{1/2}$ , possible E0 transitions from <sup>187</sup>Au decay (French) 0-32230  
Rb neutron rich isotopes, nucl. spins and mag. moments 0-47367  
<sup>A</sup>Re, A=181, 182, 187, spin polarisation, state struct. and mag. moments in rot. model 0-18194  
<sup>210</sup>Rn high spin states, decay and lifetimes, spin assignments from <sup>204</sup>Pb(<sup>3</sup>He,3n) 0-18168  
<sup>32</sup>S levels and  $J^\pi$  from <sup>32</sup>Cl  $\beta^+$  decay 0-22772  
<sup>32</sup>(n,X), 2.5-1100 keV, resonance struct. from total and capture cross sections 0-42620  
<sup>A</sup>Sb, A=121,123, levels below 2 MeV, spins, transitions and mixing ratio from (p, $\gamma$ ), (n,n' $\gamma$ ) 0-32191  
<sup>46</sup>Sc energy levels, resonances, spin and parity from <sup>45</sup>Sc(n, $\gamma$ ) 0-52673  
<sup>46</sup>Sc transition polarisation, levels and spin assignments from <sup>45</sup>Sc(n, $\gamma$ ), pol. n 0-52656  
<sup>48</sup>Sc isobaric analogue states and resonances,  $J^\pi$  from <sup>48</sup>Ca(p,p) 0-13426  
<sup>78</sup>Se high spin levels, transitions,  $J^\pi$  assignments from <sup>76</sup>Ge( $\alpha$ ,n $\gamma$ ) 0-459  
<sup>28</sup>Si levels and  $J^\pi$  from <sup>28</sup>P  $\beta^+$  decay 0-22772  
<sup>28</sup>Si, spin cutoff factors, sd shell realistic effective interactions, shell model spectra 0-18190  
Sn,  $\alpha$ -spectroscopic factors from (d, <sup>6</sup>Li) 0-534  
Sn, odd mass isotopes, low lying negative parity states, energy levels, shell model calc. 0-5076  
<sup>A</sup>Sn(p,p'), A=115, 117, 119, 18 MeV, state spin assignment, particle-vibr. coupling 0-32160  
<sup>116</sup>Sn levels,  $J^\pi$  and transitions from <sup>115</sup>Sn(n, $\gamma$ ) 0-52587  
<sup>116</sup>Sn(d,p), pol. d, 8.22 MeV, vector anal. power, p and d spin depend. effects 0-5114  
<sup>124</sup>Sn(p,p), threshold enhancement of parity violation, Born approx. 0-18191  
<sup>132</sup>Sn, energy levels, gamma transitions, spin and parity 0-9239  
<sup>132</sup>Sn level struct., lifetimes,  $\gamma$ - $\gamma$  coincidences, internal conversion from <sup>235</sup>U fission 0-52584  
<sup>87</sup>Sr high spin states,  $J^\pi$  and de-excitation from Kr( $\alpha$ ,xn) 0-42516  
<sup>177</sup>Ta spin polarisation, state struct. and mag. moments in rot. model 0-18194  
<sup>95</sup>Tc, energy levels from <sup>95</sup>Mo(p, n $\gamma$ )<sup>95</sup>Tc 0-37372  
<sup>96</sup>Tc, high spin states,  $\gamma$ -energy, intensity, coincidence, ang. distrib. and electron conversion from <sup>93</sup>Nb( $\alpha$ ,n) 0-52554  
<sup>102</sup>Tc deduced levels, tentative  $J^\pi$  and transitions from <sup>102</sup>Mo decay 0-52630  
<sup>121</sup>Te isomeric state, spin, lifetime and mag. moment from ( $\alpha$ ,n),(d,Zn) 0-47387  
<sup>132</sup>Te from fission, 10<sup>+</sup> isomeric state,  $J^\pi$  from deexcitation pattern, half life 0-460  
<sup>48</sup>Ti high spin states,  $\gamma$ -decay,  $J^\pi$  assignments, lifetimes from <sup>45</sup>Sc( $\alpha$ ,p $\gamma$ ) 0-13356  
<sup>50</sup>Ti high spin states, transitions and  $J^\pi$  values from <sup>48</sup>Ca( $\alpha$ ,Zn $\gamma$ ) 0-455  
<sup>201</sup>Tl levels, transitions and  $J^\pi$  assignments from <sup>201</sup>Pb decay 0-5099  
<sup>175</sup>Tm single proton states, rot. bands,  $J^\pi$  assignments from <sup>176</sup>Yb(t, $\alpha$ ), pol. t 0-452  
<sup>235</sup>U(n,f), thermal polarised n capture, P-odd asymmetry meas. (Russian) 0-13452  
<sup>237</sup>U levels, bands and  $J^\pi$  assignments, n binding energy from <sup>236</sup>U(n, $\gamma$ ) 0-5041  
<sup>238</sup>U(n, $\gamma$ ), 2, 24 keV, resonance averaged  $\gamma$ -spectra, level and  $J^\pi$  appls. 0-37347  
<sup>A</sup>W, A=172-175, bands and backbending,  $i_{13/2}$  neutron decoupling from Dy(<sup>16</sup>O,xn) 0-9212  
<sup>178</sup>W high spin states, yrast bands and backbending from <sup>170</sup>Er(<sup>12</sup>C,4n) 0-13352  
<sup>182</sup>W high spin states, J assignments and mixing ratios from <sup>182</sup>Re isomer decay 0-42593  
<sup>A</sup>Xe, A=129, 131, populated in ( $\alpha$ ,n $\gamma$ ), props. of low-lying levels 0-464  
<sup>A</sup>Yb(<sup>16</sup>O,<sup>16</sup>O $\gamma$ ), A=168-176, even nuclei, 58-62 MeV, Coulomb excitation, vibr. and rot. states 0-32162  
<sup>167</sup>Yb  $i_{13/2}$  band, spin alignment in the particle-rotor and cranking models 0-42536  
<sup>64</sup>Zn,  $\gamma$ -ray studies of levels above 3.1 MeV 0-32238

**nuclear spin-lattice relaxation**

- N-acetyl-L-phenylalanine methyl ester, model for amino acid side chains internal motions in peptides and proteins 0-48017  
albumin denaturation, investigation by PMR 0-3582  
alkali silicate glass, Li<sup>+</sup> motion, <sup>7</sup>Li NMR spectra, nucl. relax. 0-34804  
amino acid side chains, internal motions in peptides and proteins, N-acetyl-L-phenylalanine methyl ester model 0-48017  
anilinium halides, and anilinium sulphate, proton mag. relax. obs. 0-34800  
borate glass, Li<sup>+</sup> motion, <sup>7</sup>Li NMR spectra, nucl. relax. 0-34804  
bromobenzenes <sup>13</sup>CBr bond, spin-spin coupling const., correl. with C hybridisation s-character 0-34806  
bromobenzene liquid, NMR spin-lattice relax. time 0-25232  
chemical fast kinetics studied by NMR, review 0-55662  
chlorinated compounds, <sup>13</sup>C  $T_1$  meas. and scalar coupling const. 0-18945  
chlorobenzene, liq., spin lattice relax. time, elec. field induced charges 0-44945  
CW spectroscopy, phys. chem. lab. expt. 0-17775  
cis-decalin, shift difference between chem. exchange sites using <sup>13</sup>C  $T_1$  meas. 0-18945  
diethyl ether, liq., spin lattice relax. time, elec. field induced charges 0-44945  
dioxane, liq., spin lattice relax. time, elec. field induced charges 0-44945  
dipole-dipole reservoir of nuclei in magic angle configuration 0-11286  
EBBA, binary systems with non-nematic solutes, phase transition behaviour and <sup>1</sup>H NMR anal. 0-34174  
epoxy polymers, cured spin-spin and lattice relax., proton coupling, <sup>13</sup>C NMR obs. 0-34799  
Fischer-Tropsch wax, NMR investigation 0-7186  
p-fluoranol, <sup>19</sup>F NMR and spin-lattice relax. meas., pot. profile calc., mole. reorientation 0-29634  
9H-fluorene, soln., correl. times from <sup>13</sup>C relax. 0-23438

**nuclear spin-lattice relaxation continued**

- fluorite lattices, <sup>19</sup>F<sup>-</sup>, self-diffusion, spin lattice relax., NMR techniques 0-34801  
glasses, nuclear quadrupole spin-lattice relax., soliton-nucl. quadrupole moment interaction, temp. depend. 0-50220  
glycerol-d<sub>3</sub>(-d<sub>2</sub>), compressed viscous liq., reorientational motion, NMR obs. 0-7183  
graphite intercalation cpds. with Li, nucl. relax. times 0-44947  
ionic conductors, central component NMR relax. rates 0-29640  
lipid bilayers, D relax. rates and mol. dynamics 0-26206  
lysozyme, tryptophan residues, H exchange for D, relax., proton NMR spectra 0-35846  
magnetic props. of materials, appl. of nucl. orientation, review 0-44928  
magnetic relaxation depend. on internal motion in solid, correlations 0-25239  
mammalian cells, NMR relax. time meas. of bulk water 0-21454  
measurement, variable perturbation method 0-22408  
methanols, labelled, proton  $T_1$  in presence of intramol. rots., intermol. relax. rate 0-2656  
methyl group hinderance barrier, spin-rot. relax. times 0-53011  
methyl groups in solids, reorienting and tunnelling, spin-lattice relax. 0-50217  
molecular crystals, chem. shielding, spin-lattice, quadrupole interactions, <sup>2</sup>D NMR spin echo spectroscopy 0-34817  
monovalent ions in aq. metal ion solns., <sup>14</sup>N NMR relax. 0-20481  
nitrobenzene, liq., spin lattice relax. time, elec. field induced charges 0-44945  
NMR line profile, paramagnetic ion nuclei in magnetically conc. solid, theory 0-25238  
NMR-NQR double resonance, two-freq. methods, resonance spectrometers 0-20512  
NQR spin-lattice relax. due to mol. fragments reorientation (Russian) 0-7189  
nucleic acid bases, <sup>14</sup>N relax. and N-proton spin coupling, NH-proton spin-lattice relax. 0-26202  
phenylene sulphides, NMR relaxation for mol. motions (German) 0-11288  
phosphate glass, Li<sup>+</sup> motion, <sup>7</sup>Li NMR spectra, nucl. relax. 0-34804  
poly-p-phenylene sulphide, NMR relaxation for mol. motions (German) 0-11288  
polyacetylene and polyacetylene: AsF<sub>5</sub>, one-dimens. spin diffusion, NMR  $T_1$  and dynamic nuclear polarisation meas. 0-44946  
polyatomic fluid, local dynamics, spectroscopic studies, summer school lecture series 0-6343  
polybutadiene, mol. motion in solid and soln., <sup>13</sup>C NMR relaxation meas. (Japanese) 0-2666  
polyethylene, linear, <sup>13</sup>C spin-lattice relaxation 0-25235  
polyethylene, linear, nuclear relaxation, mol. motion (Russian) 0-44949  
polymer glassy and crystalline, relax. process characterisation, <sup>13</sup>C NMR obs. 0-34802  
polystyrene, dilute soln., <sup>1</sup>H mag. relax., selective inversion technique appl. 0-44957  
proteins, solid, PMR spin-lattice relax., mol. dynamics 0-51041  
rare earth Cu<sub>2</sub>Si<sub>2</sub>, interconfiguration fluctuation system, NMR meas. 0-15817  
rare earth systems, NMR, EPR, and Mossbauer effect, book contribs. 0-39883  
relaxation time meas., simulation, systematic and random error effects 0-37062  
ribonuclease-A, solid, PMR spin-lattice relax., mol. dynamics 0-51041  
rotating coordinate system, phenomenological approach 0-39887  
rotating frame, <sup>13</sup>C spin-lattice relax. using proton decoupled Fourier transform spectra, errors origin 0-18945  
rotating-frame measurement, modification of commercial spectrometer 0-22407  
small molecules in protein solns., spin-lattice relax. times, inversion recovery spin-echo sequence 0-21446  
spin glasses, nuclear magnetic relaxation calcs. (French) 0-34797  
spin systems under multiple pulse NMR conditions, chem. shift relax. 0-34808  
squaric acid, critical slowing down of fluctuations at phase transition, <sup>13</sup>C spin-lattice relax. 0-44948  
steady state pulse method, master eqn. for  $T_1$  NQR determ. 0-54975  
steam, supercritical, compressed, proton spin-lattice relax. time meas. 0-22403  
styrene, thermal polymerization, PMR obs. 0-3342  
superionic conductors, mag. reson., book contrib. 0-25240  
TCNQ complex, Adn TCNQ<sub>2</sub>, nuclear-spin-lattice relaxation 0-39886  
TCNQ salt, pyridinium (TCNQ)<sub>2</sub>, low temp. mag. phase transition, ESR study 0-25139  
TCNQ salts, proton nucl. relax. meas. 0-20484  
TCNQ-DIP  $\Phi_4$ , electronic diffusion coeffs. in chains, proton spin-lattice relax. and dynamic nucl. polarisation 0-25241  
TCNQ-NMP, incomplete charge transfer, NMR relax. and line-shift meas. 0-20485  
tetraalkylammonium halides, mol. reorientation, spin lattice relax. time study 0-18875  
tetrahedral four spin  $1/2$  systems, Zeeman and tunnel system reson., coupled and uncoupled relax. 0-50214  
thermodynamics of nuclear spins 0-54964  
transition metal complexes, vibronic coupling and spin relax. NMR decay rate study 0-18870  
trichlorophosphazoperfluoro-1,1-dimethylethane, cryst., <sup>19</sup>F NMR and mol. mobility, fluorination influence 0-34809  
trimethylammonium cobalt trichloride dihydrate, Ising-like system, nucl. spin-lattice relax. of <sup>1</sup>H and <sup>35</sup>Cl 0-29638  
triptycene, soln., correl. times from <sup>13</sup>C relax. 0-23438  
TTF-TCNQ, interchain tunnelling effect on nucl. spin-lattice relax. time, interchain coupling of CDW 0-20163  
variable nutation WEFT, biochemical appl. 0-20482  
AgClO<sub>3</sub>, structural phase transition, <sup>35</sup>Cl NQR meas. 0-15819  
Al small particle, NMR study, Knight shift, spin-lattice relax. time, supercond. effects 0-39710  
As, pulsed NQR, bonding, bond angle distrib. obs. in different phases 0-54984  
<sup>13</sup>C NMR in solids, high-resolution 0-34802  
Co complex, tris(ethylenediamine)cobalt(III) ion in complex anion solns., <sup>59</sup>Co NMR relax. obs. 0-25234  
Co(II)-containing aq. electrolyte soln., nucl. dip. relax., hydration shell (Russian) 0-54966



## nuclear spin-lattice relaxation continued

- (Co<sub>1-x</sub>M<sub>x</sub>)B, M=Mn or Fe, paramag., spin echo NMR spectra, ferro-mag. transition, spin-lattice relax. 0-29645  
 Cr<sub>1-x</sub>V<sub>x</sub>, nucl. spin relax., spin fluctuation effect 0-34811  
 CsCoCl<sub>3</sub>, Ising like antiferromag., mag. phase transition, <sup>133</sup>Cs NMR 0-7184  
 Cu complex, Cu(II) dimers, temp. depend. PMR relax., singlet-triplet separation determ. 0-43073  
 Cu-Cs diluted deuterated Tutton salts, electron non-Zeeman system, nuclear relaxation study 0-44951  
 Cu(NO<sub>3</sub>)<sub>2</sub>·2<sup>1</sup>/<sub>2</sub>H<sub>2</sub>O, singlet ground state system, mag. props. 0-44850  
 CuSO<sub>4</sub>·5H<sub>2</sub>O, S=1/2 antiferromag. Heisenberg chain, spin dynamics 0-11285  
 Fe<sup>2+</sup> compounds, Mossbauer spectra, spin-lattice relax. effects 0-50239  
 FeF<sub>3</sub>, canted antiferromag., spin echo spectra of <sup>57</sup>Fe and <sup>19</sup>F nuclei 0-2662  
 GaP:Te(S), nucl. relax. rel. to donor density 0-11284  
 o-H<sub>2</sub> molecules in solid nonmagnetic host, nucl. spin lattice relax. times calc. 0-20483  
 H(UO<sub>2</sub>PO<sub>4</sub>)<sub>4</sub>H<sub>2</sub>O, solid, fast hydrogen ion diffusion, NMR relax. time meas. 0-2205  
<sup>3</sup>He, adsorbed, on MgO, nucl. mag. relax. props. 0-49457  
<sup>3</sup>He film, submonolayer and multilayer, adsorbed on Grafoil, pulsed NMR study 0-49456  
<sup>3</sup>He-<sup>4</sup>He mixtures, anomalous 0-54463  
 In<sub>1-x</sub>Sn<sub>x</sub>, molten mixture, NMR, reson. shifts, relax. rates, quadrupole relax. 0-2654  
 K<sub>2</sub>Co(CN)<sub>6</sub>, NMR spin lattice relax. of <sup>59</sup>Co rel. to Co(CN)<sub>6</sub> octahedra vibr. modes 0-39885  
 KLiSO<sub>4</sub>, <sup>7</sup>Li NMR, spin-lattice relax. (Chinese) 0-39884  
 K<sub>2</sub>MnF<sub>4</sub>, nucl. spin-magnon relax. time, temp. depend., NMR study 0-25117  
 K<sub>2</sub>NiF<sub>4</sub>, nucl. spin-magnon relax. time, temp. depend., NMR study 0-25117  
 K<sub>2</sub>Pt(CN)<sub>4</sub>Br<sub>0.30</sub>·3H<sub>2</sub>O, dynamic <sup>195</sup>Pt NMR meas. below metal-insulator transition 0-34810  
 K<sub>2</sub>PtCl<sub>6</sub>, K<sub>2</sub>ReCl<sub>6</sub>, K<sub>2</sub>SnCl<sub>6</sub>, solid state phase transitions, lattice vibr., NMR and NQR obs. 0-34814  
<sup>83</sup>Kr, nucl. mag. relax. meas. in gas 0-43072  
 La, FCC, NMR 4.2 to 296K, mag. susceptibility and sp. ht. 0-15813  
 LaNi<sub>5</sub>-H, with small Cr additions, NMR parameters (Russian) 0-29637  
 β-LaNi<sub>5</sub>-Al, hydrides, H diffusion, NMR studies 0-15298  
 LiH, solid, anion and cation diffusion, NMR relax. and linewidth obs., Schottky disorder 0-15815  
 α-LiIO<sub>3</sub>, <sup>7</sup>Li NMR, spin-lattice relax., spurious reson. (Chinese) 0-39884  
 Li<sub>6</sub>In<sub>2</sub>O<sub>6</sub>, pseudo-two-dimens. electrolytic solid, Li ion mobility, NMR study (French) 0-34235  
 LiNH<sub>4</sub>SO<sub>4</sub>, nuclear spin lattice and effective proton relaxation, phase transitions 0-54965  
 LiNbO<sub>3</sub>:Fe, Mossbauer spectra quadrupole doublet asymmetry 0-44960  
 Li<sub>7</sub>NbO<sub>6</sub>, pseudo-two-dimens. electrolytic solid, Li ion mobility, NMR study (French) 0-34235  
 Li<sub>6</sub>SnO<sub>6</sub>, pseudo-two-dimens. electrolytic solid, Li ion mobility, NMR study (French) 0-34235  
 methane, solid, librational tunnelling and proton relax. temp. 0-38969  
 ND<sub>4</sub>ClO<sub>4</sub>, level-crossing relax. study of MD<sub>4</sub><sup>+</sup> ion tunnelling freq. 0-7185  
 ND<sub>4</sub>ClO<sub>4</sub>, librational tunnelling and proton relax. temp. 0-38969  
 (ND<sub>4</sub>)<sub>2</sub>PtCl<sub>6</sub>, level-crossing relax. study of MD<sub>4</sub><sup>+</sup> ion tunnelling freq. 0-7185  
 NH<sub>3</sub>, magnetic relaxation rates for microwave spectrum and contributions to linewidth 0-5564  
 NH<sub>4</sub>HF<sub>2</sub>, powder, proton and fluorine 2nd moments meas., 77-395K 0-34803  
 (NH<sub>4</sub>)<sub>2</sub>PbCl<sub>6</sub>, librational tunnelling and proton relax. temp. 0-38969  
 (NH<sub>4</sub>)<sub>2</sub>SnCl<sub>6</sub>, <sup>35,37</sup>Cl NQR, Raman spectra and spin lattice relax., hindered rot. 0-54974  
 N<sub>2</sub>O dissolved in liq. cryst., NMR, relax. times 0-25233  
 NaCl:Sr, dimer and trimer aggregate formation by NMR, ionic cond. and dielectric losses 0-15094  
 Na<sub>2</sub>In<sub>2</sub>Sn<sub>1-x</sub>S<sub>2</sub>, intercalation-substitution compounds, NMR study 0-44952  
 NaNO<sub>2</sub>, size effect and spin-lattice relax. of <sup>14</sup>N 0-20480  
 Na<sub>2</sub>WO<sub>3</sub>, Knight shift, spin-lattice and spin-spin relax., high press. NMR obs. 0-50211  
 Nb, NMR study up to 1700K, Knight shift and spin-lattice relax. time 0-2653  
 Nb, proton diffusion, NMR obs., 120-480K 0-34812  
 (NbCl<sub>4</sub>Br<sub>6-n</sub>)<sup>-</sup> complexes in acetonitrile soln., <sup>93</sup>Nb spin relax. and mag. shielding 0-44944  
 NbS<sub>2</sub>, intercalation with pyridine, nucl. spin-lattice relax. meas. 0-54962  
 Ni-b, hyperfine interactions from 6 to 730K, <sup>15</sup>N NMR 0-29372  
 Ni<sub>1-x</sub>Si<sub>x</sub>, electronic states of Si NMR study 0-50216  
 PF<sub>3</sub>Br<sub>2</sub>, spin systems under multiple pulse NMR conditions, chem. shift relax. 0-34808  
 Pb<sub>1-x/2</sub>Mo<sub>6</sub>Se<sub>7.5</sub>, Chevrel phase supercond., NMR study 0-49989  
 PbSnF<sub>4</sub>, fast ionic cond. of F<sup>-</sup> ions, NMR study (French) 0-39345  
 RbCaF<sub>3</sub>, cubic to tetragonal phase transition, <sup>87</sup>Nb NMR meas. 0-7187  
 Rb<sub>2</sub>ZnCl<sub>4</sub>, spin-lattice relax. in incommensurable phase, phason and amplitudon excitations 0-50213  
 Si-Au, solid soln., influence of precip. on relax. of <sup>29</sup>Si nucleus 0-11287  
 SiH<sub>4</sub>, magnetisation relax., appl. of theory of spin-lattice relax. 0-50214  
 TaH<sub>x</sub>, H diffusion and electronic struct., pulsed NMR obs. 0-54967  
 TaS<sub>2</sub>, intercalation with pyridine, nucl. spin-lattice relax. meas. 0-54962  
 TaS<sub>2</sub>(NH<sub>3</sub>)<sub>x</sub>, NMR spectral densities and two-dimens. diffusion 0-50215  
 β-TiFeH<sub>1.03</sub>, H diffusion, NMR meas. 0-10707  
 TiH<sub>x</sub>, H diffusion, NMR obs. 0-34813  
 Ti<sub>1-x</sub>Nb<sub>x</sub>H<sub>1.94</sub>, electronic struct. MNR meas. 0-15439  
 TiS<sub>2</sub>(NH<sub>3</sub>)<sub>1.0</sub>, NMR spectral densities and two-dimens. diffusion 0-50215  
 TlBr melts, Tl doped and pure, stoichiometric, nucl. spin relax. 0-25236  
 UO<sub>2</sub>(NO<sub>3</sub>)<sub>2</sub>, aq. soln., pulsed NMR relax. time, <sup>235</sup>U enrichment depend. 0-2658  
 V<sub>2</sub>Ge, A-15 cpds., nucl. mag. relax. in normal and supercond. state 0-49993  
 V<sub>1-x</sub>Pt<sub>x</sub>(Ga<sub>2</sub>)(Si<sub>2</sub>), A-15 cpds., nucl. mag. relax. in normal and supercond. state 0-49993  
 V<sub>2</sub>Si, NMR meas. near struct. transform. (Russian) 0-44942  
 V<sub>2</sub>Si, NMR of <sup>51</sup>V above and below 21K struct. transition (Russian) 0-34796

## nuclear spin-spin relaxation see spin-spin relaxation

## nuclear structure

- see also form factors (nuclear); nuclear binding energy; nuclear charge; nuclear density; nuclear energy level transitions; nuclear energy levels; nuclear forces; nuclear isomerism; nuclear isospin; nuclear matter; nuclear moments; nuclear polarisation; nuclear shape; nuclear size; nuclear spectroscopic factors; nuclear spin and parity; nuclear structure theory  
 A=111 nuclei, nuclear struct. data sheets to February 1979 0-9193  
 A=84 nuclei, nuclear struct. data sheets to March 1979 0-9191  
 A=87 nuclei, nuclear struct. data sheets to January 1979 0-9192  
 data sheets, recent references, Jan. to April 1979 0-5039  
 data tables, May to August 1979 references 0-41953  
 electron scatt. theory, EM struct. from DWBA and other models 0-5133  
 modern atomic and nuclear physics (book) 0-11  
 Pauli's exclusion principle for strong interactions in hadrons, nuclei, and astrophysics 0-37206  
 properties from alpha scatt. studies (Hungarian) 0-18159  
 quarks and leptons, high energy and nuclear physics interface 0-41974  
 spectroscopy, publications produced in USSR 0-22186  
 A=101 nuclei, nuclear struct. data sheets to May 1979 0-41954  
 A=103 nuclei, nuclear struct. data sheets to July 1979 0-41955  
 A=196 nuclei, nuclear structure data sheets to Sept. 1978 0-41956  
<sup>71</sup>Br, prod. in proton spallation reactions, nuclear structure influence on yields of product nuclei 0-22794  
<sup>74</sup>Rb, prod. in proton spallation reactions, nuclear structure influence on yields of product nuclei 0-22794  
 nuclear structure theory  
 see also generator coordinate method; HF calculations; nuclear models; nuclear reaction and scattering theory; RPA calculations  
 Op shell nuclei, effective interaction spin-tensor decomposition 0-32198  
 A=12 polarised β-decay, nuclear Dirac wave function test 0-5060  
 A=15 mag. moments, nuclear Dirac wave function test 0-5060  
 A=16-58, charge, proton and neutron density distrib. calc. 0-22680  
 A=24-60, yrast lines using Strutinsky method, empirical fusion bands 0-42514  
 A=42 isotopic spin triplet, Coulomb energies and shifts, microscopic calcs. 0-9200  
 A=4-16, monopole giant resonances, state density radii and compressibility using hyperspherical functions (Russian) 0-27615  
 A=60-140, spherical nuclei, two phonon admixture effect on M1 resonance (Russian) 0-5105  
 A=60-260 nuclei, violated Wigner SU(4) symmetry reconstruction from mass data (Russian) 0-37336  
 A=60-80 even-even nuclei, collective motions and band structs. 0-9202  
 asymmetric rotator, yrast states, wobbling freq., boson representation 0-32167  
 backbenders, rot. energy expressions and least squares fitting 0-27531  
 band level staggering in doubly-odd nuclei, evidence for predicted phase change 0-32144  
 boson and fermion systems, eigenvalue spectra widths, symmetry, Wigner coeffs. 0-18213  
 Brueckner-Bethe calculations of nuclear matter 0-22718  
 coherent rot. states, quantum flow pattern and vortex struct. 0-22656  
 cold nuclear matter, stationary finite amplitude motions, quantum shock waves and solitons 0-42573  
 collective angular momentum in classical mechanics 0-4516  
 compound nucleus nonstatistical struct., runs tests as indicators 0-506  
 conference on neutron capture gamma ray spectroscopy, Upton, USA. (Sep. '78) 0-36780  
 conference on nuclear interactions, Canberra, Australia (Aug.-Sep. 1978) 0-4476  
 Coulomb displacement energies, isobaric analogue resonances, TDHF calcs. 0-42518  
 Coulomb effect in rotating nuclei in the Thomas-Fermi approach 0-47355  
 damped oscillator approach to nuclear structure 0-27569  
 deformed nuclei, even-even, phonon space and giant resonances (Russian) 0-52641  
 dense neutron and nuclear matter, spin and isospin stability 0-22737  
 density matrix, harmonic oscill. approx. 0-13391  
 density matrix for arbitrary spin, equations of motion for new SU(n) parameters 0-52592  
 dipole sum rule schematical eval., collective isovector quadrupole strength 0-47428  
 dynamical symmetries in nuclei 0-9249  
 E0 conversion, reduced probability, quadrupole moment effects 0-18235  
 E1-giant dipole resonance, strength function pygmy anomaly, nonstatistical background coupling 0-37358  
 effective form factor pot. due to unbound core after direct process, asymptotic behaviour 0-27560  
 energy weighted electonuclear sum rules, centre-of-mass corrections 0-5091  
 even nuclei, 2<sup>+</sup> excited states quadrupole moments, energy weighted sum rule appl. 0-9229  
 even-even deformed nuclei, collective K<sup>π</sup>=0<sup>+</sup> states, realistic boson expansion comparison 0-5043  
 even-even spherical nuclei, neutron strength function, spin depend., quasi-particle-phonon model (Russian) 0-42561  
 even-odd mass difference ratio, mass and binding energy formula 0-47361  
 exchange mag. moments, meson exchange currents, field theoretical approach 0-52574  
 excitation energies, calc. by energy density method 0-47425  
 Fermi systems, semi-infinite, surface props., thickness and energy 0-52600  
 finite Fermi system correlation energy, fast configuration interaction approach 0-22739  
 finite nuclei and inhomogeneous infinite systems, ground states, FHNC method extension 0-22736  
 G-matrix equation and nuclear forces 0-9242  
 Gamow state vectors as functionals over subspaces of the nuclear space 0-32227  
 giant dipole resonance, particle-hole calcs., M1 strength 0-22785  
 ground state deformation energy, rot. band inertial parameter depend. 0-18185  
 ground-state proton-neutron occupancies in the f-p shell 0-13381  
 group symmetries in nuclear struct., book 0-41963  
 hadrons, extended, second-quantisation of strongly interacting fields 0-13270



## nuclear structure theory continued

Hamiltonians, semiclassical approx., spin-indep. pots. 0-32208  
Hartree-Fock and linear response, coordinate space representation and gradient iteration 0-18216  
Hartree-Fock calcs., fast iterative procedure 0-47414  
Hartree-Fock-Bogolubov eqns., exact soln. 0-27582  
hole states in nuclear matter, single-particle potential 0-32150  
ideal fermions in boson expansions 0-42565  
impure nuclear matter with  $\Lambda$ , binding energy, functional variational approach 0-22744  
inelastic electron scatt., nuclear charge and current spatial struct. 0-5134  
infinite nuclear matter, correlated basis functions method 0-22721  
infinite nuclear matter ambiguities, harmonic oscillator and infinite well solns. 0-22742  
interacting boson model for collective states in even even nuclei 0-22715  
isobar degrees of freedom, binding energy from BHF approx. 0-22734  
isobar degrees of freedom in nuclear matter, binding, NN interactions and  $2\pi$  exchange 0-22735  
Judek effect and nuclear hidden colour excitations in heavy cosmic ray-nucleus reactions 0-27567  
large amplitude collective motion, field theory, excitation energies 0-22665  
level density of nuclei and the superconductive-type pair interaction (*Russian*) 0-13383  
light nuclei, hyperspherical functions for size, excited states, compressibility, binding energy 0-22679  
light nuclei, isospin mixing, charge depend. nuclear forces and Coulomb interactions 0-5056  
magic nuclei, microscopic model incorporating 2p2h configuration (*Russian*) 0-13392  
many body effective interaction theory problem, comparison with atoms 0-47406  
mesonic processes and quarks in nuclei 0-42564  
microscopic versus empirical effective interactions in a single j shell 0-18210  
Monte Carlo methods in quantum many-body problems 0-22727  
N identical particles, Rayleigh-Ritz principle complement for energy spectrum 0-5074  
neutron, alpha and nuclear matter, ground vacuum states 0-22738  
neutron and nuclear matter, variational calc. models 0-22724  
neutron matter, pair condensation, variational theory using correlated basis functions 0-32220  
nuclear, matter,  $V^8$  models, variational calcs. for binding energy and density 0-42571  
nuclear critical opalescence, pion field and condensation 0-42559  
nuclear Dirac phenomenology and the  $\Lambda$ -nucleus potential, anomalous mag. moment 0-37344  
nuclear forces, charge dependence and nuclear struct. effects, nuclear charge distrib. 0-32197  
nuclear forces, nonrelativistic quark model study, resonating group method 0-47403  
nuclear kinetics, quasiclassical method, and angular distribution of nucleons 0-22777  
nuclear matter, Brueckner Bethe and variational calcs. review, nuclear saturation problem 0-22745  
nuclear matter, charge constrained coherent pion states from transversing fast nucleon 0-27585  
nuclear matter, fermion hypernetted chain variational calc. 0-22725  
nuclear matter, Hugenholtz Van Hove theorem and density depend. effective interactions 0-32219  
nuclear matter, optimised Jastrow correlations for Fermi liquids 0-32223  
nuclear matter, three-body problem, variational and Bethe-Faddeev methods 0-27586  
nuclear matter binding energy expansion convergence in Brueckner-Bethe-Goldstone theory 0-488  
nuclear matter binding energy from low density expansions, Brueckner-Hartree-Fock approx. 0-22720  
nuclear matter equation of state, relativistic quantum field theory of neutron stars 0-5088  
nuclei far from  $\beta$ -stability, exotic nuclei 0-5075  
nucleon-nucleus potential at low and intermediate energy in a Dirac-Hartree model 0-5070  
odd mass nuclei in  $1f_{7/2}$ , level density and spacings from resonance data anal. 0-18206  
odd-odd nuclei, pn multiplets  $x=l(l+1)$  energy depend., parabolic rule, nuclear states 0-13379  
odd-odd nuclei, role of tensor force as an effective interaction 0-37332  
one-body dissipation and nuclear dynamics, TDHF calcs. 0-52597  
one-dimensional many-boson systems, with attractive delta interactions, ground state energy 0-27071  
one-dimensional TDHF eqn. numerical soln. with and without collision term 0-5083  
open shell nuclei by seniority and reduced isospin projections 0-47415  
pairing properties and superconductivity, semiclassical treatment, local density approx. of nuclear gap 0-32188  
Paris NN pot. parametrisation, phase shifts, nuclear matter binding energy 0-47405  
parity non-conservation review 0-32207  
particle-number-projected mass tensor 0-9220  
pion condensation, field theoretic many-body system 0-22703  
pion dispersion relation in nuclear matter 0-42572  
proton-proton potential models obtained from the Virginia phase-shift analysis 0-47401  
QCD phenomenology, quarks and gluons in medium energy nuclear physics 0-42563  
quantum number projection, general theory, particle number and ang. momentum 0-27565  
quark lattice and QCD in nuclei 0-5101  
quasiparticle spectra near the yrast line 0-453  
radiative strength distrib. with energy, E1, M1 giant resonances, particle-hole calcs. 0-37349  
rapidly rotating nuclei, high spin rot. including shell fluctuations, semiclassical description 0-47348  
realistic NN pot. construction for three body systems and nuclear matter 0-22699  
relativistic mean field theories, correlation effects estimate 0-5073  
relativistic two-body forces in many-body systems, Weinberg and Yukawa interactions 0-32203  
ring diagrams in nuclear matter, many-body forces contrib.,  $\rho$  and  $\pi$  exchange 0-22740  
second class current upper limit from  $\beta$ -decay data 0-47404

## nuclear structure theory continued

self-consistent pseudopots. in thermodynamic limit, correlation field, nuclear matter single particle orbitals 0-9253  
semi-infinite nuclear matter calc., nuclear density oscillations 0-22681  
semi-infinite nuclear medium, kinetic energy density, simple approx., giant monopole resonance 0-32222  
single particle orbitals, Coriolis attenuation problem, pairing plus recoil model 0-32159  
solid like aspect with alternating layer spin and  $\pi$  condensation 0-22733  
spin-unsaturated subshells and the nucleon-nucleus optical-model spin-orbit potential 0-18259  
strongly bound  $\pi^-$  nuclear states, vel. depend. pot. binding, pionic atoms 0-37331  
symmetries and statistical behavior in fermion systems in nuclei 0-9248  
TDHF approximation and exact Schrodinger dynamics, Taylor series comparison 0-42568  
TDMF phase, unique implication of variational principle 0-27583  
three parameter rotational formula, physical meaning, rot. and vibr. limits 0-18157  
three particle level spectrum, Thomas theorem and Efimov effect, N/D eqns. 0-42562  
time-dependent Hartree-Fock dynamics and phase transition in Lipkin-Meshkov-Glick model 0-52598  
transitional nuclei, single particle and collective degrees of freedom coupling (*Russian*) 0-13345  
uniform extended Fermi medium, correlated basis functions, graphical anal., integral eqn. methods 0-22722  
unitary pole expansion for hard core pots., negative zero eigenvalues contrib. to t-matrix 0-9243  
variational calculation in truncated bases, unbounded operators effect 0-27568  
weak, EM and strong interactions in the nucleus 0-4978  
Young's diagram for nuclear excited states 0-42566  
yrast band, backbending, canonical formalism (*French*) 0-52555  
 $\Delta$ -propagation in nuclear matter, Pauli principle effects 0-32221  
(n, $\gamma$ ) gamma ray spectra calc. 0-52620  
 $\pi$ N scattering amplitude in nuclear matter, quantum field theory approach 0-42570  
 $^{212}\text{At}$ , relative  $\alpha$ -decay width and excited levels, nuclear field theory 0-47437  
 $^{212}\text{Ba}$ , A=130, 132, 134, 136, levels and EM props., ang. momentum projected quasiboson model 0-5067  
 $^{212}\text{Be}$  deformed nucleus, continuum states in strong coupling model 0-22682  
 $^{12}\text{C}$  M1 (15.11 MeV) form factor, evidence for nuclear pion field critical opalescence 0-32232  
 $^{12}\text{C}(n,n)$ , <17 MeV, resonating group calcs., phase shifts and differential cross sections 0-32275  
 $^{40}\text{Ca}$ , finite nuclear props. in relativistic quantum field theory, mass and p densities 0-9219  
 $^{52}\text{Cr}$ , lf nucleon orbit RMS radii from transfer data 0-27544  
 $^{63}\text{Cu}$ , A=65,67,68, energy levels, core coupling model calcs. 0-9238  
Dy,  $\Delta N=2$  coupling problem 0-47412  
 $^{164}\text{Er}$ , A=156, 164, aligned positive parity bands from rot. aligned model 0-9209  
Gd,  $\Delta N=2$  coupling problem 0-47412  
 $^{146}\text{Gd}$ , spherical HFB calcs. for Z=64 shell closure 0-22716  
 $^{154}\text{Gd}$  multiphonon vibr. bands, dynamic deformation theory 0-5035  
 $^3\text{H}$  binding energy, 3N bound state with separable interactions, Faddeev theory corrections 0-13388  
 $^3\text{H}$ , energy levels using ATMS method and realistic nuclear forces 0-22707  
 $^3\text{H}$ , three-particle bound states for partly nonlocal interactions with continuum bound states 0-32206  
 $^3\text{H}$  wave function anal. form from Faddeev eqn.,  $^3\text{He}$  form factor 0-47410  
 $^3\text{H}$  binding energy using phenomenological  $\Lambda N$  pots. 0-9254  
 $^3\text{He}$  charge form factor, 3N bound state with separable interactions, Faddeev theory corrections 0-13388  
 $^3\text{He}$  charge form factors at high momentum transfer, relativistic interactions, N form factors 0-32205  
 $^4\text{He}$  binding energy,  $\Delta(3-3)$  effects, reaction matrix calc.,  $\Delta$  degrees of freedom 0-9218  
 $^4\text{He}$ , energy levels using ATMS method and realistic nuclear forces 0-22707  
 $^4\text{He}$  mixed symmetry state admixture from  $^3\text{He}(n,\gamma)$  (*Russian*) 0-37378  
 $^4\text{He}$ , parity mixing below 30 MeV excitation energy for  $\Delta T=0,1$  transitions 0-52604  
 $^4\text{He}$ - $^4\text{H}$  binding energy difference, bound states, exact four body calc. 0-9255  
 $^{16}\text{O}$ , A=166, 168, 170, 172, yrast states, quadrupole moments and B(E2) values, microscopic calcs. 0-32147  
 $^{180}\text{Hf}$  band crossing and giant backbending 0-32156  
 $^{123}\text{I}$ , bands and decay props., core-particle coupling and polarisation effects 0-13354  
 $^{26}\text{Mg}$  ( $\alpha,\alpha$ ), 104 MeV, oblate-prolate effects in struct. and reactions 0-9225  
 $^{91}\text{Nb}$ , energy spectra and EM props. using broken pair model 0-499  
 $^{93}\text{Nb}$  B(EA) transitions, quasiparticle-phonon multiplet, nuclear field theory for superfluid nuclei 0-47427  
 $^{20}\text{Ne}$  low lying states, configuration mixing calcs. with basis states from variational method 0-22693  
Ni doubly even nuclei, eqns. of motion method, pairing correlations, ground state energies 0-52585  
 $^{15}\text{O}$ , normal parity levels from P-model calcs. with realistic NN interaction (*Russian*) 0-32194  
 $^{16}\text{O}$  and  $\text{Sd}$  shell nuclei, binding energy from realistic Hamiltonians and spectral distrib. theory 0-22678  
 $^{16}\text{O}$ ,  $\Delta(3,3)$  excitations and effective 3-nucleon forces 0-27561  
 $^{16}\text{O}$  ground state and binding energy, microscopic calc. with realistic NW interaction (*Russian*) 0-5052  
 $^{16}\text{O}$ , odd parity levels, correlated basis functions method 0-22721  
 $^{16}\text{O}$  region, effect operators, number conserving set generalisation 0-42555  
 $^{18}\text{O}$  1.98 MeV  $2^+$  state static quadrupole moment, from nuclear sum rules 0-13374  
Pb region, mag. moments and M1, M2 and M4 values, self consistent calcs. 0-47371  
 $^{208}\text{Pb}$ , finite nuclear props. in relativistic quantum field theory, mass and p densities 0-9219



**nuclear structure theory continued**

- <sup>208</sup>Pb, isoscalar giant multipole resonances, simple macroscopic model, damping mechanisms 0-42617
- <sup>149</sup>Pm,  $\beta$ -decay, nucl. matrix elements, calc.,  $\gamma$ -transitions 0-52628
- <sup>212</sup>Po levels and  $J^\pi$ , weak coupling calc. using realistic matrix elements 0-5068
- <sup>A</sup>Pt, A=190, 192, 194, levels and  $\gamma$ -transition reduced probab., interacting boson model 0-18196
- Sm,  $\Delta N=2$  coupling problem 0-47412
- <sup>154</sup>Sm giant multipole resonance fragmentation among two-phonon states 0-18260
- Sn, deep h-lc state fragmentation, strength functions, giant resonances, quasiparticle phonon model 0-37320
- Sn isotopes, quantum number projection, particle number projection 0-27566
- <sup>A</sup>Sn, A=116, 118, 120, 122, 124, 0<sup>+</sup>, 2<sup>+</sup> and 4<sup>+</sup> states 1 number conserving approach 0-22694
- Sn( $\alpha,\alpha'$ ), even-even isotopes, nuclear struct. effects in microscopic theory 0-37391
- <sup>12</sup>C mean life, Pauli exclusion principle validity for nucleons 0-18233
- <sup>51</sup>V, 1f nucleon orbit RMS radii from transfer data 0-27544
- <sup>89</sup>Y, energy spectra and EM props. using broken pair model 0-499
- <sup>69</sup>Zn, energy levels, core coupling model calcs. 0-9238
- Zr even isotopes, quadrupole moments and E2 transition rates, broken pair approx. 0-52579

**nuclear track emulsions**

- automatic rotary diaphragm for microphotometer 0-22415
- cellulose nitrate track detector, effect of  $\gamma$ -radiation on bulk etching rate 0-885
- development probability, AgBr grain diameter depend. 0-9056
- heavy ion track width, Katz's theory 0-32578
- muon deep inelastic scatt. event location 0-27906
- particle track detectors, trends and developments (*Hungarian*) 0-18755
- proton interactions at 28 GeV (*Korean*) 0-18299
- secondary ionisation, delta-ray effects 0-881
- sensitivity centre variation with AgBr grain diameter 0-9055
- small-grain development of emulsion monofilms for electron-microscope autoradiography (*Russian*) 0-297
- supralinear photographic emulsions, radiobiological aspects 0-26290
- tissuelike medium  $\alpha$  trajectory heavy secondary ion ejection 0-9466
- tissuelike medium  $\alpha$  trajectory production of  $\delta$ -rays 0-9465
- AgBr, nucl. emulsion, latent image form., grain diameter depend. 0-9453
- Ag( $K^-,K^0$ ), cascade hypernucleus identification in nuclear emulsion 0-52603
- Br( $K^-,K^0$ ), cascade, hypernucleus identification in nuclear emulsion 0-52603
- He nuclei emission in 7.5 to 200 GeV hadron interactions (*Russian*) 0-9325
- <sup>16</sup>O induced reactions in nuclear emulsions at 2.1 GeV/nucleon, multiplicity distrib. of white and grey tracks (*Spanish*) 0-47495

**nucleation**

see also crystal growth; crystallisation

- A + A<sub>n</sub>  $\rightleftharpoons$  A<sub>n+1</sub><sup>\*</sup>, cluster dynamics, classical trajectory study 0-3316
- alloy decomposition kinetics, Johnson-Mehl-Avrami (JMA) formula appl. 0-16263
- anisotropic nuclei, kinetics of formation (*Russian*) 0-29149
- atomic cluster, free energy, chem. pot. and surface energy, microscopic capillarity approx. 0-5654
- beam-addressable optical display using supersaturated vapour photonucleation 0-4691
- biotite, deform. and recrystallisation in Woodroffe Thrust mylonite zone 0-21739
- boiling delay, unsteady heat transfer with phase transition 0-48690
- book, current topics in material science 0-46747
- $\alpha$ -brass, 70:30, cold-worked, recrystallised grains nucleation on heating 0-29998
- brass, 70:30, rolled, nucleation and annealing texture development 0-45320
- chemical systems, non-equilib., mol. dynamics studies of long range and short range fluctuations 0-21318
- cholesteric nonanoate, isothermic crystallisation, microscopic exam. (*Polish*) 0-10651
- cholesteryl capricinate spherulite growth rate and nucleation rate, optical method (*Polish*) 0-10652
- classical nucleation theory, test on cryst. nucleation in Li<sub>2</sub>O-SiO<sub>2</sub> glass 0-1939
- cloud chamber, low-pressure tissue-equivalent gas for  $\alpha$ -particle tracking 0-9462
- cloud chamber, thermal diffusion, continuous flow parallel plate type, analysis w.r.t. atm. water droplet growth 0-36416
- cloud droplet growth studies, optical motion control appl. to Atmospheric Cloud Physics Laboratory 0-12634
- coherent phase form. at stress concentrators, effect of dislocation splitting, dislocation pile-ups, and phase elastic moduli (*Russian*) 0-49356
- condensation, homogeneous, cluster size distrib., stochastic model 0-22311
- conference, phase transformations in metallurgy, York, England (Apr. 1979) 0-2994
- cosmic dust, grains sudden nucleation and growth in supernova and nova ejecta 0-26941
- crystal nucleation and symmetry, interaction pots. effect 0-34169
- defect clusters, nucleation and growth due to energetic particle radiation, chemical rate reaction theory, computer program 0-49263
- dielectric crystallisation kinetics, electric field effect, nucleation 0-19919
- diffusional crystal growth mechanisms 0-3059
- droplets nucleation in finite systems, theory and computer simulation 0-26038
- electrochemical phase formation 0-55309
- electrocrystallisation, nucleation, phase form., symposium, Southampton, England (Dec. 1977) 0-51942
- electrolyte, binary, cryst. growth kinetics during precipitation 0-49149
- electron-hole plasma nucleation, time evolution 0-49616
- gas bubbles in solids, simultaneous hetero- and homogeneous nucleation model 0-2066
- glass transition, soft-sphere model, mol. dynamics study 0-49343
- glass-ceramics and photosensitive glass, microstructure rel. to properties (*German*) 0-38926
- grain boundary crack nucleation, and growth under low cyclic stresses, dislocation mechanism 0-19811
- grain boundary migration vacancy generation, and drag force 0-15090

**nucleation continued**

- graphite nucleation, role of pre-heat treatments (*Japanese*) 0-35220
- homogeneous, and heterogeneous nucleation processes for substance of different crystn. struct. 0-49144
- homogeneous, classification of spontaneous condensation processes 0-6500
- homogeneous nucleation kinetics, steady state solns. 0-50873
- ice nucleation by fluid-breaking metaldehyde particles (*Chinese*) 0-12468
- industrial crystallisation, conference, Warsaw, Poland (Sept. 1978) 0-46737
- interstellar grains formation, time-depend. nucleation theory 0-26946
- ion-implanted bubble garnet film, vel. asymmetry during stripe head propagation 0-39834
- ionic crystals, precipitation from aq. solns., induction period 0-50882
- ions, mol. clustering, gaseous-condensed state, nucleation and solvation 0-28129
- Johnson-Mehl and cellular microstructure, comparative analysis, computer simulation 0-54392
- liquids, saturated, boundaries of region of existence of nucleate boiling, thin film breakdown 0-48695
- martensite nucleation at dislocations, elasticity model 0-55393
- martensitic transformation, nucleation time estimate 0-29954
- metal film, nucleation controlled interaction with Si substrate, silicide form. 0-10711
- metal films, on alkali halide substrates, nucleation and growth, surface study techniques, review 0-10809
- metastable state relaxation, critical point region nucleation in thermodynamic systems (*Russian*) 0-13026
- Nimonic PE16, He injected, bubble-void transitions in Ni ion bombard. 0-34095
- non-spherical nuclei, nucleation kinetics, high pressure effects 0-19730
- nuclear track detectors, X-ray anal. of microcrystallite nucleation 0-890
- nucleate pool boiling, meas. of void frequency distrib. and profiles using neutron beams 0-27691
- octaphenylcyclotetrasiloxane, phase behaviour and nucleation kinetics 0-29168
- precipitation processes, study by particle site anal. 0-50883
- premartensitic phenomena, nucleation, shape memory effect, review 0-3041
- rate, relationship between experimentally determined and true values 0-54343
- review, nucleation 0-49143
- review, nucleation theory for high and low supersaturations 0-49142
- sapphire:Ti<sup>4+</sup>, plastically deformed, precipitation hardening, TEM study 0-7592
- secondary nucleation, formation, survival and growth of nuclei 0-50540
- secondary nucleation kinetics 0-19945
- size dependent growth systems, effective nucleation rate 0-38972
- solid phase reactions, modelling using population balance approach 0-11874
- solids, amorphous and crystalline, condensing from gas phase, nucleation, growth and transform. 0-24745
- steel, austenite hot deformation influence on phase transformations 0-7606
- steel, austenitic type 347, nucleation and growth of creep cavities 0-40513
- steel, C martensitic, tempering induced decomposition and segregation, atom probe study 0-3112
- steel, Mo-Cr (3 wt.%), CrC formation in isochronal tempering, electron microscope study 0-7584
- steel, stainless, He effects on microstruct. in ion-irrad. 0-29078
- steel, stainless, martensite formation, in situ obs. 0-25692
- steel, stainless, martensite nucleation, in situ electron microscope obs. 0-7572
- steel, stainless, martensite nuclei obs., role of defects in nucleation 0-25693
- steel, type FV548, 1 MeV electron irradiated, influence of pre-injected He on void nucleation and growth 0-34054
- steel, unkillied deep drawing sheets, influence of N content on recrystn. (*German*) 0-40376
- steel, W-Cr (3 wt.%), CrC formation in isochronal tempering, electron microscope study 0-7584
- step decoration on cryst. surfaces, conditions 0-15349
- stereological counting measurements, use in testing growth rate theories 0-16311
- sulphate particle formation by heteromol. nucleation and condensation in cavities 0-26183
- TGS, domain nucleation in AC elec. fields 0-34867
- thin film growth, nucleation kinetics, coalesc. of mobile nuclei 0-6671
- thin films, vapour deposited, saturation cluster density, general formula 0-15408
- transition metal, bimetallic cluster, photoselective bimetallic aggregation, review 0-53182
- two phase alloy hardening by second phase particle coalescence 0-7591
- two-dimensional, simulation using kinetic Ising model 0-54156
- water supercooled droplets, on ice substrate after low speed collision, freezing behaviour, cryst. struct. 0-29152
- water vapour, photoinduced nucleation expt. 0-2149
- water-isobutyric acid (2,6-lutidine) mixtures, critically quenched, phase separation and coalescence 0-24581
- water-methanol (n-propanol), binary mixtures, nucleation 0-44305
- YIG, hot spraying to give fine, free flowing, sinterable powder 0-20865
- Ag epitaxial films, grain boundary struct. evolution during recrystn., interface energy effect (*Russian*) 0-15387
- Ag epitaxial growth, cluster mobilities, in-situ electron microscopes obs. 0-15407
- Al alloys, continuous precipitation, nucleation, spinodal decomposition 0-3061
- Al epitaxial films, grain boundary struct. evolution during recrystn., interface energy effect (*Russian*) 0-15387
- Al-Mg-Si, nucleation and precipitation growth on dislocations, electron microscope studies 0-3064
- Al<sub>2</sub>(SO<sub>4</sub>)<sub>3</sub>.K<sub>2</sub>SO<sub>4</sub>.24H<sub>2</sub>O, secondary nucleation rate under agitation 0-50541
- Al<sub>2</sub>(SO<sub>4</sub>)<sub>3</sub>(NH<sub>4</sub>)<sub>2</sub>SO<sub>4</sub> or AlNH<sub>4</sub>(SO<sub>4</sub>)<sub>3</sub>.12H<sub>2</sub>O, size dependent growth systems, effective nucleation rate 0-38972
- Al<sub>2</sub>TiO<sub>5</sub> powders, decomposition kinetics using nucleation and growth-rate constants (*Japanese*) 0-35156
- Au epitaxial films, grain boundary struct. evolution during recrystn., interface energy effect (*Russian*) 0-15387
- Au epitaxial growth, cluster mobilities, in-situ electron microscopes obs. 0-15407



## nucleation continued

- BaMoO<sub>4</sub>, single crystals, habit modification, growth kinetics in silica gel 0-20777  
 BaO-SiO<sub>2</sub>, glass ceramic, growth and nucleation kinetics 0-7528  
 Bi<sub>2</sub>Te<sub>3</sub>, anodic oxide films, two-dimens. nucleation and growth 0-11807  
 CaCO<sub>3</sub>, nucleation mechanism accompanying Ostwald ripening 0-50641  
 CaCO<sub>3</sub>, with perfect struct., temp. depend. of rate of twinning 0-10561  
 Ca(NO<sub>3</sub>)<sub>2</sub>-H<sub>2</sub>O system, induction period supercooling depend. meas. 0-19918  
 Cd films, nucleation and growth, props. 0-29878  
 Co-Ga  $\beta^2$  quenched single crystals, annealing-out of point defects 0-55426  
 Cu alloys, continuous precipitation, nucleation, spinodal decomposition 0-3061  
 Cu-B(25 wt.%) (Japanese) 0-55402  
 Cu-Be-Co(0.1,0.2 wt.%), discontinuous precipitation (Japanese) 0-55402  
 Cu-Cr (0.55 wt.%), crystallography of precipitates, strain field study 0-25699  
 Cu-Ni-Al, review 0-7564  
 Cu-Ti, dil. alloy, cellular precipitates, nucleation, TEM study 0-3069  
 $\beta$ -Cu-Ti, dil. alloy, growth phenomena associated with precipitation, TEM study 0-3070  
 Cu-Zn-Al, memory alloy wire and ribbon reversible martensitic transformation, ageing effect, review 0-7564  
 CuSO<sub>4</sub>·5H<sub>2</sub>O, secondary nucleation and growth in a fluidized bed 0-50542  
 Fe alloy type G18, martensitic  $\gamma \rightarrow \alpha$  transformation, dislocation pile-ups,  $\epsilon$  phase nucleation (Russian) 0-55396  
 Fe, BCC, void nucleation following electron irradiation 0-29054  
 Fe-C, proeutectoid ferrite nucleation kinetics at austenite grain boundaries 0-55405  
 Fe-Mn-V-C austenitic steel, discontinuous precipitation, morphological changes 0-3078  
 Fe-N, nucleation and precipitation growth on dislocations, electron microscopy studies 0-3064  
 Fe-Ni (29 wt.%), martensite nucleation at dislocations, elasticity model 0-55393  
 Fe-Ni-C (31, 0.28 wt.%), crossings of thin plate martensites, TEM obs. 0-25756  
 Fe-Zn, crystallographic relations by X-ray diffraction 0-24408  
 FeOCl-pyridine intercalate, mechanism, nucleation and diffusion 0-49420  
 GaSe, anodic oxide films, two-dimens. nucleation and growth 0-11807  
 Ge, amorphous film, laser pulse annealing 0-15006  
 Ge, electron-hole drops, non-isothermal nucleation 0-44514  
 H<sub>2</sub>O droplet growth in presence of soluble gases, expts. 0-21807  
<sup>4</sup>He, isotopically pure superfluid, vortex nucleation 0-44378  
 In epitaxial growth, cluster mobilities, in-situ electron microscopes obs. 0-15407  
 KCl, influence of collisions on cryst. growth and secondary nucleation under conditions of meas. crystn. 0-50544  
 LiF, radiation induced voids, formation on dislocations 0-15159  
 Li<sub>2</sub>O-SiO<sub>2</sub> glass, cryst. nucleation, test of classical nucleation theory 0-1939  
 Mo, BCC, void nucleation following electron irradiation 0-29054  
 Mo-Zr, heavy ion irradiated, void swelling, phase instability 0-29084  
 NO<sub>2</sub>, heat transfer in boiling on surface of vertical cylindrical rod 0-48706  
 NO<sub>2</sub>-HNO<sub>3</sub>-H<sub>2</sub>O clusters, gas phase, thermodynamic quantities, mass spectra obs. 0-50875  
 Na smoke particles, nucleation and growth, light scatt. study 0-35580  
 Nb, BCC, void nucleation following electron irradiation 0-29054  
 Ni base superalloy,  $\gamma$ -precipitation influence on recrystallisation 0-29955  
 Ni, epitaxial growth, on NiO(100), by low pressure hydrogen reduction (French) 0-11578  
 Ni-based superalloys, TEM obs. of cellular transformation products 0-3045  
 Ni-Co-Cr superalloy, powder produced, necklace struct. development 0-40395  
 Ni-Ti (9.6 wt.%), mag. study on phase decomposition (Japanese) 0-15758  
 Ni<sub>4</sub>Mo, coherent phase form. at stress concentrators (Russian) 0-49356  
 Ni(NH<sub>4</sub>)<sub>2</sub>(SO<sub>4</sub>)<sub>2</sub>·6H<sub>2</sub>O, precipitation from equimolar aqueous solns., kinetics study 0-7848  
 Pb, variations of energy of the (111) torsion joint as a function of the angle of torsion in metallic seeds [dendritic structure] (French) 0-25682  
 PbS epitaxial growth, cluster mobilities, in-situ electron microscopes obs. 0-15407  
 Pd, epitaxial growth, cluster mobilities, in-situ electron microscopes obs. 0-15407  
 Pd, two-dimens. nucleus form. on Ag (111), UHV electron microscope obs. 0-10760  
 SF<sub>6</sub>-Ar, condensing flow, gasdynamic and IR meas. 0-6501  
 Si, CVD on SiO<sub>2</sub> and Si<sub>3</sub>N<sub>4</sub> substrates, nucleation in SiH<sub>4</sub>-HCl-H<sub>2</sub> system at high temp. 0-49538  
 Si, epitaxial layer, growth mechanism from ion-molecular beams 0-2299  
 Si:H amorphous film, plasma-deposited, growth morphology and defects 0-44128  
 Si-Co interface metal-semiconductor transition, rel. to first compound nucleation 0-24771  
 SiC, epitaxial film, effect of impurities on polymorphism during growth 0-15414  
 $\alpha$ -SiC, single crystals, phase struct. rel. to heat treatment, nucleation 0-38991  
 SiO<sub>2</sub>-Na<sub>2</sub>O-CaO glass, phase separation characts., melting atmosphere effect 0-44141  
 Sn droplets, on Bi, Zn and Al, heterogeneous nucleation 0-44294  
 Sn polymorphic transformations ( $\beta \rightarrow \alpha$ ), effect of impurities, exam. 0-7557  
 Ti-Al-Sn (5, 2.5 wt.%), annealing of near-basal hydrides 0-20989  
 TiAl<sub>3</sub> crystals dissolution in pure Al liq., grain refinement of  $\alpha$ -Al solid-solution by Ti addition 0-35178  
 ZnC<sub>2</sub>O<sub>4</sub>·2H<sub>2</sub>O, crystn. kinetics by precipitation 0-50884

## nuclei see nucleus

## nuclei with mass number 1 to 5

- <sup>3</sup>Li states, phase shift anal. of <sup>3</sup>He(d,d) 0-47382  
 A=3 systems, charge form factor and bound nucleon polarisation 0-22708  
 A=3-4 hypernuclei, binding energy anal., A-N pot., scatt. length and effective range 0-9256  
 A=4-16, monopole giant resonances, state density radii and compressibility using hyperspherical functions (Russian) 0-27615

## nuclei with mass number 1 to 5 continued

- A<100, average E1/M1 strength ratio 0-52621  
 baryon-antibaryon nuclei 0-22709  
 realistic NN pot. construction for three body systems and nuclear matter 0-22699  
 three particle level spectrum, Thomas theorem and Efimov effect, N/D eqns. 0-42562  
 three-nucleon system, bound state calc. program PERFECT 0-13390  
 (e,e), A=2, 3, 4, scaling laws in relativistic impulse approx. model, spin effects 0-52662  
 ( $\gamma$ ,X), A=2, 3, 4, photonuclear and EM interactions 0-22816  
<sup>2</sup>H( $\pi$ ,pp), pion absorpt., effect of  $\rho\pi$  exchange currents (Korean) 0-47402  
 t formation average cross sections in ( $\alpha$ ,t) and (d,t) 0-42670  
<sup>1</sup>H, possibility of thermonuclear fuel in relativistic plasma in B(p,  $2\alpha$ ) $\alpha$  reaction (Russian) 0-37573  
<sup>3</sup>B(p,  $2\alpha$ ) $\alpha$ , possibility of thermonuclear fuel in relativistic plasma (Russian) 0-37573  
 H<sup>+</sup>, upper limit from P- and T-violating interactions in hyperfine struct., mol. beam reson. expt. on TIF 0-53019  
 H<sup>+</sup>, value from electric dipole hyperfine struct. calc. of TIF 0-53162  
 H(d,d), 2 GeV, polarised d, tensor and vector asymmetries 0-9285  
<sup>1</sup>H( $\bar{n}$ ,X), annihilation, 1.4 GeV/c,  $\pi^{\pm}$ , p emission angles, momentum and multiplicity distrib. 0-532  
<sup>1</sup>H(n,d) $\pi^0$ , 459, 648, 802 MeV, relative diff. cross section and ang. distrib. 0-52671  
<sup>1</sup>H(n, $\gamma\gamma$ )<sup>2</sup>H, cross section upper limit 0-52683  
<sup>1</sup>H(n,n)p, 210-495 MeV, free elastic scatt., phase shift anal. 0-52676  
<sup>1</sup>H(n,p), pol. n and p, 220-495 MeV, free elastic scatt., D<sub>1</sub> and P parameters 0-52674  
<sup>1</sup>H(n,p), pol. n and p, 220-495 MeV, free elastic scatt., Wolfenstein parameters R<sub>1</sub>, A<sub>1</sub> 0-52675  
<sup>1</sup>H(n, $\pi^0$ )<sup>2</sup>H, nuclear forces charge symmetry test 0-5071  
<sup>2</sup>H( $\gamma$ , $\pi$ ), theoretical and expt. results. 0-42698  
<sup>2</sup>H, distant ENDOR obs. of partially deuterated succinic acid 0-23445  
<sup>2</sup>H  $\gamma$ -energy and binding energy from <sup>1</sup>H(n, $\gamma$ ) 0-52564  
<sup>2</sup>H, NMR relax. and mol. dynamics in lipid bilayers 0-26206  
<sup>2</sup>H neutron binding energy and n mass excess from <sup>1</sup>H(n, $\gamma$ ) 0-47362  
<sup>2</sup>H<sup>3</sup>H $\mu \rightarrow$ He+n+ $\mu^-$ +17.6 MeV, muonic catalysis in synthesis reactions (Russian) 0-52706  
<sup>2</sup>H+p(n), differential cross sections, Coulomb penetration factor in DWBA calc. (Chinese) 0-27603  
<sup>2</sup>H(<sup>2</sup>H,n)<sup>3</sup>He, fusion through metallic D 0-13517  
<sup>2</sup>H( $\alpha$ , $\alpha$ )<sup>2</sup>H, 6 to 14 MeV, cross section meas. 0-27655  
<sup>2</sup>H( $\alpha$ , $\alpha$ n), quasi-elastic scatt., direct reaction unitarised impulse approx. 0-42674  
<sup>2</sup>H( $\alpha$ ,np)<sup>3</sup>He, differential cross section and polarisation, three body model 0-47460  
<sup>2</sup>H(d,n), 13.6, 24.3 MeV, 0° absolute differential cross section 0-27649  
<sup>2</sup>H(d,n), 290, 460 keV, neutron polarisation, ang. depend. 0-42632  
<sup>2</sup>H(d,n)<sup>2</sup>He, 1.5-15.5 MeV, tensor anal. power, charge symmetry violation in mirror reaction 0-13368  
<sup>2</sup>H(d,p)<sup>3</sup>H, 13.4, 17 MeV, pol. d, anal. power direct reaction and isospin symmetries 0-515  
<sup>2</sup>H(d,p)<sup>3</sup>H, 1.5-15.5 MeV, tensor anal. power, charge symmetry violation in mirror reaction 0-13368  
<sup>2</sup>H(e,e'p), single hole state momentum distrib. 0-22674  
<sup>2</sup>H(e,e), EM interactions and mag. sum rules 0-42639  
<sup>2</sup>H(e,e), energy weighted sum rules, almost realistic NN pot. anal. (Russian) 0-13465  
<sup>2</sup>H(e, $\pi$ ), total cross section from square reaction matrix element (Russian) 0-32271  
<sup>2</sup>H( $\gamma$ ,  $\pi^-$ )2p, target asymmetry and effective neutron polarisation, polarised d 0-9286  
<sup>2</sup>H( $\gamma$ , $\pi^+$ ) photoexcitation in  $\Delta(1236)$  region 0-22813  
<sup>2</sup>H( $\gamma$ , $\pi^0$ ), coherent photoprod., binding effects and threshold amplitude calc. 0-32264  
<sup>2</sup>H( $\gamma$ , $\pi^0$ ), cross section and threshold effects using dynamical  $\gamma$ N $\rightarrow$ N $\pi^0$  model 0-27627  
<sup>2</sup>H( $\gamma$ , $\pi^+$ )2n, threshold to 22 MeV, bremsstrahlung yield and total cross section 0-9288  
<sup>2</sup>H( $\gamma$ , $\pi$ ), threshold photoprod. cross sections, elementary nucleonic amplitudes 0-22812  
<sup>2</sup>H(n, np)n, 17 to 27 MeV, neutron-neutron scattering length determination, Monte Carlo analysis 0-13476  
<sup>2</sup>H( $\bar{p}$ , $\bar{p}$ )p, neutral current cross section for reactor  $\bar{\nu}$  0-5129  
<sup>2</sup>H(p,2p)n, 23, 39.5 MeV, noncoplanar reaction, breakup cross section 0-530  
<sup>2</sup>H(p,2p)n, 28.6 MeV, breakup cross sections in collinear geometry 0-9296  
<sup>2</sup>H(p, $\pi^+$ ), 800 MeV, pion prod. with spectator neutron, cross section 0-9294  
<sup>2</sup>H(p,n)2p, pol. n and p, 10.6-15.1 MeV, transverse polarisation transfer at 0° 0-42630  
<sup>2</sup>H(p,p'), 0.6-25 GeV, backward emitted proton inclusive spectra, short range correlation 0-32281  
<sup>2</sup>H(p,p), backscattering, large momentum transfers,  $\pi$  exchange effects 0-5143  
<sup>2</sup>H(p,n)<sup>3</sup>H, 12.5 MeV, angular distrib. of p-n final state interaction 0-52672  
<sup>2</sup>H(p,n)p, 1.67 GeV/c, secondary particle ang. distrib. and correlations (Russian) 0-27646  
<sup>2</sup>H(p, $\pi^+$ )<sup>2</sup>H, 400, 470, 600 MeV, differential cross section using isobar model 0-9291  
<sup>2</sup>H( $\pi$ ,p), reactive two body contrib. to pion-nucleus optical pot. 0-9313  
<sup>2</sup>H( $\pi$ , $\pi$ ), expt. and theoretical work, present status, model testing,  $\pi$ N interaction 0-42699  
<sup>2</sup>H( $\pi$ , $\pi$ ), high energy total cross section in Glauber model 0-18346  
<sup>2</sup>H( $\pi$ , $\pi$ ), medium energy elastic scatt. amplitudes, covariant multiple scatt. model convergence test 0-42710  
<sup>2</sup>H( $\pi$ , $\pi$ ), polarised d, dibaryon resonance signals in excitation functions 0-9181  
<sup>2</sup>H( $\pi$ , $\pi$ ), relativistic description,  $\pi$ N waves, NN rescatt.,  $\rho$ -exchange,  $\pi$  absorption and emission 0-9310  
<sup>2</sup>H( $\pi^-$ ,  $\pi^-$ ), 552 MeV/c, elastic differential cross section Glauber theory anal. (Russian) 0-52700  
<sup>2</sup>H( $\pi^-$ ,  $\pi^-$ )p, 438 GeV/c, break up process, kinematic variables, np final state interaction (Russian) 0-52701  
<sup>2</sup>H( $\pi^-$ ,  $\pi^-$ ), 1.57, 1.66 and 1.76 GeV/c elastic back scatt. cross section energetic shape struct. (Russian) 0-47510



## nuclei with mass number 1 to 5 continued

- $^2\text{H}(\pi^+, \pi^-)\text{X}^-$ , 2.6 GeV/c, d proton screening correction and Glauber parameter 0-9175  
 $^2\text{H}(\pi^+, \pi^+)$ , tensor polarisation and cross section at  $180^\circ$  0-5116  
 $^2\text{H}(\pi^+, \pi^+)$ , 340 MeV/c, reaction mechanisms and isospin effects 0-32306  
 $^3\text{H}$  binding energy, 3N bound state with separable interactions, Faddeev theory corrections 0-13388  
 $^3\text{H}$ , energy levels using ATMS method and realistic nuclear forces 0-22707  
 $^3\text{H}$  isobaric analogue state excitation, cross section from  $^3\text{He}(\pi^-, \pi^0)$  0-42544  
 $^3\text{H}$  neutron binding energy 0-47362  
 $^3\text{H}$  neutron binding energy from  $^1\text{H}(n, \gamma)$  0-52564  
 $^3\text{H}$  wave function anal. form from Faddeev eqn.,  $^3\text{He}$  form factor 0-47410  
 $^3\text{H}(\text{He}, \text{X})$ , 50, 65, 78 MeV, quasifree scattering and quasifree reaction processes 0-13486  
 $^3\text{H}(d, n)$ , pol. d, below 6.75 MeV, tensor anal. power 0-42633  
 $^3\text{H}(e, e')2n$ , realistic NN interactions, three body variational wave functions, spectral functions 0-47470  
 $^3\text{H}(e, e')\text{X}$ ,  $\text{X}=\text{p}$  or  $\text{n}$ , coincidence reactions, electrodisintegration cross sections 0-22823  
 $^3\text{H}(\gamma, \text{X})$  two- and three-body photodisintegration cross sections 0-32263  
 $^3\text{H}(\gamma, \pi^0)$ , polarisation effects 180 to 700 MeV, impulse approx. calcs. (Russian) 0-37368  
 $^3\text{H}(\gamma, \pi^0)^3\text{H}$ , polarisation effects 180 to 700 MeV, impulse approx. calcs. (Russian) 0-37368  
 $^3\text{H}(\gamma, \text{xn})$ ,  $\text{x}=1$  or  $2$ , photodisintegration cross sections 0-22817  
 $^3\text{H}(\mu, \nu)3n$ , transitions from bound to continuum three nucleon states 0-5128  
 $^3\text{H}(\rho, \gamma)^3\text{He}$ , intermediate energy, ang. distrib., reaction amplitude and  $^3\text{He}$  vertices 0-22835  
 $^3\text{H}(\pi^+, \pi^+)$ , 232-252 MeV charge exchange differential cross section 0-37401  
 $^3\text{H}$  binding energy using phenomenological  $\Delta\text{N}$  pots. 0-9254  
 $^3\text{H}(e^+, e^+)\text{H}$ , s-wave scatt., effective range expansion 0-47467  
 $^3\text{H}(\pi, \pi)\Delta(1236)$  resonance region, Watson multiple scatt. series. integral eqns. 0-37402  
 $^3\text{He}$  charge form factor, 3N bound state with separable interactions, Faddeev theory corrections 0-13388  
 $^3\text{He}$  charge form factor with Reid soft core pot. 0-13389  
 $^3\text{He}$  charge form factors at high momentum transfer, relativistic interactions, N form factors 0-32205  
 $^3\text{He}$ , Coulomb energy, charge symmetry breaking 0-27564  
 $^3\text{He}$  elastic breakup in  $^3\text{He}(\text{p}, \text{d})$  0-52685  
 $^3\text{He}$  form factor from  $^3\text{H}$  wave function anal. form 0-47410  
 $^3\text{He}$  prod. in  $\text{Br}, \text{Ag}+\text{p}$  in 24 GeV/c reacts., role of pick-up processes 0-27632  
 $^3\text{He}$ , rigorous bounds for charge densities from form factor data 0-5055  
 $^3\text{He}$  spectroscopic strengths from  $^{13}\text{C}(\text{Li}, \text{t})$  0-47390  
 $^3\text{He}$ , trinucleon bound state problem, binding energy, form factors and mag. moment 0-22710  
 $^3\text{He}(\text{He}, \text{X})$  50, 65, 78 MeV, quasifree scattering and quasifree reaction processes 0-13486  
 $^3\text{He}(\text{He}, \text{d}^3\text{He})$ , three body break up reaction energy spectra, computer program 0-27593  
 $^3\text{He}(\text{He}, \text{p}^3\text{He})$ , three body break up reaction energy spectra, computer program 0-27593  
 $^3\text{He}(d, \text{p})$ , pol. d, below 6.75 MeV, tensor anal. power 0-42633  
 $^3\text{He}(e, e')\text{p}$  electrodisintegration by 1200 MeV electrons (Russian) 0-37370  
 $^3\text{He}(e, e)$ , charge formfactors, second Born approx. and pole model 0-18155  
 $^3\text{He}(e, e')$ , 0.1-14 GeV, deep inelastic inclusive scatt. response functions and momentum distrib. 0-42640  
 $^3\text{He}(e, e')\text{X}$ ,  $\text{X}=\text{p}$  or  $\text{n}$ , coincidence reactions, electrodisintegration cross sections 0-22823  
 $^3\text{He}(e, e)$ , 3-15 GeV, inclusive scatt. 0-13464  
 $^3\text{He}(\gamma, n)$ , photodisintegration cross sections 0-22817  
 $^3\text{He}(\gamma, \text{p})^3\text{H}$ , intermediate energy, ang. distrib., reaction amplitude and  $^3\text{He}$  vertices 0-22835  
 $^3\text{He}(\gamma, \pi^0)$ , cross section and threshold effects using dynamical  $\gamma\text{N} \rightarrow \text{N}\pi^0$  model 0-27627  
 $^3\text{He}(\gamma, \pi^0)$ , polarisation effects 180 to 700 MeV, impulse approx. calcs. (Russian) 0-37368  
 $^3\text{He}(\gamma, \pi^0)^3\text{He}$ , polarisation effects 180 to 700 MeV, impulse approx. calcs. (Russian) 0-37368  
 $^3\text{He}(\gamma, \pi^+)^3\text{H}$ , Fermi motion and off-shell effects, impulse approx. 0-27626  
 $^3\text{He}(\gamma, \pi)$ , threshold photoprod. cross sections, elementary nucleonic amplitudes 0-22812  
 $^3\text{He}(n, \gamma)$ , thermal, effective cross section (Russian) 0-37378  
 $^3\text{He}(\text{p}, \text{p})$ , pol. p, 0.3-1.0 MeV, differential cross section, anal. power, and phase shifts 0-42629  
 $^3\text{He}(d, d)$ , 17-45 MeV, differential cross section and tensor and power ang. distrib. 0-42631  
 $^3\text{He}(d, d)$ , pol. d, 20 MeV, optical pot. strong tensor term, anal. powers 0-37364  
 $^3\text{He}(d, d)$  pol. d, 17-43 MeV, vector anal. power, highly excited six nucleon system 0-47458  
 $^3\text{He}$  binding energy,  $\Delta(3-3)$  effects, reaction matrix calc.,  $\Delta$  degrees of freedom 0-9218  
 $^3\text{He}$ , energy levels using ATMS method and realistic nuclear forces 0-22707  
 $^3\text{He}$  ground state, energy and wave function, static Hartree-Fock calcs. 0-47414  
 $^3\text{He}$  magnetometer, optically pumped (Japanese) 0-8434  
 $^3\text{He}$  mixed symmetry state admixture from  $^3\text{He}(n, \gamma)$  (Russian) 0-37378  
 $^3\text{He}$ , parity mixing below 30 MeV excitation energy for  $\Delta T=0, 1$  transitions 0-52604  
 $^3\text{He}$ , shell model calcs. 0-13393  
 $^3\text{He}$ , soft-core radial wave function, photo-disintegration calculation 0-18209  
 $^3\text{He}$  system,  $\text{O}^+$  states, microscopic wave function 0-463  
 $^3\text{He}(\text{He}, \text{He})$ , 60.2, 113.1 MeV, ang. distrib., optical and coupled channel anal., cross sections 0-47492  
 $^3\text{He}(\alpha, \alpha)$ , composite particle scatt., generator coordinate and natural boundary condition methods 0-13489  
 $^3\text{He}(d, d)$ , pol. d, 12-17 MeV, differential cross sections, anal. powers, phase shift anal. 0-13449

## nuclei with mass number 1 to 5 continued

- $^4\text{He}(d, \text{pn})^4\text{He}$ , differential cross section and polarisation, three body model 0-47460  
 $^4\text{He}(e, e)$ , elastic scatt., spectroscopic information and form factors 0-9260  
 $^4\text{He}(\gamma, 2d)$ , 30-35 MeV,  $2^+$  state search (Russian) 0-42553  
 $^4\text{He}(\gamma, n)$ , 30-35 MeV,  $2^+$  state search (Russian) 0-42553  
 $^4\text{He}(\gamma, \text{pn})^2\text{H}$  reaction, distribution along Treiman-Yang angle (Russian) 0-27628  
 $^4\text{He}(\gamma, \pi^0)$ , differential cross section, complex momenta theory for nondiffractive processes (Russian) 0-32266  
 $^4\text{He}(\gamma, \pi^0)$ , polarisation effects 180 to 700 MeV, impulse approx. calcs. (Russian) 0-37368  
 $^4\text{He}(\text{p}, ^3\text{He})$ ,  $^2\text{H}$ , large momentum transfers,  $\pi$  exchange effects 0-5143  
 $^4\text{He}(2p, 2p)$ , 250, 350, 500 MeV, cross section energy depend., DWIA calcs. 0-37375  
 $^4\text{He}(2p, 2p)$ , pol. nucleon quasi-elastic scatt., nuclear wave function and model tests 0-42656  
 $^4\text{He}(p, d)$ , intermediate energies, pion exchange currents in DWBA anal. 0-32199  
 $^4\text{He}(p, d)$  pickup reaction, isobar configurations and short range correlations 0-22798  
 $^4\text{He}(p, d)^3\text{He}$ , 770 MeV, multiple-scattering approach 0-27636  
 $^4\text{He}(p, d)^3\text{He}$ , large momentum transfers,  $\pi$  exchange effects 0-5143  
 $^4\text{He}(p, \pi^+)$ , pion prod. operator non-relativistic approx. 0-27640  
 $^4\text{He}(p, p)$ , 45-65 MeV, phase shift anal. 0-22832  
 $^4\text{He}(\pi, \pi)$ , (3,3) region, multiple scatt. theory study by optical pot. method (Russian) 0-13509  
 $^4\text{He}(\pi, \pi)$ , low energy, first order optical pot., Pauli principle corrections, nuclear binding 0-27675  
 $^4\text{He}(\pi^-, \pi^-\text{X})^3\text{H}$ , 5 GeV, nucleon isobar prod. and knockout 0-42709  
 $^4\text{He}$ , 16.7 MeV states energy calc. using mixed cluster representation 0-27555  
 $^5\text{He}$  energy levels deduced from  $d(t, t)d$  0-47488  
 $^5\text{He}(\text{p}, \text{p})$ ,  $A=3, 4$ , backscattering, large momentum transfers,  $\pi$  exchange effects 0-5143  
 $^5\text{He}(\pi, \pi)$ ,  $A=3, 4$ , low energy scatt. length and phase calcs. 0-47508  
 $^5\text{He}$ ,  $^4\text{H}$  binding energy difference, bound states, exact four body calc. 0-9255  
 $^5\text{He}(e^+, e^+)\text{He}$ , s-wave scatt., effective range expansion 0-47467  
 $^5\text{He}(\gamma, \text{pr})$ , photoexcitation in  $\Delta(1236)$  region 0-22813  
 $^5\text{Li}$ , cluster model study using generator coord. method on  $^3\text{He}+\text{p}$  scatt. 0-27581  
 $^5\text{Li}(3/2^-)$  tensor polarisation from  $^2\text{H}(\alpha, \alpha\text{n})\text{p}$  0-13450

## nuclei with mass number 6 to 19

- $^{16}\text{O}(\gamma, \text{N})$ , photonuclear sum rules from continuum calcs., dependence on residual interactions 0-22807  
 $^{18}\text{F}$  levels,  $J^\pi$  and ang. distrib. DWBA anal. of  $^{19}\text{F}(p, d)$  0-42545  
 $A=10-58$ , neutron separation energies, self consistent set from  $(n, \gamma)$  reaction 0-52563  
 $A=11, 12$ , energy levels, transitions and resonances, compilation 0-46743  
 $A=12$  polarised  $\beta$ -decay, nuclear Dirac wave function test 0-5060  
 $A=15$  mag. moments, nuclear Dirac wave function test 0-5060  
 $A=15-18$ , effective interaction from coupled cluster many-body method extension 0-22701  
 $A=16$  to  $40$ , mag. moments, shell model calcs, mesonic exchange current effects, book contrib. 0-479  
 $A=16-58$ , charge, proton and neutron density distrib. calc. 0-22680  
 $A=18$ , multiple scattering, three-particle one-hole nuclear effective interaction 0-13384  
 $A=19-31$  odd nucleii,  $K^\pi=1/2^-$  bands, spectroscopic factors and transitions 0-32151  
 $A=4-16$ , monopole giant resonances, state density radii and compressibility using hyperspherical functions (Russian) 0-27615  
 $A=6-44$ , gamma-ray transition strengths, data tables 0-37345  
 $A=8$  fragment products from  $K^-$ +emulsion nuclei 0-52695  
 $A<100$ , average  $E1/M1$  strength ratio 0-52621  
 $A\leq 28$ , giant quadrupole resonance,  $E2$  intensity distrib., from  $(\alpha, \alpha')$ , DWBA anal. (Hungarian) 0-52642  
 $A\leq 57$  nuclei,  $E2, M1$  multipole mixing ratios 0-22751  
even-even nuclei,  $z=6$  to  $100$ , probable members of quasi-bands in spherical and deformed regions 0-13357  
light nuclei, alpha cluster model, 3-body problem 0-32217  
thermonuclear reaction rate data for intermediate mass nuclei 0-31427  
 $(e, e)$ , low-q,  $A=14$  nuclei, isospin  $T=2, 1$  and 0 collective resonances, shell model 0-510  
 $(\gamma, \text{X})$ ,  $A=14$  nuclei, isospin  $T=2, 1$  and 0 collective resonances, shell model 0-510  
 $(\pi, \gamma)$ ,  $A=14$  nuclei, isospin  $T=2, 1$  and 0 collective resonances, shell model 0-510  
 $^6\text{Li}(p, n)$ , 144 MeV, one pion exchange and PCAC expt. test 0-528  
 $^6\text{B}(p, \pi^+)$ ,  $A=10, 11, 0.5-10$  MeV, total cross sections near pion Coulomb barrier 0-32280  
 $^{10}\text{B}$ ,  $\alpha$ -transfer reactions, spectroscopic factors, exact finite range DWBA anal. 0-13372  
 $^{10}\text{B}$  levels,  $J^\pi$  and ang. distrib. from  $^9\text{Be}(\text{He}, d)$  0-42546  
 $^{10}\text{B}$   $T=1$  states,  $\gamma$ -transition strengths, lifetimes, branching and mixing ratios from  $^9\text{Li}(\alpha, \alpha)$  0-27594  
 $^{10}\text{B}$  transitions and levels from  $^{11}\text{B}(\gamma, n\gamma')$  (Russian) 0-13433  
 $^{10}\text{B}$ , triaxial deformation in shell model non-central forces, projected HF calc. 0-13367  
 $^{10}\text{B}+^{10}\text{B}$ , fusion below Coulomb barrier, quantum mechanical barrier penetration model anal. 0-18361  
 $^{10}\text{B}(\text{He}, \text{He})$ , optical potentials and volume integrals, mass and energy dep. 0-52686  
 $^{10}\text{B}(d, ^2\text{He})$ , 55 MeV, cross sections,  $^2\text{He}$  energy spectra and ang. distrib. 0-18321  
 $^{10}\text{B}(p, \pi^+)$ , 320-605 MeV, cross sections, pion exchange model anal. 0-27676  
 $^{11}\text{B}$  analogue of  $^{11}\text{C}$  6478 keV state, lifetime from  $^7\text{Li}(\alpha, \gamma)$  0-5092  
 $^{11}\text{B}, (\alpha, \text{X})$ , 116 MeV, heavy ion-alpha in-plane correlations 0-18343  
 $^{11}\text{B}$ ,  $M2$  giant resonance calcs. from  $(e, e'), (\pi^-, \gamma), (\mu^-, \nu)$  0-22784  
 $^{11}\text{B}$  states, spectroscopic factors from DWBA anal. of  $^{12}\text{C}(p, 2p)$  0-5057  
 $^{11}\text{B}$ , struct. study of  $2\alpha+t$  system in orthogonality condition model, level energies and parity 0-5080  
 $^{11}\text{B}_{\alpha\rightarrow\pi}+^{11}\text{C}^*$ , produced in  $p$ +emulsion nuclei reacts. (Russian) 0-9297  
 $^{11}\text{B}+^{10,11}\text{B}$ , fusion below Coulomb barrier, quantum mechanical barrier penetration model anal. 0-18361  
 $^{11}\text{B}(e, e')$ ,  $E1$  transitions to unnatural parity states 0-22758



## nuclei with mass number 6 to 19 continued

- <sup>11</sup>B( $\gamma, n\gamma$ ) 30 MeV giant dipole resonance decay, <sup>10</sup>B transitions (*Russian*) 0-13433
- <sup>11</sup>B(p,n)<sup>11</sup>C, shell model anal. of polarisation-analysing power differences 0-22804
- <sup>11</sup>B, aligned,  $\beta$ -ang. distrib. and alignment correction coeffs., axial vector currents 0-5097
- <sup>14</sup>B, mass excess and excited states from <sup>14</sup>C(<sup>14</sup>C, <sup>14</sup>B) 0-42676
- Be, neutron spectra from p,d, <sup>3</sup>He collisions 0-524
- Be(<sup>40</sup>Ca,X), 212 MeV/amu, neutron rich nuclide yields from <sup>48</sup>Ca fragmentation 0-27660
- <sup>4</sup>Be, M2 giant resonance calcs. from (e,e'), ( $\pi^-$ ,  $\gamma$ ), ( $\mu^-$ ,  $\nu$ ) 0-22784
- <sup>7</sup>Be excitation functions from <sup>6</sup>Li(<sup>3</sup>He, d) 0-18223
- <sup>7</sup>Be  $\alpha$ -cluster spectroscopic factors, DWBA anal. from (d, <sup>6</sup>Li) 0-52571
- <sup>8</sup>Be cross sections and ang. distrib., direct knockout model anal. of <sup>12</sup>C( $\pi^+$ ,  $\pi^+$ ) (*Russian*) 0-27620
- <sup>8</sup>Be isospin mixed 2<sup>+</sup> doublet, level parameters from <sup>4</sup>He( $\alpha$ ,  $\alpha$ ) 0-27556
- <sup>7</sup>Be lowest negative parity state, shell and cluster model calcs. from <sup>7</sup>Li(p,p), <sup>8</sup>Be lowest negative parity state, shell and cluster model calcs. 0-18205
- <sup>8</sup>Be, Skyrme-type interactions, spectroscopy of light nuclei, density dependent Hartree-Fock 0-22717
- <sup>8</sup>Be spontaneous fission pot. energy curve, cluster shell model (*Chinese*) 0-22867
- <sup>8</sup>Be, 2s<sub>1/2</sub> state obs. in <sup>10</sup>B(t,  $\alpha$ ) 0-22691
- <sup>9</sup>Be deformed nucleus, continuum states in strong coupling model 0-22682
- <sup>9</sup>Be(K,  $\pi$ ), narrow  $\Sigma$ -hypernuclear states, estimated widths, quantum number assignments 0-42576
- <sup>9</sup>Be(e,e'), single hole state momentum and energy distrib. 0-22674
- <sup>9</sup>Be(e,e), longitudinal form factor for 1/2<sup>+</sup> resonance 0-22682
- <sup>9</sup>Be( $\gamma$ , X), charged particle emission in (e,e') reaction, virtual phonon theory 0-13460
- <sup>9</sup>Be( $\gamma$ , n) cross section, strong coupling model 0-22682
- <sup>9</sup>Be( $\gamma$ ,  $\pi^-$ ), 100-800 MeV, cross section, surface prod. model anal. 0-47466
- <sup>9</sup>Be( $\gamma$ ,  $\pi^+$ ), threshold to 175 MeV, total cross sections, DWIA anal. 0-13459
- <sup>9</sup>Be( $\gamma$ ,  $\pi$ ), photoabsorption and sum rules, structure, RMS radius, polarisability and exchange parameters 0-22686
- <sup>9</sup>Be(n,n) pseudolevel eval. validation 0-22697
- <sup>9</sup>Be(p,  $\alpha$ )X, direct knockout model for fragmentation, (p,  $\alpha$ ) predictions 0-18275
- <sup>9</sup>Be(p,  $\pi^-$ ), 0.5-10 MeV, total cross sections near pion Coulomb barrier 0-32280
- <sup>9</sup>Be(p,  $\pi^+$ ), 320-605 MeV, cross sections, pion exchange model anal. 0-27676
- <sup>9</sup>Be( $\pi$ , X), X= $\gamma$ ,  $\gamma\gamma$ , e<sup>+</sup>e<sup>-</sup>, rare pion absorption modes, theoretical and expt. results 0-42698
- <sup>10</sup>Be near threshold state from <sup>7</sup>Li(t, <sup>9</sup>Li) (*Russian*) 0-13484
- <sup>10</sup>Be<sub>XX</sub>, four body dynamical eqns. in Faddeev-Yakubovsky formalism 0-47419
- <sup>11</sup>Be, Hartree-Fock calculations of nuclear bulk properties with density- and starting-energy dependent effective interaction 0-9246
- Be(d,n), activation cross-section, integral tests, dosimeter appl. 0-32553
- Be(p,X), 200, 300 GeV/c direct photon prod.,  $\eta/\pi^0$  and  $\gamma/\pi^0$  prod. ratios 0-27618
- Be(p,X), 400 GeV/c, light ion backward prod., invariant cross section 0-32279
- Be(p,  $\pi$ X), x=1, 2, 640 MeV, energetic backward p emission, inclusive differential cross section 0-9290
- <sup>13</sup>B hypernucleus, spin determ. from <sup>12</sup>B-<sup>12</sup>C\*+ $\pi^-$  0-27589
- <sup>11</sup>Bu(p,  $\alpha$ ) $\alpha$ , sputtering yield meas. (*Japanese*) 0-25513
- C (n,n), pol. n, 16.1 MeV, differential cross section, optical model fit 0-32259
- C+p(d,  $\alpha$ )(<sup>12</sup>C), 4.2 GeV/N, multiple  $\pi^-$  prod., mean multiplicity (*Russian*) 0-27647
- C(<sup>20</sup>Ne,  $\pi^+$ X), 400 MeV/N, pion prod. doubly differential cross sections and ang. distrib. 0-32299
- C(<sup>16,17</sup>O, <sup>16,17</sup>O), two centre shell model, molecular single particle states at level crossings 0-47354
- <sup>12</sup>C, A=13,14, M2 giant resonance calcs., from (e,e'), ( $\pi^-$ ,  $\gamma$ ), ( $\mu^-$ ,  $\nu$ ) 0-22784
- <sup>12</sup>C, A=13,14, neutron binding energy from <sup>1</sup>H(n,  $\gamma$ ) 0-52564
- <sup>12</sup>C, A=13,14 neutron binding energy 0-47362
- <sup>12</sup>C(<sup>16</sup>O, X), A=12, 13 exit channel competition for some residual nucleus 0-47499
- <sup>12</sup>C(p,  $\pi^+$ ), A=12, 13, 0.5-10 MeV, total cross sections near pion Coulomb barrier 0-32280
- <sup>12</sup>C( $\pi$ ,  $\pi^+$ ), A=12, 13, ~180 MeV, isospin mixing, levels, excitation functions and ang. distrib. 0-42543
- <sup>12</sup>C levels and resonance,  $\gamma$ -ray excitation curves from (p,  $\alpha$ ), (p,  $\gamma$ ) 0-9280
- <sup>12</sup>C negative parity states lifetime limits and transition strengths from <sup>10</sup>B(p,  $\gamma$ ) 0-5092
- <sup>12</sup>C, production by cyclotron, biomedical appls. (*French*) 0-56216
- (<sup>12</sup>C, X), A=12-19, total fusion cross sections and fusion barrier parameters 0-9322
- <sup>12</sup>C (<sup>16</sup>O, <sup>16</sup>O), 19-23 MeV, intermediate width structs., ang. correlations, spins 0-13431
- <sup>12</sup>C ( $\pi$ , X), X= $\gamma$ ,  $\gamma\gamma$ , e<sup>+</sup>e<sup>-</sup>, rare pion absorption modes, theoretical and expt. results 0-42698
- <sup>12</sup>C ( $\pi^+$ ,  $\pi^+$ d), 180 MeV, cross-section ratios 0-32308
- <sup>12</sup>C ( $\pi^+$ ,  $\pi^+$ t), 180 MeV, cross section ratios 0-32308
- <sup>12</sup>C  $\alpha$ -cluster spectroscopic factors, DWBA anal. of (d, <sup>6</sup>Li) 0-52571
- <sup>12</sup>C,  $\alpha$ -transfer reactions, spectroscopic factors, exact finite range DWBA anal. 0-13372
- <sup>12</sup>C,  $\alpha$ -transfer spectroscopic factors for O<sup>+</sup>, 2<sup>+</sup> and 4<sup>+</sup> states, transitions from (d, <sup>6</sup>Li) 0-13370
- <sup>12</sup>C, centre-of-mass spuriousity in continuum shell-model calculations 0-32210
- <sup>12</sup>C, electric quadrupole strength, giant quadrupole resonance 0-52575
- <sup>12</sup>C energy levels from (p,d) 0-42667
- <sup>12</sup>C, excited state decay, axion emission search 0-32235
- <sup>12</sup>C, excited state struct.,  $\alpha$ -particle model 0-47385
- <sup>12</sup>C, isoscalar giant quadrupole resonances, RPA calcs., E2 strength fragmentation, spectroscopic factors 0-13437
- <sup>12</sup>C M1 (15.11 MeV) form factor, evidence for nuclear pion field critical opalescence 0-32232
- <sup>12</sup>C p<sub>0</sub> channel E2 strength from <sup>11</sup>B(p,  $\gamma$ ) pol p. 0-22790

## nuclei with mass number 6 to 19 continued

- <sup>12</sup>C, Skyrme-type interactions, spectroscopy of light nuclei, density dependent Hartree-Fock 0-22717
- <sup>12</sup>C $\rightarrow$  $\pi^-$  + <sup>12</sup>N, produced in p+emulsion nuclei reacts. (*Russian*) 0-9297
- <sup>12</sup>C, 3 $\alpha$  model, composite particle interactions, Pauli principle (*Russian*) 0-18214
- <sup>12</sup>C+<sup>10,11</sup>B, fusion below Coulomb barrier, quantum mechanical barrier penetration model anal. 0-18361
- <sup>12</sup>C+<sup>12</sup>C, 250-1000 MeV/N, intranuclear cascade calcs. for multiplicity and cross sections 0-32300
- <sup>12</sup>C+<sup>12</sup>C, 2.8-6.3 MeV, total fusion cross section, S-factor 0-22877
- <sup>12</sup>C+<sup>12</sup>C, low energy, HFB and generator coordinate self consistent microscopic approach 0-42679
- <sup>12</sup>C+<sup>12</sup>C system, nuclear molecule microscopic description, HF and coupled channel calcs. 0-13493
- <sup>12</sup>C+<sup>9</sup>Be, 11.4 MeV cm energy, p, d, t,  $\alpha$  production 0-9302
- <sup>12</sup>C+<sup>9</sup>Be, parabolic repulsion potential, optical model 0-22782
- <sup>12</sup>C+n, 60 kev-20 MeV, average energy per ion pair, calc. 0-22841
- <sup>12</sup>C+p(d,  $\alpha$ ), transparency in composite particle-nucleus reactions 0-9273
- <sup>12</sup>C(<sup>12</sup>C, <sup>12</sup>C) intermediate struct. resonances, <sup>24</sup>Mg giant isoscalar quadrupole fission/fusion doorway states 0-37410
- <sup>12</sup>C(<sup>12</sup>C, <sup>12</sup>C)<sup>12</sup>C\*, O<sub>2</sub><sup>+</sup>, 3<sub>1</sub><sup>-</sup>, 4<sub>1</sub><sup>+</sup> state excitation functions, resonance structures 0-42616
- <sup>12</sup>C(<sup>12</sup>C, <sup>12</sup>C), gross struct., barrier top resonance model calc. 0-9279
- <sup>12</sup>C(<sup>12</sup>C, <sup>12</sup>C), intermediate resonance, coupled channels calcs. 0-42611
- <sup>12</sup>C(<sup>12</sup>C, <sup>12</sup>C), 13-14.1 MeV, Coulomb barrier resonance parameter direct determ., J<sup>+</sup> assignments 0-513
- <sup>12</sup>C(<sup>12</sup>C, <sup>12</sup>C), elastic scatt., incoming wave boundary condition model calcs. 0-47504
- <sup>12</sup>C(<sup>12</sup>C, p)X, 800 MeV/N, fireball and preequilibrium cross sections,  $\pi$  condensation proximity influence 0-27659
- <sup>12</sup>C(<sup>12</sup>C,  $\alpha$ ), 12-31.5 MeV, inclusive  $\alpha$ -particle yield, resonant like structs. 0-42691
- <sup>12</sup>C(<sup>16</sup>O, <sup>12</sup>C\*), 45-53 MeV, <sup>12</sup>C\* m-substate population, spin alignment and excitation functions 0-42615
- <sup>12</sup>C(<sup>20</sup>Ne, <sup>20</sup>Ne), back angle scatt. systematics, structured excitation functions and oscillatory ang. distrib. 0-32295
- <sup>12</sup>C(<sup>24</sup>Mg, <sup>24</sup>Mg), back angle scatt. systematics, structured excitation functions and oscillatory ang. distrib. 0-32295
- <sup>12</sup>C(<sup>3</sup>He, <sup>3</sup>He), 119 MeV, optical pot. parameters energy and mass depend. 0-32289
- <sup>12</sup>C(<sup>3</sup>He, <sup>3</sup>He), optical potentials and volume integrals, mass and energy dep. 0-52686
- <sup>12</sup>C(<sup>3</sup>He, pd), 90 MeV, angular correlations, elastic break-up of <sup>3</sup>He 0-52685
- <sup>12</sup>C(<sup>40</sup>Ar, X), 213 MeV/N, relativistic fragmentation, microscope and macroscopic calcs., np correlation 0-13495
- <sup>12</sup>C(<sup>40</sup>Ca, <sup>40</sup>Ca), 90° and 180° excitation functions energy depend., DWBA anal. 0-42582
- <sup>12</sup>C(<sup>6</sup>Li, <sup>6</sup>Li), 153 MeV, isoscalar giant quadrupole resonances 0-13440
- <sup>12</sup>C(<sup>6</sup>Li, d)<sup>16</sup>O\*, 18-28 MeV, configuration mixing effect and cross sections, zero range DWBA 0-42692
- <sup>12</sup>C(<sup>9</sup>Be, <sup>9</sup>Be), ang. distrib. from pick-up model anal. (*Russian*) 0-37396
- <sup>12</sup>C(<sup>9</sup>Be,  $\alpha$ )<sup>17</sup>O, ang. distrib. from pick-up model anal. of cluster transfer (*Russian*) 0-37396
- <sup>12</sup>C(K,  $\pi^-$ ), <sup>12</sup>C\*, 800 MeV/c, ang. distrib. from DWIA calcs. 0-32225
- <sup>12</sup>C(K,  $\pi$ ), narrow  $\Sigma$ -hypernuclear states, estimated widths, quantum number assignments 0-42576
- <sup>12</sup>C(K<sup>+</sup>, K<sup>+</sup>), Glauber model anal. 0-42697
- <sup>12</sup>C(K<sup>+</sup>, K<sup>+</sup>), kaon-nucleus coupling const. from scatt. amplitudes 0-32304
- <sup>12</sup>C( $\alpha$ ,  $\alpha$ ), generalised optical potentials 0-22781
- <sup>12</sup>C(d, <sup>3</sup>He), 55 MeV, cross sections, <sup>3</sup>He energy spectra and ang. distrib. 0-18321
- <sup>12</sup>C(e, e'), eN interaction in quasifree scatt., nonrelativistic Hamiltonian through 4th order 0-47469
- <sup>12</sup>C(e, e'), quasifree scatt., spin-orbit distortion of emerging nucleon 0-52664
- <sup>12</sup>C(e,e'), deuteron knock-out yield, contrib. to inelastic scatt. cross section (*Russian*) 0-27621
- <sup>12</sup>C(e,e'), cross sections from DWIA, optical, and shell model calcs. (*Russian*) 0-32270
- <sup>12</sup>C(e,e), 180° scatt., transverse inelastic form factors and spectra, collective 2<sup>+</sup> state 0-9261
- <sup>12</sup>C(e,e), elastic scatt., spectroscopic information and form factors 0-9260
- <sup>12</sup>C(e,e), electroexcitation cross sections, incoherent superposition of single nucleon processes 0-32269
- <sup>12</sup>C(e,e), 12.71 and 15.11 MeV level struct. and isospin mixing from form factors 0-32186
- <sup>12</sup>C(e,  $\pi$ ), total cross section from square reaction matrix element (*Russian*) 0-32271
- <sup>12</sup>C( $\gamma$ ,  $\pi^-$ p), final state interaction, plane and distorted wave momentum distrib. 0-18286
- <sup>12</sup>C( $\gamma$ , N), photoneuclear sum rules from continuum calcs., dependence on residual interactions 0-22807
- <sup>12</sup>C( $\gamma$ , p), up to 0.25 GeV, from bremsstrahlung  $\gamma$ -quanta (*Russian*) 0-5123
- <sup>12</sup>C( $\gamma$ ,  $\pi^-$ ), 160-250 MeV, total cross section from elementary Hamiltonian model 0-18292
- <sup>12</sup>C( $\gamma$ ,  $\pi^-$ ), ( $\gamma$ ,  $\pi^-$ p), knockout p interaction, optical model and quasifree  $\pi$  photoprod. mechanism (*Russian*) 0-42638
- <sup>12</sup>C( $\gamma$ ,  $\pi^-$ ), threshold to 360 MeV, total cross sections in  $\Delta$  region 0-13457
- <sup>12</sup>C( $\gamma$ ,  $\pi^-$ ), total cross section calc. in impulse approx. 0-13458
- <sup>12</sup>C( $\gamma$ ,  $\pi^-$  p), 340-380 MeV, quasi-free photoprod., impulse and shell model anal. (*Russian*) 0-5124
- <sup>12</sup>C( $\gamma$ ,  $\pi^-$ )<sup>12</sup>B<sub>g.s.</sub>, 0-4 MeV, pion photoprod. cross section 0-42637
- <sup>12</sup>C( $\mu$ ,  $\nu$ )<sup>12</sup>B, Hartree Fock wavefunction, correlations, pseudoscalar coupling constant, capture rates, recoil nuclear polarisation 0-22774
- <sup>12</sup>C(n, X), compound resonance decay based on bound and metastable single nucleon states (*Russian*) 0-5107
- <sup>12</sup>C( $\bar{n}$ , X), annihilation, 1.4 GeV/c,  $\pi^\pm$ , p emission angles, momentum and multiplicity distrib. 0-532
- <sup>12</sup>C(n,n), <17 MeV, resonating group calcs., phase shifts and differential cross sections 0-32275
- <sup>12</sup>C( $\nu$ ,  $\nu$ ), ( $\bar{\nu}$ ,  $\bar{\nu}$ ), 15.11 MeV state excitation, cross sections, level decay 0-9258
- <sup>12</sup>C(p, X), 50 MeV, effective cross sections for charged particles in outgoing channel 0-18294



## nuclei with mass number 6 to 19 continued

- $C(p,n)$ , 144 MeV, one pion exchange and PCAC expt. test 0-528  
 $C(p,n)$ , 62, 120 MeV, isobaric analogue states, differential cross sections 0-18202  
 $C(p,p')$ , 1 GeV, proton polarisation in natural parity level excitation (Russian) 0-42634  
 $C(p,p')$ , 62, 120 MeV, isobaric analogue states, differential cross sections 0-18202  
 $C(p,p')$ , 800 MeV, multistep processes, ang. distrib., Glauber model anal. 0-47475  
 $C(p,p')$  proton polarisation and natural parity level excitations (Russian) 0-5144  
 $C(p,p')^{12}C^*$ , pol. p., 19-23 MeV, giant resonances as doorway states, virtual excitation 0-5102  
 $C(p,p)$ , 100-2200 MeV, total and reaction cross sections from optical pot. 0-18303  
 $C(p,p)$ , 144 MeV, elastic scatt. cross sections, optical pot. 0-42660  
 $C(p,p)$ , 40-75 MeV, polarisation meas., differential cross sections 0-52840  
 $C(p,p)$ , 50-160 MeV, energy depend. optical pot. 0-22830  
 $C(p,p)$ , optical potential, spin-orbit term 0-52668  
 $C(p,p)$ , pol. p., 450-600 keV, Mott-Schwinger interaction existence, anal. power 0-22805  
 $C(p,p)$  spin 0-spin 1/2 phase shift anal. discrete ambiguities 0-18307  
 $C(p,py)$ , bremsstrahlung cross section near 1.7 MeV resonance, Feshbach-Yennie approx. 0-42662  
 $C(p,pn)$ , pol. nucleon quasi-elastic scatt., nuclear wave function and model tests 0-42656  
 $C(\pi^-, \pi p)^{11}B$ , knockout reaction, cross section ratio  $\sigma(\pi^-, \pi^+ p)/\sigma(\pi^-, \pi^- p)$  meas. 0-32254  
 $C(\pi, X)$ , angular distrib. of inelastic diffusion of  $\pi^\pm$  (French) 0-47507  
 $C(\pi, X)$ , deep inelastic,  $\pi$  and  $\Delta$  optical pot. effects, semiclassical transport model 0-52698  
 $C(\pi, n)$ , total cross section, density distrib. and ray bending effects 0-47509  
 $C(\pi^-, 2\gamma)$ , doubly radiative capture theory, branching ratio and ang. correlations 0-9314  
 $C(\pi^-, \gamma)$ , pion<sup>-</sup> radiative capture probab. (Russian) 0-42538  
 $C(\pi^-, \gamma)^{12}B^*$ , excitation of collective states, shell model 0-22652  
 $C(\pi^-, X)$ , 40 GeV/c, secondary neutron average number, charge exchange coeffs., n inelasticity coeffs. (Russian) 0-32132  
 $C(\pi^-, n)$ , stopped pion, neutron energy spectra, mean energies and multiplicities 0-9311  
 $C(\pi^-, \pi^-)^{12}C^*$ , 20 to 40 GeV/c, semicoherent elastic scatt. 0-5174  
 $C(\pi^+, d)^{10}C$ , PWBA differential cross section (Chinese) 0-27673  
 $C(\pi^+, \pi^+)$ , 100-291 MeV, cross sections and ang. distrib., spin and isospin transfer 0-52697  
 $C(\pi^+, \pi^+)$ , 40 MeV, differential cross sections and strength parameters, optical model fit 0-18347  
 $C(\pi^+, d)$ , DWBA cross section formula, PWBA differential cross section (Chinese) 0-22861  
 $C(\pi^+, \pi^-)$ , model Coulomb corrections in eikonal 0-5171  
 $C(\pi^+, \pi^+)$ , 290 MeV, double charge exchange cross sections 0-18348  
 $C(\pi^+, \pi N)$ , 40-600 MeV, excitation functions and absolute cross sections 0-18226  
 $C(\pi^+, \pi^0)$ , angle integrated cross section, optical pot., n and p radius differences 0-32307  
 $C$  cascade hypernucleus, decay into two ordinary hypernuclei,  $^{13}C-^4Be+^3He+Q$  by  $\Xi^- p \rightarrow \Lambda^0 \Lambda^0$  0-52603  
 $C$ , chemical shifts for halomethanes 0-1002  
 $C$ , giant quadrupole resonance blocking mechanism 0-13437  
 $C$ , NMR data bank, DARC PLURIDATA system 0-30298  
 $C$ , photoexcited giant dipole resonance, continuum shell model anal. 0-18266  
 $C$  satellites use in proton spectra of oriented mols. 0-18872  
 $C$ , shielding consts. and anisotropy of NMR shielding tensor, modified CNDO/S calcs. (French) 0-32610  
 $C$ , simultaneous multinucl. NMR by alternate scan recording of  $^{31}P$  and  $^{13}C$  spectra 0-26426  
 $C$  spectroscopic factors, cross sections DWBA anal. optical model parameters from  $^{12}C(^{16}O, X)$  0-13371  
 $C$  spin-lattice relax. using proton decoupled Fourier transform spectra, errors origin 0-18945  
 $C$ , TOF transmission meas. of neutron resonances 0-37374  
 $C(^{12}C, ^{12}C)$ , mixed parity neutron orbits, coupled channel theory with adiabatic assumption 0-9304  
 $C(^{12}C, ^{12}C)$  15, 87 MeV, elastic transfer exchange amplitude, coupled reaction channel and DWBA calcs. 0-32298  
 $C(^{12}C, ^{24}Mg)$ , 3.05-6.88 MeV, fusion cross section energy depend., optical anal. 0-42724  
 $C(^4He, ^4He)$ , optical potentials and volume integrals, mass and energy dep. 0-52686  
 $C(\gamma, n)$ , 7.6-24 MeV, photoneutron ang. distrib., level scheme and  $J^\pi$  assignments 0-466  
 $C(p, \alpha)^{10}B$ , 65 MeV, pol. p., DWBA form factor 0-52559  
 $C(p, d)$ , 200, 500 MeV, differential cross section scaling, reaction mechanism 0-42625  
 $C(p, d)$ , 800 MeV, cross sections, DWBA anal. 0-42667  
 $C(p, \gamma)$ , pol. p., 6.25-17.0 MeV, anal. power and cross section ang. distrib., E1, E2 amplitudes 0-47461  
 $C(\pi, \pi)$ , 162 MeV, pure n and p transitions, differential cross sections 0-5040  
 $C(\pi^+, \pi^+)$ , near  $\pi N$  (3,3) resonance, 180 MeV, collective states and cross sections 0-13507  
 $C$  beam prod. from isotopically enriched sputter targets 0-23221  
 $C$  spectroscopic factors, cross sections DWBA anal. optical model parameters from  $^{12}C(^{16}O, X)$  0-13371  
 $C(^{12}C, X)$ , 40-57 MeV, strong resonant behaviour in inelastic and transfer channels,  $\gamma$ -yields 0-52644  
 $C(\alpha, \gamma)^{16}O$  and onset of core He flash in low-mass stars 0-51735  
 $C$  0.74 MeV  $5/2^+$  state g-factor, shell model interpretation from  $^3H(^{13}C, p)$  0-32176  
 $C$  beta decay transition rates and half life,  $^{15}N$  excited states and transitions 0-18248  
 $C+^9Be$ , parabolic repulsion potential, optical model 0-22782  
 $C$ , giant isoscalar monopole state energies in generator coordinate method 0-37317  
 $C(d, d)$ , 4.3, 6.3, 8.9 GeV/c, secondary momentum spectra, multiple scatt. model anal. (Russian) 0-27650  
 $C(\gamma, \gamma)$ , neutron capture  $\gamma$ -ray Rayleigh scatt. 0-52661  
 $C$  low lying excited states, ang. distrib. from  $^{12}C(K^-, \pi^-)$  0-32226

## nuclei with mass number 6 to 19 continued

- $C(n, n)$ , total cross sections below 2 MeV, R-matrix fits to data 0-13466  
 $C(p, X)$  (Russian) 0-52649  
 $C(p, X)$ , 400 GeV/c, light ion backward prod., invariant cross section 0-32279  
 $C(p, X)$ , 70 GeV/c,  $\pi^\pm$ ,  $K^\pm$ ,  $p$ ,  $\bar{p}$  prod. with  $p_T=0.5-2.5$  GeV/c cross sections, yield ratios (Russian) 0-52681  
 $C(p, p)$ , 640 MeV, proton pair quasifree knock-out 0-22795  
 $C(p, p')$ , 0.6-25 GeV, backward emitted proton inclusive spectra, short range correlation 0-32281  
 $C(p, xpX)$ ,  $x=1, 2$ , 640 MeV, energetic backward p emission, inclusive differential cross section 0-9290  
 $C(\pi^-, X)$ , 3 GeV/c, n inclusive spectra, neutron yield (Russian) 0-13510  
 $F(^{20}Ne, \pi^+ X)$ , 400 MeV/N, pion prod. doubly differential cross sections and ang. distrib. 0-32299  
 $^A F$ ,  $A=18, 19$ , E2 transition rates calc., shell model with effective interaction and charges 0-47423  
 $^{18}F$  integrated cross sections to excited residual states from  $^{19}F(\gamma, n)$  0-18200  
 $^{18}F J^\pi=3^-$  doublet at 6241 keV, isospin mixing from (p,  $\gamma$ ), (p,  $\alpha$ ), ( $\alpha, \gamma$ ) ( $^{14}N, \alpha$ ) 0-511  
 $^{18}F$  levels and resonances, cross sections in R-matrix formalism from  $^{18}O(p, \alpha)$  0-18267  
 $^{18}F$ , semi-microscopic calc. of  $\alpha$ -cluster states, shell model approx. 0-465  
 $^{19}F$ , coupled channel orthogonality condition model 0-47384  
 $^{19}F$ , energy levels from  $\alpha$ - $^{15}N$  and t- $^{16}O$  coupled channel orthogonality condition model 0-37326  
 $^{19}F$  final state selective population, triton clustering from band anal. from ( $^{7}Li, t$ ), ( $^{7}Li, ^3He$ ) 0-9306  
 $^{19}F$  level struct., ang. distrib. anal. using DWBA of  $^{17}O(^3He, p)$  0-9232  
 $^{19}F$  levels, resonances and phase shifts, resonating group calcs. from  $^{15}N(\alpha, \alpha)$  0-32189  
 $^{19}F$  low lying band state lifetimes, stopping power, transition strengths from  $^{15}N(\alpha, \gamma)$  0-42585  
 $^{19}F+^{28}Si$  spin orbit pot., single folding model and cluster model 0-9196  
 $F(d, X)$ ,  $X=^7Li, ^7Be$ , 13.6 MeV, diff. cross sections,  $^3He$  cluster direct transfer (Russian) 0-52650  
 $F(d, \alpha)^{17}O$ , 1.8 to 3.0 MeV, vector analysing ability using polarised deuterons (Russian) 0-32288  
 $F(d, d)^{19}F$ , 1.8 to 3.0 MeV, vector analysing ability using polarised deuterons (Russian) 0-32288  
 $^{19}F(n, \alpha)^{16}O$ , average cross sections in  $^{235}U$  fission neutron spectrum 0-22828  
 $^{19}F(n, p)^{19}O$ , average cross sections in  $^{235}U$  fission neutron spectrum 0-22828  
 $^{19}F(n, X)$ , annihilation, 1.4 GeV/c,  $\pi^\pm$ , p emission angles, momentum and multiplicity distrib. 0-532  
 $^{19}F(p, p)$ , 17.5 and 30 MeV, low lying level cross-sections, coupled-channel method 0-42649  
 $^{20}F$  cross sections and anal. power, compound nucleus contrib. Ericson fluctuations from  $^{18}O(d, p)$ , pol. d 0-22803  
 $^6He$ ,  $\beta$  decay cross sections 0-27880  
 $^6He$ , density distribution function of nucleons 0-22650  
 $^{10}He$  isotope search in  $^{232}Th$  target nucleus spallation (Russian) 0-5110  
 $^6Li(\alpha, \alpha)$ , 59 MeV, elastic and inelastic, differential cross section systematic anal. 0-22845  
 $^6Li$ , EM form factors and spectroscopic factors in phenomenological cluster models 0-496  
 $^6Li$  energy levels from (p, d) 0-42667  
 $^6Li$  excited states,  $D(\alpha, \alpha)D$  cross-sections,  $\alpha$ -d systems 0-47491  
 $^6Li$ , quantitative microlocation in the brain by a (n,  $\alpha$ ) nuclear reaction 0-41353  
 $^6Li+\alpha$  system, exchange effects, resonating-group study 0-9240  
 $^6Li(^4He, ^4He)$ , excitation functions 0-18223  
 $^6Li(^4He, d)^7Be$ , 2-6 MeV, cross section meas. rel. to fusion reactor first wall 0-13791  
 $^6Li(^4He, \alpha)$ , 2.9 MeV, quasifree reaction,  $^2H(^4He, \alpha)$  contrib., cluster motion 0-13485  
 $^6Li(^4He, \pi^-)^7C$ , 910 MeV, doubly coherent  $\pi$  prod. 0-13487  
 $^6Li(d, ^2He)$ , 55 MeV, cross sections,  $^2He$  energy spectra and ang. distrib. 0-18321  
 $^6Li(d, \alpha)$ , 100-180 keV, low energy cross sections, astrophysical region extrapolation 0-22843  
 $^6Li(d, p)$ , 100-180 keV, low energy cross sections, astrophysical region extrapolation 0-22843  
 $^6Li(e, e)$ , charge formfactors, second Born approx. and pole model 0-18155  
 $^6Li(e, e)$ , 140-330 MeV, 3.65 MeV  $0^+$  state form factor at high momentum transfer 0-495  
 $^6Li(e, e)$ , elastic scatt., spectroscopic information and form factors 0-9260  
 $^6Li(e, e)$ , electroexcitation cross sections, incoherent superposition of single nucleon processes 0-32269  
 $^6Li(\gamma, \gamma)^6Li^*(3.56 \text{ MeV})$ , partial photoproduction reactions, large momentum transfer anal., form factor choice 0-22808  
 $^6Li(\gamma, \pi^+)^6Li^*(3.56 \text{ MeV})$ , partial photoproduction reactions, large momentum transfer anal., form factor choice 0-22808  
 $^6Li(n, \alpha)^3H$ , 23 keV cross section, absolute meas., ang. distrib. 0-18305  
 $^6Li(p, ^3He)$ , 0.1-3.0 MeV, absolute differential and total cross sections, astrophysical S-factor 0-27642  
 $^6Li(p, X)$ , 400 GeV/c, light ion backward prod., invariant cross section 0-32279  
 $^6Li(p, \gamma)$ , 200-1200 keV, cross section 0-13478  
 $^6Li(p, p)$ , 144 MeV, elastic scatt. cross sections, optical pot. 0-42660  
 $^6Li(p, p)$ , 590 MeV,  $\alpha$ -d motion, impulse distrib., cluster momentum distrib. 0-52679  
 $^7Li 3/2^-$  state from  $^6Li(n, -\alpha)$  0-18297  
 $^7Li$ ,  $d\sigma(p, p'd)/d\sigma(p, nd)$ , 670 MeV, cross section ratio, cluster model estimate 0-22829  
 $^7Li$ , M2 giant resonance calcs. from (e, e'), ( $\pi^-, \gamma$ ), ( $\mu^-, \nu$ ) 0-22784  
 $^7Li$  NMR, spin-lattice relax. in  $KLiSO_4$  and  $\alpha$ - $LiIO_3$  (Chinese) 0-39884  
 $^7Li$ , NMR in solid  $LiH$  0-15815  
 $^7Li(^3He, t)^7Be$ , 2-6 MeV, cross section meas. rel. to fusion reactor first wall 0-13791  
 $^7Li(K^-, \pi)$ , narrow  $\Sigma$ -hypernuclear states, estimated widths, quantum number assignments 0-42576  
 $^7Li(d, t)$ , 12 MeV, nuclear vertex constant in peripheral model for virtual decay  $^7Li \rightarrow \alpha + t$  0-18295  
 $^7Li(d, p)$ , 0.7-3.4 MeV, absolute total cross section,  $^8Li$   $\beta$ -decay half life 0-13483  
 $^7Li(e, X)$ ,  $X=^6He, ^6Li$ , 108-198 MeV, ang. distrib. and cross sections 0-42647



## nuclei with mass number 6 to 19 continued

- <sup>7</sup>Li( $\gamma, \pi^-$ ), threshold to 360 MeV, total cross sections in  $\Delta$  region 0-13457
- <sup>7</sup>Li( $\gamma, \pi^-$ ), total cross section calc. in impulse approx. 0-13458
- <sup>7</sup>Li( $\gamma, t$ ), <50 MeV, total and differential cross sections, levels, cluster model calcs. 0-32265
- <sup>7</sup>Li(n,n') $\alpha$ T, three body sequential reactions, kinetics modelling 0-37371
- <sup>7</sup>Li(p,  $\alpha$ ), 45 MeV, nuclear vertex constant in peripheral model for virtual decay  $^7\text{Li} \rightarrow \alpha + t$  0-18295
- <sup>7</sup>Li(p,d), 800 MeV, cross sections, DWBA anal. 0-42667
- <sup>7</sup>Li(p,n)<sup>6</sup>Be as therapy neutron source especially for small cyclotrons 0-26335
- <sup>8</sup>Li  $\beta$ -decay half life from <sup>7</sup>Li(d,p) 0-13483
- <sup>9</sup>Li,  $\beta$  decay cross sections 0-27880
- <sup>6</sup>Li( $\gamma, \pi$ ), A=6, 7 0-22686
- <sup>6</sup>Li(n,x), A=6, 7, 14.6 MeV, ang. distrib. and cross sections for <sup>6,7</sup>Li, <sup>6</sup>He products 0-42650
- <sup>11</sup>Li,  $\beta$ -delayed two neutron radioactivity 0-18247
- <sup>12</sup>N, aligned,  $\beta$ -ang. distrib. and alignment correction coeffs., axial vector currents 0-5097
- <sup>12</sup>N ground state electric quadrupole moment from <sup>12</sup>C( $\gamma, \pi$ ), <sup>12</sup>N ground state electric quadrupole moment (Russian) 0-42538
- <sup>13</sup>N isobaric analogue state excitation, cross sections from <sup>13</sup>C( $\pi^+, \pi^0$ ) 0-42544
- <sup>13</sup>N, production by cyclotron, biomedical appls. (French) 0-56216
- <sup>13</sup>N, quadrupole strength, from <sup>12</sup>C(p, $\gamma$ )<sup>13</sup>N, semi-direct capture model calcs. 0-47370
- <sup>14</sup>N  $1^+$  state cross sections, effective two nucleon interaction, isovector tensor component from <sup>14</sup>C(p,n) 0-18208
- <sup>14</sup>N,  $\alpha$ -transfer reactions, spectroscopic factors, exact finite range DWBA anal. 0-13372
- <sup>14</sup>N,  $\alpha$ X, 156 MeV, heavy ion-alpha in-plane correlations 0-18343
- <sup>14</sup>N, energy levels up to 11.05 MeV, transitions and resonance decay from <sup>13</sup>C(p, $\gamma$ ) 0-47376
- <sup>14</sup>N, M2 giant resonance calcs. from ( $e, e'$ ), ( $\pi^-, \gamma$ ), ( $\mu^-, \nu$ ) 0-22784
- <sup>14</sup>N NMR, single cryst., separation of dipolar and quadrupolar splittings, new technique 0-25217
- <sup>14</sup>N spectroscopic factors, cross sections DWBA anal. optical model parameters from <sup>12</sup>C(<sup>16</sup>O, X) 0-13371
- <sup>15</sup>N(<sup>6</sup>Li, <sup>6</sup>Li'), 153 MeV, isoscalar giant quadrupole resonances 0-13440
- <sup>14</sup>N(d,  $\alpha$ ), pol. d., vector anal. capacity energy and ang. depend. 0-18281
- <sup>14</sup>N(e,e) in storage ring, elastic form factor 0-22819
- <sup>14</sup>N( $\gamma, n_0$ )<sup>13</sup>N, 17 to 26 MeV, angular distrib., giant dipole resonance, single-particle nuclear model 0-52659
- <sup>14</sup>N( $\gamma, \pi^-$ )<sup>14</sup>O, 145-325 MeV, Gamow-Teller suppression and M1 radiative widths 0-52609
- <sup>14</sup>N(n, $\alpha$ )<sup>11</sup>B, 12-18 MeV, pickup of three nucleons, distorted wave approx. 0-22793
- <sup>14</sup>N(n, $\gamma$ ),  $\gamma$ -ray energies, calibration standards 0-52613
- <sup>14</sup>N(p, X), 50 MeV, effective cross sections for charged particles in outgoing channel 0-18294
- <sup>14</sup>N(p,n), 144 MeV, one pion exchange and PCAC expt. test 0-528
- <sup>14</sup>N(p,p), 144 MeV, elastic scatt. cross sections, optical pot. 0-42660
- <sup>14</sup>N(p, $\pi^+$ ), 0.5-10 MeV, total cross sections near pion Coulomb barrier 0-32280
- <sup>14</sup>N( $\pi^-, n$ ), stopped pion, neutron energy spectra, mean energies and multiplicities 0-9311
- <sup>15</sup>N  $3/2^-$  state spin alignment and polarisation, 1/2-spin orbit interaction from <sup>27</sup>Al, <sup>88</sup>Sr(<sup>16</sup>O, <sup>15</sup>N) 0-27622
- <sup>15</sup>N excited states and transitions from <sup>15</sup>C beta decay 0-18248
- <sup>15</sup>N integrated cross sections to excited residual states from <sup>19</sup>F( $\gamma, \alpha$ ) 0-18200
- <sup>15</sup>N low lying states, cross sections and anal. power, transitions, spectroscopic factors from <sup>14</sup>N(d,p), pol. d 0-32183
- <sup>15</sup>N, neutron binding energy 0-47362
- <sup>15</sup>N, neutron binding energy from <sup>1</sup>H(n, $\gamma$ ) 0-52564
- <sup>15</sup>N states, cross sections and lifetimes, EM decay strengths from 3 and 4 particle transfers 0-9237
- <sup>15</sup>N-<sup>13</sup>C spin-spin coupling constants calc. using SCF and INDO method 0-32609
- <sup>15</sup>N(n',n)<sup>15</sup>N, continuum random phase approx. 0-27635
- <sup>15</sup>N(p,p), 18-44 MeV, differential cross sections, phase shift anal., energy depend. 0-47481
- <sup>17</sup>N levels and ang. distrib. meas., shell model calcs. from <sup>15</sup>N(t,p) 0-9233
- <sup>18</sup>N, mass excess and excited states from <sup>14</sup>C(<sup>18</sup>O, <sup>18</sup>N) 0-42676
- <sup>18</sup>Ne analogue and nonanalogue states,  $\pi$  double charge exchange form factors from <sup>18</sup>O( $\pi^+, \pi^-$ ) 0-13405
- <sup>18</sup>Ne cross section, excitation function and double isobaric analogue state from <sup>18</sup>O( $\pi^+, \pi^-$ ) 0-27596
- <sup>19</sup>Ne, final state selective population, triton clustering from band anal. from <sup>16</sup>Li(<sup>6</sup>Li,t) 0-9306
- <sup>20</sup>Ne resonances, J $^\pi$ , excitation functions and branching ratio from <sup>19</sup>F(p, $\gamma$ ) 0-22787
- <sup>20</sup>Ne+<sup>12</sup>C orbiting dinuclear system, inelastic scatt. cross section 0-22854
- <sup>20</sup>Ne(<sup>12</sup>C, <sup>12</sup>C), symmetry and shell struct. effects on absorption, precompound states 0-27666
- N(p,X), 340, 660 MeV, ang. distrib., proton quasi-elastic knockout (Russian) 0-52649
- <sup>16</sup>O, A=17, 19, level scheme, two-step transfer contri., coupled channel anal. from O(<sup>13</sup>C,X) 0-32181
- <sup>16</sup>O, A=18, 19, E2 transition rates calc., shell model with effective interaction and charges 0-47423
- <sup>16</sup>O(<sup>4</sup>He, <sup>4</sup>He), A=16, 18, optical potentials and volume integrals, mass and energy dep. 0-52686
- <sup>16</sup>O, normal parity levels from P-model calcs. with realistic NN interaction (Russian) 0-32194
- <sup>16</sup>O, production by cyclotron, biomedical appls. (French) 0-56216
- <sup>16</sup>O and Sd shell nuclei, binding energy from realistic Hamiltonians and spectral distrib. theory 0-22678
- <sup>16</sup>O,  $\alpha$ -transfer reactions, spectroscopic factors, exact finite range DWBA anal. 0-13372
- <sup>16</sup>O, bound isobars  $\Delta(1236)$ , single particle energies, wave functions (Chinese) 0-52562
- <sup>16</sup>O, Brueckner-Hartree-Fock approach, variational definition of single particle pot. 0-32170
- <sup>16</sup>O, centre-of-mass spuriousity in continuum shell-model calculations 0-32210
- <sup>16</sup>O collective and giant multipole states, Brueckner RPA particle-hole state description 0-32169

## nuclei with mass number 6 to 19 continued

- <sup>16</sup>O,  $\Delta(3,3)$  excitations and effective 3-nucleon forces 0-27561
- <sup>16</sup>O E1 and p<sub>0</sub> channel E2 strength from <sup>15</sup>N(p, $\gamma$ ) 0-22790
- <sup>16</sup>O, electric quadrupole strength, giant quadrupole resonance 0-52575
- <sup>16</sup>O, energy calcs., Jastrow variational method extension, FAHT cluster expansion 0-22677
- <sup>16</sup>O excited  $0^+$  levels 0-42551
- <sup>16</sup>O form factor effects, zero range DWBA calcs. from <sup>18</sup>O(p,t) 0-491
- <sup>16</sup>O, giant isoscalar monopole state energies in generator coordinate method 0-37317
- <sup>16</sup>O ground state and binding energy, microscopic calc. with realistic NW interaction (Russian) 0-5052
- <sup>16</sup>O, Hartree-Fock calculations of nuclear bulk properties with density- and starting-energy dependent effective interaction 0-9246
- <sup>16</sup>O high spin states, J $^\pi$  and  $\alpha$ -decay branching ratios from <sup>12</sup>C(<sup>12</sup>C, <sup>8</sup>Be) 0-18166
- <sup>16</sup>O induced reactions in nuclear emulsions at 2.1 GeV/nucleon, multiplicity distrib. of white and grey tracks (Spanish) 0-47495
- <sup>16</sup>O, isoscalar giant quadrupole resonances, RPA calcs., E2 strength fragmentation, spectroscopic factors 0-13437
- <sup>16</sup>O levels and ang. distrib., <sup>3</sup>He spectroscopic strengths, Hauser-Feshbach/DWBA anal. of <sup>13</sup>C(<sup>6</sup>Li,t) 0-47390
- <sup>16</sup>O, M2 giant resonance calcs. from ( $e, e'$ ), ( $\pi^-, \gamma$ ), ( $\mu^-, \nu$ ) 0-22784
- <sup>16</sup>O magnetic dipole strength 0-37385
- <sup>16</sup>O, monopole vibration damping, TDHF calcs. 0-22667
- <sup>16</sup>O, odd parity levels, correlated basis functions method 0-22721
- <sup>16</sup>O, pion condensation effects, RPA calcs. (Chinese) 0-47407
- <sup>16</sup>O region, effect operators, number conserving set generalisation 0-42555
- <sup>16</sup>O, Skyrme-type interactions, spectroscopy of light nuclei, density dependent Hartree-Fock 0-22717
- <sup>16</sup>O states, J $^\pi$  from <sup>12</sup>C(<sup>12</sup>C,  $\alpha\alpha$ ) 0-22660
- <sup>16</sup>O+<sup>16</sup>O, fusion cross section gross struct., excitation functions, coupled channel method 0-52705
- <sup>16</sup>O+<sup>4</sup>He, group theory appl. to reaction studies 0-9276
- <sup>16</sup>O+p(d, $\alpha$ ), transparency in composite particle-nucleus reactions 0-9273
- <sup>16</sup>O(<sup>10,11</sup>B, <sup>10,11</sup>B), 33.7-49.5 MeV, mag. distrib., ground state quadrupole moment contrib. 0-42689
- <sup>16</sup>O(<sup>12</sup>C,X), sub-barrier energies, fusion cross section, static and dynamic deformation effects 0-42729
- <sup>16</sup>O(<sup>16</sup>O, <sup>12</sup>C)<sup>20</sup>Ne, reaction mechanism by polarisation meas. 0-9301
- <sup>16</sup>O(<sup>16</sup>O, <sup>16</sup>O), gross struct., barrier top resonance model calc. 0-9279
- <sup>16</sup>O(<sup>16</sup>O, <sup>16</sup>O), Coulomb field effects using generalised JWKB method 0-13504
- <sup>16</sup>O(<sup>16</sup>O, <sup>16</sup>O), elastic scatt., incoming wave boundary condition model calcs. 0-47504
- <sup>16</sup>O(<sup>16</sup>O, <sup>16</sup>O), symmetry and shell struct. effects on absorption, precompound states 0-27666
- <sup>16</sup>O(<sup>16</sup>O,X), total fusion cross sections and fusion barrier parameters 0-9322
- <sup>16</sup>O(<sup>3</sup>He, <sup>3</sup>He), pol. <sup>3</sup>He, 33.3 MeV, differential cross section and anal. power, optical pots. 0-42627
- <sup>16</sup>O(<sup>3</sup>He, x), pol. <sup>3</sup>He, x=d or  $\alpha$ , 33 MeV, anal. power and cross sections 0-42628
- <sup>16</sup>O(<sup>6</sup>Li, <sup>6</sup>Li'), 153 MeV, isoscalar giant quadrupole resonances 0-13440
- <sup>16</sup>O(<sup>8</sup>Be, <sup>3</sup>He)<sup>20</sup>Ne\*, sub-Coulomb alpha transfer cross sections 0-37394
- <sup>16</sup>O( $0^+$ )=<sup>16</sup>N( $0^-$ ), beta decay and muon capture rate ratio, mesonic exchange currents 0-42594
- <sup>16</sup>O( $\alpha$ , <sup>12</sup>C), 90.3 MeV, cross sections and systematics multi- $\alpha$ -cluster transfer implications 0-42675
- <sup>16</sup>O( $\alpha$ ,  $\alpha$ ), 28-33.6 MeV, forward peaking variation, DWBA with optical pots., ang. distrib. 0-13488
- <sup>16</sup>O( $\alpha$ ,  $\alpha$ ), giant isoscalar quadrupole resonance,  $\alpha$ -over p-decay ratio, SU(3) and shell model 0-27608
- <sup>16</sup>O( $\alpha$ , d), 1.12 MeV, forward peaking variation, DWBA with optical pots., ang. distrib. 0-13488
- <sup>16</sup>O(d,p), 12 MeV, stripping reaction differential cross section, d distortion effect (Japanese) 0-22796
- <sup>16</sup>O( $e, e'$ ), single hole state momentum and energy distrib. 0-22674
- <sup>16</sup>O( $e, e$ ), elastic scatt., spectroscopic information and form factors 0-9260
- <sup>16</sup>O( $e, e$ ), spectroscopic amplitude determ. 0-5127
- <sup>16</sup>O( $e, e$ ), T=1 level form factors, Helm model, pion photoprod. and muon capture appls. 0-52553
- <sup>16</sup>O( $\gamma, n$ ), 25-45 MeV, isovector giant quadrupole resonance evidence, E2 cross section 0-18268
- <sup>16</sup>O( $\gamma, n$ ) total photoneutron cross sections 0-42619
- <sup>16</sup>O( $\gamma, p$ )<sup>15</sup>N up to 120 MeV, cross-sections, energy levels (Russian) 0-47465
- <sup>16</sup>O( $\gamma, \pi^+$ ), differential cross section from elementary Hamiltonian model 0-18292
- <sup>16</sup>O( $\gamma, \pi^+$ ), threshold to 175 MeV, total cross sections, DWIA anal. 0-13459
- <sup>16</sup>O( $\mu, \nu$ ), recoil nucleus odd and even tensor orientations, general expressions 0-13451
- <sup>16</sup>O(n,n), elastic cross section, microscopic calc. 0-531
- <sup>16</sup>O(p, X), 50 MeV, effective cross sections for charged particles in outgoing channel 0-18294
- <sup>16</sup>O(p, $\alpha$ )<sup>13</sup>N, in-cyclotron <sup>13</sup>N prod., water loop target 0-23201
- <sup>16</sup>O(p,p'), 1 GeV, proton polarisation in natural parity level excitation (Russian) 0-42634
- <sup>16</sup>O(p,p'), 135 MeV, high spin particle-hole states, 4 $^-$  states 0-9217
- <sup>16</sup>O(p,p'), proton polarisation and natural parity level excitations (Russian) 0-5144
- <sup>16</sup>O(p,p'), 135 MeV, 4 $^-$  particle-hole states, J $^\pi$  ambiguity removal 0-5036
- <sup>16</sup>O(p,p), 100-2200 MeV, total and reaction cross sections from optical pot. 0-18303
- <sup>16</sup>O(p,p), 20-50 MeV differential cross section, polarisation ang. distrib., optical model exchange terms 0-27638
- <sup>16</sup>O(p,p), 50-160 MeV, energy depend. optical pot. 0-22830
- <sup>16</sup>O(p, $\pi^+$ ), 0.5-10 MeV, total cross sections near pion Coulomb barrier 0-32280
- <sup>16</sup>O( $\pi, \gamma n$ ), direct and resonance reaction unified shell model, n,  $\gamma$  spectra 0-52696
- <sup>16</sup>O( $\pi, \pi$ ),  $\sim$ 180 MeV, isospin mixing, levels, excitation functions and ang. distrib. 0-42543
- <sup>16</sup>O( $\pi, \pi$ ), T-matrix from isobar-hole model, many-body corrections, optical pot. parameter 0-9312
- <sup>16</sup>O( $\pi, \pi$ ), three-body model of  $\pi$ N interaction using finite binding pots. 0-42707



## nuclei with mass number 6 to 19 continued

- <sup>16</sup>O( $\pi^-, n$ ), stopped pion, neutron energy spectra, mean energies and multiplicities 0-9311  
<sup>16</sup>O( $\pi^-, \pi^+$ ), 40 MeV, differential cross sections and strength parameters, optical model fit 0-18347  
<sup>16</sup>O(t,p), centre of mass corrections to DWBA overlap factors 0-18319  
<sup>17</sup>O, cross sections to ground, 0.87 and 5.09 MeV states, neutron strength from <sup>16</sup>O(d,p) 0-5066  
<sup>17</sup>O levels, resonances, J<sup>π</sup> and radiative width from <sup>14</sup>N(t,γ) 0-47389  
<sup>17</sup>O, NQR spectrum of H<sub>2</sub>O 0-9620  
<sup>17</sup>O, TOF transmission meas. of neutron resonances 0-37374  
<sup>17</sup>O(<sup>11</sup>B, Li), 115 MeV, shell and semiclassical reaction model anal. 0-13494  
<sup>17</sup>O(<sup>12</sup>C, Be), 115 MeV, shell and semiclassical reaction model anal. 0-13494  
<sup>17</sup>O(<sup>13</sup>C, <sup>10</sup>B), 105 MeV, shell and semiclassical reaction model anal., <sup>20</sup>F spins 0-13494  
<sup>17</sup>O(e,e), mag. scatt., form factors, HF calcs., core polarisation effects 0-42579  
<sup>17</sup>O(γ,n), 8.5-39.7 MeV, cross section, giant dipole and pygmy resonance decays 0-42619  
<sup>17</sup>O(γ,n), cross section, Lane-Lynn radiative capture mechanisms 0-52660  
<sup>18</sup>O, 1.98 MeV 2<sup>+</sup> state static quadrupole moment, from nuclear sum rules 0-13374  
<sup>18</sup>O, heavy ion excitation, single particle and core polarisation amplitude interference 0-5117  
<sup>18</sup>O integrated cross sections to excited residual states from <sup>19</sup>F(γ,p) 0-18200  
<sup>18</sup>O level gamma decay from <sup>17</sup>O(n,γ) 0-52623  
<sup>18</sup>O(<sup>18</sup>O, <sup>18</sup>O), symmetry and shell struct. effects on absorption, precompound states 0-27666  
<sup>18</sup>O(p,p), 18-44 MeV, differential cross sections, phase shift anal., energy depend. 0-47481  
<sup>18</sup>O(π,X), angular distrib. of inelastic diffusion of π<sup>±</sup> (French) 0-47507  
<sup>18</sup>O(π,π<sup>±</sup>), 164 MeV, yrast state and level excitation, DWIA calcs., shell model context 0-42526  
<sup>19</sup>O, pairing correlation effects (Chinese) 0-47420  
<sup>19</sup>O(p,X), 340, 660 MeV, ang. distrib., proton quasi-elastic knockout (Russian) 0-52649  
<sup>1</sup>u2C mean life, Pauli exclusion principle validity for nucleons 0-18233

## nuclei with mass number 20 to 38

- A=10-58, neutron separation energies, self consistent set from (n,γ) reaction 0-52563  
A=16 system, weak nuclear form factors of 0<sup>+</sup>-0<sup>-</sup> transitions, nuclear struct. effects 0-18246  
A=16 to 40, mag. moments, shell model calcs, mesonic exchange current effects, book contrib. 0-479  
A=16-58, charge, proton and neutron density distrib. calc. 0-22680  
A=19-31 odd nuclei, K<sup>π</sup>=1/2<sup>-</sup> bands, spectroscopic factors and transitions 0-32151  
A=24-60, yrast lines using Strutinsky method, empirical fusion bands 0-42514  
A=6-44, gamma-ray transition strengths, data tables 0-37345  
A<100, average E1/M1 strength ratio 0-52621  
A≤28, giant quadrupole resonance, E2 intensity distrib., from (α, α'), DWBA anal. (Hungarian) 0-52642  
A≤57 nuclei, E2, M1 multipole mixing ratios 0-22751  
even-even nuclei, z=6 to 100, probable members of quasi-bands in spherical and deformed regions 0-13357  
thermonuclear reaction rate data for intermediate mass nuclei 0-31427  
(n,X), fast n, <sup>3</sup>He emission cross sections for A=27-115 0-13475  
Al(Ne,X), 400 MeV/N, direct vs. thermal particle emission, inclusive cross sections 0-52688  
<sup>26</sup>Al low energy resonances, decay and J<sup>π</sup> assignments, branching ratios from <sup>25</sup>Mg(p,γ) 0-42624  
<sup>26</sup>Al/<sup>26</sup>Mg isobars, separation via negative ion mass spectroscopy 0-31146  
<sup>27</sup>Al (<sup>14</sup>N, X), 70, 100 MeV, deep inelastic, charged reaction products ang. correlations, 3-body kinematics 0-5162  
<sup>27</sup>Al, J<sup>π</sup>=5/2 state, cross section and analysing power ang. distrib. 0-18296  
<sup>27</sup>Al, resonance strengths from <sup>26</sup>Mg(p,γ) 0-22786  
<sup>27</sup>Al+<sup>16</sup>O, 34-81 MeV, total fusion-evaporation cross sections, fusion barrier 0-5190  
<sup>27</sup>Al+d(α), 12-50 MeV, t formation average cross sections 0-42670  
<sup>27</sup>Al(<sup>12</sup>C, <sup>12</sup>C), 14-25 MeV, 180° scatt. excitation function and ang. distrib. struct. 0-32253  
<sup>27</sup>Al(<sup>16</sup>O,X), 88 MeV, inelastic scatt. and multinucleon transfer, Q-value depend. 0-42690  
<sup>27</sup>Al(<sup>3</sup>He, <sup>3</sup>He), 119 MeV, optical pot. parameters energy and mass depend. 0-32289  
<sup>27</sup>Al(<sup>3</sup>He, He), optical potentials and volume integrals, mass and energy dep. 0-52686  
<sup>27</sup>Al(α,X), 20, 40 MeV/N, α breakup yield, fragment yield ratios 0-9300  
<sup>27</sup>Al(γ,p), cross sections and proton energy spectra from (e,e'p) 0-13461  
<sup>27</sup>Al(γ,p)<sup>26</sup>Mg, energy and angular distribution (Korean) 0-18289  
<sup>27</sup>Al(p,α)<sup>26</sup>Mg, finite-range cluster-model description, DWBA approach 0-52667  
<sup>27</sup>Al(p,α)X, direct knockout model for fragmentation, (p,α) predictions 0-18275  
<sup>27</sup>Al(p,p), 100-2200 MeV, total and reaction cross sections from optical pot. 0-18303  
<sup>27</sup>Al(π,π<sup>±</sup>p), 255 MeV, quasielastic knockout, proton yield, σ(π<sup>+</sup>)/σ(π<sup>-</sup>) cross section ratio 0-32305  
<sup>28</sup>Al E1 transitions and partial radiative widths from <sup>27</sup>Al(n,γ) 0-52618  
<sup>28</sup>Al ground state doublet ang. distrib., direct charge exchange model anal. from <sup>28</sup>Si(<sup>18</sup>O, <sup>18</sup>F) 0-9307  
<sup>28</sup>Al levels, spins and γ-rays, multipole mixing from <sup>27</sup>Al(n,γ), pol. thermal 0-47398  
<sup>28</sup>Al, neutron binding energy precision meas. 0-18182  
Al(d,d), 4.3, 6.3, 8.9 GeV/c, secondary momentum spectra, multiple scatt. model anal. (Russian) 0-27650  
Al(μ<sup>+</sup>, X) energetic charged particle spectrum, integrated yield 0-18293  
Al(p,X), 400 GeV/c, light ion backward prod., invariant cross section 0-32279  
Al(p,X), 70 GeV/c, π<sup>±</sup>, K<sup>±</sup>, p, p prod. with p<sub>T</sub>=0.5-2.5 GeV/c cross sections, yield ratios (Russian) 0-52681  
Al(p,pxX), x=1, 2, 640 MeV, energetic backward p emission, inclusive differential cross section 0-9290

## nuclei with mass number 20 to 38 continued

- Ar isotopes, spallation ratios and prod. cross sections from (p, spallation) 0-9284  
<sup>36</sup>Ar α-cluster spectroscopic factors, DWBA anal. of (d, <sup>6</sup>Li) 0-52571  
<sup>36</sup>Ar, delayed proton and alpha emission, transition energies, levels, J<sup>π</sup>, from <sup>36</sup>K decay 0-52629  
<sup>36</sup>Ar, electric quadrupole strength, giant quadrupole resonance 0-52575  
<sup>38</sup>Ar high spin state density, γ-decay mode, deformed states from <sup>35</sup>Cl(α,py) 0-32168  
<sup>38</sup>Ar levels, J<sup>π</sup> and transition strengths, DWBA anal. of <sup>40</sup>Ar(p,t) 0-47378  
<sup>38</sup>Ar resonance strengths from <sup>37</sup>Cl(p,γ) 0-22786  
Cl (Ar, π<sup>±</sup>X), 250, 400 MeV/A, pion yield near threshold 0-18344  
<sup>32</sup>Cl, β<sup>+</sup> decay, delayed particle emission, <sup>32</sup>S levels and J<sup>π</sup> 0-22772  
<sup>35</sup>Cl, contrib. to fast neutron dose to the human body 0-51263  
<sup>35</sup>Cl, resonance strengths from <sup>34</sup>S(p,γ) 0-22786  
<sup>37</sup>Cl(α,γ), 2.9-5.2 MeV, excitation function competition cusps, Mauser-Feshbach calcs. 0-13404  
<sup>37</sup>Cl(v,e)<sup>37</sup>Ar, shell model cross section calc., appl. to cosmic ray and background elimination (Russian) 0-5131  
<sup>20</sup>F spins from <sup>17</sup>O(<sup>13</sup>C, <sup>10</sup>B) 0-13494  
<sup>4</sup>K, A=37,39, levels, excitation and microscopic form factors, DWBA calcs. from Ca(p,α) 0-32185  
<sup>36</sup>K, β-decay, delayed proton and alpha emission <sup>36</sup>Ar levels, J<sup>π</sup>, transitions 0-52629  
<sup>38</sup>K low lying 1<sup>+</sup>, T=0 states, DWBA anal. of <sup>40</sup>Ca(p,<sup>3</sup>He) 0-470  
<sup>4</sup>Mg(<sup>3</sup>He, <sup>3</sup>He), A=24,25,26, optical potentials and volume integrals, mass and energy dep. 0-52686  
<sup>4</sup>Mg(Li, Li), A=24, 26, 88 MeV, optical potentials, phenomenological and microscopic 0-52687  
<sup>4</sup>Mg(α, <sup>12</sup>C), A=24, 26, 90.3 MeV, cross sections and systematics multi-α-cluster transfer implications 0-42675  
<sup>24</sup>Mg hole states, transitions and spectroscopic factors, DWBA anal. of <sup>24</sup>Mg(p,d) 0-32161  
<sup>24</sup>Mg, <sup>16</sup>O+α cluster model, energy level structure 0-18215  
<sup>24</sup>Mg 2<sup>+</sup> state quadrupole moment from <sup>208</sup>Pb(<sup>24</sup>Mg, <sup>24</sup>Mg) 0-9230  
<sup>24</sup>Mg (α,α<sup>12</sup>C), 120 MeV, symmetric fission, resonances and average partial widths 0-42714  
<sup>24</sup>Mg (γ,p), 17-30 MeV, giant dipole resonances and transitions, shell effects (Russian) 0-13434  
<sup>24</sup>Mg continuum states, branching ratios from <sup>12</sup>C(<sup>16</sup>O, α) 0-22661  
<sup>24</sup>Mg, electric quadrupole strength, giant quadrupole resonance 0-52575  
<sup>12</sup>C, giant isoscalar quadrupole fission/fusion doorway states from <sup>12</sup>C(<sup>12</sup>C, <sup>12</sup>C) 0-37410  
<sup>24</sup>Mg ground state band from <sup>12</sup>C(<sup>12</sup>C,X) 0-42727  
<sup>24</sup>Mg high spin selectivity, critical ang. momentum effects from <sup>10</sup>B(<sup>16</sup>O,d) 0-13366  
<sup>24</sup>Mg high spin states from selective compound reactions, stat. anal. from <sup>10</sup>B(<sup>16</sup>O,d) 0-18180  
<sup>24</sup>Mg, K<sup>π</sup>=0<sup>+</sup>, K<sup>π</sup>=3<sup>-</sup> bands, radiative and α-widths from (α,γ), (<sup>16</sup>O,α) 0-18173  
<sup>24</sup>Mg low lying K-band from <sup>28</sup>Si α-decay 0-47438  
<sup>24</sup>Mg nuclear molecular resonances in <sup>12</sup>C-<sup>12</sup>C system from <sup>12</sup>C(<sup>16</sup>O,α), 0-13430  
<sup>24</sup>Mg rot. band termination, level lifetimes from <sup>12</sup>C(<sup>16</sup>O, α) 0-18174  
<sup>24</sup>Mg yrast and high spin states up to 24 MeV, ang. distrib. from <sup>10</sup>B(<sup>16</sup>O, d) 0-18175  
<sup>24</sup>Mg yrast line, Strutinsky type cranking calc., pairing correlation inclusion 0-13355  
<sup>24</sup>Mg(<sup>13</sup>C, <sup>13</sup>C'), 35 MeV, γ-rays and spin flip 0-18189  
<sup>24</sup>Mg(e,e), elastic scatt., spectroscopic information and form factors 0-9260  
<sup>24</sup>Mg(γ,p), cross sections and proton energy spectra from (e,e'p) 0-13461  
<sup>24</sup>Mg(γ,p), up to 0.25 GeV, from bremsstrahlung γ-quanta (Russian) 0-5123  
<sup>24</sup>Mg(p,p'), 0.8 GeV, rot., γ and β bands, ground state deformation, DWBA, coupled channels anal. 0-9198  
<sup>24</sup>Mg(p,p), 20, 40, 800 MeV, γ-vibr. band, coupled channels anal. 0-9194  
<sup>24</sup>Mg(p,p'), 40 MeV, two step pickup-stripping process, negative parity states 0-32256  
<sup>24</sup>Mg(p,p), 15 MeV, excitation functions 0-22825  
<sup>24</sup>Mg(p,p), 18-44 MeV, differential cross sections, phase shift anal., energy depend. 0-47481  
<sup>25</sup>Mg(e,e), 180° scatt., magnetisation distrib., mag. multipole moments 0-9228  
<sup>26</sup>Mg, 2<sup>+</sup> state quadrupole moment in band mixed HF model 0-52578  
<sup>26</sup>Mg (α,α), 104 MeV, oblate-prolate effects in struct. and reactions 0-9225  
<sup>26</sup>Mg(p,π<sup>+</sup>), isobar configuration effects, p→Δ<sup>0</sup>π model, ang. distrib. (Chinese) 0-47484  
<sup>27</sup>Mg energy levels, spectroscopic factors, DWBA, Hauser-Feshbach anal. from <sup>26</sup>Mg(d,p) 0-52581  
<sup>28</sup>Mg radionuclide yield from <sup>27</sup>Al(α,3p) and <sup>26</sup>Mg(α,2p) 0-32290  
Na(Ne,X), 800 MeV/N, direct vs. thermal particle emission, inclusive cross sections 0-52688  
Na(<sup>20</sup>Ne, π<sup>+</sup>), 800 MeV/N, doubly differential cross sections and ang. distrib. 0-9305  
Na(<sup>20</sup>Ne, π<sup>+</sup>X), 400 MeV/N, pion prod. doubly differential cross sections and ang. distrib. 0-32299  
<sup>21</sup>Na deduced levels and cross sections from <sup>12</sup>C(<sup>12</sup>C,t) 0-469  
<sup>22</sup>Na, effective interactions for dominant shell-model configurations: ds-shell example 0-32204  
<sup>23</sup>Na, 14.7 MeV neutron capture cross-section measurements with activation technique 0-32282  
<sup>23</sup>Na level α-spectroscopic strengths assuming direct cluster transfer from <sup>19</sup>F(<sup>4</sup>Li,d) 0-27552  
<sup>23</sup>Na, nuclear relax. correl. times in polymethacrylic acid 0-50212  
<sup>23</sup>Na(<sup>3</sup>He, <sup>3</sup>He), optical potentials and volume integrals, mass and energy dep. 0-52686  
<sup>23</sup>Na(n, α)<sup>20</sup>F, average cross sections in <sup>235</sup>U fission neutron spectrum 0-22828  
<sup>23</sup>Na(n, p)<sup>23</sup>Ne, average cross sections in <sup>235</sup>U fission neutron spectrum 0-22828  
<sup>24</sup>Na fragment ang. and energy distrib., two-step model anal. of <sup>19</sup>Au(p,X) 0-52678  
<sup>24</sup>Na<sup>m</sup>, 1<sup>+</sup> isomer, mag. moment 0-32177  
Ne+Ne, classical many-body model for heavy ion collisions 0-536  
<sup>20</sup>Ne α-cluster spectroscopic factors, DWBA anal. of (d, <sup>6</sup>Li) 0-52571  
<sup>20</sup>Ne, α-transfer reactions, spectroscopic factors, exact finite range DWBA anal. 0-13372



## nuclei with mass number 20 to 38 continued

- <sup>20</sup>Ne breakup cross section, direct mechanism, DWBA anal. of <sup>40</sup>Ca(<sup>20</sup>Ne,<sup>16</sup>O) 0-18276
- <sup>20</sup>Ne continuum states, J<sup>π</sup> and branching from <sup>12</sup>C(<sup>12</sup>C, αα) 0-22660
- <sup>20</sup>Ne E1 resonance from <sup>19</sup>F(p,γ) pol. p 0-22790
- <sup>20</sup>Ne, electric quadrupole strength, giant quadrupole resonance 0-52575
- <sup>20</sup>Ne excitation functions, resonance search from <sup>10</sup>B(<sup>14</sup>N,α) 0-27614
- <sup>20</sup>Ne from <sup>16</sup>O(<sup>16</sup>O,<sup>12</sup>C)<sup>20</sup>Ne, polarisation measurements 0-9301
- <sup>20</sup>Ne high spin states, J<sup>π</sup> and α-decay branching ratios from <sup>16</sup>O(<sup>12</sup>C,<sup>8</sup>Be) 0-18166
- <sup>20</sup>Ne high spin states, J<sup>π</sup> assignments from <sup>16</sup>O(<sup>6</sup>Li,d) 0-18167
- <sup>20</sup>Ne, high-spin states and shell struct. 0-47342
- <sup>20</sup>Ne levels, J<sup>π</sup>, branching ratio and EM transition rates from <sup>16</sup>O+α 0-42540
- <sup>20</sup>Ne, levels, J<sup>π</sup> and ang. distrib. from <sup>18</sup>O(t,p) 0-18204
- <sup>20</sup>Ne levels and branching ratio from <sup>12</sup>C(<sup>16</sup>O, αα) 0-22661
- <sup>20</sup>Ne low lying states, configuration mixing calcs. with basis states from variational method 0-22693
- <sup>20</sup>Ne non-isolated resonances, excitation functions and ang. distrib. from <sup>20</sup>Na(p,α) (Chinese) 0-22788
- <sup>20</sup>Ne, nuclear current from cranked HF solns. 0-9241
- <sup>20</sup>Ne, Skyrme-type interactions, spectroscopy of light nuclei, density dependent Hartree-Fock 0-22717
- <sup>20</sup>Ne states, J<sup>π</sup>, differential cross sections and ang. distrib. from <sup>16</sup>O(α,α') 0-18203
- <sup>20</sup>Ne+<sup>12</sup>C, 6.3-13.8 MeV, total fusion cross section, S-factor, γ-yields 0-22877
- <sup>20</sup>Ne+<sup>20</sup>Ne, 250-1000 MeV/N, intranuclear cascade calcs. for multiplicity and cross sections 0-32300
- <sup>20</sup>Ne(<sup>20</sup>Ne,X), 132 MeV, TDHFB calc. for total fusion cross section 0-13521
- <sup>20</sup>Ne(d,d), pol. d, 10-12 MeV, cross section, coupled channel and fluctuations anal. 0-27617
- <sup>20</sup>Ne(e,e,α), EM induced α emission, α spectroscopic amplitudes, anal. solvable model 0-32267
- <sup>20</sup>Ne(γ,α), EM induced α emission, α spectroscopic amplitudes, anal. solvable model 0-32267
- <sup>20</sup>Ne(γ,n) cross sections and giant resonance struct. 0-13441
- <sup>21</sup>Ne, energy moments, sd shell realistic effective interactions, shell model spectra 0-18190
- <sup>21</sup>Ne states cross section, coupled channel and fluctuations anal. from <sup>20</sup>Ne(d,p) 0-27617
- <sup>21</sup>Ne structure, differential cross sections from <sup>27</sup>Al(α,<sup>8</sup>B) 0-5153
- Ne(<sup>2</sup>p,p), 0.6-25 GeV, backward emitted proton inclusive spectra, short range correlation 0-32281
- <sup>22</sup>O, Hartree-Fock calculations of nuclear bulk properties with density- and starting-energy dependent effective interaction 0-9246
- <sup>A</sup>P, A=31, 33, levels and transition j-depend., DWBA anal. for Si(<sup>19</sup>F,<sup>16</sup>O) 0-42542
- <sup>28</sup>P, β<sup>+</sup> decay, delayed particle emission, <sup>28</sup>Si levels and J<sup>π</sup> 0-22772
- <sup>29</sup>P resonance coherence widths from <sup>28</sup>Si(p,p), pol. p 0-32258
- <sup>29</sup>P high spin two nucleon states decay props. from <sup>28</sup>Si(α, dγ) 0-13402
- <sup>31</sup>P NMR analysis of intact tissue 0-26432
- <sup>31</sup>P, NMR in phospholipids 0-5644
- <sup>31</sup>P, resonance strengths from <sup>30</sup>Si(p,γ) 0-22786
- <sup>31</sup>P, shielding consts. and anisotropy of NMR shielding tensor, modified CNDO/S calcs. (French) 0-32610
- <sup>31</sup>P, simultaneous multinucl. NMR by alternate scan recording of <sup>31</sup>P and <sup>13</sup>C spectra 0-26426
- <sup>32</sup>P, half-life and mean beta disintegration energy determ by low-temp calorimetry 0-5094
- <sup>32</sup>S compound nucleus formation and deexcitation entrance channel effects from <sup>16</sup>O+<sup>16</sup>O, <sup>12</sup>C+<sup>20</sup>Ne 0-549
- <sup>32</sup>S, contrib. to fast neutron dose to the human body 0-51263
- <sup>32</sup>S, electric quadrupole strength, giant quadrupole resonance 0-52575
- <sup>32</sup>S levels and J<sup>π</sup> from <sup>32</sup>Cl β<sup>+</sup> decay 0-22772
- <sup>32</sup>S levels and spectroscopic factors from pickup DWBA anal. of <sup>33</sup>S(<sup>3</sup>He,α) 0-9235
- <sup>32</sup>S, nuclear radii, energy density and HF-BCS methods 0-47363
- <sup>32</sup>S(α,<sup>12</sup>C), 90.3 MeV, cross sections and systematics multi-α-cluster transfer implications 0-42675
- <sup>32</sup>S(e,e), elastic scatt., spectroscopic information and form factors 0-9260
- <sup>32</sup>S(n,X), 2.5-1100 keV, resonance struct. from total and capture cross sections 0-42620
- <sup>32</sup>S(n,γ), fast n, doorway structs. and single particle resonances, microscopic treatment 0-52646
- <sup>32</sup>S(n,γ), non-statistical effects in shell model calcs. 0-32274
- <sup>32</sup>S(n,γ), single particle resonances and doorway states, K matrix formalism 0-37384
- <sup>32</sup>S(n,n), 2-3 MeV neutrons studied using assoc. particle TOF spectrometer 0-13468
- <sup>32</sup>S(n,n), 5 MeV, elastic and inelastic scatt., differential cross-sections, model anal. (Russian) 0-42668
- <sup>32</sup>S(π,π), total cross section, density distrib. and ray bending effects 0-47509
- Si isotopes deformed nuclei, stability, shape, Hartree-Fock calcs. (Russian) 0-52568
- Si+<sup>16</sup>O, 34-81 MeV, total fusion-evaporation cross sections, fusion barrier 0-5190
- <sup>A</sup>Si(<sup>12</sup>C,X), 20-49 MeV, A=28-30, complete fusion cross sections, excitation function weak struct. 0-5188
- <sup>A</sup>Si(<sup>16</sup>O,X), 21-61 MeV, A=28-30, complete fusion cross sections, excitation function weak struct. 0-5188
- <sup>28</sup>Si 8<sup>+</sup> state, level systematics and energy spectra from <sup>25</sup>Mg(<sup>12</sup>C,<sup>9</sup>Be) 0-42528
- <sup>28</sup>Si (e,f), K=2 symmetry intermediate state 0-47514
- <sup>28</sup>Si α-doorway states in α-decay to <sup>24</sup>Mg low lying K-band 0-47438
- <sup>28</sup>Si, isoscalar giant quadrupole resonances, RPA calcs., E2 strength fragmentation, spectroscopic factors 0-13437
- <sup>28</sup>Si levels and J<sup>π</sup> from <sup>28</sup>P β<sup>+</sup> decay 0-22772
- <sup>28</sup>Si p3/2 neutron resonance γ-decay, partial rad. widths from Si(n,γ) 0-52617
- <sup>28</sup>Si, resonance strengths from <sup>27</sup>Al(p,γ) 0-22786
- <sup>28</sup>Si resonance wave functions and differential cross sections from <sup>27</sup>Al(p, n), (p, p), (p, α) 0-18261
- <sup>28</sup>Si, spin cutoff factors, sd shell realistic effective interactions, shell model spectra 0-18190
- <sup>28</sup>Si+<sup>16</sup>O, fusion oscillations, evaporation residue gamma yields, cross section 0-42725
- <sup>28</sup>Si+<sup>6</sup>Li, parabolic repulsion potential, optical model 0-22782

## nuclei with mass number 20 to 38 continued

- <sup>28</sup>Si(<sup>12</sup>C,<sup>12</sup>C), 19-48 MeV, ang. distrib., cross sections and optical parameters 0-5157
- <sup>28</sup>Si(<sup>12</sup>C,<sup>12</sup>C), 27.8-31.5 MeV, elastic and inelastic excitation functions, fine struct., statistical anal. 0-18269
- <sup>28</sup>Si(<sup>12</sup>C,<sup>12</sup>C), entrance channel resonances, backward angle scatt., elastic scatt. enhancement 0-27612
- <sup>28</sup>Si(<sup>15</sup>N,<sup>14</sup>N), 44 MeV, modified optical pot. from backward elastic scatt. 0-32255
- <sup>28</sup>Si(<sup>15</sup>N,<sup>16</sup>O), 44 MeV, modified optical pot. from backward elastic scatt. 0-32255
- <sup>28</sup>Si(<sup>16</sup>O,<sup>16</sup>O), 30-32.7 MeV, elastic and inelastic excitation functions, fine struct., statistical anal. 0-18269
- <sup>28</sup>Si(<sup>16</sup>O,<sup>16</sup>O), entrance channel resonances, backward angle scatt., elastic scatt. enhancement 0-27612
- <sup>28</sup>Si(<sup>18</sup>O,X), 56 MeV, multinucleon transfers, ang. distrib., distorted wave and shell model anal. 0-27663
- <sup>28</sup>Si(<sup>18</sup>F,<sup>18</sup>O), 60 MeV, exact finite range DWBA and CCBA calcs. 0-538
- <sup>28</sup>Si(<sup>20</sup>Ne, X), 120 MeV, linear response theory anal., frictional coeffs. and energy dissipation 0-13502
- <sup>28</sup>Si(<sup>9</sup>Be,<sup>9</sup>Be), 45, 60 MeV cross sections, ang. distrib., Wegner plot, optical and double folding anal. 0-47497
- <sup>28</sup>Si(α,<sup>12</sup>C), 90.3 MeV, cross sections and systematics multi-α-cluster transfer implications 0-42675
- <sup>28</sup>Si(α,α'), c=charged particle, 150 MeV, isoscalar giant quadrupole resonance struct. 0-13438
- <sup>28</sup>Si(d,p), 8.05 MeV, stripping reaction differential cross section, d distortion effect (Japanese) 0-22796
- <sup>28</sup>Si(e,e), elastic scatt., spectroscopic information and form factors 0-9260
- <sup>28</sup>Si(γ, p), 18.1-29 MeV, giant dipole resonance, contrib. from various configs. 0-18264
- <sup>28</sup>Si(n,γ), fast n, doorway structs. and single particle resonances, microscopic treatment 0-52646
- <sup>28</sup>Si(n,γ), single particle resonances and doorway states, K matrix formalism 0-37384
- <sup>28</sup>Si(n,n'), 13.9 MeV, spin flip probability from 1.78 MeV state, direct theory 0-9234
- <sup>28</sup>Si(n,n), 5 MeV, elastic and inelastic scatt., differential cross-sections, model anal. (Russian) 0-42668
- <sup>28</sup>Si(p,p), pol. p, 12-18 MeV, cross section, anal. power and states, <sup>29</sup>P resonance coherence widths 0-32258
- <sup>28</sup>Si(π,X), angular distrib. of inelastic diffusion of π<sup>±</sup> (French) 0-47507
- <sup>28</sup>Si(π,π), 162 MeV, elastic and inelastic ang. distrib., optical and PWIA anal. 0-42706
- <sup>29</sup>Si excitation functions from <sup>27</sup>Al(<sup>3</sup>He,p) 0-47493
- <sup>29</sup>Si neutron resonance, γ-spectra, partial and total radiative widths from <sup>28</sup>Si(n,γ) 0-42578
- <sup>30</sup>Si, 2<sup>+</sup> state quadrupole moment in band mixed HF model 0-52578
- <sup>30</sup>Si first excited state, static quadrupole moment from <sup>208</sup>Pb(<sup>30</sup>Si,<sup>30</sup>Si) 0-13373
- <sup>30</sup>Si(d,p), pol.d, 1.9-2.5 MeV, anal. power excitation function anomaly 0-5118
- S(n,γ), on-line gamma anal. using Ge detector 0-52624

## nuclei with mass number 39 to 58

- A=10-58, neutron separation energies, self consistent set from (n,γ) reaction 0-52563
- A=16 to 40, book, moments, shell model calcs, mesonic exchange current effects, book contrib. 0-479
- A=16-58, charge, proton and neutron density distrib. calc. 0-22680
- A=24-60, yrast lines using Strutinsky method, empirical fusion bands 0-42514
- A=40 to 56, two-nucleon transfer reactions, coupled channel formalism for isospin depend. optical pot. 0-42609
- A=40-56, spectroscopy props. using pure configuration shell model (Chinese) 0-42584
- A=40-80, yrast props. and high spin isomers, cranking plus Strutinsky formalism 0-32152
- A=42 isotopic spin triplet, Coulomb energies and shifts, microscopic calcs. 0-9200
- A=6-44, gamma-ray transition strengths, data tables 0-37345
- A<100, average E1/M1 strength ratio 0-52621
- A≤57 nuclei, E2, M1 multipole mixing ratios 0-22751
- even-even nuclei, z=6 to 100, probable members of quasi-bands in spherical and deformed regions 0-13357
- thermonuclear reaction rate data for intermediate mass nuclei 0-31427
- (n,X), fast n, <sup>3</sup>He emission cross sections for A=27-115 0-13475
- (p,n) excitation functions for A=45 to 80, proton optical pot. at sub-Coulomb energies 0-9292
- Ar isotopes, spallation ratios and prod. cross sections from (p, spallation) 0-9284
- <sup>A</sup>Ar, A=45,46, β-decay, <sup>A</sup>K, A=45,46, levels, lifetimes and transitions 0-42597
- <sup>40</sup>Ar+<sup>40</sup>Ar, 250-1000 MeV/N, intranuclear cascade calcs. for multiplicity and cross sections 0-32300
- <sup>40</sup>Ar(γ, xp yn), 9-29 MeV, cross sections in giant resonance region, particle decay modes 0-13462
- <sup>40</sup>Ar(p,p), 18-44 MeV, differential cross sections, phase shift anal., energy depend. 0-47481
- Ca+Ca, classical many-body model for heavy ion collisions 0-536
- <sup>A</sup>Ca, (A=43-46), pairing force, seniority number 0-27563
- <sup>A</sup>Ca, A=40, 42-44, 48, pionic X-rays, strong interaction and isotope shifts, π-nuclear optical pot. 0-53169
- <sup>A</sup>Ca, A=40, 48, neutron densities and single particle struct. 0-32165
- <sup>A</sup>Ca, A=40,48, nuclear radii, energy density and HF-BCS methods 0-47363
- <sup>A</sup>Ca(<sup>3</sup>Li,<sup>3</sup>Li'), A=40, 44, 48, 153 MeV, isoscalar giant quadrupole resonances 0-13440
- <sup>A</sup>Ca(<sup>3</sup>Li,<sup>3</sup>Li'), A=40, 48, 88 MeV, optical potentials, phenomenological and microscopic 0-52687
- <sup>A</sup>Ca(γ,X), A=42, 44, 48, photoneutron and photoproton cross section systematics 0-13463
- <sup>A</sup>Ca(π<sup>+</sup>, π<sup>+</sup>), A=40,44,48, 290 MeV, double charge exchange cross sections 0-18348
- <sup>A</sup>Ca=A=40, 48, Hartree-Fock calculations of nuclear bulk properties with density- and starting-energy dependent effective interaction 0-9246
- <sup>40</sup>Ca (α,α'), 104 MeV, giant resonance ang. distrib., L-transfer contrib. 0-27610
- <sup>40</sup>Ca (π<sup>+</sup>, π<sup>+</sup>), model Coulomb corrections in eikonal 0-5171



## nuclei with mass number 39 to 58 continued

- <sup>40</sup>Ca, electric quadrupole strength, giant quadrupole resonance 0-52575  
<sup>40</sup>Ca, finite nuclear props. in relativistic quantum field theory, mass and p densities 0-9219  
<sup>40</sup>Ca, monopole vibration damping, TDHF calcs. 0-22667  
<sup>40</sup>Ca resonance strengths from <sup>39</sup>K(p,γ) 0-22786  
<sup>40</sup>Ca, weak s resonance γ-ray decay in negative parity low lying levels 0-27591  
<sup>40</sup>Ca + <sup>6</sup>Li, parabolic repulsion potential, optical model 0-22782  
<sup>40</sup>Ca + p(d,α) transparency in composite particle-nucleus reactions 0-92773  
<sup>40</sup>Ca(<sup>16</sup>O, <sup>16</sup>O), A=10,11, angular distrib., Woods-Saxon and double-folding optical models 0-52691  
<sup>40</sup>Ca(<sup>13</sup>C, <sup>13</sup>C), 108 MeV, nuclear continuum investigation 0-13506  
<sup>40</sup>Ca(<sup>16</sup>O, p)<sup>55</sup>Co, 39 to 89 MeV reaction cross section 0-47496  
<sup>40</sup>Ca(<sup>16</sup>O, <sup>16</sup>O), 60 MeV, long range absorption and optical model effects from strong inelastic coupling 0-535  
<sup>40</sup>Ca(<sup>16</sup>O, <sup>16</sup>O), rot. band of molecular resonances, generator coordinate model 0-13428  
<sup>40</sup>Ca(<sup>16</sup>O, X), 40-214 MeV, fusion and elastic scatt. cross sections, optical anal. 0-32314  
<sup>40</sup>Ca(<sup>17</sup>O, <sup>17</sup>O), 61 MeV, elastic and inelastic, microscopic single folding model anal. 0-52692  
<sup>40</sup>Ca(<sup>20</sup>Ne, X), 44.1-70.4 MeV, fusion and elastic scatt. cross sections, evaporation residues 0-550  
<sup>40</sup>Ca(<sup>3</sup>He, x), pol. <sup>3</sup>He, x=d or α, 33 MeV, anal. power and cross sections 0-42628  
<sup>40</sup>Ca(<sup>3</sup>He, He), optical potentials and volume integrals, mass and energy dep. 0-52686  
<sup>40</sup>Ca(<sup>3</sup>He, He), pol. <sup>3</sup>He, 33.3 MeV, differential cross section and anal. power, optical pots. 0-42627  
<sup>40</sup>Ca(<sup>40</sup>Ar, <sup>40</sup>Ar), 191, 236, 272 MeV, elastic cross sections, optical and Fresnel model anal. 0-22858  
<sup>40</sup>Ca(<sup>40</sup>Ar, X), 191, 263, 272 MeV, strongly damped collision cross sections, product energies 0-32291  
<sup>40</sup>Ca(<sup>40</sup>Ca, X), 10 MeV/N, charged particle emission Q-value depend. 0-47503  
<sup>40</sup>Ca(<sup>40</sup>Ca, X), 400 MeV, fragment energy spectra struct., giant resonances, direct process 0-47452  
<sup>40</sup>Ca(<sup>40</sup>Ca, X), deep inelastic, doubly differential cross section, spectra struct. 0-5103  
<sup>40</sup>Ca(<sup>9</sup>Be, <sup>9</sup>Be), 45, 60 MeV cross sections, ang. distrib., Wegner plot, optical and double folding anal. 0-47497  
<sup>40</sup>Ca(K<sup>+</sup>, K<sup>+</sup>), Glauber model anal. 0-42697  
<sup>40</sup>Ca(α, α), (<sup>6</sup>Li, <sup>6</sup>Li), velocity of refined folding model approaches 0-541  
<sup>40</sup>Ca(α, <sup>13</sup>C), 90.3 MeV, cross sections and systematics multi-α-cluster transfer implications 0-42675  
<sup>40</sup>Ca(α, α), 6-18 MeV, resonances, anomalous large angle scatt. and quasi-molecular states 0-27613  
<sup>40</sup>Ca(α, α), entrance channel resonances, backward angle scatt., elastic scatt. enhancement 0-27612  
<sup>40</sup>Ca(α, α), giant isoscalar quadrupole resonance, α-over p-decay ratio, SU(3) and shell model 0-27608  
<sup>40</sup>Ca(e, e), cross sections, model independ. charge density 0-27548  
<sup>40</sup>Ca(e, e), elastic scatt., spectroscopic information and form factors 0-9260  
<sup>40</sup>Ca(n, γ), mechanism in 3s size resonance, radiative width statistical and valence effects 0-37388  
<sup>40</sup>Ca(n, n), 11-26 MeV, differential cross sections, global optical model anal. 0-18298  
<sup>40</sup>Ca(n, n), 2-3 MeV neutrons studied using assoc. particle TOF spectrometer 0-13468  
<sup>40</sup>Ca(p, p), 20-50 MeV differential cross section, polarisation ang. distrib., optical model exchange terms 0-27638  
<sup>40</sup>Ca(π<sup>+</sup>, π<sup>+</sup>), 40 MeV, differential cross sections and strength parameters, optical model fit 0-18347  
<sup>40</sup>Ca(t, p), centre of mass corrections to DWBA overlap factors 0-18319  
<sup>41</sup>Ca 1f<sub>7/2</sub> neutron radial distrib., single particle, orbits, RMS radii from <sup>40</sup>Ca(<sup>13</sup>C, <sup>12</sup>C) 0-42532  
<sup>41</sup>Ca giant dipole resonance, isospin struct., direct-semidirect anal. from <sup>40</sup>K(p, γ) 0-47449  
<sup>42</sup>Ca high spin state density, γ-decay mode, deformed states from <sup>39</sup>K(α, pγ) 0-32168  
<sup>48</sup>Ca beam prod. from isotopically enriched sputter targets 0-23221  
<sup>48</sup>Ca fragmentation at 212 MeV/amu in Be(<sup>48</sup>Ca, X) 0-27660  
<sup>48</sup>Ca(<sup>12,13</sup>C, X), elastic, inelastic and single nucleon transfer excitation functions, <sup>48</sup>Ca levels 0-13492  
<sup>48</sup>Ca(<sup>6</sup>Li, <sup>6</sup>Li), (α, α), velocity of refined folding model approaches 0-541  
<sup>48</sup>Ca(p, p), 1 GeV, elastic scatt. differential cross section calc. 0-47480  
<sup>39</sup>Cl, charge state study prod. by (n,d) in liquid Ar ionization chamber (Russian) 0-9298  
<sup>39</sup>Cl excited states and transitions from <sup>39</sup>S decay 0-42595  
<sup>39</sup>Cl, charge state study prod. by (n,p) in liquid Ar ionization chamber (Russian) 0-9298  
<sup>55</sup>Co f-wave resonances, inelastic p amplitudes, analogue state spectroscopic factors from <sup>54</sup>Fe(p, pγ) 0-47451  
<sup>55</sup>Co, resonance decays, branching ratios and analogue resonances from <sup>54</sup>Fe(p, γ) 0-52643  
<sup>57</sup>Co, Mossbauer gamma-X-ray coincidence meas. 0-14041  
<sup>58</sup>Co decay, student expt. 0-12875  
<sup>4</sup>Cr (d,d), pol. d, A=52, 54, 12 MeV, cross sections, anal. powers, global optical model anal. 0-47459  
<sup>4</sup>Cr(n, X), A=50, 52-54, 14 MeV, X=p,n,p,α,n,α,<sup>3</sup>He, production cross-sections 0-42648  
<sup>4</sup>Cr high spin states, yrast levels and 6<sup>-</sup> isomeric state from <sup>40</sup>Ca(<sup>10</sup>B, np) 0-454  
<sup>51</sup>Cr, bands, levels, EM transitions, J<sup>π</sup>, branching and mixing ratios from <sup>48</sup>Ti (γ, nγ) <sup>51</sup>Cr and <sup>51</sup>V(p, nγ) <sup>51</sup>Cr 0-52606  
<sup>52</sup>Cr, if nucleon orbit RMS radii from transfer data 0-27544  
<sup>52</sup>Cr high spin states, transitions and J<sup>π</sup> values from <sup>50</sup>Ti(α, Znγ) 0-455  
<sup>52</sup>Cr(<sup>12,13</sup>C, X), elastic, inelastic and single nucleon transfer excitation functions, <sup>52</sup>Cr levels 0-13492  
<sup>52</sup>Cr(α, α), 8-18 MeV, cross sections, search for giant dipole resonance 0-9281  
<sup>52</sup>Cr(d, p) <sup>52</sup>Cr, Coulomb stripping, 2.12-2.48 MeV, DWBA anal., spectroscopic strengths 0-516  
<sup>52</sup>Cr(d, p) <sup>52</sup>Cr, deuteron break-up model anal. of cross-section, vector analysing power and angular correlation 0-27648  
<sup>52</sup>Cr(γ, X), photoneutron and photoproton cross section systematics 0-13463

## nuclei with mass number 39 to 58 continued

- <sup>52</sup>Cr(γ, γ), 35 MeV, 2<sup>+</sup> state deexcitation γ-rays, differential cross sections, deformation (Russian) 0-13406  
<sup>52</sup>Cr(γ, γ), up to 12 MeV, highly excited spin-1 resonances, γ-transitions 0-13427  
<sup>52</sup>Cr(n, n), 1.77 to 3 MeV, validity of Wick's inequality in the calculation of the lower limits of the differential elastic cross sections 0-5137  
<sup>52</sup>Cr(π, X), angular distrib. of inelastic diffusion of π<sup>±</sup> (French) 0-47507  
<sup>52</sup>Cr levels, J<sup>π</sup>, γ-transitions and 1626 eV resonance from <sup>52</sup>Cr(n, γ) 0-42610  
<sup>52</sup>Cr(γ, p) <sup>52</sup>V, cross-section, 14.4-27 MeV, isospin splitting 0-520  
<sup>54</sup>Cr levels, transitions, T<sub>1/2</sub>, J<sup>π</sup>, shell model anal. from <sup>51</sup>V(α, pγ) 0-47381  
<sup>54</sup>Cr(p, γ), 1.0-3.8 MeV, γ-yields, cross sections, predicted (p, n) cross section, Stat. anal. 0-5136  
<sup>54</sup>Cr deduced levels and spins, from <sup>54</sup>Cr(d<sub>pol</sub>, p), cross section and vector analysing power 0-52684  
Fe isotopes, cross sections for charged particle prod. by 14 MeV neutrons, data compilation 0-9289  
<sup>54</sup>Fe, A=54-56, high spin states, energy levels, spectroscopic factors, EM props., shell model 0-47359  
<sup>54</sup>Fe(α, α'), A=54, 58, 8-18 MeV, cross sections, search for giant dipole resonance 0-9281  
<sup>54</sup>Fe(d, d), pol. d, A=54, 56, 12 MeV, cross sections, anal. powers, global optical model anal. 0-47459  
<sup>54</sup>Fe(n, X) A=54, 56, 57, transmission and capture meas. 0-18313  
<sup>54</sup>Fe(n, γ), A=54, 56, 57, mechanism in 3s size resonance, radiative width statistical and valence effects 0-37388  
<sup>54</sup>Fe, α-cluster spectroscopic factors, DWBA anal. of (d, <sup>6</sup>Li) 0-52571  
<sup>54</sup>Fe high spin states, transitions and J<sup>π</sup> values from <sup>52</sup>Cr(α, Znγ) 0-455  
<sup>54</sup>Fe(<sup>12,13</sup>C, X), elastic, inelastic and single nucleon transfer excitation functions, <sup>54</sup>Fe levels 0-13492  
<sup>54</sup>Fe(p, α) <sup>51</sup>Mn, 21 MeV analogue state, excitation 0-13471  
<sup>54</sup>Fe(α, α'), coupled channels calc., capture cross section, GQR decay modes 0-27654  
<sup>54</sup>Fe(γ, X), photoneutron and photoproton cross section systematics 0-13463  
<sup>54</sup>Fe(n, γ), cross section, resonance and background interference 0-18310  
<sup>54</sup>Fe(p, p), 39, 62 MeV, DWBA anal., collective spectra, direct process contrib. (Russian) 0-13408  
<sup>54</sup>Fe deduced levels, from <sup>54</sup>Fe(d<sub>pol</sub>, p), cross section and vector analysing power 0-52684  
<sup>54</sup>Fe Zp<sub>1/2</sub> neutron orbit radius isotope shift from DWBA anal. of <sup>54</sup>Fe(t, d) 0-32172  
<sup>56</sup>Fe, search for giant quadrupole resonance 0-9281  
<sup>56</sup>Fe, shell model wave functions from <sup>56</sup>Fe(p, α) 0-32211  
<sup>56</sup>Fe(<sup>6</sup>Li, X), 75 MeV, Z=1 or 2 fast particle prod. mechanism above Coulomb barrier 0-42687  
<sup>56</sup>Fe(e, e'), 0.1-14 GeV, deep inelastic inclusive scatt. response functions and momentum distrib. 0-42640  
<sup>56</sup>Fe(γ, γ), up to 12 MeV, highly excited spin-1 resonances, γ-transitions 0-13427  
<sup>56</sup>Fe(n, n), 1.77 to 3.0 MeV, validity of Wick's inequality in the calculation of the lower limits of the differential elastic cross sections 0-5137  
<sup>56</sup>Fe(p, p), 100-2200 MeV, total and reaction cross sections from optical pot. 0-18303  
<sup>57</sup>Fe, (n, γ), cross section, 2.5-200 keV, s-wave resonances 0-18309  
<sup>57</sup>Fe(n, X) transmission data up to 400 keV, J<sup>π</sup> value for resonances 0-18311  
<sup>57</sup>Fe(n, γ) capture and total cross section meas. below 325 keV, resonance parameters 0-18314  
<sup>57</sup>Fe(n, X), resonance capture cross section s- and p-wave radiative widths 0-47476  
<sup>56</sup>Fe(e, e), nuclear radius, core polarisation and isotope shifts, muonic X-rays 0-22685  
<sup>56</sup>Fe(n, X), 3 eV-1 MeV transmission meas., resonance anal. 0-18316  
<sup>56</sup>Fe(n, γ) cross-section meas. principal resonance parameters 0-18312  
<sup>56</sup>Fe(n, γ), on-line gamma anal. using Ge detector 0-52624  
<sup>56</sup>Fe(n, n), pol. n, 16.1 MeV, differential cross section, optical model fit 0-32259  
<sup>56</sup>Fe(p, spallation), 0.08-24 GeV, Ar isotopes, spallation ratios and prod. cross sections 0-9284  
<sup>4</sup>K (Ar, π<sup>+</sup> X), 250, 400 MeV/A, pion yield near threshold 0-18344  
<sup>4</sup>K, A=37,39, levels, excitation and microscopic form factors, DWBA calcs. from Ca(p, α) 0-32185  
<sup>4</sup>K, A=45,46, levels, lifetimes and transitions from Ar β-decay 0-42597  
<sup>39</sup>K, contrib. to fast neutron dose to the human body 0-51263  
<sup>39</sup>K states and spectroscopic strengths DWBA anal. of <sup>40</sup>Ca(<sup>7</sup>Li, <sup>8</sup>Be) 0-5069  
<sup>39</sup>K(<sup>12</sup>C, <sup>12</sup>C), 54, 63 MeV, angular distrib., Woods-Saxon and double-folding optical models 0-52691  
<sup>40</sup>K, γ-ray energies meas. for Ge(Li) detector calibration 0-27865  
<sup>40</sup>K, naturally occurring, gamma-ray emission energies 0-52811  
<sup>40</sup>K mass excess and states from <sup>40</sup>Cu(<sup>7</sup>Li, Be) 0-9221  
<sup>55</sup>Mn low lying states, DWBA anal., shell model wave functions from <sup>56</sup>Fe(p, α) 0-32211  
<sup>55</sup>Mn, 14.7 MeV neutron capture cross-section measurements with activation technique 0-32282  
<sup>55</sup>Mn, energy levels, bound state mean lifetimes and spins from <sup>54</sup>Cr(p, γ) 0-42586  
<sup>55</sup>Mn(<sup>3</sup>He, 3n) <sup>55</sup>Co, nuclear medicine appl. 0-36132  
<sup>55</sup>Mn(n, X), 14 MeV, X=p,n,p,α,n,α,<sup>3</sup>He, production cross-sections 0-42648  
Ni doubly even nuclei, eqns. of motion method, pairing correlations, ground state energies 0-52585  
<sup>58</sup>Ni A=57-59, f<sub>7/2</sub> hole configuration effects, shell model calcs. 0-22670  
<sup>58</sup>Ni, A=58, 64, neutron densities and single particle struct. 0-32165  
<sup>58</sup>Ni, A=58, 60, search for giant quadrupole resonance 0-9281  
<sup>58</sup>Ni(<sup>3</sup>He, <sup>3</sup>He), A=58, 60, 62, 64, 119 MeV, optical pot. parameters energy and mass depend. 0-32289  
<sup>58</sup>Ni(<sup>40</sup>Ca, fusion), A=58, 60, 62, 113-170 MeV, fusion cross sections and excitation functions 0-32315  
<sup>58</sup>Ni(e, e'), 102 MeV, A=58, 60, E1-E4 giant multipole resonance comparison, shell model anal. 0-42614  
<sup>58</sup>Ni(n, X) A=58, 60, transmission data, resonance anal. 0-18317  
<sup>58</sup>Ni(n, n'), A=58-64, <4 MeV, gamma prod. and inferred cross sections 0-525  
<sup>58</sup>Ni(n, n), A=58, 60, 62, 64, 5 MeV, differential cross sections, optical, statistical and coupled channel anal. (Russian) 0-37377  
<sup>58</sup>Ni(p, π<sup>+</sup>), A=58, 64, 660 MeV, pion energy spectra, isotopic effects (Russian) 0-42669



## nuclei with mass number 39 to 58 continued

- <sup>56</sup>Ni excitation functions from <sup>40</sup>Ca(<sup>16</sup>O,X) fusion 0-18362  
<sup>57</sup>Ni, fine structure of hole-state analogues, isospin mixing 0-13401  
<sup>58</sup>Ni, cross sections for charged particle prod. by 14 MeV neutrons, data compilation 0-9289  
<sup>58</sup>Ni, HFB and dynamic anal., collective motion, zero point energy correction 0-18161  
<sup>58</sup>Ni, nuclear radii, energy density and HF-BCS methods 0-47363  
<sup>58</sup>Ni + p, 1 GeV, alpha-particle decay channels 0-22826  
<sup>58</sup>Ni(<sup>16</sup>O,X), 100 MeV, deep inelastic, fragment spin polarisation and alignment,  $\gamma$ -rays 0-18284  
<sup>58</sup>Ni(<sup>3</sup>He,<sup>3</sup>He), optical potentials and volume integrals, mass and energy dep. 0-52686  
<sup>58</sup>Ni(<sup>7</sup>Li,<sup>7</sup>Li'), 19 MeV, first 2<sup>+</sup> states Coulomb-nuclear interference, optical and DWBA anal. 0-22852  
<sup>58</sup>Ni( $\alpha$ ,X), 20, 40 MeV/N,  $\alpha$  breakup yield, fragment yield ratios 0-9300  
<sup>58</sup>Ni( $\alpha$ , $\alpha'$ c), 150 MeV, c=charged particle, particle decay from isoscalar giant resonance region 0-13439  
<sup>58</sup>Ni( $\alpha$ ,tp), double differential cross section, t-p ang. correlation function, direct breakup 0-22797  
<sup>58</sup>Ni(d,d), pol. d, 12 MeV, cross sections, anal. powers, global optical model anal. 0-47459  
<sup>58</sup>Ni(d,p)<sup>59</sup>Ni, deuteron break-up model anal. of cross-section, vector analysing power and angular correlation 0-27648  
<sup>58</sup>Ni(e,e'), 120-264 MeV, J<sup>+</sup>=6<sup>+</sup>, 5.125 MeV state isoscalar character, form factors, transition strengths 0-9262  
<sup>58</sup>Ni( $\gamma$ , $\gamma$ ), M1 strength isospin splitting for dipole ang. distrib. states 0-13412  
<sup>58</sup>Ni(n,n), 1.77 to 3.0 MeV, validity of Wick's inequality in the calculation of the lower limits of the differential elastic cross sections 0-5137  
<sup>58</sup>Ni(n,X) transmission and capture data up to 120 keV 0-18311  
<sup>58</sup>Ni(p,p), pol. p, 40 MeV, elastic and inelastic, asymmetries and differential cross sections (*Russian*) 0-27623  
<sup>58</sup>Ni( $\pi$ , $\pi$ ), 162 MeV, elastic and inelastic ang. distrib., optical and PWIA anals. 0-42706  
<sup>58</sup>Ni(n, $\gamma$ ), cross-section meas. principal resonance parameters 0-18312  
<sup>58</sup>Ni(n, $\gamma$ ), on-line gamma anal. using Ge detector 0-52624  
<sup>59</sup>Sc decay, half life, <sup>59</sup>Sc excited states and transitions 0-42595  
<sup>59</sup>Sc fragment differential ranges and energy spectra from <sup>238</sup>U(p,X), reaction mechanisms 0-42666  
<sup>41</sup>Sc resonance strengths from <sup>40</sup>Ca(p, $\gamma$ ) 0-22786  
<sup>41</sup>Sc-<sup>41</sup>Ca Coulomb displacement energy, HF calcs. 0-42527  
<sup>45</sup>Sc(n, $\gamma$ ), mechanism in 3s size resonance, radiative width statistical and valence effects 0-37388  
<sup>46</sup>Sc, beta decay half life 0-47435  
<sup>46</sup>Sc energy levels, resonances, spin and parity from <sup>45</sup>Sc(n, $\gamma$ ) 0-52673  
<sup>46</sup>Sc level deexcitation, E1 and M1 absolute radiative widths from <sup>46</sup>Sc(n, $\gamma$ ) 0-52622  
<sup>46</sup>Sc transition polarisation, levels and spin assignments from <sup>45</sup>Sc(n, $\gamma$ ), pol. n 0-52656  
<sup>46</sup>Sc Gamow-Teller strength, ang. distrib., from <sup>48</sup>Ca (<sup>3</sup>He,t) 0-42589  
<sup>46</sup>Sc isobaric analogue states and resonances, J<sup>+</sup> from <sup>48</sup>Ca(p,p) 0-13426  
<sup>46</sup>Sc(p, spallation), 0.08-24 GeV, Ar isotopes, spallation ratios and prod. cross sections 0-9284  
<sup>46</sup>Ti(<sup>3</sup>He, pnx), <sup>48</sup>V positron source prep. for annihilation radiation line-shapes, positron lifetimes meas. 0-876  
<sup>46</sup>Ti(d,d), pol. d, A=46, 48, 50, 12 MeV, cross sections, anal. powers, global optical model anal. 0-47459  
<sup>46</sup>Ti, A=46, 48, 50, pionic X-rays, strong interaction and isotope shifts,  $\pi$ -nuclear optical pot. 0-53169  
<sup>46</sup>Ti(<sup>7</sup>Li,<sup>7</sup>Li'), A=46, 48, 17 MeV, first 2<sup>+</sup> states Coulomb-nuclear interference, optical and DWBA anal. 0-22852  
<sup>46</sup>Ti( $\Gamma$ ,X), A=46, 48, 50, photoneutron and photoproton cross section systematics 0-13463  
<sup>46</sup>Ti(n,X), A=46-50, 14 MeV, X=p,n',p, $\alpha$ ,n,<sup>3</sup>He, production cross-sections 0-42648  
<sup>46</sup>Ti(n, $\gamma$ ) A=46, 47, 49, 50, 45 MeV, cross section meas., resonance parameters 0-18315  
<sup>46</sup>Ti, fp-shell nuclei struct., effect of core-excitation and  $\alpha$ -clustering correl. 0-9245  
<sup>46</sup>Ti(d,d), 7.10 MeV, ang. distrib., DWBA and Hauser Feshbach anal. 0-47377  
<sup>47</sup>Ti levels, DWBA and Hauser Feshbach anal., compound nucleus cross sections from <sup>46</sup>Ti(d,p) 0-47377  
<sup>48</sup>Ti high spin states,  $\gamma$ -decay, J<sup>+</sup> assignments, lifetimes from <sup>45</sup>Sc( $\alpha$ , $\gamma$ ) 0-13356  
<sup>48</sup>Ti(p,p), 1 GeV, elastic scatt. differential cross section calc. 0-47480  
<sup>49</sup>Ti, mag. form factors, core polarisation and exchange current effects 0-13409  
<sup>49</sup>Ti nuclear levels from n-capture  $\gamma$ -rays in <sup>50</sup>Ti( $\gamma$ ,n) 0-37327  
<sup>49</sup>Ti( $\gamma$ , $\gamma$ ), nuclear levels from n-capture  $\gamma$ -rays 0-37327  
<sup>50</sup>Ti high spin states, transitions and J<sup>+</sup> values from <sup>48</sup>Ca( $\alpha$ ,Zn $\gamma$ ) 0-455  
<sup>50</sup>Ti(<sup>12,13</sup>C,X), elastic, inelastic and single nucleon transfer excitation functions, <sup>49</sup>Ti levels 0-13492  
<sup>50</sup>Ti( $\gamma$ ,X), photoneutron and photoproton cross sections, giant dipole resonance isospin splitting 0-13442  
<sup>51</sup>Ti Zp<sub>1/2</sub> neutron orbit radius isotope shift from DWBA anal. of <sup>50</sup>Ti(t,d) 0-32172  
<sup>51</sup>Ti(p, spallation), 0.08-24 GeV, Ar isotopes, spallation ratios and prod. cross sections 0-9284  
<sup>51</sup>V, lf nucleon orbit RMS radii from transfer data 0-27544  
<sup>51</sup>V,  $\gamma$ -strength function,  $\gamma$ -ray spectra, average resonance method from <sup>50</sup>Ti(p, $\gamma$ ) 0-9257  
<sup>51</sup>V, mag. form factors, core polarisation and exchange current effects 0-13409  
<sup>51</sup>V+d( $\alpha$ ), 12-50 MeV, t formation average cross sections 0-42670  
<sup>51</sup>V(<sup>3</sup>He,pd), 90 MeV, angular correlations, elastic breakup of <sup>3</sup>He 0-52685  
<sup>51</sup>V( $\alpha$ ,t), absolute normalisation from spin depend. sum rule anal. 0-27652  
<sup>51</sup>V(n,X), 14 MeV, X=p,n',p, $\alpha$ ,n,<sup>3</sup>He, production cross-sections 0-42648  
<sup>51</sup>V(n, $\gamma$ ), circular polarisation, ang. distrib. meas. 0-32285

## nuclei with mass number 59 to 89

- A=24-60, yrast lines using Strutinsky method, empirical fusion bands 0-42514  
A=40-80, yrast props. and high spin isomers, cranking plus Strutinsky formalism 0-32152  
A=60, nuclear data sheets, levels and transitions 0-31433

## nuclei with mass number 59 to 89 continued

- A=60-140, spherical nuclei, two phonon admixture effect on M1 resonance (*Russian*) 0-5105  
A=60-80 even-even nuclei, collective motions and band structs. 0-9202  
A=64, nuclear data sheets, levels and transitions 0-31434  
A=71, nuclear data sheets, levels, J<sup>+</sup> and transitions 0-31428  
A=76-79 charge dispersion curve from <sup>232</sup>Th(p,f) 0-18349  
A=84 nuclei, nuclear struct. data sheets to March 1979 0-9191  
A=87 nuclei, nuclear struct. data sheets to January 1979 0-9192  
A<100, average E1/M1 strength ratio 0-52621  
even-even and odd A nuclei, nuclear shapes and motions, review 0-5054  
even-even nuclei, z=6 to 100, probable members of quasi-bands in spherical and deformed regions 0-13357  
even-even spherical nuclei, 2<sup>+</sup> state deformation parameter from (p,p) and EM excitation 0-27549  
thermonuclear reaction rate data for intermediate mass nuclei 0-31427  
(n, $\gamma$ ), A=75 to 103,  $\gamma$ -strength functions and stat. model cross section calcs. 0-52612  
(n,X), fast n, <sup>3</sup>He emission cross sections for A=27-115 0-13475  
(p,n), 2.5-5.8 MeV, A=89-130, cross sections, sub-Coulomb proton anomalous optical pot. 0-32278  
(p,n) excitation functions for A=45 to 80, proton optical pot. at sub-Coulomb energies 0-9292  
<sup>69</sup>As, A=69-72, <sup>3</sup>S<sub>1/2</sub> ground state hyperfine struct. and nuclear moments 0-32853  
<sup>69</sup>As, A=70, 72, level scheme, transitions, J<sup>+</sup> and lifetimes from Ge(p,n $\gamma$ ) 0-22695  
<sup>69</sup>As, A=79,81, Q-values and mass excess from Se(d,<sup>3</sup>He) 0-9222  
<sup>76</sup>As, beta decay, level scheme for <sup>76</sup>Se from  $\gamma\gamma$  coincidence meas. 0-22754  
<sup>76</sup>As, level structure, transitions and J<sup>+</sup>, from <sup>76</sup>Ge(p,n $\gamma$ ) 0-47379  
Br, emulsion nuclei, 28 GeV proton interactions (*Korean*) 0-18299  
Br+C(O), 0.2-4.2 GeV/N, compression phenomena and Mach shock waves 0-22851  
Br(HI,X), 0.2-4.2 GeV/N, nonperipheral collisions, forward-backward asymmetry, compression phenomena 0-18329  
<sup>81</sup>Br, A=87-89,  $\beta$ -delayed neutron emission probabilities, half-life 0-52634  
<sup>71</sup>Br, prod. in proton spallation reactions, nuclear structure influence on yields of product nuclei 0-22794  
<sup>76</sup>Br, <sup>77</sup>Br, production from decay of cyclotron produced <sup>76</sup>Kr and <sup>77</sup>Kr 0-52799  
<sup>76</sup>Br, Coriolis distorted bands, common g<sub>9/2</sub> parentage in N=41 nuclei 0-13349  
<sup>77</sup>Br collective bands, lifetimes, spins and E2 transition probabilities from <sup>66</sup>Ni(<sup>16</sup>O, 2n $\gamma$ ) 0-13415  
<sup>77</sup>Br E2 transition probabilities and mean lives from <sup>64</sup>Ni(<sup>16</sup>O, 2n $\gamma$ ) 0-13414  
<sup>78</sup>Br, high-spin states, from <sup>77</sup>Se( $\alpha$ ,2np), decay into isomers 0-52569  
<sup>79</sup>Br(<sup>32</sup>S,X), 153-184 MeV, fission like processes around A<sub>CN</sub>=100, mass distrib. strong change 0-9318  
<sup>79</sup>Br( $\alpha$ ,2n)<sup>81</sup>Rb-<sup>81m</sup>Kr production excitation functions and thick target yield curves 0-12253  
<sup>80</sup>Br( $\alpha$ ,X), annihilation, 1.4 GeV/c,  $\pi^+$ , p emission angles, momentum and multiplicity distrib. 0-532  
<sup>81</sup>Br(<sup>3</sup>He,3n)<sup>81</sup>Rb-<sup>81m</sup>Kr production excitation functions and thick target yield curves 0-12253  
<sup>88</sup>Br  $\beta$ -decay, <sup>88</sup>Kr level scheme and transitions, delayed neutrons 0-42600  
Br( $\alpha$ ,X) 0-22851  
Co, cross sections for charged particle prod. by 14 MeV neutrons, data compilation 0-9289  
<sup>59</sup>Co, deformation effect of aligned target, fast-neutron transmission 0-47364  
<sup>59</sup>Co, mag. form factors, core polarisation and exchange current effects 0-13409  
<sup>59</sup>Co, neutron capture cross section meas. 0-5147  
<sup>59</sup>Co(<sup>32</sup>S,X), 153-184 MeV, fission like processes around A<sub>CN</sub>=100, mass distrib. strong change 0-9318  
<sup>59</sup>Co(<sup>3</sup>He, <sup>3</sup>He), 119 MeV, optical pot. parameters energy and mass depend. 0-32289  
<sup>59</sup>Co(n,2n), isomeric cross-section ratio and excitation function, mixed-powder method and gamma-ray spect. 0-47472  
<sup>59</sup>Co(n, $\alpha$ ), excitation function, mixed-powder method and gamma-ray spect. 0-47472  
<sup>59</sup>Co(n,n' $\gamma$ ), level transitions, deexcitations and lifetimes 0-18222  
<sup>60</sup>Co gamma ray sources, exposure efficiency dependence on distance, theoretical interpretation (*Czech*) 0-850  
<sup>60</sup>Co, neutron scatt. cross section meas., parameters of neutron levels 0-5147  
<sup>62</sup>Co differential from <sup>66</sup>Zn ( $\alpha$ , <sup>8</sup>B) 0-5153  
Co(e,e), nuclear radius, core polarisation and isotope shifts, muonic X-rays 0-22685  
Co(p, spallation), 0.08-24 GeV, Ar isotopes, spallation ratios and prod. cross sections 0-9284  
Cu(<sup>20</sup>Ne, $\pi^+$ ), 800 MeV/N, doubly differential cross sections and ang. distrib. 0-9305  
Cu(<sup>20</sup>Ne,  $\pi^+$ X), 400 MeV/N, pion prod. doubly differential cross sections and ang. distrib. 0-32299  
<sup>63</sup>Cu, A=65,67,68, energy levels, core coupling model calcs. 0-9238  
<sup>63</sup>Cu(p,p), A=63,65, 100-2200 MeV, total and reaction cross sections from optical pot. 0-18303  
<sup>63</sup>Cu levels and transition j-depend., DWBA anal. of <sup>60</sup>Ni(<sup>19</sup>F, <sup>16</sup>O) 0-42542  
<sup>63</sup>Cu( $\gamma$ ,p), up to 0.25 GeV, from bremsstrahlung  $\gamma$ -quanta (*Russian*) 0-5123  
<sup>64</sup>Cu  $\beta^-$  and  $\beta^+$ -decays, K-shell ionisation probabilities, X-ray spectra 0-42592  
<sup>64</sup>Cu  $\beta^-$  decay, K-shell autoionis. 0-956  
<sup>64</sup>Cu, extraction from reactor-irrad.  $\alpha$ -phthalocyanine target 0-35563  
<sup>64</sup>Cu levels and transitions, stat. anal. of <sup>64</sup>Ni(p,  $\gamma$ ) (*Russian*) 0-5104  
<sup>65</sup>Cu analogue resonance direct n decay, stat. anal. from <sup>64</sup>Ni(p,n $\gamma$ ) (*Russian*) 0-5104  
<sup>65</sup>Cu levels and transitions,  $\gamma$ -strength function using average resonance capture from <sup>64</sup>Ni(p, $\gamma$ ) 0-13411  
<sup>65</sup>Cu(<sup>32</sup>S,X), 153-184 MeV, fission like processes around A<sub>CN</sub>=100, mass distrib. strong change 0-9318  
<sup>69</sup>Cu Q-values and mass excess from <sup>70</sup>Zn(d,<sup>3</sup>He) 0-9222  
Cu(e,e), nuclear radius, core polarisation and isotope shifts, muonic X-rays 0-22685  
Cu( $\gamma$ , $\gamma$ ), neutron capture  $\gamma$ -ray Rayleigh scatt. 0-52661



## nuclei with mass number 59 to 89 continued

- Cu( $\mu$ , X), energetic charged particle spectrum, integrated yield 0-18293  
 Cu(n,  $\gamma$ ), on-line gamma anal. using Ge detector 0-52624  
 Cu(n, n), 14.2 MeV, polarisation in forward angle scatt. 0-18282  
 Cu(n, n), pol. n, 16.1 MeV, differential cross section, optical model fit 0-32259  
 Cu(p, X), 400 GeV/c, light ion backward prod., invariant cross section 0-32279  
 Cu(p, X), 70 GeV/c,  $\pi^+$ ,  $K^+$ , p,  $\bar{p}$  prod. with  $p_T=0.5-2.5$  GeV/c cross sections, yield ratios (Russian) 0-52681  
 Cu(p, p'), 0.6-25 GeV, backward emitted proton inclusive spectra, short range correlation 0-32281  
 Cu(p, spallation), 0.08-24 GeV, Ar isotopes, spallation ratios and prod. cross sections 0-9284  
 Cu(p, pX),  $x=1, 2, 640$  MeV, energetic backward p emission, inclusive differential cross section 0-9290  
 Cu( $\pi^-$ , X), 3 GeV/c, n inclusive spectra, neutron yield (Russian) 0-13510  
 Cu( $\pi^-$ , spallation) 0.6, 0.9, 12 GeV, T=1/2 resonances, Na, Sc and Co rel. yields 0-5109  
<sup>59</sup>Fe deduced levels and spins, from <sup>58</sup>Fe(d, pol. p), cross section and vector analysing power 0-52684  
 Fe(n, n), MeV elastic and inelastic cross sections meas. 0-32277  
<sup>59</sup>Ga, A=73, 75, Q-values and mass excess from Ge(d, <sup>3</sup>He) 0-9222  
<sup>61</sup>Ga, A=79-83,  $\beta$ -delayed neutron emission probabilities, half-life 0-52634  
<sup>67</sup>Ga  $\gamma$ - and X-ray emission probabilities and half-life obs. 0-32242  
<sup>69</sup>Ga(n, n'), fast n, levels, J<sup>π</sup>, transitions and mixing ratios, statistical anal. (Russian) 0-13382  
<sup>71</sup>Ga(v, e<sup>-</sup>)<sup>71</sup>Ge, shell model cross section calc., appl. to cosmic ray and background elimination (Russian) 0-5131  
<sup>72</sup>Ga, 3<sup>-</sup>2<sup>+</sup> first forbidden beta transitions,  $\beta$ - $\gamma$  ang. correlation, nuclear matrix elements 0-42599  
<sup>74</sup>Ge(p, p), A=72, 74, 100-2200 MeV, total and reaction cross sections from optical pot. 0-18303  
<sup>66</sup>Ge levels, lifetimes and mixing ratio, in-beam  $\gamma$ -spectroscopy from <sup>58</sup>Fe(<sup>14</sup>N, np $\gamma$ ) 0-42541  
<sup>66</sup>Ge states and decay scheme, polarisations J<sup>π</sup> and ang. distrib. from <sup>58</sup>Ni(<sup>10</sup>B, np $\gamma$ ) 0-22692  
<sup>68</sup>Ge multiple band struct., g<sub>9/2</sub> orbital, level lifetimes from <sup>58</sup>Ni(<sup>12</sup>C, 2p) 0-13358  
<sup>69</sup>Ge high spin states, EM props., Branching and mixing ratios from <sup>58</sup>Mn(<sup>16</sup>O, pn) 0-13347  
<sup>72</sup>Ge levels pop. in <sup>82</sup>N(<sup>6</sup>Li, pn), in beam gamma-ray spectroscopy 0-47343  
<sup>74</sup>Ge(<sup>32</sup>S, X), 153-184 MeV, fission like processes around A<sub>CN</sub>=100, mass distrib. strong change 0-9318  
<sup>76</sup>Ge( $\pi^+$  xn)<sup>76</sup>As, 100, 180 MeV, product formation cross section 0-42705  
 Ge( $\gamma$ , e<sup>-</sup>), near threshold, variable energy source, total cross section (French) 0-37367  
 Kr even isotopes, collective levels and B(E2) values, IBA calcs. 0-27539  
<sup>84</sup>Kr, A=74, 76, rot. bands, band crossing and backbending 0-18176  
<sup>84</sup>Kr, A=74-82, even-even isotopes, B(E2) values and collectivity, interacting boson approx. 0-27537  
<sup>84</sup>Kr, A=76, 78, 80, yrast states and band struct., backbending from Zn(<sup>12</sup>C, 2n) 0-13359  
<sup>84</sup>Kr, A=78, 80, quasi- $\gamma$  bands and negative parity levels from Br(p, 2n $\gamma$ ) 0-456  
<sup>74</sup>Kr, charged particle evaporation following form. from <sup>58</sup>Ni+<sup>16</sup>O 0-47453  
<sup>78</sup>Kr band struct., level scheme, from  $\gamma$ - $\gamma$ -coincidence from <sup>65</sup>Cu(<sup>16</sup>O, 2np) 0-18177  
<sup>78</sup>Kr band struct., in-beam  $\gamma$ -rays from <sup>68</sup>Zn(<sup>12</sup>C, 2n) 0-22672  
<sup>78</sup>Kr high spin levels, bands and transitions, level lifetimes from <sup>68</sup>Zn(<sup>12</sup>C, Zn) 0-42525  
<sup>78</sup>Kr high spin states, transitions and lifetimes from (<sup>16</sup>O, 2np), (<sup>19</sup>F, 2n $\alpha$ ), (<sup>16</sup>O, 2n), (<sup>12</sup>C, 2n) 0-27534  
<sup>84</sup>Kr+n, capture cross section meas. in Triton reactor (French) 0-18308  
<sup>88</sup>Kr level scheme and transitions, delayed neutrons from <sup>88</sup>Br  $\beta$ -decay 0-42600  
<sup>89</sup>Mo mass even and excited states from <sup>92</sup>Mo(<sup>3</sup>He, <sup>6</sup>He) 0-42531  
 Ni doubly even nuclei, eqns. of motion method, pairing correlations, ground state energies 0-52585  
 Ni giant resonances using virtual and real photons 0-22791  
 Ni isotopes, cross sections for charged particle prod. by 14 MeV neutrons, data compilation 0-9289  
<sup>58</sup>Ni A=57-59, f<sub>7/2</sub> hole configuration effects, shell model calcs. 0-22670  
<sup>58</sup>Ni, A=58, 64, neutron densities and single particle struct. 0-32165  
<sup>58</sup>Ni, A=58, 60, search for giant quadrupole resonance 0-9281  
<sup>58</sup>Ni, A=61, 63, fine structure of hole-state analogues, isospin mixing from (p, d) 0-13401  
<sup>58</sup>Ni(<sup>3</sup>He, <sup>3</sup>He), A=58, 60, 62, 64, 119 MeV, optical pot. parameters energy and mass depend. 0-32289  
<sup>58</sup>Ni(<sup>40</sup>Ca, fusion), A=58, 60, 62, 113-170 MeV, fusion cross sections and excitation functions 0-32315  
<sup>58</sup>Ni( $\alpha$ ,  $\gamma$ ), A=62, 64, 4.5-8.6 MeV, excitation function competition cusps, Mauser-Feshbach calcs. 0-13404  
<sup>58</sup>Ni( $\alpha$ , n), A=62, 64, 5.3-8.7 MeV, excitation function competition cusps, Mauser-Feshbach calcs. 0-13404  
<sup>58</sup>Ni(e, e'), 102 MeV, A=58, 60, E1-E4 giant multipole resonance comparison, shell model anal. 0-42614  
<sup>58</sup>Ni(n, X) A=58, 60, transmission data, resonance anal. 0-18317  
<sup>58</sup>Ni(n,  $\gamma$ ), A=58-64, <4 MeV, gamma prod. and inferred cross sections 0-525  
<sup>58</sup>Ni(n, n), A=58, 60, 62, 64, 5 MeV, differential cross sections, optical, statistical and coupled channel anal. (Russian) 0-37377  
<sup>58</sup>Ni(p,  $\pi^+$ ), A=58, 64, 660 MeV, pion energy spectra, isotopic effects (Russian) 0-42669  
<sup>59</sup>Ni deduced levels, from <sup>58</sup>Ni(d, pol. p), cross section and vector analysing power 0-52684  
<sup>60</sup>Ni, 1173 keV transition M3/M2 mixing ratio meas. 0-52608  
<sup>60</sup>Ni deduced levels from <sup>58</sup>Fe(<sup>16</sup>O, <sup>14</sup>C)<sup>60</sup>Ni, DWBA anal., spectroscopic strengths 0-47380  
<sup>60</sup>Ni+n, total and differential cross-sections, optical-statistical and coupled-channel models 0-13472  
<sup>60</sup>Ni( $\alpha$ ,  $\alpha'$ ), 8-18 MeV, cross sections, search for giant dipole resonance 0-9281  
<sup>62</sup>Ni( $\gamma$ , X), 19.2-26.2 MeV, photoneutron and photoproton spectra, giant dipole resonance-decay, isospin conservation 0-13443

## nuclei with mass number 59 to 89 continued

- Ni(e, e), nuclear radius, core polarisation and isotone shifts, muonic X-rays 0-22685  
 Ni(p, spallation), 0.08-24 GeV, Ar isotopes, spallation ratios and prod. cross sections 0-9284  
 Rb, fission products, precise Q<sub>B</sub> values (German) 0-37354  
 Rb neutron rich isotopes, nucl. spins and mag. moments 0-47367  
 Rb relative and indep. fission yields from <sup>235</sup>U(n, f) 0-27679  
<sup>85</sup>Rb, A=83, 84, 86 prod. cross sections and recoil props. from (p, X) 0-9295  
<sup>74</sup>Rb, prod. in proton spallation reactions, nuclear structure influence on yields of product nuclei 0-22794  
<sup>78</sup>Rb  $\beta$ -decay half lives of isomeric and ground state from (<sup>16</sup>O, 3n) 0-27534  
<sup>83</sup>Rb, level structure, gamma angular and time distrib. from <sup>81</sup>Br( $\alpha$ , 3n) 0-52583  
<sup>83</sup>Rb high spin states, positive and negative parity bands from (<sup>6</sup>Li, 3n), ( $\alpha$ , 2n) 0-18178  
<sup>83</sup>Rb(<sup>32</sup>S, X), 153-184 MeV, fission like processes around A<sub>CN</sub>=100, mass distrib. strong change 0-9318  
<sup>87</sup>Rb-<sup>87</sup>Sr+neutrons, nucleon charge conservation, improved test 0-5098  
<sup>85</sup>Se, A=75, 77, 79, 81, levels and ang. distrib., spectroscopic factors from Se(p, d) 0-22696  
<sup>84</sup>Se(d, d), A=76, 78, 80, 82, pol. d, 12 MeV, cross sections, anal. powers, global optical model anal. 0-47459  
<sup>75</sup>Se, yield for various reactions and chem. processing 0-36131  
<sup>74</sup>Se, collective excitations in the interacting boson model (Russian) 0-5044  
<sup>74</sup>Se quasi- $\gamma$  bands and negative parity levels from <sup>75</sup>As(p, 2n $\gamma$ ) 0-456  
<sup>74</sup>Se, decay, electric monopole transitions 0-22752  
<sup>76</sup>Se, level scheme from  $\gamma$  coincidence meas. of <sup>76</sup>As decay 0-22754  
<sup>76</sup>Se( $\pi^-$  xn)<sup>76</sup>As, 100, 180 MeV, product formation cross section 0-42705  
<sup>78</sup>Se high spin levels, transitions, J<sup>π</sup> assignments from <sup>76</sup>Ge( $\alpha$ , n $\gamma$ ) 0-459  
<sup>84</sup>Sm, A=150, 152, E2:M1 multipole mixing ratio, sign change in A=150 region 0-493  
 Sr, fission products, precise Q<sub>B</sub> values (German) 0-37354  
<sup>84</sup>Sr, A=80, 82, 84-86, levels and transitions from Kr(<sup>3</sup>He, n) 0-18201  
<sup>80</sup>Sr ground state mass from Kr(<sup>3</sup>He, n) 0-18201  
<sup>84</sup>Sr high spin states, J<sup>π</sup> and de-excitation from Kr( $\alpha$ , xn) 0-42516  
<sup>84</sup>Sr quasi- $\gamma$  bands and negative parity levels from <sup>87</sup>Rb(p, 2n $\gamma$ ) 0-456  
<sup>87</sup>Sr, mag. form factors, core polarisation and exchange current effects 0-13409  
<sup>88</sup>Sr(d, p), pol. d, excitation curve isospin anomaly, neutron single particle resonances 0-27595  
<sup>89</sup>Sr, soil analysis using total sample decomp. 0-35808  
 Y, fission products, precise Q<sub>B</sub> values (German) 0-37354  
 Y isotopes, Hauser Feshbach calcs., of neutron cross sections 0-22839  
<sup>89</sup>Y, 14.7 MeV neutron capture cross-section measurements with activation technique 0-32282  
<sup>89</sup>Y, energy spectra and EM props. using broken pair model 0-499  
<sup>89</sup>Y high spin states and decay scheme from <sup>87</sup>Rb( $\alpha$ , 2n $\gamma$ ) 0-32166  
<sup>89</sup>Y, spin-spin relax. times in solns. 0-2657  
<sup>89</sup>Y(<sup>3</sup>He, <sup>3</sup>He), 119 MeV, optical pot. parameters energy and mass depend. 0-32289  
<sup>89</sup>Y(<sup>40</sup>Ar, X), 237 MeV, ang. momentum transfer in deep inelastic reactions 0-5156  
<sup>89</sup>Y( $\pi$ ,  $\pi'$ ), 163, 240 MeV, giant resonance pionic excitation 0-52561  
<sup>89</sup>Yb(<sup>32</sup>S, X), 153-184 MeV, fission like processes around A<sub>CN</sub>=100, mass distrib. strong change 0-9318  
<sup>64</sup>Zn(p, p), A=66, 68, 20-50 MeV differential cross section, polarisation ang. distrib., optical model exchange terms 0-27638  
<sup>64</sup>Zn,  $\gamma$ -ray studies of levels above 3.1 MeV 0-32238  
<sup>64</sup>Zn, search for giant quadrupole resonance 0-9281  
<sup>68</sup>Zn(<sup>6</sup>Li, pn) in beam gamma-ray spectroscopy of <sup>72</sup>Ge levels 0-47343  
<sup>68</sup>Zn, energy levels, core coupling model calcs. 0-9238  
 Zn(e, e), nuclear radius, core polarisation and isotone shifts, muonic X-rays 0-22685  
 Zr-region, two nucleon transfer reactions, spectroscopic amplitudes, form factors, ang. distrib. 0-22779

## nuclei with mass number 90 to 149

- <sup>116</sup>Sn(d, d), polarised d, 8.22 MeV, anal. power 0-5114  
<sup>145</sup>Sm neutron separation and level exciton (n,  $\gamma$ ) and (d, p) correlations 0-22756  
 A=111 nuclei, nuclear struct. data sheets to February 1979 0-9193  
 A=131 isobaric nuclides, formation in <sup>238</sup>U(p, X) 0-9293  
 A=140, nuclear data sheets, levels and transitions 0-31435  
 A=60-140, spherical nuclei, two phonon admixture effect on M1 resonance (Russian) 0-5105  
 A<100, average E1/M1 strength ratio 0-52621  
 A~150 transitional region, collective props., interacting boson model 0-2/538  
 deformed rare earth nuclei, bandcrossing in K $\neq$ 0 bands, backbending 0-9204  
 even actinides, two-nucleon transfer, first 0<sup>+</sup> collective state excitation, spectroscopic factor (Russian) 0-42530  
 even-even nuclei, z=6 to 100, probable members of quasi-bands in spherical and deformed regions 0-13357  
 even-even rare earths, microscopic quadrupole and hexadecapole moments 0-13376  
 even-even spherical nuclei, 2<sub>1</sub><sup>+</sup> state deformation parameter from (p, p) and EM excitation 0-27549  
 fission products yield from <sup>239</sup>Pu(n, f) 0-27678  
 high angular momentum fusion compound nucleus deexcitation, high spin states, rare earths 0-9259  
 N=50 isotones, transition probabilities, 1p<sub>3/2</sub> and 0f<sub>5/2</sub> hole excitation effects 0-47431  
 rare earth nuclei, high spin states from (HI, xn) reactions, discrete  $\gamma$ -transitions 0-5050  
 Sn Z=50 region isotopes, system struct calcs. 0-18192  
 Z=55-63, odd proton nuclei, low lying even parity states 0-27551  
 (n,  $\gamma$ ), A=75 to 103,  $\gamma$ -strength functions and stat. model cross section calcs. 0-52612  
 (n,  $\gamma$ ), A=94-190, resonance capture, low lying level population fluctuations,  $\gamma$ -rays 0-52619  
 (n, X), fast n, <sup>3</sup>He emission cross sections for A=27-115 0-13475  
 (p, n), 2.5-5.8 MeV, A=89-130, cross sections, sub-Coulomb proton anomalous optical pot. 0-32278  
 A=101 nuclei, nuclear struct. data sheets to May 1979 0-41954  
 A=103 nuclei, nuclear struct. data sheets to July 1979 0-41955



## nuclei with mass number 90 to 149 continued

- Ag ( $\alpha, x$ ), 0.2-4.2 GeV/N, compression phenomena and Mach shock waves 0-22851
- Ag, emulsion nuclei, 28 GeV proton interactions (*Korean*) 0-18299
- Ag+C(O), 0.2-4.2 GeV/N, compression phenomena and Mach shock waves 0-22851
- $^A$ Ag, A=104, 106, levels,  $J^\pi$ , and isobaric analogue resonances from Pd(p,n) 0-32180
- $^A$ Ag, A=105, 107, positive parity band, mixing and branching ratios lifetimes from ( $^{16}\text{O}, 2\text{np}$ )( $^{14}\text{N}, \text{n}$ ) 0-9197
- $^A$ Ag, A=113, 115,  $\beta$ -decay,  $^{113}, ^{115}\text{Cd}$  low lying  $7/2^-$  state lifetime, triaxial rotor interpretation 0-47432
- $^A$ Ag, A=99, 101, 103, levels, transitions and  $J^\pi$  from Cd decay, Pd(p,2n $\gamma$ ) 0-47383
- $^A$ Ag( $^{86}\text{Kr}, X$ ), A=107, 109, 620 MeV, deep inelastic scatt., ang. momentum transfer,  $\gamma$ -ray multiplicities 0-27665
- $^A$ Ag(p,n), A=107, 109, 2.0-6.7 MeV, cross sections, Hauser-Feshbach optical calcs. for p absorption systematics 0-47483
- $^A$ Ag(p,p), A=107, 109, 2.0-6.7 MeV, cross sections, Hauser-Feshbach optical calcs. for p absorption systematics 0-47483
- $^{106}\text{Ag}^m$  decay, IC and  $\gamma$ -rays,  $^{106}\text{Pd}$  energy states and  $J^\pi$  0-18197
- $^{107}\text{Ag}$  high spin states,  $J^\pi$  assignments, polarisations and transitions from ( $^7\text{Li}, 4\text{n}\gamma$ ), ( $^6\text{Li}, 3\text{n}\gamma$ ) 0-27536
- $^{107}\text{Ag}+^{40}\text{Ar}$ , deep inelastic transfer, decay of binary nuclear system 0-22848
- $^{107}\text{Ag}+^{40}\text{Ar}$ , deep inelastic transfer, decay of binary nuclear system 0-22848
- $^{107}\text{Ag}(\text{n}, \gamma)$   $^{108}\text{Ag}^m$ , in stainless-steel structure of high-power nuclear reactors 0-42747
- $^{107}\text{Ag}(\text{n}, \text{n})$ , 0.25-4.5 MeV, total, elastic and inelastic cross sections, optical-statistical anal. 0-27639
- $^{107}\text{Ag}(\text{p}, \alpha X)$ , 20-45 MeV,  $\alpha$  spectra, exciton model anal. 0-18306
- $^{108}\text{Ag}$  transition multipolarity and conversion electrons from  $^{107}\text{Ag}(\text{n}, \text{e}^-)$  0-52627
- $^{108}\text{Ag}^m$ , prod. in nuclear reactors by thermal neutron capture in stainless-steel structure 0-42747
- $^{109}\text{Ag}$  ( $^{40}\text{Ar}, X$ ),  $\alpha$ -decay amplification in superdeformed nuclei, high ang. momentum deexcitation 0-22776
- $^{109}\text{Ag}+^{40}\text{Ar}$ , deep inelastic transfer, decay of binary nuclear system 0-22848
- $^{109}\text{Ag}+^{40}\text{Ar}$ , deep inelastic transfer, decay of binary nuclear system 0-22848
- $^{110}\text{Ag}$  low lying states, decay scheme and  $T_{1/2}$  from  $^{109}\text{Ag}(\text{n}, \gamma)$  0-47393
- $^{110}\text{Ag}$  low-lying levels, from  $^{109}\text{Ag}(\text{n}, \gamma)$  obs. 0-47422
- $^{108\text{m}}\text{Ag}$ ,  $\gamma$ -ray energies meas. for Ge(Li) detector calibration 0-27865
- Ag(p, $\alpha$ )X, direct knockout model for fragmentation, (p, $\alpha$ ) predictions 0-18275
- Ag(p,f), 600 MeV, fragment energies, cross sections level density and barrier heights 0-42723
- Ar(HI,X) 0.2-4.2 GeV/N, nonperipheral collisions, forward-backward asymmetry, compression phenomena 0-18329
- $^A$ Ba, A=130, 132, 134, 136, levels and EM props., ang. momentum projected quasiboson model 0-5067
- $^{126}\text{Ba}$  backbending, shell model calc., pair realignment and Coriolis antipairing 0-32164
- $^{131}\text{Ba}$ , decay, electric monopole transitions 0-22752
- $^{135}\text{Ba}^m$  yield in  $^{131}\text{Cs}(\alpha, \text{pn})$  and  $^{139}\text{La}(\text{p}, \alpha \text{n})$  reactions, depend. on energy of bombarding energy 0-5151
- $^{138}\text{Ba}$ , 14.7 MeV neutron capture cross-section measurements with activation technique 0-32282
- $^{138}\text{Ba}(\gamma, \pi^- \text{xn})\text{La}$ , 150-300 MeV, pion production cross sections calc. 0-9287
- $^{138}\text{Ba}(\text{n}, \gamma)$ , 30 keV, capture cross sections, stellar nucleosynthesis 0-42663
- $^{139}\text{Ba}$  level scheme,  $J^\pi$  and  $\gamma$ -transitions from  $^{139}\text{Cs}$   $\beta$ -decay 0-42590
- Br, isomer ratios in fission fragments at high excitation 0-32261
- Cd,  $\alpha$ -spectroscopic factors from ( $^6\text{Li}$ ) 0-534
- Cd decay and half life,  $^A$ Ag A=99, 101, 103, levels, transitions and  $J^\pi$  0-47383
- $^A$ Cd, A=113, 115 from  $^{113}, ^{115}\text{Ag}$   $\beta$ -decay 0-47432
- $^A$ Cd, A=107, 109, 111, from Pd( $\alpha, 3\text{n}\gamma$ )Cd, high spin states obs. 0-450
- $^A$ Cd, A=111, 115, deeply bound hole state transition strength giant resonance, DWBA anal. of (p,d) 0-47426
- $^A$ Cd(n, $\text{n}\gamma$ ) A=114, 116, energy levels, spins, and gamma-ray multipole mixing ratios investig. 0-52580
- $^{100}\text{Cd}(\text{d}, \text{p})$ , pol. d, excitation curve isospin anomaly, neutron single particle resonances 0-27595
- $^{104}\text{Cd}$ ,  $\beta^+$ (EC+ $\beta^+$ ) probability ratio, EC decay energies, mass excesses 0-27543
- $^{106}\text{Cd}(\text{p}, \text{p}')$ , 10, 12 MeV, compound nucleus lifetime by X-ray spectroscopy 0-22831
- $^{109}\text{Cd}$  EC decay data revision 0-5095
- $^{109}\text{Cd}$ , production in nuclear reactors by neutron irradiation of  $^{107}\text{Ag}$  0-52798
- $^{110}\text{Cd}$ , collective excitations in the interacting boson model (*Russian*) 0-5044
- $^{111}\text{Cd}$ , elec. quadrupole moment from elec. field gradients of trans-dimethyl organometallic moieties 0-29371
- $^{111}\text{Cd}$ , excitation by photon less positron annihilation, isomeric  $\gamma$ -transitions (*Russian*) 0-5089
- $^{111}\text{Cd}^m$ , nuclear orientation in Zn and Be, 245 keV state quadrupole moment, half-life 0-37324
- $^{111}\text{Cd}(\gamma, \gamma)$ , isomeric states excitation, integral cross sections 0-27528
- $^{114}\text{Cd}$ , neutron binding energy precision meas. 0-18182
- $^{117}\text{Cd}$  isomer decay,  $^{117}\text{In}$  level scheme,  $J^\pi$  and transitions 0-32193
- Cd(d,xn),  $E_d \leq 27.5$  MeV, cross sections for form. of  $^{114\text{m}}\text{In}$  and  $^{116\text{m}}\text{In}$  0-13482
- $^A$ Ce(n, $\gamma$ ), A=140, 142, 30 keV, capture cross sections, stellar nucleosynthesis 0-42663
- $^{135}\text{Ce}$ , yrast cascade dipole component from  $^{122}\text{Sn}^{16}\text{O}, 4\text{n}$ ) 0-9266
- $^{140}\text{Ce}$   $\gamma$ -spectra, E1 and M1 hindrance factors from  $^{143}\text{Nd}(\text{n}, \gamma\alpha)$  0-37386
- $^{143}\text{Ce}$  quasi- $f_{7/2}$  low lying states spectroscopic factors, cluster-vibr. model from  $^{142}\text{Ce}(\text{d}, \text{p})$  0-47391
- $^{144}\text{Ce}$ , e- $\gamma$  and e-e coincidences, improved detection system 0-52605
- $^{144}\text{Ce}$  levels from  $^{144}\text{La}$  decay 0-13417
- $^{144}\text{Ce}$ , low energy conversion lines resolution using fast discriminator cct. 0-5450
- Ce( $\gamma, \text{n}$ ), 30 to 140 MeV, partial photoneutron cross section, total cross section approx. 0-22809
- Cs neutron rich isotopes, nucl. spins and mag. moments 0-47367
- Cs relative and independ. fission yields from  $^{235}\text{U}(\text{n}, \text{f})$  0-27679

## nuclei with mass number 90 to 149 continued

- $^A$ Cs, A=141-145,  $\beta$ -delayed neutron emission probabilities, half-life 0-52634
- $^{114}\text{Cs}$   $\beta$ -decay, half life and branching ratio,  $^{114}\text{Xe}$  excited states and  $\gamma$ -rays 0-47436
- $^{131}\text{Cs}$ , 133.5 keV state, electric quadrupole interaction 0-32228
- $^{133}\text{Cs}(\alpha, \text{pn})$   $^{135\text{m}}\text{Ba}$ ,  $^{135\text{m}}\text{Ba}$  yield depend. on energy of bombarding particle 0-5151
- $^{137}\text{Cs}$ , 10 GeV proton spallation for transmutation of radioactive waste, calc. of transmutation number 0-13470
- $^{137}\text{Cs}$ , gamma source, Poisson and Brockwell-Moyal freq. distrib.,  $\chi^2$ -square test 0-5430
- $^{139}\text{Cs}$   $\beta$ -decay,  $^{139}\text{Ba}$  level scheme,  $J^\pi$  and  $\gamma$ -transitions 0-42590
- $^{139}\text{Cs}$  level scheme,  $J^\pi$  and  $\gamma$ -transitions from  $^{139}\text{Xe}$   $\beta$ -decay 0-42590
- $^{148}\text{Dy}$ , p single particle states and pairing force calcs., high spin states 0-42522
- $^{145}\text{Eu}$  high spin and isomeric states, transitions, weak coupling from  $^{144}\text{Sm}(\alpha, 2\text{n}\gamma)$  0-13348
- $^{145}\text{Eu}$  high spin core coupled states and transitions from  $^{142}\text{Nd}(^6\text{Li}, 3\text{n}\gamma)$  0-42520
- $^{145}\text{Eu}$  high spin states,  $J^\pi$  and transitions from ( $^7\text{Li}, 4\text{n}\gamma$ ) and ( $^6\text{Li}, 3\text{n}\gamma$ ) 0-47350
- $^{145}\text{Eu}$  level and transition effects on  $^{145}\text{Gd}$  decay anomalies 0-32244
- $^A$ Gd, A=150-156, E2:M1 multipole mixing ratio, sign change in A=150 region 0-493
- $^{145}\text{Gd}$  EC/ $\beta^+$ -decay branching ratio anomalies,  $^{145}\text{Eu}$  level and transition effects 0-32244
- $^{146}\text{Gd}$ , p single particle states and pairing force calcs., high spin states 0-42522
- $^{146}\text{Gd}$ , spherical HFB calcs. for Z=64 shell closure 0-22716
- $^{147}\text{Gd}^m$  high spin yrast trap, oblate deformation and quadrupole moment 0-32157
- $^A$ I, A=137-139,  $\beta$ -delayed neutron emission probabilities, half-life 0-52634
- $^{121}\text{I}$  mass excess, energy levels and single particle strength distrib. from  $^{120}\text{Te}$  ( $^3\text{He}, \text{d}$ ) 0-5053
- $^{123}\text{I}$ , bands and decay props., core-particle coupling and polarisation effects 0-13354
- $^{123}\text{I}$ , isomer shift calibration of  $^{29}\text{I}$  and  $^{127}\text{I}$ , lifetime variations in electron capture decay 0-39925
- $^{125}\text{I}$ , electron capture decay lifetime, calibration of Mossbauer isomer shift of  $^{127}\text{I}$  and  $^{129}\text{I}$  0-39922
- $^{127}\text{I}$ , 14.7 MeV neutron capture cross-section measurements with activation technique 0-32282
- $^{127}\text{I}(\text{n}, \text{n}\gamma)$ , fast n,  $\gamma$ -ang. distrib., level ang. momenta 0-18224
- $^{127}\text{I}(\text{p}, \text{p})$ , 100-2200 MeV, total and reaction cross sections from optical pot. 0-18303
- $^{129}\text{I}$  in transition metals, calibration of Mossbauer isomer shift 0-20520
- $^{129}\text{I}$ , internal conversion electron and Mossbauer spectra, calibration of isomer shift 0-39921
- $^{138}\text{I}$ ,  $\beta$ -decay scheme, population of  $^{137}\text{Xe}$  and  $^{138}\text{Xe}$  levels, delayed neutron obs. 0-27600
- $\text{I}(\text{n}, \text{n})$ , pol. n, 16.1 MeV, differential cross section, optical model fit 0-32259
- $^A$ In, A=113, 115, excitation by photon less positron annihilation, isomeric  $\gamma$ -transitions (*Russian*) 0-5089
- $^A$ In, A=127-132,  $\beta$ -delayed neutron emission probabilities, half-life 0-52634
- $^{109}\text{In}$  high spin states, transitions, isomeric state, negative parity bands from  $^{107}\text{Ag}(\alpha, 2\text{n}\gamma)$  0-451
- $^{114}\text{In}$ , deeply bound hole state transition strength giant resonance, DWBA anal. of (p,d) 0-47426
- $^{114}\text{In}$ , internal conversion on outer electron shells, 191 keV E4 transition 0-42587
- $^{115}\text{In}$ , elec. quadrupole moment from elec. field gradients of trans-dimethyl organometallic moieties 0-29371
- $^{115}\text{In}(\gamma, \gamma)$ , isomeric states excitation, integral cross sections 0-27528
- $^{115}\text{In}(\text{n}, \gamma)$ , effective cross section dependence on thermal neutron temp. 0-547
- $^{115}\text{In}(\text{p}, \text{n})$ , 2.0-6.7 MeV, cross sections, Hauser-Feshbach optical calcs. for p absorption systematics 0-47483
- $^{115}\text{In}(\text{p}, \text{p})$ , 2.0-6.7 MeV, cross sections, Hauser-Feshbach optical calcs. for p absorption systematics 0-47483
- $^{117}\text{In}$  level scheme,  $J^\pi$  and transitions from  $^{117}\text{Cd}$  isomer decay, unified model anal. 0-32193
- $^{114\text{m}}\text{In}$ , prod. in Cd(d,xn) reactions,  $E_d \leq 27.5$  MeV, cross sections 0-13482
- $^{116\text{m}}\text{In}$ , prod. in Cd(d,xn) reactions,  $E_d \leq 27.5$  MeV, cross sections 0-13482
- $\text{In}(\gamma, \gamma)$ , neutron capture  $\gamma$ -ray Rayleigh scatt. 0-52661
- $^{138}\text{La}/^{139}\text{La}$  nuclear electric quadrupole moment ratio, laser RF double reson. obs. 0-23447
- $^{131}\text{La}$ - $^{131}\text{I}$  decay scheme,  $\gamma$ , X-ray and conversion electron spectra (*Russian*) 0-32241
- $^{138}\text{La}$ , naturally occurring, gamma-ray emission energies 0-52811
- $^{138}\text{La}$ , radioactive decay meas., half life,  $\gamma$  energies 0-13418
- $^{139}\text{La}$ , level props., Coulomb excitation obs. 0-13378
- $^{139}\text{La}^{86}\text{Kr}, X$ , TDHF fusion calcs., fusion cross sections 0-37409
- $^{139}\text{La}^{86}\text{Kr}, X$ , 505, 610, 710 MeV, TDHF calcs., fusion behaviour 0-9323
- $^{139}\text{La}(\text{n}, \gamma)$ , non-statistical capture, radiative widths,  $\gamma$ -ray doorway state model 0-37389
- $^{139}\text{La}(\text{p}, \text{pn})$   $^{135\text{m}}\text{Ba}$ ,  $^{135\text{m}}\text{Ba}$  yield depend. on energy of bombarding particle 0-5151
- $^{139}\text{La}(\text{p}, \text{f})$ , 600 MeV, fragment energies, cross sections level density and barrier heights 0-42723
- $^{140}\text{La}$ , beta decay half life 0-47435
- $^{144}\text{La}$ , radioactive decay meas., half life,  $^{144}\text{Ce}$  levels 0-13417
- Mo stable isotope eval., 5 keV-5 meV neutrons, rel. to reactor structural steel 0-13620
- $^A$ Mo, A=92, 94-98, 100, muonic atomic X-ray transitions, nuclear charge radii 0-27545
- $^A$ Mo, A=94, 96, 98, multiparticle states, method of generalised seniority 0-22759
- $^A$ Mo, A=94, 97 deeply bound hole state transition strength giant resonance, DWBA anal. of (p,d) 0-47426
- $^A$ Mo( $^4\text{He}, ^3\text{He}$ ), A=92, 94, 96, 98, 100, 110 MeV, giant quadrupole resonance isotopic depend. 0-9282
- $^A$ Mo(n, $\gamma$ ) A=98, 100 resonance parameters, capture  $\Gamma$ -rays and reaction mechanism 0-18272



## nuclei with mass number 90 to 149 continued

- <sup>100</sup>Mo(p,n), A=94-96, 98, 1.7-6.7 MeV, total cross sections, p strength functions, optical model anal. 0-18301
- <sup>100</sup>Mo(p,p'), (A=92,94), 20 MeV, polarisation effects on nuclear excited states (*Russian*) 0-27645
- <sup>102</sup>Mo(N,N)<sup>102</sup>Mo, optical model anal. 0-47473
- <sup>102</sup>Mo(d,p), pol. d, excitation curve isospin anomaly, neutron single particle resonances 0-27595
- <sup>102</sup>Mo(n,n), 7-26 MeV, differential cross sections, global optical model anal. 0-18298
- <sup>104</sup>Mo, direct neutron decay of analogue resonances 0-22824
- <sup>108</sup>Mo static quadrupole moment of first 2<sup>+</sup> state from ( $\alpha,\alpha'$ ), (<sup>16</sup>O,<sup>16</sup>O) 0-5061
- <sup>108</sup>Mo(d,p), (d,n), (d, $\alpha$ ), activation analysis, excitation functions 0-22842
- <sup>109</sup>Mo isobaric analogue resonances, activation analysis, excitation functions of <sup>108</sup>Mo + d reactions 0-22842
- <sup>102</sup>Mo,  $\beta$ -decay, T<sub>1/2</sub>, <sup>102</sup>Tc deduced levels, tentative J <sup>$\pi$</sup>  and transitions 0-52630
- Mo(n,X), 2 keV-20 MeV cross sections, coherent optical and statistical model calcs. 0-18318
- <sup>101</sup>Nb, 17<sup>1/2</sup> state, g-factor meas. 0-32179
- <sup>101</sup>Nb, energy spectra and EM props. using broken pair model 0-499
- <sup>103</sup>Nb B(E<sub>2</sub>) transitions, quasiparticle-phonon multiplet, nuclear field theory for superfluid nuclei 0-47427
- <sup>103</sup>Nb, mag. form factors, core polarisation and exchange current effects 0-13409
- <sup>103</sup>Nb + d( $\alpha$ ), 12-50 MeV, t formation average cross sections 0-42670
- <sup>103</sup>Nb( $\alpha$ , X), 15-72 MeV, excitation functions and spallation cross-sections 0-18274
- <sup>103</sup>Nb(e,e), 180° scatt., magnetisation distrib., mag. multipole moments 0-9228
- <sup>103</sup>Nb(p, $\alpha$ X), 20-45 MeV,  $\alpha$  spectra, exciton model anal. 0-18306
- <sup>103</sup>Nb(p,n)<sup>103</sup>Mo, direct neutron decay of analogue resonances of <sup>94</sup>Mo 0-22824
- <sup>104</sup>Nb level density, neutron spectra and ang. distrib. nonequilibrium processes from <sup>94</sup>Zr(p,n) (*Russian*) 0-37376
- <sup>107</sup>Nb high spin analogue resonance near N=50 neutron shell, DWBA anal. of <sup>96</sup>Zr(<sup>3</sup>He,d) 0-42613
- Nd(<sup>16</sup>O,<sup>16</sup>O), 40-48 MeV, even nuclei, 2<sup>+</sup> state E2 transition probabilities and quadrupole moments 0-18234
- <sup>141</sup>Nd + n, A=143,145, capture cross section meas. in Triton reactor (*French*) 0-18308
- <sup>144</sup>Nd capture states partial  $\alpha$ -decay widths from <sup>143</sup>Nd(n, $\gamma\alpha$ ) 0-37328
- <sup>144</sup>Nd, excited states calculation, phenomenological models: band-mixing, vibrational-rotational and interacting-boson model 0-22653
- <sup>144</sup>Nd levels and transitions,  $\gamma$ -ray spectra from <sup>144</sup>Pr<sup>m</sup> $\beta$ -decay (*French*) 0-18250
- <sup>147</sup>Nd, beta spectrum, hard component 0-22769
- <sup>147</sup>Nd decay, <sup>147</sup>Pm levels, transitions,  $\gamma\gamma$ -coincidences and IC electrons 0-18243
- <sup>148</sup>Nd from <sup>148</sup>Pr  $\beta$ -decay, low lying energy levels, quasi band description 0-5096
- <sup>148</sup>Nd(n, $\gamma$ )<sup>149</sup>Nd $\rightarrow$ <sup>149</sup>Pm, energy levels 0-27592
- <sup>149</sup>Nd $\rightarrow$ <sup>149</sup>Pm, energy level study 0-27592
- <sup>141</sup>P(n, $\gamma$ ), resonance parameters, s-wave radiative and reduced neutron widths 0-47471
- Pd, even isotopes, low lying collective states, IBA 0-27540
- <sup>105</sup>Pd, A=106, 108, collective excitations in the interacting boson model (*Russian*) 0-5044
- <sup>105</sup>Pd, 1592 keV E0 transition T<sub>1/2</sub> meas. using e- $\gamma$  coincidence 0-22762
- <sup>105</sup>Pd, K-electron capture decay, double K-shell vacancy creation 0-22773
- <sup>106</sup>Pd energy states and J <sup>$\pi$</sup>  from <sup>106</sup>Ag<sup>m</sup> decay 0-18197
- <sup>106</sup>Pd levels, J <sup>$\pi$</sup> , transitions, unique parity states, and spectroscopic factors from <sup>108</sup>Pd(n, $\gamma$ ) 0-42547
- <sup>110</sup>Pd(<sup>208</sup>Pb, X), 1.18-1.28 GeV, charge equil. time scale, relaxation time 0-18188
- <sup>110</sup>Pd(<sup>208</sup>Pb, X), 1.2 GeV, central collisions, neutron rich nucleon flow, mass, charge and energy 0-18337
- <sup>143</sup>Pm high spin states, J <sup>$\pi$</sup> , transitions, isomer g-factors from (d,2N), ( $\alpha$ ,2N) 0-32154
- <sup>143</sup>Pm, p single particle states and pairing force calcs., low lying levels 0-42522
- <sup>143</sup>Pm,  $\beta$ -decay, branching ratio and K-shell autoionisation 0-42598
- <sup>147</sup>Pm levels, transitions,  $\gamma\gamma$ -coincidences and IC electrons from <sup>147</sup>Nd decay 0-18243
- <sup>149</sup>Pm,  $\beta^-$  decay, <sup>149</sup>Sm level scheme 0-22750
- <sup>149</sup>Pm,  $\beta$ -decay, nucl. matrix elements, calc.,  $\gamma$ -transitions 0-52628
- <sup>149</sup>Pm, energy levels from <sup>149</sup>Nd beta decay 0-27592
- <sup>149</sup>Pm high spin states and bands, rot. description and in-beam study from <sup>150</sup>Nd(p,2n $\gamma$ ) 0-32153
- <sup>149</sup>Pm single proton states, spin assignments, spectroscopic factors from <sup>150</sup>Sm(t, $\alpha$ ), pol.t 0-18170
- <sup>140</sup>Pr, deeply bound hole state transition strength giant resonance, DWBA anal. of (p,d) 0-47426
- <sup>141</sup>Pr(n, $\gamma$ ), circular polarisation, ang. distrib. meas. 0-32285
- <sup>141</sup>Pr(n, $\gamma$ ), non-statistical capture, radiative widths,  $\gamma$ -ray doorway state model 0-37389
- <sup>143</sup>Pr<sup>m</sup> $\beta$ -decay, <sup>144</sup>Nd levels and transitions,  $\gamma$ -ray spectra (*French*) 0-18250
- <sup>143</sup>Pr  $\beta$ -decay to <sup>148</sup>Nd,  $\gamma$ -spectra energy levels, isomerism 0-5096
- Rb neutron rich isotopes, nucl. spins and mag. moments 0-47367
- <sup>85</sup>Rb, A=92-96,  $\beta$ -delayed neutron emission probabilities, half-life 0-52634
- <sup>85</sup>Rb, A=96,98,  $\beta$ -decay schemes and total energies, mass excess and separation energies 0-27601
- <sup>94</sup>Rb  $\beta$ -delayed n decay, <sup>93</sup>Sr excited state depopulation  $\gamma$ -rays, n coincidence 0-52631
- <sup>94</sup>Rh decay, T<sub>1/2</sub>, <sup>94</sup>Ru levels and  $\gamma$ -transitions 0-18244
- <sup>103</sup>Rh(e,e'), 350-800 keV, isomer Coulomb excitation cross sections 0-22659
- <sup>103</sup>Rh(n, $\gamma$ ), cross-sections above 2.6 keV 0-32276
- <sup>103</sup>Rh(n, $\gamma$ ), 0.5-3.0 MeV,  $\gamma$ -spectra strength functions 0-32240
- Ru, even isotopes, low lying collective states, IBA 0-27540
- <sup>100</sup>Ru, A=96, 98, 100, multiparticle states, method of generalised seniority 0-22759
- <sup>100</sup>Ru(<sup>16</sup>O,<sup>16</sup>O'), 36-45 MeV, A=96, 98, 100, 102, 104, first 2<sup>+</sup> excited state quadrupole moment 0-47374
- <sup>100</sup>Ru( $\alpha,\alpha'$ ), 8.5-9.5 MeV, A=96, 98, 100, 102, 104, first 2<sup>+</sup> excited state quadrupole moment 0-47374
- <sup>100</sup>Ru(n, $\gamma$ ), A=100-104, cross-sections above 2.6 keV 0-32276

## nuclei with mass number 90 to 149 continued

- <sup>100</sup>Ru(p,p'), A=96, 98, 5-8 MeV, level schemes, transitions, vibr. state, mixing ratios 0-18199
- <sup>94</sup>Ru levels and  $\gamma$ -transitions from <sup>94</sup>Rh decay 0-18244
- <sup>97</sup>Ru populated in <sup>88</sup>Sr(<sup>13</sup>C, 3n $\gamma$ ), band-like structures 0-32146
- <sup>98</sup>Ru decay scheme from <sup>99</sup>Tc<sup>m</sup>  $\beta$ -decay 0-42596
- <sup>102</sup>Ru 2<sup>+</sup> state quadrupole moment, reorientation effects and multiple Coulomb excitation from ( $\alpha,\alpha'$ ), (<sup>16</sup>O,<sup>16</sup>O) 0-5063
- Sb isomer ratio, high spin trapping from ( $\alpha,\alpha'$ )( $\alpha$ , pn) 0-22655
- Sb, isomer ratios in fission fragments at high excitation 0-32261
- <sup>121</sup>Sb, A=119,122, level density, neutron spectra and ang. distrib. nonequilibrium processes from Sn(p,n) (*Russian*) 0-37376
- <sup>121</sup>Sb, A=121,123, levels below 2 MeV, spins, transitions and mixing ratio from (p, $\gamma$ ), (n,n' $\gamma$ ) 0-32191
- <sup>121</sup>Sb, A=123,125,127,129, cross-sections, ang. distrib., spectroscopic factors, DWBA anal. of Te(t, $\alpha$ ) 0-52572
- <sup>124</sup>Sb, A=134,135,  $\beta$ -delayed neutron emission probabilities, half-life 0-52634
- <sup>124</sup>Sb(n,2n), A=121,123, 12.8-18.1 MeV, activation cross sections 0-47477
- <sup>113</sup>Sb, 15 MeV excitation, average nucl. lifetime determ. 0-43164
- <sup>113</sup>Sb mean nuclear lifetime from X-ray spectrum in <sup>112</sup>Sn(p,p') 0-9267
- <sup>121</sup>Sb, elec. quadrupole moment from elec. field gradients of trans-dimethyl organometallic moieties 0-29371
- <sup>124</sup>Sb(n, $\gamma$ )<sup>125</sup>Sb, reactor neutron capture cross section of 60.3-day <sup>124</sup>Sb 0-13469
- <sup>136</sup>Sm, A=148, 150, 152, 154, 156, excited states of transitional region nuclei, rot. bands (*Russian*) 0-52556
- <sup>136</sup>Sm(<sup>16</sup>O,X), 60-75 MeV, A=148, 150, 152, 154 deformation effects on fusion 0-18360
- <sup>136</sup>Sm(<sup>20</sup>Ne, <sup>20</sup>Ne), 70 MeV, A=148, 150, 152, Coulomb polarisation pot., coupled channel calcs. 0-22855
- <sup>136</sup>Sm(<sup>86</sup>Kr,X), A=144, 154, 490 MeV, transfer reactions and associated  $\gamma$ -multiplicity moments 0-18342
- <sup>144</sup>Sm, p single particle states and pairing force calcs., high spin states 0-42522
- <sup>144</sup>Sm(<sup>13</sup>C,<sup>13</sup>C'), 108 MeV, nuclear continuum investigation 0-13506
- <sup>144</sup>Sm(n, $\gamma$ ), resonance and thermal n,  $\gamma$ -spectra, recent expt. review, non-statistical effects 0-37383
- <sup>147</sup>Sm + n, capture cross section meas. in Triton reactor (*French*) 0-18308
- <sup>147</sup>Sm(n,  $\alpha$ )<sup>144</sup>Nd, 12 to 18 MeV, energy and angular distribution of  $\alpha$ -particles, statistical, pre-equilibrium and knock-on models 0-13477
- <sup>148</sup>Sm compound states partial  $\alpha$ -widths,  $\alpha$ -spectra of <sup>147</sup>Sm(n, $\alpha$ ) 0-47392
- <sup>149</sup>Sm, level scheme following <sup>149</sup>Pm  $\beta^-$  decay 0-22750
- Sn,  $\alpha$ -spectroscopic factors from (d, <sup>6</sup>Li) 0-534
- Sn, deep h-l state fragmentation, strength functions, giant resonances, quasiparticle phonon model 0-37320
- Sn isotopes, quantum number projection, particle number projection 0-27566
- Sn isotopes, relation between interacting boson approx. and quasiparticle formalism 0-32216
- Sn, neutron cross section, filtered neutron beam technique, Doppler effect 0-52670
- Sn, odd mass isotopes, low lying negative parity states, energy levels, shell model calc. 0-5076
- Sn odd-mass isotopes, hole-state analogues, line broadening and Coulomb displacement energies 0-52560
- <sup>118</sup>Sn (t, $\alpha$ ), 4.75-5.25 MeV, A=112, 116, 118, 120, 124, single proton states RMS radius 0-13350
- <sup>118</sup>Sn, A=106,108,  $\beta^+/(EC+\beta^+)$  probability ratio, EC decay energies, mass excesses 0-27543
- <sup>118</sup>Sn, A=111,115,119, neutron hole distrib., IAS and spectroscopic factors from Sn(<sup>3</sup>He, $\gamma$ ) 0-42519
- <sup>118</sup>Sn, A=116, 118, 120, 122, 124, 0<sup>+</sup>, 2<sup>+</sup> and 4<sup>+</sup> states 1 number conserving approach 0-22694
- <sup>118</sup>Sn, A=116, 124, neutron densities and single particle struct. 0-32165
- <sup>118</sup>Sn(n,n) A=116, 124, 11, 24 KeV, differential cross sections, global optical model anal. 0-18298
- <sup>118</sup>Sn(p,p'), A=115, 117, 119, 18 MeV, state spin assignment, particle-vibr. coupling 0-32160
- <sup>118</sup>Sn(p, $\pi^-$ ), A=112, 124, 660 MeV, pion energy spectra, isotopic effects (*Russian*) 0-42669
- <sup>106</sup>Sn excited states from <sup>106</sup>Co (<sup>3</sup>He,3n), coincidence experiments 0-52607
- <sup>112</sup>Sn(p,p'), 20.51, 25.0 MeV, energy levels, excitation functions and ang. distrib. 0-32184
- <sup>116</sup>Sn levels, J <sup>$\pi$</sup>  and transitions from <sup>115</sup>Sn(n, $\gamma$ ) 0-52587
- <sup>116</sup>Sn(<sup>40</sup>Ar,X) 187, 222, 340 MeV, fusion cross sections, direct and evaporative p and  $\alpha$  prod., evaporation, fission 0-13518
- <sup>116</sup>Sn(d,p), pol. d, 8.22 MeV, vector anal. power, p and d spin depend. effects 0-5114
- <sup>117</sup>Sn(p,d), polarised p, 12.9 MeV, anal. power 0-5114
- <sup>117</sup>Sn(p,p), polarised p, 12.9 MeV, anal. power 0-5114
- <sup>118</sup>Sn(<sup>6</sup>Li,<sup>6</sup>Li'), 153 MeV, isoscalar giant quadrupole resonances 0-13440
- <sup>118</sup>Sn( $\gamma$ p), up to 0.25 GeV, from bremsstrahlung  $\gamma$ -quanta (*Russian*) 0-5123
- <sup>118</sup>Sn(p, $\alpha$ X), 20-45 MeV,  $\alpha$  spectra, exciton model anal. 0-18306
- <sup>118</sup>Sn(p,t), ang. distrib. and cross sections full finite range CCBA anal. 0-5141
- <sup>119</sup>Sn, 23.87 keV level half-life 0-47433
- <sup>119</sup>Sn elec. quadrupole moment from elec. field gradients of trans-dimethyl organometallic moieties 0-29371
- <sup>119</sup>Sn( $\gamma$ n), giant mag. dipole resonance location, photoneutron polarisation method 0-37357
- <sup>120</sup>Sn  $\gamma$ -spectra, E1 and M1 hindrance factors from <sup>123</sup>Te(n, $\gamma\alpha$ ) 0-37386
- <sup>120</sup>Sn, nuclear K-X-ray satellites, Z=50-83, by  $\alpha$ -bombard., 17.5-22.5 MeV 0-42984
- <sup>120</sup>Sn(<sup>40</sup>Ar,X), deeply inelastic collisions, form factors, microscopic calcs. 0-18339
- <sup>120</sup>Sn( $\pi,\pi^-$ ), total cross section, density distrib. and ray bending effects 0-47509
- <sup>123</sup>Sn, deeply bound hole state transition strength giant resonance, DWBA anal. of (p,d) 0-47426
- <sup>124</sup>Sn(<sup>32</sup>S,xn), continuum  $\gamma$  rays, linear polarisation, feeding high spin yrast states in <sup>151,2</sup>Dy 0-497
- <sup>124</sup>Sn(p,p), threshold enhancement of parity violation, Born approx. 0-18191
- <sup>132</sup>Sn, energy levels, gamma transitions, spin and parity 0-9239
- <sup>132</sup>Sn level struct., lifetimes,  $\gamma\gamma$  coincidences, internal conversion from <sup>235</sup>U fission 0-52584



## nuclei with mass number 90 to 149 continued

- $\text{Sn}(\alpha, \alpha')$ , even-even isotopes, nuclear struct. effects in microscopic theory 0-37391
- $\text{Sn}(d, {}^6\text{Li})\text{Cd}$ , alpha-cluster pickup reactions, spectroscopic factors and reduced widths 0-534
- $\text{Sn}(\gamma, n)$ , 30 to 140 MeV, partial photoneutron cross section, total cross section approx. 0-22809
- $\text{Sn}(p, X)$ , 70 GeV/c,  $\pi^+$ ,  $K^+$ ,  $p$ ,  $\bar{p}$  prod. with  $p_T=0.5-2.5$  GeV/c cross sections, yield ratios (*Russian*) 0-52681
- ${}^{87}\text{Sr}$ ,  $A=96, 98$ ,  $\beta$ -decay schemes and total energies, mass excess and separation energies 0-27601
- ${}^{90}\text{Sr}$ , soil analysis using total sample decomp. 0-35808
- ${}^{93}\text{Sr}$  excited state depopulation  $\gamma$ -rays,  $n$  coincidence from  ${}^{94}\text{Rb}$   $\beta$ -delayed  $n$  decay 0-52631
- ${}^{147}\text{Tb}$ ,  $A=147, 148$ , high spin particle-hole states, octupole M2/E3 isomers from  ${}^{151}\text{Eu}(\alpha, xn)$  0-18171
- ${}^{147}\text{Tb}$ ,  $p$  single particle states and pairing force calcs., low lying levels 0-42522
- ${}^{149}\text{Tb}$ , high spin states obs. 0-18158
- ${}^{147}\text{Tc}$ ,  $A=93-96$ , excitation functions and isomer ratios from  ${}^{93}\text{Nb}(\alpha, xn)$  ( $x=1$  to 4) 0-492
- ${}^{93}\text{Tc}$  high spin analogue resonance near  $N=50$  neutron shell, DWBA anal. of  ${}^{92}\text{Mo}({}^3\text{He}, d)$  0-42613
- ${}^{95}\text{Tc}$ , energy levels from  ${}^{95}\text{Mo}(p, n\gamma)$   ${}^{95}\text{Tc}$  0-37372
- ${}^{96}\text{Tc}$ , high spin states,  $\gamma$ -energy, intensity, coincidence, ang. distrib. and electron conversion from  ${}^{93}\text{Nb}(\alpha, n)$  0-52554
- ${}^{99}\text{Tc}$ ,  $\beta$ -decay, branching ratio and  $K$ -shell autoionisation 0-42598
- ${}^{99}\text{Tc}$ ,  $\beta$ -decay,  $\beta$ -branching,  ${}^{99}\text{Ru}$  decay scheme 0-42596
- ${}^{99}\text{Tc}$ ,  $\beta$  decay constant, chemical state effect 0-42591
- ${}^{99}\text{Tc}+n$ , capture cross section meas. in Triton reactor (*French*) 0-18308
- ${}^{100}\text{Tc}$  low lying and isomeric levels, transitions and mean lines from  ${}^{100}\text{Mo}(p, n\gamma)$  0-42548
- ${}^{102}\text{Tc}$  deduced levels, tentative  $J^\pi$  and transitions from  ${}^{102}\text{Mo}$  decay 0-52630
- $\text{Te}$  isomer ratio, high spin trapping from  $\text{Sn}(\alpha, 3n)$  0-22655
- ${}^{124}\text{Te}$ ,  $A=117, 119, 121$ , collective excitations, high spin states and transitions from  $(\alpha, Zn)(d, Zn)({}^3\text{He}, 3n)$  0-13346
- ${}^{124}\text{Te}$ ,  $A=127, 129, 131$ , ground state mag. moments 0-5059
- ${}^{124}\text{Te}^m$ ,  $A=125, 127, 129, 11/2^-$  isomeric state magnetic moments 0-42537
- ${}^{124}\text{Te}$  isomeric state, spin, lifetime and mag. moment from  $(\alpha, n)(d, Zn)$  0-47387
- ${}^{124}\text{Te}$  capture states partial  $\alpha$ -decay widths from  ${}^{123}\text{Te}(n, \gamma\alpha)$  0-37328
- ${}^{124}\text{Te}$ , deeply bound hole state transition strength giant resonance, DWBA anal. of  $(p, d)$  0-47426
- ${}^{132}\text{Te}({}^{32}\text{S}, xn)$ , continuum  $\gamma$  rays, linear polarisation, feeding high spin yrast states in  ${}^{156-8}\text{Er}$  0-497
- ${}^{130}\text{Te}(n, \gamma)$ , resonance and thermal  $n, \gamma$ -spectra, recent expt. review, non-statistical effects 0-37383
- ${}^{132}\text{Te}$   $2^+$  level, shell model calc., Lanczos and Householder method comparison 0-22711
- ${}^{132}\text{Te}$  from fission,  $10^+$  isomeric state,  $J^\pi$  from deexcitation pattern, half life 0-460
- ${}^{132}\text{Te}$  low lying levels and EM props., shell model description 0-42549
- $\text{Te}(d, {}^6\text{Li})\text{Sn}$ , alpha-cluster pickup reactions, spectroscopic factors and reduced widths 0-534
- $\text{Xe}$  prod. cross sections with protons of 320-590 MeV, nuclear medicine appl. 0-36133
- ${}^{114}\text{Xe}$ ,  $A=129, 131$ , populated in  $(\alpha, n\gamma)$ , props. of low-lying levels 0-464
- ${}^{114}\text{Xe}$  excited states and  $\gamma$ -rays from  ${}^{114}\text{Cs}$   $\beta$ -decay 0-47436
- ${}^{116}\text{Xe}$  level scheme and yrast band, in-beam  $\gamma$ -study from  ${}^{106}\text{Cd}({}^{12}\text{C}, 2n)$  0-13360
- ${}^{125}\text{Xe}$   $11/2^- \rightarrow 9/2^-$  transition in odd parity band from  ${}^{124}\text{Te}(\alpha, 3n)$  0-9203
- ${}^{125}\text{Xe}$  odd and even parity band structs., level lifetimes from  ${}^{125}\text{Te}({}^3\text{He}, 3n\gamma)$  0-27533
- ${}^{129}\text{Xe}$ , excited state lifetimes by delayed coincidence method 0-18231
- ${}^{135}\text{Xe}$ , poisoning of IRT reactor, optimisation of operation regime (*Russian*) 0-37473
- ${}^{136}\text{Xe}(n, \gamma)$ , resonance and thermal  $n, \gamma$ -spectra, recent expt. review, non-statistical effects 0-37383
- ${}^{137}\text{Xe}$ , populated in  ${}^{138}\text{I}$   $\beta$ -decay, delayed neutrons feeding excited states obs. 0-27600
- ${}^{138}\text{Xe}+{}^{181}\text{Ta}$ , deep inelastic transfer, decay of binary nuclear system 0-22848
- ${}^{139}\text{Xe}$   $\beta$ -decay,  ${}^{139}\text{Cs}$  level scheme,  $J^\pi$  and  $\gamma$ -transitions 0-42590
- ${}^{139}\text{Xe}$ , populated in  ${}^{138}\text{I}$   $\beta$ -decay, level scheme 0-27600
- ${}^{91}\text{Y}$ , beta ray generated bremsstrahlung yield const. 0-42588
- ${}^{98}\text{Y}^*$ ,  $\beta$ -decay schemes and total energies, mass excess and separation energies 0-27601
- ${}^{91}\text{Y}$  primary  $\gamma$ -rays and binding energies from  ${}^{90}\text{Zr}(n, \gamma)$  0-52566
- $\text{Zr}$  even isotopes, quadrupole moments and E2 transition rates, broken pair approx. 0-52579
- $\text{Zr}$  isotopes, Hauser Feshbach calcs., of neutron cross sections 0-22839
- $\text{Zr}$  neutron separation energies from  $(d, t)$  and  $(d, p)$  reactions 0-47489
- $\text{Zr}$ -region, two nucleon transfer reactions, spectroscopic amplitudes, form factors, ang. distrib. 0-22779
- ${}^{94}\text{Zr}$  ( $p, p$ ),  $A=92, 94, 2-6.5$  MeV, optical and Lane model anal. comparison 0-18302
- ${}^{94}\text{Zr}$ ,  $A=90, 92$  and  $94$ , charge densities and single-particle structure 0-9224
- ${}^{94}\text{Zr}$ ,  $A=91, 92, 94$ , binding energy and primary  $\gamma$ -ray intensities from  $\text{Zr}(n, \gamma)$  0-52565
- ${}^{94}\text{Zr}$ ,  $A=92, 94, 96$ , multiparticle states, method of generalised seniority 0-22759
- ${}^{94}\text{Zr}({}^3\text{He}, {}^3\text{He})$ ,  $A=90, 92, 119$  MeV, optical pot. parameters energy and mass depend. 0-32289
- ${}^{94}\text{Zr}(d, p)$ , pol. d.,  $A=90, 91$ , excitation curve isospin anomaly, neutron single particle resonances 0-27595
- ${}^{94}\text{Zr}(p, n)$ ,  $A=92, 94, 1.7-6.7$  MeV, total cross sections,  $p$  strength functions, optical model anal. 0-18301
- ${}^{94}\text{Zr}(p, p')$ , ( $A=90, 92$ ), 20 MeV, polarisation effects on nuclear excited states (*Russian*) 0-27645
- ${}^{94}\text{Zr}(p, p')$ ,  $A=94, 96, 11.2-13.4$  MeV, anal. power and excitation function  $T^\gamma$  fluctuations 0-42626
- ${}^{90}\text{Zr}$  neutron absorption, multipole giant resonance contrib. to optical pot. imaginary part 0-18263
- ${}^{90}\text{Zr}$ , nuclear radii, energy density and HF-BCS methods 0-47363
- ${}^{90}\text{Zr}$ , proton orbit sizes and E0 matrix element for 2 lowest  $0^+$  states 0-27546
- ${}^{90}\text{Zr}({}^{13}\text{C}, {}^{13}\text{C}')$ , 108 MeV, nuclear continuum investigation 0-13506

## nuclei with mass number 90 to 149 continued

- ${}^{90}\text{Zr}({}^3\text{He}, pd)$ , 90 MeV, angular correlations, elastic break-up of  ${}^3\text{He}$  0-52685
- ${}^{90}\text{Zr}({}^6\text{Li}, {}^6\text{Li}')$ , 153 MeV, isoscalar giant quadrupole resonances 0-13440
- ${}^{90}\text{Zr}(\alpha, X)$ , 20, 40 MeV/ $N$ ,  $\alpha$  breakup yield, fragment yield ratios 0-9300
- ${}^{90}\text{Zr}(n, n)$ , 11 MeV, differential cross sections, global optical model anal. 0-18298
- ${}^{90}\text{Zr}(\pi^+, \pi^+)$ , 40 MeV, differential cross sections and strength parameters, optical model fit 0-18347
- ${}^{90}\text{Zr}(t, p)$ , centre of mass corrections to DWBA overlap factors 0-18319
- ${}^{92}\text{Zr}$  level struct. and reduced spectroscopic factors from  ${}^{91}\text{Zr}(d, p)$  0-32192
- ${}^{92}\text{Zr}$ , neutron binding energy precision meas. 0-18182
- ${}^{92}\text{Zr}(N, N)$   ${}^{92}\text{Zr}$ , optical model anal. 0-47473
- ${}^{92}\text{Zr}(p, \text{pol. A})$   ${}^{89}\text{Y}$ , finite-range cluster-model description, DWBA approach 0-52667

## nuclei with mass number 150 to 189

- $A=167-196$ , product cross sections from  ${}^{197}\text{Au}(\pi^+, \text{spallation})$  0-27619
- $A=150$  transitional region, collective props., interacting boson model 0-27538
- deformed rare earth nuclei, bandcrossing in  $K \neq 0$  bands, backbending 0-9204
- even actinides, two-nucleon transfer, first  $0^+$  collective state excitation, spectroscopic factor (*Russian*) 0-42530
- even-even rare earths, microscopic quadrupole and hexadecapole moments 0-13376
- high angular momentum fusion compound nucleus deexcitation, high spin states, rare earths 0-9259
- $N=82-86$ , high spin isomers, gamma spectroscopy 0-47358
- rare earth nuclei, high spin states from  $(\text{HI}, xn)$  reactions, discrete  $\gamma$ -transitions 0-5050
- $Z=55-63$ , odd proton nuclei, low lying even parity states 0-27551
- $(n, \gamma)$ ,  $A=94-190$ , resonance capture, low lying level population fluctuations,  $\gamma$ -rays 0-52619
- ${}^{187}\text{Au}$ ,  $A=189, 191, 193$ , high spin states and transitions, isomeric states from  $\text{Ir}(\alpha, xn\gamma)$  0-5038
- ${}^{187}\text{Au}$  decay,  ${}^{187}\text{Pt}$ , levels,  $J^\pi$ ,  $T_{1/2}$ , possible E0 transitions (*French*) 0-32230
- ${}^{198}\text{Au}$  gamma-ray strength functions from spectrum fitting method from  ${}^{197}\text{Au}(n, \gamma)$  0-52616
- ${}^{137}\text{Ba}({}^{32}\text{S}, {}^{32}\text{S}')$ ,  $A=130, 132, 134, 136, 72-80$  MeV,  $2_1^+$  state mag. moments 0-47373
- $\text{CC}^{158}\text{Dy}$  high spin states B(E2) values, IBA model test from  ${}^{26}\text{Ne}({}^{136}\text{Xe}, 4n)$   $\text{CC}^{158}\text{Dy}$  high spin states B(E2) values, IBA model test 0-27541
- $\text{CC}^{168}\text{Er}$  high intrinsic excitation levels,  $\gamma$ -decay props. from  ${}^{167}\text{Er}(n, \gamma)$  0-52588
- ${}^{137}\text{Ce}({}^{32}\text{S}, {}^{32}\text{S}')$ ,  $A=106, 108, 110, 112, 114, 116, 72-80$  MeV,  $2_1^+$  state mag. moments 0-47373
- $\text{Dy}$ , deformed nuclei, quasicontinuum  $\gamma$ -spectrum, M1, E1, E2 components 0-498
- $\text{Dy}$ ,  $\Delta N=2$  coupling problem 0-47412
- $\text{Dy}$  even isotopes, aligned Stockholm band intrinsic spin  $I_0^{\text{eff}}$  0-13363
- $\text{Dy}$ , quadrupole moment calc. using HF method (*Russian*) 0-13375
- ${}^{151}\text{Dy}$ , ( $A=151, 152$ ), high spin yrast states,  $\gamma$ -ray polarisation in  $({}^{32}\text{S}, n)$  reactions 0-497
- ${}^{151}\text{Dy}$  levels, bands and transitions, in-beam  $\gamma$ -rays from  ${}^{142}\text{Nd}({}^{12}\text{C}, 3n\gamma)$  0-458
- ${}^{152}\text{Dy}$ , collective bands and absence of yrast traps 0-9207
- ${}^{152}\text{Dy}$  high spin isomeric states, g-factors from  ${}^{140}\text{Ce}({}^{16}\text{O}, 4n)$  0-13377
- ${}^{152}\text{Dy}$  high spin isomers, yrast states and level lifetimes from  $({}^{15}\text{N}, 4n)$ ,  $({}^{16}\text{O}, 4n)$  0-13361
- ${}^{152}\text{Dy}$  high spin struct., in beam  $\gamma$  meas. from  $({}^{15}\text{N}, 4n)$ ,  $({}^{16}\text{O}, 4n)$  0-18179
- ${}^{152}\text{Dy}$ , rotation along axis of symmetry 0-448
- ${}^{152}\text{Dy}$  yrast continuum  $\gamma$ -ray multipolarity via polarisation meas. from  ${}^{140}\text{Ce}({}^{16}\text{O}, 4n)$  0-9264
- ${}^{152}\text{Dy}$  yrast traps, isomers and oblate deformations from  ${}^{124}\text{Te}({}^{32}\text{S}, 4n)$  0-13362
- ${}^{153}\text{Dy}$ , populated in  ${}^{153}\text{Ho}$   $\beta$ -decay, lower excited states 0-22765
- ${}^{156}\text{Dy}$  high spin states,  $\gamma$ -ang. distrib., lifetimes and feeding times from  ${}^{148}\text{Nd}({}^{19}\text{C}, 5n)$  0-13364
- ${}^{156}\text{Dy}$  high spin states lifetimes and feeding times, quadrupole moments from  ${}^{24}\text{Mg}({}^{136}\text{Xe}, 4n)$  0-32239
- ${}^{159}\text{Dy}$ , yrast-band of odd nuclei 0-22651
- ${}^{160}\text{Dy}$  anomalous  $\gamma$ -L X-ray directional correlations from  ${}^{160}\text{Tb}$  decay 0-52610
- ${}^{162}\text{Dy}({}^{136}\text{Xe}, {}^{136}\text{Xe}')$ , 547, 612 MeV, high spin state energies and reduced transition probabilities 0-18232
- ${}^{164}\text{Dy}$  multipole mixing in  $\gamma$  to ground bands from  ${}^{163}\text{Dy}(n, \gamma)$  0-52615
- ${}^{164}\text{Dy}+n$ , capture cross section meas. in Triton reactor (*French*) 0-18308
- ${}^{164}\text{Dy}({}^{40}\text{Ar}, X)$  222, 340 MeV, fusion cross sections, direct and evaporative  $p$  and  $\alpha$  prod., evaporation, fission 0-13518
- ${}^{165}\text{Dy}$ , neutron binding energy precision meas. 0-18182
- ${}^{166}\text{Dy}$  decay,  ${}^{166}\text{Ho}$  low lying levels and transitions, 54.24 keV level mag. moment 0-13380
- $\text{Er}$  (*Russian*) 0-13375
- $\text{Er}$  even isotopes, aligned Stockholm band intrinsic spin  $I_0^{\text{eff}}$  0-13363
- $\text{Er}$  yrast levels, spin alignment, populated by preequilibrium  $(\alpha, xn\gamma)$  reactions 0-52557
- ${}^{167}\text{Er}$ , ( $A=154, 155$ ), rotational struct. at high spins 0-457
- ${}^{167}\text{Er}$ , ( $A=156, 157, 158$ ), high spin yrast states,  $\gamma$ -ray polarisation in  $({}^{32}\text{S}, xn)$  reactions 0-497
- ${}^{167}\text{Er}$ ,  $A=156, 164$ , aligned positive parity bands from rot. aligned model 0-9209
- ${}^{153}\text{Er}$  360 ns yrast trap,  $\gamma$  transitions and lifetimes from  ${}^{144}\text{Sm}({}^{12}\text{C}, 3n)$  0-9205
- ${}^{154}\text{Er}$ , collective bands and absence of yrast traps 0-9207
- ${}^{154}\text{Er}$  yrast trap and transitions, decay scheme from  $({}^{64}\text{Ni}, 4n)$ ,  $({}^{16}\text{O}, 4n)$  0-9206
- ${}^{158}\text{Er}$ , back-bending phenomenal, rotating potential (*Chinese*) 0-47357
- ${}^{160}\text{Er}$  high spin yrast states and transitions from  ${}^{152}\text{Sm}({}^{13}\text{C}, 5n)$  0-9208
- ${}^{164}\text{Er}$  deformed nucleus, excited rot. bands, selfconsistent HFB treatment 0-42515
- ${}^{164}\text{Er}$  rot. states, HF and HFB self consistent calc. with Skyrme interaction 0-22662
- ${}^{166}\text{Er}$ , 2-quasiparticle states obs. 0-18198
- ${}^{166}\text{Er}({}^{86}\text{Kr}, X)$ , 600 MeV, deeply inelastic, alignment of transferred ang. momentum, discrete  $\gamma$ -ray ang. correlations 0-47498



## nuclei with mass number 150 to 189 continued

- <sup>160</sup>Er(<sup>86</sup>Kr,X), 12.1 MeV/u, dynamical splitting of projectilelike fragments 0-42685
- <sup>160</sup>Er(<sup>86</sup>Kr,X), 8.18 MeV/amu, energy loss and nucleon exchange 0-18323
- <sup>160</sup>Er(<sup>86</sup>Kr,X), statistical fluctuations in dissipative collisions, multidifferential cross sections 0-37399
- <sup>160</sup>Er(<sup>86</sup>Kr,X) 6-8 MeV, dynamic equilib. process observables, energy dissipation, mass, ang. momentum 0-18336
- <sup>160</sup>Er( $\gamma,\gamma$ ), 15 MeV, elastic and nuclear Raman scatt. 0-22811
- <sup>160</sup>Er, neutron binding energy precision meas. 0-18182
- <sup>160</sup>Eu ( $n,\alpha$ ), A=153, 154, 155, total neutron cross sections, effect on reactor chars. 0-32284
- <sup>160</sup>Eu, A=151, 152, 153, 154, 155, excited states of transitional region nuclei, rot. bands (Russian) 0-52556
- <sup>160</sup>Eu(N,  $\gamma$ ), A=151, 153, cross sections, time of flight spectra, scintillation detectors 0-27634
- <sup>152</sup>Eu, decay, gamma transitions and probabilities of beta transitions 0-22768
- <sup>152</sup>Eu, isomeric levels and transitions, Nilsson model 0-18195
- <sup>152</sup>Eu, X-ray emission probabilities per decay 0-14027
- <sup>152</sup>Eu<sup>m</sup> ( $n,n'$ ), thermal neutron acceleration by isomeric nuclei (Russian) 0-52680
- <sup>152</sup>Eu+n, capture cross section meas. in Triton reactor (French) 0-18308
- <sup>154</sup>Eu(p,p'), 12 MeV, ground band rot. states, deformation parameters, coupled channels anal. 0-9195
- Gd,  $\Delta N=2$  coupling problem 0-47412
- Gd, quadrupole moment calc. using HF method (Russian) 0-13375
- <sup>154</sup>Gd, A=152, 154, 156, 158, excited states of transitional region nuclei, rot. bands (Russian) 0-52556
- <sup>154</sup>Gd( $n,\gamma$ ), A=154, 156-8, 2, 24 keV, resonance averaged  $\gamma$ -spectra, level and J<sup>+</sup> appls. 0-37347
- <sup>154</sup>Gd, collective bands and absence of yrast traps 0-9207
- <sup>150</sup>Gd, high spin states, pairing correlations and nuclear shape, HFB approach 0-42517
- <sup>152</sup>Gd, populated in <sup>152</sup>Eu decay, gamma transition and IC 0-22768
- <sup>154</sup>Gd ( $\alpha, xn$ ), 47-130 MeV, reaction cross section 0-22844
- <sup>154</sup>Gd ( $\alpha, xn$ ), deformed Dy quasicontinuum spectrum, M1, E1, E2 components 0-498
- <sup>154</sup>Gd multiphonon vibr. bands, dynamic deformation theory 0-5035
- <sup>156</sup>Gd, excited states calculation, phenomenological models: band-mixing, vibrational-rotational and interacting-boson model 0-22653
- <sup>158</sup>Gd, excited states calculation, phenomenological models: band-mixing, vibrational-rotational and interacting-boson model 0-22653
- <sup>158</sup>Gd+n, capture cross section meas. in Triton reactor (French) 0-18308
- <sup>160</sup>Gd(<sup>12</sup>C, $\alpha$ ), 120, 200 MeV, average  $\alpha$ -multiplicities, incomplete fusion and breakup 0-27661
- <sup>160</sup>Gd(<sup>12</sup>C, $\alpha$ ), 90-200 MeV, incomplete fusion, fast  $\alpha$  prod. absolute cross sections 0-18359
- <sup>160</sup>Gd( $\alpha, xn$ ), 47-130 MeV, reaction cross section 0-22844
- Hf, quadrupole moment calc. using HF method (Russian) 0-13375
- Hf-Os region, high lying states, Nilsson strength fragmentation 0-42539
- <sup>160</sup>Hf, A=166, 168, 170, 172, yrast states, quadrupole moments and B(E2) values, microscopic calcs. 0-32147
- <sup>160</sup>Hf(HI,xn), A=170-173, two and three quasiparticle isomers, rot. bands, decays and lifetimes 0-9211
- <sup>171</sup>Hf, hindered electric dipole transitions and lifetimes from (HI,xn) reactions 0-9263
- <sup>171</sup>Hf one- and three-quasiparticle states, high spin rot. bands from (<sup>16</sup>O,5n), (<sup>13</sup>C,4n) 0-18163
- <sup>172</sup>Hf EC decay, <sup>172</sup>Lu levels, transitions and J<sup>+</sup> values 0-18249
- <sup>172</sup>Hf yrast band and high spin states, 22<sup>+</sup>→20<sup>+</sup> transition, band crossing from <sup>160</sup>Gd(<sup>16</sup>O,4n) 0-42523
- <sup>175</sup>Hf multi-quasiparticle states and bands, isomeric states, lifetimes from <sup>170</sup>Er(<sup>6</sup>Be,4n) 0-9213
- <sup>180</sup>Hf band crossing and giant backbending 0-32156
- <sup>185</sup>Hg<sup>m</sup>, and <sup>186m</sup>-<sup>191m</sup>Hg, nucl. spins, on-line quantum beat spectrosc. determ. 0-9562
- <sup>188</sup>Hg, HF calc., shape and lowest band struct., B(E2) values 0-32148
- <sup>140</sup>Ho, A=153, 160, isomeric levels and transitions, Nilsson model 0-18195
- <sup>153</sup>Ho-<sup>153</sup>Dy, decay scheme, lifetimes 0-22765
- <sup>165</sup>Ho, nuclear K-X-ray satellites, Z=50-83, by  $\alpha$ -bombard., 17.5-22.5 MeV 0-42984
- <sup>165</sup>Ho(<sup>86</sup>Kr,X), 620 MeV, deep inelastic scatt., ang. momentum transfer,  $\gamma$ -ray multiplicities 0-27665
- <sup>165</sup>Ho(p, $\alpha$ X), 20-45 MeV,  $\alpha$  spectra, exciton model anal. 0-18306
- <sup>165</sup>Ho( $\pi,\pi$ ), aligned deformed nuclei, cross sections and diffractive minima from eikonal approx. 0-22860
- <sup>166</sup>Ho, internal hyperfine field obs. using  $\beta$ - $\gamma$  directional correl. 0-32229
- <sup>166</sup>Ho low lying levels and transitions, 54.24 keV level mag. moment from <sup>160</sup>Dy decay 0-13380
- <sup>185</sup>Ir levels excited in ( $\alpha, xn$ ) reactions 0-9231
- <sup>185</sup>Ir levels populated in <sup>185</sup>Pt<sup>m+8</sup> decay 0-9269
- <sup>185</sup>Lu( $n,\gamma$ ), A=175, 176, 30 keV, capture cross sections, stellar nucleosynthesis, <sup>176</sup>Lu cosmic clock 0-42663
- <sup>157</sup>Lu, short lived  $\alpha$  emitter,  $\alpha$  energy, T<sub>1/2</sub> and branching ratio 0-501
- <sup>169</sup>Lu, radioactive decay, gamma ray and conversion electron spectra 0-22766
- <sup>169</sup>Lu, radioactive decay scheme 0-22767
- <sup>172</sup>Lu levels, transitions and J<sup>+</sup> values from <sup>172</sup>Hf EC decay 0-18249
- <sup>176</sup>Lu  $\beta$ -decay half life 0-52633
- <sup>176</sup>Lu( $n,\gamma$ ), effective cross section dependence on thermal neutron temp. 0-547
- <sup>177</sup>Lu, excited state lifetimes by delayed coincidence method 0-18231
- <sup>178</sup>Lu isomeric states and spins, transition probability from <sup>181</sup>Ta( $n,\alpha$ ) 0-52582
- Nd(<sup>16</sup>O,<sup>16</sup>O), 40-48 MeV, even nuclei, 2<sup>+</sup> state E2 transition probabilities and quadrupole moments 0-18234
- <sup>150</sup>Nd(<sup>20</sup>Ne,X), 115, 130 MeV,  $\gamma$ -continuum multiplicity distrib., yrast bump 0-9265
- <sup>180</sup>Nd(<sup>12</sup>C,xn), deformed Dy quasicontinuum spectrum, M1, E1, E2 components 0-498
- <sup>180</sup>Os, A=186, 188, 190, 192, rigid asymmetric rotor model descript., E2 and E4 props. 0-13403
- <sup>180</sup>Os( $n,\gamma$ ), A=186-188, 2.6-800 keV, capture Maxwellian cross sections, galactic nucleosynthesis 0-42664
- <sup>188</sup>Os, muonic resonance spectra, deduced isomer shifts and electric moments 0-18948
- <sup>189</sup>Os(t,  $\alpha$ ) <sup>188</sup>Re, 15.1 MeV, <sup>188</sup>Re energy level obs. 0-47487
- <sup>184</sup>Pb isotope identification from Sm(<sup>40</sup>Ca,xn) 0-32302

## nuclei with mass number 150 to 189 continued

- <sup>140</sup>Pd(<sup>32</sup>S,<sup>32</sup>S), A=102, 104, 106, 108, 110, 72-80 MeV, 2<sup>+</sup> state mag. moments 0-47373
- <sup>185</sup>Pt<sup>m+8</sup> decay, population of <sup>185</sup>Ir levels 0-9269
- <sup>187</sup>Pt, levels, J<sup>+</sup>, T<sub>1/2</sub>, possible E0 transitions from <sup>187</sup>Au decay (French) 0-32230
- <sup>187</sup>Re, A=181, 182, 187, magnetic moments meas. by PAC 0-22688
- <sup>187</sup>Re, A=181, 182, 187, spin polarisation, state struct. and mag. moments in rot. model 0-18194
- <sup>187</sup>Re, A=183, 184, nuclear K-X-ray satellites, Z=50-83, decay scheme 0-42984
- <sup>182</sup>Re isomer decay mag. moment, <sup>182</sup>W high spin states, J assignments and mixing ratios 0-42593
- <sup>187</sup>Re, decay const. determ. from <sup>187</sup>Re-<sup>187</sup>Os systematics in meteorites 0-41778
- <sup>187</sup>Re low lying level struct. and transitions, E2/E1 mixing ratios from <sup>187</sup>W decay 0-27557
- <sup>188</sup>Re, energy levels obs., form. by <sup>189</sup>Os(t,  $\alpha$ ) <sup>188</sup>Re 0-47487
- Sm,  $\Delta N=2$  coupling problem 0-47412
- Sm isotopes, shape transition, s-d IBA model Hamiltonian struct. 0-32173
- <sup>148</sup>Sm, A=148, 150, 152, 154, 156, excited states of transitional region nuclei, rot. bands (Russian) 0-52556
- <sup>148</sup>Sm(<sup>16</sup>O,X), 60-75 MeV, A=148, 150, 152, 154 deformation effects on fusion 0-18360
- <sup>148</sup>Sm(<sup>20</sup>Ne, <sup>20</sup>Ne), 70 MeV, A=148, 150, 152, Coulomb polarisation pot., coupled channel calcs. 0-22855
- <sup>148</sup>Sm(<sup>86</sup>Kr,X), A=144, 154, 490 MeV, transfer reactions and associated  $\gamma$ -multiplicity moments 0-18342
- <sup>150</sup>Sm, excited states calculation, phenomenological models: band-mixing, vibrational-rotational and interacting-boson model 0-22653
- <sup>151</sup>Sm,  $\beta$ -decay, branching ratio and K-shell autoionisation 0-42598
- <sup>151</sup>Sm, gamma spectra, energy levels (Dutch) 0-47430
- <sup>152</sup>Sm ( $n,n$ ), 2.4-7.2 MeV, inelastic and elastic optical model and deformation parameter depend. (Russian) 0-13481
- <sup>152</sup>Sm, populated in <sup>152</sup>Eu decay, gamma transitions and IC 0-22768
- <sup>154</sup>Sm giant multipole resonance fragmentation among two-phonon states 0-18260
- <sup>154</sup>Sm(<sup>16</sup>O,X), 153 MeV, angular momentum transfer in incomplete-fusion reactions 0-9320
- <sup>154</sup>Sm(<sup>40</sup>Ar,X), 222, 340 MeV, fusion cross sections, direct and evaporative p and  $\alpha$  prod., evaporation, fission 0-13518
- <sup>154</sup>Sm( $\alpha,\alpha$ ), 50 MeV, long range absorption and optical model effects from strong inelastic coupling 0-535
- <sup>154</sup>Sm(p,p'), 35 MeV, ground state rot. band and multipole moment 0-32178
- Ta+p(d)( $\alpha$ )(<sup>12</sup>C), 4.2 GeV/N, multiple  $\pi^-$  prod., mean multiplicity (Russian) 0-27647
- <sup>177</sup>Ta, magnetic moments meas. by PAC 0-22688
- <sup>177</sup>Ta spin polarisation, state struct. and mag. moments in rot. model 0-18194
- <sup>181</sup>Ta, nuclear K-X-ray satellites, Z=50-83, by  $\alpha$ -bombard., 17.5-22.5 MeV 0-42984
- <sup>181</sup>Ta+<sup>12</sup>C, 4.2 GeV/N, identical pion<sup>-</sup> interference effect, generation range determ. (Russian) 0-42695
- <sup>181</sup>Ta+<sup>138</sup>Xe, deep inelastic transfer, decay of binary nuclear system 0-22848
- <sup>181</sup>Ta+<sup>40</sup>Ar, deep inelastic transfer, decay of binary nuclear system 0-22848
- <sup>181</sup>Ta+<sup>86</sup>Kr, deep inelastic transfer, decay of binary nuclear system 0-22848
- <sup>181</sup>Ta(<sup>14</sup>N,X), 85-115 MeV, cross sections, preequilibrium  $\alpha$ -particle emission 0-42680
- <sup>181</sup>Ta( $\gamma,n$ ) photoneutron absorpt. cross section meas. 20.9 to 837.8 keV (German) 0-5122
- <sup>181</sup>Ta( $n,\gamma$ ), 30 keV, capture cross sections, stellar nucleosynthesis 0-42663
- <sup>181</sup>Ta(p,4n) <sup>178</sup>W radionuclide production and purification 0-12252
- Ta( $\gamma,\gamma$ ), neutron capture  $\gamma$ -ray Rayleigh scatt. 0-52661
- Ta( $\gamma,n$ ), 30 to 140 MeV, partial photoneutron cross section, total cross section approx. 0-22809
- Ta(p,X), 400 GeV/c, light ion backward prod., invariant cross section 0-32279
- Ta(p,p'), 0.6-25 GeV, backward emitted proton inclusive spectra, short range correlation 0-32281
- <sup>159</sup>Tb, neutron resonances, time-of-flight spectra 0-27633
- <sup>159</sup>Tb(<sup>14</sup>N,X), 85-115 MeV, cross sections, preequilibrium  $\alpha$ -particle emission 0-42680
- <sup>159</sup>Tb(p,f), 600 MeV, fragment energies, cross sections level density and barrier heights 0-42723
- <sup>160</sup>Tb  $\beta$ -decay, oriented nuclei,  $\gamma$  transitions multipole mixing parameters 0-18240
- <sup>160</sup>Tb decay, <sup>160</sup>Dy anomalous  $\gamma$ -L X-ray directional correlations 0-52610
- <sup>153</sup>Tm, short lived  $\alpha$  emitter,  $\alpha$  energy, T<sub>1/2</sub> and branching ratio 0-501
- <sup>169</sup>Tm, excited state lifetime meas. 0-32237
- <sup>169</sup>Tm, high resolution meas. of anisotropic directional correl. between  $\gamma$ -rays and KX rays 0-32243
- <sup>169</sup>Tm, nuclear K-X-ray satellites, Z=50-83, by  $\alpha$ -bombard., 17.5-22.5 MeV 0-42984
- <sup>169</sup>Tm(<sup>14</sup>N,X) 85-115 MeV, cross sections, preequilibrium  $\alpha$ -particle emission 0-42680
- <sup>169</sup>Tm(p, $\alpha$ X), 20-45 MeV,  $\alpha$  spectra, exciton model anal. 0-18306
- <sup>169</sup>Tm gamma-ray strength functions from spectrum fitting method from <sup>169</sup>Tm( $n,\gamma$ ) 0-52616
- <sup>170</sup>Tm( $n,\gamma$ ), 0.5-3.0 MeV,  $\gamma$ -spectra strength functions 0-32240
- <sup>175</sup>Tm single proton states, rot. bands, J<sup>+</sup> assignments from <sup>176</sup>Yb(t, $\alpha$ ), pol. 0-452
- W, quadrupole moment calc. using HF method (Russian) 0-13375
- <sup>140</sup>W, A=172-175, bands and backbending, i<sub>1/2</sub> neutron decoupling from Dy(<sup>16</sup>O,xn) 0-9212
- <sup>140</sup>W, A=173, 175, hindered electric dipole transitions and lifetimes from (HI,xn) reactions 0-9263
- <sup>140</sup>W, A=174, 175 quasicontinuum  $\gamma$ -rays yrast cascade dipole component, moment of inertia from Dy(<sup>16</sup>O, xny) 0-47424
- <sup>140</sup>W, A=184, 186, rigid asymmetric rotor model descript., E2 and E4 props. 0-13403
- <sup>170</sup>W high spin states, yrast bands and backbending from <sup>170</sup>Er(<sup>12</sup>C,4n) 0-13352
- <sup>180</sup>W ground and K=2<sup>-</sup> octupole band ang. momenta coupling, lifetimes from <sup>181</sup>Ta(p,2ny) 0-9214



nuclei with mass number 150 to 189 continued

- <sup>182</sup>W high spin states, J assignments and mixing ratios from <sup>182</sup>Re isomer decay 0-42593  
<sup>183</sup>W(<sup>12</sup>C,X), 77-167 MeV, fusion cross sections, direct and evaporative p and  $\alpha$  prod., evaporation, fission 0-13518  
<sup>183</sup>W( $\alpha,\alpha'$ ), 15 MeV, level and band Coulomb excitation, B(E2) values 0-32233  
<sup>186</sup>W, 14.7 MeV neutron capture cross-section measurements with activation technique 0-32282  
<sup>187</sup>W decay, <sup>187</sup>Re low lying level struct. and transitions, E2/E1 mixing ratios 0-27557  
W( $\alpha,\alpha'e^+e^-$ ), 1.0-2.5 MeV,  $e^+e^-$  pair prod. search 0-27637  
W(n,n), pol. n, 16.1 MeV, differential cross section, optical model fit 0-32259  
W(p,X), 400 GeV, particle mean multiplicities 0-13473  
W(p,p $e^+e^-$ ), 1.0-2.5 MeV,  $e^+e^-$  pair prod. search 0-27637  
<sup>132</sup>Xe+n, capture cross section meas. in Triton reactor (French) 0-18308  
Yb, quadrupole moment calc. using HF method (Russian) 0-13375  
<sup>A</sup>Yb, A=160, 161, backbending, multiple band crossing freq. and alignment from Sm(<sup>16</sup>O,3n) 0-47347  
<sup>A</sup>Yb, A=161, 162, 166, yrast cascade dipole component from Sm(<sup>16</sup>O,4n) 0-9266  
<sup>A</sup>Yb, A=164, 166, high spin yrast states and transitions from Gd(<sup>13</sup>C,5n) 0-9208  
<sup>A</sup>Yb, A=166, 168, 170, backbending and moment of inertia in HFB cranking method 0-42521  
<sup>A</sup>Yb, A=169-x,  $\gamma$  de-excitation and ang. momentum distrib. after fast  $\alpha$ -emission from <sup>159</sup>Tb(<sup>14</sup>N, $\alpha$ nxn) 0-18228  
<sup>A</sup>Yb(<sup>16</sup>O,<sup>16</sup>O $\gamma$ ), A=168-176, even nuclei, 58-62 MeV, Coulomb excitation, vibr. and rot. states 0-32162  
<sup>A</sup>Yb(<sup>40</sup>Ca,<sup>40</sup>Ca $\gamma$ ), A=170,172,174, 168 MeV, rotational g-factor meas. using transient field interactions 0-18193  
<sup>160</sup>Yb double backbending and rot. states, HFB cranking model anal. 0-32155  
<sup>161</sup>Yb quasicontinuum  $\gamma$ -rays yrast cascade dipole component, moment of inertia from Sm(<sup>16</sup>O, xny) 0-47424  
<sup>163</sup>Yb high spin states, HF self consistent calc. with Skyrme interaction, cranking approach 0-9210  
<sup>162</sup>Yb rot. states, HF and HFB self consistent calc. with Skyrme interaction 0-22662  
<sup>163</sup>Yb  $i_{1/2}$  band, spin alignment in the particle-rotor and cranking models 0-42536  
<sup>169</sup>Yb, populated in <sup>169</sup>Lu decay, meas. of  $\gamma$ -ray and conversion electron spectra 0-22766  
<sup>169</sup>Yb populated in <sup>169</sup>Lu decay,  $\gamma$ -ray and conversion electron spectra 0-22767  
<sup>170</sup>Yb(n, $\gamma$ ), 10-70 keV capture cross-section 0-27631  
<sup>172</sup>Yb, muonic resonance spectra, deduced isomer shifts and electric moments 0-18948  
<sup>173</sup>Yb octupole band, particle vibrational alignment from <sup>170</sup>Er ( $\alpha$ ,2n) 0-13351  
<sup>173</sup>Yb M1 transitions from 636 keV level, multipole mixture parameters, penetration effect 0-18220  
<sup>176</sup>Yb(p,p $\gamma$ ), 35 MeV, ground state rot. band and multipole moment 0-32178

nuclei with mass number 190 to 219

- A=167-196, product cross sections from <sup>197</sup>Au( $\pi^+$ , spallation) 0-27619  
A=190, Nilsson strength fragmentation, quadrupole and hexadecapole deformations 0-47394  
A=204, nuclear data sheets, levels, J<sup>π</sup> and transitions 0-31429  
A=212, nuclear data sheets, levels, J<sup>π</sup>, transitions 0-31430  
even-even and odd A nuclei, nuclear shapes and motions, review 0-5054  
preactinide nuclei, fission excitation functions and fission barrier height, liquid drop model 0-47513  
(n, $\gamma$ ), A=94-190, resonance capture, low lying level population fluctuations,  $\gamma$ -rays 0-52619  
(n, $\gamma$ ), interacting boson and Nilsson model tests, Pt-Os transition region 0-37380  
<sup>208</sup>(N, $\gamma$ ), pol. N, anal. power and giant multipole resonances, direct-semidirect model 0-18265  
A=196 nuclei, nuclear structure data sheets to Sept. 1978 0-41956  
<sup>A</sup>At, A=209, 210, production by photospallation of <sup>232</sup>Th and <sup>238</sup>U 0-52797  
<sup>208</sup>At energy levels and transitions, IC electrons from <sup>208</sup>Rn decay 0-18242  
<sup>212</sup>At high spin states, decay, g factor, J<sup>π</sup> assignments, level energies from <sup>208</sup>Pb(<sup>12</sup>C,3n) 0-5042  
<sup>212</sup>At, relative  $\alpha$ -decay width and excited levels, nuclear field theory 0-47437  
Au(<sup>40</sup>Kr,X), 724 MeV, deeply inelastic, <sup>4</sup>He, <sup>1</sup>H emission, fragment spin, semiempirical method 0-47366  
<sup>A</sup>Au, A=189, 191, 193, high spin states and transitions, isomeric states from Ir( $\alpha$ ,xny) 0-5038  
<sup>A</sup>Au A=190, 192, 194, levels, J<sup>π</sup>, isomers and rot. aligned bands from Ir( $\alpha$ ,xn) 0-9215  
<sup>196</sup>Au energy levels and Q-value from <sup>197</sup>Au( $\gamma$ ,n) 0-37329  
<sup>197</sup>Au, 14.7 MeV neutron capture cross-section measurements with activation technique 0-32282  
<sup>197</sup>Au, nuclear K-X-ray satellites, Z=50-83, by  $\alpha$ -bombard, 17.5-22.5 MeV 0-42984  
<sup>197</sup>Au+<sup>136</sup>Xe, 1064 MeV, fragment spin orientation from continuum  $\gamma$ -ray anisotropy meas. 0-22853  
<sup>197</sup>Au+<sup>40</sup>Ar, deep inelastic reactions, isotopic distrib., n excess degree of freedom relaxation 0-9308  
<sup>197</sup>Au+d( $\alpha$ ), 12-50 MeV, t formation average cross sections 0-42670  
<sup>197</sup>Au(<sup>A</sup>Xe,X), A=129, 132, 136, damped collision, proton and neutron exchange correlations 0-18335  
<sup>197</sup>Au(<sup>A</sup>Xe,X), A=129, 132, 136, <787 MeV, light and heavy fragment N/Z ratios 0-32292  
<sup>197</sup>Au(<sup>132</sup>Xe,X), damped collisions, charge distrib. second moments and giant E1 quantal fluctuations 0-27547  
<sup>197</sup>Au(<sup>14</sup>N,X), 85-115 MeV, cross sections, preequilibrium  $\alpha$ -particle emission 0-42680  
<sup>197</sup>Au(<sup>40</sup>Ar,X), 222, 340 MeV, fusion cross sections, direct and evaporative p and  $\alpha$  prod., evaporation, fission 0-13518  
<sup>197</sup>Au(<sup>40</sup>Ar,X), 240 MeV, fragment shape deformation in deep inelastic collisions 0-47365  
<sup>197</sup>Au(<sup>63</sup>Cu,X), 400 MeV, neutron multiplicity in deep inelastic collisions 0-18324

nuclei with mass number 190 to 219 continued

- <sup>197</sup>Au(<sup>63</sup>Cu,X), 9.6 MeV/A, quasi elastic, deep inelastic and fission like ang. distrib. 0-18334  
<sup>197</sup>Au(<sup>6</sup>Li, X), 75 MeV, Z=1 or 2 fast particle prod. mechanism above Coulomb barrier 0-42687  
<sup>197</sup>Au(<sup>84</sup>Kr,X), 9.6 MeV/A, quasi elastic, deep inelastic and fission like ang. distrib. 0-18334  
<sup>197</sup>Au(<sup>86</sup>Kr,X), 620 MeV, deep inelastic scatt., ang. momentum transfer,  $\gamma$ -ray multiplicities 0-27665  
<sup>197</sup>Au(<sup>86</sup>Kr,X) 612 MeV,  $\gamma$ -ray circular polarisation 0-13453  
<sup>197</sup>Au(HI,X), 60-120 MeV complete fusion cross sections from fission fragment ang. distrib. 0-13516  
<sup>197</sup>Au( $\alpha,\alpha'$ ), 120 MeV, isoscalar resonance excitation, low lying transitions, DWBA calc. 0-512  
<sup>197</sup>Au(n, $\gamma$ ), effective cross section dependence on thermal neutron temp. 0-547  
<sup>197</sup>Au(n,n)<sup>197m</sup>Au, E<sub>n</sub>=3 and 14.1 MeV, form. cross sections of short-lived isomer, cyclic activation technique 0-32283  
<sup>197</sup>Au(p,X)<sup>149</sup>Tb, target fragmentation momentum transfer, collective tube model, collectivity effects 0-37359  
<sup>198</sup>Au, 411 keV transition energy, absolute meas. rel. to He-Ne laser freq. (Czech) 0-22755  
<sup>198</sup>Au level spin assignments from  $\gamma$  ang. distrib. and circular polarisation from <sup>197</sup>Au(n, $\gamma$ ) 0-52570  
<sup>198</sup>Au, populated in <sup>198</sup>Au(n, $\gamma$ ), high energy transitions 0-22878  
<sup>198</sup>Au(n, $\gamma$ ), 0.5-3.0 MeV,  $\gamma$ -spectra strength functions 0-32240  
<sup>199</sup>Au, populated in <sup>198</sup>Au(n, $\gamma$ ), high energy transitions 0-22878  
<sup>200</sup>Be(<sup>136</sup>Xe,X), statistical fluctuations in dissipative collisions, multidifferential cross sections 0-37399  
Bi+Xe, 1.13 GeV, deep inelastic nuclear reaction, electronic 1sr vacancy prod., compound nucleus 0-27662  
Bi(Kr,X), strongly damped collisions, classical dynamical model with shape deformation 0-27658  
Bi(Xe,X), strongly damped collisions, classical dynamical model with shape deformation 0-27658  
<sup>204</sup>Bi excited states,  $\gamma$  rays, conversion electrons and  $\gamma\gamma$  coincidences from <sup>204</sup>Po, EC 0-18241  
<sup>208</sup>Bi two-particle, two-hole configuration, levels, J<sup>π</sup> and excitation energies from <sup>210</sup>Bi<sup>m</sup>(p,t) 0-32190  
<sup>209</sup>Bi low lying levels and spectroscopic factors, EFR-DWBA anal. of <sup>208</sup>Pb(<sup>7</sup>Li, <sup>6</sup>He) 0-32182  
<sup>209</sup>Bi(<sup>14</sup>N,X), 85-115 MeV, cross sections, preequilibrium  $\alpha$ -particle emission 0-42680  
<sup>209</sup>Bi(<sup>6</sup>Li,X), 60-156 MeV, break-up fragment transfer, cross sections, recoil ranges 0-13491  
<sup>209</sup>Bi(<sup>84</sup>Kr, X), TDHF fusion calcs., fusion cross sections 0-37409  
<sup>209</sup>Bi(HI,X), 60-120 MeV complete fusion cross sections from fission fragment ang. distrib. 0-13516  
<sup>209</sup>Bi( $\alpha$ ,X), 20, 40 MeV/N,  $\alpha$  breakup yield, fragment yield ratios 0-9300  
<sup>209</sup>Bi( $\alpha$ ,X), 69.2, 140 MeV, scatt. and fission reaction mechanisms, cross sections 0-18350  
<sup>209</sup>Bi( $\alpha,\alpha'$ ), 120 MeV, isoscalar resonance excitation, low lying transitions, DWBA calc. 0-512  
<sup>209</sup>Bi(n,n), 50, 100, 200 MeV, eikonal scatt. by complex pots., cross sections 0-27643  
Bi(d,d), 4.3, 6.3, 8.9 GeV/c, secondary momentum spectra, multiple scatt. model anal. (Russian) 0-27650  
Hf-Os region, high lying states, Nilsson strength fragmentation 0-42539  
<sup>A</sup>Hg, A=198, 200, rigid asymmetric rotor model descript., E2 and E4 props. 0-13403  
<sup>A</sup>Hg, quadrupole moment, change between first 5/2<sup>-</sup> states for A=197,199, shell model anal. 0-52576  
<sup>A</sup>Hg( $\alpha,\alpha'$ ), A=198, 200, 204, 16-27 MeV backward scatt., collective states 0-13365  
<sup>191</sup>Hg<sup>m</sup> and <sup>190m-185m</sup>Hg, nucl. spins, on-line quantum beat spectrosc. determ. 0-9562  
<sup>200</sup>Hg, neutron binding energy precision meas. 0-18182  
<sup>201</sup>Hg missing f<sub>5/2</sub> state Coulomb excitation, level scheme, J<sup>π</sup>, transitions using ( $\alpha,\alpha'$ ), (<sup>16</sup>O, <sup>16</sup>O) 0-47386  
Hg(n,n), pol. n, 16.1 MeV, differential cross section, optical model fit 0-32259  
<sup>192</sup>Ir levels, resonances and low energy  $\gamma$ -rays from <sup>191</sup>Ir(n, $\gamma$ ) 0-47397  
Os even nuclei, spin exspn. Hamiltonian, quadrupole moments 0-5058  
<sup>A</sup>Os, A=186, 188, 190, 192, rigid asymmetric rotor model descript., E2 and E4 props. 0-13403  
<sup>A</sup>Os, A=191,193, ground state spectroscopic quadrupole moment meas. 0-27553  
<sup>190</sup>Os, collective states and static quadrupole moment, boson expansion theory 0-47346  
Os(tp), 17 MeV, two neutron transfer strength, O(6) limiting symmetry in IBA, Pt comparison 0-32287  
Pb region, mag. moments and M1, M2 and M4 values, self consistent calcs. 0-47371  
Pb(<sup>12</sup>C,X) 3.6 GeV proton emission invariant cross sections (Russian) 0-13500  
Pb(<sup>20</sup>Ne, $\pi^+$ ), 800 MeV/N, doubly differential cross sections and ang. distrib. 0-9305  
Pb(<sup>20</sup>Ne,  $\pi^+$ X), 400 MeV/N, pion prod. doubly differential cross sections and ang. distrib. 0-32299  
Pb(Xe,X), deep inelastic,  $\delta$ -electron emission, reaction time effects 0-32293  
<sup>A</sup>Pb, A=197, 198, low energy  $\gamma$ -transitions and level lifetimes from <sup>186</sup>W(<sup>16</sup>O, xn) 0-18221  
<sup>A</sup>Pb, A=200,206, 12<sup>+</sup> isomer states, quadrupole moments 0-27554  
<sup>A</sup>Pb, A=205-207, neutron hole states, spectroscopic factors, DWBA anal. of Pb(<sup>3</sup>He, $\alpha$ ) 0-47352  
<sup>A</sup>Pb, A=206-209, nuclear K-X-ray satellites, Z=50-83, by  $\alpha$ -bombard., 17.5-22.5 MeV 0-42984  
<sup>A</sup>Pb( $\alpha,\alpha'$ ), A=204, 206, 208, 16-27 MeV backward scatt., collective states 0-13365  
<sup>A</sup>Pb( $\alpha,\alpha'$ ), A=206, 208, 120 MeV, isoscalar resonance excitation, low lying transitions, DWBA calc. 0-512  
<sup>A</sup>Pb(e,e'), A=204, 206-208, levels and inelastic cross sections 0-22698  
<sup>A</sup>Pb( $\gamma$ ,n), A=206, 208, levels using tagged photons 0-23245  
<sup>201</sup>Pb decay, <sup>201</sup>Tl levels, transitions and J<sup>π</sup> assignments 0-5099  
<sup>205</sup>Pb multipole resonance E1-E2 and E1-M1 interference from <sup>206</sup>Pb( $\gamma$ ,n) 0-32251  
<sup>206</sup>Pb, population of 0<sup>+</sup>, alpha-decay of <sup>210</sup>Po 0-22775  
<sup>207</sup>Pb parity assignments and M1 radiative strength from <sup>206</sup>Pb(n,n) 0-52614



## nuclei with mass number 190 to 219 continued

- <sup>207</sup>Pb(e,e), magnetisation distrib. from elastic mag. form factors, core polarisation, exchange currents 0-47372
- <sup>208</sup>Pb( $\gamma$ ,n), 7632 keV level photoexcitation, cross section and  $J^\pi$  0-37330
- <sup>208</sup>Pb(Ar,  $\pi^+$ X), 250, 400 MeV/A, pion yield near threshold 0-18344
- <sup>208</sup>Pb( $\alpha$ , $\alpha'$ ), 100-172 MeV, giant monopole resonance evidence from strong energy depend. 0-13432
- <sup>208</sup>Pb and neighbouring nuclei, shell model calcs. with correlated pairs basis 0-22712
- <sup>208</sup>Pb core with valence nucleon or hole, mag. props., exchange currents, electron scatt. 0-22689
- <sup>208</sup>Pb, fast neutron scatt. and capture, microscopic isovector optical pot. test 0-52682
- <sup>208</sup>Pb, finite nuclear props. in relativistic quantum field theory, mass and p densities 0-9219
- <sup>208</sup>Pb, isoscalar giant multipole resonances, simple macroscopic model, damping mechanisms 0-42617
- <sup>208</sup>Pb isoscalar giant reson., decay scheme 0-9277
- <sup>208</sup>Pb M1, E1, M2, E2 localised  $\gamma$ -ray strengths from <sup>207</sup>Pb(n, $\gamma$ ) 0-37350
- <sup>208</sup>Pb, neutron densities and single particle struct. 0-32165
- <sup>208</sup>Pb, nuclear radii, energy density and HF-BCS methods 0-47363
- <sup>208</sup>Pb + <sup>208</sup>Ne(<sup>40</sup>Ar), 250-1000 MeV/N, intranuclear cascade calcs. for multiplicity and cross sections 0-32300
- <sup>208</sup>Pb + <sup>58</sup>Ni(<sup>90</sup>Zr), fission phenomena in deep inelastic collisions 0-5186
- <sup>208</sup>Pb(<sup>136</sup>Xe,X), 7 MeV/u, composite system lifetime from  $\delta$ -electron distrib., sticking times 0-540
- <sup>208</sup>Pb(<sup>13</sup>C, <sup>12</sup>C), 108 MeV, nuclear continuum investigation 0-13506
- <sup>208</sup>Pb(<sup>16</sup>O, <sup>16</sup>O), elastic scatt., exponential optical pots. 0-42681
- <sup>208</sup>Pb(<sup>16</sup>O, <sup>16</sup>O), 315 MeV, continuous spectrum and giant resonance excitation, coherent state model test 0-32252
- <sup>208</sup>Pb(<sup>16</sup>O,X), 80-313 MeV, optical model anal., dynamic shape or density changes 0-18186
- <sup>208</sup>Pb(<sup>40</sup>Ar,X), deeply inelastic collisions, form factors, microscopic calcs. 0-18339
- <sup>208</sup>Pb(<sup>6</sup>Li,X), 60-156 MeV, break-up fragment transfer, cross sections, recoil ranges 0-13491
- <sup>208</sup>Pb(<sup>86</sup>Kr,X), 610 MeV, deep inelastic ang. momentum transfer from sequential fission fragments 0-18325
- <sup>208</sup>Pb(N,N), <30 MeV, microscopic optical pot. in nuclear struct. approach, HF field 0-527
- <sup>208</sup>Pb( $\alpha$ , $\alpha'$ ), 65 MeV, inclusive reaction, giant resonance background, heavy ion model anal. 0-5150
- <sup>208</sup>Pb( $\alpha$ , $\alpha'$ ), 172 MeV, strongly excited giant monopole resonance 0-18273
- <sup>208</sup>Pb(e,e'), E2 transitions of fragmented isoscalar quadrupole giant resonance 0-22758
- <sup>208</sup>Pb(e,e'), 60 MeV, backward scatt., 2 $\hbar\omega$  M1 excitation search 0-32234
- <sup>208</sup>Pb(e,e'), giant multipole resonance excitation, particle-hole interaction 0-22789
- <sup>208</sup>Pb( $\gamma$ ,n), 9.5-12 MeV, photoneutron ang. distrib., struct. below giant resonance 0-13444
- <sup>208</sup>Pb( $\gamma$ ,n) giant mag. dipole resonance location, photoneutron polarisation method 0-37357
- <sup>208</sup>Pb( $\gamma$ ,p), up to 0.25 GeV, from bremsstrahlung  $\gamma$ -quanta (Russian) 0-5123
- <sup>208</sup>Pb(n, $\gamma$ ), fast, direct-semidirect and pure resonance model calcs. 0-47486
- <sup>208</sup>Pb(n,n), 7-26 MeV, differential cross sections, global optical model anal. 0-18298
- <sup>208</sup>Pb(p,P), pol. p, 9, 10 MeV, vol. integrals for optical pots., real symmetry pot. 0-42659
- <sup>208</sup>Pb( $\gamma$ , $\gamma$ ),  $\gamma$ -ray ang. distrib., asymmetry effects through IAR, direct-semidirect model 0-42581
- <sup>208</sup>Pb(p,p'), 39, 62 MeV, DWBA anal., collective spectra, direct process contrib. (Russian) 0-13408
- <sup>208</sup>Pb(p,p), 100-2200 MeV, total and reaction cross sections from optical pot. 0-18303
- <sup>208</sup>Pb(p,p), 20-50 MeV differential cross section, polarisation ang. distrib., optical model exchange terms 0-27638
- <sup>208</sup>Pb(p,t) <sup>208</sup>Pb(3 $^+$ ), pol. p, 22 MeV, anal. power and (p,d)(d,t) sequential transfer processes 0-5119
- <sup>208</sup>Pb( $\pi$ , $\pi$ ), 255 MeV, quasielastic knockout, proton yield,  $\sigma(\pi^+)/\sigma(\pi^-)$  cross section ratio 0-32305
- <sup>208</sup>Pb( $\pi$ , $\pi$ ), 162 MeV, elastic and inelastic ang. distrib., optical and PWIA anal. 0-42706
- <sup>208</sup>Pb( $\pi$ , $\pi$ ), total cross section, density distrib. and ray bending effects 0-47509
- <sup>208</sup>Pb( $\pi^+$ , $\pi^+$ ), 40 MeV, differential cross sections and strength parameters, optical model fit 0-18347
- <sup>208</sup>Pb(t,p), centre of mass corrections to DWBA overlap factors 0-18319
- <sup>209</sup>Pb excited states and 3/2 $^-$  resonances, shell model, calcs. from <sup>208</sup>Pb(n,n) 0-18262
- <sup>210</sup>Pb ground state decay 0-47429
- Pb( $\alpha$ ,X), 3.6 GeV proton emission invariant cross sections (Russian) 0-13500
- Pb( $\gamma$ , n), 30 to 140 MeV, partial photoneutron cross section, total cross section approx. 0-22809
- Pb( $\mu$ , X), energetic charged particle spectrum, integrated yield 0-18293
- Pb(n,n), 13.7-15 MeV, differential cross section energy depend., meas. and optical model 0-18304
- Pb(n,n), 14.0-17.4 MeV, neutron polarisation, ang. depend. diffraction struct. 0-18283
- Pb(n,n), 14.2 MeV, polarisation in forward angle scatt. 0-18282
- Pb(n,n), pol. n, 16.1 MeV, differential cross section, optical model fit 0-32259
- Pb(p,X), 70 GeV/c,  $\pi^+$ , K $^+$ , p,  $\bar{p}$  prod. with  $p_T=0.5-2.5$  GeV/c cross sections, yield ratios (Russian) 0-52681
- Pb(p,xpX), x=1, 2, 640 MeV, energetic backward p emission, inclusive differential cross section 0-9290
- Pb( $\pi$ , X), 3 GeV/c, n inclusive spectra, neutron yield (Russian) 0-13510
- <sup>210</sup>Po, EC, <sup>204</sup>Bi excited states,  $\gamma$  rays, conversion electrons and  $\gamma\gamma$  coincidences 0-18241
- <sup>210</sup>Po, alpha-decay, population of 0 $^+$  of <sup>206</sup>Pb 0-22775
- <sup>212</sup>Po levels and  $J^\pi$ , weak coupling calc. using realistic matrix elements 0-5068
- <sup>212</sup>Po, shell model  $\alpha$ -spectroscopic factors 0-32245
- Pt, even mass, ground and gamma band EM transition rates, asymmetric rotor model 0-32231
- <sup>191</sup>Pt, A=190, 192, 194, levels and  $\gamma$ -transition reduced probab., interacting boson model 0-18196
- <sup>191</sup>Pt, A=192, 194, 196, rigid asymmetric rotor model descript., E2 and E4 props. 0-13403

## nuclei with mass number 190 to 219 continued

- <sup>191</sup>Pt, A=192, 194, 196, states,  $J^\pi$ , ang. distrib. and transitions, DWBA anal. of Pt(p,t) 0-468
- <sup>190</sup>Pt, collective excitations in the interacting boson model (Russian) 0-5044
- <sup>196</sup>Pt (<sup>20</sup>Ne, <sup>20</sup>Ne'), excited states, lifetime meas. using recoil-distance method 0-13413
- <sup>196</sup>Pt (<sup>58</sup>Ni, <sup>58</sup>Ni'), excited states, lifetime meas. using recoil-distance method 0-13413
- <sup>196</sup>Pt, collective states and static quadrupole moment, boson expansion theory 0-47346
- <sup>196</sup>Pt negative parity states in partially decoupled bands,  $\gamma$ -transitions from <sup>195</sup>Pt(n, $\gamma$ ) 0-47360
- <sup>196</sup>Pt, O(6) symmetry of interacting boson approx. model in shape transition 0-27550
- Pt(l,p), 17 MeV, two neutron transfer strength, O(6) limiting symmetry in 1BA, Os comparison 0-32287
- Ra A (<sup>218</sup>Po) adsorption to monodispersed aerosol 0-32535
- <sup>208</sup>Rn decay, <sup>208</sup>At energy levels and transitions, IC electrons 0-18242
- <sup>210</sup>Rn high spin states, decay and lifetimes, spin assignments from <sup>204</sup>Pb(<sup>6</sup>Be,3n) 0-18168
- <sup>211</sup>Rn, production by photospallation of <sup>232</sup>Th and <sup>238</sup>U 0-52797
- <sup>191</sup>Th, A=212, 213, 214, decay energies and half lives from <sup>176</sup>Hf(<sup>40</sup>Ar,X) 0-47440
- <sup>191</sup>Tl, A=199, 200 cross section and excitation function statistical anal. from <sup>197</sup>Au( $\alpha$ ,xn) (Rumanian) 0-22846
- <sup>192</sup>Tl high spin band struct. and transitions, isomeric state from <sup>181</sup>Ta(<sup>16</sup>O,xn $\gamma$ ) 0-47353
- <sup>194</sup>Tl high spin states, excitation functions, I $^\pi=8^-$  isomeric state from <sup>181</sup>Ta(<sup>16</sup>O,5n) 0-32163
- <sup>199</sup>Tl, production by <sup>197</sup>Au( $\alpha$ , 2n) reaction, medical appls. 0-51245
- <sup>201</sup>Tl  $\gamma$ - and X-ray emission probabilities and half-life obs. 0-32242
- <sup>201</sup>Tl levels, transitions and  $J^\pi$  assignments from <sup>201</sup>Pb decay 0-5099
- <sup>204</sup>Tl, beta ray generated bremsstrahlung yield consts. 0-42588
- <sup>204</sup>Tl,  $\beta$ -decay, branching ratio and K-shell autoionisation 0-42598
- <sup>205</sup>Tl, electric dipole interaction energy from electric dipole hyperfine struct. calc. of TlF 0-53162

## nuclei with mass number 220 or higher

- <sup>239</sup>Pu(n,f), thermal, fission product yield 0-27678
- A=221, nuclear data sheets, levels,  $J^\pi$ , transitions 0-31431
- A=225, nuclear data sheets, levels,  $J^\pi$ , transitions 0-31432
- actinide nuclei, photo- and electro-fission cross sections and yields, giant resonances 0-5187
- CANDU-PHW, neutron group cross sections in resolved resonance region calcs. 0-13573
- even actinides, lowest 0 $^+$  state excitation, collective phonon state, spectroscopic factors from (p,t), (t,p) 0-13410
- Z=103, 105, 107 element prod. from heavy ion fusion, cross sections from statistical model 0-32313
- (n,f) simulated cross sections for exotic actinide nuclei 0-544
- <sup>232</sup>Th( $\alpha$ ,  $\alpha'$ ), coupled channel Born anal. of deformation correl 0-5149
- <sup>227</sup>Ac, spontaneous fission, neutron emission 0-37405
- <sup>227</sup>Ac, high pressure meas. of gamma transitions 0-18225
- <sup>241</sup>Am( $\gamma$ , $\delta$ ) 7-26 MeV, A=241,243, photofission cross section in E1 giant resonance region (Russian) 0-5182
- <sup>241</sup>Am(n,f), thermal, sub-barrier fission fragment energy correlations for A=241, 243 0-42715
- <sup>240</sup>Am $^m$ , spontaneously fissioning isomer optical shift in pumped <sup>8</sup>Sr/<sup>10</sup>P $_{7/2}$  transition, nuclear deformation 0-27971
- <sup>241</sup>Am, gamma ray spectra of reactor fuels 0-42577
- <sup>241</sup>Am-Be neutron spectrum, (n,p) reaction average cross-sections 0-22827
- <sup>241</sup>Am(n,f), 14.8 MeV, mass yield distrib., and absolute fission yield, isomer ratios 0-18352
- <sup>242</sup>Am, mag. dipole moment-atomic electron satellite states, influence on E0 conversion 0-18236
- <sup>241</sup>Am, absolute yields of 43.5, 74.7 and 117.8 keV photons 0-32568
- <sup>241</sup>Am( $\alpha$ ,f), fragment mass distrib., and yield, statistical anal. (Russian) 0-5183
- <sup>241</sup>Am(n,f), thermal neutron induced fission cross section 0-37403
- <sup>242</sup>Am, high pressure meas. of gamma transitions 0-18225
- <sup>240</sup>Bk, A=240, 242, electron capture, delayed fission prob. and fission barrier height (Russian) 0-42722
- <sup>241</sup>Cf, A=244, 248, fission barrier heights from  $\beta$ -delayed fission,  $\beta$ -strength functions struct. 0-5184
- <sup>241</sup>Cf, A=250, 252, 254, spontaneous fission fragment kinetic energy and neutron multiplicity meas. 0-42717
- <sup>250</sup>Cf(d,d'), 15 MeV, vibr. states,  $J^\pi$  and reduced transition probabilities 0-47351
- <sup>251</sup>Cf fission-neutron spectrum unfolding experiment 0-13514
- <sup>252</sup>Cf neutron sources, appls. of activation anal., review 0-18728
- <sup>252</sup>Cf, spontaneous fission, fragment slowing in gases 0-22875
- <sup>252</sup>Cf spontaneous fission, meas. of fission neutron spectra 0-22873
- <sup>252</sup>Cf, spontaneous fission, scission point configuration, evaluation anal. 0-37361
- <sup>252</sup>Cf(n, $\gamma$ ), neutron capture gamma expt. equipment designs 0-52832
- <sup>252</sup>Cf(sf), energy dissipation in fission, comments 0-42719
- <sup>252</sup>Cf(sf), scission, energy dissipation magnitude during descent from saddle point 0-42718
- <sup>252</sup>Cf, spontaneous fission, fission barriers and products 0-18355
- <sup>256</sup>Cf spontaneous fission, mass and kinetic energy distrib. from <sup>254</sup>Cf(t,p) 0-47518
- <sup>240</sup>Cm, A=246,248, fission isomer rot. spectra I $^2$ (1+1) $^2$  correction 0-18229
- <sup>240</sup>Cm(n,f), A=224,246, 0.3-45 MeV, near threshold fission cross section, energy depend. (Russian) 0-37406
- <sup>240</sup>Cm, fission barrier heights from  $\beta$ -delayed fission,  $\beta$ -strength functions struct. 0-5184
- <sup>240</sup>Cm(n,f), thermal neutron induced fission, mass yield obs. 0-32309
- <sup>240</sup>Cm(<sup>216</sup>U,X), 7.5 MeV/amu, three particle exclusive meas. for exit channels fission fragment ang. distrib. 0-13513
- <sup>240</sup>Cm excited and single particle states,  $\gamma$ -transitions from <sup>248</sup>Cm(n, $\gamma$ ) 0-47399
- <sup>240</sup>Cm, A=244, 246, 248, electron capture, delayed fission prob. and fission barrier height (Russian) 0-42722
- <sup>240</sup>Cm, A=255,256, fission barrier first peak height, pot. energy surface struct. 0-42720
- <sup>240</sup>Cm fission coincidence data from d, t, and <sup>3</sup>He induced reactions 0-42720



## nuclei with mass number 220 or higher continued

- <sup>242</sup>Fm, A=258, 259, spontaneous fission, fission barriers and products 0-18355
- <sup>242</sup>Fm(n,f), A=253, 255, 257, 259, fission mass distrib. transition, liquid drop and shell model calcs. 0-32310
- <sup>242</sup>Fm(s,f), A=254, 256, 258, 260, fission mass distrib. transition, liquid drop and shell model calcs. 0-32310
- <sup>248</sup>Fm, fission barrier heights from  $\beta$ -delayed fission,  $\beta$ -strength functions struct. 0-5184
- <sup>255</sup>Fm, fission barrier first peak height, pot. energy surface struct. 0-42720
- <sup>257</sup>Fm, spontaneous fission fragment kinetic energy and neutron multiplicity meas. 0-42717
- <sup>258</sup>Fm, nuclear pressure and fission fragment mass distrib. 0-18356
- <sup>258</sup>Fm spontaneous fission, mass and kinetic energy distrib. from <sup>258</sup>Md<sup>m</sup> decay 0-47518
- <sup>259</sup>Fm spontaneous fission,  $T_{1/2}$  and kinetic energies from <sup>257</sup>Fm(t,p) 0-47517
- <sup>259</sup>Md, A=248, 250, electron capture, delayed fission prob. and fission barrier height (Russian) 0-42722
- <sup>258</sup>Md isomer, EC decay, <sup>258</sup>Fm spontaneous fission, mass and kinetic energy distrib. 0-47518
- <sup>237</sup>Np, criticality anal., possible utilisation in fission reactors 0-621
- <sup>237</sup>Np fission and capture cross sections in GCFR neutron spectra 0-37404
- <sup>237</sup>Np, gamma ray spectra of reactor fuels 0-42577
- <sup>237</sup>Np, quasi-stationary state decay through two bump barrier (Russian) 0-13420
- <sup>237</sup>Np( $\alpha$ ,f), fragment mass distrib., and yield, statistical anal. (Russian) 0-5183
- <sup>238</sup>Np levels, resonances and transitions from <sup>237</sup>Np(n, $\gamma$ ) 0-52589
- <sup>238</sup>Np, high pressure meas. of gamma transitions 0-18225
- <sup>231</sup>Pa, A=236, 238, strength function of  $\beta$ -transitions 0-22764
- <sup>231</sup>Pa, high pressure meas. of gamma transitions 0-18225
- <sup>233</sup>Pa, high pressure meas. of gamma transitions 0-18225
- <sup>233</sup>Pa(n,f), cross sections, semi-empirical formula 0-22864
- <sup>208</sup>Pb(<sup>40</sup>Ca, $\gamma$ ), nuclear pressure and fission fragment mass distrib. 0-18356
- Pu-Th-U, neutron group cross sections in resolved resonance region calcs. 0-13573
- <sup>242</sup>Pu, A=238,240, fission isomer rot. spectra  $I^2(1+1)^2$  correction 0-18229
- <sup>242</sup>Pu, A=238 to 241, gamma ray spectra of reactor fuels 0-42577
- <sup>242</sup>Pu/<sup>238</sup>U, A=240, 242, fission cross section ratio meas. 0.127 to 7.4 MeV 0-5180
- <sup>232</sup>Pu, fission barrier heights from  $\beta$ -delayed fission,  $\beta$ -strength functions struct. 0-5184
- <sup>239</sup>Pu fission single particle isomers, half lives and isomeric ratio from <sup>239</sup>Pu( $\gamma$ ,2n) 0-18181
- <sup>239</sup>Pu(n,f), 10 eV-100 keV, fission cross section 0-27681
- <sup>239</sup>Pu, absolute fission yield meas. by track-etch-cum- $\gamma$ -spectrometry method 0-27859
- <sup>239</sup>Pu, high pressure meas. of gamma transitions 0-18225
- <sup>239</sup>Pu( $\alpha$ ,f), 19-27 MeV, integral and differential cross sections, anisotropy energy depend. (Russian) 0-37407
- <sup>239</sup>Pu(n,f), undisturbed resonance integral determ., and neutron flux meas. 0-5453
- <sup>239</sup>Pu(n,X), nuclear reaction statistical model parameters (Russian) 0-18280
- <sup>239</sup>Pu(n,X), thermal n, gamma spectra from capture, fission and fission products 0-37352
- <sup>239</sup>Pu(n,f), 0.005-0.4 eV, fission fragment average kinetic energies in resonance region 0-18358
- <sup>239</sup>Pu(n,f), cross section, parameter testing in statistical model (Russian) 0-52653
- <sup>239</sup>Pu(n,f), effective cross section dependence on thermal neutron temp. 0-547
- <sup>239</sup>Pu(n,f) 0-37405
- <sup>239</sup>Pu(n,f) 0.009-0.6 eV cross-section, Westcott factor 0-546
- <sup>240</sup>Pu fission total kinetic energy release, excitation energy depend., scission point anal. of <sup>241</sup>Pu(<sup>He</sup>,af) 0-18351
- <sup>240</sup>Pu, hexadecapole shape isomeric state, shell correction method fission barrier calcs. 0-545
- <sup>242</sup>Pu half life relative to <sup>238,239</sup>Pu,  $\alpha$ -activity and atom ratios 0-5100
- <sup>242</sup>Pu+n, 10 keV-20 MeV, ENDF/B-V cross sections 0-22837
- <sup>242</sup>Pu( $\alpha$ ,f), fragment mass distrib., and yield, statistical anal. (Russian) 0-5183
- <sup>246</sup>Pu excited states, mass excess and shell gap, L=0 transition from <sup>244</sup>Pu(t,p) 0-9236
- <sup>242</sup>Pu( $\gamma$ , $\gamma$ ) 12.754 MeV, Delbruck scatt., Coulomb correction terms, differential cross sections 0-27629
- <sup>242</sup>Pu(n,f), 0-18 MeV, prompt neutron spectrum, evaporation model (Chinese) 0-42721
- <sup>225</sup>Ra rotational band level diagram from  $\alpha$ -decay and conversion electrons 0-18156
- <sup>226</sup>Ra decay chain,  $\gamma$ -ray energies meas. for Ge(Li) detector calibration 0-27865
- <sup>222</sup>Rn, and its descendants, radioactivity in low atmosphere, pollution-dust dynamics (Rumanian) 0-12524
- <sup>222</sup>Rn, release to atm. due to UK coal combustion, annual rate of release determ. 0-17143
- <sup>224</sup>Rn-<sup>224</sup>Fr-<sup>224</sup>Ra decay,  $\gamma$ -rays IC electrons and e $\gamma$  coincidences 0-18239
- Th-U, neutron group cross sections in resolved resonance region calcs. 0-13573
- Th-U-Pu, neutron group cross sections in resolved resonance region calcs. 0-13573
- <sup>228</sup>Th, high pressure meas. of gamma transitions 0-18225
- <sup>230</sup>Th(n, $\gamma$ ), 680-1050 keV, fission barriers and cross sections, fragment ang. distrib. 0-18357
- <sup>231</sup>Th, rotational band level diagram from  $\alpha$ -decay and  $\gamma$ -transitions 0-18156
- <sup>232</sup>Th(e, $\gamma$ ), 7-65 MeV, absolute electrofission cross sections, fragment ang. distrib. 0-5185
- <sup>232</sup>Th, fission barrier heights from  $\beta$ -delayed fission,  $\beta$ -strength functions struct. 0-5184
- <sup>232</sup>Th, mirror hybrid reactors 0-42860
- <sup>232</sup>Th, neutron cross section meas. 0-526
- <sup>232</sup>Th, photofission, determ. of neutron multiplicities 0-32311
- <sup>232</sup>Th target nucleus spallation, <sup>10</sup>He isotope search (Russian) 0-5110
- <sup>232</sup>Th+<sup>40</sup>Ar(<sup>63</sup>Cu), deep inelastic reactions, isotopic distrib., n excess degree of freedom relaxation 0-9308

## nuclei with mass number 220 or higher continued

- <sup>232</sup>Th+n, 0.1-18 eV, neutron total cross section determ. 0-22838
- <sup>232</sup>Th(<sup>16</sup>O, $\gamma$ ), transfer induced fission, excitation functions and cross sections 0-13515
- <sup>232</sup>Th(<sup>19</sup>F, $\gamma$ ), transfer induced fission, excitation functions and cross sections 0-13515
- <sup>232</sup>Th( $\alpha$ , $\alpha'$ ), 120 MeV, isoscalar giant resonances, DWBA anal. 0-42621
- <sup>232</sup>Th( $\alpha$ , $\alpha'$ ), total kinetic energy release 0-27682
- <sup>232</sup>Th( $\alpha$ ,f), 19-27 MeV, integral and differential cross sections, anisotropy energy depend. (Russian) 0-37407
- <sup>232</sup>Th( $\alpha$ ,x), 140 MeV, spallation and fission product yields 0-13512
- <sup>232</sup>Th( $\gamma$ ,f), deep subthreshold photofission, double humped fission barrier anal., shape isomer 0-5179
- <sup>232</sup>Th(n,f), cross sections, semi-empirical formula 0-22864
- <sup>232</sup>Th(n, $\gamma$ ), effective cross section dependence on thermal neutron temp. 0-547
- <sup>232</sup>Th(p,f), 35-85 MeV, light mass nuclide charge dispersion curves for A=76-79 0-18349
- <sup>232</sup>Th(p,X), 10-100 MeV, spallation residue excitation functions, fissionability 0-18353
- <sup>232</sup>Th(p,f), 9.5-17 MeV, symmetric to asymmetric mass ratios for fragments 0-5178
- <sup>232</sup>Th(p,p'), 35 MeV, ground state rot. band and multipole moment 0-32178
- <sup>232</sup>Th( $\pi^-$ ,f), resting pions, delayed fission search (Russian) 0-52704
- U (M,f), muon excitation probabilities, muonic atoms, Schrodinger eqn. 0-47515
- U-Th, neutron group cross sections in resolved resonance region calcs. 0-13573
- U+<sup>20</sup>Ne, quark matter, signature in nuclear fireball model 0-37395
- U(Ne,X), 250, 400 MeV/N direct vs. thermal particle emission, inclusive cross sections 0-52688
- U(Ne,n)X, 337 MeV/N inclusive double differential neutron prod. cross sections 0-32294
- <sup>235</sup>U, A=235, 236, 238, determ. of neutron multiplicities 0-32311
- <sup>235</sup>U, A=236, 238, strength function of  $\beta$ -transitions, probability of delayed fission 0-22764
- <sup>235</sup>U, A=236,238, fission isomer rot. spectra  $I^2(1+1)^2$  correction 0-18229
- <sup>235</sup>U( $\alpha$ , $\alpha'$ ), A=234, 236, 238, coupled channel Born anal. of deformation correl 0-5149
- <sup>235</sup>U( $\alpha$ ,f), A=235,238, 19-27 MeV, integral and differential cross sections, anisotropy energy depend. (Russian) 0-37407
- <sup>235</sup>U( $\gamma$ ,f), A=235, 236, 238, deep subthreshold photofission, double humped fission barrier anal., shape isomer 0-5179
- <sup>235</sup>U(n,X), A=233, 235, thermal n, gamma spectra from capture, fission and fission products 0-37352
- <sup>232</sup>U half-life from specific and relative activity methods 0-9270
- <sup>232</sup>U, high pressure meas. of gamma transitions 0-18225
- <sup>232</sup>U high spin states and ground state rot. band from <sup>232</sup>Th( $\alpha$ ,n $\gamma$ ) 0-47349
- <sup>233</sup>U fission by polarised neutrons, P odd asymmetry of emitted fragments (Russian) 0-18354
- <sup>233</sup>U, gamma ray spectra of reactor fuels 0-42577
- <sup>233</sup>U( $\alpha$ ,X), 28-140 MeV, scatt. and fission reaction mechanisms, cross sections 0-18350
- <sup>233</sup>U(n,f), effective cross section dependence on thermal neutron temp. 0-547
- <sup>235</sup>U, absolute fission yield meas. by track-etch-cum- $\gamma$ -spectrometry method 0-27859
- <sup>235</sup>U, muonic, fission studies, target preparation 0-23217
- <sup>235</sup>U, thermal neutron irr., fission product decay power calc. 0-22868
- <sup>235</sup>U<sup>m</sup> prod. by nuclear excitation by electron transition in plasma 0-22668
- <sup>235</sup>U( $\gamma$ ,f), 12-70 MeV bremsstrahlung, product yields and  $\gamma$ -spectra 0-42716
- <sup>235</sup>U( $\gamma$ ,f), 20 MeV, long range  $\alpha$ -particle spectrum 0-47516
- <sup>235</sup>U(n,2n), threshold to 13 MeV, cross section meas. by Gd loaded liquid scintillator 0-52669
- <sup>235</sup>U(n, $\alpha$ ), thermal fission neutron spectrum 0-42712
- <sup>235</sup>U(n,f), 0.6, 7 MeV, fission neutron spectra meas. 0-22872
- <sup>235</sup>U(n,f), effective cross section dependence on thermal neutron temp. 0-547
- <sup>235</sup>U(n,f), fission fragment average kinetic energies in resonance region 0-18358
- <sup>235</sup>U(n,f), sensitivity of decay power to uncertainties in estimated decay data 0-22932
- <sup>235</sup>U(n,f), thermal, appl. of  $\bar{v}$  constraint to fission product yields 0-22874
- <sup>235</sup>U(n,f), thermal, Rb and Cs relative and independ. fission yields 0-27679
- <sup>235</sup>U(n,f), time correlated associated particle method, CAMAC experiment 0-52702
- <sup>236</sup>U fission shape isomer,  $\gamma$ -decay from <sup>238</sup>U( $\gamma$ ,2n) 0-18230
- <sup>236</sup>U fission total kinetic energy release from <sup>235</sup>U(d,pf) 0-27682
- <sup>236</sup>U, giant E2 isoscalar resonance determ. 0-27607
- <sup>236</sup>U low lying levels from <sup>4-</sup> isomer decay in (n,e), (n, $\gamma$ ) 0-47396
- <sup>236</sup>U, nuclear matter density distrib., in asymmetric two centre shell model 0-32209
- <sup>236</sup>U, nuclear pressure and fission fragment mass distrib. 0-18356
- <sup>236</sup>U( $\alpha$ , $\alpha'$ ), total kinetic energy release 0-27682
- <sup>236</sup>U(n,f), fast n, fragment mass and kinetic energy distrib. (Russian) 0-5181
- <sup>237</sup>U levels, bands and J $^\pi$  assignments, n binding energy from <sup>236</sup>U(n, $\gamma$ ) 0-5041
- <sup>237</sup>U virtual photon excited state decay and total cross section of <sup>238</sup>U(e,n) 0-22757
- <sup>238</sup>U(e,f), 7-65 MeV, absolute electrofission cross sections, fragment ang. distrib. 0-5185
- <sup>238</sup>U, mirror hybrid reactors 0-42860
- <sup>238</sup>U, muonic, fission studies, target preparation 0-23217
- <sup>238</sup>U neutron cross sections evaluation for incident neutron energies up to 4 keV 0-5146
- <sup>238</sup>U, neutron resonance parameters, time-of-flight spectroscopy 0-47375
- <sup>238</sup>U thin self supporting foils 0-9440
- <sup>238</sup>U+<sup>20</sup>Ne(<sup>40</sup>Ar), 250-1000 MeV/N, intranuclear cascade calcs. for multiplicity and cross sections 0-32300
- <sup>238</sup>U+<sup>32</sup>S(<sup>40</sup>Ar), deep inelastic reactions, isotopic distrib., n excess degree of freedom relaxation 0-9308
- <sup>238</sup>U+<sup>58</sup>Ni(<sup>70</sup>Zr), fission phenomena in deep inelastic collisions 0-5186
- <sup>238</sup>U(<sup>16</sup>O,f) 20 MeV/N, light particle spectra in central and peripheral collisions 0-5177
- <sup>238</sup>U(<sup>184</sup>W,f), Coulomb fission excitation function, cross section 0-5176



**nuclei with mass number 220 or higher continued**

- $^{238}\text{U}$ ( $\alpha$ ,X), 7.42 MeV/u, charge, kinetic energy and ang. distrib. of products 0-539  
 $^{238}\text{U}$ ( $^{238}\text{U}$ ,X), 7.5 MeV/amu, three particle exclusive meas. for exit channels fission fragment ang. distrib. 0-13513  
 $^{238}\text{U}$ ( $^{238}\text{U}$ ,X), 7.5 MeV/A, 3-dimens. TDHF-BCS model calcs., possible fission 0-52694  
 $^{238}\text{U}$ ( $^{238}\text{U}$ ,X), damped collision, proton and neutron exchange correlations 0-18335  
 $^{238}\text{U}$ ( $^{48}\text{Ca}$ , $\gamma$ ), nuclear pressure and fission fragment mass distrib. 0-18356  
 $^{238}\text{U}$ ( $^{56}\text{Fe}$ ,X), 538 MeV, binary coincident fragments, fragment mass and energy, fission following fusion 0-548  
 $^{238}\text{U}$ (Hf,f), Coulomb fission cross sections from coupled channel calcs. 0-9319  
 $^{238}\text{U}$ (P,X), 11.5 GeV, heavy fragment energies and masses, reaction mechanism 0-5140  
 $^{238}\text{U}$ ( $\alpha$ ,f), 100-1000 MeV, resonance production 0-52658  
 $^{238}\text{U}$ ( $\alpha$ ,f), fragment mass distrib., and yield, statistical anal. (Russian) 0-5183  
 $^{238}\text{U}$ (e,e'), 87.5 MeV, deformed fissionable nucleus, giant multiple resonances and isovector states 0-42612  
 $^{238}\text{U}$ (e,e'), 5.5-9 MeV, fission fragment ang. distrib. DWBA anal., low lying fissioning levels 0-42713  
 $^{238}\text{U}$ ( $\gamma$ ,f), 12-70 MeV bremsstrahlung, fragment mass and energy distrib. 0-27680  
 $^{238}\text{U}$ ( $\gamma$ ,f), 20 MeV, fission product yields, charge distrib. 0-42533  
 $^{238}\text{U}$ ( $\gamma$ , $\gamma$ ), 15 MeV, elastic and nuclear Raman scatt. 0-22811  
 $^{238}\text{U}$ (n,f), 14.5 MeV, neutron emission, mass distrib. and energetics 0-47512  
 $^{238}\text{U}$ (n,f), 7 MeV, fission neutron spectra meas. 0-22872  
 $^{238}\text{U}$ (n, $\gamma$ ), 2, 24 keV, resonance averaged  $\gamma$ -spectra, level and J<sup>\*</sup> appls. 0-37347  
 $^{238}\text{U}$ (n, $\gamma$ ), cross section and resonance shape, gas molecule vibr. effects 0-42661  
 $^{238}\text{U}$ (n, $\gamma$ ), effective cross section dependence on thermal neutron temp. 0-547  
 $^{238}\text{U}$ (p,X), 0.8-11.5 GeV, formation of A=131 isobaric nuclides 0-9293  
 $^{238}\text{U}$ (p,X), 0.8-400 GeV, Sc fragment differential ranges and energy spectra 0-42666  
 $^{238}\text{U}$ (p,X), 400 GeV/c, unusual backward enhancement in product ang. distrib. 0-514  
 $^{238}\text{U}$ (p,f), 9.5-17 MeV, symmetric to asymmetric mass ratios for fragments 0-5178  
 $^{238}\text{U}$ (p,f) 12 MeV, estimation of neutron yield from individual fragment in medium-excitation fission 0-542  
 $^{238}\text{U}$ (p,p'), 22 MeV, rot. band, multipole deformation parameters from coupled channel anal. 0-13369  
 $^{238}\text{U}$ (p,p'), 35 MeV, ground state rot. band and multipole moment 0-32178  
 $^{238}\text{U}$ ( $\pi^-$ , f), resting pions, delayed fission search (Russian) 0-52704  
 $^{239}\text{U}$ , neutron binding energy precision meas. 0-18182  
 $\text{U}(\gamma,\gamma)$ , neutron capture  $\gamma$ -ray Rayleigh scatt. 0-52661  
 $\text{U}(\gamma,n)$ , 30 to 140 MeV, partial photoneutron cross section, total cross section approx. 0-22809  
 $\text{U}(n,f)$ , 0-18 MeV, prompt neutron spectrum, evaporation model (Chinese) 0-42721  
 $\text{U}(p,f)$ , 600 MeV, fragment energies, cross sections level density and barrier heights 0-42723  
 $\text{U}(\pi^-,X)$ , 3 GeV/c, n inclusive spectra, neutron yield (Russian) 0-13510

**nucleic acids** see *macromolecules*

**nucleon interactions** see *hyperon-nucleon interactions; kaon-nucleon interactions; lepton-nucleon interactions; muon-nucleon interactions; neutrino-nucleon interactions; nucleon-nucleon interactions; nucleon-nucleus reactions; photon-nucleon interactions; pion-nucleon interactions*

**nucleon-nucleon interactions**

- see also *nucleon-nucleon scattering; proton-proton interactions*  
 $(\pi,\pi^-)$ , inelastic scatt. in Fermi liquid, nucleon-nucleon interaction effects 0-22862  
backward production on nuclei and the tube model, comments 0-52544  
constituent quark model and production of particles from nuclear targets 0-380  
many body effective interaction theory problem, comparison with atoms 0-47406  
meson exchange 0-32195  
nonrelativistic QCD, short range NN interaction 0-32200  
nuclear collisions, pion multiplicity and nonlinear effects in pion production, NN inelastic interactions (Russian) 0-52637  
nuclear forces, nonrelativistic quark model study, resonating group method 0-47403  
one boson exchange model, OZI rule, nucleon-nucleon-boson coupling 0-32066  
one-boson-exchange-potential model of baryon-baryon scatt. 0-13295  
Paris NN pot. parametrisation, phase shifts, nuclear matter binding energy 0-47405  
realistic NN pot. construction for three body systems and nuclear matter 0-22699  
Reid soft core potential, low-rank separable matrix formalism 0-22704  
resonance-nucleon and particle beam-nucleon scatt. cross sections (Russian) 0-32115  
separable nucleon-nucleon potentials and minimal relativity 0-27495  
valence nucleon effective interactions 0-9244  
NN charge symmetry breaking, nn and pp scatt. length difference, meson mixing 0-13325  
nN in nuclei, 200 GeV/c, inclusive backward prod., collective tube model 0-47338  
NN interaction in pion exchange, nuclear matter and pion condensation, review 0-42557  
NN $\rightarrow$ N(N $\pi$ ) diffractive dissociation process, one pion Regge-pole exchange amplitude (Russian) 0-42491  
NN $\rightarrow$ N $\pi$ N, 9 GeV/c, isospin cross sections, differential anal. 0-431  
NN potential, imaginary part 0-32118  
NN potential short range behaviour with the quark model 0-47409  
NN resonances and total cross sections, expt. evidence review 0-42558  
NN short range interaction, six quark symmetry props., nucleon colour mag. attraction (Russian) 0-42411  
NN $\rightarrow$ X, nuclear size dependence of particle prod., hydrodynamical model 0-22593  
Np $\rightarrow$ (N $\pi$ )p, diffraction dissociation, absorptive effects 0-5009

**nucleon-nucleon interactions continued**

- p(p)N,  $\psi$  hadronic prod., lepton pair ang. distrib., cross section  $\chi$  contribution 0-42487  
pd $\rightarrow$  $\pi^+$ , 750 MeV, T=1 NN phase shifts and total cross section 0-22630  
pN, 28 GeV in Cu, prompt neutrinos and penetrating particles 0-47336  
pN, 29.4 GeV,  $\Sigma$  and  $\Xi$  prod. ratios 0-42457  
pN, 300 GeV, quark fragmentation functions in additive model 0-37222  
pN, 400 GeV/c in emulsion, ang. and rapidity distrib. 0-32140  
pN, dilepton production by pol. protons, parity violating, asymmetry, Weinberg-Salam calcs. 0-42488  
pN, pN, 200 GeV/c, dimuon prod. cross section, Drell-Yan predictions, struct. functions 0-37300  
pN, W boson and lepton pair prod. off nuclei, cross section enhancement 0-5014  
pN in Fe, 400 GeV/c, bottom meson prod. search in multimuo final states 0-47334  
pN $\rightarrow$  $\Lambda^0$ X, 28.5 GeV/c,  $\Lambda^0$  polarisation 0-32137  
pN $\rightarrow$  $\mu$ X, 350 GeV p-Fe collisions, prompt muon prod. rate 0-37311  
pN $\rightarrow$  $\pi^0$ X, 200-400 GeV/c, inclusive  $\pi^0$  prod. over large  $X_T$  and  $X_F$  ranges 0-37310  
pN $\rightarrow$  $\pi$ X, intermediate  $\bar{p}$  contrib. to backward  $\pi$  prod. (Russian) 0-13326

**nucleon-nucleon scattering**

- see also *neutron-proton scattering; nucleon-nucleon interactions; proton-proton scattering*  
resonance degrees of freedom in the two-nucleon system 0-5072  
Saito potential, off-energy-shell unitarity 0-18207  
spin effects, QCD quark and gluon interactions 0-22577  
two component Pomeron,  $\pi$ N, kN, NN forward scatt. amplitudes 0-37245  
Nd $\rightarrow$ (N $\pi$ )d, ISR energies, single and coherent nucleon diffraction dissociation 0-22640  
NN elastic scatt. with one boson exchange, Bethe-Salpeter eqn. 0-42485  
NN potentials for bound and scattering states 0-47323  
NN system, quasi-nuclear over-threshold resonance, annihilation effects (Russian) 0-27521  
pN, high energy polarised scatt. particle struct. studies, book 0-41952

**nucleon-nucleus reactions**

- for *inelastic nucleon-nucleus scattering*, see "nucleon-nucleus scattering"  
see also *neutron-nucleus reactions; nucleon-nucleon interactions; proton-nucleus reactions*  
cluster production in hadron-nucleus interaction at cosmic-ray energies 0-13467  
inelastic collisions of light nuclei and nucleon-nucleus collisions, dynamical model (Russian) 0-37356  
nuclear matter, charge constrained coherent pion states from transversing fast nucleon 0-27585  
off energy two body t-matrix in the R-matrix theory (Russian) 0-22780  
(N,X), complex shell model, narrow resonances and bound states (Chinese) 0-42622  
 $^2\text{H}+\text{p}(n)$ , differential cross sections, Coulomb penetration factor in DWBA calc. (Chinese) 0-27603

**nucleon-nucleus scattering**

- see also *neutron-nucleus scattering; nucleon-nucleon scattering; proton-nucleus scattering*  
nucleon optical pot., spin-orbit term 0-27606  
 $\Delta(33)$  interaction with nucleus, effective shell model pot., pion scatt. test 0-32202

**nucleons**

- see also *neutrons; protons*  
dimensions, mass, elec. and mag. moments (French) 0-13305  
elastic form factor, exclusive and almost exclusive process asymptotic behaviour, renormalisation group 0-42464  
structure function determination from  $\mu$ N inclusive scatt. meas. 0-42472  
SU(5) grand unification, nucleon lifetime, bag model calc. 0-52450

**nucleosynthesis**

- anomalous nuclei, primordial synthesis 0-46719  
cosmic ray source material synthesis, evidence from Ne, Mg and Si isotopes meas. 0-51631  
cosmological, conventional and unconventional 0-46722  
D-D cross sections for thermonuclear synthesis 0-18608  
galactic nucleosynthesis, rel. to metal-poor stars O abundances 0-36610  
galaxy chemical evolution, O and N abundance 0-46680  
isotopic anomalies from neutron reactions during stellar explosive C burning 0-12651  
massive stars, effects of binary evolution on heavy elements prod. 0-46534  
massive stars and metal production 0-51741  
massive stars nucleosynthesis, effect of mass loss on chemical yields 0-36614  
meteorites, isotope abundance anomalies, astrophysical implications 0-46511  
noble gases isotopic anomalies in Murchison meteorite, evidence for stellar condensates 0-41772  
reactions producing D, T, and  $^3\text{He}$  in advanced stellar evolution, cross sections 0-56815  
resonant thermonuclear reaction rate integrals, closed-form evaluation and approximation considerations 0-8535  
s-process and nuclear correction factor for Re/Os cosmochronology 0-17485  
s-process calcs. and Ba II stars 0-56824  
s-process nucleosynthesis in giant stars, implications of Ti isotopic abundance ratios 0-26840  
s-process nucleosynthesis in U Aquarii, rel. to extraordinary comp. 0-17588  
stellar, A>20 nuclei in advanced stellar evolution and supernovae 0-41817  
stellar nucleosynthesis, cosmochronology after Allende 0-4462  
stellar nucleosynthesis, effect of mass loss by stellar wind on Galaxy chemical enrichment 0-41814  
stellar nucleosynthesis in irregular and blue compact galaxies, rel. to chemical comp. and evolution 0-36711



**nucleosynthesis continued**

- supernovae nucleosynthesis, implications for solar system origin 0-17509  
 thermonuclear flashes on accreting neutron stars 0-31321  
 Tycho supernova, Type I supernova, nucleosynthesis rel. to remnant elemental abundances 0-46635  
 (n, $\gamma$ ) for A=138-181, stellar nucleosynthesis and s-process neutron flux 0-42663  
<sup>26</sup>Al nucleosynthesis, astrophysical aspects of <sup>25</sup>Mg(p, $\gamma$ ) 0-42624  
 H burning in C-O dwarf degenerate envelope 0-17585  
 He, C-O dwarf degenerate envelope (*Russian*) 0-17585  
 He core flash onset and <sup>12</sup>C( $\alpha,\gamma$ )<sup>16</sup>O in low-mass stars 0-51735  
 He shell burning, thermal pulses in accreting white dwarf 0-22009  
 He shell flashes in red supergiants, convective penetrations and observable effects 0-51755  
 Li in weak G-band stars, spallative origin 0-51752  
 Li production by weak G-band stars, results from abundance meas. 0-41819  
 Mg, stellar nucleosynthesis rel. to isotopic abundances in G and K dwarf stars 0-51757  
 N, in planetary nebula in irregular galaxy NGC 6822, abundance and nucleosynthesis 0-41867  
<sup>22</sup>Ne anomalous abundance in Orgueil meteorite, evidence for presolar grains 0-41773  
 O, in supernova remnant in NGC 4449, abundance rel. to nucleosynthesis 0-56895  
<sup>A</sup>Os(n, $\gamma$ ), A=186-188, 2.6-800 keV, capture Maxwellian cross sections, galactic nucleosynthesis 0-42664

**nucleus**

- see also hypernuclei; nuclei with mass number 150 to 189; nuclei with mass number 190 to 219; nuclei with mass number 1 to 5; nuclei with mass number 20 to 38; nuclei with mass number 220 or higher; nuclei with mass number 39 to 58; nuclei with mass number 59 to 89; nuclei with mass number 6 to 19; nuclei with mass number 90 to 149  
 No entries

**number theory**

- see also digital arithmetic  
 education, Fibonacci numbers, recurrence relation soln., combinatorics function anal. 0-51988

**numerical analysis**

- see also approximation theory; curve fitting; difference equations; error analysis; finite element analysis; function approximation; functional analysis; functional equations; interpolation; iterative methods; Monte Carlo methods  
 Abel integral eqn. inversion in astrophysical problems 0-26732  
 aerodynamics, discrete vortices method and multidimensional singular integral eqns. theory 0-19421  
 air-H<sub>2</sub>O injection into permeable bed for underground coal gasification, numerical model 0-30359  
 airdroplet flight in air, drift loss from spray cooling pond, numerical estimation 0-19471  
 amplified spontaneous emission in spherical and disk-shaped laser media 0-1177  
 atmosphere numerical model, modified forward-backward scheme for two-grid-interval noise 0-26575  
 atmosphere O<sub>3</sub> production transport and distribution, numerical simulations with global general circulation model 0-56544  
 atmosphere spectral energetics, determ. via numerical filtering anal. 0-26577  
 atmospheric pollution, photochemical numerical model 0-40943  
 atom models, ionisation time depend. under intense EM fields 0-32683  
 band struck. in 1-D, continued fraction approach 0-6694  
 Baneberry nucl. explosion, numerical simulation 0-841  
 beam-like lattice trusses, prediction of thermoelastic and free vibration responses 0-14566  
 beams, dynamic plastic response, rotatory inertia and transverse shear effects 0-5947  
 blunt body, boundary and wake, supersonic viscous gas flow, numerical soln. 0-38441  
 blunt body, unsteady supersonic flow, grid characteristic method 0-38442  
 cavitation gas bubble in compressible liquid, influence of inhomogeneous sound field on motion 0-6131  
 cavities, advanced numerical anal. of 2-D time depend. free convection 0-43704  
 celestial mechanics, rectilinear isosceles restricted problem, numerical study 0-4242  
 composite, laminate, crack normal to interface, impact response 0-14628  
 composite, layered, Love wave diff. by stress-free crack in plane interface 0-33501  
 compressed air energy storage, anal. of moist air cycling in porous rock reservoirs 0-30575  
 control jets, gasdynamic features, 3-D subsonic and supersonic flows 0-6112  
 convection, natural, three-dimens. analysis in inclined channel with square cross section 0-14546  
 convection, turbulent, numerical models based on unsteady Navier-Stokes eqns. 0-38415  
 Coulomb off shell two body amplitudes, numerical computation 0-46858  
 critical phenomena, renormalisation group theory, numerical method for calc. of free energy and correl. length of generalised Ising model 0-4664  
 crystallisation, directed, 2-D approx., numerical soln. 0-15021  
 current generation by RF travelling waves in tokamaks, numerical anal. 0-1800  
 cylinder, circ., impulsively started from rest, heat transfer, numerical anal. 0-10248  
 dielectric relaxation, Williams-Watts type, normalised complex permittivity, num. table 0-7287  
 discrete kinetic theory, maths. and numerical aspects, Couette flow appls. 0-19413  
 duct, curved transition type, three-dimens. turbulent subsonic flow calc. 0-38498  
 duct noise radiation, aircraft turbojet and turbofan engines 0-23834  
 duct with abrupt enlargement, transonic flow, self-excited oscills., model calcs. 0-28522  
 earth mantle connection, numerical anal. 0-51371  
 elastic linear collisions, dynamic solns., for teaching 0-17769  
 electromagnetic fields, Green function selection and effects on matrix condition 0-14271  
 electron beam, relativistic, fields excited near plane magnetodielectric slab 0-18986

**numerical analysis continued**

- EPR spectra, significance plots use 0-22409  
 external disturbance transformation into boundary layer waves 0-28523  
 extremum position and confidence limits, determ. of absorpt. max. in wide bands 0-22188  
 FBR safety calculations, numerical mixing errors in Eulerian calculations of coupled thermohydrodynamic motions 0-47553  
 fibrous composite, thermal crack propagation anal. 0-10205  
 fission reactor LOCA, AA 0-18528  
 flexural deformation of structural anisotropic domes composed of cylindrical shells 0-19260  
 flow, Ekman boundary layer, incompressible, nonlinear stability, numerical soln. 0-38378  
 flow, in pipe, turbulent, perturbed by sudden enlargement 0-19354  
 flow, in two-dimens. channel, turbulent, with separation 0-19356  
 flow, inviscid, hyperbolic, computational algorithms tests 0-27140  
 flow, past arbitrary body, unsteady, inviscid incompressible, numerical soln. 0-28509  
 flow, rotating, nonstationary eqns. soln., appl. to flow between discs 0-28516  
 flow, separating incompressible laminar boundary layer, over smooth step of small height 0-19325  
 flow, viscous, time-dependent, integral representation approach to simulation 0-38375  
 flow between concentric rot. spheres, nonlinear, axisymmetric 0-19412  
 flow through porous media, 2-D nonisothermal filtration 0-6137  
 galactic cosmic ray modulation, numerical models of particle drift effect on cosmic ray transport 0-31180  
 galaxy triaxial model, nonexistence of three-dimensional tube orbits around intermediate axis 0-22046  
 Galileo's two bodies falling through air, numerical anal. for teaching 0-17755  
 gas centrifuge, numerical anal. of weakly compressible rotating flows 0-47726  
 gas dynamics, self-adapted algorithms 0-38432  
 Gaussian integrals, evaluation by backwards recursion or Taylor expansion 0-31488  
 geophysical prospecting, galvanic effects calc. via method of sub-areas 0-56348  
 geothermal steam pipeline network, numerical simulation 0-40822  
 gravity 5° mean anomalies, recovery from ATS 6/Geos 3 satellite to satellite range-rate obs. 0-41366  
 Hamiltonian, Henon-Heiles, survey and applications to related examples 0-8917  
 heart valves, blood flow, vortex-grid method 0-41105  
 heavy particle scatt. in solids, classical deflection ang. using Brinkman pot., numerical calc. 0-11525  
 horizontal falling wire, max. strain due to instantaneous avert of its ends 0-28418  
 hydrodynamic neutral stability curves, analytic approach, book contrib. 0-1529  
 hydrodynamic stability computation, algorithm construction 0-19329  
 hypersonic boundary layer eqns. including chemical reactions, numerical error control, book contrib. 0-1699  
 ideal gas in ejector nozzles, theory of combined flow of high/low pressure streams 0-6123  
 inelastic numerical analysis for quasistatic and dynamic problems 0-19233  
 inhomogeneous materials, elastic deform. under multiaxial stress, analytical relations 0-44247  
 internal waves, nonlinear, stationary, in shallow seas, anal. for Baltic Sea 0-17292  
 interstellar turbulent 0-56910  
 jet, axisymmetric free shear flow with Reynolds stress closure 0-19469  
 large strain inelastic anal., dynamic problems 0-38278  
 laser with saturable absorber, stationary state, nondiffusive approx. 0-19076  
 latent heat solar energy storage system, heat transfer eqns., numerical soln. 0-55926  
 Lotka-Volterra eqns. with stochastic approx., numerical soln. 0-8912  
 magnetic domain wall mass at high vel., numerical anal. 0-11217  
 magnetosphere time-dependent heat energy eqns., numerical soln. 0-21875  
 maximum likelihood method, for galaxies distrib. determ. in clusters 0-56954  
 micromagnetism, numerical calcs. 0-11222  
 migmatite rise, numerical expts. based on continuum dynamics 0-51381  
 molecular dynamic simulation, event scheduling 0-49069  
 monsoon circulations simulation 0-21812  
 multi-frequency EM system, numerical modelling 0-56623  
 multidimensional unsteady laminar flames, scaling transformations for numerical computations 0-19522  
 multiple quadratic regressions, programmable desk calculators in the laboratory 0-42048  
 N-two level atoms, interaction with radiation field in restricted rotating wave approx., numerical anal. 0-5714  
 Navier-Stokes eqns., viscous incompressible liquid flow in plane channel 0-23985  
 Navier-Stokes equation, incompressible, soln. using primitive variables 0-6017  
 nonisoplanatic spectral instruments, num. correction of images formed 0-249  
 nonlinear heat conduction efficient soln. method using modified Crank-Nicolson method 0-1402  
 nonlinear internal waves, turbulence, numerical anal. 0-14721  
 nonlinear resonant propagation of two concomitant optical pulses interacting with three-level atomic system, num. modelling 0-9942  
 nonlinear thermal bending of shallow sandwich shells and flat plates 0-5936  
 nonlinear viscoelasticity, a method of successive approxs., based on nonlinear correspondence principal 0-5953  
 nonstationary viscous flow of thermally conductive gas around semi-infinite plate, numerical anal. 0-6104  
 one-dimensional, in continua, non-propagative modes (*Japanese*) 0-4539  
 oxidation kinetics, C by CO<sub>2</sub>, in Fe-C melts (*Russian*) 0-40680  
 permeable boundaries in multidimensional unsteady flow 0-38490  
 perturbed Stormer problem, long periodic solns. families 0-17440  
 pipes, hydraulic, with nonlinear boundaries, transient waves 0-43722  
 pipes, turbulence and heat exchange 0-24094  
 planetary system accumulation model, numerical expts. results (*Russian*) 0-8557



## numerical analysis continued

plasma trans-relativistic shock relations, numerical solns. 0-31202  
 plate, infinite, with circular disc, tensile and compressive stress problems 0-38255  
 plate bending, numerical soln. by general boundary integral formulation 0-1422  
 plates, annular, dynamic stability numerical soln. (*Polish*) 0-10173  
 plates, thick, thermally loaded, 3-D anal. 0-33459  
 protostellar envelopes of masses 3  $M_{\odot}$  and 10  $M_{\odot}$ , struct. and hydrodynamic evolution 0-36616  
 quantum pendulum under periodic perturbation, stochastic behaviour 0-8834  
 radiant heat exchange modelling in rectangular chamber with attenuating medium 0-33433  
 radiative transfer in diatomic gas, vibr. nonequil., probabilistic modelling 0-33434  
 radiative transfer in nonplane geometry media, approx. and num. methods of eqns. soln. 0-33431  
 radionuclide movement from hypothetical nuclear waste repository 0-16853  
 rarefied gas dynamics projection and variational methods 0-6189  
 rectangular plate, supported at arbitrary number of points, modal constraint method 0-23947  
 Schrodinger equation, solution by hand-held calculator using Euler method of numerical integration 0-52052  
 sea ice, dynamic thermodynamic model 0-51432  
 simplex method solution of inverse ionospheric problem 0-26619  
 sinusoidal complex object with a small phase modulation, Fresnel diffr. patterns, self-imaging 0-43256  
 solar cells, 3-D modelling of comb-shaped cells 0-50973  
 solar corona quasi-static loops, numerical modelling with uniform energy input 0-21958  
 solar heating system components, optimal insulation, numerical sensitivity anal. 0-35745  
 solar stills, design and thermodynamic parameters, numerical anal. 0-55914  
 space probe or meteorite reentry, mass loss and shape change with radiative heating 0-31198  
 spectral line formation in axisymmetric moving envelopes, numerical method and appl. to YY Orionis stars 0-41813  
 star clusters, evolution, Fokker-Planck eqn. numerical integration 0-36675  
 star escape from isolated clusters, numerical methods (*Polish*) 0-26922  
 star formation process simulation, hydrostatic models evolution (*Polish*) 0-21998  
 stars, rigidly rotating, secular instabilities in general relativity, numerical results 0-4342  
 stellar adiabatic non-radial oscillations with moderate or large  $l$ , numerical anal. 0-56819  
 stellarator toroidal field production by modular systems 0-10441  
 Stirling cycle machine anal. using nodal anal. techniques, review 0-30532  
 Stirling heat engine design, isothermal second order calc. method 0-30533  
 stress analysis, elastic half space containing embedded rigid block 0-23890  
 supercritical accretion discs winds struct. and appearance, numerical models 0-21984  
 supersonic blunt body flow of viscous perfect gas and nonequilib. gas mixture 0-28578  
 supersonic flow, linearised, improved higher-order panel method 0-6082  
 supersonic inlet, flowfield computation using bicharacteristics method with shock wave fitting 0-38443  
 suspension deposition in entrance of a diffuser, electrostatic and gravitational effects, laminar flow 0-14785  
 suspensions, deposition in channel entrance, combined influence of diffusion, electricity and gravity 0-1674  
 Takagi-Taupin equations, boundary conditions in numerical integration, appl. to Bragg and Laue cases 0-1886  
 thermoelastoplastic solution for a circular solid cylinder subjected to heating and cooling 0-5952  
 Tokamak, effect of fuel pellet injection velocity on energy parameters 0-32490  
 Tokamak, electrostatic drift waves, numerical anal. of instability and transport 0-48871  
 Tokamaks, high- $\beta$ , MHD stability limits 0-28643  
 transient elasto-dynamic response of circular crack in thick plate under torsion 0-5993  
 transonic free jet, overexpanded two-dimens., eqns. formulation and soln. method 0-6109  
 transonic small-disturbance theory, leading-edge singularity, num. integration methods eval. 0-6080  
 turbulence computation, bispectral meas. 0-38382  
 turbulent boundary layer, nominally steady, two-dimens., vel. and temp. profile prediction method 0-1624  
 turbulent flow, annular, with inner cylinder rot., computation 0-1544  
 turbulent shear flow, large eddy simulation 0-38390  
 turbulent transport eqns. soln. by accurate numerical method 0-28498  
 turbulent two-dimens. recirculating flow, numerical model calcs. 0-19358  
 two-phase flow, two-fluid model calculations, stability problems 0-19489  
 unsteady aerodynamic modelling for arbitrary motions 0-19433  
 Venus rotation, possible dynamical evolution since formation 0-56742  
 vibration analysis of two-layered beam, with unconstrained viscoelastic layer damping (*Japanese*) 0-5968  
 viscoelasticity, nonlinear, stress relaxation, Volterra integral equation, numerical analysis 0-53646  
 viscoelasticity differential eqn. method approximation, for solving dynamic viscoelastic problems 0-14585  
 viscous gas flow computation, grid point condensation, high-order schemes 0-36866  
 weather forecasting, assessment of model initial conditions using satellite imagery 0-31084  
 Wendroff type discrete inequalities and their applications 0-17786  
 wing, 3-dimens. boundary layer calc. method 0-1622  
 wing, supersonic gas flow, numerical method and routine 0-38440  
 CO<sub>2</sub>-N<sub>2</sub>-He, vol. discharge, negative ions effect 0-14956  
 H II regions gas dynamics, two-dimensional axisymmetric calcs. 0-12791  
 HF chemical lasers, numerical anal. of laser generation conditions 0-9872  
 H<sub>2</sub>O, energy levels, triat. large amplitude vibrs. model appl. 0-23392

## numerical control

see also computerised numerical control; digital control; machine tools  
 diamond turning system evolution 0-1369

## numerical methods

see also convergence of numerical methods; predictor-corrector methods  
 aerodynamics, one-dimensional unsteady flow, hyperbolic initial-boundary value problems solution (*German*) 0-6095  
 alpha particle orbits in radially nonuniform slender plasma column, multi-group rep. 0-53921  
 apodizing filters for optimum Sparrow resolution in coherent systems with annular aperture 0-53435  
 atmospheric numerical model (*French*) 0-21814  
 bifurcation theory, applic. to premixed laminar flame modelling 0-16681  
 chemically reacting flows in porous media, numerical solns. 0-43801  
 chemically reactive boundary layer problems with relaxation processes, Enskog-Chapman method modification (*Russian*) 0-19523  
 coarse-mesh eqns. for the numerical soln. of 2nd-order transport eqn. 0-47527  
 complete EM field of dielectric lossy fibre excited by dipole source, numerical calc. 0-43427  
 composite slab with variable cond., transient heat cond. anal. using collocation method 0-10106  
 convective dispersive equation, movement of chemical pollutants in groundwater 0-16855  
 crack stress intensity factor determ., using numerical method (*Italian*) 0-14625  
 creep, numerical solution methods 0-14582  
 creeping flow in closed cylindrical cavity, numerical calculation 0-16976  
 crystal growth, diffusive, numerical soln. accounting for growth rate and surface tension anisotropy 0-33912  
 deconvolution method for X-ray spectra from hot plasma 0-54030  
 differential equations, second-order, degenerative, boundary-value problem solution, asymptotic expansion (*German*) 0-32  
 differential equations solution, free boundary conditions (*German*) 0-35  
 differential equations solution, generalised splines and linear multistage formulae (*German*) 0-34  
 direct reduction method, transfer theory soln. 0-22309  
 drift wave equations, numerical solution by invariant bedding 0-10374  
 elastic prismatic bar, with rigid ends, lower and upper bounds for torsional rigidity 0-48568  
 elasto-hydrodynamic problems for rough bodies with non-Newtonian lubrications (*Ukrainian*) 0-24054  
 electric dipole fields in conducting media, calc. by numerical methods 0-18957  
 electron beam, relativistic, high-current, in microwave linear accelerator, transient behaviour 0-32541  
 Euler-Maclaurin summation rule, anal. of unsteady thermal stress problems 0-48580  
 exterior linear elliptic problem, numerical method, appl. to 2-dimens. wave resistance 0-28485  
 Fermat number transform for microwave holography data processing 0-43298  
 fission gas behaviour model, intragranular, nonequilibrium behaviour, numerical integration 0-32345  
 fluid bifurcation phenomena numerical anal. (*French*) 0-19319  
 fluid dynamics, conference, Tbilisi, USSR (June 1978) 0-17717  
 fluid dynamics, numerical simulation 0-17805  
 Fokker-Planck equatn. solutn. 0-18622  
 fusion reactor blankets, MHD coolant flows, 3-D model 0-23119  
 gas dynamics, numerical investigation by net-characteristic method 0-19420  
 gas flows, selfgravitating, thermodynamic processes and radiation, numerical method 0-14848  
 geosphere transport model for WIPP site, radioactive waste repository 0-16854  
 Hartree-Fock wave function, numerical technique overcoming exchange blowup 0-9485  
 heat transfer optimal control problem, finite element and conjugate grad. methods 0-19220  
 high temp., transport process soln. 0-19559  
 holographic numerical optical processor configurations 0-48194  
 hybrid random choice method for viscous boundary layer 0-38461  
 hydrodynamic stability problems with time-depend. boundary conditions, numerical simulation methods, review 0-19411  
 impulse load effects, EPIC-3 code anal. 0-19293  
 incompressible finite elasticity, method for numerical soln. of problems (*French*) 0-42062  
 inviscid barotropic vorticity eqn., soln. by finite difference, finite element and pseudospectral method 0-43687  
 Ising square frustration model, numerical study of ground state correl. 0-34638  
 isotropic thin shells with circular hole, stress state, numerical investigation 0-48586  
 Korteweg-de Vries equation, numerical methods of solution, difference and transform schemes, accuracy 0-46833  
 Lagrangian method for transonic flow Euler eqns. 0-38435  
 LMFBR, neutron streaming through control rod followers, diffusion coeff. by numerical integration 0-13636  
 LPE layer growth from undercooled melts, numerical model 0-6665  
 maximum entropy method confidence limits 0-22284  
 melt, temp. field calc. by numerical implicit method 0-44342  
 metals, metallic deformation, improved boundary-integral eqn. calc. method 0-28437  
 multi-dimensional solidification, dominated by thermal cond., similarity calc. method 0-38243  
 multicompartment system simulation 0-55976  
 natural three-dimensional convection, strongly implicit algorithms 0-33422  
 neutron transport theory, spatial approximation methods for the  $S_N$  equations in  $x, y$  geometry 0-47525  
 nonlinear medium, mag. field calc. by differential grid method (*Ukrainian*) 0-4555  
 Numerov scheme for Schrodinger eqn. soln. 0-52046  
 ocean waves generation, propagation and dissipation spectral simulation model 0-31060  
 oceanographic circulation partial differential equatns. solution 0-21864  
 optical fibre mode-coupling phenomena anal. using matrix method, accuracy 0-23803  
 optical processing systems, seminar, Huntsville, USA (May 1979) 0-46732



**numerical methods continued**

- oscillators, nonlinear stochastic, triangular wave, optimally controlled, Weiner process and Poisson process, numerical studies 0-52128
- panel method, improved high-order, for linearised supersonic flow 0-6082
- parallel jets systems, aerodynamics calc. (*Bulgarian*) 0-28543
- plane elastostatic boundary value problems, integral operators, eigenvalue num. calc. 0-36848
- plasma, submillimetre diagnostics, active, of Ar arc, data numerical anal. 0-48979
- plastic flow pattern smoothing 0-7625
- plates, thin, converged stress solns. by extended field method 0-38306
- Poisson's equation, linear and nonlinear numerical solution including spatially variable dielectric const. 0-6825
- Poisson summation formula, generalisations 0-4565
- radiative transfer in rectangular enclosures, six-flux model evaluation 0-1415
- radioactive waste migration, groundwater environment, hydrodynamic dispersion in transport models 0-17146
- rotational flow, steady and unsteady, fluid in finite cylindrical container 0-14708
- Schrodinger equation, applications of perturbation theory to numerical integration methods 0-12926
- separated flows, upwind and central difference schemes 0-28539
- shell enclosures, temp. distrib. calcs. under thermal radiation, numerical calcs. 0-38241
- shock wave diffraction on plane with semicircular cylindrical roughness, numerical integration (*Ukrainian*) 0-22201
- space truss analysis in post-buckling range in dual load method 0-38298
- spherical X-ray wave, dynamic diffraction theory, numerical results 0-38867
- spinning wavy axisymmetric body, three-dimens. flow 0-38422
- stenosed tube, numerical solns. of Navier Stokes problems 0-16975
- Stokes stream function, direct soln. method 0-64
- subsurface nuclear waste disposal, groundwater modelling 0-16852
- supersonic laminar viscous flow, partial differential eqns., separation 0-24062
- Tikhonov regularizing algorithm for nonlinear inverse heat cond. problem 0-23862
- torsion problem for elastic cylinder with holes, integral eqn. method soln. 0-36849
- transient laser radiation, stochastic process near an instability point, numerical solution 0-23658
- transonic flow past swept wing, soln. by finite volume method 0-19431
- truncation method, stability of solns. in electrodynamics (*Ukrainian*) 0-31532
- two-layer shallow water flow, internal and surface waves, numerical anal. 0-19472
- unhomogeneous bars, normal mode response, stress anal. by boundary operator method 0-19239
- vertical jet under gravity, Riemann-Hilbert problem, numerical soln. 0-36858
- vibrational analysis, of thin cylindrical shell 0-5969
- viscous flow, non-Navier Stokes computations, parabolic and thin layer approx. 0-48666
- waveguide theory, cylindrical inhomogeneity in homogeneous medium of infinite extent, guided EM field computation 0-14274
- yrast-band of odd nuclei 0-22651
- $\Theta_2^4$  quantum field theory, numerical methods, anharmonic oscillator approx. 0-52390
- $^3\text{He}$ , superfluid B phase, spin wave breathers, double sine-Gordon equations 0-15329

**numerical methods, convergence** *see convergence of numerical methods***Nyquist criterion**

- plasma cyclotron instability with anisotropic kinetic temp., Nyquist diagrams (*Chinese*) 0-28627

**Nyquist noise** *see thermal noise***occultations**

- 13 Egeria, occultation of SAO 92603, photoelectric obs. rel. to minor planet possible satellite 0-46460
- AGK3 +0°1022 by Juno, obs. 0-26773
- Be stars, emission shell diameter meas. possibility by lunar occultation method 0-56839
- composite spectrum stars susceptible to lunar occultation, identification list of 68 stars 0-26908
- Crab Nebula, lunar occultation obs. at 114 and 26.3 MHz, small-scale struct. 0-46627
- 65 Cybele, occultation of AGK3 +19°599, 1979 October 17, obs. 0-31237
- Ganymede, stellar occultation obs. by Voyager 1 rel. to exospheric atmosphere 0-26792
- Juno, occultation of AGK3 +0°1022 re-analyzed 0-41757
- 18 Melpomene, occultation of SAO 114159, secondary extinction event obs. rel. to 1978 (18) 1, possible satellite 0-56749
- 9 Metis occultation of SAO 80950, Guianan obs. 0-31236
- Neptune, 1980 February 10, no occultation event, revised calcs. 0-26805
- Pallas, occultation of SAO 120836, 1973 February 6, reliability of obs. 0-46460
- planetary atmosphere HF radio occultation meas., phase screen concept 0-56735
- planets, atmosphere exponential turbulence and light bending during oscillation 0-17513
- PSR 0525+21 occulted by solar corona, Faraday rot. at 1720 MHz 0-46526
- radiosource occultation obs. and near-surface lunar plasma 0-8559
- S255, H II region, by Moon, CO emission small-scale struct. obs. 0-46637
- AQ Sagittarii, C star, ang. dia. from lunar occultation meas. 0-22008
- SAO 158687 by Uranus, obs. rel. to Uranian upper atmosphere struct. 0-17547
- stars, by asteroids, satellites discovery 0-4286
- Uranus, by Moon, 1977 February 10, radius, limb darkening and polar brightening at 6900 Å 0-17545
- Uranus occultation of SAO 158687, obs. rel. to upper atmosphere mean temp. and temp. vars. 0-46477
- Venus, nightside ionosphere, Pioneer orbiter radio occultations 0-46441
- Venus atmosphere, model from radio, radar and occultation obs. 0-46420
- Voyager 1, radio occultation by Jupiter and atmosphere and ionosphere preliminary profiles 0-26791
- Voyager 2 by solar corona, 1979 August, signals ang. and spectral broadening 0-51639

**ocean water** *see seawater***ocean waves**

- 12 m discus and NOMAD buoy hull transfer function computations 0-46303
- acoustic remote sensing of surface waves, theory 0-12564
- aerodynamic drag of sea surface, role of high freq. gravity waves 0-26536
- airflow above waves, numerical simulation (*Russian*) 0-4076
- annual Rossby wave in tropical N. Pacific Ocean, obs. 0-51421
- N. Atlantic, internal wavefield-mean flow interaction 0-36309
- Baltic Sea, two-dimensional seiches theory 0-8323
- baroclinic Rossby waves asymptotic behaviour taking into account Earth's curvature 0-8321
- beach, uniform bore, surf and run-up 0-21779
- Benguela Current, anomalously high waves region 0-51434
- buoy wave data analyses noise correction functions and error sources 0-46302
- capillary and gravity wave development in two-layer fluid (*Russian*) 0-12421
- coastal, near breakwater, physical and numerical modelling 0-51401
- coastal wavestaff system 0-46324
- coastal zone, wave setup and backwash due to local thermal wind-field disturbances 0-36371
- continental shelf waves, generation by alongshore vars. in bottom topography 0-51424
- continental shelf waves, scatt. by isolated topographic irregularities 0-51423
- correlation function and averaged power of radar signals reflected from sea waviness 0-46190
- data buoy wave meas. system malfunction detection 0-46304
- data buoy wideband wave directional spectra, real-time telemetry 0-46305
- deep ocean internal waves, dynamics 0-26517
- Douglas Channel, Canada, waves in Kitimat Inlet generated by submarine slide 0-51417
- Eady waves, effects of vertical eddy viscosity 0-51404
- edge wave in stratified sea with sloping bottom (*French*) 0-31045
- edge waves, wavelengths rel. to shoreline periodicities 0-12375
- edge waves on complex beach profile, theory 0-31025
- Ekman layer, stationary transport generated by waves (*Russian*) 0-17276
- energy conversion techniques and subsystems 0-45627
- equatorial Kelvin and inertio-gravity waves in zonal shear flow 0-26520
- equatorial trapped waves, vertical eigenvalue problem 0-56477
- equatorial undercurrent effect on equatorial waves 0-26519
- generation, propagation and dissipation spectral simulation model 0-31060
- geomag. fields, towed magnetometer investigation 0-3923
- Ghana shelf fortnightly wave, characts. 0-26515
- gravity wave-stream function relationships, variation approach 0-36318
- Gulf of Alaska SeaSat Experiment synthetic aperture radar wave imagery 0-46199
- harbour wave pattern, model with directional wave spectra (*Polish*) 0-17288
- Hawaii tsunami simulation, open boundary reflection interference 0-17232
- heat exchange between sea and atmosphere (*Russian*) 0-56479
- height and dominant wavelength obtained from Geos-3 altimeter study 0-4024
- height measurements using GEOS 3 radar altimeter data 0-8452
- heights and wind speed from Geos 3 data 0-4079
- high sea state, wave height measurements from Geos-3 radar altimeter data, aircraft and ship data—a comparison 0-4025
- imaging and wavelength meas. by aerial photography 0-46323
- interaction with atmospheric sound waves, model (*Russian*) 0-12402
- internal ocean waves, book contrib. review 0-21781
- internal solitary waves near turning point 0-46188
- internal wave effect on surface gravity wave spectrum (*Russian*) 0-21776
- internal wave field, vertical coherence from towed sensors 0-36310
- internal waves, acoustic reverberation data 0-41562
- internal waves, relationship with wind field variability 0-31052
- internal waves meas. with electrical contact device 0-12566
- inviscid barotropic vorticity eqn., soln. by finite difference, finite element and pseudospectral method 0-43687
- Krishnapatnam nearshore zone, wave conditions and wave-induced long-shore currents 0-41449
- linearly stratified fluid, gravitational collapse of mixed region 0-33653
- magnetic gradient fluctuations caused by internal waves 0-56491
- maximum height of wind waves, theory 0-41458
- measurement and data anal., by Naval Coastal Systems Center (NCSC) environmental measuring system 0-12570
- microwave emission at 37 GHz, wind effects 0-12414
- mixed fluid, nonlinear internal wave formation from gravitational collapse 0-33619
- modulation characteristics of surface waves 0-51416
- momentum flux and wave spectra, air-sea interaction obs. of Long Island, New York 0-26513
- monochromatic waves, obliquely incident on plane beach, instabilities 0-17275
- multi-component wave data, directional spectra extraction var. technique 0-26637
- nonlinear internal motion in open sea, obs. using range-gated Doppler sonar 0-51422
- nonlinear internal waves in a rotating ocean 0-26534
- nonlinear stationary internal and surface waves in shallow seas, propag. 0-17292
- nonlinear waves in closed basin, random behaviour 0-26557
- North Sea, wave height statistics using hindcast wave data 0-17273
- ocean wind wave analysis instruments 0-26640
- pack ice attenuation of waves 0-36332
- Paradip Port, India, wave characts. 0-41450
- parametrical wave prediction model 0-17272
- phase velocity, propagation direction 0-28521
- propagating inertial and internal waves, refl. at rigid boundary rel. to induced drift currents 0-51403
- propagation theories for water waves, variational principles 0-24043
- radar impulse reflection from nonlinear random sea 0-12416
- radar remote sensing, minimisation of ionospheric disturbance 0-21857
- radar returns from rough sea 0-51408
- random field fluctuations of near-water atm. layer and upper ocean layer, linear filtration errors 0-12425



## ocean waves continued

- random gravity wave mathematical representation 0-46198
- reef effects, model study 0-4043
- refraction by circular island, model 0-36316
- ripple growth to swell, ang. momentum conservation explanation 0-56478
- Rossby wave interactions and stability in rot. two-layer fluid on  $\beta$ -plane 0-10257
- Rossby waves, effects of vertical eddy viscosity 0-51404
- Rossby waves in a baroclinic ocean, exact soln. (*Russian*) 0-21775
- rotating stratified fluid, an exact soln. for edge waves 0-4038
- sand barrier beach shoreline accumulative section, protective dune ridge morphodynamics (*Russian*) 0-36287
- sand barrier beach shoreline transit section, protective dune ridge morphodynamics (*Russian*) 0-36286
- sand tracer dispersion under progressive water waves, laboratory and field obs. 0-46170
- sea state, influence on marine geoid spectrum 0-3904
- sea state, significant wave height extracted by algorithms 0-4023
- sea state, surface roughness slope density calcs. from Geos-3 data 0-4022
- sea-echo Doppler spectra, sample-averaged, accuracy of parameter extraction 0-51561
- SEASAT altimeter wave height comparisons 0-46201
- semidiurnal internal waves in Polygon-70 test area of Atlantic, spatial characts. 0-31051
- short pulse radar ocean wave sensing, preliminary results 0-46315
- significant wave height, comments on airborne profilometer problems 0-4026
- solitary Rossby waves in two-layer system, theory 0-17293
- spectral decomposition of short gravity wave systems 0-36319
- spectral model, verification results using wave height study 0-4027
- standing equatorial wave modes, in bounded oceanic basins 0-51420
- stationary temperature boundary layers generation by surface waves (*Russian*) 0-1611
- subsea sensor on offshore mooring platform, for wave anal. 0-26641
- subsurface bubble clouds caused by breaking waves 0-46185
- surf zone, breaking wave energetics 0-12415
- surface characteristics affecting acoustic scatt. 0-46194
- surface distortion analysis, laser beam spreading 0-8332
- surface reflection by underwater ridges 0-4034
- surface wave prediction model for varying wind fields 0-12408
- surface waves meas., using resistance wave gauge, accuracy and calibration 0-24110
- surface wind wave related turbulence meas. by impeller current meter array 0-46301
- surge wave height determination, graphical method 0-56485
- swell decay in shallow water, ang. momentum conservation explanation 0-56478
- synthetic aperture radar imagery rel. to surface structure 0-46197
- tidal waves in channel, energy dissipation due to bottom friction and eddy losses 0-31058
- topographic Rossby waves generated off continental shelf, kinetic energy on shelf 0-51425
- topographic Rossby waves off E. Australia, shelf circulation identification and role 0-26518
- transient waves generated by a moving oscillatory pressure on a sloping beach 0-56476
- tsunami, 1978 June 12, Miyagi Prefecture, Japan (*Japanese*) 0-41401
- tsunami, damping in stratified ocean with rough bottom (*Russian*) 0-21651
- tsunami, due to Izu-Oshima-kinkai earthquake, Jan. 1978, source mechanism 0-41393
- tsunami, generation and propag., simulation using shallow water eqns. 0-41407
- tsunami, response of bay water (*Japanese*) 0-41399
- tsunami along Mie coast, central Japan, 1707 and 1854 records (*Japanese*) 0-41402
- tsunami caused by Izu-Oshima-kinkai earthquake, Jan. 1978, source mechanism (*Japanese*) 0-41392
- tsunami from Sanriku earthquake, 1933 March 2, initial motion rel. to dislocation model 0-31000
- tsunami with Miyagiken-oki 1978 June 12 earthquake (*Japanese*) 0-41400
- tsunamis propagation, finite difference simulation, book contrib. 0-3956
- vertical diffusion driving mechanism in Oslofjord, tidal origins 0-26531
- wavenumber spectrum, effects on laser beam refl. from sea surface 0-31121
- wind energy transfer to near-inertial waves, calc. 0-4017
- wind wave elevation sensor array system 0-46322
- wind waves, high-freq. spectra meas. in presence of currents in shallow sea 0-31053
- wind waves, statistical model for groups 0-12409
- wind-generated sea waves, interaction with tidal currents 0-51428
- wind-wave layer, temp. fluctuations (*Russian*) 0-51410
- wind-wave tank, microscopic and macroscopic surface structs. growth and decay rates 0-48726

## oceanic crust

- Acoustically-Navigated Geological Undersea Surveyor, for Mid-Atlantic Ridge appl. 0-4120
- Agulhas Basin of S.Atlantic, seafloor spreading history, geomag. study 0-21696
- ancient oceanic lithosphere, mag. props. as alteration indicators, Othris ophiolite example 0-8297
- Andaman Sea crust, seismotectonics and tectonic history 0-8283
- aseismic ridges, isostasy anal. 0-3971
- N.Atlantic crustal structure, deep drilling results 0-26478
- N.Atlantic Mesozoic crust reconstruction 0-51365
- Atlantic mid-oceanic ridge, axial temp. profile and crustal struct. 0-26476
- NE Atlantic Ocean, bathymetry of continental margin around British Isles 0-12372
- Atlantic Ocean, history of growth and topography of ocean bottom 0-3993
- Atlantic Ocean south of Bermuda, geophys. survey within Mesozoic mag. anomaly sequence 0-26492
- S.Atlantic oceanic crust in Mesozoic and subsequent evolution, mag. and gravity data 0-21699
- Mid Atlantic Ridge crest, geological and geophys. investigations 0-8284
- Atlantic S.E. of Azores, crustal struct. rel. to mag. anomalies and bathymetry 0-51384
- central Baffin Bay, sea-floor spreading 0-51373

## oceanic crust continued

- Baltic Sea, continuous underwater gamma-survey 0-12377
- basalt-seawater reactions chemical exchange, Fe, Mn, and S species results 0-17294
- basaltic pillars, in collapsed lava pools on deep ocean floor 0-3991
- basalts, elec. resistivity meas. 0-21713
- basalts geochemistry from back-arc spreading centre, East Scotia Sea 0-3989
- Bay of Islands ophiolite complex, Newfoundland, seismic vel. struct 0-21688
- Beaufort Sea area, earthquake data, tectonic setting and stress study 0-3931
- Blake Escarpment, ocean geoid estimation using Geos 3 satellite altimetry data 0-3902
- borehole magnetometer data interpretation 0-21625
- Campbell Plateau and Lord Howe Rise, plate tectonics of SE.Gondwanaland 0-17244
- Canadian continental margins, evolution and geophys. features 0-8274
- Caroline Plate, petrochem. of troughs and crustal accretion 0-12385
- Ceylon-Cocos Zone, thermal regime and nascent island arc 0-56418
- S.China Sea, 1965 October 7, intraplate thrust earthquake 0-26461
- Coral Sea basin tectonic evolution from marine mag. anomaly data 0-21698
- Cuvier Basin, off W.Australia, crust form. by rifting, seismic study 0-12368
- deep sea sediment cores, Au, Pd, Ir, Mn sources, neutron activation anal. 0-17247
- deep-sea basalts, clinopyroxenes chemistry statistical anal. 0-41437
- deep-sea basalts, He and Xe as measure of magmatic differentiation 0-31040
- deep-sea hydrothermal site on strike-slip fault, discovery 0-21710
- Early Cretaceous remanent spreading centre in central Pacific Basin 0-21706
- Eltanin fault zone, Pacific Ocean, crustal struct. from petrographic data 0-12376
- Falkland-Agulhas Fracture Zone, ridge-crest offset history 0-26490
- Galapagos Rift, submarine thermal springs 0-8295
- Galapagos Rift at 86°W, regional morphological and struct. anal. 0-26491
- Galapagos Rift at 86°W, rift valley sheet flows, collapse pits and lava lakes 0-21708
- Galapagos Rift at 86°W, sealed topography and magmatic episodes 0-21681
- Galapagos Rift at 86°W, volcanism struct. and evolution of rift valley 0-21707
- Galapagos Rift hydrothermal mounds, obs. with DSRV Alvin and detailed heat flow studies 0-51383
- geomorphology of sea floor and glacial morphogenesis of W.Spitsbergen underwater margins 0-26494
- Guaymas Basin, Gulf of California, heat flow at spreading centres 0-41411
- Gulf of Aden and Afar, mag. anomaly map and plate tectonics 0-56364
- central Gulf of California, heat flow meas. 0-3968
- Hawaiian Island chain, volcanism linear migration from Kauai shield-building volcanism age 0-36281
- Hawaiian Islands, isostasy and lithosphere flexure 0-26485
- Hawaiian-Emperor seamount chain, geoid heights derived from Geos 3 altimeter data 0-3899
- Hellenic trench system, subduction to transform motion, Seabeam survey 0-8285
- high velocity layer, vel. indicating garnet comp. 0-17251
- hot spring created by drill hole 0-55951
- Iceland, crust of oceanic affinity, borehole results 0-8264
- Iceland Plateau, deep crust and mantle struct. from surface waves dispersion 0-41413
- Indian Ocean, model of evolution rel. to breakup of Gondwanaland 0-41428
- intraplate seismicity on bathymetric features, 1968 Emperor Trough earthquake 0-30997
- isostasy at midocean ridge crests 0-31022
- Juan de Fuca Ridge crest, E.Pacific, tectonic topography compensation 0-56448
- Kane fracture zone of central Atlantic 0-21668
- Kerguelen Islands area, geoid determined from Geos 3 altimeter data correl. with sea bottom topography 0-3900
- Laccadive uplifting zone, crustal struct., gravity field modelling (*Russian*) 0-3966
- layer 2, low-temp. seawater-basalt interaction rel. to S distrib. 0-41432
- lithosphere flexure and uplifted atolls, comment 0-26486
- magma series erupted in different marine tectonic settings, trace element anal. 0-21667
- magnetic anomalies of seafloor spreading rel. to geochemistry 0-56345
- magnetic anomalies recorded during deep-water mag. surveys, statistical anal. 0-36233
- Marcus-Necker Ridge, volcanic rocks comp. and stages of development 0-36282
- marginal and interarc basins, volcanic evolution 0-8271
- marginal basins, formation rel. to relative plate motions 0-41427
- Mid-Atlantic Ridge, FAMOUS area basalt glasses regional var. and petrogenesis 0-31041
- mid-ocean ridge basalts, density var. rel. to magma mixing and primitive lavas scarcity 0-56460
- mid-oceanic ridge axes, topography and tectonics from fluid dynamic models 0-41433
- Middle America Trench offshore Guatemala, seismic refr. and refl. meas. 0-26493
- Mozambique Channel, crustal struct., seismology study 0-51362
- N.Norway, continental margin crustal struct. and tectonic history 0-51360
- Norwegian-Greenland sea, thermal evolution in sea floor spreading model 0-56427
- Ontong Java and Manihiki Pacific oceanic plateaus, seismic struct. 0-21680
- ophiolitic peridotites structures, role of young lithosphere thrusting in subduction zones 0-56446
- SW.Pacific basin, reverberant subbottom layers distrib. 0-8290
- Pacific Ocean, Pn waves propag. rel. to lower lithosphere struct. 0-26459
- Pacific Ocean basin, volcanic history since Jurassic, crustal loading study 0-46165
- Pacific Ocean bottom sediments, interstitial waters B content 0-36289
- E.Pacific Rise, metalliferous sediments three-dimensional distrib. 0-21705



## oceanic crust continued

- E.Pacific Rise, struct. of crust, volcanism periodicity and magma flow 0-17243
- E.Pacific Rise, young cratered volcanoes pairs 0-12374
- Papua New Guinea-Solomon Islands region, 1964-1973 earthquakes, seismotectonics 0-8270
- Parace Vela Basin, E.Philippine Sea, evolution and chronology 0-41431
- plate bending at trenches, mechanical models constraints from earthquakes 0-41426
- random magnetisation, effect on coherence of short-wavelength marine mag. anomalies 0-36225
- Reykjanes Ridge, mid-Atlantic 59°/°N, seismic crustal struct. 0-56423
- ridge crests, hydrothermal activity rel. to ocean major and minor elements balance, Galapagos data 0-41459
- ridge crests, metal-rich deposits form. 0-41430
- rift valley formation over oceanic ridge, upwelling flow model of topographic profile (*Chinese*) 0-8280
- Rockall Bank, N.Atlantic, seismic struct., synthetic reconstruction 0-21670
- seismic wave field assoc. with fine structured Moho in continents and oceans 0-12361
- seismological techniques, two-chip multichannel methods 0-56632
- seismometer stationed on ocean bed, self-contained unit with mag. recorder (*Russian*) 0-36410
- South China Sea basin, crustal struct. from profiler-sonobuoy meas. 0-8291
- structure from refraction expts. 0-3952
- submarine lithosphere, geophys., geochem. and petrological model 0-3994
- submarine pillow basalts, seafloor weathering effects on geomag. palaeointensities determ. 0-3927
- Tamayo transform fault, E.Pacific Rise, deep tow study 0-51361
- thermal evolution of ocean ridge, affected by spreading rate 0-56424
- thermal evolution of passive continental margin 0-56427
- trench outer rise width, model of crust thickness as function of age 0-56426
- Tyrrhenian Sea rifting, Rayleigh wave dispersion evidence 0-56445
- volcanic material alteration in marine sediments, SE.Pacific Ocean 0-3990
- Walvis Ridge, lithospheric struct. from Rayleigh wave dispersion 0-41412
- Walvis Ridge, S. Atlantic, gravity anomalies and origin 0-21682
- U abundance, heat flow implications, basalt fission track anal. 0-8287

## oceanographic equipment

- see also oceanographic techniques; water pollution detection and control*
- 12 m discus and NOMAD buoy hull transfer function computations 0-46303
- 32 kW Doppler sonar for ocean internal wave meas. 0-46296
- Aanderaa Ni-coated current meter, pressure-induced direction error 0-4121
- Acoustically-Navigated Geological Undersea Surveyor, for Mid-Atlantic Ridge appl. 0-4120
- Benthic Untethered Multipurpose Platform for underwater acoustic TV 0-46319
- buoy wave data analyses noise correction functions and error sources 0-46302
- coastal wavestaff system 0-46324
- data buoy wave meas. system malfunction detection 0-46304
- data buoy wideband wave directional spectra, real-time telemetry 0-46305
- data logger for recording slow sea oscillations, solid-state 0-36414
- deep towed seismic profiling system, multichannel hydrophone array, sub-bottom oceanic structure study appl. 0-26550
- Doppler sonar, range-gated, obs. of strongly nonlinear internal motion in open sea 0-51422
- Doppler sonar ocean current profiles 0-46311
- drift buoys, drogued, appl. to coastal flow meas. in N.Gulf of Alaska 0-51431
- Drifting Oceanographic Profile Buoy with minimum vertical motion 0-46306
- errors in profiling instruments, analysis 0-8445
- estuarine current meter data acquisition microcomputer system 0-46265
- expendable bathythermograph digital recording and display system 0-46318
- free vehicle grab respirometer for deep-sea sediments O<sub>2</sub> uptake and nutrient exchange meas. 0-3564
- holographic microvelocimeter, ocean particle dynamics meas. 0-12567
- intelligent terminals and calculators, as alternative to minicomputer systems 0-12553
- Inverted Echo Sounder for ocean thermal structural variations and currents 0-46312
- lidar, scanning bathymetric system for nautical, near-shore charting 0-8463
- long tow-wire complex vibration obs. and empirical drag law 0-46309
- magnetometer for sea floor temporal mag. variation meas. 0-51581
- microwave radiometers, ice movement measurement (*Danish*) 0-26624
- Moored Acoustic Buoy System suspended Kevlar array technology 0-43572
- multichannel wide-range oceanographic sonar 0-46295
- Naval Coastal Systems Center (NCSC) environmental measuring system 0-12570
- ocean wind wave elevation sensor array system 0-46322
- pneumopress, for extracting interstitial water from marine sediments 0-26643
- pressure tolerant electronic systems 0-46317
- propeller Vector Measuring Current Meter development 0-46313
- radar altimeter height and timing bias report 0-46326
- range resolved Brillouin scattering using pulsed laser 0-38055
- resources and meas. techniques, conference, San Diego (1979) 0-41943
- scanning sensor for real-time optical mapping 0-8464
- sea surface contour airborne radar as remote sensing instrument 0-51562
- sea-floor mapping in real time, sonar-microprocessor equipment 0-26646
- SeaSat scanning multichannel microwave radiometer 0-46248
- sediment free-fall penetrometer with Doppler telemetry 0-46320
- seismometer hydrophones for deep ocean bottom deployment 0-51582
- Spar Buoy Oceanographic Telemetry System 0-46307
- Spar Buoy Oceanographic Telemetry System software engineering 0-46308
- submerged self-contained buoy station, expt. launchings 0-26642
- submersible data acquisition system SCRIBE 0-46266
- surface meteorological buoy and aircraft VHF link 0-46298

## oceanographic equipment continued

- tide gauge for shallow-water, fast-response characts. 0-26639
- tiltmeter, appl. to ice shelves tidal flexure meas. 0-31050
- tow system with depth control, hydrographic and current meas. 0-17403
- towed instruments carrier, for hydrophysical research 0-36423
- transmissometer for profiling and moored observations in water 0-8462
- transparency meter, Se photocell device, for biological activity 0-8442
- underwater acoustic pulse compression system, signal processing methods 0-56630
- Vaisala-Brunt frequency vertical fine struct. meas. in Mediterranean Sea 0-26537
- vector averaging current meters, moored, for vertical temp. gradients meas. 0-12561
- velocity sensor, calibration equipment and technique, oceanographic appls. 0-8447
- velocity sensor for three-dimensional turbulence meas. 0-46314
- versatile oceanographic data-logger 0-46264
- Visible and Infrared Radiometer evaluation from SeaSat-A surface temp. obs. 0-46325
- wave analysis instruments 0-26640
- wind-wave tank, microscopic and macroscopic surface structs. growth and decay rates 0-48726
- YVETTE, free-fall shear profiler 0-31124
- Nd:YAG Q-switched laser for bathymetry 0-8461

## oceanographic techniques

- see also oceanographic equipment; water pollution detection and control*
- acoustic remote sensing of high-frequency internal waves 0-41562
- acoustic stratigraphy of carbonate sediments, fine scale detail 0-21709
- acoustic tomography, for large scale monitoring 0-4119
- biological life forms recording, using CCD colour TV camera 0-51301
- chemical tracer studies, implications of multiple components transport through thermohaline diffusive interfaces 0-12396
- conservation calculations in natural coordinates, example from Baltic Sea 0-51433
- coral and shell dating 0-12434
- directional spectra extraction from multi-component wave data, var. technique 0-26637
- dynamic ocean data, acquisition and display by portable real-time mini-computer system 0-12552
- eddy models, environmental effect prediction anal. 0-4146
- EM sounding of sea ice, visit to Arctic and Antarctic Research Institute, Leningrad 0-4504
- environmental data files, quick guide 0-12551
- estuarine hydrography and sedimentation, measurement techniques, book 0-36788
- freely sinking probe horizontal velocity meas. interpretation 0-46321
- Gauss-Markov models of ocean currents for error analysis of inertial navigation system 0-36411
- geomagnetic depth sounding using sea floor magnetometer system 0-51581
- Geos 3 altimetry, anal. for regional sea surface model in Tasman and Coral seas 0-3903
- geostrophic ocean currents determ. independently of reference level, inverse technique 0-51574
- HF sky wave radar remote sensing of sea state, minimisation of ionospheric disturbance 0-21857
- horizontal mixing measurement, Hay-Pasquill method testing in Baltic Sea 0-17290
- ice shelves tidal flexure measurement, near tiltmeter appl. 0-31050
- internal waves meas. with electrical contact device 0-12566
- mapping using observational data (*Russian*) 0-17416
- marine particulate plume density and distrib., acoustic assessment 0-45843
- marine pollution, data collection 0-3545
- marine sediments probed by acoustic array, penetration conditions (*French*) 0-33324
- Mellor-Durbin theory, appl. to marine thermocline evolution 0-4041
- microwave remote sensing, radiative transfer eqns. 0-21855
- microwave remote sensing 0-56612
- nautical, near-shore charting, laser appls. 0-8463
- ocean wave geomag. fields, towed magnetometer investigation 0-3923
- optical interferometry, water vertical density structure meas. (*Russian*) 0-51569
- palaeogeographic reconstruction, H<sub>2</sub>S levels stagnation coeff. appl. 0-36291
- parametrical wave prediction model 0-17272
- particle dynamics meas. using holographic microvelocimeter 0-12567
- passive radiometry of ocean, radio meteorology colloquium, Victoria, British Columbia, Canada (1978 June 14 to 21) 0-46724
- PFM fibre-optic video transmission to and from undersea vehicles 0-46310
- Project Kiwi One, S.Pacific Ocean acoustic cross-section 0-36330
- radar altimetry for remote sensing of ocean surface circulation 0-46189
- radionavigation systems appl., available systems survey, modes and accuracy 0-36408
- remote sensing, particulate Fe mapping in ocean acid waste dump 0-56497
- remote sensing of ocean color 0-8460
- remote temperature sounding in thin surface layer (*Russian*) 0-4138
- RPV, high-altitude, for environmental appls. 0-17470
- sea depth, coding via sedimentary deposits (*Russian*) 0-17383
- sea floor relief mapping considerations 0-46169
- sea foam produced by storms, microwave remote sensing of storm intensity 0-41528
- sea ice internal forces, local values determ. from mean stresses 0-31056
- sea state, significant wave height extracted by algorithms 0-4023
- sea surface topography, altimeter data analysis by sequential filter 0-4145
- sea surface topography obs. with Geos 3 altimeter data 0-3908
- sea suspended material and chlorophyll conc., estimation from outgoing radiation spectrum meas. from helicopter 0-36333
- sea-echo Doppler radar, accuracy of parameter extraction 0-51561
- sea-surface temperatures in tropical Pacific, satellite determ. and climatological usefulness 0-31044
- SEASAT synthetic aperture microwave-imaging radar expt., overview 0-46267
- sediments, acoustic anisotropy due to overburden press. 0-56455
- seismic profiling, continuous, with two receiver systems, effective vels. determ. 0-31150



**oceanographic techniques continued**

- short arc adjustment model technique for oceanic geoid determination, satellite altimetry 0-21830  
 short pulse radar ocean wave sensing, preliminary results 0-46315  
 small-scale turbulence and stratification study, via towed instruments carrier 0-36423  
 surface current mapping by Coastal Ocean Dynamics Radar 0-46316  
 surface temp. determ., satellite data processing (*Russian*) 0-17417  
 surface water, remotely sensed by microwave radiometry 0-36428  
 surface waves meas., using resistance wave gauge, accuracy and calibration 0-24110  
 surface wind wave related turbulence meas. by impeller current meter array 0-46301  
 surge wave height determination, graphical method 0-56485  
 suspended solids measurement, test of diffuse reflectance models 0-8453  
 synthetic aperture radar imagery rel. to surface structure 0-46197  
 temperature by coral Sr/Ca ratio 0-12568  
 temperature gradient meas. in sea, anal. of two methods 0-31149  
 underwater acoustic pulse compression system, signal processing methods 0-56630  
 US scattering method for small-scale turbulence study 0-26540  
 Vaisala-Brunt frequency vertical fine struct. meas. in Mediterranean Sea 0-26537  
 velocity calc., improved Stommel-Schott method 0-41561  
 velocity determination from hydrographic data 0-17415  
 velocity sensor, calibration equipment and technique, oceanographic appls. 0-8447  
 wave analysis, using subsurface sensor on offshore mooring platform 0-26641  
 wave height measurements using GEOS 3 radar altimeter data 0-8452  
 wave height profiling, depth sounding, laser beam reflection method, sea surface wavenumber effects 0-31121  
 wave imaging and wavelength meas. by aerial photography 0-46323  
<sup>134</sup>Cs and <sup>137</sup>Cs as tracers in water and sediments 0-3541

**oceanography**

- see also *ocean waves; seawater; sediments; tides*  
 acid waste dump, particulate Fe mapping 0-56497  
 acoustic parabolic wave theories and applications 0-51436  
 acoustic signal coherence limits in random ocean environment 0-46193  
 Adriatic Sea, chem. parameters, spring and winter time obs. 0-41447  
 N. Adriatic Sea, Green's function of Laplace's tidal eqn. 0-17291  
 advective mixed-layer model with imposed surface heating and wind stress 0-12395  
 Alaskan continental shelf, sea ice ridging 0-12410  
 ancient shorelines from stone rosettes 0-26489  
 Antarctic Circumpolar Current, geotrophic barotropic volume transport 0-36305  
 Arctic Basin, ice movements, external factors 0-26541  
 Arctic leads, atmos. boundary layer turbulence spectra obs. 0-56588  
 Arctic Ocean sea ice, snow and ice cover conditions 0-26547  
 Arctic sea ice, 1953-77 period fluctuations 0-36314  
 arctic sea ice extent rel. to interannual atmospheric var. 0-41501  
 NW Atlantic, absolute vel. calc. 0-41561  
 Atlantic, anomalous bottom water south of Grand Banks due to turbidity current activity 0-4042  
 S. Atlantic, Antarctic Intermediate Water, modal props. 0-36306  
 NE tropical Atlantic, current data (*Russian*) 0-17378  
 E. central Atlantic, horizontal temp. in upper ocean layer (*Russian*) 0-17283  
 NE tropical Atlantic, hydrochemical structure (*Russian*) 0-17284  
 N. Atlantic, internal wavefield-mean flow interaction 0-36309  
 N. Atlantic, pressure field along W. margin 0-12412  
 NW Atlantic, surface temp. features, 1975-7, satellite obs. 0-51412  
 NE tropical Atlantic, thermohaline structure (*Russian*) 0-17281  
 N. Atlantic, transient response, model studies 0-12405  
 NE Atlantic, wind and ocean circulation, climatic var., Little Ice Age 0-8422  
 Mid-Atlantic Bight, coastal longshore pressure gradient 0-12411  
 S. Atlantic Bight, Hg flux meas. 0-4046  
 Mid-Atlantic Bight, mean circulation 0-36317  
 Atlantic coastal waters, optical coherence loss meas. 0-8333  
 N. Atlantic deep water, production since Miocene, sediment evidence 0-46186  
 tropical Atlantic near W. Africa coast, optical studies (*Russian*) 0-17285  
 NE Atlantic Ocean, bathymetry of continental margin around British Isles 0-12372  
 W. Atlantic Ocean, equatorial, subthermocline countercurrents 0-51426  
 Atlantic Ocean, history of growth and topography of ocean bottom 0-3993  
 NW Atlantic Ocean, oceanic geoid and tides derived from Geos 3 satellite data 0-3901  
 Atlantic Ocean, spatial characts. of semidiurnal internal waves in Polygon-70 test area 0-31051  
 Atlantic S.E. of Azores, crustal struct. rel. to mag. anomalies and bathymetry 0-51384  
 atmosphere heat exchange with ocean, influence of waves (*Russian*) 0-56479  
 atmospheric boundary layer, heat transfer with ocean, reef effects, AMTEX 1975 obs. 0-26567  
 atmospheric shortwave and longwave radiative flux, mid-ocean obs. 0-12547  
 Azov Sea, USSR, hummocking of floating ice, distrib. 0-26549  
 Baffin Bay, oil seepage from seabed during 1976, August 0-12400  
 Baja California coast, sea level vars. and currents 0-36321  
 Baltic Sea, salt transports determ. from conservation calculations in natural coordinates 0-51433  
 Baltic Sea, two-dimensional seiches theory 0-8323  
 Baltic Sea horizontal mixing, Lagrangian and Eulerian meas. 0-17290  
 Barents Sea sediments, continuous seismic profiling with two receiver systems 0-31150  
 barrier island breach morphology and dynamics, study in stability 0-12371  
 barrier island configuration, coastal currents altering shape 0-17289  
 bay water response to tsunami (*Japanese*) 0-41399  
 beach configurations, seasonal patterns and sediment transport 0-31026  
 beach deposits sedimentary material differentiation and bedding form. dynamico 0-26496  
 Benard convection, very viscous fluid, theory 0-10236  
 Benguela Current, anomalously high waves region 0-51434  
 Bering Sea, hydrographic features of deep water 0-31061

**oceanography continued**

- E. Bering Sea, structural front in ice free conditions 0-8317  
 Bering Sea shelf sediments, denitrification estimates 0-12433  
 Bight of Abaco, Bahamas, algorithmic tidal study, expt. and harmonic anal. 0-8319  
 Bight of Abaco, Bahamas, tidal model comparison with data 0-4035  
 Black Sea, H<sub>2</sub>S and O<sub>2</sub> zone boundaries rel. to water mass dynamics (*Russian*) 0-12435  
 Blake Escarpment, ocean geoid estimation using Geos 3 satellite altimetry data 0-3902  
 boundary layer mixing, reinterpretation of entrainment process in laboratory expts. 0-51405  
 Boussinesq turbulence, statistical theory, appl. to thermocline erosion 0-48713  
 Bristol Bay, Alaska, lateral water mass interaction study 0-26521  
 British Isles region, EM induction by analogue model 0-56368  
 California coast, 1941-1978, land and sea level changes 0-21610  
 California Current during last 8000 years, model reconstruction 0-41457  
 chemistry, major and minor elements balances, role of ridge crest hydrothermal activity from Galapagos data 0-41459  
 Chesapeake Bay, subtidal sea level var., rel. to atm. forcing 0-26530  
 Chesapeake Bay, winter 1975 wind-driven circulation 0-36313  
 chlorophyll, gradient map from high-altitude ocean colour scanner data 0-26551  
 circulation, hyperbolic partial differential equatns. numerical solution 0-21864  
 coastal current driven by wind, transient state 0-51439  
 coastal surface water temp., spatial var. during upwelling 0-36322  
 coastal upwelling region off Oregon, vertical and cross-shelf flow meas. 0-12397  
 coastal zone, statistical forecasting of local thermal wind-field disturbances freq. 0-36371  
 Cochín backwater, India, estuarine water, particulate heavy metal content 0-7964  
 Cochín Harbour mouth, India, hydrographic characts. and tidal prism 0-41452  
 conference, April 1980, Birmingham, England 0-56474  
 continental shelf off Sierra Leone and Liberia, mesoscale flow anomalies 0-26524  
 continental shelf waters, kinetic energy from topographic Rossby waves generated off shelf 0-51425  
 continental shelf waves, generation by alongshore vars. in bottom topography 0-51424  
 continental shelf waves, scatt. by isolated topographic irregularities 0-51423  
 convection, simple theoretical and expt. study, geophysical appl. and analogies 0-24018  
 coral C isotope composition, rel. to environmental factors 0-46202  
 coral reef water, O isotope composition rel. to evaporation and precipitation 0-46202  
 cosmogenic isotopes, vertical turbulent diffusion 0-12428  
 coupled ocean-atmosphere expt., ocean response, rel. to climate 0-12430  
 currents, synoptic-scale, numerical model 0-12424  
 currents generated by heat and momentum fluxes through surface, numerical simulation 0-26535  
 currents in mid-ocean, geostrophic balance 0-17268  
 deep sea sediments, benthic mixing study using radioactive tracers 0-8294  
 Delmarva coast, USA, shoreline periodicity and offshore shoals 0-56457  
 depth simulation, analogue/hybrid technique 0-36336  
 developing turbulent surface shear layer model 0-12417  
 Drake Passage, 1975 currents and temps. 0-36307  
 Drake Passage, Antarctica, polar front motions in horizontal temp. gradients 0-4037  
 dredger spoil, dumping ground obs., motion of fine particles with current 0-17287  
 drift current/slope current interaction 0-21780  
 drift currents, induced by propagating inertial and internal waves refl. at rigid boundary 0-51403  
 drift-slope current interaction, Conf., Tokyo, Japan (May 1979) 0-31411  
 drift-slope current interaction 0-36334  
 drifter data analysis, sampling rate and random position error effects 0-26527  
 drifting sea ice, inertial period motions (*Japanese*) 0-36327  
 Earth annual wobble, affected by wind stressed sea level 0-36221  
 ecological significance of solar UV radiation 0-45974  
 eddies and the general circulation of model gyres 0-56490  
 Ekman pumping to geostrophic flow, water mass props. determ. 0-56489  
 electric currents induced in insulated oceans 0-51407  
 E. England coast, storm surge (1978 January 11 to 12) 0-12419  
 enhanced pole tide rel. to Chandler wobble period and damping 0-21778  
 equatorial trapped waves, vertical eigenvalue problem 0-56477  
 estuaries, <sup>15</sup>O distrib. 0-26532  
 estuarine and coastal waters, suspended particles surface charge 0-36331  
 estuarine mixing implications of Fe, Mn and organic material dissolved in river water 0-17296  
 finite depth stratified flow over topography on a beta-plane 0-6128  
 Florida continental shelf, rain-formed mixed layer 0-36323  
 flow, vel. determ. from hydrographic data 0-17415  
 foam produced by storms, microwave remote sensing of storm intensity 0-41528  
 frontal generation, mixing and mutual intrusion mechanism model 0-26522  
 Galapagos sea floor sediments, hydrothermal mounds, stratigraphy and chem. 0-26497  
 Garonne-Gironde river estuary system, radioactive tracing of physiochemical behaviour of Zn (OH)<sub>2</sub> (*French*) 0-7994  
 geomagnetic lunar daily var. at Alibag, oceanic and ionospheric dynamos contrib. 0-26444  
 Geos 3 project, review 0-4224  
 geostrophic ocean currents determ. independently of reference level, inverse technique 0-51574  
 Gironde inlet and Pertuis of Maumusson, estuarine waters seaward dispersion, remote sensing study (*French*) 0-8324  
 Global Weather Experiment, observational phase through first special observing period 0-51543  
 Glomar Challenger drilling ship, experience and prospects 0-21711  
 gravity anomalies in N. Atlantic and Indian Oceans, recovery from Geos 3 altimetry data 0-3905  
 Guinea Gulf northern coast, sea temp. and level, Msf tide propag. 0-4033



## oceanography continued

- Gulf of Alaska, coastal circulation, precipitation and runoff effects 0-36312  
 N.Gulf of Alaska, coastal flow from dynamic topography and satellite-tracked drogued drift buoys 0-51431  
 NE.Gulf of Alaska, continental shelf bottom press. and current anal. 0-8318  
 NE Gulf of Alaska, processes affecting suspended matter distrib. and transport 0-12398  
 Gulf of Alaska SeaSat Experiment 14.6 GHz scatterometer surface wind obs. 0-46200  
 Gulf of Alaska SeaSat Experiment synthetic aperture radar wave imagery 0-46199  
 central Gulf of California, thermal waters discharges rel. to terrestrial heat flow meas. 0-3968  
 Gulf of Elat (Aqaba), seasonal temp. and salinity vars. 0-31047  
 Gulf of Genova, effect of low freq. winds on sea level and currents 0-8322  
 Gulf of Lions, surface currents, spatial structure (*Russian*) 0-17277  
 W.Gulf of Maine winter circulation current and press. obs. 0-51430  
 Gulf of Mexico, surface water circulation, 1973-7 obs. 0-51415  
 W.Gulf of Oman, bathymetry rel. to tectonics 0-8279  
 Gulf of Suez, possible water-layer seismic multiple refls. and head waves 0-56400  
 Gulf Stream, Hg distrib. 0-7965  
 Gulf stream, surface boundaries measured by Geos 3 radar altimetry and IR data 0-4021  
 Gulf Stream, vel. fluctuations during Late Cenozoic rel. to climate 0-12432  
 Gulf Stream cyclonic ring, 'Allen', 1976-7 obs. 0-51413  
 Gulf Stream seaward deflection; bottom topography effects 0-36308  
 Haicheng Earthquake, 1975, precursory sea level changes (*Chinese*) 0-51331  
 Hawaiian-Emperor seamount chain, geoid heights derived from Geos 3 altimeter data 0-3899  
 heat flux, effect on wintertime of W. Europe 0-26542  
 hot spring created by drill hole 0-55951  
 hurricane sea surface wind speed, L-band radar backscatt. obs. 0-56561  
 hydrodynamic model of upper ocean frontal dynamics, development and anal. 0-4028  
 hydrodynamic model of upper ocean frontal dynamics 0-4029  
 ice, melting in sea water, model, Antarctic ice shelf and iceberg appl. 0-4036  
 ice age climate and sea level at ~95000 BP 0-51444  
 ice cover, drifting, relationship between mean stresses and internal forces local values 0-31056  
 ice from glaciers, melting process (*German*) 0-33606  
 ice shelves tidal flexure, meas. by tiltmeter 0-31050  
 India, W. continental shelf,  $\text{CaCO}_3$ ,  $\text{Mg}^{2+}$ , and  $\text{Ca}^{2+}$  content 0-8289  
 India, W. continental shelf, marine sediment  $\text{P}_2\text{O}_5$  content 0-8288  
 W.India coast, upwelling, geopotential anomaly study 0-56482  
 W.India continental shelf, topography and sediments 0-56454  
 Indian, palaeotemps. during Brunhes epoch from sediment core study 0-12429  
 Indian, sea levels in western equatorial region rel. to tides, meteorology and ocean circulation 0-4018  
 NW.Indian Ocean, eddy in Somali Basin associated with monsoon 0-51414  
 W.Indian Ocean, equatorial currents meas. 0-12427  
 infinite  $\beta$ -plane ocean model, response to atmospheric forcing 0-4031  
 inshore and offshore profile, statistical determination 0-56458  
 internal waves, relationship with wind field variability 0-31052  
 internal waves causing geomagnetic gradient fluctuations 0-56491  
 introductory dynamic oceanography, book 0-4044  
 Joint Air-Sea Interaction (JASIN) Experiment 1978, general review 0-4113  
 JONSWAP 1973, surface wave prediction model for varying wind fields 0-12408  
 Kerguelen Islands area, geoid determ. from Geos 3 altimeter data 0-3900  
 Krishnapatnam nearshore zone, wave conditions and wave-induced long-shore currents 0-41449  
 Kuroshio in East China Sea, variations of surface velocity from (1965-75) (*Chinese*) 0-31049  
 Kuroshio meander, theory 0-4019  
 light scattering of layer, affected by underlying surface (*Russian*) 0-12403  
 linear prediction models, review 0-56590  
 lipid composition of marine aerosols, sea surface microlayer and subsurface water 0-17297  
 Lower Strathern, Scotland, sea-level changes of early Flandrian 0-56484  
 lunar  $\text{O}_2$  tide, contrib. to geomag. lunar daily var. at Alibag 0-56355  
 $\text{M}_2$  ocean tide parameters and Moon's meas. longit. decel. from artificial satellite orbit data 0-31048  
 Mangalore coast, India, 1976-7 nearshore water conditions 0-8315  
 old Mangalore Port, India, sediment transport and siltation of navigational channel 0-56488  
 old Mangalore port, seasonal vars. in estuarine and oceanic waters hydrographic conditions 0-41451  
 marine gravity modelling, considerations of indirect effect (geoid undulation effect) 0-3907  
 marine thermocline evolution, study using Mellor-Durbin theory 0-4041  
 E.Mediterranean, during glacial max., surface temp. and salinity from foraminifera in sediments 0-41456  
 Mediterranean harbour tidal harmonic constants 0-41448  
 Mediterranean outflow, deep circulation in Gulf of Cadiz 0-17270  
 Mediterranean outflow mixing 0-17269  
 Mediterranean Sea, hydrological regime during glacial periods (*French*) 0-4040  
 E.Mediterranean Sea, T and  $\text{O}_2$  profiles 0-17298  
 mesoscale eddies in mid-ocean, simulated dynamic balances, model 0-26525  
 Mesoscale horizontal turbulence (*Russian*) 0-12423  
 meteoroid ablation spheres in abyssal clay 0-46500  
 microwave emissivity of sea surface, roughened by wind 0-46184  
 Late Miocene, water depths shallowing rel. to C isotope stratigraphy in New Zealand marine sediments 0-26479  
 monochromatic waves, obliquely incident on plane beach, instabilities 0-17275  
 Monterey Bay, optical props., spectral values 0-8327

## oceanography continued

- navigation problems in oceanographic research (*Russian*) 0-17286  
 Newfoundland, depositional environments and benthos of the continental slope and rise 0-3987  
 nonlinear coastal and equatorial jets, theory 0-51427  
 nonlinear internal motion in open sea, obs. using range-gated Doppler sonar 0-51422  
 North Atlantic Drift, decline rel. to rapid ice-sheet growth and last glaciation initiation 0-51530  
 North Sea floor, lunar type features explanation 0-31028  
 Norwegian continental shelf, topographically trapped vortex 0-31046  
 ocean-atmosphere coupled model, atmospheric feedback 0-12500  
 ocean-atmosphere coupled model, tropical sea surface temp. anomaly effect 0-12418  
 oceanic fronts, optical and particulate matter properties 0-51418  
 oil-rich layer at 200 metre depth, obs. in N.Atlantic and Caribbean 0-56498  
 Okhotsk Sea coast of Hokkaido in winter, ocean currents (*Japanese*) 0-36326  
 Oregon continental shelf currents, spring transition 0-41453  
 Oslofjord, vertical diffusion driving mechanism, internal tidal waves, model 0-26531  
 SE.Pacific, Antarctic Intermediate Water, modal props. 0-36306  
 midlatitude N. Pacific, optimum oceanographic network design 0-36315  
 N.Pacific, size distrib. of suspended particles in surface water 0-4047  
 tropical Pacific, trace gases, ITCZ and ocean currents 0-41509  
 N.Pacific Basin, simulation studies for oceanic anomalies, atm.-ocean link 0-8316  
 N.Pacific Cenozoic sedimentation history 0-31027  
 N.Pacific mesoscale phenomena, oceanographic model and acoustic survey comparison 0-46195  
 S.Pacific Ocean, acoustic cross-section (Project Kiwi One) 0-36330  
 tropical Pacific Ocean, climatological usefulness of satellite-determined sea-surface temps. 0-31044  
 Pacific Ocean, early Pliocene deep thermal struct. 0-56492  
 Pacific Ocean, Mn distrib. 0-56494  
 Pacific Ocean, telluric current channelling rel. to EM induction in Vancouver Island region 0-56356  
 N.Pacific Ocean, tropical, annual Rossby wave obs. 0-51421  
 N.Pacific Ocean, west, depth, var. of temp., salinity and sound vel. meridional gradients 0-51429  
 Pacific Ocean bottom sediments, interstitial waters B content 0-36289  
 Pacific Ocean waters, nitrate N distrib. 0-31065  
 E.Pacific Rise, hydrothermal vents on seabed issuing  $\text{H}_2$  and methane 0-41422  
 N.W.Pacific surface currents 0-26548  
 packice drift, oceanic boundary layer effect, model 0-26528  
 palaeocurrent indicators in deep-sea sediments 0-3992  
 Paradip Port, India, wave characts. 0-41450  
 passive radiometry of ocean, radio meteorology colloquium, Victoria, British Columbia, Canada (1978 June 14 to 21) 0-46724  
 physical and biological sciences, conf., Japan (Mar. 1979) 0-17714  
 planetary boundary layer, wind driven current, temp. profile, model 0-26526  
 pollution, dynamically passive impurity propag. in sea surface layer 0-31063  
 Polygon-70 in Atlantic Ocean, internal tidal structure (*Russian*) 0-51411  
 radar returns from sea ice, freq. characts. (*Japanese*) 0-36328  
 radionavigation with global Omega system, hydrophysical research appls. (*Russian*) 0-17418  
 refractive index microstruct. from diffusive and turbulent ocean mixing 0-56486  
 regional sea surface model in Tasman and Coral seas, Geos 3 altimeter data anal. 0-3903  
 resources and meas. techniques, conference, San Diego (1979) 0-41943  
 Rio Grande Rise, marine sediments and erosional canyons of late Cainozoic 0-56456  
 Rosenstiel School of Marine and Atmospheric Science, University of Miami, review 0-8755  
 rotating fluid, vortices formation near reson. for elastoid-inertia waves 0-12473  
 rotating stratified fluid, an exact soln. for edge waves 0-4038  
 Sargasso Sea, internal wave field, vertical coherence 0-36310  
 Sargasso Sea, optical transfer function meas. 0-8328  
 sea ice, dynamic thermodynamic model 0-51432  
 sea ice, EM sounding by Arctic and Antarctic Research Institute, Leningrad 0-4504  
 sea ice-ocean temp. oscillator model, nonlinear analysis 0-12413  
 sea level during ice age, and Antarctic ice surge theory 0-51525  
 sea level during last 18000 years, retreat of Antarctic ice sheet 0-41455  
 sea level in Late Pleistocene, USA Atlantic shoreline sediments 0-26543  
 sea level vars. rel. to contemporary crustal movements in Canada 0-8273  
 sea surface topography, altimeter data analysis by sequential filter 0-4145  
 sea surface topography and ocean geoid, Geos 3 investigation 0-3906  
 sea surface topography obs. with Geos 3 altimeter data 0-3908  
 sea use plan concepts and criteria 0-46203  
 sea-surface microlayer,  $^{210}\text{Pb}$  and  $^{210}\text{Po}$  enrichment obs. 0-56496  
 seasonal thermocline, temp. field fine structure (*Russian*) 0-17278  
 seasonal thermocline models, dissipation effect 0-4030  
 sediments, acoustic anisotropy due to overburden press. 0-56455  
 shallow sea thermal structure, during heating and storms (*Russian*) 0-56480  
 shelf circulation, vertical structure 0-36320  
 shelf water/slope water front in Middle Atlantic, summertime synoptic var. 0-12407  
 Shinnecock Inlet, radiometric sea surface temp. distrib. 0-41454  
 shoreline periodicities, spectral anal. rel. to edge waves 0-12375  
 small-scale turbulence and stratification study, via towed instruments carrier 0-36423  
 solitary Rossby waves in two-layer system, theory 0-17293  
 Somali Current, eddy form., wind effects model 0-26523  
 sound pulse generation by explosion, region of nonlinear effects 0-56493  
 Southern Hemisphere oceans, mean annual poleward energy transports 0-51406  
 SS 0-3904  
 St. Lawrence Estuary turbidity maximum, sediment, salinity, suspended matter study 0-4015  
 standing equatorial wave modes, in bounded oceanic basins 0-51420  
 stepwise stratified ocean, temp. gradient meas. methods 0-31149



**oceanography continued**

- Stokes' drift in presence of oscillatory and residual currents, theory 0-17267
- storm surge theory, in stratified sea 0-51437
- Straits of Kerch, water exchange calcs. 0-26545
- stratified flow around three-dimens. barrier 0-48769
- stratified rotating fluid, vortex created by mass transfer 0-12401
- surface circulation, remote sensing with radar altimetry 0-46189
- surface circulation and the distribution of pelagic tar and plastic 0-16856
- surface layer rel. to atmospheric temp. and humidity (*Russian*) 0-17282
- surface ocean current response to wind, quadratic and linear laws 0-26529
- surface temp., canonical correl. method study 0-26593
- surface wind obs., SeaSat scatterometer/scanning radiometer/altimeter comparison 0-46249
- surface wind-driven flow 0-46187
- Sverdrup transport and ocean circulation 0-36324
- synoptic disturbances, evolution (*Russian*) 0-12422
- synoptic eddies, Atlantic polygon 70 studies 0-26544
- synoptic eddies, remote sensing data (*Russian*) 0-12420
- synoptic eddy charact., variability (*Russian*) 0-17280
- temperature vertical gradients, meas. via moored vector averaging current meters 0-12561
- thermal anomalies numerical study with dynamic model 0-17271
- thermal energy, conversion to electricity (*French*) 0-21389
- thermocline affecting vertical distrib. of oscills. (*Russian*) 0-21777
- thermocline and mixed layer, model of seasonal evolution 0-26546
- thermocline model (*Russian*) 0-51409
- thermohaline diffusive interfaces, multiple components transport 0-12396
- tidal flows, turbulence in depth-limited boundary layer 0-12406
- tidal interactions in region of large bottom slope, NW Africa, JOINT-1 obs. 0-4016
- tidal power schemes of West Bengal, siltation estimation 0-31059
- tropical cyclone-ocean model, mutual response 0-4032
- turbulence, small-scale, horizontal struct. statistical charact. (*Russian*) 0-4020
- turbulence, small-scale, study by acoustic scatt. method 0-26540
- turbulence stratification and vertical current vel. gradients vars. in Strait of Tunis 0-26539
- turbulence vertical struct. charact. 0-12426
- turbulent Ekman layer, struct. of homogeneous ocean surface layer 0-51438
- typhoon Tess wake vertical struct. in upper layer of Pacific Ocean 0-26538
- underwater irradiance in Norwegian and Barents Sea, relation to water temp. 0-31055
- underwater sound, analysis of acoustical effects of receiver and source motions at short ranges in deep ocean channel 0-10063
- underwater sound, computations of strength and diffraction parameters for real and canonical oceans 0-33320
- underwater sound, deep ocean LF attenuation data, review 0-33318
- underwater sound, derivation of wave eqn. in inhomogeneous ocean 0-33313
- underwater sound, effects of tidally varying sound speed on propag. over sloping ocean bottom 0-10062
- underwater sound, experimental studies of attenuation in sediments 0-10067
- underwater sound, fluctuations in reciprocal acoustic transmission in midocean environment 0-10069
- underwater sound, hydrophone shadowing by seamounts 0-33308
- underwater sound, influence of cyclonic eddies on short-range transmission 0-33316
- underwater sound, influence of range dependence of ocean bottom on adiabatic approximation 0-10066
- underwater sound, mode interactions in isovelocity ocean of uniformly varying depth 0-33321
- underwater sound, plane-wave reflection loss model including sediment rigidity 0-33311
- underwater sound, ratio of compressional wave vel. to shear wave vel. and Poisson's ratios in sediments and rocks 0-12404
- underwater sound, volume scattering strengths and zooplankton distributions at acoustic frequencies between 0.5 and 3 MHz 0-33317
- underwater sound 0-33312
- underwater sound amplitude fluctuations due to temp. microstructure 0-19140
- underwater sound in North Pacific, variation of vertical directionality of noise with depth 0-19130
- underwater sound in range-dependent ocean, examination of multipath processes within context of adiabatic mode theory 0-19134
- upper ocean, spatial variability, influence on ocean acoustics 0-51435
- upwelling, dynamic data acquisition and display by portable real-time minicomputer system 0-12552
- upwelling off SW India coast 0-56481
- Vaisala-Brunt frequency vertical fine struct. meas. in Mediterranean Sea 0-26537
- Venice, sea-lagoon exchange in modified tide regime 0-12431
- vertical buoyancy flux, atmospherically induced 0-4039
- vertical eddy viscosity, effects on Rossby and Eady waves 0-51404
- vertical mixing and chimney-like formations 0-36311
- Weddell Sea drift ice, pushed north by barrier winds 0-26514
- West Flower Gardens coral reef, effect on waves 0-4043
- wind driven currents, regression coeffs. and bottom stress anal. 0-8320
- wind waves, high-freq. spectra meas. in presence of currents in shallow sea 0-31053
- wind-driven circulation, finite element anal. 0-56487
- wind-driven flow in zonal channel, with stratification and bottom topography 0-51402
- wind-generated sea waves, interaction with tidal currents 0-51428
- wind-wave layer, temp. fluctuations (*Russian*) 0-51410
- wind-wave tank, microscopic and macroscopic surface structs. growth and decay rates 0-48726
- World Ocean, waters heat and salt content 0-31054
- CO<sub>2</sub> cycling in environment, non-proportionality between flux and reservoir content 0-46261
- CO<sub>2</sub> from fossil fuel burning, deep-sea injections and atmospheric response 0-31090
- CO<sub>2</sub> solution in ocean surface waters, role of homogeneous buffer factor 0-21783
- Ca<sup>2+</sup> in seawater 0-31064
- H<sub>2</sub>S levels, stagnation coeff. and appl. in palaeogeographic reconstruction 0-36291

**oceanography continued**

- Mn nodules, quant. distrib. and metal content (*Japanese*) 0-8292
- Mn nodulus and micronodules of NW Atlantic, rare earth element study 0-46167
- NO<sub>3</sub><sup>-</sup>, PO<sub>4</sub><sup>3-</sup>, Si(OH)<sub>4</sub>, ratios in Moroccan upwelling region 0-4045
- N<sub>2</sub>O composition of Pacific surface water 0-51519
- Nd isotopic composition of sediments of different oceans 0-21704
- <sup>18</sup>O in equatorial Pacific core, glacial time scales and climate 0-21817
- <sup>90</sup>Sr and T in N. Pacific surface water during 1974, conc. meas. 0-26181
- OCR see optical character recognition
- octet theory see SU<sub>3</sub> theory
- ODMR see microwave-optical double resonance
- oecology see ecology
- OH<sup>-</sup> centres
- No entries
- ohmic contacts
- space charge limited current with diffusion theory, for exponential trap distribution 0-10992
- n-Al<sub>1-x</sub>Ga<sub>1-x</sub>As, Au-based ohmic contacts TEM obs. 0-34509
- Au-Ge contacts to n-GaAs layers with SiO<sub>2</sub> overlayer, ohmic props. 0-2467
- Ga<sub>1-x</sub>Al<sub>x</sub>As, ohmic contacts, metallisation systems 0-25010
- GaAs DH laser, alloying of ohmic contacts, Nd:YAG laser irradi. 0-43357
- n-GaAs nonalloyed ohmic contacts of TiPtAu by pulse-electron-beam annealed Se implants 0-2466
- GaAs, review of ohmic contacts fabrication 0-49901
- n-GaAs, ultra low resistance 0-20307
- In-CdS-In structure, volt-ampere charact., carrier tunnelling emission (*Russian*) 0-49914
- InP-metal, elec. and metallurgical props., heat treatment effects 0-34514
- Ni/Au-Ge/GaAs contact system, alloying behaviour, microprobe AES and X-ray diffr. 0-54548
- a-Si:H sputtered films, ohmic contacts by H depletion, H diffusion 0-34511
- ohmmeters
- see also electric resistance measurement
- relative-error determination in instrument checking 0-17961
- transistorised, reading range extension using op. amp. (*French*) 0-42207
- very high resistance measurement, meas. device using operational amplifiers 0-42240
- oil refining
- unleaded petrol, improving octane rating using gasohol 0-30329
- oil technology
- see also oil refining
- Arctic oil spillage response techniques 0-46204
- continuous oil-in-water meas. by towed fluorometer 0-45846
- in situ oil shale technological developments, review 0-30354
- Ninian Field drilling platform construction, assoc. weather forecasting 0-41522
- reserves and resources, production and transport problems (*German*) 0-26102
- resources in US, estimation of undiscovered sites 0-21361
- seismic prospecting techniques for oil resources (*French, English*) 0-21362
- shale oil, in situ retorts, computer simulation of ignition with hot inert gas 0-30356
- shale oil in situ extraction processes, US DOE 1979 R and D program 0-40812
- shale retort dispersion, effect of particle size distrib. and flow nonuniformities 0-28560
- shale retort flow nonuniformities c.f. numerical predictions 0-28492
- shale retorts, multi-dimens. simulation of flow nonuniformities in fissured porous media 0-28559
- sonic interface detection for multiproduct liquid transportation by pipeline, developments 0-33382
- undersea resources and related topics, world-wide survey 0-35622
- world oil resource estimates (1949-79) (*French, English*) 0-21365
- oiling (lubrication) see lubrication
- oils, insulating see insulating oils
- omega mesons
- $e^+e^- \rightarrow \pi^+\pi^-(\pi^0\omega)$ ,  $\rho'(1250)$  description, EM form factors, bound states, N/D method (*Russian*) 0-42465
- masses in QCD lattice gauge theory 0-4928
- $\gamma p$ , 46-180 GeV,  $\omega$ -meson photoprod. cross section,  $\omega\gamma$  coupling constant 0-13319
- $K^0, K^0$  transmission regeneration on deuterons and neutrons, 10 to 50 GeV/c 0-4985
- $K_1 p \rightarrow K_1 p$ , 5 to 10 GeV, differential cross-section,  $\omega$  Regge trajectory 0-22637
- $\omega(1670) \rightarrow B\pi$ , decay mode cross section from  $K^+p$  backward prod. 0-37257
- $\omega$ - $\phi$ -baryonium mixing model 0-32072
- $p p$ , 200 GeV/c in Be, inclusive  $\omega$  prod. at large  $p_T$ ,  $\eta'$  prod. upper limit 0-52547
- $p p$ , ISR energies, inclusive high  $p_T$   $\omega^0$  and  $\eta'$  prod. 0-42504
- $p p$  annihilation, low energy, prompt  $e^+e^-$ ,  $\omega^0$  and  $\eta^0$  prod., inclusive prod. rates 0-42506
- $p p \rightarrow \omega^0 p$ , 1950 MeV/c<sup>2</sup>, coupling with  $p p \rightarrow 5\pi$  0-27517
- $\pi\omega \rightarrow \pi\omega$ ,  $\rho'(1250)$  meson and two channel  $\pi\pi$ ,  $\pi\omega$  problem, N/D method (*Russian*) 0-37297
- $\pi^- p \rightarrow \omega n$ , 15-40 GeV/c, cross sections and density matrix elements (*Russian*) 0-37302
- $\pi\pi \rightarrow \pi\omega$ ,  $\rho'(1250)$  meson and two channel  $\pi\pi$ ,  $\pi\omega$  problem, N/D method (*Russian*) 0-37297
- $\rho$ - $\omega$  mixing, quark mass differences 0-37243
- $\tau \rightarrow \pi\omega$ , decay width and form factor calc. using vector dominance hypothesis (*Russian*) 0-47271
- $w^+$  baryonium mixing, dual S-matrix approach to baryonium 0-52526
- omegatrons see cyclotrons
- one-dimensional conductivity
- A15 compounds as Jahn-Teller systems, multiple band electron-phonon transport theory 0-24902
- anomalies due to two mechanisms of electron phonon interaction (*Russian*) 0-34430
- antiferromagnetic Hubbard chain, interband absorpt., Peierls dimerisation, excitonic effects 0-25072
- charge density waves, impurity pinning 0-6819
- charge transfer salts, soliton model for dielectric permeability 0-40036



## one-dimensional conductivity continued

cobalt platino-oxalate, one-dimens. conductors, prep., struct. and elec. cond. 0-24900  
 conference, Dubrovnik, Yugoslavia, (Sep. 1978) 0-12853  
 copper platino-oxalate, one-dimens. conductors, prep., struct. and elec. cond. 0-24900  
 Coulomb gas in strong mag. field analogy with electron gas with backward scatt. 0-24817  
 dibenzotetrathiafulvalene cation radical salts, cryst. struct. by X-ray anal., rel. to elec. props. 0-24436  
 1,4-dibromonaphthalene, k-k scatt., exciton dephasing time-resolved phosphoresc. obs. 0-11458  
 disordered one-dimensional conductors, elec. props., coherence length, impurity effects 0-24903  
 disordered one-dimensional conductors, interacting electron thermodynamics (*Russian*) 0-54679  
 disordered systems, one dimensional, electron transmission and wave propagation 0-24907  
 disordered systems, one dimensional nonvanishing zero temp. static cond. 0-29396  
 distorted one dimensional system with bond disorder, electron density of states, CPA calcs. 0-24778  
 electron gas, one dimensional, dynamic interaction screening, spin and charge density wave instabilities 0-24819  
 electron-electron interactions in physics of one dimensional conductors 0-24895  
 electron-electron scattering in quasi-one dimens. metals 0-10957  
 energy and charge transport theory (*German*) 0-15506  
 Fermi gas, one dimensional with backward scatt., gap renormalisation 0-24818  
 Fermi gas, one-dimensional theory, correlation functions 0-22278  
 Fermi one dimensional gas with long range potential, renormalisation group, exchange, Umklapp interactions 0-2351  
 frequency dependent conductivity, theory of many-body effects 0-44575  
 Frohlich model dynamics, Green's function anal. 0-20170  
 HMTSF-TNAP, microwave cond. at 35 GHz 0-24963  
 HMTSF-TNAP, transport props. 0-20165  
 Hubbard model, one-dimens., extended,  $2k_F$  and  $4k_F$  correl. functions, computer renormalisation group calcs., appl. to one-dimens. conductors 0-54625  
 impurity effects on ordered phases 0-24905  
 incommensurate CDW 0-20174  
 incommensurate Peierls-Frohlich system, fluctuation cond., Green's function calc. 0-24886  
 incommensurate sliding CDW 0-20156  
 Landau model, anisotropic one dimens., correl. length complex order parameter amplitude fluctuation effect 0-46995  
 linear-chain conductors review 0-24887  
 magnesium platino-oxalate, one-dimens. conductors, prep., struct. and elec. cond. 0-24900  
 magnetic transition in one-dimens. electron system with attractive interaction in mag. field 0-7072  
 metal, phonon drag and sliding CDW 0-20173  
 molecular crystals, electronic struct., mol. orbital theory 0-54588  
 narrow band quasi-one-dimensional metals, exchange-correlation effects on plasmons and on CDW instability 0-44525  
 NMP-TCNQ, X-ray diffuse scatt., and cond. study 0-49701  
 nonlinear one-dimens. Hamiltonian dynamics for lattice distortion 0-20171  
 one dimensional Fermi gas model in relation to spin and field theoretical models 0-24816  
 one-dimensional conductors, conductivity peaks, Peierls transitions (*Russian*) 0-49700  
 one-dimensional Hubbard model, Friedel oscills. around a nonmagnetic impurity 0-25073  
 optical properties of one-dimensional conductors, review 0-45106  
 organic charge transfer crystals, transport props., phase transitions, mol. dynamic (*German*) 0-39507  
 organic metals, transport theory, electron-phonon scatt. 0-20161  
 organic semiconductors, resonant states, mag. excitations and impurities 0-24839  
 organic solids, dimer level splitting, hopping integral calc. using PPP Hamiltonian 0-24890  
 orientational metal-insulator phase transitions in quadrupolar strands with itinerant electrons 0-15455  
 Peierls dielectric, one dimensional, selftrapped excitations in Peierls-Frohlich state (*Russian*) 0-54678  
 Peierls instability, dynamics, structural energy, pseudopot. calc. 0-54676  
 Peierls transition temp. and 0K energy gap, mean field theory calc. 0-24782  
 phase ordering in quasione-dimensional system, phase ordering (*Japanese*) 0-2352  
 phenomenological equations of motion for electrons, phonons and librions 0-10955  
 photoemission from organic mol. crystals, book contrib. 0-16158  
 polyacetylene:AsF<sub>6</sub>, X-ray absorpt. meas. of mol. struct., orientation and charge transfer 0-25486  
 polyacetylene, semiconducting and metallic, thermoelec. props. 0-40884  
 polyacetylene and derivatives, chemically doped, elec., chem. and phys. props. 0-24912  
 polyacetylene film, doped, transport props. 0-24913  
 polyacetylene film, partially oriented, anisotropic elec. cond., quasi-one-dimens. behaviour of fully oriented doped material 0-11112  
 polydiacetylene, cryst., one-dimens. conjugated semicond., vibronic coupling, Fano interference effects 0-34939  
 quantum particle in one-dimensional potentials with incommensurate periods 0-34345  
 quasi one-dimensional spin lattice coupled system, collective modes 0-24896  
 rubidium platino-oxalate, one-dimens. conductors, prep., struct. and elec. cond. 0-24900  
 sine-Gordon chain, cond., finite damping correction 0-46993  
 spin-Peierls transition in mag. field, phonon freq., Heisenberg model calcs. 0-25151  
 superconductivity, response functions, from renormalisation group theory 0-54829  
 symmetry, role on props. of quasi-one dimensional systems 0-24916  
 TCNQ, generalised Wigner lattices and band motion effects 0-24815  
 TCNQ, lattice softening mechanism 0-6481  
 TCNQ, salt, DBTTF-TCNQ, elec. resistivity and thermoelec. power meas. 0-20193

## one-dimensional conductivity continued

TCNQ alkali salt, spin-Peierls transition 0-29395  
 TCNQ complex, Adn TCNQ<sub>2</sub>, nuclear-spin-lattice relaxation 0-39886  
 TCNQ complex formed from cation (methyl-1-N-ethyl benzimidazolium)<sup>+</sup> conductivity transition 0-10954  
 TCNQ complex with 5-phenyl-[1-thiol]-3-selenol-2-thione, charge-transfer salt, cryst. and mol. struct. 0-33986  
 TCNQ complexes with ferrocenes, charge transfer type, struct. and mag. props. 0-24439  
 TCNQ complexes with N-methyl derivatives of pyridine, cond. and thermoelec. power meas., band model anal. 0-10952  
 TCNQ salt, (N-methylphenazinium)<sub>x</sub>(phenazine)<sub>1-x</sub>, 1 band filling, carrier mobility and disorder effects 0-24904  
 TCNQ salt, (NMe<sub>3</sub>H)(I)(TCNQ), one-dimens. semicond. with metal-like cond. 0-24909  
 TCNQ salt, (NMP)<sub>0.5</sub>(phenazine)<sub>0.5</sub> TCNQ, transport props. 0-24891  
 TCNQ salt, (TSeF)<sub>x</sub>(TTF)<sub>1-x</sub>-TCNQ, struct., elec. and mag. props. review 0-20158  
 TCNQ salt, acridinium (TCNQ)<sub>2</sub> low temp. heat capacity, Debye temp. 0-2180  
 TCNQ salt, HMTTF-TCNQ, sp. ht., 30 to 80K 0-24614  
 TCNQ salt, HMTTF-TCNQ, three-dimens. ordering, Ginzburg-Landau model for Peierls instability 0-20160  
 TCNQ salt, K-TCNQ, high and low temp. phases, dielec. const. 0-34844  
 TCNQ salt, MEM(TCNQ)<sub>2</sub>, phase transition electronic struct. interpretation 0-24781  
 TCNQ salt, MEM(TCNQ)<sub>2</sub>, phase transitions, elec. cond., ESR, mag. susceptibility study 0-24981  
 TCNQ salt, MTPA (TCNQ)<sub>2</sub>, IR refl., dielec. function and cond. 0-34924  
 TCNQ salt, N-propyl-quinolinium(TCNQ)<sub>2</sub>, defect conc. depend. phase transition 0-44577  
 TCNQ salt, NMP<sub>0.63</sub>phenazine<sub>0.37</sub>TCNQ, mag. susceptibility, 0.03-4.2K 0-25191  
 TCNQ salt, NPQn (TCNQ)<sub>2</sub>, neutron irradi. induced defect concentration depend. phase transition 0-29449  
 TCNQ salt, pyridinium (TCNQ)<sub>2</sub>, low temp. mag. phase transition, ESR study 0-25139  
 TCNQ salt, Qn(TCNQ)<sub>2</sub>, non-Ohmic cond. 0-20169  
 TCNQ salt, Qn(TCNQ)<sub>2</sub>, thermoelec. power and cond., large Coulomb repulsion model 0-24893  
 TCNQ salt, Qn (TCNQ)<sub>2</sub>, configurational entropy, thermoelec. power meas. 0-34432  
 TCNQ salt, quinolinium, electron spin location, elec., mag., and thermal props. 0-25189  
 TCNQ salt, quinolinium (TCNQ)<sub>2</sub>, mag. chain double resonance study, deuteration 0-25250  
 TCNQ salt, quinolinium (TCNQ)<sub>2</sub>, transport props. 0-24891  
 TCNQ salt, TEA (TCNQ)<sub>2</sub>, anomalous conductivity, conductivity transitions 0-15508  
 TCNQ salt, tetramethylhexamethylenediammonium-TCNQ-iodine, elec. and mag. props., struct., specific heat 0-24898  
 TCNQ salt, TMTSF-DMTCNQ, cond. and thermopower meas. 0-20165  
 TCNQ salt, TMTSF-DMTCNQ, mag. susceptibility meas. under press. 0-29521  
 TCNQ salt, TMTSF-TCNQ, microwave cond. at 35 GHz 0-24963  
 TCNQ salt, TSeF-TCNQ, Peierls transition and CDW ordering, X-ray study 0-20101  
 TCNQ salt in aqueous media, electrochem. behavior 0-6976  
 TCNQ salts, aminopyridinium (TCNQ)<sub>2</sub>, elec. and mag. props., 4.2 to 300K 0-24889  
 TCNQ salts, anomalous infra-red activity and the determination of electron-molecular vibration coupling constants 0-25389  
 TCNQ salts, charge transfer and cond. 0-20164  
 TCNQ salts, conducting, Raman spectra, estimation of degree of charge transfer from vibrational frequencies 0-50344  
 TCNQ salts, ionene polycation-TCNQ salts, elec. cond. rel. to polycation struct. 0-34428  
 TCNQ salts, n-methylacridium (TCNQ)<sub>2</sub>, 2,2'-bipyridinium (TCNQ)<sub>2</sub> and Qn(TCNQ)<sub>2</sub>, with asymmetric donors, mag. susceptibility, 0.035-4.2K 0-25190  
 TCNQ salts, polymer composites, elec. cond. 0-20157  
 TCNQ salts with heterocyclic amines and hydroquinone form. via redox reaction 0-26013  
 TCNQ- $\phi_6$ DTP, chemisorbed O<sub>2</sub> effects on mag. susceptibility 0-15679  
 TCNQ-HMTSF, de Haas-Shubnikov oscills. 0-10956  
 TCNQ-NMP, transport props. 0-24891  
 TCNQ-TTF, chemisorbed O<sub>2</sub> effects on mag. susceptibility 0-15679  
 TEA(TCNQ)<sub>2</sub>, elec. cond. and thermoelec. power under hydrostatic press. 0-11024  
 tetraphenyldithiadipyranilidene-iodine, synthesis and cond. props. 0-24910  
 tetraselenatetracene cation radical salts, cryst. struct. by X-ray anal., rel. to elec. props. 0-24436  
 tetraselenatetracene chloride, elec. cond. below 1K (*Russian*) 0-6820  
 (TMTSF)<sub>2</sub>PF<sub>6</sub>, one dimens. conductor, superconds., resist. meas. and mag. field effects (*French*) 0-44753  
 (TMTSF)<sub>2</sub>PF<sub>6</sub>, organic one-dimensional superconductor, transition temp. 0-44754  
 TMTTF-TCNQ, quasi one-dimens. conductor, diffusive hopping, theory 0-54677  
 TMTTF-TCNQ crystals grown from several organic solvents 0-25544  
 Tomonaga model, response function calc. method 0-22279  
 transport processes, isothermal method for static cond. of electrons 0-29373  
 TSeF-TCNQ, Kohn anomaly of metallic state, X-ray diffuse scatt. meas. 0-19887  
 TSeF-TCNQ, nonlinear electronic transport, microwave harmonic mixing obs. 0-20168  
 TSeF-I<sub>2</sub>, physical props., elec. cond. 0-24908  
 $\alpha$ TTF:Br, transport and mag. props., effect of doping 0-24934  
 TTF(MBDT) spin-Peierls transition, mag. exchange interactions, mag. props. 0-25138  
 (TTF)CuS<sub>4</sub>C<sub>4</sub>(CF<sub>3</sub>)<sub>4</sub>, spin Peierls system, mag. field effects 0-7123  
 TTF-Cu bis-dithiolenes, dimer, mol. displacements at 4.2K 0-10539  
 TTF-halides, conductors with chain struct., lattice phonons and distortions, incommensurability transitions 0-24549  
 TTF-SCN, quasi one-dimens. conductor, CDW phase transform., X-ray scatt. study 0-24594  
 TTF-TCNQ, anal. of harmonic microwave mixing 0-44635  
 TTF-TCNQ, and related compounds, low temp. irradi. effects 0-24906



**one-dimensional conductivity continued**

- TTF-TCNQ, and related cpds., elastoresistivity by strain gauge technique 0-24892
- TTF-TCNQ, anharmonic props., temp. (press.) depend., rel. to naphthalene and anthracene 0-15200
- TTF-TCNQ, charge transfer change with press. 0-39564
- TTF-TCNQ, cond. in phase transition region 0-24979
- TTF-TCNQ, controlled defects effect on microwave cond. and dielec. function 0-24885
- TTF-TCNQ, elastic neutron scatt. evidence for charge transfer change at high power 0-2163
- TTF-TCNQ, elec. cond. and spin susceptibility, press. and temp. depend. 0-24894
- TTF-TCNQ, electron-electron interaction as source of metallic resist. 0-20162
- TTF-TCNQ, electron-molecular distortion coupling near Peierls transition, IR spectra obs. 0-25390
- TTF-TCNQ, fluctuation cond. and commensurability pinning 0-34429
- TTF-TCNQ, impurity effects on CDW fluctuations 0-44576
- TTF-TCNQ, interchain tunnelling effect on nucl. spin-lattice relax. time, interchain coupling of CDW 0-20163
- TTF-TCNQ, IR reflectance in conducting phase 0-25388
- TTF-TCNQ, Matthiessen's rule, effective defect resistivity 0-6821
- TTF-TCNQ, non-linear elec. transport by pinned CDW 0-20172
- TTF-TCNQ, nonlinear electronic transport, microwave harmonic mixing obs. 0-20168
- TTF-TCNQ, organic metal, Van der Waals donor stacking 0-15037
- TTF-TCNQ, phase transitions and CDW state, controlled disorder effects 0-15507
- TTF-TCNQ, phase transitions and CDW state, induced defect depend., transport and mag. studies 0-24980
- TTF-TCNQ, physical properties, reviews (*Japanese*) 0-24883
- TTF-TCNQ, temp. depend. of phonon frequencies at constant vol. 0-10616
- TTF-TCNQ, two-chain Fermi gas, response behaviour 0-2381
- TTF-TCNQ, X-ray irradi., transverse cond. 0-6432
- TTF-TCNQ and related compounds, cryst. struct., organisation, dimensionality, interchain disorder 0-19790
- TTF-TCNQ family, donor stack dominance of transport props. 0-20166
- TTF-TCNQ series, cryst. struct., elec. cond., and EPR meas., steric factor effects 0-19789
- TTFCuBDT, spin-Peierls transition in spin 1/2 Heisenberg chains, RPA calcs. 0-25150
- TTT<sub>2</sub>(I<sub>3</sub>)<sub>1+x</sub>, physical props., elec., mag. and optical meas. 0-24908
- TTT<sub>2</sub>I<sub>3-5-x</sub>Br<sub>x</sub>, chem. impurities and neutron irradi. induced defects, effects on DC cond. 0-49699
- TTT<sub>2</sub>I<sub>3+x</sub>, thermoelec. power and metal-semicond. transition 0-34431
- TTT<sub>2</sub>I<sub>3</sub>, charge transfer salt, Coulomb effects, Madelung energy calcs. 0-19747
- TTT<sub>2</sub>I<sub>3</sub>, chem. impurities and neutron irradi. induced defects, effects on DC cond. 0-49699
- TTT<sub>2</sub>I<sub>3</sub>, quasi one-dimens. organic metal, elec. cond. and thermoelec. power 0-24899
- (TTT)<sub>2</sub>I<sub>3+x</sub>, struct., X-ray diffuse scatt. study 0-24437
- TTT cation radical salts, cryst. struct. by X-ray anal., rel. to elec. props. 0-24436
- TTTI<sub>x</sub>Br<sub>1.5-x</sub>, optical and transport props. 0-24911
- two-band system, coexistence of dielec. and supercond. ordering 0-10853
- valence bond theory of narrow band conductors 0-24777
- Ba<sub>4</sub>I, cyclodextrin, quasi-one-dimens. cpd., synthesis, elec. and mag. props. 0-2380
- Co<sub>0.83</sub>[Pt(C<sub>2</sub>O<sub>4</sub>)<sub>2</sub>].6H<sub>2</sub>O, cond., dielec. const., microwave obs. 0-44636
- Co<sub>0.83</sub>[Pt(C<sub>2</sub>O<sub>4</sub>)<sub>2</sub>].6H<sub>2</sub>O, quasi-one-dimens. conductor, Peierls distortion and superlattice, X-ray study 0-29397
- Fe<sub>2</sub>I, cyclodextrin, quasi-one-dimens. cpd., synthesis, elec. and mag. props. 0-2380
- Hg<sub>3-5</sub>AsF<sub>6</sub>, linear chain compound, mag. field induced residual resist., anisotropic supercond. 0-24897
- Hg<sub>3-5</sub>AsF<sub>6</sub>, one dimens. fluctuations and chain ordering transform 0-24593
- Hg<sub>3-5</sub>AsF<sub>6</sub>, one dimensional phonons and chain ordering 0-24544
- Hg<sub>3-5</sub>AsF<sub>6</sub>, quasi one-dimensional, anomalous magnetoresistance 0-24884
- Hg<sub>3-x</sub>AsF<sub>6</sub>, linear chain metallic cpd., square Fermi surface model for conduction 0-6822
- K<sub>2</sub>Pt(CN)<sub>4</sub>, quasi-one-dimens. Peierls system, phonon dispersion and neutron scatt., calc. 0-24550
- K<sub>2</sub>Pt(CN)<sub>4</sub>Br<sub>0.3</sub>2H<sub>2</sub>O, linear cond., <sup>195</sup>Pt NMR evidence of low lying non-linear excitation 0-44933
- K<sub>2</sub>Pt(CN)<sub>4</sub>Br<sub>0.3</sub>3H<sub>2</sub>O, quasi one-dimens. conductor, EPR linewidth 0-54938
- K<sub>1.75</sub>Pt(CN)<sub>4</sub>1.5H<sub>2</sub>O, Raman scatt. and luminesc. studies 0-25394
- K<sub>1.75</sub>[Pt(CN)<sub>4</sub>]1.5H<sub>2</sub>O, elec. cond. studies, Peierls transition 0-24901
- β-LiAlSiO<sub>4</sub>, eucryptite, one-dimensional ionic conductor, neutron scatt. study 0-49361
- NbS<sub>3</sub>, transport props. 0-20175
- NbS<sub>3</sub>(Se<sub>3</sub>), Peierls distortion, electron diff. obs. 0-39503
- NbS<sub>3</sub>(Se<sub>3</sub>), phase transitions and elec. props. 0-20178
- NbSe<sub>2</sub>(2H), intercalated with TCNQ, elec. resistivity temp. behaviour anomaly (*Russian*) 0-10953
- NbSe<sub>2</sub>/Fe (2H), pure and doped, magnetoresist. and elec. resist. temp. depend. rel. to CDW form. 0-44574
- NbSe<sub>3</sub> and Nb<sub>1-x</sub>Ta<sub>x</sub>Se<sub>3</sub>, thermoelec. power meas., 10-300K 0-20177
- NbSe<sub>3</sub>, CDW form., non-linear props., temp. and press. depend. 0-49753
- NbSe<sub>3</sub>, Fermi surface, press. effects, Shubnikov-de Haas effect meas. at 1.5K 0-20068
- NbSe<sub>3</sub>, metallic, non-ohmic cond., CDW pinning 0-39563
- NbSe<sub>3</sub>, quasi one-dimens. conductor, CDW phase transform., X-ray scatt. study 0-24594
- NbSe<sub>3</sub>, transport props. 0-20175
- NbSe<sub>3</sub>, two band model and galvanomagnetic study 0-20176
- Ni complex, (1,4,5,8,9,12,13,16-octamethyltetradbenzporphinato nickel)<sup>2+</sup> (I<sub>3</sub>), atomic limit of Hubbard model and polarons 0-39860
- Pt chain compounds, one dimens. conductors, Fermi wavevector determ., X-ray scatt. obs. 0-44187
- (SN)<sub>x</sub>, brominated, struct. and elec. props. 0-24914
- (SN)<sub>x</sub> halogenated derivatives, cond. and magnetoresist., 4.2-300K 0-24915
- (SN)<sub>x</sub>, supercond., fluctuation cond., crit. mag. fields 0-39712
- (SN)<sub>x</sub>Br, X-ray absorpt. meas. of mol. struct., orientation and charge transfer 0-25486

**one-dimensional conductivity continued**

- (Sn)<sub>x</sub> superconducting polymer, elec. cond., heat capacity and optical props. 0-7028
- TCNQ salt, TSeF-TCNQ, anal. of harmonic microwave mixing 0-44635
- (TSeT)<sub>2</sub>Cl, metallic phases 0-20159
- TTF-TCNQ, pure and irradi., nonlinear transport, ESR study, 1.2-4.2K 0-20167
- TTT<sub>2</sub>I<sub>3</sub>, neutron irradi. induced defects and chemical impurity effects on DC cond. 0-39565
- TaS<sub>3</sub>, transport props. 0-20175
- TaSe<sub>3</sub>(Se<sub>3</sub>), phase transitions and elec. props. 0-20178
- TaSe<sub>3</sub>, transport props. 0-20175
- Tl<sub>2</sub>Mo<sub>6</sub>Se<sub>6</sub>, one dimensional supercond. crystal struct., resist. and upper crit. field 0-50016
- one-dimensional conductors** *see one-dimensional conductivity*
- online literature searching** *see information retrieval*
- online operation**  
*used for systems software in online and real-time systems but for hardware aspects see real-time systems*  
*see also interactive systems; real-time systems*  
 gas chromatography-mass spectrometry data system, research-oriented, principles and applics. 0-40770  
 NMR in undergrad. instruction, general purpose microcomputers use for hypothetical spectra synthesis 0-42009  
 particle-particle correlation experiment, on-line four parameter anal. system (*Chinese*) 0-42910
- Onsager relations** *see thermodynamics*
- Onsager theory of dielectrics** *see dielectric properties of substances*
- opacimeters** *see turbidimetry*
- opallescence**  
*see also critical opalescence*  
 No entries
- OPDAR** *see optical radar*
- operating amplifiers** *see operational amplifiers*
- operating systems (computers)**  
*see also distributed processing*  
 RSX-11M appl. to X-ray diffr. and fluoresc. anal. 0-322
- operational amplifiers**  
 acoustic temp. indicator, consisting of temp. sensitive resistor and operational amplifiers (*Spanish*) 0-13061  
 electrochemical analysis, use of operational amplifiers 0-21335  
 ohmmeter reading range extension using noninverting op. amp. (*French*) 0-42207  
 photodiode sensor, camera shutter control appl. (*German*) 0-52341
- operator training** *see training*
- optic mode of crystals** *see lattice dynamics*
- optical aberrations** *see aberrations*
- optical activity** *see optical rotation*
- optical auroras** *see aurora*
- optical character recognition**  
 coherent OCR system using spatial light modulator (*Japanese*) 0-14291  
 development trends (*Czech*) 0-14457  
 holography technique appl., using optical spatial filter (*Japanese*) 0-5699  
 scan system for encoding and tabulation of visually scored sleep data 0-8197  
 spatial filter correlator, coherent optical matched, for microfilm data base word recognition 0-43279
- optical coherent transients**  
*see also photon echo*  
 free-induction decay, 100 ps time scale, laser freq. switching method 0-19074  
 many-pulsed excitation of optical coherent responses under large inhomogeneous line broadening (*Russian*) 0-48358  
 multilevel molecular system, coherent pulse propag. effects 0-9968  
 naphthalene:pentacene, picosec. optical coherence obs. 0-14400  
 naphthalene:pentacene, zero-phonon transition bottlenecks, photon echo detect. 0-33092  
 nutational photon echo 0-28283  
 particle motion effect on transient optical phenomena 0-1283  
 photon echoes, picosec., stimulated from accumulated grating 0-33092  
 rotary echoes, Bloch eqns. perturbative solns. 0-43407  
 ruby, optical free induction decay modulation and absorpt. line struct. due to superhyperfine interaction 0-33091  
 spectroscopy, superhigh resolution, using coherent phenomena 0-22445  
 subnanosecond optical free-induction decay with novel laser freq. shifting 0-38075  
 T<sub>2</sub> as collision time, dephasing time, or reciprocal linewidth, for teaching 0-27075  
 three-level molecular system, cooperative evolution, transient effects of dephasing and relax. 0-28184  
 time-correlated picosecond laser pulses generation, rapid sampling of optical relax. phenomena 0-9969  
 time-resolved laser saturation spectroscopy and coherent transients survey 0-9965  
 two-level atomic system, superfluoresc. fluctuations 0-23651  
 [<sup>15</sup>NH<sub>3</sub>], modulated coherent Raman beats 0-23464  
 H<sub>2</sub>O, relaxation by IR and microwave coherent transients 0-28092  
 I<sub>2</sub>, coherent optical transients and optical dephasing in mol. collisions 0-9966  
 KCl:KReO<sub>4</sub>, CO<sub>2</sub> pulse generation by free induction decay 0-53388  
 LaF<sub>3</sub>:Pr<sup>3+</sup>, optical transition, spin decoupling and magic angle line narrowing 0-28286  
 NH<sub>3</sub>, relaxation by IR and microwave coherent transients 0-28092  
 NH<sub>3</sub>, two-photon coherent transients, expts. 0-19073  
 Na, two-photon transition, distinction of competing processes in nonlinear resonant freq. mixing 0-33080  
 O<sub>2</sub>, relaxation by IR and microwave coherent transients 0-28092  
 OCS, relaxation by IR and microwave coherent transients 0-28092  
 SF<sub>6</sub>, model system, coherent pulse propag. effects 0-9968  
 SF<sub>6</sub>, nonradiative collisionless dephasing rate, two-photon coherent transient meas. 0-14176
- optical collimators**  
 alignment techniques by optical means 0-1341  
 autocollimation apparatus to test manufacturing quality of aspherical mirror profile 0-10053  
 autocollimator, photo-electric, calibration with laser interferometer system and microcomputer 0-1304  
 error compensators, calc. procedure 0-28296



**optical collimators continued**

- monochromatic MTF computation program 0-14451
- optoelectronic goniometers, linearity and sensitivity ranges increase 0-23786
- radioisotope imaging, optimal collimator design parameters for dynamic spatial resolution 0-17087
- scintillation camera/high energy collimator system, misleading results with a bar phantom image 0-12237
- X-ray diagnostic equipment, method and algorithm for adjusting 0-30852

**optical communication**

- see also *optical links*
- conference, Amsterdam, Netherlands (Sep. 1979) 0-46733
- development trends (*Czech*) 0-14457
- digital fibre optical communication system, average error probability calc. 0-53228
- electro-optics, conference, Utrecht, Netherlands (Oct. 1978) 0-31420
- error probability calc. in communication channel with intersymbol interf. 0-53227
- extraterrestrial laser signals detect. likelihood, instrumentation 0-4276
- fibre, development, advantages and applications 0-53410
- fibre cable attenuation and input and output efficiency 0-14469
- fibre cable transmission and strength improvement technology 0-28347
- fibre communication applications, trends and implications 0-33211
- fibre communications history and prospects 0-9994
- fibre optic communication, progress review of fibre design, low-loss and low-dispersion (*German*) 0-28325
- fibre optic systems, development during next decade 0-1329
- fibre optic telecommunication appls. 0-1330
- fibre optics appl., 1979 status and development trends 0-53408
- fibre technology and information transmission props. (*German*) 0-10010
- fibre transmission in TE<sub>01</sub> mode 0-53432
- fibre transmission technology, single mode systems in 1.0 to 1.8  $\mu$ m region, review 0-38105
- fibre-optic communication systems, devices and ccts., book 0-38123
- fibre-optic system appls., review of benefits 0-43480
- laser engineering and appls., conf., Washington, USA (May-June 1979) 0-1216
- laser modulator for HF laser communication links 0-48311
- laser propagation statistics in Montreal area 0-4099
- LW fibre-optic, InGaAsP/InP lasers and detectors 0-9885
- monomode waveguides developments 0-48404
- optical fibre transmission characteristics measurement appl. 0-53409
- quantum effects in communication theory 0-1147
- seawater transmission props. for underwater laser communication 0-33069
- signal detection characteristics, evolution of influence of destabilising factors 0-9825
- single-mode fibre cabling for low-loss communication 0-53467
- three-layer waveguides for wideband optical communication lines 0-28310
- timing error tolerant waveforms in optical fibre systems 0-14293
- tracking system for space laser communication 0-33068
- two-photon coherent states, quantum meas. realisable with photoemissive detectors 0-53220
- wavefront sensing using white light sources 0-1146

**optical communication equipment**

- see also *optical waveguides*
- 800 Mb/s fibre transmission test using low-loss and low-dispersion single-mode cable 0-10001
- acousto-optic planar guided-wave Bragg modulators, integrated optic communication appls. 0-38131
- bandwidth of distorted multimode waveguides excited by laser sources 0-43436
- bistable optical device, transient response and applications 0-33214
- characts. and appl. survey (*Flemish*) 0-5836
- circulator, polarization-independent, configuration method 0-38095
- circulator for optical fibre transmission, using Faraday rotator and Glan-Taylor prisms 0-23769
- connector, low loss index matched optical connector 0-48452
- data transmitter, laser and LED comparison (*German*) 0-14432
- data-bus system paired optical-fibre switch 0-23791
- demultiplexer, using diffraction grating, for FDM fibre transmission system 0-5845
- demultiplexer using concave grating, 0.7 to 0.9  $\mu$ m, expt. results 0-38099
- demultiplexer using Si echelette grating 0-53422
- electro-optical channel waveguide switch for computer communication bus 0-9987
- electrooptic diffraction modulator, large-aperture 0-33179
- electrooptical oscillator, integrated cutoff modulation 0-48424
- fibre, modal noise, dependence on source coherence and fibre length 0-48402
- fibre cable, measurement calc. of stranding pitch using stranded wire theory 0-10036
- fibre communication, elimination of polarisation in optical isolators 0-5844
- fibre communication receivers 0-43460
- fibre communication systems, computer design aids 0-28350
- fibre optic communication cable, commercial development review 0-1331
- fibre optic communication systems, utilisation of optoelectronic devices 0-1328
- fibre optic connectors, update on standardisation 0-5830
- fibre PCM repeaters with low power requirements, design and operation (*German*) 0-28315
- fibre splicing and connection techniques (*Italian*) 0-38097
- fibre transmission systems, active and passive devices 0-43463
- fibre voice transmission using unmodulated transmission of AF, telephone terminal sets (*German*) 0-28314
- fibre-based system, for analogue data transmission (*German*) 0-23781
- fibres and components, development and performance 0-53411
- GaAs laser diodes for optical communication transmission (*German*) 0-28252
- graded index rod lens applications in optical fibre communications 0-14485
- high-density low-loss optical fibre unit and cable 0-53468
- III-V semiconductor emitters and detectors for 1.0-1.6  $\mu$ m fibre-optic communications 0-10007
- injection laser quantum noise in optical fibre communication systems 0-48259
- integrated branching filter using three-dimens. input waveguide, nonradiative condition 0-38130

**optical communication equipment continued**

- integrated optics in later generation systems 0-43487
- laser beam deflector, electromechanical, for data transmission through free atmosphere (*German*) 0-38053
- laser diode appl., TJS, single-mode oscill. with low threshold currents 0-14355
- laser-fibre transverse coupling and front-mirror monitoring for feedback control of laser transmitters 0-33151
- LED coupling to optical fibre, efficiency 0-48416
- long-wavelength optical communication laser diodes and LED, 1  $\mu$ m range 0-48448
- LW receivers using avalanche photodiodes 0-10043
- metal-Ge Schottky barrier quantum detectors, optoelectronic props. 0-13146
- micro-optic directional coupler, aberration losses 0-48395
- microoptic grating multiplexers, optical isolators, fibre-optic communication applications 0-48408
- monolithically integrated optical repeater, fabrication and characts. 0-28353
- multiplexer using blazed grating, 1.1 to 1.5  $\mu$ m, for WDM transmission system 0-38100
- multiplexers/demultiplexers for single-fibre WDM transmission 0-43475
- multiwavelength monolithic integrated fibre-optic terminal development 0-33243
- Network 2000, use of optical communication technology 0-1306
- p-i-n/FET hybrid optical receiver 0-33158
- plastic fibre-optic assemblies 0-14433
- pulsed light source with thin-film modulator, fabrication and characts. 0-43467
- reed-type routing switch for multimode optical fibres 0-53463
- review of market trends and products 0-28319
- semiconductor devices for fibre transmission systems, reliability tests 0-43464
- semiconductor junction laser module for optical fibre communications, temp. compensation 0-5757
- semiconductor junction lasers, simultaneous feedback control of bias and modulation currents for injection lasers 0-43332
- semiconductor laser, electrooptically tuned external-cavity CW, FM optical communication appl. 0-14351
- semiconductor laser, pattern effect minimization at high-rate pulse modulation 0-19059
- standardisation of components, EIA P-6 committee 0-1352
- switch, four-way optical fibre, mechanically operated 0-53464
- transmitters for fibre communication systems 0-43459
- transmitting and receiving devices, laser light and fibre optics techniques (*German*) 0-5827
- waveguides development strategy, Poland (*Polish*) 0-48438
- waveguides technology, components and systems (*German*) 0-33168
- AlGaAs DH laser preamplifier to improve optical receiver sensitivity 0-53316
- (AlGa)As oxide-defined strip lasers, self-sustained oscillations, ageing effects, appl. to communication systems 0-32991
- CO<sub>2</sub> 10.6  $\mu$ m laser, freq. modulation and demodulation 0-43378
- (Ga,In)(As,P) DH lasers, 1.55  $\mu$ m, low-threshold current densities 0-1221
- (GaAl)As DH stripe contact injection lasers, local attached data fibre link appls. 0-19044
- Ga<sub>1-x</sub>Al<sub>x</sub>As buried heterostructure lasers for analogue communication 0-48297
- Ga<sub>1-x</sub>Al<sub>x</sub>As junction-up TJS laser electron injection efficiency improvement 0-48300
- Ga<sub>1-x</sub>Al<sub>x</sub>As-GaAs narrow stripe laser for improved communication performance 0-48299
- GaAs LED modulation bandwidth, influence of inhomogeneous current density distrib. 0-9993
- GaAs MESFET, optical detector appl., sensitive high-speed device 0-13143
- GaAs-GaAlAs laser, practical appls. 0-1212
- GaAs<sub>1-x</sub>Sb<sub>x</sub> photodiode structures, current-voltage characts., photo-EMF spectra 0-29472
- GaInAsP/InP DH lasers, direct modulation charact. meas. by sharp pulse method 0-1245
- GaInAsP-InP lasers and detectors, 1.1 to 1.3  $\mu$ m, fibre optics appls. 0-14360
- InGaAs/InP p-i-n small area photodiodes, fabrication, characts. and performance in 274 Mb/s receivers at 1.31 microns 0-53415
- InGaAsP InP DH lasers, optical power and wavelength stabilisation 0-38036
- InGaAsP laser, single-mode CW ridge waveguide, emitting at 1.55 micron for optical fibre links 0-9883
- InGaAsP/InP heterostruct. lasers as optical source, CW operation at room temp. 0-1220
- InGaAsP-InP dual wavelength LED 0-15589
- InGaAsP-InP:Mg LEDs, for high-bit-rate optical communication systems 0-5823
- Nd<sup>3+</sup> ion miniature phosphate glass lasers with high ion concentration 0-19038

**optical constants**

- see also *light absorption; reflectivity; refractive index*
- absorbing films, optical parameters determ. by ellipsometry 0-254
- biological materials, VUV and visible obs. 0-30762
- laser annealing, optical constants, ellipsometry observation 0-34024
- MgSiO<sub>3</sub>, Mg<sub>2</sub>SiO<sub>4</sub>, vapour condensed, mid IR optical props. 0-31337
- micellar solution, micellisation kinetics, pressure-jump and stopped-flow methods 0-45564
- optical glasses, development and manufacturing processes 0-53393
- quartz, far IR ordinary-ray optical constants 0-45025
- quartz, nonlinear polarisation plane rotation due to ruby laser irradi. (*Russian*) 0-53390
- semiconductor, optical props. with electron temp. superlattice (*Russian*) 0-34879
- thermoregulating plasma coatings, UV irradi. influence on optical parameters (*Russian*) 0-40259
- zero-gap semicond., IR absorption coeff., theoretical anal. 0-20641
- $\beta$ -AgI thin film, exciton spectrum 0-55216
- As<sub>2</sub>Se<sub>3</sub> chalcogenide semicond. film, thermooptical transitions with photostructural transformations (*Russian*) 0-16016
- Bi<sub>2</sub>(Te<sub>1-x</sub>S<sub>x</sub>)<sub>3</sub> film, optical const. meas., Shamir-Graff method evaluation 0-11489
- Co film, optical props. by self-consistent photometric technique 0-55217



**optical constants continued**

- Co<sub>1-x</sub>Fe<sub>x</sub>Si, elec. and optical props. 0-49740  
 Cr, fine particle solar absorber, effective medium theory 0-21396  
 CuFeS<sub>2</sub> single crystal, optical reflectivity spectrum 0-40129  
 FeBr<sub>3</sub>, Faraday rotation in pulsed mag. field, linear absorpt. const. 0-45041  
 Fe<sub>2</sub>O<sub>3</sub>, haematite, anal. of refl. spectrum by Kramers-Kronig relations 0-16058  
 GaAs, oxide film, microscopy with an ellipsometric arrangement 0-17998  
 Ge<sub>0.3</sub>As<sub>0.7</sub>Se<sub>0.5</sub>, IR optic materials, characteristics (*German*) 0-38081  
 GeS<sub>2</sub>, IR optic materials, characteristics (*German*) 0-38081  
 H<sub>2</sub>O, liquid, far IR optical const. meas. with optically pumped laser 0-40082  
 InP, reflection spectra, optical functions, exciton peaks (*Russian*) 0-50372  
 InSe, optical props. from 2-25 eV 0-29760  
 KCl coloured crystal, susceptibility variation calculations 0-55055  
 KNdP<sub>4</sub>O<sub>12</sub>, laser emission cross sections, fluorescence spectra, radiative lifetimes, quantum efficiency 0-23694  
 LaB<sub>6</sub> film, prep. by electron beam evaporation, and optical and elec. props. 0-20793  
 LiNbO<sub>3</sub>, optical const. determ. by background stimulated Raman scatt. 0-48336  
 LiNdP<sub>4</sub>O<sub>12</sub>, laser emission cross sections, fluorescence spectra, radiative lifetimes, quantum efficiency 0-23694  
 NaCl surface with adsorbed water layer, absorpt. and thickness meas. 0-16001  
 NaNdP<sub>4</sub>O<sub>12</sub>, laser emission cross sections, fluorescence spectra, radiative lifetimes, quantum efficiency 0-23694  
 Na<sub>2</sub>O·Al<sub>2</sub>O<sub>3</sub>·10TiO<sub>2</sub>, crystallized bronze, chem. comp., morphology, optical and thermal props. (*Japanese*) 0-16172  
 Ni, electronic structure and optical const. by inelastic electron scatt. 0-7451  
 Ni, optical const., influence of temp. and relation to bandstruct. 0-25403  
 Ni, optical spectrum, anomalous temp. depend. around T<sub>c</sub>, band struct. 0-40128  
 PbMoO<sub>4</sub>, Faraday rotation, interband optical transitions (*Russian*) 0-55071  
 PbTe film, optical const., support roughness effect 0-2882  
 PrB<sub>6</sub> film, prep. by electron beam evaporation, and optical and elec. props. 0-20793  
 Si<sub>1-x</sub>Au<sub>x</sub> amorphous films, IR absorpt. spectra 0-16034  
 SmB<sub>6</sub> film, prep. by electron beam evaporation, and optical and elec. props. 0-20793  
 Ti-Ni, martensite transform. B2-B19', optical props. and electron struct. (*Russian*) 0-34878  
 TiO<sub>2</sub>-Cu, anodic, effect of Cu on optical props., rel. to possible appl. in solar energy conversion 0-16115  
 UO<sub>2</sub>, liquid, reactor safety research, laser experiments (*German*) 0-42787

**optical couplers**

- 16-channel star coupler for fibre optic data links 0-43450  
 35 Mb/s optical fibre cable transmission using IR LED optocouplers 0-33156  
 acoustooptic hydrophone, coupled waveguide, using intensity modulation 0-14431  
 advantages of design with optoelectronic couplers (*Rumanian*) 0-33165  
 communication, conference, Amsterdam, Netherlands (Sep. 1979) 0-46733  
 connector, 2 male plugs and central lens receptacle, 10 min. field installation, less than 1 dB loss 0-43470  
 curved dielectric waveguides, coupling characteristics, coupled-mode equations 0-48455  
 data bus system optical coupler with light conducting fibres (*German*) 0-43438  
 directional couplers with weighted coupling 0-9992  
 fiber array, end preparation and fusion splicing with CO<sub>2</sub> laser 0-10051  
 fiber-optic safety closure with deflector 0-53425  
 fibre, modal noise, dependence on source coherence and fibre length 0-48402  
 fibre, theory and design 0-38122  
 fibre angular scrambling star couplers 0-53465  
 fibre butt coupling in aligned vee-grooves 0-53429  
 fibre connector for keyboard lens finger detection 0-19095  
 fibre connectors, wavelength dependent transmission loss 0-5825  
 fibre demountable connector, triple-ball connector using fibre-bead location 0-43431  
 fibre demountable connector using injection-moulded thermoplastics 0-53472  
 fibre lightguide connector with spring clip 0-23802  
 fibre optic connectors, 1979 design approaches 0-43437  
 fibre optic connectors, update on standardisation 0-5830  
 fibre optic connectors developments, cancellation of coupling mismatches 0-1332  
 fibre optic coupler use 0-28344  
 fibre optic coupling using tapered microlens, high efficiency (*Korean*) 0-43449  
 fibre optics communications, 1979 status and development trends 0-53408  
 fibre rod lens connector design and applications 0-53473  
 fibre Y-branch, low-loss 0-10004  
 fibre-optic communication systems, measurement techniques for passive optical components 0-1354  
 fibre-optic connector design, using resilient alignment mechanisms 0-48399  
 fibre-optic coupling techniques (*German*) 0-28330  
 fibre-optic interconnection design and performance 0-14436  
 fibre-photodiode alignment by etched Si structure 0-53430  
 future trends and problems 0-28319  
 Gaussian beams, waveguided, coupled by misaligned or curved grating effect 0-33228  
 grating coupler fabrication in waveguide photoresist. (*Czech*) 0-28354  
 injection laser diode coupling to planar waveguide 0-33245  
 integrated bistable optical multivibrator using electro-optically controlled directional coupler switches 0-19111  
 integrated directional coupler modulator, 1 Gbit/s 0-38125  
 integrated directional coupler switches, modulators and filters using Δβ reversal techniques, review 0-38132  
 integrated optical prism-waveguide dual coupler theory and exptl. performance 0-33236

**optical couplers continued**

- IR emitting diodes, high radiance, analysis of radiation coupling into optical fibre 0-14473  
 laser diode-to-diffused waveguide coupling efficiency, waveguide mode asym. effects 0-9990  
 laser-fibre transverse coupling and front-mirror monitoring for feedback control of laser transmitters 0-33151  
 micro-optic directional coupler, aberration losses 0-48395  
 microlenses to improve LED-to-fibre optical coupling and alignment tolerance 0-19088  
 monomode fibers developments, for optical communications 0-48404  
 multimode glass fibres 0-48405  
 multimode W-type fibres, steady-state characts. 0-5818  
 nematic liquid crystal adjustable access couplers for fibre-optic switching 0-33217  
 optical fibre splicing by butt-joint method, multi-glass-rod optical-fibre splicers made by drawing technique 0-53413  
 passive components for integrated-optics signal processing 0-48466  
 phase diffraction grating as laser beam coupler, radiation parameters monitoring 0-10033  
 polarisation-independent optical circulator coupled with multimode fibres 0-43430  
 polarisation-independent optical directional coupler switch using weighted coupling 0-28352  
 semiconductor laser beam coupling efficiency into fibre, matching element misalignment influence 0-48432  
 semiconductor laser optical isolator in laser-to-fibre coupling module 0-48267  
 shape memory effect alloy connector for optical fibres 0-53475  
 single fibre optic connector design and development 0-53474  
 single-mode fibres and integrated optical components, novel method of coupling, appls. 0-43442  
 single-mode optical fibre coupling techniques using microscopic lenses 0-53462  
 single-mode optical fibres, 1.3 μm, ceramic capillary connector with 0.3 dB loss 0-23778  
 slab-type waveguides, mode coupling via dichroic absorpt. of M centres 0-33178  
 spherical end faced coupling fibre fabrication by selective etching/melting 0-53492  
 star couplers, low-loss refl. type, for optical-fibre distrib. systems 0-1301  
 stepped switched optical directional couplers with unequal section lengths 0-33235  
 survey, coupling parameters and techniques (*German*) 0-38108  
 tee-coupler for single-mode fibres 0-10000  
 thick film optical waveguide integration with fibre-optic connectors 0-33246  
 waveguide components and systems (*German*) 0-33168  
 waveguide tapers for optical coupling of optical fibres, appls. (*German*) 0-38107  
 As<sub>2</sub>S<sub>3</sub> amorphous film waveguide and grating coupler 0-53448  
 GaAs film optical components, prep. by MBE using Si shadow masking technique 0-28358  
 GaAs integrated LED/sphere-lens source for optical fibres, coupling efficiency calcs. 0-43433  
 LiNbO<sub>3</sub>, Ti diffused, optical directional couplers, characts. 0-33145  
 LiNbO<sub>3</sub>:Ti waveguide directional coupler switches, optically-induced cross-talk 0-48417
- optical design techniques**  
*see also optical instruments*  
 antireflection coating, three-layer, refractive index optimum combination 0-28306  
 aperiodic spacious objects imaging, influence of AF sinusoidal phase deformations of wavefront (*Czech*) 0-14290  
 aspheric optics developments and appl. 0-5813  
 aspheric reflecting systems, geometrical design 0-38083  
 aspherical area shape predeterm. method (*German*) 0-28294  
 astronomical telescope design and construction technology 0-31211  
 astronomy, extreme values algorithm for automatic design (*Chinese*) 0-8544  
 catoptric objective design, testing (*German*) 0-53400  
 collimator monochromatic MTF computation program 0-14451  
 contemporary optical design, aspects 0-23766  
 Cooke triplet, air-spaced anastigmatic quadruplet design 0-1291  
 Cooke triplet derivative of five-element config., design 0-33111  
 cost reduction in manufacturing 0-1361  
 dichroic multilayer mirror for 16 μm region, design and fabrication 0-5808  
 diffraction gratings, review of Japanese research 0-10018  
 diffraction point spread function second moment as image quality criterion 0-9818  
 double Gauss basic lenses, design (*German*) 0-53398  
 elastic tools for finishing optical components with noncircular cylindrical surfaces 0-28368  
 element fabrication and assembly, centration errors 0-9980  
 factor analysis methods for designing complicated optical systems 0-28303  
 fibre optic sensor for photoelectric recording, design 0-28338  
 filter, narrow bandpass, for far IR, using double half wave designs 0-33173  
 Fresnel lens, colour-corrected linear convex, for solar concentration 0-45640  
 geodesic aspherical perfect lens, general sol. for integrated optics 0-10049  
 geodesic lenses, axially symmetric, geometrical theory 0-33238  
 geodesic lenses, aberration-corrected rounded edge, profile calcs. 0-10048  
 gradient index imaging lens and system status 0-14420  
 gradient index imaging system theory 0-14294  
 gradient index optical imaging systems, topical meeting, Rochester, USA (May 1979) 0-12851  
 gradient index spherical lens design for selfcoupled optical pickup system 0-14427  
 graphical ray tracing for conic surfaces 0-5683  
 high-volume optical component tolerance/specification relationship 0-48383  
 holographic concave grating design 0-1153  
 holographic lens system, method for wave aberrations calc. 0-28175  
 inhomogeneous planar dielec. waveguides for integrated optics structs., synthesis (*Russian*) 0-38135



**optical design techniques continued**

- interference coating, with narrow reflection bands, design (*Russian*) 0-43472
- interference filters, multilayer, design method 0-48396
- interference polarizers on plane-parallel substrates 0-1336
- IR lens system, large diameter, for pyroelec. vidicon 0-19086
- lens CAD, three-lens zoom system 0-43424
- lens compensators for testing concave mirrors of astron. telescopes, design 0-28305
- lens design, automatic, algorithm for accelerating convergence 0-38085
- lens design parameters, 35 mm format enlarging lenses, survey 0-13168
- Luneburg guided-wave optical thin-film lens, fabrication technique and props. 0-33223
- merit function, diffr. based, for automatic lens design (*Chinese*) 0-5809
- metal mirror design and mounting specifications 0-48388
- metal optics, reflective system specifications 0-48387
- microobjectives, reflected light, image glare coeff. depend. on design parameters 0-28302
- microscope scanning stage, motion rectilinearity determ., method and device 0-10055
- mirror systems, coupling props. determ. 0-53396
- multilayer nonabsorbent coating reflectivity computation program 0-28293
- multilayers, polarisation avoidance or enhancement 0-43255
- multiple-pass Raman gain cell 0-48334
- non-coaxial aspherical IR optical system, automatic design (*Chinese*) 0-5810
- nonimaging concentrator design as second stages with image-forming first-stage concentrators 0-50933
- nonimaging solar concentrator design, cavity enhancement by controlled directional scattering 0-45631
- pancratic apochromatic objectives, variable focal length, design 0-53404
- paraboloid epimirror for microscope illuminator, design 0-28304
- paraxial optical systems, nomographic diagrams for design and anal. 0-48377
- photocopier lens array design, Wood lens and gradient index fibre comparison 0-14479
- photographic gradient singlet, total aberrations 0-13177
- plane mirror system synthesis using biquaternions 0-9982
- plano-cylindrical Fresnel plastic lens, design and performance analysis as solar collector 0-53403
- plastic optical component specification 0-48362
- prisms dimensional design, rhombic, with and without computer (*Czech*) 0-53431
- radial refractive index gradient optical element, off-axis aberrations 0-14423
- ray tracing through tilted and decentred optical surfaces, computer program 0-33120
- reference mirror for alignment of optical instruments 0-10054
- reflecting optical system, seventh order design 0-48378
- reflector design, rotationally symmetrical, with aid of physical model (*Slovak*) 0-38088
- simplified optical system design using graphs 0-48379
- skew ray tracing with the TI-59, programmable calculator 0-48141
- solar concentrators, design variables, optical efficiency, heat loss coefficient and heat removal factor 0-7927
- solar energy, photo-optical instrumentation, [Conf. San Diego, CA, USA Aug. 1978] 0-7926
- solar energy concentrators, low cost-low ratio systems design 0-7928
- solar simulator design for testing solar collectors 0-50996
- stigmats using two curved Fresnel surfaces 0-38084
- system and component specifications, seminar, Washington, USA (Apr. 1979) 0-46731
- tapered light guide condenser design approach 0-33218
- telephoto apochromat lenses, design 0-31924
- tolerancing plan activities and documents 0-48382
- two-lens afocal compensators in high-resolution lens objectives, design 0-33125
- variable-focus objectives, use of aspherical surfaces 0-33124
- vector transformation by system of four plane mirrors 0-9981
- visual optical system specification and test procedures 0-48385
- visual system quantitative tolerance specification and standard development 0-48384
- waveguides with prescribed propag. const., design 0-48419
- wideband archival optical storage technology assessment 0-43283
- with equal optical thicknesses of layers, theoretical design, dielectric interference film, with equal optical thicknesses of layers, theoretical design (*Russian*) 0-43471
- zoom null lens design for optical component and system testing 0-23811
- zoom projection lens, optical level system, paraxial characts. 0-53399
- Ti/KCl/Ti low absorpt. antireflection coatings for KCl surfaces 0-38078

**optical detection of ENDOR** see *ENDOR; optical double resonance*

**optical detection of magnetic resonance (EPR)** see *microwave-optical double resonance*

**optical detection of magnetic resonance (radiofrequency)** see *magnetic double resonance; optical double resonance*

**optical dispersion**

see also *optical constants*

- alpha-power graded-core fibre dispersion, closed-form approximation 0-1320
- bistability, beyond mean-field theory 0-43408
- Brewster cases, generalised interface with uniaxial media, dispersion rels. (*German*) 0-5682
- continuous wavelength interferometry for measuring dispersion of complex refractive index 0-22423
- dielectric coating, highly dispersive artificial dielectric utilising metal spheres 0-5690
- dielectric waveguides, dispersion props., approx. formulas 0-14444
- elliptical multimode fibres, whispering and bouncing mode evaluation 0-10015
- fibre, low-loss graded index, produced by double crucible technique 0-48449
- fibre dispersion measurement, nonreciprocity noise in fibre gyroscopes 0-1346
- fibre single mode characterisation by LP<sub>11</sub> mode radiation pattern 0-23790
- fibre technology and information transmission props. (*German*) 0-10010
- fibre waveguide, chromatic dispersion effect on pulses of arbitrary coherence 0-1317

**optical dispersion continued**

- fibres, graded-index fibre cables, transmission meas. in 1.2 to 1.6  $\mu\text{m}$  range 0-10037
- fibres, min. dispersion at 1.55 micron for single-mode step-index fibres 0-10006
- fibres, modal dispersion with composite  $\alpha$ -profile graded-index core 0-9998
- fibres, mode dispersion, material dispersion and profile dispersion in graded-index single-mode fibres 0-14443
- fibres, single-mode, wavelength dispersion characts. (*Japanese*) 0-33162
- fibres, single-mode dispersion-free long-span, pulse broadening meas. 0-53417
- Fraunhofer diffraction of Gaussian beam at a straight edge 0-53205
- frequency-modulation spectroscopy: a new method for measuring weak absorptions and dispersions 0-42262
- glass film and shell wall thickness meas., white light interferometric meas., dispersion effect 0-4757
- graded-index optical fibres, compensation of profile dispersion 0-1316
- infrared microwaveguides with a mode-guiding layer of chalcogenide glass 0-28329
- inhomogeneous planar dielec. waveguides for integrated optics structs., synthesis (*Russian*) 0-38135
- injection laser quantum noise in optical fibre communication systems 0-48259
- IR reflection spectrum, dispersion formula fitting, Kramers-Kronig anal. 0-50311
- liquid, pure, organic and inorganic, Verdet const., pulsed mag. field meas. 0-16012
- multimode and single-mode optical fibre guides with rectangular cores 0-33220
- multimode fibre links, intermodal dispersion reduction by mode-delay equalising methods 0-48400
- multimode fibre with refr. index gradient distrib., pulse dispersion 0-10022
- multimode fibres, dispersion characts. from baseband freq. response meas. using InGaAsP laser beam 0-1308
- multimode step-index fibres, effect of waveguide struct. on material dispersion meas. 0-1311
- normal reflectance of conductors and insulators, dispersion relations and sum rules 0-29706
- optical fibre, graded index, intermodal dispersion meas. 0-38115
- optical fibre, high bandwidth graded-index, propag. const. meas. related to material props. 0-38103
- optical fibre, measurement of attenuation and dispersion 0-33185
- poly[(R)-oxypropylene], opt. rot. dispersion and vac. UV circular dichroism 0-40084
- pulse dispersion in a clad lens-like medium 0-53445
- ring cavity, dispersive bistability in homogeneously broadened systems 0-14306
- ring laser gyro, dispersion and gas flow effects 0-1267
- ruby, Cr<sup>3+</sup> ion doped, R-line region, absorpt. spectrum, dispersion rel. to mag. field 0-2732
- scattered radiation spatial structure statistical characts., optical thickness, particle conc. depend. 0-5694
- self-filtering S-type strip waveguides 0-33219
- single-mode fibre, 14 km long, with low attenuation at 1.2 to 1.32  $\mu\text{m}$ , MCVD fabrication 0-53461
- spatially dispersive media, optical boundary value problem 0-45024
- spatially dispersive medium, exciton polaritons, absorption theory 0-54618
- spliced graded-index fibres, 11.7 km link, measured and predicted transmission characts. 0-14454
- step-index fibres, multimode silicone-clad, mode dispersion 0-33142
- step-index monomode fibre, mode dispersion anal. of approx. for propag. const. 0-1307
- surface waves, interface with uniaxial media, dispersion rels. (*German*) 0-5682
- switching in dispersive optical bistability, anomalous behaviour 0-23740
- thin film rib waveguide, numerical anal. by mode-matching method 0-48421
- thin-film strip waveguide on dielectric substrate, optical dispersion 0-53478
- trapezoidal cross-section dielectric waveguides, mode dispersion by effective-index method 0-9999
- trichloroacetonitrile, IR dispersion, complex refractive index and permittivity, time correl. function 0-45057
- visibility, definition, confirmation using marine optics data 0-23633
- water-methanol(ethanol)(acetic acid), liq., Verdet const., pulsed mag. field meas. 0-16012
- waveguide mode with arbitrary anisotropy, dispersion relation 0-5840
- Al(PO<sub>3</sub>)<sub>2</sub>-NaF-LiF glasses, mixed-alkali effect 0-19715
- CuCl, anomalously slow group velocity of upper branch polariton 0-10893
- (Er,Tb,Gd<sub>3</sub>)Fe<sub>2</sub>O<sub>12</sub> plate, pseudouniaxial, domain struct., magneto-optical obs. 0-11221
- GaAs, refr. index and induced birefringence dispersion 0-2717
- Gd-La alloy, optical freq. cond. in 0.5-3.1 eV range, paramag.-ferromag. transition 0-29761
- Na vapour doublet, dispersion free point, cooperative phased-array radiation 0-53352
- PbI<sub>2</sub>, excitons in spatially dispersive medium, absorption theory 0-54618
- SiO<sub>2</sub>, fused, refractive index dispersion, thermal history depend. 0-25331
- SiO<sub>2</sub> single-mode optical fibre, wavelength dispersion characts. in low-loss region 0-53423
- SiO<sub>2</sub>:Ge single-mode fibres, dispersion meas., pulse synchronisation technique 0-48410
- SiO<sub>2</sub>-based single mode optical fibres, dispersion minimisation 0-9997

**optical double resonance**

see also *microwave-optical double resonance*

- absorption spectra in optical triple resonance 0-38069
- atom, AC Stark effect, fluoresc., in modulated laser beams, two-photon stepwise excitation 0-42989
- atom, two- and three-level, transition in stochastic field, saturation and Stark splitting 0-9546
- diatomic molecules, sub-Doppler laser spectrosc. 0-52320
- p-dibromobenzene crystal nucl. spin polarisation cross. relax. study 0-29647
- p-dichlorobenzene, in p-dibromobenzene, optical detection of Cl NQR in mag. field 0-50228



**optical double resonance continued**

- ethylene, IR double reson. obs., external-resonator controlled Raman laser pumped by CW CO laser 0-9624  
 fluoromethane-d<sub>3</sub>, matrix isolated, vibr. energy transfer at low temps. 0-37860  
 fluoromethane-d<sub>3</sub>, vibr. energy transfer at low temps., inert gas and N<sub>2</sub> matrix obs. 0-9706  
 formaldehyde-d<sub>2</sub>, 733  $\mu$ m line, Autler-Townes effect in laser interacting with RF field 0-53269  
 formaldehyde-d<sub>2</sub> vapour, IR-UV double resonance 0-43078  
 glyoxal, singlet-triplet coupling, double reson. and level-anticrossing spectroscopy 0-48053  
 halo-alkanes, IR-microwave double resonance, book contrib. 0-54997  
 microwave spectroscopy, modern aspects, book 0-51973  
 modern aspects, theoretical and expt. considerations, book contrib. 0-54997  
 NMR under optical pumping conditions 0-25253  
 nonlinear resonant propagation of two concomitant optical pulses interacting with three-level atomic system, num. modelling 0-9942  
 propynal, energy dispersion and relax., laser IR-visible double reson. 0-48023  
 propynal, energy dispersion and relax., laser IR/visible double reson. obs. 0-53028  
 propynal, internal energy distrib., collisional effects, IR-vis. double reson. obs. 0-14159  
 resonance scattering methods in atomic spectroscopy 0-53167  
 RF saturation spectroscopy, optical nucl. polarisation detect., excited state NMR and ESR transition mechanisms 0-54995  
 Stark splitting, optical dynamic, Zeeman degeneracy 0-37774  
 sub-Doppler technique, appl. to small mols. 0-52339  
 subpicosecond spectroscopy, tunable probe, spectral dynamics 0-23429  
 three-level system, double-reson. self-induced transparency, numerical integration 0-28288  
 triatomic molecules, sub-Doppler laser spectrosc. 0-52320  
 CO, collision-induced reorientation, direct meas. by IR double reson. 0-32800  
 ClO<sub>2</sub>, laser-microwave double reson. of  $\nu_1$  band 0-48022  
<sup>138</sup>La/<sup>139</sup>La nuclear electric quadrupole moment ratio, laser RF double reson. obs. 0-23447  
 LaF<sub>3</sub>:Pr<sup>3+</sup>, spectroscopic and relaxation character of <sup>3</sup>P<sub>0</sub>-<sup>3</sup>H<sub>4</sub> transition, photon echo 0-39897  
 Li<sub>2</sub>, optical-optical double reson.,  $\Sigma_g^+$  state mil. consts. 0-53027  
 NH<sub>3</sub>, IR-microwave double resonance, book contrib. 0-54997  
 SF<sub>6</sub>, highly excited, time-resolved IR absorpt. obs. 0-9666  
 SF<sub>6</sub>, IR double reson. with tunable diode laser 0-14160  
 SF<sub>6</sub>, laser-irrad., high-resolution double-reson. spectroscopy, collisionless multiphoton dissoc. 0-9623  
 SF<sub>6</sub>, multiple-photon excited, double reson. spectroscopy 0-53030

**optical elements**

- see also diffraction gratings; fibre optics; mirrors; monochromators; optical collimators; optical fibres; optical films; optical filters; optical isolators; optical modulation; optical prisms; optical waveguides; optical zone plates  
 adaptive optical components, seminar, Washington USA (Apr. 1979) 0-31421  
 aspherical, manufacturing and testing techniques development, use of computer (Italian) 0-48467  
 aspherical surfaces, holographic methods of testing, review 0-33257  
 Babinet compensator, appl. in optical testing 0-33251  
 beam divider and mirror expt., amplitude correlation method for optical polarisation meas. 0-53206  
 beam splitter, birefringent, polarisation-independent 0-5814  
 beam splitter, position in Michelson interferometer, form. of bands of equal thickness 0-52298  
 birefringent, rotating, and achromatic quarter wave plates, appl. to ellipsometry and photoelasticity (French) 0-14278  
 circulator, polarization-independent, configuration method 0-38095  
 component manufacture and evaluation, seminar, Los Angeles, USA (Jan. 1979) 0-12850  
 contamination modelling, photometric characts. estimation 0-48429  
 diffuser for Fourier transform hologram recording 0-43285  
 diffuser with pseudorandom phase sequence [hologram recording] 0-14298  
 discrete component Sagnac optical rate sensor, error sources 0-1342  
 dye, bleachable no.3955, relax. time meas., laser passive shutter appl. 0-23759  
 elastic tools for finishing optical components with noncircular cylindrical surfaces 0-28368  
 elliptic polarisation, Stokes parameters, vector trihedron, optical element evaluation 0-53209  
 fabrication and assembly, centration errors 0-9980  
 grids of fine W wire, production, use in IR spectroscopy, polarization interferometry 0-9052  
 half-screen, shadow cast when illuminated by Gaussian beam, props. 0-28156  
 high-energy, IR laser component optical characterisation techniques 0-14347  
 high-volume optical component tolerance/specification relationship 0-48383  
 imaging polarizer with spherical mirrors for VUV radiation 0-48375  
 integrated polariser, reduced cladding-medium, fabricated in ion-exchanged guides 0-14489  
 interference polarizer with large entrance aperture, characts. 0-43453  
 interference polarizers on plane-parallel substrates 0-1336  
 iris diaphragm with straight leaf edge, mechanism accuracy 0-28337  
 laser beam simple submicrosecond optical chopper 0-14373  
 laser induced damage in optical materials, symposium, Boulder, USA (Sep. 1978) 0-31417  
 laser optical component props. depend. on material flow props. (Russian) 0-38047  
 MBBA liquid crystal wedge as a polarizing element and its use in shear-wave interferometry 0-53444  
 plasma shutter for CO<sub>2</sub> laser, transmission cut-off time depend. on breakdown intensity 0-6259  
 plastic optical component specification 0-48362  
 polariser + crystal plate + analyser system, passage of light 0-10023  
 quartz:Ge attenuator for 0.25 to 1  $\mu$ m band, with attenuation coeff. up to 10<sup>5</sup> 0-48415  
 radial refractive index gradient optical element, off-axis aberrations 0-14423

**optical elements continued**

- reflector, 90 degrees, ray transfer matrix 0-33184  
 shutter, controllable phototropic, synchronization of single pulse ruby laser 0-23699  
 spectral shared aperture beam splitter for high-energy laser systems 0-14477  
 system and component specifications, seminar, Washington, USA (Apr. 1979) 0-46731  
 tapered gradient index rod, geometrical optics and imaging props. 0-14280  
 wide aperture optical shutter with saturating filter at 1.06  $\mu$ m 0-53457  
 CaF<sub>2</sub>, window for optical high press. cell at high temp., characts. (German) 0-47999  
 InSb-NiSb eutectic, struct. and optical props., IR polariser appl. 0-45078  
 W wire grids, FIR performance and appl. 0-10012  
 ZnS CVD window, IR lattice absorption, phonon assignments and image spoiling 0-33104

**optical fibres**

- 1.6 km half-duplex optical data link 0-14470  
 6-fibre cable with polyurethane covered steel wire central support, optical links appl. 0-43470  
 35 Mb/s optical fibre cable transmission using IR LED optocouplers 0-33156  
 800 Mb/s fibre transmission test using low-loss and low-dispersion single-mode cable 0-10001  
 800 Mbit/s digital transmission expt. (Japanese) 0-33164  
 acoustic modulation of light propagation 0-33209  
 acrylic coating, surface tension effects 0-53487  
 air-pollution monitoring fibre network system for wide area by optical absorption method 0-10002  
 alignment tool 0-23814  
 alkali germanosilicate glasses, water extraction for making graded index optical fibres 0-28361  
 alpha-power graded-core fibre dispersion, closed-form approximation 0-1320  
 angular scrambling star couplers 0-53465  
 applications as transmission medium, review 0-14456  
 arbitrary index profile, formula for TE<sub>01</sub> cutoff freq. 0-48418  
 arc fusion splicing of low-loss single-mode fibres 0-53489  
 arc splicing unit (German) 0-19115  
 axial refractive index depression in modified CVD preforms and fibres, interf. microscopy obs. 0-1319  
 backscatter attenuation measurements, optimised technique 0-53447  
 backscattering technique, appl. in fibre diagnostics and attenuation meas. 0-33188  
 bandwidth of distorted multimode waveguides excited by laser sources 0-43436  
 bandwidth of multimode fibres, calc. from refr. index profile meas. 0-5817  
 bandwidth spectrum of multimode fibres, depend. on refr. index profile 0-9985  
 bend loss radiation 0-33187  
 book, current topics in material science 0-46747  
 butt coupling in aligned vee-grooves 0-53429  
 cable attenuation and input and output efficiency 0-14469  
 cable specifications, fibre optic cable selection problem 0-28320  
 cable termination methods 0-53419  
 cable transmission and strength improvement technology 0-28347  
 Canadian government research, role and development in communications 0-43481  
 characteristics measurements, review 0-43458  
 chromatic signal distortion depend. on coherence of optical carrier 0-1317  
 circulator for optical fibre transmission, using Faraday rotator and Glan-Taylor prisms 0-23769  
 clad parabolic-index square-law, perturbation anal. 0-33190  
 clad with Teflonlike plastic coating, press. sensitivity 0-33149  
 classification, transmission modes and principles 0-43428  
 coated fibre and cable unit structure optimisation 0-53466  
 coating structure for microbending loss minimisation 0-28346  
 communication, conference, Amsterdam, Netherlands (Sep. 1979) 0-46733  
 communication appl., 1979 status and development trends 0-53408  
 communication applications, microoptic grating multiplexers, optical isolators 0-48408  
 communication applications, trends and implications 0-33211  
 communication cable, commercial development review 0-1331  
 communication cable manufacture 0-23794  
 communication cables, measurement of baseband transfer function 0-1355  
 communication fibre waveguide fabrication techniques 0-1322  
 communication fibres and components, development and performance 0-53411  
 communication receivers 0-43460  
 communication system apps., review of benefits 0-43480  
 communication system components characts. and appl. (Flemish) 0-5836  
 communication system transmitters 0-43459  
 communication systems, computer design aids 0-28350  
 communication systems, development during next decade 0-1329  
 communication systems, development of fibres 0-53458  
 communication systems, devices and ccts., book 0-38123  
 communication systems, elimination of polarisation depend. in optical isolators 0-5844  
 communication systems, measurement techniques for passive optical components 0-1354  
 communication systems, use of integrated optics 0-43487  
 communications, progress review of fibre design, low-loss and low-dispersion (German) 0-28325  
 communications history and prospects 0-9994  
 communications systems, review of worldwide development 0-43468  
 complete EM field of dielectric lossy fibre excited by dipole source, numerical calc. 0-43427  
 component developments 0-1356  
 compound glass fibres, mode-dependent effects, total loss decomposition, absorpt. and scatt. losses 0-53437  
 connector, low loss index matched optical connector 0-48452  
 connector design, using resilient alignment mechanisms 0-48399  
 connector for keyboard lens finger detection 0-19095  
 connector for single-mode fibres, low-loss detachable (Japanese) 0-33163  
 connectors, update on standardisation 0-5830



**optical fibres continued**

- connectors, wavelength dependent transmission loss 0-5825  
 connectors 1979 design approaches 0-43437  
 connectors developments, cancellation of coupling mismatches 0-1332  
 connectors theory and design 0-38122  
 cooling, convective, during high speed coating 0-23815  
 couplers, fibre optics applications 0-28344  
 coupling between single-mode fibres and integrated optical components, novel method and appls. 0-43442  
 coupling efficiency and surface damage threshold for giant and free-running laser pulses 0-33212  
 coupling efficiency of semicond. laser beam into fibre, matching element misalignment influence 0-48432  
 coupling parameters and techniques, survey (*German*) 0-38108  
 coupling techniques (*German*) 0-28330  
 coupling using tapered microlens, high efficiency (*Korean*) 0-43449  
 cutting tool 0-1360  
 cutting tool 0-33255  
 cylindrical optical fibre transmission and guided mode behaviour 0-28348  
 data bus system optical coupler with light conducting fibres (*German*) 0-43438  
 data transmission links (*Danish*) 0-10009  
 data-bus system paired optical-fibre switch 0-23791  
 deformation of cable sheath by bending in plastic range, loss anal. 0-43477  
 demountable connector using injection-moulded thermoplastics 0-53472  
 development, advantages and applications 0-53410  
 development for long wavelengths (*Danish*) 0-14434  
 differential interferometry, optical characteristics determination 0-48397  
 digital fibre optical communication system, average error probability calc. 0-53228  
 digital optical fibre system, 4-level, using LED, meas. at 68 Mbit/s 0-1313  
 m-dinitrobenzene, electrooptic cryst., growth in monomode optical fibres 0-55288  
 dispersion chars. from baseband freq. response meas. using InGaAsP laser beam 0-1308  
 doped-silica optical fibres, nuclear radiation effects 0-33172  
 dual beam fibre optic time-of-flight spectrometer 0-52347  
 electronic interconnection system design 0-5828  
 elliptical dielectric waveguides, higher-mode cutoff 0-43432  
 elliptical multimode fibres, whispering and bouncing mode evaluation 0-10015  
 elliptical selectively excited, near-field distrib. 0-48401  
 elliptical step-index multimode fibre, rays and modes 0-14442  
 elliptically clad borosilicate single-mode, strain birefringence 0-33148  
 end preparation and fusion splicing of fibre array with CO<sub>2</sub> laser 0-10051  
 error probability calc. in communication channel with intersymbol interf. 0-53227  
 evaluation of normalised cutoff frequencies in radially inhomogeneous fibres, perturbation theory 0-43434  
 fabrication, vapour-phase axial deposition, simultaneous dehydration with consolidation 0-23780  
 fabrication by vapour phase axial deposition, 1.3  $\mu$ m, low-loss and wide bandwidth 0-38136  
 Faraday effect in single-mode optical fibre using injection DH laser light source 0-48245  
 fatigue strength meas. of screen tested fibres 0-19098  
 fibre-photodiode alignment by etched Si structure 0-53430  
 field distribution of a point source inside a lossy optical fibre 0-10044  
 field measurement of splice loss applying backscattering method 0-19091  
 filled 10-fibre cable, epoxy/fibreglass central strength member, optical links appl. 0-43470  
 fluidised bed probing using optical fibres 0-19533  
 fundamental mode propag. on fibres of arbitrary cross section 0-43443  
 gamma irradiated, radii and refr. index changes 0-1338  
 germanosilicate, single polarisation, strain birefringence 0-1314  
 glass, analogue data transmission system (*German*) 0-23781  
 glass, production methods for optical communications (*German*) 0-23813  
 glass fibre development, large-core, for military appls. 0-48451  
 glass fibre for optical communications, statistics of tensile strength (*German*) 0-38121  
 glass fibre thickness meas. and control system in production (*German*) 0-10052  
 glass fibre waveguide,  $\gamma$ -irrad., reversible optical bleaching of induced absorb. 0-14462  
 glass fibre guides, for lighwave communication, fabrication and characterisation 0-50586  
 graded core W-type fibre and its propagation characteristics 0-1334  
 graded fibres with non-circular index contours, core fields 0-14455  
 graded glass fibre, effect of shape of refractive index profile, on distortion 0-33197  
 graded index, intermodal dispersion meas. 0-38115  
 graded index diameter determ. from backward scattered pattern 0-5820  
 graded index fibre optical loss meas. using dummy fibre 0-5819  
 graded index fibres made by vapour phase axial deposition, refr. index profile 0-48477  
 graded index P<sub>2</sub>O<sub>5</sub> doped CVD fabricated silica fibres, reduction of OH-ion conc. 0-1310  
 graded index rod lens applications in optical fibre communications 0-14485  
 graded monomode fibres and planar waveguides, analytical characterisation 0-43435  
 graded noncircular multimode, attenuation const. of leaky modes 0-33160  
 graded noncircular multimode fibres, leaky modes, analytical ray theory 0-33192  
 graded weakly guiding fibres, fundamental HE<sub>11</sub> modes 0-43444  
 graded-index, compensation of profile dispersion 0-1316  
 graded-index, for optical transmission system field trial, investigation of MCVD and VAD processes 0-43462  
 graded-index, propag. consts. and group delays 0-23770  
 graded-index fibre, spatial degree of coherence 0-53441  
 graded-index fibre cables, transmission meas. in 1.2 to 1.6  $\mu$ m range 0-10037  
 graded-index fibre link, baseband bandwidth estimation for spliced system, empirical formula 0-53460  
 graded-index fibre transmission characteristic computation 0-1321  
 graded-index fibre with polynomial-profile core, propag. constants of guided modes 0-10005
- optical fibres continued**  
 graded-index fibres, analytical relations between model power distrib. and near-field intensity 0-9995  
 graded-index monomode fibres with elliptical cross-section, birefringence 0-53416  
 graded-index multimode, distortion of light signals 0-19092  
 graded-index with polynomial profiles, propag. characts. 0-38118  
 guided-wave optical systems and devices, seminar, Washington, USA (April 1979) 0-31418  
 gyroscope, based on Sagnac effect, background and development (*German*) 0-48431  
 high bandwidth graded-index, propag. consts. meas. related to material props. 0-38103  
 high-density low-loss optical fibre unit and cable 0-53468  
 inhomogeneous circular waveguide, asymptotic eigenvalues 0-53442  
 injection laser diode, single freq., for integrated optics and fibre optic appls. 0-1237  
 integrated LED/sphere-lens source for optical fibres, coupling efficiency calcs. 0-43433  
 interconnection design and performance 0-14436  
 IR emitting diodes, high radiance, analysis of radiation coupling into optical fibre 0-14473  
 jacketed optical fibre residual stress diagnosis, pulse delay technique 0-53469  
 jelly-filled optical fibre cable fabrication and characteristics 0-53490  
 laser-fibre transverse coupling and front-mirror monitoring for feedback control of laser transmitters 0-33151  
 light source coherence meas. and fibre modal noise simulation by Michelson interferometer 0-48324  
 light transmission mechanism in optical fibres, communications appl. 0-43469  
 lightguide connector with spring clip 0-23802  
 local normal modes, superlattice modes, ideal modes 0-14466  
 long fibre, mirror and hollow dielec. lightguides, photometric characts. 0-33201  
 loss increase due to stranding in optical cables 0-38117  
 losses, spectral and length-depend. attenuation meas. using two-channel backscatter anal. 0-33159  
 low loss optical fibre waveguide, ionizing radiation effect on attenuation 0-38112  
 low loss optical fibre waveguide, radiation induced transmission loss behaviour, review 0-38111  
 low V-number., secondary maxima in far-field radiation pattern 0-33182  
 low-loss graded index, produced by double crucible technique 0-48449  
 low-loss high-numerical-aperture, fabrication by vapour-phase axial deposition 0-1315  
 low-loss optical fibre production with high numerical aperture 0-48450  
 low-loss single-mode fibres, elliptical and circular core, laser gyro appl. 0-1344  
 LW communication, InGaAsP/InP lasers and detectors 0-9885  
 manufacture, properties, optical links appl. 0-23793  
 measurement of attenuation, numerical aperture and input-output radiation profile 0-33186  
 measurement of attenuation and dispersion 0-33185  
 measurement of refractive-index profiles in optical-fibre preforms by spatial-filtering technique 0-48403  
 measurement procedure quality, standards 0-1351  
 measurement techniques for physical characts. 0-1353  
 mechanical deformation meas. by light scatt. method 0-14452  
 mechanical strength, fractographical analysis, review (*Japanese*) 0-35319  
 mechanical stresses effect on transmission 0-10032  
 mechanical testing of fibres and cables 0-3285  
 mechanically operated four-way optical fibre switch 0-53464  
 metal-free cables for wide temp. range appl. 0-23795  
 micro-light guide photometry of biological tissues 0-46005  
 microbending loss evaluation, arbitrary-index single mode fibres 0-48411  
 microbending loss evaluation, core index profile effects arbitrary-index single mode optical fibres 0-48412  
 microlenses to improve LED-to-fibre optical coupling and alignment tolerance 0-19088  
 minimum dispersion at 1.55 micron for single-mode step-index fibres 0-10006  
 modal dispersion with composite  $\alpha$ -profile graded-index core 0-9998  
 modal noise, dependence on source coherence and fibre length 0-48402  
 modal noise anal. and meas. 0-10003  
 mode conversion caused by splices of graded index fibres 0-1340  
 mode dispersion, material dispersion and profile dispersion in graded-index single-mode fibres 0-14443  
 mode-coupled multimode, baseband transmission theory based on scattering matrix 0-14468  
 monomode, fabrication, characterization and cabling for transmission in 1.2-1.6  $\mu$ m range 0-10042  
 monomode, optical communications developments 0-48404  
 multimode, anal. of propag. characts. and field distrib. in guided modes, review 0-43441  
 multimode, effect of microbending on light propag. (*French*) 0-53406  
 multimode, energy description of propagation of monochromatic radiation 0-38116  
 multimode, irregular, with fluctuation focusing, ray calcs. of power loss 0-33195  
 multimode, mode conversion coeffs. meas. 0-53433  
 multimode, mode-coupling phenomena anal. using matrix method, accuracy 0-23803  
 multimode, optical characts. meas. by backscatt. 0-23801  
 multimode, principles and performance of tapping elements 0-48405  
 multimode and single-mode optical fibre guides with rectangular cores 0-33220  
 multimode average intensity distrib. of laser light far-field radiation patterns at end face 0-53459  
 multimode delay compensation in fibres with profile distortions 0-33143  
 multimode fibre, pass band depend. on excitation conditions 0-48433  
 multimode fibre links, intermodal dispersion reduction by mode-delay equalising methods 0-48400  
 multimode fibre optimum refractive index profiles 0-14435  
 multimode fibre routing reed switch improvement 0-53463  
 multimode fibre with refr. index gradient distrib., pulse dispersion 0-10022  
 multimode fibres, arbitrary index profile, propag. mode anal. using ray optics adiabatic approx. 0-53418  
 multimode fibres, mode conversion coeff. meas. (*Portuguese*) 0-23797



**optical fibres continued**

multimode step index, effect of waveguide struct. on material dispersion meas. 0-1311  
 multimode W-type fibres, steady-state characts. 0-5818  
 multiwavelength monolithic integrated fibre-optic terminal development 0-33243  
 narrow band high power laser radiation transmission through fibres, non-linear optical processes 0-53443  
 nematic liquid crystal adjustable access couplers for fibre-optic switching 0-33217  
 Network 2000, use of optical communication technology 0-1306  
 optoacoustic effect observation using piezoceramic transducer 0-48423  
 optoelectronic devices facilitate fibre optic communication systems 0-1328  
 paper tape data transmission, wavelength multiplexing 0-43454  
 parabolic-index multimode, mode power distribution meas. method 0-14439  
 PCM repeaters with low power requirements, design and operation (*German*) 0-28315  
 plasma activated CVD, influence of substrate temp. 0-48475  
 plastic, polystyrene core material, 140 dB/km transmission loss at 670 nm 0-19093  
 plastic fibre-optic assemblies 0-14433  
 polarisation-independent optical circulator coupled with multimode fibres 0-43430  
 polymer protective coatings for glass fibres, materials and techniques 0-33252  
 polystyrene, and copolymers, spectral characts. 0-14461  
 power-law graded-index, core/cladding power distrib., propag. const. and group delay 0-48420  
 power-law refractive index profile, scalar modal eigenvalues and group delays 0-28322  
 preform fabrication in axial direction by vapour phase axial deposition, continuous process 0-43473  
 preparation by Ar plasma augmented vapour deposition 0-48478  
 progress in optical waveguide process and materials, review 0-23768  
 proof-tester for optical glass fibres 0-53412  
 quartz-glass large-diameter core and polymer cladding, prod. technology, low losses 0-14463  
 quasiparabolic index profile, propag. characts., perturbation anal. (*French*) 0-33189  
 radiation damage, nuclear pulsed thermal radiation effects, hardening techniques 0-33170  
 refractive index measurement (*Japanese*) 0-10020  
 refractive index profile, effect on fibre bandwidth 0-23773  
 refractive index profile models 0-14453  
 refractive index profile synthesis using algorithm for inverse Sturm-Liouville problem 0-28351  
 refractive-index profile and cross-sectional geometry of preform, nondestructive determ. 0-1312  
 reinforcement, primary coat using modified silicone, transmission characts 0-38098  
 remote detection of CARS employing fibre optic guides 0-9984  
 research projects at IROE Institute (Firenze) (*Italian*) 0-56668  
 review of market trends and products 0-28319  
 ribbon cable cutting tool 0-19113  
 ribbon splicing with vacuum-assisted injection mould 0-53491  
 rod lens connector design and applications 0-53473  
 rod-in-tube method, modified, for low-loss silica fibres manufacture (*Japanese*) 0-33253  
 self-focusing, matching elements calc. 0-28339  
 Selfoc conically graded medium, aberration anal. 0-1142  
 semi-automatic machine for hot splicing glass fibres for optical communication 0-23818  
 semiconductor laser couple, lasing spectra 0-1202  
 shape memory effect alloy connector 0-53475  
 sheathed fibres, excess loss due to coated resin shrinking at low temp. 0-43476  
 side illuminated, noncircular cross section effect on forward scatt. pattern 0-33150  
 silica optical fibres, large core polymer clad, electron-beam and  $\gamma$ -ray effects 0-33171  
 silicone double-layer coating with double cone nozzle in-line with optical fibre drawing 0-53488  
 silicone resin clad fibre technology, optical and mech. props. 0-28349  
 single fibre optic connector design and development 0-53474  
 single mode, anal. of propag. characts. and field distrib. in guided modes, review 0-43441  
 single mode, preparation and transmission properties 0-33204  
 single mode, refractive index profile meas., focusing method 0-33144  
 single mode fibre characterisation by  $LP_{11}$  mode radiation pattern 0-23790  
 single mode fibre transmission characts. and refr. index profile meas. from exit radiation pattern 0-9986  
 single mode optical fibre polarisation stabilisation 0-33154  
 single-mode, low-loss, for 1.55  $\mu$ m operation (*Japanese*) 0-33161  
 single-mode, splicing method based on discharge fusion (*Japanese*) 0-28317  
 single-mode, wavelength dispersion characts. (*Japanese*) 0-33162  
 single-mode cable, evaluation of characts. (*Japanese*) 0-28316  
 single-mode dispersion-free long-span fibres, pulse broadening meas. 0-53417  
 single-mode fibre, 14 km long, with low attenuation at 1.2 to 1.32  $\mu$ m, MCVD fabrication 0-53461  
 single-mode fibre cabling for low-loss communication 0-53467  
 single-mode fibre lightguide, phase of coherent signal, temp. and stress effects 0-33208  
 single-mode low-loss silica fibre prep., 10 km long 0-48476  
 single-mode optical fibre coupling techniques using microscopic lenses 0-53462  
 single-mode optical fibres, 1.3  $\mu$ m, ceramic capillary connector with 0.3 dB loss 0-23778  
 slit light guide design, fibre optics (*German*) 0-53420  
 snap-in fibre-optic aligners 0-1325  
 spherical end faced coupling fibre fabrication by selective etching/melting 0-53492  
 spherical surface, coupling to LED, efficiency 0-48416  
 spliced graded-index fibres, 11.7 km link, measured and predicted transmission characts. 0-14454  
 splicing and connection techniques (*Italian*) 0-38097  
 splicing and sheath jointing expts. 0-23806

**optical fibres continued**

splicing by butt-joint method, multi-glass-rod optical-fibre splicers made by drawing technique 0-53413  
 spring steel cutter for glass fibres 0-48468  
 standardisation of components, EIA P-6 committee 0-1352  
 star couplers, low-loss refl. type, for optical-fibre distrib. systems 0-1301  
 step index, mode conversion due to scattering from off-axis inhomogeneity, Green's function analysis 0-10045  
 step-index fibres, multimode silicone-clad, mode dispersion 0-33142  
 step-index fibres with microbending, bandwidth 0-23775  
 step-index monomode fibre, mode dispersion anal. of approx. for propag. const. 0-1307  
 step-index optical fibre, scatt. from off-axis inhomogeneity, radiation loss 0-43446  
 step-index single-mode fibres, birefringence in limit of weak guidance and slight ellipticity 0-1309  
 stimulated Raman scattering dynamics by Stokes component detect. 0-14394  
 strain measurement in coated optical fibres and cables using resistance wire 0-23804  
 stranding pitch, numerical calc. using stranded wire theory 0-10036  
 strength distribution description using upper and lower limits 0-53470  
 sum frequency generation of visible light, Q-switched mode-locked Nd:YAG laser excitation 0-43399  
 switch with electrostatic deflection cantilever 0-53427  
 tape twist induced stress estimation and reduction by pretwisting 0-53471  
 technology and information transmission props. (*German*) 0-10010  
 tee-coupler for single-mode fibres 0-10000  
 Telecom Australia optical fibre communications, fibre research and measurement technique developments 0-43456  
 telecommunication appls. of fibre optic systems 0-1330  
 telecommunication network, role of fibre optics 0-43484  
 telecommunication system components, status of development 0-43485  
 tensile strength, preparation conditions influence 0-33205  
 theory, basic principles and equations, multimode and single-mode fibre characteristics 0-43457  
 thick film optical waveguide integration with fibre-optic connectors 0-33246  
 timing error tolerant waveforms in optical fibre systems 0-14293  
 transmission characteristics measurement using backscatter technique, power decay separation from fibre imperfection contribution appl. 0-53409  
 transmission expts. at 1.3  $\mu$ m wavelength (*Japanese*) 0-28318  
 transmission in  $TE_{01}$  mode 0-53432  
 transmission of 565 Mbit/s signals on coaxial cables and optical waveguides 0-43483  
 transmission of communications, laser light and fibre optics techniques (*German*) 0-5827  
 transmission properties (*Czech*) 0-1305  
 transmission systems, active and passive devices 0-43463  
 transmission systems, development progress 0-43482  
 transmission systems, reliability tests on optical semiconductor devices 0-43464  
 transmission technology, single mode systems in 1.0 to 1.8  $\mu$ m region, review 0-38105  
 triple-ball connector using fibre-bead location 0-43431  
 two-mode, temporal spreading of pulse 0-33183  
 undersea cables, small, recent experiences 0-14488  
 uniform asymptotic theory 0-28323  
 uniform theory of inhomogeneous waveguide modes near cut-off 0-28324  
 VAD cables, characts. 0-43461  
 vapour phase axial deposition, OH content reduction by flame hydrolysis control 0-48474  
 voice transmission using unmodulated transmission of AF, telephone terminal sets (*German*) 0-28314  
 W-shaped fibre waveguide with rectangular core and two-layer shell, eigenmodes 0-28340  
 waveguide for time-of-flight spectra 0-23767  
 waveguide tapers for optical coupling of optical fibres, appls. (*German*) 0-38107  
 wavelength-division multiplexing transmission via single fibre, multiplexer design 0-33222  
 weakly guiding, modal propagation for arbitrary cross sectional shape 0-10014  
 Y-branch, low-loss 0-10004  
 AgBr single-crystal IR optical fibres, growth from melt 0-53449  
 $GeO_2-P_2O_5-SiO_2$  glass fibre, incorporation of OH in modified CVD process 0-50560  
 $In_{0.53}Ga_{0.47}As$  p-i-n photodiodes, for long-wavelength fibre-optic systems 0-5826  
 $Na_2O-K_2O-GeO_2-SiO_2-As_2O_3$  glass, water extraction for making graded index optical fibres 0-28361  
 $P_2O_5-SiO_2$  clad low-loss monomode fibres for 1.2 to 1.6  $\mu$ m, modified CVD prep. 0-48479  
 $PbF_2-AlF_3$  glass, optical props., crystn. and thermal expansion 0-48367  
 $SiO_2$  clad, elongation, force depend., deviations from linearity 0-45334  
 $SiO_2$  silica glass fibre CVD manufacture and characteristics 0-28345  
 $SiO_2$  single-mode optical fibre, wavelength dispersion characts. in low-loss region 0-53423  
 $SiO_2-Ge$  single-mode fibres, dispersion meas., pulse synchronisation technique 0-48410  
 $SiO_2-GeO_2/SiO_2$ ,  $SiO_2/SiO_2-B_2O_3$ , glass fibre waveguides,  $\gamma$ -radiation optical stability 0-23799  
 $SiO_2$ -based single-mode, dispersion minimisation over wide spectral range 0-9997  
 $SiO_2-GeO_2$ , 21.2 km graded-index VAD fibre with low loss and wide bandwidth 0-53414  
 $SiO_2-GeO_2$ , preform prep., particulate mass transfer mechanism in modified CVD, thermophoresis 0-2955  
 $SiO_2-GeO_2$  particles, deposition props. in flame hydrolysis reaction for optical fibre fabrication 0-48470  
 $SiO_2-P_2O_5$  cladding vapour-phase axial deposition fibres at 1.3  $\mu$ m and 1.6  $\mu$ m 0-9996

**optical films**

see also antireflection coatings  
 absorbing films, optical parameters determ. by ellipsometry 0-254  
 absorption light filters, thin-film 0-19101  
 absorption measurement by 1.06  $\mu$ m laser calorimeter 0-33066  
 absorptive laser damage analysis by Weibull distrib. 0-33061



## optical films continued

coating requirements in United States military specifications 0-48365  
 coating technique and refractive index meas. 0-43488  
 dichroic multilayer mirror for 16  $\mu\text{m}$  region, design and fabrication 0-5808  
 dielectric coating, highly dispersive artificial dielectric utilising metal spheres 0-5690  
 dielectric interference film, with equal optical thicknesses of layers, theoretical design (*Russian*) 0-43471  
 dielectric laser mirror production with variable transmissivity (*Russian*) 0-14362  
 dielectric multilayers, optical and geometrical thickness monitoring using monochromatic maximeter, substrate effects (*French*) 0-38140  
 dielectric thin film deposition by CW  $\text{CO}_2$  laser, optical and struct. props. 0-7506  
 DOBAMBC, chiral smectic C-phase ferroelectric liq. crystal film, classical X-Y system, props. 0-44123  
 fibre coating structure for microbending loss minimisation 0-28346  
 Fresnel formula for dielectric multilayer mirrors 0-33118  
 inhomogeneous interface laser mirror coatings, durability improvement 0-1252  
 interference coating, with narrow reflection bands, design (*Russian*) 0-43472  
 interference filters, multilayer, design method 0-48396  
 interference polarizers on plane-parallel substrates 0-1336  
 ion polishing for diamond-turned mirror dielectric coating adhesion 0-1370  
 ion polishing of optical coatings, for multilayer interf. systems and integrated optics 0-33261  
 IR multilayer partial mirrors effective from 1.3 to 16  $\mu\text{m}$ , GeSe/KRS-6 and GeSe/NaF 0-9978  
 laser beam indicator/visualiser made from new thermochromic material 0-9976  
 laser coating, UV damage obs. 0-33056  
 laser coating materials, 100 ns pulsed laser damage at 2.7 and 3.8  $\mu\text{m}$  0-33057  
 laser induced damage in optical materials, symposium, Boulder, USA (Sep. 1978) 0-31417  
 laser rate calorimetry analysis with coating absorption 0-33050  
 metal oxide layers, obtained by cathode and HF sputtering, light scatt. and refr. index reduction 0-29877  
 multilayer coating performance, thin-film volume or interface absorption effect calc. 0-33130  
 multilayer nonabsorbent coating reflectivity computation program 0-28293  
 multilayer structure devices, nonideal, computation of optical props. 0-5684  
 multilayers, polarisation avoidance or enhancement 0-43255  
 organic thin film refractive index adjustment by absorbing dyes 0-43413  
 oscillating beam spectrometer for organic thin film transmission 0-18022  
 oxide single and multi-layer optical coatings, light scattering reduction and meas. 0-48381  
 photochromic film waveguide, acousto-optical props., integrated optics appl. 0-33207  
 photoimaging system based on photopolymerisation in cryst. coatings 0-40716  
 pulsed laser damage determ., optical techniques 0-33060  
 quarter wave multilayer monitoring, optical props. change rel. to error compensation 0-38139  
 quarter-wave dielectric reflector, spectral absorbance approximation 0-33131  
 rare earth fluorides,  $\text{CeF}_3$ ,  $\text{PrF}_3$ ,  $\text{LaF}_3$ , coating materials for IR laser components 0-33105  
 refractive index and thickness, algorithm for determ. on basis of ellipsometric meas. 0-34881  
 refractive index variation for given reflectivity, analytic soln. to synthesis problem 0-34996  
 selective optical properties, for enhanced output and radiation spectrum correction, light sources appl. (*Russian*) 0-48372  
 sputtered, production and props. (*Hungarian*) 0-53483  
 stray light performance, surface and system scatt. characteristic specification 0-48389  
 system and component specifications, seminar, Washington, USA (Apr. 1979) 0-46731  
 transparent film on absorbing substrate, optimum angle of incidence for monochromatic interference 0-43254  
 UV coating, damage resistance 0-33047  
 vacuum deposition, improved film quality, progress in vacuum generation and deposition technology 0-35101  
 waveshifter coatings for fluorescent radiation convertors 0-32574  
 Al reflective coating, reflectance in UV and visible 0-28307  
 $\text{Al}_2\text{O}_3$  facet coating, self-pulsation stabilisation and initial degradation elimination in (Al,Ga)As laser 0-43347  
 As-S glassy film, photobrightening effect 0-11498  
 $\text{As}_2\text{Se}_3$  film on  $\text{CaF}_2$ , interface and bulk absorption meas. 0-35001  
 Au film on Al, reflectance and absorpt. obs. 0-7426  
 $\text{BiF}_3$  coating materials for IR laser components 0-33105  
 $\text{BiI}_3$  coating materials for IR laser components 0-33105  
 $\text{CeO}_2$  coating of laser optical components, electron microscope obs. 0-43342  
 $\text{Cr}_2\text{O}_3$ -Cr black, on Ni, defects and their effect on props. 0-39474  
 $\text{GeO}_2$  optical props., rel. to possible appl. in holography 0-29816  
 $\text{In}_2\text{O}_3$  film reactive sputtering gas composition and film growth rate (*Russian*) 0-50554  
 $\text{In}_2\text{O}_3$  transparent conductive coating production 0-35092  
 $\text{In}_2\text{O}_3$ , transparent heat mirror formation by ion plating on ambient temp. substrates and props. 0-25578  
 $\text{KGaF}_4$  coating materials for IR laser components 0-33105  
 NaF film on  $\text{CaF}_2$ , interface and bulk absorption meas. 0-35001  
 NaF film on ZnSe plate, absorption coeff. ATR spectroscopy 0-35000  
 $\text{PbF}_2$ -TiI graded coatings on KCl laser windows, photoacoustic spectroscopy 0-33052  
 Pt evaporated film, optical props. meas. in VUV, 220 to 150  $\text{\AA}$  0-45159  
 $\text{SiO}_2$ , amorphous, dispersion of refr. index and chem. comp. 0-7429  
 $\text{SiO}_2$ , durable, ion plating onto plastics, optical and mech. props. 0-38141  
 Te facet coating, for side lobe suppression in far field of AlGaAs DH stripe laser 0-5744  
 $\text{TiO}_2$ , reactively sputtered optical coating for inertial confinement fusion laser components 0-23705  
 $\text{TiO}_2$ - $\text{SiO}_2$  multilayered film striped optical filters, optical props. and fabrication of RF sputtering 0-10030

## optical films continued

$\text{TiO}_2$  durable, ion plating onto plastics, optical and mech. props. 0-38141  
 TiI coatings on KCl laser windows, photoacoustic spectroscopy 0-33052  
 $\text{VO}_2$  film as holographic recording medium, diffr. efficiency 0-28180  
 $\text{WO}_3$  film, evaporated, mech. of elec. cond. 0-44747  
 ZnS films prepared by thermal evaporation in vac., nature of defects 0-10835

**optical filters**  
 see also light absorption; optical films; optical isolators; spatial filters  
 absorption light filters, thin-film 0-19101  
 acoustooptic tunable filter for staring IR sensor, performance 0-36407  
 aperture, partially apodised, diffracted field characts. 0-48139  
 apertures with Straudel Class of pupil functions, var. apodisation 0-23616  
 apodizing filters for optimum Sparrow resolution in coherent systems with annular aperture 0-53435  
 atmospheric transmittance meter, absolute filter device 0-51584  
 birefringent filter improvements, field of view effects 0-14428  
 certification of neutral light filters using spectrophotometers in UV, visible and near IR regions 0-273  
 conversion filters for scientific photography 0-48394  
 deconvolution techniques applied to astronomical images 0-46407  
 didymium glass filters for spectrophotometer wavelength scale calibration 0-43417  
 diplexer reflection type periodic filter, elliptic response 0-43474  
 electronographic photometry, narrow-band high spatial resolution, astron. appls. (*French*) 0-46408  
 Fabry-Perot interference filters, neutron irradi. effects 0-14437  
 fibre and integrated optical devices for signal processing 0-33233  
 height and flow velocity, optical pseudo-colour processing (*Japanese*) 0-9826  
 integrated branching filter using three-dimens. input waveguide, nonradiative condition 0-38130  
 integrated directional coupler switches, modulators and filters using  $\Delta\beta$  reversal techniques, review 0-38132  
 interference filter, transparency, effect of harmonic variation of layer thickness 0-28326  
 interference filter for submillimetre astronomy 0-48393  
 interference filters, multilayer, design method 0-48396  
 interference polarization filters, crystal plate orientation depend. of spectral background 0-48426  
 IR multilayer interference filter manufacture, supposed longwave limit 0-9989  
 isotropic medium, nonlinear refr. index, self-induced polarisation rot. 0-5802  
 Kaiser filters, window function, equivalent pass band, incoherent optical transfer function 0-1323  
 laser beam indicator/visualiser made from new thermochromic material 0-9976  
 laser engineering and appls., conf., Washington, USA (May-June 1979) 0-1216  
 luminescence filters, efficiency for Nd:glass lasers 0-1213  
 metallic mesh interference filters, low temp. narrowbandpass 0-14430  
 metallized polyester film as a solar filter 0-51666  
 Michelson interferometer, use as selective filter for stratospheric trace gas concs. meas. 0-17408  
 multi-element interference filter, far IR, generalised treatment 0-33174  
 multilayers, polarisation avoidance or enhancement 0-43255  
 multiplexer design for optical wavelength-division multiplexing transmission via single fibre 0-33222  
 narrow band interf., optical props. as function of incidence angle and polarisation 0-19102  
 narrow bandpass, for far IR, using double half wave designs 0-33173  
 nonquarterwave multilayer, optical monitoring with minicomputer allowing thickness error correction 0-23774  
 nonquarterwave multilayer, wideband optical monitoring during deposition 0-28309  
 optical spatial filtering, of visualised results of flaw detection monitoring, rational regions of appl. 0-7751  
 photographic light sources, characteristics and parameter definition using graphical method for correct choice of compensating filters (*German*) 0-52342  
 quarter wave multilayer monitoring, optical props. change rel. to error compensation 0-38139  
 reflected-light fluorescence microscope, LABOVAL 2a.fl, for routine and research 0-56300  
 rhomb laser beam sampler, two-grating, inherent aberration correction, inverse filter description 0-37954  
 ring laser, solid state, with intracavity bleachable filter, conditions for CW stimulated emission 0-14368  
 saw-tooth wave target, modulation by optical system with triang. and assoc. filters 0-9817  
 second- and higher-order waveguide grating filters, refl., transmission and loss coeffs. meas. 0-19110  
 second- and higher-order waveguide grating filters, spectral response calcs. 0-19109  
 semiconductor iso-index coupled-wave electrooptic filter 0-1324  
 spatial, pattern recognition by means of holography (*Japanese*) 0-5699  
 spectrophotometer, cutoff system for filtering out higher spectral orders in 400 to 200  $\text{cm}^{-1}$  region 0-28334  
 spectrophotometer-type filters of highest possible performance, 2.5-40  $\mu\text{m}$  0-14438  
 sputtered films production and props. (*Hungarian*) 0-53483  
 tunable narrow-band thin-film waveguide grating filters, performance 0-38124  
 wide aperture optical shutter with saturating filter at 1.06  $\mu\text{m}$  0-53457  
 Ag halide emulsion colouring, k-value and sensitivity relationship (*German*) 0-7815  
 $\text{As}_2\text{S}_3$  thin films, vacuum deposited on Ge and PbS, sealing props. and TEM 0-35097  
 GaAs-polyethylene mixture, optical transmission spectra, IR filter prep. using computer appl. 0-2763  
 $\text{TiO}_2$ - $\text{SiO}_2$  multilayered film striped optical filters, optical props. and fabrication of RF sputtering 0-10030

optical free induction decay see optical coherent transients

## optical frequency conversion

see also optical harmonic generation; optical parametric devices  
 degenerate 4-wave mixing in plasmas 0-24179  
 dye laser, difference frequency generation, degree of conversion depend. on linewidth 0-48347



**optical frequency conversion continued**

- fifth order atomic optical nonlinearities in multiphoton resonances 0-28275
- integrated coherent IR generator, difference freq. generation in nonlinear optical waveguide 0-33084
- IR image nonlinear conversion allowing for turbulent atm. influence 0-23751
- IR source, tunable, efficient 0-5789
- N two-level atoms, quantum theory of nonlinear optical phenomena 0-5790
- nonlinear adaptive system, characteristic purposes 0-28273
- nonlinear crystals for frequency conversion of optical radiation, review (*Russian*) 0-38068
- optical fibre, sum-freq. generation of visible light 0-43399
- parametric frequency up-conversion with stochastic pumping, canonical model 0-53368
- phase distortion compensation by three-freq. parametric interaction 0-23750
- phasematching of freq.-conversion processes induced by additional selective pump 0-28271
- polarization converters for 2-freq. optical interferometers 0-18005
- resonant parametric optical conversion in gases (*Russian*) 0-48351
- SHG in crystals, two-photon radiation absorpt. effect 0-9950
- signal detuning, effects on phase conjugation 0-23748
- three-wave interactions in randomly inhomogeneous dispersive media (*Russian*) 0-53364
- three-wave mixing, multiplicative stochastic processes in statistical physics appl. 0-22289
- tunable laser resources development and appl., laser pulse width meas. 0-48262
- two-photon field nonlinear optical efficiency, sum freq. generation 0-9949
- up-conversion with stochastic pumping, exactly soluble model 0-23744
- upconversion, three-freq. parametric, beam focusing effects 0-48340
- urea crystal, efficient phase-matched SHG and sum freq. mixing 0-14391
- vision, IR nonlinear perception in 800-1355 nm range 0-12123
- $\text{Ag}_3\text{AsS}_3$ , proustite upconverter, effect of temp. on phase match angle characts. 0-5799
- Be, 4-wave sum mixing around H Lyman- $\alpha$  0-23747
- CdS, biexciton, low intensity nonlinear coherent mixing study 0-49619
- CdSe, down-conversion of picosecond IR source, 10 to 20  $\mu\text{m}$  tuning range 0-5793
- $\text{Hg}_{1-x}\text{Cd}_x\text{Te}$ , nonlinear optical effects 0-14389
- n-InSb, spin resonant four-wave mixing, CW meas. and transient effects 0-48344
- $\text{LiIO}_3$ , simultaneous stimulated Raman scatt. and optical freq. mixing using three-mirror config. 0-48342
- $\text{LiNbO}_3$  crystal and ruby lasers in difference freq. laser, tunable MM range emission 0-5764
- $\text{LiNbO}_3$ , SHG, two-photon radiation absorpt. effect 0-9950
- $\text{LiNbO}_3$  three-dimens. optical waveguide, parametric difference freq. generation 0-48335
- Na, two-photon transition, distinction of competing processes in nonlinear resonant freq. mixing 0-33080
- Na vapour, effective freq. conversion of radiation 0-28278
- Na vapour, reson. freq. conversion by two-photon reson. pumping 0-28277
- Nd laser, emission freq. conversion by method of reson. pumping of active media 0-1206
- Si, degenerate four wave mixing of 1.06  $\mu\text{m}$  laser radiation 0-5794

**optical glass**

- apochromatic pancratic objective components, primary chromatic coeffs. 0-28298
- boundary with  $\text{CS}_2$ , optical bistability at nonlinear interface 0-33094
- communication fibre waveguide fabrication techniques 0-1322
- compound glass fibres, mode-dependent effects, total loss decomposition, absorpt. and scatt. losses 0-53437
- cylinder refractive index variation by field-assisted ion exchange 0-14500
- development and manufacturing processes 0-53393
- didymium glass filters for spectrophotometer wavelength scale calibration 0-43417
- ellipsometric study of zone of contact 0-4754
- fibre production methods for optical communications, review (*German*) 0-23813
- fibre technology and information transmission props. (*German*) 0-10010
- fibre waveguide,  $\gamma$ -irrad., reversible optical bleaching of induced absorpt. 0-14462
- finishing with small-grained diamond grinding wheels (*German*) 0-38137
- flint, dense and ultradense, acousto-optical props. and appl. (*Russian*) 0-2721
- fluorophosphate and fluoroberyllate glass laser damage thresholds and solid inclusions 0-33054
- fluorophosphate laser glass, highly homogeneous, production 0-14411
- gradient index lens fabrication by molecular stuffing 0-14499
- gradient index material models and exptl. verification 0-16002
- gradient index SELFOC lens, aberration improvement 0-14425
- gravity glass, IR emissivity, 673-1673K 0-24623
- greasy films on glass, due to everyday handling, effect on optical transmittance 0-27329
- ground, surface height and correlation length from reflection scatt. of laser light (*French*) 0-54491
- inhomogeneous glass sintering, self stresses producing bulk flow, optical wave guide appl. 0-14448
- IR materials for measuring radiant flux, IKS glass (*Russian*) 0-48366
- IR permeable materials (*German*) 0-38081
- IR spectral emissivity and absorpt. coeff. at 600 to 1700K 0-16018
- K8, bending strength, sample dimension effects 0-9975
- K8, foam form. and suppression methods during polishing 0-28364
- light effects, history of development of photosensitive and polychromatic glasses 0-40080
- multicomponent Schott, proton-induced colouring 0-9974
- ophthalmic lenses, thin, chemtempered, strength meas. by drop-ball testing 0-5811
- phosphate laser glasses, review 0-9888
- photochromic, electron-hole separation, influence on recombination probability 0-11445
- photochromic, spectral characts. control 0-16073
- photochromic, thermo-optic transitions 0-50307
- photochromic glass, coloration kinetics, isothermal relax., and spectral sensitivity using spectrosensitometer 0-27358

**optical glass continued**

- photochromic glass, with Ag halides:Cu formation and theoretical models, review 0-43418
- photosensitive glass, microstruct. rel. to props. (*German*) 0-38926
- planar waveguide, fabricated by ion exchange in glass, refractive index profile 0-14460
- polished, 1.064  $\mu\text{m}$  laser damage threshold rel. to pulse duration and surface roughness 0-33055
- polishing with  $\text{ZrO}_2$ - $\text{SiO}_2$  powder mixture 0-28367
- polychromatic, induced colour by optical/thermal treatment 0-34954
- polychromatic thick lens glass selection (*German*) 0-23763
- quartz glass, spectral absorpt., 3000-4000K 0-25401
- quartz glass, spectral absorpt. coeff., 0.25 to 1.25  $\mu\text{m}$  and 1300 to 1700K 0-20622
- quenching, horizontal, technological parameters rel. to optical properties 0-45264
- Raman scattering and nonlinear refr. index 0-2749
- refractive index freq. depend., dispersion eqn. calc. 0-40083
- silicate Fe activated glass, diffraction trating recording by UV laser 0-5842
- soda lime glass gradient index variation by ion exchange and migration 0-14412
- solar glass components, specularly meas. using Fourier transform anal. 0-5804
- space glass technology (*German*) 0-40317
- stained glass, Ag- and Cu-, optical waveguide effect (*Japanese*) 0-14471
- thermal diffusivity of silicate glasses in range 0-600°C, influence of  $\text{TiO}_2$  0-29233
- thermophysical props., temp. wave methods 0-24624
- torsional deform. above  $T_g$  under low stresses, temp. effect 0-21052
- torsional deform. above  $T_g$  under low stresses of type K8 0-25804
- toughening of coloured glass, spectral characts. 0-43416
- waveguide, fabrication in glass by effusion 0-5850
- waveguide, in-plane scatt. and loss mechanisms 0-33216
- waveguides, diffused glass, graded refractive index, anisotropy 0-33210
- Ag halide, photochromic glass, optically induced anisotropy 0-1282
- Ag halide photochromic centres, isothermal relaxation kinetics 0-16072
- AgCl photochromic glass, additional absorpt. spectrum, ellipsoidal model of colour centres 0-40142
- As-S glassy film, photobrightening effect 0-11498
- As-Se chalcogenide glass, optical const. photoinduced changes mechanism 0-7321
- $\text{CdO-GeO}_2\text{-Ti}_2\text{O}_5$  photochromic glass for optical information retention media 0-33108
- Cu halide based photochromic glasses, spectral props. 0-29708
- $\text{GeO}_2\text{-P}_2\text{O}_5\text{-SiO}_2$  glass fibre, incorporation of OH in modified CVD process 0-50560
- $\text{K}_2\text{O-BaO-SiO}_2\text{-Nd}^{3+}$  glasses, absorption and fluoresc. spectra, density 0-25417
- $\text{Na}_2\text{O-BaO-SiO}_2\text{-Nd}^{3+}$  glasses, absorption and fluoresc. spectra, density 0-25417
- Nd glasses, GLS-1 and GLS-22, luminesc. band, forced transition cross sections, laser meas. 0-40152
- $\text{PbF}_2\text{-AlF}_3$  glass, optical props., crystn. and thermal expansion 0-48367
- $\text{PbF}_2\text{-AlF}_3$  glass, prep. and props. 0-49120
- $\text{PbO-SiO}_2$  glass, use of  $\text{Na}_2\text{S}_2\text{O}_5\cdot 5\text{H}_2\text{O}$  in polishing 0-33258
- $\text{SiO}_2$ , fused, shock compressed, refractive index, density, and polarisability behaviour 0-50295
- $\text{SiO}_2\text{-GeO}_2\text{-SiO}_2$ ,  $\text{SiO}_2\text{-SiO}_2\text{-B}_2\text{O}_3$ , glass fibre waveguides,  $\gamma$ -radiation optical stability 0-23799

**optical harmonic generation**

see also lasers

- bistable steady states in optical subharmonic generation, Wigner distrib. 0-53370
- double-pass frequency doubler for Nd:glass laser, phase optimisation 0-9962
- dye laser oscillator-amplifier system second harmonic generation using laser-flashlamp hybrid pumping 0-14359
- dye lasers, mode-locked, exponential SHG autocorrelation function rel. to pulse to pulse var. 0-9920
- efficient generation, state of art 0-33090
- fast transform calcs., appl. to SHG with depletion and diffraction 0-53376
- inhomogeneous nonlinear elements, coherent frequency doubling (*Russian*) 0-5795
- intracavity SHG, phase effects 0-1276
- IR source, tunable, efficient 0-5789
- laser plasma, SHG, review 0-53993
- laser with nonlinear active medium, transient intracavity SHG, giant pulse generation 0-9948
- liquid, laser radiation second harmonic intensity meas. 0-48338
- lithium formate biaxial crystal, nonlinear conical refr. obs. in harmonic generation 0-23745
- nonlinear adaptive system, characteristic purposes 0-28273
- nonlinear crystals for frequency conversion of optical radiation, review (*Russian*) 0-38068
- phosphate glass laser, statistical props. and stabilisation 0-48266
- Raman scattering of light by polaritons, reviews 0-34928
- rare earth titanates, pseudoperovskite struct., nonlinear spectral and luminesc. characts. 0-29771
- rare-earth formates, second optical harmonic generation 0-43403
- second harmonic beam anal., laser pulses duration 0-1275
- second-harmonic, in nonlinear crystals with longitudinally nonuniform refr. index, efficiency 0-43402
- SHG, effect of partial mode locking 0-9960
- SHG, heating effects, absorpt. coeffs. and temp. variation of refr. index difference 0-14390
- SHG, polarisation effects 0-48350
- SHG intracavity generation, phase effects, harmonic feedback case 0-9945
- subharmonic generation, multiplicative stochastic processes in statistical physics appl. 0-22289
- subMM radiation, monochromatic, simple tunable source 0-5788
- surface plasmons, counterpropagating, for coherent SHG 0-33081
- synchronous nonlinear interaction between waves on Bragg diff. in media with periodic struct. (*Russian*) 0-14399
- third harmonic generation, spatial modes effect 0-43400
- three-wave interactions in randomly inhomogeneous dispersive media (*Russian*) 0-53364



**optical harmonic generation continued**

- two photon reson. third harmonic generation, quantised field theory 0-43397  
 urea, electro-optical coeffs. meas., rel. to nonlinear optics calcs. 0-34889  
 urea crystal, efficient phase-matched SHG and sum freq. mixing 0-14391  
 vector matching ang. width 0-9946  
 $\text{Bi}_2\text{Sn}_2\text{O}_7$ , polymorphic phase transition, X-ray, DSC, SHG, dielec. and optical obs. 0-44163  
 GaP ribbon waveguide, vapour-grown, phase-matched SHG 0-48339  
 $\text{HgGa}_2\text{S}_4$ , melt growth, optical props. and SHG,  $\text{HgS-HgGa}_2\text{S}_4$  phase diagram 0-50548  
 $\text{n-InSb}$ , optical SHG in rectang. waveguide 0-43401  
 $\text{KH}_2\text{PO}_4$ , efficient high-energy SHG of triaxial flashlamp-pumped dye laser 0-38061  
 $\text{KNbO}_3$ , SHG with  $\text{Ga}_{1-x}\text{Al}_x\text{As}$  lasers 0-5785  
 Kr gas, tunable narrow-band coherent VUV source for Lyman- $\alpha$  region 0-38070  
 $\text{La}_2\text{Ti}_2\text{O}_7$ , ferroelects., nonlinear optical props. 0-33086  
 $\text{LiCsSO}_4$ , thermal and dielec. props. 0-34860  
 $\text{LiIO}_3$ , crystal inside cavity of 1064 nm YAG: $\text{Nd}^{3+}$  laser, optical SHG (*Russian*) 0-28272  
 $\text{LiKSO}_4$ , thermal and dielec. props. 0-34860  
 $\text{LiNbO}_3$ , doubly resonant intracavity SHG of 1153 nm radiation with stabilization on HFS components of  $^{121}\text{I}$ , 0-33077  
 $\text{LiNbO}_3$ , optical consts. determ. by background stimulated Raman scatt. 0-48336  
 $\text{LiNbO}_3$ , SHG, refr. index induced optical inhomogeneity effect 0-9951  
 $(\text{NH}_4)_2\text{BeF}_4$ , ferroelectric, incommensurate phase, nonlinear optical props., SHG study (*Russian*) 0-33089  
 Na, magnetically induced SHG, intensity saturation 0-1273  
 Na, spontaneous field induced optical SHG, multiphoton ionisation 0-14395  
 Na vapour, two-photon resonant fifth harmonic generation 0-53374  
 NaCl, additively coloured, SHG 0-1274  
 Nd:glass laser system with parametric freq. conversion 0-1277  
 $\text{RbH}_2\text{PO}_4$ , for tunable frequency-doubled CW dye laser 0-53372  
 $\text{Rb}_2\text{K}_{1-x}\text{H}_2\text{PO}_4$ , 90° phase matching in freq. doubling, appl. to lasers 0-33088  
 $\text{SF}_6$ , multiphoton absorpt. meas. by third harmonic generation 0-1036  
 $\text{Sr}_2\text{Nb}_2\text{O}_7$ , ferroelects., nonlinear optical props. 0-33086  
 Ti vapour, ruby laser third harmonic generation, flowing degree influence 0-48348

**optical images**

see also aberrations

- acoustic wave visualisation using Koster prism 0-5701  
 annular apertures, imaging performance, apodization and MTF 0-23625  
 aperiodic specious objects influence of AF sinusoidal phase deformations of wavefront (*Czech*) 0-14290  
 aperture, partially apodised, diffracted field characts. 0-48139  
 aperture ratio of optical devices (*Russian*) 0-1140  
 apertures with Straudel Class of pupil functions, var. apodisation 0-23616  
 apodisation and image contrast rel. to MTF 0-32920  
 apodisation for max. Strehl ratio and specified Rayleigh limit of resolution 0-28170  
 apodized optical systems, frequency response and point image irradiance distrib. 0-9819  
 apodizing filters for optimum Sparrow resolution in coherent systems with annular aperture 0-53435  
 astrophysical applications of image restoration, conf., Bordeaux, France (Mar. 1979) 0-41935  
 atmospheric turbulence effects on optical and IR image form. (*French*) 0-46257  
 biimidazole+leuco dye photochem. reaction, modulation by photopolymerisation 0-40714  
 biological material, laser stereometry light-scatt. technique, cardiac images 0-56310  
 coded-aperture images, pre-folded Fourier filter reconstruction 0-53222  
 coherent optical system, impulse response for image multiplication by spatial sampling filtration 0-33126  
 coherently illuminated objects, image improvement (*Russian*) 0-28168  
 colour coding of spatial freq. using incoherent optical processing 0-37956  
 colour reproduction, of images obtainable by two-primary colour projections 0-12125  
 complex degree of coherence expansion, image intensity data, object reconstruction 0-32906  
 conference, Bad Harzburg, Germany (June 1979) 0-51951  
 conjugate image appearance in volume reflection hologram 0-28181  
 correlation, real-time high-resolvance, by Bragg diff. in saturable absorbers 0-48159  
 Correlation image formation with an axicon 0-48162  
 deblurring system using diffraction gratings 0-43274  
 detail sharpness and its quantitative expression (*Czech*) 0-1141  
 diffraction at straight edge, partially coherent illum., aberrations (*Chinese*) 0-43267  
 diffraction limited image from obs. through irregular atmosphere (*Ukrainian*) 0-9814  
 diffraction theory of image form. 0-9822  
 diffuser for Fourier transform hologram recording 0-43285  
 double-slit object illuminated with ultrasound-modulated laser light, resolution 0-37959  
 education, perspective distortion in photography, eye as simple lens 0-17734  
 electrographic instrumentation for ultraviolet imaging and spectrography 0-46399  
 evaluation criteria for optical systems (*German*) 0-43268  
 field wavefunction, analytic properties in optics 0-1138  
 formation in photosensitive layers on highly conductive substrates 0-43419  
 Fresnel images, depth of focus 0-1145  
 gradient index fibre array development and imaging props. 0-14483  
 gradient index imaging lens and system status 0-14420  
 gradient index imaging system theory 0-14294  
 gradient index optical imaging systems, topical meeting, Rochester, USA (May 1979) 0-12851  
 gratings, embedded, optical imaging calc., Fourier optics methods appl. (*German*) 0-23805  
 grey-scale texture anal. and use of co-occurrence matrices 0-43276

**optical images continued**

- hologram, reflection, real image reconstruction, resolving power and diff. efficiency 0-53237  
 holographic image formation, coherent transfer functions and resolution 0-43292  
 illumination with a moving light source 0-23632  
 image formation theory, work of D.S. Rozhdestvenskii 0-18999  
 incoherent imaging system, diff. images asymptotic behavior 0-1139  
 instrument image evaluation by multitarget array detection 0-1362  
 isoplanatic degradation of tilt correction and short-term imaging systems 0-53219  
 isoplanatic optical systems, partially coherent image form. through random absorbing media 0-14292  
 isoplanatism in optical systems, image form. 0-1144  
 lake monsters, prod. by image distortion due to atmospheric refr. 0-46259  
 least-squares wave front errors of minimum norm 0-48137  
 lens-array photography, longitudinal distortion compensation, integral image reconstruction 0-52345  
 linear line screen for image reproduction, analysis 0-32925  
 long-distance multimode waveguide image transmission in coherent light 0-48435  
 metal-photosemiconductor-insulator multilayered structure, charge pattern formation during recharging 0-47129  
 metal-photosemiconductor-insulator multilayered structure, optical image recording,  $\text{As}_2\text{Se}_3$  photosensitive element 0-42286  
 microscope, effect of magnification distrib. between objective and eyepiece on image quality 0-18013  
 models of optical systems 0-9821  
 moments of images aberrated by turbulences undersampling errors in meas. 0-1137  
 moving object imagery using large aperture telescope arrays 0-53225  
 multicolour reflection holograms, improved image techniques 0-48184  
 multislit spatial filtered pseudocolour holographic imaging 0-53236  
 non-imaging optical design principals, appl. to solar energy concentrators 0-7928  
 nonisoplanatic spectral instruments, num. correction of images formed 0-249  
 nonlinear optical processing with Fabry-Perot interferometers containing phase recording media 0-48158  
 optical transfer measure, system relations, appl. wide field microscopy and microelectronic photolithography (*German*) 0-9815  
 optimisation by apodisation filters in optical systems with residual aberrations 0-53223  
 optoelectronic devices and optical imaging techniques, book 0-27059  
 parabolic gradient index lens, SELFOC, chromatic aberration in imaging system 0-14422  
 paraxial coherent, apodization by interposing masks in pupil plane (*French*) 0-23630  
 phase-inverting grating construction, use in deblurring filters 0-48398  
 photographic lens, image quality improvement 0-47123  
 photomaging system based on photopolymerisation in cryst. coatings 0-40716  
 polarizer with spherical mirrors for VUV radiation 0-48375  
 quality criteria, OTF, modular transfer function, phase transfer function (*German*) 0-53221  
 quasars, image doubling assoc. with absorpt. systems 0-22112  
 remote sensing, evaluation of atmospheric effect on aerospace information 0-4101  
 representation using genetic geometrical functions 0-5702  
 rotation and magnification, optical system 0-48376  
 scanning microscopes, partially coherent and confocal, imaging of periodic structs. 0-5700  
 scanning of image-carrying light beams with acousto-optic deflection cell 0-14459  
 Scophony light valve, comparison with flying spot scanner 0-33147  
 sector templates for determining the contrast transfer of imaging systems 0-32924  
 self-image techniques, optical computing 0-18998  
 Selfoc conically graded medium, aberration anal. 0-1142  
 shadowgraph apparatus, phase struct. visualisation by crossed statistical amplitude rasters (*Russian*) 0-5846  
 shift, Adamar transform appl. (*Russian*) 0-1134  
 sinusoidal complex object with a small phase modulation, Fresnel diff. patterns, self-imaging 0-43256  
 solar concentrator image characteristics, non-uniform intensity distrib. 0-55816  
 solar glass components, specularly meas. using Fourier transform anal. 0-5804  
 speckle interferometry, wideband, true imaging of astronomical objects 0-53226  
 speckle patterns in white light images, average contrast meas. 0-9808  
 statistical image anal., 3 parameter probability distrib. density function 0-43266  
 stellar speckle interferometry data processing method 0-17498  
 Strehl intensity applicability as image quality criterion (*German*) 0-28166  
 surface orientation determ. from multiple images, photometric method 0-52163  
 tapered gradient index rod, geometrical optics and imaging props. 0-14280  
 teaching, holographic experiments on optical imaging 0-12872  
 three-beam interference images, sinusoidal complex object with phase modulation 0-53208  
 tone reproduction analysis with square, circular and concentric-ring patterned screens 0-53229  
 virtual image display using Fresnel lenses 0-1295  
 visual analyser space-frequency filter harmonisation with statistics of images 0-30726  
 visual optical line spread width judgement, merits of Gaussian moment 0-16924  
 visual optical line spread width judgement, merits of Gaussian moment 0-16923  
 visual simulation and image realism, seminar, San Diego, USA (Aug. 1978) 0-3639  
 wavefront reconstruction method, plane waveguide hologram coupled system 0-5708  
 wavefront sensing using white light sources 0-1146  
 waveguides with prescribed propag. consts., design 0-48419



**optical images continued**

- Wigner distribution function, optical production, speech signal analysis 0-48521
- V<sub>2</sub>O<sub>5</sub> FTIROS thermochromic materials, colour and visual contrast 0-33100

**optical information processing**

see also spatial filters

- 2-D image processing applications of acoustooptical devices 0-53231
- A/D conversion, parallel real-time, using liq. cryst. light valve 0-53451
- achromatic interferometers for white light optical processing and holography 0-53234
- acousto-optical devices for real- and near-real-time signal processing 0-10024
- analytic Fourier optics, information encoding by complex zeros 0-23628
- astronomical images, coherent optical processing expts. (Russian) 0-12675
- automatic pattern processor for simple and complex interference patterns 0-13129
- bistable element array generation by liquid crystal light valve and optical feedback 0-48442
- bistable optical device, transient response and applications 0-33214
- bistable TV-optical feedback system using optical flip-flops 0-53354
- Bragg imaging in the reflection mode and designs for improved optics 0-17040
- clip-correlator, for fluorescence correlation experiments (Russian) 0-42270
- coherent optical hybrid space- and time-integrating spectrum analysis 0-48177
- coherent optical image amplification by injection locked dye amplifier 0-19041
- coherent optical processor for vehicle tracking and identification using laser diode light sources 0-37957
- coherent space-variant processing, 2D, using temporal holography, theory 0-23624
- conference, Bad Harzburg, Germany (June 1979) 0-51951
- correlator with shift invariant linear matched filter 0-37962
- cylindrical lens systems described by operator algebra 0-38086
- cylindrical lenses, rotation of parallel fan of light, matrix representation 0-38089
- decoders based on controlled transparencies (Russian) 0-28321
- deconvolution techniques applied to astronomical images 0-46407
- development trends (Czech) 0-14457
- digital image processing, local filtering methods (French) 0-46406
- digital processing aerial images, conf., Huntsville, Alabama, USA (May 1979) 0-48165
- elastomer storage device evaluation for optical signal processing 0-48444
- electrooptical processor, iterative colour-multiplexed 0-23792
- fibre and integrated optical devices for signal processing 0-33233
- fibre-optic delay line signal processing devices 0-48443
- fluorescence intensity correlation, photon counting using clip-correlator (Russian) 0-42271
- Fourier beam system, double, data recording and processing appl. (Russian) 0-28165
- frequency-variant signal waveform processing using 2-D optical processors 0-48178
- galaxy redshifts survey, data reduction techniques 0-22074
- gas, Stark tunable, mirrorless optical bistability and optical limiting, obs. 0-38056
- geodesic lens design for integrated optics signal processing 0-33247
- gratings optical imaging, embedded, for meas. by moire fringes (German) 0-23805
- grey-scale texture anal. and use of co-occurrence matrices 0-43276
- guided-wave optical signal processing, diode laser sources and photodetectors 0-48465
- guided-wave optical systems and devices, seminar, Washington, USA (April 1979) 0-31418
- guided-wave signal transformers, synthesis 0-1358
- Hadamard and M-sequence transforms are permutationally similar 0-32921
- half-tone images, histograms meas. 0-23631
- height and flow velocity, optical pseudo-colour processing (Japanese) 0-9826
- holographic numerical optical processor configurations 0-48194
- hybrid image processing for feature extraction and constant variance enhancement 0-53224
- hybrid image processing trends and prospects 0-32927
- image deblurring using diffraction gratings 0-43274
- image representation using genetic geometrical functions 0-5702
- image rotation and magnification, optical system 0-48376
- image shifts, Adamar transform appl. (Russian) 0-1134
- incoherent diffraction correlator with a holographic filter 0-37955
- incoherent extended source appl., Fourier holography in white light 0-37960
- incoherent image optical matched filtering 0-14286
- information storage, seminar, Washington, USA (Apr. 1979) 0-41942
- integrated optical data processor, satellite data processing appls. 0-48458
- integrated optical prism-waveguide dual coupler theory and exptl. performance 0-33236
- inverse problems, source feature determination 0-14296
- IR heterodyne detect. of stars, atm. turbulence effects, corrections (French) 0-46409
- Kaiser filters, window function, equivalent pass band, incoherent optical transfer function 0-1323
- Landsat imagery, planimetric restitution using Zeiss Stereotop 0-56648
- laser engineering and appls., conf., Washington, USA (May-June 1979) 0-1216
- least squares image restoration 0-37961
- least-mean-square spatial filter for IR sensors 0-38092
- linear line screen for image reproduction, analysis 0-32925
- local image restoration by a least-squares method 0-14289
- Mach-Zehnder interferometric switch for integrated optical multivibrators 0-53479
- materials for optical storage and reproduction 0-33109
- medical, flashing tomosynthesis: three-dimensional X-ray imaging 0-26325
- microchannel spatial light modulator as storage medium 0-43479
- modular arithmetic inner product processor optical implementation 0-48170
- multichannel signal processing using acoustooptic techniques 0-19160

**optical information processing continued**

- multiplex holographic representations of space-variant optical processors 0-48192
- nonlinear optical processing with Fabry-Perot interferometers containing phase recording media 0-48158
- operations achievable, real-time devices, systems and applications 0-9816
- optical/digital pattern recognition automated system 0-48175
- optoelectronic devices, digital data processing, review 0-19106
- particle population statistical inference from scattered light 0-37950
- passive components for integrated-optics signal processing 0-48466
- petrographic characterization of coal using automatic image analysis 0-18002
- phase shift plate analysis and design (Russian) 0-5696
- phase-inverting grating construction, use in deblurring filters 0-48398
- photoelectric converters, one-coordinate, signal processing algorithm 0-33199
- pulsed light source with thin-film modulator, fabrication and characts. 0-43467
- quality enhancement, adaptive methods (Russian) 0-28163
- quantitative image analysis, appls. using sequential transforms. 0-23627
- quantitative image analysis, theory and instrumentation 0-23626
- real 1D signal convolution and correlation by freq. plane filtering 0-32919
- residue number optical processor design concepts 0-48168
- residue-based optical processor 0-48169
- sampled/raster displays, assessment of information visibility using signal detection model 0-19002
- sampling theorems in polar coordinates 0-28169
- SAW and optical signal processing techniques compared 0-48173
- scene matching methods 0-48167
- scene matching with feature detection 0-48166
- self-image techniques, optical computing 0-18998
- side-entry surface acousto-optic interaction signal processor 0-48174
- signal processing activities of United States Army 0-48172
- signal processing research programme of United States Air Force 0-48171
- space-blur bandwidth product in correlator performance evaluation 0-43270
- spatial filtration in coherent optics system, amplitude and phase spectra analysis (Russian) 0-28164
- spatial frequency determination, selected interference schemes 0-48146
- spatial light modulator, using KD<sub>2</sub>PO<sub>4</sub> and Se photoconductor, optical processing appl. 0-9988
- spatial light modulator, using oil film deform. by surface tension var. 0-5831
- spatially orthogonal optical information transfer system, design and anal. (Chinese) 0-43275
- speckle interferometry, wideband, true imaging of astronomical objects 0-53226
- spherically symmetric object reconstruct. from slit-imaged emission 0-23634
- statistical image anal., 3 parameter probability distrib. density function 0-43266
- stellar speckle interferometry data processing method 0-17498
- stereology conference, Salzburg, Austria (Sep. 1979) 0-22134
- surface modal deformation sensor for heterodyne interferometry 0-31859
- surface orientation determ. from multiple images, photometric method 0-52163
- systems, seminar, Huntsville, USA (May 1979) 0-46732
- time integrating acousto-optic signal processors 0-48176
- two-dimensional linear transforms, generalized, in optical processing 0-9824
- two-dimensional optical information correlation reduction in course of photoelectric registration 0-19000
- velocity distribution measuring system, 2D, using multiple line detectors and correlation analysis 0-14851
- video disc information retrieval by optical readout 0-43284
- visualisation of periodic amplitudes and phase structures (Russian) 0-1135
- wavefront reconstruction method, plane waveguide hologram coupled system 0-5708
- Wigner distribution function, optical production, speech signal analysis 0-48521
- Wigner distribution function and its application to first-order optics 0-37958
- Wigner distribution function display using coherent optical processor 0-48160
- X-ray tomography, non-computed, using coherent light reconstruction 0-17116
- Bi<sub>12</sub>SiO<sub>20</sub> electrooptic crystals, vol. phase holograms, light diffr. and non-linear image processing 0-37972
- Bi<sub>12</sub>SiO<sub>20</sub> photoelectret, in optical processing and X, γ ray imaging 0-23764
- CdO-GeO<sub>2</sub>:Ti<sub>2</sub>O photochromic glass for optical information retention media 0-33108
- GaAs signal processing optical electronic devices 0-33242
- InAs/LiNbO<sub>3</sub> structure, SAW generated transverse acoustoelectric voltage, image scanning and signal processing appl. 0-49826
- Sr<sub>0.61</sub>Ba<sub>0.39</sub>Nb<sub>2</sub>D<sub>6</sub>, photoinduced birefr. 0-7325
- VO<sub>2</sub> thin film semiconductor-metal transition applications 0-49835

**optical instrument testing**

see also aberrations

- aspherical systems manufacturing and testing techniques development, use of computer (Italian) 0-48467
- endoscopes, equipment for checking optical and illum. characts. 0-56157
- image evaluation by multitarget array detection 0-1362
- laser gyro evaluation plan and test results 0-9934
- microscope scanning stage, motion rectilinearity determ., method and device 0-10055
- mirror flatness meas. using group of line light sources (Japanese) 0-1294
- movie projector objective lenses, standardisation of optotechnical parameters and testing methods 0-28301
- reference mirror for alignment of optical instruments 0-10054
- spatial and energy parameters of optical instrument, criteria for performance evaluation 0-33259
- zoom null lens design for optical component and system testing 0-23811



**optical instruments**

- see also *colorimeters; coronagraphs; ellipsometers; holographic instruments; light interferometers; optical microscopes; optical prisms; photometers; polarimeters; refractometers*
- angular meas. instrum. in engineering 0-13119
- apparatus for optical measurements under conditions of hydrostatic pressure up to 2 kbar at temperatures  $\leq 25\text{K}$  0-22379
- aspheric optics developments and appl. 0-5813
- aspheric optics production costs, instrumental and photographic applications 0-28308
- comparator, for fine sieves evaluation 0-37068
- cryostat with optical high-pressure chamber 0-31767
- dark adaptometer, normative and clinical data 0-41019
- dilatometer, for thermal expansion coeff. determ. of fibres, films and polymers 0-45454
- discrete component Sagnac optical rate sensor, error sources 0-1342
- economic potential of optical instrument developments 0-31841
- endoscopic contour technique for meas. dimensions of object detail (*German*) 0-31839
- flow cytometer, high-resolution, based on net flow configuration 0-8223
- influence on the polarisation of light 0-52290
- Knollenberg light scattering counters, response to doublet latex aerosols 0-37152
- laser retinoscope using He-Ne laser light source 0-41159
- linear dimensions meas. instrum. 0-13118
- magneto-optical effects meas., Kerr and Faraday, with accuracy up to  $0.001^\circ$  0-47087
- manufacturing standardisation and unitisation 0-9016
- measurement equipment development tendencies 0-13117
- medical and biological instruments 0-21517
- microprocessor-based optical multichannel analyser 0-33167
- MTF measurement of low light level devices 0-33221
- nonisoplanatic spectral instruments, num. correction of images formed 0-249
- Ophthalmometron, refractive error meas. cycloplegia effect 0-41002
- optical fibre, measurement of attenuation and dispersion 0-33185
- passive ring cavity optical rotation sensor, drift performance 0-1343
- profilometer, fast versatile, for surface roughness of workpieces meas. 0-37069
- pulsed light rangefinder, amplitude error in presence of signal fluctuations 0-28332
- quantitative image analysis, theory and instrumentation 0-23626
- Royco aerosol particle counter 225, data processing system and modified system props. 0-37005
- scan system for encoding and tabulation of visually scored sleep data 0-8197
- shadow optical method for turbulent flow microstruct. investig., stat. analysis problems 0-19534
- solar selective surfaces instrumentation for high temp. and hemispherical meas. 0-4756
- theodolite, type 2T, highly unified instrum. 0-13120
- tonometer, applanation, for intraocular pressure meas. 0-30833
- transmissometers for atmospheric visual range monitors 0-13122
- Zeiss Stereotop, appl. to Landsat imagery planimetric restitution 0-56648

**optical interferometers** see *light interferometers***optical isolators**

- diode lasers, struct. simplification 0-1209
- fibre communication, elimination of polarisation in optical isolators 0-5844
- fibre-optic communication applications, microoptic grating multiplexers, optical isolators 0-48408
- fog, laser light nonlinear transmission 0-1256
- pinhole plasma shutter for optical isolation in high-power glass lasers 0-23733
- semiconductor laser optical isolator in laser-to-fibre coupling module 0-48267

**optical Kerr effect**

- 4-cyano-4'(n-amy)-diphenyl, isotropic phase, induced molecular orientation relaxation time, Kerr effect (*Russian*) 0-19699
- intracavity absorbing gas Kerr nonlinearity rel. to dye laser emission spectral condensation 0-53286
- IR to visible AC Kerr efficient switches using liquid  $\text{O}_2$  and liquid  $\text{CS}_2$  0-19078
- liquids 0-23761
- nitrobenzene, oscill. optically induced Kerr kinetics 0-1286
- polarisation-sensitive nonlinear spectroscopy, improved geometry 0-1285
- Raman-induced Kerr effect with nonmonochromatic waves 0-48359
- $\text{CS}_2$ , liq., struct. and equilib. optical props. 0-45026
- $\text{CS}_2$ -glass boundary, optical bistability at nonlinear interface 0-33094
- $\text{H}_2\text{O}$ , liq., pulsed elec. field applied to sharp point, prebreakdown field 0-6308

**optical links**

- see also *optical communication equipment*
- 1.6 km half-duplex optical data link 0-14470
- 35 Mb/s optical fibre cable transmission using IR LED optocouplers 0-33156
- 565 Mbit/s signal transmission on optical waveguides 0-43483
- 800 Mbit/s digital transmission expt. (*Japanese*) 0-33164
- atmospheric optical communication line operating under photon counting conditions, adaptation to turbulence 0-9930
- atmospheric optical communication link, laser beam size 0-33064
- CERN Super Proton Synchrotron, beam observation via optical transmission system 0-38119
- coupling of fibre optic data links 0-43450
- development trends (*Czech*) 0-14457
- digital optical fibre system, 4-level using LED, meas. at 68 Mbit/s 0-1313
- fibre, graded-index, baseband bandwidth estimation for spliced system, empirical formula 0-53460
- fibre cables, 10-fibre filled, 6-fibre, connector for field installation 0-43470
- fibre communications systems, review of worldwide development 0-43468
- fibre developments 0-53458
- fibre optic connectors developments, cancellation of coupling mismatches 0-1332
- fibre optic undersea cables, small, recent experiences 0-14488
- fibre transmission system field trial, investigation of MCVD and VAD processes 0-43462
- fibre transmission systems, active and passive devices 0-43463

**optical links continued**

- fibre-optic communication applications, microoptic grating multiplexers, optical isolators 0-48408
- fibre-optic communication system appls., review of benefits 0-43480
- fibre-optic communication systems, devices and ccts., book 0-38123
- fibre-optic data transmission links (*Danish*) 0-10009
- fibre-optic systems, measurement techniques for passive optical components 0-1354
- fibre-optic transmission expts. at  $1.3\ \mu\text{m}$  wavelength (*Japanese*) 0-28318
- fibre-optic transmission systems, development progress 0-43482
- light transmission mechanism in optical fibres, communications appl. 0-43469
- long distance communications, fibre optic developments (*Norwegian*) 0-1318
- multimode fibre links, intermodal dispersion reduction by mode-delay equalising methods 0-48400
- multiwavelength monolithic integrated fibre-optic terminal development 0-33243
- over-the-horizon optical propagation in a maritime environment 0-41547
- paper tape data transmission, wavelength multiplexing, optical fibres 0-43454
- PCM 480 digital transmission system for Deutsche Bundespost 0-38120
- PFM fibre-optic video transmission to and from undersea vehicles 0-46310
- spliced graded-index fibres, 11.7 km link, measured and predicted transmission characts. 0-14454
- Telecom Australia optical fibre communications, fibre research and measurement technique developments 0-43456
- telecommunication network, role of fibre optics 0-43484
- VAD fibre cables, characts. 0-43461
- waveguides technology, components and systems (*German*) 0-33168

**optical mark reading** see *mark scanning equipment***optical masers** see *lasers***optical materials**

- see also *glass; optical films; optical glass*
- trans-4-alkylcyclohexane carboxylic acids, visible and UV spectroscopy transparent matrix 0-45102
- dichromated gelatin as holographic storage medium 0-43303
- m-dinitrobenzene, electrooptic cryst., growth in monomode optical fibres 0-55288
- EM sensor window materials, particulate erosion 0-38080
- gradient index material profiles and chromatic props. 0-14409
- gradient index optical imaging systems, topical meeting, Rochester, USA (May 1979) 0-12851
- information storage, seminar, Washington, USA (Apr. 1979) 0-41942
- integrated and guided wave optics, materials and fabrication techniques 0-23809
- ion bombardment of materials containing alkali metals or alkaline earths, chem. sensitisation 0-3227
- IR absorption measurement, interference calorimetric method, effect of crystal thermo-optic props. 0-47096
- IR materials for measuring radiant flux (*Russian*) 0-48366
- IR-optical material surface breakdown, adsorbed water evaporation model 0-35020
- jelly-filled optical fibre cable fabrication and characteristics 0-53490
- laser beam damage thresholds of  $\text{CO}_2$  fusion laser optics 0-38050
- laser damage in optical materials at  $1.06\ \mu\text{m}$  0-28263
- laser induced damage in optical materials, symposium, Boulder, USA (Sep. 1978) 0-31417
- laser window construction, for type 300.1  $\text{TEM}_{00}$  He-Ne laser (*Rumanian*) 0-9898
- leucosapphire, crystal growth by Kyropoulos method, temp. effect on structural and optical quality 0-20784
- leucosapphire large crystals, anomalies in block struct. formation 0-9972
- matched filter correlator memory techniques and capacity 0-43280
- metal optics, reflective system specifications 0-48387
- rare-earth formates, second optical harmonic generation 0-43403
- refractive index data interpretation, collection of program library 0-55056
- sapphire, shock compressed, refractive index, density, and polarisability behaviour 0-50295
- selective absorber coatings for enhanced photothermal energy collection 0-12027
- storage and reproduction materials 0-33109
- storage medium specification and performance trends, review 0-43415
- system and component specifications, seminar, Washington, USA (Apr. 1979) 0-46731
- thermochromic material, vanadium oxides mixture, appl. to laser beam indicator/visualiser 0-9976
- thermoplastic photoconductor tape performance for optical recording 0-43305
- transparent dielectric with metallic inclusions, light pulse shape effect on optical breakdown threshold 0-20588
- transparent materials, laser irradiated, in-depth and surface temp. meas. by Moire-Schlieren technique 0-53392
- transparent optical materials, laser induced damage and lattice strain due to lattice defects 0-48315
- waveguide process and materials, review of progress 0-23768
- window, composite vacuum-tight, for IR and visible observations, strength and IR transmission 0-48406
- $\text{BaF}_2$  crystal, refr. index temp. increments meas. 0-33098
- $\text{BaF}_2$ , large optical crystals, quality 0-33097
- $\text{BaF}_2$ , piezo-optical coeffs. meas. at  $0.6328, 1.15$  and  $3.39\ \mu\text{m}$  0-34888
- $\text{Ba}_2\text{Sr}_{1-x}\text{Nb}_2\text{O}_6$  crystals, optical defects and edge dislocation distributions 0-19806
- Be mirrors, props. and fabrication procedures 0-38138
- Be substrate for lightweight mirror, surface quality and thermal props. 0-23762
- $\text{Bi}_2\text{SiO}_{20}$  electrooptic crystals, vol. phase holograms, light diffr. and nonlinear image processing 0-37972
- $\text{CaF}_2$  antireflection coated,  $3.8\ \mu\text{m}$  CW laser damage threshold obs. 0-33053
- $\text{CaF}_2$ , fine-grained, forging and bulk optical props. 0-33103
- $\text{CaF}_2$ , large optical crystals, quality 0-33097
- $\text{CaF}_2$ , piezo-optical coeffs. meas. at  $0.6328, 1.15$  and  $3.39\ \mu\text{m}$  0-34888
- $\text{CaF}_2$ , press forged, mech. and optical props. 0-38079
- $\text{CdSe}$ , two-photon absorption, laser calorimetric obs. 0-33076
- $\text{CdTe}$ , cryogenic refractive indices and temp. coeffs. meas. 0-7319
- $\text{CdTe}$  two-photon absorption, laser calorimetric obs. 0-33076
- $\text{CsBr}$ , cryogenic temp. IR refractive index obs. 0-7320



**optical materials continued**

- CsI, cryogenic temp. IR refractive index obs. 0-7320  
 Ge demand evaluation and supply comparison 0-33106  
 Ge IR optical characteristics and performance requirements 0-48363  
 HgGa<sub>2</sub>S<sub>4</sub>, melt growth, optical props. and SHG, HgS-HgGa<sub>2</sub>S<sub>4</sub> phase diagram 0-50548  
 KCl, bulk and surface absorption comparison, 9.2 to 10.85  $\mu$ m 0-33051  
 KCl surface texture and optical props. after forging between polished dies 0-33102  
 LiF mech. and optical props. rel. to forging conditions 0-33101  
 LiF, press forged, mech. and optical props. 0-38079  
 Mo laser mirror, optical and metallurgical characterisation 0-33129  
 NaCl, bulk and surface absorption comparison, 9.2 to 10.85  $\mu$ m 0-33051  
 NaCl, laser-induced damage threshold variations 0-14380  
 NaCl surface with adsorbed water layer, absorpt. and thickness meas. 0-16001  
 SrF<sub>2</sub> antireflection coated, 3.8  $\mu$ m CW laser damage threshold obs. 0-33053  
 SrF<sub>2</sub> fusion-cast prism refractive index obs., 0.2138 to 11.475  $\mu$ m 0-34882  
 SrF<sub>2</sub> piezo-optical coeffs. meas. at 0.6328, 1.15 and 3.39  $\mu$ m 0-34888  
 SrTiO<sub>3</sub> electro-optic crystals, mechanical grinding and polishing 0-48471  
 TiBr-TiI, TiBr-TiCl, KRS-5 and KRS-6 crystals, optical losses, laser calorimetric meas. 0-9973  
 TiBr-TiI, TiCl-TiBr, KRS-5 and KRS-6 crystals, refr. index temp. increments meas. 0-33098  
 V<sub>2</sub>O<sub>5</sub>, FTIROS thermochromic materials, colour and visual contrast 0-33100  
 Y<sub>2</sub>O<sub>3</sub> sintered pieces, optical transmittance 0-40561  
 ZnS CVD IR material specifications 0-48364  
 ZnS CVD window, IR lattice absorption, phonon assignments and image spoiling 0-33104  
 ZnSe CVD IR material specifications 0-48364  
 ZnSe crystal, refr. index temp. increments meas. 0-33098  
 ZrSiO<sub>4</sub>, single cryst. growth from soln. in melt, solvent system selection 0-55285

**optical microscopes**

- see also optical microscopy*  
 annular lenses in microscopes, imaging props., calcs. 0-22426  
 attachment for low temp. operation 0-47099  
 coherent optical processor with interference contrast microscope input 0-43281  
 confocal scanning microscope, imaging modes 0-42257  
 confocal scanning microscope with high-aperture immersion lenses, imaging characts. 0-42256  
 EPIQUANT automatic structure analyser for inclusion investigs. in free-cutting steel 0-55609  
 image quality, effect of magnification distrib. between objective and eyepiece 0-18013  
 interference microscope with electronic image formation (*Slovak*) 0-31862  
 inverted, differential interference contrast, appl. to study of in vitro perfused nephron 0-51303  
 laser Raman spectrometer, 180° microscope sampling and viewing attachment 0-13150  
 microscope-spectrophotometer, computer processed, for measurement of absorption spectra of rock-forming minerals 0-18010  
 MORPHOQUANT automatic microscope image analyser, universal program system 0-56160  
 ophthalmological instruments and eye models in teaching, training and education 0-51993  
 paraboloid epimirror for microscope illuminator, design 0-28304  
 polarisation adapter, for transparent material anisotropy and internal stresses meas. 0-31863  
 reflected-light fluorescence microscope, LABOVAL 2a.fl, for routine and research 0-56300  
 scanning, based on electron beam pumped CdS laser 0-31864  
 scanning, operation and appls. 0-47098  
 scanning, using semiconductor laser with longitudinal electron pumping 0-18012  
 scanning IR microscope, photodetector field of view correction using additional mirror 0-52304  
 scanning laser microscope, electron beam excited 0-52303  
 scanning microscopes, resolution criteria rel. to radiation detection technique 0-33388  
 scanning stage, motion rectilinearity determ., method and device 0-10055  
 selection criteria w.r.t. applications 0-13132  
 stereoscopic microscopes, domestic, review 0-27342  
 surgical, model 310, photographic documentation in eye operations 0-56161  
 three dimensional, tracking of bacterial dispersal 0-30965  
 three-coordinate workshop meas. machines 0-27280  
 tilt stage for stereoscopy 0-21587  
 tracking microscope, design and operation 0-36214  
 VERTICAL with interference contrast equipment after NOMARSKI for gonorrhoea types classification 0-56301

**optical microscopy**

- see also optical microscopes*  
 n-alkane, long chain, syntactic coalescences between monoclinic and orthorhombic polymorphs 0-10520  
 p-alkoxy-phenyl-p-acryloyloxy benzoate polymers, mesomorphic struct. 0-38905  
 anthracene crystals, growth in melts of cholesteryl-caproate-anthracene system 0-2943  
 bidirectional illumination and viewing, living cells 0-51304  
 book, advances in optical and electron microscopy, vol.7 0-31437  
 bordered surface layers, Mossbauer and metallographic anal. 0-50769  
 ceramic, brittle, specimen prep. for optical and SEM obs. (*German, English*) 0-35457  
 computer-controlled double-beam scanning microspectrophotometry for rapid microscopic image reconstructions 0-18008  
 crystallography, optical, book 0-12862  
 Cunil MNA13-3, Mn addition effect on props. 0-21035  
 dielectric films, CW CO<sub>2</sub> laser-deposited, optical and struct. props. 0-7506  
 diffraction analysis, in microscopy 0-32926  
 electrocrystallisation, recent progress in electrochem. and physical methods (*French*) 0-7510  
 ellipsometric arrangement for microscopical obs. 0-17998  
 glass bead epoxy resin, direct obs. of debonding at crack tips 0-3167

**optical microscopy continued**

- graphite nodule growth, kinetics and rate controlling process (*Japanese*) 0-35203  
 Hastelloy X, grain size effect. creep and creep-rupture (*Japanese*) 0-16382  
 high-speed autoradiography, evaluation of effectiveness 0-47100  
 histopathological information obtained from US tissue signatures and microscopy of biopsy samples 0-51195  
 holographic interference microscope, MGI-1 0-5706  
 industrial, qualitative and quantitative surface testing 0-9033  
 lymphocytes, living and dead, mag. props. and mag. sedimentation 0-35925  
 matched spatial filter optimisation for diatom recognition 0-48180  
 metal oxides, high temperature interactions with Re 0-16665  
 meteorite Zaisho, Japanese pallasite, mineralogical and petrographical study 0-46509  
 meteorites, identification of ordered FeNi 0-8604  
 microfluorometric measurements of DNA dye complex using cryostat 0-17949  
 microkymography, and related techniques 0-36215  
 microscope photometry, appls. in materials science 0-21236  
 microscope photometry in studies of molecular struct. of carbonized bitumens and pyrobitumens 0-18011  
 microstructures micrographs digital simulation 0-19679  
 neural histological section, computer-assisted mapping 0-30963  
 Nylon-6, injection moulded, struct. and morphology 0-38949  
 object delineation program 0-41338  
 optical transfer measure, system relations, appl. wide field microscopy and microelectronic photolithography (*German*) 0-9815  
 Permalloy, magnetic head wear resistance and surface charact. against magnetic tape (*Japanese*) 0-35335  
 petrographic characterization of coal using automatic image analysis 0-18002  
 PMMA, thermochem. instability at Pt sphere inclusions caused by CW laser beam 0-29689  
 polycarbonate, effect of mol. weight on craze shape and fracture toughness 0-25858  
 polycarbonate, fatigue crack propag., mol. wt. depend. 0-50700  
 polycrystals, deform. during cooling, revealed by deposited graphite layer (*Polish*) 0-25755  
 polyesters, thermotropic, quiescent crystn. 0-38937  
 polyethylene, crystn. under high pressure 0-38946  
 polyethyleneterephthalate, crystallised from thin layer melts, temp. depend. of morphology 0-54149  
 polyethyleneterephthalate, foil, optical microscopy and low angle light scattering 0-55210  
 polystyrene-co-divinylbenzene microgels in dimethylformamide, diffusion coeff., viscosity and mol. wt. meas. 0-30286  
 projection system with brightness amplifier, laser appl., for medicine and biology 0-36060  
 projection system with quantum amplifier 0-33116  
 PVC, rigid, craze and yield zones in fracture 0-50701  
 quantitative image analysis, theory and instrumentation 0-23626  
 quartz, defects growth, study by X-ray diffr. topography (*French*) 0-39095  
 reflectance microscopy of coal, considerations involved in automation 0-18001  
 reflection microdensitometry, optical principles and practical solutions 0-4790  
 Rene 95, as hot isostatically pressed (HIP) and HIP+forged, low cycle fatigue 0-25854  
 roughness meas. by reflected-light microscope (*German*) 0-31861  
 scanning microscopes, partially coherent and confocal, imaging of periodic structs. 0-5700  
 semiconductors, dislocation structure, optical microscopy obs. techniques 0-24458  
 Sendust alloy, magnetic head wear resistance and surface characts. against mag. tape (*Japanese*) 0-35335  
 small objects, detection using liq. cryst. method, expt. using graphite powder as model object 0-9034  
 spirals, growth and dissolution from liq. state 0-15027  
 steel, 0.2 to 0.8% C, ferrite-pearlite transformation, tensile strength, cooling rate effect 0-7549  
 steel, alloy structural, anomalous grain growth 0-20984  
 steel, austenitic, Cr-Ni (25, 20 wt.%) recrystallisation and sigma phase formation 0-35211  
 steel, austenitic stainless, 18-8, effect of H on martensitic transformation (*Chinese*) 0-55394  
 steel, austenitic stainless, ferritic, single phase ferritic solidification in welds, exam. 0-7546  
 steel, austenitic stainless, Ni-alloyed, Cr<sub>2</sub>N precipitation, interface struct. and morphology 0-11644  
 steel, austenitic stainless, precipitates and grain orientation by non aqueous electrolyte potentiostatic etching method (*Japanese*) 0-15102  
 steel, C1020, dual phase, mech. behaviours and structs. (*Korean*) 0-25779  
 steel, C, transform. kinetics, heat cond. and elastic-plastic stresses during quenching (*Japanese*) 0-25688  
 steel, Cr and Ni-Cr, cyclic re-austenitizing 0-35222  
 steel, Cr-Mo(20, 1 wt.%), creep rupture tests, at 500°C loading times up to 300000 hours (*German*) 0-25828  
 steel, Cr-Mo (2.25, 1 wt.%), small changes effect in impurity elements, creep life 0-25790  
 steel, Cr-Ni (1.47, 1.48 wt.%), lath martensite microstruct. and props., cold rolling effect 0-55422  
 steel, Cr-Ni-Ti (18, 8, 0.7 wt.%), creep rupture tests, at 500°C loading times up to 300000 hours (*German*) 0-25828  
 steel, CrMo(W)V, creep rupture tests, at 500°C loading times up to 300000 hours (*German*) 0-25828  
 steel, high Si dual-phase, mech. props and microstruct. anal. 0-40444  
 steel, hot deformed austenite, transition from discontinuous to continuous formation of pearlite (*German*) 0-35214  
 steel, low-C-Si, LS1.2, LS1.5, phase transformation 0-45302  
 steel, martensitic, age hardening with Cu, Nb additions, exam. of hardness 0-7681  
 steel, Mn-Cr-B (1.46, 1.03, 0.003 wt.%) 0-55422  
 steel, Ni-Co-Mo (17.55, 8.02, 4.92 wt.%) maraging, lath martensite microstruct. and props., cold rolling effect 0-55422  
 steel, plain C, creep rupture tests, at 500°C loading times up to 300000 hours (*German*) 0-25828  
 steel wire, high C, fatigue and fracture 0-55531



**optical microscopy continued**

steels, C, quenched and tempered, struct.-prop. relationships 0-7599  
steels, structural St 37-2, cleavage fracture, report 0-25868  
stereoscopic method of viewing internal structures in resin-embedded biological specimens 0-21586  
Teflon foils, cryst. struct. and texture changes due to polarisation process (Polish) 0-35209  
texture anal. of sinter struct., appl. to Ca ferrites in sinters of rich Fe ores 0-18009  
thermoplastic, partially crystalline, microscopic methods of struct. anal. (German, English) 0-30198  
TV microscopy and cinephotomicrography with Zeiss Axiomat 0-27343  
ultramicrospectrophotometry techniques in intravital microcirculatory studies 0-21589  
uses, differences from electron microscope 0-13186  
wetting, exam. of accompanying size effect (Russian) 0-6596  
Ag, (211)[111] single crystals, shear band effects on rolling deformation 0-50651  
Ag-Zn (2 to 12 wt.%) containing several metals, internal oxidation (Japanese) 0-16570  
AgCl, surface crystallisation, due to colloid adsorption 0-54544  
Al alloy, type 2024-T3, fatigue deformation and crack growth, holographic study 0-25836  
Al-Cr(Zr), simultaneous recrystallisation and precipitation (French) 0-16313  
Al-Cu-Zn system, solid-phase reactions, phase diagram 0-50603  
Al<sub>2</sub>O<sub>3</sub> bicrystals, grain boundary obs. 0-39106  
Al<sub>2</sub>O<sub>3</sub>, grinding and polishing, quantitative control and optimization (German, English) 0-35460  
 $\beta$ -Al<sub>2</sub>O<sub>3</sub>:MgO, strength and delayed fracture behaviour 0-35290  
CaCO<sub>3</sub>, calcite, gel grown crystals, spirals on rhombohedral faces 0-7486  
Co, corrosion in Ar-SO<sub>2</sub> atmospheres, scale struct. obs. (Japanese) 0-55568  
Cu alloy, superplastic, microscopic examination of internal void formation 0-16383  
Cu-Al-Ni, mixed powder compacts, Ni content influence in sintering behaviour (Japanese) 0-35130  
Cu-Al-Ni-Fe system, corrosion behaviour in sea water 0-45421  
Cu-Ni-Bi-(Al) (30.0,5,(0.2-2) wt.%), Al addition effect on grain boundary reaction (Japanese) 0-54254  
Cu-Ti (4 wt.%), isothermal transformation, electron and optical microscopy obs. of microstructure 0-16307  
Fe, ductile, with different secondary struct., abrasive wear (German) 0-25871  
Fe-Cu-Ni (2, 5 wt.%), interphase precipitation obs. in assoc. with Widmanstätten ferrite lateral growth 0-40365  
Fe-Mn (15(24)(30)wt.%), high hydrostatic pressure influence on stress-strain curve 0-25805  
Fe-Mn-C, variation of martensite morphology with Mn and C composition 0-50635  
Fe-Mn-Ti alloys, austenitic, precipitation strengthened 0-25714  
Fe-Ni (31 wt.%), thermoelastic martensite obs. 0-3052  
Fe-V-C (0.3, 0.05 wt.%), interphase precipitation obs. in assoc. with Widmanstätten ferrite lateral growth 0-40365  
GaAs, ellipsometer equipment used for microscopical arrangement 0-17998  
GaAs layers, from gas phase, impurity influence on growth micromechanism 0-45237  
n-GaAs-n-GaN, diffusion growth kinetics, morphology and electrical properties 0-20294  
GaP, dislocation structure, optical microscopy obs. 0-24458  
InP/InGaAsP/InP double heterostructure, grown on InP(111)B substrate, threading dislocation multiplication 0-54237  
InSb:Se, exam. of defects in crystal 0-6423  
KCl(Br)(I), single cryst., quenched, microstruct. around indentations 0-7628  
LiF-AlF<sub>3</sub>-NaF-AlF<sub>3</sub>-Al<sub>2</sub>O<sub>3</sub> system, phase equilibrium, X-ray diffr., DTA, quenching, optical microscopy study 0-50610  
LiNdP<sub>2</sub>O<sub>12</sub>, grown by top seeded pulling technique, possible laser material 0-25542  
Li<sub>2</sub>O-SiO<sub>2</sub> glass, bulk crystals, SEM and optical microscope studies 0-44142  
Na<sub>2</sub>O-NaF-CaO-ZnO<sub>1-x</sub>-Al<sub>2</sub>O<sub>3</sub>-SiO<sub>2</sub>, opal glasses, strength, surface composition 0-30066  
Na<sub>3</sub>W<sub>3</sub>O<sub>10</sub>F<sub>4</sub>, single cryst., prep., optical and dielec. studies (French) 0-15994  
Ni, C precipitation 0-29958  
Ni, pure, anomalous grain growth 0-20984  
Ni-Co-Cr superalloy, powder produced, necklace struct. development 0-40395  
Ni-Ta-Al system, phase equilibria and diagram, electron probe, X-ray diffr. anal. 0-29927  
Ni-Ti (1.6, 7.64 wt.%), monophasic high temp. scaling, metallography study 0-21159  
Ni<sub>3</sub>Al-Ni<sub>3</sub>Nb, eutectic, temp. and thermal cycling influence on oxidation 0-45417  
Ni<sub>3</sub>Al-Ni<sub>3</sub>Nb eutectic, directionally solidified, high-temp. oxidation mechanism 0-16544  
Ni<sub>73</sub>Fe<sub>27</sub>O<sub>4</sub>, precipitation of  $\alpha$ -Fe<sub>2</sub>O<sub>3</sub>, optical microscopy, SEM and TEM studies (French) 0-11650  
PbTiO<sub>3</sub>, single cryst., He<sup>+</sup> backscatt. shoulder spectra struct., domain struct. 0-35048  
Si, ion-implanted, period surface struct. in laser annealing, new expt. evidence 0-29836  
Si, thermally induced microdefect form., C and O role 0-11439  
SiC, high period polytype at interface of two interacting spirals 0-20041  
SiC, impurity redistrib. and anomalous grain growth effects during polytypic transform. 0-15033  
Si<sub>3</sub>N<sub>4</sub>-AlN-Al<sub>2</sub>O<sub>3</sub>-SiO<sub>2</sub>-Y<sub>2</sub>O<sub>3</sub>, phase equilibrium study by X-ray diffr. and optical microscopy 0-50614  
SiO<sub>2</sub>-base cores, for superalloys, high temp. characterisation 0-10640  
Sn droplets, on Bi, Zn and Al, heterogeneous nucleation 0-44294  
steel, Cr-Ni, ferrite precip. (Japanese) 0-35187  
ThO<sub>2</sub>, sintered, fracture props. studied by Hertzian indentation technique 0-50703  
Ti-Al-H, H effect on mech. props. and lattice constants 0-21036  
Ti-Al-Sn-Zr-Mo (6.2,4.6 wt.%),  $\alpha$ - $\beta$  type 6246, fusion zone fracture behaviour in weldments 0-30093  
Ti-Al-V (6.4 wt.%), to H effect on fracture props. and microstruct. 0-40512

**optical microscopy continued**

Ti-Al-V-Sn (6.6,2 wt.%),  $\alpha$ - $\beta$  type 662, fusion zone fracture behaviour in weldments 0-30093  
Ti-Al-Zr-Mo alloy 685, phase at  $\alpha/\beta$  interface (French) 0-25661  
Ti-Al(Mo), swaged and recrystallized, grain growth 0-3092  
U core fuel elements, of A-1 reactor, volume growth (Czech) 0-27745  
UO<sub>2</sub>-zircaloy-4, reaction kinetics at high temps., O<sub>2</sub> diffusion 0-16667  
Zn-Al (22 at.%) eutectic, superplastic, microscopic examination of internal void formation 0-16383  
ZnO, film for solar cell appl. structural, optical and elec. props. 0-2294  
 $\alpha$ -Zr, H terminal solid solubility, optical metallographic study 0-34195

**optical model (nuclear) see nuclear optical model**

**optical modulation**

4-bit digitally driven integrated optical amplitude modulator for data processing 0-53476  
acousto-optic planar guided-wave Bragg modulators, integrated optic communication appls. 0-38131  
acousto-optic polarisation modulator, 200 to 2400 nm transmission band (Russian) 0-14472  
acousto-optical laser beam intensity modulator (Slovenian) 0-43429  
acousto-optical modulator, metrological certification of photodetection devices 0-23727  
acoustooptic hydrophone, coupled waveguide, using intensity modulation 0-14431  
acoustooptic modulator, reduction of thermal distortion of diffracted light 0-5837  
acoustooptical modulators, computer controlled laser interferometer 0-56294  
active pulse shaping in ps domain using fast Pockel cell and GaAs switch 0-28257  
airborne laser scanner, modulation techniques 0-5770  
alkali halide, ReO<sub>4</sub><sup>-</sup> doped, saturable absorber at 10.6  $\mu$ m 0-53384  
arbitrary profile beam, diffr. by periodically modulated layer 0-43252  
birefringence measurement using photoelastic modulator 0-31838  
broadband optical modulator for laser range finder (Russian) 0-53424  
coherent OCR system using spatial light modulator (Japanese) 0-14291  
coherent pulse propagation, or pulse generation from zero-area pulse 0-48352  
convex beam integrator for laser beam shaping, heat treating appl. 0-53346  
cutoff modulator using Ti-diffused LiNbO<sub>3</sub> waveguide 0-9991  
decoders based on controlled transparencies (Russian) 0-28321  
dye CW lasers, RF tuning 0-1243  
dye ring laser, flashlamp pumped, injection of N<sub>2</sub> laser excited oscillator beam 0-5754  
electro-optic guided-wave A/D convertor, high speed 0-33234  
electro-optic modulator, servo controlled, for CW laser power stabilisation and control 0-19060  
electro-optic multimode waveguide modulator or switch 0-23783  
electro-optic waveguide modulators, capacitance of electrode system rel. to modulation efficiency (Russian) 0-1359  
electrochromic ATR prism modulator 0-43440  
electrooptic diffraction modulator, large-aperture 0-33179  
electrooptic nonlinear devices with two feed signals, operation characts. 0-14441  
electrooptical oscillator, integrated cutoff modulation 0-48424  
ellipsometry, modulation error 0-255  
Fabry-Perot cavity, optical pulse tailoring and termination by self-sweeping 0-23760  
ferroelectric ceramic-photoconductor structure, as optically controlled transparency 0-28343  
fibre-optic delay line signal processing devices 0-48443  
FM optical communications, using electrooptically tuned semicond. lasers 0-14351  
Fraunhofer diffraction of apertures, analogy with SSB modulation 0-48138  
frequency modulation by p-i-n structure, optical waveguide with moving walls 0-19099  
gas laser, modulation method, for relative excitation level, cavity bandwidth and at. temp 0-5771  
hybrid field-effect liquid crystal light valve, sensitometry control 0-23788  
hydrophone, moving fibre optic, based on intensity-modulation mech. 0-43455  
III-V nitride semiconductors, physical properties and appls. in integrated optics (Czech) 0-28355  
injection diode modulated laser pulse generator and digital control cct. (Russian) 0-14372  
integrated directional coupler modulator, 1 Gbit/s 0-38125  
integrated directional coupler switches, modulators and filters using  $\Delta\beta$  reversal techniques, review 0-38132  
interferometer signal processing by acoustooptic correlation devices, radio astronomy applications 0-8543  
interlocked solid-state lasers, radiation intensity modulation for precision meas. 0-1250  
laser, passive mode locking, two laser amplifiers with slow saturable absorber 0-33041  
laser alphanumeric character generator for line printer and COM 0-33067  
laser beam, electro-optical and acousto-optical devices comparison 0-43380  
laser beam scanning by acousto-optic deflector array 0-10017  
laser beam simple submicrosecond optical chopper 0-14373  
laser diode, modulated, with short external cavity, single mode operation 0-5756  
laser engineering and appls., conf., Washington, USA (May-June 1979) 0-1216  
laser modulator for HF laser communication links 0-48311  
laser velocimetry using acousto-optical modulators 0-33715  
light source coherence meas. and fibre modal noise simulation by Michelson interferometer 0-48324  
liquid crystal electro-optic valve testing using laser light (French) 0-28311  
Mach-Zehnder waveguide modulators in Ti-diffused LiNbO<sub>3</sub> 0-33203  
magneto-optic bounce-cavity modulator, direct AM 0-5769  
matched holographic filters with Pockels readout optical modulators 0-53456  
methanol far-IR laser, optically pumped, intracavity polarization modulation 0-23726  
microchannel spatial light modulator as storage medium 0-43479  
microwave light modulator (Chinese) 0-33169



# optical modulation continued

mode locked lasers, effects of narrow-free-spectral-range etalons 0-38041  
multibeam acousto-optic modulator efficiency stabilisation 0-43439  
multifrequency Bragg acousto-optic deflector, laser beam AM suppression 0-53426  
nematic liquid crystal light modulator, scanning mode of operation 0-33200  
noncoherent optical signals coding, double-scanning monochromator appl. (Russian) 0-5697  
optical coherence modulation by two ultrasonic waves 0-1120  
optical fibres, acoustic modulation of light propagation 0-33209  
parametric generation of picosecond light pulses with an energy conversion greater than 50% 0-53377  
pendulum effect influence on optical modulation of diffr. electron beam in cryst. (Russian) 0-55219  
photoelastic isodynes method, stress components meas. using scatt. light modulation 0-14638  
photon counting distribution, modulation effect 0-43307  
photosensitive MIS structure in contact with nematic liq. cryst., light spatial modulation 0-48436  
physical principles and Czechoslovak development (Czech) 0-19090  
picosecond light continua generation depending on various nonlinear processes 0-33095  
picosecond spectroscopy, methods and appls., laser mode-locking 0-42263  
planar waveguide, isotropic, polarisation conversion by Bragg deflection, expt. results 0-48462  
PLZT electrooptic ceramic, electron beam surface charging, rel. to optical modulation 0-6952  
polariser + crystal plate + analyser system, passage of light 0-10023  
PROM, diffr. efficiency 0-14467  
pulsed light source with thin-film modulator, fabrication and characts. 0-43467  
ruby, optical free induction decay modulation and absorpt. line struct. due to superhyperfine interaction 0-33091  
ruby laser, negative feedback, cavity Q insertion effect on parameters of modulated pulses 0-43376  
ruby lasers, freq. synchronisation and locking by passive modulator 0-1249  
saw-tooth wave target, modulation by optical system with triang. and assoc. filters 0-9817  
Scophony light valve, comparison with flying spot scanner 0-33147  
sector templates for determining the contrast transfer of imaging systems 0-32924  
semiconductor injection laser, intensity pulsation enhancement by self focusing 0-48253  
semiconductor laser, pattern effect minimization at high-rate pulse modulation 0-19059  
sinusoidal complex object with a small phase modulation, Fresnel diffr. patterns, self-imaging 0-43256  
space-time light modulator for laser radiation control 0-48310  
spatial light modulator, using  $KD_2PO_4$  and Se photoconductor, optical processing appl. 0-9988  
spatial light modulator, using oil film deform. by surface tension var. 0-5831  
spatial light modulator with CCD address 0-48445  
spectrum analyzer, time- and space-integrating 0-9983  
sub-mm-wave laser interferometer, use of low-inertia semiconductor structs. to modulate radiation 0-31848  
sub-picosecond optical pulses, generation and meas. 0-23731  
subnanosecond optical free-induction decay with novel laser freq. shifting 0-38075  
thin-film waveguide with liq. cryst. boundary modulation of refr. index, mode switching 0-23800  
three-beam interference images, sinusoidal complex object with phase modulation, interferometric gratings 0-53208  
transverse light modulator, improvement of permissible incident angle 0-5843  
ultrasound modulated laser light, resolution of illuminated double-slit object 0-37959  
wavefront reversal and short pulse generation using steady-state stimulated Brillouin scatt. 0-53381  
waveguide light modulator, using Raman-Nath diffr. of vol. acoustic wave 0-48437  
[ $^{15}NH_3$ ], modulated coherent Raman beats 0-23464  
AlGaAs DH diode laser, ps optical pulse generation with RF modulated 0-9882  
As $_2$ S $_3$ , film waveguide, acoustooptic deflection and modulation of light by stationary phase grating struct. 0-5841  
Bi $_{12}$ GeO $_{20}$ , mechanism of creation of internal fields and photoelectret effect 0-25290  
Bi $_{12}$ SiO $_{20}$ , mechanism of creation of internal fields and photoelectret effect 0-25290  
CO $_2$  laser, internal modulation 0-23728  
CO $_2$  laser intracavity freq. modulation, transient behaviour 0-14374  
CO $_2$  laser line, electro-optic frequency shift (Chinese) 0-43379  
CO $_2$  TEA oscillator, injection mode-locking using N $_2$  laser-controlled semicond. switching of 10- $\mu$ m radiation 0-1247  
CS $_2$  travelling wave Kerr cell, ultrafast pulse shaping and picosecond rise time elec. pulses 0-33152  
GaAlAs injection laser, monolithic integration with Schottky-gate FET 0-48275  
GaAs DH laser, self-induced modulation, noise, instability 0-48250  
GaAs LED modulation bandwidth, influence of inhomogeneous current density distrib. 0-9993  
GaInAsP/InP DH lasers, direct modulation charact. meas. by sharp pulse method 0-1245  
GaInAsP-InP mesa substrate buried heterostruct. injection laser, fabrication and lasing props. 0-53319  
GaP-AlGaP, stripe-geometry electrooptical modulator 0-23798  
n-Ge, IR absorption by hot carrier 0-40087  
Ge, p-n junction, IR radiation modulation, light absorption by injected current carriers (Russian) 0-10013  
HF chemical laser beam, phase fluctuation meas. 0-48317  
He-I $_2$  laser, sequential separate multicolour output operation (Japanese) 0-28205  
I photodissociation laser, stimulated emission pulse temporal characts. with active-medium gain control 0-28226  
KD $_2$ PO $_4$  r $_{63}$  laser modulator (Chinese) 0-28260  
KrF $_2$  excimer laser, passive mode-locking using saturable absorber dyes 0-1244

# optical modulation continued

LiNbO $_3$  electrooptic device, interdigitally electroded, acoustic reson. 0-19097  
LiNbO $_3$  microwave laser beam electro-optic modulators using rectangular waveguides, 1.0 to 10 GHz 0-43381  
LiNbO $_3$  waveguide and modulator form. by ion implantation 0-48469  
LiNbO $_3$ /Ti waveguide thin film electrooptic Bragg modulator, bistable optical element 0-10034  
LiTaO $_3$  fast electro-optic deflector, arbitrarily shaped optical pulsed generation 0-53421  
LiTaO $_3$ /Cu waveguide, electro-optic control of radiation loss in off-axial propagation 0-23789  
Na atomic vapour, Doppler-broadened system, degenerate four-wave mixing, line shape and strength angular depend. 0-43391  
Na vapour doublet, dispersion free point, cooperative phased-array radiation 0-53352  
Nd:glass laser with US modulated emission 0-48309  
Nd:YAG laser, CW, with high output coupling modulation 0-9917  
PLZT spatial light modulator for a 1-D hologram memory 0-37963  
Si rubber as electro-optic material for optical hydrophones 0-43412  
**optical modulators** see modulators; optical modulation  
**optical noise measurement**  
amplifier, lock-in, with synchronous filter, construction (Japanese) 0-28362  
fibre modal noise anal. and meas. 0-10003  
light flux fluctuations, limiting factors in photoelectric meas. 0-13136  
light source coherence meas. and fibre modal noise simulation by Michelson interferometer 0-48324  
long-pathlength interferometry accuracy and noise problems 0-31860  
GaAlAs lasers, return-beam-induced noise generation model 0-48244  
**optical parametric amplifiers**  
degenerate, photon-anticorrelation effect calc. 0-33079  
IR grating tuned (1.9-2.4  $\mu$ m) picosec. travelling wave generator 0-5793  
laser optical inhomogeneity cancellation using parametric convertor 0-33049  
N two-level atoms, quantum theory of nonlinear optical phenomena 0-5790  
plasma laser pulse amplifier using induced Raman or Brillouin processes 0-1279  
two-photon resonant four-wave parametric amplification 0-48341  
LiO $_3$ , appl. to cancellation of optical inhomogeneities in Nd:glass laser 0-33049  
LiNbO $_3$ , double-pass config., parametric generation of single picosecond tunable pulses 0-19067  
LiNbO $_3$ , picosecond IR-continuum generation by 3-photon parametric amplification 0-23746  
**optical parametric devices**  
see also optical parametric amplifiers; optical parametric oscillators  
incoherent four-photon parametric processes 0-48349  
nonlinear adaptive system, characteristic purposes 0-28273  
picosecond light pulse parametric generation with energy conversion greater than 50% 0-53377  
upconversion, three-freq. parametric, beam focusing effects 0-48340  
Ag $_3$ AsS $_3$ , proustite upconverter, effect of temp. on phase match angle characts. 0-5799  
LiNbO $_3$ , double-pass config., parametric generation of single picosecond tunable pulses 0-19067  
**optical parametric oscillators**  
see also lasers  
incoherent four-photon parametric processes 0-48349  
injection tuning, theoretical study 0-19069  
intracavity absorption spectroscopy theory with singly resonant optical parametric oscillator 0-23742  
IR source, tunable, efficient 0-5789  
subnanosecond pumped, near to middle IR 0-19072  
 $\alpha$ -HIO $_3$ , pumped by high stability phosphate glass laser second harmonic 0-48266  
KH $_2$ PO $_4$ , parametric generation of picosecond light pulses with an energy conversion greater than 50% 0-53377  
LiNbO $_3$ , synchronously pumped, design and operation 0-14388  
LiNbO $_3$  three-dimens. optical waveguide, parametric difference freq. generation 0-48335  
Ti vapour, coherent anti-Stokes scatt. four-photon parametric oscill. 0-9959  
**optical phase conjugation**  
adaptive optics technology status and prospects 0-33132  
benzaldehyde, wavefront reprod. obs. by stimulated Brillouin, Raman scatt. 0-53369  
compensation for phase distortions by three-freq. parametric interaction 0-23750  
degenerate four-frequency interaction, compensation of phase distortions 0-53380  
Doppler-free spectroscopy and wave-front conjugation by four-wave mixing of monochromatic waves 0-28265  
dye solution, laser illuminated, nonlinear interactions (Russian) 0-28266  
dye solution amplifying dynamic holograms, wavefront reversal 0-48331  
irregular phase objects, dynamic interferometry, differential holography using phase conjugate refl. 0-37969  
laser amplifying medium, beam spatial struct. reproduction inaccuracy with reversing mirror 0-14379  
laser engineering and appls., conf., Washington, USA (May-June 1979) 0-1216  
laser resonator with phase conjugate mirrors, modes 0-14392  
laser system with phase conjugation, stimulated Mandelstam-Brillouin scatt. 0-5786  
MBEA, nematic liq. cryst. isotropic phase, phase-conjugate refl. by degenerate four-wave mixing 0-43389  
mirrors, phase-conjugate, for optical resonators, degenerate four-wave mixing 0-43393  
nearly degenerate four-wave mixing, transient analysis 0-53359  
nematic layers, optical phase difference and capacitance, elec. and mag. field depend. 0-28911  
phase distortion compensation 0-43392  
pump wave wavefront reversal in Brillouin mirror, influence of certain radiation parameters 0-9961  
reflection, phase-conjugate, using TEM $_{00}$  pump beams 0-48327  
signal detuning, effects on phase conjugation 0-23748  
spatial polarisation wavefront reversal in four-photon interaction 0-9956  
stimulated Brillouin and Raman scatt., phase conjugated wavefronts 0-5791



**optical phase conjugation continued**

- stimulated scattering, reprod. of light field weak components 0-5792
- three-photon mixing wave conjugation, effect of strong wave front distrib. 0-5783
- wavefront reversal and short pulse generation using steady-state stimulated Brillouin scatt. 0-53381
- wavefront reversal by stimulated Brillouin scatt., four-wave process 0-53382
- wavefront reversal in four wave mixing with angular tilting of reversal wave 0-38057
- wavefront reversal of fields using nonlinear optics methods 0-9958
- weak beam wavefront inversion in stimulated light scatt. 0-5798
- $\text{Bi}_{12}\text{SiO}_{20}$ , phase-conjugate wavefront refl. depend. on dynamic hologram spatial freq. 0-53358
- $\text{CS}_2$ , wavefront reprod. obs. by stimulated Brillouin, Raman scatt. 0-53369
- CdTe, backward degenerate four-wave mixing obs. 0-53361
- InSb, degenerate four-wave mixing obs. at 5K 0-53355
- $\text{LiNbO}_3$ , complex conjugate wavefront generation via degenerate four-wave mixing 0-48329
- $\text{LiTaO}_3$ , complex conjugate wavefront generation via degenerate four-wave mixing 0-48329
- $\text{LiTaO}_3$ , time depend. phase inhomogeneity compensation via degenerate four-wave mixing 0-53353
- Na atomic vapour, Doppler-broadened system, degenerate four-wave mixing, line shape and strength angular depend. 0-43391
- Na vapour doublet, dispersion free point, cooperative phased-array radiation 0-53352
- Ni complex, BDN, saturable absorber, degenerate four-wave mixing, amplification and phase conjugation 0-43394

**optical prisms**

- axicon and related optical component diagnostic techniques 0-14417
- design methodology, dimensional, with and without computer (Czech) 0-53431
- dielectric film refractive index meas., synchronous angle integrated optical method 0-15976
- electro-optic waveguide deflector performance characteristics 0-33213
- electrochromic ATR prism modulator 0-43440
- electrooptic waveguide array deflectors, performance criteria and limitations 0-5821
- Glan-Taylor prisms and Faraday rotator, circulator for optical fibre transmission 0-23769
- image filtering using prism and incoherent light (French) 0-14450
- inclined prism three-point meas. reliability (German) 0-28359
- integrated optical prism-waveguide dual coupler theory and exptl. performance 0-33236
- interleaved glass layer prism for semiconductor mask testing 0-43425
- Koster prism for progressive acoustic wavefront visualisation 0-5701
- multiplexer design for optical wavelength-division multiplexing transmission via single fibre 0-33222
- perspex, refr. index meas., crit. angle method, student expt. 0-12873
- prismatic double monochromator 0-23796
- Raman laser, CW fibre, bandwidth reduction using prisms, gratings and etalons 0-53366
- raster focusing-prism and light guide pump system for  $\text{NH}_3$  laser 0-9905
- SISAM employing contracircular design, adjustment by prism system 0-31894
- spectroscopic resolution increased with separated gratings and prisms 0-43271
- surface waveguide electrooptical deflector, high-resolution, prism model 0-48454
- waxicons for high-power chemical lasers, interferogram analysis 0-14418
- $\text{SrF}_2$  fusion-cast prism refractive index obs., 0.2138 to 11.475  $\mu\text{m}$  0-34882

**optical projectors**

- autostereoscopic displays using stereo-pair of projected images 0-1296
- colour transparency projector/scanner and printer 0-52343
- enlarger analyser using Si-blue photoamplifier IC 0-42288
- glass industry, applications of gauges and optical projectors 0-21249
- image digitiser system design 0-48441
- laser application in brightness amplifier, for medicine and biology 0-36060
- lens-array photography, longitudinal distortion compensation, integral image reconstruction 0-52345
- microscopic image projection system with quantum amplifier 0-33116
- movie projector objective lenses, standardisation of optotechnical parameters and testing methods 0-28301
- multispectral photography appl. using MKF-6 camera and MSP-4 projector 0-56633
- noncoherent optical projection system input holograms (Russian) 0-14297
- review and appls. of new laboratory projectors 0-22459
- system transfer function definition and performance testing (Hungarian) 0-14413
- tapered light guide condenser design approach 0-33218
- three-dimensional optical display unit 0-1297
- uniform test picture for all projection equipment (German) 0-27328
- zoom projection lens, optical level system, paraxial characts. 0-53399

**optical properties of substances**

- see also acousto-optical effects; birefringence; brightness; cathodochromism; colour; dichroism; dielectric function; electro-optical effects; electrochromism; magneto-optical effects; optical constants; optical Kerr effect; optical rotation; optical saturation; optical susceptibility; photochromism; piezo-optical effects; pleochroism; reflectivity; thermo-optical effects
- acetylene smoke particles, agglomerated, optical extinction meas. at 0.5145 and 10.6  $\mu\text{m}$  0-48155
- amorphous and liquid semiconductors, conference, Cambridge, MA, USA (Aug. 1979) 0-41933
- constitutive relations in photomechanics 0-43251
- cylinders, perfectly conducting arrays, transport prop. investig. 0-13011
- dielectrics, electric, optical and acoustic interactions from Lagrangian representation, book 0-2715
- gas mixtures, IR absorpt. theory using hard sphere model (Russian) 0-14879
- kinetic effects in an optically excited gas 0-1721
- layered materials and intercalates, International Conference, Nijmegen, Netherlands (Aug. 1979) 0-36771
- optomechanical characts. determ., polarisation device application, by compensation method 0-40643

**optical properties of substances continued**

- polyethylene tubes and sheets, light resistance investigation under natural climatic conditions 0-21127
  - Au-Ag-Cu, optical props. study using automatic nulling spectroellipsometer 0-55058
  - Na vapour, induced optical anisotropy (Russian) 0-38526
  - Na vapour in inert gas, effect of oxidant on optical props. 0-1736
- optical pumping**
- see also lasers; multiphoton spectra
  - acetylene, multiphoton vacuum UV photodissoc. obs. and interpret. 0-11939
  - aliphatic tertiary amines, laser action feasibility, emission spectra, two photon excitation 0-23683
  - alkali metal-He quantum magnetometer 0-17965
  - alkyl iodides, UV photodissoc., time-resolved obs. of  $\text{I}^2\text{P}_{1/2}$  reactions 0-11940
  - atomic RF spectroscopy, nonlinear and parametric effects, review 0-18816
  - BBOT dye, vapour phase, optical props. (Japanese) 0-9879
  - bromomethane, multiphoton vacuum UV photodissoc. obs. and interpret. 0-11939
  - bromotrifluoromethane, FIR laser action obs. at 823, 883  $\mu\text{m}$  0-14321
  - carbon tetrafluoride laser, optically pumped, freq. tuning 0-28208
  - carbon tetrafluoride optically pumped laser, stimulated emission stabilisation and tuning 0-9866
  - CW intracavity dye laser spectroscopy, enhancement, pumping power depend. 0-13155
  - diatomic molecule, two identical 3-level atoms, excitation spectrum 0-23476
  - diphenyl with pyrene cryst., self induced transparency self stimulated excitation (Russian) 0-14403
  - dispersive medium, incoherent, coherent stimulated Raman scatt. with multimode pump (Russian) 0-38063
  - Doppler-free Raman spectroscopy and suppression of laser-induced mol. Doppler broadened transitions 0-9638
  - dressed molecule, RF field, saturated absorpt. obs. 0-9648
  - dye laser, CW, technology developments and appl. 0-43383
  - dye laser, freq. shifting using stimulated Raman scatt. in  $\text{H}_2$ , tunable UV source 0-9963
  - dye laser, heating effect minimization 0-1198
  - dye laser, injection-locked pumped by Xe ion laser, 4-mirror ring-cavity 0-48280
  - dye laser, narrow-band pulsed, for nonlinear spectroscopy, pumping by Nd:YAG laser 0-53318
  - dye laser, PMMA modular matrix pulse width influence on power output 0-28247
  - dye laser, pulsed output, mode locking with synchronous-pumping 0-5760
  - dye laser, radial distrib. of pumping in coaxial cell with external irradi. 0-53308
  - dye laser, short resonator, tunable, pumped by travelling wave  $\text{N}_2$  laser 0-48291
  - dye laser, tunable, flashlamp pumped, ultra-narrow bandwidth 0-9897
  - dye laser, unstable ring resonator,  $\text{N}_2$  laser pumped 0-53326
  - dye laser, with high levels of coherent excitation, lasing characteristics 0-28229
  - dye laser oscillator-amplifier system second harmonic generation using laser-flashlamp hybrid pumping 0-14359
  - dye laser pumping, characts. using KrF excimer laser at 248 nm 0-1199
  - dye laser pumping, inductive storage bank transfer to flash lamp discharge 0-5742
  - dye lasers, synchronous pumping, extension of spectral range 0-5731
  - dye lasers pumped by XeF, KrF excimer lasers (Chinese) 0-1234
  - dye ring laser, flashlamp pumped, injection of  $\text{N}_2$  laser excited oscillator beam 0-5754
  - dye solution, laser illuminated, light field phase conjugation, nonlinear interactions (Russian) 0-28266
  - dye solution, nonlinear fluoresc. meas., two-photon pumping by low power laser 0-48037
  - dye solutions and their mixtures, excitation by Cu vapour laser, laser action 0-28230
  - dyes, 266 nm pumped, tuning ranges in near UV, 390 to 333 nm 0-48239
  - electron scattering by Coulomb potential in Born approx., bremsstrahlung statistics 0-5665
  - electron spin polarised targets for polarised ion beam prod. 0-27851
  - energy transfer dye lasers and laser induced intermol. and intramol. energy transfer processes 0-9647
  - ethylene, excited with parametric oscillator, vibr. relax. obs. and interpret. 0-9702
  - ethylene, line selective excitation with  $\text{CO}_2$  laser light and vibr. relax. 0-9705
  - ethylene dimer,  $\text{CO}_2$  laser induced photodissoc., pulsed mol. beam obs., van der Waals bond 0-9660
  - excimer lasers, optically pumped CW 0-14322
  - flash lamp drive circuit discharge currents, Fourier anal. 0-23695
  - fluoromethane, excited state rot. spectroscopy and kinetics, appl. of tunable sub-MM sources 0-14162
  - fluoromethane, laser pumped, vibr. states collision dynamics fluoresc. obs. 0-53104
  - fluoromethane, molecular pumping, thermal lens phenomena 0-9708
  - fluoromethane DFB gas laser, construction and operation 0-23715
  - fluoromethane TEM<sub>00</sub> far IR laser with integrated pump laser 0-43348
  - fluoromethane- $\text{d}_3$ , vibr. energy transfer at low temps., inert gas and  $\text{N}_2$  matrix obs. 0-9706
  - formaldehyde, multiphoton dissoc. by  $\text{CO}_2$  laser, intensity/fluence depend. 0-11913
  - formaldehyde- $\text{d}_2$ , 733  $\mu\text{m}$  line, Autler-Townes effect in laser interacting with RF field 0-53269
  - Freon 14, roto-vibr. mol. laser, low-temp. performance 0-9871
  - frequency up-conversion with stochastic pumping, exactly soluble model 0-23744
  - gas laser, modulation method, for relative excitation level, cavity bandwidth and at temp 0-5771
  - high gain amplifiers, gain meas. technique 0-1208
  - high-repetition-rate short-pulse gas discharge for discharge pumping gas lasers 0-1233
  - homonuclear molecules, vibrs. excitation by IR radiation 0-28068
  - iodomethane, RF field dressed mol. saturated absorpt. obs. 0-9648
  - IR Doppler free molecular spectroscopy, two photon coherence and pumping 0-48052



# optical pumping continued

laser pump fluctuations, influence on resonance fluoresc. radiation intensity correlation 0-37981  
laser specific and thermal reactions classifications 0-11919  
laser spectroscopy of unstable isotopes, nucl. props. determ. from atomic spectra using fast beams 0-9720  
laser utilizing self-terminating transitions, CW stimulated emission possibility 0-14329  
laser-controlled unimolecular and bimolecular processes, field-depend. rate const. 0-11906  
laser-induced chemical processes, optical selection of reagent orientation 0-11914  
laser-induced processes in molecules, conf., Edinburgh, Scotland (Sept. 1978) 0-9577  
methane, energy transfer obs. using excitation of fund., overtone and combination bands 0-9704  
methanol assignment of weak FIR laser lines 0-14320  
methanol far-IR laser, optically pumped, intracavity polarization modulation 0-23726  
methanol-d, CO<sub>2</sub> laser pumped, CW laser lines obs. 0-53272  
methyl alcohol, optically pumped, new CW FIR laser lines meas. and assignments 0-48224  
methyl fluoride Raman FIR laser, high-intensity CO<sub>2</sub> laser pumping, new emission lines 0-23675  
methyl fluoride-d<sub>3</sub>, optically pumped sub-MM wave laser 0-23676  
molecular species in defined quantum states, laser studies of relax. and reaction 0-11918  
multilevel molecular system, coherent pulse propag. effects 0-9968  
multiphoton ionisation, simple model, transition rates 0-953  
Na<sub>2</sub>, laser-excited, emission bands obs. in visible and IR 0-48036  
nitromethane+H<sub>2</sub> reaction, CO<sub>2</sub> laser initiated, mechanism and yield 0-11912  
nonequilibrium dissoc., Morse oscill. rigid rotator system, master eqn. soln. 0-40682  
nonlinear selection of optical radiation on refl. from stimulated Mandelstam-Brillouin scatt. mirror (*Russian*) 0-28280  
nonresonant excitation, ensemble of two-level systems, rel. to multiphoton spectra, polyatomic mols. 0-5585  
nucleic acid-dye complexes, energy transfer obs. using laser-induced fluorescence 0-12054  
parametric amplification, four-wave, two-photon reson. 0-48341  
parametric frequency up-conversion with stochastic pumping, canonical model 0-53368  
phase-conjugate reflection using TEM<sub>00</sub> pump beam 0-48327  
phaseshifting of freq.-conversion processes induced by additional selective pump 0-28271  
photochemistry in solid state, IR lasers appl. 0-11929  
photofragment spectroscopy of mol. ions using fast ion beams 0-9755  
photon antibunching in single atom fluoresc., rel. to wave packet reduction in detection process 0-52928  
polarisation spectroscopy and forward scatt., in Na gas 0-52336  
polyatomic molecule, anharmonic model for mol. photoexcitation 0-9669  
polyatomic molecule, collisionless multiphoton dissoc., threshold behaviour, nonthermal theory 0-11905  
polyatomic molecule, multiphoton absorpt. resons., dynamic Stark splitting 0-9670  
polyatomic molecule, multiphoton dissoc. dynamics, classical model 0-11904  
polyatomic molecule, multiple-photon IR laser pumping, collisional effects 0-9668  
polyatomic molecule, ultrafast vibr. using laser light pulses 0-9699  
polyatomic molecules, IR laser sensitised chem. reactions 0-11910  
POPOP dye vapour lasers, optical and electron beam pumping, review 0-48237  
propynal, IR photochem. in electronically excited state 0-11923  
Raman amplifier with broadband pumping, gain enhancement 0-43398  
Raman laser, external-resonator controlled, pumped by CW CO laser, mol. spectroscopy uses 0-9624  
resonance scattering methods in atomic spectroscopy 0-53167  
resonant electronic-vibrational energy transfer and use in pumping IR mol. lasers 0-9700  
rhodamine 6G laser amplifier pumped by N<sub>2</sub> laser, sub nsec pulse generation 0-1232  
rhodamine 6G-isopropyl or ethyl alcohol solution, flashlamp pumped laser, photochem. effects 0-53287  
roto-vibrational molecular laser scaling, CO<sub>2</sub>-TEA laser pumped 0-5728  
ruby, optically excited, diffusion of bottlenecked 29 cm<sup>-1</sup> phonons 0-6472  
ruby, optically induced two-phonon processes connecting <sup>2</sup>E states 0-25443  
ruby, phonons, at 29 cm<sup>-1</sup>, stimulated emission 0-45114  
ruby, resonance interaction of electronic two-level states and short-wave phonon radiation 0-24551  
ruby laser, generation, amplification of high power picosecond pulses depend. on superluminescence 0-53305  
ruby laser, graphical method for pumping coeff. estimation 0-14343  
saturation spectroscopy including collisional effects, for three-level atomic system 0-37099  
solid laser, active element thermal lens focal distance meas. by interf. method 0-48268  
stimulated Raman scattering, spatial structure of first Stokes component 0-14398  
stimulated Raman scattering with spatially inhomogeneous pump, enhanced gain 0-28279  
Stokes radiation spatial characts. in stimulated scattering, saturation conditions 0-53379  
sub-Doppler laser spectroscopy of mol. ions in fast ion beams 0-9655  
superradiance in Raman light scatt., pump depletion effect 0-9957  
p-terphenyl, substituted, dye laser and spectral characts., output power, conversion efficiency 0-23681  
tertiary amines, lasing action feasibility, excited state absorpt., two step photoionisation 0-23682  
sym-tetrazine, isotope selective mol. spectroscopy and isotopically pure mols. prod. with dye laser 0-11926  
thermal lens phenomena in mol. pumping expts., time-resolved geom. optics approach 0-9708  
three level system, nonlinear coherent effects, nonabsorpt. reson. 0-946  
three two-level atoms system, continuously incoherently-pumped, radiation rate, spectrum 0-5716  
three-level molecular system, cooperative evolution, transient effects of dephasing and relax. 0-28184

# optical pumping continued

three-level molecular system, populations, rate equations 0-37975  
time-correlated picosecond laser pulses generation, rapid sampling of optical relax. phenomena 0-9969  
two-level molecular systems, increased inversion efficiency 0-23657  
two-photon resonant four-wave mixing with non-monochromatic waves 0-38066  
water, laser-induced ionisation, quantum yield, temp. and wavelength depend. 0-11924  
Al<sub>0.5</sub>Ga<sub>0.5</sub>As-GaAs, CW 300k quantum-well heterojunction laser, optical and injection pumping operation 0-5735  
<sup>240</sup>Am<sup>m</sup>, spontaneously fissioning isomer optical shift in pumped <sup>85</sup>Sr<sub>2</sub>→<sup>10</sup>P<sub>7/2</sub> transition, nuclear deformation 0-27971  
BCl<sub>3</sub>+methane reaction, laser-induced, vibr. excitation influence on reactivity, isotope selectivity 0-11921  
Ba, efficient ionis. by reson. laser pumping 0-32685  
Ba, laser saturation spectroscopy, atomic-resonance absorption transitions 0-47121  
Ba, reson. transition, laser saturation spectroscopy with optical pumping 0-52334  
Ba+SO<sub>2</sub>→BaO+SO reaction, laser-induced fluoresc. obs., vibronic distrib. of BaO, collisional energy depend. 0-11917  
Br<sub>2</sub>, photolytic cage effect in high-press. gases, laser wavelength depend. 0-11925  
C<sub>2</sub>, low lying a<sup>3</sup>Π<sub>u</sub> state produced in intense IR field, fluoresc. and quenching obs. 0-11931  
CH<sub>2</sub>, photoprod. from ketene, singlet-triplet energy separation and vibronic level obs. 0-11936  
CO, hole burning in single quantum power spectrum due to Autler-Townes splitting 0-9671  
CO, isotopically enriched, Ar matrix isolation, laser-included vibr. fluoresc. 0-9707  
CO-Ar-(N<sub>2</sub>), C<sub>2</sub> and CN form. by optical pumping, room temp. 0-16701  
CO-NO mixtures, Ar matrix isolation, laser-included vibr. fluoresc. 0-9707  
CO<sub>2</sub>, optically pumped laser, simultaneous lasing in bands of sequence 0-5725  
Ca, efficient ionis. by reson. laser pumping 0-32685  
Ca+CCl<sub>4</sub>→CaCl+CCl<sub>3</sub> reaction, laser-induced fluoresc. obs. 0-11916  
Cd, electron impact, 6<sup>2</sup>D<sub>5/2</sub> and 7<sup>1</sup>P<sub>1</sub> level mixing 0-37889  
CdHg, excimer kinetics and transmission meas. 0-37832  
CdS, two-photon-excitation, tunable laser emission, luminesc. processes 0-55127  
Ce:LiYF<sub>4</sub>, tunable UV laser at 325, 309 nm, KrF laser excitation 0-38022  
Co:MgF<sub>2</sub>, laser, broadly tunable CW operation, output powers, optical pumping 0-32995  
Cs, cooperative cascade emission transitions 0-14120  
Cs, optical pumping with second resonance light 0-23376  
D enrichment by CW vibr. photochem. of methane, economic aspects 0-11920  
D<sub>2</sub>O, optical pumping using CO<sub>2</sub> CW capillary waveguide laser 0-48278  
EuCrO<sub>3</sub>, long term mag. ordering, antiferromagnetic resonance study (*Russian*) 0-54953  
F+CH<sub>3</sub>I(CF<sub>3</sub>I)(ICI) reactions, product state analysis using laser-induced fluoresc. 0-11915  
Ge, immersed in liquid He, optical pumping to generate first and second sound 0-6581  
HCN (001)+HCN(Ar)(N<sub>2</sub>)(CO<sub>2</sub>)(CO), relax. rate consts., using Cs vap. IR source 0-9696  
HF CW optically resonance-pumped laser 0-43356  
HF+HF(H<sub>2</sub>)(D<sub>2</sub>)(CO<sub>2</sub>)(isobutene), vibr. relax. dye laser pumping effects 0-9703  
H<sub>2</sub><sup>+</sup>(HD<sup>+</sup>), IR photodissoc. cross sections, calc. and simulation expt. 0-9659  
HN<sub>3</sub> high energy density laser using unstable resonator CO<sub>2</sub> laser pump 0-53327  
He, 2<sup>3</sup>S<sub>1</sub> metastable state, interactions, optical pumping investig. 0-23377  
He, low discharge, low press., excitation transfer and quenching of n=3 excited states 0-38743  
He I glow discharge, low-press., quenching of singlet states by N<sub>2</sub> 0-49030  
He+Na<sub>3</sub>, optically pumped state to state differential cross sections for rot. transitions, rainbow phenomena 0-5609  
<sup>4</sup>He magnetometer characteristics and operating principles (*Japanese*) 0-8434  
Hg, optically pumped positive column, E-I characts. 0-44035  
Hg<sub>2</sub> excimers, photoassoc., spectroscopy and kinetic processes of high-lying vibronic states, laser appls. 0-9649  
Hg<sub>1-x</sub>Cd<sub>x</sub>Te, photolum. and optical pumping 0-50424  
HgTl optically excited excimers, upper state kinetics 0-37831  
I chemical laser, four-level model (*Korean*) 0-28224  
I nanosecond single pulse laser, open electric discharge pumping 0-5763  
I<sub>2</sub>, produced in UV photodissoc. of alkyl iodides, time-resolved obs. of I(<sup>2</sup>P<sub>1/2</sub>) reactions 0-11940  
I<sub>2</sub> molecule pumped by Cu vapour laser, pulsed stimulated emission due to electronic transitions 0-14330  
I<sub>2</sub>, photolytic cage effect in high-press. gases, laser wavelength depend. 0-11925  
I<sub>2</sub> UV laser, quartz flashlamp pumped, pulse-periodic operation 0-53279  
ICl selective photoaddition to acetylene, isotope enrichment, influence of press., buffer and wavelength 0-11927  
KF, F<sub>2</sub><sup>+</sup>-centre excited-state absorption spectrum, rel. to H<sub>2</sub><sup>+</sup> model 0-16066  
KXe, dye laser induced emission, excimer bands and uses 0-9650  
Kr, g-factors meas. by optical pumping and mag. reson. 0-14246  
Li atomic beam, spin-polarisation by dual-freq. optical pumping 0-43003  
Li<sub>2</sub>, circular polarisation of emission, influence of nucl. hyperfine interactions and elastic collisions 0-9635  
Li<sub>2</sub>, collisional depolarisation and rot. energy transfer, laser-induced fluorescence obs. 0-9698  
Li<sub>2</sub>+inert gas, collision induced transition rate consts., two-laser spectrosc. 0-9629  
LiF crystal with F<sub>2</sub><sup>+</sup> centres, periodic pulsed tunable laser, Nd laser second harmonic excited 0-38021  
LiF with stable F<sub>2</sub><sup>+</sup> centres, F<sub>2</sub><sup>+</sup> colour centre generation accumulation, tunable laser production (*Russian*) 0-28238  
LiNdP<sub>6</sub>O<sub>12</sub> glass-clad rectangular waveguide, laser performance 0-32996  
NH<sub>3</sub>+H rot. energy transfer in vibronic levels, absolute transfer rates 0-9701  
NH<sub>3</sub>, efficient energy extraction by superradiant emission 0-53271



**optical pumping continued**

- NH<sub>3</sub> laser, optically pumped, freq. tuning 0-28208  
 NH<sub>3</sub> laser, resonantly pumped, for spectroscopy 0-48277  
 NH<sub>3</sub> laser with focusing-prism raster and light-guide pump system 0-9905  
 NH<sub>3</sub> sensitiser, excitation in MW region using CO<sub>2</sub> laser, pumping models 0-11911  
 Ni:MgF<sub>2</sub> laser, broadly tunable CW operation, output powers, optical pumping 0-32995  
 NO<sub>2</sub> excited, fluoresc. spectrum, IR multiphoton vibr. pumping, photon absorpt. probability distrib. study 0-18854  
 NO<sub>2</sub> laser-induced fluoresc. quenching rate const. and lifetimes 0-11930  
 Na atomic vapour, Doppler-broadened system, degenerate four-wave mixing, line shape and strength angular depend. 0-43391  
 Na, laser saturation spectroscopy, atomic-resonance absorption transitions 0-47121  
 Na, reson. transition, laser saturation spectroscopy with optical pumping 0-52334  
 Na, two-photon absorpt. processes, polarisation selection rules 0-9574  
 Na vapour, reson. freq. conversion by two-photon reson. pumping 0-28277  
 Na<sub>2</sub>, ground state, vibr.-rot. relax., optical pumping transients obs. 0-28067  
 NaK dimer formed in supersonic beam, laser-induced emission 0-9636  
 Nd<sup>3+</sup>, Cr<sup>3+</sup>-glass, nonradiative energy transfer from Cr to Nd, optical pumping efficiency improvement 0-33001  
 Nd laser, emission freq. conversion by method of reson. pumping of active media 0-1206  
 Nd, lasers, efficiency enhancement by pump radiation conversion in luminesc. liq. 0-48293  
 Nd pulsed garnet lasers, pulse repetition frequency, optimal operating regime 0-53303  
 Nd<sup>3+</sup> miniature laser principles, materials and integrated optical design 0-33004  
 Ne, 2p 3s<sup>3</sup>P<sub>0</sub> state, optical pumping, g-factor, metastability exchange cross section 0-947  
 O, metastable <sup>3</sup>S-state, optical pumping 0-32678  
 O<sub>2</sub><sup>+</sup>, predissociated b<sup>2</sup>Σ<sub>g</sub><sup>-</sup> state, high resolution laser spectroscopy in fast ion beam 0-9656  
 O<sub>3</sub>, multiphoton dissociation dynamics, classical model 0-11904  
 OCS, roto-vibr. mol. laser, low-temp. performance 0-9871  
 S<sub>2</sub> mol. B<sup>2</sup>Σ<sub>u</sub><sup>-</sup> → X<sup>3</sup>Σ<sub>g</sub><sup>-</sup> fluorescence induced by N<sub>2</sub> laser (*Japanese*) 0-14175  
 SF<sub>6</sub> and S<sub>2</sub>F<sub>10</sub>, absorpt. of intense laser radiation, vibr. excitation 0-9667  
 SF<sub>6</sub> and S<sub>2</sub>F<sub>10</sub>, multiple-photon IR laser pumping, collisional effects 0-9668  
 SF<sub>6</sub>, highly excited, time-resolved IR absorpt. obs. 0-9666  
 SF<sub>6</sub>, model system, coherent pulse propag. effects 0-9968  
 SF<sub>6</sub>, multiple photon excitation, collisionless 0-53079  
 SF<sub>6</sub>, photon-enhanced dissociative electron attachment 0-9749  
 SF<sub>6</sub>, resonant single-photon dissociation route using prelim. electron excitation 0-9662  
 SF<sub>6</sub>, time-resolved IR absorpt. meas. using injection-locked single mode TEA CO<sub>2</sub> laser 0-9665  
 Si: Au donor and acceptor centre obs. using IR absorpt. and dynamic nucl. polarisation with optical pumping 0-54639  
 Sr, efficient ionis. by reson. laser pumping 0-32685  
 Ti, 6<sup>3</sup>P<sub>1/2</sub> - 6<sup>3</sup>P<sub>1/2</sub> transition, population inversion 0-950  
 Ti, hyperfine struct. optical pumping, O-O transition perturbation 0-949  
 Ti, in gas discharge, optical self pumping, hyperfine struct., microwave-optical spectroscopy 0-32680  
 Ti, optical excitation, Landau-Zener nonlinearity, fluoresc. obs. (*Russian*) 0-52948  
 Xe, g-factors meas. by optical pumping and mag. reson. 0-14246  
 ZnO, two-photon-excitation, tunable laser emission, luminesc. processes 0-55127

**optical quantum generators** *see lasers***optical radar**

- see also remote sensing by laser beam*  
 aerosol meas. by lidar, error analysis and simulation 0-26617  
 aerosol pattern recognition (*Japanese*) 0-51028  
 air pollutants, laser spectroscopic detection 0-17366  
 atmospheric aerosol, use of lidars, laser rangefinders 0-51580  
 atmospheric particulate concentration, rise of smoke plumes, application of lidar 0-51026  
 atmospheric remote sensing by aerosol lidar backscatter (*Dutch*) 0-4110  
 atmospheric sounding, lidar characts., optical system parameters effect 0-33065  
 atmospheric visibility using lidar 0-31141  
 correlator, Malvern, based on photon correlation and laser scattering spectroscopy, development and appl. 0-5741  
 differential absorption lidar at 724 nm water vapour line 0-17384  
 excimer laser application to laser-radar obs. of stratospheric O<sub>3</sub> 0-17410  
 fast-response photodetector for atm. sounding, photometric properties 0-51585  
 gas absorption lines, half width and intensity, lidar remote probing technique (*Russian*) 0-21844  
 geometrical form factor in laser radar eqn., experimental determ. 0-36391  
 high accuracy distance measurement by two-wavelength pulsed laser sources 0-192  
 laser engineering and appls., conf., Washington, USA (May-June 1979) 0-1216  
 lidar observations of Labadie Power Plant plume, particulate density and behaviour obs. 0-55956  
 LIDAR teledetection and measurement of minority atmospheric constituents for pollution control (*French*) 0-7992  
 Mason method for lidar temp. profiling, computer simulation 0-21827  
 meteorological phenomena observation, mobile computerised laser radar system 0-56644  
 mobile lidar system for atmospheric gaseous pollutant meas. 0-35814  
 multifrequency lidar, sounding of lower-stratospheric aerosol microstruct. 0-56645  
 power detected by receiver, narrowly collimated beam backscattered by reflector in turbulent atm. 0-32918  
 radiation effect on laser system performance 0-38054  
 Raman lidar for industrial atmospheric pollutant remote analysis 0-12047  
 refractive effects of atmosphere on 10.6 μm lidar 0-36392  
 Space Shuttle lidar, OH radical in upper atmosphere, meas. 0-51590

**optical radar continued**

- troposphere, pressure and temp. meas. by lidar differential absorpt., influence of laser emission spectral width (*French*) 0-41554  
 tunable dye lasers for pollution monitoring 0-3562  
 wind meas. from orbit using lidar system 0-4114

**optical resolving power**

- see also optical instrument testing*  
 acousto-optic deflector, resolution criteria 0-43265  
 apodisation for max. Strehl ratio and specified Rayleigh limit of resolution 0-28170  
 apodizing filters for optimum Sparrow resolution in coherent systems with annular aperture 0-53435  
 degenerate four-frequency interaction, compensation of phase distortions 0-53380  
 diode laser, near and far field characterization 0-48242  
 double-slit object illuminated with ultrasound-modulated laser light, resolution 0-37959  
 far IR interferometric spectrometer, sampling comb generation and precision 0-47122  
 grating monochromator, real instrumental function 0-43452  
 hologram, reflection, real image reconstruction, resolving power and diff. efficiency 0-53237  
 holographic image and plate substrate quality relationship 0-48193  
 holographic image formation, coherent transfer functions and resolution 0-43292  
 holography, super resolution technique in Fresnel transform holography 0-9840  
 image correlation, real-time high-resolvance, by Bragg diff. in saturable absorbers 0-48159  
 IR interferometric spectrometer, slow scan, resolution and performance 0-42274  
 lithographic coated polyester panchromatic plate system 0-13172  
 Michelson inclined mirror interferometer, high spectral resolution, gaseous D<sub>2</sub>O-H<sub>2</sub>O-HDO mixture, absorpt. meas. 0-9023  
 photographic materials (*Russian*) 0-42292  
 ruled steel grating system for length meas. 0-13039  
 scanning microscopes, resolution criteria rel. to radiation detection technique 0-33388  
 spectral instrument choice in plasma and flame emission spectrometry of traces 0-35613  
 spectroscopic resolution increased with separated gratings and prisms 0-43271  
 surface waveguide electrooptical deflector, high-resolution, prism model 0-48454  
 EUO film for thermomagnetic recording, anisotropy of resolving power 0-20404

**optical rotation**

- see also Faraday effect; Kerr magneto-optical effect; rotational isomerism*  
 alkali metal vapour, induced optical anisotropy in laser radiation field (*Russian*) 0-38525  
 benzene, magneto-optic rotatory dispersion curves 0-45040  
 1-chloro-2-methylbutane, conformer depend. C-Cl stretching vibrs., Raman optical activity spectrum simulation 0-14146  
 cholesteric liquid crystals, apparent rotatory power (*French*) 0-50294  
 cholesteric liquid crystals, asymmetric synthesis failure using bimolecular reactions 0-44115  
 chromophores, semiempirical rules in circular dichroism, Cotton effect sign correl. with stereochem. 0-1006  
 circularly polarised laser radiation frequency shifting via rotating half-wave retardation plate 0-9800  
 crystallography, optical, book 0-12862  
 doped cubic crystals, resonance absorption region, self-induced rot. of polarisation 0-2805  
 elliptically polarised Gaussian beams, nonlinear precession 0-28269  
 gyroanisotropic crystal light polarisation states, Cauchy problem 0-20609  
 isotropic medium, nonlinear refr. index, self-induced polarisation rot. 0-5802  
 lattice dynamical theory of optical activity in crystals 0-34883  
 liquid crystal polarization rotator for intermodulation spatial-bandwidth reduction holography 0-53439  
 low value rotation angles, detection and measurement (*Rumanian*) 0-22418  
 magnetoelectric susceptibilities, phenomenological rules for computation 0-55068  
 methyl torsion modes, vibrational optical activity, inertial contrib. 0-5524  
 molecules, optically active mirror systems, parity-violating effects of weak interactions 0-52455  
 nonlinear polarisation resonances in a continuum, optical activity, spin-orbit interactions (*Russian*) 0-53391  
 oscillating electric dipole contrib. to light scatt. and interpret. in terms of polarisability and hyperpolarizability 0-53212  
 (+)-(S)-2-phenyl-3,3-dimethylbutane, optical activity, circular dichroism, polarisability model 0-43082  
 poly-thio-1-N,N-diethylaminomethylethylene, optically active samples, <sup>13</sup>C NMR spectra 0-28127  
 polynucleotide, double-stranded, conform. inhomogeneity of sugar-phosphate chain rel. to compact particle optical activity 0-35839  
 pseudoisocyanine bound by sulphated polysaccharides, dil. aq. soln., visible and circular dichroism spectra 0-45107  
 PT asymmetry and four-fold EM degeneracy lifting, appl. to ring laser mode splitting, optical prop. effects 0-23606  
 quartz, nonlinear polarisation plane rotation due to ruby laser irradi. (*Russian*) 0-53390  
 resonance medium, induced dichroism and gyrotropy 0-9971  
 resonant degenerate four-wave mixing, polarisation rotation and thermal motion 0-5779  
 Stokes relations in optically active media, macroscopic reversibility principle appl. 0-53207  
 tryptophan, stereoselective energy transfer induced by circularly polarised light 0-1010  
 Bi, neutral current-induced parity nonconserving optical rot., Dirac-HF calcs. 0-47948  
 Bi, vapour, optical rot., parity nonconservation 0-23353  
 Bi, vapour, optical rot., parity nonconservation expts. 0-23354  
 Co complex, C0(l-sparteine)Cl<sub>2</sub>, IR circular dichroism spectra, vibr.-electronic interaction 0-55074  
 Cs, 7P<sub>3/2</sub>-6S<sub>1/2</sub> transition, photon-echo quantum beats obs. 0-23373  
 CsCuCl<sub>3</sub>, cryst., gyrotropy, anomalous dispersion curves 0-2719



# optical rotation continued

- FeBr<sub>3</sub>, Faraday rotation in pulsed mag. field, linear absorpt. const. 0-45041
- KLiSO<sub>4</sub>(Cr), uniaxial crystals, circular dichroism and optical activity 0-45029
- Na laser oriented atoms, refl. by non-disorienting surfaces, optical activity detect. 0-55252
- Na vapour, diffusion coeff. of oriented atoms in buffer gases 0-53908
- Ni complex, Ni(l-sparteine)Cl<sub>2</sub>, IR circular dichroism spectra, vibr.-electronic interaction 0-55074
- NiSO<sub>4</sub>·6H<sub>2</sub>O, uniaxial crystals, circular dichroism and optical activity 0-45029
- Pb<sub>5</sub>GeO<sub>4</sub>(VO<sub>4</sub>)<sub>2</sub>, centrosymmetric crystals, induced linear electrogyration 0-45039
- Pb<sub>5</sub>SiO<sub>4</sub>(VO<sub>4</sub>)<sub>2</sub>, centrosymmetric crystals, induced linear electrogyration 0-45039
- SF<sub>6</sub>, polarization-rotation and thermal-motion studies via resonant degenerate four-wave mixing 0-5779
- Te, optical activity, de Haas-van Alphen oscillations and cond. band parameters 0-54605
- Te, optically active crystals, circular photogalvanic effect 0-54739
- Zn complex, Zn(l-sparteine)Cl<sub>2</sub>, IR circular dichroism spectra, vibr.-electronic interaction 0-55074

# optical saturable absorption

- alkali halide, ReO<sub>4</sub><sup>-</sup> doped, saturable absorber at 10.6 μm 0-53384
- atom, three-level, saturation spectroscopy including collisional effects 0-37099
- bistability, dispersive, beyond mean-field theory 0-43408
- diphenyl butadiene, absorption recovery lifetime, use in UV mode-locked lasers 0-19075
- DODCI dye dissolved in glycerine, time delayed picosecond pulse transmission obs. 0-48355
- Doppler-free intracavity polarization spectroscopy using elliptically polarized light 0-5537
- dressed molecule, RF field, saturated absorpt. obs. 0-9648
- dye, bleachable no.3955, relax. time meas., laser passive shutter appl. 0-23759
- dye, bleaching, coherence time meas. of laser radiation 0-23739
- dye bleaching, no. 3955 in soln., relaxation and correlation times meas. 0-28281
- dye laser, mode-locked CW, subpicosecond pulse generation with slow saturable absorber 0-9915
- dye ultrafast saturable absorbers for Nd lasers 0-53386
- Fabry-Perot cavity, instabilities for coherently driven absorber 0-53387
- glass fibre waveguide, γ-irrad., reversible optical bleaching of induced absorpt. 0-14462
- image correlation, real-time high-resolvance, by Bragg diffr. in saturable absorbers 0-48159
- iodomethane, RF field dressed mol. saturated absorpt. obs. 0-9648
- laser, passive mode locking, two laser amplifiers with slow saturable absorber 0-33041
- laser, photon distrib. with 1st-order phase-transition analogy 0-23659
- laser with saturable absorber, near threshold, correlation functions, renormalised Fokker-Planck eqn. 0-48208
- laser with saturable absorber, stationary state, nondiffusive approx. 0-19076
- laser-radiofrequency double quantum saturation spectroscopy 0-48105
- methane, frequency stabilisation of 0.633 μm line with 3.39 μm line locked to saturated absorpt. line 0-28258
- methane absorption cell for He-Ne ring laser, power resonances 0-28255
- methane E-component saturated absorpt. for stabilising He-Ne laser, quantum freq. standard 0-9901
- methanol, excited by CO<sub>2</sub> laser, sub-Doppler optoacoustic spectrum 0-5545
- methyl iodide FIR laser gas, passive Q-switching of CO<sub>2</sub> laser 0-1246
- molecular gases, saturation of light absorption 0-14401
- phosphate glass laser, statistical props. and stabilisation 0-48266
- polarisation spectroscopy, Doppler free intracavity 0-52335
- POPOP laser, bleaching of vapour 0-19027
- ring cavity, dispersive bistability in homogeneously broadened systems 0-14306
- ring laser, solid state, with intracavity bleachable filter, conditions for CW stimulated emission 0-14368
- ruby, optical free induction decay modulation and absorpt. line struct. due to superhyperfine interaction 0-33091
- ruby, optical hole burning, Stark and pump-probe studies 0-48356
- ruby lasers, freq. synchronisation and locking by passive modulator 0-1249
- spectroscopy, superhigh resolution, using coherent phenomena 0-22445
- time-correlated picosecond laser pulses generation, rapid sampling of optical relax. phenomena 0-9969
- TOPOT, 1,4-bi[2-(5-p-tolylloxazolyl)]benzene laser, bleaching of vapour 0-19027
- transient in absorptive optical bistability, analytical treatment 0-19077
- two-level atomic system, weak probe field absorption spectra in coherent laser field 0-23758
- two-level atoms, saturation in chaotic field 0-37982
- wave beam distortion by thermal self-interaction in droplet medium 0-19082
- wide aperture optical shutter with saturating filter at 1.06 μm 0-53457
- Ag halide, photochromic glass, optically induced anisotropy 0-1282
- AgCl photochromic glass, additional absorpt. spectrum, ellipsoidal model of colour centres 0-40142
- Ar laser emission under passive mode-locking conditions, temporal structure 0-9923
- Ba, reson. absorpt. transitions, laser saturation spectroscopy with optical pumping 0-47121
- CO<sub>2</sub>, excited by CO<sub>2</sub> laser, sub-Doppler optoacoustic spectrum 0-5545
- Cu, Doppler-free laser spectroscopy in hollow cathode discharge 0-9537
- Ge<sub>30</sub>S<sub>70</sub> glass film, Ag photodoping sensitivity 0-39121
- H<sub>2</sub>O absorption lines at ruby laser wavelengths, saturation effect 0-4098
- He, 3<sup>2</sup>D-2<sup>3</sup>P<sub>0</sub> line, press. broadening studies by saturated absorpt. techniques 0-52939
- I<sub>2</sub>, hyperfine transition saturation intensities, saturated absorpt. technique 0-43208
- I<sub>2</sub>, multiwavelength stabilisation of an Ar-Kr ion laser 0-28282
- I<sub>2</sub>, stabilisation of He-Ne laser, wavelength meas. 0-28264
- I<sub>2</sub> stabilised He-Ne laser, practical approach to design and construction 0-19051

# optical saturable absorption continued

- <sup>127</sup>I<sub>2</sub>, hyperfine structure components, stabilization of doubly resonant intracavity SHG of 1153 nm radiation 0-33077
- <sup>129</sup>I<sub>2</sub> absorption cell, freq. stabilisation of He-Ne 0.63 μm laser 0-53333
- KBr:Na(Rb)(Cs), microcrystalline powders, isothermal decay of colour centres 0-2804
- KrF excimer laser, passive mode-locking using saturable absorber dyes 0-1244
- Na, D-line saturation, under high power laser illumination 0-32653
- Na, reson. absorpt. transitions, laser saturation spectroscopy with optical pumping 0-47121
- Ni complex, BDN, degenerate four-wave mixing, amplification and phase conjugation 0-43394
- Ni complex, BDN II in tetrahydrothiophene-1,1-dioxide, saturation behaviour, Q-switching appl. 0-48354
- SF<sub>6</sub>, collisions, laser spectroscopy investig. 0-9697
- SiF<sub>4</sub> molecule, saturated absorpt. of CO<sub>2</sub> laser radiation 0-37811
- Te, optical bleaching near fundamental absorpt. edge at 80K 0-28287
- ZnIn<sub>2</sub>S<sub>4</sub> single cryst., intense radiation effect on optical transmission, absorpt. saturation 0-53385

# optical saturation

- see also optical saturable absorption
- atomic transition in stochastic field, saturation and Stark splitting 0-9546
- bidirectional laser amplifiers, amplified spontaneous emission intensity fluctuations 0-37988
- cresyl violet, rot. diffusion, picosec. saturation spectrosc. obs. 0-5634
- diffracted stimulated emission induced by coherent crossed laser beams for conc. meas. 0-35585
- fluoromethane, optically pumped laser, IR-FIR transferred Lamb dip spectra 0-1193
- free electron laser, classical theory 0-23655
- free electron laser, saturation behaviour from barrier reflection 0-9846
- gas, Stark tunable, mirrorless, optical bistability and optical limiting, obs. 0-38056
- homogeneously broadened three level atoms, intense standing wave saturated, spatial inhomogeneity, mode competition 0-23646
- hyper-Raman scattering, saturation effects, resonant three photon processes 0-38069
- intrinsic waveguide, in medium with saturated nonlinearity, theory 0-14405
- IR laser Stark spectroscopy, RF elec. field modulation effects 0-52989
- laser fields, stochastically fluctuating, saturation and Stark splitting of resonant transitions 0-53245
- laser resonator gain saturation, interf. effects 0-37987
- laser-induced atom-atom collision line shape 0-9691
- lasing system, three-level one-dimens., saturation effects 0-53253
- methanol, optically pumped laser, IR-FIR transferred Lamb dip spectra 0-1193
- molecule, saturation spectroscopy using tunable spin flip Raman laser, review 0-55762
- ring laser, two-mode, intensity fluctuations 0-33038
- spectroscopy, developments and applics. (Japanese) 0-4777
- Stokes radiation spatial characts. in stimulated scattering, saturation conditions 0-53379
- three-photon vector model, resonant coherent interaction (Chinese) 0-43306
- time-resolved laser saturation spectroscopy and coherent transients survey 0-9965
- two-photon saturation effect on ordinary Raman scatt. 0-9967
- Ba, reson. transition, laser saturation spectroscopy with optical pumping 0-52334
- CO laser with selective resonator, gain saturation law, lasing transition efficiency 0-48227
- CO<sub>2</sub> waveguide laser, saturation parameter 0-9856
- Cs, multiphoton ionis. cross sections, absolute meas. evaluation 0-14122
- He-Ne travelling wave laser, spontaneous emission spectra, 3.39 μm region 0-37995
- KrF electron-beam-excited amplifier, master-oscillator power-amplifier expt. for gain coeff. and saturation intensity determ. 0-48222
- Na, magnetically induced SHG, intensity saturation 0-1273
- Na, reson. transition, laser saturation spectroscopy with optical pumping 0-52334
- Na vapour, saturation holes meas. using FM spectrosc. 0-42262
- TI vapour, coherent anti-Stokes scatt. four-photon parametric oscill. 0-9959
- Xe-He source, intensity fluctuations of amplified spontaneous emission at 3.51 μm 0-32957

# optical self-focusing

- see also electrostriction; Kerr electro-optical effect; self-trapping
- beams of elliptic cross-section, crit. modes 0-19081
- coaxial atomic and light beams, simultaneous self-focusing and self channeling (Russian) 0-28292
- distortions, nonlinear, of scanning light beams 0-14407
- ferroelectric, with anomalously high dielec. const., self-focusing of EM wave 0-14408
- fibre, self-focusing, matching elements calc. 0-28339
- intrinsic waveguide, in medium with saturated nonlinearity, theory 0-14405
- laser amplifier with spatial filters, optimal length and operating conditions 0-48323
- laser beams, elliptically shaped Gaussian, nonlinear propagation 0-43409
- laser beams, self-focusing in nonlinear media 0-48360
- liquid crystal laser self-focusing, effect of spatially dispersed nonlinearity 0-38908
- nonlinear pressure forces for laser radiation in plasma, experimental confirmation 0-28682
- picosecond light continua generation depending on various nonlinear processes 0-33095
- self-focusing media, filament form 0-28291
- soliton solutions, light beam self-action in nonlinear media 0-14404
- solitons, laser physics appls. 0-48333
- steady-state self-focusing and filamentation in presence of longit. inhomogeneity 0-19079
- stimulated Raman scatt. thresholds for ultra-short excitation 0-33078
- stimulated Raman scattering, wavefront reconstruction and self-focusing 0-23752
- Ba, vapour, laser excited, anomalous conical emission and self focusing 0-43411



**optical self-focusing continued**

- InSb, low-power nonlinear refraction effect on laser beam propagation 0-5801
- Nd laser, with mirror plasma-optical Q-switch (*Russian*) 0-33028
- Nd:glass laser amplifiers, self-focusing and suppression by spatial filtering 0-14406
- Nd<sup>3+</sup> phosphate glass laser, brightness enhancement by spatial filtering in amplifying channel 0-48321

**optical storage devices**

- see also holographic storage*
- buffer store, liquid crystal image convertor appl. 0-33166
- disc, data recording using diode laser 0-19001
- elastomer storage device evaluation for optical signal processing 0-48444
- holographic colour video memories, recording and playback technique 0-9833
- holographic memory devices, optoelectronic ROM memory, injection laser appls. in construction (*Polish*) 0-19007
- memory readout by superluminescent diode with integrated photodetector 0-32922
- microchannel spatial light modulator as storage medium 0-43479
- thermoplastic photoconductor tape performance 0-43305
- three- and four-dimensional photoacoustic store readout 0-48413

**optical stores**

- see also holographic storage*
- bistable TV-optical feedback system using optical flip-flops 0-53354
- conference, Bad Harzburg, Germany (June 1979) 0-51951
- frequency-domain nonvolatile optical storage scheme 0-43282
- information storage, seminar, Washington, USA (Apr. 1979) 0-41942
- matched filter correlator memory techniques and capacity 0-43280
- materials for optical storage and reproduction 0-33109
- medium specification and performance trends, review 0-43415
- microscopically rough substrate local smoothing for optical storage 0-14288
- organic charge transfer salt process for high-density video storage 0-43269
- surface polariton use 0-48414
- wideband archival optical storage technology assessment 0-43283
- As-Se, relation between glass-transition temp. and optical memory-eraser temp. 0-10650
- As<sub>2</sub>S<sub>3</sub>, relation between glass-transition temp. and optical memory-eraser temp. 0-10650

**optical susceptibility**

- see also nonlinear optical susceptibility*
- benzene, derivatives, calc. of second-order susceptibility, using electronic spectra data 0-29756
- structural phase transition induced refractive index changes in crystals. 0-16000
- three-level system, interacting with two strong EM fields, steady-state population distrib. and complex susceptibility 0-37978
- DyAsO<sub>4</sub>, first-order cooperative Jahn-Teller phase transition, dielec. suscept. studies 0-19940
- Fe<sub>2</sub>O<sub>3</sub>, magnetite, magnetoelc. effect at 77K and cryst. symm. 0-29593
- GaAs:Be, ion-implanted, IR refl. and transmission meas. 0-34908
- KCl coloured crystal, susceptibility variation calculations 0-55055
- KD<sub>2</sub>PO<sub>4</sub>, Rayleigh scatt. and narrow central component, depend. on scatt. wave vector direction 0-29747
- KH<sub>2</sub>PO<sub>4</sub> type crystals, transverse elc. susceptibilities 0-50273
- W (001), surface phase transition, electronic contribs., surface susceptibility, ab initio self-consistent thin-film energy band calc. 0-29255

**optical systems**

- see also adaptive optics*
- aberration approximation using wave, transverse and longit. values (*Russian*) 0-28167
- adaptive optical components, seminar, Washington USA (Apr. 1979) 0-31421
- alignment mechanism, testing by interferometric method 0-53454
- aperiodic spacous objects imaging, influence of AF sinusoidal phase deformations of wavefront (*Czech*) 0-14290
- apodized optical systems with third-order spherical aberrations, MTF 0-9823
- aspheric reflecting systems, geometrical design 0-38083
- aspherical, manufacturing and testing techniques development, use of computer (*Italian*) 0-48467
- aspherical surface measurement (*Hungarian*) 0-38087
- automatic correction of optical systems by accurate ray tracing (*Spanish*) 0-53401
- automatic correction of optical systems by accurate ray tracing (*Spanish*) 0-53402
- coherent, impulse response for image multiplication by spatial sampling filtration 0-33126
- coherent optical image processing system, expts. and astronomical appls. (*Russian*) 0-12675
- coherent speckle interferometry system, for stars cold satellites searching (*Russian*) 0-12672
- compound elliptical concentrator, geometrical vector flux field 0-33119
- conference, Bad Harzburg, Germany (June 1979) 0-51951
- cryogenic and contamination effects 0-38113
- cylindrical lens systems described by operator algebra 0-38086
- diffraction analysis, in microscopy 0-32926
- diffraction dispersing systems with scarcely altering spectral line curvature (*Russian*) 0-1292
- dye laser demonstration system, educational appl. (*German*) 0-51994
- error compensators, calc. procedure 0-28296
- evaluation criteria and problems, review (*German*) 0-43268
- factor analysis methods for designing complicated optical systems 0-28303
- field correctors, for astronomical telescopes at better observing sites 0-4257
- focal-reducer system, for slitless fieldspectroscopy 0-36504
- gradient index fibre array for photocopying machine 0-14482
- gradient index imaging lens and system status 0-14420
- gradient index imaging system theory 0-14294
- gradient index optical imaging systems, topical meeting, Rochester, USA (May 1979) 0-12851
- hologram lens system, astigmatism and coma reduction 0-53238
- image optimisation by apodisation filters in optical systems with residual aberrations 0-53223
- image quality criteria, modular transfer function, phase transfer function (*German*) 0-53221
- image rotation and magnification, optical system 0-48376

**optical systems continued**

- immersion optics in multichannel photoelectric systems 0-53405
  - integrated optics long-term role in optical and electronic systems 0-33232
  - isoplanatism, image form. 0-1144
  - laser system, high energy, thermally induced optical distortion 0-38051
  - lobster-eye optical configuration, appl. in X-ray telescopes 0-17491
  - merit function, diffr. based, for automatic lens design (*Chinese*) 0-5809
  - moire gratings strain meas., long time high temperature appl. 0-38361
  - narrow-field receiver system, spherical aberration effect on radiation power losses 0-28299
  - non-coaxial aspherical IR optical system, automatic design (*Chinese*) 0-5810
  - optical transfer measure, system relations, appl. wide field microscopy and microelectronic photolithography (*German*) 0-9815
  - optomechanical scanner, noise analysis 0-47090
  - paraxial optical systems, nomographic diagrams for design and anal. 0-48377
  - plasma temperature field determ., asymmetrical, spectral method (*Czech*) 0-38704
  - polariser + crystal plate + analyser system, passage of light 0-10023
  - ray tracing through tilted and decentred optical surfaces, computer program 0-33120
  - remote sensing system specification using computer image simulation 0-48439
  - reversed Cassegrain, seventh-order design of a reflecting optical system 0-48378
  - scanning system with multifaceted mirror, tracking sweep 0-33123
  - shadowgraph apparatus, phase struct. visualisation by crossed statistical amplitude rasters (*Russian*) 0-5846
  - simulator for UHF antennas 0-26742
  - stigmats using two curved Fresnel surfaces 0-38084
  - stray light performance, surface and system scatt. characteristic specification 0-48389
  - Strehl intensity applicability as image quality criterion (*German*) 0-28166
  - surface damage from fusion experimental lasers, high fluence and contamination effects 0-38049
  - system and component specifications, seminar, Washington, USA (Apr. 1979) 0-46731
  - telecentric imaging system focus detector 0-53397
  - telecentric system condenser alignment 0-33115
  - tolerancing plan activities and documents 0-48382
  - vacuum monochromator low-temp. attachment construction and optics 0-31764
  - visual optical system specification and test procedures 0-48385
  - visual system quantitative tolerance specification and standard development 0-48384
  - wave aberrations caused by misalignments of aspherics, and their elimination 0-33127
  - zoom lens focusing system (*Japanese*) 0-31922
  - zoom projection lens, optical level system, paraxial characts. 0-53399
- optical telescopes** *see telescopes*
- optical television recording** *see telerecording*
- optical testing**
- see also optical instrument testing; optical workshop techniques*
  - alignment mechanism, testing by interferometric method 0-53454
  - aspheric surface contour meas. machine and computer system 0-14494
  - aspherical surface interferometric testing using dual computer-generated holograms 0-9830
  - aspherical surfaces, holographic methods of testing, review 0-33257
  - astronomical telescope concave mirrors, design of lens compensators for testing 0-28305
  - autocolimation apparatus to test manufacturing quality of aspherical mirror profile 0-10053
  - automatic pattern processor for simple and complex interference patterns 0-13129
  - axicon and related optical component diagnostic techniques 0-14417
  - Babinet compensator, appl. in optical testing 0-33251
  - characterisation for IR diamond-turned aspherical elements 0-1373
  - coating surfaces of optical components, reflection coeff. meas. 0-28366
  - coherent-optical materials testing for vibration pattern and defect discrimination (*German*) 0-30181
  - component manufacture and evaluation, seminar, Los Angeles, USA (Jan. 1979) 0-12850
  - dielectric multilayers, optical and geometrical thickness monitoring using monochromatic maximeter, substrate effects (*French*) 0-38140
  - far IR optics testing and specification for night vision thermal imaging 0-48440
  - fast aspheric mirror figure control by profile monitor, wire tester and null lens 0-14419
  - fibre characteristics testing, differential interferometry 0-48397
  - film pulsed laser damage determ., optical techniques 0-33060
  - heliostat facets, optical characterisation 0-53485
  - high-energy, IR laser component optical characterisation techniques 0-14347
  - high-energy laser diffraction grating evaluation approach 0-14474
  - high-energy laser mirror thermal distortion test facility 0-14348
  - high-performance telescope aspheric mirror test error budget 0-48386
  - inclined prism three-point meas. reliability (*German*) 0-28359
  - interferogram aberration evaluation program 0-13130
  - interferogram fringe pattern reduction, automated system 0-47097
  - interferometer, real-time shearing, quality factors testing appl. 0-37081
  - laser fusion Optical Evaluation Laboratory, Antares CO<sub>2</sub> laser system 0-14346
  - laser interferometer for routine aspheric surface testing 0-14495
  - lens, large-size, simplified MTF meas. (*Japanese*) 0-33121
  - lens quality measurement using lateral shearing interferometer (*German*) 0-22425
  - lens surface quality testing at Zeiss factory (*German*) 0-33113
  - lens system evaluation, use of OTF for image anal. 0-53481
  - liquid crystal electro-optic valve testing using laser light (*French*) 0-28311
  - microscope polarisation adapter, for transparent material anisotropy and internal stresses meas. 0-31863
  - mirror optical scatter meas. specification proposal 0-48390
  - mirror production and testing, low-scatter, low-loss mirrors for laser gyros 0-1272
  - multiactuator deformable mirror evaluations 0-14416
  - off-axis parabolic mirror fabrication for laser function expt. 0-1374
  - ophthalmic lenses, thin, chemtempered, static load strength testing 0-5812



**optical testing continued**

- ophthalmic lenses, thin, chemtempered, strength meas. by drop-ball testing 0-5811
- projection system transfer function definition and performance testing (*Hungarian*) 0-14413
- quarter wave multilayer monitoring, optical props. change rel. to error compensation 0-38139
- quasi-Ronchigrams for interpreting wave-front and glass-error slopes 0-37078
- Ronchi test, fringe sharpening 0-53480
- Ronchi test, practical formulae and experimental verification 0-43490
- Ronchi test formulae, theory 0-23817
- rotational symmetric aspheric in compensated interferometers, computer-generated-holography testing 0-33128
- shearing interferogram evaluation improvement (*German*) 0-27339
- solar concentrators, luminescent, operation theory and performance evaluation techniques 0-7913
- solar simulator design for testing solar collectors 0-50996
- spherical aberration measurement of photographic lenses, using solid-state image sensor 0-23812
- surface contaminant generation and bidirectional reflectance distrib. function meas. 0-14493
- surface quality standards based on total integrated scatt. 0-48391
- system and component specifications, seminar, Washington, USA (Apr. 1979) 0-46731
- thermal blooming cell design for adaptive optics evaluation 0-33096
- unequal path interferometer, alignment and use as optical test tool 0-9031
- visual optical system specification and test procedures 0-48385
- wave aberrations caused by misalignments of aspherics, and their elimination 0-33127
- wavefront analysis, automatic real-time meas. of interferograms, technique 0-9029
- waxicons for high-power chemical lasers, interferogram analysis 0-14418
- zoom null lens design for optical component and system testing 0-23811
- Si, diffraction grating, rectangular profile, fabricated from single cryst. 0-38093

**optical transfer function**

- acousto-optic heterodyning image processor 0-5833
- annular apertures, imaging performance, apodization and MTF 0-23625
- annular lenses in microscopes, imaging props., calcs. 0-22426
- aperiodic spaciuous objects imaging, influence of AF sinusoidal phase deformations of wavefront (*Czech*) 0-14290
- apodisation and image contrast rel. to MTF 0-32920
- apodized optical systems with third-order spherical aberrations, MTF 0-9823
- atmosphere modulation transfer function, vel. to IR speckle interferometry 0-31216
- C-CD, charge transfer inefficiency effect on MTF, compensation techniques 0-10026
- channel plate in image tube, MTF 0-19108
- coherent optical system, impulse response for image multiplication by spatial sampling filtration 0-33126
- collimator monochromatic MTF computation program 0-14451
- computed tomography scanner geometry optimisation 0-46037
- computerised tomography, computer assisted determ. of OTF 0-46030
- diffraction analysis, in microscopy 0-32926
- diffraction point spread function, second moment as image quality criterion 0-9818
- Electroitus, detective quantum efficiency 0-42307
- fibre-optic communication cables, measurement of baseband transfer function 0-1355
- gamma camera data, evaluation in moving organ exam. 0-30845
- holographic image formation, coherent transfer functions and resolution 0-43292
- holographic recording medium, optimal linear transfer function determ. 0-23635
- image optimisation by apodisation filters in optical systems with residual aberrations 0-53223
- image quality criteria, modular transfer function, phase transfer function (*German*) 0-53221
- imaging system, incoherent, diff. images asymptotic behavior 0-1139
- interferogram fringe pattern reduction, automated system 0-47097
- interferometer, real-time shearing, quality factors testing appl. 0-37081
- isoplanatic degradation of tilt correction and short-term imaging systems 0-53219
- isoplanatic optical systems, partially coherent image form. through random absorbing media 0-14292
- lens, large-size, simplified MTF meas. (*Japanese*) 0-33121
- lens design data, OTF numerical calc. (*Korean*) 0-19085
- lens system evaluation, use of OTF for image anal. 0-53481
- lithography, optical and electron-beam, MTF evaluation 0-4801
- mammography, detective quantum efficiency anal. of electrostatic imaging and screen-film imaging 0-41232
- mass-produced camera objectives, effects of cosmetic defects 0-47135
- merit function, diff. based, for automatic lens design (*Chinese*) 0-5809
- microdensitometer flare, methodology for quantifying 0-52293
- monochromator, total spread function description of props. 0-19100
- MTF measurement of low light level devices 0-33221
- optical transfer measure, system relations, appl. wide field microscopy and microelectronic photolithography (*German*) 0-9815
- projection system transfer function definition and performance testing (*Hungarian*) 0-14413
- radiographic imaging system OTF 0-17085
- radiographic system, OTF as means of evaluation of image characts. (*German*) 0-35450
- radiography, metal screen-film detector MTF at megavoltage X-ray energies 0-30868
- radiography, rare-earth screens, effect of P X-rays 0-30867
- reflection microdensitometry, optical principles and practical solutions 0-4790
- retinal diffusion and eye optics quality, OTF and light scatt. characterisation 0-41004
- satellite retroreflector arrays 0-5778
- saw-tooth wave target, modulation by optical system with triang. and assoc. filters 0-9817
- schlieren instrument, amplitude transfer charact., Monte Carlo method 0-28336
- schlieren techniques represented by phase contrast function 0-9813

**optical transfer function continued**

- sector templates for determining the contrast transfer of imaging systems 0-32924
- spatial and energy parameters of optical instrument, criteria for performance evaluation 0-33259
- systems with small residual aberrations, schlieren effects (*German*) 0-32923
- visibility, definition, confirmation using marine optics data 0-23633
- visual stimulus device for characterizing temporal MTFs in man 0-51204
- X-ray focal spot, MTF, modified meas. method 0-37149
- X-ray TV chain MTF and image quality determ. factors 0-36126
- xeroradiographic imaging linearity and MTF applicability 0-4825

**optical variables control**

- injection laser output regulation by NTC resistor cct. 0-14353
- simultaneous feedback control of bias and modulation currents for injection lasers 0-43332

**optical variables measurement**

- see also *colorimetry; densitometry; light velocity measurement; optical noise measurement; photometry; polarimetry; Q-factor measurement; refractive index measurement; streak photography; turbidimetry*
- absorption coefficient, precise meas. of small change (*Japanese*) 0-4749
- amplitude correlation method for optical polarisation meas. 0-53206
- apparatus for optical measurements under conditions of hydrostatic pressure up to 2 kbar at temperatures  $\leq 25\text{K}$  0-22379
- birefringence measurement using photoelastic modulator 0-31838
- camera lens performance, routine checking system 0-277
- depolarisation ratio of light scattered by compressed gases, meas. apparatus 0-38527
- diffuse reflectance meas. for buildings 0-27334
- dispersion in single-mode optical fibres pulse synchronisation meas. technique 0-48410
- fibre backscatter attenuation measurements, optimised technique 0-53447
- fibre Y-branch, low-loss, attenuation and far-field meas. 0-10004
- film optical constns. meas., Shamir-Graff method evaluation 0-11489
- frequency, direct method for visible light 0-47041
- gain measurement technique for high gain amplifiers 0-1208
- glossiness of curved surface, physical and psychological, meas. method 0-37074
- graded index fibre optical loss meas. using dummy fibre 0-5819
- interlocked solid-state lasers, radiation intensity modulation for precision meas. 0-1250
- IR pulse laser intensity profiles meas. (*Japanese*) 0-22413
- laser beam diameter meas. methods survey, safety aspects 0-53348
- laser beam interferometric wavelength measurements through post-detection signal processing 0-42254
- laser cavity resonator, photon lifetime and reflectance meas., phase-shift method 0-38039
- laser heterodyne apparatus for measuring small angle scattering from particles 0-1261
- laser radiation in liquid second harmonic intensity meas. 0-48338
- laser radiation pulse, based on semiconductor radiators 0-23710
- laser radiation pulse length meas., discussion 0-1259
- laser radiation pulse width, from solid-state meas. lasers 0-23736
- laser wavelength measurements, review of recent developments 0-48320
- layer surfaces, reflectivity at  $3.39\text{ }\mu\text{m}$ , meas. method, relevance to pipelines 0-52340
- light intensity variations, metal-halide discharge lamps appl. to film lighting 0-4796
- microwave to visible frequency synthesis 0-48319
- mirror optical scatter meas. specification proposal 0-48390
- mode power distribution meas. method for multimode parabolic-index fibres 0-14439
- MTF measurement of low light level devices 0-33221
- multimode optical fibres, mode conversion coeffs. meas. 0-53433
- optical fibre, measurement of attenuation, numerical aperture and input-output radiation profile 0-33186
- optical fibre, measurement of attenuation and dispersion 0-33185
- optical fibres, baseband freq. response meas. by modulated InGaAsP laser beam, dispersion characts. 0-1308
- phase measurement in real time using photodetector array, Fourier transform computation 0-9013
- picosecond light pulse, meas. techniques (*Japanese*) 0-52291
- precision loss measurement of photoelectric pulse signals using microcomputer 0-13142
- reflectance and transmittance, arrangement for accurate meas. (*German*) 0-31844
- reflection coefficient meas., effect of light beam collimation 0-18003
- reflectivity, mirror arrangement for meas. by changing incident angle 0-18000
- rotation angles in polarised light, detection and measurement (*Rumanian*) 0-22418
- semiconductor and dielectric optical nonuniformity, spatial distrib. determ. 0-13116
- spectral response, pulsed measurement, test set-up and apparatus, shortcomings and planned improvements 0-45695
- sub-picosecond optical pulses, generation and meas. 0-23731
- surface brightness, newly developed reflectometer appl. (*German*) 0-42253
- surface modal deformation sensor for heterodyne interferometry 0-31859
- surface quality standards based on total integrated scatt. 0-48391
- Thermophysical method for optical characts. determ. of scatt. medium 0-9014
- waveguide properties, components and systems for optical links (*German*) 0-33168
- waveguides meas. procedure quality, standards 0-1351
- CO<sub>2</sub> laser transition absolute freqs. by multiplication of difference freqs. 0-37992

**optical waveguide components**

- see also *optical couplers; optical isolators*
- acousto-optical devices, critical assessment and development trends (*Czech*) 0-23777
- active and passive devices for fibre transmission systems 0-43463
- circulator, polarisation independ., for optical fibre transmission systems 0-23779
- circulator, polarization-independent, configuration method 0-38095
- circulator for optical fibre transmission, using Faraday rotator and Glan-Taylor prisms 0-23769
- colinear interaction between acoustic and optical waves in planar waveguide, radiation into substrate 0-53452



**optical waveguide components continued**

deflector using chalcogenide amorphous film on graded index  $\text{LiNbO}_3$  waveguide 0-48463  
 diplexer reflection type periodic filter, elliptic response 0-43474  
 directional couplers and phase shifters for guided-wave signal transformers, synthesis 0-1358  
 electro-optic multimode waveguide modulator or switch 0-23783  
 electro-optic waveguide deflector performance characteristics 0-33213  
 electro-optic waveguide modulators, capacitance of electrode system rel. to modulation efficiency (*Russian*) 0-1359  
 electrooptic waveguide array deflectors, performance criteria and limitations 0-5821  
 fibre optics components and integrated optics 0-1356  
 fibre tapers for optical coupling of optical fibres, appls. (*German*) 0-38107  
 fibre-optic communication systems, devices and ccts., book 0-38123  
 geodesic aspherical perfect lens, general sol. for integrated optics 0-10049  
 geodesic lenses, aberration-corrected rounded edge, profile calcs. 0-10048  
 geodesic optical lens prod. by anisotropic etching 0-10047  
 guided-wave signal transformers, synthesis 0-1358  
 lenses, Bragg and Luneburg type 0-10050  
 lenses, review (*Japanese*) 0-10019  
 Mach-Zehnder waveguide modulators in Ti-diffused  $\text{LiNbO}_3$  0-33203  
 micro lenses to improve LED-to-fibre optical coupling and alignment tolerance 0-19088  
 modulators, switches and deflectors, physical principles and Czechoslovak developments (*Czech*) 0-19090  
 second- and higher-order waveguide grating filters, refl., transmission and loss coeffs. meas. 0-19110  
 second- and higher-order waveguide grating filters, spectral response calcs. 0-19109  
 tunable narrow-band thin-film waveguide grating filters, performance 0-38124  
 CdS semiconducting thin-film optical waveguide polariser 0-33180

**optical waveguide theory**

see also *guided light propagation*  
 alpha-power graded-core fibre dispersion, closed-form approximation 0-1320  
 anisotropic graded index waveguide, acoustooptic interaction efficiency freq. depend. 0-23776  
 asymmetric dielectric-slab waveguide, beam mode scatt. characts. 0-38114  
 asymmetric three-layer optical waveguide, radiation losses due to discontinuities 0-53446  
 asymmetric three-layered slab waveguide, leaky TE modes 0-43447  
 asymmetrical, 2-dimensional, application of the equivalent-index method to DH diode lasers 0-23772  
 bandwidth of distorted multimode waveguides excited by laser sources 0-43436  
 bandwidth spectrum of multimode fibres, depend. on refr. index profile 0-9985  
 Bragg mirror reflectance, dielectric waveguide inhomogeneity effect 0-28356  
 clad parabolic-index square-law dielectric waveguide, perturbation anal. 0-33190  
 colinear interaction between acoustic and optical waves in planar waveguide, radiation into substrate 0-53452  
 complete EM field of dielectric lossy fibre excited by dipole source, numerical calc. 0-43427  
 conic and quasi-conic profile, calc. and construction (*Rumanian*) 0-28331  
 corrugated dielectric waveguide, radiation loss calcs. for TM polarisation 0-43445  
 corrugated dielectric waveguide, second order stop band numerical study 0-23807  
 corrugated waveguide, guided mode diffrr., coupled-wave eqns. 0-48434  
 curved slab waveguide, excitation 0-14445  
 cylindrical inhomogeneity in homogeneous medium of infinite extent, guided EM field numerical computation 0-14274  
 cylindrical optical fibre transmission and guided mode behaviour 0-28348  
 dielectric fibres of arbitrary cross-section, fundamental mode propag. 0-43443  
 diffused waveguide, acoustooptic interaction efficiency of TE modes, freq. depend. 0-53455  
 diffused waveguide, attenuation characteristics of TE modes and surface scatt. 0-5822  
 diffused waveguide, refractive index profile determ. by inverse scatt. theory 0-5838  
 dispersion properties, approx. formulas 0-14444  
 dispersion relation for waveguide mode with arbitrary anisotropy 0-5840  
 elliptical dielectric waveguides, higher-mode cutoff 0-43432  
 elliptical fibres, selectively excited, near-field distrib. 0-48401  
 elliptical multimode fibres, whispering and bouncing mode evaluation 0-10015  
 envelope wave stability 0-43410  
 fibre, arbitrary index profile, formula for  $\text{TE}_{01}$  cutoff freq. 0-48418  
 fibre, elliptical step-index multimode fibre, rays and modes 0-14442  
 fibre, modal noise, dependence on source coherence and fibre length 0-48402  
 fibre, power-law graded-index, core/cladding power distrib., propag. const. and group delay 0-48420  
 fibre, power-law refractive index profile, scalar modal eigenvalues and group delays 0-28322  
 fibre, quasiparabolic index profile, propag. characts., perturbation anal. (*French*) 0-33189  
 fibre, two-mode, temporal spreading of pulse 0-33183  
 fibre and film waveguides, local normal modes, superlocal modes, ideal modes 0-14466  
 fibre loss increase due to stranding in optical cables 0-38117  
 fibre optics, uniform asymptotic theory 0-28323  
 fibre refractive index profile, effect on fibre bandwidth 0-23773  
 fibre refractive index profile models 0-14453  
 fibre tapers for optical coupling of optical fibres, appls. (*German*) 0-38107  
 fibre waveguide, chromatic signal distortion depend. on optical carrier coherence 0-1317  
 fibres, graded-index with polynomial profiles, propag. characts. 0-38118  
 fibres, min. dispersion at 1.55 micron for single-mode step-index fibres 0-10006

**optical waveguide theory continued**

fibres, modal dispersion with composite  $\alpha$ -profile graded-index core 0-9998  
 fibres, mode dispersion, material dispersion and profile dispersion in graded-index single-mode fibres 0-14443  
 fibres, mode-coupled multimode, baseband transmission theory based on scattering matrix 0-14468  
 fibres, weakly guiding and slightly elliptical, birefringence expression using perturbation theory 0-1309  
 field distribution of a point source inside a lossy optical fibre 0-10044  
 flexible IR waveguides, high-power transmission 0-48409  
 frequency modulation by p-i-n structure, optical waveguide with moving walls 0-19099  
 gas waveguide laser, mode comp. of radiation 0-28192  
 gas-dielectric optical waveguide, general azimuthal asymmetry, loss evaluation 0-53453  
 Gaussian beams, waveguided, coupled by misaligned or curved grating effect 0-33228  
 graded core W-type fibre and its propagation characteristics 0-1334  
 graded fibres with non-circular index contours, core fields 0-14455  
 graded glass fibre, effect of shape of refractive index profile, on distortion 0-33197  
 graded index fibres, mode conversion caused by splices 0-1340  
 graded index fibres, propag. const. and group delays 0-23770  
 graded monomode fibres and planar waveguides 0-43435  
 graded noncircular multimode fibres, leaky modes, analytical ray theory 0-33192  
 graded weakly guiding fibres, fundamental  $\text{HE}_{11}$  modes 0-43444  
 graded-index fibre, spatial degree of coherence 0-53441  
 graded-index fibre transmission characteristic computation 0-1321  
 graded-index fibre with polynomial-profile core, propag. constants of guided modes 0-10005  
 graded-index fibres, analytical relations between model power distrib. and near-field intensity 0-9995  
 graded-index monomode fibres with elliptical cross-section, birefringence 0-53416  
 inhomogeneous medium, two-dimens., light propag. problems rel. to thermodynamic waveguide development 0-32914  
 inhomogeneous planar dielec. waveguides for integrated optics structs., synthesis (*Russian*) 0-38135  
 intrinsic waveguide, in medium with saturated nonlinearity, theory 0-14405  
 laser diode-to-diffused waveguide coupling efficiency, waveguide mode asym. effects 0-9990  
 long fibre, mirror and hollow dielec. lightguides, photometric characts. 0-33201  
 long-distance multimode waveguide image transmission in coherent light 0-48435  
 modal propagation for arbitrary cross sectional shape 0-10014  
 multimode and single-mode optical fibre guides with rectangular cores 0-33220  
 multimode fibre, pass band depend. on excitation conditions 0-48433  
 multimode fibres, arbitrary index profile, propag. mode anal. using ray optics adiabatic approx. 0-53418  
 multimode irregular fibre, with fluctuation focusing ray calcs. of power loss 0-33195  
 multimode W-type fibres, steady-state characts. 0-5818  
 multimode fibres, energy description of propagation of monochromatic radiation 0-38116  
 optical fibre, multimode, mode-coupling phenomena anal. using matrix method, accuracy 0-23803  
 particle motion in potential channel, waveguide-optical analogy 0-12942  
 permittivity profile of inhomogeneous planar waveguide, determ. from mode spectrum (*Czech*) 0-28312  
 planar anisotropic structures, waveguiding properties (*Czech*) 0-28313  
 planar waveguide, isotropic, polarisation conversion by Bragg deflection coupled mode theory 0-48461  
 pulse dispersion in a clad lens-like medium 0-53445  
 S-shaped dielectric waveguide, guided leaky waves 0-28341  
 self-filtering multilayer S-waveguides with absorption and radiation losses 0-38102  
 signal distortion, intensity distrib., single and coupled waveguides 0-33202  
 single mode fibers, microbending loss evaluation, core index profile effects 0-48412  
 single mode fibres, arbitrary-index, microbending loss evaluation 0-48411  
 step index fibres, mode conversion due to scattering from off-axis inhomogeneity, Green's function analysis 0-10045  
 step-index fibres with microbending, bandwidth 0-23775  
 step-index monomode fibre, mode dispersion anal. of approx. for propag. const. 0-1307  
 step-index optical fibre, scatt. from off-axis inhomogeneity, radiation loss 0-43446  
 surface waveguide electrooptic deflector, high-resolution, prism model 0-48454  
 tapered optical waveguide structs., mode coupling in terms of local modes 0-38126  
 thin film, using Maxwell EM theory (*Czech*) 0-33229  
 thin film rib waveguide, numerical anal. by mode-matching method 0-48421  
 thin-film strip waveguide on dielectric substrate, optical dispersion 0-53478  
 three-layer waveguides for wideband optical communication lines 0-28310  
 TM mode in Eckart-Epstein optical strip guides, exact solution 0-10046  
 transversally nonhomogeneous waveguide EM wave propagation, using variational methods (*Czech*) 0-33155  
 trapezoidal cross-section dielectric waveguides, mode dispersion by effective-index method 0-9999  
 uniform theory of inhomogeneous waveguide modes near cut-off 0-28324  
 whispering-gallery waves, polarisation and losses along twisted trajectories 0-9798  
 $\text{LiNbO}_3$ , Ti diffused waveguide, leaky mode loss coeffs., calc. 0-19094

**optical waveguides**

see also *optical fibres*; *optical waveguide components*; *optical waveguide theory*  
 acousto-optic light modulator, using Raman-Nath diffrr. of vol. acoustic wave 0-48437  
 acousto-optic tunable TE-TM mode convertor on diffused waveguide 0-53477



**optical waveguides continued**

aperture-type light conductor, photometric charact., computerised calc. by Monte Carlo method (*Russian*) 0-1339  
 blanks, thermal and elastic stresses in a cylinder 0-1447  
 channel waveguide array in fan-out pattern for high resolution optical imaging 0-38129  
 channel waveguide arrays coupled to integrated CCD 0-33244  
 characteristics determination, far-field radiation patterns, semiconductor laser structure appl. 0-48407  
 chemical laser, electronic phototransition, with thermal initiation by shock wave 0-53283  
 circular dielectric screened three-layer waveguide, cut-off characteristics and modal inversion 0-1303  
 composite light-controlled waveguide struct., polystyrene film with methyl red dye as active medium 0-14464  
 composite waveguide laser with end-fire excitation, output characts. 0-23738  
 conference, Bad Harzburg, Germany (June 1979) 0-51951  
 conic and quasi-conic profile, calc. and construction (*Rumanian*) 0-28331  
 curved waveguide, with parabolic refr. index profile over cross section, light propag. 0-19104  
 curved waveguide, with refr. index varying over cross section, light propag. 0-19103  
 design of waveguides with prescribed propag. constns. 0-48419  
 development strategy, Poland (*Polish*) 0-48438  
 diffraction grating form. on optical waveguide surface, ion-beam etching through photoresist mask 0-14492  
 evanescent fields, use in obs. of laser radiation effects on mammalian cells 0-12183  
 fabrication in glass by effusion 0-5850  
 fibres, evaluation of normalised cutoff frequencies in radially inhomogeneous fibres, perturbation theory 0-43434  
 film thickness and refractive index, accurate meas. by symmetric prism wave couplers (*Chinese*) 0-2885  
 flexible IR waveguides, high-power transmission 0-48409  
 fluoromethane DFB gas laser, construction and operation 0-23715  
 GaAs epitaxial layer photoelastic channel optical waveguides 0-48457  
 glass waveguide, in-plane scatt. and loss mechanisms 0-33216  
 graded refractive index, diffused glass waveguide, anisotropy 0-33210  
 guided-wave optical systems and devices, seminar, Washington, USA (April 1979) 0-31418  
 hollow lightguides for H lamp, optical and operational characts. 0-53395  
 holography with guided optical waves, expt. techniques and results 0-28173  
 III-V nitride semiconductors, physical properties and appls. in integrated optics (*Czech*) 0-28355  
 index profile determ. methods 0-1337  
 infrared microwaveguides with a mode-guiding layer of chalcogenide glass 0-28329  
 inhomogeneous glass sintering, self stresses producing bulk flow 0-14448  
 integrated coherent IR generator, difference freq. generation in nonlinear optical waveguide 0-33084  
 integrated optic Bragg spectrum analyser design 0-33237  
 integrated waveguide-hologram memory design approach 0-32940  
 ion exchanged, thin film overlay effect on mode props. 0-33191  
 ion-exchanged, influence on step-index profile, double alkali effect 0-5824  
 ion-exchanged optical waveguide repeatability improved by melt dilution 0-53493  
 laser beam intensity fluctuations, waveguide channel with large-scale random inhomogeneities 0-33194  
 laser gyro applications 0-1345  
 laser-induced damage in diffused waveguide 0-9925  
 light pipes, timing errors evaluation 0-5445  
 light polarisation in twisted tape lightguides and braided cylindrical liquid-filled lightguides (*Russian*) 0-19107  
 LiNbO<sub>3</sub> single-mode planar waveguides for integrated optics, fabrication (*Korean*) 0-43448  
 materials and fabrication techniques for integrated and guided wave optics 0-23809  
 MBE, device appls. 0-25570  
 optics for electronic engineers (*Japanese*) 0-38106  
 passive components for integrated-optics signal processing 0-48466  
 photochromic film waveguide, acousto-optical props., integrated optics appl. 0-33207  
 photoconductive detector with integrated waveguide struct. 0-48456  
 photorecombination laser, shock wave triggered, waveguide mode optical gain 0-5730  
 planar, fabricated by ion exchange in glass, refractive index profile 0-14460  
 planar anisotropic structures, waveguiding properties (*Czech*) 0-28313  
 planar optics, goals, methods, potential appl., principles and trends 0-33231  
 planar waveguide, isotropic, polarisation conversion by Bragg deflection, expt. results 0-48462  
 polyethylene, O-type, loss characts. at 337  $\mu\text{m}$  0-33175  
 progress in optical waveguide process and materials, review 0-23768  
 raster focusing-prism and light guide pump system for NH<sub>3</sub> laser 0-9905  
 rectangular, propagation losses at 10.6  $\mu\text{m}$  for distributed feedback appl. 0-38101  
 scattering, out-of-plane, in sputtered optical waveguides 0-38127  
 self-filtering S-type strip waveguides 0-33219  
 single-mode ring-type, EM propag. characts. (*Russian*) 0-38104  
 slab-type, mode coupling via dichroic absorpt. of M centres 0-33178  
 stained glass, Ag- and Cu-, optical waveguide effect (*Japanese*) 0-14471  
 Stokes radiation spatial characts. in stimulated scattering, saturation conditions 0-53379  
 strip guides, Eckart-Epstein type, exact soln. for TM mode propagation 0-10046  
 tapered light guide condenser design approach 0-33218  
 technology, components and communication systems (*German*) 0-33168  
 thick film optical waveguide integration with fibre-optic connectors 0-33246  
 thin film, theory, technology and appl. (*Czech*) 0-33229  
 thin film dielectric waveguide with emitting diffr. grating, inhomogeneity in thickness 0-48425  
 thin-film laser with a two-dimensional diffraction grating 0-9906  
 thin-film laser with spatially separated multiple-frequency outputs 0-43368  
 thin-film waveguide with liq. cryst. boundary modulation of refr. index, mode switching 0-23800

**optical waveguides continued**

trapezoidal cross-section dielectric waveguides, mode dispersion by effective-index method 0-9999  
 underground beam-guide lines with periodic light beam corrections 0-33196  
 wavefront reconstruction method, plane waveguide hologram: coupled system 0-5708  
 (AlGa)As CW narrow stripe injection laser with induced waveguide, expt. props. 0-32988  
 (AlGa)As DH narrow stripe injection laser with rigid waveguide, expt. props. 0-32987  
 AlGaAs rib waveguides, characts. 0-33177  
 AlGaAs-GaAs transverse mode stabilised plano-convex waveguide laser made by single step LPE 0-48274  
 Al<sub>1-x</sub>Ga<sub>x</sub>As buried heterostruct. laser, fabrication, optical props. and reliability 0-53322  
 Al<sub>1-x</sub>Ga<sub>x</sub>As, fabrication of mesa-type waveguides by laser irradi. 0-5849  
 Al<sub>2</sub>O<sub>3</sub> optical waveguide, fabrication by reactive Al sputtering in O<sub>2</sub>-Ar atm. 0-33262  
 As<sub>2</sub>S<sub>3</sub> amorphous film waveguide and grating coupler 0-53448  
 As<sub>2</sub>S<sub>3</sub> film waveguide, acoustooptic deflection and modulation of light by stationary phase grating struct. 0-5841  
 BN fabricated CO<sub>2</sub> CW capillary waveguide laser for optically pumping D<sub>2</sub>O 0-48278  
 CO<sub>2</sub> laser, saturation parameter 0-9856  
 CO<sub>2</sub> waveguide laser, design and performance characts. 0-9909  
 CO<sub>2</sub> waveguide laser, gain and saturation (*Rumanian*) 0-23667  
 CO<sub>2</sub> waveguide laser amplifier, using short BeO ceramic discharge tube, gain meas. 0-33027  
 CdSe<sub>1-x</sub> photosemiconductor, optically controlled deflector based on thin-film waveguide 0-33206  
 (GaAl)As buried-heterostructure laser with buried optical guide, highly efficient operation 0-1219  
 Ga<sub>1-x</sub>Al<sub>x</sub>As buried heterostructure lasers for analogue communication 0-48297  
 Ga<sub>1-x</sub>Al<sub>x</sub>As stripe laser with stable transverse mode structure 0-48298  
 Ga<sub>1-x</sub>Al<sub>x</sub>As symmetrised epitaxial variable-gap waveguide, coherent radiation generation 0-38018  
 Ga<sub>1-x</sub>Al<sub>x</sub>As transverse mode DH laser with inbuilt plano-convex waveguide 0-48296  
 Ga<sub>1-x</sub>As<sub>1-x</sub>P<sub>1-x</sub>InP, room temp. electron-beam-pumped laser with dielec. waveguide, output characts. 0-5761  
 GaP ribbon waveguide, vapour-grown, phase-matched SHG 0-48339  
 He-Ne optical waveguide amplifier, operation 0-43363  
 InGaAsP-InP DH laser with self-aligned struct., oscillation characts. 0-38017  
 LiBi<sub>1-x</sub>Nd<sub>x</sub>P<sub>1-x</sub>O<sub>12</sub> waveguide laser layer epitaxially grown on LiNdP<sub>4</sub>O<sub>12</sub> substrate 0-23709  
 LiNbO<sub>3</sub> graded index loaded with chalcogenide amorphous film, light deflector 0-48463  
 LiNbO<sub>3</sub> microwave laser beam electro-optic modulators using rectangular waveguides, 1.0 to 10 GHz 0-43381  
 LiNbO<sub>3</sub> ridge struct. fabrication by CF<sub>4</sub> plasma etching 0-28357  
 LiNbO<sub>3</sub> three-dimens. optical waveguide, parametric difference freq. generation 0-48335  
 LiNbO<sub>3</sub> Ti-diffused waveguide for cutoff modulator 0-9991  
 LiNbO<sub>3</sub> waveguide and modulator form. by ion implantation 0-48469  
 LiNbO<sub>3</sub> waveguide formation using organometallic solns. as diffusion sources 0-23810  
 LiNbO<sub>3</sub>:Ti diffused, fabrication problems (*Japanese*) 0-33256  
 LiNbO<sub>3</sub>:Ti narrow ridge optical waveguides and electro-optical, ion-bombardment-enhanced etching 0-38133  
 LiNbO<sub>3</sub>:Ti planar and channel optical waveguides, Ti diffusion coeff. meas. 0-19096  
 LiNbO<sub>3</sub>:Ti waveguide, in-plane scatt. obs. and countermeasures 0-33215  
 LiNbO<sub>3</sub>:Ti waveguide, operation of geodesic lens, anisotropic and curvature losses 0-48453  
 LiNbO<sub>3</sub>:Ti waveguide thin film electrooptic Bragg modulator, bistable optical element 0-10034  
 LiNbO<sub>3</sub>:Ti waveguide and cryst., absorpt. loss and photorefractive index changes 0-48368  
 LiNbO<sub>3</sub>:Ti waveguide directional coupler switches, optically-induced cross-talk 0-48417  
 LiNdP<sub>4</sub>O<sub>12</sub> glass-clad rectangular waveguide, laser performance 0-32996  
 LiTaO<sub>3</sub>, Czochralski growth technique, light guide prod. by Nb diffusion (*German*) 0-20783  
 LiTaO<sub>3</sub>:Cu waveguide, electro-optic control of radiation loss in off-axial propagation 0-23789  
 LiTaO<sub>3</sub>:Ti, diffused waveguide prep., parameters determ. 0-14465  
 Nb<sub>2</sub>O<sub>5</sub> waveguide, in-plane scatt. and loss mechanisms 0-33216  
 PbO-SiO<sub>2</sub> interdiffusion layer optical waveguide, prep. and props. 0-43489  
 SiO<sub>2</sub>, ion implanted, fused, refr. index profiles 0-54272  
 Ta<sub>2</sub>O<sub>5</sub>, collinear interaction between acoustic and optical waves in planar waveguide, radiation into substrate 0-53452

**optical workshop techniques**

acrylic coating, surface tension effects 0-53487  
 air bearing and diamond machine design 0-1365  
 alkali germanoscintillator glasses, water extraction for making graded index optical fibres 0-28361  
 antireflection coatings, thickness monitoring during deposition 0-19114  
 antireflection coatings applied from metal-organic derived liquid precursors 0-5847  
 arc fusion splicing of low-loss single-mode fibres 0-53489  
 aspherical surface diamond turning machine development 0-1372  
 aspherical systems manufacturing and testing techniques development, use of computer (*Italian*) 0-48467  
 aspherics precision manufacture with programmed microelectronic control 0-1368  
 autocollimation apparatus to test manufacturing quality of aspherical mirror profile 0-10053  
 blazed ion-etched holographic grating, prod. methods, optical props. (*Japanese*) 0-10021  
 coating technique and refractive index meas. 0-43488  
 cold light production by high vacuum deposition of multilayer interference coatings (*German*) 0-53486  
 communication fibre waveguide fabrication techniques 0-1322  
 component manufacture and evaluation, seminar, Los Angeles, USA (Jan. 1979) 0-12850



**optical workshop techniques continued**

- computer-controlled machine tool for diamond-turned surface accuracy improvement 0-1367  
 computer-controlled polisher for small-tool fabrication of mirrors 0-14496  
 concave stigmatic grating mech. prod. on spherical surface 0-38109  
 contact lens fabrication and fitting, state of art and science 0-12311  
 contact problem soln. in optical surface shaping 0-33260  
 cost reduction in manufacturing 0-1361  
 crystal surface finishing using diamond cup grinding wheels (*German*) 0-19112  
 diamond machined optical surface specification 0-48472  
 diamond turning, Honeywell Corporation facilities 0-5852  
 diamond turning air-bearing spindle and eddy-current motor 0-5851  
 diamond turning and precision engineering 0-1364  
 diamond turning machine characteristics and turned surface microtopography 0-33263  
 diamond turning optical surfaces on electroless Ni 0-1375  
 diffraction grating form. on optical waveguide surface, ion-beam etching through photoresist mask 0-14492  
 diffraction grating generation for integrated optics, interference method 0-48460  
 diffraction grating production, review of Japanese research 0-10018  
 diffraction gratings, photoresist and GaAs, exposure and etching time optimisation 0-23816  
 double-layer antireflection coatings for plastic lenses, evaporation coating process 0-14491  
 double-layer coating with double cone nozzle in-line with optical fibre drawing 0-53488  
 elastic tools for finishing optical components with noncircular cylindrical surfaces 0-28368  
 element fabrication and assembly, centration errors 0-9980  
 end preparation and fusion splicing of fibre array with CO<sub>2</sub> laser 0-10051  
 fibre, low-loss graded index, produced by double crucible technique 0-48449  
 fibre alignment tool 0-23814  
 fibre and cable splicing and sheath jointing expts. 0-23806  
 fibre arc splicing unit (*German*) 0-19115  
 fibre cutting tool 0-1360  
 fibre cutting tool 0-33255  
 fibre fabrication by vapour phase axial deposition, 1.3  $\mu\text{m}$ , low-loss and wide bandwidth 0-38136  
 fibre high speed coating, forced convective cooling 0-23815  
 fibre plasma activated CVD, influence of substrate temp. 0-48475  
 fibre preparation by Ar plasma augmented vapour deposition 0-48478  
 fibre ribbon splicing with vacuum-assisted injection mould 0-53491  
 fibre waveguides with large-diameter core and low optical losses, prod. technology 0-14463  
 fibre-optic sintered plates, micropore sealing, vac. tightness improvement 0-28333  
 fibres, low-loss, manufacture, modified rod-in-tube method (*Japanese*) 0-33253  
 filter, nonquarterwave multilayer, optical monitoring with minicomputer allowing thickness error correction 0-23774  
 filter, nonquarterwave multilayer, wideband optical monitoring during deposition 0-28309  
 glass, polishing with ZrO<sub>2</sub>-SiO<sub>2</sub> powder mixture 0-28367  
 glass cylinder refractive index variation by field-assisted ion exchange 0-14500  
 glass development and manufacturing processes 0-53393  
 glass fibre development, large-core, for military appls. 0-48451  
 glass fibre production methods for optical communications, review (*German*) 0-23813  
 glass fibre thickness meas. and control system in production (*German*) 0-10052  
 glass fibre vapour phase axial deposition, OH content reduction by flame hydrolysis control 0-48474  
 glass finishing with small-grained diamond grinding wheels (*German*) 0-38137  
 graded index fibres made by vapour phase axial deposition, refr. index profile 0-48477  
 gradient index lens fabrication by molecular stuffing 0-14499  
 holographic grating blazing techniques comparison 0-53438  
 holographic grating production by laser irradiation of photoresist (*German*) 0-33254  
 integrated polariser, reduced cladding-medium, fabricated in ion-exchanged guides 0-14489  
 interference polarizer with large entrance aperture, characts. 0-43453  
 ion polishing for diamond-turned mirror dielectric coating adhesion 0-1370  
 ion polishing of optical coatings, for multilayer interf. systems and integrated optics 0-33261  
 ion-exchanged optical waveguide repeatability improved by melt dilution 0-53493  
 IR multilayer interference filter manufacture, supposed longwave limit 0-9989  
 jelly-filled optical fibre cable fabrication and characteristics 0-53490  
 lens, high performance, manufacturing methods (*German*) 0-53482  
 lens, water soluble cryst., protective coating to aid polishing 0-33250  
 lens polishing and shaping techniques (*German*) 0-33114  
 LiNbO<sub>3</sub> single-mode planar waveguides for integrated optics, fabrication (*Korean*) 0-43448  
 linear motor slide drive system for optical machining 0-1366  
 low-loss optical fibre production with high numerical aperture 0-48450  
 Luneburg guided-wave optical thin-film lens, fabrication technique and props. 0-33223  
 materials and fabrication techniques for integrated and guided wave optics 0-23809  
 MBE, device appls. 0-25570  
 mirror coatings, selective reflectors, and antireflection coatings for nonlinear optics, chemical method 0-28300  
 mirror production and testing, low-scatter, low-loss mirrors for laser gyros 0-1272  
 NC diamond turning system evolution 0-1369  
 off-axis parabolic mirror fabrication for laser function expt. 0-1374  
 plastic gradient index lens fabrication and image evaluation 0-14426  
 precision machining, seminar, San Diego, USA (Aug. 1978) 0-1363  
 precision machining commercialisation for military economy 0-1371  
 resin polishers, holders, and tools 0-33248

**optical workshop techniques continued**

- semi-automatic machine for hot splicing glass fibres for optical communication 0-23818  
 single-mode low-loss silica fibre prep., 10 km long 0-48476  
 single-mode optical fibre coupling techniques using microscopic lenses 0-53462  
 spherical end faced coupling fibre fabrication by selective etching/melting 0-53492  
 sputtered films production and props. (*Hungarian*) 0-53483  
 thin and polished section preparation status and trends (*German*) 0-28360  
 tolerancing tradeoffs for mass production economies 0-48473  
 toroidal mirror optical polisher 0-5848  
 transmission grating fabrication, photochemical replication for space astronomy 0-14490  
 vacuum deposition, improved film quality, progress in vacuum generation and deposition technology 0-35101  
 waveguide, fabrication in glass by effusion 0-5850  
 waveguide fabrication by CW Ar laser irradiation of Al<sub>x</sub>Ga<sub>1-x</sub>As 0-5849  
 waveguide holography, expt. techniques and results 0-28173  
 waveguide process and materials, review of progress 0-23768  
 zone plate production by laser irradiation of photoresist. (*German*) 0-23782  
 AgBr single-crystal IR optical fibres, growth from melt 0-53449  
 Al spherical mirror generation with single point diamond cutting tool 0-33249  
 Al<sub>x</sub>Ga<sub>1-x</sub>As buried heterostruct. laser, fabrication, optical props. and reliability 0-53322  
 Al<sub>x</sub>Ga<sub>1-x</sub>As-GaAs, DH integrated optics development 0-33240  
 Be mirrors, props. and fabrication procedures 0-38138  
 GaAs film optical components, prep. by MBE using Si shadow masking technique 0-28358  
 GaAs:Zn, diffusion of Zn by two-temp. method, LED fabrication 0-49416  
 GaInAsP-InP DH lasers made by melt-back method, operating characteristics 0-48287  
 GaP ribbon waveguide, vapour-grown, phase-matched SHG 0-48339  
 LiNbO<sub>3</sub> geodesic lens fabrication by single-point diamond turning 0-33239  
 LiNbO<sub>3</sub>, ridge struct. fabrication by CF<sub>4</sub> plasma etching 0-28357  
 LiNbO<sub>3</sub>, waveguide formation using organometallic solns. as diffusion sources 0-23810  
 LiNbO<sub>3</sub>:Ti diffused, optical waveguide, fabrication problems (*Japanese*) 0-33256  
 Mo sputtering for laser mirror refurbishment 0-14498  
 Ni plated aspheric metal mirror fabrication for IR optical systems 0-14497  
 P<sub>2</sub>O<sub>5</sub>-SiO<sub>2</sub> clad low-loss monomode fibres for 1.2 to 1.6  $\mu\text{m}$ , modified CVD prep. 0-48479  
 PbF<sub>2</sub>, antireflection coating deposition technique, 2.87  $\mu\text{m}$  laser damage threshold 0-33264  
 PbO-SiO<sub>2</sub> glass, use of Na<sub>2</sub>S<sub>2</sub>O<sub>3</sub>·5H<sub>2</sub>O in polishing 0-33258  
 PbO-SiO<sub>2</sub> interdiffusion layer optical waveguide, prep. and props. 0-43489  
 Si, diffraction grating, rectangular profile, fabricated from single cryst. 0-38093  
 SrTiO<sub>3</sub> electro-optic crystals, mechanical grinding and polishing 0-48471  
 TiI/KCl/TiI low absorpt. antireflection coatings for KCl surfaces 0-38078  
 TiI-PbF<sub>2</sub> graded-index film coating technique and results 0-33265
- optical zone plates**  
 diffraction patterns, white light, of amplitude and phase zone plates 0-14449  
 Fourier transformation, qualitative and semiquantitative, using noncoherent system 0-5698  
 Fresnel zone plate support UV window as lens and monochromator 0-1326  
 image rotation and magnification, optical system 0-48376  
 linear zone plates, optically produced 0-1299  
 production by laser irradiation of photoresist. (*German*) 0-23782  
 profiled, chromatic props. 0-43451  
 profiled, chromatic props. calc. 0-28328
- optics**  
 see also aberrations; adaptive optics; atmospheric optics; fibre optics; Fourier transform optics; geometrical optics; holography; integrated optics; nonlinear optics; optical elements; physical optics; quantum optics  
 conference, Bad Harzburg, Germany (June 1979) 0-51951  
 conference, trends in physics, York, England (Sep. 1978) 0-31416  
 Institute of Optics, Univ. of Rochester, 1929-79, brief commemorative 0-4501  
 ocean optics, conf. proceedings (San Diego, 30-31 August 1978) 0-8325  
 Optical Society of America meeting, Rochester, USA (Oct. 1979) 0-12841  
 Raman effect, combinational scatt. of light, discovery and history 0-27101  
 review of recent advances 0-28155
- optimal control**  
 see also game theory; maximum principle  
 dynamic systems, equations of motion canonical transform 0-36843  
 heat transmission between bodies in contact 0-19223  
 nonlinear noisy sine wave oscillator 0-27218  
 nuclear reactor, digital control using linear quadratic Gaussian regulator 0-37554  
 nuclear reactor, Xe spatial oscillation, time optimal control 0-32320  
 oscillators, nonlinear stochastic, triangular wave, optimally controlled, Wiener process and Poisson process, numerical studies 0-52128  
 physiology system models, breathing control example 0-41058  
 plate heating, optimal fast response control under temp. field gradient constraints 0-38232  
 transonic potential flow finite element method program stability 0-24045
- optimal systems**  
 initial temp. distrib. determ. by optimal dynamic filtering 0-19208  
 plasma accelerator, three-rail type, one cluster regime, optimum length 0-6288
- optimisation**  
 see also mathematical programming; minimax techniques; minimisation  
 acoustic energy optimisation using secondary sources (*French*) 0-53518  
 air-core Tokamak, optimisation of ohmic heating coil configurations 0-14914



**optimisation continued**

- aircraft landing trajectories of minimum noise (*Spanish*) 0-53546  
 analytic radial orbitals, optimisation on variational parameters 0-42941  
 astronomical images optimal classification into stars or galaxies, Bayesian approach 0-21920  
 astronomical observations errors, optimum linear estimation of mathematical expectation and standard deviation (*Russian*) 0-12673  
 Brayton-Rankine binary cycles in HTGRs 0-22904  
 Brunswick plant post-startup optimization 0-23048  
 chemical analysis, simplex optimisation calcs., high speed algorithms 0-40767  
 circular ring, inner boundary shapes, optimised, diametral compression 0-38369  
 composite materials, hybrid, 3-layered plates, optimisation 0-20996  
 design optimisation of solar energy district, systems anal. of external energy supply 0-30398  
 diseases, communicable, anal./control, novel model 0-30634  
 double Gauss basic lenses, design (*German*) 0-53398  
 elastic ribbed plate, optimal design 0-14578  
 energy storage systems, compressed air, w.r.t. economics 0-26167  
 gasdynamic laser, CO, energy characts. 0-23665  
 geothermal power plants flash cycle optimisation, analytical expression in terms of temp. only 0-40894  
 GFRP sheet moulding compound, influence of cure time restrictions, on minimum weight design of double layer panels 0-11623  
 grating profile optimization, inverse scattering methods 0-48142  
 gravitational-wave resonant antennas, optimum filtering and sensitivity 0-8545  
 heat treatment regimes anal. and optimisation using simplex proportional designs 0-25734  
 holographic recording medium, optimal linear transfer function determ. 0-23635  
 holographic spatial filter, CAD (*Russian*) 0-28171  
 ICRF heating in PLT 0-28742  
 IRT reactor, optimisation of operation regime (*Russian*) 0-37473  
 laminates, fibre-reinforced, optimum design under natural frequency restraints 0-53688  
 layered thin composites, optimum design and strength 0-10210  
 LMFBFR, development and Pu allocation, optimal policies 0-725  
 LMFBFR, fuel cycle cost optimisation anal. of core design modifications 0-22900  
 lubrication, hydrodynamic, free boundary problem including surface tension 0-19542  
 maximum-likelihood method, measuring baseline coordinate vectors of multielement radio interferometer 0-26753  
 metal-composite shell, three-layer, stochastic formulation of optimisation using heuristic methods 0-38268  
 microcalorimeters, conductive, limiting potentialities, anal. 0-17942  
 molecular geometry optimisation with explicit inclusion of electron correl. 0-37748  
 multiple dipole heart generator location optimisation in simple torso model 0-41277  
 nonlinear transfer processes, optimisation (*Russian*) 0-8934  
 nuclear reactor, multigoal fuel cycle optimization including nonproliferation objectives 0-52764  
 optimal nodal point distribution for improved accuracy in computational fluid dynamics 0-48670  
 optimization of practical stability problems 0-5966  
 positron emission computerised tomography, optimisation of system design parameters 0-26347  
 PWR, development and Pu allocation, optimal policies 0-725  
 PWR fuel assembly design 0-821  
 quantum systems control, pure states and mean values 0-22210  
 radioisotope thermoelec. generators, design optimisation program 0-40880  
 reconstruction angles in CT 0-8178  
 remote sensing, multispectral information volume optimisation in natural formations studies 0-4118  
 satellites integration and test phase (*French*) 0-17464  
 seasonal reservoir, optimal releases, deterministic case 0-8362  
 shell, reinforced plastic, optimisation with allowance for geometrically nonlinear factors 0-38270  
 solar heating system components, optimal insulation anal. 0-35745  
 solar heating system economic evaluation and optimisation 0-35644  
 solar thermal collector, fixed, design optimisation 0-40905  
 steel ingot, state of viscoelastic-plastic stress deformation, in process of solidification (*Russian*) 0-45295  
 Stirling free piston engine technology and appls., design optimisation 0-35723  
 stochastic gradient problems, error of estimation of direction 0-22282  
 storage reservoir analysis, mass-curve techniques, systems and perspective 0-8457  
 thermal conductivity detector, with a narrow packed column 0-22355  
 torsional vibrators, design by computer optimisation (*Japanese*) 0-33405  
 vibrating beam, distrib. of additive damping 0-38310  
 vibration simulating system 0-53729  
 vibration-simulating systems, rel. to efficiency and cost 0-53728  
 vibrations simulator design, random, wide-band 0-53731  
 WPDCC, systems analysis appl. 0-26182  
 X-ray spectrometer for energy-dispersive XFA using X-ray tubes in combination with secondary targets 0-30316

**optimum control** *see* optimal control

**photoacoustic spectroscopy** *see* photoacoustic spectroscopy

**optoelectronic devices**

*see also photoelectric devices*

- biomedical target tracker for limb movement meas. and anal. 0-56166  
 colour sensing optoelectronic device, neural mechanism modelling 0-12128  
 couplers, advantages of design and appl. trends (*Rumanian*) 0-33165  
 digital data processing, review 0-19106  
 extended part diameter meas. contactless instrument (*Russian*) 0-27270  
 goniometer, linearity and sensitivity ranges increase 0-23786  
 holographic memory devices, optoelectronic ROM memory, injection laser appls. in construction (*Polish*) 0-19007  
 III-V semiconductors, radiative recomb. and related phenomena, conference, Prague, Czechoslovakia (Sept. 1979) 0-51940  
 IR technology, radiator and detector designs (*German*) 0-22430  
 long-term role in optical and electronic systems 0-33232  
 MBE process and problem areas, review 0-10815  
 mechanical laws, optoelectronic apparatus for classroom demonstrations 0-46773

**optoelectronic devices continued**

- metrological provisions for optophysical measuring instrums. 0-8953  
 photogram meas. system using optoelectronic convertor of linear coordinates 0-17917  
 reference mirror for alignment of optical instruments 0-10054  
 retinal hue signal generation, optoelectronic robot model 0-3647  
 GaAlAsSb/GaSb alloys, prep. and optoelectronic device appl. 0-25587  
 GaAs and related cpds., conference, St. Louis, MO, USA (Sept. 1978) 0-8737

**OPW calculations**

- anisotropic normal metal, thermopower calc. 0-24879  
 Hartree-Fock energy bands using OPW method 0-10856  
 Al, Fermi surface under homogeneous strain, local pseudopot. model 0-29308  
 Al-Ga(Ag), dil, Hall coeff. by OPW Fermi surface model 0-6816  
 C, amorphous, inelastic electron scatt., valence electron contrib. 0-55240  
 CdS, band structure calcs. by modified orthogonalised plane wave (MOPW) method 0-54609  
 LiH, solid, Hartree-Fock energy band calc. using OPW method 0-10856  
 Te, trigonal, self-consistent ground state,  $X_{\alpha}$  calcs. 0-54604  
 $\text{TiS}_2$ , valence density of states 0-44465  
 $\text{ZnS}$ , band structure calcs. by modified orthogonalised plane wave (MOPW) method 0-54609  
 $\text{ZrS}_2$ , valence density of states 0-44465

**orbital calculation methods**

- see also APW calculations; atomic orbitals calculations; EHT calculations; GTO calculations; GTO calculations; HMO calculations; KKR calculations; LCAO calculations; molecular orbitals calculations; NDO calculations; OPW calculations; PNO calculations; PPP calculations; STO calculations*  
 ab initio effective core pot. method appl. to  $\text{F}_2$ ,  $\text{Cl}_2$  and  $\text{LiCl}$  0-32625  
 addition theorems of spatial functions, multicentre integrals of arbitrary atomic functions, symmetry and analytical struct. (*German*) 0-37729  
 atom, valence electrons local-density theory of exchange and correlation energies 0-52854  
 atomic correlation energies calc., Wilson's scaling parameter evaluation 0-5486  
 atomic two-parameter exponential-type basis functions 0-52847  
 Combination of Atomic Boxes MO model, development and testing 0-32592  
 comparison of classical analytic theories for the motion of artificial satellites 0-8515  
 contracted Gaussian basis set for correl. wave functions, appl. struct. and energies 0-52881  
 Coulomb interaction integrals bounds 0-52856  
 coupled cluster many electron theory, unitary group formulation 0-52859  
 density functional theory, quantum mech. system, accurate pot. and energy functionals 0-52849  
 diagram approach to character formulas for finite and compact groups 0-36888  
 effective convergence to complete orbital bases and at HF limit through systematic Gaussian primitive sequences 0-14065  
 electron correlation calculations, scaling and Pade approximants rel. to perturbation series 0-5487  
 electron density calc., approx. differential eqn. 0-47864  
 equation of motion-Green's function and CI methods comparison, appls. 0-47841  
 equations of motion Green's function methods, higher order terms, ionisation pots. 0-52891  
 equations of motion Green's function methods, higher order terms, ionisation pots., CI comparison 0-52892  
 extension of Gauss' method for the solution of Kepler's equation 0-8524  
 finite electron no. system, approx. Green's-functions algebraic formulations 0-47849  
 gravity gradiometers mounted on satellites used to improve orbit estimation 0-8523  
 Hamiltonians, effective, appl. to atomic pot. transferability in hydrocarbons 0-42933  
 Hartree-Fock energies, scaled  $1/Z$  expansion, integral eqns. 0-47886  
 incomplete basis set problem, virtual orbitals and CIBS expansion of HF energies 0-52844  
 LMO population calc. method from given SCF eigenvector matrix, appls. 0-14063  
 local multigaussian FSGO one-determinant wave functions, energy gradient expression 0-23282  
 MNDO semiempirical calcs. accuracy rel. to current MO methods 0-47893  
 molecular open shells, RHF treatment without Lagrange multipliers 0-32589  
 Newton-Raphson scheme, comparison with super-C I, for complete active space SCF method 0-47904  
 orthonormality constrained orbital optimisation technique 0-5465  
 polar molecule, excited state MCSCF wave functions, BeO appl. 0-47916  
 Singer polymal tempering methods 0-52845  
 two-electron atom, exchange and correlation pots., density functional theory 0-52848

**orbitals, atomic** *see* atomic structure

**orbitals, molecular** *see* molecular energy levels

**order, long-range** *see* long-range order

**order, short-range** *see* short-range order

**order-disorder changes** *see* order-disorder transformations

**order-disorder transformations**

*see also polymorphic transformations*

- adsorbed monolayer, classification of continuous order-disorder transitions 0-19910  
 adsorbed monolayers, order-disorder transitions, classification and characterisation, review 0-52149  
 alkali halide, electric-dipole ordering of tunnelling impurity centres 0-2215  
 alkylammonium zinc tetrachloride cpds., high temp. phase transitions 0-54372  
 alloy, FCC closed packed, ordering-type transitions 0-2140  
 alloys, binary, BCC, order-disorder transform., three-body interaction effects 0-39257  
 alloys, concentrated, local atomic arrangements, associated with ordering, review 0-50632  
 alloys,  $\text{DO}_{22}$  and  $\text{L1}_0$  superstructures, atomic ordering, multicenter approx., order-disorder transition 0-38990



## order-disorder transformations continued

- alloys, interstitial solid solns., HCP, ordering type transitions within thermodynamics theory framework 0-49162  
 alloys,  $Li_2$  and  $Li_0$  superstructure atomic ordering phase diagrams, order-disorder transition 0-38989  
 alloys, transformation kinetics 0-2138  
 ammonium halides, cryst., H bonding, order-disorder phenomena 0-6379  
 antiferroelectric model dynamics, order-disorder transition, correl. functions and polarisation waves (*Russian*) 0-50282  
 Brightsey S, lattice contraction during ageing 0-3030  
 ceramics, local atomic arrangements, associated with ordering, review 0-50632  
 cluster phenomena, displacive to order disorder crossover 0-10629  
 conference, phase transformations in metallurgy, York, England (Apr. 1979) 0-2994  
 critical dynamics below  $T_c$  0-27256  
 critical dynamics far from equilibrium 0-27258  
 crystal layer order-disorder structures 0-38981  
 crystals with dislocations, phase transitions of the second kind, dislocation superparamagnetism (*Russian*) 0-1957  
 diethylammonium cadmium tetrachloride, first order phase transition, optical phonon line broadening, spin-phonon coupling model 0-7335  
 disorder parameter, phase transition theory, rel. to entropy 0-52146  
 electron irradiation effects on kinetics of order-disorder transformations 0-34056  
 ethane submonolayer on graphite, struct. and melting, elastic neutron scatt. 0-29266  
 FCC lattices, ordered superstruct., phase diagrams, cluster variation calc. 0-39256  
 ferroelastic transitions, order parameter symm., free energy expansions 0-49164  
 flexible polymer chain in nematic solvent, phase diagram (*French*) 0-39253  
 glass-fibre reinforced PET, order-disorder transitions during extrusion 0-50633  
 graphite intercalation compound  $C_{24}K$ , order-disorder transition, X-ray study 0-33922  
 Heusler alloys, order-disorder transitions, intermediate model 0-54341  
 ice, phase transition from disordered VII phase to ordered VIII phase 0-19911  
 intrinsic and extrinsic central peak properties, review 0-34168  
 laser instability, example from synergetics 0-9848  
 layer systems, intercalates, phase transforms., CDW and mass density waves 0-39281  
 metal-H, phase transitions 0-50631  
 Nimonic 80A, lattice contraction during ageing 0-3030  
 PAC method appl. (*German*) 0-2679  
 phase ordering, in quasi-one-dimensional system, review (*Japanese*) 0-2352  
 phase transition in BCC hard sphere lattice gas with second neighbour exclusions 0-160  
 plastic flow, order-disorder transform. effect on creep, traction and relaxation (*French*) 0-35180  
 Potts model, first order phase transitions, Monte Carlo renormalisation group method 0-34645  
 quantum crystals, discontinuous orientational phase transitions, thermodynamics, isotope effects 0-6590  
 quantum optics, transition phenomena, review 0-32944  
 refractive index changes induced by struct. transitions 0-16000  
 solid solutions binary, order-disorder transitions, long range order parameter and chemical potential 0-6487  
 steel, Si, commercial, ordering after heat treatment, Mossbauer meas. 0-7556  
 symmetry, of order-disorder structures 0-38982  
 system with nonconserved order parameter, influence of heat cond. on relax. of unstable states 0-10637  
 ternary oxides, short-range order and superstructures 0-49159  
 TGS, proton and deuteron NMR anal. of temp. depend. 0-33919  
 thiourea, phonon modes near order-disorder transforms., hard-core modes due to pseudospin-phonon coupling 0-44285  
 thiourea, phonon modes near phase transitions, IR and Raman spectra 0-45084  
 triangular and honeycomb lattice gases, order-disorder transitions to  $2 \times 2$  struct. 0-4674  
 TTF-TCNQ, Landau free energy function, CDW-libron interaction, sp. ht. near phase transitions 0-19963  
 two dimensional periodic lattice, electron ordering, CDW-disordered state transition, Hubbard model (*Russian*) 0-6754  
 X-ray powder patterns of order-disorder structs. 0-38864  
 AgAu, quenched, short range order effects on specific heat 0-29181  
 AgCrS<sub>2</sub>, mixed conductor props., near order-disorder transition temp. 0-44675  
 AgI, phase transition, statics and local dynamics, mean field and Mori theory 0-39347  
 $\alpha$ -AgI, superionic, continuous order-disorder transition, Raman spectroscopic evidence 0-45070  
 Ag<sub>2</sub>SI, superionic cond., phase transition and cryst. structs., sp. ht., neutron and X-ray diffr. obs. 0-10662  
 Al-Mn, metastable  $Li_0$  phase, transformations, mag. struct., TEM study 0-3029  
 $\beta$ -Al<sub>2</sub>O<sub>3</sub>, stoichiometric, Raman and IR spectra, Frenkel defects, order-disorder transition and cation cond. 0-55086  
 Al<sub>2</sub>O<sub>3</sub>-SiO<sub>2</sub> system, andalusite and kyanite powders, shock induced transformations 0-45301  
 As, condensed layers, low temp. allotropic phase transition (*Russian*) 0-54553  
 Au<sub>3</sub>Cd, order-disorder phase transform., X-ray diffr. anal. (*Russian*) 0-45297  
 B-transition metal thin films, amorphous to cryst. transformation 0-7563  
 C, structure change, during thermal ordering, radiation disordering 0-54283  
 C<sub>24</sub>Cs and C<sub>36</sub>Cs, graphite intercalated, ordering of intercalant layers, X-ray diffuse scatt. 0-44182  
 C<sub>8</sub>Cs, intercalation cpd., theory of order-disorder phase transitions 0-19908  
 C<sub>12</sub>K, graphite intercalated, two-dimens. structurally disordered phases, X-ray diffr. profiles 0-44181  
 C<sub>8</sub>Li, intercalate ordering in first stage graphite-Li 0-6380  
 C<sub>8</sub>Li, theory of order-disorder phase transitions 0-19908  
 (CO(NO)<sub>2</sub>CL)<sub>2</sub>, order-disorder struct., X-ray data 0-39037

## order-disorder transformations continued

- C<sub>8</sub>Rb, intercalation cpd., theory of order-disorder phase transitions 0-19908  
 CaBSi<sub>2</sub>O<sub>6</sub>, B=Mg, Fe<sup>3+</sup>, Al, pyroxenes, order-disorder interpretation 0-38987  
 CaHPO<sub>4</sub>, monetite, low-temp. ordering of H atoms, X-ray and neutron diffr. study at 145K 0-39022  
 Cd<sub>65</sub>Hg<sub>35</sub> and Cd<sub>55</sub>Hg<sub>45</sub>, X-ray study of cryst. struct. and thermal expansion 0-24405  
 Cs<sub>2</sub>PbCu(NO<sub>2</sub>)<sub>6</sub>, one-dimensional stacking order 0-28941  
 Cu-Al (21 at.%) transition state, tempered and quenched alloy (*French*) 0-55392  
 Cu<sub>3</sub>Au, metastable states domain existence, phase transition ordering energy, press. effect (*Russian*) 0-45303  
 Cu<sub>3</sub>Au, radiation disorder model of phase stability 0-16297  
 Cu<sub>3</sub>Au-Cu<sub>3</sub>Pd(Pt), quasibinary system, order-disorder transform., superlattice form. 0-2159  
 Cu<sub>3</sub>Ga, transition state between long range order and short range order, model, computer simulation (*French*) 0-49371  
 Cu<sub>0.9</sub>In<sub>2.1</sub>Se<sub>4</sub>, transition state and domain struct. by electron microscopy and diffr. studies 0-15095  
 Fe-Al, optical props. rel. to order-disorder transformations 0-29736  
 Fe-C-Mn-Si (4, 2, 1.5 wt.%), cast wire, influence of B addition on struct. and elec. cond. (*Russian*) 0-55391  
 Fe-Co, order-disorder transformation, metallography, ordering kinetics 0-3026  
 Fe-Co-Si, BCC solid soln. interchange energies, high temp. neutron diffr. 0-29166  
 Fe-Co-V, ordered and disordered, dynamic ageing (*French*) 0-16355  
 Fe-Pt, plastic deform. effect on struct. singularities and mag. props. (*Russian*) 0-44892  
 Fe-V, order-disorder transition and  $\sigma$ -phase form. 0-7555  
 Fe<sub>3</sub>Al, exam. of hyperfine field variations with order state 0-6800  
 Fe<sup>2+</sup>BSi<sub>2</sub>O<sub>6</sub>, B=Mg, Fe<sup>3+</sup>, Al, pyroxenes, order-disorder interpretation 0-38987  
 Fe<sub>25</sub>Pd<sub>50</sub>Au<sub>25</sub>, atomic ordering influence on mag. props. and elec. resistance (*Russian*) 0-7551  
 GaAs (110) surface, O<sub>2</sub> interaction, order-disorder effects, LEED, UPS anal. 0-6634  
 H, chemisorbed on Ni (111), order-disorder transition, cluster-variation method 0-15372  
<sup>4</sup>He, monolayer adsorbed on Kr-plated graphite, possible Ising transition 0-34298  
 Hg<sub>3-2</sub>AsF<sub>6</sub>, one dimens. fluctuations and chain ordering transform 0-24593  
 Hg<sub>3-2</sub>AsF<sub>6</sub>, space group symmetry and phase ordering 0-6396  
 Hg<sub>1-x</sub>Mn<sub>x</sub>Te(S)(Se), EPR of Mn<sup>2+</sup>, order-disorder transitions 0-50176  
 K<sub>2</sub>PbCu(NO<sub>2</sub>)<sub>6</sub>, phase transitions induced by Jahn-Teller effect, uniaxial stress effects 0-6512  
 MgBSi<sub>2</sub>O<sub>6</sub>, B=Mg, Fe<sup>3+</sup>, Al, pyroxenes, order-disorder interpretation 0-38987  
 Mg<sub>3</sub>Cd, order-disorder transformation kinetics 0-2138  
 Mn<sub>5</sub>Ge<sub>3</sub>Mn<sub>2</sub>Si<sub>3</sub>, electrical resistivity meas., order-disorder transition 0-10945  
 NH<sub>3</sub> halides, acoustic anomalies above critical temps., volume magnetostriiction type terms 0-2123  
 NH<sub>4</sub>Br<sub>2</sub>Cl<sub>1-x</sub>, cryst., order-disorder phase transitions, US investig. 0-6378  
 NH<sub>4</sub>Cl, doped and undoped, spontaneous polarisation at order-disorder phase transition 0-25281  
 NH<sub>4</sub>Cl,  $\lambda$ -type phase transition, hypersonic study using Brillouin scatt. 0-34165  
 NH<sub>4</sub>Cl, Raman scatt. of light on limiting and nonlimiting dipole vibr. 0-11402  
 $\alpha$ -NH<sub>4</sub>HgCl<sub>3</sub>, Raman study of phase transition (*French*) 0-11378  
 NaBSi<sub>2</sub>O<sub>6</sub>, B=Mg, Fe<sup>3+</sup>, Al, pyroxenes, order-disorder interpretation 0-38987  
 NaO<sub>2</sub>, elastic interaction, role in disordered-pyrite to ordered-pyrite phase transition 0-19739  
 NaO<sub>2</sub>, physical mechanisms of phase transitions 0-6381  
 $\alpha$ -NaSbS<sub>2</sub>, cryst. struct. and  $\beta$ - $\alpha$  phase transform. features 0-33961  
 Ni-Al, spinodal decomposition, atom probe field ion microscopy study 0-3028  
 Ni-Mo (10.7 wt.%) alloy, ordering energy calc. 0-10522  
 Ni<sub>3</sub>Fe, order-disorder transition phase diagram, Mossbauer meas. 0-39995  
 Ni<sub>3</sub>Mn, partially ordered, spin-wave dispersion relation, inelastic neutron scatt. meas. 0-20394  
 NiSe film, vac. deposited, phase transformation, electron microscope studies 0-2302  
 Pd, H(D) interstitial interactions rel. to diffusion and ordering transition 0-34249  
 PdFe<sub>1-x</sub>Cr<sub>x</sub>, ordering alloys, elec. resist., temp. depend. (*Russian*) 0-24866  
 phase transition in transverse field with deform. depend., phonon anomaly separation KH<sub>2</sub>PO<sub>4</sub> 0-39258  
 Pt-Ir, structural phase transform., ion field emission microscopy obs. (*Russian*) 0-50628  
 RbAg<sub>4</sub>I<sub>3</sub>, phase transition, statics and local dynamics, mean field and Mori theory 0-39347  
 RbCaF<sub>3</sub>, struct., phase transitions, neutron diffr. study 0-33918  
 Si<sub>3</sub>N<sub>4</sub> films, struct. 0-54545  
 SiO<sub>2</sub>-Li<sub>2</sub>O-K<sub>2</sub>O-ZnO glass ceramic, prep., phase transformations and physical props. 0-45299  
 SnCl<sub>2</sub>·2H<sub>2</sub>O, order-disorder transition, neutron diffr. study, lattice statistical model 0-24558  
 SnCl<sub>2</sub>·2H<sub>2</sub>O, protonic cond. in layered single cryst. 0-19983  
 SnCl<sub>2</sub>·2H<sub>2</sub>O, quasi two-dimensional, DC protonic cond., crit. contrib. near order-disorder transition temp. 0-44362  
 Ta<sub>2</sub>D, neutron diffr. meas. of disorder-order phase transitions 0-29947  
 Ta<sub>2</sub>H, ordered, distortion-induced superstruct. modulation, from X-ray scatt. 0-49186  
 TbAl<sub>3</sub>, polytypism occurrence 0-44164  
 (Ti<sub>1-x</sub>V<sub>x</sub>)O<sub>7</sub>, order-disorder and metal-insulator transition theory 0-24802  
 (Ti<sub>1-x</sub>V<sub>x</sub>)O<sub>7</sub>, order-disorder and metal-insulator transitions 0-39504  
 Ti-Bi system, phase transitions near Ti<sub>3</sub>Bi, elec. props. meas. 0-35181  
 V-H(D), metallographic and thermal differential anal., potential for H energy storage appls. 0-45281  
 V-Mn, equiatomic, ordering kinetics and antiphase domain coarsening 0-7559



## order-disorder transformations continued

- V<sub>2</sub>D<sub>3</sub>, ordered, distortion-induced superstruct. modulation, from X-ray scatt. 0-49186  
 Va<sub>2</sub>D<sub>3</sub>, neutron diffr. meas. of disorder-order phase transitions 0-29947

ores *see* minerals

organic acids *see* organic compounds

## organic compounds

- see also* DNA; free radicals; macromolecules; organic semiconductors; organometallic compounds; plastics; polymers; proteins; Rochelle salt; waxes  
 [1-pyrenyl-(CH<sub>2</sub>)<sub>n</sub>-N(CH<sub>3</sub>)<sub>3</sub>]<sup>+</sup>Cl<sup>-</sup>, intracellular fluorescence quenching 0-9627  
 2,4-hexadiyne-1,6 diol bis(p-toluene sulphonate) ester, demonstration of high mobility 0-20212  
 3-amino- and 4-amino-N-methylphthalimide, effect of orientational-relax. processes in fluoresc. kinetics 0-18886  
 4-octyl-4-cyano-biphenyl, nematic to smectic A phase transition texture changes, thermoelectrooptic effect 0-49098  
 1,1'-Bis[phenylglyoxylol]-ferrocen, mol. and cryst. struct. (German) 0-10538  
 1,3-butadiene-1-one, spectroscopic consts., IR and microwave spectra, prep. 0-18859  
 S,S'-dimethyldithiocarbonate, pot. for rot. about C(sp<sup>2</sup>)-S bonds, electron diffr. obs. 0-23572  
 E,E-1,4-diphenylbutadiene-(1,3), isomerisation, reaction quantum yields, exciting light bandwidth influence study (German) 0-21310  
 3,3,3-trifluoropropene, struct. and vibr. spectra, IR, Raman polarisation study 0-18845  
 acetaldehyde, adsorbed on Al<sub>2</sub>O<sub>3</sub>, inelastic electron tunnelling spectra, surface vibr. struct. determ. 0-35572  
 acetaldehyde, Coriolis resonance bands in IR spectrum 0-47995  
 acetaldehyde, first triplet state geometry, fragmentation into free radicals 0-47915  
 acetaldehyde + H<sub>2</sub>(N<sub>2</sub>)(CO<sub>2</sub>), rot. line broadening, mol. quadrupole moments calc. 0-28065  
 acetaldehyde formation on radiolysis of ethanol formaldehyde systems (Russian) 0-55684  
 acetamide, aqueous solution, ultrasonic velocity measurement 0-19878  
 acetamide, geometry from ab initio calcs., rel. to formamide, N-methylformamide, and N-methyl acetamide 0-23338  
 acetamide, IR spectra, amino group inversion transitions and pot. functions 0-43041  
 acetate radical CIDEP, appl. of ns time-resolved EPR in pulse radiolysis 0-43075  
 acetic acid, -d<sub>1</sub>(=d<sub>4</sub>) liquid, molecular motion, proton spin echo study (Russian) 0-32745  
 acetic acid, adsorbed on Al<sub>2</sub>O<sub>3</sub>, inelastic electron tunnelling spectra, surface vibr. struct. determ. 0-35572  
 acetic acid, chemisorption on goethite, IR spectra 0-7855  
 acetic acid, Cl<sub>2</sub> absorpt. kinetics in presence of homogeneous catalysts 0-11876  
 acetic acid, ionised, pot. energy profiles for unimol. reactions 0-43210  
 acetic acid, permeation of large unilamellar vesicle membranes, <sup>1</sup>H NMR obs. 0-8031  
 acetic acid amides, polarisabilities and π-π\* transitions, dipole interaction calcs. 0-23411  
 acetic acid-acetone mixture, physical parameters 0-2716  
 acetic acid-aniline (pyridine) complex, in CCl<sub>4</sub>, dielec. polarisation 0-29675  
 acetic acid-formic acid, 'dimer', tritium β<sup>-</sup>-decay causing H<sup>+</sup> transfer, ab initio MO calc. 0-3391  
 acetic acid-methanol-tetrahydrofuran-d<sub>3</sub>, superimposed intermolecular spin exchange reactions, NMR lineshape theory 0-32740  
 acetic acid-pyridine, H-bonding, proton transfer, isolated system, solvent effect, MO calc. 0-55629  
 acetic acid-water, liq., Verdet const., pulsed mag. field meas. 0-16012  
 acetic anhydride, multiphoton dissociation, CH<sub>2</sub> and C<sub>2</sub> prod., fluence depend. meas. 0-5586  
 acetone, electrification during laminar flow in metal pipe 0-6954  
 acetone, isothermal Joule-Thomson coeff. 0-43828  
 acetone, liq., C-C stretching mode relax., Fermi reson. influence 0-25352  
 acetone, transient pressure-drop fluctuations in electroviscous effect 0-15286  
 acetone in mixed protic-aprotic solns., C=O stretching, IR spectra 0-45056  
 acetone-d<sub>6</sub>, multiphoton dissociation, recomb. to ethane 0-3371  
 3d-acetonitrile, cryst. struct., <sup>14</sup>N NQR free induction decay times meas. 0-54985  
 acetonitrile, in liq. phase, Ramon band profiles, calc. using IR intensities 0-2741  
 acetonitrile, possible source of amino acids on primitive Earth 0-4112  
 acetonitrile, quadratic force fields, MOCIC pot. functions calcs. 0-5475  
 acetonitrile, soln., high press., mol. reorientation, correl. times, depolarised Rayleigh scatt. obs. 0-29748  
 acetonitrile molecule dissociation in IR field, laser-induced fluoresc. obs. 0-53075  
 acetonitrile solvent for poly[(R)-oxypropylene], effect on opt. rot. dispersion and vac. UV circular dichroism 0-40084  
 acetonitrile-water mixture, electrolyte transfer, thermodynamic props. 0-3395  
 acetophenone, highly purified, luminesc. props. 0-32764  
 acetophenone enolate anion radicals, substituted, electron photodetachment cross sections, reson. states 0-1030  
 N-acetyl-L-phenylalanine methyl ester, model for amino acid side chains internal motions in peptides and proteins 0-48017  
 acetylcholine, dielectric transient response following UV-irradiation 0-51166  
 acetylcholine receptor molecules heterogeneity of clonal muscle cells surfaces 0-16910  
 acetylene, absorption spectrum, LiF F<sub>2</sub><sup>+</sup>-centre laser intracavity spectroscopy appl. 0-32999  
 acetylene, adsorption and decomp. on Ni (111), high resolution EELS study 0-40739  
 acetylene, angular dependent photoelectron spectral meas. 0-28060  
 acetylene, catalytic decomposition, STEM of catalyst particles 0-24328  
 acetylene, core ionised, core-excited and shake-up states, ab initio MRD-CI methods 0-42950  
 acetylene, electron momentum distrib. in π orbitals from (e,2e) expts. 0-14239

## organic compounds continued

- acetylene, electron propagator theory for mol. electron binding energies and photoionis. intensities 0-47848  
 acetylene, LMO population calc. method appl., from given SCF eigenvector matrix 0-14063  
 acetylene, magnetic susceptibility, frost model wavefunctions with p-type Gaussians 0-5477  
 acetylene, mol. and cluster Auger spectrum calc., SCF core-valence-valence spectra 0-48045  
 acetylene, multiphoton vacuum UV photodissoc. obs. and interpret. 0-11939  
 acetylene, multipole moments and polarisabilities, SCF calcs. 0-5471  
 acetylene, photoelectron spectrum, satellite line intensity, photon energy depend. 0-53042  
 acetylene, prod. by coal gasification process, development and economics 0-30338  
 acetylene, selective photoaddition of ICl, isotope enrichment, influence of press., buffer and wavelength 0-11927  
 acetylene, surface interaction with transition metal atoms, MO calc. 0-6623  
 acetylene, tropospheric and lower stratospheric vertical profiles 0-4073  
 acetylene, vibr. intensities, G sum rule appls. 0-32776  
 acetylene + Br<sub>2</sub>, laser-induced photochemistry 0-45498  
 acetylene + N<sub>2</sub>, reaction rate consts., pulse radiolysis obs. 0-35508  
 acetylene(-d<sub>1</sub>,d<sub>2</sub>), integrated IR intensities 0-23457  
 acetylene dimer, ab initio HF calc. for 64 conformers. 0-23333  
 acetylene photopolymers, presence in Jupiter stratosphere 0-31244  
 acetylene smoke, optoacoustic meas. of absorpt. at 0.5145, 10.6 μm 0-43060  
 acetylene smoke particles, agglomerated, optical extinction meas. at 0.5145 and 10.6 μm 0-48155  
 acetylene smoke particles, optoacoustic meas. 0-50895  
 acetylene submonolayer-covered Ni<sub>4</sub>(111), surface phonons obs. by EELS 0-39403  
 acetylene type acid corrosion inhibitors, elongation effect on Fe polarised wire 0-55590  
 acetylene-d<sub>1</sub>, vibr. bands, IR spectrum in region of bending fundamental ν<sub>4</sub> 0-23418  
 acetylene/H<sub>2</sub> mixing ratio in Neptune stratosphere 0-51692  
 acetylenic hydrocarbons, cyclohexane soln., structureless fluoresc. 0-5575  
 acoustic spectroscopy, H bonds investigation, N-butyl acetamide association in solns. 0-5891  
 acridine, aqueous soln., laser induced two-photon ionisation investig. 0-32780  
 acridine orange in ethanol, soln., excited single state lifetimes, aggregates, visible luminesc. spectra, conc. depend. 0-55172  
 Acridine Orange rot. diffusion from absorpt. relax. 0-1008  
 acrolein, excitation, ionisation and electron affinity, expts., HAM/3 calcs. 0-18790  
 acrylic acid doped polystyrene film, elec. cond. and activation energy conc. depend. 0-15631  
 acrylonitrile, IR multiphoton dissociation, C<sub>2</sub> prod. and quenching obs. 0-11931  
 acrylonitrile, multiple photon dissociation, photofragment spectroscopy by laser-induced fluoresc. 0-11937  
 adamantane, elastic props., press. depend. rel. to intermol. forces 0-54297  
 adamantane, Ising, diffuse scatt., hard-core correl., weak-graph method 0-49137  
 adamantane, plastic cryst., thermolum. curves 0-2876  
 adamantane, plastic cryst. lattice vibr. study of phase transition 0-7355  
 adenine tautomers, relative stabilities, nonempirical MO calcs. 0-21442  
 adenosine 5'-diphosphate, interactions with myosin, intermolecular spin diffusion study 0-18951  
 adenylate kinase, photokinetic microassay using the firefly luciferase reaction 0-56306  
 adipic acid crystals, H bonds, harmonic couplings, IR vibr. modes, isotope effect origin 0-34902  
 adsorption on Bi 0-20038  
 L-alanine:Cu(II), EPR and ligand-ENDOR measurements 0-44907  
 β-alanine, aqueous solution, ultrasonic velocity measurement 0-19878  
 albumin reticulated with rhodopsin, membrane permeabilities, dynamic, meas. under non-equilib. conditions 0-46107  
 alcohol, alternate liquid fuel development, for diesel engines and gas turbines 0-55782  
 alcohol fuel production from biomass 0-55773  
 alcohol fuel production from wood, Brazil, ethanol and methanol 0-30328  
 alcohol-unassociated active component liquid mixtures, associated soln. theory, thermodynamic parameters 0-7836  
 alcohols, assoc. liq., viscous props. 0-2186  
 alcohols, dil. aqueous solns., isentropic compressibility behaviour from sound vel. meas., dissolution mechanism 0-30269  
 alcohols, glass, electron trapping, pulse radiolysis obs. 0-30264  
 alcohols, H-bond system, liq., high-press. effect 0-49080  
 alcohols, OH-stretching vibr. band in overtone region, IR-Fourier spectral investig. (German) 0-976  
 alcohols, saturated, bonded and nonbonded, quantum chem. calcs. 0-9514  
 aliphatic alcohol, thermodynamics of adsorption at air/aqueous soln. interface 0-10752  
 aliphatic alcohols, glass transitions 0-54357  
 aliphatic ethers-HF, H bonded complex, gas phase, first overtone reconstruction 0-43040  
 aliphatic liquid crystals, trans, trans-cyclohexyl cyclohexanoates, synthesis, mesomorphic phases 0-44121  
 aliphatic perfluorocarbons, electron attachment, fragmentation 0-12 eV 0-5618  
 aliphatic tertiary amines, laser action feasibility, emission spectra, two photon excitation 0-23683  
 alkali metal dicarboxylates, H bonding and motion, incoherent inelastic neutron scatt. spectroscopy 0-48095  
 n-alkane, long chain, syntactic coalescences between monoclinic and orthorhombic polymorphs 0-10520  
 n-alkane, OCS solute, rot. relax., solvent hydrodynamic props., Raman and IR spectra 0-45055  
 alkane chains in liquids, rot. and torsional dynamics, Riemann tensor theory 0-54084  
 n-alkane crystal test for porphyrin, phototautomerism IR spectral obs. 0-34963  
 alkane hydrocarbon + Cd, <sup>3</sup>P<sub>0,1,2</sub> state distrib., E to V,R transfer 0-28088  
 n-alkane pollutants, N.Atlantic gas and particle concs. in troposphere 0-7969



## organic compounds continued

- alkanes, and cycloalkanes, saturated hydrocarbon chains PMR characterisation (*Portuguese*) 0-5562  
 n-alkanes, dielec. permittivity and pVT data 0-44996  
 n-alkanes, liq. mixtures, thermodynamics 0-55700  
 alkanes, liquid, chain reorientation, Brownian dynamics simulation, comparison of models 0-49067  
 n-alkanes, longitudinal acoustic modes, Raman intensities 0-32718  
 alkanes, solubility in liquid O<sub>2</sub>, estimation by Preston-Prausnitz method 0-39285  
 1-alkanols, liq., H-bond order temp. depend. from Hildebrand rule 0-7838  
 alkene+N, reaction rate consts., pulse radiolysis obs. 0-35508  
 alkenes, IR absorpt. curves calc. using standard fragments computer library 0-982  
 alkenes, solubility in liquid O<sub>2</sub>, estimation by Preston-Prausnitz method 0-39285  
 trans-p-n-alkoxy- $\alpha$ -methyl cyanophenyl cinnamates, elastic consts. and orientational order parameters 0-44244  
 alkoxy-cyanobiphenyls, isotropic phase, Cotton-Mouton effect 0-16013  
 p-n-alkoxybenzoic acid, elec. cond. anisotropy of nematic structs. 0-1928  
 N-alkyl amides in H<sub>2</sub>O, dioxan solns., Kerr consts. 0-2727  
 alkyl benzenes, jet-cooled, intramol. vibr. relax., reson. fluoresc. and excitation obs. 0-14152  
 alkyl benzoates, phosphoresc. and fluoresc. spectra in organic matrices 0-32756  
 alkyl cyanobiphenyls, pretransitional behaviour, alkyl chain length depend., light scatt. in isotropic phase 0-44301  
 alkyl iodides, two-photon reson. ionis. spectra 0-28071  
 2-alkyl pyridine N-oxides, effects on photosynthesizing membranes, near photosystem II, hydrophobic pocket 0-55999  
 alkyl substituted diacetylene radical cations, optical emission and photoelectron spectra, fragmentation decay 0-53004  
 4-alkyl-3-phenyl-3,4-dihydrocoumarins cis- and trans-, <sup>13</sup>C NMR spectra 0-43067  
 3-nalkyl-6-(4-n-alkyloxy-phenyl)-1,2,4,5-tetrazines, stable dyestuffs with liq. cryst. props. 0-19693  
 alkyl-cyanobiphenyls, isotropic phase, Cotton-Mouton effect 0-16013  
 di-alkylammonium copper tetrachloride, weakly discontinuous phase transition, linear birefringence obs. 0-11362  
 alkylammonium zinc tetrachloride cpds., high temp. phase transitions 0-54372  
 alkylcyano-cyclohexyl-cyclohexanoates, nematic and smectic mesophases 0-19692  
 alkylcyanobiphenyls, far IR absorpt. in nematic and isotropic phases, order parameter determ. (*French*) 0-50330  
 trans-4-alkylcyclohexane carboxylic acids, visible and UV spectroscopy transparent matrix 0-45102  
 alkylcyclohexyl-cyclohexyl-cyclohexanoates, nematic and smectic mesophases 0-19692  
 trans-4-n-alkylcyclohexylbenzylamines, synthesis and mesomorphic props. 0-44116  
 trans-bis(N-1-alkyliminodiacetato)-chromate(III) complexes, luminesc. spectra 0-1020  
 alkylidides, UV photodissoc., time-resolved obs. of I(<sup>2</sup>P<sub>1/2</sub>) reactions 0-11940  
 N-alkylpyridium halides, molten, and mixtures with AlCl<sub>3</sub>, density, elec. cond. and viscosity meas. 0-24630  
 1-alkynes+O(<sup>3</sup>P), CO prod., vibr. population distrib., rate consts., laser reson. absorpt. technique 0-40676  
 allene, laser induced reaction, energy distrib. 0-16710  
 allene(-d<sub>2</sub>), IR absorption intensities 0-1026  
 allyl isocyanide, state-selected, visible absorption spectra and photoisomerisation kinetics 0-11879  
 allyl radical, doublet state, open shell RPA unitary group formulation, Hartree Fock stability eqns. 0-52860  
 aluminium and boron hydrides of titanium(III) bis-cyclopentadienyl, exam. of catalytic props. 0-30278  
 amidofluorosulphuric acid, and Hg salt, IR spectra (*French*) 0-18858  
 amines, saturated, bonded and nonbonded, quantum chem. calcs. 0-9514  
 amino acid anal. by ion exchange chromatography 0-11986  
 amino acid protonation ab initio Hartree-Fock-Roothaan SCF calcs. 0-9503  
 amino acid radiolysis, geochem. and cosmochem. implications 0-45975  
 amino acid residues, contacting, ligand binding rate dependence on specific microdynamics 0-51031  
 amino acid side chains, internal motions in peptides and proteins, N-acetyl-L-phenylalanine methyl ester model 0-48017  
 amino acid valine, heavy ion induced desorption, time-of-flight mass spectra anal. 0-54509  
 amino acids in meteorite, carbonaceous chondrite 0-26822  
 2-amino-5-chloropyridine, IR absorption, vibr. assignments 0-979  
 6-amino-7-hydroxy-4-methylcoumarin solutions, additions effect on fluoresc. 0-2833  
 p-aminobenzoic acid hydrochloride, X-ray cryst. struct. determ. 0-39063  
 $\gamma$ -aminobutyric acid, aq. soln., low freq. vibrs. Raman spectra obs. 0-987  
 ammonium tartrate, triboluminescence and cryst. fracture dynamics 0-50437  
 cAMP-induced structural changes in membranes, rel. to acetylcholinesterase activity 0-30674  
 $\alpha$ -amylase isoenzymes, formation in germinating wheat,  $\gamma$ -irrad. effect 0-56143  
 $\Delta^5$ -androster-3-ol-17-one, polycryst., NMR, selection of nonprotonated C resonances 0-50201  
 aniline, laser two-photon ionisation in mol. beam and bulk gas phase 0-18891  
 aniline, nonlinear second-order optical susceptibility 0-9947  
 aniline+carbon tetrachloride, binary liquid mixtures, excess free vol. calcs. 0-34202  
 aniline-cyclohexane, crit. mixture with shear flow, light scatt. obs. 0-6521  
 aniline-HBr, ferroelasticity, orthorhombic to monoclinic phase transition, X-ray scatt. 0-39276  
 anilines, substituted, in benzene soln., dielectric relax. time, dipole moment 0-50259  
 anilines, substituted, in nonpolar solvent, dielec. relax. obs. 0-55022  
 anilinium halides, and anilinium sulphate, proton mag. relax. obs. 0-34800  
 p-anisidine, single cryst. growth from cyclohexane-water immiscible system 0-40244

## organic compounds continued

- anisylidenebenzidine, particle size distrib. function, electrooptical diffusion method for determ. 0-8956  
 18-annulene, geometrical parameters, STO-3G ab initio calc. 0-52867  
 anthracene,  $\gamma$ -irradiation influence on defects, luminesc. study (*Russian*) 0-55185  
 anthracene, anharmonic props., temp. (press.) depend., rel. to TTF-TCNQ 0-15200  
 anthracene, charge storage and trapping levels, TSC studies 0-6875  
 anthracene, chemical thermodynamic props. 0-21312  
 anthracene, coherent exciton scatt. and recomb. 0-39510  
 anthracene, isotopically mixed cryst., exciton dynamics 0-29329  
 anthracene, laser excited single crystal, numerical anal. for TSC results (*Japanese*) 0-34464  
 anthracene, mag. susceptibility anisotropies, high field <sup>2</sup>H NMR quadrupolar effects obs. 0-25225  
 anthracene, photocond. spectrum induced by excitons (*Japanese*) 0-29440  
 anthracene, photogeneration of charge carriers through two photon excitation 0-11033  
 anthracene, polarisation energy of localised charge 0-15034  
 anthracene, protection against radiation damage, exciton effects 0-29055  
 anthracene, single cryst., photocond. threshold, excitation spectrum 0-44639  
 anthracene, single crystal, photoconductivity quantum yield, experimental validation of fund. theory 0-6909  
 anthracene, soln. and melt, second vibronic transition, spectroscopic characts., effective field dispersion calcs. 0-55102  
 anthracene, time-resolved transient photocond. obs. 0-6892  
 anthracene, trapping effects on emission-limited current flow 0-29413  
 anthracene, triplet-exciton fine struct., high resolution optical meas. 0-45099  
 anthracene, TSC and carrier retrapping 0-39599  
 anthracene, vapour, fluoresc. spectra, mol. vibr. freq. reson. laser IR irradiation, quenching 0-18883  
 anthracene, with pentracene and tetracene impurities, laser-pulse-excited luminesc. 0-7408  
 anthracene anion+dimethylaniline cation, recombination reaction in soln., time-resolved mag. field effect 0-3308  
 anthracene crystals,  $\alpha$ -particle induced scintillation, mag. field effects 0-40161  
 anthracene crystals, growth in melts of cholesteryl-caproate-anthracene system 0-2943  
 anthracene crystals, nonlinear fluorescence quenching, recomb. of free excitons 0-7397  
 anthracene derivative, Langmuir-Blodgett multilayer film, semiconducting props., optical and elec. meas. 0-11122  
 anthracene dimer anion, charge reson. transition anal. 0-42931  
 anthracene film, effect of struct. on luminesc. quenching (*Russian*) 0-7411  
 anthracene intramolecular excimer in 1,3-dianthrylpropane, direct obs. 0-48029  
 anthracene Langmuir film, lightly substituted, electrolum., photolum. and electroabsorption 0-20726  
 anthracene single cryst., Frenkel exciton spectra at dielectric and conducting layer interfaces 0-44510  
 anthracene single crystals, effect of  $\gamma$ -irrad. on photolum. (*Russian*) 0-2852  
 anthracene vapour, optically induced dynamic gratings 0-28289  
 anthracene-Au interface exciton luminescence Frenkel exciton metallic quenching (*Russian*) 0-50421  
 anthracene-PDMA, weak donor-acceptor complexes, electron mobility model 0-15511  
 anthracene-pyromellitic dianhydride, mol. charge transfer cryst., Raman scatt. meas. 0-29743  
 anthracene-pyromellitic dianhydride complex, optical and photoelectric props. (*Russian*) 0-15570  
 anthracene-quartz interface exciton luminescence, Frenkel exciton metallic quenching (*Russian*) 0-50421  
 anthracene-tetracyanobenzene 1:1 charge transfer complex, low temp. phase, cryst. struct. 0-6397  
 anthracene-tetracyanobenzene cryst., triplet exciton annihilation, time correlated delay fluoresc., ODMR 0-39895  
 anthracene-tetracyanobenzene crystals, deuteration effect on phase transition, triplet state EPR study 0-50163  
 anthraquinone, electrochromism, display devices, multiplexing 0-45037  
 9,10-anthraquinones,  $\Pi$ - $\Pi^*$  electronic transitions, substituent effects calcs. 0-28006  
 4-(9-anthryl)-N,N-dimethylaniline, fluoresc., dipole moments and polarisabilities 0-1019  
 anthracene crystals, thermal expansion meas. by quartz dilatometer 0-34212  
 L-arginine L-ascorbate, X-ray cryst. struct. determ. 0-35826  
 aromatic, absolute fluorescence quantum yield, calorimetric determ. 0-43092  
 aromatic compounds, oxidative bromination, chem. oscils. 0-3335  
 aromatic compounds, reduction by KC<sub>24</sub> intercalation compound 0-3306  
 aromatic esters, phosphoresc. and fluoresc. spectra in organic matrices 0-32756  
 aromatic hydrocarbon, centrosymmetric, two photon excited upper state fluoresc. spectra, reson. fluoresc. and vibr. mode selectivity 0-18878  
 aromatic hydrocarbon in soln., excited electronic state vibr. relax., time resolved fluoresc. 0-48024  
 aromatic hydrocarbons,  $\pi$ -ionisation energies correl. with free electron MO energies 0-14073  
 aromatic hydrocarbons, IR spectra and high-pressure phase transitions 0-10659  
 aromatic hydrocarbons, mol. polarisability, INDO calc. 0-52886  
 aromatic hydrocarbons, proton chemical shifts, localised  $\pi$ -bond model calcs. 0-43070  
 aromatic hydrocarbons, singlet-triplet conversion at low temp. 0-43094  
 aromatic hydrocarbons, solubility in liquid O<sub>2</sub>, estimation by Preston-Prausnitz method 0-39285  
 aromatic hydrocarbons-amine,  $\pi$ - $\pi$  complexes, intermolecular interactions 0-43134  
 aromatic isolated mol. nonradiative conversion, internal and S-T conversion, vibr. excitation and fluoresc. quantum yield 0-43095  
 aromatic molecules, and derivatives, radiationless conversion processes, regularities 0-14171  
 aromatic rigid soln. phosphoresc. promotion by I<sup>-</sup> 0-50387  
 aryl ammonium hydrogen difluorides, IR vibr. spectra and NMR reson. obs. 0-34788



## organic compounds continued

- ascorbic acid, action with perhydroxyl radicals, radiolytic study 0-35523  
 L-ascorbic acid, cryst. isolated OH oscillators, IR absorption, temp. and H-bond effects 0-7351  
 astatotyronine and astato-iodotyronine, prep. and stability 0-55687  
 atactic polypropylene waste, pyrolytic conversion to fuel oil 0-35627  
 atom-pair interactions in molecules, semi-empirical MO calc. 0-915  
 aza-aromatic molecules, intersystem crossing, quantum interference effects 0-53037  
 azabenzene dimers, C, N, H atom-atom pot. parameters, dispersion energy calcs. 0-23489  
 azaheterocyclic molecules, radiationless conversion processes, regularities 0-14171  
 7-azaindole dimers, photoautomerisation by double proton transfer, fluoresc. kinetics 0-11880  
 aziridine, ab initio calcs., appl. of convergent SCF procedure 0-47875  
 azo dyes, photoanisotropy, effect on holographic reconstruction (*Russian*) 0-42290  
 azoalkanes, cyclic, quenching of 1,5-dimethylnaphthalene fluoresc., micelle system probe 0-35578  
 azobenzene, derivatives, photoelectron spectra, ionisation pot., electronic struct. determ. 0-1024  
 trans-azobenzene,  $S_2 \rightarrow S_0$  fluoresc. 0-28044  
 azomethane + OH, rate const. meas. 0-7771  
 azulene, induced circular dichroism of  $\pi-\pi^*$  bands in presence of (+)-nopinone 0-53058  
 azulene-fluoranthene, soln., triplet energy transfer, delayed fluoresc. study of  $S_2 \rightarrow S_0$  0-23331  
 barium stearate film, in Al/(Al<sub>2</sub>O<sub>3</sub>)-BaSt/Sn struct., internal voltage temp. variation 0-20326  
 BBOA, polymorphism, radiothermoluminescence and differential scanning calorimetric study 0-24570  
 BBOA, smectic B phase, fluidlike mol. dynamics, Raman scatt. study 0-20630  
 BBOA, smectic liq. cryst. glass-supercooled transition and Debye temp., <sup>57</sup>Fe Mossbauer effect 0-54999  
 BBOT dye, vapour phase, optical props. (*Japanese*) 0-9879  
 benzaldehyde, electronic spectra, Cl and F substitution effects 0-23456  
 benzaldehyde, wavefront reprod. obs. by stimulated Brillouin, Raman scatt. 0-53369  
 $\pi\pi^*$ benzaldehyde, zero field splitting and sublevel decay rates, deuteration and host effect 0-37750  
 benzaldehyde-biacetyl system, self-quenching and electronic energy transfer obs. 0-5571  
 benzaldehydes, o- and m-substituted fluoro- and chloro- forms, rot. isomerism,  $n\pi^*$  spectra obs. 0-5631  
 benzaldehydes, para-halogenated, IR and Raman spectra, vibr. assignments, thermodynamic functions 0-14139  
 1,2-benzanthracene in polystyrene films, delayed luminesc. decay kinetics 0-43088  
 benzene, <sup>13</sup>C substituted, mass selective two-photon ionis., mass spectroscopy obs. 0-9651  
 benzene,  $\pi$  electron system, excitation energy, appl. of MBPT 0-52876  
 benzene, adsorbed at metal surface, obs. of vibrational modes 0-6649  
 benzene, adsorbed on porous vycor glass, adsorp. spectrum 0-9615  
 benzene, adsorption on Ir (111), electronic transitions sensitivity to molecule-surface orientation, energy loss spectra 0-45184  
 benzene, and methyl derivatives, <sup>1</sup>E<sub>1u</sub> N-V state mag. moments, MCD obs. 0-23575  
 benzene, bromination on zeolite adsorption complex, Raman spectroscopic anal. 0-16670  
 benzene, chem. shielding tensor obs. using proton-enhanced <sup>13</sup>C reson. in He-cooled probe 0-17978  
 benzene, chemisorption on Ni (111) and (100), vibr. EELS study 0-39436  
 benzene, critical heat flux of saturated natural convection boiling with heating from below 0-10114  
 benzene, cryst., IR and Raman intensity of lattice vibrs., theory 0-11381  
 benzene, derivatives, calc. of second-order susceptibility, using electronic spectra data 0-29756  
 benzene, doubly charged ion fragmentation, ion kinetic energy spectrum peaks, collision gas sensitive 0-40679  
 benzene, elec. dipole forbidden states, high resolution electron impact obs. 0-43195  
 benzene, electrification during laminar flow in metal pipe 0-6954  
 benzene, gas, liq. and crit., cation mobility 0-48842  
 benzene, ground state props., coupled cluster and MBPT methods appl. 0-47881  
 benzene, high-order stimulated Raman scatt. obs. (*Chinese*) 0-45053  
 benzene, in liquid binary mixtures of optically anisotropic molecules, depolarized Rayleigh scatt. 0-40122  
 benzene, LMO population calc. method appl., from given SCF eigenvector matrix 0-14063  
 benzene, local mode combination bands and local mode mixing 0-27999  
 benzene, low concs. in air, determ. by gas chromatographic method (*German*) 0-21429  
 benzene, magneto-optic rotatory dispersion curves 0-45040  
 benzene, molecule translational mobility in depolarised Raman spectra 0-14150  
 benzene, noncrossing and degeneracy in Hubbard models 0-14096  
 benzene, optoacoustic spectroscopy using cell with ultimate corrosion resistance 0-42269  
 benzene, plasma polymerisation in glow discharge, thin film IR and free radical EPR obs. 0-2964  
 benzene, SCF-EHT polarisability calc. 0-47895  
 benzene, schlieren method for the determination of electric field distributions in dielectrics 0-31720  
 benzene, solid, fluoresc. decay times and quantum yields, rel. to vap. phase 0-55154  
 benzene, solid, ion implantation, chem. effects 0-55635  
 benzene, stimulated Raman scatt., anti-Stokes components, class-II radiation cones 0-28276  
 benzene, T<sub>1</sub>-S<sub>0</sub> intersystem crossing vibronic interactions IR absorpt. spectrum obs. 0-28042  
 benzene, thermal lensing effect, absorptivity meas. at 607 nm 0-34900  
 benzene, topological resonance energy, rel. to cyclobutadiene 0-5462  
 benzene, UV photoelectron spectra, valence electron shake up approx. methods 0-18788  
 benzene, zero- and four-photon NMR coherence, selective excitation 0-23439

## organic compounds continued

- benzene-(cyclohexane), second virial coeff. meas. using new apparatus 0-44289  
 benzene-(d<sub>1</sub>,d<sub>2</sub>,d<sub>4</sub>), two-photon <sup>1</sup>B<sub>2u</sub>-<sup>1</sup>A<sub>1g</sub> spectrum, deuterium effect 0-32788  
 benzene and deuterates, highly vibr. excited intramolecular V-V transfer, visible and photoacoustic spectra 0-32729  
 benzene aqueous hetero-azeotrope mixture, condensation heat transfer coeff. (*German*) 0-33425  
 benzene in dilute cyclohexane solution, fluoresc. quenching on pulsed proton irradi., temp. depend. 0-21307  
 benzene in PMA and PEA, penetrant diffusion, statistical mech. model 0-44352  
 benzene in solution, rotational motion, Raman study 0-44104  
 benzene-chlorobenzene, benzene-toluene, perfect binary liquid mixtures on silica gel, adsorption thermodynamics 0-44428  
 benzene-cyclohexane-butanol, evaluation of US vel. 0-38201  
 benzene-cyclohexane-ethanol, evaluation of US vel. 0-38201  
 benzene-cyclohexane-methanol, evaluation of US vel. 0-38201  
 benzene-ethanol-water-(NH<sub>4</sub>)<sub>2</sub>SO<sub>4</sub>, liq. mixture, near tricrit. pt., thermodynamic model and sum rules 0-34196  
 benzene-hexa-n-alkylanoates, disc-like molecules, miscibility studies of mesophases 0-19696  
 benzene-hexafluorobenzene, liq., mol. interactions 0-28907  
 benzene-hexafluorobenzene mixture, percolation model of electron and hole mobility 0-29452  
 benzene-I<sub>2</sub> mixture, N<sub>2</sub> and Ar matrix isolated magnetic circular dichroism spectrum 0-5567  
 benzene-p-dioxan, mixtures, mol. reorientation and assoc., depolarised Raman scatt. obs. 0-7341  
 benzene-p-ylene, excess vol., enthalpies, Gibbs free energies 0-44335  
 benzene-similar liquids, US attenuation in 10 to 1300 MHz range 0-39229  
 benzene-tetrahydrofuran, soln., excess thermodynamic props. and interactions, US vel. and density meas. 0-39288  
 benzene-toluene, perfect binary liquid mixtures on silica gel, adsorption thermodynamics 0-44428  
 benzene-water-ethanol-(NH<sub>4</sub>)<sub>2</sub>SO<sub>4</sub>, liq. mixture, near tricrit. pt., light scatt. and sum rules 0-34933  
 benzenoid system intercalation with AsF<sub>5</sub>, EPR, NMR and X-ray diff. obs. 0-19775  
 benzil, excited electronic states; conformational relax., time resolved matrix isolation spectral obs. 0-32701  
 benzil, structural transition model, cryst. symm. spontaneous strain components 0-2161  
 benzil crystals, mol. triboluminesc. meas. 0-40172  
 benzo(a)pyrene, determ. in water using spectrofluorimetry 0-7997  
 benzoate/benzotriazole mixture, for corrosion inhibition of Fe in ethanediol/water soln., synergistic effect 0-45425  
 1,3-benzodioxole, geometry electronic absorpt. spectra 0-971  
 benzoic acid, IR absorpt. spectra, fundamental assignments 0-5542  
 benzoic acid, single cryst. growth from nitrobenzene-water immiscible system 0-40244  
 benzoin containing system, photosensitized free radical polymerisation 0-7825  
 benzonitrile, HCN elimination, ion kinetic energy spectrum peaks, collision gas sensitive 0-40679  
 benzonitrile, vibronic spectrum, semiempirical method 0-43031  
 benzophenone containing system, photosensitized free radical polymerisation 0-7825  
 benzophenone L in dibromodiphenylether, benzophenone triplet state, nanosecond resolved ODMR, freq.-agile techniques appl. 0-34825  
 benzophenone-N,N-dimethylaniline, intramolecular exciplex systems, laser photolysis obs. 0-35550  
 p-benzoquinones, chlorinated, transferable force field for in-plane vibrs. 0-964  
 2-benzoylpyridine crystals, lowest triplet state, optically detected EPR 0-15827  
 2-benzoylpyridine crystals, optical spectra of lowest triplet state 0-16081  
 benzyl acetate, phosphoresc. and fluoresc. spectra in organic matrices 0-32756  
 benzyl benzoate, supercooled, depolarised lines in quasielastic light scatt. 0-45095  
 benzyl bromide and chloride, bond orders estimation, bond polarisability derivative 0-32594  
 benzyl cyanides,  $\alpha$ -substituted, in dil. soln., dielec. absorpt. obs., enthalpy of activation 0-55019  
 benzyl fluoride, mol. struct., NMR and gas electron diffraction obs., ab initio and mol. mechanics calcs. 0-23574  
 benzyl propionate, phosphoresc. and fluoresc. spectra in organic matrices 0-32756  
 benzyl viologen, mechanism of electrochromism (*Japanese*) 0-34893  
 $\Delta^6$ -bicyclo[3.2.0]heptene, microwave spectrum and dipole moment 0-9591  
 biimidazole + leuco dye photochem. reaction, modulation by photopolymerisation 0-40714  
 bile acid hepatobiliary kinetics, compartmental model validity 0-30971  
 binary liquid mixtures, excess free vol. calcs. 0-34202  
 binary system forming simple association complexes, liq. diffusivities prediction 0-34216  
 biomotrifluoromethane, multiphoton dissoc., isotopically selective 0-28113  
 biotin, NMR of <sup>13</sup>C, spectrum assignment 0-26204  
 (biphenol)<sup>+</sup>/(biphenol)<sup>-</sup> ion-radical pair, ODMR, hyperfine struct. (*Russian*) 0-15829  
 biphenyl, diamagnetism and thermal motion 0-25076  
 biphenyl, heat capacity near phase transition regions 0-44330  
 biphenyl, incommensurable phases, obs. of excitations, inelastic neutron scatt. 0-49334  
 biphenyl, vibr. level classification by Longuet-Higgins group 0-43030  
 biphenyl single crystals,  $\gamma$ -ray induced radicals, EPR and optical absorpt. studies 0-44921  
 biphenylbenzoates, synthesis, mesomorphic, and thermodynamic props. 0-44117  
 biphenyls, polychlorinated, gas chromatographic anal. using electron capture detector (*Japanese*) 0-55764  
 bipyridines, torsional isomerisation of biologically active bicyclic molecules 0-27996  
 2,2'-bipyrimidine, in nematic solvent, conformation, ab initio and PMR determ. 0-47869  
 biradical metal chelates, rot. motion in polar solvents, rel. to ESR line-shape 0-27994



## organic compounds continued

- bis(benzonitrile)trichloromonoovanadium(V), *cryst.*, stacking faults (French) 0-49238
- bis(p-toluene sulphonate)diacetylene, monomer and polymer, solid state phase transformation, far IR transmission spectra obs. 0-55077
- bis (methylammonium) tetrachlorometallates (II), IR spectra and phase transitions of 10-25 kbar at 25°C 0-10658
- 4,4'-bisubstitutedoxy quaterphenyl, dye laser pumping characts. using KrF excimer laser at 248 nm 0-1199
- borazine, triplet instability, RPA calculations 0-27938
- bromal, in benzene soln., dielec. relax., loss, and dipole moment 0-2692
- bromobenzene, optoacoustic spectroscopy using cell with ultimate corrosion resistance 0-42269
- bromobenzenes <sup>13</sup>CBr bond, spin-spin coupling consts., correl. with C hybridisation s-character 0-34806
- p-bromochlorobenzene, vibr. relax., Raman active phonons temp. depend. 0-29139
- bromoform, solid, phase transform., dielec. dispersion and differential scanning calorimetric obs. 0-24582
- bromoform liquid, NMR spin-lattice relax. time 0-25232
- bromomethane, mol. Rydberg transitions mag. circular dichroism 0-43081
- bromomethane, multiphoton vacuum UV photodissoc. obs. and interpret. 0-11939
- bromomethane, vibr., rot. and translational energy exchange, semiclassical theory 0-48067
- bromomethyl methyl ether, microwave spectra, quadrupole computing effect 0-18848
- bromomethyl methyl ether, microwave spectra, quadrupole coupling effect 0-14135
- bromomethylsilane, microwave spectra, quadrupole computing effect 0-18848
- bromomethylsilane, microwave spectra, quadrupole coupling effect 0-14135
- 1-bromopropane, photoionisation mass spectrometry 0-40779
- bromotrichloromethane, <sup>13</sup>C isotope selectivity press. depend., multiphoton IR photolysis 0-45523
- bromotrifluoromethane, CW optically pumped, FIR laser action obs. at 823, 883  $\mu$ m 0-14321
- bromotrifluoromethane, E-species force consts., using L-F approx. method, HLFS applicability 0-962
- butadiene, electron momentum distrib. in  $\pi$  orbitals from (e,2e) expts. 0-14239
- butadiene, LMO population calc. method appl., from given SCF eigenvector matrix 0-14063
- butadiene, singlet and triplet state, open shell RPA unitary group formulation, Hartree Fock stability eqns. 0-52860
- 1,3-butadiene+N<sub>2</sub>, reaction rate consts., pulse radiolysis obs. 0-35508
- butadiynyl in IRC+10216, N=12-11 doublet study 0-51829
- n-butane, impurity in liq. and solid neopentane, effect on electron mobility and electron-ion recomb. 0-24984
- n-butane in liq. solvents, conformational structure 0-28115
- n-butane-N<sub>2</sub>(CO<sub>2</sub>) mixtures, viscosity, diffusion coeffs. 0-1722
- 1-butanethiol, simulated ab initio MO method calcs. 0-47867
- butanethiol, volume change on melting and reduced Lindemann's relation 0-29151
- n-butanol, natural convection from temp. fields in spherical partially filled vessel 0-1561
- 1-butanol, permitt., dielec. time domain spectroscopy, total transmission method study 0-27323
- n-butanol in ethyl methyl ketone, measurements of US vel. and density for determination of excess props. 0-37910
- butanol-methylethyl ketone, soln., excess thermodynamic props. and interactions, US vel. and density meas. 0-39288
- n-butanol-water-Ca (SCN)<sub>2</sub> system with hypercrit. point, US absorpt. 0-49306
- trans-2-butene, Ar matrix, TEA CO<sub>2</sub> laser irr. photoisomerisation study 0-21303
- cis-2-butene, charge transfer mass spectra and photoelectron spectra 0-40778
- cis-butene, ozonolysis, radical form., matrix ESR spectrosc. 0-16653
- butene isomers, gaseous, density and temp. effects on electron mobilities 0-33725
- butene-1, solubility in liq. N<sub>2</sub> 0-39286
- N-n-butoxybenzylidene-n-butylaniline, US propag. near nematic-smectic A transition, mag. field effect 0-39266
- N-p-butoxybenzylidene-p-n-octylaniline, smectic A-B transition, birefringence pretransitional behaviour 0-15226
- butyl alcohol, pumping down curve, P(t), rel. to adsorption isotherm (Japanese) 0-52249
- tert-butyl alcohol in nonpolar solvents, liq. struct. from dielectric studies 0-38894
- t-butyl bromide, elec. cond., temp. depend. in liq. and plastic phases 0-1944
- t-butyl chloride, elec. cond., temp. depend. in liq. and plastic phases 0-1944
- n-butyl chloride, glass transition rel. to press. depend. of viscosity 0-34171
- t-butyl chloride +Cs<sup>+</sup>, reactive scatt., stripping model, ang. and energy distrib. 0-35510
- t-butyl chloride-d<sub>3</sub> and -d<sub>2</sub>, polymorphism, Raman spectra 0-20617
- t-butyl cyanide-HF, hydrogen bonded heterodimer, spectroscopic consts. from IR and microwave spectra 0-43039
- tert-butyl formate-d<sub>3</sub>, Fermi reson. parameters meas. attempt 0-48103
- butyl iodide, two-photon reson. ionis. spectra 0-28071
- butyl radical +O<sub>2</sub>, reaction rate consts. meas. 0-45490
- p-n-butyl-p'-methylhydroxyazobenzene/p-n-butylheptanoylazoxybenzene mixture, temp. depend. of elec. cond. 0-1925
- butyl-PBD laser, tunable narrow-band coherent VUV source for Lyman- $\alpha$  region 0-38070
- n-butylamine, second virial coeff. meas. using new apparatus, 40°C 0-44289
- butylbenzene-nitrobenzene binary mixtures, with weak charge transfer interactions, thermodynamic props. 0-54360
- caesium propanoate, solid state transitions and melting process, diff. and conductometric meas. 0-10670
- caesium trichloroacetate, temp. depend. of <sup>31</sup>Cl NQR spectra 0-20495
- calcium formate, intermolecular shielding contributions, proton mag. shielding 0-34783
- calcium tartrate tetrahydrate:Cr<sup>3+</sup>, optical absorpt. spectrum, *cryst.* field parameters 0-16067
- organic compounds continued
- calcium tartrate tetrahydrate:Cu<sup>2+</sup>, spin-orbit coupling, optical absorpt. spectra 0-45120
- capsular polysaccharide antigen, structure investig. by <sup>13</sup>C NMR 0-35828
- carbazole, birefr. meas., 20 to 190°C, crystal-to-crystal phase transform. 0-45031
- carbenes, triplet state g-tensors and hyperfine coupling tensors 0-52895
- carbocyanine dye lasers, synchronous pumping, extension of spectral range 0-5731
- carbohydrates, reactions with hydrated electrons and hydroxyl radicals, rate constants obs. 0-50825
- carbon tetrabromide, ordered phases, polymorphism obs. 0-54217
- carbon tetrachloride, adsorption on Fe (100), AES, LEED, work function, and thermal desorption study 0-15376
- carbon tetrachloride, binary liquid mixtures, excess free vol. calcs. 0-34202
- carbon tetrachloride, charge exchange mass spectra 0-43177
- carbon tetrachloride, clusters, collision induced polarisability, mol. frame distortion 0-32798
- carbon tetrachloride, internucl. parameters meas. using total scatt. of fast electrons 0-32857
- carbon tetrachloride, M-X bond flexibility, by compliance scheme 0-37805
- carbon tetrachloride, ordered phases, polymorphism obs. 0-54217
- carbon tetrachloride, solid, Raman study of phase transition and dynamic struct. 0-34916
- carbon tetrachloride, US vel., 265-435K 0-6464
- carbon tetrachloride+Ca reaction, laser-induced fluoresc. obs. 0-11916
- carbon tetrachloride aqueous hetero-azeotrope mixture, condensation heat transfer coeff. (German) 0-33425
- carbon tetrachloride with aromatic amines mixture, theoretical evaluation of US vel. 0-39224
- carbon tetrachloride-GaCl<sub>3</sub>-Nd<sup>3+</sup> nontoxic liquid phosphor system, synthesis 0-55157
- carbon tetrachloride-I<sub>2</sub> soln., ps dye laser excitation, fluoresc. and resonance Raman emission 0-28021
- carbon tetrachloride-water soln., fundamental H<sub>2</sub>O IR spectrum, liq. struct. 0-23419
- carbon tetrafluoride, clusters, collision induced polarisability, mol. frame distortion 0-32798
- carbon tetrafluoride, weak absorpt. spectra of  $\nu_2+\nu_4$  vibr. using CO<sub>2</sub> laser 0-5762
- carbon tetrafluoride+4% O<sub>2</sub> plasma, Si etch rate uniformity 0-40568
- carbon tetrafluoride laser, emission spectrum in 16 micron range, CO<sub>2</sub> laser stimulation 0-9870
- carbon tetrafluoride laser, optically pumped, freq. tuning 0-28208
- carbon tetrafluoride optically pumped laser, stimulated emission stabilisation and tuning 0-9866
- carbon tetraiodide, ordered phases, polymorphism obs. 0-54217
- carbonic anhydride, active site substrate binding, environmental effects, CNDO and SCF LCAO calcs. 0-8002
- carbonized bitumens and pyrobitumens, studies of molecular struct. using microscope photometry 0-18011
- carbonyl sulphide, roto-vibrational molecular laser scaling, CO<sub>2</sub>-TEA laser pumped 0-5728
- carboranes, small cage, antipodal H-H coupling 0-1003
- carboxyl groups, -COO<sup>-</sup>, -COOH, -COOCH<sub>3</sub>, bond lengths and angles relations 0-53158
- carnauba wax, thermoelectret, lattice parameter changes at elevated temps. 0-29674
- $\beta$ -carotene, Franck-Condon effects in resonance Raman spectra and excitation profiles 0-14129
- catechol borane, geometry, electronic absorpt. spectra 0-971
- CBOOA, isotropic, nematic, smectic-A phases, Brillouin scatt. 0-11421
- cellulose membranes bearing ATPase, permeabilities, dynamic, meas. under non-equilib. conditions 0-46107
- charge transfer salt process for high-density video storage 0-43269
- charge-transfer salts, comparison of ESR spectra 0-50164
- charged excitonic complexes, coupled states, exciton interaction with charge carriers study 0-20090
- chemistry courses, unified approach to teaching of struct. and bonding 0-17732
- chloral hydrate, phase transform. rate, <sup>35</sup>Cl NQR rate 0-54983
- o-chloranil, adsorbed on phthalocyanine films, effect on surface photovoltage 0-34485
- chlorin, electronic struct. props. and photosynthesis 0-16902
- 6-chloro-2,4-dimethoxypyrimidine, <sup>35</sup>Cl NQR, Zeeman effect 0-18874
- 2-chloro-1,3,2-dioxo-arsolane, temp. depend. of NQR spectra parameters of <sup>75</sup>As and <sup>35</sup>Cl 0-20494
- 2-chloro-1,3,2-X, Y-arsolanes, temp. depend. of NQR spectra parameters of <sup>75</sup>As and <sup>35</sup>Cl 0-20494
- 1-chloro-2-methylbutane, conformer depend. C-Cl stretching vibr., Raman optical activity spectrum simulation 0-14146
- 2-chloro-2-nitropropane, far IR-microwave estimation of binary collision approx. 0-55095
- chloro-hydrocarbons, interaction between atmospheric pollutants (French) 0-7976
- 2-chloro-p-nitroaniline, in benzene soln., dipole moment from solute relax. time-solvent viscosity relation 0-37905
- chloroacetylene decomposition, unimolecular lifetime and relative translational energy distrib. 0-25994
- o-chloroaniline-iso-octane, crit. system, comp. depend. of absorpt., US obs. (German) 0-19879
- o-chloroaniline-n-heptane, crit. system, comp. depend. of absorpt., US obs. (German) 0-19879
- chlorobenzene, liq., spin lattice relax. time, elec. field induced charges 0-44945
- chlorobenzene, optoacoustic spectroscopy using cell with ultimate corrosion resistance 0-42269
- chlorobenzene ion fragmentation, kinetic shift and phenyl ion heat at formation, photoelectron-photoion coincidence meas. 0-25998
- chlorobenzene-bromobenzene, perfect binary liquid mixtures on silica gel, adsorption thermodynamics 0-44428
- chlorobenzene-cis-decalin mixtures, phase transitions and dielec. behaviour study in 77-330K 0-29680
- chlorobenzenes, substituted, NQR freqs. 0-20504
- chlorobenzenes determination by gas chromatography with photoionis. detection, air and biological samples 0-35809
- p-chlorobenzylidene-p-n-pentylaniline, metastable phases formed by rapid cooling of mesophase, IR and Raman spectra and DSC obs. 0-34919



**organic compounds continued**

chlorocyclohexane, US relaxation 0-24540  
 chlorodifluoroethane, CW laser induced reactions, activation energies, temps. and rate consts 0-40710  
 chlorodifluoroethane, CW laser-induced reaction, vibr. rate enhancement obs. 0-11922  
 chlorodifluoromethane, IR multiphoton dissociation, CF<sub>2</sub> form., time-resolved optical absorption obs. 0-16702  
 chlorodifluoromethane, photoacoustic spectra meas. at CO<sub>2</sub> laser wavelengths 0-18849  
 chloroethane, reson. multiphoton dissociation 0-53077  
 chlorofluoroethane, multiphoton dissociation under CO<sub>2</sub> laser irradiation, decomposing mol. energy distrib. 0-30251  
 chlorofluoromethanes, laser photolysis, product vibr. relax. rates and diffusion coeffs. 0-55680  
 chlorofluoromethylene radical, gas phase laser-induced fluorescence spectroscopy 0-14173  
 chloroform, charge exchange mass spectra 0-43177  
 chloroform, isothermal Joule-Thomson coeff. 0-43828  
 chloroform, optical constants and dispersion eqns. 0-30762  
 chloroform, second virial coeff. meas. using new apparatus 0-44289  
 chloroform HV polarisation and space charge obs. (Russian) 0-25277  
 chloroform-d<sub>0</sub>(-d<sub>1</sub>), Raman and IR intensity anal. 0-18857  
 chloroform-He(Ar)(N<sub>2</sub>) gaseous compressed mixture, mol. reorientation, Raman spectra 0-23422  
 chloroform-p-dioxan and chloroform-benzene mixtures, mol. reorientation and assoc., depolarised Raman scatt. obs. 0-7341  
 chloroform-paraffin system chem. changes after <sup>60</sup>Co γ-irradiation, dosimetry appl. 0-30258  
 chloromethane, charge exchange mass spectra 0-43177  
 chloromethane, vibr., rot. and translational energy exchange, semiclassical theory 0-48067  
 chloromethane+OH, mean collision cross sections from microwave spectroscopy 0-1046  
 chloromethane in atmosphere, biomass burning as source 0-26586  
 chloromethanes, VUV fluoresc., UV multiphoton dissociation 0-28076  
 chloromethyl formate(-d<sub>1</sub>,d<sub>2</sub>,d<sub>3</sub>), gas, solid. and liq., IR spectra assignments and struct. 0-32715  
 chloromethyl oxirane, microwave spectra and conformations of cis and gauche-2 forms 0-5534  
 m-chloronitrobenzene, cryst., low freq. vibrs., polarised Raman and IR spectra study (French) 0-16029  
 m-chloronitrobenzene, molecular crystals, translational and orientational vibr. determ. 0-55103  
 chloropentafluoroethane, multiphoton dissociation, crossed laser and mol. beam obs. 0-11908  
 o-chlorophenol+o(m)-toluidine, H-bonded mol. complex, microwave absorpt., dipole moment and relax. times 0-14134  
 chlorophenols in surface waters, 1976-7 obs. in Netherlands 0-16858  
 4-chlorophenoxy aluminium dibromide, intramolecular configs., nucl. quadrupole double reson. obs. 0-34821  
 chlorophyll-pheophytin pigment associations, conc. effects, luminesc., absorpt. spectra and dichroism obs. 0-1007  
 chlorophyll a, electronic struct. props. and photosynthesis 0-16902  
 chlorophyll concentration in sea, estimation from outgoing radiation spectrum meas. from helicopter 0-36333  
 chlorophyll photo-oxidation, role of singlet-excited and triplet states 0-51156  
 chlorophyll special pair models, reaction centres 0-3574  
 chlorophyll spectral forms, Chlamydomonas mutants with inactive photosynthesis 0-51054  
 chlorophyll-a, conc. quenching rel. to functional charge transfer 0-30666  
 chlorophyll-a (b), dimerisation, fluoresc. and ODMR study 0-18876  
 chlorophylls a and b and pheophytins, fluoresc. and phosphoresc. 0-12057  
 2-chloropropane, photoionisation mass spectrometry 0-40779  
 1-chloropropane 0-40779  
 chloroquine-biopolymer binding interactions, PMR effects 0-55982  
 N-5'-chlorosalicylideneaniline, photochromism and thermochromism, NQR spectra, temp. and UV irradiation. depend. 0-54968  
 chlorotrifluoromethane, IR rovibr. spectrum (German) 0-47998  
 chlorotrifluoroethylene, multiphoton dissociation, fragment energy partitioning 0-55681  
 chlorotrifluoromethane, E-species force consts., using L-F approx. method, HLF applicability 0-962  
 chlorpromazine, automated synthesis of <sup>11</sup>C-labelled radiopharmaceuticals 0-17133  
 cholecalciferol, UV dependent synthesis in a green plant 0-35860  
 cholesteric esters, effect of nature of organic solvent on gamma radiolysis 0-7835  
 cholesterol, liq. cryst., synthesis and light refl. props. (German) 0-10497  
 cholesterol, dielectric props. under UV excitation 0-6912  
 cholesterol, dielectric transient response following UV-irradiation 0-51166  
 cholesterol, optical constants and dispersion eqns. 0-30762  
 cholesteryl alkanoyl esters, effect on red-green transition temp. of cholesteryl nonanoate (decanoate) 0-19924  
 cholesteryl decanoate, effect of cholesteryl alkanoyl esters on red-green transition temp. 0-19924  
 cholesteryl methyl carbonate, liq. cryst., low-ang. X-ray diffraction obs., solid and liq. 0-49093  
 cholesteryl nonanoate, effect of cholesteryl alkanoyl esters on red-green transition temp. 0-19924  
 cholic acid, dielectric props. under UV excitation 0-6912  
 cholic acid, dielectric transient response following UV-irradiation 0-51166  
 choline phosphate calcium chloride tetrahydrate, struct., conformation, metal coordination, model for membrane surface interactions 0-15085  
 chromium formate, mol., Hartree-Fock instability of SCF wavefunctions 0-9492  
 chromophores, biochemical, in cosmic dust, contrib. to interstellar UV extinction 0-26945  
 chromophores, semiempirical rules in circular dichroism, Cotton effect sign correl. with stereochem. 0-1006  
 chrysene, mag. susceptibility anisotropies, high field <sup>2</sup>H NMR quadrupolar effects obs. 0-25225  
 citric acid monohydrate, triboluminescence and cryst. fracture dynamics 0-50437  
 coatings, development (French) 0-30127  
 cobalt(II) metalloporphyrin, Z-ray photoelectron spectra satellites 0-5582  
 cobalt(III) complexes, mixed glycylglycinate, synthesis and config. (French) 0-2005

**organic compounds continued**

cobalt naphthalate electret, thermally stimulated discharge, 55-75°C 0-25279  
 cobalt platino-oxalate, one-dimens. conductors, prep., struct. and elec. cond. 0-24900  
 cobalt stearate, monomolecular layer, electron escape depth, XPS (Japanese) 0-11532  
 COC test of tricriticality 0-10648  
 cofacial diporphyrins, electron transfer reactions following picosecond excitation, CT state lifetimes, optical difference spectra 0-25995  
 complex, nuclear relaxation influence on stimulated emission 0-48019  
 conductors, narrow band, valence bond theory 0-24777  
 conjugated cpds., aromaticity determ. by topological reson. energy method 0-42915  
 conjugated hydrocarbon, graph theoretical formulation of London diamag. 0-27919  
 COOB, solid state dimorphism and cryst.-smectic transition, Raman study 0-45063  
 copper(II) metalloporphyrin, Z-ray photoelectron spectra satellites 0-5582  
 copper complex CuBr<sub>2</sub> (pyrimidine)<sub>2</sub>, mag. susceptibility and magnetisation curve, 1.2-4.2K 0-11177  
 copper dipyrindine dichloride, dynamic shift of the ESR field 0-2630  
 copper formate tetrahydrate, ferrielectricity 0-2706  
 copper formate urea hydrate, two dimens. antiferromagnet, EPR, temp. depend. 0-54937  
 copper phthalocyanin, thin film, thermal behaviour (Japanese) 0-24753  
 copper phthalocyanine film, photoelectrochem. behaviour on SnO<sub>2</sub> electrodes 0-15626  
 copper platino-oxalate, one-dimens. conductors, prep., struct. and elec. cond. 0-24900  
 copperporphyrin, metastable quartet state radiative decay 0-23453  
 coronene, an ordered struct. 0-19786  
 coronene, excited state Faraday values mag. circular dichroism spectra and MO CI calcs. 0-18877  
 coronene, luminesc., spin-orbit coupling perturbation by metal chlorides (German) 0-1021  
 coronene, mag. susceptibility anisotropies, high field <sup>2</sup>H NMR quadrupolar effects obs. 0-25225  
 coronene, protection against radiation damage, exciton effects 0-29055  
 coronene trimer radical cation, spin densities in CH<sub>3</sub>Cl<sub>2</sub>-CH<sub>3</sub>NO<sub>2</sub> solvent mixture, -100°C 0-5565  
 corrosion inhibitor efficiency for Zn 0-40589  
 coumarin, geometry, electronic absorpt. spectra 0-971  
 coumarin 102, excited state protonation kinetics, laser pH jump and picosecond spectroscopy 0-25992  
 coumarin in water and heavy water, fast neutron response 0-845  
 coumarine 1-rhodamine 6G-water-Triton X100, micellar dye soln., energy transfer 0-45581  
 o-cresol, binary liquid mixtures, excess free vol. calcs. 0-34202  
 cresyl violet, luminesc. quantum yield standard for red, calorimetric obs. 0-190  
 cresyl violet, rot. diffusion, picosec. saturation spectrosc. obs. 0-5634  
 cresyl violet 620, injection locked dye amplifier, coherent optical image amplification 0-19041  
 cresyl violet in ethanol soln., and dye mixtures, excitation by Cu vapour laser 0-28230  
 cryptolepine derivatives, absorpt. and fluoresc. obs. of photodecomp. processes, dye laser relevance 0-55686  
 crystal violet, prereson. Raman spectra 0-32721  
 crystals, quantitative validity domains of single scattering approximations 0-28888  
 CTA-DNA crystal growth and morphology 0-26198  
 cyan pigment photoconducting, electric field-induced fluoresc. quenching 0-34967  
 cyanine dyes for spectral sensitization of evaporated AgBr layers 0-26035  
 4-cyano-4'-(n-amy)-diphenyl, isotropic phase, induced molecular orientation relaxation time, Kerr effect (Russian) 0-19699  
 p-cyano-p'-pentylbiphenyl/p-pentylbenzoic acid, mixture, induced smectic phase, dielec. props. 0-6498  
 cyanoacetylene, cyanoacetylene in interstellar clouds, obs. 0-46634  
 cyanoacetylene, vibrational excitation in Orion molecular cloud 0-22067  
 cyanobiphenyls, nematic, dielec. consots. and diamag. anisotropies 0-7253  
 cyanobutadiene, interstellar, in Heiles 2 dust cloud, emission distrib. rel. to NH<sub>3</sub> emission 0-17641  
 cyanobutadiene (HC<sub>3</sub>N), interstellar, obs. in Taurus 0-26957  
 cyanocyclohexylcyclohexanes, nematic, dielec. consots. and diamag. anisotropies 0-7253  
 cyanoacetylene (HC<sub>3</sub>N), interstellar, obs. in (Heiles's cloud 2) 0-22054  
 N-cyanoguanidine, structure, microwave transitions 0-973  
 cyanogen azide, electron-density maps of bent bonds 0-1084  
 cyanogen fluoride, fund., hot bands, laser microwave two photon and double reson. spectroscopy 0-32752  
 2-cyanoguanidine, electron-density maps of bent bonds 0-1084  
 cyanomethane-HF, hydrogen bonded heterodimer, spectroscopic consts. from microwave spectrum 0-43038  
 4-cyanophenyl 4-n-pentylbenzoate, electrical Kerr effect studies 0-25339  
 p-cyanophenyl-p'-caproyloxybenzoate, charge carrier behaviour, thermal depolarisation current study 0-7283  
 cyanophenylcyclohexanes, nematic, dielec. consots. and diamag. anisotropies 0-7253  
 cyanopolynes, interstellar, and related molecules, synthesis 0-12793  
 3-cyanopyridine, NQR Zeeman obs., crystal packing 0-54978  
 cyanuril chloride, quadrupole spin echo envelope EFG tensor axisymmetry in mag. field 0-20497  
 cyclic monocarboxylic acid radicals, ring inversion barriers, EPR 0-53025  
 cyclobutadiene, noncrossing and degeneracy in Hubbard models 0-14096  
 cyclobutadiene, topological resonance energy, rel. to benzene 0-5462  
 cyclobutane, MS-Xa-MT study 0-52906  
 1,1-cyclobutane dicarboxylic acids and K salts, IR and Raman vibr. spectra (French) 0-2758  
 cyclobutane-d<sub>0</sub>(d<sub>2</sub>), cryst. modifications, low. freq. Raman and IR spectra 0-7342  
 cyclobutane-t, chem. activated by nucl. recoil reaction, energy transfer interpret. 0-25985  
 cyclobutene, strong collision and thermal decomp. on surface, variable encounter method calcs. 0-50885  
 cycloheptanone, photolysis, CIDNP effects 0-18869



## organic compounds continued

cycloheptatriene, and substituted forms, vibr. highly excited, steady-state photoisomerisation 0-16704  
 cyclohexadiene, shock compression, dynamic high press. eqns. of state 0-6450  
 cyclohexane, adsorption and decomp. on Ni (111), high resolution EELS study 0-40739  
 cyclohexane, conform. equilb., CNDO/2 calcs. on six-membered rings 0-23336  
 cyclohexane, neutron irradiation, radical distribution, ESR study (*Japanese*) 0-44920  
 cyclohexane, plastic and liquid crystal phase, rot. correl. func. by Raman spectroscopy 0-23403  
 cyclohexane, reactions catalysed by Pt surfaces with variable kink concs., surface O<sub>2</sub> effects 0-35576  
 cyclohexane, shock compression, dynamic high press. eqns. of state 0-6450  
 cyclohexane+n-heptyl alcohol, measurements of US vel. and related parameters 0-38200  
 cyclohexane+toluene, energy transfer, pulse radiolysis obs. 0-16714  
 cyclohexane aqueous hetero-azeotrope mixture, condensation heat transfer coeff. (*German*) 0-33425  
 cyclohexane in ethyl methyl ketone, measurements of US vel. and density for determination of excess props. 0-37910  
 cyclohexane solvent for poly[(R)-oxypropylene], effect on opt. rot. dispersion and vac. UV circular dichroism 0-40084  
 cyclohexane-aniline, crit. mixture with shear flow, light scatt. obs. 0-6521  
 cyclohexane-aniline mixture, shear induced transition to mean-field crit. behaviour 0-7364  
 cyclohexane-benzene, second virial coeff. meas. using new apparatus 0-44289  
 cyclohexane-d<sub>6</sub>(d<sub>6</sub>), plastic crystal phase transition, mol. reorientation, Raman scatt. phonon spectra 0-20631  
 cyclohexane-I<sub>2</sub> soln., ps dye laser excitation, fluoresc. and resonance Raman emission 0-28021  
 cyclohexane-transdecalin mixture, percolation model of electron and hole mobility 0-29452  
 cyclohexene, reactions catalysed by Pt surfaces with variable kink concs., surface O<sub>2</sub> effects 0-35576  
 cyclohexene, shock compression, dynamic high press. eqns. of state 0-6450  
 cyclopentadienyl radical, pot. surface and vibronic states, ab initio CI calcs. 0-47897  
 cyclopentene, mol., pot. functions of bending modes 0-9753  
 cyclopropane, 3e-orbital, electron momentum distrib., mol. distortions effects 0-18773  
 cyclopropane, electron momentum distrib. in  $\pi$  orbitals from (e,2e) expts. 0-14239  
 cyclopropane, laser induced reaction, energy distrib. 0-16710  
 cyclopropane, partial vibr. energy transfer map 0-32760  
 cyclopropane, thermal unimol. isomerisation, vibr. energy transfer, diffusion cloud method 0-26001  
 cyclopropane, vibr. intensities, G sum rule appls. 0-32776  
 cyclopropane+inert gas, reactant decomp., rot.-vibr. energy transfer, relax. analytic soln. 0-55650  
 1,1-cyclopropane-d<sub>2</sub>, isomerisation transient vibr. energy distrib., collisional relax., variable encounters method 0-50836  
 cyclopropene, photoionisation and threshold photoelectron-photoion coincidence study 0-53062  
 cyclopropene fragment ions, from photoionisation, efficiency curves, isomerisation 0-53062  
 cyclopropyl bromide, IR absorption, Raman scatt., assignments, thermodynamic functions 0-984  
 DL-cysteine, phase transition obs. at 10°C (*French*) 0-49355  
 cytosine monohydrate, deuterated, neutron diff. cryst. struct. determ. 0-54215  
 decalin, liq. and glass mol. motion, kinematic and electrodynamic solns. 0-25293  
 cis-decalin, shift difference between chem. exchange sites using <sup>13</sup>C T<sub>1</sub> meas. 0-18945  
 n-decane, emulsion drop, efficiency of capture by bubble in noninertial flotation 0-11956  
 decane on Teflon FEP, effect of drop size on contact angle 0-2245  
 deoxycholic acid, lyotropic and thermotropic phase transitions, clathrate form. 0-49341  
 di-(2,2,6,6-tetramethyl-4-piperidinyl-1-oxyl)-suberate, spin densities, polarised neutron diff. meas. 0-50037  
 di-butyl-sebacate, HV evaporation, mass transfer in evaporating space (*Japanese*) 0-50558  
 p,p'-di-n-alkoxyazobenzene series, C<sub>1</sub>-C<sub>7</sub>, submillimetre wave absorpt. investig. 0-34910  
 diacetylene, obs. of  $\nu_4$  band near 3 microns 0-47977  
 diacetylene, single cryst., photopolymerisation, intermediate states, struct. changes 0-30235  
 diacetylhydrazine, <sup>14</sup>N NQR echo envelope slow beats 0-29643  
 diacrylate fissure sealants, film charact., dentistry appl. 0-12306  
 di-alkyl-cyclohexyl-cyclohexanoates, nematic and smectic mesophases 0-19692  
 dialkylammonium copper tetrachloride, ferromagnetic layer compound, magnetostatic mode excitation 0-29538  
 dialkylaniline derivatives, twisted intramol. charge transfer states, dual fluoresc. obs. and form., dipole moments 0-18881  
 p-diazoquinone, photodecomp. 0-7827  
 dibenzofuran, cryst., phosphoresc. spectra and ODMR meas. 0-11470  
 dibenzofuran-fluorene, mixed cryst., phosphoresc. spectra and ODMR meas. 0-11470  
 dibenzotetrathiafulvalene cation radical salts, cryst. struct. by X-ray anal., rel. to elec. props. 0-24436  
 meso-2,3-dibromo-1,4-dichlorobutane, rot. isomerism, IR and Raman spectra 0-981  
 p-dibromobenzene, crystal nucl. spin polarisation cross relax. study 0-29647  
 dibromodifluoromethane, UV laser fluoresc. and photochem., CF<sub>2</sub>, CF and Br<sub>2</sub> fluoresc. obs. 0-16703  
 p-dibromodiphenylether surface, normal and ultra-Brewster refl. spectra 0-25400  
 1,2-dibromooethane, volume change on melting and reduced Lindemann's relation 0-29151  
 dibromomaleic acid thioanhydride, mol. and cryst. structs., X-ray obs. (*German*) 0-44199

## organic compounds continued

1,4-dibromonaphthalene, highly disordered quasi-one-dimens., excitation transport 0-34961  
 1,4-dibromonaphthalene, k-k scatt., exciton dephasing time-resolved phosphoresc. obs. 0-11458  
 p,p'-dibutyl-azobenzene, DIBAB, light scatt. studies (*Dutch*) 0-33885  
 dibutyl-phenyl-benzoyloxy-benzoate, nematic liq. cryst., rot. barrier, PCIL0 and CNDO/2 calcs. 0-33874  
 dicalcium lead propionate, ferroelec., annealed, crit. exponents, dielec. const. temp. depend. 0-55050  
 dicarbaclosododecaboranes, icosahedral, electron transfer phenomena in isolated borane units 0-18871  
 dicarbonitrile-anthracene solutions, absorpt. and emission spectra, solvent influence 0-43083  
 dichelated protohaeme, model haemoglobin cpd., Mossbauer spectra 0-16904  
 dichloride 2,4'-bis (trimethylammonium-acetamide)-benzal-fluorene, thin layers, behaviour in electric field (*Rumanian*) 0-35108  
 1,1-dichloro-1-nitroethane, dil. soln. in benzene, dielec. relax. study 0-29679  
 dichloroanilines, vibr. assignments, Raman spectra obs., thermodynamic functions 0-52992  
 9,10-dichloroanthracene, monoclinic, photocond. carrier mobility 0-39630  
 p-dichlorobenzene, <sup>35</sup>Cl powder Zeeman NQR, injection and phase locked NQR spectrometer 0-54979  
 p-dichlorobenzene, expansivity, determ. by calorimetric compression from 0 to 400 MPa 0-44339  
 p-dichlorobenzene, in p-dibromobenzene, optical detection of Cl NQR in mag. field 0-50228  
 p-dichlorobenzene, vibr. relax., Raman active phonons temp. depend. 0-29139  
 4,4'-dichlorobenzophenone, phase changes, Raman spectra (*French*) 0-2756  
 3,4-dichlorobromobenzene, liq., laser Raman spectrum, LF band assignments 0-48002  
 dichlorodifluoromethane, infrared multiphoton processes, apparent step cross-sections, pulse spatial structure, irradiation techniques 0-32792  
 dichlorodifluoromethane, threshold multiphoton dissociation, Cl<sub>2</sub> elimination 0-9653  
 dichlorodifluoromethane, UV photolysis, free radical emission 0-30263  
 1,2-dichloroethane, conformer equilibrium by effusive beam-matrix IR spectroscopy 0-48100  
 1,1-dichloroethane, tilt-effect and interference with rel. sign determination in weak irradi. expts. 0-32742  
 1,2-dichloroethane, volume change on melting and reduced Lindemann's relation 0-29151  
 trans-1,2-dichloroethylene, Ar matrix, TEA CO<sub>2</sub> laser irradi. photoisomerisation study 0-21303  
 dichlorofluoromethane, IR absorpt. spectra, 1155-1163 cm<sup>-1</sup> 0-37807  
 dichlorofluoromethane, photoacoustic spectra meas. at CO<sub>2</sub> laser wavelengths 0-18849  
 dichloromethane, charge exchange mass spectra 0-43177  
 dichloromethane, high press. and temp. IR absorpt. spectra, stretching fundamentals (*German*) 0-47999  
 dichloromethane, solidified, solubility in liq. N<sub>2</sub> at 77.4K 0-10673  
 3,5-dichloronitrobenzene, NQR line, Zeeman effect 0-28034  
 3,5-dichlorophenoxy aluminiumdibromide, intramolecular configs., nucl. quadrupole double reson. obs. 0-34821  
 3,6-dichloropyridazine, liq. and solid soln. spectra, fundamental freqs. and assignments 0-5541  
 4,6-dichloropyrimidine, <sup>35</sup>Cl NQR, Zeeman effect 0-18874  
 dicyanodiacetylene radical cation, photoelectron and emission spectra 0-5558  
 didodecyltrimethylammonium bromide-benzene inverted micelles, solubilisation of pyrene-3-sodium sulphate 0-3417  
 diene-iron tricarbonyl complexes,  $\pi$ -orbital perturbation energies, ionisation energies; UV photoelectron spectra 0-32775  
 diethyl ether, liq., spin lattice relax. time, elec. field induced charges 0-44945  
 diethyl phthalate, enhanced arcing as function of organic exposure and arc current 0-38778  
 3,3'-diethyl-oxadiazabicyclopentadiene iodide, model-locking of picosecond transverse-flow flashlamp-pumped dye laser 0-38025  
 7-diethylamino-4-trifluoromethyl coumarin, dye laser pumping characts. using KrF excimer laser at 248 nm 0-1199  
 diethylammonium cadmium tetrachloride, first order phase transition, optical phonon line broadening, spin-phonon coupling model 0-7335  
 diethylammonium copper tetrachloride, <sup>63</sup>Cu NMR, hyperfine interactions 0-54956  
 diethylammonium copper tetrachloride, ferromag., static and dynamic mag. props. 0-50074  
 diethylammonium manganese chloride, antiferromag., low temp. luminesc. spectra, magnetoelastic effect 0-2810  
 diethylammonium manganese chloride, planar Heisenberg magnet, spin diffusion, EPR study 0-15793  
 3,3'-diethylthiacarbocyanine iodide-rhodamine-6G-sodium lauryl sulphate, soln., premicellar region, energy transfer 0-20685  
 diffusion of radical-ion pairs, spatial distrib., electron spin echo obs. 0-29622  
 difluorocarbene,  $\bar{A}^1B_1-\bar{X}^1A_1$  system spectrosc. and photophysics 0-5577  
 1,2-difluoroethane, internal rotation temp. frozen in supersonic jet, matrix IR spectroscopy 0-9594  
 1,1-difluoroethane, rot. relax., anharmonic shifts and excited state absorpt. 0-43154  
 1,1-difluoroethylene, diode-laser heterodyne spectrosc. meas. 0-43051  
 difluoroethylenes, plasma polymerisation, ESCA characterisation of polymers 0-21283  
 difluoromethylborane, microwave spectra and struct. obs. 0-43036  
 diformylhydrazine, <sup>14</sup>N NQR echo envelope slow beats 0-29643  
 diglycine nitrate, cryst. growth, dielec. and electromech. props. 0-2701  
 p-dihalobenzenes, apparent NQR spin-spin relax. times obs. 0-54991  
 4,4-dihexyloxybenzene, nematic liq. cryst., alignment on surfactant treated obliquely evaporated surfaces 0-49092  
 5,6-dihydro-6-methyluracil, X-ray irradi., free radical form; ESR spectra obs. 0-50189  
 2,5-dihydrofuran, mol., pot. functions of bending modes 0-9753  
 dihydroxycarbene, singlet and triplet state rot. pot. surfaces 0-32627  
 1,2-diiodobenzene, vibr. spectra, packing calcs. and crystal structure investig. 0-28938  
 diimide, electron-density maps of bent bonds 0-1084



## organic compounds continued

- diiodomaleic acid thioanhydride, mol. and cryst. structs., X-ray obs. (*German*) 0-44199
- 2,2-dimethoxypropane, enthalpy of hydrolysis meas., microprocessor-controlled system 0-22361
- N,N-dimethyl acrylamide ( $-d_3, d_6, d_9$ ), force field, IR and Raman spectra obs. 0-47979
- dimethyl ammonium copper chloride, spin dynamics near crit. pt. 0-7112
- dimethyl ammonium copper manganese tetrachloride, EPR study (*German*) 0-54941
- dimethyl ether, condensed multilayers, electron bombard. effects, AES line-shape anal., XPS, and desorption meas. 0-7450
- dimethyl ether, review of microwave spectrum, tabulated data 0-51965
- dimethyl ether-HF H-bonded complex, cubic force consts. calcs. 0-47868
- dimethyl oxalate, oriented cryst. film, polarised IR spectrum 0-29730
- dimethyl tin difluoride, solid, methyl group motion, neutron scatt. study 0-10607
- dimethyl urea, aqueous solution, ultrasonic velocity measurement 0-19878
- dimethylamino radical +  $O_2(NO)(NO_2)$ , reaction rate constants, FTIR obs. 0-16652
- dimethylammonium cadmium tetrabromide, room temp. struct. 0-29000
- dimethylammonium cadmium tetrachloride-type compounds, theory struct. phase transitions 0-10668
- dimethylammonium copper chloride bromide, mag. props., pulsed NMR expts. 0-11292
- dimethylammonium copper tetrachloride, ferromag., static and dynamic mag. props. 0-50074
- dimethylammonium iron tetrachloride, Mossbauer study of struct. phase transition 0-39278
- dimethylammonium manganese chloride, antiferromag., low temp. luminesc. spectra, magnetoelastic effect 0-2810
- dimethylammonium manganese tetrachloride, phonon density of states, expt. and calc. 0-54323
- dimethylammonium manganese tetrachloride- $d_6$ , structural and mag. phase transitions, neutron scatt. and AC susceptibility meas. 0-44825
- N,N-dimethylaniline + carbon tetrachloride, binary liquid mixtures, excess free vol. calcs. 0-34202
- dimethylaniline cation + anthracene anion, recombination reaction in soln., time-resolved mag. field effect 0-3308
- 2,6-dimethylbenzoic acid,  $^1H$  chem. shift recovery from combined multiple pulse NMR and sample spinning 0-32738
- 2,3-dimethylbuta-1,3-diene, IR, Raman spectra, torsional pot. function, thermodynamic function 0-43046
- 1,5-dimethylnaphthalene, fluoresc. quenching by cyclic azoalkanes, micelle system probe 0-35578
- 5,10-dimethylphenazine, in 3-methylpentane (ethanol) (PMMA), radiationless processes, temp. depend. 0-43087
- 3,5-dimethylphenol formaldehyde resin carbon, catalytic graphitisation from various metals 0-11871
- N,N-dimethylselenourea, deuterated forms and methyl derivatives, fundamental IR vibr. assignments 0-961
- dimethylsulphoxide, effects on water struct., Raman and IR spectral study 0-14143
- 1,4-bis(2,5-dimethylstyryl)benzene, lasing characts. on UV  $N_2$  laser excitation 0-32979
- dimethylsulphoxide- $d_6$ , Jeener-Brockaert three-pulse sequence, inhomogeneous lineshapes second rank spin interactions 0-39891
- N,N-dimethylthiourea, deuterated forms and methyl derivatives, fundamental IR vibr. assignments 0-961
- N,N-dimethyltrichloroacetamide, two-site exchange system, total line shape anal. 0-35519
- 1,3-dimethyluracil, non-hydrogen bonding crystal, radical formation 0-35552
- m-dinitrobenzene, electrooptic cryst., growth in monomode optical fibres 0-55288
- 1,5-dinitronaphthalene, diamag. cryst., mag. axis, struct. interpretation 0-50039
- 2,2-dinitropropane- $d_0(-d_6)$ , phase polymorphism, vibrational assignments, IR and Raman study 0-16031
- dinitrotoluene isomers, occurrence and determ. in seawater 0-7966
- dioctyl phthalate plasticised pentaplast, thermal treatment effect on props. 0-40324
- diolefins, substituted, topochemically controlled solid-state polymerization 0-35532
- 1,4-dioxadiene, mol., pot. functions of bending modes 0-9753
- p-dioxane, aq. soln., excess molar heat capacities, 298.15K, US vel. obs. 0-6523
- 1,4-dioxane, conform. equilib., CNDO/2 calcs. on six-membered rings 0-23336
- dioxane, liq., spin lattice relax. time, elec. field induced charges 0-44945
- dioxane based gel, scintillation yield and mechanisms involved study (*French*) 0-52816
- dioxane solutions, radioluminescence quenching in mixtures of solvents (*Russian*) 0-55192
- dipalmitoyl lecithin elastic monolayer, dynamic surface potentials 0-3603
- dipalmitoyl phosphatidylcholine vesicles, appl. of depolarised light scatt. theory from hollow spherical particles 0-45946
- diphenyl:pyrene, self induced transparency under nonreson. excitation, luminesc. and stimulated emission 0-11436
- diphenyl:pyrene, stimulated emission at 0-0 transition, 4.2K 0-11437
- diphenyl butadiene, absorption recovery lifetime, use in UV mode-locked lasers 0-19075
- diphenyl with pyrene cryst., self induced transparency self stimulated excitation (*Russian*) 0-14403
- 1,8-diphenyl-1,3,5,7-octatetraene, high press. fluoresc. studies of radiative and nonradiative processes 0-1011
- 1,6-diphenyl-1,3,5-hexatriene, high press. fluoresc. studies of radiative and nonradiative processes 0-1011
- 9,10-diphenylanthracene-toluene, soln., electron beam pulse radiolysis, energy transfer 0-7808
- diphenylethylene, UV spectra, quantum-mechanical investigation of isomerisation pathways 0-43065
- diphenylhaloselenium radical trapped in single crystals, FSR, struct. 0-44919
- 1,6-diphenylhexatriene, lower excited states fluoresc. quenching 0-1016
- 5,10-diphenylphenazine, in 3-methylpentane (ethanol) (PMMA), radiationless processes, temp. depend. 0-43087
- 4-diphenylphosphorylstibenes, fluoresc., photodimerisation 0-1015
- diphenylselenone crystals, gamma irradiation, ESR study of trapped phenylselenonyl radical 0-44917

## organic compounds continued

- dipropionyl peroxide, photochemical production of ethyl radical 0-3373
- dipropylammonium manganese tetrachloride, and tetrabromide, two-dimens. antiferromagnet, spin canting and exchange 0-34620
- 2,5-distyrylpyrazine, absorpt., Raman and fluoresc. spectrosc. 0-28049
- distyrylpyrazine, topochemically controlled solid-state polymerization 0-35532
- dithioformic acid, pot. for rot. about  $C(sp^2)-S$  bonds, ab initio calc. 0-23572
- divinyl benzene, topochemically controlled solid-state polymerization 0-35532
- divinyl benzene suspension, dielectrophoresis 0-3362
- dyenes, acyclic, non-conjugated, UPS comparison, obs. and calc. 0-32772
- DMSO- $PdCl_2$  complex semi-empirical INDO calc. of bonding 0-32611
- DNA-acridine dye complex, fluorescence studies 0-37921
- DOBAMBC, chiral smectic, flexoelectric effect and polarisation props. (*Russian*) 0-15002
- DOBAMBC, chiral smectic C-phase ferroelectric liq. crystal film, classical X-Y system, props. 0-44123
- DOBAMBC, dielec. props. near ferroelec. smectic A to C transition 0-45015
- DOBAMBC, ferroelec. liq. cryst., helical struct., elec. field depend. (*Japanese*) 0-38910
- DOBAMBC, smectic liquid crystal, ferroelectric, colour switching in elec. field 0-29719
- DODCI + malachite green (DQOCI), electronic energy transfer obs. 0-5633
- DODCI dye dissolved in glycerine, time delayed picosecond pulse transmission obs. 0-48355
- dodecane-tributyl phosphate solns., radiolysis, liquid products 0-40723
- DQOCI + DODCI, electronic energy transfer obs. 0-5633
- dulcitol, X-irrad., 4.2K, electron traps, alkoxy hyperfine coupling, ENDOR obs. 0-50863
- durane-naphthalene melt, exciton diffusion, percolation approach 0-2390
- dye, bleachable no.3955, relax. time meas., laser passive shutter appl. 0-23759
- dye, bleaching, coherence time meas. of laser radiation 0-23739
- dye, excited mol. decay near metal surface, energy transfer to plasmon surface polaritons 0-50440
- dye bleaching, no. 3955 in soln., relaxation and correlation times meas. 0-28281
- dye indicators of membrane pot., review 0-21594
- dye laser materials, PPP calcs., ground and excited states, triplet yields and efficiency 0-37743
- dye layer, adsorbed on ZnO cryst., charge transfer 0-49815
- dye molecules, two-photon absorpt. in laser fields with arbitrary statistical characts. (*Russian*) 0-37842
- dye solution, fluorescent, contact with metal electrodes, photovoltage generation, comprehensive model 0-40871
- dye solution, laser illuminated, light field phase conjugation, nonlinear interactions (*Russian*) 0-28266
- dye solution, nonlinear fluoresc. meas., two-photon pumping by low power laser 0-48037
- dye solution amplifying dynamic holograms, wavefront reversal 0-48331
- dye solutions, picosecond flash photolysis and very fast processes 0-30249
- dye ultrafast saturable absorbers for Nd lasers 0-53386
- dyes, absolute fluorescence quantum yield, calorimetric determ. 0-43092
- dyes, absorbing, for organic thin film refractive index adjustment 0-43413
- E. coli, light scatt., ribosomal subunit diffusion coeffs. 0-21438
- EBBA, binary systems with non-nematic solutes, phase transition behaviour and  $^1H$  NMR anal. 0-34174
- EBBA, metastable phases formed by rapid cooling of mesophase, IR and Raman spectra and DSC obs. 0-34919
- EBBA, polymorphism, radiothermoluminescence and differential scanning calorimetric study 0-24570
- EDTA-methylene blue photogalvanic cell, solar energy conversion and storage appl. 0-21406
- n-eicosane, freezing, control by natural convection 0-39262
- emulsion, hexadecane- $H_2O$ -butanol-Brij 96, drop dia., comp. depend. light scatt. obs. 0-45573
- emulsion, hexadecane- $H_2O$ -pentanol-Tween 60, drop dia., comp. depend. light scatt. obs. 0-45573
- eosin, photoacoustic spectra in soln. 0-9606
- epoxysilicon organic tar DFM-135 cement composition, internal friction meas. by composite oscill. method (*Russian*) 0-54312
- epoxytitanosilicon organic tar TK-75 cement composition internal friction meas. by composite oscill. method (*Russian*) 0-54312
- Erythrosine B, rot. diffusion from absorpt. relax. 0-1008
- ethane, ground state parameters and IR absorpt. spectra 0-47986
- ethane,  $H^+$ ,  $H_2^+$ , and  $H_3^+$  kinetic energy distrib., electron impact dissociation, time of flight mass spectra 0-32843
- ethane, liq., correl. function modelling, third order memory function method 0-7339
- ethane, localised molecular orbitals, orthogonal transformations calcs. 0-47892
- ethane, multipole moments and polarisabilities, SCF calcs. 0-5471
- ethane, nuclear spin-spin coupling consts., vicinal proton-proton coupling calcs. 0-32737
- ethane, shift of electronic spectrum during dissociation, CNDO calc. 0-37759
- ethane, thermodynamic props., use of high press. recycle-flow calorimeter 0-42228
- ethane, tropospheric and lower stratospheric vertical profiles 0-4073
- ethane, two-stage diagonalisation of Hamiltonian in CNDO/2 method 0-42946
- ethane, vibr. intensities, G sum rule appls. 0-32776
- ethane + CsF, rot. inelastic collisions, mol. beam meas. 0-1049
- ethane- $(d_6, d_3, d_1)$ , electro-optical parameters from IR intensities, least-squares calc. 0-9584
- ethane derivatives, diastereoselective form. and symm. props., semirigid mol. model 0-48099
- ethane gas, electron-mol. collision freqs. from breakdown data in crossed mag. field 0-43835
- ethane submonolayer on graphite, struct. and melting, elastic neutron scatt. 0-29266
- ethane- $Ar(N_2)$  binary and ternary mixtures, dielec. const., excess vol. 0-7254
- ethane- $CO_2(N_2)(SF_6)$  (tetrafluoromethane) mixtures, viscosity, diffusion coeffs. 0-1722
- ethane/ $H_2$  mixing ratio in Neptune stratosphere 0-51692



## organic compounds continued

ethanol, adsorbed on  $\text{Al}_2\text{O}_3$ , inelastic electron tunnelling spectra, surface vibr. struct. determ. 0-35572  
 ethanol, critical heat flux of saturated natural convection boiling with heating from below 0-10114  
 ethanol, glassy, electron trap relaxation model 0-15470  
 ethanol,  $\text{H}^\bullet$ ,  $\text{H}_2^\bullet$ , and  $\text{H}_3^\bullet$  kinetic energy distrib., electron impact dis-soc. ionisation, time of flight mass spectra 0-32843  
 ethanol, ion internal energy selection by angle-resolved mass spectrometry 0-53164  
 ethanol, surface reaction with Cu (100), EELS study 0-16728  
 ethanol fuel, octane booster for inferior regular unleaded gasoline 0-55783  
 ethanol fuel production from municipal cellulosic wastes using enzymatic hydrolysis 0-55779  
 ethanol glass, trapped and solvated electrons produced in presence of applied electric field 0-7379  
 ethanol vapour, isothermal Joule-Thomson coefficient, equation of state 0-24119  
 ethanol-benzene- $(\text{NH}_4)_2\text{SO}_4$ -water, liq. mixture, near tricrit. pt., light scatt. and sum rules 0-34933  
 ethanol-benzene-water- $(\text{NH}_4)_2\text{SO}_4$ , liq. mixture, near tricrit. pt., thermo-dynamic model and sum rules 0-34196  
 ethanol-normal hexane mixture, percolation model of electron and hole mobility 0-29452  
 ethanol-water, liq., Verdet const., pulsed mag. field meas. 0-16012  
 ethanol-water mixture, nonlinear acoustic coeff. meas., 0-50°C (French) 0-34142  
 ethene, optical synchrotron-Cherenkov radiation threshold effects 0-28154  
 ethers, saturated, bonded and nonbonded, quantum chem. calcs. 0-9514  
 N-p-ethoxybenzylidene-p'-cyanoaniline, nematic, mol. reorientation in DC elec. field, IR ATR spectra study 0-45064  
 ethoxyhexyltolan, Raman spectra, molecular conformational instability, internal field effects 0-54127  
 ethoxyoctyltolan, Raman spectra, molecular conformational instability, internal field effects 0-54127  
 p-p-ethoxyphenylazophenyl hexanoate, dielec. relax. in stable and metas-table solid phases 0-34851  
 ethyl acetate, multiphoton dissoc. by  $\text{CO}_2$  laser beam 0-7811  
 ethyl acetate, photoacoustic spectra meas. at  $\text{CO}_2$  laser wavelengths 0-18849  
 ethyl alcohol, electrification during laminar flow in metal pipe 0-6954  
 ethyl chlorophyllide a, electronic struct. props. and photosynthesis 0-16902  
 ethyl formate, microwave rot. spectrum, centrifugal distortion effects 0-52979  
 ethyl iodide, two-photon reson. ionis. spectra 0-28071  
 ethyl methyl ketone+cyclohexane, measurements of US vel. and density for determination of excess props. 0-37910  
 ethyl methyl sulphide, low freq. vibr. spectra, methyl torsional pot. func-tions and internal rot. 0-5543  
 ethyl methylketone+n-butanol, measurements of US vel. and density for determination of excess props. 0-37910  
 ethyl phenyl acetate, phosphoresc. and fluoresc. spectra in organic matrices 0-32756  
 ethyl radical,  $^{13}\text{C}_\alpha$  and  $\text{H}^\bullet$  hyperfine interactions, EPR spectra, vibr. anal. 0-23443  
 ethyl radical decomposition, mol. dynamics, trajectory studies 0-7780  
 ethyl vinyl ether, laser induced reaction, energy distrib. 0-16710  
 ethyl-trimethyl phosphines,  $(\text{C}_2\text{H}_5)_3\text{-P}(\text{E}^{\text{VB}}(\text{CH}_3)_3)_n$  ( $\text{E}^{\text{VB}}=\text{C}, \text{Si}, \text{Sn}$ ;  $n=0,1,2,3$ ), ( $^1\text{H}$ ,  $^{13}\text{C}$ ,  $^{29}\text{Si}$ ,  $^{31}\text{P}$ ,  $^{119}\text{Sn}$ ) NMR 0-32744  
 ethylacetate, CW laser induced reactions, activation energies, temps. and rate consts. 0-40710  
 N-ethylacridone, cryst. and mol. struct. 0-33988  
 ethylammonium tetrachloromanganate, dielec. props. in phase transition region 0-55011  
 ethylbenzene-nitrobenzene binary mixtures, with weak charge transfer interactions, thermodynamic props. 0-54360  
 ethylbenzocarbazole, soln., luminesc., effect of electronic excitation energy vibr. 0-55174  
 N-ethylcarbazole, soln., laser induced ionic photodissoc., transient polyelectrolyte form. 0-53068  
 ethyldiaminetetraacetate in the scala media, effect on cochlear pots. 0-16952  
 ethylene, adsorption and decomp. on Ni (111), high resolution EELS study 0-40739  
 ethylene, autoionisation and photoemitted electron ang. distrib., cylindrical mirror analyser study 0-18049  
 ethylene, core ionised, core-excited and shake-up states, ab initio MRD-CI methods 0-42950  
 ethylene, dehydrogenated adsorption on Ni (111), thermal desorption and AES study 0-29274  
 ethylene, electron affinities,  $\pi^*$  anion, bond lengths, electron transmission spectroscopy study 0-18925  
 ethylene, electron momentum distrib. in  $\pi$  orbitals from (e,2e) expts. 0-14239  
 ethylene, excited with parametric oscillator, vibr. relax. obs. and interpret. 0-9702  
 ethylene, Hartree-Fock energy and Moller-Plesset perturbation energy, harmonic vibr. freq. 0-52852  
 ethylene, ion ejection mass resolution test of wideband freq.-swept marginal oscillator detector for ion cyclotron reson. spectrometer 0-9069  
 ethylene, IR double reson. obs., external-resonator controlled Raman laser pumped by CW  $\text{CO}$  laser 0-9624  
 ethylene, IR multiphoton excitation, optoacoustic meas. 0-1038  
 ethylene, line selective excitation with  $\text{CO}_2$  laser light and vibr. relax. 0-9705  
 ethylene, magnetic susceptibility, frost model wavefunctions with p-type Gaussians 0-5477  
 ethylene, mol. and cluster Auger spectrum calc., SCF core-valence-valence spectra 0-48045  
 ethylene, mol. ion, mass spectra ion intensity internal energy depend., quasi equilibrium theory calcs. 0-53163  
 ethylene, multiphoton dissoc.,  $\text{CH}_2$  and  $\text{C}_2$  prod., fluence depend. meas. 0-5586  
 ethylene, multipole moments and polarisabilities, SCF calcs. 0-5471  
 ethylene, obtained from gas cylinder, particle size distrib. 0-55723  
 ethylene, ozonolysis, intermediate struct., multiconfig. SCF CI calcs. 0-18803  
 ethylene, ozonolysis, radical form., matrix ESR spectrosc. 0-16653

## organic compounds continued

ethylene, photoassisted decomposition at room temp. over  $\text{Pt/TiO}_2$  0-55703  
 ethylene, photoelectron spectrosc., ang. depend. 0-9641  
 ethylene, planar dissociation, electronic rearrangement, states, bonds, ab initio multiconfigurational SCF calcs. 0-27937  
 ethylene, quasidegeneracy and effective Hamiltonians, canonical trans-formation cluster expansion formalism 0-52888  
 ethylene, solid, phase diagram and NMR at high press. 0-11279  
 ethylene, solubility in liq.  $\text{N}_2$  0-39286  
 ethylene, surface interaction with transition metal atoms, MO calc. 0-6623  
 ethylene, UV photoelectron spectra, valence electron shake up approx. methods 0-18788  
 ethylene, vibr. intensities, G sum rule appls. 0-32776  
 ethylene( $-\text{d}_4$ ), Rydberg states assignments, electron energy loss spectra 0-53153  
 (ethylene) $_n$ , mol. crystals, quantum theory, mol. tight binding method calcs. 0-49572  
 ethylene adsorbed on Ag, photon-induced field ionisation mass spectroscopy 0-6639  
 ethylene cation, state geometries, electronic vibr. coupling consts., HF calcs., comparison with Xalpha calcs. 0-27946  
 ethylene dimer,  $\text{CO}_2$  laser induced photodissoc., pulsed mol. beam obs., van der Waals bond 0-9660  
 ethylene glycol, conformational anal., photoelectron spect. 0-43107  
 ethylene glycol on Teflon FEP, effect of drop size on contact angle 0-2245  
 ethylene oxide,  $^{13}\text{C}$  and D variants,  $\text{T}_2$ -relax.,  $2_{20}2_{11}$  rot. transition by microwave pulse spectrometer 0-47976  
 ethylene oxide, gas, EPR rot. transitions,  $\text{T}_1$  and  $\text{T}_2$  relax. 0-9622  
 ethylene V state, ab initio study of spatial extension 0-27952  
 ethylene-butane matrix, D atom bombardment, ethyl radical proton exchange reaction, indirect ESR obs. 0-16700  
 ethylene- $\text{O}_2$ , thermal electron attachment meas., microwave cond., pulse radiolysis 0-28592  
 ethylenediamine, solvated electrons, optical spectra and model potentials 0-30318  
 ethylmethylaniline, low freq., vibr. spectra, methyl torsional pot. functions, mol. struct. 0-43045  
 ethylperoxy radical+ $\text{NO}_2$ , reaction rate const. meas. 0-21262  
 excimer laser organic material forming quasi-one-dimensional crystals 0-23673  
 2-exo-acetoxy-7-anti-dinitrophenylthionorbornane, mol. and cryst. struct. 0-2007  
 fatty acid systems, Langmuir multilayer film, structure-dependent carrier transport obs. (Japanese) 0-20339  
 fatty acids, unsaturated, containing peroxide oxidation products, free radicals formed on UV irradi. 0-51165  
 fatty alcohol solid monolayers in  $\text{H}_2\text{O}$ , interface struct., model 0-54505  
 ferriochrome A, selective excitation double Mossbauer meas. 0-8015  
 1,1'-ferrocenedicarboxylic acid, triclinic, X-ray and neutron cryst. and mol. struct. determ. at 78 and 298K 0-29008  
 ferrous porphyrin, intermediate ( $S=1$ ) spin state, PMR characterisation 0-48014  
 flavanthrene molecules, stationary stochastic adparticle flip-flop as a precursor to surface diffusion 0-15371  
 p-fluoraniil,  $^{19}\text{F}$  NMR and spin-lattice relax. meas., pot. profile calc., mole. reorientation 0-29634  
 fluoranthene, single cryst. and in fluorene matrix, polarised absorption spectra, assignments 0-55122  
 fluoranthene-Rose Bengal, singlet-singlet energy transfer in Manoxol OT-cyclohexane-water 0-9531  
 fluorene: acridene, radical pair form. from excited states, optical nucl. polarisation obs. 0-14155  
 fluorene:pyrene- $\text{d}_{10}$ , exciton-guest, triplet-triplet annihilation, impurity traps effects 0-25433  
 fluorene:pyrene- $\text{d}_{10}$  cryst., magnetic resonance absorpt. of host-guest triplet paired centres 0-34750  
 fluorene,  $\gamma$ -irrad., void form. 0-2068  
 fluorene, cryst., phosphoresc. spectra and ODMR meas. 0-11470  
 fluorene, single cryst., dielec. matrix suspension, electroluminesc. 0-2862  
 9H-fluorene, soln., correl. times from  $^{13}\text{C}$  relax. 0-23438  
 fluorescein dye laser, solvation effects on tunability 0-53285  
 fluorescent molecules, stimulated spectra, excited state intramol. vibrs. 0-32717  
 fluorinated ethylenes, valence bond polar parameters, IR intensities, MO calc. 0-28013  
 fluoroacetylene, fund. and hot bands, laser microwave two-photon and double reson. spectroscopy 0-32752  
 fluoroanilines, isomers, thermodynamic functions and fundamental vibr. freqs. 0-9581  
 fluorobenzene, optoacoustic spectroscopy using cell with ultimate corrosion resistance 0-42269  
 fluorobenzene cations, fluoresc. quantum yields and lifetimes, electronic state relax. processes 0-48027  
 fluorobenzene radical cations, matrix laser fluoresc. spectra 0-1009  
 fluorobenzenes, negative ion states, comments and reply 0-32599  
 fluorocarbon foil, fluoroplast, homogeneity study (Polish) 0-35278  
 fluorocarbon-hydrocarbon mixtures press. second virial coeff., graph theory prediction 0-43823  
 fluorocarbons, press. second virial coeff., graph theory prediction 0-43823  
 fluorocarbons, press. second virial coeffs., walks on graphs method 0-7841  
 fluoroethanes, IR multiphoton dissoc., HF vib. energy distrib. 0-53073  
 fluoroethyl radical, unimol. dissoc., pot. energy characts. and energy parti-tioning calcs. 0-45488  
 fluoroethylenes, electron affinities,  $\pi^*$  anions, bond lengths, electron trans-mission spectroscopy study 0-18925  
 fluoroethylenes, IR multiphoton dissoc., HF vib. energy distrib. 0-53073  
 fluoroethylenes, variable angle photoelectron spectra, ionisation pot. asym-metry parameter 0-28064  
 fluoroform, quadratic force fields, MOCIC pot. functions calcs. 0-5475  
 fluoromethane,  $\nu_3$  band Lamb dips, effects of RF elec. field modulation on Stark spectra 0-52989  
 fluoromethane, excited state rot. spectroscopy and kinetics, appl. of tunable sub-MM sources 0-14162  
 fluoromethane, laser pumped, vibr. states collision dynamics fluoresc. obs. 0-53104  
 fluoromethane, laser pumped molecular lasers, sub MM laser expts. 0-1192



## organic compounds continued

fluoromethane, molecular pumping, thermal lens phenomena 0-9708  
 fluoromethane, optically pumped laser, IR-FIR transferred Lamb dip spectra 0-1193  
 fluoromethane+fluoromethane, collisionally induced relax. processes and vibr. energy transfer 0-53107  
 fluoromethane+HCl, IR spectra, intermol. interactions 0-9605  
 fluoromethane+OCS, rot. relax. parameters, microwave spectra linewidth parameters 0-28009  
 fluoromethane+SO<sub>2</sub>, collisionally induced relax. processes and vibr. energy transfer 0-53107  
 fluoromethane DFB gas laser, construction and operation 0-23715  
 fluoromethane TEM<sub>00</sub> far IR laser with integrated pump laser 0-43348  
 fluoromethane-d<sub>2</sub>, matrix isolated, vibr. energy transfer at low temps. 0-37860  
 fluoromethane-d<sub>3</sub>, vibr. energy transfer at low temps., inert gas and N<sub>2</sub> matrix obs. 0-9706  
 fluorometh.HF, H-bonded complex, ab initio calcs. (*French*) 0-52866  
 2-fluoronaphthalene, disordered form, thermal expansion, neutron and X-ray diffr. study 0-24621  
 2-fluoronaphthalene-2-naphthol system, phase relations, X-ray diffr. and DTA study 0-45287  
<sup>18</sup>F-5-fluorouracil; synthesis and purification by fractional sublimation 0-17134  
 fly ash and trace organic compounds anal., from municipal incinerators 0-45584  
 formaldehyde<sup>+</sup>, excited state dissociation, nonadiabatic interactions, conical and Jahn-Teller intersections, classical trajectory method 0-25997  
 formaldehyde, ab initio calcs., appl. of convergent SCF procedure 0-47875  
 formaldehyde, adiabatic CI pot. surface LCAO calc., gradient determ., mol. dynamics 0-48056  
 formaldehyde, atmos. composition, air over N.Germany coast, obs. 0-26584  
 formaldehyde, atomisation and bond energies, LMO calc., conjugation contrib. 0-9496  
 formaldehyde, bond polarity effect on other bonds and lone pairs, LMO calc. 0-9495  
 formaldehyde, ground state, potential energy surface 0-42967  
 formaldehyde, interstellar, excitation, effects of microwave background radiation observed spectrum 0-36681  
 formaldehyde, interstellar, form. rel. to interstellar dust new model 0-26934  
 formaldehyde, interstellar, kinematics and distrib. near Cone nebula and NGC 2264 IR source 0-4418  
 formaldehyde, microwave-microwave double resonance 0-53029  
 formaldehyde, multiphoton dissociation by CO<sub>2</sub> laser, intensity/fluence depend. 0-11913  
 formaldehyde, multiphoton dissociation, intensity depend. 0-28073  
 formaldehyde, predissociation, reson. multiphoton dissociation 0-53077  
 formaldehyde, solid soln. in Xe, precipitation, IR spectra obs. 0-45059  
 formaldehyde, T<sub>2</sub>-relax., rot. transitions, time resolved spectra, microwave pulsed spectrometer study 0-18846  
 formaldehyde, triplet instability, RPA calculations triplet instability, RPA calculations 0-27938  
 formaldehyde, triplet state g-tensors and hyperfine coupling tensors 0-52895  
 formaldehyde, vibrational band intensities of <sup>1</sup>A<sub>2</sub>-<sup>1</sup>A<sub>1</sub> transition, ab initio calc. 0-43028  
 formaldehyde+O, absolute rate consts., discharge flow and flash photolysis reson. fluoresc. meas. 0-55648  
 formaldehyde decomposing to H<sub>2</sub>+CO, reaction path Hamiltonian 0-45486  
 formaldehyde in giant molecular clouds, H<sub>2</sub> densities and <sup>12</sup>C/<sup>13</sup>C ratio 0-51837  
 formaldehyde in NGC 5128 (Centaurus A), 14 GHz absorpt. obs. 0-17657  
 o-formaldehyde in rho Ophiuchi dark cloud, excitation temp. and optical depths 0-51846  
 formaldehyde-<sup>13</sup>C, A<sup>1</sup>A<sub>2</sub>-X<sup>1</sup>A<sub>1</sub> system, UV absorpt. spectra, rot. anal. 0-9614  
 formaldehyde-d<sub>1</sub>, detect. in interstellar clouds 0-8670  
 formaldehyde-d<sub>1</sub> (-d<sub>2</sub>), single vibronic levels, fluoresc. emission, radiative lifetimes and vibr. relax 0-23521  
 formaldehyde-d<sub>2</sub>, reson. multiphoton dissociation 0-53077  
 formaldehyde-d<sub>2</sub> 733 μm line, Autler-Townes effect in laser interacting with RF field 0-53269  
 formaldehyde-d<sub>2</sub> vapour, IR-UV double resonance 0-43078  
 formaldehyde-H<sub>2</sub>O complex, IR spectrum in solid Ar, N<sub>2</sub> matrix 0-43042  
 formaldehyde.H<sub>2</sub>S(H<sub>2</sub>O) complexes, ab initio SCF MO calcs., binding energy dispersion contrib. 0-27967  
 formamide, geometry from ab initio calcs., rel. to N-methylformamide, acetamide, and N-methylacetamide 0-23338  
 formamide, IR spectra, amino group inversion transitions and pot. functions 0-43041  
 formamide, liq., vac. UV optical and dielec. meas. 0-25329  
 formamide, photoelectron spectrum, Green's function calcs., satellite lines 0-28061  
 (formamide)<sub>n</sub>, mol. crystals, quantum theory, mol. tight binding method calcs. 0-49572  
 formamide dimer, tritium β<sup>-</sup>-decay causing H<sup>+</sup> transfer, ab initio MO calc. 0-3391  
 formate esters-d<sub>1</sub>, Fermi reson. parameters 0-48103  
 formic acid, <sup>13</sup>C NMR spectra and relax. under intermediate decoupling power conditions 0-20515  
 formic acid, adsorption and surface reaction on metals 0-40741  
 formic acid, chemisorption and decomp. on Cu (100), EELS study 0-16729  
 formic acid, conform. hypersurface determ. and analysis 0-1078  
 formic acid, electron-density maps of bent bonds 0-1084  
 formic acid, H bonding, electronic struct., geometries, moments, dimerisation energies, charge distrib., pseudopotential calcs. 0-27942  
 formic acid, vibr. states, rot. and Coriolis parameters IR Fourier transform spectra 0-32709  
 formic acid amides, polarisabilities and π-π\* transitions, dipole interaction calcs. 0-23411  
 formic acid corrosion of ferritic steel, electrochem. pot. and Mo additions effect (*French*) 0-45439  
 formic acid dimer, tritium β<sup>-</sup>-decay causing H<sup>+</sup> transfer, ab initio MO calc. 0-3391

## organic compounds continued

formyl chloride, equilib. geometries and one-electron props., ab initio calcs. 0-47878  
 formyl fluoride, and isotopic forms, mol. struct., from electron diffr. and microwave data 0-23570  
 formyl fluoride, equilib. geometries and one-electron props., ab initio calcs. 0-47878  
 formyl radical, -d<sub>0</sub>, (-d<sub>1</sub>), first ionis. pot., photoelectron spectrosc. determ. 0-48039  
 formyl radical, electronic struct., dissociation energy and pot. energy surface many body perturbation theory and couple cluster doubles calc. 0-23296  
 formyl radical, laser mag. reson. spectrum at 5.3 micron 0-47981  
 Freon 123-d and natural 123, selective absorpt. cross section at 10.2 and 10.6 μm 0-5546  
 Freon 14, roto-vibr. mol. laser, low-temp. performance 0-9871  
 Freon F-13V1, specific heat standards choice and certification, for liquids and vapours in 90 to 273.15K range 0-23877  
 Freon gas flow around blunt object, bow shock instability 0-10266  
 Freon plasma, Si plasma etching, microelectronics appls. 0-3080  
 fucose, optical constants and dispersion eqns. 0-30762  
 furan, adsorbed on NaCl, evidence of new condensed phase, IR spectra (*French*) 0-16028  
 furan, photoacoustic spectra meas. at CO<sub>2</sub> laser wavelengths 0-18849  
 galvinoxyl radical in phenol matrix, ESR spectra 0-54950  
 gelatine, effect on lifetime and formation of latent image in photographic layers (*Russian*) 0-3389  
 glutaric acid-polyoxyethylene eutectic, melting and crystn. 0-28924  
 glycerin, aq. soln., heat transfer in oscillating liquid-filled cylinders 0-10117  
 glycerine, thermal diffusivity, constant-rate heating method (*Japanese*) 0-6570  
 glycerol, cryst. and glassy states, sp.ht. 0-2176  
 glycerol, Mossbauer and neutron scatt. 0-20559  
 glycerol, natural convection from temp. fields in spherical partially filled vessel 0-1561  
 glycerol-d<sub>3</sub> (-d<sub>2</sub>), compressed viscous liq., reorientational motion, NMR obs. 0-7183  
 1-glyceryl 1-octanoate-water-CsCl, Cs<sup>+</sup>H<sub>2</sub>O interaction in lamellar phase, NMR quadrupole splitting and chemical shift 0-50209  
 γ-glycine, cryst. struct. by neutron diffr. at 83K and 298K 0-35825  
 α-glycine, deuterated, low freq. intermol. modes, neutron diffr. obs. 0-15086  
 glycine silver nitrate, dielec. relax. in paraelec. and ferroelec. phases 0-29678  
 glyoxal, internal conversion, energy redistrib. 0-53036  
 glyoxal, singlet-triplet coupling, double reson. and level-anticrossing spectroscopy 0-48053  
 glyoxal, vibr. energy redistrib. following internal conversion 0-23452  
 glyoxal (<sup>1</sup>A<sub>1</sub>), fluoresc. quantum yields, radiative and nonradiative lifetimes 0-32759  
 guanidinium aluminium sulphate hexahydrate:Fe<sup>3+</sup>, EPR spectra, angular var. calc. 0-54940  
 guanidinium vanadium sulphate hexahydrate, singlet ground state system, low temp. mag. props. 0-44843  
 guanine tautomers, relative stabilities, nonempirical MO calcs. 0-21442  
 haeme proteins and metalloporphyrins, redox chem. and oxygen binding 0-3573  
 haemoglobin, dielectric transient response following UV-irradiation 0-51166  
 halides, aryl and aryl-alkyl 193 nm photodissoc., fragment translational energy distrib. 0-48048  
 halo-alkanes, IR-microwave double resonance, book contrib. 0-54997  
 haloaceneaphthenes in n-heptane, quasi-line phosphoresc. spectra, vibronic spin-orbit interaction 0-43096  
 haloacetylene cations, electron impact excitation A→X band system assignment 0-32766  
 haloanilines+thionine triplets, electron transfer reaction, radical yield meas. 0-3330  
 halobenzenes, aqueous molar solubilities and partitioning, 25°C obs., rel. to melting pts. 0-40803  
 halocarbons, atmospheric global distrib., sources and sinks, rel. to O<sub>3</sub> depletion 0-4088  
 halomethane+Hg, <sup>3</sup>P<sub>1</sub>-state total quenching 0-52927  
 halomethane+O(<sup>1</sup>D), direct reaction in flow system 0-3333  
 halomethanes, <sup>13</sup>C chem. shifts, trigonal additivity procedure 0-1002  
 halomethanes, synchrotron radiation photoabsorption cross sections, Rydberg states 0-28033  
 halomethanes, UV multiphoton dissociation, photofragment fluoresc. 0-14165  
 halomethanes in troposphere and stratosphere, O<sub>3</sub> depletion 0-16866  
 halonaphthalenes, intersystem crossing-singlet excited state to triplet state spin sublevel 0-53035  
 2-haloacrylates, liq., dielec. relax. and permittivity 0-15948  
 HBPA, smectic liq. cryst. glass-supercooled transition and Debye temp., <sup>57</sup>Fe Mossbauer effect 0-54999  
 heart cytosol, aspartate transaminase, electron density map interpretation 0-55990  
 heptafluoroiodopropane, photodissoc., appl. in I ring laser 0-48236  
 n-heptane, electrification during laminar flow in metal pipe 0-6954  
 n-heptane, Townsend primary and secondary ionisation coeffs. and sparking voltages 0-1732  
 n-heptyl alcohol in tetrachloromethane, cyclohexane, measurements of US vel. and related parameters 0-38200  
 4-n-heptyl-4'-β-cyanovinylbiphenyl, liq. cryst., isotropic mechanism of mol. rot., dielec. permitt. meas. 0-10491  
 4-n-heptyl-4'-cyanobiphenyl, linear dichroism spectra in nematic and isotropic phases 0-25336  
 4-heptyl-4'-cyanobiphenyl, nematic liq. cryst., alignment on surfactant treated obliquely evaporated surfaces 0-49092  
 p-heptyl-p'-cyanobiphenyl, refractive index, dielec. const., mag. susceptibility, orientational ordering (*Dutch*) 0-33884  
 4-n-hexyloxyphenyl 4-n-hexyloxybenzoate, liquid crystal, freezing polarisation, electret effect (*Polish*) 0-10496  
 heteroaromatic molecules, planar, orientation and phosphoresc. polarisation in stretched film 0-14169  
 heteroaromatic molecules, radiationless conversion processes, regularities 0-14171  
 heterocyclic liquids, US attenuation in 10 to 1300 MHz range 0-39229  
 heterocyclic N compounds, radiationless transitions, isotope effects 0-48033



## organic compounds continued

- heterocyclic N-containing compounds, crysts., intermol. pots. calcs. 0-49169  
 hexachlorobenzene, quadrupole spin echo envelope EFG tensor axisymmetry in mag. field 0-20497  
 hexachloroethane, orthorhombic, neutron struct. refinement 0-29009  
 hexafluoro ethyl cation fragmentation, mass spectrometry 0-53070  
 hexafluoroacetone, IR multiphoton decomposition, press., fluence, wavelength, temp. depend. 0-7809  
 hexafluoroacetone, IR multiphoton dissociation, isotopic selectivity and yield, temp. effect 0-53069  
 hexafluorobenzene, in liquid binary mixtures of optically anisotropic molecules, depolarized Rayleigh scatt. 0-40122  
 hexafluorobenzene-benzene, liq., mol. interactions, IR and Raman line-shape obs. 0-28907  
 hexafluorobenzene-benzene mixture, percolation model of electron and hole mobility 0-29452  
 hexafluorobutene, vibrational broadening, dense fluid region, Raman and NMR study 0-43056  
 hexafluoroethane, RF discharge chemistry, added H<sub>2</sub> effect 0-33832  
 hexafluoropropene, struct. and vibr. spectra, IR, Raman polarisation study 0-18845  
 hexamethyldisiloxane-Ar, glow discharge positive column ion mass spectra identification 0-38834  
 n-hexane, liq. trapped electron photoionis., photocond. 0-2418  
 hexane, liquid, chain reorientation, Brownian dynamics simulation, comparison of models 0-49067  
 n-hexane, mass selective storage mass spectra by quadrupole ion storage mass spectrometer 0-52351  
 n-hexane, shock compression, dynamic high press. eqns. of state 0-6450  
 n-hexane, Townsend primary and secondary ionisation coeffs. and sparking voltages 0-1732  
 n-hexane induced changes in visual evoked pots. and ERG of industrial workers 0-45886  
 hexane-ethanol mixture, percolation model of electron and hole mobility 0-29452  
 n-hexane-nitrobenzene crit. mixture, in ultracentrifuge, dynamic phenomena 0-44310  
 hexane-nitrobenzene soln., dielec. permitt. in two-phase region 0-2682  
 hexane-nitrobenzene solution, double-scatt. light intensity near critical point of mixing (*Russian*) 0-55117  
 n-hexatriacontane, cryst., orthorhombic modification, vibr. spectra 0-50314  
 n-hexatriacontane, suitability as model cpd. for cond. band struct. of polyethylene 0-16131  
 hexatriacontane single cryst., elec. cond. and dielec. breakdown 0-6849  
 n-hexyl 4'-n-decyloxybiphenyl-4-carboxylate, smectic C phase, tilt angle using electron reson. spectroscopy 0-33886  
 4-n-hexyl-4-cyanobiphenyl, liq. cryst., isotropic mechanism of mol. rot., dielec. permitt. meas. 0-10491  
 4-n-hexyloxybenzylidene-4'-n-hexylaniline, liquid crystal, exam. of orientation order of dissolved molecules 0-44112  
 p-hexyloxyphenyl-p-pentoxybenzoate, nematic liq. cryst., elec. discharge meas. of persistent internal polarisation 0-10488  
 histidine quenching of fluoresc. of tryptophan, indole solns. rel. to pH 0-2826  
 histones, H2A and H4, effect of molecular interactions on fluorescence intensity 0-51032  
 HMTSF-TNAP, microwave cond. at 35 GHz 0-24963  
 HMTSF-TNAP, one-dimens. conductor, transport props. 0-20165  
 HOAB, chain ordering model 0-24357  
 HOAB, thermotropic mesophase, DMR chain segments assignment 0-24356  
 horseradish peroxidase, transport in  $\gamma$ -irrad. brain tissue 0-41119  
 humic acid sorption of actinide cations, effect on radioactive waste storage 0-13715  
 hydrazine derivatives, adsorption on Al surface, inhibiting dissoln. in HCl soln. 0-50759  
 hydrazine monohydrate, <sup>14</sup>N NQR, echo envelope modulation obs. 0-50218  
 hydrazoic acid, electron-density maps of bent bonds 0-1084  
 hydrazones, protonation energy and basic strength 0-37719  
 hydrocarbon bearing anticlines, pattern space of seismic anomalies, location tool and theory 0-17234  
 hydrocarbon chains, stability of lyotropic phases 0-24359  
 hydrocarbon liquids, electrostatically charged, incendivity of sparks from surface 0-6303  
 hydrocarbon liquids, streamer breakdown in divergent field 0-25308  
 hydrocarbon permeation through polyethylene membrane 0-30281  
 hydrocarbon turbulent diffusion flame, flame-zone model anal. 0-16684  
 hydrocarbons, atmospheric global distrib., sources and sinks, rel. to O<sub>3</sub> depletion 0-4088  
 hydrocarbons, bond functions, for ab initio calcs. 0-5469  
 hydrocarbons, coating nuclear fuel particles for HTR (*German*) 0-18585  
 hydrocarbons, conjugated, heat of formation and reson. energies 0-7839  
 hydrocarbons, diffusion, sorption, solubility, permeation in polyvinyltrimethylsilane (*Russian*) 0-6564  
 hydrocarbons, dipole moments, NDDO calcs. 0-47894  
 hydrocarbons, effective Hamiltonians for atomic pot. transferability 0-42933  
 hydrocarbons, electric polarisability, in excited singlet and triplet states (*Bulgarian*) 0-52897  
 hydrocarbons, formation on metal surfaces in fusion reactors 0-21322  
 hydrocarbons, gas phase oxidations and pyrolysis, wall-less reactor technique 0-45500  
 hydrocarbons, glass transitions, cellulose blotter/torsion pendulum technique, for relax. determ. 0-54357  
 hydrocarbons, heavy liq., vapour press. and enthalpies of vaporisation by group-contrib. method 0-40726  
 hydrocarbons, liquid, high-field carrier transport at pre-breakdown and breakdown regions 0-25305  
 hydrocarbons, long chain, interstellar formation mechanism expt. 0-46653  
 hydrocarbons, mol. Raman intensities calcs. 0-52993  
 hydrocarbons, NMR parameters, chem. shielding, <sup>13</sup>C chem. shifts 0-23435  
 hydrocarbons, normal, mass-spectrometric fragmentation processes, quantum field theory 0-40782  
 hydrocarbons, pool boiling, heat transfer, surface roughness effect 0-48705  
 hydrocarbons, press. second virial coeff., graph theory prediction 0-43823

## organic compounds continued

- hydrocarbons, press. second virial coeffs., walks on graphs method 0-7841  
 hydrocarbons, reactions, rate consts., temp. depend., photolysis, high temp. fast flow reactor technique 0-42231  
 hydrocarbons, saturated, bonded and nonbonded, quantum chem. calcs. 0-9514  
 hydrocarbons, saturated open-chain, transport behaviour of excess electrons and props. 0-39643  
 hydrocarbons, shock compression, dynamic high press. eqns. of state 0-6450  
 hydrocarbons, sorption, diffusion, solubility in polyvinyltrimethylsilane rel. to temp. (*Russian*) 0-6565  
 hydrocarbons, vibr. intensities, G sum rule appls. 0-32776  
 hydrocarbons decomposition reaction, with Ta and  $\alpha$ -Hf, surface segregation influence of O<sub>2</sub> or N<sub>2</sub> 0-55654  
 hydrocarbon chain synthesis in interstellar clouds, ion-molecule scheme 0-12786  
 hydroquinone, oxidation of centre of photographic development, electrochem. kinetics (*Russian*) 0-3367  
 15-hydroxy prostaglandin dehydrogenase activity in tissues of mice, X-irrad. effects 0-51169  
 8-hydroxy quinoline, single cryst. growth from cyclohexane-water immiscible system 0-40244  
 2-hydroxy-3-(2-undecyl, pentadecyl or heptadecyl amidoethylamine) propane-1-triethyl ammonium hydroxides, acid-corrosion inhibitors, effect on corrosion of low C steel in HCl 0-50761  
 hydroxy-tetraazaindenes for photographic emulsion supersensitization 0-3384  
 hydroxyapatite, automated scan of X-ray powder diffraction pattern 0-22492  
 2-hydroxybenzophenone, excitation singlet, internal H<sup>+</sup> transfer, visible spectra 0-32728  
 ortho-hydroxybenzophenone, soln., intramol. proton transfer and energy relax. photostability, transient absorption obs. 0-28032  
 3-hydroxyflavone, excited state proton transfer, luminesc. 0-35818  
 tris(hydroxymethyl)aminomethane, enthalpy of reaction meas. microprocessor-controlled system 0-22361  
 hydroxymethylene radical cation stability, CH<sub>2</sub>O<sup>+</sup> isomers, ab initio MO study 0-42965  
 hypohalites, electron structure, stability and reactivity 0-14086  
 IBPBAC, smectic phases, self-diffusion coeffs., radiotracer meas. 0-49394  
 imidazole, Z-irrad., EPR study of H exchange 0-40718  
 imidazoles, reaction with photochemically generated  $\alpha$ -hydroxyalkyl radicals, EPR study 0-35558  
 imipramine, automated synthesis of <sup>11</sup>C-labelled radiopharmaceuticals 0-17133  
 indenol[2,1-a]indene, in glassy media, phosphoresc., heavy atom effects 0-55153  
 indigo dyes, triplet state config., laser flash absorpt. spectrosc. obs. 0-5557  
 indium oxine (<sup>111</sup>In), cell damage resulting from labelling rat lymphocytes and HeLa S3 cells 0-56145  
 indole soln. containing histidine, fluoresc. rel. to soln. pH 0-2826  
<sup>11</sup>C- $\alpha$ -p-iodoanilinophenylacetone, conc. of activity in brain 0-3776  
 o-iodohippurate, <sup>131</sup>I labelled, in vitro stability 0-16668  
 iodomethane, RF field dressed mol. saturated absorpt. obs. 0-9648  
 iodomethane, vibr., rot. and translational energy exchange, semiclassical theory 0-48067  
 iodomethane+F, IF product internal rot.-vibr. distrib., fluoresc. obs. 0-48078  
 iodomethane+F reactions, product state analysis using laser-induced fluorescence 0-11915  
 iodomethane-d<sub>3</sub>, Stark tuned level crossings and saturated absorpt., RF elec. field modulation effects 0-52989  
 1-iodopropane, photoionisation mass spectrometry 0-40779  
 iodoseptofluoropropane photodissoc. laser, refr. index distrib. fields, double exposure holography 0-9873  
 iodotrifluoromethane, E-species force consts., using L-F approx. method, HLFs applicability 0-962  
 iodotrifluoromethane, IR multiphoton dissoc., source of trifluoromethyl radicals 0-26036  
 ions, pot. energy profiles for unimol. reactions 0-43210  
 iron (4,7-dimethyl-di-1,10-phenanthroline)(NCS)<sub>2</sub>, spin state transition, X-ray and Mossbauer obs. 0-7195  
 iron formate dihydrate, higher order term of uniaxial anisotropy (*Japanese*) 0-2571  
 iron phthalocyanine cathode, performance in fuel cells with H<sub>2</sub>SO<sub>4</sub> electrolyte 0-21293  
 isobutane+methylal+Ar, drift properties of tubular drift chambers in high magnetic fields 0-53917  
 isobutene+HF, vibr. relax. dye laser pumping effects 0-9703  
 isobutylene, photoelectron spectrosc., ang. depend. 0-9641  
 isobutyric acid and water, shear viscosity of critical mixture, amplitude ratios 0-2188  
 isobutyric acid-water, crit. mixture, conc. fluctuation mean relax. time, US absorpt. and vel. meas 0-29163  
 isobutyric acid-water, crit. mixture 0-24601  
 isobutyric acid-water, mixture, heat of transport, crit. exponent 0-15277  
 isobutyric acid-water mixture critically quenched, phase separation and coalescence 0-24581  
 isocyanates, nonbonding and  $\pi$ -orbital interactions, photoelectron spectra 0-32774  
 isocyanic acid, molecular structure and centrifugal distortion constants 0-47974  
 isooctane-nitromethane, liq. mixture, coexistence curve, refr. index meas. 0-10655  
 isopropyl alcohol, glass transition rel. to press. depend. of viscosity 0-34171  
 isoquinoline, dil. soln., dielec. absorpt., relax. and thermodynamic parameters meas. 0-50258  
 isothiocyanic acid, H<sup>15</sup>NCS, HN<sup>13</sup>CS and HNC<sup>34</sup>S, ground state spect. constants and molecular struct. 0-47973  
 isothiocyanic acid, interstellar detect. in Sagittarius B2, mm wave spectrum 0-41878  
 isothiothiocyanates, nonbonding and  $\pi$ -orbital interactions, photoelectron spectra 0-32774  
 isotopically mixed organic solid, electronic energy transfer, Anderson transition 0-44545  
 isotopically modified compounds, nomenclature 0-3294



## organic compounds continued

- in Jilin meteorite 0-17557  
kerogen-like compounds, possible presence in Trojan asteroids 0-56751  
ketene,  $\text{CH}_3$  photoproduct, wavelength depend. 0-11936  
ketene, multiphoton dissociation,  $\text{CH}_2$  and  $\text{C}_2$  prod., fluence depend. meas. 0-5586  
ketocyanines alcohol solns., spectral-luminesc. props. 0-2835  
ketones, effect of polyethylene, environmental stress relax. study 0-45336  
ketones, solns., IR absorpt. band parameters rel. to temp. 0-2762  
lactam-lactim tautomeric equilibria, quantum chem. calcs. 0-50833  
laser, limiting length, stimulated radiation reabsorpt. by unexcited and excited singlet mols. 0-48240  
lasers, organic cpds. as active media (*Russian*) 0-38015  
lead formate, intermolecular shielding contributions, proton mag. shielding 0-34783  
lecithin, optical constants and dispersion eqns. 0-30762  
leuco dye+biimidazole photochem. reaction, modulation by photopolymerisation 0-40714  
lindane, organic water pollutant, influence of detergents on hydrosolubility and suspension (*French*) 0-7961  
linear chain cpds., diffuse  $4k_F$  refls., small intramolecular Coulomb interaction 0-34376  
lipid composition of marine aerosols, sea surface microlayer and subsurface water 0-17297  
lipid function in excitable membranes 0-12095  
lipid-rhodopsin interactions in photoreceptor membranes 0-12094  
lipids in aquatic sediments, Recent and ancient 0-51583  
liquid, simple, struct. exam. and scatt. data interpret. 0-54096  
liquids, interdependence of specific acoustic impedance and surface tension (*Polish*) 0-39223  
liquids, thermal conductivity meas., radiant heat exchange effect 0-19996  
lithium acetate dihydrate, nearly free methyl rotors, rot. energy states, nucl. reson. props. 0-34784  
lithium ammonium tartrate monohydrate, isostructure with lithium potassium tartrate monohydrate:  $\text{Mn}^{2+}$ , EPR obs. 0-29607  
lithium ammonium tartrate monohydrate, Raman spectra, anomalous low-lying response 0-2746  
lithium formate biaxial crystal, nonlinear conical refr. obs. in harmonic generation 0-23745  
lithium formate monohydrate, thermal dehydration, dislocation effects 0-3331  
lithium perfluoro-octanoate-water, liquid crystal,  $^{19}\text{F}$  multipulse NMR obs. 0-34795  
lithium potassium tartrate monohydrate:  $\text{Mn}^{2+}$ , isomorphism with lithium ammonium tartrate monohydrate, EPR obs. 0-29607  
long chain paraffins, thermodynamic functions, Monte Carlo method appl. (*German*) 0-19962  
low frequency anharmonic vibrations, pot. function determ., Raman and IR spectra obs. 0-52997  
lucensomycin interacting with phosphatidylcholine-cholesterol vesicles, PMR obs. 0-40954  
2,6-lutidine-water mixture, critically quenched, phase separation and coalescence 0-24581  
lyotropic nematic liquid crystals, mag. susceptibility, mol. aggregation meas. 0-19690  
magenta pigment, photoconducting, electric field-induced fluoresc. quenching 0-34967  
magnesium platino-oxalate, one-dimens. conductors, prep., struct. and elec. cond. 0-24900  
malachite green+DODCI, electronic energy transfer obs. 0-5633  
malonic acid, phase transition at 360K, IR study 0-44311  
malononitrile, displacive phase transition, 294.7K, Raman and Brillouin-Rayleigh scatt. obs. 0-16047  
manganese zinc formate dihydrate, two-dimens. antiferromag., anomalous crit. phenomena, neutron scatt. and PMR obs. 0-50104  
Manoxol OT-cyclohexane-water reversed micellar system, singlet-singlet energy transfer 0-9531  
MBAB, liq. cryst., Brillouin-Mandelstam light scatt. and refr. index 0-55119  
MBBA, dielectric permitt. rel. to molecular props., effect of anisotropy of medium and local field 0-25270  
MBBA, dynamic critical behaviour in NLC above nematic-isotropic transition 0-49096  
MBBA, HF electrohydrodynamic instability in NLC (*Russian*) 0-54130  
MBBA, metastable phases formed by rapid cooling of mesophase, IR and Raman spectra and DSC obs. 0-34919  
MBBA, nematic, EHD transitions, white noise effects 0-6159  
MBBA, nematic liq. crys., refractive index distrib. and mol. alignment in electro-optical effect (*Japanese*) 0-20613  
MBBA, nematic liq. cryst., nonlinear optical suscept. using light combination scatt. (*Russian*) 0-38064  
MBBA, nematic liq. cryst. isotropic phase, phase-conjugate refl. by degenerate four-wave mixing 0-43389  
MBBA, nematic liquid crystal, omeotropically aligned thin slice, dielectric permeability (*Italian*) 0-6354  
MBBA, nematic liquid crystals, wave number spectrum of dissipative structures 0-38904  
MBBA, nematic-isotropic transition, intermolecular forces, IR  $\text{N}_2\text{O}$  mol. probe obs. 0-29155  
MBBA, pure and mixed with benzene (chlorobenzene), nematic-isotropic transition, US absorpt., visual hysteresis 0-54355  
MBBA, refractive index, dielec. const., mag. susceptibility, orientational ordering (*Dutch*) 0-33884  
MBBA-BBCA-cholesteryl chloride, field induced nematic-cholesteric relax. processes, transient helical pitch 0-38906  
MBBA-n-heptane system, thermodynamic functions in lattice model (*Russian*) 0-33887  
MBBA/EBBA, nematic, mol. interaction energy 0-33881  
MBBA/EBBA binary liquid crystal mixture, US absorpt. and vel. dispersion, phase transition and alignment effects (*Korean*) 0-29121  
2-mercaptobenzimidazole, corrosion inhibition on Cu, XPS and X-ray induced Auger spectra obs. 0-40600  
2-mercaptobenzothiazole, corrosion inhibition on Cu, XPS and X-ray induced Auger spectra obs. 0-40600  
merocyanine dyes, non-photochromic, for autoprocesor reprography system 0-35555  
metaldehyde, cloud seeding expts., Fujian province, China (*Chinese*) 0-46235  
metaldehyde particles, fluid-breaking, ice nucleation (*Chinese*) 0-12468  
metallo-octaethyl porphyrins, I oxidation products, metallic cond., EPR and reson. Raman spectra 0-29610

## organic compounds continued

- metalloporphyrins, photoelectrochemical props. 0-50991  
metalloporphyrins, reson. Raman spectra, intra- and inter-manifold couplings interference 0-28020  
methane,  $3\nu_3$  band in Saturn's atm., seasonal phenomena detect. 0-26803  
methane, 7300 Å band obs. of Uranus disk structure 0-17544  
 $^{13}\text{C}$ -methane,  $\nu_1$  fund., quasi-CW inverse Raman spectra 0-48004  
methane,  $\nu_1$  line contour anomalous behaviour on pressure changes (*Russian*) 0-43052  
methane,  $\nu_3=1$  state, dipole moment and IR-radiofrequency double reson. spectra 0-14161  
methane,  $\nu_3$  P(6) transition, Doppler-free intracavity polarisation spectroscopy 0-5537  
methane,  $\nu_4$  band, high resolution spectrosc. 0-5529  
methane,  $\nu_4$  band Q-branch spectrum 0-5530  
methane,  $\nu_4$  fundamental, Q and R branch absolute line intensities 0-5539  
methane, (methane-Xe)(methane- $\text{NH}_3$ ), mol. relax., optoacoustic reson. meas. 0-27351  
methane, ab initio calcs., appl. of convergent SCF procedure 0-47875  
methane, absorption spectrum,  $\text{LiF F}_2^+$ -centre laser intracavity spectroscopy appl. 0-32999  
methane, adsorbed on graphite, NMR pulsed field gradient method, diffusion coeff. meas. 0-15362  
methane, adsorbed on graphite, orientational phases, Monte Carlo calc. 0-2263  
methane, adsorption on BN and graphite in first monolayer domain, thermodynamic props. (*French*) 0-29275  
methane, adsorption on graphite, substrate deform. meas. 0-54520  
methane, adsorption potential on NaCl cryst. surface 0-24739  
methane, bonding, electron pairs, size and shape parameters, Gaussian basis set MO calcs. 0-27935  
methane, clusters, collision induced polarisability, mol. frame distortion 0-32798  
methane, combustible gas production from organic wastes using bacteria 0-7898  
methane, compressed gas, apparatus for depolarisation ratio meas. of scatt. light 0-38527  
methane, compressibility isotherms, thermodynamic props., 0 to 150°C 0-6196  
methane, CW vibr. photochem. for D enrichment, economic aspects 0-11920  
methane, desorption, from Cu surface, production and meas. of atomically clean surface environment 0-52250  
methane, elastic and inelastic electron scatt. differential cross section, obs. and calc., struct., binding energy 0-28110  
methane, electron pair interactions calcs. 0-23298  
methane, electron transmission function and mean energy per ion pair, obs. 0-23566  
methane, electronic density, multiple scatt. method, muffin-tin approx. 0-27924  
methane, energy transfer obs. using excitation of fund., overtone and combination bands 0-9704  
methane, fluid, electron mobility, density and temp. effects 0-10351  
methane, frequency stabilisation of 0.633 $\mu\text{m}$  line with 3.39 $\mu\text{m}$  line locked to saturated absorpt. line 0-28258  
methane,  $\text{H}^+$ ,  $\text{H}_2^+$ , and  $\text{H}_3^+$  kinetic energy distrib., electron impact dissociation, time of flight mass spectra 0-32843  
methane, high-resolution CARS, press. depend. of intensity 0-9964  
methane, identification in atmosphere of Triton from IR spectrum 0-21945  
methane, intradoppler CARS saturation spectroscopy 0-43057  
methane, ion internal energy selection by angle-resolved mass spectrometry 0-53164  
methane, IR spectral atlas for 1120-1800  $\text{cm}^{-1}$  region 0-23415  
methane, large angle elastic and inelastic electron scatt. differential cross section, exchange corrections 0-28111  
methane, line profile of coherent radiation in separated fields due to  $\text{F}_2^{(2)}$  transition 0-37835  
methane, liq., drift vel. of excess electrons 0-54744  
methane, liq., mol. dynamics simulation using singularity-free algorithm 0-54116  
methane, liquid, Brillouin scatt. obs., US vel. and absorpt. 0-45085  
methane, mol. and cluster Auger spectrum calc., SCF core-valence-valence spectra 0-48045  
methane, narrow reson., elastic scatt., spectroscopic studies 0-53094  
methane, nuclear spin-spin coupling consts., finite perturbation-CI calcs. 0-5563  
methane, nuclear steam reforming for coal gasification 0-55775  
methane, obs. in IR spectra of Uranus, Neptune and Titan (0.8 to 2.5 microns) 0-21946  
methane, photoelectron ang. distrib., near threshold to 30 eV, photon energy depend. 0-53045  
methane, pulsed photoacoustic Raman spectrosc., gaseous trace anal. 0-40769  
methane, rotational partition function, isotope effects 0-14130  
methane, saturated absorpt. reson. shape, geometry and field intensity effects (*Russian*) 0-32778  
methane, scaled Raman pulse compression experiments at 248 nm, KrF pump laser 0-38071  
methane, slow electron scatt., rigid mol. model with exchange and polarisation 0-43194  
methane, solid, discontinuous orientational phase transitions, thermodynamics, isotope effects 0-6590  
methane, solid, high press. NMR obs. 0-50214  
methane, solid, Raman spectra and II-III phase transition 0-2745  
methane, steam reforming for H production, kinetic anal. 0-35788  
methane, stimulated Raman scatt. obs. 0-53003  
methane, stored energy needed to ignite by discharger from charged person 0-54063  
methane, thermodynamic perturbation theory 0-14985  
methane, torsional ground state splitting in cryst. field 0-15019  
methane, vibration-rotation energies,  $2\nu_2$  and  $\nu_2+\nu_4$  bands 0-47963  
methane, vibration-rotation energies of harmonic and combination levels 0-47962  
methane, volcanic hydrothermal vents from E. Pacific rise,  $\text{H}_2$  and  $\text{CH}_4$  content 0-41422  
methane+Ar, rot. compound state reson. 0-28090  
methane+ $\text{BCl}_3$  reaction, laser-induced, vibr. excitation influence on reactivity, isotope selectivity 0-11921



## organic compounds continued

- methane + Be<sup>+</sup> collisions, autoionising core-excited Be II states, alignment prod. 0-14204  
 methane + Cd(5<sup>3</sup>P<sub>0,1</sub>), absolute quenching cross sections 0-5604  
 methane + CH<sub>3</sub><sup>+</sup>, condensation reactions mechanism 0-25996  
 methane + Cl(<sup>2</sup>P) → CH<sub>3</sub> + HCl, reaction rate const., laser flash photolysis-resonance fluoresc. kinetic study 0-45485  
 methane + CO, vibr. relax. rates, energy transfer 0-37862  
 methane + d<sub>2</sub>, Ar vibr.-vibr. energy transfer process diagnostics 0-32807  
 methane + H<sub>2</sub>O, interaction energy calc. using minimal basis sets 0-9678  
 methane + I, excited atoms, quenching time resolved reson. fluoresc., isotope effects 0-32656  
 methane + Kr liquid mixtures, intermol. forces effect on phase diagram and excess props., perturbation theory 0-39287  
 methane + NO<sup>+</sup>, reaction rate consts. meas. 0-7782  
 methane + O, photochem. reaction, high temp., rate coeff. meas. 0-16699  
 methane + O(2<sup>1</sup>D<sub>2</sub>), collisional deactivation meas., 295K, rel. to atmospheric processes 0-16663  
 methane + O(<sup>1</sup>D), direct reaction in flow system 0-3333  
 methane + Xe liquid mixtures, intermol. forces effect on phase diagram and excess props., perturbation theory 0-39287  
 methane-(d<sub>1</sub>, d<sub>2</sub>, d<sub>3</sub>), electro-optical parameters from IR intensities, least-squares calc. 0-9584  
 methane absorption cell for He-Ne ring laser, power resonances 0-28255  
 methane adsorbed on γ-Al<sub>2</sub>O<sub>3</sub>, γ-radiolysis 0-3375  
 methane adsorbed on graphite basal plane, first order melting transition, triple point 0-2269  
 methane aerosol, possible presence in Uranus clouds 0-31253  
 methane and methane-d<sub>4</sub>, low energy electron impact dissociation, autoionisation 0-9744  
 methane cell for freq., stabilised He-Ne ring laser, operating characts. 0-14366  
 methane E-component saturated absorpt. for stabilising He-Ne laser, quantum freq. standard 0-9901  
 methane frost, presence of Pluto from 1.5 to 2.5 μm spectrum obs. 0-56765  
 methane gas—C(dissolved) + 2H<sub>2</sub> (gas), kinetics on Fe and Fe-Ni surface 0-55712  
 methane gas plumes, in atmosphere, tracking via acoustic sounder 0-55968  
 methane in condensed inert gas matrices, optical excitation of rotational transition, far IR absorption spectra 0-37808  
 methane in Jupiter atmosphere, abundance deduced from absorpt. bands in refl. sunlight 0-56758  
 methane in marine sediments, profiles 0-12373  
 methane in Titan atmosphere, visible and near IR spectrum 0-46471  
 methane reforming by nuclear steam for coal hydrogasification 0-30325  
 methane-air flame, stimulated Raman scatt. obs. 0-53003  
 methane-air flames, meas. of temp. and OH conc. 0-16687  
 methane-air flames, OH conc. profile 0-35534  
 methane-air mixtures, ignition energy by capacitive discharge (*French*) 0-10446  
 methane-Ar, cryogenic fluid mixture, transport phenomena, shear viscosity (*Russian*) 0-29198  
 methane-Ar, liq., drift vel. of excess electrons 0-54744  
 methane-Ar(N<sub>2</sub>) binary and ternary mixtures, dielec. const., excess vol. 0-7254  
<sup>13</sup>C-methane-d<sub>4</sub>O, annealed, spin conversion and proton 2nd moment time-depend. 0-11283  
 methane-d<sub>1</sub>, ν<sub>3</sub> band anal., 7.6 micron 0-47980  
 methane-d<sub>1</sub>, laboratory rotational spectrum and upper limits on abundance in (OMC-1) 0-56705  
 methane-d<sub>4</sub>, ν<sub>2</sub> and ν<sub>4</sub> IR bands meas. and anal. 0-18851  
 methane-d<sub>4</sub>, low temp. phase, X-ray study (*Russian*) 0-33985  
 methane-d<sub>4</sub>, selectively excited, cooling, vibr.-vibr., vibr.-translational relax. 0-33723  
 methane-d<sub>4</sub>, solid, thermodynamic props. calc. using significant structures method, 6 to 87K 0-24616  
 methane-ethane liq. mixture, phase equilb., heat of mixing, vol. change, data evaluation 0-15233  
 methane-H<sub>2</sub> mixture properties for hydrogen supplementation of natural gas 0-45781  
 methane-O<sub>2</sub> mixture, laser initiated combustion 0-55661  
 methane/H<sub>2</sub> mixing ratio in Neptune stratosphere 0-51692  
 methanes + CsF, rot. inelastic collisions, mol. beam meas. 0-1049  
 methanethiol + Cl<sub>2</sub>, laser-initiated chain reactions, rates, mechanisms, chemiluminesc. obs. 0-55651  
 methanol, absorption spectrum, LiF F<sub>2</sub><sup>+</sup>-centre laser intracavity spectroscopy appl. 0-32999  
 methanol, adsorption in GaAs(110) surface, UPS study 0-6632  
 methanol, condensed multilayers, electron bombard. effects, AES line-shape anal., XPS, and desorption meas. 0-7450  
 methanol, excited by CO<sub>2</sub> laser, sub-Doppler optoacoustic spectrum 0-5545  
 methanol, H bonding, electronic struct., geometries, moments, dimerisation energies, charge distrib., pseudopotential calcs. 0-27942  
 methanol, ion internal energy selection by angle-resolved mass spectrometry 0-53164  
 methanol, laser-induced decomp., comparative obs. using pulsed HF and CO<sub>2</sub> lasers 0-11888  
 methanol, mol., nucl. spin-spin coupling const., Hartree-Fock calc. 0-9618  
 methanol, mol. and cluster Auger spectrum calc., SCF core-valence-valence spectra 0-48045  
 methanol, multiphoton absorpt. of intense HF laser radiation 0-23475  
 methanol, optically pumped, assignment of weak FIR laser lines 0-14320  
 methanol, optically pumped laser, IR-FIR transferred Lamb dip spectra 0-1193  
 methanol, second virial coeff. meas. using new apparatus 0-44289  
 methanol, solar thermal energy storage utilising CaCl<sub>2</sub>-methanol thermochem. cycle 0-30587  
 methanol, solubility in liquid O<sub>2</sub>, estimation by Preston-Prausnitz method 0-39285  
 methanol, solvated electrons, optical spectra and model potentials 0-30318  
 methanol, surface reaction with Cu (100), EELS study 0-16728  
 methanol, UV multiphoton dissociation, photofragment fluoresc. 0-14165  
 methanol (d<sub>3</sub>), OH stretch fund., torsion-rot. levels, IR spectra obs. 0-32711  
 methanol and deuterates, H<sup>+</sup>, H<sub>2</sub><sup>+</sup>, and H<sub>3</sub><sup>+</sup> kinetic energy distrib., electron impact dissociation, ionisation, time of flight mass spectra 0-32843

## organic compounds continued

- methanol dimer, intermol. function from ab initio calcs. 0-32629  
 methanol far-IR laser, optically pumped, intracavity polarization modulation 0-23726  
 methanol glass solvated electrons, EPR, <sup>1</sup>H spin flip satellites, geometrical model 0-7146  
 methanol laser, twin optically pumped far IR, use in plasma diagnostics 0-54049  
 methanol optically pumped laser, frequency instability meas. at 70.5 and 118 μm 0-1254  
 methanol vapour, isothermal Joule-Thomson coefficient, equation of state 0-24119  
 methanol-2-methyltetrahydrofuran mixed glasses, annealed, γ-ray produced electrons transfer from IR to bisible traps 0-11440  
 methanol-d<sub>1</sub>(-d<sub>4</sub>), far-IR internal rotation spectrum 0-47989  
 methanol-d<sub>3</sub>(d<sub>1</sub>) in freon 11, self-associated, OH frequency temp. depend. 0-37809  
 methanol-d, CO<sub>2</sub> laser pumped, CW laser lines obs. 0-53272  
 4:1 methanol-ethanol, glass transition rel. to press. depend. of viscosity 0-34171  
 methanol-H<sub>2</sub>O mixture, evaporating droplets in air, temp. modelling (*German*) 0-2243  
 methanol-water, binary mixtures, nucleation 0-44305  
 methanol-water, liq., Verdet const., pulsed mag. field meas. 0-16012  
 methanol-water mixture, nonlinear acoustic coeff. meas., 0-50°C (*French*) 0-34142  
 methanols, labelled, proton T<sub>1</sub> in presence of intramol. rots., intermol. relax. rate 0-2656  
 methionine, automated synthesis of <sup>14</sup>C-labelled radiopharmaceuticals 0-17133  
 methionine sulfoxide in protein, <sup>13</sup>C NMR anal., method and expt. obs. 0-56305  
 2-methoxycyclobutane, mol. struct., electron diffraction obs. 0-1065  
 3-methoxybenzanthrone in ethanol, photoprolytic reactions, spectra, rate consts. and lasing thresholds 0-43327  
 methyl 4(1-pyrenyl)butyrate, decreased stabilisation energy of excimers and exciplexes in polymer matrices 0-25431  
 N-methyl acetamide, geometry from ab initio calcs., rel. to formamide, N-methylformamide and acetamide 0-23338  
 methyl alcohol, molecular FIR laser design, freq. tunable by Stark effect 0-5750  
 methyl alcohol, optically pumped, new CW FIR laser lines meas. and assignments 0-48224  
 methyl alcohol, photoacoustic spectra meas. at CO<sub>2</sub> laser wavelengths 0-18849  
 methyl amine, photodissoc. products, Doppler spectroscopy 0-53124  
 methyl ammonium chloride, Raman spectra, 70 to 300K, H stretching vibrs. 0-20628  
 methyl bromide, I-reson. perturbations in overtone and combination vibr. systems 0-52962  
 methyl chloride, charge distrib., substituents effect 0-905  
 methyl chloride, vacuum UV absorpt. spectrosc., Rydberg transitions obs. 0-5561  
 methyl chloride in stratosphere, conc. profile up to 32 km. altitude 0-36368  
 methyl compounds, rotational tunnelling, temp. dependence 0-38970  
 methyl cyanide, molecular FIR laser design, freq. tunable by Stark effect 0-5750  
 methyl fluoride, charge distrib., substituents effect 0-905  
 methyl fluoride, molecular FIR laser design, freq. tunable by Stark effect 0-5750  
 methyl fluoride Raman FIR laser, high-intensity CO<sub>2</sub> laser pumping, new emission lines 0-23675  
 methyl fluoride-d<sub>3</sub>, optically pumped sub-MM wave laser 0-23676  
 methyl formate, microwave spectra, rot. consts., moments and struct., radio astronomy appl., review 0-17637  
 methyl formate(-d<sub>1</sub>, d<sub>2</sub>, d<sub>3</sub>), mol. vibr. spectrum, struct., beginning with PCICO calc. (*French*) 0-23401  
 methyl group hindrance barrier, spin-rot. relax. times 0-53011  
 methyl groups in solids, reorienting and tunnelling, spin-lattice relax. 0-50217  
 methyl groups in solids, tunnelling freq. for internal rotation in pot. function 0-49134  
 methyl halides, force consts. evaluation using gp. vibrs. and centrifugal distortion consts. 0-9580  
 methyl halides, mol. force fields, IR intensities, and vibr. props. 0-47879  
 methyl iodide, liq., A<sub>1</sub> modes, vibr. relax., temp. depend. Raman spectra obs. 0-32806  
 methyl iodide, molecular FIR laser design, freq. tunable by Stark effect 0-5750  
 methyl iodide, Rydberg states, quantum defect theory applic. 0-32700  
 methyl iodide FIR laser gas, passive Q-switching of CO<sub>2</sub> laser 0-1246  
 methyl iodide-d<sub>3</sub> (-d<sub>3</sub>), two-photon reson. ionis. spectra 0-28071  
 methyl isocyanide, laser initiated thermal isomerisation, time behaviour of CN radicals 0-11887  
 methyl mercaptan, interstellar detect. in Sagittarius B2, mm wave spectrum 0-41877  
 methyl mercaptans, atmospheric, determ. using automatic odour analyser (*Japanese*) 0-50924  
 methyl nitrite, internal rotation temp. frozen in supersonic jet, matrix IR spectroscopy 0-9594  
 methyl radical in sodium acetate, EPR spectra, anisotropic hyperfine interaction, rot. tunnelling 0-34775  
 methyl substituted antimony chlorides, (CH<sub>3</sub>)<sub>3</sub>SbCl<sub>3-x</sub>, lone pair electrons, <sup>121</sup>Sb Mossbauer spectroscopy study 0-39984  
 methyl sulphoxide, photoacoustic spectra meas. at CO<sub>2</sub> laser wavelengths 0-18849  
 methyl thionine chloride, intramol. vibr. spectra 0-977  
 methyl torsion modes, vibrational optical activity, inertial contrib. 0-5524  
 methyl transfer reactions, Marcus theory 0-21279  
 methyl vinyl sulphide, syn-gauche equilb., force field and ab initio calcs., microwave and Raman spectra 0-23573  
 5-methyl-10-phenylphenazine, in 3-methylpentane (ethanol) (PMMA), radiationless processes, temp. depend. 0-43087  
 1-and 2-methyl-anthraquinone radicals, EPR 'reduced' spectra 0-23444  
 α-methyl-D-glucopyranoside, X-irrad., ESR and ENDOR study of free radicals 0-45526  
 6-methyl-mercaptopurine, cryst., light sensitive free radical EPR after electron irradiation 0-7167



## organic compounds continued

- N-methylacetamide, structure, Raman spectroscopy and neutron diffr. obs. (French) 0-7343
- N-methylacetamide in organic solns., dielec. const., dipole moments, monomer-dimer equilb. 0-40031
- methylacetylene, quadratic force fields, MOCIC pot. functions calcs. 0-5475
- methylamine, multiphoton discoc., N isotope separation 0-35553
- methylamine, multiple photon dissoci.,  $\text{NH}_2$  fragments, laser-excited fluoresc. obs. 0-11938
- methylamine, multiple-photon dissociation, laser induced fluoresc. photofragment detect. 0-37840
- methylammonium chromium selenate dodecahydrate crystals, dielectric relaxation 0-40043
- methylanilines, far IR spectra, pot. energy barriers 0-43043
- methylated benzene+tetracyanobenzene, fluorescent exciplex form., electronic relax. 0-5573
- 7-methylbicyclo[2.2.1]-hept-2-ene-5-one, config., microwave spectrosc. obs. 0-9593
- methylcyclohexane, dense liq., self-diffusion and viscosity 0-15278
- methylchlorosilane, Stark effect and microwave-microwave double reson., struct. (German) 0-47975
- methylene, singlet-triplet separation, relativistic corrections 0-32618
- methylene+ $\text{H}_2$ →methane, ab initio CI calc. on SCF level, insertion reaction min. energy path 0-7774
- methylene blue, effect on colour attenuation in Cherenkov radiation (Spanish) 0-7432
- methylene chloride HV polarisation and space charge obs. (Russian) 0-25277
- methylene isoelectronic radical, separation of two lowest states, comparison with  $\text{NH}_2^+$  0-53047
- methylene peroxide, multiconfig. SCF CI calcs. 0-18803
- methylene radical, classical stretching dynamics 0-23400
- methylene radical, vibronic bands obs. in pulsed supersonic jet 0-28024
- methylene radicals, rotational transitions, laser mag. resonance spectra 0-5538
- 3-methyleneoxetane, electron structure, orbital-O interaction, MO calcs., UV photoelectron spectra 0-28058
- methyl ethyl ketone-butanol, soln., excess thermodynamic props. and interactions, US vel. and density meas. 0-39288
- N-methylformamide, cis-isomer rot. struct., IR absorpt. spectrosc. obs. 0-14138
- N-methylformamide, geometry from ab initio calcs., rel. to formamide, acetamide, and N-methyl acetamide 0-23338
- methylidyne, interstellar, obs. in AFGL IR sources 0-51856
- methylidyne (CH), interstellar, abundance and column density in post-shock gas 0-56911
- 3-methylpentane-nitroethane, crit. conc. fluctuations, nonexponential decay 0-44309
- 3-methylpentane-nitroethane crit. mixture, dynamical scaling for sound propag. 0-49305
- 2-methylPOPOP, soln., anisotropic fluoresc. of prolate mol. (German) 0-1018
- 1-methylpyrene, fluoresc. quenching by  $\text{Cu}^{2+}$  in micellar system, general kinetic model 0-32753
- $\alpha$ -methylstyrene, photoinduced ionic polymerisation 0-7828
- 2-methyltetrahydrofuran-methanol mixed glasses, annealed,  $\gamma$ -ray produced electrons transfer from IR to bisible traps 0-11440
- 3-methylthiomethylpropionate, liq., dielec. relax. and permittivity 0-15948
- methoxy radical, electronic absorpt. spectra, visible, vibr. freqs., vibronic intensities and oscill. strengths 0-28025
- mineral oil-polystyrene mixture, viscosity and normal stress coeff. 0-44349
- mirex in lake Ontario sediments, circulation simulation 0-26556
- molecular crystal, band structure, excitonic processes, trap distrib. 0-6720
- molecular solid, film, 0-15 eV electron transmission spectra 0-35023
- molecular spectroscopy book 0-27051
- molecules, incorporation in electrodeposited films, stereomicroscopic method for obs. 0-2288
- di-molybdenum cyclopentadienyl tri-carbonyl, dual luminesc., ps pulse excitation 0-32754
- molybdenum formate, mol., Hartree-Fock instability of SCF wavefunctions 0-9492
- 12-molybdophosphoric acid, determ. of Mo content by NAA and AAS 0-15148
- monocarboxylic acids in meteorite, Murchison carbonaceous chondrite isomer struct. 0-26823
- monocrotaline sulphite hydrochloride, struct., space groups from X-ray crystallography (Chinese) 0-49210
- monofluoromethane+Ar, vibr.-vibr. energy transfer process diagnostics 0-32807
- monophenyl phosphate in aq. soln., pulse radiolysis obs. 0-30261
- monoterpene hydrocarbons in rural atmospheres, gas chromatography/mass spectrometric anal. 0-17336
- monothioformic acid, pot. for rot. about  $\text{C}(\text{sp}^2)\text{-S}$  bonds, ab initio calc. 0-23572
- morpholine, centrifugal distortion consts., microwave spectrum 0-5531
- myristyltrimethylammonium bromide, micelle size, press. dependence, photon correlation spectrosc. 0-11953
- N-acetyl-L-leucine, single crystals, X-ray induced free radicals 0-45525
- n-alcohol short chain molecules, optical investig. of mol. motions 0-40123
- n-alkane short chain molecules, optical investig. of mol. motions 0-40123
- [n]-alkanes, cryst., vibr. correl. splitting and chain packing 0-7338
- naphtene hydrocarbons, solubility in liquid  $\text{O}_2$ , estimation by Preston-Prausnitz method 0-39285
- naphthalene: pentacene, picosec. optical coherence obs. 0-14400
- naphthalene, adsorbed on silica gel surface, biphasic photochemistry, time-resolved spectra 0-30252
- naphthalene, and deuterio derivatives, fluoresc., absorpt. spectra under Shpol'skii conditions 0-2825
- naphthalene, anharmonic props., temp. (press.) depend., rel. to TTF-TCNQ 0-15200
- naphthalene, charge separation during cryst. growth, Costa Ribeiro effect 0-7316
- naphthalene, dimer triplet state line shape, small excitons 0-48041
- naphthalene, fluorescence and absorpt. spectra, deviations from Condon approx. 0-28004
- naphthalene, melting of rotational degrees of freedom near cryst.-liq. transition 0-54352

## organic compounds continued

- naphthalene, microcryst. and evaporated film, excimer emission 0-2823
- naphthalene, phonon eigenvectors, neutron scatt. intensities determ. 0-44271
- naphthalene, polarisation energy of localised charge 0-15034
- naphthalene, pure and deuterated, band-hopping mobility transition 0-6833
- naphthalene, quantitative structural studies by means of the energy-dispersive method with X-rays from a storage ring 0-24314
- naphthalene, single crystal, anomaly in permittivity due to thermoelectric space charge 0-7258
- naphthalene, soln. and melt, second vibronic transition, spectroscopic characts., effective field dispersion calcs. 0-55102
- naphthalene, space charge transport 0-20209
- naphthalene, triplet exciton annihilation and triplet spin relax. 0-29792
- naphthalene, triplet state time evolution after radiationless transition, initial vibronic distrib. effects 0-23450
- naphthalene, UV spectra and extinction coeffs. for  $\text{S}_0\text{-S}_1$  absorption 0-18866
- naphthalene, vibr. dephasing and Raman active localised internal mode temp. depend. 0-45060
- (naphthalene) $^+$ (naphthalene) $^+$  radical pairs, ESR absorption, optical detection 0-7166
- naphthalene anions, electron affinities, transition energy, comparison for gaseous liquid and solid 0-29731
- naphthalene crystals, nonlinear fluorescence quenching, recomb. of free excitons 0-7397
- naphthalene in nonpolar solvent, vibr. and reorientational relax., correl. function 0-45065
- naphthalene single crystals, surface active substances effect on plastic flow 0-44248
- naphthalene-adipic acid system, crystal growth from melt,  $\text{V-}\Delta\text{T}$  and  $\text{V-}\lambda$  relations 0-19734
- naphthalene- $\text{d}_8$  crystal, with isotopic impurities, Rashba effect, luminescence spectra, impurity states 0-29768
- naphthalene-He photoionis. plasma,  $\text{CO}_2$  additive effect 0-10359
- naphthalimide derivatives, solutions, lasing characts. in green spectral region, photostability 0-32978
- naphthyl, excited electronic states; conformational relax., time resolved matrix isolation spectral obs. 0-32701
- naphthalene: pentacene, zero-phonon transition bottlenecks, photon echo detect. 0-33092
- nematic liquid crystal, Merck 389, polymorphism, radiothermoluminescence and differential scanning calorimetric study 0-24570
- neopentane, adsorbed on graphite ( $\text{TiO}_2$ ), NMR pulsed field gradient method, diffusion coeff. meas. 0-15362
- neopentane, solid and liq., effect of n-butane impurity on electron mobility and electron-ion recomb. 0-24984
- neopentane, virial coefficient, meas. at various temps. using differential Burnett apparatus 0-22373
- neopentane- $\text{O}_2$ , thermal electron attachment meas., microwave cond., pulse radiolysis 0-28592
- niacin, biologically active forms, radiometric microbiologic assay 0-17208
- nickel(II) metalloporphyrin, Z-ray photoelectron spectra satellites 0-5582
- nickel acetate tetrahydrate:  $\text{Mn}^{2+}$ , EPR spectra, angular var. calc. 0-54940
- nicotine, automated synthesis of  $^{14}\text{C}$ -labelled radiopharmaceuticals 0-17133
- nigrosin black dye-Teflon spheres-water dispersion, turbid, laser backscatt. 0-1129
- Nile Blue, subpicosecond spectroscopy, tunable probe, spectral dynamics 0-23429
- nitriles, solns., IR absorpt. band parameters rel. to temp. 0-2762
- 3-nitro-o-anisidine, in benzene soln., dipole moment from solute relax. time-solvent viscosity relation 0-37905
- p-nitroaniline, binding energy, XPS obs. 0-37833
- p-nitroaniline, nonlinear second-order optical susceptibility 0-9947
- p-nitroaniline, valence and core photoionisation, spectral lines, many body effects 0-47853
- nitrobenzene, in acetone-isopropanol soln., Rayleigh scatt. and viscosity 0-5550
- nitrobenzene, liq., spin lattice relax. time, elec. field induced charges 0-44945
- nitrobenzene, nonlinear second-order optical susceptibility 0-9947
- nitrobenzene, oscill. optically induced Kerr kinetics 0-1286
- nitrobenzene, polarised, simultaneous variation of dielec. const. and discharge current, room temp. to beyond melting point 0-11314
- nitrobenzene, quenching and inhibition of orthopositronium 0-35002
- nitrobenzene, temp. depend. of electro-optic Kerr coeff. 0-2725
- nitrobenzene-hexane, soln., dielec. permitt. in two phase region 0-2682
- nitrobenzene-hexane solution, double-scatt. light intensity near critical point of mixing (Russian) 0-55117
- nitrobenzene-n-heptane, crit. mixture, conc. fluctuation mean relax. time, US absorpt. and vel. meas 0-29163
- nitrobenzene-n-hexane crit. mixture, in ultracentrifuge, dynamic phenomena 0-44310
- p-nitrobenzoic acid: rare earth laser materials, vibr. spectra, wavelength 125 to 500 nm 0-2769
- N-nitrodimethylamine- $\text{d}_6$ -( $\text{d}_6$ ), structural phase transition, Raman study 0-34911
- nitroethane-3-methylpentane, crit. conc. fluctuations, nonexponential decay 0-44309
- nitroethane-3-methylpentane mixture, crit. temp. press. variation 0-15235
- nitroethane-isoctane, crit. mixture, conc. fluctuation mean relax. time, US absorpt. and vel. meas 0-29163
- nitroethane-isooctane mixture, crit. temp. press. variation 0-15235
- nitroethane-isooctane mixture, depolarised Rayleigh scatt. near crit. point 0-45089
- nitromethane, shocked, utilisation of thermal ignition-time data for vol. of activation determ. 0-16683
- nitromethane+ $\text{H}_2$  reaction,  $\text{CO}_2$  laser initiated, mechanism and yield 0-11912
- nitromethane molecule dissociation in IR field, laser-induced fluoresc. obs. 0-53075
- nitromethane-isooctane, liq. mixture, coexistence curve, refr. index meas. 0-10655
- 4-nitrophenyl 4-n-octyloxybenzoate, electrical Kerr effect studies 0-25339
- 4-nitrophenyl 4-n-octyloxybenzoate, space group unit-cell and crystallographic props. 0-6399
- 4-nitrophenyl 4-n-pentyloxybenzoate, electrical Kerr effect studies 0-25339



## organic compounds continued

- 4-nitrophenyl-4'-alkoxybenzoates, incommensurate smectic A phase 0-10647  
 nitrosomethane, ground state and nonvertical  $n-\pi^*$  excitation energy calcs. 0-18804  
 nitroxyl radical, cationic surfactant, intramolecular fluorescence quenching of [1-pyrenyl-(CH<sub>2</sub>)<sub>6</sub>-N(CH<sub>3</sub>)<sub>3</sub>]<sup>+</sup>Cl<sup>-</sup> 0-9627  
 NMP-TCNQ, X-ray diffuse scatt., and cond. study 0-49701  
 nonane, liquid, chain reorientation, Brownian dynamics simulation, comparison of models 0-49067  
 nonelectrolyte aqueous solutions, temp. of max. density rel. to partial compressibility, struct. strengthening 0-30270  
 nonpolar binary mixture, partial molar vol. prediction from Lee-Kesler eqn. of state 0-10632  
 nonpolar liquids, far infrared absorption 0-50331  
 nonylammonium bromide, micellar aggregation number, <sup>13</sup>C NMR chemical shift conc. depend. 0-48016  
 (+)-nopinone induced circular dichroism of azulene  $\pi-\pi^*$  bands 0-53058  
 $\alpha$ -NPO, fluoresc. spectrum light quenching factor wavelength depend. 0-18882  
 nucleic acid bases, <sup>14</sup>N relax. and N-proton spin coupling, NH-proton spin-lattice relax. 0-26202  
 nucleic acid bases, Zn<sup>2+</sup> binding, ab initio SCF (pseudopot.) calcs. 0-12052  
 nucleic acid solutions, dye-tagged, electrically induced fluorescence polarised component change meas. 0-32863  
 nucleic acid-TCNQ complex, charge transfer interaction 0-3576  
 nucleic acids, electronic absorpt. and emission spectra 0-55989  
 nucleic acids, H<sub>2</sub> exchange kinetics and internal motions 0-21440  
 nucleic bases, interactions and self-organisation, ionisation and solvent salt comp. effects 0-55985  
 nucleotide bases, electronic absorpt. and emission spectra 0-55989  
 nucleotides, interactions and self-organisation, ionisation and solvent salt comp. effects 0-55985  
 octafluoronaphthalene, phase transitions at elevated press., Raman and mid-IR spectroscopy obs. 0-45062  
 octane, fragmental and molecular orbitals, CNDO/2 approx. calcs. 0-42947  
 octane, melting surface, ablation in impingement region of water jet 0-14766  
 octane, pore filling of wetproofed electrode 0-40702  
 octaphenylcyclotetrasiloxane, phase behaviour and nucleation kinetics 0-29168  
 4-n-octyl-4'-cyano-diphenyl, appl. in detection of graphite powder particles by optical microscopy 0-9034  
 4'-n-octyl-4-cyanobiphenyl, chain ordering model 0-24357  
 4'-n-octyl-4-cyanobiphenyl, thermotropic mesophase, DMR chain segments assignment 0-24356  
 p-n-octyl-p'-cyanobiphenyl, thermally addressed liq. cryst. display, light scatt. and contrast 0-34892  
 4-n-octyloxybenzoyloxy-4'-cyanostilbene, re-entrant polymorphism, nematic-smectic A-nematic-smectic A, X-ray study 0-34172  
 n-p-octyloxybenzylidene-p-toluidine, dielectric behaviour in nematic mesophase at RF 0-34842  
 p-octyloxyphenyl-p'-pentyloxybenzoate, charge carrier mobility and cond. in nematic and isotropic phases 0-44347  
 p-octyloxyphenyl-p-pentyloxybenzoate, nematic liq. cryst., elec. discharge meas. of persistent internal polarisation 0-10488  
 oil, lubricating, radn. effects and radn. dosimetry appl. 0-2069  
 oil-polymer mixture, acoustic attenuation CW meas., tissue simulation appl. 0-35961  
 olefins, zwitterionic states, polaris. and vibronic interactions 0-32620  
 oligocarbonatemetacrylates, and their cross-linked polymers, thermophysical characts., temp. depend. anal. 0-19721  
 oligoesters, effect of mol. architecture on dispersion props of TiO<sub>2</sub> in non-aqueous liquids 0-40751  
 oligomers, polymer-derived, mass spectral charact. 0-37916  
 olive oil, melting surface, ablation in impingement region of water jet 0-14766  
 one-dimensional and two-dimensional conductors, optical props. of small organic metal particles 0-45106  
 organic carbon analysis, automation 0-45592  
 organic dielectric layered structures quasi two dimensional conductors (Russian) 0-33989  
 organic water pollutant, DDT, influence of detergents on hydrosolubility and suspension (French) 0-7961  
 organo-arsenic compounds, (CF<sub>3</sub>)<sub>2</sub>AsSCH<sub>3</sub> and (CF<sub>3</sub>)<sub>2</sub>AsSeCH<sub>3</sub>, gas phase IR and liq. Raman spectra, normal coord. anal. (German) 0-32725  
 organochlorine, pesticide residual levels, pollution in Sathiar reservoir water, mud and organisms 0-45828  
 organonitrogen molecules, synthesis in interstellar clouds, ion-molecule scheme 0-12786  
 organophosphorus compounds, (CF<sub>3</sub>)<sub>2</sub>PSCH<sub>3</sub> and (CF<sub>3</sub>)<sub>2</sub>PSeCH<sub>3</sub>, gas phase IR and liq. Raman spectra, normal coord. anal. (German) 0-32725  
 organophosphorus pesticide residual levels, pollution in Sathiar reservoir water, mud and organisms 0-45828  
 organosilane coupling agent interphase of glass-fibre reinforced plastics, molecular organisation 0-44195  
 organosilicon binder, for prod. of spalling-resistant quartz glass based ceramic 0-40313  
 ovalene, isolated ultra cold mol., intermediate level structure of S<sub>2</sub> state 0-28048  
 ovalene, vibrational quasicontinuum threshold, spectrosc. criterion 0-52972  
 2'-oxaindan (dihydroisobenzofuran) spiropyran, photochromic transforms, spectrokinetic study 0-30259  
 oxalate esters, low intensity long duration chemilum., disposable lighting device appl. 0-11488  
 oxazine dyes, comparative photostability 0-3376  
 oxazole scintillator solns., two- and three-component, laser emission spectra 0-32980  
 3-oxetanone, electron structure, orbital-O interaction, MO calcs., UV photoelectron spectra 0-28058  
 oxyloxycyanobiphenyl, nematic-smectic-A transition, high-resolution 0-10649  
 p-terphenyl, positronium and thermal defects 0-24496  
 [p]-quinquaphenyl film between metal electrodes, memory switching 0-2484

## organic compounds continued

- PAA, cryst. phase transitions, intermolecular motion, Raman and inelastic neutron scatt. spectra 0-2164  
 PAA, homologous series, isotropic phase, mol. self diffusion by spin echo method 0-44109  
 PAA, light scatt. near cryst. to nematic transition 0-16046  
 PAA, nematic, adjustable domain struct. in inhomogeneous elec. field, electro-optic props. obs. 0-10494  
 PAA, nematic liq. cryst., elec. field effects, neutron diffr. study 0-28912  
 PAA, nematic liq. cryst., rot. barrier, PCIO and CNDO/2 calcs. 0-33874  
 PAA, refractive index, dielec. const., mag. susceptibility, orientational ordering (Dutch) 0-33884  
 palladium porphyrin, in n-alkane crystal, Zeeman and crystal field effects, absorpt. vibr. anal. 0-7372  
 palladium-octaethylporphyrin, gas phase delayed fluoresc. and phosphoresc., triplet excimer formation 0-18884  
 PAP, cryst. phase transitions, intermolecular motion, Raman and inelastic neutron scatt. spectra 0-2164  
 paraaminophenol and paraphenylenediamine analogue molecular complex, free radicals of developers, EPR obs. (Russian) 0-7814  
 paradibromobenzene-paradichlorobenzene solid solutions, mol. cryst., NQR study 0-25242  
 paradichlorobenzene-paradibromobenzene solid solutions, mol. cryst., NQR study 0-25242  
 n-paraffin, crystals, phase transitions, statistical theory 0-44290  
 paraffin, liquid, interface with photoconductor, carrier injection 0-24970  
 paraffin plate heat storage element, fusion, periodic solidification, heat transfer kinetics (French) 0-40913  
 paraffin thermal storage by sensitive, latent heat, (French) 0-40917  
 paraffin wax, two-phase Stefan problem solns. 0-43594  
 paraterphenyl, dye laser pumping characts. using KrF excimer laser at 248 nm 0-1199  
 pelagic tar, ocean distribution and surface circulation 0-16856  
 penicillins, semi-synthetic, radiation sterilisation 0-17064  
 pentacene, vibrational quasicontinuum threshold, spectrosc. criterion 0-52972  
 pentacene films, luminesc., struct. 0-11461  
 pentacene in naphthalene, intersystem crossing rates following single-mode laser excitation 0-43085  
 pentane, liquid, chain reorientation, Brownian dynamics simulation, comparison of models 0-49067  
 n-pentane, Townsend primary and secondary ionisation coeffs. and sparking voltages 0-1732  
 pentane isomeric vapours, electron transport mechanisms, density induced transition 0-24122  
 pentanol activity in bulk phases, distribution and surface activity (French) 0-24712  
 pentofuranosyl nucleosides, isomeric, <sup>1</sup>H NMR coupling consts., SCF FPT INDO approx. calc. 0-14156  
 p-pentoxy-benzylidene-alkylaniline series, smectic phases, dielec. anisotropy 0-55010  
 4-n-pentyl-phenylthiol-4'-alkoxybenzoate, homologous series, specific heat meas., nematic-smectic-A tricritical point 0-15227  
 pentyloxybiphenyl, liquid crystal, isotropic phase, surface induced ordering, birefringence obs. 0-14998  
 4-pentylphenyl-4'-benzoyloxybenzoate/TBBA system, smectic A<sub>1</sub>-smectic A<sub>2</sub> transition, X-ray diffr. obs. 0-44303  
 peptide analysis by field desorption mass spectrometry using pretreated Si emitter 0-55751  
 perchloro-3-cyclopentenone, <sup>35</sup>Cl NQR Zeeman obs. 0-54981  
 perchlorohydrocarbons, crystn., intermol. potential-function models 0-49168  
 perdeuterio-N-1-oxyl-2,2,6,6-tetramethyl-4-piperidiny l maleimide, spin label, biological EPR 0-32746  
 perdeuterobenzophenone, in 4,4'-dibromodiphenylether, cross-relax., microwave pulse obs. 0-53031  
 perfluorocarbons,  $\gamma$ -irrad. solns., mag. field effect on fluoresc. 0-55677  
 perfluorodimethylcyclohexane, retrograde vapour, shock wave induced condensation 0-34177  
 perhalonitrosomethanes, gas phase IR spectra, assignments, isomerism 0-28017  
 perylene in n-heptane cryst., polarised fluoresc. 0-1017  
 perylene-tetracene in liquid crystals, temp. depend. of absorption and fluoresc. (German) 0-18887  
 pesticides, chlorinated, gas chromatographic anal. using electron capture detector (Japanese) 0-55764  
 Phase V, nematic, transient response to redirected mag. field, EPR study 0-33879  
 phenacyl halides, IR spectra,  $\delta$ (CH<sub>2</sub>) vibr. correlation with structs. (French) 0-23417  
 phenanthrene, chemical thermodynamic props. 0-21312  
 phenanthrene, planar normal vibr. calcs. 0-5525  
 phenazine, dimer triplet state line shape, small excitons 0-48041  
 $\alpha$ -phenazine, multiple scattering, secondary reflections and their interference 0-33856  
 p-phenitidine, in benzene soln., dipole moment from solute relax. time-solvent viscosity relation 0-37905  
 phenol, cryst., mol. vibr., factor group splittings 0-16021  
 phenol formaldehyde resin carbon, catalytic graphitisation from various metals 0-11871  
 phenoxy radical dimer, reversible diffusion controlled dissoc., detailed equilib. principle 0-7770  
 (+)-(S)-2-phenyl-3,3-dimethylbutane, optical activity, circular dichroism, polarisability model 0-43082  
 phenyl-trimethine-merocyanine, X-ray diffr. exam. of cryst. and mol. struct. 0-6398  
 phenylcyclohexanes, alkylamino substituted, synthesis and mesomorphic props. 0-44120  
 phenylene sulphides, NMR relaxation for mol. motions (German) 0-11288  
 pheophytin-a (b), dimerisation, fluoresc. and ODMR study 0-18876  
 pheophytin-chlorophyll, pigment associations, conc. effects, luminesc., absorpt. spectra and dichroism obs. 0-1007  
 phosphamides, carcinostatic, <sup>14</sup>N NQR, electron distrib. and bonding configs. 0-48018  
 phosphates, cellular, heteronucl. two-dimens. NMR as conform. probe 0-3590  
 phosphatidylcholine-cholesterol vesicles interacting with lucensomycin, PMR obs. 0-40954



## organic compounds continued

- phospholipid inter- and intra-molecular interactions, PCIOCC and pot. function calc. 0-3570
- phospholipid membrane, polar head motion, NMR and EPR linewidth study using TCNQ<sup>-</sup> ion-radical (*French*) 0-45865
- phospholipids, <sup>31</sup>P NMR, slow-motional lineshapes for very anisotropic rot. diffusion 0-5644
- phosphors, surface impregnation of Al<sub>2</sub>O<sub>3</sub> anodised film, fluoresc. spectrum (*Japanese*) 0-55170
- photo-electron-microscope pictures of organic samples on metal supports 0-26431
- phthalan, geometry, electronic absorpt. spectra 0-971
- phthalic acid, IR absorpt. spectra, fundamental assignments 0-5542
- phthalimide acetyl derivatives in polar solvents, luminesc. kinetics and phosphoresc. quenching 0-18885
- phthalimide derivatives, hidden vibr. band determ. method, fluorescence and excitation spectra meas. 0-40158
- phthalimide derivatives, solutions, lasing characts. in green spectral region, photostability 0-32978
- phthalocyanides, thermal stability, DTA (*German*) 0-11945
- phthalocyanine films, metal-free, adsorbed o-chloranil effect on surface photovoltage 0-34485
- phthalocyanine metal-free, photoconducting, electric field-induced fluoresc. quenching 0-34967
- phthalocyanine sensitization of Se photoreceptors, charge decay characts. 0-15630
- $\alpha$ -phthalocyanine target, reactor-irrad., extraction rate and mechanism of <sup>64</sup>Cu 0-35563
- phthalocyanine-halogen complexes, elec. props. 0-29424
- phthalocyanine-metal interfaces, surface photovoltage 0-20308
- pigment associations, conc. effects, luminesc., absorpt. spectra and dichroism obs. 0-1007
- pigment crystalline soln., electrically induced fluorescence polarised component change meas. 0-32863
- pinacyanol dye, adsorbed on CdS substrate, aggregation effect on mol. electronic states 0-37757
- 1,4-piperazine, conform. equilib., CNDO/2 calcs. on six-membered rings 0-23336
- piperidine solution of PbI<sub>2</sub>, crystn. of intercalation cryst. 0-16170
- pitch, coal-derived low-volatile residues, glass transition, rheological props., DSC anal. 0-39331
- pitch and coke-pitch disperse system, viscoelastic props. 0-1500
- pivalic acid, liq. and plastic crysts., <sup>13</sup>C NMR chem. shift, temp. depend. 0-2652
- pivalophenone, organic soln., triplet reactivity solvent depend., flash photolysis study 0-11902
- plasticizer effect on electric strength of polystyrene 0-29688
- pleochroic dyes, dissolved in nematic liq. crysts., guest-host interactions, appl. to electrooptic displays 0-44113
- PMMA, circular plates, thermoviscoelastic anal. of a thermorheologically simple material 0-10161
- PNAOBA, type C smectic liq. crysts., electrohydrodynamic instability 0-1927
- poly(N-vinylcarbazole), space charge effects on triboelec. charge exchange 0-54763
- poly- $\gamma$ -benzyl-L-glutamate, sidechain order parameters, <sup>2</sup>H NMR meas. 0-1923
- poly- $\gamma$ -benzyl-L-glutamate helices, optical activity 0-48113
- poly-N-benzamide, lyotropic liq. crystals, viscosity anisotropy 0-10693
- polyacetylene, doped and neutral, resonance Raman scatt. 0-55107
- polyacetylene, pristine and acceptor doped isomers, EPR, DC cond., evidence against solitons 0-15782
- polyacrylamide gel, automated scanning of <sup>14</sup>C 0-17221
- polyamine iodide/AgI solid electrolytes, conc. depend. of elec. cond. 0-24647
- polychlorinated biphenyls, pollutants, radiation degradation in organic solvents, H<sub>2</sub>O 0-30262
- polydiacetylene, cryst., one-dimens. conjugated semicond., vibronic coupling, Fano interference effects 0-34939
- polyene chromophores, band broadening in electronic-vibr. absorpt. spectra 0-28003
- polyenes, symmetric, combinatorial enumeration of chemical isomers 0-28114
- polyethersulphone, thin film TLD, skin dosimetry appl. 0-52790
- polyethylene: octadecanol, contact charging and donor impurity conc. relationship 0-20286
- polyethylene, in toluene, pressure crystallised, swelling behaviour, rel. to densities 0-2167
- polyethylene glycol, effect on photographic film during fast development (*Russian*) 0-45533
- polyisobutylene, circular plates, thermoviscoelastic anal. of a thermorheologically simple material 0-10161
- polymeric conjugated hydrocarbons, energy gap estimation, graph-theoretical approach 0-24789
- polymers formed in Fischer-Tropsch and Miller-Urey reactions, N isotope fractionation 0-46496
- polymethine cyanine dyes, vibronic energy relax., picosec. spectrosc. obs. 0-5526
- polymethine cyanine dyes, viscosity depend. fluoresc. lifetime using synchronously operated ps streak camera 0-28041
- polymethine dye behaviour in lasers, efficiency and photoisomer generation 0-14335
- polymethine dye laser, near IR, optimal molecular struct. and lasing characteristics 0-19026
- polymethylene, extended chain, C-H stretching band struct., Fermi reson., Raman spectrum 0-5552
- polynaphthoquinone-SO<sub>2</sub>-I<sub>2</sub> system for H<sub>2</sub>O decomposition for H<sub>2</sub> production 0-16825
- polynucleotides, double helical, conformation, pairwise pot. function calcs. 0-53173
- polynucleotides, interactions and self-organisation, ionisation and solvent salt comp. effects 0-55985
- polypeptides,  $\alpha$ -helical,  $\pi$ - $\pi^*$  absorpt. and circular dichroism spectra 0-23398
- polypeptides, in aq. poly(L-glutamic acid) soln., helix-coil transition, US relax. times 0-45849
- polysaccharide components dissolved into chlorite liquor according to the variation of treating conditions (*Japanese*) 0-3291
- polystyrene, amorphous, failure in methanol and ambient air 0-3165
- polystyrene-chloranil molecular complex, glass-rubber and liquid-liquid transitions 0-45002

## organic compounds continued

- polystyrene-PMMA-benzene, soln., polystyrene diffusion, photon correl. spectroscopy 0-34220
- polysubstituted peri-condensed compounds, combinatorial enumeration of chemical isomers 0-28114
- polyvinyl alcohol, effect on lifetime and formation of latent image in photographic layers (*Russian*) 0-3389
- polyvinylalcohol, gel macromol. gel layer formed on ultrafiltration tubular membrane, charact. 0-14260
- polyvinylcarbazole-trinitrofluorenone, organic photoconductor, photoinduced paramag. centres 0-25188
- polyvinylidene fluoride film as diaphragm material for electroacoustic transducer 0-10100
- POPOP, fluoresc. spectrum light quenching factor wavelength depend. 0-18882
- POPOP, soln., anisotropic fluoresc. of prolate mol. (*German*) 0-1018
- POPOP+Ar+N<sub>2</sub>, electron beam excited, energy transfer mechanisms 0-23497
- POPOP dye vapour lasers, optical and electron beam pumping, review 0-48237
- POPOP laser, bleaching of vapour 0-19027
- POPOP vapour, optically induced dynamic gratings 0-28289
- POPOP vapour, picosecond generation of radiation 0-48238
- porphin in host n-alkane crystals, phototautomerism, IR spectral obs. 0-34963
- porphine, electronic struct. props. and photosynthesis 0-16902
- porphins orientation in n-alkane Shpolskii hosts, spectra 0-48035
- potassium butyl xanthate, X-ray cryst. struct. determ. 0-33987
- potassium hydrogen malonate, deuterate, NQR data (I=1) from ENDOR expts. 0-54994
- potassium hydrogen oxalate, oriented single cryst., Raman spectra with very strong H-bonding 0-25359
- potassium oxalate, anhydrous, phase II, vibr. spectra and cryst. struct. 0-34901
- potassium oxalate, EPR of Mn<sup>2+</sup> and VO<sup>2+</sup> 0-39858
- potassium oxalate monohydrate:VO<sup>2+</sup>, cryst., IR absorpt. 0-55134
- potassium p-chloranil, solvated with acetone, X-ray cryst. struct. determ. 0-39062
- praseodymium  $\beta$ -ketoesters, Pr<sup>3+</sup>, visible spectrum, interaction, intensity and bonding parameters 0-993
- progesterone in crude serum extracts, radioimmunoassay using <sup>3</sup>H and <sup>125</sup>I labelled tracers 0-56185
- l-proline monohydrate single cryst., X-irrad., ESR and ENDOR study of radicals 0-45528
- propan-1-ol, ion internal energy selection by angle-resolved mass spectrometry 0-53164
- propane, diffusion flame, coherent spectral interference from C<sub>2</sub>, CARS spectra 0-43404
- propane, graphite hollow cathode glow discharge C conc. determ. 0-44032
- propane, ion internal energy selection by angle-resolved mass spectrometry 0-53164
- propane, mol. ion, mass spectra ion intensity internal energy depend., quasi equilibrium theory calcs. 0-53163
- propane, vapour-liquid and vapour-solid equilb. data, mass spectroscopic tracer pulse chromatography 0-37115
- propane, vibr. intensities, G sum rule appls. 0-32776
- propane-N<sub>2</sub>(CO<sub>2</sub>), mixtures, viscosity, diffusion coeffs. 0-1722
- propane-O<sub>2</sub> flame, microwave-emission plasma diagnostics 0-45503
- 2-propanol, dielec. time domain spectroscopy, total transmission method study 0-27323
- 1-propanol, glassy, electron trap relaxation model 0-15470
- l-propanol, glassy, electron trapping, pulse radiolysis obs. 0-30264
- n-propanol, sparking pot. and ionis. coeffs. 0-1864
- n-propanol-water, binary mixtures, nucleation 0-44305
- propene, catalytic oxidation, modification of V<sub>2</sub>O<sub>5</sub>(001) surface (*French*) 0-45557
- propenyl chloride, IR bands, torsional struct. 0-28018
- $\beta$ -propiolactone, electron structure, orbital-O interaction, MO calcs., UV photoelectron spectra 0-28058
- propionic acid, adsorbed in thin film tunnel junctions, hydrogenation and deuteration, IETS obs. 0-45547
- propylbenzene-nitrobenzene, binary mixtures, with weak charge transfer interactions, thermodynamic props. 0-54360
- N-p-propoxybenzylidene-p-pentylaniline, Williams domains, interference study 0-44114
- p-propoxysalicylidene-p'-butylaniline cryst. and mol. struct., intramolecular bonding 0-44197
- isopropyl chloride, torsional pot. function, far IR and Raman obs. 0-28022
- propyl iodide, two-photon reson. ionis. spectra 0-28071
- propylene, electron impact ionisation and dissociation 0-37894
- propylene, equations of state, search procedure, based on step-wise least-squares technique 0-19900
- propylene, mol. dissociation on bombardment by low energy electrons 0-43845
- propylene, solubility in liq. N<sub>2</sub> 0-39286
- propylene carbonate-LiClO<sub>4</sub> solution, composition of passivation layers on Li electrode (*French*) 0-11899
- propylene glycols, dielec. props., chain length effect 0-44995
- 1,3-propylenediammonium manganese tetrachloride, vibr. study of phase transitions, IR and Raman spectra 0-40103
- propynal, energy dispersion and relax., laser IR-visible double reson. 0-48023
- propynal, energy dispersion and relax., laser IR/visible double reson. obs. 0-53028
- propynal, internal energy distrib., collisional effects, IR-vis. double reson. obs. 0-14159
- propynal, IR photochem. in electronically excited state 0-11923
- proton chemical shifts, combined pulse NMR and magic-angle spinning 0-44934
- Prussian blue analogues, Mossbauer spectra 0-15898
- pyromellitic and dianhydride, intermolecular shielding contributions, proton mag. shielding intermolecular shielding contributions, proton mag. shielding 0-34783
- PTZ:PMDA, purification, growth, struct., optical and elec. props. 0-54216
- PVC-chlorinated, piping for secondary criticality control of fissable solns. 0-13607
- PVC/coal blends, fluidized bed combustion of plastic waste with coal, removal of HCl 0-30347
- pyrazine, cryst. phases, entropy changes and struct. implications 0-54397



## organic compounds continued

- pyrazine, dispersion induced circular dichroism, determ. of mag. dipole allowed transitions 0-14163  
 pyrazine, excited and  $N_{1s}$  ionised states, ab initio calcs. broken orbital symm. 0-27931  
 pyrazine, triplet-triplet absorpt. related to state splitting 0-47917  
 pyrazine, vibronic and spin-orbit coupling interaction 0-14126  
 pyrazine ( $-d_4$ ), single vibronic level fluoresc. spectra, rel. to vibronic coupling 0-28043  
 pyrazine ( $-d_4$ ) vapour, single vibronic level fluoresc. from n,  $\pi^*$  0-37827  
 pyrazine adsorbed on electrode, surface enhanced Raman spectra, symmetry and polarisability changes 0-50310  
 pyrene, adsorbed on silica gel surface, biphasic photochemistry, time-resolved spectra 0-30252  
 pyrene, band structure, excitonic processes, trap distrib. 0-6720  
 pyrene, positronium and thermal defects 0-24496  
 pyrene-3-sodium sulphate solubilised in didodecylmethylammonium bromide-benzene inverted micelles 0-3417  
 pyrene-sodium 5-[1-pyrenyl]pentanoate intramolecular excimer formation in CTAC and SDS micelles, fluoresc. probe 0-16733  
 pyridazine,  $\pi$  bond order calc. using U(3) basis algebra 0-18810  
 pyridine, adsorbed on Ag, Raman intensity enhancement using surface plasmons 0-7334  
 pyridine, adsorbed on Ag electrodes, ang. resolved Raman spectra 0-16017  
 pyridine, adsorbed on  $Al_2O_3$ , surface acidity meas. 0-35611  
 pyridine, adsorbed on Cu(Au) electrode, angle-resolved Raman spectroscopy 0-52991  
 pyridine, adsorption on Cu (110), angle-resolved photoemission, selection rules 0-40231  
 pyridine, adsorption on Ir (111), electronic transitions sensitivity to molecule-surface orientation, energy loss spectra 0-45184  
 pyridine, chemisorption on goethite, IR spectra 0-7855  
 pyridine, dispersion induced circular dichroism, determ. of mag. dipole allowed transitions 0-14163  
 pyridine, intercalation cpd. with  $TaS_2$ ,  $NbS_2$ , nucl. spin-lattice relax. meas. 0-54962  
 pyridine+carbon tetrachloride (o-cresol), binary liquid mixtures, excess free vol. calcs. 0-34202  
 pyridine adsorbed on Ag, reson. Raman scatt. 0-25380  
 pyridine and salts, deuterium NQR, double reson. method, ring charge distrib. 0-53015  
 pyridine cation radical in trichlorofluoromethane matrix, gamma irradi., EPR and optical obs. 0-23442  
 pyridine intercalation with  $FeOCl$ , mechanism, nucleation and diffusion 0-49420  
 pyridine iodine complexes, charge transfer complexes, vibr. spectra, laser Raman obs. 0-52990  
 pyridine-acetic acid, H-bonding, proton transfer, isolated system, solvent effect, MO calc. 0-55629  
 pyridine- $d_5$ , physisorbed thin film on Ag surface, enhanced Raman scatt. study 0-20620  
 pyridine- $H_2O$ , bonding, double quadrupole reson. obs. 0-32749  
 pyridine-HCl complex, self assoc., intermolecular interactions, matrix isolation vibr. spectra obs. Raman and IR spectra 0-52995  
 pyridine- $I_2$ ( $Br_2$ ) charge transfer complexes, vibr. spectra, vibronic contrib., intensity enhancement 0-53048  
 di- $\alpha$ -pyridyl hydroperchlorates, intramol. H bonds, steric conditions and polarisability obs. 0-53160  
 pyrimidine  $N_2O$  aq. solns., dimer formation in  $\gamma$ -radiolysis, chromatographic obs. 0-7785  
 pyrocatechol, oxidation pots., correl. of V-I characts. and photographic developing power (Russian) 0-45534  
 Pyronine G rot. diffusion from absorpt. relax. 0-1008  
 quasi one dimensional charge transfer salts, soliton model for dielectric permeability 0-40036  
 p-quaterphenyl, polycryst. thin layer-metal sandwich, elec. cond. 0-34526  
 p-quaterphenyl oriented layers, charge carrier transport, hopping model 0-2506  
 quercetin, excited state proton transfer, luminesc. 0-35818  
 quinoline, dil. soln., dielec. absorpt., relax. and thermodynamic parameters meas. 0-50258  
 quinoline, in binary solvents, phosphorescent and fluorescence 0-7409  
 quinoline+carbon tetrachloride, (o-cresol) binary liquid mixtures, excess free vol. calcs. 0-34202  
 quinoline-isoquinoline, dil. soln., dielec. absorpt., relax. and thermodynamic parameters meas. 0-50258  
 quinoxaline guest molecule in p-dibromobenzene crystal nucl. spin polarisation cross relax. study 0-29647  
 R-113, refrigerant, critical heat flux of saturated natural convection boiling with heating from below 0-10114  
 radioactive waste, microbial prod. of tritiated and  $^{14}C$  methane 0-45868  
 randomised X-ray powder diffraction patterns, adjustable sample holder 0-6317  
 rare earth ethyl sulphates: $Ce^{3+}$ , Kramers ions, virtual phonon exchange, field theoretic formalism 0-20137  
 rare-earth formates, second optical harmonic generation 0-43403  
 refractive indices, and optical anisotropies of some monoclinic and orthorhombic crystals. 0-50287  
 resorcin, Raman line intensity as function of mol. orientation 0-11383  
 retinyl acetate, high press. fluoresc. studies of radiative and nonradiative processes 0-1011  
 rhodamine, CARS spectroscopy, vibr. spectra of electronic states 0-27964  
 rhodamine 101, quenching of emission in methanol and latex particle suspensions 0-3374  
 rhodamine 4C, in ethanol soln., rot. relax. time using ps. spectroscopy technique 0-1013  
 rhodamine 590 picosecond transverse-flow flashlamp-pumped dye laser 0-38025  
 rhodamine 640, subpicosecond spectroscopy, tunable probe, spectral dynamics 0-23429  
 rhodamine 6G, aqueous soln., absorpt. spectra, ground and triplet state photoprotonation pH depend. 0-42961  
 rhodamine 6G, B in ethanol soln., and dye mixtures, excitation by Cu vapour laser 0-28230  
 rhodamine 6G, dye laser pumping characts. using KrF excimer laser at 248 nm 0-1199  
 rhodamine 6G, fluoresc. polarisation, solvent effects 0-32755  
 rhodamine 6G, orientated relax. times, streak camera meas. 0-14168  
 rhodamine 6G, photoacoustic spectra in soln. 0-9606  
 rhodamine 6G, rot. diffusion from absorpt. relax. 0-1008

## organic compounds continued

- rhodamine 6G and rhodamine B adsorbed on  $AlH_3$ , luminesc. spectra during  $AlH_3$  photolysis 0-55171  
 rhodamine 6G laser amplifier pumped by  $N_2$  laser, sub nsec pulse generation 0-1232  
 rhodamine 6G soln. in ethanol, luminesc. liq., pump radiation conversions to enhance laser efficiency 0-48293  
 rhodamine 6G-coumarine 1-water-Triton X100, micellar dye soln., energy transfer 0-45581  
 rhodamine 6G-isopropyl or ethyl alcohol solution, flashlamp pumped laser, photochem. effects 0-53287  
 rhodamine B, 6G, resonance CARS line shape, scatt. processes in ground or excited states 0-48043  
 rhodamine B, doping density dependent attachment on  $TiO_2$  electrodes 0-54777  
 rhodamine B, injection locked dye amplifier, coherent optical image amplification 0-19041  
 rhodamine B, tunable freq. doubled CW laser using  $RbH_2PO_4$  cryst. 0-53372  
 rhodamine B and 6G, fluoresc. decay time meas. in different solns. 0-9637  
 rhodamine B surface state hole traps, surface photovoltage meas. 0-39654  
 rhodamine dye polar frozen solns., luminesc. broadening 0-2834  
 rhodamine dyes in soln., bleaching, electronic and vibr. absorpt. spectra, fluoresc. 0-42960  
 rhodamine-6G-3,3'-diethylthiacarbocyanine iodide-sodium lauryl sulphate, soln., premicellar region, energy transfer 0-20685  
 t-RNA, rot. relax. time,  $10^{-8}$ s range Fabry-Perot and photoelectron time of arrival method 0-21437  
 Rose Bengal-fluoranthene, singlet-singlet energy transfer in Manoxol OT-cyclohexane-water 0-9531  
 rubidium platino-oxalate, one-dimens. conductors, prep., struct. and elec. cond. 0-24900  
 rubidium propanoate, solid state transitions and melting process, diff. and conductometric meas. 0-10670  
 rubrene, orthorhombic cryst. photogenerated carriers, transit time meas. 0-49811  
 rubrene, sensitised photooxidation of 1,3-diphenylisobenzofuran solns.,  $S_1$  excited state  $O_2$  quenching 0-45529  
 rubrene thin layer and flow cells, steady DC electrogenerated chemilum. 0-55205  
 salicylic acid, IR absorpt. spectra, fundamental assignments 0-5542  
 salicylidene-2-chloroaniline, photochromism and thermochromism, NQR spectra, temp. and UV irradi. depend. 0-54968  
 sandwich compounds, prep. from free atoms of metals (French) 0-21281  
 saturated hydrocarbons, adsorption on alumina 0-26053  
 scandium octaethylporphyrin,  $\mu$ -oxo bridged dimer, triplet states and geometrys, ODMR obs. 0-9625  
 scandium octaethylporphyrin, triplet states and geometrys, ODMR obs. 0-9625  
 Schiff's base compounds, double axis, Siamese Twin type liq. crystals., thermal and X-ray obs. 0-39312  
 selenophene, flash photolysis, transient absorpt. spectra 0-14153  
 L-serine-L-ascorbic acid, X-ray cryst. struct. determ. 0-35827  
 serotonin effect on cytochrome c soln. optical props. after UV irradi. 0-30663  
 1-silabicyclo 2,2,2 octane, double-min. skeletal torsion, microwave spectroscopy 0-47972  
 silicon oil, thermal diffusivity, constant-rate heating method (Japanese) 0-6570  
 silver thioamides, precip., electron microscope and potentiometric studies, growth of photosensitive crystals. 0-33107  
 silylacetylene, centrifugal distortion consts., thermodynamic functions 0-47959  
 sodium acetate trihydrate, press. depend. of methyl tunnelling motion 0-10603  
 sodium cholate-decanol, soln., aggregate form., comp. and dynamics 0-45575  
 sodium decanoate-n-decanol-water system, lamellar G-phase, orientational-order, EPR investigation 0-24355  
 sodium decyl sulphate/water/decanol/ $Na_2SO_4$ , lyotropic mesophase, mag.-oriented, X-ray diff. obs. 0-1921  
 sodium di-2-ethylhexyl suphosuccinate in  $H_2O$ -n-heptane micellar soln., neutron small-angle scatt. (French) 0-26059  
 sodium dodecylsulphate, micellar system, 1-methylpyrene quenching by  $Cu^{2+}$ , general kinetic model 0-32753  
 sodium dodecylsulphate micelle, intramolecular fluorescence quenching of [1-pyrenyl-( $CH_2$ ) $_n$ -N( $CH_3$ ) $_3$ ] $^+Cl^-$  by cationic surfactant nitroxyl radical 0-9627  
 sodium hexanoate, micellar aggregation number,  $^{13}C$  NMR chemical shift conc. depend. 0-48016  
 sodium hydrogen oxalate monohydrate, oriented single cryst., Raman spectra with very strong H-bonding 0-25359  
 sodium lauryl sulphate micelles, chlorophyll-a, soln., dilution expts., solubilisation anal. 0-35587  
 sodium lauryl sulphate-3,3'-diethylthiacarbocyanine iodide-rhodamine-6G, soln., premicellar region, energy transfer 0-20685  
 sodium octanoate, micellar aggregation number,  $^{13}C$  NMR chemical shift conc. depend. 0-48016  
 sodium oxalate, cryst. struct. rel. to those of  $SnC_2O_4$ ,  $Na_2Sn(C_2O_4)_2$  (French) 0-2004  
 sodium salicylate-toluene, singlet-singlet energy transfer in Manoxol OT-cyclohexane-water 0-9531  
 sodium tin oxalate, cryst. struct. rel. to those of  $Na_2C_2O_4$ ,  $SnC_2O_4$  (French) 0-2004  
 solar energy conversion, photoelectrochemical cells, chlorophyll sensitised reactions 0-7948  
 solutes in liquids, conc. determ. by (n, $\alpha$ ) and (n, $\gamma$ ) reacts., scintillation counting 0-35602  
 sorbitol, X-irrad., 4.2K, electron traps, alkoxy hyperfine coupling, ENDOR obs. 0-50863  
 spiropyrans, photochromic, thermophotodegradation for autoproccessor reprography system 0-35555  
 squaric acid, critical slowing down of fluctuations at phase transition,  $^{13}C$  spin-lattice relax. 0-44948  
 squaric acid, two-dimens. antiferroelec., temp. depend. of order parameter, birefr. obs. 0-11351  
 steam-gas system, joint use of nucl. and organic fuels 0-40807  
 stearic acid film, in MIM struct., AC cond. and dielec. props., freq. depend. 0-55030



## organic compounds continued

- stearic acid-calcium stearate monomolecular films, multilayer deposition 0-54550
- stearyl alcohol, H bonding effects on skeletal optical and longitudinal acoustical modes 0-34914
- stilbene, cis→trans photoisomerisation rate const., direct meas. 0-30250
- stilbene, cis- and trans-, picosecond flash photolysis, intramol. charge-reson. transition obs. 0-7810
- trans-stilbene, in glassy media, phosphoresc., heavy atom effects 0-55153
- trans-stilbene, time resolved fluoresc. in ps. regime 0-14164
- stilbene derivatives containing 2-pyrazoline and 1,3,4-oxadiazole groups, spectral-luminescent props. 0-7394
- strontium acetate hemihydrate:  $Mn^{2+}(Cu^{2+})$ , EPR, spin Hamiltonian anal. and unit cell symmetry 0-29603
- strontium calcium tartrate tetrahydrate, gel grown mixed single crystals, defect characterisation 0-2027
- strontium formate dihydrate:  $Cr^{3+}$ , optical absorption spectrum 0-50380
- styrene, plasma polymerisation in glow discharge, thin film IR and free radical EPR obs. 0-2964
- styrene, thermal polymerization, PMR obs. 0-3342
- styrene anions, electron affinities, transition energy, comparison for gaseous liquid and solid 0-29731
- styrene divinylbenzene, viscosity meas. during radical copolymerisation 0-3344
- substituted benzoic acids, PMR study 0-39881
- subtilisin charge-relay system, electrostatic pot. map, STO transferable bond calc. 0-3571
- succinic acid, partially deuterated,  $^1H$  and  $^2H$  distant ENDOR obs. of mol. struct. parameters 0-23445
- succinic acid and its alkaline salts in aqueous soln., Raman and IR spectra (French) 0-32723
- succinonitrile, defects in plastic phase, positron annihilation obs. 0-11504
- succinonitrile, plastic, diffuse scatt., hard-core correl., weak-graph method 0-49137
- succinonitrile, plastic phase, mol. motions correlation times, incoherent neutron scatt. 0-49138
- sucrose, mathematical model of crystn. rate in pure solns. 0-49151
- sucrose, polycryst., NMR, selection of nonprotonated C resonances 0-50201
- sugar, triboluminescence and cryst. fracture dynamics 0-50437
- sugar char, EPR in transition range 0-34751
- sulphate cellulose prod. waste water, radiation treatment (Russian) 0-55688
- sulphides, interacting mechanisms with Fe and Cu surfaces rel. to friction and lubrication behaviour 0-45546
- sulphononaphthols, rapid pH and  $\Delta\mu H^+$  jump by short laser pulse 0-16709
- surfactant molecules reorientation on electrode surface, electrochem. kinetics 0-45522
- surfactant-water liquid crystal phases, review 0-28913
- TANOL, free radical, spin flopping transition, temp. depend., mag. anisotropy energy 0-54890
- D-tartaric acid, cryst. struct., 35-295K, by X-ray diffr. 0-22369
- dl-tartaric acid, radiation products, ESR-ENDOR OBS. 0-55682
- tartaric acid, triboluminescence and cryst. fracture dynamics 0-50437
- tartaric acid salts, and deuterated forms, irradi-crysts., primary reactions, EPR obs. 0-3370
- tetrakis(ethyl isocyanide) platinum(II) tetracyanoplatinate(II), cryst. data, X-ray powder anal. 0-2003
- TBBA liquid crystal, self diffusion coeffs., neutron diffr. and NMR study 0-19689
- TBPA, liq. cryst., smectic F phase, X-ray diffr. obs. 0-44122
- TCNQ $^-$ , ESR probe for phospholipid membrane polar head motion study (French) 0-45865
- TCNQ, charge transfer complexes, changes in valence electronic structure 0-7477
- TCNQ, generalised Wigner lattices and band motion effects 0-24815
- TCNQ, lattice softening mechanism 0-6481
- TCNQ, salt, DBTTF-TCNQ, elec. resistivity and thermoelec. power meas. 0-20193
- TCNQ alkali salt, spin-Peierls transition 0-29395
- TCNQ complex, Adn TCNQ $_2$ , nuclear-spin-lattice relaxation 0-39886
- TCNQ complex formed from cation (methyl-1-N-ethyl benzimidazolium) $^+$  conductivity transition 0-10954
- TCNQ complex with 5-phenyl-[1-thiol]-3-selenol-2-thione, charge-transfer salt, cryst. and mol. struct. 0-33986
- TCNQ complexes with ferrocenes, charge transfer type, struct. and mag. props. 0-24439
- TCNQ complexes with N-methyl derivatives of pyridine, cond. and thermoelec. power meas., band model anal. 0-10952
- TCNQ dimers, extended Huckel hamiltonian supermol. CNDOS calcs. 0-27953
- TCNQ intercalated 2H-NbSe $_2$ , elec. resistivity temp. behaviour anomaly (Russian) 0-10953
- TCNQ salt, (N-methylphenazinium) $_x$ (phenazine) $_{1-x}$ , 1 band filling, carrier mobility and disorder effects 0-24904
- TCNQ salt, (NMe $_2$ H)(I)(TCNQ), one-dimens. semicond. with metal-like cond. 0-24909
- TCNQ salt, (NMP) $_{0.5}$ (phenazine) $_{0.5}$  TCNQ, transport props. 0-24891
- TCNQ salt, (NMP) $_x$ (phen) $_{1-x}$ (TCNQ), thermoelectric power temp. depend. 0-15548
- TCNQ salt, (TSeF) $_x$ (TTF) $_{1-x}$ -TCNQ, struct., elec. and mag. props., review 0-20158
- TCNQ salt, acridinium (TCNQ) $_2$  low temp. heat capacity, Debye temp. 0-2180
- TCNQ salt, HMTTF-TCNQ, sp. ht., 30 to 80K 0-24614
- TCNQ salt, HMTTF-TCNQ, three-dimens. ordering, Ginzburg-Landau model for Peierls instability 0-20160
- TCNQ salt, K-TCNQ, high and low temp. phases, dielec. const. 0-34844
- TCNQ salt, K-TCNQ, single crystal, charge transfer band interpretation, refl. spectrum obs. 0-25353
- TCNQ salt, MEM(TCNQ) $_2$ , phase transition electronic struct. interpretation 0-24781
- TCNQ salt, MEM(TCNQ) $_2$ , phase transitions, elec. cond., ESR, mag. susceptibility study 0-24981
- TCNQ salt, MTPA (TCNQ) $_2$ , IR refl., dielec. function and cond. 0-34924
- TCNQ salt, N-n-butyl-quinolinium (TCNQ) $_2$ , ESR spectrum fine struct. splitting 0-44904
- TCNQ salt, N-propyl-quinolinium(TCNQ) $_2$ , defect conc. depend. phase transition 0-44577

## organic compounds continued

- TCNQ salt, NMP $_{0.63}$ phenazine $_{0.37}$ TCNQ, mag. susceptibility, 0.03-4.2K 0-25191
- TCNQ salt, NMP-TCNQ, electronic struct., SCF calc., total energy polarisation effects 0-15469
- TCNQ salt, NPQn (TCNQ) $_2$ , neutron irradi. induced defect concentration depend. phase transition 0-29449
- TCNQ salt, polyvinylcarbazole-TCNQ complex, elec. cond. meas. 0-34456
- TCNQ salt, pyridinium (TCNQ) $_2$ , low temp. mag. phase transition, ESR study 0-25139
- TCNQ salt, Qn(TCNQ) $_2$ , non-Ohmic cond. 0-20169
- TCNQ salt, Qn(TCNQ) $_2$ , one-dimens. spin glass with antiferromag. exchange, Knight shift meas. 0-25231
- TCNQ salt, Qn(TCNQ) $_2$ , thermoelec. power and cond., large Coulomb repulsion model 0-24893
- TCNQ salt, Qn (TCNQ) $_2$ , configurational entropy, thermoelec. power meas. 0-34432
- TCNQ salt, quinolinium, electron spin location, elec., mag., and thermal props. 0-25189
- TCNQ salt, quinolinium (TCNQ) $_2$ , mag. chain double resonance study, deuteration 0-25250
- TCNQ salt, quinolinium (TCNQ) $_2$ , transport props. 0-24891
- TCNQ salt, TEA (TCNQ) $_2$ , anomalous conductivity, conductivity transitions 0-15508
- TCNQ salt, tetramethylhexamethylenediammonium-TCNQ-iodine, elec. and mag. props., struct., specific heat 0-24898
- TCNQ salt, TMTSF-DMTCNQ, cond. and thermopower meas. 0-20165
- TCNQ salt, TMTSF-DMTCNQ, mag. susceptibility meas. under press. 0-29521
- TCNQ salt, TMTSF-TCNQ, microwave cond. at 35 GHz 0-24963
- TCNQ salt, TSeF-TCNQ, Peierls transition and CDW ordering, X-ray study 0-20101
- TCNQ salt, TTF $_{1-x}$ TSeF $_x$ -TCNQ, mol. substitutional disorder 0-24438
- TCNQ salt in aqueous media, electrochem. behavior 0-6976
- TCNQ salts, aminopyridinium (TCNQ) $_2$ , elec. and mag. props., 4.2 to 300K 0-24889
- TCNQ salts, anomalous infra-red activity and the determination of electron-molecular vibration coupling constants 0-25389
- TCNQ salts, charge transfer and cond. 0-20164
- TCNQ salts, conducting, Raman spectra, estimation of degree of charge transfer from vibrational frequencies 0-50344
- TCNQ salts, ionene polycation-TCNQ salts, elec. cond. rel. to polycation struct. 0-34428
- TCNQ salts, n-methylacridium (TCNQ) $_2$ , 2,2'-bipyridinium (TCNQ) $_2$  and Qn(TCNQ) $_2$ , with asymmetric donors, mag. susceptibility, 0.035-4.2K 0-25190
- TCNQ salts, polymer composites, elec. cond. 0-20157
- TCNQ salts, proton nucl. relax. meas. 0-20484
- TCNQ salts with heterocyclic amines and hydroquinone form. via redox reaction 0-26013
- TCNQ solids, quasi-one and -two dimensional materials crystal growth (Japanese) 0-35073
- TCNQ- $\phi_6$ DTP, chemisorbed O $_2$  effects on mag. susceptibility 0-15679
- TCNQ-DIP  $\Phi_4$ , electronic diffusion coeffs. in chains, proton spin-lattice relax. and dynamic nucl. polarisation 0-25241
- TCNQ-HMTSF, de Haas-Shubnikov oscils. 0-10956
- TCNQ-NMP, incomplete charge transfer, NMR relax. and line-shift meas. 0-20485
- TCNQ-NMP, transport props. 0-24891
- TCNQ-TTF, chemisorbed O $_2$  effects on mag. susceptibility 0-15679
- TEA(TCNQ) $_2$ , elec. cond. and thermoelec. power under hydrostatic press. 0-11024
- technetium glucoheptonate, prep. using formamidine sulfonic acid 0-51252
- TEM, appl. to organic crystals 0-2327
- ternary gas mixture, natural convection, naphthalene sublimation appl. 0-6511
- ternary liquid mixtures, evaluation of US vel. 0-38201
- terpenes, IR absorption bands of  $\alpha$ - and  $\beta$ -pinenes above forests 0-12539
- o-terphenyl, dipolar solutes, reorientational motions, dielectric relax. below glass transition 0-19706
- o-terphenyl, liq. and glassy, dynamics of dissolved ferrocene, Mossbauer obs. 0-55000
- p-terphenyl, narrow bandwidth pulsed UV laser, 3350 to 3450 Å 0-38032
- p-terphenyl, substituted, dye laser and spectral characts., output power, conversion efficiency 0-23681
- p-terphenyl, triplet exciton annihilation and triplet spin relax. 0-29792
- p-terphenyl polycrystalline layers, AC cond. 0-44746
- tertiary amines, laser action feasibility, excited state absorpt., two step photoionisation 0-23682
- tertiarybutylisocyanide-borane, vibr., rot. const., moment of inertia, microwave spectra obs. 0-32706
- testosterone, dielectric props. under UV excitation 0-6912
- testosterone, dielectric transient response following UV-irradiation 0-51166
- tetra-n-butylammonium halide-MnCl $_2$  melts, density, elec. cond., and viscosity 0-24631
- tetraalkylammonium bromide soln., conductance and viscosity, temp. and concentration depend. 0-6531
- tetraalkylammonium halides, mol. reorientation, spin lattice relax. time study 0-18875
- meso-1,2,3,4-tetrabromobutane, IR and Raman spectral studies 0-32722
- 1,1,2,2-tetrabromoethane, dil. soln. in benzene, dielec. relax. study 0-29679
- tetrabromomethane, adsorption on Fe (100), AES, LEED, work function, and thermal desorption meas. 0-39422
- tetrabromomethane, in disordered phases, IR active mode Raman line shape, dipole-dipole interaction 0-9603
- tetrabutylammonium iodide, in aq. proline soln., elec. conductance investigation 0-10692
- tetrabutylammonium iodide/I solid/liquid electrolyte interface, impedance study 0-26031
- tetracene, amorphous film, TSC meas., carrier traps 0-2496
- tetracene, organic insulator action spectra of photocurrent 0-34482
- tetracene, trapping effects on emission-limited current flow 0-29413
- tetracene, vibrational quasicontinuum threshold, spectrosc. criterion 0-52972
- tetracene in liquid crystal, temp. depend. of absorption and fluoresc. (German) 0-18887



## organic compounds continued

tetracene surface states, electric field effects, exciton-charge carrier interactions (*Russian*) 0-24989  
 tetracene-Kr(Xe), intramol. intersystem crossing in supersonic beam, external heavy atom effect 0-14167  
 tetrachlorobenzene, dimer triplet state line shape, small excitons 0-48041  
 1,2,4,5-tetrachlorobenzene, excited triplet state dimer, intermol. exchange integral, isotope effect 0-15826  
 1,2,4,5-tetrachlorobenzene, triplet excitons, high. mag. field, spin-lattice relax. study 0-20517  
 meso-1,2,3,4-tetrachlorobutane, IR and Raman spectral studies 0-32722  
 tetrachloroisophthalonitrile, vapour press. by effusion method, solid phase eqn. of state 0-49350  
 tetrachloromethane, fluid vibr. spectra, repulsive force depend. line broadening (*Russian*) 0-47970  
 tetrachloromethane+n-heptyl alcohol, measurements of US vel. and related parameters 0-38200  
 tetrachloromethane-cyclohexane liq. mixtures, heat of transport, Dufour effect 0-44344  
 tetracyanobenzene+methylated benzene, fluorescent exciplex form., electronic relax. 0-5573  
 s-tetracyanobenzene+p-xylene, photoassoc., exciplex form., excitation energy and isotope depend., vibr. effects 0-55634  
 tetradecanoic acid monolayers, liq.-expanded/liq.-condensed phase changes press., effect of temp. diff. between liq. substrate and air 0-54476  
 di-(tetraethylammonium)tetrahalomanganate, mag. circular and linear dichroism obs. 0-29725  
 tetraethylene glycol dodecyl ether-H<sub>2</sub>O, binary micellar solns. and emulsions, dielec. behaviour 0-44994  
 tetraethylene glycol dodecyl ether-H<sub>2</sub>O-heptane, binary micellar solns. and emulsions, dielec. behaviour 0-44994  
 tetrafluoromethane, compressed gas, apparatus for depolarisation ratio meas. of scatt. light 0-38527  
 tetrafluorodilithetane, IR photolysis, multiphoton dissoc. models 0-30253  
 tetrafluoromethane, bond length and chemical shielding, NMR lineshape anal. of multipspin system 0-32741  
 tetrafluoromethane, elastic and inelastic electron scatt. differential cross section, obs. and calc., struct., binding energy 0-28110  
 tetrafluoromethane, gas, DID Rayleigh and Raman depolarised scatt., lattice-gas model 0-10356  
 tetrafluoromethane, in disordered phases, IR active mode Raman line shape, dipole-dipole interaction 0-9603  
 tetrafluoromethane, intermolecular pot., lattice energy and heat of sublimation 0-38995  
 tetrafluoromethane, M-X bond flexibility, by compliance scheme 0-37805  
 tetrafluoromethane, RF discharge chemistry, added H<sub>2</sub> effect 0-33832  
 tetrafluoromethane, vap. press., triple pt. to 173K 0-6522  
 tetrafluoromethane+CO, vibr. relax. rates, energy transfer 0-37862  
 tetrafluoromethane adsorbed on graphite, adsorption isotherms, crit. temps. (*French*) 0-34312  
 tetrafluoromethane-trifluoromethane-chlorotrifluoromethane, vapour-liq. equilib. compositions, calc. 0-19925  
 tetrahydrofuran, reversible intercalation in graphite-alkali metal lamellar cpds. 0-16211  
 tetrahydrofuran-benzene, soln., excess thermodynamic props. and interactions, US vel. and density meas. 0-39288  
 tetramethyl orthocarbonate, enthalpy of hydrolysis meas., microprocessor-controlled system 0-22361  
 tetramethylammonium hexabromotellurate, far IR and Raman spectra and phase transitions 0-11376  
 tetramethylammonium iodide, in aq. proline soln., elec. conductance investigation 0-10692  
 tetramethylammonium tetrachlorozincate, ferroelec., incommensurate-commensurate transition, neutron scatt. study 0-40073  
 tetramethylammonium tetrachlorozincate, low temp. phases, superstruct., X-ray study 0-39065  
 tetramethylammonium zinc tetrachloride, <sup>13</sup>C NMR and PMR study of incommensurate phase transition 0-34863  
 2,2,3,3-tetramethylbutane,  $\gamma$ -irrad., EPR spectrum assignment 0-15800  
 2,2,3,3-tetramethylbutane, radiolysis, radical prods., EPR obs. 0-32747  
 tetramethylethylene, photoelectron spectrosc., ang. depend. 0-9641  
 tetramethylsilane, IR and visible spectral intensity data and the universal intensity concept 0-28066  
 tetramethylsilane, liq., electron drift vel. saturation, skeletal vibr. 0-34451  
 tetramethylsilane, local mode combination bands and local mode mixing 0-27999  
 tetraphenylchlorin-d<sub>0</sub>, -d<sub>1</sub>, lowest triplet state, intersystem crossing rates, temp. and isotope effects 0-48026  
 tetraphenyldithiadipyranilene-iodine, synthesis and cond. props. 0-24910  
 meso-tetraphenylporphine, potential parameters of H migration tunnel rates calcs. 0-5600  
 tetraphenylporphyrin, dispersion induced circular dichroism, determ. of mag. dipole allowed transitions 0-14163  
 tetraphenylporphyrin, free base in PVC matrix, excited state props., electrochromism obs. 0-37815  
 tetraphersylanionium-tetraphenylborate assumption for single ion thermodynamics in amphiprotic and dipolar-aprotic solvents 0-55675  
 tetraselenotetracene cation radical salts, cryst. struct. by X-ray anal., rel. to elec. props. 0-24436  
 tetraselenotetracene thiocyanate complex, X-ray struct. anal. 0-2006  
 tetraselenotetracene chloride, elec. cond. below 1K (*Russian*) 0-6820  
 tetrathiotetracene, charge transfer state parameters, evaluation by mag. field effect (*Russian*) 0-10924  
 sym-tetrazine, isotope selective mol. spectroscopy and isotopically pure mols. prod. with dye laser 0-11926  
 sym-tetrazine, isotopic isomers, spectroscopic obs. 0-53009  
 s-tetrazine, mol., pot. functions of bending modes 0-9753  
 s-tetrazine in n-hexane, picosecond time-resolved fluoresc., vibr. relax. 0-48025  
 tetrazine-Ar, van der Waals bond, nonstatistical vibr. energy distrib., photochemical reaction effects 0-30255  
 TGFB, high press. influence on anomalous specific heat, tricritical point 0-25322  
 TGS:(CuSO<sub>4</sub>), internal friction 0-44257  
 TGS:Cr single cryst., lattice defect influence on critical behaviour 0-25315  
 TGS:Fe<sup>3+</sup>, crystals and their aq. solns., ESR 0-39862  
 TGS:nitroanilines, permittivity, elec. cond. and Curie temp. 0-25273  
 TGS, domain nucleation in AC elec. fields 0-34867

## organic compounds continued

TGS, effect of edge dislocations on shapes of moving domain boundary 0-20602  
 TGS, exponential switching by sidewise domain wall motion 0-29703  
 TGS, ferroelec. domain struct., polarisation obs. (*Chinese*) 0-20603  
 TGS, ferroelectric transition, neutron diff. obs. 0-25324  
 TGS, proton and deuteron NMR anal. of temp. depend. 0-33919  
 TGS, pyroelec. single cryst., elec. field meas., thermally stimulated charges 0-45012  
 TGS  $\gamma$ -ray irrad. cryst., heat capacity anomalies near phase transition (*Russian*) 0-49375  
 TGS pyroelectric detector, compared with W-C point contact, appl. to temporal coherence meas. of HCN laser 0-31871  
 TGS X-irradiated, paramag. relax. spin-echo study 0-7168  
 TGSe:Cu<sup>2+</sup>, EPR ang. depend., coord. of Cu<sup>2+</sup>, Cu-ligand bond obs. and ferroelec. transition anomaly 0-7156  
 TGSe, deuterated, thermal and dielectric props. at high hydrostatic press. 0-34864  
 thiaalkanes pure crystals, thermal press. coeffs. and expansivity at 298.15K 0-49381  
 thiazine dye-Fe photoelectrochem. cells for H<sub>2</sub> production, cell instabilities 0-16814  
 thiirene and deuteroderivatives, Fourier transform IR spectra using Ar matrix isolation, vibr. band assignments 0-14142  
 thioacetamide, IR spectra, amino group inversion transitions and pot. functions 0-43041  
 thiocyanate complexes at Ag electrode surface, Raman spectroscopic study 0-37813  
 thiocyanates, nonbonding and  $\pi$ -orbital interactions, photoelectron spectra 0-32774  
 thioformaldehyde-d<sub>0</sub>, -d<sub>2</sub>, A<sub>1</sub>A<sub>2</sub>-X<sub>1</sub>A<sub>1</sub> vis. absorpt. system, rot. anal. 0-5559  
 thioindigo dyes, triplet state config., laser flash absorpt. spectrosc. obs. 0-5557  
 thiomethoxyl anion, and deuterate, electron photodetachment, affinities, vibr. freq. and spin-orbit splitting 0-53063  
 thionine triplet+haloanilines, electron transfer reaction, radical yield meas. 0-3330  
 thiophene, US and hypersonic investigations of vibrational relaxation 0-33377  
 thiophosgene, B<sup>1</sup>A<sub>1</sub>-state, photophys., fluoresc. lifetime meas. 0-53033  
 l-thioproline single cryst., X-irrad., ESR and ENDOR study of radicals 0-45528  
 thiourea, lock-in phase transform. 0-29698  
 thiourea, phonon modes near order-disorder transforms., hard-core modes due to pseudospin-phonon coupling 0-44285  
 thiourea, phonon modes near phase transitions, IR and Raman spectra 0-45084  
 thorium oxalate, natural, separation of <sup>228</sup>Ra 0-45600  
 thromboxane, evidence against prostaglandin hairpin conformation 0-3585  
 thymine aq. and N<sub>2</sub>O solns., radiolysis products anal. 0-30257  
 thymine damage in chromatin from heated cells after X-irrad., excision obs. 0-45980  
 thymine monoanions in soln., tautomer identification by laser Raman spectroscopy 0-14148  
 thyroxine, free, radioimmunoassay with prebound anti-T<sub>4</sub> microcapsules 0-46014  
 tin oxalate, cryst. struct. rel. to those of Na<sub>2</sub>C<sub>2</sub>O<sub>4</sub>, Na<sub>2</sub>Sn(C<sub>2</sub>O<sub>4</sub>)<sub>2</sub> (*French*) 0-2004  
 TMMC:Cu, dynamic props. using local-moment pair correl. functions 0-15728  
 TMMC:Cu, EPR lines, dynamic effect of low-symmetric spin distrib. 0-39854  
 TMMC:Cu, EPR linewidth freq. depend., spin dynamics 0-15794  
 TMMC, classical Heisenberg antiferromagnet, one-dimens., dynamic props., review 0-15737  
 TMMC, EPR lines in one-dimensional mag. systems, dynamic effect of low-symmetric spin distrib. 0-39853  
 TMMC, linear Heisenberg antiferromagnet, EPR half-field transitions 0-15792  
 TMMC, one dimensional antiferromagnet, EPR expts. 0-20454  
 TMMC, one-dimensional antiferromag., solitons, neutron inelastic-scatt. meas. 0-44810  
 TMMC, one-dimensional paramag., anomalous freq. depend. of EPR linewidth 0-15784  
 TMMC, quasi-1D antiferromag., mag. phase diagram 0-2573  
 TMMC, XY-Ising crossover transition, quasi-elastic neutron scatt. obs. 0-44826  
 (TMTSF)<sub>2</sub>PF<sub>6</sub>, one dimens. conductor, superconds., resist. meas. and mag. field effects (*French*) 0-44753  
 (TMTSF)<sub>2</sub>PF<sub>6</sub>, organic one-dimensional superconductor, transition temp. 0-44754  
 TMTSF-DMTCNQ, metallic state, transport props. 0-24974  
 TMTTF-TCNQ, quasi one-dimens. conductor, diffusive hopping, theory 0-54677  
 TMTTF-TCNQ crystals grown from several organic solvents 0-25544  
 toluene, 91<sup>2+</sup> ion fragmentation, ion kinetic energy spectrum peaks, collision gas sensitive 0-40679  
 toluene, electronic-vibr. spectra calcs., Franck-Condon and Herzberg-Teller approx. 0-37735  
 toluene, gas, liq. and crit., cation mobility 0-48842  
 toluene, molecule translational mobility in depolarised Raman spectra 0-14150  
 toluene, optoacoustic spectroscopy using cell with ultimate corrosion resistance 0-42269  
 toluene, shock compression, dynamic high press. eqns. of state 0-6450  
 toluene, two-photon ionisation spectrum, of <sup>1</sup>L<sub>b</sub>-S<sub>0</sub> transition 0-14180  
 toluene+cyclohexane, energy transfer, pulse radiolysis obs. 0-16714  
 toluene+OH, rate constant under simulated atmospheric conditions 0-50846  
 toluene polymerisation in CC N<sub>2</sub> afterglow, chem. reactions rel. to plasma props 0-3346  
 toluene-9,10-diphenylanthracene, soln., electron beam pulse radiolysis, energy transfer 0-7808  
 toluene-brine microemulsion, liquid interfacial tension meas. from scatt. light intensity 0-20012  
 toluene-bromobenzene, perfect binary liquid mixtures on silica gel, adsorption thermodynamics 0-44428  
 toluene-chlorobenzene, benzene-toluene, perfect binary liquid mixtures on silica gel, adsorption thermodynamics 0-44428



## organic compounds continued

toluene-nitrobenzene binary mixtures, with weak charge transfer interactions, thermodynamic props. 0-54360  
 toluene-sodium salicylate, singlet-singlet energy transfer in Manoxol OT-cyclohexane-water 0-9531  
 o-toluidine+carbon tetrachloride, binary liquid mixtures, excess free vol. calcs. 0-34202  
 o(m)-toluidine+o-chlorophenol, H-bonded mol. complex, microwave absorpt., dipole moment and relax. times 0-14134  
 m-toluidine+o-cresol, binary liquid mixtures, excess free vol. calcs. 0-34202  
 tomato bushy stunt virus crystals, appl. of oscillation method to data collection 0-14961  
 TOPOT, 1,4-bi[[2-(5-p-tolyloxazoyl)]benzene laser, bleaching of vapour 0-19027  
 TOPOT, fluoresc. spectrum light quenching factor wavelength depend. 0-18882  
 toxin, penicillium roqueforti, struct. and absolute configuration 0-39064  
 transdecane-cyclohexane mixture, percolation model of electron and hole mobility 0-29452  
 tri-i-propylgermylamine, and isotopomers, IR and Raman spectra, normal coord. anal. (*German*) 0-32716  
 tri-n-propylamine, low ionis. pot. effect on vol. discharge with UV preionis. 0-44065  
 tri-p-tolylamine and its paramag. radical cation, disordered mol. solid, direct obs. of superexchange 0-39848  
 tri-p-tolylamine doped polycarbonate amorphous film, elec. and mag. props 0-49959  
 s-triazine, triplet instability, RPA calculations 0-27938  
 tribromotrifluoroethane, IR and Raman spectra, normal coord. anal. (*German*) 0-32726  
 trichloroacetonitrile, IR dispersion, complex refractive index and permittivity, time correl. function 0-45057  
 1,3,5-trichloro-2,4,6-trifluorobenzene radical cation,  $B^2A_2' \rightarrow X^2E''$  laser-induced fluoresc. spectra 0-14172  
 trichloroacetic acid molecular compounds, intramolecular configs., nucl. quadrupole double reson. obs. 0-34821  
 3,4,5-trichloroaniline, polymorphism,  $^{35}\text{Cl}$  NQR 0-54163  
 1,2,3-trichlorobenzene, oriented mols.,  $^{13}\text{C}$  satellites use in proton spectra,  $T_c$ -structure 0-18872  
 1,1,2-trichloroethane, phase-modulated spin echoes, derivation of pure absorpt. spectra 0-22410  
 trichloroethane+OH—H<sub>2</sub>O+CH<sub>2</sub>CCl<sub>3</sub>, rate const. and tropospheric chem. 0-16658  
 trichloroethane + OH, 1,1,1- and 1,1,2-isomers, reaction kinetics 298-460K, lower atmos. chem. 0-16657  
 trichloroethylene aqueous hetero-azeotrope mixture, condensation heat transfer coeff. (*German*) 0-33425  
 trichlorofluoromethane, 8-12  $\mu\text{m}$  band model calcs. 0-43112  
 trichlorofluoromethane, 8-12  $\mu\text{m}$  bands intensities, temp. depend. 0-43048  
 trichlorofluoromethane,  $^{19}\text{F}$  spin-rot. tensors, appl. to liq.-phase rot. diffusion 0-43068  
 trichloromethane glass:O<sub>2</sub>,  $^{17}\text{O}$ , NQR by proton double reson., broad reson. assignments 0-53014  
 2,3,4-trichlorophenol, AX spin system, two-dimens. J-resolved NMR, spin decoupling 0-31823  
 trichlorophosphazoperfluoro-1,1-dimethylethane, cryst.,  $^{19}\text{F}$  NMR and mol. mobility, fluorination influence 0-34809  
 trichlorotrifluoroethane, IR and Raman spectra, normal coord. anal. (*German*) 0-32726  
 1,2,3-trichlorotrimethylbenzene, disordered mol. solid, electrodynamic influences on dielec. absorption 0-40040  
 tricresylphosphate, appl. of spectroscopic methods for surface anal. in area of lubrication (*French*) 0-26095  
 triethylacetic acid, high resolution  $^1\text{H}$  and  $^{13}\text{C}$  NMR spectra at liquid-solid phase transition 0-11281  
 triethylamine-perfluoro-T-butanol, photoelectron and Rydberg bands, UV spectra study 0-18865  
 triethylenediamine, plastic cryst., thermolum. curves 0-2876  
 triethylenediamine complexes, structural relationships (*French*) 0-54213  
 triethylsilylamine, and isotopomers, IR and Raman spectra, normal coord. anal. (*German*) 0-32716  
 trifluoroacetic acid-water, molecular dynamics simulation of chemical reactions in solution 0-40673  
 trifluoroethanol solvent for poly[(R)-oxypropylene], effect on opt. rot. dispersion and vac. UV circular dichroism 0-40084  
 trifluoroacetates, methyl and ethyl, intramol. relax. at microwave freqs. 0-55020  
 trifluoroethane-(d<sub>3</sub>), IR and Raman spectra, normal coord. anal. (*German*) 0-32726  
 trifluoroiodomethane, isotopic sensitivity of IR laser photodissociation 0-7805  
 trifluoroiodomethane, molecular vibration energy stochasticization in intense IR laser field by Raman spectroscopy (*Russian*) 0-14149  
 trifluoroiodomethane, multiphoton dissoc., isotopically selective 0-28113  
 trifluoroiodomethane, multiphoton IR excitation and dissoc. (*Russian*) 0-35562  
 trifluoroiodomethane, multiple IR photon excitation and dissoc., primary characts. 0-11909  
 trifluoroiodomethane, photolysis in I laser, chem. kinetics 0-48235  
 trifluoroiodomethane, pyrolysis in Ar:O<sub>2</sub> matrix, forming trifluoromethylperoxy radical 0-50845  
 trifluoroiodomethane, UV absorpt. spectrum broadening by laser-induced vibr. excitation 0-53050  
 trifluoroiodomethane+F, IF product internal rot.-vibr. distrib., fluoresc. obs. 0-48078  
 trifluoroiodomethane+F reactions, product state analysis using laser-induced fluoresc. 0-11915  
 trifluoroiodomethane+O, vel. distrib. and cross section, reactive scatt. 0-26011  
 trifluoromethane, D ultrahigh single-step enrichment by CO<sub>2</sub> laser photolysis 0-45527  
 trifluoromethane, RF discharge chemistry, added H<sub>2</sub> effect 0-33832  
 trifluoromethyl chloride, IR multiphoton dissociation, isotopic selectivity and yield, temp. effect 0-53069  
 trifluoromethyl hypofluorite+Kr( $^3\text{P}_2$ ), KrF\* bound-free oscill. emission spectra calc. 0-7799  
 trifluorotriiodoethane, IR and Raman spectra, normal coord. anal. (*German*) 0-32726

## organic compounds continued

trimethyl orthoacetate, enthalpy of hydrolysis meas. microprocessor-controlled system 0-22361  
 trimethyl phosphate,  $^{31}\text{P}$  normal Fourier transform spectra, line narrowing, selective population transfer induced 0-31827  
 trimethylacetic acid, high resolution  $^1\text{H}$  and  $^{13}\text{C}$  NMR spectra at liquid-solid phase transition 0-11281  
 trimethylamine, adsorption on Mo (100), adsorbed O effect, LEED and AES obs. 0-39443  
 trimethylammonium cobalt trichloride dihydrate, Ising-like system, nucl. spin-lattice relax. of  $^1\text{H}$  and  $^{55}\text{Co}$  0-29638  
 trimethylchlorosilane, chemisorption on goethite, IR spectra 0-7855  
 trimethylene sulphoxide, ring puckering vibr., IR spectra obs. 0-32710  
 trimethylenemethane, ground state triplet, HFS, EPR obs. 0-50188  
 trimethylethylene, photoelectron spectrosc., ang. depend. 0-9641  
 triphenyl-(triphenylgermanylperoxy)silane, cryst. and mol. struct. 0-39066  
 triphenylene, excited state Faraday values mag. circular dichroism spectra and MO CI calcs. 0-18877  
 triphenylene-(d<sub>12</sub>), lowest T<sub>1</sub>[ $^3A_2'(\pi\pi^*)$ ] state vibronic coupling 0-47955  
 tripropylamine admixtures, influence on optical characteristics of CO<sub>2</sub> laser 0-23669  
 triptycene, soln., correl. times from  $^{13}\text{C}$  relax. 0-23438  
 trisarcosine calcium chloride crystals, ferroelec., electrooptic and ferroelastic props. 0-34865  
 trishydrazyl radical in s-butylbenzene, slowly slowly tumbling triradicals EPR 0-32748  
 Triton X100-water-coumarine 1-rhodamine 6G, micellar dye soln., energy transfer 0-45581  
 2-tromopropane, tilt-effect and interference with rel. sign determination in weak irradi. expts. 0-32742  
 tropolone vibr. spectra and proton tunneling 0-28014  
 tryptophan, stereoselective energy transfer induced by circularly polarised light 0-1010  
 tryptophan soln. containing histidine, fluoresc. rel. to soln. pH 0-2826  
 TSeF-TCNQ, Kohn anomaly of metallic state, X-ray diffuse scatt. meas. 0-19887  
 TSeF-TCNQ, nonlinear electronic transport, microwave harmonic mixing obs. 0-20168  
 TSeT-I<sub>2</sub>, physical props., elec. cond. 0-24908  
 $\alpha\text{TTF}:\text{Br}$ , transport and mag. props., effect of doping 0-24934  
 TTF(MBDT) spin-Peierls transition, mag. exchange interactions, mag. props. 0-25138  
 (TTF)Cu<sub>5</sub>C<sub>4</sub>(CF<sub>3</sub>)<sub>4</sub>, spin Peierls system, mag. field effects 0-7123  
 TTF and derived cpds., intramolecular vibr. and vibronic effects, IR and Raman spectra 0-25387  
 TTF derivatives, smectic and nematic, for liq. cryst. device appl. 0-54124  
 TTF halides, charge transfer effect on internal modes, Raman scatt. 0-25392  
 TTF-Cu bis-dithiolene, dimer, mol. displacements at 4.2K 0-10539  
 TTF-Cu<sub>5</sub>C<sub>4</sub>(CF<sub>3</sub>)<sub>4</sub>, spin-Peierls system, high-field phase 0-39816  
 TTF-halides, conductors with chain struct., lattice phonons and distortions, incommensurability transitions 0-24549  
 TTF-SCN, quasi one-dimens. conductor, CDW phase transform., X-ray scatt. study 0-24594  
 TTF-TCNQ, anal. of harmonic microwave mixing 0-44635  
 TTF-TCNQ, and related compounds, low temp. irradi. effects 0-24906  
 TTF-TCNQ, and related cpds., elastoresistivity by strain gauge technique 0-24892  
 TTF-TCNQ, and related cpds., lattice modulations, X-ray diffuse scatt. obs. 0-19787  
 TTF-TCNQ, anharmonic props., temp. (press.) depend., rel. to naphthalene and anthracene 0-15200  
 TTF-TCNQ, antiferroelectric ordering of TCNQ ion elec. polarisation 0-20598  
 TTF-TCNQ, charge transfer change with press. 0-39564  
 TTF-TCNQ, charge transfer determ. from spectral line shift using Raman scatt. 0-25392  
 TTF-TCNQ, cond. in phase transition region 0-24979  
 TTF-TCNQ, controlled defects effect on microwave cond. and dielec. function 0-24885  
 TTF-TCNQ, deuterated, isotope effect on mag. susceptibility 0-25080  
 TTF-TCNQ, divergent mag. responses at 2k<sub>F</sub> and structural phase transitions 0-20376  
 TTF-TCNQ, effect of benzene ring substitution on supercon. and metallic props. 0-20193  
 TTF-TCNQ, elastic neutron scatt. evidence for charge transfer change at high power 0-2163  
 TTF-TCNQ, elec. cond. and spin susceptibility, press. and temp. depend. 0-24894  
 TTF-TCNQ, electron-electron interaction as source of metallic resist. 0-20162  
 TTF-TCNQ, electron-electron interactions in physics of one dimensional conductors 0-24895  
 TTF-TCNQ, electron-molecular distortion coupling near Peierls transition, IR spectra obs. 0-25390  
 TTF-TCNQ, fluctuation cond. and commensurability pinning 0-34429  
 TTF-TCNQ, impurity effects on CDW fluctuations 0-44576  
 TTF-TCNQ, interchain tunnelling effect on nucl. spin-lattice relax. time, interchain coupling of CDW 0-20163  
 TTF-TCNQ, IR reflectance in conducting phase 0-25388  
 TTF-TCNQ, Landau free energy function, CDW-libron interaction, sp. ht. near phase transitions 0-19963  
 TTF-TCNQ, Matthiessen's rule, effective defect resistivity 0-6821  
 TTF-TCNQ, non-linear elec. transport by pinned CDW 0-20172  
 TTF-TCNQ, nonlinear electronic transport, microwave harmonic mixing obs. 0-20168  
 TTF-TCNQ, organic metal, Van der Waals donor stacking 0-15037  
 TTF-TCNQ, Peierls transition temp. and 0K energy gap, mean field theory calc. 0-24782  
 TTF-TCNQ, phase transitions and CDW state, controlled disorder effects 0-15507  
 TTF-TCNQ, phase transitions and CDW state, induced defect depend., transport and mag. studies 0-24980  
 TTF-TCNQ, physical properties, reviews (*Japanese*) 0-24883  
 TTF-TCNQ, pinned CDW in very far IR 0-25391  
 TTF-TCNQ, temp. depend. of phonon frequencies at constant vol. 0-10616  
 TTF-TCNQ, two-chain Fermi gas, response behaviour 0-2381  
 TTF-TCNQ, X-ray irradi., transverse cond. 0-6432



## organic compounds continued

- TTF-TCNQ analogues, TTF-TCNQ and METTF-TCNQ, cryst. struct., X-ray anal. 0-19788
- TTF-TCNQ and derivatives, 1.8 to 40K, three dims. state, specific heats 0-44333
- TTF-TCNQ and related compounds, cryst. struct., organisation, dimensionality, interchain disorder 0-19790
- TTF-TCNQ family, donor stack dominance of transport props. 0-20166
- TTF-TCNQ series, cryst. struct., elec. cond., and EPR meas., steric factor effects 0-19789
- TTFCuBDT, spin-Peierls transition in spin 1/2 Heisenberg chains, RPA calcs. 0-25150
- TTT-(I<sub>3</sub>)<sub>2</sub>, physical props., elec., mag. and optical meas. 0-24908
- TTT<sub>2</sub>I<sub>3</sub>-Br<sub>3</sub>, chem. impurities and neutron irradi. induced defects, effects on DC cond. 0-49699
- TTT<sub>2</sub>I<sub>3</sub>+Br<sub>3</sub>, thermoelec. power and metal-semicond. transition 0-34431
- TTT<sub>2</sub>I<sub>3</sub>, charge transfer salt, Coulomb effects, Madelung energy calcs. 0-19747
- TTT<sub>2</sub>I<sub>3</sub>, chem. impurities and neutron irradi. induced defects, effects on DC cond. 0-49699
- TTT<sub>2</sub>I<sub>3</sub>, quasi one-dimens. organic metal, elec. cond. and thermoelec. power 0-24899
- (TTT)<sub>2</sub>I<sub>3</sub>+Br<sub>3</sub>, struct., X-ray diffuse scatt. study 0-24437
- TTT cation radical salts, cryst. struct. by X-ray anal., rel. to elec. props. 0-24436
- TTT salts, IR spectra, mixed-valence salts 0-40121
- TTTI<sub>2</sub>Br<sub>1.5</sub>-X, optical and transport props. 0-24911
- TU-20 turbine oil, 4-methyl-2,6-di-tert-butylphenol determ., using IR spectrophotometry (*Polish*) 0-13161
- di-tungsten cyclopentadienyl tri-carbonyl, dual luminesc., ps pulse excitation 0-32754
- tyrosine, polycryst., NMR, selection of nonprotonated C resonances 0-50201
- undecane, liquid, chain reorientation, Brownian dynamics simulation, comparison of models 0-49067
- unsaturated P-containing peroxides, electron structure, stability and reactivity 0-14086
- uracil in carbonaceous chondrites, Murchison, Murray and Orgueil meteorites 0-31261
- uracil monoanions in soln., tautomer identification by laser Raman spectroscopy 0-14148
- uranin in ethanol soln., and dye mixtures, excitation by Cu vapour laser 0-28230
- uranyl hexafluoroacetylacetonate tetrahydrofuran, IR laser photodissoc., O and U isotope selective 0-50868
- urea, electro-optical coeffs. meas., rel. to nonlinear optics calcs. 0-34889
- urea, electrochem. removal, basis for a regenerative dialysis system 0-26417
- urea, quantitative structural studies by means of the energy-dispersive method with X-rays from a storage ring 0-24314
- urea adducts, crystn., geometry of urea-cation bonding 0-39061
- urea antimony fluoride, X-ray cryst. struct. determ. (*French*) 0-44196
- urea crystal, efficient phase-matched SHG and sum freq. mixing 0-14391
- urea mixed and adsorption mixed crystals and epitaxial growth from solns., trachit and habit (*German*) 0-38973
- uridine 5'-phosphate (Na salt), NO<sub>2</sub> species in an irradi. single crystal, EPR obs. 0-40719
- US relaxation of aqueous mixtures of methanol and ethanol (*French*) 0-6468
- vanadyl bisacetylacetonate, polarised X-ray absorption and double refraction 0-50459
- vapour sorption on PVC and polystyrene powders, glassy-state relaxation induction and meas. 0-44415
- vinyl bromide, mol. struct., from gas-phase electron diff. and microwave data 0-23571
- vinyl bromide-d<sub>3</sub>, <sup>13</sup>CBr bond, coupling consts., correl. with C hybridisation s-character 0-34806
- n-vinyl carbazole, radiation induced polymerization ESH study 0-7817
- n-vinyl carbazole-acrylamide, post radiation induced polymerisation 0-7818
- n-vinyl carbazole-acrylamide, radiation induced polymerization, monomer crystallinity effects 0-7819
- vinyl isocyanate, and vinylcyano ether, geometry and conform., ab initio minimal STO-3G MO calcs. 0-23337
- vinyl mercaptan -d<sub>0</sub>, -d<sub>1</sub>, anti rotamer, conform., microwave spectrum 0-9592
- vinyl mercaptan -d<sub>0</sub>, -d<sub>1</sub>, synrotamer, conform., microwave spectrum 0-5535
- 2-vinylanthracene, conform. conversion kinetics, fluoresc. 0-9631
- vinylcyano ether, and vinyl isocyanate, geometry and conform., ab initio minimal STO-3G MO calcs. 0-23337
- volatile trace organics, aqueous environmental samples, head space anal. 0-40763
- water dodecane potassium oleate hexanol, micro emulsion, Rayleigh scatt., micellisation (*French*) 0-43055
- water toluene sodium dodecylsulfate butanol, micro emulsion, Rayleigh scatt., micellisation (*French*) 0-43055
- xanthene dyes, hidden vibr. band determ. method, fluorescence and excitation spectra meas. 0-40158
- xanthene dyes, internal heavy atom effect on radiative and non-radiative rate consts. 0-32765
- xanthine, planar autoassoc. energy 0-53086
- xanthine oxidase (dehydrogenase), EPR, mag. spin-spin dipolar interaction 0-53026
- p-xylene, electronic-vibr. spectra calcs., Franck-Condon and Herzberg-Teller approx. 0-37735
- p-xylene, liq., heat capacity rel. to temp. 0-44335
- xylene, liq., interface with photoconductor, carrier injection 0-24970
- p-xylene, melting surface, ablation in impingement region of water jet 0-14766
- p-xylene+s-tetracyanobenzene, photoassoc., exciplex form., excitation energy and isotope depend., vibr. effects 0-55634
- n-xylene dissociation, C precipitate with preferred orientation [100] (*Russian*) 0-45484
- xylideneaniline-p'-benzonitri 0-44328
- xylytol, X-irrad., 4.2K, electron traps, alkoxy hyperfine coupling, ENDOR obs. 0-50863
- yeast phosphoglycerate kinase crystals, rotation camera data, empirical method correction for absorpt. and decay effects 0-14962

## organic compounds continued

- yellow pigment, photoconducting, electric field-induced fluoresc. quenching 0-34967
- zinc(II) metalloporphyrin, Z-ray photoelectron spectra satellites 0-5582
- zinc stearate lubricant, admixed, effect on Fe sintered compact, shrinkage and mech. props. 0-45402
- zinc stearate lubricant effect on Fe powder compact, apparent density, mixing, and friction 0-45403
- Ag complexes, Ag(II) porphyrins, picosec. flash photolysis, transient absorpt. 0-52976
- Ar-methyl chloride, mol. beam elec. reson. spectrosc. 0-23477
- Ar-Xe-tetrachloromethane, self-sustained electrophotolysed discharge in compressed gas 0-38003
- Ba<sub>2</sub>I<sub>2</sub> cyclodextrin, quasi-one-dimens. cpd., synthesis, elec. and mag. props. 0-2380
- C chain molecules in interstellar clouds, form. schemes 0-26935
- CBr<sub>2</sub> emission in solid Ar, laser excitation spectra and lifetimes 0-48034
- CBrCl emission in solid Ar, laser excitation spectra and lifetimes 0-48034
- CD<sup>+</sup>, A<sup>1</sup>Π, rot.-vibr. population distrib. 0-23396
- CF<sub>3</sub>, CF<sub>3</sub><sup>+</sup>, and CF<sub>3</sub><sup>+</sup>, optimised struct. and bonding, ab initio SCF MO calc. 0-23334
- CF<sub>3</sub>(<sup>3</sup>B<sub>1</sub>) energy distrib., from triplet-triplet CF<sub>2</sub>(<sup>3</sup>B<sub>1</sub>) annihilation and C<sub>2</sub>F<sub>4</sub> vuv photolysis 0-50861
- CF<sub>3</sub><sup>+</sup>CO, core ionisation phenomena, nonempirical LCAO MO SCF investig. 0-37906
- CF<sub>3</sub>NO-CF<sub>3</sub>NO, photodissociation dynamics, two-photon laser-induced fluorescence study 0-43122
- CH, B<sup>2</sup>Σ<sup>-</sup> state predissoc., calcs. and time resolved spectrosc. 0-23576
- CH, CD, interstellar, A-doublet population inversion by collisions 0-22065
- CH, CH<sup>+</sup> towards Cepheus OB2 association, interstellar lines obs. 0-22052
- CH, prod. by multiphoton dissoc. of organic compounds 0-5586
- CH<sub>2</sub>, A<sup>1</sup>Π, rot.-vibr. population distrib. 0-23396
- CH<sub>2</sub><sup>+</sup>, in interstellar diffuse clouds, prod. by interstellar shock waves 0-56898
- CH<sub>2</sub><sup>+</sup> polar molecular ion, electron vibr.-rot. excitation (*Russian*) 0-1053
- CH<sub>2</sub><sup>+</sup>, predissociated levels obs. 0-37838
- CH<sub>2</sub><sup>+</sup>, sub-Doppler laser spectroscopy using fast ion beams 0-9655
- CH<sub>2</sub>+p-H<sub>2</sub>(He), collisional pumping of A-doublet transitions, pot. energy surface 0-23516
- CH<sub>2</sub> molecular beam source 0-37908
- CH<sub>2</sub>, photoprod. from ketene, singlet-triplet energy separation and rovibronic level obs. 0-11936
- CH<sub>2</sub><sup>+</sup>, <sup>4</sup>A<sub>2</sub> states, large CI wavefunctions, non-adiabatic coupling matrix elements 0-37744
- CH<sub>2</sub><sup>+</sup>, <sup>4</sup>A<sub>2</sub>(2,3) states, unimolecular decay, nonadiabatic interactions, transition probability as function of Massey parameter 0-35503
- CH<sub>3</sub> average internal excitation formed in F+CH<sub>3</sub>I(CF<sub>3</sub>I), fluoresc. obs. 0-48078
- CH<sub>3</sub>+O<sub>2</sub>-OH+H<sub>2</sub>CO, 368K, rate const. upper limit 0-7771
- CH<sub>3</sub><sup>+</sup>+CH<sub>3</sub>(NH<sub>3</sub>)(H<sub>2</sub>S), condensation reactions mechanism 0-25996
- CH<sub>3</sub><sup>+</sup>CO, core ionisation phenomena, nonempirical LCAO MO SCF investig. 0-37906
- CX<sub>n</sub> radical, (X=H,D; n=1,2,3), thermodynamic function in ideal gas state 0-14871
- <sup>13</sup>C/<sup>12</sup>C ratio analysis in organic materials by mass spectrometry (*Portuguese*) 0-7875
- CaSO<sub>4</sub>/Tm/polythene mixture, thermoluminesc. response to fast neutrons 0-5340
- ClFCS, second excited singlet state photophysics, laser excitation obs. 0-32758
- Cl<sub>2</sub>PNC(ClF<sub>3</sub>)<sub>2</sub>, cryst., <sup>35</sup>Cl NQR obs. of molecular reorientations between unequal potential wells 0-54989
- Co complexes, EXAFS obs. 0-998
- Co(II) Schiff base complexes, structure and bonding, book contrib. 0-972
- Co(II)-octaethylporphyrin, Mossbauer emission spectra 0-8020
- Cu complex, 1,2-ethanediammonium tetrachlorocuprate, layered struct. mag. susceptibility 0-7094
- Cu complexes, EXAFS obs. 0-998
- Cu(II) iminodiacetates in aqueous solution, gamma-ray radiolysis 0-35560
- dimethylammonium manganese tetrachloride, 2D Heisenberg antiferromag., spin wave anal. 0-54879
- Eu(III) complexes, f-f transition probabilities, ligand polarisation model, anisotropic contribs. 0-53049
- FeCl<sub>4</sub> in organic solvents, dilute, ESR linewidths (*German*) 0-11258
- Fe<sub>2</sub>I<sub>2</sub> cyclodextrin, quasi-one-dimens. cpd., synthesis, elec. and mag. props. 0-2380
- HCC-H+C=C dissoci., trajectory calcs., random vibr. excitation 0-45491
- HCCN, a cyanocarbene, geom. struct., electron correl. effects 0-1077
- HCOH, prediction, potential energy surface for ground state of formaldehyde 0-42967
- HCS<sup>+</sup>-CSH<sup>+</sup>, struct. and stability, ab initio SCF calcs., CNDO calcs. 0-32608
- H<sub>2</sub>O-organic aerosol-n-heptane reverse-type micellar soln., neutron small-angle scatt. (*French*) 0-26059
- HOBHA, thermotropic mesophase, DMR chain segments assignment 0-24356
- I<sub>2</sub>-aromatic complexes, photodissociation, I-aromatic complex in soln. formation ps laser studies 0-40711
- Li soaps, n.C<sub>13</sub>-n.C<sub>20</sub>, phase transition temps. and enthalpies, DSC obs. 0-45544
- methane cation, Jahn-Teller distortion 0-48098
- methane, solid, librational tunnelling and proton relax. temp. 0-38969
- Mg-chlorin, electronic struct. props. and photosynthesis 0-16902
- Mg-meso-tetraphenylporphine-coated glass electrode, in photogalvanovoltaic cell (*Chinese*) 0-40865
- Mg-porphine, electronic struct. props. and photosynthesis 0-16902
- Na-fluorescein, glycerol-alcohol soln., luminesc. decay time, conc. depend. 0-34960
- Na<sub>3</sub>Pr(C<sub>4</sub>H<sub>4</sub>O<sub>3</sub>)<sub>2</sub>.2NaClO<sub>4</sub>.6H<sub>2</sub>O, single cryst., forbidden A<sub>1</sub>→A<sub>1</sub> transition, mag. field induced intensification 0-50302
- Ni complexes, Ni(II) porphyrins, picosec. flash photolysis, transient absorpt. 0-52976
- Ni(CN)<sub>2</sub>-dodecylamine, lamellar paraffinic system, phase transitions, wide-line NMR obs. (*French*) 0-44929
- trans-Ni(S<sub>2</sub>N<sub>2</sub>CH<sub>3</sub>)<sub>2</sub>, IR and Raman spectra, normal coord. anal. 0-28019



**organic compounds continued**

- O-containing compounds, dipole moments, NDDO calcs. 0-47894  
 pyrene, UV spectra and extinction coeffs. for  $S_0 \rightarrow S_1$  absorption 0-18866  
 Ru complex, Creutz-Taube ion, ground state, single crystal EPR obs. of mixed valence Ru dimer ion 0-34766  
 Si compounds, free mol. chemical shift, binding energy and Auger spectra 0-32782  
 TCNQ salt, TSeF-TCNQ, anal. of harmonic microwave mixing 0-44635  
 TGS, ferroelec. cryst., complex permittivity at microwave freq. and high press. 0-2685  
 TGSe, ferroelec. cryst., complex permittivity at microwave freq. and high press. 0-2685  
 TGSe:Cu<sup>2+</sup>, EPR studies 0-7153  
 (TSeT)<sub>2</sub>Cl, one-dimens. conductor, metallic phases 0-20159  
 TTF-TCNQ, pure and irradiated, nonlinear transport, ESR study, 1.2-4.2K 0-20167  
 TTT<sub>2</sub>I<sub>3</sub>, neutron irradiation induced defects and chemical impurity effects on DC cond. 0-39565  
 UO<sub>2</sub>HCONH<sub>2</sub>·0.5H<sub>2</sub>O, prep., cryst. struct. and charact. 0-29010  
 Zn II complex, hexaimidazole-zinc(II) dichloride tetrahydrate:Cr(III), D-tensor orientation, charge-compensation vacancies 0-50172

**organic insulating materials**

- see also *insulating oils; paper; plastics; rubber; silicones; varnish; waxes*  
 epoxy resin based composites, superconducting magnet insulators, gamma-ray radiation effects 0-24495  
 epoxy resins, phenomena and mechanisms of tree inception 0-29687  
 glass-epoxy laminate, superconducting magnet insulators, gamma-ray radiation effects 0-24495  
 hydrocarbon liquids, streamer breakdown in divergent field 0-25308  
 PET, ionic cond. current rel. to neutralisation at polymer-metal interface at elevated temps. 0-24664  
 PMMA, immersion in high press. gaseous media, breakdown characts. for direct voltages with ripple 0-45009  
 polycarbonate, plastic insulation for cryogenic power cable, exam. of dielectric, tensile props. 0-25823  
 polyester (Mylar), plastic insulation for cryogenic power cable, exam. of dielectric, tensile props. 0-25823  
 polyethylene:NaCl, internal field strength, Raman spectra obs. 0-40061  
 polyethylene, electrical capacitance under high DC elec. field 0-54705  
 polyethylene, microwave dielec. losses variation rel. to different sample treatments 0-25881  
 polyethylene, plastic insulation for cryogenic power cable, exam. of dielectric, tensile props. 0-25823  
 polyethylene, space charge injected from electrode at low temps., luminesc. obs. 0-25464  
 polyethylene, voltage-induced charge transfer and its effects on tree initiation 0-25307  
 polyethylene cables carrying DC current, TSC and space charge effects (French) 0-40042  
 polyethylenes, dielec. losses, for use in AC superconducting power transmission lines 0-25302  
 polymer films, superconducting magnet insulators, gamma-ray radiation effects 0-24495  
 polymer irradiation by high energy electron beams, industrial applications 0-3210  
 polymers, book 0-7257  
 polymers, charge carrier species determ. using interfacial phenomena 0-24978  
 polymers, streamer breakdown in divergent field 0-25308  
 polypropylene, plastic insulation for cryogenic power cable, exam. of dielectric, tensile props. 0-25823  
 polypropylene film, in MIM struct., electroforming 0-25019  
 polypropylene films, meas. of dielectric losses at cryogenic temps. 0-25301  
 polypropylene-polyurethane laminates, meas. of dielectric losses at cryogenic temps. 0-25301  
 polysulphone, plastic insulation for cryogenic power cable, exam. of dielectric, tensile props. 0-25823

**organic molecule configurations**see also *isomerism*

- 1,1'-Bis[phenylglyoxyl]-ferrocene, mol. and cryst. struct. (German) 0-10538  
 S,S'-dimethylthiocarbonate, pot. for rot. about C(sp<sup>2</sup>)-S bonds, electron diff. obs. 0-23572  
 3,3-trifluoropropene, struct. and vibr. spectra, IR, Raman polarisation study 0-18845  
 acetaldehyde, first triplet state geometry, fragmentation into free radicals 0-47915  
 acetic acid-pyridine, H-bonding, proton transfer, isolated system, solvent effect, MO calc. 0-55629  
 acetylene, angular dependent photoelectron spectral meas. 0-28060  
 acetylene dimer, ab initio HF calc. for 64 conformers. 0-23333  
 alkyl benzenes, jet-cooled, intramol. vibr. relax., reson. fluoresc. and excitation obs. 0-14152  
 alkyl cyanobiphenyls, pretransitional behaviour, alkyl chain length depend., light scatt. in isotropic phase 0-44301  
 4-alkyl-3-phenyl-3,4-dihydrocoumarins cis- and trans-, <sup>13</sup>C NMR spectra 0-43067  
 amides, geometry from ab initio calcs. 0-23338  
 amidofluorosulphuric acid, and Hg salt, IR spectra (French) 0-18858  
 p-aminobenzoic acid hydrochloride, X-ray cryst. struct. determ. 0-39063  
 18-annulene, geometrical parameters, STO-3G ab initio calc. 0-52867  
 L-arginine L-ascorbate, X-ray cryst. struct. determ. 0-35826  
 aromatic five-membered heterocyclic ring system, covalent radii determ. method 0-23332  
 benzaldehyde, electronic spectra, Cl and F substitution effects 0-23456  
 1,3-benzodioxole, geometry, electronic absorpt. spectra 0-971  
 benzophenone-N,N-dimethylaniline, intramolecular exciplex systems, laser photolysis obs. 0-35550  
 benzyl fluoride, mol. struct., NMR and gas electron diffraction obs., ab initio and mol. mechanics calcs. 0-23574  
 Δ<sup>6</sup>-bicyclo[3.2.0]heptene, microwave spectrum and dipole moment 0-9591  
 biomolecule conformational anal., solvent effects 0-3583  
 biopolymer soln., heat capacity, conformational props. temp. depend. 0-8009  
 2,2'-bipyrimidine, in nematic solvent, conformation, ab initio and PMR determ. 0-47869  
 bovine trypsinogen, low-temp. study, effect on flexibility, temp. factor, mosaic spread, extinction and diffuse scattering 0-54214  
 n-butane in liq. solvents, conformational structure 0-28115

**organic molecule configurations continued**

- t-butyl cyanide-HF, hydrogen bonded heterodimer, spectroscopic consts. from IR and microwave spectra 0-43039  
 capsular polysaccharide antigen, structure investig. by <sup>13</sup>C NMR 0-35828  
 carbon tetrachloride, clusters, collision induced polarisability, mol. frame distortion 0-32798  
 carbon tetrachloride, internucl. parameters meas. using total scatt. of fast electrons 0-32857  
 carbon tetrafluoride, clusters, collision induced polarisability, mol. frame distortion 0-32798  
 catechol borane, geometry, electronic absorpt. spectra 0-971  
 1-chloro-2-methylbutane, conformer depend. C-Cl stretching vibr., Raman optical activity spectrum simulation 0-14146  
 chloroethane, reson. multiphoton dissociation 0-53077  
 chloromethyl formate-(d<sub>1</sub>,d<sub>2</sub>,d<sub>3</sub>), gas, solid. and liq., IR spectra assignments and struct. 0-32715  
 chloromethyl oxirane, microwave spectra and conformations of cis and gauche-2 forms 0-5534  
 cholesteric liquid crystals, light reflection by crystals with tilted molecular struct. 0-29713  
 cholesterogens, non-sterol, odd-even effect in helix 0-19701  
 choline phosphate calcium chloride tetrahydrate, struct., conformation, metal coordination, model for membrane surface interactions 0-15085  
 chromophores, semiempirical rules in circular dichroism, Cotton effect sign correl. with stereochem. 0-1006  
 cobalt(III) complexes, mixed glycyglycinate, synthesis and config. (French) 0-2005  
 collisional activation mass spectra 0-48106  
 coumaran, geometry, electronic absorpt. spectra 0-971  
 N-cyanofornimine-d<sub>2</sub>, struct., microwave transitions 0-973  
 cyanogen azide, electron-density maps of bent bonds 0-1084  
 2-cyanoguanidine, electron-density maps of bent bonds 0-1084  
 cyanomethane-HF, hydrogen bonded heterodimer, spectroscopic consts. from microwave spectrum 0-43038  
 cyclobutane, MS-Xa-MT study 0-52906  
 cyclohexane, conform. equilib., CNDO/2 calcs. on six-membered rings 0-23336  
 difluoromethylborane, microwave spectra and struct. obs. 0-43036  
 dihydroxycarbene, singlet and triplet state rot. pot. surfaces 0-32627  
 diimide, electron-density maps of bent bonds 0-1084  
 1,4-dioxane, conform. equilib., CNDO/2 calcs. on six-membered rings 0-23336  
 diphenylethylene, UV spectra, quantum-mechanical investigation of isomerisation pathways 0-43065  
 diphenylhaloselenium radical trapped in single crystals, FSR, struct. 0-44919  
 dithioformic acid, pot. for rot. about C(sp<sup>2</sup>)-S bonds, ab initio calc. 0-23572  
 ethane, nuclear spin-spin coupling consts., vicinal proton-proton coupling calcs. 0-32737  
 ethyl methyl sulphide, low freq. vibr. spectra, methyl torsional pot. functions and internal rot. 0-5543  
 N-ethylacridone, cryst. and mol. struct. 0-33988  
 ethylene cation, state geometries, electronic vibr. coupling consts., HF calcs., comparison with Xalpha calcs. 0-27946  
 ethylene glycol, conformational anal., photoelectron spect. 0-43107  
 ethylene V state, ab initio study of spatial extension 0-27952  
 2-exo-acetoxy-7-anti-dinitrophenylthionorbornane, mol. and cryst. struct. 0-2007  
 Fe-fragment crystals, low-temp. study, effect on flexibility, temp. factor, mosaic spread, extinction and diffuse scattering 0-54214  
 ferrocene, metal to ring distance, ab initio MO SCF calcs. 0-47870  
 ferrocene, triclinic, struct. anal. at 101, 123 and 148K 0-19785  
 1,1'-ferrocenedicarboxylic acid, triclinic, X-ray and neutron cryst. and mol. struct. determ. at 78 and 298K 0-29008  
 fluorobenzenes, negative ion states, comments and reply 0-32599  
 fluoromethane-HF, H-bonded complex, ab initio calcs. (French) 0-52866  
 formaldehyde, adiabatic CI pot. surface LCAO calc., gradient determ., mol. dynamics, equilib. geometry 0-48056  
 formaldehyde-d<sub>2</sub>, reson. multiphoton dissociation 0-53077  
 formic acid, conform. hypersurface determ. and analysis 0-1078  
 formic acid, electron-density maps of bent bonds 0-1084  
 formic acid, H bonding, electronic struct., geometries, moments, dimerisation energies, charge distrib., pseudopotential calcs. 0-27942  
 formyl chloride, equilib. geometries and one-electron props., ab initio calcs. 0-47878  
 formyl fluoride, and isotopic forms, mol. struct., from electron diff. and microwave data 0-23570  
 formyl fluoride, equilib. geometries and one-electron props., ab initio calcs. 0-47878  
 formyl radical, electronic struct., dissociation energy and pot. energy surface many body perturbation theory and couple cluster doubles calc. 0-23296  
 γ-glycine, cryst. struct. by neutron diff. at 83K and 298K 0-35825  
 gramicidin A in biomembrane channel, IR spectroscopic obs. 0-16901  
 haemoglobin, sickling deer type III, macromol. struct. refinement by restrained least-squares and interactive graphics 0-28870  
 halides, aryl and aryl-alkyl 193 nm photodissoc., fragment translational energy distrib. 0-48048  
 heparin, in soln., small angle X-ray scattering 0-14993  
 hexafluoropropene, struct. and vibr. spectra, IR, Raman polarisation study 0-18845  
 histones H<sub>2</sub>A and H<sub>4</sub>, mixed solns., oligomer structs. 0-30648  
 HOAB, chain ordering model 0-24357  
 hydrazoic acid, electron-density maps of bent bonds 0-1084  
 hydrocarbon chains, stability of lyotropic phases 0-24359  
 hydroxymethylene radical cation stability, CH<sub>2</sub>O<sup>+</sup> isomers, ab initio MO study 0-42965  
 indigo dyes, triplet state config., laser flash absorpt. spectrosc. obs. 0-5557  
 isocyanic acid, molecular structure and centrifugal distortion constants 0-47974  
 isothiocyanic acid, H<sup>15</sup>NCS, HN<sup>13</sup>CS and HNC<sup>34</sup>S, ground state spect. constants and molecular struct. 0-47973  
 liquid crystal, theoretical foundations of chain ordering props. 0-38907  
 liquid crystal, thermotropic mesophase, DMR chain segments assignment 0-24356  
 methane, clusters, collision induced polarisability, mol. frame distortion 0-32798



**organic molecule configurations continued**

- methane, elastic and inelastic electron scatt. differential cross section, obs. and calc., struct., binding energy 0-28110  
 methanol, H bonding, electronic struct., geometries, moments, dimerisation energies, charge distrib., pseudopotential calcs. 0-27942  
 2-methoxycyclobutane, mol. struct., electron diff. obs. 0-1065  
 methyl chloride, charge distrib., substituents effect 0-905  
 methyl fluoride, charge distrib., substituents effect 0-905  
 methyl formate, microwave spectra, rot. consts., moments and struct., radio astronomy appl., review 0-17637  
 methyl formate(-d<sub>1</sub>,d<sub>2</sub>,d<sub>3</sub>), mol. vibr. spectrum, struct., beginning with PCILC calc. (French) 0-23401  
 methyl vinyl sulphide, syn-gauche equilb., force field and ab initio calcs., microwave and Raman spectra 0-23573  
 methylanilines, far IR spectra, pot. energy barriers 0-43043  
 7-methylbicyclo[2.2.1]-hept-2-ene-5-one, config., microwave spectrosc. obs. 0-9593  
 methyldichlorosilane, Stark effect and microwave-microwave double reson., struct. (German) 0-47975  
 methylene peroxide, multiconfig. SCF CI calcs. 0-18803  
 3-methyleneoxetane, electron structure, orbital-O interaction, MO calcs., UV photoelectron spectra 0-28058  
 monothioformic acid, pot. for rot. about C(sp<sup>2</sup>)-S bonds, ab initio calc. 0-23572  
 4'-n-octyl-4-cyanobiphenyl, chain ordering model 0-24357  
 organic compounds, low freq. anharmonic vibr., pot. function determ., Raman and IR spectra obs. 0-52997  
 organosilane coupling agent interphase of glass-fibre reinforced plastics, molecular organisation 0-44195  
 ovalene, isolated ultra cold mol., intermediate level structure of S<sub>2</sub> state 0-28048  
 3-oxetanone, electron structure, orbital-O interaction, MO calcs., UV photoelectron spectra 0-28058  
 paramagnetic systems, multiple internal motions, nucl. spin dipolar relax. obs. 0-28037  
 pentofuranosyl nucleosides, isomeric, <sup>1</sup>H NMR coupling consts., SCF FPT INDO approx. calc. 0-14156  
 peptide and glycopeptide research methods 0-51307  
 perchloro-3cyclopentenone, <sup>35</sup>Cl NQR Zeeman obs. 0-54981  
 perhalonitrosomethanes, gas phase IR spectra, assignments, isomerism 0-28017  
 phenyl-trimethine-merocyanine, X-ray diff. exam. of cryst. and mol. struct. 0-6398  
 phosphamides, carcinostatic, <sup>14</sup>N NQR, electron distrib. and bonding configs. 0-48018  
 phthalan, geometry, electronic absorpt. spectra 0-971  
 1,4-piperazine, conform. equilb., CNDO/2 calcs. on six-membered rings 0-23336  
 polyacetylene, pristine and acceptor doped isomers, EPR, DC cond., evidence against solitons 0-15782  
 polyatomic mol. gas phase spectra, struct., review and tabulation 0-14136  
 polyenes, symmetric, combinatorial enumeration of chemical isomers 0-28114  
 polyethylene, dielec. props. rel. to mol. struct. 0-29681  
 polyethylene, lightly crosslinked, processed under mol. orient., struct., props., review 0-38957  
 polymethine cyanine dyes, vibronic energy relax., picosec. spectrosc. obs. 0-5526  
 polymethine dye laser, near IR, optimal molecular struct. and lasing characteristics 0-19026  
 polystyrene and model cpds., conformational struct. influence on normal modes of benzene ring, Raman study 0-14144  
 polysubstituted peri-condensed compounds, combinatorial enumeration of chemical isomers 0-28114  
 potassium butyl xanthate, X-ray cryst. struct. determ. 0-33987  
 potassium p-chloranil, solvated with acetone, X-ray cryst. struct. determ. 0-39062  
 β-propiolactone, electron structure, orbital-O interaction, MO calcs., UV photoelectron spectra 0-28058  
 p-propoxysalicylidene-p'-butylaniline cryst. and mol. struct., intramolecular bonding 0-44197  
 proteins, model building procedure 0-51036  
 PVC, reduced, dielec. props. rel. to mol. struct. 0-29681  
 pyrazine, excited and N<sub>1s</sub> ionised states, ab initio calcs. broken orbital symm. 0-27931  
 pyrazine (-d<sub>4</sub>) vapour, single vibronic level fluoresc. from n, π\* 0-37827  
 pyrazine absorbed on electrode, surface enhanced Raman spectra, symmetry and polarisability changes 0-50310  
 pyridine-acetic acid, H-bonding, proton transfer, isolated system, solvent effect, MO calc. 0-55629  
 di-α-pyridyl hydroperchlorates, intramol. H bonds, steric conditions and polarisability obs. 0-53160  
 rhodamine 6G, orientated relax. times, streak camera meas. 0-14168  
 ring current theories in NMR 0-53020  
 scandium octaethylporphyrin, μ-oxo bridged dimer, triplet states and geometrys, ODMR obs. 0-9625  
 scandium octaethylporphyrin, triplet states and geometrys, ODMR obs. 0-9625  
 L-serine-L-ascorbic acid, X-ray cryst. struct. determ. 0-35827  
 stereoisomer generation, specification and enumeration, config. symmetry group appl. 0-1079  
 succinic acid, partially deuterated, <sup>1</sup>H and <sup>2</sup>H distant ENDOR obs. of mol. struct. parameters 0-23445  
 TCNQ complex with 5-phenyl-[1-thiol]-3-selenol-2-thione, charge-transfer salt, cryst. and mol. struct. 0-33986  
 tetraselenotetracene thiocyanate complex, X-ray struct. anal. 0-2006  
 thioindigo dyes, triplet state config., laser flash absorpt. spectrosc. obs. 0-5557  
 thioketen, microwave spectrum, substitution structure and dipole moment 0-975  
 thromboxane, evidence against prostaglandin hairpin conformation 0-3585  
 toxin, penicillium roqueforti, struct. and absolute configuration 0-39064  
 1,2,3-trichlorobenzene, oriented mol., <sup>13</sup>C satellites use in proton spectra, r<sub>r</sub>-structure 0-18872  
 triphenyl-(triphenylgermanylperoxy)silane, cryst. and mol. struct. 0-39066  
 urea adducts, crystn., geometry of urea-cation bonding 0-39061  
 urea antimony fluoride, X-ray cryst. struct. determ. (French) 0-44196  
 valence-nonbonded H atoms interaction and two-centre contrib. to total energy of mol. 0-32624

**organic molecule configurations continued**

- valinomycin conformation in a phospholipid bilayer, <sup>1</sup>H NMR obs. 0-40958  
 vinyl bromide, mol. struct., from gas-phase electron diff. and microwave data 0-23571  
 vinyl isocyanate, and vinylcyano ether, geometry and conform., ab initio minimal STO-3G MO calcs. 0-23337  
 vinyl mercaptan -d<sub>0</sub>, -d<sub>1</sub>, anti rotamer, conform., microwave spectrum 0-9592  
 vinyl mercaptan -d<sub>0</sub>, -d<sub>1</sub>, synrotamer, conform., microwave spectrum 0-5535  
 vinylcyano ether, and vinyl isocyanate, geometry and conform., ab initio minimal STO-3G MO calcs. 0-23337  
 xanthine, planar autoassoc. energy 0-53086  
 Ar-methyl chloride, mol. beam elec. reson. spectrosc. 0-23477  
 CF<sub>3</sub>, CF<sub>2</sub><sup>+</sup>, and CF<sub>3</sub><sup>+</sup>, optimised struct. and bonding, ab initio SCF MO calc. 0-23334  
 HCCN, a cyanocarbene, geom. struct., electron correl. effects 0-1077  
 HCS<sup>+</sup>-CSH<sup>+</sup>, struct. and stability, ab initio SCF calcs., CNDO calcs. 0-32608  
 methane cation, Jahn-Teller distortion 0-48098

**organic molecule electronic structure** see *molecular electronic states*

**organic semiconductor materials** see *organic semiconductors*

**organic semiconductors**

- 2,4-hexadiyne-1,6 diol bis(p-toluene sulphonate) ester, demonstration of high mobility 0-20212  
 2,4-hexadiyne-1, 6-diol, bis(p-toluene sulphonate), dark-current meas. 0-15520  
 anthracene, charge storage and trapping levels, TSC studies 0-6875  
 anthracene, isotopically mixed cryst., exciton dynamics 0-29329  
 anthracene, laser excited single crystal, numerical anal. for TSC results (Japanese) 0-34464  
 anthracene, photocond. spectrum induced by excitons (Japanese) 0-29440  
 anthracene, photogeneration of charge carriers through two photon excitation 0-11033  
 anthracene, single cryst., photocond. threshold, excitation spectrum 0-44639  
 anthracene, single crystal, photoconductivity quantum yield, experimental validation of fund. theory 0-6909  
 anthracene, single crystals, TSC excited by Q-switched ruby laser 0-29417  
 anthracene, surface photovoltage 0-2419  
 anthracene crystal, resonance secondary emission, Raman scatt. in exciton absorpt. region (Russian) 0-40120  
 anthracene crystals, α-particle induced scintillation, mag. field effects 0-40161  
 anthracene crystals, nonlinear fluorescence quenching, recomb. of free excitons 0-7397  
 anthracene derivative, Langmuir-Blodgett multilayer film, semiconducting props., optical and elec. meas. 0-11122  
 anthracene film, effect of struct. on luminesc. quenching (Russian) 0-7411  
 anthracene film, electroabsorption spectra obs. 0-50301  
 anthracene single crystals, effect of γ-irrad. on photolum. (Russian) 0-2852  
 anthracene-pyromellitic dianhydride complex, optical and photoelectric props. (Russian) 0-15570  
 biopolymers, role in biochemical phenomena, book contrib. 0-12053  
 copper phthalocyanine film, photoelectrochem. behaviour on SnO<sub>2</sub> electrodes 0-15626  
 9,10-dichloroanthracene, monoclinic, photocond. carrier mobility 0-39630  
 films, relax. currents, polarisation and depolarisation currents obs. 0-49764  
 naphthalene, pure and deuterated, band-hopping mobility transition 0-6833  
 naphthalene crystals, nonlinear fluorescence quenching, recomb. of free excitons 0-7397  
 one-dimensional, resonant states, mag. excitations and impurities 0-24839  
 p-terphenyl, positronium and thermal defects 0-24496  
 pentacene, surface photovoltage 0-2419  
 photoelectrode processes and effects (German) 0-26145  
 phthalocyanine films, metal-free, adsorbed o-chloranil effect on surface photovoltage 0-34485  
 phthalocyanine-metal interfaces, surface photovoltage 0-20308  
 polycene quinone radical polymers, elec. props. described by variable range hopping model 0-44588  
 polyacetylene:AsF<sub>6</sub>, thermal decomp. kinetics, elec. cond., ESCA and mass spectra 0-50830  
 polyacetylene, doping with AsF<sub>6</sub>, mechanism, effect on elec. cond. and spectra 0-24473  
 polyacetylene, phototransport effects 0-44653  
 polyacetylene, pristine and acceptor doped isomers, EPR, DC cond., evidence against solitons 0-15782  
 polyacetylene, pure and heavily doped, optical and IR studies, electronic struct. calcs. 0-7347  
 polyacetylene, semiconducting and metallic, thermoelec. props. 0-40884  
 cis-polyacetylene, static lattice calcs. for crystals 0-10509  
 polyacetylene and derivatives, chemically doped, elec., chem. and phys. props. 0-24912  
 polyacetylene film, (CH)<sub>x</sub>, synthesis, struct. and elec. props., doped materials, review 0-15623  
 polyacetylene film, partially oriented, anisotropic elec. cond., quasi-one-dimens. behaviour of fully oriented doped material 0-11112  
 polyacetylene photoelectrochemical solar cell, fabrication and efficiency 0-50954  
 polyaromatics, elec. cond. correl. with chem. struct. and synthesis, charge transfer complexes (German) 0-15514  
 polycarbonate:tri-p-tolylamine amorphous film, elec. and mag. props. 0-49959  
 polydiacetylene, cryst., one-dimens. conjugated semicond., vibronic coupling, Fano interference effects 0-34939  
 polydiacetylenes, photocond. action spectrum of single crystals, charge transport obs. 0-15557  
 polyene, one-dimensional chain, Raman scatt., one-phonon final states and many-body effects 0-34913  
 polyenes, compensation temp. 0-39625  
 polyethylene, oxidised, charge carrier, transport phenomena 0-15515  
 polymer, conjugated, synthesis and elec. props., review 0-15513



**organic semiconductors** continued

- polyvinylcarbazole-trinitrofluorenone, organic photoconductor, photoinduced paramag. centres 0-25188  
 pyrene, positronium and thermal defects 0-24496  
 p-quaterphenyl, polycryst. thin layer-metal sandwich, elec. cond. 0-34526  
 rhodamine B surface state hole traps, surface photovoltage meas. 0-39654  
 TCNQ, salt, DBTTF-TCNQ, elec. resistivity and thermoelec. power meas. 0-20193  
 TCNQ complexes with N-methyl derivatives of pyridine, cond. and thermoelec. power meas., band model anal. 0-10952  
 TCNQ salt,  $(\text{NMe}_2\text{H})(\text{I})(\text{TCNQ})$ , one-dimens. semicond. with metal-like cond. 0-24909  
 TCNQ salt,  $(\text{NMP})_x(\text{phen})_{1-x}(\text{TCNQ})$ , thermoelectric power temp. depend. 0-15548  
 TCNQ salt, K-TCNQ, high and low temp. phases, dielec. const. 0-34844  
 TCNQ salt, Rb-TCNQ-II, two carrier cond. 0-44625  
 TCNQ salt in aqueous media, electrochem. behavior 0-6976  
 TEA(TCNQ)<sub>2</sub>, elec. cond. and thermoelec. power under hydrostatic press. 0-11024  
 p-terphenyl polycrystalline layers, AC cond. 0-44746  
 tetracene, amorphous film, TSC meas., carrier traps 0-2496  
 tetracene, surface photovoltage 0-2419  
 tetracene surface states, electric field effects, exciton-charge carrier interactions (*Russian*) 0-24989  
 $\alpha$ TTF:Br, transport and mag. props., effect of doping 0-24934  
 TTF-TCNQ, semicond., driven oscils. of carrier conc. 0-15551  
 TTF-TCNQ and derivatives, 1.8 to 40K, three dimens. state, specific heats 0-44333  
 TTT film, hopping cond. AC and DC meas. and EPR 0-11111  
 xerographic photoconductors, bimolecular recomb., reciprocity failure 0-49798

**organometallic compounds**

- antireflection coatings derived from liquid precursors 0-5847  
 benzenetricarbonylchromium, neutron inelastic scatt. spectrum and valence force field 0-48096  
 cyclopentadienyl  $\text{Ho}(\text{III})$ , cyclooctadienyl sandwich compound, mag. circular dichroism and absorption spectra, anal. 0-23449  
 1,1'-diacetylferrocene, <sup>57</sup>Fe Mossbauer effect, probe study of smectic liq. cryst. glass-supercooled transition and Debye temp. 0-54999  
 dimethyl aluminium hydride dimer, electron density distrib., electrostatic mol. pot. anal. 0-52885  
 dimethyl di(trifluoromethyl) germanium, and perdeuterated analogues, vibr. spectra, normal coord. anal. (*German*) 0-5547  
 trans-dimethyl organometallic moieties, nuclear elec. quadrupole moment from elec. field gradients 0-29371  
 dimethyl stannous chloride di(pyridine 1-oxide), <sup>119</sup>Sn Mossbauer spectra, elec. field gradient 0-15909  
 dimethyl tin diisothiocyanate, <sup>119</sup>Sn Mossbauer spectra, elec. field gradient 0-15909  
 ethyl-trimethylstannyl phosphines,  $(\text{C}_2\text{H}_5)_3\text{P}[\text{Sn}(\text{CH}_3)_3]_n$ , ( $n=0,1,2,3$ ), (<sup>1</sup>H, <sup>13</sup>C, <sup>29</sup>Si, <sup>31</sup>P, <sup>119</sup>Sn) NMR 0-32744  
 ferrocene, cryst., stable low-temp. phase 0-34185  
 ferrocene, dynamics in liquid and glassy o-terphenyl, Mossbauer obs. 0-55000  
 ferrocene, metal to ring distance, ab initio MO SCF calcs. 0-47870  
 ferrocene, triclinic, struct. anal. at 101, 123 and 148K 0-19785  
 ferrocene derivatives, mixed and averaged valence types, Mossbauer spectra 0-15906  
 ferrocene related compounds,  $\text{C}_5\text{R}_5\text{Fe}(\text{I})\text{-C}_6\text{R}'_6$  paramag. sandwiches, Mossbauer study 0-39982  
 fluxional, solid state chem. exchange, <sup>13</sup>C NMR magic angle spinning 0-7775  
 hexaphenylene mercury, bright-field imaging of single heavy atoms in an electron microscope with superconducting lens system 0-10472  
 intermolecular interaction, Mossbauer spectra 0-15899  
 methyl tri(trifluoromethyl) germanium, and perdeuterated analogues, vibr. spectra, normal coord. anal. (*German*) 0-5547  
 methylmercuric halides, partially oriented, <sup>1</sup>H and <sup>13</sup>C NMR obs. 0-23437  
 methylmercury nitrate, in nematic and lyotropic liq. crystals,  $r_a$ -struct. and anisotropy of Hg-C coupling const. 0-43071  
 Mossbauer spectra of spin crossover 0-15903  
 neptunium cyclopentadienyl compounds,  $(\text{C}_5\text{H}_5)_3\text{NpX}$ , ( $\text{X}=\text{F}, \text{Cl}, \text{Br}, \text{I}, (\text{SO}_4)_{1/2}$ ), mag. susceptibility 0-11152  
 organo-tin polymer films, glow discharge prep., comp. determ. by XPS and AES 0-35109  
 organosilicon binder, for prod. of spalling-resistant quartz glass based ceramic 0-40313  
 phosphines, substituted,  $\gamma$ -irrad. EPR spectra and struct. of free radicals 0-29623  
 rare earth complexes, with organometallic bonding, formation and props., book contrib. 0-43204  
 sandwich complexes, mag. props., effective Hamiltonian method 0-37731  
 tri-i-propylgermylamine, and isotopomers, IR and Raman spectra, normal coord. anal. (*German*) 0-32716  
 tri-t-butylstannyl hydroxide, Mossbauer spectrum, tin coordination (*German*) 0-32716  
 tri-t-butylstannylamine, and isotopomers, IR and Raman spectra, normal coord. anal., Mossbauer spectrum (*German*) 0-32716  
 triethylsilylamine, and isotopomers, IR and Raman spectra, normal coord. anal. (*German*) 0-32716  
 trifluoromethyl trimethyl germanium (tin)(lead), and perdeuterated analogues, vibr. spectra, normal coord. anal. (*German*) 0-5547  
 trimethyl tin cyanide, <sup>119</sup>Sn Mossbauer spectra, elec. field gradient 0-15909  
 trimethyl-indium trimethyl phosphine adduct, cc InP VPE with new metallorganic compound 0-55278  
 Fe organometallics, interaction of naked Fe atoms with small mols., Mossbauer study of bonding in products 0-43080

**organs (artificial body)** see *artificial organs***origin of elements** see *element origin***origin of life** see *evolution (biological)***orthicons** see *television camera tubes***orthogonalised plane wave calculations** see *OPW calculations***orthosis** see *orthotics***orthotics**see also *prosthetics*

- audible training aid for visually impaired infants, motion activated 0-36193  
 balloon pump counterpulsation, increasing operational safety 0-3869  
 blood circulation apparatus, improved electromechanical drive regulator 0-3871  
 blood oxygenation perfusion system for treatment of acute respiratory failure in infants 0-3866  
 circulation-assist, steady state anal. of press. and flow 0-17193  
 circulatory assist apparatus, stabilisation of gas vol. in pneumatic transmission unit 0-3863  
 communication/control systems for motor impaired people, standardisation 0-17198  
 earphone cushion, comparison between one-piece model 51 and conventional two-piece MS-41AR cushion 0-51123  
 electrophrenic respiration, feedback control of tidal vol. (*Japanese*) 0-41316  
 EMG activated spatial morse code general purpose communication device 0-30946  
 extracorporeal circulation apparatus using thermoelec. heat regulating systems 0-3870  
 extracorporeal circulation equipment, automatic control 0-3865  
 extracorporeal circulation system, energy parameters of temp. stabilisation system 0-3867  
 haemodialysis, single-needle, recirculation anal. 0-41320  
 heart assist blood pump, counterpulsation dynamics simulation 0-16996  
 hip guidance articulations, principles and practice 0-3873  
 lower-limb orthoses, force-line visualisation system 0-17200  
 mobility aid for blind people based on US sensing 0-56290  
 motorized shoe for submaximal assist 0-56289  
 myofeedback control system, design 0-51296  
 orthopaedic engineering in Oxford 0-17187  
 Oxford external fracture fixator, anal. of fixation 0-17188  
 rehabilitation engineering (*Japanese*) 0-12304  
 SCRIBE, system to help the badly handicapped, using a microprocessor (*French*) 0-56282  
 speech synthesizer for severely handicapped children, portable 0-56154  
 weak speech amplification device with suppression of respiration noise 0-30929  
 wheelchair seat evaluation by time-lapse and quantitative thermography of skin after sitting 0-51205

**oscillations**see also *circuit oscillations; electromagnetic oscillations; harmonic oscillators; harmonics; liquid oscillations; piezoelectric oscillations; plasma oscillations; resonance; stability; vibrations; waves*

- aerofoil, oscillating, viscous incompressible flow, finite element anal. 0-38427  
 asteroid orbits in vicinity of 1:3 commensurability with Jupiter, semi-major access oscils. (*Russian*) 0-36486  
 atom spin transition, nonadiabatic, in time-depend. mag. field 0-9576  
 Bowditch flow, spin-up, angular momentum adjustment 0-28511  
 capsules, neutrally buoyant, in Lake Tahoe, oscils. damping 0-12438  
 cavitation gas bubble in compressible liquid, influence of inhomogeneous sound field on motion 0-6131  
 chemical reaction, oscillating, entrainment by periodic light pulses of variable freq. (*French*) 0-35551  
 corona discharge, positive, sound effects 0-28858  
 coupled, demonstration using permanent magnets 0-42015  
 cracks, circular, forced torsional oscillations at low frequencies 0-53703  
 cryogenic system, thermally driven acoustic oscillation, stability limit 0-8992  
 damping, light, influence of eigenvalues (*German*) 0-31490  
 drag reduction of an oscillating flat plate with an interface film 0-10268  
 dynamic axisymmetrical elasticity problems soln. using factorised differential systems of second-order accuracy (*Russian*) 0-8796  
 dynamical system construction from pre-assigned family of solns. 0-39  
 Earth, viscoelastic, free oscillations attenuation theory 0-21652  
 education, sprung pendulum, anal. of nonlinear coupling 0-51987  
 forced, lower bound on forcing amplitude for stability, third order nonlinear system 0-52013  
 forced oscillations experiment for students 0-17780  
 gas, in multicylinder fluid machinery manifolds, lumped parameter descriptions 0-19511  
 gas flow into duct, self-excited oscillations 0-33647  
 inertia-buoyancy oscillations in hurricanes, excitation and relation to spiral bands 0-56538  
 infinite pendulum system, finite controllability 0-31494  
 interstellar medium in stellar component gravitational field, oscillations (*Russian*) 0-41883  
 Josephson self-resonant modes analysis, using mechanical analogue model (*Chinese*) 0-34563  
 Kolmogorov eqn., separation of variables, applied to oscill. Brownian motion 0-36945  
 Liapunov's periodic motions at heavy rigid body with fixed point (*Russian*) 0-22190  
 Lissajous figures, mechanical system, for student demonstration 0-31459  
 mechanical oscillations amplifier 0-13069  
 1 Monocerotis,  $\delta$  Scuti star, oscillation modes from photoelectric radial vels. and BVRI photometry 0-51787  
 neural net temporal oscillations, cortical neurons interactions model 0-3636  
 nonlinear two-degree-of-freedom system, internally resonanced, forced vibrs. 0-36838  
 oscillators in convective biperiodic regime, velocity oscils. 0-53759  
 pipe containing flowing fluid, forced oscillations (*Russian*) 0-38304  
 pipelines with liquid, stability and oscillations 0-14612  
 plane two-dimensional motion in acoustic medium caused by kinematic excitation, Laplace transform study (*Russian*) 0-43503  
 plates, pre-stressed, 3-D problems, basis systems of homogeneous solns. (*Ukrainian*) 0-10177  
 Poincaré cycles of the linear chain of oscillators 0-4662  
 proton (antiproton) storage ring, incoherent motion damping by dissipative elements 0-5419  
 spindle unit on test stand, wheel failure 0-19277  
 spiral flow between coaxial cylinders, branching and stability loss 0-19406  
 stars, adiabatic non-radial oscillations with moderate or large l 0-56819



**oscillations continued**

- stars, oscill. freqs. line broadening due to convective fluctuations 0-31293  
 stellar motion, z-oscill. theory rel. to force field normal to galactic plane 0-46669  
 stochastic properties of complex nonlinear oscillation regimes 0-8919  
 Sun, structure from global studies of 5-min. oscills. 0-26838  
 sunspot chromosphere, radial vel. and brightness oscills. regimes (*Russian*) 0-51727  
 synchrotron, effects of induced voltage and forces of space charge on motion (*Bulgarian*) 0-47792  
 turbomachinery ring chamber, oscillatory behaviour of confined ring vortex 0-6075  
 viscoelastic rod, forced longitudinal oscillations, thermomechanical coupling effect 0-19274  
 wedge oscillations in confined vesicle (*Russian*) 0-43651  
 white dwarfs seismological theory for 1  $M_{\odot}$  model with crystalline core 0-17577  
 wing, in transonic flow, unsteady airloads and flow linearisation 0-19426  
 He, thermoacoustic oscillations in nonuniformly heated tubes 0-33441  
 He transfer line, oscillation damper 0-37041

**oscillator strengths**

- acetic acid amides, polarisabilities and  $\pi$ - $\pi^*$  transitions, dipole interaction calcs. 0-23411  
 alkali homonuclear dimers, quasi-static wing profiles of self-broadening reson. lines 0-48042  
 alkali metal, oscillator strengths, nonlocal Simons pot. anal. 0-32795  
 alkali metal atom, Rydberg state emission oscill. strength minima 0-32662  
 alkali metal atom, Rydberg state Stark struct. 0-37754  
 alkali metal atom, transition oscillator strengths in discontinuous and continuous spectra, review 0-52937  
 astrophysical objects, general aspects 0-12656  
 atom, rel. oscill. strengths determ. by combined absorption/emission meas., Ti appl. 0-37784  
 atoms, ground and excited states, polarisability and scaling, oscillator strength, continuum spectrum contribution 0-27923  
 atoms, singly excited states, oscillator strengths, ab initio calcs. 0-920  
 beam-foil lifetime measurement, cascading problem, ANDC method use and error limits 0-14249  
 bounds on van der Waals coeffs., oscillator strength sum rules 0-27941  
 C IV, optical oscillator strength 0-47941  
 diatomic molecules, excitation energies, oscillator strengths, many body approach, eqns. of motion method 0-47969  
 diphenylethylene, UV spectra, quantum-mechanical investigation of isomerisation pathways 0-43065  
 dipole properties and dispersion energies additivity, using atoms and small mol. models 0-53091  
 Drude oscillator model, atomic and molecular props. for different oscillator freq. 0-37846  
 electron impact spectroscopy, low-energy aspects, book contrib. 0-14243  
 fast electron collision, K, L, M-shell generalised oscillator strengths and ionisation cross section, Hartree-Slater calc. 0-53141  
 formic acid amides, polarisabilities and  $\pi$ - $\pi^*$  transitions, dipole interaction calcs. 0-23411  
 group IV homologous ions, oscillator strength trends 0-42991  
 heavy ions, beam-foil decay curves for reson. transitions, simulation 0-9721  
 hydrocarbons, vibr. intensities, G sum rule appls. 0-32776  
 lanthanide(III) complexes, f-f transition intensities, general theory of solvent effect 0-18811  
 measurement using reson. Faraday effect in monochromatic light 0-23363  
 methoxy radical, electronic absorpt. spectra, visible, vibr. freqs., vibronic intensities and oscill. strengths 0-28025  
 molecular crystal, surface exciton levels, radiation corrections 0-34962  
 nonlinear polarisation resonances in a continuum, optical activity, spin-orbit interactions (*Russian*) 0-53391  
 particle stopping power meas., mean excitation energy from oscillator strength distrib. 0-9481  
 photosynthetically relevant mols., electronic structural props. 0-16902  
 polar semiconductor, exciton, energies, oscillator strengths, and phonon side bands 0-44512  
 polar semiconductors, exciton-phonon interactions, optical absorpt. spectra, theory 0-49614  
 polyatomic molecules, excitation energies, oscillator strengths, many body approach, eqns. of motion method 0-47969  
 relativistic effects in central field approximation, RELAC method and use 0-9520  
 relativistic effects introduction, ab initio methods 0-9519  
 relativistic RPA calcs. for He(Be)(Mg)(Zn)(Ne) isoelectronic series 0-47925  
 Tokamak impurity problems, atomic and mol. struct. and collision data, review 0-43959  
 Ag, ionisation energies and oscill. strengths calcs. 0-5488  
 $\beta$ -AgI thin film, exciton spectrum 0-55216  
 Al II to Al VI, beam-foil obs. from 1100 to 1900 Å, lifetimes and oscillator strengths 0-14108  
 Al II to Al VI, beam-foil obs. from 300 to 2000 Å, mean lives and oscillator strengths 0-14109  
 Al IX to Al XI, beam-foil obs. of lifetimes and oscillator strengths, 300 to 1000 Å 0-14110  
 Ar IV to Ar XII, beam-foil obs. of lifetimes and oscillator strengths, spectral identifications, 400-2000 Å (*French*) 0-9555  
 Ar, reson. transition oscill. strengths, rel. to electron impact 0-27985  
 Ar XV, wavefunctions and oscill. strengths, CI calcs. 0-23317  
 As, L-shell soft X-ray emission spectra, oscillator strengths 0-32651  
 As XXV, 2p-4d and 2p-4s transition arrays, wavelengths and oscillator strengths 0-47933  
 B I, weighted oscillator strengths for elec. dipole and forbidden transitions, data tables 0-37779  
 Be I, weighted oscillator strengths for elec. dipole and forbidden transitions, data tables 0-37779  
 Be isoelectronic sequence, highly ionised, beam-foil obs. of oscillator strengths for EI transitions 0-14112  
 Br, L-shell soft X-ray emission spectra, oscillator strengths 0-32651  
 C I, weighted oscillator strengths for elec. dipole and forbidden transitions, data tables 0-37779  
 C, optical oscillator strengths, independent particle model, excited state wave functions, LS coupling and Born approx. 0-32674  
 CO, X-ray K-absorpt. spectra, reson. obs., near fine struct. 0-37817

**oscillator strengths continued**

- CO<sub>2</sub>, valence shell ionic photofragmentation, oscill. strengths, EELS and electron-ion coincidence meas. 0-37879  
 Ca XVII, wavefunctions and oscill. strengths, CI calcs. 0-23317  
 Ca+inert gas, collision-induced dipole transitions assoc. with high-lying states 0-37866  
 Cl ions, multiply-charged, beam-foil obs. of allowed L-shell transitions 0-14113  
 Cr II lines,  $A_{mn}$  transition probabilities 0-14099  
 Cs, oscillator strengths in principal series, Rozhdestvenskii hook obs. 0-37760  
 Cs, photoabsorption oscillator strengths,  $17 < n < \infty$  transitions, interpolation formula 0-9559  
 Cs( $5D_{3/2, m=1/2}$ )+inert gas, dipole-induced transitions, pot. curves, oscillator strength 0-32816  
 Cu, isoelectronic series, semi-empirical oscillator strengths, lifetime, transition probability 0-32672  
 Cu, L-shell soft X-ray emission spectra, oscillator strengths 0-32651  
 Cu XXI, 2p-4d and 2p-4s transition arrays, wavelengths and oscillator strengths 0-47933  
 Cu<sup>+</sup>, reson. transition, effect of correl. in 3d<sup>n</sup> core, HF calcs. 0-47911  
 Cu-like ions, EI transitions, wavelengths, oscillator strengths and transition probabilities, data tables 0-37780  
 Fe II, oscillator strengths derived from solar spectrum, choice of solar model atmosphere 0-56791  
 Fe XXII, allowed transition CI wave functions, oscill. strengths and transition probabilities 0-32664  
 Fe XXII, intercomb. transitions, oscill. strengths, transition probs., rel. to solar spectra 0-52935  
 Fe XXIII, wavefunctions and oscill. strengths, CI calcs. 0-23317  
 Fe XXIV, oscillator strengths, electron impact excitation collision strengths, solar flare spectra appl. 0-32647  
 Fe<sup>+</sup>, gf values determ. in laboratory, for solar studies 0-42994  
 Ga, L-shell soft X-ray emission spectra, oscillator strengths 0-32651  
 Ga XXIII, 2p-4d and 2p-4s transition arrays, wavelengths and oscillator strengths 0-47933  
 GaSe, electron-phonon interaction and optical props. 0-34942  
 H, photoionisation cross sections elec. field-induced oscills. 0-955  
<sup>4</sup>He, soft-core radial wave function, photo-disintegration calculation 0-18209  
 Hg vapour, absorpt. spectrum, 1849 Å line, self-broadening, interatomic interaction (*French*) 0-32661  
 I VI and I VII, beam-foil obs. of lifetimes, spectral assignments, 400 to 1300 Å 0-9556  
 I VII, beam-foil lifetime meas., cascading problem 0-14249  
 InSe, spin orbit split off valence bands, exciton transitions, Hopfield's quasibicubic model, visible absorpt. spectrum 0-50370  
 KCl(Br)(I):Eu<sup>2+</sup>, single cryst. optical absorpt. spectra 0-45117  
 Kr VIII, beam-foil decay curves for reson. transitions simulation 0-9721  
 Kr XXXIII and Kr XXXIV, beam-foil obs. of transition wavelengths and oscillator strengths 0-14115  
 Li, electron impact excitation, 15-190 eV, generalised oscill. strengths, differential cross sections 0-23556  
 Li isoelectronic series, relativistic pseudopot. appl. in HF calcs. 0-27960  
 LiF:OH crystals, X-irradiated, H centres formation and annealing 0-54226  
 Mg I isoelectronic sequence, intercombination line oscillator strengths 0-23360  
 Mg IX, wavefunctions and oscill. strengths, CI calcs. 0-23317  
 N I, weighted oscillator strengths for elec. dipole and forbidden transitions, data tables 0-37779  
 N III, electron impact excitation cross sections, generalised oscillator strengths, Born approx. 0-18928  
 N isoelectronic sequence ions, theoretical EUV oscillator strengths and electron scatt. data 0-51649  
 N V, optical oscillator strength 0-47941  
 N<sub>2</sub>, N K-shell excitation, high-resolution electron energy loss spectra 0-53152  
 N<sub>2</sub>, triplet-triplet transitions, Einstein-A coeffs., oscill. strengths, lifetimes, theory and experiment comparison 0-47876  
 N<sub>2</sub>, X-ray K-absorpt. spectra, reson. obs., near fine struct. 0-37817  
 N<sub>2</sub>H<sub>3</sub> radical, lowest two electronic states 0-925  
 NO, N K-shell excitation, high-resolution electron energy loss spectra 0-53152  
 N<sub>2</sub>O, N K-shell excitation, high-resolution electron energy loss spectra 0-53152  
 N<sub>2</sub>O, valence shell ionic photofragmentation, oscill. strengths, EELS and electron-ion coincidence meas. 0-37879  
 Na isoelectronic series, oscill. strengths, effective orbital quantum no. method 0-9521  
 Na, measurement using reson. Faraday effect in monochromatic light 0-23363  
 NaCl:Eu<sup>2+</sup>, single cryst. optical absorpt. spectra 0-45117  
 Ne, 2p<sup>6</sup>(<sup>1</sup>S<sub>0</sub>) ground state electron impact excitation cross sections 0-23558  
 Ne, isoelectronic sequence, excitation energy and oscillator strength, level crossing anomaly, relativistic RPA calc. 0-14077  
 Ne, reson. transition oscill. strengths, rel. to electron impact 0-27985  
 O I, weighted oscillator strengths for elec. dipole and forbidden transitions, data tables 0-37779  
 O III, optical oscillator strengths for astrophysically interesting lines 0-32660  
 O IV, electron-impact excitation cross sections 0-14236  
 OH, band oscill. strength, rot. excitation effects 0-23460  
 PbI<sub>2</sub>, visible exciton spectrum, exciton-phonon interactions, dielectric const. and oscill. strengths 0-25405  
 Rb, ionisation energies and oscill. strengths calcs. 0-5488  
 Rb, L-shell soft X-ray emission spectra, oscillator strengths 0-32651  
 RbCl(Br):Eu<sup>2+</sup>, single cryst. optical absorpt. spectra 0-45117  
 S IV, P-, D-, S-states, oscillator strengths, transition strengths, CI calcs. 0-922  
 Si, glow discharge deposited, optical spectra, reflectance, dielectric function and oscillator strength 0-11492  
 Si isoelectronic sequence, CI calcs. of oscillator strengths, L-S framework 0-14089  
 Si XI, wavefunctions and oscill. strengths, CI calcs. 0-23317  
 Sn, oscillator strengths and hyperfine splitting of 5<sup>2</sup>D<sub>1</sub><sup>0</sup> and 6<sup>3</sup>P<sub>2</sub><sup>0</sup> levels, line absorpt. meas. 0-18818  
 Sr, L-shell soft X-ray emission spectra, oscillator strengths 0-32651  
 TaSe<sub>2</sub>(2H), plasmon behaviour at charge density wave onset 0-10900  
 Th II, oscillator strengths calc. 0-27982



**oscillator strengths continued**

- Tl<sub>2</sub>AsS<sub>4</sub>, optical phonons, Raman and refl. spectra 0-11400  
 Xe, s-p transitions, Stark const. and oscill. strengths, shock tube meas. 0-18822  
 Xe VIII, beam-foil lifetime meas., cascading problem 0-14249  
 Zn I isoelectronic series, 4s4p<sup>2</sup> lifetimes meas. 0-42998  
 Zn, L-shell soft X-ray emission spectra, oscillator strengths 0-32651  
 Zn XXII, 2p-4d and 2p-4s transition arrays, wavelengths and oscillator strengths 0-47933  
 ZrO, B<sup>II</sup> state radiative lifetimes, transition rates and oscillator strengths, reson. fluoresc. decay 0-28053

**oscillators**

- see also *Gunn oscillators; microwave oscillators; parametric oscillators; radiofrequency oscillators; relaxation oscillators; tunnel diode oscillators; variable-frequency oscillators*  
 convective bi-periodic regime, velocity oscils. 0-53759  
 coupled oscillators, nonlinear, with slow, nonexplicitly time-depend. evolution 0-52009  
 electrooptical oscillator, integrated cutoff modulation 0-48424  
 Frohlich steady state model, asymptotic solns. 0-21435  
 harmonic general time depend., quantal fluctuations and invariant operators 0-36898  
 hydraulic lines, wave phenomena, coupled vibrations in bending and branching lines 0-14778  
 linear oscillator, vibrations, excitation by stationary random force (*Russian*) 0-27116  
 macroscopic oscillator motion parameter meas., quantum restrictions (*Russian*) 0-12943  
 multidimensional infinite mechanical oscill. system, resonance and controllability 0-33444  
 nonlinear noisy sine wave oscillator, optimal control 0-27218  
 nonlinear oscillators, limit cycle, chaotic response 0-148  
 nonlinear oscillators, normal modes, uncoupling and stability 0-27115  
 nonlinear stochastic, triangular wave, optimally controlled, Weiner process and Poisson process, numerical studies 0-52128  
 parameter-dependent system, energy soln. method 0-8828  
 quasimonochromatic self-oscillations, phase self-stabilisation 0-18973  
 SAW, physical props. and communication signals processing applications and devices 0-38162  
 SAW devices, appls. of amorphous magnetic-layers 0-28389  
 waves in nonlinear media, Poincare normal form method 0-36875

**oscillograms** see *oscillographs***oscillograph recorders** see *oscillographs***oscillographs**

- see also *cathode-ray oscilloscopes*  
 exploding wires expts., oscillograms processing with aid of microcomputer and main-frame computer (*Russian*) 0-28854  
 steel, low strength, impact tests with oscillography, exam. of fracture toughness using new method 0-21215

**oscilloscopes, cathode-ray** see *cathode-ray oscilloscopes***Oseen method** see *flow***osmium**

- see also *nuclei with .....*  
 atomic vibr. and fermion behaviour of HCP metals 0-6474  
 electrical resistivity and thermal diffusivity meas. 0-15495  
 impurity in Cu-Ni sulphidised alloys, behaviour during carbonylation (*Russian*) 0-40584  
<sup>186</sup>Os and <sup>187</sup>Os neutron capture cross sections rel. to Re/Os cosmochronology 0-17485  
<sup>187</sup>Os, muonic resonance spectra, deduced isomer shifts and electric moments 0-18948  
<sup>187</sup>Re-<sup>187</sup>Os systematics in meteorites, rel. to solar system early chronology and Galaxy age 0-41778

**osmium alloys**

- see also *osmium compounds*  
 Cr-Os, magnetic transition T-P-C diagram, triple points (*Russian*) 0-54895  
 Fe-Os, antiferromag. ordering, hyperfine fields 0-15867  
 Nb<sub>2</sub>Os, A-15 struct. <sup>93</sup>Nb NQR spectra 0-20496  
 Nb<sub>2</sub>Os, X-ray M<sub>IV,V</sub> emission bands (*Russian*) 0-45170  
 Os-Hf, dil., <sup>177</sup>Hf Mossbauer transition, electric quadrupole interaction 0-39928  
 W-Os system films, condensation temp., conc., and phase comp. effect on struct. and props. (*Russian*) 0-24749

**osmium compounds**

- see also *osmium alloys*  
 double oxides, elec. cond. 0-34438  
 CO<sub>2</sub>/<sup>192</sup>OsO<sub>4</sub> laser, absolute light oscill. freq., universal const. variation meas. possibilities (*Russian*) 0-5723  
 OsO<sub>4</sub>, HFS and fine struct., saturation spectroscopy obs. visible spectra 0-53008  
 OsO<sub>4</sub>, spectroscopy using tunable high-pres. CO<sub>2</sub> waveguide laser 0-43054

**osmosis**

- see also *membranes*  
 biological longitudinal transport, electroosmotic model 0-45870  
 cellulose acetate, reverse osmosis membranes, ion mobility, diffusion coeff., elec. resist. obs. 0-45550  
 cellulose acetate-g-polyacrylamide membranes, radiation grafted, appl. in water desalination by reverse osmosis 0-45548  
 coal liquids characterisation, analytical use of dialysis 0-30334  
 corneal environment, osmotic responses to contact lenses 0-12078  
 electrodialysis and its applications 0-55702  
 electroosmosis as distinguished from electrophoresis 0-45514  
 glassy polymer, solvent osmotic stresses, prediction of Case II transport kinetics 0-26049  
 muscle cell osmotic state and membrane permselectivity repeated microwave irradiation effects quantitation 0-56131  
 nephron functioning, diffusion and selective osmosis (*French*) 0-45864  
 Osmo-Hydro power, salinity gradient energy conversion feasibility and system design 0-45721  
 Osmo-Hydro power systems, technical feasibility and economics of salinity power 0-40893  
 polyelectrolyte in solution, variation of contrast, neutron forward scatt. calc. (*French*) 0-54104  
 polyelectrolyte solution, thermodynamic props. determ. from Donnan equil. obs. 0-7846  
 polymer, non-ion-exchange type, electrolyte solubility (*Russian*) 0-54391  
 polymer membrane, transport of organic liqs., review 0-16720

**osmosis continued**

- polyphenylquinoxaline-cellulose acetate, battery separator membrane, diffusion meas. 0-35574  
 polystyrene, diethyl malonate soln., near-crit., osmotic compressibility, correlation length, scaled functions 0-11422  
 reverse, desalination plants using solar and wind powered pumps (*French*) 0-55807  
 suspension of charged particles in ionic solutions, elec. cond. 0-7866  
 water in single capillary, electrokinetic and rheological parameters 0-10220  
 wind powered brackish water purification by electrodialysis and reverse osmosis 0-35630  
 Co bi-univalent cpds., soln., activity coeffs., osmotic coeffs., water activity, Gibbs energy, molality depend. 0-51963  
 Cu bi-univalent cpds., soln., activity and osmotic coeffs., H<sub>2</sub>O activity, Gibbs energy, molality depend. 0-51964  
 Dy(ClO<sub>4</sub>)<sub>3</sub>, osmotic coeffs. 0-45556  
 Er(ClO<sub>4</sub>)<sub>3</sub>, osmotic coeffs. 0-45556  
 FeCl<sub>2</sub>, soln., activity coeffs., osmotic coeffs., water activity, Gibbs energy, molality depend. 0-51963  
 Gd(ClO<sub>4</sub>)<sub>3</sub>, osmotic coeffs. 0-45556  
 Gd(NO<sub>3</sub>)<sub>3</sub>, osmotic coeffs. 0-45556  
<sup>3</sup>He-<sup>4</sup>He, superfluid, osmotic and mag. props., review (*French*) 0-10733  
 Ho(ClO<sub>4</sub>)<sub>3</sub>, osmotic coeffs. 0-45556  
 La(ClO<sub>4</sub>)<sub>3</sub>, osmotic coeffs. 0-45556  
 Lu(ClO<sub>4</sub>)<sub>3</sub>, osmotic coeffs. 0-45556  
 Mn bi-univalent cpds., soln., activity and osmotic coeffs., H<sub>2</sub>O activity, Gibbs energy, molality depend. 0-51964  
 NaCl-KCl, aq. solns., isopiestic studies, 383 to 474K 0-21320  
 Nd(ClO<sub>4</sub>)<sub>3</sub>, osmotic coeffs. 0-45556  
 Nd(NO<sub>3</sub>)<sub>3</sub>, osmotic coeffs. 0-45556  
 Ni bi-univalent cpds., soln., activity coeffs., osmotic coeffs., water activity, Gibbs energy, molality depend. 0-51963  
 Pb bi-univalent cpds., soln., activity and osmotic coeffs., H<sub>2</sub>O activity, Gibbs energy, molality depend. 0-51964  
 Pr(ClO<sub>4</sub>)<sub>3</sub>, osmotic coeffs. 0-45556  
 Sm(ClO<sub>4</sub>)<sub>3</sub>, osmotic coeffs. 0-45556  
 Sm(NO<sub>3</sub>)<sub>3</sub>, osmotic coeffs. 0-45556  
 Tm(ClO<sub>4</sub>)<sub>3</sub>, osmotic coeffs. 0-45556  
 Yb(ClO<sub>4</sub>)<sub>3</sub>, osmotic coeffs. 0-45556

**osmotic pressure** see *osmosis***otology** see *ear***ovens**

- see also *domestic appliances; electric heating*  
 self-cleaning catalyst, 'SC ceramic coating' (*Japanese*) 0-55557

**overcurrent protection**

- 900 mW solar battery construction and characteristics (*German*) 0-12008  
 superconducting magnets, superconducting switch 0-9007

**Overhauser effect**

- see also *nuclear Overhauser effect*  
 dielectrics, solid, dipole electron-nucleus interaction, review 0-29649  
 polyacetylene, dynamic nuclear polarisation of protons (*French*) 0-43217  
 spin system, X<sub>3</sub>{A} experiment 0-25251

**overhead line conductors**

- steel-Al bimetallic wire for overhead lines, manufacturing methods 0-16247

**overhead lines**

- see also *power overhead lines*  
 HV lines, noise, publications review (*Czech*) 0-23827

**overvoltage protection**

- long spark-gaps, breakdown voltage (*French*) 0-33828  
 spark gaps, electrode shape influence on SF<sub>6</sub> dielectric strength (*Czech*) 0-10444

**oxidation**

- see also *anodisation; combustion; corrosion; reduction (chemical)*  
 acrylic fibres, oxidative stabilisation, moisture sensitivity 0-16524  
 actinides, oxidation potential 0-5495  
 alloys, passivable, role of oxide films in stress corrosion cracking initiation 0-50762  
 aromatic compounds, oxidative bromination, chem. oscils. 0-3335  
 ascorbic acid, action with perhydroxyl radicals, radiolytic study 0-35523  
 chalcopryrite, electrooxidation in ACI, stoichiometry and reaction mechanism, Cu extraction appl. (*French*) 0-16231  
 chlorophyll photo-oxidation, role of singlet-excited and triplet states 0-51156  
 copper molybdates, oxidation, reduction and thermal decomp. mechanisms 0-50847  
 CrMoV, surface coating to prevent oxidation during high temp. AE 0-16539  
 cytochrome C, immobilised, investigs. using magnetic micromixer attachment for SPECORD UV VIS spectrophotometer 0-56302  
 defect theory and processes, review 0-2009  
 deformation effects in nuclear reactors and mech. structures 0-3211  
 diffusion laws in solids, phenomenological 0-39341  
 1,3-diphenylisobenzofuran solns., rubrene sensitised photooxidation, S<sub>1</sub> excited state O<sub>2</sub> quenching 0-45529  
 ferritic alloy DT02, oxidation behaviour in CO<sub>2</sub> or Ar with H<sub>2</sub>O and H<sub>2</sub>, 823-123K 0-3249  
 graphite, ATJS, tensile strength, oxidation effects up to 2500K 0-3209  
 graphite AlCl<sub>3</sub> intercalation compound, electrochem. characterisation method 0-55666  
 graphite oxidation and coolant chemistry of CEGB gas-cooled reactors 0-42774  
 haeme proteins and metalloporphyrins, redox chem. and oxygen binding 0-3573  
 high temperature metallic species, absorpt. and fluoresc., high temp. fast flow reactor technique 0-42231  
 hydrocarbons, gas phase oxidations and pyrolysis, wall-less reactor technique 0-45500  
 Inconel 600, oxide layer, mechanical impedance meas. method 0-45444  
 I (*French*) 0-11984  
 lanthanides, oxidation potential 0-5495  
 lubricants, ester-type, thin-film test for meas. of oxidation and evaporation 0-40626  
 membrane damage caused by light irradiation of fluorescent concanavalin A 0-56123  
 metal, laser heating kinetics, influence of oxide film interf. effects 0-11841



## oxidation continued

metal-slag interface, interaction under diffusion conditions, impurity oxidation (*Russian*) 0-35390  
 metals, sintering, surface oxide layer effects, oxide dissolution process, anal. 0-11588  
 methanol oxidation mechanisms at Pt electrodes in acid electrolytes in methanol-air fuel cells 0-45661  
 3-methoxybenzanthrone in ethanol, photoprotolytic reactions, spectra, rate consts. and lasing thresholds 0-43327  
 mordenite-hosted redox reactions 0-55939  
 Ni, oxidation in air, 50-150°C, film growth obs. using AES and contact resist. 0-3242  
 nuclear reactor core meltdown, chemical reacts. between core melt and concrete 0-13588  
 oxidising metal heating by periodically pulsed CO<sub>2</sub> laser 0-7445  
 Permalloy, magnetic head wear resistance and surface charact. against magnetic tape (*Japanese*) 0-35335  
 Permalloy films, oxidation effects on atmospheric corrosion, AES, XPS and ion sputtering anal. 0-11829  
 polyacetylene, doping with AsF<sub>5</sub>, mechanism, effect on elec. cond. and spectra 0-24473  
 1,4-polybutadiene, oxidation stabilisation by singlet O<sub>2</sub> quencher 4-(1-imidazolyl)-phenol 0-16677  
 polyethylene, cross-linked, thermal oxidation stability, influence of Cu 0-30128  
 polyethylene, high density, carrier trapping, X-ray induced TSC 0-11005  
 polyethylene coating on galvanized steel, thermal oxidation affect on adhesion (*German*) 0-35419  
 polymer, photo-oxidation 0-3380  
 polymer coatings for corrosion protection, electrochem. techniques for performance monitoring 0-3234  
 polymer melt, oxidative stability determ. technique 0-45412  
 polystyrene, props. changes upon photooxidation 0-30123  
 propene, catalytic oxidation, modification of V<sub>2</sub>O<sub>5</sub>(001) surface (*French*) 0-45557  
 pyrocarbon, oxidation behaviour at high temps. 0-55551  
 pyrocatechol, oxidation pots., correl. of V-I characts. and photographic developing power (*Russian*) 0-45534  
 pyrographite, elec. resist., during electrochem. insertion of H<sub>2</sub>SO<sub>4</sub> (*French*) 0-2437  
 rare earth oxides, binary, struct. and props., book contrib. 0-45292  
 rare earths, purification, laser methods 0-16712  
 retinals, prod. and quenching of singlet oxidation 0-35840  
 rhodamine 6G, aqueous soln., absorpt. spectra, ground and triplet state photoprotonation pH depend. 0-42961  
 rhodamine dyes in soln., bleaching, electronic and vibr. absorpt. spectra, fluoresc. 0-42960  
 Sendust alloy, magnetic head wear resistance and surface characts. against mag. tape (*Japanese*) 0-35335  
 silicides, oxidation and hot corrosion resistance kinetics 0-25896  
 SIMS, solid surface investig. applications (*Rumanian*) 0-49510  
 smouldering discharge at O<sub>3</sub> liq. surface in N<sub>2</sub>, thin solid pellicle formation of N<sub>2</sub>O<sub>5</sub> 0-38827  
 space charge effects on steady-state transport in oxide films 0-11124  
 steel, alloy, carburisation, internal oxidation of excess carbides (*Russian*) 0-25903  
 steel, alloy cladding, oxidation behaviour in GCFR He environment 0-16594  
 steel, austenitic stainless, fretting wear in air and CO<sub>2</sub> at elevated temps. 0-21119  
 steel, austenitic stainless, oxidation and spalling resistance 0-30133  
 steel, Cr-Mn-C-Si (20, 14, 0.2, 0 to 3 wt.%), high-temp. oxidation (*Russian*) 0-25904  
 steel, Cr-Mo (2.25, 1 wt.%), oxidation effect on hold time fatigue behaviour 0-30161  
 steel, Fe<sub>3</sub>O<sub>4</sub>, transformation to Fe<sub>3</sub>O<sub>4</sub> in oxide scales conversion kinetics 0-7561  
 steel, stainless, ferritic, 430 Zr, oxidation, forming and mech. props. 0-11680  
 steel, stainless, gas liberation in vacuum, depend. on oxidation process (*Russian*) 0-25901  
 steel, stainless, oxidation resistance, effect of C, Zr, Ti and Nb 0-35394  
 steel, stainless 316 0-16606  
 steels, austenitic stainless, Cl and H<sub>2</sub>S effect on oxidation resist. 0-45418  
 steels, oxidation of structural steels in gas-cooled reactors 0-45447  
 submarine pillow basalts, mag. minerals oxidation rel. to geomag. palaeointensities determ. 0-3927  
 surface structure, distribution of defects, LEED 0-44402  
 TCNQ salts with heterocyclic amines and hydroquinone form. via redox reaction 0-26013  
 tissue, animal, lyophilised, paramagnetic centres 0-30681  
 transition metal oxides, surface oxidation, study by AES 0-45175  
 water, photoassisted oxidation at TiO<sub>2</sub>:Be electrodes 0-30502  
 wear frictional heating and oxidation theory 0-44255  
 Zircaloy oxidation, improved evaluation model 0-32349  
 Zircaloy-2 claddings, oxidation reaction kinetics in steam environment in temp. range 1273-1673K 0-35401  
 Zircaloy-4, anomalous oxide growth during transient temp. oxidation 0-50773  
 Zircaloy-4, oxidation in steam, 900-1500°C, kinetics 0-3241  
 Zn-salt, molten system, separation of Hf and Zr 0-11884  
 Ag-Zn (2 to 12 wt.%) containing several metals, internal oxidation (*Japanese*) 0-16570  
 Al, chemisorption of O, O-Al and O-O bond lengths, surface extended X-ray absorpt. fine struct. 0-29267  
 Al, clean and oxidised surfaces, secondary electron spectrum, EELS and AES, comparison 0-55237  
 Al clean films, O<sub>2</sub> interaction study using synchrotron-radiation-induced-photoemission 0-55709  
 Al in (NH<sub>4</sub>)<sub>2</sub>CO<sub>3</sub> solutions, to form amorphous self-supporting vac.-tight Al<sub>2</sub>O<sub>3</sub> films 0-16177  
 Al magnetron sputtering target, oxidation in Ar/O<sub>2</sub> mixtures 0-55291  
 Al, negative corona 0-40593  
 Al, oxidation, influence on deformation map 0-40599  
 Al, pitting mechanism, obs. using Engell-Stolica potentiostatic method 0-25905  
 Al, surface energy and adhesion props. 0-10774  
 Al-based coatings, for high temp. alloys, process development and props. 0-40614  
 Al-Cu (1 to 10 wt.%), vapour deposited films, ion scattering spectrometry characterisation 0-15386

## oxidation continued

Al-Mg, oxidation induced stresses, dislocation network form., HVEM obs 0-14978  
 Al+O<sub>2</sub> reaction, surface chemiluminesc. study 0-55708  
 Al<sub>2</sub>O<sub>3</sub>, plasmachemical synthesis, oxidised from metals, exam. of props. 0-2984  
 Au-Cu, oxidation kinetics of Cu out of Au soln. at 50-150°C 0-21171  
 BN ceramic with organosilicon polymer additions, strength and oxidation resistance 0-20880  
 BaB<sub>2</sub>H<sub>12</sub>·10H<sub>2</sub>O, struct. dehydration, intermediate phases and thermooxidative degradation 0-33951  
 BaF<sub>2</sub>, formation and growth of oxidation centres result of O<sup>2-</sup> diffusion 0-7706  
 BaTeO<sub>3</sub>, oxidation, X-ray powder anal. (*French*) 0-15080  
 Be, implanted D and He, interaction and radiation enhanced oxidation 0-39120  
 (Bi, Sb)<sub>2</sub>Te<sub>3</sub> solid soln., semiconductor film, oxidation, electrophysical props. 0-45407  
 Bi film, vac. evaporated, thermally oxidised, struct. by electron diffr. and TEM obs. 0-6678  
 Bi, oxidation kinetics 0-25914  
 Bi-Pb(Te)(Sn)(Ti)(In)(Sb), dilute, oxidation kinetics 0-25914  
 Bi<sub>2</sub>Mo<sub>2</sub>O<sub>9</sub>, thermal decomp. rel. to catalytic oxidation 0-35520  
 C fibre reinforced, C oxidation behaviour, rate-controlling steps 0-55550  
 C fibres and C fibre reinforced epoxy phenol, oxidation, effect on props. 0-40574  
 C oxidation kinetics, in Fe-C melts by CO<sub>2</sub> (*Russian*) 0-40680  
 C refractories, alkali attack as catalyst for oxidation 0-40562  
 C, vitreous, tensile strength, oxidation effects up to 2500K 0-3209  
 CO, over Ir, tracer studies on reaction path and kinetics of CO oxidation 0-7857  
 CS<sub>2</sub>, COS, atmospheric, oxidation as SO<sub>2</sub> sources 0-4085  
 CaB<sub>2</sub>H<sub>12</sub>·10H<sub>2</sub>O, struct. dehydration, intermediate phases and thermooxidative degradation 0-33951  
 CaF<sub>2</sub>:Mn<sup>2+</sup>, fluorite, radiation and thermal redox processes 0-55678  
 CaTeO<sub>3</sub>, oxidation, X-ray powder anal. (*French*) 0-15080  
 CdS films, amorphous and polycrystalline, microinclusion distrib. of high resist. phase and residual cond. 0-7008  
 CdTe, clean and oxidised surfaces, surface states, low-energy EELS study 0-11522  
 CdUO<sub>4</sub>, phase transforms., anomalous oxidation state change 0-54369  
 Co<sup>3+</sup> complex, ammoniated zeolite, oxygenated product form., electronic spectrosc. obs. 0-991  
 Co-Cr (up to 25 wt.%), sulphidation and oxidation in Ar-SO<sub>2</sub>, effects of increase in Cr content 0-11839  
 Co-Mn (0 to 45 wt.%), high temp. oxidation 0-35371  
 Co-Ni-Cr-Al-Ta, S-57 alloy hot corrosion, cyclic oxidation, depth of attack determinations 0-11837  
 Co-Ni-Cr-W-Fe, HA-188 alloy, hot corrosion, cyclic oxidation, depth of attack determinations 0-11837  
 Co-superalloy, cast, high temperature fatigue behaviour 0-40485  
 Co-VC (12 wt.%), directionally solidified eutectic, oxidation 0-11821  
 Co<sub>30</sub>Ni<sub>70</sub>, oxidation study by Auger electron spectroscopy (*Ukrainian*) 0-7711  
 Cr (100), adsorption of O<sub>2</sub> and initial oxidation at room temp. 0-20034  
 Cr-Fe alloy (up to 50%), hardness, oxidation and electronic constitution 0-30154  
 Cr-Ti/MgO-NbC(TaC) dispersion-strengthened, high temp. wear and oxidation resist. 0-25877  
 Cr-Ti/NbC(TaC) dispersion-strengthened, high temp. wear and oxidation resist. 0-25877  
 Cu, (100) single crystal surface 0-11846  
 Cu (100) surface, interaction with O<sub>2</sub>, AES, EELS, LEED and work function studies 0-24731  
 Cu, diffusion/oxidation through Au, rate-controlling step 0-34240  
 Cu, epitaxy in aq. oxidation of (001) single crystal 0-11844  
 Cu-Fe (0.2 at.%), clustering, precipitation, and oxidation, 298 to 919K, Mossbauer study 0-7242  
 Cu-Fe (0.2 at.%), surface oxidation, Mossbauer obs. 0-55564  
 Cu-Ga, high dislocation density alloys and oxide precipitated struct., NMR, spin echo 0-39892  
 Cu-MgO, dispersion hardened alloys, prep. and props. 0-40291  
 Cu-Mn(Ti)(Sn)(Si), dil., oxide film form. in ammoniacal Cu(II) solns., AES obs. 0-45415  
 Cu-Ni, annealing effect on oxidation kinetics, reduction in vacancy level 0-50760  
 Cu-Ni (0.1 to 51 wt.%), oxidation, diffusion kinetics in porous inner layers 0-16546  
 Cu-Si, high dislocation density alloys and oxide precipitated struct., NMR, spin echo 0-39892  
 CuO, plasmachemical synthesis, oxidised from metals, exam. of props. 0-2984  
 Fe, aerosoled ultrafine particles oxidation 0-21183  
 Fe and Fe-Cr alloys, friction behaviour in oxygen, development of wear-protective oxides and influence on sliding friction 0-30111  
 Fe, cast, anodic polarisation in slag melt (*Russian*) 0-45513  
 Fe colloidal dispersion, mag. props., struct. and oxidation 0-34699  
 Fe, deoxidation of liq. by Al, Mossbauer meas. 0-20553  
 Fe, initial oxidation kinetics using proton-induced X-ray emission 0-35618  
 Fe, oxidation in NaCl soln., ferric oxide film form. 0-25898  
 Fe, passivity in aq. soln., correlation with mol. struct. 0-16541  
 Fe pellets, re-oxidation at high temp., growth of needle-like haematite crystals 0-35431  
 Fe powder, sponge and atomized types, steam oxidation, pore closure and surface hardness 0-45441  
 Fe powder compacts, surface oxidation influence on shrinkage anisotropy 0-50574  
 Fe, sponge, oxidation kinetics by nuclear  $\gamma$ -resonance method (*Russian*) 0-40681  
 Fe-Al, electron-beam-induced surface oxidation, HVEM obs. 0-14978  
 Fe-Cr, Auger electron and appearance pot. spectroscopic study of surfaces 0-11520  
 Fe-Cr (24 wt.%), low temperature, oxidation, kinetics, oxide morphology 0-11838  
 Fe-Cr alloys, NaClO<sub>3</sub> and NaCl effects on corrosion behaviour in hot NaOH soln. (*Japanese*) 0-35407  
 Fe-Cr-Al (0.3 wt.%), oxidation behaviour at high temps. (*Japanese*) 0-35404  
 Fe-Cr-Al-Y, high temp. corrosion depend. on Y, oxidation, stress growth (*Russian*) 0-40588  
 Fe-Cr-Al(-Y), isothermal oxidation behaviour at 1200°C, SEM 0-50755



oxidation continued

Fe-Cr-Al(Y), thermal cycling influence on oxidation behaviour at 1200°C, SEM 0-50756  
 Fe-Cr-Al(Y) alloys, oxide grain morphology and growth mechanism 0-3239  
 Fe-Cu (75 ppm), internal oxidation, local struct. determ. by EXAFS 0-25916  
 Fe-Hf (Si) (Ti) (V), molten, gaseous O<sub>2</sub> absorption 0-11836  
 Fe-Ni-Cr, austenitic with dispersed phases, oxidation 0-16540  
 Fe-Ni-Cr base alloy, oxidation and hot corrosion (*Chinese*) 0-21149  
 Fe-Ni-Cr melts, O solubility (*Russian*) 0-15250  
 Fe-O-V melts, phase equilib. (*Russian*) 0-16273  
 Fe-Si protective oxide film form. 0-11818  
 Fe-Si-B, surface tension, density, and oxidation kinetics 0-20028  
 Fe-Si(Al), oxide layer form. during annealing, AES in-depth anal. (*German*) 0-16576  
 Fe<sup>2+</sup>Cr<sub>x</sub><sup>3+</sup>Al<sub>1-x</sub><sup>3+</sup>O<sub>4</sub><sup>2-</sup>, finely divided, oxidation kinetics 0-50848  
 (Fe<sup>2+</sup>Fe<sub>1-x</sub><sup>3+</sup>M<sub>x</sub><sup>3+</sup>)O<sub>4</sub><sup>2-</sup> (M<sup>3+</sup>=Al<sup>3+</sup>, Cr<sup>3+</sup>), oxidation to γ lacunar spinels, rate law vs. O<sub>2</sub> press. 0-50849  
 Fe<sub>1-x</sub>O, surface struct., XPS study 0-20759  
 Fe<sub>2</sub>O<sub>3</sub>, plasmochemical synthesis, oxidised from metals, exam. of props. 0-2984  
 Fe<sub>2</sub>O<sub>3</sub>, magnetite, oxidation mechanism during roasting of nodules (*Russian*) 0-40567  
 Fe<sub>2</sub>O<sub>4</sub> powder, oxidation to γ-Fe<sub>2</sub>O<sub>3</sub>, coercivity changes 0-44864  
 FeS<sub>2</sub>, oxidation, Mossbauer spectroscopic and magnetokinetic studies, 400-500°C 0-44880  
 GaAs (110), adsorption of O<sub>2</sub>, oxide form., XPS/UPS study 0-49497  
 GaAs (110), coadsorption of Cs and O<sub>2</sub>, initial oxidation, soft XPS obs. 0-10793  
 GaAs (110), initial oxidation, XPS and AES study 0-11542  
 GaAs (110), O chemisorption, surface EXAFS meas. 0-50460  
 GaAs (110), optical technique, detection of external reflectivity change on oxidation 0-6939  
 GaAs (110), reconstruction and oxidation initial stages, ab initio calc. 0-49473  
 GaAs (110), with ultrathin Al and Cs overlayers, O<sub>2</sub> adsorption, comparative studies 0-50740  
 GaAs (110) surface, O<sub>2</sub> interaction, order-disorder effects, LEED, UPS anal. 0-6634  
 GaAs (110) surfaces, ordered and disordered, O<sub>2</sub> adsorption, XPS meas. 0-49498  
 GaAs hydrothermal oxidation kinetics, exam. 0-40566  
 GaAs, microscopy with an ellipsometric arrangement 0-17998  
 GaAs, oxidation, initial process and oxide/semicond. interface formation 0-50739  
 GaAs, oxidation in multipole plasma, MOS elec. props. 0-44737  
 GaAs, shallow-homojunction solar cell by MBE, conversion efficiency 0-30476  
 GaAs, thermal oxide film growth and characterisation 0-11808  
 GaAs, XPS study of native oxides on surface 0-16141  
 GaAs:Cs, oxidation process, UPS obs. 0-50511  
 GaAs-GaAs oxide interface layer characterisation by spectroscopic ellipsometry 0-50738  
 GaAs-oxide interfaces, local atomic and electronic struct., high resolution XPS 0-49927  
 GaP (110), initial oxidation, XPS and AES study 0-11542  
 GaSb (110), initial stages, photoemission study 0-16529  
 Ge dissolution by oxidation and solvation, hole injection effect 0-26051  
 Ge, oxidation of clean cleaved (111) surfaces, EELS and AES 0-3230  
 GeCl<sub>4</sub> hydrolysis and oxidation kinetics for graded-index fibre vapour phase axial deposition 0-48477  
 Ge(111)2×1, oxide layer, surface states detect optical reflectivity obs. 0-50368  
 H production from coal using steam-Fe process, development status 0-55942  
 H<sub>2</sub>, production by solar energy, homogeneous photoredox system 0-3387  
 Hf, microstructural study (*French*) 0-45436  
 HfB<sub>2</sub>, oxidation in O<sub>2</sub> atmosphere, exam. 0-11814  
 Hg<sub>1-x</sub>Cd<sub>x</sub>Te, anodic oxide films, formation and props. 0-3212  
 In film, oxidation, XPS excited by Zr Mγ radiation 0-40236  
 In film, RF plasma oxidised, surface analysis using ESCA 0-50742  
 InAs anodic oxide films prep. and props. 0-55553  
 InP (110), initial stages, photoemission study 0-16529  
 InP hydrothermal oxidation kinetics, exam. 0-40566  
 InP, thermal oxidation, growth rate and comp. of oxide 0-55555  
 InSb (110), initial oxidation, XPS and AES study 0-11542  
 InSb, charact. and phys. props., review (*Japanese*) 0-39576  
 K<sub>1+x</sub>Fe<sub>1-x</sub>Ga<sub>1-x</sub>O<sub>17</sub>, electron hopping and excitation at room temp., <sup>51</sup>Fe Mossbauer spectra 0-25257  
 LaB<sub>6</sub>, high temp. interaction with O<sub>2</sub>, AES and mass desorption expts. 0-7698  
 LaCrO<sub>3</sub>, vaporization in oxidizing atmos. 0-24579  
 Mg clean films, O<sub>2</sub> interaction study using synchrotron-radiation-induced-photoemission 0-55709  
 Mg+O<sub>2</sub>=MgO+O, shock-tube study of evap. and oxidation kinetics 0-16651  
 MgB<sub>2</sub>H<sub>12</sub>·10H<sub>2</sub>O, struct. dehydration, intermediate phases and thermooxidative degradation 0-33951  
 MgO, plasmochemical synthesis, oxidised from metals, exam. of props. 0-2984  
 MgO:Li, enhancement of elec. cond. by oxidation 0-44600  
 MgO-C in melts, corrosion resist., rel to oxidation, porosity, content 0-40578  
 Mg<sub>2</sub>SiO<sub>4</sub>, forsterite, decorated dislocations 0-54245  
 Mo, oxidation kinetics, Mossbauer study 0-40005  
 Mo<sub>2</sub>B<sub>3</sub>-based alloys, mech. props., rel. to appl. as electrodes in electros-park machining 0-21174  
 Na<sub>3</sub>AlF<sub>6</sub> film, evaporated, electron bombard. effect on secondary electron emission, Auger peak shifts 0-2903  
 Na<sub>2</sub>O particles, effect on optical props. of Na vapour 0-1736  
 Na<sub>2</sub>O-B<sub>2</sub>O<sub>3</sub>-Au glasses, Au solubility, oxidation state and opt. absorpt. 0-44321  
 Nb alloys, cold worked, chemothermal strengthening, internal oxidation 0-35229  
 Nb, oxide growth and oxide coatings, XPS and AES studies 0-50765  
 Nb, pure, reaction with gas residual in vacuum, physicochem. props. effect 0-16587  
 Nb-alloys, reaction with gas residual in vacuum, physicochem. props. effect 0-16587

oxidation continued

Nb-NbO<sub>2</sub>-Pb Josephson tunnel junctions, fabrication using FR glow discharge oxidation 0-34559  
 Nb-V oxidation in air, rate determining process (*Russian*) 0-21170  
 Nb-V-Cr, Nb-V, and Nb-Cr, oxidation resist., Cr and V effects (*Russian*) 0-40585  
 Ni (110), chemisorption of O<sub>2</sub> and initial oxidation, AES, EELS, and work function meas. 0-54523  
 Ni amalgam, anodic polarisation in alkaline soln. 0-11823  
 Ni, inner layer of high temp. oxide scale, metallographic obs. 0-3240  
 Ni, oxidation transport processes using tracers in growing NiO scales 0-25913  
 Ni surface, oxidation, structural changes, low energy ion scatt. study 0-35423  
 Ni-Al spraying powders, alumina and aluminide formation 0-25920  
 Ni-Al-Cr<sub>2</sub>C<sub>3</sub>, eutectic, directionally solidified, high-temp. oxidation 0-50775  
 Ni-Au alloy, oxidation in air, 50-150°C, film growth obs. using AES and contact resist. 0-3242  
 Ni-Co-Cr-Al-Y, plasma-arc-sprayed, metallurgical characts. and oxidation behaviour 0-40618  
 Ni-Cr-Al-ThO<sub>2</sub>, hot corrosion, cyclic oxidation depth of attack determinations 0-11837  
 Ni-Cr-Co-Mo-Al, IN-67 alloy, hot corrosion, cyclic oxidation, depth of attack determinations 0-11837  
 Ni-Nb alloys, oxidation at high temp., high energy ion backscattering anal. (*Japanese*) 0-35405  
 Ni-Si-B powder, oxidation at 850°C, SEM, ESCA, and elec. cond. meas. 0-7717  
 Ni-Ti (1.6, 7.64 wt.%), monophase high temp. scaling, metallography study 0-21159  
 Ni<sub>3</sub>Al-Ni<sub>3</sub>Nb, eutectic, temp. and thermal cycling influence on oxidation 0-45417  
 Ni<sub>3</sub>Al-Ni<sub>3</sub>Nb eutectic, directionally solidified, high-temp. oxidation mechanism 0-16544  
 NiO, plasmochemical synthesis, oxidised from metals, exam. of props. 0-2984  
 Ni(100), oxidation, UPS obs. 0-6648  
 P, amorphous, stability in air, XPS study, comparison with cryst. polymorphs 0-25517  
 Pb/Au/Pb, Josephson junction, oxide formation process, ellipsometric meas. (*Japanese*) 0-11561  
 Pb-In and Pb-In/Au, Josephson junction, oxide formation process, ellipsometric meas. (*Japanese*) 0-11561  
 PbInAu film, RF plasma oxidised, surface analysis using ESCA 0-50742  
 PbS, oxidation, PbSO<sub>4</sub> distrib. in products (*Polish*) 0-25883  
 Pb<sub>1-x</sub>Sn<sub>x</sub>Te anodic oxide film form. conditions, IR absorpt. spectra 0-11494  
 Pb<sub>2</sub>Sn<sub>1-x</sub>Te, thin film, appl. of Mossbauer method 0-45410  
 PdH<sub>2</sub> layer, galvanostatic desorption of hydrogen, quantitative theory 0-40694  
 Ph, Josephson junction, oxide formation process, ellipsometric meas. (*Japanese*) 0-11561  
 Pt, hydrocarbon reactions catalysed by surfaces with variable kink concs., surface O<sub>2</sub> effects 0-35576  
 Pt resistance thermometer, oxidation problems 0-52206  
 Pt, surfaces, oxidation by electrosorpt., of H<sub>2</sub>, effect of soluble prods. (*German*) 0-55717  
 Pt, XPS spectra study 0-3254  
 Pu, radioactive waste, oxidation by radiation, effect on migration rate 0-13714  
 Si, (111) surface, oxide formation, AES and EELS meas. 0-3232  
 Si, and Si:H, amorphous, sputter deposited, O<sub>2</sub> incorporation during and after fabrication 0-49541  
 Si and Si:H amorphous films, porosity and oxidation of evap., sputtered and plasma-deposited films 0-10838  
 Si Czochralski wafers, thermally oxidized, stacking fault distrib., O conc. depend. 0-2042  
 Si double polycrystalline VLSI devices, low temp. differential oxidation 0-16521  
 Si film removal using anodic oxidation, determination of active impurity distrib. 0-40583  
 Si, impurity redistribution during single oxidation step, computer program calc. 0-2060  
 Si, in HCl/O<sub>2</sub> ambients, phase separation and Na passivation in thermal oxides 0-3219  
 p-Si inversion-channel photoelectric cell characteristic (*Russian*) 0-49941  
 Si, microwave O<sup>+</sup> plasma, magnetoactive, for oxidation of Si 0-38831  
 Si oxidation in O<sub>2</sub>-H<sub>2</sub>-HCl mixture, kinetics, SiO<sub>2</sub> film props. 0-40569  
 Si, oxidation with trichloroethylene additive to eliminate oxidation induced stacking faults 0-39118  
 Si, oxidation-induced stacking faults, nucleation mechanism 0-15122  
 Si, oxidation-induced stacking faults, influence of annealing ambient on shrinkage kinetics 0-29035  
 Si, stacking fault growth, oxidation-induced, HCl and interstitial effects 0-49241  
 Si, steam oxidation, low temp., high press., oxide growth kinetics and props. 0-16523  
 Si substrate for Pb, Sb, and Bi silicate films, form. kinetics and props. 0-35358  
 Si, surface oxidation, in wet O<sub>2</sub> environment 0-3410  
 Si, thermal oxidation in O<sub>2</sub>-trichloroethylene mixture, 900, 1000 and 1100°C 0-3221  
 Si, thermal oxidation in wet O<sub>2</sub>/trichloroethylene mixtures at 1200°C 0-16522  
 Si wafer, automatic meas. system for resist. profiles 0-39574  
 Si:As implanted emitters, oxidizing drive-in ambient deleterious effect 0-2044  
 Si:B, lateral effect of oxidation on B diffusion 0-29217  
 Si:B, redistrib. of B during thermal oxidation, numerical and analytical calcs. 0-49259  
 Si:P, ion-implanted, carrier conc. reduction caused by wet O<sub>2</sub> oxidation 0-10565  
 Si:P film, CVD polycrystalline, low press. and atmos. press., oxidation 0-3214  
 Si:P(As)(B)-SiO<sub>2</sub> interface oxidation kinetics, high doping levels, experiment 0-11828  
 Si-Al-O-N, oxidation mechanisms 0-40570  
 Si-Al(Ti)C, sintered, exam. of props. 0-25644  
 Si-B based CVD coating for gas turbine blading, props. 0-40615



## oxidation continued

- Si-B system, liq., surface tension, density, and oxidation kinetics, 1410-1700°C 0-20011  
Si-based coatings, for high temp. alloys, process development and props. 0-40614  
p-Si-Mn contact, barrier height, oxidation effects 0-34510  
Si-SiO<sub>2</sub>, bonding at (111) interface, stoichiometry and kinetics, synchrotron radiation photoemission spectroscopy 0-24744  
Si-SiO<sub>2</sub>, ESR centres, interface states and oxide fixed charge 0-2474  
Si-SiO<sub>2</sub>, impurity redistrib. during oxidation, numerical soln. including interfacial fluxes 0-25888  
Si-SiO<sub>2</sub>, interface, reconstructing states 0-49925  
Si-SiO<sub>2</sub>, interface defect states obs. by constant capacitance DLTS 0-49924  
Si-SiO<sub>2</sub>, interface, backscattering-channelling study 0-34320  
Si-SiO<sub>2</sub>, interface, effect of oxidation time and temp. using AES 0-35359  
Si-SiO<sub>2</sub>, interface, oxidation stacking faults, growth rel. to self-diffusion 0-49239  
Si-SiO<sub>2</sub>, interface layer characterisation by spectroscopic ellipsometry 0-50738  
Si-SiO<sub>2</sub>, interface oxidation kinetics, high doping levels, theory 0-11827  
Si-SiO<sub>2</sub>, interface state density, dependence on thermal oxidation process variables 0-15607  
Si-SiO<sub>2</sub>, interfaces, local atomic and electronic struct., high resolution XPS 0-49927  
Si-SiO<sub>2</sub>, interfacial region on TCE/O<sub>2</sub> and CCl<sub>4</sub>/O<sub>2</sub> oxidised Si, struct. and comp. 0-50741  
Si-undoped poly Si interface, in oxidation process, defects generation 0-40571  
SiC, chem. stability, mech. and thermal props. rel. to appls. 0-21103  
SiC, oxidation and corrosion behaviour, formation of protective SiO<sub>2</sub> coatings (German) 0-25885  
SiC, oxidation and hot corrosion resistance kinetics 0-25896  
SiC, reactions with oxidising atms. 0-11812  
SiC, resist. to oxidation and corrosion at high temps. (German) 0-35357  
SiCl<sub>4</sub> hydrolysis and oxidation kinetics for graded-index fibre vapour phase axial deposition 0-48477  
SiH<sub>4</sub>, low temp. oxidation, film growth rates, IR absorption spectra 0-15399  
Si<sub>3</sub>N<sub>4</sub> films, struct. and oxidation characts. 0-54545  
Si<sub>3</sub>N<sub>4</sub>, oxidation and hot corrosion resistance kinetics 0-25896  
Si<sub>3</sub>N<sub>4</sub>-CeO<sub>2</sub>, surface stress development during oxidation 0-50736  
Si<sub>3</sub>N<sub>4</sub>-MgO, compressive creep, oxidation induced compositional change 0-50676  
Si<sub>3</sub>N<sub>4</sub>-Y<sub>2</sub>O<sub>3</sub>, hot-pressed, oxidation kinetics 0-16520  
Si<sub>3</sub>N<sub>4</sub>-Y<sub>2</sub>O<sub>3</sub> ceramic, thermal degradation, C impurity effect 0-50708  
SiO<sub>2</sub>, vitreous film on Si, defect struct. comparison with crystalline SiO<sub>2</sub> and Si-O bond nature 0-54557  
Si(111)2x1, oxide layer, surface states detec., optical reflectivity obs. 0-50368  
Sn, clean and oxidised, Auger spectra expt., fine structure anal. 0-29831  
Sn<sub>1-x</sub>Pb<sub>x</sub>Se(Te) thin films, resistance to oxidation, Mossbauer study 0-39986  
SrB<sub>2</sub>H<sub>12</sub>·10H<sub>2</sub>O, struct. dehydration, intermediate phases and thermooxidative degradation 0-33951  
T, metal and alloys, mechanical props., electrochemistry, oxidation and corrosion resist., conference, Nantes, France (Nov. 1978) 0-41932  
Ta, formation of Ta<sub>2</sub>O<sub>5</sub> on GaAs, interface props. 0-49935  
Ta<sub>2</sub>O<sub>5</sub>, reactive DC sputtering deposited films with magnetron-plasmatron, mechanical elec., optical props. 0-25566  
Ti alloys, oxidation resist., 400 to 800°C 0-50768  
Ti, clean and oxidised surfaces, refl., 2-25 eV 0-55123  
Ti, hydriding, surface condition and environment influence 0-35380  
Ti, interaction with O<sub>2</sub>, resist. and work function changes obs. 0-45431  
Ti, oxidation under hydrothermal cond. to produce brookite (Japanese) 0-35433  
Ti, oxide film form. during thermal treatment, morphological and struct. study (French) 0-50766  
Ti, oxide layer growth by dry oxidation at 25°C, ESCA obs. (French) 0-45434  
Ti-Al alloy thin film, anodic voltage-time dependence obs. (Polish) 0-55574  
Ti-Al-Sn-Zr-Mo-Si (6, 2, 4, 2, 0.1 wt.%), effect of elevated temperature and environment on fatigue crack growth 0-40486  
Ti-Cu thin films, oxidation kinetics in air at 100 to 300°C, meas. 0-40590  
Ti+O<sub>2</sub> reaction, surface chemiluminesc. study 0-55708  
TiB<sub>2</sub>, electric arc melting prep. and oxidation props. 0-20860  
TiC reactively sputtered coatings on Ni-Cr-Mo-Ti (19,11,3 wt.%), adherence, XPES and wear study 0-25565  
TiC sputtered coatings on Ti-Al-V (6,4 wt.%), adherence, XPES and wear study 0-25565  
TiC-Fe-Cr powder mixture, exam. of milling condition effects 0-16237  
TiN, from high-temp. reaction of NH<sub>3</sub> and TiCl<sub>4</sub>, physicochem. props. 0-55334  
TiN, synthesised in SHF discharge plasma, exam. of props. (Russian) 0-7524  
TiN<sub>x</sub>, oxidation mechanism 0-25912  
TiO<sub>2</sub>, plasmachemical synthesis, oxidised from metals, exam. of props. 0-2984  
TiO<sub>2</sub>, reactive DC sputtering deposited films with magnetron-plasmatron, mechanical elec., optical props. 0-25566  
(U,Pu)C, controlled oxidation for head-end step reprocessing 0-5308  
(U,Pu)O<sub>2</sub>, oxidation rates 0-37557  
UO<sub>2</sub>, oxidation rates 0-37557  
UO<sub>2</sub> pellet surfaces, β-UO<sub>2.33</sub> formation in air at 229 to 275°C, X-ray diff. study 0-35362  
U<sub>2</sub>O<sub>8</sub>, oxidation rates 0-37557  
USb, UPS and XPS, surface oxidation 0-7465  
V, oxidised in air during laser irradiation, switching effect (Russian) 0-24977  
V-Si, strengthening by internal oxidation 0-55424  
V-Zr, strengthening by internal oxidation 0-55424  
W surface wetting by liquid Cu depend. on preliminary surface treatment (Russian) 0-35388  
W, thermal and anodic oxidation, production of WO<sub>3</sub> layer semiconductor electrode 0-35544  
W-Al<sub>2</sub>O<sub>3</sub> cermet films, oxide evaporation deposited on Mo, Ti, Al<sub>2</sub>O<sub>3</sub> substrates, struct., props. 0-25581  
W-Cu-(Ti)(Zr), exam. of mech. props. as function of temp., composition, and oxidation props. 0-16472

## oxidation continued

- W-B<sub>2</sub>-based alloys, mech. props., rel. to appl. as electrodes in electrospray machining 0-21174  
WC-Co, composition and oxidation resistance of coatings deposited by thermal diffusion, using TiB<sub>2</sub> (Bulgarian) 0-45430  
WC-Co, phase comp. and oxidation resist. of coatings deposited by thermal diffusion using TiB<sub>2</sub> 0-21173  
W<sub>2</sub>C, oriented struct. transform. to W, FEM and TEM obs. 0-30124  
WSi<sub>2</sub> sputtered film on Si and SiO<sub>2</sub> substrate, thermal oxidation kinetics 0-3208  
(Zn,Cd)S:Cu,Al, luminesc. efficiency deterioration due to surface oxidation by (NH<sub>4</sub>)<sub>2</sub>Cr<sub>2</sub>O<sub>7</sub> thermal decomp. 0-29810  
Zn, oxidation kinetics in O<sub>2</sub>-CO<sub>2</sub>-SO<sub>2</sub> gas mixture rel. to elec. cond. of ZnO 0-34448  
ZnFe<sub>2</sub>O<sub>4</sub>-Fe<sub>2</sub>O<sub>4</sub> solid solns., form. of α-Fe<sub>2</sub>O<sub>3</sub> during oxidation 0-25889  
ZnO, plasmachemical synthesis, oxidised from metals, exam. of props. 0-2984  
ZnS:Ag, luminesc. efficiency deterioration due to surface oxidation by (NH<sub>4</sub>)<sub>2</sub>Cr<sub>2</sub>O<sub>7</sub> thermal decomp. 0-29810  
ZnSe(Te), clean and oxidised surfaces, surface states, low-energy EELS study 0-11522  
ZnTeO<sub>3</sub>, oxidation, X-ray powder anal. (French) 0-15080  
Zr, integral emittance, during high temp. heating and oxidation (Russian) 0-39327  
Zr-Hf (2.2 wt.%), oxidation kinetics in flowing CO<sub>2</sub>, 873 to 1173K 0-16596  
Zr-Hf (2.2 wt.%), oxidation kinetics in flowing CO<sub>2</sub> at high temp. 0-47575  
Zr-Nb (2.25 wt.%), oxidation kinetics in flowing CO<sub>2</sub>, 873 to 1173K 0-16596  
Zr-Nb-Sn (3.0, 1.0 wt.%), oxidation kinetics in flowing CO<sub>2</sub>, 873 to 1173K 0-16596  
Zr-Nb-Sn (3 wt.%, 1 wt.%) 0-47575  
Zr-Nb (2.5 wt.%), oxidation kinetics in flowing CO<sub>2</sub> at high temp. 0-47575  
Zr-Ni, surface layer, segregation of ferromag. Ni, magnetooptic investigation 0-2256  
Zr-Ni-H<sub>x</sub> (x=2.8 to 3), surface layer, segregation of ferromag. Ni, magnetooptic investigation 0-2256  
ZrB<sub>2</sub>, electric arc melting prep. and oxidation props. 0-20860  
ZrB<sub>2</sub>, oxidation in O<sub>2</sub> atmosphere, exam. 0-11814  
ZrB<sub>2</sub>-SiC-C(-V)(-Nb), refractory cermet, hot pressing and oxidation resist. 0-3231
- oxide coated cathodes**  
see also thermionic electron emission  
elementary discharge of the electric arc at slightly oxidated cathode (Polish) 0-19663  
ionisation gauges, heated cathodes, emission characteristics, selection (German) 0-236  
Al, cold, vapour deposited, for He-Ne lasers, performance improvement by Cu addition 0-5748
- oxygen**  
see also nuclei with .....  
δ<sup>18</sup>O, variations in snow on Devon Island ice cap, NWT, Canada 0-4050  
abundance in galaxies 0-8686  
abundance in H II regions 0-46680  
activity in liquid Pb and Sb from electrochem. meas. 0-55695  
activity meas. in liquid Na, development of electrolytic probes 0-18550  
adsorbed c(2x2) on Cu (001), surface geometry determ. by deep-core-level XPS 0-40224  
adsorbed half monolayer on W (100), surface reconstruction, struct. props. 0-44421  
adsorbed layers on graphite, heat capacity meas. 0-49511  
adsorbed on Al (100), Xa-scatt. wave cluster approach 0-49851  
adsorbed on Be, secondary ion emission, coverage dependence 0-35043  
adsorbed on Be, secondary-ion emission energy depend. 0-50502  
adsorbed on clean metal surfaces, sputtering effects, combined analytical techniques 0-35047  
adsorbed on Cu (001), Ar<sup>+</sup> bombarded, particle ejection, ang. depend. 0-50489  
adsorbed on Cu (110), low-energy ion bombardment investigation 0-34302  
adsorbed on Fe surface, effect on chem. reaction kinetics 0-55572  
adsorbed on metal-sapphire interface, effect on shear strength 0-49485  
adsorbed on Ni (110) and Ir (110), surface struct. anal. using hybridisation model 0-44423  
adsorbed on Pd (111) surface, UPS and thermal desorpt. characts. 0-54754  
adsorbed on Pt, reaction with H<sub>2</sub> 0-49514  
adsorbed on stepped W (100) surface, electron stimulated desorption ion ang. distrib. 0-20035  
adsorbed on W, coverage degree meas. by ion induced secondary electron emission 0-55251  
adsorption, ion-induced, on Cu (110) 0-54510  
adsorption, on Cu (100) single crystal surface, oxidation 0-11846  
adsorption and field-desorption on GaAs and GaP surfaces, FEM studies 0-34304  
adsorption and reaction with CO on IR (110), transient study 0-30284  
adsorption of Cs+O on GaAs (111) epitaxial film, ellipsometric study 0-29282  
adsorption on (111) surface, possible ordered struct. 0-44412  
adsorption on Ag(111) and polycrystalline surfaces, LEED, AES and energy loss spectra 0-34310  
adsorption on Al, interatomic Auger transition spectroscopy 0-11521  
adsorption on clean InSb (110), AES, LEED, RHEED and field effect meas. 0-49501  
adsorption on Cr (100) and initial oxidation at room temp. 0-20034  
adsorption on Cs-covered GaAs (110) 0-10793  
adsorption on Cu (100) surface, EELS study 0-2260  
adsorption on Cu (110), adsorbed layer reaction with CO, ellipsometry, AES, LEED study 0-6635  
adsorption on Cu (110) and surface reaction with CO 0-15373  
adsorption on Cu (111), surface band energy shift, angle-resolved UPS study 0-40228  
adsorption on ErFe<sub>2</sub> surface, effect studied by spin polarised photoemission 0-29854  
adsorption on GaAs (110), oxide form., XPS/UPS study 0-49497  
adsorption on GaAs (110), surface photovolt. spectroscopy 0-49499  
adsorption on GaAs (110) ordered and disordered surfaces, XPS meas. 0-49498



## oxygen continued

adsorption on Gd-Co, Gd-Fe amorphous films, effect on perpendicular anisotropy 0-34713  
 adsorption on InP (110), low coverage, SIMS study 0-49500  
 adsorption on Ir, field emission energy distrib. spectra 0-25535  
 adsorption on LaB<sub>6</sub> (100) surface, UPS and LEED study 0-49519  
 adsorption on MgO during  $\alpha$ -irrad., thermostimulated surface cond. obs. 0-34499  
 adsorption on MgO-CoO, EPR, volumetric investig. 0-10782  
 adsorption on Mo, metastable He de-excitation spectroscopy and UPS study 0-34314  
 adsorption on Mo (100), AES, LEED, work function, and desorption meas. 0-6654  
 adsorption on Ni {100}, low energy ion scatt. study 0-39420  
 adsorption on Ni (100), effects on secondary electron spectra 0-50480  
 adsorption on PbS (100) surface, electronic struct., UPS study 0-54756  
 adsorption on Pt, surface composition, AES and temp. programmed desorption meas. 0-34313  
 adsorption on Re, effect of struct. defects, steps and kinks 0-29269  
 adsorption on reconstructed GaAs (100) surfaces, ang. resolved photoemission from surface states 0-16143  
 adsorption on Sc and Lu surfaces, effect on reflection EELS 0-20742  
 adsorption on Si (111) surface, atomic steps and residual gas effects 0-54517  
 adsorption on SiO<sub>2</sub>, effect on EPR spectra of surface defects 0-7163  
 adsorption on SnO<sub>2</sub>, desorpt., ESR and cond. meas 0-10790  
 adsorption on U and Th, XPS study 0-7473  
 adsorption on W(111), angle resolved electron stimulated desorption, LEED and AES 0-6645  
 adsorption on W (110)(112) and Mo (110), work function and thermal stability 0-44427  
 arterial PO<sub>2</sub> continuous meas. 0-56240  
 atom, 1304 angstrom absolute emission cross section from CO(CO<sub>2</sub>) UV photodissoc. 0-32652  
 atom, beam-foil excited <sup>4</sup>P state, delayed coincidence Auger electron lifetime meas. 0-14117  
 atom, chemisorption on Cu, cluster theory 0-29264  
 atom, chemisorption on Ni, cluster theory 0-29264  
 atom, dipole properties and dispersion energies additivity, using atoms and small mol. models 0-53091  
 atom, distrib. in lower thermosphere assuming tidal effects, one dimens. nonstationary diffusion-photochemical model 0-4160  
 atom, electron impact ionisation, differential and total cross-sections 0-18935  
 atom, ground and excited state, laser-induced photolysis of ozone reactions 0-11928  
 atom, K $\alpha$  spectrum, intensity of high energy peak as function of oxide layer thickness 0-936  
 atom, many electron autoionisation states, perturbation theory Z-expansion, numerical results 0-52863  
 atom, metastable <sup>5</sup>S-state, optical pumping 0-32678  
 atom, photoionisation cross sections and ang. distrib., outer p subshell 0-9572  
 atom, photoionisation cross-section calc., 304 and 584 Å 0-43015  
 atom, SCF electron-gas local-spin-density model including correlation 0-9488  
 atom, two-photon absorpt., auroral transition relax. obs. (Japanese) 0-47954  
 atom+1-alkyne, CO prod., vibr. population distrib., rate consts., laser reson. absorpt. technique 0-40676  
 atom and molecule, photoionis. and photoabsorpt. cross sections for aerodynamic calcs., data tables 0-41599  
 barley seeds, minimum  $\gamma$ -exposure and O<sub>2</sub> concs. to produce post irradi. O<sub>2</sub> damage enhancement 0-30779  
 blood monitoring, intraarterial vs. transcutaneous monitoring in newborn infants 0-56266  
 blood O<sub>2</sub> monitoring, combined system for transcutaneous and intravascular determ. of partial press. 0-56241  
 BWR, H<sub>2</sub> and O<sub>2</sub> monitoring in containment and off-gas systems 0-32414  
 capacitive discharge, high-freq. gas overheating suppression 0-38856  
 catalytic surface activity, LaNi<sub>5</sub> surface segregation (German) 0-51008  
 cellular O<sub>2</sub> enhancement ratio, hypothesis test and microdosimetric implications 0-26212  
 chemisorbed in TTF-TCNQ and  $\phi_4$ DTP-TCNQ, effect on mag. susceptibility 0-15679  
 chemisorbed on Ag film, reflectance and elec. resist. changes 0-11495  
 chemisorbed on Ni (100), rapid LEED intensity meas. 0-44420  
 chemisorbed on Si (111), electronic struct. tight-binding calc., XPS and UPS meas. 0-49845  
 chemisorbed on Si (111) surface, electron states by AES 0-54747  
 chemisorbed on W (110), island form. and condensation 0-49517  
 chemisorbed overlayers on Al (111), angle-resolved photoemission, band struct. 0-40229  
 chemisorption, on Si (III) surface, appl. of UPS ultra high vacuum apparatus (Japanese) 0-37125  
 chemisorption, on stepped Ru (~001) cryst., 300K, LEED and AES obs. 0-11947  
 chemisorption in non-polar cpd. semicond. surfaces,  $\pi$ -bonding contrib. 0-6631  
 chemisorption on Al, photon and electron emission as indicators of intermediate states 0-39439  
 chemisorption on Al, site determ. by LEED 0-39421  
 chemisorption on Al (111), O-Al and O-O bond lengths, surface extended X-ray absorpt. fine struct. 0-29267  
 chemisorption on and initial oxidation of Nb (110) and (750) 0-44408  
 chemisorption on CaO and MgO, adsorboluminescence from surface F-centres 0-20723  
 chemisorption on GaAs (110), surface EXAFS meas. 0-50460  
 chemisorption on GaP (110), initial steps, electronic surface states 0-49844  
 chemisorption on LaB<sub>6</sub>, time of flight atom-probe FIM study 0-6652  
 chemisorption on Ni (110) and initial oxidation, AES, EELS, and work function meas. 0-54523  
 chemisorption on Ti (0001), valence band struct., XPS and UPS study 0-35062  
 chemisorption on TiC (001) surface, change in work function 0-29461  
 chemisorption props. and catalytic activities of Pt surfaces with variable kink concs. 0-35576  
 coadsorption with CO on Ru (001), uptake and flash desorption meas. 0-39450

## oxygen continued

coadsorption with H<sub>2</sub> on Rh (111) below 140K 0-29276  
 coadsorption with Xe on W (110) and (100), work function and thermal desorption meas. 0-39448  
 coadsorption with Zr on W(100) 0-6653  
 coating, on Al thin film, effect on supercond. 0-7026  
 codeposition with Cs on W (110), Cs<sub>2</sub>O form. 0-44425  
 deposition in a mesh-packed cold trap 0-22905  
 desorption from CdS and CdSe films, heating depend. 0-24737  
 desorption from Nb in a vacuum, thermodynamic props. calcs. (Russian) 0-54501  
 desorption from Ta in a vacuum, thermodynamic props. calcs. (Russian) 0-54501  
 determination, in BN, heat treatment temp. depend., neutron activation anal. obs. 0-16356  
 determination, in minerals, anal. of C and O<sub>2</sub>, ZAF correction procedure (French) 0-11983  
 determination in Zn dust by 14 MeV neutron activation anal. (Japanese) 0-11977  
 diatomic mols., internal partition functions for O<sub>2</sub>, N<sub>2</sub>, NO and their ions, max. summation indices 0-27995  
 diffusion, facilitated, in muscle tissues 0-56327  
 diffusion in  $\alpha$ -Ti, atomic jumping model 0-44366  
 diffusivity in TiO<sub>2</sub>(-Cr<sub>2</sub>O<sub>3</sub>) rutile, Cr<sub>2</sub>O<sub>3</sub> effects, depth profile meas. by SIMS 0-24651  
 diploid yeast, O<sub>2</sub> effect in killing by photon irrads. of different energies 0-36018  
 discharge, conditions, self-consistent electron energy distrib. functions calc. 0-38746  
 discharge plasma, metastable states role, two-step ionisation, electron densities and transition pts. 0-44019  
 dissolved in Fe-Ni liq. alloys, thermodynamic props., electrochem. meas. 0-30244  
 dissolved O<sub>2</sub> in rivers, reliability parameter in probabilistic programming models 0-26179  
 dissolved O<sub>2</sub> in water, pollution indices, automatic analyser (Japanese) 0-35812  
 Earth atmosphere, O<sub>3</sub> and O<sub>2</sub> photolysis, translationally hot O(<sup>3</sup>P) energy distrib. 0-21811  
 electrocatalytic O<sub>2</sub> evolution on reactively sputtered electrochromic IrO films 0-26125  
 electrochemical measurement transducers, actual distribution of errors 0-45605  
 electron backscattering coeffs., 100 eV to 5 keV 0-9750  
 electron irradi. effect on electrolum., defects form. and quenching obs. 0-55194  
 electron lateral diffusion to mobility ratio 0-6203  
 electrotransport in La 0-24674  
 evolution on Teflon bonded NiCo<sub>2</sub>O<sub>4</sub> porous electrodes 0-30247  
 evolution reaction kinetics on NiLa<sub>2</sub>O<sub>4</sub> electrochem. electrodes 0-30430  
 filtered neutron beam of 2.35 MeV 0-27848  
 gas, electron and negative ion swarms 0-28595  
 gas, electron mobility to lateral diffusion coeff. ratio 0-43836  
 gas, influence on field emission of glassy C tips 0-11543  
 glow discharge, DC, particle concs. calc. 0-1859  
 impurity in amorphous Ge film, depth profiling by SIMS 0-39480  
 impurity in CaF<sub>2</sub> crystals, influence on elec. cond. 0-2431  
 impurity in d-transition metals, integration with large-angle grain boundaries 0-39148  
 impurity in liquid Fe, influence on short-range order struct. (Russian) 0-38901  
 impurity in Si, equil. of dissolved C and O with CO in ambient atm. 0-1949  
 impurity in ZnS single crystals, determ. by fast neutron activation anal. 0-15142  
 incorporation in Ni HCP and amorphous RF sputtered films, ESCA obs. 0-10832  
 inhalation automatic control for patients with respiratory failure 0-17181  
 intravascular O<sub>2</sub> continuous monitoring, electrochem. sensor 0-56238  
 intravascular PO<sub>2</sub> probe routine appl., practical experience 0-56239  
 ion, in Fe(Ni)(Co), transient mag. field discontinuity 0-24515  
 ion-surface impact, X-ray prod., 5 MeV/amu, projectile X-ray prod. by 5 MeV/amu deuterons (oxygen ions), projectile Z depend. depend. 0-42982  
 ions, beam-foil excitation, relative initial populations, lifetime curves 0-14210  
 ions, beam-foil spectra 0-42977  
 isotope separation, supersonic molecular beam technique using RF spectroscopy, mag. reson. 0-47725  
 left ventricle time-varying capacitance model, driving energy and cardiac O<sub>2</sub> consumption (Japanese) 0-21486  
 liberation from electrolytic Ni during vacuum heating, Mossbauer spectra (Russian) 0-35594  
 liquid, Brillouin scatt. obs., US vel. and absorpt. 0-45085  
 liquid, estimation of solubility of solidified substances by Preston-Prausnitz method 0-39285  
 liquid, for efficient IR AC Kerr switches 0-19078  
 liquid, mol. correl. functions, effective pair pot. evaluation 0-10476  
 liquid, possible active media in high-power Raman lasers 0-19028  
 liquid, stimulated Raman scatt., vibr.-translational relax. rate, schlieren technique meas. 0-9955  
 lung, duck, O<sub>2</sub> and CO<sub>2</sub> exchange and cardiopulmonary control interaction model 0-3600  
 lung, intrapulmonary haematocrit maldistrib., effect on O<sub>2</sub>, CO<sub>2</sub>, inert gas exchange 0-8033  
 in metal-poor stars, O abundances from O I IR triplet 0-36610  
<sup>13</sup>C-methane-d<sub>1</sub>:O, annealed, spin conversion and proton 2nd moment time-depends. 0-11283  
 methane-O<sub>2</sub> mixture, laser initiated combustion 0-55661  
 molecular cluster formation, in rarefied nozzle flowfield 0-5639  
 molecular electron attachment in non-self-maintained discharge, plasma decay obs. 0-43844  
 molecular gas, K-shell photoabsorption coeffs., 500-600 eV 0-9617  
 molecule, (0-0) atmospheric band, laboratory discharge lamp source 0-4148  
 molecule,  $b^{\infty}_g + X^{\infty}_g$  electronic transition, absorpt. coeffs. and transition moments 0-43061  
 molecule, C<sup>2</sup> $\Delta_g - a^1\Delta_g$  band system, vibr. anal. 0-5556  
 molecule, dipole properties and dispersion energies additivity, using atoms and small mol. models 0-53091



## oxygen continued

- molecule, distrib. in lower thermosphere assuming tidal effects, one dimens. nonstationary diffusion-photochemical model 0-4160  
 molecule, electron impact vibr. excitation, direct and stepwise, rate coeffs. 0-5630  
 molecule, electronic struct., self-consistent pseudopot. calc. 0-9508  
 molecule, K-shell, excitation and ionisation, vibr. struct., electron energy loss spectra obs. 0-18943  
 molecule, light polarisability parameters, Raman scatt. ang. meas. 0-37814  
 molecule, low energy electron impact dissociative ionis.,  $O^{2+}$  form. and energy distrib. 0-5626  
 molecule, metastable, laser-induced photolysis of ozone reactions 0-11928  
 molecule, metastable, sensitisation of  $SO(^1\Delta_g, ^1\Sigma_g^+)$  chemiluminescence 0-26016  
 molecule, metastable level electron impact excitation, resonances (*Russian*) 0-43198  
 molecule, microwave spectrum, press. broadening 0-23412  
 molecule,  $MSX\alpha$  calc., partial wave expansion, binding energy and orbital energy 0-37738  
 molecule, multiconfig. Hartree-Fock calcs. convergence 0-47901  
 molecule, photoelectron ang. distrib., photon energy depend., 16-25 eV 0-53046  
 molecule, photoexcitation and photoionisation cross sections, HF Gaussian method 0-53064  
 molecule, photoionisation, partial channel cross-sections calcs. 0-53061  
 molecule, polarisability tensor anisotropy, Raman spectra differential scatt. cross section 0-18860  
 molecule, relaxation by IR and microwave coherent transients 0-28092  
 molecule, singlet states, quenching by  $O_2(N_2)$ , shock tube study 0-23511  
 molecule, thermal decomposition, vibr.-rot. state depletion, Monte Carlo calc. 0-35506  
 molecule, three-body electron attachment in pure and He discharge 0-24245  
 molecule, vacuum UV molecular photoabsorpt. cross-section meas. 0-37096  
 molecule electron impact dissociation rel. to  $O_3$  generation in air-fed ozonisers 0-3323  
 monitoring instruments, trace oxygen measurement 0-52181  
 nucleosynthesis in supernova remnant in NGC 4449, spectrophotometric evidence 0-56895  
 $O_2$ ,  $CO_2$  and heat transport in the placenta, construct. and usefulness of models 0-3604  
 Orion Nebula, Ne, S and O abundances from fine-struct. lines obs. 0-4410  
 in Orion Nebula peripheral regions, O/H ratio and O ionisation 0-36686  
 overlayer, ( $2\times 2$ ), on Ir (111) surface, LEED study 0-2264  
 oximeter for spectrophotometric monitoring of arterial  $O_2$  saturation in the fingertip 0-41161  
 permeability in hard elastic polypropylene films, extension effects 0-40412  
 phase equilibria near 298K, Raman spectral study of solid and fluid 0-19937  
 pionic atom, isotope effects, 1s state energy shift and line broadening for  $^{16}O^{18}O$  pair (*German*) 0-48107  
 plasma, carbon tetrafluoride+4%  $O_2$ , Si etch rate uniformity 0-40568  
 plasma, electron beam energy branching, discrete energy loss method 0-48905  
 plasma impurity, flux on wall of DITE Tokamak 0-28688  
 pneumocytes, isolated type II, effects of high  $O_2$  exposure on bioenergetics 0-30685  
 precipitation in dislocation-free Si, IR and TEM obs. 0-29173  
 precipitation in Si, 1000°C TEM, IR absorpt. and X-ray studies 0-34194  
 premixed  $H_2-O_2-N_2$  laminar flames, temp. profile, comparison of spectroscopic meas. 0-42227  
 prod. and props. in liq. Ar and  $N_2$ , by  $N_2O$  photodissociation 0-43063  
 quenching of rubrene  $S_1$  excited state in 1,3-diphenylisobenzofuran soln. photooxidation 0-45529  
 radiobiological effect, molecular and cellular basis 0-26211  
 rare earth-transition metal alloy thin films vapour deposition, influence of gaseous phase on mag. props. (*Polish*) 0-39820  
 reactive sputtering of Sn cathode, ion formation (*Japanese*) 0-50494  
 recombining atomic plasmas, population inversion 0-32679  
 red blood cell shape, optimality,  $O_2$  diffusion approach 0-30693  
 skeletal muscle, canine, blood flow and  $O_2$  uptake obs. in acute anaemia 0-45930  
 solar O abundance, influence of diffusion 0-4318  
 solid,  $\alpha$ - $\beta$  transition, mag. susceptibility (*Russian*) 0-6592  
 solid,  $\beta$ -phase, mag. excitations spectrum (*Russian*) 0-7101  
 solid, magnetic props. theory for Heisenberg system (*Russian*) 0-54900  
 solid, transformation charact. and orientation relations 0-33917  
 solubility in Fe-Si melts (*Russian*) 0-15252  
 solubility in liq. U and composition of lower phase boundary of  $UO_2$  at 1950K 0-49366  
 steel, C, friction faces, S, O content, secondary ion-ion emission obs. 0-55545  
 submonolayer-covered Ni (111), surface phonons obs. by EELS 0-39403  
 surface interaction with Cu (100), AES, EELS, LEED and work function studies 0-24731  
 thermochemical prod. by  $H_2O$  decomposition using solar energy 0-40919  
 thermosphere, annual var. from Aeros Nims data 0-12578  
 thermosphere, atomic oxygen content, 100-160 km, new spectral method 0-41578  
 transeutaneous  $O_2$  and skin blood flow, laser system for simultaneous meas. 0-26321  
 triple point, determination at low temp. (*Japanese*) 0-31749  
 Zircaloy- $O_2$  phase diagram 0-3003  
 $O_3+OCS$ , gas, EPR of rot. transitions,  $T_1$  press. depend. 0-9621  
 Al-O (100), extended appearance potential fine struct. anal., LEED study 0-50467  
 $Al_{0.5}Ga_{0.5}As$ :O surface layer, on GaAs p-n junction, surface recomb. current reduction 0-49878  
 Br+ $O_2(NO)$ , quencher paramagnetism, deactivation rate const., spin-orbit relax. study 0-21263  
 CO-He-( $O_2$ ), glow discharge ion cluster in positive column, ion mass spectra diagnostics 0-38752  
 $CO_2-O_2-H_2O$ , photodissoc. and photodetachment of negative ions 0-14182  
 $CaF_2:O_2^-$ ,  $OH^-$ , ion incorporation by reaction with surrounding atm. 0-55143

## oxygen continued

- $CdS:Li$ , O film, chemical bath deposited, photocond. and optical props., O trap level 0-2426  
 Cu-Ge-O, phase diagram and thermodynamics, electrochem. study 0-50617  
 $Fe^{3+}-O^{2-}$ , overlap and covalency contrib. to zero field splitting, LCAO-MO calc. 0-24850  
 GaAs,  $O^+$  implantation, energy levels, photoluminesc. 0-24838  
 GaAs thin film, effect of O on thin film compositions obtained by secondary ion emission 0-26079  
 GaAs:Cr, O, effect of O in photoluminesc. meas. 0-29799  
 GaAs:Cr, O, semi-insulating, photocond. anal. of levels 0-20243  
 GaAs:O, annealing effects, optical absorpt. and I-V characts. 0-29037  
 GaAs:O, electronic struct., multiple-scatt.  $X\alpha$  mol. cluster model 0-15445  
 GaAs:O, field depend. of radiative recomb. 0-20700  
 GaAs:O, implantation, effect on LPE growth and elec. props. 0-24477  
 n-GaAs:O, photocond. associated with deep level at 0.4 eV 0-44640  
 GaP, deep  $O^-$  state, model impurity calc. 0-6780  
 GaP:N,O epitaxial struct., luminesc. study of degradation during heat treatment 0-45139  
 GaP:O, photoionisation of deep impurity levels 0-34386  
 GaP:O, two-electron  $O^-$  state evidence, ODMR, IR emission, phonon replicas 0-15828  
 Ge:Li,O, EPR and piezospectroscopy 0-25338  
 Ge:O, shallow defects, PTIS meas. 0-24971  
 H-O electrochemical matrix-type cells, growth and elec. props. study 0-26027  
 $H_2+O_2$  on polycryst. Ni surface, SIMS and thermal desorption meas. 0-40742  
 $KZnF_3:(Fe^{3+}-O^{2-})$ , overlap and covalency contrib. to zero field splitting, LCAO-MO calc. 0-24850  
 $Mn^{2+}-O^{2-}$ , overlap and covalency contrib. to zero field splitting, LCAO-MO calc. 0-24850  
 $N_2$ -Ar- $O_2$  system, vapour-liq. equilib. 0-54358  
 $N_2-O_2$  mixture, impulse breakdown processes at low press. 0-44021  
 $N_2+O_2$ , binary diffusion coeff. pressure depend. meas. 0-43826  
 NaCl crystals with dipole O colour centres, radiation colouring and holographic recording 0-48187  
 NaCl:O, hologram recording, colloidal type centre transformation (*Russian*) 0-55147  
 Ni (001)/CO(O) system, adsorbate geometries determ. from final state scattering in X-ray photoemission 0-54488  
 Ni-Cu, liq., activity meas. of  $O_2$  by EMF method (*Japanese*) 0-54408  
 O ( $O^+$ ) ( $O^{2+}$ ), Rayleigh and Compton X-ray scatt. cross sections in plasma 0-43884  
 O, adsorbed on metals, ion impact desorption, adsorption energy depend. 0-39442  
 O concentration in mesosphere, inference from positive ion comp. data 0-8405  
 O I, nightglow spectra correl. to atmos. Na density 0-41585  
 O I, weighted oscillator strengths for elec. dipole and forbidden transitions, data tables 0-37779  
 O I 5577 Å and 6300 Å, laboratory discharge lamp source for lines of known width 0-4148  
 O I 5577 Å line nightglow, intensity var., related to solar tides (*Russian*) 0-12585  
 O I 6300 Å in type A aurora rays, emission intensification 0-4163  
 O I 7774 Å line in O6 to G2 stars, equivalent widths and narrow-band photometry 0-8621  
 O I forbidden 6300 Å airglow at mag. equator, rel. to vertical E×B plasma drift vel. 0-36435  
 O II dielectronic recombination through the forbidden levels, in low density and  $T_e$  highly ionised plasma 0-43850  
 O III, electron impact excitation of semi-forbidden transitions 0-48092  
 O III, optical oscillator strengths for astrophysically interesting lines 0-32660  
 O III, Z 0-43972  
 O III forbidden line in Seyfert galaxy NGC 1068, high-resolution profile 0-46665  
 O IV, electron-impact excitation cross sections 0-14236  
 O IV, intersystem multiplet as density indicator for solar plasmas 0-31264  
 O IV 1402.5 Å semi-forbidden line, identification with 1400 Å emission feature in quasi-stellar objects 0-12825  
 O in lower ionosphere, conc. determ. by fluoresc. technique 0-36434  
 O,  $O_2$  distribution in lower thermosphere 0-4159  
 O silent discharge, excited species reactions,  $O_3$  form., discharge channel characts., numerical simulation 0-38813  
 O V,  $2s3p\ ^3P_1-2s^2\ ^1S_0$  intercombination line transition probabilities 0-18823  
 O V, independent particle pots. comparison 0-52846  
 O VI, electron ionisation cross sections of excited atoms and ions 0-43186  
 O VI, in plasma, ion electron collisional radiative recomb. coeffs., bottleneck calc. 0-53942  
 O VI in OB-type stars stellar winds, P Cygni line profiles obs. 0-8630  
 O VII, ground-state electron impact excitation strengths, close-coupling calcs. 0-23561  
 O VIII, and isoelectronic series, in laser-produced plasma, Balmer fine struct. (broadening) 0-48860  
 O VIII emission line detect. from M87 in Virgo cluster 0-26977  
 $O^+$  and  $O_2^+$ , beam-foil excitation, optical radiation obs. 0-9724  
 $O^+$ , beam-foil excitation, absolute Auger yield meas. 0-14203  
 $O^+$ , from exploding fast mol. ions, Auger spectra 0-32781  
 $O^+$  in Jupiter inner magnetosphere, forbidden emission detect. 0-51687  
 $O^+$  reson. line regularities in plasma Stark widths and shifts 0-43881  
 $O^{2+}$  reactions with atoms or molecules of ionospheric importance, lab. meas. 0-26004  
 $O^{2+}$ , solar wind spectrum, ion frequencies and velocities (*German*) 0-51636  
 $O^{2+}$ , solar wind spectrum, ion frequencies and velocities (*German*) 0-51636  
 O/C ratio in massive stars, core convection effects 0-17579  
 O/H abundance ratio determ. in Galaxy from H II regions radio obs. 0-36692  
 O-Ar pot. parameters, from CO in Ar matrix, empirical evaluation 0-48057  
 O-orbital interaction 3-methyleneoxetane, struct., MO calcs., UV photoelectron spectra obs. 0-28058  
 O-orbital interaction in 3-oxetanone, struct., MO calcs., UV photoelectron spectra obs. 0-28058



## oxygen continued

- O-orbital interaction in  $\beta$ -propiolactone, struct., MO calcs., UV photoelectron spectra obs. 0-28058  
O-treated polystyrene, interaction with vapour-deposited Cr and Ni atoms 0-3407  
O+C(N), K-shell excitation, Auger electron spectrosc. obs. 0-9715  
O+formaldehyde, absolute rate consts., discharge flow and flash photolysis reson. fluoresc. meas. 0-55648  
O+H<sub>2</sub>O(methane/halomethane), direct reaction in flow system 0-3333  
O+H<sub>2</sub>→OH+H, pot. surface, HF calc. 0-16669  
O+methane, photochem. reaction, high temp., rate coeff. meas. 0-16699  
O+N<sub>2</sub>, excitation and deactivation at above-thermal energies 0-43171  
O+N<sub>2</sub><sup>+</sup>, collision, correl. diagram calcs. 0-23504  
O+NO, chemiluminesc., absolute rate const., O<sub>3</sub> effect 0-45507  
O+NO, vibr. relaxation of NO, laser induced IR fluoresc. study 0-9626  
O+N(D), associative ionisation 0-4161  
O+O, K-shell excitation, Auger electron spectrosc. obs. 0-9714  
O+O<sub>2</sub>, quenching of O(S) state, rate coeff. 0-41581  
O+O<sub>2</sub>→O<sub>3</sub>, Hartley band during formation, metastable states, vibr. excitation and relax. 0-55632  
O+O<sub>3</sub>, collisionally induced relax. processes and vibr. energy transfer 0-53107  
O+O<sub>3</sub> reaction, vibr. enhancement 0-30215  
O+OH, direct rate meas. 0-30217  
O+trifluoriodomethane, vel. distrib. and cross section, reactive scatt. 0-26011  
O<sup>-</sup>+Ne(Ar)(Kr), 0.2-1 keV, elastic and inelastic reduced differential cross-sections 0-32829  
O<sup>-</sup>+SF<sub>6</sub>→SF<sub>5</sub>+F+O, electron affinity of SF<sub>5</sub> radical 0-45495  
O<sup>+</sup>+H<sub>2</sub>, linear approach, pot. energy surface for H<sub>2</sub>O<sup>+</sup> 0-47922  
O<sup>+</sup>+inert gas, potential energy curves from elastic scatt. cross sections 0-23502  
O<sup>+</sup>+Ne, pot. energy curves, nonadiabatic coupling matrix elements 0-53110  
O<sup>2+</sup>+H, charge transfer rate coeff. and astrophysical appls. 0-56701  
O<sup>2+</sup>+H<sup>+</sup>, <sup>3</sup>P<sub>1</sub> fine structure transitions 0-37864  
O<sup>5+</sup>+Ti, ratio of single K-shell ionisation cross section to double K-shell ionisation cross section 0-53119  
O<sup>8+</sup>+Ar, bound- and continuum-state electron capture in gas, strong correlations 0-9730  
O<sup>8+</sup>+H(1s)(He(1s<sup>2+</sup>)), electron capture into n,l excited states 0-23543  
O<sub>2</sub>, <sup>3</sup>P<sub>g</sub> states, large CI wavefunctions, non-adiabatic coupling matrix elements 0-37744  
O<sub>2</sub> analyser, OTOX 90, operation, and multipoint monitoring 0-55736  
O<sub>2</sub> and WO<sub>2</sub> adsorption on W (110) 0-34317  
O<sub>2</sub>, chemisorption on Cu, cluster theory 0-29264  
O<sub>2</sub>, chemisorption on Ni, cluster theory 0-29264  
O<sub>2</sub> consumption of mouse, effects of microwaves and environmental temp. 0-51161  
O<sub>2</sub> diffusion into mammalian cells following ultrahigh dose rate irradiation 0-30694  
O<sub>2</sub> discharge, O<sub>3</sub> production 0-38780  
O<sub>2</sub> dissolved in Ar, mol. orientation, Raman spectrosc. obs. 0-52994  
O<sub>2</sub>, electron attachment kinetics in flames 0-3349  
O<sub>2</sub>, impurity in alkali halides, reorientation, linear dichroism (*Russian*) 0-45127  
O<sub>2</sub> in chloroform and carbon tetrachloride solns., sensitized luminesc. 0-32762  
O<sub>2</sub>, photodissoc. and spectral absorpt. in stratosphere and mesosphere 0-51497  
O<sub>2</sub> photofragment, produced by O<sub>3</sub> photolysis at 266 nm 0-50865  
O<sub>2</sub>, predissoc. of B<sup>2</sup>Σ<sub>g</sub><sup>-</sup> state, Rydberg-valence crossing model 0-1032  
O<sub>2</sub> profiles in E.Mediterranean Sea, meas. 0-17298  
O<sub>2</sub>, Schumann-Runge band system in sunspots UV spectrum 0-12735  
O<sub>2</sub> sensitisation of CHO cells at ultrahigh dose rates 0-36000  
O<sub>2</sub>, total X $\alpha$  energy, LCAO calc., rel. to local density models 0-32607  
O<sub>2</sub>, UV absorpt. into <sup>3</sup>P<sub>g</sub> state, calc., atmos. opacity 0-12582  
O<sub>2</sub>, UV nightglow emission meas. 0-41590  
O<sub>2</sub> zone in Black Sea, boundary determ. rel. to water mass dynamics (*Russian*) 0-12435  
O<sub>2</sub><sup>+</sup>, electron impact dissoc. recomb., pot. energy curves calcs. 0-53150  
O<sub>2</sub><sup>+</sup>, first negative system, high-resolution photofragment spectroscopy 0-47971  
O<sub>2</sub><sup>+</sup>, in winter anomalous D-region over Sardinia (40°N), prod. rates 0-21871  
O<sub>2</sub><sup>+</sup>, mobility in CO<sub>2</sub> 0-43834  
O<sub>2</sub><sup>+</sup>, photofragment spectroscopy using fast ion beams 0-9755  
O<sub>2</sub><sup>+</sup>, predissociated b<sup>2</sup>Σ<sub>g</sub><sup>-</sup> state, high resolution laser spectroscopy in fast ion beam 0-9656  
O<sub>2</sub><sup>+</sup>, sub-Doppler laser spectroscopy using fast ion beams 0-9655  
O<sub>2</sub><sup>+</sup>, auroral ionosphere spectral emission process 0-41577  
O<sub>2</sub>-<sup>85</sup>Kr-Xe, liquefaction, retention of <sup>85</sup>Kr from fission exhaust gases, separation technique (*German*) 0-27753  
O<sub>2</sub>-CO<sub>2</sub> (ethylene)(neopentane), thermal electron attachment meas., microwave cond., pulse radiolysis 0-28592  
O<sub>2</sub>-He, binary diffusion coeffs., press. depend., 300 and 323K, Thorne's eqn. 0-1724  
O<sub>2</sub>+Ar, binary diffusion coeff. pressure depend. meas. 0-43826  
O<sub>2</sub>+B, chemiluminesc. metal oxide formation 0-35509  
O<sub>2</sub>+butyl radical, reaction rate consts. meas. 0-45490  
O<sub>2</sub>+CH<sub>3</sub>→OH+H<sub>2</sub>CO, 368K, rate const. upper limit 0-7771  
O<sub>2</sub>+CO<sub>2</sub>, Senftleben-Beenakker effect, saturation field, Kohler-Raum theory and obs. 0-28596  
O<sub>2</sub>+dimethylamino radical, reaction rate constants, FTIR obs. 0-16652  
O<sub>2</sub>+H<sub>2</sub>, on Pd (111), mol. beam relax. and isotopic exchange meas. 0-35575  
O<sub>2</sub>+H(F), quantum reactive scatt. theory, 3-dimens. 0-55637  
O<sub>2</sub>+He\*(<sup>2</sup>S), (<sup>2</sup>S), ion pair form., ion beam neutralisation reionisation spectroscopy 0-53120  
O<sub>2</sub>+inert gas, reactant decomp., rot.-vibr. energy transfer, relax. analytic soln. 0-55650  
O<sub>2</sub>+Kr<sup>2+</sup>(Xe<sup>2+</sup>)(C<sup>2+</sup>), charge transfer reaction rate consts. 0-7779  
O<sub>2</sub>+N, plasma jet, NO synthesis, chem. kinetics anal., model 0-38728  
O<sub>2</sub>+N<sup>+</sup>, NO<sup>+</sup>(a<sup>3</sup>Σ<sup>+</sup>) ion prod. 0-7784  
O<sub>2</sub>+NO<sup>+</sup>, reaction rate consts. meas. 0-7782  
O<sub>2</sub>+Na(3p<sup>3</sup>P<sub>3/2</sub>), electronic energy quenching dynamics, crossed beam expt. 0-9683  
O<sub>2</sub>+negative ion, electron-loss cross sections 0-37877  
O<sub>2</sub>+O, quenching of O(S) state, rate coeff. 0-41581  
O<sub>2</sub>+O<sub>2</sub>(H<sub>2</sub>), vibr. energy transfer, collinear and 3-dimens. rate consts. 0-48065

## oxygen continued

- O<sub>2</sub>+O<sub>2</sub>(N<sub>2</sub>), IR spectral absorpt. induced by press. in atmos. (*Russian*) 0-56600  
O<sub>2</sub>+OH(A<sup>2</sup>Σ<sup>+</sup>), quenching rates and fluoresc. efficiency, rel. to atmosphere 0-14199  
O<sub>2</sub>+inert gas, rot. energy transfer, centrifugal sudden approx. 0-27933  
O(<sup>1</sup>D, <sup>3</sup>P) isoelectronic series, Sternheimer valence shielding and anti-shielding factors 0-18807  
O(<sup>1</sup>D) quantum yields from laser flash photolysis of O<sub>3</sub> in fall-off region 0-45524  
O(<sup>1</sup>D) quenching in Earth atmosphere, translationally hot O(<sup>3</sup>P) energy distrib. 0-21811  
O(<sup>1</sup>D)+Ar(Kr)(Xe), inelastic collisions, spin-orbit coupling 0-5605  
O(<sup>1</sup>D)+O<sub>3</sub>, UV photolysis, O(<sup>3</sup>P) prod., rate consts. determ. 0-55636  
O(<sup>1</sup>D<sub>2</sub>)+CO(<sup>1</sup>Σ<sup>+</sup>), collisional quenching, energy transfer processes 0-23501  
O<sub>2</sub>(<sup>1</sup>Δ<sub>g</sub>)+O<sub>3</sub>, UV photolysis, O(<sup>3</sup>P) prod., rate consts. determ. 0-55636  
O(<sup>3</sup>P, D)+H<sub>2</sub>(<sup>1</sup>Σ<sub>g</sub><sup>+</sup>)→H<sub>2</sub>O, potential energy surfaces, extended basis first-order CI study 0-7776  
O(<sup>3</sup>P) atom yield in radiolysis of water by <sup>2</sup>H<sup>+</sup> and <sup>4</sup>He<sup>2+</sup> 0-35556  
O(<sup>3</sup>P), translationally hot, in Earth atmosphere, energy distrib. function 0-21811  
O(<sup>3</sup>P)+H<sub>2</sub>→OH+H, potential energy surface, theory 0-45492  
O(<sup>1</sup>S), absolute quantum yield meas. by XeO luminesc. in CO<sub>2</sub>, N<sub>2</sub>O photolysis 0-35561  
O(<sup>1</sup>S), auroral production sources determ. from rocket and satellite meas. 0-26662  
O(<sup>3</sup>S)+inert gas, de-excitation cross sections 0-53118  
O(<sup>3</sup>S)+O<sub>2</sub>→O(<sup>1</sup>S)+O<sub>2</sub>, reson. radiation 0-53122  
<sup>15</sup>O activity decay determ. of cerebral perfusion rate after photon activation 0-26341  
<sup>15</sup>O production for nuclear medicine use 0-30889  
<sup>15</sup>O, serial positron imaging, assess. of pulmonary embolism resolution rates 0-3789  
<sup>17</sup>O, <sup>1</sup>H, <sup>2</sup>H in muscle water, study of spin-lattice and spin-spin relax. times 0-21443  
<sup>17</sup>O, NQR at natural isotope abundance, double reson. new techniques, review 0-53013  
<sup>17</sup>O nuclear quadrupole double resonance spectroscopy, line shapes and examples 0-31820  
<sup>17</sup>O/<sup>16</sup>O, <sup>18</sup>O/<sup>16</sup>O in Chainpur meteorite, meas., rel. to D conc. in early Solar system 0-36518  
<sup>18</sup>O in equatorial Pacific core, glacial time scales and climate 0-21817  
<sup>18</sup>O in estuaries 0-26532  
<sup>18</sup>O/<sup>16</sup>O, groundwater seepage, control Kentucky karst 0-8370  
<sup>18</sup>O/<sup>16</sup>O geochemistry, of potassic igneous rocks from Roccamonfina volcano, Roman comagmatic region, Italy, 0-41420  
<sup>18</sup>O/<sup>16</sup>O ratio analysis in carbonates by mass spectrometry (*Portuguese*) 0-7875  
<sup>18</sup>O/<sup>16</sup>O ratios in granites from British Late Caledonian 0-36276  
<sup>18</sup>O/<sup>16</sup>O trends, Middle Pliocene climate change in W.Mediterranean 0-26605  
<sup>18</sup>O-D relationship for atmospheric precip., global climatic interpretation 0-17331  
O<sub>2</sub>\*+O<sub>3</sub>, UV photolysis, O(<sup>3</sup>P) prod., rate const. determ. 0-55636  
O(2<sup>1</sup>D<sub>2</sub>)+N<sub>2</sub>(O<sub>2</sub>)(N<sub>2</sub>O)(CO<sub>2</sub>)(H<sub>2</sub>O)(methane), collisional deactivation meas., 295K, rel. to atmospheric processes 0-16663  
O(3p<sup>3</sup>P), population and depopulation of O(3p<sup>3</sup>P) in supersonic freejet of O<sub>2</sub>-seeded Ar plasma 0-42958  
O(3p<sup>3</sup>P), population and depopulation in supersonic freejet of O<sub>2</sub>-seeded Ar plasma 0-42958  
O<sub>2</sub>(b<sup>2</sup>Σ<sub>g</sub><sup>-</sup>, v'=4, N', F') predissociation fragments, ang. distrib., separation energies 0-5588  
O<sub>2</sub><sup>+</sup>(b<sup>2</sup>Σ<sub>g</sub><sup>-</sup>) predissociation, branching ratio determ. 0-14181  
O<sub>2</sub>(c<sup>2</sup>Σ<sub>g</sub><sup>-</sup>), in Ar(Kr)(Ar-Kr) matrices, multiphonon vibr. relax. time-resolved emission obs. 0-18861  
Pd melting point, effect of surrounding O<sub>2</sub> 0-27299  
S<sup>+</sup>+O<sub>2</sub>→SO<sup>+</sup>+O+0.26 eV, rate consts. kinetic energy depend., drift tube meas. 0-7778  
Si, Czochralski crystals, O microsegregation, swirl defect distrib., growth rate depend. meas. 0-39295  
Si, dislocation free, C and O impurity clouds, heat treatment influence on light scatt. 0-6427  
Si thin film, effect of O on thin film compositions obtained by secondary ion emission 0-26079  
Si wafer O interstitial IR absorption spectrometry, multiple reflection correction 0-55131  
Si:O, electrical activity due to heat treatment, Hall effect meas. 0-15543  
Si:H,F,O amorphous, plasma deposited, comp. and optical props. 0-50441  
Si:O, amorphous, sputtered, influence of O and deposition conditions 0-54693  
n-Si:O, charge carrier scattering on neutral centres 0-49762  
Si:O, comparison of depth profiling techniques 0-29048  
Si:O, cryst., donor form. during annealing, elec. resist. study 0-49653  
Si:O, electrical and infrared spectroscopic investigations 0-34389  
Si:O, evaporated amorphous film, effect of O<sub>2</sub> on props., ESR spectra 0-11265  
Si:O, impurity conc. profiles, scanning IR absorpt. using semicond. laser 0-50376  
Si:O, ion-implanted between 2 and 20 MeV, range and range straggling 0-44241  
Si:O, striated impurity distrib. calc. in melt-grown crystals 0-24488  
Si:O:H amorphous, plasma-deposited, electronic and struct. props. 0-50391  
Si:O wafer, annealed, surface- and inner-microdefects, TEM obs. 0-54236  
SiC, thin film, effect of O on thin film compositions obtained by secondary ion emission 0-26079  
T 0-41588  
Ta-O, steady state O<sub>2</sub> solubility (*German*) 0-44322  
UC:O, sample prep. method importance in O determ. (*Japanese*) 0-23100  
V:O, neutron irradi., void form., 673-1073K 0-29066  
V:O, purification and plastic props. 0-25810

## oxygen compounds

- bridged complexes, vibr. and electronic props., reson. Raman spectra appl. 0-52996  
fluoride-oxide slags, elec. cond., Al and Si addition agents influence (*Russian*) 0-39572



## oxygen compounds continued

- OH, interstellar, abundance and column density in post-shock gas 0-56911  
 OH main lines, IR pumping in Mira variable stars and OH-IR sources 0-46632  
 organic, dipole moments, NDDO calcs. 0-47894  
 oxides, interaction between point defects and dislocations, cryst. plasticity 0-15149  
 oxides, liquid, surface tension calc. (*Russian*) 0-15335  
 oxides, point defects diffusion coeffs. calc. (*Japanese*) 0-15302  
 COS, atmospheric, oxidation as  $\text{SO}_2$  source 0-4085  
 COS in atmosphere, biomass burning as source 0-26586  
 $\text{CaF}_2\cdot\text{O}_2$ ,  $\text{OH}^-$ , ion incorporation by reaction with surrounding atm. 0-55143  
 HOCl, photolysis product of  $\text{Cl}_2\text{-O}_3\text{-H}_2$  dil. mixtures, absolute integrated IR band intensities 0-26033  
 LiF:OH crystals, X-irradiated, H centres formation and annealing 0-54226  
 LiF:OH<sup>-</sup>, IR spectra 0-20676  
 LiF:OH,  $\gamma$ -irrad., colour centre lasing at 0.84-1.13  $\mu$  at 300K 0-5739  
 $\text{N}_2\text{O}_4\rightleftharpoons 2\text{NO}_2\rightleftharpoons 2\text{NO}+\text{O}_2$ , working fluid for power-producing thermodynamic cycles 0-13536  
 $\text{O}_2^+\text{AsF}_6^-$ , thermal decomposition, Raman spectra study, free radical mechanism 0-55652  
 OCS, electron elastic scatt., 0 to 100 eV 0-23547  
 OCS, gas, EPR of rot. transitions,  $T_1$  press. depend. 0-9621  
 OCS, high-intensity laser photolysis at 157 nm,  $\text{S}^1\text{S}$  prod., photoionisation, and loss, laser appl. 0-21306  
 OCS in Ar soln., IR spectra, solvent shifts, vibr. band assignment and anharmonic force consts. 0-9607  
 OCS, in atmosphere, contrib. to stratospheric aerosols and climate 0-41524  
 OCS, microwave-microwave double resonance 0-53029  
 OCS, motion, regular and irregular spectra, theory 0-9590  
 OCS photodissociation,  $\text{S}^1\text{S}$  prod. and props. in liq. Ar and  $\text{N}_2$  0-43064  
 OCS, relaxation by IR and microwave coherent transients 0-28092  
 OCS, rot.-vibr. levels and semiclassical energy levels 0-37804  
 OCS, roto-vibr. mol. laser, low-temp. performance 0-9871  
 OCS, spectroscopic reference freqs. in 9.5  $\mu\text{m}$  band, heterodyne freq. meas. 0-18850  
 OCS, stratosphere content, solar spectra meas. by 12 km altitude aircraft 0-41486  
 OCS, third order coupling coeffs. for two phonon absorpt. 0-10621  
 OCS<sup>+</sup>, photodissociation cross section, UV and visible spectral obs. 0-28077  
 OCS+ $\text{H}_2(\text{CO}_2)$  (fluoromethane), rot. relax. parameters, microwave spectra linewidth parameters 0-28009  
 OCS+He(Ne)(Ar)(Kr)(H<sub>2</sub>)(O<sub>2</sub>)(CO<sub>2</sub>), gas, EPR of rot. transitions,  $T_1$  press. depend. 0-9621  
 OCS+N<sub>2</sub><sup>+</sup> 0-48063  
 OCS+nonpolar perturbation,  $J=1\rightarrow 2$  microwave line press. broadening 0-9644  
 OCS+Si(Ge), SiS and GeS multiple collision chemiluminesc., intercombination systems 0-45505  
 OCSe photolysis producing Se, using high efficiency ArF laser source 0-33032  
 $\text{OCl}_2^+$ , radical cation, struct. and electronic props., ab initio RHF SCF MO calc. 0-52883  
 OH 1612 MHz survey at high declinations 0-4452  
 OH (8, 3), nightglow spectra correl. to atmos. Na density 0-41585  
 OH, A-X system, rot. transition probabilities 0-43027  
 OH,  $\text{A}^2\Sigma^+-\text{X}^2\Pi$  system, vibrational and rotational levels, transition probability determ. 0-43034  
 OH and trace gases, laser induced fluorescence system for aircraft appl. 0-36425  
 OH, atmospheric, vibr. excited states, time and altitude vars. 0-41589  
 OH, band oscill. strength, rot. excitation effects 0-23460  
 OH column densities in stratosphere from far IR rotational lines 0-36367  
 OH conc. meas. in flat methane-air flames 0-16687  
 OH concentration profile in methane-air flames 0-35534  
 OH emission and absorption in H II region (*Russian*) 0-36733  
 OH emission obs. of Lynds 134 dark nebula 0-22062  
 OH formation in  $\text{H}_2\text{-NO}$  flame, OH collisional broadening parameter, curve of growth method 0-53052  
 OH impurities in  $\text{GeO}_2\text{-P}_2\text{O}_5\text{-SiO}_2$  glass fibre made by modified CVD process 0-50560  
 OH in southern globular clusters, maser emission upper limits 0-22047  
 OH, interstellar, new main line maser obs. with probable Zeeman pattern 0-56908  
 OH, interstellar, towards galactic centre, absorbing clouds struct. determ. using regularisation method 0-17505  
 OH maser sources, accurate position meas. 0-46646  
 OH maser sources, interstellar, radiative transport effects on inversion 0-17681  
 OH, nonthermal main lines in interstellar dust clouds and OH abundance 0-36683  
 OH, OD, interstellar, A-doublet population inversion by collisions 0-22065  
 OH, prod. by photolysis, A-doublets, population, rot. states, hyperfine struct., microwave spectra 0-32694  
 OH radical, matrix-isolated, from  $\text{H}_2$  oxidation on Pt, laser diagnostics 0-5572  
 OH radical concentration in troposphere, determ. via atmospheric  $^{14}\text{CO}$  meas. (*German*) 0-8419  
 OH radical in upper atmosphere, meas. using lidar from Space Shuttle 0-51590  
 OH radical lifetime in comets at 1 AU 0-46488  
 OH rotational temp. determ., successive approx. 0-23389  
 OH, Simon-Parr-Finlan potential appls. 0-18785  
 OH type I maser source G 109.7+2.2 near Herbig-Haro object (*Russian*) 0-17684  
 OH<sup>-</sup> and rare earth doped solid 0-7398  
 OH<sup>-</sup> impurity in  $\text{BaTiO}_3$ , IR spectra meas. 0-20679  
 OH<sup>-</sup>, mobility in polyester, from ionic injection current at strong diffusion 0-2210  
 OH<sup>+</sup>, Simon-Parr-Finlan potential appls. 0-18785  
 OH-HF, H-bonded complex, ab initio calcs. (*French*) 0-52866  
 OH+ $\text{Co}(\text{NH}_3)_5\text{Br}^{2+}$ , polyelectrolyte catalysis, high pressure effect 0-55657

## oxygen compounds continued

- OH+ $\text{H}_2$ , pot. energy surface, barrier heights and transition state geometry, POL-CI calc. 0-55649  
 OH+ $\text{H}_2\text{O}(\text{NO}_2)(\text{CH}_3\text{Cl})(\text{N}_2)(\text{He})$ , mean collision cross sections from microwave spectroscopy 0-1046  
 OH+ $\text{H}_2\rightarrow\text{H}_2\text{O}+\text{H}$ , rate constant, ab initio calc. 0-45478  
 OH+NO radical-molecule reactions, relax. and rate consts. 0-11918  
 OH+ $\text{NO}_2+\text{M}\rightarrow\text{HNO}_3+\text{M}$ , rate constant under simulated atmospheric conditions 0-50846  
 OH+N(O), direct rate meas. 0-30217  
 OH+p- $\text{H}_2(\text{He})$ , collisional pumping of A-doublet transitions, pot. energy surface 0-23516  
 OH+toluene, rate constant under simulated atmospheric conditions 0-50846  
 OH+trichloroethane, 1,1,1- and 1,1,2-isomers, reaction kinetics, 298-460K, lower atmos. chem. 0-16657  
 OH+trichloroethane $\rightarrow\text{H}_2\text{O}+\text{CH}_2\text{CCl}_3$ , rate const. and tropospheric chem. 0-16658  
 OH( $\text{A}^2\Sigma^+$ )+ $\text{N}_2(\text{O}_2)(\text{H}_2\text{O})(\text{air})$ , quenching rates and fluoresc. efficiency, rel. to atmosphere 0-14199  
 OH( $^2\Pi_{3/2}$ ,  $v=1$ ), population inversion of A doublets in microwave spectrum 0-974  
 ON+azomethane, rate const. meas. 0-7771  
 OSC, N<sub>2</sub>O, submillimetre rot. lines, press. shifts 0-23463  
 $^{17}\text{O}$ , isotropic hyperfine coupling consts. in small radicals 0-52894  
 PuO, nuclear oxide fuel anal., coulometry, emission anal., chromatography, X-ray anal. 0-18420  
 UO, nuclear oxide fuel anal., coulometry, emission anal., chromatography, X-ray anal. 0-18420
- ozone  
 A<sub>1</sub> ground state, dipole moment function, ab initio SCF and CI calcs. 0-32628  
 absorption coefficients for backscatter UV expt. 0-46254  
 air, negative corona current O<sub>3</sub> density depend., 46-87 kPa 0-1852  
 air pollution in NE USA, ozone source study 0-41482  
 atmosphere, Be distrib. within E. United States high press. systems rel. to stratospheric O<sub>3</sub> contrib. 0-4072  
 atmosphere, distribution vars. rel. to urban heat island circulation in St. Louis 0-51488  
 atmosphere, perturbed, O<sub>3</sub> cones. rel. to thermal struct. and relaxation rates 0-8408  
 atmosphere, pollution effects on O<sub>3</sub> layer, numerical modelling 0-40943  
 atmosphere, seasonal and interannual vars., Nimbus 4 BUW expt. 0-41506  
 atmosphere content during March-April 1976 stratospheric warming 0-12494  
 atmosphere content rel. to 0-26607  
 atmosphere content rel. to solar activity 0-41488  
 atmosphere O<sub>3</sub> production transport and distribution, numerical simulations with global general circulation model 0-56544  
 atmosphere ozone content, July-Sept. 1978, Belgium 0-12484  
 atmosphere total O<sub>3</sub> content, 1964-75, season and latitude depend. 0-41534  
 atmospheric composition, air over N. Germany coast, obs. 0-26584  
 atmospheric O<sub>3</sub> vertical distrib., shortened version of Umkehr ob. method 0-8430  
 depletion in troposphere and stratosphere by halomethanes 0-16866  
 Dobson total content meas., atmospheric aerosol effects 0-12463  
 Earth atmosphere, O<sub>3</sub> and O<sub>2</sub> photolysis, translationally hot O(<sup>3</sup>P) energy distrib. 0-21811  
 form. in silent discharge, excited species reactions, discharge channel characts., numerical simulation 0-38813  
 formation and control strategy options for Sydney, precursor distrib. 0-16859  
 formation by heated corona wires of electrostatic precipitator 0-47081  
 formation dynamics in cities 0-31112  
 generation in air-fed ozonisers 0-3323  
 IR absorption spectrum using CO<sub>2</sub> TEA laser injection locked, tunable single longitudinal mode operation 0-33018  
 mesosphere, lower, O<sub>3</sub> number density profile 0-41579  
 molecule, Hartley band during formation, metastable states, vibr. excitation and relax. 0-55632  
 molecule, inertia defects and dipole moments by kinetic consts. method 0-928  
 molecule, multiphoton dissociation dynamics, classical model 0-11904  
 molecule, open-shell SCF secular eqn., iterative algorithm soln. 0-52868  
 molecule, photolysis, laser flash, O(<sup>3</sup>D) quantum yields in fall-off region 0-45524  
 molecule isotope effects, complete quartic force field calc., algorithm 0-37736  
 ozonograms, Oct.-Dec. 1978, Uccle, Belgium (*French, Flemish*) 0-21797  
 ozonosphere and N<sub>2</sub>O pollution from fertilisers 0-36370  
 ozonosphere reactions affected by CO<sub>2</sub> stratosphere cooling 0-36369  
 photodissociation rate under ozonosphere conditions 0-40722  
 photolysis, laser-induced, reactions of O(<sup>3</sup>P), O(<sup>3</sup>D) and O<sub>2</sub>(<sup>1</sup>D) 0-11928  
 photolysis, primary products electronic and vibr. state distrib. 0-50865  
 production in homogeneous O<sub>2</sub> discharge 0-38780  
 production in unipolar HF discharge 0-1855  
 sea breeze affecting surface level conc., Wallops Island, Virginia 0-51473  
 smouldering discharge at O<sub>3</sub> liq. surface in N<sub>2</sub>, thin solid pellicle formation of N<sub>2</sub>O<sub>2</sub> 0-38827  
 solar MUV photometer, rocket borne, stratospheric ozone concentration measurement 0-52292  
 stratosphere, laser-radar obs. using excimer lasers 0-17410  
 stratosphere, perturbing influences, 1955-75 catalogue 0-41502  
 stratosphere and troposphere content, circumpolar airliner flight obs. 0-51475  
 stratosphere composition, implications of OH+trichloroethane reactions 0-16657  
 surface concentration forecasts for polluted areas, Model Output Statistics appl. 0-12035  
 transport by planetary waves, mechanistic model of stratosphere 0-8402  
 trichloromethane glass:O<sub>3</sub>,  $^{17}\text{O}$ , NQR by proton double reson., broad reson. assignments 0-53014  
 troposphere, differential absorption lidar meas. 0-12554  
 troposphere, O<sub>3</sub> photochemical prod. and influence on climate 0-36365  
 variations in Auckland, comparison between city and urban regions 0-17350  
 Ar-O<sub>3</sub> Van der Waals complex, struct. and props., RF and microwave obs. 0-32704



## ozone continued

- Cl<sub>2</sub>-O<sub>3</sub>-H<sub>2</sub> dilute mixtures, photolysis products, Fourier Transform IR kinetic obs. 0-26033  
 NO+O<sub>3</sub>, O<sub>3</sub> effect, chemiluminesc., absolute rate const. 0-45507  
 O+O<sub>3</sub> reaction, vibr. enhancement 0-30215  
 O<sub>3</sub>-Ar(CO), photorecombination laser, shock wave triggered, waveguide mode optical gain 0-5730  
 O<sub>3</sub>+B, chemiluminesc. metal oxide formation 0-35509  
 O<sub>3</sub>+Fe(CO)<sub>5</sub>, modulated chemiluminesc. by CO addition 0-40692  
 O<sub>3</sub>+NO<sub>2</sub>→NO<sub>2</sub>\*+O<sub>2</sub>→NO<sub>2</sub>+hν+O<sub>2</sub>, chemiluminesc., translational and rot. energy effects 0-30218  
 O<sub>3</sub>+Ni(CO)<sub>4</sub>, modulated chemiluminesc. by CO addition 0-40692  
 O<sub>3</sub>+O, collisionally induced relax. processes and vibr. energy transfer 0-53107  
 O<sub>3</sub>+O(Δ<sub>g</sub>)(O<sub>2</sub>\*), UV photolysis, O(3P) prod., rate consts. determ. 0-55636  
 O<sub>3</sub>+O(1D), UV photolysis, O(3P) prod., rate consts. determ. 0-55636

## ozonosphere

- chlorofluorocarbon residence times in stratosphere, two-dimens. model 0-45834  
 chlorofluoromethane induced O<sub>3</sub> depletion, atmos. chem. theory 0-51477  
 composition of middle atm., in situ meas. 0-17339  
 halocarbons, hydrocarbons and SF<sub>6</sub>, global distrib., sources and sinks, rel. to O<sub>3</sub> depletion 0-4088  
 laser-radar obs. using excimer lasers 0-17410  
 ozonograms, July-Sept. 1978, Belgium 0-12484  
 ozonograms, Oct.-Dec. 1978, Uccle, Belgium (*French, Flemish*) 0-21797  
 perturbing influences, 1955-75 catalogue 0-41502  
 planetary waves, mechanistic model of O<sub>3</sub> transport 0-8402  
 season and latitude depend. of total O<sub>3</sub> content, 1964-75 period 0-41534  
 solar activity affecting total O<sub>3</sub> content of atmos. 0-41488  
 solar activity fluctuations, reln. to variation in O<sub>3</sub> conc. and layer temp. 0-31110  
 solar cycle-O<sub>3</sub> relationships 0-17342  
 stratospheric warming, March-April 1976, tropical O<sub>3</sub> content, 35-60 km altitude 0-12494  
 CO<sub>2</sub> cooling of atmos. affecting O<sub>3</sub> content of stratosphere 0-36369  
 HOCl involvement 0-26033  
 N<sub>2</sub>O from fertilisers and O<sub>3</sub> content of stratosphere, latitudinal effects 0-36370  
 O<sub>3</sub> content effects on troposphere radiative energy balance 0-51466  
 O<sub>3</sub>, UV photodissoc. rate, expt. and theory 0-40722  
 OH<sup>+</sup> trichloroethane reaction rel. to O<sub>3</sub> content 0-16657

## P invariance

- 1/2<sup>+</sup>, baryons, vector mesonic decay, charm changing mode, SU(4) and SU(8) 0-47283  
 atom, heavy, parity non-conserving E1 matrix elements, many body calcs. 0-47924  
 atom, metastable, sensitivity and level crossing role in parity nonconservation meas. 0-43005  
 atoms, photoionisation cross sections, electron correl. reson. struct., relax. effects many body perturbation calcs. 0-47852  
 baryon nonleptonic decay, light-like reduction formula and derivation of PC and PV Lee-Sugawara relation 0-32032  
 broken symmetries at high temperature 0-42357  
 dynamically broken-gauge theories, P and T violation in QCD 0-9093  
 elastic electron scatt. and atom parity nonconservation caused by nuclear parity violation 0-27427  
 electron-hadron interactions, P-invariance, lepton, quark anapolar moments with pol. e (*Russian*) 0-52518  
 EM interactions, gauge formulation, SU<sub>c</sub>(2) internal symmetry and P- and CP-violation (*Russian*) 0-42368  
 extended relativity, T-violation and new particle 0-37182  
 Higgs bosons, effects on experimental observables, and fermion mass scale 0-32061  
 inclusive lepton pair prod., P violation, quark-parton model in Weinberg-Salam theory, QCD 0-37217  
 ions, multiply charged, highly excited states, parity nonconservation effects 0-52898  
 lepton-nucleus scattering, bremsstrahlung and neutral currents 0-32268  
 magnetic monopoles, PT-invariant theory of massive dually charged particles, Dirac-like eqn. 0-52429  
 molecules, parity-violating effects of weak interactions 0-52455  
 neutrino fluxes from rotating black holes and thermal radiation, parity violating effects 0-22034  
 nonleptonic weak interaction, SU(4) symmetry struct., parity violating Hamiltonian 0-52456  
 nuclear force, parity violating, unified treatment 0-47400  
 nuclei, parity non-conservation review 0-32207  
 P and T violating electromagnetic interaction of the quark in the instanton field 0-52430  
 parity nonconservation, discovery and nondiscovery, history 0-370  
 parity violating asymmetries in polarized electron scattering from p, d, e 0-9111  
 parity violating neutral currents, radiative corrections, Weinberg-Salam and left-right symmetric models 0-52451  
 parity violating neutral currents in two-photon and autoionisation atomic transitions 0-32034  
 PT asymmetry and four-fold EM degeneracy lifting, appl. to ring laser mode splitting 0-23606  
 quark-lepton correspondence in neutral current interactions 0-27450  
 relativistic QFT, spontaneous symmetry violations 0-52411  
 SU(2), unification of isospin and hypercharge, electroweak interactions of leptons 0-27439  
 unified model for atomic parity violation and neutral currents in gauge theories 0-4912  
 ed elastic scatt., P-odd effects due to neutral weak currents, cross sections (*Russian*) 0-13312  
 ed scatt., P-violation calc. in weak interaction theory 0-42469  
 e<sup>+</sup>e<sup>-</sup>, weak corrections to three-jet angular distributions 0-22629  
 e<sup>+</sup>e<sup>-</sup>→μ<sup>+</sup>(τ<sup>+</sup>)μ<sup>-</sup>(τ<sup>-</sup>), neutral current couplings, lepton polarisation, p violation in SU(2)×U(1) model 0-4975  
 eN interactions, parity nonconservation, SU(2)<sub>L</sub>×SU(2)<sub>R</sub>×U(1) gauge model anal., Z boson decay widths 0-47302  
 ep, high Q<sup>2</sup>, QCD corrections to parity-violating asymmetries 0-22618  
 ep deep inelastic scatt., parity violation and neutral currents 0-22559  
 γN→l<sup>+</sup>l<sup>-</sup>X, pol. γ, neutral current effect, Weinberg Salam model calcs., p violation 0-5000  
 γN→l<sup>+</sup>l<sup>-</sup>X, polarisation effects on P-violating asymmetry in Weinberg-Salam model 0-32055

## P invariance continued

- np→dγ radiative capture, relativistic effects, parity violation, Weinberg-Salam model (*Russian*) 0-32120  
 pN, dilepton production by pol. protons, parity violating, asymmetry, Weinberg-Salam calcs. 0-42488  
 pp, pp, polarised and unpolarised, jet cross sections vector boson signals, QCD-weak interference 0-5026  
 p<sup>0</sup>-electroproduction, parity violating effects 0-9178  
 Bi, neutral current-induced parity nonconserving optical rot., Dirac-HF calcs. 0-47948  
 Bi, vapour, optical activity, Faraday effect, parity nonconservation, mag. transitions (*Russian*) 0-55070  
 Bi, vapour, optical rot., parity nonconservation 0-23353  
 Bi, vapour, optical rot., parity nonconservation expts. 0-23354  
 H<sub>2</sub> ortho-para transition as means of observing weak interaction parity nonconservation (*Russian*) 0-900  
 NH<sub>3</sub> inverse level doubling mol., space and combined parity nonconservation (*Russian*) 0-52879  
 TIF, P- and T-violating interactions in hyperfine struct., mol. beam reson. expt. 0-53019  
<sup>23</sup>U fission by polarised neutrons, P odd asymmetry of emitted fragments (*Russian*) 0-18354

## p-n heterojunctions

- Anderson theory, proposal for new approach 0-6961  
 carrier behaviour in p-n junctions at high current densities 0-6968  
 chalcogenide glass-GaAs(InP) p-n junction, fabrication, characterization, switching 0-49892  
 characteristics, impact on field of semiconductors (*Polish*) 0-39664  
 effective band edges, due to quantum and grading effects 0-20305  
 II-IV p-n amorphous heterojunction, phenomenological model 0-54769  
 III-V compound heterojunctions, recomb. vel., appl. to Al<sub>1-x</sub>Ga<sub>x</sub>As-GaAs<sub>1-x</sub>Sb<sub>x</sub> solar cells (*Korean*) 0-54771  
 III-V semiconductor heterostructures, growth and dissolution kinetics by LPE 0-49543  
 III-V semiconductors, p-n heterostructures, epitaxial growth techniques, appl. to optoelectronics, review 0-54770  
 III-V semiconductors, radiative recomb. and related phenomena, conference, Prague, Czechoslovakia (Sept. 1979) 0-51940  
 multilayer semiconductor structure, current noise 0-20302  
 solar cells, cryst. and polycryst. band structure and photocurrent collection 0-21402  
 solar cells, heterojunction thin films, survey or semi-conductor combinations 0-50974  
 solar cells appl., props. obs. by electron beam induced currents 0-3518  
 superinjection in structs. with separate p-n and heterojunctions 0-50427  
 AlGaAs electroluminescent heterostructures, LPE, appl. to LED fabrication 0-55308  
 AlGaAs-GaAs heterostructures, luminescent characts., efficiency and radiative lifetime conc. depend. 0-55151  
 (AlGa)As-GaAs solar cells, theoretical perform. of multi-layer grid patterns 0-55846  
 Al<sub>1-x</sub>Ga<sub>x</sub>As-GaAs, p-n heterojunction laser, low temp. operation 0-1204  
 Al<sub>1-x</sub>Ga<sub>x</sub>As-GaAs, p-n heterostruct. laser, tunnel injection and phonon-assisted recomb. 0-5733  
 Al<sub>1-x</sub>Ga<sub>x</sub>As-GaAs heterostructures, MO-CVD, phonon assisted recomb. and stimulated emission 0-1205  
 Al<sub>1-x</sub>Ga<sub>x</sub>As-GaAs<sub>1-x</sub>Sb<sub>x</sub> solar cells, appl. of recomb. vel. at III-V cpd. heterojunctions (*Korean*) 0-54771  
 n-CdGeP<sub>2</sub>-p-CdGeAs<sub>2</sub> heterojunction photocells, polarisation-sensitive 0-11075  
 n-CdIn<sub>2</sub>S<sub>4</sub>/p-CuInSe<sub>2</sub> heterostructure, form. and photovolt. meas. 0-10831  
 CdS heterojunction solar cells by CVD method 0-45685  
 CdS/Cu<sub>2</sub>S heterojunction solar cells, optimal material props. theory and experimental verification 0-45686  
 CdS-CdTe-Te, effect of low cond. CdTe interlayer on charact. 0-44721  
 CdS-PbS, photoresistive props. 0-6970  
 CdS-Te, effect of low cond. CdTe interlayer on charact. 0-44721  
 CdTe-CdS, closed-tube vapour growth 0-55302  
 Cd<sub>1-x</sub>Zn<sub>x</sub>S/Cu<sub>2</sub>S thin film heterojunction solar cells, operational charact. 0-45687  
 Cd<sub>1-x</sub>Zn<sub>x</sub>S-p-GaAs, electrical and photovolt. props. 0-29466  
 Cu<sub>2</sub>S-CdS heterojunction solar cell, interface recomb. vel. determ. by capacitance/collection efficiency variation 0-50959  
 Cu<sub>2</sub>S-Zn<sub>1-x</sub>Cd<sub>x</sub>, heterojunction, composition meas. near interface using aqueous ion-exchange 0-29465  
 Cu<sub>2</sub>S/CdS heterostructures, heat treated, capacitance voltage meas. anal. 0-20292  
 Cu<sub>2</sub>S-CdS p-n heterojunction solar cells, props., Burstein-Moss effects 0-21404  
 Cu<sub>2</sub>S-CdS heterojunction solar cells spectral distrib. and photocapacitance 0-55864  
 Cu<sub>2</sub>S-CdS solar cells, SEM parameter meas. for space charge region recombination 0-16808  
 Cu<sub>2</sub>S(Se)-CdS(Se) p-n heterophotoelements of optronic converters, props. on X-irrad. of scintillator 0-34505  
 GaAlAs based, integrated optics appl., technology advancements and heterostructure types (*Slovak*) 0-33226  
 GaAlAs p-n heterostructures, current-flow mechanisms, luminesc. spectra 0-20298  
 Ga<sub>1-x</sub>Al<sub>x</sub>As, p<sup>+</sup>-n-n<sup>+</sup> heterostructure, distrib. of injected carriers, forward V-I characts. (*Russian*) 0-6973  
 Ga<sub>1-x</sub>Al<sub>x</sub>As-GaAs heterojunctions grown by metallorganic CVD 0-15599  
 GaAs n-p solar cells, theoretical perform. of multi-layer grid patterns 0-55846  
 GaAs solar cell structs., photoluminesc. props. 0-50958  
 GaAs/Al<sub>1-x</sub>Ga<sub>x</sub>As heterostruct., anomalous elec. and optical characts. 0-2865  
 GaAs/III-V solid soln. heterostructure composition profile by photoemission microanalysis 0-44717  
 GaAs-Al<sub>1-x</sub>Ga<sub>x</sub>As, negative differential resist., real-space electron transfer 0-6958  
 GaAs-Al<sub>1-x</sub>Ga<sub>x</sub>As, heterojunction and superlattice, magnetophonon reson., polaron mass 0-44715  
 GaAs-Al<sub>1-x</sub>Ga<sub>1-x</sub>As superlattice, electronic props. 0-11080  
 GaAs-AlAs, heterostructure, effects of cation order on energy bands 0-11081  
 GaAs-AlGaAs heterojunction superlattices, electron mobilities 0-29473  
 GaAs-AlGaAs heterojunction superlattices, obs. of intersubband excitations in multilayer two dimensional electron gas 0-29753



**p-n heterojunctions continued**

- GaAs-Ga<sub>1-x</sub>Al<sub>x</sub>As heterostructures, quantum size effect in superlattices, electronic props. 0-29471  
 GaAs-Ga<sub>1-x</sub>Al<sub>x</sub>As variable gap p-n junction, variable gap and photo EMFs 0-15596  
 GaAs-GaAlAs, superlattice, subband related anisotropy in negative magnetoresistivity 0-11082  
 GaAs-GaAlAs (100) interfaces, carrier transport coeffs., tight binding calc. 0-49889  
 GaAs-Ge<sub>1-x</sub>(GaAs)<sub>x</sub> n-p heterojunctions, hydrostatic press. effect on elect. and photoelectric props. 0-20304  
 p-(GaAs)<sub>x</sub>(ZnSe)<sub>1-x</sub>nn<sup>+</sup> GaAs, avalanche heterojunctions, inverse branch of volt ampere charact. (*Russian*) 0-6974  
 Ga<sub>1-x</sub>In<sub>x</sub>Sb-Ga<sub>1-x</sub>In<sub>x</sub>Sb, heterojunction parameters 0-50550  
 Ga<sub>1-x</sub>In<sub>x</sub>Sb p-n junction photodiode fabrication, sensitivity as 1 to 2.5  $\mu$ m detectors (*Japanese*) 0-52311  
 Ge-GaAs, (100) interface, electronic struct. calc. 0-49861  
 Ge-GaAs heterojunction, interface geometry, model 0-49879  
 Ge-GaAs heterojunctions, effect of  $\gamma$ -radiation on current-voltage charact. (*Russian*) 0-2459  
 Ge-GaAs interface, electronic struct. of Ge overlayers on (100) GaAs 0-49880  
 Ge-GaAs structure, electronic struct., ang.-resolved photoemission obs. 0-49881  
 Ge-ZnSe, (100) interface, electronic struct. calc. 0-49861  
 HgSe/CdSe lattice-matched heterostructs. as Schottky barriers, CVD epitaxial growth and elec. props. 0-49877  
 InAs-GaSb (110), electronic states, Green's function technique, tight binding approx. 0-49855  
 In<sub>0.53</sub>Ga<sub>0.47</sub>As-InP heterostructure, LPE growth 0-11582  
 InGaAsP/InP DH, vapour phase growth by dual-growth-chamber method 0-50559  
 InGaAsP-InP, LPE grown, impurity effect on surface morphology 0-29291  
 InGaAsSb, LPE growth, and appl. in GaSb/AlGaAsSb/InGaAsSb/AlGaAsSb/GaSb DH 0-16205  
 In<sub>0.3</sub>Sn<sub>0.7</sub>Si, current mechanisms and barrier height 0-11083  
 n-In<sub>0.3</sub>O<sub>0.7</sub>p-InP solar cell, photovolt. effects 0-12014  
 InP-CdS, integrated optics appl., prep. and props. (*Slovak*) 0-33225  
 InP-CdSnP<sub>2</sub>, integrated optics appl., prep. and props. (*Slovak*) 0-33225  
 InP-InGaAs, integrated optics appl., prep. and props. (*Slovak*) 0-33225  
 InP-InGaAsP, integrated optics appl., prep. and props. (*Slovak*) 0-33225  
 (In<sub>1-x</sub>Sn<sub>x</sub>)<sub>2</sub>O<sub>3</sub>-Si-N solar cell efficiency and elec. props. 0-35676  
 In<sub>2-x</sub>Sn<sub>2x-3</sub>O<sub>3-y</sub>CdTe(InP) photovoltaic heterojunctions, surface and interface studies, efficiency 0-45691  
 NiO:Li-O-ZnO, contact resist., effect of water vapour 0-34506  
 PbS-Si heterojunction, struct. and comp. 0-54530  
 PbS-Si heterojunction detector, direct injection readout 0-4765  
 Pb<sub>1-x</sub>Sn<sub>x</sub>Te LPE grown heterostructures, dislocation etch pitch, interfaces 0-2023  
 PbTe surfaces, Te coating, struct. and junction charact. 0-50743  
 Se-Ag<sub>2</sub>Se, electrically controlled negative differential conductance mechanism 0-44720  
 Se-Ag<sub>2</sub>Se, heterojunction with memory, transient switching characteristics 0-44718  
 Si, n-p-n heterojunction transistor 0-6959  
 Si-As<sub>2</sub>S<sub>3</sub> heterojunctions, hole transport obs. in vitreous As<sub>2</sub>S<sub>3</sub> 0-49727  
 Si-CdS, detector for integrated optics appl. (*Czech*) 0-33227  
 p-Si-In<sub>2-x</sub>Sn<sub>2x-3</sub>O<sub>3-y</sub> solar cells, thermal degradation mechanisms 0-55841  
 Si-SiC, photovoltaic effect of sheet Si dip-coated on graphite substrate 0-29442  
 SnO<sub>2</sub>/n-Si spray-deposited solar cells 0-12007  
 SnO<sub>2</sub>-GaSe heterojunction photocell, fine struct. of photo-EMF spectra 0-6967  
 SnO<sub>2</sub>-Si, heterojunction solar cells, anomalous photocurrent 0-3515  
 SnO<sub>2</sub>-Si heterojunctions, elec. and photovoltaic props. 0-26141  
 SnO<sub>2</sub>-Si solar cells, electron-beam deposited, struct., photovolt. props. 0-50956  
 SnO<sub>2</sub>-SiO<sub>2</sub>-n-Si heterojunction, cheap solar elements for ground-based appls. 0-40860  
 Zn<sub>1-x</sub>Cd<sub>x</sub>S/GaAs heterojunction solar cells, meas. of minority carrier diffusion length 0-26158  
 ZnSe-GaAs narrow junction lasers 0-43334

**p-n homojunctions**

- back surface field semiconductor junction, temp. depend. of open circuit photovoltage 0-15593  
 hyperabrupt junction, C-V index, junction parameters depend. 0-49876  
 integrated tandem solar cell performance 0-3521  
 n<sup>+</sup>-n-p high-low-emitter junction solar cell, open-circuit voltage in conc. sunlight 0-50957  
 p-n-n<sup>+</sup> structures containing deep traps, double injection currents 0-15592  
 polyacetylene, doped, p-n junction, elec. props., review (*Japanese*) 0-29410  
 semiconductor, deep impurities, exptl. techniques (*Japanese*) 0-15476  
 Si p<sup>+</sup>pn<sup>+</sup> junction, diffusion of transition elements, anomalous behaviour 0-29044  
 solar cells, CdTe, shallow homojunctions, characteristics and surface resistance influences 0-45690  
 solar cells, power conversion efficiency monitoring 0-50989  
 variable-gap, recomb. currents 0-20303  
 Al<sub>1-x</sub>Ga<sub>x</sub>Sb-Zn, impurity diffusion, p-n junction depth 0-24678  
 Ga<sub>1-x</sub>Al<sub>x</sub>As p-n structure, charge-storage diode, variable-gap 0-11076  
 GaAs, electroepitaxy and thermal LPE growth, elec. charact. 0-2290  
 GaAs homojunction LED, mechanical stress induced degradation 0-2860  
 GaAs, shallow homojunction solar cell, resist. to 1 MeV electron radiation 0-50953  
 GaAs, shallow-homojunction solar cell by MBE, conversion efficiency 0-30476  
 GaAs solar cells on Ge substrates, thin film shallow homojunction struct., quantum efficiencies 0-35677  
 GaAs, surface recomb. current reduction with Al<sub>0.5</sub>Ga<sub>0.5</sub>As:O surface layer 0-49878  
 GaAs:Si p-n light-emitting struct., soln. of general minority carrier transport eqn. 0-15597  
 GaAs:Si p-n struct., effect of growing conditions on distrib. of recomb. parameters 0-39668  
 GaAs<sub>1-x</sub>Sb<sub>x</sub> photodiode structures, current-voltage charact., photo-EMF spectra 0-29472

**p-n homojunctions continued**

- GaP, electron traps around dislocations in p-n junction and metal-semicond. struct. 0-34388  
 GaP:N(N,O) epitaxial struct., luminesc. study of degradation during heat treatment 0-45139  
 GaP:ZnO, electron irradi. effect on electrolum., defects form. and quenching obs. 0-55194  
 Ge, epitaxial-diffusion p-n junction, inductive props. in secondary breakdown 0-15598  
 Ge, IR radiation modulation, light absorption by injected current carriers (*Russian*) 0-10013  
 Ge p-n junctions with hot carriers, current amplification, elec. domain form. 0-6966  
 Ge-Si alloy, Sb-diffused, TSC 0-20289  
 HgCdTe Schottky barrier diode and n-p diffused junction IR detectors, comparison 0-9039  
 Hg<sub>1-x</sub>Cd<sub>x</sub>Te photodiodes, implanted n<sup>+</sup>-p, improved performance using insulated field plates 0-52309  
 InAs<sub>1-x</sub>Sb<sub>x</sub> p-n junctions, avalanche multiplication 0-6965  
 n-InP, p-n junction form. by Be ion implantation 0-29474  
 InSb, minority carrier injection in mag. field, recomb. radiation obs. 0-11078  
 InSb p-n junctions, diffused, avalanche multiplication and impact ionisation 0-15595  
 Pb<sub>1-x</sub>Ge<sub>x</sub>Te, ferroelec. constants, C-V and C-T charact. of abrupt p-n junctions 0-25323  
 Pb<sub>1-x</sub>Ge<sub>x</sub>Te, ferroelectric phase transition effect on forbidden band width 0-24794  
 PbSnTe(Se) Schottky barrier diode and n-p diffused junction IR detectors, comparison 0-9039  
 Si, amorphous, p-n junction devices, barrier profile effect on elec. props. 0-49890  
 Si, amorphous films, ion implanted, elec. and photocond. props. 0-49717  
 Si beam epitaxy for epitaxial film growth and p-n junction formation in high vacuum 0-16187  
 Si, charge carrier recomb. at dislocations, combined SEM and TEM study 0-15105  
 Si, detector for integrated optics appl. (*Czech*) 0-33227  
 Si diffused horizontal homojunction solar cells, effects of junction depth and impurity conc. 0-55877  
 Si, ellipsometric method of temp. meas. rel. to secondary breakdown (*Russian*) 0-11074  
 Si epitaxial structures, junction layer width and impurity conc. estimates (*Russian*) 0-49893  
 Si, high-voltage, elec. props. by optical scanning 0-6969  
 Si, ion-implanted, lapping and staining techniques, junction depth determ. 0-29468  
 Si, p<sup>+</sup>-n junction, irradi. with  $\alpha$ -particles, defect form 0-24509  
 Si, p<sup>+</sup>-n junction diodes, flow fluence S implanted unequal defect densities, dynathermal obs. 0-20293  
 Si p-n diode, 1/f noise calc., free carrier mobility interpretation 0-54774  
 Si p-n homoepitaxial junctions, elec. and struct. charact. 0-6662  
 Si p-n junction local temp. meas. using pulsed SEM, induced-current mode 0-54775  
 Si, p-n junctions, neutron transmutation doping, breakdown process 0-15600  
 Si, polycryst.-single cryst. p<sup>+</sup>-n and n<sup>+</sup>-p junctions, elec. charact. 0-11077  
 Si solar cell array with concentration, design and development 0-45700  
 Si solar cells, polycrystalline n<sup>+</sup>/p, computer model of spectral response and photocurrent 0-55853  
 Si surface layers, impurities, elec. and photoelec. props. 0-2298  
 Si, technology and physics, review 0-34353  
 Si:As, p-n junction form. by laser annealing, space charge region, effects on reverse current 0-54772  
 Si:Au, p<sup>+</sup>-n junction, quantitative study of Au atoms by TSC method 0-2458  
 Si:Au(Pt), heavily doped, gradual p<sup>+</sup>-n junctions, trap levels (*French*) 0-34392  
 Si:B,P, double implanted layer, n-p-n struct., single pulse laser annealing 0-49247  
 Si:H, amorphous, in p<sup>+</sup>-i-n<sup>+</sup> struct., hole diffusion length meas. 0-44712  
 Si:H, amorphous, p<sup>+</sup>-i-n<sup>+</sup> struct. solar cells, material parameters and deposition condition optimisation study for higher efficiencies 0-45676  
 Si:H, amorphous and crystalline, hydrogenation and dehydrogenation, luminesc. spectra 0-11477  
 Si:P dislocation p-n junctions, capacitive props. 0-20300  
 n-Si:Pd Schottky diodes photocapacitance meas., photon and carrier capture cross sections 0-20309  
 Si:Zn, p-n-n<sup>+</sup> and p-n-p struct., reson. charact. of impedance near excitation threshold of recomb. waves 0-20301  
 SiC reverse biased p-n junctions, prebreakdown violet luminesc. 0-7420  
 SiC:Al<sup>+</sup> p-n junctions, elec. props., defect effects 0-15594  
 ZnSe:Cu, I ceramic, injection electroluminesc. of p-n microjunctions 0-40163

**p-n junctions**

- see also p-n heterojunctions; p-n homojunctions  
 boundary conditions 0-20295  
 deep level properties measurement, capacitance spectrometer (*German*) 0-15471  
 electrical parameters, optical derivative meas. 0-2455  
 electron-phonon scatt. 0-24997  
 heavily doped device, collection efficiency and surface recomb. vel. modulation 0-20291  
 hot carrier junctions, current-voltage charact., effect of space charge defects 0-25001  
 impurity ions, overcharging, effect on movement in p-n junction (*Russian*) 0-11079  
 linearly graded, linearly graded, characterisation 0-6962  
 minority carrier diffusion length meas. by short-circuit current ratio 0-31849  
 P<sup>+</sup>-P-N<sup>+</sup> junctions, thermocapacitive behaviour (*Spanish*) 0-2457  
 photoconverter, bilateral sensitivity, n<sup>+</sup>-p-p<sup>+</sup> structure, volt-ampere charact. under illumination 0-40855  
 potential step meas. by SIMS 0-34503  
 recombination phenomena as function of temp. and applied voltage (*Polish*) 0-53294  
 short circuit, SEM investigation 0-6957  
 solar cell, photoinjected carrier lifetime meas. by reverse voltage pulse response 0-45664



**p-n junctions continued**

- solar cell, two-stage, fraction of radiation usefully converted, power prod. efficiency 0-30477
- solid state physics rel. to solar cells, review 0-49601
- solid-state electronics, introductory theory, book 0-22160
- temperature measurement using several junctions (*Polish*) 0-13075
- three-frequency parameter systems, equivalent conductivities, partially opened p-n junctions (*Russian*) 0-24998
- transition region anal. using quasi-equilibrium assumptions 0-6963

**P-V-T relations** *see equations of state***pacemakers**

- see also patient treatment*
- asynchronous cardiostimulators, increasing interference immunity 0-3868
- automated test system developments 0-30944
- batteries, neutron radiography investigation of electrolyte, USA National Bureau of Standards 0-56179
- battery characteristic meas. microcalorimeter 0-30936
- battery internal loss characterisation calorimeter 0-30934
- battery microcalorimetric testing 0-30933
- battery self-discharge process assessment by microcalorimetry 0-30935
- cardiac pacemaker, high-reliability hybrid IC procurement 0-30942
- cardiac pacemaker reliability technology workshop, Gaithersburg, USA (Oct. 1977) 0-27038
- cardiac pacemaker semiconductor component reliability trends 0-30943
- cardiac pacemaker treatment principles and experience 0-8213
- Dutch development of medical physics (*Dutch*) 0-3877
- electrostatic discharge sensitivity grouping 0-30941
- endocardial electrode lead and pacemaker failure, actuarial analysis 0-30945
- implanted electrodes, signal source impedance 0-56275
- medical electronics, new forms and techniques 0-3856
- microprocessor-controlled dual-channel stimulator 0-56279
- NDT by holographic interferometry and optical correl. 0-40659
- patient stimulator 0-41322
- power source, Li-I hermetically-sealed cells, long life expectancy 0-40850
- programmable pacemaker with digital memory (*Chinese*) 0-36192
- respiration linked cardiac pacemaker system 0-26416
- tachycardia termination system, microcomputer-based 0-56280
- vector cardiograph for pacemaker pulse display 0-41325
- Li-I<sub>2</sub> pacemaker battery electrolyte exam. by neutron radiography 0-30940
- Li-I<sub>2</sub> pacemaker cell end-of-life characteristic approximation 0-30937
- Li-I<sub>2</sub> power cell accelerated discharge test for battery longevity model 0-30938
- Li-SOCl<sub>2</sub> battery for implantable cardiac pacemakers 0-30939

**packaging**

- see also encapsulation; modules*
- weights and measures, conference, Washington (1978) 0-27260

**packing** *see packaging***pair algebra** *see algebra***pair annihilation, electron** *see electron-positron interactions***pair breaking, Cooper** *see Cooper pairs***pair production, electron** *see electron pair production***pairing, Cooper** *see Cooper pairs***pairs, electron** *see electron pairs***palaeomagnetism**

- N.America, palaeopoles and palaeolatitudes, displaced terrains 0-12367
- ancient oceanic lithosphere, mag. props. as alteration indicators, Othris ophiolite example 0-8297
- Antarctic igneous rocks, palaeomag. and K-Ar age 0-12332
- E.Antarctic, Mesozoic lava flows in Dronning Maud Land 0-30984
- Appalachians, Newark Trend igneous rocks, palaeomagnetism 0-51320
- Archaean rocks from Superior Geotraverse, regional palaeomagnetism 0-30980
- Archaean Shelley Lake granite, <sup>40</sup>Ar-<sup>39</sup>Ar dating of magnetizations 0-30982
- Arkansas, St. Joe Limestone, Early Carboniferous 0-21628
- book, palaeomagnetism and plate tectonics 0-36789
- Botwood Group and Mount Peyton Batholith, Newfoundland, orogenic history 0-3917
- N.Calcareous Alps, Permo-Triassic red sandstone 0-56358
- Cambro-Ordovician redbeds, Armorican Massif, France and Channel Islands, palaeomag. 0-21617
- Campbell Plateau and Lord Howe Rise, plate tectonics of SE.Gondwanaland 0-17244
- Canary Island palaeomagnetism, and continental margin evolution 0-56363
- China, Quaternary magnetic stratigraphy (*Chinese*) 0-56359
- continental plates pre-Tertiary velocities from palaeomag. data 0-21848
- Cretaceous and Eocene mag. pole positions, Turkish tuffs 0-31020
- data analysis, angle in Fisher distrib. that will be exceeded by given probability 0-51325
- data analysis, Fisher's precision parameter 0-51326
- data analysis, modes of directional data 0-56352
- Denchai Basalt, N.Thailand, paleomagnetism, age and geochemistry 0-41421
- Devonian Onondaga limestone (New York), palaeomagnetism re-examination 0-3928
- Early Cretaceous magnetic stratigraphy, Italian Umbrian carbonate rocks 0-36229
- Earth radius expansion, effect on palaeomagnetic data 0-56422
- geomagnetic field palaeointensity, determ. at heated rock contact by step-wise remagnetisation method 0-21619
- Himalayan basic volcanic formation, palaeomagnetic study 0-51328
- Holocene lake sediments, N.Poland, palaeomag. 0-21616
- Indian apparent polar wandering rel. to India-Asia collision 0-26452
- intensity variation, over last 10000 years, archaeomagnetic record 0-36237
- IRM of Yellowstone Group comparison with DRM of Pearllette ash beds 0-21624
- Japan, Permian greenstones, geological significance 0-21629
- Jersey, Gt.Britain, volcanics and dykes remanent magnetisation 0-46125
- Keweenaw diabase dikes from N.Michigan 0-51321
- Lake Tahoe, California-Nevada, sediments, palaeomag. and sedimentological studies 0-41371
- Late Pleistocene and Holocene dry lake deposits, Mexico, palaeomag. record 0-21618
- lava flows of Mt. Etna, partial self-reversal and NRM 0-46126

**palaeomagnetism continued**

- Lewisian foreland, NW.Scotland, central zone palaeomag. rel. to tectonics 0-26443
- Lower and Middle Cambrian sedimentary rocks, Desert Range, Nevada, palaeomag. rel. to polar wander 0-21620
- Lower Palaeozoic polar wander for Europe 0-46125
- N.Maine, USA, Devonian rocks and W. limit of Avalon microcontinent 0-41373
- marine short-wavelength mag. anomalies coherence, effect of random crustal magnetisation 0-36225
- meteorite impact site, Slate Islands, Canada, shock remanent magnetisation 0-30986
- Monteregian intrusives, Quebec, palaeomagnetic polarity pattern 0-26438
- Morocco, volcanic rock palaeomagnetism and K-Ar dating (*French*) 0-51322
- North America Early Carboniferous palaeomag. field rel. to N. Appalachians tectonics 0-8249
- Notre Dame Bay lamprophyre dikes, Newfoundland rel. to Atlantic opening 0-26440
- palaeointensities determ. from submarine pillow basalts, effects of seafloor weathering 0-3927
- palaeointensity and thermoluminescence measurements on Cretan kilns from 1300 to 2000 BC 0-36232
- phanerozoic polar wander curve for India 0-51328
- Precambrian polar wandering rel. to plate tectonics 0-31024
- Rose Hill Formation, USA, Middle Silurian pole position 0-56353
- San Vincenzo, Tuscany, study of Pliocene rhyolite 0-56357
- Scandinavian Caledonides, gabbro complex palaeomag., plate rot. or polar shift theories 0-21615
- Seal Group rocks, Quebec, magnetisation study 0-3918
- secular variation periods, spectral anal. of archaeomagnetic data 0-41372
- shock-diminished remanence at Charlevoix impact structure, Quebec 0-26441
- Sila nappes (Calabria), palaeomag. evidence for non-Apeninian origin 0-56369
- St-Urbain and other Grenville palaeopoles 0-26442
- Superior Geotraverse symposium (Toronto, 1978 October 23-26) 0-27029
- S.W.Sweden, Permian multiple intrusion dykes in Bohuslan, mag. studies 0-36228
- Swedish rapakivi suite, palaeomag. study rel. to Proterozoic tectonics of Baltic Shield 0-56346
- Tertiary volcanics from Sardinia 0-56343
- Tertiary volcanics of Sardinia 0-46127
- Thunder Bay Late Quaternary sediments, palaeomagnetic record from remanent mag. meas. 0-17230
- Tibetan Plateau underthrust by India, palaeomagnetic constraints 0-56449
- Umfaville Gabbro, Ontario, palaeomag. study and K-Ar age 0-12330
- Upper Precambrian sedimentary rocks, Desert Range, Nevada, palaeomag. rel. to polar wander 0-21621
- Upper Proterozoic apparent polar wander, analogous loops from Laurentia, Fennoscandia and Africa 0-56360
- Varanger peninsula, Norway, Late Precambrian dolerite dykes 0-30989
- volcanic rocks in Lesser Antilles island arc, palaeomagnetic survey and age determ. 0-8265
- S.Wales, Lower Cambrian Caerfai Bay Shales, diagenetic magnetisation 0-36227
- Zijderveld vector diagrams, use in multicomponent palaeomag. studies 0-17420

**palladium***see also nuclei with .....*

- abundance in stone and Fe meteorites, mass spectroscopy 0-8601
- adsorbed CO on (210) surface, inclined bonding config., electron stimulated desorption and LEED obs. 0-39430
- adsorbed layer on W FEM tips, conc. determ. by nucl. microanal. (*French*) 0-29860
- adsorption of CO, geometrical struct., LEED and high-resolution EELS study 0-20037
- adsorption of Xe on (110) surface, anomalous 5p photoemission 0-7471
- adsorption of Xe on Pd(110) surface AES, UPS, LEED, work function, flash desorption 0-6633
- atom, K $\beta$ /K $\alpha$  rel. intensity obs. 0-32665
- atom, XPS and XES, dynamical effects 0-52924
- Auger peaks, M<sub>45</sub>N<sub>45</sub>N<sub>45</sub> transition, influence of surface environment 0-7447
- catalyst, on glass, used in electroless deposition, proton backscattering anal. 0-16749
- chemisorption of H, bond nature 0-34297
- chemisorption of H, embedded cluster model 0-39427
- coating, on stainless steel, interdiffusion at reactor wall temps., Rutherford backscatt. obs. 0-39361
- confined geometry, p-wave supercond. or itinerant ferromag. 0-11129
- crystallite morphology, surface struct., electron microscopy obs. 0-29257
- dilute alloys, electronic struct. calc. using KKR method 0-15438
- elastic consts. 4 to 300K 0-6455
- electrical resistivity, temp. depend. data 0-51967
- electrode, evaporation rate from cathode spot in vac. arcs. 0-49024
- electrodeposited layers, props., deposition parameters influence (*German*) 0-20808
- electrodes for electrolytic H prod., reaction kinetics 0-30434
- electron-phonon parameters and supercond. p-state pairing 0-25041
- epitaxial growth, cluster mobilities, in-situ electron microscopes obs. 0-15407
- film, high dose Si<sup>+</sup> ion implantation, silicide phases, backscatter spectra 0-19820
- film, on Si, ion-induced intermixing 0-15420
- film, two-dimens. nucleus form. on Ag (111), UHV electron microscope obs. 0-10760
- film on Si, Xe ion beam induced form. of PdSi 0-10800
- film on Si substrate, laser irradi., cellular struct. and silicide form. 0-10710
- film with defects, field-induced resist. min. 0-11050
- films, evaporated, resist and thermolec. power, annealing effects 0-39684
- interatomic pair potential, phonon spectra 0-33927
- melting point determ., effect of surrounding O<sub>2</sub> 0-27299
- nuclear acoustic resonance from 4-200K 0-25247
- overlayers, on Nb, form. of Pd (111) surface states and reson. d-levels, photoemission obs. 0-50523
- pair potentials calc., appl. to point defect props. 0-19798



**palladium continued**

- positron lifetime spectra, influence of adsorbed H 0-25480  
 powder, sponge, sintering shrinkage kinetics 0-29900  
 scattering, adsorption, and absorpt. of H<sub>2</sub> and D<sub>2</sub> on (111) surface, mol. beam study 0-29277  
 superconducting transition temperature, ab initio calc. 0-25036  
 surface, (100), ( $\sqrt{2} \times \sqrt{2}$ )R45°, S layer, adsorbate induced surface reson. obs. in photoemission 0-7470  
 surface, (111), adsorbed O<sub>2</sub>, UPS and thermal desorpt. characts. 0-54754  
 surface, coverage and desorption of CO flash desorption spectrum 0-49493  
 surface (100), CO monolayers, electronic states, tight-binding method appl. 0-49564  
 surface (111), H<sub>2</sub>+O<sub>2</sub> reaction, mol. beam relax. and isotopic exchange meas. 0-35575  
 surface (111)(110), H adsorption, inert model 0-50889  
 XPS, electronic struct. 0-7464  
 AgBr-Pd(II), photolysis-induced trapping behaviour, EPR study 0-54949  
 Al-Al oxide-Pd tunnel junctions, exposed to H<sub>2</sub>, inelastic electron tunnelling spectra 0-20327  
 Au/Pd, bicrystals, in situ relax. of interphase interfaces 0-39455  
 Pd, H(D) interstitial interactions rel. to diffusion and ordering transition 0-34249  
 Pd/Ni/Cr layered catalyst for H<sub>2</sub>-O<sub>2</sub> recombination in BWR coolant 0-18504  
 Pd/Si interface, chem. and struct. props. during silicide form., AES and TEM obs. 0-49430  
 Pd/W (110), metastable 2D condensations, epitaxy, growth modes, exp. techniques, book contrib. 0-49558  
 Pd-amorphous Si thin film interaction, metal rich Pd-silicide formation 0-2284  
 Pd-H, incoherent phase transition, lattice gas model 0-29171  
 Pd-H system, review of props., book contrib. 0-24605  
 Pd-H system, electronic struct. of H, mol. cluster and pseudojellium models 0-24832  
 Pd-Si (111) interface, microscopic Pd<sub>2</sub>Si form., UPS obs. 0-24743  
 Pd-TiO<sub>2</sub>, Schottky barrier, work function depend. on adsorbed species 0-54782  
 Pd-ZnO Schottky-barrier diode, H<sub>2</sub> sensitivity 0-11085  
 n-Si/Pd Schottky diodes photocapacitance meas., photon and carrier capture cross sections 0-20309

**palladium alloys**

see also palladium compounds

- Ag-Pd, surface comp. changes under ion bombardment, AES study 0-55250  
 controllable hydrogen phase nakle, hardening and phase-strengthening 0-16323  
 rare earth alloys RPd<sub>2</sub>X<sub>2</sub> (X=Si,Ge), cryst. struct. 0-1964  
 Al-Pd eutectic, microstruct. morphology 0-3018  
 Au/AuPd, bicrystals, in situ relax. of interphase interfaces 0-39455  
 Au-Pd, dil., Friedel d-reson. scatt. and elec. resists. 0-44566  
 Au-Pd, surface comp. changes under ion bombardment, AES study 0-55250  
 CePd<sub>2</sub>-Er(Gd)(Yb), dil., EPR spectra 0-25201  
 Cu-Pd, mag. susceptibility and electronic struct. of ordering (Russian) 0-11161  
 Cu-Pd, surface comp. changes under ion bombardment, AES study 0-55250  
 Cu-Pd, surface structures, LEED obs. 0-10761  
 Cu<sub>2</sub>Au-Cu<sub>3</sub>Pd, quasibinary system, order-disorder transform., superlattice form. 0-2159  
 Cu<sub>3</sub>Pd<sub>17</sub>, Cu<sup>+</sup> (Au<sup>+</sup>) ion-bombarded, displacement cascades and disordered zones, TEM studies 0-15167  
 Er,Ce<sub>1-x</sub>Pd<sub>3</sub>, cryst. field spectra, neutron scatt. study 0-50047  
 ErPd<sub>3</sub>, specific heat at low temp. 0-20413  
 EuPd<sub>2</sub>, elec. field gradient, spin echo NMR meas. 0-20509  
 EuPd<sub>2</sub>, indirect exchange, spin echo NMR meas. 0-15822  
 Fe-Cr-Pd, Pd alloying effects on passivation 0-35373  
 Fe-Pd, anomalous elec. cond. near mag. phase transition point,  $\alpha$  to  $\gamma$  phase transition 0-15722  
 Fe-Pd, residual resist., s-d hybridisation effect 0-39559  
 Fe-Pd crystalline alloy, positive large linear magnetostriction 0-25173  
 Fe<sub>25</sub>Pd<sub>75</sub>Au<sub>25</sub>, atomic ordering influence on mag. props. and elec. resistance (Russian) 0-7551  
 Fe<sub>2</sub>Pd<sub>82-x</sub>Si<sub>18</sub>, amorphous, magnetisation, magnetoresist., spin glass and ferromag. phases 0-34697  
 Nb-Pd, impurity diffusion and vacancy-impurity binding energy 0-15307  
 Ni-Cu alloy, surface comp. and catalysis 0-54489  
 Ni-Fe-Pd thin films, mag., surface and corrosion props. 0-34707  
 Ni-Pd, anodic behaviour, potentiodynamic current density and impedance potential meas. (German) 0-25925  
 Ni-Pd surfaces, electrochem. passive film form. and comp. determ. by SEM, SIMS, XPS 0-39401  
 Ni-Pd-H, film, struct. and phases formed, when Ni, Pd are sputtered in H 0-29289  
 NiCoPd, anodic dissolution, SFE effect (German) 0-25924  
 Pb-Pd, diffusion of Au, de-enhancement by Pd impurities 0-19990  
 Pd alloy-H system, review of props., book contrib. 0-24605  
 Pd Ni, effect of hydrogenation on thermopower 0-39562  
 Pd-Ag, Fermi energy influence on soln. behaviour of H, B and C (German) 0-44323  
 Pd-Ag, influence of adsorbed H on positron lifetime spectra 0-25480  
 Pd-Ag, thin layer, deposited on glass or Si substrate, X-ray microanalysis (French) 0-50902  
 Pd-Ag electrical resistivity, thermo-EMF and thermal diffusivity at high temps. (Russian) 0-6808  
 Pd-Ag microwires, electrical resistance, influence of gaseous environment in heat treatment (Russian) 0-20146  
 Pd-Ag-Si alloys, amorphous, crystn. kinetics, DSC meas. 0-1933  
 Pd-Ag(V), H mobility and solubility, appearance pot. spectra obs. 0-55231  
 Pd-Al, transition metal group VIII aluminide, NMR near equiatomic composition (Russian) 0-20479  
 Pd-Au:H<sub>2</sub>(D<sub>2</sub>), thermodynamic props. at 555 and 700K, vibr. freqs. and excess entropies 0-29186  
 Pd-Au-Si, amorphous films, RF sputter deposition, composition and thermal behaviour 0-55292  
 Pd-C, dil., C segregation to single cryst. surfaces 0-39301  
 Pd-C (graphite), adhesion and wettability of graphite (Russian) 0-20008

**palladium alloys continued**

- Pd-Co, dilute, extraordinary Hall effect meas., 2-250K 0-34420  
 Pd-Co, very dil., Mossbauer emission spectra of <sup>57</sup>Co, relax. effects 0-29656  
 Pd-Cu, influence of adsorbed H on positron lifetime spectra 0-25480  
 Pd-Cu-Si, laser melting and splat quenching to form foils for TEM obs. 0-29986  
 Pd-Fe, molecular field distribution function in disordered Ising model (Russian) 0-54859  
 Pd-Fe, resist. min. 0-11050  
 Pd-Fe, scatt. and transmission Mossbauer spectra near Curie temp. 0-15864  
 Pd-Fe-Mn, dil. alloy, high press. study 0-34600  
 Pd-Fe-Mn, ferromag. and spin-glass props; comment 0-2591  
 Pd-H, low temp. transport props., heterogeneous-mixture model 0-24871  
 Pd-H dilute alloy, de Haas-van Alphen oscill. freq., absolute amplitude, Dingle temp. 0-49575  
 Pd-H thin film system, phase diagrams using quartz crystal thickness monitor 0-7537  
 Pd-H-Gd, dil., ESR exam. of low temp. region of phase diagram, and electronic props. 0-29930  
 Pd-H(D), superconductivity and electron-phonon interaction 0-49975  
 Pd-H(D), thermal expansion and lattice anharmonicity 9 to 270K 0-39241  
 Pd-Mn, Curie temp. and magnetisation, vol. depend. 0-34629  
 Pd-Mn, dil. alloy, very temp. magnetisation 0-34692  
 Pd-Mn(Fe), mag. ordering phenomena, neutron scatt. obs. 0-44812  
 Pd-Ni, dil., resist. min. 0-11050  
 Pd-Pt surface, adsorbed Xe, 5p photoemission, local surface struct. influence 0-2920  
 Pd-Sb film, rhombohedral phase, cryst. struct. electron diff. determ. 0-39008  
 Pd-Si amorphous films, RF and DC sputter deposition, composition and thermal behaviour 0-55292  
 Pd-Si glasses, changes in density of states with alloys comp., UPS obs. 0-50531  
 Pd-Si-Fe amorphous alloy, Mossbauer spectra, struct. and bonding 0-7224  
 Pd-V, alloy and bilayer, silicide form. solid phase reaction with Si 0-6568  
 Pd-W/Si, contact reactions, backscattering, X-ray diff. meas. 0-20040  
 Pd-Zn, L<sub>10</sub> type intermetallic phase, X-ray diff. study of lattice compression 0-49182  
 Pd-Zr, metallic glasses, valence band struct. investigation 0-11533  
 Pd<sub>0.96</sub>Ag<sub>0.04</sub>, phonon dispersion curves at 296K 0-24546  
 Pd<sub>2</sub>Ag<sub>1-x</sub>, possibility of superconductivity 0-10862  
 PdAgFe, ferromag., Curie temp. depend. on susceptibility, non-mean field theory 0-44829  
 PdAl-Fe(Ni), phase diagrams, eutectic points and solubility (Russian) 0-40333  
 Pd<sub>2</sub>AlCu-PdAl system, interactions and solid-state transforms (Russian) 0-16272  
 (Pd<sub>1-x</sub>Au<sub>x</sub>)<sub>0.99</sub>Co<sub>0.01</sub>, mag. hyperfine interaction for impurity Co atoms (Russian) 0-7078  
 $\gamma$ -Pd<sub>8</sub>Co<sub>43</sub>, X-ray cryst. struct. determ. 0-54172  
 PdCo, effect of hydrogenation on thermopower 0-39562  
 Pd<sub>0.775</sub>Cu<sub>0.06</sub>Si<sub>0.165</sub> glass, optical props. in energy range 0.67 to 5.6 eV 0-34872  
 Pd<sub>77.5</sub>Cu<sub>6</sub>Si<sub>16.5</sub>, metallic glass, composition, mech. props., simulation 0-49117  
 Pd<sub>77.5</sub>Cu<sub>6</sub>Si<sub>16.5</sub> metallic glass wire, cold drawing 0-50650  
 Pd<sub>77.5</sub>Cu<sub>6</sub>Si<sub>16.5</sub>, ternary miscibility gap, simulation, dispersed phase composite form. 0-54379  
 Pd<sub>2</sub>Fe foil, L<sub>12</sub> superstructure, antiphase boundary orientation and energy 0-39112  
 PdFe<sub>1-x</sub>Cr<sub>x</sub> ordering alloys, elec. resist., temp. depend. (Russian) 0-24866  
 Pd<sub>0.98</sub>Fe<sub>0.01</sub>Gd<sub>0.01</sub>, ferromag., Pd-Gd exchange const. and Pd polarisation, neutron scatt. meas. 0-25122  
 (Pd<sub>0.9965</sub>Fe<sub>0.0035</sub>)Mn<sub>0.05</sub>, ferromag. and spin-glass props. 0-2590  
 PdFeRh, ferromag., Curie temp. depend. on susceptibility, non-mean field theory 0-44829  
 PdH<sub>x</sub>-Fe, dil., Kondo system, local moment hyperfine studies, Mossbauer expt. 0-39908  
 PdH<sub>x</sub>(D<sub>x</sub>) films, electron-phonon coupling, elec. cond. obs. 0-50011  
 PdIn, refractive index, reflectivity and band struct., APW calcs. 0-40139  
 Pd(M<sub>2</sub>Co), giant moments, Mossbauer study of <sup>57</sup>Fe 0-44969  
 Pd<sub>2</sub>Mn, disordered, mag. correls., neutron scatt. study 0-50105  
 Pd<sub>2</sub>MnIn<sub>1-x</sub>Sb<sub>x</sub>, Heusler alloy, mag. order obs. 0-29528  
 Pd<sub>2</sub>MnSn, ferromag. Heusler alloy, electronic struct., spin polarisations, theory 0-54598  
 Pd<sub>2</sub>Mn<sub>0.95</sub>Sn<sub>1.05</sub>, hyperfine mag. fields, Mossbauer spectra 0-15870  
 Pd<sub>2</sub>MnSn<sub>1-x</sub>Sb<sub>x</sub>, Mossbauer spectra, mag. hyperfine field 0-15868  
 Pd<sub>60</sub>Ni<sub>20</sub>Si<sub>20</sub>, amorphous, struct., high resolution electron microscopy 0-1969  
 (Pd,Pt<sub>1-x</sub>)<sub>3</sub>Fe atomically ordered alloy, thermoelectric power, carrier energy spin shift, mag. props. 0-29394  
 Pd<sub>0.9</sub>Rh<sub>0.1</sub>, lattice dynamics, inelastic neutron scatt. meas. at 296K 0-29135  
 PdSb, XPS, electronic struct. 0-7464  
 PdSi, amorphous, structural relaxation enhancement following stress reduction 0-3118  
 PdSi, formation by Xe ion beam bombard. of Pd film on Si substrate 0-10800  
 Pd<sub>2</sub>Si, epitaxial film on Si, <sup>4</sup>He ion channelling meas. and RHEED anal. 0-10834  
 Pd<sub>2</sub>Si, formation at Pd-Si (111) interface, UPS obs. 0-24743  
 Pd<sub>2</sub>Si, on Si substrate, thermally induced Si accumulation, AES study 0-24718  
 Pd<sub>80</sub>Si<sub>20</sub>, amorphous, elec. resist. and magnetoresist. 0-49693  
 Pd<sub>80</sub>Si<sub>20</sub>, amorphous, structural changes with neutron irradi., X-ray scatt. obs. 0-33898  
 Pd<sub>80</sub>Si<sub>20</sub> metallic glass, high-resolution XPS study, electronic state struct. 0-29846  
 Pd<sub>80</sub>Si<sub>20</sub>, metallic glass, composition, mech. props., simulation 0-49117  
 PdSiCu, amorphous, US attenuation and vel. studies 0-19881  
 Pd<sub>18</sub>Si<sub>14</sub>Cu<sub>6</sub>, glass, changes in density of states with alloys comp. UPS obs. 0-50531  
 Pd<sub>80</sub>Si<sub>7</sub>Cu<sub>13</sub>, glass, changes in density of states with alloys comp., UPS obs. 0-50531  
 Pd<sub>82-x</sub>V<sub>x</sub>Si<sub>18</sub>, metallic glasses, effect of press. on elec. resist. 0-6805



**palladium alloys continued**

- PdZr, amorphous, supercond., US props. 0-44765  
 Pt-Pd melts, surface tension and density (*Russian*) 0-39388  
 TbPd<sub>3</sub>, specific heat at low temp. 0-20413  
 Ti-Pd (0.15 wt.%), IMI-260, strain rate effect on mech. behaviour 0-3153  
 UPd<sub>3</sub>, crystalline elec. field studies using neutron inelastic scatt. at NRCN 0-10931  
 YbPd-YbAg system, valency state, Yb behaviour (*French*) 0-45277

**palladium compounds**

see also *palladium alloys*

- double oxides, elec. cond. 0-34438  
 layer, galvanostatic desorption of hydrogen, quantitative theory 0-40694  
 mixed valence-mixed metal compounds, ionic crystals, longitudinal lattice modes, Raman spectroscopy 0-40099  
 palladium-octaethylporphyrin, gas phase delayed fluoresc. and phosphoresc., triplet excimer formation 0-18884  
 porphyrin, in n-alkane crystal, Zeeman and crystal field effects, absorpt. vibr. anal. 0-7372  
 Fe<sub>2</sub>Pd<sub>8-10</sub>Si<sub>18</sub> metallic glass, mag. phase diagram, weak ferromagnet-spin glass transition 0-54893  
 Ni-Pd-H, film, struct. and phases formed, when Ni, Pd are sputtered in H 0-29289  
 Pd complex, linear ionic mixed valence cpd., IR and resonance Raman spectra rel. to lattice modes 0-25393  
 Pd complex, Pd<sup>II</sup>(CNCH<sub>3</sub>)<sub>6</sub>(PF<sub>6</sub>)<sub>2</sub>, vibr. spectra, M-M bonds. (*French*) 0-47997  
 Pd-H-Gd, dil., ESR exam. of low temp. region of phase diagram, and electronic props. 0-29930  
 Pd<sub>2</sub>B, and other Pd<sub>2</sub>B<sub>x</sub> cpds., cryst. chem. 0-19769  
 Pd<sub>2</sub>B, cryst. struct., X-ray diffr. study 0-54204  
 PdF<sub>2</sub> fluorite-type form, mag. props., structure studies (*French*) 0-34187  
 PdH<sub>0.97</sub>, high press. modification, cryst. and mag. props. 0-38988  
 PdGdH, diagram of state elec. props., indirect exchange interaction, EPR study (*Russian*) 0-50179  
 PdH, supercond., book contrib. 0-25037  
 β-PdH<sub>0.66</sub>, elastic consts. 4 to 300K, Debye temp. 0-6455  
 PdH<sub>0.97</sub>Fe(Cr), supercond. transition temp. depression, coexistent mag. behaviour 0-49976  
 PdH<sub>1.18</sub>, PdH<sub>1.20</sub>, prep., cryst. struct., chem. comp. determ. by thermal decomp. 0-34334  
 α-PdH<sub>x</sub>, electronic states and Fermi surface props. 0-29310  
 α-PdH<sub>x</sub>, impurity motion, neutron scatt. obs. 0-24682  
 PdH<sub>x</sub>, incoherent phase transition, lattice gas model 0-29171  
 PdH<sub>x</sub>Co(Fe), diffusion and interstitial site occupancy, Mossbauer spectra 0-20555  
 PdO, electronic struct., XPS and UPS study 0-35061  
 Pd(S<sub>2</sub>N)<sub>2</sub>, IR and Raman spectra, normal coord. anal. 0-28019  
 Pd<sub>2</sub>Si, form. from solid phase reaction between Si and Pd-V 0-6568

p.a.m. see *pulse amplitude modulation*

**paper**

see also *paper industry*

- elastic properties, inhomogeneity with reference to basis wt. depend. of elastic moduli (*Japanese*) 0-2110  
 gravure and embossed papers, printability prediction by time series anal. 0-15345  
 laser pulse, position determ. using ordinary paper 0-33046  
 mechanical strength anisotropy, NDT determ., using radiowave method 0-25969  
 non-impregnated, non-destructive breakdowns 0-55035  
 polyethylene resin coated paper formulation for photography 0-4794

**paper industry**

- photographic pulp quality control using He-Ne laser scanning system (*German*) 0-3272

paraelectric materials see *dielectric materials*

**paraelectric resonance**

- nonstationary tunnelling state paraelectric resonance, weak photon coupling (*Russian*) 0-34869  
 KCl:CN<sup>-</sup>, paraelectric reson. study, tunnelling parameters and elec. dipole moment 0-25326

**parallel processing**

- holographic numerical optical processor configurations 0-48194  
 image processing, digital, parallel logic device and half-adder circuit 0-10027  
 residue-based optical processor 0-48169  
 signal processing research programme of United States Air Force 0-48171

paralleled resonator filters see *band-pass filters*

**paramagnetic-antiferromagnetic transitions**

see also *Neel temperature*

- intermediate valence, mag. susceptibility and mag. instabilities 0-39532  
 semiconductor, magnetic phase transitions in impurity band (*Russian*) 0-50097  
 Dy, resistivity anomalies at mag. transitions, sp.ht. 0-39785  
 Dy<sub>1.2</sub>Mo<sub>0.8</sub>S<sub>8</sub>, low temp. heat capacity anomaly rel. to antiferromag. transition in supercond. state 0-25044  
 ErFeO<sub>3</sub>, weak ferromag., high freq. props. in ordering region of spin system, antiferromag. reson. study (*Russian*) 0-2644  
 Eu<sub>2</sub>Sb<sub>3</sub>, cryst. struct., elec. and mag. props. 0-33958  
 Fe-Mn mag. contributions to γ-ε phase transformations 0-25694  
 GdCrO<sub>3</sub>, EPR linewidth, Neel point to 700K 0-39849  
 Gd<sub>1.2</sub>Mo<sub>0.8</sub>S<sub>8</sub>, low temp. heat capacity anomaly rel. to antiferromag. transition in supercond. state 0-25044  
 K<sub>2</sub>FeCl<sub>4</sub>(H<sub>2</sub>O), phase diagram, antiferromag., paramag. and spin flop phases 0-44831  
 K<sub>2</sub>FeO<sub>4</sub>, antiferromag., critical fluctuations obs. using Mossbauer spectroscopy 0-39955  
 Mn-Cu alloy, volume effect, paramagnetic-antiferromagnetic and structural transition, lattice consts. 0-39007  
 MnO, antiferromagnetic-paramagnetic phase transition at high press. 0-39778  
 MnTe, resistivity anomalies at mag. transitions, sp.ht. 0-39785  
 PrSb, pressure-induced antiferromag., neutron scatt. study 0-39750  
 TbBe<sub>13</sub>, magnetic structure at low temps., antiferromagnetic, neutron diffraction study (*French*) 0-39743  
 Tb<sub>1.2</sub>Mo<sub>0.8</sub>S<sub>8</sub>, low temp. heat capacity anomaly rel. to antiferromag. transition in supercond. state 0-25044  
 TbP, mag. excitations above antiferromag. ordering temp., inelastic neutron scatt. obs. 0-50112

**paramagnetic-antiferromagnetic transitions continued**

- TbP, neutron scatt. study above paramagnetic-antiferromagnetic transition temp. 0-11159  
 UO<sub>2</sub>, crystalline elec. field studies using neutron inelastic scatt. at NRCN 0-10931  
 V<sub>2</sub>O<sub>3+x</sub>, 0 ≤ x ≤ 0.08, mag. and elec. props. 0-49833  
 V<sub>2</sub>O<sub>5</sub>, spin order, one-dimensional, Neel transition 0-39799  
 YCrO<sub>3</sub>, EPR linewidth, Neel point to 700K 0-39849

paramagnetic Curie temperature see *Curie temperature*

**paramagnetic-ferromagnetic**

transitions see *ferromagnetic-paramagnetic transitions*

**paramagnetic properties of substances**

see also *paramagnetic resonance; paramagnetism*

- alkali metal-transition metal double molybdates, susceptibility, 90-800K, moments (*French*) 0-39734  
 anthracene crystals, α-particle induced scintillation, mag. field effects 0-40161  
 borate glass: Ni, absorption spectra, mag. props., coordination behaviour (*German*) 0-40147  
 di-(2,2,6,6-tetramethyl-4-piperidinyl-1-oxyl)-suberate, spin densities, polarised neutron diffr. meas. 0-50037  
 ferrocene related compounds, C<sub>5</sub>R<sub>5</sub>Fe(I)-C<sub>6</sub>R'<sub>6</sub> paramag. sandwiches, Mossbauer study 0-39982  
 graphite intercalation cpds., mag. susceptibility, tight-binding model 0-44796  
 graphite intercalation cpds. with alkali metal, interlayer screening and mag. susceptibility 0-44794  
 graphite-alkali metal intercalation cpds., large anisotropy and stage depend. 0-44795  
 guanidinium vanadium sulphate hexahydrate, singlet ground state system, low temp. mag. props. 0-44843  
 lanthanide complexes, paramag., and shift reagents, NMR, book contrib. 0-53023  
 lymphocytes, living and dead, mag. props. and mag. sedimentation 0-35925  
 metal borides, MM'<sub>2</sub>B<sub>4</sub> (M=Y,R; M'=Os,Ir), mag. meas., Curie Weiss behaviour 0-20375  
 metals, polarised neutron studies of the field induced magnetisation 0-25084  
 Na<sub>2</sub>V<sub>2</sub>Ti<sub>6</sub>O<sub>16</sub>, characterisation and mag. props., 90-800K, Na<sub>x</sub>Ti<sub>6</sub>O<sub>8</sub> bronze isotypes (*French*) 0-39735  
 neptunium cyclopentadienyl compounds, (C<sub>5</sub>H<sub>5</sub>)<sub>3</sub>NpX, (X=F, Cl, Br, I, (SO<sub>4</sub>)<sub>1/2</sub>), mag. susceptibility 0-11152  
 organic paramagnetic systems, multiple internal motions, nucl. spin dipolar relax. obs. 0-28037  
 phosphate glass: Ni, absorption spectra, mag. props., coordination behaviour (*German*) 0-40147  
 polarised neutrons in condensed matter [conference, Zaborow, Poland (Sept. 1979)] 0-22136  
 rare earth dodecaborides, mag. susceptibility temp. depend., 90-1200K 0-20374  
 rare earth intermetallic compounds with Cu<sub>3</sub>Au structure, crystal field splitting 0-54663  
 rare earth metasilicates, R<sub>2</sub>(SiO<sub>3</sub>)<sub>3</sub>, mag. susceptibility, temp. depend., 77-800K 0-20372  
 rare earth molybdates, cryst. growth, cryst. chem., and phys. props., book contrib. 0-44194  
 rare earth oxides, binary, struct. and props., book contrib. 0-45292  
 rare earth-iron, RFe<sub>2</sub>, Laves phase intermetallics, ordered and paramagnetic phases, mean field exchange consts. 0-50084  
 spin cross-relaxation, temp. depend. of transition probability 0-25184  
 steel, austenitic stainless, magnetic susceptibility and magnetisation, low temp. 0-25102  
 steel, Cr-Ni-Mo-V, magnetic induction, struct. dependence (*Czech*) 0-50141  
 TCNQ complexes with ferrocenes, charge transfer type, struct. and mag. props. 0-24439  
 TCNQ salt, tetramethylhexamethylenediammonium-TCNQ-iodine, elec. and mag. props., struct., specific heat 0-24898  
 TCNQ salt, TMTSF-DMTCNQ, mag. susceptibility meas. under press. 0-29521  
 TMMC, one-dimensional paramag., anomalous freq. depend. of EPR linewidth 0-15784  
 transition metal borides, narrow band types, electronic density of states, many-electron Hubbard model calcs. 0-20064  
 transition metals, photoemission spectra, core-level satellite struct. 0-29855  
 transition metals and alloys, 3d, Hall effect, electron scatt. processes 0-34419  
 TTF-TCNQ, phase transitions and CDW state, controlled disorder effects 0-15507  
 TTT<sub>2</sub>(I<sub>3</sub>)<sub>x</sub>, physical props., elec., mag. and optical meas. 0-24908  
 Al<sub>2</sub>O<sub>3</sub>:V<sup>3+</sup>, magnetocaloric effect in high magnetic fields 0-25140  
 (Al<sub>2</sub>O<sub>3</sub>:Fe<sub>2</sub>O<sub>3</sub>):Cr<sup>3+</sup>, (0.04 mol.% Fe<sub>2</sub>O<sub>3</sub>), paramag., cross relax., annealing temp. effect from Mossbauer meas. 0-44983  
 BH,  $\Sigma^+$  ground state, mag. susceptibility, paramag. contrib., large config. interaction wave function calcs. 0-47899  
 CdF<sub>2</sub>:Cu, paramagnetic centre coordination, g-tensor orientation by anisotropy of <sup>19</sup>F ENDOR 0-54993  
 Cd<sub>1-x</sub>In<sub>x</sub>Cr<sub>2</sub>Se<sub>4</sub>, electric, photoelectric and mag. props., metal-semicond. transition (*Russian*) 0-34738  
 Cd<sub>1-x</sub>Mg<sub>x</sub>, magnetic susceptibility anisotropy, press. effects, electronic phase transitions (*Russian*) 0-54869  
 CdPS<sub>3</sub>, layered, organometallic intercalates, X-ray diffr., optical absorpt. and mag. props. 0-45103  
 Ce, liq., 4f electron susceptibility temp. depend. 0-20378  
 CeCu<sub>2</sub>Si<sub>2</sub>, strong Pauli paramagnetism, superconductivity obs. 0-29499  
 CeSn<sub>3</sub>, polarised neutron study of induced magnetisation 0-34594  
 CeX (X=P, As, Sb, Bi), neutron inelastic scatt. expts. 0-19674  
 Co, FCC, self-diffusion and isotope effect, influence of mag. order-disorder transition 0-29205  
 Co-V, solid and liq., mag. susceptibility and electronic struct. 0-39738  
 Co<sub>1-x</sub>Cu<sub>x</sub>Cr<sub>2</sub>S<sub>4</sub>, paramag. susceptibility 0-20373  
 (Co<sub>1-x</sub>Mn<sub>x</sub>)B, M=Mn or Fe, paramag., spin echo NMR spectra, ferro-mag. transition, spin-lattice relax. 0-29645  
 (Co<sub>1-x</sub>Mn<sub>x</sub>)<sub>2</sub>B, 0 ≤ x ≤ 1, magnetisation, lattice consts., press. depend. of Curie temp. 0-7137  
 CoS<sub>2</sub>:Se<sub>x</sub>, conc. and temp. effects on metamagnetic transition 0-15716  
 Cr, Hartree band struct., Fermi surface, nesting wave vector 0-49583  
 Cr-Co-V alloys, dil., elec. resist. min. 0-54680



## paramagnetic properties of substances continued

- Cr-Ni(V), dil., mag. susceptibility, 77 to 400K (*Russian*) 0-50066  
 Cr<sub>0.5</sub>NbSe<sub>2</sub>, cryst. struct., metallic cond., mag. and phys. props. (*French*) 0-33956  
 CrSe<sub>2</sub>, layered, phys. and elec. props. 0-44594  
 Cs fluid, metallic and nonmetallic, mag. props. 0-44799  
 Cs<sub>3</sub>K<sub>2</sub>Br<sub>6</sub>(Cl<sub>6</sub>)(F<sub>6</sub>), Cs<sub>2</sub>NaTmF<sub>6</sub> and Cs<sub>3</sub>RbTmF<sub>6</sub>, mag. behaviour 2.9 to 251.3K, cryst. field levels, ang. overlap model (*German*) 0-29520  
 Cs<sub>3</sub>KYbF<sub>6</sub>, mag. behaviour, 3.5-251.3K (*German*) 0-50041  
 Cs<sub>3</sub>NaYbF<sub>6</sub>, mag. behaviour, 3.5-251.3K (*German*) 0-50041  
 Cs<sub>3</sub>NaYbF<sub>6</sub>, mag. behaviour, 3.5-251.3K (*German*) 0-50041  
 Cs<sub>3</sub>RbYbF<sub>6</sub>, mag. behaviour, 3.5-251.3K (*German*) 0-50041  
 Cu-Fe, dilute, low temp. heat capacity in mag. field, superparamagnetism 0-39804  
 CuF<sub>3</sub>, <sup>63</sup>Cu NQR meas. 0-50219  
 Cu<sub>2</sub>O-CuO-MoO<sub>3</sub>, subsolidus phase diagram, mag. props. 0-50615  
 Dy, Curie-Weiss law anisotropy, paramag. susceptibility meas. 0-15686  
 Dy<sub>2</sub>Ga<sub>2</sub>O<sub>12</sub>, crystal field effect on paramag. props. of Dy<sup>3+</sup> ion 0-50040  
 Er<sub>2</sub>Te<sub>3</sub>, magnetic susceptibility meas., cryst. field interpretation 0-11156  
 ErVO<sub>4</sub>, produced by Er<sub>2</sub>O<sub>3</sub>+VO<sub>2</sub> high-press. reaction, cryst. struct. and mag. props. meas. 0-19773  
 ErVO<sub>4</sub>, phonon resistivity mag. field depend. in paramag. phase 0-2226  
 EuX(X=O,S,Se) 0-20635  
 EuX(X=O,S,Se), spin-disorder-induced Raman scatt. from phonons, theory 0-20636  
 Fe complex, tetraphenylporphyrinate iron III bromide, mag. props., zero-field splitting 0-34584  
 Fe, paramagnetic, orbital magnetic susceptibility calc. 0-7075  
 Fe-B, amorphous paramag. alloys, hyperfine field distrib., Mossbauer study 0-39958  
 Fe-Ni, thermal expansion, ferromagnetic-paramagnetic transition (*Russian*) 0-54412  
 Fe-Ni, thermodynamic props., anomalous 0-39313  
 Fe-Ni ordered phase in meteorites, Mossbauer studies 0-41776  
 Fe-Ni-P-B, amorphous paramag. alloys, hyperfine field distrib., Mossbauer study 0-39958  
 Fe-Ni-Si-B, amorphous paramag. alloys, hyperfine field distrib., Mossbauer study 0-39958  
 Fe-Ni(Co), solid and liq., paramag. susceptibility and electron struct., 800-1800°C (*Russian*) 0-25081  
 Fe-Si amorphous film, struct. and crystallisation, Mossbauer study 0-11300  
 Fe<sub>2</sub>, magnetism, randomised exchange field theory 0-39733  
 FeAs, Mossbauer spectra of paramag. and ferromag. states, helimagnetic spin ordering 0-7197  
 (Fe<sub>0.5</sub>Ni<sub>0.5</sub>)-Co, solid and liq., paramag. susceptibility and electron struct., 800-1800°C (*Russian*) 0-25081  
 (Fe<sub>2</sub>Ni<sub>100-x</sub>)<sub>30</sub>P<sub>10</sub>B<sub>10</sub>, amorphous, elec. resist., 2 to 300K, composition depend. 0-44562  
 Fe<sub>2</sub>Ni<sub>100-x</sub>P<sub>14</sub>B<sub>6</sub> (x=0, 20, 40, 60, 80), metallic glass, low temp. sp. ht. 0-2588  
 (Fe<sub>1-x</sub>Ni<sub>x</sub>)<sub>77</sub>Si<sub>10</sub>B<sub>13</sub> amorphous alloy system, saturation mag. moment, Curie temp., mag. susceptibility 0-39753  
 FeOOH:Cl(F), quadrupole interaction, Mossbauer spectra 0-15895  
 20Fe<sub>2</sub>O<sub>3</sub>.80[3B<sub>2</sub>O<sub>3</sub>(1-x)PbO.xGeO<sub>2</sub>] glass, phys. props. 0-49119  
 FeS<sub>2</sub> (marcasite), temp. depend. mag. susceptibility 0-20391  
 Fe<sub>3-x</sub>Ti<sub>2</sub>O<sub>4</sub>, Mossbauer spectra in paramag. phase 0-39943  
 (Fe<sub>1-x</sub>V<sub>x</sub>)-Ge, magnetic and X-ray studies 0-1966  
 Hf(Fe<sub>1-x</sub>Co<sub>x</sub>)<sub>2</sub>, mag. props., Mossbauer spectra and magnetisation meas. 0-39948  
 HfSe<sub>2-x</sub>Te<sub>x</sub> and HfTe<sub>2-x</sub>, elec. resist. and mag. suscept. studies 0-44599  
 Hg<sub>1-x</sub>Mn<sub>x</sub>Te, mag. susceptibility, 2.4 to 300K 0-20379  
 HoNi<sub>5</sub>, ferromag., magnetisation and paramag. susceptibility 0-25082  
 Ho<sub>2</sub>Y<sub>1-x</sub>Sb<sub>x</sub>, mag. props. 0-34634  
 K, Pauli susceptibility and Knight shift meas., electron wave functions 0-44937  
 K<sub>2</sub>CuCl<sub>4</sub>.2H<sub>2</sub>O, paramag. single cryst., PMR temp. depend., hyperfine const. and exchange interaction (*Korean*) 0-29630  
 KCuF<sub>3</sub>, <sup>63</sup>Cu NQR meas. 0-50219  
 La, FCC, NMR 4.2 to 296K, mag. susceptibility and sp. ht. 0-15813  
 LaNi<sub>1-x</sub>Mn<sub>x</sub>O<sub>3</sub>, <sup>55</sup>Mn NMR study, magnetisation meas., ferromag. and Pauli paramag. components 0-7191  
 La<sub>1-x</sub>Tb<sub>x</sub>Ag(Sn<sub>3</sub>)(Al<sub>2</sub>), paramag. anisotropy of Tb<sup>3+</sup> in cubic cryst. field 0-15687  
 Li-transition metal dioxide intercalation compounds, mag. props., decomposition effects 0-25075  
 LiTmF<sub>4</sub>, strongly isotropic Van Vleck paramag., nucl. spin interaction (*Russian*) 0-34792  
 MgO:Mn<sup>2+</sup>, clustering of mag. ions, study method 0-11155  
 Na<sub>2</sub>Co<sub>2</sub>Ti<sub>2</sub>O<sub>4</sub>F<sub>2</sub>, characterisation and mag. props., 90-800K, Na<sub>x</sub>Ti<sub>4</sub>O<sub>8</sub> bronze isotypes (*French*) 0-39735  
 Na<sub>2</sub>Cr<sub>2</sub>Ti<sub>2</sub>O<sub>4</sub>F<sub>2</sub>, characterisation and mag. props., 90-800K, Na<sub>x</sub>Ti<sub>4</sub>O<sub>8</sub> bronze isotypes (*French*) 0-39735  
 Na<sub>2</sub>FeTi<sub>2</sub>O<sub>4</sub>F<sub>2</sub>, characterisation and mag. props., 90-800K, Na<sub>x</sub>Ti<sub>4</sub>O<sub>8</sub> bronze isotypes (*French*) 0-39735  
 Na<sub>2</sub>Ni<sub>2</sub>Ti<sub>2</sub>O<sub>4</sub>F<sub>2</sub>, characterisation and mag. props., 90-800K, Na<sub>x</sub>Ti<sub>4</sub>O<sub>8</sub> bronze isotypes (*French*) 0-39735  
 Nb-S system, phase relations at high temp., elec. and mag. props. 0-29932  
 Nd<sub>2</sub>Eu<sub>1-x</sub>B<sub>6</sub> solid solution, mag. susceptibility, lattice parameters, Weiss temp. 0-29535  
 Ni-Co, solid and liq., paramag. susceptibility and electron struct., 800-1800°C (*Russian*) 0-25081  
 Ni-Cu, Ni-rich, temp. depend. resist. 0-10943  
 Ni-Ti, Ni-rich, temp. depend. resist. 0-10943  
 Ni-V, solid and liq., mag. susceptibility and electronic struct. 0-39738  
 PbSe, electron gas magnetisation, energy band parameters determ., use of Faraday effect 0-45047  
 PbSe, Faraday effect and electron gas magnetisation, Kane two band model calcs. (*Russian*) 0-34899  
 Pb<sub>1-x</sub>Sn<sub>x</sub>Te, Faraday effect and electron gas magnetisation, Kane two band model calcs. (*Russian*) 0-34899  
 Pb<sub>1-x</sub>Sn<sub>x</sub>Te: Mn, Mn mag. and elec. active states, mag. impurity behaviour 0-44627  
 Pd-Co, dilute, extraordinary Hall effect meas., 2-250K 0-34420  
 Pd<sub>80</sub>Si<sub>20</sub>, amorphous, elec. resist. and magnetoresist. 0-49693  
 Pr compounds, Van Vleck paramagnets, mag. props., anisotropy from NMR anal. 0-54862  
 Pr-Nd (5 at.%), paramag. excitation spectrum, CPA calc. 0-50043  
 PrNi<sub>3</sub>, metallic Van Vleck paramag., nucl. interactions, NMR meas. 0-44953

## paramagnetic properties of substances continued

- RbCuF<sub>3</sub>, <sup>63</sup>Cu NQR meas. 0-50219  
 SeSi, paramag. susceptibility 0-50035  
 Si, electron-hole drops, nonequilibrium paramagnetism 0-6749  
 Si:B, heavily doped, paramagnetic props., anomalous hole spin susceptibility (*Russian*) 0-54861  
 Si:Cr<sup>3+</sup> EPR spectra and spin state population inversion with unpolarised optical lighting (*Russian*) 0-44909  
 Sm<sub>2</sub>S<sub>4</sub>, mag. susceptibility meas., valence state of Sm 0-15684  
 Sr<sub>2</sub>Fe<sub>2</sub>Ru<sub>2</sub>O<sub>4</sub> solid soln., Mossbauer spectrosc. study 0-50235  
 SrRFeO<sub>4</sub>, (R=La,Pr,Nd), Mossbauer spectra, spin reorientation 0-15880  
 TbNi<sub>5</sub>, ferromag., magnetisation and paramag. susceptibility 0-25082  
 TbP, mag. excitations above antiferromag. ordering temp., inelastic neutron scatt. obs. 0-50112  
 TbP, neutron scatt. study above paramagnetic-antiferromagnetic transition temp. 0-11159  
 Tb<sub>2</sub>Y<sub>1-x</sub>Sb<sub>x</sub>, elec. resist., cryst. field and exchange interaction contribs. 0-39556  
 Tc, paramagnetic form factor, polarised neutron diffr. study 0-39745  
 Th<sub>2</sub>Fe<sub>3</sub>, Mossbauer spectra, mag. props. 0-15852  
 Ti<sub>0.5</sub>NbSe<sub>2</sub>, cryst. struct., metallic cond., mag. and phys. props. (*French*) 0-33956  
 TiCoF<sub>3</sub>, paramagnetic, nonmagnetic atomic nuclei spin density, NMR study 0-29633  
 Ti<sub>2</sub>Cr<sub>2</sub>O<sub>7</sub>, Ti<sub>2</sub>Mn<sub>2</sub>O<sub>7</sub>, pyrochlore type, synthesis and physical props. 0-33963  
 Ti<sub>2</sub>Se<sub>1-x</sub>, liquid semiconductor, diamagnetism and paramagnetism, dangling bond paramag. centres, mag. susceptibility obs. 0-44797  
 U(Co<sub>2</sub>Ni<sub>1-x</sub>)<sub>2</sub>, cryst. struct. and mag. props. at 4.2K 0-54175  
 UGe<sub>2</sub>, magnetisation density, neutron scatt. meas. 0-50038  
 U(OH)<sub>2</sub>SO<sub>4</sub>, mag. susceptibility, heat capacity anomalies at 21K 0-11151  
 UPd<sub>3</sub>, crystalline elec. field studies using neutron inelastic scatt. at NRCN 0-10931  
 U<sub>2</sub>Si, crystalline elec. field studies using neutron inelastic scatt. at NRCN 0-10931  
 USn<sub>3</sub>, crystalline elec. field studies using neutron inelastic scatt. at NRCN 0-10931  
 V, orbital magnetic susceptibility calc. 0-7075  
 (V<sub>1-x</sub>Cr<sub>x</sub>)<sub>2</sub>Si, mag. susceptibility, 4.2 to 320K, density of states model 0-7035  
 V<sub>1-x</sub>Fe<sub>x</sub>, low temp. sp. ht. and mag. props. 0-2548  
 V<sub>1-x</sub>Fe<sub>x</sub>H<sub>n</sub>, low temp. sp. ht. and mag. props. 0-2548  
 V<sub>0.5</sub>NbSe<sub>2</sub>, cryst. struct., metallic cond., mag. and phys. props. (*French*) 0-33956  
 V<sub>3</sub>O<sub>5</sub>, high-temp. phase transition, resistivity, valence photoelectron spectra 0-49357  
 V<sub>3</sub>O<sub>7</sub>, microscopic mag. props., NMR 0-7177  
 V<sub>2</sub>S<sub>8</sub>, paramag. cryst., struct. factors using polarised neutron diffr. 0-15691  
 Y<sub>2</sub>Cr<sub>2</sub>O<sub>7</sub>, Y<sub>2</sub>Mn<sub>2</sub>O<sub>7</sub>, pyrochlore type, synthesis and physical props. 0-33963  
 Y<sub>2</sub>Er<sub>1-x</sub>Al<sub>2</sub>, paramag. anisotropy 0-39737  
 Y<sub>6</sub>(Fe<sub>1-x</sub>Mn<sub>x</sub>)<sub>23</sub>, struct. and mag. props. 0-25083  
 YFe<sub>2</sub>O<sub>4</sub>, Mossbauer spectra of <sup>51</sup>Fe in antiferromag. and paramag. states 0-15834  
 (Y<sub>1-x</sub>Gd<sub>x</sub>)Co<sub>2</sub>, spin echo NMR of mag. states 0-7190  
 YNi<sub>3</sub>, loss of ferromagnetism after H<sub>2</sub> absorpt., Pauli paramag. props. 0-34588  
 YbS<sub>1.387</sub>, magnetic and thermal props. 0-34586  
 ZnCr<sub>2</sub>Se<sub>4</sub>:Mn, paramagnetic, giant cubic anisotropy 0-7073  
 Zr, magnetic form factor, field-induced, polarised neutron scatt. meas. 0-50044  
 Zr<sub>1-x</sub>Nb<sub>x</sub>Zn<sub>2</sub>, microscopic mag. props., NMR investigation 0-15807

## paramagnetic resonance

- see also acoustic paramagnetic resonance; CESR; CIDEP; electron spin-lattice relaxation; ENDOR; EPR line breadth; paramagnetic resonance of colour centres; paramagnetic resonance of free radicals; paramagnetic resonance of ions and impurities; spin echo (EPR); spin-spin relaxation  
 adamantane ceramic, structural, thermophysical and electrophysical props. 0-6918  
 alternating magnetic field meas. using EPR 0-52277  
 amorphous and liquid semiconductors, conference, Cambridge, MA, USA (Aug. 1979) 0-41933  
 anisotropic fluid, diffusion, EPR spin exchange and nuclear spin relax., theory 0-34753  
 anthracene-tetracyanobenzene crystals, deuteration effect on phase transition, triplet state EPR study 0-50163  
 bounded medium, nonlinear paramagnetic reson., limit cycle solns. 0-19071  
 crystal field theory, finite symmetry adaptation in spectroscopy 0-43032  
 dating of minerals by EPR method 0-36415  
 digital data acquisition using microprocessor 0-17975  
 DNA conformation, influence of intermol. interactions 0-16900  
 dynamic magnetoresonance effects in solids 0-20447  
 ferredoxin, soluble, investigation of 2 forms from pea leaves 0-45851  
 glauconite group minerals, Norwegian-Greenland basin, age determ. by EPR and Mossbauer spectra 0-26467  
 graphite, EPR, effect of motional averaging, anisotropy, skin effect rel. to heat treatment and neutron irradiation (*French*) 0-34752  
 intensity operator and its use in exact analysis of EPR line intensities 0-20448  
 Jahn-Teller effect, intermediate, in orbital triplet, effect on EPR 0-34756  
 Ka-band EPR/ENDOR spectrometer, modified, obs. of electron spin echoes at 35 GHz 0-13113  
 low temperature spectra, inexpensive quick-freeze technique 0-9012  
 magnetic field modulator, EPR radiospectrometer having discrete set of modulation frequencies 0-52285  
 methanol dehydrogenase, enzyme, electron spin echo, 35 GHz 0-13113  
 methanol glass solvated electrons, EPR, <sup>1</sup>H spin flip satellites, geometrical model 0-7146  
 microemulsions, struct. aspects, using dielec. relax. and spin label techniques 0-26199  
 molecular motion dynamics in crystal influence on spectral parameters of NQR, NMR and EPR 0-20486  
 molecules or clusters, interpretation of data from Mossbauer, ESR, susceptibility, optical and XPS meas. 0-37825  
 montmorillonite group minerals, Norwegian-Greenland basin, age determ. by EPR and Mossbauer spectra 0-26467



**paramagnetic resonance continued**

nanosecond time-resolved EPR in pulse radiolysis via spin echo method 0-43075  
 organic charge-transfer salts, comparison of ESR spectra 0-50164  
 paramagnetic crystal resonator dynamics, low temp. anomalies (*Russian*) 0-7147  
 polyacetylene, pristine and acceptor doped isomers, EPR, DC cond., evidence against solitons 0-15782  
 polyacetylene, thin film, ESR study, effects of O<sub>2</sub>, NO and halogens 0-25186  
 polyarylenealkyls, colour, EPR, electron density delocalisation degree determ. (*Russian*) 0-7152  
 polypropylene fibres,  $\gamma$ -irrad., microstruct. changes in glassy-high elastic state transition (*Rumanian*) 0-49347  
 polyvinylcarbazole-trinitrofluorenone, organic photoconductor, photoinduced paramag. centres 0-25188  
 $\alpha$ -quartz, hydrogenic trapped hole species, EPR studies 0-44915  
 quartz, muonium EPR transitions by muon-spin rot. 0-29668  
 'reduced' spectra calc. 0-23444  
 review of magnetic resonance, book contrib. 0-11242  
 rotation of US plane of polarisation under ESR saturation conditions 0-29123  
 saturation spectrum, effect of strong microwave field 0-15785  
 significance plots use in spectra interpret. 0-22409  
 solutions, bibliography of 1975-76 literature 0-51979  
 spin glass, EPR frequency and mag. transverse susceptibility with remanent magnetisation (*French*) 0-7145  
 spin Hamiltonian, perturbation treatment, M=0 electronic state, HFS of triplet state EPR 0-25185  
 superionic conductors, mag. reson., book contrib. 0-25240  
 TCNQ salt, N-n-butyl-quinolinium (TCNQ)<sub>2</sub>, ESR spectrum fine struct. splitting 0-44904  
 TCNQ salt, quinolinium, electron spin location, elec., mag., and thermal props. 0-25189  
 TCNQ salt, tetramethylhexamethylenediammonium-TCNQ-iodine, elec. and mag. props., struct., specific heat 0-24898  
 TCNQ salts, aminopyridinium (TCNQ)<sub>2</sub>, elec. and mag. props., 4.2 to 300K 0-24889  
 time resolved EPR spectroscopy, stopped flow EPR apparatus for biological appl. 0-36206  
 TTF(MBDT) spin-Peierls transition, mag. exchange interactions, mag. props. 0-25138  
 TTF-TCNQ series, cryst. struct., elec. cond., and EPR meas., steric factor effects 0-19789  
 As<sub>2</sub>Te<sub>3</sub>, amorphous, defect and impurity states, hopping cond. obs., EPR meas. 0-54650  
 C, amorphous, diamond-like 3-fold coord. 0-50323  
 Cd(CIO<sub>4</sub>)<sub>2</sub> irradiated single crystal, ESR and annealing, trapped defect centre 0-55141  
 GaAs (100) surface struct. determ. by LEED, UPS, and EPR 0-49475  
 Ge amorphous film, effects of alloying halogen atoms 0-49670  
 Ge, neutron irradiated, positron annihilation, ESR and resist. meas. 0-15160  
 Ge powder, diamag., strong mag. particle form., mag. props., EPR (*Russian*) 0-54863  
 Ge-S, amorphous, photocond., photo-induced ESR, optical edge shift 0-49809  
 Ge-S amorphous film, defect states, ESR 0-49670  
 GeSe<sub>2</sub>, amorphous film, photocond., photo-induced ESR, optical edge shift 0-49809  
<sup>199</sup>Hg optically oriented atom interaction with cell wall paramag. centres 0-37762  
<sup>127</sup>I atoms in Xe matrices, EPR spectrum 0-1005  
 InSb (110) surface struct. determ. by LEED, UPS, and EPR 0-49475  
 InSb, electron spin relaxation 0-25187  
 Li<sub>2</sub>O-LiCl-B<sub>2</sub>O<sub>3</sub> system, fast Li<sup>+</sup> ion vitreous superconductors, EPR study (*French*) 0-11269  
 (NH<sub>4</sub>)<sub>2</sub>BeF<sub>4</sub>,  $\gamma$ -irrad. cryst., F<sub>2</sub><sup>-</sup> ions, ESR meas. 0-34770  
 OCS, gas, EPR of rot. transitions, T<sub>1</sub> press. depend. 0-9621  
 OCS+He(Ne)(Ar)(Kr)(H<sub>2</sub>)(O<sub>2</sub>)(CO<sub>2</sub>), gas, EPR of rot. transitions, T<sub>1</sub> press. depend. 0-9621  
 Se, glassy, pure and K-doped, photolum. and optically induced ESR 0-50398  
 Si, amorphous, spin depend. recomb., luminesc. and light induced ESR 0-50393  
 Si, amorphous, structural defects EPR 0-25208  
 Si amorphous film, dangling bond ESR, light-induced quenching 0-50162  
 Si, amorphous film, RF-sputtered, influence of O<sub>2</sub> and deposition conditions, elec. cond., IR absorpt. and ESR 0-2949  
 Si, deformed, photo-EPR of dislocations 0-11267  
 Si, ESR in neutron transmutation doped samples 0-20462  
 Si implanted layers, interaction of defects and impurities stimulated by induced ionisation, ESR 0-11270  
 Si, laser annealed, EPR and cyclotron resonance 0-34773  
 Si surface interacting with adsorbed gases, paramag. props., EPR study 0-34772  
 Si:As, implanted through SiO<sub>2</sub> films, elec. props., defect struct. 0-54264  
 Si:B, heat treatment centres changes, EPR obs. 0-29601  
 Si:H, amorphous, defect creation and H evolution 0-50392  
 Si:H, amorphous, exodiffusion of H, EPR expts. 0-49102  
 Si:H, amorphous, light-induced ESR and photoluminesc., dangling bonds with positive correl. energy 0-50161  
 Si:H film, amorphous, bombarded, defects, luminesc. and ESR meas. 0-34977  
 Si:H(D), amorphous films, CVD, post-hydrogenation 0-54552  
 Si-H, amorphous, plasma-deposited, H evolution and defect creation 0-44914  
 Si-SiO<sub>2</sub> interface, light induced reson. centres, photocond. reson., EPR obs. 0-50184  
 Si<sub>3</sub>As<sub>2</sub>-H, amorphous system, struct. and defects, Raman and EPR meas. 0-49103  
 SiO-B<sub>2</sub>O<sub>3</sub> composite dielec. films, EPR, dangling bonds and dielec. loss 0-11246  
 SiO<sub>2</sub>, vitreous, heat treatment effect on viscosity and struct. 0-19714  
 TTF-TCNQ, pure and irrad., nonlinear transport, ESR study, 1.2-4.2K 0-20167  
 ZnCrFeO<sub>4</sub>, ferrite spinel, unsupported and SiO<sub>2</sub> supported, structural and catalytic studies 0-44191  
 ZnTe (110) surface struct. determ. by LEED, UPS, and EPR 0-49475

**paramagnetic resonance of colour centres**

inc. other defects involving initial vacancy or interstitial formation  
 alkali halides, <sup>14</sup>N impurities, molecular point defects, EPR isotropic hyperfine triplets 0-2636  
 alkali halides, spin lattice relax. and g-shift 0-15799  
 diamond: Sb, ion implanted, defect study using optical absorpt. and EPR 0-24480  
 diamond, type-IIa, electron irrad., EPR spectrum 0-25210  
 nonmetallic crystals, ENDOR of impurity centres 0-25249  
 quartz, synthetic, electron beam irrad., defect form., annealing and migration effects, ESR obs. 0-50180  
 quartz, synthetic, electron beam irrad.-induced interstitial ion mobility, ESR centres and IR spectra meas. 0-39153  
 silicate glass, dangling bond states 0-24846  
 AgBr:Pd(II), photolysis-induced trapping behaviour, EPR study 0-54949  
 AgCl, paramagnetic S-centres, saturation props., ESR meas. 0-50181  
 $\beta$ -Al<sub>2</sub>O<sub>3</sub>-K<sub>2</sub>O(Na<sub>2</sub>O)(H<sub>2</sub>O)<sup>+</sup>, ESR of paramag. defects in cond. planes 0-29617  
 B-C system, struct. of paramag. centres 0-20460  
 BaO-Al<sub>2</sub>O<sub>3</sub>-B<sub>2</sub>O<sub>3</sub>:Ag, X-ray irrad., atomic centre interactions, EPR spectra 0-25207  
 BaSO<sub>4</sub>, X-ray irrad., electron and holes traps, g-factors, ESR obs. 0-50183  
 BaTiO<sub>3</sub>, H<sub>2</sub>-reduced, elec. cond. mechanism, EPR, resist. and Seebeck coeff. meas. 0-10976  
 CaF<sub>2</sub>:U, U<sup>3+</sup> centres, nonoctahedral symmetry 0-11266  
 CaSO<sub>4</sub>,  $\gamma$ -irradiated, ESR and bleaching studies of radical ion centres 0-2637  
 GaP:Fe(Cr), photo-ESR of annealed crystals, 0-15795  
 Ge,Se<sub>1-x</sub>, amorphous, excitation spectra of photolum. fatigue and creation of paramag. centres 0-50402  
 KBr:Na, U-centres, HFS and g-factor, EPR spectra 0-39869  
 KCN:HCN<sup>-</sup>, structural props. using ESR 0-25205  
 KCl:Ga(In), ESR of impurity centres, impurity optical absorpt. bands 0-29618  
 KCl:H, dichroic H- and U-centres by polarised bleaching of interstitial H, ESR study 0-29766  
 KCl:SnCl<sub>2</sub>, X-ray irrad., polarised luminesc. and EPR study of Sn<sup>3+</sup> centres 0-39868  
 KCl:Sr, triplet state of F<sub>2</sub>-centres, ESR spectra 0-29616  
 KClO<sub>4</sub>, X-irrad. induced paramag. defects, ESR study 0-24493  
 LiF, V<sub>i</sub> centre (F<sub>2</sub><sup>-</sup>) identification, ESR spectrum anal. 0-7164  
 MoO<sub>3</sub>, amorphous films, EPR of Mo<sup>3+</sup> centres 0-34771  
 NaCl:Ga(In), ESR of impurity centres, impurity optical absorpt. bands 0-29618  
 NaCl:Li, U-centres, HFS consts., g-factor, EPR spectra 0-39869  
 RbCl:Na, U-centres, HFS consts., g-factors, EPR spectra 0-39869  
 Si, divacancies orientation induced by IR light, EPR spectra 0-25209  
 Si, electron irrad., two-vacancy defect EPR 0-29619  
 Si-SiO<sub>2</sub>, ESR centres, interface states and oxide fixed charge 0-2474  
 Si-SiO<sub>2</sub> interface, electrically active paramag. centres detect., photocond. reson. obs. 0-50185  
 SiO<sub>2</sub>, dangling bond states 0-24846  
 SiO<sub>2</sub>, glass, <sup>29</sup>Si hyperfine struct. of E' centre, microwave saturation props. 0-7165  
 SiO<sub>2</sub>, glass, irrad., EPR of Al E' centres 0-11268  
 SiO<sub>2</sub>, vitreous, low temp. thermal props. and intrinsic defects 0-29057  
 WO<sub>3</sub> films, ESR study after colouring by H<sub>2</sub> injection and after bleaching in air 0-39867

**paramagnetic resonance of conduction electrons see CESR****paramagnetic resonance of free radicals**

AA 0-25212  
 acetate radical CIDEP, appl. of ns time-resolved EPR in pulse radiolysis 0-43075  
 agriculture applications 0-56298  
 alcohols, glassy, diffusion of radical-ion pairs, spatial distrib., electron spin echo obs. 0-29622  
 benzene, plasma polymerisation in glow discharge, thin film IR and free radical EPR obs. 0-2964  
 biomolecules, conformation and struct., ESR, NMR and optical meas. 0-26201  
 biphenyl single crystals,  $\gamma$ -ray induced radicals, EPR and optical absorpt. studies 0-44921  
 biradical metal chelates, rot. motion in polar solvents, rel. to ESR line-shape 0-27994  
 cis-butene, ozonolysis, radical form., matrix ESR spectrosc. 0-16653  
 coronene trimer radical cation, spin densities in CH<sub>3</sub>Cl<sub>2</sub>-CH<sub>3</sub>NO<sub>2</sub> solvent mixture, -100°C 0-5565  
 cyclic monocarboxylic acid radicals, ring inversion barriers, EPR 0-53025  
 cyclohexane, neutron irradiation, radical distribution, ESR study (*Japanese*) 0-44920  
 5,6-dihydro-6-methyluracil, X-ray irrad., free radical form; ESR spectra obs. 0-50189  
 dihydrouracil, EPR study of light- and temp.-induced free radical conversions 0-35824  
 1,3-dimethyluracil, non-hydrogen bonding crystal, radical formation 0-35552  
 diphenylhaloselenium radical trapped in single crystals, FSR, struct. 0-44919  
 diphenylselenone crystals, gamma irradiation, ESR study of trapped phenylselenonyl radical 0-44917  
 DNA costacking nucleotides,  $\gamma$ -irrad., charge-migration phenomena, EPR obs. 0-36015  
 ethyl radical, <sup>13</sup>C <sub>$\alpha$</sub>  and H<sup>+</sup> hyperfine interactions, EPR spectra, vibr. anal. 0-23443  
 ethyl radical proton exchange reaction with ethylene matrix, indirect ESR obs. 0-16700  
 ethylene, ozonolysis, radical form., matrix ESR spectrosc. 0-16653  
 fast reaction kinetics meas. by ESR of free radicals 0-21286  
 fatty acids, unsaturated, containing peroxide oxidation products, free radicals formed on UV irrad. 0-51165  
 G 0-44099  
 galvinoxyl radical in phenol matrix, ESR spectra 0-54950  
 halide dioxide radical form., H<sub>2</sub>O<sub>2</sub> decomposition of halide-coated surface, EPR obs. 0-7851  
 n-hexyl 4'-n-decyloxybiphenyl-4-carboxylate, smectic C phase, tilt angle using electron reson. spectroscopy 0-33886  
 imidazole, X-irrad., H exchange study 0-40718  
 imidazoles, reaction with photochemically generated  $\alpha$ -hydroxyalkyl radicals, EPR study 0-35558



**paramagnetic resonance of free radicals continued**

- 4-(1-imidazolyl)-phenol, ESR spectra 0-16677  
intracellular membrane microviscosity, rat liver and hepatoma 27  
0-30675  
methyl radical in sodium acetate, EPR spectra, anisotropic hyperfine interaction, rot. tunnelling 0-34775  
1-and 2-methyl-anthraquinone radicals, EPR 'reduced' spectra 0-23444  
 $\alpha$ -methyl-D-glucopyranoside, X-irrad., ESR and ENDOR study of free radicals 0-45526  
6-methyl-mercaptopurine, cryst., light sensitive free radical EPR after electron irrad. 0-7167  
N-acetyl-L-leucine, single crystals, X-ray induced free radicals 0-45525  
(naphthalene)<sup>+</sup> radical pairs, ESR absorption, optical detection 0-7166  
paraaminophenol and paraphenylenediamine analogue molecular complex, free radicals of developers, EPR obs. (Russian) 0-7814  
peptides and derivatives, mol. electron acceptor groups 0-30637  
perdeuterio-N-1-oxyl-2,2,6,6-tetramethyl-4-piperidyl maleimide, spin label, biological EPR 0-32746  
Phase V, nematic, transient response to redirected mag. field, EPR study 0-33879  
phosphines, substituted,  $\gamma$ -irrad. EPR spectra and struct. of free radicals 0-29623  
photolytic generation of transient radicals for EPR spectroscopy 0-11271  
PMMA, neutron irradiation, radical distribution, ESR study (Japanese) 0-44920  
polyethylene, low-density,  $\gamma$ -irrad., spin trapping reaction 0-39873  
polyethylene, neutron irradiation, radical distribution, ESR study (Japanese) 0-44920  
polypropylene, electron bombarded, radical formation, piezoelectric and pyroelectric effects, ESR study 0-7169  
polypropylene, electron bombarded electret, trapped charges ESR study 0-7170  
protein, radical limiting conc. on UV irrad. at 77K, effect of luminesc. quenchers 0-30662  
PTFE, peroxy radical labelled, temp. dependent rots., EPR obs. 0-28125  
pyridine cation radical in trichlorofluoromethane matrix, gamma irrad., EPR and optical obs. 0-23442  
sodium decanoate-n-decanol-water system, lamellar G-phase, orientational-order, EPR investigation 0-24355  
styrene, plasma polymerisation in glow discharge, thin film IR and free radical EPR obs. 0-2964  
dl-tartaric acid, radiation products, ESR-ENDOR OBS. 0-55682  
tartaric acid salts, and deuterated forms, irrad.-crysts., primary reactions, EPR obs. 0-3370  
TCNQ<sup>-</sup>, ESR probe for phospholipid membrane polar head motion study (French) 0-45865  
2,2,3,3-tetramethylbutane,  $\gamma$ -irrad., EPR spectrum assignment 0-15800  
2,2,3,3-tetramethylbutane, radiolysis, radical prods., EPR obs. 0-32747  
TGS X-irradiated, paramag. relax, spin-echo study 0-7168  
l-thioproline single cryst., X-irrad., ESR and ENDOR study of radicals 0-45528  
tissue, animal, lyophilised, paramagnetic centres 0-30681  
trimethylenemethane, ground state triplet, HFS, EPR obs. 0-50188  
TTT<sub>2</sub>(I<sub>2</sub>)<sub>1+x</sub>, physical props., elec., mag. and optical meas. 0-24908  
uridine 5'-phosphate (Na salt), NO<sub>2</sub> species in an irrad. single crystal 0-40719  
n-vinyl carbazole, radiation induced polymerization ESH study 0-7817  
AlH<sup>+</sup> radical cation, EPR matrix isolation obs., hyperfine components calcs. 0-14158  
AsF<sub>3</sub> intercalation with graphite and benzenoid systems, EPR, NMR and X-ray diffr. obs. 0-19775  
BeO-P<sub>2</sub>O<sub>5</sub>-RO(R<sub>2</sub>O) (R=Li,Na,K,Mg,Ca,Sr,Ba) glasses, gamma irrad., cation modifier effect on radiation centre formation 0-40720  
CO<sub>2</sub>-O<sub>2</sub> radical, on MgO surface, ESR spectrum, mobility effects 0-43076  
Fe(NO<sub>3</sub>)CO radical, form. by Fe(CO)<sub>5</sub> photolysis in NO soln., EPR spectrum 0-53024  
H<sub>2</sub>SO<sub>4</sub>, frozen soln., EPR of trapped H-atoms produced by UV and X-irrad. 0-3369  
KPF<sub>6</sub>, temp. depend. hyperfine interactions of trapped pyramidal radicals 0-44918  
K<sub>2</sub>SO<sub>4</sub>·(NH<sub>4</sub>)<sub>2</sub>SO<sub>4</sub>, X-irrad., EPR of NH<sub>3</sub><sup>+</sup> 0-11272  
MgO surface, mobile (CO<sub>2</sub>-O<sub>2</sub>)<sup>-</sup> radical, ESR spectrum 0-43076  
MgTiO<sub>3</sub>, ESR study of Fe<sup>3+</sup> 0-50173  
(NH<sub>4</sub>)<sub>1-x</sub>·Cs<sub>x</sub>SO<sub>4</sub> mixed cryst., EPR of NH<sub>3</sub><sup>+</sup> and SeO<sub>3</sub><sup>-</sup> radicals 0-50190  
(NH<sub>4</sub>)<sub>1-x</sub>·Rb<sub>x</sub>SO<sub>4</sub> mixed cryst., EPR of NH<sub>3</sub><sup>+</sup> and SeO<sub>3</sub><sup>-</sup> radicals 0-50190  
NaClO<sub>4</sub>, aq. glass, formation of trapped H-atoms and electrons on X-irrad. 0-35559  
NaClO<sub>4</sub>, frozen soln., EPR of trapped H-atoms produced by UV and X-irrad. 0-3369  
NaOH, frozen soln., EPR of trapped H-atoms produced by UV and X-irrad. 0-3369  
l-proline monohydrate single cryst., X-irrad., ESR and ENDOR study of radicals 0-45528

**paramagnetic resonance of ions and impurities**

- see also paramagnetic resonance of iron group ions and impurities;  
paramagnetic resonance of palladium and platinum group ions and impurities; paramagnetic resonance of rare earth ions and impurities  
angular variation, calc. using Feynman's theorem 0-54940  
clustering of mag. ions, study method 0-11155  
diamond, exchange interaction of N paramag. centres, spin density delocalisation 0-39847  
diamond, synthetic, N impurity effect on strength characts. and thermal stability 0-11726  
exchange interaction caused by elementary excitations in solids, temp. depends. 0-25193  
fluorene:pyrene-d<sub>10</sub> cryst., magnetic resonance absorpt. of host-guest triplet paired centres 0-34750  
graphite lamellar cpds. with Li, K, Rb, HNO<sub>3</sub> and SO<sub>3</sub>, EPR studies 0-44902  
hyperfine structure, low symmetry effects, calc. 0-50165  
ions in <sup>55</sup>Si<sub>2</sub> ground state, ESR line with 3.33 isotropic g-factor 0-15787  
quartz, alpha particle induced radiation defects, EPR and thermoluminescence study 0-20461  
quintet transition, exact axial reson. fields calc., rel. to powder spectra 0-2622

**paramagnetic resonance of ions and impurities continued**

- spin-glass, dirty, paramag. reson. 0-11264  
transition metal systems, ESR studies, polarised absorption, ligand field model, group theory applications 0-43077  
As<sub>2</sub>Se<sub>3</sub>, amorphous, defect states, exptl. study. 0-54645  
 $\beta$ -B<sub>2</sub>C, rhombohedral, EPR meas. partly resolved absorpt. spectra 0-20449  
CaF<sub>2</sub>:U, charge conversion of U<sup>3+</sup>, ESR spectra 0-7150  
CaF<sub>2</sub>:U<sup>4+</sup>, EPR hyperfine struct. 0-15781  
CaO:Li, thermally quenched, generation of Li<sup>0</sup> centres 0-50382  
CaSe:Pb, luminesc. and EPR props. of Pb centres 0-55168  
CdS, donors, EPR and spin-lattice relax., Faraday rot. meas. 0-54939  
Cs<sub>2</sub>ZrCl<sub>6</sub>:Np<sup>4+</sup>, EPR data interpretation for octahedral  $\Gamma_8$  state in cubic cryst. field 0-2634  
Cs<sub>2</sub>ZrCl<sub>6</sub>:Np<sup>4+</sup>, EPR of np<sup>4+</sup> ground state 0-44903  
GaP, electron irrad., EPR of antisite-impurity defect 0-25211  
Ge:Li,O, EPR and piezospectroscopy 0-25338  
He, liquid, EPR of negative ions, antiferromagnetic transition possibility (Russian) 0-15322  
K<sub>2</sub>Cr<sub>2</sub>O<sub>7</sub> single crystals, X-irrad., EPR spectra 0-2638  
KD<sub>2</sub>(SeO<sub>3</sub>)<sub>2</sub>, ferroelastic transition, EPR 0-7148  
KPO<sub>3</sub>-Fe<sub>2</sub>O<sub>3</sub> glasses,  $\gamma$ -irrad., ESR 0-50182  
MgO-CoO, high surface area, O<sub>2</sub> adsorpt., EPR, volumetric investigs. 0-10782  
Si, (111) surface, low press. baked, dominant interactions and average distances between paramag. centres 0-15783  
n-Si, EPR linewidth, Orbach relax. process, conc. depend. 0-44901  
Si, EPR of quenched-in defects 0-29620  
Si, ion implanted, spin density effect on laser annealing 0-11517  
Si, ion-implanted polycrystalline film, defect build-up efficiency 0-2054  
Si, vacancies and interstitials 0-29015  
Si:H, electron states 0-29355  
Si:O, amorphous, sputtered, influence of O and deposition conditions 0-54693  
Si:O, evaporated amorphous film, effect of O<sub>2</sub> on props., ESR spectra 0-11265  
Si:P, amorphous, CVD, defect compensation, ESR meas. 0-54644  
Si:P<sup>+</sup>, Zeeman energy transfer at surface layer 0-11247  
Si<sub>100-x</sub>Al<sub>x</sub>, RF sputtered, amorphous, props. 0-34754  
SnO<sub>2</sub> surface, interactions with O<sub>2</sub>, H<sub>2</sub>O and H<sub>2</sub>, desorpt., ESR and cond. meas. 0-10790  
SrTiO<sub>3</sub>, structural phase transition, intrinsic and extrinsic central peak properties 0-34168  
ZnFeO<sub>4</sub>, ferrite spinel, structural and catalytic studies 0-44191
- paramagnetic resonance of iron group ions and impurities**  
agriculture applications 0-56298  
L-alanine:Cu(II), EPR and ligand-ENDOR measurements 0-44907  
 $\alpha$ -B, rhombohedral, magnetic props. and ESR spectra 0-20452  
copper pyridine dichloride, dynamic shift of the ESR field 0-2630  
diacetylene, single cryst., photopolymerisation, intermediate states, struct. changes 0-30235  
diethylammonium manganese chloride, planar Heisenberg magnet, spin diffusion, EPR study 0-15793  
dimethyl ammonium copper manganese tetrachloride, EPR study (German) 0-54941  
Fe particles in glass-like C matrix, identification and props. 0-11229  
ferredoxin, from Clostridium pasteurianum, Mossbauer effect, ESR, and mag. susceptibility meas. 0-40961  
ferredoxin synthetic analogues, [Fe<sub>4</sub>S<sub>4</sub>(SR)<sub>4</sub>]<sup>3-</sup> clusters, Mossbauer effect, EPR, and mag. props. 0-41057  
ferredoxin-like centres, membrane bound, in photosystem I of blue-green algae, Mossbauer and EPR study 0-40974  
guanidinium aluminium sulphate hexahydrate:Fe<sup>3+</sup>, EPR spectra, angular var. calc. 0-54940  
lithium potassium tartrate monohydrate: Mn<sup>2+</sup>, isomorphism with lithium ammonium tartrate monohydrate, EPR obs. 0-29607  
metallo-octaethyl porphyrins, I oxidation products, metallic cond., EPR and reson. Raman spectra 0-29610  
MgO:Cr<sup>3+</sup>, single cryst., ESR linewidth 0-29605  
nickel acetate tetrahydrate:Mn<sup>2+</sup>, EPR spectra, angular var. calc. 0-54940  
potassium oxalate, EPR of Mn<sup>2+</sup> and VO<sup>2+</sup> 0-39858  
review of 1974 literature 0-11253  
Rochelle salt, VO<sup>2+</sup>-doped, EPR study 0-34762  
ruby, Cr<sup>3+</sup> ESR transition influence on <sup>27</sup>Al, distant ENDOR and dynamic nucl. polarisation 0-2664  
ruby, ESR and NMR correl. line broadening effect assoc. with external mag. field inhomogeneities 0-50227  
ruby, spin-strain coupling tensor meas. US modulated EPR obs. 0-50170  
S=1, singlet ground state systems, mag. props. 0-11157  
silicate glass, NiFe<sub>2</sub>O<sub>4</sub> precipitation process, ESR study, effective g value, transition temp. 0-25194  
sodium iron fluorophosphate glasses, EPR and Mossbauer resonance study 0-39968  
stalactites, chem. decomp., ESR obs. 0-15788  
strontium acetate hemihydrate:Mn<sup>2+</sup> (Cu<sup>2+</sup>), EPR, spin Hamiltonian anal. and unit cell symmetry 0-29603  
tC FeCr<sub>2</sub>S<sub>4-x</sub>Se<sub>x</sub>, chalcospinel, ESR spectrum and paramag. susceptibility 0-15789  
TGS:Fe<sup>3+</sup>, crystals and their aq. solns., ESR 0-39862  
TGSe:Cu<sup>2+</sup>, EPR ang. depend., coord. of Cu<sup>2+</sup>, Cu-ligand bond obs. and ferroelec. transition anomaly 0-7156  
TMMC:Cu, EPR lines, dynamic effect of low-symmetric spin distrib. 0-39854  
TMMC:Cu, EPR linewidth freq. depend., spin dynamics 0-15794  
TMMC, EPR lines in one-dimensional mag. systems, dynamic effect of low-symmetric spin distrib. 0-39853  
TMMC, linear Heisenberg antiferromagnet, EPR half-field transitions 0-15792  
TMMC, one dimensional antiferromagnet, EPR expts. 0-20454  
transition metal ions in solids 0-51968  
valency assessment, appl. to ceramics and glass industries (German) 0-34757  
YAG crystals, EPR spectra of V<sup>2+</sup> ions, ion energy levels 0-7157  
AgCl:Ni, double quantum EPR transition, superhyperfine struct. 0-7154  
 $\alpha$ -Al<sub>2</sub>O<sub>3</sub>:Co,H, Co and proton ENDOR, IR and optical spectra charge compensator nature and defect struct. 0-44956  
As<sub>2</sub>S<sub>3</sub>:Fe, glass, photolum. and ESR, Fe impurities as non-radiative recomb. centres 0-29788  
(As<sub>2</sub>Te<sub>3</sub>)<sub>1-x</sub>Mn<sub>x</sub>, defect and impurity states, EPR meas. 0-54650



**paramagnetic resonance of iron group ions and impurities continued**

- $\text{Ba}_2(\text{PO}_4)_3\text{Cl}$  with substituted  $\text{CrO}_4^{2-}$ , ESR study 0-2629  
 $\text{BaTiO}_3$ , antiferro. in EPR spectra of  $\text{Fe}^{3+}$  ions (*Russian*) 0-11257  
 $\text{BaTiO}_3\text{:Cu}$ , Cu ion as electron trap, rel. to Curie temp.,  $\Gamma_{15}$  phonon freezing 0-25318  
 $\text{BaTiO}_3\text{:Fe}^{3+}$ , local position of  $\text{Fe}^{3+}$  in ferroelec. phases, EPR study 0-25196  
 $\beta\text{-Cu}_2\text{V}_2\text{O}_8$ , mag. and spectroscopic study, semiconductor to metal transition 0-2628  
 $\text{CaCo}_2$ , aragonite, EPR of  $\text{Mn}^{2+}$  impurities, orthorhombic spin-Hamiltonian parameters 0-2631  
 $\text{CaO:V}^{3+}$  orbital triplet, intermediate Jahn-Teller effect, APR 0-34758  
 $\text{CaO-MnO}$  system, solid soln. form. and analysis 0-28996  
 $\text{Ca(OH)}_2\text{:Ni}^{2+}$  single cryst., X-irrad.,  $\text{Ni}^{2+}$  EPR, g-factors and point-charge model 0-2626  
 $\text{CdBr}_2\text{:Co}$ , spectroscopic studies of interactions 0-29769  
 $\text{CdCl}_2\text{:Co}$ , spectroscopic studies of interactions 0-29769  
 $\text{Cd}_{1-x}\text{Mn}_x\text{Te}$ , EPR, mag. crit. point 0-39851  
 $\text{Cd}_2\text{Nb}_2\text{O}_7$ ,  $\text{Mn}^{2+}$  ESR, hyperfine interaction const., ferroelectric domain orientation 0-54943  
 $\text{CdTe:Cr}$ , impurity photoionisation transitions, EPR meas. 0-39857  
Co Schiff base complex,  $\text{N,N'}$ -ethylene-bis (salicylideneiminato)-Co II pyridine doped in Znsalenpy crystal, ENDOR, EPR studies 0-34819  
 $\text{Co}_2\text{Mg}_{1-x}\text{O}$ , solid solution, EPR of  $\text{Co}^{2+}$  (*Russian*) 0-11251  
 $\text{CsZnCl}_4\text{:Cu}^{2+}$ , electron spin echo, 35 GHz 0-13113  
 $\text{Cs}_2\text{ZnCl}_4\text{:Cu}^{2+}$ , single cryst. and powdered single cryst., EPR, linear elec. field effect 0-11250  
Cu complex, catena- $\mu$ -isothiocyanato-( $\text{N'}$ -pyridylmethylene- $\text{N''}$ -salicyloylhydrazinato- $\text{NN'O}$ ) copper (II), EPR and visible spectra 0-5566  
Cu complex, Cu-glycine in water, EPR spectral parameters, temp. depend. 0-2623  
Cu complex, halocuprates, ferromagnetic insulator, two-dimens. Heisenberg layers, mag. susceptibility 0-50068  
Cu complex with L-phenylalanine amino acid, ESR spectra and magnetic susceptibility measurement 0-34761  
 $\text{CuCl}_2\cdot 2\text{H}_2\text{O}$ , submillimetre ESR meas. using pulsed high mag. field 0-44905  
 $\text{Cu(NH}_3)_5(\text{ClO}_4)_2$ , ( $n=4$  or  $5$ ), EPR parameters and dilatometry 0-39850  
 $\text{Cu(NH}_3)_4\text{SO}_4\cdot \text{H}_2\text{O}$ , submillimetre ESR meas. using pulsed high mag. field 0-44905  
 $\alpha\text{-Cu}_2\text{V}_2\text{O}_8$ , EPR and mag. susceptibility meas. 0-2627  
Fe complex, ferrous pseudo-tetrahedral compounds, paramag. relax., Mossbauer spectra 0-15869  
 $\text{FeCl}_4^-$  in organic solvents, dilute, ESR linewidths (*German*) 0-11258  
 $\text{Fe(III)}$  Laeme complex, EPR g-value anal. 0-30657  
 $\text{Fe}_{1-x}\text{Mn}_x\text{Cl}_2$ , disordered, Mn spin excitations by microwave absorption at high freqs. 0-34759  
 $\text{Fe(N}_3)_2$ , paramag. relax. in trigonal bipyramidal environment, Mossbauer spectra 0-15871  
 $20\text{Fe}_2\text{O}_3\cdot 80[3\text{B}_2\text{O}_3\cdot (1-x)\text{PbO}\cdot x\text{GeO}_2]$  glass, phys. props. 0-49119  
 $\text{FeSiF}_6\cdot 6\text{H}_2\text{O}$ , submillimetre EPR and zero field spectra, spin Hamiltonian 0-29604  
GaAs:Cr, optically induced transient EPR phenomena 0-50168  
GaAs:Cr, semi-insulating, Cr charge states conc., EPR determ. 0-20450  
GaP:Fe, heat treated, EPR spectra, struct. defects 0-7158  
GaP:Fe, photo-EPR study  $\text{Fe(3d}^6)$  centres and deep electron traps 0-44910  
GaP:Fe(Cr), photo-ESR of annealed crystals 0-15795  
 $\text{GdCrO}_3$ , EPR linewidth, Neel point to 700K 0-39849  
 $\text{Gd(Rh}_{1-x}\text{Fe}_x)_3$ ,  $x\leq 0.15$ , magnetisation and EPR studies 0-34767  
 $(\text{Ge}_{1/3}\text{Se}_{2/3})_{100-x}\text{Ni}_x$ , ESR, rel. to elec. cond. 0-7155  
 $(\text{Ge}_{30}\text{Se}_{70})_{32}\text{Te}_{32}\text{As}_{32}\text{O}_{100-x}\text{Ni}_x$ , ESR, rel. to elec. cond. 0-7155  
 $\text{Hg}_{1-x}\text{Mn}_x\text{Te(S)}(\text{Se})$ , EPR of  $\text{Mn}^{2+}$ , order-disorder transitions 0-50176  
 $\text{KCl:Fe(CN)}_6^{4-}$ , electron irradi., Mossbauer and ESR study 0-7238  
 $\text{KCl:V}^{2+}$ , EPR spectra above 300K 0-34765  
 $\text{KNbO}_3\text{:Fe}$ , orthorhombic, EPR of  $\text{Fe}^{3+}$  0-39861  
 $\text{K}_2\text{O-B}_2\text{O}_3\text{:Mn}^{2+}$  glass, fine struct. parameter distrib., EPR meas. 0-11256  
 $\text{K}_2\text{O-BaO-B}_2\text{O}_3$  glasses, ESR detection of immiscibility rel. to Cu II ions 0-20916  
 $\text{K}_2\text{PbCu(NO}_2)_6$ , uniaxial stress, EPR meas. 0-20455  
 $\text{K}_2\text{SO}_4\text{:MnO}_4^-$ , electronic struct. by ESR 0-44906  
 $\text{KTaO}_3\text{:Fe}^{3+}$ , local phase transition, EPR line temp. broadening (*Russian*) 0-54944  
 $\text{KZnF}_3\text{:V}^{2+}$ , calc. of  $t_{2g}$  antibonding mol. orbital in  $|\text{VF}_6|^{14}$ , rel. to ESR 0-50174  
 $\text{LiNbO}_3\text{:Cu}^{2+}$ , EPR and optical spectra 0-20453  
 $\text{Li}_2\text{O-B}_2\text{O}_3\text{:Mn}^{2+}$  glass, fine struct. parameter distrib., EPR meas. 0-11256  
 $\text{LiSO}_4\cdot \text{H}_2\text{O:Cr}^{3+}$ , single cryst., EPR and optical absorpt. spectra 0-39855  
 $\text{MgCl}_2\text{:Co}$ , spectroscopic studies of interactions 0-29769  
 $\text{MgIn}_2\text{S}_4\text{:Co(Cr)}$ , EPR powder spectra 0-25197  
 $\text{MgO:Cr}$ , Co, optical and ESR studies 0-50175  
 $\text{MgO:Cr}^{3+}$  ( $\text{Mn}^{2+}$ ) spin Hamiltonian parameters, lattice expansion and vibr. effects 0-24851  
 $\text{MgO:Mn}^{2+}$ , clustering of mag. ions, study method 0-11155  
 $\text{Mn}^{2+}$  EPR spectra in glasses with  $g_{\text{eff}}=4.29$  computer simulation 0-34764  
 $\text{Mn}^{2+}\text{-Cu}^{2+}$  coupled pair, ESR spectrum, strong isotropic exchange model 0-29606  
 $\text{Mn,Mg}_{1-x}\text{O}$ , solid solution EPR, mag. interactions (*Russian*) 0-44908  
 $\text{MnO}$ , EPR spectra of ceramic and epitaxial monocrystalline thin film samples (*Russian*) 0-11252  
 $(\text{Mo}_x\text{V}_{1-x})_2\text{O}_8$ , mag. and spectroscopic investigation 0-25206  
 $(\text{NH}_4)_2\text{Co(SO}_4)_2\cdot 6\text{H}_2\text{O}$ , submillimetre ESR meas. using pulsed high mag. field 0-44905  
 $(\text{NH}_4)_2\text{CuCl}_4\cdot 2\text{H}_2\text{O}$ , submillimetre ESR meas. using pulsed high mag. field 0-44905  
 $(\text{NH}_4)_2\text{Rb}_{1-x}\text{Al(SO}_4)_2\cdot 12\text{H}_2\text{O:Cr}^{3+}$  EPR study, effect of monovalent ions on trigonal distortion 0-11255  
 $(\text{NH}_4)_2\text{SO}_4\text{:Cu}^{2+}$ , ESR parameters, effect of pH of mother soln., trapping sites 0-15791  
 $(\text{NH}_4)_2\text{SO}_4\text{:VO}^{2+}$ , EPR spectrum, temp. depend. 110-300K 0-11249  
 $(\text{NH}_4)_x\text{Tl}_{1-x}\text{Al(SO}_4)_2\cdot 12\text{H}_2\text{O:Cr}^{3+}$ , zero field splitting, g-values, EPR spectra obs. 0-50169  
Na-Fe fluorophosphate glass, EPR and Mossbauer resonance study 0-15838

**paramagnetic resonance of iron group ions and impurities continued**

- $\text{NaCl:Mn}^{2+}$ ,  $\text{CN}^-$ , EPR spectrum rel. to  $\text{Mn}^{2+}$ -vacancy- $\text{CN}^-$  complex 0-54942  
 $\text{NaCl:V}^{2+}$ , EPR spectra above 300K 0-34765  
 $\text{NaF:Mn}^{2+}$ , VUV absorpt. spectrum and EPR 0-55142  
 $\text{Na}_2\text{O-B}_2\text{O}_3\text{:Cu}^{2+}\text{ZZ}$  0-34760  
 $\text{Na}_2\text{O-B}_2\text{O}_3\text{:Mn}^{2+}$  glass, fine struct. parameter distrib., EPR meas. 0-11256  
 $\text{Na}_2\text{O} \cdot 3\text{B}_2\text{O}_3 \cdot x\text{Fe}_2\text{O}_3$ , borate glass,  $\text{Fe}^{3+}$  spin state and distrib. meas. 0-39966  
Ni complex, (1,4,5,8,9,12,13,16-octamethyltetradenzporphinato nickel) $^{++}$  ( $\text{I}_3^-$ ), atomic limit of Hubbard model and polarons 0-39860  
 $\text{Ni}_2\text{Mg}_{1-x}\text{O}$ , EPR in magnetocentrated solid solution (*Russian*) 0-39856  
 $\text{Ni(NH}_3)_6\text{I}_2$ , EPR of  $\text{Ni}^{2+}$  ion near structural phase transformation 0-11248  
 $\text{Ni(NH}_3)_4(\text{SO}_4)_2\cdot 6\text{H}_2\text{O}$ ,  $\text{Mn}^{2+}$  doped, EPR study 0-34763  
 $\text{NiSO}_4\cdot 7\text{H}_2\text{O}$ ,  $\text{Mn}^{2+}$  doped, EPR study 0-34763  
 $\text{NiSiF}_6\cdot 6\text{H}_2\text{O}$ , EPR line shape, Tanaka-Kondo method 0-29602  
Pb ceramic glaze,  $\text{Cu}^{2+}$  doped,  $\text{Pb}^{2+}$  release 0-49101  
 $\text{PbO-B}_2\text{O}_3\text{:Cu}^{2+}$ , glasses, ESR and optical absorpt. 0-34760  
 $\text{RbIn(MoO}_4)_2\text{:Fe}^{3+}$  monocrystals, EPR spectrum in the phase transition neighbourhood 0-2624  
 $\text{RbMgF}_3\text{:Mn}^{2+}$ , spin Hamiltonian, HFS and  $\text{Mn}^{2+}$  site occupation, struct. implications (*French*) 0-50167  
 $\text{Rb}_2\text{Mn}_2\text{Mg}_{1-x}\text{F}_4$ , spin dynamics near percolation threshold, EPR study 0-39859  
 $\text{Rb}_2\text{PbCu(NO}_2)_6$ , uniaxial stress, EPR meas. 0-20455  
Si, Jahn-Teller  $\text{Mn}^0$  centre ESR spectrum, depend. on axial press. 0-44911  
 $\text{Si:Cr}^{3+}$  EPR spectra and spin state population inversion with unpolarised optical lighting (*Russian*) 0-44909  
 $\text{Si:Fe}$ , interstitial form., Au dopant effect 0-29611  
 $\text{Si:Mn(Fe)(Ni)}$  amorphous films, ESR and elec. cond. 0-50171  
 $\text{SnTe:Mn}$ , EPR as probe of phase transitions 0-15790  
 $\text{SrO:Ni}^{2+}$ , noncentral Jahn-Teller ion, energy minimum localisation, ESR study 0-25198  
 $\text{SrTiO}_3$ , EPR of  $\text{Fe}^{3+}\text{-V}_O$  centre, above  $T_c$  0-39870  
 $\text{SrTiO}_3\text{:Cr}^{3+}$ , nonlinear Jahn-Teller coupling, local dynamics, near struct. transition 0-2625  
 $\text{SrTiO}_3\text{:V}$ , Jahn-Teller impurity,  $\text{V}^{4+}$  EPR 0-29608  
 $\text{TGSe:Cu}^{2+}$ , EPR studies 0-7153  
 $\text{TiO}_2\text{:Fe}$ , rutile, ESR meas. 0-54945  
 $\text{TiO}_2\text{:Fe}^{3+}$ , microwave second harmonic generation and freq. conversion 0-50166  
 $\text{TiO}_2\text{:V(Cr)(Mn)(Fe)}$ , impurity levels, photocurrent and ESR meas. 0-29346  
 $\text{Ti}_2\text{O}_7$  and  $(\text{Ti}_{1-x}\text{V}_x)_4\text{O}_7$ , metal-insulator transitions, EPR, elec. and mag. props. 0-2336  
 $\text{VO}^{2+}$  EPR in solids, review 0-11254  
 $\text{V}_2\text{O}_5$  amorphous films, CVD prep., structural characts. 0-49114  
 $\text{YCrO}_3$ , EPR linewidth, Neel point to 700K 0-39849  
Zn II complex, hexaimidazole-zinc(II) dichloride tetrahydrate:Cr(III), D-tensor orientation, charge-compensation vacancies 0-50172  
 $\text{ZnGa}_2\text{O}_4\text{:Fe}^{3+}(\text{Mn}^{2+})$ , EPR, spin Hamiltonian parameters 0-25195  
 $\text{ZnO-B}_2\text{O}_3\text{:Cu}^{2+}$ , glasses, ESR and optical absorpt. 0-34760  
 $\text{ZnS:Fe}$ , luminesc. and ESR investigations 0-2822  
 $\text{ZnS:Fe}^{3+}$ , spin-lattice relax., expt. evidence for optical phonons 0-20451  
 $\text{ZnS:Mn}^{2+}$ , spin-lattice relaxation, EPR, optical phonons 0-39852  
 $\text{ZnSe:Ga,As}$ , characts. of simultaneous incorporation, by  $\text{Mn}^{2+}$  ESR and X-ray fluoresc. anal. 0-34017  
 $\text{ZnSiF}_6\cdot 6\text{H}_2\text{O:Mn}^{2+}$ , ESR spectrum, effect of uniaxial compression 0-29609  
 $\text{ZnSiF}_6\cdot 6\text{H}_2\text{O}$ , spin-phonon interaction between  $\text{Ni}^{2+}$  ions, phonon bottleneck effects, splitting parameters (*Russian*) 0-15796  
 $\text{ZnSiF}_6\cdot 6\text{H}_2\text{O:V}^{2+}$ , spin-lattice relax. at normal and high press. 0-2632

**paramagnetic resonance of palladium and platinum group ions and impurities**

- $S=1$ , singlet ground state systems, mag. props. 0-11157  
transition metal ions in solids 0-51968  
 $\text{Al}_2\text{O}_3\text{:Mo}^{3+}$ , zero field splitting study by ESR 0-7159  
 $\text{CaMoO}_4\text{:Mo}^{3+}$ , g-factor, ground state, line broadening, EPR obs. 0-39863  
 $\text{MgO:Pt}^{3+}$ , Jahn-Teller effect in EPR spectrum 0-7160  
 $\text{NaCl:K}_2\text{IrCl}_6$  electron irradi., ligand field anal., EPR obs. 0-29612  
 $\text{Nb}_2\text{O}_5$ , B-form single crystals, ESR of  $\text{Mo}^{3+}$  and  $\text{W}^{5+}$ , site symmetry 0-54946  
Ru complex, Creutz-Taube ion, ground state, single crystal EPR obs. of mixed valence Ru dimer ion 0-34766  
 $\text{WO}_3$  electron density map of  $\text{W}^{5+}$  polarons, EPR and optical absorpt. obs. 0-44912

**paramagnetic resonance of rare earth ions and impurities**

- lanthanide and actinide ions, review of 1974 literature 0-11253  
metallic rare earths, conference, St. Pierre-de-Chartreuse, France (Sept. 1978) 0-12844  
 $\text{Pb}_3\text{Ge}_2\text{O}_{11}\text{:Gd}^{3+}$ , ESR spectra, electric-field effect and reversible permittivity 0-29614  
rare earth complexes, formation and props., book contrib. 0-43204  
rare earth intermetallics,  $\text{RAl}_2\text{-Gd(Er)(Dy)(Nd)}$ , dil., ( $\text{R=La, Yb, Lu}$ ), EPR and mag. susceptibility 0-15797  
rare earth ions in solids 0-51968  
rare earth systems, NMR, EPR, and Mossbauer effect, book contribs. 0-39883  
rare earth trichloride hexahydrate  $\text{Gd}^{3+}$  EPR, linear point charge model predictions 0-25200  
Ag-Dy, dil., thin films, ESR spectra, stress effects 0-39866  
Au-Er, dil., cold-worked, EPR expts. 0-39864  
 $\text{BaY}_2\text{F}_8\text{Nd}^{3+}(\text{Ho}^{3+})(\text{Er}^{3+})(\text{Yb}^{3+})$ , ESR spectra and spin-lattice relax. 0-11263  
 $\text{CaF}_2\text{:Eu}$ , oxidation and reduction of Eu, EPR and optical studies 0-25199  
 $\text{CaF}_2\text{:Pr}^{2+}$ , EPR data interpretation for octahedral  $\Gamma_8$  state in cubic cryst. field 0-2634  
 $\text{CaMoO}_4\text{:Er}^{3+}$ , phase relax. time rel. to g-factor anisotropy, electron spin echo obs. 0-29615  
 $\text{CaWO}_4$ ,  $\text{Yb}^{3+}$ ,  $\text{Nd}^{3+}$  phase relaxation electron spin echo spectra 0-29613  
 $\text{CaWO}_4\text{:Yb}^{3+}(\text{Nd}^{3+})$ , phase relax. time rel. to g-factor anisotropy, electron spin echo obs. 0-29615  
 $\text{CePd}_3\text{-Er(Gd)(Yb)}$ , dil., EPR spectra 0-25201



**paramagnetic resonance of rare earth ions and impurities continued**

- Er(PO<sub>3</sub>)<sub>3</sub> glass, Faraday resonance effect in pulsed mag. field, optical freq. EPR (*Russian*) 0-2734  
 EuAsO<sub>4</sub>·Gd, dynamical interactions, EPR meas. 0-7162  
 EuB<sub>6</sub>, pure single crystals, magnetic and electric props. 0-11260  
 EuVO<sub>4</sub>·Gd, dynamical interactions, EPR meas. 0-7162  
 Gd<sup>3+</sup> in R<sub>2</sub>(SO<sub>4</sub>)<sub>3</sub>·8H<sub>2</sub>O, (R=Pr, Nd, Sm, Eu, Yb and Y), EPR 0-20458  
 Gd<sub>3</sub>Al<sub>6</sub>, amorphous film, spin glass, microwave mag. resonance, freq. dependence 0-39798  
 Gd(Rh<sub>1-x</sub>Fe<sub>x</sub>)<sub>2</sub>, x≤0.15, magnetisation and EPR studies 0-34767  
 HoVO<sub>4</sub>·Gd, indirect superhyperfine interaction, EPR line width meas. 0-2633  
 La<sub>2</sub>Eu<sub>1-x</sub>B<sub>6</sub>, EPR linewidth conc. depend., Sr<sub>x</sub>Eu<sub>1-x</sub>B<sub>6</sub> comparison, exchange interaction in EuB<sub>6</sub> 0-20457  
 LaNi<sub>2</sub>-Gd, dil., ESR spectra, fine struct. and random stresses 0-25203  
 LiErF<sub>6</sub>, EPR studies, lowest levels of rare-earth ions, submillimetre freq. 0-39865  
 LiHoF<sub>4</sub>, EPR studies, lowest levels of rare-earth ions, submillimetre freq. 0-39865  
 LiTbF<sub>4</sub>, EPR studies, lowest levels of rare-earth ions, submillimetre freq. 0-39865  
 LiYF<sub>4</sub>·Dy<sup>3+</sup>(Yb<sup>3+</sup>)(Er<sup>3+</sup>), ESR, nonlinear effect of elec. field 0-2635  
 Na<sub>3</sub>Sc<sub>2</sub>V<sub>2</sub>O<sub>12</sub>·Yb<sup>3+</sup>, EPR of Yb<sup>3+</sup> in octahedral sites 0-54948  
 NdCl<sub>3</sub>·6H<sub>2</sub>O·Gd<sup>3+</sup>, EPR spectra, angular var. calc. 0-54940  
 PbF<sub>2</sub>·Gd<sup>3+</sup>, EPR and ENDOR of Gd<sup>3+</sup> at cubic sites 0-7161  
 PbMo<sub>8</sub>S<sub>8</sub>·Gd, EPR meas. (*French*) 0-54947  
 PbMo<sub>8</sub>S<sub>8</sub>·Gd<sup>3+</sup>, powder EPR spectra, cryst. field, supercond. energy gap 0-34769  
 Pb<sub>3</sub>(PO<sub>4</sub>)<sub>2</sub>·Gd<sup>3+</sup>(Eu<sup>2+</sup>), EPR spectra of α- and β-phases 0-11261  
 Pd-H-Gd, dil., ESR exam. of low temp. region of phase diagram, and electronic props. 0-29930  
 PdGdH, diagram of state elec. props., indirect exchange interaction, EPR study (*Russian*) 0-50179  
 PrNi<sub>5-x</sub>Gd<sub>x</sub>, nucl. cooling agent, relax. and exchange, EPR and NMR study 0-25237  
 RbCaF<sub>3</sub>·Gd<sup>3+</sup>, O<sub>h</sub><sup>1</sup>-D<sub>4h</sub><sup>18</sup> struct. transition, ESR obs. 0-50178  
 RbCdF<sub>3</sub>·Gd<sup>3+</sup>, O<sub>h</sub><sup>1</sup>-D<sub>4h</sub><sup>18</sup> struct. transition, ESR obs. 0-50178  
 RbCl:Eu<sup>2+</sup>, EPR of <sup>139</sup>Eu<sup>2+</sup> and <sup>151</sup>Eu<sup>2+</sup> 0-11259  
 RbCl:Eu<sup>2+</sup>, tetragonal sites, spin Hamiltonian parameters, EPR and UV absorpt. spectra obs. 0-50177  
 ScAl<sub>2</sub>-Er(Dy)(Nd), dil., EPR and mag. susceptibility 0-15797  
 ScH<sub>2</sub>-Er, ESP determ. of proton locations 0-34768  
 SmB<sub>6</sub>, mixed valence cpd., EPR and heat capacity obs., metal-semicond. behaviour 0-20456  
 SmCl<sub>3</sub>·6H<sub>2</sub>O·Gd<sup>3+</sup>, X-ray band EPR lines, exact anal. using intensity operator 0-20448  
 SnMo<sub>8</sub>S<sub>8</sub>·Gd, EPR meas. (*French*) 0-54947  
 SnMo<sub>8</sub>S<sub>8</sub>·Gd<sup>3+</sup>, powder EPR spectra, cryst. field, supercond. energy gap 0-34769  
 SrCl<sub>2</sub>·Gd<sup>3+</sup>, small dielec. particles, cryst. field size effects 0-44913  
 Sr<sub>2</sub>Eu<sub>1-x</sub>B<sub>6</sub>, EPR linewidth conc. depend., La<sub>x</sub>Eu<sub>1-x</sub>B<sub>6</sub> comparison, exchange interaction in EuB<sub>6</sub> 0-20457  
 SrF<sub>2</sub>·Gd<sup>3+</sup>, Na<sup>+</sup>(Kr<sup>+</sup>)(Rb<sup>+</sup>)(Ag<sup>+</sup>), EPR of orthorhombic Gd<sup>3+</sup>-univalent metal ion complexes 0-11262  
 ThH<sub>2</sub>:Er<sup>3+</sup>, EPR of Er localised electron mag. states, Kondo effect 0-25202  
 Th<sub>2</sub>H<sub>11</sub>:Er<sup>3+</sup>, EPR of Er localised electron mag. states, Kondo effect 0-25202  
 ThOS:Gd<sup>3+</sup>, EPR study, g-factor and cryst. field parameters 0-25204  
 YAl<sub>2</sub>-Er, dil., EPR, Er<sup>3+</sup> ground state 0-15798  
 YAl<sub>2</sub>-Er(Dy)(Nd), dil., EPR and mag. susceptibility 0-15797  
 YbBe<sub>3</sub>, mag. props. and EPR meas. 0-11175  
 YbCl<sub>3</sub>·6H<sub>2</sub>O, paramag. relax., Mossbauer spectra 0-20536

**paramagnetism**

- see also *paramagnetic properties of substances*  
 anisotropic paramagnet, statistical mechanics using second order Green's function theory 0-25074  
 anisotropic paramagnet with exchange-bond dilution, sixth freq. moments 0-44789  
 classical paramagnet, wavelength-depend. fluctuations in mag. field 0-7069  
 clustering of mag. ions, study method 0-11155  
 electron spin density functional gradient expansion, local approx. calcs. 0-44792  
 electron state density for narrow-band model with Coulomb interaction 0-10852  
 Heisenberg paramagnet, exchange bond dilution, freq. moments of spin correl. function 0-50030  
 impurities, influence on saturation of NQR lines 0-20491  
 intracellular water, effect of paramag. impurities on proton spin-lattice relax. 0-51134  
 isotope separation, supersonic molecular beam technique using RF spectroscopy, mag. reson. 0-47725  
 metal, polarised neutron inelastic and quasi-elastic scattering 0-50045  
 one-dimensional electron system, with attractive interaction in mag. field, paramag. transition 0-7072  
 plasma, penetration of external RF mag. field 0-6225  
 polarisation analysis of diffuse neutron scattering from magnetic systems 0-25098  
 relativistic paramagnetism, statistical mechanics in strong mag. field 0-17865  
 S=1, singlet ground state systems, mag. props. 0-11157  
 spin glasses, phase transition, mag. susceptibility, specific heat, Ising model calcs. (*Russian*) 0-34671  
 spin waves, classical approach 0-29519  
 type II superconductor, giant-vortex state, temp. depend. 0-7051  
 uniaxial Heisenberg antiferromagnet, phase diagrams 0-15730

**parameter estimation**

- adaptive control and parameter identification, applic. to nuclear reactor systems 0-22970  
 cardiovascular system, identification and parameter estimation 0-35947  
 distribution function parameters determ. in real time, instrument description 0-202  
 exchange parameters in compartmental models, identification, biomedical appls. (*French*) 0-42044  
 limb function discrimination performance using EMG parameter identification 0-8220  
 nuclear reactor systems, appl. of stable adaptive schemes 0-13635

**parameter estimation continued**

- nuclear reactors, process monitoring and parameter estimation, multivariate signal analysis algorithms 0-47585  
 optokinetic reflex, mathematical model 0-41008  
 pulmonary blood flow estimation, Ljung's algorithm sensitivity 0-56107  
 respiratory system, human, modelling and parameter estimation 0-12169  
 solar thermal systems long-term performance predictions using closed-form solutions 0-30556  
 systemic arterial bed, quantitative evaluation by parameter estimation of a simple model 0-56094  
 tissue parameter identification by digital processing of real-time US clinical cardiac data 0-51191
- parameter identification** see *parameter estimation*
- parametric amplifiers**  
 see also *acoustic parametric amplifiers; microwave parametric amplifiers; optical parametric amplifiers*  
 Josephson junction parametric inductance fluctuations, upconverter 0-25052
- parametric devices**  
 see also *acoustic parametric devices; microwave parametric devices; optical parametric devices*  
 certain ineffective parametric interactions 0-43396
- parametric oscillators**  
 see also *acoustic parametric oscillators; microwave parametric oscillators; optical parametric oscillators*  
 external-noise-driven, multiplicative stochastic processes in statistical physics appl. 0-22289
- parametric up-convertors** see *parametric devices*
- parametric varactor diodes** see *varactors*
- parametrons** see *parametric oscillators*
- parcel post** see *postal services*
- Pariser-Parr-Pople calculations** see *PPP calculations*
- parity**  
 see also *baryon spin and parity; lepton spin and parity; meson spin and parity; nuclear spin and parity; P invariance*  
 heavy atom, parity violation in forbidden mag. transitions, chiral absorpt. of polarized light and circular dichroism in crossed DC fields 0-23370  
 L-amino acids, weak neutral currents and biological stereoselection 0-26196  
 muonic atoms, long range parity violating interaction from γ-Z<sup>0</sup> conversion 0-48108  
 γ\*N→ψN, gluon momentum, spin, parity and coupling 0-42395
- parking control** see *traffic control*
- partial differential equations**  
 see also *boundary value problems; wave equations*  
 acoustic wave propagation in isotropic viscous weakly compressible medium, eqn. limits problem (*French*) 0-8808  
 Bachlund problem, Lie algebra bundles (*French*) 0-18085  
 beam, rotating slender, bending vibrs., Galekin method anal. 0-1465  
 Belousov-Zhabotinskii reaction, existence of solitary travelling wave solns. 0-35525  
 black holes, construction of metric and vector pot. perturbations 0-8647  
 buckled states of spherical shell under uniform external pressure, asymptotic methods and Newton's method 0-43635  
 circular loop induced eddy current distrib. and loss calc. 0-9771  
 coherent waves in nonlinear medium, nonresonant interaction, eqns. system development and examples (*Czech*) 0-24149  
 complex potential eqns., all solns. to nonlinear system 0-46795  
 complex potential equations, special relativity, and complexified Minkowski space-time 0-52018  
 conservation equation, numerical soln. by variational approach, mass transfer problem appl. (*French*) 0-19317  
 convection, natural, transient and steady-state numerical solns. 0-10119  
 deep fast trapping dielectric, SCL current injection 0-6862  
 discrete kinetic theory, maths. and numerical aspects, Couette flow appls. 0-19413  
 dissipative operators for infinite classical systems and equilibrium 0-12982  
 dynamic axisymmetrical elasticity problems soln. using factorised differential systems of second-order accuracy (*Russian*) 0-8796  
 dynamical system construction from pre-assigned family of solns. 0-39  
 education, Schrodinger eqn. for free particle, wave packet spreading in coord. representation 0-17736  
 elastic-viscoplastic proportional combined twist and stretch of circular bar of rate sensitive material 0-23912  
 elastostatics, error estimates of finite element approx. 0-8793  
 electrodynamic aspects of electrophotography (*Japanese*) 0-13170  
 elliptic, grid generation, automatic mesh-point clustering 0-31487  
 elliptic 2nd order problems, soln. using global element methods 0-46805  
 first-order, energy description of propagation of monochromatic radiation along multimodal fibre 0-38116  
 flow, in two-dimens. channel, turbulent, with separation 0-19356  
 Fokker-Planck, numerical soln. 0-18622  
 gas dynamics, numerical investigation by net-characteristic method 0-19420  
 Gel'fand-Levitan kernel for 3-D Schrodinger eqn. 0-36892  
 generalized symmetries of nonlinear partial differential equations, Lie derivatives 0-4886  
 Green's function for surface physics, partial differential eigenvalue eqn. 0-6929  
 heat conduction, Sommerfeld problem generalisation for one-dimens. ring 0-5908  
 heat conduction, unidimensional, inverse Cauchy problem solution, coeff. identification (*German*) 0-33419  
 heat conductivity, two-dimensional inverse problems solution (*German*) 0-1404  
 homogeneous viscoelastic mixtures, speed of sound 0-33272  
 Huygens principle for equations dissociating into factors 0-31581  
 hyperbolic, analogue/hybrid soln. 0-36336  
 hyperbolic balance laws in continuum physics 0-4525  
 hyperbolic in oceanographic circulation, numerical soln. 0-21864  
 incompressible flows in three dimensions, finite-difference methods 0-33554  
 incompressible liquid oscills. in variable cross section viscoelastic tube due to pulsating press. 0-31519  
 Jaulent-Miodek family of nonlinear evolution eqns., Hamiltonian formulation 0-31511  
 Kolmogorov direct equation, solution, Galerkin measures (*Russian*) 0-46981



**partial differential equations continued**

- Kolmogorov eqn., separation of variables, applied to oscill. Brownian motion 0-36945  
 Kolmogorov eqn., separation of variables 0-36835  
 Korteweg de Vries equation, Pade approximants, soliton solns. 0-42071  
 linear partial differential eqns. describing transport phenomena, soln. technique 0-13004  
 magnetic field problems, numerical techniques 0-32878  
 membrane and plate vibrations, functionals method for lateral vibr. freqs. determ. (*Japanese*) 0-12918  
 meromorphic solutions of nonlinear partial differential equations and many-particle completely integrable systems 0-31523  
 metals, heating by concentrated energy sources, simple analytical expressions (*Russian*) 0-38215  
 MHD, transient phenomena, simultaneous solns. to coupled gasdynamic-EM equations of motion 0-6157  
 moving boundary problems, weak soln. 0-179  
 multi-dimensional two-phase flow finite difference solutn. 0-18564  
 non-linear transport equations: Properties deduced through transformation groups 0-4680  
 non-Noether invariant origin, relation to Euler eqn. transformation props. 0-31493  
 nonhomogeneous medium, backwards heat eqn. soln. approx., partial differential eqn. 0-53611  
 nonlinear, appls. 0-4510  
 nonlinear transformations for partial differential eqns. 0-42043  
 nonmagnetic conductors, three-dimensional eddy current calc. (*French*) 0-14270  
 nonsteady filtration of two immiscible liquids alternative to kDv-Burgers eqn. 0-6019  
 ocean waves generation, propagation and dissipation spectral simulation model 0-31060  
 oscillators, nonlinear stochastic, triangular wave, optimally controlled, Weiner process and Poisson process, numerical studies 0-52128  
 parabolic, with M-matrices, iterative processes comparison, w.r.t. rate of convergence (*German*) 0-1405  
 plasma high temp. transport process, numerical soln. 0-19559  
 plate, eigenvalue problem, bidimensional approximation (*French*) 0-33445  
 quasilinear parabolic system, chemical reaction study 0-7759  
 Reynold's equation, free boundary problem in hydrodynamic lubrication including surface tension 0-19542  
 Schlesinger systems, isomonodromy deformation, integrable Hamiltonian systems 0-22229  
 shells of revolution, variable thickness, stress state determ. 0-38275  
 shock structure, numerical, nonlinear corrections for difference schemes in conservation form 0-36878  
 shock tube flows, unsteady non-equilibrium, discretisation of boundary layer terms 0-14742  
 sine-Gordon eqn. separable solutions in terms of Painleve transcendent 0-52037  
 solitary wave solns. of classical nonlinear field eqns., for teaching 0-17756  
 supersonic laminar viscous flow, numerical soln., separation 0-24062  
 supersonic plane flow past a curved wedge, quasi-linear hyperbolic systems (*French*) 0-10261  
 tetrachloromethane-cyclohexane liq. mixtures, heat of transport, Dufour effect 0-44344  
 throughflow between rotating and stationary disk calc., using Goertler series, finite difference method appl. (*Japanese*) 0-6064  
 Tokamak transport eqns., nonlinear partial differentials, soln. technique 0-19556  
 transfer theory, numerical soln. by direct reduction method 0-22309  
 transonic flow fast implicit procedure 0-19430  
 transonic potential flow, finite element method solutn. 0-24045  
 turbulence, isotropic two-dimensional, energy dissipation, correl. relationships and Taylor length scale 0-19334  
 vibration analysis of two-layered beam, with unconstrained viscoelastic layer damping (*Japanese*) 0-5968  
 Voigt functions analysis, appl. to astrophys. spectral line profiles and neutron cross sections 0-22879  
 weather forecasting nonlinear evolutionary problems, finite element methods appl. 0-21865  
 whale biothermal mathematical model 0-12059  
 zeros of polynomial satisfying second order linear partial differential equation 0-12889  
<sup>3</sup>He, superfluid B phase, soliton-like spin waves 0-44385

**partial discharges**

- dielectrics, inhomogeneous, breakdown model 0-50268  
 epoxy treeing breakdown, slit model 0-15970  
 ice and ice-silica compound system, electrical breakdown at cryogenic temps. 0-45007  
 in insulation, dielectric internal discharge, apparent charge evaluation (*Polish*) 0-19659  
 liquid dielectric gassing rate and discharge energy loss meas. 0-15965  
 PMMA, ageing characts., sub-atm. pressure partial discharge obs. 0-1867  
 polyethylene, electrical tree growth anal. using simultaneous meas. of light intensity and partial discharges 0-45008  
 spectra meas. by multichannel amplitude analyser system (*Italian*) 0-33847

**particle accelerator accessories**

- see also storage rings*  
 automatic radioisotope production devices adapted to a medical cyclotron 0-12260  
 chopper buncher system for tandem Van de Graaff 0-13989  
 electron injector in HV terminal, control and protection system 0-27836  
 electrostatic wire septums, leakage field 0-5423  
 heavy ion facility, target production 0-23213  
 laser polarimeter for  $e^+e^-$  beam polarisation meas. in storage ring 0-14019  
 linear accelerators, plasma waveguides appl. as accelerating structures 0-9438  
 wiggler, helical wiggler and free electron laser (*Japanese*) 0-37658  
 C stripper foil, lifetime meas. 0-23216  
 C stripper foil preparation, under heavy ion bombardment 0-18717  
 C stripper foils, ethylene cracking in glow discharge, irradiation lifetimes 0-23207  
 C stripper foils, lifetime enhancement by slackening technique 0-23186

**particle accelerators**

- see also beam handling equipment; beam handling techniques; cyclotrons; electron accelerators; electron ring accelerators; electrostatic accelerators; linear accelerators; proton accelerators; synchrotrons*  
 conical accelerator, plasma cluster vel. calc., snow-plough and erosive models (*Russian*) 0-27839  
 crystal accelerator, radiative energy loss 0-23611  
 decommissioning, radioactive waste management 0-18720  
 heavy ion accelerator facilities in Europe, review 0-42880  
 high energy accelerators, superconducting dipole magnets with high field uniformity, development and investigation (*Russian*) 0-5416  
 historical review, impact on scientific culture 0-868  
 ion, atomic collision processes rel. to vacuum system, review 0-54290  
 ion, small-size direct-action 0-23184  
 ion accelerator systems for ion implantation research 0-32540  
 laser radiation-surface launching of macroscopic particles 0-6290  
 medical, international standards 0-51272  
 modern atomic and nuclear physics (book) 0-11  
 negative ions from accelerated hydrogen clusters, fusion ignition appl. 0-13883  
 next generation, possibility of multinational sponsorship 0-47791  
 nonlinear crystal, optical acceleration of charged particles by 'rectified' light 0-23610  
 radiation exposure, proper design of cooling and ventilation systems 0-5350  
 radiobiological studies in space and at ground-based accelerators 0-41266  
 Sandia particle beam fusion accelerator facilities 0-37592  
 synchrotron radiation, techniques and appls., book 0-5668  
 synchrotron radiation source, book contrib. 0-5421  
 toroidal resonator excitation by uniformly moving charge 0-18726  
 H<sup>+</sup> cluster ion beam high power injector 0-13889

**particle backscattering**

- see also electron energy loss spectra*  
 AES, backscattering factor, Monte Carlo method calc. 0-7449  
 air electron backscattering coeffs., 100 eV to 5 keV 0-9750  
 anodic oxide superficial layer, X-ray emission spectrometry and ion backscattering (*French*) 0-49482  
 backscattering spectrometry and related analytical techniques 0-50505  
 beta-ray backscatt. from thick targets 0-32567  
 Boltzmann equation, appl., electron transmission, secondary electron emission (*French*) 0-20740  
 coherent X-ray generation from CO<sub>2</sub> laser backscattered relativistic electron beam 0-53252  
 coincidence measurements between scattered particles and X-rays to obtain high depth and mass resolution 0-54278  
 diamond/Sb, ion implanted under channelling conditions, depth profile, distribution tail 0-2057  
 electron, backscatt. by solids 0-2906  
 electron gas, 1-D, 2-D Coulomb gas, and 2-D epitaxial monolayer problems, family of mappings 0-34346  
 electron probe microanalysis, quantitative, 4-40 keV, electron backscatt. coeff. meas. 0-35608  
 EM analyser control, automatic registration of the back-scattered ions 0-18042  
 gas flow detector, back-scatter-type, conversion electron Mossbauer spectrometry 0-37680  
 Inconel 625, plasma nitriding, hardness meas., Rutherford backscatt. surface anal. 0-45442  
 ion backscattering under planar channelling conditions, ion-atom pot. and stopping power 0-24519  
 ion beam monitoring using thin self-supporting reference foils 0-50911  
 ion scattering from solid surfaces, single scatt. and ion neutralization (*Japanese*) 0-50500  
 material analysis technique using 2 MeV <sup>4</sup>He<sup>+</sup> ions (*Chinese*) 0-35590  
 Monte Carlo analysis of backscattering and sputtering in vacuum systems 0-235  
 nuclear microprobe anal. of stable isotope tracers spatial distrib. 0-50909  
 photon backscattered ang. distrib. for oblique incidence (*Rumanian*) 0-47456  
 planar channelling, oscill. behaviour of backscatt. spectra from small depths 0-6447  
 radiation device, layer thickness measurement by backscattered radiation 0-47829  
 Rutherford 180° backscatt. anomaly in solid, Monte Carlo simulation 0-45189  
 Rutherford backscatt. standard for ion beam expts. 0-50496  
 Rutherford backscattering spectrometry, signal overlap subtraction, surface struct. studies 0-50486  
 Rutherford spectra anal 0-50497  
 Rutherford spectrometry, comparison of depth profiling techniques of O in Si 0-29048  
 sample contamination, by sputtering, during ion implantation 0-54274  
 SEM, magnetic contrast, type-2, isolation by lock-in technique 0-13184  
 solid target, anomalous enhancement of 180° backscatt. yields for light ions 0-45188  
 steel, stainless, with Pd coating, interdiffusion at reactor wall temps., Rutherford backscatt. obs. 0-39361  
 surface topology using Rutherford backscattering 0-47015  
 Ag-Cu couple, grain boundary diffusion of Ag through Cu film, Rutherford backscattering obs. 0-34252  
 Al, electron backscatter fractions, exptl. determ. 0-18617  
 Al, electron transmission, secondary electron emission, appl. of Boltzmann equation (*French*) 0-20740  
 Al, fission fragment backscatt. 0-16138  
 Al, heavy ion ranges, 120 keV Pb ions backscatt. obs. 0-19855  
 Al, primary electron backscatter yield using material model parameters 0-39184  
 Al, surface exfoliation and blistering induced by He ion bombard. in energy range 10-80 keV 0-39173  
 Al, thick anodised films, O conc. determ. using non Coulomb H ion backscatt. 0-55753  
 Al-silicide-Si systems with CoSi<sub>2</sub>, Pt<sub>3</sub>Ni<sub>1-x</sub>Si, and MoSi<sub>2</sub> as silicide, diffusion, compound form., and microstructure 0-34253  
 Al<sub>2</sub>O<sub>3</sub>, O conc. determ. using non Coulomb H ion backscatt. 0-55753  
 Au,  $\alpha$ -particle Rutherford spectra anal. 0-50497  
 Au film, interface reaction with n-type Ga<sub>0.7</sub>Al<sub>0.3</sub>As and GaAs 0-39482  
 Au, fission fragment backscatt. 0-16138  
 Au, primary electron backscatter yield using material model parameters 0-39184



**particle backscattering continued**

- Au, stopping powers and backscatt. charge fractions for 20-150 keV  $H^+$  and  $He^+$  0-42907  
 Be, implanted D and He, interaction and radiation enhanced oxidation 0-39120  
 Be, surface hardening by B ion implantation, Rutherford backscatt. obs. 0-16604  
 C with Au and Al implants, Rutherford backscatt. standard 0-50496  
 CdS, clean surface, AES and LEED exam. 0-10762  
 CdTe, surface characterisation by high resolution Rutherford backscatt. 0-25511  
 Co, effect on surface roughness on backscattering spectra 0-47016  
 Cu, electron backscatter fractions, exptl. determ. 0-18617  
 Cu, fission fragment backscatt. 0-16138  
 $^{57}Fe$  backscatt. electron Mossbauer spectroscopy 0-29661  
 GaAs, 40 keV  $N^+$  implantation, disorder profiles meas. by Rutherford backscatt. and channelling 0-54270  
 GaAs, ion implanted, laser induced recrystn. and damage, ion backscatt. and Raman scatt. obs. 0-49248  
 GaAs, ion-implanted, laser pulse annealing of amorphous surface layer, TEM 0-55436  
 GaAs, surface characterisation by high resolution Rutherford backscatt. 0-25511  
 GaSb, elastic scatt. of  $He^+$  ions by atomic chains, screening 0-2915  
 Ge, proton energy loss, 0.1-1.0 MeV 0-42909  
 He ions, electrostatic anal., electronic reduction of charge state energy doublets 0-27870  
 InAs-GaSb superlattices, crystallography, Rutherford backscatt. and channelling obs. 0-49533  
 Mo, proton energy loss, 0.1-1.0 MeV 0-42909  
 $MoS_2$ , clean surface, AES and LEED exam. 0-10762  
 Nb, electron backscattering coeffs., 100 eV to 5 keV 0-9750  
 Nb, (001) surface, low energy  $H^+$  and  $He^{++}$  ion refl., computer simulation 0-11524  
 Nb film on Si, Ar ion bombard.,  $NbSi_3$  form. 0-10709  
 Nb thin films on Si substrate, intermixing, ion induced silicide formation 0-34101  
 Ni-In, ion-implanted, impurity defect interaction and diffusion, Rutherford backscatter and TDPAC expts. 0-34039  
 Ni-Nb alloys, oxidation at high temp., high energy ion backscattering anal. (Japanese) 0-35405  
 $NiSi_2$ , epitaxial film on Si,  $^4He$  ion channelling meas. and RHEED anal. 0-10834  
 O $_2$ , electron backscattering coeffs., 100 eV to 5 keV 0-9750  
 PbS, clean surface, AES and LEED exam. 0-10762  
 PbS film, vac. deposited, optical and phys. props. 0-2315  
 $PbTiO_3$ , single cryst.,  $He^+$  backscatt. shoulder spectra struct., domain struct. 0-35048  
 Pd, catalyst on glass, used in electroless deposition, proton backscattering anal. 0-16749  
 Pd film, high dose  $Si^+$  ion implantation, silicide phases, backscatter spectra 0-19820  
 Pd film on Si, Xe ion beam induced form. of  $PdSi$  0-10800  
 Pd-amorphous Si thin film interaction, metal rich Pd-silicide formation 0-2284  
 Pd-V, alloy and bilayer, silicide form. solid phase reaction with Si 0-6568  
 Pd $_2$ Si, epitaxial film on Si,  $^4He$  ion channelling meas. and RHEED anal. 0-10834  
 PtSi, epitaxial film on Si,  $^4He$  ion channelling meas. and RHEED anal. 0-10834  
 Si, 40 keV  $N^+$  implantation, disorder profiles meas. by Rutherford backscatt. and channelling 0-54270  
 Si (100), self-ion implanted, laser annealing, channelling and TEM meas. 0-24466  
 Si (110) surface peak anal. by 100-350 keV protons 0-55247  
 Si, (111) surface, low energy  $H^+$  and  $He^{++}$  ion refl., computer simulation 0-11524  
 Si, amorphous films, characterisation by Rutherford backscatt. spectrometry 0-50498  
 Si, and Si:H, amorphous, sputter deposited,  $O_2$  incorporation during and after fabrication 0-49541  
 Si, heavy ion ranges, 120 keV Pb ions backscatt. obs. 0-19855  
 Si, implanted annealed layers, amorphised structure formation mechanism and crystallographic nature 0-29091  
 Si, ion implantation and pulsed laser annealing of group III and group V dopants, supersat. alloy form. 0-54267  
 Si, ion implanted, spin density effect on laser annealing 0-11517  
 Si, proton energy loss, 0.1-1.0 MeV 0-42909  
 Si, surface radiation damage cross sections, influence of distortions 0-6442  
 Si:As, high-dose implanted, irradiation time and subsequent heat treatment effects on laser annealing 0-29041  
 Si:As, implanted, thermal diffusion of As 0-39352  
 Si:As, ion-implanted, CW IR laser annealing 0-34022  
 Si:As sputter rate meas. SIMS combination with Rutherford backscatter 0-21334  
 Si:Au Ar ion implant gettering obs. by MOS and Rutherford backscatt. techniques 0-39119  
 Si:B, self-interstitials location by Rutherford backscatt. of channelled ions 0-2101  
 Si:B ion implantation, large-angle proton scatt., anal. using Promiss protonograph 0-19823  
 Si:F, amorphous, thermal stability, comparison with Si:D 0-49542  
 Si:Ge, regrowth behaviour from backscatt. and channelling meas. 0-2300  
 Si:N, ion implantation, refractive index, IR spectra, ion range and straggling meas. 0-34020  
 Si:P, diffusion-doped laser irradiation effects, electrical reactivation of P 0-39124  
 Si:Pt, depth depend. of atomic mixing by ion beams 0-29837  
 Si/Pd-W, contact reactions, backscattering, X-ray diffr. meas. 0-20040  
 Si-H, amorphous, H three-dimens. distrib., ion-induced AES and Rutherford backscattering 0-44132  
 Si-SiO $_2$  interface, backscattering-channelling study 0-34320  
 Si+Ga $^{3+}$  ion implantation at high current density, lattice disorder, proton backscattering 0-34085  
 SiC(6H), ion-implanted, laser-induced recrystallization and defects 0-44221  
 Ti film, solid state reaction with Si or SiO $_2$  substrates, backscatt. anal. 0-34257  
 TiC film, CVD, on WC, diffusion processes, ion beam anal. 0-49424

**particle backscattering continued**

- TiO $_2$  layer form. by anodic oxidation, characterisation using  $^4He$  backscatt. (French) 0-45433  
 V thin film-amorphous Si interface, V silicide formation, backscattering diffraction meas. 0-2285  
 W (001) surface structure by MeV ion backscattering, channelling 0-6605  
 W (110), ionisation of hyperthermal Na atoms, temp. depend. 0-50504  
 WO $_3$  amorphous film, sublimed under different conditions, elec. transport props. 0-7015  
 (Y,Sm,Lu,Cu) $_3$ (Fe,Ge) $_5$ O $_{12}$ , ion implanted, hard bubble suppression 0-11238  
 ZnS, clean surface, AES and LEED exam. 0-10762

**particle beam diagnostics**

- accelerator linear, intense electron beam transient radial motion 0-9434  
 AGS slow extracted beam, size meas. 0-37672  
 Arnold diffusion, numerical studies in Nekhoroshev region 0-37668  
 Arnold diffusion in near-integrable Hamiltonian systems with three degrees of freedom 0-37665  
 beam spot measurements and beam divergence 400 keV electron accelerator 0-877  
 bunched beams, transport, second order aberrations 0-52801  
 collective-effect electron acceleration 0-14016  
 conference, storage ring beam-beam interactions and nonlinear dynamics, Upton, NY, USA (March 1979) 0-36758  
 direct energy conversion optimisation with charged particle parabolic trajectories 0-37585  
 double cylindrical electrostatic sector as an ion energy analyzer 0-23208  
 electron accelerator, electron current density distribution, approx. formula (Japanese) 0-14032  
 electron beam, pulsed high-intensity, self-focusing in low press. gas 0-32899  
 electron beam, relativistic, diocotron instability 0-27853  
 electron cloud confinement, radial and longitudinal distrib. determ. 0-14928  
 electron relativistic beam in synchrotron, ang. spread of vel. using undulator radiation electron 0-14021  
 electron ring optical diagnostics using synchrotron radiation and light scattering meas. 0-5405  
 elliptical beam inside non-confocal elliptic vacuum chamber, potential 0-47799  
 fringing field effects in a cylindrical condenser 0-52821  
 generalised coordinate variation on crossing cyclotron gap (French) 0-37657  
 heavy-ion accelerator, dimensions of electron ring meas. by synchrotron radiation 0-42877  
 high current beam, bunching, autoacceleration in slow wave system 0-52805  
 invariant tori and cantori, variational principles 0-37666  
 ISABELLE, bunched beams, instability threshold 0-37652  
 ISABELLE, linear and nonlinear beam-beam effects 0-37656  
 ISABELLE, nonlinear beam-beam interaction, computer model 0-37654  
 KAM surfaces computed from the Henon-Heiles Hamiltonian 0-37664  
 liquid H chamber Lyudmila, electronic apparatus for expanded diagnostic system 0-23265  
 MeV cluster ion beam diagnostics by calorimetry and time of flight spectra 0-13882  
 particle dynamics computer modelling, alternating phase focusing LINAC (Russian) 0-23234  
 photon beam characts. of 20 MV accelerator for radiation therapy appls. 0-26430  
 polarised heavy ion beams, polarisation monitors 0-27910  
 proton polarisation meas. for  $^{12}C(p,p)$  at 40-75 MeV 0-52840  
 relativistic beam contraction in necked mag. field 0-9436  
 RF field induced by a charged beam in a multigap resonator 0-52804  
 second coordinate measurement in drift chamber using charge division method 0-27856  
 SPEAR I, beam-beam limit simulation 0-37655  
 stable and unstable beam motions, mathematical statements 0-37663  
 stochastic cooling of particle beams, review 0-37675  
 storage rings, beam-beam interaction, radical diffusion simulation 0-37653  
 storage rings, beam-beam interactions, perturbation method solns. 0-37667  
 transverse beam instability in a resonator section, multimode approx. 0-52803  
 $\pi^-$  discrimination and absolute counting for nucl. capture at rest expts. 0-5432  
 He beam, magnetic spectrom. meas. using automatic tracking NMR system 0-27869  
 P ions, charge distrib., 72-123 MeV 0-27849

**particle beams**

- see also atomic beams; beam handling techniques; electron beams; ion beams; molecular beams; particle beam diagnostics; particle optics  
 bunching in cyclic focusing channel 0-23229  
 effusive beam source, heterogeneous reaction type, chem. equilib. 0-52362  
 electron beam interaction with target, integral eqns. (Ukrainian) 0-32549  
 high-power neutral beam, spectral resolution by optical diagnostics 0-33819  
 monochromatic and polarised photon beam at Frascati 0-23239  
 neutral beam generation, negative ion revolving multiple beam instabilities (French) 0-47798  
 neutron, non-monochromatic, spin flipper with prolonged working area 0-37673  
 neutron beam experiments (Japanese) 0-27684  
 relativistic, injected into strong mag. field, cross-section limiting 0-5427  
 relativistic beam contraction in necked mag. field 0-9436  
 relativistic collimated particle beam ave. particle energy meas., difference method 0-14049  
 relativistic self-pinch beam, radial expansion with distrib. energy, anal. 0-19609  
 beam prod. from isotopically enriched sputter targets 0-23221  
 $^{48}Ca$ , beam prod. from isotopically enriched sputter targets 0-23221



# particle counters *see counters*

## particle counting

counting of microscopic particles in disperse systems (aerosols, colloids etc.)

Knollenberg light scattering counters, response to doublet latex aerosols 0-37152

Royco aerosol particle counter 225, data processing system and modified system props. 0-37005

## particle detectors

*see also bubble chambers; ionisation chambers; particle track visualisation; position sensitive particle detectors; streamer chambers*

$\Delta E$ -E sample particle identification with wide dynamic range 0-14058

air showers for  $10^4$  to  $10^6$  particles, lateral distrib. of EM component, detection 0-17459

channel plate electron multipliers, single electron detection and timing 0-9458

charged particle spectrometer telescope 0-42895

cosmic ray muons and neutrinos, deep underwater detectors 0-8546

dead time meas. of individual detecting system 0-9470

electronics in nuclear science and technology 0-9347

focusing ion detector and mass filter for use with time-of-flight vel. distrib. measurements 0-4819

ion detector, electro-optical, for spark source mass spectrometry 0-42246

neutron detection, using  $Dy_2O_3$  activation detectors 0-887

neutron detectors for in-core flux monitoring 0-5297

neutron spherical survey meter response 0-18679

nuclear failed fuel element detection by delayed neutrons using solid state track-etch technique 0-5249

nuclear radiation detection lab., desk top calculators 0-36821

nuclear track detector, appl. as neutron dosimeter, response to standard neutron sources 0-5342

peak detector circuits, use with single-particle detectors and multichannel analysers 0-37707

plastic track detectors, method of producing thin sheets of proton-sensitive CR-39 0-35155

proton spectrometer/polarimeter for photoreactions below 1 GeV 0-18751

PWR neutron flux detectors, reliability tests (French) 0-32403

random summing in multi-detector counting system meas. radionuclide mixtures 0-36097

solid state nuclear track detectors, review 0-37696

superheated superconducting detectors, magnetic field dependence 0-27893

Cu as activation detector for thermal neutron meas. 0-52814

MgO dielectric detector characteristics 0-27898

## particle focusing *see focusing; particle optics*

## particle lenses, electrostatic *see electrostatic lenses*

## particle lenses, magnetic *see magnetic lenses*

## particle optics

*see also aberrations; beam handling techniques; electrodynamics; electron optics; ion optics; particle beam diagnostics*

beam trajectories through einzel lens for linear accelerator ion source (Japanese) 0-18718

bunched beams, transport, second order aberrations 0-52801

charged particle beam focusing, collimation and deflection 0-48132

dipole particle dynamics, integrable problems 0-18980

elliptical beam inside non-confocal elliptic vacuum chamber, potential 0-47799

high-power neutral beam, spectral resolution by optical diagnostics 0-33819

linac injection system beam dynamics, computer simulation 0-13989

mass-separator beam, quadrupole focusing lens system 0-47801

neutral beam injectors, multi-aperture extraction systems 0-42301

neutral beam line for plasma heating, stray particle loss near deflection magnet 0-47794

neutron holography, using Fresnel zone plate encoding 0-48131

quadrupole lenses with sector magnets, nonzero emittance beam focusing conditions 0-23612

two-dimensional electrostatic field construction for energy analysis 0-9796

## particle range *see energy loss of particles*

## particle scattering *see collision processes; energy loss of particles; particle backscattering; potential scattering; radiation effects; transport processes*

## particle separators

HV deflection condenser operated under high vac. conditions 0-27861

neutron velocity selector, high resolution, applic. to materials research (German) 0-47803

solar wind spectrometer, ion frequencies and velocities (German) 0-51636

velocity filter SHIP, efficiency for unsolved evaporation residues 0-23244

## particle size

acoustic particle agglomeration due to hydrodynamic collision between monodisperse aerosols 0-26191

aerosol, atmospheric, at S.Pole, size distrib. and concs. obs. 0-41484

aerosol, atmospheric, large particles in convective storm environment 0-41512

aerosol over Milwaukee, theoretical and meas. size distrib. 0-7970

aerosol particle content study at cloud edges and in clear atmosphere (Russian) 0-21794

aerosol particle size distrib. meas. in stratosphere 0-51578

aerosol particles attached to falling snow crystals, size distrib. 0-17362

aerosols, urban, in Nagoya area, size distrib. and Si and Al concs. 0-26581

aerosols from urban and desert regions in Israel, size distrib. 0-41503

aerosols with Junge size distrib., IR extinction 0-51537

anisylidenebenzidine, particle size distrib. function, electrooptical diffusion method for determ. 0-8956

atmosphere pollution aerosol, particle size spectra rel. to cloud modification effects 0-56571

atmospheric aerosols, particle size distrib. evolution via Brownian coagulation, num. simulation 0-41513

atmospheric precipitation, particle-size depend. of optical array precip. probe response 0-51577

bituminous surfaces, review of aggregate selection criteria for improved wear and skid resist. 0-7689

bone, mechanical properties rel. to density and mineral phase orientation and particle size 0-16989

$\eta$  Carinae, silicate grains size distrib. in Homunculus Nebula 0-4382

## particle size continued

ceramic, ultrafine powder, prod. by cryochemical, freeze drying, spray drying or soln. techniques 0-55336

clouds, drop size spectra modification by urban pollution aerosol, physical demonstration 0-56571

coal liquefaction, particle size distrib. as function degree of coal conversion 0-35626

coherent precipitates, particle size distrib. influence on extra-resist. 0-49689

colloid, electrooptical diffusion method for determ. 0-8956

colloids, concentrated, appl. of modern concepts in liquid state theory 0-40750

colloids, structure determ. by neutron diffr. and small angle scatt. 0-40748

crystallite with screw dislocation, determination of particle size and distortion 0-15098

crystallites, with step displacement, particle sizes and distortion determ., by means of X-rays (German) 0-14960

dendritic particle characterisation of automatic methods 0-25590

diamond, suspension, particle size distrib. function electrooptical diffusion method for determ. 0-8956

dispersed particles in matrix, coarsening 0-30288

dispersion coarsening, computer simulations 0-30289

distribution, continuity eqn. 0-55406

ethylene, obtained from gas cylinder, particle size distrib. 0-55723

extraction replica evaluation, Ashby-Ebeling model analysis (Czech) 0-49062

fine particle clusters, mass distrib. and growth process, expt. 0-26937

floatation of small particles, capture by bubble, theory 0-11959

fluidised bed reactor discrete cut particle size distributions, calc. 0-14812

granular materials, packing parameters, calc. from particle size anal. results 0-19294

graphite, suspension, particle size distrib. function electrooptical diffusion method for determ. 0-8956

hexamethylcyclotrisilazane film, plasma-polymerised, TEM study 0-44456

highly dispersed systems, phase size effect 0-6488

interface-controlled to diffusion-controlled coarsening kinetics, particle size distrib. 0-7579

interstellar, UV scatt. props. and size distrib. 0-26932

interstellar charged dust grains, radii rel. to motion in interplanetary space 0-4300

interstellar dust grains, size rel. to temp. fluctuations 0-26938

interstellar grain size, polarimetric obs. of four deviating stars 0-12792

interstellar grains, shape and size rel. to near IR linear polarisation wavelength depend. 0-51833

interstellar particle size distribution from linear polarisation calcs. 0-12787

jets produced by shaped explosive charges, particle size distribution in breakup 0-23957

Jupiter atmosphere aerosol, particle size and conc. from 0.6 to 1.1  $\mu$  spectrophotometry 0-46468

magnetic particle inspection oxides, evaluation 0-40657

mathematical modelling of growth of spherical metallic particles during photographic development process (Russian) 0-50871

metallic, surface tension depend. on size, vaporisation time (Russian) 0-34290

Nimonic, IN100,  $\gamma'$  precipitates, casting conditions effect on morphology 0-7548

oil shale retort dispersion, effect of particle size distrib. and flow nonuniformities 0-28560

organic pollutants, particle size distrib. in urban, rural and seashore aerosols 0-55958

Ostwald ripening, effect of precipitate vol. fraction 0-40356

polydisperse system, particle-size distrib. functions, determ. from SAS data by indirect transformation method 0-38860

polystyrene aerosols, monodisperse, depend. of attachment rate of  $^{220}\text{Rn}$  and  $^{222}\text{Rn}$  decay products 0-41256

polystyrene lattice, emulsions-polymerised, particle size determ. by soap titration 0-40753

polyvinyl alcohol, in water-ethanol mixture, processes of structure formation 0-10482

polyvinyl alcohol/vinyl acetate copolymer, in water-ethanol mixture, processes of structure formation 0-10482

powders, particle nonequiality effect on size distrib. meas. in pulse conductometric anal. 0-20833

powders and sintered bodies, particle size distributions from chord and area distributions (German, English) 0-35126

quartz, grinding and surface treatment by ball mill in cetyl alcohol (Japanese) 0-25890

Saturn C-ring, particle size from IR brightness and eclipse cooling obs. 0-56763

spherical particle in free-fall, time-to-complete-dissolution prediction 0-15245

steel, stainless, creep ductility, intergranular particle size and spacing effect 0-40461

steel, stainless, creep ductility, signal phase influence 0-55478

suspension, filtration in porous membranes, pore and particle size distrib. correl. (Japanese) 0-3418

suspension, in nonpolar dispersion media, particle size and number conc. meas. 0-9082

suspensions, creeping flow, hindered settling, particle shape effect 0-14797

transition metal clusters, particle size rel. to bulk metallic props. 0-44490

two phase alloy hardening by second phase particle coalescence 0-7591

ultrafine particles, production using cryopump (Japanese) 0-52252

YIG, hot spraying to give fine, free flowing, sinterable powder 0-20865

Ag ultrafine particles, effect of truncation of size distrib. 0-49562

Ag-Sn (6(8.2)(11) wt.%), splat-quenched, X-ray line broadening 0-40397

AgI aerosols, particle size influence on cryst. struct. 0-2000

Al-Si crystals, work hardened, softening and creep rates on annealing 0-11663

n-Bi<sub>2</sub>Te<sub>2.88</sub>Se<sub>0.12</sub>, extrusion deformed, powder dispersion degree influence on thermal and elec. props. (Russian) 0-39366

Cr, fine particle solar absorber, effective medium theory 0-21396

Cr-Co-Fe, chromindur alloy, field heat treatment, and mag. props. 0-35354

$\beta$ -Cu phthalocyanine electrophotographic props. rel. to particle size (Japanese) 0-13171

Cu powder, electrodeposition prep. conditions, statistical anal. 0-20828

Fe, atomised powder, props. 0-25600



**particle size continued**

- Fe powder, atomised, effect on props. of pressed and sintered material 0-11601  
 Fe-Ni-C, atomized, O/C ratio effect, particle size on annealing kinetics, physicochemical props. 0-20832  
 Fe-Si (3 wt.%), grain growth inhibition by MnS spherical particles with size distrib. 0-35218  
 Fe<sup>2+</sup>-Cr<sub>x</sub><sup>3+</sup>-Al<sub>2-x</sub><sup>3+</sup>-O<sub>4</sub><sup>2-</sup>, finely divided, oxidation kinetics 0-50848  
 Fe<sub>2</sub>O<sub>3</sub> powder, oxidation to γ-Fe<sub>2</sub>O<sub>3</sub>, coercivity changes 0-44864  
 α-FeOOH ultrafine particle NGR spectra, size distrib. and surface effects 0-11299  
 FeS<sub>2</sub>, oxidation, Mossbauer spectroscopic and magnetokinetic studies, 400-500°C 0-44880  
<sup>115</sup>In aerosol generation technique for atm. tracer obs. 0-26190  
 KCl:TiCl<sub>3</sub>, lattice defects, X-ray line profile obs. 0-24455  
 LiAlO<sub>2</sub>, fine particle size, heat treatment synthesis, molten carbonate fuel cell appl. 0-21395  
 MgO powders, hot pressing, mechanisms 0-40300  
 MgO, single cryst., order hardening by large precipitated vol. fraction of spinel particles 0-3085  
 Na smoke particles, nucleation and growth, light scatt. study 0-35580  
 NaCl aqueous aerosols, fixation and microscopic sizing 0-16734  
 Ni powders, stereological appl. in study of compacting process, elec. and mech. props. (French) 0-40286  
 Ni wire plasma sputtering with W particles, coagulation, struct. and particle size (Russian) 0-40260  
 Ni-SiO<sub>2</sub> supported catalysts, particle size, H<sub>2</sub> chemisorption, Mossbauer study 0-7219  
 Ni-ZrO<sub>2</sub>, electron-beam-evaporated condensate, cold deform. and annealing effects on microstruct. 0-16331  
 Pb powder size and shape distribution via image anal. 0-16221  
 p-Sb<sub>0.48</sub>Bi<sub>0.52</sub>Te<sub>3</sub>, extrusion deformed, powder dispersion degree influence on thermal and elec. props. (Russian) 0-39366  
 Se, amorphous, vac. deposition on polymer substrates, use of temp. gradient vac. coating device 0-35099  
 Ta powder, cathodic electrodeposit, effect of electrolyte composition and process parameters, on particle size distribution 0-16233  
 TiO<sub>2</sub>-ZrO<sub>2</sub>, submicron powders, vapour phase production from TiCl<sub>4</sub>-ZrCl<sub>4</sub>-O<sub>2</sub> system 0-40301  
 W powders, influence of geometrical props. on compaction (Russian) 0-20818  
 W/Cu powders, liq. phase sintering, particle rearrangement 0-45253  
 WC-Co powder, prep. by direct carburisation of WO<sub>3</sub> in presence of Co<sub>2</sub>O<sub>3</sub> 0-50573

**particle size measurement**

- aerosol beam instruments, nozzle inlet design 0-6183  
 aerosol particle size meas. by microcomputer-modified elec. analyser 0-40756  
 aerosols, monodisperse, 0.1-0.4 μm, size meas. by polarisation ratio of 90° scatt. light 0-40754  
 aerosols, size meas. by optical methods, review 0-40746  
 air pollution detector, condensation nucleus counter 0-55967  
 airborne, inertial sizing using laser velocimeter method 0-53901  
 atmospheric precipitation size distrib., small-particle response of optical array probe 0-51577  
 biological sound scatterers in water, acoustic size measurement 0-38199  
 colloid of submicron particles, ultrasonically induced birefringence technique 0-30290  
 continuum source particle beam properties, comput. modelling 0-26062  
 dispersed system, simultaneous determ. of refr. index and particle size from scattered radiation characts. 0-27335  
 dispersion, liq.-liq., new drop size distrib. mass. technique 0-3419  
 distribution parameters, estimation using forward scatt. techniques 0-36974  
 drop size measurement methods, review 0-17916  
 electron beam particulate analysis of air samples 0-40785  
 electrooptical diffusion method, determ. colloidal particle size distrib. function 0-8956  
 fine particle granulometric analysis, sieve and pulse methods (German) 0-22502  
 growing bubbles on heated plate, meas. using computerised image anal. system 0-22322  
 image dissector for size and position of statically suspended particles 0-26616  
 Knollenberg light scattering counters, response to doublet latex aerosols 0-37152  
 laser diffraction appl., particle and droplet size distributions meas. 0-17925  
 micropowder, cyclic classification, using variable electric field, device design 0-36982  
 Mie theory calculations, particle sizing appl. 0-14282  
 polydisperse particle size distrib. function, angularly scatt. light intensity profile meas. 0-13040  
 powder and sintered material particles, dimension and shape evaluation by SEM 0-40278  
 precipitation processes, study by particle site anal. 0-50883  
 remote sensing of size distrib., anomalous diffraction approx. solns. 0-17386  
 Royco aerosol particle counter 225, data processing system and modified system props. 0-37005  
 sieves, automatic, for particle size analysis 0-52380  
 spectrometer, Doppler shift, for research and calibration 0-4827  
 spherical particle velocity and size meas., crossed-beam light scatt. interferometry 0-47011  
 suspension, in nonpolar dispersion media, particle size and number conc. meas. 0-9082  
 suspensions, colloidal, radiometric method for particulate processes characterisation, theory 0-45578  
 suspensions, colloidal, radiometric method for particulate processes characterisation, expt. 0-45579  
 techniques for different branches of physics 0-1113  
 virtual impactor for particle classif. and generation of test aerosols with narrow size distrib. 0-30626  
 Zircaloy-4, microstrain and particle size meas. by Warren-Averbach method 0-55420  
 H<sub>2</sub>SO<sub>4</sub> aerosol particle size measured by impaction method 0-31134  
 Na vapour, particle size meas. using anemometer 0-13195

**particle sources**

- see also ion sources; neutron sources; radioactive sources  
 cluster beam generation of strong flux intensity using a slit nozzle (Japanese) 0-52361  
 electron, HV glow discharge as plasma electron source, characts. 0-44031  
 electron and ion beam generation at high power, review 0-13988  
 electron beam production, hollow cathode discharge as electron beam generator 0-44039  
 low energy positron beams, spin polarisation 0-9442  
 photon, electron and positron prod. from primary proton beams, Monte Carlo calcs. 0-32555  
 polarised positron, electron production by colliding photon beams in storage ring 0-5426  
 positron beam generation at low energy 0-5422  
 synchrotron orbital radiation, wiggler, helical wiggler and free electron laser (Japanese) 0-37658  
<sup>48</sup>V positron source prep. for annihilation radiation lineshapes, positron lifetimes meas. 0-876

**particle spectrometers**

- see also alpha-particle spectrometers; beta-ray spectrometers; electron spectrometers; gamma-ray spectrometers; neutron spectrometers; X-ray spectrometers  
 Amsterdam 500 MeV high duty factor electron scatt. facility, status report 0-23191  
 Cerenkov, total-absorption, characts. investigated with gamma-quantum, electron and positron beams 0-23242  
 electronic device for reduction of charge state energy doublets in electrostatic anal. of backscatt. He ions 0-27870  
 focal plane, large hybrid detectors, electric field uniformity improvements 0-37684  
 ionisation chamber, fission fragment atomic number identification 0-27863  
 ionisation chamber, multiplate, with intrinsic background reduction, response to photofission 0-37685  
 magnetic spectrometers, cosmic ray muons multiple scatt. 0-4215  
 neutral-particle analyzer system, multichannel, for anal. of charge-exchange flux from magnetically-confined plasma 0-4804  
 neutron capture gamma and electron spectroscopy, instruments and techniques 0-37695  
 nuclear reaction-emitted charged particle mag. spectrograph, multi-ang. 0-5429  
 pion non-dispersive low energy spectrom. 0-14038  
 pion spectrom. for meas. electro- and photo-pion spectra in high background environment 0-27868  
 positron annihilation investigation apparatus, review 0-23240  
 He beam, magnetic spectrom. meas. using automatic tracking NMR system 0-27869  
 Xe filled proportional scintillation detector for charged particles 0-32572

**particle track visualisation**

- see also bubble chambers; cloud chambers; nuclear track emulsions; scintillation chambers; spark chambers; streamer chambers  
 air showers for 10<sup>4</sup> to 10<sup>6</sup> particles, lateral distrib. of EM component, detection 0-17459  
 automated method for fission-fragment track density determ. in solid state track detection using MAGMO-1 system 0-42891  
 cellulose nitrate, <sup>6</sup>Li enriched, neutron detection props. 0-52828  
 CR-39 plastic, electrochemical etching, dosimetry appl. 0-52824  
 drift chambers in high-energy gamma-ray telescope 0-41726  
 ethylene-tetrafluoroethylene copolymer, chem. etching of fission tracks 0-896  
 fast neutron induced tracks in plastics, comparison using electrochem. etching 0-23154  
 fission track registration technique for U conc. determ. in water samples 0-12565  
 fission track-etch-cum-γ-spectrometry method for absolute fission yield meas. 0-27859  
 glass detections, thermometry 0-37031  
 glasses, effect of pre-irradiation and condition on etching 0-37702  
 ionising particle beam interactions with liquids, acoustic effect, laser beam simulations 0-23262  
 LR115 red cellulose nitrate personnel neutron rem dosimeter, design 0-52826  
 minerals, fission fragment range and closing temp. for track retention 0-41566  
 neutrino interactions in vertical emulsion target of hybrid apparatus 0-5126  
 neutron response of solid state nuclear track detector 0-27876  
 non etching polymers, fluorescent and dyed tracks, state of art 0-47825  
 nuclear failed fuel element detection by delayed neutrons using solid state track-etch technique 0-5249  
 nuclear particle track detectors, trends and developments (Hungarian) 0-18755  
 nuclear track detector, appl. as neutron dosimeter, response to standard neutron sources 0-5342  
 photographic tracking method, association with laser fringe anemometry 0-38512  
 polycarbonate foil, α-particle track prod., electrochemical etching 0-52825  
 polycarbonate track detector, electrochemically etched, meas. of low neutron fluences 0-32577  
 polyester foil neutron track detection, dosimeter appl. 0-5439  
 polyethylene-terephthalate track detector, electrochemically etched, meas. of low neutron fluences 0-32577  
 polymeric detector particle track diameter rel. to etching time (French) 0-9463  
 proton-sensitive CR-39 for plastic track detectors, method of producing thin sheets 0-35155  
 rem-dose measurement of mixed p-n radiation using solid state detectors of fission fragments 0-36137  
 soda lime glass track registration, HF etching conditions effect 0-52815  
 solid state nuclear track detectors, review 0-37696  
 TRIGA core, gamma dose meas. by plastic detectors 0-9381  
 vidicon systems, time digitiser in CAMAC format 0-14062  
 X-ray anal. of microcrystallite nucleation and detection threshold 0-890

**particle tracks**

- see also energy loss of particles  
 apatite, fission track retention as functions of heating time during isothermal expts. 0-36420



**particle tracks continued**

- bubble chamber, CERN HPD, finite spot size in ionisation meas. 0-27892
- charged particle track evaluation, distance distrib. and intratrack dose 0-26368
- corona counter, determ. of U content in solid waste mats. by  $\alpha$ -detection (Russian) 0-27904
- electron interactions, low-energy, single and twin biological targets 0-12195
- electron track end effects in water 0-11932
- emulsion nuclei, 28 GeV proton interactions (Korean) 0-18299
- fission track data reports standardisation 0-31436
- fission track dating method, standard error estimation 0-36419
- fission track dating technique 0-36417
- fission track retention as function of heating time during isothermal expts. 0-36420
- heavy ion track width in nucl. emulsion, Katz's theory 0-32578
- heavy-particle track structure rel. to radical physical distrib. and chemical effects 0-11933
- nuclear tracks, etched, statistical distrib. of quadratic holes on planar surface, computer simulation 0-37705
- single atom detection 0-9475
- structure analysis advantages over classical microdosimetry 0-26284
- tissuelike medium  $\alpha$  trajectory heavy secondary ion ejection 0-9466
- tissuelike medium  $\alpha$  trajectory production of  $\delta$ -rays 0-9465

**particle velocity analysis**

- see also energy loss of particles; ion mobility; mass spectrometers; particle spectrometers
- No entries

**particles, elementary see elementary particles****parton model**

- $\eta_c$  prod. cross section ratio in quark parton model (Korean) 0-27466
- asymptotic freedom and parton model appl. to leptonic processes 0-4959
- asymptotically free parton model, struct. function transverse momentum behaviour, SU(3) gauge model 0-27469
- deep inelastic scatt., field theoretical description, QCD, quark-parton, and light cone algebra (Russian) 0-42388
- deep inelastic structure functions and the quark parton model 0-4992
- fragmentation functions beyond leading order in QCD 0-13282
- hadron+hadron, jet production, large transverse momentum 0-42503
- hadron EM interactions, review 0-412
- hadron high energy struct. models (Hungarian) 0-4924
- hadron microstructure, de Sitter microuniverse, relativistic Hooke group and nonrelativistic quark model 0-27480
- hadron-lepton deep inelastic scatt., review, book contrib. 0-47260
- hard processes, parton model and QCD, review 0-47258
- high  $p_T$  jet pairs, parton-parton scattering and  $\pi$  quark struct. functions 0-47248
- hydrodynamic theory of high energy interactions (German) 0-406
- inclusive lepton pair prod., P violation, quark-parton model in Weinberg-Salam theory, QCD 0-37217
- intermediate vector boson, hadron-hadron collisions, Weinberg-Salam model 0-9186
- jet quantum number, identification model 0-42423
- jet quantum number identification event by event, original parton and gluon jets 0-52466
- jet-mass effects and high- $p_T$  jet production 0-52473
- kinematical scale breaking in high  $p_T$  interactions, parton fragmentation function 0-367
- massive lepton pair hadroproduction, QCD and parton model anal. 0-42421
- multiperipheral parton model, Reggeisation and dual unitarisation 0-37249
- pseudoscalar mesons, EM mass shifts, quark-parton model, SU<sub>3</sub> quark triplet 0-42459
- QCD, parton cross sections, infrared and mass singularity regularisation 0-32075
- QCD, parton distrib. function, transverse momenta, axial gauge ladder model 0-27467
- QCD extended leading logarithm approx. for inclusive distrib. and lepton pair prod. 0-379
- QCD multijet model, universal quark-jet fragmentation in soft hadronic reactions 0-13285
- quark masses and structure functions 0-22585
- quark parton model with large parton  $k_T$  0-42412
- relativistic oscillator formalism for hadron struct. and props. 0-9144
- scattering, deep inelastic, energy flow and energy correlations, perturbative QCD, infrared safety 0-27465
- Sterman-Weinberg formula for quark jets and gluon jets, leading log version, master equation 0-22552
- vector meson production in pp interactions, constituent-interchange model 0-22579
- virtual photon-nucleon scatt. anal. for spin 1/2 parton in covariant parton model 0-4966
- weak and EM phenomenology, gauge theoretical prospective, charm and flavour conservation 0-4916
- ed deep inelastic scatt. cross sections, quark-parton model with broken scaling (Russian) 0-32109
- $e^+e^-$  hadrons, scaling and quark struct. 0-425
- $e^+e^- \rightarrow \gamma +$  hadrons, high energy, lepton radiation and  $\gamma$  struct. functions, quark parton model 0-32113
- $e^+e^-$  hadrons, 13-31.6 GeV, gluon bremsstrahlung evidence, seagull effect, one sided jet broadening 0-430
- ep, deep inelastic scatt. cross sections, quark-parton model with broken scaling (Russian) 0-32109
- ep, high  $Q^2$ , QCD corrections to parity-violating asymmetries 0-22618
- $\mu N \rightarrow \mu X$ , broken colour gauge theory of integer charge quarks 0-13313
- $\nu_\mu(\bar{\nu}_\mu)N$ , charm meson prod. and decay, lepton inclusive distrib., c-quark fragmentation function (Russian) 0-52493
- $\nu N$ , deep-inelastic, electromagnetic radiative corrections 0-22602
- pp, 5.7 GeV/c, parton-cluster model, hadron struct. and non-diffractive collision impact parameters struct. 0-27454
- pp $\rightarrow l^+l^-X$ , QCD corrections to Drell-Yan formula 0-22578

**Paschen-Back effect see Zeeman effect****passivation**

- alloys, passivable, role of oxide films in stress corrosion cracking initiation 0-50762
- anodic oxide superficial layer, X-ray emission spectrometry and ion back-scattering (French) 0-49482

**passivation continued**

- Incoloy 600 and 800, surface film in hot conc. NaOH, XPS study 0-11824
- metal, corrosion pit initiation and growth, salt film form. 0-16563
- metal AC anodic dissolution rate, effect of  $H^+$  evolution (Russian) 0-16693
- metals, electrocrystallisation and passivation kinetics, multiple stationary states and dissipative structs. theory (French) 0-7804
- metals, precipitate films, ion selectivity effects on passivation and corrosion 0-35377
- review, passivity, in metals and alloys 0-50750
- steel, austenitic stainless, anodic polarization, Cr content effect 0-35382
- steel, low alloy, influence of accelerated weathering on corrosion 0-55565
- steel, stainless, ferritic, passivity in 1N HCl, X-ray photo-electron spectroscopic study 0-11817
- steel, stainless, type 304, corrosion fatigue and stress corrosion cracking, in boiling NaOH 0-7719
- steel, stainless 304, stress corrosion, high temp. electrochemical studies 0-30146
- surfactant adsorption on metal surface, effect on electrochem. reaction kinetics 0-40703
- TJS single-mode junction-up laser passivated with Si<sub>3</sub>N<sub>4</sub> film, life tests 0-19045
- Al brass condenser tubes, XPS study of protective layers 0-35383
- Al, cathodic polarization 0-21153
- Al, pitting mechanism, obs. using Engell-Stolica potentiostatic method 0-25905
- Al-Si<sub>3</sub>N<sub>4</sub>-Si struct., surface energy bands under step function illumination 0-49840
- Cu, passivation using protective glassy layers at 500°C 0-3246
- Cu-Ni alloys 706 and 715, corrosion in flowing sea water, dissolved sulfide effect 0-35379
- Fe and Fe alloys, passive films studied using AES combined with ion sputtering technique 0-35378
- Fe, corrosion and passivation in presence of halide ions in aq. solns. 0-50758
- Fe, dissolution and passivation, effect of phosphate and chromate corrosion inhibitors 0-21152
- Fe, in H<sub>2</sub>HO<sub>4</sub>, model for anodic dissolution 0-35545
- Fe, mechanism of action of weak acids and their salts on passivation by O<sub>2</sub> 0-50886
- Fe, passive, semicond. model for oxide film 0-2493
- Fe, passive films and phosphate layers, sputtering rate evaluation in glow discharge lamp 0-45443
- Fe, passivity in aq. soln., correlation with mol. struct. 0-16541
- Fe, pure, Auger anal. of passive films in neutral aq. soln. 0-16605
- Fe pyrophoric powders, stabilising layer form. during passivation, saturation moment meas. 0-44865
- Fe surface, nitride layer formation, activated surface, passivation 0-16577
- Fe-Cr alloys, NaClO<sub>3</sub> and NaCl effects on corrosion behaviour in hot NaOH soln. (Japanese) 0-35407
- Fe-Cr alloys, passivation films, modulation spectroscopy study 0-3244
- Fe-Cr-Pd, Pd alloying effects on passivation 0-35373
- Fe-Cr(Mo), passivated single crystal, selective dissolution and surface enrichment 0-16543
- Fe-Mo (5 wt.%), Auger anal. of passive films in neutral aq. soln. 0-16605
- Fe-Mo alloys, pitting 0-16549
- Fe-Ni-Cr-P-B amorphous alloy, localized corrosion 0-16559
- Ga<sub>1-x</sub>Al<sub>x</sub>As junction-up TJS laser electron injection efficiency improvement 0-48300
- Ga<sub>x</sub>Al<sub>1-x</sub>P high-temp. solar cell with 0.3 eV band gap 0-21400
- GaAs MESFET, possible use of anodic Al<sub>2</sub>O<sub>3</sub> for passivation, elec. props. of GaAs-Al<sub>2</sub>O<sub>3</sub> interface 0-49934
- GaAs MIS structs., nitride-based passivation for reduced surface state density 0-16537
- GaAs p-n junction, surface recomb. current reduction with Al<sub>0.5</sub>Ga<sub>0.5</sub>As:O surface layer 0-49878
- GaAs, surface, electron struct. and Fermi level pinning by O<sub>2</sub> and metals 0-11066
- GaAs surface passivation by GaO<sub>x</sub>N<sub>y</sub> films and multilayer systems 0-11809
- GaSb, surface, electron struct. and Fermi level pinning by O<sub>2</sub> and metals 0-11066
- InP, surface, electron struct. and Fermi level pinning by O<sub>2</sub> and metals 0-11066
- Li electrode, passivation layer, in LiClO<sub>4</sub>-propylene carbonate solution, composition (French) 0-11899
- Mo<sub>2</sub>C, corrosion and electrochem. props. in aq. H<sub>2</sub>SO<sub>4</sub>, HCl, HNO<sub>3</sub> and KOH solns. 0-11813
- Ni, dissolution and passivation in acid environment, effect of P (French) 0-45440
- Ni-Pd, anodic behaviour, potentiodynamic current density and impedance potential meas. (German) 0-25925
- Pb, aq. corrosion film, IR and Raman spectroscopy 0-55567
- PbO<sub>2</sub>, plate of Pb-acid battery, thermopassivation 0-3507
- PbTe surfaces, Te coating, struct. and junction characts. 0-50743
- SiO<sub>2</sub>, evaporated amorphous film, effect of O<sub>2</sub> on props., ESR spectra 0-11265
- Si<sub>3</sub>N<sub>4</sub> CVD for thin film passive components fabrication for high temp. instrumentation 0-40266
- Si<sub>3</sub>N<sub>4</sub> planar plasma deposition system, productivity increase for semiconductor device manufacture 0-40269
- SiO<sub>x</sub>, grown in HCl/O<sub>2</sub> ambients, phase separation and Na passivation 0-3219
- Sn plate, lacquer adhesions of passivation films, adhesion, ESCA exam. of constitution and effects 0-40776
- Sn-plate passivation films, TEM struct. obs. 0-45416
- Ti anode, Pt-Ir coated, corrosion and passivation behaviour in Cu electro-winning appl. 0-55573
- Ti, anodic behaviour, steady-state, in conc. HCl 0-45515
- Ti in acidic chloride solns., anodic dissolution and passivation 0-35541
- Ti, passive oxide layer form. in H<sub>2</sub>SO<sub>4</sub>, ageing with and without photoexcitation (French) 0-45432
- Ti, repassivation and pitting corrosion 0-30143
- Ti-Al-V (6, 4 wt.%), repassivation and pitting corrosion 0-30143

**passive filters**

- acoustic filters with open end, finite element prediction of transmission characts. 0-33349



**passive filters continued**

- elastic surface waves propag., characts. for SAW filters, book contrib. 0-1378
- magnetostatic wave transversal filters, status report 0-28394
- SAW, design and expt. results (*Czech*) 0-19201
- SAW, narrow band transversal types and interdigital transducers, review 0-28395
- SAW, physical props. and communication signals processing applications and devices 0-38162
- SAW, synthesis, limitations of phys. model in terms of number of fingers and material const. 0-28399
- SAW delay line filters, wideband, low insertion loss, VHF band 0-28398
- SAW filter design and implementation, book contrib. 0-1394
- SAW filter design for TV, CATV and radar appls. 0-53579
- SAW filters, design, construction, appl., book 0-1393
- SAW filters, electrode-withdrawal weighted method for reducing sidelobes 0-5875
- SAW filters, low insertion loss, using multiphased unidirectional transducers 0-28397
- SAW GHz quartz transversal filters, fabrication limits and characteristics 0-43562
- SAW grating-resonator filter, behaviour of unidirectional transducers 0-5877
- SAW metallic gratings, equivalent circuit of step discontinuity, rel. to SAW devices 0-33389
- SAW resonator filters, improved temp. stability using multiple coupling paths 0-19175
- SAW transversal, interdigital transducer models for accurate design implementation 0-28396
- SAW transversal filters, status report 0-28394
- SAW transversal filters, synthesis using interdigital transducer models 0-5897
- SAW TV IF filter, temp. stable ZnO/Pyrex glass substrate 0-43566
- shallow bulk acoustic wave delay line filters, narrowband and wideband implementations 0-28400

**patient care**

- anaesthesiology, characts. of elec. currents 0-46093
- breathing ratemeter for neonatal intensive care 0-41311
- computed tomography, cost of technically improved diagnostic images 0-17084
- ECG three-dimensional recording technique 0-41274
- intensive care ventilator, microcomputer-controlled 0-51292
- microprocessor-based tilting bed for blood pressure control 0-26412
- obstetric computer system for intensive care of mother and foetus during labour (*German*) 0-3857
- optometry, future of public and community health 0-12084
- vision research laboratory, clinically oriented, tasks and goals 0-12083
- O<sub>2</sub> inhalation automatic control for patients with respiratory failure 0-17181

**patient diagnosis**

- see also biomedical ultrasonics; electrocardiography; electroencephalography; medical diagnostic computing; radiography; radioisotope scanning and imaging; scanning radiography
- abdominal diagnosis, combined, complementary appl. of echoscopy, echotomography and echography 0-21507
- abdominal ultrasonography, clinical appl. 0-30826
- acoustic diagnostic technique for prosthetic fixation evaluation 0-21510
- acoustic microscopy of excised tissue 0-17041
- aneurysm detection using one-bit correl. 0-17175
- arterial stenoses, fluid mechanics 0-35948
- automated patient testing 0-46088
- ballistocardiograms, statistical pattern recognition 0-26408
- blood cell anal., weighted chi-squared test 0-30925
- blood cell electrophoretic mobility study, semi-automatic system 0-3851
- blood flow echography using Doppler techniques (*French*) 0-26303
- bone elemental analysis by prompt  $\gamma$ -ray spectra due to <sup>252</sup>Cf neutron irradi. 0-17065
- Bragg imaging in the reflection mode and designs for improved optics 0-17040
- brain stem electric response audiometry and middle ear effusion 0-56151
- brain stem transmission time and auditory nerve response 0-45917
- breast cancer connective tissue content correl. with US attenuation 0-45997
- breast carcinoma detect. by US Doppler signals 0-8110
- breast malignant tumour, freq. depend. US attenuation, fast Fourier transform technique 0-45996
- breast thermography, use of liq. cryst. sheets 0-41166
- breast tissue characterisation in vivo by US TOF computed tomography 0-51186
- breast tumour detection by US Doppler blood-flow signals 0-46001
- broadband US tomography 0-26311
- cancer, microwave techniques for diagnosis 0-26320
- cardiology, appl. of US in echography and bioecholocation, progress and prospects 0-21509
- cardiology, pulsed Doppler velocimetry, clinical appls. 0-46003
- cardiology, US real time system for simultaneous image displays 0-41148
- carotid obstruction detect. by supraorbital opacity pulses 0-51200
- carpal tunnel syndrome, palmar conduction time of median and ulnar nerves 0-12075
- chest radiography screening for employees in nuclear industry 0-26342
- chest X-ray automated screening, texture anal. of lung fields 0-41228
- chromosome-classification system based on banding technique 0-36199
- clinical microwave focusing thermography 0-3771
- computed tomography, spectral artefact correction and determ. of electron density and at. no. 0-51231
- computed tomography of liver, comparison with nucl. medicine scans 0-17109
- computed tomography of liver and biliary tract 0-17108
- computed tomography of thorax and abdomen, clinical study 0-17107
- computer-aided tomography and US, conf., Haifa, Israel, (Aug. 78) 0-27035
- computerised fluoroscopy for non-invasive cardiovascular imaging 0-17121
- computerised tomography, dynamic spatial reconstructor, high temporal resolution scanner 0-51235
- computerised tomography, X-ray, Rotate/Rotate type whole body scanner using direct magnification 0-21565
- computerised tomography in pulmonary nodule diagnosis 0-17110
- contact lens wearer diagnostic testing 0-12312
- coronary artery disease, early detect. by nonlinear anal. of ECG 0-26410

**patient diagnosis continued**

- cytogenetics, applications of photomicrography 0-21577
- diazotype radiographic duplicating system as diagnostic aid 0-8137
- dyslexia, detect. by computerised brain mapping 0-36185
- ECG, classification in terms of spectral characts. 0-56264
- ECG body surface potential mapping, improved diagnostic technique 0-26409
- echoencephalography, US pulsatile, prototype instrument and trial obs. (*Russian*) 0-17174
- echographic diagnosis of lesions of the abdominal aorta and lymph nodes 0-17033
- echography, real time, contrib. to diagnosis and management of palpable breast lumps 0-17027
- electro oculography, computerised diagnostic system 0-21566
- electronic linear-scanning US diagnostic equipment, high resolution 0-30813
- electronic radiography, computerised, for early detect. of vascular disease 0-41226
- electroradiographic image laser readout 0-41225
- electrostatic X-ray imaging, book contrib. 0-36112
- elementary particles from 1 GeV range accelerators, medicine appl. (*German*) 0-41210
- EM methods for medical diagnosis, review 0-36063
- EM strip transmission line energy coupler, for medical diagnostic appls. 0-17045
- EMG F response, radicular injury evaluation 0-3852
- epilepsy of late onset, visual and computer-assisted assessment 0-12294
- evaluation of diagnostic tests 0-17180
- eye, human, holographic diagnosis 0-12209
- fluoroscopic image recording using multiframed camera 0-51234
- fluoroscopy, automatic brightness control operating protocols and effect on image quality 0-17120
- glaucoma, optic disc changes meas. using retinal stereophotogrammetry 0-3757
- hand pathology, role of thermography 0-8120
- hearing defect diagnosis using electro-cochleographic methods (*Dutch*) 0-3855
- heart rate monitor cct., construction 0-30920
- heavy ion radiography 0-17122
- high technology medical equipment, Angioscan, Cardiac Output Computer, Medishield Analyser, Tomographic Scanner 0-36171
- histopathological information obtained from US tissue signatures and microscopy of biopsy samples 0-51195
- imaging, conf., San Diego, USA, (Aug 1978) 0-17025
- imaging, electronics developments 0-51285
- imaging systems, non-silver halide, recent developments and pot. 0-41223
- imaging techniques, book 0-12861
- imaging techniques, developments, review 0-26324
- impedance plethysmography, origin of impedance changes measured in the human calf 0-56269
- in-vivo activation analysis, diagnostic technique 0-56210
- joint inflammation, radioisotope X-ray fluoresc. technique obs. 0-56184
- kidney, intra-operative X-ray diagnostics in detection and localization of residual concretions 0-41202
- laser fluorescence bronchoscope for occult lung tumor localisation 0-30832
- laser medicine development trends 0-51198
- leg electrical impedance freq. characts. (*Japanese*) 0-56252
- leukaemia, rel. to blood U conc., meas. method using thermal neutron induced fission 0-21532
- lingual tactile sensory system, automated instrumentation for research 0-8205
- liver, comparison of scintigraphy, US and computerised tomography scanning 0-17105
- lung, small airway disease, possible diagnosis by pulmonary resistance meas. 0-30744
- maculopathy, Friedmann quantitative analyser for study of posterior pole disease (*Italian*) 0-17172
- magnification mammography evaluation 0-17124
- malignant melanomas, value of IR thermography 0-36062
- mammographic imaging, historical review in terms of image quality and reduced radiation dose 0-41229
- mammography, detective quantum efficiency anal. of electrostatic imaging and screen-film imaging 0-41232
- mammography reliability for early breast cancer detection 0-8127
- mammography techniques comparison, in vitro studies of breast microcalcification detectability 0-41230
- mammography with magnification and grids: detail visibility and dose measurements 0-41231
- mass spectrometry and metabolite profiling in study of human diseases 0-51289
- median nerve lesion localisation, usefulness of F-wave conduction time, post mastectomy patient 0-56267
- metabolite mapping by <sup>31</sup>P NMR in whole animals, diagnosis appl. 0-36211
- microwave scanner for soft tissue tumour detect. 0-17054
- multiple sclerosis diagnosis using cerebral evoked response and optokinetics 0-36183
- mutual impedivity spectrometry 0-17046
- neural diseases, quantitative EOG and CT obs. 0-36070
- neuroradiography by NMR imaging 0-51197
- NMR imaging, and biomedical appls. 0-46006
- NMR imaging, book contrib. 0-36064
- NMR in cancer, FONAR scan of live human abdomen 0-8122
- NMR limb blood flowmeter, clinical appls. 0-17178
- NMR technique 0-8121
- NMR zeugmatographic imaging of heart and lungs 0-17053
- non-invasive technology assessment, multiple endpoints 0-17179
- ocular photography, accessory fill-in flash for the Nikon photo-slit lamp 0-36056
- ocular tonometry through sonic excitation and laser Doppler velocimetry 0-56152
- optical instruments for medicine and biology 0-21517
- paediatric pneumogram patterns 0-3749
- paediatric radiology, image intensifier fluorography 0-41201
- pancreatic disease, short circuit current rat jejunum bioassay 0-8204
- pap smear inspection, segmentation approach 0-8124
- phonocardiogram detection algorithm using spectral tracking 0-41151
- phonocardiogram quantitative anal. for murmur detect. 0-56270
- plethysmograph, automatic venous occlusion device 0-17176



**patient diagnosis continued**

- pneumoconiosis, suspicious, recognition with aid of pulmonary function meas. 0-21567  
 prostate US sectional pictures, pattern recognition for tumour diagnosis 0-51194  
 radiographic  $\text{CaWO}_4$  intensifying screen, meas. of X-ray induced light photons emitted 0-41218  
 radiographic contrast improvement using fore-and-aft rotating aperture wheel device 0-41227  
 radiographic image formation, perceptual eval. of phys. parameters, computer-simulated images 0-41222  
 radiographic screen-film system evaluation, intensity vs. time scale sensitometry 0-41219  
 radiographic screen-film system evaluation, sensitometric method 0-41220  
 radiography, anal. of making, reading and reporting films, rel. to equipment design 0-17123  
 radiography, computed, contrast-detail-dose evaluation 0-41221  
 radiography, detection of bars and discs in quantum noise [radiography] 0-41042  
 radiography, micro-dose system 0-51233  
 radiography, patient exposure 0-46066  
 radiography, X-ray spectra determ., high intensity 0-41217  
 radiography equipment, idealised, for routine chest exams., specifications and requirements 0-46034  
 radiography screen-film combination selection 0-46047  
 radioimmunoassay as aid to diagnosis, review (*French*) 0-21522  
 radiosaturation diagnostic methods (*Slovenian*) 0-30863  
 retinal resolving power meas. by laser interferometry 0-36066  
 signal analysis applied to medical imaging 0-17038  
 skeletal demineralisation osteopathy, quantitative diagnosis, review (*German*) 0-30872  
 skin lesion Mn, Cu and Zn conc. meas. by neutron activation 0-17063  
 Sono Diagnost R multi-element scanner, use for upper abdomen US diagnostics 0-17028  
 SonoChromascope, US B-scan image acquisition, display and recording 0-30818  
 stability of human stance, meas. using vectorstabilograph 0-41275  
 thermographic diagnosis, high resolution dynamic method, detector system 0-41167  
 thermography, eval. of distortion 0-3750  
 Thoramat-automatic thoracic radiography unit experience 0-12212  
 tissue characterisation, static and moving, high spatial resolution US meas. techniques 0-51187  
 tissue parameter identification by digital processing of real-time US clinical cardiac data 0-51191  
 transkull transmission of axisymm. focused US beams, 0.5 to 1 MHz 0-51184  
 transrectal echographical ultrasound system, prostate, seminal vesicles and bladder exam. 0-41153  
 traumatised patient diagnostic radiology requirements 0-8128  
 tympanometry in neonates 0-3651  
 ultrasonography of the kidney in 1979 (*French*) 0-56149  
 upper airways in newborn and infants, X-ray physiological exam. using Orbiskop 0-8130  
 urodynamic combination EMG and functional X-ray exam. technique 0-8131  
 US, human abdominal tissue phantom 0-51152  
 US, linear-filter model for signal transmission process 0-17026  
 US, newer clinical imaging appls. 0-30825  
 US, signal processing 0-36049  
 US, tissue simulators 0-51153  
 US, transmission tomography by reconstruction compared with pulse-echo imaging, tissue-equiv. test objects 0-51154  
 US computed tomography of breast, progress 0-51196  
 US delay technique using phased array imaging system 0-30810  
 US diagnosis, basic principles 0-17037  
 US diagnosis, F mode images for any diagnostic plane utilising microcomputer and light pen 0-41147  
 US diagnostic techniques, basic principles (*Dutch*) 0-3744  
 US digitiser/processor for extraction of clinical parameters from Doppler-shift waveforms 0-36042  
 US dynamic imaging, high resolution 0-17042  
 US echo probes, flexible, and prospects for use in oncology 0-56147  
 US echography (*French*) 0-26305  
 US images corrected for refr. and attenuation, comparison of high resolution methods 0-30817  
 US imaging of neoplasms 0-17032  
 US imaging over view, appls. and future trends 0-48536  
 US imaging techniques (*French*) 0-26304  
 US impediography, quantitative characterisation of lesions in vivo 0-17039  
 US real-time diagnostic system 0-30819  
 US tissue analysis, comprehensive system 0-51189  
 US tissue characterisation, conf., Gaithersburg, USA (Jun. 1977) 0-41940  
 US tomography, refr. index and attenuation images rel. to breast tissue types 0-17036  
 US use in medicine and biology 0-4481  
 venous occlusion plethysmography for the detection of venous thrombosis 0-56268  
 video photography in computed tomography and US imaging, film selection 0-41224  
 vision, time-varying response anomalies 0-16935  
 visual evoked response meas. using versatile pattern-reversal stimulator 0-17177  
 X-ray appls., equipment development trends (*German*) 0-3751  
 X-ray beam characteristic time vars. meas. using solid state devices 0-46048  
 X-ray image intensifiers, quantum noise meas. 0-46033  
 X-ray tube performance characteristic rel. to radiologic image quality 0-17125  
 $\text{O}_2$  monitoring, intraarterial vs. transcutaneous monitoring in newborn infants 0-56266

**patient monitoring**

see also electrocardiography; electroencephalography

- acoustic method for monitoring healing of human long bones 0-21511  
 amputee monitoring system for rehabilitation programmes, assessment 0-17167  
 anaesthesia stage indicator, signal divider 0-3858

**patient monitoring continued**

- aortic ejection click and first heart sound description 0-30827  
 arterial blood pressure noninvasive monitoring by US imaging and phonocuff-sphygmomanometry 0-36180  
 arterial  $\text{PO}_2$  continuous meas. 0-56240  
 arterial pressure automatic indirect monitor 0-56231  
 blood gas continuous monitoring, current trends 0-56237  
 blood pressure long-term recordings, fast data reduction, hybrid system 0-41278  
 brain retraction pressure monitoring, meas. system for surgical procedures 0-21563  
 cardiac dysrhythmia anal., automated systems, review of difficulties 0-17164  
 cardiachometer histogram indicator, prototype 0-41268  
 deep tissue temp. monitoring by ultraminiature thermistors 0-3761  
 ECG, long-term recording on mag. tape 0-56243  
 ECG long term monitoring, automatic detect. of cardiac arrhythmias 0-3850  
 ECG slow wave real-time anal., hardware implementation of selective Bouilland transform. 0-56233  
 ECG three-dimensional recording technique 0-41274  
 EEG, automatic recognition of inter-ictal epileptic activity in prolonged recordings 0-3838  
 electrocardiodynamic continuous monitoring method 0-8195  
 electrocardioscopes, appl. and designs 0-41304  
 esophageal accelerometers, use in monitoring cardiovascular system 0-26403  
 eye-zz 0-56244  
 fever alarm device using telemetry 0-21556  
 glioblastoma tumour volume monitoring, autopsy rel. to computerised tomography meas. 0-21526  
 haemodynamic parameters monitoring by SOLO, an interactive minicomputer based bedside monitor 0-26392  
 hand pathology, role of thermography 0-8120  
 high technology medical equipment, Angioscan, Cardiac Output Computer, Medishield Analyser, Tomographic Scanner 0-36171  
 idiopathic scoliosis, adolescent, monitoring with Moire fringe photography 0-17047  
 intracranial pressure monitoring in neurotraumatology 0-17156  
 intravascular  $\text{O}_2$  continuous monitoring, electrochem. sensor 0-56238  
 intravascular  $\text{PO}_2$  probe routine appl., practical experience 0-56239  
 IR recording retinoscope for accommodation monitoring 0-36055  
 IR telemetry system for surgical patient monitoring 0-30836  
 knee ligament damage monitoring by acoustic emission, canine model 0-41149  
 medical electronics, new forms and techniques 0-3856  
 microcomputer-based pulmonary wedge pressure measurements 0-26391  
 monitor using Walsh transform on standard microprocessor 0-26399  
 muco-ciliary transport monitoring method using  $^{99m}\text{Tc}$  colloid, bronchiectatic patient appl. 0-30840  
 multiple pregnancies, problems in US monitoring 0-41145  
 neurology monitoring system for stroke patients 0-26394  
 obstetric computer-aided monitoring system (*German*) 0-41300  
 oximeter for spectrophotometric monitoring of arterial  $\text{O}_2$  saturation in the fingertip 0-41161  
 perfusion blood temp. monitoring, zero-heat-flow transducer 0-8201  
 physiological profiling, automated, in acute ill patients 0-30914  
 physiological signal on-line anal., multiple microprocessor system 0-26389  
 pressure transducer performance, effect of zero offset changes 0-56255  
 pulse rate monitor, digital, IR absorpt. detect. 0-26322  
 ROM based ECG monitor 0-26401  
 scintillation probe detector in assessment of cardiovascular disease 0-3800  
 static charge sensitive bed, method for recording body movements during sleep 0-3840  
 temperature distribution, using temp. depend. of US vel. 0-45994  
 $\text{O}_2$ , intraarterial vs. transcutaneous monitoring in newborn infants 0-56266  
 $\text{O}_2$  monitoring, combined system for transcutaneous and intravascular determ. of partial press. 0-56241

**patient treatment**

see also biomedical ultrasonics; radiation therapy; surgery

- air compressor used in system for treatment of decubitus ulcers, noise reduction 0-48513  
 biofeedback control of skin potential level 0-21572  
 blood oxygenation perfusion system for treatment of acute respiratory failure in infants 0-3866  
 bone healing, elec. stimulation of growth, treatment of non-union and delayed fractures 0-17044  
 bone healing, elec. stimulation of growth in treatment of non-union, review 0-17043  
 bone healing augmentation by electric currents and fields 0-8116  
 bone marrow transplant patients, clean room and laminar air flow room microbiology 0-26411  
 bone remodelling beneath internal fixation plates of varying stiffness, parametric study 0-16990  
 cancer treatment by hyperthermia (*French*) 0-17024  
 cardiac arrhythmias management, automated feedback control of drug therapy 0-41307  
 cardiac pacemaker treatment principles and experience 0-8213  
 cardiac pacing, signal source impedance of implanted electrodes 0-56275  
 coordination therapy electronic aid using pattern recognition methodology 0-56276  
 deaf people, computer generated speech training patterns 0-51290  
 diabetes mellitus, devices for control of continuous insulin infusion 0-17184  
 diabetes mellitus, public policy toward evaluation of control devices 0-17185  
 electrical stimulation and callus (*Japanese*) 0-12204  
 electrode-induced bone growth, function of implanted cathodes 0-41312  
 electrophrenic respiration, feedback control of tidal vol. (*Japanese*) 0-41316  
 EMG assisted relaxation training with hyperkinetic children 0-21571  
 EMG biofeedback training in low back pain treatment 0-21570  
 EMG feedback therapy after stroke, efficacy obs. 0-30927  
 endosteal implants, alveolar bone growth enhancement by elec. stimulation, dog expts. 0-26413  
 extraction wound non-invasive treatment by EM stimulation, dog expt. 0-17049



**patient treatment continued**

- eye, abnormal movements control method using audio feedback 0-41156  
 femoral shaft fractures, early weight-bearing treatment using cast-brace, biomechanics 0-16985  
 functional electrical stimulation of the upper limb, joint moment charting 0-41310  
 haemodialysis, PIXE meas. of trace element transport 0-36102  
 haemofiltration, appls. and limitations in clinical use (*German*) 0-21568  
 haemofiltration as alternative to conventional chronic dialysis (*German*) 0-21569  
 heart temporary artificial elec. stimulation 0-56272  
 laser medicine development trends 0-51198  
 LF interference current therapeutic apparatus (*Bulgarian*) 0-26314  
 Marat, Jean Paul, medical use of electricity, historical note 0-17781  
 paralysis, electric field control electrode for stimulation of peripheral nerve 0-21515  
 parametric biostimulation, mag. field calcs. 0-36054  
 photographic appls. in medical treatment and litigation 0-36189  
 skeletal muscle const.-vel. contractions by sequential stimulation of muscle efferents 0-41309  
 speech synthesis, portable equipment (*French*) 0-51291  
 spinal-cord stimulation in multiple sclerosis, electronic aspects 0-41313  
 stomatology, needle holder for intraosseous infusion 0-3859  
 tissue regeneration by electric potentials 0-41308  
 vascular bed modelling, optimal dialysis appl. 0-30758  
 ventricular defibrillation, transthoracic 100 kg calf, truncated and untruncated exponential stimuli 0-41306  
 visual deprivation studies rel. to therapy of strabismus, amblyopia and learning disorders 0-12081  
 visual therapy at home for constant esotropia with anomalous correspondence 0-8207

**pattern classification** *see* **pattern recognition****pattern recognition**

- see also computerised pattern recognition; speech recognition*  
 astronomical data reduction problem, appl. 0-8554  
 atom + diatom trajectories, collinear, pattern recognition appl. to  $H_2 + F(I)$ ,  $He + H_2^+$  0-45481  
 ballistocardiograms, statistical pattern recognition 0-26408  
 biological specimen recognition with partially matched spatial filter 0-46113  
 biomedical signal modelling and recognition, system identification approach 0-51286  
 chest X-ray automated screening, texture anal. of lung fields 0-41228  
 coherent optical correlation techniques, review 0-43277  
 coherent optical processor for vehicle tracking and identification using laser diode light sources 0-37957  
 coherent optical processor with interference contrast microscope input 0-43281  
 coordination therapy electronic aid using pattern recognition methodology 0-56276  
 digital processing aerial images, conf., Huntsville, Alabama, USA (May 1979) 0-48165  
 earthquake prediction, pattern recognition as a method of data analysis 0-4157  
 ECG, QRS detection accuracy rel. to anal. of HF components 0-17158  
 EEG automatic classification, Kullback-Leibler nearest neighbour rules 0-46079  
 fission reactor surveillance appls. (*French*) 0-37477  
 hand radiographs, congenital abnormalities classification 0-30870  
 holographic pattern recognition for 'simple' objects 0-53230  
 image representation using genetic geometrical functions 0-5702  
 landscape multispectral data, Karhunen-Loove analysis 0-48164  
 mass spectra, computer-aided classif., pattern recognition techniques, decision-tree approach 0-40774  
 matched filters for optical signal and pattern recognition 0-48392  
 moving object imagery using large aperture telescope arrays 0-53225  
 neural multiunit signals, educable waveform recognition system for sorting unit discharges 0-51312  
 neural net properties rel. to image processing algorithm 0-40993  
 neuronal waveforms, optimal recognition 0-56003  
 optical information storage, seminar, Washington, USA (Apr. 1979) 0-41942  
 optical scene matching methods 0-48167  
 overlapping-cell clustering algorithm, biomedical appls. 0-30926  
 pap smear inspection, segmentation approach 0-8124  
 peak identification in spectral analysis program 0-37706  
 phonocardiogram automatic classification, linear predictive anal. processing (*Japanese*) 0-36036  
 photoelastic fringe pattern analyzer, computer aided 0-38359  
 scene matching with feature detection 0-48166  
 scene principal vector analysis by multiple spatial filtering 0-48179  
 shape descriptors, Fourier-Walsh, radiographic image processing appls. 0-8153  
 side scan sonar data, adaptive sample set construction 0-43554  
 spatial light modulator, using  $KD_2PO_4$  and Se photoconductor, optical processing appl. 0-9988  
 steel, austenitic stainless, pipe welds, US inspection pattern recognition reflector classification feasibility study 0-16615  
 visual systems, fly, response properties 0-41021  
 $H_2 + F(I)$ , collinear trajectories, pattern recognition 0-45481  
 $He + H_2^+$ , collinear trajectories, pattern recognition 0-45481

**Patterson diagrams** *see* **crystallography; X-ray crystallography calculation methods****p.c.m.** *see* **pulse-code modulation****p.c.m. links** *see* **pulse-code modulation links****Peierls instability**

- antiferromagnetic Hubbard chain, interband absorpt., Peierls dimerisation, excitonic effects 0-25072  
 coulomb electron interaction and Peierls instability near the period doubling (*Russian*) 0-34343  
 disordered one-dimensional system, electron density of states and Peierls transition (*Russian*) 0-29304  
 electronic and spin Peierls transition, gap eqns. 0-24801  
 Fermi system, quasi-one-dimensional, electronic density of states (*Russian*) 0-6755  
 incommensurate Peierls-Frohlich system, fluctuation cond., Green's function calc. 0-24886  
 layered materials, struct. changes rel. to CDW, TEM, electron diffr., dichalcogenides appl. 0-39042

**Peierls instability continued**

- one-dimensional conductors, conductivity peaks, Peierls transitions (*Russian*) 0-49700  
 one-dimensional conductors, incommensurate CDW 0-20174  
 one-dimensional conductors, Peierls instability, dynamics, structural energy, pseudopot. calc. 0-54676  
 one-dimensional conductors, Peierls transition temp. and 0K energy gap, mean field theory calc. 0-24782  
 one-dimensional metal, phonon drag and sliding CDW 0-20173  
 one-dimensional metals, incommensurate sliding CDW 0-20156  
 organic linear chain cpds., diffuse  $4k_F$  refls., small intramolecular Coulomb interaction 0-34376  
 orientational metal-insulator phase transitions in quadrupolar strands with itinerant electrons 0-15455  
 phase transition in BCC hard sphere lattice gas with second neighbour exclusions 0-160  
 quasi one-dimensional spin lattice coupled system, collective modes 0-24896  
 spin-Peierls transition, mag. field effects 0-39796  
 spin-Peierls transition in mag. field, phonon freq., Heisenberg model calcs. 0-25151  
 spinless fermion systems, Coulomb repulsion, bond alternation, Peierls distortion, HF approx. 0-44524  
 TCNQ alkali salt, spin-Peierls transition 0-29395  
 TCNQ salt, HMTTF-TCNQ, three-dimens. ordering, Ginzburg-Landau model for Peierls instability 0-20160  
 TCNQ salt, MEM(TCNQ)<sub>2</sub>, phase transition electronic struct. interpretation 0-24781  
 TCNQ salt, pyridinium (TCNQ)<sub>2</sub>, low temp. mag. phase transition, ESR study 0-25139  
 TCNQ salt, Qn(TCNQ)<sub>2</sub>, thermoelec. power and cond., large Coulomb repulsion model 0-24893  
 TCNQ salt, TSeF-TCNQ, Peierls transition and CDW ordering, X-ray study 0-20101  
 TMTSF-DMTCNQ, metallic state, transport props. 0-24974  
 TMTTF-TCNQ, quasi one-dimens. conductor, diffusive hopping, theory 0-54677  
 TTF(MBDT) spin-Peierls transition, mag. exchange interactions, mag. props. 0-25138  
 (TTF)CuS<sub>2</sub>C<sub>4</sub>(CF<sub>3</sub>)<sub>4</sub>, spin Peierls system, mag. field effects 0-7123  
 TTF-Cu bis-dithiolenes, dimer, mol. displacements at 4.2K 0-10539  
 TTF-TCNQ, charge transfer change with press. 0-39564  
 TTF-TCNQ, electron-molecular distortion coupling near Peierls transition, IR spectra obs. 0-25390  
 TTF-TCNQ, physical properties, reviews (*Japanese*) 0-24883  
 TTFCuBDT, spin-Peierls transition in spin 1/2 Heisenberg chains, RPA calcs. 0-25150  
 TTT<sub>2</sub>(I<sub>3</sub>)<sub>1+x</sub>, physical props., elec., mag. and optical meas. 0-24908  
 two-band system, coexistence of dielec. and supercond. ordering 0-10853  
 X-Y quasi-one-dimens. system anisotropic, spin-Peierls phase transition, tricritical point 0-25142  
 Co<sub>0.83</sub>[Pt(C<sub>2</sub>O<sub>4</sub>)<sub>2</sub>].6H<sub>2</sub>O, quasi-one-dimens. conductor, Peierls distortion and superlattice, X-ray study 0-29397  
 K<sub>1.75</sub>Pt(CN)<sub>4</sub>·1.5H<sub>2</sub>O, Raman scatt. and luminesc. studies 0-25394  
 K<sub>1.75</sub>[Pt(CN)<sub>4</sub>].1.5H<sub>2</sub>O, elec. cond. studies, Peierls transition 0-24901  
 NbS<sub>2</sub>(Se<sub>2</sub>), Peierls distortion, electron diffr. obs. 0-39503  
 PbTe, CDW in strong mag. fields, Peierls-type transition 0-34362  
 Pt chain compounds, one dimens. conductors, Fermi wavevector determ., X-ray scatt. obs. 0-44187  
 TaS<sub>3</sub>, transport props. 0-20175

**Peltier effect**

- degenerate semiconductors, longitudinal thermo-EMF in quantising mag. field, scatt. mechanism (*Russian*) 0-24960  
 solar-powered solid-state heat transfer device based on photovolt. and Peltier effects 0-217  
 transient behaviour of thermoelectric coolers with high current pulse and finite cold junction 0-27290  
 GaAs:Sn, dopant segregation during liq. phase electroepitaxy 0-54384  
 HgI<sub>2</sub> thin sections with Peltier-cooled preamplification for X-ray spectrosc. 0-324  
 Si<sub>1-x</sub>B<sub>x</sub>H, amorphous films, thermopower and cond. for mixed band and broad tail state cond. 0-49786

**PEM effect** *see* **photoelectromagnetic effects****Pendellosing fringes** *see* **X-ray crystallography****pendulums**

- see also time measurement*  
 double with varying length, probabilistic characteristics of solns. (*Polish*) 0-8781  
 education, sprung pendulum, anal. of nonlinear coupling 0-51987  
 experimental design and statistical analysis of data, measurement of period of simple pendulum 0-42017  
 gyropendulum, aperiodic single rotor 0-14561  
 quantum, representation of canonical relns. 0-42084  
 quantum pendulum under periodic perturbation, stochastic behaviour 0-8834  
 ring of torsion coupled overdamped pendulums, nucleation theory of overdamped soliton motion 0-12899  
 simple, large-amplitude, Fourier anal., for teaching 0-17767  
 simple, with uniformly shortening string length, behaviour 0-27111  
 torsion pendulums, Collette anal. 0-22349

**penetration depth (superconductivity)**

- frequency dependence of penetration depth of elec. field (*Russian*) 0-34548  
 junction, superconductor-normal metal-supercond., impurities in normal metal layer, pair penetration depth determ. 0-29508  
 longitudinal electric field in superconductors and oscillations 0-15664  
 scattering model for DC Josephson effect, penetration depth 0-54838  
 strong-coupling superconductors, press. coeffs. of critical field, Ginzburg-Landau parameter, penetration depth 0-54833  
 superconducting contacts, critical currents, density, penetration depth 0-25059  
 superconducting round wire, flux distribution and hysteresis loss 0-34570  
 type I superconductor, first stage magnetisation and metastable migration field in slab 0-15655  
 type II superconductors, flux-line cutting 0-7055  
 Al-formvar superconductive junction, Ginzburg's generalised jellium model 0-15663  
 La particles, supercond. props. (*Russian*) 0-7018



**Penning ionisation**

- atomic metastable states, props., energy transfer mechanisms, exptl. techniques 0-27921
- discharge, HV, ionis. average freq. in anode sheath 0-44012
- ion source, Penning discharge type, HF instabilities 0-43997
- kinetic reactions, pulsed afterglow technique obs. in Ar-II plasma 0-48854
- molecular metastable states, props., energy transfer mechanisms, exptl. techniques 0-27921
- tripropylamine admixtures, influence on optical characteristics of CO<sub>2</sub> laser 0-23669
- Ar+He\*(1s2s,<sup>3</sup>S), Penning ionis., multichannel calcs. 0-53111
- CS+He, Penning ionisation, CS<sup>+</sup>(B<sup>2</sup>Σ<sup>+</sup>→A<sup>2</sup>Π<sub>i</sub>) fluoresc., flowing afterglow 0-14197
- H<sub>2</sub>+He (metastable), Penning ionisation (*French*) 0-1060
- He, 2<sup>3</sup>S<sub>1</sub> metastable state, interactions, optical pumping investig. 0-23377
- He-N<sub>2</sub>, de excitation rate consts., energy transfer, pulse radiolysis obs. 0-30303
- He+group II metal atoms, gas discharge plasma, Penning ionisation, cross section anal. 0-33735
- He(2<sup>3</sup>S<sub>1</sub>)+Ca(Sr)(Ba), coherent <sup>2</sup>P<sub>3/2</sub> levels excitation by Penning ionis., Hanle effect 0-5520
- He(2s<sup>3</sup>S<sub>1</sub>)+Sr, alignment of ions in Penning collisions, polarised emission obs. 0-25533
- Kr afterglow plasma, electron energy distrib. funtion 0-38748
- Kr\*+Ar\*, metastables, chemi-ionis., merging beams. 0.01-10 eV 0-14198
- LiF(Cl)(Br) film, electron emission under metastable He and Ne atom impact 0-20747
- N<sub>2</sub>+He\*, Penning ionisation, ejected electron spectra obs. 0-48074
- NaF(Cl) film, electron emission under metastable He and Ne atom impact 0-20747
- Sn<sup>+</sup>(5s5p<sup>2</sup>)<sup>4</sup>P<sub>1/2</sub> level, lifetime and Lande g-factor (*French*) 0-52938
- Zn<sup>+</sup>-He, positive column laser discharge, upper and lower state densities, Penning collision 0-32964

**penny-shaped cracks**

- branching criterion, invalidity of proof based on energy balance arguments 0-33536
- cylinder, weakened by penny-shaped cracks, thermoelastic stresses 0-10191
- elastic cylinder bonded to elastic surrounding material 0-19285
- elastic fracture mechanics, boundary integral eqn. anal. 0-14622
- finite orthotropic cylinder with penny-shaped crack, transient response under torsion 0-48640
- infinite transversely isotropic solid containing penny shaped crack, stress intensity factor (*French*) 0-43663
- longitudinal wave interactions at interface of two bonded dissimilar elastic solids 0-33532
- porous media, liquid saturated, disc-like crack development by hydraulic rupture (*Russian*) 0-19286
- thick plate under torsion, transient elasto-dynamic response 0-5993
- torsional oscillations at low frequencies 0-53703

**pentary algebra** *see algebra***perception (hearing)** *see hearing***periodic system of elements***see also elements (chemical)*

No entries

**peripheral equipment (computers)** *see computer peripheral equipment***peripheral models***see also multiperipheral models*

- deuteron wave functions, relativistic, π-NN coupling 0-22595
- exchange degeneracy breaking, hadronic selection rules 0-37248
- hadron photoproduction nondiffractive processes, review, book contrib. 0-47313
- hamiltonian for the nonrelativistic two-fermion bound state 0-13273
- meson exchange, relativistic corrections, book contrib. 0-475
- meson exchange currents, conservation principles, symmetries, book contrib. 0-473
- meson theory of nuclear vector and axial vecotr exchange currents, review, book contrib. 0-474
- multiperipheral parton model, Reggeisation and dual unitarisation 0-37249
- nucleonic form factor, pion exchange, model 0-22608
- one boson exchange model, OZI rule, nucleon-nucleon-boson coupling 0-32066
- one-boson-exchange-potential model of baryon-baryon scatt. 0-13295
- D<sup>+</sup> decay, Cabibbo suppression, strong 20-plet dominance and W exchange 0-42453
- e<sup>+</sup>e<sup>-</sup>→l<sup>+</sup>l<sup>-</sup> via many-vector boson exchange, cross sections from unified models 0-22597
- γp, low energy scatt., one-particle exchange model 0-22617
- NN elastic scatt. with one boson exchange, Bethe-Salpeter eqn. 0-42485
- NN narrow meson resonances near threshold, theoretical approaches 0-9157
- NN potentials for bound and scattering states 0-47323
- NN spectrum in pot. models, meson exchange forces 0-9156
- np→pn, 5-25 GeV/c, charge exchange scatt., πNN vertex function, one pion exchange 0-37291
- pp→(π<sup>+</sup>n)p, π energy and transverse momentum distrib., DHD model with nucleon exchange (*Russian*) 0-13327
- pp→nn, 5-25 GeV/c, charge exchange scatt., πNN vertex function, one pion exchange 0-37291
- pp→π<sup>+</sup>X, large p<sub>T</sub> processes, pion exchange model anal. (*Russian*) 0-27527
- pp reaction, exchange current corrections π and ρ exchange 0-26733
- pp scattering amplitudes, 6 GeV, phase shift anal. 0-37290
- π d→ρ<sup>+</sup>π d, 9 GeV exchange Deck model anal. 0-47322
- π n→ρ<sup>+</sup>π n, 9 GeV exchange Deck model anal. 0-47322
- πNN form factor, Δ(1236) contrib., calc. 0-22609
- π p→π<sup>+</sup>X, large p<sub>T</sub> processes, pion exchange model anal. (*Russian*) 0-27527
- N\*(1236) propagator, momentum depend. in N\*-excitation current 0-27559

**peripheral speed** *see velocity***peristaltic flow**

pumping by a lateral bending wave 0-53862

**Permalloy**

alloyed with refractory metal borides, mech. props., rel. to appl. as electrodes in electrosark machining 0-21174

**Permalloy continued**

- conductor crossing effect on bubble propagation margins 0-29588
- demagnetisation eigenfunctions anal. of linear transverse magnetisation in long, thin stripes 0-34687
- FCC, mag. anisotropy induced by cold rolling 0-11188
- film, coercive force associated with domain boundary displacement (*Russian*) 0-50151
- film, coercivity control 0-15764
- film, domain nucleation using low intensity US 0-34731
- film, domain wall mass and energy, wall vel. depend. calc. 0-2614
- film, multi- and single-layer, reson. curves subjected to tangential mag. reversals (*Russian*) 0-50195
- film, oxidation effects on atmospheric corrosion, AES, XPS and ion sputtering anal. 0-11829
- films, Faraday rotation effect dispersion 0-40092
- l-bar elements, magnetostatic effects, unifying overview of domain and continuum results 0-44853
- magnetic head wear resistance and surface characts. against mag. tape (*Japanese*) 0-35335
- Permalloy, pressing velocity effect on quality of compacts 0-20834
- Permalloy-Rh, film, influence of Rh on corrosion resist. and mag. props. 0-3235
- Permalloy-SiO<sub>2</sub>-Schott glass, bubble propagation struct. 0-34719
- powders, electric pulse shaping and sintering 0-25605
- proton radiation effects, Mossbauer obs. 0-40008
- RF sputtered films, struct.-sensitive mag. props. 0-34705
- solid boring for mag. head appl., wear resist. and microhardness 0-21172
- thin film cores, domain wall motion and flux patterns, Kerr magneto-optic effect obs. 0-34721
- Ti-Permalloy films, interdiffusion, Auger anal. and X-ray diffr. obs., degradation of mag. props. 0-34251

**permanent magnet motors**thermodynamic motor, dynamic characts. and stable operation (*Japanese*) 0-16840**permanent magnets**

- development and appls. 0-27320
- flux stability enhancement, by thermomechanical treatments, inertial guidance systems appl. 0-50144
- multipole, oriented rare earth cobalt materials 0-37925
- oscillations, coupled, demonstration using permanent magnets 0-42015
- plane permanent magnet system field distrib. model (*Russian*) 0-28133
- pull force magnitude, ferrite particle struct. effect 0-31815
- rare earth, physics and technology 0-20433
- repelling force system, with cylindrical rare-earth magnets, dynamic characts., forced vibrations of one-degree-of-freedom system (*Japanese*) 0-4744
- single crystal permanent magnet, industrial technology and equipment for manufacturing process 0-35075
- sintered permanent magnets, development history, magnetic and physical props., appl. 0-29901
- temperature dependences meas., automated apparatus for -150 to 300°C range 0-31809
- testing parameters selection, meas. errors determ. 0-52280
- Co-mishmetal-rare earth alloys for high energy permanent magnets, manufacture technology (*Polish*) 0-35132
- Cr-Co-Fe, chromindur alloy, field heat treatment, and mag. props. 0-35354
- Cr-Co-Fe permanent magnet anisotropic alloys, plastic deform., ageing, particle alignment temp. 0-35254
- Cu-Ni-Fe, permanent magnet, temp. effect 0-34701
- Fe-Cr-Co, permanent magnet, temp. effect 0-34701
- Nd,Pr,Sm,Co, permanent magnets, coercive force, low-temp. annealing influence (*Russian*) 0-39812
- Sm(Pr)-Co, sintered, cryst. phases (*Russian*) 0-39004
- SmCO<sub>5</sub> based permanent magnets, props. and cryst. orientation (*Russian*) 0-20431
- SmCo<sub>5</sub>, permanent magnet stability, during long-term ageing (*Chinese*) 0-55428
- SmCo<sub>5</sub>, sintered permanent magnet manufacture 0-20838
- Sm(Co<sub>0.81</sub>Cu<sub>0.19</sub>Fe<sub>0.04</sub>)<sub>6.9</sub> and Sm(Co<sub>0.84</sub>Cu<sub>0.16</sub>)<sub>6.9</sub> powders, mag. props. (*Russian*) 0-20434
- Sm(Co<sub>0.86-x</sub>Cu<sub>0.14</sub>Fe<sub>x</sub>)<sub>7</sub>, permanent magnet, sintering and heat treatment effects 0-39817

**permeability**

- acrylonitrile-methylacrylate-acrylamide latexes graft copolymerised onto PVA, for haemodialysis membranes (*Japanese*) 0-12297
- alkaline earth silicate glasses, morphology effects on props. 0-49118
- biomembranes, potential, rel. to surface pot., ionic permeab. 0-35853
- brain vascular permeability, effect of π<sup>-</sup> irradiation in neonatal rats 0-26275
- cellophane membrane, polarised, electret transport props., permeability coeff. 0-7860
- electrolytes, solid oxide, elec. props., study methods (*French*) 0-22386
- ethylene-vinyl alcohol copolymer membranes for haemodialysis, prep. conditions and props. (*Japanese*) 0-12299
- glass sintered powder porous bodies, liq. penetration mechanism (*Japanese*) 0-53853
- graphite, CO<sub>2</sub> permeability meas. up to 41 bars 0-29176
- haemodialysis membranes, permeability and rejection coeffs. 0-26207
- hydrogel of high water content as a material for the soft contact lens (*Japanese*) 0-12300
- kaolinite membranes, anion permeation 0-11952
- limiting relative law of heat and mass transfer and friction, permeability parameter effect 0-23999
- mammal cell junction, permeability of cell-to-cell membrane channel 0-51061
- membrane permeabilities, dynamic, meas. under non-equilib. conditions, appls. 0-46107
- membrane selectivity, influence of particle/pore size ratio 0-11946
- metal powders, vacuum treatment, method of calc. evacuation time and permeability 0-20827
- muscle cell osmotic state and membrane permselectivity repeated micro-wave irrads. effects quantitation 0-56131
- poly-n-hexyl L-glutamate, sorption and permeation mechanism 0-26048
- polyethylene films, fibres, radiation initiated graft polymerisation of acrylonitrile, initiation rate rel. to props. (*Russian*) 0-7531
- polyethylene membrane, permeation of hydrocarbons 0-30281
- polymer, glassy, gas sorption and transport, review 0-15360
- polymer, high, gas permeability meas. techniques 0-14854



**permeability continued**

- polypropylene films, hard elastic, gas permeability, extension effects 0-40412  
 polyvinyltrimethylsilane, diffusion, sorption, solubility, permeation of hydrocarbons, Xe (*Russian*) 0-6564  
 porous deep drawn conical shells 0-11728  
 porous medium, foaming, liquid and gas relative permeabilities 0-33669  
 PTFE, Ne, Ar, Xe and He diffusion and solubility 0-6561  
 PVC, chlorinated, fibres, radiation initiated graft polymerisation of acrylonitrile, initiation rate rel. to props. (*Russian*) 0-7531  
 solid electrolyte dielectric permeability, phase transition to superionic state (*Russian*) 0-49403  
 spectrin-actin monolayer, adsorbed at Hg-H<sub>2</sub>O interface, ionic permeability 0-12064  
 steel, stainless, permeation by <sup>2</sup>H(<sup>3</sup>H) in fusion reactor, oxide film influence 0-34241  
 steel, stainless types 321-SS and 430-SS, alumina coated, H<sub>2</sub> permeation 0-34244  
 tight junction disruption and recovery after sublethal  $\gamma$ -irrad. 0-36027  
 unsteady state meas. method 0-53895  
 vascular walls, physical theory of permeability rel. to atherogenesis, mech. effects 0-16908  
 Al<sub>2</sub>O<sub>3</sub>, permeability and solubility of H<sub>2</sub>, 1200-1450°C 0-39351  
 Al<sub>2</sub>O<sub>3</sub> sintered tubes, H<sub>2</sub> permeability 0-24675  
 Fe, permeation by H in fusion reactor 0-34242  
 H<sub>2</sub> in liquid Na reactor coolant, effect of O<sub>2</sub> 0-614  
 SiC, permeability and solubility of H<sub>2</sub>, 1200-1450°C 0-39351  
 T permeation through steam generator alloys 0-34250  
 Ti, permeation of H plasma reduced by layer of interstitially built  $\epsilon$ -Ti<sub>2</sub>N 0-16566

**permeability (magnetic) see magnetic permeability****permeability measurement (magnetic) see magnetic permeability measurement****permittivity***see also electric strength*

- acetamides, N-methyl-, N,N-dimethyl-, in organic solns., dielec. const., dipole moments, monomer-dimer equilib. 0-40031  
 alkali halide, electric-dipole ordering of tunnelling impurity centres 0-2215  
 alkali halide crystals, high freq. dielectric const. press. derivative model calcs., electronic polarisation 0-7255  
 n-alkanes, dielec. permittivity and pVT data 0-44996  
 anilines, substituted, in benzene soln., dielectric relax. time, dipole moment 0-50259  
 anilines, substituted, in nonpolar solvent, dielec. relax. obs. 0-55022  
 benzil, structural transition model, cryst. symm. spontaneous strain components 0-2161  
 benzyl cyanides,  $\alpha$ -substituted, in dil. soln., dielec. absorpt. obs., enthalpy of activation 0-55019  
 binary dielectric mixture relative permittivity formulae compared 0-15939  
 bone, human cortical, US properties and microtexture 0-51144  
 brain tissue, dog, dielectric props. between 0.01 and 10 GHz 0-16915  
 bromal, in benzene soln., dielec. relax., loss, and dipole moment 0-2692  
 bromoform, solid, phase transform., dielec. dispersion and differential scanning calorimetric obs. 0-24582  
 1-butanol, permitt., dielec. time domain spectroscopy, total transmission method study 0-27323  
 tert-butyl alcohol in nonpolar solvents, liq. struct. from dielectric studies 0-38894  
 carnauba wax, polarised, simultaneous variation of dielec. const. and discharge current, room temp. to beyond melting point 0-11314  
 celcian, with CaF<sub>2</sub> and ZnO additives, props. obs. (*Bulgarian*) 0-50579  
 ceramics, TiO<sub>2</sub> based, variation of dielectric constant and resistivity with temp. 0-2683  
 chiral smectic liquid cryst., ferroelectric, flexoelectric effects, dielectric const. 0-33877  
 complex, normalised, for Williams-Watts type of dielec. relax., num. table 0-7287  
 composite medium, with regular struct., dielec. props. 0-20576  
 cryogenic gases and liquids, dielectric breakdown 0-40051  
 cubic array of identical spheres, dielec. const. calc. 0-25271  
 p-cyano-p'-pentylbiphenyl/p-pentylbenzoic acid, mixture, induced smectic phase, dielec. props. 0-6498  
 cyanobiphenyls, nematic, dielec. consots. and diamag. anisotropies 0-7253  
 cyanocyclohexylcyclohexanes, nematic, dielec. consots. and diamag. anisotropies 0-7253  
 cyanophenylcyclohexanes, nematic, dielec. consots. and diamag. anisotropies 0-7253  
 dicalcium lead propionate, ferroelec., annealed, crit. exponents, dielec. const. temp. depend. 0-55050  
 1,1-dichloro-1-nitroethane, dil. soln. in benzene, dielec. relax. study 0-29679  
 dielectric friction in plasma, harmonic oscillator and rigid dipole dielectrics 0-53928  
 dielectric negative static permittivity possibility (*Russian*) 0-50253  
 dielectric relaxation data representation by Havriliak-Negami formalism 0-15950  
 diglycine nitrate, cryst. growth, dielec. and electromech. props. 0-2701  
 dipolar fluids, equilib. statistical mechanics, struct., dielec. and thermodynamic props. 0-6345  
 dipolar liquid, dielectric function rel. to microscopic correlation function 0-7290  
 dipolar molecules, zero-THz liq. phase dielec. absorpt. and rot. Langevin eqn. 0-40032  
 dielectrics and dielectrics, conf., Sao Carlos, Brazil, Sept. (1975) 0-7251  
 epoxy resin, curing investigation by polarisation current method 0-3345  
 epoxy resin systems, synthesis review, phys. and mech. props. at low temps. 0-25650  
 p-p'-ethoxyphenylazophenyl hexanoate, dielec. relax. in stable and metastable solid phases 0-34851  
 ethylammonium tetrachloromanganate, dielec. props. in phase transition region 0-55011  
 ferroelectric, with anomalously high dielec. const., self-focusing of EM wave 0-14408  
 ferroelectric plate, polarisation distribution, permittivity, domain structure 0-29704  
 fluid, of hard-spheres, with dipoles and quadrupoles, integral eqns. approx. 0-24334
- permittivity continued**  
 glycine silver nitrate, dielec. relax. in paraelec. and ferroelec. phases 0-29678  
 2-haloopropionates, liq., dielec. relax. and permittivity 0-15948  
 hard sphere fluid, dielectric const., Monte Carlo simulations, mol. dynamics calcs. 0-28897  
 heavy ice Ih (D<sub>2</sub>O ice), dielec. props. 0-29671  
 4-n-heptyl-4'- $\beta$ -cyanovinylbiphenyl, liq. cryst., isotropic mechanism of mol. rot., dielec. permitt. meas. 0-10491  
 p-heptyl-p'-cyanobiphenyl, refractive index, dielec. const., mag. susceptibility, orientational ordering (*Dutch*) 0-33884  
 heterogeneous matrix system, generalised conductivity and loss, tangent 0-7289  
 4-n-hexyl-4-cyanobiphenyl, liq. cryst., isotropic mechanism of mol. rot., dielec. permitt. meas. 0-10491  
 hydrocarbons, saturated open-chain, transport behaviour of excess electrons and props. 0-39643  
 ice, dielectric const., Onsager-Slater theory and unit model, Bjerrum defects 0-11310  
 incommensurate lattice, energy gap in phonon spectrum. role of Coulomb forces, dielec. props. 0-44269  
 inhomogeneous planar dielec. waveguides for integrated optics structs., synthesis (*Russian*) 0-38135  
 insect, Periplaneta americana, pyroelectric coeff. and permittivity obs. 0-51315  
 interferometric microwave spectroscopy, modern aspects, book contrib. 0-52330  
 ionic crystal, electronic dielectric const. first and second electronic dielectric const., effective charge parameters 0-29669  
 laser with inhomogeneous active medium, emission asymmetry 0-28191  
 layered random media, remote sensing, radiative-transfer theory 0-36413  
 leaves of rhododendron and encephalarts, pyroelectric coeff. and permittivity obs. 0-51315  
 longitudinal permittivity, crystal in strong EM field, light absorpt. and emission effect 0-15938  
 lossy dielectric material containing short randomly distributed metal fibres 0-20584  
 marble, LF dielectric props. 0-34843  
 MBBA, dielectric permitt. rel. to molecular props., effect of anisotropy of medium and local field 0-25270  
 MBBA, nematic liquid cryst., omeotropically aligned thin slice, dielectric permeability (*Italian*) 0-6354  
 MBBA, refractive index, dielec. const., mag. susceptibility, orientational ordering (*Dutch*) 0-33884  
 metal surface, adatom pair interaction asymptotics, degenerate electron gas permittivity 0-29281  
 methylammonium chromium selenate dodecahydrate crystals, dielectric relaxation 0-40043  
 3-methylthiomethylpropionate, liq., dielec. relax. and permittivity 0-15948  
 mixture of dipolar hard spheres, dielec. props. 0-24335  
 molecular crystals, polariton spectra and lattice dynamics 0-49313  
 naphthalene, single crystal, anomaly in permittivity due to thermoelectric space charge 0-7258  
 nematic liquid crystals, molecular mechanisms of dielec. polarisation and relaxation 0-34846  
 nematic liquid crystals, multicomponent mixtures, dielec. props. 0-38909  
 nematic liquid crystals, dielec. polarisation and relax., mol. mechanisms 0-29673  
 nitrobenzene, polarised, simultaneous variation of dielec. const. and discharge current, room temp. to beyond melting point 0-11314  
 nitrobenzene-hexane, soln., dielec. permitt. in two phase region 0-2682  
 NLC, high frequency electrohydrodynamic instability, permittivity, elec. cond. (*Russian*) 0-49099  
 Nylon 7-7 and 11, dielectric const. and dielectric relax. 0-25294  
 n-p-octyloxybenzylidene-p-toluidine, dielectric behaviour in nematic mesophase at RF 0-34842  
 oil shale from Piceance Creek Basin, Colorado, microwave radiation method 0-12378  
 one-dimensional conductors, disordered, elec. props., coherence length, impurity effects 0-24903  
 PAA, refractive index, dielec. const., mag. susceptibility, orientational ordering (*Dutch*) 0-33884  
 Pb<sub>3</sub>Ge<sub>3</sub>O<sub>11</sub>Gd<sup>3+</sup>, ESR spectra, electric-field effect and reversible permittivity 0-29614  
 p-pentoxyl-benzylidene-alkylaniline series, smectic phases, dielec. anisotropy 0-55010  
 physiological sample, fusion progression during rapid freezing for electron microscopy 0-3884  
 plasma, radiative, with anisotropic permittivity, developing wavefronts 0-43896  
 Poisson's equation, linear and nonlinear numerical solution including spatially variable dielectric const. 0-6825  
 polar semiconductor, exciton-dispersion 0-6741  
 poly(vinylidene fluoride) films, poled, piezoelec. activity and field-induced cryst. struct. transitions 0-20592  
 polyacetylene:1, electric props. in semicond. and metallic regions 0-29432  
 polyacrylate solutions, dielec. relaxation 0-40045  
 polyamide 6 (polycapromide), temp. depend. of complex permittivity rel. to moisture content 0-50251  
 polycarbonate, plastic insulation for cryogenic power cable, exam. of dielectric, tensile props. 0-25823  
 polydimethylsiloxane, crystalline and amorphous, characterised by DTA, polarised light microscopy, dielectric relax. 0-25295  
 polydimethylsiloxane liquid film, non-pure, dielec. behaviour 0-29672  
 polyester (Mylar), plastic insulation for cryogenic power cable, exam. of dielectric, tensile props. 0-25823  
 polyethylene, dielec. props. rel. to mol. struct. 0-29681  
 polyethylene, plastic insulation for cryogenic power cable, exam. of dielectric, tensile props. 0-25823  
 polyethylene-terephthalate, field-controlled photogeneration and carrier trapping 0-25285  
 polymer coatings for corrosion protection, electrochem. techniques for performance monitoring 0-3234  
 polymers, book 0-7257  
 polymers, electrical phenomena, nature and appl., book contrib. 0-50254  
 polypropylene, plastic insulation for cryogenic power cable, exam. of dielectric, tensile props. 0-25823  
 polypropylene sulphide, atactic chains, dipole moments, dielec. const. meas. 0-23584



## permittivity continued

- polysulphone, plastic insulation for cryogenic power cable, exam. of dielectric, tensile props. 0-25823  
 polytetrahydrofuran film, electrochemically prepared between Pt and Au electrodes, AC elec. props. 0-40062  
 polyvinylidene fluoride, dielec. props. and phase transitions (*French*) 0-55008  
 polyvinylidene fluoride magnetoelectret, AF and RF charge and dielectric characts. 0-40038  
 prefluorinated polymer, DuPont Krytox 143-AB, viscoelastic and dielectric props. 0-1503  
 2-propanol, dielec. time domain spectroscopy, total transmission method study 0-27323  
 propylene glycols, dielec. props., chain length effect 0-44995  
 PVC, reduced, dielec. props. rel. to mol. struct. 0-29681  
 $\alpha$ -quartz, complex dielec. const. at audio freqs., 5.5 to 380K 0-25272  
 quasi one dimensional charge transfer salts, soliton model for dielectric permeability 0-40036  
 radiation of uniformly moving charge on nonstationary layer 0-32893  
 rubber, styrene butadiene, dielectric const. and loss, lignin content depend. 0-29670  
 sapphire, complex dielec. const. at audio freqs., 5.5 to 380K 0-25272  
 schlieren method for the determination of electric field distributions in dielectrics 0-31720  
 semiconductors, doped, insulator-metal transition, dielec. const. enhancement on insulating side 0-20087  
 semiconductors, doped, insulator-metal transition, dielec. constant enhancement on insulating side 0-20088  
 shallow impurity centres near Curie point, influence of dielec. nonlinearity on temp. depend. of ionisation energy 0-10916  
 spin-phonon system, transition to self-trapping 0-10606  
 Stockmayer molecules, two dimens. fluid, static props., dielec. const. mol. dynamics calcs. 0-54094  
 suspensions, concentrated, of shell-spheres, dielectric theory, interfacial polarisation, anal. of biological cell suspensions 0-45563  
 suspensions, dielectric separation of solid particles 0-16213  
 suspensions of ellipsoidal particles covered with shell, dielec. behaviour, rel. to biological cells 0-51057  
 TCNQ salt, K-TCNQ, high and low temp. phases, dielec. const. 0-34844  
 TCNQ salt, N-propyl-quinolinium(TCNQ)<sub>2</sub>, defect conc. depend. phase transition 0-44577  
 TCNQ salt, NPQn (TCNQ)<sub>2</sub>, neutron irradiated defect concentration depend. phase transition 0-29449  
 1,1,2,2-tetrabromoethane, dil. soln. in benzene, dielec. relax. study 0-29679  
 tetrabutylammonium iodide, in aq. proline soln., elec. conductance investigation 0-10692  
 tetraethylene glycol dodecyl ether-H<sub>2</sub>O, binary micellar solns. and emulsions, dielec. behaviour 0-44994  
 tetraethylene glycol dodecyl ether-H<sub>2</sub>O-heptane, binary micellar solns. and emulsions, dielec. behaviour 0-44994  
 tetramethylammonium iodide, in aq. proline soln., elec. conductance investigation 0-10692  
 TGS:Cr single cryst., lattice defect influence on critical behaviour 0-25315  
 TGS:nitroanilines, permittivity, elec. cond. and Curie temp. 0-25273  
 TGSe, deuterated, thermal and dielectric props. at high hydrostatic press. 0-34864  
 trichloroacetonitrile, IR dispersion, complex refractive index and permittivity, time correl. function 0-45057  
 trifluoroacetates, methyl and ethyl, intramol. relax. at microwave freqs. 0-55020  
 trisarcosine calcium chloride crystals, ferroelec., electrooptic and ferroelastic props. 0-34865  
 TTF-TCNQ, interchain tunnelling effect on nucl. spin-lattice relax. time, interchain coupling of CDW 0-20163  
 water, normal and heavy, glass-transition temp., crystn. temp., and dielec. const. 0-15229  
 waveguide, inhomogeneous planar, profile determ. from mode spectrum (*Czech*) 0-28312  
 X- and  $\gamma$ -ray region dielectric permittivity, review 0-44998  
 zeolite-S layers, high-temp. activated dipole moments in S clusters (*Russian*) 0-20575  
 Ag<sub>2</sub>AsS<sub>3</sub>, proustite, light effects on dielec. props., elec. resist. 0-49816  
 AgNbO<sub>3</sub>, cryst. growth and phase transitions 0-40243  
 $\beta$ -AgSbS<sub>2</sub>, phase transitions, electrophysical props. 0-44316  
 Al-TeO<sub>2</sub>-Al, field-assisted cond. mechanism 0-11105  
 As<sub>2</sub>Se<sub>3</sub> glass, rel. to microwave elec. cond. 0-49793  
 Ba<sub>0.9</sub>Ca<sub>0.1</sub>Fe<sub>2</sub>O<sub>7</sub> glasses, semicond., cond. models, electronic props., 77-800K 0-54688  
 Bi<sub>1-x</sub>Si<sub>x</sub>,  $\beta$  rhombohedral, conduction mechanism, thermoelectric props. 0-24932  
 BaF<sub>2</sub>, dielec. const., 5.5 to 400K 0-50249  
 Ba<sub>1-x</sub>Sr<sub>x</sub>Nb<sub>2</sub>O<sub>6</sub> (x=0.27 to 0.54) exam. of freq. dependence of permittivity diffuse ferroelectric phase transition kinetics 0-2703  
 BaTiO<sub>3</sub>, single crystals, dielec. spectrum 0-25275  
 BaTiO<sub>3</sub>:La<sub>2</sub>O<sub>3</sub> and BaTiO<sub>3</sub>:La<sub>2</sub>O<sub>3</sub>:3TiO<sub>2</sub> capacitor, permittivity ageing obs. (*Korean*) 0-25325  
 Bi-NbO<sub>3</sub>-Bi system, Schottky barrier effects in transport and dielec. props. 0-29486  
 Bi-Sb, semiconducting, lattice dielec. const., comp. depend. 0-39516  
 Bi<sub>2</sub>O<sub>3</sub> film, dielec. meas. 0-2696  
 Bi<sub>2</sub>Ti<sub>3</sub>O<sub>12</sub> ceramics, ferroelectric, hot-forged, grain orientation and dielectric props. 0-40076  
 Bi<sub>2</sub>WO<sub>6</sub>, ionic cond. and relaxation polarisation, capacitance, losses 0-24657  
 CaCO<sub>3</sub>, calcite, complex dielec. const. at audio freqs., 5.5 to 380K 0-25272  
 CaF<sub>2</sub>, dielec. const., 5.5 to 400K 0-50249  
 CaF<sub>2</sub>:Na, vacancy motion activation vol., complex dielec. const. meas. 0-39356  
 CaTiO<sub>3</sub>-CaTiSiO<sub>5</sub>, sintering and dielectric props. 0-40307  
 CdS:Cu binder layer, photoactive, AC impedance meas. 0-25299  
 CdS:Li film, optical props. 0-2886  
 CeF<sub>3</sub> film, in MIM struct., dielec. props. (*Czech*) 0-25309  
 Co<sub>0.33</sub>(Pt(C<sub>2</sub>O<sub>4</sub>)<sub>2</sub>).6H<sub>2</sub>O, cond., dielec. const., microwave obs. 0-44636  
 Cs(B<sub>1-x</sub>W<sub>x-3</sub>)O<sub>9</sub> (B=Na, Ca, Co, Ni, Cd, Ga, Bi, Nb, Ta) cryst. struct., temp. dielec. anomalies 0-1998  
 CsD<sub>2</sub>PO<sub>4</sub>, dielec. props., press. and temp. depend. 0-25317  
 CsH<sub>2</sub>PO<sub>4</sub>, dielec. props., press. and temp. depend. 0-25317  
 CsH<sub>2</sub>PO<sub>4</sub>, ferroelec., critical behaviour of dielec. constant 0-34845

## permittivity continued

- CuFeS<sub>2</sub>, single crystal, optical reflectivity spectrum 0-40129  
 EuSe, annealed, AC conductivity and dielectric anomaly 0-34445  
 EuSe, polarisability of shallow donors, permittivity meas. 0-24833  
 Fe-Ge, characteristic energy losses and optical props. 0-29834  
 GaSe, long wavelength IR refl. spectra 0-11401  
 Ge:Sb, low-freq., low temp. dielec. behaviour below metal-insulator transition 0-50250  
 Ge-S-Se system, glass-forming, struct. and props. 0-19713  
 HCN crystals, polarisation spectra and lattice dynamics 0-49313  
<sup>3</sup>He-<sup>4</sup>He equimolar mixtures, excess vol., temp. and density depend. (*Russian*) 0-39380  
 Hg<sub>1-x</sub>Cd<sub>x</sub>Te, anodic oxide films, formation and props. 0-3212  
 K(B<sub>1-x</sub>W<sub>x-3</sub>)O<sub>9</sub> (B=Na, Ca, Co, Ni, Cd, Ga, Bi, Nb, Ta) cryst. struct., temp. dielec. anomalies 0-1998  
 KCl, colloidal suspension, radiowave dielec. dispersion 0-11311  
 KDY(WO<sub>4</sub>)<sub>2</sub>, Jahn-Teller transition, permittivity behaviour 0-55012  
 KNbO<sub>3</sub>, dielec. spectrum rel. to polarisation effects 0-15984  
 KNbO<sub>3</sub>, elec. and thermoelec. props., influence of O defects 0-29401  
 K<sub>2</sub>SeO<sub>4</sub>, Raman scatt. and dielec. props. 0-11313  
 K(Ta,Nb)O<sub>3</sub> ceramic, prep. and electro-optical props. 0-25620  
 La<sub>0.9</sub>Ca<sub>0.7</sub>CrO<sub>3</sub> polar semiconductor, elec. props., slight reduction effect 0-20183  
 (Li,Na,K) (Nb,Ta)O<sub>3</sub>, pseudo-binary and ternary systems quenched metastable glassy and cryst. phases 0-29935  
 LiCl, colloidal suspension, radiowave dielec. dispersion 0-11311  
 LiCsO<sub>4</sub>, thermal and dielec. props. 0-34860  
 LiF films, polycrystalline and single-cryst., comparative study of phonons by electron spectroscopy 0-25505  
 $\alpha$ -LiIO<sub>3</sub>, ion migration polarisation phenomena, current correlation function (*Chinese*) 0-6539  
 $\alpha$ -LiIO<sub>3</sub>, surface polariton spectroscopy, frustrated total reflection method (*Russian*) 0-49628  
 LiKSO<sub>4</sub>, thermal and dielec. props. 0-34860  
 MgF<sub>2</sub>, complex dielec. const. at audio freqs., 5.5 to 380K 0-25272  
 MgO, dielec. const., 5.5 to 400K 0-50249  
 N<sub>2</sub>-Ar(methane)(ethane) binary and ternary mixtures, dielec. const., excess vol. 0-7254  
 (NH<sub>4</sub>)<sub>2</sub>BeF<sub>4</sub>, gamma-ray effects obs. (*Japanese*) 0-11349  
 NH<sub>4</sub>HSO<sub>4</sub>, ferroelectric powder dielectric behaviour particle size depend. 0-55046  
 NH<sub>4</sub>IO<sub>3</sub>.2H<sub>2</sub>O, dielec. constant, elec. cond. phase transition and cryst. struct. 0-1999  
 Na vapour, induced optical anisotropy (*Russian*) 0-38526  
 Na<sub>0.5</sub>Bi<sub>0.5</sub>TiO<sub>3</sub>, dielectric const. thermal hysteresis, ferroelectric-antiferroelectric transitions 0-50281  
 NaBrO<sub>3</sub>, surface polariton spectroscopy, frustrated total reflection method (*Russian*) 0-49628  
 NaCl(Br) (F) (I), lattice dynamics and statics, three-body-force shell model 0-49323  
 NaNO<sub>2</sub>, incommensurate-and-antiferroelectric phase transition, amplitude mode, ultrasonic study 0-39227  
 NaNbO<sub>3</sub>, elec. and thermoelec. props., influence of O defects 0-29401  
 Na<sub>2</sub>W<sub>2</sub>O<sub>7</sub>F<sub>6</sub>, single cryst., prep., optical and dielec. studies (*French*) 0-15994  
 Nb, anodic oxidation, open circuit transient anal., dielec. and elec. props. of oxide film 0-3245  
 Ne, dielectric constant near liquid-vapour critical point 0-50252  
 P-Se-Tl system glasses, polarisation, refr. index and dielec. const. meas. 0-20608  
 PLZT ceramics, diffuse phase transitions and thermodynamics 0-29694  
 PLZT ceramics, ferroelectric and struct. transitions, crystallographic, thermal, and dielec. anal. 0-29693  
 PLZT ceramics, phase transitions induced by elec. fields 0-29695  
 2PbFe<sub>1/2</sub>Nb<sub>1/2</sub>O<sub>3</sub>-PbFeReO<sub>6</sub>, comp., struct., dielec. and mag. props. 0-2704  
 2PbFe<sub>1/2</sub>Ta<sub>1/2</sub>O<sub>3</sub>-Ba<sub>2</sub>FeReO<sub>6</sub>, comp., struct., dielec. and mag. props. 0-2704  
 2PbFe<sub>1/2</sub>Ta<sub>1/2</sub>O<sub>3</sub>-PbFeReO<sub>6</sub>, comp., struct., dielec. and mag. props. 0-2704  
 Pb<sub>3</sub>(Ge,Si)<sub>3</sub>O<sub>11</sub>, dielec. and elec. props., 20 to 250°C 0-29697  
 Pb<sub>3</sub>GeO<sub>7</sub>, dielectric thin film, obtained by sedimentation, exam. of dielectric props. and structure 0-2282  
 Pb<sub>2</sub>Ge<sub>2</sub>O<sub>11</sub>, photodielectric effects, Curie temp., permittivity and polarisation 0-40034  
 Pb<sub>2</sub>(Ge<sub>1-x</sub>Si<sub>x</sub>)<sub>2</sub>O<sub>11</sub> solid solutions, dielec. props., ferroelec. phase transitions 0-15988  
 PbHAsO<sub>4</sub>, ferroelec., far IR and microwave dielec. props. 0-55108  
 PbHPO<sub>4</sub>, microwave permitt. and far IR refl. spectra in paraelec. and ferroelec. phases 0-40033  
 PbI<sub>2</sub>, visible exciton spectrum, exciton-phonon interactions, dielectric const. and oscil. strengths 0-25405  
 PbMg<sub>1/3</sub>Nb<sub>2/3</sub>O<sub>3</sub>, dielec. props. under high hydrostatic pressure near phase transition point 0-44997  
 Pb(Mn<sub>1/2</sub>Ta<sub>1/2</sub>)O<sub>3</sub>, ceramic, for thermal and dielectric isolation at low temp. 0-39365  
 Pb<sub>1-x</sub>Sn<sub>x</sub>Te, (x<0.35), permittivity and soft modes, carrier density and comp. effects 0-7256  
 Pb<sub>0.94</sub>Sr<sub>0.06</sub>(Ti<sub>0.47</sub>Zr<sub>0.53</sub>)O<sub>3</sub>-NiO, modified, dielec. and piezoelec. props. 0-11342  
 Pb<sub>2</sub>TaMnO<sub>6</sub>, reaction of form. from oxides, ferroder. props. 0-55326  
 PbTe very thin epitaxial films, transmission and refl. spectra, 1 to 5 eV, dielec. const. calc. 0-7430  
 PbTe-SnTe compound semiconductors, lattice instability by mm-wave magnetoplasma refl. 0-54336  
 PbTiO<sub>3</sub>, anomalies in elec., photoelectric and mechanical props. 0-55051  
 PbTiO<sub>3</sub>, ferroelectric thin films, fabrication by RF sputtering, characts. 0-40261  
 PbTiO<sub>3</sub>-La<sub>2</sub>O<sub>3</sub>.3TiO<sub>2</sub>, struct. and dielec. props. 0-54200  
 Pb(Zr,Ti)O<sub>3</sub> ceramic, interconnected porous, props. 0-43579  
 Pb(Zr,Ti)O<sub>3</sub> thin films, fabrication and characterisation electron-beam deposition 0-16188  
 Pb(Zr,Ti)O<sub>3</sub> thin film, ferroelec., fabrication by RF sputtering (*Japanese*) 0-25560  
 Pb(Zr,Ti)O<sub>3</sub>:Cr<sub>2</sub>O<sub>3</sub> ceramic, electrical cond. and dielectric const. meas. 0-2389  
 PbZrO<sub>3</sub>, phase transitions, X-ray, dielec., and thermal anal. 0-45020  
 PbZrO<sub>3</sub>, pyroelectric detector, low temp. behaviour, expt. 0-31869  
 1-xPbZrO<sub>3</sub>-xPbSc<sub>0.9</sub>Nb<sub>0.1</sub>O<sub>3</sub>, 0≤x≤1, phase transitions, X-ray, dielec., and thermal anal. 0-45020



**permittivity continued**

- Pb( $Zr, Ti_{1-x}$ )O<sub>3</sub> films, ion beam deposition, struct., dielec. and ferroelec. props. 0-20788  
 Rb(B,W<sub>1-x</sub>)O<sub>9</sub> (B=Na, Ca, Co, Ni, Cd, Ga, Bi, Nb, Ta) cryst. struct., temp. dielec. anomalies 0-1998  
 RbHSO<sub>4</sub>, acoustic and dielectric props. near phase transition 0-55053  
 RbHSO<sub>4</sub>, dielec. dispersion near ferroelec. phase transition 0-2684  
 RbHSO<sub>4</sub>, isotope effect, dielec. const. and spin polarisation investigation 0-20574  
 RbHSeO<sub>4</sub>, successive phase transitions 0-15985  
 SbNbO<sub>3</sub> single crystals, pure and doped, growth and pyroelec. and ferroelec. props 0-40248  
 SbSi, cryst., low temp. dielec. anomalies and domain struct. 0-40035  
 Si oxide film, porous Si layer oxidation, dielec. props. 0-55556  
 Sn<sub>2</sub>P<sub>2</sub>S<sub>6</sub>, illumination effect on soft mode and dielectric props., luminesc. study (*Russian*) 0-50420  
 Sr<sub>0.6</sub>Ba<sub>0.39</sub>Nb<sub>0.6</sub>O<sub>6</sub>, electromechanical props., permittivity, elastic compliance, piezoelectric moduli 0-29691  
 SrF<sub>2</sub>, dielec. const., 5.5 to 400K 0-50249  
 SrF<sub>2</sub>:Er, activation vol. for interstitial motion, dielec. const. meas. 0-49412  
 SrTiO<sub>3-x</sub>In contacts, differential capacitance, elec. field depend. permittivity effect 0-54779  
 TGS, ferroelec. cryst., complex permittivity at microwave freq. and high press. 0-2685  
 TGSe, ferroelec. cryst., complex permittivity at microwave freq. and high press. 0-2685  
 Ta<sub>2</sub>O<sub>5</sub>, reactive DC sputtering deposited films with magnetron-plasmatron, mechanical elec., optical props. 0-25566  
 TiO<sub>2</sub>, reactive DC sputtering deposited films with magnetron-plasmatron, mechanical elec., optical props. 0-25566  
 TiO<sub>2</sub>-Ti<sub>2</sub>O<sub>3</sub>-P<sub>2</sub>O<sub>5</sub>, glass form., struct. and elec. props. 0-44592  
 TiO<sub>2</sub>:Cr<sub>2</sub>O<sub>3</sub>, dielec. const., AC and DC resist. 0-20186  
 TiH<sub>2</sub>PO<sub>4</sub> and TiD<sub>2</sub>PO<sub>4</sub>, dielec. props. under hydrostatic press. up to 7 kbar 0-29696  
 W, anodic oxidation, open circuit transient anal., dielec. and elec. props. of oxide film 0-3245  
 ZnO-Bi<sub>2</sub>O<sub>3</sub>-CoO-MnO-Sb<sub>2</sub>O<sub>3</sub> (97.5, 0.5, 0.5, 1.0 mole%), exam. of elec. props. at different annealing temps. 0-3099

**permittivity measurement**

- anisotropic dielectrics parameter meas. using resonance of waveguide-dielectric system 0-27274  
 anisotropy meas. at microwave freq., experimental results 0-52279  
 anisotropic specimen, dielectric const., NDT 0-35475  
 biological liquids at microwave freqs. 0-26424  
 biological substances at RF and microwave frequencies 0-52275  
 capacitor for wide-range dielectric constant meas. on fluids 0-4737  
 cavity method of dielectric constant meas., freq. and mode errors 0-13103  
 complex dielec. const., wide-range dynamic measurements using microcomputer control techniques 0-22383  
 complex permittivity of liquids at mm/cm wavelengths, quadratic convergence curve fitting technique 0-13097  
 dielectrophoretic, effects of sample size 0-13094  
 dielectrophoretic levitation method 0-52264  
 EM waves, parallel polarised, equal reflectance at normal and oblique incidence, dielec. const. meas. 0-1119  
 ground, determination using EM methods, review 0-22382  
 heterogeneous dielectric, resistivity and static dielec. permittivity determ. in linearly time depend. elec. field 0-52268  
 high precision measuring device 0-4742  
 homopolar devices, rotation of DC glow discharge, Doppler shift of spectral lines 0-33838  
 human serum and erythrocyte microwave complex permittivity meas. 0-3889  
 insulating materials, three-terminal cell for meas. over wide freq. and temp. ranges 0-37053  
 liquid and solid complex permittivity meas., rectangular waveguide method 0-15941  
 liquids, complex dielectric const., modified Hippel method (*German*) 0-31801  
 liquids, modified microwave cavity perturbation techniques 0-42239  
 liquids with high dielectric losses, 300 MHz to 6 GHz (*German*) 0-13106  
 low-loss solid dielectric meas., automated resonance substitution systems 0-15957  
 microwave measurement of materials with high permittivity using waveguide measuring line 0-47080  
 microwave measurement using cavity perturbation technique 0-31802  
 microwave Michelson interferometer improvement operating at 140 GHz 0-31854  
 oil composition analysis by means of cracking, permittivity thermal dependences obs. (*Czech*) 0-46289  
 open resonator methods for microwave permittivity meas. 0-15942  
 piezoelectric film, third-order piezoelec. and dielec. const. meas. using surface acoustic waves (*Japanese*) 0-55042  
 relative dielectric constant for insulators in range 1-10 GHz, State Special Standard 0-13037  
 small liquid biological sample microwave complex permittivity meas. 0-17222  
 soil, SW measurement of dielec. const. and conductivity 0-22388  
 solids and liquids, dielec. characts., temp. depend., laboratory installation for meas. 0-37051  
 standard specimens, class 1, for dielectric constant, certification methods 0-13036  
 substrate dielectric constants, standard specimens 0-13038  
 test scheme design 0-13101  
 thin film permittivity and thickness determ. using differential-gap varying method (*Japanese*) 0-4739  
 USSR state standard for 0.2-1 GHz range 0-9004  
 water film, between muscovite sheets, permittivity change meas. method, 20-70°C 0-55009  
 CsFeF<sub>4</sub>, struct. phase transition at 250K 0-10663  
 KCl far IR complex permittivity meas. by dispersive Fourier transform spectroscopy, 7 to 300K 0-15940  
 LiNbO<sub>3</sub> piezoelectric coeff. and permittivity meas., small-sample method 0-15981

**personnel**

- see also education; management; teaching; training  
 computer-assisted-learning agency, staffing needs and position in vertical organisational struct. of educational institution 0-42007

**personnel continued**

- consumer electricity supply demands fulfilment and ensuring full employment (*German*) 0-36831  
 nuclear power stations, radiation dosage determination, monitoring and control for personnel safety (*German*) 0-842  
 Phenix plant operations and modifications (*French*) 0-47615  
 social effects of microelectronics (*Dutch*) 0-20

**perturbation techniques**

- see also control system analysis; control system synthesis  
 atomic configuration interactions, appl. of unitary group methods 0-27958  
 atoms, photoionisation cross sections, electron correl. reson. struct., relax. effects many body perturbation calcs. 0-47852  
 convection, forced, laminar, wedge flow with separation 0-1523  
 electron correlation calculations, scaling and Pade approximants rel. to perturbation series 0-5487  
 human head EM induced field and power absorption, ellipsoidal model 0-3724  
 methane+Ar, rot. compound state resons. 0-28090  
 molecular configuration interactions, appl. of unitary group methods 0-27958  
 neutron streaming along fusion reactor ducts, perturbation and variational corrections 0-23143  
 nuclear spin-spin coupling const., finite perturbation-CI calcs. 0-5563  
 plate temp. dependent props. under linear temp. distrib., thermoelastic problem for crack 0-48579  
 Signorini's perturbation procedure in elasticity, branching of solutions 0-27134  
 soliton perturbations, variational calcs. 0-46825  
 HgI<sub>2</sub>, relativistic effects, photoelectron spectra, Hartree-Fock-Slater method, perturbation theory approach 0-27962  
 I<sub>2</sub>, relativistic effects, photoelectron spectra, Hartree-Fock-Slater method, perturbation theory approach 0-27962

**perturbation theory**

- see also quantum theory  
 1/N perturbation theory, large orders by inverse scatt. in 1-dimens., anharmonic oscillators 0-22214  
 $\sigma$  models, nonlinear, perturbative approach to symmetry restoration 0-37163  
 acetaldehyde, Coriolis resonance bands in IR spectrum 0-47995  
 adiabatic perturbations of solitons and shock waves 0-46830  
 algebraic aspects of perturbation theories 0-31539  
 algebraic methods, so(4,2) algebraic soln. of H ground state in strong mag. field 0-47845  
 alkali metal ion, with filled shell, dipole polarisability 0-9501  
 n-alkanes, longitudinal acoustic modes, Raman intensities 0-32718  
 Anderson model, asymmetric 0-6766  
 anharmonic oscillator, computation of energy eigenvalues of Hamiltonian 0-12925  
 anharmonic oscillator, energy level calcs., double well potential summable series 0-17819  
 anisotropic crystal impurity states, perturbative theory 0-34390  
 asymmetric Anderson Hamiltonian, perturbation expansion 0-6687  
 asymptotic estimate of perturbation theory at large orders, anharmonic oscillator,  $\Phi$  field theory 0-4585  
 asymptotic estimates in perturbation theory, Yukawa and  $g_0^4$  theory 0-4873  
 atom, dynamic multipole polarisability, hydrodynamic model, variational approximations 0-23340  
 atom, hyperfine shift and interatomic pots. in inert buffer gas, alkali atoms and H 0-5491  
 atom, open-shell, effective electron-electron interaction, many-body perturbation theory, C appl. 0-47843  
 atom+charged particle, autoionisation state decay 0-9565  
 atom+ion slow collisions, K-shell excitation of relativistic atoms 0-48073  
 atom with partially-filled shell, relativistic theory, secular operator renormalisation (*Russian*) 0-52896  
 atomic collisions, quasiclassical theory, transition between spatially degenerate levels 0-43150  
 atomic correlation energies calc., Wilson's scaling parameter evaluation 0-5486  
 atomic double vacancy states, correl. photon and electron transition, perturbation theory 0-27968  
 atomic systems, many-electron autoionisation states, transition probability and autoionisation rate, perturbation theory Z-expansion 0-52863  
 atomic systems, many-electron autoionising states, Z-expansion energy calcs. 0-909  
 benzene,  $\pi$  electron system, excitation energy, appl. of MBPT 0-52876  
 Bloch equations solution in presence of varying B<sub>1</sub> field, selective pulse analysis 0-25222  
 Borel summability, improvement on Watson's theorem,  $\phi_2^4$  appl. 0-52394  
 boson quantum thermodynamical system in one space dimension, high-order perturbation expansion 0-4636  
 bound state energy levels, quantum mechanical formalism, convergent perturbation theory (*Russian*) 0-4573  
 bound states, semiclassical, in one-dimension, perturbation formalism 0-12937  
 bremsstrahlung of vector particle in nucl. field 0-37198  
 CARS in condensed phases, perturbation theory of third-order nonlinear susceptibility 0-14393  
 linear Chapman-Enskog procedure, evolution equations of hydrodynamic variables 0-49075  
 charge equations of motion in perturbation theory quadratic approx., betatron oscils. 0-37661  
 charged particles in single wave fields, adiabatic and stochastic motion 0-9795  
 classical, of good action-angle variables, applic. to semiclassical eigenvalues and collisional energy transfer 0-23481  
 coherent multiphoton intense interactions, convergent perturbation anal. 0-1037  
 conference on hadron struct. and lepton-hadron interactions, Cargèse, France (July 1977) 0-4473  
 correlation energy, many-body Rayleigh-Schrodinger perturbation theory calcs., exclusion principle violation 0-52890  
 coupled neutron-nuclide problems, time depend. generalised perturbation theory 0-32322  
 Davidson's algorithm with and without perturbation corrections 0-27570  
 dense Fermi systems, generalised perturbation theory, ground and low excited states 0-22741



**perturbation theory continued**

dense liquids and gases, one-component systems, isothermal eqn. of state using thermodynamic perturb. theory (*Russian*) 0-49335  
 diagrammatic, correlation energy, triply excited state contrib., water appl. 0-18774  
 diagrammatic many-body perturbation theory applicable to arbitrary model spaces 0-47844  
 diagrammatic many-body perturbation theory for general model spaces 0-18780  
 diatomic molecule, Stark effect calcs., rigid rotator rotational levels in asymmetric potential well 0-5580  
 diatomic molecules, Stark effect variational and perturbational calcs. 0-1022  
 diblock copolymer solution, second virial coeff., perturbation theory 0-29148  
 differentially rotating gaseous polytropes, second-order perturb. theory 0-21990  
 dipolar liquids, hypernetted-chain eqn., perturbation theory soln. 0-49072  
 dipole interaction of an oscillator with scalar field 0-94  
 Dirac equation, approx. soln. using partitioning technique, appl. to H(1s, 2s, 2p) 0-23284  
 direct-gap crystals, one-photon absorpt., Keldysh and perturbation formulas 0-20607  
 disordered electronic system, scaling theory of localization and non-ohmic effects in two dimensions 0-44539  
 doublet with singlet ground state electronic system, long range interaction energy, CNDO approx. 0-53089  
 Drude oscillator model, atomic and molecular props. for different oscillator freq. 0-37846  
 education, two-electron atom, 1snl excited levels, ionisation energy calc., perturbation, Schrödinger eqn. methods 0-17728  
 electron+atom potential scatt. in low freq. laser field, perturbation theory 0-43191  
 electron gas, jellium model, dynamic correlations, first-order perturbation theory 0-44527  
 electron propagator theory for mol. electron binding energies and photoionisation intensities 0-47848  
 electron transfer cross-section, second Born approx. 0-48080  
 energy transfer and two-centre optical transitions in OH<sup>-</sup> and rare earth double-doped solid 0-7398  
 envelope wave stability 0-43410  
 EPR spin Hamiltonian, perturbation treatment, M=0 electronic state, HFS of triplet state EPR 0-25185  
 ethane, nuclear spin-spin coupling consts., vicinal proton-proton coupling calcs. 0-32737  
 fermion self-energy calculation, covariant formulation of relativistic Hamiltonian theory (*Russian*) 0-9087  
 ferromagnetic resonance in anisotropic Heisenberg model, magnon-magnon, phonon-magnon interactions (*Russian*) 0-11274  
 ferromagnetic semiconductor, theory review 0-20369  
 Feynman path integrals, conference, Marseille, France, 1978 0-31422  
 fluid, hard dumbbell mols., reference pot., perturbation theories, spherical reference systems 0-28898  
 fluid with nearly spherically symmetric molecules, thermodynamic perturbation theory 0-14985  
 focusing of waves in anisotropic plane-layered medium, analytical solns. of Maxwell's eqns. 0-32890  
 formyl radical, electronic struct., dissociation energy and potential energy surface many body perturbation theory and couple cluster doubles calc. 0-23296  
 fragmentation functions beyond leading order in QCD 0-13282  
 Frenkel-Kontorova system, discreteness effects, perturbation formalism, Peierls pot. and kink vel. reduction 0-34001  
 gauge copies, Abelian and non-Abelian cases 0-47170  
 gauge invariance and pseudoperurbations 0-22545  
 generalized bound-state perturbation theory 0-17748  
 glow discharge in diatomic molecular gas, electronic excitation rate, vibr. temp. influence 0-19633  
 halogen ion, with filled shell, dipole polarisability 0-9501  
 Hamiltonian, zero-order, for many-body perturbation theory 0-9483  
 harmonic oscillator with  $\lambda x^M$  perturbation 0-27161  
 harmonic time depend. oscillator with damping and perturbative force 0-82  
 HF subsystems, long range induction and dispersion interactions 0-53092  
 hot nonuniform magnetised plasma wave propag. theory, Vlasov eqn. perturbation expansion 0-33768  
 hydrides, single-centre perturbation theory calcs. 0-5470  
 incomplete basis set problem, virtual orbitals and CIBS expansion of HF energies 0-52844  
 induction energy, coupled Hartree-Fock calcs. 0-43139  
 intense field QED in continuous medium, appl. to Thomson scatt. and Cherenkov radiation 0-27435  
 intermolecular forces, ab initio calcs. applicability and accuracy 0-18898  
 3x3 inverse scattering transform, soliton perturb. scheme 0-27151  
 ionic crystal, Sternheimer antishielding factors of F<sup>-</sup>, Cl<sup>-</sup>, Br<sup>-</sup> and I<sup>-</sup>, approx. free- and cryst.-ion pot. influence 0-39544  
 ions, electron impact excitation, close-coupling formalism, perturbative treatment 0-48091  
 ions, multiply charged, level lifetimes relativistic calc., S-matrix approach 0-7942  
 Jupiter, and Saturn natural vibration spectrum, rot. effects, calc. 0-8583  
 Keldysh's perturbation formalism 0-13217  
 Klein-Gordon charged particles, perturbation theory for non-equilibrium stat. Green's functions 0-31994  
 Korteweg-de Vries equation, Pade approximants, soliton solns. 0-42071  
 Korteweg-de Vries eqns., perturbed solns. and soliton production 0-42074  
 Kramers theory of friction and vel. in chemical kinetics 0-50826  
 Langmuir solitons, non-neutral soln. 0-33763  
 light scattering by a pair of conjugate nonspherical particles 0-32912  
 linear zero-spin fields in external gravit. and scalar fields, perturbation theory 0-31969  
 linearisation stability and globally singular change of variables 0-31629  
 liquid, perturbation theory for soft core pot., radial distrib. function 0-6333  
 liquid metals, radial distrib. function and thermodynamic characts., interparticle interaction pot. (*Russian*) 0-49086  
 liquid mixtures, intermol. forces effect on phase diagram and excess props., perturbation theory 0-39287  
 liquids with noncentral interactions, struct. contrib., perturbation method and partition function separation 0-24341  
 LMFBR heterogeneous core, sensitivity anal. 0-22935

**perturbation theory continued**

logarithmic perturbation expansions, appl. to H in multipole field 0-37720  
 long wavelength spin susceptibility from particle-particle scattering, logarithmic temp. control 0-7124  
 LWR, first order perturbation methods in sensitivity anal. 0-37425  
 many body perturbation theory fourth order calc. of correl. energy 0-14087  
 many body systems, Anderson model, localisation phenomena, state variable randomness, perturbation theory 0-29297  
 many fermion systems, asymptotic nature of perturbation theory 0-46967  
 many-body perturbation theory, symmetry-adapted, wave operator matrix elements 0-23311  
 Mayer cluster function and quantum two-body t matrix 0-17859  
 MBBA/EBBA, nematic, mol. interaction energy 0-33881  
 meson+meson cross sections in QCD (*Russian*) 0-4968  
 metal, FCC, covalent component of electron density and energy (*Russian*) 0-28945  
 metal surface, perturbative calc. of elec. field 0-45108  
 metals, atomic displacements near impurities and many-particle interactions (*Russian*) 0-24553  
 metals, localised moment interaction, Alexander-Anderson model, perturbation expansion 0-29524  
 MIM diodes, negative differential resistance, stimulated inelastic tunnelling theory 0-49951  
 molecular fluid, computer simulation of liquid-vapour surface 0-54478  
 molecular fluids, ref. system selection and average Mayer-function perturbation theory 0-38891  
 molecular geometry optimisation with explicit inclusion of electron correl. 0-37748  
 molecular hyperpolarisabilities, HF calc. with correlation method, appl. to HF mol. 0-23342  
 molecular polarisability, scaling and Pade approximants, many-body perturbation theory 0-42952  
 molecular vibration excitation on resonant electron scatt., time-perturbation method (*Russian*) 0-14242  
 molecules, ground state props., coupled cluster and MBPT methods appl. 0-47881  
 molecules, isotopically tagged, normal vibr. freq. calc., eigenvalue behaviour, perturbation theory obs. 0-52973  
 molecules, two criteria for labelling approx. treatments as fully quantal ones 0-23289  
 Mossbauer relaxation theory 0-39954  
 multiply charged ions, relativistic perturbation theory appls. 0-23323  
 neutrino, Maxwell, and scalar fields in the cylindrical magnetic or plasma universe 0-120  
 neutron transport eqn., homogenised diffusion approx. 0-47522  
 nonlinear diffusion-reaction with autocatalysis and saturation law, single perturbation approach 0-35502  
 nonlinear harmonic oscillator, perturbation theory 0-19272  
 nonlinear periodic waves stability in plasmas 0-38615  
 nuclei, transitional, pairing rotations and quadrupole modes 0-18165  
 nuclei acid base stacked dimer, origin of excimer states in extended Huckel method 0-35832  
 one-dimensional band calculations using perturbation theory 0-44460  
 one-dimensional molecular crystals, electronic struct., mol. orbital theory 0-54588  
 one-dimensional particle-in-the-box problem, perturbation theory illustration using champagne bottle situation 0-36816  
 open shell polarisation propagator, for doublet-doublet transitions calcs. 0-27939  
 operator polynomials, divisors, perturbation theory 0-36905  
 optical fibre, quasiparabolic index profile, propag. characts., perturbation anal. (*French*) 0-33189  
 optical fibre birefringence, in limit of weak guidance and slight ellipticity 0-1309  
 optical fibres, evaluation of normalised cutoff frequencies in radially inhomogeneous fibres, perturbation theory 0-43434  
 optical rotary echoes, Bloch eqns. perturbative solns. 0-43407  
 optical waveguide, asymmetric dielectric-slab, beam mode scatt. characts. 0-38114  
 optical waveguides, index profile determ. methods 0-1337  
 orbit-orbit interaction, new tensor expansion, matrix and graphical forms 0-14064  
 organic molecules, quadrupole moments, dipole quadrupole A and C polarisabilities, perturbation theory anal. 0-27934  
 particle motion in two waves, numerical study 0-8914  
 pentofuranosyl nucleosides, isomeric, <sup>1</sup>H NMR coupling consts., SCF FPT INDO approx. calc. 0-14156  
 phase grating, 3-dimens., electrodynamic perturbation theory for light diff. 0-28327  
 phonon scattering by spherical defect aggregates 0-24552  
 photon splitting into three components by electron in quantised plane EM field 0-18101  
 photonuclear sum rules from continuum calcs., dependence on residual interactions 0-22807  
 plasma, ion-acoustic solitary wave, third-order corrections, reductive perturbation method 0-43898  
 polarisation spectroscopy, Doppler free intracavity 0-52335  
 polyatomic molecules, radiationless conversion processes, regularities 0-14171  
 polyatomic mols., nuclear charge model and valence force consts. prediction 0-43022  
 potential scattering, classical, small-ang., anisotropic, for Lennard-Jones (2n, n) pot. 0-1043  
 pulse dispersion in a clad lens-like medium 0-53445  
 QCD<sub>2</sub>, fermionic Green function and functional determinant, closed representation 0-13269  
 QCD, two jet process noncollinearity in first order perturbation theory 0-22567  
 QCD perturbation theory for confined quarks and gluons 0-401  
 QFT, perturbation theory at large orders 0-32022  
 quantum fermion thermodynamic system, high-order perturbation expansion 0-4635  
 quantum system, jarring and corresponding stimulated transitions 0-17839  
 quark stars, possible existence, 2nd order perturbation theory 0-26889  
 quasi-periodic motion, asymptotic expansion method 0-17877  
 radial reduced Coulomb Green's function 0-31559  
 random Ising magnet, phase diagrams 0-7065



**perturbation theory continued**

- rays calculation in inhomogeneous magnetoactive ionosphere by perturbation method 0-21874
- relativistic atomic systems, perturbation theory appls. 0-23323
- renormalized operator form of quantum action principle 0-42314
- rotating stars, perturb. and stability, eigenvalues and perturb. theory 0-46538
- scattering theory, nonsingular potential, scatt. length by iterative-perturbation method 0-27160
- Schrodinger equation, applications of perturbation theory to numerical integration methods 0-12926
- Schrodinger equation, energy approximants and perturbation theory 0-22232
- Schrodinger equation, perturbation problem, two-level atom interacting with EM field 0-52056
- Schrodinger equation, radial one-dimens., second order perturbative numerical calcs. 0-31580
- screened Coulomb pot., perturbation theory and hypervirial theorem, sixth order atom energy levels 0-14071
- second-order matrix elements, variational methods 0-12936
- shielding problems, higher order generalized theory 0-47731
- simple fluids, semiempirical calcs. using perturbation theory 0-28892
- sine-Gordon breather soliton dynamics, rel. to special relativity 0-46801
- single-particle density matrix, perturbation expansion 0-54635
- small overdense plasma particle Thomson-like RF scatt., linear perturbation theory 0-48858
- soliton evolution, perturbation effects 0-46824
- spectral analysis of wave perturbations in D-layer and F-layer 0-21873
- spherically symmetric space-times, even parity junction conditions for perturbations 0-31628
- Stark effect, perturbation and variation treatments, appl. to H(1s) reson. 0-14105
- stochastic behaviour of quantum pendulum under periodic perturbations 0-8834
- stochastic dynamical systems, kinetic eqn. derivation based on cumulant function props. 0-12995
- stochastic properties of complex nonlinear oscillation regimes 0-8919
- storage rings, beam-beam interactions, perturbation method solns. 0-37667
- superconducting small metal particles ground state energy and orbital mag. susceptibility 0-49983
- supergraphs, loop calculations 0-13229
- system influenced by time dependent electric field, fourth order variation perturbation theory 0-22230
- transition metal complexes, octahedral substituted, ligand-fluid splittings, accidental degeneracy origin 0-10932
- 3d transition metal ions in crystals, Jahn-Teller coupling constants calcs. 0-49679
- transition moments, vibrational, of diatomic and polyatomic mols., elec. and mech. anharmonicity influences 0-23459
- transition probability, second order, time-independent perturbation asymptotic formalism 0-27159
- transverse wave packet, 3-dimens., nonlinear evolution in hot plasma, ion-acoustic wave effect 0-43899
- two-electron ions, ground state, quadratic Stark effect 0-37775
- two-electron systems, pair function calcs. 0-32590
- UHFS model, CI, CC, and MBPT approaches, appl. to weak  $\delta$ - $\delta^*$  bonds and  $\delta$ - $\delta^*$  excitation 0-32585
- urea, electro-optical coeffs. meas., rel. to nonlinear optics calcs. 0-34889
- vacuum polarisation in intense EM fields, perturbation theory, renormalisation group calcs. (Russian) 0-52444
- Van der Pol oscillator, renormalised perturbation theory 0-27225
- variational principle for spinning liquid-filled solid bodies 0-43609
- vector resonator mode synthesis, from scalar results 0-43374
- waveguide, clad parabolic-index square-law dielectric, perturbation anal. 0-33190
- weakly bound particle ionisation, perturbation theory series convergence in alternating field 0-4575
- weakly dissipative system, higher order approx. in reductive perturbation method, shock wave appl. 0-14743
- Wigner's (2n+1) rule in MBPT 0-42095
- xanthine, planar autoassoc. energy 0-53086
- Yukawa fluid used as reference system in perturbation theory 0-6334
- AgBr, exciton absorpt. at high excitation rates 0-2343
- AgBr:Li<sup>+</sup>(Na<sup>+</sup>), impurity induced IR absorpt. 0-7386
- Ar, inner electron energy characteristics, validity of Hartree-Fock-Pauli approx. 0-42957
- Ar, liq., struct. factor calc., perturbation treatment using Lennard Jones (6, 12) pot. 0-10483
- BH, PE curve, spectroscopic consts., perturbation theory appl. 0-23341
- BNC=BCN, isomerisation energy/barrier correlation, rel. to HNC(LiNC) 0-50840
- Be-like system, numerical many-body perturbation calcs. using multiconfig. model space 0-47907
- CO<sub>2</sub>, rot.-vibr. bands, absorpt. coeff. calc. method, Fermi reson. effect on spectral lines 0-32696
- CdCl<sub>2</sub>, deformation densities, relativistic effect 0-42928
- CdMnTe, exciton ground state, magnetic field influence 0-54616
- F<sub>2</sub>, PE curve, spectroscopic consts., perturbation theory appl. 0-23341
- GaAs, impurity states and core excitons, binding energies, perturb. theory 0-49659
- Ge, amorphous, molecular liquid model and electronic structure 0-54133
- Ge, dispersion law of indirect excitons 0-24805
- H atom, energy level calcs. in superstrong mag. field 0-37737
- H, bond energy, chem. substitution influence 0-37718
- H, Stark effect, dispersion relation, asymptotic formulae, ionis. rate, perturbation theory calc. 0-14106
- H<sup>+</sup> chemical shifts, INDO calcs. 0-32743
- H-like atoms, Stark effect and perturbation approxs. 0-52932
- H<sub>2</sub>, polarisability, finite field MC SCF calcs. 0-14075
- H<sub>2</sub> predissociation probabilities of  $4p\pi^1\Pi_u^+ \nu \geq 1$  levels, dissoc. channels interference 0-28074
- HCNO, vertical ionisation pot., Koopmans' theorem, perturbation connections calcs. 0-42966
- HD, nucl. spin coupling const., MBPT theory calcs. 0-28035
- HN<sub>3</sub>, vertical ionisation pot., Koopmans' theorem, perturbation connections calcs. 0-42966
- HNCO, vertical ionisation pot., Koopmans' theorem, perturbation connections calcs. 0-42966
- HNC=HCN, isomerisation energy/barrier correlation, rel. to LiNC(BNC) 0-50840

**perturbation theory continued**

- H<sub>2</sub>O, many body perturbation theory fourth order calc. of correl. energy 0-14087
- HOCN, vertical ionisation pot., Koopmans' theorem, perturbation connections calcs. 0-42966
- He, film, Brownian motion, boundary layers and quantised vortex prod. 0-6579
- He, isoelectronic series, ground state specific mass shift, HF variation perturbation calc. 0-47889
- He+He<sup>2+</sup>, single and double electron capture, high vels., independent electron approx. calc. 0-18923
- HgCl<sub>2</sub>, deformation densities, relativistic effect 0-42928
- K-Rb, liq., form factors and transport coeffs., pseudopot. perturb. theory 0-44561
- KH<sub>2</sub>PO<sub>4</sub>-type crystal, LF dynamics 0-10602
- Kr, inner electron energy characteristics, validity of Hartree-Fock-Pauli approx. 0-42957
- LiH, many body perturbation theory fourth order calc. of correl. energy 0-14087
- LiNC type molecules, Born-Oppenheimer approx. applicability 0-32603
- LiNC=LiCN, isomerisation energy/barrier correlation, rel. to HNC(BNC) 0-50840
- Li<sup>2</sup>(S), open shell polarisation propagator, for doublet-doublet transitions calcs. 0-27939
- N<sub>2</sub>, liq., thermodynamic props., perturbation theory with hard dumbbell reference system 0-14991
- N<sub>2</sub>, PE curve, spectroscopic consts., perturbation theory appl. 0-23341
- <sup>14</sup>N, spherical ground state nuclear quadrupole interaction, Breit interaction, relativistic perturbation theory 0-42939
- Na-K(Cs), liq., form factors and transport coeffs., pseudopot. perturb. theory 0-44561
- Ne, atomic struct. calc., symmetry adapted pair functions, Rayleigh Schrodinger HF variational perturbation theory 0-42944
- P<sub>1</sub> radical, b<sup>3</sup> $\Pi_g$ -a<sup>3</sup> $\Sigma_u^+$  transition, perturbed by <sup>1</sup> $\Sigma_g^+$  state (French) 0-18855
- Rb, ground state, hyperfine struct., relativistic many-body calcs. 0-23322
- Rb, photoionis. cross section, elec. field depend. 0-37796
- Si, amorphous, molecular liquid model and electronic struct. 0-54133
- Si, dispersion law of indirect excitons 0-24805
- Si, impurity states and core excitons, binding energies, perturb. theory 0-49659
- Xe, inner electron energy characteristics, validity of Hartree-Fock-Pauli approx. 0-42957
- Xe, liq. struct. factor calc., perturbation treatment using Lennard Jones (6, 12) pot. 0-10483
- ZnCl<sub>2</sub>, deformation densities, relativistic effect 0-42928

**petrol engines see internal combustion engines****petroleum industry**

- petro-chemical industrial plants, piping networks, noise abatement 0-28381
- solar enhanced oil recovery; an assessment of economic feasibility 0-40832
- US flowmeters, petroleum and similar fluids 0-43804

**petroleum refining see oil refining****p.f.m. see pulse frequency modulation****pH**

- aerosol of Sudan Gezira airstream, chem. composition and pH 0-51518
- albumin, adsorption on SiO<sub>2</sub>, 0-10777
- 6-amino-7-hydroxy-4-methylcoumarin solutions, additions effect on fluoresc. 0-2833
- coumarin 102, excited state protonation kinetics, laser pH jump and picosecond spectroscopy 0-25992
- DNA-Au (III) interaction, rate consts., activation energies, pH, spectrophotometric obs. 0-30228
- indole soln. containing histidine, fluoresc. rel. to soln. pH 0-2826
- liquids for cooling and index matching of Nd:glass laser systems 0-33015
- motor reactivity, isolated heart of grass snake, pH and temp. effects 0-26219
- peptides and derivatives, mol. electron acceptor groups 0-30637
- poly (N',N'-terephthaloil-L-lysine) membrane for artificial red blood cells, interaction with serum proteins (Japanese) 0-12061
- potential-pH diagram, improved algorithms for computer generation, max. constriction method 0-26019
- purple membrane suspensions, light-induced conductivity changes, pH and temp. effects 0-51157
- rain and snow, release of S and nitrogen oxides by burning fossil fuels 0-26590
- rain interacting with rock partially covered by lichen 0-17302
- rhodamine 6G, aqueous soln., absorpt. spectra, ground and triplet state photoprotonation pH depend. 0-42961
- seawater, pH distrib. rel. to transparency 0-31057
- silver thioamides, precip., electron microscope and potentiometric studies, growth of photosensitive crystals 0-33107
- skin tissue pH electrodes for clinical applications 0-36175
- solution, <sup>89</sup>Y spin-spin relax. times, no pH depend. 0-2657
- steel, C, corrosion inhibition by 2-ethylamino-ethanol in aerated 3% NaCl soln., pH effect 0-21160
- sulphononaphthols, rapid pH and  $\Delta\mu\text{H}^+$  jump by short laser pulse 0-16709
- tryptophan soln. containing histidine, fluoresc. rel. to soln. pH 0-2826
- water quality monitoring, modular system (German) 0-26186
- Fe(OH)<sub>3</sub>-Fe(OH)<sub>2</sub> suspension system, potential-pH diagram 0-55728
- IrO<sub>2</sub> film, anodic, electrochromism, pH effects on corrosion stability, coloration and bleaching mech. 0-2726
- (NH<sub>4</sub>)<sub>2</sub>SO<sub>4</sub>:Cu<sup>2+</sup>, ESR parameters, effect of pH of mother soln., trapping sites 0-15791
- PbCO<sub>3</sub>, cryst. growth, Liesegang ring form., pH effect 0-49140
- ZrO<sub>2</sub>, isoelec. points, effect of pH on electrophoretic mobility 0-35548

**pH control**

- development of pH monitoring systems, limitations 0-3421
- neutralisation process, self-tuning control 0-30242
- Fe, mechanism of action of weak acids and their salts on passivation by O<sub>2</sub> 0-50886

**pH factor see pH****pH measurement**

- development of pH monitoring systems, limitations 0-3421
- glass microelectrode, for pH meas. 0-21291
- Al<sub>2</sub>O<sub>3</sub> surface, acidity, rel. to topochem., IR determ., adsorption method 0-35611



**pH measurement continued**

Li<sub>2</sub>SiO<sub>3</sub> glass pH meter electrode performance (*German*) 0-40695  
 Na<sub>2</sub>SiO<sub>3</sub> glass pH meter electrode performance (*German*) 0-40695

**phase angle meters** *see phase meters***phase conjugation (optical)** *see optical phase conjugation***phase-contrast microscopy** *see microscopy***phase control**

two-wavelength optical phase control system 0-33140  
 HF chemical laser phase control servo system 0-33063

**phase diagrams**

*see also phase equilibrium; phase transformations*

<sup>3</sup>He, solid, two parameter model of mag. and thermal props., spin exchange 0-49461  
 adsorbed layers, two dimensional incommensurate crystal theory, thermodynamics (*Russian*) 0-49524  
 alloy, binary, crystallisation kinetics, temperature dependence, kinetic phase diagrams 0-16294  
 alloys, binary, BCC, order-disorder transform., three-body interaction effects 0-39257  
 alloys, binary, kinetic crystallisation diagrams, given finite diffusion coeff. (*Russian*) 0-40341  
 alloys, Li<sub>2</sub> and Li<sub>10</sub> superstructure atomic ordering phase diagrams, order-disorder transition 0-38989  
 alloys, phase analysis by Mossbauer spectra 0-15922  
 azeotropic and two terminal solid solution type binary diagrams, synthesis 0-19901  
 benzene-hexa-n-alkylanoates, disc-like molecules, miscibility studies of mesophases 0-19696  
 binary alloys, diagrams of state, component interaction parameters (*Russian*) 0-55354  
 binary alloys, diagrams of state, component interaction parameters, computer calcs. (*Russian*) 0-55355  
 bond percolation in anisotropic square lattice 0-46989  
 catastrophe theory, phase diagram classification 0-22313  
 classification by catastrophe theory 0-17905  
 critical isomorphous  $\gamma \rightleftharpoons \alpha$  transition, phase equilibrium curve (*Russian*) 0-55397  
 critical points, catastrophe polynomials 0-8946  
 critical points and transitions, in phase diagram, geometrical relation (*Japanese*) 0-24568  
 crystal growth, macroscopic equil. and transport concepts, book 0-27054  
 diamond, 'melting' to solid metallic C phase above graphite triple point 0-15236  
 electron crystal in strong mag. field, phase diagram, normal mode anal. 0-44287  
 epoxy resin, cure history effect on dynamic mech. props. 0-54356  
 ethylene, solid, phase diagram and NMR at high press. 0-11279  
 eutectic crystal-melt system, interphase boundary struct., Monte Carlo method study 0-1950  
 FCC lattices, ordered superstruct., phase diagrams, cluster variation calc. 0-39256  
 flexible polymer chain in nematic solvent, phase diagram (*French*) 0-39253  
 2-fluoronaphthalene-2-naphthol system, phase relations, X-ray diff. and DTA study 0-45287  
 gas, thermodynamic props. review 0-31694  
 Heisenberg spin systems, two-dimensional, phase diag., renormalisation group approach to phase diag. 0-4847  
 heterogeneous system, melting, enthalpy and phase relations (*Czech*) 0-45543  
 Ising model in 1-D with random transverse field at T=0, real space renormalisation group method 0-4656  
 Kondo lattice, phase diagram 0-7077  
 lipid mixtures, phase transitions, theoretical model 0-8032  
 liquid crystal symmetry and thermodynamic states, review 0-0493  
 magmatic rocks, anchiutectic comp. 0-12381  
 metal-H, phase transitions 0-50631  
 metal-semimetal alloy, phase diagram computation from thermodynamic functions 0-40329  
 metallic glasses, structure and formation, thermodynamic props., cluster relaxation approx. 0-54143  
 metals, phase analysis by Mossbauer spectra 0-15922  
 microemulsions, phase diagram and homogeneity gap, light scatt. and viscosity meas. 0-16736  
 multi-ion system, strong electrolytes, phase diagrams and solubilities calcs. 0-25665  
 multicomponent alloys, phase diagram calc. program from thermodynamic data 0-3008  
 petrological melts and glasses, Fe-containing, Niggli's diagram 0-34170  
 polyester-organic solvent mixtures, phase diagrams, eutectic props., devitrification, crystn. (*French*) 0-3015  
 polymer, multicomponent, homopolymer blends, macroscopic phase separation 0-45289  
 polystyrene, cyclohexane soln., coil-globule transition 0-54110  
 Potts q-state model, variational renormalisation group approach 0-31679  
 random Ising magnet, phase diagrams 0-7065  
 rare earth hydrides, props., book contrib. 0-45291  
 rare earth oxides, binary, struct. and props., book contrib. 0-45292  
 rare earth oxides, mixed, phase relations and struct., book contrib. 0-45293  
 semiconductors, chemical thermodynamics, review 0-55692  
 sine-Gordon chain, T $\neq$ 0, commensurability, phase-torque eqn. of state 0-39251  
 steel, carbide and nitride phases dissolution (*Russian*) 0-20888  
 steel, Cr-C and C, carbide coating by CVD, interlayer form. 0-11574  
 steel, Cr-Mn, metastable constitution diagram and phase transforms. (*Russian*) 0-50590  
 steel, low-C-Si, LS1.2, LS1.5, phase transformation 0-45302  
 steel, stainless, Cr-Ni-Mo-N, phase diagrams 0-35161  
 superconducting composites, bronze process, metallurgy 0-3004  
 superconducting ferromagnet, magnetic ordering, spin wave dispersion (*Russian*) 0-54818  
 ternary polymer systems, diffusion controlled formation of porous structures 0-7539  
 ternary systems containing more than three phases, eutectic like and peritectic like reactions 0-29928  
 ternary systems with two component solid phases, eutectic, peritectic curve eqns. (*Russian*) 0-54344

**phase diagrams continued**

thermosetting materials, formation and props., phase diagram and torsion pendulum anal. 0-55381  
 transition metal alloys with rare earths or actinides, binary system constitution diagram interrelations (*Russian*) 0-7535  
 transition metal carbonitrides, physicochem. props., comp. depend. 0-55370  
 transition metal hydrides, struct. change from metal struct., due to interaction of metal with H 0-49196  
 transition metal hydrides, synthesis and physicochemical props., conf., Moscow, USSR (Jan. 1978) 0-27032  
 transition metal-H systems under high H pressure, phase diagrams, electrical cond., mag. props. 0-29923  
 transition metal-hydrogen systems, eqn. for multiplateau isotherm, lattice expansion role 0-39252  
 transition metal-rare earth-B systems, phase diagrams and struct. considerations 0-16286  
 triangular and honeycomb lattice gases, order-disorder transitions to 2X2 struct. 0-4674  
 triple points, 180° Rule, Butterfly model 0-8945  
 type equations for binary equil. curves, ternary system polythermic sections 0-39250  
 water-isobutyric acid, crit. mixture 0-24601  
 YIG, hot spraying to give fine, free flowing, sinterable powder 0-20865  
 Zircaloy-O<sub>2</sub> phase diagram 0-3003  
 Ag<sub>7</sub>AsSe<sub>6</sub>, thermal, crystallographic and elec. props. (*French*) 0-40338  
 Ag<sub>7</sub>AsSe<sub>6</sub>, thermal, crystallographic and elec. props. (*French*) 0-40338  
 Al-B(-C) system, synthesis and struct. of boride phases 0-45282  
 Al-Cu-Zn system, solid-phase reactions, phase diagram 0-50603  
 Al-Ga-Ge, thermodynamic props. of mixing of binary systems, phase diagram 0-45275  
 Al-Ga-Sb ternary phase diagram, calc., DTA and LPE expts. 0-29931  
 Al-Ge-Sn, thermodynamic props. of mixing of binary systems, phase diagram 0-45275  
 Al-Mg-Zn alloys, liq./solid phase equilibria determ. (*German*) 0-50601  
 Al-Sr-Nd phase diagram (*Russian*) 0-20893  
 Al-Ti-Fe, ternary phase diagram, computer calculations 0-45274  
 Al<sub>4</sub>C<sub>3</sub>-Be<sub>2</sub>C-SiC system, phase equilibria 0-45284  
 Al<sub>2</sub>O<sub>3</sub>-AlN phase diagram and reaction sintering of transparent cubic ALON spinel 0-25669  
 Al<sub>2</sub>O<sub>3</sub>-B<sub>2</sub>O<sub>3</sub>-SiO<sub>2</sub> system, liq. phase calc. for commercial quartzite powders 0-25671  
 Al<sub>2</sub>O<sub>3</sub>-Dy<sub>2</sub>O<sub>3</sub> phase diagram at high temps. (*Japanese*) 0-50619  
 Al<sub>2</sub>O<sub>3</sub>-Er<sub>2</sub>O<sub>3</sub> system, high temp. phase diagrams 0-40340  
 Al<sub>2</sub>O<sub>3</sub>-Eu<sub>2</sub>O<sub>3</sub> system, phase diagram at high temp. (*Japanese*) 0-40339  
 Al<sub>2</sub>O<sub>3</sub>-Gd<sub>2</sub>O<sub>3</sub> system, high temp. (*Japanese*) 0-45290  
 Al<sub>2</sub>O<sub>3</sub>-Ho<sub>2</sub>O<sub>3</sub> system, high temp. phase diagrams 0-40340  
 Al<sub>2</sub>O<sub>3</sub>-P<sub>2</sub>O<sub>5</sub>-H<sub>2</sub>O system, phase diagram 0-3014  
 As-Te-Ga system, glass-forming region and props. 0-25674  
 Au-Zn, (55 to 88 at.%), equil. diagram, X-ray diff. obs. 0-25660  
 B<sub>4</sub>C, melting and phase homogeneity range 0-20911  
 B<sub>2</sub>O<sub>3</sub>-BaO, liquid immiscibility region, equilibration and quenching expts. 0-45288  
 B<sub>2</sub>S<sub>3</sub>-Ti<sub>2</sub>S system, phase diagram and verification 0-35165  
 B<sub>2</sub>Se<sub>3</sub>-Ti<sub>2</sub>Se<sub>3</sub> system, phase diagram 0-35165  
 BaPO<sub>3</sub>F-Al<sub>2</sub>O<sub>3</sub>-B<sub>2</sub>O<sub>3</sub> system, liq. phase separation, IR spectra, microstruct. 0-29940  
 Be-Li-V, phase diagram, metallurgical aspects for fusion blanket use 0-32467  
 Bi-O system, phase equil., diagram (*German*) 0-55380  
 Bi<sub>2</sub>O<sub>3</sub>-AlPO<sub>4</sub>, phase equil. 0-35168  
 Bi<sub>2</sub>O<sub>3</sub>-SiO<sub>2</sub>(GeO<sub>2</sub>), metastable phases form., crystn. conditions, melt viscosity and density effects 0-35167  
 C, noncrystalline conversion to diamond, diffusion conversion enhanced rate due to shock compression 0-39221  
 CaCl<sub>2</sub>-Ca phase diagram, DTA study (*French*) 0-25672  
 CaO-Ga<sub>2</sub>O<sub>3</sub> phase diagram and Czochralski melt growth of CaGa<sub>2</sub>O<sub>4</sub> 0-29934  
 CaO-MgO-Al<sub>2</sub>O<sub>3</sub>-SiO<sub>2</sub>, quartz sand-dolomite-magnesia-clay based glasses, crystn. 0-20915  
 CaO-MgO-ZrO<sub>2</sub>-SiO<sub>2</sub> refractories, phase diagram 0-11634  
 CaO-Nd<sub>2</sub>O<sub>3</sub>-Fe<sub>2</sub>O<sub>3</sub>-Al<sub>2</sub>O<sub>3</sub> system, solid-state reactions 0-35173  
 CaO-P<sub>2</sub>O<sub>5</sub>-H<sub>2</sub>O system, phase diagram at 200°C 0-45286  
 Cd-Hg-Te, phase diagram, computer estimation 0-20903  
 Cd-Pb, high pressure effects, eutectic temp. 0-55361  
 Cd-Sb-Sn ternary system, phase equil. 0-16266  
 CdO-WO<sub>3</sub> phase diagram and prep. of CdWO<sub>4</sub> single crystals 0-29933  
 CdSb-ZnSb, crystallisation characts., phase diagram 0-55383  
 CdSnP<sub>2</sub> crystal growth, DTA obs. of Cd-Sn-CdSnP<sub>2</sub> phase diagram 0-24394  
 CdTe-Au system, phase diagram rel. to doping 0-16282  
 CdTe-CdSb system solid soln. single crystals, forbidden band width determ., comp. depend. 0-55083  
 CdTe-ZnS system, phase diagram and solid solubility 0-20909  
 CdTe-ZnS ternary mutual system, phase diagram 0-20904  
 Ce-Ga system, phase equil. and cryst. struct. of phases 0-35159  
 Co-V (10 to 23 wt.%) system, phase constitution, X-ray and elec. resist. meas. 0-3007  
 CoTe<sub>2</sub>-GeTe<sub>2</sub> phase diagram, from thermal, X-ray, microstructural analyses 0-55367  
 Cr-Mo-N system, at high-pressure, temp., X-ray anal., phase diagram 0-50607  
 Cr-Ni-O, computer-assisted anal. and calcs. of phase diagrams 0-25667  
 Cr-Os, magnetic transition T-P-C diagram, triple points (*Russian*) 0-54895  
 Cr-rare earth alloys, liquid phase, topology in diagrams of state (*Russian*) 0-54121  
 Cs-O system, phase diagram and O<sub>2</sub> potential 0-3011  
 CsCl-TiCl<sub>4</sub> solid soln., determ. and computation of phase diagram 0-55379  
 Cs<sub>3</sub>R<sub>2</sub>X<sub>2</sub> (=Sc,Y,Ho-Lu, X=Cl and R=Sc,Sm-Lu, X=Br), prep. and Guinier-Simon X-ray study 0-49204  
 Cu, shock compressed, release isentropes, eqn. of state at high energy density (*Russian*) 0-54340  
 Cu-Al-Ni, mixed powder compacts, Ni content influence in sintering behaviour (*Japanese*) 0-35130  
 Cu-Ge-O, phase diagram and thermodynamics, electrochem. study 0-50617  
 Cu-Mn-P alloys, phase diagram (*Russian*) 0-20891  
 Cu-Nb-Sn system, phase equilibria and supercond. props. (*Russian*) 0-50589



## phase diagrams continued

- Cu-Ni-Sn, liq. alloy, calc. and anal. of mixing enthalpies (*German*) 0-44325  
 Cu-Ni-Zn system, tie lines in a two phase region 0-24404  
 Cu-Zr alloys, isothermal transformation diagram 0-20902  
 Cu<sub>3</sub>Au-Cu<sub>3</sub>Pd(Pt), quasibinary system, order-disorder transform., superlattice form. 0-2159  
 CuBr-AgI system, ionic cond. and phase diagram 0-2198  
 (CuInTe)<sub>1-x</sub>(ZnTe)<sub>x</sub>, phase diagram and cryst. growth of CuZn<sub>2</sub>InTe from ZnCl<sub>2</sub> flux 0-16287  
 Cu<sub>2</sub>MnAl, Heusler alloy, decomposition at 360°C 0-7536  
 Cu<sub>2</sub>Mo<sub>6</sub>S<sub>8</sub> system, low temp. modifications (*French*) 0-50606  
 CuO-Cu<sub>2</sub>O-TiO<sub>2</sub>, phase equilibria, thermodynamics of Cu<sub>3</sub>TiO<sub>4</sub> phase 0-55374  
 Cu<sub>2</sub>O-CuO-MoO<sub>3</sub>, subsolidus phase diagram, mag. props. 0-50615  
 Cu<sub>2</sub>S-Ti<sub>2</sub>S system, phase diagram 0-20906  
 Cu<sub>2-x</sub>Te, x<0.22, phase diagram, electronic and ionic cond. meas. 0-6917  
 Dy-Er, Kaufman approach to calc. of intra-rare earth phase diagrams 0-25657  
 Dy-Ho, Kaufman approach to calc. of intra-rare earth phase diagrams 0-25657  
 ErFe<sub>2</sub>H<sub>8</sub>, pressure-composition-temperature phase diagram 0-3010  
 Fe,  $\alpha$ -,  $\gamma$ -, liq., thermodynamic data (*German*) 0-40328  
 Fe-Al, ordering and phase separations (*Japanese*) 0-50595  
 Fe-As, phase equilib. diagram (*German*) 0-16280  
 Fe-C, diffusion of Sn, microprobe anal. of intermediate phases (*French*) 0-50596  
 Fe-C system, mixing variables, activities and entropies calc., short range order model (*German*) 0-25655  
 Fe-Co-Mo ternary system, phase diagram (*Russian*) 0-16269  
 Fe-Cr-O, computer-assisted anal. and calcs. of phase diagrams 0-25667  
 Fe-Mn-Sb, phase comp. 0-16267  
 Fe-Ni-Co-Mo phase diagram and structure (*Russian*) 0-20899  
 Fe-Ni-O, computer-assisted anal. and calcs. of phase diagrams 0-25667  
 Fe-Zn, crystallographic relations by X-ray diffr. 0-24408  
 Fe-Zn, phase diagram, DTA, EDAX, X-ray diffr. study 0-50602  
 FeO, wüstite, invariant points between stable and metastable phases, T-P-X diagram (*French*) 0-29938  
 FeO-Fe<sub>2</sub>O<sub>3</sub>-SiO<sub>2</sub> system, molten, struct. using high temp. X-ray method (*Japanese*) 0-14992  
 FeO-Fe<sub>2</sub>O<sub>3</sub>-SiO<sub>2</sub> system, molten, struct. by high temp. X-ray diffr. 0-49084  
 FeO-FeS, mag. susceptibility, eutectic phase diagram (*Russian*) 0-15682  
 Fe<sub>2</sub>O<sub>3</sub>-Fe<sub>2</sub>O<sub>4</sub>-Fe<sub>2</sub>SiO<sub>4</sub> system, haematite-magnetite-fayalite nodules, stressed state parameters (*Russian*) 0-40336  
 Fe<sub>2</sub>O<sub>4</sub>-Co<sub>3</sub>O<sub>4</sub> spinels, phase diagram anal., thermodynamic props. 0-3009  
 Fe<sub>2</sub>O<sub>4</sub> phase comp. on equil. heating to 3300K (*Russian*) 0-16285  
 FeOOH, crystal growth in FeSO<sub>4</sub> solution with NaOH or NH<sub>4</sub>OH as precipitant, phase diagrams (*Chinese*) 0-44158  
 Fe<sub>2</sub>Pd<sub>2-x</sub>Si<sub>8</sub> metallic glass, mag. phase diagram, weak ferromagnet-spin glass transition 0-54893  
 FeS-MnS system, pseudobinary phase diagram 0-50777  
 Fe<sub>3</sub>Se<sub>4</sub>, Fe<sub>7</sub>Se<sub>8</sub>, phase gap, Mossbauer spectra 0-20552  
 Ga-As-Sb system, two- and three-phase fields obs. 0-55373  
 Ga-Ge-Sn, thermodynamic props. of mixing of binary systems, phase diagram 0-45275  
 Ga<sub>2</sub>S<sub>3</sub>-PbS system, phase diagram and crystallographic study (*French*) 0-29937  
 Gd-Y, Kaufman approach to calc. of intra-rare earth phase diagrams 0-25657  
 Ge-GaAs, crystallisation at superhigh cooling rates 0-54349  
 Ge-Si-Ga(In) system glasses, photoinduced changes 0-24365  
<sup>3</sup>He, A-phase slab, mag.-field-induced cellular superflow, periodic texture 0-24706  
 Hf-Be, coupled phase diagrams and thermochemical descriptions 0-25656  
 Hf-M-B systems (M=Rh,Ir), phase equilib. and cryst. structs. 0-15072  
 Hf-Ni(Cu)-Ge, alloys, phase diagrams and cryst. struct. (*Russian*) 0-25658  
 HgGa<sub>2</sub>S<sub>4</sub>-HgS, rel. to melt growth of HgGa<sub>2</sub>S<sub>4</sub> 0-50548  
 In-Pb-Sn system, thermal anal. 0-35162  
 In<sub>2</sub>Ga<sub>1-x</sub>P<sub>x</sub>As<sub>1-x</sub>InP, LPE, lattice matching, phase 0-54350  
 K<sub>2</sub>O<sub>2</sub>-O system, thermodynamic props. 0-29184  
 K<sub>2</sub>O-Fe<sub>2</sub>O<sub>3</sub>-SiO<sub>2</sub>, subsolidus sector of phase diagram, X-ray obs. 0-40335  
 Kr absorption on graphite, monolayer regime phase diagram 0-49507  
 (Li,N<sub>a</sub>,K) (Nb,Ta)O<sub>3</sub>, pseudo-binary and ternary systems quenched metastable glassy and cryst. phases 0-29935  
 LiBO<sub>2</sub>-In<sub>2</sub>O<sub>3</sub>, phase composition, mag. props, elec. cond. 0-55365  
 LiF-AlF<sub>3</sub>-Na<sub>3</sub>AlF<sub>6</sub>-Al<sub>2</sub>O<sub>3</sub> system, phase equilibrium, X-ray diffr., DTA, quenching, optical microscopy study 0-50610  
 Li<sub>2</sub>K(IO<sub>3</sub>) in LiIO<sub>3</sub>-KIO<sub>3</sub> system, lattice parameter, equil. and metastable phase diagram (*Chinese*) 0-7538  
 Li<sub>2</sub>O-Nd<sub>2</sub>O<sub>3</sub>-P<sub>2</sub>O<sub>5</sub> phase diagram, LiNdP<sub>4</sub>O<sub>12</sub> single crystal growth 0-25668  
 Li<sub>2</sub>O-SiO<sub>2</sub>, glass ceramics, phase transformation processes 0-3025  
 Li<sub>2</sub>O-TiO<sub>2</sub>, liquidus phase relations, Bridgman-Stockbarger crystal growth of Li<sub>2</sub>Ti<sub>2</sub>O<sub>7</sub> 0-25548  
 Li<sub>2</sub>V<sub>2</sub>O<sub>6</sub> (0.1<x<1.0), phase relationship in ambient temperature system 0-20912  
 Mg-Ag-Cu, phase comp. in Mg-rich region (*Russian*) 0-40331  
 Mg-Ga-In(Tl) and Mg-In-Tl, phase diagrams and electrochem. props. (*Russian*) 0-40330  
 Mg-Li-Ga(Ge)(In)(Tl)(Pb), phase diagram, isothermal cross section (*Russian*) 0-20900  
 Mg-Sm, phase diagram and mech. props. (*Russian*) 0-20892  
 Mg-Tb, (up to 45 wt.%), phase diagram, and mech. preps. 0-16277  
 Mg-Y-Cd, phase equilibria and mech. props. (*Russian*) 0-20894  
 Mg-Y-Zn alloys, phase equilib. (*Russian*) 0-16271  
 MgO-Al<sub>2</sub>O<sub>3</sub>-SiO<sub>2</sub>, glass ceramics, phase transformation processes 0-3025  
 MgO-CaMgSiO<sub>4</sub>-(Al<sub>0.5</sub>Cr<sub>0.5</sub>)<sub>2</sub>O<sub>3</sub>(Al<sub>2</sub>O<sub>3</sub>)(Cr<sub>2</sub>O<sub>3</sub>), spinel phase, phase equilibrium relations and spinel bonding 0-55376  
 Mn-Cu, alloying behaviour and high damping capacity 0-35160  
 Mn-Fe-C, melts, activities of Mn at 1673K 0-50597  
 Mn-Fe-C, phase instability 0-11628  
 Mn-Fe-Si-C, melts, activities of Mn at 1673K 0-50597  
 Mn-Si-C, melts, activities of Mn at 1673K 0-50597  
 Mn-Ti-Fe, ternary phase diagram, computer calculations 0-45274  
 Mn<sub>0.394</sub>Ti<sub>0.606</sub>-O-S system, 1380 and 1485K, phase equilib. study 0-50616  
 MnAs, generalised P-T phase diagram, mag. and structural phase transition 0-39780

## phase diagrams continued

- Mn<sub>1-x</sub>Fe<sub>x</sub>As, magnetic transition under high press., exchange striction model calcs. (*Russian*) 0-50096  
 Mn<sub>2</sub>O<sub>4</sub>-Co<sub>3</sub>O<sub>4</sub> spinels, phase diagram anal., thermodynamic props. 0-3009  
 Mo-Cr, fusibility diagram (*Russian*) 0-20897  
 Mo-TiC-Ni phase equilibria, subsolidus temp., metallographic and X-ray anal. 0-16278  
 (Na,Cl)(F,Cl,I) quaternary reciprocal system, calc. of phase diagrams 0-25666  
 NaCl-LiCl mixed crystals, Au decoration study of solid-melt interface, phase separation 0-15026  
 NaCl-NaBr-TeO<sub>2</sub>, condition diagram, thermographic obs. (*Russian*) 0-55377  
 NaF-YF<sub>3</sub> system, fusibility diagram, quasibinary section of NaF-YF<sub>3</sub>-YOF system characts. 0-55371  
 Na<sub>2</sub>O-B<sub>2</sub>O<sub>3</sub>-SiO<sub>2</sub>-Yb(Tb), luminesc. cooperative processes, glass struct. and comp. effect 0-16101  
 Nb-Ga-Fe ternary system, phase equil. at 1000°C, supercond. transition temp. 0-35158  
 Nb-Ge-Cu, phase equil. and supercond. props. (*Russian*) 0-40332  
 Nb-Ge-Ni, phase composition and superconducting props., influence of Ni (*Russian*) 0-20898  
 Nb-Pt-O system, phase equilibria, diagram, unit cell parameters, supercond. 0-55352  
 Nb-Rh, radiation disorder model of phase stability 0-16297  
 Nb-Si diagram of state, melting temp., polymorphic transform. temp. (*Russian*) 0-50594  
 NbH(D), structs. phase diagrams, morphologies, prep. methods, book contrib. 0-25675  
 Nd, magnetoresistance, mag. struct., elec. resistance at low temps. (*Russian*) 0-54936  
 Nd-Pr, Kaufman approach to calc. of intra-rare earth phase diagrams 0-25657  
 Ni-Al-Ti-(W) (Cr) (Co) (Mo) (Ta) (Nb), heat resist., solidification range 0-35177  
 Ni-Ta-Al system, phase equilibria and diagram, electron probe, X-ray diffr. anal. 0-29927  
 Ni-W-C(Nb) system,  $\gamma$  to ( $\gamma$ +W) phase boundary calcs. using Wigner method (*Russian*) 0-54346  
 Ni<sub>3</sub>Fe, order-disorder transition phase diagram, Mossbauer meas. 0-39995  
 PLZT, ferroelectric phase transitions, phase state identification 0-45018  
 Pb, shock compressed, release isentropes, eqn. of state at high energy density (*Russian*) 0-54340  
 Pb-Sn system, soft solder, elec. and thermal cond. at low temps., superconducting transition temp. 0-20150  
 Pb<sub>2</sub>SiO<sub>4</sub>-PbSiO<sub>3</sub>, Raman and IR spectra of crystalline phases 0-3013  
 PbTiO<sub>3</sub>-PbZrO<sub>3</sub>-based multicomponent ferroelec. solid solns., morphotropic transitions and comp-temp. phase diagrams 0-55047  
 Pd-H and Pd alloy-H systems, review of props., book contrib. 0-24605  
 Pd-H thin film system, phase diagrams using quartz crystal thickness monitor 0-7537  
 Pd-H-Gd, dil., ESR exam. of low temp. region of phase diagram, and electronic props. 0-29930  
 PdAl-Fe(Ni), phase diagrams, eutectic points and solubility (*Russian*) 0-40333  
 Pd<sub>3</sub>AlCu-PdAl system, interactions and solid-state transforms (*Russian*) 0-16272  
 PdGdH, diagram of state elec. props., indirect exchange interaction, EPR study (*Russian*) 0-50179  
 PdH<sub>x</sub>, incoherent phase transition, lattice gas model 0-29171  
 Pr-Ga (0 to 50 at.%), phase diagram and cryst. structs. of intermetallic cryst. 0-3002  
 Pu binary alloys, periodical depend. of equilibrium distrib. coeffs. of Pu admixtures on atomic number of admixture 0-18419  
 Re-Cu-Al phase diagram, X-ray structural and microscopic anal. (*Russian*) 0-20895  
 SbCl<sub>3</sub>, phase diagram to 43 kbar 0-2144  
 Sc-[Co,Ni,Cu]-Ga, phase equilibria, diagrams of state, X-ray, microstructural study (*Russian*) 0-55356  
 Sc-H, p-T phase diagram and influence of H pressure, on decomposition temp., DTA exam. 0-29929  
 Sc-M-B systems (M=Rh,Ir), phase equilib. and cryst. structs. 0-15072  
 Sc-Rh-Si system, partial phase diagram, X-ray diffr. and microprobe anal. 0-25659  
 ScRu<sub>2</sub>B<sub>4</sub>, superconducting and crystallographic data 0-33968  
 Si-Al-B-O-N, calc. of phase diagrams from data set 0-55362  
 Si-Al-Zr-O-N, calc. of phase diagrams from data set 0-55362  
 Si<sub>3</sub>N<sub>4</sub>-Al<sub>2</sub>O<sub>3</sub>-AlN, isothermal sections, free energy of formation 0-55363  
 Si<sub>3</sub>N<sub>4</sub>-Si<sub>3</sub>N<sub>2</sub>O<sub>5</sub>-Mg<sub>2</sub>SiO<sub>4</sub>, melting and eutectic studies 0-45285  
 SiO<sub>2</sub>-Al<sub>2</sub>O<sub>3</sub>-Si<sub>3</sub>N<sub>4</sub>, isothermal sections, free energy of formation 0-55363  
 Sn-F system, partial phase diagram construct. in Sn-SnF<sub>4</sub> region (*French*) 0-50605  
 Sn<sub>1-x</sub>SnF<sub>2</sub> system, phase diagram construct. (*French*) 0-50605  
 Sn<sub>2</sub>Sb<sub>2</sub>So, cryst. struct. (*French*) 0-1991  
 SnTe, polymorphism, high press. and temp., X-ray diffr. study 0-54375  
 Sr<sub>2</sub>EuFeO<sub>5</sub>-SrO-PbO, quasi-ternary system comp. diagram, rel. to Sr<sub>2</sub>FeO<sub>5</sub>, Sr<sub>2</sub>AlO<sub>5</sub>, cryst. growth 0-20776  
 SrSi<sub>3</sub>, phase diagram, 10 to 40 kbar, 600 to 1200°C, polymorphic transform. 0-29165  
 Ta-O, steady state O<sub>2</sub> solubility (*German*) 0-44322  
 TaH(D), structs. phase diagrams, morphologies, prep. methods, book contrib. 0-25675  
 Tb-Er, Kaufman approach to calc. of intra-rare earth phase diagrams 0-25657  
 Tb-Ho, Kaufman approach to calc. of intra-rare earth phase diagrams 0-25657  
 Te-In alloys, direct reaction calorimetric study, 737 to 1340K (*French*) 0-49382  
 Ti alloys, metallurgical characterisation using thermolec. power meas. (*French*) 0-45462  
 Ti-Be, coupled phase diagrams and thermochemical descriptions 0-25656  
 Ti-Be, metallic glass form. and props. 0-16219  
 Ti-Be-Zr, coupled phase diagrams and thermochemical descriptions 0-25656  
 Ti-Co, radiation disorder model of phase stability 0-16297  
 Ti-Co(Ni) alloys, absorpt. of H<sub>2</sub>, press.-composition-temp. relationships, enthalpy, entropy 0-2267  
 Ti-O system, intermediate oxide thermodynamics under equilibrium press. 0-55351



# phase diagrams continued

Ti-Ru, radiation disorder model of phase stability 0-16297  
 Ti-TiC-TiN system, phases 0-20905  
 $\alpha$ -Ti-V(Al)(Sn), Mossbauer spectra, metastable  $\theta$ - and  $\omega$ -phases 0-20556  
 Ti-Zr-W-(Al) alloys, phase struct. and props. (Russian) 0-16270  
 TiC-TiN, physicochem. props., comp. depend. 0-55370  
 $(\text{Ti}_{1-x}\text{V}_x)_2\text{O}_7$ , elec. cond. and phase diagram near metal-insulator transition 0-11054  
 Ti-Pb-S system, phase diagram quasibinary  $\text{Ti}_2\text{S}$ -PbS section obs. 0-55372  
 $\text{TiGaS}_2$ - $\text{TiGaSe}_2$ , phase and composition-property diagrams 0-55366  
 $\text{TiInS}_2$ - $\text{TiInSe}_2$ , phase and composition-property diagrams 0-55366  
 $\text{Ti}_3\text{VS}_4$ , growth of inclusion free crystals, for surface wave and bulk wave acoustic devices 0-25549  
 $\text{TmSe}_{1-x}\text{Te}_x$ , phase relationships and press. induced transitions 0-19771  
 U, liq.,  $\text{O}_2$  solubility and comp. of lower phase boundary of  $\text{UO}_2$  at 1950K 0-49366  
 U-Zr-O system, phase formation, phase equilibrium 0-16667  
 V-H(D), metallographic and thermal differential anal., potential for H energy storage appls. 0-45281  
 $\text{V}_{1-x}\text{Cr}_x\text{Si}$ ,  $x=0$  to 3, struct., supercond. and mag. props. 0-1962  
 $\text{V}_{1-x}\text{Fe}_x\text{O}_{2-x}\text{F}_x$ ,  $0 < x < 0.2$ , phase diagrams,  $^{57}\text{Fe}$ -Mossbauer spectra, X-ray diff. studies (German) 0-29663  
 VH(D), struct. phase diagrams, morphologies, prep. methods, book contrib. 0-25675  
 $\text{VO}_2$ -CrNbO<sub>4</sub>, solid solns., synthesis and phase diagram 0-35171  
 W-Hf-C, phase equilb. 0-55348  
 $\text{Y}_{1-x}\text{Gd}_x\text{Fe}_2\text{O}_{12}$ , mag. phase diagrams, mag. transitions, exchange interaction (Russian) 0-54896  
 Zn-Sn-Hg, diagram of state, melting temp., peritectic and eutectic phases (Russian) 0-55350  
 $\text{ZnAs}_2$ -ZnSe(ZnTe) solid solutions, single cryst., phase equilb. and props. 0-16283  
 $\text{Zn}_3\text{P}_2$ , stoichiometry deviation from phase diagram 0-35164  
 $\text{ZnS}$ -MnS-CuInS<sub>2</sub>, subsolidus equilb., phase diagrams 0-3016  
 $\text{ZnSiP}_2$ , crystal growth, DTA obs. of Sn-Zn-ZnSiP<sub>2</sub> phase diagram 0-24394  
 ZnTe, TEM obs. of precipitates, shape of Te solidus line 0-25703  
 Zr-Be, coupled phase diagrams and thermochemical descriptions 0-25656  
 Zr-Be, metallic glass form. and props. 0-16219  
 Zr-M-B systems (M=Rh,Ir), phase equilb. and cryst. structs. 0-15072  
 Zr-M-H (M=V, Cr, Mn, Fe, Co, Ni), synthesis at high pressure, props 0-29924

# phase equilibrium

see also phase diagrams; phase transformations; solutions  
 alcohol-unassociated active component liquid mixtures, associated soln. theory, thermodynamic parameters 0-7836  
 alloys systems, ternary, phase equilibria calc., line compounds 0-10638  
 aluminosilicate glass, phase separated, phase characterization by STEM and X-ray microanal. 0-50643  
 azeotropic and two terminal solid solution type binary diagrams, synthesis 0-19901  
 binary systems, diffusion coeffs., stochastic theory of nonideal behaviour 0-44346  
 ceramic technology, DTA appl. 0-20913  
 condensed systems, phase equilibria, 400-1100°C, DTA method 0-218  
 critical isomorphous  $\gamma \rightleftharpoons \alpha$  transition, phase equilibrium curve (Russian) 0-55397  
 crystal growth, macroscopic equilb. and transport concepts, book 0-27054  
 ferrite systems, thermodynamic stability, dissociation and phase relations (Japanese) 0-55378  
 glass workability rel. to melting history, microstruct., apparent liquidus temp., mechanical props. 0-11633  
 glasses, liq.-phase separated, phase comp., temp. depend. 0-16289  
 growing phase diffusivity determ. 0-24641  
 hard rod system, improved lattice model, nematic and isotropic phases 0-33882  
 inhomogeneous fluid in rigid container, equilb. states stability 0-44392  
 liquid mixtures, intermol. forces effect on phase diagram and excess props., perturbation theory 0-39287  
 liquid-liquid equilibrium data, prediction 0-54367  
 liquid-liquid-ideal vap., isothermal condition, 3-phase equilb. line special point (Russian) 0-54345  
 liquid-vapour equilibrium, azeotropic props. meas., differential tensimetric titration appl. (Russian) 0-54363  
 metals and alloys, martensitic transitions accompanied by interactions between phases (Russian) 0-7568  
 metastable phases, in metals, ion implantation review 0-49254  
 methane-ethane liq. mixture, phase equilb., heat of mixing, vol. change, data evaluation 0-15233  
 mixtures, vapour-liquid equilibria, mixing rules in equations of state 0-19902  
 mixtures containing polar substances, corresponding states principle use in crit. states calc. 0-39196  
 multicomponent mixtures, phase envelopes and crit. points calc. 0-54337  
 multicomponent vapours-condensed phases, equilb., computer modelling 0-44288  
 nitrobenzene-hexane, soln., dielec. permitt. in two phase region 0-2682  
 nitromethane-isooctane, liq. mixture, coexistence curve, refr. index meas. 0-10655  
 periclase-spinel refractories, phase conversions up to 1720°C 0-25670  
 phthalocyanides, thermal stability, DTA (German) 0-11945  
 propane, vapour-liquid and vapour-solid equilb. data, mass spectroscopic tracer pulse chromatography 0-37115  
 rare earth garnets, prep. and props. book contrib. 0-44193  
 rare earth systems,  $\text{RCO}_3\text{H}_2$  (R=Ce, Pr, Tb, Dy, Er), phase equilibria, from dissociation isotherms 0-50591  
 refractories, castable, X-ray powder diff. meas. of phase composition, and flexural strength 0-3449  
 simple solid family of phase states (Russian) 0-15216  
 steel, austenite-martensitic, struct. changes during plastic deform., mutual influence of phases (Russian) 0-30015  
 steel, low C, dual phase, impact props., microstruct. element influence 0-40525  
 steel, solubility of W and Mo in Ti(C,N), 0-16276  
 ternary systems, diffusion coeffs., stochastic theory of nonideal behaviour 0-44346  
 tetrafluoromethane-trifluoromethane-chlorotrifluoromethane, vapour-liq. equilb. compositions, calc. 0-19925

# phase equilibrium continued

transition metal-hydrogen systems, eqn. for multiplateau isotherm, lattice expansion role 0-39252  
 tricritical coexistence in three dimensions, multicomponent limit 0-19907  
 type equations for binary equilb. curves, ternary system polythermic sections 0-39250  
 unstable compounds, free energy of formation calcs., FORTRAN program for ternary phase equilibria. 0-10683  
 vapour-liquid equilibria, algorithm for calcs. 0-19903  
 vapour-liquid equilibria, and intermol. forces, semi-empirical approach 0-54359  
 vapour-liquid equilibria correlation and prediction 0-2141  
 vapour-liquid equilibrium, supercritical components, standard state fugacities 0-15230  
 $3\text{PbO} \cdot \text{GeO}_2$ , X-ray and electron diff. exam. (German) 0-11632  
 Ag-Fe, dil., ion implanted, phase comp., Mossbauer study 0-7244  
 Ag-rare earth alloys, Ag-rich, phase equilb. 0-45276  
 $\text{AgZr}_2(\text{PO}_4)_3$  system, phase charact. at different temps. 0-29936  
 Al-Ge (6.8 at.%), quenching from mushy state for production of metastable phases 0-35223  
 Al-Mg-Zn alloys, liq./solid phase equilibria determ. (German) 0-50601  
 Al-Mn, direct chill-cast, struct. changes during heat treating (German) 0-40408  
 Al-Mn(Cr), quenched, thermal stability (Russian) 0-20976  
 $\text{Al}_2\text{C}_3$ -Be<sub>2</sub>C-SiC system, phase equilibria 0-45284  
 $\text{Al}_2\text{O}_3$ -B<sub>2</sub>O<sub>3</sub>-SiO<sub>2</sub> system, liq. phase calc. for commercial quartzite powders 0-25671  
 $\text{Al}_2\text{O}_3$ -SiO<sub>2</sub> system, solid state transform. of andalusite to mullite 0-16281  
 Ar, gas-liquid-solid equilibrium, eqn. of state 0-24563  
 Ar, phase transition, anharmonic cryst.-gas transition 0-6510  
 Au-Fe, dil., ion implanted, phase comp., Mossbauer study 0-7244  
 B and borides, conference, Varna, Bulgaria (Oct. 1978) 0-12842  
 $\text{BBr}_2\text{-PbCl}_2\text{-H}_2$ , gas phase equilb. comp. 0-35166  
 $\text{BPO}_4$ -SiO<sub>2</sub> system, new data to prevent B<sub>2</sub>O<sub>3</sub> or P<sub>2</sub>O<sub>5</sub> loss at elevated temp. 0-20914  
 BaTiO<sub>3</sub>-CeO<sub>2</sub> liquid immiscibility region, X-ray diff. anal. 0-50611  
 Bi-Bi<sub>3</sub>(BiBr<sub>3</sub>) liquid binary mixtures, phase separation under press. 0-34183  
 CO<sub>2</sub>, vapour-liquid and vapour-solid equilb. data, mass spectroscopic tracer pulse chromatography 0-37115  
 Ca<sub>2</sub>Nb<sub>2</sub>O<sub>7</sub>-Sm<sub>2</sub>NbO<sub>7</sub> system, phase equilb. 0-20907  
 CaO-Fe<sub>2</sub>O<sub>3</sub>-Al<sub>2</sub>O<sub>3</sub> system, solid soln. of Ca<sub>2</sub>Fe<sub>2(1-x)</sub>Al<sub>2x</sub>O<sub>5</sub> (Russian) 0-16284  
 CaO-SiO<sub>2</sub> glass, two phase region, expt. and thermodynamic data 0-16288  
 Ca<sub>2</sub>SiO<sub>4</sub>-CaMgSiO<sub>4</sub>, T phase, review 0-50612  
 Ce-Mn-Cu systems, phase equilibria at 600 and 400°C (Ukrainian) 0-11625  
 CeMg<sub>11</sub>V(Cr)(Mn)(Fe)(Co), hydriding and appl. in H<sub>2</sub> storage 0-51009  
 Co-Ge-Te system 0-20908  
 Co-Ti (22 at.%), amorphous eutectic phase 0-55360  
 Co<sub>2</sub>Ge<sub>3</sub>, solid and liquid, physicochemical props. and structure 0-39548  
 B-C-Te phase, thermodynamic study by Galvanic cell meas. 0-29190  
 Cr-Si-Cu, struct. and supercond., Cu influence 0-50592  
 Cs-Cr-O system, phase equilibrium 0-3012  
 Cu alloy solid solution condensed films, influence of alloying components on phase composition and lattice spacing (Russian) 0-20047  
 Cu-Fe, dil., ion implanted, phase comp., Mossbauer study 0-7244  
 Cu-Ge-O, phase diagram and thermodynamics, electrochem. study 0-50617  
 Cu-U-O system, equilb. relationships (German) 0-35163  
 CuO-Cu<sub>2</sub>O-TiO<sub>2</sub>, phase equilibria, thermodynamics of Cu<sub>3</sub>TiO<sub>4</sub> phase 0-55374  
 Dy<sub>2</sub>B<sub>3</sub>, prep. and props., DTA study 0-20859  
 Fe-As-Su-Si (Cr)(Mn) melts, As and Sn distrib., Si, Cr, and Mn influence (Russian) 0-16274  
 Fe-C-Cr, pearlite reaction kinetics 0-3006  
 Fe-C-Cr, thermodynamics and phase equilibria near eutectoid temp. 0-3005  
 Fe-Mn mag. contributions to  $\gamma \rightarrow \epsilon$  phase transformations 0-25694  
 Fe-Ni heterogeneous alloys, ferrite, martensite and austenite phase distrib., effect on mech. props. 0-45363  
 Fe-Ni-Al-Co-Ti base alloys, highly coercive, phase comp., Mossbauer meas. 0-39996  
 Fe-Ni-C, plastic deform. effect on austenite stabilisation (Korean) 0-21021  
 Fe-O-V melts (Russian) 0-16273  
 Fe-TiB<sub>3</sub>, phase composition, secondary ion-ion emission study (Russian) 0-20896  
 Fe-V<sub>2</sub>O<sub>3</sub>, rel. to deoxidation of Fe by V (Russian) 0-16275  
 Fe-Zn intermetallics, initial stages of form. (Russian) 0-20889  
 Ga-Bi liquid binary mixtures, phase separation under press. 0-34183  
 Gd-Fe-B ternary systems, phase equilibria and cryst. struct. (Ukrainian) 0-11626  
 GdCrO<sub>3</sub>-GdAlO<sub>3</sub> solid solutions 0-20887  
 Ge-S-Cu, phase separation in melt centrifugal quenching 0-25701  
 In-As system, exam. of thermodynamic consistence of models, and QCE approx. for activity coeffs. (German) 0-24615  
 InAs-InP, phase equilb. and dissoc. 0-35170  
 K<sub>2</sub>O-BaO-B<sub>2</sub>O<sub>3</sub> glasses, ESR detection of immiscibility rel. to Cu II ions 0-20916  
 K<sub>2</sub>O-V<sub>2</sub>O<sub>5</sub>-Al<sub>2</sub>O<sub>3</sub> melt, soln. of Al<sub>2</sub>O<sub>3</sub> single crystal 0-20910  
 K<sub>2</sub>O<sub>4</sub>TiO<sub>2</sub>, new fibrous phase 0-20917  
 LaOF-LaF<sub>3</sub>, high pressure phase transitions 0-55368  
 Li-LiH two-phase equil. system, vaporis. diagram at high temps. 0-19926  
 Li-Na liquid binary mixtures, phase separation under press. 0-34183  
 LiF-AlF<sub>3</sub>-Na<sub>3</sub>AlF<sub>6</sub>-Al<sub>2</sub>O<sub>3</sub> system, phase equilibrium, X-ray diff., DTA, quenching, optical microscopy study 0-50610  
 Li<sub>2</sub>O-V<sub>2</sub>O<sub>5</sub>-Al<sub>2</sub>O<sub>3</sub> melt, soln. of Al<sub>2</sub>O<sub>3</sub> single crystal 0-20910  
 Mg-Ni-W-Co-Al-Cr alloy KhN56VMKYu, Al effect on excess Mg phase 0-29926  
 Mg-Y-Al alloys, phase equilb. (Russian) 0-20890  
 Mn-Fe-C, phase instability 0-11628  
 Mn-Si, liq. alloys, equilibria between MnO-SiO<sub>2</sub>-CaO-MgO slags 0-10639  
 Mn<sub>0.394</sub>Ti<sub>0.606</sub>-O-S system, 1380 and 1485K, phase equilb. study 0-50616  
 MnZn ferrite, Ti substituted, vacancy contents and phase equilibria 0-29012  
 Mo-Al-Ge, new compounds, structure and props. 0-39003



**phase equilibrium continued**

- Mo-Hf-C-Ni, electrochemical phase composition anal., precip. of HfC phase (*Russian*) 0-20901  
 Mo-Si-Cu, struct. and supercond., Cu influence 0-50592  
 MoSi<sub>2</sub>-CrSi<sub>2</sub>, phase equilib., struct. and props. 0-50608  
 N<sub>2</sub>-Ar-O<sub>2</sub> system, vapour-liq. equilib. 0-54358  
 N<sub>2</sub>-Kr-Xe, liquefaction, retention of <sup>85</sup>Kr from fission exhaust gases, separation technique (*German*) 0-27753  
 Na<sub>2</sub>O-B<sub>2</sub>O<sub>3</sub> glass-forming melts, thermodynamic functions 0-25673  
 Na<sub>2</sub>O-SiO<sub>2</sub>, (5.3, 94.7 wt.%) glass, liq.-phase separated, struct., heat treatment effect 0-16359  
 Na<sub>2</sub>O-V<sub>2</sub>O<sub>5</sub>-Al<sub>2</sub>O<sub>3</sub> melt, soln. of Al<sub>2</sub>O<sub>3</sub> single crystal 0-20910  
 Na<sub>2</sub>O-V<sub>2</sub>O<sub>5</sub>-(VO<sub>2</sub>)<sub>2</sub>-V<sub>2</sub>O<sub>3</sub>, phase comp. and equilib. 0-35172  
 Na<sub>2</sub>O.y(Al<sub>1-x</sub>Fe<sub>x</sub>)<sub>2</sub>O<sub>3-m</sub>, β"-Al<sub>2</sub>O<sub>3</sub> phase stability, lattice constants 0-45283  
 Nb-Pt-O system, phase equilibria, diagram, unit cell parameters, supercond. 0-55352  
 Nb-S system, phase relations at high temp., elec. and mag. props. 0-29932  
 Nb-Si-Cu, struct. and supercond., Cu influence 0-50592  
 Nb-Sn(Al)(Ga)(Ge)(Si)-C, phase equilib. and supercond. 0-50593  
 Nd-Fe-B ternary systems, phase equilibria and cryst. struct. (*Ukrainian*) 0-11626  
 Nd<sub>2</sub>O<sub>3</sub>-HfO<sub>2</sub> system, phase relationships 0-35169  
 Ne-H<sub>2</sub> mixture, liquid vapour phase equilib., sound vel., compressibility, thermodynamic perturbation theory obs. (*Russian*) 0-39306  
 Ni-Mo (20.8 wt.%), order, heat treatment effects 0-40406  
 Ni-Ta-Al system, phase equilibria and diagram, electron probe, X-ray diffr. anal. 0-29927  
 Ni<sub>3</sub>Ge<sub>3</sub>, solid and liquid, physicochemical props. and structure 0-39548  
 NiO-CuO, equilibrium relations 0-55375  
 O<sub>2</sub>, phase equilibria near 298K, Raman spectral study of solid and fluid 0-19937  
 O<sub>2</sub>-<sup>85</sup>Kr-Xe, liquefaction, retention of <sup>85</sup>Kr from fission exhaust gases, separation technique (*German*) 0-27753  
 Pb melts, As and Sn distrib., Si, Cr, and Mn influence (*Russian*) 0-16274  
 Pb-Se-As-Ge, phase separation in melt centrifugal quenching 0-25701  
 Pb(Zr,Ti)O<sub>3</sub>, thermodynamic properties and formation data 0-29939  
 Pd-Ag, Fermi energy influence on soln. behaviour of H, B and C (*German*) 0-44323  
 Se-(Co,Ni,Cu)-Ga, phase equilibria, diagrams of state, X-ray, microstructural study (*Russian*) 0-55356  
 Si-Al-B-O-N, calc. of phase diagrams from data set 0-55362  
 Si-Al-O-N, mullite like cpd. comp., EPMA, X-ray and chem. anal. obs. (*Japanese*) 0-35175  
 Si-Al-Zr-O-N, calc. of phase diagrams from data set 0-55362  
 α/β-Si<sub>3</sub>N<sub>4</sub>, formation during nitridation of Si 0-50609  
 Si<sub>3</sub>N<sub>4</sub>-AlN-Al<sub>2</sub>O<sub>3</sub>-SiO<sub>2</sub>-Y<sub>2</sub>O<sub>3</sub>, phase equilibrium study by X-ray diffr. and optical microscopy 0-50614  
 Si<sub>3</sub>N<sub>4</sub>-Mg-SiO<sub>2</sub>-Si<sub>3</sub>N<sub>4</sub>-N<sub>2</sub>O, compressive creep, composition effect 0-50674  
 Si<sub>3</sub>N<sub>4</sub>-SiO<sub>2</sub>-ZrN-ZrO<sub>2</sub>, X-ray diffr. phase anal. and reactions Si<sub>3</sub>N<sub>4</sub>+ZrO<sub>2</sub>, SiO<sub>2</sub>+ZrN 0-50613  
 SiO<sub>2</sub>-Na<sub>2</sub>O-CaO (13, 11 wt.%) glass, phase separation, SiO<sub>2</sub> purity effect 0-44144  
 SiO<sub>2</sub>-Na<sub>2</sub>O-CaO glass, phase separation characts., melting atmosphere effect 0-44141  
 Sm-Fe-B ternary systems, phase equilibria and cryst. struct. (*Ukrainian*) 0-11626  
 SrO-Fe<sub>2</sub>O<sub>3</sub> system, non-existence of single phase SrFe<sub>2</sub>O<sub>4</sub>, Mossbauer expts. 0-29178  
 Ta-Si-Cu, struct. and supercond., Cu influence 0-50592  
 TaSi<sub>2</sub>-CrSi<sub>2</sub>, phase equilib., struct. and props. 0-50608  
 Ti-Al-Mo-Cr-Fe, distrib. of Sn, Zr between phases, temp effect. 0-55357  
 Ti-Al-Zr-Mo alloy 685, phase at α/β interface (*French*) 0-25661  
 Ti-Al(Fe) microprobe anal. of alloying addition distrib. 0-55358  
 Ti-O system, intermediate oxide thermodynamics under equilibrium press. 0-55351  
 Ti-V-Mo-Cr system, β-phase stability 0-55353  
 TiSi<sub>2</sub>-CrSi<sub>2</sub>, phase equilib., struct. and props. 0-50608  
 Ti(Zr,Hf)-Gd-B system, phase equilib. 0-11629  
 Ti-Se liquid binary mixtures, phase separation under press. 0-34183  
 Ti<sub>2</sub>S-SnS, phase equilibria exam. 0-55369  
 U-UNi<sub>3</sub>-UCO<sub>2</sub> system, phase equilibria, lattice constants (*German*) 0-50598  
 U-Zr-O system, phase formation, phase equilibrium 0-16667  
 V-Si-Cu, struct. and supercond., Cu influence 0-50592  
 V-Sn(Al)(Ga)(Ge)(Si)-C, phase equilib. and supercond. 0-50593  
 V<sub>3-x</sub>Cr<sub>3-x</sub>Si<sub>x</sub>, x=0 to 3, struct., supercond. and mag. props. 0-1962  
 V<sub>13</sub>O<sub>24</sub> long-period Magneli phase as product of V<sub>6</sub>O<sub>11</sub>-V<sub>7</sub>O<sub>13</sub> periodic microsyntactic intergrowth 0-50618  
 VS through V<sub>3</sub>S<sub>4</sub>, nonstoichiometric, phase relations and thermodynamics 0-29188  
 W-Si-Cu, struct. and supercond., Cu influence 0-50592  
 YOF-YF<sub>3</sub>, high pressure phase transitions 0-55368  
 YbCr<sub>1-x</sub>Al<sub>x</sub>O<sub>3</sub> solid solutions 0-20887  
 Zr-Fe, Mossbauer spectra parameters of Zr<sub>2</sub>Fe particles (*Russian*) 0-29654  
 Zr-Fe-Cu-W, Mossbauer spectra parameters of Zr<sub>2</sub>Fe particles (*Russian*) 0-29654  
 Zr-Nb-Ga, phase equilibria 800°C (*Ukrainian*) 0-35157  
 Zr-Se-Ga, phase equilibria 800°C (*Ukrainian*) 0-35157  
 ZrO<sub>2</sub>, substoichiometric, thermodynamic props. at lower phase boundary 0-29185  
 ZrO<sub>2</sub>-SiO<sub>2</sub>-αAl<sub>2</sub>O<sub>3</sub> mixed powders, solid state reactions 0-40337

**phase equilibrium diagrams** *see phase diagrams***phase-locked loops**

- discriminator, five channels, automatic meas. of whistler dispersion (*Japanese*) 0-31143  
 lasers, coherently combined, phase lock control considerations 0-5743

**phase measurement**

- forced oscillations experiment for students 0-17780  
 microwave interference signals from 0 to n.360° for plasma density meas. (*German*) 0-6278  
 optical phase measurement in real time using photodetector array, Fourier transform computation 0-9013  
 phase-angle differences, up to 100 MHz meas. devices classification 0-52269  
 photoacoustic spectroscopy in solids, phase measurement, appl. to nonradiative transitions, optical absorpt. 0-31885

**phase measurement continued**

- RF phase bridge, use of piezoelectric resonators 0-4732  
 stellar interferometry, phase effect detect. and appl. to orbit of α Aurigae (Capella) (*French*) 0-36508

**phase meters**

- phase-angle differences meas., up to 100 MHz meas. devices classification 0-52269

**phase modulation**

- see also phase shift keying*  
 baseline ripple reduction by quasi-optical phase modulation, mm radio spectra 0-56710  
 ferroelectric ceramic-photoconductor structure, as optically controlled transparency 0-28343  
 spin-echo Fourier transform NMR spectroscopy, multiple pulse technique 0-37063  
 GaP-AlGaP, stripe-geometry electrooptical modulator 0-23798

**phase regulation** *see phase control***phase shift circuits** *see phase shifters***phase shift keying**

- two-phase PSK modulator employing SAW delay line, fundamental performance 0-33398

**phase shift microphones** *see microphones***phase shifters**

- digital phase-shifter for multiple quantum NMR 0-17974  
 electro-optic waveguide deflector performance characteristics 0-33213  
 musical appls., digital phase shifter using Bell Labs digital filter module 0-5884  
 optical for guided-wave signal transformers, synthesis 0-1358

**phase space methods**

- free electron lasers, boundary deform. and Robinson-Liouville theorem 0-48202  
 granulation due to mode-mode coupling in plasma turbulence simulation 0-38651  
 heat transfer in linear harmonic chain, nonequilib. steady states, information theoretic approach 0-19214  
 turbulence kinetic theory, fundamental soln. 0-27137

**phase transfer function** *see optical transfer function***phase transformations**

- see also critical fluctuations; heat of transformation; isothermal transformations; liquid crystal phase transformations; liquid-vapour transformations; phase diagrams; phase equilibrium; solid-liquid transformations; solid-state phase transformations; solid-vapour transformations; spinodal decomposition; vapourisation*  
 φ<sup>3</sup> theory, three dims. second order phase transitions, infrared singularities 0-37161  
 absorbed layer, commensurate-incommensurate transition 0-49494  
 acoustooptical effects of cooling liquid, absorption of flashlamp radiation with phase transition in medium 0-5868  
 adiabatic and isothermal order-parameter susceptibilities and the thermal diffusion mode 0-36962  
 adsorbate layer, phase transition theory, review 0-44433  
 adsorbed layers, two-dimensional phase transitions, review 0-39419  
 anisotropic system, random field conjugate to non-crit. variable, effect on phase transition 0-13022  
 binary alloy freezing, non-equilibrium thermodynamic processes 0-34167  
 biomembrane, phase changes and determination methods (*Czech*) 0-3599  
 black hole thermodynamics, second order phase transitions 0-46897  
 catastrophe indices and fourth checkpoint second-order transitions 0-52147  
 CDW ordered state in coupled chains of BGD model, props. 0-6756  
 chemical fluctuations near nonequilibrium phase transitions to nonuniform states 0-45542  
 colloids, statistical mechanics approach 0-40749  
 commensurability in one-dimensional lattices at finite temperature 0-42156  
 commensurate-incommensurate phase transitions on restricted substrate area 0-49513  
 conference on dynamical critical phenomena, Geneva (Apr. 1979) 0-27040  
 conformal-invariant field theory, anomalous dimensions, coupling consts. 0-4870  
 critical phenomena, catastrophe theory appl. 0-8948  
 critical thermodynamics, phase transition in transverse field with deform. depend., phonon anomaly separation 0-39258  
 Dicke model phase transition, thermodynamic Green's function method 0-5715  
 DNA, phase transition, ψ transition of single coils 0-26200  
 DTA, thermal curve interpretation 0-45599  
 electron-vibration system, nonequilib. first-order type phase transition 0-9633  
 energy storage unit sizing for air-based solar heating systems 0-7922  
 FCC lattice, phase transitions of fully frustrated models 0-29517  
 finite system, order parameter and sp. ht. for epitaxial ordering renormalisation-group calc. 0-17862  
 fourth checkpoint for second-order transitions 0-27248  
 Gibbs ensembles equivalence, phase transitions 0-134  
 Goldstone theorem in classical statistical mech., correl. function nonvanishing boundary terms as phase transition origin 0-27253  
 grain boundary migration vacancy generation, and drag force 0-15090  
 group structure for general lattice systems and surface tension 0-4675  
 hadronic matter, Pomeron and critical temp. 0-22566  
 hard-core lattice gas with tricrit. point, phase transition behaviour 0-8926  
 Heisenberg spin 1 system assembly with tunneling, phase transitions, thermodynamic behavior 0-4667  
 Higgs lattice abelian model, finite temp. behaviour 0-13260  
 highly dispersed systems, phase size effect 0-6488  
 hyaluronate solns., cooperative phase transitions, review 0-45850  
 Ising frustration pots., phase transition 0-52142  
 Ising lattice, thermal relaxation, nonideal behaviour, stochastic theory 0-22312  
 Ising model for monolayers of coadsorbed atoms, phase transitions 0-19909  
 Ising model two-dimensional with periodically distributed frustration, rigorous props. 0-46987  
 Ising O(2), O(3) and O(4) spin systems, Hamiltonian string-coupling expansions 0-20426  
 kink dynamics in one-dimens. double-well field theory 0-39247



**phase transformations continued**

- laser system qualitative change in threshold range, analogy with phase transition (*Czech*) 0-32949  
 lattice 2-D models with isotropic short range interactions and continuous symmetries 0-36949  
 lattice gauge theories, strong coupling phase large space-time dimension, Ising model 0-27397  
 layered spin systems, phase transitions, partition functions and binary correlation functions 0-50133  
 Lennard-Jones type one-dimens. system, Van der Waals type eqn. of state 0-24562  
 light scattering near phase transitions in solids, review 0-29752  
 lipid mixtures, phase diagrams, theoretical model 0-8032  
 long chain molecule, crystals, phase transitions, statistical theory 0-44290  
 metastable state relaxation, critical point region nucleation in thermodynamic systems (*Russian*) 0-13026  
 monolayer, anomalous thermal effects, statistical mechanics 0-15367  
 monolayer, interfacial, thermodynamic treatment, excess quantities, adsorbed and spread layers 0-40732  
 multicomponent, multiphase systems near critical point, phase volume behaviour 0-15212  
 nonequilibrium phase transitions in presence of external non-white noise 0-42182  
 nucleation rate, relationship between experimentally determined and true values 0-54343  
 O(N)  $\sigma$ -model, two-dimens., mag. susceptibility, phase transitions and high temp. expansion 0-47177  
 phase diagram classification by catastrophe theory 0-17905  
 planetary formation as adiabatic phase transition, isocentropic model 0-26763  
 polyacrylamide, gels and single chains, phase transitions and crit. behaviour 0-40759  
 polymers solns., cooperative phase transitions, review 0-45850  
 polystyrene sphere crystals, in aqueous suspensions, solid-like phase transition 0-50893  
 Potts model, Monte Carlo simulation in three dims. 0-163  
 Potts model, quenched bond disorder, single-bond effective interaction approx. 0-27229  
 Potts model, three-state, phase transition continuity 0-22302  
 pressure in lattice systems, differentiability props. 0-31677  
 pseudo-first-order phase transitions in one dimension 0-22270  
 random Ising model on Cayley tree, phase transition 0-42150  
 renormalisation group anal. in 2D Coulomb gas, sine-Gordon theory and XY model 0-36950  
 renormalisation group eqns. and thermodynamic anomalies near tricritical point (*Russian*) 0-13027  
 representation generating theorems and interaction of improper quantities with order parameter 0-4682  
 small cluster formation, fifth state of matter 0-39304  
 spin systems and lattice theories, phase diagrams and critical points of continuous transitions 0-22528  
 Stephan problem, one dimens., direct and inverse solns. 0-14552  
 structural stability in physics (conference, Tübingen, Germany, May and Dec. 1978) 0-8739  
 structural stability in statistical mechanics 0-8932  
 superconductivity and elementary particles theory, review 0-4911  
 superradiance phase transition problem, applicability of Wang-Hion method 0-31695  
 surface tension and phase transition in lattice systems 0-27226  
 temperature wave analysis method 0-15217  
 theory, electron density of states tail, profile in Gaussian random field 0-6691  
 thermoelectric electret, Costa Ribeiro effect 0-7272  
 thermodynamic nonlinear fluctuation-dissipation theory 0-36963  
 two-dimensional system, phase transitions and metal-insulator transitions 0-2143  
 water, Ising lattice model with directional bonding, renormalisation group study 0-28894  
 X-Y model, gauge theory analogue, 4-D self-dual gauge model, phases and transitions 0-27399  
 $\text{AlPO}_4$ , high temp. behaviour up to liq. state, phase relations, X-ray diffr. and therm. anal. study (*French*) 0-10660  
 $\text{NbO}_x$ , phase comp. on heating 2000-4000K 0-21267

**phase transitions** *see phase transformations***phased arrays (antenna)** *see antenna phased arrays***phased locked oscillators** *see parametric oscillators***phi mesons**

- mass compilation study 0-52552  
 $K^+p$ , 32 GeV/c,  $\rho$ ,  $K^*$ ,  $\phi$  inclusive prod., quark fusion model 0-32135  
 $\omega$ - $\phi$  baryonium mixing model 0-32072  
 $\phi \rightarrow \pi^+\pi^-$ ,  $\pi$  form factor,  $\phi$  peak, unitarity and gluonic corrections 0-22615

**philosophical aspects***see also humanities*

- Aristotelian philosophy, J.B. van Helmont's attack 0-31474  
 catastrophe theory's role in natural philosophy, definition of science 0-8772  
 chemical evolution far from equilibrium, concepts (*French*) 0-7761  
 clock synchronisation, distant simultaneity 0-27125  
 concept acceptance in scientific research phlogiston theory example 0-27102  
 dimensional analysis 0-27263  
 EM vector pot., physical interpretation 0-46772  
 essentialism, relative 0-42041  
 Francesco Patrizi da Cherso's concept of space and its later influence 0-31478  
 frontiers of time 0-12886  
 general relativity and the conceivability of time travel 0-27192  
 human brain functions and foundations of science 0-27103  
 increasing weight of falling bodies, Aristotle's conclusion 0-46770  
 liquidons and gasons, continuity of state historical controversies 0-12882  
 mathematical models role in natural sciences (*Afrikaans*) 0-8771  
 mathesis universalis, philosophers conception from Descartes for Leibniz 0-31479  
 physical constants, epistemological, historical and general investig. 0-12884  
 physical theories, formal analysis; inductive inference, physical states, truth and physical states 0-12883  
 physics, foundation problems 0-12856  
 physics models, nature and purpose 0-42023

**philosophical aspects continued**

- probability foundations, modal frequency interpretation 0-12885  
 propensity theory, hidden variables, coin tossing appl. 0-42040  
 quantum logic, props. of states 0-12947  
 quantum logic interpretation of orthocomplemented quasi modular lattice 0-12950  
 quantum mech. foundations, conditional probability of a generalised probability theory 0-12949  
 quantum mechanics, meas. problem 0-12948  
 quantum probability in logical space 0-31579  
 radioactivity and quantum mechanics unification, probabilistic conceptions 0-12946  
 relativity, special theory, foundational problems 0-12906  
 science and the humanities, The Two Cultures gap, teaching 0-41979  
 Solubility Data Project, IUPAC venture 0-19  
 space, time, geometric style of explanation 0-18  
 special theory of relativity, relative simultaneity 0-27126  
 statistical mechanics, nonequilibrium, review 0-12983  
 Tao of Physics, course in modern physics and Eastern mystical philosophy 0-17730

**phonographs** *see gramophones***phonon bottleneck** *see phonons***phonon-defect interactions***see also lattice localised modes*

- diamond, thermal cond. at low temp., correl. with IR absorpt. features 0-49435  
 dislocation-phonon interaction in cryst. with anisotropic slip system 0-29137  
 glasses, thermal cond. rel. to diffusion process due to phonon-defect interaction 0-34259  
 phonon scattering by spherical defect aggregates 0-24552  
 point defect formation in weak shock wave front (*Russian*) 0-6401  
 Al, lattice thermal cond. at low temps., Ashcroft pseudopotential method 0-19897  
 Cu, defect-phonon perturbations after neutron irradi., neutron scatt. study 0-44278  
 Cu, vacancy, lattice vibrs., reson. and localised modes 0-39236  
 $\alpha$ -Fe, vacancy, lattice vibrs., reson. and localised modes 0-39236  
 GaAs, phonon assisted tunnel emission of electrons from deep levels 0-25532  
 $^3\text{He}$ , solid, low temp. thermal cond., structural crystalline defects 0-2240  
 $^4\text{He}$ , solid, boundary limited thermal cond., Poiseuille phonon flow 0-2241  
 K, thermomagnetic and thermoelectric properties, phonon scatt. processes 0-29390  
 KCl:CN $^-$ , phonon-defect interaction, Brillouin scatt. obs. 0-34935  
 (La,Gd)Al $_2$ , normal and supercond. state, US attenuation, freq. depend. and mechanisms 0-49992  
 Si:Sn, thermal conductivity, Hall mobility depend. on Sn conc., phonon-defect scatt. 0-29232

**phonon dispersion relations**

- Al $_5$  type compound, props. and one-dimensionality 0-2530  
 alkali metal, Ashcroft pseudopotential, unified study of props. 0-39239  
 alkali metals, axially symmetric model 0-34152  
 binary alloy, of simple metals, pseudopotential approach 0-44464  
 cooperative Jahn-Teller T-systems dynamics vibronic excitation branches 0-10934  
 crystal with interstitials, lattice dynamics 0-2128  
 dichalcogenide layer compounds, interface plasmon-phonon interactions, transverse cond. 0-49641  
 graphite intercalation cpds., Raman scatt. and IR refl., review 0-45066  
 HCP metals, lattice dynamics, local pseudopotential approach, dielectric functions 0-34151  
 insulators, book, showing curves for over 100 cpds. 0-51970  
 kinetics of phonon system with almost linear dispersion law (*Russian*) 0-29136  
 metal, cubic, Sharma-Joshi model, correl. exchange effects 0-10613  
 molecular rare-gas solids, dispersion relations in central force rigid atom model 0-2131  
 noble metals, energy wave number charact., by reson. model 0-10612  
 noble metals, phonon dispersion relation in resonant model potential 0-6473  
 optical activity in crystals, lattice dynamical theory 0-34883  
 orbit degenerate electron state localised at point defect, T-term multimode Jahn-Teller effect (*Russian*) 0-15490  
 Peierls dielectric, one dimensional, selftrapped excitations in Peierls-Frohlich state (*Russian*) 0-54678  
 phonon scattering by spherical defect aggregates 0-24552  
 polariton Fermi resonance, Raman spectra in band of many-particle states 0-25374  
 polyethylene, H bonding effects on skeletal optical and longitudinal acoustical modes 0-34914  
 polysulphur nitride, Kohn anomalies in phonon dispersion 0-24555  
 rare earth intermediate valence systems, neutron scatt., review 0-49674  
 semiconductor superlattice, phonon spectrum, effect of strong elec. field, parametric reson. 0-44273  
 spectroscopy of high-frequency phonons, transport phenomena, review 0-49325  
 superionic conductors, struct. and dynamical props., X-ray and neutron scatt. studies, book contrib. 0-24433  
 transition metal, BCC, phonon dispersion relations, Fieles five-const. model calc. 0-34150  
 transition metals, lattice excitations, classical models 0-29132  
 two-parameter dynamical model, appl. to Ag and Al 0-10597  
 Ag halides, quadrupolar deformability theory by tight binding method 0-10614  
 Ag, lattice dynamics, ion-ion and ion-electron interactions 0-49321  
 Ag, pseudopot. optimised form for phonon dispersion study 0-10611  
 Al, lattice vibrations, seven parameter non-central force model 0-44270  
 Ar, solid, lattice dynamics calc. using energy band theory 0-49320  
 Au, lattice dynamics, ion-ion and ion-electron interactions 0-49321  
 Be, phonon spectrum from inelastic coherent scatt. of cold neutrons 0-10617  
 $\text{C}_8\text{K(Rb)}$ , graphite intercalated, phonon dispersion relations and Raman spectra 0-44272  
 $\text{CaF}_2\text{:Dy}^{3+}$ , cubic cryst. field effects 0-2368  
 $\text{CdGa}_2\text{Se}_4$ , IR refl. spectra, optical phonon dispersion 0-29746  
 $\text{CrCl}_3$ , phonon dispersion curves 0-2130  
 Cs-Graphite, interaction ordered and disordered cpd., Raman spectra 0-11393



**phonon dispersion relations continued**

- Cu, lattice dynamics, ion-ion and ion-electron interactions 0-49321  
 Cu, lattice specific heat, from two-parameter lattice dynamical model with dispersion 0-10678  
 D<sub>2</sub>, solid, phonon absorption line shape as function of density 0-50329  
 EuS, phonon anomalies and electron-lattice coupling 0-39490  
 Eu<sub>1-x</sub>S<sub>x</sub> (X=Sr,Gd), spin-disorder-induced Raman scatt. from phonons, theory 0-20636  
 EuX (X=O,S,Se), spin-disorder-induced Raman scatt. from phonons, theory 0-20636  
 α-Fe, lattice wave dispersion, lattice consts., elastic consts. 0-24545  
 Fe<sub>2</sub>TiO<sub>4</sub>, cooperative Jahn-Teller effect, neutron scatt. study 0-49678  
 GaAs-AlGaAs superlattice, selective transmission of HF phonons 0-34154  
 GaP, lattice dynamics, phonon freq. meas., valence-force-field overlap shell model 0-15205  
 GaP, polariton dispersion, IR reflection spectroscopy 0-11415  
 GaSe, long wavelength IR refl. spectra 0-11401  
 Ge, phonon dispersion and microscopic screening, extreme tight-binding model 0-49324  
 H<sub>2</sub>, phonon absorption line shape as function of density 0-50329  
<sup>4</sup>He, superfluid, phonon dispersion 0-10722  
 Hf, HCP, lattice dynamics, thermal and elastic props., model 0-34155  
 K, helicon-phonon interaction for oblique propagation, dispersion relation 0-49315  
 KCl(Br)(I), lattice dynamics, bond-bending force model 0-54322  
 KI, relationship between fourth moments in molten state and phonon freq. in solid phase 0-10477  
 KNbO<sub>3</sub>, ferroelec. phase, phonon dispersion relations and lattice dynamics calcs., comparison with expt. 0-49319  
 KNbO<sub>3</sub>, tetragonal phase, inelastic neutron scatt. 0-19676  
 K<sub>2</sub>Pt(CN)<sub>4</sub>, quasi-one-dimens. Peierls system, phonon dispersion and neutron scatt., calc. 0-24550  
 LaNbO<sub>4</sub>, Raman scatt. and fluoresc. spectra 0-20625  
 LiNbO<sub>3</sub>, ferroelec. phase, phonon dispersion relations and lattice dynamics calcs., comparison with expt. 0-49319  
 NH<sub>3</sub>, phonon dispersion curves, phonon lifetimes, anharmonic effects 0-15202  
 NaCl(Br) (F) (I), lattice dynamics and statics, three-body-force shell model 0-49323  
 NaClO<sub>4</sub>, Brewster type surface mode dispersion, IR refl. meas. 0-11415  
 Nb-Zr, acoustic phonon anomalies and superstructure, neutron inelastic scatt. meas. 0-19892  
 Ne, solid, lattice dynamics calc. using energy band theory 0-49320  
 Pb<sub>3</sub>(PO<sub>4</sub>)<sub>2</sub>, ferroelastic phase transition, inelastic neutron scatt. (French) 0-24584  
 Pd<sub>0.96</sub>Ag<sub>0.04</sub>, phonon dispersion curves at 296K 0-24546  
 Pd<sub>0.9</sub>Rh<sub>0.1</sub>, lattice dynamics, inelastic neutron scatt. meas. at 296K 0-29135  
 Rb, lattice vibrations, seven parameter non-central force model 0-44270  
 RbBr, harmonic and anharmonic props. from phonon dispersion at three temps. 0-39235  
 SO<sub>2</sub>, lattice dynamics, rigid mol. model 0-44266  
 SeCl<sub>3</sub>, phonon dispersion curves 0-2130  
 Se and Te, homology of phonons, scaling formalism for phonon freqs. 0-54326  
 Se, trigonal, force field calc. 0-54328  
 Se, trigonal, low temp. sp. ht. and elastic consts., piezoelec. effect influence on phonons 0-54404  
 Se, trigonal, vitreous and red amorphous, phonon density of states comparison 0-54329  
 Si, pseudopotential calculation of phonon dispersion curves 0-10620  
 SiC (1 OH), phonon spectrum, dispersion curves energy discontinuity and vibr. modes, IR spectra obs. 0-44274  
 SmS, phonon anomalies and electron-lattice coupling 0-39490  
 Sm<sub>0.75</sub>Y<sub>0.25</sub>S, phonon anomalies and electron-lattice coupling 0-39490  
 Sm<sub>0.75</sub>Y<sub>0.25</sub>S, intermediate valence compound, phonon investigation by neutron scatt. 0-6476  
 Sm<sub>0.75</sub>Y<sub>0.25</sub>S, mixed valence, phonon dispersion theory 0-34153  
 Te and Se, homology of phonons, scaling formalism for phonon freqs. 0-54326  
 Th, lattice dynamics, unpaired forces 0-15201  
 TiCl<sub>3</sub>, phase transition, phonon dispersion curves 0-2130  
 TiSe<sub>2</sub>, lattice dynamics, charge density waves transverse phonon dispersion curves, model 0-49322  
 TiSe<sub>2</sub>(S<sub>2</sub>) (1T), electronic and vibronic struct. 0-44500  
 Ti<sub>3</sub>AsS<sub>4</sub>, optical phonons, Raman and refl. spectra 0-11400  
 UAl<sub>3</sub>, elastic consts., temp. and mag. field depend. 0-55450  
 USb, neutron inelastic scatt. meas., phonon spectra, mag. response, anisotropy 0-50065  
 VI<sub>3</sub>, lattice dynamics and ionic charge 0-10615  
 W, lattice wave dispersion, lattice consts., elastic consts. 0-24545  
 YS, phonon anomalies and electron-lattice coupling 0-39490  
 ZnO, polariton dispersion, IR reflection spectroscopy 0-11415  
 ZnP<sub>2</sub>, second-order vibr. spectra and dispersion of phonon branches 0-25376  
 Zr, BCC, phonon vibrs., pseudopot. method 0-15204

**phonon drag**

- anisotropic normal metal, thermopower calc. 0-24879  
 graphite, carrier mobility, temp. depend. determ. from magnetoresist. expts. 0-11009  
 graphite, electron-phonon interactions, rel. to elec. transport 0-34156  
 graphite, neutron irradiation, electron transport, annealing study 0-39165  
 superconductors, thermoelectric and acoustoelectric effects, influence of mutual drag of excitations and phonons 0-44761  
 Bi, phonon-drag low temperature thermoelectric refrigeration 0-22366  
 Bi-Sn, thermopower from 50 mK to 25K 0-24880  
 K, thermomagnetic and thermoelectric properties, phonon scatt. processes 0-29390  
 (SN)<sub>x</sub>, thermopower from 0.15 to 4.2K 0-34427  
 YIG, phonon viscosity effect on dislocation motion 0-24450

**phonon-electron interactions** *see electron-phonon interactions***phonon-exciton interactions**

- anthracene-Au interface exciton luminescence Frenkel exciton metallic quenching (Russian) 0-50421  
 anthracene-quartz interface exciton luminescence, Frenkel exciton metallic quenching (Russian) 0-50421  
 1,4-dibromonaphthalene, substitutionally disordered, energy localisation, optical and ODMR spectra of triplet Frenkel excitons 0-54996  
 electron-hole droplet cloud, role of thermalisation phonons 0-49617

**phonon-exciton interactions continued**

- exciton physics, review, book contrib. 0-44517  
 excitons, book 0-41951  
 ferroelectrics, absorption edge anomalies in phase transitions 0-2718  
 molecular crystal, one-dimensional model, exciton-phonon and phonon-impurity interactions 0-24542  
 molecular crystal trapping processes, exciton-phonon coupling 0-39505  
 molecular crystals, two particle exciton-phonon interactions, optical absorpt. line shapes theory 0-55120  
 organic charge transfer crystals, transport props., phase transitions, mol. dynamic (German) 0-39507  
 phenazine, substitutionally disordered, energy localisation, optical and ODMR spectra of triplet Frenkel excitons 0-54996  
 polar semiconductors, exciton-phonon interactions, optical absorpt. spectra, theory 0-49614  
 polar semiconductors, hot exciton scatt. accompanied by transitions to excited states, phonon interactions 0-44516  
 semiconductor, bound excitons, review, book contrib. 0-44519  
 semiconductor, resonant Raman and Brillouin spectroscopy, review, book contrib. 0-49624  
 semiconductors, exciton light absorpt. band formation, linear and quadratic exciton acoustic phonon interactions (Russian) 0-34368  
 semiconductors, excitons in mag. field, exciton-phonon interaction 0-24806  
 surface exciton polaritons, book contrib., review 0-49623  
 variational solns. for energy and correl. functions 0-10601  
 AgBr:Cl, exciton-phonon interaction, reson. Raman scatt. vs photolum. 0-29798  
 CdSe, polarisation correl. of resonant Raman scatt. or hot luminesc. 0-25384  
 CuCl, phonon interaction of excitonic molecule 0-50316  
 CuCl, Urbach rule at excitonic absorpt. edge, theoretical model tests 0-50299  
 Cu<sub>2</sub>O, exciton-phonon dynamics, reson. Raman scatt. 0-11406  
 p-GaAs, hot exciton luminesc., LO phonon Raman scatt. 0-11474  
 GaSe, exciton-phonon bound state, photocond. and visible absorpt. spectra obs. 0-50369  
 GaTe, exciton polariton effect on absorpt. edge, absorpt. and refl. spectra, 4.2 to 300K 0-20664  
 Ge, exciton and electron-hole drop entrainment by nonequilib. phonons 0-6751  
 NaI, motion of free excitons and their self-localisation 0-2342  
 PbI<sub>2</sub>, visible exciton spectrum, exciton-phonon interactions, dielectric const. and oscill. strengths 0-25405  
 TiCl<sub>3</sub>, Urbach rule at excitonic absorpt. edge, theoretical model tests 0-50299  
 Xe, crystalline, polariton effects, reflectivity, absorpt., and resonant luminesc. spectra calcs. 0-20095  
 Xe, solid, self-trapped exciton emission bands 0-20697  
 Zn,Cd<sub>1-x</sub>S, resonance Raman scatt. involving exciton complexes 0-16039

**phonon-impurity interactions***see also lattice localised modes*

- absorption and emission spectra, of impurities in solids, bandshapes, moments 0-45122  
 alkali halide, ReO<sub>4</sub><sup>-</sup> doped, saturable absorber at 10.6 μm 0-53384  
 crystal with interstitials, lattice dynamics 0-2128  
 disordered systems, time dependent spectral transfer, Monte Carlo calc. 0-11464  
 fluorite and antiferroite structs., (110) surface vibr. modes, dynamics and adiabatic potential 0-6613  
 fluorite type struct., impurity defect interaction in boundary layer, adiabatic approx. 0-6614  
 impurity pinning, phonon localization, in incommensurate modulated lattices 0-39238  
 ionic crystals with intermediate polaron coupling, magneto-optical effects in shallow F-centres 0-20615  
 Jahn-Teller multimode effect for E-term with strong vibronic coupling, IR and Raman spectra band shapes 0-20139  
 Kramers ions, virtual phonon exchange, field theoretic formalism 0-20137  
 laminary crystal, phonon spectrum and local vibrations (Russian) 0-10623  
 metal, BCC quantum diffusion model of light interstitial atoms 0-2212  
 metal, diffusion of H(D), slow neutron scatt. obs., review 0-34248  
 metals, ferromagnetic, nonmagnetic impurity hyperfine field temp. depend. 0-34402  
 molecular crystal, one-dimensional model, exciton-phonon and phonon-impurity interactions 0-24542  
 multimode Jahn-Teller effect for E-term with strong vibronic coupling, local and resonant states 0-24858  
 nonlinear impurity electron-phonon oscillations 0-49327  
 oscillator, highly-excited, decay in cryst. vibr. interaction 0-10600  
 paraelectric resonance of nonstationary tunnelling states (Russian) 0-34869  
 semiconductor or insulator, impurity optical spectra, p-phonon processes 0-16061  
 Cr antiferromagnetic with nonmagnetic impurities, mag. susceptibility using two band model 0-2559  
 CuBr:Cl(I), lattice-dynamical study of impurity modes 0-29129  
 CuCl:Br(I), lattice-dynamical study of impurity modes 0-29129  
 CuI:Br(Cl), lattice-dynamical study of impurity modes 0-29129  
 GaN:Zn, VPE grown, optical cross sections, photoluminesc. and optical absorpt. meas. 0-55160  
 GaN:Zn, VPE growth, photoluminesc. rel. to doping conditions 0-55159  
 n-Ge, magnetothermal cond., 4.2K 0-24688  
 Ge:Ga(In), resonant phonon interaction with localised acceptor levels 0-6784  
 KBr:CN<sup>-</sup> 0-49316  
 KCl:CN<sup>-</sup>, coherent admixtures of phonons with impurity librionic excitations, neutron scatt. study 0-49316  
 K(H<sub>1-x</sub>D<sub>x</sub>)<sub>2</sub>PO<sub>4</sub> polarised impurity cluster effects in light scatt. expts. 0-29716  
 Ni film, phonon transport into SrF<sub>2</sub> substrate, diffusive scatt. at impurities 0-49487  
 Si:Sn, thermal conductivity, Hall mobility depend. on Sn conc., phonon-defect scatt. 0-29232  
 ZnS CVD window, IR lattice absorption, phonon assignments and image spoiling 0-33104



# phonon-magnon interactions

antiferromagnet, high frequency properties, spin wave spectra corrections magnon interactions (*Russian*) 0-54876  
antiferromagnet, phonon-magnon relaxation times, external mag. field depend. 0-44898  
elastic properties of magnetic materials, review 0-7142  
ferroelectric ferromagnet, soft modes and ferromag. reson. 0-11275  
ferromagnetic resonance in anisotropic Heisenberg model, magnon-magnon, phonon-magnon interactions (*Russian*) 0-11274  
ferromagnetic semiconductor, magnon coupling to plasmons and LA phonons, s-d model 0-29536  
magnon kinetic eqns. in parametric ultrasonically excited ferromagnets 0-44820  
metastable polarised crystals, decay kinetics, exchange magnon-phonon interactions (*Russian*) 0-7060  
metastable spin-aligned crystals, decay kinetics 0-34669  
system with two singlet levels, phonon coupling to mag. excitations 0-6470  
CdCr<sub>2</sub>Se<sub>4</sub>, spin system heating by drifting current carriers, magnon-phonon system energy transfer (*Russian*) 0-29541  
CoCl<sub>2</sub>·2H<sub>2</sub>O, antiferromag., light scatt. from phonons and magnons 0-40104  
CoCl<sub>2</sub>·2H<sub>2</sub>O, magnon-phonon interactions and two-magnon Raman scatt., magnetoelastic waves and selection rules 0-34917  
CsCoCl<sub>3</sub>, Ising like antiferromag., mag. phase transition, <sup>133</sup>Cs NMR 0-7184  
EuO, spin system heating by drifting current carriers, magnon-phonon system energy transfer (*Russian*) 0-29541  
FeCl<sub>2</sub>·2H<sub>2</sub>O, magnon-phonon interactions and two-magnon Raman scatt., magnetoelastic waves and selection rules 0-34917  
K<sub>2</sub>CoF<sub>4</sub>·Mn<sup>2+</sup>, impurity induced mag. excitations, magnon gap mode, far IR spectra obs. 0-44821  
Rb<sub>2</sub>MnCl<sub>4</sub>, layer antiferromag., optical absorpt., temp. and mag. field depend. 0-20661

# phonon-phonon interactions

*see also Umklapp process*  
Boltzmann eqn., phonon and electron transport in bounded systems 0-39545  
p-dibromodiphenylether surface, normal and ultra-Brewster refl. spectra 0-25400  
dielectric, thermal cond. at low conc. of phonon scatt. centre, freq. crossing signals 0-2224  
dielectric material, phonon thermal conductivity, Umklapp process, comparison with LiF data 0-39367  
dielectric solids, acoustic wave propagation, phonon relax. time 0-44263  
dynamic multiphoton processes as criteria for luminesc. of electronically excited centres 0-11463  
frozen media, electron transfer reactions and multiphonon transition theory 0-7812  
ice, Ih, thermal resist. near melting point meas. 0-44375  
interface three-phonon processes, Kapitza conductance and pulse expt. applications 0-2261  
ionic crystals, nonradiative multiphonon transitions in impurity centres with extremely weak electron-phonon coupling 0-25436  
kinetics of phonon system with almost linear dispersion law (*Russian*) 0-29136  
metal surface, sticking coeff. and transmission problem, quadratic phonon coupling effects 0-39424  
phonon conductivity correction due to three phonon normal processes in presence of dislocations 0-15318  
polar semiconductors, anharmonicity influence on cond. in quantising mag. field 0-2406  
polaritons, two-phonon Brillouin scattering 0-20656  
rare earth doped crystals, intra- and inter-ionic multiphonon transitions 0-34973  
rare earth ions in crystals, nonradiative processes, book contrib. 0-55188  
resonant Brillouin scattering of exciton polaritons 0-11418  
ruby, optically induced two-phonon processes connecting <sup>2</sup>E states 0-25443  
spectroscopy of high-frequency phonons, transport phenomena, review 0-49325  
uranyl salts, cryst., multiphonon relax. 0-15208  
As<sub>2</sub>Se<sub>3</sub>, photodarkening and photostructural effects, Raman, IR and NQR studies 0-16036  
CdS, Raman shift dispersion near exciton reson., two-phonon cascade processes 0-11405  
CuCl, phonon interaction of excitonic molecule 0-50316  
D<sub>2</sub>, solid, phonon absorption line shape as function of density 0-50329  
GaP, core levels, chem. shift and relaxation energy, temp. dependence 0-39520  
n-GaSb, coupled LO-phonon-plasmon modes, Raman spectrum 0-11409  
GaSe, cascade resonant Raman processes 0-25385  
H<sub>2</sub>, phonon absorption line shape as function of density 0-50329  
HIO<sub>3</sub> crystals, anharmonicity effects in Raman spectra 0-25379  
n-InSb, three-phonon assisted cyclotron harmonic transitions in magneto-photoconductivity 0-44652  
MgF<sub>2</sub>, transparent, multiphonon IR absorption spectra 0-7348  
Na, dynamical structure factor calc., High temp. 0-15047  
NaCl, single cryst., for IR dispersive refl. meas., low temp., rel. to anharmonicity calcs. 0-11371  
NaCl(Br) (F) (I), lattice dynamics and statics, three-body-force shell model 0-49323  
OCS, third order coupling coeffs. for two phonon absorpt. 0-10621  
O<sub>2</sub>(cΣ<sub>g</sub><sup>-</sup>), in Ar(Kr)(Ar-Kr) matrices, multiphonon vibr. relax., time-resolved emission obs. 0-18861  
Si, core levels, chem. shift and relaxation energy, temp. dependence 0-39520  
SiO<sub>2</sub>, core levels, chem. shift and relaxation energy, temp. dependence 0-39520  
SiO<sub>2</sub>, vitreous, multiphonon IR absorpt. 0-25381  
Y<sub>3</sub>(Al<sub>1-x</sub>Ga<sub>x</sub>)O<sub>5</sub>·Nd<sup>3+</sup>, time-resolved site-selection spectroscopy, energy transfer 0-2814  
YIG, phonon viscosity effect on dislocation motion 0-24450  
ZnP<sub>2</sub>, second-order vibr. spectra and dispersion of phonon branches 0-25376  
ZnS, cubic, IR-active phonons obs. 0-55084  
ZnTe, Se<sub>1-x</sub>, Raman phonon spectra, resonance interaction effect 0-25375

# phonon-plasmon interactions

dichalcogenide layer compounds, interface plasmon-phonon interactions, transverse cond. 0-49641  
heavily doped semiconductor, magnetoconductivity, effect of resonant phonon-plasmon coupling 0-24954  
ionic solids, surface phonon-plasmon coupling (surface plasmarons) 0-54497  
semiconductor, ionic, -oxide interface, plasmon-phonon interactions 0-44730  
Ga<sub>1-x</sub>Al<sub>x</sub>As:Te, plasmon-LO-phonon coupling, IR refl. obs. 0-50335  
n-GaAs, conduction band nonparabolicity and coupled plasmon-phonon modes, IR refl. spectra 0-55110  
GaAs, effective mass, Raman spectrum determ. 0-24797  
p-GaAs:Zn, Raman scatt. by LO phonon-plasmon coupled modes, wave vector non-conservation 0-16033  
n-HgCr<sub>2</sub>Se<sub>4</sub>, ferromagnetic semiconductor, plasmon refl., 86 to 320K 0-50346  
Pb<sub>0.8</sub>Sn<sub>0.2</sub>Te, single cryst. and epitaxial film, far IR refl. spectra, carrier density, Hall const., and plasma freq. 0-20629  
ZnO, surface phonon-plasmon coupling (surface plasmarons) 0-54497  
ZnTe, resonance Raman scatt. at high excitation levels (*Russian*) 0-55109

# phonon softening *see soft modes*

# phonons

*see also crystal surface and interface vibrations; electron-phonon interactions; lattice phonons; phonon-defect interactions; phonon dispersion relations; phonon-exciton interactions; phonon-impurity interactions; phonon-magnon interactions; phonon-phonon interactions; phonon-plasmon interactions; spin-phonon interactions; tunnelling spectra; tunnelling spectroscopy; vibrational states in disordered systems*  
<sup>4</sup>He, superfluid, one phonon excitation spectrum and interaction pot. 0-54455  
bose condensation of phonons in biological systems 0-30641  
Bose gas, weakly interacting in restricted geometries, low-temp. thermodynamics 0-34261  
Bose system, Jastrow wavefunction, hypernetted chain method 0-17866  
Fermi system, Jastrow wavefunction, hypernetted chain method 0-17866  
localisation in condensed matter, electrons, phonons and magnons 0-10905  
low temperature, effective-medium theory for Goldstone systems with off-diagonal disorder 0-19890  
one-dimensional ϕ<sup>4</sup> and double quadratic systems, kinks, quantum statistical mechanics 0-47197  
superfluidity, model Hamiltonian 0-44377  
He, liquid, first and second sound generation by immersed Ge cryst. optical pumping 0-6581  
<sup>3</sup>He-<sup>4</sup>He, liquid mixture, second sound, quantised vortex creation at constrictions, excitation model 0-44383  
<sup>3</sup>He-<sup>4</sup>He, superfluid soln., dil., low temp. props., book contrib. 0-15330  
<sup>4</sup>He, liq., ground state, wavefunctions 0-10724  
<sup>4</sup>He, liq., neutron scatt., book contrib. 0-2230  
<sup>4</sup>He, liq., two-dimensional, ground state 0-49438  
<sup>4</sup>He, liquid, condensed phase, long-range order of one- and two-body density matrices 0-10726  
<sup>4</sup>He superfluid, acoustic vibration field density of states in piecewise const. parameter media 0-6483  
<sup>4</sup>He, superfluid, two-dimens., microscopic theory, excitation spectrum and thermodynamics props. 0-24709  
<sup>4</sup>He, superfluid, viscosity and thermal conductivity (*Russian*) 0-10720

# phosphate glasses

*for iron and vanadium phosphate semiconducting glasses see amorphous semiconductors*  
alkali aluminophosphate, ionic cond. mechanism 0-15299  
alkali metal polyphosphates, vitreous IR spectra 0-16043  
alkali rare earth metaphosphate glasses, n(M<sub>2</sub>O·P<sub>2</sub>O<sub>5</sub>·(1-x)Y<sub>2</sub>O<sub>3</sub>·xTb<sub>2</sub>O<sub>3</sub>·3P<sub>2</sub>O<sub>5</sub>, M=Li, Na, K, excitation and emission spectra 0-40150  
alkaline earth phosphate (MO·Al<sub>2</sub>O<sub>3</sub>·P<sub>2</sub>O<sub>5</sub>) irradiated electret glasses, relax. of external field intensity on heating 0-25282  
cation-site interactions, vibrational spectroscopy 0-2744  
fluorophosphate and fluoroberyllate glass laser damage thresholds and solid inclusions 0-33054  
fluorophosphate laser glass, highly homogeneous, production 0-14411  
formation of glasses in various phosphate systems 0-19708  
gamma dosimetry appl. (*Slovenian*) 0-32521  
laser, statistical props. and stabilisation 0-48266  
laser glass, nonradiative energy transfer from Cr to Nd, optical pumping efficiency improvement 0-33001  
laser glasses, review 0-9888  
Li<sup>+</sup> motion, <sup>7</sup>Li NMR spectra, nucl. relax. 0-34804  
luminescence inhomogeneous line profile in Yb<sup>3+</sup> excited glasses, excitation migration, energy gap depend. 0-7407  
metaphosphates, chem. stability in water and acetic acid soln. 0-21144  
metaphosphates, vitreous, microhardness 0-25864  
optical glass, Raman scatt. and nonlinear refr. index 0-2749  
phosphate glass: Ni, absorption spectra, mag. props., coordination behaviour (*German*) 0-40147  
phosphate glass:Nd<sup>3+</sup>, highly conc., electron energy deactivation and transfer (*Russian*) 0-29802  
phosphate glass:Nd, comparison of gain with silicate glass:Nd 0-19039  
sodium iron fluorophosphate glasses, EPR and Mossbauer resonance study 0-39968  
BaO·P<sub>2</sub>O<sub>5</sub>, Nd<sup>3+</sup> luminesc. quenching by transition metal and rare earth ions 0-25449  
Ba(PO<sub>3</sub>)<sub>2</sub>-BaF<sub>2</sub>-BaCl<sub>2</sub>(BaBr<sub>2</sub>), elec. cond., mixed anion effect 0-15300  
BaPO<sub>3</sub>-F-Al<sub>2</sub>O<sub>3</sub>-B<sub>2</sub>O<sub>3</sub> system, liq. phase separation, IR spectra, microstruct. 0-29940  
BeO·P<sub>2</sub>O<sub>5</sub>-RO(R<sub>2</sub>O) (R=Li,Na,K,Mg,Ca,Sr,Ba) glasses, gamma irradi., cation modifier effect on radiation centre formation 0-40720  
CaO·P<sub>2</sub>O<sub>5</sub>-WO<sub>3</sub> glass, computer simulation of Mn<sup>2+</sup> EPR spectra 0-34764  
Ca(PO<sub>3</sub>)<sub>2</sub> glass, crystallisation below glass transition, stress effect 0-19709  
CdO·P<sub>2</sub>O<sub>5</sub> glasses, elec. props. at high elec. fields 0-39573  
CuO·V<sub>2</sub>O<sub>5</sub>-P<sub>2</sub>O<sub>5</sub> glass, elec. cond. and switching (*Japanese*) 0-34492  
Er(PO<sub>3</sub>)<sub>3</sub> glass, Faraday resonance effect in pulsed mag. field, optical freq. EPR (*Russian*) 0-2734  
K<sub>2</sub>O-Al<sub>2</sub>O<sub>3</sub>-P<sub>2</sub>O<sub>5</sub> glass, low-temp. viscosity 0-39198  
KPO<sub>3</sub>-Fe<sub>2</sub>O<sub>3</sub> glasses, γ-irrad., ESR 0-50182



**phosphate glasses continued**

- Li-Nd-La phosphate glass active elements, laser characts., comparison with Nd:YAG 0-33002  
 LiF-Al(PO<sub>3</sub>)<sub>3</sub> glass, phase decomp., X-ray diffr. and IR spectra study 0-30003  
 LiF-NaPO<sub>3</sub>-MeF<sub>x</sub> (Me=Mg, Ca, Al) glasses, IR spectroscopy study 0-16042  
 LiPO<sub>3</sub>, crystn. mechanism from melt 0-44139  
 MgO-P<sub>2</sub>O<sub>5</sub>-Fe<sub>2</sub>O<sub>3</sub> glass, Fe<sup>2+</sup>(<sup>3</sup>) impurity ions struct.-chem. state, Mossbauer data 0-40028  
 Mn<sup>2+</sup> doped, luminesc. colour change 0-7392  
 Na-Fe fluorophosphate glass, EPR and Mossbauer resonance study 0-15838  
 Na-Fe fluorophosphate glass, Mossbauer study, mag. and optical props. 0-16065  
 Na<sub>2</sub>O-Al<sub>2</sub>O<sub>3</sub>-P<sub>2</sub>O<sub>5</sub> glass, low-temp. viscosity 0-39198  
 Na<sub>2</sub>O-Al<sub>2</sub>O<sub>3</sub>-P<sub>2</sub>O<sub>5</sub>:Eu glasses, fluorescence line narrowing meas. (French) 0-34975  
 Na<sub>2</sub>O-P<sub>2</sub>O<sub>5</sub>, XPS quantitative struct. anal. 0-2917  
 Na<sub>2</sub>O(K<sub>2</sub>O)-P<sub>2</sub>O<sub>5</sub> glasses, P K-band X-ray emission spectra, state anal. 0-40190  
 Nd doped (fluoro) phosphate laser glass piezo-optic coeffs. meas. at 0.6328 and 1.15 μm 0-34888  
 Nd<sup>3+</sup>-phosphate glass laser, brightness enhancement by spatial filtering in amplifying channel 0-48321  
 P<sub>2</sub>O<sub>5</sub>, glassy, high freq. vibr. bands, central force model 0-49330  
 P<sub>2</sub>O<sub>5</sub>-Al<sub>2</sub>O<sub>3</sub>-Na<sub>2</sub>O-K<sub>2</sub>O-Li<sub>2</sub>O-(CaO+MgO) glass system, ion exchange effect on mech. props. 0-30229  
 P<sub>2</sub>O<sub>5</sub>-MO-Al<sub>2</sub>O<sub>3</sub>, (M=MgO, CaO, SrO, BaO) (45, 5 wt.%) glass, electron irradiation effect on dielec. props. 0-29056  
 PtRh5 alloy, phosphate glass addition effect on high temp. strength (German) 0-25807  
 SiO<sub>2</sub>-Li<sub>2</sub>O-K<sub>2</sub>O-ZnO-P<sub>2</sub>O<sub>5</sub>, glass ceramic, phase changes and crystn. processes 0-7562  
 TiO<sub>2</sub>-Ti<sub>2</sub>O<sub>3</sub>-P<sub>2</sub>O<sub>5</sub>, glass form., struct. and elec. props. 0-44592  
 V<sub>2</sub>O<sub>5</sub>-P<sub>2</sub>O<sub>5</sub> (70-30), electrical cond. and thermoelectric meas., Au-glass-Au sandwich 0-29403  
 WO<sub>3</sub>-P<sub>2</sub>O<sub>5</sub> alkali glasses, electrochromic, electron-ion processes 0-25341

**phosphorescence**

- see also fluorescent screens; MIDP; phosphors*  
 acetophenone, highly purified, luminesc. props. 0-32764  
 alkali hexahalogeno compounds: ReCl<sub>6</sub><sup>2-</sup> (ReBr<sub>6</sub><sup>2-</sup>), low symm. splittings in vibronic spectrum due to phase transitions 0-55161  
 alkali metal hexahalogenostannate: ReBr<sub>6</sub><sup>2-</sup>, vibronic transition  $\Gamma_7(^2T_{2g}) \rightarrow \Gamma_8(^4A_{2g})$ , intensity distrib. 0-45142  
 aromatic esters, phosphoresc. and fluoresc. spectra in organic matrices 0-32756  
 aromatic rigid soln. phosphoresc. promotion by I<sup>-</sup> 0-50387  
 aza-aromatic molecules, intersystem crossing, quantum interference effects 0-53037  
 benzaldehyde, electronic spectra, Cl and F substitution effects 0-23456  
 benzaldehyde-biacetyl system, self-quenching and electronic energy transfer obs. 0-5571  
 1,2-benzanthracene in polystyrene films, delayed luminesc. decay kinetics 0-43088  
 2-benzoylpyridine crystals, optical spectra of lowest triplet state 0-16081  
 chlorophylls a and b and pheophytins, fluoresc. and phosphoresc. 0-12057  
 coronene, luminesc., spin-orbit coupling perturbation by metal chlorides (German) 0-1021  
 dibenzofuran, cryst., phosphoresc. spectra and ODMR meas. 0-11470  
 dibenzofuran-fluorene, mixed cryst., phosphoresc. spectra and ODMR meas. 0-11470  
 1,4-dibromonaphthalene, highly disordered quasi-one-dimens., excitation transport 0-34961  
 1,4-dibromonaphthalene, k-k scatt., exciton dephasing time-resolved phosphoresc. obs. 0-11458  
 1,4-dibromonaphthalene, substitutionally disordered, energy localisation, optical and ODMR spectra of triplet Frenkel excitons 0-54996  
 ethylbenzocarbazole, soln., luminesc., effect of electronic excitation energy vibr. 0-55174  
 fluorene:pyrene-d<sub>10</sub>, exciton-guest, triplet-triplet annihilation, impurity traps effects 0-25433  
 fluorene, cryst., phosphoresc. spectra and ODMR meas. 0-11470  
 glyoxal, singlet-triplet coupling, double reson. and level-anticrossing spectroscopy 0-48053  
 haloaceneaphthenes in n-heptane, quasi-line phosphoresc. spectra, vibronic spin-orbit interaction 0-43096  
 heteroaromatic molecules, planar, orientation and phosphoresc. polarisation in stretched film 0-14169  
 hexamethylolmelamine, doped, and condensation resin, room temp. phosphoresc., thermal transforms. 0-45132  
 indeno[2,1-a]indene, in glassy media, phosphoresc., heavy atom effects 0-55153  
 intermolecular triplet excitation transfer in diffusive limit 0-28046  
 open photoreceiver, vacuum ultraviolet 0-52307  
 palladium-octaethylporphyrin, gas phase delayed fluoresc. and phosphoresc., triplet excimer formation 0-18884  
 phthalimide acetyl derivatives in polar solvents, luminesc. kinetics and phosphoresc. quenching 0-18885  
 poly(N-vinylcarbazole) film, fluoresc. and phosphoresc., energy transfer mechanism 0-16112  
 poly-N-vinylbenzocarbazole, soln., luminesc., effect of electronic excitation energy vibr. 0-55174  
 polyatomic mols., quantum beats 0-37826  
 polyvinylbenzocarbazole, weak solution, intramolecular energy transfer by singlet and triplet excitons 0-34971  
 polyvinylcarbazole, weak solutions, intramolecular energy transfer by singlet and triplet excitons 0-34971  
 porphins orientation in n-alkane Shpol'skii hosts, spectra 0-48035  
 pyrazine, excited and N<sub>1s</sub> ionised states, ab initio calcs. broken orbital symm. 0-27931  
 quinoline, in binary solvents, luminesc. props. 0-7409  
 ruby, Raman <sup>2</sup>E and phosphorescence transitions, line widths, time correl. study 0-20621  
 solid, molecular fluoresc., phosphoresc., and ODMR line narrowing 0-43084  
 trans-stilbene, in glassy media, phosphoresc., heavy atom effects 0-55153  
 substitutionally disordered, energy localisation, optical and ODMR spectra of triplet Frenkel excitons 0-54996

**phosphorescence continued**

- 1,2,4,5-tetrachlorobenzene, triplet excitons, high. mag. field, spin-lattice relax. study 0-20517  
 xanthene dyes, internal heavy atom effect on radiative and non-radiative rate consts. 0-32765  
 CaO:Ce,Gd phosphors, trap distrib., phosphoresc. decay characts. obs. 0-29773  
 CaO:Eu(Tb), phosphor, isothermal decay 0-55156  
 CaSO<sub>4</sub>:Sm phosphors, X-ray induced fluorescence and phosphorescence 0-55179  
 KBr:PO<sub>2</sub><sup>-</sup>, phosphorescence, triplet state sublevels, mixing 0-25446  
 KCl:PO<sub>2</sub><sup>-</sup>, photo-orientation, spectrosc. and ODMR obs. 0-29772  
 SO<sub>2</sub>, laser-induced phosphoresc.-excitation spectra of vibr. bands of (<sup>3</sup>B<sub>1</sub>)-(X,<sup>1</sup>A<sub>1</sub>) transition 0-18879  
 Zn<sub>2</sub>O(BO<sub>2</sub>)<sub>6</sub>:Tb, phosphoresc. study (Spanish) 0-16105  
**phosphorescence microwave double resonance** *see* PMDR  
**phosphorescence microwave photoexcitation spectroscopy** *see* PMDR  
**phosphors**  
*see also fluorescent screens; luminescence*  
 alkali earth halides, solid soln. spectroscopy, investigs. by F. Klement (Russian) 0-8767  
 alkali halide:Ti<sup>3+</sup>-like ions, triplet state lifetime, hyperfine interaction 0-2844  
 alkali halide, Ag-doped, luminesc. rel. to formation of complex compounds (Russian) 0-11454  
 alkali halides, solid soln. spectroscopy, investigs. by F. Klement (Russian) 0-8767  
 carbon tetrachloride-GaCl<sub>3</sub>-Nd<sup>3+</sup> nontoxic liquid phosphor system, synthesis 0-55157  
 EL-570 M type, electroluminesc. excitation by SAW, nonlinear effects 0-16104  
 electroluminescence intensity of EL-455s commercial phosphor, temp. depend. 0-45146  
 halophosphate, radiation stability, recombination processes effect (Russian) 0-7424  
 organic, surface impregnation of Al<sub>2</sub>O<sub>3</sub> anodised film, fluoresc. spectrum (Japanese) 0-55170  
 polyethersulphone, thin film TLD, skin dosimetry appl. 0-52790  
 rare earth activated phosphors, chemistry and physics, book contrib. 0-55187  
 stilbene derivatives containing 2-pyrazoline and 1,3,4-oxadiazole groups, spectral-luminescent props. 0-7394  
 thermoluminescence, UV dosimetry 0-853  
 thermoluminescent phosphors, thermolum. induced by 254 nm UV photons 0-55204  
 TLD phosphors, use for high-level gamma-ray dosimetry 0-13934  
 BaAl<sub>2</sub>O<sub>9</sub>:Mn, vac. UV excitation spectra, appl. to gas discharge display 0-2816  
 BaMgAl<sub>14</sub>O<sub>23</sub>:Eu<sup>2+</sup>, vac. UV excitation spectra, appl. to gas discharge display 0-2816  
 Ba<sub>3</sub>(PO<sub>4</sub>)<sub>2</sub>, ionisation of capture centres, thermolum. spectra 0-11487  
 Ba<sub>2</sub>SiO<sub>4</sub>Cl<sub>2</sub>:Eu, blue-emitting phosphor high quenching temp. 0-16076  
 BeO ceramic TLD, gamma ray response 0-23153  
 Bi<sup>3+</sup> activated phosphors, luminesc. characts. 0-2849  
 CaF<sub>2</sub>:Eu, thermolum. in presence of lanthanide impurities 0-2870  
 CaO:Ag (Au), electroluminesc. meas. 0-40162  
 CaO:Ce,Gd phosphors, trap distrib., phosphoresc. decay characts. obs. 0-29773  
 CaO:Eu(Tb), phosphor, isothermal decay 0-55156  
 CaS:Bi phosphors, UV dosimetry by thermolum. 0-55199  
 CaS:Bi<sup>3+</sup>, Na<sup>+</sup>(Li<sup>+</sup>), luminescence of associated centres (French) 0-40155  
 CaS:Mn,Ce, phosphor, fluoresc. spectrum, fine struct., <sup>4</sup>T<sub>1g</sub>(<sup>4</sup>G)→<sup>6</sup>A<sub>1</sub>(<sup>6</sup>S) transition 0-45130  
 CaS:Tb, Eu, fluoresc. spectra under X-ray excitation 0-16083  
 CaS-BaS:Cu phosphors, X-ray diffr. and fluoresc. spectra 0-40148  
 CaSO<sub>4</sub>:Ce(Eu) phosphors, fluorescence spectra, thermolum. glow curve 0-2879  
 CaSO<sub>4</sub>:Dy-KBr thermolum. phosphor, thermal neutron detect. by activation 0-32581  
 CaSO<sub>4</sub>:Sm phosphors, X-ray induced fluorescence and phosphorescence 0-55179  
 CaSO<sub>4</sub>:Tm intrinsic thermoluminescence stability for UV dosimetry 0-12262  
 CaS(Se):Eu<sup>2+</sup>, emission and excitation spectra obs. 0-55162  
 CsI(Tl), crystallophosphor, luminesc. characts., temp. and conc. depend. 0-55175  
 CsI(Tl), gamma-scintillation growth front, external elec. field effect 0-34984  
 Eu ion based, liq., using aprotic solvents 0-20686  
 GAP luminophor powders, SAW nonlinear acoustoelectro-luminescence 0-45143  
 GdB<sub>2</sub>O<sub>3</sub>:Bi<sup>3+</sup>, Tb<sup>3+</sup>, energy transfer from sensitiser to activator, intermediate role of Gd<sup>3+</sup> 0-50389  
 GdPO<sub>4</sub>:Dy<sup>3+</sup>, Bi<sup>3+</sup>(Sb<sup>3+</sup>), energy transfer from sensitiser to activator, intermediate role of Gd<sup>3+</sup> 0-50389  
 (Gd<sub>1-x</sub>Tb<sub>x</sub>)<sub>2</sub>O<sub>2</sub>S phosphor, concentration quenching of Tb<sup>3+</sup> luminesc. 0-29785  
 KBr:Ti, Jahn-Teller system, negative mag. circular polarisation in emission spectrum 0-20694  
 KCl:Ti, Jahn-Teller system, negative mag. circular polarisation in emission spectrum 0-20694  
 KI:Ti, Jahn-Teller system, negative mag. circular polarisation in emission spectrum 0-20694  
 La<sub>2</sub>O<sub>3</sub>S penetration phosphor, penetration and cathodoluminescent props. 0-20718  
 La<sub>1-x</sub>Tb<sub>x</sub>OBr phosphor, concentration quenching of Tb<sup>3+</sup> luminesc. 0-29785  
 Li<sub>2</sub>B<sub>4</sub>O<sub>7</sub>:Mn, gamma ray response 0-23153  
 LiF TLD-100 phosphor, sensitisation mechanism study, thermolum. glow peak intensity obs. 0-55202  
 MgS:Eu<sup>2+</sup>, emission and excitation spectra obs. 0-55162  
 MgS:Eu<sup>2+</sup> phosphors, anal. of absorption spectra 4f<sup>N+1</sup>→4f<sup>N</sup>5d-6s 0-7383  
 Na<sub>2</sub>ZrSiO<sub>4</sub>, scintillation props., excited by α particles 0-29809  
 Nd ion based, liq., using aprotic solvents 0-20686  
 SiC luminophor powders, SAW nonlinear acoustoelectro-luminescence 0-45143  
 (Y,Gd)BO<sub>3</sub>:Eu<sup>3+</sup>, vac. UV excitation spectra, appl. to gas discharge display 0-2816



## phosphors continued

- YAG:Ce phosphors, luminesc. efficiency, prep. and dopant effects 0-45151  
 YAG:Ce<sup>3+</sup>, photoluminescence excitation energy, crystal field and temp. effects 0-11460  
 YAG:Ce<sup>3+</sup>(Eu<sup>3+</sup>)(Gd<sup>3+</sup>)(Tb<sup>3+</sup>), cathodoluminesc. efficiency rel. to activator conc. 0-11479  
 YF<sub>3</sub>:Yb,Er, limit efficiency of transformation of IR to visible radiation 0-29784  
 Y<sub>2</sub>O<sub>3</sub>:S:Eu phosphor, luminescence saturation effects due to N<sub>2</sub> laser and cathode-ray excitation 0-40151  
 Y<sub>2</sub>O<sub>3</sub>:S:Ti<sup>3+</sup>(Eu<sup>3+</sup>) temp. and viscosity depend. of colour coords. 0-40149  
 YPO<sub>4</sub>, ionisation of capture centres, thermolum. spectra 0-11487  
 YVO<sub>4</sub>, ionisation of capture centres, thermolum. spectra 0-11487  
 (Zn,Cd)S:Cu,Al, luminesc. efficiency deterioration due to surface oxidation by (NH<sub>4</sub>)<sub>2</sub>Cr<sub>2</sub>O<sub>7</sub>, thermal decomp. 0-29810  
 ZnCdS:Ag, phosphor screen, electron beam excited, light ang. distrib., modulation transfer function 0-45150  
 Zn<sub>3</sub>Cd<sub>1-x</sub>S:Cu crystallophosphors, spectra of IR electrophotographic sensitivity (*Russian*) 0-50423  
 ZnO powders, UV luminesc. spectral distrib., comparison with single crystals, excitons role 0-55167  
 ZnO:GeO<sub>2</sub>-MnO-B<sub>2</sub>O<sub>3</sub> wideband cathodoluminescent phosphor 0-55196  
 ZnO-SiO<sub>2</sub> system, struct. and phase comp. of luminescent Zn orthosilicate 0-19951  
 ZnS, excited phosphor, IR stimulation and quenching of luminesc., review (*Russian*) 0-11455  
 ZnS film production, for luminophors, method and apparatus (*Bulgarian*) 0-7499  
 ZnS, IR stimulation and quenching of luminesc., review (*Russian*) 0-11455  
 ZnS, voltage and temp. dependence of pre-breakdown electroluminescence 0-45147  
 ZnS, voltage depend. of electrolum. brightness 0-45148  
 ZnS:Ag, luminesc. efficiency deterioration due to surface oxidation by (NH<sub>4</sub>)<sub>2</sub>Cr<sub>2</sub>O<sub>7</sub>, thermal decomp. 0-29810  
 ZnS:Ag, luminesc. of surface glow centres 0-29782  
 ZnS:Ag,Cl, embedded in HBO<sub>3</sub>-glass matrix, blue electrolum. 0-55195  
 ZnS:Al,Cu(Ag)(Au) phosphors, luminesc. excitation spectra and exciton struct. 0-55164  
 ZnS:Al(Te) phosphors, luminesc. excitation spectra and exciton struct. 0-55165  
 ZnS:Cu crystallophosphors, spectra of IR electrophotographic sensitivity (*Russian*) 0-50423  
 ZnS:Mn<sup>2+</sup> phosphors, luminesc. excitation spectra and exciton struct. 0-55164  
 ZnS:Ne, implanted single crystals, photolum. and bombardment effect, thermolum. curve obs. 0-55166  
 ZnS:Pb, ionisation mechanism of field trapping centres 0-45156  
 ZnS-CdS:Ag, Ni, temp. sensitive, biological effects of microwaves determ. appl. 0-36186  
 ZnSe, Gudden-Pohl effect, release of electrons from traps 0-45149  
 Zn<sub>3</sub>Si<sub>2</sub>O<sub>7</sub>:Mn phosphor, efficiency enhancement by AlPO<sub>4</sub> substitution 0-11452

## phosphorus

see also nuclei with .....

- adsorption on GaAs (110), UPS and EELS study, tight-binding calcs. 0-49496  
 adsorption on Ni, coadsorbed Pb or Sn, AES study 0-54521  
 adsorption on Ni (100), effects on secondary electron spectra 0-50480  
 allotropic modifications, muonic X-ray intensities, computer analysis 0-23577  
 amorphous, red, far IR absorpt. spectra 0-34923  
 amorphous, red, photolum. props. and band gap 0-50403  
 amorphous, stability in air, XPS study, comparison with cryst. polymorphs 0-25517  
 amorphous, US attenuation and sound vel. meas., 4.2 to 300K; 0-49308  
 amorphous, vibrational excitations of defect sites 0-49332  
 amorphous red P, Raman scattering 0-11416  
 atom, highly ionised, beam foil radiative lifetimes and EUV spectrum 0-32671  
 atom, np<sup>2</sup>(n+1)s excited-state config. quadrupole moments, Sternheimer shielding factor 0-37755  
 atom, SCF electron-gas local-spin-density model including correlation 0-9488  
 crystalline to amorphous transition, thermodynamic functions 0-54354  
 deep diffusion into Si, expt. results 0-54437  
 diffusion in Si, radn. enhanced 0-29216  
 diffusion into Si from spin-on SiO<sub>2</sub>:P film 0-2050  
 Ge:P, radiation-accelerated diffusion 0-6559  
 impurity in Ni, dissolution and passivation in acid environment, effect of P (*French*) 0-45440  
 ions, charge distrib., 72-123 MeV 0-27849  
 muonic allotropes, muonic Roentgen intensities (*German*) 0-53168  
 Raman vibr. spectra and bonding 0-11411  
 steel, Cr-Mo (2.25, 1 wt.%), SCC and temper brittleness, P grain boundary segregation effect 0-55571  
<sup>32,33</sup>P incorporated in DNA, transmutation effects 0-26283  
 BN:P film, effect of CVD parameters on props. 0-25571  
 CdSe:P, implanted, electroreflexion obs. 0-40089  
 CdTe:P, annealing induced lattice defects, TEM obs. 0-2010  
 GaAs:P, form. of GaAs<sub>1-x</sub>P<sub>x</sub> by diffusion 0-54389  
 Ge, high-purity, with Al, B and P, residual impurities, photothermal cond. 0-24965  
 Ge:P, growth atm. effect on struct. microdefect form. 0-20779  
 Ge:P, impurity photocond. spectra under uniaxial compression 0-44656  
 (In+InP) melt, critical undercooling determ. and P content change after annealing (*Slovak*) 0-55430  
 P II, CI calcs. of oscillator strengths, L-S framework 0-14089  
 P XII, beam-foil obs. of oscillator strengths for E1 transitions 0-14112  
 P<sup>+</sup>, reson. line regularities in plasma Stark widths and shifts 0-43881  
 P<sub>2</sub>, intersystem transition obs. in absorpt. spectrum 0-48008  
 P<sub>2</sub> radical, b<sup>1</sup>Π<sub>g</sub>-a<sup>3</sup>Σ<sub>u</sub><sup>+</sup> transition, perturbed by I<sup>2</sup>Σ<sub>g</sub><sup>+</sup> state (*French*) 0-18855  
 P<sub>2</sub><sup>+</sup>, electronic states pot. energy curves, dissociation energy, ionisation pot., curve fitting 0-32796  
<sup>31</sup>P, muonic, 3d-2p X-ray transition 0-9764  
<sup>31</sup>P NMR applications to cells 0-46110

## phosphorus continued

- <sup>31</sup>P, NMR obs. of lipid bilayer head group, orientational order and rotational diffusion 0-21451  
<sup>32</sup>P, comparison with <sup>47</sup>Ca in profile scanning of skeletal disease 0-51218  
 Si, neutron transmutation doping, <sup>31</sup>P conc. meas. 0-19833  
 Si, P<sup>+</sup> implantation, induced disorders. 0-6422  
 Si:B,P, anomalous diffusion 0-29229  
 Si:B,P, double implanted layer, n-p-n struct., single pulse laser annealing 0-49247  
 Si:H,P, amorphous, heavily hydrogenated, high gap state densities 0-49803  
 Si:P, amorphous, CVD, defect compensation 0-54644  
 Si:P, appl. of ion implantation systems, high throughput 0-34029  
 Si:P, BF<sub>3</sub><sup>+</sup> ion implantation, anomalous carrier profiles 0-2048  
 Si:P, defect annealing, ionisation effects, DLTS meas. 0-24483  
 Si:P, determ. of P content in high-purity Si using meas. of Mo in 12-molybdophosphoric acid by NAA and AAS 0-15148  
 Si:P, diffusion of P impurities stimulated by gas discharge Ar plasma, low temp. 0-6560  
 Si:P, diffusion-doped laser irradiation effects, electrical reactivation of P 0-39124  
 Si:P, diffusivity, strain-induced band gap narrowing, E-centres 0-29228  
 Si:P, doped by neutron transmutation, lattice defects 0-34018  
 Si:P, effect of impurities on solar cell performance 0-55848  
 Si:P, film, polycrystalline, low press. CVD, resist. meas. 0-2494  
 Si:P, glow discharge deposited amorphous film, UV absorpt. spectra 0-25420  
 Si:P, heavily doped, glow-discharge-produced, elec. and optical props 0-2497  
 Si:P, heavily doped, mag.-field depend. of sp. ht. 0-29183  
 Si:P, high resolution study of group V impurities absorption 0-7388  
 Si:P, implanted, pulsed electron beam annealing, Hall effect and sheet resist. meas. 0-34467  
 Si:P, ion implanted film, elec. prop. impurity depend. 0-24467  
 Si:P, ion-implanted, carrier conc. reduction caused by wet O<sub>2</sub> oxidation 0-10565  
 Si:P, laser annealing, photoluminesc. study 0-2049  
 Si:P, neutron irradi. crystals, qualitative distrib. of P using autoradiography 0-24486  
 Si:P, piezoelectroscopic studies of bound multiexciton complexes 0-16006  
 Si:P, polycryst., CVD, elec. activation of impurities, EPR obs. 0-34774  
 Si:P, proton enhanced diffusion, vacancies diffusion length 0-29226  
 Si:P, satellite of bound excitons, transient decay 0-11466  
 Si:P, uniaxially stressed, impurity-assisted intervalley scatt., photoluminesc. obs. 0-34979  
 Si:P, variable range hopping at very low temp. 0-49736  
 Si:P CVD films, ion-implanted, doping effect on elec. props. 0-2495  
 Si:P diffused solar cells, laser treatment to dissolve diffused P precipitates 0-45667  
 Si:P dislocation p-n junctions, capacitive props. 0-20300  
 Si:P epitaxial layer, incorporation conc. depend. of P from silane-phosphine-H<sub>2</sub> mixture 0-2053  
 Si:P film, CVD polycrystalline, low press. and atmos. press., oxidation 0-3214  
 Si:P film, polycryst. pulsed electron beam annealing 0-10566  
 Si:P high temp. impurity diffusion via vacancies and self-interstitials 0-24667  
 Si:P non-Fickian diffusion, parameter depend. on doping level and impurity gradient (*German*) 0-54440  
 Si:P polycrystalline thin film, plasma annealing, effect on elec. props. 0-7005  
 Si:P solar cells, improved P diffusion using laser treatment 0-55850  
 Si:P<sup>+</sup>, Zeeman energy transfer at surface layer 0-11247  
 Si:P<sup>+</sup> ion implanted single crystals, secondary defects development during annealing 0-44228  
 Si-H,P, in situ prepared amorphous film, photoemission studies 0-35060  
 Si-P MOS devices, time dependence of depletion region formation at cryogenic temp. 0-34522  
 SiO<sub>2</sub>:P, diffusion from spin-on source 0-44367  
 SiO<sub>2</sub>:P thin films, plasma deposition in prod. planar reactor and P doping 0-2966  
 SmS:P, neutron irradi., semiconductor-metal transition 0-24975  
<sup>99m</sup>Tc radiopharmaceuticals, As for P substitution, bone-seeking agent analogues 0-51250  
 ZnO:<sup>31</sup>P<sup>+</sup> implanted nonlinear resistor production and characteristics (*Russian*) 0-49252  
 ZnTe:P, pure and doped, electron and exciton excited states of neutral donor 0-34393

## phosphorus compounds

- air pollutants, conc. meas. with flame photometric apparatus 0-16883  
 phosphate working in direct flow plasma reactor (*Russian*) 0-55663  
 polyacetylene:PF<sub>6</sub>, metallic, band theory 0-49570  
 Al<sub>2</sub>O<sub>3</sub>-P<sub>2</sub>O<sub>5</sub>-H<sub>2</sub>O system, phase diagram 0-3014  
 BBr<sub>3</sub>-PCl<sub>3</sub>-H<sub>2</sub>, gas phase equilib. comp. 0-35166  
 CaO-P<sub>2</sub>O<sub>5</sub>-H<sub>2</sub>O system, phase diagram at 200°C 0-45286  
 CdO-P<sub>2</sub>O<sub>5</sub> glasses, elec. props. at high elec. fields 0-39573  
 KCl:PO<sub>2</sub><sup>+</sup>, photo-orientation, spectrosc. and ODMR obs. 0-29772  
 KCl:PO<sub>2</sub><sup>+</sup>, triplet state, level anticrossing and pseudonuclear Zeeman effect, microwave ODMR 0-39896  
 KH<sub>2</sub>PO<sub>4</sub>, press. and deuteration effects on static ferroelec. props., four-point cluster approx. 0-34861  
 K<sub>2</sub>O-Al<sub>2</sub>O<sub>3</sub>-P<sub>2</sub>O<sub>5</sub> glass, low-temp. viscosity 0-39198  
 K<sub>2</sub>O-Ga<sub>2</sub>O<sub>3</sub>-P<sub>2</sub>O<sub>5</sub>-H<sub>2</sub>O, reactions, 150-500°C 0-35514  
 Li<sub>2</sub>O-Nd<sub>2</sub>O<sub>3</sub>-P<sub>2</sub>O<sub>5</sub> phase diagram, LiNdP<sub>4</sub>O<sub>12</sub> single crystal growth 0-25668  
 100(Li<sub>2</sub>O.2SiO<sub>2</sub>).3P<sub>2</sub>O<sub>5</sub>, directionally solidified, thermal and mech. props. (*Japanese*) 0-16295  
 Na<sub>2</sub>O-Al<sub>2</sub>O<sub>3</sub>-P<sub>2</sub>O<sub>5</sub> glass, low-temp. viscosity 0-39198  
 Na<sub>2</sub>O(K<sub>2</sub>O)-P<sub>2</sub>O<sub>5</sub> glasses, P K-band X-ray emission spectra, state anal. 0-40190  
 P-O bond parachors 0-14247  
 P-S, amorphous, glass transition and specific heat, intermolecular bond saturation 0-15011  
 P-Se, amorphous, glass transition and specific heat, intermolecular bond saturation 0-15011  
 P-Se glasses, solubility, photostimulated changes 0-24602  
 P-Se-Te system glasses, mag. susceptibility and opt. props. 0-25079  
 P-Se-Tl glasses, NMR of <sup>31</sup>P and <sup>205</sup>Tl 0-15812  
 P-Se-Tl system glasses, polarisation, refr. index and dielec. const. meas. 0-20608



**phosphorus compounds continued**

- PCl<sub>3</sub>, mol. orbital calcs. core-valence approx. scheme 0-42927  
 PCl<sub>3</sub>-HgCl<sub>2</sub>; Raman spectra, solid and melt, species identification (*German*) 0-45083  
 PF<sub>3</sub> (PF<sub>3</sub>), pot. energy curves and dissoc. energy, Hulbert-Hirschfelder calc. 0-30210  
 PF<sub>3</sub>, mol. geometry calcs. using centrifugal distortion const. 0-18841  
 PF<sub>3</sub>-graphite intercalation cpds., prep. and props. 0-40686  
 PF<sub>3</sub>Br<sub>2</sub>, spin systems under multiple pulse NMR conditions, chem. shift relax. 0-34808  
 PF<sub>3</sub>H(D), vibr. spectra and normal coordinate anal., Raman and IR spectra 0-14147  
 PH<sub>2</sub>, X<sup>2</sup>P<sub>2</sub>-state, rot. laser mag. reson. spectrosc. 0-28038  
 PH<sub>3</sub>, dipole moment in ground and excited states, submm. spectrum obs. 0-28056  
 PH<sub>3</sub>, equilibrium structure and harmonic force field, ab initio calc. 0-9502  
 PH<sub>3</sub>, IR spectrum rel. to absorpt. in Jupiter 5 μm window 0-31243  
 PH<sub>3</sub>, liq. and solid, Raman spectra., vibr. correl. functions, rot. motions 0-55087  
 PH<sub>3</sub>, NMR shielding consts. and mag. susceptibilities, coupled HF with extended GTO basis 0-5480  
 PH<sub>3</sub>, X-ray K-fluoresc. obs. of electronic struct. 0-37818  
 PH<sub>3</sub>, equilibrium structure and harmonic force field, ab initio calc. 0-9502  
 PHD<sub>2</sub>, vibr. dephasing in liq. and solid PD<sub>3</sub>, calcs. 0-19884  
 P<sub>2</sub>H<sub>4</sub>, synthesis and struct. 0-54201  
 PMO<sub>3</sub>O<sub>3</sub>, model vibr. freqs. 0-23408  
 PO, in Ar matrix, IR and UV absorpt. spectra 0-47985  
 PO, electron structure rel. to synthesis and utilisation of ATP 0-40955  
 PO<sub>4</sub> groups in biomembrane models, quantum-chemical investigation of cation motion mech. 0-30678  
 PO<sub>4</sub><sup>3-</sup>, NO<sub>3</sub><sup>-</sup>, Si(OH)<sub>4</sub>, ratios in Moroccan upwelling region 0-4045  
 P<sub>2</sub>O<sub>5</sub>, marine sediment content, India, W. continental shelf 0-8288  
 P<sub>2</sub>O<sub>5</sub>-SiO<sub>2</sub> clad low-loss monomode fibres for 1.2 to 1.6 μm, modified CVD prep. 0-48479  
 POCl<sub>3</sub> reaction with ZrCl<sub>4</sub> in O<sub>2</sub>, for ZrP<sub>2</sub>O<sub>7</sub> prep. 0-21272  
 POCl<sub>3</sub>-SnCl<sub>4</sub>(ZrCl<sub>4</sub>)(TiCl<sub>4</sub>), splitting of Sm<sup>3+</sup> near IR absorpt. bands 0-2750  
 POF<sub>3</sub>, level anticrossing effects, vibr., laser Stark spectra obs. 0-32771  
 PON, synthesis and struct. 0-54201  
 SiC filament reinforced phosphate foam ceramics, bending strength 0-11716  
 SiO<sub>2</sub>-Li<sub>2</sub>O-K<sub>2</sub>O-ZnO-P<sub>2</sub>O<sub>5</sub>, glass ceramic, phase changes and crystn. processes 0-7562  
 Sn<sub>2</sub>P<sub>2</sub>S<sub>6</sub>, illumination effect on soft mode and dielectric props., luminesc. study (*Russian*) 0-50420

**phosphosilicate glasses**

- optical single-mode fibre with low attenuation, MCVD fabrication 0-53461  
 GeO<sub>2</sub>-P<sub>2</sub>O<sub>5</sub>-SiO<sub>2</sub> glass fibre, incorporation of OH in modified CVD process 0-50560  
 SiO<sub>2</sub>-P<sub>2</sub>O<sub>5</sub> cladding vapour-phase axial deposition fibres at 1.3 μm and 1.6 μm 0-9996

**photoacoustic effect**

- chiral compound, circular dichroism, polarisation modulated photoacoustic spectroscopy 0-18018  
 ferromagnetic resonance detection 0-20463  
 FIR laser, optically pumped, nearly transparent power monitors 0-5773  
 gas, acoustical theory 0-1729  
 laser beam moving over fluid surface, sound radiation from thermal sources 0-38161  
 laser generation of sound in fluid half-space with 2 types of boundary roughness 0-15194  
 laser-generated US waves, freq. spectrum 0-53537  
 liquid acoustical theory 0-1729  
 liquid half-space bounded by solid layer, optical generation of sound 0-38158  
 microscopy, principle and appl. to semiconductor industry 0-14525  
 optical fibre, photoacoustic effect obs. using piezoceramic transducer 0-48423  
 photoacoustic exciter, nonlinear limit on efficiency 0-28406  
 polymer film, thickness effect on magnitude of photoacoustic signals 0-11969  
 polymethine dye solution, photoacoustic response 0-6465  
 semiconductor, determ. of bulk and surface absorption coeffs. 0-4781  
 solids, review (*Japanese*) 0-31887  
 sound generation by laser, nonlinear theory of thermal mechanism 0-38147  
 sound generation by long laser pulses incident on liquid surface 0-5900  
 steel, C, EM excitation of US at high temps. 0-33412  
 subsurface structure detection by scanning photoacoustic microscopy 0-6323  
 teaching approach, rel. to wave physics 0-42003  
 thermo-optical generation of nonsteady acoustic fields 0-15193  
 three- and four-dimensional photoacoustic store readout 0-48413  
 three-dimensional heat flow 0-48840  
 Fe, foil, ferromagnetic resonance detection by photoacoustic effect 0-20463  
 I<sub>2</sub>, vibr.-translational relax., collisional predissoc., opto-acoustic effect obs. 0-43157  
 Si, photoacoustic signal changes assoc. with crystallinity, recrystallisation after laser annealing 0-16127

**photoacoustic spectroscopy**

- acetylene smoke, photoacoustic meas. of absorpt. at 0.5145, 10.6 μm 0-43060  
 acetylene smoke particles, photoacoustic meas. 0-50895  
 air pollution monitoring, spectrophone measurement of absorpt. coeffs. at CO<sub>2</sub> laser wavelengths 0-26193  
 analytical applications, direct exam. of solid and liq. samples 0-7886  
 background signal in photoacoustic detector 0-31913  
 benzene and deuterates, highly vibr. excited intramolecular V-V transfer, visible and photoacoustic spectra 0-32729  
 cell design and characteristics for photoacoustic spectroscopy of condensed matter 0-52326  
 chlorodifluoromethane, photoacoustic spectra meas. at CO<sub>2</sub> laser wavelengths 0-18849  
 chrysotile asbestos, photoacoustic spectrum using CW HF laser 0-7980  
 circular differential photoacoustic spectroscopy 0-47114  
 corrosion resistant photoacoustic cell for spectrosc. of liquids 0-42269

**photoacoustic spectroscopy continued**

- dichlorodifluoromethane, photoacoustic spectra meas. at CO<sub>2</sub> laser wavelengths 0-18849  
 diesel smoke particles, photoacoustic meas. 0-50895  
 eosin, photoacoustic spectra in soln. 0-9606  
 ethyl acetate, photoacoustic spectra meas. at CO<sub>2</sub> laser wavelengths 0-18849  
 ethylene, IR multiphoton excitation, photoacoustic meas. 0-1038  
 experimental apparatus (*Japanese*) 0-31903  
 fluoromethane, optically pumped laser, IR-FIR transferred Lamb dip spectra 0-1193  
 furan, photoacoustic spectra meas. at CO<sub>2</sub> laser wavelengths 0-18849  
 Helmholtz resonance cells for dye laser excited spectra 0-9048  
 Helmholtz resonator as photoacoustic detector 0-31896  
 impurity microconcentrations in liquids analysis using opto-acoustic effect 0-50916  
 insulator, mag. transition sp. ht. anomaly, photoacoustic meas. 0-4773  
 IR spectroscopy of solids and liquids 0-13163  
 liquid film, micron thick, photoacoustic spectroscopy using pulsed dye laser 0-42265  
 liquids, linear and nonlinear absorpt., photoacoustic determ. (*German*) 0-37090  
 liquids acoustic relaxation mechanism, using coherent photoacoustic spectroscopy scheme 0-5890  
 metal, photoacoustic phase angle meas. for subsurface struct. 0-28388  
 methane, (methane-Xe)(methane-NH<sub>3</sub>), mol. relax., photoacoustic reson. meas. 0-27351  
 methanol, optically pumped laser, IR-FIR transferred Lamb dip spectra 0-1193  
 methanol excited by CO<sub>2</sub> laser, sub-Doppler photoacoustic spectrum 0-5545  
 methyl alcohol, photoacoustic spectra meas. at CO<sub>2</sub> laser wavelengths 0-18849  
 methyl sulphoxide, photoacoustic spectra meas. at CO<sub>2</sub> laser wavelengths 0-18849  
 phase measurement, appl. to nonradiative transitions, optical absorpt., in solids 0-31885  
 polarization modulated, for measurement of circular dichroism 0-18018  
 polymer film, thickness effect on magnitude of photoacoustic signals 0-11969  
 polystyrene film, Fourier-transformed IR photoacoustic spectra 0-34993  
 pulsed photoacoustic Raman spectrosc., gaseous trace anal. 0-40769  
 rare earth ions in aq. solns., photoacoustic spectroscopy using pulsed dye laser for micron thick film 0-42265  
 rhodamine 6G, photoacoustic spectra in soln. 0-9606  
 Rosencwaig-Gersho theory, extension to include sample coating effects 0-52319  
 semiconductor, determ. of bulk and surface absorption coeffs. 0-4781  
 solids, optical absorption spectra determ. of CdS, KMnO<sub>4</sub> and rare-earth elements 0-13160  
 solids, review (*Japanese*) 0-31887  
 solids immersed in transparent liquids 0-22452  
 techniques, general description 0-31884  
 theory, techniques and appls., book contrib. 0-9050  
 time-domain, nonradiative lifetime meas. of condensed phases 0-55232  
 toxic gas monitor based on laser photoacoustic spectrometer (*German*) 0-12046  
 C particulate, airborne, photoacoustic and absorption spectrum using tunable dye laser 0-4102  
 CO<sub>2</sub>, excited by CO<sub>2</sub> laser, sub-Doppler photoacoustic spectrum 0-5545  
 CO<sub>2</sub>, pure rotational stimulated Raman photoacoustic spectroscopy 0-32724  
 CdS, phonon-coupled photoacoustic spectroscopy 0-54317  
 Dy<sub>2</sub>O<sub>3</sub>, powdered cryst., high resolution photoacoustic spectroscopy 0-31898  
 Er<sub>2</sub>O<sub>3</sub>, powdered cryst., high resolution photoacoustic spectroscopy 0-31898  
 GaAs, ion implanted and laser-annealed, photoacoustic meas. 0-47117  
 Ge, laser irradiation, photoacoustic detection 0-2901  
 HD, ν=0 to ν=5 rot.-vibr. band, photoacoustic spectrosc. obs. 0-9589  
 H<sub>2</sub>O, D<sub>2</sub>O, visible absorpt. meas., pulsed dye laser photoacoustic spectroscopy 0-11426  
 Ho<sub>2</sub>O<sub>3</sub>, photoacoustic spectra using Helmholtz reson. cells 0-9048  
 Ho<sub>2</sub>O<sub>3</sub>, powdered cryst., high resolution photoacoustic spectroscopy 0-31898  
 I<sub>2</sub>, Doppler-free photoacoustic spectra 0-995  
 Li, seeded flames, excitation, laser radiation absorpt., sound vel., opto-acoustic effects obs. 0-43345  
 N<sub>2</sub>O, pure rotational stimulated Raman photoacoustic spectroscopy 0-32724  
 Na seeded flames, excitation, laser radiation absorpt., sound vel., opto-acoustic effects obs. 0-43345  
 PbF<sub>2</sub>-TlI graded coatings on KCl laser windows 0-33052  
 TlI coatings on KCl laser windows 0-33052  
 ZnSe laser windows and coatings on CaF<sub>2</sub> 0-33052

**photobleaching** *see optical saturable absorption***photocapacitance**

- see also photodielectric effect*  
 III-V semiconductors, deep level defects, review 0-24841  
 Al-Si<sub>3</sub>N<sub>4</sub>-Si struct., surface energy bands under step function illumination 0-49840  
 Al<sub>0.5</sub>Ga<sub>0.5</sub>As, DX photocond. centres, photocapacitance and DLTS meas. 0-11044  
 CdS Schottky barrier solar cells, spectral distrib. and photocapacitance 0-55864  
 GaAs grown by VPE using organometallic method, deep trap levels 0-10923  
 GaAs microcharacterisation for device appls. 0-10922  
 GaAs, optical cross sections associated with deep levels, O centre obs. 0-6777  
 GaAs<sub>0.65</sub>P<sub>0.35</sub>, gamma irradiated, deep level study using DLTS and photocapacitance methods (*Japanese*) 0-49665  
 n-GaP, deep state controlled minority carrier lifetime 0-20211  
 Ge MIS photocapacitive IR detector 0-47106  
 Si, positively charged divacancy photoionisation cross section by photocapacitance meas. 0-6901  
 n-Si:Pd Schottky diodes photocapacitance meas., photon and carrier capture cross sections 0-20309  
 Si-SiO<sub>2</sub>-Si<sub>3</sub>N<sub>4</sub>, internal photoemission 0-7475



# photocapacitance continued

ZnSe:Cu, deep energy levels 0-6774

ZnTe:Cu, red centre, electric and optical props. 0-20239

# photocatalysis *see catalysis*

# photocathodes

*see also photoemission*

biplanar image converter, photocathode switching 0-19105

photocathode polarisation sensitivity, two-beam interferometer expts. 0-4772

photomultipliers for BBQ applications 0-27896

reradiation effects in negative electron affinity photocathodes 0-55274

Ag-Cs<sub>2</sub>O photocathode, light absorption and photoemission 0-50510

Ag-O-Cs, Ag granules and colloidal particles on Cs<sub>2</sub>O film (*Chinese*) 0-2279

Ag-O-Cs photocathode, Ag colloidal particles and long wavelength response (*Chinese*) 0-45195

Ag-O-Cs photocathode, role of Ag colloidal particles in photoemission (*Chinese*) 0-40215

Cs<sub>2</sub>Sb photocathode, wavelength-modulated photoemission spectra 0-29857

GaAs (111) epitaxial film, adsorption of Cs, Cs+O, ellipsometric study, photocathode sensitivity 0-29282

GaAsP, negative electron affinity process obs. by laser beam scanning (*Japanese*) 0-55262

Ge photocathodes, Au absorbed photofield emission current spectral investigation 0-29856

K<sub>2</sub>Sb, photocathode material, optical and dielec. props., energy spectra, density of states calc. 0-20083

Si, negative electron affinity process obs. by laser beam scanning (*Japanese*) 0-55262

# photocells *see photoelectric cells*

# photochemistry

*see also photochromism; photodissociation; photoelectrochemical cells; photolysis; photosynthesis*

E,E-1,4-diphenylbutadiene-(1,3), isomerisation, reaction quantum yields, exciting light bandwidth influence study (*German*) 0-21310

acetone-d<sub>6</sub>, multiphoton dissoc., recomb. to ethane 0-3371

acetylene, photolytic polymerisation rel. to presence in Jupiter stratosphere 0-31244

allyl isocyanide, state-selected, visible absorption spectra and photoisomerisation kinetics 0-11879

6-amino-7-hydroxy-4-methylcoumarin solutions, additions effect on fluorescence 0-2833

atmosphere, perturbed, photochemical radiative convective model for thermal struct. and relaxation rates 0-8408

atmosphere, photochemical form. of natural organic aerosols of terrestrial origin 0-36381

atmosphere O<sub>3</sub> production transport and distribution, numerical simulations with global general circulation model 0-56544

atmosphere pollution, photochemical numerical model 0-40943

7-azaindole dimers, photoautomerisation by double proton transfer, fluorescence kinetics 0-11880

beam-addressable optical display using supersaturated vapour photonucleation 0-4691

bimimidazole+leuco dye photochem. reaction, modulation by photopolymerisation 0-40714

trans-2-butene, Ar matrix, TEA CO<sub>2</sub> laser irradiation. photoisomerisation study 0-21303

chlorin, free-base, in n-alkane matrices, photochem. hole burning, optical dephasing 0-21305

chlorophyll photo-oxidation, role of singlet-excited and triplet states 0-51156

cholecalciferol, UV dependent synthesis in a green plant 0-35860

conference, Heverlee, Belgium (July 1978) 0-3378

cryogenic solutions, spectrosc. and photochem. 0-16713

cycloheptatriene, and substituted forms, vibr. highly excited, steady-state photoisomerisation 0-16704

diacetylene, single cryst., photopolymerisation, intermediate states, struct. changes 0-30235

p-diazoquinone, photodecomp. 0-7827

trans-1,2-dichloroethylene, Ar matrix, TEA CO<sub>2</sub> laser irradiation. photoisomerisation study 0-21303

dichromated photoresist, photochem. reactions 0-7830

disfluorocarbene, A'B<sub>1</sub>-X<sup>1</sup>A<sub>1</sub> system spectrosc. and photophysics 0-5577

diolefins, substituted, topochemically controlled solid-state polymerization 0-35532

4-diphenylphosphorylstilbenes, fluoresc., photodimerisation 0-1015

dipropionyl peroxide, photochemical production of ethyl radical 0-3373

electron transfer in monolayer assemblies 0-3383

electronic phototransition CW chemical laser with thermal initiation by shock wave 0-53283

energy transfer dye lasers and laser induced intermol. and intramol. energy transfer processes 0-9647

ethyl acetate, CW laser induced reactions, activation energies, temps. and rate consts. 0-40710

ethyl radical, photochemical studies 0-3373

ethylacetate, CW laser induced reactions, activation energies, temps. and rate consts. 0-40710

fluorene: acridene, radical pair form. from excited states, optical nucl. polarisation obs. 0-14155

frequency-domain nonvolatile optical storage scheme 0-43282

hologram recording on semiconductor, photochem. etching control 0-28179

inert gas halide lasers, operation and use in photochem. 0-9860

inorganic photochemistry, review 0-3382

interstellar medium, mol. form, from grain mantles UV photolysis, laboratory analogue expts. 0-26944

IR laser applications in chemistry 0-16710

IR laser chemistry research using mol. beam (*German*) 0-55683

isomerisation, complexing, proton transfer, initiation of internal conversion processes 0-40713

isotope separation by laser photochemistry in nozzle flows with heterogeneous condensation 0-50862

Jupiter upper atmosphere, photochemical models 0-36567

labile species, electron photoejection, reaction kinetics characterisation 0-26089

laser applications, review 0-45535

laser dye mixtures, photodegradation 0-9880

laser dyes, photochemical quantum yield determ. using fluorescence data 0-55685

# photochemistry continued

laser engineering and appls., conf., Washington, USA (May-June 1979) 0-1216

laser induced reactions, activation energies, temps. and rate consts. 0-40710

laser radiation, selective action on matter, review 0-7832

laser specific and thermal reactions classifications 0-11919

laser spectroscopy, conf., San Diego, USA (Aug. 1978) 0-13153

laser studies of relaxation and reaction of species in defined quantum states 0-11918

laser-controlled unimolecular and bimolecular processes, field-depend. rate const. 0-11906

laser-induced chemical processes, optical selection of reagent orientation 0-11914

laser-induced predissociation, diatomic and polyatomic mols., photocatalytic effect 0-11907

laser-induced processes in molecules, conf., Edinburgh, Scotland (Sept. 1978) 0-9577

laser-initiated chain reactions, rates, mechanisms, chemiluminesc. obs. 0-55651

light source, immersion type, radiation utilisation factor calc. aspects (*Russian*) 0-48374

MB<sup>2</sup>-Fe<sup>2+</sup> system, solar energy utilisation (*German*) 0-45713

merocyanine dyes, non-photochromic, for autoproccessor reprography system 0-35555

metal combustion under CW CO<sub>2</sub> laser radiation action 0-30241

metalloporphyrins, photoelectrochemical props. 0-50991

methacrylate polymer, carbazolyl substituted, excimer and charge transfer complex trapping of excitons 0-34367

methane-O<sub>2</sub> mixture, laser initiated combustion 0-55661

3-methoxybenzanthrone in ethanol, photoprotolytic reactions, spectra, rate consts. and lasing thresholds 0-43327

$\alpha$ -methylstyrene, photoinduced ionic polymerisation 0-7828

naphthalene, adsorbed on silica gel surface, biphasic photochemistry, time-resolved spectra 0-30252

nitromethane+H<sub>2</sub> reaction, CO<sub>2</sub> laser initiated, mechanism and yield 0-11912

organic crystal, appl. of TEM 0-24327

organic reactions in solid state 0-21309

organic solids, one- and two-photon laser photochem., hole burning appls. 0-21304

oscillating chemical reaction, entrainment by periodic light pulses of variable freq. (*French*) 0-35551

paraaminophenol and paraphenylenediamine analogue molecular complex, free radicals of developers, EPR obs. (*Russian*) 0-7814

photoactive catalyst used in light induced photocuring of coating systems 0-7820

photoelectrochemical investigation of the influence of gelatine and polyvinyl alcohol on the formation and lifetime of a latent image in photographic layers on a ZnO base (*Russian*) 0-3389

photoimaging system based on photopolymerisation in cryst. coatings 0-40716

photoinitiated cationic polymerization by photosensitization of onium salts 0-7822

photopolymer systems, conf., Washington, USA (Nov. 1978) 0-4799

photopolymerisation, O<sub>2</sub> inhibition elimination 0-7821

photopolymerisation, dye-sensitized, activation by trialkylbenzylstannanes 0-7824

photorecombination reactions initiated by shock wave, light amplification (*Russian*) 0-38011

photosensitive layers with chromic acid salts, photochemistry (*Russian*) 0-50869

PMMA-spiropyran Langmuir monolayers, reversible photochemical strain 0-50867

polyatomic mols., multiple photon IR processes, reviews 0-43125

1,4-polybutadiene, oxidation stabilisation by singlet O<sub>2</sub> quencher 4-(1-imidazolyl)-phenol 0-16677

polyesters, photoreactive, synthesis and struct.-prop. relations 0-7826

polymer, crosslinking with X-ray irradiation, active group and heavy atom effects 0-7829

polymer, photo-oxidation 0-3380

polymer, photochromic, thermal effect in photomech. conversion 0-16706

polymer ageing through exposure to light, device (*French*) 0-30126

polymer film, photoreticulation by UV irradiation 0-40717

polymer media 0-3381

polymethylene dye behaviour in lasers, efficiency and photoisomer generation 0-14335

polymethyl isopropenyl ketons, spectrally sensitized decomposition and Deep UV resists 0-40715

polyvinylbenzocarbazole, weak solution, intramolecular energy transfer by singlet and triplet excitons 0-34971

polyvinylcarbazole, weak solutions, intramolecular energy transfer by singlet and triplet excitons 0-34971

polyvinylcinnamate, crosslink form. by photoreaction 0-7823

porphin in host n-alkane crystals, phototautomerism, IR spectral obs. 0-34963

porphyrin, free-base, in n-alkane matrices, photochem. hole burning, optical dephasing 0-21305

purple membrane of H.halobium, effect of 560 $\pm$ 570 transition and blue light on photochem. 0-30673

purple membranes from Halobacterium halobium, spectral transitions 0-12056

pyrene adsorbed on silica gel surface, biphasic photochemistry, time-resolved spectra 0-30252

quantum-chemical  $\pi$ -electron system, molecules-in-molecule model (*German*) 0-5490

rare earths, purification, laser methods 0-16712

resonant electronic-vibrational energy transfer and use in pumping IR mol. lasers 0-9700

rhodamine 101, quenching of emission in methanol and latex particle suspensions 0-3374

rhodamine 6G, aqueous soln., absorpt. spectra, ground and triplet state photoprotonation pH depend. 0-42961

rhodamine 6G-isopropyl or ethyl alcohol solution, flashlamp pumped laser, photochem. effects 0-53287

selection rules for spectra and photochemical reactions (*Chinese*) 0-21308

solar chemistry research and developments (*French*) 0-11999

solar energy conversion, photoelectrochemical cells, chlorophyll sensitised reactions 0-7948

solar energy utilisation, photoelectrochemical systems (*German*) 0-45713

solid state, IR lasers appl. 0-11929



**photochemistry continued**

- spiropyrans, photochromic, thermophotodegradation for autoprocesor reprography system 0-35555
- stilbene, cis→trans photoisomerisation rate const., direct meas. 0-30250
- s-tetracyanobenzene+p-xylene, photoassoc., exciplex form., excitation energy and isotope depend., vibr. effects 0-55634
- tetrazine-Ar, van der Waals bond, nonstatistical vibr. energy distrib., photochemical reaction effects 0-30255
- thermal chemistry as an exercise in photochem. 0-3379
- thermosphere, lower, one-dimensional diffusion-photochemical model for O and O<sub>2</sub> distrib. simulation 0-4159
- time-correlated picosecond laser pulses generation, rapid sampling of optical relax. phenomena 0-9969
- troposphere, O<sub>3</sub> photochemical prod. and influence on climate 0-36365
- tunable-diode-laser IR spectroscopy appls. 0-40798
- unimolecular decay, nonadiabatic interactions, transition probability as function of Massey parameter 0-35503
- Uranus upper atmosphere, photochemistry rel. to mean temp. and temp. vars. 0-46477
- UV radiation meas. using ferrioxalate actinometer 0-41731
- visual pigment chromophores, models, spectroscopic and photochemical studies 0-30723
- water, photoassisted oxidation at TiO<sub>2</sub>/Be electrodes 0-30502
- water, photoelectrolysis, appl. of semiconductor interface system (French) 0-6935
- BCl<sub>3</sub>+methane reaction, laser-induced, vibr. excitation influence on reactivity, isotope selectivity 0-11921
- Ba+SO<sub>2</sub>→BaO+SO reaction, laser-induced fluoresc. obs., vibronic distrib. of BaO, collisional energy depend. 0-11917
- Br<sub>2</sub>+acetylene, laser-induced photochemistry 0-45498
- CO-Ar(N<sub>2</sub>), C<sub>2</sub> and CN form. by optical pumping, room temp. 0-16701
- CO<sub>2</sub> photochem. reduction to organic fuels using photoelectrochem. solar cells 0-55880
- CS<sub>2</sub>, aerosol form. by laser, kinetics study and photoreaction products chem. nature study 0-21324
- Ca+CCl<sub>4</sub>→CaCl+CCl<sub>3</sub> reaction, laser-induced fluoresc. obs. 0-11916
- Cl<sub>2</sub>+H<sub>2</sub>(H<sub>2</sub>S)(methanethiol), laser-initiated chain reactions, rates, mechanisms, chemiluminesc. obs. 0-55651
- CsH, crystallisation in Cs+H<sub>2</sub> gas mixture, laser snow effect 0-40712
- D enrichment by CW vibr. photochem. of methane, economic aspects 0-11920
- F+CH<sub>3</sub>I(CF<sub>3</sub>I)(ICI) reactions, product state analysis using laser-induced fluoresc. 0-11915
- Fe organometallics, interaction of naked Fe atoms with small mols., Mossbauer study of bonding in products 0-43080
- Fe+N<sub>2</sub>(NH<sub>3</sub>) interaction, chemical species formed studied by Mossbauer effect 0-43080
- Ga<sub>2</sub>In<sub>2</sub>P, flat band pot., impedance meas. and photoelectrochemistry (French) 0-49894
- p-GaP electrode, photoelectrochemical effect 0-55673
- Ge-S-Ga(In) system glasses, photoinduced changes 0-24365
- Ge+Br<sub>2</sub>, surface reaction, rate-limiting step, ellipsometric and photochem. meas. 0-16730
- H photoelectrochemical prod., solar beam-assisted electrolyser applied to Yokohama marks 5 and 6 [system for hydrogen production] systems 0-45768
- H<sub>2</sub>, production by solar energy, homogeneous photoredox system 0-3387
- H<sub>2</sub>, production by solar photochemical decomposition of H<sub>2</sub>O 0-16822
- Hg<sub>2</sub>, excimers, photoassoc., spectroscopy and kinetic processes of high-lying vibronic states, laser appls. 0-9649
- ICI selective photoaddition to acetylene, isotope enrichment, influence of press., buffer and wavelength 0-11927
- K+HgBr<sub>2</sub>, laser irradi., HgBr\* form., chemiluminescence 0-55658
- KBr, additively coloured, self-enhancement of amplitude hologram (Russian) 0-9828
- MgSi<sub>2</sub>, laser irradi. induced form., cryst. microstruct. 0-35011
- NH<sub>3</sub> sensitiser, excitation in MW region using CO<sub>2</sub> laser, pumping models 0-11911
- NO<sub>2</sub>, laser-induced fluoresc. quenching rate const. and lifetimes 0-11930
- N<sub>2</sub>O, atmospheric, instantaneous global photochemical reaction rates 0-17335
- Ni complex, bis-4-dimethylaminodithiabenzylnickel, tetrachlorethane soln., photochem. and thermal stability 0-16708
- O+methane, photochem. reaction, high temp., rate coeff. meas. 0-16699
- Rh(III) complexes, luminesc. rise time meas. by wavelength shifter 0-50390
- Ru complex, ruthenium(II) tris(2,2'-bipyridine), absorption spectrum and quantum yield of formation (French) 0-5554
- Ru complex, tris(2,2'-bipyridyl)-Ru(II) complex, photoelectrochemical systems, solar energy utilisation (German) 0-45713
- SF<sub>6</sub>, photon-enhanced dissociative electron attachment, isotope selectivity 0-18939
- Ti, passive oxide layer form. in H<sub>2</sub>SO<sub>4</sub>, ageing with and without photoexcitation (French) 0-45432
- TiO<sub>2</sub>, photodesorption of H<sub>2</sub>O, pulsed-laser-dynamic-mass-spectrometer study 0-35568
- TiO<sub>2</sub> electrodes, effect of processing variables on photoelectrochem. props 0-6975
- TiO<sub>2</sub> electrodes, room temp. diffusions, capacitance, spectral response and volt-ampere characts. 0-15294
- UF<sub>6</sub>+SiH<sub>4</sub>, photoinduced reaction in low temp. SiH<sub>4</sub> matrix 0-30256
- UO<sub>2</sub><sup>2+</sup>+UO<sub>2</sub>NO<sub>3</sub><sup>+</sup>, ground and excited state interaction, struct., thermodynamic functions, photochemistry obs. 0-32779
- ZnO, photodesorption of CO<sub>2</sub>, pulsed-laser-dynamic-mass-spectrometer study 0-35568

**photochromism**

- N-5'-chlorosalicylideneaniline, photochromism and thermochromism, NQR spectra, temp. and UV irradi. depend. 0-54968
- glass, coloration kinetics, isothermal relax., and spectral sensitivity using spectroscopistometer 0-27358
- glass, light effects, history of development of photosensitive and polychromatic glasses 0-40080
- glass, photochromic, thermo-optic transitions 0-50307
- glass, spectral characts. control 0-16073
- glasses, electron-hole separation, influence on recombination probability 0-11445
- halide photochromic centres, isothermal relaxation kinetics 0-16072
- organic photochromic materials, holographic recording (Russian) 0-1161
- 2-oxaindan (dihydroisobenzofuran) spiropyrans, photochromic transforms, spectrokinetic study 0-30259

**photochromism continued**

- polymer, photochromism 0-5805
- polymer, thermal effect in photomech. conversion 0-16706
- quartz, fused, photochromic LITMO, optical props. 0-1287
- salicylidene-2-chloroaniline, photochromism and thermochromism, NQR spectra, temp. and UV irradi. depend. 0-54968
- spectrosensitometer for spectral-kinetic characts. meas. of photochromic materials 0-27358
- spirobenzopyran copolymer photochromic soln., photoviscosity effect 0-6536
- spiropyrans, photochromic, thermophotodegradation for autoprocesor reprography system 0-35555
- surface polariton use in optical storage 0-48414
- waveguide, gradient photochromic film, acousto-optical props., integrated optics appl. 0-33207
- Ag halide, photochromic glass, optically induced anisotropy 0-1282
- Ag halides:Cu in photochromic glass, formation and theoretical models, review 0-43418
- AgCl photochromic glass, additional absorpt. spectrum, ellipsoidal model of colour centres 0-40142
- As-S glassy film, photobrightening effect 0-11498
- As-Se system, chalcogenide vitreous semiconductors, darkened films, thermal and optical bleaching, light transmission obs. 0-50447
- CdO-GeO<sub>2</sub>/TiO<sub>2</sub> photochromic glass for optical information retention media 0-33108
- Cu halide based photochromic glasses, spectral props. 0-29708
- KBr F→M transform., electrostatic field control of optical information recording (Russian) 0-48370
- Se, vitreous, darkened films, thermal and optical bleaching, light transmission obs. 0-50447

**photoconducting devices**

- see also photoconductive cells; photodiodes; phototransistors
- elastomer storage device evaluation for optical signal processing 0-48444
- ferroelectric ceramic-photoconductor structure, as optically controlled transparency 0-28343
- hybrid field-effect liquid crystal light valve, sensitometry control 0-23788
- image processing, digital, parallel logic device and half-adder circuit 0-10027
- imaging systems, limitations on sensitivity 0-6907
- IR detectors, microwave-biased, noise performance 0-9037
- IR photodetector, microwave biased, module construction 0-9038
- optoelectronic devices and optical imaging techniques, book 0-27059
- photodetector with integrated waveguide struct. 0-48456
- spatial light modulator, using KD<sub>2</sub>PO<sub>4</sub> and Se photoconductor, optical processing appl. 0-9988
- switch, laser-activated, high-power switching with ps. precision 0-2416
- (Cd,Hg)Te, photoconductive detector, uncooled, for 8-14 μm region 0-31868
- CdS<sub>0.5</sub>Se<sub>0.5</sub>, picosecond optoelectronic switching 0-54734
- CdSe image convertor, liquid-crystal, hybrid optical processors appl. 0-33166
- GaAs switch, laser-activated, high-power switching with ps. precision 0-2416
- MoSe<sub>2</sub>-I<sub>2</sub>, photoelectrode, time resolved photocurrent, nanosecond excitation 0-45708
- Si disc semiconductor-insulator structure, for liq. cryst. incoherent-coherent image convertor 0-28342
- Si:As photoconductive detector for IR astronomy, responsivity and system noise 0-51665

**photoconducting materials**

- see also photoconductivity
- electrophotographic layer, electrostatic force calc. (German) 0-42285
- electrophotographic receptor, near IR sensitive 0-48369
- organic photoconductor, electric field-induced fluoresc. quenching 0-34967
- organic semiconductor photoelectrode processes and effects (German) 0-26145
- photothermoplastic recording with rapid switching 0-32941
- phthalocyanine films, metal-free, adsorbed o-chloranil effect on surface photovoltage 0-34485
- pigmented organic photoreceptors for plain paper copying 0-49824
- poly(N-vinyl carbazole) sensitisation with Se, purification effect on electrophotographic characts. 0-49825
- polyvinylcarbazole-trinitrofluorenone, organic photoconductor, photoinduced paramag. centres 0-25188
- surface charges produced in photoconductor-air gap-semicond. system, calc. 0-6905
- thermoplastic film, photoconducting, double exposure holographic interferometry using memory effect (Chinese) 0-37967
- thermoplastic photoconductor tape performance for optical recording 0-43305
- thermoplastic-photocond. device for holographic recording, diffr. efficiencies 0-5707
- TTF derivatives, smectic and nematic, for liq. cryst. device appl. 0-54124
- xerographic discharge in binder layers 0-47140
- Bi<sub>2</sub>SiO<sub>5</sub> photoelectret, in optical processing and X, γ ray imaging 0-23764
- CdIn<sub>2</sub>S<sub>4</sub>, photoconducting semiconductors, fundamental absorption edge 0-40130
- CdS, convolution voltage enhancement due to carrier transverse drift in SAW convolver 0-1381
- CdS films, precip. from soln., phase comp. change during annealing in air at 200-600°C 0-15393
- CdS, photoconductive, obs. of high intensity sound self-defocusing 0-24972
- CdS powder layers, surface pot. dark decay, moisture sorption and heat treatment effects 0-18038
- CdS:Cu,Cl film, applied voltage freq. effect on props. 0-39635
- CdS:Cu binder layer, photoactive, AC impedance meas. 0-25299
- CdS,Se<sub>1-x</sub>, photosensitive films, prep., props., and use for photodetectors 0-55298
- CdSe, photocond. film, plasma reson., IR refl. obs. 0-11037
- GaAs:Cr plane-parallel photocond. plate, oscills. in current and light intensity in laser irradiation 0-49819
- GaAs:Cr plate, illuminated, oscills. in V-I charact. 0-11038
- In<sub>1-x</sub>Sn<sub>x</sub>O<sub>3-y</sub>[SnO<sub>2</sub>]-CdSe-CdS:Cd,Cl sandwich photoconductor injection obs. (Russian) 0-54773
- Pb<sub>1-x</sub>Sn<sub>x</sub>Te film, sputtered, for IR detector appl. elec. and optical props. 0-35084



**photoconducting materials continued**

- Se-binding agent electrophotographic film characteristics and sensitivity (*German*) 0-4789  
 Si, amorphous, as photo-receptor for electrophotography 0-47126  
 Si, amorphous glow discharge films, H<sub>2</sub> content, elec. props., and photostability 0-25577  
 Si:H, amorphous, radiative recomb. by diffusion and tunnelling, photocond. quantum efficiency 0-50394  
 WO<sub>3</sub> layers, semiconductor electrodes, electrochromism and photoelectrochemistry 0-35544

**photoconductive cells**

- pulse time resolution when optical pulse shorter than photoelectron transit time, theory (*German*) 0-9035  
 richardson-Schottky type photoinjection current from photoconductor into insulating liquid 0-15608  
 transparent electrode photo-galvano-voltaic cell, using Mg-meso-tetraphenylporphine-coated glass (*Chinese*) 0-40865

**photoconductivity**

see also *photoconducting devices; photoconducting materials*

- alkaline frozen solutions, polycryst. and glassy, photocond. and radiometric obs. 0-45531  
 amorphous semiconductor, modulated photoconductivity anal. 0-44650  
 anthracene, photocond. spectrum induced by excitons (*Japanese*) 0-29440  
 anthracene, photogeneration of charge carriers through two photon excitation 0-11033  
 anthracene, single cryst., photocond. threshold, excitation spectrum 0-44639  
 anthracene, single crystal, photoconductivity quantum yield, experimental validation of fund. theory 0-6909  
 anthracene, time-resolved transient photocond. obs. 0-6892  
 anthracene-pyromellitic dianhydride complex, optical and photoelectric props. (*Russian*) 0-15570  
 Bi<sub>1-x</sub>Sb<sub>x</sub>, narrow band gap semiconductors, galvanomagnetic, optical and photoelectric props. 0-15544  
 p-CdTe, surface photovoltage spectroscopy in IR and visible range 0-39632  
 chalcogenide glasses, trap controlled transient photocond. 0-44641  
 dark current relaxation, barrier cond. mech. 0-6904  
 diamond: Li, ion implantation doped, IR photocond. 0-20249  
 9,10-dichloroanthracene, monoclinic, photocond. carrier mobility 0-39630  
 dielectric, trap-controlled transient photocond., numerical study 0-50285  
 disordered semiconductor, photon-phonon-assisted hopping, theory 0-44642  
 donors with excited states, kinetics of electron transitions 0-39600  
 electrets and dielectrics, conf., Sao Carlos, Brazil, Sept. (1975) 0-7251  
 electrode and volume controlled photocurrents 0-6908  
 electron trapping, donor state generation, photo I-V study 0-20210  
 n-GaAs:Cr(Si), deep-level extrinsic photocond. response, decay at 4.2K 0-2420  
 n-hexane, liq. trapped electron photoionis., photocond. 0-2418  
 homogeneous semiconductor, imperfections and photocond., electronic nonequilibrium behaviour 0-44667  
 imaging systems, limitations on sensitivity 0-6907  
 impurity photoconductivity and autoionisation calc. 0-44648  
 insulated crystal, primary photocurrent kinetics for simultaneous trapping and recomb. 0-6899  
 metal-RbAgI<sub>2</sub>, solid electrolyte interface, photocurrent obs. on illumination 0-34513  
 MIS tunnel diodes, photoionisation of states 0-11099  
 molecular crystals, spectroscopy, bibliography (1977) 0-7317  
 MOS diodes, minority carrier lifetime determ. from photocurrent spectra 0-49920  
 naphthalene, pure and deuterated, band-hopping mobility transition 0-6833  
 one-dimensional, semiconducting polymer, demonstration of high mobility 0-20212  
 organic xerographic photoconductors, bimolecular recomb., reciprocity failure 0-49798  
 PET, pyroelectric effects and depolarisation currents, illumination effects 0-34859  
 photocathode polarisation sensitivity, two-beam interferometer expts. 0-4772  
 photoconductor-insulator interface, carrier injection 0-24970  
 photodielectric, stationary recombination equations, analytical solutions in source limiting cases 0-44662  
 point defect electrons and vibrations, dislocation field effect, dislocation photoconduction spectrum (*Hungarian*) 0-51977  
 poly- $\gamma$ -ethyl-D-glutamate, pulsed photoconduction 0-24969  
 polyacetylene, phototransport effects 0-44653  
 polyacrylonitrile, pyrolyzed, pulsed photoconduction 0-24969  
 polydiacetylenes, photocond. action spectrum of single crystals, charge transport obs. 0-15557  
 polyenes, semicond., compensation temp. 0-39625  
 polyethylene-2,6-naphthalate, pulsed photoconduction 0-24969  
 polyethylene-terephthalate, field-controlled photogeneration and carrier trapping 0-25285  
 polymer UV photoconduction expts. and electronic props. 0-15572  
 polymers, electrical phenomena, nature and appl., book contrib. 0-50254  
 polymonochloro-p-xylylene,  $\gamma$ -ray-induced cond., hole injection effects 0-34452  
 polynaphthalene films, plasma polymerised, photovoltaic and photocond. props. 0-34479  
 polystyrene,  $\gamma$ -ray-induced cond., hole injection effects 0-34452  
 polystyrene film, in MIM struct., elec. conduction and free radicals 0-20340  
 polystyrene thin film, glow discharge formed, dark current and photocurrent obs. (*Japanese*) 0-15633  
 positive photoresists, photocond. factor rel. to composition (*Russian*) 0-42289  
 PVC thin films, pure and I doped, photoconductivity study 0-44646  
 quantum statistics of photocurrent in optimal light detector, atm. 'seeing' conditions 0-53244  
 relaxations of photoelectric conductance meas., submicrosecond (*Czech*) 0-31804  
 rubrene, orthorhombic cryst. photogenerated carriers, transit time meas. 0-49811  
 scanning background-limited IR sensor with adaptive threshold signal processing logic, performance 0-37082  
 Schottky barrier, real and ideal, photosensitivity losses 0-2452

**photoconductivity continued**

- Schottky barriers, photocurrent, recomb. losses (*Russian*) 0-2470  
 screening charge formation time at illuminated spot boundaries 0-29438  
 semiconductor, adiabatic approx. in transient donor recomb. 0-49761  
 semiconductor, capture probabilities of two deep impurity levels by photocond. decay 0-49799  
 semiconductor, deep impurities, exptl. techniques (*Japanese*) 0-15476  
 semiconductor, exciton condensation, microwave cond., book contrib. 0-11043  
 semiconductor, inhomogeneous elec. fields in oscillatory photocond. 0-2421  
 semiconductor, stationary recombination equations, analytical solutions in source limiting cases 0-44662  
 semiconductor, strong electron-lattice interaction, review (*Japanese*) 0-49664  
 semiconductor, surface electronic props., optical spectroscopic techniques, review 0-11070  
 semiconductor film, carrier temperature and density self-oscills. near instability threshold 0-11118  
 semiconductor thin films, degenerate one-valley and many-valley, photogalvanic effect calcs. 0-34487  
 semiconductors, compensated, spectral depend. of photoresponse 0-15562  
 semiconductors, influence of surface space-charge layer 0-15563  
 solar cells, electrochem. liquid-junction, Schottky barrier height, photovoltage and photocurrent 0-26162  
 solar EM radiation measurement using CdS photoresistor 0-31092  
 superlattice semiconductor impurity photoconductivity electron spectrum reconstruction 0-24966  
 surface charges produced in photoconductor-air gap-semicond. system, calc. 0-6905  
 temp. depend. of conductivity and photocond. at 632.8 nm (*Russian*) 0-44666  
 tetracene, organic insulator action spectra of photocurrent 0-34482  
 tetracene surface states, electric field effects, exciton-charge carrier interactions (*Russian*) 0-24989  
 tetrathiotetracene, charge transfer state parameters, evaluation by mag. field effect (*Russian*) 0-10924  
 transport equation for electrons in nonmonochromatic EM field 0-10937  
 wave hierarchy interpretation of multiple trapping model 0-6894  
 Ag<sub>3</sub>AsS<sub>3</sub>, proustite, light effects on dielec. props., elec. resist. 0-49816  
 AgCl(Br), crossed elec. and mag. fields, hot electrons, streaming motion, population inversion 0-44649  
 Al-GaAs-Al<sub>1-x</sub>Ga<sub>x</sub>As Schottky barrier diodes, prep., characts. 0-6948  
 Al<sub>1-x</sub>Ga<sub>x</sub>As, DX photocond. centres, photocapacitance and DLTS meas. 0-11044  
 Al<sub>1-x</sub>Ga<sub>x</sub>As: Sn(Te), persistent photocond., due to donor-related centres, symmetry 0-15558  
 AlH<sub>3</sub>, dark electrical cond., exam. 0-39624  
 AlH<sub>3</sub>, polycrystalline, photoconductivity and photochemical decomp. 0-44638  
 As-S chalcogenide glass holographic recording efficiency, photocond. and annealing effects (*Russian*) 0-15556  
 As-Se glasses, low temp. photocond. 0-49808  
 As<sub>2</sub>S<sub>3</sub> (Se<sub>3</sub>), electron irradiated, effects on elec., photoelec. and optical props. 0-49806  
 As<sub>2</sub>S<sub>3</sub>, amorphous, elec. cond. mech. obs., in bulk material and evaporated thin films (*Japanese*) 0-11028  
 As<sub>2</sub>S<sub>3</sub>(Se<sub>3</sub>):Ag glassy films, doped by photodiffusion and thermodiffusion, photocond. 0-29441  
 As<sub>2</sub>Se<sub>3</sub>, amorphous, modulated photoconductivity anal. 0-44650  
 As<sub>2</sub>Se<sub>3</sub>, amorphous, nonradiative recombination of photocarriers 0-11046  
 As<sub>2</sub>Se<sub>3</sub>, amorphous, time resolved meas. of photoinduced optical absorpt. and photocond. 0-49807  
 As<sub>2</sub>Se<sub>3</sub> amorphous thin films, illumination-induced change in contact pot. 0-20251  
 As<sub>2</sub>Se<sub>3</sub>, photosensitive layer, in metal-photosemiconductor-insulator multilayered struct., optical image recording 0-42286  
 As<sub>2</sub>Se<sub>2</sub> amorphous film, photocond., TSC, light-induced changes 0-49810  
 As<sub>2</sub>Se<sub>2</sub>, electron irradiated, effects on elec., photoelec. and optical props. 0-49806  
 As<sub>2</sub>Se<sub>1</sub>, glasses, cond. and photocond. 0-20253  
 Au-GaAs, photosensitivity losses, field and spectral depend. 0-2452  
 Au-GaAs Schottky barrier, photocurrent, recomb. losses (*Russian*) 0-2470  
 Au-oxide-GaAs struct., steady-state and transient photocurrents 0-6994  
 Au-oxide-n-GaAs structs., reverse-bias depend. photocurrent, photoionisation of surface states 0-20323  
 B, residual photoconductivity in single crystals. 0-20241  
 Bi<sub>4</sub>Si<sub>3</sub>  $\beta$  rhombohedral, conduction mechanism, thermoelectric props. 0-24932  
 Bi<sub>4</sub>Si<sub>3</sub> elec. props., medium range disorder model 0-15522  
 (Ba<sub>1-x</sub>Sr<sub>x</sub>)<sub>1-x</sub>(Nb<sub>2</sub>O<sub>6</sub>)<sub>1-x</sub>:CeO<sub>2</sub> crystals, photoelectric and photorefractive props., hologram recording 0-53239  
 BaTiO<sub>3</sub>, ferroelectric semicond. anomalous photovoltaic effect due to ionising radiation 0-29437  
 Bi<sub>12</sub>GeO<sub>20</sub>, photoelectret state 0-11315  
 Bi<sub>2</sub>O<sub>3</sub> anodic films, struct. and electronic props., photoeffects 0-44749  
 CdGa<sub>2</sub>S<sub>4</sub>, single crystals, peculiarities of photocond. in strong elec. field 0-54736  
 CdGa<sub>2</sub>Se<sub>4</sub>, struct. of valence band, photocond. and reflection spectra meas. 0-6719  
 Cd<sub>1-x</sub>Hg<sub>x</sub>Te, photothermomag. effect and photocond. in millimetre wavelength range 0-44657  
 Cd<sub>1-x</sub>In<sub>x</sub>Cr<sub>2</sub>Se<sub>4</sub>, electric, photoelectric and mag. props., metal-semicond. transition (*Russian*) 0-54738  
 CdIn<sub>2</sub>S<sub>4</sub> film, vac. deposited, growth, struct., optical and photoelectronic props. 0-10831  
 Cd<sub>1-x</sub>M<sub>x</sub>S (M=Sr, Ca, Mg, Pb, Sn), solid soln., prep. and semicond. props. 0-2383  
 Cd<sub>3</sub>P<sub>2</sub>Cl<sub>3</sub>(Br<sub>3</sub>)(I<sub>3</sub>), elec. and photoelec. props. 0-34480  
 CdS films, pure and Na doped, chemical bath deposited, photothermoelectric effect 0-6906  
 CdS laser irradi. native defect formation, influence on photoelectric props., IR luminescence (*Russian*) 0-11039  
 CdS, photoinduced sensitisation process, thermal activity (*Russian*) 0-34477  
 CdS, photosensitivity degradation mechanism due to photocurrent, photocarrier lifetime 0-6903  
 CdS, recombination electric domains, production mechanism 0-29433  
 CdS, stress-induced photolum. bands, photocond., rel. to dislocation electron states 0-25447



## photoconductivity continued

- CdS type semiconductors, bulk laser damage mechanism, photocond. meas. 0-15567  
 CdS:Ag crystals, spectral shifts of induced impurity photocond. bands 0-39633  
 CdS:Cu, dye-sensitized, photocond. and photocurrent decay time obs. 0-6893  
 CdS:CuCl<sub>2</sub>(CdCl<sub>2</sub>) sintered layer, distrib. of energy levels of local centres 0-15568  
 CdS:Li chemically deposited filter, elec. props. 0-11113  
 CdS:Li film, chemical bath deposited, photocond. and optical props. 0-2426  
 CdS:Na thin film, photoconducting props. 0-39623  
 CdS:Ni, recomb. parameters, photocond. spectra meas. (*Russian*) 0-49820  
 CdS-PbS heterojunctions, photoresistive props. 0-6970  
 CdS,Se<sub>1-x</sub>, photosensitive layer, in metal-photoconductor-insulator multilayered struct., charge pattern form. 0-47129  
 CdS,Se<sub>1-x</sub>, photosensitive films, prep., props., and use for photodetectors 0-55298  
 CdSe, dark current relaxation 0-44613  
 CdSe, pulsed Hall photoeffect, transient processes in scattering of carriers 0-15546  
 CdSe:Au impurity light absorpt. for current control in negative resistance region 0-11052  
 CdSi<sub>2</sub>:Na(Bi), single crystal, under laser excitation 0-44661  
 CdTe sputtered films, struct., photocond., and trap distrib. 0-29489  
 CdTe<sub>1-x</sub>Se<sub>x</sub>, solid solution films, prep., struct., and photocond. 0-54541  
 Cu<sub>2</sub>O, photoconductivity in IS excitonic line 0-34366  
 Fe<sub>2</sub>O<sub>3</sub>, metallic phase, photocond. and mag. permeab., photoinduced changes 0-15566  
 p-Ga<sub>1-x</sub>Al<sub>x</sub>As crystals, spectral characts. of photosensitivity, mechanism 0-44735  
 GaAs, electrical and optical props. at low temps. 0-39636  
 GaAs, electron-exciton collision influence on luminescence line profile due to bound excitons and photocond. meas. 0-29800  
 n-GaAs epitaxial film, undoped, correl. incorporation of donors, photocond. meas. at 4.2K 0-6898  
 GaAs epitaxial film recombination props. (*Russian*) 0-49812  
 GaAs epitaxial films, deep levels, impurity photocond. 0-20247  
 n-GaAs epitaxial films, residual cond. meas., struct. perfection rel. to photomemory 0-7010  
 GaAs, laser-induced bulk breakdown and free carrier generation, photocond. meas. 0-35018  
 GaAs, neutron transmutation doping, shallow donors magneto-optical effects 0-20255  
 GaAs, plastically deform., photocond., spectral response and decay process 0-29435  
 GaAs, semi-insulating, conduction model 0-10986  
 GaAs VPE layers, elec. props., semi-insulating substrates effect 0-11123  
 GaAs:Cr<sub>2</sub>O<sub>3</sub>, semi-insulating, photocond. anal. of levels 0-20243  
 GaAs:Cr plane-parallel photocond. plate, oscills. in current and light intensity in laser irradiation 0-49819  
 GaAs:Cr plate, illuminated, oscills. in V-I charact. 0-11038  
 p-GaAs:Cu, impurity photocond. and absorpt. coeff., Hall meas. 0-6770  
 n-GaAs:Ni, negative photocond. at low temps., impurity levels 0-6900  
 n-GaAs:O, photocond. associated with deep level at 0.4 eV 0-44640  
 GaAs:Si epitaxial films, elec. and photoelec. props., impurity distrib. 0-7006  
 GaAs:Te, recombination barrier, dark cond., photocond., and Hall mobility meas. 0-15559  
 GaAs-Al<sub>0.1</sub>Ga<sub>0.9</sub>As superlattice, electronic props. 0-11080  
 GaAs-AlGaAs DH laser, degradation rate rel. to photocurrent 0-28233  
 n-GaAs-electrolyte interface, surface pretreatment rel. to photocurrent, spectral response 0-3204  
 GaAs-Ga<sub>1-x</sub>Al<sub>x</sub>As variable gap p-n junction, variable gap and photo EMFs 0-15596  
 GaAs-Ge<sub>1-x</sub>(GaAs)<sub>x</sub> n-p heterojunctions, hydrostatic press. effect on elect. and photoelectric props. 0-20304  
 GaAs<sub>1-x</sub>P<sub>x</sub>:S, deep level, photoconductivity, carrier nonradiative recombination 0-20112  
 Ga<sub>1-x</sub>In<sub>x</sub>:Se, fabrication, struct., elec. and optical props. 0-44180  
 GaN:Al, VPE grown, luminesc. and elec. props. depend. on doping conc., bound excitons 0-20688  
 GaP complex band semicond. photogalvanic effect mechanism 0-11036  
 GaP, electrical and optical props. at low temps. 0-39636  
 GaP:Cu, elec. and optical props., rel. to doping and heat treatment 0-16056  
 GaP:Fe n-i-n epitaxial struct., photoconductivity, recombination scheme (*Russian*) 0-15569  
 GaSe, exciton-phonon bound state, photocond. and visible absorpt. spectra obs. 0-50369  
 GaSe, photocond., influence of stacking disorder 0-2422  
 n-GaSe, photomagnetolectric effect, photocond., in presence of traps 0-39631  
 Ge and Ge:O(Li), shallow defects, PTIS meas. 0-24971  
 Ge, electrical and optical props. at low temps. 0-39636  
 Ge, electron irradi., light-sensitive defects 0-24498  
 Ge, exciton condensation, microwave cond. below 1K, book contrib. 0-8997  
 Ge, exciton condensation, microwave cond., book contrib. 0-11040  
 Ge, exciton condensation, microwave breakdown, luminesc., book contrib. 0-11471  
 Ge, exciton microwave breakdown, electron-hole drops, book contrib. 0-11041  
 Ge, high-purity, with Al, B and P, residual impurities, photothermal cond. 0-24965  
 Ge, laser-induced bulk breakdown and free carrier generation, photocond. meas. 0-35018  
 Ge, microwave absorption by nonequilib. current carriers, book contrib. 0-11042  
 Ge, photocurrent magneto-oscillations 0-6911  
 p-Ge, photoexcited charge carrier capture by shallow impurity centres (*Russian*) 0-15571  
 n-Ge, plastically deform., dislocation state spectrum, photocond., elec. cond., and Hall const. meas. (*Russian*) 0-2362  
 n-Ge surface, chemical channel of recombination 0-39656  
 Ge:As(P)(Sb), impurity photocond. spectra under uniaxial compression 0-44656  
 Ge:Au under laser illumination, non-equilibrium conduction 0-6896  
 Ge:H, photoelec. spectra, acceptor and donor behaviour 0-29443

## photoconductivity continued

- n-Ge:Ni, recombination of hot electrons on Ni impurity centres 0-44612  
 Ge:Sb (As), isolated D<sup>-</sup> states and D<sup>-</sup> complexes in mag. fields 0-15473  
 Ge-S, amorphous, photocond., photo-induced ESR, optical edge shift 0-49809  
 GeS, interband transitions, intrinsic photocond., anisotropy 0-20244  
 Ge<sub>2</sub>S<sub>3</sub>, electron irradiated, effects on elec., photoelec. and optical props. 0-49806  
 Ge<sub>2</sub>S<sub>3</sub>-Ag contact, photoinduced diffusion of Ag in amorphous semicond. film 0-49418  
 GeSe<sub>2</sub>, amorphous film, photocond., photo-induced ESR, optical edge shift 0-49809  
 GeSe<sub>2</sub>, drift mobilities of electrons and holes, photocurrent decay meas. 0-2424  
 n-HgCdTe, photocond., Hall mobility and resist. 0-34478  
 Hg<sub>1-x</sub>Cd<sub>x</sub>Te, carrier conc., Hall effect, photocond., IR spectra meas. 0-49771  
 InAs/LiNbO<sub>3</sub> structure, SAW generated transverse acoustoelectric voltage, image scanning and signal processing appl. 0-49826  
 InAs<sub>1-x</sub>Sb<sub>x</sub> p-n junctions, avalanche multiplication 0-6965  
 InP, electrical and optical props. at low temps. 0-39636  
 InP:Fe, deep acceptor levels, photocond. meas. 0-20116  
 InP:Fe, photocond., Fe<sup>2+</sup> intracenter excitation model 0-29436  
 InP:Fe, resonance photocond. 0-44651  
 n-InSb, deformed, spectral oscills. of absorption in quantising mag. field 0-34486  
 InSb, intrinsic, photoinduced electron hole pairs, Auger lifetime, photoconductive decay obs. 0-39629  
 n-InSb, magneto-optical transitions from deep levels, photocond. obs. 0-55069  
 n-InSb, optical phonon emission in intraband magneto-optical transitions, photocond. meas. 0-34481  
 InSb p-n junctions, diffused, avalanche multiplication and impact ionisation 0-15595  
 n-InSb, photoconductive lifetime, surface pot. effects 0-11029  
 n-InSb, photoconductivity, recombination processes 0-11030  
 n-InSb, photoconductivity of laser excited hot electrons 0-11045  
 n-InSb, weakly compensated, sub MM photocond. 0-15565  
 In<sub>2</sub>Te<sub>3</sub> defect semicond., photoconductive kinetics 0-11035  
 In<sub>2</sub>Te<sub>3</sub>, photocond. and absorption spectra, polarisation dependences 0-20642  
 KNbO<sub>3</sub>, photovoltaic effect lux ampere characts., photoconductivity 0-15561  
 La<sub>2</sub>Ti<sub>2</sub>O<sub>7</sub>, ferroelects., nonlinear optical props. 0-33086  
 LiNbO<sub>3</sub>:Fe, anomalous photovoltaic effect in polarised light (*Russian*) 0-34484  
 LiNbO<sub>3</sub>:Fe, pure and doped, photocond. and dark cond. 0-29439  
 LiNbO<sub>3</sub>-CdS, layered structure, transverse acousto-electric current 0-44669  
 NaNbO<sub>3</sub>, elec. and photoelec. props. near ferroelec.-antiferroelec. phase transition 0-15989  
 Ni-Nichrome, MOM diode, breakdown effect in visible and near-IR regions 0-6999  
 Pb<sub>2</sub>As<sub>2</sub>S<sub>5</sub>, gratonite, single crystal, photoelectric props. 0-49822  
 PbO single crystals, current-voltage characts., electrom. (*Russian*) 0-2863  
 Pb<sub>1-x</sub>Sn<sub>x</sub>Se, displacive transition, temp. and press. depend., elec. meas. 0-10672  
 Pb<sub>0.78</sub>Sn<sub>0.22</sub>Te:In epitaxial layers, dislocation density, Hall effect, conductivity, photoeffects 0-25024  
 Pb<sub>1-x</sub>Sn<sub>x</sub>Te, inter- and intraband magneto-optical transitions 0-25346  
 Pb<sub>1-x</sub>Sn<sub>x</sub>Te:Cd, impurity photocond. spectra 0-6902  
 Pb<sub>1-x</sub>Sn<sub>x</sub>Te:Cd, photocond., photomag. effect, carrier lifetimes 0-44658  
 Pb<sub>1-x</sub>Sn<sub>x</sub>Te:Cd, photoelec. props., surface recomb. effect 0-44659  
 PbTe, resonant scattering, photocond. 0-6910  
 PbTiO<sub>3</sub>, anomalies in elec., photoelectric and mechanical props. 0-55051  
 Sb<sub>2</sub>Se<sub>3</sub>, photocond., photo-EMF and photodielectric effect, expts. 0-20245  
 Se, amorphous, photoconductivity quantum yield, experimental validation of fund. theory 0-6909  
 Se, trigonal single crystal, dark current relax., barrier cond. mech. 0-6904  
 Se, trigonal single crystal, peak in temp. dependence of elec. cond. 0-44663  
 Se, X-ray sensitivity, induced photocurrents, xeroradiographic meas., pair creation energy 0-22490  
 Si, amorphous, control of dihydride bond density using RF sputtering, dark anal. and photocond. 0-34327  
 Si, amorphous, photovoltaic diodes, influence of mag. field on charge transport 0-49891  
 Si, amorphous, solar cells, and photovoltaic devices (*Japanese*) 0-50965  
 Si, amorphous, transport results interpretation 0-44590  
 Si, amorphous films, ion implanted, elec. and photocond. props. 0-49717  
 Si, amorphous glow discharge films, H<sub>2</sub> content, elec. props., and photostability 0-25577  
 Si, exciton-plasma transitions, dense electron-hole system portrait composition (*Russian*) 0-49622  
 Si, influence of surface recombination rate and carrier diffusion on photocond. 0-44660  
 n-Si, irradiated with large neutron doses, defect annealing 0-19849  
 Si, kinetics, effect of exciting illumination (*Russian*) 0-11032  
 Si, laser annealing at 1.06 μm, free carrier absorpt. role 0-24964  
 Si, laser-induced bulk breakdown and free carrier generation, photocond. meas. 0-35018  
 Si, local electron irradi., Frankel pair separation, influence on photo EMF 0-44203  
 p-Si, millimetric and far-IR cond., freq.-depend. carrier relax time 0-34460  
 n-Si neutron and electron irradi., isochronous annealing influence on edge absorpt. 0-11449  
 Si p-n junctions, high-voltage, elec. props. by optical scanning 0-6969  
 Si, plastically deformed, spin-depend. charge transport 0-6895  
 Si, recomb. centre study by spin-depend. photocond. 0-49805  
 a-Si, resonant and non-resonant photoconductivity changes 0-49814  
 a-Si, resonant and non-resonant luminesc. changes theory 0-50410  
 Si solar cells, polycrystalline n<sup>+</sup>/p, computer model of spectral response and photocurrent 0-55853  
 Si, sputtered amorphous film, photocond. and electronic props., effects of annealing in plasma gas 0-44644  
 Si, temp. dependence, excitation with laser pulses (*Russian*) 0-11031



**photoconductivity continued**

- Si, temporary trap characteristic after heat treatment (*German*) 0-34459  
 Si with thermal defects, photocond., effect of annealing on elec. resist. 0-6837  
 Si: Cd  $n^+-n-n^+$  structs., photoresist. props. under exclusion conditions 0-39666  
 Si:F, H amorphous films, optical props., photoconductivity, photostructural changes 0-11034  
 Si:F, H, amorphous, glow discharge deposited elec. props. and device aspects 0-44744  
 Si:H, amorphous, excess carrier thermalisation and recomb., luminesc. decay and photocond. 0-50397  
 Si:H, amorphous, plasma-deposited, effect of DC elec. field superimposed during deposition 0-44643  
 Si:H, amorphous, RF sputtered, suitability as solar cell material 0-40864  
 Si:H, amorphous, solar cell struct., photocurrent meas., absorpt. coeff. 0-50960  
 Si:H, amorphous field induced and quenched-in excess cond. 0-24968  
 Si:H, amorphous film, prep. by plasma decomp. of  $\text{SiH}_4$  under mag. field, and characterisation 0-45239  
 Si:H, Cl(F), amorphous, photocond., dark cond. and photoluminesc. 0-49802  
 a-Si:H, spin defect and recombination influence on electronic transport 0-50409  
 Si:H,P, amorphous, heavily hydrogenated, high gap state densities 0-49803  
 Si:H amorphous films, optoelectronic behaviour depend. on impurity incorporation during plasma deposition 0-49804  
 Si:H amorphous films, photovoltaic and photocond. spectra, photoluminesc. 0-44645  
 Si:H amorphous films, photoinduced optical absorpt. and photocond. 0-50361  
 Si:H amorphous films, role of Ar in deposition process, IR absorpt. and photocond. meas. 0-50321  
 Si:H amorphous films for solar cells, optical and elec. props. of RF glow discharge deposited films 0-54576  
 Si:H amorphous sputtered film, photoluminesc., photocond. 0-20729  
 Si:H film, amorphous, photocond. imaging 0-1300  
 Si:H film, amorphous, reactively sputtered, H content effect on props. 0-49714  
 a-Si:H MIS junction, electronic struct. study by tunnelling 0-44729  
 p-Si:Mn, giant residual cond. 0-20250  
 Si:N, amorphous, prep. by RF sputtering and props. 0-44229  
 Si:Ni, capture probabilities of two deep impurity levels by photocond. decay 0-49799  
 Si:P, amorphous, CVD, defect compensation 0-54644  
 Si:SiO<sub>2</sub>, SiO<sub>2</sub> layer charging in UV irradi. of MISS struct., photoinjection currents (*Russian*) 0-39680  
 Si-SiO<sub>2</sub> interface, electrically active paramag. centres detect., photocond. reson. obs. 0-50185  
 Si-SiO<sub>2</sub> interface, light induced reson. centres, photocond. reson., EPR obs. 0-50184  
 Si-SiO<sub>2</sub>-Si<sub>3</sub>N<sub>4</sub>, internal photoemission 0-7475  
 SiH<sub>0.16</sub> amorphous films, optical props. and photocond. near optical gap 0-50443  
 SiO<sub>2</sub> film electron beam induced conductivity theory and expts. 0-15640  
 a-SiO<sub>2</sub>, transient photocond. simulations using multiple-trap model 0-49801  
 SnO<sub>2</sub>-Si, heterojunction solar cells, anomalous photocurrent 0-3515  
 SnO<sub>2</sub>-Si solar cells, electron-beam deposited, struct., photovolt. props. 0-50956  
 Sn<sub>2</sub>P<sub>2</sub>S<sub>6</sub>, illumination effect on soft mode and dielectric props., luminesc. study (*Russian*) 0-50420  
 Sr<sub>2</sub>Nb<sub>2</sub>O<sub>7</sub>, ferroelects., nonlinear optical props. 0-33086  
 SrO, luminesc. band edge, 4-6.5 eV, optical absorpt., photoluminesc., cathodoluminescence, photocond. obs. 0-50411  
 SrTiO<sub>3</sub> semicond. electrode, electrochem., photoelectrochem. props. 0-3352  
 Te, opt. props. under high press., band struct. transform. 0-55112  
 Te, photoconductivity under pulse excitation conditions 0-2425  
 TiO<sub>2</sub> electrodes in photoelectrochem. cell, photothermal effect 0-7947  
 TiO<sub>2</sub> sputtered film, photocond. and TSC meas. 0-15560  
 TiO<sub>2</sub>:V(Cr)(Mn)(Fe), impurity levels, photocurrent and ESR meas. 0-29346  
 TiGaSe<sub>2</sub>-TiGaSe<sub>2</sub>, phase and composition-property diagrams 0-55366  
 TiInSe<sub>2</sub>-TiInSe<sub>2</sub>, phase and composition-property diagrams 0-55366  
 TiInSe<sub>2</sub>(Se<sub>2</sub>), electrical cond. of single crystals with symm. and asymm. Ag-In contacts 0-6835  
 V<sub>2</sub>O<sub>5</sub> crystal, photoinduced threshold switching in VO<sub>2</sub> channel 0-29450  
 W-Ni, MOM diode, breakdown effect in visible and near-IR regions 0-6999  
 ZnO crystals, adsorbed dye laser, charge transfer, field effect and spectrally sensitised photocond. meas. 0-49815  
 ZnO, electric field dependence of photoconductivity (*Russian*) 0-49821  
 $\alpha$ -Zn<sub>2</sub>P, local centre parameters, photoelectron transition scheme, recomb. process anal. 0-44654  
 ZnS:Ag, TSC and induced impurity photoconductivity, existence of two electron trapping centres 0-44655  
 ZnS-metal interface in MIM struct., photoexcitation level assignment (*French*) 0-15622  
 ZnS,Se<sub>1-x</sub>, VPE, characterisation of defect centres by photoelectronic meas. 0-10914  
 ZnSe, cryst., elec. cond., dislocation motion effects 0-54710  
 n-ZnSe, long persistent cond. relax. and frozen cond. 0-54735  
 ZnSe/aqueous electrolyte junction, electrochem. behaviour in dark and under illum. 0-25003  
 ZnTe, photoinduced dielec. loss and capacitance changes, rel. to space charge polarisation 0-2417

**photoconductors** *see* **photoconducting materials****photocopying***see also* **electrophotography**

- exposure modulation during photoprinting of highly-contrasting negatives by electronic copier (*Russian*) 0-292  
 gradient index fibre array for photocopying machine 0-14482  
 gradient index lens array fabrication for office photocopier 0-13178  
 lens array design, Wood lens and gradient index fibre comparison 0-14479  
 pigmented organic photoreceptors for plain paper copying 0-49824

**photocurrent** *see* **photoconductivity; photoemission****photodetectors**

- coherent detection of partially coherent sources 0-47109  
 colour film densitometer with Si photodetector 0-4791  
 communication, conference, Amsterdam, Netherlands (Sep. 1979) 0-46733  
 displacement meas. of violin G-string under sinusoidal EM force 0-53540  
 distance meas. methods fundamentals, using twin diode technique (*German*) 0-13064  
 fibre optics communications, 1979 status and development trends 0-53408  
 fibre-optic delay line signal processing devices 0-48443  
 Fourier transform spectroscopy, photon and detector noise quantitative limit, definition (*German*) 0-9049  
 guided-wave optical signal processing, diode laser sources and photodetectors 0-48465  
 guided-wave optical systems and devices, seminar, Washington, USA (April 1979) 0-31418  
 III-V semiconductor emitters and detectors for 1.0-1.6  $\mu$  fibre-optic communications 0-10007  
 III-V semiconductors, p-n heterostructures, epitaxial growth techniques, appl. to optoelectronics, review 0-54770  
 integral error, matching to weighting function (*German*) 0-31876  
 integrated light-sensor device with broad operating range and enhanced-blue spectral response 0-13140  
 integrated optics appl., detectors development with and without optical coupler (*Czech*) 0-33227  
 integrated photoductive detector and waveguide struct. 0-48456  
 laser meas. appl., metrological certification, using acoustooptical modulators 0-23727  
 light-activated switch, photo-gate, pulse method of switching, circuit 0-42021  
 linearity meas. of photometric devices using two LEDs 0-17996  
 multichannel photoelectric systems, immersion optics 0-53405  
 multispectral linear array, pushbroom scan mode, satellite earth resources survey sensor appl. 0-56693  
 noncontact optical gauging by remote image tracking in production environment 0-8961  
 nonlinear photoelectric or photographic receiver signal value calc. (*German*) 0-31866  
 nonlinearity of low noise Si detectors, radiant flux ratio meas. 0-47089  
 open photoreceiver, vacuum ultraviolet 0-52307  
 optical memory readout by superluminescent diode with integrated photodetector 0-32922  
 optical phase measurement in real time using photodetector array, Fourier transform computation 0-9013  
 optical radar, logarithmic fast-response photodetector for atm. sounding, photometric properties 0-51585  
 optical receiver system, narrow-field, spherical aberration effect on radiation power losses 0-28299  
 optical/digital pattern recognition automated system 0-48175  
 optoelectronic devices and optical imaging techniques, book 0-27059  
 oscillating beam spectrometer for organic thin film transmission 0-18022  
 p-i-n laser detector, Si, wavelength and temp. depend. characts. 0-13134  
 photocathode polarisation sensitivity, two-beam interferometer expts. 0-4772  
 photodiode with IC amplifier, camera shutter control appl. (*German*) 0-52341  
 photoelectric converters, one-coordinate, signal processing algorithm 0-33199  
 photoelectron statistics, joint moment method, phase radiation 0-23647  
 quantum statistics of photocurrent in optimal light detector, atm. 'seeing' conditions 0-53244  
 spatial noise reduction in detector arrays, controlled lateral shifts 0-53436  
 spectral characteristics of MIS struct. with variable-gap semicond. 0-44735  
 spectral sensitivity meas. using two tandem monochromators (*Japanese*) 0-47107  
 telecentric imaging system focus detector 0-53397  
 thermal detectors and photodetectors, operating conditions and applications, review 0-47110  
 threshold sensitivity for semiconductor photography 0-18017  
 ultrahigh-speed photodetector design 0-47108  
 video disc information retrieval by optical readout 0-43284  
 X-ray fluorescence spectra, energy-dispersive, least-squares anal., detector response function approach 0-3457  
 Zn<sub>2</sub>P<sub>2</sub>, UV photoconductive detectors 0-4766  
 CdS,Se<sub>1-x</sub> photosensitive films, prep., props., and use for photodetectors 0-55298  
 GaAs MESFET, optical detector appl., sensitive high-speed device 0-13143  
 GaAs, planar ion-implanted avalanche photodiodes 0-22431  
 GaAs Schottky barrier diode, beat freq. generation between visible lasers 0-1253  
 Ga<sub>1-x</sub>In<sub>x</sub>As photodetectors for 1.3 micron PIN-FET receiver 0-13145  
 (Hg,Cd)Te photodiode IR detectors, planar technology 0-9043  
 (Hg,Cd)Te photodiodes, wide-bandwidth 10.6  $\mu$ m IR heterodyne detect. 0-9042  
 HgCdTe-CdTe IR detector arrays, 3 to 11  $\mu$ m, fabrication techniques 0-9041  
 Hg<sub>1-x</sub>Cd<sub>x</sub>Te Schottky barrier photodiodes, for IR detection 0-13144  
 In<sub>0.53</sub>Ga<sub>0.47</sub>As/InP avalanche photodetector 0-4764  
 Si, amorphous CVD film photodetector for picosecond pulses 0-47101  
 Si, for improved short-wavelength quantum efficiency 0-31874  
 Si photodetector, surface-barrier 0-4771  
 Si photodiode array for integrated optical spectrum analyser 0-33241  
 Si, shallow junction type, internal quantum efficiency meas. model fits, visible quantum yield 0-267

**photodielectric effect**

- cholesterol, dielectric props. under UV excitation 0-6912  
 cholic acid, dielectric props. under UV excitation 0-6912  
 haemoglobin, dielectric props. under UV excitation 0-6912  
 stationary recombination equations, analytical solutions in source limiting cases 0-44662  
 testosterone, dielectric props. under UV excitation 0-6912  
 Sb<sub>2</sub>Se<sub>3</sub>, photocond., photo-EMF and photodielectric effect, expts. 0-20245  
 ZnTe, photoinduced dielec. loss and capacitance changes, rel. to space charge polarisation 0-2417



**photodiffusion effects** *see* **Dember effect****photodiodes**

- see also avalanche photodiodes*  
 array, thermal behaviour (*French*) 0-37083  
 camera shading correction cct. used in chromosome anal. 0-56325  
 coeff. and surface conc. 0-39122  
 fibre optic communication systems, utilisation of optoelectronic devices 0-1328  
 integrated light-sensor device with broad operating range and enhanced-blue spectral response 0-13140  
 laser power radiation instability meas., of CW gas lasers 0-23704  
 linearity meas. of photometric devices using two LEDs 0-17996  
 narrow band gap semiconductor IR devices, advances 0-48464  
 optical fibre-photodiode alignment by etched Si structure 0-53430  
 optoelectronic devices and optical imaging techniques, book 0-27059  
 p-i-n laser detector, Si, wavelength and temp. depend. characts. 0-13134  
 photosensor with IC amplifier, camera shutter control appl. (*German*) 0-52341  
 reliability tests on devices for optical fibre transmission systems 0-43464  
 Schottky barrier, quantitative meas. of body motion using laser beam 0-12207  
 Schottky barrier IR detector, nomographs for parameter evaluation, 77K 0-31870  
 scintillation spectrometers, with LED and PIN photodiode, stabilising system 0-47821  
 self-scanning silicon photodiode array with microcomputer control 0-35612  
 solar power measurement, microcomputer-controlled photodiode light meter and thermistors 0-50946  
 telecentric system condenser alignment 0-33115  
 ultrahigh-speed photodetector design 0-47108  
 Al-GaAs-Al<sub>0.1</sub>Ga<sub>0.9</sub>As Schottky barrier diodes, prep., characts. 0-6948  
 Al-SiO<sub>2</sub>-Si, experimental verification of theoretical predictions 0-29485  
 Au-GaAs, photosensitivity losses, field and spectral depend. 0-2452  
 GaAs<sub>1-x</sub>Sb<sub>x</sub> photodiode structures, current-voltage characts., photo-EMF spectra 0-29472  
 GaInAs p-i-n/FET hybrid optical receiver for communication systems 0-33158  
 Ga<sub>1-x</sub>In<sub>x</sub>As photodetectors for 1.3 micron PIN-FET receiver 0-13145  
 Ga<sub>1-x</sub>Sb<sub>x</sub>p-n junction photodiode fabrication, sensitivity as 1 to 2.5  $\mu$ m detectors (*Japanese*) 0-52311  
 GaSb mesa photodetectors with very high quantum efficiency between 1.3 and 1.6  $\mu$ m 0-47102  
 Ge:Hg S-type diodes, photoelec. props. 0-6964  
 (Hg,Cd)Te n<sup>+</sup>-p photodiodes, 8 to 12  $\mu$ m IR imaging appls. 0-9044  
 (Hg,Cd)Te photodiode IR detectors, planar technology 0-9043  
 (Hg,Cd)Te photodiodes, wide-bandwidth 10.6  $\mu$ m IR heterodyne detect. 0-9042  
 HgCdTe Schottky barrier diode and n-p diffused junction IR detectors, comparison 0-9039  
 HgCdTe-CdTe IR detector arrays, 3 to 11  $\mu$ m, fabrication techniques 0-9041  
 Hg<sub>1-x</sub>Cd<sub>x</sub>Te photodiodes, implanted n<sup>+</sup>-p, improved performance using insulated field plates 0-52309  
 Hg<sub>1-x</sub>Cd<sub>x</sub>Te Schottky barrier photodiodes, for IR detection 0-13144  
 InGaAs, lattice-matched VPE on (100) InP, photodiode appl. 0-35102  
 InGaAs, VPE on (100) InP substrate, photodiodes fabricated 0-40267  
 InGaAs/InP p-i-n small area photodiodes, fabrication, characts. and performance in 274 Mb/s receivers at 1.31 microns 0-53415  
 In<sub>0.53</sub>Ga<sub>0.47</sub>As p-i-n photodiodes, for long-wavelength fibre-optic systems 0-5826  
 p-InGaAsP, on InP surface, diffusion coeff. and surface recombination velocity 0-39598  
 InGaAsP-InP photodiodes antireflectively coated with InP native oxide 0-13137  
 MoO<sub>3</sub>-Si, fabrication as function of O<sub>2</sub> partial press. 0-29464  
 PbSnTe(Se) Schottky barrier diode and n-p diffused junction IR detectors, comparison 0-9039  
 Si, amorphous, photovoltaic diodes, influence of mag. field on charge transport 0-49891  
 Si, for position-sensitive X-ray detector 0-52831  
 Si photodiode array for integrated optical spectrum analyser 0-33241  
 Si, photodiode array for radiation detection in AES and analytical appl. (*German*) 0-11992  
 Si, Schottky diodes on sputtered amorphous Si:H, light induced ageing effects, interpretation of photovoltaic stability 0-54780  
 Si:H, amorphous, Schottky diode, spectral response and hole drift mobility 0-39673

**photodisintegration**

- see also deuteron photodisintegration; photofission*  
<sup>3</sup>H( $\gamma$ ,X) two- and three-body photodisintegration cross sections 0-32263  
<sup>4</sup>He, soft-core radial wave function, photo-disintegration calculation 0-18209

**photodissociation**

- see also molecular photodissociation*  
 cryptoleurine derivatives, absorpt. and fluoresc. obs. of photodecomp. processes, dye laser relevance 0-55686  
 ortho-hydroxybenzophenone, soln., intramol. proton transfer and energy relax. photostability, transient absorption obs. 0-28032  
 ionosphere D-region, sunrise variations of negative ions and electron conc. 0-31157  
 oxazine dyes, comparative photostability 0-3376  
 polymers, synthetic, radiative degradation, chem., phys., environmental, technological effects, review 0-40948  
 I photodissociation laser, high-power, pulse amplification 0-48234  
 NH<sub>3</sub>, appl. to solar energy conversion 0-30513

**photodissociation of molecules** *see* **molecular photodissociation****photoelasticity**

- see also mechanical birefringence*  
 axisymmetric problem, simplification 0-38272  
 basic concepts 0-14637  
 birefringence measurement using photoelastic modulator 0-31838  
 birefringent, rotating, and achromatic quarter wave plates, appl. to ellipsometry and photoelasticity (*French*) 0-14278  
 circular ring, inner boundary shapes, optimised, diametral compression 0-38369  
 composites, appl. of exptl. methods to fracture 0-11869  
 constitutive relations in photomechanics 0-43251  
 crack, stress concentration near apex, elasticity theory and photoelastic expts. 0-23959

**photoelasticity continued**

- crack growth, 3-D geometric effects, implications for composite material structures 0-10204  
 crack tip mixed mode isochromatic fringe patterns 0-28464  
 cylindrical shell, stress concentration near inclined holes 0-33460  
 dielectric bodies, stress determ. using EM waves 0-38370  
 dielectric permeability sound wave induced nonlinear modulation (*Russian*) 0-16008  
 discs, static and dynamic contact conditions obs. (*Japanese*) 0-23970  
 elasto-optical detection of gravitational waves 0-126  
 elastooptical constants and refractive index, thermo-optical method for meas. 0-7327  
 epoxy resin (Araldite B), photothermoelasticity meas. by heating method 0-6000  
 error assessment using euidensity fringes 0-28475  
 fracture studies 0-38358  
 fringe pattern analyser, computer aided 0-38359  
 fringe photography, improved photograph quality 0-27364  
 GaAs epitaxial layer photoelastic channel optical waveguides 0-48457  
 glass, float, surface stress meas. by optical waveguide effect 0-43681  
 gravitational radiation detection method, elastooptical antenna, photoelastic effect 0-46947  
 holographic photoelasticity, Faradays effect appl. (*Chinese*) 0-5998  
 integrated retardation technique, rotationally symmetrical bodies, thermal stress 0-38362  
 ionic crystals, evaluation of photoelastic consts. 0-50297  
 isochromatic crack tip fringe patterns, dynamic 3-parameter method for stress intensity factors 0-38365  
 load meas. and testing (*German*) 0-19297  
 mode I stress intensity factors, method of caustics 0-38364  
 nematic liquid crystal, flexural elasticity meas. (*Dutch*) 0-34112  
 nonlinear photomechanics, birefringence in polymers, stress anal. appl. 0-33545  
 optical fibre hydrophone sensitivity, strain configs. 0-23771  
 optical fibre waveguide transmission, mechanical stresses effect 0-10032  
 optically isotropic mats., stress intensity factor determ. by dynamic method of caustics 0-33546  
 piezoelectric semiconductors, photoelasticity and acousto-optic diff. 0-29715  
 plane isotropic elastic medium, photoelastic determ. of complex stress intensity factors 0-43664  
 PMMA, glassy, photoelasticity 0-45034  
 polybutadienes, use of high modulus inclusion gauge, in stress analysis 0-21254  
 polymer, birefringent, stress intensity factor determ. 0-14633  
 polymer, brittle photoelastic, use of gelatin gels in prep. for optical polarization stress study 0-40325  
 polymer films, ultrathin, photochemical props., transducer appl. 0-37020  
 polymer granules, compression, stress state by photoelasticity method 0-10218  
 quartz, Dauphine twinning, stress-induced, acoustic emissions and photoelastic effect obs. 0-6414  
 scattered light, for meas. of stress distrib. in cubic single crystals (*Russian*) 0-7326  
 shell subjected to centrifugal force, stress anal. (*German*) 0-23900  
 stress analysis method, automatic, of photoelastic fringes 0-14639  
 stress field components measurement, integrated plane photoelastic isodynes method 0-14638  
 stress intensity factors, mixed mode, photoelastic determ., notch effects 0-14632  
 stress intensity factors, photoelastic meas. correlation, for various specimen and defect geometries (*German*) 0-53727  
 stress measurement method for crystals, appl. to Si 0-48656  
 thermal stress determ. circumferentially grooved cylinder 0-38363  
 transition metal dichalcogenides, layered, surface Brillouin scatt. obs., surface ripple and elasto-optic mechanisms 0-16048  
 US waves in liquids, photoelastic visualisation 0-28374  
 CsH<sub>2</sub>AsO<sub>4</sub>, elastic props., photoelasticity near ferroelectric phase transition 0-29107  
 Cs<sub>2</sub>NaBiCl<sub>6</sub>, optical, photoelastic, acoustooptic props. 0-55064  
 GaAs, birefringence, photoelastic consts. dispersion 0-11361  
 GaAs, surface Brillouin scattering from acoustic phonons 0-55113  
 GaP, birefringence, photoelastic consts. dispersion 0-11361  
 KCl, stress distrib., meas. by scattered light photoelasticity (*Russian*) 0-7326  
 MnF<sub>2</sub>, magnetic, thermal, elastic refraction of light, mag. order influence on refractive index (*Russian*) 0-34880  
 NaCl(Br) (F) (I), lattice dynamics and statics, three-body-force shell model 0-49323  
 PbCl<sub>2</sub> crystals, acousto-optical props. and photoelasticity 0-40085  
 RbBr(Cl)(I), evaluation of photoelastic consts. 0-50297  
 Si, appl. of photoelastic stress meas. technique 0-48656  
 Si, surface Brillouin scatt. from acoustic phonons 0-55113
- photoelectrets**  
 dielectric-photosemiconductor two component systems, photoelectret state 0-25287  
 internal counter-EMF determ. by pot. meas 0-45003  
 narrow band gap semiconductor electrophotographic processes 0-13169  
 Ba<sub>2</sub>Sr<sub>1-x</sub>Nb<sub>2</sub>O<sub>6</sub>, ferroelectric with diffused phase transition, photoelectret states 0-20583  
 Bi<sub>12</sub>GeO<sub>20</sub>, mechanism of creation of internal fields and photoelectret effect 0-25290  
 Bi<sub>12</sub>GeO<sub>20</sub>, photoelectret state 0-11315  
 Bi<sub>12</sub>SiO<sub>20</sub>, mechanism of creation of internal fields and photoelectret effect 0-25290  
 Bi<sub>12</sub>SiO<sub>20</sub> photoelectret, in optical processing and X,  $\gamma$  ray imaging 0-23764  
 CdTe film, photopolarisation 0-25286  
 PbMg<sub>1/3</sub>Nb<sub>2/3</sub>O<sub>3</sub>, ferroelectric with diffused phase transition, photoelectret states 0-20583
- photoelectric cells**  
*see also photoconductive cells; photovoltaic cells*  
 angular meas. by Fraunhofer diffraction pattern, appls. (*Japanese*) 0-52159  
 mechanical component features comparative metrology, misalignment meas. using photocell 0-31716  
 solar photoelectric conversion cost reduction (*Italian*) 0-30479  
 n-CdGeP<sub>2</sub>-p-CdGeAs<sub>2</sub> heterojunction photocells, polarisation-sensitive 0-11075  
 p-Si inversion-channel photoelectric cell characteristic (*Russian*) 0-49941



**photoelectric devices**

- see also *image sensors; photocathodes; photoconducting devices; phototubes*
- angular displacement transducer, accuracy 0-8977  
 condensation nucleus counter with digital recording 0-8448  
 fibre optic sensor for photoelectric recording, design 0-28338  
 luxmeter design using linear ICs (*Rumanian*) 0-17993  
 multichannel photoelectric systems, immersion optics 0-53405  
 scanner for spectrometer, vacuum UV molecular photoabsorpt. cross-section meas. 0-37096  
 turbidimeter (*Polish*) 0-31840  
 vernier sine-cosine angle converters, output signal eqn. 0-10031

**photoelectric effects** see *photoelectricity***photoelectric electron emission** see *photoemission***photoelectric emission** see *photoemission***photoelectric tubes** see *phototubes***photoelectricity**

- see also *Dember effect; photocapacitance; photoconductivity; photodielectric effect; photoelectrets; photoelectromagnetic effects; photoemission; photoionisation; photorefractive effect; photovoltaic effects*
- amorphous and liquid semiconductors, conference, Cambridge, MA, USA (Aug. 1979) 0-41933  
 bacteriorhodopsin generated photocurrents on planar bilayer membranes 0-51050  
 compensated semiconductor, theory of transient processes 0-24930  
 Einstein's nonrelativistic work (*Czech*) 0-27095  
 Einstein and the quantum theory, review 0-22237  
 MISS, potential barrier height determ. using photoelectric methods (*Polish*) 0-20317  
 optical information, two-dimensional, correlation reduction in course of photoelectric registration 0-19000  
 organic semiconductor photoelectrode processes and effects (*German*) 0-26145  
 p-n junction, electrical parameters, optical derivative meas. 0-2455  
 photoferroelectrics, book 0-2702  
 quantum utilizing solar energy convertor efficiency in absence of intraband thermalisation 0-26144  
 semiconductor, inhomogeneity effects on thermoelec. and photothermoelec. power meas. 0-54728  
 semiconductor-metal surface-barrier struct., photoelec. effect, theoretical anal. 0-15564  
 semiconductors, disordered, light induced stationary non-equilibrium distribution of electrons, balance equation 0-39528  
 shock compression of solids, review 0-24534  
 transition metal compounds, valence band struct., X-ray spectroscopic study 0-29319  
 As<sub>2</sub>S<sub>3</sub>-Ag system, photosensitivity depend. on As<sub>2</sub>S<sub>3</sub> thickness (*Russian*) 0-54784  
 As<sub>2</sub>S<sub>3</sub>-Ag system, photosensitivity depend. on metallic layer thickness (*Russian*) 0-54785  
 Au-Ga<sub>1-x</sub>Al<sub>x</sub>As variable-gap surface-barrier struct., photoelectric effect 0-39634  
 Cd-GeO<sub>4</sub>, n-type, prep. and photoelectronic props. 0-39628  
 CdS, and CdS<sub>1-x</sub>Se<sub>x</sub>, thermoelec. and photothermoelec. power meas., inhomogeneity effects 0-54728  
 CdS film, chemically sprayed, carrier conc. and mobility, thermoelec. and photothermoelectric meas. 0-2503  
 CdS photosensitive film production from chelated metallo-organic compounds (*Russian*) 0-49813  
 CdSe photosensitive film production from chelated metallo-organic compounds (*Russian*) 0-49813  
 CdSe:Cu impurity light absorpt. for current control in negative resistance region 0-11052  
 CuInSe<sub>2</sub>-CuInS<sub>2</sub>, solid soln., photo-EMF spectra 0-20248  
 Cu-S-CdS heterojunction, photoelectric props. 0-29467  
 GaP, transverse acoustoelec. voltage spectroscopy and photoenhanced acoustoelec. effect 0-49828  
 Ge, homopolar semiconductor, quantum efficiency 0-20254  
 Ge surface, optical charging meas., 120-300K 0-49817  
 Ge, surface recomb. before and after laser annealing, 10-μm transmission meas. 0-1247  
 Ge:Hg S-type diodes, photoelec. props. 0-6964  
 InAs, transverse acoustoelec. voltage spectroscopy and photoenhanced acoustoelec. effect 0-49828  
 InSb, MIS struct., background radiation effect on photoelec. processes 0-25015  
 Pb<sub>1-x</sub>Sn<sub>x</sub>Te, photoelec. props. 30 to 4.2K, temp. depend. of electron density 0-20246  
 Se, electroradiographic layer, radiographic contrast 0-12241  
 Si, homopolar semiconductor, quantum efficiency 0-20254  
 Si surface layers, impurities, elec. and photoelec. props. 0-2298  
 SnO<sub>2</sub>-InSe n-n heterostructures, photoelec. props., 80 to 300K 0-20297  
 Ti-TiO<sub>2</sub>-Au diode, spectral photoresponse and I-V characs. 0-15617

**photoelectrochemical cells**

- see also *solar cells*
- developments, conversion efficiency estimates for different cells 0-50993  
 hydride concentration cells for solar conversion 0-35698  
 laser applications in photoelectrochemistry for solar energy conversion 0-40873  
 liquid-junction solar cells, Schottky barrier height, photovoltage and photocurrent 0-26162  
 low cost solar cells 0-50972  
 material aspects of solar conversion systems, charge transport, energy output 0-12022  
 MB<sup>+</sup>-Fe<sup>2+</sup> system, solar energy utilisation (*German*) 0-45713  
 metal electrodes in contact with fluorescent dye solns., photovoltage generation, comprehensive model 0-40871  
 metalloporphyrins, photoelectrochemical props. 0-50991  
 n-type semiconductor anode, illum., charge transfer modes, digital simulation 0-2464  
 organic semiconductor photoelectrode processes and effects (*German*) 0-26145  
 photoelectrolysis cells, props. of oxide-based heterostruct. photoelectrodes 0-12023  
 polyacetylene photoelectrochemical solar cell, fabrication and efficiency 0-50954  
 secondary cells, Pb/acid, design and performance characteristics for remote photovoltaic applications 0-55833  
 semiconductor based, interaction of light and transport control 0-12020  
 semiconductor photoanodes, corrosion stability 0-21130

**photoelectrochemical cells continued**

- solar, function and construction of regenerative cell 0-26147  
 solar cells, design and operation, underlying theoretical principles 0-40872  
 solar cells, power conversion efficiency monitoring 0-50989  
 solar cells, semiconductor/redox electrolyte junctions, functions examples and problems 0-45714  
 solar energy conversion, chlorophyll sensitised reactions 0-7948  
 solar energy conversion, photo-electrochemical production of C-C bonds from carbon dioxide 0-21407  
 solar energy conversion and storage appl., EDTA-methylene blue cells props. obs. 0-21406  
 solar energy conversion principles, review 0-35695  
 solar energy utilisation (*German*) 0-45713  
 surface aspects 0-12021  
 thiazine dye-Fe photoelectrochem. cells for H<sub>2</sub> production, cell instabilities 0-16814  
 TTF polymer thin film batteries 0-45709  
 Ag/AgCl photogalvanic cells for solar energy conversion, basic electrochemistry 0-45715  
 Cd-S-Fe regenerative cell for photoelectrolytic H prod. 0-51016  
 CdS polycrystalline thin-film liq. junction photovolt. cell 0-50988  
 CdS(Se) photoanodes, effect of S(Se) substitution, photoelectron spectroscopy obs. 0-2463  
 CdSe electrochem. photovoltaic cells, effect of thin film electrode prep. and conc. on efficiency 0-55847  
 CdSnO<sub>3</sub>, single crystals, elec. props. 0-6978  
 Cd<sub>2</sub>SnO<sub>4</sub>, single crystals, elec. props. 0-6978  
 Fe-thionine cells 0-50993  
 Fe-thionine homo/heterogeneous cells, power output enhancement 0-45711  
 Fe-thionine homogeneous cells, power output enhancement 0-45710  
 Fe-thionine photogalvanic, cells 0-35696  
 n-Fe<sub>2</sub>O<sub>3</sub> electrodes, enhanced photoeffects by electrocatalysis and peroxide effects 0-16815  
 GaAs photoanode, using n/n<sup>+</sup> struct., power conversion efficiency 0-50990  
 n-GaAs/K<sub>2</sub>Se-K<sub>2</sub>Se<sub>2</sub>-KOH/C solar cell, Ru (III) chemisorption on photoanode, effect on performance 0-3516  
 n-GaAs/K<sub>2</sub>Se-K<sub>2</sub>Se<sub>2</sub>-KOH/C liq. junction cell, effect of Ru ion chemisorption on grain boundaries 0-55879  
 p-GaP semiconductor-electrolyte solar cells for photochemical reduction of CO<sub>2</sub> to organic fuel 0-55880  
 p-GaP-NaOH-Pt cell, H<sub>2</sub> evolution quantum efficiency potential characs. 0-55673  
 H photoelectrolytic production by H<sub>2</sub>O decomposition using sunlight, cell energetics 0-45774  
 H<sub>2</sub> production using solar energy and Zn(Mg)(Cr)(Ni) phthalocyanine dyes (*French*) 0-55936  
 LaCrO<sub>3</sub>-TiO<sub>2</sub> photoactive anode, for photoelectrolytic production of H<sub>2</sub> and electricity 0-12024  
 MoSe<sub>2</sub>-I<sup>-</sup>, photoelectrode, time resolved photocurrent, nanosecond excitation 0-45708  
 Ru complex, tris-(2,2'-bipyridyl)-Ru(II) complex, photoelectrochemical systems, solar energy utilisation (*German*) 0-45713  
 TiO<sub>2</sub> electrode, doping density dependent attachment of rhodamine B 0-54777  
 TiO<sub>2</sub> electrodes, in aq. electrolytes, surface states, photocurrent obs. 0-49895  
 TiO<sub>2</sub> electrodes in photoelectrochem. cell, photothermal effect 0-7947  
 n-TiO<sub>2</sub> photoanodes, corrosion suppression mechanism 0-2462  
 TiO<sub>2</sub> semicond. films for water photoelectrolysis 0-26146  
 TiO<sub>2</sub>, solar energy utilisation (*German*) 0-45713  
 n-TiO<sub>2</sub>:Be electrodes, photoassisted oxidation of water 0-30502  
 TiO<sub>2</sub>:H photoanodes, diffusion and surface chemistry 0-35546  
 n-TiO<sub>2</sub>-electrolyte interface, charge-transfer-controlled photocurrent 0-50992  
 TiO<sub>2</sub>-LaCrO<sub>3</sub>-GaP photoelectrochem. reactor for materials synthesis using solar energy 0-45712  
 TiO<sub>2</sub>-Si solar cell hybrid electrodes for photoelectrochem. H prod. 0-45775  
 ZnO sintered electrode, for dye-sensitised solar photocell 0-16816

**photoelectromagnetic effects**

- semiconductor, highly excited, photomagnetolectric effect under Auger recombination 0-44664  
 Shubnikov de Haas type of photomag. effect, monotonic component of quantum oscils. 0-49818  
 Cd<sub>2</sub>Hg<sub>1-x</sub>Te, effects of electron heating at low temps. 0-49823  
 Cd<sub>2</sub>Hg<sub>1-x</sub>Te, photomagnetic and galvanomagnetic effects in quantising mag. fields 0-20223  
 n-GaSe, photomagnetolectric effect, photocond., in presence of traps 0-39631  
 n-InSb, optical phonon emission in intraband magneto-optical transitions, photocond. meas. 0-34481  
 n-InSb, three-phonon assisted cyclotron harmonic transitions in magneto-photoconductivity 0-44652

**photoelectron multipliers** see *photomultipliers***photoelectron spectra**

- see also *Auger effect; photoemission; X-ray photoelectron spectra*
- acetylene, angular dependent photoelectron spectral meas. 0-28060  
 acetylene, electron propagator theory for mol. electron binding energies and photoionis. intensities 0-47848  
 acetylene, photoelectron spectrum, satellite line intensity, photon energy depend. 0-53042  
 acrolein, excitation, ionisation and electron affinity, expts., HAM/3 calcs. 0-18790  
 adsorbates, photoexcitation theory rel. to angle-resolved UPS and surface EXAFS 0-39426  
 adsorbates deep level spectroscopy, many body effects 0-39441  
 adsorbed atom on solid surface, photoemission from valence band, surface plasmon emission, model Hamiltonian calcs. 0-50525  
 adsorbed Xe layers, on Pd-Pt, Ir, and Ru, 5p photoemission, local surface struct. influence 0-2920  
 alkali graphite intercalation compound, evidence for alkali-like cond. bands 0-45201  
 alkali graphite intercalation compounds, evidence for alkali-like conduction band, UPS study 0-45208  
 alkali metal atom, outer-shell photoelectron ang. distrib. 0-37797  
 alkali metal atom, two-photon ionis. with two light beams, photoelectron polaris. 0-43011



**photoelectron spectra continued**

alkyl substituted diacetylene radical cations, optical emission and photoelectron spectra, fragmentation decay 0-53004  
 atomic and electronic struct. 0-54746  
 azobenzene, derivatives, photoelectron spectra, ionisation pot., electronic struct. determ. 0-1024  
 benzene, UV photoelectron spectra, valence electron shake up approx. methods 0-18788  
 bulk bands of solids, electron-phonon interaction effects 0-20767  
 trans-2-butene, charge transfer mass spectra and photoelectron spectra 0-40778  
 chalcogens, photoionisation cross sections and ang. distrib., outer p subshell 0-9572  
 chlorobenzene ion fragmentation, kinetic shift and phenyl ion heat at formation, photoelectron-photoion coincidence meas. 0-25998  
 collective effects, relax. and localisation of hole levels 0-52950  
 core ionisation in 3d, 4f and 5f series, rearrangement effects 0-53065  
 cyclopropene, photoionisation and threshold photoelectron-photoion coincidence study 0-53062  
 dicyanodiacetylene radical cation, photoelectron and emission spectra 0-5558  
 diene-iron tricarbonyl complexes,  $\pi$ -orbital perturbation energies, ionisation energies; UV photoelectron spectra 0-32775  
 diynes, acyclic, non-conjugated, UPS comparison, obs. and calc. 0-32772  
 ethylene, autoionisation and photoemitted electron ang. distrib., cylindrical mirror analyser study 0-18049  
 ethylene, photoelectron spectrosc., ang. depend. 0-9641  
 ethylene, UV photoelectron spectra, valence electron shake up approx. methods 0-18788  
 ethylene glycol, conformational anal., photoelectron spect. 0-43107  
 fluoroethylenes, variable angle photoelectron spectra, ionisation pot. asymmetry parameter 0-28064  
 formamide, photoelectron spectrum, Green's function calcs., satellite lines 0-28061  
 formyl radical,  $-d_0$ ,  $(-d_1)$ , first ionis. pot., photoelectron spectrosc. determ. 0-48039  
 graphite, band struct. determ. by angle-resolved photoemission 0-45203  
 graphite, photoemission, C 1s core-electron line shape, excitonic effects, Fermi energy and hole density of states 0-29848  
 graphite-alkali metal intercalation cpds., electronic props. 0-45202  
 Group IV-VI diatomic molecules, He(I) photoelectron spectra, calcs. 0-1023  
 halogens, photoionisation cross sections and ang. distrib., outer p subshell 0-9572  
 hexafluoro ethyl cation fragmentation, mass spectrometry 0-53070  
 high temp. vapours 0-52238  
 hole recoil, vibrational shake-up and photoelectron lineshapes, in mols. and solids 0-55265  
 ion fragmentation mechanisms and photoelectron spectroscopy, book contrib. 0-14179  
 isobutylene, photoelectron spectrosc., ang. depend. 0-9641  
 isocyanates, nonbonding and  $\pi$ -orbital interactions, photoelectron spectra 0-32774  
 isothiocyanates, nonbonding and  $\pi$ -orbital interactions, photoelectron spectra 0-32774  
 labile species, electron photoejection, reaction kinetics characterisation 0-26089  
 large molecule, electronic struct., photoemission and optical absorpt. spectrum, CNDO/S3 model 0-53172  
 metal conduction electron photoemission spectrum, effect of recoil on shake-up spectra, infinite summation method 0-50526  
 metal surface, chemisorption bonding anal. using PES 0-10791  
 metal surface photoemission, spatially-varying photon field effects 0-2921  
 metal-InP contacts, intermediate adsorbed layer effect on electronic props. 0-39674  
 methane, photoelectron ang. distrib., near threshold to 30 eV, photon energy depend. 0-53045  
 3-methyleneoxetane, electron structure, orbital-O interaction, MO calcs., UV photoelectron spectra 0-28058  
 negative ions, autodetachment, spectroscopy 0-23385  
 organic compounds, HeI photoelectron spectra (*Japanese*) 0-16150  
 organic ion, excited electronic state correlation with mass-spectral fragmentation pattern 0-45482  
 organic molecular crystals, photoemission, book contrib. 0-16158  
 organic molecules, UV photoelectron spectroscopy, systematic review 0-28057  
 organic samples on metal supports, origin of photo-electron-microscope pictures 0-26431  
 3-oxetanone, electron structure, orbital-O interaction, MO calcs., UV photoelectron spectra 0-28058  
 polyatomic molecule, multiphoton absorpt. resons., dynamic Stark splitting 0-9670  
 polyethylene-metal contact charging, electron transfer mechanism, PES characts. 0-35055  
 $\beta$ -propiolactone, electron structure, orbital-O interaction, MO calcs., UV photoelectron spectra 0-28058  
 rare earth pnictides, prep. and props., book contrib. 0-54212  
 rare earths, and their alloys and cpds., book contrib. 0-16157  
 t-RNA, rot. relax. time,  $10^{-9}$ s range Fabry-Perot and photoelectron time of arrival method 0-21437  
 semiconductor, surface electronic props., optical spectroscopic techniques, review 0-11070  
 semiconductor-oxide interface and Schottky barriers, photoemission and Auger spectroscopy 0-50536  
 semiconductors, photoelectron spectra and band struct., book contrib. 0-16155  
 simple metals, photoemission theory, book contrib. 0-16159  
 solids, book 0-12860  
 surface anal., deconvolution of exptl. curves (*French*) 0-16153  
 surface chemical bonding, electron spectroscopy, book contrib. 0-24992  
 TCNQ, charge transfer complexes, changes in valence electronic structure 0-7477  
 ternary semiconductor,  $A^{II}B^{III}C^{VI}$ , crystal structure effects in electronic states 0-20085  
 tetramethylethylene, photoelectron spectrosc., ang. depend. 0-9641  
 theory, techniques, and appl., book 0-8748  
 thiocyanates, nonbonding and  $\pi$ -orbital interactions, photoelectron spectra 0-32774  
 transient species, vacuum UPS, book contrib. 0-14178  
 transition metal dihalides, MS potential from a set of overlapping densities 0-52850

**photoelectron spectra continued**

transition metal monosulphides of first-row, XPES and UV PES 0-20760  
 transition metals, and their alloys and cpds., book contrib. 0-16156  
 transition metals, photoemission spectra, core-level satellite struct. 0-29855  
 triethylamine-perfluoro-T-butanol, photoelectron and Rydberg bands, UV spectra study 0-18865  
 trimethylethylene, photoelectron spectrosc., ang. depend. 0-9641  
 UPS, angle-resolved, initial state symmetries from polarisation effects 0-40227  
 UPS ultrahigh vacuum apparatus, appl. to clean and gas covered Si(III) surfaces (*Japanese*) 0-37125  
 vapours, oven heated inorganic solids, charact. technique 0-52239  
 X-ray intensity due to photoelectrons, calc. for fluorescence anal. 0-26075  
 yield from monocrystals under X-ray diffr. conditions, meas. method 0-50521  
 Ag, 4d level He II photoelectron spectra, energies and intensities 0-5511  
 Ag (100) and (111) epitaxial films, ang. depend. UPS 0-55270  
 Ag, adsorption and surface reaction of formic acid 0-40741  
 Ag-O-Cs photocathode, Ag colloidal particles and long wavelength response (*Chinese*) 0-45195  
 (AgBr)<sub>3</sub>, gas, He(I) photoelectron spectra 0-43103  
 (AgCl)<sub>3</sub>, gas, He(I) photoelectron spectra 0-43103  
 AgI, superionic conductor, density of valence states, photoelectron spectra meas. 0-25523  
 (AgI)<sub>3</sub>, gas, He(I) photoelectron spectra 0-43103  
 Al (111), ordered O overlayer, angle-resolved photoemission, band struct. 0-40229  
 Al caesiated thin film, surface plasma wave excitation by polarised light, photoemission obs. 0-50518  
 Al clean films, O<sub>2</sub> interaction study using synchrotron-radiation-induced-photoemission 0-55709  
 Al, surface broadening of 2p core level photoemission spectra 0-25524  
 Al-SiO<sub>2</sub>, surface reactions and interdiffusion, photoemission study 0-49532  
 Ar, ns- $\rightarrow$ ep photoelectrons, spin polarisation 0-37792  
 Ar, photoelectron emission, polarisation depend. on incident unpolarised VUV radiation wavelength 0-52952  
 Ar, plane polarised VUV irradi., emitted photoelectron polarisation, ang. depend. 0-47952  
 As-Se amorphous film, density of upper valence band states, annealing effects, UPS obs. 0-29845  
 Au, 4f-subshell photoionisation cross section, energy depend. from Auger and photoelectron spectra 0-35057  
 Au (100), normal and reconstructed, electronic struct. changes, ang. resolved photoemission obs. 0-25520  
 Au, photoelectron spectra, bulk and surface, rel. to band struct. 0-20770  
 Au-Si interface, valence band and core levels, Si diffusion, alloy form., photoelectron spectra obs. 0-45205  
 Ba, 5p<sub>3/2</sub> level broadening, ligand field splitting, photoelectron spectra 0-47950  
 Bi, liquid and solid, UPS, optical densities of states 0-2924  
 BrN<sub>3</sub>, VPS obs., comparison with ab initio and semi-empirical calcs. 0-53043  
 BrNCO, VPS obs., comparison with ab initio and semi-empirical calcs. 0-53043  
 C<sub>2</sub>N<sub>2</sub>, and C<sub>2</sub>N<sub>2</sub><sup>+</sup>, electronic struct. UV and PE spectra 0-23304  
 C<sub>2</sub>N<sub>2</sub>, satellite struct. of electron spectra, CI and vibronic coupling, dynamical calc. 0-53044  
 CO, photoelectron ang. distrib., photon energy depend., 16-25 eV 0-53046  
 CO<sub>2</sub>, spin polarised photoelectrons, synchrotron excited 0-43101  
 CS<sub>2</sub>, photoelectron spectrum, spin-orbit splitting, excited state form. 0-43102  
 Cd 1, 4d<sup>10</sup> subshell photoelectron ang. distrib. 0-14123  
 CdF<sub>2</sub>, electronic structure of outermost levels, UPS study 0-7468  
 CdIn<sub>2</sub>S<sub>4</sub>, electronic states, sensitivity to cryst. struct., UPS study 0-45209  
 CdS(Se) photoanodes, effect of S(Se) substitution, photoelectron spectroscopy obs. 0-2463  
 $\gamma$ -Ce, photoelectron spectra, 4f level position 0-25519  
 CIN<sub>3</sub>, VPS obs., comparison with ab initio and semi-empirical calcs. 0-53043  
 CINCO, VPS obs., comparison with ab initio and semi-empirical calcs. 0-53043  
 Co (0001) surface state, photoemission and synchrotron radiation obs., symmetry determ. 0-20771  
 Co<sub>2</sub>B, crystalline, photoemission and electronic struct. 0-2926  
 Co<sub>78</sub>P<sub>14</sub>B<sub>8</sub>, amorphous, photoemission and electronic struct. 0-2926  
 Cr (100), adsorption of O<sub>2</sub> and initial oxidation at room temp. 0-20034  
 Cs, He II  $\alpha$  5p<sup>-1</sup> photoelectron spectrum, config. interaction effects 0-5510  
 Cu, (100) and (111), surface states, d-band, angle-resolved photoemission spectra obs. 0-20768  
 Cu (100) surface, angle-resolved PES study 0-55273  
 Cu, (100) surface, UPS, two-electron reson. at 3p threshold, rel. to Ni 0-25522  
 Cu (110), adsorption of pyridine, angle-resolved photoemission, selection rules 0-40231  
 Cu (111) surface band energy shift upon adsorption of Cs and O, angle-resolved UPS study 0-40228  
 Cu (111)/Cs, adsorption-induced changes of photoemission spectra and surface electronic struct. 0-55260  
 Cu, adsorption and surface reaction of formic acid 0-40741  
 Cu, band structure and high-resolution normal emission UPS 0-6712  
 Cu, final energy bands, high energy, angle resolved photoemission 0-2327  
 Cu-Ni (100), UPS spectra, direct transition and matrix element effects 0-55268  
 Cu-Zr, metallic glasses, valence band struct. investigation 0-11533  
 (CuBr)<sub>3</sub>, gas, He(I) photoelectron spectra 0-43103  
 CuCl, UPS meas., electronic struct. 0-50529  
 (CuCl)<sub>3</sub>, gas, He(I) photoelectron spectra 0-43103  
 CuCl<sub>4</sub><sup>2-</sup>, core ionisation in 3d, 4f and 5f series, rearrangement effects 0-53065  
 Cu(111) surface, UPS at const. wavevector component 0-16151  
 ErFe<sub>2</sub>, surface, effect of H and O adsorption, spin polarised photoemission study 0-29854  
 Fe, adsorption and surface reaction of formic acid 0-40741  
 Fe, ferromagnetic, chemisorption of H, spin-spin interactions, UPS spectra calc. 0-6630  
 FeO, valence band XPS and UPS, LCAO-MO calcs. 0-45197



**photoelectron spectra continued**

- Fe(110) surface covered with C, O, N, S, CO adsorption, photoemission spectroscopy study 0-54527  
 Ga, transition from ordered solid to disordered liquid, viewed by photoemission 0-45217  
 GaAs (100), angle-resolved photoemission spectra 0-50516  
 GaAs (100) and (110), photoelectrons spin polarisation 0-11530  
 GaAs (100) surface struct. determ. by LEED, UPS, and EPR 0-49475  
 GaAs, (100) surfaces, reconstructed, ang. resolved photoemission from surface states, adsorption and annealing effects 0-16143  
 GaAs (110), adsorption of In, N, P, and As, UPS and EELS study, tight-binding calcs. 0-49496  
 GaAs (110), adsorption of O<sub>2</sub>, oxide form., XPS/UPS study 0-49497  
 GaAs (110), chemisorption of Cl, photoemission spectra and tight-binding calcs. 0-6629  
 GaAs (110), chemisorption site geometry and interface electronic struct. of Al and Ga, photoelectron spectra 0-49843  
 GaAs (110) surface, O<sub>2</sub> interaction, order-disorder effects, LEED, UPS anal. 0-6634  
 GaAs, angle-resolved photoemission and valence band dispersions 0-7469  
 GaAs, surface, electron struct. and Fermi level pinning by O<sub>2</sub> and metals 0-11066  
 GaAs, surface electron states, (110), photoemission 0-25529  
 p-GaAs: Cd, (110) cleaved surface, defect-induced surface states 0-6925  
 GaAs:Cs, oxidation process, UPS obs. 0-50511  
 GaAs/III-V solid soln. heterostructure composition profile by photoemission microanalysis 0-44717  
 GaAs-Al(Ga)(Ge), surface reactions and interdiffusion, photoemission study 0-49532  
 GaAs-Ge interface, photoemission 0-25530  
 GaAs(110) surface, adsorption of water and methanol, UPS study 0-6632  
 GaP (110), electronic surface states, initial steps of O<sub>2</sub> chemisorption 0-49844  
 GaP, cleaved (110) surface, electron surface props. 0-11067  
 GaS<sub>2</sub>Se<sub>1-x</sub>, wavefunction symm. and binding energies, synchrotron radiation photoemission spectroscopy 0-50532  
 GaSb (110), chemisorption of Cl, photoemission spectra and tight-binding calcs. 0-6629  
 GaSb (110), oxidation, initial stages, photoemission study 0-16529  
 GaSb, surface, electron struct. and Fermi level pinning by O<sub>2</sub> and metals 0-11066  
 GaSe, core level excitation effects, synchrotron radiation UPS study 0-40234  
 GaSe, photoyield reson. enhancement near Se 3d core threshold, photoelectron spectra obs. 0-45207  
 Ge (111) surface, clean and CO-covered, UPS and ion-neutralisation spectroscopy 0-10785  
 Ge photocathodes, Au adsorbed photofield emission current spectral investigation 0-29856  
 Ge:H amorphous films, photoemission spectra 0-50517  
 GeS(S<sub>2</sub>) amorphous films, photostructural changes, UPS study 0-49550  
 GeSe(Se<sub>2</sub>) amorphous films, photostructural changes, UPS study 0-49550  
 H<sub>2</sub>, photoionisation, ang. distrib. of photoelectrons 0-37834  
 H<sub>2</sub>O, electron propagator theory for mol. electron binding energies and photoionis. intensities 0-47848  
 Hg, transition from ordered solid to disordered liquid, viewed by photoemission 0-45217  
 HgF<sub>2</sub>, electronic structure of outermost levels, UPS study 0-7468  
 HgI<sub>2</sub>, relativistic effects, photoelectron spectra, Hartree-Fock-Slater method, perturbation theory approach 0-27962  
 I<sub>2</sub>, relativistic effects, photoelectron spectra, Hartree-Fock-Slater method, perturbation theory approach 0-27962  
 INCO, VPS obs., comparison with ab initio and semi-empirical calcs. 0-53043  
 In, transition from ordered solid to disordered liquid, viewed by photoemission 0-45217  
 InP (110), oxidation, initial stages, photoemission study 0-16529  
 InP, cleaved surface, angle resolved photoelectron spectroscopy 0-55258  
 InP, surface, electron struct. and Fermi level pinning by O<sub>2</sub> and metals 0-11066  
 InSb (110), chemisorption of Cl, photoemission spectra and tight-binding calcs. 0-6629  
 InSb (110) surface struct. determ. by LEED, UPS, and EPR 0-49475  
 InSe, energy band structure, chem. bond polarity, photoemission, semiempirical tight binding method 0-44504  
 Ir (100), adsorption of Xe, local surface struct., UPS study 0-39429  
 K, valence p-shell HeIIα photoelectron spectra, final state CI effects 0-14121  
 Kr, ns-εp photoelectrons, spin polarisation 0-37792  
 Kr, photoelectron emission, polarisation depend. on incident unpolarised VUV radiation wavelength 0-52952  
 LaB<sub>6</sub> (100) surface, O<sub>2</sub> adsorption, UPS and LEED study 0-49519  
 LaB<sub>6</sub>, valence band dispersions, angle-resolved photoemission 0-11536  
 Li<sub>2</sub>Br<sub>2</sub>, UPS of dimeric mol., expt. and Xα calc. 0-9640  
 LiC<sub>6</sub>, intercalated, charge-transfer and non-rigid-band effects 0-44496  
 LiC<sub>6</sub>, intercalated graphite, band struct. determ. by angle-resolved photoemission 0-45203  
 Li<sub>2</sub>Cl<sub>2</sub>, UPS of dimeric mol., expt. and Xα calc. 0-9640  
 Li<sub>2</sub>F<sub>2</sub>, UPS of dimeric mol., expt. and Xα calc. 0-9640  
 Li<sub>2</sub>I<sub>2</sub>, UPS of dimeric mol., expt. and Xα calc. 0-9640  
 LuH<sub>2</sub>, electronic struct., photoelectron spectra study 0-50527  
 Mg clean films, O<sub>2</sub> interaction study using synchrotron-radiation-induced-photoemission 0-55709  
 Mo, adsorption of CO, O<sub>2</sub>, metastable He de-excitation spectroscopy and UPS study 0-34314  
 Mo(100), adsorbed H<sub>2</sub>, photoemission rel. to surface resonances and surface reconstruction 0-44417  
 N<sub>2</sub>, photoelectron ang. distrib., photon energy depend., 16-25 eV 0-53046  
 NH<sub>3</sub>(X<sup>2</sup>B<sub>1</sub>) radical, and ND<sub>2</sub>, ionisation pot., vibr. anal., ab initio calcs. and vacuum UPS obs. 0-53047  
 NO X<sup>2</sup>Π(ν<sup>+</sup>=0), ionis. energies to NO<sup>+</sup> X<sup>1</sup>Σ<sup>+</sup>(ν=0-34), NO<sup>+</sup> mol. const., UPS obs. 0-14177  
 N<sub>2</sub>O, spin polarised photoelectrons, synchrotron excited 0-43101  
 Na, reson. two-photon ionisation via 3p<sup>2</sup>P<sub>3/2</sub> state, photoelectron ang. distrib. 0-43016  
 Na, Rydberg states, high resolution spectroscopy 0-52901  
 Na<sub>2</sub>WO<sub>3</sub>, core level photoelectron spectra, final state effects 0-50509

**photoelectron spectra continued**

- Ni (001), adsorbed c(2×2) Na overlayer, core level excitation effects, synchrotron radiation UPS study 0-40234  
 Ni (001), adsorbed Se and Te, photoelectron diffr. obs. 0-40223  
 Ni (100), chemisorption of NO, LEED, AES, UPS, and thermal desorption study 0-39449  
 Ni (111), adsorption of chalcogens, angle-resolved photoemission 0-40230  
 Ni (111), electron spin polarised photoemission spectrum 0-25525  
 Ni (111), isothermal desorption of CO, UPS study, time-resolved approach 0-39440  
 Ni, adsorbed CO, core level spectrum, satellite struct., ab initio HF-LCAO calc. 0-40233  
 Ni atoms, Xe matrix isolation, photoemission 0-27987  
 Ni, chemisorptive binding of O, CNDO calc. of potential energy curves (German) 0-44431  
 Ni, core level excitation effects, synchrotron radiation UPS study 0-40234  
 Ni, ferromagnetic, chemisorption of H, spin-spin interactions, UPS spectra calc. 0-6630  
 Ni monolayer and submonolayer films, on ZnO, UPS study 0-7472  
 Ni, near-Fermi part of energy band struct. from PES 0-2328  
 Ni, photoelectron spectra, threshold Auger emission 0-29849  
 Ni surface (111), photoyield near threshold negative-positive spin polaris. crossover 0-2922  
 Ni, UPS, two-electron reson. at 3p threshold, rel. to Cu (100) expt. 0-25522  
 Ni, valence-band photoemission spectra, self-energy corrections effect 0-11534  
 Ni(CO)<sub>4</sub>, bonding, shakeup energies, and shakeup intensities for photoelectron spectra 0-50528  
 Ni<sub>3</sub>Ti, electronic struct., Xα calc., photoelectron and AES spectra 0-20769  
 Ni(100) magnetic surface states, photoelectron spectra, surface Brillouin zones 0-6928  
 Ni(100), oxidation, UPS obs. 0-6648  
 O<sub>2</sub>, photoelectron ang. distrib., photon energy depend., 16-25 eV 0-53046  
 O<sub>2</sub>, photoexcitation and photoionisation cross sections, HF Gaussian method 0-53064  
 O<sub>2</sub>, photoionisation, partial channel cross-sections calcs. 0-53061  
 Pb, liquid and solid, UPS, optical densities of states 0-2924  
 PbS (100) surface, electronic struct., O<sub>2</sub> adsorption effects, UPS study 0-54756  
 PbS, temp. effects on valence bands, UPS study 0-11537  
 PbS(Se)(Te), photoemission interpretation 0-25531  
 PbSe, temp. effects on valence bands, UPS study 0-11537  
 Pd (100), (√2×√2)R45° s layer, adsorbate induced surface reson. obs. in photoemission 0-7470  
 Pd (111) surface, adsorbed O<sub>2</sub>, UPS and thermal desorpt. characts. 0-54754  
 Pd-Si (111) interface, microscopic Pd<sub>2</sub>Si form., UPS obs. 0-24743  
 Pd-Si glasses, changes in density of states with alloys comp., UPS obs. 0-50531  
 Pd-Zr, metallic glasses, valence band struct. investigation 0-11533  
 PdO, electronic struct., XPS and UPS study 0-35061  
 Pd<sub>18</sub>Si<sub>14</sub>Cu<sub>6</sub>, glass, changes in density of states with alloys comp. UPS obs. 0-50531  
 Pd<sub>80</sub>Si<sub>17</sub>Cu<sub>3</sub>, glass, changes in density of states with alloys comp., UPS obs. 0-50531  
 Pd(110) surface, adsorption of Xe, UPS study 0-6633  
 Pt, core level excitation effects, synchrotron radiation UPS study 0-40234  
 Pt-SrTiO<sub>3</sub> (100) interface, struct. and electronic props., AES, LEED, EELS, and UPS study 0-24986  
 Pt-SrTiO<sub>3</sub> (100) interface, Auger and photoemission studies, relax. and chem. shift effects 0-54749  
 Rb, 4p level He II photoelectron spectra, energies and intensities 0-5511  
 Rb, valence p-shell HeIIα photoelectron spectra, final state CI effects 0-14121  
 RbC<sub>8</sub>, intercalated graphite, band struct. determ. by angle-resolved photoemission 0-45203  
 Re (0001), chemisorption of CO, role of d-orbitals, angular resolved UPS and thermal desorption meas. 0-40232  
 Re<sub>2</sub>Cl<sub>6</sub>, metal cluster complexes, He(I) photoelectron spectrum, SCC DV Xα calcs., Re<sub>2</sub>Cl<sub>6</sub><sup>2+</sup> comparison 0-28063  
 Rh, band structure and photoemission from low index surfaces 0-24790  
 Ru (001), adsorption of NO, KPS, UPS, and X-ray AES meas. 0-6655  
 Sb<sub>2</sub> photoelectron spectra, visual assessment stripping program anal. 0-28062  
 (SCN)<sub>2</sub>, prep., UV photoelectron spectrum and structure 0-28059  
 SeH<sub>2</sub>, electronic struct., photoelectron spectra study 0-50527  
 SeBr<sub>2</sub>, photoelectron spectra, visual assessment stripping program anal. 0-28062  
 Si (100), intrinsic surface states, photoemission study 0-50514  
 Si (111) 7×7 surface, chemisorption of H<sub>2</sub>O, AES, EELS and UPS 0-10792  
 Si (111) 7×7 surface electronic struct., angle-resolved UPS study 0-50513  
 Si (111)-Au interface, chemically driven intermixing, UPS study 0-50533  
 Si (111)7×7 surface electronic struct., angle-resolved UPS study 0-40226  
 Si, amorphous, position of Fermi level, spectroscopic and transport determ. 0-6706  
 Si:H, amorphous, electronic struct. calc., rel. to UPS data 0-39527  
 Si:H, amorphous, surface activated, photoemission spectra, minority carrier diffusion length 0-40235  
 SiO<sub>2</sub>, amorphous and α-cristobalite cryst., band struct., photoelectron and X-ray spectra interpret. 0-24787  
 SiX<sub>4</sub> (X=Cl,H,F), chemical shifts, relax., X-ray spectra, SCF Xα calcs. 0-27928  
 SrTiO<sub>3</sub> (100) surface, struct. and electronic props., AES, LEED, EELS, and UPS study 0-24986  
 Te overlayer, c(2×2), on Ni surface, 4d levels, angle resolved photoemission cross section, atomic and solid-state effects 0-29853  
 Ti (0001), with adsorbed N (1×1) layer, underlayer geometry, electronic struct. calcs. and UPS meas. 0-54751  
 Ti-Cu dissolution mechanisms, photoelectron spectra study (French) 0-45198  
 TiC (001) surface, change in work function with chemisorption of O<sub>2</sub> and H<sub>2</sub>O 0-29461  
 TiO<sub>2</sub> (rutile), (001) and (110) faces, UPS and LEED obs. 0-45206



**photoelectron spectra continued**

- TiSe<sub>2</sub>(S<sub>2</sub>) (1T), electronic and vibronic struct. 0-44500  
 Ti, liquid and solid, UPS, optical densities of states 0-2924  
 Ti, transition from ordered solid to disordered liquid, viewed by photoemission 0-45217  
 TiI, XPS and UPS study of phase transforms. 0-45210  
 US(Se)(Te), photoelectron energy distrib. and spin polarisation, electronic and mag. props. 0-16146  
 US(Se)(Te), spin polarisation and magnetism, photoelectron study 0-40219  
 USb, UPS and XPS, surface oxidation 0-7465  
 UTe, Sb<sub>1-x</sub>, photoemission, densities of states 0-16147  
 VSe<sub>2</sub>, angle-resolved UPS, Fermi surface determ. 0-55257  
 W {110}, chemisorption of  $\beta$ -N<sub>2</sub>, underlayer mechanism 0-39432  
 W, chemisorption of halogens, UV photoelectron spectrosc. study 0-7854  
 W, secondary emission and photoemission props., effect of one-electron density of states 0-16152  
 W, surface state transferability, UPS meas. for (011) states 0-39650  
 Xe, adsorbed on Pd (110), anomalous 5p photoemission 0-7471  
 Xe, ns $\rightarrow$ sp photoelectrons, spin polarisation 0-37792  
 Xe, photoelectron studies of 5p branching ratio 0-37793  
 Xe, plane polarised VUV irr., emitted photoelectron polarisation, ang. depend. 0-47952  
 YH<sub>2</sub>, electronic struct., photoelectron spectra study 0-50527  
 Yb, valence-charge-induced Fano reson. 0-55267  
 Yb-Al, valence changes during autoionisation and Auger electron emission 0-50475  
 ZnF<sub>2</sub>, electronic structure of outermost levels, UPS study 0-7468  
 ZnIn<sub>2</sub>S<sub>4</sub>, cond. and valence band states, photoemission study 0-35054  
 ZnTe (110) surface struct. determ. by LEED, UPS, and EPR 0-49475

**photoelectron spectroscopy**

- adhesion measurement, locus of failure, bond failure in adhesive joints 0-50801  
 adsorbate on single crystal, anal. of electronic state by angle-resolved photoelectron spectroscopy 0-11541  
 adsorbed atoms, relax. shifts, satellites and sum rules 0-11539  
 aerosol sampling, chemical heterogeneity revealed by X-ray photoelectron spectroscopy 0-55970  
 cylindrical mirror analyser, design and use with synchrotron radiation, autoionisation obs. 0-18049  
 ESCA appl. to thin film production, surface analysis (*Hungarian*) 0-54537  
 gas-phase time-of-flight photoelectron spectrometer using synchrotron radiation 0-4818  
 heated vacuum monochromator for 40-280 nm spectroscopy 0-33176  
 high temp. vapours 0-52238  
 high temperature, charact. of vapours oven heated inorganic solids 0-52239  
 ion fragmentation mechanisms and photoelectron spectroscopy, book contrib. 0-14179  
 photoelectron counting statistics, theory, fully quantum, review 0-52312  
 semiconductor, electron spectroscopy techniques, review (*Japanese*) 0-49061  
 solid state spectroscopy using synchrotron radiation, book contrib. 0-7375  
 solids, review 0-55263  
 surface studies, gas press. up to 1 Torr, photoelectron spectrometer 0-4822  
 surface study of clean and adsorbate covered surfaces (*French*) 0-50519  
 synchrotron radiation appls., book contrib. 0-14035  
 theory, techniques, and appl., book 0-8748  
 transient species, vacuum UPS, book contrib. 0-14178  
 An alloys, bonding investig. 0-55263  
 Mg, K $\alpha$  radiation, X-ray photoelectron spectroscopy resolution 0-18888  
 Ni, one-electron energy investig. 0-55263

**photoemission**

- see also photoelectron spectra; photoemissive devices*  
 actinide compounds, spectroscopic techniques for electronic props. meas. 0-11427  
 alkali metal atom, heavy, polarised, circ. dichroism of ang. distrib. of photoelectrons 0-37789  
 alkali metal atom, spin polarisation of photoelectrons, one-quantum photoeffect 0-37790  
 angle-resolved photoemission, review 0-45214  
 annealing twins density, photoemission microscopy 0-35208  
 bone-ZZ 0-36144  
 cathode spot shape and kinetics, cathode photoeffect from discharge UV irradiation 0-38836  
 electron energy, distrib. calc. 0-40237  
 ferromagnet, spin polarisation of emitted photoelectrons 0-45215  
 ionosphere, general photoelectron current, meas. technique 0-12636  
 laser- or black-body radiation, strong electron coupling, limitation of Fermi-Dirac statistics 0-29843  
 metal, laser irradiated, optical and electronic emissions (*French*) 0-2919  
 metal surface cleanliness control by photoemission recording (*Russian*) 0-49839  
 metal-electrolyte boundary, elec. refl. and photoemission relationship 0-45211  
 metal-electrolyte boundary, photoemission effect on elec. refl. 0-45212  
 metallic surface state, influence of refr. of p-polarised light on photoemission 0-20772  
 metals, laser and nuclear radiation induced emission anomalies, current sources (*Russian*) 0-25536  
 metals, resonant photoemission, mech. 0-50524  
 MIS structure charge distrib., optoelectric determ. methods (*Polish*) 0-39675  
 molecular crystal, band structure, excitonic processes, trap distrib. 0-6720  
 optical communication with two-photon coherent states, quantum meas. realisable with photoemissive detectors 0-53220  
 photoelectrochemistry, laser sources use for solar energy conversion 0-40873  
 pyrene, band structure, excitonic processes, trap distrib. 0-6720  
 random alloy, optical absorption and photoemission spectra 0-45216  
 reradiation effects in negative electron affinity photocathodes 0-55274  
 scanned internal photoemission characterisation of MOS structs. and contact barriers 0-49915  
 semiconductor, photoemission meas. of surface and bulk states 0-25527  
 semiconductor-metal system, long wavelength photosensitivity edge 0-6984  
 solid state physics, conf. Munster, Germany (March 1979) 0-41941

**photoemission continued**

- solution, optical methods of studying solid-liquid interface (*French*) 0-7318  
 spectra calculation program 0-55256  
 spin and energy analysed photoemission, feasibility anal. 0-55271  
 spin-polarization measurements by Mott scattering, use of 90° spherical deflector 0-31951  
 theoretical aspects, review 0-45213  
 yield of photoelectrons, single cryst., X-ray diffr. conditions (*Japanese*) 0-16144  
 Ag-O-Cs photocathode, Ag colloidal particles and long wavelength response (*Chinese*) 0-45195  
 Ag-O-Cs photocathode, role of Ag colloidal particles in photoemission (*Chinese*) 0-40215  
 Al (100) model surface, ang. terms in optical pot. 0-55269  
 Al alloys, contamination, automated nondestructive inspection 0-16629  
 Al/III-V interfaces, photoemission 0-25526  
 Al-SiO<sub>2</sub> interface, internal photoemission and photon-assisted tunnelling 0-6982  
 Ar, electron ionisation and excitation coeffs. in low E/N region 0-48090  
 As, 3d subshell, photoionisation partial cross-section, energy depend. meas. 0-29850  
 Au, 5d and 4f subshells, photoionisation partial cross-section, energy depend. meas. 0-29850  
 Bi<sub>2</sub>O<sub>3</sub>, anodic films, struct. and electronic props., photoeffects 0-44749  
 C foils, forward photoemission and transmittance meas. 0-25516  
 Ca films, thin and ultrathin, vac. deposited, struct. and photoemission meas. 0-11538  
 Co (0001), photoemission, exchange-split energy-band dispersions 0-35059  
 Cs<sub>2</sub>Sb photocathode, wavelength-modulated photoemission spectra 0-29857  
 Cu-Al (3 wt.%), annealing twins density, photoemission microscopy 0-35208  
 Cu-CdS, Schottky barrier, Cu diffusion and photovolt. mechanism 0-6980  
 Cu-Ni, optical absorption and photoemission spectra 0-45216  
 Fe (111), photoemission, exchange-split energy-band dispersions 0-35059  
 Fe (111), spin polarised photoemission 0-45221  
 Ga, 3d subshell, photoionisation partial cross-section, energy depend. meas. 0-29850  
 GaAs (111) epitaxial film, adsorption of Cs, Cs+O, ellipsometric study, photocathode sensitivity 0-29282  
 GaAs-Ge structure, electronic struct., ang.-resolved photoemission obs. 0-49881  
 GaAs-metal interface form., chem. and electronic struct. 0-25009  
 GaAsP cathode, negative electron affinity process obs. by laser beam scanning (*Japanese*) 0-55262  
 GaAs<sub>0.62</sub>P<sub>0.38</sub>, negative electron affinity, photoemission of spin polarised electrons 0-2916  
 GaP (100), prep. of negative electron affinity surface by Cs adsorption 0-10768  
 Ge photocathodes, Au adsorbed photofield emission current spectral investigation 0-29856  
 KCl crystal, use of photoelectrons to investigate surface charges 0-2444  
 Kr, electron ionisation and excitation coeffs. in low E/N region 0-48090  
 Ni (100), spin polarised photoemission 0-45221  
 Ni (111), photoemission, exchange-split energy-band dispersions 0-35059  
 Ni (111), single crystal, spin polarisation of emitted photoelectrons 0-45215  
 Ni, (99 wt.%), annealing twins density, photoemission microscopy 0-35208  
 Ni atoms, Xe matrix isolation, photoemission 0-27987  
 Ni d-band photoemission, resonance enhancement by coupling to 3p excitation 0-20766  
 Pb, 5d subshell, photoionisation partial cross-section, energy depend. meas. 0-29850  
 Pd overlayers, on Nb, form. of Pd (111) surface states and reson. d-levels, photoemission obs. 0-50523  
 S adsorbed on Ni, photoelectron diffr. data 0-29851  
 Sb, 4d subshell, photoionisation partial cross-section, energy depend. meas. 0-29850  
 Se adsorbed on Ni, photoelectron diffr. data 0-29851  
 Si cathode, negative electron affinity process obs. by laser beam scanning (*Japanese*) 0-55262  
 Si-SiO<sub>2</sub>-Si<sub>3</sub>N<sub>4</sub>, internal photoemission 0-7475  
 SnS<sub>2</sub>, Sn4d photoionisation, second threshold 0-40222  
 Ta, photo field emission spectroscopy of band structure by He-Ne laser irr. 0-55276  
 W, four-photon photoemission, incident angle and polarisation depend. 0-40221  
 W, pure and Ba covered, photo-stimulated field emission, effect of light polarisation (*French*) 0-7480  
 Xe, electron ionisation and excitation coeffs. in low E/N region 0-48090

**photoemission spectra** *see photoelectron spectra***photoemissive devices**

- see also photocathodes; photoemission*  
 solar-cells, efficiency calc., use of negative affinity photoemitters 0-55876

**photoemissivity** *see photoemission***photofission**

- actinide nuclei, photo- and electro-fission cross sections and yields, giant resonances 0-5187  
 ( $\gamma$ ,f), linear polarised photon on even-even nuclei 0-543  
 $\Lambda$ m( $\gamma$ , $\delta$ ) 7-26 MeV, A=241,243, photofission cross section in E1 giant resonance region (*Russian*) 0-5182  
<sup>232</sup>Th, determ. of neutron multiplicities 0-32311  
<sup>232</sup>Th( $\gamma$ ,f), deep subthreshold photofission, double humped fission barrier anal., shape isomer 0-5179  
 $\Lambda$ U, A=235, 236, 238, determ. of neutron multiplicities 0-32311  
 $\Lambda$ U( $\gamma$ ,f), A=235, 236, 238, deep subthreshold photofission, double humped fission barrier anal., shape isomer 0-5179  
<sup>235</sup>U( $\gamma$ , f), 12-70 MeV bremsstrahlung, product yields and  $\gamma$ -spectra 0-42716  
<sup>235</sup>U( $\gamma$ ,f), 20 MeV, long range  $\alpha$ -particle spectrum 0-47516  
<sup>236</sup>U, giant E2 isoscalar resonance determ. 0-27607  
<sup>238</sup>U( $\alpha$ ,f), 100-1000 MeV, resonance production 0-52658  
<sup>238</sup>U( $\gamma$ ,f), 12-70 MeV bremsstrahlung, fragment mass and energy distrib. 0-27680  
<sup>238</sup>U( $\gamma$ ,f), 20 MeV, fission product yields, charge distrib. 0-42533



**photoflash lamps** *see flash lamps*

**photoglow tubes** *see phototubes*

## photogrammetry

American Society of Photogrammetry Annual Convention, Washington, USA (March 1978) 0-4149

atmosphere refraction compensation for long photographic distances 0-56339

cartography, point transfer error determ. 0-17227

Death Valley, geological interpretation from composited radar and Landsat imagery 0-56647

digital orthophoto production using scanning microdensitometers 0-41571

high intensity dot grids, for accurate area determ. 0-17225

land-use/land-cover mapping from aerial photographs 0-41569

Landsat imagery, planimetric restitution using Zeiss Stereotop 0-56648

Mapsat (Automated Mapping Satellite System), proposed parameters 0-17468

multispectral photography appl. using MKF-6 camera and MSP-4 projector 0-56633

optic disc changes meas. using retinal stereophotogrammetry, glaucoma detect. appl. 0-3757

photographic investigation of earth, RADUGA 1 experiment, results (*German*) 0-36224

saline seep detection and mapping, IR remote sensing techniques 0-4154

stereo X-ray, use in absorbed dose determ. in radiation therapy 0-12222

stereometric measurement of streambank erosion 0-17421

techniques and appls. 0-31927

W.Tennessee, wetland mapping and classification, high altitude photography 0-8340

## photographic applications

*see also photogrammetry; photolithography; remote sensing*

astronomy, cooled emulsion photography for amateurs 0-56714

ballistics, high-speed and other photographic methods 0-9068

biological objects, elec. discharges, electrographic investigation methods 0-46118

computerised tomographic image display by TV and photography 0-8129

cosmic ray expts. on ocean floor 0-36509

cytogenetics, applications of photomicrography 0-21577

demonstrations, audio-visual presentations for physicians, photography of

medical X-ray plates 0-37103

diesel engine transient fuel jet droplet photography using light pipes 0-23784

eye, operations, photographic documentation using model 310 surgical microscope 0-56161

frost blisters, growth meas. using long-term automatic time-lapse photography 0-12437

gas laser medium, large-bore CW high-energy, holographic interferometry during power extraction 0-28172

geological joints, mapping via photogrammetry and EDP appl. 0-56470

idiopathic scoliosis, adolecent, monitoring with Moire fringe photography 0-17047

immunogram recording apparatus, self-contained, modified version using Polaroid film 0-17209

interferometric gratings, three beam interf. images, sinusoidal complex object with phase modulation 0-53208

ion detector, electro-optical, for spark source mass spectrometry 0-42246

IR time-resolved spectral photography, transient broadband absorption spectra 0-18024

knee joint movement during walking, meas. method using photographic records 0-17048

laryngeal cinematography, high speed, optical/lighting system 0-17055

lightning, return stroke rise speed meas. method (*French*) 0-51493

manufacturing processes, industrial visual testing, photographic methods as technical aid (*German*) 0-31923

medical treatment and litigation 0-36189

multispectral photography, using MKF-6 camera and MSP-4 projector 0-56633

ocean wave imaging and wavelength meas. by aerial photography 0-46323

ocular photography, accessory fill-in flash for the Nikon photo-slit lamp 0-36056

oscilloscope cameras, new fast oscilloscope makes special photographic techniques redundant 0-27287

particle tracking, association with laser fringe anemometry 0-38512

rotation measurement, in-plane, speckle photography appl. 0-31714

stereoscopic instrumentation, kinematic and kinetic analysis of human wrist 0-16999

stress measurement by sandwich speckle photography (*German*) 0-10216

subspeckle size changes meas. by laser-speckle photography 0-31853

thermal spectrozonal aerial photography, capabilities and future prospects 0-18036

Al plastic flow visualisation in plain strain extrusion 0-7626

<sup>4</sup>He, superfluid, turbulence, electron photography (*French*) 0-54456

OH emissive layer, waves, atmospheric dynamical process study 0-51545

Xe discharge lamps, large, electrode temp. meas. (*Russian*) 0-47057

Xe, high power pulse gas discharges development, photographic obs. 0-14954

**photographic developers** *see photographic materials*

**photographic development** *see photographic process*

## photographic emulsions

cellulose base, extraordinary reflection halo (*German*) 0-42282

colour reproduction of objects by speckle interferometry in white light 0-47094

cooled emulsion photography for amateurs, astronomical appls. 0-56714

development probability, AgBr grain diameter depend. 0-9056

film grain size and transmittance influence on fluctuation and diffraction spectra (*German*) 0-4788

film response to 25 MV X-rays, sensitometric curves, relative dosimetry 0-52376

gels, coloured component addition, struct. form., dynamic shear modulus, viscosity meas. (*Russian*) 0-7871

Herschel effect as a rehalogenation process 0-26034

light sensitivity, effect of applied electric field (*Russian*) 0-296

monochrome photographic film densitometry errors and standards (*German*) 0-37102

monodispersive emulsions, frequency-contrast responses, resolution magnitude, sensitisation effects (*Russian*) 0-295

noise diffraction spectra 0-27368

production, effect of mixing on diffusion rate (*Russian*) 0-3388

radiography screen-film combination selection 0-46047

response relationship for holography 0-1148

## photographic emulsions continued

sensitivity centre variation with AgBr grain diameter 0-9055

sensitivity of films used in high-voltage electron microscopy 0-22474

small-grain development of emulsion monofilms for electron-microscope autoradiography (*Russian*) 0-297

supersensitisation by hydroxy-tetraazaindenes 0-3384

video photography in computed tomography and US imaging, film selection 0-41224

Ag halide emulsion colouring, k-value and sensitivity relationship (*German*) 0-7815

Ag halide emulsions, induced sensitized photodichroism 0-9061

AgBr melts, surface energy and surface tension coeffs., effect on photographic emulsion microcryst. growth rate (*Russian*) 0-47132

AgCl melts, surface energy and surface tension coeffs., effect on photographic emulsion microcryst. growth rate (*Russian*) 0-47132

**photographic filters** *see optical filters*

## photographic lenses

*see also aberrations*

aspheric optics production costs, instrumental and photographic applications 0-28308

automatic focusing systems 0-18028

chromaticity of camera lenses, spectral transmission curves analysis 0-31925

cinematographic image quality improvement, dependence of resolving power on lenses (*Russian*) 0-27371

cinematographic lenses with fixed and variable focal length, comparison of types (*Russian*) 0-27370

cinematography, OMNIMAX system using Leitz wide-angle lens, domed roof in planetarium appl. 0-276

Cooke triplet, air-spaced anastigmatic quadruplet design 0-1291

Cooke triplet derivative of five-element config., design 0-33111

design parameters, 35 mm format enlarging lenses, survey 0-13168

enlarger, Czechoslovak Opemus Standard (2) (*Czech*) 0-18034

gradient index lens array fabrication for office photocopier 0-13178

gradient singlet, total aberrations 0-13177

image quality improvement 0-47123

lens-array photography, longitudinal distortion compensation, integral image reconstruction 0-52345

mass-produced camera objectives, effects of cosmetic defects 0-47135

motion-picture and TV camera objective lenses, testing by projection 0-9060

movie projector objective lenses, standardisation of optotechnical parameters and testing methods 0-28301

optical glasses, development and manufacturing processes 0-53393

OTF, numerical calc. from lens design data (*Korean*) 0-19085

performance meas. system, routine checking film, TV cameras appl. 0-277

photocopier lens array design, Wood lens and gradient index fibre comparison 0-14479

polishing and shaping techniques (*German*) 0-33114

spherical aberration measurement using solid-state image sensor 0-23812

surface quality testing at Zeiss factory (*German*) 0-33113

telephoto apochromatic lenses, design 0-31924

wide-angle, fish-eye, lenses, optical constructions 0-18037

zoom lens focusing system (*Japanese*) 0-31922

zoom projection lens, optical level system, paraxial characts. 0-53399

**photographic light sources** *see light sources; photography*

## photographic material sensitivity

colour film densitometer with Si photodetector 0-4791

desensitising dye polarographic half-wave potential meas. 0-7802

diffraction, transmission, sensitivity at 442, 633 nm for holographic appls. (*Russian*) 0-43301

electric field effects on light sensitivity of films (*Russian*) 0-290

electron microscopy, high-voltage, film sensitivity 0-22474

emulsion supersensitisation by hydroxy-tetraazaindenes 0-3384

emulsions, effect of applied electric field on light sensitivity (*Russian*) 0-296

film grain noise, spectral density estimation, in electron microscopy (*French*) 0-9075

film response to 25 MV X-rays, sensitometric curves, relative dosimetry 0-52376

holographic interferometry, highly sensitive plates for short exposure times (*Russian*) 0-1164

ion-sensitive photographic plate evaluation using optical wedge microdensitometer (*German*) 0-42298

Kodak 649F plates, intermittent characteristic curves at 514.5 nm 0-23637

Kodak 649F plates, specular multiplexed hologram recording, diff. efficiency 0-23638

laser unconventional recording materials for He-Ne laser 0-18040

lithographic coated polyester panchromatic plate system 0-13172

monodispersive emulsions, frequency-contrast responses, resolution magnitude, sensitisation effects (*Russian*) 0-295

negative photoresists, photosensitivity (*Russian*) 0-50872

papers, spectral sensitivity, meas. of optical density in reflected light (*Russian*) 0-300

photodetector, threshold sensitivity for semiconductor photography 0-18017

photoimaging system based on photopolymerisation in cryst. coatings 0-40716

photosensitive layers with chromic acid salts, photochemistry (*Russian*) 0-50869

photothermoplastic materials, electrophotog. sensitivity, diff. efficiency (*Russian*) 0-47130

polymethyl isopropenyl ketons, spectrally sensitized decomposition and Deep UV resists 0-40715

prediction of maximum attainable sensitivity for photographic systems (*Russian*) 0-298

supralinear photographic emulsions, radiobiological aspects 0-26290

UF-VR film, exposed to soft X-rays, quantum discrimination efficiency and sensitivity 0-22499

Ag halide dry materials for laser printing appls. 0-13179

Ag halide emulsion colouring, k-value and sensitivity relationship (*German*) 0-7815

AgBr, evaporated layer, influence of sublayer on stability and photographic characteristics (*Bulgarian*) 0-42281

AgBr evaporated layers, spectral sensitization using cyanine dyes 0-26035

AgBr, evaporated layers, use as registering system (*Bulgarian*) 0-52344



**photographic material sensitivity continued**

- AgBr grains, photographic emulsion, sensitivity centre variation with grain size 0-9055  
 AgI large single crystals, gel and soln. growth and props. 0-35071  
 As<sub>2</sub>Se<sub>3</sub> layers for electrophotographic use (*German*) 0-42283  
 As<sub>2</sub>Se<sub>3</sub>, photosensitive layer, in metal-photoconductor-insulator multilayered struct., optical image recording 0-42286  
 CdS, Se<sub>1-x</sub>S<sub>x</sub>, photosensitive layer, in metal-photoconductor-insulator multilayered struct., charge pattern form. 0-47129  
 $\beta$ -Cu phthalocyanine electrophotographic props. rel. to particle size (*Japanese*) 0-13171  
 2,5-diphenyloxazole enhanced emulsion, effectiveness of light microscope autoradiography 0-47100  
 Zn<sub>1-x</sub>Cd<sub>x</sub>S:Cu crystallophosphors, spectra of IR electrophotographic sensitivity (*Russian*) 0-50423  
 ZnS:Cu crystallophosphors, spectra of IR electrophotographic sensitivity (*Russian*) 0-50423

**photographic materials**

- see also *photographic emulsions*  
 benzoin containing system, photosensitized free radical polymerisation 0-7825  
 benzophenone containing system, photosensitized free radical polymerisation 0-7825  
 camera speed diffusion transfer offset master on filmbase 0-37108  
 camera speed negative working diffusion transfer material 0-37107  
 colour positive cinefilm standardisation on sensimetric tests (*Russian*) 0-287  
 p-diazoquinone, photodecomp. 0-7827  
 diffusion transfer based negative and positive working camera speed overlay color system 0-37109  
 films, high speed, colorimetric testing of Boots 400 and Agfa CNS 400 0-18026  
 gelatin layer, in MIS struct., C-V characts. and gelatin-semiconductor interaction rel. to photographic process (*Russian*) 0-49944  
 graphic arts imaging material and laser source cost tradeoffs 0-14383  
 holographic interferometry, selection of working point on amplitude-exposure curve for uniform illumination (*Russian*) 0-1162  
 hydroquinone, oxidation of centre of photographic development, electrochem. kinetics (*Russian*) 0-3367  
 instant colour-discrimination shadowgraphic technique and film 0-9057  
 laser printing, seminar, Los Angeles, USA (Jan. 1979) 0-12852  
 laser unconventional recording materials for He-Ne laser 0-18040  
 laser-compatible materials for graphic arts 0-13180  
 mammographic dose reduction, Kodak Definix Medical rel. to Kodak Min R film (*German*) 0-12243  
 merocyanine dyes, non-photochromic, for autoproccessor reprography system 0-35555  
 $\alpha$ -methylstyrene, photoinduced ionic polymerisation 0-7828  
 optical resolving power, determ. (*Russian*) 0-42292  
 photoactive catalyst used in light induced photocuring of coating systems 0-7820  
 photoanisotropy in yellow mordant azo dyes (*Russian*) 0-42290  
 photoinitiated cationic polymerization by photosensitization of onium salts 0-7822  
 photopolymer, biaxial stress-strain test 0-40417  
 photopolymer in holographic real-time fluid flow measurement 0-6176  
 photopolymer industry in Japan 0-4800  
 photopolymer systems, conf., Washington, USA (Nov. 1978) 0-4799  
 photopolymerisation, O<sub>2</sub> inhibition elimination 0-7821  
 photopolymerisation, dye-sensitized, activation by trialkylbenzylstannanes 0-7824  
 polyester filmbase experience in motion picture industry, review 0-42278  
 polyesters, photoreactive, synthesis and struct.-prop. relations 0-7826  
 polyethylene resin coated paper formulation 0-4794  
 polymer, crosslinking with X-ray irradi., active group and heavy atom effects 0-7829  
 polymer, photochromism 0-5805  
 polymer film, photoreticulation by UV irradiation 0-40717  
 polyvinylcinnamate, crosslink form. by photoreaction 0-7823  
 pulp quality control using He-Ne laser scanning system (*German*) 0-3272  
 pyrocatechol, oxidation pots., correl. of V-I characts. and photographic developing power (*Russian*) 0-45534  
 silver thioamides, precip., electron microscope and potentiometric studies, growth of photosensitive crystals. 0-33107  
 spiropyrans, photochromic, thermophotodegradation for autoproccessor reprography system 0-35555  
 thermoplastic recording material, latent image and surface deformation (*German*) 0-42284  
 UF-VR film, exposed to soft X-rays, quantum discrimination efficiency and sensitivity 0-22499  
 Ag diffusion transfer systems, graphic arts appl. 0-37106  
 Ag, vacuum deposition, on evaporated AgBr layers, growth mechanism 0-35095  
 AgBr(I) crystals, luminesc. of individual monocrystals (*Russian*) 0-301  
 As<sub>2</sub>S<sub>3</sub>-Ag light sensitive material, development of non-interchangeability under continuous laser radiation (*Russian*) 0-50870  
 InCl powder, effect of thermal treatment on photographic props. (*Russian*) 0-291  
 TiO<sub>2</sub> transparent film photographic layers, props. (*Russian*) 0-43420

**photographic process**

- see also *photochemistry*  
 3D image, longitudinal definition of details and information density (*Russian*) 0-40721  
 biimidazole+leuco dye photochem. reaction, modulation by photopolymerisation 0-40714  
 colour negatives, commercial processing technique (*German*) 0-13173  
 colour reversal cinefilm, rapid processing technique for TV studios (*Russian*) 0-3385  
 copying process for colour reversal films (*German*) 0-30254  
 developer reuse technology and environmental protection (*Japanese*) 0-22457  
 developing and colour balancing, description of Thomson-CSF flying-spot twin format telecine (*French*) 0-37110  
 development probability, AgBr grain diameter depend. 0-9056  
 diffusion transfer based negative and positive working camera speed overlay color system 0-37109  
 emulsion supersensitisation by hydroxy-tetraazaindenes 0-3384  
 film development and the environment (*German*) 0-7806  
 film response to 25 MV X-rays, sensimetric curves, relative dosimetry 0-52376

**photographic process continued**

- Herschel effect as a rehalogenation process 0-26034  
 holograms, diffraction efficiency of recordings on high resolution photographic plates (*Rumanian*) 0-48188  
 Hurter and Driffield, photographic research, biography 0-22181  
 hydroquinone, oxidation of centre of photographic development, electrochem. kinetics (*Russian*) 0-3367  
 image enhancement using fluorescent light emission techniques 0-31928  
 interior scenes, optimum photographic representation of brightness 0-31921  
 ion-exchange wash water recycling system, pair exchange tanks, solar panels for tempering, processing laboratory appl. 0-42277  
 latent-image formation: the contribution of the Research Division, Kodak Limited, Harrow, review 0-22458  
 liquid-developed migration image fixing and abrasion resistance 0-4792  
 magnetic brush development characteristics for xerography 0-4798  
 masked antifogants, hydrolysis stability, photographic process depend. (*German*) 0-45530  
 mathematical modelling of growth of spherical metallic particles at slow diffusion stage (*Russian*) 0-50871  
 metal-photoconductor-insulator multilayered structure, charge pattern formation during recharging 0-47129  
 metal-photoconductor-insulator multilayered structure, optical image recording, As<sub>2</sub>Se<sub>3</sub> photosensitive element 0-42286  
 modular contact printer for high speed automatic additive colour cinefilm printing 0-42276  
 narrow band gap semiconductor electrophotographic processes 0-13169  
 paraaminophenol and paraphenylenediamine analogue molecular complex, free radicals of developers, EPR obs. (*Russian*) 0-7814  
 photoelectrochemical investigation of the influence of gelatine and polyvinyl alcohol on the formation and lifetime of a latent image in photographic layers on a ZnO base (*Russian*) 0-3389  
 photoimaging system based on photopolymerisation in cryst. coatings 0-40716  
 polyethylene glycol, effect on photographic film during fast development (*Russian*) 0-45533  
 reciprocity law failure, effects on exposure time and contrast 0-47124  
 reflection holograms of diffusely reflecting objects, improved efficiency 0-32939  
 rotary tube photographic processor design 0-4795  
 small-grain development of emulsion monofilms for electron-microscope autoradiography (*Russian*) 0-297  
 sound track stripe applicator, control system, colour release prints for both positive, reversal stocks appl. 0-42275  
 stabilisation of photographic image, introduction of N(CH<sub>3</sub>PO(ONa)<sub>2</sub>)<sub>3</sub>·6H<sub>2</sub>O in thiocarbamide (*Russian*) 0-302  
 thermoplastic recorder development, interaction of regular and chaotic deformation (*Russian*) 0-42291  
 thermoplastic recording development, electrocapillary effect, nonlinear distortions (*Russian*) 0-294  
 thermoplastic recording material, latent image and surface deformation (*German*) 0-42284  
 thiosulphate processing technique, cinefilms appl. (*Russian*) 0-3386  
 wetprinting, historical review 0-283  
 X-ray films, automatic development (*German*) 0-280  
 Ag diffusion transfer systems, graphic arts appl. 0-37106  
 Ag halide dry materials for laser printing apps. 0-13179  
 Ag photographic films, thermal development (*Russian*) 0-303  
 Ag, vacuum deposition, on evaporated AgBr layers, growth mechanism 0-35095  
 AgBr, nucl. emulsion, latent image form., grain diameter depend. 0-9453  
 AgX, XX (*Russian*) 0-293
- photographic recording media** see *photographic materials*
- photographic techniques** see *photography*
- photography**  
 see also *cinematography*; *colour photography*; *electrophotography*; *microphotography*; *photographic applications*; *photographic lenses*; *photographic materials*; *photographic process*; *radiography*; *streak photography*  
 automatic cameras, exposure error compensation 0-52346  
 automatic time-lapse photography, long term, for frost blisters meas. 0-12437  
 camera automation developments 0-18027  
 camera shutter control, use of photosensor with IC amplifier (*German*) 0-52341  
 education, perspective distortion in photography, eye as simple lens 0-17734  
 electrophotographic imaging of objects, in electric discharge (*Czech*) 0-37104  
 enlarger, Czechoslovak Opemus Standard (2) (*Czech*) 0-18034  
 enlarger analyser using Si-blue photoamplifier IC 0-42288  
 exposure meter for flash lamp photography 0-9058  
 film colorimetry 0-22461  
 flashgun slave trigger, using Si solar cell 0-47125  
 Hurter and Driffield, photographic research, biography 0-22181  
 image enhancement using fluorescent light emission techniques 0-31928  
 IR aerial photography for agriculture, potato blight detection 0-13174  
 IR photography on wax films at 10  $\mu$ m 0-4784  
 lens-array photography, longitudinal distortion compensation, integral image reconstruction 0-52345  
 negative print production, electron micrographs of metal shadowed materials 0-18051  
 nonlinear photoelectric or photographic receiver signal value calc. (*German*) 0-31866  
 oblique panoramic aerial photographs, geometrical characts. 0-47128  
 ophthalmic photography to prevent diabetic blindness 0-16920  
 optical flashes from double wire explosion, photographic appl. 0-1865  
 optical images of plasma objects, synchronisation with electrical parameters 0-31919  
 photodetector, threshold sensitivity for semiconductor photography 0-18017  
 photoelastic fringe photography, improved photograph quality 0-27364  
 post-development image intensification by autoradiography, technique, astron. apps. 0-26752  
 reciprocity law failure, effects on exposure time and contrast 0-47124  
 reliefographic process during signal recording (*Russian*) 0-47131  
 satellite photograph production using laser beam recorder (*German*) 0-5777  
 sound-controlled flashlamp trigger circuit (*Spanish*) 0-13175  
 underwater luminaires, technical requirements (*Russian*) 0-9064  
 UV photography and fluoresc. photography techniques 0-18033



**photography continued**

- volume holographic multiple recording on photographic plates (*German*) 0-43288
- I<sub>1</sub>, high-dispersion polarisation-labelled spectrum 0-990
- ZnCl<sub>2</sub>-oil system, simulation of steel-slag, macrophotographic method of diagnosing disperse system 0-25952

**photoionisation**

- acridine, aqueous soln., laser induced two-photon ionisation investig. 0-32780
- alkali metal atom, transition oscillator strengths in discontinuous and continuous spectra, review 0-52937
- alkyl iodides, two-photon reson. ionis. spectra 0-28071
- aniline, laser two-photon ionisation in mol. beam and bulk gas phase 0-18891
- atom, collision-induced three-photon ionization 0-23384
- atom, photoionisation from low or high excited states, radial transition integrals 0-18832
- atom, resonance multiphoton processes of laser radiation interaction 0-37800
- atom, resonant ionisation under adiabatic level inversion conditions (*Russian*) 0-32691
- atom, single photon, AC Stark splitting of bound-continuum decay 0-5502
- atom models, ionisation time depend. under intense EM fields 0-32683
- atomic cross sections, calc. using effective Feynman diagrams, in plasma 0-38566
- atomic ionisation by strong coherent EM field, nonperturbative calc. methods 0-5512
- atoms, multichannel relativistic RPA calcs. 0-9570
- atoms, photoionisation cross sections, electron correl. reson. struct., relax. effects many body perturbation calcs. 0-47852
- atoms, two-step laser selective method 0-23473
- benzene, <sup>13</sup>C substituted, mass selective two-photon ionis., mass spectroscopy obs. 0-9651
- benzene, UV photoelectron spectra, valence electron shake up approx. methods 0-18788
- bound electron photon scatt., atomic ionisation, field theoretic anal. 0-23380
- chalcogens, photoionisation cross sections and ang. distrib., outer p subshell 0-9572
- chemisorptive bonding on metal surface, PES 0-10791
- cooperative multiphoton ionisation, bistability effects, Bonifacio-Lugiato model 0-19010
- core ionisation in 3d, 4f and 5f series, rearrangement effects 0-53065
- cyclopropene, photoionisation and threshold photoelectron-photoion coincidence study 0-53062
- dense metal vapour, radiation trapping, multiphoton ionisation and reson. fluoresc. 0-32654
- diatomic molecule, resonance multiphoton processes of laser radiation interaction 0-37800
- Dirac-Slater potential, hole and exchange terms, influence on photoionisation cross-sections 0-952
- doubly charged ion formation, 2-electron multiphoton ionisation of atoms, mechanism (*Russian*) 0-5514
- electron propagator theory for mol. electron binding energies and photoionis. intensities 0-47848
- N-ethylcarbazole, soln., laser induced ionic photodissoc., transient polyelectrolyte form. 0-53068
- ethylene, UV photoelectron spectra, valence electron shake up approx. methods 0-18788
- excited state photoionisation, at. and mol. photoabsorpt. cross sections determ. 0-32783
- gas chromatography with photoionis. detection for chlorobenzenes determ. in air and biological samples 0-35809
- halogens, photoionisation cross sections and ang. distrib., outer p subshell 0-9572
- n-hexane, liq. trapped electron photoionis., photocond. 0-2418
- hydrogen atoms, threshold behaviour of multiphoton ionisation 0-954
- inert gas atom, photoionis. cross sections of excited levels, quantum defect method calcs. 0-37795
- inert gas atom + H<sup>+</sup>, electron capture, charge-state distrib. 0-32814
- inert gas plasma, free-bound continuum determ. using photoionis. cross sections calc. 0-43878
- inert gas-halogen bearing molecule three-component mixture, self-sustained electric photoionization discharge 0-54073
- inert gases, initial state wave functions for photoionisation cross-sections, multiconfigurational HF calcs. 0-47908
- inert gases, outer shell photoionisation, relativistic RPA calcs. 0-9571
- inert gases, photoabsorption to bound state and photoabsorption to continuum state (ionisation), comparison, HF calcs. 0-47910
- inert gases, photoelectron spin polarisation, ab initio calcs. 0-18833
- interference in two-channel two photon ionization 0-23381
- ion fragmentation mechanisms and photoelectron spectroscopy, book contrib. 0-14179
- K-shell photoionization of multielectron atomic systems 0-47949
- labile species, electron photoejection, reaction kinetics characterisation 0-26089
- laser pumping using self-sustained electron-photoionization discharge 0-33013
- laser radiation, selective action on matter, review 0-7832
- Li, multiphoton ionis. at ruby laser wavelength 0-9566
- mass spectrometry, of high temp. vapours 0-52238
- molecular gas, vol. discharge with UV preionisation by capillary discharge, ionis. pots. depend. 0-44065
- molecular multiphoton ionisation dynamics, rate eqn. modelling 0-48046
- molecular photoionisation cross sections, at. extrapolation, ground state inversion method appl. 0-18877
- molecular photoionisation mass spectroscopy, reson. peak shapes 0-42295
- molecule, inner-shell spectra anal., rel. to electron impact vibr. excitation 0-5629
- molecule, shape-reson. enhanced nucl. motion effects 0-1031
- molecules, techniques and discussion 0-17721
- molecules, valence and core photoionisation, spectral lines, many body effects 0-47853
- multiphoton ionisation, short time behaviour, theory appl. 0-47951
- multiphoton ionisation, simple model, transition rates 0-953
- multiphoton ionisation, theory of two strongly interacting resons. 0-52955
- naphthalene-He photoionis. plasma, CO<sub>2</sub> additive effect 0-10359
- nebulae, gaseous, photoionisation models for third period elements 0-46640

**photoionisation continued**

- parity violating neutral currents in two-photon and autoionisation atomic transitions 0-32034
- photofragment spectroscopy of mol. ions using fast ion beams 0-9755
- pinacyanol dye, adsorbed on CdS substrate, aggregation effect on mol. electronic states 0-37757
- poly N-vinylcarbazole, soln., laser induced ionic photodissoc., transient polyelectrolyte form. 0-53068
- polyatomic molecule, multiphoton absorpt. resons., dynamic Stark splitting 0-9670
- positive atomic ions with Z ≤ 30, photoabsorpt. cross sections 0-26727
- propyl halides, photoionisation mass spectrometry 0-40779
- protein, radical limiting conc. on UV irradiat. at 77K, effect of luminesc. quenchers 0-30662
- quantum beats, origin 0-52954
- quasar emission lines, photoionisation models 0-27009
- quasar spectra, photoionisation theory for H line emission from dense plasmas 0-51900
- radiative capture of an electron of a target atom by multiply charged ions 0-5617
- relativistic multichannel RPA, appls. 0-47925
- resonance ionization spectroscopy and one-atom detection 0-22441
- resonant, ground-state electron simultaneous vs. sequential two-photon absorption 0-23383
- resonant multiphoton ionisation, photon correl. effects, near reson. levels 0-43020
- rotated coordinate method use, rel. to stabilisation method 0-37845
- semiconductor, photoionisation of deep impurity levels 0-34386
- semiconductor with superlattice, optical phonon excitation by light absorpt., impurity photoionisation 0-44275
- solar chromospheric flares, H Lyman  $\alpha$  excitation by photoelectrons rel. to profile and polarisation 0-41780
- surface anal. by photon-induced field ionisation mass spectroscopy 0-40780
- synchrotron radiation source for atomic photoionisation studies in extreme UV and X-ray regions 0-43017
- tertiary amines, lasing action feasibility, excited state absorpt., two step photoionisation 0-23682
- Tokamak impurity problems, atomic and mol. struct. and collision data, review 0-43959
- toluene, two-photon ionisation spectrum, of <sup>1</sup>L<sub>y</sub>-S<sub>0</sub> transition 0-14180
- transparent dielectrics, laser damage, electron avalanche and multiphoton ionisation roles 0-35016
- volume high-pressure discharge with photoionization for laser pumping 0-54058
- water, laser-induced ionisation, quantum yield, temp. and wavelength depend. 0-11924
- Ar discharge, optogalvanic and excited state photoionisation signals, space charge effects 0-14947
- Ar, photoexcited LMM Auger processes, post-collision interaction 0-32682
- Ar, photoionisation, Auger processes, decay lifetime, line shift, profile, X-ray photoelectron spectra 0-37798
- Ar, preionised, CO<sub>2</sub> laser induced breakdown press. and pre-ionisation depend., cascade model 0-54010
- Ar-Xe-tetrachloromethane, self-sustained electrophotoionised discharge in compressed gas 0-38003
- As, 3d subshell, photoionisation partial cross-section, energy depend. meas. 0-29850
- Au, 4f-subshell photoionisation cross section, energy depend. from Auger and photoelectron spectra 0-35057
- Au, 5d and 4f subshell, photoionisation partial cross-section, energy depend. meas. 0-29850
- Ba, efficient ionis. by reson. laser pumping 0-32685
- CO<sub>2</sub> laser, photoionis. TEA type, output pulse characts. calc. 0-32953
- CO<sub>2</sub> pulsed laser with continuously tunable radiation frequency 0-48292
- CO<sub>2</sub> TEA lasers, one-step photoionisation, preionisation discharge effect on electron density 0-53256
- CO<sub>2</sub>, valence shell ionic photofragmentation, oscill. strengths, EELS and electron-ion coincidence meas. 0-37879
- Ca, efficient ionis. by reson. laser pumping 0-32685
- CaF<sub>2</sub>:Dy crystal with M centre, antiresonance line, mag. field effect 0-55138
- CdTe:Cr, impurity photoionisation transitions, EPR meas. 0-39857
- Cl, initial state wave functions for photoionisation cross-sections, multiconfigurational HF calcs. 0-47908
- Cr(CO)<sub>3</sub>, multiphoton ionisation, mol. cooling in pulsed supersonic beam 0-28070
- Cs, four-photon ionis., strongly interacting resons. theory 0-52955
- Cs, He II  $\alpha$  5p<sup>-1</sup> photoelectron spectrum, config. interaction effects 0-5510
- Cs I, pulsed 4-photon 6f-reson. ionis. 0-18831
- Cs I, three-photon 16p reson. ionis. and DC Stark effect 0-14124
- Cs, multiphoton ionis. cross sections, absolute meas. evaluation 0-14122
- Cs, oscillator strengths in principal series, Rozhdetsvenskii hook obs. 0-37760
- Cs, polarised photoelectrons produced by circ. polarised synchrotron radiation 0-18830
- Cs, resonant multiphoton ionisation, spatio-temporal effects 0-37794
- Cs, two-photon ionis., profiles of 6<sup>2</sup>S<sub>1/2</sub>-7<sup>2</sup>P<sub>1/2,3/2</sub> lines 0-958
- CuCl<sub>2</sub>, core ionisation in 3d, 4f and 5f series, rearrangement effects 0-53065
- F<sub>2</sub>, photoexcitation and ionisation cross sections, Stieltjes-Chebyshev static exchange calc. 0-53060
- Fe(CO)<sub>5</sub>, multiphoton ionisation, mol. cooling in pulsed supersonic beam 0-28070
- Ga, 3d subshell, photoionisation partial cross-section, energy depend. meas. 0-29850
- GaP:O, photoionisation of deep impurity levels 0-34386
- H in quasars, photoionisation rel. to line and continuum emission 0-27003
- H, multiphoton ionis. pot. in intense circ. polarised laser beam 0-43010
- H, photoionisation cross sections elec. field-induced oscills. 0-955
- H<sup>+</sup>, bound-free photodetachment cross-section calcs. 0-9567
- H photodetachment, Feshbach resonances 0-37753
- H<sub>2</sub>, Born-Oppenheimer Hamiltonian, resolvent matrix elements complex coord. calc. 0-52878
- H<sub>2</sub>, diabatic and reson. states, dissociative photoionisation calcs. 0-47883
- H<sub>2</sub>, photoionisation, ang. distrib. of photoelectrons 0-37834
- H<sub>2</sub>, photoionisation effective cross sections 0-43121
- He, 2<sup>1</sup>S and 2<sup>3</sup>S states, two-photon ionization 0-37791



**photoionisation continued**

- He, double photoionisation calcs., variational method 0-37734  
 He, many electron system, photoionisation and photoexcitation, at. transition strong config. interaction effect 0-47909  
 He, metastable, two-photon ionisation, multipole interference effects 0-23466  
 He, multiphoton ionis. pot. in intense circ. polarised laser beam 0-43010  
 He, photoionis. and photoabsorpt. cross sections for aeronomic calcs., data tables 0-41599  
 He<sup>+</sup>, ion+electron scatt., static exchange approx. Schwinger variational principle, photoionisation cross section 0-43192  
 Kr, twelve-photon ionis. at 10<sup>13</sup> W cm<sup>-2</sup> laser field 0-32687  
 Li, two-photon ionization spectra 0-23382  
 Li-like ions, partial photoionis. cross-sections and radiative recomb. rate coeffs. 0-52951  
 Mo<sup>29+</sup> to <sup>39+</sup>, photoionis. cross sections, radiative recomb. rate coeffs., rel. to plasma diagnostics 0-52953  
 Mo<sup>30, 12+</sup>, photoionis., relativistic RPA calc. 0-47913  
 Mo(CO)<sub>6</sub>, multiphoton ionisation, mol. cooling in pulsed supersonic beam 0-28070  
 N<sub>2</sub>, 3σ<sub>g</sub> photoionis., shape-reson.-induced non-Franck-Condon vibr. intensities 0-43120  
 N<sub>2</sub>, electric breakdown, vol. discharge with external photoionisation, plasma focus spark channel (*Russian*) 0-38738  
 N<sub>2</sub>, photoionis., shape-reson. enhanced nucl. motion effects 0-1031  
 N<sub>2</sub>, photoionis. and photoabsorpt. cross sections for aeronomic calcs., data tables 0-41599  
 NO, state selective step-wise photoionis. with mass spectroscopic ion detect. 0-43119  
 N<sub>2</sub>O, valence shell ionic photofragmentation, oscill. strengths, EELS and electron-ion coincidence meas. 0-37879  
 Na, laser temporal coherence effects in two-photon resonant three-photon ionisation 0-32686  
 Na, photoionis. cross section resons., time-dependent HF theory 0-32684  
 Na, quantum beats of hyperfine levels observed in photoionisation 0-32690  
 Na, reson. two-photon ionisation via 3p<sup>2</sup>P<sub>3/2</sub> state, photoelectron ang. distrib. 0-43016  
 Na, spontaneous field induced optical SHG, multiphoton ionisation 0-14395  
 Na, three-photon ionisation, laser bandwidth and intensity effects 0-52956  
 Na, vap. associatively ionised by CW IR laser beam (*Japanese*) 0-5515  
 Ne, 1s and 2s photoionis. cross sections, L<sup>2</sup> calc. 0-951  
 Ne II, III, and IV ground state, photoionis. cross sections, close coupling calcs. 0-5513  
 Ne II, III, IV, photoionisation cross sections calc. 0-43014  
 O and O<sub>2</sub>, photoionis. and photoabsorpt. cross sections for aeronomic calcs., data tables 0-41599  
 O, UV photoionisation cross-section calc., 304 and 584 Å 0-43015  
 O<sub>2</sub>, photoexcitation and photoionisation cross sections, HF Gaussian method 0-53064  
 O<sub>2</sub>, photoionisation, partial channel cross-sections calcs. 0-53061  
 OCS, high-intensity laser photolysis at 157 nm, S(<sup>1</sup>S) prod., photoionisation, and loss, laser appl. 0-21306  
 Pb, 5d subshell, photoionisation partial cross-section, energy depend. meas. 0-29850  
 Rb, photoionis. cross section, elec. field depend. 0-37796  
 SF<sub>6</sub>, photoionisation spectra in XUV region 0-37837  
 Sb, 4d subshell, photoionisation partial cross-section, energy depend. meas. 0-29850  
 Si:Zn, photoionisation of deep impurity levels 0-34386  
 SnS<sub>2</sub>, Sn4d photoionisation, second threshold 0-40222  
 Sr, efficient ionis. by reson. laser pumping 0-32685  
 Xe, 5s→ep photoelectron ang. distrib. near Cooper minimum 0-18834  
 Xe precursors, associative ionisation and photoionisation, relative contrib., electron density prediction 0-43858

**photolithography**

- see also masks; photoresists*  
 diffraction grating generation for integrated optics, interference method 0-48460  
 Josephson microbridges, ultrasmall, step-edge fabrication 0-49997  
 lithographic coated polyester panchromatic plate system 0-13172  
 MTF evaluation for optical and electron-beam lithography 0-4801  
 optical channel waveguide arrays coupled to integrated CCD 0-33244  
 optical transfer measure, system relations, appl. wide field microscopy and microelectronic photolithography (*German*) 0-9815  
 steel, mild, photoetched profiles 0-25907  
 thick film optical waveguide integration with fibre-optic connectors 0-33246  
 X-ray lithography with thin polymer resists, high energy irradi. and selective dissolution (*German*) 0-13167  
 Al-Cu alloy layer, photolithographically patterned, separation from substrate using plasma etching (*Slovak*) 0-45405  
 Pb-Sn Josephson junctions, small area high current density normal resistance, RC times 0-34555

**photoluminescence**

- see also fluorescence; phosphorescence*  
 alkali halide:Ti<sup>4+</sup>-like ions, triplet state lifetime, hyperfine interaction 0-2844  
 alkali halides, coloured, light amplification at activator centres 0-2795  
 anthracene, γ-irradiation influence on defects, luminesc. study (*Russian*) 0-55185  
 anthracene, with pentacene and tetracene impurities, laser-pulse-excited luminesc. 0-7408  
 anthracene crystal, resonance secondary emission, Raman scatt. in exciton absorpt. region (*Russian*) 0-40120  
 anthracene Langmuir film, lightly substituted, electrolum., photolum. and electroabsorption 0-20726  
 anthracene single crystals, effect of γ-irrad. on photolum. (*Russian*) 0-2852  
 anthracene-Au interface exciton luminescence Frenkel exciton metallic quenching (*Russian*) 0-50421  
 anthracene-pyromellitic dianhydride complex, optical and photoelectric props. (*Russian*) 0-15570  
 anthracene-quartz interface exciton luminescence, Frenkel exciton metallic quenching (*Russian*) 0-50421  
 bacteria, effect of mag. field on recomb. fluoresc. 0-35856  
 bisphenol-A-diglycidyl epoxy, light emission under high elec. field, compared with photolum. 0-25465

**photoluminescence continued**

- caesium uranyl propionate, low temp. absorpt., luminesc. spectra, intermol. interactions 0-2830  
 concentrational depolarisation by excitation energy transfer 0-2821  
 crystal luminescence, polariton mechanism, reabsorption, spatial dispersion effects, boundaries (*Russian*) 0-55186  
 decay curve simulation, finite breadth light pulse excited (*Hungarian*) 0-11473  
 diamond, GRI and UV band, fine struct. 0-20678  
 diamond, optical absorption and luminesc. spectra, review 0-2848  
 diethylammonium manganese chloride, antiferromag., low temp. luminesc. spectra, magnetoelastic effect 0-2810  
 dimethylammonium manganese chloride, antiferromag., low temp. luminesc. spectra, magnetoelastic effect 0-2810  
 diphenyl-pyrene, self induced transparency under nonreson. excitation, luminesc. and stimulated emission 0-11436  
 diphenyl-pyrene, stimulated emission at 0-0 transition, 4.2K 0-11437  
 disordered systems, time dependent spectral transfer, Monte Carlo calc. 0-11464  
 energy transfer and two-centre optical transitions in OH<sup>-</sup> and rare earth double-doped solid 0-7398  
 energy transfer between 5d electronic states 0-2808  
 filter, luminescent, efficiency for Nd:glass lasers 0-1213  
 glass:Nd<sup>3+</sup>,Cr<sup>3+</sup>, nonradiative energy transfer from Cr to Nd, optical pumping efficiency improvement 0-33001  
 hot luminescence in F centres, nonradiative quenching 0-11467  
 hot photoluminescence polarisation spectrum, photoelectron momentum distrib. function anisotropy relax. 0-7404  
 II-VI semiconductors, impurity and defect centre energy states, luminesc. meas., review 0-55150  
 II-VI semiconductors, radiation effects, optoelectric props. control 0-25458  
 impurities in solids, absorption and emission spectra, bandshapes, moments 0-45122  
 lone-pair semiconductor, defects, valence-alternation model and new directions 0-54646  
 metal, laser irradiated, optical and electronic emissions (*French*) 0-2919  
 micelle-confined molecules reaction, diffusion-controlled, luminesc. quenching, excimer form. 0-50890  
 molecular crystal, sensitised luminesc. calc. for trapping models using momentum-space theory of exciton transport 0-11447  
 molecular crystal, surface exciton levels, radiation corrections 0-34962  
 molecular excited state relaxation processes, oscillatory versus dissipative limits, education appl. 0-31468  
 naphthalene, microcryst. and evaporated film, excimer emission 0-2823  
 naphthalene-d<sub>8</sub>(d<sub>8</sub>) crystal, with isotopic impurities, Rashba effect, luminescence spectra, impurity states 0-29768  
 nitrate glass:Eu<sup>3+</sup> struct. reorganisation in glass transition interval, polarised luminesc. obs. 0-45141  
 NMR under optical pumping conditions 0-25253  
 nonequilibrium thermodynamics of luminescent processes in solids 0-50435  
 open photoreceiver, vacuum ultraviolet 0-52307  
 organic glass, electron-cation recombination; charge distrib. simulation and luminesc. kinetics 0-2855  
 orientation factor in conc. effects due to nonradiative energy transfer 0-25425  
 pentacene films, luminesc., struct. 0-11461  
 phenyl methacrylate copolymers, photoluminescent behaviour 0-25432  
 phosphate glass: Nd<sup>3+</sup>, miniature laser with high ion conc., luminesc. characts. 0-19038  
 phosphate glass:Nd<sup>3+</sup>, highly conc., electron energy deactivation and transfer (*Russian*) 0-29802  
 phosphate glass:Yb<sup>3+</sup>, excitation migration in inhomogeneous line profile, energy gap depend. 0-7407  
 phosphate glass:Mn<sup>2+</sup>, luminesc. colour change 0-7392  
 phosphate laser glasses, review 0-9888  
 pigment associations, conc. effects, luminesc., absorpt. spectra and dichroism obs. 0-1007  
 radiative electronic transitions of impurities, effects of hydrostatic press. 0-11446  
 Raman scattering, luminesc., electron-phonon interaction effects on polarisation 0-55088  
 resonance Raman scattering and luminescence of excitons in self-trapping process 0-20689  
 resonant scattering of light by slowly fluctuating localized electrons 0-7365  
 retinals, prod. and quenching of singlet oxidation 0-35840  
 rhodamine 6G and rhodamine B adsorbed on AlH<sub>3</sub>, luminesc. spectra during AlH<sub>3</sub> photolysis 0-55171  
 rhodamine 6G soln. in ethanol, luminesc. liq., pump radiation conversions to enhance laser efficiency 0-48293  
 rhodamine dye polar frozen solns., luminesc. broadening 0-2834  
 rubidium uranyl propionate, low temp. absorpt., luminesc. spectra, intermol. interactions 0-2830  
 semiconductor, bound excitons, review, book contrib. 0-44519  
 semiconductor crystals, with high quantum efficiency, minority carrier lifetime meas. (*Japanese*) 0-54711  
 semiconductor optical characterization 0-50352  
 semiconductors, heavily doped, compensated, long wavelength recomb. radiation 0-7403  
 semiconductors, p-type, mag. oscills. of momentum distribution of hot photoexcited electrons (*Russian*) 0-2854  
 semiconductors, PH luminescence band profile 0-20702  
 semiconductors, variable-gap, photoluminesc. under transient excitation conditions 0-20698  
 β-SiC, optical quenching of luminesc., acceptor ionisation energy 0-55178  
 small-polaronic glass, dynamics of optically induced props. 0-49630  
 sodium uranyl acetate (deuteroacetate) 0-2830  
 solution, rigid, luminesc. exchange promotion kinetics 0-50387  
 tetracene surface states, electric field effects, exciton-charge carrier interactions (*Russian*) 0-24989  
 transition quasilinear spectra of resonant secondary emission (*Russian*) 0-16102  
 variable-gap semiconductors, anal. of drift of recombination radiation 0-16096  
 AgBr, new shoulder in luminesc. spectra, triplet excitons 0-20706  
 AgBr:Cl, exciton-phonon interaction, reson. Raman scatt. vs photolum. 0-29798



## photoluminescence continued

- AgCl:Ni, optically detected double resonance, radiative recombination electron traps 0-20518  
 AgI large single crystals, gel and soln. growth and props. 0-35071  
 $\beta$ -AgI, luminesc. of 2H- and 4H-polytypes 0-2843  
 (AlGa)As DH, proton-stripped, proton-induced defects, photoluminesc. study 0-48251  
 (AlGa)As heterostruct., proton irradi., photoluminesc. 0-29808  
 AlGaAs-GaAs heterostructures, luminescent characts., efficiency and radiative lifetime conc. depend. 0-55151  
 Al<sub>1-x</sub>Ga<sub>x</sub>As, optically magnetised, luminescence polarisation anisotropy, hysteresis effect symmetry props. 0-34982  
 Al<sub>1-x</sub>Ga<sub>x</sub>As:N, ion implantation, in situ annealing photoluminesc. obs. 0-10567  
 Al<sub>1-x</sub>Ga<sub>x</sub>As:N<sup>+</sup>, (x=0.58), laser annealing of optically active impurities, photolum. charact. 0-20682  
 Al<sub>1-x</sub>Ga<sub>x</sub>P, photoluminescence excitation spectra, bound excitons, Al conc. depend. 0-20687  
 $\alpha$ -Al<sub>2</sub>O<sub>3</sub>, crystal defects from X-ray irradiation, F-centres, X-ray luminesc. obs. 0-55176  
 ArS, photoluminesc. in rare gas matrices 0-5568  
 As, amorphous, bulk and sputtered thin films 0-25457  
 As-Se glasses, low temp. photocond., complementary nature of photocond. and photolum. 0-49808  
 As<sub>2</sub>S<sub>3</sub>, amorphous, band to band radiative recomb. 0-25435  
 As<sub>2</sub>S<sub>3</sub>, amorphous, charged defect pair photolum. meas. 0-16078  
 As<sub>2</sub>S<sub>3</sub>, amorphous, luminesc. and optically detected ESR, photoinduced struct. change 0-50399  
 As<sub>2</sub>S<sub>3</sub>, amorphous, quantum efficiency and fatiguing behaviour of luminesc. processes 0-7402  
 As<sub>2</sub>S<sub>3</sub>, amorphous, time resolved spectroscopy of valence alternation pair luminesc. 0-50400  
 As<sub>2</sub>S<sub>3</sub>:Fe glass, photolum. and ESR, Fe impurities as non-radiative recomb. centres 0-29788  
 As<sub>2</sub>Se<sub>3</sub>, amorphous, defect states, exptl. study. 0-54645  
 a-As<sub>2</sub>Se<sub>3</sub>, doped film, photoluminescence intensity and lineshape study 0-50448  
 AuCl, luminesc., excitons 0-2839  
 BH<sub>x</sub>, photoluminesc. spectra 0-2815  
 BaAl<sub>2</sub>O<sub>4</sub>:Mn, phosphor, vac. UV excitation spectra, appl. to gas discharge display 0-2816  
 Bi<sub>2</sub>W<sub>2</sub>O<sub>9</sub>, energy transfer and luminesc. props. 0-55177  
 Bi<sub>2</sub>W<sub>2</sub>O<sub>9</sub>:Mo(Eu), energy transfer and luminesc. props. 0-55177  
 Ca<sub>2</sub>, new ground state, photolum. obs. vibr. consts., dissociation energy 0-5576  
 CaF<sub>2</sub>:Eu<sup>2+</sup>, X-ray excited luminesc., <sup>5</sup>D<sub>0</sub>-<sup>7</sup>F<sub>1</sub> transition 0-2842  
 CaI<sub>2</sub>:Pb(Mn), recomb. processes, luminesc. characts. (Russian) 0-25450  
 CaO:Bi<sup>3+</sup>(Pb<sup>2+</sup>), impurity centres vibronic spectra, lattice dynamics and electron-phonon interactions 0-7396  
 Ca<sub>2</sub>P<sub>2</sub>O<sub>7</sub>:Sb(Mn), luminesc., colouration 0-2828  
 $\beta$ -Ca<sub>2</sub>(PO<sub>4</sub>)<sub>2</sub>:Sb(Mn), luminesc., colouration 0-2828  
 CaS:Bi<sup>3+</sup>, Na<sup>+</sup>(Li<sup>+</sup>) phosphors, luminescence of associated centres (French) 0-40155  
 CaSO<sub>4</sub> phosphors:Ce(Eu)(Dy)(Tm), gamma-irradiated valency conversions in rare-earth ions 0-55198  
 CaSO<sub>4</sub>:Sm phosphors, X-ray induced fluorescence and phosphorescence 0-55179  
 CaS(Se):Eu<sup>2+</sup>, emission and excitation spectra obs. 0-55162  
 CaSe:Pb, luminesc. and EPR props. of Pb centres 0-55168  
 CdS, biexciton levels, luminescence-assisted two-photon spectra 0-29795  
 CdS, deep level IR luminescence, origin 0-20704  
 CdS, dislocation emission, photoluminesc. spectra 0-16084  
 CdS, dislocation structural optical absorpt., plastic deformation (Russian) 0-34959  
 CdS, doped laser mechanism and output study 0-43340  
 CdS, excitation spectroscopy, relation between I<sub>2</sub> bound exciton line and CdS excitonic molecule line 0-40153  
 CdS, exciton condensation, photoluminesc. spectra 0-25448  
 CdS, exciton optical and luminescence spectra characts. near dislocation slip bands 0-45111  
 CdS, high intensity excited, exciton reflection spectra, reflection struct. 0-20692  
 CdS laser irradi. native defect formation, influence on photoelectric props., IR luminescence (Russian) 0-11039  
 CdS, pure and Cl doped, stimulated emission due to indirect band-band transitions 0-7376  
 CdS single crystals, Roentgenoluminescence, exciton interactions (Russian) 0-2853  
 CdS, size effect of dense electron hole systems 0-7413  
 CdS, stress-induced photolum. bands, photocond., rel. to dislocation electron states 0-25447  
 CdS, three-photon absorpt. coeff. determ. by nonlinear luminesc. expt. 0-14384  
 CdS, time-resolved spectra of spontaneous luminesc. from high density electron-hole plasma 0-40156  
 CdS, two-photon-excitation, tunable laser emission, luminesc. processes 0-55127  
 CdS<sub>1-x</sub>Se<sub>x</sub> mixed crystals, free excitons, disorder effects 0-34365  
 CdS(Se)(Te):Co<sup>2+</sup>, IR luminesc. quenching, Co<sup>2+</sup> level position, ionisation energy 0-16079  
 CdSe, electron irradi., edge emission 0-25461  
 CdSe, high intensity excited, exciton reflection spectra, reflection struct. 0-20692  
 CdSe, luminesc. of high density electron-hole plasma at elevated temps. 0-20696  
 CdSe, polar semiconductor, collisions between hot excitons and hot electrons 0-7415  
 CdTe, electron-hole liquid formation in pure and doped crystals, luminesc. study (Russian) 0-55184  
 CdTe:Cl, electron irradi., defects 0-25460  
 CdTe:Fe(Ni), luminesc. and refl. spectra, high temp. annealing effects 0-24472  
 CdTe:In, pure and heavily doped, electron-hole liq. form., luminesc. spectra 0-10884  
 CeP<sub>2</sub>O<sub>8</sub>, IR absorpt. and luminesc. spectra 0-55079  
 CsBr, self-trapped excitons, magneto-optical props., 1.3-50K 0-49606  
 CsI, self-trapped excitons, magneto-optical props., 1.3-50K 0-49606  
 CsI:Na, electronic struct. and luminesc. 0-16080  
 CsI:Na, self-trapped exciton emission polarisation 0-49607  
 CsMnCl<sub>2</sub>·2H<sub>2</sub>O, nonequilibrium magnon population obtained by optical pumping (Russian) 0-11457

## photoluminescence continued

- CsMnF<sub>3</sub>, magnon absorption and luminesc. 0-7400  
 CsPbBr<sub>3</sub>, electronic and optical props. 0-25414  
 CsPbCl<sub>3</sub>, electronic and optical props. 0-25414  
 CuCl, donor-acceptor recomb. spectra 0-45131  
 CuCl, excitonic molecules, secondary emission under two-photon reson. excitation 0-11468  
 CuCl, luminesc. of excitonic mols. 0-2817  
 CuCl, two-photon absorpt. and luminesc., biexcitons 0-11434  
 CuGaSe<sub>2</sub>, single crystals, elect. and optical props. for solar cell appl. 0-10981  
 Er<sup>3+</sup>:Yb<sup>3+</sup> in liq. media, luminesc. cooperative sensitisation 0-2827  
 Eu<sup>3+</sup> soln., luminesc. quantum yield spectral depend. 0-2838  
 EuGa<sub>3</sub>(BO<sub>3</sub>)<sub>4</sub>, luminesc. spectra, local symmetry of rare earth ion determ. 0-16095  
 GaAlAs:Zn recombination radiation drift, charge carrier photon induced drift in varigap semicond. 0-50418  
 Ga<sub>1-x</sub>Al<sub>x</sub>As DH catastrophically degraded laser, TEM obs. of defects 0-32989  
 Ga<sub>1-x</sub>Al<sub>x</sub>As, photoluminescence, deep level trap emission capture 0-29805  
 Ga<sub>1-x</sub>Al<sub>x</sub>As-GaAs heterojunctions grown by metallorganic CVD 0-15599  
 Ga<sub>1-x</sub>Al<sub>x</sub>As-GaAs solar cells, photoluminesc. characterisation 0-3512  
 Ga<sub>1-x</sub>Al<sub>x</sub>As-GaAs double heterostructure laser diode, temp. depend. of photolum. 0-5734  
 GaAs, electrical and optical props. at low temps. 0-39636  
 p-GaAs, electron minority carrier diffusion lengths 0-29807  
 GaAs, electron-exciton collision influence on luminescence line profile due to bound excitons 0-29800  
 GaAs, epitaxial, nonequilibrium carrier relax., recombination radn. 0-7416  
 GaAs epitaxial layer, photoluminesc. defect complex 0-29804  
 GaAs, gamma and electron irradi. defect formation depend. on interface, luminescence study 0-34057  
 GaAs, holes optical orientation, luminesc. 0-25452  
 GaAs, hot photoluminescence depolarisation in mag. field, 0.4 eV energy state electron lifetime (Russian) 0-16086  
 GaAs injection lasers, amplified luminesc. 0-2824  
 GaAs LPE buffer layers for MESFET appls. 0-29887  
 n-GaAs, luminescence emitted from deep centres,  $\gamma$ -irrad. induced changes in internal quantum efficiency 0-20701  
 GaAs, MBE, undoped, growth and characterisation 0-10836  
 GaAs MBE epilayers, photoluminesc. and elec. characterisation 0-11500  
 GaAs, O<sup>+</sup> implantation, energy levels, photoluminesc. 0-24838  
 GaAs, photoluminescence, deep level trap emission capture 0-29805  
 GaAs, photoluminescence, electron-acceptor, from non-Maxwellian distrib. of photo-excited electrons 0-45138  
 GaAs, polar semiconductor, collisions between hot excitons and hot electrons 0-7415  
 GaAs, prep. of thin films by ionised-cluster beam deposition, photolum. meas. (Japanese) 0-25576  
 GaAs, radiative yield improvement by laser annealing 0-45128  
 GaAs, recombination radiation, anomalous temp. depend. 0-2847  
 n-GaAs Schottky diode 0-29781  
 GaAs solar cell structs., photolum. props. 0-50958  
 GaAs, spontaneous luminesc. due to high density electron-hole plasma under nano- and picosecond pulse excitation 0-40157  
 GaAs thin layers, MBE, growth conditions and phys. props. (German) 0-55307  
 n-GaAs VPE layers, Hall mobility, effect of Cu contamination, photolum. expts. 0-54810  
 n-GaAs vapour phase epitaxial film electrophysical props. rel. to growth temp. (Russian) 0-49961  
 GaAs:Be(C)(Ge)(Sn), MBE layers, photoluminesc. 0-29803  
 GaAs:Cr, O, effect of O in photoluminesc. meas. 0-29799  
 GaAs:Ge, ion-implanted, photoluminesc., deep emission centres 0-34965  
 GaAs:O, field depend. of radiative recomb. 0-20700  
 GaAs:Si encapsulated with AlN, Si<sub>3</sub>N<sub>4</sub> layers, photolum., annealing effects 0-20681  
 GaAs:Si layers, MBE growth, elec. and optical props., doping characts. 0-10819  
 n-GaAs:Si(Te), radiative transitions induced by modest annealing, photoluminesc. spectra 0-55158  
 GaAs:Si(Te)(S), vapour phase epitaxial grown layers, photoluminesc. and emission spectra 0-29774  
 GaAs:Zn, heavily doped, photolum. obs., above gap 0-29796  
 p-GaAs:Zn, luminescent, ion doped MBE growth 0-44436  
 GaAs-Al<sub>1-x</sub>Ga<sub>x</sub>As DH lasers, MBE grown, substrate temp. effect on current threshold 0-48243  
 GaAs-Al<sub>1-x</sub>Ga<sub>x</sub>As multilayer, photoluminesc., electron spin orientation 0-25453  
 GaAs-AlAs multilayer heterostructure laser, power and photoelectroluminescence characts. 0-53297  
 GaAs-AlGaAs photoelectroluminescent diodes, characts., radiant power 0-6972  
 GaAs-Au, quenching of exciton luminesc. by surface elec. field 0-29801  
 GaAs-Ga<sub>1-x</sub>In<sub>x</sub>P heterostruct., MBE layers, photolum. props., assessment as laser struct. 0-20705  
 GaAs<sub>0.6</sub>P<sub>0.4</sub>:N, isoelectronic tape by ion implantation and CO<sub>2</sub> laser annealing 0-24464  
 GaAs<sub>1-x</sub>P<sub>x</sub>, N implantation, characterisation by photolum. and channelling 0-54262  
 GaAs<sub>1-x</sub>P<sub>x</sub>, structural defects, optical props. effect 0-55208  
 GaAs<sub>1-x</sub>Sb<sub>x</sub>, undoped epitaxial layers, photoluminesc. meas. 0-20703  
 n-Ga<sub>1-x</sub>In<sub>x</sub>As<sub>1-y</sub>P<sub>y</sub>, photoluminesc. of epitaxial films, isovalent substitution 0-16097  
 GaN:Al, VPE grown, luminesc. and elec. props. depend. on doping conc., bound excitons 0-20688  
 GaN:Zn, VPE grown, optical cross sections, photoluminesc. and optical absorpt. meas. 0-55160  
 GaN:Zn, VPE growth, photoluminesc. rel. to doping conditions 0-55159  
 GaP, donor-acceptor pair luminesc., excitation spectroscopy 0-25440  
 GaP, electrical and optical props. at low temps. 0-39636  
 GaP:Co, deep levels, IR photoluminesc., stress effects 0-55163  
 GaP:N, electron-hole liq., luminesc. obs. 0-25438  
 GaP:N(N,O) epitaxial struct., luminesc. study of degradation during heat treatment 0-45139  
 GaP:Ni, deep traps, near IR luminesc., polarised spectra meas. 0-16077  
 GaP:Zn, luminesc., acceptor-bound multiple excitons 0-11476  
 GaSb and alloys, struct. defect, photoluminesc. 0-25459  
 p-GaSb, hot exciton luminesc., LO phonon Raman scatt. 0-11474



## photoluminescence continued

- GaSb:Te, indirect gap photolum. 0-29797  
 GaSe, direct exciton excited state hot luminescence, band struct. props. 0-55183  
 GaSe, optical excitation, excitonic spectra, stimulated luminesc. 0-40132  
 GaSe<sub>1-x</sub>S<sub>x</sub> polytypes, exciton gap energies, luminesc. study 0-54611  
 GdAlO<sub>3</sub>:Er<sup>3+</sup>, <sup>4</sup>S<sub>3/2</sub> to <sup>4</sup>I<sub>9/2</sub> transition laser action, optical and luminescence spectra 0-16082  
 Gd<sub>2</sub>O<sub>3</sub>:Bi<sup>3+</sup>, Tb<sup>3+</sup>, energy transfer from sensitiser to activator, intermediate role of Gd<sup>3+</sup> 0-50389  
 GdPO<sub>4</sub>:Dy<sup>3+</sup>, Bi<sup>3+</sup>(Sb<sup>3+</sup>), energy transfer from sensitiser to activator, intermediate role of Gd<sup>3+</sup> 0-50389  
 Gd<sub>2</sub>S<sub>3</sub>, resonance excitation of Nd<sup>3+</sup>, luminescence, absorption spectra (Russian) 0-50381  
 β-Gd<sub>2</sub>S<sub>3</sub>:Nd<sup>3+</sup>, spectroscopic props. from absorpt., photoluminesc. and excitation spectra 0-34968  
 (Gd<sub>1-x</sub>Tb<sub>x</sub>)<sub>2</sub>O<sub>3</sub>S phosphor, concentration quenching of Tb<sup>3+</sup> luminesc. 0-29785  
 Ge, biexciton and trion existence, photolum. (Russian) 0-16088  
 Ge, cyclotron resonance and radiative recomb. with laser excitation, book contrib. 0-11472  
 Ge, electrical and optical props. at low temps. 0-39636  
 Ge, electron-hole drop luminesc., phonon wind induced anomalous depend. at low mag. fields 0-34980  
 Ge, electron-hole drop motion 0-6744  
 Ge, electron-hole drop recombination radiation due to heat pulse action (Russian) 0-16087  
 Ge, electron-hole liquid, strain-confined 0-6745  
 Ge, exciton condensation, microwave breakdown, luminesc., book contrib. 0-11471  
 Ge, magnetoluminescence of electron-hole liq. 0-29790  
 Ge, nonuniformly deformed, electron-hole drop density depend. on size (Russian) 0-20092  
 Ge, stressed, metal-insulator transition, luminesc. 0-20695  
 Ge:As, recomb. of donor bound excitons, luminesc. intensity decay 0-25441  
 Ge:As(Bi), donor bound exciton luminesc. and absorpt. 0-29777  
 n-Ge:As(Sb), moderately heavily doped, electron-hole drops photoluminesc. 0-7417  
 Ge:B(Al)(Ga)(In)(Tl), binding energy, excited state spectra, photolum., semi-empirical short range pot. 0-44534  
 GeS orthorhombic layer crystals, photolum. spectra 0-2851  
 GeSe<sub>2</sub>, single crystals, 3 polymorphic forms, DTA, photolum., IR and Raman spectroscopy 0-33923  
 Ge<sub>2</sub>Se<sub>7</sub>, amorphous, excitation spectra of photolum. fatigue and creation of paramag. centres 0-50402  
 Hg<sub>1-x</sub>Cd<sub>x</sub>Te, photolum. and optical pumping 0-50424  
 α-HgS, cinnabar, reson. Raman effect and luminesc. meas. 0-50338  
 n-InAs, edge luminescence band, shape depend. on degree of doping, band gap 0-7405  
 InGaAsP, quaternary alloy, physical props. (Japanese) 0-15449  
 In<sub>1-x</sub>Ga<sub>x</sub>As<sub>1-y</sub>P<sub>y</sub> DH laser, low threshold current density, near equilibrium LPE growth 0-19040  
 InP, acceptor excited states, luminesc. spectra 0-16091  
 InP, bulk grown, selective spectroscopy, acceptor level studies 0-29778  
 InP, deep level electron traps, emission and capture props. 0-29806  
 InP, electrical and optical props. at low temps. 0-39636  
 InP, photoluminesc. of epitaxial films, isovalent substitution 0-16097  
 InP, polar semiconductor, collisions between hot excitons and hot electrons 0-7415  
 p-InP:Zn, vapour grown, prep. and props. 0-54268  
 InP-In<sub>1-x</sub>Ga<sub>x</sub>P<sub>1-y</sub>As<sub>y</sub>, heterostructure laser, single and multiple quantum-well, liquid-phase epitaxial growth 0-38031  
 InP(100) undoped homoepitaxial films grown by MBE, photoluminesc. props. 0-2809  
 InSb, electron spin levels resonant excitation, photolum. 0-25454  
 InSb p-n junction, minority carrier injection in mag. field, recomb. radiation obs. 0-11078  
 InSb, prep. of thin films by ionised-cluster beam deposition, photolum. meas. (Japanese) 0-25576  
 KBr, F-centre radiative lifetime meas. near 65K 0-25439  
 KBr:Pb, A-luminesc., 8-80K 0-2836  
 KBr:Ti, Jahn-Teller system, negative mag. circular polarisation in emission spectrum 0-20694  
 KBr(Cl)(I), electron-spin memory and magnetic-circular-dichroic effects in F-centre luminesc. 0-29794  
 KCl:Ag(In)(Tl), excitation in fund. absorpt. region, luminesc. and thermolum. 0-50433  
 KCl:Ba(Sr), Z-centre, luminesc. and absorpt. spectra obs. 0-49221  
 KCl:I, luminesc. at low temp. 0-2818  
 KCl:SnCl<sub>2</sub>, X-ray irradi., polarised luminesc. and EPR study of Sn<sup>3+</sup> centres 0-39868  
 KCl-CuCl solid solution supersaturated, precipitation, impurity aggregation 0-29174  
 KCl-Tl, Jahn-Teller system, negative mag. circular polarisation in emission spectrum 0-20694  
 KI, luminesc. lines due to n=2 free exciton state of Wannier series 0-29776  
 KI, quenched, absorpt. and emission spectra, α-centres 0-11442  
 KI:Tl, Jahn-Teller system, negative mag. circular polarisation in emission spectrum 0-20694  
 K<sub>6</sub>Nb<sub>6</sub>Si<sub>6</sub>O<sub>26</sub>, luminesc. bands, Stokes shift, rel. to crystal struct., stacking faults 0-34974  
 K<sub>8</sub>Nb<sub>8</sub>Si<sub>8</sub>O<sub>47</sub>, luminesc. bands, Stokes shift, rel. to crystal struct., stacking faults 0-34974  
 K<sub>5</sub>NdLi<sub>2</sub>F<sub>10</sub> (KNLF), spectroscopy and lasing 0-5737  
 K<sub>1.75</sub>Pt(CN)<sub>4</sub>·1.5H<sub>2</sub>O, Raman scatt. and luminesc. studies 0-25394  
 KI:Tl, excitation in fund. absorpt. region, luminesc. and thermolum. 0-50433  
 K<sub>2</sub>S, photoluminesc. in rare gas matrices 0-5568  
 La<sub>2</sub>O<sub>3</sub>-Al<sub>2</sub>O<sub>3</sub>-SiO<sub>2</sub>:Sm<sup>3+</sup>, luminesc. selective laser excitation line narrowing 0-25434  
 La<sub>1-x</sub>Tb<sub>x</sub>OBr phosphor, concentration quenching of Tb<sup>3+</sup> luminesc. 0-29785  
 LiF with stable F<sub>2</sub> centres, F<sub>2</sub><sup>+</sup> colour centre generation accumulation, tunable laser production (Russian) 0-28238  
 LiH(D), resonant Raman scattering in crystals with self-trapping excitons 0-7344  
 LiIO<sub>3</sub>, crystal, parametric superluminescence in ps band 0-11469  
 Li<sub>2</sub>N, photoluminesc. props. 0-50414  
 LiNbO<sub>3</sub>:Cr<sup>3+</sup> glass, roller quenched, crystn. kinetics 0-44143

## photoluminescence continued

- LuAlO<sub>3</sub>:Er<sup>3+</sup>, <sup>4</sup>S<sub>3/2</sub> to <sup>4</sup>I<sub>9/2</sub> transition laser action, optical and luminescence spectra 0-16082  
 MgF<sub>2</sub>, nonactivated, X-ray luminesc., 0-2832  
 MgF<sub>2</sub>, X-ray luminesc. polarisation 0-11462  
 MgO, F-centre luminesc., effects of uniaxial stress and ODMR 0-20690  
 MgS:Eu<sup>2+</sup>, emission and excitation spectra obs. 0-55162  
 N<sub>2</sub>, solid and matrix isolated mol., triplet state spectra (Russian) 0-5574  
 Na-fluorescein, glycerol-alcohol soln., luminesc. decay time, conc. depend. 0-34960  
 NaCl particle, luminesc. duration rel. to time in CO<sub>2</sub> laser beam focal zone 0-34983  
 NaCl:Ag, excitation in fund. absorpt. region, luminesc. and thermolum. 0-50433  
 NaI, motion of free excitons and their self-localisation 0-2342  
 NaI, resonant Raman scattering in crystals with self-trapping excitons 0-7344  
 NaI, thermal dissociation of photoproduced excitons at UV band edge, recomb. luminesc. obs. 0-50412  
 NaMnCl<sub>3</sub>, antiferromagnet, exciton self-localisation luminesc. and excitation spectra (Russian) 0-11456  
 Na<sub>2</sub>O-B<sub>2</sub>O<sub>3</sub>-SiO<sub>2</sub>:Yb(Tb), luminesc. cooperative processes, glass struct. and comp. effect 0-16101  
 P, amorphous, red, photolum. props. and band gap 0-50403  
 PbBr<sub>2</sub>, red luminesc., absorpt. spectra 0-2831  
 PbI<sub>2</sub> crystals, exciton condensation, excitation and luminesc. study 0-55182  
 PbI<sub>2</sub> direct gap semiconductor, exciton lifetime and condensation threshold, luminescence spectra 0-34981  
 PbI<sub>2</sub>, three-photon absorpt. coeff. determ. by nonlinear luminesc. expt. 0-14384  
 PbMg<sub>1/3</sub>Nb<sub>2/3</sub>O<sub>3</sub>, photolum. near ferroelec.-paraelec. phase transition 0-16100  
 PbSe, X-ray diffr. exam. of struct., and luminescence props. 0-55209  
 Pb<sub>1-x</sub>Sn<sub>x</sub>Te films, size quantisation, optical orientation of free carriers, polarisation props. of luminesc. 0-20725  
 Pb<sub>1-x</sub>Sn<sub>x</sub>Te:In epitaxial layers, growth, elec. props., and luminesc. 0-54542  
 RbMnF<sub>3</sub>, antiferromagnetic resonance, optical detection, luminescence 0-7174  
 S<sub>2</sub> mol. B<sup>3</sup>Σ<sub>u</sub><sup>-</sup>→X<sup>3</sup>Σ<sub>g</sub><sup>-</sup> fluorescence induced by N<sub>2</sub> laser (Japanese) 0-14175  
 Se, glassy, pure and K-doped, photolum. and optically induced ESR 0-50398  
 Si, amorphous, glow discharge, fatigue effect in luminesc., recovery by annealing 0-50416  
 Si, amorphous, spin depend. recomb., luminesc. and light induced ESR 0-50393  
 Si, amorphous, time resolved photoluminesc. near band gap 0-25445  
 Si, amorphous, time-resolved ODMR and luminesc. 0-25254  
 Si amorphous film, optical props., electronic states 0-25475  
 Si, bound multiexciton complexes, luminesc. 0-10888  
 Si, CW laser annealed, defect luminesc. 0-50388  
 Si, diamagnetism of excitons and biexcitons, recomb. spectra (Russian) 0-7412  
 Si, electron-hole droplet spatial distrib., luminesc. obs. 0-49615  
 Si, electron-hole drops, nonequilibrium paramagnetism 0-6749  
 Si, electron-hole drops, thermodynamical parameter determ. from luminescence data 0-2845  
 Si, electron-hole drops radius, luminesc. meas. 0-50415  
 Si, electron-hole liquid, free excitons, biexciton gas, luminesc. 0-6750  
 Si, excitons and electron-hole liquid, luminesc. 0-6746  
 Si, high purity, exciton lifetime, temp. depend., photoluminesc. meas. 0-44508  
 Si, neutron transmutation doping, photoluminesc. characterisation 0-11453  
 Si, piezoelectroscopic effect on zero phonon luminescence lines 0-50406  
 a-Si, resonant and non-resonant luminesc. changes theory 0-50410  
 Si:B, photolum. of heavily doped p- and n-type 0-20708  
 Si:B,In, sharp line series in near-band-edge photolum. 0-16092  
 Si:B(Al)(Ga)(In)(Tl), binding energy, excited state spectra, photolum., semi-empirical short range pot. 0-44534  
 Si:B(P), uniaxially stressed, impurity-assisted intervalley scatt., photoluminesc. obs. 0-34979  
 Si:H, amorphous, defect creation and H evolution 0-50392  
 Si:H, amorphous, excess carrier thermalisation and recomb., luminesc. decay and photocond. 0-50397  
 Si:H, amorphous, glow discharge deposited, laser annealing 0-49104  
 Si:H, amorphous, light-induced ESR and photoluminesc., dangling bonds with positive correl. energy 0-50161  
 Si:H, amorphous, luminesc., band tail states and thermalization 0-25455  
 Si:H, amorphous, radiative recomb. by diffusion and tunnelling, photocond. quantum efficiency 0-50394  
 Si:H, amorphous, radiative recomb. and luminescent processes 0-55152  
 Si:H, amorphous and crystalline, hydrogenation and dehydrogenation, luminesc. spectra 0-11477  
 Si:H, amorphous sputtered, excitation spectra and photoluminesc. 0-50396  
 Si:H, Cl(F), amorphous, photocond., dark cond. and photoluminesc. 0-49802  
 Si:H, ion-implanted, photoluminesc. spectrum 0-45129  
 a-Si:H, spin defect and recombination influence on electronic transport 0-50409  
 Si:H,F,O amorphous, plasma deposited, comp. and optical props. 0-50441  
 Si:H,P, amorphous, heavily hydrogenated, high gap state densities 0-49803  
 Si:H amorphous film, sputtered IR vibr. spectra and photolum., effects of partial evolution of H 0-44413  
 Si:H amorphous films, optoelectronic behaviour depend. on impurity incorporation during plasma deposition 0-49804  
 Si:H amorphous films for solar cells, optical and elec. props. of RF glow discharge deposited films 0-54576  
 Si:H amorphous sputtered film, photoluminesc., photocond. 0-20729  
 Si:H sputtered amorphous film, luminesc. and non-radiative decay 0-50395  
 Si:O,H amorphous, plasma-deposited, electronic and struct. props. 0-50391  
 Si:P, amorphous, CVD, defect compensation 0-54644  
 Si:P, ion-implanted and unimplanted, laser annealing, photoluminesc. study 0-2049



## photoluminescence continued

- Si:P, satellite of bound excitons, transient decay 0-11466  
 Si-H, amorphous, plasma-deposited, H evolution and defect creation 0-44914  
 SiC, (6H), radiation damaged, luminesc. 0-25462  
 SiC:Al(Ga)(B) (6H) LEDs, fabrication by rotation dipping technique, electrolum. mechanisms 0-50426  
 SiO<sub>2</sub>, amorphous and cryst., neutron irradi. and unirradi., intrinsic defect photolum. 0-50401  
 SiO<sub>2</sub>, intrinsic luminescence 0-16098  
 SnO<sub>2</sub>, semiconductor, photoluminescence, depend. on lattice temp. and excitation intensity 0-45137  
 Sn<sub>2</sub>P<sub>2</sub>S<sub>6</sub>, illumination effect on soft mode and dielectric props., luminesc. study (*Russian*) 0-50420  
 Sr<sub>1-x</sub>Eu<sub>x</sub>B<sub>2</sub>O<sub>4</sub>, luminesc. props. 0-34972  
 Sr<sub>1-x</sub>Eu<sub>x</sub>B<sub>2</sub>O<sub>7</sub>, luminesc. props. 0-34972  
 Sr<sub>1-x</sub>Eu<sub>x</sub>B<sub>2</sub>O<sub>10</sub>, luminesc. props. 0-34972  
 SrO, luminesc. band edge, 4-6.5 eV, optical absorpt., photoluminesc., cathodoluminescence, photocond. obs. 0-50411  
 SrO:Pb<sup>2+</sup>(Bi<sup>3+</sup>), impurity centres vibronic spectra, lattice dynamics and electron-phonon interactions 0-7396  
 Tb complexes, intermol. energy transfer to Eu complexes in aq. soln. 0-25426  
 Tb complexes, intermol. energy transfer to Eu complexes in aq. soln. 0-25427  
 Tb<sup>3+</sup> soln., luminesc. quantum yield spectral depend. 0-2838  
 Tb<sup>3+</sup>-Yb<sup>3+</sup> in liq. media, luminesc. cooperative sensitisation 0-2827  
 TbGa<sub>3</sub>(BO<sub>3</sub>)<sub>4</sub>, luminesc. spectra, local symmetry of rare earth ion determ. 0-16095  
 Tb(OH)<sub>3</sub>, exciton dynamics within an inhomogeneously broadened line, luminesc. spectra 0-50407  
 TbP<sub>2</sub>O<sub>14</sub>, IR absorpt. and luminesc. spectra 0-55079  
 UO<sub>2</sub>·HCONH<sub>2</sub>·0.5H<sub>2</sub>O, prep., cryst. struct. and charact 0-29010  
 Xe, crystalline, polariton effects, reflectivity, absorpt., and resonant luminesc. spectra calcs. 0-20095  
 Xe, solid, self-trapped exciton emission bands 0-20697  
 XeF fragment luminescence, during XeF<sub>2</sub> photodissoc. in solid Xe and Kr 0-3372  
 XeS, photoluminesc. in rare gas matrices 0-5568  
 (Y,Gd)BO<sub>3</sub>:Eu<sup>3+</sup>, phosphor, vac. UV excitation spectra, appl. to gas discharge display 0-2816  
 YA-O<sub>3</sub>:Er<sup>3+</sup>, pulsed laser action, <sup>4</sup>S<sub>3/2</sub> to <sup>4</sup>I<sub>9/2</sub> transition laser action, optical and luminescence spectra 0-16082  
 YAG:Ce<sup>3+</sup>, photoluminescence excitation energy, crystal field and temp. effects 0-11460  
 YAG:Eu<sup>3+</sup>, reson. fluoresc. spectra, showing multiple Eu<sup>3+</sup> sites 0-2812  
 YF<sub>3</sub>:Nd, Ce, energy transfer between 5d electronic states 0-2808  
 YF<sub>3</sub>:Tm, Nd, energy transfer between 5d electronic states 0-2808  
 YF<sub>3</sub>:Yb,Er, limit efficiency of transformation of IR to visible radiation 0-29784  
 Y<sub>2</sub>O<sub>3</sub>:S:Eu phosphor, luminescence saturation effects due to N<sub>2</sub> laser and cathode-ray excitation 0-40151  
 δ-Y<sub>2</sub>S<sub>3</sub>:Nd<sup>3+</sup>, spectroscopic props. from absorpt., photoluminesc. and excitation spectra 0-34968  
 Yb:glass, luminesc., low temp. energy transfer 0-2837  
 YbP<sub>2</sub>O<sub>14</sub> and Yb<sub>2</sub>O<sub>3</sub>Tb<sub>2</sub>P<sub>2</sub>O<sub>14</sub>, IR absorpt. and luminesc. spectra 0-55079  
 Zn,Cd<sub>1-x</sub>S:Cu, local centres responsible for photoluminescence 0-29783  
 Zn<sub>1-x</sub>Mg<sub>x</sub>Te, P doped alloys, elec. props. 0-2813  
 ZnO, biexciton levels, luminescence-assisted two-photon spectra 0-29795  
 ZnO epitaxial film on Al<sub>2</sub>O<sub>3</sub> substrate, recombination radiation in intense single photon excitation 0-7410  
 ZnO, excited states of bound excitons, photoluminesc. obs. 0-44513  
 ZnO, multiparticle exciton complexes, luminesc. spectra (*Russian*) 0-16090  
 ZnO powders, UV luminesc. spectral distrib., comparison with single crystals, excitons role 0-55167  
 ZnO, two-photon-excitation, tunable laser emission, luminesc. processes 0-55127  
 ZnO-GeO<sub>2</sub>-MnO-B<sub>2</sub>O<sub>3</sub> wideband cathodoluminescent phosphor 0-55196  
 α-Zn<sub>3</sub>P<sub>2</sub>, local centre parameters, photoelectron transition scheme, recomb. process anal. 0-44654  
 ZnS, excited phosphor, IR stimulation and quenching of luminesc., review (*Russian*) 0-11455  
 ZnS, luminescence of M-centre 0-29779  
 ZnS, single crystals, excited by laser beam and elec. field, streamer luminesc. and photolum. obs. 0-34986  
 ZnS:Ag, phosphor, luminesc. of surface glow centres 0-29782  
 ZnS:Al<sub>2</sub>Cu(Ag)(Au) phosphors, luminesc. excitation spectra and exciton struct. 0-55164  
 ZnS:Al(Te) phosphors, luminesc. excitation spectra and exciton struct. 0-55165  
 ZnS:Fe, luminesc. and ESR investigations 0-2822  
 ZnS:Mn, self-activated and Mn<sup>2+</sup> emission, high press. action 0-16093  
 ZnS:Mn<sup>2+</sup> phosphors, luminesc. excitation spectra and exciton struct. 0-55164  
 ZnS:Ne, implanted single crystals, photolum. and bombardment effect, thermolum. curve obs. 0-55166  
 ZnS(Se)(Te):Co<sup>2+</sup>, IR luminesc. quenching, Co<sup>2+</sup> level position, ionisation energy 0-16079  
 ZnSe:Ga(As), edge luminesc. 0-20699  
 ZnSe:In films, MBE growth, doping effect on photoluminesc. 0-10818  
 ZnSe:Li(Na)(Ga) doped and pure cryst., donor-acceptor bands 0-11465  
 ZnSe:Ni, evidence for exciton binding at Ni impurity sites, photolum. excitation spectrum 0-45135  
 (ZnSe)<sub>1-x</sub>(GaAs)<sub>x</sub> solid solns., photoluminescence spectra 0-40159  
 Zn<sub>2</sub>SiO<sub>4</sub>:Mn phosphor, efficiency enhancement by AlPO<sub>4</sub> substitution 0-11452  
 ZnTe crystals, secondary radiation polarization and relaxation of optical excitation 0-11399  
 ZnTe, dominant acceptors, annealing and quenching 0-24463  
 ZnTe, elec., SEM and TEM studies of impurity segregation during long annealing 0-30001  
 ZnTe, electron-phonon coupling, donor-acceptor pairs selective excitation 0-11475  
 ZnTe, luminesc., donor-acceptor-pair excitation spectroscopy 0-25456  
 ZnTe, luminescence spectra struct. surface and volume polaritons (*Russian*) 0-16089  
 ZnTe, real structure effect on luminescence and absorption spectra, dislocations 0-16085  
 ZnTe, refined, undoped, Cu acceptor, optical absorption and photoluminesc. meas. 0-34970

## photoluminescence continued

- ZnTe, unalloyed, mechanism of radiative transitions 0-50405  
 ZnTe:Ag, real structure effect on luminescence and absorption spectra, dislocations 0-16085  
 ZnTe:Al,Cl, photolum., complex acceptor, ionization energy 0-20693  
 ZnTe:As(Li), donor-acceptor pair excitation and recomb., photoluminesc. obs. 0-20691  
 ZnTe:Li, diffusion investigation by SEM and TEM 0-10706  
 ZnTe:P, pure and doped, electron and exciton excited states of neutral donor 0-34393

## photolysis

- see also photodissociation*  
 acetaldehyde, first triplet state geometry, fragmentation into free radicals 0-47915  
 atom+ molecule reaction rate meas. 0-16676  
 benzoin containing system, photosensitized free radical polymerisation 0-7825  
 benzophenone containing system, photosensitized free radical polymerisation 0-7825  
 benzophenone-N,N-dimethylaniline, intramolecular exciplex systems, laser photolysis obs. 0-35550  
 bromotrifluoromethane, <sup>13</sup>C isotope selectivity press. depend., multiphoton IR photolysis 0-45523  
 chlorodifluoromethane, IR multiphoton dissociation, CF<sub>2</sub> form., time-resolved optical absorption obs. 0-16702  
 chlorofluoromethanes, laser photolysis, product vibr. relax. rates and diffusion coeffs. 0-55680  
 chlorotrifluoroethylene, multiphoton dissociation, fragment energy partitioning 0-55681  
 cofacial diporphyrins, electron transfer reactions following picosecond excitation, CT state lifetimes, optical difference spectra 0-25995  
 complex molecules, laser induced dissociation, thermal energy effects 0-53071  
 cycloheptanone, photolysis, CIDNP effects 0-18869  
 dibromodifluoromethane, UV laser fluoresc. and photochem., CF<sub>2</sub>, CF and Br<sub>2</sub> fluoresc. obs. 0-16703  
 dichlorodifluoromethane, UV photolysis, free radical emission 0-30263  
 1,3-diphenylisobenzofuran solns., rubrene sensitised photooxidation, S<sub>1</sub> excited state O<sub>2</sub> quenching 0-45529  
 dye solutions, picosecond flash photolysis and very fast processes 0-30249  
 Earth atmosphere, translationally hot O(<sup>3</sup>P) atoms energy distrib. function 0-21811  
 ethyl acetate, multiphoton dissociation by CO<sub>2</sub> laser beam 0-7811  
 N-ethylcarbazole, soln., laser induced ionic photodissociation, transient polyelectrolyte form. 0-53068  
 ethylene, photoassisted decomposition at room temp. over Pt/TiO<sub>2</sub> 0-55703  
 fluorobenzenes, matrix laser fluoresc. spectra of radical cations 0-1009  
 free radicals, photolysis, excimer laser UV obs. 0-16711  
 hydrocarbons, reactions, rate consts., temp. depend., photolysis, high temp. fast flow reactor technique 0-42231  
 imidazoles, reaction with photochemically generated α-hydroxyalkyl radicals, EPR study 0-35558  
 interstellar grain mantles, UV photolysis rel. to mol. form., laboratory analogue expts. 0-26944  
 IR multiple-photon photolysis, fluence-depend. dissociation probabilities calc. 0-32786  
 ketene, CH<sub>3</sub> photoproduct, wavelength depend. 0-11936  
 laser photolysis installation for investigation of phototransformations of substances in nanosecond time interval 0-33006  
 laser-induced, effective manifold reduction, criteria 0-43123  
 photoelectrochemical cells, metal, electrodes in contact with fluorescent dye solns., photovoltage generation, comprehensive model 0-40871  
 photoelectrochemistry, laser sources use for solar energy conversion 0-40873  
 photoelectrolysis, basic electrode processes and appls. to H prod. from H<sub>2</sub>O 0-51016  
 pivalophenone, organic soln., triplet reactivity solvent depend., flash photolysis study 0-11902  
 poly N-vinylcarbazole, soln., laser induced ionic photodissociation, transient polyelectrolyte form. 0-53068  
 poly-2-vinylnaphthalene, soln., lowest triplet props., flash photolysis and radiolysis obs. 0-32861  
 radical generation for EPR 0-11271  
 rhodopsin, photo- and thermo-bleaching rel. to heterogeneity problem 0-41114  
 selenophene, flash photolysis, transient absorpt. spectra 0-14153  
 simple molecules, two-photon dissociation, spectrosc. obs. 0-32787  
 stilbene, cis- and trans-, picosecond flash photolysis, intramol. charge-reson. transition obs. 0-7810  
 sulphononaphthols, rapid pH and ΔμH<sup>+</sup> jump by short laser pulse 0-16709  
 tetrafluorodihietane, IR photolysis, multiphoton dissociation models 0-30253  
 trifluoromethane, D ultrahigh single-step enrichment by CO<sub>2</sub> laser photolysis 0-45527  
 uranyl hexafluoroacetylacetonate tetrahydrofuran, IR laser photodissociation, O and U isotope selective 0-50868  
 Ag complexes, Ag(II) porphyrins, picosec. flash photolysis, transient absorpt. 0-52976  
 AgBr:Pd(II), photolysis-induced trapping behaviour, EPR study 0-54949  
 AlH<sub>3</sub>, photolysis, luminesc. spectra of adsorbed rhodamine dyes 0-55171  
 AlH<sub>3</sub>, polycrystalline, photoconductivity and photochemical decomp. 0-44638  
 Ar:PH<sub>3</sub>:N<sub>2</sub>O, photolysis, HPO and PO form., IR(UV) matrix isolation spectra 0-47985  
 Br<sup>+</sup>NOBr, primary and secondary photochemistry, vibrationally excited NO, IR fluoresc. obs. 0-48030  
 Br<sub>2</sub>-CO<sub>2</sub> IR laser with Br<sup>+</sup>-CO<sub>2</sub> electronic-vibr. energy transfer as pump mechanism 0-53260  
 C<sub>2</sub>F<sub>4</sub> VUV photolysis, CF<sub>2</sub>(<sup>1</sup>B<sub>1</sub>) energy dynamics. 0-50861  
 CF<sub>3</sub>NO-CF<sub>3</sub>NO, photodissociation dynamics, two-photon laser-induced fluorescence study 0-43122  
 CO, multiphoton UV photolysis, isotope effects obs. 0-55679  
 CO<sub>2</sub>, photolysis, O(<sup>3</sup>S) absolute quantum yield spectral depend. meas. using XeO luminesc. 0-35561  
 CdI<sub>2</sub> crystals, photolysis obs. (*Russian*) 0-7833  
 Cl+NOCl, primary and secondary photochemistry, vibrationally excited NO, IR fluoresc. obs. 0-48030  
 Cl<sub>2</sub>-O<sub>2</sub>-H<sub>2</sub> dilute mixtures, photolysis products, Fourier Transform IR kinetic obs. 0-26033



**photolysis continued**

- $\text{Cl}(\text{P}) + \text{CH}_4 \rightarrow \text{CH}_3 + \text{HCl}$ , reaction rate const., laser flash photolysis-resonance fluoresc. kinetic study 0-45485  
 $\text{Cs}_2$ , two-photon dissociation, spectrosc. obs. 0-32787  
 $\text{Fe}(\text{CO})_5$ , solns. with dissolved NO, photolysis,  $\text{Fe}(\text{NO})_3\text{CO}$  form. 0-53024  
 $\text{H}_2$ , generation by water solar photolysis, large-scale impracticability 0-26172  
 $\text{HCl}-\text{Br}_2-\text{Ar}$ , flash photolytically produced  $\text{Br}^*$  to  $\text{HCl}$  electronic to vibr. and rot. energy transfer 0-48066  
 $\text{HI}$  photolysis, ESR spectrum of  $^{127}\text{I}$  atoms in  $\text{Xe}$  matrices 0-1005  
 $\text{H}_2\text{O}$  and activated C, photoassisted decomposition at room temp. over  $\text{Pt}/\text{TiO}_2$  0-55703  
 $\text{H}_2\text{O}$ , for H fuel prod. (French) 0-55776  
 $\text{H}_2\text{O}$ , for photoelectrochem.  $\text{H}_2$  production using solar energy and  $\text{Zn}(\text{Mg})(\text{Cr})(\text{Ni})$  phthalocyanine dyes (French) 0-55936  
 $\text{H}_2\text{O}$ , photochem. prod. of H using sunlight 0-45776  
 $\text{H}_2\text{O}$  photolysis using fission pumped gas lasers for H prod. 0-45810  
 $\text{H}_2\text{O}$  solar photolysis for  $\text{O}_2$ ,  $\text{H}_2$  prod. by engineering methods using biological materials (Japanese) 0-45765  
 $\text{H}_2\text{SO}_4$ , frozen soln., EPR of trapped H-atoms produced by UV and X-irrad. 0-3369  
 $\text{HgBr}$ , laser photolysis prep., laser induced fluoresc., collisional quenching processes 0-38014  
 $\text{HgBr}_2$  photolysing,  $\text{HgBr}^*$  fluorescence, steady state meas. 0-42986  
 $\text{HgCl}_2$  photolysing,  $\text{HgCl}^*$  fluorescence, steady state meas. 0-42986  
 $\text{I}$  laser, photolytically pumped, chem. kinetics 0-48235  
 $\text{IBr}-\text{CO}_2$  IR laser with  $\text{Br}^* \rightarrow \text{CO}_2$  electronic-vibr. energy transfer as pump mechanism 0-53260  
 $\text{N}_2$  dye laser flash photolysis system, 5  $\mu\text{J}$  with 3 ns time resolution 0-1211  
 $\text{NH}_3 + \text{NO}_2$ , reaction rate const. meas. 0-7772  
 $\text{NH}_3$ , UV laser photodissoc.,  $\text{NH}_2$  internal energy distrib., NH states 0-11901  
 $\text{NH}_3$ ,  $^{57}\text{Fe}$ , solid, Mossbauer study of iron bonding to solid ammonia and its photofragments 0-15833  
 $\text{NO} + \text{BrO}$ , temp. depend. kinetic study, stratospheric Br photochemistry implication 0-50866  
 $\text{N}_2\text{O}$ , photolysis,  $\text{O}(\text{S})$  absolute quantum yield spectral depend. meas. using  $\text{XeO}$  luminesc. 0-35561  
 $\text{NaClO}_4$ , frozen soln., EPR of trapped H-atoms produced by UV and X-irrad. 0-3369  
 $\text{NaOH}$ , frozen soln., EPR of trapped H-atoms produced by UV and X-irrad. 0-3369  
 $\text{Ni}$  complexes,  $\text{Ni}(\text{II})$  porphyrins, picosec. flash photolysis, transient absorpt. 0-52976  
 $\text{NiO}$  electrode for photolysis 0-40696  
 $\text{O}_2 + \text{CH}_3 \rightarrow \text{OH} + \text{H}_2\text{CO}$ , 368K, rate const. upper limit 0-7771  
 $\text{O}_3$ , laser flash photolysis,  $\text{O}(\text{D})$  quantum yields in fall-off region 0-45524  
 $\text{O}_3$ , laser-induced photolysis, reactions of  $\text{O}(\text{P})$ ,  $\text{O}(\text{D})$  and  $\text{O}_2(\text{D})$  0-11928  
 $\text{O}_3$ , primary products electronic and vibr. state distrib. 0-50865  
 $\text{O}_3$ , UV photodissoc. rate, expt. and theory 0-40722  
 $\text{O}_3 + \text{O}_2(\text{D}_g)(\text{O}_2^*)$ , UV photolysis,  $\text{O}(\text{P})$  prod., rate consts. determ. 0-55636  
 $\text{O}_3 + \text{O}(\text{D})$ , UV photolysis,  $\text{O}(\text{P})$  prod., rate consts. determ. 0-55636  
 $\text{OCS}$ , high-intensity laser photolysis at 157 nm,  $\text{S}(\text{S})$  prod., photoionisation, and loss, laser appl. 0-21306  
 $\text{OCSe}$  photolysis producing Se, using high efficiency ArF laser source 0-33032  
 $\text{OH}$ , prod. by photolysis, A-doublets, population, rot. states, hyperfine struct., microwave spectra 0-32694  
 $\text{O}(\text{D}) + \text{N}_2(\text{O}_2)(\text{N}_2\text{O})(\text{CO}_2)(\text{H}_2\text{O})(\text{methane})$ , collisional deactivation meas., 295K, rel. to atmospheric processes 0-16663  
 $\text{SCI}(\text{Br})$ , unstable radicals, matrix-isolated, IR spectra force const. (German) 0-43053  
 $\text{Se}_2$ , photolysis by UV lasers, appl. to kinetics of group VI laser systems 0-7807  
 $\text{SiF}_4$ ,  $\text{CO}_2$  laser-irrad., dissociation product fluoresc., wavelength depend. 0-11900  
 $\text{U}$  complex, bis-hexafluorocetylacetate uranyl tetrahydrofuran, laser-induced dissociation 0-53071  
 $\text{XeF}_2$ , photodissoc. yield in solid Xe and Kr, time-resolved photolum. excitation obs. 0-3372  
 $\text{XeF}_2$  photodissociation for XeF laser 0-32976  
 $\text{XeF}_2$  photolysis with VUV radiation, XeF (B,C) state prod. and kinetics 0-32975

**photomagnetic effect**

- $\text{CdCr}_2\text{Se}_4$ , ferromag. semicond., photoinduced mag. anisotropy 0-50086  
 $\text{Cd}_{1-x}\text{Hg}_x\text{Te}$ , photothermomag. effect and photocond. in millimetre wavelength range 0-44657  
 $\text{Fe}_2\text{O}_4$ , metallic phase, photocond. and mag. permeab., photoinduced changes 0-15566  
 $\text{Pb}_{1-x}\text{Sn}_x\text{Te}$ :Cd, photocond., photomag. effect, carrier lifetimes 0-44658  
 $\text{Si-SiO}_2\text{-Si}_3\text{N}_4$ , internal photoemission 0-7475

**photometers**

- see also photometry; spectrophotometers  
 Ascoris photometer, description and use 0-4256  
 astronomical, LED field stop boundary and reticle illumination control circuit 0-37070  
 automatic, new concepts for luminaire studies 0-4752  
 automatic cameras, exposure error compensation 0-52346  
 automatic rotary diaphragm for microphotometer 0-22415  
 biomedical catheterisable sensors,  $\text{PO}_2$  probes, press. transducer and photometers 0-46080  
 calorimeter, pulse gas, for vacuum UV rad. meas. 0-251  
 digital multipurpose integrating microphotometer, type TSMF-2 0-4753  
 exposure meter for flash lamp photography 0-9058  
 goniophotometer, total luminous flux meas. on radiometric base 0-42250  
 grid-gated photomultiplier photometer with subnanosecond time response, for fluorescence photobleaching recovery expts. 0-37071  
 illumination meters, metrological requirements (Hungarian) 0-17997  
 laser photometer based on boxcar integrator principle (Chinese) 0-31842  
 laser power meter, calibration, Si solar cell 0-46780  
 linearity meas. of photometric devices using two LEDs 0-17996  
 luxmeters with large measuring ranges, method for calibration 0-13123  
 optomechanical scanner, noise analysis 0-47090  
 photoelectric luxmeter using linear ICs (Rumanian) 0-17993

**photometers continued**

- rocket borne resonant absorption spectrometer and photometer for geocoronal and interplanetary He obs. 0-4155  
 solar MUV photometer, rocket borne, stratospheric ozone concentration measurement 0-52292  
 solar power measurement, microcomputer-controlled photodiode light meter and thermistors 0-50946  
 spectral reflectance and transmittance measuring apparatus for variable angle of incidence 0-250  
 spectrum microphotometer connection to PDP 11 digital processor for astronomical photographic plate meas. (Italian) 0-8550  
 tachistoscope lamp luminance meas. 0-42248  
 CdS photo resistance, light density meters (Hungarian) 0-27366

**photometric light sources**

- pulsed laser, for photometer based on boxcar integrator principle (Chinese) 0-31842  
 UV radiometric standards, gas discharges, plasma diagnostics appls. 0-47088

**photometry**

- see also brightness; colorimetry; densitometry; spectrophotometry; stellar photometry  
 AO 0235+164, BL Lacertae object, photometric obs. of optical outburst 0-56924  
 387 Aquitania, slow spinning asteroid with rot. period of nearly one day, photometric evidence 0-17529  
 asteroids, photometric method for shape and spin axis orientation determ. (Russian) 0-8581  
 astronomical IR photometry, atmospheric extinction meas. above Mauna Kea 0-12546  
 automatic LEED spot tracing method 0-10467  
 automatic reactive analysers,  $\text{H}_2\text{O}$  composition checking 0-27330  
 beam incidence angle determ. from refl. meas. (French) 0-37072  
 776 Berbericia, slow spinning asteroid with rot. period of nearly one day, photometric evidence 0-17529  
 burner, for emission flame photometry 0-17988  
 Comet Meier (1978 XXI), photoelectric BV photometry rel. to opposition effect 0-31258  
 electronographic photometry, narrow-band high spatial resolution, astron. appls. (French) 0-46408  
 emission spectrographic analysis system, minicomputer based, using scanning microphotometry 0-22436  
 energy photometry and spectral measurements of radiation detectors 0-252  
 ESO 012-G21, Seyfert 1 galaxy, spectrum, redshift, UVB photometry and X-ray identification 0-8695  
 ESO 113-IG 45 (=Fairall 9), Seyfert galaxy, spectroscopic and multiaperture photometric obs. 0-31362  
 flames, premixed, structure investig. by light intensity distrib. meas. 0-16680  
 galaxies, BV photometry rel. to galactic extinction coeff. amplitude 0-17664  
 galaxies, early-type, UVB photometry rel. to relative distance moduli 0-22080  
 galaxies, elliptical and S0, ten-colour photometry rel. to absorpt. line strengths 0-4430  
 galaxy clusters, photographic photometry (German) 0-46681  
 globular clusters, photoelectric photometry rel. to structural parameters and integrated magnitudes 0-46623  
 high-energy, IR laser component optical characterisation techniques 0-14347  
 Hurter and Driffield, photographic research, biography 0-22181  
 IC 4329A, Seyfert galaxy, photographic photometry and optical spectrum 0-36706  
 illumination engineering, contributions of luminous surfaces (Rumanian) 0-4750  
 illumination engineering measurements using photometry and spectroradiometry 0-22416  
 illuminators light distribution indication method for computerised illumination projecting (Hungarian) 0-27333  
 integrating sphere arrangement for reflectance and transmittance accurate meas. (German) 0-31844  
 interpretation process for colour film 0-42251  
 Io, M-band photometry and 5 micron variability 0-46463  
 iris diaphragm photometry, nonuniform background correction 0-12680  
 Jupiter, IR images at 5 microns wavelength during Voyager 1 encounter 0-26799  
 22 Kalliope, pole coordinates from photoelectric photometry 0-31230  
 BL Lacertae type objects, southern, optical monitoring 0-56969  
 light emitting diode, light flux meas. by photometric sphere 0-253  
 light sources, psychophysical luminous efficiency (Polish) 0-33110  
 light sources props. meas., laboratory equipment requirements and standards (Slovak) 0-17990  
 long fibre, mirror and hollow dielec. lightguides, photometric characts. 0-33201  
 luminaire photometry, new concepts using automatic photometer 0-4752  
 luminous flux meas., automatic null method (French) 0-27331  
 metallic mirror as complex rough surface, light scatt. 0-1293  
 9 Metis, pole coordinates from photoelectric photometry 0-31230  
 micro-light guide photometry of biological tissues 0-46005  
 microphotometry of biological materials, digital picture analysis 0-17991  
 microscope, appls. in materials science 0-21236  
 microscope photometry in studies of molecular struct. of carbonized bitumens and pyrobitumens 0-18011  
 Moon, photometric and polarimetric obs., 1976 April to 1977 December 0-51677  
 NAB 0137-01, quasar, UVB photometry and brightness vars. 0-56967  
 NGC 1275, photometric and spectrum vars. 0-22075  
 NGC 253, Sc-type galaxy, two-micron spectrophotometry 0-4442  
 NGC 3115, lenticular galaxy, photometry and struct. 0-36707  
 NGC 6251, radio galaxy, CCD photometry rel. to central supermassive object 0-26966  
 NGC 6902, H I rich southern supergiant spiral galaxy, optical studies 0-8680  
 44 Nysa, pole coordinates from photoelectric photometry 0-31230  
 optical element contamination modelling, photometric characts. estimation 0-48429  
 optical radar, logarithmic fast-response photodetector for atm. sounding, photometric properties 0-51585  
 Periodic Comet Ashbrook-Jackson (1978 XIV) 0-31258



# photometry continued

petrographic characterization of coal using automatic image analysis 0-18002  
 PKS 1144-379 BL Lacertae object, optical and IR photometry and optical spectrum 0-4451  
 point source lighting computation using point-by-point method (*Rumanian*) 0-17987  
 polymer relaxation props. determ. using photometric transducer method of meas. 0-3268  
 proton flux measurements using photometric calorimeter 0-4718  
 quasar, strong emission line, with redshift  $z=0.189$ , spectrum and photometry 0-8710  
 quasars, southern, optical monitoring 0-56969  
 radiant flux ratio meas., nonlinearity of low noise Si detectors 0-47089  
 reflectance microscopy of coal, considerations involved in automation 0-18001  
 rocks, photometric analyser for crystallographic orientations in thin sections 0-41560  
 S0 galaxies, luminosity distrib. perpendicular to plane of discs rel. to struct. and origin 0-36705  
 shell, internally exploded, displacement meas. by photometric method 0-14642  
 solar MUV photometer, rocket borne, stratospheric ozone concentration measurement 0-52292  
 spiral galaxies, optical surface photometry rel. to local mass-to-light ratio 0-31361  
 spiral galaxies studied at Westerbork, optical surface photometry 0-17655  
 supergiant elliptical galaxies nuclei, CCD photometry rel. to supermassive object in (NGC 6251) 0-26966  
 surface orientation determ. from multiple images, photometric method 0-52163  
 Titan, JHK photometry and suspected near IR variability 0-46469  
 total luminous flux meas. on radiometric base, goniophotometer 0-42250  
 vision, extinction photometry, entoptical scatter, model 0-51087  
 Co film, optical props. by self-consistent photometric technique 0-55217  
 H II regions, compact, in galaxy NGC 6822, new discoveries and photoelectric magnitudes 0-51854

# photomultiplier tubes see photomultipliers

# photomultipliers

grid-gated photomultiplier photometer with subnanosecond time response, for fluorescence photobleaching recovery expts. 0-37071  
 hodoscopes, scintillation, with hodoscope photomultipliers 0-47817  
 laser beam registration sensitivity to incidence angle obs. 0-31843  
 magnetic shielding for photomultiplier array in strong external field 0-32573  
 magneto-electrostatic electron multipliers, long-term efficiency changes (*German*) 0-5448  
 microchannel, with subnanosec. characts. for time meas. 0-37001  
 nuclear medicine, photomultiplier tube balance assessment 0-41196  
 photocathodes for BBO applications 0-27896  
 protection against optical overloads, electromagnetic shutter control 0-23255  
 scintillation detector, in SEM 0-52819  
 scintillation spectrometers, with LED and PIN photodiode, stabilising system 0-47821  
 single-photon counter, with 9789 QB photomultiplier (*Chinese*) 0-27332  
 wavelength shifter, coating technique 0-18760  
 GaAs single-cell radiometer for artificial satellite measurement system 0-13147

# photon counting

atmospheric optical communication line operating under photon counting conditions, adaptation to turbulence 0-9930  
 atomic vapour quantum counter, Stark tuning 0-53242  
 correlator, Malvern, based on photon correlation and laser scattering spectroscopy, development and appl. 0-5741  
 Doppler spectrum, radiation energy cumulants 0-1172  
 fast light phenomena, detection and analysis (*French*) 0-13133  
 fluorescence correlation, clip-correlator (*Russian*) 0-42270  
 fluorescence intensity correlation, photon counting using clip-correlator (*Russian*) 0-42271  
 fluorometric system, nanosec. time-resolved spectrometry with tunable dye laser and pulse-gated photon counter 0-11968  
 laser radiation scattered by atmosphere, photocount distrib. 0-9921  
 microspectrophotometer for study of single vertebrate photoreceptor cells 0-13233  
 modified-triggered photocounting and its application to optical superheterodyne spectrum analysis 0-31865  
 modulation effects on counting distrib. 0-43307  
 optimal light detector photocurrent analysis, quantum statistics, atmospheric 'seeing' conditions 0-53244  
 parametric frequency up-conversion with stochastic pumping, canonical model 0-53368  
 photoelectron counting statistics, theory, fully quantum, review 0-52312  
 photoelectron statistics, joint moment method, phase radiation 0-23647  
 photon existence testing by photoelectric counting and nonexistence of photons 0-9842  
 pyrometer, 1400K to above 2200K within 0.5K and 1.0K 0-52232  
 radiographic  $\text{CaWO}_4$  intensifying screen, meas. of X-ray induced light photons emitted 0-41218  
 resonant Raman scattering in laser fields of arbitrary strength, antibunching effects 0-23653  
 second-order coherence effects due to the superposition of two independent thermal light beams 0-23618  
 single-photon counter, with 9789 QB photomultiplier (*Chinese*) 0-27332  
 spermatozoa mobility, photon correlation study 0-12063  
 stellar objects monitoring, using TV type photon counter, minicomputer-controlled (*Russian*) 0-31212  
 threshold detection equivalence with and without dead time 0-32580  
 tunnel junction mixers, quantum limited detection 0-18015  
 two photon coherent states in degenerate four wave mixing 0-5717  
 He-Ne laser photon statistics variation with cavity length 0-53265

# photon-deuteron interactions

see also *photon-deuteron scattering*  
 $\gamma d \rightarrow \pi^0 d$ , meson-exchange currents in photomesic reactions, relativistic many-body theory 0-422  
 $\gamma d \rightarrow \pi^+ n n$ , off-energy shell photoprod. amplitudes for reactions on bound neutrons 0-421

# photon-deuteron scattering

see also *photon-deuteron interactions*  
 No entries

# photon echo

atomic system, photon echoes in standing-wave fields: time separation of spatial harmonics 0-9759  
 atomic vapour, obs. of optical echoes generated by standing-wave fields 0-23755  
 gaseous media, rephasing phenomena, generalised theory 0-23757  
 high resolution light echo angular spectroscopy, inhomogeneously broadened lines 0-43406  
 inert gas plasma, weakly ionised, photon echo relax. obs. in RF discharge 0-43986  
 modulation echo spectroscopy in double reson. mode 0-1284  
 naphthalene:pentacene, zero-phonon transition bottlenecks, photon echo detect. 0-33092  
 nutational photon echo 0-28283  
 particle motion effect on transient optical phenomena 0-1283  
 picosecond, stimulated from accumulated grating 0-33092  
 ruby, stimulated photon echo modulation 0-38074  
 stimulated photon echo under two-quantum resonance 0-28284  
 three level system, photon echo with relax. 0-43405  
 three-level system with adjacent optically allowed transitions (*Russian*) 0-33093  
 two-photon optical echo effect, appl. in nonlinear echo spectroscopy 0-48357  
 $\text{Cs}$ ,  $7P_{3/2}-6S_{1/2}$  transition, photon-echo quantum beats obs. 0-23373  
 $\text{LaF}_3:\text{Pr}^{3+}$ , optical line narrowing by nuclear spin decoupling, photon echo meas. 0-48353  
 $\text{LaF}_3:\text{Pr}^{3+}$ , spectroscopic and relaxation character of  $^3P_0-^3H_4$  transition, photon echo 0-39897  
 $\text{LaF}_3:\text{Pr}^{3+}$ , ultrahigh resolution photon echo spectroscopy 0-28285  
 $\text{Na}+\text{He}$ ,  $\text{Na}$  ( $3S_{1/2}-3P_{1/2}$ ) photon echo, collision vel. changes and dissimilar electronic states superposition 0-32803  
 $\text{YAlO}_3:\text{Pr}^{3+}$ , ultrahigh resolution photon echo spectroscopy 0-28285

# photon-hadron interactions

see also *photon-hadron scattering*; *photon-nucleon interactions*  
 generalized vector dominance, photon-hadron interaction anal., review, book contrib. 0-47265  
 hadronics props. of photons, effect of large intermediate masses in hadron-mediated photon-nucleus interaction 0-27625  
 multibody channels, review, book contrib. 0-47303  
 QCD Compton effects, quark and gluon jets 0-32101  
 $\text{SU}(4)_W$  symmetry, dibaryon coupling constants for  $\gamma$ ,  $\pi$  and baryon interactions (*Russian*) 0-13329

# photon-hadron scattering

see also *photon-hadron interactions*  
 Compton scattering amplitude constraints, below photoprod. threshold 0-32102  
 multipole polarisabilities of hadrons from Compton scatt. amplitudes 0-13311

# photon interactions see photon-deuteron interactions; photon-hadron interactions; photon-lepton interactions; photon-nucleus reactions; photon-photon interactions

# photon-lepton interactions

see also *photon-lepton scattering*  
 hydrodynamic theory of high energy interactions (*German*) 0-406  
 X-ray generation distribution formulae (*Danish*) 0-47269

# photon-lepton scattering

see also *photon-lepton interactions*  
 quasars and active galactic nuclei, magnetic flare model, magnetised accretion disc around massive black hole 0-22113

# photon-nucleon interactions

see also *photon-nucleon scattering*; *photon-proton interactions*  
 hadron photoproduction nondiffractive processes, review, book contrib. 0-47313  
 high  $p_T$  hadronic jet photoprod., QCD anal., quark and gluon jets 0-42474  
 nuclear shadowing of electromagnetic processes, vector dominance model anal., review, book contrib. 0-47266  
 physical pion low energy electro- and photoprod., Ward identity, chiral symmetry breaking struct. 0-5003  
 physical pion low energy photo- and electroprod., photoprod. phenomenology, quark mass 0-5004  
 pion production, multipole amplitudes, dispersion relations,  $\Delta(1232)$  production 0-5002  
 t-flavoured meson production in photonicuclear and pp collision 0-22623  
 virtual photon-nucleon scatt. anal. for spin 1/2 parton in covariant parton model 0-4966  
 $D^0$  prod. and decay in high energy photon interaction, mass and decay time 0-42478  
 $\gamma^* N \rightarrow \psi N$ , gluon momentum, spin, parity and coupling 0-42395  
 $\gamma d \rightarrow \pi^+ n n$ , off-energy shell photoprod. amplitudes for reactions on bound neutrons 0-421  
 $\gamma N$ , jet cross sections and quark current-photon pointlike coupling, sum rules 0-32104  
 $\gamma N \rightarrow K^+ \Sigma$ , meas. of asymmetries and cross sections using 16 GeV linearly polarised photons 0-13318  
 $\gamma N \rightarrow l^+ l^- X$ , pol.  $\gamma$ , neutral current effect, Weinberg Salam model calcs., p violation 0-5000  
 $\gamma N \rightarrow l^+ l^- X$ , polarisation effects on P-violating asymmetry in Weinberg-Salam model 0-32055  
 $\gamma n \rightarrow \pi^+ p$  reaction cross-section asymmetry in photon energy range 0.9 to 1.65 GeV (*Russian*) 0-32108  
 $\gamma N \rightarrow \pi^+ N$ , meas. of asymmetries and cross sections using 16 GeV linearly polarised photons 0-13318  
 $\gamma N \rightarrow \pi \Delta$ , meas. of asymmetries and cross sections using 16 GeV linearly polarised photons 0-13318  
 $\gamma N \rightarrow \pi \Delta$  reaction amplitude, equivalence theorems (*Russian*) 0-52522  
 $\gamma N \rightarrow \psi(3.1) + \text{anything}$ , cross section and N charmed quark composition 0-423  
 $\gamma n \rightarrow p \bar{p}$ ,  $\rho$ -meson as dormant Goldstone boson 0-368

# photon-nucleon scattering

see also *photon-nucleon interactions*; *photon-proton scattering*  
 No entries



## photon-nucleus reactions

- for inelastic photon-nucleus scattering, see "photon-nucleus scattering"  
see also photodisintegration; photon-deuteron interactions; photon-nucleon interactions
- conference on nuclear interactions, Canberra, Australia (Aug.-Sep. 1978) 0-4476
- conference on nuclear physics with EM interactions, Mainz, Germany (June 1979) 0-22145
- electro- and photoneuclear EM sum rules 0-22810
- electron pair production, cross section calc. on nuclei in range  $1 \leq Z \leq 92$  0-503
- hadron-mediated, effect of large intermediate masses 0-27625
- isobar propagation and collective effects, pion-nucleus and photoneuclear investigation 0-22676
- laser-induced resonant absorption of  $\gamma$  radiation 0-18290
- medium nuclei, photoproton spectra and preequilb. decay, microscopic theory 0-47464
- mesonic and relativistic effects in the nuclear electromagnetic interaction 0-22818
- mesonic effects in photoneuclear sum rules, book contrib. 0-476
- one-particle formalism in continuum approach for photoneuclear cross-section calcs. 0-37355
- photodisintegration and  $\pi$  photoprod. coincidence expts. at Bonn 500 MeV synchrotron 0-22815
- photon splitting cross sections in nucleus Coulomb field 0-32041
- photoneuclear reactions review, giant dipole resonances and cross sections 0-5125
- photoneuclear sum rule, spin current contribs., strong violations 0-18291
- photoneuclear sum rules from continuum calcs., dependence on residual interactions 0-22807
- real photon expts. from continuous wave accelerator 0-42635
- spin-orbit interaction, independent particle model of nuclear Fano effect 0-519
- ( $\gamma, N$ ), intermediate energies, nucleon current interactions, direct knock out mechanism 0-27624
- ( $\gamma, n$ ), nuclear spectroscopy, unbound excited level, spin, parity and width of resonance level 0-18287
- ( $\gamma, p$ ),  $>100$  MeV, using monochromatic photons, leading to final nuclear states 0-22814
- ( $\gamma, \pi$ ), few body pion photoprod. in  $\Delta$ -resonance, region 0-42636
- ( $\gamma, \pi$ ), light nuclei near threshold,  $\pi$  mass difference effects, nuclear K-matrix 0-27674
- ( $\gamma, \pi$ ),  $\pi$  electromag. processes, theoretical aspects 0-22822
- ( $\gamma, X$ ),  $A=14$  nuclei, isospin  $T=2, 1$  and  $0$  collective resonances, shell model 0-510
- ( $\gamma, X$ ),  $A=2, 3, 4$ , photoneuclear and EM interactions 0-22816
- $\gamma p \rightarrow X$ , strong interaction model anal., review, book contrib. 0-47310
- $^{27}\text{Al}(\gamma, p)$ , cross sections and proton energy spectra from (e,e'p) 0-13461
- $^{27}\text{Al}(\gamma, p)$ ,  $^{26}\text{Mg}$ , energy and angular distribution (Korean) 0-18289
- $^A\text{Am}(\gamma, \delta)$  7-26 MeV,  $A=241, 243$ , photofission cross section in E1 giant resonance region (Russian) 0-5182
- $^{40}\text{Ar}(\gamma, xp \text{ yn})$ , 9-29 MeV, cross sections in giant resonance region, particle decay modes 0-13462
- $^{197}\text{Au}(\gamma, n)$ ,  $^{196}\text{Au}$  energy levels and Q-value 0-37329
- $^{11}\text{B}(\gamma, n\gamma')$  30 MeV giant dipole resonance decay,  $^{10}\text{B}$  transitions (Russian) 0-13433
- $^{138}\text{Ba}(\gamma, \pi \text{ xn})\text{La}$ , 150-300 MeV, pion production cross sections calc. 0-9287
- $^9\text{Be}(\gamma, X)$ , charged particle emission in (e,e'X) reaction, virtual phonon theory 0-13460
- $^9\text{Be}(\gamma, n)$  cross section, strong coupling model 0-22682
- $^9\text{Be}(\gamma, \pi^+)$ , 100-800 MeV, cross section, surface prod. model anal. 0-47466
- $^9\text{Be}(\gamma, \pi^+)$ , threshold to 175 MeV, total cross sections, DWIA anal. 0-13459
- $^9\text{Be}(\gamma, \pi)$ , photoabsorption and sum rules, structure, RMS radius, polarizability and exchange parameters 0-22686
- $^{12}\text{C}(\gamma, \pi \text{ p})$ , final state interaction, plane and distorted wave momentum distrib. 0-18286
- $^{12}\text{C}(\gamma, \pi)$ ,  $^{12}\text{N}$  ground state electric quadrupole moment (Russian) 0-42538
- $^{12}\text{C}(\gamma, p)$ , up to 0.25 GeV, from bremsstrahlung  $\gamma$ -quanta (Russian) 0-5123
- $^{12}\text{C}(\gamma, \pi^-)$ , 160-250 MeV, total cross section from elementary Hamiltonian model 0-18292
- $^{12}\text{C}(\gamma, \pi^-)$ , ( $\gamma, \pi^- p$ ), knockout p interaction, optical model and quasifree  $\pi$  photoprod. mechanism (Russian) 0-42638
- $^{12}\text{C}(\gamma, \pi^-)$ , threshold to 360 MeV, total cross sections in  $\Delta$  region 0-13457
- $^{12}\text{C}(\gamma, \pi^-)$ , total cross section calc. in impulse approx. 0-13458
- $^{12}\text{C}(\gamma, \pi^- p)$ , 340-380 MeV, quasi-free photoprod., impulse and shell model anal. (Russian) 0-5124
- $^{12}\text{C}(\gamma, \pi^+)$ ,  $^{12}\text{B}_{\text{gs}}$ , 0.4 MeV, pion photoprod. cross section 0-42637
- $^{13}\text{C}$ , photoexcited giant dipole resonance, continuum shell model anal. 0-18266
- $^{13}\text{C}(\gamma, n)$ , 7.6-24 MeV, photoneutron ang. distribs., level scheme and  $J^\pi$  assignments 0-466
- $^A\text{Ca}(\gamma, X)$ ,  $A=42, 44, 48$ , photoneutron and photoproton cross section systematics 0-13463
- $\text{Ce}(\gamma, n)$ , 30 to 140 MeV, partial photoneutron cross section, total cross section approx. 0-22809
- $^{62}\text{Cr}(\gamma, X)$ , photoneutron and photoproton cross section systematics 0-13463
- $^{53}\text{Cr}(\gamma, p)$ ,  $^{52}\text{V}$ , cross-section, 14.4-27 MeV, isospin splitting 0-520
- $^{63}\text{Cu}(\gamma, p)$ , up to 0.25 GeV, from bremsstrahlung  $\gamma$ -quanta (Russian) 0-5123
- $^{19}\text{F}(\gamma, X)$ , 14-30 MeV,  $X=p, n, \alpha$ , integrated cross sections to excited residual states 0-18200
- $^{54}\text{Fe}(\gamma, X)$ , photoneutron and photoproton cross section systematics 0-13463
- $\text{Ge}(\gamma, e^+e^-)$ , near threshold, variable energy source, total cross section (French) 0-37367
- $^2\text{H}(\gamma, \pi)$ , theoretical and expt. results. 0-42698
- $^2\text{H}(\gamma, \pi^+)$ , target asymmetry and effective neutron polarisation, polarised d 0-9286
- $^2\text{H}(\gamma, \pi)$  photoexcitation in  $\Delta(1236)$  region 0-22813
- $^2\text{H}(\gamma, \pi^0)$ , coherent photoprod., binding effects and threshold amplitude calc. 0-32264
- $^2\text{H}(\gamma, \pi^0)$ , cross section and threshold effects using dynamical  $\gamma N \rightarrow N\pi^0$  model 0-27627

## photon-nucleus reactions continued

- $^2\text{H}(\gamma, \pi^+)2n$ , threshold to 22 MeV, bremsstrahlung yield and total cross section 0-9288
- $^2\text{H}(\gamma, \pi)$ , threshold photoprod. cross sections, elementary nucleonic amplitudes 0-22812
- $^3\text{H}(\gamma, \pi^0)$ , polarisation effects 180 to 700 MeV, impulse approx. calcs. (Russian) 0-37368
- $^3\text{H}(\gamma, \pi^0)^3\text{H}$ , polarisation effects 180 to 700 MeV, impulse approx. calcs. (Russian) 0-37368
- $^3\text{H}(\gamma, \pi)$ ,  $x=1$  or  $2$ , photodisintegration cross sections 0-22817
- $^3\text{He}(\gamma, n)$ , photodisintegration cross sections 0-22817
- $^3\text{He}(\gamma, p)^3\text{H}$ , intermediate energy, ang. distribs., reaction amplitude and He vertices 0-22835
- $^3\text{He}(\gamma, \pi^0)$ , cross section and threshold effects using dynamical  $\gamma N \rightarrow N\pi^0$  model 0-27627
- $^3\text{He}(\gamma, \pi^0)$ , polarisation effects 180 to 700 MeV, impulse approx. calcs. (Russian) 0-37368
- $^3\text{He}(\gamma, \pi^0)^3\text{He}$ , polarisation effects 180 to 700 MeV, impulse approx. calcs. (Russian) 0-37368
- $^3\text{He}(\gamma, \pi^+)^3\text{H}$ , Fermi motion and off-shell effects, impulse approx. 0-27626
- $^3\text{He}(\gamma, \pi)$ , threshold photoprod. cross sections, elementary nucleonic amplitudes 0-22812
- $^4\text{He}(\gamma, 2d)$ , 30-35 MeV,  $2^+$  state search (Russian) 0-42553
- $^4\text{He}(\gamma, n)$ , 30-35 MeV,  $2^+$  state search (Russian) 0-42553
- $^4\text{He}(\gamma, pn)^2\text{H}$  reaction, distribution along Treiman-Yang angle (Russian) 0-27628
- $^4\text{He}(\gamma, \pi^0)$ , differential cross section, complex momenta theory for nondiffractive processes (Russian) 0-32266
- $^4\text{He}(\gamma, \pi^0)$ , polarisation effects 180 to 700 MeV, impulse approx. calcs. (Russian) 0-37368
- $\text{He}(\gamma, \pi)$ , photoexcitation in  $\Delta(1236)$  region 0-22813
- $^6\text{Li}(\gamma, n)^6\text{Li}^*(3.56 \text{ MeV})$ , partial photoproduction reactions, large momentum transfer anal., form factor choice 0-22808
- $^6\text{Li}(\gamma, \pi^0)^6\text{Li}^*(3.56 \text{ MeV})$ , partial photoproduction reactions, large momentum transfer anal., form factor choice 0-22808
- $^7\text{Li}(\gamma, \pi^-)$ , threshold to 360 MeV, total cross sections in  $\Delta$  region 0-13457
- $^7\text{Li}(\gamma, \pi^-)$ , total cross section calc. in impulse approx. 0-13458
- $^7\text{Li}(\gamma, t)$ ,  $<50$  MeV, total and differential cross sections, levels, cluster model calcs. 0-32265
- $^A\text{Li}(\gamma, \pi)$ ,  $A=6, 7$  0-22686
- $^{24}\text{Mg}(\gamma, p)$ , 17-30 MeV, giant dipole resonances and transitions, shell effects (Russian) 0-13434
- $^{24}\text{Mg}(\gamma, p)$ , cross sections and proton energy spectra from (e,e'p) 0-13461
- $^{24}\text{Mg}(\gamma, p)$ , up to 0.25 GeV, from bremsstrahlung  $\gamma$ -quanta (Russian) 0-5123
- $^{14}\text{N}(\gamma, n)^{13}\text{N}$ , 17 to 26 MeV, angular distrib., giant dipole resonance, single-particle nuclear model 0-52659
- $^{14}\text{N}(\gamma, \pi^-)^{14}\text{O}$ , 145-325 MeV, Gamow-Teller suppression and M1 radiative widths 0-52609
- $^{20}\text{Ne}(\gamma, \alpha)$ , EM induced  $\alpha$  emission,  $\alpha$  spectroscopic amplitudes, anal. solvable model 0-32267
- $^{20}\text{Ne}(\gamma, n)$  cross sections and giant resonance struct. 0-13441
- $^{62}\text{Ni}(\gamma, X)$ , 19.2-26.2 MeV, photoneutron and photoproton spectra, giant dipole resonance-decay, isospin conservation 0-13443
- $^{16}\text{O}(\text{e,e})$ ,  $T=1$  level form factors, Helm model, pion photoprod. and muon capture appls. 0-52553
- $^{16}\text{O}(\gamma, n)$ , 25-45 MeV, isovector giant quadrupole resonance evidence, E2 cross section 0-18268
- $^{16}\text{O}(\gamma, n)$  total photoneutron cross sections 0-42619
- $^{16}\text{O}(\gamma, p)^{15}\text{N}$  up to 120 MeV, cross-sections, energy levels (Russian) 0-47465
- $^{16}\text{O}(\gamma, \pi^+)$ , differential cross section from elementary Hamiltonian model 0-18292
- $^{16}\text{O}(\gamma, \pi^+)$ , threshold to 175 MeV, total cross sections, DWIA anal. 0-13459
- $^{17}\text{O}(\gamma, n)$ , 8.5-39.7 MeV, cross section, giant dipole and pygmy resonance decays 0-42619
- $^{17}\text{O}(\gamma, n)$ , cross section, Lane-Lynn radiative capture mechanisms 0-52660
- $^A\text{Pb}(\gamma, n)$ ,  $A=206, 208$ , levels using tagged photons 0-23245
- $^{208}\text{Pb}(\gamma, n)$ , 8.5-11.4 MeV,  $^{205}\text{Pb}$  multipole resonance E1-E2 and E1-M1 interference 0-32251
- $^{207}\text{Pb}(\gamma, n)$ , 7632 keV level photoexcitation, cross section and  $J^\pi$  0-37330
- $^{208}\text{Pb}(\gamma, n)$ , 9.5-12 MeV, photoneutron ang. distribs., struct. below giant resonance 0-13444
- $^{208}\text{Pb}(\gamma, n)$  giant mag. dipole resonance location, photoneutron polarisation method 0-37357
- $^{208}\text{Pb}(\gamma, p)$ , up to 0.25 GeV, from bremsstrahlung  $\gamma$ -quanta (Russian) 0-5123
- $\text{Pb}(\gamma, n)$ , 30 to 140 MeV, partial photoneutron cross section, total cross section approx. 0-22809
- $^{239}\text{Pu}(\gamma, 2n)$ ,  $^{237}\text{Pu}$  fission single particle isomers, half lives and isomeric ratio 0-18181
- $^{28}\text{Si}(\gamma, p)$ , 18.1-29 MeV, giant dipole resonance, contrib. from various configs. 0-18264
- $^{118}\text{Sn}(\gamma, p)$ , up to 0.25 GeV, from bremsstrahlung  $\gamma$ -quanta (Russian) 0-5123
- $^{119}\text{Sn}(\gamma, n)$ , giant mag. dipole resonance location, photoneutron polarisation method 0-37357
- $\text{Sn}(\gamma, n)$ , 30 to 140 MeV, partial photoneutron cross section, total cross section approx. 0-22809
- $^{181}\text{Ta}(\gamma, n)$  photoneutron absorpt. cross section meas. 20.9 to 837.8 keV (German) 0-5122
- $\text{Ta}(\gamma, n)$ , 30 to 140 MeV, partial photoneutron cross section, total cross section approx. 0-22809
- $^A\text{Ti}(\gamma, X)$ ,  $A=46, 48, 50$ , photoneutron and photoproton cross section systematics 0-13463
- $^{50}\text{Ti}(\gamma, n)$ ,  $^{49}\text{Ti}$  nuclear levels from n-capture  $\gamma$ -rays 0-37327
- $^{50}\text{Ti}(\gamma, X)$ , photoneutron and photoproton cross sections, giant dipole resonance isospin splitting 0-13442
- $^{238}\text{U}(\gamma, 2n)$ , 4.5 MeV,  $^{236}\text{U}$  fission shape isomer,  $\gamma$ -decay 0-18230
- $\text{U}(\gamma, n)$ , 30 to 140 MeV, partial photoneutron cross section, total cross section approx. 0-22809

## photon-nucleus scattering

- see also photon-deuteron scattering; photon-nucleon scattering
- conference on nuclear physics with EM interactions, Mainz, Germany (June 1979) 0-22145
- Delbruck and Rayleigh scattering below 5 MeV 0-13456



**photon-nucleus scattering continued**

- EM interactions, high duty cycle accelerators and experimental possibilities 0-23187
- EM sum rules for  $(\gamma, \gamma)$ ,  $(e, e)$ , transitions and giant resonances 0-5090
- Rayleigh and Compton contribs. to nuclear resonance scattering of gamma rays, line inversion 0-39919
- real photon expts. from continuous wave accelerator 0-42635
- $(\gamma, \gamma)$  processes using  $(n, \gamma)$  photons 0-18288
- $(\gamma, \gamma)$ , resonance scatt., bound or unbound excited level, spin, parity and width of resonance level 0-18287
- $^{111}\text{Cd}(\gamma, \gamma)$ , isomeric states excitation, integral cross sections 0-27528
- $\text{C}(\gamma, \gamma)$ , neutron capture  $\gamma$ -ray Rayleigh scatt. 0-52661
- $^{52}\text{Cr}(\gamma, \gamma)$ , 35 MeV,  $2^+$  state deexcitation  $\gamma$ -rays, differential cross sections, deformation (*Russian*) 0-13406
- $^{54}\text{Cr}(\gamma, \gamma)$ , up to 12 MeV, highly excited spin-1 resonances,  $\gamma$ -transitions 0-13427
- $\text{Cu}(\gamma, \gamma)$ , neutron capture  $\gamma$ -ray Rayleigh scatt. 0-52661
- $^{166}\text{Er}(\gamma, \gamma)$ , 15 MeV, elastic and nuclear Raman scatt. 0-22811
- $^{56}\text{Fe}(\gamma, \gamma)$ , up to 12 MeV, highly excited spin-1 resonances,  $\gamma$ -transitions 0-13427
- $^{115}\text{In}(\gamma, \gamma)$ , isomeric states excitation, integral cross sections 0-27528
- $\text{In}(\gamma, \gamma)$ , neutron capture  $\gamma$ -ray Rayleigh scatt. 0-52661
- Ni giant resonances using virtual and real photons 0-22791
- $^{58}\text{Ni}(\gamma, \gamma)$ , M1 strength isospin splitting for dipole ang. distrib. states 0-13412
- $\text{Pu}(\gamma, \gamma)$  12.754 MeV, Delbruck scatt., Coulomb correction terms, differential cross sections 0-27629
- $\text{Ta}(\gamma, \gamma)$ , neutron capture  $\gamma$ -ray Rayleigh scatt. 0-52661
- $^{49}\text{Ti}(\gamma, \gamma)$ , nuclear levels from n-capture  $\gamma$ -rays 0-37327
- $^{238}\text{U}(\gamma, \gamma)$ , 15 MeV, elastic and nuclear Raman scatt. 0-22811
- $\text{U}(\gamma, \gamma)$ , neutron capture  $\gamma$ -ray Rayleigh scatt. 0-52661

**photon-phonon excitations** *see polaritons***photon-photon interactions**

- see also photon-photon scattering*
- helicity method, back factorisation procedure, deep inelastic config. 0-22606
- manifestation strength of colour below and above colour threshold 0-381
- polarised positron, electron production by colliding photon beams in storage ring 0-5426
- QCD, two-photon scatt. amplitudes, leading order behaviour 0-52458
- single tagged event interpretation in  $\gamma\gamma$  events, helicity formalism 0-52551
- $ee \rightarrow e\mu^+\mu^-$ , virtual photon-photon collisions, equivalent photon approx. validity 0-5033
- $e^+e^-$  calorimetric experiments,  $\gamma\gamma$  processes, tests of QCD 0-22628
- $e^+e^- \rightarrow e^+e^- + 2$  gluon jets from  $\gamma\gamma$  interactions cross section, gluon role in QCD 0-4976
- $\gamma\gamma$ , jet cross sections and quark current-photon pointlike coupling, sum rules 0-32104
- $\gamma\gamma$ -hadrons, 1-5 GeV, hadron prod. cross sections 0-37315
- $\gamma\gamma$ -X, equivalent-photon approx. for two-photon processes, role of dynamical cut-off 0-47314
- $\gamma\mu \rightarrow \mu^+\mu^-$ , cross sections,  $\gamma$  struct. function determ. 0-42473

**photon-photon scattering**

- see also photon-photon interactions*
- pair production on photon scattering by intense EM wave in homogeneous mag. field (*Russian*) 0-47227
- $e^+e^- \rightarrow e^+e^-$  gg, gluon jet polarisation in photon-photon scatt., QCD test 0-52550

**photon polarisation**

- monochromatic polarised photon source from Compton backscattered laser light on electrons 0-52800
- $\gamma$  source generation and properties, review 0-14029
- np-d $\gamma$  radiative capture, relativistic effects, parity violation, Weinberg-Salam model (*Russian*) 0-32120
- $\pi N \rightarrow \mu^+\mu^- X$ , longitudinal photon polarisation from helicity ang. distrib. 0-5025
- qg $\rightarrow 1^+$ , high  $P_T$  photon polarisation as QCD test 0-4934
- Ar+K, photon emission polarisation anal., coincidence studies 0-5614
- K+He, photon emission polarisation anal., coincidence studies 0-5614
- K+Kr, photon emission polarisation anal., coincidence studies 0-5614
- K+Ne, photon emission polarisation anal., coincidence studies 0-5614
- K+Xe, photon emission polarisation anal., coincidence studies 0-5614

**photon-proton interactions**

- see also photon-proton scattering*
- jets as source for observed increase in  $\gamma\gamma$  cross-section 0-22620
- $\gamma\gamma$ , 46-180 GeV,  $\omega$ -meson photoprod. cross section,  $\omega\gamma$  coupling constant 0-13319
- $\gamma\mu \rightarrow h^+X$ , large  $p_T$  photoprod., perturbative QCD test 0-37276
- $\gamma\mu \rightarrow K^+\Lambda$ , meas. of asymmetries and cross sections using 16 GeV linearly polarised photons 0-13318
- $\gamma\mu \rightarrow \pi^+\pi^+$ , multipole anal. in region of first reson. 0-22622
- $\gamma\mu \rightarrow \pi^+\pi^+$  section asymmetry, pion-proton twin birth contribution (*Russian*) 0-47308
- $\gamma\mu \rightarrow \text{ppp}$ , threshold -4.8 GeV, elastic photoprod. cross section 0-52521
- $\gamma\mu \rightarrow \pi\pi$ , multipole anal. in region of first reson. 0-22622
- $\gamma\mu \rightarrow \pi^0 X$ , invariant cross section at large  $p_T$ , hard scatt. model 0-22621
- $\gamma\mu \rightarrow \pi^0 p$ , 1.4 GeV, differential cross section meas. 0-42476
- $\gamma\mu \rightarrow \pi^0 X$ , duality and finite energy sum rules 0-42477
- $\gamma\mu \rightarrow \pi N$  multipole isotopic anal., soln. irregular behaviour near  $P_{33}$  resonance (*Russian*) 0-5005
- $\mu p \rightarrow \pi$ , threshold to 450 MeV, energy depend. multipole anal. 0-32110
- $\pi^+$  prod., 1300-2300 MeV, meas. of double polarisation parameters 0-13317

**photon-proton scattering**

- see also photon-proton interactions*
- quark loop contrib. to photon total cross sections 0-4999
- $\gamma p$ , low energy scatt., one-particle exchange model 0-22617
- $\gamma p$  scatt. in  $\Delta(1236)$  resonance region, dispersion relation anal. 0-18140

**photon scattering** *see photon-deuteron scattering; photon-hadron scattering; photon-lepton scattering; photon-nucleus scattering; photon-photon scattering***photon transport theory**

- absorption, k-photon, unsaturated, exact soln. of master eqn. 0-37984
- earth, radiation transport for neutron and  $\gamma$ -ray point sources above air-ground interface 0-32526
- electron beam fusion of D-T pellets, neutronics and photonics 0-52781
- ENDF/B-V nuclear data for shielding appls., energy balance anal. 0-47745

**photon transport theory continued**

- fusion reactor shielding experiment, cross-section sensitivity calcs., one- and two-dimensional models 0-27799
- gamma buildup factors for photons in air, water, iron, moments method code 0-27828
- gamma-ray albedo data, removal of negative albedo terms 0-5347
- LWR lattices, Monte Carlo radiation transport program for reactor bundle gamma transport and energy deposition analysis 0-22915
- pulsed source, distrib. of scattered  $\gamma$ -radiation, unsteady transport 0-27830
- radiation dose deposition calcs. in human marrow 0-26365
- radiation protection studies expt. and theoretic results comparison 0-47750
- Tokamak fusion test reactor, dose rates from induced activity in test cell 0-23144
- $\gamma$ -ray scatt. in air, anal. by discrete ordinates transport codes 0-32525
- Li, T breeding performance eval., multigroup neutron and photon transport calc. 0-13831
- $\text{LiO}_2$ , T breeding performance eval., multigroup neutron and photon transport calc. 0-13831
- $\text{Li}_2\text{Pb}_2$ , T breeding performance eval., multigroup neutron and photon transport calc. 0-13831

**photons**

- see also cosmic ray photons; gamma-rays; light; photon transport theory; X-rays*
- ballistic theory of light based on EM force laws and Newtonian mechanics 0-50
- behaviour in high intensity coherent laser beams 0-28185
- dosimetry standardisation in Germany 0-5353
- Einstein and the quantum theory, review 0-22237
- fission in intense laser fields and nuclear Coulomb field, QED test 0-4895
- form factor, asymptotic behaviour in QED 0-18096
- hadronic props., effect of large intermediate masses in hadron-mediated photon-nucleus interaction 0-27625
- spin, relation to isospin, strangeness and charm 0-37183
- structure function determ. in  $\gamma p \rightarrow \mu^+\mu^- X$  expts. 0-42473
- structure functions parametrisation 0-37267

**photonuclear reactions** *see photon-nucleus reactions***photophoresis**

No entries

**photoplasticity**

- KCl,  $\gamma$ -irrad., photoplastic effect and internal friction aftereffect 0-24529
- NaCl,  $\gamma$ -irrad., photoplastic effect and internal friction aftereffect 0-24529
- ZnSe, cryst., elec. cond., dislocation motion effects 0-54710

**photorefractive effect**

- acousto-optical devices for real- and near-real-time signal processing 0-10024
- holographic grating form. in photorefractive cryst. with arbitrary electron transport lengths 0-1151
- $(\text{Ba}_{1-x}\text{Sr}_x)_2(\text{Nb}_2\text{O}_6)_2\text{CeO}_2$  crystals, photoelectric and photorefractive props., hologram recording 0-53239
- GeO film, optical props., rel. to possible appl. in holography 0-29816
- $\text{La}_2\text{Ti}_2\text{O}_7$ , ferroelects., nonlinear optical props. 0-33086
- $\text{LiNbO}_3$ , pure and Fe doped, photorefract. temp. and light intensity depend. 0-50288
- $\text{LiNbO}_3/\text{Fe}$ , anomalous photovoltaic effect in polarised light (*Russian*) 0-34484
- $\text{LiNbO}_3/\text{Fe}$ , local photodeform. and photorefract. 0-16003
- $\text{LiNbO}_3/\text{Fe}$ , photorefract.,  $\gamma$ -irrad. influence, polarisation-optic and holographic obs. 0-11359
- $\text{LiNbO}_3/\text{Fe}$ , pulsed photorefr. process for hologram recording 0-53235
- $\text{LiNbO}_3/\text{Ti}$  waveguide and cryst., absorpt. loss and photorefractive index changes 0-48368
- $\text{LiNbO}_3/\text{Ti}$  waveguide directional coupler switches, optically-induced cross-talk 0-48417
- $\text{LiTaO}_3/\text{Fe}$  crystal, holographic storage process 0-32942
- $\text{Sr}_2\text{Nb}_2\text{O}_7$ , ferroelects., nonlinear optical props. 0-33086

**photoresistors**

- impurity photoresistor in interferometer, threshold charact. 0-31856
- CdS photoresistor for measuring solar EM radiation 0-31092
- $\text{CdS}_x\text{Se}_{1-x}$  photosensitive films, prep., props., and use for photodetectors 0-55298

**photoresists**

- see also electron resists*
- contact printing method utilising heated photoresist adhesive prop. for hologram copying 0-5704
- dichromated photoresist, photochem. reactions 0-7830
- diffraction grating form. on optical waveguide surface, ion-beam etching through photoresist mask 0-14492
- diffraction gratings, photoresist and GaAs, exposure and etching time optimisation 0-23816
- holographic grating production by laser irradiation of photoresist (*German*) 0-33254
- image formation in photosensitive layers on highly conductive substrates 0-43419
- nonlinear optical processing with Fabry-Perot interferometers containing phase recording media 0-48158
- optical waveguide, grating coupler fabrication (*Czech*) 0-28354
- photopolymer industry in Japan 0-4800
- photosensitivity of negative photoresists (*Russian*) 0-50872
- plasma etching methods for semicond. struct. and devices (*Slovak*) 0-40564
- polymer, thin, high energy irrad. and selective dissolution, X-ray lithography (*German*) 0-13167
- polymethyl isopropenyl ketones, spectrally sensitized decomposition and Deep UV resists 0-40715
- positive photoresists, photocond. factor rel. to composition (*Russian*) 0-42289
- zone plate production by laser irradiation of photoresist. (*German*) 0-23782

**photosphere**

- active regions and X-ray bright points, birthplaces 0-12739
- faculae, 5000 Å continuum diagnostics 0-4315
- faculae, models 0-12716
- faculae and sunspots, mag. field effects on solar luminosity 0-46515
- faculae intensity, centre to limb var. 0-21967



**photosphere continued**

- fine structure, no correlation between brightness and radial obs. (*Russian*) 0-17564
- granulation, convection models, book contrib. 0-4329
- granulation, dark dot form. in cell 0-31274
- granulation, speckle interferometric obs. (*French*) 0-46523
- granulation, spectral props. of random arrays 0-12727
- granulation morphology and granule spatial distrib. 0-26830
- granule diameters near penumbra 0-8607
- granule fragmentation, morphological study in Ca II K-line 0-56799
- light absorption in photospheric layers, eclipse limb darkening obs. (*French*) 0-8612
- limb emission lines near Ca II H and K, spatial intensity vars. obs. 0-51720
- magnetic field rearrangement, rel. to disparities brusques of solar filaments (*Russian*) 0-51726
- 'microturbulent' velocity and damping const., introductory review (*Russian*) 0-12719
- model atmosphere, rel. to solar Fe abundance and Fe II lines oscillator strengths 0-56791
- oscillations depth depend. 0-31275
- photosphere-chromosphere transition region, spectra during eclipse June 30 1973 0-8614
- proton flux influenced by photosphere mag. field 0-41672
- spectral line profiles, acoustic wave effects 0-46517
- spectral line profiles for Na I and O I, acoustic wave effects 0-17558
- sunspot magnetic fields higher rot. rate at photosphere, Doppler meas. 0-46516
- sunspot moats, lifetimes from magnetograph obs. 0-21966
- sunspot model, radiation transfer theory 0-21964
- sunspot structure, vars. correl. with Earth climate 0-31272
- sunspots, magneto-optical effects rel. to linearly polarised intensity distrib. obs. with vector magnetograph 0-21965
- sunspots and mag. flux tube physics, connective overstability in mag. field in downdraft 0-21960
- sunspots and magnetic flux tubes physics, umbral dots and longitudinal overstability 0-26825
- surface (capillary) waves, props. (*Russian*) 0-12726
- temperature at chromosphere photosphere boundary, from emission spectrum in far infrared (*German*) 0-51721
- turbulence (*French*) 0-31270
- UV continuum high resolution photographic obs. 0-17565
- velocity fields, large-scale, from Doppler line shift obs. 0-12730
- velocity fields and spectral line shift obs. interpretation 0-51714
- vertical motion in intense mag. flux tube, slender tube approx. 0-31278
- wave propagation in nonisothermal atmosphere, rel. to solar five minute oscils. 0-31276
- C III 1909 Å and Si III 1892 Å emission lines, echelle obs. 0-31277
- Fe abundance, determ. from weak Fe I Fraunhofer lines with microturbulence and damping (*Russian*) 0-12720
- Fe I lines, equivalent widths and microturbulent vels. determ. (*Russian*) 0-51719

**photosynthesis**

- algae in cylindrical photoreactor, radiation intensity and absorption profiles (*German*) 0-3610
- bacteria, effect of mag. field on recomb. fluoresc. 0-35856
- bacteria, mechs. of charge separation 0-30684
- bacteriochlorophyll a, triplet state energy and lifetime 0-30682
- bacteriopheophytin a, triplet state energy and lifetime 0-30682
- bacteriorhodopsin Br570, bathochromic shift of absorpt. band in external elec. field 0-35838
- bacterium Chromatium minutissimum, linear dichroism of oriented chromatophores and pigment-protein complexes 0-35841
- bioconversion of solar energy, review 0-45720
- biomass energy conversion, energy sources for rural development 0-30509
- chlorophyll, photosystem 2, activation energy and lifetime of fluoresc. 0-35842
- chlorophyll special pair models, reaction centres 0-3574
- chlorophyll spectral forms, Chlamydomonas mutants with inactive photosynthesis 0-51054
- chlorophyll-a, conc. quenching rel. to functional charge transfer 0-30666
- chloroplast, mag. relax. of water protons and state of water photodissociation system 0-51133
- cytochrome C, immobilised, investigs. using magnetic micromixer attachment for SPECORD UV VIS spectrophotometer 0-56302
- dye/detergent system, model for energy transfer in photosynthetic unit 0-20685
- electron flow, photosynthetic and respiratory, in dual functional bacterial membrane 0-16914
- electron transport and energy migration in higher plants 0-40976
- electronic structural props. of mols. relevant to photosynthesis 0-16902
- energy conversion radiation enhancement using surface polaritons 0-7941
- entropy changes in energy bioconversion 0-3609
- fluorescence picosec. kinetics in chromatophores and reaction centres from R.sphaeroides, 295 to 80K 0-35857
- kinetics under saturating light 0-35858
- membrane, photosynthesising, near photosystem II, hydrophobic pocket 0-55999
- pigment molecule organisation and interaction in reaction centres of Rhodospseudomonas viridis 0-35843
- redox conversion kinetics in the electron transport chain 0-40950
- Rhodospseudomonas sphaeroides, growth yield in light-anaerobic and dark-aerobic cultures 0-3608
- solar energy utilisation via plant photosynthesis 0-3491
- soybean plants, radiation-stressed, photosynthesis and photophosphorylation rel. to photoassimilate export 0-56140
- technoeconomic analysis of an photosynthesis energy factory as an integrated bioconversion system 0-30510
- thylakoid membrane, in plant cell, electron microscopy 0-26210
- H biological photoprod. using sunlight, review 0-45777
- H biological prod. by solar energy conversion, coupling of hydrogenase and chloroplast photosystems 0-45778
- H prod. by H<sub>2</sub>O solar photolysis methods based on photosynthesis (*Japanese*) 0-45765
- H synthetic chloroplasts 0-30508
- H<sub>2</sub> gas, photosynthesis prod. by green algae, turnover times and pool sizes 0-16821

**photothermal conversion**

- see also solar absorber-convertors
- heat generation for multipurpose utilization systems by heat of dilution converted from solar energy 0-55915
- solar thermal power system, 10 MWe pilot central receiver design concept 0-16792
- Ni cermet selective absorbers, photothermal conversion appls. 0-21413

**phototransistors**

- optoelectronic devices and optical imaging techniques, book 0-27059
- photoelectric convertor for automated spectral measurements 0-22449
- GaAs MESFET, optical detector appl., sensitive high-speed device 0-13143

**phototubes**

- see also photocathodes; photomultipliers
- light flux fluctuations, limiting factors in photoelectric meas. 0-13136

**photovoltaic cells**

- see also solar cells
- 5 kW photovoltaic generator system, analysis, design and realisation 0-45704
- 100 kW peak photovoltaic power system, design, construction and capabilities 0-45705
- AlSiO<sub>2</sub>-Si photodiode, experimental verification of theoretical predictions 0-29485
- antireflection coatings applied from metal-organic derived liquid precursors 0-5847
- desalination plant coupling to solar conversion system, technical and economic evaluation 0-55804
- distributed photovoltaic systems for electricity generation, economic and technologic feasibility 0-55906
- economic power generation, photovoltaic modules fabrication cost analysis 0-45674
- electron beam induced currents appl., topotaxiality and dead region determ. 0-3518
- energy conversion radiation enhancement using surface polaritons 0-7941
- grid lines, optimal design to reduce conductive losses 0-7945
- materials, fabrication and research for low cost photovoltaic solar cells 0-55838
- monolithic solar cell panel of amorphous Si 0-45666
- Moss relation between refr. index and energy gap of semiconductors rel. to photovoltaic solar cells 0-11357
- multi-bandgap concentrator cells, Si and Al<sub>x</sub>Ga<sub>1-x</sub>As systems, operation with spectrum splitting filter 0-45698
- operation using solar simulator lamp 0-42004
- photoconverter, bilateral sensitivity, n<sup>+</sup>-p-p<sup>+</sup> structure, volt-ampere characts. under illumination 0-40855
- photovoltaic concentrator cells development project, developments, performances and future trends 0-45699
- photovoltaic power systems, equipment performance and manufacturing techniques improvements and system design problems for telecommunication applications 0-55843
- photovoltaic solar energy conversion [conf. Berlin, West Germany, April 79] 0-30482
- polyacetylene photoelectrochemical solar cell, fabrication and efficiency 0-50954
- power loss in photovoltaic arrays due to mismatch in cell characteristics 0-16802
- review of US DOE R and D program 0-55874
- satellite generators, low-orbit, D2B and Signe 3, performances comparison 0-3524
- solar arrays and DC motors, direct coupling theory 0-3523
- solar cell arrays, DC to AC power conversion and utility interfacing, techniques, requirements and components used 0-45703
- solar cell developments and new appls., cost effectiveness 0-16800
- solar cell efficiency calc., using irradiance-transmittance solar spectrum 0-26137
- solar cell electricity, future development prospects, research projects and new appls. 0-16798
- solar cell spectral response characterisation, 400 to 1000 nm 0-35675
- solar cells, for satellite solar power systems, developments and future trends 0-45694
- solar cells, photovoltage source in photocond. materials due to comp. and doping var. 0-7938
- solar cells, SnO<sub>2</sub>-SiO<sub>2</sub>-n-Si heterojunction, cheap solar elements for ground-based appls. 0-40860
- solar cells, thin film, performance analysis employing loss minimisation of essential characteristics 0-45682
- solar energy, review using rational units 0-30389
- solar generators, ampere-hour efficiency, charging and discharge power 0-29434
- solar photovoltaic cells production technology, future systems efficiency and cost effectiveness 0-16799
- solar photovoltaic electricity generation in India 0-21381
- solar photovoltaic energy system, 25 kWp, for agricultural appl., performance anal. 0-30491
- solar photovoltaic generators using optical concentration, current status and development trends review 0-45697
- solar photovoltaic modules, physical and electrical degradation in terrestrial environment 0-30492
- solar photovoltaic power systems for rural areas of developing countries 0-50967
- solar photovoltaic systems, design for intermediate-sized appls. 0-30490
- solar powered electrodialysis, water desalination appl. 0-55805
- solar space power generators, past developments and future trends 0-45693
- space heating, photovoltaic and thermal collector system design and testing 0-45675
- spectral response, pulsed measurement, test set-up and apparatus, shortcomings and planned improvements 0-45695
- table top pulsed solar simulator, design and construction, for testing solar cell arrays powering artificial satellites 0-45696
- terrestrial flat plate photovoltaic modules, environmental testing 0-30560
- terrestrial solar generators, design, fabrication, testing and economic power generation 0-45672
- terrestrial solar modules, sandwich type glass encapsulation, climatic parameters effect, economic anal. 0-45673
- thermophotovoltaic energy convertor, development of new Si cells 0-12016
- transparent electrode photo-galvano-voltaic cell, using Mg-meso-tetraphenylporphine-coated glass (*Chinese*) 0-40865
- CdS heterojunction solar cells by CVD method 0-45685



**photovoltaic cells continued**

- CdS solar photovoltaic panels, deposited by spray pyrolysis, film and junction structure studies 0-45689  
 CdS/Cu<sub>2</sub>S heterojunction solar cells, optimal material props. theory and experimental verification 0-45686  
 CdS/Cu<sub>2</sub>S solar cell, design and fabrication 0-30481  
 CdS-Cu<sub>2</sub>S solar cells, screen printed, prep. and photovoltaic props. 0-40863  
 CdSe MIS thin film solar cell 0-45688  
 Cd<sub>1-x</sub>Zn<sub>x</sub>S/Cu<sub>2</sub>S thin film heterojunction solar cells, operational charact. 0-45687  
 Cu<sub>1-x</sub>Ag<sub>x</sub>InS<sub>2-x</sub>Se<sub>2x</sub> for solar photovoltaic cells 0-10982  
 Cu<sub>2</sub>S/CdS, developments, appls., and economics of solar photovoltaic conversion (*German*) 0-26132  
 Cu<sub>2-x</sub>S/CdS heterostructures, heat treated, capacitance voltage meas. anal. 0-20292  
 Ga<sub>1-x</sub>Al<sub>x</sub>As:Si photoelectric convertors, broadband varizone creation 0-40856  
 GaAs, developments, appls., and economics of solar photovoltaic conversion (*German*) 0-26132  
 GaAs photovoltaic solar system, appl. in electric utility system 0-55875  
 GaAs-GaAlAs LPE grown, parameters dependence upon impurity concentration and temp. performances for series resistance reduction 0-45692  
 In<sub>2</sub>O<sub>3</sub>-SnO<sub>2</sub>/SiO<sub>2</sub>/Si diode solar cells, loss mechanisms, characts., band struct. 0-26135  
 In<sub>2-x</sub>Sn<sub>x</sub>O<sub>3-y</sub>-CdTe(InP) photovoltaic heterojunctions, surface and interface studies, efficiency 0-45691  
 Si, amorphous and solar cells (*Japanese*) 0-50965  
 Si, developments, appls., and economics of solar photovoltaic conversion (*German*) 0-26132  
 Si, for tristimulus colorimeter (*German*) 0-17994  
 Si photoelectric convertors, photoelectric parameters under illumination 0-40857  
 Si photoelectric convertors, bilateral sensitivity, optical characts. anal. 0-40858  
 Si, polycryst. solar cells, production problems (*Rumanian*) 0-21398  
 Si solar cell array with concentration, design and development 0-45700  
 Si solar cells, developments (*French*) 0-55845  
 Si solar cells for cathode protection of submerged marine structures 0-40859  
 Si solar cells with concentrating collectors and integrated heat use system 0-45701  
 Si solar concentration cells, concentrated sunlight effects, experimental results, interpretation 0-35690  
 Si terrestrial photovoltaic systems, historical developments and current research and development trends 0-45702  
 Si:H, amorphous, p<sup>+</sup>-i-n<sup>+</sup> struct. solar cells, material parameters and deposition condition optimisation study for higher efficiencies 0-45676  
 Si:H, amorphous, RF sputtered, Schottky barrier solar cells, photovoltaic props. and capacitance-voltage charact. 0-45678  
 Si:H, amorphous, Schottky barrier solar cell, degradation mechanisms affecting stability and operation 0-45680  
 Si/Si-Ge alloy, amorphous, solar cell, multijunction structure, increased conversion efficiencies, low cost 0-45677  
 SnO<sub>2</sub>-GaSe heterojunction photocell, fine struct. of photo-EMF spectra 0-6967  
 SnO<sub>2</sub>-Si heterojunctions, elec. and photovoltaic props. 0-26141  
 SnO<sub>2</sub>-Si solar cells, electron-beam deposited, struct., photovolt. props. 0-50956

**photovoltaic effects**

see also Dember effect

- amorphous semiconductor (*Japanese*) 0-54737  
 anthracene, surface photovoltage 0-2419  
 back surface field semiconductor junction, temp. depend. of open circuit photovoltage 0-15593  
 p-CdTe, surface photovoltage spectroscopy in IR and visible range 0-39632  
 copper phthalocyanine film, photoelectrochem. behaviour on SnO<sub>2</sub> electrodes 0-15626  
 ferroelectric, photovoltaic current, general formula (*Russian*) 0-39627  
 ferroelectric-photoconductor two component systems, photoelectret state 0-25287  
 Fokker-Planck eqn., kinetic effects due to detailed equilibrium violation, elastic scatt. (*Russian*) 0-31687  
 metalloporphyrins, photoelectrochemical props. 0-50991  
 MIS, and amorphous materials (*Japanese*) 0-54737  
 pentacene, surface photovoltage 0-2419  
 phthalocyanine films, metal-free, adsorbed o-chloranil effect on surface photovoltage 0-34485  
 phthalocyanine-metal interfaces, surface photovoltage 0-20308  
 PLZT ferroelectric ceramic, anomalous bulk photovoltaic effect and cond. (*Russian*) 0-54733  
 polyacetylene, phototransport effects 0-44653  
 polynaphthalene films, plasma polymerised, photovoltaic and photocond. props. 0-34479  
 rhodamine B surface state hole traps, surface photovoltage meas. 0-39654  
 semiconductor-electrolyte interface, phenomenological theory and expt. confirmation 0-15601  
 semiconductor surface probing using scanned photovoltage techniques 0-49915  
 solar-powered solid-state heat transfer device based on photovolt. and Peltier effects 0-217  
 tetracene, surface photovoltage 0-2419  
 vibron ferroelectric, intrinsic anomalous photovoltaic effect (*Russian*) 0-44665  
 Au-CdS, Schottky junction, surface defects, photovoltaic, piezoelectric and V-I characteristics (*French*) 0-49898  
 BaTiO<sub>3</sub>, ferroelectric semicond. anomalous photovoltaic effect due to ionising radiation 0-29437  
 n-CdIn<sub>2</sub>S<sub>3</sub>/p-CuInSe<sub>2</sub> heterostructure, form. and photovolt. meas. 0-10831  
 CdTe film, photopolarisation 0-25286  
 CdTe sputtered films, struct., photocond., and trap distrib. 0-29489  
 Cu-CdS, Schottky barrier, Cu diffusion and photovolt. mechanism 0-6980  
 Cu<sub>2</sub>S-CdS solar cells in backwall configuration, model of photovoltaic effect 0-55861  
 Cu<sub>2-x</sub>S-CdS p-n heterojunction solar cells, props., Burstein-Moss effects 0-21404

**photovoltaic effects continued**

- GaAs (110), adsorption of O<sub>2</sub>, H<sub>2</sub>, H<sub>2</sub>O and H<sub>2</sub>S, surface photovolt. spectroscopy 0-49499  
 GaAs microcharacterisation for device appls. 0-10922  
 p-GaAs-Cd<sub>1-x</sub>Zn<sub>x</sub>S heterojunctions, elec. and photovolt. props. rel. to growth technique 0-29466  
 GaAs-Ga<sub>1-x</sub>Al<sub>x</sub>As, variable band gap, photo-EMF 0-20296  
 GaAs-Ga<sub>1-x</sub>Al<sub>x</sub>As variable gap p-n junction, variable gap and photo-EMFs 0-15596  
 GaAs<sub>1-x</sub>Sb<sub>x</sub> photodiode structures, current-voltage characts., photo-EMF spectra 0-29472  
 GaSe, photovoltaic spectra 0-20240  
 GaSe:Cu(Cd, Sb), photovoltaic spectra 0-20240  
 In<sub>1-x</sub>Ga<sub>x</sub>Sb-Au, photovoltaic effect and Schottky barriers 0-49897  
 KNbO<sub>3</sub>, photovoltaic effect lux ampere characts., photoconductivity 0-15561  
 LiNbO<sub>3</sub>:Fe, anomalous photovoltaic effect in polarised light (*Russian*) 0-34484  
 Mn ferrites, photogalvanomagnetic effects 0-34483  
 Pb<sub>1-x</sub>Ge<sub>x</sub>Te, ferroelectric phase transition effect on forbidden band width 0-24794  
 Pb<sub>1-x</sub>Sn<sub>x</sub>Te, surface photo-EMF under laser excitation conditions 0-6897  
 Sb<sub>2</sub>Se<sub>3</sub>, photocond., photo-EMF and photodielectric effect, expts. 0-20245  
 Si, amorphous, p-n junction devices, barrier profile effect on elec. props. 0-49890  
 Si, amorphous, photovoltaic diodes, influence of mag. field on charge transport 0-49891  
 Si dip-coated on graphite substrate, Si-SiC p-n heterojunctions 0-29442  
 Si, electron irradi. induced defects, bulk photo-EMF meas. 0-39160  
 Si, polycryst., elec. and photovolt. props., grain size effects 0-49800  
 Si, Schottky diodes on sputtered amorphous Si:H, light induced ageing effects, interpretation of photovoltaic stability 0-54780  
 Si solar cells, photoelectric effect and principles of operation and efficiency 0-50983  
 Si surface, electron states, surface photovoltage spectroscopy study, doping effects 0-49860  
 Si:H, amorphous, Schottky diode, spectral response and hole drift mobility 0-39673  
 Si:H amorphous films, photovoltaic and photocond. spectra, photoluminesc. 0-44645  
 Si-CdSe n-n heterojunction, photovoltage sign reversal, energy band profile (*Korean*) 0-29469  
 SiH<sub>4</sub>, amorphous reactively sputtered films, in Pd Schottky barrier devices, photovoltaic props. 0-49910  
 SnO<sub>2</sub>-GaSe heterojunction photocell, fine struct. of photo-EMF spectra 0-6967  
 SnO<sub>2</sub>-Sb<sub>2</sub>S<sub>3</sub>-Sn structures, photovoltaic effects (*Korean*) 0-44647  
 Te, optically active crystals, circular photogalvanic effect 0-54739  
 Te, photovoltaic effect in thin films, 10.6 μ, prep. methods 0-20252  
 Zn<sub>3</sub>P<sub>2</sub> bulk and thin film, UV reflectivity spectra, photovoltaic effects, optical consts. 0-25472  
 Zn<sub>3</sub>P<sub>2</sub>, direct and indirect optical transitions, metal-Zn<sub>3</sub>P<sub>2</sub> contact photovoltage response 0-25402  
 ZnS-metal interface in MIM struct., photoexcitation level assignment (*French*) 0-15622  
 ZnSiP<sub>2</sub>-In Schottky diode, photovoltaic spectra 0-2423

**photovoltaic generators, solar** see photovoltaic cells; solar cells

**phthalocyanines** see organic compounds

**physical chemistry**

- see also chemical analysis; chemical equilibrium; chemical reactions; chemical structure; crystal chemistry; electrochemistry; nuclear chemistry; pH; photochemistry; radiation chemistry; radiochemistry; solvated electrons; surface chemistry; thermochemistry  
 laser spectroscopy applications, conf., Anaheim, USA (Mar. 1978) 0-36781  
 phase change derivation, phys. chem. textbook assumption removal 0-17772

**physical data, collections of** see collections of physical data

**physical instrumentation control**

- AC calorimetry technique (*Japanese*) 0-27306  
 aerosol electrical analyser, microcomputer-modified, for particle size anal. 0-40756  
 astronomical mirror horizontal control, deforms. calc. 0-17494  
 Atmospheric Cloud Physics Laboratory on Shuttle/Spacelab, droplets optical motion control appl. 0-12634  
 autocollimator, photo-electric, calibration with laser interferometer system and microcomputer 0-1304  
 automated, qualitative anal. 0-22497  
 automatic rotary diaphragm for microphotometer 0-22415  
 CAMAC, 2-D anal. of spectroscopic data, electronics 0-5460  
 CAMAC I/O module based on Signetics 8X300 microcontroller 0-47835  
 CAMAC spectroscopic data anal., programming techniques 0-5461  
 chromatograph, microcomputer controlled GC with data processor and printer-plotter (*Japanese*) 0-50921  
 chromatography, automatic liquid sample injector for GC, syringe-type (*Japanese*) 0-50923  
 chromatography, nonlinear detector response quantification with lab. automation system 0-40775  
 circular dichroism spectrophotometer, near IR, microprocessor controlled 0-22454  
 Cs beam freq. standard, servo-control system anal. 0-42201  
 electron injector in HV terminal, control and protection system 0-27836  
 EM analyser control, automatic registration of the back-scattered ions 0-18042  
 Enraf-Nonius CAD-4 diffractometer, mechanical design, computer control and system performance 0-24318  
 flowmeter, gas, low speed, constant gas flow production (*Hungarian*) 0-1702  
 flowmeter calibration, microcomputer-controlled flow rigs 0-10320  
 gas chromatograph development, temp. control system (*Japanese*) 0-50922  
 gas chromatography-mass spectrometry data system, research-oriented, principles and appls. 0-40770  
 HPLC, two-pump gradient, accuracy and reproducibility 0-16742  
 instrumentation and control technology, decentralisation, past developments and future trends 0-4701  
 laboratory data acquisition and control system based on Commodore PET microcomputer 0-204  
 laser, radiation pulses formation and stabilisation 0-23735



**physical instrumentation control continued**

- laser gyrometer, accuracy increase by automatic output signal correction (*Russian*) 0-215
- laser system, He-Ne, automatic frequency trimming circuit (*Russian*) 0-1217
- lasers, coherently combined, phase lock control considerations 0-5743
- Marx's composite oscillator method, automated, for internal friction and Young's modulus meas. 0-37151
- measuring projector for bubble chamber film, minicomputer on-line system 0-27878
- microcomputer-controlled visual stimulator for eye movement and visual evoked pots. study 0-41350
- MORPHOQUANT automatic microscope image analyser, universal program system 0-56160
- neutron depolarisation meas., exptl. set up and process program 0-18771
- neutron diffractometer, four-circle, single cryst., automatic control using FORTRAN software 0-38876
- NIM-controlled rabbit system 0-18731
- NMR, pulse type, programmable pulse sequence generator 0-17979
- NMR spectrometer, for quantitative analysis, microprocessor-controlled digital integrator 0-11971
- NMR spectrometer, programming device for control of frequency synthesizers 0-22400
- NQR spectrometer, programming device for a spin-echo installation 0-17972
- NQR spectrometer, weak signal relax. meas. with Sigma type digital storage device, pulse-train program blocks 0-17970
- odour analyser, automatic, for atmospheric sulphide anal. (*Japanese*) 0-50924
- particle physics expts., on-line data acquisition system using PDP-11 computers 0-27913
- photomultiplier protection against optical overloads, electromagnetic shutter control 0-23255
- plasma position detection and control, in Tokamaks, interferometric method 0-1850
- polariscope interactive control system to evaluate stresses 0-19299
- potentiometric analyser, automated, with selective electrodes, microcomputer control 0-40773
- potentiometric analysis with ion-selective electrodes, computer automation 0-3424
- radiospectrometer, automatic thermostatic control, using Diapazon variator 0-47160
- Schmidt telescope at Campo Imperatore, automatic control using PDP 11 processor (*Italian*) 0-8541
- SIMS, computerised system for energy spectra determ. 0-3423
- solar flat-plate collector loops with on-off control, anal. of dynamic behaviour (*French*) 0-55901
- spectrometer, grazing-incidence, automatic scanning system 0-14250
- spectrophotometer for multielement atomic spectrum anal. under computer control 0-27357
- spectrophotometers, microprocessor based data acquisition and control system 0-22335
- thermal diffusivity meas. system using microprocessor (*French*) 0-14559
- UV spectrometers, on OSO-8, computer-controlled, mission operations 0-41723
- vacuum apparatus (*Czech*) 0-52256
- X-ray diffractometer, HAG 4/A universal instrument, applic. versatility of basic software 0-52375

**physical metallurgy** *see metallurgy***physical optics**

- critical angle scattering of light by air bubble in water, approx. 0-9797
- diffraction catastrophes, optical caustics 0-9801
- Gaussian beam, plane-wave-type expansion, errors incurred 0-48312
- gradient index imaging system theory 0-14294
- models of optical systems 0-9821
- principles for electronic engineers (*Japanese*) 0-9799
- surface waveguide electrooptical deflector, high-resolution, prism model 0-48454

**physics***see also physics computing*

- Australian Institute of Physics conf., 1979 0-4477
- David Ausubel learning theory as reference system for content organisation in physics 0-22172
- education, physical sciences in medicine diploma 0-31444
- electronics technology development, teaching 0-31470
- International Centre for Theoretical Physics, objectives and scope 0-12839
- medical applications of physical methods (*Polish*) 0-12048
- metrology, scope and relationship with physics 0-52153
- models, nature and purpose 0-42023
- problem-solving, teaching and understanding 0-8752
- Soviet physics, review articles, book 0-46742

**physics computing***see also computerised instrumentation; spectroscopy computing*

- acoustic field in finite cuboidal spaces, computer-aided geometrical field analysis of directional props. 0-19157
- acoustical holography, digital reconstruction and computer graphics display 0-23842
- adsorption, density functional theory, computer simulation 0-24735
- air coils, magnetostatic field FFT calcs., linear system theory 0-32868
- air showers for  $10^4$  to  $10^6$  particles, lateral distrib. of EM component, detection, data handling 0-17459
- air-based solar heating systems with phase-change energy storage, performance anal. using computer simulation 0-35762
- airborne noise, personal calculator program for A-weighted sound pressure level and noise ratings 0-23828
- airborne plume dispersion, 2-D computer hydrodynamic simulations 0-45837
- aircraft design technology, fluid dynamics computer program assessment data base 0-1637
- alkali chlorides, thin film, crystal-vacuum (100) surface, mol. dynamics computer simulation 0-34288
- alkali halides, thin films, crystal-vacuum (110) interfaces, mol. dynamics computer simulation 0-34289
- alloys systems, ternary, phase equilibria calc., line compounds 0-10638
- ANALYT, analytic extrapolations towards interior points from a cut, applic. to elementary particle scatt. theory 0-12952
- ANISN code for calc. of neutron bomb rad. penetration in air 0-47743
- associated Legendre polynomial  $P_L^M(x)$ , Chebyshev expansion 0-8774

**physics computing continued**

- atom, Breit interaction between electrons, calc. angular coeffs., computer program 0-18779
- atomic, molecular, and solid-state theory, collisions, quantum statistics, symposium, Florida, USA (March 1979) 0-51946
- atomic shells, internal conversion coefficients, numerical solution of Dirac equation 0-47434
- audiometry, threshold, optimum crossings and time-window validation 0-19187
- Auto-Resonant acceleration, computer simulation of linear and nonlinear wave growth phenomena 0-9439
- automated method for fission-fragment track density determ. in solid state track detection using MAGMO-1 system 0-42891
- azimuthal scanning method, allowance for X-ray absorpt. in single-crystal diffractometry 0-38874
- barytes concrete, gamma ray buildup factors, PIPE code 0-27823
- BASIC overlay for CAMAC data and command handling 0-18772
- BCC metals, plastic deform., computer simulation 0-40456
- Bessel functions,  $Y_p(x)$  and  $J_p(x)$ , of real order and argument, calc. prog. 0-8776
- binary alloys, diagrams of state, component interaction parameters, computer calcs. (*Russian*) 0-55355
- BIODOSE, chronic radioactive release assessment 0-13710
- BIOT2, heat conduction, three-dimens. code (*Hungarian*) 0-43593
- BKWAWE, program, calculation of 1-dimensional shock wave propagation 0-38448
- blunt-body boundary layers, three dimensional, surface curvature effects 0-1520
- Bragg reflections, ang. positions calcs. by computer program 0-38863
- brittle material, fast crack propagation, computer simulation 0-38331
- bubble chamber film meas. automisation in Spiral reader system 0-14045
- CAMAC diagnostic module for on-line monitoring of CAMAC integrity 0-5459
- CAMAC high rate data acquisition system 0-23281
- cavitation failure, incorporating cavity nucleation with strain, computer program 0-16451
- chain molecules in soln., thermodynamic props. related to chem. pot. 0-3394
- COBRA-IV, multi-dimens. simulation of flow nonuniformities in fissured porous media 0-28559
- COL, Laue patterns, cylindrical, flat transmission or flat back-reflection Laue photographs, calc. of crystal orientation 0-19670
- collective modes in solids, computer simulation 0-54325
- composite fracture with bonding strength defects between components, computer simulation 0-11771
- computational fluid mechanics, book 0-1517
- CONAN code, effects of evaporation and condensation on LMFBR post-accident containment response 0-47637
- critical two-phase flow, nonequilibrium vapour production model, K-FIX 0-52719
- crystal growth, from soln., implication for industrial crystn. 0-49147
- crystal surface, (1n0), stepped relief machine model 0-34283
- curve fitting to data with low statistics 0-9471
- cyclotrons, superconducting, spiral electric gap effects on ion orbits, computer program calc. 0-52795
- data acquisition system on-line, for particle physics expts. using PDP-11 computers 0-27913
- defect clusters, nucleation and growth due to energetic particle radiation, chemical rate reaction theory, computer program 0-49263
- defect coordinate determ. by calibration of AE method 0-35473
- defect displacement field construction from angular dislocation segments, electron microscope image simulation 0-6325
- dendritic particle characterisation of automatic methods 0-25590
- dense liquids and their mixtures, mol. dynamics, numerical algorithm 0-28890
- densities of states, computational algorithm 0-44466
- diamagnetic susceptibility calculation using Pascal's consts., BASIC program 0-37717
- dielectric, freq. crossing signals in thermal cond., extension to high conc. of phonon scatt. centres using computer anal. 0-2224
- dielectric, solid, energetic struct. of traps, from SCL currents 0-24941
- dielectric thin film refractive index and thickness, algorithm for determ. on basis of ellipsometric meas. 0-34881
- diffusion, chemical, highly defective solids, steady-state computer simulation method for lattice gas 0-49401
- dilute frustrated lattice, spin-glass ordering, triangle and FCC lattices, Monte Carlo simulation 0-15746
- dislocation image in X-ray plane wave topography 0-54234
- dislocation segment oscillations, internal props., point obstacle collisions, glide plane motion (*Russian*) 0-39088
- DOT-III, anal. of  $^{60}\text{Co}$   $\gamma$ -ray scatt. in air 0-32525
- drift-flux model of LMFBR Na boiling transient 0-47636
- dynamic electric and magnetic field evolutions, visualisation using computer graphics display 0-46776
- dynamic fatigue tests, statistical reproducibility of crack propag. parameter 0-25842
- dynamic heat transfer meas. at Mach 8, digital Fourier anal., boundary layer transition 0-14682
- ECSIMPACT, version of IMPACT for CDC machines with ex-core memory, electron impact 0-18924
- elastic coefficients of fourth order, independent, for 32 cryst. classes (*French*) 0-34117
- elasticity, pot.-type singular integral approx. algorithm 0-27132
- elastomers, tackiness, fracture mechanics theory (*French*) 0-38344
- electrocrystallisation, chess board type computer simulation 0-54157
- electron collision theory, asymptotic soln. calc. program 0-53129
- electron diffraction computer simulation for one-dimens. studies (*French*) 0-1902
- electron micrographs, computer-aided anal. 0-4813
- electron microscope image contrast of small dislocation loops and stacking fault tetrahedra 0-6326
- electron motion in elec. and mag. fields, student lab and computing studies 0-27076
- electron solid, two-dimens., shear modulus and melting, temp. depends. 0-158
- electron transport, discrete ordinates calc. using standard  $S_n$  neutron transport codes 0-46998
- electron-image calculation system, interactive, for use in electron microscopy 0-24325
- elementary particle physics, use of database management systems 0-899



# physics computing continued

environmental radiation dose assessment of a growing nuclear industry 0-3553  
environmental radioactive releases from nuclear installations, computer simulation of effects 0-3550  
equations of state, search procedure, based on step-wise least-squares technique 0-19900  
exact finite range DWBA form factor for heavy-ion induced nuclear reactions, calc. program adaption 0-9271  
externally cracked cylinder, elastoplastic response anal. by method of lines, computer program 0-28435  
fatigue, cumulative damage, under random loads algorithm of hysteresis loop counting 0-21064  
fatigue life prediction, computer based 0-21251  
fatigue life predictions using computer modelling, cyclic stress/strain curves 0-19290  
FERDOR, neutron spectrum unfolding, optimised smoothing 0-27860  
fibrous material failure kinetics, internal stresses, computer simulation (*Russian*) 0-40479  
fission fragments, kinetic energies and fly-off angles, ionisation method of meas., online numerical processing (*Russian*) 0-52838  
fission reactor and plasma nonlinear optimisation algorithms 0-18623  
fission reactor poisoning by Xe and Sa, transient anal. using XESAMO code (*Spanish*) 0-52749  
fixed mirror solar concentrator, optical-thermal performance anal. 0-30392  
flame, mutual ion neutralisation 0-35537  
flow, inviscid, hyperbolic, computational algorithms tests 0-27140  
flow field, multiply connected, curvilinear coords. and macro-elements 0-19318  
flow field meas., near nozzle outlet using laser Doppler anemometer 0-28582  
flow probe output digital processing, appl. to cylinder wake characts. 0-19541  
flowmeter standard orifice plate calc., for meas. flowrate of liquids, gases and vapours 0-1714  
FLUID, Galerkin method program, viscoelastic fluid flow in fixed geometry 0-14750  
fluid, Monte Carlo calculations, optimisation of sampling algorithms 0-54099  
fluid and structural dynamics, transient 3-D potential flow problems, SING-S 0-48668  
fluid dynamics, transient 3-D potential flow problems and dynamic response of surrounding structures, singularity method, SING 0-48667  
flux-corrected transport algorithm, rezoning technique 0-31516  
fracture toughness testing, elastoplastic range, computer simulation 0-21217  
free convection mass transfer from downward facing horizontal plates, analog soln. 0-43706  
Frenkel pair formation in solids, due to passage of relativistic electrons, computer simulation (*Russian*) 0-6402  
frozen core Hartree-Fock program for atomic discrete and continuous states 0-9509  
fusion power plant simulation model 0-13865  
fusion reactor materials, appl. of dynamical computer models to high energy cascades 0-34046  
gas dynamic flow fields with discontinuities, computational method checking test 0-36864  
gas dynamics, self-adapted algorithms 0-38432  
gas lasers, computer modelling, at. and mol. processes 0-23661  
gas-liquid surface of mol. fluids, mol. dynamics computer simulations 0-39387  
glass, refractive index freq. depend., dispersion eqn. calc. 0-40083  
glass surface, ellipsometric study of zone of optical contact 0-4754  
graded-index fibre transmission characteristic computation 0-1321  
grain boundary segregation, computer simulation using Mie type interatomic pot. 0-54259  
grain growth, chem. driven, during liq. phase sintering, computer simulation 0-55427  
grid generation, automatic mesh-point clustering elliptic partial differential eqns, grid generation, automatic mesh-point clustering 0-31487  
growing bubbles on heated plate, meas. using computerised image anal. system 0-22322  
haemoglobin, sickling deer type III, macromol. struct. refinement by restrained least-squares and interactive graphics 0-28870  
HEAP, heat energy anal. of cavity-type solar receivers 0-30548  
heat exchange modelling of marine two stroke compression ignition engines 0-30529  
heavy ion radiation transport computer codes for thick targets 0-39180  
HEPROP, programs for the calculation of thermophysical and thermodynamic props. of He 0-6529  
high-speed shaping of free-flowing materials 0-25591  
hologram, computer generated, 3D reconstructed images, characts. 0-43297  
holographic interferograms, computer anal. for nondestructive testing 0-9836  
hybrid thermal energy storage system, transient simulation 0-30588  
hybrid thermal energy storage with water systems, eval. using analytical models 0-30589  
hydration, hydrophobic, of nonpolar mols. in dilute aq. soln., Monte Carlo simulation 0-3314  
hydrodynamic stability computation, algorithm construction 0-19329  
hydrodynamics codes, Eulerian and Lagrangian, pressure iteration, multi-grid method 0-53738  
hydrodynamics computer codes, limited compressibility 0-53803  
hydrogen-bonded liquids, HF, H<sub>2</sub>O, NH<sub>3</sub>, computer simulation, intermolecular potentials 0-38890  
image reconstruction formulae, computer implementation 0-52179  
image reconstruction from projections 0-52178  
inclusive backward proton cross sections, calc. program adaptation 0-9185  
interferogram aberration evaluation program 0-13130  
internal conversion data anal., nuclear parameter determ. 0-52626  
inverse pole figures, calc. method on digital computer 0-20950  
ion scattering from single crystals, computer simulation 0-2911  
Ising ferromagnets, correlation decay, zero-field susceptibility, mass gap 0-50116  
isobar nuclei, separation of alkali and alkaline earth elements using surface ion source 0-37688  
isotropic thin shells with circular hole, stress state, numerical investigation 0-48586

# physics computing continued

Johnson-Mehl and cellular microstructure, comparative analysis, computer simulation 0-54392  
K-FIX, critical two-phase flow, nonequilibrium vapour production model 0-52719  
laser fusion targets, X-ray meas. using least squares fitting 0-32425  
lattice disorientations 0-28936  
lattice dynamics of group IV semiconductors using an adiabatic bond charge model 0-10599  
lens CAD, three-lens zoom system 0-43424  
light pulse excited decay curve simulation, finite breadth (*Hungarian*) 0-11473  
light scattering by dielectric particles, statistical theory 0-32913  
linac injection system beam dynamics 0-13989  
liquid metals, viscosity calc. using microinhomogeneous struct. model (*Russian*) 0-15284  
liquid radial distribution functions, method of reducing termination errors 0-24332  
liquid-liquid solubility, critical phenomena in binary mixtures 0-54376  
liquid-vapour interface, fluid phase coexistence, Monte Carlo computer simulation 0-49349  
LMFBR critical assembly, neutron diffusion calc., DB<sup>2</sup> transverse leaking predictions 0-13529  
magnet shimming, using computer routine 0-245  
magnetic bubble domain Bloch lines motion, computer simulation 0-54916  
magnetostatic problems, soln. by MAGGY2 problem package 0-28134  
magnetron ion sputtering, thin film layers deposition uniformity investigation (*Russian*) 0-20787  
magnox fuel cladding, surface struct. data acquisition and processing system 0-898  
many-electron atoms, one-electron operators, Z-expansion of matrix elements 0-9489  
matter modelling conf. Anaheim, USA (Mar. 1978) 0-51954  
measuring projector for bubble chamber film, minicomputer on-line system 0-27878  
melting and freezing, computer simulation of simple systems using array processor 0-54353  
metallic system, compound formation rel. to heat of mixing 0-55689  
metals, heating by concentrated energy sources, simple analytical expressions (*Russian*) 0-38215  
methane, liq., mol. dynamics simulation using singularity-free algorithm 0-54116  
microcomputer controlled UV ozone calibrator 0-13149  
micromagnetism, numerical calcs. 0-11222  
microphysics to macrochemistry, discrete simulations, review 0-54102  
microprocessor applications in deformation processes (*German*) 0-40627  
microstructures simulation, based on optical electron and field-ion microscopy 0-19679  
Micu-type invariants of simple Lie algebras 0-12934  
Mie theory calculations, particle sizing appl. 0-14282  
minicomputer-based gamma spectrum analysis system SAMPO78 0-14043  
mixing of multicomponent solids, mixing index and contact number estimation by spot sampling 0-16214  
modeling of a thermal wall panel using phase change materials 0-35758  
molecular crystals, optimum packing in atom-atom approx., algorithm and computer program 0-1960  
molecular fluid, computer simulation of liquid-vapour surface 0-54478  
molecular fluid, hard-core triatomic, Monte Carlo simulations 0-38880  
molecular rotational spectra, assignment by double reson. technique, computer program 0-32751  
Monte Carlo analysis of backscattering and sputtering in vacuum systems 0-235  
Monte Carlo radiation transport program for reactor bundle gamma transport and energy deposition analysis 0-22915  
MORSE code, neutral particle transport in toroidal plasma 0-33750  
multicomponent alloys, phase diagram calc. program from thermodynamic data 0-3008  
multicomponent vapours-condensed phases, equilib., computer modelling 0-44288  
multilayer nonabsorbent coating reflectivity computation program 0-28293  
multilayer structure devices, nonideal, computation of optical props. 0-5684  
Nairi-K use in multichannel installation for activation meas. 0-23271  
NATOF-2D for Na flow transient anal. in LMFBR 0-47633  
near-field jet entrainment, overlaid viscous/inviscid model, BOAT computational model 0-19457  
neutron balance and flux distrib. calc. for Oklo natural fission reactor (*French*) 0-21767  
neutron bomb radiation protection, calc. of rad. penetration in air using ANISN code 0-47743  
neutron experiments, Braunschweig accelerator facility, data acquisition and anal. 0-47806  
neutron scatt., automatic data processing (*Russian*) 0-54079  
neutron spectrum unfolding, optimised smoothing, FERDOR method 0-27860  
neutron transport, anisotropic scattering treatment using improved comput. code (*Japanese*) 0-13526  
neutron transport, transverse buckling effects in 2-D calcs. 0-32318  
neutron transport eqn., response matrix finite element soln. 0-13527  
neutron transport eqn. cylindrical and spherical geometries, characteristics formulation in CHART program 0-5197  
neutron transport theory, S<sub>N</sub> calcs. using ANL DIF3D diffusion code 0-47526  
non-crystalline materials, hole struct. of computer models 0-49109  
normal coordinate calcs., computer program for Z-matrix determ. 0-23388  
nuclear elastic scatt. with optical potential, complex angular momentum methods, poles and zeros of S-matrix, REGGE 0-47445  
nuclear K-X-ray satellites, Z=50-83 cascade anal. algorithm 0-42984  
nuclear physics course, computer simulation techniques 0-36823  
nuclear radiation detection lab., desk top calculators 0-36821  
nuclear reactor kinetics, computational methods and computer codes for space-dependent transient analysis 0-52716  
nucleation in finite systems, theory and computer simulation 0-26038  
optical interference fringe location by digital scanning methods 0-13128  
optimal nodal point distribution for improved accuracy in computational fluid dynamics 0-48670



- physics computing continued**  
orbital pairs, transformation into localised pairs, use of FORTRAN for angle selection 0-27922  
organic scintillator efficiency using Monte Carlo code 0-889  
Ostwald ripening, effect of precipitate vol. fraction 0-40356  
oxidation kinetics, C by CO<sub>2</sub> in Fe-C melts (*Russian*) 0-40680  
PALLAS-2DCV, anal. of <sup>60</sup>Co  $\gamma$ -ray scatt. in air 0-32525  
parametric biostimulation, mag. field calcs. 0-36054  
partial vapour pressure calculation, phase comp. of Nb oxides on heating 2000-4000K 0-21267  
particle dispersion coarsening, computer simulations 0-30289  
particle dynamics computer modelling, alternating phase focusing LINAC (*Russian*) 0-23234  
particle scattering amplitude, analytic extrapolations, EMZERO 0-47221  
particle tracks, time digitiser in CAMAC format 0-14062  
particle-particle correlation experiment, on-line four parameter anal. system (*Chinese*) 0-42910  
perturbation stable cell comparison technique 0-49133  
phase diagram, of metal-semimetal alloy, from thermodynamic functions 0-40329  
photoelastic fringe pattern analyzer, computer aided 0-38359  
photoemission spectra calculation program 0-55256  
PIPE, barytes concrete, gamma ray buildup factors 0-27823  
plane triangular element, stress-strain finite dynamic element, FORTRAN IV program 0-53  
plasma, chemical reactions, rate coeffs., database creation, DATSTOR 0-48846  
plasma, chemical species, number density variation with time, numerical model, PLASKEM 0-48845  
plasma, collisionless drift modes, graphical method for finding complex roots of nonlinear eqn. 0-33762  
plasma, cross-field electron heat transport due to high frequency electrostatic waves, simulation 0-53932  
plasma, laser produced, ionisation process computer simulation code, atomic transition processes 0-28764  
plasma, neutral atom transport, computer code SPUDNUT 0-48962  
plasma, submillimetre diagnostics, active, of Ar arc, data numerical anal. 0-48979  
plasma drifting, cold or hot, radiation potential of immersed point antenna, DRFT computation 0-14906  
plasma of given chemical content, chemical reactions, computer generation, REACS 0-48844  
plasma turbulence simulation, phase space granulation due to mode-mode coupling 0-38651  
PLOMAC, plot program for 0-19669  
point defects short term annealing, simulation, in  $\alpha$ -Fe 0-54282  
polar semiconductors, hot exciton scatt. accompanied by transitions to excited states, phonon interactions 0-44516  
polarisation meas. with high press. He scintillation counter 0-14061  
polyethylene, crystalline, twist disclination formation and longitudinal motion of defects 0-19810  
polymer crystal, conformational energy calcs., appl. to defect props. 0-54154  
polymer melts, crystallisation models, Avrami eqn. extension 0-19723  
positron annihilation ang. correl. curves anal. using ANNIH program 0-37709  
potential-pH diagram, improved algorithms for computer generation, max. constriction method 0-26019  
powder least-squares program, POWLS 0-1892  
prism dimensional design, rhombic (*Czech*) 0-53431  
product operators, closed basic diagram generation program 0-8817  
proportional counter data acquisition system 0-42913  
PWR, Xe-induced spatial flux transient, anal. and control, parameter identification 0-18441  
quantitative image analysis, appls. using sequential transforms. 0-23627  
quantum liquids and crystals, computer modelling 0-54472  
quantum mechanical measurements, simulation using programmable pocket calculator 0-41982  
radiation damage in fusion reactors, computer expts. on Nb 0-13839  
radiation damage produced by energetic heavy particles, computer simulation (*Japanese*) 0-29094  
radiation damage simulation in amorphous Fe 0-34045  
radiation dosimetry, standardised radioactive decay data sets 0-13945  
radiation transport in Earth for neutron and gamma-ray point sources above an air-ground interface 0-32526  
radioactive waste geologic repositories, computer anal. of long-term radiation hazards 0-18483  
radiographs processing 0-3259  
rare earth compounds, binary, regression eqns., for calc. props. from electron struct. 0-39498  
ray tracing program, CUPID, for continuously varying refracting media 0-18990  
ray tracing through tilted and decentred optical surfaces, computer program 0-33120  
reactor fuel pin performance anal., COMETHE III-K code 0-13605  
REDUCE, Feynman diagrams, dimensionally regularised, symbolic evaluation, quantum gravity application 0-13259  
refractive index data interpretation, collection of program library 0-55056  
resonance analysis of neutron transmission data, least square fitting program REFIT 0-22840  
Rietveld neutron profile refinement, interactive computer system, POWDER 0-1900  
rolling of complex metal sections, unified anal. function of surface of strain focus (*Russian*) 0-21017  
rolling texture formation, computer simulation in HCP and orthorhombic metals 0-3095  
SAS-3D analysis of natural-convection boiling behavior in the sodium boiling test facility 0-47635  
SAS-3D evaluation of LMFBR boiling of decay-heat levels in FFTF 0-47634  
SCAM, Stirling cycle anal. model of compressible flow 0-35717  
Schrödinger equation, solution by hand-held calculator 0-52052  
segment description, of unique set of reflections to data collection and data reduction 0-1881  
selective solar absorbers, reflectance calcs. for inhomogeneous surfaces 0-12029  
shale oil, in situ retorts, computer simulation of ignition with hot inert gas 0-30356  
simulation of sputter broadening in impurity depth profiling 0-2908  
simulation plasma, boundary conditions in magnetic field 0-10392
- physics computing continued**  
SINDA heat transfer modelling for thermionic converter array 0-40886  
SIR program, use of negative quartets 0-24304  
skew ray tracing with the TI-59, programmable calculator 0-48141  
small angle X-ray scatt., slit height smearing correction prog. 0-10456  
small angle X-ray scatt., slit height smearing correction prog. 0-10457  
solar collectors, tubular, computerised performance simulation 0-55903  
solar radiation levels on tilted surfaces, computer model validation 0-35641  
solar receivers, cavity-type, HEAP computer simulation program for heat energy anal. 0-30548  
solid solution hardening, statistical behaviour analysis (*Japanese*) 0-11658  
solid state detection spectra, fast analysis, LIZA program 0-37706  
solitons, computer calcs. 0-46832  
speckle, non-Gaussian, correlated weak scatterers, computer simulation 0-28159  
spherical Bessel function  $j_l(r)$ , Chebyshev series 0-8775  
spherical X-ray wave, dynamic diffr. theory, numerical results 0-38867  
spin-glass, two-dimensional Ising model, low temp. dynamic props. 0-20425  
SPODE, Monte Carlo radiation transport code, comparison of electron transport models 0-23030  
SPS, real-time control system, operating system principles 0-875  
steel, high strength sheets, finite element anal. of crack propag. expts. 0-40498  
steel, parts, stress calcs. during cooling, program system THEPLA (*German*) 0-35237  
stereoprojections for crystals of all symgonies computer program Mir-1 (*Ukrainian*) 0-24299  
Stirling Laboratory Research Engine, preliminary test results 0-35717  
structural phase transition, intrinsic and extrinsic central peak properties, review 0-34168  
structures, dynamic instability region, computation by finite element method 0-23927  
STRUKTURA, program system for cryst. struct. investigations 0-44071  
SUNSPOT, sensitivity anal. of direct gain passive solar space heating systems 0-35647  
surface semichannelling effects on spatial distrib. of reflected ions, computer simulation for Cu 0-35030  
teaching, Newtonian motion anal. using micro-computer simulations (*Japanese*) 0-31462  
teaching, two-dimens. Brownian motion simulation on micro-computer (*Japanese*) 0-31461  
textures, deformation, eulerian simulation 0-3096  
thermal blooming: round beam vs square beam, computer study 0-38076  
thermal conduction of solids, temperature stochastic field in cylinder, digital simulation algorithm (*Polish*) 0-17879  
thermochemical water splitting cycles for H prod., thermodynamic anal. and optimisation 0-45766  
three body break up reaction energy spectra, computer program 0-27593  
three-nucleon system, bound state calc. program PERFECT 0-13390  
Tokamak, neutral beam injection, low density ignition scenarios 0-48937  
Tokamak fusion reactors, pulsed electrical power systems, computer design and simulation 0-13827  
torsional vibrators, design by computer optimisation (*Japanese*) 0-33405  
train noise, prediction of equivalent mean energy level from relatively short parts of railway lines 0-38172  
transport properties of dilute gas mixtures, calc. prog. 0-10342  
TRNSYS, transient simulation of hybrid thermal energy storage system 0-30588  
Trombe-Michel wall using phase change materials, solar energy collection and thermal storage, computer anal. 0-55909  
turbulent transport eqns. soln. by accurate numerical method 0-28498  
underwater sound, model for determining significance of beam pattern side lobes in fluid flow measurement 0-19136  
unstable compounds, free energy of formation calcs., FORTRAN program for ternary phase equilibria. 0-10683  
vapour pressure measurement, torsion-effusion method, automatic data acquisition 0-52188  
viscoelastic material, stress-strain behaviour, mathematical simulation (*German*) 0-1442  
viscometric data from Brookfield RVT viscometer, conversion to shear stress-shear rate relationship 0-1495  
viscous supersonic flow over external axial corners, shock and bubble generation computation 0-14734  
void sink strength depend. on mutual recombination, point defect loss to fixed sinks 0-33995  
water, liq., Monte Carlo studies of struct., review 0-54101  
water, thermodynamic props., computer programme calcs. (*French*) 0-54409  
water pollution by radioactive waste, computer anal. of relative potential hazards 0-21422  
X-ray, neutron, and electron diffr., radial distrib. anal., computer program 0-28875  
X-ray crystallographic computations for students using programmable calculator 0-36811  
X-ray diffractometer, HAG 4/A universal instrument, applic. versatility of basic software 0-52375  
X-ray diffractometer controlled by laboratory automation module 0-317  
X-ray powder diffraction, computer automation 0-1899  
X-ray powder diffraction anal., Guinier camera, film densitometry and search match procedures 0-3454  
X-ray powder diffraction data, search-match system 0-28874  
X-ray small angle scattering, curve anal., by triaxial body models using graphic display model 0-28873  
X-ray spectroscopy, equivalent wavelength representation and secondary fluoresc. calcs., minicomputer program 0-321  
X-ray traverse topographs, computer simulation on basis of Green function method 0-49044  
XESAMO code for Xe and Sa poisoning transient anal. in fission reactors (*Spanish*) 0-52749  
Zircaloy-Z, thermal diffusion of H, numerical soln. with computer (*Korean*) 0-19989  
zone plate, profiled, chromatic props. 0-43451  
<sup>60</sup>Co  $\gamma$ -ray scatt. in air, anal. by discrete ordinates transport codes 0-32525  
Al, phonon anharmonic response, neutron-scatt. test of computer calcs. 0-44281  
Al-Ga-Ge, thermodynamic props. of mixing of binary systems, phase diagram 0-45275  
Al-Ga(Ag), dil. Hall coeff. by OPW Fermi surface model 0-6816



**physics computing continued**

- Al-Ge-Sn, thermodynamic props. of mixing of binary systems, phase diagram 0-45275  
 Al-Ti-Fe, ternary phase diagram, computer calculations 0-45274  
 Al<sub>2</sub>O<sub>3</sub>, Czochralski bulk flow, in microgravity, digital simulation 0-28934  
 Au film (001) surface, computer modelling of high resolution TEM images 0-6330  
 BaF<sub>2</sub>, ionic conductivity meas., computer anal. point defect parameters 0-54429  
 Be-Cu dynode, depth profiling anal. of surface layer 0-2253  
 CaO, (100) surface struct. using LEED meas. and rumpled ionic models 0-20019  
 Cd-Hg-Te, phase diagram, computer estimation 0-20903  
 Cl<sub>2</sub>, liquid-vapour surface, computer simulation 0-54478  
 Cr, paramagnetic, Hartree band struct., Fermi surface, nesting wave vector 0-49583  
 Cr-Ni-O, computer-assisted anal. and calcs. of phase diagrams 0-25667  
 Fe-Cr-O, computer-assisted anal. and calcs. of phase diagrams 0-25667  
 Fe-Ni-C (0.15, 0.05 wt.%) pore formation kinetics during crystallisation, FORTRAN study (*Russian*) 0-54158  
 Fe-Ni-O, computer-assisted anal. and calcs. of phase diagrams 0-25667  
 Ga-Ge-Sn, thermodynamic props. of mixing of binary systems, phase diagram 0-45275  
 GaP, temp. depend. of Fermi Level, calc. 0-39491  
 Ge(Li) detector, calc. of gamma-ray efficiency 0-37693  
 Hf-Be, coupled phase diagrams and thermochemical descriptions 0-25656  
 InP, temp. depend. of Fermi Level, calc. 0-39491  
 MgF<sub>2</sub>-Ag (Al)(Cu)(Au) film substrate tunable external-reflector retarder, computer based anal. 0-53407  
 Mn<sup>2+</sup> EPR spectra in glasses with  $\epsilon_{\text{eff}}=4.29$  computer simulation 0-34764  
 Mn-Ti-Fe, ternary phase diagram, computer calculations 0-45274  
 N<sub>2</sub>, dense gas near metallic target, laser spark (*Russian*) 0-38682  
 N<sub>2</sub>, liquid-vapour surface, computer simulation 0-54478  
 (NH<sub>4</sub>)<sub>2</sub>BeF<sub>4</sub>,  $\gamma$ -irrad. cryst., F<sub>2</sub><sup>-</sup> ions, ESR meas. 0-34770  
 NaCl aqueous soln., mol. dynamics simulation, central force model 0-49077  
 Nb, (001) surface, low energy H<sup>+</sup> and He<sup>++</sup> ion refl., computer simulation 0-11524  
 Nb, neutron bombarded, defect size distrib. influence on hardening (*Russian*) 0-10580  
 Nb<sub>3</sub>Sn fatigue effects in unidirectional composites, computer simulated model 0-35289  
 Ni based superalloys, sigma phase prediction techniques 0-7567  
 Pd sponge powder, sintering shrinkage kinetics 0-29900  
 Si, (111) surface, low energy H<sup>+</sup> and He<sup>++</sup> ion refl., computer simulation 0-11524  
 Si solar cells, polycrystalline n<sup>+</sup>/p, computer model of spectral response and photocurrent 0-55853  
 Si:H, amorphous, density of states determ. using field effect 0-49937  
 Si-Al-B-O-N, calc. of phase diagrams from data set 0-55362  
 Si-Al-Zr-O-N, calc. of phase diagrams from data set 0-55362  
 Si<sub>3</sub>N<sub>4</sub>-Al<sub>2</sub>O<sub>3</sub>-AlN, isothermal sections, free energy of formation 0-55363  
 a-SiO<sub>2</sub>, transient photocond. simulations using multiple-trap model 0-49801  
 SiO<sub>2</sub>-Al<sub>2</sub>O<sub>3</sub>-Si<sub>3</sub>N<sub>4</sub>, isothermal sections, free energy of formation 0-55363  
 Tb(OH)<sub>3</sub>, powder and single crystal, mag. props. 0-2558  
 Ti-Be, coupled phase diagrams and thermochemical descriptions 0-25656  
 Ti-Be-Zr, coupled phase diagrams and thermochemical descriptions 0-25656  
 TiS, vaporisation chemistry and thermodynamics, computer-automated simultaneous Knudsen-torsion effusion 0-48837  
 U neutron criticality, solid angle computations using computer code 0-13726  
<sup>235</sup>U(n,f), time correlated associated particle method, CAMAC experiment 0-52702  
 W/Cu powders, liq. phase sintering, particle rearrangement 0-45253  
 Zr-Be, coupled phase diagrams and thermochemical descriptions 0-25656

**physics fundamentals**

- see also *classical field theory; complementarity; cosmology; elementary particles; fundamental law tests; mechanics; quantum field theory; quantum theory; relativity; thermodynamics; units (measurement)*  
 causal structure and four-momenta conservation law (*Rumanian*) 0-46887  
 causal theory, removal of Einstein's objections to quantum theory, unification 0-31572  
 dimensional analysis 0-27263  
 Dirac's large-number hypothesis, angular momentum for Regge trajectory with  $n=2$  0-18091  
 formalisation of physical theories 0-12883  
 fractionally charged ions, search in He gas 0-8954  
 inversion problems, information theoretical approach 0-27210  
 molecular computer, biophys. rel. to phys. of real world 0-30630  
 physical operations, diagram operations 0-46846  
 proton half life, Dirac approach to large number coincidences 0-27501  
 Rydberg const., direct freq. determ. by two-photon mm spectroscopy 0-43018  
 symmetry breaking, and nature of weak interactions 0-27428  
 Universe isotropy and homogeneity, origin 0-22125  
 $e^+e^- \rightarrow l^+l^-$ ,  $l=3$ ,  $\mu$ ,  $\tau$ , charged lepton universality test 0-32091

**physiological models**

- see also *brain models; neurophysiology; physiology*  
 arterial stenosis model, pulsatile flowfield downstream 0-17001  
 articular surfaces, math. representation of position 0-3685  
 auditory function, linear system model 0-51127  
 auditory nerve, effect of response suppression on exposure to 2-tone stimuli 0-51115  
 bile acid hepatobiliary kinetics, compartmental model validity 0-30971  
 binocular vision, fusional vergence eye movements rel. to fixation disparity 0-56031  
 bioelectric rhythms represented by coupled synthesized relax. oscillators 0-26218  
 biomembrane, quantum-chemical investigation of cation motion mech. 0-30678  
 blood flow, post-stenotic turbulent wall pressure fluctuations 0-16994  
 blood flow through small diameter tubes, two-fluid model 0-3667  
 blood mass flow distrib., aortic arch atherosclerotic formations effect 0-16995  
 blood unsteady flow curved elastic tube model 0-16998

**physiological models continued**

- bone, anisotropy of Young's modulus, fibre-reinforced composite model 0-35944  
 bone, stress generated pots., linear piezoelec. model 0-3688  
 brain, planning and problem solving mechanisms 0-45877  
 cardiac chemical power, appl. of power, work and efficiency eqns. to left ventricular energetics in man 0-16912  
 cardiac chemical power, derivation of chem. power eqn. and determ. of eqn. const. 0-16911  
 cardiac contractile filament and series elastic work and power, mathematical model 0-16981  
 cardiac left ventricle, contractile filament stress rel. to wall stress 0-56096  
 cardiac muscle force-velocity relation, anal. in time domain 0-35943  
 cardiovascular system as fluid cct., elec. network analogue 0-30759  
 cell division, model relating cell deformation to elastic props. of cell membrane 0-3606  
 cell representation by an elec. circuit, voltage gain 0-40977  
 cell survival dependence on radiation quality, models and exptl. data analysis 0-26287  
 cells laser Doppler meas., scattering characts. of intersecting beams (*Russian*) 0-3874  
 chlorophyll special pair models, reaction centres 0-3574  
 colour sensing optoelectronic device, neural mechanism modelling 0-12128  
 compartmental models, identification of exchange parameters, biomedical appls. (*French*) 0-42044  
 compartmental models with delays, physical realisability 0-7998  
 counterpulsation dynamics simulation, rel. to heart assist. blood pump 0-16996  
 cyprinid retina, model of function at outer plexiform layer 0-12103  
 disturbed cell renewal systems, simulation by microprocessor system 0-35859  
 dynamic phantom for radionuclide cardiology 0-12232  
 ECG sources in a 2D anisotropic activation model 0-40994  
 EEG analysis by all-pole model 0-41287  
 EEG potential, theory, model with thin meninges 0-51283  
 elbow flexion-extension and forearm pronation-supination for elbow endoprosthesis design 0-3682  
 electrokinetic phenomena in biology, book contrib. 0-12326  
 electronic neuron model incorporating both active and passive responses 0-8040  
 electrophysiological research animal model, chronically instrumented 0-26323  
 EM dosimetry for human and animal models, numerical techniques review 0-36142  
 EM energy deposition for realistic model of man, numerical calc. 0-12180  
 EMG power spectra linking to recruitment and rate coding 0-3616  
 enzymatic active transport model 0-51049  
 ERG, effects of conducting media inhomogeneities 0-51078  
 eye, direction-selective cells formation modelling in developing retina 0-30721  
 eye, human, adaptive model using accommodation index 0-51073  
 eye, retinal photoreceptor model, FET cct. realisation 0-56027  
 femoral components, probability model for fracture taking into account patient's age 0-41070  
 G 0-26263  
 gastro-intestinal tract, physiological signals, spectral analysis, autoregressive technique appl. 0-41269  
 haemodialyser, lumped-parameter model, simulation of artificial kidney-patient system 0-56281  
 head heating by EM waves, human and infrahuman models 0-56125  
 hearing nonlinearities model described by active processes with saturation at 40 dB 0-56058  
 heart, mech. model, role of pericardium 0-35938  
 heart rate and blood pressure biofeedback theoretical models review 0-16974  
 human head EM induced field and power absorption, ellipsoidal model 0-3724  
 human motion and force sensory mechanism model 0-8094  
 inert gas transport in the microcirculation, isobaric supersaturation risk 0-45939  
 intrathoracic airway models, impedance during low-freq. periodic flow 0-41077  
 IPFM neural model, input-output anal., spike regularity and record length effects 0-56016  
 joint differential mobility meas., periodontal ligament and temporomandibular joint 0-8093  
 joint lubrication model, nonporous compliant bearing, effects of cartilage stiffness and lubricant viscosity 0-3692  
 knee joint, anatomy, menisci load carrying capacity, expts. using four-spring model 0-41067  
 knee joint, menisci load carrying capacity 0-41068  
 left heart and systemic circulation, 2-stage identification scheme 0-41071  
 left ventricle model, diastolic pressure-vol. relations and wall pressure distrib., fibre extension 0-8079  
 left ventricle time-varying capacitance model, driving energy and cardiac O<sub>2</sub> consumption (*Japanese*) 0-21486  
 left ventricular wall force, comparison of models used in calc. 0-56093  
 leg, human dynamic nonlinear finite element model 0-35949  
 lipid mixtures, phase transitions, phase diagrams, theoretical model 0-8032  
 locomotion, human, dynamic modelling 0-8095  
 long-latency reflex pathway dynamics, monkey 0-30706  
 lung, duck, O<sub>2</sub> and CO<sub>2</sub> exchange and cardiopulmonary control interaction model 0-3600  
 lung, human, with uneven ventilation, gas transport (*Japanese*) 0-3700  
 lung, intrapulmonary haematocrit maldistrib., effect on O<sub>2</sub>, CO<sub>2</sub>, inert gas exchange 0-8033  
 lung, ventilation-perfusion inequality, susceptibility of different gases 0-8089  
 lung compartmental models, steady state inert gas exchange 0-26249  
 lung compartmental models, transient inert gas exchange 0-26251  
 lung models, inert gas elimination studies without mixed venous partial pressures 0-26250  
 lung phantom, dynamic, use as educational tool 0-8757  
 lung ventilation model, radioactive tracer tidal breathing 0-56095  
 mathematical, muscle commands from nervous system in normal walking (*French*) 0-51071  
 membrane excitability mechanisms, book contrib. 0-12062



**physiological models continued**

- morphogenesis and biological differentiation, computer simulation 0-30691
- motoneurone model with early inactivation, after hyperpolarisation conductance time-course and repetitive firing 0-40987
- multicompartment system simulation 0-55976
- multiple dipole heart generator location optimisation in simple torso model 0-41277
- muscle, contractile element behaviour as force and shortening generator, Hill's model 0-3681
- muscle, linear systems model, EMG recordings of muscular contract., estimations of active-state 0-3623
- myofibrils, contracting, tension fluctuations and their interpretation 0-41065
- nephron functioning model (*French*) 0-36218
- nerve action potential model 0-30697
- nerve axon adsorption model, action pot. and excitation currents, volt. clamp test 0-56018
- nerve fibre conduction vel. distrib., estimation from action pots. 0-3633
- network analysis of biological systems, review 0-30635
- neural coding schemes, integrate-to-threshold anal. 0-35868
- neuron firing threshold model, empirical examination 0-56014
- neuron mathematical model, freq. characts. (*Japanese*) 0-35866
- neuronal impulse generation, modulation of point processes 0-30698
- neuronal synapses, information processing, electrical neuronal model design (*Korean*) 0-35865
- neuronal template-matching mechanism for sensory search with olfactory bulb, anal. 0-56069
- neurons, synergism and antagonism caused by electrical synapse 0-30696
- ophthalmological instruments and eye models in teaching, training and education 0-51993
- optimal control, breathing model example 0-41058
- oviductal egg transport, stochastic model 0-51059
- Parkinson tremor generation, linear modelling of possible mechanisms 0-3615
- particle flow behaviour in branching vessels models, vortices in 90° T-junctions 0-16971
- pattern generation in lobster stomatogastric ganglion, pyloric network simulation 0-12076
- peristaltic reflex dynamics model 0-56080
- phantom model techniques, biological effects of EM radiation appl. 0-8239
- phantom models of man, head resonance, numerical solns. and expt. results 0-12181
- phosphatidylcholine bilayers, artificial, interaction with C-reactive protein 0-3579
- placenta models, heat, O<sub>2</sub> and CO<sub>2</sub> transport, construct. and usefulness of models 0-3604
- polymer chain, uniform, elastic, possible conformational states 0-37913
- primary visual cortex, orientation selectivity development models, normally and dark reared kittens 0-41007
- prolate spheroidal mammalian models, EM near-field irr., long wavelength anal. 0-41115
- protein transport across endothelial membrane 0-3601
- pulmonary radiograph interpretation, review of models used 0-36089
- pulsatile flow in arteries simulation, utilitarian approach 0-3669
- pupillary escape, positive off-diagonal kernels as correlates of dynamic process 0-26229
- Purkinje fibers, delay, block, oneway conduction model 0-21462
- radiation therapy, equivalence of quantitative models for tumour response 0-30770
- radiobiological simulation by supralinear photographic emulsions 0-26290
- random neural nets, experimental studies 0-12077
- renal arteries model, human, qualitative and quantitative flow studies (*German*) 0-21483
- respiration effects model, left ventricular performance 0-3670
- respiratory rhythm generation, mathematical model, respiratory neuron classification 0-35873
- respiratory system, human, mechanics of regulation 0-41102
- respiratory system, human, modelling and parameter estimation 0-12169
- retinal horizontal cells, nonlinear characts. of spatial summation in receptive field, model 0-26232
- retinal hue signal generation, optoelectronic robot model 0-3647
- retinal model, layered visual processing 0-16925
- retinal neurons, catfish, spatiotemporal testing and modelling 0-41005
- retinotectal projection development, Gierer-Meinhardt eqns. appl. 0-56022
- retinotectal projection development, mathematical model (*Japanese*) 0-21467
- RF EM plane wave incident on a man model, energy absorpt. by and fields in calcs. 0-56115
- RF higher-frequency energy absorpt. by biological models, geometrical optics calcs. 0-56116
- rhythmic heart-cell clusters, fluctuations in interbeat interval, membrane voltage noise role 0-30705
- Schwann cell layer of squid axon, diffusion models 0-40985
- skin, cumulative radiation effect, cell survival description 0-30771
- skin rheological behaviour, expt. results and struct. model 0-16968
- speech production, physiology and acoustical props. of vocal system (*Japanese*) 0-26242
- stochastic neuron models, multi-input-output information transmission 0-30707
- synovial fluid boundary lubrication model, structuring of boundary water 0-35950
- systemic arterial bed, quantitative evaluation by parameter estimation of a simple model 0-56094
- temperature distrib. in microwave-irradiated cylinders simulating living tissues 0-3760
- thermoregulation mechanism model, human 0-8028
- thyroid cells in culture as radiobiological model, sheep, culturing method 0-41327
- timbre differences, functional model (*German*) 0-30733
- tissue induced EM power distribution in closed environment 0-3725
- tissue model, two-layer, theoretical anal. of diffuse reflectance 0-35956
- tissue response to retraction during open-heart surgery 0-26254
- tissue simulation, acoustic attenuation CW meas. in oil-polymer mixture 0-35961
- tracheobronchial clearance of inhaled particles in man 0-8080
- vascular bed modelling, optimal dialysis appl. 0-30758
- ventricle, left, human, geometric modelling, using biplane cineangiograms 0-35955

**physiological models continued**

- vertebra, dynamical response analysis 0-3684
- vertebral response to laminectomy, finite element model 0-41090
- vesicular transport and endothelial membrane interaction, theoretical models 0-45869
- vision, Broca-Sulzer effect, combined temporal and spatial unified model 0-35893
- visual pigment chromophores, models, spectroscopic and photochemical studies 0-30723
- visual system, inhomogeneous model predictions, detect. of local, extended spatial stimuli 0-45894
- whale biothermal mathematical model 0-12059
- Ba treated nerve cells, generation of long potential waves 0-56002
- Ba-treated nerve cells, reduced systems, qualitative anal. of model generating long potential waves 0-26213
- <sup>18</sup>F, skeletal tracer kinetics in rats, evaluation of model 0-56188
- Na channel fluctuations, phys. nature, microscopic model 0-35869
- Na exchange in tissue, incorporating diffusion effects into multicompartment models using digital simulation 0-3611
- O<sub>2</sub>, facilitated diffusion in muscle tissues 0-56327
- PuO<sub>2</sub> aerosol, acute inhalation, predictive model of early mortality 0-36028
- THO, prediction of flux from air to plant leaves 0-26381

**physiological optics see vision****physiology**

- see also blood; haemodynamics; hearing; neurophysiology; physiological models; speech; vision
- blink reflex studies in stroke patients, role of dynamic sensory perception 0-3641
- blood pressure control, racial differences 0-30757
- bone, X-irrad., histopathological and physiological changes, rabbit expts. 0-51171
- cardiovascular response to acute aquatic and treadmill exercise in the untrained rat 0-8085
- exercise physiology in teenagers and asthmatic children 0-12170
- eye, abnormal movements control method using audio feedback 0-41156
- eye, pursuit after-nystagmus obs. 0-41018
- eye, smooth pursuit movements rel. to perceived motion 0-3649
- eye and retina development in kittens 0-12113
- eye blink rate, human, long-term trends 0-35879
- eye convergence and divergence, large and sustained improvement after short isometric exercise 0-8049
- eye convergence insufficiency rel. to school achievement 0-8048
- eye divergence excess, prevalence and management 0-35877
- eye movements, additivity of fusional vergence and pursuit eye movements 0-35884
- eye movements in paralysed cats induced by drugs and sympathetic stimulation 0-51083
- eye torsion in response to tilted visual stimulus 0-45891
- IR recording retinoscope for accommodation monitoring 0-36055
- isobaric gas counterdiffusion in rabbit eye 0-30718
- jaw action of lizard, mechanical significance of streptostyly 0-51143
- macromolecular thermodynamics and its possible relevance in physiology 0-53176
- multiplexing system for measuring physiological responses 0-56292
- nasal mucous velocity and airflow resistance, effect of exercise in normal subjects 0-8088
- ocular peripheral saccades, latency obs. 0-12089
- ocular physiology review 0-56023
- optokinetic reactions in man elicited by localised retinal motion stimuli 0-45889
- patient physiologic profiling, automated, in acute ill patients 0-30914
- pCM telemetry for physiological data 0-36059
- psychophysiological function of the human eye (*Czech*) 0-21472
- psychophysiological techniques applied to aircraft design and other operational problems 0-26384
- pupil responses, human, instrumentation for automated study 0-36164
- retinal image stabilisation 0-12088
- saccadic system, anal. by double step stimuli 0-41014
- space research, biology and medicine 0-41265
- spatial localisation during pursuit eye movements 0-51081
- stereoscope vergence, convergence and divergence independence obs. 0-30714
- subcutaneous tissue gas space pressure during superficial isobaric counterdiffusion 0-30968
- vagina, rats, delay of constant light-induced persistent oestrus by 24-hour time cues 0-12182
- vision, compensatory eye movements to miniature rotations, rabbit, retinal image stability implications 0-45890
- vision fixation disparity rel. to rapid prism adaption 0-16929
- visual accommodation in infants, photorefractive study 0-56028
- wind speed limits to work under hot environments for clothed men 0-8030
- CO<sub>2</sub> responses of conscious rabbits at ambient temps. of 5, 20 and 35°C 0-56085

**pi mesons see pions****pick-up reactions**

- heavy ion induced deep inelastic transfer, decay of binary nuclear system 0-22848
- neutron pickup reactions to (i<sub>13/2</sub>)<sup>2</sup> bands, theoretical rot. signatures, back-bending 0-52558
- (d, <sup>6</sup>Li), 54.25 MeV, α-cluster spectroscopic factors, DWBA anal. 0-52571
- (p,d), 52 MeV, deeply bound hole state transition strength giant resonance, DWBA anal. 0-47426
- Ag + p, role of pick-up processes in prod. of fast t and <sup>3</sup>He 0-27632
- Br + p, role of pick-up processes in prod. of fast t and <sup>3</sup>He 0-27632
- <sup>13</sup>C(p,d), 200, 500 MeV, differential cross section scaling, reaction mechanism 0-42625
- <sup>13</sup>C(p,d), 800 MeV, cross sections, DWBA anal. 0-42667
- <sup>40</sup>Ca(Li,<sup>6</sup>Be), 34 MeV, <sup>39</sup>K states and spectroscopic strengths DWBA anal. 0-5069
- <sup>4</sup>He(p,d) pickup reaction, isobar configurations and short range correlations 0-22798
- <sup>4</sup>He(p,d)<sup>3</sup>He, 770 MeV, multiple-scattering approach 0-27636
- <sup>7</sup>Li(p,d), 800 MeV, cross sections, DWBA anal. 0-42667
- <sup>24</sup>Mg(p,p'), 40 MeV, two step pickup-stripping process, negative parity states 0-32256
- <sup>14</sup>N(n,α)<sup>11</sup>B, 12-18 MeV, pickup of three nucleons, distorted wave approx. 0-22793



**pick-up reactions continued**

- $^{33}\text{S}$  ( $^3\text{He}, \alpha$ ), 15 MeV,  $^{32}\text{S}$  levels and spectroscopic factors from pickup DWBA anal. 0-9235  
 $^{28}\text{Si}$  ( $^{15}\text{N}, ^{16}\text{O}$ ), 44 MeV, modified optical pot. from backward elastic scatt. 0-32255  
 $\text{Sn}(\text{d}, ^6\text{Li})\text{Cd}$ , alpha-cluster pickup reactions, spectroscopic factors and reduced widths 0-534  
 $\text{Te}(\text{d}, ^6\text{Li})\text{Sn}$ , alpha-cluster pickup reactions, spectroscopic factors and reduced widths 0-534

**pick-up tubes, television** *see television camera tubes***pick-ups**

- corona discharge, positive, sound effects 0-28858  
 piezoelectric, for pulsed pressures meas. 0-31778  
 pressure pick-up with Si column strain-gauge convertor 0-31732  
 rotation-angle pick-up, for goniometer, using precision variable resistor 0-47047  
 speed meas., contactless, of running strips or bands, transit time determ. (German) 0-14862

**pickups** *see pick-ups***pictorial bandwidth compression** *see bandwidth compression***picture processing**

- see also computerised picture processing; pattern recognition*  
 2-D image processing applications of acoustooptical devices 0-53231  
 acousto-optic heterodyning image processor, OTF 0-5833  
 additive-obtained moire patterns (German) 0-47017  
 Algebraic Reconstruction Techniques, modifications 0-3774  
 astronomical image processing, atmospheric turbulence effects, interferometer data technique 0-12679  
 astronomical images, coherent optical processing expts. (Russian) 0-12675  
 astronomical images optimal classification into stars or galaxies, Bayesian approach 0-21920  
 astronomical plates for iris diaphragm photometry, nonuniform background correction 0-12680  
 biomedical image processing, state of art (Japanese) 0-56251  
 brain computer tomograms, shape anal. in isodence lesion characterisation 0-8152  
 coded-aperture images, pre-folded Fourier filter reconstruction 0-53222  
 colour reproduction of objects by speckle interferometry in white light 0-47094  
 detector array spatial noise reduction, controlled lateral shifts 0-53436  
 diagnostic imaging systems, non-silver halide, recent developments and pot. 0-41223  
 difference detection by digitised moire pattern processing 0-52156  
 diffraction limited image from obs. through irregular atmosphere (Ukrainian) 0-9814  
 digital processing aerial images, conf., Huntsville, Alabama, USA (May 1979) 0-48165  
 electron microscope image analysis 0-31947  
 electron microscope image contrast and localized signal selection techniques 0-37126  
 electron microscopy, image processing, optical diffraction and filtering, fast Fourier transforms 0-30956  
 electron microscopy, image processing by linear integration technique, periodic structures obs. (Japanese) 0-52363  
 eye movement research, data collection using on-line computers 0-41329  
 hybrid image processing for feature extraction and constant variance enhancement 0-53224  
 hybrid processors, liquid-crystal convertor appl., incoherent-to-coherent 0-33166  
 image digitiser system design 0-48441  
 image edge enhancement 0-43273  
 Landsat imagery, planimetric restitution using Zeiss Stereotop 0-56648  
 least squares image restoration 0-37961  
 linear line screen for image reproduction, analysis 0-32925  
 local image restoration by a least-squares method 0-14289  
 medical imaging appls. 0-17038  
 microphotometry of biological materials, digital picture analysis 0-17991  
 microwave scattering parameter imagery of isolated canine kidney 0-3755  
 neural net properties rel. to image processing algorithm 0-40993  
 nuclear medicine, image processing system 0-41174  
 nuclear medicine, sigma scan, method for enhancement of statistically significant differences 0-36096  
 optical hybrid image processing trends and prospects 0-32927  
 optical matched filter correlator memory techniques and capacity 0-43280  
 phase-inverting grating construction, use in deblurring filters 0-48398  
 quantitative microscopy, object delineation program 0-41338  
 radioisotope angiocardigraphic image, left ventricular contour extraction and vol. computation (Japanese) 0-3798  
 scene matching methods 0-48167  
 scene matching with feature detection 0-48166  
 tone reproduction analysis with square, circular and concentric-ring patterned screens 0-53229  
 transverse analogue tomography, cross-sectional imaging of X-rays 0-56201  
 US dynamic imaging, high resolution 0-17042  
 US image processing device status and prospects 0-48446  
 US medical image digital processing methods (Chinese) 0-30805  
 US tissue analysis, comprehensive system 0-51189  
 vision, problems in matching images to the eye—effects of pictorial noise 0-51113  
 wavefront registration and volume object image reconstruction by stimulated Raman scatt. (German) 0-53367  
 $\text{LiNbO}_3:\text{Fe}$ , nonlinear image processing in 3-dimens. hologram 0-14303

**picture tubes, television** *see television picture tubes***PID control** *see three-term control***piecewise-linear techniques**

- Steiner surface, piecewise surface approx., finite element calcs., isoparametric method 0-12881

**piezo-magneto-optical effects** *see magneto-optical effects; piezo-optical effects***piezo-optical effects**

- see also piezoreflectance*  
 adamantane, plastic cryst. lattice vibr. study of phase transition 0-7355  
 alkali halides, linear dichroism spectra, stress-induced, reorientation of  $\text{O}_2^-$  and  $\text{NO}_2^-$  impurity ions (Russian) 0-45127

**piezo-optical effects continued**

- Brillouin scattering in reflection and transmission modes, rel. to intense acoustic flux, relation linearity test 0-45098  
 cholesteric liquid crystals, light reflection by crystals with tilted molecular struct. 0-29713  
 diamond, optical absorption lines, GR4 and GR8, effect of uniaxial stress 0-34956  
 dielectrics, electric, optical and acoustic interactions from Lagrangian representation, book 0-2715  
 fibre optic waveguide transmission, mechanical stresses effect 0-10032  
 heavy water, piezo- and elasto-optic props. under high press. 0-50296  
 ice VI, OH stretching peak freq. press. depend., Raman spectra using diamond anvil cell 0-16023  
 optical fibres, acoustic modulation of light propagation 0-33209  
 optomechanical properties determ., polarisation device application, by compensation method 0-40643  
 PMMA, piezobirefringence, optical and mech. relaxations, temp. depend. 0-34885  
 $\alpha$ -quartz, ferroelastic hysteresis 0-19869  
 quartz, natural, gamma-irradiated, stress effect on thermolum. sensitivity 0-11482  
 single-mode fibre lightguide, phase of coherent signal, temp. and stress effects 0-33208  
 stress measurement method for crystals, appl. to Si 0-48656  
 toluene sulphonate diacetylene polymer, vibr. modes, strain depend. using Raman spectra 0-20626  
 $\text{Al}_2\text{O}_3:\text{Cr}^{3+}$  shock compression, absorpt. spectra 0-20675  
 $\alpha\text{-Al}_2\text{O}_3:\text{Cr}^{3+}$ , stress-induced linear dichroism in  $^3\text{A}_2(^3\text{T}_1)-^3\text{T}_2$  transition, Jahn-Teller effect 0-34884  
 $\alpha\text{-Al}_2\text{O}_3:\text{V}^{3+}$ , stress-induced linear dichroism in  $^3\text{A}_2(^3\text{T}_1)-^3\text{T}_2$  transition, Jahn-Teller effect 0-34884  
 $\text{As}_2\text{S}_3$  glass, press. effect on optical props. 0-50363  
 $\text{As}_2\text{S}_4$ , effects of pressure and temp. on phonons, Raman scattering study 0-7360  
 $\text{BaF}_2$ , piezo-optical coeffs. meas. at 0.6328, 1.15 and 3.39  $\mu\text{m}$  0-34888  
 $\text{CaF}_2$ , piezo-optical coeffs. meas. at 0.6328, 1.15 and 3.39  $\mu\text{m}$  0-34888  
 $\text{CdS}$ , stress-induced photolum. bands, photocond., rel. to dislocation electron states 0-25447  
 $\text{CdS}$ , thermal equilb. phonon populations, acoustic intensity meas. by Brillouin scatt. intensity obs. 0-45098  
 $\text{CdTe}$ , transmission spectrum under uniaxial compression 0-29714  
 $\text{GaAs}$ , thermal equilb. phonon populations, acoustic intensity meas. by Brillouin scatt. intensity obs. 0-45098  
 $\text{GaAs}$ , transmission spectrum under uniaxial compression 0-29714  
 $\text{GaP}$ , S-bound exciton stress depend. 0-29333  
 $\text{Ge}$ , biexciton and trion existence, photolum. (Russian) 0-16088  
 $\text{Ge}$ , stressed, metal-insulator transition, luminesc. 0-20695  
 $\text{Ge}:\text{Li}, \text{O}$ , EPR and piezospectroscopy 0-25338  
 $\text{n-InSb}$ , deformed, spectral oscills. of absorption in quantising mag. field 0-34486  
 $\text{MnF}_2$ , birefringence variation on uniaxial compression (Russian) 0-34887  
 $\text{N}_2$ , solid, Raman spectroscopy up to 374 kbar 0-7353  
 $\text{NH}_4\text{Br}$  and  $\text{NH}_4\text{I}$ , Raman scatt., 1 bar-7 kbar, 86-295 K 0-34909  
 $\text{Nd}$  doped (fluoro) phosphate laser glass piezo-optic coeffs. meas. at 0.6328 and 1.15  $\mu\text{m}$  0-34888  
 $\text{S}_2\text{N}_4$ , effects of pressure and temp. on phonons, Raman scattering study 0-7360  
 $\text{Si}$ , appl. of photoelastic stress. meas. technique 0-48656  
 $\text{Si}$ , diamagnetism of excitons and biexcitons, recomb. spectra (Russian) 0-7412  
 $\text{Si}$ , piezospectroscopic effect on zero phonon luminescence lines 0-50406  
 $\text{Si}$  rubber as electro-optic material for optical hydrophones 0-43412  
 $\text{Si}:\text{B}(\text{Li})\text{P}$ , piezospectroscopic studies of bound multiexciton complexes 0-16006  
 $\text{Si}:\text{B}(\text{P})$ , uniaxially stressed, impurity-assisted intervalley scatt., photoluminesc. obs. 0-34979  
 $\text{SrF}_2$ , piezo-optical coeffs. meas. at 0.6328, 1.15 and 3.39  $\mu\text{m}$  0-34888  
 $\text{Sr}_2\text{Nb}_2\text{O}_7$ , optical mode softening in incommensurate phase 0-7352  
 $\text{Te}$ , intervalence band absorption, press. and defects influence 0-55149  
 $\text{Te}$ , opt. props. under high press., band struct. transform. 0-55112  
 $\text{TeO}_2$ , elastic wave parametric instability kinetics in dielectrics (Russian) 0-45035  
 $\text{TiO}_2$ , energy band struct., uniaxial stress depend. 0-2334  
 $\text{ZnS}:\text{Mn}$ , self-activated and  $\text{Mn}^{2+}$  emission, high press. action 0-16093  
 $\text{ZnSe}:\text{Cr}$ , piezodichroism due to reorientation of Jahn-Teller centres 0-11363

**piezoelectric devices**

- see also crystal resonators; piezoelectric transducers*  
 accelerometers (German) 0-22334  
 Bleustein-Gulyaev waveguides with gratings, anal. Bleustein-Gulyaev waveguides with gratings, anal. 0-1391  
 deformable mirrors with bimorph actuators 0-33135  
 detector for photoacoustic microscopy, principle and appl. to semiconductor industry 0-14525  
 discrete actuator deformable mirror 0-33133  
 earphone, piezoelectric plastic film transducer theory 0-43582  
 equivalent cct. parameters calc. for radially polarised piezoceramic sphere 0-14538  
 Fabry-Perot scanning interferometer with piezoelec. spacers, appl. to solar UV spectrum 0-12678  
 high dynamic pressure measurements in solids 0-47070  
 light beam control appl. (Czech) 0-19090  
 mirror translator, piezoelec., stabilisation of narrow-bandwidth CW dye laser 0-33036  
 monolithic deformable mirror/heat exchanger unit evaluation 0-33139  
 multiactuator deformable mirror evaluations 0-14416  
 noise cancelling microphone with piezoelectric plastic diaphragm, coupled oscillator theory 0-43581  
 pick-up, for pulsed pressures meas. 0-31778  
 reactor diagnosis by acoustic meas. methods, magnetostrictive and piezoelec. high-temp.-resistant sensors 0-32411  
 relays, multilayer plates bending, anal. 0-40064  
 strain gauges, biaxial gauge factors 0-52185  
 three- and four-dimensional photoacoustic store readout 0-48413  
 three-actuator deformable water-cooled mirror 0-33134  
 US focusing device with IDT on thin piezoelectric plate 0-1398  
 vibrators, elec. steered line array, US probe characts. 0-35486  
 xerographic cascade flow, carrier bead velocity distribution meas. probe 0-47136



piezoelectric effects *see piezoelectricity*

## piezoelectric materials

- see also piezoelectric semiconductors; piezoelectric thin films; piezoelectricity*
- acoustic transverse wave polarisation and energy flow in external static fields 0-19123
- ceramic resonators, eigencoupling state space vector representation 0-2697
- ceramics, bimorph element for loudspeakers props. and manufacture (*Japanese*) 0-53597
- finite amplitude SAW distorted rippling profiles, optical probing obs. 0-34287
- high temp. US generation, piezoelectric material and adhesive props. 0-43586
- piezoceramics, energy dissipation in high-freq. cyclic loading 0-15779
- polypropylene, electron bombarded, radical formation, piezoelectric and pyroelectric effects, ESR study 0-7169
- polyvinylidene fluoride, piezoelec., pyroelec., and improper ferroelec. 0-7301
- polyvinylidene fluoride, poling process effect on fine struct. 0-7285
- polyvinylidene fluoride, polycryst. ferroelec., microstruct., piezoelec. and pyroelec. props. 0-7303
- polyvinylidene fluoride, struct. study, piezoelec. and pyroelec. props. 0-7300
- polyvinylidene fluoride films, corona-poled, piezoelectricity (*Japanese*) 0-55040
- PVDF dielectric, piezoelec. and pyroelectric props. rel. to crystalline forms 0-15982
- PZT/polymer composites, simplified fabrication 0-40323
- quartz, crystal growth in fluoride environment, growth features and props. 0-6373
- $\alpha$ -quartz, ferroelastic hysteresis 0-19869
- quartz, smoky,  $\gamma$ -irrad., electric dipolar echoes 0-20604
- quartz lattice constants, impurity effects 0-39034
- quartz plates, acoustic reson. vibr., Berg-Barrett X-ray diffr. method 0-40063
- $\alpha$ -quartz plates vibrating in thickness, doubly rotated, zero polarizing effect 0-55038
- quartz resonators, thickness-mode, thermal stress effects on reson. freq., theory 0-50272
- quartz wedge, reflection, transmission and conversion of normally incident SAW 0-2257
- thermopiezoelectric material, monoclinic symmetry, surface wave propag. 0-44403
- tourmaline, elastic const. by US phase-comparison method 0-2108
- tourmaline, resonator, electroelastic constants, elec. field induced freq. shift study 0-20597
- BaTiO<sub>3</sub>, piezoceramic, elastic normal wave propagation, phase transitions (*Russian*) 0-40067
- Bi<sub>12</sub>GeO<sub>20</sub>, finite amplitude SAW distorted rippling profiles, optical probing obs. 0-34287
- K<sub>2</sub>SeO<sub>4</sub>, elastic compliance anomalies 0-45010
- LiF, compressed crystals, inhomogeneous elec. field due to piezoelectric effect 0-55044
- Li<sub>2</sub>GeO<sub>3</sub>, acoustic props., intrinsic piezoeffect, US absorpt. coeffs. (*Russian*) 0-29692
- LiHSeO<sub>3</sub>, X-ray cryst. struct. determ. 0-28966
- $\alpha$ -LiIO<sub>3</sub>, neutron diffr. intensity enhancement under DC field, investig. 0-10462
- $\alpha$ -LiIO<sub>3</sub>, single crystals, light diffr. under DC field 0-11367
- LiNbO<sub>3</sub>, crystals, elec. field influence on hypersonic wave propag. 0-44668
- LiNbO<sub>3</sub> interfaces, SAW reflection, light scatt. meas. 0-34286
- LiNbO<sub>3</sub>, piezoceramic, elastic normal wave propagation, phase transitions (*Russian*) 0-40067
- LiNbO<sub>3</sub>, piezoelectric coeff. and permittivity meas., small-sample method 0-15981
- LiNbO<sub>3</sub>, piezoelectric plate, direct and indirect elastic wave excitation (*Russian*) 0-34858
- LiNbO<sub>3</sub>, SAW convergence props. 0-24726
- LiNbO<sub>3</sub>, SAW conversion to bulk plate modes in shallow gratings 0-1385
- LiNbO<sub>3</sub>, SAW propagation and scatt., finite difference anal. 0-20595
- LiNbO<sub>3</sub>, substrate for InSb films, prep. and props. 0-35093
- LiNbO<sub>3</sub>, Y-cut, plasma ion-acoustic waves excitation by piezoelectric surface acoustic wave 0-10381
- LiNbO<sub>3</sub>-CdSe structure, electroacoustic effects and signal convolution 0-10098
- LiTaO<sub>3</sub>, crystals, elec. field influence on hypersonic wave propag. 0-44668
- NH<sub>4</sub>NbF<sub>6</sub>, successive phase transitions, dielec. and optical props. obs. 0-50275
- Na<sub>2</sub>W<sub>3</sub>O<sub>7</sub>F<sub>4</sub>, phase transitions obs. (*French*) 0-6516
- Pb(Ti, Zr)O<sub>3</sub>, piezoelectric-ferroelectric ceramic, polarisation processes, X-ray obs. 0-34847
- PbTiO<sub>3</sub> ceramics, temp.-compensated, for SAW appl. 0-15355
- PbTiO<sub>3</sub>-Pb(Fe<sub>1/2</sub>Nb<sub>1/2</sub>)O<sub>3</sub>-PbZrO<sub>3</sub>, with additions, exam. of electrical characteristics 0-2698
- Pb(Zr,Ti)O<sub>3</sub> ceramic, interconnected porous, props. 0-43579
- Pb(Zr,Ti-x)O<sub>3</sub>, high density, sol-gel technique prep., piezoelec. props. 0-20596
- SO<sub>2</sub>, lattice dynamics, rigid mol. model 0-44266
- Sr<sub>0.5</sub>Pb<sub>0.5</sub>(Zr<sub>0.545</sub>Ti<sub>0.455</sub>)O<sub>3</sub>, piezoelec. resonator, preparation and props. (*Rumanian*) 0-28402
- Ti<sub>2</sub>VS<sub>4</sub>, growth of inclusion free crystals, for surface wave and bulk wave acoustic devices 0-25549
- ZnO films US transducers obtained by DC diode sputtering, dielec. breakdown props. 0-40066
- ZnO, piezoelec. films produced by gas transport reaction, US excitation efficiency 0-2700

## piezoelectric oscillations

- energy trapping methods of thickness extension and thickness shear modes 0-15980
- nonsymmetric vibrations of piezoelectric ceramic rings polarized along the thickness 0-7299
- quartz plates, acoustic reson. vibr., Berg-Barrett X-ray diffr. method 0-40063
- thermopiezoelectricity, general eqns. 0-7297
- thin piezoceramic discs with split electrodes, asymmetric vibrs. 0-34857

piezoelectric resonators *see crystal resonators*

piezoelectric semiconductor materials *see piezoelectric semiconductors*

## piezoelectric semiconductors

- acoustoelectric interactions on cylindrical surfaces 0-6914
- cyclotron resonance linewidth, quantum-limit 0-7171
- degenerate semiconductors, hot electron transport in parabolic energy bands, kinetic theory, transport coeffs. 0-29412
- magnetised heavily doped piezoelectric semicond., hybrid mode parametric excitation 0-29427
- oscillations of piezosemiconductor plates, charged particle beam modulated, energy losses (*Russian*) 0-2259
- photoelasticity and acousto-optic diffr. 0-29715
- piezoelectric semiconductor SAW convolver, convolution voltage enhancement due to carrier transverse drift 0-1381
- SAW convolver, convolution voltage enhancement due to carrier transverse drift 0-1381
- SAW convolver, effect of transverse drift of carriers on operation, theory and expt. 0-14529
- sound attenuation, effect of strong doping 0-2120
- stimulated Brillouin scatt. in magnetised semiconductor plasma 0-33085
- surface phonon acoustoelectric interaction, elastic anisotropy effects 0-6610
- US attenuation, polarisation of Maxwell-Wagner relaxation oscillators 0-44670
- US parametric amplification effects, contributions to nonlinear material coefficients 0-34144
- wave discontinuities, growth 0-34488
- weakly inhomogeneous, theory of sound absorption 0-15574
- Ag<sub>3</sub>SbS<sub>4</sub>, electron absorption and dispersion of ultrasound velocity 0-15197
- CdS, acoustoelectronic current SHG 0-6916
- CdS crystal, SAW amplification, bulk and acoustic noise 0-39637
- CdS SAW convolver, effect of transverse drift of carriers on operation 0-14529
- Cds, photoconductive, convolution voltage enhancement due to carrier transverse drift in SAW convolver 0-1381
- (CuCr<sub>2</sub>S<sub>4</sub>)<sub>x</sub>-(Cu<sub>0.5</sub>In<sub>0.5</sub>Cr<sub>2</sub>S<sub>4</sub>)<sub>1-x</sub> solid solution, piezoelectric effect, X-ray struct. anal. (*Russian*) 0-15978
- Cu<sub>0.5</sub>In<sub>0.5</sub>Cr<sub>2</sub>S<sub>4</sub>, piezoelectric effect, X-ray struct. anal. (*Russian*) 0-15978
- GaAs, high press. electron transport props., three band model 0-15516
- n-GaAs, non-equilibrium acoustic phonon generation by hot electrons 0-6477
- n-InSb, helicons, parametric decay 0-34472
- n-InSb, SBS of laser radiation in presence of mag. field, ion acoustic wave nonlinearity 0-45091
- Se, trigonal, low temp. sp. ht. and elastic const., piezoelec. effect influence on phonons 0-54404
- Te, dislocations influence on galvanomag. props. 0-54722
- piezoelectric thin films**
- polar polymer, piezoelectricity and pyroelectricity 0-7267
- poly(vinylidene fluoride), piezoelec. response depend. on phase I vol. fraction 0-20593
- poly(vinylidene fluoride), poled, piezoelec. activity and field-induced cryst. struct. transitions 0-20592
- $\beta$ -poly(vinylidene fluoride), single cryst. orientation, piezoelec. 0-20591
- poly(vinylidene fluoride), strong piezoelec. under high press. annealing 0-11344
- poly(vinylidene fluoride) piezoelectric film, Lamb and shear wave propagation (*French*) 0-44256
- polyvinylidene fluoride, polarisation and depolarisation processes 0-11318
- polyvinylidene fluoride, uniaxially stretched and corona poled, piezoelec. meas. 0-25311
- silk fibroin, oriented, piezoelec. const. temp. dispersions 0-11345
- third-order piezoelectric and dielec. const. meas. using surface acoustic waves (*Japanese*) 0-55042
- vinylidene fluoride/tetrafluoroethylene copolymer, piezoelect. and pyroelect. response rel. to dipole polarisation 0-7267
- LiNbO<sub>3</sub>, spontaneous parametric scatt. line profile, IR absorpt. coeffs. 0-25377
- LiNbO<sub>3</sub>:Na<sup>+</sup>(Co<sup>2+</sup>, Zr<sup>4+</sup>), LPE growth from Li<sub>2</sub>O-V<sub>2</sub>O<sub>5</sub> flux, X-ray and acoustic characterisation 0-15383
- ZnO films US transducers obtained by DC diode sputtering, dielec. breakdown props. 0-40066
- ZnO, SAW devices appl. for HF range (*Japanese*) 0-53598

## piezoelectric transducers

- acoustic microscope appl. 0-1387
- acousto-optic devices, transducer bandwidth, layer thickness determ. (*Chinese*) 0-53593
- annular array search units, potential appl. in conventional US testing systems 0-35446
- biological and medical appls. 0-19205
- bolt-clamped Langevin type transducer, effect of surface conditions on performance (*Japanese*) 0-48543
- broadband piezotransducers, comparative anal. and power ratings 0-5904
- ceramic cylinders, short axially polarized annular, calculation of equivalent circuit parameters 0-5901
- development trends and appl. (*German*) 0-52186
- electroacoustic transducers using piezoelectric polyvinylidene fluoride films for diaphragm material 0-10100
- electromagnetic cavity resonator, excitation and detection of acoustic waves 0-33399
- electronically scanned US diagnostic systems, electromechanical coupling coeff. for plank-shaped transducers 0-33383
- farfield angular radiation pattern generated from arrayed piezoelectric transducers using finite element anal. 0-33401
- flowmeter appl., Danfoss 0-6172
- force-frequency measuring gauge based on oscillating quartz crystal 0-31727
- frequency response, meas. using an acoustooptic modulator 0-38023
- HF vibration measurement using time-average electronic speckle pattern interferometry system 0-37966
- hydrophones using piezoelectric polymer, for large receiver arrays 0-14540
- interdigital transducer models for synthesis of SAW transversal filters 0-5897
- LAW transducer made with LiNbO<sub>3</sub> 0-5854
- materials, high-temp. long duration appl. 0-43586
- micropositioning appl. (*German*) 0-8967
- miniature, for transient soft body contact stress problems 0-8975



**piezoelectric transducers continued**

- noise suppression and prevention for shock and vibration meas. 0-22353  
 optimisation using acoustic emission transducers 0-48539  
 piezoceramic, optoacoustic effect obs., in optical fibre 0-48423  
 polymer film, piezoelec. and pyroelec. response rel. to dipole polarisation 0-7267  
 pressure meas. appl., up to  $6 \times 10^4$  N/m<sup>2</sup> 0-31785  
 pulse-driven, fundamental characts. 0-38210  
 reciprocity calibration of acoustic emission transducers 0-28401  
 reciprocity technique for estimating the diffuse-field sensitivity of piezoelectric transducers 0-48538  
 reflex hammer with piezoelec. cryst. for accurate reflex latency meas. 0-3839  
 surface excited, operation in radiation mode 0-33407  
 surface excited, operation in reception mode 0-33408  
 surface-skimming bulk wave excitation, analysis using Green's function formulation 0-53519  
 transformation factor, effect of DC field 0-5903  
 unidirectional transducer used in SAW grating-resonator filter, behaviour 0-5877  
 US, for acoustic emission measurement in NDT 0-28375  
 US inclined probe, construction improvements 0-33411  
 US pulsed fields, from thick piezoelectric disc immersed in petrol (*French*) 0-53512  
 US transducer, thick, operating as radiator or receiver, performance characts. 0-35484  
 US transducer, US energy meas. for echography 0-36044  
 US transducers, energy and spectral evaluations of broadband excitation 0-35485  
 US transducers, surface-driven, input impedance calc. 0-35493  
 wideband, US field intensity meas. appl. (*Russian*) 0-38209  
 wideband excitation of surface elastic waves in microwave range 0-10105  
 Mn low-impedance stress gauges for precision measurement in severe shock-wave environments 0-38367  
 Pb(Zr,Ti)O<sub>3</sub> ceramic, interconnected porous, props. 0-43579  
 Si miniature biomedical piezoresistive pressure transducer (*German*) 0-37016  
 Si piezoresistive accelerometer power transfer factor (*German*) 0-37017  
 Si piezoresistive coefficient calc. and meas. (*German*) 0-39571  
 ZnO films US transducers obtained by DC diode sputtering, dielec. breakdown props. 0-40066  
<sup>67</sup>Zn spectrometer, double freq. interferometer for absolute velocity calibration of piezoelectric transducer 0-37146

**piezoelectricity**

- see also electrostriction; piezoelectric devices; piezoelectric materials; piezoelectric oscillations  
 acoustoelectrical waves, double refl. and birefr. in piezoelec. cryst. 0-11047  
 anisotropic media, piezomagnetolectric effects 0-25174  
 bending of piezoelectric multilayer plates with uniform elec. field, anal. 0-40064  
 bone, human cortical, US properties and microtexture 0-51144  
 bone, strain-related potentials, freq. depend., effect of meas. system parameters 0-16991  
 bone, stress generated pots., linear piezoelec. model 0-3688  
 charge storage, charge transport and electrostatics conference, Kyoto, Japan (Oct. 78) 0-7252  
 cholesteric liquid crystals, electrodynamics, continuum theory 0-6356  
 collagen structures, piezoelec. effect, in rel. to mol. struct. 0-41100  
 dielectrics, deformable, polarisation gradient elasticity theory; coupled mechano-electric fields 0-55037  
 diglycine nitrate, cryst. growth, dielec. and electromech. props. 0-2701  
 DOBAMBC, chiral smectic, flexoelectric effect and polarisation props. (*Russian*) 0-15002  
 electrets and dielectrics, conf., Sao Carlos, Brazil, Sept. (1975) 0-7251  
 electrical discharge from arbitrarily deformed bodies, theory (*Ukrainian*) 0-11341  
 electroacoustic echo, phase amplitude depend. (*Russian*) 0-7298  
 ferroelectric theory and dynamics, optical, acoustic electro-optical props., Brillouin zone struct. 0-11347  
 insulating crystals, piezoelec. potentials of dislocations 0-20594  
 molecular crystals, polariton spectra and lattice dynamics 0-49313  
 nonlinear electroacoustics, fundamentals and appl. 0-34489  
 polar polymer, piezoelectric response rel. to dipole polarisation 0-7267  
 polar polymer, piezoelectricity and pyroelectricity 0-7267  
 polyacrylonitrile, elec. polarisation 0-7275  
 polymer film transducer, piezoelec. and pyroelec. response rel. to dipole polarisation 0-7267  
 polymers, electrical phenomena, nature and appl., book contrib. 0-50254  
 polypropylene, electron bombarded, radical formation, piezoelectric and pyroelectric effects, ESR study 0-7169  
 polyvinylidene fluoride, piezoelectric effect formation due to injection process, TSC (*French*) 0-34856  
 polyvinylidene fluoride, thermodynamical model, applications (*French*) 0-39315  
 polyvinylidene fluoride films, corona-poled, piezoelectricity (*Japanese*) 0-55040  
 polyvinylidene fluoride films, stretched and rolled, electrostriction and piezoelectric effects (*Japanese*) 0-55041  
 PVFD, electret, polarisation process 0-7273  
 PZT/polymer composites, simplified fabrication 0-40323  
 rare earth compounds, RNbMTa<sub>2</sub>O<sub>15</sub> (R=rare earth, M=K, Rb, Tl, Cs), relative stability of struct. types, and piezoelec. props. (*French*) 0-49206  
 semi-infinite crystal, surface wave solns. nonexistence example 0-6611  
 shock compression of solids, review 0-24534  
 slab with dissipative characteristics, disturbances 0-25310  
 spinning disc of radially inhomogeneous piezoelectric material, transient voltages and stresses 0-55039  
 surface modes, acoustic wave propagation in piezoelec. crystals 0-20026  
 thermo-piezoelectric material, time depend. harmonically changing plane wave propag. anal. 0-15977  
 thermo-piezoelectricity, of polarised annular disc, deformation due to prescribed temp. distrib. 0-2699  
 thickness vibration of piezoelectric plate, natural freq. spectrum 0-15979  
 thin anisotropic layer, electroelastic equilibrium 0-28429  
 tourmaline, resonator, electroelastic constants, elec. field induced freq. shift study 0-20597  
 vinylidene fluoride/tetrafluoroethylene copolymer, piezoelect. and pyroelect. response rel. to dipole polarisation 0-7267

**piezoelectricity continued**

- Au-CdS, Schottky junction, surface defects, photovoltaic, piezoelectric and V-I characteristics (*French*) 0-49898  
 Ca<sub>2</sub>MTa<sub>2</sub>O<sub>15</sub> (M=K, Rb, Tl, Cs), relative stability of struct. types, and piezoelec. props. (*French*) 0-49206  
 Cd<sub>2</sub>MTa<sub>2</sub>O<sub>15</sub> (M=K, Rb, Tl, Cs), relative stability of struct. types, and piezoelec. props. (*French*) 0-49206  
 CsCuCl<sub>3</sub>, piezoelectricity, Jahn-Teller type phase transform. 0-40065  
 CsH<sub>2</sub>AsO<sub>4</sub>, elastic props., photoelasticity near ferroelectric phase transition 0-29107  
 GaP-Ag(Au), Schottky barrier, stress effects on elec. props. 0-34512  
 HCN crystals, polarisation spectra and lattice dynamics 0-49313  
 K<sub>2</sub>Mn<sub>2</sub>(SO<sub>4</sub>)<sub>3</sub>, elastic props. using piezoelec. reson. and US vel. meas. 0-15180  
 LiF, compressed crystals, inhomogeneous elec. field due to piezoelectric effect 0-55044  
 Li<sub>2</sub>GeO<sub>3</sub>, acoustic props., intrinsic piezoeffect, US absorpt. coeffs. (*Russian*) 0-29692  
 LiNbO<sub>3</sub> piezoelectric plate, direct and indirect elastic wave excitation (*Russian*) 0-34858  
 NaCl, electric field induced by homogeneous stresses 0-11343  
 Pb<sub>0.94</sub>Sr<sub>0.06</sub>(Ti<sub>0.47</sub>Zr<sub>0.53</sub>)O<sub>3</sub>-NiO, modified, dielec. and piezoelec. props. 0-11342  
 PbTiO<sub>3</sub>-Pb(Fe<sub>1/2</sub>Nb<sub>1/2</sub>)O<sub>3</sub>-PbZrO<sub>3</sub>, with additions, exam. of electrical characteristics 0-2698  
 Pb(Zr,Ti)O<sub>3</sub> ceramics, space charge field meas. by ferroelec. domain switching current, piezoelec. reson. freq. ageing characts. 0-7296  
 Pb(Zr,Ti)O<sub>3</sub> ceramic, interconnected porous, props. 0-43579  
 SiO<sub>2</sub>, and SiO<sub>0.7</sub>, amorphous sputtered thin film, US anomalies, 0.5-300K 0-34145  
 Sr<sub>0.61</sub>Ba<sub>0.39</sub>Nb<sub>2</sub>O<sub>6</sub>, electromechanical props., permittivity, elastic compliance, piezoelectric moduli 0-29691  
 Sr<sub>2</sub>MTa<sub>2</sub>O<sub>15</sub> (M=K, Rb, Tl, Cs), relative stability of struct. types, and piezoelec. props. (*French*) 0-49206  
 Te, piezoelectrical free-carrier scatt. by screw dislocations, Hall effect and cond. meas. 0-24926  
 ZnO, piezoelec. films produced by gas transport reaction, US excitation efficiency 0-2700

**piezoreflectance**

- graphite, magnetoreflexion under press., Landau level transitions 0-50303

**piezoresistance**

- hexagonal metals, deformed, resistivity changes calcs. 0-44564  
 metal-GaAs(GaP), Schottky barrier diodes, elec. props. under mech. stress 0-11087  
 minerals, up to 60 kbar (*German*) 0-31032  
 MOSFET, piezoresistivity effects and use as press. transducers 0-4695  
 Schottky-barrier structs., surface barrier current instability, uniaxial crystal compression 0-20310  
 shock compression of solids, review 0-24534  
 strain gauges, biaxial gauge factors 0-52185  
 Al, resistivity, press. depend., calc. 0-20151  
 Ba I-Ba II phase boundary, Ba I fusion curve peak at high press. (*Russian*) 0-2165  
 Bi whiskers, electron transition on simple extension, elec. resist. and magnetoresist. meas. (*Russian*) 0-29422  
 Cd<sub>2</sub>Hg<sub>1-x</sub>Te, low temp. piezoresistance, Hall effect, elec. cond., plastic flow 0-6844  
 CdS, even acoustoelec. current due to Lamb waves, freq. depend. 0-20256  
 CdS, plastically deformed cryst. with dislocation slip band, residual cond. 0-6839  
 Cr-Co (4.0 at.%) alloy, antiferromag., disappearance of resist. min. under press., and press. coeff. of T<sub>N</sub> 0-10960  
 EuO, magnetic semiconductor, piezoresistance effect, 4.2 to 300K 0-34450  
 Fe<sub>2</sub>SiO<sub>4</sub>, elec. cond. under defined thermodynamic activities, up to 20 kbar, 340-1100°C 0-6832  
 GaP, scatt. mech., mobility tensor 0-6826  
 P-Ge, acceptor wavefunctions in spherical approx. and piezoresist. 0-29405  
 Ge, low-temp. dislocation cond. mechanism in plastically-deformed pure samples 0-15527  
 n-Ge, piezoresistance under mechanical stress, rel. to cond. band minima 0-6836  
 Ge, plastically deformed low temp. cond. (*Russian*) 0-6831  
 p-Ge, uniaxial compression influence on carrier heating by weak electric field 0-10978  
 n-Ge:Au piezoresistance in presence of deep levels, stress anisotropy 0-10979  
 InP, transferred electron effects under high press. 0-34453  
 n-InSb, elec. cond., press. dependence 0-6830  
 n-InSb, Hall effect and magnetoresist. in extreme quantum limit, stress depend. 0-11021  
 p-InSb, negative magnetoresist. under press. 0-20224  
 InSb:Si(Se)(Te), reson. states and reson. scatt., elec. props. 0-49738  
 MgSiO<sub>3</sub>, elec. cond. under defined thermodynamic activities up to 20 kbar, 340-1100°C 0-6832  
 NbCl<sub>4</sub>, high press. elec. resistivity 0-29404  
 NbO, high press. elec. resistivity, semiconductor to semiconductor transition 0-29404  
 NbO<sub>2</sub>, high press. elec. resistivity, phase transition 0-29404  
 NbSe<sub>3</sub>, Fermi surface, press. effects, Shubnikov-de Haas effect meas. at 1.5K 0-20068  
 Ni<sub>2</sub>SiO<sub>2</sub>, elec. cond. under defined thermodynamic activities, up to 20 kbar, 340-1100°C 0-6832  
 PbO, compressed powder magnetoresistance and apparent carrier mobility 0-35669  
 Pb<sub>1-x</sub>Sn<sub>x</sub>Se, band struct. and transport props., hydrostatic press. effects 0-15452  
 Pb<sub>1-x</sub>Sn<sub>x</sub>Te:In, carrier spectroscopic g-factors, magnetoresistance, temp. depend. 0-6705  
 Pd<sub>2-x</sub>V<sub>x</sub>Si<sub>18</sub>, metallic glasses, effect of press. on elec. resist. 0-6805  
 n-Si, drag thermoelec. power, anisotropy parameter determ., piezoresist. meas. 0-20235  
 Si piezoresistive coefficient calc. and meas. (*German*) 0-39571  
 Si, plastically deformed, spin-depend. charge transport 0-6895  
 n-Si, shear deformed, Smith-Herring and mobility change piezoresistance 0-6842  
 Si:P dislocation p-n junctions, capacitive props. 0-20300



**piezoresistance continued**

- SiC polytypes deformed, resist. anisotropy in (0001) plane 0-20198  
 Te:Sb, impurity states and impurity conduction, hydrostatic pressure 0-39521  
 TiS<sub>2</sub>, elect. resist. at room temp., press. depend. to 80 kbar 0-49730

**piezoresistive devices** *see piezoelectric devices***piles (nuclear fission)** *see fission reactors***pinch effect**

- $\theta$ -pinch energy loss, electron temp. meas. by Thomson laser scatt. (Chinese) 0-54028  
 Belt Pinch IIa, transport phenomena, density profiles 0-24219  
 belt pinches, transport and radiation studies 0-28798  
 belt shaped screw pinch, reactor design study 0-13857  
 diffuse, equilb. density and mag. field profiles determ. using magnetoacoustic oscills. 0-48986  
 diffuse, magnetoacoustic equilibria, circ. cylindrical, internal modes stability 0-43957  
 diffuse pinch, electrothermal stability anal. of fully ionised plasma 0-43901  
 diffuse pinch, energy equilb., classical scalar cond. and neo-classical models 0-24208  
 electrode discharge, nonhydrodynamic pinch compression, kinetics and D<sup>+</sup> focusing (Russian) 0-38689  
 Eta-Beta II, reverse field pinch toroidal machine, design parameters 0-13851  
 field reversed theta pinch, model for angular rotation 0-37596  
 fusion reactors, design, and alternative fusion concepts, systems studies 0-27805  
 H-pinch discharge, quasistationary, EM characts. and energy balance, erosion plasma generator 0-19630  
 HBTX1A experimental reversed field pinch machine, parameters and layout 0-13850  
 high-beta, hard core, magneto-viscous resistive tearing of cylindrical flux surfaces 0-1831  
 inert gas high-current discharges, Z-pinch dynamic and radiative characts. 0-19631  
 ion self-pinch formulae 0-1833  
 LASL toroidal reversed-field pinch programme, energy loss meas. 0-23127  
 magnetoacoustic oscillations in a finite-beta current carrying plasma column 0-1771  
 magnetoacoustic wave, absorpt. in high-beta plasma (German) 0-10430  
 pinch-tormac, device using theta pinches and tormac-like end sections 0-24213  
 plasmatron channel, spatial-temporal pulsations of arc plasma pinch 0-24210  
 reverse field pinch, Faraday rot. diagnostics for internal mag. field 0-43976  
 reversed field pinch, expt. and comp. studies 0-23128  
 reversed field pinch machines, plasma stability anal. 0-24214  
 reversed field pinches, mag. field meas. in plasma toroidal systems 0-49004  
 reversed-field pinch, formation, relaxation and heating studies 0-24215  
 reversed-field pinch, in STP-1, using new external-field programming, MHD instability 0-28803  
 screw pinch, finite Larmor radius stabilisation, resonant particle effects 0-54020  
 screw-pinch configs., collisionless, hybrid-kinetic stability props. of high-beta plasmas 0-43871  
 screw-pinch high- $\beta$  Tokamak, field generation using transverse rotating mag. field 0-19606  
 self-pinch beam, with distributed energy, radial expansion 0-19609  
 sharp boundary Vlasov-fluid screw pinch, free and forced  $m=0$  oscillations 0-38636  
 spheromak plasma config. form. by combined Z- and  $\theta$ -pinch discharges 0-43955  
 stabilizing passive shell and active feedback windings in reverse field pinch fusion reactors 0-18666  
 super pinch in thermonucl. microexplosion, gamma-ray laser pumping 0-28186  
 theta, plasma heating mechanism obs. and analysis (Japanese) 0-1818  
 theta pinch, hot linear, end plugging effect on stability and parameters 0-24223  
 theta pinch, linear, end losses, stoppering, instabilities and heating 0-24224  
 theta pinch, linear, with strong and fast rising mag. field 0-24222  
 theta pinch, mag. pulse penetration, Alfvén velocity scaling 0-33803  
 theta pinch, N<sup>2</sup>,  $\pi$ ,  $\pi^+$  lines Stark broadening, He(II) line diagnostics 0-24249  
 theta pinch, plugged, thermal end loss 0-1836  
 theta pinch, radial oscills. of plasma density and mag. field, light scatt. and probe obs. 0-14937  
 theta pinch, rigidly rotating, Vlasov fluid stability 0-28794  
 theta-pinch, collisionless, high-beta, anisotropy-driven EM modes, finite Larmor radius effects 0-1830  
 theta-pinch, electron heating in turbulent neutral layer (Russian) 0-10361  
 theta-pinch, neutral current sheet, electron energy distrib. meas. 0-43954  
 theta-pinch, reverse field expts., equilibrium, confinement, stability 0-28787  
 theta-pinch, strong fast growing mag. field, pre-ionisation effects (Russian) 0-33800  
 thin skin pinch, anisotropic conducting wall effect on instabilities 0-28800  
 Tokamaks, transport losses, computer modelling and scaling 0-28612  
 toroidal magnetic pumping method, efficiency (Russian) 0-10401  
 toroidal reversed field pinch reactor, engineering desing 0-13856  
 Z discharge between electrodes, relax., toroidal config. possibility 0-28802  
 Z-pinch, dense plasma, H $\alpha$  line profile, density meas. 0-43987  
 Z-pinch, fast discharge, plasma target form., laser irradi. 0-38683  
 Z-pinch, mag. field fast recomb. through plane pinch current sheet 0-38695  
 Z-pinch, rotating, energy balance (Russian) 0-14924  
 Z-pinch plasma, interaction with CO<sub>2</sub> laser radiation 0-48919  
 Z-pinch of intense energy density driven by high-voltage storage lines 0-24216

**pin cushion distortion** *see aberrations***Piobert lines** *see Luder's bands***pion-baryon interactions**

- see also pion-baryon scattering; pion-hyperon interactions; pion-nucleon interactions*  
 SU(4)<sub>w</sub> symmetry, dibaryon coupling constants for  $\gamma$ ,  $\pi$  and baryon interactions (Russian) 0-13329

**pion-baryon scattering**

- see also pion-baryon interactions; pion-hyperon scattering; pion-nucleon scattering*  
 pion-charmed baryon scatt. and coupling strengths, superconvergence sum rules 0-52532

**pion decay**

- decay constant, EM form factor, quark EM self-energy on QCD 0-37242  
 radiative decay amplitude, low-energy expansion, currents, sum rules 0-52509  
 $\pi \rightarrow e \nu \gamma$ , isospin violation in form factor, induced by current quark mass 0-32069  
 $\pi^0 \rightarrow 2\gamma$ , Han-Nambu and SUB quark models, modified, appl. to spin statistics 0-22562  
 $\pi^0 \rightarrow 3\gamma$ , C-noninvariant decay, branching ratio upper limit 0-47297  
 $\pi^0 \rightarrow 4\gamma$  allowed decay search, branching ratio upper limit 0-47298  
 $\pi^0 \rightarrow \gamma \gamma$ ,  $\mu e$  universality and  $\mu$  number nonconservation in rare decays 0-42445  
 $\pi^0 \rightarrow \chi \gamma$ , in 2x-dimensional space time 0-52510  
 $\pi^+ \rightarrow \mu^+ \nu$ , muon momentum, weak interactions and lepton number conservation 0-42444  
 $\pi^+ \rightarrow \mu^+ \nu$ ,  $\mu e$  universality and  $\mu$  number nonconservation in rare decays 0-42445  
 $\pi^+ \rightarrow \mu^+ \nu$ , muon momentum meas. 0-37253  
 $\pi^\pm \rightarrow e^\pm \nu$ , Higgs bosons, effects on experimental observables, and fermion mass scale 0-32061  
 $\pi^\pm \rightarrow \mu^\pm \nu$ , Higgs bosons, effects on experimental observables, and fermion mass scale 0-32061

**pion-hyperon interactions**

- see also pion-hyperon scattering*  
 No entries

**pion-hyperon scattering**

- see also pion-baryon interactions*  
 No entries

**pion interactions** *see lepton-hadron interactions; meson-meson interactions; photon-hadron interactions; pion-baryon interactions; pion-nucleus reactions; pion-pion interactions***pion-nucleon interactions**

- see also pion-nucleon scattering; pion-proton interactions*  
 chiral symmetry and pion condensation, review book contrib. 0-437  
 constituent quark model and production of particles from nuclear targets 0-380  
 deep inelastic scatt., total cross section unitarity bound 0-37294  
 inelastic scatt. in Fermi liquid, nucleon-nucleon interaction effects 0-22862  
 non-perturbative effects, quantum field theory, modified normalisation conditions 0-9089  
 nuclear matter, quasiclassical model of meson condensation (Russian) 0-5086  
 quark jet multiple production in  $\pi$ -Al collisions 0-9188  
 $N\pi$  dynamics, medium energy, dispersion relations, isobar expansion for  $\pi N$  0-4917  
 $N\pi\pi$  medium energy dynamics from  $\pi N$ , isobar model rescatt. corrections 0-4918  
 $\pi$ -nucleus interactions, 40 GeV/c, multiparticle production 0-5173  
 $\pi^\pm U$  interaction at 55 GeV/c, search for long lived heavy mesons (Russian) 0-5029  
 $\pi^- d \rightarrow \pi^- pn$  final state interactions and d breakup for 438 MeV/c  $\pi^-$  impulse (Russian) 0-18145  
 $\pi^- d \rightarrow \pi^+ X^-$ , 2.6 GeV/c, d proton screening correction and Glauber parameter 0-9175  
 $\pi N$ ,  $\psi$  hadronic prod., lepton pair ang. distrib., cross section  $\chi$  contribution 0-42487  
 $\pi N$  coupling in  $\Delta(1231)$  isobar region, pion index of refraction, self-energy in low density limit 0-42554  
 $\pi N$  low energy partial wave anal., cross sections,  $\Delta^0$  and  $\Delta^{++}$  0-52531  
 $\pi N \rightarrow \mu^+ \mu^- X$ , longitudinal photon polarisation from helicity ang. distrib. 0-5025  
 $\pi N \rightarrow \pi^+ \pi^- N$ , 4-17 GeV/c,  $\rho^0$  and f prod. mech. 0-436  
 $\pi^- n$ , 40 GeV/c, secondary neutron average number, charge exchange coeffs., n inelasticity coeffs. (Russian) 0-32132  
 $\pi^- N$ ,  $\Delta$  hyperon prod. cross section, momentum and ang. distrib. (Russian) 0-42497  
 $\pi^- N$  in Be, 150, 175 GeV/c, high mass muon pair prod., Drell-Yan QCD corrections 0-13343  
 $\pi^- n \rightarrow \rho^0 \pi^-$ , 9 GeV exchange Deck model anal. 0-47322  
 $\pi^+ n \rightarrow p X$ , 100 to 400 GeV/c, slow-proton prod., Regge trajectory 0-22646  
 $\pi^\pm N$ , 200 GeV/c, dimuon prod. cross section, Drell-Yan predictions, struct. functions 0-37300  
 $\pi N$  form factor; relativistic calc. of  $\Delta(1232)$  contribution to imaginary part (Korean) 0-47292  
 $^3H(\pi^+ \pi^-)$ , 232-252 MeV charge exchange differential cross section 0-37401

**pion-nucleon scattering**

- see also pion-nucleon interactions; pion-proton scattering*  
 Padé approximants and  $\pi N$  scattering 0-22634  
 partial wave amplitudes coupled channel anal. 0-42495  
 partial wave analysis 0-42494  
 quantum field theory approach, standard reduction techniques, calc. of scatt. amplitude 0-42570  
 two component Pomeron,  $\pi N$ ,  $kN$ ,  $NN$  forward scatt. amplitudes 0-37245  
 $\pi d$  polarised scatt., dibaryon resonance signals in excitation functions 0-9181  
 $\pi N$ , null plane current anticommutators, sum rules and apps. 0-52436  
 $\pi N$  low energy partial wave anal., cross sections,  $\Delta^0$  and  $\Delta^{++}$  0-52531  
 $\pi N$  off shell scatt. near  $\Delta$  resonance, parameter free form factor 0-9168  
 $\pi N$  scatt., isospin violation from  $\pi^0 \eta$  mixing, partial wave anal.,  $N^*(1540)$  struct. 0-27426  
 $^3He(\pi, \pi^+)$   $\Delta(1236)$  resonance region, Watson multiple scatt. series. integral eqns. 0-37402



## pion-nucleus reactions

for inelastic pion-nucleus scattering, see "pion-nucleus scattering"

see also pion-nucleon interactions

channelling, modulation of high energy interactions 0-37373

charged particle yields from  $\pi^-$  capture in biologically significant materials 0-12201

conference on high energy physics and nuclear struct. Vancouver, Canada (Aug. 1979) 0-41936

emulsion nuclei, 20 TeV, balloon-borne chamber, Monte Carlo simulation 0-9309

isobar propagation and collective effects, pion-nucleus and photonuclear investigation 0-22676

nuclear critical opalescence, pion field and condensation 0-42559

pion condensation and the pion-nuclear interaction, book contrib. 0-485

pion condensation in nuclear matter, book contrib. 0-484

proton semileptonic decay in nuclei, pion attenuation 0-47286

reaction mechanisms, nuclear environment and models 0-42700

total cross section treatment for (3,3) resonance region 0-42703

$^2\text{H}(\pi^+, \text{pp})$ , pion absorpt., effect of  $\rho\omega$  exchange currents (Korean) 0-47402

$(\pi^+, \text{d})$ , DWBA cross section (Chinese) 0-27673

$(\pi, \gamma)$ ,  $A=14$  nuclei, isospin  $T=2, 1$  and  $0$  collective resonances, shell model 0-510

$(\pi, \gamma)$ ,  $\gamma$ -transitions on and off line 0-37912

$(\pi, \gamma)$ , inverse pion photoprod., level struct. determ. 0-22863

$(\pi, \gamma)$ ,  $\pi$  electromag. processes, theoretical aspects 0-22822

$(\pi, \gamma)$ ,  $1p$  nuclei  $M2$  giant resonance calcs. 0-22784

$(\pi, \text{nn})$ ,  $S$ -wave and  $p$ -wave absorptive pion-nucleus optical pot. 0-27677

$(\pi^+, \pi^0)$ , isobar-doorway model optical pot. appl. to isospin nonzero nuclei 0-52699

$(\pi, X)$ , 50-300 MeV, pion reaction mode status, absorption and inelastic scatt. 0-42701

$(\pi, X)$ , 1.75-6.5 GeV/c, total inelastic and knock-out cross sections, nuclear RMS radius (Russian) 0-32175

$(\Pi, X)$ , in emulsion, 50 GeV, charged particle multiplicity obs. 0-5172

$(\pi, X)$  slow pion capture in deformed nuclei, effects on high spin state excitation 0-18345

$\pi^-$  capture at rest, exptl. method for pion discrimination and absolute counting 0-5432

$\pi^3\text{He}^3\text{He}$  coupling on basis of PCAC 0-32196

$\text{Al}+\pi^-$ , 40 GeV/c, multiparticle production 0-5173

$^{27}\text{Al}(\pi, \pi^0 p)$ , 255 MeV, quasielastic knockout, proton yield,  $\sigma(\pi^+)/\sigma(\pi^-)$  cross section ratio 0-32305

$\text{Al}(\pi, X)$ , quark jet multiple production 0-9188

$^{197}\text{Au}(\pi^+, \text{spallation})$ , 100-300 MeV, cross sections for products  $A=167-196$  0-27619

$^9\text{Be}(\pi, X)$ ,  $X=\gamma, \gamma\gamma, e^+e^-$ , rare pion absorption modes, theoretical and expt. results 0-42698

$\text{C}+\pi^-$ , 5 GeV/c, pp correlations (Russian) 0-9316

$\text{C}+\pi^-$ , elastic and coherent cross-section at 40 GeV/c using propane bubble chamber 0-27524

$\text{C}+\pi^-$  40 GeV/c, multiparticle production 0-5173

$^{12}\text{C}(\pi, X)$ ,  $X=\gamma, \gamma\gamma, e^+e^-$ , rare pion absorption modes, theoretical and expt. results 0-42698

$^{12}\text{C}(\pi^+, \pi^0 d)$ , 180 MeV, cross-section ratios 0-32308

$^{12}\text{C}(\pi^+, \pi^0 t)$ , 180 MeV, cross section ratios 0-32308

$^{12}\text{C}(\pi, \pi p)$ ,  $^{11}\text{B}$ , knockout reaction, cross section ratio  $\sigma(\pi^+, \pi^0 p)/\sigma(\pi^-, \pi^0 p)$  meas. 0-32254

$^{12}\text{C}(\pi, X)$ , angular distrib. of inelastic diffusion of  $\pi^\pm$  (French) 0-47507

$^{12}\text{C}(\pi, X)$ , deep inelastic,  $\pi$  and  $\Delta$  optical pot. effects, semiclassical transport model 0-52698

$^{12}\text{C}(\pi, 2\gamma)$ , doubly radiative capture theory, branching ratio and ang. correlations 0-9314

$^{12}\text{C}(\pi, \gamma)$ , pion $^-$  radiative capture probab. (Russian) 0-42538

$^{12}\text{C}(\pi, \gamma)$ ,  $^{12}\text{B}^*$ , excitation of collective states, shell model 0-22652

$^{12}\text{C}(\pi, X)$ , 40 GeV/c, secondary neutron average number, charge exchange coeffs.,  $n$  inelasticity coeffs. (Russian) 0-32132

$^{12}\text{C}(\pi, n)$ , stopped pion, neutron energy spectra, mean energies and multiplicities 0-9311

$^{12}\text{C}(\pi^+, \pi^0 \alpha)$ , 60 MeV,  $^8\text{Be}$  cross sections and ang. distrib., direct knockout model anal. (Russian) 0-27620

$^{12}\text{C}(\pi^0 d)$ , DWBA cross section formula, PWBA differential cross section (Chinese) 0-22861

$^{12}\text{C}(\pi^+, \pi^+)$ , 290 MeV, double charge exchange cross sections 0-18348

$^{12}\text{C}(\pi^+, \pi N)$ , 40-600 MeV, excitation functions and absolute cross sections 0-18226

$^{13}\text{C}(\pi^+, \pi^0)$ , angle integrated cross section, optical pot.,  $n$  and  $p$  radius differences 0-32307

$^{13}\text{C}(\pi^+, \pi^0)$ , 150 MeV, single charge exchange, isobaric analogue state excitation, cross sections 0-42544

$^{14}\text{C}(\pi^+, \pi^+)$ ,  $A=40, 44, 48$ , 290 MeV, double charge exchange cross sections 0-18348

$\text{C}(\pi, X)$ , 3 GeV/c,  $n$  inclusive spectra, neutron yield (Russian) 0-13510

$^{52}\text{Cr}(\pi, X)$ , angular distrib. of inelastic diffusion of  $\pi^\pm$  (French) 0-47507

$\text{Cu}+\pi^-$  40 GeV/c, multiparticle production 0-5173

$\text{Cu}(\pi, X)$ , 3 GeV/c,  $n$  inclusive spectra, neutron yield (Russian) 0-13510

$\text{Cu}(\pi^-)$ , spallation 0.6, 0.9, 12 GeV,  $T=1/2$  resonances, Na, Sc and Co rel. yields 0-5109

$^{76}\text{Ge}(\pi^+ \text{xn})$ ,  $^{76-78}\text{As}$ , 100, 180 MeV, product formation cross section 0-42705

$^2\text{H}(\pi, p)$ , reactive two body contrib. to pion-nucleus optical pot. 0-9313

$^2\text{H}(\pi, \pi^0 p)$ , 438 GeV/c, break up process, kinematic variables,  $np$  final state interaction (Russian) 0-52701

$^2\text{H}(\pi^+, \pi^-)X$ , 2.6 GeV/c,  $d$  proton screening correction and Glauber parameter 0-9175

$^2\text{H}(\pi^+, \pi^+)$ , 340 MeV/c, reaction mechanisms and isospin effects 0-32306

$^3\text{He}(\pi, \pi^0)$ , 200 MeV, single charge exchange, isobaric analogue state excitation, cross sections 0-42544

$^4\text{He}(\pi, \pi^+ X)$ ,  $^3\text{H}$ , 5 GeV, nucleon isobar prod. and knockout 0-42709

$^{14}\text{N}(\pi, n)$ , stopped pion, neutron energy spectra, mean energies and multiplicities 0-9311

$^{16}\text{O}(\pi, \gamma n)$ , direct and resonance reaction unified shell model,  $n, \gamma$  spectra 0-52696

$^{16}\text{O}(\pi, n)$ , stopped pion, neutron energy spectra, mean energies and multiplicities 0-9311

$^{16}\text{O}(\pi, X)$ , angular distrib. of inelastic diffusion of  $\pi^\pm$  (French) 0-47507

$^{18}\text{O}(\pi, \pi^-)$ ,  $^{18}\text{Ne}$  cross section, excitation function and double isobaric analogue state 0-27596

## pion-nucleus reactions continued

$^{18}\text{O}(\pi^+, \pi^-)$ , 164 MeV,  $^{18}\text{Ne}$  analogue and nonanalogue states,  $\pi$  double charge exchange form factors 0-13405

$\text{Pb}+\pi^-$  40 GeV/c, multiparticle production 0-5173

$^{208}\text{Pb}(\pi, \pi^0 p)$ , 255 MeV, quasielastic knockout, proton yield,  $\sigma(\pi^+)/\sigma(\pi^-)$  cross section ratio 0-32305

$\text{Pb}(\pi^+, X)$ , 3 GeV/c,  $n$  inclusive spectra, neutron yield (Russian) 0-13510

$^{76}\text{Se}(\pi, \text{xn})$ ,  $^{76-78}\text{As}$ , 100, 180 MeV, product formation cross section 0-42705

$^{28}\text{Si}(\pi, X)$ , angular distrib. of inelastic diffusion of  $\pi^\pm$  (French) 0-47507

$^{232}\text{Th}(\pi, \pi^-)$ , resting pions, delayed fission search (Russian) 0-52704

$^{238}\text{U}(\pi, \pi^-)$ , resting pions, delayed fission search (Russian) 0-52704

$\text{U}(\pi^-, X)$ , 3 GeV/c,  $n$  inclusive spectra, neutron yield (Russian) 0-13510

## pion-nucleus scattering

see also pion-nucleon scattering

Born series rearrangement in model space, resolvent operator expansion 0-13422

microscopic theory, review 0-47511

multiple Coulomb scattering angle meas. 50 to 200 GeV/c 0-9315

pion condensation in nuclear matter, book contrib. 0-484

$\Delta(33)$  interaction with nucleus, effective shell model pot., pion scatt. test 0-32202

$(\pi, \pi)$ ,  $A>2$  nuclei, three rung ladder graph, singularity curves 0-32303

$(\pi, \pi)$ , light nuclei near threshold,  $\pi$  mass difference effects, nuclear K-matrix 0-27674

$(\pi, \pi)$ , relativistic Schrodinger and Klein-Gordon optical models, off-shell sensitivity 0-5175

$(\pi, \pi)$  elastic scatt., reaction mechanisms, structure information and neutron radii 0-42702

$(\pi, \pi)$ ,  $1p$  shell targets, DWIA calcs., strong transitions, isospin effects 0-42708

$(\pi, \pi)$ , collective transitions, giant resonances, isospin content and spin transfer 0-42580

$(\pi, \pi')$ , particle-hole state excitation, field theory calcs. (Russian) 0-37318

$(\pi, \pi)$  many body QFT framework anal., final state particle-hole correlations 0-13508

$(\pi, X)$ , 50-300 MeV, pion reaction mode status, absorption and inelastic scatt. 0-42701

$^{14}\text{C}(\pi, \pi)$ ,  $A=12, 13$ ,  $\sim 180$  MeV, isospin mixing, levels, excitation functions and ang. distrib. 0-42543

$^{12}\text{C}(\pi, \pi)$ , total cross section, density distrib. and ray bending effects 0-47509

$^{12}\text{C}(\pi^+, \pi^-)$ ,  $^{12}\text{C}^*$ , 20 to 40 GeV/c, semicoherent elastic scatt. 0-5174

$^{12}\text{C}(\pi^+, \pi^+)$ , 100-291 MeV, cross sections and ang. distrib., spin and isospin transfer 0-52697

$^{12}\text{C}(\pi^+, \pi^+)$ , 40 MeV, differential cross sections and strength parameters, optical model fit 0-18347

$^{12}\text{C}(\pi^+, \pi^+)$ , model Coulomb corrections in eikonal 0-5171

$^{13}\text{C}(\pi, \pi)$ , 162 MeV, pure  $n$  and  $p$  transitions, differential cross sections 0-5040

$^{13}\text{C}(\pi^+, \pi^+)$ , near  $\pi N$  (3,3) resonance, 180 MeV, collective states and cross sections 0-13507

$^{40}\text{Ca}(\pi^+, \pi^+)$ , model Coulomb corrections in eikonal 0-5171

$^{40}\text{Ca}(\pi^+, \pi^+)$ , 40 MeV, differential cross sections and strength parameters, optical model fit 0-18347

$^2\text{H}(\pi, \pi)$ , expt. and theoretical work, present status, model testing,  $\pi N$  interaction 0-42699

$^2\text{H}(\pi, \pi)$ , high energy total cross section in Glauber model 0-18346

$^2\text{H}(\pi, \pi)$ , medium energy elastic scatt. amplitudes, covariant multiple scatt. model convergence test 0-42710

$^2\text{H}(\pi, \pi)$ , polarised  $d$ , dibaryon resonance signals in excitation functions 0-9181

$^2\text{H}(\pi, \pi)$ , relativistic description,  $\pi N$  waves,  $NN$  rescatt.,  $\rho$ -exchange,  $\pi$  absorption and emission 0-9310

$^2\text{H}(\pi, \pi^-)$ , 552 MeV/c, elastic differential cross section Glauber theory anal. (Russian) 0-52700

$^2\text{H}(\pi, \pi^-)$ , 1.57, 1.66 and 1.76 GeV/c elastic hack scatt. cross section energetic shape struct. (Russian) 0-47510

$^2\text{H}(\pi^+, \pi^+)$ , tensor polarisation and cross section at  $180^\circ$  0-5116

$^2\text{H}(\pi, \pi)$ , (3,3) region, multiple scatt. theory study by optical pot. method (Russian) 0-13509

$^4\text{He}(\pi, \pi)$ , low energy, first order optical pot., Pauli principle corrections, nuclear binding 0-27675

$^A\text{He}(\pi, \pi)$ ,  $A=3, 4$ , low energy scatt. length and phase calcs. 0-47508

$^{16}\text{O}(\pi, \pi)$ , aligned deformed nuclei, cross sections and diffractive minima from eikonal approx. 0-22860

$^{58}\text{Ni}(\pi, \pi)$ , 162 MeV, elastic and inelastic ang. distrib., optical and PWIA anal. 0-42706

$^{16}\text{O}(\pi, \pi)$ ,  $\sim 180$  MeV, isospin mixing, levels, excitation functions and ang. distrib. 0-42543

$^{16}\text{O}(\pi, \pi)$ , T-matrix from isobar-hole model, many-body corrections, optical pot. parameter 0-9312

$^{16}\text{O}(\pi, \pi)$ , three-body model of  $\pi N$  interaction using finite binding pots. 0-42707

$^{16}\text{O}(\pi^+, \pi^+)$ , 40 MeV, differential cross sections and strength parameters, optical model fit 0-18347

$^{18}\text{O}(\pi, \pi)$ , 164 MeV, yrast state and level excitation, DWIA calcs., shell model context 0-42526

$^{208}\text{Pb}(\pi, \pi)$ , 162 MeV, elastic and inelastic ang. distrib., optical and PWIA anal. 0-42706

$^{208}\text{Pb}(\pi, \pi)$ , total cross section, density distrib. and ray bending effects 0-47509

$^{208}\text{Pb}(\pi^+, \pi^+)$ , 40 MeV, differential cross sections and strength parameters, optical model fit 0-18347

$^{32}\text{S}(\pi, \pi)$ , total cross section, density distrib. and ray bending effects 0-47509

$^{28}\text{Si}(\pi, \pi)$ , 162 MeV, elastic and inelastic ang. distrib., optical and PWIA anal. 0-42706

$^{120}\text{Sn}(\pi, \pi)$ , total cross section, density distrib. and ray bending effects 0-47509

$^{89}\text{Y}(\pi, \pi)$ , 163, 240 MeV, giant resonance pionic excitation 0-52561

$^{90}\text{Zr}(\pi, \pi^+)$ , 40 MeV, differential cross sections and strength parameters, optical model fit 0-18347

pion-pion interactions

see also pion-pion scattering

form factor and propagator bounds (German) 0-37265

$\pi\pi \rightarrow \text{KK}$ , low energy cross sections (Chinese) 0-52535

$\pi\pi \rightarrow \pi\omega$ ,  $\rho(1250)$  meson and two channel  $\pi\pi$ ,  $\pi\omega$  problem, N/D method (Russian) 0-37297



**pion-pion scattering**

see also *pion-pion interactions*

- elastic scatt., asymptotic total cross sections and positivity 0-13334  
 $\pi\pi$  elastic scatt., exclusive and almost exclusive process asymptotic behaviour, renormalisation group 0-42464  
 $\pi\pi \rightarrow \pi\pi$ ,  $\rho(1250)$  meson and two channel  $\pi\pi$ ,  $\pi\omega$  problem, N/D method (Russian) 0-37297  
 $\pi^+\pi^0$  scatt., axiomatic constraint optimality, lower bounds 0-32124

**pion production**

- black holes in binary stellar systems,  $\pi$  meson prod. and gamma emission during accretion 0-17608  
 charged current induced weak one pion prod., form factors from PCAC 0-18129  
 cosmic ray-nucleus reacts., 20 TeV, balloon-borne chamber, Monte Carlo simulation 0-9309  
 $e^+e^- \rightarrow \pi^+\pi^-$  ( $\pi^0\omega$ ),  $\rho(1250)$  description, EM form factors, bound states, N/D method (Russian) 0-42465  
 electropion prod., deep inelastic scatt. and struct. from electron coincidence expts. at Stanford 0-22821  
 expanding fireball in high energy heavy ion reactions, pion radiation 0-5155  
 hadron+hadron, high-energy, inclusive spectra of secondary pions, Feynman scaling and statistical model 0-42502  
 hadron+hadron, jet production, large transverse momentum 0-42503  
 heavy ion collisions, pion prod. depend. on pion charge 0-37392  
 heavy ion collisions, pion spectra, Coulomb distortion in final state EM interaction 0-13497  
 nuclear collisions, pion multiplicity and nonlinear effects in pion production, NN inelastic interactions (Russian) 0-52637  
 nuclear multi-particle rescatt. effects, cumulative  $\pi$ , p, K prod. (Russian) 0-52638  
 phase space critical surface of pions produced in inclusive  $\pi^-p$  interactions (Russian) 0-18154  
 photoproduction in  $E < 450$  MeV region, dispersion relations, CT invariance, review, book contrib. 0-47311  
 photoproduction in large cosmic-ray showers 0-4214  
 physical pion low energy electro- and photoprod., Ward identity, chiral symmetry breaking struct. 0-5003  
 physical pion low energy photo- and electroprod., photoprod. phenomenology, quark mass 0-5004  
 pionisation influence on beam hardness, beam evolution eqns. for hadronic processes (Russian) 0-42407  
 relativistic light ion collisions, two-fireball model improvements, p and  $\pi$  spectra 0-5158  
 ( $d,\pi$ ), 4.2, 4.5 GeV/N, pion multiplicities and theoretical models, review 0-42657  
 DD  $\rho\pi$ , 1300 to 2300 MeV,  $\pi^0$  photoproduction, double polarisation parameters 0-13317  
 ( $e,e\pi$ ),  $\pi$  electromag. processes, theoretical aspects 0-22822  
 $e^+e^- \rightarrow \pi^+\pi^- \gamma$ , virtual electrons bremsstrahlung photon, Feynman diagrams, Weizsacker-Williams approx. 0-52484  
 $e^+e^- \rightarrow \pi^+\pi^-$ , near threshold,  $\pi$  form factor (Russian) 0-4996  
 ep, 20.5 GeV, inclusive  $\pi^0$  electroprod. in deep inelastic region 0-52520  
 ep  $\rightarrow eN\pi$ ,  $\gamma^+p \rightarrow \pi^+(1231)$  vertex transition form factor (Russian) 0-37269  
 ep  $\rightarrow \pi^0X$ , duality and finite energy sum rules 0-42477  
 $\eta^0\pi^0$  mixing effects and  $\Delta S=1$  nonleptonic weak decays 0-4991  
 ( $\gamma,\pi$ ), few body pion photoprod. in  $\Delta$ -resonance, region 0-42636  
 ( $\gamma,\pi$ ), light nuclei near threshold,  $\pi$  mass difference effects, nuclear K-matrix 0-27674  
 ( $\gamma,\pi$ ),  $\pi$  electromag. processes, theoretical aspects 0-22822  
 ( $\gamma, \pi X$ ), 4.2, 4.5 GeV/N, pion multiplicities and theoretical models, review 0-42657  
 $\gamma d \rightarrow \pi^0 d$ , meson-exchange currents in photomesic reactions, relativistic many-body theory 0-422  
 $\gamma d \rightarrow \pi^+ n n$ , off-energy shell photoprod. amplitudes for reactions on bound neutrons 0-421  
 $\gamma n \rightarrow \pi^+ p$  reaction cross-section asymmetry in photon energy range 0.9 to 1.65 GeV (Russian) 0-32108  
 $\gamma N \rightarrow \pi^+ n$ , meas. of asymmetries and cross sections using 16 GeV linearly polarised photons 0-13318  
 $\gamma N \rightarrow \pi^0 \Delta$ , meas. of asymmetries and cross sections using 16 GeV linearly polarised photons 0-13318  
 $\gamma N \rightarrow \pi^0 \Delta$  reaction amplitude, equivalence theorems (Russian) 0-52522  
 $\gamma N \rightarrow \pi^0 \Delta(1232)$ , multipole amplitudes, dispersion relations 0-5002  
 $\gamma p \rightarrow \pi^+ n$ , multipole anal. in region of first reson. 0-22622  
 $\gamma p \rightarrow \pi^+ n$  section asymmetry, pion-proton twin birth contribution (Russian) 0-47308  
 $\gamma p \rightarrow \pi^+ n$ , multipole anal. in region of first reson. 0-22622  
 $\gamma p \rightarrow \pi^0 X$ , invariant cross section at large  $p_T$ , hard scatt. model 0-22621  
 $\gamma p \rightarrow \pi^0 p$ , 1.4 GeV, differential cross section meas. 0-42476  
 $\gamma p \rightarrow \pi^0 X$ , duality and finite energy sum rules 0-42477  
 $\gamma p \rightarrow \pi^0 X$  multipole isotopic anal., soln. irregular behaviour near  $P_{33}$  resonance (Russian) 0-5005  
 $K^- d \rightarrow \pi^0 \Delta p$ ,  $\Sigma N$  bound state and  $\Delta p$  enhancement 0-47326  
 $K^- p \rightarrow (K\pi\pi)^- p$ , 4.2 GeV/c, partial wave anal. in Q region 0-13330  
 $k p \rightarrow \pi^+ \pi^- X$ , partial wave anal. in  $\Lambda(1520)$  region,  $\Lambda$  partial decay widths (Russian) 0-32131  
 $K^- p \rightarrow pK^0 \pi^- \pi^0$ , 10 GeV/c, dynamical mechanism from cluster anal. (Russian) 0-42499  
 $K^+ p \rightarrow \pi^0 X$ , 32 GeV/c, inclusive and semi-inclusive distributions of  $\pi^0$  0-27525  
 $K^0 p \rightarrow K^0 \pi^+ \pi^- p$ , up to 17 GeV/c,  $Q^0 \cdot Q^0$  prod., cross sections 0-32129  
 IN-1  $\pi X$ , semi-inclusive deep inelastic scatt. cross sections, higher twist effects 0-32105  
 NN  $\rightarrow \pi N$ , 9 GeV/c, isospin cross sections, differential anal. 0-431  
 NP  $\rightarrow (N\pi)p$ , diffraction dissociation, absorptive effects 0-5009  
 np  $\rightarrow d\pi^0$ , nuclear forces charge symmetry test 0-5071  
 NN dynamics, medium energy, dispersion relations, isobar expansion for  $\pi N$  0-4917  
 NN medium energy dynamics from  $\pi N$ , isobar model rescatt. corrections 0-4918  
 $\nu, \bar{\nu}$  charged current induced one pion weak prod., I=1/2 resonant contrib. 0-47274  
 $\nu(\bar{\nu})$  charged current induced one  $\pi$  prod., model total cross sections 0-4979  
 $\nu n \rightarrow \nu n \pi^0$ , neutral current induced one-pion production, Weinberg-Salam structure 0-52454  
 $\nu n \rightarrow \nu p \pi^-$ , neutral current induced one-pion production, Weinberg-Salam structure 0-52454

**pion production continued**

- $\nu p \rightarrow \nu n \pi^+$ , neutral current induced one-pion production, Weinberg-Salam structure 0-52454  
 $\nu p \rightarrow \nu p \pi^0$ , neutral current induced one-pion production, Weinberg-Salam structure 0-52454  
 $\nu p \rightarrow \pi$ , threshold to 450 MeV, energy depend. multipole anal. 0-32110  
 ( $p,\pi$ ), 4.2, 4.5 GeV/N, pion multiplicities and theoretical models, review 0-42657  
 ( $p,\pi$ ), exclusive single nucleon transfer, theoretical status 0-42652  
 ( $p,\pi^+$ ), 8-16 MeV, inclusive cross sections near threshold, A depend. 0-27644  
 ( $p,\pi^+$ ), light nuclei, 0.5-10 MeV, total cross sections near pion Coulomb barrier 0-32280  
 ( $p,\pi$ ) in emulsion, 70 GeV/c, Lorentz invariant kinematical anal. 0-47474  
 ( $p,X$ ), 70 GeV/c (Russian) 0-52681  
 p-nucleus 0.8-4.89 GeV collisions, energy depend. of  $180^\circ$  prod. of  $\pi^+$  0-22834  
 pd, rescattering effects in 19 GeV/c interactions,  $\Delta\Delta$  component of D 0-42500  
 pD annihilation, pion rescatt. effect at intermediate energies 0-5010  
 pd  $\rightarrow \pi^+ \pi^- d$ , interference phenomena in coherent production, nucleon diffractive amps., helicity-flip 0-47329  
 pd  $\rightarrow \pi^+ X$ , 750 MeV, T=1 NN phase shifts and total cross section 0-22630  
 pn  $\rightarrow \pi p \pi^-$ , 2.98 GeV/c,  $\bar{\Delta}^{--}$  prod. in additive quark model framework 0-52529  
 pN  $\rightarrow \pi^0 X$ , 200-400 GeV/c, inclusive  $\pi^0$  prod. over large  $X_T$  and  $X_F$  ranges 0-37310  
 pN  $\rightarrow \pi X$ , intermediate  $\bar{p}$  contrib. to backward  $\pi$  prod. (Russian) 0-13326  
 pp, 405 GeV/c, pion local number distrib. fluctuations, higher order correlations 0-18152  
 pp  $\rightarrow (\pi^+ n)p$ ,  $\pi$  energy and transverse momentum distrib., DHD model with nucleon exchange (Russian) 0-13327  
 pp collision inclusive spectra, fast pionisation at high energies, z-scaling (Russian) 0-47339  
 pp  $\rightarrow d\pi^+$ , 0.8 GeV, differential cross section and polarisation asymmetries 0-27519  
 pp  $\rightarrow d\pi^+$ , 750 MeV, T=1 NN phase shifts and total cross section 0-22630  
 pp  $\rightarrow \Delta^{++} \pi^-$ , 4 GeV/c, mass spectra, ang. distrib. and momentum transfer (Russian) 0-42489  
 pp jet prod.,  $\pi^0$  fragments, jet fragmentation function and momentum 0-443  
 pp  $\rightarrow \pi^+$ , large transverse momentum jets investig. at 52.4, 62.7 GeV 0-18151  
 pp  $\rightarrow \pi^0 X$ , scaling in the mean hypothesis and Feynman variable energy depend. 0-42501  
 pp  $\rightarrow \pi^0 + X$ , secondary neutral pion-nucleon flux ratio at atm. top 0-8500  
 pp  $\rightarrow \pi^0 \pi^0$ , up to 10 GeV/c, correlation of momentum of  $\pi^0$  pairs 0-5011  
 pp  $\rightarrow \pi^0 \pi^0 X$ , ISR  $\pi^0\pi^0$  azimuthal correlation data, comments 0-52543  
 pp  $\rightarrow \pi^0 d$ , 400-800 MeV, anal. by neutron exchange,  $\Delta N$  intermediate states, diproton resonances 0-27518  
 pp  $\rightarrow \pi^+ d$ , di-proton resonances 0-22631  
 pp  $\rightarrow \pi^+ d$ ,  $N\Delta(1232)$  state contrib., K matrix theory anal. 0-5013  
 pp  $\rightarrow \pi^+ d$ , SIS, 578 MeV, pol. beam and target, spin depend. parameters 0-42651  
 pp  $\rightarrow \pi^+ \pi^- \pi^+ \pi^- \pi^0$ , 1950 MeV/c<sup>2</sup>, experimental evidence 0-27516  
 pp  $\rightarrow \pi^+ \pi^- \pi^+ \pi^- \pi^0$ , 1950 MeV/c<sup>2</sup>, properties evidence for  $pp \rightarrow \omega^0 \rho^0$  0-27517  
 pp  $\rightarrow \pi^0 X$  reaction, quark-quark inelastic collision model (Russian) 0-32141  
 pp  $\rightarrow \pi X$ ,  $\sqrt{s}=63$  GeV, high momentum meson correlations 0-32138  
 pp  $\rightarrow \pi X$ , QCD radiation and mean scaling, longitudinal and transverse momentum 0-42405  
 $\pi^- d \rightarrow \pi^+ X^-$ , 2.6 GeV/c, d proton screening correction and Glauber parameter 0-9175  
 $\pi^+ d$ , 15 GeV/c, many-pion prod. and resonant prod. cross sections 0-22642  
 $\pi N \rightarrow \pi^+ \pi^- N$ , 4-17 GeV/c,  $\rho^0$  and f prod. mech. 0-436  
 $\pi^- p$ , 200, 300 GeV, relative  $\pi^+$ ,  $K^+$ , p,  $\bar{p}$  prod., charge ratios, high  $p_T$  0-47335  
 $\pi^- p$ , 40 GeV/c, multi-pion systems and transverse momenta, differential cross sections (Russian) 0-32142  
 $\pi^- p \rightarrow \pi^- \pi^- \pi^+ p$ , 63, 94 GeV/c,  $A_2$  meson prod. from partial wave anal. 0-37303  
 $\pi^- p \rightarrow \pi^- \pi^- \pi^+ p$ , 63, 94 GeV/c,  $A_1$  meson existence from partial wave anal. 0-37304  
 $\pi^- p \rightarrow \pi^- \pi^- \pi^+ p$ , 63, 94 MeV/c,  $A_3$  meson,  $3\pi$  resonances in  $2^-$  partial waves 0-37305  
 $\pi^- p \rightarrow \pi^- \pi^- \pi^+ n$ , 203-357 MeV, integrated cross section, chiral symmetry breaking parameter 0-32125  
 $\pi^- p \rightarrow \pi^- \pi^- \pi^+ n$ , below 1400 MeV, PS11 contrib. threshold K-matrix, chiral symmetry breaking 0-32126  
 $\pi^- p \rightarrow \pi^- \pi^+ \pi^+ n$ , narrow epsilon resonance under rho 0-5021  
 $\pi^- p \rightarrow \pi^0 \pi^0 n$ , 200, 240 MeV, total near-threshold cross section, isotopic amplitudes (Russian) 0-37296  
 $\pi^- p \rightarrow \pi^0 \pi^0 n$ , 6, 8, 12 GeV,  $\pi^0 \pi^0$  S wave and I=0 amplitude 0-18144  
 $\pi^- p \rightarrow \pi^- \pi^+ X^-$ , 2.6 GeV/c, d proton screening correction and Glauber parameter 0-9175  
 $\pi^- p \rightarrow \pi^- \pi^+ \pi^- n$ ,  $\pi\pi$  scatt. partial wave anal. f, g and h mesons 0-5015  
 $\pi^+ p \rightarrow \pi^+ \pi^- \pi^+ \pi^-$ , narrow epsilon resonance under rho 0-5021  
 $\pi^+ p \rightarrow \pi^+ \pi^- \pi^+ \pi^-$ , 16 GeV/c, dynamical mechanism from cluster anal. (Russian) 0-42499  
 $\psi(3100)$  decay, inclusive  $\gamma$  and  $\pi^0$  momentum spectra, direct  $\gamma$  prod. at large x 0-42466  
 $\tau \rightarrow \nu \mu \pi$  decay parameters from PCAC and current algebra,  $A_1$  characts. 0-37314  
 (Ar,  $\pi^- X$ ), 800 MeV/A,  $\pi^-$  energy and ang. distrib., firebreak and hard scatt. model anal. 0-13498  
 $^{10}\text{B}(\pi,\pi^+)$ , 320-605 MeV, cross sections, pion exchange model anal. 0-27676  
 $^{138}\text{Ba}(\gamma,\pi^- \text{xn})\text{La}$ , 150-300 MeV, pion production cross sections calc. 0-9287  
 $^9\text{Be}(\gamma,\pi^+)$ , 100-800 MeV, cross section, surface prod. model anal. 0-47466  
 $^9\text{Be}(\gamma,\pi^+)$ , threshold to 175 MeV, total cross sections, DWIA anal. 0-13459  
 $^9\text{Be}(\gamma,\pi)$ , photoabsorption and sum rules, structure, RMS radius, polarisability and exchange parameters 0-22686



**pion production continued**

- $^9\text{Be}(\pi^+, \pi^-)$ , 320-605 MeV, cross sections, pion exchange model anal. 0-27676  
 $(C, \pi^-X)$ , 800 MeV/A,  $\pi^-$  energy and ang. distrib., firestreak and hard scatt. model anal. 0-13498  
 $C+p(d, \alpha)^{12}\text{C}$ , 4.2 GeV/N, multiple  $\pi^-$  prod., mean multiplicity (*Russian*) 0-27647  
 $^{12}\text{C}(\pi X)$ , 4.2, 4.5 GeV/N, pion multiplicities and theoretical models, review 0-42657  
 $^{12}\text{C}(\epsilon, \pi)$ , total cross section from square reaction matrix element (*Russian*) 0-32271  
 $^{12}\text{C}(\gamma, \pi^-p)$ , final state interaction, plane and distorted wave momentum distrib. 0-18286  
 $^{12}\text{C}(\gamma, \pi^-)$ , 160-250 MeV, total cross section from elementary Hamiltonian model 0-18292  
 $^{12}\text{C}(\gamma, \pi^-)$ ,  $(\gamma, \pi^-p)$ , knockout  $p$  interaction, optical model and quasifree  $\pi$  photoprod. mechanism (*Russian*) 0-42638  
 $^{12}\text{C}(\gamma, \pi^-)$ , threshold to 360 MeV, total cross sections in  $\Delta$  region 0-13457  
 $^{12}\text{C}(\gamma, \pi^-)$ , total cross section calc. in impulse approx. 0-13458  
 $^{12}\text{C}(\gamma, \pi^-p)$ , 340-380 MeV, quasi-free photoprod., impulse and shell model anal. (*Russian*) 0-5124  
 $^{12}\text{C}(\gamma, \pi^-)^{12}\text{B}_{gs}$ , 0-4 MeV, pion photoprod. cross section 0-42637  
 $\text{Cl}(\text{Ar}, \pi^+X)$ , 250, 400 MeV/A, pion yield near threshold 0-18344  
 $\text{Cu}^{20}\text{Ne}, \pi^+$ , 800 MeV/N, doubly differential cross sections and ang. distrib. 0-9305  
 $^1\text{H}(n, d)\pi^0$ , 459, 648, 802 MeV, relative diff. cross section and ang. distrib. 0-52671  
 $^1\text{H}(n, \pi^0)^2\text{H}$ , nuclear forces charge symmetry test 0-5071  
 $^1\text{H}(p, \pi^+)^2\text{H}$ , SIS, 578 MeV, pol. beam and target, spin depend. parameters 0-42651  
 $^2\text{H}(\epsilon, \pi)$ , total cross section from square reaction matrix element (*Russian*) 0-32271  
 $^2\text{H}(\gamma, \pi^0)$ , coherent photoprod., binding effects and threshold amplitude calc. 0-32264  
 $^2\text{H}(\gamma, \pi^0)$ , cross section and threshold effects using dynamical  $\gamma N \rightarrow N\pi^0$  model 0-27627  
 $^2\text{H}(\gamma, \pi^+)2n$ , threshold to 22 MeV, bremsstrahlung yield and total cross section 0-9288  
 $^2\text{H}(\gamma, \pi^-)$ , threshold photoprod. cross sections, elementary nucleonic amplitudes 0-22812  
 $^2\text{H}(p, d\pi^+)$ , 800 MeV, pion prod. with spectator neutron, cross section 0-9294  
 $^2\text{H}(p, \pi^+)^3\text{H}$ , 400, 470, 600 MeV, differential cross section using isobar model 0-9291  
 $^3\text{H}(\gamma, \pi^0)^3\text{H}$ , polarisation effects 180 to 700 MeV, impulse approx. calcs. (*Russian*) 0-37368  
 $^3\text{He}(\gamma, \pi^0)$ , cross section and threshold effects using dynamical  $\gamma N \rightarrow N\pi^0$  model 0-27627  
 $^3\text{He}(\gamma, \pi^0)$ , polarisation effects 180 to 700 MeV, impulse approx. calcs. (*Russian*) 0-37368  
 $^3\text{He}(\gamma, \pi^+)$ , He, polarisation effects 180 to 700 MeV, impulse approx. calcs. (*Russian*) 0-37368  
 $^3\text{He}(\gamma, \pi^+)^3\text{H}$ , Fermi motion and off-shell effects, impulse approx. 0-27626  
 $^3\text{He}(\gamma, \pi^-)$ , threshold photoprod. cross sections, elementary nucleonic amplitudes 0-22812  
 $^4\text{He}(\gamma, \pi^0)$ , differential cross section, complex momenta theory for nondiffractive processes (*Russian*) 0-32266  
 $^4\text{He}(\gamma, \pi^0)$ , polarisation effects 180 to 700 MeV, impulse approx. calcs. (*Russian*) 0-37368  
 $^4\text{He}(p, n\pi^+)$ , pion prod. operator non-relativistic approx. 0-27640  
 $\text{K}(\text{Ar}, \pi^+X)$ , 250, 400 MeV/A, pion yield near threshold 0-18344  
 $\text{Li}^{12}(\text{He}, \pi^+)^{12}\text{C}$ , 910 MeV, doubly coherent  $\pi$  prod. 0-13487  
 $\text{Li}(\gamma, \pi^0)^6\text{Li}^*(3.56 \text{ MeV})$ , partial photoproduction reactions, large momentum transfer anal., form factor choice 0-22808  
 $^7\text{Li}(\gamma, \pi^-)$ , threshold to 360 MeV, total cross sections in  $\Delta$  region 0-13457  
 $^7\text{Li}(\gamma, \pi^-)$ , total cross section calc. in impulse approx. 0-13458  
 $^8\text{Li}(\gamma, \pi^-)$ ,  $A=6, 7$  0-22686  
 $^{20}\text{Mg}(p, \pi^+)$ , isobar configuration effects,  $p \rightarrow \Delta^0 \pi$  model, ang. distrib. (*Chinese*) 0-47484  
 $^{14}\text{N}(\gamma, \pi^-)^{14}\text{O}$ , 145-325 MeV, Gamow-Teller suppression and M1 radiative widths 0-52609  
 $\text{Na}^{20}\text{Ne}, \pi^+$ , 800 MeV/N, doubly differential cross sections and ang. distrib. 0-9305  
 $(\text{Ne}, \pi^-X)$ , 800 MeV/A,  $\pi^-$  energy and ang. distrib., firestreak and hard scatt. model anal. 0-13498  
 $^{20}\text{Ne}, \pi^+X$ , 400 MeV/N, pion prod. doubly differential cross sections and ang. distrib. 0-32299  
 $^{58}\text{Ni}(p, \pi^+)$ ,  $A=58, 64, 660$  MeV, pion energy spectra, isotopic effects (*Russian*) 0-42669  
 $^{16}\text{O}(\pi X)$ , 4.2, 4.5 GeV/N, pion multiplicities and theoretical models, review 0-42657  
 $^{16}\text{O}(\epsilon, \pi)$ ,  $T=1$  level form factors, Helm model, pion photoprod. and muon capture appls. 0-52553  
 $^{16}\text{O}(\gamma, \pi^-)$ , differential cross section from elementary Hamiltonian model 0-18292  
 $^{16}\text{O}(\gamma, \pi^+)$ , threshold to 175 MeV, total cross sections, DWIA anal. 0-13459  
 $\text{Pb}^{20}\text{Ne}, \pi^+$ , 800 MeV/N, doubly differential cross sections and ang. distrib. 0-9305  
 $^{208}\text{Pb}(\text{Ar}, \pi^+X)$ , 250, 400 MeV/A, pion yield near threshold 0-18344  
 $\text{pp}$ , 5.7 GeV/c, nonannihilation channels  $\Delta^{++}, \Delta^+, \Delta^0, \Delta^-$  prod. cross sections 0-27515  
 $\text{pp} \rightarrow \pi^+ \pi^-$ , 5.7 GeV/c, two-pion correl., interference effects 0-32116  
 $^{118}\text{Sn}(p, \pi^+)$ ,  $A=112, 124, 660$  MeV, pion energy spectra, isotopic effects (*Russian*) 0-42669  
 $\text{Ta}+p(d, \alpha)^{12}\text{C}$ , 4.2 GeV/N, multiple  $\pi^-$  prod., mean multiplicity (*Russian*) 0-27647  
 $^{181}\text{Ta}+^{12}\text{C}$ , 4.2 GeV/N, identical pion $^-$  interference effect, generation range determ. (*Russian*) 0-42695

**pion-proton inclusive interactions**

- hadronic multiple prod. and average charged multiplicity, strato-gluon mechanism in  $\text{pp}$ ,  $\text{Kp}$ ,  $\pi\text{p}$  (*Chinese*) 0-22586  
phase space critical surface of pions produced in inclusive  $\pi^-p$  interactions (*Russian*) 0-18154  
 $\pi^-p$ , 147 GeV/c, neutral particle prod.,  $\text{K}_S, \Lambda, \bar{\Lambda}, \gamma$ , multiplicity scaling form 0-22645

**pion-proton inclusive interactions continued**

- $\pi^-p$ , 200, 300 GeV, relative  $\pi^+, \text{K}^+, p, \bar{p}$  prod., charge ratios, high  $p_T$  0-47335  
 $\pi^-p$ , 40 GeV/c, multi-pion systems and transverse momenta, differential cross sections (*Russian*) 0-32142  
 $\pi^-p \rightarrow \gamma X$ , large angle real photon prod. at large  $p_T$ , QCD anal. 0-22644  
 $\pi^-p \rightarrow \text{K}_S^0, \Lambda, \bar{\Lambda}$ , prod. in 16 GeV/c interactions 0-37308  
 $\pi^-p \rightarrow pX$ , inclusive backward proton cross sections, calc. program adaptation 0-9185  
 $\pi^-p \rightarrow \pi^0 X$ , large  $p_T$  processes, pion exchange model anal. (*Russian*) 0-27527  
 $\pi^+p$ , 10.5 GeV, inclusive and direct photon prod. 0-5024  
 $\pi^+p$ , 32 GeV/c, elastic scatt. and multiplicities, total and differential cross sections (*Russian*) 0-52548  
 $\pi^+p$ , 32 GeV/c, inclusive strange particle prod.,  $\Sigma^+, \text{K}_S^0, \Lambda$  and  $\bar{\Lambda}$  cross sections 0-52541  
 $\pi^+p \rightarrow \text{K}_S^0 X$ , 147 GeV/c, cross-section, scaling 0-52539  
 $\pi^+p \rightarrow \Lambda X$ , 147 GeV/c, cross-section, scaling 0-52539

**pion-proton interactions**

- see also pion-proton inclusive interactions; pion-proton scattering  
 $\pi^-p \rightarrow \delta^- p, \pi^+ \pi^- \pi^+ \gamma\gamma$  backgrounds produced near the  $\delta^-$  mass region 0-9182  
meson resonances, new, search in  $\mu$  channel in 11.46 GeV/c interactions 0-22641  
quasi-potential reconstruction, scatt. theory inverse problems (*Russian*) 0-5016  
strange axial vector meson non-diffractive prod. in  $\text{Kp}$  and  $\pi\text{p}$  interactions 0-32122  
 $\eta \rightarrow \mu^+ \mu^- \gamma$ , in  $\pi^-p$  interactions at 25 and 33 GeV/c, form factors (*Russian*) 0-4984  
 $\pi\text{p}$ , beauty prod. total cross section from perturbative QCD 0-32080  
 $\pi\text{p} \rightarrow 2\pi^+ \pi^- \pi^0$ , diffractive dissociation at 16 GeV (*Russian*) 0-22639  
 $\pi^-p$ , 25, 33 GeV/c, mass spectrum,  $\eta \rightarrow \mu^+ \mu^- \gamma$ , branching ratio 0-27498  
 $\pi^-p$ , 40 GeV/c, secondary neutron average number, charge exchange coeffs.,  $n$  inelasticity coeffs. (*Russian*) 0-32132  
 $\pi^-p, \chi_1$  P-wave charmonium states, hadronic prod. cross section 0-37292  
 $\pi^-p$  Drell-Yan lepton pair prod. processes,  $\pi$  structure function and scaling phenomena 0-405  
 $\pi^-p \rightarrow \eta' n$ , rare decay modes near production threshold of  $\eta^-$  0-9171  
 $\pi^-p \rightarrow \eta n$ , Reggeon field theory, behaviour of  $A_2$  trajectory 0-22594  
 $\pi^-p \rightarrow \text{K}^0 \Lambda$ , 1375 to 2375 MeV, new results and anal. 0-438  
 $\pi^-p \rightarrow \text{K}^0 \Lambda^0$  up to 2.375 GeV/c, resonance parameters, partial wave anal. 0-32133  
 $\pi^-p \rightarrow \text{K}^0 \phi$ , 1395 to 2375 MeV/c, differential cross-section and polarisation meas. 0-9183  
 $\pi^-p \rightarrow \text{K}^0 \text{K}^0 n$ , S-wave anal., scalar mesons and branching ratios 0-13328  
 $\pi^-p \rightarrow \omega n$ , 15-40 GeV/c, cross sections and density matrix elements (*Russian*) 0-37302  
 $\pi^-p \rightarrow \text{pp} \pi$ , 18 GeV,  $\text{pp}$  resonant state partial wave anal. 0-32134  
 $\pi^-p \rightarrow \phi n$ , quark line rule, violations 0-52530  
 $\pi^-p \rightarrow \pi^+ \pi^- \pi^+ p$ , 63, 94 GeV/c,  $A_2$  meson prod. from partial wave anal. 0-37303  
 $\pi^-p \rightarrow \pi^+ \pi^- \pi^+ p$ , 63, 94 GeV/c,  $A_1$  meson existence from partial wave anal. 0-37304  
 $\pi^-p \rightarrow \pi^+ \pi^- \pi^+ p$ , 63, 94 MeV/c,  $A_3$  meson,  $3\pi$  resonances in  $2^-$  partial waves 0-37305  
 $\pi^-p \rightarrow \pi^+ \pi^- \pi^+ n$ , 203-357 MeV, integrated cross section, chiral symmetry breaking parameter 0-32125  
 $\pi^-p \rightarrow \pi^+ \pi^- \pi^+ n$ , below 1400 MeV, PS11 contrib. threshold K-matrix, chiral symmetry breaking 0-32126  
 $\pi^-p \rightarrow \pi^+ \pi^- \pi^+ n$ , narrow epsilon resonance under rho 0-5021  
 $\pi^-p \rightarrow \pi^+ \pi^- \pi^0 n$ , 200, 240 MeV, total near-threshold cross section, isotopic amplitudes (*Russian*) 0-37296  
 $\pi^-p \rightarrow \pi^0 \pi^0 n$ , 6, 8, 12 GeV,  $\pi^0 \pi^0$  S wave and  $I=0$  amplitude 0-18144  
 $\pi^-p \rightarrow \pi^+ X^-$ , 2.6 GeV/c, d proton screening correction and Glauber parameter 0-9175  
 $\pi^-p \rightarrow \pi^+ \pi^- \pi^+ n$ ,  $\pi\pi$  scatt. partial wave anal. f, g and h mesons 0-5015  
 $\pi^-p \rightarrow \psi n$ , generalised Veneziano models 0-22638  
 $\pi^+p$ , 10 to 16 GeV/c, hypercharge-exchange reactions 0-13335  
 $\pi^+p \rightarrow 3\pi^+ \pi^- n$ , diffractive dissociation at 16 GeV (*Russian*) 0-22639  
 $\pi^+p \rightarrow (\pi^+ \text{pp}) p$ , 50 GeV/c, narrow baryonium states, diffractive prod. cross sections 0-442  
 $\pi^+p \rightarrow \pi^+ \pi^- \pi^+ \Delta^{++}$ , narrow epsilon resonance under rho 0-5021  
 $\pi^+p \rightarrow \text{pp} \pi^+ \pi^+$ , 16 GeV/c, clustering, multidimens. study using Yang variables 0-5020  
 $\pi^+p \rightarrow \text{pp} \pi^+ \pi^+$ , 16 GeV/c, dynamical mechanism from cluster anal. (*Russian*) 0-42499  
 $\Pi^-p \rightarrow \bar{p} d$ ,  $\bar{p}$  prod. obs. near 3.75 GeV/c threshold momentum 0-52533

**pion-proton scattering**

- see also pion-proton interactions  
impact parameter representation (*Russian*) 0-5019  
 $\pi\text{p}$ , quark-diquark elastic scatt., diquark fragments, large transverse momentum baryon production 0-47330  
 $\pi^-p$ , elastic and coherent cross-section at 40 GeV/c using propane bubble chamber 0-27524  
 $\pi^-p$  elastic scatt., 450-560 MeV, polarisation parameter (*Russian*) 0-37295  
 $\pi^-p$  elastic scatt. at 490 and 600 MeV, polarisation parameter meas. (*Russian*) 0-42496  
 $\pi^-p$  elastic scatt. near  $\eta$  threshold, cusp discontinuity, nonspin-flip elastic amplitude 0-22635  
 $\pi^+p$ , 32 GeV/c, elastic scatt. and multiplicities, total and differential cross sections (*Russian*) 0-52548  
 $\pi^+p$  backward elastic scatt., 30-90 GeV/c, cross section  $u$  and momentum depend. 0-18146

**pion scattering** see lepton-hadron scattering; meson-meson scattering; photon-hadron scattering; pion-baryon scattering; pion-nucleus scattering; pion-pion scattering

**pions**

- $\sigma$  model,  $\text{SU}_2 \times \text{SU}_2$ , modified Goldberger-Treiman relation, pseudoscalar form factor 0-27421  
axial vector form factor from current algebra,  $\pi$  PCAC and covariant threshold electroprod. amps. 0-414  
biomedical experiences with  $\pi^-$ , conf., Brugg-Windsch, Switzerland (Dec. 1978) 0-22138  
dimensions, mass, elec. and mag. moments (*French*) 0-13305  
dosimetry, in vivo, using Al activation 0-46060  
EM mass shifts, quark-parton model,  $\text{SU}_3$  quark triplet 0-42459  
EM props., dressed quark model (*Russian*) 0-52508



**pions continued**

- form factor, expt. behaviour, influence of left-hand cut on second Riemann sheet 0-13304
- high  $p_T$  jet pairs, parton-parton scattering and  $\pi$  quark struct. functions 0-47248
- longitudinal struct. function, exclusive and almost exclusive process asymptotic behaviour, renormalisation group 0-42464
- masses in QCD lattice gauge theory 0-4928
- QCD exclusive processes,  $\pi$ ,  $K$ ,  $\rho$  form factors, hadronic wavefunction evolution eqns. 0-18135
- Santilli's model for hadron constituents number, computation simple approach 0-42389
- structure function, comparison between results from ep-epX and Kuti-Weisskopf model (Russian) 0-13291
- structure function and scaling phenomena in Drell-Yan lepton pair prod. processes 0-405
- structure function from nucleon low energy relation 0-52507
- $SU_3$  couplings of scalar mesons to two pseudoscalars,  $S^*$  to  $\pi\pi$  and  $\epsilon$  to  $KK$  0-22580
- Thomas-Fermi type picture of EM struct. 0-9170
- $e^+e^- \rightarrow \pi^+\pi^-$ , near threshold,  $\pi$  form factor (Russian) 0-4996
- $\pi^-$ , absorpt. length in Fe in range  $15 < E < 140$  GeV 0-894
- $\pi^-$ , effect on brain vascular permeability of neonatal rats 0-26275
- $\pi^-$ , effects on mouse embryo pronuclear zygote stage 0-26274
- $\pi^-$ , energy deposition spectra and radiation therapy appl. 0-26363
- $\pi^-$ , long-term effects on female mice rel. to X-rays 0-26273
- $\pi^-$ , pre-clinical studies at TRIUMF 0-26264
- $\pi^-$ , RBE and OER values from Vicia Faba root growth inhibition obs. 0-26271
- $\pi^-$ , suitability for use in radiotherapy, radiobiological obs. 0-26338
- $\pi^-$  and  $\pi^+$ , stopping density distrib. in 1 and 2 dimensions 0-26340
- $\pi^-$  radiation therapy dose calcs., Monte Carlo computer program 0-46061
- $\pi N$  coupling in  $\Delta(1231)$  isobar region, pion index of refraction, self-energy in low density limit 0-42554

**pipe diffusion** see *diffusion in solids***pipeline processing**

- multiple microprocessors for continuous patient monitoring 0-26389

**pitch detection** see *acoustic variables measurement***PIXE** see *ion microprobe analysis***plages** see *Sun***planet Mercury** see *Mercury (planet)***planetary atmospheres**

- absorption line variation across planetary disc with inhomogeneous atm. 0-8569
- angular momentum of seasonally condensing atmospheres, appl. to Mars 0-26735
- diffuse reflection, adding algorithm for Markov chain radiative transfer formalism 0-21902
- dust grains in outer planetary magnetospheres, physical and dynamical processes 0-41745
- energy balance of rot. planet in solar flux 0-26765
- entry probes heat shield ablation, C excited electronic states contrib. to transport props. 0-23326
- exponential turbulence and light bending during occultation 0-17513
- giant planet, convective instability of fluid layers 0-56754
- giant planet atmospheres, IR radiation, review 0-8568
- HF radio occultation meas., phase screen concept 0-56735
- ice evaporation rel. to ice-covered rivers on Mars 0-17526
- Io, SHF radioemission and radiation belts (Russian) 0-36565
- Io interacting with jovian magnetosphere, model 0-36563
- Io Na cloud, distrib. implications 0-46464
- Jupiter, atmosphere coloration due to Si compounds 0-51689
- Jupiter, atmosphere optical parameters latit. vars. from 0.6 to 1.1  $\mu$  spectrophotometry 0-46468
- Jupiter, atmospheric comp. and cloud struct. deduced from absorpt. bands in refl. sunlight 0-56758
- Jupiter, atmospheric comp. rel. to near IR spectral albedo 0-31242
- Jupiter, circulation and thermal regime, survey 0-8584
- Jupiter, comp. and temp. struct. from Voyager 1 IR obs. 0-26790
- Jupiter, cosmic ray ionization 0-17538
- Jupiter, EM noise and radiowave propag. below 100 kHz in atm., equatorial region 0-26782
- Jupiter, high spectral resolution obs. between 30 and 50  $\mu m$  0-46462
- Jupiter, IR radiation absorpt. induced by press., mol. collision between  $CO_2$ ,  $N_2$ ,  $O_2$  (Russian) 0-56600
- Jupiter, mag. tail, traversal by Voyager 2 and Saturn, 1981 prospects 0-12706
- Jupiter, magnetoplasma disc, struct. and props. 0-12704
- Jupiter, magnetosphere, 1.79-2.15 MeV protons residence lifetimes in equatorial region 0-26785
- Jupiter, magnetosphere, energetic electrons ten-hour modulation phase 0-26784
- Jupiter, magnetosphere, low-energy charged particle environment, Voyager 1 first look 0-26797
- Jupiter, magnetosphere corotation lag, inertial limit, theory 0-41660
- Jupiter, magnetospheric effects of Io's wobbling flux tube and surface cond. 0-26783
- Jupiter, mean temp. struct. from far IR spectral obs. 0-17540
- Jupiter,  $NH_3$ , spatial distrib. from optical band strengths and curves of growth 0-46386
- Jupiter,  $PH_3$  absorpt. in 5  $\mu m$  window 0-31243
- Jupiter, quasi-geostrophic model of circulation 0-41761
- Jupiter, radio emission, mag. field, energisation, comparison with pulsars 0-46466
- Jupiter, S Nebula, temp. anisotropy 0-17539
- Jupiter, temporal characts., IR obs., north-south temp. asymm. 0-41760
- Jupiter, upper atmosphere temperature, Voyager 1 meas. 0-17536
- Jupiter, Voyager 1, photographic obs. of atmosphere struct. and motions 0-26788
- Jupiter, Voyager 1 EUV obs. 0-26792
- Jupiter, Voyager 1 results 0-4293
- Jupiter atmosphere, origin of differential rot. 0-46467
- Jupiter atmosphere and ionosphere, Voyager 1 preliminary radio profiles 0-26791
- Jupiter cloud configurations, Pioneer and Voyager obs. interpretation in time-depend. framework 0-26787
- Jupiter cloud morphology, monitoring by 5 micron IR imaging during Voyager 1 encounter 0-26799
- planetary atmospheres continued**
- Jupiter clouds spectropolarimetry, lines equivalent widths information content 0-31215
- Jupiter diffuse aurora, influence of plasma injection from Io 0-4289
- Jupiter inner magnetosphere,  $O^+$  forbidden emission detect. 0-51687
- Jupiter magnetosphere, electron pitch-angle diffusion by whistler mode waves near Io plasma torus 0-4290
- Jupiter magnetosphere, plasma and mag. field perturbations due to Galilean satellites perturbations 0-46465
- Jupiter magnetosphere, S plasma discontinuities 0-4291
- Jupiter magnetosphere, theory of Io-modulated decametric radio S-bursts (Russian) 0-8582
- Jupiter magnetosphere, Voyager 1 obs. of energetic ions and electrons 0-26798
- Jupiter magnetosphere, Voyager 1 planetary radio astronomy obs. 0-26796
- Jupiter magnetosphere, Voyager 1 plasma wave obs. 0-26795
- Jupiter magnetosphere, Voyager 1 studies preliminary results 0-26793
- Jupiter magnetosphere plasma observations, Voyager 1 initial results 0-26794
- Jupiter magnetosphere-satellite interactions, aspects of energetic charged particle loss 0-36566
- Jupiter spectrum, obs. from 1500 to 2000  $\text{\AA}$  with IUE 0-56752
- Jupiter stratosphere, acetylene photopolymers aerosol 0-31244
- Jupiter upper atmosphere, photochemical models 0-36567
- Jupiter zonal flow, baroclinic instabilities 0-31245
- magnetosphere boundary layer phenomena 0-36776
- magnetospheres, props. of dust in plasma environment 0-26930
- magnetospheres and radio emissions, conf. Snowmass, Colorado, USA (Aug. 1978) 0-41939
- Mars, atmosphere density long-term vars. rel. to watery past 0-17527
- Mars, atmosphere opacity, 1977 obs. from Viking 0-41753
- Mars, chemical composition deduced from twilight glow obs. 0-56739
- Mars, crater ejecta emplacement, atmos. effects 0-56747
- Mars, cusp of magnetosphere, to explain Mars 5 mag. and plasma obs. 0-51685
- Mars, lower atmosphere modelling, multilayer radiative transfer 0-46451
- Mars, magnetosphere, effect of Deimos 0-41752
- Mars, N atom loss rate, calc. 0-46452
- Mars, palaeoclimate and enhanced atmospheric  $CO_2$  0-46450
- Mars, photoelectrons caused by solar photons of less than 80  $\text{\AA}$  0-56744
- Mars, released volatiles 0-17524
- Mars, soil transport by winds 0-31228
- Mars, south polar region eolian features rel. to polar vortex, seasonal var. 0-31227
- Mars, thermal radiative transfer, numerical modelling 0-8574
- Mars, travelling thermal wave effect on circulation 0-8388
- Mars, upper atmosphere absorption of solar UV, interaction model 0-56746
- Mars, wind blown deposits, silt-clay electrostatic aggregates 0-21940
- Mars, windblown particle abrasion, erosion of quartz and basaltic sand 0-17525
- mass spectrometry, for atmos. composition 0-8518
- Mercury, magnetosphere model 0-36531
- Mercury magnetosphere and mag. field, Mariner 10 obs. and theory 0-36530
- mixed fluid, nonlinear internal wave formation from gravitational collapse 0-33619
- Neptune, mixing ratios of methane, ethane and acetylene in stratosphere 0-51692
- Neptune, props. from IR spectrum from 0.8 to 2.5 microns 0-21946
- origin, Pioneer Venus gas comp. meas. implications 0-51678
- origin, theory based on protoplanetary cloud history 0-12549
- Pluto, surface and atmosphere from 1.4-1.9  $\mu m$  spectrum 0-46480
- radiative transfer albedo problem in inhomogeneous isotropically scatt. atmospheres 0-36398
- radiative transfer in atmosphere of finite optical thickness, standard problem 0-51646
- radiative transfer in spherical shell atmospheres, appl. to Venus, line form. level 0-17487
- radiowaves refraction attenuation 0-4280
- remote sounding, new inversion method 0-12677
- Saturn, at. H cloud formed by photo sputtering of ring ice 0-46475
- Saturn, atmospheric comp. rel. to near IR spectral albedo 0-31242
- Saturn, ionosphere, chem. and phys. props., model calcs. 0-26801
- Saturn, magnetopause influenced by Jupiter's mag. tail 0-12706
- Saturn, Pioneer 11 investig. 0-46476
- Saturn, seasonal phenomena from  $P_3$  methane band obs. 0-26803
- Saturn atmosphere, origin of differential rot. 0-46467
- scattering cross section of radiowaves reflected from planet with spherically symmetrical atmosphere 0-21935
- space probe or meteorite reentry, mass loss and shape change with radiative heating 0-31198
- thermal escape of molecules, non-Maxwellian effects 0-46419
- Titan, 16-30  $\mu m$  spectroscopy 0-56760
- Titan, optical props. and vertical distrib. of aerosols in atmosphere 0-46471
- Uranus, props. from IR spectrum from 0.8 to 2.5 microns 0-21946
- Uranus clouds, particle comp. 0-31253
- Uranus upper atmosphere, mean temp. and temp. vars. 0-46477
- Uranus upper atmosphere, struct. from SAO 158687 occultation obs. 0-17547
- Venus, acoustic-gravity waves in thermosphere 0-17520
- Venus, atmospheric tidal torque rel. to rot. dynamic evolution since form. 0-56742
- Venus, bow shock observations, 4th Dec. 1978 0-41747
- Venus, chemical composition deduced from twilight glow obs. 0-56739
- Venus, cloud microstructure 0-46431
- Venus, cloud optical properties and atmos. layered struct. 0-51681
- Venus, cloud structure, high-contrast UV detail 0-51682
- Venus, composition and structure, Pioneer results 0-46230
- Venus, cyclic and diurnal vars. in thermosphere and exosphere 0-51683
- Venus, dayside ion densities 0-46444
- Venus, electron obs. and ion flows, Pioneer orbiter plasma analyzer expt. 0-46448
- Venus, hothouse theory of recent cosmological catastrophe 0-41749
- Venus, implications of  $^{36}Ar$  excess 0-12700
- Venus, ionosphere,  $CO_2$  and  $CO$  electron vibr. cooling rates 0-41750
- Venus, ionosphere, ion comp., photochemical and thermal diffusion control 0-46445
- Venus, ionosphere, thermal structure and energy influx 0-46443



## planetary atmospheres continued

- Venus, ionospheric diurnal ion comp. vars., Pioneer orbital meas. 0-46440  
 Venus, IR radiation absorpt. induced by press., mol. collision between  $\text{CO}_2$ ,  $\text{N}_2$ ,  $\text{O}_2$  (*Russian*) 0-56600  
 Venus, lightning discharges, frequency of occurrence 0-56743  
 Venus, magnetic field and magnetosphere 0-56737  
 Venus, magnetosphere, solar wind interaction 0-41687  
 Venus, model from radio, radar and occultation obs. 0-46420  
 Venus, net radiation meas. by Pioneer small probe 0-46435  
 Venus, nightside ionosphere, electron temp. and density models 0-46442  
 Venus, nightside ionosphere, formation process, ionization, mixing ratios 0-41751  
 Venus, nightside ionosphere, Pioneer orbiter radio occultations 0-46441  
 Venus, NO production by lightning in clouds, odd N chem. reactions 0-26768  
 Venus,  $\text{O}_2(^1\Delta)$  airglow and nightglow emission 0-17515  
 Venus, photoelectrons caused by solar photons of less than 80 Å 0-56744  
 Venus, Pioneer gas chromatograph analyses, laboratory simulation 0-46362  
 Venus, Pioneer meas. of physical props. up to 200 km altitude (*French*) 0-46421  
 Venus, Pioneer nephelometer expts. results 0-46430  
 Venus, Pioneer Venus results, surface and atmosphere 0-17523  
 Venus, radar obs. of atmos., soil and relief 0-36537  
 Venus, radiative transfer, line form. level 0-17487  
 Venus, retrograde zonal winds below clouds 0-46436  
 Venus, role of gaseous  $\text{S}_2$ ,  $\text{S}_3$ ,  $\text{S}_4$  and  $\text{H}_2\text{S}$  0-17518  
 Venus, rotation of upper atmosphere (*French*) 0-36534  
 Venus, scattered solar radiation, day sky spectrum, Venera meas. 0-56573  
 Venus, scattering coeff. from Venera 9 and 10 photometry 0-8572  
 Venus, spin evolution 0-46423  
 Venus, stratospheric large-scale turbulence, model 0-12699  
 Venus, struct. and comp. from refl. sunlight polarisation calc. and obs. 0-36533  
 Venus, sulphur chemical cycles, involving S, sulphite, sulphide and sulphate 0-50837  
 Venus, sunlight absorption 0-46434  
 Venus, temp., cloud structure and dynamics from IR remote sensing 0-46429  
 Venus, thermal contrast from Pioneer probe data 0-46229  
 Venus, thermal radiative transfer, numerical modelling 0-8574  
 Venus, thermal radiometry by Venera 9 and 10 of cloud tops 0-46424  
 Venus, thermosphere during daytime, nitrogen chemistry 0-17517  
 Venus, tidal theory and torque balance 0-46422  
 Venus, turbulence from Pioneer multiprobe radio scintillations 0-46437  
 Venus, ultraviolet photometry and cloud struct., Venera obs. 0-56738  
 Venus, upper atm. temp. and dynamics from Pioneer Orbiter IR radiometer meas. 0-26766  
 Venus, upper atmosphere neutral gas comp., diurnal vars. 0-46427  
 Venus, UV cloud images from pioneer orbiter 0-46432  
 Venus, UV markings, Venera 9 cloud top data analysis 0-17521  
 Venus, UV nightglow and thermospheric circulation 0-46428  
 Venus, whistler mode wave absorption in ionosphere 0-46446  
 Venus atmospheric precipitation, props. and possibilities of detect. 0-56741  
 Venus bow shock, depend. on solar wind strength 0-41748  
 Venus bow shock, Pioneer magnetometer obs. 0-36535  
 Venus cloud cover, obs. by Venera 9 orbiter 0-51680  
 Venus clouds, UV absorbers, Pioneer data 0-46433  
 Venus clouds spectropolarimetry, lines equivalent widths information content 0-31215  
 Venus daytime ionosphere, two-freq. radio transillumination data using Venera-9, 10 probes 0-21936  
 Venus exosphere, hot hydrogen origin 0-36536  
 Venus radiative transfer of solar radiation, model based on Venera 10 data (*Russian*) 0-12698  
 Venus thermosphere, Ar isotope abundances upper limits 0-4281  
 HD 4-0 and 5-0 bands, absorption strengths in outer planet atmospheres 0-43059

## planetary nebulae

- 8 to 13 micron spectrophotometry, of six planetary nebulae 0-22057  
 Abell 30, Abell 78, unusual central struct. obs. 0-51855  
 central stars, UV spectral obs. from TD-1 satellite 0-31300  
 central stars of planetary nebulae, kinematics 0-51762  
 detection rates in globular clusters 0-26950  
 dust model for IR emission 0-56900  
 ESO/Uppsala survey of ESO (B) Atlas of S. sky, pt. VII 0-56722  
 formation, role of Mira-type pulsation 0-26928  
 G339.2-0.4, supernova remnant or planetary nebula, radio and optical obs. 0-22104  
 galactic centre field, planetary nebulae and Wolf-Rayet stars identifications 0-8674  
 galactic centre planetary nebulae, radio search, implications of flux density distrib. 0-56913  
 IC 3568, struct. and internal extinction 0-31338  
 IC 418, IR spectra, heated dust emission, atomic emission lines 0-46629  
 IC 418, near-IR spectroscopic obs. 0-4421  
 IC 418, search for absorpt. in CO fourth positive system 0-46647  
 kinematics, radial vel. meas. in galactic anticentre direction 0-46633  
 kinematics of galactic objects 0-26948  
 low excitation planetary nebulae of small ang. size, spectral studies 0-17646  
 M2-9, compact planetary nebula, search for 1612 MHz OH maser 0-12774  
 NGC 1360, central star radial vel. obs. 0-4350  
 NGC 4361, unusual high excitation nebula, theoretical model, chem. comp. 0-22060  
 NGC 650/0-17639  
 NGC 6527, 7027, [O III] 88.35 microns and [O I] 63.2 microns fine struct. lines search 0-12794  
 NGC 6572, IR spectra, heated dust emission, atomic emission lines 0-46629  
 in NGC 6822, irregular galaxy, planetary nebula spectrophotometry and comp. 0-41867  
 NGC 7027, charge transfer reaction rate rel. to forbidden Ne II 12.8  $\mu$  emission 0-56701  
 NGC 7027, dust model for IR emission 0-56900  
 NGC 7027, effect of dust on [O II] emission 0-8667

## planetary nebulae continued

- NGC 7027, Mg abundance gradient 0-41875  
 NGC 7027, struct. from electronographic obs. 0-12789  
 photoionisation models for gaseous nebulae with optically thin condensations 0-36693  
 physical parameters, from absolute flux densities for emission lines in 6000-11000 Å range 0-51857  
 runaway planetary nebula ejection from M32 0-46626  
 HM Sagittae, variable emission object, spectrophotometry 0-17599  
 stellar planetary nebulae, southern, with emission lines, observational data 0-41843  
 stellar planetary nebulae, VLA obs. 0-22056  
 Webb Society handbook 0-8743
- planetary rings** see *planetary satellites*
- planetary satellite atmospheres** see *extraterrestrial atmospheres; planetary satellites*
- planetary satellites**  
 see also *Moon*  
 1980 S 2, new Saturnian satellite, discovery and possible orbital periods 0-46473  
 asteroid satellites, discovery from occultations of stars 0-4286  
 axisymmetric, periodic motion rel. to centre of mass in evolutionary circular orbit 0-21899  
 Callisto, evolution and surface age 0-56755  
 Callisto, surface affected by internal processes 0-21944  
 65 Cybele, occultation of AGK3+19°599, discovery of 1979 (65) 1 possible satellite 0-31237  
 Deimos, effect on magnetosphere of Mars 0-41752  
 Deimos, spectral evidence for carbonaceous chondrite surface comp. 0-41754  
 Deimos, surface features map and props. 0-31224  
 Enceladus, near IR spectra and JHK photometry 0-56761  
 Europa, liquid water layer beneath ice crust, model 0-26780  
 formation of regular satellite systems and major planet rings 0-41746  
 Galilean satellites, Amalthea, Voyager 1 results 0-4293  
 Galilean satellites, orbits from numerical integration (*French*) 0-26779  
 Galilean satellites, positions obtained in 1978 at ESO-La Silla (*French*) 0-21943  
 Galilean satellites magnetospheres, plasma and mag. field perturbations 0-46465  
 Galilean satellites volcanism and rotation, influence of Jupiter mag. field 0-31247  
 Ganymede, evolution and surface age 0-56755  
 Ganymede, stellar occultation obs. by Voyager 1 rel. to exospheric atmosphere 0-26792  
 Ganymede, surface affected by internal processes 0-21944  
 gravitational heating of interior during form. process 0-36529  
 Hyperion, near IR spectra and JHK photometry 0-56761  
 Iapetus, near IR reflectivity of dark and light faces 0-26800  
 icy satellites, mass-radius relationships 0-31222  
 Io, 5 micron variability 0-46463  
 Io, contrib. to Jupiter low-energy charged particle environment, Voyager 1 first look 0-26797  
 Io, contrib. to Jupiter magnetosphere energetic ions and electrons, Voyager 1 obs. 0-26798  
 Io, currently active volcanism discovery 0-26789  
 Io, evidence of  $\text{SO}_2$  from UV obs. 0-36561  
 Io, flux tube wobbling and surface cond. effects on Jupiter's decametric emission and magnetosphere 0-26783  
 Io, interaction with Jupiter mag. field, Voyager 1 preliminary results 0-26793  
 Io, IR refl. spectra, 2.8-5.2  $\mu\text{m}$  0-56756  
 Io, melting by tidal dissipation 0-4292  
 Io, plasma injection influence on diffuse Jovian aurora 0-4289  
 Io, plasma sheath electrons rel. to Jupiter modulated decametric radio S-bursts (*Russian*) 0-8582  
 Io, SHF radioemission and radiation belts (*Russian*) 0-36565  
 Io, sulphur chemical cycles, involving S, sulphite, sulphide and sulphate 0-50837  
 Io, surface and environs, magmatic-volatile model 0-17537  
 Io, volcanism, sulphur as volatile material 0-51688  
 Io and Jovian radio S-bursts source of 2.5-35 MHz radiation 0-36562  
 Io interacting with jovian magnetosphere, model 0-36563  
 Io Na cloud, distrib. implications 0-46464  
 Io Na cloud, solar radiation press. as cause of east-west asymmetries 0-36560  
 Io plasma torus, electrons pitch-angle diffusion by whistler mode waves 0-4290  
 Io plasma torus, Voyager 1 EUV spectrum obs. 0-26792  
 Io plasma torus, Voyager 1 plasma waves obs. 0-26795  
 Io plasma torus, Voyager 1 radio astronomy obs. 0-26796  
 Jupiter, Galilean from Voyager spacecraft 0-56759  
 Jupiter, Galilean satellites, 1975-6 astrometric obs. 0-4288  
 Jupiter, narrow rings, origin and location 0-56764  
 Jupiter, orbital and solar resonance of inner three Galilean satellites 0-56753  
 Jupiter, ring system, Voyager 2 obs. 0-12707  
 Jupiter, surface meteoroid bombardment effects on satellite light curves 0-26786  
 Jupiter, Voyager 1 photographic obs. of ring, Amalthea and Galilean satellites 0-26788  
 Jupiter, Voyager 1 encounter, general description of planet and satellites environment 0-12642  
 Jupiter, Voyagers 1 and 2, general results 0-17542  
 Jupiter faint satellites, astrometric obs. during 1976 to 1977 opposition 0-26778  
 Jupiter magnetosphere-satellite interactions, aspects of energetic charged particle loss 0-36566  
 Jupiter major satellites, thermal structs. from Voyager 1 IR obs. 0-26790  
 magnetic moments, two predictions from scaling law test 0-21934  
 18 Melpomene, occultation of SAO 114159, secondary extinction event obs. rel. to 1978 (18) 1, possible satellite 0-56749  
 Mimas and Tethys, orbital theory including perturb. 0-36568  
 minor planet satellite observations, reliability 0-46460  
 Nereid (Neptune II), ephemeris (1980 March 2 to September 8) 0-46481  
 Oberon, near IR spectra and JHK photometry, mass and dia. measurement 0-56761  
 Phobos, surface features map and props. 0-31224  
 Phobos, Viking 1 Orbiter, encounter, trajectory analysis 0-12641



**planetary satellites continued**

- Phobos and Deimos orbital evolution 0-26770
- Phobos surface grooves, hybrid origin 0-31229
- Phoebe, near IR spectra and JHK photometry 0-56761
- Pluto, Charon, account of discovery 0-12708
- Pluto, satellite obs. (*Czech*) 0-31252
- Pluto-Charon, tidal evolution 0-26806
- Saturn, 1979 S 3, discovery of possible satellite 0-26802
- Saturn, F-ring and new satellite, Pioneer II discoveries 0-8585
- Saturn, narrow rings, origin and location 0-56764
- Saturn, outer ring and five possible new satellites discovery 0-46472
- Saturn, outer ring search, 1979 November obs. 0-17543
- Saturn, rings, four colour phase curves, analysis 0-4295
- Saturn, rings, International Planetary Patrol obs. and data reduction 0-4294
- Saturn, satellite surfaces and interiors, review 0-4297
- Saturn, satellites and exterior ring obs. (1980 Feb.-March) 0-51690
- Saturn, surface meteoroid bombardment effects on satellite light curves 0-26786
- Saturn's rings, thickness caused by satellite and solar perturb. and planetary precession 0-36569
- Saturn B-ring, optical reflectance polarimetry interpretation 0-31248
- Saturn innermost satellites, separations and times of elongation, (1980 February 29 to March 18) 0-56762
- Saturn ring E, inferences from obs. of radiation belt particles 0-41762
- Saturn rings, 3 mm obs. and props. 0-46470
- Saturn rings, ice photo-sputtered to form at. H cloud 0-46475
- Saturn rings, IR brightness and eclipse cooling obs. 0-56763
- Saturn rings, Pioneer 11 investig. 0-46476
- Saturn rings, vertical struct. and thickness 0-4296
- thermal evolution of small planetary bodies, convection modes 0-26764
- three-body problem, doubly-averaged elliptical restricted, trajectories 0-46376
- Titan, 16-30  $\mu\text{m}$  spectroscopy 0-56760
- Titan, IR spectrum from 0.8 to 2.5 microns 0-21946
- Titan, optical props. and vertical distrib. of aerosols in atmosphere 0-46471
- Titan, suspected near IR variability 0-46469
- Titan (Saturn VI) eclipse, 1979 December 20, photometric obs. 0-31250
- Titan atmosphere, photochemical aerosols identification 0-31249
- Titan atmosphere, photochemical models 0-36567
- Titania, near IR spectra and JHK photometry, mass and dia. measurement 0-56761
- Triton, diameter and reflectance, spectral and radiometric obs. 0-17546
- Triton, satellite with atmosphere, IR spectrum obs. 0-21945
- true circular orbit 0-46368
- Umbriel, near IR spectra and JHK photometry, mass and dia. re-assessment 0-56761
- Uranus, narrow rings, origin and location 0-56764
- Uranus e ring, precession 0-26804
- Uranus rings, as volatile material in satellite orbits, model 0-26807
- Venus, dust ring possibility from Venera 9 and 10 spectroscopy 0-8573

**planetoids see asteroids****planets**

- see also asteroids; comets; Earth; Jupiter; Mars; Mercury (planet); Neptune; planetary satellites; Pluto; Saturn; Uranus; Venus*
- accretion rates, implications of  $^{36}\text{Ar}$  excess on Venus 0-12700
- accumulation model, numerical expts. results (*Russian*) 0-8557
- AGU conference, June 1979, Washington, DC, USA 0-8732
- American Astron. Soc., Division for Planetary Sciences, 11th-Annual meeting (Clayton, Missouri, 23-26 October 1979) 0-36760
- angular momentum and magnetic moment from superheavy hadrons 0-26843
- asteroids and planets X, conference (Tucson, March 1979) 0-31406
- core cooling by subsolidus mantle convection 0-36278
- dynamism in interior driven by gravitational settling 0-36246
- electrically-conducting fluid, mag. flux linkage, planetary dynamo theory 0-8536
- electrically-conducting fluid, mag. flux linkage, relativistic case, planetary dynamo theory 0-12655
- energy balance of rot. planet with atmosphere in solar flux 0-26765
- ephemerides, effect of star catalogue coord. system orientation errors (*Russian*) 0-51640
- equatorial parameters determ., theory 0-4282
- eucrite parent asteroid, bulk composition, planetary evolution bearing 0-56786
- extrasolar planets, astrometric photoelectric detection equipment 0-56882
- extrasolar systems, search strategies 0-46615
- formation, implications of origin of large interstellar grains towards  $\rho$  Ophiuchi 0-41870
- formation as adiabatic phase transition, isentropic model 0-26763
- formation from solar nebulae, mass transprt processes in rotating dust cloud 0-8556
- four-body problem, restricted planetary case 0-41742
- giant gaseous protoplanets, interaction with primitive solar nebula 0-56727
- giant planet evolution, theory 0-56734
- giant planets, representation of perturbations due to Pluto (*French*) 0-26724
- gravitational heating of interior during form. process 0-36529
- gravitational spectra, determ. from planetary orbiters tracking 0-41744
- gravitational spectra from direct measurements 0-30978
- interstellar planetesimals, capture by solar system rel. to terrestrial catatrophism 0-31043
- lithosphere global TRM in presence of central dipole field, theory 0-31223
- lunar and planetary science, ninth conference, Houston, Texas, (1978 March 13 to 17) 0-17711
- magnetic field, hydromagnetic phenomena described by elec. currents 0-36495
- magnetic field as probe of interior structure 0-36528
- magnetic field origin, conf., Nov. 1978, Texas USA 0-36234
- magnetic fields, cosmological interpretation 0-46714
- magnetic moments, two predictions from scaling law test 0-21934
- mass-radius relations for cold spherical body, relativistic effects 0-26730
- motion reproduced by planetary gear mechanisms 0-4258
- orbit determ. by Lambert 0-42024
- origin of planetary systems, model comparisons 0-17508
- osculating elements reduction to proper elements for entire solar system 0-21897

**planets continued**

- periodic systems dynamical coupling, particular case of homographic soln. 0-36480
- perturbations of Quadrantid meteor stream, rel. to long-term orbital evolution 0-17551
- protoplanetary disc nebula disruption by T Tauri-like solar wind 0-36516
- radio source mapping using VLBI (*Japanese*) 0-21927
- radiowaves reflected from planet with spherically symmetrical atmosphere 0-21935
- reflectance meas. in thermal emission region, thermal component removal 0-17497
- relativistic celestial mechanics, astron. meas. and coord. systems 0-36481
- rotation, ang. moments mass depend. rel. to self-similarity 0-36490
- spin angular momentum distrib. explanation 0-41741
- stars cold satellites searching via speckle interferometry, coherent optical system appl. (*Russian*) 0-12672
- stars possessing Earthlike planets, prevalence in Universe 0-41735
- surface scattering of bistatic radar signals 0-41743
- survival following supernovae in planetary systems 0-56860
- terrestrial planets, core formation 0-17514
- thermal evolution of small planetary bodies, convection modes 0-26764
- Titius-Bode law, Piagetian learning cycle for astronomy study unit 0-51985
- turbulent thermal convection in presence of rot. and mag. field, stellar and planetary dynamos appl. 0-6042
- $^{15}\text{N}/^{14}\text{N}$  ratio rel. to solar nebula differentiation 0-36519

**planimeters see area measurement****planning**

- see also town and country planning*
- acoustic planning of plants, technical and economic advantages 0-3561
- computed tomography, USA government regulation of use 0-17104
- computerised tomography planning issues (in 1975 and 1976) 0-17103
- electron beam dosimetry for treatment planning 0-3817
- energy, in Arab world, with aid of computer 0-26122
- energy demand and conservation in USA, National Energy Plan impact 0-26121
- European computer network, engineering design computer packages, teaching 0-31465
- neutron radiotherapy planning and radiation quality definition 0-12246
- optical system tolerancing plan activities and documents 0-48382
- sea use plan concepts and criteria 0-46203
- space research, computerised planning in ESA 0-4223
- space research, forward-looking financial planning in ESA 0-4221
- space research, investment planning in ESA 0-4222

**plants (industrial) see industrial plants****plants (power) see power plants****plasma**

- see also electromagnetic wave propagation in plasma; plasma-beam interactions; plasma impurities; plasmons; relativistic plasmas; solid-state plasma*
- antenna in magnetoplasma, radiation patterns 0-43933
- astronomical plasmas, dielectronic recombination review 0-46391
- astrophysical, super-Alfvénic particle streaming 0-31206
- astrophysical compressible plasma, current sheet self-similar resistive decay 0-1755
- astrophysical plasmas, charge transfer rel. to Si lines appl. as spectral diagnostics 0-41717
- astrophysical self-gravitating plasma with finite ion gyroviscosity effects rotating layer instability 0-56706
- at mag. equator, rel. to vertical E×B plasma drift vel. 0-36435
- atmosphere, phenomena induced by charged particle beams obs. 0-17443
- atomic level population of plasma, Jeffries' level population ratios and Seaton's cascade matrix 0-52934
- auroral plasma, electrostatic V-shocks approximate equipotentials 0-21870
- circumterrestrial plasma faraday inverse effect (*Russian*) 0-4190
- collisionless magnetized cosmic plasmas, non-resistive electric potential drops 0-31204
- Comet Morehouse (1908 III) tail, helical waves theory 0-4305
- comet tails, hydromagnetic models 0-56773
- cometary plasma acceleration, role of mag. structs. 0-46486
- conference, trends in physics, York, England (Sep. 1978) 0-31416
- conference on ionised gas physics, Dubrovnik, Yugoslavia (Aug.-Sept. 1978) 0-36779
- conference on phenomena in ionised gases, Grenoble, France (July 1979) 0-36767
- cosmic plasma environments, immersed dust props. 0-26930
- near-Earth plasma, 0 to 100 keV, quantitative models review 0-36459
- electrons, from heated oxide cathode, multiphoton laser absorption 0-6224
- energy build-up and release in astrophysical plasmas 0-46395
- Galilean satellites magnetospheres, plasma and mag. field perturbations 0-46465
- geophysical compressible plasma, current sheet self-similar resistive decay 0-1755
- geophysical self-gravitating plasma with finite ion gyroviscosity effects rotating layer instability 0-56706
- gravitating magnetised plasma, nonlinear Poynting flux 0-26736
- high  $\beta$  plasmas, hydromagnetic waves propag. and damping 0-17482
- impurity ions on rational magnetic surfaces, convection and diffusion, collisional multifluid model 0-28615
- intercluster intergalactic medium, theory for expanding cosmologies 0-4426
- intergalactic plasma, rel. to diffuse X-ray background spectrum from 3 to 50 keV 0-41916
- interplanetary medium, solar type III radio bursts nonlinear stability 0-26826
- interplanetary plasma inhomogeneities, anisotropy (*Russian*) 0-36468
- interplanetary plasma turbulence spectrum, determ. from radio sources scintillation spectra 0-46361
- interplanetary shock waves in turbulent medium, energetic particles interaction 0-4210
- ionosphere, artificial excitation of plasma inhomogeneities 0-36450
- ionosphere, drifting plasmon simulation, electrostatic waves 0-53965
- ionosphere, equatorial, plasma density bubbles obs. by (ESRO-4) 0-4194
- ionosphere, ion cyclotron waves critical-level behaviour 0-6238
- ionosphere, lower hybrid drift instability 0-46343
- ionosphere, plasma motion in depleted regions at equator 0-12605
- ionosphere, rapid subauroral ion drifts obs. by Atmosphere Explorer C 0-4188



## plasma continued

- ionosphere, subsonic wave-ionised plasma interaction, electron density study 0-4183  
 ionosphere, thermal parametric instability at freqs. close to electron gyrofreq. 0-46344  
 ionosphere/magnetosphere, coherent anomalous resist. in region of electrostatic shocks 0-4189  
 Jupiter, magnetosphere, low-energy charged particle environment, Voyager 1 first look 0-26797  
 Jupiter inner magnetosphere, O<sup>+</sup> forbidden emission detect. 0-51687  
 Jupiter ionosphere, peak electron concs. from Voyager 1 preliminary radio profiles 0-26791  
 Jupiter magnetosphere, electron pitch-angle diffusion by whistler mode waves near Io plasma torus 0-4290  
 Jupiter magnetosphere, influence of Io plasma injection on Jovian diffuse aurora 0-4289  
 Jupiter magnetosphere, S plasma discontinuities 0-4291  
 Jupiter magnetosphere, theory of Io-modulated decametric radio S-bursts (Russian) 0-8582  
 Jupiter magnetosphere, Voyager 1 planetary radio astronomy obs. 0-26796  
 Jupiter magnetosphere plasma observations, Voyager 1 initial results 0-26794  
 near-Jupiter plasma, Voyager 1 plasma wave obs. 0-26795  
 laboratory and space plasmas, conference, Nagoya, Japan (1977 December 8 to 9) 0-4470  
 magnetopause, plasma acceleration evidence for reconnection 0-26701  
 magnetosphere, Alfvén waves excitation by bouncing electron beams rel. to nightside mag. pulsations 0-4203  
 magnetosphere, current instability on short wave drift oscils., nonlinear theory (Russian) 0-53981  
 magnetosphere, double layers and electrostatic shocks review 0-36460  
 magnetosphere, plasma parameters along satellite trajectories 0-8490  
 magnetosphere, toroidal line resons. rel. to continuous (Pc 3,4) pulsations in European sector 0-21877  
 near-Earth plasma, elec. fields penetration along geomag. force lines, electrostatic approach applicability 0-4178  
 neutron star interior plasma, mag. field rel. to pulsar periods long-term changes 0-22029  
 neutron star magnetosphere, plasma dynamics and accretion, fate of sinking filaments 0-51798  
 nonlinear optimisation algorithms 0-18623  
 NP 0532 magnetosphere, cyclotron instability rel. to origin of radiation (Russian) 0-8645  
 particle acceleration in collisionless shocks, astrophysical systems 0-31208  
 particles of disperse material, and plasma fluxes, heat exchange calcs. (Russian) 0-23997  
 pinch, thin skin type, anisotropic conducting wall effect on instabilities 0-28800  
 plasmopause, spontaneous polarization of a turbulent magnetized plasma 0-19580  
 pulsar magnetosphere, magnetoactive plasma equilb. in gravit. field (Russian) 0-26895  
 pulsar magnetospheres, narrowband versus broadband emission processes rel. to luminosities 0-51797  
 pulsar magnetospheres, propag. effects in shearing field-free plasma rel. to microstruct. 0-17483  
 pulsar magnetospheres, stellar-wind model for plasma-EM fields 0-22031  
 quasars, theory of H line emission from dense plasmas 0-51900  
 radiation opacity in dense plasma 0-26731  
 radio sources, double, extragalactic, plasmons ejection models rel. to source separation depend. on redshift 0-22096  
 radio sources, extended, extragalactic, MHD instabilities and electron accel. 0-27000  
 radio sources, physical conditions in compact heads 0-51892  
 solar atmosphere, electrostatic ion-cyclotron heating 0-51708  
 solar atmosphere, mag. flux ropes equilb. and stability (Russian) 0-8617  
 solar atmosphere, type III radio bursts fundamental emission 0-36603  
 solar corona, fast electrons stream free dispersal with nonsteady injection 0-17568  
 solar corona, hydromagnetic surface waves dissipation 0-21904  
 solar corona magnetic traps, plasma instability periodical regimes (Russian) 0-8616  
 solar corona quasi-static loops, numerical modelling with uniform energy input 0-21958  
 solar coronal loops, thermal instabilities in magnetically confined plasmas 0-36600  
 solar flares, compressible mag. field reconnection theory 0-6226  
 solar flares, electron beam diagnostic 0-26827  
 solar flares, Fe XXIV-XXV X-ray lines wavelengths rel. to hot plasma motions 0-21973  
 solar flares, Fe XXV dielectronic satellite line spectra as measure of non-thermal electron energy distribns. 0-21911  
 solar flares, plasma column merging, simulation expt. (Japanese) 0-31269  
 solar flares, plasma equilb. conditions from high-resolution X-ray spectra 0-26837  
 solar flares, protons stochastic accel. 0-21953  
 solar flares collective plasma effects assoc. with particle streams continuous injection model 0-21954  
 solar flares nonthermal electron beams, reverse currents effects on dynamics and X-ray bremsstrahlung 0-51711  
 solar plasmas density determination, N III and O IV intersystem multiplets appl. 0-31264  
 solar type III radio burst sources, plasma wave clumping origin 0-21959  
 solar wind, current sheets resistive instabilities 0-4218  
 solar wind, MHD solitons theory 0-4217  
 solar wind, obs. of flows associated with hot heavy ions 0-51635  
 solar X-ray flares, Skylab obs. rel. to physical parameter profiles 0-17561  
 space plasma, mass discrimination effects in mass spectrometers ion and neutral extraction 0-4230  
 space plasma, non-ducted whistler-mode signal parametric decay 0-6239  
 spin-flip and normal synchrotron radiation from rot. charge in mag. plasma 0-28153  
 SS 433, plasma clouds props. and nature of system (Russian) 0-36647  
 stellar, rotating Hall plasma, self gravitational instability, MHD stability 0-14890  
 stellar interiors, thermonuclear reaction rate enhancement due to strong screening, ionic mixtures case 0-36613  
 stream, electron distribution function, probe diagnostics 0-14935  
 superradiation from non-ideal plasmas in electric field 0-38568

## plasma continued

- Tycho supernova remnant, X-ray line emission rel. to plasma ionisation equilb. 0-46636  
 upper atmosphere and solar-terrestrial relations, introduction to aerospace environment, book 0-8466  
 X-ray pulsars atmospheres, possible vacuum signature in spectra 0-27015  
 Ar discharge, population processes of 4p levels, perturbation influence 0-38565  
 Ar-Br<sub>2</sub> positive column at. state densities 0-44007  
 CO<sub>2</sub>-N<sub>2</sub>-He, vol. discharge, negative ions effect 0-14956  
 H<sub>2</sub> pulsed arc, dense plasma, Balmer spectrum near photorecombination threshold, press. depend. 0-38569  
 H $\alpha$ (D $\alpha$ ) plasma red shift meas. in Ar arc, ion dynamic depend. 0-10364  
 Hg, liq. sound vel. near metal-nonmetal transition, up to 1600°C and 2000 kg/cm<sup>2</sup> 0-39222  
 Kr afterglow plasma, electron energy distrib. function 0-38748

## plasma accelerators see collective accelerators

## plasma applications

- see also plasma arc spraying; plasma deposition; plasma devices  
 chemistry, nonequilibrium plasma, diat. mol. excited state population in diffusion approx. 0-19553  
 cutting with additional heating of plasma-forming gas 0-24267  
 direct flow plasma reactor, working of phosphate (Russian) 0-55663  
 element mass separation mechanism in plasma discharge in intersecting fields (Russian) 0-14943  
 etching, end point detection by optical emission spectroscopy 0-50733  
 ferrite reduction using plasma methods (Russian) 0-7700  
 flow of gas meas., with fluctuating pressures and temperatures, transit time of spark charged plasma cloud determ. (German) 0-14861  
 fluorescence spectrometry, inductively coupled plasmas as excitation sources 0-43999  
 glass thermopollishing, by use of low temp. plasma radiation (Russian) 0-45406  
 integrated circuit, plasma-removal of polymeric layers 0-1851  
 isotope separation, impulse plasma centrifuge with circulation, theory (Russian) 0-38553  
 isotope separation by ponderomotive force effect near ion-cyclotron reson. 0-43998  
 laser with plasma Q-switch 0-28259  
 metal oxide reduction using plasma methods (Russian) 0-7700  
 neutral beam production using negative ions 0-28696  
 oxidation of Si, magnetoactive O<sup>+</sup> plasma 0-38831  
 plasmochemical synthesis, powder dispersion control 0-55332  
 plasmochemical synthesis, powdered infusible compounds, props. 0-55330  
 restoration, evaporation and melting of materials in high temp. gas flow (Russian) 0-39271  
 ruby laser, power enhancement by intracavity plasma 0-53330  
 semiconductor structures and devices, plasma etching methods (Slovak) 0-40564  
 steel, austenitic stainless, high N, plasma arc remelting, processing parameters and props. 0-16336  
 theoretical scaling laws, implications 0-28805  
 AlN, plasmochemical synthesis, powder dispersion control 0-55332  
 AlN powder, synthesis in low-temp. plasma 0-16257  
 Ar plasma, inductive coupled, pyrolysis of hydrocarbons for coating nuclear fuel particles (German) 0-18585  
 BN, high-temp. plasmochem. synthesis, control of props. 0-55333  
 H plasmochemical prod. by H<sub>2</sub>O decomposition in non-equilib. plasma 0-45773  
 H prod. from CO<sub>2</sub>+steam, plasmochem. cycle 0-45772  
 Li, isotope separation by plasma centrifuge, static characts. anal. (Japanese) 0-5326  
 W, heat resistant particles in low temp. Ar plasma, heating, melting, vapourisation (Russian) 0-40384  
 Xe-He(Ne), gas mixture, element and isotope separation in impulse plasma centrifuge (Russian) 0-38725

## plasma arc sprayed coatings

- adhesion, ASTM test 0-50812  
 electronic and domestic appl., cooking plates with high abrasion and corrosion resistance (Japanese) 0-55558  
 Nichrome-silicate glass-CaF<sub>2</sub> multicomponent self-lubricating coating, prep. by plasma spraying, and props. 0-40604  
 powder sprayed materials, control of mech. props. 0-11560  
 Al, effect of Si substrate surface conditions and impact velocity of sprayed particles 0-21145  
 Al sintered powder coatings, form. and behaviour under particle bombard. 0-35029  
 Al-Si coatings, form. and behaviour under particle bombard. 0-35029  
 Al<sub>2</sub>O<sub>3</sub>, form. and behaviour under particle bombard. 0-35029  
 Be, erosion rates under H<sup>+</sup> ion bombard., fusion reactor appls. 0-39179  
 Cr<sub>x</sub>C<sub>y</sub>(Ni-Cr), for gas cooled reactor heat exchangers, factors affecting performance 0-40609  
 Ni, effect of Si substrate surface conditions and impact velocity of sprayed particles 0-21145  
 Ni-Co-Cr-Al-Y, metallurgical characts. and oxidation behaviour 0-40618  
 (NiCo)-Cr-Al-Y/ZrO<sub>2</sub>-Y<sub>2</sub>O<sub>3</sub> plasma sprayed ceramic coating for turbine engine components 0-40616  
 Nichrome, plasma spray coatings, relaxation phenomena 0-19876  
 TiB<sub>2</sub>, erosion rates under H<sup>+</sup> ion bombard., fusion reactor appls. 0-39179  
 TiC, erosion rates under H<sup>+</sup> ion bombard., fusion reactor appls. 0-39179  
 VBe<sub>12</sub>, erosion rates under H<sup>+</sup> ion bombard., fusion reactor appls. 0-39179  
 W, effect of Si substrate surface conditions and impact velocity of sprayed particles 0-21145  
 W, plasma spray coatings, relaxation phenomena 0-19876  
 Zr-based thermal barrier coating evaluation 0-40619

## plasma arc spraying

- electronic and domestic appl., cooking plates with high abrasion and corrosion resistance (Japanese) 0-55558  
 glow discharge cleaning effectiveness rel. to base material atomisation rate (Russian) 0-20797  
 Nichrome-silicate glass-CaF<sub>2</sub> multicomponent self-lubricating coating, prep. by plasma spraying, and props. 0-40604  
 ZrO<sub>2</sub> powders, stabilised, for plasma spray-coatings 0-20869  
 Mo-N, nonporous metal production accompanying arc plasma nitriding (Russian) 0-7712  
 Ni-Al thermally reactive powder, particle heating dynamics during plasma deposition 0-16179



**plasma-beam interactions**

- see also *electromagnetic wave propagation in plasma; plasma production and heating by laser beam*
- beam instabilities, periodic regimes (*Russian*) 0-53999
- beam-induced currents in toroidal plasma 0-28808
- Cerenkov interaction between obliquely propagating whistler wave and electron beam, computer simulation 0-43937
- charge exchange meas. in Tokamak plasma, active beam method 0-48991
- cold beam-weakly collisional plasma, amplitude oscills. destruction 0-28695
- column embedded by rotating ion beam 0-28690
- deflagration wave in slab target, form. by ion beam 0-28628
- deflagration wave in spherical target, form. by ion beam 0-28629
- deuteron beam relaxation, charge exchange, instability, in 2-component Tokamak (*Russian*) 0-53997
- discharge dynamics, calculations of plasma energy and particle balance 0-28847
- double beam interaction with plasma theory 0-48901
- efficiency, wave HF press. effects (*Russian*) 0-10395
- electron beam, Coulomb collisions in mag. field, polarised radiation enhancement (*Russian*) 0-54002
- electron beam, fast, relax. in thermionic converter, cross sections energy depend. 0-43939
- electron beam, fluid treatment of runaway electrons in strong elec. fields 0-33812
- electron beam, freely propagating, ion oscill. excitation (*Russian*) 0-1815
- electron beam, high energy, relax. in weakly ionised plasma with few collisions (*Russian*) 0-14909
- electron beam, high-current, causing press. reduction in air afterglow 0-28867
- electron beam, low current passage through gases, peculiarities 0-38812
- electron beam, relativistic, anomalous energy deposition into solid low-Z target 0-48906
- electron beam, relativistic, diocotron modes, magnetic shear stabilisation 0-54006
- electron beam, relativistic, excitation of rippled plasma resonators 0-48902
- electron beam, relativistic, interaction with air 0-48904
- electron beam, relativistic instability in variable dissipation level plasma (*Russian*) 0-19594
- electron beam fusion of D-T pellets, neutronics and photonics 0-52781
- electron beam generated electron plasma oscillations, quenching by low freq. externally applied wave 0-24160
- electron beam heating of a mirror confined plasma, diode mag. field gradient effect 0-54009
- electron beam in isotropic plasma, EM wave radiation 0-19591
- electron beam instability in solar type III radio bursts, nonlinear stabilisation 0-26826
- electron beam penetration, double layer form., Buneman and Pierce instabilities, collisionless regime 0-10398
- electron beam propagation in plasma channels for ICF reactors 0-1812
- electron beam waves+plasma waves, nonlinear interactions 0-38670
- electron beam-plasma discharge, characts. in crossed elec. and mag. fields (*Russian*) 0-10396
- electron beam-plasma discharge, of initially neutral gas 0-54004
- electron beam-plasma interaction, in strong Langmuir turbulence region (*Russian*) 0-1811
- electron beam-plasma interactions in turbulence regime, phenomenological model 0-6260
- electron beam-plasma low freq. instability, cyclotron oscills. (*Russian*) 0-33783
- electron beam-plasma system, explosive instability 0-1813
- electron beams, stability in plasma 0-1814
- electron flux-driven ion acoustic instability in Q-machine, probe diagnostics 0-33765
- electron oscillation in radial potential well effect on beam interactions (*Russian*) 0-14912
- electron stopping model and secondary-electron distrib. in weakly ionised gas 0-6263
- electron stream, sheared, in semi-infinite plasma, reson. instability 0-48868
- electron-beam inertial confinement expts. at Valduc (*French*) 0-48907
- electron-beam scattering in partially ionised He(Ar), diagnostic technique 0-28824
- EM radiation, direct generation mechanism in beam-plasma system 0-54007
- energy balance in PLT Tokamak 0-28733
- energy transfer in laser (or particle) beam produced plasmas 0-38680
- explosive magnetic field generation due to EM incident radiation, laser plasma mechanism 0-6253
- fast electron beam, suppression in plasma in strong EM wave field (*Russian*) 0-53998
- fast ion beam, Alfvén wave excitation in Tokamak (*Russian*) 0-53999
- fast ions, behaviour during H-neutral-beam-injection in large Tokamak plasma 0-28713
- fast ions in laser-produced plasma, nonlinear plasma-wave interaction 0-24183
- field reversal experiment in 2XIB 0-28732
- fusion device surface effects on neutral beam injector and beam direct converter operation 0-47719
- fusion plasma in beam driven Tokamak, Fokker-Planck/transport analyses 0-28826
- fusion reactor, beam-driven bumpy torus 0-42859
- fusion reactor, TFTR Tokamak, plasma generation and confinement 0-42864
- fusion reactor, two-component and hot-ion Tokamaks 0-42863
- fusion reactor cavity design, compact electron beam or light ion beam reactor using nonspherical blast waves 0-9405
- fusion reactor cavity gas response to particle beam target explosions 0-37602
- fusion-neutron production in D-beam-heated PLT plasmas 0-28807
- heating in toroidal plasmas 0-24239
- high current relativistic electron beam retardation distance (*Russian*) 0-14911
- high toroidal mode number stability of beam-induced tensor press. Tokamak 0-10378
- hot plasma, space pot. distrib. meas. by fast neutral beam method 0-48970
- ICF reactor mats., particle-beam-driven, critical environmental considerations 0-32444

**plasma-beam interactions continued**

- implosion, by pulsed electron beam accelerator, 4TW, laser and X-ray obs. 0-1816
- impurity injected beam, edge cooling by super-banana limiter 0-43940
- ion acceleration in plasma by steady state field, UV and X-ray laser amplification 0-28187
- ion beam, 60 MeV, high-press. plasma production, electron props. diagnostics (*French*) 0-10407
- ion beam, parametric excitation of ion acoustic (electrostatic ion cyclotron) waves 0-38591
- ion beam, velocity-modulated, steepening and breaking in phase space 0-54005
- ion beam scattering by ion-acoustic turbulence 0-6262
- ion beam system, 4-wave interaction, positive (negative) energy electrostatic ion waves 0-48884
- ion beam with rotational and axial motion, thermal equilibrium props. 0-53934
- ion beam-plasma system wave propag. in cylindrical geometry 0-38592
- ion beam-plasma system with nonisothermal electrons, ion-acoustic solitary waves 0-33784
- ion beam-slab target interaction, deflagration waves form. 0-24184
- ion beam-spherical target, deflagration wave 0-28694
- ion beam-stabilisation of ion acoustic instability in Q-machine 0-33766
- ion cyclotron waves and high-energy protons, nonlinear interaction in Earth's magnetosphere (*Russian*) 0-17444
- ion ring, field-reversed, anomalous decay of induced electron current 0-24206
- megavolt and megampere diagnostic techniques for pulsed power particle beam fusion drivers 0-49010
- neutral beam generation, negative ion revolving multiple beam instabilities (*French*) 0-47798
- neutral beam injection, neutron prod. in Maxwellian D ion plasma, ion temp. diagnostics appls. 0-49005
- neutral beam injection expts. on Tokamak plasma at ORNL 0-28809
- neutral beam injection heating in JIPP-II Tokamak 0-28710
- neutral beam injection heating in Tokamaks, review 0-28729
- neutral beam injection in JIPP T-II, investig. 0-28810
- neutral beam injection in Tokamaks, review of technology progress 0-28731
- neutral beam injection systems based on negative ions, review 0-42852
- neutral beam injector, simulation of neutral particle transport 0-37600
- neutral beam production using negative ions 0-28696
- neutral beam-sustained field reversed mirror fusion test facility 0-43962
- neutral beam-sustained tandem mirror reactors, fusion power reactor and fusion-fission hybrid reactor 0-42856
- neutral injection heating of CLEO stellarator—theory and experiment 0-28755
- neutral injection heating of Cleo stellarator 0-28714
- neutral injection instability, kinetic, criteria for anisotropic plasma 0-38627
- neutral injection parameters and beam line design for TEXTOR 0-28811
- neutral-beam-driven current evolution in Tokamak plasmas 0-28712
- neutron flux pumped gamma-ray laser 0-28186
- non-self sustained discharge current, gas purity effects 0-38845
- nonlinear evolution of the bump-on-tail instability for electron beam in plasma 0-6248
- particle and momentum source response of Tokamak plasma 0-6261
- particle-beam fusion experiments for fusion ignition, pellet compression and long solenoid approaches, breakeven experiments 0-47720
- peripheral suppressor grid recovery systems for Tokamaks 0-28813
- plasma confinement, relativistic electron beam ring experiments 0-28691
- polarized light interferometer for laser fusion studies 0-31855
- production and flow of plasma in ion beams 0-28624
- pulsed non self maintained discharge, ionisation, high electron beam current effects (*Russian*) 0-14951
- quasilinear relaxation of dissipative instability of relativistic beam in bounded plasma 0-38671
- radiation emission from electron beam excited strongly turbulent plasma 0-53943
- radiative collapse of a relativistic electron-positron plasma to ultrahigh densities 0-14929
- relativistic electron beam, combined reson. in corrugated waveguide (*Russian*) 0-10394
- relativistic electron beam, D-D target, thermonucl. reaction, neutron and proton prod. 0-37575
- relativistic electron beam, irr. of anode foil plasma, ion accel. (*Russian*) 0-54000
- relativistic electron beam, propag. in vac., ion accel. from anode plasma 0-47790
- relativistic electron beam, slow space-charge wave propag. 0-1115
- relativistic electron beam, Vlasov eqn. in plasma medium 0-14910
- relativistic electron beam induced heating 0-43942
- relativistic electron beam induced turbulence and heating, review 0-38672
- relativistic electron beam initiated plasma, optical meas. (*Japanese*) 0-48914
- relativistic electron beam injection into plasma, development of dissipative two-stream instability 0-19593
- relativistic electron beam rot. in plasma, coherent curvature radiation, two-stream instability 0-19590
- relativistic electron beam transmission through strong mag. field in gases 0-48900
- relativistic electron beam-EM wave interaction under autoresonance conditions (*Russian*) 0-54001
- resonator, electron-beam excited, explosive instability 0-28693
- rF instabilities driven by neutral beam injection, review 0-28757
- runaway electrons, enhanced drag by radiation 0-10397
- space-charge wave instability of spiral beam-plasma system in nonuniform mag. field 0-1760
- spiral beam-plasma system, instability, effect of nonuniformity of mag. field 0-48899
- stationary discharge, ionisation, high electron beam current effects (*Russian*) 0-14951
- strongly magnetised plasma collisional relax. of ion beam 0-33785
- surface oscillation cyclotron excitation, electron beam cyclotron instability (*Russian*) 0-54008
- Tokamak, flux-conserving cylindrical equilib. evolution with adiabatic compression and beam heating 0-28799
- Tokamak, impurity control by neutral-beam injection 0-32494
- Tokamak, neutral beam injection, low density ignition scenarios 0-48937
- Tokamak, neutral beam-heated, parametric scaling 0-10406



# plasma-beam interactions continued

Tokamaks, neutral-beam injection, USA research 0-27808  
torsatrons, neutral beam injection calcs. 0-48949  
transverse Cherenkov mode nonlinear stabilisation by external mag. field 0-38642  
Twin Beam Mirror, effect of hot beam injection angle 0-48939  
ultrarelativistic beam quasilinear relativistic plasma relax. in strong mag. field, magnetobremstrahlung (*Russian*) 0-38669  
ultrarelativistic particle beam in relativistic plasma, emission due to mag. bremsstrahlung 0-46390  
wave dispersion in presence of relativistic beam 0-19592  
wave-particle interaction in the late beam-plasma instability 0-28692  
waveguide, plasma-filled, two-stream instability nonlinear evolution, numerical simulation 0-43938  
wide electron beam, quasielastic relax. into finite thickness plasma layer (*Russian*) 0-54003  
Au pellet fusion target-particle beam system, radiative opacity 0-10365  
H(D) neutral beam injection expts., PLT and ISX 0-28812  
N<sub>2</sub>, electron beam sustained high press. discharge, time behaviour of recomb. coeff. 0-10447  
O<sub>2</sub>, electron beam energy branching, discrete energy loss method 0-48905

# plasma collision processes

see also plasma transport processes; plasma-wall interactions  
acceleration effects in resonant interaction of laser beam and ions 0-10390  
air, weakly-ionised, secondary electron distrib., produced by electron source distrib. 0-6211  
alpha-particle heating in an open-field-line plasma 0-48908  
ambipolar electron and ion diffusion in collisional plasma in RF electric field 0-6220  
amplitudes oscillations destruction in weakly collisional plasma-cold beam system 0-28695  
arc plasma, temp. meas. by submillimeter diagnostic technique 0-38853  
atomic and molecular processes involving ionic-covalent nonadiabatic coupling, review 0-38535  
atomic cross sections, calc. using effective Feynman diagrams 0-38566  
atomic ion-electron recomb. in presence molecules, appl. to HCl 0-28601  
atomic processes for mag. fusion research, data status, review 0-42851  
ballooning and tearing instabilities 0-28651  
beam-plasma system, electron relax. in weakly ionised plasma with few collisions (*Russian*) 0-14909  
bottleneck calculation for collisional radiative recomb. coeffs. for Li-like ions 0-53942  
broadening of free-bound radiation thresholds, expt. results for Cl<sup>-</sup>, I<sup>-</sup> and Br<sup>-</sup> 0-53940  
charge exchange meas. in Tokamak plasma, active beam method 0-48991  
chemical reactions, rate coeffs., database creation, DATSTOR 0-48846  
chemical reactions in plasma of given chemical content, computer generation, REACS 0-48844  
chemical species within plasma, number density variation with time, numerical model, PLASKEM 0-48845  
classical oscillators, parametrically excited, appl. to plasma interactions 0-33729  
cold-banket systems, boundary layer analysis 0-28605  
column and surrounding liq. interaction, quantitative anal. under quasiisothermal conditions 0-38788  
current instability on short wave drift oscills., nonlinear theory (*Russian*) 0-53981  
cylindrical pellet in plasma, ablation flow linear stability anal. 0-1738  
DC plasma jet, NO synthesis, chem. kinetics obs. 0-38728  
dense plasma XUV transition Doppler broadening suppression, collisional-radiative model 0-19614  
deuteron beam relaxation, charge exchange, instability, in 2-component Tokamak (*Russian*) 0-53997  
diagnostic techniques for fluctuations 0-49002  
diatomic molecules vibr. excited state population in nonequilib. plasma, rel. to plasma chem. 0-19553  
dielectric response and energy loss in intermediate quantum plasma 0-38541  
dielectron recombination, secondary ionis. effects (*Russian*) 0-53922  
dielectronic recombination through the forbidden levels, low density and T<sub>e</sub> highly ionised plasma 0-43850  
discharge, molecular dissociation on bombardment by low energy electrons 0-43845  
discharge plasma, diffusion regime, elec. sheath theory 0-1810  
drift and trapped electron instabilities, in systems with mag. shear 0-28648  
drift instability, electrostatic current-driven, scaling law for high density and high current Tokamaks 0-38691  
drift instability, local and nonlocal theories comparison 0-19574  
drift wave turbulence, dissipative, current driven, in Tokamak plasma 0-38587  
elastic electron+neutral atom in weakly ionised plasma unstable modes anal. 0-38606  
electrical conductivity of high-density, shock-heated Ar and Xe plasmas 0-38557  
electron beam, Coulomb collisions in mag. field, polarised radiation enhancement (*Russian*) 0-54002  
electron distribution function, electron-electron interaction effects in external field 0-1739  
electron distribution relaxation numerical study for CO<sub>2</sub>-N<sub>2</sub>-He discharges 0-54070  
electron energy distrib. function, Coulomb collision effects, in Xe plasma 0-38532  
electron energy loss by ionisation and excitation of atoms in plasma 0-33732  
electron fluctuation spectrum and drift instabilities in partially ionised plasmas, collision freq. effects 0-53924  
electron hole-electron hole interactions in magnetised plasma loaded waveguide 0-38661  
electron hole-Korteweg-de Vries soliton interactions in magnetised plasma loaded waveguide 0-38661  
electron impact width of plasma lines, approximative semiclassical formula 0-43972  
electron plasma, impurity screening effects in intermediate degeneracy region 0-14882  
electron stopping model and secondary-electron distrib. in weakly ionised gas 0-6263

# plasma collision processes continued

electron-ion recombination coefficient: in afterglow, continuity equation, numerical solution 0-28598  
electron-ion recombination in ambient electron and neutral gases 0-38531  
electron-neutral collision effects on ionisation wave in He plasma 0-43846  
electrothermal stability anal. of fully ionised plasma, diffuse pinch 0-43901  
energy loss due to binary collisions in a relativistic plasma 0-24127  
energy transfer collision freq. in turbulently heated plasma with ion-acoustic instability 0-10399  
explosive instability of one dimensional weak mag. field (*Russian*) 0-14896  
fast electron beam, suppression in plasma in strong EM wave field (*Russian*) 0-53998  
fast ion deceleration in accretion column 0-38530  
finite bandwidth radiation, nonlinear dissipation near electron cyclotron harmonic resonances 0-28670  
free electron recombination, arbitrary nonequilibrium stationary distribution calcs. (*Russian*) 0-53947  
free expansion of slightly ionized plasma (*Russian*) 0-1740  
fusion possibilities and plasma confinement and interactions in mag. conf. Tokamak, review (*French*) 0-54017  
fusion reaction rate increase in plasma strongly perturbed by longitudinal wave 0-27815  
glow discharge plasma, corpuscular diagnostic method of metastable atoms, review (*Czech*) 0-24241  
guided waves in hot collisional uniaxial plasma 0-53995  
He I and II radiation enhancement in mag. field, nonlocal thermodynamic equilib. 0-10366  
high melting particle heating, melting and vaporisation in hot gas 0-6201  
impurity ions on rational magnetic surfaces, convection and diffusion, collisional multifluid model 0-28615  
inert gas afterglow, excimer form., VUV emission obs. at low press. 0-38755  
inert gas plasma, weakly ionised, photon echo relax. obs. in RF discharge 0-43986  
inert gas stationary afterglow obs. of singly charged atomic ions, three-body rate coeffs. 0-38757  
ion+molecule, interstellar species form. radiative assoc., reaction types 0-31348  
ion+neutral atom collisions, partially ionised plasma, turbulence, power spectrum var. with press. 0-38645  
ion and electron temps. equilibration rate, quantum effects 0-24133  
ion beam scattering by ion-acoustic turbulence 0-6262  
ion composition of plasma of pulsed discharge in He, H<sub>2</sub><sup>+</sup> current time evolution 0-54046  
ion excited level population probabilities, steady- vs. quasisteady-state models 0-24128  
ion excited level population probabilities, steady-state, appl. to H-like ions 0-19552  
ion scatt., suprathermal, by partially ionised impurities, measurement of Z<sub>eff</sub> 0-54039  
ion sources, fundamental and special physical processes 0-32559  
ion-sound soliton-resonant particle interactions (*Russian*) 0-14880  
ionisation dynamics of CO<sub>2</sub> laser prod. plasma, spectrosc. obs. 0-43968  
ionisation of H plasma in uniform elec. field (*Russian*) 0-53923  
ions, electron impact excitation close-coupling formalism, perturbative treatment 0-48091  
ions, positive, dielectronic recomb. in plasma generalised cascade theory 0-43851  
kinetic reactions, pulsed afterglow technique obs. in Ar-II plasma 0-48854  
laser target, Monte Carlo (hybrid) suprathermal electron transport 0-24200  
laser-fusion regime, plasma transport, extension of Braginskii system of fluid equations 0-53935  
long time confinement of pure electron plasma, max. confinement time 0-48954  
long-wavelength modes and anomalous transport in toroidal magnetoplasmas 0-28613  
low ionised anisothermal plasma, ionising electron collision kinetics (*German*) 0-33730  
magnetic pulse penetration into plasma, theta pinch geometry, Alfvén velocity scaling 0-33803  
magnetic trap, with helical mag. axis, plateau and banana diffusion regimes 0-10425  
microcanonically distributed plasma, reduced distrib. functions 0-28604  
Microwave reflexion in rectangular waveguides by high pressure RF plasma columns 0-43975  
modes and ballooning in magnetically confined plasmas 0-28650  
neutral atom transport, computer code SPUDNUT 0-48962  
nonideal plasma, elem. excitations and macroscopic props., review 0-43842  
nonlinear dielectric perturbation, wave and particle interactions 0-38593  
ohmic heating of plasmas in closed magnetic systems 0-28756  
particle and momentum source response of Tokamak plasma 0-6261  
particle dynamics in low freq. EM waves, magnetosphere particle flux in inhomogeneous plasma 0-1804  
particle orbit in magnetic field, guiding-centre Hamiltonian, arbitrary gyration 0-1834  
ponderomotive effects and magnetic field generation in radiation plasma interaction 0-28680  
ponderomotive laser effects in collisional plasma transport 0-38562  
positive column, metastable atom radial transport at various electron distrib., atom+atom collision effects 0-44037  
positive column of glow discharge of electronegative gas, molecular excitation and ionisation by electron collisions 0-49031  
propane-air laminar flame plasmas interaction with microwave TM<sub>010</sub> mode in combustion bomb cavity 0-53939  
pulsed limiter discharge, multicomponent nonideal plasma, chem. composition 0-19657  
quasistatic theory for negative ion free-bound radiation threshold broadening 0-53941  
radiowaves interaction, thermic excitation of parametric instability, controlled 0-24164  
resonant charge exchange, polarisation effect 0-43859  
resonant ion charge exchange collective modes 0-33736  
RF discharge, electrode sheath 0-44052  
RF driven currents in steady state Tokamak reactors 0-28687  
rotational and gas temps., rel. in low press. mol. plasma 0-6215



**plasma collision processes continued**

- self-sustained gas discharge, mol. vibr. relax. effect on thermal stability 0-10358  
 sheath edge theory is weakly ionised collision dominated plasma 0-43935  
 silent discharge, excited species reactions, discharge channel characts., numerical simulation 0-38813  
 single atomic collision relative level populations, thermal equil. 0-1743  
 single particle motion in 1-component strongly coupled plasma 0-48847  
 solar emission lines of NeV, MgVII, SiIX, SXI, population levels as function of electron density and temp. 0-21963  
 spectral line profile of low-press. afterglow plasma in mag. field 0-6285  
 strongly magnetised plasma collisional relax. of ion beam 0-33785  
 submillimetre diagnostics, active, of Ar arc, data numerical anal. 0-48979  
 supersonic colliding plasma jets, hot dense plasma formation, hydrodynamic model (*Russian*) 0-38676  
 thermal ionisation, single-step ionis. role, diffusion approx. 0-43843  
 thermodynamical functions for dense multicomponent plasmas, electron-proton plasma appl. 0-38548  
 three-body electron attachment to O in nonself maintained discharge (*Russian*) 0-14881  
 Tokamaks, divertor, refuelling methods, pellet-plasma interaction 0-28841  
 trapped electron instability, turbulence, unstable mode dynamics anal. 0-33761  
 turbulence induced by plasma-electric current interaction in focus expt., laser diagnostics 0-24171  
 two electron temp. plasma, collisional and Landau damping of ion-acoustic waves 0-19572  
 two-electron capture processes in plasma containing multiply charged ions 0-43854  
 two-particle effective pot., for dense hydrogenous plasma near 10K 0-38533  
 Ar afterglow, line radiation of plasma in early afterglow 0-38745  
 Ar hollow cathode arc, in mag. field up to 2 kOe, plasma parameters 0-6306  
 Ar, plasma column of hollow cathode arc, collisional model of ion system 0-38749  
 Ar, weakly-ionised, collisional drift instability 0-53977  
 CO discharge, electron energy distrib. and kinetic coeffs., ground-state mols. 0-43867  
 CO discharge, electron energy distrib. and kinetic coeffs., vibr. excited mols. 0-43868  
 CO<sub>2</sub>-He-Cs glow discharge, quenching cross section of resonant Cs(6P) state by CO<sub>2</sub> mols. 0-43860  
 CO<sub>2</sub>-(He) discharge, UV-initiated, electron ion recomb. and CO<sub>2</sub> dissociation 0-44068  
 Cr, gas-phase, plasma, sputtering and beam-foil excitations 0-32820  
 Cr ions in Tokamak plasmas, spectroscopy and atomic physics 0-53938  
 Cs, nonideal plasma press. ionisation, short range forces, thermodynamic props. 0-33733  
 Cs plasma discharge, positive column constriction, ion conversion effect 0-44020  
 D+T, guiding centre distrib. spatial separation, reaction rate enhancement 0-33737  
 Eu<sup>+</sup> metastable states in discharge plasma, anomalously high speed deexcitation, modulation of induced radiation obs. 0-44014  
 F<sub>2</sub>, electron dissociative attachment rate consts. at 300 and 500K in discharge 0-43849  
 Fe ions in Tokamak plasmas, spectroscopy and atomic physics 0-53938  
 H Balmer lines, plasma-broadening in wall-stabilised arc, low electron density 0-43891  
 H I (3<sup>1</sup>P<sup>o</sup>-2<sup>1</sup>S) line, Stark broadening parameters, modified adiabatic theory, electron scatt. phase shifts 0-43879  
 H<sub>1</sub> in hot plasma, elementary excitation spectrum, exchange and polarisation effects 0-43892  
 H line Stark broadening, role of ion dynamics simulation 0-24144  
 H<sub>2</sub> glow discharge with variable degrees of dissociation, diffusion theory of positive column 0-44018  
 H<sub>2</sub> monoplasmatron arc plasma, electrokinetic parameters space distrib. (*Russian*) 0-53925  
 H<sub>2</sub>-He, hollow cathode effect in cylindrical geometry (*French*) 0-33842  
 H<sub>2</sub>+He(Ne), gas discharge plasma, H<sub>2</sub> dissociation excitation, cross section anal. 0-33735  
 HCl, in nonequilibrium plasma, electron energy distrib. function and dissociation kinetics 0-11882  
 H<sub>2</sub>(D<sub>2</sub>), electron dissociative attachment rates, rot. (vibr.) excitation depend. 0-43848  
 He (n=3, 4) singlet states quenching by N<sub>2</sub> in low-press. glow discharge 0-49030  
 He flow discharge, intermediate press., positive column conc. of ions and metastables 0-44017  
 He glow discharge, low press., excitation transfer and quenching of n=3 excited states 0-38743  
 He-like ions, spectral broadening in plasma, theory, high-Z 0-6223  
 He-Ne gas mixture plasma, role of charge exchange in form. of optical props. 0-28600  
 He+group II metal atoms, gas discharge plasma, Penning ionisation, cross section anal. 0-33735  
 He<sup>+</sup> recombination, high-temp., in plasma jet (*French*) 0-43861  
 HeI, low density suprathermal field fluctuations and high energy electrons 0-1847  
<sup>3</sup>He-Hg (-Kr)+<sup>3</sup>He(n,p)T, high press. plasma excitation, luminesc. spectra 0-38719  
 Hg+Hg, gas discharge plasma, collision cross section anal. 0-33735  
 K<sup>+</sup> discharge plasma, K<sub>2</sub> excited mols. form. by K(4P) collisions 0-44013  
 K<sup>+</sup> ion formation in low press. K discharge plasma 0-43862  
 Kr gas discharge plasma, electron impact depolarization 0-43847  
 Mg, hollow cathode discharge, excitation mechanisms of triplet state atoms and decay obs. 0-44015  
 Mo<sup>29+</sup> to <sup>39+</sup>, photoionisation, cross sections, radiative recomb. rate coeffs., rel. to plasma diagnostics 0-52953  
 Mo<sup>32+</sup>, dielectronic recomb. rate coeffs. in plasma 0-43853  
 Mo<sup>38+</sup>, dielectronic recomb. rate coeffs. in plasma 0-43852  
 N discharge, externally maintained, instability growth time, associative ionisation 0-6254  
 N<sub>2</sub>, beam and glow discharge type, macroscopic props., kinetic eqns. 0-43864  
 N<sub>2</sub>, diffuse plasma, population densities of triplet states, correl. with electron impact processes 0-43966

**plasma collision processes continued**

- N<sub>2</sub>, electron beam sustained high press. discharge, time behaviour of recomb. coeff. 0-10447  
 N<sub>2</sub> plasma, electronic excitation levels in gas-discharge 0-24280  
 N<sub>2</sub> positive column, superelastic collisions and electron distrib. function 0-1858  
 NF<sub>3</sub>, electron dissociative attachment rate consts. at 300 and 500K in discharge 0-43849  
 Ne, 2p levels prod. by dissociation recomb. in afterglow, recomb. coeff., level population 0-43855  
 Ne afterglow plasma, 2p levels collisional transfer coeffs., laser excitation obs. 0-43856  
 Ne, excited atoms reactions in pure afterglow, plasmas using resonance absorpt. spectrometry 0-33835  
 Ne gas discharge plasma, electron impact depolarization 0-43847  
 Ne, low ionised anisothermal plasma, ionising electron collision kinetics (*German*) 0-33731  
 Ne Townsend discharge, Ne<sub>2</sub><sup>+</sup> form. and destruction 0-38747  
 Ne-N<sub>2</sub>, energy transfer, H<sup>+</sup> ion beam produced plasma, ion density and temp. 0-38539  
 Ni ions in Tokamak plasmas, spectroscopy and atomic physics 0-53938  
 O<sub>2</sub> discharge, conditions, self-consistent electron energy distrib. functions calc. 0-38746  
 O<sub>2</sub> electron attachment in non-self-maintained discharge, plasma decay obs. 0-43844  
 SF<sub>6</sub> axially blown arc, current-zero behaviour, theoretical model 0-38789  
 Ti plasma impurity, atom-electron collisions in inner discharge column (*Russian*) 0-38529  
 U<sup>+</sup>+U(U<sup>+</sup>)(U<sup>2+</sup>), elastic scatt. in plasma, interaction pots. and momentum transfer 0-38534  
 Xe afterglow, radiative and collisional deexcitation of reson. states, absorpt. and emission obs. 0-38742  
 Xe, in gas discharge, collisional excitation, radiation lifetimes, macroscopic alignment obs. 0-33734  
 Xe, plasma shock front, elementary processes 0-19581  
 Xe precursors, associative ionisation and photoionisation, relative contrib., electron density prediction 0-43858  
 Xe<sub>2</sub><sup>+</sup> excimer form. in pulsed discharge, visible emission obs. 0-38754  
 Zn, gas-phase, plasma, sputtering and beam-foil 0-32820

**plasma confinement**

- see also magnetic traps; pinch effect; plasma focus; plasma impurities; plasma-wall interactions  
 additional heating in Tokamaks, specific diagnostics review 0-28753  
 Alcator Tokamak, energy balance, MHD activity 0-28838  
 alpha-particle heating in high density D-T plasma 0-28735  
 anomalous electron pseudo-classical transport with coherent electrostatic wave propag. 0-24137  
 anomalous turbulent resistivity at high drift vels., rel. to confinement and fluctuations in toroid 0-24139  
 ASDEX divertor Tokamak, status and design principles 0-13847  
 atomic processes for mag. fusion research, data status, review 0-42851  
 ball lightning, turbulent plasma sphere, rel. to confinement in fusion reactor 0-32516  
 ballooning instability in bumpy torus, hot electron annulus effect 0-53983  
 beam-induced currents in toroidal plasma 0-28808  
 Belt Pinch Screw Reactor, neutronics characteristics 0-18624  
 blanket boundary layer, high-density gas, localised drift mode stability 0-43956  
 Bohm-type thermal losses from high-β plasma 0-38679  
 bumpy torus, NBT-1, effective toroidal curvature, error field, electron beam diagnostics 0-24237  
 Cherenkov adsorption of azimuthal EM travelling waves, magnetoactive heating and containment (*Russian*) 0-38675  
 collisionless drift waves in Tokamaks analytic eigenvalue eqns. 0-6246  
 column, confinement by ablation front from cold gas plug 0-28793  
 compact toroidal configuration, heating and confinement principles 0-24185  
 conference, fusion technology, Padova, Italy (Sep. 1978) 0-8741  
 conference on fusion reactor materials [Miami Beach, Florida, Jan. 1979] 0-31407  
 conference on fusion research and plasma physics, Innsbruck, Aug. 1978 0-27033  
 diffuse pinch, energy equilib., tensor cond. model 0-24209  
 diffusion in toroidal traps, anomalous electron viscosity (*Russian*) 0-48956  
 diffusion reduction by plasma rotation and ion dissipative effects 0-38696  
 discharge, light emission efficiency, electrostatic confinement effects 0-33752  
 DITE phase II neutral injection system investig. 0-28814  
 DIVA, metal-impurity, confinement, discharges 0-28843  
 drift and trapped electron instabilities, in systems with mag. shear 0-28648  
 drift instability, current-driven, sheared mag. field, finite-beta effect on transport 0-28617  
 drift instability, electrostatic current-driven, scaling law for high density and high current Tokamaks 0-38691  
 drift motion in curved mag. field with rot. transform 0-1754  
 drift waves, shear damping in large aspect ratio Tokamak 0-6242  
 EBT reactor, new design arising from plasma research 0-27806  
 ECR ion source, extracted ions charge state distrib., confinement times 0-24268  
 electrode discharge, nonhydrodynamic pinch compression, kinetics and D<sup>+</sup> focusing (*Russian*) 0-38689  
 electrode power loading in high current ion sources 0-27858  
 electron beam inertial confinement thermonuclear fusion 0-27803  
 electron beam propagation in plasma channels for ICF reactors 0-1812  
 electron beam ring, relativistic, toroidal magnetic configs. 0-28691  
 electron cyclotron frequency expts. in 15X-B Tokamak, temp. rel. to heating power 0-48912  
 electron-beam inertial confinement expts. at Valduc (*French*) 0-48907  
 electrostatic confinement of a plasma torus in a magnetic field (*Russian*) 0-1825  
 electrostatic levitation, control and transport in high rate, low cost production of inertial confinement fusion targets 0-47723  
 electrostatic Trivelpiece-Gould modes in a torus 0-38609  
 ELMO bumpy torus, ambipolar diffusion 0-38552  
 ELMO Bumpy Torus, electron cyclotron heating, density and temp. 0-28780



## plasma confinement continued

EM field orthonormal decomposition, duality and complex vectorial space in anisotropic media 0-28754  
 energy balance in PLT Tokamak 0-28733  
 equilibria in elongated field-reversed plasma 0-14926  
 equilibrium, in  $l=2$  stellarator, mag. bump effects (*Russian*) 0-54019  
 equilibrium and stability, strong magnetic shear effect, anal. 0-14925  
 equilibrium in highly collisional toroidal regime 0-28796  
 external conducting sheets, stability effects on mag. contained plasmas 0-1787  
 fast ions, behaviour during H-neutral-beam-injection in large Tokamak plasma 0-28713  
 fast wave heating via mode conversion and ICRF scaling 0-28815  
 fast-magnetosonic-wave heating of the conceptual NUWMAK Tokamak reactor 0-6264  
 FE Tokamak, ray trajectory and ion absorption of LH waves 0-28671  
 field reversal experiment in 2XIIIB 0-28732  
 field reversed mirror configuration, sustaining a toroidal current 0-28804  
 field reversing electron and proton layers, recent results 0-28789  
 finite-beta effects on drift wave turbulence and particle confinement 0-38652  
 flute oscillation suppression, regulator synthesis (*Russian*) 0-24212  
 Frascati Tokamak, 1MJ plasma focus dynamics, neutron production scaling 0-24220  
 FT Tokamak, electron energy replacement time and total energy containment time 0-28836  
 fusion plasma in beam driven Tokamak, Fokker-Planck/transport analyses 0-28826  
 fusion possibilities and plasma confinement and interactions in mag. config. Tokamak, review (*French*) 0-54017  
 fusion reactor, gas insulated plasma boundary layers, ballooning modes stability 0-10415  
 fusion reactor, reversed-field-pinch, superconducting windings 0-27804  
 fusion reactor divertor collector plate, pot. drop across electrostatic plasma sheath 0-13833  
 fusion reactors, design, and alternative fusion concepts, systems studies 0-27805  
 fusion reactors, divergent impulsive crossflow over packed columnar arrays 0-47702  
 fusion reactors, magnetic confinement research developments 0-13844  
 fusion Tokamak reactor, driven, two-component and hot ion, modes of operation 0-42863  
 fusion-neutron production in D-beam-heated PLT plasmas 0-28807  
 guiding centre orbits and topology of noncircular axisymm. Tokamak plasmas 0-6227  
 gyrotron for electron-cyclotron heating in large Tokamaks 0-28751  
 heating in toroidal plasmas 0-24239  
 heavy ion beam inertial confinement fusion, US programme 0-23136  
 helical system, MHD instabilities 0-1829  
 high beta MHD theory, stellarator equilibrium and stability, mirror traps and reverse field machines 0-28778  
 high beta Tokamak heating 0-28730  
 high toroidal mode number stability of beam-induced tensor press. Tokamak 0-10378  
 high- $\beta$  flux-conserving equilibria, with supercond. metal shell, stability anal. 0-10428  
 high-temp. regimes, simulation and confinement scaling 0-38673  
 hybrid reactors, fuel production for fission reactors, fuel cycle options 0-27812  
 ICF reactor, first wall protection schemes 0-32437  
 ICF reactor fuel pellet fabrication techniques and quality factors, optical systems 0-32436  
 ICF reactors, material implications of design and system studies 0-32431  
 ICF targets, laser driven, materials problems 0-32438  
 ICF targets, semiconductor process technology for mass production 0-32439  
 inertial confinement fusion, A-FLINT advanced-fuel pellet design 0-23125  
 inertial confinement fusion at NRL, laser and ion drivers 0-23131  
 inertial confinement fusion at Osaka, laser energy drivers, REB fusion research 0-23135  
 inertial confinement fusion gains using collective model for electrodynamic laser compressions 0-23138  
 inertial confinement fusion research at Los Alamos, recent progress 0-23133  
 inertial confinement fusion target, density in fuel region by activation anal. 0-33807  
 inertial-confinement ion-beam wet-wood-burner fusion neutron source 0-32489  
 internal disruption in Tokamak, relax. oscills., self-consistent model (*Russian*) 0-53957  
 internal helical modes,  $m>1$ , in Tokamak with small shear and high plasma press. (*Russian*) 0-10371  
 ion ring, field-reversed, anomalous decay of induced electron current 0-24206  
 ion sources, large vol. mag. multipole development 0-27857  
 ISX-A Tokamak, plasma confinement and impurity flow reversal 0-28770  
 ISX-B Tokamak, intense heating, plasma position and current, feedback control modeling 0-33802  
 JIPP T-II torus, neutral gas injection and plasma current control, suppression of major disruption 0-28839  
 kink instabilities of a field reversed ion ring with a toroidal magnetic field 0-1758  
 kink instability, internal MHD, sufficient cond. (*Chinese*) 0-43897  
 laser compression of inertially confined plasmas, future energy developments 0-23120  
 laser fusion, plasma confinement, laser compression, Li activation (*German*) 0-52783  
 laser-fusion plasma confinement,  $\alpha$ -emission recoil force effect 0-6275  
 low frequency parametric processes in magnetically confined plasmas 0-28827  
 low-Z impurities radiation during RF heating in ATC 0-28816  
 lower hybrid waves, ray trajectory and ion absorpt. in Tokamak 0-28667  
 magnetic field measurement in toroidal plasma systems 0-49004  
 magnetically confined plasma, high temp., transport processes, numerical soln. 0-19559  
 magnetically confined plasmas, ballooning modes 0-6231  
 magneto-viscous resistive tearing of cylindrical flux surfaces 0-1831  
 magnetoacoustic oscills., in toroidal plasma, comparison with cylindrical plasmas, numerical calcs. 0-33760

## plasma confinement continued

magnetohydrostatic equilibria, circ. cylindrical, internal modes stability, in diffuse pinch 0-43957  
 magnetosonic resonance heating in the Erasmus Tokamak 0-28720  
 materials development for fusion 0-33804  
 MHD equilibria, secular instability in mag. quadrupole field 0-53982  
 MHD equilibria in mag. quadrupole field, secular instability 0-10427  
 MHD equilibrium and stability, triangular deformation elliptic cross section (*Chinese*) 0-53950  
 MHD equilibrium and stability in three dimens. configurations 0-28776  
 mirror machine, enhanced plasma confinement by MHD oscillation 0-24205  
 modes and ballooning in magnetically confined plasmas 0-28650  
 neutral beam injection expts. on Tokamak plasma at ORNL 0-28809  
 neutral beam injection heating in Tokamaks, review 0-28729  
 neutral beam injection in JIPP T-II, investig. 0-28810  
 neutral beam injection in Tokamaks, review of technology progress 0-28731  
 neutral injection parameters and beam line design for TEXTOR 0-28811  
 neutral-beam-driven current evolution in Tokamak plasmas 0-28712  
 non-neutral plasmas, confinement props. 0-38688  
 nonlinear kink instabilities in Tokamaks surrounded by force-free fields 0-43909  
 Ohmic current driven MHD instability in Heliotron-D device 0-38640  
 ohmic heating of plasmas in closed magnetic systems 0-28756  
 oscillations of radially confined round beam, stability and distrib. function 0-53966  
 paramagnetism in RF mag. field, expt., theory and simulation 0-6225  
 particle orbit in magnetic field, guiding-centre Hamiltonian, arbitrary gyration 0-1834  
 peripheral suppressor grid recovery systems for Tokamaks 0-28813  
 Petula Tokamak, Transit Time Magnetic Pumping heating 0-28739  
 pinch-tormac, device using theta pinches and tormac-like end sections 0-24213  
 PLT Tokamak, neutral beam heating 0-28701  
 PLT Tokamak, ohmically heated plasmas, radiation, impurity effects, instability and particle transport 0-28833  
 poloidal rotation velocity determ. in FT-1 Tokamak (*Russian*) 0-19565  
 preionisation in discharge regime in Tokamak (*Russian*) 0-54018  
 Pulsator Tokamaks, modulated runaway losses and effects of helical dipole field 0-28845  
 pulsed Tokamak reactor, poloidal mag. field design 0-13858  
 pure electron plasma long time confinement, max. confinement time 0-48954  
 radiation losses from T-10 Tokamak, pyroelectric detect. (*Russian*) 0-53936  
 renormalised Vlasov turbulence 0-19579  
 reversed magnetic fields induced by a rotating e-beam 0-28790  
 RF flux control of toroidal plasma 0-38582  
 RFC-XX, cusp end plugging MW quasi-steady wide band RF system 0-13880  
 runaway electron diffusion and power balance in Tokamak moderate density discharges 0-28609  
 screw-pinch high- $\beta$  Tokamak, field generation using transverse rotating mag. field 0-19606  
 segmented compact Tokamak reactor, poloidal field coil system 0-13866  
 semi-stellarator field stabilization of Tokamak plasma 0-6245  
 shape stability for plasma in standing EM field 0-28795  
 sheaf instability at moderate densities, anomalous ion heating (*Russian*) 0-43922  
 shear Alfvén wave heating experiments in heliotron D 0-28716  
 skin current heating of toroidal plasma 0-28715  
 SLPX, supercond. long pulse expt., design features 0-13854  
 soft X-ray emission from Tokamak low  $\beta$  mag. confinement systems 0-48959  
 spheromak, toroidal reactor low aspect ratio limit 0-23139  
 spheromak plasma config. form. by combined Z- and  $\theta$ -pinch discharges 0-43955  
 spheromaks, nonlinearly stable equilibrium statistical states 0-53975  
 stability in toroidal axisymmetric system (*German*) 0-28792  
 stellarator, high- $\beta$  equilibria with three helical beta fields, numerical expt. 0-10426  
 stellarator, Saturn, current-free transport processes, drift modes effect 0-19605  
 stellarator geometry, superbanana orbits for 3.5 MeV alpha particles 0-24231  
 T-10, ohmic heating, plasma confinement study 0-28768  
 T-11 Tokamak, neutral beam injection, plasma heating and stability 0-28702  
 T-tube plasma, influence of boundary layer on H<sub>2</sub> line 0-48862  
 tearing modes, unified theory 0-19607  
 tearing modes with mag. braiding 0-10429  
 TFR 600 Tokamak, plasma confinement, low effective plasma charge 0-28769  
 theoretical scaling laws, implications 0-28805  
 theta-pinch, collisionless, high-beta, anisotropy-driven EM modes, finite Larmor radius effects 0-1830  
 Tokamak, Alcator, electron cyclotron emission, polarisation freq. depend. 0-33808  
 Tokamak, confinement and stability, effects of shaping and compression of plasma 0-28772  
 Tokamak, electron cyclotron heating, Bernstein modes, Vlasov dispersion relation 0-33809  
 Tokamak, flux-conserving cylindrical equilib. evolution with adiabatic compression and beam heating 0-28799  
 Tokamak, high beta, transport and radiation studies 0-28798  
 Tokamak, high-beta, equilibria and  $m=1$  kink ballooning mode nonlinear evolution 0-24236  
 Tokamak, internal kink mode, numerical study 0-48953  
 Tokamak, major disruption suppression by tearing modes stabilisation 0-10422  
 Tokamak, noncircular cross-section, high- $\beta$ , anisotropic equilib. 0-24238  
 Tokamak, plasma paramagnetism, expt. obs 0-54021  
 Tokamak, PLT, current profile evolution effect on plasma-limiter interaction and energy confinement time 0-10420  
 Tokamak, PLT, fast-wave heating of two-ion plasma through minority cyclotron reson. damping 0-24194  
 Tokamak, runaway electron instability, non-thermal microwave radn. 0-1842  
 tokamak, stochastic ion heating by lower hybrid wave 0-28707



**plasma confinement** continued

- Tokamak, Tuman-2A, plasma compression particle diagnostics, density and temp. (*Russian*) 0-38677
- Tokamak, weakly localized two-dimensional drift modes 0-53970
- Tokamak (Alcator), driven lower-hybrid waves, light scatt. study 0-1835
- Tokamak discharge, transient behaviour, electrohydrodynamical model 0-48952
- Tokamak fusion devices, likelihood of success 0-52784
- Tokamak fusion reactor, TFTR, plasma generation and confinement 0-42864
- Tokamak fusion reactors, doublet research, plasma shape control, MHD stability 0-28837
- Tokamak limiter, surface observation, infrared techniques 0-38693
- Tokamak orbits, topology 0-28806
- Tokamak power plants, impact of technology and maintainability on economic aspects 0-27807
- Tokamak reactor with high-temperature blanket 0-27809
- Tokamak reactors, prod. of noncircular discharge, ohmic heating expts. (Doublet III) 0-52785
- Tokamak toroidal field coils, reduction of bending moments 0-47697
- tokamak-like equilibria at beta close to unity 0-19604
- Tokamaks, CT-8, mag. field design (*Chinese*) 0-43995
- Tokamaks, high- $\beta$ , expt. and comp. studies 0-23128
- Tokamaks, high-beta, heating, confinement, dynamics studies 0-24218
- Tokamaks, lower hybrid resonance cones 0-28791
- Tokamaks, magnetic islands, tearing modes 0-28846
- Tokamaks, neutral-beam injection, USA research 0-27808
- Tokamaks, nonlinear drift tearing modes 0-53971
- Tokamaks, transport losses, computer modelling and scaling 0-28612
- Tokamaks with iron core transformer, self-consistent MHD equilibria 0-19608
- Tokapole II, poloidal divertor, plasma production and confinement studies 0-18602
- toroidal, azimuthal plasmas rot., classical transport processes, hydrodynamic eqn. (*Russian*) 0-33746
- toroidal, edge cooling by super-banana limiter, injected impurity beam orbits 0-43940
- toroidal axisymmetric equilibria, particle diffusion by mag. perturbations 0-14927
- toroidal cross section,  $\alpha$ -particle confinement 0-1828
- toroidal discharge, minimum energy state 0-44058
- toroidal plasma, compression, appl. of plasma focus device 0-43996
- toroidal plasma, convective cells and transport anal. 0-24229
- toroidal plasma, eigenvalue problem and nonlinear evolution of kink modes 0-24234
- toroidal plasma, resistive MHD mode and sawtooth oscill., nonlinear evolution 0-24235
- toroidal plasma, vertical displacement instability (*Chinese*) 0-1824
- toroidal plasma compression by imploding plasma liner 0-33811
- toroidal reactors, confinement scaling, effect on economy and unit size 0-13860
- toroidal stellarator, single particle motion, computer code 0-28818
- toroidal system, MHD plasma control by feedback and HF fields 0-28781
- transverse convective ion transport in Tokamak, kinetic description 0-6214
- VLF heating methods, thermonuclear prospects, review 0-28738
- weakly-ionised plasma diffusion in apparatus with spatial axis (*Russian*) 0-1826
- Ar full circle arc, mass flow field investig. 0-38797
- D diffusion studies by pulsed injection in Tokamak plasma 0-28611
- D-He, confined by levitating supercond. ring, neutron effects 0-47715
- D-D fusion reactor plasmas, pure and catalysed, thermal stability 0-24207
- D-T Tokamak, high-density, ohmically-heated, transport calcs. 0-24142
- D<sub>2</sub> fusion reactors, catalysed, power balance calc., plasma confinement 0-42847
- H(D) neutral beam injection expts., PLT and ISX 0-28812

**plasma containment** see *plasma confinement***plasma density**

- air, flowing, glow discharge, negative ion density increase with press. 0-28821
- air-water vapour mixture, electron conc. and conductivity behind strong shock wave 0-48890
- alpha-particle heating in high density D-T plasma 0-28735
- ambipolar electron and ion diffusion in collisional plasma in RF electric field 0-6220
- anomalous conductivity and electron heating, in two-stream unstable plasma 0-6219
- anomalously resistive phase, spiky density fluctuations and relax oscill., microwave scatt. obs. 0-38547
- arc, plasma parameters, probe and spectral meas. 0-24273
- arc plasma, atmospheric, electron density meas. by two-wavelengths interferometry (*Japanese*) 0-38720
- astrophysical plasma, highly ionized, ionization equilib. validity 0-21906
- at. emission obs. of plasma props. 0-19021
- atmospheric pressure plasma flow, boundary layer charged particle density profiles 0-38571
- beam-plasma discharge, characts. in crossed elec. and mag. fields (*Russian*) 0-10396
- Belt Pinch IIa, transport phenomena, density profiles 0-24219
- Brillouin backscatt. depend. on density scale lengths near crit. density 0-43888
- broadening of free-bound radiation thresholds, expt. results for Cl<sup>-</sup>, I<sup>-</sup> and Br<sup>-</sup> 0-53940
- bundle divertor, Tokamak plasma, scrape off layer density decrease, model 0-28851
- caviton generation in plasma reson. region (*Russian*) 0-53926
- cavitons, highly nonlinear states in plasmas, expt. obs. 0-6233
- cavitons in laser irradiated fusion plasmas, EM wave propag., supersonic density humps 0-24178
- continuous optical discharge, diagnostics 0-43947
- corona, discharge pulses, field strength and electron density calcs. 0-38814
- critical density surface, CO<sub>2</sub> laser radiation reson. absorption and surface instability 0-48859
- current sheet generation in rarefied plasma, mag. flux plasma trap appls. 0-38698
- cyclotron harmonic waves props. from perpendicular dispersion relation 0-38612

**plasma density** continued

- cyclotron self-absorption in two-temp. plasma, temp. and density meas. 0-48987
- D-T plasma model, uniqueness and linear stability of operating points 0-14897
- Debye screening modifications in ponderomotive effects 0-33777
- determination of equilb. density using magnetoacoustic oscills. in diffuse pinch 0-48986
- diagnostics, scattered radiation intensity fluctuation method (*Russian*) 0-14932
- diffuse pinch, energy equilb., classical scalar cond. and neo-classical models 0-24208
- discharge, RF, gamma regime, ionis. balance and plasma characts., model 0-44022
- discharge, running striation excitation, metastable atoms lifetime influence 0-38760
- discharges, high current, press., conductivity meas. 0-38793
- DITE phase II neutral injection system investig. 0-28814
- DIVA, scrape off layer, multigrid energy analyser applications 0-33818
- double-layer, steady-state, fluid theory 0-43873
- drift-dissipative waves, weakly ionised plasma, column steady state 0-38613
- ECR as a diagnostic for mirror trap plasma 0-38709
- eigenmodes, universal, in collisionless plasma slab 0-38581
- electron and at. excited states densities in laser prod. He plasma 0-38710
- electron beam, relativistic, with inhomogeneous ion density, self-consistent model 0-43247
- electron beam controlled discharge, cathode density waves 0-38798
- electron cyclotron frequency sub-harmonic effect on wave absorpt. in Tokamak Thor 0-28686
- electron cyclotron heating in Tokamaks: experiments and prospects 0-28749
- electron density, meas. in unmagnetised plasma, self-oscill. probe method 0-19611
- electron density, multi-pulse ruby laser recording of temporal evolution by light scatt. 0-14938
- electron density determ. by globally convergent method for partially ionised plasma 0-53929
- electron density fluctuations in cold plasma, effective dielec. permeability (*Russian*) 0-32882
- electron density meas. by EM wave propag. in magnetised plasma column 0-43974
- electron density meas. by far IR laser beam deflection 0-48966
- electron density meas. in shock generated plasma by light interferometry 0-48981
- electron density variation influence on excitation temp. in rapidly varying plasma 0-38537
- electron oscillation in radial potential well effect on beam interactions (*Russian*) 0-14912
- electron plasma, impurity screening effects in intermediate degeneracy region 0-14882
- electron temp. meas., continuous, automatic, using double Langmuir probe 0-43977
- electron temperature and density in Ar behind reflected shock waves 0-38549
- electron temperature and electron density in low density magnetised plasma by probe method 0-48848
- electron wave, guided, on planar plasma slab, propag. and attenuation characts., dissipative processes 0-38608
- electrostatic turbulence, variable density and pressure, two-fluid model and geostrophic approx. 0-53986
- ELMO Bumpy Torus, electron cyclotron heating, density and temp. 0-28780
- EM resonant properties of laser-prod. plasmas 0-43928
- EM wave resonant absorption, due to DC mag. field parallel to density gradient 0-19563
- EM wave self action during modulation instability (*Russian*) 0-14905
- EM wave self-action during thermal modulation instability of high hybrid oscills. (*Russian*) 0-53980
- equilibrium in highly collisional toroidal regime 0-28796
- expansion into vacuum, ion acceleration 0-6228
- explosive magnetic field generation due to EM incident radiation, laser plasma mechanism 0-6253
- Faraday rot. meas. in high- $\beta$  fusion expts., plasma electron density and mag. field determ. 0-49008
- fast IR laser interferometry, electronic density fluctuation meas. 0-49000
- first wall materials, effect on Tokamak plasmas 0-38692
- fluctuations, microwave scatt. obs. 0-48851
- focal region of intense laser beam in tenuous plasma, spatial and temporal electron and ion density variations 0-53989
- free electron recombination, arbitrary nonequilibrium stationary distribution calcs. (*Russian*) 0-53947
- fusion mirror reactors, finite orbit treatment of plasma buildup 0-37631
- fusion possibilities and plasma confinement and interactions in mag. config. Tokamak, review (*French*) 0-54017
- fusion reactor, gas insulated plasma boundary layers, ballooning modes stability 0-10415
- fusion reactors, superheating-diffusion instability, thermonuclear burn 0-32500
- fusion Tokamak experiments, H(D) recycling model, influence on discharge behaviour 0-10393
- fusion-neutron production in D-beam-heated PLT plasmas 0-28807
- glow discharge instability in N<sub>2</sub>-CO<sub>2</sub> non self sustained ionisation source, mechanism 0-38819
- Grill phase tracking during density increase in Tokamaks 0-28762
- He I and II radiation enhancement in mag. field, nonlocal thermodynamic equilb. 0-10366
- heterodyne CO<sub>2</sub>-laser interferometer with direct phase readout for meas. electron line densities in plasmas 0-1848
- high current relativistic electron beam retardation distance (*Russian*) 0-14911
- high density directed plasma, source, design, characts., numerical model 0-38538
- high melting particle heating, melting and vapourisation in hot gas 0-6201
- high pressure optical discharges, density and temp. meas. 0-48931
- holographic study of laser prod. plasma at 10.6  $\mu$ m 0-38685
- hydrodynamic wave description including electron spin 0-38643
- ICRF heating in TFR, preliminary obs. and further development prospects 0-28741
- ICRF heating optimisation in PLT 0-28742
- impedance of magneto-acoustic wave launching antenna 0-24180



# plasma density continued

interferometry techniques for high  $\beta$ -plasma density meas., holographic and coupled cavity laser methods 0-49006  
internal disruption in Tokamak, relax. oscills., self-consistent model (*Russian*) 0-53957  
ion acoustic soliton propag. in two-electron temp. plasma 0-33767  
ion beam-created high-press. plasma, electron props. diagnostics (*French*) 0-10407  
ion beam-plasma system wave propag. in cylindrical geometry 0-38592  
ion composition of plasma of pulsed discharge in He,  $H_2^+$  current time evolution 0-54046  
ion cyclotron wave, in density stratified magnetoplasma, crit. level behaviour 0-6238  
ion oscillation excitation by freely propagating electron beam (*Russian*) 0-1815  
ion pressure discharge theory in the strong ionisation regime 0-38734  
ion temp. and density meas. in direct current octopole by induced optical fluoresc. 0-14939  
ion-acoustic instability, ion tail formation and saturation 0-38610  
ion-acoustic turbulence-plasma interactions and electron spectrum in electric fields 0-38617  
ionisation instability mode of plasma accelerator, probe method for electron distrib. function determ. 0-19612  
ionosphere, gradient-drift instability, nonlinear effects 0-36455  
ionosphere, lower hybrid drift instability 0-46343  
ionospheric plasma disturbance due to earthquakes and volcanic eruptions 0-36453  
JAERI Tokamak, Ti coating for improved plasma characts. 0-24232  
jet carrying solid particles, electrophysical props. 0-24134  
JIPP T-II Tokamak, current density profile control 0-32493  
JIPP T-II tokamak plasma, Mo impurity diffusion during  $H_2$  gas puffing 0-28602  
L-2 stellarator, current equilibrium and effective ion charge 0-24228  
laser created plasma, interferometer for electron density meas. 0-48983  
laser emission intensity reduction near solid target surface (*Russian*) 0-38681  
laser interferometer, optoelectronic modulation for electron density variation meas. in IR 0-4762  
laser plasmas, wave absorpt. and superreflectivity due to EM struct. resonances 0-24177  
laser produced plasma, structure of XUV emitting regions 0-54038  
laser produced plasma density profile meas. using Wollaston prism interferometer 0-48973  
laser spark absorpt. and laser pulse contraction meas. using dye lasers 0-48988  
laser target, Monte Carlo (hybrid) suprathermal electron transport 0-24200  
laser-compressed plasma, density measurement by X-ray line shift (*German*) 0-48967  
laser-irradiated glass shell plasma, electron temp. and density, Si X-ray emission diagnostics (*Chinese*) 0-38718  
laser-irradiated plasma, soliton form. at crit. density 0-6267  
laser-produced plasma, electron density meas. using holographic microinterferometer 0-43964  
laser-produced plasma, ion acceleration in presence of density profile steepening 0-14923  
low-Z impurities radiation during RF heating in ATC 0-28816  
lower hybrid wave accessibility, effect of density gradient 0-1794  
lower hybrid waves, quasi-optical beam self-action in magnetoplasma 0-38657  
magnetic mirror, injected plasma particle refl. (trapping), quiescent (turbulent) plasma 0-48955  
magnetic mirror trap, open, with min. B, LF oscills. 0-38708  
magnetic pulse penetration into plasma, theta pinch geometry, Alfvén velocity scaling 0-33803  
measurement using microwave interference signals from 0 to  $n.360^\circ$  phase meas. (*German*) 0-6278  
metal vapour production by sputtering in hollow-cathode discharge 0-1868  
metal vapour-inert gas arc discharges, heavy particle distrib. 0-38782  
microwave beam interaction, intense, with low temp. plasma flow, space distrib. 0-38578  
microwave dynamic interaction, probe diagnostics 0-19584  
Microwave reflexion in rectangular waveguides by high pressure RF plasma columns 0-43975  
molecular lines role in plasma satellites,  $H_2$  ( $He_2$ ) obs. 0-44053  
multi-chord particle diagnostics of a plasma column (*Russian*) 0-1840  
multiposition Thomson scatt., determ. of electron density and temp. profiles 0-48977  
naphthalene-He photoionis. plasma,  $CO_2$  additive effect 0-10359  
neutral atom distribution near wall, temp. grad. effect 0-19555  
neutral density profile, absolute meas. by  $H_\alpha$  line reson. fluorescence 0-24250  
neutral injection heating of Cleo stellarator 0-28714  
neutral injection parameters and beam line design for TEXTOR 0-28811  
neutral-beam-driven current evolution in Tokamak plasmas 0-28712  
non-stationary resonant reflectivity of plasmas, model calcs. 0-14903  
nonideal plasma, elem. excitations and macroscopic props., review 0-43842  
normal atom conc. determ. by resonance line broadening with Hg press. 0-43883  
ohmic heating in Frascati Tokamak, preliminary results 0-28734  
plasma, magnetised, double-layer characts. meas. 0-43874  
plateau effect on inverse bremsstrahlung 0-43894  
profiling by interferometry with rapid spatial scanning, and Thomson scatt. of short laser 0-49014  
pulsed limiter discharge, multicomponent nonideal plasma, chem. composition 0-19657  
pulsed micro-discharges, optical interferometry obs. 0-38804  
quasi steady high beta plasma in multiple mirror machine, density oscill., stability obs. 0-28663  
radiation induced shock tube flow nonuniformities in ionising Ar 0-43865  
radiation intensity calcs. in vacuum UV region (*Russian*) 0-48861  
radiative collapse of a relativistic electron-positron plasma to ultrahigh densities 0-14929  
rarefied plasma flow, degree of nonisothermality, probe meas. 0-24243  
recovery electric strength, effect of plasma parameters 0-6294  
resonance fluorescence method for plasma diagnostics, at. density and temp. meas. 0-49001  
resonant absorption in Ar plasma at thermal equilib. 0-1799

# plasma density continued

reverse field pinch, Faraday rot. diagnostics for internal mag. field 0-43976  
rotation influence on kink instability, compressibility (*Russian*) 0-48887  
runaway electron diffusion and power balance in Tokamak moderate density discharges 0-28609  
runaway relativistic electron scatt. on oscills. in Tokamak (*Russian*) 0-48849  
Saha equation, first order estimate for He plasma 0-19554  
self similar cooling wave, effective thermal cond. (*Russian*) 0-14908  
sheaf instability at moderate densities, anomalous ion heating (*Russian*) 0-43922  
single particle motion in 1-component strongly coupled plasma 0-48847  
solar flar spectra, high dielectronic satellite lines analysis for plasma props. calc. 0-12728  
solar plasmas density determination, N III and O IV intersystem multiplets appl. 0-31264  
solar transition zone, electron density, energy balance and press. from EUV spectra 0-21957  
source, dielec. chamber, plasma flow characts. optimisation 0-38574  
spectroscopic effects in dense and ultradense plasmas, review 0-43990  
stimulated Brillouin backscatter saturation for long  $CO_2$  laser pulses 0-19582  
stimulated Brillouin scatt., saturated steady-state refl., density depend. 0-53945  
stratified plasma, obliquely propag. extraordinary microwave Budden tunnelling 0-48895  
submillimetre diagnostics, active, of Ar arc, data numerical anal. 0-48979  
supercritical density profiles of  $CO_2$ -laser-irradiated microballoons 0-14918  
superradiation from non-ideal plasmas in electric field 0-38568  
supersonic jet, ionisation in Mach disc, submillimeter laser interferometry diagnostics 0-14934  
surface modes in magnetized fully ionized plasma 0-38550  
surfatron produced electron density and temp. microwave meas. 0-43965  
target impurity effect on laser produced expansion, ion spectrography 0-43945  
theoretical scaling laws, implications 0-28805  
thermonuclear dense plasma, neutron diagnostics, book contrib. 0-24253  
theta pinch,  $N^{+2+3+}$  lines Stark broadening, He(II) line diagnostics 0-24249  
theta pinch, radial oscills. of plasma density and mag. field, light scatt. and probe obs. 0-14937  
Thompson scattering for electron beam and plasma diagnostics (*Russian*) 0-54031  
Thomson scatt. pathways calibration, rel. to diagnostics (*French*) 0-43886  
Thomson scattering with high background level of plasma scattering 0-43979  
Tokamak, neutral beam-heated, parametric scaling 0-10406  
Tokamak, Thomson scatt. diagnostics, far IR lasers development, review 0-24242  
Tokamak TFR, Thomson scattering system based on two-detector spectrometers 0-32426  
Tokamaks, density upper limit from thermal stability data 0-18600  
transition layer between two magnetized plasmas 0-24136  
tubular flow reactor, ion density and  $Z_{eff}$  profiles, neutral beam attenuation technique 0-6282  
Tuman-2A, plasma compression particle diagnostics, density and temp. (*Russian*) 0-38677  
UHF discharge plasma, parametrically excited relaxation oscills. 0-53978  
UHF discharge with preliminary locally ionised gaseous medium 0-38851  
vacuum arc in Cu cathode region, current parameters, theory 0-54068  
W VII-A stellarator, Ohmic heating, energy and particle confinement 0-24226  
wave heating at electron cyclotron harmonics in toroidal plasmas 0-28727  
whistler wave trapping in density crest 0-53984  
Z-pinch plasma, interferometry 0-6277  
Al resonance line profiles, influence of boundary layer of Al-seeded shock heated plasma 0-43876  
Ar, decaying plasma arc, electron disappearance mechanism 0-38765  
Ar hollow cathode arc, in mag. field up to 2 kOe, plasma parameters 0-6306  
Ar, plasma arc, dynamic charact., electron energy relaxation effect 0-38774  
Ar, plasma column of hollow cathode arc, collisional model of ion system 0-38749  
Ar plasma density meas. by Langmuir probe and microwave interferometer 0-28819  
Ar, positive column, contracted, electron density, temp., elec. field, line emission 0-6311  
Ar, positive column, contracted, balance equations anal. 0-6312  
Ar, stream electrons, at atm. press., electrical parameters (*Russian*) 0-53930  
Ar-Xe, shock wave dynamic compression, thermodynamic props. (*Russian*) 0-53931  
ArI, highly excited atomic levels, spectral-line-blending study in high-density plasma 0-48969  
beta measurements in high- $\beta$  fusion experiments from magnetic flux and luminosity profiles 0-49007  
C arc in air, electron density meas. by  $CO_2$  laser interferometry (*Japanese*) 0-28822  
 $CO-N_2-He$ , nucl. reactor active zone, plasma and sustained discharge props. 0-5729  
 $Cl_2$ -arc, low temp., visible and IR continuum radiation 0-38784  
Cu vapour laser, non heated, kinetic processes 0-37999  
D-T Tokamak, high-density, ohmically-heated, transport calcs. 0-24142  
 $D_2$  plasma, isolated,  $CO_2$  laser-produced, holographic interferometry diagnostics 0-24254  
 $DyI_3$ -Hg arc discharge plasma, spectroscopic study 0-54033  
H arc, electron density, interferometric determ., refr. index calc. in high press. 0-24284  
H Balmer lines, plasma-broadening in wall-stabilised arc, low electron density 0-43891  
H,  $H_\alpha$  line profile as plasma density meas. 0-43987  
 $H^-$ , density meas. by photodetachment 0-48976  
 $H_2$  monoplasmatron arc plasma, electrokinetic parameters space distrib. (*Russian*) 0-53925  
 $H_2$ , plasma, resonance fluorescence diagnostics 0-48971



**plasma density continued**

- He discharge, medium press., contraction mechanism, inhomogeneous heating 0-44024  
 He discharge, RF, plasma parameters and volt-ampere characts., two discharge regimes 0-44016  
 He, electron distribution function relaxation in high freq. gas breakdown (*Russian*) 0-14957  
 He flow, RF discharge test obs. 0-44028  
 He I line profiles, ion motion effect in low electron density plasma 0-43877  
 He positive column comp. at intermediate press. 0-19646  
 He pulsed arc, Thomson scatt. diagnostics 0-24297  
 Kr glow discharge, electron energy distrib. function, electrical characts. investig. 0-24279  
 Kr-Cl<sub>2</sub> mixture, glow discharge positive column, electron energy distrib. and rates of inelastic processes, negative Cl ions form. 0-19632  
 N discharge, externally maintained, instability growth time, associative ionisation 0-6254  
 N<sub>2</sub> afterglow, chem. reactions rel. to plasma props, appl. to toluene polymerisation 0-3346  
 N<sub>2</sub> arc plasma, stabilised by gas injection, thermochem. nonequil., particle excitation, vibr. temps. 0-19634  
 N<sub>2</sub>, dense gas near metallic target, laser spark (*Russian*) 0-38682  
 N<sub>2</sub>, diffuse plasma, population densities of triplet states, correl. with electron impact processes 0-43966  
 N<sub>2</sub> discharge, electron shock wave formation, numerical simulation 0-38777  
 N<sub>2</sub> plasma, spatial distrib. in transverse-discharge supersonic stream, continuum theory and probe meas. 0-48866  
 N<sub>2</sub> positive corona into spark, prebreakdown phase, spectroscopic anal. 0-38790  
 N(<sup>2</sup>D,<sup>2</sup>P) metastable ats. prod. in N<sub>2</sub> DC glow discharge 0-38758  
 Ne-N<sub>2</sub>, energy transfer, H<sup>+</sup> ion beam produced plasma, ion density and temp. 0-38539  
 O<sub>2</sub> discharge plasma, metastable states role, two step ionisation, electron densities and transition pts. 0-44019  
 SiH<sub>4</sub> discharge, low pressure, plasma parameters, relevance to Si film deposition 0-44030  
 Ti density, in DC sputtering discharge by atomic absorpt. spectroscopy 0-43973  
 Xe discharges, electrodeless, UHF in waveguide rel. to DC characts. 0-38762  
 Xe precursors, associative ionisation and photoionisation, relative contrib., electron density prediction 0-43858  
 Xe, s-p transitions, Stark consts. and oscill. strengths, shock tube meas. 0-18822

**plasma deposited coatings**

- organo-tin polymer films, glow discharge prep., comp. determ. by XPS and AES 0-35109  
 polyacrylonitrile, adhesion to plastics 0-50745  
 polymer film, adhesion to plastics 0-50745  
 polysiloxane plasma polymerised film growth on GaAs substrate, dry etching process 0-25575  
 polystyrene, adhesion to plastics 0-50745  
 temperature measurement of spherical or near-spherical particles in plasma stream 0-21138  
 thermoregulating plasma coatings, UV irradiation influence on optical parameters (*Russian*) 0-40259  
 VLSI multilayer metallisation interlayer dielectrics, CVD films 0-45235  
 Ag, electron beam plasma sputtered coatings on KCl substrate, islet struct. (*Russian*) 0-39460  
 Al, electron beam plasma sputtered coating, islet struct. (*Russian*) 0-39460  
 Al-Zn-Mg plasma sputtered, mech. props. rel. to heat treatment (*Russian*) 0-40387  
 As<sub>2</sub>-S<sub>3</sub>, hydrogenated chalcogenide glasses, prep. by plasma decomposition 0-49735  
 As<sub>2</sub>-Se<sub>3</sub>, hydrogenated chalcogenide glasses, prep. by plasma decomposition 0-49735  
 B films, prep. by H reduction of BCl<sub>3</sub>, struct. and hardness 0-54543  
 B, protective coatings for first wall, prep. by means of low press. plasma CVD 0-35103  
 B<sub>2</sub>Cy, protective coatings for first wall, prep. by means of low press. plasma CVD 0-35103  
 C, diamond-like, produced by RF glow discharge of hydrocarbon gases, props. and coating rates 0-21146  
 i-C, hard coating preparation by ion beam methods 0-25579  
 CrO<sub>2</sub>, plasma deposition of crystals and their characterisation 0-20800  
 Cr-C, hard coating preparation by ion beam methods 0-25579  
 Fe<sub>2</sub>N, hard coating preparation by ion beam methods 0-25579  
 Fe<sub>2</sub>O<sub>3</sub>, plasma sputtered coatings, oxide dissociation, coating props., struct. and composition (*Russian*) 0-54577  
 HfO<sub>2</sub>, plasma deposition of crystals and their characterisation 0-20800  
 Re, films, from Re<sub>2</sub>(CO)<sub>10</sub> vapour decomp. 0-20799  
 Si, amorphous, glow-discharge, optically detected mag. reson., annealing and substrate temp. effects 0-20519  
 Si, amorphous, photovoltaic cell, plasma deposited, horizontally multilayered struct. 0-50964  
 Si amorphous film, film, glow discharge deposited, refl. spectra and dielec. function 0-50360  
 Si, amorphous glow discharge films, H<sub>2</sub> content, elec. props., and photostability 0-25577  
 Si and Si:H amorphous films, porosity and oxidation of evap., sputtered and plasma-deposited films 0-10838  
 Si films, polycryst., glow discharge deposited below 250°C, struct. and morphology 0-49535  
 Si, glow discharge film decomposed from silane, on amorphous substrate, elec. cond., RHEED study 0-20044  
 Si:F,H, amorphous, glow discharge deposited elec. props. and device aspects 0-44744  
 Si:H, amorphous, defect creation and H evolution 0-50392  
 Si:H, amorphous, dopant conc., glow discharge optical spectroscopy 0-49546  
 Si:H, amorphous, exodiffusion of H, EPR expts. 0-49102  
 Si:H, amorphous, glow discharge deposited, thermal dehydrogenation, IR spectra 0-44442  
 Si:H, amorphous, glow discharge deposited, laser annealing 0-49104  
 Si:H, amorphous, plasma deposited, cond. adsorbate and insulating layer effects 0-49749

**plasma deposited coatings continued**

- Si:H, amorphous, plasma-deposited, effect of DC elec. field superimposed during deposition 0-44643  
 Si:H, amorphous, prep. by RF glow discharge decomp. of SiH<sub>4</sub>, optical props. and H conc. 0-15416  
 Si:H, amorphous film, prep. by plasma decomp. of SiH<sub>4</sub> under mag. field, and characterisation 0-45239  
 Si:H<sub>2</sub>F<sub>2</sub>O amorphous, plasma deposited, comp. and optical props. 0-50441  
 Si:H amorphous film, microstruct., SEM and TEM obs. 0-10801  
 Si:H amorphous film, plasma-deposited, growth morphology and defects 0-44128  
 Si:H amorphous film, plasma-deposited, elec. and comp. heterogeneity 0-44745  
 Si:H amorphous film, prop. by glow discharge deposition, and plasma parameter effects on props. 0-45240  
 Si:H amorphous films, role of Ar in deposition process, IR absorpt. and photocond. meas. 0-50321  
 Si:O,H amorphous, electronic and struct. props. 0-50391  
 Si:P, heavily doped, glow-discharge-produced, elec. and optical props. 0-2497  
 Si-H, amorphous, on Nb or W, spectrally selective absorber, IR spectra 0-26164  
 Si-H, amorphous, plasma-deposited, H evolution and defect creation 0-44914  
 Si-H, amorphous, thermal stability and decomp. kinetics 0-24758  
 Si<sub>3</sub>As<sub>1-x</sub>H<sub>x</sub>, amorphous system, struct. and defects, Raman and EPR meas. 0-49103  
 SiN<sub>x</sub>, composition and characterisation, optical and elec. props. 0-15401  
 Si<sub>3</sub>N<sub>4</sub>, hard coating preparation by ion beam methods 0-25579  
 Si<sub>3</sub>N<sub>4</sub>:H, film, impurity profile determ. by 1.2 MeV proton-proton scatt. 0-49256  
 ThO<sub>2</sub>, plasma deposition of crystals and their characterisation 0-20800  
 Ti<sub>3</sub>N<sub>4</sub> plasma condensation on steel and carbide (*Russian*) 0-20796  
 ZrO<sub>2</sub>, plasma deposition of crystals and their characterisation 0-20800
- plasma deposition**  
 benzene, plasma polymerisation in glow discharge, thin film IR and free radical EPR obs. 0-2964  
 ceramics coating by physical vapour deposition processes (*Japanese*) 0-55306  
 film deposition, ion beam techniques 0-11564  
 inorganic thin films, review 0-50564  
 macroparticles elimination from plasma stream, using curved plasma duct 0-33826  
 optical fibre plasma activated CVD, influence of substrate temp. 0-48475  
 optical fibre preparation by Ar plasma augmented vapour deposition 0-48478  
 polymeric electret films, produced in HF discharge, props. (*Russian*) 0-20578  
 polymerisation on solid substrate in RF discharge 0-2963  
 polymorphous thin film production in HF discharge 0-1855  
 semiconductor IC production, plasma CVD equipment for insulating films 0-25572  
 sputtering, particle velocity and disperse composition (*Russian*) 0-40258  
 styrene, plasma polymerisation in glow discharge, thin film IR and free radical EPR obs. 0-2964  
 thin film growth measurement using galvanically separated quartz monitor probe (*German*) 0-11576  
 CeO<sub>2</sub>, plasma deposition of crystals and their characterisation 0-20800  
 Cr coatings, plasma-chemical deposition using transport reactions (*Russian*) 0-16191  
 GaN, deposition from plasma reactor, organo-metallic and donor-acceptor complex exchange in HF plasma 0-38839  
 HfO<sub>2</sub>, plasma deposition of crystals and their characterisation 0-20800  
 Ni wire plasma sputtering with W particles, coagulation, struct. and particle size (*Russian*) 0-40260  
 Si film, glow discharge deposition, SiH<sub>4</sub> discharge parameters obs. 0-44030  
 Si:H, amorphous, control and anal. of deposition, using plasma spectroscopy 0-45230  
 Si:H, amorphous film, prep. by plasma decomp. of SiH<sub>4</sub> under mag. field, and characterisation 0-45239  
 Si:H, plasma-deposited amorphous film, proton mag. reson. 0-44931  
 Si:H amorphous film, prop. by glow discharge deposition, and plasma parameter effects on props. 0-45240  
 Si:H amorphous films, optoelectronic behaviour depend. on impurity incorporation during plasma deposition 0-49804  
 Si<sub>3</sub>N<sub>4</sub> passivation planar plasma deposition system, productivity increase 0-40269  
 SiO<sub>2</sub> nonporous film, plasma deposition method, appl. to semicond. device manufacture (*Russian*) 0-16197  
 SiO<sub>2</sub> thin films, plasma deposition in prod. planar reactor 0-2966  
 ThO<sub>2</sub>, plasma deposition of crystals and their characterisation 0-20800  
 ZrO<sub>2</sub>, plasma deposition of crystals and their characterisation 0-20800

**plasma devices**

- see also *magnetohydrodynamic converters; plasma diodes; plasma focus; plasma guns; stellarators; Tokamak devices*  
 accelerator with pre-ionised Cs, closed electron drift, and extended accel. zone, I-V characts. 0-14944  
 arc, DC, wall-stabilised, plasma source for biological soln. spectrochem. anal. 0-41343  
 arc, low press., large cross section anode plasma with constricted channels, broad electron beam prod. 0-38840  
 bimetallic electrodes for plasma torches, Cu to W joining methods 0-24266  
 branch divertor for Tokamaks (*Russian*) 0-54051  
 bundle divertor, Tokamak plasma, scrape off layer density decrease, model 0-28851  
 centrifuge, isotope and element separation mechanism 0-6291  
 chemical reactors for surface layer removal, regime parameters (*Russian*) 0-54050  
 chromatograph/mass spectrometer column overload prevention valve 0-16748  
 cluster accelerator, external mag. field influence 0-6287  
 conference on fusion research and plasma physics, Innsbruck, Aug. 1978 0-27033  
 current multiplier, gas discharge device, current amplification 0-49018  
 DITE phase II neutral injection system investig. 0-28814  
 double plasma and other synthesised plasma devices, adjustment of ion energy distribution 0-19625



## plasma devices continued

- ECR ion source, extracted ions charge state distrib., confinement times 0-24268  
 equilibrium of plasma without shell, impurities outside coronal equilibrium and hollow profiles, MAKOKOT code 0-28774  
 field reversed mirror configuration, sustaining a toroidal current 0-28804  
 focus discharge in Mather accelerator 0-24257  
 furnaces, mineralogy and extractive metallurgy appls. (*French*) 0-28849  
 fusion reactor, beam and plasma direct converters 0-42861  
 generator arc chamber, hydrodynamic struct. 0-1817  
 gyrotron 50 GHz design considerations 0-28728  
 gyrotron for electron-cyclotron heating in large Tokamaks 0-28751  
 gyrotron power source development in MM wavelength range 0-28852  
 gyrotrons, space charge phenomena 0-28868  
 Heliotron D, shear Alfvén wave heating expts. 0-28716  
 high-current multirod-cathode, influence of absorption effects on characts. 0-20756  
 HV glow discharge as plasma electron source, characts. 0-44031  
 ICP torch design method, using hydrodynamic flow patterns 0-24256  
 inductively coupled plasma-AES, present and future position in analytical chem., review 0-7887  
 ion source, cold cathode, for mass spectrometry 0-42293  
 ion source, IBM-5, without external mag. field 0-5428  
 ion sources, large vol. mag. multipole development 0-27857  
 ion-acoustic instability oscillations in collisionless single ended Q-machine 0-38731  
 JIPP T-II, lower hybrid wave heating 0-28722  
 JIPP T-II, neutral beam injection, investig. 0-28810  
 laser pulse amplifier using induced Raman or Brillouin processes 0-1279  
 Levitron, fluctuations, diffusion and beam-induced currents 0-28616  
 light sources of high radiation intensity 0-19084  
 materials development for fusion 0-33804  
 MHD generator, coal-fired, mol. beam mass spectrometric sampling system 0-52358  
 MHD generator, open cycle, with shaped magnetic induction, theory of nonuniform electrical conduction 0-28831  
 multipole, appl. to provide source for magnetized plasma column 0-33810  
 peripheral suppressor grid recovery systems for Tokamaks 0-28813  
 pulsator, accumulation of impurities and stability behaviour in high density regime 0-28835  
 pulsed erosion jet, energy characts., heat flow distribution (*Russian*) 0-33825  
 reflex tetrode, ion beam extraction anal. 0-48903  
 RF plasma torch, temp. distribution and EM field, one dimensional analysis, using finite element method 0-24264  
 source, dielec. chamber, plasma flow characts. optimisation 0-38574  
 stationary magnetoplasma dynamic source, elec. and thermal characteristics 0-14915  
 switch, grid-controlled Cs-Ba discharge, spontaneous current cutoff 0-19626  
 thermonuclear ignition by means of compact devices (*Italian*) 0-52778  
 three-rails accelerator, one cluster regime 0-6288  
 torch, reduced size inductively coupled, operation mode and detection limit 0-43994  
 torch plasmatron, high-freq., burning regimes (*Russian*) 0-38723  
 toroidal plasmas, axisymmetric, high mode number stability 0-28642  
 H, atomic beam prod. at. 90 to 500 eV from surface plasma source 0-38729  
 ZrD, electrodes with externally ignited vacuum arc, source of D<sup>+</sup> ions 0-33845

## plasma diagnostic techniques

- see also plasma probes  
 active beams for charge exchange meas., Tokamak plasma diagnostics appls. 0-48991  
 active particle beam systems for meas. of plasma pot., current and impurity profiles 0-48990  
 active spectroscopy of 4-photon scatt. in cold plasma (*Russian*) 0-1839  
 Agat, streak image camera with picosecond time resolution used in plasma investig. 0-38717  
 arc plasma flow, velocimetry methods 0-43992  
 arcs characts. meas. temp. and particle densities determ. (*French*) 0-19651  
 atom temperature measurements using thermal diffusion 0-43985  
 atomic profile determ., Fourier analysis, deconvolution of Fabry-Perot interferograms (*French*) 0-48972  
 collective electric field fluctuations of two-temp. electron gas nonthermal plasma 0-43882  
 collective oscills. in toroidal plasma, microwave scatt. diagnostic technique, review 0-48863  
 corpuscular diagnostic method of metastable atoms in glow discharge plasma, review (*Czech*) 0-24241  
 current transport at the surface of a hollow cathode, current distrib. technique 0-54048  
 density and mag. field profile determs. in diffuse pinch using magnetoacoustic oscills. 0-48986  
 density meas. by Langmuir probe and microwave interferometer 0-28819  
 density measurement of laser-compressed plasma, X-ray line shift (*German*) 0-48967  
 density profiling by interferometry with rapid spatial scanning, and Thomson scatt. of short laser pulse 0-49014  
 digital spectral techniques in plasma fluctuation diagnostics 0-49003  
 diode, field-emission type, Thomson-scatt. diagnostics 0-43988  
 echo effect, appl. to particle distrib. function regeneration (*Russian*) 0-14933  
 ECR as a diagnostic for mirror trap plasma 0-38709  
 electron beam in solar flares, diagnostic 0-26827  
 electron current component meas. method for hollow cold cathode 0-54043  
 electron density determ. by globally convergent method for partially ionised plasma 0-53929  
 electron density meas. by EM wave propag. in magnetised plasma column 0-43974  
 electron density meas. in shock generated plasma by light interferometry 0-48981  
 electron energy distrib. function measurement by probe, cct. for potential fluctuation compensation in plasma 0-54041  
 electron temp., time and space var., determ. from electron cyclotron emission meas. in Tokamak plasma 0-48996

## plasma diagnostic techniques continued

- electrons nonthermal energy distrib. meas., Fe XXV dielectronic satellite spectra appl. 0-21911  
 Faraday rot. diagnostics of laser gas discharge plasma 0-43981  
 field visualisation technique applied to sub-mm diagnostics of axisymmetric plasma 0-43980  
 flame, microwave-emission diagnostics, propane-O<sub>2</sub> flame obs. 0-45503  
 fluctuations, methods for diagnostics 0-49002  
 formation dynamics of underexpanded supersonic erosive laser plasma flare, high speed techniques 0-48923  
 formation of plasma in fusion devices, at. and plasma processes, diagnostic techniques 0-48915  
 free-free transitions, multiphoton, energy absorption laser pulse shape-independ. 0-43184  
 hard X-ray energy and flux meas. for 50 keV to 10 MeV range 0-48992  
 holographic microinterferometer to meas. plasma electron densities and other transparent objects 0-43964  
 holographic time-differential cine interferometry of gas discharge plasma 0-38716  
 hot plasma, space pot. distrib. meas. by fast neutral beam method 0-48970  
 impurity concentrations on wall during Tokamak discharges, laser probing technique 0-49013  
 incoherent Thomson scattering techniques 0-48999  
 inert gas hollow cathode arc, mol. beam sampling of metastable atoms as electron temp. probe 0-43967  
 inert gas plasma, weakly ionised, photon echo relax. obs. in RF discharge 0-43986  
 insulator surface flashover in vacuum, electro-optical meas. 0-38823  
 interferometer for electron density meas. on laser created plasma 0-48983  
 interferometry techniques for high  $\beta$ -plasma density meas., holographic and coupled cavity laser methods 0-49006  
 ion scatt., suprathermal, by partially ionised impurities, measurement of  $Z_{\text{eff}}$  0-54039  
 ion temperature profile meas. using charge-exchange neutral anal. 0-48850  
 Knudsen converter low energy electron reflection from thermionic cathode, mag. field depend. 0-19627  
 laser amplitude calibration from Raman spectra, for diagnostics (*Russian*) 0-38702  
 laser fusion diagnostics, techniques and appl. 0-49009  
 laser interferometer, optoelectronic modulation for electron density variation meas. in IR 0-4762  
 laser produced plasma density profile meas. using Wollaston prism interferometer 0-48973  
 laser-ZZ, review 0-48975  
 lasers, far IR, developed for Tokamak plasma Thomson scatt. diagnostics, review 0-24242  
 low temp. plasma diagnostics by reson. Rayleigh scatt. 0-48980  
 luminescence spectroscopy for gases excited by products of neutron nuclear reactions 0-26074  
 magnetic field determ. from charged particle beam defl. 0-28825  
 magnetic field measurement in toroidal plasma systems 0-49004  
 magnetically insulated ion diode, ion beam diagnostics 0-48974  
 magnetobremstrahlung emission, in toroidal plasma, electron diagnostics 0-48997  
 megavolt and megampere diagnostic techniques for pulsed power particle beam fusion drivers 0-49010  
 metal halide discharges, horizontal burning, parameter meas. techniques 0-38802  
 MHD power generators, combustion products plasma characterisation, generator channel flow, diagnostic techniques 0-43993  
 microcoded, aperture imaging, appl. to laser plasma diagnosis 0-24251  
 microwave interference signals from 0 to  $n.360^\circ$  phase meas. for plasma density meas. (*German*) 0-6278  
 microwave plasma detector system for gas chromatography/emission spectroscopy in environmental pollution studies 0-26070  
 microwave propag. const. determ. in temperate plasma, slab line technique 0-53992  
 Microwave reflexion in rectangular waveguides by high pressure RF plasma columns 0-43975  
 mirror machine diagnostics 0-48958  
 MM and subMM wave appl. in 100-1000 GHz range 0-17962  
 molecular lines role in plasma satellites, H<sub>2</sub>(He<sub>2</sub>) obs. 0-44053  
 monochromators, grazing incidence and normal incidence, intensity calibration in VUV for plasma diagnostics 0-48995  
 multi-pulse ruby laser recording of temporal evolution of electron density and temp. 0-14938  
 multiposition Thomson scatt., determ. of electron density and temp. profiles 0-48977  
 neutral-particle analyzer system, multichannel, for anal. of charge-exchange flux from magnetically-confined plasma 0-4804  
 neutron production in Maxwellian D ion plasmas, ion temp. diagnostics appls. 0-49005  
 optical image synchronisation with electrical parameters 0-31919  
 optical scattering of light by atoms, techniques theory 0-54044  
 optical systems for diagnostics of laser produced plasmas 0-10434  
 optically thick plasma, two-dimens. radiation restoration rel. to local diagnostics 0-43885  
 particle densities, neutral and charged, using electron beam scatt., in partially ionised He(Ar) 0-28824  
 particle-beam fusion experiments for fusion ignition, pellet compression and long solenoid approaches, breakeven experiments 0-47720  
 photographic UF-VR film, exposed to soft X-rays, quantum discrimination efficiency and sensitivity 0-22499  
 position detection and control, in Tokamaks, interferometric method 0-1850  
 pulse hollow cathode discharge, time resolved high resolution spectroscopy 0-38759  
 ram effect for conducting cylinder in drifting plasma 0-54029  
 ray phase determ., probing radiation transmittivity modulus for plasma column 0-38658  
 refraction into a nonlinear medium: wave profiles and hysteresis 0-43395  
 resonance fluorescence diagnostics, of high temp. H<sub>2</sub> plasma 0-48971  
 resonance fluorescence method for plasma diagnostics, at. density and temp. meas. 0-49001  
 reverse field pinch, Faraday rot. diagnostics for internal mag. field 0-43976  
 rotation meas. by perturbed mag. field phase slip between X-ray and field detectors 0-48982



**plasma diagnostic techniques continued**

- sampling techniques for long-wavelength electron wave dispersion evolution meas. 0-6283
- scattered radiation intensity fluctuation method (*Russian*) 0-14932
- soft X-ray analysers for pulsed-source emissions 0-31957
- soft X-ray emission from Tokamak low  $\beta$  mag. confinement systems 0-48959
- solar emission lines of NeV, MgVII, SiIX, SXI, population levels as function of electron density and temp. 0-21963
- solar plasmas density determination, N III and O IV intersystem multiplets appl. 0-31264
- Spacelab Picpab expt., phenomena induced by charged particle beams obs. 0-17443
- spatial imaging detector system for pulsed plasma extreme ultraviolet diagnostics 0-33821
- spectral method for temperature field determ., in asymmetrical plasmas (*Czech*) 0-38704
- spectroscopic effects in dense and ultradense plasmas, review 0-43990
- spectroscopy techniques development, review 0-43991
- submillimetre diagnostics, active, of Ar arc, data numerical anal. 0-48979
- subMM compensation-type interferometer to receive probing radiation for optically dense plasmas 0-54037
- surfatron produced electron density and temp. microwave meas. 0-43965
- temporal and spatial meas. of RF electric field in magnetized plasma using emissive probe 0-54042
- thermoanemometric sounding, ion energy accommodation coeff. meas. in rarefied plasma 0-16722
- Thompson scattering for electron beam and plasma diagnostics (*Russian*) 0-54031
- Thomson scatt. pathways calibration, rel. to diagnostics (*French*) 0-43886
- Thomson scattering, 4-channel spectral analyser 0-31905
- three-mirror image rotator use in laser produced plasma expt. 0-33814
- Tokamak fusion reactor, TFTR, plasma generation and confinement 0-42864
- Tokamak plasmas, measurement of electron cyclotron emission using fast response InSb subMM detector 0-27347
- UV radiometric standards, gas discharges, plasma diagnostics appls. 0-47088
- XUV emission as a diagnostic of laser-heated plasmas 0-48994
- Z-pinch, dense plasma, H $\alpha$  line profile, density meas. 0-43987
- Al coated glass microballoon targets for laser implosion expt., search for shell disintegration 0-33792
- Ar plasma radiation obs., line and continuous spectra (*French*) 0-19619
- H-like ions in laser-produced plasma, Balmer fine struct. (broadening) 0-48860
- He non-equilib. plasma diagnostics, PLTE model and steady state attainment 0-38715
- Mo<sup>29+</sup> to <sup>39+</sup> photoionis. cross sections, radiative recomb. rate coeffs., rel. to plasma diagnostics 0-52953
- Nd:YAG laser multipass cell for Raman scatt. diagnostics 0-1231

**plasma diagnostics**

- see also *plasma density; plasma diagnostic techniques; plasma diagnostics by laser beam; plasma temperature*
- absorption in laser-produced plasma expts. 0-14931
- acoustic noise in electric arcs, arc temp. meas. appl. (*French*) 0-28865
- additional heating in Tokamaks, specific diagnostics review 0-28753
- air, DC point-to-plane elec. discharge, temp. patterns, Michelson interferometry 0-54061
- air, flowing glow discharge, negative ion density, probe and gasdynamic thermometer diagnostics 0-28821
- air discharge, HF, bipolar, reduced-pressure, elec. macroparameter diagnostics 0-1854
- Alcator, electron cyclotron emission, polarisation freq. depend. 0-33808
- Alcator A Tokamak, spatial profiles of light impurity ions 0-48948
- alkali metal, dense arc plasma, elec. and heat conds., two-probe diagnostics 0-38560
- alkali-metal hollow cathode arc, low-pressure, current limiting 0-6304
- anomalous conductivity and electron heating, in two-stream unstable plasma 0-6219
- anomalous glow discharge Faraday dark space, electron vel. distrib., Langmuir probe meas. 0-44040
- anomalous turbulent resistivity at high drift vels., rel. to confinement and fluctuations in toroid 0-24139
- anomalous turbulent resistivity at high drift vels., toroidal plasma 0-24138
- anomalously resistive phase, spiky density fluctuations and relax oscill., microwave scatt. obs. 0-38547
- arc, electrical characts., effects of laminar and turbulent flows 0-1870
- arc, of Cs-film coated hollow cathode, intermediate press. operation 0-6305
- arc, plasma parameters, probe and spectral meas. 0-24273
- arc hollow cathode, diagnostics 0-44043
- arc plasma, temp. meas. by submillimetre diagnostic technique 0-38853
- arc plasma electron density meas., high-pressure, by strioscopy and IR absorption (*French*) 0-19620
- Balmer H $\beta$  line profiles, mag. field effects on afterglow plasma 0-1849
- beam-plasma discharge, characts. in crossed elec. and mag. fields (*Russian*) 0-10396
- Blumlein-type transverse fast discharge, voltage meas. 0-19642
- Brillouin backscatt. depend. on density scale lengths near crit. density 0-43888
- broadening of free-bound radiation thresholds, expt. results for Cl<sup>-</sup>, I<sup>-</sup> and Br<sup>-</sup> 0-53940
- bumpy torus, NBT-I, effective toroidal curvature, error field, electron beam diagnostics 0-24237
- charge exchange neutrals, spectrum, meas. in rot. plasma 0-38706
- charge exchange neutrals detection based on H<sub>2</sub><sup>+</sup> negative surface ionisation on ThO<sub>2</sub> 0-6280
- circuit breaking arc column electrical conductivity meas., microcomputer appl. (*French*) 0-28864
- coefficients of viscosity of a gaseous plasma 0-43875
- coherent four-wave scatt. 0-28681
- cold cathode arc starting, probe and high speed photography obs. 0-38832
- continuous emission, ionisation potential lowering and total excitation cross section of atmospheric thermal plasma 0-38705
- continuous optical discharge, diagnostics 0-43947
- corona, discharge pulses, field strength and electron density calcs. 0-38814

**plasma diagnostics continued**

- current disruption, in Tokamak plasmas, schlieren signal meas. from millimetre waves 0-48998
- current generation by electrostatic travelling waves in collisionless magnetised plasma 0-53976
- current-driven collisionless drift instability 0-14893
- cyclotron harmonic waves props. from perpendicular dispersion relation 0-38612
- cyclotron radiation from magnetically confined plasmas, review 0-38722
- cyclotron self-absorption in two-temp. plasma, temp. and density meas. 0-48987
- data acquisition system assembly for pulsed fusion experiments 0-49011
- dense plasma, spectral series degeneracy 0-19622
- dense plasma XUV transition Doppler broadening suppression, collisional-radiative model 0-19614
- density fluctuations, microwave scatt. obs. 0-48851
- density profile of Z-pinch plasma, interferometry 0-6277
- diffuse pinch, energy equilib., tensor cond. model 0-24209
- diffusion of charged particles along mag. neutral line 0-6218
- discharge, capillary pulse type, spectral chronographic-equidensitometric diagnostics 0-44055
- discharge, hollow-cathode type, cathode fall width determ. with fixed shadow probe 0-24292
- DIVA, scrape off layer, multigrid energy analyser applications 0-33818
- divertor fluxes in stellarators and torsatrons, azimuthal distrib. 0-6216
- Doppler temp. measurements in TFR Tokamak using spectral scanning in VUV, monochromator design 0-38703
- drift and current flow of charged particle along mag. neutral line 0-1749
- drift wave spectra modulation due to HF fields 0-38624
- duoplasmatron anode plasma, ion temp. 0-6292
- ECR fundamental ordinary mode absorption and emission, in PLT 0-43943
- electrical conductivity of high-density, shock-heated Ar and Xe plasmas 0-38557
- electrical conductivity of nonideal high-pressure plasma, Ar arc IR continuum absorption obs. 0-38558
- electron and at. excited states densities in laser prod. He plasma 0-38710
- electron and heavy particle temp. difference in Ar arc, laser interferometry 0-38766
- electron beam controlled discharge, cathode density waves 0-38798
- electron beam current meas. in gas 0-38523
- electron beam-formed plasma potential, two-electrode probe diagnostics (*Russian*) 0-1841
- electron cyclotron emission in steady state inhomogeneous plasma 0-48864
- electron cyclotron frequency expts. in 15X-B Tokamak, temp. rel. to heating power 0-48912
- electron cyclotron heating in Tokamaks: experiments and prospects 0-28749
- electron cyclotron resonance plasma, production of multiply-charged ions, X-rays and charge state distrib. meas. 0-43941
- electron density, temp., and distrib. function, in ion beam-created high-pressure plasma (*French*) 0-10407
- electron density meas. by EM wave propag. in magnetised plasma column 0-43974
- electron distribution function, plasma stream, probe diagnostics 0-14935
- electron distribution relaxation numerical study for CO<sub>2</sub>-N<sub>2</sub>-He discharges 0-54070
- electron long-wavelength wave dispersion evolution meas., sampling technique 0-6283
- electron temp. meas., continuous, automatic, using double Langmuir probe 0-43977
- electron temperature measurements from cyclotron emission in T-10 Tokamak 0-19617
- electron-beam inertial confinement expts. at Valduc (*French*) 0-48907
- electrostatic waves in drifting ionospheric simulation 0-53965
- EM trap confinement, microwave investig. (*Russian*) 0-10416
- emission from plasma formed in proton beam collision with Al target 0-53946
- energy balance in PLT Tokamak 0-28733
- energy distribution of electrons heated by laser light absorpt., simulation and test particle methods 0-48963
- ERASMUS Tokamak data acquisition system, program struct. 0-49012
- Faraday rot. meas. in high- $\beta$  fusion expts., plasma electron density and mag. field determ. 0-49008
- flow over flat plate, flush probe studies 0-1845
- flush probe studies of plasma flow over flat plate 0-24147
- focus dynamics with powerful laser interaction during MHD stage, diagnostics 0-48924
- fusion experiments application conf., Varenna, Italy (Sept. 1978) 0-48989
- fusion plasma, RF phased waveguide heating, thermal eddies form. 0-24193
- fusion plasma in beam driven Tokamak, Fokker-Planck/transport analyses 0-28826
- fusion possibilities and plasma confinement and interactions in mag. config. Tokamak, review (*French*) 0-54017
- gas filled microballoon targets, laser produced implosion dynamics 0-24198
- generator arc chamber, hydrodynamic struct. 0-1817
- glass microballoon imploded by laser, X-ray transmission analysis (*French*) 0-54011
- graphite hollow cathode glow discharge C conc. determ. 0-44032
- grid influence, on low-voltage Cs arc plasma in 3-electrode system 0-38844
- Hall effect in toroidal discharge, investig. 0-38701
- He I and II radiation enhancement in mag. field, nonlocal thermodynamic equilib. 0-10366
- heating experiments, diagnostics, turbulent heating example 0-49015
- heating mechanism obs. and analysis, with fast theta pinch (*Japanese*) 0-1818
- HF discharge, near electrode region, spectra 0-38833
- high current, high pressure, discharges, conductivity meas. 0-38793
- high-power neutral beam, spectral resolution by optical diagnostics 0-33819
- hollow cathode glow discharge, state of equilib., spectroscopic meas. 0-19647
- impurity density in DITE Tokamak, soft X-ray meas. 0-19616
- impurity deposition in ISX-Tokamak, time resolved measurements 0-38694



# plasma diagnostics continued

inert gas afterglow, excimer form., VUV emission obs. at low press. 0-38755  
inert gas halides, excimer emission from electron beam produced plasma 0-43887  
inert gas stationary afterglow obs. of singly charged atomic ions, three-body rate coeffs. 0-38757  
inhibited electron thermal cond. in plasma from microwave laser irradiation, laser intensity threshold Z-depend. 0-48928  
ion beam scattering by ion-acoustic turbulence 0-6262  
ion charge distribution, in 10.6 micron heated laser induced plasma, X-ray diagnostics 0-6271  
ion composition of plasma of pulsed discharge in He, H<sub>2</sub><sup>+</sup> current time evolution 0-54046  
ion composition of pulsed discharge plasma, optical, probe, mass spectroscopic anal. 0-33840  
ion current from Penning discharge ion source, depend. on mag. field and anode diameter 0-54072  
ion-acoustic dissemination in moving plasma jet 0-38707  
ion-acoustic instability, electron flux driven, in Q-machine, probe diagnostics 0-33765  
ion-acoustic instability stabilisation by ion beam in Q-machine, probe diagnostics 0-33766  
ion-acoustic waves in two electron temp. plasma, collisional and Landau damping 0-19572  
ionisation dynamics of CO<sub>2</sub> laser prod. plasma, spectrosc. obs. 0-43968  
ions, multiply ionised, electron impact line width, semiclassical formula 0-43972  
IR thermography of high-power neutral beam target 0-33820  
jet, absolute spectral brightness measurement 0-28832  
JIPP T-II, electron cyclotron emission meas. using double-pass optical spectrometer 0-54035  
JIPP T-II tokamak plasma, Mo impurity diffusion during H<sub>2</sub> gas puffing 0-28602  
JIPP-T-II Tokamak plasma, time resolved spatial profiles of impurities 0-48950  
kinetic reactions, pulsed afterglow technique obs. in Ar-II plasma 0-48854  
Knudsen arc ignition, plasma form. kinetics, spectroscopic and probe obs. 0-38808  
Langmuir turbulence meas., forbidden transition satellites 0-38714  
Langmuir waves, driven by electron-ion decay instability, scattered spectrum 0-43970  
laser plasma, backscattered light pulse shape depend. 0-10431  
laser produced plasma, structure of XUV emitting regions 0-54038  
laser radiation energy loss to resonantly accelerated ions X-ray meas. of energy distrib. 0-10413  
laser thermonuclear fusion, shell target parameters meas. using X-ray schlieren method 0-14942  
laser-irradiated glass shell plasma, electron temp. and density, Si X-ray emission diagnostics (*Chinese*) 0-38718  
laser-produced multiple-charged ions, pressure dependence, microwave meas. (*Japanese*) 0-10412  
laser-produced plasma, spectral line shape and intensity, multicharged ion obs. 0-10435  
laser-produced plasma, X-ray spectrometry, for energy transport diagnostics (*French*) 0-43982  
light impurities, diagnostics in T-4 Tokamak plasma (*Russian*) 0-10432  
low frequency parametric processes in magnetically confined plasmas 0-28827  
lower hybrid cones, trajectory meas., mag. field line determ. 0-33817  
lower hybrid wave propag. and parametric decay in WEGA Tokamak 0-28725  
Lyman- $\alpha$ , line broadening calc. 0-43984  
magnetic diverters for experimental Tokamaks and fusion reactors 0-18621  
magnetic field strength meas. in high density plasma, spectrosc. method 0-1843  
magnetic mirror experiments, measuring MeV ions from fusion reactions 0-6281  
magnetic mirror trap, open, with min. B, LF oscils. 0-38708  
magnetic pickup for spontaneous magnetic fields meas. near laser plasma 0-24246  
microwave dynamic interaction, probe diagnostics 0-19584  
microwave heating in ELMO Bumpy Torus, anal. 0-28829  
molecular beam mass spectrometric sampling system, ion concs. in coal-fired MHD plasmas 0-52358  
moving arc, microcrater current and spectral fluctuations, simultaneous meas. 0-38828  
multi-chord particle diagnostics of a plasma column (*Russian*) 0-1840  
multicharged ions, in laboratory plasma, spectroscopy 0-24255  
N<sup>2+</sup>, <sup>2+</sup>, <sup>3+</sup> lines Stark broadening, He(II) line diagnostics in theta pinch plasma 0-24249  
negative grid pulse effects, on Knudsen Cs arc discharge plasma 0-38843  
neutral density profile, absolute meas. by H <sub>$\alpha$</sub>  line reson. fluorescence 0-24250  
nonideal plasma, measured props. and nonideality influence 0-43869  
nonlinear pressure forces for laser radiation in plasma, experimental confirmation 0-28682  
optical measurements on plasma initiated by a relativistic electron beam (*Japanese*) 0-48914  
paramagnetism in RF mag. field, expt., theory and simulation 0-6225  
parametric decay spectrum of heating near LH frequency in Petula 0-28761  
parametric heating near lower hybrid frequency in Petula 0-28760  
parametric instabilities in weakly-inhomogeneous hot plasmas 0-28828  
partial discharge spectra meas. by multichannel amplitude analyser system (*Italian*) 0-33847  
particle distribution function, diagnosis using echo effect (*Russian*) 0-14933  
PDX Tokamak, Ti density meas. using Ti XVII forbidden line 0-32496  
Penning discharge ion source with hollow cathode, HF instabilities 0-43997  
polarized light interferometer for laser fusion studies 0-31855  
poloidal rotation velocity determ. in FT-1 Tokamak (*Russian*) 0-19565  
polyethylene, laser-prod. plasma, space-resolved extreme UV emission 0-54015  
polyethylene, X-ray emission spectra of CO<sub>2</sub> laser-irrad. targets, nonlinear processes 0-33793  
positive corona electrode, negative ion counterflow, elec. field strength meas. 0-38817

# plasma diagnostics continued

pulsed EUV diagnostics using spatial imaging detector system 0-33821  
pulsed micro-discharges, optical interferometry obs. 0-38804  
radiation intensity calcs. in vacuum UV region (*Russian*) 0-48861  
radiation losses from T-10 Tokamak, pyroelectric detect. (*Russian*) 0-53936  
rarefied plasma flow, degree of nonisothermality, probe meas. 0-24243  
ray tracing near electron cyclotron reson., finite temp. effect 0-53994  
resonance cone trajectory, focused, nonlinear modification, probe diagnostics 0-10379  
resonance scattering in an argon high current low pressure discharge 0-38735  
resonant absorption in Ar plasma at thermal equilib. 0-1799  
RF sputtering, impedance matching networks, experimental and design information 0-50555  
RF voltage in plasma probe sheath, effect on electron energy distrib. meas. 0-54045  
rotating high current arc, hot wake investigation 0-1862  
runaway electron instability, non-thermal microwave radn. 0-1842  
shock-heated dense plasma, continuum radiation and optical transmittance diagnostics 0-24202  
solar flares, Fe XXI 1354 Å obs. from Skylab rel. to ionisation equilib. calcs. 0-21956  
space charge field, spatio-temporal distrib. determ. in breakdown 0-38771  
space charge phenomena in gyrotrons 0-28868  
spatially resolved suprathermal X-ray emission from laser-fusion targets 0-48984  
spectral diagnostics of plasma object with known contours 0-1846  
spectral line emission from C-H plasmas generated by TEM<sub>10</sub> laser pulses 0-43969  
spectral line profile of low-pressure afterglow plasma in mag. field 0-6285  
spectral lines of laser produced plasma, space depend. shift 0-6268  
spectroscopic diagnostics of plasmas in space and the laboratory 0-38721  
spontaneous magnetic field, target size and struct. depend. 0-1819  
strong Langmuir turbulence for electron plasma waves, plasma diagnostics appl. 0-48889  
supercritical density profiles of CO<sub>2</sub>-laser-irradiated microballoons 0-14918  
superradiation from non-ideal plasmas in electric field 0-38568  
surfatron produced electron density and temp. microwave meas. 0-43965  
symmetrical implosion system, charged reaction products, electrostatic field effects 0-32499  
T-10 Tokamak, plasma X-ray emission 0-28840  
T-tube plasma, influence of boundary layer on H <sub>$\alpha$</sub>  line 0-48862  
temperature determination from H<sub>2</sub> and D<sub>2</sub> molecular band intensities in low pressure plasma 0-37896  
temperature meas. in inhomogeneous plasmas appl. of Bartels' theory of radiation 0-53948  
TFR, ICRF heating obs. by all metal antenna 0-18606  
TFR 600, <sup>2</sup>H ion flux, temp., and density meas. 0-48940  
thermal end loss from plugged theta pinch 0-1836  
thermonuclear dense plasma, neutron diagnostics, book contrib. 0-24253  
thermonuclear fusion plasmas, elem. processes and role of atomic, ionic and mol. data 0-14916  
theta-pinch, neutral current sheet, electron energy distrib. meas. 0-43954  
Thompson scattering for electron beam and plasma diagnostics (*Russian*) 0-54031  
Tokamak, DITE, arcing, time-resolved meas. 0-10436  
Tokamak, PLT, fast-wave heating of two-ion plasma through minority cyclotron reson. damping 0-24194  
Tokamak (Alcator), driven lower-hybrid waves, light scatt. study 0-1835  
Tokamak plasma spectroscopic diagnostics, Fe ion resonance-line intensity meas. 0-48993  
Tokamaks, electron freq. rad. spontaneous emission 0-53944  
toroidal discharge, optical meas. of primary avalanche 0-54059  
trapped electrons, test charge pot. in single wave case 0-24247  
Tuman-2A, plasma compression particle diagnostics, density and temp. (*Russian*) 0-38677  
two phase flow, particle velocity optical meas. (*Russian*) 0-54032  
unstable turbulent ionisation waves, two dimensional Fourier spectroscopy 0-38646  
vacuum arc in Cu cathode region, current parameters, theory 0-54068  
weakly-ionised plasma diffusion in apparatus with spatial axis (*Russian*) 0-1826  
whistler wave trapping in density crest 0-53984  
X-ray deconvolution method from hot plasmas 0-54030  
Al, laser-prod. plasma, space-resolved extreme UV emission 0-54015  
Al reflective target, momentum and energy transfer pulse duration/polarisation depend., torsion pendulum diagnostics 0-43952  
Al, X-ray emission spectra of CO<sub>2</sub> laser-irrad. targets, nonlinear processes 0-33793  
Ar arc discharge, parameters variation during extinction obs., by spectroscopy and laser interferometry (*French*) 0-19653  
Ar DC magnetron discharge, spectroscopic obs. 0-44010  
Ar, decaying plasma arc, electron disappearance mechanism 0-38765  
Ar discharge, population processes of 4p levels, perturbation influence 0-38565  
Ar, HF discharge, arc type, spectral parameters 0-1873  
Ar high density plasma, highly excited atomic levels, spectral-line-blending study 0-48969  
Ar hollow cathode arc, in mag. field up to 2 kOe, plasma parameters 0-6306  
Ar low temp. plasma flow, interaction with intense microwave beam 0-38654  
Ar, positive column, contracted, electron density, temp., elec. field, line emission 0-6311  
Ar, sputtering glow discharge, metastable and reson. states density meas. (*French*) 0-14955  
Ar, stream electrons, at atm. press., temp. and conc. from study of electrical parameters (*Russian*) 0-53930  
Ar-air arc, stabilised, spectroscopic methods of temp. meas. (*Russian*) 0-38854  
Ar-hexamethyldisiloxane, glow discharge positive column ion mass spectra identification 0-38834  
C spectra from CO<sub>2</sub> laser prod. plasmas 0-38711  
CN molecular bands in N<sub>2</sub> and air-O<sub>2</sub> arcs, CN origin, band identification 0-38803  
CO-Ar, glow discharge, ion cluster in positive column, ion mass spectra diagnostics 0-38752



## plasma diagnostics continued

- CO-He(-O<sub>2</sub>), glow discharge ion cluster in positive column, ion mass spectra diagnostics 0-38752  
 CO<sub>2</sub> lasers, CO<sub>2</sub>-CO-N<sub>2</sub>-He, ionisation wave, slow changes, dispersion curves 0-38822  
 CO<sub>2</sub> plasma, atm. press. opt. props., 400-1200 nm spectral range and 10<sup>3</sup>-2×10<sup>4</sup> K temp. 0-33753  
 CO<sub>2</sub>-laser radiation filamentation in underdense H<sub>2</sub> plasma, X-ray diagnostics 0-14941  
 Cl<sub>2</sub>-arc, low temp., visible and IR continuum radiation 0-38784  
 Cr from Tokamak-produced plasma, 2s<sup>2</sup>2p<sup>k</sup>-2s2p<sup>k+1</sup> transitions in F I to Be I isoelectronic sequences 0-37765  
 Cs thermionic convertor, pulsed, plasma parameters, operating characts. 0-6293  
 Cs-Ba, high current Knudsen arc discharge, spontaneous extinction, optical diagnostics 0-44044  
 Cs-CO<sub>2</sub>-He glow discharge, quenching cross section of resonant Cs(6P) state by CO<sub>2</sub> mols. 0-43860  
 DyI<sub>1</sub>-Hg arc discharge plasma, spectroscopic study 0-54033  
 Eu<sup>+</sup> metastable states in discharge plasma, anomalously high speed deexcitation, modulation of induced radiation obs. 0-44014  
 Fe from Tokamak-produced plasma, 2s<sup>2</sup>2p<sup>k</sup>-2s2p<sup>k+1</sup> transitions in F I to Be I isoelectronic sequences 0-37765  
 H Balmer lines, plasma-broadening in wall-stabilised arc, low electron density 0-43891  
 H high power arc, standard source of continuum radiation, 53-92 nm 0-44054  
 H<sup>-</sup>, density meas. by photodetachment 0-48976  
 H<sub>2</sub> plasma reactor design, heat transfer and flow 0-38697  
 H<sub>2</sub> pulsed arc, dense plasma, Balmer spectrum near photorecombination threshold, press. depend. 0-38569  
 He(Da) plasma red shift meas. in Ar arc, ion dynamic depend. 0-10364  
 He, afterglow produced by microwave surfguide, spectroscopic diagnostic, electron and He<sub>2</sub> rot. temp. 0-44042  
 He, duoplasmatron arc, ionisation meas., line intensity ratios 0-54060  
 He, fast electron energy distrib. in positive column and negative glow 0-38764  
 He glow discharge, n=3 sublevel quenching and energy transfer, laser perturbation method 0-44060  
 He glow discharge, negative-luminesc. plasma, electron energy distrib. from line intensities and probe obs. 0-49033  
 He I line profiles, ion motion effect in low electron density plasma 0-43877  
 He I plasma lines, Stark broadening, quantum mechanical calcs. 0-43880  
 He pulsed arc, Thomson scatt. diagnostics 0-24297  
 He-Cu discharge, Cu ion laser, at. emission obs. of plasma props. 0-19021  
 He-N<sub>2</sub> plasma, N<sub>2</sub> B<sup>3</sup>Π<sub>g</sub> state excitation, role of long lived states, luminesc. 0-37829  
 He<sub>2</sub><sup>+</sup> recombination, high-temp., in plasma jet (French) 0-43861  
 HeI, low density suprathermal field fluctuations and high energy electrons 0-1847  
<sup>3</sup>He-Hg (-Kr) + <sup>3</sup>He(n,p)T, high press. plasma excitation, luminesc. spectra 0-38719  
 Hg, optically pumped positive column, E-I characts. 0-44035  
 Hg plasma flow, electron temp. determ. from partial LTE populations 0-24248  
 Hg-Ar, HF discharge, electron energy distrib. and atom ionisation processes 0-44048  
 K plasma in arc and capillary devices, optical props. 0-24244  
 K<sub>2</sub><sup>+</sup> ion formation in low press. K discharge plasma 0-43862  
 Kr-Cl<sub>2</sub> mixture, glow discharge positive column, electron energy distrib. and rates of inelastic processes, negative Cl ions form. 0-19632  
 Mn XVII to Mn XXII ions spectrum emitted by Tokamak produced plasma 0-10437  
 N I plasma jet, spectroscopic diagnostics, Stark broadening and shift, study 0-38727  
 N<sub>2</sub><sup>+</sup>, spectral line breadth in molecular nonequilibrium plasma (Russian) 0-48044  
 N<sub>2</sub> afterglow, chem. reactions rel. to plasma props, appl. to toluene polymerisation 0-3346  
 N<sub>2</sub> arc, magnetically stabilised cross-flow, temp. and flow fields meas. 0-54054  
 N<sub>2</sub>, diffuse plasma, population densities of triplet states, correl. with electron impact processes 0-43966  
 N<sub>2</sub> glow discharge, neutral components comp., mass spectroscopy study (Russian) 0-10439  
 N<sub>2</sub> plasma, non-equilib., excited species, vibr.-rot. anal. fluoresc. obs. 0-54034  
 N<sub>2</sub> positive corona into spark, prebreakdown phase, spectroscopic anal. 0-38790  
 N<sub>2</sub> vibrational levels stepwise excitation, effect on electron energy balance in He-N<sub>2</sub>-CO<sub>2</sub> discharge 0-54071  
 N<sub>2</sub>-Ar corona discharge, convection and mixing, atm. press., mass spectra obs. 0-1853  
 N<sup>(2)D</sup>, P metastable ats. prod. in N<sub>2</sub> DC glow discharge 0-38758  
 Ne, discharge, excitation mechanisms investig. using radial distrib. of excited atoms 0-38744  
 Ne, discharge, low-press., atom densities of first excited state 0-38750  
 Ne, excited atoms reactions in pure afterglow, plasmas using resonance absorpt. spectrometry 0-33835  
 Ne Townsend discharge, Ne<sub>2</sub><sup>+</sup> form. and destruction 0-38747  
 Ne, Townsend discharge afterglow, decay rate of metastable ats. 0-44011  
 Ne-Ar discharge, transient cathoporesis, time depend. 0-38753  
 Ni from Tokamak-produced plasma, 2s<sup>2</sup>2p<sup>k</sup>-2s2p<sup>k+1</sup> transitions in F I to Be I isoelectronic sequences 0-37765  
 Pb, X-ray emission spectra of CO<sub>2</sub> laser-irrad. targets, nonlinear processes 0-33793  
 Pt, laser produced plasma, Ni-like X-ray spectrum 0-43983  
 SF<sub>6</sub> plasma column, in Maecker type arc, diagnostics and model (French) 0-19652  
 Si III, EUV spectra in solar transition zone rel. to energy balance and press. 0-21957  
 Si lines as spectral diagnostics for astrophysical plasmas, effect of charge transfer 0-41717  
 Si:H, amorphous, control and anal. of deposition, using plasma spectroscopy 0-45230  
 Ti density, in DC sputtering discharge by atomic absorpt. spectroscopy 0-43973  
 Ti, laser-prod. plasma, space-resolved extreme UV emission 0-54015

## plasma diagnostics continued

- Ti spectral line excitation by 100 eV electrons in inner discharge column (Russian) 0-38529  
 Tl, axial distrib. in unipolar arc discharge, influence of Li conc. 0-19656  
 Tl-Xe, electric discharge excitation of Tl in high-press. Xe 0-49025  
 Xe discharges, electrodeless, UHF in waveguide rel. to DC characts. 0-38762  
 Xe, plasma column in flashtube, characts. and parameters 0-54053  
 Xe-He plasma, plasma parameters determ. 0-54047  
 Xe<sub>2</sub><sup>+</sup> excimer form. in pulsed discharge, visible emission obs. 0-38754  
 Zn I, relative populations in arc, sputtering and gas phase collisions 0-934
- plasma diagnostics by laser beam  
 absorption, z-depend., stimulated backscatter processes in laser plasma 0-43944  
 air, laser-induced breakdown over long distances 0-33795  
 air gap, drift vel. meas. of ionized particles 0-24298  
 Alcator Tokamak, IR laser probing 0-10433  
 amplitude calibration from Raman spectra (Russian) 0-38702  
 arc plasma, atmospheric, electron density meas. by two-wavelengths interferometry (Japanese) 0-38720  
 arcs characts. meas. temp. and particle densities determ. (French) 0-19651  
 atomic absorption spectra, high freq. Stark effect 0-23359  
 density profiling by interferometry with rapid spatial scanning, and Thomson scatt. of short laser pulse 0-49014  
 diode, field-emission type, Thomson-scatt. diagnostics 0-43988  
 effective cross section and space charge, preionised gas laser induced breakdown 0-48930  
 electron density meas. by far IR laser beam deflection 0-48966  
 electron temperature meas. by Thomson laser scatt., θ-pinch energy loss (Chinese) 0-54028  
 far IR lasers, development for Thomson scatt. diagnostics of Tokamak plasma, review 0-24242  
 fast IR laser interferometry, electronic density fluctuation meas. 0-49000  
 free-free transitions, multiphoton, energy absorption laser pulse shape-independent 0-43184  
 glass targets, laser-produced plasma X-ray spectral lines identification (Chinese) 0-54036  
 heterodyne CO<sub>2</sub>-laser interferometer with direct phase readout for meas. electron line densities in plasmas 0-1848  
 holographic microinterferometer to meas. plasma electron densities and other transparent objects 0-43964  
 holographic study of laser prod. plasma at 10.6 μm 0-38685  
 implosion, by pulsed electron beam accelerator, 4TW, laser and X-ray obs. 0-1816  
 impurity concentrations on wall during Tokamak discharges, laser probing technique 0-49013  
 incoherent Thomson scattering techniques 0-48999  
 ion temp. and density meas. in direct current octopole by induced optical fluoresc. 0-14939  
 laser created plasma, interferometer for electron density meas. 0-48983  
 laser fusion diagnostics, techniques and appl. 0-49009  
 laser implosion microballoons, X-ray line radiation diagnostics (Chinese) 0-6279  
 laser spark absorpt. and laser pulse contraction meas. using dye lasers 0-48988  
 laser-heated plasma with large temp. gradient, ion acoustic turbulence, reduced thermal cond. 0-53987  
 magnetic field diagnosis by scatt. radiation spectral comp. (Russian) 0-28823  
 magnetic field measurement in toroidal plasma systems 0-49004  
 methanol laser, twin optically pumped far IR, use in plasma diagnostics 0-54049  
 MHD plasma, by holographic interferometry and Fourier filter correlation, Hungarian progress report 0-48965  
 multi-pulse ruby laser recording of temporal evolution of plasma parameters by light scatt. 0-14938  
 multiframing interferometer and appl. to plasma focus expt. 0-4761  
 multiple-pass laser heating of a short plasma column 0-38684  
 probing radiation Raman scatt. (Russian) 0-19618  
 resonant CO<sub>2</sub> laser radiation absorption and surface instability at crit. density surface 0-48859  
 SHG in laser plasma, review 0-53993  
 spectroscopy techniques development, review 0-43991  
 supersonic jet, ionisation in Mach disc, submillimeter laser interferometry diagnostics 0-14934  
 theta pinch, radial oscills. of plasma density and mag. field, light scatt. and probe obs. 0-14937  
 Thomson scatt. pathways calibration, rel. to diagnostics (French) 0-43886  
 Thomson scattering, rot. Raman calibration 0-1844  
 Thomson scattering with high background level of plasma scattering 0-43979  
 Tokamak electron density meas., non-interferometric FIR scheme 0-14936  
 tubular flow reactor, ion density and Z<sub>eff</sub> profiles, neutral beam attenuation technique 0-6282  
 turbulence induced by plasma-electric current interaction in focus expt., laser diagnostics 0-24171  
 Z-pinch plasma, interaction with CO<sub>2</sub> laser radiation 0-48919  
 Ar arc discharge, parameters variation during extinction obs. (French) 0-19653  
 Ar discharge, optogalvanic and excited state photoionisation signals, space charge effects 0-14947  
 Ar, hollow cathode arc discharge, collective scatt. meas., turbulence 0-48978  
 C arc in air, electron density meas. by CO<sub>2</sub> laser interferometry (Japanese) 0-28822  
 CO<sub>2</sub> laser, pulsed low-pressure far IR, appls. 0-53332  
 Cu, laser-produced plasma X-ray spectral lines identification (Chinese) 0-54036  
 D<sub>2</sub> plasma, isolated, CO<sub>2</sub> laser-produced, holographic interferometry diagnostics 0-24254  
 Fe-Ar low press. flow discharge, axial density profiles of sputtered cathode atoms 0-49029  
 H arc, electron density, interferometric determ., refr. index calc. in high press. 0-24284  
 H atoms, Rayleigh scatt. from n=2 states, fusion plasma diagnostics appls. 0-43002  
 H<sub>2</sub> plasma, resonance fluorescence diagnostics 0-48971



**plasma diagnostics by laser beam continued**

- HCN laser, temporal coherence meas., comparison of TGS pyroelec. detector with W-C point contact diode 0-31871  
 He ( $n=3, 4$ ) singlet states quenching by  $N_2$  in low-pres. glow discharge 0-49030  
 $Mo^{13+}$ , determination of spectrum using low-inductance spark and laser-produced plasma 0-19610  
 Ne afterglow plasma, 2p levels collisional transfer coeffs., laser excitation obs. 0-43856  
 Xe, s-p transitions, Stark const. and oscill. strengths, shock tube meas. 0-18822

**plasma diodes**

- collective ion acceleration in diode with insulated anode 0-14005  
 diode, field-emission type, Thomson-scatt. diagnostics 0-43988  
 duoplasmatron anode plasma, ion temp. 0-6292  
 electron processes, in collisionless diode, linear theory 0-38730  
 field reversing E-layers, translation and compression in magnetically insulated diode 0-14017  
 foil-less, appl. to rel. beam accel. from pulsar polar cap 0-17604  
 high current short bremsstrahlung pulse sources 0-5400  
 inert gas duoplasmatron, ion source 0-32560  
 magnetically insulated diode, controlling hollow electron beam current with shielding beam 0-9437  
 magnetically insulated diode, superdense MeV proton beam generation 0-14017  
 magnetically insulated diodes for prod. of intense proton beams 0-14004  
 magnetically insulated ion diode, ion beam diagnostics 0-48974  
 periplasmatron, neutral beam injectors, multi-aperture extraction systems 0-42301  
 plasmatron, high-power elec. arc AC generator, phys. processes and parameters 0-19623  
 plasmatron, coaxial, transversely blown electric arc (*Russian*) 0-24265  
 plasmatron, high freq. torch discharge calcs., burning regimes (*Russian*) 0-38723  
 plasmatron channel, spatial-temporal pulsations of arc plasma pinch 0-24210  
 plasmatron gas average enthalpy, forced heat exchange calcs. (*Russian*) 0-38724  
 plasmatron melting arc in Ar and  $CO_2$  atmosphere, performance characts., MHD calcs. (*Russian*) 0-38573  
 plasmatron with interelectrode insert, characts. 0-44009  
 thermal cathode, emission cooling (*Russian*) 0-54052  
 X-ray source, high power microsecond electron beam 0-52378  
 H<sub>2</sub> monoplasmatron arc plasma, electrokinetic parameters space distrib. (*Russian*) 0-53925

**plasma filled waveguides**

- collisionless plasma, microwave electron acceleration, waveguide obs. 0-43932  
 corrugated, relativistic electron beam interaction, combined reson. (*Russian*) 0-10394  
 discrete modes of a system subject to an inhomogeneous, high-frequency force 0-43237  
 electron wave, guided, on planar plasma slab, propag. and attenuation characts., dissipative processes 0-38608  
 EM wave propagation, effect of inhomogeneities 0-19585  
 enhanced radiation beams from three annular plasma layers coaxial line excitation 0-53996  
 fusion plasma, RF phased waveguide heating, thermal eddies form. 0-24193  
 Grill phase tracking during density increase in Tokamaks 0-28762  
 harmonic generation at microwave frequency in bounded magnetoplasma 0-48897  
 hot collisional uniaxial plasma, guided waves, TM mode dispersion rel. 0-53995  
 ICR heating in T-10 Tokamak under weak dissipation conditions 0-28759  
 ICRF heating in Macrotron Tokamak 0-28744  
 impedance of magneto-acoustic wave launching antenna 0-24180  
 linear accelerators, plasma waveguides appl. as accelerating structures 0-9438  
 lower hybrid region, antenna impedance 0-28664  
 lower hybrid self-trapping at RF gas breakdown 0-38850  
 lower hybrid wave heating in JIPP T-II 0-28722  
 magnetised plasma loaded waveguide, interaction between solitary structures 0-38661  
 microwave harmonic generation in plasma-filled waveguide 0-1798  
 Microwave reflexion in rectangular waveguides by high pressure RF plasma columns 0-43975  
 nonlinear distortion of amplitude-modulated microwave 0-28683  
 nonlinear electron plasma waves in magnetised plasma waveguide 0-38662  
 nonlinear lower-hybrid waveguide in plasma, stability 0-19578  
 parametric decay spectrum of heating near LH frequency in Petula 0-28761  
 resonator, electron-beam excited, explosive instability 0-28693  
 slow-fast mode conversion effect on lower hybrid slow mode excitation 0-28668  
 solitary structures in magnetised plasma loaded waveguide 0-48878  
 two-stream instability, nonlinear evolution, numerical simulation 0-43938  
 UHF discharge with preliminary locally ionised gaseous medium 0-38851  
 wave heating at electron cyclotron harmonics in toroidal plasmas 0-28727

**plasma flow**

- see also *plasma focus; plasma magnetohydrodynamics*  
 arc lamps, Hg vertical, Hg plus I, metal halide, convection effects study 0-6299  
 arc nozzle clogging theory 0-38791  
 arc plasma flow, velocimetry methods 0-43992  
 astrophysical plasma, highly ionized, ionization equilib. validity 0-21906  
 atmospheric pressure plasma flow, boundary layer charged particle density profiles 0-38571  
 auroral plasma, turbulent acceleration by electrostatic waves (*Russian*) 0-53952  
 Bohm-type thermal losses from high- $\beta$  plasma 0-38679  
 Buneman-Farley instability, nonlinear decay interactions 0-38616  
 centrifuges, fluid flow analysis, third-order differential equation solution (*Japanese*) 0-53949  
 coaxial channel flow of accelerators and compressors, two-dimens., simulation 0-19566

**plasma flow continued**

- collisionless plasma, expansion into vac., ion accel., instability devel. electron heat flow 0-38575  
 constricted glow discharge in transverse air flow 0-24278  
 continuous optical discharge, diagnostics 0-43947  
 convective cell formation and EM drift wave turbulence 0-24168  
 critical surface, enhanced stimulated Brillouin scatt. due to light refl. 0-1750  
 density plateau effect on inverse bremsstrahlung 0-43894  
 diffusion in toroidal traps, anomalous electron viscosity (*Russian*) 0-48956  
 diffusion reduction by plasma rotation and ion dissipative effects 0-38696  
 discharge under transverse convection conditions 0-24272  
 EM field induced resultant drift inwards from boundary, in D-T plasma 0-38577  
 expansion into vacuum, ion acceleration 0-6228  
 flush probe studies of plasma flow over flat plate 0-24147  
 free-burning arcs, simple theory 0-6297  
 fusion reactors, divergent impulsive crossflow over packed columnar arrays 0-47702  
 gas discharge, perturbation by longitudinal turbulence 0-24271  
 generator arc chamber, hydrodynamic struct. 0-1817  
 guiding center orbits and topology of noncircular axisymm. Tokamak plasmas 0-6227  
 heat exchange of low-temp. plasma with wall, longitudinal mag. field effect 0-33781  
 high density directed plasma, source, design, characts., numerical model 0-38538  
 ion beam extraction from flowing plasma 0-18044  
 ion source, high current, plasma supply to extraction region, theory and expt. 0-14023  
 ionised gas, nonequilibrium, supersonic, corner expansion flow, physical aspects 0-1639  
 ionised mixture, dense, binary, dynamical props., statistical mechs. 0-43895  
 ionosphere, plasma flow, var. in topside and F-layer, ionospheric-protonospheric interaction model calcs. 0-4180  
 ionospheric rocket-borne mass spectrometer, Monte Carlo prediction of +ve ion collection 0-8459  
 JIPP T-II tokamak plasma, Mo impurity diffusion during H<sub>2</sub> gas puffing 0-28602  
 laser supported absorption waves, momentum transfer to surface, flowfield model 0-14921  
 laser-fusion regime, plasma transport, extension of Braginskii system of fluid equations 0-53935  
 laser-irradiated solid target, nonlinear dynamics 0-28767  
 linear gasdynamic confinement system 0-48957  
 macroparticles elimination from plasma stream, using curved plasma duct 0-33826  
 magnetic mirror, injected plasma particle refl. (trapping), quiescent (turbulent) plasma 0-48955  
 magnetoacoustic disturbance, hydrodynamic instability in nonuniform plasma flow (*Russian*) 0-1766  
 mass separation in rotating weakly ionised plasma (*Russian*) 0-1745  
 metal surface, high-intensity laser beam interaction 0-19600  
 MHD converter channel flow 0-24261  
 microwave beam interaction, intense, with low temp. plasma flow, space distrib. 0-38578  
 nonlinear interactions and hydrodynamics in HF field (*Russian*) 0-53951  
 numerical methods in fluid dynamics, conference, Tbilisi, USSR (June 1978) 0-17717  
 photoabsorption convection in horizontal tube, unsteady-state convection, num. investig. 0-33594  
 poloidal rotation velocity determ. in FT-1 Tokamak (*Russian*) 0-19565  
 probe meas. of flow over flat plate 0-1845  
 production and flow of plasma in ion beams 0-28624  
 pulsed erosion jet, energy characts., heat flow distribution (*Russian*) 0-33825  
 pulsed laser-generated impulse on a surface in supersonic flow 0-48917  
 radiation induced shock tube flow nonuniformities in ionising Ar 0-43865  
 radiation pressure dominated plasma flow 0-1763  
 ram effect for conducting cylinder in drifting plasma 0-54029  
 rarefied plasma flow, degree of nonisothermality, probe meas. 0-24243  
 rotating plasma, charge exchange neutrals, spectrum 0-38706  
 seeded combustion gas near cold electrodes, MHD boundary layer 0-48865  
 self-gravitating plasma with finite ion gyroviscosity effects rotating layer instability 0-56706  
 self-similar expansion of a plasma into a vacuum 0-28623  
 Shuttle/Spacelab platform in near Earth ionospheric plasma, aerodynamics 0-8517  
 source, dielec. chamber, plasma flow characts. optimisation 0-38574  
 Sun, adiabatic flow in coronal loops 0-56803  
 supersonic dense stream, shock braking processes, radiation-gasdynamic obs. 0-19635  
 Thompson scattering for electron beam and plasma diagnostics (*Russian*) 0-54031  
 Tokamak, noncircular cross-section, high- $\beta$ , anisotropic equilib. 0-24238  
 Tokamaks and reactors, appl. of bundle divertors, collisionless exhaust flow 0-27814  
 toroidal plasma, convective cells and transport anal. 0-24229  
 turbulent acceleration by electrostatic waves, in Earth's auroral plasma (*Russian*) 0-53952  
 turbulent stream of high temp. gas with particles, modelling (*Russian*) 0-38572  
 two fluid theory for flow of fully ionised plasma, initial value problem (*German*) 0-53954  
 two phase flow, particle velocity optical meas. (*Russian*) 0-54032  
 UHF discharge with preliminary locally ionised gaseous medium 0-38851  
 velocity driven modes in dense partially ionized plasmas, stability aspects 0-1792  
 viscosity of H plasma (*Russian*) 0-53953  
 vortex, heating and cooling dynamics (*Russian*) 0-1753  
 Ar arcs in supersonic flow, numerical analysis 0-38776  
 Ar full circle arc, mass flow field investig. 0-38797  
 Ar low temp. plasma flow, interaction with intense microwave beam 0-38654  
 H<sub>2</sub> plasma reactor design, heat transfer and flow 0-38697  
 He, RF discharge test obs. 0-44028  
 Hg plasma flow, electron temp. determ. from partial LTE populations 0-24248



**plasma flow continued**

- N<sub>2</sub> arc, magnetically stabilised cross-flow, temp. and flow fields meas. 0-54054
- N<sub>2</sub> plasma, spatial distrib. in transverse-discharge supersonic stream, continuum theory and probe meas. 0-48866
- N<sub>2</sub>H<sub>4</sub> production from NH<sub>3</sub> in atmospheric press. electron-beam controlled discharge 0-38799
- TiC plasma-chemical synthesis, depend. on geometric and flow rate parameters (*Russian*) 0-40677

**plasma focus**

- current structure, fast particle generation (*Russian*) 0-48913
- discharge in Mather accelerator 0-24257
- discharges, electron and deuteron beam energy spectra 0-24262
- dynamics with powerful laser interaction during MHD stage, diagnostics 0-48924
- Frascati Tokamak, 1MJ plasma focus dynamics, neutron production scaling 0-24220
- neutron emission parameters 0-24221
- neutron yield scaling lasers, recent research 0-24263
- prepulse discharges in high current accelerator diodes with double shaping line 0-5399
- self-trapped cylindrical laser beams, radial intensity profile and nonlinear wavenumber shift 0-1802
- sheath driven targets, simulation 0-48898
- toroidal plasma, compression, appl. of plasma focus device 0-43996
- turbulence induced by plasma-electric current interaction in focus expt., laser diagnostics 0-24171
- upper-hybrid reson. absorpt. of laser in plasma focus, backscatter 0-28621
- N<sub>2</sub> electric breakdown, vol. discharge with external photoionisation, plasma focus spark channel (*Russian*) 0-38738

**plasma generation see plasma production****plasma guns**

- analysis for plasma guns for spraying 0-38732
- arc plasma gun for metal cutting, transient performance, obs. 0-49017

**plasma heating**

- see also *plasma focus; plasma production and heating by laser beam*
- 2XIIIB magnetic mirror device, neutral beam injection 0-28782
- active burn control of nearly ignited plasmas 0-48909
- additional heating in Tokamaks, specific diagnostics review 0-28753
- air-core Tokamak, optimisation of ohmic heating coil configurations 0-14914
- Alfven and magnetoacoustic wave heating for fusion plasmas 0-24188
- Alfven wave heating, nonlinear processes 0-28718
- Alfven wave heating in toroidal plasma 0-28740
- alpha particle orbits in radially nonuniform slender plasma column, multi-group rep. 0-53921
- alpha-particle heating in an open-field-line plasma 0-48908
- alpha-particle heating in high density D-T plasma 0-28735
- anomalous turbulent resistivity at high drift vels., rel. to confinement and fluctuations in toroid 0-24139
- anomalous turbulent resistivity at high drift vels., toroidal plasma 0-24138
- ASDEX, 30 kA ohmic heating system, tests and performance 0-13848
- atmospheric positive streamer corona, primary wave emission, secondary electron emission 0-44008
- atomic processes for mag. fusion research, review 0-42851
- Berkeley multicusp ion source for use with TFTR neutral beam injector, characts. 0-54040
- Bohm-type thermal losses from high- $\beta$  plasma 0-38679
- charged particle acceleration and diffusion in stochastic mag. field 0-43872
- Cherenkov adsorption of azimuthal EM travelling waves, magnetoactive heating and containment (*Russian*) 0-38675
- CLEO stellarator, heating, confinement and fluctuations 0-24225
- collective phenomena and anomalous resistance, electron current drift velocity (*Russian*) 0-24140
- collisionless plasma, microwave electron acceleration, waveguide obs. 0-43932
- compact fusion ignition experiments, designs, numerical computation 0-13853
- compact toroidal configuration, heating and confinement principles 0-24185
- compression by profiled explosion, neutron output 0-13782
- conference on fusion research and plasma physics, Innsbruck, Aug. 1978 0-27033
- current structure, fast particle generation (*Russian*) 0-48913
- currents in short pulsed high current electron beam injection into initially neutral gases 0-33749
- cutting with additional heating of plasma-forming gas 0-24267
- cyclotron self-absorption in two-temp. plasma, temp. and density meas. 0-48987
- cylindrical ion implosion fusion using radially convergent beams 0-23137
- diagnostics, turbulent heating example 0-49015
- discharge dynamics, calculations of plasma energy and particle balance for T-10 Tokamak 0-28847
- DIVA, scrape off layer, multigrad energy analyser applications 0-33818
- double plasma and other synthesised plasma devices, adjustment of ion energy distribution 0-19625
- Doublet III, neutral beam injection system, overview and status 0-13868
- Doublet III, neutral beam injection system, parametric study 0-13869
- drift cone instability suppression by electron heating in adiabatic traps (*Russian*) 0-53959
- dynamics of heating and cooling of a plasma vortex (*Russian*) 0-1753
- EBT reactor, new design arising from plasma research 0-27806
- ECR fundamental ordinary mode absorption and emission, in PLT 0-43943
- electron beam, quasilinear relaxation of dissipative instability of relativistic beam in bounded plasma 0-38671
- electron beam controlled discharge, cathode density waves 0-38798
- electron beam fusion of D-T pellets, neutronics and photonics 0-52781
- electron beam heating of a mirror confined plasma, diode mag. field gradient effect 0-54009
- electron beam inertial confinement thermonuclear fusion 0-27803
- electron beam propagation in plasma channels for ICF reactors 0-1812
- electron cyclotron frequency expts. in ISX-B Tokamak, temp. rel. to heating power 0-48912
- electron cyclotron heating, Bernstein modes, Vlasov dispersion relation 0-33809

**plasma heating continued**

- electron cyclotron heating and wave trajectory in toroidal plasmas 0-28726
- electron cyclotron heating in Elmo bumpy torus, review 0-28750
- electron cyclotron heating in Tokamaks: experiments and prospects 0-28749
- electron cyclotron heating in toroidal plasmas, wave trajectories 0-38678
- electron cyclotron heating of high- $\beta$  toroidally confined plasmas, ISX-B expt. 0-37588
- electron cyclotron resonance plasma, metal surface cleaning (*Japanese*) 0-16572
- electron heating and anomalous conductivity, in two-stream unstable plasma 0-6219
- electron heating by Langmuir waves, with induced I-s scatt. (*Russian*) 0-10403
- electron-beam inertial confinement expts. at Valduc (*French*) 0-48907
- ELMO bumpy torus, ambipolar diffusion 0-38552
- ELMO Bumpy Torus, electron cyclotron heating, density and temp. 0-28780
- EM field orthonormal decomposition, duality and complex vectorial space in anisotropic media 0-28754
- energy balance in PLT Tokamak 0-28733
- energy transfer in laser (or particle) beam produced plasmas 0-38680
- explosive instability collision mode stabilisation by drifting effects, Thirring instability (*Russian*) 0-43920
- fast ions, behaviour during H-neutral-beam-injection in large Tokamak plasma 0-28713
- fast wave heating via mode conversion and ICRF scaling 0-28815
- fast-magnetosonic-wave heating of the conceptual NUWMAK Tokamak reactor 0-6264
- Fermi acceleration and RF heating 0-33790
- field reversal experiment in 2XIIIB 0-28732
- FT Tokamak, RF additional heating system 0-13879
- FT-1 Tokamak, lower hybrid plasma heating 0-28700
- fusion device surface effects on neutral beam injector and beam direct convertor operation 0-47719
- fusion plasma, RF phased waveguide heating, thermal eddies form. 0-24193
- fusion plasma in beam driven Tokamak, Fokker-Planck/transport analyses 0-28826
- fusion reactor cavity design, compact electron beam or light ion beam reactor using nonspherical blast waves 0-9405
- fusion reactors, neutral beam design for plasma heating 0-13836
- fusion-neutron production in D-beam-heated PLT plasmas 0-28807
- Grill phase tracking during density increase in Tokamaks 0-28762
- gyrotron 50 GHz design considerations 0-28728
- gyrotron for electron-cyclotron heating in large Tokamaks 0-28751
- heating expts. in Japan, summary 0-28737
- heating in toroidal plasmas 0-24239
- heavy ion beam inertial confinement fusion, US programme 0-23136
- Heliotron D, RF heating, equilibrium and stability 0-28777
- HF heating in Tokamaks and stellarators, review 0-28736
- HF plasma generation, electron heating, nonlinear kinetic theory 0-44041
- high beta Tokamak heating 0-28730
- high current relativistic electron beam retardation distance (*Russian*) 0-14911
- high melting particle heating, melting and vaporisation in hot gas 0-6201
- high power microwave pulse interaction with thermally ionised laboratory plasma 0-10409
- high power MM wave source-gyrotron (*Japanese*) 0-23654
- high power neutral injectors, review 0-18656
- high-temp. regimes, simulation and confinement scaling 0-38673
- ICR heating in T-10 Tokamak under weak dissipation conditions 0-28759
- ICRF heating, preliminary results in DIVA 0-28758
- ICRF heating in Macrotron Tokamak 0-28744
- ICRF heating in TFR, preliminary obs. and further development prospects 0-28741
- ICRF heating of D<sup>+</sup> plasma with H<sup>+</sup> minority component in DIVA 0-18601
- ICRF heating of H-D Tokamak plasma under harmonic resonance 0-28719
- ICRF heating of toroidal plasma, linearly- rel. to circ.-polarised RF field efficiency 0-28711
- ICRF heating optimisation in PLT 0-28742
- implosion liner fusion, USA expt. and theoretical studies 0-23129
- impurity effects and control, neutral beam injection, computational models for large Tokamaks 0-28773
- inertial confinement fusion at NRL, laser and ion drivers 0-23131
- inertial-confinement ion-beam wet-wood-burner fusion neutron source 0-32489
- ion beam-slab target interaction, deflagration waves form. 0-24184
- ion cyclotron heating by azimuthally rotating RF fields, in toroidal plasma 0-28721
- ion cyclotron waves, oscillating two-stream instability, RF heating of tokamak plasma 0-1779
- ion heating by current driven turbulence in inhomogeneous plasma 0-33791
- ISX-B Tokamak, intense heating, plasma position and current, feedback control modeling 0-33802
- JFT-2 Tokamak, plasma heating near lower hybrid frequency 0-28698
- Langmuir turbulence, statistical theory 0-38647
- Langmuir wave excitation by two pumping waves, convective instability (*Russian*) 0-14904
- LHR frequency range waves interactions in octopole Tokamak 0-28724
- long time confinement of pure electron plasma, max. confinement time 0-48954
- low frequency heating wave, parametric instabilities induction in mag. confined plasma 0-24187
- low frequency parametric processes in magnetically confined plasmas 0-28827
- lower hybrid cones, trajectory meas., mag. field line determ. 0-33817
- lower hybrid heating experiments in JFT-2 Tokamak 0-28747
- lower hybrid heating in toroids, US experimental program, review 0-28748
- lower hybrid resonance heating in WEGA Tokamak, effectiveness study 0-28746
- lower hybrid resonance heating theory of Tokamak plasmas 0-28745
- lower hybrid wave heating, quasilinear effects 0-28763
- lower hybrid wave heating in Doublet IIA 0-28723
- lower hybrid wave heating in JIPP T-II 0-28722



**plasma heating continued**

- lower hybrid wave propag. and parametric decay in WEGA Tokamak 0-28725
- lower hybrid waves, filamentation and spatial attenuation in Tokamaks 0-28665
- lower hybrid waves, nonlinear behaviour, near linear mode-conversion-point 0-53963
- lower hybrid waves, ray trajectory and ion absorpt. in Tokamak 0-28667
- magnetic mirror, injected plasma particle refl. (trapping), quiescent (turbulent) plasma 0-48955
- magnetoacoustic oscillation excitation in strongly inhomogeneous plasma 0-38641
- magnetoacoustic oscillations, parametric decay in cylindrical plasma 0-24157
- magnetoplasma, intense EM wave absorption, numerical results 0-43890
- magnetosonic resonance heating in the Erasmus Tokamak 0-28720
- materials development for fusion 0-33804
- MHD equilibrium and stability, triangular deformation elliptic cross section (*Chinese*) 0-53950
- microwave heating in ELMO Bumpy Torus, anal. 0-28829
- microwave heating of plasma in EM trap (*Russian*) 0-10400
- motional impedance and heating of low resistive plasmas 0-14913
- neutral beam generation, negative ion revolving multiple beam instabilities (*French*) 0-47798
- neutral beam injection, fuelling profiles effect on plasma transport props. 0-19596
- neutral beam injection, impurity contaminated Tokamak 0-9403
- neutral beam injection, RF instabilities, review 0-28757
- neutral beam injection expts. on Tokamak plasma at ORNL 0-28809
- neutral beam injection heating in JIPP-II Tokamak 0-28710
- neutral beam injection heating in Tokamaks, review 0-28729
- neutral beam injection in JIPP T-II, investig. 0-28810
- neutral beam injection in Tokamaks, review of technology progress 0-28731
- neutral beam injection systems based on negative ions, review 0-42852
- neutral beam injection USA research 0-27808
- neutral beam line for plasma heating, stray particle loss near deflection magnet 0-47794
- neutral injection heating of CLEO stellarator-theory and experiment 0-28755
- neutral injection heating of Cleo stellarator 0-28714
- neutral injection parameters and beam line design for TEXTOR 0-28811
- neutral-beam-driven current evolution in Tokamak plasmas 0-28712
- neutron production in Maxwellian D ion plasma, ion temp. diagnostics appls. 0-49005
- non-stochastic heating of magnetized plasma by electrostatic wave 0-10405
- nonlinear effects in propagation of lower hybrid waves in a plasma 0-10380
- nonlinear stability problems, two-time method, dissipation scalings, ohmic heating 0-53967
- octupole, lower hybrid heating and mode conversion 0-6265
- ohmic heating in Frascati Tokamak, preliminary results 0-28734
- ohmic heating of plasmas in closed magnetic systems 0-28756
- Ohmic pumping by means of externally driven tearing modes 0-28706
- oscillations, in lower-hybrid range, of bounded plasma 0-24162
- paramagnetism in RF mag. field, expt., theory and simulation 0-6225
- parametric decay spectrum of heating near LH frequency in Petula 0-28761
- parametric heating near lower hybrid frequency in Petula 0-28760
- parametric instabilities and ion heating in a two-ion species plasma 0-28708
- Petula Tokamak, lower hybrid waves, plasma heating and nonlinear effects 0-28697
- Petula Tokamak, transit time magnetic pumping 0-24186
- PLT, start-up phase, volt-second consumption 0-18603
- PLT Tokamak, neutral beam heating 0-28701
- PLT Tokamak, ohmically heated plasmas, radiation, impurity effects, instability and particle transport 0-28833
- prepulse discharges in high current accelerator diodes with double shaping line 0-5399
- pulsed erosion jet, energy characts., heat flow distribution (*Russian*) 0-33825
- radiation due to gas layer impact against obstacle at very high vel. 0-19602
- radiowaves interaction, thermic excitation of parametric instability, controlled 0-24164
- relativistic electron beam induced heating 0-43942
- relativistic electron beam induced turbulence and heating, review 0-38672
- relativistic electron beams as plasma heating mechanism for solenoid systems 0-24190
- reversed-field pinch, formation, relaxation and heating studies 0-24215
- RF and neutral beam heating of current-free stellarators 0-28853
- RF electric fields in ion cyclotron excitation of multispecies plasma 0-1803
- RF energy coupling by magneto-acoustic waves in toroidal plasma 0-28743
- RF heating in ATC, low-Z impurity radiation 0-28816
- RF heating limitations, Alfvén's critical ionisation velocity phenomena 0-28717
- RF heating of magnetized rarefied plasma 0-24195
- RF intense heating, energy confinement 0-38674
- RF plasma heating, effect of wall corrugations on lower hybrid wave spectrum 0-33787
- RF plasma heating, stochasticity role 0-28752
- Sandia Labs. particle beam fusion programme 0-23134
- self similar cooling wave, effective thermal cond. (*Russian*) 0-14908
- sheaf instability at moderate densities, anomalous ion heating (*Russian*) 0-43922
- shear Alfvén wave heating experiments in heliotron D 0-28716
- shock heated plasma, Al-seeded, boundary layer influence on Al I reson. line profiles 0-43876
- shock waves, implosive and re-explosive, plasma parameters 0-48891
- shock-heated dense plasma, continuum radiation and optical transmittance diagnostics 0-24202
- shock-heated high-density Ar(Xe) plasmas, elec. cond. 0-38557
- skin current heating of toroidal plasma 0-28715
- solar corona, loop heating by fast mode MHD waves 0-41801
- solar quiescent prominences, heating and cooling, calc. 0-12738

**plasma heating continued**

- stochastic ion heating by a perpendicularly propagating electrostatic wave 0-10410
- stochastic ion heating by electrostatic wave in sheared mag. field 0-28705
- stochastic ion heating by lower hybrid wave 0-28707
- stratified plasma, obliquely propag. extraordinary microwave Budden tunnelling 0-48895
- subsonic electron fluid and small spark formation 0-38792
- Sun, quasiperiodic microwave bursts and adiabatic heating 0-51713
- T-10, ohmic heating, plasma confinement study 0-28768
- T-11 Tokamak, neutral beam injection, plasma heating and stability 0-28702
- tearing mode instabilities and suppression by lower hybrid fields 0-28666
- TFR, ICRF heating obs. by all metal antenna 0-18606
- theoretical scaling laws, implications 0-28805
- thermonuclear fusion plasmas, elem. processes and role of atomic, ionic and mol. data 0-14916
- thermonuclear ignition by means of compact devices (*Italian*) 0-52778
- theta pinch, fast, plasma macroscopic behaviour obs. and analysis (*Japanese*) 0-1818
- theta pinch, linear, end losses, stoppering, instabilities and heating 0-24224
- theta pinch plasma, absorpt. of magnetoacoustic waves (*German*) 0-10430
- theta-pinch, electron heating in turbulent neutral layer (*Russian*) 0-10361
- theta-pinch, neutral current sheet, electron energy distrib. meas. 0-43954
- theta-pinch, strong fast growing mag. field, pre-ionisation effects (*Russian*) 0-33800
- TNS fusion reactors, negative-ion neutral-beam system design for plasma heating 0-13837
- Tokamak, flux-conserving cylindrical equilb. evolution with adiabatic compression and beam heating 0-28799
- Tokamak, heating by pulsed elec. fields, hot ion prod. 0-24192
- Tokamak, lower hybrid heating to ignition 0-18605
- Tokamak, neutral beam injection, low density ignition scenarios 0-48937
- Tokamak, neutral beam-heated, parametric scaling 0-10406
- Tokamak, octupole, obs. of RF driven plasma current 0-48910
- Tokamak, PLT, fast-wave heating of two-ion plasma through minority cyclotron reson. damping 0-24194
- Tokamak, RF heating by lower-hybrid wave electron Landau damping 0-19595
- Tokamak, Vlasov plasmas, geometrical optics approach to electron-cyclotron frequency heating 0-14917
- Tokamak fusion reactor, steady-state, lower hybrid wave-driven, design constraints 0-10424
- Tokamak fusion reactors, doublet research, plasma shape control, MHD stability 0-28837
- Tokamak heating by fast magnetosonic wave excitation 0-24189
- Tokamak installation, supplementary RF heating (*Czech*) 0-24258
- Tokamak plasma, RF power coupling antennae for ion cyclotron heating 0-13878
- Tokamak plasma power coupling by 500 KW RF amplifier 0-13877
- Tokamak power reactor, steady state, lower hybrid wave driven 0-48945
- Tokamak reactors, prod. of noncircular discharge, ohmic heating expts. (Doublet III) 0-52785
- Tokamak with poloidal divertor, discharge startup 0-48942
- Tokamaks, high-beta, heating, confinement, dynamics studies 0-24218
- Tokamaks, non-circular, shaping and internal structure 0-28842
- topside ionosphere, ion heating by electrostatic ion cyclotron waves 0-12606
- Tormac, confinement system, magnetoacoustic heating studies 0-24217
- toroidal magnetic pumping method, efficiency (*Russian*) 0-10401
- toroidal reactors,  $\alpha$  heating 0-13861
- torsatrons, neutral beam injection calcs. 0-48949
- TORTUR I, heating by current driven turbulence 0-24191
- Transit Time Magnetic Pumping heating in Petula Tokamak 0-28739
- Tuman-2A, plasma compression particle diagnostics, density and temp. (*Russian*) 0-38677
- Tuman-2A Tokamak, ohmic heating and compression of plasma 0-28703
- turbulent heating, flat top electron distrib. effect, with ion-acoustic instability 0-10399
- VLF heating methods, thermonuclear prospects, review 0-28738
- W VII-A stellarator, Ohmic heating, energy and particle confinement 0-24226
- wave heating at electron cyclotron harmonics in toroidal plasmas 0-28727
- waveguide array for lower hybrid wave excitation 0-48911
- Wega Tokamak, lower hybrid heating 0-28699
- Z-pinch of intense energy density driven by high-voltage storage lines 0-24216
- Al foil in quartz dust, electrical explosion for accelerator application 0-6314
- CO<sub>2</sub> laser, semi-self-sustained discharge, optical homogeneity, mol. gas heating 0-37990
- D source, magnetically insulated, pulsed, peak beam parameters 0-32548
- D-D fusion reactor plasmas, pure and catalysed, thermal stability 0-24207
- D-T plasmas, ignition toroidal expt., equilibrium configs. and heating 0-28704
- D-T Tokamak, high-density, ohmically-heated, transport calcs. 0-24142
- D<sub>2</sub> plasma, compression by microfusion explosion, expt. biconical system 0-13783
- DT-Pu plasma, neutron induced fission, plasma heating effect 0-27800
- H<sub>2</sub>, highly turbulent, produced by magnetically rotated arc 0-38769
- He discharge, medium press., contraction mechanism, inhomogeneous heating 0-44024
- K plasma, magnetic-mirror-trapped, heating with array of hot W wires 0-33789
- N<sub>2</sub> discharge, anomalous heating (*Russian*) 0-1866
- N<sub>2</sub>, discharge, excitation efficiency of rot. and vibr. levels, heating due to elastic collisions and relax. 0-38751
- Xe, electron gas shock heated, associative ionisation and photoionisation, rel. contribs. 0-43858
- Xe, plasma shock front, elementary processes 0-19581

**plasma impurities**

see also plasma-wall interactions

active particle beam systems for meas. of plasma pot., current and impurity profiles 0-48990



## plasma impurities continued

- Alcator A Tokamak, spatial profiles of light impurity ions 0-48948  
 atomic processes for mag. fusion research, review 0-42851  
 bundle divertor, Tokamak plasma, scrape off layer density decrease, model 0-28851  
 concentrations on wall during Tokamak discharges, laser probing technique 0-49013  
 conference on fusion research and plasma physics, Innsbruck, Aug. 1978 0-27033  
 deposition of plasma impurities, in ISX-Tokamak, time resolved measurements 0-38694  
 DITE Tokamak, impurity density, soft X-ray meas. 0-19616  
 DIVA, metal-impurity, confinement, discharges 0-28843  
 electron plasma, impurity screening effects in intermediate degeneracy region 0-14882  
 equilibrium of plasma without shell, impurities outside coronal equilibrium and hollow profiles, MAKOKOT code 0-28774  
 first wall materials, effect on Tokamak plasmas 0-38692  
 flux and differential wall changes, in Alcator-A Tokamak, surface probes 0-38664  
 fusion possibilities and plasma confinement and interactions in mag. config. Tokamak, review (*French*) 0-54017  
 fusion reactor plasma impurity control using neutral gas blankets 0-13835  
 high-pressure atomic and molecular impurities, preionisation by UV irradiation of surface discharge 0-38847  
 ICRF heating, preliminary results in DIVA 0-28758  
 ICRF heating in TFR, preliminary obs. and further development prospects 0-28741  
 impurity control and plasma transport in plasma-edge region 0-13832  
 injected beam, edge cooling by super-banana limiter 0-43940  
 ion scat., suprathermal, by partially ionised impurities, measurement of  $Z_{\text{eff}}$  0-54039  
 ion-drift wave eigenmodes in sheared mag. field, impurity effects 0-43911  
 ions on rational magnetic surfaces, convection and diffusion, collisional multifluid model 0-28615  
 ISX Tokamak, arcing obs. 0-33836  
 ISX-A Tokamak, plasma confinement and impurity flow reversal 0-28770  
 ISX-B impurity study program, in situ Tokamak expts. 0-37589  
 ISX-B noncircular Tokamak for expts. on the physics of high- $\beta$  toroidally confined plasmas 0-37588  
 ISX-B Tokamak for impurity study expts., program objectives 0-37587  
 JIPP T-II tokamak plasma, Mo impurity diffusion during  $H_2$  gas puffing 0-28602  
 JIPP T-II torus, neutral gas injection and plasma current control, suppression of major disruption 0-28839  
 JIPP-T-II Tokamak plasma, time resolved spatial profiles of impurities 0-48950  
 light impurities, diagnostics in T-4 Tokamak plasma (*Russian*) 0-10432  
 low-Z impurities radiation during RF heating in ATC 0-28816  
 macroparticles elimination from plasma stream, using curved plasma duct 0-33826  
 metal-seeded rotating plasma 0-1746  
 naphthalene-He photoionis. plasma,  $CO_2$  additive effect 0-10359  
 neutral beam injection expts. on Tokamak plasma at ORNL 0-28809  
 neutral beam injection heating in JIPP-II Tokamak 0-28710  
 PLT Tokamak, ohmically heated plasmas, radiation, impurity effects, instability and particle transport 0-28833  
 pulsator, accumulation of impurities and stability behaviour in high density regime 0-28835  
 surface erosion from plasma solid interaction 0-38665  
 T-10, ohmic heating, plasma confinement study 0-28768  
 T-10 Tokamak, plasma X-ray emission 0-28840  
 T-12 Tokamak with two axisymmetric divertors, characteristics of divertor 0-28844  
 TFR 600 Tokamak, plasma confinement, low effective plasma charge 0-28769  
 Tokamak, DITE, impurity ion concentrations and diffusion, spectroscopic measurement 0-28771  
 Tokamak, DITE, plasma and impurity fluxes on walls 0-28688  
 Tokamak, impurity control by neutral-beam injection 0-32494  
 Tokamak, PLT, current profile evolution effect on plasma-limiter interaction and energy confinement time 0-10420  
 Tokamak collisional plasmas, poloidal asymmetry of impurity spectral line emission 0-32485  
 Tokamak fusion devices, secondary ion emission, appl. to impurity control 0-37584  
 Tokamak impurity problems, atomic and mol. struct. and collision data, review 0-43959  
 Tokamak limiter, surface observation, infrared techniques 0-38693  
 Tokamak plasmas containing momentum sources, impurity transport 0-48935  
 Tokamak reactor, impurity diversion through ambient boundary layer flow 0-19603  
 Tokamak scrape-off plasma, metal impurity recycling effect 0-10421  
 Tokamaks, large, impurity effects and control, neutral beam injection, computational models 0-28773  
 Tokamaks and reactors, applic. of bundle divertors, collisionless exhaust flow 0-27814  
 C component determ. in He and propane glow discharges 0-44032  
 D-T plasmas, ignition toroidal expt., equilibrium configs. and heating 0-28704  
 H isotope trapping, materials exposed to high power discharges in PLT 0-37576  
 H-like ions in laser-produced plasma, Balmer fine struct. (broadening) 0-48860  
 He-like ions, spectral broadening in plasma, theory, high-Z 0-6223  
 InI, in AC metal halide discharge, atomic plasma charact., a priori method 0-44034  
 NaI, in AC metal halide discharge, atomic plasma charact., a priori method 0-44034  
 Ti, atom-electron collisions in inner discharge column (*Russian*) 0-38529  
 Ti density meas. in PDX Tokamak using Ti XVII forbidden line 0-32496  
 TII, in AC metal halide discharge, atomic plasma charact., a priori method 0-44034

## plasma in solids see solid-state plasma

## plasma instability

see also plasma oscillations

- air, discharge, high-current, nanosecond, explosive cathode processes and contraction 0-10449  
 Alfvén-ion-cyclotron instability for axially bounded plasma 0-1788  
 alpha particles interaction with mag. plasma fluctuations in D-T reactor 0-24204  
 amplitudes oscillations destruction in weakly collisional plasma-cold beam system 0-28695  
 anisotropic plasma, cyclotron and electrostatic instabilities criteria 0-38627  
 anomalous absorption of UHF radiation in electron cyclotron resonance range (*Russian*) 0-1807  
 anomalous plasma transport due to electron temp. gradient instability 0-33813  
 anomalous Tokamak radial transport, large mode number tearing and twisting modes 0-1747  
 auroral plasma, turbulent acceleration by electrostatic waves (*Russian*) 0-53952  
 ballooning and tearing instabilities 0-28651  
 ballooning criterion for multipoles 0-43915  
 ballooning instability boundaries in circular Tokamak 0-6241  
 ballooning instability in bumpy torus, hot electron annulus effect 0-53983  
 ballooning limit of non-circular small aspect ratio Tokamak 0-28801  
 ballooning modes, MHD theory, applic. to JET 0-28639  
 ballooning trapped electron mode, linear and nonlinear theory 0-28656  
 ballooning trapped-electron mode overlapping many rational surfaces 0-28618  
 beam plasma system, interaction efficiency, wave HF press. effects (*Russian*) 0-10395  
 bump-in-tail instability-generated turbulence, phase space -granulation due to mode-mode coupling 0-38651  
 Buneman and Pierce instability, double layer form. in collisionless plasma 0-10398  
 Buneman-Farley instability, nonlinear decay interactions 0-38616  
 Bunemann instability in presence of mag. field 0-6234  
 CLEO stellarator, heating, confinement and fluctuations 0-24225  
 coherent waves in nonlinear medium, nonresonant interaction, eqns. system development and examples (*Czech*) 0-24149  
 cold mantle plasma current and mag. curvative driven modes, non-adiabatic stability anal. 0-33772  
 collisional drift instability, local and nonlocal theories comparison 0-19574  
 collisionless drift modes in sheared slab geometry, stability props. 0-1786  
 collisionless plasma, expansion into vac., ion accel., instability devel. electron heat flow 0-38575  
 conductor, MHD kink instability 0-6307  
 confined waves with ergodic ray trajectories, instability condition 0-14894  
 convective cell excitation by Bernstein waves (*Russian*) 0-53961  
 convective instability, harmonic generation and anomalous absorpt. in pumping wave decay (*Russian*) 0-14889  
 cool regions in relativistic plasmas: thermal instabilities 0-17486  
 coupled intensity deviations from stationary nonlinear state, space and time soln. 0-48882  
 current disruption, in Tokamak plasmas, schlieren signal meas. from millimetre waves 0-48998  
 current driven collisional drift and Alfvén instabilities in sheared mag. field 0-1795  
 current instability on short wave drift oscills., nonlinear theory (*Russian*) 0-53981  
 current-driven collisionless drift instability 0-14893  
 cyclotron instability, quasilinear relativistic plasma relax. in strong mag. field, magnetobremstrahlung (*Russian*) 0-38669  
 cyclotron instability in magnetosphere of pulsar NP 0532, rel. to origin of radiation (*Russian*) 0-8645  
 cyclotron instability with anisotropic kinetic temp., Nyquist diagrams (*Chinese*) 0-28627  
 cyclotron maser instability, quasi-linear theory, calc. of microwave generation efficiency 0-1783  
 cyclotron maser instability in intense hollow electron beams, effect of energy and axial momentum spreads 0-1782  
 cylindrical pellet in plasma, ablation flow linear stability anal. 0-1738  
 D-T plasma model, uniqueness and linear stability of operating points 0-14897  
 Debye screening modifications in ponderomotive effects 0-33777  
 decay dissipative instability of surface Langmuir wave in semibounded plasma (*Russian*) 0-38583  
 decay instability of laser radiation in a magnetoplasma 0-1781  
 dense relativistic electron gas, EM response in strong mag. fields, particle polarisation, mode struct. 0-43963  
 deuteron beam relaxation, charge exchange, instability, in 2-component Tokamak (*Russian*) 0-53997  
 diffuse pinch, energy equilib., classical scalar cond. and neo-classical models 0-24208  
 disruption, tearing and kink modes, limit of safety factor in JFT-2 Tokamak 0-38589  
 disruptions, internal, precursors of, tearing mode 0-28652  
 dissipative instability, quasilinear relax. of relativistic electron beam in metal sheath bounded plasma 0-38671  
 dissipative instability of 1-dimens. force-free mag. field (*Russian*) 0-53956  
 dissipative trapped particle instability, Connor-Hastie-Taylor transformation (*Russian*) 0-33759  
 divertor injection Tokamak experiment, plasma stability, energy and particle transport, and hydrogen recycling 0-28834  
 double layer, existence and stability of trapped Langmuir modes 0-6236  
 drift and trapped electron instabilities, in systems with mag. shear 0-28648  
 drift cone instability suppression by electron heating in adiabatic traps (*Russian*) 0-53959  
 drift cyclotron loss-cone mirror instability, HF mag. field interaction 0-6249  
 drift instability, current-driven, sheared mag. field, finite-beta effect on transport 0-28617  
 drift instability, electrostatic current-driven, scaling law for high density and high current Tokamaks 0-38691  
 drift mode, localised, in high density gas blanket boundary layer 0-43956



# plasma instability continued

drift wave instability, current-driven 0-1770  
drift wave instability, nonlocal collisionless, toroidal curvature effects 0-38588  
drift wave stability and transport theory in fusion systems 0-28653  
drift wave turbulence, dissipative; current driven, in Tokamak plasma 0-38587  
drift waves, instability in AC elec. field, wave growth rate and dispersion relation 0-48886  
drift waves, stabilisation by lower hybrid waves of finite wavenumber 0-53968  
drift waves, strongly dispersive, modulation instability, convective cell formation 0-38635  
drift-cone instabilities in mirror-confined plasma 0-28630  
drift-dissipative instability, excitation suppression by weak transverse mag. field (*Russian*) 0-33829  
eigenmodes, universal, in collisionless plasma slab 0-38581  
electric arc, self magnetic field, kink instability, plasma jets production (*Polish*) 0-19662  
electron beam, relativistic, diocotron instability 0-27853  
electron beam, relativistic, diocotron modes, magnetic shear stabilisation 0-54006  
electron beam, relativistic instability in variable dissipation level plasma (*Russian*) 0-19594  
electron beam in circ. waveguide electrostatic instability in rippled magnetic field 0-19588  
electron beam-plasma low freq. instability, cyclotron oscills. (*Russian*) 0-33783  
electron beam-plasma system, explosive instability 0-1813  
electron beams, relativistic, striations in density distrib. rel. to plasma column instability 0-24154  
electron current driven ion wave instability, excitation, electrode type effects 0-38603  
electron cyclotron instability on Jupiter rel. to diffuse aurora, influence of plasma injection from Io 0-4289  
electron fluctuation spectrum and drift instabilities in partially ionised plasmas, collision freq. effects 0-53924  
electron heat conductivity, magnetic field line diffusion 0-28641  
electron runaway affect on ordinary and extraordinary modes in inhomogeneous plasma 0-28669  
electron-ion decay instability in laser prod. plasma, backscatter diagnostics 0-43944  
electron-ion two-stream unstable plasma, anomalous cond., electron heating 0-6219  
electron-plasma waves excited by cavity modulation instability investigation 0-19567  
electronegative gas glow discharge, plasma instability boundary conditions (*Russian*) 0-38739  
electrophotoinised discharge, inert gases-halide mols. laser mixtures, current voltage characts. 0-38821  
electrostatic bounce modes in mirror plasmas 0-1790  
electrostatic ion cyclotron electron drift instability anal. using linear Vlasov dispersion reln. 0-1780  
electrostatic ion cyclotron waves and ion acoustic waves, parametric instabilities 0-38591  
electrostatic ion-cyclotron instability in solar atmosphere, rel. to coronal heating 0-51708  
electrostatic Trivelpiece-Gould modes in a torus 0-38609  
electrothermal stability anal. of fully ionised plasma, diffuse pinch 0-43901  
EM field orthonormal decomposition, duality and complex vectorial space in anisotropic media 0-28754  
EM wave parametric decay to electrostatic wave, mode coupling of modulational instabilities 0-24161  
EM wave self action during modulation instability (*Russian*) 0-14905  
EM wave self-action during thermal modulation instability of high hybrid oscills. (*Russian*) 0-53980  
EM waves, extraordinary parametric decay into two upper hybrid plasmons 0-43904  
energetic particle trapping by Alfvén wave instabilities 0-31205  
energy lifetime of plasma, T-3 scaling law, in Tokamaks 0-28635  
enhanced losses due to collisionless drift waves, dynamic stabilisation effects 0-14888  
equilibrium and stability, iron core influence in fusion reactor TFR 600 0-23150  
equilibrium of plasma without shell, impurities outside coronal equilibrium and hollow profiles, MAKOKOT code 0-28774  
expansion into vacuum, ion acceleration 0-6228  
explosive instability collision mode stabilisation by drifting effects, Thirring instability (*Russian*) 0-43920  
explosive instability of one dimensional weak mag. field (*Russian*) 0-14896  
explosive magnetic field generation due to EM incident radiation, laser plasma mechanism 0-6253  
external conducting sheets, stability effects on mag. contained plasmas 0-1787  
filamentation instability of laser beam in inhomogeneous plasma, preferential heating 0-19568  
flute, laser produced plasma column in uniform mag. field 0-38687  
flute instability, hollow axisymmetric mirror, MHD stable, multipole field stabilization (*Russian*) 0-33801  
fusion energy program, mirror approach 0-42855  
fusion possibilities and plasma confinement and interactions in mag. conf. Tokamak, review (*French*) 0-54017  
fusion reactor, field-reversed mirror 0-42857  
fusion reactor, gas insulated plasma boundary layers, ballooning modes stability 0-10415  
fusion reactor, using toroidally-linked mirrors 0-42858  
fusion reactors, field reversed mirrors 0-43961  
fusion reactors, superheating-diffusion instability, thermonuclear burn 0-32500  
g×B instability in finite Larmor radius plasma, multiple time scale anal. 0-53972  
generalized lower-hybrid-drift instability and modified two-stream instability, unified theory 0-1777  
glow discharge instability in N<sub>2</sub>-CO<sub>2</sub> non self sustained ionisation source, mechanism 0-38819  
helical modes, of solar mag. flux ropes (*Russian*) 0-8617  
helical perturbation in Tokamak, freq. entrapment (*Russian*) 0-10369  
helical system, current-carrying, m=1 reconnecting mode, nonlinear calc. 0-6243

# plasma instability continued

Heliotron D, RF heating, equilibrium and stability 0-28777  
high beta MHD theory, stellarator equilibrium and stability, mirror traps and reverse field machines 0-28778  
high beta stellarator, l=2,3 helical fields, stabilisation effects 0-28779  
high beta stellarator stability theory 0-28797  
high density plasma in multiple mirror, low freq. instability 0-48870  
high pressure, HF discharges and DC arcs in H<sub>2</sub>(D<sub>2</sub>)(inert gas), instability obs. 0-38807  
high toroidal mode number stability of beam-induced tensor press. Tokamak 0-10378  
high-β flux-conserving equilibria, with supercond. metal shell, stability anal. 0-10428  
hollow cathode arc with reduced gas flow, operation mode 0-38783  
hollow cathode glow discharge, state of equilb., spectroscopic meas. 0-19647  
hydromagnetic surface waves, dissipation by reson. conversion 0-21904  
ICRF heating, preliminary results in DVA 0-28758  
internal disruption in Tokamak, relax. oscills., self-consistent model (*Russian*) 0-53957  
internal feedback caused by variation of plasma pot. in bounded plasma 0-43906  
internal helical modes, m>1, in Tokamak with small shear and high plasma press. (*Russian*) 0-10371  
internal m=1 helical mode, feedback suppression in Tokamak 0-19577  
ion acoustic, strongly magnetised plasma collisional relax. of ion beam 0-33785  
ion beam-plasma system wave propag. in cylindrical geometry 0-38592  
ion cyclotron waves, oscillating two-stream instability, RF heating of tokamak plasma 0-1779  
ion loss due to low frequency instabilities 0-6217  
ion ring, field-reversed, anomalous decay of induced electron current 0-24206  
ion wave, rel. to Brillouin backscatter saturation in underdense plasma target 0-14886  
ion-acoustic, in turbulent plasma, ion-tail form. effect on resistivity 0-10360  
ion-acoustic, in turbulently heated plasma, flat top electron distrib. effect 0-10399  
ion-acoustic instability, electron flux driven, in Q-machine, probe diagnostics 0-33765  
ion-acoustic instability, ion tail formation and saturation 0-38610  
ion-acoustic instability oscillations in collisionless single ended Q-machine 0-38731  
ion-acoustic instability stabilisation by ion beam in Q-machine, probe diagnostics 0-33766  
ion-drift wave eigenmodes in sheared mag. field, impurity effects 0-43911  
ionisation instability mode of plasma accelerator, probe method for electron distrib. function determ. 0-19612  
ionosphere, instabilities and fine struct. 0-21869  
ionosphere, lower hybrid drift instability 0-46343  
JAERI Tokamak, Ti coating for improved plasma characts. 0-24232  
JIPP T-II torus, neutral gas injection and plasma current control, suppression of major disruption 0-28839  
Kelvin-Helmholtz instability in comet tails, appl. to helical waves in Comet House (1908 III) 0-4305  
kink instabilities of a field reversed ion ring with a toroidal magnetic field 0-1758  
kink instability, internal MHD, sufficient cond. (*Chinese*) 0-43897  
Landau modes, higher order, in water-bag and 2-Maxwellian plasmas 0-38601  
Langmuir oblique solitons, self-contraction in free path regime (*Russian*) 0-43921  
Langmuir oscills., modulational instability, in EM wave field 0-38618  
Langmuir running wave instability and damping, at different amplitudes and phase velocity 0-38620  
Langmuir soliton solns. with high nonlinearities, energy principle 0-24156  
Langmuir standing waves instability, one dimens., soliton and collapse, numerical expt. 0-38619  
Langmuir turbulence, statistical theory 0-38647  
Langmuir turbulence, strong, transition (*French*) 0-28674  
Langmuir wave excitation by two pumping waves, convective instability (*Russian*) 0-14904  
Langmuir waves, driven by electron-ion decay instability, scattered spectrum 0-43970  
laser-plasma interaction, spiken lifetime 0-14922  
Levitron, fluctuations, diffusion and beam-induced currents 0-28616  
localised drift-Alfvén mode instability due to current density gradient 0-19571  
localised pumping-excited waves, parametric instability, nonlinear stage 0-38622  
long-wavelength modes and anomalous transport in toroidal magnetoplasmas 0-28613  
longitudinal plasma wave, threshold amplitude for onset of instability 0-1793  
low frequency heating wave, parametric instabilities induction in mag. confined plasma 0-24187  
low frequency parametric processes in magnetically confined plasmas 0-28827  
lower hybrid drift, laser produced plasma column in uniform mag. field 0-38687  
lower hybrid heating experiments in JFT-2 Tokamak 0-28747  
lower hybrid waves, modulation instability growth rates 0-48881  
lower hybrid waves in toroidal discharge, parametric decay 0-38596  
magnetic field generation by intense Langmuir plasma waves 0-38623  
magnetic field measurement in toroidal plasma systems 0-49004  
magnetic mirror, injected plasma particle refl. (trapping), quiescent (turbulent) plasma 0-48955  
magnetic piston interaction with nonmagnetised plasma 0-38630  
magnetically confined plasmas, ballooning modes 0-6231  
magnetized plasma parametric resonance in non-monochromatic pump-wave 0-38598  
magneto-viscous resistive tearing of cylindrical flux surfaces 0-1831  
magnetoacoustic disturbance, hydrodynamic instability in nonuniform plasma flow (*Russian*) 0-1766  
magnetoacoustic oscillations, parametric decay in cylindrical plasma 0-24157  
magnetoacoustic oscills., in toroidal plasma, comparison with cylindrical plasmas, numerical calcs. 0-33760



## plasma instability continued

- magnetosphere, proton-cyclotron harmonics, instability due to anti-loss core proton distrib. 0-56678  
 marginal stability in solar flares, assoc. with particle streams continuous injection model 0-21954  
 MHD eqn., stability, transport calc. for high-beta Tokamaks 0-28848  
 MHD equilibria, secular instability in mag. quadrupole field 0-53982  
 MHD equilibria in mag. quadrupole field, secular instability 0-10427  
 MHD equilibrium and stability, triangular deformation elliptic cross section (*Chinese*) 0-53950  
 MHD equilibrium and stability in three dimens. configurations 0-28776  
 MHD generator, conductivity and power output ionization stability, and boundary layer effects 0-1752  
 MHD instabilities in extended extragalactic radio sources, rel. to electron accel. 0-27000  
 MHD instabilities in helical system 0-1829  
 MHD kink stability, convection effects, MHD boundary layer anal. 0-1762  
 MHD stability criteria for localised displacements 0-28645  
 microwave dynamic interaction, probe diagnostics 0-19584  
 microwave heating in ELMO Bumpy Torus, anal. 0-28829  
 mirror drift cone stability simulation with loss-cone ions 0-1789  
 mirror fusion test facility 0-43962  
 mirror-drift-cone instability, nonlocal hybrid-kinetic stability anal. 0-24230  
 modes and ballooning in magnetically confined plasmas 0-28650  
 modulation instability and plasma electrodynamic characteristics 0-38621  
 modulational instability produced by Langmuir turbulence in a magnetic field 0-1759  
 multiple-mirror plasmas, MHD stabilisation 0-6244  
 neutral beam generation, negative ion revolving multiple beam instabilities (*French*) 0-47798  
 non self sustained repetitively pulsed discharge in  $N_2$ - $CO_2$  and  $N_2$ , instability obs. 0-38820  
 nonideal plasma, elem. excitations and macroscopic props., review 0-43842  
 nonlinear electrostatic 4-wave interaction, positive (negative) energy waves, explosive instability 0-48884  
 nonlinear evolution of the bump-on-tail instability for electron beam in plasma 0-6248  
 nonlinear helical perturbation in Tokamak, dynamics, mag. probe obs. (*Russian*) 0-53958  
 nonlinear kink instabilities in Tokamaks surrounded by force-free fields 0-43909  
 nonlinear lower-hybrid waveguide in plasma, stability 0-19578  
 nonlinear mode coupling instability saturation, bifurcations and strange behaviour 0-48873  
 nonlinear periodic waves stability in plasmas 0-38615  
 nonlinear stability problems, two-time method, dissipation scalings, ohmic heating 0-53967  
 nonuniform Langmuir fields, evolution and modulation instability 0-38599  
 octupole, lower hybrid heating and mode conversion 0-6265  
 Ogra-3 mirror device, loss mechanism due to cyclotron instabilities 0-28788  
 Ohmic current driven MHD instability in Heliotron-D device 0-38640  
 ohmic heating of plasmas in closed magnetic systems 0-28756  
 open traps, axially symmetric, transverse particle losses 0-28784  
 ordinary EM waves hydrodynamic instability, rel. to Jupiter Io-modulated decametric radio S-bursts (*Russian*) 0-8582  
 oscillating two-stream instability, rel. to solar type III radio bursts nonlinear stability 0-26826  
 oscillations, in lower-hybrid range, of bounded plasma 0-24162  
 oscillations of radially confined round beam, stability and distrib. function 0-53966  
 parametric decay instabilities in UHF discharge due to inhomogeneity parallel to pump field 0-19644  
 parametric instabilities and ion heating in a two-ion species plasma 0-28708  
 parametric instabilities in weakly-inhomogeneous hot plasmas 0-28828  
 parametric instability, drift waves convective cells, shear nonlinear excitation (*Russian*) 0-38585  
 parametric instability development, supplementary plasma ionisation (*Russian*) 0-24150  
 parametric instability saturation by electrostatic daughter wave nonlinear decay 0-53945  
 parametric wave excitation in bounded systems 0-6252  
 Penning discharge ion source with hollow cathode, HF instabilities 0-43997  
 periodical regimes in solar mag. traps, rel. to solar radio pulsations (*Russian*) 0-8616  
 Pierce and Buneman instability, double layer form. in collisionless plasma 0-10398  
 pinch, reversed-field type, in STP-1, using new external-field programming, MHD instability 0-28803  
 plasmatron with interelectrode insert, characts. 0-44009  
 PLT Tokamak, ohmically heated plasmas, radiation, impurity effects, instability and particle transport 0-28833  
 poloidal mode ballooning of trapped electron instability 0-28657  
 precursor whistler mode plasma turbulence formation in parallel shock waves 0-24172  
 pulsar electron-positron plasma (*Russian*) 0-36656  
 pulsar polar caps as foil-less diodes, nonneutral relativistic beam accel. 0-17604  
 pulsator, accumulation of impurities and stability behaviour in high density regime 0-28835  
 Pulsator Tokamaks, modulated runaway losses and effects of helical dipole field 0-28845  
 quasi steady high beta plasma in multiple mirror machine, density oscill., stability obs. 0-28663  
 Rayleigh-Taylor instability in toroidal plasma compression by imploding plasma liner 0-33811  
 real gas discharge, thermodynamic stability 0-38852  
 relativistic electron beam injection into plasma, development of dissipative two-stream instability 0-19593  
 relativistic electron beam rot. in plasma, coherent curvature radiation, two-stream instability 0-19590  
 relativistic transverse cold plasma waves, nonlinear, linearly polarised, stability 0-6235  
 resistive MHD instabilities of current sheets, appl. to solar wind 0-4218  
 resistive tearing  $m=1$  instability turbulent modification 0-43916

## plasma instability continued

- resonant  $CO_2$  laser radiation absorption and surface instability at crit. density surface 0-48859  
 resonant instability of semi-infinite plasma with sheared electron stream 0-48868  
 resonator, electron-beam excited, explosive instability 0-28693  
 reversed field pinch machines, plasma stability anal. 0-24214  
 rF instabilities driven by neutral beam injection, review 0-28757  
 rotating Hall plasma, self gravitational instability, MHD stability 0-14890  
 rotation influence on kink instability, compressibility (*Russian*) 0-48887  
 rotation of magnetised nonuniform plasma, MHD ordering 0-33756  
 rotational stabilization of a spiral instability in a plasma with an immobile boundary 0-38644  
 runaway electron instability, non-thermal microwave radn. 0-1842  
 screw pinch, finite Larmor radius stabilisation, resonant particle effects 0-54020  
 screw-pinch configs., collisionless, hybrid-kinetic stability props. of high-beta plasmas 0-43871  
 self-gravitational instability of plasma rotating layer, effects of finite ion gyroviscosity 0-56706  
 self-sustained gas discharge, mol. vibr. relax. effect on thermal stability 0-10358  
 semi-stellarator field stabilization of Tokamak plasma 0-6245  
 shape stability for plasma in standing EM field 0-28795  
 sheaf instability at moderate densities, anomalous ion heating (*Russian*) 0-43922  
 shear Alfvén wave, heat flux instability 0-43893  
 sheath, approx. model analysis of steady state situation 0-43934  
 sideband instability in large amplitude wave, computer simulation 0-38602  
 slow-fast mode conversion effect on lower hybrid slow mode excitation 0-28668  
 solar wind kinetic instability due to electron nonthermal props. 0-41691  
 solitary kinetic Alfvén wave stability, one dimensional nonlinear case 0-1776  
 space-charge wave instability of spiral beam-plasma system in nonuniform mag. field 0-1760  
 spectral distrib., modulation of plasma noise 0-38648  
 spheroidal low aspect ratio plasma configurations, MHD equilibrium and stability 0-1791  
 spheromaks, nonlinearly stable equilibrium statistical states 0-53975  
 spiral beam-plasma system, instability, effect of nonuniformity of mag. field 0-48899  
 stability of Bernstein-Greene-Kruskal equilibria, spatially inhomogeneous Vlasov equilibrium 0-1778  
 stabilizing passive shell and active feedback windings in reverse field pinch fusion reactors 0-18666  
 stimulated Raman and Brillouin scatt., static mag. field effects 0-6258  
 stochastic instability theory applies. to nonlinear plasma systems, review (*Czech*) 0-38580  
 striations in narrow He-Ne discharges 0-38736  
 surface oscillation cyclotron excitation, electron beam cyclotron instability (*Russian*) 0-54008  
 T-11 Tokamak, neutral beam injection, plasma heating and stability 0-28702  
 tandem mirror physics, fusion plasma confinement 0-43960  
 tearing, twisting and ballooning modes in finite- $\beta$  plasmas 0-28649  
 tearing instability, current shear effect in relativistic stream superposition model 0-24155  
 tearing instability in cylindrical plasma configurations (*Russian*) 0-10370  
 tearing mode instabilities and suppression by lower hybrid fields 0-28666  
 tearing mode mag. island struct. rot., diagnostics theory 0-48982  
 tearing modes, unified theory 0-19607  
 tearing modes with mag. braiding 0-10429  
 tearing-mode instability, Alfvén pulse-excited, mag. field lines reconnection dynamics (*Russian*) 0-1768  
 tearing-mode instability in a field-reversed ion layer 0-53969  
 temperature gradient drift wave eigenmodes stability in sheared mag. field 0-43914  
 thermal convection instabilities of spherically symmetric plasmas (*Chinese*) 0-1774  
 thermal instabilities in magnetically confined plasmas, appl. to solar coronal loops 0-36600  
 thermal modulation instability in a weakly ionized plasma, nonlinear stage (*Russian*) 0-38586  
 thermic excitation of parametric instability, controlled, radiowaves interaction 0-24164  
 thermomagnetic instability of inhomogeneous plasma (*Russian*) 0-28660  
 thermonuclear cone microinstabilities and anomalous alpha-particle losses in Tokamaks 0-28636  
 theta pinch, hot linear, end plugging effect on stability and parameters 0-24223  
 theta pinch, linear, end losses, stoppering, instabilities and heating 0-24224  
 theta pinch, rigidly rotating, Vlasov fluid stability 0-28794  
 theta-pinch, reverse field expts., equilibrium, confinement, stability 0-28787  
 TO-1 Tokamak, kink instability, feedback stabilisation 0-28634  
 Tokamak, confinement and stability, effects of shaping and compression of plasma 0-28772  
 Tokamak, high-beta, equilibria and  $m=1$  kink ballooning mode nonlinear evolution 0-24236  
 Tokamak, internal kink mode, numerical study 0-48953  
 Tokamak, major disruption suppression by tearing modes stabilisation 0-10422  
 Tokamak discharge, transient behaviour, electrohydrodynamical model 0-48952  
 Tokamak fusion reactors, doublet research, plasma shape control, MHD stability 0-28837  
 Tokamak thermonuclear reactor, MHD modes drift phenomena, kinetic method (*Russian*) 0-1827  
 Tokamaks, ballooning modes and pressure limits 0-28647  
 Tokamaks, feedback stabilisation of magnetic islands 0-28638  
 Tokamaks, high- $\beta$ , MHD stability limits 0-28643  
 Tokamaks, high-pressure, MHD-mode stability, high wave number 0-28644  
 Tokamaks, magnetic islands, tearing modes 0-28846  
 Tokamaks, MHD beta limits, dependence on current density and pressure profiles, num. calc. 0-28637  
 Tokamaks, non-circular, shaping and internal structure 0-28842



**plasma instability continued**

- Tokamaks, non-circular, stability and beta limits 0-28646
- Tokamaks, nonlinear drift tearing modes 0-53971
- Tokamaks with large-aspect-ratio, stability, two-fluid dissipative theory 0-28640
- toroidal axisymmetric system (*German*) 0-28792
- toroidal plasma, eigenvalue problem and nonlinear evolution of kink modes 0-24234
- toroidal plasma, vertical displacement instability (*Chinese*) 0-1824
- toroidal plasmas, axisymmetric, high mode number stability 0-28642
- toroidal plasmas, MHD instabilities 0-38579
- toroidal system, MHD plasma control by feedback and HF fields 0-28781
- transverse Cherenkov mode nonlinear stabilisation by external mag. field 0-38642
- trapped electron instability, turbulence, unstable mode dynamics anal. 0-33761
- trapped electron shear-Alfven instability, stabilisation by temp. gradient 0-28599
- Tuman-2A Tokamak, ohmic heating and compression of plasma 0-28703
- turbulence induced by plasma-electric current interaction in focus expt., laser diagnostics 0-24171
- turbulent convective transport in a plasma 0-28606
- two-stream instability in plasmas with arbitrary orientation of magnetic field 0-41715
- ultralow frequency oscill. in trapped electron regime 0-1784
- unstable continuous spectrum and ballooning modes 0-19569
- unstable turbulent ionisation waves, two dimensional Fourier spectroscopy 0-38646
- variational methods for complex eigenfrequencies 0-28631
- velocity driven modes in dense partially ionized plasmas, stability aspects 0-1792
- W VII-A stellarator,  $m=2$  mode at  $q=2$  0-24227
- wave growth, stability anal., particle distrib. functions and transport theory 0-43903
- wave heating at electron cyclotron harmonics in toroidal plasmas 0-28727
- wave-particle interaction in the late beam-plasma instability 0-28692
- waveguide, plasma-filled, two-stream instability nonlinear evolution, numerical simulation 0-43938
- weakly inhomogeneous magnetic field amplification by plasma wave 0-24166
- weakly ionised plasma in DC field, non-zero neutrals temp., unstable modes anal. 0-38606
- whistlers, scattering, nonlinear, by lower hybrid and ion Bernstein modes 0-43929
- Zakharov equations derivation for higher electron non-linearities in Langmuir collapse dynamics 0-43919
- Ar hollow cathode arc, in mag. field up to 2 kOe, plasma parameters 0-6306
- Ar, weakly-ionised, collisional drift instability 0-53977
- Ar-N<sub>2</sub>(CO), non-self-sustained discharge instability, negative differentiated cond. (*Russian*) 0-38740
- Co<sub>2</sub>:He:N, glow discharge instability in afterglow 0-6313
- Cu II, laser construction and performance, novel hollow cathode discharge structs. 0-38000
- D-D fusion reactor plasmas, pure and catalysed, thermal stability 0-24207
- D-D plasma interaction with relativistic electron beam, thermonucl. reaction, neutron and proton prod. 0-37575
- D-T plasmas, ignition toroidal expt., equilibrium configs. and heating 0-28704
- He spark, cathode spot conversion kinetics 0-44067
- N discharge, externally maintained, instability growth time, associative ionisation 0-6254
- N, glow discharge instability in afterglow 0-6313
- SF<sub>6</sub> gas, dispersion relation of spontaneous oscill., unstable regions 0-1875

**plasma interactions** see *plasma collision processes*

**plasma jets**

- absolute spectral brightness measurement 0-28832
- aerosol jet, electrophysical props. 0-24134
- air plasma jet of induction plasma generator, SiO<sub>2</sub> particle movement and heating (*Russian*) 0-7522
- atomic emission spectroscopy, discharge current and gas flow rate influence (*Czech*) 0-26081
- DC plasma jet, NO synthesis, chem. kinetics obs. 0-38728
- electric arc, self magnetic field, kink instability, plasma jets production (*Polish*) 0-19662
- flame, heat transfer to stationary sphere 0-33824
- H plasma jet, calc. of temp. and trajectory of particles in nonisothermal jet (*Russian*) 0-7514
- heat transfer to rotating water-cooled cylindrical wall (*French*) 0-28850
- heterogeneous medium, interactions of laser radiation 0-28765
- ion-acoustic dissemination in moving plasma jet 0-38707
- low temperature, decomposition and reduction of SiO<sub>2</sub> (*German*) 0-45499
- powder condensation growth, math. model of jet-plasma treatment process (*Russian*) 0-7513
- pulsed erosion jet, energy characts., heat flow distribution (*Russian*) 0-33825
- rarefied plasma flow, degree of nonisothermality, probe meas. 0-24243
- source, dielec. chamber, plasma flow characts. optimisation 0-38574
- spectral analysis of fission reactor materials 0-19624
- supersonic, damaging of metals, mech. momentum role 0-2065
- supersonic, ionisation in Mach disc, submillimeter laser interferometry diagnostics 0-14934
- supersonic colliding plasma jets, hot dense plasma formation, hydrodynamic model (*Russian*) 0-38676
- Ar magnetoplasma dynamic arcjet, recomb. lasing 0-48218
- ArH exciplex emission obs. in rarefied Ar-H<sub>2</sub> plasma jet (*French*) 0-48054
- He<sub>2</sub><sup>+</sup> recombination, high-temp., in plasma jet (*French*) 0-43861
- N I plasma jet, spectroscopic diagnostics, Stark broadening and shift, study 0-38727
- TiC plasma-chemical synthesis, depend. on geometric and flow rate parameters (*Russian*) 0-40677

**plasma magnetohydrodynamics**

- Alcator A Tokamak, disruptive MHD activity during plasma current rise 0-32487
- Alcator Tokamak, energy balance, MHD activity 0-28838

**plasma magnetohydrodynamics continued**

- Alfven pulse-excited instability in neutral sheet, mag. field lines reconnection dynamics (*Russian*) 0-1768
- Alfven waves, nonlinear self-precession and wavenumber shift 0-10389
- Alfven-ion-cyclotron instability for axially bounded plasma 0-1788
- arc tunnel, formation of high speed quasisteady plasma flow (*Japanese*) 0-10367
- arc voltage-current characts., MHD eqns. anal. 0-38815
- channel with Hall and ion slip currents, forced convective heat transfer 0-33823
- charged particles drifts in mag. field with arbitrary spatial var. 0-46382
- coal-fired MHD generator, molecular beam mass spectrometric sampling system 0-52358
- coaxial channel flow of accelerators and compressors, two-dimens., simulation 0-19566
- collective plasma effects in solar flares, assoc. with particle streams continuous injection model 0-21954
- column embedded by rotating ion beam, instability 0-28690
- compressible magnetic-field reconnection 0-6226
- conference on fusion research and plasma physics, Innsbruck, Aug. 1978 0-27033
- current disruption, in Tokamak plasmas, schlieren signal meas. from millimetre waves 0-48998
- current sheet in compressible plasma, self-similar resistive decay 0-1755
- diagnostics by holographic interferometry and Fourier filter correlation 0-48965
- diffusion due to mag. field fluctuations 0-1761
- discharge dynamics, calculations of plasma energy and particle balance 0-28847
- disruptions, internal, precursors of, tearing mode 0-28652
- drift motion in curved mag. field with rot. transform 0-1754
- electron gas with external mag. field, Vlasovs equation with mollified density 0-1756
- electron heat conductivity, magnetic field line diffusion 0-28641
- energy lifetime of plasma, T-3 scaling law, in Tokamaks 0-28635
- equilibria, secular instability in mag. quadrupole field 0-53982
- equilibrium and stability in three dims. configurations 0-28776
- explosive instability of one dimensional weak mag. field (*Russian*) 0-14896
- flow, numerical simulation 0-6229
- focus dynamics with powerful laser interaction during MHD stage, diagnostics 0-48924
- general relativistic plasma sphere with central gravitating mass, MHD eqns. 0-6276
- generator, local characts., transverse current inhomogeneity in MHD channel 0-24146
- glow discharge, MHD gas movement near anode spots 0-1869
- Heliotron D, RF heating, equilibrium and stability 0-28777
- high beta MHD theory, stellarator equilibrium and stability, mirror traps and reverse field machines 0-28778
- high beta stellarator,  $I=2.3$  helical fields, stabilisation effects 0-28779
- hollow axisymmetric mirror, MHD stable, multipole field stabilization (*Russian*) 0-33801
- hydrodynamic wave description including electron spin 0-38643
- hydromagnetic rarefaction waves and free expansion in collision-free strongly magnetised plasma 0-38594
- instability, secular, in mag. quadrupole field, of MHD equilibria 0-10427
- internal  $m=1$  helical mode, feedback suppression in Tokamak 0-19577
- interplanetary plasma wave propagation, magnetoacoustic wave transverse to mag. field 0-12629
- ion acoustic wave radiation due to oscill. point charge (*French*) 0-43900
- ionosphere, vertical displacement during substorms 0-4184
- ISX-A Tokamak, plasma confinement and impurity flow reversal 0-28770
- JET, ballooning modes, MHD theory 0-28639
- kink instabilities of a field reversed ion ring with a toroidal magnetic field 0-1758
- kink instability, internal MHD, sufficient cond. (*Chinese*) 0-43897
- kink stability, convection effects, MHD boundary layer anal. 0-1762
- long-wavelength modes and anomalous transport in toroidal magnetoplasmas 0-28613
- magnetic flux ropes on Sun, equilib. and stability (*Russian*) 0-8617
- magnetic islands coalescence 0-19564
- magnetic pulse penetration into plasma, theta pinch geometry, Alfven velocity scaling 0-33803
- magneto-viscous resistive tearing of cylindrical flux surfaces 0-1831
- magnetoacoustic disturbance, hydrodynamic instability in nonuniform plasma flow (*Russian*) 0-1766
- magnetohydrostatic equilibria, circ. cylindrical, internal modes stability, in diffuse pinch 0-43957
- magnetospheric simulation expts. 0-46347
- MHD equilibrium and stability, triangular deformation elliptic cross section (*Chinese*) 0-53950
- MHD generator, characteristics improvement, using current parallel to magnetic field 0-1751
- MHD generator, conductivity and power output ionization stability, and boundary layer effects 0-1752
- mirror machine, enhanced plasma confinement by MHD oscillation 0-24205
- modulational instability produced by Langmuir turbulence in a magnetic field 0-1759
- multiple-mirror plasmas, MHD stabilisation 0-6244
- nonequilibrium plasma, two-temp., expanding in disc-shaped channel, hypersonic MHD interactions 0-10368
- nonlinear stability problems, two-time method, dissipation scalings, ohmic heating 0-53967
- numerical simulation, variational approach 0-28625
- perturbations for finite magnetic Reynolds number 0-1757
- pinch, reversed-field type, in STP-1, using new external-field programming, MHD instability 0-28803
- plasma column, influence of external mag. axial field on an autocompression, review (*Rumanian*) 0-24148
- plasmastron melting arc in Ar and CO<sub>2</sub> atmosphere, performance characts., MHD calcs. (*Russian*) 0-38573
- power generators, combustion products plasma characterisation, generator channel flow, diagnostic techniques 0-43993
- relativistic degenerate electron plasma, dielectric response in mag. field, plasma oscillations 0-54022
- residual force equation soln. by three dims. code 0-28622
- resistive MHD instabilities of current sheets, appl. to solar wind 0-4218



**plasma magnetohydrodynamics continued**

- rotating plasma, weakly ionised, rot. vel. and ion cond., obs. and MHD theory 0-38576
- rotation of magnetised nonuniform plasma, MHD ordering 0-33756
- screw pinch, finite Larmor radius stabilisation, resonant particle effects 0-54020
- seeded combustion gas near cold electrodes, MHD boundary layer 0-48865
- self-gravitational instability of plasma rotating layer, effects of finite ion gyroviscosity 0-56706
- shear Alfvén wave, heat flux instability 0-43893
- shear Alfvén wave heating experiments in heliotron D 0-28716
- shock waves in turbulent medium, energetic particles interaction 0-4210
- space-charge wave instability of spiral beam-plasma system in nonuniform mag. field 0-1760
- spheroidal low aspect ratio plasma configurations, MHD equilibrium and stability 0-1791
- stability criteria for localised displacements 0-28645
- stability in toroidal axisymmetric system (*German*) 0-28792
- stable MHD fluctuations theory development (*Russian*) 0-24145
- stationary magnetoplasma dynamic source, elec. and thermal characteristics 0-14915
- supersonic conducting gas stream, interaction with mag. field, numerical simulation 0-6230
- surface hydromagnetic waves, dissipation 0-21904
- TFR 600 Tokamak, plasma confinement, low effective plasma charge 0-28769
- theoretical plasma mechanics, book 0-27048
- theta pinch, radial oscills. of plasma density and mag. field, light scatt. and probe obs. 0-14937
- Thomson scattering, rot. Raman calibration 0-1844
- Tokamak, high-beta, equilibria and  $m=1$  kink ballooning mode nonlinear evolution 0-24236
- Tokamak, high-beta, MHD eqn., stability, transport calc. 0-28848
- Tokamak, internal kink mode, numerical study 0-48953
- Tokamak discharge, transient behaviour, electrohydrodynamical model 0-48952
- Tokamak doublet geometry, shape control of doublets 0-48943
- Tokamak fusion reactors, doublet research, plasma shape control, MHD stability 0-28837
- Tokamak orbits, topology 0-28806
- Tokamak thermonuclear reactor, MHD modes drift phenomena, kinetic method (*Russian*) 0-1827
- Tokamaks, ballooning modes and pressure limits 0-28647
- Tokamaks, high- $\beta$ , MHD stability limits 0-28643
- Tokamaks, high-pressure, MHD-mode stability, high wave number 0-28644
- Tokamaks, large, impurity effects and control, neutral beam injection, computational models 0-28773
- Tokamaks, MHD beta limits, dependence on current density and pressure profiles, num. calc. 0-28637
- Tokamaks, non-circular, shaping and internal structure 0-28842
- Tokamaks, non-circular, stability and beta limits 0-28646
- Tokamaks with iron core transformer, self-consistent MHD equilibria 0-19608
- Tokamaks with large-aspect-ratio, stability, two-fluid dissipative theory 0-28640
- toroidal plasma, eigenvalue problem and nonlinear evolution of kink modes 0-24234
- toroidal plasma, resistive MHD mode and sawtooth oscill., nonlinear evolution 0-24235
- toroidal plasmas, axisymmetric, high mode number stability 0-28642
- toroidal plasmas, MHD instabilities 0-38579
- toroidal system, MHD plasma control by feedback and HF fields 0-28781
- Transit Time Magnetic Pumping heating in Petula Tokamak 0-28739
- turbulence, two dimens. stationary states in non-dissipative limit 0-24169
- two-dimensional mag. flux shell model for MHD simulations of cylindrically symmetric plasmas 0-1838
- vacuum arc retrograde motion in mag. field, Hall effect study 0-6315
- Ar magnetoplasma dynamic arcjet, recomb. lasing 0-48218

**plasma measurement techniques** *see plasma diagnostic techniques***plasma oscillations***see also plasma waves*

- Alfvén and magnetoacoustic wave heating for fusion plasmas 0-24188
- alpha particles interaction with mag. plasma fluctuations in D-T reactor 0-24204
- anomalous absorption of UHF radiation in electron cyclotron resonance range (*Russian*) 0-1807
- anomalously resistive phase, spiky density fluctuations and relax oscill., microwave scatt. obs. 0-38547
- axial eigenmodes for long- $\lambda_{||}$  waves in plasmas bounded by sheaths 0-28655
- coated semiconductor spheres, surface modes, plasmon oscills. 0-54730
- collective oscills. in toroidal plasma, microwave scatt. diagnostic technique, review 0-48863
- constricted glow discharge in transverse air flow 0-24278
- current instability on short wave drift oscills., nonlinear theory (*Russian*) 0-53981
- dielectric friction in plasma, harmonic oscillator and rigid dipole dielectrics, collective plasma oscills. 0-53928
- disruption, tearing and kink modes, limit of safety factor in JFT-2 Tokamak 0-38589
- drift oscillation spectra, LF, modification in HF elec. pump field (*Russian*) 0-1767
- drift-dissipative waves, weakly ionised plasma, column steady state 0-38613
- echo oscillations in relativistic plasma (*Russian*) 0-53990
- electron beam generated electron plasma oscillations, quenching by low freq. externally applied wave 0-24160
- electron beam-plasma low freq. instability, cyclotron oscills. (*Russian*) 0-33783
- electron cyclotron heating in toroidal plasmas, wave trajectories 0-38678
- electron cyclotron reson. in inhomogeneous mag. field integral eqn. (*Russian*) 0-33758
- electron oscillation in radial potential well effect on beam interactions (*Russian*) 0-14912
- electrostatic waves in drifting ionospheric simulation 0-53965
- EM wave self-action during thermal modulation instability of high hybrid oscills. (*Russian*) 0-53980

**plasma oscillations continued**

- explosive emission diode, plasma pot. oscills., probe diagnostics 0-6284
- flute oscillations suppression, regulator synthesis (*Russian*) 0-24212
- FT-1 Tokamak, lower hybrid plasma heating 0-28700
- HF oscillations and electron beam relax. in homogeneous gas-discharge plasma 0-38614
- internal disruption in Tokamak, relax. oscills., self-consistent model (*Russian*) 0-53957
- ion cyclotron waves, oscillating two-stream instability, RF heating of tokamak plasma 0-1779
- ion oscillation excitation by freely propagating electron beam (*Russian*) 0-1815
- ion-acoustic instability oscillations in collisionless single ended Q-machine 0-38731
- ion-cyclotron, non-electrostatic, spontaneous excitation, threshold electron drift 0-38625
- ionisation waves, half subharmonic excitation in glow discharge, positive column 0-44006
- Langmuir oscillation collapse in supersonic regime, forbidden energy (*Russian*) 0-14895
- Langmuir oscills., modulational instability, in EM wave field 0-38618
- Langmuir turbulence, modulation perturbation spectrum 0-33776
- Langmuir waves, induced nonthreshold scatt. on HF oscills. in inhomogeneous plasma (*Russian*) 0-53960
- Langmuir waves, nonperiodic oscillations 0-48888
- localised pumping-excited waves, parametric instability, nonlinear stage 0-38622
- lower-hybrid range oscillations in bounded plasma 0-24162
- magnetic mirror trap, open, with min. B, LF oscills. 0-38708
- magnetoacoustic, used for equilb. plasma density and mag. field profile determs. 0-48986
- magnetoacoustic oscillation excitation in strongly inhomogeneous plasma 0-38641
- magnetoacoustic oscillations in a finite-beta current carrying plasma column 0-1771
- magnetoacoustic oscills., in bounded plasmas, viscous damping 0-38605
- magnetoacoustic oscills., in toroidal plasma, comparison with cylindrical plasmas, numerical calcs. 0-33760
- mirror machine, enhanced plasma confinement by MHD oscillation 0-24205
- modulational instability produced by Langmuir turbulence in a magnetic field 0-1759
- nonlinear lower-hybrid waveguide in plasma, stability 0-19578
- Ogra-3 mirror device, loss mechanism due to cyclotron instabilities 0-28788
- oscillating two-stream and parametric decay instabilities in a weakly magnetized plasma 0-38637
- parametrically excited relaxation oscills. in UHF discharge 0-53978
- Penning discharge ion source with hollow cathode, HF instabilities 0-43997
- potential double layers, highly nonlinear states in plasmas, expt. obs. 0-6233
- probkotron plasma stabilisation system, automatic, against flute oscills. (*Russian*) 0-24211
- Pulsator Tokamaks, modulated runaway losses and effects of helical dipole field 0-28845
- quasi steady high beta plasma in multiple mirror machine, density oscill., stability obs. 0-28663
- relativistic degenerate electron plasma, dielectric response in mag. field, plasma oscillations 0-54022
- relativistic isotropic plasma, EM and electrostatic oscills. 0-54026
- relaxational oscillations of plasma wave energy, in solar mag. traps (*Russian*) 0-8616
- runaway relativistic electron scatt. on oscills. in Tokamak (*Russian*) 0-48849
- sharp boundary Vlasov-fluid screw pinch, free and forced  $m=0$  oscillations 0-38636
- stability and distrib. function influence on eigenoscillations 0-53966
- surface oscillation cyclotron excitation, electron beam cyclotron instability (*Russian*) 0-54008
- T-10, ohmic heating, plasma confinement study 0-28768
- T-12 Tokamak with two axisymmetric divertors, characteristics of divertor 0-28844
- theta pinch, radial oscills. of plasma density and mag. field, light scatt. and probe obs. 0-14937
- Tokamak, confinement and stability, effects of shaping and compression of plasma 0-28772
- Tokamaks, feedback stabilisation of magnetic islands 0-28638
- Tokamaks, magnetic islands, tearing modes 0-28846
- toroidal plasma, resistive MHD mode and sawtooth oscill., nonlinear evolution 0-24235
- UHF discharge with preliminary locally ionised gaseous medium 0-38851
- ultralow frequency oscill. in trapped electron regime 0-1784
- viscous damping of magnetoacoustic oscillations in cold, bounded cylindrical plasma 0-24151
- wave dispersion in presence of relativistic beam 0-19592
- whistler wave, large amplitude oscillation by high power microwaves 0-43913
- whistler wave trapping in density crest 0-53984
- Co,  $K\beta_{1,3}$  X-ray emission spectra, low energy plasmon satellites 0-19560
- Cs-Ba discharge, high-current, low-press., spontaneous current cutoff 0-19626
- Cu,  $K\beta_{1,3}$  X-ray emission spectra, low energy plasmon satellites 0-19560
- D-T plasmas, ignition toroidal expt., equilibrium configs. and heating 0-28704
- SF<sub>6</sub> gas, dispersion relation of spontaneous oscill., unstable regions 0-1875

**plasma probes***see also Langmuir probes*

- Berkeley multicusp ion source for use with TFTR neutral beam injector, characts. 0-54040
- DC probe voltage deviation caused by probe current drawing across plasma resistance, compensation cct. 0-54041
- diagnostic techniques for fluctuations 0-49002
- diffusion type, cylindrical, in mag. field, floating pot. calc. 0-10438
- discharge, luminesc. lamp. external and internal probe meas. 0-43978
- electric field measurement in corona discharges 0-33822
- electric probe in weakly ionised and rarefied plasma (*Russian*) 0-24252
- electrical conductivity of low-temp. alkali plasma, weak probing signal method meas. 0-48968



**plasma probes continued**

- electron density, meas. in unmagnetised plasma, self-oscill. probe method 0-19611  
 electron distribution function in ionis. instability mode of plasma accelerator 0-19612  
 electron temperature and electron density in low density magnetised plasma by probe method 0-48848  
 electrostatic probe characteristics in a magnetic field, ellipsoidal probe in diffusion regime 0-33815  
 emissive probe using CO<sub>2</sub> laser-heated emission of electrons from C-coated metal surface 0-6270  
 explosive emission diode, plasma pot. oscills., probe diagnostics 0-6284  
 field visualisation technique applied to sub-mm diagnostics of axisymmetric plasma 0-43980  
 flame measurements, probe material effect on results 0-19613  
 formation of plasma in fusion devices, at. and plasma processes, diagnostic techniques 0-48915  
 glow discharge, investigation with cylindrical hollow cathode in Ne and He (*Russian*) 0-28856  
 ion current and charact. by non-self-maintained ionisation 0-38713  
 ionospheric plasma probe measurements, commutable source of ref. voltages 0-31192  
 laser fusion diagnostics, techniques and appl. 0-49009  
 microwave, hemispherical monopole, characts. 0-19621  
 neutral beam probe, ion temp. meas. (*Japanese*) 0-19615  
 nonlinear effects in the vicinity of a radiofrequency probe 0-48985  
 nonlinear helical perturbation in Tokamak, dynamics, mag. probe obs. (*Russian*) 0-53958  
 positive ion extraction by an anodic orifice probe 0-38712  
 RF probe sheath, finite thickness effect 0-43971  
 RF voltage in plasma probe sheath, effect on electron energy distrib. meas. 0-54045  
 shooting, for high-density plasma 0-33816  
 space potential location, in large Debye length stationary plasma 0-14940  
 temporal and spatial meas. of RF electric field in magnetized plasma using emissive probe 0-54042  
 theta pinch, radial oscills. of plasma density and mag. field, light scatt. and probe obs. 0-14937  
 two-electrode probe, electron beam-formed plasma, pot. diagnostics (*Russian*) 0-1841  
 He glow discharge, negative-luminesc. plasma, electron energy distrib. from line intensities and probe obs. 0-49033  
 N<sub>2</sub> plasma, spatial distrib. in transverse-discharge supersonic stream, continuum theory and probe meas. 0-48866

**plasma production**

- see also *exploding wires and foils; plasma production and heating by laser beam*  
 anodic plasma production and ion acceleration in coaxial diode with mag. insulation (*Russian*) 0-10402  
 arc, vac., fast plasma jet production from cathode spot 0-6309  
 atmospheric positive streamer corona, primary wave emission, secondary electron emission 0-44008  
 beam discharge for apparatus with spatial axis, weakly ionised plasma diffusion (*Russian*) 0-1826  
 coaxial lower hybrid plasma source capable of producing pulsed plasmas 0-33788  
 current structure, fast particle generation (*Russian*) 0-48913  
 currents in short pulsed high current electron beam injection into initially neutral gases 0-33749  
 dielectric surfaces in evacuated cavities, plasma release due to electron irradi., transport characts. 0-33786  
 electric discharge, in air, pulsed, high-density, between parallel plates 0-1857  
 electron beam, relativistic, anomalous energy deposition into solid low-Z target 0-48906  
 electron beam, relativistic, interaction with air 0-48904  
 electron beam in gas, current meas. 0-38523  
 electron beam-formed plasma potential, two-electrode probe diagnostics (*Russian*) 0-1841  
 electron cyclotron resonance plasma, production of multiply-charged ions, X-rays and charge state distrib. meas. 0-43941  
 electron density meas. in shock generated plasma by light interferometry 0-48981  
 electron distribution function and ionisation in space-depend. theory 0-38545  
 emission from plasma formed in proton beam collision with Al target 0-53946  
 explosion induced compression, neutron yield optimisation in crucial systems 0-5328  
 explosive instability collision mode stabilisation by drifting effects, Thirring instability (*Russian*) 0-43920  
 extended high-current discharge, initiation by long laser spark (*Russian*) 0-10404  
 flow and production in ion beam 0-28624  
 formation of plasma in fusion devices, at. and plasma processes, diagnostic techniques 0-48915  
 generator arc chamber, hydrodynamic struct. 0-1817  
 H-pinch discharge, quasistationary, EM characts. and energy balance, erosion plasma generator 0-19630  
 high current short bremsstrahlung pulse sources 0-5400  
 high melting particle heating, melting and vaporisation in hot gas 0-6201  
 implosion, by pulsed electron beam accelerator, 4TW, laser and X-ray obs. 0-1816  
 inert gas halides, excimer emission from electron beam produced plasma 0-43887  
 insulator surface flashover in vacuum, electro-optical meas. 0-38823  
 ion beam-created high-press. plasma, electron props. diagnostics (*French*) 0-10407  
 ion source, two-stage discharge type, operational characts. 0-47797  
 ion-acoustic instability, electron flux driven, in Q-machine, probe diagnostics 0-33765  
 ion-acoustic instability stabilisation by ion beam in Q-machine, probe diagnostics 0-33766  
 Knudsen arc ignition, plasma form. kinetics, spectroscopic and probe obs. 0-38808  
 microwave discharge, supersonic flow in waveguide, electron densities, possible laser 0-38842  
 microwave O<sup>+</sup> plasma, magnetoactive, for oxidation of Si 0-38831

**plasma production continued**

- microwave plasma production at atm. press., surface wave propag. method 0-10408  
 motional impedance and heating of low resistive plasmas 0-14913  
 multiple-wire implosion in transmission line generators, hot plasma efficient prod. 0-48929  
 nonideal plasma, measured props. and nonideality influence 0-43869  
 optical measurements on plasma initiated by a relativistic electron beam (*Japanese*) 0-48914  
 prepulse discharges in high current accelerator diodes with double shaping line 0-5399  
 pulsed erosion jet, energy characts., heat flow distribution (*Russian*) 0-33825  
 reflex tetrode, ion beam extraction anal. 0-48903  
 relativistic electron beam, anomalous interaction with solid target 0-28709  
 sheath driven targets, simulation 0-48898  
 shock wave induced fusion, multiple refraction problems in layered medium 0-5330  
 shock wave produced plasma, electron and ion thermal diffusion effects 0-48891  
 stationary magnetoplasma dynamic source, elec. and thermal characteristics 0-14915  
 supersonic colliding plasma jets, hot dense plasma formation, hydrodynamic model (*Russian*) 0-38676  
 surfatron produced electron density and temp. microwave meas. 0-43965  
 thermonuclear fusion plasmas, elem. processes and role of atomic, ionic and mol. data 0-14916  
 Tokamak fusion reactor, TFTR, plasma generation and confinement 0-42864  
 Tokapole II, poloidal divertor, plasma production and confinement studies 0-18602  
 Al foil in quartz dust, electrical explosion for accelerator application 0-6314  
 Ar-liquid K cathode arc, dense plasma prod., cathode erosion rate estimation (*French*) 0-44056  
 Ar-Xe plasma, shock wave dynamic compression, thermodynamic props. (*Russian*) 0-53931  
 Cr from Tokamak-produced plasma, 2s<sup>2</sup>2p<sup>k</sup>-2s2p<sup>k+1</sup> transitions in F I to Be I isoelectronic sequences 0-37765  
 D-fusion, shock wave induced, Ar admixture optimisation 0-5329  
 D-T plasma, thermonuclear reaction product kinetics effect on parameters 0-5327  
 Fe from Tokamak-produced plasma, 2s<sup>2</sup>2p<sup>k</sup>-2s2p<sup>k+1</sup> transitions in F I to Be I isoelectronic sequences 0-37765  
 H<sub>2</sub>, solid pellet ablation in plasma 0-19589  
 He, afterglow produced by microwave surfaguide, spectroscopic diagnostic, electron and He<sub>2</sub> rot. temp. 0-44042  
 Ne-N<sub>2</sub>, energy transfer, H<sup>+</sup> ion beam produced plasma, ion density and temp. 0-38539  
 Ni from Tokamak-produced plasma, 2s<sup>2</sup>2p<sup>k</sup>-2s2p<sup>k+1</sup> transitions in F I to Be I isoelectronic sequences 0-37765  
 O<sub>2</sub>, electron beam energy branching, discrete energy loss method 0-48905
- plasma production and heating by laser beam**  
 absorption, z-depend., stimulated backscatter processes 0-43944  
 absorption in laser-produced plasma expts. 0-14931  
 aerosol, plasma production by CO<sub>2</sub> laser beam, brightening channel 0-6272  
 air, laser-induced breakdown over long distances 0-33795  
 air, optical breakdown, initiation by absorbing water droplets 0-10352  
 air, optical breakdown near metal target by laser beam 0-6209  
 alkali hydride arc, laser initiated, H<sup>+</sup> production 0-32550  
 ANTARES and advanced CO<sub>2</sub> laser-fusion systems 0-32502  
 backscattered light pulse shape depend. 0-10431  
 beat heating in plasmas using CO<sub>2</sub> lasers 0-43950  
 cavitons in laser irradiated fusion plasmas, EM wave propag., supersonic density humps 0-24178  
 conference on fusion reactor materials [Miami Beach, Florida, Jan. 1979] 0-31407  
 continuous optical discharge, diagnostics 0-43947  
 curvature effects in laser plasma interactions 0-43948  
 Debye screening modifications in ponderomotive effects 0-33777  
 decay instability of laser radiation in a magnetoplasma 0-1781  
 dense plasma XUV transition Doppler broadening suppression, collisional-radiative model 0-19614  
 density measurement of laser-compressed plasma, X-ray line shift (*German*) 0-48967  
 density profile meas. using Wollaston prism interferometer 0-48973  
 dielectric medium, optically transparent, avalanche ionis., recomb. effect 0-7295  
 dynamic response to laser modulations, in CW laser prod. Cs plasma 0-14920  
 effective cross section and space charge, preionised gas laser induced breakdown 0-48930  
 electric field pattern calcs. in laser produced plasma (*German*) 0-54014  
 electron and at. excited states densities in laser prod. He plasma 0-38710  
 electron-energy transport in laser-produced plasmas 0-6266  
 EM resonant properties of laser-prod. plasmas 0-43928  
 emission of multiply charged ions from plasma produced by CO<sub>2</sub> laser 0-9445  
 energy distribution of electrons heated by laser light absorpt., simulation and test particle methods 0-48963  
 energy transfer in laser (or particle) beam produced plasmas 0-38680  
 explosive magnetic field generation due to EM incident radiation, laser plasma mechanism 0-6253  
 explosive-pusher-type laser compression experiments with neon-filled microballoons 0-23132  
 fast electrons, X-rays and ions, motion evaluation 0-19557  
 fast ions in laser-produced plasma, nonlinear plasma-wave interaction 0-24183  
 filamentation instability of laser beam in inhomogeneous plasma, preferential heating 0-19568  
 focus dynamics with powerful laser interaction during MHD stage, diagnostics 0-48924  
 formation dynamics of underexpanded supersonic erosive laser plasma flare, high speed techniques 0-48923  
 fusion, developments for future energy involving lasers 0-23120  
 fusion energy generation, plasma confinement, laser compression, Li activation (*German*) 0-52783



- plasma production and heating by laser beam continued  
 fusion plasma confinement,  $\alpha$ -emission recoil force effect 0-6275  
 fusion plasma simulation, hydrodynamical behaviour (*Chinese*) 0-1823  
 fusion targets, six-beam irradiation and implosion, laser focus depend. 0-14919  
 gas breakdown model 0-1821  
 gas filled microballoon targets, laser produced implosion dynamics 0-24198  
 glass microballoon imploded by laser, X-ray transmission analysis (*French*) 0-54011  
 glass shell target, electron temp. and density, Si X-ray emission diagnostics (*Chinese*) 0-38718  
 glass target, spherical-shell, energy absorpt., expt. determ. 0-54016  
 glass targets, laser-produced plasma X-ray spectral lines identification (*Chinese*) 0-54036  
 glass-CO<sub>2</sub>-hybrid laser system for plasma prod. and heating in mag. traps 0-24196  
 heat flux limitation by magnetic field curvature in laser-plasma interaction 0-43951  
 heat front penetration depth, heat transport wavelength depend. 0-48926  
 Helios gas laser system, ICF expt. program as LASL 0-32501  
 heterogeneous medium, interactions of laser radiation 0-28765  
 high power laser appl. (*French*) 0-13785  
 high pressure optical discharges, density and temp. meas. 0-48931  
 high-Z disc targets, 1.06  $\mu$ m laser radiation interaction 0-6269  
 holographic study of laser prod. plasma at 10.6  $\mu$ m 0-38685  
 hot spot distribution, significance in interpretation of laser produced plasma expts. 0-1820  
 hybrid-wavelength laser system, spherical solid target, computer anal. 0-48920  
 ice, surface, interaction of laser burst, possible appl. 0-7444  
 ICF reactor fuel pellet fabrication techniques and quality factors, optical systems 0-32436  
 ICF reactors, pellet and laser beam space-time interaction system study 0-13802  
 ICF targets, laser driven, materials problems 0-32438  
 ICF targets, semiconductor process technology for mass production 0-32439  
 inertial confinement fusion at NRL, laser and ion drivers 0-23131  
 inertial confinement fusion at Osaka, laser energy drivers, REB fusion research 0-23135  
 inertial confinement fusion gains using collective model for electrodynamic laser compressions 0-23138  
 inertial confinement fusion research at Los Alamos, recent progress 0-23133  
 inertial confinement fusion research system of high power lasers (*Japanese*) 0-5324  
 inhibited electron thermal cond. in plasma from microwave laser irradiation, laser intensity threshold Z-depend. 0-48928  
 inhomogeneous laser-generated plasma, resonantly enhanced elec. field props. 0-33796  
 instabilities in laser produced plasma column in uniform mag. field 0-38687  
 intense field QED in continuous medium, appl. to Thomson scatt. and Cherenkov radiation 0-27435  
 inverse-bremsstrahlung absorption rate in an intense laser field 0-24201  
 ion acceleration in presence of density profile steepening 0-14923  
 ion emission from laser plasma, longit. mag. field effects (*Russian*) 0-54012  
 ionisation dynamics of CO<sub>2</sub> laser prod. plasma, spectrosc. obs. 0-43968  
 ionisation process computer simulation code, atomic transition processes 0-28764  
 KMSF laser implosion fusion programme, neutron yield and peak fuel density 0-23130  
 L-2 stellarator, solid H<sub>2</sub> pellet injection parameters and effects 0-28775  
 Langmuir soliton generation at crit. density with HF pump 0-6267  
 Langmuir waves, driven by electron-ion decay instability, scattered spectrum 0-43970  
 laser diagnostics, probing radiation Raman scatt. (*Russian*) 0-19618  
 laser driven fusion, teaching approach 0-42012  
 laser driven plasma, vacuum insulation against suprathermal electrons 0-18598  
 laser emission intensity reduction near solid target surface (*Russian*) 0-38681  
 laser fusion, interaction and transport processes, continuous pulse shaping 0-28766  
 laser fusion, suprathermal electron transport, dual treatment 0-18599  
 laser fusion implications of resonance absorption and associated electrostatic field pressure 0-24176  
 laser fusion microsphere targets, nondestructive anal. using rot. Raman spectroscopy 0-50896  
 laser implosion microballoons, X-ray line radiation diagnostics (*Chinese*) 0-6279  
 laser induced thermonuclear fusion, turbulent mixing effect on shell target compression (*Russian*) 0-5332  
 laser interaction and implosion at Centre d'Etudes de Limeil 0-24197  
 laser plasmas, wave absorpt. and superreflectivity due to EM struct. resonances 0-24177  
 laser radiation energy loss to resonantly accelerated ions 0-10413  
 laser spark absorpt. and laser pulse contraction meas. using dye lasers 0-48988  
 laser supported absorption waves, momentum transfer to surface, flowfield model 0-14921  
 laser systems for high temp. plasma prod. 0-19599  
 linear discharge, laser initiated, electron density meas. by far IR laser beam deflection 0-48966  
 luminar-combustion wave, shock parameters near detonation threshold 0-6256  
 magnetothermal phenomena (*Russian*) 0-33798  
 maximum energy flux in collisionless plasma, comparison with free molecular gas motion 0-6221  
 metal surface, high-intensity laser beam interaction 0-19600  
 metal surface micro-inhomogeneity effect on optical breakdown of gas 0-48922  
 metal vaporisation centres, erosion accompanying simultaneous action of laser emission and ultrasound (*Russian*) 0-7442  
 metal vapour production by sputtering in hollow-cathode discharge 0-1868  
 microdiscs, energy transport to rear surface under high laser irradiation. 0-33797  
 Monte Carlo (hybrid) suprathermal electron transport 0-24200  
 plasma production and heating by laser beam continued  
 multicharged plasma, heated by laser radiation, ionis. and recomb. 0-19597  
 multiple-charged ions, pressure dependence (*Japanese*) 0-10412  
 multiple-pass laser heating of a short plasma column 0-38684  
 non-linear theory of collective processes in laser-pellet interaction and soliton generation 0-24199  
 nonlinear dynamics of laser irradiated solid target 0-28767  
 nonlinear inverse bremsstrahlung and heated-electron distributions 0-48927  
 NOVA laser facility and future programs for fusion reactor ignition 0-37590  
 nuclear fusion, 1979 development trends and supercompression (*Czech*) 0-23122  
 nuclear pumped laser fusion blanket optimisation in space and time 0-37616  
 optical system for laser induced plasma compression 0-14382  
 optical systems for diagnostics of laser produced plasmas 0-10434  
 planar laser explosion near a target in air 0-19601  
 polyethylene, laser-prod. plasma, space-resolved extreme UV emission 0-54015  
 polyethylene, laser-produced plasma, momentum transfer and interaction phenomena of high power CO<sub>2</sub> laser 0-48921  
 polyethylene, X-ray emission spectra of CO<sub>2</sub> laser-irradiated targets, nonlinear processes 0-33793  
 pulse shaping effects on interaction processes in laser prod. plasmas 0-43946  
 pulsed laser-generated impulse on a surface in supersonic flow 0-48917  
 PVA target, spherical-shell, energy absorpt., expt. determ. 0-54016  
 reactor-laser for disintegrating thermonuclear plasma 0-19598  
 reflection of laser plasma from hot shield, expt. 0-33782  
 review of laser radiation interaction phenomena 0-43953  
 screening of graphite, polished Al targets in air, CO<sub>2</sub> laser radiation refl. 0-25500  
 self-generated magnetic field distrib., near laser-plasma reson. interaction region 0-10414  
 SHG in laser plasma 0-53993  
 spatially resolved suprathermal X-ray emission from laser-fusion targets 0-48984  
 spectral line emission from C-H plasmas generated by TEM<sub>10</sub> laser pulses 0-43969  
 spectral line shape and intensity, multicharged ion obs. on laser-produced plasma 0-10435  
 spectral lines in plasma, space depend. shift 0-6268  
 spectroscopic observation of laser produced plasma, XUV emitting region struct. 0-54038  
 spikon lifetime 0-14922  
 spontaneous mag. field form. in laser plasma, opto-electric effect (*Russian*) 0-54013  
 spontaneous magnetic field, target size and struct. depend. 0-1819  
 spontaneous magnetic field generation associated with laser-produced plasmas in presence of ambient gas 0-10411  
 stimulated Brillouin backscatter saturation for long CO<sub>2</sub> laser pulses 0-19582  
 stimulated Raman and Brillouin scatt., static mag. field effects 0-6258  
 striated filamentary sparks produced by a CO<sub>2</sub> TEA laser 0-24288  
 supercritical density profiles of CO<sub>2</sub>-laser-irradiated microballoons 0-14918  
 superthermal electrons, temp. and fraction estimation 0-1822  
 symmetrical implosion system, charged reaction products, electrostatic field effects 0-32499  
 target impurity effect on laser produced expansion, ion spectrography 0-43945  
 TEA-CO<sub>2</sub> laser pulse interaction with dense H plasma 0-38683  
 TEA-CO<sub>2</sub> laser-metallic target system, plasma target coupling 0-48925  
 temperature gradient-caused ion acoustic turbulence and reduced thermal cond. 0-53987  
 thin target in air, pulse-laser heating 0-2902  
 three-mirror image rotator use in laser produced plasma expt. 0-33814  
 triggered solid dielectric switches with low jitter and inductance 0-54066  
 triggered switching of solid insulated spark gap 0-54065  
 two-dimensional Lagrangian calculation of a laser-heated solenoid 0-54027  
 upper-hybrid reson. absorpt. of laser in plasma focus, backscatter 0-28621  
 water, interaction of laser bursts, possible appl. 0-7444  
 X-ray source for synchrotron radiation research and microradiography 0-320  
 X-ray spectrometry of laser-plasma, energy transport diagnostics (*French*) 0-43982  
 Z-pinch plasma, interaction with CO<sub>2</sub> laser radiation 0-48919  
 Al coated glass microballoon targets for laser implosion expt., search for shell disintegration 0-33792  
 Al foil, burn-through by laser-driven ablation 0-33794  
 Al, IR laser reflectance, anomalous absorpt., plasma ignition 0-7439  
 Al, laser-prod. plasma, space-resolved extreme UV emission 0-54015  
 Al, laser-produced plasma, momentum transfer and interaction phenomena of high power CO<sub>2</sub> laser 0-48921  
 Al reflective target, momentum and energy transfer pulse duration/polarisation depend., torsion pendulum diagnostics 0-43952  
 Al surface, pulsed CO<sub>2</sub> laser interaction at oblique incidence 0-48916  
 Al, X-ray emission spectra of CO<sub>2</sub> laser-irradiated targets, nonlinear processes 0-33793  
 Ar, preionised, CO<sub>2</sub> laser induced breakdown press. and pre-ionisation depend., cascade model 0-54010  
 C spectra from CO<sub>2</sub> laser prod. plasmas 0-38711  
 CO<sub>2</sub> laser plasma shutter, transmission cut-off time depend. on breakdown intensity 0-6259  
 CO<sub>2</sub> laser-heated electron emission from C-coated metal surface, appl. to emissive probe meas. 0-6270  
 CO<sub>2</sub> laser-induced plasma heated at 10.6 micron, nonequilibrium ionis. 0-6271  
 CO<sub>2</sub> laser-produced plasma-initiated neutral gas recomb. lasers 0-48286  
 Cu, laser-produced plasma X-ray spectral lines identification (*Chinese*) 0-54036  
 D fuel pellets, laser acceleration for injection into thermonuclear reactor (*Russian*) 0-52779  
 D pellet, ionisation by Nd laser irradiation. 0-43949  
 D, shell target compression on laser heating (*Russian*) 0-47718  
 D<sub>2</sub> plasma, isolated, CO<sub>2</sub> laser-produced, holographic interferometry diagnostics 0-24254



**plasma production and heating by laser beam continued**

- DT reaction rate in laser fusion pellets, effect of high energy ion loss 0-32495  
 N<sub>2</sub>, dense gas near metallic target, laser spark (*Russian*) 0-38682  
 N<sub>2</sub>, dense molecular gas, breakdown due to laser radiation, numerical simulation 0-38686  
 Pb, X-ray emission spectra of CO<sub>2</sub> laser-irrad. targets, nonlinear processes 0-33793  
 Pt, laser produced plasma, Ni-like X-ray spectrum 0-43983  
 Ti, laser-prod. plasma, space-resolved extreme UV emission 0-54015  
 YAG:Nd laser pulses, mutual exchanges with plasma (*German*) 0-48918

**plasma sheaths**

see also *plasma confinement*

- air, discharge, high-current, nanosecond, explosive cathode processes and contraction 0-10449  
 anode sheath in a strong transverse magnetic field 0-6310  
 arc, transient, contracted, cold-cathode, in mag. field, characts. 0-24291  
 arc discharge, high current, anode near-electrode layer, spot formation and sheath breakdown 0-38835  
 axial eigenmodes for long- $\lambda$  waves in plasmas bounded by sheaths 0-28655  
 discharge, RF, gamma regime, ionis. balance and plasma characts., model 0-44022  
 discharge plasma, diffusion regime, elec. sheath theory 0-1810  
 edge theory is weakly ionised collision dominated plasma 0-43935  
 effective boundary conditions for plasma in mag. field near electrode 0-38668  
 electrode, geometrically developed electron refl. at plasma boundary, kinetic coeff. 0-24182  
 fusion reactor divertor collector plate, pot. drop across electrostatic plasma sheath 0-13833  
 integro-differential eqns., nonlinear, nonlocal, soln. formalism 0-43936  
 Io, plasma sheath electrons rel. to Jupiter modulated decametric radio S-bursts (*Russian*) 0-8582  
 low temp. dense plasma electrode phenomena, review 0-33743  
 magnetosheath effects on cylindrical Langmuir probes 0-28820  
 metal vapour production by sputtering in hollow-cathode discharge 0-1868  
 nonlinear effects in the vicinity of a radiofrequency probe 0-48985  
 nonselfmaintained discharge, current voltage characts. 0-44045  
 Penning-type HV discharge, ionis. average freq. in anode sheath 0-44012  
 probe, diffusion type, cylindrical, in mag. field, floating pot. calc. 0-10438  
 probe ion current and charact. by non-self-maintained ionisation 0-38713  
 pulsar polar caps as foil-less diodes, nonneutral relativistic beam accel. 0-17604  
 RF discharge, electrode sheath 0-44052  
 RF probe sheath, finite thickness effect 0-43971  
 RF sheath in self-sustained plasmoids, size and disappearance analysis 0-44026  
 RF voltage in plasma probe sheath, effect on electron energy distrib. meas. 0-54045  
 solid surface interaction, electrostatic sheath equations, inc. heating, ion mobility and ion recomb. 0-1808  
 spherical antenna covered with isotropic plasma layer, radiation characts. 0-14907  
 stability, approx. model analysis of steady state situation 0-43934  
 targets, sheath driven, simulation 0-48898  
 thermionic converters sheath operating mechanism effects 0-30507  
 Al plasma anodisation forming voltage limitation mechanism (*Japanese*) 0-16579  
 Cs-Ba discharge, high-current, low-press., spontaneous current cutoff 0-19626  
 H<sub>2</sub>, solid, ablation by magnetised plasma, semi-empirical calc. 0-38666  
 He spark, cathode spot conversion kinetics 0-44067

**plasma shock waves**

- air-water vapour mixture, electron conc. and conductivity behind strong shock wave 0-48890  
 blast waves produced by a time-dependent energy source 0-14898  
 compressible magnetic-field reconnection 0-6226  
 compression by profiled explosion, neutron output 0-13782  
 critical surface, enhanced stimulated Brillouin scatt. due to light refl. 0-1750  
 deflagration wave formed by ion beam in spherical target 0-28694  
 electrical conductivity of high-density, shock-heated Ar and Xe plasmas 0-38557  
 electron density meas. in shock generated plasma by light interferometry 0-48981  
 electron temperature and density in Ar behind reflected shock waves 0-38549  
 electrostatic, double layer stability 0-6236  
 electrostatic shocks in ionosphere/magnetosphere, role of coherent anomalous resistivity 0-4189  
 electrostatic V-shocks in auroral plasma, approximate equipotentials 0-21870  
 fast ion deceleration in accretion column 0-38530  
 Fermi acceleration by shock waves in astrophysical plasmas 0-31207  
 fusion reactor cavity design, compact electron beam or light ion beam reactor using nonspherical blast waves 0-9405  
 interplanetary medium, type II radiobursts and shock waves 0-56690  
 luminar-combustion wave, shock parameters near detonation threshold 0-6256  
 magnetic piston interaction with nonmagnetised plasma 0-38630  
 MHD shock waves in turbulent medium, energetic particles interaction 0-4210  
 nonlinear-wave propagation in a proton-electron plasma coupled with a strong radiation field 0-48872  
 photodetonation and supersonic radiation wave propag. in Xe plasma (*Russian*) 0-10385  
 precursor whistler mode plasma turbulence formation in parallel shock waves 0-24172  
 radiation induced shock tube flow nonuniformities in ionising Ar 0-43865  
 second-kind explosive shock wave propagating after implosive shock wave collapse 0-48891  
 shock-heated dense plasma, continuum radiation and optical transmittance diagnostics 0-24202  
 solitary quasishock compression waves in vel.-modulated ion beam (*Russian*) 0-28679  
 structure, at re-entry speeds, in Ar 0-43927

**plasma shock waves continued**

- supersonic dense stream, shock braking processes, radiation-gasdynamic obs. 0-19635  
 supersonic jet, ionisation in Mach disc, submillimeter laser interferometry diagnostics 0-14934  
 Thomson scattering, rot. Raman calibration 0-1844  
 trans-relativistic shock relations, numerical solns. 0-31202  
 Al foil, burn-through by laser-driven ablation 0-33794  
 Ar-Xe, shock wave dynamic compression, thermodynamic props. (*Russian*) 0-53931  
 D<sub>2</sub> plasma, compression by microfusion explosion, expt. biconical system 0-13783  
 N<sub>2</sub> discharge, electron shock wave formation, numerical simulation 0-38777  
 Xe, plasma shock front, elementary processes 0-19581  
 Xe precursors, associative ionisation and photoionisation, relative contrib., electron density prediction 0-43858

**plasma simulation**

- anomalous electron pseudo-classical transport with coherent electrostatic wave propag. 0-24137  
 anomalous plasma transport due to electron temp. gradient instability 0-33813  
 ballooning instability in bumpy torus, hot electron annulus effect 0-53983  
 Cerenkov interaction between obliquely propagating whistler wave and electron beam, computer simulation 0-43937  
 coaxial channel flow of accelerators and compressors, two-dimens., simulation 0-19566  
 critical surface, enhanced stimulated Brillouin scatt. due to light refl. 0-1750  
 cross-field electron heat transport due to high frequency electrostatic waves 0-53932  
 desorption of TiD<sub>2</sub> films formed during simulated Tokamak gettinger cycles 0-34296  
 diffusional expansion across mag. field, modelling problem (*Russian*) 0-48964  
 EBTR, parametric anal. of thermonuclear burn dynamics and energy balance 0-37597  
 electric double layer form. and dynamics, simulation 0-48855  
 electron beam-plasma interactions in turbulence regime, phenomenological model 0-6260  
 electron cross-field heat transport caused by HF electrostatic wave 0-28619  
 electrostatic waves in drifting ionospheric simulation 0-53965  
 energy distribution of electrons heated by laser light absorpt., simulation and test particle methods 0-48963  
 focal region of intense laser beam in tenuous plasma, spatial and temporal electron and ion density variations 0-53989  
 fusion reactors, field reversed mirrors 0-43961  
 guiding center plasma with gravitational or gradient drifts 0-38632  
 gyrating charged particle beam compression, modeling with finite circuit element code 0-14930  
 heat transport, computer simulation 0-28817  
 ion acoustic wave, large amplitude, initial freq. shift 0-28661  
 Langmuir wave evolution, three dimensional kinetic model, Vlasov eqn. calcs. 0-43923  
 laser fusion simulation, hydrodynamical behaviour (*Chinese*) 0-1823  
 laser produced, ionisation process computer simulation code, atomic transition processes 0-28764  
 laser-target, Monte Carlo (hybrid) suprathermal electron transport 0-24200  
 linear multipole, plasma simulation, finite element model 0-1837  
 magnetic field effects, boundary conditions 0-10392  
 maximum energy flux in collisionless plasma, comparison with free molecular gas motion 0-6221  
 MHD, numerical simulation, variational approach 0-28625  
 MHD channel flow, numerical simulation 0-6229  
 mirror drift cone stability simulation with loss-cone ions 0-1789  
 neutral atom transport, computer code SPUDNUT 0-48962  
 numerical simulation in fluid dynamics 0-17805  
 paramagnetism in RF mag. field, expt., theory and simulation 0-6225  
 phase space granulation due to mode-mode coupling, in instability generated turbulence 0-38651  
 runaway electrons, enhanced drag by radiation 0-10397  
 runaway electrons in strong elec. fields, fluid treatment 0-33812  
 sheath driven targets, simulation 0-48898  
 sideband instability in large amplitude wave, computer simulation 0-38602  
 silent discharge, excited species reactions, discharge channel characts., numerical simulation 0-38813  
 supersonic conducting gas stream, interaction with mag. field, numerical simulation 0-6230  
 TEA-CO<sub>2</sub> laser pulse interaction with dense H plasma 0-38683  
 Tokamak, high-beta, equilibria and m=1 kink ballooning mode nonlinear evolution 0-24236  
 tokamak-like equilibria at beta close to unity 0-19604  
 toroidal plasma, eigenvalue problem and nonlinear evolution of kink modes 0-24234  
 toroidal plasma, resistive MHD mode and sawtooth oscill., nonlinear evolution 0-24235  
 toroidal stellarator, single particle motion, computer code 0-28818  
 Townsend discharge, macroscopic quantities, Boltzmann eqn. and Monte Carlo calcs. 0-38848  
 two-dimensional Lagrangian calculation of a laser-heated solenoid 0-54027  
 two-dimensional mag. flux shell model for MHD simulations of cylindrically symmetric plasmas 0-1838  
 waveguide, plasma-filled, two-stream instability nonlinear evolution, numerical simulation 0-43938  
 Ar-Xe, shock wave dynamic compression, thermodynamic props. (*Russian*) 0-53931  
 D-He, driven Tokamak fusion reactor, plasma parametric studies and appl. 0-42865  
 H line Stark broadening, role of ion dynamics simulation 0-24144

**plasma temperature**

- AC discharges between isolated electrodes, gas temp. depend. 0-38800  
 active burn control of nearly ignited plasmas 0-48909  
 air, DC point-to-plane elec. discharge, temp. patterns, Michelson interferometry 0-54061



## plasma temperature continued

Alcator A Tokamak, disruptive MHD activity during plasma current rise 0-32487  
 anisotropic plasma, cyclotron and electrostatic instabilities criteria 0-38627  
 arc, plasma parameters, probe and spectral meas. 0-24273  
 arc plasma, electron and heavy particle temp. difference 0-38766  
 arc plasma, temp. meas. by submillimeter diagnostic technique 0-38853  
 asymmetrical plasma diagnostics, by spectral method (*Czech*) 0-38704  
 at. emission obs. of plasma props. 0-19021  
 atom temperature measurements using thermal diffusion 0-43985  
 atomic ion-electron recomb. in presence molecules, appl. to HCl 0-28601  
 collective electric field fluctuations of two-temp. electron gas nonthermal plasma 0-43882  
 collective phenomena and anomalous resistance, electron current drift velocity (*Russian*) 0-24140  
 column and surrounding liq. interaction, quantitative anal. under quasiisothermal conditions 0-38788  
 continuous emission, ionisation potential lowering and total excitation cross section of atmospheric thermal plasma 0-38705  
 continuous optical discharge, diagnostics 0-43947  
 current structure, fast particle generation (*Russian*) 0-48913  
 cyclotron instability with anisotropic kinetic temp., Nyquist diagrams (*Chinese*) 0-28627  
 cyclotron self-absorption in two-temp. plasma, temp. and density meas. 0-48987  
 D-T plasma model, uniqueness and linear stability of operating points 0-14897  
 Debye screening modifications in ponderomotive effects 0-33777  
 determination from H<sub>2</sub> and D<sub>2</sub> molecular band intensities in low pressure plasma 0-37896  
 diagnostics, scattered radiation intensity fluctuation method (*Russian*) 0-14932  
 diffuse pinch, energy equil., classical scalar cond. and neo-classical models 0-24208  
 discharge, capillary pulse type, spectral chronographic-equidensitometric diagnostics 0-44055  
 discharge, RF, gamma regime, ionis. balance and plasma characts., model 0-44022  
 discharges, high current, press., conductivity meas. 0-38793  
 DIVA, scrape off layer, multigrid energy analyser applications 0-33818  
 double-layer, steady-state, fluid theory 0-43873  
 drift-dissipative waves, weakly ionised plasma, column steady state 0-38613  
 duoplasmatron anode plasma, ion temp. 0-6292  
 EBT expts., simple annulus power balance 0-48947  
 ECR as a diagnostic for mirror trap plasma 0-38709  
 ECR fundamental ordinary mode absorption and emission 0-43943  
 electric field pattern calcs. in laser produced plasma (*German*) 0-54014  
 electrical conductivity of high-density, shock-heated Ar and Xe plasmas 0-38557  
 electron cyclotron frequency expts. in 15X-B Tokamak, temp. rel. to heating power 0-48912  
 electron plasma, impurity screening effects in intermediate degeneracy region 0-14882  
 electron temp., time and space var., determ. from electron cyclotron emission meas. in Tokamak plasma 0-48996  
 electron temp. meas., continuous, automatic, using double Langmuir probe 0-43977  
 electron temperature, multi-pulse ruby laser recording of temporal evolution by light scatt. 0-14938  
 electron temperature and density in Ar behind reflected shock waves 0-38549  
 electron temperature and electron density in low density magnetised plasma by probe method 0-48848  
 electron temperature meas. by Thomson laser scatt.,  $\theta$ -pinch energy loss (*Chinese*) 0-54028  
 electron temperature measurements from cyclotron emission in T-10 Tokamak 0-19617  
 electronegative gas glow discharge, plasma instability boundary conditions, electron temp. (*Russian*) 0-38739  
 ELMO Bumpy Torus, electron cyclotron heating, density and temp. 0-28780  
 equilibrium in highly collisional toroidal regime 0-28796  
 excitation temperature of rapidly varying plasma 0-38537  
 expansion into vacuum, ion acceleration 0-6228  
 fast electron convective heat transfer and thermal escape (*Russian*) 0-1744  
 free electron recombination, arbitrary nonequilibrium stationary distribution calcs. (*Russian*) 0-53947  
 free-burning arcs, simple theory 0-6297  
 fusion mirror reactors, finite orbit treatment of plasma buildup 0-37631  
 fusion possibilities and plasma confinement and interactions in mag. conf. fig. Tokamak, review (*French*) 0-54017  
 fusion reactors, superheating-diffusion instability, thermonuclear burn 0-32500  
 fusion research plasma temp. increase 0-18607  
 gradient drift wave eigenmodes stability in sheared mag. field 0-43914  
 He I and II radiation enhancement in mag. field, nonlocal thermodynamic equil. 0-10366  
 high pressure optical discharges, density and temp. meas. 0-48931  
 high-temp. regimes, simulation and confinement scaling 0-38673  
 ICRF heating in TFR, preliminary obs. and further development prospects 0-28741  
 impedance of magneto-acoustic wave launching antenna 0-24180  
 inert gas hollow cathode arc, mol. beam sampling of metastable atoms as electron temp. probe 0-43967  
 internal disruption in Tokamak, relax. oscills., self-consistent model (*Russian*) 0-53957  
 ion acoustic soliton propag. in two-electron temp. plasma 0-33767  
 ion acoustic wave radiation due to oscill. point charge (*French*) 0-43900  
 ion and electron temps. equilibration rate, quantum effects 0-24133  
 ion beam-created high-press. plasma, electron props. diagnostics (*French*) 0-10407  
 ion pressure discharge theory in the strong ionisation regime 0-38734  
 ion temp. and density meas. in direct current octopole by induced optical fluoresc. 0-14939  
 ion temperature, neutral beam probe meas. (*Japanese*) 0-19615  
 ion temperature profile meas. using charge-exchange neutral anal. 0-48850

## plasma temperature continued

ionosphere, electron temp. distrib., approx. expressions using vertical rockets data 0-12599  
 ionosphere, lower hybrid drift instability 0-46343  
 jet, absolute spectral brightness measurement 0-28832  
 JFT-2 Tokamak, radiation loss meas. using thin-film thermometer 0-47698  
 JIPP T-II, electron cyclotron emission meas. using double-pass optical spectrometer 0-54035  
 Langmuir wave excitation by two pumping waves, convective instability (*Russian*) 0-14904  
 laser-heated plasma with large temp. gradient, ion acoustic turbulence, reduced thermal cond. 0-53987  
 laser-irradiated glass shell plasma, electron temp. and density, Si X-ray emission diagnostics (*Chinese*) 0-38718  
 LASL toroidal reversed-field pinch programme, energy loss meas. 0-23127  
 linear gasdynamic confinement system 0-48957  
 low-Z impurities radiation during RF heating in ATC 0-28816  
 maximum energy flux in collisionless plasma, comparison with free molecular gas motion 0-6221  
 microwave beam interaction, intense, with low temp. plasma flow, space distrib. 0-38578  
 multi-chord particle diagnostics of a plasma column (*Russian*) 0-1840  
 multicharge heavy ion emission from strong-current low induction discharge plasma (*Russian*) 0-14033  
 multicomponent multiply ionised plasma, mean radiation paths calc. 0-33754  
 multiposition Thomson scatt., determ. of electron density and temp. profiles 0-48977  
 neutral atom distribution near wall, temp. grad. effect 0-19555  
 neutral beam injection heating in JIPP-II Tokamak 0-28710  
 neutron production in Maxwellian D ion plasmas, ion temp. diagnostics appls. 0-49005  
 nonideal plasma, elem. excitations and macroscopic props., review 0-43842  
 nonthermal electron energy distrib. measured by Fe XXV satellite lines 0-21911  
 normal atom conc. determ. by resonance line broadening with Hg press. 0-43883  
 ohmic heating in Frascati Tokamak, preliminary results 0-28734  
 positive column, electron temp. with two- and three-body vol. recomb. 0-19645  
 pulsed erosion jet, energy characts., heat flow distribution (*Russian*) 0-33825  
 quantum effects on temp. relax. 0-28603  
 radiation intensity calcs. in vacuum UV region (*Russian*) 0-48861  
 ram effect for conducting cylinder in drifting plasma 0-54029  
 rarefied plasma flow, degree of nonisothermality, probe meas. 0-24243  
 ray tracing near electron cyclotron reson., finite temp. effect 0-53994  
 recovery electric strength, effect of plasma parameters 0-6294  
 resonance fluorescence method for plasma diagnostics, at. density and temp. meas. 0-49001  
 resonant absorption in Ar plasma at thermal equil. 0-1799  
 reverse field pinch, Faraday rot. diagnostics for internal mag. field 0-43976  
 rotational and gas temps., rel. in low press. mol. plasma 0-6215  
 runaway electron diffusion and power balance in Tokamak moderate density discharges 0-28609  
 self similar cooling wave, effective thermal cond. (*Russian*) 0-14908  
 sheaf instability at moderate densities, anomalous ion heating (*Russian*) 0-43922  
 shock-heated dense plasma, continuum radiation and optical transmittance diagnostics 0-24202  
 solar flares, Fe XXI 1354 Å obs. from Skylab rel. to ionisation equil. calcs. 0-21956  
 solar transition zone, electron density, energy balance and press. from EUV spectra 0-21957  
 submillimetre diagnostics, active, of Ar arc, data numerical anal. 0-48979  
 superradiation from non-ideal plasmas in electric field 0-38568  
 supersonic dense stream, shock braking processes, radiation-gasdynamic obs. 0-19635  
 surfatron produced electron density and temp. microwave meas. 0-43965  
 T-tube plasma, influence of boundary layer on H<sub>2</sub> line 0-48862  
 temperature meas. in inhomogeneous plasmas appl. of Bartels' theory of radiation 0-53948  
 TFR 600, <sup>2</sup>H ion flux, temp., and density meas. 0-48940  
 TFR plasma temp. measurement using spectral scanning in VUV, monochromator design 0-38703  
 theoretical plasma mechanics, book 0-27048  
 thermonuclear dense plasma, neutron diagnostics, book contrib. 0-24253  
 theta pinch, N<sup>2+</sup>, <sup>3+</sup> lines Stark broadening, He(II) line diagnostics 0-24249  
 Thompson scattering for electron beam and plasma diagnostics (*Russian*) 0-54031  
 Thomson scatt. pathways calibration, rel. to diagnostics (*French*) 0-43886  
 Thomson scattering with high background level of plasma scattering 0-43979  
 Tokamak, neutral beam-heated, parametric scaling 0-10406  
 Tokamak, PLT, fast-wave heating of two-ion plasma through minority cyclotron reson. damping 0-24194  
 Tokamak, Thomson scatt. diagnostics, far IR lasers development, review 0-24242  
 Tokamak fusion reactor, ignited operation regimes 0-10423  
 Tokamak fusion reactor, steady-state, lower hybrid wave-driven, design constraints 0-10424  
 Tokamak power reactor, steady state, lower hybrid wave driven 0-48945  
 Tokamak scrape-off plasma, metal impurity recycling effect 0-10421  
 Tokamak TFR, Thomson scattering system based on two-detector spectrometers 0-32426  
 transition layer between two magnetized plasmas 0-24136  
 Tuman-2A, plasma compression particle diagnostics, density and temp. (*Russian*) 0-38677  
 two electron temp. plasma, collisional and Landau damping of ion-acoustic waves 0-19572  
 UHF discharge with preliminary locally ionised gaseous medium 0-38851  
 wave dispersion in presence of relativistic beam 0-19592  
 weakly ionised plasma in DC field, non-zero neutrals temp., unstable modes anal. 0-38606



**plasma temperature continued**

- whistler damping near electron gyrofreq. due to cold-plasma injection, rel. to magnetosphere 0-28659
- Ar decaying arc, numerical simulation 0-38767
- Ar, decaying plasma arc, electron disappearance mechanism 0-38765
- Ar full circle arc, mass flow field investig. 0-38797
- Ar hollow cathode arc, in mag. field up to 2 kOe, plasma parameters 0-6306
- Ar, plasma arc, dynamic charact., electron energy relaxation effect 0-38774
- Ar plasma radiation obs., line and continuous spectra (*French*) 0-19619
- Ar, stream electrons, at atm. press., electrical parameters (*Russian*) 0-53930
- CO<sub>2</sub> plasma, atm. press. opt. props., 400-1200 nm spectral range and  $10^{-2} \times 10^4$  K temp. 0-33753
- CO<sub>2</sub>-(He) discharge, UV-initiated, electron ion recomb. and CO<sub>2</sub> dissoc. 0-44068
- Cl<sub>2</sub>-arc, low temp., visible and IR continuum radiation 0-38784
- DyI<sub>3</sub>-Hg arc discharge plasma, spectroscopic study 0-54033
- H plasma plane and cylindrical layer emission field calc. (*Russian*) 0-33755
- H<sub>2</sub> plasma, resonance fluorescence diagnostics 0-48971
- H<sub>2</sub> plasma reactor design, heat transfer and flow 0-38697
- H<sub>2</sub>(D<sub>2</sub>), electron dissociative attachment rates, rot. (vibr.) excitation depend. 0-43848
- He, afterglow produced by microwave surfguide, spectroscopic diagnostic, electron and He, rot. temp. 0-44042
- He discharge, medium press., contraction mechanism, inhomogeneous heating 0-44024
- He discharge, RF, plasma parameters and volt-ampere characts., two discharge regimes 0-44016
- He positive column, magnetised, temps. of charged particles, nonlinear effect of ions, waves 0-44023
- He pulsed arc, Thomson scatt. diagnostics 0-24297
- Hg plasma flow, electron temp. determ. from partial LTE populations 0-24248
- N<sub>2</sub> afterglow, chem. reactions rel. to plasma props, appl. to toluene polymerisation 0-3346
- N<sub>2</sub> arc plasma, stabilised by gas injection, thermochem. nonequil., particle excitation, vibr. temps. 0-19634
- N<sub>2</sub>, diffuse plasma, population densities of triplet states, correl. with electron impact processes 0-43966
- N<sub>2</sub> discharge, electron shock wave formation, numerical simulation 0-38777
- N<sub>2</sub> plasma, non-equilib., excited species, vibr.-rot. anal. fluoresc. obs. 0-54034
- N<sub>2</sub> positive corona into spark, prebreakdown phase, spectroscopic anal. 0-38790
- Ne-N<sub>2</sub>, energy transfer, H<sup>+</sup> ion beam produced plasma, ion density and temp. 0-38539
- SF<sub>6</sub> axially blown arc, current-zero behaviour, theoretical model 0-38789
- SF<sub>6</sub> plasma column, in Maecker type arc, diagnostics and model (*French*) 0-19652
- SiH<sub>4</sub> discharge, low pressure, plasma parameters, relevance to Si film deposition 0-44030
- Xe discharges, electrodeless, UHF in waveguide rel. to DC characts. 0-38762
- Xe, s-p transitions, Stark const. and oscill. strengths, shock tube meas. 0-18822

**plasma theory**

see also *Debye-Huckel theory*

- anisotropic plasma, kinetic evolution theory 0-28608
- arc, laminar flow, equilib. composition deviation 0-24274
- atomic and molecular processes involving ionic-covalent nonadiabatic coupling, review 0-38535
- atomic cross sections, calc. using effective Feynman diagrams 0-38566
- atomic processes for mag. fusion research, data status, review 0-42851
- atomic transitions, dense plasma, modified quantum defect method, Ar appl. 0-38570
- ballistic wave transformation kinetic effects (*Russian*) 0-38584
- bifurcation numerical method (*French*) 0-24129
- bottleneck calculation for collisional radiative recomb. coeffs. for Li-like ions 0-53942
- bounded medium, nonlinear parametric reson., limit cycle solns. 0-19071
- bremstrahlung emission coefficient in the dipole approx., in magnetised plasma 0-19562
- classical oscillators, parametrically excited, appl. to plasma interactions 0-33729
- coefficients of viscosity of a gaseous plasma 0-43875
- cold-banket systems, boundary layer analysis 0-28605
- collective radio-emission from plasmas 0-46392
- collisionless magnetized cosmic plasmas, non-resistive electric potential drops 0-31204
- complex dielectric function long wave limit, Coulomb systems with bound states, elec. cond. 0-33738
- compressible magnetic-field reconnection 0-6226
- conductance theory of nonideal plasmas 0-33745
- continuous emission, ionisation potential lowering and total excitation cross section of atmospheric thermal plasma 0-38705
- Coulomb bridge graphs in  $2+\epsilon$  dimensions 0-24131
- coupled intensity deviations from stationary nonlinear state, space and time soln. 0-48882
- current generation by electrostatic travelling waves in collisionless magnetised plasma 0-53976
- current sheet in compressible plasma, self-similar resistive decay 0-1755
- D-T plasma model, uniqueness and linear stability of operating points 0-14897
- Debye thermodynamics for the two-dimensional one-component plasma 0-43866
- dense relativistic electron gas, EM response in strong mag. fields, particle polarisation, mode struct. 0-43963
- dielectric friction in plasma, harmonic oscillator and rigid dipole dielectrics, collective plasma oscils. 0-53928
- dielectric response and energy loss in intermediate quantum plasma 0-38541
- discharge plasma, diffusion regime, elec. sheath theory 0-1810
- discharges, high-freq., unipolar and electrodeless capacitively-coupled, excited at atm. press., appls. 0-1861
- dispersion function, multipole approx., modified asymptotic Pade method 0-48853
- plasma theory continued
  - double-layer, steady-state, fluid theory 0-43873
  - effective dielectric permeability of cold plasma with electron density fluctuations (*Russian*) 0-32882
  - electroionised discharges, theory 0-38816
  - electromagnetic fields of non-equilibrium plasmas 0-6210
  - electron cyclotron emission in steady state inhomogeneous plasma 0-48864
  - electron density determ. by globally convergent method for partially ionised plasma 0-53929
  - electron distribution function and ionisation in space-depend. theory 0-38545
  - electron distribution in a free HF plasma column, anomalous skin effect (*Russian*) 0-1741
  - electron distribution relaxation numerical study for CO<sub>2</sub>-N<sub>2</sub>-He discharges 0-54070
  - electron dynamics in random field, dense Hg plasma conductivity appl. 0-14885
  - electron energy distribution function in very nonuniform elec. field 0-38556
  - electron kinetic eqn. for plasma with strong inter-ion interaction and electron exchange correlation 0-48857
  - electron kinetics in const. and varying field (*Russian*) 0-53927
  - electron plasma waves, toroidal Trivelpiece-Gould modes 0-33770
  - electron processes, in collisionless diode, linear theory 0-38730
  - electron waves, beat radiation 0-43314
  - electron waves beat-driven optical free electron laser 0-43315
  - electron-ion recombination in ambient electron and neutral gases 0-38531
  - electrophysical properties of non-equilibrium aerosol plasma 0-38543
  - elementary processes and chem. reactions, review (*Czech*) 0-24126
  - elliptic problems involving a free boundary 0-24130
  - equation of state, activity expansion (*Chinese*) 0-43863
  - excitation of high-frequency waves with mixed polarization by streaming energetic electrons 0-1773
  - excitation temperature of rapidly varying plasma 0-38537
  - fast electron convective heat transfer and thermal escape (*Russian*) 0-1744
  - fast Langmuir solitons existence in non-equilibrium plasma 0-38604
  - fusion reactor, time-dependent tandem mirror confinement, start-up and alpha particle build-up 0-10419
  - galactic masers, role of plasma effects in generating high-vel. and symmetric spectral features 0-31378
  - generalised Ohm's law, for unsteady state of partially ionised gases 0-38542
  - He I and II radiation enhancement in mag. field, nonlocal thermodynamic equilb. 0-10366
  - HF plasma generation, electron heating, nonlinear kinetic theory 0-44041
  - high density directed plasma, source, design, characts., numerical model 0-38538
  - high melting particle heating, melting and vaporisation in hot gas 0-6201
  - highly degenerate multicomponent plasma thermodynamic props. 0-33739
  - inert gas plasma, free-bound continuum determ. using photoionis. cross sections calc. 0-43878
  - inverse-bremstrahlung absorption rate in an intense laser field 0-24201
  - ion excited level population probabilities, steady- vs. quasisteady-state models 0-24128
  - ion excited level population probabilities, steady-state, appl. to H-like ions 0-19552
  - ion pressure discharge theory in the strong ionisation regime 0-38734
  - ion-sound soliton-resonant particle interactions (*Russian*) 0-14880
  - ionisation of H plasma in uniform elec. field (*Russian*) 0-53923
  - kinetic equation, for plasma in strong high freq. EM field 0-38540
  - kinetic equation including strong fields and inhomogeneities 0-38544
  - kinetic reactions, pulsed afterglow technique obs. in Ar-II plasma 0-48854
  - Landau-Fokker-Planck eqn., for arbitrary statistics, relativistic and nonrelativistic case 0-36935
  - Langmuir soliton EM wave scatt., theory (*Russian*) 0-38564
  - Langmuir solitons, transverse instability 0-6250
  - Langmuir turbulence, statistical theory 0-38647
  - laser-irradiated plasma, soliton form, at crit. density 0-6267
  - laser-plasma interaction, spikon lifetime 0-14922
  - low pressure Ar plasmas near wall, kinetics study (*French*) 0-28689
  - low voltage inert gas arc theory 0-38809
  - lower hybrid resonance heating theory of Tokamak plasmas 0-28745
  - magnetic field, force-free, resistive evolution, in cylindrical geometry 0-6212
  - magnetic piston interaction with nonmagnetised plasma 0-38630
  - magneto-viscous resistive tearing of cylindrical flux surfaces 0-1831
  - magnetoactive plasma, effect on a plane disc, impedance calcs. 0-1809
  - mechanics, book 0-27048
  - Mossbauer effect in magnetised plasma, applic. to gamma-ray lasers 0-28186
  - multicomponent multiply ionised plasma, mean radiation paths calc. 0-33754
  - negative grid pulse effects, on Knudsen Cs arc discharge plasma 0-38843
  - neutral beam production using negative ions 0-28696
  - nonideal plasma, elem. excitations and macroscopic props., review 0-43842
  - nonideal plasma, measured props. and nonideality influence 0-43869
  - nonisothermal rarefied plasma, transport processes and Lenard-Balescu eqn. 0-6222
  - nonlinear coupling of three waves in non-uniform plasma 0-6237
  - nonlinear dielectric perturbation, wave and particle interactions 0-38593
  - nonlinear-wave propagation in a proton-electron plasma coupled with a strong radiation field 0-48872
  - one component plasma, dynamical struct. factor, collective modes 0-28607
  - one component plasma fluid, derivation of eqn. of state in strong coupling 0-33741
  - one-component plasma, internal energy, mean spherical approx., asymptotic form 0-1742
  - optical measurements on plasma initiated by a relativistic electron beam (*Japanese*) 0-48914
  - optical scattering of light by atoms, techniques theory 0-54044
  - optically thick plasma, two-dimens. radiation restoration rel. to local diagnostics 0-43885
  - oscillations, in lower-hybrid range, of bounded plasma 0-24162
  - paramagnetism in RF mag. field, expt., theory and simulation 0-6225



## plasma theory continued

- particle orbit in magnetic field, guiding-centre Hamiltonian, arbitrary gyration 0-1834  
 particle-wave interactions, cyclotron reson. vel. shift, wave propag. effects 0-33774  
 photon escape probabilities for Stark-broadened Lyman series lines 0-24143  
 photon soliton and fine structure due to nonlinear Compton scattering 0-10363  
 planetary and stellar magnetospheres, conf., Snowmass, Colorado, USA (Aug. 1978) 0-41939  
 pulsed current voltage characteristics of a thermally produced plasma 0-38554  
 quasioptics and anisotropic and dispersive media 0-38567  
 quasistatic theory for negative ion free-bound radiation threshold broadening 0-53941  
 radiative plasma with anisotropic permittivity, developing wavefronts 0-43896  
 real gas discharge, thermodynamic stability 0-38852  
 reflex triode system, generation of intense microwave radiation by relativistic electron beam 0-14887  
 regularised long wave equation, numerical studies 0-53964  
 relativistic electron power law spectra in random mag. field 0-24240  
 relativistic plasma, kinetic equation, fully convergent 0-54025  
 relativistic transverse cold plasma waves, nonlinear, linearly polarised, stability 0-6235  
 resistivity, of turbulent plasma, with ion-acoustic instability, ion-tail form. effect 0-10360  
 resonance cone surface, nonlinear eqn. modification for magnetised plasma 0-33740  
 resonant absorption in Ar plasma at thermal equil. 0-1799  
 resonant charge exchange, polarisation effect 0-43859  
 runaway electron diffusion and power balance in Tokamak moderate density discharges 0-28609  
 Saha equation, first order estimate for He plasma 0-19554  
 self-generated magnetic fields and harmonic emission 0-38546  
 slightly ionised inert gas plasma, hollow arc discharge in cylindrical hollow cathode, theory 0-38810  
 small overdense plasma particle Thomson-like RF scatt., linear perturbation theory 0-48858  
 solar emission lines of NeV, MgVII, SiIX, SXI, population levels as function of electron density and temp. 0-21963  
 solar transition zone, electron density, energy balance and press. from EUV spectra 0-21957  
 solid surface interaction, electrostatic sheath equations, inc. heating, ion mobility and ion recomb. 0-1808  
 spin polarisation in mag. field (*Russian*) 0-33744  
 sputtered atoms, LTE in excitation process 0-35037  
 stochastic equations of motion for plasma particles 0-38551  
 strongly coupled multicomponent plasmas, statics and thermodynamics 0-33742  
 temperature relaxation, quantum effects 0-28603  
 test particle potential in external homogeneous magnetic field 0-43870  
 thermal equilibrium, single atomic collision relative level populations 0-1743  
 thermodynamical functions for dense multicomponent plasmas, electron-proton plasma appl. 0-38548  
 thermodynamics and correlation functions 0-24132  
 thermonuclear fusion plasmas, elem. processes and role of atomic, ionic and mol. data 0-14916  
 thermonuclear plasma, H<sub>2</sub> fuel pellet ablation, atomic processes effect 0-18596  
 thermonuclear reactions in laser fusion, emitted particle spectra, Monte Carlo calcs. (*Russian*) 0-52780  
 theta-pinch, collisionless, high-beta, anisotropy-driven EM modes, finite Larmor radius effects 0-1830  
 Tokamak fusion reactor, ignited operation regimes 0-10423  
 transverse convective ion transport in Tokamak, kinetic description 0-6214  
 transverse wave packet, 3-dimens., nonlinear evolution in hot plasma, ion-acoustic wave effect 0-43899  
 turbulent heating, flat top electron distrib. effect, with ion-acoustic instability 0-10399  
 turbulent plasma, anomalous EM wave electron radiation 0-43889  
 two-particle effective pot., for dense hydrogenous plasma near 10K 0-38533  
 velocity autocorrelation function in a strongly coupled, magnetized, pure electron plasma 0-6213  
 virial pressure of classical one-component plasma 0-38536  
 Vlasov plasma, linearisation, optimal control 0-53920  
 wave packets in dispersive media, main signal and precursor approx. 0-24158  
 weakly ionised plasma in DC field, non-zero neutrals temp., unstable modes anal. 0-38606  
 weakly-ionised, three-component, ionis. equil. instability 0-10877  
 Z-pinch, rotating, energy balance (*Russian*) 0-14924  
 Zakharov equations derivation for higher electron non-linearities in Langmuir collapse dynamics 0-43919  
 Al resonance line profiles, influence of boundary layer of Al-seeded shock heated plasma 0-43876  
 Ar-Xe, shock wave dynamic compression, thermodynamic props. (*Russian*) 0-53931  
 ArI, highly excited atomic levels, spectral-line-blending study in high-density plasma 0-48969  
 C plasma, continuous absorpt. coeffs. 0-10362  
 CO discharge, electron energy distrib. and kinetic coeffs., ground-state mols. 0-43867  
 CO<sub>2</sub>-N<sub>2</sub>-He, vol. discharge, negative ions effect 0-14956  
 Cr ions in Tokamak plasmas, spectroscopy and atomic physics 0-53938  
 Cs, dense plasma near saturation line elec. cond. 0-38559  
 Fe ions in Tokamak plasmas, spectroscopy and atomic physics 0-53938  
 H I (3P<sup>0</sup>-2S) line, Stark broadening parameters, modified adiabatic theory, electron scatt. phase shifts 0-43879  
 H II region, H137 $\beta$ /109 $\alpha$  intensity ratio interpretation 0-31344  
 H<sub>2</sub> in hot plasma, elementary excitation spectrum, exchange and polarisation effects 0-43892  
 H<sub>2</sub>, pair correlations down to r=0 0-14883  
 H<sup>+</sup> affinity radiation, theoretical study of negative absorption 0-38001  
 N<sub>2</sub>, beam and glow discharge type, macroscopic props., kinetic eqns. 0-43864  
 N<sub>2</sub> discharge, anomalous heating (*Russian*) 0-1866

## plasma theory continued

- N<sub>2</sub> positive column, superelastic collisions and electron distrib. function 0-1858  
 N<sub>2</sub> vibrational levels stepwise excitation, effect on electron energy balance in He-N<sub>2</sub>-CO<sub>2</sub> discharge 0-54071  
 Na isoelectronic sequence, dielectronic recombination rate coeffs., 2-10<sup>3</sup> eV 0-10357  
 Ni ions in Tokamak plasmas, spectroscopy and atomic physics 0-53938  
 O<sub>2</sub> discharge, conditions, self-consistent electron energy distrib. functions calc. 0-38746  
 O<sub>2</sub> glow discharge, DC, particle concs. calc. 0-1859  
 Xe, arc, wall-stabilised, dynamic analysis, radiation transport 0-44066  
 Xe, plasma shock front, elementary processes 0-19581  
 Xe precursors, associative ionisation and photoionisation, relative contrib., electron density prediction 0-43858
- plasma thermocouples** see *plasma devices; thermocouples*
- plasma torches** see *plasma devices*
- plasma transport processes**  
 see also *Vlasov equation*  
 accelerator, conical, plasma cluster vel. calc., snow-plough and erosive models (*Russian*) 0-27839  
 active particle beam systems for meas. of plasma pot., current and impurity profiles 0-48990  
 air gap, drift vel. meas. of ionized particles 0-24298  
 air-water vapour mixture, electron conc. and conductivity behind strong shock wave 0-48890  
 alkali metal, dense arc plasma, elec. and heat conds., two-probe diagnostics 0-38560  
 alkali-metal hollow cathode arc, low-press. current limiting 0-6304  
 alpha particle orbits in radially nonuniform slender plasma column, multi-group rep. 0-53921  
 alpha-particle heating in an open-field-line plasma 0-48908  
 ambipolar electron and ion diffusion in collisional plasma in RF electric field 0-6220  
 anisotropic plasma, kinetic evolution theory 0-28608  
 anomalous conductivity and electron heating, in two-stream unstable plasma 0-6219  
 anomalous electron pseudo-classical transport with coherent electrostatic wave propag. 0-24137  
 anomalous glow discharge Faraday dark space, electron vel. distrib., Langmuir probe meas. 0-44040  
 anomalous plasma transport due to electron temp. gradient instability 0-33813  
 anomalous Tokamak radial transport, large mode number tearing and twisting modes 0-1747  
 anomalous turbulent resistivity at high drift vels., rel. to confinement and fluctuations in toroid 0-24139  
 anomalous turbulent resistivity at high drift vels., toroidal plasma 0-24138  
 arc, of Cs-film coated hollow cathode, intermediate press. operation 0-6305  
 arc nozzle clogging theory 0-38791  
 Asperator NP-3, toroidal device with nonplanar mag. axis, current equil. 0-48932  
 atom-molecule anisotropic interaction pot. influence on transport cross sections, appl. to He-alkali dimer 0-9677  
 ball lightning, turbulent plasma sphere, model eqns. for current and heat flux 0-32516  
 ballooning trapped-electron mode overlapping many rational surfaces 0-28618  
 Belt Pinch IIa, transport phenomena, density profiles 0-24219  
 belt pinches, transport and radiation studies 0-28798  
 bumpy torus plasma, weak vertical mag. field effect on fluctuation induced transport 0-48946  
 charged particle acceleration and diffusion in stochastic mag. field 0-43872  
 charged particle drift motion under resonance conditions 0-38611  
 classical transport processes in azimuthally rot. plasma (*Russian*) 0-33746  
 coefficients of viscosity of a gaseous plasma 0-43875  
 coherent anomalous resistivity, in region of ionosphere/magnetosphere electrostatic shocks 0-4189  
 cold turbulent plasma blanket, anomalous heat transport 0-18604  
 cold-banket systems, boundary layer analysis 0-28605  
 collective electric field fluctuations of two-temp. electron gas nonthermal plasma 0-43882  
 collective ion acceleration by relativistic electron cloud (*Russian*) 0-48961  
 collective phenomena and anomalous resistance, electron current drift velocity (*Russian*) 0-24140  
 collisional divertor scrape-off layer in Tokamak, plasma transport 0-28614  
 collisionless drift modes, graphical method for finding complex roots of nonlinear eqn. 0-33762  
 compact fusion ignition experiments, designs, numerical computation 0-13853  
 complex dielectric function long wave limit, Coulomb systems with bound states, elec. cond. 0-33738  
 conductance theory of nonideal plasmas 0-33745  
 conference on fusion research and plasma physics, Innsbruck, Aug. 1978 0-27033  
 convective cell excitation by Bernstein waves (*Russian*) 0-53961  
 convective cells of drift waves, plasma with shear, nonlinear excitation mechanism (*Russian*) 0-38585  
 convective instability, harmonic generation and anomalous absorpt. in pumping wave decay (*Russian*) 0-14889  
 corona, multifluid behaviour between elec.-stressed spherical cathode and spherical anode 0-10443  
 cross-field electron heat transport due to high frequency electrostatic waves 0-53932  
 current disruption, in Tokamak plasmas, schlieren signal meas. from millimetre waves 0-48998  
 current fluctuations, discharge contractions, in combustion products plasma 0-14953  
 current generation by electrostatic travelling waves in collisionless magnetised plasma 0-53976  
 current instability on short wave drift oscills., nonlinear theory (*Russian*) 0-53981  
 current sheet in compressible plasma, self-similar resistive decay 0-1755  
 current sheets resistive MHD instabilities, appl. to solar wind 0-4218



**plasma transport processes continued**

current structure, fast particle generation (*Russian*) 0-48913  
 current transport at the surface of a hollow cathode, current distrib. technique 0-54048  
 currents in short pulsed high current electron beam injection into initially neutral gases 0-33749  
 curvature effects in laser plasma interactions 0-43948  
 cyclotron radiation transport in plasmas by neutron transport techniques 0-38660  
 cyclotrons resonance maser, Vlasov-Maxwell eqns., guided wave field theory 0-14309  
 dielectric response and energy loss in intermediate quantum plasma 0-38541  
 dielectric surfaces in evacuated cavities, plasma release due to electron irradi., transport characts. 0-33786  
 diffuse pinch, energy equilib., classical scalar cond. and neo-classical models 0-24208  
 diffuse pinch, energy equilib., tensor cond. model 0-24209  
 diffusion, quasilinear, in solar mag. traps, rel. to plasma instability periodic regimes (*Russian*) 0-8616  
 diffusion due to mag. field fluctuations 0-1761  
 diffusion in toroidal traps, anomalous electron viscosity (*Russian*) 0-48956  
 diffusion of charged particles along mag. neutral line 0-6218  
 diffusion reduction by plasma rotation and ion dissipative effects 0-38696  
 diffusion spreading of weak inhomogeneities in ionospheric according to electrostatic approx. 0-4187  
 diffusional expansion across mag. field, modelling problem (*Russian*) 0-48964  
 discharge current, in electrodeless RF discharges in gas mixtures 0-44029  
 discharge plasma, diffusion regime, elec. sheath theory 0-1810  
 discharges, high current, press., conductivity meas. 0-38793  
 DIVA, metal-impurity, confinement, discharges 0-28843  
 divertor fluxes in stellarators and torsatrons, azimuthal distrib. 0-6216  
 divertor injection Tokamak experiment, plasma stability, energy and particle transport, and hydrogen recycling 0-28834  
 double-layer, steady-state, fluid theory 0-43873  
 drift and current flow of charged particle along mag. neutral line 0-1749  
 drift and trapped electron instabilities, in systems with mag. shear 0-28648  
 drift instability, current-driven, sheared mag. field, finite-beta effect on transport 0-28617  
 drift loss cone instability in inhomogeneous mag. field 0-48934  
 drift wave stability and transport theory in fusion systems 0-28653  
 drift wave turbulence and convective cell formation 0-43925  
 drift waves, instability in AC elec. field, wave growth rate and dispersion relation 0-48886  
 EBT, neoclassical transport 0-32488  
 EBT, radial transport in collisionless electron regimes 0-32491  
 electric double layer form. and dynamics, simulation 0-48855  
 electric double layer motion 0-33751  
 electric field pattern calcs. in laser produced plasma (*German*) 0-54014  
 electrical conductivity of high-density, shock-heated Ar and Xe plasmas 0-38557  
 electrical conductivity of low-temp. alkali plasma, weak probing signal method meas. 0-48968  
 electrical conductivity of nonideal high-press. plasma, Ar arc IR continuum absorption obs. 0-38558  
 electrode discharge, nonhydrodynamic pinch compression, kinetics and D<sup>+</sup> focusing (*Russian*) 0-38689  
 electron beam propagation in plasma channels for ICF reactors 0-1812  
 electron cross-field heat transport caused by HF electrostatic wave 0-28619  
 electron current component meas. method for hollow cold cathode 0-54043  
 electron distribution function, electron-electron interaction effects in external field 0-1739  
 electron distribution in a free HF plasma column, anomalous skin effect (*Russian*) 0-1741  
 electron drift threshold for nonelectrostatic ion cyclotron oscils. spontaneous excitation 0-38625  
 electron dynamics in random field, dense Hg plasma conductivity appl. 0-14885  
 electron energy distribution function in very nonuniform elec. field 0-38556  
 electron energy radial distrib., in molecular gas discharge plasmas (*French*) 0-48852  
 electron heat conductivity, magnetic field line diffusion 0-28641  
 electron holes, theory, anal. soln. 0-48879  
 electron kinetic eqn. for plasma with strong inter-ion interaction and electron exchange correlation 0-48857  
 electron oscillation in radial potential well effect on beam interactions (*Russian*) 0-14912  
 electron temperature meas. by Thomson laser scatt.,  $\theta$ -pinch energy loss (*Chinese*) 0-54028  
 electron-energy transport in laser-produced plasmas 0-6266  
 electronegative gas plasma, negative ion ambipolar diffusion coeffs. 0-44046  
 electrostatic probe characteristics in a magnetic field, ellipsoidal probe in diffusion regime 0-33815  
 ELMO bumpy torus, ambipolar diffusion 0-38552  
 ELMO Bumpy Torus, electron cyclotron heating, density and temp. 0-28780  
 EM field induced resultant drift inwards from boundary, in D-T plasma 0-38577  
 EM field orthonormal decomposition in anisotropic media, duality and vector space 0-28620  
 EM resonant properties of laser-prod. plasmas 0-43928  
 energy lifetime of plasma, T-3 scaling law, in Tokamaks 0-28635  
 enhanced losses due to collisionless drift waves, dynamic stabilisation effects 0-14888  
 fast electron convective heat transfer and thermal escape (*Russian*) 0-1744  
 fast electrons, X-rays and ions, motion evaluation in laser produced plasma 0-19557  
 field reversed mirrors, fusion product energy distrib. 0-37595  
 formation of plasma in fusion devices, at. and plasma processes, diagnostic techniques 0-48915  
 free trajectory derivation of (Bohm) diffusion coeff., comments and reply 0-1748

**plasma transport processes continued**

fusion inertial confinement plasmas, energetic charged fusion product slowing 0-37594  
 fusion plasma in beam driven Tokamak, Fokker-Planck/transport analyses 0-28826  
 fusion possibilities and plasma confinement and interactions in mag. conf. Tokamak, review (*French*) 0-54017  
 fusion reactor inertial confinement pellets, neutronics modelling 0-37593  
 guiding centre orbits and topology of noncircular axisymm. Tokamak plasmas 0-6227  
 heat exchange of low-temp. plasma with wall, longitudinal mag. field effect 0-33781  
 heat transport, computer simulation 0-28817  
 heat wave propagation in fully ionised plasma (*Russian*) 0-24141  
 heating in toroidal plasmas 0-24239  
 HF oscillations and electron beam relax. in homogeneous gas-discharge plasma 0-38614  
 high density directed plasma, source, design, characts., numerical model 0-38538  
 high density plasma interaction with a strong EM wave, Green's function method calcs. 0-48885  
 high melting particle heating, melting and vaporisation in hot gas 0-6201  
 high-temp. regimes, simulation and confinement scaling 0-38673  
 higher-order Chapman-Enskog theory for electrons 0-38561  
 hollow cathode arc with reduced gas flow, operation mode 0-38783  
 hot plasma resistivity, minimum cutoff 0-28610  
 hydromagnetic rarefaction waves and free expansion in collision-free strongly magnetised plasma 0-38594  
 ICRF heating in TFR, preliminary obs. and further development prospects 0-28741  
 impurity control and plasma transport in plasma-edge region 0-13832  
 impurity effects and control, neutral beam injection, computational models for large Tokamaks 0-28773  
 impurity ions on rational magnetic surfaces, convection and diffusion, collisional multifluid model 0-28615  
 inert gases, metastable atom diffusion, state decay, VUV obs. from discharge afterglow 0-44061  
 ion acceleration in anode foil plasma, irradi. by relativistic electron beams (*Russian*) 0-54000  
 ion acceleration in coaxial diode with mag. insulation (*Russian*) 0-10402  
 ion acoustic wave radiation due to oscill. point charge (*French*) 0-43900  
 ion beam with rotational and axial motion, thermal equilibrium props. 0-53934  
 ion composition of plasma of pulsed discharge in He, H<sub>2</sub><sup>+</sup> current time evolution 0-54046  
 ion current from Penning discharge ion source, depend. on mag. field and anode diameter 0-54072  
 ion current in electron beam-formed plasma, two-electrode probe meas. (*Russian*) 0-1841  
 ion heating by current driven turbulence in inhomogeneous plasma 0-33791  
 ion loss due to low frequency instabilities 0-6217  
 ion motion, superadiabatic and stochastic, in mirror-machine plasma, in presence of electrostatic wave 0-53933  
 ion pressure discharge theory in the strong ionisation regime 0-38734  
 ion ring, field-reversed, anomalous decay of induced electron current 0-24206  
 ion-acoustic instability, electron flux driven, in Q-machine, probe diagnostics 0-33765  
 ion-acoustic instability stabilisation by ion beam in Q-machine, probe diagnostics 0-33766  
 ion-sound soliton-resonant particle interactions (*Russian*) 0-14880  
 isotope separation, HF stationary discharge, travelling mag. field, barodifusion separation 0-44049  
 isotope separation, impulse plasma centrifuge with circulation, theory (*Russian*) 0-38553  
 isotope separation by ponderomotive force effect near ion-cyclotron reson. 0-43998  
 jet carrying solid particles, electrophysical props. 0-24134  
 kinetic reactions, pulsed afterglow technique obs. in Ar-II plasma 0-48854  
 Langmuir oblique solitons, self-contraction in free path regime (*Russian*) 0-43921  
 Langmuir wave evolution, three dimensional kinetic model, Vlasov eqn. calcs. 0-43923  
 laser driven plasma, vacuum insulation against suprathermal electrons 0-18598  
 laser fusion, interaction and transport processes, continuous pulse shaping 0-28766  
 laser fusion, suprathermal electron transport, dual treatment 0-18599  
 laser plasma, magnetothermal phenomena (*Russian*) 0-33798  
 laser produced plasma, heat front penetration depth, heat transport wavelength depend. 0-48926  
 laser target, Monte Carlo (hybrid) suprathermal electron transport 0-24200  
 laser-fusion regime, plasma transport, extension of Braginskii system of fluid equations 0-53935  
 laser-produced plasma, X-ray spectrometry, for energy transport diagnostics (*French*) 0-43982  
 Levitron, fluctuations, diffusion and beam-induced currents 0-28616  
 linear gasdynamic confinement system 0-48957  
 long time confinement of pure electron plasma, max. confinement time 0-48954  
 long-wavelength modes and anomalous transport in toroidal magnetoplasmas 0-28613  
 longitudinal current generation and relax. in stellarator (*Russian*) 0-10418  
 low pressure HF discharge, anomalous cond. mag. field effects 0-44047  
 magnetic diverters for experimental Tokamaks and fusion reactors 0-18621  
 magnetic field, force-free, resistive evolution, in cylindrical geometry 0-6212  
 magnetic field effects, boundary conditions, computer simulation 0-10392  
 magnetic mirrors Hamiltonians of particle motion, canonical transforms. 0-33748  
 magnetic trap, with helical mag. axis, plateau and banana diffusion regimes 0-10425  
 magnetically confined plasma, high temp., transport processes, numerical soln. 0-19559  
 magnetised column, drift dissipative waves, LF oscils., anomalous diffusion and equilib. 0-33769



## plasma transport processes continued

magnetised plasma, double-layer characts. meas. 0-43874  
 magneto-electrostatic reactor, power gain factor 0-48933  
 magneto-viscous resistive tearing of cylindrical flux surfaces 0-1831  
 magnetoplasma, intense EM wave absorption, numerical results 0-43890  
 mass separation in rotating weakly ionised plasma (*Russian*) 0-1745  
 maximum energy flux in collisionless plasma, comparison with free molecular gas motion 0-6221  
 megavolt and megampere diagnostic techniques for pulsed power particle beam fusion drivers 0-49010  
 metal surface, high-intensity laser beam interaction 0-19600  
 metal-seeded rotating plasma 0-1746  
 MHD channel with Hall and ion slip currents, forced convective heat transfer 0-33823  
 MHD eqn., stability, transport calc. for high-beta Tokamaks 0-28848  
 MHD equilibria, secular instability in mag. quadrupole field 0-53982  
 MHD generator, characteristics improvement, using current parallel to magnetic field 0-1751  
 MHD generator, conductivity and power output ionization stability, and boundary layer effects 0-1752  
 microcanonically distributed plasma, reduced distrib. functions 0-28604  
 motion of the cathode spot of a vacuum arc 0-54069  
 multicomponent plasma, ion-acoustic resist. 0-10383  
 negative grid pulse effects, on Knudsen Cs arc discharge plasma 0-38843  
 neutral atom transport, computer code SPUDNUT 0-48962  
 neutral beam injection, fuelling profiles effect on plasma transport props. 0-19596  
 neutral beam injector, simulation of neutral particle transport 0-37600  
 neutral-beam-driven current evolution in Tokamak plasmas 0-28712  
 non-linear transport equations: Properties deduced through transformation groups 0-4680  
 non-self sustained discharge current, gas purity effects 0-38845  
 nonideal plasma, elem. excitations and macroscopic props., review 0-43842  
 nonideal plasma, measured props. and nonideality influence 0-43869  
 nonisothermal rarefied plasma, transport processes and Lenard-Balescu eqn. 0-6222  
 nonlinear inverse bremsstrahlung and heated electron distributions 0-43930  
 nonlinear inverse bremsstrahlung and heated-electron distributions 0-48927  
 nonlinear kink instabilities in Tokamaks surrounded by force-free fields 0-43909  
 nonselfmaintained discharge, current voltage characts. 0-44045  
 ohmic heating in Frascati Tokamak, preliminary results 0-28734  
 ohmic heating of plasmas in closed magnetic systems 0-28756  
 open traps, axially symmetric, transverse particle losses 0-28784  
 PLT Tokamak, ohmically heated plasmas, radiation, impurity effects, instability and particle transport 0-28833  
 poloidal mode ballooning of trapped electron instability 0-28657  
 ponderomotive laser effects in collisional plasma transport 0-38562  
 positive column, metastable atom radial transport at various electron distrib., atom+atom collision effects 0-44037  
 positive column, metastable atom transport, excitation rate radial variation, flux to wall calc. 0-44038  
 positive-ion distribution in a strong electric field, steady state kinetic eqn. 0-33844  
 prepulse discharges in high current accelerator diodes with double shaping line 0-5399  
 pulsed current voltage characteristics of a thermally produced plasma 0-38554  
 pure electron plasma, waves and transport 0-38563  
 quasi neutral plasma expansion, fluid model approach 0-33747  
 randomly inhomogeneous cond. medium in mag. field 0-19558  
 renormalised Vlasov turbulence 0-19579  
 resistivity, anomalous, in turbulently heated plasma with ion-acoustic instability 0-10399  
 resistivity, of turbulent plasma, with ion-acoustic instability, ion-tail form. effect 0-10360  
 resistivity phenomena in multi-ion plasma with ion-acoustic turbulence 0-48856  
 RF discharge, electrode sheath 0-44052  
 RF driven currents in steady state Tokamak reactors 0-28687  
 RF voltage in plasma probe sheath, effect on electron energy distrib. meas. 0-54045  
 rotating plasma, weakly ionised, rot. vel. and ion cond., obs. and MHD theory 0-38576  
 runaway relativistic electron scatt. on oscills. in Tokamak (*Russian*) 0-48849  
 screw-pinch configs., collisionless, hybrid-kinetic stability props. of high-beta plasmas 0-43871  
 self similar cooling wave, effective thermal cond. (*Russian*) 0-14908  
 shock wave produced plasma, electron and ion thermal diffusion effects 0-48891  
 single particle motion in 1-component strongly coupled plasma 0-48847  
 skin current heating of toroidal plasma 0-28715  
 spheromak plasma config. form. by combined Z- and  $\theta$ -pinch discharges 0-43955  
 stationary turbulence regions and anomalous resist. in magnetosphere plasma 0-38649  
 steady-state currents driven by collisionally damped lower-hybrid waves 0-38639  
 steady-state Tokamak reactors with RF driven currents 0-27818  
 stellarator, Saturn, current-free transport processes, drift modes effect 0-19605  
 stellarator geometry, superbanana orbits for 3.5 MeV alpha particles 0-24231  
 surfatron produced electron density and temp. microwave meas. 0-43965  
 Tandem mirror reactors, anomalous and classical transport effect 0-13862  
 tandem mirrors, analytic approx. to resonant plateau transport coeff. 0-32486  
 target impurity effect on laser produced expansion, ion spectrography 0-43945  
 tearing instability, current shear effect in relativistic stream superposition model 0-24155  
 tearing modes with mag. braiding 0-10429  
 test particle potential in external homogeneous magnetic field 0-43870  
 thermal conductivity, reduced in laser-heated plasma with large temp. gradient 0-53987

## plasma transport processes continued

thermal convection instabilities of spherically symmetric plasmas (*Chinese*) 0-1774  
 thermionic converter, ignited mode, internal phenomena and output characteristics (*Japanese*) 0-3527  
 thermionic convertor, ignited mode, electron energy distrib. meas. of Cs plasma (*Japanese*) 0-3528  
 thermionic convertors, effect of electron thermal conductivity, theory 0-40892  
 thermonuclear cone microinstabilities and anomalous alpha-particle losses in Tokamaks 0-28636  
 theta-pinch, electron heating in turbulent neutral layer (*Russian*) 0-10361  
 theta-pinch, neutral current sheet, electron energy distrib. meas. 0-43954  
 time-dependent transport processes, for two-component plasma 0-38555  
 Tokamak, anomalous diffusion of  $\alpha$ -particles due to trapped ion mode 0-48951  
 Tokamak, DITE, impurity ion concentrations and diffusion, spectroscopic measurement 0-28771  
 Tokamak, effect of fuel pellet injection velocity on energy parameters 0-32490  
 Tokamak, electrostatic drift waves, numerical anal. of instability and transport 0-48871  
 Tokamak, high beta, transport and radiation studies 0-28798  
 Tokamak, neutral beam-heated, parametric scaling 0-10406  
 Tokamak, physics of burn control 0-37599  
 Tokamak, PLT, current profile evolution effect on plasma-limiter interaction and energy confinement time 0-10420  
 Tokamak, small ignition, with neutral injection heating, transport calculations 0-9409  
 Tokamak device, eddy currents induced in vacuum vessel, anal. 0-1832  
 Tokamak doublet geometry, shape control of doublets 0-48943  
 Tokamak fusion reactor, steady-state, lower hybrid wave-driven, design constraints 0-10424  
 Tokamak fusion reactors, doublet research, plasma shape control, MHD stability 0-28837  
 Tokamak plasmas containing momentum sources, impurity transport 0-48935  
 Tokamak refuelling by pellet injection, transport processes effects 0-38699  
 Tokamak scrape-off plasma, metal impurity recycling effect 0-10421  
 Tokamak transport eqns., nonlinear partial differentials, soln. technique 0-19556  
 Tokamak with poloidal divertor, discharge startup 0-48942  
 tokamak-like equilibria at beta close to unity 0-19604  
 Tokamaks, divertor, refuelling methods, pellet-plasma interaction 0-28841  
 Tokamaks, magnetic islands, tearing modes 0-28846  
 Tokamaks, transport losses, computer modelling and scaling 0-28612  
 Tokamaks with shear, scaling law for trapped ion anomalous diffusion 0-32492  
 toroidal axisymmetric equilibria, particle diffusion by mag. perturbations 0-14927  
 toroidal plasma, convective cells and transport anal. 0-24229  
 toroidal plasma, Monte Carlo treatment for neutral particle transport 0-33750  
 toroidal plasma, resistive MHD mode and sawtooth oscill., nonlinear evolution 0-24235  
 torsatrons, neutral beam injection calcs. 0-48949  
 transition layer between two magnetized plasmas 0-24136  
 transverse convective ion transport in Tokamak, kinetic description 0-6214  
 trapped electron instability, turbulence, unstable mode dynamics anal. 0-33761  
 trapped electron shear-Alfven instability, stabilisation by temp. gradient 0-28599  
 Tuman-2A Tokamak, ohmic heating and compression of plasma 0-28703  
 turbulent convective transport in a plasma 0-28606  
 two phase flow, particle velocity optical meas. (*Russian*) 0-54032  
 vacuum arc in Cu cathode region, current parameters, theory 0-54068  
 variable property heat transfer to single sphere in high temp. surroundings 0-14884  
 viscosity, rel. to hydromagnetic surface waves dissipation 0-21904  
 Vlasov plasmas, geometrical optics approach, Tokamak appl. 0-14902  
 wave growth, stability anal., particle distrib. functions and transport theory 0-43903  
 weakly-ionised plasma diffusion in apparatus with spatial axis (*Russian*) 0-1826  
 Wigner distribution function, transport equations, inhomogeneous dispersive medium 0-53214  
 Z-pinch, mag. field fast recomb. through plane pinch current sheet 0-38695  
 Ar afterglow, line radiation of plasma in early afterglow 0-38745  
 Ar arcs in supersonic flow, numerical analysis 0-38776  
 Ar, decaying arc, electron cooling, diffusion, ionisation and recombination processes 0-33841  
 Ar decaying arc, numerical simulation 0-38767  
 Ar full circle arc, mass flow field investig. 0-38797  
 Ar hollow cathode arc, in mag. field up to 2 kOe, plasma parameters 0-6306  
 Ar, stream electrons, at atm. press., temp. and conc. from study of electrical parameters (*Russian*) 0-53930  
 Ar-N<sub>2</sub>(CO), non-self-sustained discharge instability, negative differentiated cond. (*Russian*) 0-38740  
 CO discharge, electron energy distrib. and kinetic coeffs., ground-state mols. 0-43867  
 CO discharge, electron energy distrib. and kinetic coeffs., vibr. excited mols. 0-43868  
 Co<sub>2</sub>:He:N, glow discharge instability in afterglow 0-6313  
 Cs, dense plasma near saturation line elec. cond. 0-38559  
 D diffusion in the Tokamak plasma, pulsed injection obs. 0-28611  
 D-T Tokamak, high-density, ohmically-heated, transport calcs. 0-24142  
 H, HF discharge, gas breakdown, electron diffusion eqn. exact soln. 0-19658  
 H<sub>2</sub> glow discharge with variable degrees of dissociation, diffusion theory of positive column 0-44018  
 He, electron distribution function relaxation in high freq. gas breakdown (*Russian*) 0-14957  
 He I line profiles, ion motion effect in low electron density plasma 0-43877  
 He pulsed arc, Thomson scatt. diagnostics 0-24297



# plasma transport processes continued

- Hg low-pressure arc, positive column, heat flow processes 0-24135
- N<sub>2</sub> glow discharge instability in afterglow 0-6313
- N<sub>2</sub>, beam and glow discharge type, macroscopic props., kinetic eqns. 0-43864
- N<sub>2</sub> discharge, anomalous heating (*Russian*) 0-1866
- N<sub>2</sub> positive corona into spark, prebreakdown phase, spectroscopic anal. 0-38790
- N<sub>2</sub>, stationary beam discharge plasma, electron kinetics 0-38775
- Ne, positive column contraction under diffusion-recombination conditions 0-24293
- Ne-Ar discharge, transient cathodoluminescence, time depend. 0-38753
- Ne-H-H<sub>2</sub> mixture, positive column characts. and comparison with approx. diffusion theory 0-44025
- SF<sub>6</sub> axially blown arc, current-zero behaviour, theoretical model 0-38789
- SF<sub>6</sub> gas blast breaker, current zero meas. 0-38795
- Xe, electrical conductivity beyond critical point, intermediate density between gas plasma and solid (*Russian*) 0-20265
- Xe-He(Ne), gas mixture, element and isotope separation in impulse plasma centrifuge (*Russian*) 0-38725

# plasma turbulence

- acoustic waves dispersion in turbulent medium 0-10384
- Alfvén turbulence in extended extragalactic radio sources, rel. to electron accel. 0-27000
- Alfvén wave turbulence in solar flares, rel. to protons stochastic accel. 0-21953
- anomalous absorption of UHF radiation in electron cyclotron resonance range (*Russian*) 0-1807
- anomalous EM wave electron radiation 0-43889
- anomalous turbulent resistivity at high drift vels., rel. to confinement and fluctuations in toroid 0-24139
- anomalous turbulent resistivity at high drift vels., toroidal plasma 0-24138
- anomalously resistive phase, spiky density fluctuations and relax oscill., microwave scatt. obs. 0-38547
- arc column in free turbulent jet, electric field strength 0-49021
- arc in channel with distributed gas flow, positive column anal. (*Russian*) 0-14949
- ball lightning, turbulent plasma sphere, model eqns. for current and heat flux 0-32516
- ballooning trapped electron mode, linear and nonlinear theory 0-28656
- bump-in-tail instability-generated turbulence, phase space -anulation due to mode-mode coupling 0-38651
- collective phenomena and anomalous resistance, electron current drift velocity (*Russian*) 0-24140
- Compton scattering of transverse waves by relativistic electrons, effect on plasma turbulent reactors 0-51644
- convective cell excitation by Bernstein waves (*Russian*) 0-53961
- density fluctuations, microwave scatt. obs. 0-48851
- diagnostic techniques for fluctuations 0-49002
- diagnostics, turbulent heating example 0-49015
- diffusion coefficients of low frequency electromagnetic turbulent plasma 0-28677
- digital spectral techniques in plasma fluctuation diagnostics 0-49003
- discharges, high current, press., conductivity meas. 0-38793
- drift wave turbulence, dissipative, current driven, in Tokamak plasma 0-38587
- drift wave turbulence, nonlinear behaviour and turbulence spectra 0-19573
- drift wave turbulence and convective cell formation 0-43925
- electron beam-plasma interactions in turbulence regime, phenomenological model 0-6260
- electron long-wavelength wave dispersion evolution meas. in turbulent column 0-6283
- electrostatic ion cyclotron turbulence in ionosphere/magnetosphere, rel. to coherent anomalous resistivity 0-4189
- electrostatic turbulence, variable density and pressure, two-fluid model and geostrophic approx. 0-53986
- electrostatic Vlasov turbulence, iterative soln. 0-10375
- electrostatic waves, turbulent acceleration in Earth's auroral plasma (*Russian*) 0-53952
- EM drift wave turbulence and convective cell form. 0-24168
- energetic particles, interaction with shock wave front in turbulent medium 0-4210
- finite bandwidth radiation, nonlinear dissipation near electron cyclotron harmonic resonances 0-28670
- finite-beta effects on drift wave turbulence and particle confinement 0-38652
- formation of plasma in fusion devices, at. and plasma processes, diagnostic techniques 0-48915
- gas discharge, perturbation by longitudinal turbulence 0-24271
- guiding center plasma with gravitational or gradient drifts 0-38632
- heat exchange of low-temp. plasma with wall, longitudinal mag. field effect 0-33781
- heating, turbulent, flat top electron distrib. effect, with ion-acoustic instability 0-10399
- high freq. rad. field in turbulent plasma 0-38648
- hydromagnetic turbulence in high  $\beta$  plasmas, collisionless damping by hydromagnetic waves 0-17482
- instability induced by plasma-electric current interaction in focus expt., laser diagnostics 0-24171
- interchange mode turbulence, spectral cascade processes 0-33775
- ion acoustic, resistivity phenomena in multi-ion plasma 0-48856
- ion acoustic turbulence in laser-heated plasma with large temp. gradient 0-53987
- ion beam scattering by ion-acoustic turbulence 0-6262
- ion cyclotron wave turbulence, nonlinear effects, lab. expt., magnetosphere appl. 0-24170
- ion heating by current driven turbulence in inhomogeneous plasma 0-33791
- ion-acoustic instability, ion tail formation and saturation 0-38610
- ion-acoustic turbulence-plasma interactions and electron spectrum in electric fields 0-38617
- Langmuir, adiabatic interaction with ion-acoustic waves (*Russian*) 0-1765
- Langmuir oscillation collapse in supersonic regime, forbidden energy (*Russian*) 0-14895
- Langmuir oscills., modulational instability, in EM wave field 0-38618
- Langmuir turbulence, large-scale, renormalisation group method 0-38650
- Langmuir turbulence, modulation perturbation spectrum 0-33776

# plasma turbulence continued

- Langmuir turbulence, statistical theory 0-38647
- Langmuir turbulence, strong, transition (*French*) 0-28674
- Langmuir turbulence in galactic masers, role in generating high-vel. and symmetric spectral features 0-31378
- Langmuir turbulence meas., forbidden transition satellites 0-38714
- Langmuir turbulence of relativistic plasma in strong mag. field (*Russian*) 0-28678
- Langmuir wave evolution, three dimensional kinetic model, Vlasov eqn. calcs. 0-43923
- Langmuir wave turbulence in solar type III radio bursts, nonlinear stabilisation 0-26826
- Langmuir waves, induced nonthreshold scatt. on HF oscills. in inhomogeneous plasma (*Russian*) 0-53960
- Langmuir waves, nonperiodic oscillations 0-48888
- laser diagnostics, probing radiation Raman scatt. (*Russian*) 0-19618
- localised pumping-excited waves, parametric instability, nonlinear stage 0-38622
- low pressure plasma, two-dimens. turbulent convection 0-28676
- magnetic mirror, injected plasma particle refl. (trapping), quiescent (turbulent) plasma 0-48955
- magnetosonic turbulence in interplanetary medium, evidence from plasma inhomogeneities anisotropy (*Russian*) 0-36468
- MHD, two dimens. turbulence, stationary states in non-dissipative limit 0-24169
- modulational instability produced by Langmuir turbulence in a magnetic field 0-1759
- multicomponent plasma, ion-acoustic resist. 0-10383
- nonideal plasma, elem. excitations and macroscopic props., review 0-43842
- nonlinear interaction of intense HF EM field with Langmuir waves in turbulent plasma 0-53988
- ohmic heating of plasmas in closed magnetic systems 0-28756
- parametric turbulence of particles emitted by a laser plasma (*Russian*) 0-53985
- planar Langmuir solitons, 3-dimens., stability 0-46827
- plasma convective cells of drift waves, plasma with shear, nonlinear excitation mechanism (*Russian*) 0-38585
- precursor whistler mode plasma turbulence formation in parallel shock waves 0-24172
- radiation emission from electron beam excited strongly turbulent plasma 0-53943
- relativistic electron beam induced turbulence and heating, review 0-38672
- renormalised Vlasov turbulence 0-19579
- resistive tearing  $m=1$  instability turbulent modification 0-43916
- resistivity, of turbulent plasma, with ion-acoustic instability, ion-tail form. effect 0-10360
- Rossby wave turbulence, nonlinear behaviour and turbulence spectra 0-19573
- runaway electron diffusion and power balance in Tokamak moderate density discharges 0-28609
- solitons, laser physics appls. 0-48333
- solitons, nonlinear normal mode theory 0-48875
- spontaneous polarization of a turbulent magnetized plasma 0-19580
- stationary turbulence regions and anomalous resist. in magnetosphere plasma 0-38649
- statistical theory, quantum mechanical approach 0-43926
- stellarator, Saturn, current-free transport processes, drift modes effect 0-19605
- stream of high temp. gas with particles, modelling (*Russian*) 0-38572
- strong Langmuir turbulence for electron plasma waves, plasma diagnostics appl. 0-48889
- strong turbulence fluctuations in partially ionised plasma, power spectrum var. with press. 0-38645
- subsonic electron fluid and small spark formation 0-38792
- sum rules and collective modes in a turbulent plasma 0-6255
- theta-pinch, electron heating in turbulent neutral layer (*Russian*) 0-10361
- Tokamaks, disruptions and turbulence 0-28675
- TORTUR I, heating by current driven turbulence 0-24191
- transport in plasma, turbulent, convective, kinetic equations 0-28606
- trapped electron instability, turbulence, unstable mode dynamics anal. 0-33761
- trapped electrons, test charge pot. in single wave case 0-24247
- turbulent plasma, wave scintillations, fourth-order moment eqn., astrophys. appl. 0-46381
- unstable turbulent ionisation waves, two dimensional Fourier spectroscopy 0-38646
- whistler mode turbulence in Jupiter magnetosphere, Voyager 1 plasma wave obs. 0-26795
- whistler mode turbulence near Io plasma torus, electron pitch-angle diffusion 0-4290
- Zakharov equations derivation for higher electron non-linearities in Langmuir collapse dynamics 0-43919
- Ar arcs in supersonic flow, numerical analysis 0-38776
- Ar, hollow cathode arc discharge, collective scatt. meas., turbulence 0-48978
- H<sub>2</sub>, produced by magnetically rotated arc 0-38769

# plasma-wall interactions

- see also plasma impurities
- blanket boundary layer, high-density gas, localised drift mode stability 0-43956
- current disruption, in Tokamak plasmas, schlieren signal meas. from millimetre waves 0-48998
- deflagration wave in slab target, form. by ion beam 0-28628
- deflagration wave in spherical target, form. by ion beam 0-28629
- discharge, light emission efficiency, electrostatic confinement effects 0-33752
- electrostatic sheath equations, inc. heating, ion mobility, and ion recomb. 0-1808
- external conducting sheets, stability effects on mag. contained plasmas 0-1787
- fusion device surface effects on neutral beam injector and beam direct converter operation 0-47719
- fusion reactor divertor collector plate, pot. drop across electrostatic plasma sheath 0-13833
- fusion reactor first wall materials, surface resist. 0-42853
- fusion technology, surface studies 0-23149



- plasma-wall interactions continued**  
 fusion Tokamak experiments, H(D) recycling model, influence on discharge behaviour 0-10393  
 heat exchange of low-temp. plasma with wall, longitudinal mag. field effect 0-33781  
 heat transfer to rotating water-cooled cylindrical wall (*French*) 0-28850  
 impurity concentrations on wall during Tokamak discharges, laser probing technique 0-49013  
 impurity flux and differential wall changes, in Alcator-A Tokamak, surface probes 0-38664  
 inert gas, low-pressure discharge, electron energy distrib., elec. field and electron wall loss effects 0-24294  
 low pressure Ar plasmas near wall, kinetics study (*French*) 0-28689  
 magnetic field effects, computer simulation 0-10392  
 magnetoactive plasma, effect on a plane disc, impedance calcs. 0-1809  
 MHD generator, local characts., transverse current inhomogeneity in MHD channel 0-24146  
 neutral injection parameters and beam line design for TEXTOR 0-28811  
 oscillations, low frequency, growth, limit of safety factor in JFT-2 Tokamak 0-38589  
 pellet ablation in plasma 0-19589  
 positive column, metastable atom transport, excitation rate radial variation, flux to wall calc. 0-44038  
 reflection coeffs. for light ion-surface interaction, review (*Russian*) 0-38663  
 reflection of laser plasma from hot shield, expt. 0-33782  
 scrape-off layer in Tokamak with divertor, plasma transport 0-28614  
 self similar cooling wave, effective thermal cond. (*Russian*) 0-14908  
 sheath, integro-differential eqns., nonlinear, nonlocal, soln. formalism 0-43936  
 sheath edge theory is weakly ionised collision dominated plasma 0-43935  
 substance evaporation into DC arc plasma, kinetics (*Ukrainian*) 0-33780  
 surface erosion, sputtering, unipolar arcs, heat pulses 0-38665  
 surface excitations in metal-contiguous isotropic electron plasma 0-38667  
 TEXTOR, plasma wall interaction experimental studies, design features 0-13845  
 TEXTOR, plasma-wall interaction study reactor, mechanical struct. design 0-13846  
 Tokamak, DITE, plasma and impurity fluxes on walls 0-28688  
 Tokamak, PLT, current profile evolution effect on plasma-limiter interaction and energy confinement time 0-10420  
 Tokamak fusion reactor, impurity control and plasma transport in plasma-edge region 0-13832  
 Tokamak impurity problems, atomic and mol. struct. and collision data, review 0-43959  
 Tokamak reactors and structural materials 0-32428  
 viscous damping of magnetoacoustic oscillations in cold, bounded cylindrical plasma 0-24151  
 Al foil, burn-through by laser-driven ablation 0-33794  
 H<sub>2</sub> plasma reactor design, heat transfer and flow 0-38697  
 H<sub>2</sub> solid, ablation by magnetised plasma, semi-empirical calc. 0-38666
- plasma waves**  
*see also magnetohydrodynamic waves; plasma oscillations; plasma shock waves*  
 acoustic waves dispersion in turbulent medium 0-10384  
 Alfvén, long, circ. polarised, 2-component nonlinear Schrödinger eqn. calcs. 0-48883  
 Alfvén and magnetoacoustic wave heating for fusion plasmas 0-24188  
 Alfvén pulse-excited instability in neutral sheet, mag. field lines reconnection dynamics (*Russian*) 0-1768  
 Alfvén wave accelerated particles, bremsstrahlung radiation losses rel. to self-similar soln. for distrib. function 0-56702  
 Alfvén wave heating, nonlinear processes 0-28718  
 Alfvén wave heating in toroidal plasma 0-28740  
 Alfvén wave turbulence in solar flares, rel. to protons stochastic accel. 0-21953  
 Alfvén waves, circular polarisation, propagation in mag. field, spiky soliton 0-28662  
 Alfvén waves, circularly polarised, spiky soliton soln. to nonlinear evolution eqn. 0-38590  
 Alfvén waves, exact, nonlinear, existence of solitons 0-24159  
 Alfvén waves, nonlinear self-precession and wavenumber shift 0-10389  
 Alfvén-ion-cyclotron instability for axially bounded plasma 0-1788  
 Alfvénic particle streaming in astrophysical plasmas 0-31206  
 anomalous absorption of UHF radiation in electron cyclotron resonance range (*Russian*) 0-1807  
 atmospheric positive streamer corona, primary wave emission, secondary electron emission 0-44008  
 auroral kilometric radiation coherent generation by nonlinear beatings between electrostatic waves 0-26691  
 auroral plasma, turbulent acceleration by electrostatic waves (*Russian*) 0-53952  
 axial eigenmodes for long- $\lambda_{\parallel}$  waves in plasmas bounded by sheaths 0-28655  
 ballistic wave transformation kinetic effects (*Russian*) 0-38584  
 ballooning trapped-electron mode overlapping many rational surfaces 0-28618  
 beat heating in plasmas using CO<sub>2</sub> lasers 0-43950  
 Bernstein modes in electron cyclotron heating of Tokamak, Vlasov dispersion eqn. 0-33809  
 Bernstein waves, convective cell excitation (*Russian*) 0-53961  
 bounded medium, nonlinear parametric reson., limit cycle solns. 0-19071  
 Buneman-Farley instability, nonlinear decay interactions 0-38616  
 caviton generation in plasma reson. region (*Russian*) 0-53926  
 cavitons in laser irradiated fusion plasmas, EM wave propag., supersonic density humps 0-24178  
 Cerenkov interaction between obliquely propagating whistler wave and electron beam, computer simulation 0-43937  
 coherent waves in nonlinear medium, nonresonant interaction, eqns. system development and examples (*Czech*) 0-24149  
 cold electron plasma waves, parametric decay, convective loss effect 0-38634  
 collisionless drift modes, graphical method for finding complex roots of nonlinear eqn. 0-33762  
 collisionless drift modes in sheared slab geometry, stability props. 0-1786  
 collisionless drift wave in Vlasov plasma, nonlocal anal. 0-43910  
 collisionless drift waves in Tokamaks analytic eigenvalue eqns. 0-6246  
 confined waves with ergodic ray trajectories, instability condition 0-14894  
 coupling of waves in cold nonuniform magnetoplasma 0-43918
- plasma waves continued**  
 cross-field electron heat transport due to high frequency electrostatic waves 0-53932  
 current driven collisional drift and Alfvén instabilities in sheared mag. field 0-1795  
 current generation by electrostatic travelling waves in collisionless magnetised plasma 0-53976  
 cyclotron harmonic wave, props. prediction from perpendicular dispersion relation 0-1772  
 cyclotron harmonic waves props. from perpendicular dispersion relation 0-38612  
 cyclotron waves in bounded magnetoplasma 0-48869  
 cylindrical soliton-like waves, slow and fast, obs. 0-28654  
 decay instability of laser radiation in a magnetoplasma 0-1781  
 deflagration wave in slab target, form. by ion beam 0-28628  
 deflagration wave in spherical target, form. by ion beam 0-28629  
 dielectric response and energy loss in intermediate quantum plasma 0-38541  
 digital spectral techniques in plasma fluctuation diagnostics 0-49003  
 dispersion function for anisotropic longitudinal waves 0-14891  
 disruptions, internal, precursors of, tearing mode 0-28652  
 drift dissipative, LF oscills., anomalous diffusion and equilib. 0-33769  
 drift instability, electrostatic current-driven, scaling law for high density and high current Tokamaks 0-38691  
 drift wave, collisional, nonlinear evolution, successive bifurcations to chaotic state 0-33773  
 drift wave equations, numerical solution by invariant bedding 0-10374  
 drift wave instability, current-driven 0-1770  
 drift wave instability, nonlocal collisionless, toroidal curvature effects 0-38588  
 drift wave linear dispersion eqn. including temp. fluctuation 0-10376  
 drift wave spectra modulation due to HF fields 0-38624  
 drift wave stability and transport theory in fusion systems 0-28653  
 drift wave turbulence, dissipative, current driven, in Tokamak plasma 0-38587  
 drift wave turbulence and convective cell formation 0-43925  
 drift waves, convective cells, nonlinear excitation mechanism with shear (*Russian*) 0-38585  
 drift waves, instability in AC elec. field, wave growth rate and dispersion relation 0-48886  
 drift waves, nonlinear behaviour and turbulence spectra 0-19573  
 drift waves, shear damping in large aspect ratio Tokamak 0-6242  
 drift waves, single mode, low freq., with captured electrons, spatial struct. (*Russian*) 0-10372  
 drift waves, stabilisation by lower hybrid waves of finite wavenumber 0-53968  
 drift waves, strongly dispersive, modulation instability, convective cell formation 0-38635  
 drift waves, wave action 0-43908  
 drift-dissipative waves, weakly ionised plasma, column steady state 0-38613  
 drifting plasma, radiation potential of immersed point antenna 0-14906  
 E×B effects on nonlinear mode-converted lower-hybrid waves, derivation of nonlinear differential eqn. 0-1785  
 eigenmodes, universal, in collisionless plasma slab 0-38581  
 electric field meas., forbidden transition satellites in turbulent plasma 0-38714  
 electron, stability anal. 0-6240  
 electron beam controlled discharge, cathode density waves 0-38798  
 electron beam waves+plasma waves, nonlinear interactions 0-38670  
 electron beam-plasma system, explosive instability 0-1813  
 electron classical motion in wave of slowly varying amplitude 0-28658  
 electron current driven ion wave instability, excitation, electrode type effects 0-38603  
 electron cyclotron absorption of the ordinary wave at normal incidence 0-19570  
 electron cyclotron heating and wave trajectory in toroidal plasmas 0-28726  
 electron cyclotron heating in toroidal plasmas, wave trajectories 0-38678  
 electron diamagnetic drift, RF flux control of toroidal plasma 0-38582  
 electron heating by Langmuir waves, with induced l-s scatt. (*Russian*) 0-10403  
 electron long-wavelength wave dispersion evolution meas., sampling technique 0-6283  
 electron plasma waves, in water-bag and 2-Maxwellian plasmas 0-38601  
 electron plasma waves, toroidal Trivelpiece-Gould modes 0-33770  
 electron wave, guided, on planar plasma slab, propag. and attenuation characts., dissipative processes 0-38608  
 electron waves, beat radiation 0-43314  
 electron waves, excitation long low waveguiding circuit, expts. 0-1775  
 electron waves beat-driven optical free electron laser 0-43315  
 electrostatic, nonlinear 4-wave interaction, positive (negative) energy waves, explosive instability 0-48884  
 electrostatic daughter wave nonlinear decay, causing parametric instability saturation 0-53945  
 electrostatic ion cyclotron electron drift instability anal. using linear Vlasov dispersion reln. 0-1780  
 electrostatic ion cyclotron waves, nonlinear steepening 0-31175  
 electrostatic ion cyclotron waves and ion acoustic waves, parametric instabilities 0-38591  
 electrostatic Trivelpiece-Gould modes in a torus 0-38609  
 electrostatic Vlasov turbulence, iterative soln. 0-10375  
 electrostatic wave, HF, causing cross-field electron heat transport 0-28619  
 electrostatic wave propag., anomalous electron pseudo-classical transport 0-24137  
 electrostatic waves, turbulent acceleration in Earth's auroral plasma (*Russian*) 0-53952  
 electrostatic waves in drifting ionospheric simulation 0-53965  
 EM drift wave turbulence and convective cell form. 0-24168  
 EM ion waves in cold relativistic plasmas, astrophys. appl. 0-21910  
 EM standing wave and two-wave reson. interaction, precessional rot. and nonlinear effects 0-48892  
 EM wave distribution in inhomogeneous plasma containing random irregularities 0-38633  
 EM wave in nonuniform magnetostatic field, pondermotive effect, Hamiltonian theory 0-19575  
 EM wave parametric decay to electrostatic wave, mode coupling of modulational instabilities 0-24161  
 EM waves, extraordinary parametric decay into two upper hybrid plasmons 0-43904



## plasma waves continued

EM waves excited in rippled plasma resonator by relativistic electron beam 0-48902  
energetic particle trapping by Alfvén wave instabilities 0-31205  
enhanced losses due to collisionless drift waves, dynamic stabilisation effects 0-14888  
exact solitary ion acoustic waves in a magnetoplasma 0-6247  
excitation of high-frequency waves with mixed polarization by streaming energetic electrons 0-1773  
explosive instability collision mode stabilisation by drifting effects, Thirring instability (*Russian*) 0-43920  
extraordinary mode wave damping near electron cyclotron freq. in Tokamak 0-53979  
fast ion beam, Alfvén wave excitation in Tokamak (*Russian*) 0-53999  
fast wave heating via mode conversion and ICRF scaling 0-28815  
fast-magnetosonic-wave heating of the conceptual NUWMAK Tokamak reactor 0-6264  
finite amplitude solitary Alfvén waves 0-53973  
finite amplitude wave, regeneration beyond opacity barrier (*Russian*) 0-10387  
finite bandwidth radiation, nonlinear dissipation near electron cyclotron harmonic resonances 0-28670  
finite-beta effects on drift wave turbulence and particle confinement 0-38652  
FT-1 Tokamak, lower hybrid plasma heating 0-28700  
generalized lower-hybrid-drift instability and modified two-stream instability, unified theory 0-1777  
growing waves, energy density calcs. 0-53974  
growth, stability anal., particle distrib. functions and transport theory 0-43903  
guiding center plasma with gravitational or gradient drifts 0-38632  
helical waves in tail of Comet Morehouse (1908 III), WKB approximation theory 0-4305  
Heliotron D, RF heating, equilibrium and stability 0-28777  
HF pressure, effect on efficiency of beam-plasma interaction (*Russian*) 0-10395  
HF quasinonochromatic waves, charged particle drift motion under resonance conditions 0-38611  
hot nonuniform magnetised plasma, wave propag. near singular regions 0-38628  
hot nonuniform magnetised plasma wave propag. theory, Vlasov eqn. perturbation expansion 0-33768  
hydrodynamic wave description including electron spin 0-38643  
hydromagnetic rarefaction waves and free expansion in collision-free strongly magnetised plasma 0-38594  
hydromagnetic surface waves, dissipation 0-21904  
hydromagnetic waves in high  $\beta$  plasmas, propag. and damping 0-17482  
ICRF heating, preliminary results in DIVA 0-28758  
ICRF heating in Macrotron Tokamak 0-28744  
ICRF heating of H-D Tokamak plasma under harmonic resonance 0-28719  
impedance of magneto-acoustic wave launching antenna 0-24180  
inhomogeneous nonlinear medium and time-varying medium, decay. interaction of wave packets 0-14386  
inhomogeneous plasma, approx. of confluence by reson. 0-43907  
interchange mode turbulence, spectral cascade processes 0-33775  
interplanetary plasma wave propagation, magnetoacoustic wave transverse to mag. field 0-12629  
ion acoustic, adiabatic interaction with Langmuir waves (*Russian*) 0-1765  
ion acoustic soliton propag. in two-electron temp. plasma 0-33767  
ion acoustic wave, large amplitude, initial freq. shift 0-28661  
ion acoustic wave damping changes in noisy plasma 0-33757  
ion acoustic wave radiation due to oscill. point charge (*French*) 0-43900  
ion beam-plasma system wave propag. in cylindrical geometry 0-38592  
ion cyclotron wave, in density stratified magnetoplasma, crit. level behaviour 0-6238  
ion cyclotron wave turbulence, nonlinear effects, lab. expt., magnetosphere appl. 0-24170  
ion cyclotron waves, oscillating two-stream instability, RF heating of tokamak plasma 0-1779  
ion cyclotron waves and high-energy protons, nonlinear interaction in Earth's magnetosphere (*Russian*) 0-17444  
ion heating by current driven turbulence in inhomogeneous plasma 0-33791  
ion loss due to low frequency instabilities 0-6217  
ion motion, superadiabatic and stochastic, in mirror-machine plasma, in presence of electrostatic wave 0-53933  
ion wave, rel. to Brillouin backscatter saturation in underdense plasma target 0-14886  
ion-acoustic, collisional and Landau damping in two electron temp. plasma 0-19572  
ion-acoustic dissemination in moving plasma jet 0-38707  
ion-acoustic instability, ion tail formation and saturation 0-38610  
ion-acoustic instability oscillations in collisionless single ended Q-machine 0-38731  
ion-acoustic solitary wave, third-order corrections, reductive perturbation method 0-43898  
ion-acoustic solitary waves, in ion beam-plasma systems with isothermal electrons 0-33784  
ion-acoustic solitary waves (*Czech*) 0-1764  
ion-acoustic solitons, temporal development, initial value problem; 0-33771  
ion-acoustic surface wave spectrum in nonisothermal plasma (*Russian*) 0-53962  
ion-acoustic turbulence-plasma interactions and electron spectrum in electric fields 0-38617  
ion-acoustic wave interaction with longitudinal plasma wavepacket 0-1793  
ion-acoustic waves excitation by 0-10381  
ion-drift wave eigenmodes in sheared mag. field, impurity effects 0-43911  
ion-sound resonances in crossed external electric and mag. fields 0-28626  
ion-wave fluctuation in turbulent plasma, anomalous EM wave electron radiation 0-43889  
ionisation wave, effect of electron neutral collisions in He plasma 0-43846  
ionosphere, nonlinear Landau damping 0-8474  
Langmuir, adiabatic interaction with ion-acoustic waves (*Russian*) 0-1765  
Langmuir, induced scattering on particles in external field 0-38648

## plasma waves continued

Langmuir modes, trapped, in double layer, existence and stability 0-6236  
Langmuir oblique solitons, self-contraction in free path regime (*Russian*) 0-43921  
Langmuir oscillation collapse in supersonic regime, forbidden energy (*Russian*) 0-14895  
Langmuir running wave instability and damping, at different amplitudes and phase velocity 0-38620  
Langmuir soliton EM wave scatt., theory (*Russian*) 0-38564  
Langmuir soliton generation at crit. density, laser-irrad. plasma 0-6267  
Langmuir soliton solns. with high nonlinearities, energy principle 0-24156  
Langmuir solitons, transverse instability 0-6250  
Langmuir standing waves instability, one dimens., soliton and collapse, numerical expt. 0-38619  
Langmuir wave, large amplitude, initial freq. shift 0-24167  
Langmuir wave collapse, Wentzel-Kramers-Brillouin model 0-38600  
Langmuir wave evolution, three dimensional kinetic model, Vlasov eqn. calcs. 0-43923  
Langmuir wave excitation by relativistic electron beam (*Russian*) 0-19594  
Langmuir wave excitation by two pumping waves, convective instability (*Russian*) 0-14904  
Langmuir wave induced scatt. in turbulent plasma in strong external HF EM field 0-53988  
Langmuir wave turbulence in solar type III radio bursts, nonlinear stabilisation 0-26826  
Langmuir waves, driven by electron-ion decay instability, scattered spectrum 0-43970  
Langmuir waves, induced nonthreshold scatt. on HF oscills. in inhomogeneous plasma (*Russian*) 0-53960  
Langmuir waves, intense mag. field generation 0-38623  
Langmuir waves, nonperiodic oscillations 0-48888  
Langmuir waves, upconversion of ion-sound impossible 0-41716  
Langmuir waves in solar corona, excitation by fast electrons stream 0-17568  
laser supported absorption waves, momentum transfer to surface, flowfield model 0-14921  
LHR frequency range waves interactions in octopole Tokamak 0-28724  
Liapunov stability of generalized Langmuir solitons 0-38631  
localised drift-Alfvén mode instability due to current density gradient 0-19571  
longitudinal wave perturbation, producing increased fusion reaction rate 0-27815  
longitudinal waves in relativistic plasma (*Russian*) 0-54023  
low frequency heating wave, parametric instabilities induction in mag. confined plasma 0-24187  
lower hybrid, random spectrum, resistive tearing  $m=1$  instability turbulent modification 0-43916  
lower hybrid, waveguide launching 0-10391  
lower hybrid cones, stability anal. 0-48880  
lower hybrid region, antenna impedance 0-28664  
lower hybrid self-trapping at RF gas breakdown 0-38850  
lower hybrid wave, linear amplification and absorption 0-28673  
lower hybrid wave accessibility, effect of density gradient 0-1794  
lower hybrid wave excitation by active-passive waveguide array 0-48911  
lower hybrid wave heating, quasilinear effects 0-28763  
lower hybrid wave heating in Doublet IIA 0-28723  
lower hybrid wave heating in JIPP T-II 0-28722  
lower hybrid wave propag. and parametric decay in WEGA Tokamak 0-28725  
lower hybrid waves, collisionally damped, driving steady state electron currents 0-38639  
lower hybrid waves, filamentation and spatial attenuation in Tokamaks 0-28665  
lower hybrid waves, in Petula Tokamak, plasma heating and nonlinear effects 0-28697  
lower hybrid waves, modulation instability growth rates 0-48881  
lower hybrid waves, nonlinear behaviour, near linear mode-conversion point 0-53963  
lower hybrid waves, ray trajectories and ion absorpt. in Tokamaks 0-28671  
lower hybrid waves, ray trajectory and ion absorpt. in Tokamak 0-28667  
lower hybrid waves, stochastic ion heating 0-28707  
lower hybrid waves in toroidal discharge, parametric decay 0-38596  
lower-hybrid wave excitation in RF fusion plasma heating, thermal eddies form. 0-24193  
lower-hybrid waves, Tokamak RF heating by electron Landau damping 0-19595  
magnetised plasma, backscatt. of laser beam from electrostatic waves 0-33779  
magnetised plasma, double-layer characts. meas., wave trapping 0-43874  
magnetized plasma parametric resonance in non-monochromatic pump-wave 0-38598  
magnetosonic disturbance, hydrodynamic instability in nonuniform plasma flow (*Russian*) 0-1766  
magnetosonic oscillations, parametric decay in cylindrical plasma 0-24157  
magnetosonic oscills., in bounded plasmas, viscous damping 0-38605  
magnetosonic resonance heating in the Erasmus Tokamak 0-28720  
microwave heating of plasma in EM trap (*Russian*) 0-10400  
minority cyclotron resonance damping in PLT two-ion plasma, fast-wave heating 0-24194  
monochromatic whistler wave, nonlinear evolution in nonuniform mag. 0-43912  
multicomponent plasma, ion-acoustic resist. 0-10383  
non uniform Langmuir fields, evolution and modulation instability 0-38599  
non-linear theory of collective processes in laser-pellet interaction and soliton generation 0-24199  
non-linear wave interaction in plasma column, calcs. 0-1769  
non-stochastic heating of magnetized plasma by electrostatic wave 0-10405  
nonlinear coupling of three waves in non-uniform plasma 0-6237  
nonlinear effects in the vicinity of a radiofrequency probe 0-48985  
nonlinear electron plasma waves in magnetised plasma waveguide 0-38662  
nonlinear evolution of longitudinal wavepacket 0-1793  
nonlinear interactions and hydrodynamics in HF field (*Russian*) 0-53951  
nonlinear ion-acoustic wave emission from magnetised plasma boundary 0-38638



**plasma waves continued**

nonlinear ion-acoustic waves, interactions in cold plasma 0-38607  
 nonlinear kinetic equation, structural stability, soliton collisions 0-10382  
 nonlinear magnetoacoustic waves in weakly inhomogeneous plasma 0-48867  
 nonlinear mode coupling instability saturation, bifurcations and strange behaviour 0-48873  
 nonlinear monochromatic wave growth in plasma-filled waveguide with electron beam 0-43938  
 nonlinear periodic waves stability in plasmas 0-38615  
 nonlinear plasma waves in solar atmosphere, rel. to type III radio bursts fundamental emission 0-36603  
 nonlinear polarized standing waves in a cold-electron overdense plasma 0-24163  
 nonlinear stability problems, two-time method, dissipation scalings, ohmic heating 0-53967  
 nonlinear three-wave interaction in magnetoplasma column 0-24152  
 nonlinear wave interaction in magnetoplasma column, experimental results 0-24153  
 nonlinear wave interactions and critical fluctuations 0-38626  
 nonlinear waves in magnetised plasma, periodicity anal. 0-43902  
 nonlinear-wave propagation in a proton-electron plasma coupled with a strong radiation field 0-48872  
 Ohmic pumping by means of externally driven tearing modes 0-28706  
 oscillating two-stream and parametric decay instabilities in a weakly magnetized plasma 0-38637  
 oscillations, in lower-hybrid range, of bounded plasma 0-24162  
 parametric decay of non-ducted whistler-mode signal 0-6239  
 parametric instabilities and ion heating in a two-ion species plasma 0-28708  
 parametric instabilities in weakly-inhomogeneous hot plasmas 0-28828  
 parametric wave excitation in bounded systems 0-6252  
 parametrically excited surface waves, phase mismatch 0-24165  
 particle dynamics in low freq. EM waves, magnetosphere particle flux in inhomogeneous plasma 0-1804  
 particle-wave interactions, cyclotron reson. vel. shift, wave propag. effects 0-33774  
 Penning discharge ion source with hollow cathode, HF instabilities 0-43997  
 plasmapause, electrostatic waves near upper hybrid resonance freq. 0-12616  
 plasmon dispersion, correlation correction 0-43917  
 ponderomotive force in interaction between ion wave and HF elec. field 0-10373  
 pulsar magnetospheres, relativistic MHD wind or plasma wave 0-31317  
 pumping wave decay, convective instability, harmonic generation and harmonic generation (*Russian*) 0-14889  
 pure electron plasma, waves and transport 0-38563  
 quasilinear theory 0-19576  
 regularised long wave equation, numerical studies 0-53964  
 relativistic nonlinear electron cyclotron waves in plasmas 0-10377  
 relativistic plasma, nonlinear wave modulational instability with nonlinear Landau damping (*Russian, English*) 0-53955  
 relativistic transverse cold plasma waves, nonlinear, linearly polarised, stability 0-6235  
 resonance cone trajectory, focused, nonlinear modification, probe diagnostics 0-10379  
 resonance conversion of amplitude-modulated transverse to monochromatic wave 0-6251  
 RF coupling loops, transmission line approx. 0-28672  
 RF energy coupling by magneto-acoustic waves in toroidal plasma 0-28743  
 rF instabilities driven by neutral beam injection, review 0-28757  
 Rossby waves, nonlinear behaviour and turbulence spectra 0-19573  
 rotation influence on kink instability, compressibility (*Russian*) 0-48887  
 self-generated magnetic fields and harmonic emission 0-38546  
 self-gravitational instability of plasma rotating layer, growth rates wave number depend. 0-56706  
 sheaf instability at moderate densities, anomalous ion heating (*Russian*) 0-43922  
 shear Alfvén wave heating experiments in heliotron D 0-28716  
 sideband instability in large amplitude wave, computer simulation 0-38602  
 skin-effect, anomalous, in bounded plasmas 0-24173  
 slow space-charge wave propag. on relativistic electron beam 0-1115  
 slow-fast mode conversion effect on lower hybrid slow mode excitation 0-28668  
 solitary kinetic Alfvén wave stability, one dimensional nonlinear case 0-1776  
 solitons, cylindrical ion-acoustic, propagation characts. 0-28632  
 solitons, nonlinear normal mode theory 0-48875  
 space charge wave propagation along moving magnetoplasma slab 0-38700  
 spatial collapse, highly nonlinear states in plasmas, expt. obs. 0-6233  
 spatial lower hybrid wave echoes, characts. 0-38597  
 stationary turbulence regions and anomalous resist. in magnetosphere plasma 0-38649  
 stellarator, Saturn, current-free transport processes, drift modes effect 0-19605  
 stochastic ion heating by electrostatic wave in sheared mag. field 0-28705  
 strong Langmuir turbulence for electron plasma waves, plasma diagnostics appl. 0-48889  
 subsonic electron fluid and small spark formation 0-38792  
 surface Langmuir wave decay dissipative instability in semibounded plasma (*Russian*) 0-38583  
 surface waves, LF, in cylindrical nonisothermal plasma column 0-6232  
 tearing mode instabilities and suppression by lower hybrid fields 0-28666  
 temperature gradient drift wave eigenmodes stability in sheared mag. field 0-43914  
 theoretical plasma mechanics, book 0-27048  
 theta pinch plasma, absorpt. of magnetoacoustic waves (*German*) 0-10430  
 Tokamak, electrostatic drift waves, numerical anal. of instability and transport 0-48871  
 Tokamak, lower hybrid heating to ignition 0-18605  
 Tokamak, octopole, obs. of RF driven plasma current 0-48910  
 Tokamak (Alcator), driven lower-hybrid waves, light scatt. study 0-1835  
 Tokamak fusion reactor, steady-state, lower hybrid wave-driven, design constraints 0-10424

**plasma waves continued**

Tokamak fusion reactors, doublet research, plasma shape control, MHD stability 0-28837  
 Tokamak heating by fast magnetosonic wave excitation 0-24189  
 Tokamak power reactor, steady state, lower hybrid wave driven 0-48945  
 Tokamak thermonuclear reactor, MHD modes drift phenomena, kinetic method (*Russian*) 0-1827  
 Tokamaks, lower hybrid resonance cones 0-28791  
 Tokamaks, nonlinear drift tearing modes 0-53971  
 topside ionosphere, ion heating by electrostatic ion cyclotron waves 0-12606  
 toroidal plasmas, MHD instabilities 0-38579  
 transverse wave packet, 3-dimens., nonlinear evolution in hot plasma, ion-acoustic wave effect 0-43899  
 trapped electron shear-Alfvén instability, stabilisation by temp. gradient 0-28599  
 Trivelpiece-Gould wave, excitation in magnetised plasma by slow waveguiding cct. 0-14892  
 two Maxwellian plasma, electron plasma wave, higher order Landau modes 0-38601  
 two-temperature plasma, field eqn. of electron wave 0-28633  
 unstable turbulent ionisation waves, two dimensional Fourier spectroscopy 0-38646  
 upper hybrid solitons, in warm magnetised plasma, kinetic anal. 0-38595  
 upper-hybrid reson. absorpt. of laser in plasma focus, backscatter 0-28621  
 viscous damping of magnetoacoustic oscillations in cold, bounded cylindrical plasma 0-24151  
 VLF excitation in ionosphere due to electron beam injection 0-12603  
 Warm nonuniform plasma, stress tensor for high freq. wave propag. 0-33764  
 water bag plasma, electron plasma wave, higher order Landau modes 0-38601  
 wave dispersion in presence of relativistic beam 0-19592  
 wave packets in dispersive media, main signal and precursor approx. 0-24158  
 weakly inhomogeneous magnetic field amplification by plasma wave 0-24166  
 weakly localized two-dimensional drift modes 0-53970  
 whistler mode waves near 10 plasma torus, electron pitch-angle diffusion 0-4290  
 whistler wave, large amplitude oscillation by high power microwaves 0-43913  
 whistler wave propagation in narrow density trough 0-38629  
 whistler wave trapping in density crest 0-53984  
 Ar, positive column, progressive and regressive ionisation waves (*French*) 0-43905  
 He glow discharge plasma, ionis. waves in positive column 0-1876  
 He, low-press. weakly ionised magnetoplasma, acoustic wave generation 0-44059  
 He positive column, magnetised, temps. of charged particles, nonlinear effect of ionis. waves 0-44023  
 Ne hot cathode discharge plasma, second order harmonic surface wave generation 0-38849  
 SF<sub>6</sub> gas, dispersion relation of spontaneous oscill., unstable regions 0-1875

**plasmatoms** see plasma diodes

**plasmoids** see plasma

**plasmons**

see also phonon-plasmon interactions; solid-state plasma

acoustic wave interactions due to deformation potential (*Russian*) 0-15356  
 adsorbed atom on solid surface, photoemission from valence band, surface plasmon emission, model Hamiltonian calcs. 0-50525  
 adsorbed atoms, relax. shifts, satellites and sum rules in electron spectroscopies 0-11539  
 adsorbed atoms and molecules XPS, many-body effects 0-55266  
 adsorbed molecules, surface plasmon enhanced light absorption 0-40176  
 bimetallic junctions, interface plasmon modes, theoretical anal. 0-54767  
 charged particles surface excitation system, ground-state energy 0-15462  
 coated semiconductor spheres, surface modes, plasmon oscils. 0-54730  
 cooperative emission of excited mol. monolayer into surface plasmons of metallic substrate 0-20666  
 coupling of molecules to surface plasmons in resonant elastic scattering 0-20102  
 dielectric layer, natural EM oscillations excitation by stream of electrons or EM field 0-34378  
 dispersive metals, metal, spatially dispersive, EM waves and plasmons, propagation 0-15549  
 electrochromic ATR prism modulator 0-43440  
 electron gas, jellium model, dynamic correlations, first-order perturbation theory 0-44527  
 electron gas, two-dimensional, two-component, high-freq. cond. 0-29428  
 EM waves, extraordinary parametric decay into two upper hybrid plasmons 0-43904  
 ferromagnetic semiconductor, magnon coupling to plasmons and LA phonons, s-d model 0-29536  
 ferromagnetic semiconductors, acoustic plasmons 0-7098  
 ferromagnetic semiconductors, Raman scattering of light on plasmon excitations 0-2738  
 graphite, X-ray scatt. from small particles at zero k 0-11505  
 graphite film, secondary electron emission and EELS rel. to plasmons 0-50481  
 graphite intercalation cpds., dispersion relations of intercalate modes 0-34379  
 graphite-FeCl<sub>3</sub> intercalation cpd., electronic excitation spectrum, high resolution EELS meas. 0-45182  
 Hubbard, half-filled band model, local field correction to plasmon freq. 0-24823  
 ion, near metal surface, friction parameter and Brownian motion 0-15584  
 jellium surface, hydrodynamic model of linear response, nonretarded limit 0-44526  
 laminated systems, two dimensional and surface plasmon mixing (*Russian*) 0-15466  
 Langmuir oscillation collapse in supersonic regime, forbidden energy (*Russian*) 0-14895  
 liquid, surface CARS 0-1280  
 metal, plasmon dispersion effect in (e,2e) process with atomic electron knockout 0-2904



**plasmons continued**

- metal, surface plasmon light emission due to low energy electron irradiation 0-34997
- metal, ultrasoft XPS, plasmon satellite intensity 0-35058
- metal circular cylinders, inhomogeneous, non-radiative surface plasmon-polariton modes 0-29455
- metal conduction electron photoemission spectrum, effect of recoil on shake-up spectra, infinite summation method 0-50526
- metal films, optical excitation, review 0-45106
- metal surface, electron-plasmon interaction 0-39649
- metal surface, fast ion scatt. by plasmons, theory 0-45190
- metal surface, plasmon mechanism for energy loss, dissociation and orientation of fast ions excited by grazing collisions 0-11523
- metal surface energy, gradient corrections in interpolation formulae, surface plasmons 0-2441
- metal-electrolyte boundary, electrostatics in visible and near UV range, microscopic effects 0-45521
- metallic surface, dispersion of surface plasmons 0-2440
- metallic surface, electrostatics, microscopic effects (*Russian*) 0-6936
- metals, collective modes of void-surface coupled systems, surface plasmons 0-49642
- metals, electronic transport eqns., optical cond., number conserving relaxation time approx. calcs. 0-49681
- Mg, K X-ray emission spectra, double plasmon high energy satellite 0-11510
- molten salt, possibility of plasmon mode obs., struct. dynamics 0-10477
- organic thin film refractive index adjustment by absorbing dyes 0-43413
- quasi-one-dimensional metals, narrow-band, exchange-correlation effects on plasmons and on CDW instability 0-44525
- Raman intensity enhancement, of pyridine adsorbed on Ag, by surface plasmons 0-7334
- semiconductor, local fields, nonuniform charge distrib. 0-24826
- semiconductor, natural EM oscillations excitation by stream of electrons or EM field 0-34378
- semiconductor superlattice, plasma oscills. in strong elec. field 0-44637
- semiconductor superlattices, electroplasma parametric resonance 0-34475
- simple metals, photoemission theory, book contrib. 0-16159
- simple metals, plasmon dispersion anal. from electron gas dielectric response 0-6761
- solid-liquid interface, optical methods of study (*French*) 0-7318
- spectrum and damping, collisionless absorpt. threshold nonlinear phenomena (*Russian*) 0-49646
- superlattice, plasma oscill. under strong high freq. elec. field 0-10904
- surface plasmons, counterpropagating, for coherent SHG 0-33081
- surface roughness effect on image potential electron energy loss, plasmon electron scatt. 0-54748
- two atom surface coupling, double reson. at plasmon freq., collective effects 0-34934
- uniaxial crystal foil, electron energy loss probability at oblique incidence 0-25506
- X-ray plasmon scattering plasmon cut off wave vector electron exchange energy effect 0-50458
- Ag, electroreflectance spectroscopy, longitudinal surface plasmons 0-40137
- Ag, surface and volume plasmon light emission due to low energy electron scatt. 0-40177
- Ag surfaces, Cs and Cs-O covered, surface plasma waves, ATR study 0-39451
- Ag/organic dye, excited mol. decay near metal surface, energy transfer to plasmon surface polaritons 0-50440
- BN, chem. bonding and electronic struct., AES and SIMS meas. 0-50512
- B<sub>2</sub>O<sub>3</sub>, chem. bonding, electronic struct., ESCA, Auger, and SIMS spectra 0-50512
- Be adsorbed layers on W(100) and (100), work function and loss spectra meas. surface and bulk plasmons 0-6638
- BeO, X-ray emission spectra, double plasmon high energy satellites 0-29829
- Co and its cpds., X-ray K-absorpt. edge shifts, plasmon energies correlation 0-20734
- Cr and its cpds., X-ray K-absorpt. edge shifts, plasmon energies correlation 0-20734
- Cr<sub>2</sub>O<sub>3</sub>, low energy X-ray emission satellite, unpaired electron and plasmon effects 0-35007
- Cu and its cpds., X-ray K-absorpt. edge shifts, plasmon energies correlation 0-20734
- GaAs, epitaxial film, amorphous and polycrystalline, vol. plasmon energy and linewidth, electron scatt. obs. 0-50482
- Gd, X-ray absorpt. edge, plasmon excitation 0-7437
- H<sub>2</sub>BO<sub>3</sub>, chem. bonding, electronic struct., ESCA, Auger, and SIMS spectra 0-50512
- InSb, epitaxial film, amorphous and polycrystalline, vol. plasmon energy and linewidth, electron scatt. obs. 0-50482
- InSb surface magnetoplasma wave struct. 0-6934
- LuH<sub>2</sub>, electronic struct., photoelectron spectra study 0-50527
- Mg, plasmon-loss intensities in XPS, EELS and Auger spectra 0-10902
- Mo, foil, electron energy loss spectra 0-7452
- Na film, slow electron bombarded, light radiation 0-40168
- Na, X-ray emission spectra, double plasmon high energy satellites 0-29829
- Nb, foil, electron energy loss spectra 0-7452
- Nb<sub>2</sub>Ge, disordered superconductor, T<sub>c</sub> depression by acoustic plasmon overdamping 0-7020
- Ni and its cpds., X-ray K-absorpt. edge shifts, plasmon energies correlation 0-20734
- P, amorphous, stability in air, XPS study, comparison with cryst. polymorphs 0-25517
- ScH<sub>2</sub>, electronic struct., photoelectron spectra study 0-50527
- Si, inversion layer, temp. depend. of subband energies, exchange and correlation effects 0-20281
- Si, plasmon dispersion relation, local microscopic field effects 0-20103
- Ta, foil, electron energy loss spectra 0-7452
- TaSe<sub>2</sub> (2H), optical absorpt., band struct., plasmons, and CDW 0-45104
- TaSe<sub>2</sub> (2H), plasmon behaviour at charge density wave onset 0-10900
- TiCl<sub>3</sub>, role of electron-hole interaction in optical spectra, review 0-45113
- V, foil, electron energy loss spectra 0-7452
- YH<sub>2</sub>, electronic struct., photoelectron spectra study 0-50527
- Zn and its cpds., X-ray K-absorpt. edge shifts, plasmon energies correlation 0-20734

plastic after-flow *see recovery-creep*plastic afterflow *see recovery-creep***plastic crystals**

- adamantane, Ising, diffuse scatt., hard-core correl., weak-graph method 0-49137
- adamantane, plastic cryst. lattice vibr. study of phase transition 0-7355
- adamantane, thermolum. curves 0-2876
- t-butyl bromide, elec. cond., temp. depend. in liq. and plastic phases 0-1944
- t-butyl chloride, elec. cond., temp. depend. in liq. and plastic phases 0-1944
- t-butyl chloride-d<sub>0</sub> and -d<sub>3</sub>, polymorphism, Raman spectra 0-20617
- cyclobutane-d<sub>0</sub>(d<sub>3</sub>), cryst. modifications, low. freq. Raman and IR spectra 0-7342
- cyclohexane, plastic and liquid crystal phase, rot. correl. func. by Raman spectroscopy 0-23403
- cyclohexane-d<sub>0</sub>(d<sub>3</sub>), plastic crystal phase transition, mol. reorientation, Raman scatt. phonon spectra 0-20631
- cyclohexanol plastic cryst. phase, glass transition temp., press. depend. 0-49135
- 2,2-dinitropropane-d<sub>0</sub>(-d<sub>3</sub>), phase polymorphism, vibrational assignments, IR and Raman study 0-16031
- glass transition temp., press. depend. 0-49135
- methane-d<sub>3</sub>, solid, thermodynamic props. calc. using significant structures method, 6 to 87K 0-24616
- neopentane, solid and liq., effect of n-butane impurity on electron mobility and electron-ion recomb. 0-24984
- octaphenylcyclotetrasiloxane, phase behaviour and nucleation kinetics 0-29168
- orientationally disordered cryst., diffuse scatt., hard-core correl., weak-graph method 0-49137
- pivalic acid, liq. and plastic crystals, <sup>13</sup>C NMR chem. shift, temp. depend. 0-2652
- polyethylene oxide, peculiarities of struct. form. near below the melting point 0-54150
- succinonitrile, defects in plastic phase, positron annihilation obs. 0-11504
- succinonitrile, plastic, diffuse scatt., hard-core correl., weak-graph method 0-49137
- succinonitrile, plastic phase, mol. motions correlation times, incoherent neutron scatt. 0-49138
- tetrabromomethane, in disordered phases, IR active mode Raman line shape, dipole-dipole interaction 0-9603
- tetrafluoromethane, in disordered phases, IR active mode Raman line shape, dipole-dipole interaction 0-9603
- triethylenediamine, thermolum. curves 0-2876
- trimethylacetic acid, high resolution <sup>1</sup>H and <sup>13</sup>C NMR spectra at liquid-solid phase transition 0-11281
- KCN, plastic phase, Raman scatt. spectra (*French*) 0-11379
- NaCN, diffuse scatt., hard-core correl., weak-graph method 0-49137
- NaCN, plastic phase, Raman scatt. spectra (*French*) 0-11379

**plastic deformation**

- see also Bauschinger effect; buckling; creep; ductility; elastoplasticity; kink bands; Luder's bands; necking; plastic flow; serrated yielding; shape memory effects; slip; superplasticity*
- acrylonitrile-butadiene-styrene copolymers, micromechanism of deform. and rupture (*German*) 0-35276
- activation volume stress depend. 0-54304
- adiabatic, shearing phenomena, review 0-50692
- AGR fuel cladding, development of high strength, ductile stainless steel alloys 0-45367
- Al-alloys, influence of strain path on mech. props., orthogonal tensile paths 0-30035
- alkaline silicate glass, surface layers, plasticity and microcrack formation, electron microscopy (*German*) 0-40469
- alloys, brittle and plastic, energetic strength theories (*Bulgarian*) 0-38296
- alloys, hot plastic strain, stress-strain-time dependences (*Russian*) 0-40430
- andalusite, shock-loaded, deform. 0-19873
- anharmonic atomic chain breakup, molecular dynamics calcs., deformation dynamics 0-29117
- anisotropic metal blanks, plastically deformable, stress/strain relations (*Russian*) 0-1438
- BCC metals, plastic deform., computer simulation 0-40456
- BCC single crystals, plastic deformation localisation 0-54303
- beams, dynamic plastic behaviour, rot. inertia and transverse shear influence 0-48601
- beams, dynamic plastic response, rotatory inertia and transverse shear effects 0-5947
- beams, inelastic bending under time varying moments, state variable approach 0-28439
- bimetal rolling, calc. of strains by variational method (*Polish*) 0-45323
- blanks clogged into conical matrix, stability anal. (*Russian*) 0-43636
- $\alpha$ -brass, dislocation struct., deform. (*Polish*) 0-24454
- brass, M63, yield stress decrease in compression, rel. to previous elongation (*Polish*) 0-50665
- $\alpha$ - $\beta$  brass, two phase bccrystal, deform. and fracture at 450K 0-16409
- $\alpha$ - $\beta$  brass, two phase bccrystals, deform. and fracture at 150K 0-16388
- brass  $\alpha$ - $\beta$  two-phase bccrystals, interface sliding studies 0-54248
- buckling strength of orthogonally stiffened plates under uniaxial compression 0-5964
- Burgers circuits associated with generalized distortions 0-2014
- butt joint, tensile bond strength, effect of aspect ratio 0-50823
- calcite, sound emission on dislocation annihilation (*Russian*) 0-54246
- carbonate rock, interrelation of flow or fracture and phase transition during deform. 0-51389
- cellulose, nitrated, strength, deform. and disintegration, influence of stable free nitroxyl radicals 0-11717
- ceramic nuclear fuels, mech. props. at compressive deformation 0-651
- ceramic powder, thermal stresses during spheroidisation process (*Russian*) 0-40386
- chromorheology, new exptl. method 0-48658
- circular bar of rate sensitive material, elastic-plastic tension-torsion 0-48602
- columns, Beck and Leipholz types, stability, shear deformation and rot. inertia effects 0-48610
- crack tip, plastic yielding modelling by inclined slip planes 0-33472
- crack tips, yielding on inclined planes 0-33525
- creeping structures with load variations above shakedown limit, boundary solns. 0-10156
- cubic single crystals, hardness meas. by spherical indentation 0-16622



**plastic deformation continued**

cylindrical tubes or shells, mild steel, quasi-static piercing 0-45351  
 deformable solids, fracture and hardening kinetics 0-35210  
 deformation mechanism maps 0-3143  
 diamond lattice, dynamic symmetry and plastic deform. 0-24527  
 differential geometry of deformed crystals 0-19867  
 diffusion welded joints, creep deformation effect on characts. 0-25806  
 dislocation and disclination kinetics, macroscopic theory (*Russian*) 0-49225  
 dislocation ensembles, local heating at low temps., parallel glide planes, temp. distribution (*Russian*) 0-29020  
 dislocations, state of art review, book contrib. 0-39089  
 dispersed media, shock compressibility, brittle destruction 0-49303  
 EBR-II 0-13598  
 elastic-plastic media, nonisothermal, finite deformations, constitutive equations and numerical soln. 0-31503  
 elastic-viscoplastic proportional combined twist and stretch of circular bar of rate sensitive material 0-23912  
 elastoplastic fracturing structures, boundary value rate problem, extremum theorems 0-48596  
 elastoplastic strip or half-plane under moving load, residual stresses and plastic zones 0-53645  
 elastoplastic system, dynamic deformation, internal state variables and internal forces 0-53660  
 elastoplastically deformed strengthened material, stress deformed state during rolling (*Russian*) 0-54299  
 elastoplasticity finite element anal. for large strains, natural factor displacement method 0-14580  
 endochronic plasticity, appl. to structural dynamic response of radioactive waste containers 0-16407  
 epoxy impregnated superconducting composites, mech. props., strain effect at 4K 0-25822  
 epoxy resin, Cl-containing, relation between static and dynamic deform. characts 0-3137  
 epoxy resin, deform. rate depend. of mech. props. at cryogenic temps. 0-55456  
 equivalent minimal stress in forming processes (*French*) 0-38277  
 extrusion process using orthotropy concept of Hill, kinematically determined problems in rigid-ideal plastic (*German*) 0-1445  
 failure, effect of deep wedge shaped notches of small flank angle 0-48593  
 fatigue crack propagation, new measurement and observation techniques 0-45463  
 fibre reinforced complex structural mouldings, accurate stretch data for reinforcement, deform. 0-11694  
 fibre reinforced complex structural mouldings, accurate stretch data for reinforcement, deform. 0-16375  
 fibre reinforced composites densification in free forging, exam. of specific work and kinetics 0-16218  
 fibre reinforced nonlinearly elastic matrix, unidirectionally reinforced, deform., strength, and failure 0-3134  
 filament reinforced hypoeutectoid C steel, strength characts. after deform. and quenching 0-35271  
 filamentary crystals, complex stressed state, method of investigating mech. props. 0-3264  
 fission reaction fuel, kinematic hardening rule of plasticity 0-42764  
 girder, circ-arc bow type, ultimate strength, plasticity (*Japanese*) 0-43631  
 glass fibre reinforced plastic, failure due to deform., optical investigation method (*Russian*) 0-35437  
 glass fibre reinforced plastic, strain disintegration under repeated static load 0-11756  
 glass fibre reinforced plastics, relation between matrix vol. changes and mech. props. 0-11715  
 glass-fibre reinforced Al, highly deformed, microstruct. and mech. props. (*German*) 0-55489  
 grain boundary crack nucleation, and growth under low cyclic stresses, dislocation mechanism 0-19811  
 granular medium, mixed characteristic problem 0-23914  
 hard metals, roll deform. effect on separating forces in cold strip rolling 0-35212  
 heteroepitaxial film deformation, causes and countermeasures (*Russian*) 0-49561  
 heteroepitaxial system, dislocation struct. at stress meas., theory 0-2017  
 hexagonal metals, deformed, resistivity changes calcs. 0-44564  
 hollow circular cylinder, expansion and contraction, strain softening with finite elastoplastic strain (*French*) 0-38283  
 homogeneous simple strain in elastic-plastic media, necessary and sufficient conditions 0-28427  
 honeycomb based composite, deform. theory 0-35250  
 integral inequality and plastic torsion anal. 0-10155  
 Invar, dislocation motion anomaly 0-10554  
 iron, pure, tensile deformation behaviour under high pressure (*Japanese*) 0-16381  
 isotropic and anisotropic raw materials, plastic pot. (*German*) 0-33474  
 j integral applications for short fatigue cracks at notches 0-38332  
 Kester peak, plastic deform. effects (*Russian*) 0-29118  
 laminar blocks with plastic deformations, instability 0-43629  
 large strain inelastic anal., dynamic problems 0-38278  
 lattice defects influence on axial shadow figure (*Russian*) 0-25508  
 localisability of deformations theory, representation 0-10163  
 mechanical surface structure damage, action of plastic deformations (*French*) 0-30011  
 metal, BCC, polycrystalline aggregate, prediction of plastic props., deformation by {111} pencil glide 0-11731  
 metal, deformed in pressing process, temp. field modelling (*Russian*) 0-53602  
 metal, FCC, deformation mechanism under high hydrostatic pressure (*Ukrainian*) 0-25758  
 metal, FCC, polycrystn., fatigued, behaviour model during plastic deformation (*German*) 0-21023  
 metal, FCC or BCC, dislocation annihilation during tensile and cyclic deform. and limits of dislocation densities 0-34007  
 metal, plastic impact, energy absorbed by elastic waves 0-5972  
 metal, single phase FCC, cyclic deform. long range stress changes 0-54308  
 metal electroplastic deformation meas. pulse generator (*Russian*) 0-25931  
 metal forming process, forming conditions and material characts. 0-30032  
 metal particles produced by gas evaporation, form., growth and interaction 0-16220

**plastic deformation continued**

metal strip, high-speed compression, force parameters determ. (*Russian*) 0-21016  
 metal strip, porous, elastic aftereffect in cold rolling 0-11689  
 metal strip, sintered, rolling, algorithm for force and geometric parameters calc. 0-11727  
 metallic crystal, thermomechanical deform., analytical description 0-49391  
 metallic materials, deformation process, stage-by-stage nature investigation using acoustic emission (*Russian*) 0-40434  
 metals, BCC, dislocation processes, straining expts., electron microscope obs. 0-29025  
 metals, brittle and plastic, energetic strength theories (*Bulgarian*) 0-38296  
 metals, deformation resistance, rel. between uniaxial stress state and breaking stresses in shear 0-3147  
 metals, dynamic compression testing, mech. behaviour 0-40464  
 metals, FCC, yield threshold at 4.2K, effect on strain-hardening curve (*Russian*) 0-50671  
 metals, hot plastic deform., stress/strain/time relations (*Russian*) 0-20968  
 metals, in-situ deform., 200 kV STEM study 0-47155  
 metals, mechanical props., testing and modelling 0-25811  
 metals, metallic deformation, improved boundary-integral eqn. calc. method 0-28437  
 metals, volumetric plastic deform., kinematic and static parameter calcs. (*Russian*) 0-34124  
 metals porous, mean principal stress in rolling without lateral expansion 0-25803  
 microstrains distrib. in macroinhomogeneous fields (*Russian*) 0-21018  
 Mossbauer absorbers, deformation induced texture 0-7214  
 Nimonic alloy reinforced Al, Cu and brass, laminated composites, low-temp creep singularities, structural defect changes (*Russian*) 0-11696  
 notch-tip geometry, influence on stress and strain distrib. 0-33535  
 nuclear reactor core materials, plastic deform. constitutive eqns. 0-35259  
 Nylon 6, plasticized with  $\text{NH}_3$ , deformation by solid-state extrusion 0-25736  
 ophiolitic peridotites structures, role of young lithosphere thrusting in subduction zones 0-56446  
 optical glass K8, torsional deform. above  $T_g$  under low stresses, temp. effect 0-21052  
 optical glass K8, torsional deform. above  $T_g$  under low stresses 0-25804  
 orthotropic spherical shells under blast loading, plastic response 0-33477  
 overthrust faulting, model of const. thickness overthrust on visco-plastic sole 0-51378  
 pentaplast, plasticized, thermal treatment effect on props. 0-40324  
 phenylene, deformability in physiological salt soln. 0-12305  
 pipe containing water, pressure pulse propagation 0-33475  
 pipe stability and plastic deform. under external couples 0-19259  
 plane strain deformation of strain rate sensitive materials, finite element anal. 0-1441  
 plane-strain formulation of elastic-plastic constitutive laws 0-23918  
 plastic foil, Li ferrite clad, thermal deform. (*Polish*) 0-30002  
 plate, annular, limiting load determ. 0-38295  
 plate of plastic material, dynamic deflection 0-23915  
 plates, rectangular, hinge-supported, eccentrically applied, ultimate point load, kinematic solutions 0-53638  
 PMMA with stress-raising flaw, deform. 0-25799  
 p-polyamide based organic fibres, effect of temp. and deform. time, on deform. strength props. 0-11720  
 polyamide-polyoxirane copolymers, mechanical properties evaluated 0-11700  
 polybutene-1 film, deform. mechanism, rheo-optical meas. 0-21041  
 polybutene-1 film, tubular-extended, anal. of orientational and form birefringence 0-29712  
 polycapromide, oriented, molecular rearrangements during deformation, IR spectra exam. 0-7644  
 polycrystalline metal, detect. using photoacoustic microscope 0-35435  
 polycrystals, deform. during cooling, revealed by deposited graphite layer (*Polish*) 0-25755  
 polycrystals, single phase, stress strain relations by X-ray diffraction (*Russian*) 0-5999  
 polyethylene, cryst., transverse deform. and transverse movement of defects 0-38958  
 polyethylene, deformation, Hartree-Fock SCF calcs. 0-18949  
 polyethylene, doubly oriented, low density, deformation and structure, exam. 0-11705  
 polyethylene, high mol. wt., deformability in physiological salt soln. 0-12305  
 polyethylene, hip joint prosthetic component deformation meas. by holographic interferometry (*German*) 0-12302  
 polyethylene, low density,  $\alpha$  mgch. dispersion in relation to spherulite deform. mech. 0-25781  
 polyethylene, oriented, shear strain, effect on struct., props. (*Russian*) 0-7656  
 polyethylene, ultra-oriented high density, shrinkage as meas. of deformation efficiency 0-40398  
 polyethylene, ultradrawn, electron microscope exam. of struct. after annealing 0-11662  
 polyethylene crystals, plastic deformation, molecular mech., TEM obs. 0-21022  
 polymer endoprosthetic joint, fatigue life 0-40521  
 polymer film re-stretching, elasto-plastic behaviour calc., using finite element analysis (*Japanese*) 0-7621  
 polymers, anal. of mechanics of solid phase extrusion 0-39204  
 polymers, filled, light scattering in deformation 0-11718  
 polystyrene, isotactic crystals, plastic deformation, molecular mech., TEM obs. 0-21022  
 polyurethane, filled, relation between static and dynamic deform. characts. 0-3137  
 porous bodies, anal. using plasticity theory 0-25802  
 porous metal, yield stress variation during cold deformation 0-16395  
 porous metal gauze materials, struct. and hydraulic characts. 0-11729  
 precipitate hardened material, intergranular cavity growth inhibition 0-50677  
 PVC, rigid, craze and yield zones in fracture 0-50701  
 PVC, stress relaxation in macrodeformation range 0-16370  
 PWR fuel cladding, long ballooning deformation following LOCA 0-660  
 quartz, US absorption, influence of plastic deform. and electrostatic field (*Russian*) 0-39226  
 refractory metals, mech. props. and diffusion figures (*Russian*) 0-40436



# plastic deformation continued

reinforced composites, strength and deformation anisotropy, numerical characts. 0-38285

Rene 95, as hot isostatically pressed (HIP) and HIP+forged, low cycle fatigue 0-25854

rigid perfectly plastic strip, plane strain compression between parallel dies with slipping friction 0-48603

rigid-plastic dynamics, large deformation, extremum, principle 0-53642

rings, plastic, large deforms., plasticity and hardening effects 0-43627

rod, cantilevered, with attached mass at end, plastic deform. under seismic effect (*Russian*) 0-53653

rolling, determ. of stress distrib. in rolled material 0-48651

rolling, inhomogeneous deformation model 0-48650

rough surface, plastic deformation in mechanical contact 0-14583

rubber, strain-energy density function 0-25773

rubberlike materials, finite plane strain deformations, finite element anal. 0-28438

sapphire:Ti<sup>4+</sup>, plastically deformed, precipitation hardening, TEM study 0-7592

sea ice, plastic deform. rel. to dynamic thermodynamic model 0-51432

shape-memory alloys, props. and appl. 0-30049

shear band formation models, in rolling and extrusion 0-3152

sheet drawing, slip line field for mid-plane cracking or splitting 0-50648

sheet metal deformation, criteria for determ. of deformation limit G (*German*) 0-21000

shell, internally exploded, displacement meas. by photometric method 0-14642

shell, shallow spherical, plastic deformation under explosive loading 0-14589

single crystals, fatigued age-hardenable, dislocation structure (*German*) 0-54247

slip, non-crystallographic, in cubic cryst., algebraic determ. (*French*) 0-2112

smooth pipe bend, plastic limit moment under in-plane bending 0-23906

soil mechanics, elastoplastic deformation, volumetric constitutive equation 0-53655

speckle correlation and interferometry for planar deformation analysis (*Dutch*) 0-32930

spherical shell, shallow radially ribbed, stress state, struct. parameters influence 0-14581

split Hopkinson pressure bar use in obtaining dynamic stress/strain data at const. strain rates (*Japanese*) 0-16630

statistical-kinematic analysis and limit equilibrium of systems with unilateral constraints 0-1451

steel, 11423, cyclic stress anal. within hysteresis loop (*Czech*) 0-30031

steel, 18H2N4WA, hot-worked, kinetics of austenite grain growth, rel. to deformation degree (*Polish*) 0-45322

steel, 3Kh2V8F, brittleness depend. on high temp. deform. at high stress. temp. (*Russian*) 0-50698

steel, 50N29 type, self-consistent junctions and spatial relative organisation 0-19750

steel, acoustic-emission analysis of fracture-toughness tests 0-55596

steel, alloy, high speed, cutting tools, carbide heterogeneity change during hot extrusion 0-16390

steel, alloy, high speed, type R18, hot deformation and recrystn. 0-16391

steel, alloy 40Kh, sulphide cracking resistance, strengthening method influence 0-55577

steel, austenite hot deformation influence on phase transformations 0-7606

steel, austenitic, Cr-Mn, metastable, plasticity, contrib. of martensitic transform. during deform. (*Russian*) 0-30018

steel, austenitic, high-temp. crack resist., B and Mo influence (*Russian*) 0-16435

steel, austenitic Cr-Mn, M<sub>23</sub>C<sub>6</sub> carbide precipitates comp., heat and thermomech. treatment influence (*Russian*) 0-40361

steel, austenitic stainless, 08Kh18N10T, hot-worked precipitation kinetics and struct. of dispersed phases, Ti effect 0-29964

steel, austenitic stainless, 12Kh18N10T, deformed, phase comp. and props. after prolonged heating 0-30040

steel, austenitic stainless, fusion reactor blanket struct. material, low cycle fatigue behaviour 0-30073

steel, austenitic stainless, microdeform. meas. using method of grids 0-55615

steel, austenitic stainless, stacking fault effect on martensitic transform. during plastic deform. (*Russian*) 0-25696

steel, austenitic stainless wires, phenomenology of cold twisted deformation (*French*) 0-21030

steel, austenite-martensitic, struct. changes during plastic deform., mutual influence of phases (*Russian*) 0-30015

steel, C, deformation strength and strain rate depend. under plain strain state (*Japanese*) 0-30028

steel, C, effect of pre-straining on torsional fracture strain (*Japanese*) 0-3183

steel, C, failure mechanisms in impact fatigue 0-40493

steel, C, fracture dynamics at high frequency loading (*Czech*) 0-45391

steel, C, natural reinforced composite 0-30039

steel, C, naval, corrosion in harbour anaerobic sediments, rolling direction and tensile stress effects 0-30135

steel, C, naval, corrosion in natural seawater, rolling direction and tensile stress effects 0-30134

steel, C, pearlite grade ShKh15, struct. transformations, hot plastic strain influence (*Russian*) 0-20927

steel, C, strain ageing and fatigue limit 0-40378

steel, C content effect on annealing texture, plastic anisotropy and mechanical props. 0-29976

steel, cast structural, heat treatment and mech. working influence on mech. props. (*Russian*) 0-40392

steel, Ck45, tension-compression tests, cyclic, macroscopic changes of length (*German*) 0-40424

steel, Ck 45, cylindrical bodies rolling over one another, plastic deformations caused by frictional forces 0-11735

steel, Co-Cr-Ni-Mo-Mn (39.65, 20.25, 15.33, 7.08, 1.9 wt.%) carbide formation during tempering after plastic deformation 0-16330

steel, Cr-Mo-V, biaxial cyclic deformation behaviour 0-21057

steel, Cr-Mo-V and stainless, biaxial cyclic deformation behaviour 0-16431

steel, Cr-Ni (1.47, 1.48 wt.%), lath martensite microstruct. and props., cold rolling effect 0-55422

steel, Cr-Ni-Mo, dynamic and static softening behaviour at hot forming temp. (*German*) 0-25728

# plastic deformation continued

steel, deform. resist., softening effects, analytical depend. calcs. (*Russian*) 0-49293

steel, deform. resist. during continuous hot rolling (*Russian*) 0-55462

steel, deformation and stresses during elongation, application of Ludwig eqn. (*German*) 0-40475

steel, ductile fracture in presence of elongated sulphides (*French*) 0-45394

steel, eutectoid, anisothermal strain with phase transform., effect on tensile strength (*Russian*) 0-40431

steel, flat bars, stress meas. and calc. around drilled hole, with hole-gage-rosettes aid (*German*) 0-25757

steel, grain boundary strengthening mechanism 0-35207

steel, high alloy, strain induced martensite and austenite influence on crack formation (*Russian*) 0-21007

steel, high Si dual-phase, mech. props and microstruct. anal. 0-40444

steel, hollow cylinder, thick walled, effect of thermomech. treatment 0-11674

steel, HT60, fatigue crack propag. work coeff. 0-16422

steel, hypereutectoid, austenite dissociation depend. on strain at intercritical temps., pearlite transform. (*Russian*) 0-40362

steel, Kh2G2P, high-temp. plastic strain influence on austenite transformation kinetics (*Russian*) 0-21004

steel, low C, appl. of microbeam X-ray technique to plastic zone size evaluation 0-3199

steel, low C, plastic deformation by pencil glide, r-values and yield loci 0-7654

steel, medium C, deform. hardening, plasticising action of Sn-Zn melts 0-55415

steel, medium C, isothermally quenched, high-temp. deform. effects on struct. and props. (*Russian*) 0-25760

steel, mild, orientation distribution function, representation of texture and slip directions 0-11665

steel, mild, plastic deform. around fatigue cracks, X-ray microbeam and recrystn. studies 0-35258

steel, mild, tensile and cyclic loading effect in Barkhausen noise 0-40560

steel, mild, tensile deformation, behaviour under high pressure (*Japanese*) 0-16381

steel, Mn, Mn influence on martensitic transform in presence of strain (*Russian*) 0-20934

steel, Mn-Cr-B (1.46, 1.03, 0.003 wt.%) 0-55422

steel, Ni(9 wt.%), isothermal bainitic transform., thermomechanical effects on mech. props. (*German*) 0-40383

steel, Ni-Co-Mo (17.55, 8.02, 4.92 wt.%) maraging, lath' martensite microstruct. and props., cold rolling effect 0-55422

steel, Ni-Cr-Mo, quenched and tempered, notched bar tensile tests (*German*) 0-35247

steel, pearlitic, heat-resist., secondary phase precipitation, deform., and fracture during creep (*Russian*) 0-50669

steel, plastic deform. effect on third-order elastic moduli, dislocation anharmonism (*Russian*) 0-50786

steel, plastic deformation, C distrib. (*Ukrainian*) 0-50668

steel, plastic deformation and cryst. texture in equibiaxial expsn. 0-7653

steel, plastic deformation zone, caused by crack, extent determ. with microhardness, surface roughness, measurements (*French*) 0-7682

steel, plastically deformed, force and speed criteria interactions during hot rolling (*Russian*) 0-55463

steel, quasi-cleavage fracture (*Chinese*) 0-21060

steel, stainless, clad Al, sandwich sheet material, forming limits 0-3131

steel, stainless, cold plastic deform. effect on struct. and props. 0-29113

steel, stainless, EBR-II fuel pin cladding, obs. of in-reactor creep and swelling 0-13600

steel, stainless, failure analysis at elevated temperatures 0-55499

steel, stainless, FBR fuel pin cladding strain under transient testing 0-18425

steel, stainless, fibre reinforced Al alloy, exam. of deformation, fracture and forging behaviour 0-11681

steel, stainless, in-reactor deformation and fracture behaviour of EBR-II driver fuel cladding 0-42769

steel, stainless, martensite nuclei obs., role of defects in nucleation 0-25693

steel, stainless, sensitised type 304, cyclic loading effect of SCC susceptibility in water 0-45428

steel, stainless, single crystals, shear cracks, electron microscope study 0-40522

steel, stainless, spherical shell with reinforced holes, local stability 0-50686

steel, stainless AISI 316, biaxial cyclic deformation behaviour 0-21057

steel, stainless SUS 304, fatigue crack propag. work coeff. 0-16422

steel, stainless type 03Kh13AG19, deformation temp. influence on dislocation struct. (*Russian*) 0-11698

steel, stainless type 304 L, mech. behaviour under constant stress associated with cyclic strain 0-25767

steel, stress and strain intensity, determ. after plastic deform. using microhardness meas. 0-40641

steel, stress relaxation in cyclic deformation 0-3119

steel, tempered, high strength, internal stresses and mech. props. 0-3200

steel, thread rolled, Moire fringe method for examining local deform. zones 0-21220

steel, type 12KhN4MDA, deformation and fracture props. on extension and twisting (*Russian*) 0-55504

steel, type 1Kh17N2, white zone formation and props. during friction in vac. (*Russian*) 0-40542

steel, type 4340, shear-band temp. meas. 0-48655

steel, types 45 and U8, plastically deformed, magnetoelastic props. (*Russian*) 0-44893

steel, V containing dual-phase, yielding and strain ageing, early stages 0-25794

steel, Zn coated, cold rolling influence on struct. and deform. of diffusional layer (*Russian*) 0-55465

steel, Zn coated strips, plastic deformation. influence on struct. and quality- (*Russian*) 0-40377

steel 20, deformation process, stage-by-stage nature investigation using acoustic emission (*Russian*) 0-40434

steel fatigue in surface active media, adsorption facilitation mech. 0-55586

steel granular model material, equipment for shear deform. investigation (*German*) 0-35449

steel ingot, state of viscoelasticoplastic stress deformation, in process of solidification (*Russian*) 0-45295

steel tubes, square section, collapse in bending 0-25792



## plastic deformation continued

- steels, austenitic stainless, crack propag. rates under high-temp. low cycle fatigue conditions 0-21088
- steels, heat-treated, nature of high sensitivity to stress raisers 0-21051
- steels, hot forming property and struct. (*German*) 0-25730
- steels, hot plastic strain, stress-strain-time dependences (*Russian*) 0-40430
- steels 2Kh13 and 20Kh1M1FTR, sulphide cracking resistance, strengthening method influence 0-55577
- stee, austenitic stainless, deformation process, stage-by-stage nature investigation using acoustic emission (*Russian*) 0-40434
- stored energy, and increment in heat capacity due to plastic deform. 0-54302
- strain trajectories of constant curvature for plastic deformation 0-48591
- stress dip technique for effective stress determination in cyclic straining 0-2113
- stress/strain relation, rate and temp. depend., analytic formulation 0-40466
- stretched plate with noncircular hole, stability anal. (*Ukrainian*) 0-53661
- structural phase transition induced refractive index changes in crystals. 0-16000
- superconducting transition, effect on jump-like deform. (*Russian*) 0-34538
- superconductors, plastic deformation, Cooper pair scatt. model 0-39709
- supersonic gas jet, penetration into the ground (*Russian*) 0-28544
- surface damage, plastic deformation cause in fatigue, wear, fretting and rolling fatigue 0-40537
- surface dislocation anal. of plastically bent cryst. 0-2019
- tension test, computer simulation, effect of testing conditions 0-7729
- tension tests, analysis of misalignment 0-11864
- thermoplastic body at finite deformations, incompressible plastic deformation (*Russian*) 0-53651
- thermoplastic recorder development, interaction of regular and chaotic deformation (*Russian*) 0-42291
- thermoplastics, structural changes during deformation, rel. to impact resistance 0-25800
- thin film bicrystals, dislocation interaction, with grain boundaries during plastic deform. electron microscopy technique 0-54281
- Timoshenko shells with curved openings elastic-plastic deformation under impulsive loading 0-33483
- toluene sulphamate diacetylene polymer, vibr. modes, strain depend. using Raman spectra 0-20626
- Tresca type plastic material, simple shear deform. with combined work hardening (*Japanese*) 0-35206
- two layered parallelepiped under large elastoplastic deformations, deformation instability 0-33499
- unidirectionally reinforced composites, large deflection, plastic constitutive relations 0-43624
- viscoplastic thin walled systems, stability (*Russian*) 0-1452
- welding, transient longitudinal strain changes meas. 0-16332
- X-ray analysis methodology appl., wide-angle (*German*) 0-3283
- Zircaloy PWR fuel cladding, balloon deformation during LOCA 0-659
- Zircaloy reactor fuel cladding tubes, high temp. deformation model with nonlinear temps. 0-661
- Zircaloy tubing, I<sub>2</sub> stress corrosion cracking, pellet cladding interaction mechanism (*German*) 0-16565
- Zircaloy-2, deformation and fracture behaviour, uniaxial tension test in I<sub>2</sub> environment 0-13580
- Zircaloy-2, iodine environment, plane strain tension test 0-22944
- Zircaloy-2, neutron irradiated, inhomogeneous deformation behaviour 0-50679
- Zircaloy-4, microstrain and particle size meas. by Warren-Averbach method 0-55420
- Zircaloy-4 fuel cladding axial deform. in PWR LOCA 0-13585
- Ag, (211)[111] single crystals, shear band effects on rolling deformation 0-50651
- Ag-Cu (8 wt.%), deformed, free energy changes in process of discontinuous precipitation 0-3054
- Ag-Cu (8 wt.%), plastic deform. effect on discontinuous precipitation 0-3053
- Al alloy 2219-T87, sheet, fatigue tested, fracture surface rotation mechanism 0-11764
- Al alloy stress/strain curve, in reverse loading process (*Japanese*) 0-7622
- Al cell structures produced by cycling and monotonic creep 0-55452
- Al, cold-worked, plastically deformed, internal friction spectrum, Haseguti peaks associated with dislocations 0-7618
- Al, crit. resolved shear stress, orientation depend. 0-21001
- Al crystal, lattice rotation during tensile deform., X-ray diffr. meas. 0-49231
- Al, cyclic torsional deformation, final texture 0-7595
- Al, defects formed during cryst. growth or by plastic deform., X-ray transmission topography obs. (*Russian*) 0-25761
- Al, deformed in tension, elec. cond. changes at 78 and 283K, grain boundary effect (*Japanese*) 0-30029
- Al, electron drag on mobile dislocations at low temps., strain rate, temp., and field depend. 0-19808
- Al films, appl. of current noise technique for dislocation processes 0-35442
- Al, grain boundary sliding and deformation mechanism maps 0-3128
- Al, He bubble behaviour during high plastic deform. 0-29087
- Al, lattice resistance stress, Bordoni relax., microdeform. and US attenuation results 0-25747
- Al, oxidation, influence on deformation map 0-40599
- Al, plastic deform. effect on third-order elastic moduli, dislocation anharmonism (*Russian*) 0-50786
- Al rings, deformation modes under static axial compression 0-25768
- Al sheet D16AT, plastic strain distrib. at crack tip by coordinate-grid method 0-16400
- Al, type 2014-T6, shear-band temp. meas. 0-48655
- Al, vacuum condensate, struct. and mech. props. depend. on deposition conditions 0-15417
- Al wire, hot and cold deformation drawing strengthened, thermal EMF study (*Russian*) 0-54674
- Al-Ag (40 wt.%), deformed, free energy changes in process of discontinuous precipitation 0-3054
- Al-Ag (40 wt.%), plastic deform. effect on discontinuous precipitation 0-3053
- Al-alloy, type 6351 and 6061, stress relaxation in cyclic deformation 0-3119
- Al-alloy, type PA6, under complex cyclic loading, behaviour of stress strain diagrams 0-16372
- plastic deformation continued
- Al-Cu (4 wt.%) partially coherent precipitation hardened alloy, high temp. cyclic deform. 0-25710
- Al-Cu full coherent precipitation hardened alloy, high temp. cyclic deform. 0-25711
- Al-Cu-Mg, acoustic emission during tensile testing 0-7632
- Al-Cu-Mg, type 2036, deformation at ageing temp., effect on struct. and props. 0-7605
- Al-Cu-Ni, alloy RR 350,  $\theta'$ -hardened, deform. induced microstructural instability, high temps. 0-16321
- Al-CuAl<sub>2</sub> eutectic, heat treatment and interlamellar spacing effect on tensile deformation 0-29979
- Al-Mg, acoustic emission during tensile testing 0-7632
- Al-Mg, ageing process, effects of Ag additions and pressure (*Russian*) 0-45321
- Al-Mg spherical shell with reinforced holes, local stability 0-50686
- Al-Mg<sub>2</sub>Si(1.42 wt.%), aged, dislocation structs. caused by plastic deformation 0-25786
- Al-Mg-Si, DTA exam. after small and medium deform. 0-21002
- Al-rare earth alloys, granules, rolling to form foil, exam. 0-20825
- Al-Si, deformed, local lattice rotations at second phase particles 0-25709
- Al-Zn (3.9 wt.%), single crystals, fatigued age-hardenable, dislocation structure (*German*) 0-54247
- Al-Zn (40/50)(65) wt.%, deformed, free energy changes in process of discontinuous precipitation 0-3054
- Al-Zn (40/50)(65) wt.%, plastic deform. effect on discontinuous precipitation 0-3053
- Al-Zn-Mg, plastic deform. influence on structural transform. and mechanical props. (*Russian*) 0-7623
- Al<sub>4</sub>Cu<sub>9</sub>, rhombohedral  $\gamma$ -brass, direct imaging of struct. and structural defects 0-15115
- Al<sub>8</sub>Mn<sub>3</sub>, rhombohedral  $\gamma$ -brass, direct imaging of struct. and structural defects 0-15115
- Al<sub>2</sub>O<sub>3</sub>, dynamic deform., stress-wave response 0-21020
- Au-Ni-Cu-Zn, white gold, metallographic struct., heat treatment and plastic working effect 0-40403
- B<sub>2</sub>O<sub>3</sub>, vitreous, torsional deform. above T<sub>g</sub> under low stresses, temp. effect 0-21052
- B<sub>2</sub>O<sub>3</sub>, vitreous, torsional deform. above T<sub>g</sub> under low stresses 0-25804
- Be, polycryst. plasticity, cleavage strength, ductility transition temp. 0-44250
- Be, wire, elec. cond., heat treatment and strain effects (*Russian*) 0-24870
- Be-bronze BrB2, struct. and phase transform. during mechano-thermal treatment (*Russian*) 0-11667
- n-Bi<sub>2</sub>Te<sub>2.8</sub>Se<sub>0.12</sub>, extrusion deformed, powder dispersion degree influence on thermal and elec. props. (*Russian*) 0-39366
- C fibre reinforced plastic multilayer laminate, strength and deform. (*Russian*) 0-30019
- C fibre reinforced plastic, deform. and failure using AE method (*Russian*) 0-40630
- CaF<sub>2</sub> antireflection coated, 3.8  $\mu$ m CW laser damage threshold obs. 0-33053
- CaF<sub>2</sub>, plastic deform, work hardening regions, TEM obs. 0-3140
- Cd, electronic properties depend. on 2<sup>1/2</sup>-th order phase transition under high press. (*Russian*) 0-11128
- Cd-Zn single crystals, crit. resolved shear stress at low temps. 0-3138
- Cd,Hg<sub>1-x</sub>Te, correlation between structural and chemical inhomogeneity (*Russian*) 0-49484
- CdS, deformed, dislocation struct., TEM obs. 0-54250
- CdS, dislocation structural optical absorpt., plastic deformation (*Russian*) 0-34959
- CdS, plastically deformed cryst. with dislocation slip band, residual cond. 0-6839
- Co, deformed, microstruct. singularities in pre-transform. temp. range (*Russian*) 0-45347
- Co, internal friction anomalies in spin reorientation temp. range (*Russian*) 0-49299
- Co-Fe, internal friction anomalies in spin reorientation temp. range (*Russian*) 0-49299
- Co-Ni, deformed and isochronally annealed, positron lifetimes, annihilation at dislocation trapped monovacancy 0-55221
- Co-Ni alloy, slip charact., and fatigue, FCC twinning and FCC to HCP martensite transform. effect 0-35182
- Cr bronze Sn, recrystn. props., hot rolling, annealing, polygonisation (*Russian*) 0-55419
- Cr-Co-Fe permanent magnet anisotropic alloys, plastic deform., ageing, particle alignment temp. 0-35254
- Cr-Ni VKh-4 alloy, deformation and fracture mechanism investigation (*Russian*) 0-11738
- CsCl, twin form. by compressive stress during phase transform. 0-49358
- CSl, exam. of kinking process, using cholesteric liquid crystals 0-7629
- Cu, cold rolling, mechanical props., ageing, annealing, recrystallisation, plastic strain (*Russian*) 0-35202
- Cu cyclic torsional deformation, final texture 0-7595
- M-1Cu, deformation process, stage-by-stage nature investigation using acoustic emission (*Russian*) 0-40434
- Cu, deformed, defects, thermal relaxation, positron experiments (*German*) 0-50455
- Cu, elastic modulus and internal friction during plastic deform., dislocation props. determ. 0-35244
- Cu, electron drag on mobile dislocations at low temps., strain rate, temp., and field depend. 0-19808
- Cu, electron irradi. at 100K, comparison of irradi. hardening with dislocation vel. 0-54284
- Cu, fatigued single crystals., temp. depend. of saturation stress and dislocation substruct. 0-44211
- Cu, friction mechanism, HV TEM expts. 0-35341
- Cu, MIE, yield stress decrease in compression, rel. to previous elongation (*Polish*) 0-50665
- Cu, microplastic deform. and amplitude depend. of internal friction (*Russian*) 0-45349
- Cu, polycrystn., stress relaxation in cyclic deformation 0-3119
- Cu, single crystals., fatigued, random strain amplitude cycling 0-3146
- Cu, single crystals., hysteresis behaviour implications rel. to fatigue, plastic strain cycling 0-3191
- Cu, vacuum condensate, struct. and mech. props. depend. on deposition conditions 0-15417
- Cu, virgin surface, contact formation and cohesion, influence of multiple contacting (*Russian*) 0-40548
- Cu wires, electrolytic, Young's modulus, working temp. effects 0-50667



## plastic deformation continued

- Cu-Ag (8 wt.%), deformed, free energy changes in process of discontinuous precipitation 0-3054
- Cu-Ag (8 wt.%), plastic deform. effect on discontinuous precipitation 0-3053
- Cu-Al, single crystals, hysteresis behaviour implications rel. to fatigue, plastic strain cycling 0-3191
- Cu-Al, vacuum condensate, struct. and mech. props. depend. on deposition conditions 0-15417
- Cu-Al-Ni, long period martensite phases, X-ray diffr. obs. 0-7571
- Cu-Al-Ni(Mn), duplex shape memory effect after nonuniform plastic deform. (Russian) 0-25759
- Cu-Au, cold worked solid solution, flow stress and activation volume 0-16393
- Cu-Au(Ni)(Zn), elastic modulus and internal friction during plastic deform., dislocation props. determ. 0-35244
- Cu-Be (2 wt.%), plastic deformation influence on ageing, granular microhardness (Russian) 0-55474
- Cu-Be-Ni-Ti-Mg bronze, alloying element influence on minimum thermo EMF, cold working (Russian) 0-34426
- Cu-Co (2 wt.%), single crystals, fatigued age-hardenable, dislocation structure (German) 0-54247
- Cu-Ga, high dislocation density alloys and oxide precipitated struct., NMR, spin echo 0-39892
- Cu-Ge single cryst. containing heavily faulted regions, X-ray diffr. profiles 0-24462
- Cu-Nb-Sn, multifilamentary supercond. composite wires, fabrication on laboratory scale and mech. props. 0-29897
- Cu-Ni, cold worked solid solution, flow stress and activation volume 0-16393
- Cu-Ni-Sn (10, 6 wt.%), temp. depend. of yield stress and work hardening 0-21026
- Cu-Si, high dislocation density alloys and oxide precipitated struct., NMR, spin echo 0-39892
- Cu-SiO<sub>2</sub>, deformed, lattice rotations at second phase particles 0-25709
- Cu-Zn, cold worked solid solution, flow stress and activation volume 0-16393
- $\beta$ -Cu-Zn-Al (27.5, 4.0 wt.%), strain induced martensite, exam. of structure, microstructure 0-7648
- Cu<sub>2</sub>O, thermal activation of plastic deform. (French) 0-16394
- Fe, deformed, deep trapping states for H<sub>2</sub> 0-29045
- Fe, deformed, defects, thermal relaxation, positron experiments (German) 0-50455
- Fe, electroplated with soft Fe coating, fatigue fracture, struct. characts. 0-55524
- Fe, grade EA, plastically deformed, magnetoelastic props. (Russian) 0-44893
- Fe, high purity single crystals, thermally activated slip deformation between 4.2 and 300K 0-25801
- Fe, point defect estimation from specific heat and volume in plastically deformed pure metals (Russian) 0-54223
- Fe single crystals, size effect on slip deformation ability at very low temps. 0-21049
- Fe, sintered, strength and elongation, rel. to density 0-30047
- $\alpha$ -Fe, strengthening kinetics due to deformation ageing, impurity atom sources (Russian) 0-55435
- Fe, US oscillatory stress superimposition effects on deformation 0-35287
- Fe whiskers, elastically and plastically deformed, mag. domain structs. 0-15752
- $\alpha$ -Fe, yield point behaviour for extremely inhomogeneous deformation (German) 0-55453
- $\alpha$ -Fe, yield point behaviour in homogeneous plastic deformation (German) 0-35248
- Fe-Al, deformed, low temp. recovery of elec. resist. (Russian) 0-7697
- Fe-Cr-Mo (26, 1 wt.%), single crystals and polycrystals, strain rate influence on low cycle fatigue props. 0-3126
- Fe-Cr-Ni austenitic alloy, cold deformed,  $\alpha$ - $\gamma$  transition, calorimetric study (Russian) 0-55390
- Fe-Mn (-C), Mn influence on martensitic transform in presence of strain (Russian) 0-20934
- Fe-Mn (15/24)(30)wt.%, high hydrostatic pressure influence on stress-strain curve 0-25805
- Fe-Ni (23 wt.%), struct., composition changes during  $\alpha$  to  $\gamma$  transform., martensite plastic deformation influence (Russian) 0-11642
- Fe-Ni single crystal, lattice strain induced by anisotropic distrib. of M<sub>2</sub> (Japanese) 0-35262
- Fe-Ni solid solution, deformation mechanism, softening phenomena, dislocation-solute atom interactions (French) 0-45344
- Fe-Ni-C, plastic deform. effect on austenite stabilisation (Korean) 0-21021
- Fe-Ni-C (31, 0.1 wt.%), pre-deformation and temp. effect on transformation-deformation behaviour 0-3127
- Fe-Ni-C (31, 0.28 wt.%), crossings of thin plate martensites, TEM obs. 0-25756
- Fe-Pt, plastic deform. effect on struct. singularities and mag. props. (Russian) 0-44892
- Fe-Si, maze domains upon appl. of horizontal mag. field or mech. tension 0-11218
- Fe-Si, microplastic deform. and amplitude depend. of internal friction (Russian) 0-45349
- Fe-Si (3 wt.%), fatigue crack propag. work coeff. 0-16422
- Fe-Si (3 wt.%), single crystals and polycrystals, strain rate influence on low cycle fatigue props. 0-3126
- Fe-Si (3 wt.%), US oscillatory stress superimposition effects on deformation 0-35287
- Fe-Si (3 wt.%) locally deformed, EM loss depend. on cryst. struct. and orientation (Russian) 0-7694
- GaAs, deep radiation centres from heat treatment,  $\gamma$ -irrad., deform., probability of nonradiative electronic transitions 0-50408
- n-GaAs, deform. produced deep levels, DLTS meas. 0-54634
- GaAs, during deformation, acoustic emission rel. to cracks, dislocations 0-35441
- GaAs, plastically deform., photocond., spectral response and decay process 0-29435
- GaP, birefringence observations of strain and plastic deform. 0-50678
- Ge, low-temp. dislocation cond. mechanism in plastically-deformed pure samples 0-15527
- n-Ge, plastically deform., dislocation state spectrum, photocond., elec. cond., and Hall const. meas. (Russian) 0-2362
- Ge, plastically deformed low temp. cond. (Russian) 0-6831
- Ge, self-diffusion, dynamical recovery 0-29215

## plastic deformation continued

- Ge uniaxially deformed, cyclotron resonance of RF field heated hot holes, (Russian) 0-44925
- Ge<sub>2</sub>N<sub>2</sub>O, pressure induced tetrahedral tilting and deform. 0-24415
- KCl,  $\gamma$ -irrad., photoplastic effect and internal friction aftereffect 0-24529
- KCl, US plastic deform., dislocation struct. 0-19809
- KCl(Br)(I), single cryst., quenched, microstruct. around indentations 0-7628
- LiF, crystal, electron emission under uniaxial compression 0-7483
- LiF, plastic strain accompanying local rise in surface temp., of natural shear (Russian) 0-6411
- Mg, pure, Bordoni relax. behaviour after plastic deformation 0-20997
- MgO, crack propagation during in-situ deform., plastic zone formation 0-16468
- MgO, crystal, electron emission under uniaxial compression 0-7483
- MgO, hot-pressed, elasticity props. of polycrystals and single crystals 0-54301
- MgO single cryst., internal stresses and dislocation mobility, stress relaxation method 0-6413
- MgO(Al<sub>2</sub>O<sub>3</sub>), spinel, plastic deformation at 400°C 0-40453
- Mg<sub>2</sub>SiO<sub>4</sub>, forsterite, decorated dislocations 0-54245
- Mg<sub>2</sub>SiO<sub>4</sub>, microhardness variation, exam. using Vicker indenter 0-25849
- Mn-Y-Zn-Cd alloy, phase equilibria, plastic deformation, microhardness (Russian) 0-40334
- MnF<sub>2</sub>, piezo-optical effect, birefringence variation on uniaxial compression (Russian) 0-34887
- Mo alloys, dispersion-strengthened, plastic deform. and hardness, temp. depend. 0-3087
- Mo deformed single crystals, struct. state and dislocation splitting (Russian) 0-29029
- Mo, dislocation (100) density variation, deformation effects, dislocation stability (Russian) 0-15108
- Mo, dislocation structure inhomogeneity in electromachining crater zone, rel. to plastic deform., dynamic recovery (Russian) 0-16326
- Mo, orientation distrib. function depend. on deform. during cold rolling (Russian) 0-50647
- Mo single crystals, simulating initial stage of deformation in fatigue loading 0-35328
- Mo, single crystals, pressure magnitude influence in hydroextrusion on plastic strain mechanism (Russian) 0-21009
- Mo, single crystals, work hardening and softening in cyclic strain 0-20957
- Mo, sintered, fusion reactor blanket struct. material, low cycle fatigue behaviour 0-30073
- Mo-V-C, hot-worked, substructural hardening and high-temp. strength (Russian) 0-25731
- NaCl, crystal, electron emission under uniaxial compression 0-7483
- NaCl, electric field induced by homogeneous stresses 0-11343
- NaCl,  $\gamma$ -irrad., photoplastic effect and internal friction aftereffect 0-24529
- NaCl, hydrostatically compressed crystals, in easy glide stage, plastic deformation 0-7630
- NaCl, moving dislocations, interaction with defects, elec. effects meas. in plastic deformation (Hungarian) 0-10572
- NaCl, plastic deformation influence on shape recovery effects 0-6684
- NaCl whiskers, plastification in elec. field (Russian) 0-21010
- Na<sub>2</sub>O-SiO<sub>2</sub>-(B<sub>2</sub>O<sub>3</sub>) glass, torsional deform. above T<sub>g</sub> under low stresses 0-25804
- Nb and Nb-Zr (1 wt.%), fusion reactor blanket struct. material, low cycle fatigue behaviour 0-30073
- Nb, deformed,  $\alpha$ -peak in internal friction spectra 0-16368
- Nb, fusion reactor first wall material, cyclic deform. tests 0-30074
- Nb, local heating during abrupt strain, catastrophic slip band formation 0-7652
- Nb, plastic deformation effects on superconducting specific heat transition 0-20352
- Nb-H system, temp.-stimulated acoustic emission, hydride precip. 0-3044
- Nb-Zr-C (0.1, 0.01 wt.%) plastic deform. influence on electronic state of Nb atoms 0-40463
- Nb-Zr-C alloys, plastic deform. and annealing, dislocation struct. (Russian) 0-20951
- NbC, deformation behaviour during rubbing in wide temp. range 0-16486
- Nb<sub>3</sub>Sn fatigue effects in unidirectional composites, computer simulated model 0-35289
- NbTi, superconducting multifilamentary conductors, crit. current density, bending effects (German) 0-39727
- Ni, 200, high temp. cyclic deformation and hardening 0-21055
- Ni alloy, recryst. after hot deform. (German) 0-25716
- Ni, deformed, struct. form. during annealing, Ni<sub>3</sub>Al type ordered phase precipitation (Russian) 0-45325
- Ni, dislocation intersection and solution strengthening, effect of solute on obstacle profiles 0-7590
- Ni, dislocation structure parameter determ. due to plastic deformation (Russian) 0-54242
- Ni, dispersion strengthened, high-temp. cyclic deformation 0-21056
- Ni, electrical resistance in DC mag. field after ultrasonic deform. (Russian) 0-54671
- Ni, grain boundary sliding and deformation mechanism maps 0-3128
- Ni, high temperature cyclic deformation 0-16429
- Ni, high-purity, softening of strained single crystals (Russian) 0-40499
- Ni, point defect estimation from specific heat and volume in plastically deformed pure metals (Russian) 0-54223
- Ni, powder, subjected to vibratory milling, exam. of plastic deformation, recrystallisation, sintering 0-16234
- Ni single crystal, stretched, electron microscope exam. of deformation cell structure during polygonization (German) 0-7651
- Ni, transport of H, effect of plastic deformation 0-21044
- Ni/Cr-Fe-C, Inconel, dislocation intersection and solution strengthening, effect of solute on obstacle profiles 0-7590
- Ni-base superalloy, microscopic inhomogeneity of plastic strain influence on fatigue cracks (German) 0-40470
- Ni-Co, dislocation intersection and solution strengthening, effect of solute on obstacle profiles 0-7590
- Ni-Cr, deformed, struct. form. during annealing, Ni<sub>3</sub>Al type ordered phase precipitation (Russian) 0-45325
- Ni-ThO<sub>2</sub>, dispersion strengthened, high temperature cyclic deformation 0-16430
- Ni-Ti(Fe), neutron irradiated, thermally activated deform. 0-6438
- Ni-W surfaces in contact, deform. and adhesion at very low loads 0-39457



**plastic deformation continued**

- Ni-Zn ferrite, grain size depend. of grain boundary sliding (*Japanese*) 0-15120  
 Ni<sub>3</sub>Fe, nondislocation origin friction stress in alloys, deformation hardening 0-21050  
 Ni<sub>3</sub>Fe<sub>7</sub>O<sub>4</sub>, precipitation of  $\alpha$ -Fe<sub>2</sub>O<sub>3</sub>, optical microscopy, SEM and TEM studies (*French*) 0-11650  
 NiPt, short-range order, effect of plastic deform., electron diffr. anal. (*Russian*) 0-24403  
 Pb, dislocation electron drag coeff. temp. depend., internal friction method, superconducting state 0-29031  
 Pb, SO type, commercial purity, local deform. meas., using Moire method 0-21219  
 Pb, thermal conductivity, in normal and supercond. states, 0.6-7.5K (*Russian*) 0-6815  
 Pb, virgin surface, contact formation and cohesion, influence of multiple contacting (*Russian*) 0-40548  
 Pb, work hardening, and recovery rates during steady state deformation, temp. and stress effect 0-45319  
 Pb-In (5%), supercond. mobile dislocation density, instantaneous flux change meas. 0-15670  
 (SN), deform. and defects, lattice strain, fibrillation 0-3139  
 Sb, electronic band struct. changes due to plane straining effects (*Russian*) 0-54602  
 p-Sb<sub>1.48</sub>Bi<sub>0.52</sub>Te<sub>3</sub>, extrusion deformed, powder dispersion degree influence on thermal and elec. props. (*Russian*) 0-39366  
 Si, deformed, photo-EPR of dislocations 0-11267  
 Si, plastically deformed, spin-depend. charge transport 0-6895  
 Si, polycrystalline, recrystn. after plastic deform. and annealing 0-3145  
 Si, self-diffusion, dynamical recovery 0-29215  
 Si wafers, scribing and subsequent fracture 0-11743  
 SrF<sub>2</sub> antireflection coated, 3.8  $\mu$ m CW laser damage threshold obs. 0-33053  
 Ti alloys, fatigue crack propagation resistance, grain size effect, exam. 0-11765  
 Ti commercially pure VTI-0, heterogeneity of strain field 0-35286  
 Ti, IMI-125, strain rate effect on mech. behaviour 0-3153  
 Ti, metal and alloys, compression at high strain rate, deformation anal. 0-25769  
 Ti, plastic deform. dynamics, mech. characts. and phys. props., effect of O<sub>2</sub> (*French*) 0-45353  
 Ti, point defect estimation from specific heat and volume in plastically deformed pure metals (*Russian*) 0-54223  
 Ti, pure plate, silver band formation in ductile fracture process (*Japanese*) 0-16445  
 Ti-6Al-4V, stress distrib. for steady axisymmetric extrusion 0-3103  
 Ti-Al-Mo-Sn alloy, elastically and plastically deformed, positron annihilation meas. of deformation 0-21038  
 Ti-Al-V (6, 4 wt.%), temp. distrib. for steady axisymmetric extrusion 0-11670  
 Ti-Al-V (6, 4 wt.%), temp. distrib. for steady axisymmetric extrusion numerical results 0-11671  
 Ti-Al-V(Sn) alloys, plastic deformation and fracture characts. at low temps. (*Russian*) 0-7624  
 Ti-Mo-Zr-Sn (11.5, 6, 4.5 wt.%), metastable beta III phase, recrystallization and grain growth 0-3091  
 Ti-Ni, effect of alloying on crit. points and martensitic transform. hysteresis 0-20935  
 Ti-Pd (0.15 wt.%), IMI-260, strain rate effect on mech. behaviour 0-3153  
 TiC, deformation behaviour during rubbing in wide temp. range 0-16486  
 TiC layers, on steel and cemented carbides, load-bearing capacities 0-40606  
 TiC-TiB<sub>2</sub>, strength and antifriction props. over wider range of concs. 0-50673  
 TiO<sub>2</sub> rutile single crystals, stoichiometric, dynamic strain ageing 0-50661  
 (U, Pu)C, ceramic fuel, plastic deform. behaviour at stress changes 0-35261  
 UO<sub>2</sub>-PuO<sub>2</sub>, ceramic fuel, plastic deform. behaviour at stress changes 0-35261  
 V, and V-H, fusion reactor first wall material, cyclic deform. tests 0-30074  
 V, purification and plastic props. 0-25810  
 V<sub>2</sub>Si, plastic deform. effect on supercond. props. 0-29500  
 W, powder, subjected to vibratory milling, exam. of plastic deformation, recrystallisation, sintering 0-16234  
 W surface layer struct. during milling, plastic deform., failure (*Russian*) 0-40586  
 W-Cu, porous material, skeletal type, produced by liquid phase sintering, exam. of mech. strength, determ. resistance 0-16245  
 W-Ni compact, sintering behaviour and workability (*Japanese*) 0-20822  
 WC, deformation behaviour during rubbing in wide temp. range 0-16486  
 WC-Co, elastic and plastic charact. 0-35280  
 WC-Co and WC-Co-TaC-TiC-NbC cemented carbides, microstructure, high temp. deformation, uniaxial plastic compression 0-40451  
 W<sub>2</sub>C and WC, plastic deform. under bending, 800-2200°C (*French*) 0-55482  
 Zn bicrystals, grain boundary slip in deform. 0-34008  
 Zn, density of basal dislocations, rel. to deforming stress, 1.5-300K (*Russian*) 0-29028  
 Zn polycryst., compressive strength, temp. and strain rate effects 0-16616  
 Zn polycrystals, deformation, grain sizes effect at room temp. (*Czech*) 0-45359  
 Zn single crystals, temp. and strain rate effects on strength, slip and twinning 0-16373  
 Zn, stacking faults, plastic deformation, due to laser beam irradi. (*Russian*) 0-15121  
 Zn, strengthening by electroplastic strain, surfactant effect (*Russian*) 0-20953  
 Zn-Al eutectoid alloy sheets, creep bulging 0-1439  
 Zr<sub>3</sub>Al, neutron irradi. effect on tensile props. 0-3156  
 Zr<sub>3</sub>Al, tensile props., surface preparation depend. 0-3155  
 ZrC-ZrB<sub>2</sub>, strength and antifriction props. over wider range of concs. 0-50673

**plastic flow**

- see also ductility; Luder's bands; necking; rheology  
 adiabatic plastic deformation, shearing phenomena, review 0-50692  
 $\beta + \gamma$  brass, two-phase, acoustic emission from  $\beta'$  plastic flow and  $\gamma$  cracking 0-16452

**plastic flow continued**

- bulk moulding compound, flow state, closing speed effect (*Japanese*) 0-55469  
 constitutive equations derivation from Clausius-Duhem inequality 0-46804  
 crack tip plastic zone, thermal props. calcs. 0-7659  
 cylindrical shell, thick-walled, effect of non-homogeneity on plastic flow, numerical calc. 0-19248  
 dislocations model, compatibility with transient and steady state creep (*Italian*) 0-33487  
 Drucker postulate verification at high temp. 0-30025  
 Dugdale model validity limits for thin cracked plates under biaxial loading 0-43667  
 forming limit curve for bending processes 0-7627  
 fracture and plasticity, lattice-statics approach, review 0-39212  
 hot strip rolling simulation, by hot torsion technique 0-29990  
 isotropic strain hardening theory (*Russian*) 0-38279  
 lamination, hydrodynamic analogy, utilisation of current function (*French*) 0-19292  
 laser optical component props. depend. on material flow props. (*Russian*) 0-38047  
 metal, anisotropic, description of history dependent plastic flow behaviour 0-11732  
 metals, rolling of complex sections, unified anal. function of surface of strain focus (*Russian*) 0-21017  
 naphthalene single crystals, surface active substances effect on plastic flow 0-44248  
 polyethylene, high density, hydrostatic extrusion behaviour 0-50649  
 polyolefins, plastic flow, yield limit rel. to press. (*Russian*) 0-7657  
 Prandtl punch problem for case with eccentric forces (*Russian*) 0-23965  
 rigid/linear-hardening materials, axially symmetric radial flow 0-48604  
 steel, mild, annealed, plastic flow under proportional and non-proportional straining 0-40465  
 trigonal monocrystals, classes 3 and  $\bar{3}$ , plastic potential and yield stress (*Russian*) 0-29109  
 viscoplasticity with singular yield surfaces, side and corner flow rules, finite element applications 0-48594  
 Al alloys, stress-strain state after treatment by pressure, moire strip method appl. (*Russian*) 0-40648  
 Al and annealed alloy 5086, plain strain extrusion, photographic appl. 0-7626  
 Al, numerical smoothing of flow patterns 0-7625  
 Al, polycrystalline, acoustic emission energy release, grain size and flow stress depend. 0-11722  
 Al-Cu-Zr (6, 0.4 wt.%), superplastic flow activation energy 0-11701  
 Be, polycryst., plasticity and cleavage, yield and flow stresses 0-44249  
 Cd<sub>2</sub>Hg<sub>1-x</sub>Te, low temp. piezoresistance, Hall effect, elec. cond., plastic flow 0-6844  
 Cu-Au, cold worked solid solution, flow stress and activation volume 0-16393  
 Cu-Ge, single cryst., dislocation motion obstacles, effective strength 0-15107  
 Cu-Ni, cold worked solid solution, flow stress and activation volume 0-16393  
 Cu-Zn, cold worked solid solution, flow stress and activation volume 0-16393  
 Fe, cast, ductile, strain rate and temp., influence on strength, elongation and deformation (*Japanese*) 0-45356  
 Fe, H<sub>2</sub> charged, depend. of softening on specimen size, charging current density and strain rate 0-16455  
 Fe, quenched-in hydrogen, yield stress decrease of prestrained specimens 0-16454  
 Fe, softening and hardening by H<sub>2</sub> charging during tensile deformation 0-16453  
 Fe-Co(-V), plastic flow, order-disorder transform. effect on creep, traction and relaxation (*French*) 0-35180  
 Ge<sub>30</sub>Si<sub>70</sub>, hot press sintering 0-50572  
 LiF single crystals, glide band sources, work hardening 0-34126  
 MgAl<sub>2</sub>O<sub>4</sub> spinel, single cryst., fracture behaviour, temp. depend. 0-40503  
 Mo-Ti-Zr, alloy TZM, polycrystalline, anal. of elastic anisotropy and microyielding 0-30050  
 Ni<sub>3</sub>Fe, ordered, monocrystals, thermally activated deform. processes 0-50684  
 Ni<sub>49</sub>Fe<sub>29</sub>P<sub>14</sub>B<sub>6</sub>Si<sub>2</sub> glass, flow and failure 0-40438
- plastic strain** see plastic deformation
- plastic theory** see plasticity
- plasticity**  
 see also elastoplasticity; photoplasticity; superplasticity  
 alloys, brittle and plastic, energetic strength theories (*Bulgarian*) 0-38296  
 anisotropic hardening of initially orthotropic materials 0-33488  
 boundary value problem in general theory (*Russian*) 0-28441  
 constitutive equations derivation from Clausius-Duhem inequality 0-46804  
 Cosserat continuum, non-Reimannian geometrical theory of imperfections 0-53639  
 crack tips, yielding on inclined planes 0-33525  
 crystals, with diamond struct., vacancy formation energy rel. to plastic state transition temp. (*Russian*) 0-19795  
 diamond, optically active centre effect on strength props. 0-40462  
 dynamic plasticity experiments, review 0-35288  
 elastic-plastic body, weakened by double periodic slit system, antiplane strain 0-53657  
 endochronic plasticity, appl. to structural dynamic response of radioactive waste containers 0-16407  
 fatigue crack propag., plastic wake zone effect investigated with optical interference technique 0-55502  
 fracture mechanics, K<sub>IC</sub> values determ. in elastic-plastic material behaviour range 0-45376  
 glass, viscoplastic, gas-vapour interlayer problem 0-49490  
 glass-fibre reinforced PET, order-disorder transitions during extrusion 0-50633  
 heat transfer problem in plastic injection moulding 0-38242  
 isotropic and anisotropic raw materials, plastic pot. (*German*) 0-33474  
 isotropic material in plane stress, piecewise linear theory, plasticity 0-43622  
 isotropic plastic behaviour, role of body rotation in mathematical models 0-28432  
 kinematic hardening models, use in multi-axial cyclic plasticity 0-25717  
 lattice-statics approach, review 0-39212  
 limit load theory of ideally plastic body, duality problems 0-19254



# plasticity continued

localisability of deformations theory, representation 0-10163  
low cycle fatigue and plasticity testing, specimen verification 0-30202  
lubricant, shear rheological behaviour at high press. 0-35342  
medium with nonlinear uploading, plastic wave propag. 0-23913  
metal, cutting rel. to plasticity theory 0-16610  
metals, brittle and plastic, energetic strength theories (*Bulgarian*) 0-38296  
metals, viscoplastic behaviour anal. 0-6457  
metals and alloys, fatigue behaviour, vacuum effect, review 0-35309  
non-linear uniaxial integral constitutive equation incorporating rate effects, creep and relaxation 0-28436  
orthotropic dilatant bodies, plasticity theory, plane problems (*Russian*) 0-23910  
orthotropic strip, stress intensity factors and crack opening displacements 0-53710  
oxides, interaction between point defects and dislocations, cryst. plasticity 0-15149  
plane plasticity theory based on shear synthesis (*Russian*) 0-38281  
polymeric materials, inelasticity degrees estimation, hysteresis friction model appl. rel. to US testing 0-3136  
porous bodies, plastic deform. anal. using plasticity theory 0-25802  
problem soln. by symbolic computer processing of formulae 0-17803  
rigid perfectly plastic strip, plane strain compression between parallel dies with slipping friction 0-48603  
rolling process, math. model based on plasticity theory (*Russian*) 0-16335  
shells, thin, torispherical and internally pressurised, plastic collapse 0-28440  
sludge, cohesive, dynamic props. (*Japanese*) 0-45580  
steel, 3Kh2V8F, brittleness depend. on high temp. deform. at high stress. temp. (*Russian*) 0-50698  
steel, austenitic Mn-Ni ageing, alloying element influence on struct. and mechanical props. (*Russian*) 0-35256  
steel, C, corrosion cracking by sulphide, effect on props. 0-55587  
steel, high-temp. isothermic combined heat treatment and mech. working influence on struct. and mech. props. of 60S2 (*Russian*) 0-20969  
steel, killed ingots, freezing process, liq. core movement (*Russian*) 0-20921  
steel, low C, cyclic plasticity and low cycle fatigue life in variable amplitude loading 0-16433  
steel, low C, type 17G2SF, crack critical opening evaluation using plasticity diagram 0-45382  
steel, low-alloy, props. with nitride and Cu hardening at low temps. (*Russian*) 0-40372  
steel, martensitic low C, development and props. (*Russian*) 0-20933  
steel, mild, precracked Charpy bars, plasticity spread 0-16415  
steel, plasticity indices in anisothermal extension (*Russian*) 0-16378  
steel, rail, AE use for mech. tests 0-35467  
steel, stainless, wire, cold drawing 0-50650  
steel, ultra-high strength, H induced delayed plasticity and cracking 0-21100  
steel boiler tubes, Cr-Ni-Mo, austenisation conditions effects obs. 0-3151  
steel inclusions and plasticity, crystn. conditions influence (*Russian*) 0-20923  
steel transformer, Mossbauer atomic struct. anal., decarburising annealing, cold rolling (*Russian*) 0-11294  
steels, spring, 60S2A and 50KhFA, heat treatment and mech. working effect on mech. props. (*Russian*) 0-20962  
stress-strain relation anal. using anisotropic hardening plastic pot. 0-19250  
thermoplastic body at finite deformations, incompressible plastic deformation (*Russian*) 0-53651  
visco plastic torsion, prismatic bar, finite element solution 0-38282  
viscoplastic incompressible media, static and kinematic load limits 0-28430  
viscoplastic medium, wave-barrier interaction 0-14609  
viscoplastic thin walled systems, stability (*Russian*) 0-1452  
viscoplasticity with singular yield surfaces, side and corner flow rules, finite element applications 0-48594  
work hardening, plastic constitutive equations (*Japanese*) 0-25718  
Al, electroplastic effect 0-7647  
Al-Zn-Mg plasma sputtered, mech. props. rel. to heat treatment (*Russian*) 0-40387  
Al-Zn-Mg-Cu-Co (6.5, 2.5, 1.5, 0.4 wt.%), fatigue crack propag. 0-55521  
AlN powder, plasma-chem. and self-propag. high-temp. thermoplastic slips, synthesis 0-25633  
Al<sub>2</sub>O<sub>3</sub>:Cr<sub>2</sub>O<sub>3</sub>(Ti<sub>2</sub>O<sub>3</sub>), dopant influence on struct. and mech. props. 0-24471  
Be-bronze BrB2, struct. and phase transform. during mechano-thermal treatment (*Russian*) 0-11667  
Cu-Al<sub>2</sub>O<sub>3</sub>, dispersion strengthened, plasticity qualities, fractographical analysis (*Czech*) 0-50680  
MgAl<sub>2</sub>O<sub>4</sub>, microplasticity at room temp., dislocations, TEM study 0-19805  
MgO, compressive stress-strain behaviour at high temps. 0-25774  
MgO-MgAl<sub>2</sub>O<sub>4</sub>(FeCr<sub>2</sub>O<sub>4</sub>), thermoplastic and thermophys. props. for steel vacuuming installations 0-35281  
Mo, fatigue charact., effect of Ni and Re surface doping on mech. props. (*Russian*) 0-7660  
Mo, mechanical props. and dislocation struct., mag. field effect 0-54935  
Mo-B, Mo-B-Fe(Ni), microalloying influence on mechanical props., cold rolling, plasticity (*Russian*) 0-40502  
Mo-Hf (0.3 wt.%), strength, plasticity and microhardness, internal nitriding effect (*Russian*) 0-40433  
Mo-Mn alloy, plasticity, fracture, strength depend. on C content (*Russian*) 0-35257  
Nb, mechanical props. and dislocation struct., mag. field effect 0-54935  
Ni, high temp. plasticity, oxide inclusion effect 0-50681  
Ni-Al-Ti(Nb), heat-resisting dispersion-hardening alloys, props. and struct.,  $\gamma$ -phase comp. influence (*Russian*) 0-20943  
Ni-Cr alloy, Kh20N80, inclusions and plasticity, crystn. conditions influence (*Russian*) 0-20923  
Ni-Cr-Ti(Al), effect of ultrasound on crystallisation, dendritic structure, and plasticity (*Russian*) 0-11637  
Pd<sub>77.5</sub>Cu<sub>16.5</sub> metallic glass wire, cold drawing 0-50650  
Si, plastic properties, internal friction, dislocation motion (*Russian*) 0-54305  
TiN powder, plasma-chem. and self-propag. high-temp. thermoplastic slips, synthesis 0-25633

# plasticity continued

V, plasticity and strength change in temp. range 20 to 1000°C impurity effects 0-35235  
W surface layer struct. during milling, plastic deform., failure (*Russian*) 0-40586

## plastics

see also glass fibre reinforced plastics; polymers  
CR-39, proton-sensitive, method of producing thin sheets for plastic track detectors 0-35155  
double-layer antireflection coatings for plastic lenses, evaporation coating process 0-14491  
electrophotographic layer, electrostatic force calc. (*German*) 0-42285  
fibre-optic glass manufacture using polypropylene sump pumps 0-14410  
foamed, shock absorbing capacity determ. (*German*) 0-19877  
foil, Li ferrite clad, thermal deform. (*Polish*) 0-30002  
foil prod. by extrusion blowing (*German*) 0-20786  
formvar-Al superconductive junction, Ginzburg's generalised jellium model 0-15663  
glass plastics, strength criteria 0-10208  
gradient index lens fabrication and image evaluation 0-14426  
injection-moulded thermoplastics for demountable optical fibre connectors 0-53472  
ion plating 0-16533  
modular solar energy collector with reticulated foam 0-16833  
molecular electronics appl. 0-6355  
optical component specification 0-48362  
optical fibre clad with Teflonlike plastic coating, press. sensitivity 0-33149  
organic fibre reinforced plastics, failure 0-11774  
pentaplast, plasticised, thermal treatment effect on props. 0-40324  
Perspex magneto-electret, equiv. elec. field calc. from thermally stimulated discharge current 0-7259  
perspex prism, refr. index meas., crit. angle method, student expt. 0-12873  
Perspex pyramid electret, thermally stimulated discharge currents 0-2688  
photothermoplastic recording with rapid switching 0-32941  
pigmented, elec. cond. depend. on mech. stress (*German*) 0-20264  
plasticised cellulose acetate sheet, post-yield fracture 0-25859  
Plexiglas, thin slab, microwave beam displacement upon transmission 0-1107  
PMMA fracture toughness, flame-retardant additive effect obs. 0-16470  
poly(vinylidene fluoride) orientation, solid state deformation by coextrusion 0-40394  
polymeric fibre-reinforced plastic, creep prediction from components props. 0-40448  
prestrain effect on dynamic modulus of elasticity and attenuation coeff. in nonconducting materials 0-29110  
PVC, plasticised, foam growth, thermomech. anal. 0-3416  
PVC compositions, influence of formulation on the compounding and rheological props. 0-40321  
PVC magnetoelectrets, mag. susceptibility 0-2687  
reinforced, anisotropic, stress distrib., using mm region of EM waves 0-25968  
residual stresses in shells of revolution, cut-out element method glass-plastic composite, thermoelectric residual stresses in shells of revolution, cut-out element method 0-38271  
scintillator excited by <sup>60</sup>Co  $\gamma$ -rays, absolute radioluminesc. yield meas. 0-2829  
shell, elastic cylindrical, optimisation with allowance for geometrically nonlinear factors 0-38270  
Teflon foils, cryst. struct. and texture changes due to polarisation process (*Polish*) 0-35209  
tensile and flexural testing device, incorporating an impactor (*German*) 0-3276  
thermomechanical reliability, rel. to transmission media applic. 0-40666  
thermoplastic, partially crystalline, microscopic methods of struct. anal. (*German, English*) 0-30198  
thermoplastic based composites, mean stiffness 0-11693  
thermoplastic beams, constant stress, design 0-38248  
thermoplastic film, photoconducting, double exposure holographic interferometry using memory effect (*Chinese*) 0-37967  
thermoplastic foil, US welded, IR detection for measuring temp. distrib. (*Polish*) 0-22362  
thermoplastic recorder development, interaction of regular and chaotic deformation (*Russian*) 0-42291  
thermoplastic recording material, latent image and surface deformation (*German*) 0-42284  
thermoplastics, reinforced testing by dynamic mech. anal. 0-16626  
thermoplastics, structural changes during deformation, rel. to impact resistance 0-25800  
thermosetting materials, formation and props., phase diagram and torsion pendulum anal. 0-55381  
viscoelastic anisotropic, creep 0-35249  
waste, pyrolysis to produce organic raw materials (*German*) 0-3307  
Al<sub>2</sub>O<sub>3</sub> ceramics, with thermoplastic bond, prep. 0-45254

## plastics industry

multicomponent, multipoint infrared ambient air monitor, microcomputer-controlled 0-40945

## plates (anodes) see anodes

## plating (electroplating) see electroplating

## platinum

see also nuclei with .....  
adsorbed H<sub>2</sub>O on (100) surfaces, bonding, electron energy loss spectra 0-34311  
adsorbed H on (111) surface, vibr. modes, EELS study 0-15377  
adsorption of CO, low temp. vibr. mode, site occupation, electron energy loss spectra 0-29263  
adsorption of CO, O<sub>2</sub>, NH<sub>3</sub>, surface composition, AES and temp. programmed desorption meas. 0-34313  
adsorption of CO and D<sub>2</sub>, absolute coverage meas. using nucl. microanal. 0-54511  
adsorption of HI on (111) and (100) surfaces, superlattice form., LEED, AES, and thermal desorption studies 0-55715  
adsorption of water, H<sub>2</sub> and reaction between H<sub>2</sub> and adsorbed O 0-49514  
atom ground state configurations, isotope shifts and fine struct. anal., visible and UV spectra 0-42987  
catalytic H<sub>2</sub> oxidation, OH radical form., laser diagnostics 0-5572  
chemisorption, pot. energy function of two H atoms around Pt atom protruding from metallic Pt surface 0-10781



## platinum continued

- chemisorption of H, bond nature 0-34297  
 chemisorption of H, embedded cluster model 0-39427  
 cluster, conduction electron density oscils., NMR spin-echo meas., indirect exchange interaction 0-44954  
 core level excitation effects, synchrotron radiation UPS study 0-40234  
 crowding conversion to dumbbell, two-interstitial model, thermal neutron irradi. 0-33992  
 crystallite morphology, surface struct., electron microscopy obs. 0-29257  
 desorption, associative from mixed adlayers of O and N 0-54512  
 electrode, evaporation rate from cathode spot in vac. arcs. 0-49024  
 electrodes, nonlinear AC and DC polarisation obs. 0-56247  
 EM isotope separation and in-beam electron spectroscopy, Pt target preparation 0-52812  
 EXAFS Debye-Waller factors 0-45168  
 film, discontinuous, adsorption of alkali halide mols., effect on elec. cond. 0-2487  
 film, evaporated, optical props. meas. in VUV, 220 to 150 Å 0-45159  
 film, on Si, ion-induced intermixing 0-15420  
 film, spike effects of heavy ion sputtering 0-35034  
 film, work function changes upon water contamination 0-44705  
 film coatings for Mo tips, film characterisation by atom probe FIM atomic clusters, voids 0-33863  
 films, optical props. and radiation stability 0-34999  
 foil, crystal struct. as function of substrate temp. during deposition 0-18742  
 interatomic pair potential, phonon spectra 0-33927  
 interstitial thermal conversion study by elec. cond. meas. 0-15096  
 ion plating on  $\alpha+\beta$  Ti alloy Ti-6242, creep property improvement 0-16408  
 microvoid form., gaseous impurity atom effects, positron annihilation study 0-49275  
 nucleate and film boiling in travelling wave regime 0-19231  
 oxidation, XPS spectra study 0-3254  
 pair potentials calc., appl. to point defect props. 0-19798  
 plasma, laser produced, Ni-like X-ray spectrum 0-43983  
 polycrystalline, He ion refl. (Russian) 0-35051  
 radiolytic product detection by Pt electrode rest potential 0-11973  
 resistance temperature probes, constructional types and state of technique (German) 0-52213  
 resistance thermometer, heat shock influence on elec. cond. and thermophysical props. (Russian) 0-52210  
 resistance thermometer, oxidation problems 0-52206  
 spherical inclusions in polymethyl methacrylate, thermochem. instability caused by CW laser beam 0-29689  
 stepped surface, adsorbed H, adsorption sites study by EELS 0-49521  
 stepped surface, high freq. vibr. modes, cluster recursion method calcs. 0-6615  
 superconducting transition temperature, ab initio calc. 0-25036  
 surface, (111), identification of adsorbed OH species 0-49509  
 surface, (111), Xe direct inelastic scatt. with trapping-desorption scatt., vel. and ang. distrib. 0-16140  
 surface, AR thermal accommodation coeffs., 300 to 1350K 0-30272  
 surface, coverage and desorption of CO flash desorption spectrum 0-49493  
 surface (110), reconstructed, LEED-AES study, O<sub>2</sub> treatment effect 0-39398  
 surface (111), H adsorption, inert model 0-50889  
 surface (111), LEED, quantitative anal. 0-44085  
 surface (997), terrace bending obs. from He beam scatt. 0-40202  
 surface reconstruction, physical realisation of two-dimensional Ising and X-Y model 0-15351  
 surfaces, oxidation by electrosorpt., of H<sub>2</sub>, effect of soluble prods. (German) 0-55717  
 surfaces with variable kink concs., catalysed hydrocarbon reactions, surface O<sub>2</sub> effects 0-35576  
 vapour deposited coating, on Ir and W, defects and their effect on props. 0-39474  
 VPE, on Au, crit. thickness of pseudomorphic film growth, substrate size depend. (Russian) 0-29286  
 wire, single vacancy form., activation energy meas. 0-49212  
 XPS, electronic struct. 0-7464  
 Cr<sub>2</sub>O<sub>3</sub>/γ-Fe<sub>2</sub>O<sub>3</sub>/Pt electrode, two layer oxide surface film anal. by modulation spectroscopy (Japanese) 0-11491  
 D exchange reaction between H<sub>2</sub> and water a hydrophobic catalyst supporting Pt 0-30208  
 MgO:Pt<sup>2+</sup>, Jahn-Teller effect in EPR spectrum 0-7160  
 Pt<sup>181</sup>/Hf, interaction of implanted impurity with radiation induced lattice defects, TDPAC meas. 0-24494  
 Pt/polymer/metal capacitors, electroforming and elec. cond. 0-54800  
 Pt/TiO<sub>2</sub> catalyst for photoassisted decomposition at room temp. of H<sub>2</sub>O and ethylene 0-55703  
 Pt-Au, thick film, adherence meas. and evaluation 0-50813  
 Pt-SrTiO<sub>3</sub> (100) interface, struct. and electronic props., AES, LEED, EELS, and UPS study 0-24986  
 Pt-SrTiO<sub>3</sub> (100) interface, Auger and photoemission studies, relax. and chem. shift effects 0-54749  
 Se:K, glassy, photolum. and optically induced ESR 0-50398  
 Si:Pt, depth depend. of atomic mixing by ion beams 0-29837  
 Si:Pt, electron and hole capture, DLTS obs. 0-49661  
 Si:Pt, heavily doped, gradual p<sup>+</sup>-n junctions, trap levels (French) 0-34392

## platinum alloys

- see also platinum compounds  
 ordered equiatomic, lattice specific heat meas., Debye temp. 0-54396  
 rare earth alloys, RPt<sub>2</sub>X<sub>2</sub> (X=Si,Ge), cryst. struct. 0-1964  
 rare earth intermetallics, RPt, (R=Gd, Tb, Dy, Ho, Er, Tm), structs. and mag. props. 0-50069  
 Al-Pt<sub>1-x</sub>Ni<sub>x</sub>-n-Si system, Schottky-barrier height 0-34520  
 Al-Pt<sub>1-x</sub>Ni<sub>x</sub>-Si system, diffusion, compound form., and microstructure 0-34253  
 Au-Pt, cold worked, impurity conc. rel. to internal friction Bordoni peak, solid soln. hardening mech. 0-16363  
 Co-Pt, atomic ordering props. and domain growth in strong pulsed mag. field (Russian) 0-54918  
 Co-Pt, films, electrolytic deposition conditions over large comp. range (French) 0-45242  
 Co-Pt film, electrodeposited, saturation mag. induction, mag. anisotropy and coercive field meas. (French) 0-2610

## platinum alloys continued

- CoPt<sub>3</sub>, electrolytic films, saturation mag. induction, coercive fields, thickness depend. (French) 0-44883  
 Cu<sub>3</sub>Au-Cu<sub>3</sub>Pt, quaternary system, order-disorder transform., superlattice form. 0-2159  
 Eu<sub>0.95</sub>Ba<sub>0.05</sub>Pt<sub>2</sub>, <sup>151</sup>Eu Mossbauer studies at high press. 0-39923  
 EuPt<sub>2</sub>, <sup>151</sup>Eu Mossbauer studies at high press. 0-39923  
 EuPt<sub>2</sub>, elec. field gradient, spin echo NMR meas. 0-20509  
 EuPt<sub>2</sub>, indirect exchange, spin echo NMR meas. 0-15822  
 Fe-Pt, plastic deform. effect on struct. singularities and mag. props. (Russian) 0-44892  
 Fe-Pt (22-24 at.%) austenite, long range order parameter, temp. depend. 0-40353  
 Fe-Pt Invar alloy, magnetocryst. anisotropy energy, itinerant electron model 0-54884  
 Fe-Pt-SiO<sub>2</sub>, supported catalysts, Mossbauer spectra 0-11296  
 FePt, non-linear local environment effect, Mossbauer effect of <sup>57</sup>Fe and <sup>195</sup>Pt 0-39910  
 (Gd<sub>1-x</sub>R<sub>x</sub>)(Co<sub>1-y</sub>Pt<sub>y</sub>)<sub>5</sub>, origin of hyperfine fields acting on Gd, Mossbauer study 0-44967  
 Hg<sub>2</sub>Pt, <sup>199</sup>Hg Mossbauer meas., isomer shift and quadrupole splitting calcs. 0-28039  
 Mn<sub>1-x</sub>Fe<sub>x</sub>Pt<sub>3</sub>, noncollinear mag. structs., neutron diffr. anal. (Russian) 0-25087  
 Nb-Pt-O system, phase equilibria, diagram, unit cell parameters, supercond. 0-55352  
 Nb<sub>2</sub>Pt, A-15 struct. <sup>93</sup>Nb NQR spectra 0-20496  
 Nb<sub>2</sub>Pt, X-ray M<sub>IV</sub>V emission bands (Russian) 0-45170  
 Ni-Pd, mag. form. factor, polarised neutron diffr. meas. 0-29525  
 Ni-Pt, magnetic moment distrib., diffuse neutron scatt. meas. 0-34593  
 Ni-Pt, short-range order parameter calc. in pseudopot. approx. (Russian) 0-49183  
 Ni-Pt disordered alloy, off-diagonal, T-matrix itinerant electron ferromagnetism calcs. 0-25067  
 NiPt, short-range order, effect of plastic deform., electron diffr. anal. (Russian) 0-24403  
 NiPt<sub>2</sub>Ge<sub>2</sub>, cryst. struct. (German) 0-44171  
 Pd-Pt surface, adsorbed Xe, 5p photoemission, local surface struct. influence 0-2920  
 (Pd,Pt<sub>1-x</sub>)<sub>2</sub>Fe atomically ordered alloy, thermoelectric power, carrier energy spin shift, mag. props. 0-29394  
 Pt-Al(In)(Sn) alloys, Fermi energy influence on thermodynamic props. (German) 0-24619  
 Pt-C, dil., C segregation to single cryst. surfaces 0-39301  
 Pt-C (graphite), adhesion and wettability of graphite (Russian) 0-20008  
 Pt-Cu, ESCA study 0-2923  
 Pt-Cu, surface composition, XPS (Portuguese) 0-24722  
 Pt-Cu alloys, ESCA determ. of electronic struct. 0-34352  
 Pt-Fe alloy foils prep. by electrodeposition of Fe 0-35113  
 Pt-Ir, structural phase transform., ion field emission microscopy obs. (Russian) 0-50628  
 Pt-Ir coated Ti anode, corrosion and passivation behaviour in Cu electro-winning appl. 0-55573  
 Pt-Pd (Co)(Su)(Al)(Si) melts, surface tension and density (Russian) 0-39388  
 Pt-Rh, elec. cond., temp. influence (Russian) 0-39549  
 Pt-Rh, surface comp. determ. by ion scatt. spectroscopy 0-6602  
 Pt-Rh-W (30, 8 wt.%), intergranular embrittlement by Se vapour 0-3185  
 Pt-Sn/Al<sub>2</sub>O<sub>3</sub> catalyst, Mossbauer effect, reactivity 0-11298  
 PtBi, XPS, electronic struct. 0-7464  
 γ-Pt<sub>2</sub>Cd<sub>40(41)</sub>, X-ray cryst. struct. determ. 0-54172  
 Pt<sub>2</sub>Mn, mag. excitation dispersion relation 0-25090  
 Pt<sub>2</sub>Mn<sub>2</sub>Cr<sub>1-x</sub> alloys, mag. props. 0-2562  
 Pt<sub>2</sub>Mn<sub>2</sub>Cr<sub>1-x</sub>, electronic specific heat meas. comparison with band model calcs. 0-54400  
 PtMnSb, hyperfine mag. field at Cd impurity, TDPAC study 0-39906  
 PtRh5 alloy, phosphate glass addition effect on high temp. strength (German) 0-25807  
 PtSi, epitaxial film on Si, <sup>4</sup>He ion channelling meas. and RHEED anal. 0-10834  
 ThPt, valence bands, XPS spectra 0-50520  
 Ti-Pt-Au, nonalloyed ohmic contacts to n-GaAs by pulse-electron beam annealed Se implants 0-2466  
 UPt, valence bands, XPS spectra 0-50520  
 V<sub>1-x</sub>Pt<sub>x</sub>, A-15 cpds., nucl. mag. relax. in normal and supercond. state 0-49993  
 YbPt-YbAu system, valency state, Yb behaviour (French) 0-45277

## platinum compounds

- see also platinum alloys  
 chain compounds, one dimens. conductors, Fermi wavevector determ., X-ray scatt. obs. 0-44187  
 double oxides, elec. cond. 0-34438  
 mixed valence-mixed metal compounds, ionic crystals, longitudinal lattice modes, Raman spectroscopy 0-40099  
 tetrakis(ethyl isocyanide) platinum(II) tetracyanoplatinate(II), cryst. data, X-ray powder anal. 0-2003  
 Co<sub>0.83</sub>[Pt(C<sub>2</sub>O<sub>4</sub>)<sub>2</sub>].6H<sub>2</sub>O, cond., dielec. const., microwave obs. 0-44636  
 Co<sub>0.83</sub>[Pt(C<sub>2</sub>O<sub>4</sub>)<sub>2</sub>].6H<sub>2</sub>O, quasi-one-dimens. conductor, Peierls distortion and superlattice, X-ray study 0-29397  
 H<sub>2</sub>Pt(OH)<sub>6</sub>, platinum acid, X-ray cryst. struct. determ. 0-28967  
 K<sub>2</sub>Pt(CN)<sub>4</sub>, Peierls transition temp. and 0K energy gap, mean field theory calc. 0-24782  
 K<sub>2</sub>Pt(CN)<sub>4</sub>, quasi-one-dimens. Peierls system, phonon dispersion and neutron scatt., calc. 0-24550  
 K<sub>2</sub>Pt(CN)<sub>4</sub>Br<sub>0.3</sub>2.2H<sub>2</sub>O, linear cond., <sup>195</sup>Pt NMR evidence of low lying non-linear excitation 0-44933  
 K<sub>2</sub>Pt(CN)<sub>4</sub>Br<sub>0.30</sub>3H<sub>2</sub>O, dynamic <sup>195</sup>Pt NMR meas. below metal-insulator transition 0-34810  
 K<sub>2</sub>Pt(CN)<sub>4</sub>Br<sub>0.3</sub>3H<sub>2</sub>O, spin-lattice model for elastic anomalies 0-15179  
 K<sub>2</sub>Pt(CN)<sub>4</sub>Br<sub>0.3</sub>3H<sub>2</sub>O, quasi one-dimens. conductor, EPR linewidth 0-54938  
 K<sub>1.75</sub>Pt(CN)<sub>4</sub>1.5H<sub>2</sub>O, Raman scatt. and luminesc. studies 0-25394  
 K<sub>1.75</sub>[Pt(CN)<sub>4</sub>]1.5H<sub>2</sub>O, elec. cond. studies, Peierls transition 0-24901  
 Pt complex, [Pt(en)<sub>2</sub>][Pt(en)<sub>2</sub>Cl<sub>2</sub>](ClO<sub>4</sub>)<sub>4</sub>, reson. Raman spectra 0-2760  
 Pt complex, linear ionic mixed valence cpd., IR and resonance Raman spectra rel. to lattice modes 0-25393  
 Pt complex, Pt<sup>II</sup>(CNCH<sub>3</sub>)<sub>4</sub>(PF<sub>6</sub>)<sub>2</sub>, Pt<sup>II</sup>(CNCH<sub>3</sub>)<sub>6</sub>(PF<sub>6</sub>)<sub>2</sub>, and Pt<sup>II</sup>Pd<sup>II</sup>(CNCH<sub>3</sub>)<sub>6</sub>(PF<sub>6</sub>)<sub>2</sub>, vibr. spectra, M-M bonds. (French) 0-47997



**platinum compounds continued**

- Pt complex, tris[bis(1,2-diaminoethane)Pt(II)dichlorobis(1,2-diaminoethane)]Pt(IV)tetrakis[tetrachlorocuprate(I)], cryst. and mol. struct. 0-28964  
 Pt complexes, chain cpds., orientational antiphase struct., X-ray scatt. determ. 0-24435  
 Pt<sub>3</sub>B, Pt<sub>2</sub>B, and other Pt<sub>3</sub>B<sub>2</sub> cpds., cryst. chem. 0-19769  
 PtCl<sub>2</sub><sup>2-</sup>, electronic struct., SCF Xalpha ESCA spectrum assignment 0-23339  
 PtCl<sub>2</sub>(NH<sub>3</sub>)<sub>2</sub>, cis- and trans-isomers, electronic struct., SCF-Xα study 0-18795  
 Pt(H)(D), pot. energy curves, r-centroids, Franck Condon factors, rot. depend. 0-28082  
 Pt(IV), reduction to Pt(II), X-ray irradi., Ar ion bombardment, XPS obs. 0-35573  
 PtO<sub>2</sub>, sputtered film, optical props. under H<sub>2</sub> reduction 0-20728  
 PtTe, electronic struct., self-consistent and non-self-consistent band calcs. 0-44499

**pleochroism**

- see also dichroism*  
 dyes, dissolved in nematic liq. crystals., guest-host interactions, appl. to electrooptic displays 0-44113

**plexiglas *see plastics*****plotters**

- Bruel and Kjaer acoustic level recorder type 2306, interfacing to a digital computer for a graphical output 0-53572  
 chromatography, data processor with thermal printer-plotter for GC and LC (*Japanese*) 0-50920  
 coordinatograph, precision, 120×120, accuracy of applicability 0-52158  
 graphics calculator system using X-Y recorder and computer as digitiser 0-13046  
 stress-strain diagrams, tensile testing 0-3269

**plugs (electric) *see electric connectors*****Pluto**

- Charon, account of discovery 0-12708  
 Charon, tidal evolution 0-26806  
 diameter meas. by speckle interferometry 0-41763  
 encounter possibility in extraplanetary mission 0-17466  
 geocentric positions for the 1974-8 period 0-46478  
 IR spectrum, 1.5 to 2.5 μm obs. 0-56765  
 orbital motion, theory and perturbations of giant planets (*French*) 0-26724  
 satellite observation (*Czech*) 0-31252  
 surface and atmosphere from 1.4-1.9 μm spectrum 0-46480

**plutonium**

- see also nuclei with .....*  
*see also fission of plutonium*  
 advanced MX fuels, Pu depletion by vapour-phase transport in carbothermic reduction processes 0-815  
 air monitor with background compensation system 0-27824  
 borehole assay using delayed-neutron activation anal. 0-21419  
 breeder reactor fuel, remote fabrication program, France 0-13748  
 dosimetry, calibration of whole-body counters 0-21547  
 FBR fuel remote fabrication development at PNC 0-13749  
 glove boxes, Pu-contaminated, size reduction and waste packaging 0-18469  
 isotope separation and ratios, neutron irradi. of natural U in Japan Material Testing Reactor (*Japanese*) 0-52730  
 isotopes, in soil, determination using alpha-spectrometry 0-45601  
 lung Pu of pronghorn antelope near a nuclear fuel reprocessing plant 0-30906  
 LWR recycling of Pu in (Th,Pu)O<sub>2</sub> fuels, economic viability 0-18576  
 Manhattan project workers, 32-year medical follow-up 0-26379  
 neutron analysis in solid waste 0-42840  
 nuclear fuel, burn-up, chemical separation, ion exchange 0-42746  
 radiation protection and monitoring of personnel handling Pu reactor fuels 0-5389  
 radioactive target preparation and characterisation 0-18734  
 radioactive waste, oxidation by radiation, effect on migration rate 0-13714  
 radioactive waste, Pu contaminated incinerator facility, decontamination and decommissioning 0-13987  
 radioactive waste, transport, environmental impact 0-779  
 radioactive waste monitoring, anal. of enhanced variance and twin gate methods 0-5454  
 radionuclides decomposition in glaciers 0-40934  
 specific heat, Debye temp. 0-15258  
 vapour pressure determ. 1724 to 2219K by Knudsen effusion technique 0-654  
<sup>239</sup>Pu sample irradi. in EBR-II, calc. and exptl. anal. 0-22947  
<sup>241</sup>Am(n,X), Japan Material Testing Reactor, separation of transuranium elements (*Japanese*) 0-52731  
<sup>238,239,240</sup>Pu, concs. in arthropods at a nuclear facility 0-30905  
 Pu-enriched LWR fuels, remote fabrication at Belgonucleaire 0-13754  
<sup>238</sup>Pu<sup>4+</sup>, <sup>239</sup>Pu<sup>6+</sup>, <sup>239</sup>Pu<sup>4+</sup>, <sup>239</sup>Pu<sup>6+</sup>, alpha uptake rel. to isotope and oxidation state 0-30692  
<sup>239</sup>Pu, <sup>240</sup>Pu, concs. in fish and seawater from Kwajalein Atoll 0-26380  
<sup>239</sup>Pu direct enrichment of LWR assemblies in a fusion hybrid 0-37604  
<sup>239</sup>Pu, effect on mouse haemopoietic stem cells 0-51174  
<sup>239</sup>Pu, polymeric, effects on erythrocyte survival in mice 0-45973

**plutonium alloys**

- binary alloys, periodical depend. of equilibrium distrib. coeffs. of Pu admixtures on atomic number of admixture 0-18419  
 Ag-Pu (0.5 wt.%) deposited profiles, homogeneity, from hexagonal point source array 0-25559  
 PuFe<sub>2</sub>, Mossbauer diffrr., combination type maxima, hyperfine interactions on nuclei 0-25263

**plutonium compounds**

- see also plutonium alloys*  
 slab tanks for criticality control, neutron multiplication calc. 0-13606  
 (U,Pu)O<sub>2</sub> fuel, remote fabrication experience in FRG 0-13753  
 (Pu,U)O<sub>2</sub>, oxidation rates 0-37557  
 (Pu-Th)O<sub>2</sub>, FBR fuel pellet fabrication, control of O<sub>2</sub>-to-metal ratio 0-13760  
 Pu(C, N), lattice parameter variation at low temp., thermal exspn. 0-15046  
 PuC, lattice parameter variation at low temp., thermal exspn. 0-15046  
 PuC<sub>0.82(1.49)</sub>, high temp. enthalpies 0-49384  
 PuC<sub>x</sub> (x=0.8, 1.44, 1.67), low temp. sp. ht., mag. ordering obs. 0-49372

**plutonium compounds continued**

- PuGa, cryst. and powder diffrr. data at room temp. 0-28982  
 PuN, lattice parameter variation at low temp., thermal exspn. 0-15046  
 Pu(NO<sub>3</sub>)<sub>4</sub>, solution concentrator equipment for criticality safety 0-18432  
 Pu(NO<sub>3</sub>)<sub>4</sub>-nitric acid soln., direct denitration in screw calciner 0-37567  
 PuO, nuclear oxide fuel anal., coulometry, emission anal., chromatography, X-ray anal. 0-18420  
 PuO<sub>2</sub>, spectroscopic data rel. to thermodynamic functions 0-34208  
 PuO<sub>2</sub> aerosol, acute inhalation, predictive model of early mortality 0-36028  
 PuO<sub>2</sub> air transportable package PAT-1, dose rate and criticality calcs. 0-13938  
 PuO<sub>2</sub>, Mossbauer resonance 0-20554  
 PuO<sub>2</sub> nuclear fuel, eqn. of state and thermodynamic props. 0-13592  
 PuO<sub>2</sub>, spectroscopic data rel. to thermodynamic functions 0-34208  
 PuO<sub>2</sub>, thermal and transport props., electronic contrib. 0-15432  
 PuO<sub>2</sub>C<sub>2</sub>O<sub>4</sub>, Mossbauer resonance 0-20554  
 PuP, lattice distortions in ferromag. phase, X-ray obs. 0-15774  
<sup>238</sup>PuO<sub>2</sub>, uniformly dense aerosols prod. by gas phase neutralisation of acidic droplets 0-26427  
<sup>239</sup>Pu citrate, internally deposited, pot. genetic dose, influence of testicular microanatomy 0-36147  
<sup>239</sup>PuO<sub>2</sub>, inhalation by mouse, effect on pulmonary clearance of S. aureus 0-36013  
 (Th,Pu)O<sub>2</sub> nuclear fuels, economic viability of Pu recycling in LWR 0-18576  
 (U,Pu)O<sub>2</sub>, LMFBR fuel pin lattices, calcs. of k<sub>eff</sub> valves 0-13569  
 (U, Pu)C, LMFBR carbide fuel cladding damage anal. at TREAT 0-13602  
 (U,Pu)C, self-diffusion meas. 0-6544  
 (U,Pu)N, self-diffusion meas. 0-6544  
 (U,Pu)O<sub>2</sub> FBR fuel cycle, review 0-47682  
 (U,Pu)O<sub>2</sub>, FBR fuel pellets, gel-supported precipitation conversion and prep. 0-813  
 (U,Pu)O<sub>2</sub>, FBR fuel pellet fabrication, control of O<sub>2</sub>-to-metal ratio 0-13760  
 (U,Pu)O<sub>2</sub>, FBR fuel pin thermal design, effect of fuel stoichiometry 0-18570  
 (U,Pu)O<sub>2</sub> fuel, criticality control, critical mass meas., fission rate distrib. by solid state dosimetry 0-13723  
 (U,Pu)O<sub>2</sub> fuel performance, effect of O<sub>2</sub>-metal ratio 0-13762  
 (U,Pu)O<sub>2</sub> fuel-cladding chemical interaction, effect of O<sub>2</sub>-metal ratio 0-13763  
 (U,Pu)O<sub>2</sub> GCFR fuel behaviour, effect of O<sub>2</sub>-metal ratio 0-18569  
 (U,Pu)O<sub>2</sub> LWR high burnup fuels, remote fabrication and performances 0-13755  
 (U,Pu)O<sub>2</sub> powder, FBR fuel prep. by Au/PuC coprecipitation process 0-814  
 (U<sub>1</sub>Pu)O<sub>2</sub>+x, O<sub>2</sub> chem. diffusion (*French*) 0-49427

**PMDR**

- benzophenone L in dibromodiphenylether, benzophenone triplet state, nanosecond resolved ODMR, freq.-agile techniques appl. 0-34825  
 2-benzoylpyridine crystals, lowest triplet state, optically detected EPR 0-15827  
 1,2,4,5-tetrachlorobenzene, excited triplet state dimer, intermol. exchange integral, isotope effect 0-15826  
 KCl:PO<sub>2</sub><sup>2-</sup>, photo-orientation, spectrosc. and ODMR obs. 0-29772

**PMPS *see PMDR*****p.m.r. *see proton magnetic resonance*****pneumatic control equipment**

- flow-generated noise through pipe walls, transmission at acoustic pipe coincidence 0-53767  
 noise characteristics of control valves 0-53562

**pneumodynamics**

- see also lung*  
 area under max. expiratory flow-vol. curve, meas. using analogue device 0-41284  
 breath dispersion patterns, exptl. model study 0-51139  
 breathing pattern and ventilatory response to CO<sub>2</sub> in divers 0-45934  
 breathing ratemeter for neonatal intensive care 0-41311  
 breathing responses to increased transrespiratory press., man and guinea pig obs. 0-30741  
 bronchial elasticity and air flow, mathematical anal. 0-45942  
 cardiac effects of increased lung vol. and decreased pleural press., man 0-41073  
 cardiopulmonary readjustments in passive tilt 0-56084  
 cardiopulmonary stress testing in children 0-30911  
 cardiovascular effects of positive-pressure ventilation in normal subjects 0-41081  
 diffusing capacity at different lung vols., breath holding and rebreathing obs. 0-30739  
 divers, large lungs, functional characts. 0-3680  
 elastic recoil, use of exponential function 0-8090  
 electrophrenic respiration, feedback control of tidal vol. (*Japanese*) 0-41316  
 expiratory flow rate, influence on closing vol. meas. 0-35934  
 expiratory flow-volume curves, configuration variability for maximum expiration 0-3677  
 flow-volume curves of excised right and left rabbit lungs 0-3673  
 forced oscillatory parameters of the canine respiratory system with altered vagal tone 0-56082  
 frequency response measurement technique for press., vol. and flow transducers 0-41344  
 functional residual capacity, breath-by-breath variation obs. 0-45938  
 gas exchange in normal and abnormal lungs, effects of inspiratory flow pattern 0-45936  
 gas exchange kinetics determinants during exercise, dog expts. 0-45932  
 hypocalcaemia in normal subjects, pattern and mechanism of airway response 0-30738  
 inert gas elimination studies without mixed venous partial pressures 0-26250  
 intensive care ventilator, microcomputer-controlled 0-51292  
 intrathoracic airway models, impedance during low-freq. periodic flow 0-41077  
 intrathoracic airways mechanics in normal man, sex and age diffs. 0-3676  
 lung, human, with uneven ventilation, gas transport (*Japanese*) 0-3700  
 lung compartmental models, steady state inert gas exchange 0-26249  
 lung compartmental models, transient inert gas exchange 0-26251  
 lung dead space vol. meas. 0-35935



**pneumodynamics continued**

- lung phantom, dynamic, use as educational tool 0-8757
- magnetopneumographic measurement of particle conc. and clearance in the lung 0-21514
- mechanics of the lung (*Japanese*) 0-41094
- microcomputer-based data acquisition and analysis system for CO<sub>2</sub> rebreathing studies 0-36161
- nasal mucous velocity, effect of exercise in normal subjects 0-8088
- oscillatory respiratory resistance in pregnancy and during lying-in 0-56081
- peripheral asynchronous time constants, comparative study of techniques 0-26256
- perivascular pressure measurements by wick-catheter technique in isolated dog lobes 0-35932
- physiology system models, breathing control example 0-41058
- pleural pressure and lung vol. obs., anesthetised hamster 0-30749
- pressure transducers, differential, air-filled, dynamic characts. 0-3879
- pressure transducers, gas-filled, effects of gas density on freq. response 0-56249
- pressure-volume relationship of fetal rhesus monkey lung, effect of betamethasone 0-41079
- pulmonary function measurements, aid in diagnosis of suspicious pneumoconiosis 0-21567
- pulmonary function parameter meas. system for small animals 0-8227
- pulmonary interdependence of gas transport 0-41076
- pulmonary measurement system, HP model 47804A 0-36163
- pulmonary resistance, human, effect of freq. and gas physical props. 0-30744
- pulmonary vascular interdependence in isolated dog lobes, continuum mechs. anal. 0-3671
- pulmonary vascular resistance, longitudinal distrib., and lung inflation in hypoxia 0-56086
- radioactive tracer tidal breathing, lung ventilation model, radioactive tracer tidal breathing 0-56095
- regional ventilatory clearance, estimation by Xe scintigraphy 0-30854
- respiratory impedance and derived parameters in young children by forced random noise 0-30745
- respiratory impedance measurement, direct-display oscill. method 0-36174
- respiratory resistance fractionation in young children, expt. obs. 0-56087
- respiratory resistance freq. dependence, health children 0-41075
- respiratory system, human, mechanics of regulation 0-41102
- respiratory system, human, modelling and parameter estimation 0-12169
- specific airway resistance changes meas. technique 0-8228
- spirogram, forced, transit-time anal., healthy children and adults 0-8082
- thoracoabdominal mechanics during relaxed and forced vital capacity 0-30740
- vagal blockade effects on lung mechs. in normal man 0-8081
- ventilation abnormalities detection using <sup>133</sup>Xe, washout rel. to single-breath imaging 0-41183
- ventilation and regional vols. distrib. in excised canine lobes, gravitational deform. 0-30747
- ventilation and ventilatory pattern maturation in normal sleeping infants 0-35933
- ventilation regional phase differences demonstration by breath sounds 0-8087
- ventilation-perfusion inequality, susceptibility of different gases, theoretical anal. 0-8089
- ventilatory function testing, appl. of versatile microcomputer 0-41291
- ventilatory phonetics, analogic 0-51131
- ventilatory phonotory conflict, investigation using glottoscope 0-51145
- ventilatory response to CO<sub>2</sub> obs., sprint swimmers (*Japanese*) 0-8077
- volume of lung, reduction during behavioural active sleep in newborns 0-45935
- CO, single breath diffusing capacity in man, meas. by rapid CO anal. 0-46115
- CO uptake in respiration, computer aided measuring system (*German*) 0-3875
- CO<sub>2</sub> responses of conscious rabbits at ambient temps. of 5, 20 and 35°C 0-56085
- HeO<sub>2</sub>, breathing, dogs, mechanisms of increased max. expiratory flow 0-56083

**PNO calculations**

- ArH<sup>+</sup>, <sup>1</sup>Σ<sup>+</sup> ground state, molecular const. calc. from pot. curves 0-9680

**Pockels effect**

- active pulse shaping in ps domain using fast Pockel cell and GaAs switch 0-28257
- insulator surface flashover in vacuum, electro-optical meas. 0-38823
- IR pulsed radiation production using 2.25 cm<sup>2</sup> aperture Pockels cell system 0-5806
- optical wave conjugation by three photon mixing, effect of strong wave front distrib. 0-5783
- PROM, diff. efficiency 0-14467

**point contacts**

- alkali metals, point contacts, current-voltage characts. at liq. He temps. 0-39663
- electrical transport, influence of mech. modulation 0-2481
- metal whisker point contact junctions, tunnelling and rectification characts. 0-6955
- metals, ferromagnetic, point contact spectroscopy, electron-magnon interactions (*Russian*) 0-54766
- subMM wave mixing in metal-metal and metal semiconductor point contact diodes 0-4769
- Cu-Zn heterocontacts, microcontact spectra (*Russian*) 0-34502
- Gd, microcontact magnon spectra, electron-magnon interaction (*Russian*) 0-54768
- Ge p-n junctions with hot carriers, current amplification, elec. domain form. 0-6966
- Ho, microcontact magnon spectra, electron-magnon interaction (*Russian*) 0-54768
- Nb superconducting point contact, high freq. props. in far IR 0-54840
- Tb, microcontact magnon spectra, electron-magnon interaction (*Russian*) 0-54768
- W-C, compared with TGS pyroelec. detector, appl. to temporal coherence meas. of HCN laser 0-31871
- W-Ni, MBM diode, resist. depend. of detected signals 0-2482

**point defect scattering**

- used for carrier scattering by point defects
- degenerate semiconductors, longitudinal thermo-EMF in quantising mag. field, scatt. mechanism (*Russian*) 0-24960

**point defect scattering continued**

- optical properties of band charge carriers, nonlinear, rel. to carrier scattering by lattice defects 0-29399
- organic molecular crystal, temp.-independ. mobilities, elec. field and defect scatt. effects 0-10963
- semiconductor, carrier scatt. and mobility transient processes, pulsed Hall photoeffect 0-15546
- n-Ge, deform. induced point defects, Hall coeff. meas. 0-19800

**point defects**

- see also colour centres; interstitials; point defect scattering; vacancies (crystal)
- alkali halides, <sup>14</sup>N impurities, molecular point defects, EPR isotropic hyperfine triplets 0-2636
- alkaline earth halide crystals, thermal transport of charged point defects 0-15293
- alkaline earth oxides, point defect props., band struct., lattice simulation calc. 0-19797
- coatings, defects and their effect on props. 0-39474
- concentration monitoring during low-temp. irradiations and anneals 0-7741
- covalent semiconductors, electronic struct. of localised defects, review 0-44535
- cubic crystal edge and screw dislocation-point defect elastic interactions 0-15151
- diamond, defects and impurities 0-29017
- diamond, optical absorption and luminesc. spectra, review 0-2848
- dislocation field effect, dislocation photoconduction spectrum (*Hungarian*) 0-51977
- dislocation interaction with point obstacle in non-uniform stress field, localised force approx. 0-15150
- elastic interactions between defects and interfaces 0-39147
- elastic interactions in semi-infinite medium 0-39146
- electrolytes, solid oxide, elec. props., study methods (*French*) 0-22386
- electronic structure, formation energies and diffusion parameters 0-2009
- fission reactor materials, defect trapping and solute segregation in irradiated alloys 0-13603
- fission reactor materials, point defect nucleation and growth, rate theory model for simultaneous clustering 0-13604
- n-InSb, acceptor effect of plastic bending 0-6885
- interaction mechanism, long range forces, incompressible continuous media 0-54232
- intrinsic point defect-impurity atom mobile complex form., influence on defect diffusive fluxes 0-2063
- ion axial channelling analytical model, point defect scatt. 0-39192
- ion bombardment, electron microscopical anal. of surface effects and volume defects, review (*Rumanian*) 0-29093
- ionic crystals, electronic and vibr. props. of point defects, book 0-51962
- irradiation effects, void nucleation, swelling, creep, rate eqns. 0-49274
- metal, fatigued, relationship between stress and point defect cluster density 0-10592
- migration into dislocation loops, finite difference calc. 0-54225
- molecular crystals, semi-infinite, with surface point defect, exciton states 0-20271
- orbit degenerate electron state localised at point defect, T-term multimode Jahn-Teller effect (*Russian*) 0-15490
- oxides, interaction between point defects and dislocations, cryst. plasticity 0-15149
- oxides, point defects diffusion coeffs. calc. (*Japanese*) 0-15302
- plastically deformed crystal, lattice defects influence on axial shadow figure (*Russian*) 0-25508
- point defect interactions due to static lattice displacements, continuum and lattice theory approach 0-39082
- rare earth metals, HCP, point defect production during electron irradi. at low temp. 0-49273
- screening of fields of static distortions 0-6797
- semiconductors, electron states of point defects 0-39526
- shielded point defect potential well calcs. using Poole-Frenkel effect 0-20122
- shock wave formation of point defects (*Russian*) 0-6401
- stress induced absorption, and emission by grain boundaries 0-39081
- thin foil point defect profile rel. to dislocation loop growth during HV electron microscope irradi. 0-2018
- transparent optical materials, laser induced damage and lattice strain due to lattice defects 0-48315
- Al, dislocation and point defect interactions, US study under quasistatic stress (*French*) 0-2061
- (AlGa)As DH, proton-stripped, proton-induced defects, photoluminesc. study 0-48251
- AlGaAs-GaAs double heterostructure laser lifetime, point defect generation model calcs. 0-32992
- BaF<sub>2</sub>, ionic conductivity meas., computer anal. point defect parameters 0-54429
- Bi<sub>2</sub>Se<sub>3</sub>:Hg point defects in crystal lattice, Hall coefficient and IR spectra determ. 0-55129
- CdO, point defect props., band struct., lattice simulation calc. 0-19797
- Cu, inhomogeneous clustering of radiation damage after neutron irradiation between 200 and 400°C 0-15161
- α-Fe, radiation induced displacement cascade, short term annealing, computer simulation 0-54282
- Ge, neutron irradiated, positron annihilation, ESR and resist. meas. 0-15160
- n-InAs, electron irradi., rel. to thermal and electrophysical props. (*Russian*) 0-39154
- InAs:Te(Se)(S), intrinsic pt. struct. defects 0-33998
- InGaAsP-InP, double heterostructure laser lifetime, point defect generation model calcs. 0-32992
- InSb films, melt-grown, point defect effect on elec. props., 77-300K 0-2502
- KCl:KF:Pb<sup>2+</sup>, point defects, ionic thermal currents and optical meas. 0-6403
- β-Li-Al, lattice parameters, density, defect struct. 0-24440
- LiF, radiation induced voids, formation on dislocations 0-15159
- Mo, neutron bombard., radiation damage, electron microscopy obs. (*Russian*) 0-44235
- NaCl preirradiation effect on proton channelling, thermoluminescence study 0-19860
- NaCl-NaF:Pb<sup>2+</sup>(Eu<sup>2+</sup>)(Zn<sup>2+</sup>)(Mn<sup>2+</sup>)(Sn<sup>2+</sup>), point defect ionic thermal current and optical meas. 0-6403
- Si, neutron irradi., point defects photopopulation and photoionis., IR spectra meas. 0-25423



**point defects continued**

- Si, packing defects, change in size during heat treatment 0-39079  
 Si single crystal surface, He<sup>+</sup> bombardment, damage production, defect diffusion 0-39181  
 Si with thermal defects, photocond., effect of annealing on elec. resist. 0-6837  
 Si, zone melting, swirl defects A-type as source of dislocation generation on macroscopic scale 0-25554  
 Si:B, lateral effect of oxidation on B diffusion 0-29217  
 TiO<sub>2</sub>, rutile single crystals, stoichiometric, dynamic strain ageing 0-50661  
 V<sub>2</sub>Si, plastic deform. effect on supercond. props. 0-29500  
 ZnTe, refined, undoped, Cu acceptor, optical absorption and photoluminesc. meas. 0-34970  
 Zr, point defect migration into dislocation loops, finite difference calc. 0-54225  
 Zr-base alloys, annealed specimens, irradiation growth 0-49276  
 ZrO<sub>2</sub>:Cu, point defects, electrochem. characterisation 0-35599

**point groups** *see crystal atomic structure***point of sale systems**

- hologram scanner for POS bar code symbol reader 0-48182

**point to point radio links** *see radio links***Poiseuille flow**

- Brownian particle diffusion in shear induced convection, Poiseuille flow 0-33591  
 channel flow, finite amplitude, instability shear layer parallel flow, cellular motion 0-1601  
 Fermi liquid viscosity in finite geometry 0-24702  
 Hagen-Poiseuille, of microthermopolar fluids in circular pipe 0-24092  
 inhomogeneous liquid, spin echo signal shape (*Russian*) 0-50225  
 internal separated flows at large Reynolds number, Poiseuille flow development in channel 0-53755  
 local similarity solutions and their limitations 0-33675  
 MHD Poiseuille perturbed pipe flow in nonuniform axisymmetric mag. field, anal. 0-24104  
 parallel-plate channel, theory of capillary rise of liq. 0-28567  
 particle distribution in Poiseuille flow of suspension in micropolar fluid model 0-10314  
 plane, transition to turbulence and finite amplitude disturbances 0-33558  
 plane turbulent Couette-Poiseuille flow, asymptotic anal. 0-33674  
 rarefied gas dynamics projection and variational methods 0-6189  
 turbulence theory, review 0-4536  
 turbulent shear flow, large eddy simulation 0-38390  
 vertical cylindrical tube, theory of capillary rise of liq. 0-28567  
 viscoelastic fluid flow between eccentric cylinders 0-1652  
 water, flow through circular pipe, pulsed NMR study 0-28566  
<sup>3</sup>He, solid, low temp. thermal cond., structural crystalline defects 0-2240  
<sup>4</sup>He, solid, boundary limited thermal cond., Poiseuille phonon flow 0-2241

**Poisson ratio**

- blood vessels, medium sized, mech. characts. 0-41101  
 cylindrical shell, circumferentially cracked, transverse shear effect 0-28472  
 elastic cylinder, end resonance under axisymmetric vibr. (*Ukrainian*) 0-23932  
 isotropic materials, rod shaped, elastic moduli and Poisson ratio determ. method 0-55606  
 metals, radiation effects on elasticity and elastic moduli, yield stress 0-2078  
 optical waveguide blanks, thermal and elastic stresses in a cylinder 0-14447  
 plastic, glass-reinforced bottoms with a filler, rigidity 0-15183  
 plastic plates, B-, organic-fibre, glass-fibre reinforced, optimization 0-20996  
 rock, mech. props. rel. to cooling (*Japanese*) 0-31036  
 softwoods, transverse Poisson's ratio and Young's modulus (*Japanese*) 0-2111  
 steel, stainless type 304, elastic const. variability, US vel. meas. 0-55446  
 viscoelasticity, instantaneous moduli, determ. from long-term static test results 0-38286  
 C fibre reinforced plastic, moduli meas. (*Russian*) 0-39199  
 Se, vitreous, elastic coeffs. about glass transition temp. US study (*French*) 0-19865

**polar cap absorption** *see ionospheric electromagnetic wave propagation***polar cap flow** *see airglow***polar semiconductor materials** *see polar semiconductors***polar semiconductors**

- see also ferroelectric semiconductors; piezoelectric semiconductors*  
 conduction states, pseudopot. and tight-binding calcs. 0-24785  
 conductivity in quantising mag. field, anharmonicity effect 0-2406  
 electron-hole liquid, electron-phonon interactions 0-6739  
 electron-hole system, interaction with phonons 0-6738  
 exciton, energies, oscillator strengths, and phonon side bands 0-44512  
 exciton-dispersion, influence of optical phonons 0-6741  
 exciton-phonon interactions, optical absorpt. spectra, theory 0-49614  
 excitons in mag. field, exciton-phonon interaction 0-24806  
 hot exciton scatt. accompanied by transitions to excited states, phonon interactions 0-44516  
 nonlinear transport, field-dependent relaxation time 0-6866  
 photoexcited, carrier and optical phonon distrib. time evolution 0-34158  
 surface, energy levels and geometry, theory 0-49481  
 p-Te, impact ionization rate of holes at 77K 0-10993  
 AgBr, polar semiconductor, electron-hole liquid, electron-phonon interactions 0-6739  
 CdS(Se), polar semiconductor, electron-hole liquid, electron-phonon interactions 0-6739  
 CdSe, collisions between hot excitons and hot electrons 0-7415  
 GaAs, collisions between hot excitons and hot electrons 0-7415  
 GaP, polar semicond., radiative recomb., electron-phonon interaction effects, calc. 0-49631  
 GaP, polar semiconductor, electron-hole liquid, electron-phonon interactions 0-6739  
 GaSe, direct exciton excited state hot luminescence, band struct. props. 0-55183  
 InP, collisions between hot excitons and hot electrons 0-7415  
 La<sub>0.9</sub>Ca<sub>0.7</sub>CrO<sub>3</sub>, polar semiconductor, elec. props., slight reduction effect 0-20183  
 SiC, polar semiconductor, electron-hole liquid, electron-phonon interactions 0-6739

**polar semiconductors continued**

- ZnO, polar semiconductor, electron-hole liquid, electron-phonon interactions 0-6739  
 ZnSe, polar semicond., radiative recomb., electron-phonon interaction effects, calc. 0-49631

**polarimeters**

- see also polarimetry*  
 astronomical polarimeter, stellar photometric appl. for interstellar grain size meas. 0-12792  
 automatic polariscope interactive control system to evaluate stresses 0-19299  
 Cary 60 spectropolarimeter, conversion into fast circular dichroism instrum. for use with standard rapid reaction techniques 0-52296  
 gamma ray, 100 to 800 keV, high resolution 0-52839  
 High Altitude Observatory Coronagraph/Polarimeter on the Solar Maximum Mission 0-51662  
 high-speed scanning polarimeter for study of kinetics of polarisation processes 0-31845  
 laser polarimeter for e<sup>+</sup> e<sup>-</sup> beam polarisation meas. in storage ring 0-14019  
 microscope polarisation adapter, for transparent material anisotropy and internal stresses meas. 0-31863  
 neutron depolarisation meas., exptl. set up and process program 0-18771  
 neutron polarimeter, 3-D calibration procedure 0-18770  
 optophysical and physicochemical meas. instrum. 0-13121  
 proton spectrometer/polarimeter for photoreactions below 1 GeV 0-18751  
 spectrophotometer universal cryostat attachment 0-31765  
 spectrum scanning Stokes polarimeter for solar work 0-51663  
 Stern-Gerlach, for measuring polarisation of cold neutron beams 0-37679  
 Ultraviolet Spectrometer and Polarimeter on Solar Maximum Mission 0-51661  
 Ar, liquid, scintillating target, fast neutron polarisation analyser 0-47833  
 C, proton analysing power, 300-560 MeV 0-23279  
<sup>3</sup>He(d,p)<sup>4</sup>He, polarimeter for deuteron beams 0-47834

**polarimetry**

- see also ellipsometry; polarimeters*  
 acousto-optic polarisation modulator, use in dynamic ellipsometry, polarimetry (*Russian*) 0-14472  
 circular ring, inner boundary shapes, optimised, diametral compression 0-38369  
 EM noiselike radiation, noncoherent polarimetry anal. 0-1111  
 gravitational radiation detection method, elastooptical antenna, photoelastic effect 0-46947  
 Jupiter clouds spectropolarimetry, lines equivalent widths information content 0-31215  
 neutron polariser-analyser efficiency meas. by spin flip meas. 0-27911  
 optical measurement technique using He-Ne stabilised transverse Zeeman laser 0-48272  
 optomechanical properties determ., polarisation device application, by compensation method 0-40643  
 photocathode polarisation sensitivity, two-beam interferometer expts. 0-4772  
 proton polarisation meas. for <sup>12</sup>C(p,p) at 40-75 MeV 0-52840  
 radio sources Faraday rotation measures, computation method 0-4263  
 stress measurement, polarisation device application, by compensation method 0-40643  
 Venus clouds spectropolarimetry, lines equivalent widths information content 0-31215

**polarisability**

- see also atomic polarisability; molecular polarisability*  
 alkali halide, optoelectronic props. 0-25330  
 alkali metal halide, electronic strain polarisability consts. 0-29677  
 carbazole, birefr. meas., 20 to 190°C, crystal-to-crystal phase transform. 0-45031  
 ionic crystal, electronic dielectric const. first and second electronic dielectric const., effective charge parameters 0-29669  
 ionic crystals, evaluation of photoelastic consts. 0-50297  
 linear aggregates, small, polarisability determ., CNDO method and analytical models (*French*) 0-29298  
 sapphire, shock compressed, refractive index, density, and polarisability behaviour 0-50295  
 semiconductor, electronic polarizability as function of Penn gap 0-49638  
 semiconductor, nonlinear optical props. 0-25333  
 semiconductor compounds, electronic polarisability rel. to energy gap 0-10524  
 solute-solute-solvent interaction, dielec. behaviour problems, review 0-25298  
 pp-γγ annihilation, influence on sum rule proton polarisability 0-18143  
 BaO-K<sub>2</sub>O-VO<sub>2</sub>-SiO<sub>2</sub>, glass, elec. cond. rel. to ion polarisability, polarons 0-49729  
 BaO-La<sub>2</sub>O<sub>3</sub>-VO<sub>2</sub>-SiO<sub>2</sub>, glass, elec. cond. rel. to ion polarisability, polarons 0-49729  
 Cs<sub>2</sub>NaRCl<sub>6</sub>, R=Pr<sup>3+</sup>, Eu<sup>3+</sup>, Tb<sup>3+</sup>, Tb<sup>3+</sup>, crystal field, ligand polarisability contributions 0-39536  
 FeS<sub>2</sub>, pyrite, semiconducting props., energy gap press. and lattice parameter depend., Mossbauer obs. 0-44494  
<sup>4</sup>He, polarisability, second and third virial coeffs. meas. 4.2 to 27.1K 0-43825  
 KD<sub>2</sub>PO<sub>4</sub>, Rayleigh scatt. and narrow central component, depend. on scatt. wave vector direction 0-29747  
 MnO, dielec. behaviour, Dick and Overhauser shell model calcs. 0-45001  
 NiO, dielec. behaviour, Dick and Overhauser shell model calcs. 0-45001  
 SiO<sub>2</sub>, fused, shock compressed, refractive index, density, and polarisability behaviour 0-50295

**polarisation**

- see also beta-ray polarisation; deuteron polarisation; dielectric polarisation; electron spin polarisation; gamma-ray polarisation; light polarisation; neutron polarisation; nuclear polarisation; photon polarisation; polarisation in elementary particle interactions; polarisation in elementary particle scattering; polarisation in nuclear reactions and scattering; proton polarisation*  
 √ collapse and locality 0-372  
 Abell 2256, X-ray cluster of galaxies, radio emission linear polarisation 0-36726  
 air, due to Compton electrons excited by γ-quanta pulse, radial electric fields 0-21805  
 B2 1502+28, head-tail galaxy in Abell 2022, Westerborg obs. of spectral index and polarisation distrib. 0-36727



**polarisation continued**

- B 0844+31, extended radio galaxy, polarisation distrib. from multifreq. obs. 0-56963  
 4C+36.11, extragalactic source, Faraday rot. in S232 rel. to mag. field strength 0-51840  
 3C 310, extended radio galaxy, multifreq. intensity and polarisation obs. 0-51890  
 Cassiopeia A, intensity and polarisation at 9 mm wavelength 0-36732  
 circumterrestrial plasma Faraday inverse effect (*Russian*) 0-4190  
 crystal acoustics, linear and nonlinear 0-5855  
 V1057 Cygni, OH line polarisation rel. to Zeeman splitting 0-36629  
 Earth crust, in situ induced polarisation meas. at Yerington mine, Nevada 0-51323  
 Earth induced polarisation soundings interpretation, freq.-effect transform function definition and appl. 0-56624  
 Earth-space radio signals, depolarisation rel. to ice particle orientation and alignment changes 0-17330  
 electron polarisation by circularly polarised EM waves in storage ring 0-14020  
 EM wave propagation in inhomogeneous media, 'W'-shape transients, modified ray tracing technique appl. 0-48119  
 extragalactic radiosources, mag. field orientation evidence 0-46690  
 gravitational waves, polarisation in Yang's gravitational field (*Chinese*) 0-17850  
 H Lyman  $\alpha$  in solar chromospheric flares, direct collisional excitation rel. to profile and polarisation 0-41780  
 heavy ion beams, polarisation monitors 0-27910  
 W Hydrae, OH masers polarisation obs. and suspected Zeeman splitting 0-36632  
 interstellar OH main line maser, circular polarisation and probable Zeeman pattern 0-56908  
 ion beam prod. from optically pumped electron spin polarised targets 0-27851  
 Ising model, infinite metastable states 0-34577  
 laser technology, parallel plate, hard seal technique 0-1225  
 low energy positron beams, spin polarisation 0-9442  
 M31, polarised radio emission distrib. rel. to large-scale mag. field 0-41899  
 methyl halides, mol. force fields, IR intensities, and vibr. props. 0-47879  
 microwave crosspolarization, effects of sizes of nonspherical raindrops 0-21790  
 microwave crosspolarization on satellite to Earth path, effect of rain 0-21789  
 molecular crystal, polarisation energy of localised charge, appl. to anthracene and naphthalene 0-15034  
 neutron, exact spin rotation by precession 0-32584  
 Orion A, 22 GHz water line outburst linear polarisation 0-8703  
 parallel conductors in external field 0-28136  
 particle polarisation meas., set of efficient estimators 0-27909  
 picosecond spectroscopy, anal. using polarisation method 0-13152  
 plane waves, difference between polarisation and coherence 0-8805  
 plasma, polarisation freq. depend. of electron cyclotron emission 0-33808  
 plasma, resonant charge exchange, polarisation effect 0-43859  
 polyatomic gas, plane Couette flow in Knudsen regime, wall induced polarisation 0-19443  
 pulsar microstructure, propag. effects in shearing field-free plasma 0-17483  
 pulsars, individual pulse-polarisation patterns and quasi-transverse propag. theory 0-46591  
 radio recombination lines from H II region NGC 2024, search for linear polarisation 0-41872  
 radio sources, linear polarisation catalogue 0-51671  
 radio sources, superluminal, circular and linear polarisation in mag. dipole model 0-56959  
 radio sources Faraday rotation measures, computation method 0-4263  
 radiowave propag. crosspolarisation and attenuation meas. at 11.6 GHz using theoretical rain model, canting angle distrib. 0-4070  
 rotation of US plane of polarisation under ESR saturation conditions 0-29123  
 satellite retroreflector arrays 0-5778  
 solar metre-wave radio emission, wave ducting rel. to polarisation and source positions 0-21978  
 solar type III radio bursts, fundamental emission and polarisation 0-36603  
 solar type U radio bursts, polarisation evolution 0-26834  
 synchrotron, spin flip by adiabatic passage of depolarisation resonances 0-5415  
 Taurus A, intensity and polarisation at 9 mm wavelength 0-36732  
 terrestrial electricity, induced polarisation induced potentials and derivatives rel. to deep sounding (*German*) 0-56626  
 terrestrial electricity, source field polarisation 0-56356  
 thermorigid dielectrics, nonlinear thermodynamic theory 0-10149  
 Vela supernova remnant, rot. measure and turbulent struct. 0-51836  
 Vela X supernova remnant, radio polarisation maps 0-56909  
 whistlers, effect of Earth-ionosphere waveguide propagation on polarisation and arrival angles 0-36457  
 white dwarfs, magnetic, circular polarisation prod. by cyclotron absorpt. 0-4351  
 X-ray dynamic diffraction, polarisation states in Laue case 0-28878  
 X-ray pulsars, vacuum polarisation effect rel. to radiative transfer and X-ray spectra 0-27015  
 X-ray radiation emitted near black holes, polarisation features 0-46700  
 X-rays, tuneable polarisers 0-315  
 CO<sub>2</sub>, laser excitation by RF discharge with rot. elec. field, linear and circular polarisation 0-37991  
 Cygnus A, intensity and polarisation at 9 mm wavelength 0-36732  
 Kr gas discharge plasma, electron impact depolarization 0-43847  
 Li<sub>2</sub>, circular polarisation of emission, influence of nucl. hyperfine interactions and elastic collisions 0-9635  
 Li<sub>2</sub>, collisional depolarisation and rot. energy transfer, laser-induced fluorescence obs. 0-9698  
 Ne gas discharge plasma, electron impact depolarization 0-43847  
 Pt electrodes, nonlinear AC and DC polarisation obs. 0-56247  
 SiO 86.2 GHz maser, astronomical sources polarisation props. 0-4449

**polarisation in elementary particle interactions**

- electron-hadron interactions, P-invariance, lepton, quark anapolar moments with pol. e (*Russian*) 0-52518  
 electroproduction, polarised, flavour singlet coefficient functions, QCD corrections, sum rules 0-47301  
 hadronic interactions, review 0-52527

**polarisation in elementary particle interactions continued**

- hadrons interacting, isospin-spin polarisations, dynamical characts. 0-32035  
 QCD structure function relation between deep inelastic  $\nu$  reactions and polarised electroprod. 0-37221  
 ed $\rightarrow$ epn, polarised deuteron disintegration, virtual nucleon density matrix formalism (*Russian*) 0-52519  
 e $^+e^- \rightarrow N^+N^*$ , weak neutral current effects for polarised e $^+e^-$  pair 0-37287  
 e $^+e^- \rightarrow W^+W^-$ , polarisation amplitudes 0-42484  
 e $^+e^- \rightarrow ZZ$ , polarisation amplitudes 0-42484  
 eN deep inelastic polarised scatt., QCD corrections 0-52517  
 ep deep inelastic scatt., pol. p and e, straton model, sum rule (*Chinese*) 0-42475  
 $\gamma N \rightarrow K^+\Sigma$ , meas. of asymmetries and cross sections using 16 GeV linearly polarised photons 0-13318  
 $\gamma N \rightarrow l^+l^-X$ , polarisation effects on P-violating, asymmetry in Weinberg-Salam model 0-32055  
 $\gamma N \rightarrow \pi^+n$ , meas. of asymmetries and cross sections using 16 GeV linearly polarised photons 0-13318  
 $\gamma N \rightarrow \pi\Delta$ , meas. of asymmetries and cross sections using 16 GeV linearly polarised photons 0-13318  
 $\gamma p \rightarrow K^+\Lambda$ , meas. of asymmetries and cross sections using 16 GeV linearly polarised photons 0-13318  
 $\gamma p \rightarrow \pi^+\pi^+$  section asymmetry, pion-proton twin birth contribution (*Russian*) 0-47308  
 $Kp \rightarrow \Sigma^+\pi^-$ , 500 MeV/c, meas. of polarised  $\Sigma^+$  magnetic moment 0-22614  
 $p\alpha$ , 1300 to 2300 MeV,  $\pi^0$  photoproduction, double polarisation parameters 0-13317  
 pd, polarised pn total cross sections 0-22633  
 pN, dilepton production by pol. protons, parity violating, asymmetry, Weinberg-Salam calcs. 0-42488  
 $pN \rightarrow \Lambda^0 X$ , 28.5 GeV/c,  $\Lambda^0$  polarisation 0-32137  
 pp, 28 GeV, in H, D, Be, inclusive  $\Lambda$  polarisation 0-47337  
 $pp \rightarrow \Lambda(K^0)X$ , 12 GeV/c, beam polarisation induced asymmetries 0-42507  
 $pp \rightarrow \pi^+d$ , SIS, 578 MeV, pol. beam and target, spin depend. parameters 0-42651  
 $pp \rightarrow \pi d$ ;  $\pi^+$  negative parity assignment 0-32117  
 $\pi^- p \rightarrow K^+\Sigma^0$ , 1395 to 2375 MeV/c, differential cross-section and polarisation meas. 0-9183  
 $\rho^0$  electroproduction, parity violating effects 0-9178  
 $W^0$  effects in e $^+e^-$  interactions on a $^-$  resonances 0-42386
- polarisation in elementary particle scattering**  
 hadrons, multipole polarisabilities from Compton scatt. amplitudes 0-13311  
 e-p, scatt. and polarisation matrices (*German*) 0-27508  
 ed scatt., P-violation calc. in weak interaction theory 0-42469  
 e $^+e^- \rightarrow e^+e^-$  gg, gluon jet polarisation in photon-photon scatt., QCD test 0-52550  
 ep scatt., longitudinal cross section and asymmetries for jets in leptoproduction 0-32106  
 $K^+n$ , 0.851 to 1.351 GeV, polarisation parameter meas. 0-42498  
 $K^-p$  elastic scatt., 0.955, 1.272 GeV/c, polarisation parameter meas. 0-37299  
 pN, high energy polarised scatt. particle struct. studies, book 0-41952  
 pp, polarised 6 GeV scatt., spin depend. forces in eikonal model 0-37246  
 $\bar{p}p$ , pp high energy elastic scatt., cross section rise and polarisation, Regge model (*Russian*) 0-37301  
 $\pi d$  elastic scatt., 142-256 MeV, dibaryon resonance interference with Faddeev amplitudes 0-32123  
 $\pi^-p$  elastic scatt., 450-560 MeV, polarisation parameter (*Russian*) 0-37295  
 $\pi^-p$  elastic scatt. at 490 and 600 MeV, polarisation parameter meas. (*Russian*) 0-42496
- polarisation in nuclear reactions and scattering**  
<sup>116</sup>Sn(d,d), polarised d, 8.22 MeV, anal. power 0-5114  
 collective tube model of high energy proton scatt. on polarised nuclei 0-32273  
 conference on heavy ion reaction dynamical props., Johannesburg, S.Africa (Aug. 78) 0-17715  
 elastic and quasi-elastic polarised heavy ion collision theory, semi-quantal description 0-18330  
 Ericson fluctuations in polarised (p,p) reactions (*Rumanian*) 0-5113  
 heavy ion collision polarisation, damping mechanism approach via elementary excitation modes 0-18338  
 knock-out reactions, polarisation phenomena in the presence of strong absorption (*Russian*) 0-37360  
 lepton-nucleus scattering, bremsstrahlung and neutral currents 0-32268  
 neutron and nuclear polarisation expts., spin depend. of neutron cross-sections, mag. moments, radiation capture of neutrons (*Russian*) 0-52654  
 nucleus-nucleus pot., static polarisation effects, nuclear shapes 0-5154  
 polarised nucleus fission, parity nonconservation mechanism, rot. state mixing (*Russian*) 0-37408  
 stopped muons, macroscopic polarisation (Hanle) signals 0-5130  
 (d,d), pol. d, 12 MeV, A=46-82, cross sections, anal. powers, global optical model anal. 0-47459  
 ( $\gamma$ , $\gamma$ ), linear polarised photon on even-even nuclei 0-543  
 ( $n$ , $\gamma$ ), spin assignments using polarised beams and gamma spectroscopy 0-37323  
 ( $n$ , $n$ ), pol. n, 16.1 MeV, differential cross section, optical model fit 0-32259  
 (p, p), 1 GeV, polarisation data, Glauber anal. spin-orbit parameters, matter distrib. 0-52655  
 (p,p), 600, 750 MeV, polarisation and cross section, Glauber model calc., NN matrix test 0-47485  
 (p,p), elastic, inelastic polarised and unpolarised, intermediate energy study review 0-42653  
 (p,p), pol. p, sd, fp shell nuclei, 65 MeV, effective two-body interaction range 0-32201  
 (p,t), pol. p, strong ground state transitions, anomalous anal. power, direct and sequential processes 0-5115  
 (p,X), experimental information review, polarisation phenomena 0-42655  
 (t,t), A=40-208, 17 MeV, pol. t, cross sections and anal. powers, optical anal. 0-47462  
<sup>208</sup>(N, $\gamma$ ), pol. N, anal. power and giant multipole resonances, direct-semidirect model 0-18265  
<sup>107</sup>Ag high spin states, J $^\pi$  assignments, polarisations and transitions from (<sup>7</sup>Li,4n $\gamma$ ), (<sup>6</sup>Li,3n $\gamma$ ) 0-27536



## polarisation in nuclear reactions and scattering continued

- <sup>27</sup>Al,  $J^\pi=5/2$  state, cross section and analysing power ang. distrib. 0-18296
- <sup>27</sup>Al(p, $\alpha$ )<sup>24</sup>Mg, finite-range cluster-model description, DWBA approach 0-52667
- <sup>28</sup>Al levels, spins and  $\gamma$ -rays, multipole mixing from <sup>27</sup>Al(n, $\gamma$ ), pol. thermal 0-47398
- <sup>197</sup>Au + <sup>136</sup>Xe, 1064 MeV, fragment spin orientation from continuum  $\gamma$ -ray anisotropy meas. 0-22853
- <sup>197</sup>Au(<sup>66</sup>Kr,X) 612 MeV,  $\gamma$ -ray circular polarisation 0-13453
- <sup>198</sup>Au level spin assignments from  $\gamma$  ang. distrib. and circular polarisation from <sup>197</sup>Au(n, $\gamma$ ) 0-52570
- <sup>10</sup>B(n, $\alpha$ )<sup>7</sup>Li, thermal polarised n capture, P-odd asymmetry meas. (Russian) 0-13452
- <sup>11</sup>B(p,n)<sup>11</sup>C, shell model anal. of polarisation-analysing power differences 0-22804
- <sup>9</sup>Be( $\gamma$ , $\pi$ ), photoabsorption and sum rules, structure, RMS radius, polarisability and exchange parameters 0-22686
- <sup>12</sup>C p<sub>0</sub> channel E2 strength from <sup>11</sup>B(p, $\gamma$ ) pol. p. 0-22790
- <sup>12</sup>C(p, $\gamma$ )<sup>13</sup>N, pol. p, 10-17 MeV, <sup>13</sup>N electric quadrupole strength semi-direct capture model calcs. 0-47370
- <sup>12</sup>C(p,p'), 1 GeV, proton polarisation in natural parity level excitation (Russian) 0-42634
- <sup>12</sup>C(p,p'), natural parity level excitation (Russian) 0-5144
- <sup>12</sup>C(p,p')<sup>12</sup>C\*, pol. p., 19-23 MeV, giant resonances as doorway states, virtual excitation 0-5102
- <sup>12</sup>C(p,p), 40-75 MeV, polarisation meas., differential cross sections 0-52840
- <sup>12</sup>C(p,p), pol. p, 450-600 keV, Mott-Schwinger interaction existence, anal. power 0-22805
- <sup>12</sup>C(p,pn), pol. nucleon quasi-elastic scatt., nuclear wave function and model tests 0-42656
- <sup>13</sup>C(p, $\alpha$ )<sup>10</sup>B<sub>gs</sub>, 65 MeV, pol. p, DWBA form factor 0-52559
- <sup>13</sup>C(p, $\gamma$ ), pol. p, 6.25-17.0 MeV, anal. power and cross section ang. distrib., E1, E2 amplitudes 0-47461
- <sup>40</sup>Ca(<sup>3</sup>He, x), pol. <sup>3</sup>He, x=d or  $\alpha$ , 33 MeV, anal. power and cross sections 0-42628
- <sup>40</sup>Ca(<sup>3</sup>He,<sup>3</sup>He), pol. <sup>3</sup>He, 33.3 MeV, differential cross section and anal. power, optical pots. 0-42627
- <sup>40</sup>Ca(p,p), 20-50 MeV differential cross section, polarisation ang. distrib., optical model exchange terms 0-27638
- C(n,n), total cross sections below 2 MeV, R-matrix fits to data 0-13466
- <sup>59</sup>Co, deformation effect of aligned target, fast-neutron transmission 0-47364
- <sup>54</sup>Cr(d,pol,p), cross section and vector analysing power, <sup>54</sup>Cr deduced levels and spins 0-52684
- Cu(n,n), 14.2 MeV, polarisation in forward angle scatt. 0-18282
- (d,p), A=88-106, pol. d, excitation curve isospin anomaly, neutron single particle resonances 0-27595
- <sup>152</sup>Dy( $\alpha$ ,xn $\gamma$ ), A=162,164, Er yrast levels, spin alignment 0-52557
- <sup>152</sup>Dy yrast continuum  $\gamma$ -ray multipolarity via polarisation meas. from <sup>140</sup>Ce(<sup>16</sup>O,4n) 0-9264
- <sup>19</sup>F(d, $\alpha$ )<sup>17</sup>O, 1.8 to 3.0 MeV, vector analysing ability using polarised deuterons (Russian) 0-32288
- <sup>19</sup>F(d,d)<sup>19</sup>F, 1.8 to 3.0 MeV, vector analysing ability using polarised deuterons (Russian) 0-32288
- <sup>20</sup>F cross sections and anal. power, compound nucleus contrib. Ericson fluctuations from <sup>18</sup>O(d,p), pol. d 0-22803
- <sup>54</sup>Fe(d,pol,p), A=54,58, cross section and vector analysing power, <sup>55,59</sup>Fe deduced levels 0-52684
- <sup>66</sup>Ge states and decay scheme, polarisations  $J^\pi$  and ang. distrib. from <sup>58</sup>Ni(<sup>10</sup>B,pn $\gamma$ ) 0-22692
- <sup>1</sup>H(d,d), 2 GeV, polarised d, tensor and vector asymmetries 0-9285
- <sup>1</sup>H(n,p), pol. n and p, 220-495 MeV, free elastic scatt., D, and P parameters 0-52674
- <sup>1</sup>H(n,p), pol. n and p, 220-495 MeV, free elastic scatt., Wolfenstein parameters R<sub>1</sub>, A<sub>1</sub> 0-52675
- <sup>1</sup>H(p, $\pi^+$ )<sup>2</sup>H, SIS, 578 MeV, pol. beam and target, spin depend. parameters 0-42651
- <sup>2</sup>H( $\alpha$ ,np)<sup>4</sup>He, differential cross section and polarisation, three body model 0-47460
- <sup>2</sup>H(d,n), 290, 460 keV, neutron polarisation, ang. depend. 0-42632
- <sup>2</sup>H(d,n)<sup>3</sup>He, 1.5-15.5 MeV, tensor anal. power, charge symmetry violation in mirror reaction 0-13368
- <sup>2</sup>H(d,p)<sup>3</sup>H, 13.4, 17 MeV, pol. d, anal. power direct reaction and isospin symmetries 0-515
- <sup>2</sup>H(d,p)<sup>3</sup>H, 1.5-15.5 MeV, tensor anal. power, charge symmetry violation in mirror reaction 0-13368
- <sup>2</sup>H( $\gamma$ ,  $\pi^-$ )2p, target asymmetry and effective neutron polarisation, polarised d 0-9286
- <sup>2</sup>H(p,n)2p, pol. n and p, 10.6-15.1 MeV, transverse polarisation transfer at 0° 0-42630
- <sup>2</sup>H( $\pi$ , $\pi$ ), polarised d, dibaryon resonance signals in excitation functions 0-9181
- <sup>2</sup>H( $\pi$ , $\pi$ ), relativistic description,  $\pi$ N waves, NN rescatt.,  $\rho$ -exchange,  $\pi$  absorption and emission 0-9310
- <sup>2</sup>H( $\pi^+$ ,  $\pi^+$ ), tensor polarisation and cross section at 180° 0-5116
- <sup>2</sup>H(d,n), pol. d, below 6.75 MeV, tensor anal. power 0-42633
- <sup>2</sup>H( $\gamma$ , $\pi^+$ ), polarisation effects 180 to 700 MeV, impulse approx. calcs. (Russian) 0-37368
- <sup>3</sup>H( $\gamma$ , $\pi^0$ )<sup>3</sup>H, polarisation effects 180 to 700 MeV, impulse approx. calcs. (Russian) 0-37368
- (<sup>3</sup>He, <sup>3</sup>He), pol. <sup>3</sup>He, vector and tensor polarisation, closed form description 0-37363
- <sup>3</sup>He(d,d), 0.32-5.0 MeV, anal. power, scatt. amps., <sup>5</sup>Li states, phase shift anal. 0-47382
- <sup>3</sup>He(d,p), pol. d, below 6.75 MeV, tensor anal. power 0-42633
- <sup>3</sup>He( $\gamma$ , $\pi^0$ ), polarisation effects 180 to 700 MeV, impulse approx. calcs. (Russian) 0-37368
- <sup>3</sup>He( $\gamma$ , $\pi^0$ )<sup>3</sup>He, polarisation effects 180 to 700 MeV, impulse approx. calcs. (Russian) 0-37368
- <sup>3</sup>He(p,p), pol. p, 0.3-1.0 MeV, differential cross section, anal. power, and phase shifts 0-42629
- <sup>4</sup>He (d,d), 17-45 MeV, differential cross section and tensor and power ang. distrib. 0-42631
- <sup>4</sup>He (d,d), pol. d, 20 MeV, optical pot. strong tensor term, anal. powers 0-37364
- <sup>4</sup>He (d,d) pol. d, 17-43 MeV, vector anal. power, highly excited six nucleon system 0-47458
- <sup>4</sup>He(d,d), pol. d, 12-17 MeV, differential cross sections, anal. powers, phase shift anal. 0-13449

## polarisation in nuclear reactions and scattering continued

- <sup>4</sup>He(d,pn)<sup>4</sup>He, differential cross section and polarisation, three body model 0-47460
- <sup>4</sup>He( $\gamma$ , $\pi^+$ ), polarisation effects 180 to 700 MeV, impulse approx. calcs. (Russian) 0-37368
- <sup>4</sup>He(p,2p), pol. nucleon quasi-elastic scatt., nuclear wave function and model tests 0-42656
- <sup>163</sup>Ho( $\pi$ , $\pi$ ), aligned deformed nuclei, cross sections and diffractive minima from eikonal approx. 0-22860
- <sup>5</sup>Li (3/2<sup>-</sup>) tensor polarisation from <sup>2</sup>H( $\alpha$ , np) 0-13450
- (<sup>6</sup>Li, <sup>6</sup>Li) pol. <sup>6</sup>Li, vector and tensor polarisation, closed form description 0-37363
- <sup>6</sup>Li(n,t)<sup>4</sup>He, thermal polarised n capture, P-odd asymmetry meas. (Russian) 0-13452
- <sup>6</sup>Li( $\gamma$ , $\pi$ ), A=6, 7 0-22686
- <sup>90</sup>Mo(p,p'), (A=92,94), 20 MeV, polarisation effects on nuclear excited states (Russian) 0-27645
- <sup>14</sup>N(d,  $\alpha$ ), pol. d, vector anal. capacity energy and ang. depend. 0-18281
- <sup>15</sup>N 3/2<sup>-</sup> state spin alignment and polarisation, 1/2-spin orbit interaction from <sup>27</sup>Al, <sup>88</sup>Sr(<sup>16</sup>O, <sup>15</sup>N) 0-27622
- <sup>15</sup>N low lying states, cross sections and anal. power, transitions, spectroscopic factors from <sup>14</sup>N(d,p), pol. d 0-32183
- <sup>20</sup>Ne E1 resonance from <sup>19</sup>F(p, $\gamma$ ) pol. p 0-22790
- <sup>20</sup>Ne(d,d), pol. d, 10-12 MeV, cross section, coupled channel and fluctuations anal. 0-27617
- <sup>21</sup>Ne states cross section, coupled channel and fluctuations anal. from <sup>20</sup>Ne(d,p) 0-27617
- <sup>58</sup>Ni(<sup>16</sup>O,X), 100 MeV, deep inelastic, fragment spin polarisation and alignment,  $\gamma$ -rays 0-18284
- <sup>58</sup>Ni(d,pol,p), cross section and vector analysing power, <sup>59</sup>Ni deduced levels 0-52684
- <sup>58</sup>Ni(p,p), pol. p, 40 MeV, elastic and inelastic, asymmetries and differential cross sections (Russian) 0-27623
- <sup>16</sup>O E1 and p<sub>0</sub> channel E2 strength from <sup>15</sup>N(p, $\gamma$ ) 0-22790
- <sup>16</sup>O(<sup>16</sup>O,<sup>12</sup>C)<sup>20</sup>Ne, reaction mechanism by polarisation meas. 0-9301
- <sup>16</sup>O(<sup>3</sup>He, <sup>3</sup>He), pol. <sup>3</sup>He, 33.3 MeV, differential cross section and anal. power, optical pots. 0-42627
- <sup>16</sup>O(<sup>3</sup>He, x), pol. <sup>3</sup>He, x=d or  $\alpha$ , 33 MeV, anal. power and cross sections 0-42628
- <sup>16</sup>O( $\mu$ , $\nu$ ), recoil nucleus odd and even tensor orientations, general expressions 0-13451
- <sup>16</sup>O(p,p'), 1 GeV, proton polarisation in natural parity level excitation (Russian) 0-42634
- <sup>16</sup>O(p,p'), proton polarisation and natural parity level excitations (Russian) 0-5144
- <sup>16</sup>O(p,p), 20-50 MeV differential cross section, polarisation ang. distrib., optical model exchange terms 0-27638
- <sup>17</sup>O(e,e), mag. scatt., form factors, HF calcs., core polarisation effects 0-42579
- <sup>18</sup>O, heavy ion excitation, single particle and core polarisation amplitude interference 0-5117
- <sup>20</sup>Pb(e,e), magnetisation distrib. from elastic mag. form factors, core polarisation, exchange currents 0-47372
- <sup>208</sup>Pb( $\gamma$ ,n) giant mag. dipole resonance location, photoneutron polarisation method 0-37357
- <sup>208</sup>Pb(p,P'), pol. p, 9, 10 MeV, vol. integrals for optical pots., real symmetry pot. 0-42659
- <sup>208</sup>Pb(p,p), 20-50 MeV differential cross section, polarisation ang. distrib., optical model exchange terms 0-27638
- <sup>208</sup>Pb(p,t)<sup>208</sup>Pb(3<sup>+</sup>), pol. p, 22 MeV, anal. power and (p,d)(d,t) sequential transfer processes 0-5119
- Pb(n,n), 14.0-17.4 MeV, neutron polarisation, ang. depend. diffraction struct. 0-18283
- Pb(n,n), 14.2 MeV, polarisation in forward angle scatt. 0-18282
- <sup>149</sup>Pm single proton states, spin assignments, spectroscopic factors from <sup>150</sup>Sm(t, $\alpha$ ), pol. t 0-18170
- <sup>141</sup>Pr(n, $\gamma$ ), circular polarisation, ang. distrib. meas. 0-32285
- <sup>45</sup>Sc(n,pol, $\gamma$ ), <sup>46</sup>Sc energy levels, resonances, spin and parity 0-52673
- <sup>45</sup>Sc transition polarisation, levels and spin assignments from <sup>45</sup>Sc(n, $\gamma$ ), pol. n 0-52656
- <sup>28</sup>Si(p,p), pol. p, 12-18 MeV, cross section, anal. power and states, <sup>29</sup>P resonance coherence widths 0-32258
- <sup>30</sup>Si(d,p), pol. d, 1.9-2.5 MeV, anal. power excitation function anomaly 0-5118
- <sup>45</sup>Sm(<sup>20</sup>Ne, <sup>20</sup>Ne), 70 MeV, A=148, 150, 152, Coulomb polarisation pot., coupled channel calcs. 0-22855
- <sup>116</sup>Sn(d,p), pol. d, 8.22 MeV, vector anal. power, p and d spin depend. effects 0-5114
- <sup>117</sup>Sn(p,d), polarised p, 12.9 MeV, anal. power 0-5114
- <sup>117</sup>Sn(p,p), polarised p, 12.9 MeV, anal. power 0-5114
- <sup>119</sup>Sn( $\gamma$ ,n) giant mag. dipole resonance location, photoneutron polarisation method 0-37357
- <sup>149</sup>Tb, high spin states obs. 0-18158
- <sup>175</sup>Tm single proton states, rot. bands,  $J^\pi$  assignments from <sup>176</sup>Yb(t, $\alpha$ ), pol. t 0-452
- <sup>233</sup>U fission by polarised neutrons, P odd asymmetry of emitted fragments (Russian) 0-18354
- <sup>235</sup>U(n,f), thermal polarised n capture, P-odd asymmetry meas. (Russian) 0-13452
- <sup>51</sup>V(n, $\gamma$ ), circular polarisation, ang. distrib. meas. 0-32285
- <sup>64</sup>Zn(p,p), A=66,68, 20-50 MeV differential cross section, polarisation ang. distrib., optical model exchange terms 0-27638
- <sup>64</sup>Zr(p,p'), (A=90,92), 20 MeV, polarisation effects on nuclear excited states (Russian) 0-27645
- <sup>64</sup>Zr(p,p'), A=94,96, 11.2-13.4 MeV, anal. power and excitation function T<sub>1</sub> fluctuations 0-42626
- <sup>92</sup>Zr(p,pol,A)<sup>89</sup>Y, finite-range cluster-model description, DWBA approach 0-52667

polariscopes see polarimeters

## polaritons

- crystal luminescence, polariton mechanism, reabsorption, spatial dispersion effects, boundaries (Russian) 0-55186
- damped surface polaritons at a boundary between isotropic crystals 0-2346
- degenerate semiconductor, with surface depletion layer, surface polaritons, hydrodynamical model 0-6752
- p-dibromodiphenylether surface, normal and ultra-Brewster refl. spectra 0-25400
- Dicke model, modification for long wave photons 0-1169



**polaritons continued**

dielectric films, transition layer vibr., resonance region auxiliary surface polaritons (*Russian*) 0-2347  
 energy conversion radiation enhancement using surface polaritons 0-7941  
 exciton spectroscopy, polariton dispersion 0-54613  
 Fermi-resonance, EM wave dispersion 0-2344  
 ferrimagnet, polaritons, mag. susceptibility 0-7095  
 ferroelectrics of order-disorder type 0-10894  
 hybrid bulk-surface polaritons 0-49626  
 hybrid bulk-surface polaritons 0-49627  
 kinematical polariton levels resulting from excitons, interaction, optical absorption line broadening 0-10892  
 localised electron nonequilibrium vibration interaction secondary radiation spectrum 0-2778  
 metal circular cylinders, inhomogeneous, non-radiative surface plasmon-polariton modes 0-29455  
 MIM tunnel junctions, roughened, photon emission, calc. 0-44738  
 molecular crystals, polariton spectra and lattice dynamics 0-49313  
 multi-component, reflectance spectrum, internal struct. of excitons, review, book contrib. 0-44518  
 one-dimensional two-band model, free electron-hole pairs and exciton-polariton 0-29331  
 optical activity in crystals, lattice dynamical theory 0-34883  
 parametric excitation of phonons in field of strong EM wave 0-2133  
 Raman scattering of light by polaritons, reviews 0-34928  
 Raman spectra in band of many-particle states at polariton Fermi reson. 0-25374  
 resonant Brillouin scattering via exciton-polaritons, theory 0-50353  
 semiconducting films, exciton polariton attenuation, spatial dispersion effect 0-20097  
 semiconductor, two-phonon Brillouin scattering 0-20656  
 semiconductor, Wannier excitons, fine structure, lineshape and dispersion, review 0-44520  
 semiconductor epitaxial layer, polariton wave packet propag. in exciton reson. 0-2345  
 semiconductor with superlattice, optical phonon excitation by light absorpt., impurity photoionisation 0-44275  
 semiconductors, resonant Raman scatt. from exciton-polaritons (*Japanese*) 0-50349  
 surface, linear photon and two photon absorpt. 0-49863  
 surface, nonlinear optical spectroscopy, stationary and nonstationary, theory (*German*) 0-6922  
 surface exciton polaritons, book contrib., review 0-49623  
 surface polariton frequency shift, cryst. surface and dielec. function depend. 0-44522  
 surface polariton use in optical storage 0-48414  
 Wannier exciton-polaritons, real space wave eqn. 0-39508  
 Ag/organic dye, excited mol. decay near metal surface, energy transfer to plasmon surface polaritons 0-50440  
 $\beta$ -AgI, polariton dispersion curves, Raman spectra 0-29338  
 CdS, excitonic polariton reflectance, B-exciton and k-linear term 0-7369  
 CdS, Raman shift dispersion near exciton reson., two-phonon cascade processes 0-11405  
 CdS, reson. Brillouin scatt. of exciton polaritons 0-11418  
 CdS, resonance hyper-Raman light scatt. on optical photons (*Russian*) 0-14396  
 CdS, virtually excited biexcitons polaritons dispersion, two photon Raman scatt. 0-45067  
 CdTe, reson. Raman scatt. by excitonic polaritons 0-11396  
 Cu halides, phonon anomalies for  $\text{Cu}^+$  at off-centre sites, dynamical model and Raman meas. 0-10618  
 CuBr, dispersion of multicomponent exciton polaritons, hyper-Raman emission spectra 0-20096  
 CuCl, anomalously slow group velocity of upper branch polariton 0-10893  
 CuCl, exciton luminesc., reabsorpt. and polariton effects 0-50430  
 CuCl, excitonic mol., two-photon excitation via polariton state 0-54612  
 CuCl, excitonic polariton, picosecond time of flight meas. 0-29337  
 CuCl, fission of relaxed excitonic mols. into upper and lower branch polaritons induced by  $M_1$  emission 0-11380  
 CuCl, propagation process of polaritons (*Japanese*) 0-24809  
 $\text{Cu}_2\text{O}$ , sample thickness depend. of exciton polariton absorption coeff. 0-34941  
 GaAs, exchange interaction, analytical and nonanalytical parts, from polariton spectra in mag. fields 0-50367  
 GaAs, intrinsic, on degenerate n-Ge, surface polaritons, hydrodynamical model 0-6752  
 GaAs, reson. Brillouin scatt. of exciton polaritons 0-11418  
 GaP, polariton dispersion, IR reflection spectroscopy 0-11415  
 GaP, surface polariton linear photon and two photon absorpt. 0-49863  
 GaP, surface polaritons, light scattering studies, effect of surface roughness 0-6753  
 GaTe, exciton polariton effect on absorpt. edge, absorpt. and refl. spectra, 4.2 to 300K 0-20664  
 GaTe, exciton polariton effect on absorpt. edge, thickness depend. of absorpt. 0-20665  
 Ge-type semiconductors, two-photon parametric excitation of phonons 0-29339  
 HCN crystals, polariton spectra and lattice dynamics 0-49313  
 $\text{HfO}_3$ , polariton Fermi-resonance and dissociated phonon states (*Russian*) 0-20634  
 HgI<sub>2</sub>, red anisotropic polariton dispersion, reson. Brillouin scatt. 0-7366  
 InP, exchange interaction, analytical and nonanalytical parts, from polariton spectra in mag. fields 0-50367  
 $\alpha$ - $\text{LiIO}_3$ , surface polariton spectroscopy, frustrated total reflection method (*Russian*) 0-49628  
 $\text{LiNbO}_3$ , spontaneous parametric scatt. line profile, IR absorpt. coeffs. 0-25377  
 $\text{NaBrO}_3$ , surface polariton spectroscopy, frustrated total reflection method (*Russian*) 0-49628  
 n-Si, surface polaritons in DC current 0-34369  
 $\text{SrTiO}_3$ , hyper Raman scatt. on polaritons, polariton branches (*Russian*) 0-50334  
 Xe, crystalline, polariton effects, reflectivity, absorpt., and resonant luminesc. spectra calcs. 0-20095  
 $\text{ZnO}$ , excitonic mol. transitions, optical gain and induced absorpt. spectra 0-11438  
 $\text{ZnO}$ , polariton dispersion, IR reflection spectroscopy 0-11415  
 $\text{ZnSe}$ , relaxation processes in Raman scattering and exciton luminescence under resonant excitation 0-25386

**polaritons continued**

$\text{ZnTe}$ , relaxation processes in Raman scattering and exciton luminescence under resonant excitation 0-25386  
 $\text{ZnTe}$ , luminescence spectra struct. surface and volume polaritons (*Russian*) 0-16089

**polarization in elementary particle interactions** *see polarisation in elementary particle interactions*

**polarization in elementary particle scattering** *see polarisation in elementary particle scattering*

**polarographs** *see polarography*

**polarography**

*see also voltammetry (chemical analysis)*

adsorption at soln.-electrode interface, AC polarographic data anal., computer program 0-3400  
 biomedical catheterisable sensors,  $\text{PO}_2$  probes, press. transducer and photometers 0-46080  
 desensitising dye polarographic half-wave potential meas. 0-7802  
 difference polarography, review of method, instrumentation 0-26078  
 liquid chromatography, use of electrochemical detection methods 0-50906  
 polyphenylquinoxaline-cellulose acetate, battery separator membrane, diffusion meas. 0-35574  
 sensor with microwave indicator electrode, exam. of design 0-21340  
 thermal energy, electrochem. conversion using cells with reversal of pot. with temp. 0-26124

**polarons**

*see also small polaron conduction*

alkali metal halide, laser damage morphology simulation 0-35015  
 2-benzoylpyridine crystals, lowest triplet state, optically detected EPR 0-15827  
 conducting molecular crystals, atomic limit and polarons 0-39860  
 degenerate semiconductors, heavy hole-phonon bound states for valence band with degeneracy point (*Russian*) 0-15461  
 electron-phonon interactions, dressed electron construction, Brillouin-Wigner and Tamm-Dancoff approaches 0-49629  
 Frohlich polaron, mean field theory, phase transitions 0-34371  
 ionic crystals with intermediate polaron coupling, magneto-optical effects in shallow F-centres 0-20615  
 ionisation of polarons, temp. depend. dispersion self-energy approach 0-34370  
 kinetic equation for dynamic system (*Russian*) 0-54619  
 orbit degenerate electron state localised at point defect, T-term multimode Jahn-Teller effect (*Russian*) 0-15490  
 particle-field interaction, classical version of polaron-like models 0-46834  
 polar dielectrics, triplet two electron states 0-24810  
 polar lattice coupling, effect of excitons 0-24811  
 polar liquid, additional electron delocalised state, optical excitation calcs. 0-54622  
 polar semiconductor, exciton-dispersion 0-6741  
 resonance Raman scattering in systems with localised carriers 0-7356  
 self-trapped acoustic polaron with site diagonal and off-diagonal electron-phonon interaction 0-2348  
 semiconducting crystal, phonons and localisation at impurities 0-24812  
 semiconductor, core excitons, binding energy in effective mass approx. 0-24808  
 semiconductor, ferromag., bound mag. polaron form., anomalous carrier density mag. field depend. 0-49774  
 semiconductor physics in high mag. fields, review (*Japanese*) 0-50192  
 semiconductors, elementary excitations in disordered systems with localised electrons, polarons (*Russian*) 0-49632  
 shallow impurity centres near Curie point, influence of dielec. nonlinearity on temp. depend. of ionisation energy 0-10916  
 small-polaronic glass, dynamics of optically induced props. 0-49630  
 strong coupling theory, variational approach 0-54621  
 surface, surface self-trapped states (*Japanese*) 0-2445  
 transport equation soln. in strong alternating elec. field 0-39596  
 tunnelling of small polarons, thermally assisted, computer anal. 0-2391  
 $\text{AgCl}(\text{Br})$ , crossed elec. and mag. fields, hot electrons, streaming motion, population inversion 0-44649  
 $\text{BaO}$ , electronic struct. of  $V^-$  and related centres 0-2355  
 $\text{CaO}$ , electronic struct. of  $V^-$  and related centres 0-2355  
 CdS, polaron IR cyclotron reson. 0-25347  
 CdSe, polaron IR cyclotron reson. 0-25347  
 $\text{Fe}_2\text{O}_3$ , neutron diffuse scatt. due to mol. polarons 0-15460  
 $\text{GaAs-Al}_x\text{Ga}_{1-x}\text{As}$ , heterojunction and superlattice, magnetophonon reson., polaron mass 0-44715  
 GaSe, electron-phonon interaction and optical props. 0-34942  
 $\text{LiNbO}_3$  crystals, polaron character of colour centres 0-2013  
 $\text{LiNbO}_3:\text{Fe}$ , X-ray and  $\gamma$ -ray irradiation effects on Fe charge state, Mossbauer study 0-40013  
 Ni complex, (1,4,5,8,9,12,13,16-octamethyltetradbenzporphinato nickel) $^{+2}$  ( $\text{I}_3^-$ ), atomic limit of Hubbard model and polarons 0-39860  
 Si, inversion layer, polaron model for localisation 0-20280  
 $\text{SrO}$ , electronic struct. of  $V^-$  and related centres 0-2355  
 $\text{Ti}_2\text{O}_7$  and  $(\text{Ti}_{1-x}\text{V}_x)_4\text{O}_7$ , metal-insulator transitions, EPR, elec. and mag. props. 0-2336  
 $(\text{Ti}_{1-x}\text{V}_x)_4\text{O}_7$ , elec. cond. and phase diagram near metal-insulator transition 0-11054  
 $\text{WO}_3$ , electron density map of  $\text{W}^{5+}$  polarons, EPR and optical absorpt. obs. 0-44912  
 n-ZnSe crystals, electron scatt. mechanisms, high mobility 0-34433  
 $\text{ZnTe}$ , valence band parameters and free exciton reduced mass, free exciton magnetoreflectance 0-45046

**poles and zeros**

analytic extrapolations towards interior points from a cut, applic. to elementary particle scatt. theory 0-12952  
 Bessel functions, infinite systems of nonlinear equations containing zeros 0-46786  
 neutron, charge form factor zeros 0-413  
 orthogonal polynomials, nonlinear eqns. for zeros 0-12888  
 partial scattering amplitude, analytic extrapolations, EMZERO 0-47221  
 plasma, collisionless drift modes, graphical method for finding complex roots of nonlinear eqn. 0-33762  
 polynomial satisfying linear second order partial differential equation, properties of zeros 0-12889

**polishing**

*see also electrolytic polishing*

aspherics precision manufacture with programmed microelectronic control 0-1368  
 brass, magnetoabrasive machining, optimum conditions 0-30172



**polishing continued**

- carbides, sintered, sample prep. for metallographic structural anal. 0-13048  
 ceramic, specimen prep., time saving methods (*German, English*) 0-35459  
 computer-controlled polisher for small-tool fabrication of mirrors 0-14496  
 fast aspheric mirror figure control by profile monitor, wire tester and null lens 0-14419  
 glass thermopolishing, by use of low temp. plasma radiation (*Russian*) 0-45406  
 hard and brittle materials, microsection prep. technotry and polishing systems (*German, English*) 0-11859  
 ion polishing for diamond-turned mirror dielectric coating adhesion 0-1370  
 lens, water soluble cryst., protective coating to aid polishing 0-33250  
 metal, frictional forces during polishing in vacuum 0-28365  
 metal, two-way polishing, thermal stresses and surface quality (*Russian*) 0-30151  
 metallographic specimens, automatic machine and procedure for prep. 0-13050  
 metallography, quantitative methodology (*French*) 0-30205  
 Metglas 2826 ribbons, ferromagnetic resonance and SEM obs. 0-15804  
 off-axis parabolic mirror fabrication for laser function expt. 0-1374  
 optical coating ion polishing 0-33261  
 optical glass, K8, foam form. and suppression methods during polishing 0-28364  
 optical glass, polishing with  $ZrO_2-SiO_2$  powder mixture 0-28367  
 resin polishers, holders, and tools 0-33248  
 steel, low C, fatigue endurance limit, metallurgical technology and mech. treatment effect 0-55536  
 thin and polished section preparation status and trends (*German*) 0-28360  
 toroidal mirror optical polisher 0-5848  
 wear test specimen, metallographic technique 0-35496  
 Al, transfer etch control in chemical polishing 0-16599  
 $Al_2O_3$ , grinding and polishing, quantitative control and optimization (*German, English*) 0-35460  
 Au-Er, dil., cold-worked, EPR expts. 0-39864  
 Cu mirror, surface defect layer form. on mech. polishing 0-33122  
 Fe-Ni-Mn (20, 5 wt.%), surface martensite, crystallography and morphology 0-40354  
 n-GaAs-electrolyte interface, surface pretreatment rel. to photocurrent, spectral response 0-3204  
 KCl surface texture and optical props. after forging between polished dies 0-33102  
 MgO crystals, etching and polishing, inorganic or organic acids effect 0-40573  
 Mn-Zn ferrite single crystals, mech. polishing effect on mag. props. (*Japanese*) 0-16569  
 PbO- $SiO_2$  glass, use of  $Na_2S_2O_3 \cdot 5H_2O$  in polishing 0-33258  
 n-Si, exoelectron emission, effect of surface polishing rel. to defect distrib. in surface layer 0-40239  
 Si, local mechanical defects, annealing and effect on autoepitaxial growth (*Russian*) 0-7701  
 $SiO_2-Na_2O-CaO-MgO-Fe_2O_3-Al_2O_3-SO_3-Sn$  thermally polished, exam. of strength of surfaces 0-25887  
 $SrTiO_3$  electro-optic crystals, mechanical grinding and polishing 0-48471  
 YAG brittleness anisotropy, microcrack formation due to surface treatment 0-40526

**pollution**

- see also air pollution; pollution detection and control; water pollution; water treatment  
 chemical migration of radionuclides in soil 0-17144  
 dosimetry, environmental radiation meas., instrument calibration 0-9426  
 enriched heavy minerals in sand grains, enhanced natural radiation exposure (*German*) 0-51018  
 Florida,  $^{238}U$  and  $^{226}Ra$  in phosphates 0-30615  
 gamma-emitting activation products, plant uptake of  $^{59}Fe$ ,  $^{58}Co$ ,  $^{54}Mn$  and  $^{65}Zn$  0-30614  
 light pollution at Sacramento Peak Observatory, effect on night sky brightness 0-12545  
 light pollution over Jena, night sky brightening at Karl-Schwarzschild Observatory 0-51533  
 milk radioactive fallout monitoring in Britain 0-12283  
 noise, subjective annoyance by low level sound, sound character as a physical attribute 0-35902  
 non-proportionality between flux and reservoir content 0-46261  
 nuclear power plant, environmental radioactivity and dosage models (*Spanish*) 0-32518  
 photographic film development techniques, environmental pollution appl. (*German*) 0-7806  
 radiation research, lab. contamination in the early period 0-42031  
 radioactive waste storage, interaction of actinides and humic acid 0-13715  
 radioactive contamination of biosphere, explosion and power plant influence (*Hungarian*) 0-21548  
 radioactive impact of nuclear facilities, preoperational evaluation 0-3534  
 radioactive material migration in soil, hydrologic transport model 0-16848  
 radioactive waste, geochemical aspects of radionuclide migration from waste repositories 0-13711  
 radioactive waste, geological disposal, chemical factors controlling environmental actinide sorption 0-13713  
 radioactive waste, geological long-term disposal of high-level, Sweden 0-13712  
 radioactive waste storage, Am sorption on major rock-forming minerals 0-13716  
 radioactive waste storage, migration of  $^{137}Cs$  in Magenta dolomite by aquifer 0-13718  
 radioactive waste storage, mineral-contributed anion effects on the retention of trivalent actinides in the environment 0-13717  
 radiological impact of the Rhein-Maas region from nuclear facilities under normal operation 0-3535  
 radionuclide absorption through damaged and undamaged skins of guinea pigs 0-26383  
 radionuclide migration through soils 0-16849  
 radionuclide transport through geologic media, one-dimens. model 0-786  
 simulated, T content in organs, and DNA of rat liver cells, after doses of tritiated food, protein or water 0-56226

**pollution continued**

- synthetic fuel production, environmental effects 0-21417  
 transportation effects, public, future outlook 0-35621  
 trench leachates, low-level radioactive waste disposal sites, organic carbon content 0-17145  
 tritium in rabbits after ingestion of freeze-dried tritiated food and tritiated water 0-21549  
 $CO_2$  cycling in environment, non-proportionality between flux and reservoir content 0-46261  
 $CO_2$  pollution, role of homogeneous buffer factor in  $CO_2$  solution in ocean surface waters 0-21783  
 $^{137}Cs$  whole-body content in a normal New Mexico population 1956-1977 0-26382  
 $^{210}Po$  and  $^{210}Pb$  concs. in liver and kidneys of cattle 0-30904  
 $^{238}U$ ,  $^{239}Pu$ , concs. in arthropods at a nuclear facility 0-30905  
 Pu in lungs of pronghorn antelope near a nuclear fuel reprocessing plant 0-30906  
 Pu, Manhattan project workers, 32-year medical follow-up 0-26379  
 Pu radioactive waste, oxidation by radiation, effect on migration rate 0-13714  
 Pu radioactive waste, transport, environmental impact 0-779  
 Rn, diffusion coefficient and exhalation rate from building materials, meas. technique 0-4694  
 $^{222}Rn$  releases associated with cultivation of agricultural land 0-16850  
 S, man-made sources influence on NE United States S cycle 0-26178
- pollution detection and control**  
 see also air pollution detection and control; noise abatement; remote sensing; waste disposal; water pollution detection and control; water treatment  
 conductometric instruments metrological monitoring, for environmental contaminants control 0-55973  
 environmental analysis, recent advances, book 0-41961  
 environmental problems, nuclear power stations prospects (*Hungarian*) 0-13742  
 field desorption mass spectrometry, appl. to biochemistry, medicine, and environmental science 0-35592  
 Gulf of Taganrog salinity, after restriction of exchange with Sea of Azov 0-36335  
 ion chromatography appl., on-stream, impact on energy conservation 0-55737  
 MHD conversion, pollutant emissions and controls 0-30613  
 polychlorinated biphenyls, pollutants, radiation degradation in organic solvents,  $H_2O$  0-30262  
 problems and numerical data 0-3536  
 radioactive, nuclear power stations safety, Czechoslovak practices (*Slovak*) 0-13632  
 radiochemical neutron activation anal. of environmental matrices for Hg and noble metals 0-16889  
 remote monitoring of all types of environmental pollution, promising trends 0-35811  
 sediment pollution by Hg and As, instrumental neutron activation and atomic abs. spectrometric anal. 0-16890  
 soil,  $^{89}Sr$  and  $^{90}Sr$  determ. using total sample decomp. 0-35808  
 standard reference materials, based on river sediment and urban particulate matter (SRM 1645 and SRM 1648) 0-21831  
 surface treatment, ionic deposition and electron bombardment industrial equipment (*French*) 0-7699  
 trace analysis in gases by laser-induced schlieren technique 0-3436  
 $^{14}C$  low level liq. scintillation counting using small vol. teflon-Cu vial 0-16887  
 Hg pollution of Mediterranean sediments around Alexandria, Egypt 0-3538  
 $^{131}I$  in milk, rapid method of detect. 0-46106  
 Pu borehole assay using delayed-neutron activation anal. 0-21419
- polonium**  
 see also nuclei with .....  
 chemical bonding in group V and VI elements and compounds with tetradymite structure 0-15036  
 haloes in rocks, use in geochronology 0-56468  
 $^{210}Po$  and  $^{210}Pb$  concs. in liver and kidneys of cattle 0-30904  
 $^{210}Po$ , galvanic deposition at rotating Ni disk electrode 0-55314  
 $^{210}Po/^{210}Pb$  atmospheric ratio, modification by volcanic emissions 0-41507  
 Ra A ( $^{218}Po$ ) adsorption to monodispersed aerosol 0-32535
- polonium compounds**  
 No entries
- polyelectrolytes** see electrolytes; polymers
- polymer films**  
 see also dielectric thin films; insulating thin films  
 acrylic coating, surface tension effects 0-53487  
 adhesive bonds breaking under high vacuum, light and electron emission, spectral comp. obs. 0-55190  
 aromatic copolyesters, charge storage props., electret stability 0-7277  
 benzene, polymerised, plasma polymerisation in glow discharge, thin film IR and free radical EPR obs. 0-2964  
 biophenol-A-polycarbonate, liquid induced crystallisation 0-30125  
 carrier transport meas. 0-6874  
 cellulose, in metal coated, sandwich system, spontaneous elec. current induced by heating 0-40700  
 cellulose acetate films, light scatt., tensile creep, desalination 0-16050  
 cellulose film, moisture effect on phys. and mech. props. 0-40450  
 coatings for corrosion protection, electrochem. techniques for performance monitoring 0-3234  
 dielectric electret effect, homo and heterocharge charge distribution 0-11317  
 elasto-plastic deformation calc. in re-drawing stretched film, finite element analysis appl. (*Japanese*) 0-7621  
 electret, absorpt. and relax. of charge 0-6942  
 electret, charge distrib., generalized model 0-6873  
 electret films, produced in HF discharge, props. (*Russian*) 0-20578  
 electron irradiation controlled form., elec. props. 0-15635  
 electropolymerisation, in aq. medium, book contrib. 0-50778  
 electropolymerisation, on electrodes, book contribs. 0-50854  
 ESCA of films on Au, sample charging phenomena 0-20764  
 etching and cleaning by plasma treatment 0-1855  
 glass fibre protective coatings, materials and techniques 0-33252  
 glow discharge polymerised, conditions for attaining perfect self-healing breakdown 0-20590  
 hexamethylcyclotrisilazane film, plasma-polymerised, TEM study 0-44456



## polymer films continued

- integrated circuit, plasma-removal of polymeric layers 0-1851  
 memorised mechanical birefringence (*French*) 0-43677  
 metal-polymer, electron irradi. controlled form., elec. props. 0-15635  
 metallized polyester film as a solar filter 0-51666  
 nylon 6, frictional electrification between metal and polymer, depend. on temp. and friction speed, contrib. of mol. motion of polymer to electrification 0-6953  
 optoacoustic signal, thickness effect on signal magnitude 0-11969  
 organo-tin polymer films, glow discharge prep., comp. determ. by XPS and AES 0-35109  
 orientation evaluation of noncrystalline chain, with polarised fluorescence method (*Japanese*) 0-6368  
 pentaplast, plasticised, thermal treatment effect on props. 0-40324  
 PET, in MIM struct., injection current enhancement at metal insulator interface, theory 0-49953  
 photopolymer, biaxial stress-strain test 0-40417  
 photoreticulation by UV irradiation 0-40717  
 plasma deposited, adhesion to plastics 0-50745  
 plasma polymerisation on solid substrate in RF discharge 0-2963  
 plasticised cellulose acetate sheet, post-yield fracture 0-25859  
 PMMA, solvent cast, surface characts., chromatographic study 0-20020  
 PMMA, surface charge decay and TSC 0-11328  
 PMMA-spiropyran Langmuir monolayers, reversible photochemical strain 0-50867  
 polar, piezoelectricity and pyroelectricity 0-7267  
 polar polymer, piezoelectricity and pyroelectricity 0-7267  
 poly(ethyl-methacrylate), surface charge decay and TSC 0-11328  
 poly(n-butyl-methacrylate), surface charge decay and TSC 0-11328  
 poly(N-vinylcarbazole), fluoresc. and phosphoresc., energy transfer mechanism 0-16112  
 poly(N-vinylcarbazole) layers, supermol. struct. effect on elec. props. 0-44606  
 poly(vinyl bromide), surface charge decay and TSC 0-11328  
 poly(vinylidene fluoride), phase-III, IR study 0-20624  
 poly(vinylidene fluoride), piezoelec. response depend. on phase I vol. fraction 0-20593  
 poly(vinylidene fluoride), poled, piezoelec. activity and field-induced cryst. struct. transitions 0-20592  
 $\beta$ -poly(vinylidene fluoride), single cryst. orientation, piezoelec. 0-20591  
 poly(vinylidene fluoride), strong piezoelec. under high press. annealing 0-11344  
 poly(vinylidene fluoride), surface charge decay and TSC 0-11328  
 poly- $\gamma$ -benzyl-L-glutamate, monolayers, struct. studies, IR, ATR, and TEM obs. 0-44396  
 poly-N-vinylcarbazole, in polymer film, excimer fluoresc., high press. effects 0-34966  
 polyacetonitrile film, in Pt/polymer/metal capacitors, electroforming and elec. cond. 0-54800  
 polyacetylene, (CH)<sub>x</sub>, synthesis, struct. and elec. props., doped materials, review 0-15623  
 polyacetylene, doped, transport props. 0-24913  
 polyacetylene, doped film, elec. cond. 0-24921  
 polyacetylene, ESR study, effects of O<sub>2</sub>, No and halogens 0-25186  
 polyacetylene, nascent morphology obs. 0-24379  
 polyacetylene, partially oriented, anisotropic elec. cond., quasi-one-dimens. behaviour of fully oriented doped material 0-11112  
 polyacetylene, semiconducting and metallic, thermoelec. props. 0-40884  
 polyacetylene and derivatives, chemically doped, elec., chem. and phys. props. 0-24912  
 polyacrylonitrile, plasma deposited, adhesion to plastics 0-50745  
 st-1,2-polybutadiene, oriented film, anisotropic C 1s XUV absorpt. spectra 0-55207  
 polybutene-1 film, deform. mechanism, rheo-optical meas. 0-21041  
 polybutene-1 film, tubular-extended, anal. of orientational and form birefringence 0-29712  
 polycarbonate:tri-p-tolylamine amorphous film, elec. and mag. props 0-49959  
 polycarbonate thin films, solution-grown, dielectric relaxations 0-55029  
 polychlorotrifluoroethylene, electret, TSC 0-7266  
 polyester ultrathin films, photochemical props., transducer appl. 0-37020  
 polyethylene, C filled, ultrathin films, photochemical props., transducer appl. 0-37020  
 polyethylene, cross-linked, thermal oxidation stability, influence of Cu 0-30128  
 polyethylene, drawn, dielec. breakdown and morphological struct., dichroic ratio 0-25813  
 polyethylene, elec. empulse breakdown strength, rel. to rate of drawing 0-15960  
 polyethylene, electrets, polarisation obs. and influence of wax impurities, TSC obs. and analysis (*French*) 0-44999  
 polyethylene, elongated,  $\gamma$ -irrad., TSC meas. 0-11324  
 polyethylene, high and low density, depolarisation thermocurrent study, relax. modes 0-7263  
 polyethylene, high density, carrier trapping, X-ray induced TSC 0-11005  
 polyethylene, high density, corona charged, thermally stimulated surface pot. 0-11327  
 polyethylene, lightly crosslinked, processed under mol. orient., transparent film prep. 0-38957  
 polyethylene, linear, quenching of thin films to amorphous state 0-28929  
 polyethylene, soln.-cast, low energy electron scatt. obs. of band struct. 0-16131  
 polyethylene film, dielec. breakdown sites 0-50266  
 polyethylene film, effect of corona generated excited molecules on surface pot. decay 0-6941  
 polyethylene film, oriented, soln. growth 0-45244  
 polyethylene films, radiation initiated graft polymerisation of acrylonitrile, initiation rate rel. to props. (*Russian*) 0-7531  
 polyethylene films 4 to 100  $\mu$ m, thickness meas. (*Japanese*) 0-52160  
 polyethylene oxide, peculiarities of struct. form. near below the melting point 0-54150  
 polyethylene resin coated paper formulation for photography 0-4794  
 polyethylene terephthalate, corona charged, surface voltage decay mechanism, TSC meas. 0-11326  
 polyethylene terephthalate, elec. cond. and space charge accumulation 0-10998  
 polyethylene terephthalate, space charge quantity meas. by Maxwell stress method 0-22389  
 polyethylene terephthalate electrets, formed by electron injection, TSC meas., space charge drift 0-11321  
 polyethylene terephthalate thin films, electronic mobility 0-15634

## polymer films continued

- polyethylene-terephthalate, field-controlled photogeneration and carrier trapping 0-25285  
 polyethyleneterephthalate, crystallised from thin layer melts, temp. depend. of morphology 0-54149  
 polyethyleneterephthalate, foil, optical microscopy and low angle light scattering 0-55210  
 polyimide substrate foils for nuclear targets 0-18739  
 polyimides, ultrathin films, photochemical props., transducer appl. 0-37020  
 polymer matrix composites, component interaction mass spectrometry investigation (*Russian*) 0-35511  
 polynaphthalene films, plasma polymerised, photovoltaic and photocond. props. 0-34479  
 polyphenylacetylene, phys. struct., AC and DC cond. 0-44750  
 polypropylene electrets corona charged at high temp., TSC study 0-7261  
 polypropylene film, corona-charged, TSC and space charges 0-40041  
 polypropylene film, in MIM struct., electroforming 0-25019  
 polypropylene films, hard elastic, gas permeability, extension effects 0-40412  
 polypropylene films, meas. of dielectric losses at cryogenic temps. 0-25301  
 polypropylene thin stretched foils, appl. as ionisation chamber windows 0-18764  
 polysiloxane plasma polymerised film growth on GaAs substrate, dry etching process 0-25575  
 polystyrene, frictional electrification between metal and polymer, depend. on temp. and friction speed, contrib. of mol. motion of polymer to electrification 0-6953  
 polystyrene, glow discharge polymerised, conditions for attaining perfect self-healing breakdown 0-20590  
 polystyrene, plasma deposited adhesion to plastics 0-50745  
 polystyrene, styrene plasma polymerisation in glow discharge, thin film IR and free radical EPR obs. 0-2964  
 polystyrene, TSC and dielectric props. (*Japanese*) 0-15632  
 polystyrene amorphous film, cyclically fatigued, molecular behaviour 0-35310  
 polystyrene film, acrylic acid doped, elec. cond. and activation energy conc. depend. 0-15631  
 polystyrene film, delayed luminesc. decay kinetics of 1,2-benzanthracene 0-43088  
 polystyrene film, Fourier-transformed IR photoacoustic spectra 0-34993  
 polystyrene film, in MIM struct., elec. conduction and free radicals 0-20340  
 polystyrene film, temp.-stress depend. of rupture life under hydrostatic pressure 0-16467  
 polystyrene films on metal substrates, electrode effect on carrier injection, TSC, I-V characts. 0-34463  
 polystyrene thin film, glow discharge formed, dark current and photocurrent obs. (*Japanese*) 0-15633  
 polytetrahydrofuran, electrochemically prepared between metal electrodes, DC elec. props. 0-39695  
 polytetrahydrofuran, electrochemically prepared between Pt and Au electrodes, AC elec. props. 0-40062  
 polytetrahydrofuran film, in Pt/polymer/metal capacitors, electroforming and elec. cond. 0-54800  
 polyvinyl butyral film, charge storage mechanism, TSC expts. 0-25280  
 polyvinylacetate, in MIM struct., DC cond. phenomena 0-25020  
 polyvinylidene fluoride, birefr. change induced by elec. field 0-55065  
 polyvinylidene fluoride, dielectric relax. mechanism 0-55023  
 polyvinylidene fluoride, polarisation and depolarisation processes 0-11318  
 polyvinylidene fluoride, uniaxially stretched and corona poled, piezoelec. meas. 0-25311  
 polyvinylidene fluoride films, corona-poled, piezoelectricity (*Japanese*) 0-55040  
 polyvinylidene fluoride films, field depend. depolarisation behaviour 0-20580  
 polyvinylidene fluoride films, stretched and rolled, electrostriction and piezoelectric effects (*Japanese*) 0-55041  
 polyvinylidene fluoride magnetoelectret, AF and RF charge and dielectric characts. 0-40038  
 PTFE electrets corona charged at high temp., TSC study 0-7261  
 PVA, matrix for Pr<sup>3+</sup> spectra 0-7331  
 PVC, solution-grown, between Al electrodes, AC elec. props. 0-15619  
 PVC, surface charge decay and TSC 0-11328  
 PVC thin films, pure and I doped, photoconductivity study 0-44646  
 PVDF, film, polymorphism induced by poling and annealing 0-24372  
 PVDF dielectric, piezoelec. and pyroelectric props. rel. to crystalline forms 0-15982  
 pyroelectric polymer film for electron microscope sample preparation, rapid cooling effects (*German*) 0-13185  
 Raman, spectroscopy of thin films, integrated optical techniques 0-22432  
 silk fibroin, oriented, piezoelec. const. temp. dispersions 0-11345  
 solar energy materials, transparent, optical characts. investigation 0-20724  
 solar-energy concentrator, foam-film parabolic-cylindrical, surface fabrication 0-21372  
 solvent cast, optical anisotropy origin 0-20610  
 styrene-acrylonitrile copolymer film, multiple relax. obs. using TSC 0-45000  
 superconducting magnet insulators, gamma-ray radiation effects 0-24495  
 Teflon, negatively corona charged, new model of isothermal charge transport 0-34536  
 Teflon, TSC studies of carrier trapping and mobility 0-7016  
 Teflon FEP, annealed electret, charge stability 0-6943  
 Teflon-FEP, film, plate-electret, construction and use in condenser type headphone 0-5907  
 thermoplastic film, photoconducting, double exposure holographic interferometry using memory effect (*Chinese*) 0-37967  
 transducer, piezoelec. and pyroelec. response rel. to dipole polarisation 0-7267  
 TTF polymer thin film batteries 0-45709  
 vinyl chloride-vinyl acetate copolymer film, dielec. relax. and thermally stimulated depolarisation current meas. 0-11336  
 vinyl chloride-vinyl acetate copolymer film between metal electrodes, depolarisation current studies 0-2691  
 vinylidene fluoride-tetrafluoroethylene copolymer, two types of pyroelectricity 0-11346  
 vinylidene fluoride/tetrafluoroethylene copolymer, piezoelec. and pyroelec. response rel. to dipole polarisation 0-7267  
 GaAs-(SN)<sub>x</sub>, solar cell fabrication and efficiency 0-26143



**polymer melts**

blended resins, flow charact. (*Japanese*) 0-24059  
 crystallisation, deformation effects 0-10504  
 crystallisation from melt at large undercoolings, kinetics 0-28925  
 crystallisation models, Avrami eqn. extension 0-19723  
 elastic, uniform extension by const. force, rheology 0-43682  
 elongational behaviour in const. elongation rate, tensile stress and tensile force expts. 0-38372  
 elongational properties, microscopic stretch history 0-23981  
 flow, unsteady, in rotary devices 0-24061  
 harmonic distortions, under nonlinear periodic deform. 0-28482  
 heat transfer problem in plastic injection moulding 0-38242  
 high mol. wt. polymer melts, viscoelastic props., relaxation and retardation spectra 0-19310  
 irreversibility assumption of network disentanglement, effects on elastic recoil predictions 0-6006  
 longitudinal flow of periodically deformed polymers 0-6008  
 LPDE melt, tensile stress overshoot in uniaxial extension, single integral constitutive eqn. 0-1507  
 non-linear model, constitutive equation testing with free. vol. relax. spectrum 0-6011  
 oxidative stability determ. technique 0-45412  
 particulate mixing, fluid dynamics, rheological and energetic considerations 0-43686  
 polybutadiene, hydrogenated, linear and star branched, melt rheology 0-23978  
 polydimethylsiloxane film, non-pure, dielec. behaviour 0-29672  
 polydispersity, estimation from rheological data 0-6535  
 polyesters, thermotropic, quiescent crystn. 0-38937  
 polyethylene, foam growth, thermomech. anal. 0-3416  
 polyethylene, high-density, polymer melt, shear stress at wall 0-19450  
 polyethylene, linear, melt props. correl. with chain length distrib. (*Russian*) 0-37920  
 polyethylene, linear, melt rheology 0-23976  
 polyethylene, low density, temp. depend. of the elongational behaviour 0-6012  
 polyethylene, low-density, viscosity and viscoelasticity, filler effect 0-10222  
 polyethylene, plastic flow, yield limit rel. to press. (*Russian*) 0-7657  
 polyethylene melt, lightly crosslinked, crystn. under uniaxial compression, stretching 0-38957  
 polyethylene-polyoxymethylene mixtures connection of melt thermodynamic props. with solid state struct. (*Russian*) 0-54152  
 polyoxymethylene-copolyamide mixtures, melt rheological props., extrudate microstruct. (*Russian*) 0-7530  
 polypropylene, plastic flow, yield limit rel. to press. (*Russian*) 0-7657  
 polypropylene glycol, low freq., multiple relaxation behaviour, dielectric and dynamic Kerr-effect techniques 0-29682  
 polystyrene meas. of elongation props. with universal extensional rheometer 0-6004  
 polystyrene melt, carbon-black filled, rheological study 0-48665  
 polystyrene melt, linear viscoelastic props. influence of molecular wt. distrib. 0-19309  
 polystyrene melts, wetting kinetics for spreading of viscous sessile drops 0-15338  
 polystyrene-mineral oil mixture, viscosity and normal stress coeff. 0-44349  
 polystyrene melts, stresses and birefringence in intermittent shear flows 0-19308  
 polytrifluorochloroethylene, rheological props. (*Russian*) 0-6015  
 polyvinylcyclohexane, plastic flow, yield limit rel. to press. (*Russian*) 0-7657  
 PVC, plasticised, foam growth, thermomech. anal. 0-3416  
 quasistatic bulk strength meas., specially built apparatus 0-7737  
 rheological props., effects of hydrostatic press. 0-48663  
 rheology, characterised by mol. int. distrib., review 0-1504  
 saturated liquid polydielectrics, secondary electron emission and energy loss spectra 0-55239  
 self-diffusion, review 0-29193  
 spike-strain test relevance for network connectivity destruction by deformation 0-6001  
 stabilisation of foams (*French*) 0-21323  
 triblock copolymer, model for rheology 0-23979  
 CaCO<sub>3</sub> filled polymer melts, viscous props. 0-19311

**polymer solutions**

acrylonitrile Na methallylsulphonate copolymer electrolytes in dimethylformamide, gel permeation chromatography appl. 0-21345  
 annular two-phase flow of non-Newtonian liqs. and gases, press. drop and gas vol. fraction 0-10286  
 apparent scaling laws for polymer dimensions in poor solvent, too high excluded volume exponents 0-28901  
 aqueous polymer solns., shear stress and normal stress meas. using cone-and-plate rheogoniometer 0-1496  
 binary polymeric mixtures, soln. viscosities meas. 0-54423  
 biopolymer soln. heat capacity, conformational props. temp. depend. 0-8009  
 biopolymers, conditions of liquid crystal formation 0-30642  
 birefringence lines in elongational flow (*French*) 0-25337  
 Brownian motion, fluctuation-dissipation theorem 0-46980  
 butadiene-acrylonitrile copolymer liquid, viscosity (*Japanese*) 0-39334  
 carbowax in benzene, evaporation, vapour press. determ. from gaseous diffusion coeff. 0-10654  
 cellulose acetate, conc., light scatt. studies 0-16050  
 colloid stability near repulsive wall 0-21326  
 concentrated, viscous function, hyperelasticity and viscoelasticity 0-48662  
 cooperative phase transitions 0-45850  
 crystallisation, deformation effects 0-10504  
 diblock copolymer solution, second virial coeff., perturbation theory 0-29148  
 diffusion and self-diffusion phenomena, review 0-15273  
 diffusion coefficients, limiting, of high mol. weight solutes 0-24626  
 dilute, chain mol. dynamics and transport processes 0-14989  
 dilute, equilibrium theory (*German*) 0-33872  
 dilute, Hartree self-consistent field analysis 0-5648  
 dilute, Kramers-Giesekus stress tensor 0-6105  
 dilute, turbulent flow behaviour in annulus 0-33633  
 dilute branched polymers, statistics, field theory 0-22303  
 dilute polymer liquids, time-temperature superposition principle 0-6005  
 dissolution rates and polymer-solvent system phenomena (*German*) 0-13167

**polymer solutions continued**

dynamic storage and loss compliances determ. from creep data 0-5948  
 dynamical polymer coil overlap, NMR model 0-23583  
 dynamical scaling, neutron spin echo obs. 0-14990  
 dynamics including side group motion, free draining limit 0-48111  
 elastic moduli meas., rheological spectrophasemeter, with digital display 0-33547  
 electrical phenomena, nature and appl., review 0-50254  
 electrically induced fluorescence polarised component change meas. 0-32863  
 (ethylene-co-vinyl alcohol)-g-ethylene oxide graft copolymers, sol. behaviour 0-19682  
 fibre suspension, dil., mechanistic aspects of drag reduction in turbulent pipe flow 0-6102  
 filled, normal stresses and hyperelasticity under simple shear flow 0-1506  
 flexible chain, entanglement effects in segmental motion, dielec. obs. 0-40050  
 flexible macromolecules, flow-induced crystallisation, nonhomogeneous shear rates effect 0-38952  
 flexible polymer chain in nematic solvent, phase diagram (*French*) 0-39253  
 flow anomalies, narrow slits between rotating and stationary discs (*Russian*) 0-19454  
 flow birefringence, in time dependent field 0-7323  
 flow in exit region of tube, jet swell problem 0-38452  
 free energy of mixing, modelling, critical exponents 0-44106  
 free polymer+latex, dispersion flocculation, equilib. anal. 0-45574  
 freely jointed polymer chain, with excluded vol. interaction, Monte Carlo studies 0-10475  
 frequency dependent energetics, Orwell-Stockmayer hopping model 0-24346  
 heparin, in soln., small angle X-ray scattering 0-14993  
 HPAM solns., anomalous defect pressure in laminar orifice flows 0-48664  
 hyaluronate solns., cooperative phase transitions, review 0-45850  
 hydraulic resistance of channels calc. (*Russian*) 0-38451  
 hydroxypropylmethyl cellulose soln., drag reduction by centre line fibre injection 0-14749  
 intrinsic viscosity, mol. wt. and temp. dependence 0-34222  
 intrinsic viscosity of dilute and moderately concentrated polymer solns. 0-48753  
 isocyanate polymers, partitioning between isotropic and anisotropic phases 0-24343  
 laminar flow on inclined plane, edge effects 0-19451  
 light scattering, dynamic behaviour obs. 0-55727  
 light scattering, polydispersity and internal modes of motion 0-20651  
 light scattering charact. of thermodynamic props., solvent and mol. wt. effect 0-16717  
 low eddy friction polymer soln. hydrodynamics 0-53818  
 macromolecular system, critical branching, a statistical theory 0-3413  
 net repulsive van der Waals forces between different particles, macromolecular, or biological cells in liqs., appls. 0-34274  
 network in solution, free energy of deform. 0-38900  
 non-ion-exchange, solubility of electrolytes (*Russian*) 0-54391  
 non-linear model, constitutive equation testing with free. vol. relax. spectrum 0-6011  
 Nylon-6, shish-kebab struct., obtained from quiescent soln. by self seeding 0-15017  
 partially labelled chains, neutron scatt. obs. 0-38899  
 phenyl methacrylate copolymers, photoluminescent behaviour 0-25432  
 piperylene-acrylonitrile copolymers, polymerisation, monomer composition rel. to copolymer struct. (*Russian*) 0-5651  
 plane interface between two viscoelastic superposed cond. fluids, instability in mag. field 0-1694  
 PMMA, diffusion coeffs. and thermodynamic props., conc. depend. 0-15274  
 poly(aminiumphosphate)s, mol. wts., and cond. studies 0-14264  
 poly(butyl acrylate) solutions, dielec. relaxation 0-40045  
 poly(butyl methacrylate) solutions, dielec. relaxation 0-40045  
 poly(isobutyl methacrylate) solutions, dielec. relaxation 0-40045  
 poly(vinyl methyl ether)-polystyrene mixture, electric field depend. of cloud point temp., laser scatt. meas. 0-6519  
 poly (ar-methylstyrene)s, steric effects on excimer formation, fluorescence spectra exam. 0-25430  
 poly-2-vinylnaphthalene, soln., lowest triplet props., flash photolysis and radiolysis obs. 0-32861  
 poly-4-vinyl-pyridine, solns. in ethanol, spin label obs. of local density of monomer units and mol. dynamics 0-44099  
 poly-4-vinylpyridine N-oxide, aqueous, solns., IR spectra 0-2761  
 poly- $\gamma$ -benzyl-L-glutamate in dioxane solution, relax. mechanisms, light scatt. spectra 0-20659  
 poly-N-vinylbenzocarbazole, soln., luminesc., effect of electronic excitation energy vibr. 0-55174  
 poly-N-vinylcarbazole, soln., picosecond time-resolved fluoresc. by pulse radiolysis 0-28122  
 poly-p-aminobenzhydride terephthalamide in dimethyl sulphoxide soln., rheological study 0-43683  
 poly-p-phenyleneterephthalamide solns., rheological props. comparison with nylon 6,6 soln. 0-6007  
 polyacrylamide, gels and single chains, phase transitions and crit. behaviour 0-40759  
 polyacrylamide single chain in acetone-water mixtures, coil-globule transition obs. 0-1098  
 polyacrylamide solutions, viscous behaviour 0-2185  
 polyacrylamide weak soln., wall turbulent flow 0-38450  
 polyacrylamide-fluorescein conjugates, fluoresc. polarisation, high press. obs. 0-20683  
 polyacrylamide-maltose, aq. soln., capillary flow, thermal noise, low freq. oscils. 0-48754  
 polyacrylamides-water-glycerol, streaming birefringence in extensional flow 0-6013  
 polyacrylonitrile-dimethylformamide soln., viscoelasticity and shear modulus meas. (*German*) 0-38374  
 polyazomethines, dil. soln. props. 0-19972  
 polyazomethines in H<sub>2</sub>SO<sub>4</sub>, lyotropic nematic phase, threaded textures (*French*) 0-19691  
 polycapraamide, US degradation in H<sub>2</sub>SO<sub>4</sub> soln. 0-15191  
 polyelectrolyte+physiologically active substance complexation, stability, kinetics (*Russian*) 0-8006  
 polyelectrolyte complexes, nonstoichiometric, solubility in water (*Russian*) 0-55674



## polymer solutions continued

- polyelectrolyte complexes, nonstoichiometric water-soluble structure (*Russian*) 0-54112  
 polyelectrolyte in solution, variation of contrast, neutron forward scatt. calc. (*French*) 0-54104  
 polyelectrolyte soln., small ion self-diffusion, Manning's limiting law derivation 0-54416  
 polyelectrolyte solution, polyion-polyion interaction effects, computer simulation 0-35817  
 polyelectrolyte solution, thermodynamic props. determ. from Donnon equil. obs. 0-7846  
 polyester-organic solvent mixtures, phase diagrams, eutectic props., devitrification, crystn. (*French*) 0-3015  
 polyethersulphone dissolution in chloroform 0-21353  
 polyethylene glycol, aqueous, solns., IR spectra 0-2761  
 polyethylene oxide, aq. soln., capillary flow, thermal noise, low freq. oscils. 0-48754  
 polyethylene oxide, aq. soln., mech. props. in parallel superposed flows, geometric effects 0-19448  
 polyethylene-co-vinyl alcohol-g-ethylene oxide aq. soln., surface tension (*Japanese*) 0-24716  
 polyisobutene solns., X-ray scatt., Kratky cone collimation 0-19681  
 polyisobutylene in cetane, hyperelasticity, filler effect 0-10223  
 polyisobutylene soln., NMR, chain segment motions 0-20475  
 polyisobutylene solutions, viscous behaviour 0-2185  
 polyisocyanides, solns., struct. and acidification 0-19915  
 polymethine dye solution, optoacoustic response 0-6465  
 polymethylene coils in solution, dimension and shape, computer simulation (*Russian*) 0-54111  
 polyphenyl ether in benzene, evaporation, vapour press. determ. from gaseous diffusion coeff. 0-10654  
 polypropylene sulphide, atactic chains, dipole moments, dielec. const. meas. 0-23584  
 polypropylene sulphide in athermal solvent, viscosity-temp. coeffs. 0-34933  
 polystyrene, cyclohexane soln., coil-globule transition 0-54110  
 polystyrene, diethyl malonate soln., near-crit., osmotic compressibility, correlation length, scaled functions 0-11422  
 polystyrene, dilute soln.,  $^1\text{H}$  mag. relax., selective inversion technique appl. 0-44957  
 polystyrene, ion cyclohexane, mol. dimens. near theta point 0-54105  
 polystyrene, soln., macromol. dynamics, us relax. 0-19882  
 polystyrene, swollen network in benzene, pendent chains, influence on thermodynamic and viscoelastic props. 0-28481  
 polystyrene in benzene and decalin, diffusion coeff., solvent effect 0-19971  
 polystyrene in chlorinated biphenyl, flow birefringence on appl. of step-shear strain 0-25335  
 polystyrene solution, flow birefringence, in time dependent field 0-7323  
 polystyrene solutions, viscous behaviour 0-2185  
 polystyrene suspension, laminar flow, augmentation of heat and mass transfer, correl. of data 0-53840  
 polystyrene-Aroclor 1254, streaming birefringence in extensional flow 0-6013  
 polystyrene-co-divinylbenzene microgels in dimethylformamide, diffusion coeff., viscosity and mol. wt. meas. 0-30286  
 polystyrene-decalin solns., flow irregularity obs. in theta conditions 0-38453  
 polystyrene-PMMA-benzene, soln., polystyrene diffusion, photon correl. spectroscopy 0-34220  
 polystyrene-polyisoprene two-block copolymer soln., conformation, small angle neutron scattering, X-ray diffraction, review (*Rumanian*) 0-6348  
 polyurethanes, linear, in physiological soln., degradation by ester hydrolysis (*Russian*) 0-40690  
 polyurethanes, vapour press. of solvent above swollen crosslinked networks rel. to rubber elasticity theory 0-45536  
 polyvinyl alcohol, atactic, thermoelasticity of networks swollen in water, polymer-diluent interactions 0-29102  
 polyvinyl alcohol, in water-ethanol mixture, processes of structure formation 0-10482  
 polyvinyl alcohol/vinyl acetate copolymer, in water-ethanol mixture, processes of structure formation 0-10482  
 polyvinylalcohol, aqueous, solns., IR spectra 0-2761  
 polyvinylbenzocarbazole, weak solution, intramolecular energy transfer by singlet and triplet excitons 0-34971  
 polyvinylcarbazole, weak solutions, intramolecular energy transfer by singlet and triplet excitons 0-34971  
 polyvinylpyrrolidone, aqueous, solns., IR spectra 0-2761  
 poly((R)-oxypropylene), opt. rot. dispersion and vac. UV circular dichroism 0-40084  
 pseudoisocyanine bound by sulphated polysaccharides, dil. aq. soln., visible and circular dichroism spectra 0-45107  
 PVC, diffusion coeffs. and thermodynamic props., conc. depend. 0-15274  
 random coil, radial distrib. function calcs. 0-44101  
 rheological props. in flow through porous media 0-53819  
 rheologically anomalous fluids, flow in porous media 0-53851  
 rheology, characterised by mol. int. distrib., review 0-1504  
 rodlike, and flexible chain polyamide conc. solns., comparison of rheological props. 0-6007  
 rotating disc in polymer solutions under a turbulent regime 0-33634  
 second normal stress difference, meas. 0-43747  
 sedimentation velocity in ultracentrifugation, absolute mol. at. and mol. heterogeneity determ. (*German*) 0-14261  
 self-diffusion, review 0-29193  
 solution, second virial coeff., segment cloud model, chain length and branching study 0-24559  
 solvent osmotic stresses, prediction of Case II transport kinetics 0-26049  
 specific heat, conform. effects 0-24607  
 spirobenzopyran copolymer photochromic soln., photoviscosity effect 0-6536  
 stabilisation of foams (*French*) 0-21323  
 styrene-acrylonitrile copolymer in dimethyl formamide, methyl ethyl ketone and benzene, diffusion coeff., solvent effect 0-19971  
 styrene-butadiene block copolymers, in dil. soln., extrapolation methods for intrinsic viscosity 0-24636  
 surface tension, theoretical estimation 0-44394  
 2,4,6,8-tetraphenylnonane soln., macromol. dynamics, us relax. 0-19882  
 US waves absorption in vinyl-series polymer solutions 0-15192  
 vinyl alcohol-vinyl acetate copolymers, mol. architecture and physicochem. props. 0-44103  
 viscosities of dilute polymer solutions in nematic liquids 0-29199

## polymer solutions continued

- viscosity, method for meas. of conc. solns. at high temps. 0-19535  
 viscosity rel. to mol. mass (*Russian*) 0-2190  
 weak polymer solution in smooth pipes, turbulent wall motions 0-14823  
 xanthane, dilute solns., viscosity rel. to temp., shear rate (*French*) 0-39332  
 zero-shear viscosity estimates from falling sphere data 0-19306  
 Al soap solutions, viscous behaviour 0-2185
- polymerisation**  
 acrylonitrile, radiation initiated graft polymerisation on polyethylene films, fibres, PVC fibres (*Russian*) 0-7531  
 alkali metal polyphosphates, vitreous IR spectra 0-16043  
 benzene, plasma polymerisation in glow discharge, thin film IR and free radical EPR obs. 0-2964  
 benzoin containing system, photosensitized free radical polymerisation 0-7825  
 benzophenone containing system, photosensitized free radical polymerisation 0-7825  
 biimidazole+leuco dye photochem. reaction, modulation by photopolymerisation 0-40714  
 bromostyrene-crosslinked polyester, craze resistance 0-35421  
 butyl acrylate-vinyl acetate, two-stage emulsion polymerisation, forced compatibility (*Russian*) 0-44950  
 carbonization, polymeric aspects 0-2972  
 deformation of viscoelastic solids, depth of polymerisation 0-40414  
 diacetylene, single cryst., photopolymerisation, intermediate states, struct. changes 0-30235  
 diacetylenes, urethane substituted, polymer conversions in  $\gamma$ -ray polymerisation 0-26014  
 1,6-dicarbazolyl hexadiyne, solid-state polymerisation, monomer to polymer phase transformations 0-38948  
 dipoxide-diamine network polymers, reaction mechanism investigation using gel permeation chromatography 0-40789  
 difluoroethylenes, plasma polymerisation, ESCA characterisation of polymers 0-21283  
 diolefins, substituted, topochemically controlled solid-state polymerization 0-35532  
 electric phenomena, book 0-46746  
 electroinitiated, on electrodes, book contrib. 0-50854  
 electroinitiated, polymer film coating in aq. medium, book contrib. 0-50778  
 epoxide compound, polymerisation in non-uniform magnetic field, exam. of structural changes 0-7791  
 epoxy resin, curing investigation by polarisation current method 0-3345  
 ethylene vinylacetate copolymers, prep., props. and appls. 0-35154  
 feedstock projection for petrochemicals 0-2991  
 flexible polymer chain in nematic solvent, phase diagram (*French*) 0-39253  
 glass fibre reinforced plastic cylindrical shells, temp. stresses developing during polymerisation 0-40326  
 graft copolymerization by macrozwitterion mechanism 0-21285  
 heterodisperse polymers ease of fabrication, dependence on mol. wt. distribution 0-35530  
 impact resistant styrene copolymers, control of morphology and props. (*Bulgarian*) 0-35153  
 methyl methacrylate-styrene copolymers,  $^{13}\text{C}$  NMR 0-20473  
 $\alpha$ -methylstyrene, photoinduced ionic polymerisation 0-7828  
 $\alpha$ -methylvinyl alkyl ethers, polymerisation mechanism,  $^1\text{H}$ -,  $^{13}\text{C}$ -NMR 0-48112  
 network formation, pre-gel intramol. reaction and gelation, shear moduli and glass transition 0-45501  
 network formation, relaxational props. variation 0-38961  
 organic reactions in solid state 0-21309  
 organo-tin polymer films, glow discharge prep., comp. determ. by XPS and AES 0-35109  
 photoimaging system based on photopolymerisation in cryst. coatings 0-40716  
 photoinitiated cationic polymerization by photosensitization of onium salts 0-7822  
 photopolymer systems, conf., Washington, USA (Nov. 1978) 0-4799  
 photopolymerisation,  $\text{O}_2$  inhibition elimination 0-7821  
 photopolymerisation, dye-sensitized, activation by trialkylbenzylstanmanes 0-7824  
 piperylene-acrylonitrile copolymers, polymerisation, monomer composition rel. to copolymer struct. (*Russian*) 0-5651  
 plasma polymerisation on solid substrates, thin film form in RF discharge 0-2963  
 plasma-initiated biradical polymerisation 0-3343  
 PMMA coated frit powder prep. corona-charging props. (*Japanese*) 0-25891  
 poly (N,N-dipropylacrylamide), 'feathered' polymer resin, prep. from suspension 0-35533  
 poly-1,6-di-p-toluenesulphonyloxy-2,4-hexadiyne, thermal polymerisation, Raman spectra 0-35531  
 poly- $\beta$ -substituted vinyl ethers, cationic polymeris., stereochem. 0-21284  
 poly-thio-1-N,N-diethylaminomethylethylene, optically active samples,  $^{13}\text{C}$  NMR spectra 0-28127  
 polyacetylene film synthesis, review 0-15623  
 polyacrylonitrile, copolymerisation with poly-2-hydroxyethyl methacrylate rel. to crystallinity 0-38935  
 polyacrylonitrile, single cryst. formation, during soln. polymerisation, struct. determ. 0-38938  
 polyaramatics, synthesis, correl. with elec. cond. (*German*) 0-15514  
 polyether-urethane elastomers, crosslinked, three dimensional polymerisation, kinetics, gel. form., mech. props. (*Russian*) 0-7792  
 polyethylene, nascent, electron microscope study 0-38940  
 polyethylene, obtained from heterogeneous Ziegler-Natta catalysts, cryst. morphology and growth 0-38941  
 polyethylene catalyst,  $\text{TiCl}_4\text{-MgCl}_2$ , struct. and mechanism 0-11951  
 polynaphthalene films, plasma polymerised, photovoltaic and photocond. props. 0-34479  
 polyoxymethylenes, determ. of crystalline fraction from X-ray diffraction 0-44150  
 polysiloxane plasma polymerised film growth on GaAs substrate, dry etching process 0-25575  
 radiation processing, conf., Miami, FL, USA (Oct. 1978) 0-36772  
 semiconductive conjugated polymers, synthesis and elec. props., review 0-15513  
 styrene, plasma polymerisation in glow discharge, thin film IR and free radical EPR obs. 0-2964



# polymerisation continued

- styrene, thermal polymerization, PMR obs. 0-3342
- styrene divinylbenzene, viscosity meas. during radical copolymerisation 0-3344
- textile industry, agitating type polymerizer, synthetic resins and fibres manufacturing process 0-3341
- thermosetting materials, formation and props., phase diagram and torsion pendulum anal. 0-55381
- toluene polymerisation in CC N<sub>2</sub> afterglow, chem. reactions rel. to plasma props 0-3346
- n-vinyl carbazole, radiation induced polymerization ESH study 0-7817
- n-vinyl carbazole-acrylamide, post radiation induced polymerisation 0-7818
- n-vinyl carbazole-acrylamide, radiation induced polymerization, monomer crystallinity effects 0-7819
- vinyl chloride, US monitoring of local phase transitions 0-33299
- As-S, amorphous, glass transition and specific heat, intermolecular bond saturation 0-15011
- C black-graft polymers crosslinked with epoxy resin, electrical props. (Japanese) 0-24920
- Na<sub>2</sub>O-SiO<sub>2</sub> melts, cryoscopic struct. study 0-14994
- P-S, amorphous, glass transition and specific heat, intermolecular bond saturation 0-15011
- (SN)<sub>2</sub>\* radicals polymerisation to (SN)<sub>x</sub> in thin films, optical spectra 0-16656
- SiO<sub>2</sub> polymerisation and deposition from dil. solns., kinetics, 5-180°C 0-7790

# polymers

- see also elastomers; filled polymers; glass fibre reinforced plastics; glass transition; plastics; polymer films; polymer melts; polymer solutions; rubber
- 2,4-hexadiene-1, 6-diol, bis(p-toluene sulphonate), dark-current meas. 0-15520
- ABS resin, craze growth and fracture 0-50705
- acetal copolymer, notches effect on fatigue strength 0-25857
- acetylene photopolymers, presence in Jupiter stratosphere 0-31244
- acetylferrocene-furfural resins in glass like C matrix, Fe particles synthesis and props. 0-11229
- acrylamide-acrylic acid (acrylic acid salts) copolymers, composition determ., IR spectra (Russian) 0-7358
- acrylic, denture base, tensile testing 0-16621
- acrylic surgical bone cement fracture behaviour 0-56277
- acrylonitrile-butadiene-styrene copolymers, micromechanism of deform. and rupture (German) 0-35276
- acrylonitrile-methylacrylate-acrylamide latexes graft copolymerised onto PVA, for haemodialysis membranes (Japanese) 0-12297
- ACS blender and chlorine containing polymers, electrostatic property 0-54764
- adhesion phenomena and influence of various factors, work of adhesion (Polish) 0-3292
- adhesives, thermosetting acrylic, electron beam curing 0-16634
- adsorbed layer, on particles in suspension, thickness meas. by mag. birefringence 0-42191
- adsorbed plasma proteins, Fourier transform IR spectrometry 0-16899
- aged glasses, enthalpic state determ. by scanning calorimetry 0-6528
- ageing through exposure to light, device (French) 0-30126
- amorphous, diffusion of large penetrant molecules 0-15305
- amorphous, influence of space network of linkages on acoustical props. 0-19194
- amorphous, super-glass transition processes, damping process 0-24573
- amorphous polymer multiple dielectric relaxation, time-correlation function representation 0-15951
- amphiphilic-polymer liquid crystal, NaCl conc. influence on struct., X-ray diff. study 0-44126
- anion exchange resins for Pu recovery from nitric acid waste 0-681
- Araldite D cured with triethylenetetramine, fracture stability 0-30070
- aramid/epoxy composite, tensile test 0-11778
- aromatic polyamide fibre, sputter etching 0-21147
- biocompatibility evaluation by cell culture method (Japanese) 0-12301
- bioelectrets, occurrence of electret state and appl. in mol. biophysics and bioengineering 0-8007
- bioelectrochemistry and bioenergetics (book) 0-8749
- biomedical engineering textbook for undergraduates 0-8750
- biopolymer, electronic-conformation interactions 0-3588
- biopolymer chain, uniform, elastic, possible conformational states 0-37913
- biopolymer chains, intramol. react., enzyme catalysis appl., review 0-40953
- biopolymer constituents, protonation, ab initio Hartree-Fock-Roothaan SCF calcs. 0-9503
- biopolymer soln. heat capacity, conformational props. temp. depend. 0-8009
- birefringent, stress intensity factor determ. 0-14633
- bis(p-toluene sulphonate)diacetylene, monomer and polymer, solid state phase transformation, far IR transmission spectra obs. 0-55077
- bisphenol-A-diglycidyl epoxy, light emission under high elec. field, compared with photolum. 0-25465
- blends, two-component, glass transition, calorimetric investig. (Russian) 0-39268
- blood proteinpolymer interfacial behaviour, influence of hydrophilic-hydrophobic type of microphase separated struct. (Japanese) 0-12051
- branched and crosslinked molecules, mol. description of dynamics 0-9767
- brittle photoelastic, use of gelatin gels in prep. for optical polarization stress study 0-40325
- bromostyrene-crosslinked polyester, craze resistance 0-35421
- cellophane membrane, polarised, electret transport props., permeability coeff. 0-7860
- cellulose, mechanochem. degradation 0-40371
- cellulose, New Zealand kauri, <sup>13</sup>C/<sup>12</sup>C dating for last millennium 0-21819
- cellulose, nitrated, strength, deform. and disintegration, influence of stable free nitroxyl radicals 0-11717
- cellulose, phase transitions, kinetics of precipitation from diluted cadoxen solns. 0-7845
- cellulose, thermally stimulated discharge studies 0-11329
- cellulose acetate, I, doping effect on elec. props. 0-49757
- cellulose acetate, reverse osmosis membranes, ion mobility, diffusion coeff., elec. resist. obs. 0-45550
- cellulose acetate-g-polyacrylamide membranes, radiation grafted, appl. in water desalination by reverse osmosis 0-45548

# polymers continued

- cellulose blotter/torsion pendulum technique, for relax. determ. 0-54357
- cellulose esters, plasticiser effects on mech. and dielec. relax. 0-40047
- chain conform., small-angle neutron scatt. obs. (Polish) 0-10511
- chain cyclisation, lattice embedded model, discrete scatt. series representation 0-48109
- chain dynamics, ang. correl. function decay by multiple rot. pot. diffusion 0-3569
- chain in solution, mol. dynamics obs. 0-5643
- chainlike systems, Coulombic contributions, LCAO-SCF-CO method, Fourier representations 0-32862
- chains, electronic correl., similarities with Mott insulators, AMO method (French) 0-24775
- charge absorption and transport in polymer wetted by insulating liquid subjected to electric field 0-6534
- charge carrier species determ. using interfacial phenomena 0-24978
- charge movement study using capacitance-voltage characts. of MIS struct. (French) 0-39575
- chromium phosphinate polymer, one-dimensional antiferromagnet, spin-flop 0-50131
- coating, vibration-damping, for constructions, theory 0-10178
- colloidal plates, parallel, polymer adsorption, excluded volume effects, polymer-solvent interactions 0-45568
- composite materials, fracture kinetics 0-11770
- conference, nonmetallic materials and composites at low temps., Munich, Germany, July 1978 0-22139
- configurational properties of athermal self-avoiding polymer chains at intermediate to high concentrations 0-18950
- conformational energy calcs., appl. to defect props. of polymer cryst. 0-54154
- conjugated hydrocarbons, energy gap estimation, graph-theoretical approach 0-24789
- constitutive relations in photomechanics 0-43251
- contact angle at solid-water interface 0-20010
- copolymer model with alternating spins, kinetics 0-9768
- corona charged polyethylene thermally stimulated current and surface potential decay obs. 0-15945
- corona charged PVF<sub>2</sub> α<sub>c</sub> relaxation obs. 0-15956
- crack growth kinetics in uniaxially extended specimen (Russian) 0-1483
- crosslinked, probabilistic theory of structural and physical characteristics 0-5649
- crosslinking with X-ray irradi., active group and heavy atom effects 0-7829
- crystal, hydrostatic compressibility, H<sub>2</sub> bonding effect on anisotropy 0-25782
- crystalline, broadline PMR spectra, math. separation procedure 0-2647
- crystalline, elastic modulus, strength, rel. to crystallite shape 0-45335
- crystalline, stress transmission 0-35240
- crystallinity, kinetic and morphological aspects (French) 0-1942
- crystallinity determ. by thermal method (Russian) 0-38966
- cycloaliphatic polyimides, oriented, thermomech. props., synthesis (Russian) 0-55443
- damage accumulation problem (Russian) 0-21053
- defocus transmission electron microscopy 0-28927
- deformable solids, fracture and hardening kinetics 0-35210
- deformation of viscoelastic solids, depth of polymerisation 0-40414
- detector particle track diameter rel. to etching time (French) 0-9463
- diacetylenes, urethane substituted, polymer conversions in γ-ray polymerisation 0-26014
- 1,6-dicarbazolyl hexadiene, solid-state polymerisation, monomer to polymer phase transformations 0-38948
- dielectric properties, study by capacity method, strip electrodes capacity calc. 0-25327
- dielectric relaxation, theory, appl. of derived dielec. loss formula 0-50262
- diepoxide-diamine network polymers, chem. props. and average mol. wt. 0-37915
- diffuse boundary thicknesses, determ. by small angle X-ray scattering 0-38947
- diffusion of simple penetrants in polymers, statistical mechanical model 0-10704
- diphilic polyelectrolytes, aqueous solns., Wilhelm method 0-10745
- dynamic storage and loss compliances determ. from creep data 0-5948
- elastic and creep moduli meas. by contact methods 0-11852
- elastic modulus, temp. depend. 0-39202
- elasticity of chains 0-3116
- electret, charge dissipation, transport mechanisms 0-7268
- electrets and dielectrics, conf., Sao Carlos, Brazil, Sept. (1975) 0-7251
- electric phenomena, book 0-46746
- electrical phenomena, nature and appl., review 0-50254
- electrical props., book 0-7257
- electrochemical mass transfer between rough surfaces and solutions containing drag-reducing polymers 0-19447
- electronic conductivity, bulk controlled mechanism 0-20182
- endoprosthetic joint, fatigue life 0-40521
- entangled, ternary blends of monodisperse homopolymers, viscoelastic props. 0-19301
- entangled monodisperse polymers kinetic network model for nonlinear viscoelastic flow props. 0-28538
- epichlorohydrin/bisphenol A epoxy polymer concrete, viscoelastic props. 0-45340
- Epikote 828 cured with tetraethylenepentamine, fracture stability 0-30070
- epoxide resins, amine-hardened, heat distortion, glass transition temps., chem. cure 0-44302
- epoxies, stress-enhanced chemiluminesc. 0-40628
- epoxy (Araldite B), photothermoelasticity meas. by heating method 0-6000
- epoxy based structural adhesives, time-temp. cure behaviour, torsional braid anal. 0-55621
- epoxy impregnated superconducting composites, mech. props., strain effect at 4K 0-25822
- epoxy polymers, cured spin-spin and lattice relax., proton coupling, <sup>13</sup>C NMR obs. 0-34799
- epoxy polymers, dense-network, elastic deform. rel. to props. (Russian) 0-40468
- epoxy resin, Cl-containing, relation between static and dynamic deform. characts. 0-3137
- epoxy resin, cure history effect on dynamic mech. props. 0-54356
- epoxy resin, curing investigation by polarisation current method 0-3345
- epoxy resin, deform. rate depend. of mech. props. at cryogenic temps. 0-55456



## polymers continued

- epoxy resin, heat generated by fatigue (*Spanish*) 0-11736  
 epoxy resin, mag. susceptibility, constant mag. field effect 0-11154  
 epoxy resin, meas. of glass transition temp., linear viscoelasticity 0-29157  
 epoxy resin, mobility of sorbed water, low resolution PMR method 0-11276  
 epoxy resin, rubber modified, positron annihilation 0-29825  
 epoxy resin, time-temp. superposition of creep data, linear viscoelastic props. 0-30045  
 epoxy resin clad metal, corrosion charact. by electrical resist. and capacitance meas. (*German*) 0-30171  
 epoxy resin compositions, shrinking and thermal tension estimation using ferrite sensors (*Polish*) 0-35456  
 epoxy resin cross linked with aliphatic polyamines, struct. and dynamic mech. props. (*Japanese*) 0-38956  
 epoxy resin EhDT-10, temp.-time rel. of strength 0-25798  
 epoxy resin systems, synthesis review, phys. and mech. props. at low temps. 0-25650  
 epoxy resins, correlation between valence energies and low temp. flexibility 0-25815  
 epoxy resins, fracture props. study at cryogenic temps. 0-25869  
 epoxy resins, mech. and elec. low temp. props. 0-25814  
 epoxy resins, phenomena and mechanisms of tree inception 0-29687  
 epoxy resins, struct. changes under mag. field action 0-40516  
 epoxy treeing breakdown, slit model 0-15970  
 epoxy-metal joints, environmental fracture and effects of shrinkage stresses 0-16635  
 epoxy-paper, flashover behaviour at low temps. 0-25882  
 ethylene copolymers, partially cryst. pseudoeutectoid, swelling, thermodynamics 0-39311  
 ethylene copolymers with acrylic monomers, NMR investig. (*Russian*) 0-54959  
 ethylene vinylacetate copolymers, prep., props. and appls. 0-35154  
 ethylene-tetrafluoroethylene copolymer, chem. etching of fission tracks 0-896  
 ethylene-vinyl alcohol copolymer membranes for haemodialysis, prep. conditions and props. (*Japanese*) 0-12299  
 ethyleneterephthalate-ethylene glycol copolyester/15% polyglycol, semicryst. melting and glass transitions 0-49346  
 extrusion, solid phase, anal. of mechanics 0-39204  
 fibre-reinforced plastic, creep prediction from components props. 0-40448  
 fibrils, formation by flow-induced crystallisation 0-33908  
 flammability, heat transfer meas., moving wire technique 0-3347  
 flashover behaviour, of spacers at low temps. 0-25882  
 flexible macromolecules, flow-induced crystallisation, nonhomogeneous shear rates effect 0-38952  
 Fourier anal. of X-ray diffr. patterns 0-15016  
 Fourier transform IR spectroscopy, use in polymer research as vibr. spectroscopy tool 0-55744  
 fraction exponential function use for viscoelastic behaviour (*Russian*) 0-53652  
 fracture and crazing under plain strain (*Japanese*) 0-25850  
 fracture of material with initial defects 0-38339  
 free radicals determ., on polymer surfaces, using spectroscopic method (*German*) 0-7892  
 friction pair with metal, temp. calc. under severe friction 0-40550  
 frictional properties, crystn. effect 0-40551  
 gas permeability measurement in high polymers, techniques and detectors 0-14854  
 gel, magic angle rot. H NMR spectra meas. by variable temp. probe 0-31830  
 gel permeation chromatography, appl. to polymer characterisation 0-16740  
 gelation site-bond percolation, low-density series anal. of uncorrelated limit 0-4657  
 gels, with liq. cryst. solvents, theory 0-11963  
 glass, isobaric vol. and enthalpy recovery, transparent multiparameter theory 0-24375  
 glass, specific heat discontinuity at glass transition 0-19954  
 glass transition temp., dilatometric and dielectric relaxation data 0-6497  
 glass transition temperature, rel. to mol. wt. 0-34176  
 glass-forming polymer, paramag. spin-lattice interactions 0-7149  
 glass-transition temps., mol. wt. effect, thermodynamic theory 0-19920  
 glass/epoxy composite, tensile test 0-11778  
 glass/polymer/glass plate in temp. field, failure 0-43674  
 glassy, gas sorption and transport, review 0-15360  
 glassy, generality of plastic fracture process 0-35321  
 glassy, sheets and spheres, gel diffusion with discontinuous swelling 0-44354  
 glassy, stress analysis aspects of crazing 0-21148  
 glassy and crystalline relax. process characterisation,  $^{13}\text{C}$  NMR obs. 0-34802  
 granules, compression, stress state 0-10218  
 graphite-epoxy composites, moisture profile meas. using nucl. reaction anal. 0-55760  
 gutta percha, partially hydrogenated,  $^{13}\text{C}$  NMR 0-20472  
 hard disc necklaces, rigid and nonrigid models, mol. dynamics 0-43219  
 heterodisperse, molecular weight distribution rel. to ease of fabrication 0-35530  
 hexamethylmelamine, doped, and condensation resin, room temp. phosphoresc., thermal transforms. 0-45132  
 HF density of states 0-6689  
 high molecular weight, glass transition temp. and crit. props. 0-39265  
 high-modulus, behaviour in solid state, nonlinear irreversible thermodynamic approach 0-44154  
 homopolymer, theory of 1D adsorpt. on to 0-51034  
 hopping transport, microscopic rate equations 0-39580  
 hydrogels, two-component, elasticity theory and compress. meas. 0-44246  
 2-hydroxy, 3-allyl, 4,4'-dimethoxybenzophenone, methyl methacrylate copolymer, excitation singlet, internal  $\text{H}^+$  transfer, visible spectra 0-32728  
 impact resistant styrene copolymers, control of morphology and props. (*Bulgarian*) 0-35153  
 inelasticity, estimation using hysteresis friction model 0-7617  
 inelasticity degrees, estimation, hysteresis friction model appl. rel. to US testing 0-3136  
 ion exchange resins, macroporous rapid method of rating total void volume 0-21208  
 irradiated, crosslinking density effect on glass transition (*German*) 0-34175  
 irradiation by high energy electron beams, industrial applications 0-3210

## polymers continued

- Ising model equivalent 0-37914  
 izod polystyrene, influence of dimensions in mech. props. (*German*) 0-21039  
 Kapton (polyimide), insulators for superconducting magnets, effect of low temp. irradiation 0-25817  
 Kapton H, discharge area scaling and surface/subsurface damage due to electron beam irradi. 0-34853  
 Kevlar 29 and 49, aramid fibres, microvoid obs. 0-38960  
 large molecule, electronic struct., photoemission and optical absorpt. spectrum, CNDO/S3 model 0-53172  
 latex particles, surfactant adsorpt., electrokinetic investig. 0-3363  
 light and Raman scattering obs. of high press. phases (*Japanese*) 0-2773  
 linear, struct. disordered, electron localisation 0-29359  
 linear chains, excluded vol. problem 0-5650  
 linear self interacting chains, configurational props. 0-23586  
 linear self interacting chains, internal distrib., radius of gyration 0-23587  
 matrix, decreased stabilisation energy of excimers and exciplexes 0-25431  
 mechanical relaxation, nonlinear (*Russian*) 0-40467  
 mechanochemical degradation 0-40371  
 medical applications review, book contrib. 0-12307  
 membrane, transport of organic liqs., review 0-16720  
 methacrylate polymer, carbazoyl substituted, excimer and charge transfer complex trapping of excitons 0-34367  
 $\alpha,\omega$ -methoxy-poly(ethylene oxide) effect of swelling on longitudinal acoustic mode 0-29739  
 methyl methacrylate-styrene copolymer, dielec. characts. change rel. to composition 0-25296  
 methyl methacrylate-styrene copolymers,  $^{13}\text{C}$  NMR 0-20473  
 $\alpha$  methyl styrene-acrylonitrile, molecular mass determ., solubility studies (*German*) 0-23590  
 microcrack enlargement in heterogeneous materials, conc. criterion 0-11769  
 microtoming for structure analysis 0-40665  
 mixed amorphous system, correlation of Tg, glass transition 0-24574  
 mobility edge, classical solns. and crit. exponents 0-10936  
 molecular dynamics, review of Brownian motion theory 0-23589  
 molecular dynamics simulation of struct. 0-28923  
 molecularly doped, carrier drift, percolation approach 0-2390  
 Monte Carlo renormalisation group for polymers 0-42148  
 multichain polymer system, simulating dynamic and equilib. props. 0-53179  
 multicomponent inhomogeneous system, diffusion with moving boundaries and swelling at const. volume 0-44353  
 multicomponent polymer homopolymer blends, macroscopic phase separation 0-45289  
 multiple dielectric relax. processes, mol. aspects, book contrib. 0-50264  
 Mylar, discharge area scaling and surface/subsurface damage due to electron beam irradi. 0-34853  
 mylar, implantation of positrons from  $^{22}\text{Na}$  0-16118  
 Mylar (polyester), insulators for superconducting magnets, effect of low temp. irradiation 0-25817  
 network, crosslinks and trapped entanglements, two-network model 0-38962  
 network, crystn. and form. through crystn., crystallinity influence on radiation induced form. 0-38964  
 network, permanently crosslinked, topological struct. and macroscopic behaviour 0-37919  
 network, Riemann's metric degeneration to graph metric demonstration, chain entanglement problems 0-38963  
 network, small-angle neutron scatt. obs. of mol. behaviour 0-37918  
 network entanglement contribution to rubber elasticity 0-39203  
 network formation, pre-gel intramol. reaction and gelation, shear moduli and glass transition 0-45501  
 network formation, relaxational props. variation 0-38961  
 network formation, struct. and mech. props., computer simulation 0-38965  
 networks, deformation free energy, vol. depend. 0-40454  
 networks, diffusion mechanism and model, local conform. change 0-15288  
 NMR, review 0-11277  
 Nomex (nylon paper), insulators for superconducting magnets, effect of low temp. irradiation 0-25817  
 nonvinyl polymers, diffusion of simple penetrants, statistical mechanical model 0-6556  
 nylon, H-bridge interactions, far IR spectra study 0-11374  
 nylon 66, fatigue crack propagation, effect of moisture 0-3166  
 nylon 66, stress-enhanced chemiluminesc. 0-40628  
 nylon 66 films, superstructural ordering 0-15344  
 nylon 6,  $\alpha$ -form, crystal struct. and molecular packing 0-33905  
 Nylon 6, injection moulded, residual stresses 0-38950  
 Nylon 6, injection moulded, yield stress and fracture toughness 0-38951  
 Nylon 6, oriented, extensional deformation, and effects 0-7613  
 nylon 6, oriented glassy, mol. wt. influence on cryst. rate 0-44156  
 Nylon 6, plasticized with  $\text{NH}_3$ , deformation by solid-state extrusion 0-25736  
 nylon 6-inorganic salt mixtures, glass transition temp. 0-19921  
 nylon 6-LiCl mixtures, DC cond. and struct., Lill effects 0-44149  
 Nylon 7-7 and 11, dielectric const. and dielectric relax. 0-25294  
 nylon-12, roll-ZZ (*Japanese*) 0-54707  
 Nylon-6, injection moulded, struct. and morphology 0-38949  
 Nylon-6 fibre, crystal struct., WAXS obs. 0-15015  
 Nylons, inorganic salt influence on fracture 0-30119  
 Nylons, morphology and crack propag. in inorganic salts 0-30118  
 off-lattice chains, Monte Carlo anal. of excluded vol. problem 0-5647  
 oil-polymer mixture, acoustic attenuation CW meas., tissue simulation appl. 0-35961  
 oligoethylene glycol, crystallisation kinetics in presence of tetrachloromethane, NMR investig. (*Russian*) 0-54153  
 oligomers, polymer-derived, mass spectral charact. 0-37916  
 one dimensional polymers, compositional disorder, approx. band struct., self consistent virtual crystal approx. 0-39486  
 one-dimensional semiconducting polymer, demonstration of high mobility 0-20212  
 optically active cold-setting, for models of composite materials in thermal stresses investigation 0-40639  
 organotextolite, in plane state of stress, temp. depend. variant of strength 0-40449  
 orientation of plane of large cracks prod. by laser pulses 0-11753  
 oriented, partly cryst., macromols. in amorphous regions, length, mobility 0-49132



# polymers continued

packing coefficient determ. from acoustical meas. data 0-38959  
partially crystalline, comparative evaluation of various prep. techniques for morphology visualisation 0-13049  
partially labelled chains, neutron scatt. obs. 0-38899  
PCBM, thermal and sp. ht., temp. depend. anal. rel. to oligomer base 0-19721  
PCDM, thermal and sp. ht., temp. depend. anal. rel. to oligomer base 0-19721  
PECM, thermal and sp. ht., temp. depend. anal. rel. to oligomer base 0-19721  
PCGM, thermal and sp. ht., temp. depend. anal. rel. to oligomer base 0-19721  
penetrant diffusion, statistical mech. model 0-44351  
pentaplast, crystn. effect on frictional props. 0-40551  
perfluoro polyether, vacuum use as pump fluid 0-52251  
PET, effect of liquid aliphatic compounds on mech. props. 0-55488  
PET, glassy polymer, local struct. determ. 0-33904  
PET, intrinsic birefringence 0-29711  
PET, ionic cond. current rel. to neutralisation at polymer-metal interface at elevated temps. 0-24664  
PET, ionizing radiation effect on life (*German*) 0-19853  
PET, oriented, extensional deformation, and effects 0-7613  
PET, penetrant diffusion, statistical mech. model 0-44352  
PET, pyroelectric effects and depolarisation currents, illumination effects 0-34859  
PET fibre, anisotropy of dielectric relaxation 0-25297  
PET fibres, amorphous, exam. of birefringence 0-11360  
PFTE wear, combined rotating and linear motion effects 0-3201  
phenylene, deformability in physiological salt soln. 0-12305  
photo-oxidation 0-3380  
photochemistry 0-3381  
photochromic polymer, thermal effect in photomech. conversion 0-16706  
photochromism in bulk polymers 0-5805  
photopolymer in holographic real-time fluid flow measurement 0-6176  
plastic clad metal, corrosion charact. by electrical resist. and capacitance meas. (*German*) 0-30171  
PMMA, ageing characts., sub-atm. pressure partial discharge obs. 0-1867  
PMMA, amorphous polymer, Rayleigh scattering of Mossbauer  $\gamma$ -rays 0-39926  
PMMA, and related cpds., ionic charge carriers, dielec. studies 0-25291  
PMMA, atactic, elastic strain detection by X-ray scatt. 0-25751  
PMMA, atactic, FT IR spectrum,  $^{18}\text{O}$  substitution effects 0-23581  
PMMA, C-H stretching and bending vibs., IR spectra, selective deuteration 0-23582  
PMMA, coating on metal backing, thermophys. characts., expt. determ. technique 0-4707  
PMMA, crack growth rate effect, fracture surface structure 0-16466  
PMMA, electret, dielectric meas. at ultralow freq. by reheating 0-4741  
PMMA, flashover behaviour at low temps. 0-25882  
PMMA, glassy, photoelasticity 0-45034  
PMMA, immersion in high press. gaseous media, breakdown characts. for direct voltages with ripple 0-45009  
PMMA, laser damage mechanism rel. to viscoelastic props. 0-55233  
PMMA, neutron irradiation, radical distribution, ESR study (*Japanese*) 0-44920  
PMMA, nondestructive acoustic elec. field probe meas. 0-47076  
PMMA, partial draining of low-molecular weight polymers with flexible chains 0-23592  
PMMA, piezobirefringence, optical and mech. relaxations, temp. depend. 0-34885  
PMMA, thermochem. instability at Pt sphere inclusions caused by CW laser beam 0-29689  
PMMA, uniaxial tension, fractographic anal. of crack growth kinetics 0-40519  
PMMA, unstable crack propagation in liq. environment, fractographic study 0-30155  
PMMA, viscoelastic props. in plastic zone, cooling rate effect 0-40418  
PMMA, water drops, effect of drop size on contact angle 0-2245  
PMMA coated frit powder prep., corona-charging props. (*Japanese*) 0-25891  
PMMA dental biomaterials, fracture toughness testing 0-50800  
PMMA fracture toughness, flame-retardant additive effect obs. 0-16470  
PMMA modular matrix dye laser, pulse width influence on power output 0-28247  
PMMA notched beam, fracture due to central impact 0-16426  
PMMA plano-cylindrical Fresnel lens, design and performance analysis as solar collector 0-53403  
PMMA sheets, flame spread in laminar forced oxidising gas flow 0-35535  
PMMA with stress-raising flaw, deform. 0-25799  
PMMA-latex particles in benzene light scatt., appl. of liquid state theory 0-40750  
PMMA-steel pair, temp. calc. under severe friction 0-40550  
poly(2,6-dimethyl-1,4-phenylene oxide)/poly(styrene-co-p-chlorostyrene) blends, tensile props. modelling 0-19868  
poly(4-methyl pentene-1), US props., glass transition, Gruneisen parameters 0-54316  
poly(4-methylpentene-1), isotactic, permanganic etchant for TEM obs. 0-21132  
poly( $\alpha$ -methylvinyl alkyl ether)s,  $^1\text{H}$ -,  $^{13}\text{C}$ -NMR spectra, stereoregularity 0-48112  
poly( $\gamma$ -methyl L-glutamate), electric conduction mechanism (*Japanese*) 0-54696  
poly( $\gamma$ -n-amylyl L-glutamate), crystal transition, X-ray diffr. exam. of structure 0-24374  
poly( $\gamma$ -n-butyl L-glutamate), crystal transition, X-ray diffr. exam. of structure 0-24374  
poly( $\gamma$ -n-ethyl L-glutamate), crystal transition, X-ray diffr. exam. of structure 0-24374  
poly( $\gamma$ -n-propyl L-glutamate), crystal transition, X-ray diffr. exam. of structure 0-24374  
poly( $\epsilon$ -caprolactone)-PVC system, Fourier transform infrared spectroscopic exam. 0-25361  
poly(alkyl methacrylate)s, corona charged, decay of surface charge and TSC (*Japanese*) 0-54712  
poly(ethylene oxide), partial draining of low-molecular weight polymers with flexible chains 0-23592  
poly(ethylene-oxide), isothermal growth, thickening, melting, bilayer crystals, and chain end effects 0-38939

# polymers continued

poly(halo-N-vinylcarbazoles):2,4,7-trinitro-9-fluorenone charge transfer complexes, dark DC cond. 0-39626  
poly(L-histidine), molecular motions in solid state, NMR and dielec. meas. 0-11332  
poly(m-xylylene adipamide), crystallised by water absorption, morphology (*Japanese*) 0-24378  
poly(N-vinyl carbazole) sensitisation with Se, purification effect on electrophotographic characts. 0-49825  
poly(N-vinylcarbazole), glass transition temp., mol. wt. relation 0-19922  
poly(pyromellitimide), shock-induced electrical activity, mechanically induced bond scission model 0-50256  
poly(tetramethylene terephthalate), IR obs. of reversible stress induced crystal-crystal phase transition 0-20627  
poly(tetramethylene terephthalate), struct., X-ray obs. 0-19725  
poly(vinyl pyrrolidone), silicone grafted, for contact lenses, surface props. and stability of thin tear film 0-17194  
poly(vinylidene fluoride) piezoelectric film, Lamb and shear wave propagation (*French*) 0-44256  
poly( $\gamma$ -methyl L-glutamate) film, oriented, conduction anisotropy meas. (*Japanese*) 0-54707  
poly( $\text{N}^{\text{H}}$ ,  $\text{N}^{\text{F}}$ -terephthaloyl-L-lysine) membrane for artificial red blood cells, interaction with serum proteins (*Japanese*) 0-12061  
poly(N,N-dipropylacrylamide), 'feathered' polymer resin, prep. from suspension 0-35533  
poly N-vinylcarbazole, soln., laser induced ionic photodissoc., transient polyelectrolyte form. 0-53068  
poly-1,6-di-p-toluenesulphonyloxy-2,4-hexadiyne, thermal polymerisation, Raman spectra 0-35531  
poly-1,6-dip-toluenesulphonyloxy-2,4-hexadiyne single cryst., twinning 0-33906  
poly-2-hydroxyethyl methacrylate, copolymerisation with polyacrylonitrile rel. to crystallinity 0-38935  
poly-2-hydroxyethyl methacrylate, dielectric  $\gamma$  relaxation 0-34850  
poly-4-methylpentene-1, elastic parameters, US velocity meas. at 2.1-240K 0-40415  
poly- $\gamma$ -ethyl-D-glutamate, pulsed photoconduction 0-24969  
poly- $\epsilon$ -caprolactum, semicryst. melting and glass transitions 0-49346  
poly-L-glutamic acid-poly-L-leucine block copolymers, association colloids 0-26064  
poly-n-butyl isocyanate, helical wormlike chain, dipole moment, elec. birefringence, elec. dichroism, statistical mech. calcs. 0-14262  
poly-n-hexyl L-glutamate, sorption and permeation mechanism 0-26048  
poly-N-vinylcarbazole, in polymer film, excimer fluoresc., high press. effects 0-34966  
poly-p-phenylene sulphide, NMR relaxation for mol. motions (*German*) 0-11288  
poly-thio-1,1-N,N-diethylaminomethylethylene, optically active samples,  $^{13}\text{C}$  NMR spectra 0-28127  
polyacene quinone radical polymers, elec. props. described by variable range hopping model 0-44588  
polyacetylene:AsF<sub>5</sub>, Hall effect meas. 0-24955  
polyacetylene:AsF<sub>5</sub>, thermal decomp. kinetics, elec. cond., ESCA and mass spectra 0-50830  
polyacetylene:AsF<sub>5</sub>, X-ray absorpt. meas. of mol. struct., orientation and charge transfer 0-25486  
polyacetylene:AsF<sub>5</sub>(AsF<sub>6</sub>)(SbF<sub>6</sub>)(PF<sub>6</sub>), metallic, band theory 0-49570  
polyacetylene:I, electric props. in semicond. and metallic regions 0-29432  
polyacetylene:I, NMR investigation of struct. 0-39011  
polyacetylene, band struct. valence Hamiltonian minimal STO-3G basis calc., nonempirical model pot. 0-54596  
polyacetylene, bond length alternation and energy gap, intermediate exciton formalism 0-29305  
polyacetylene, Coulomb repulsion, bond alternation, Peierls distortion, HF approx. 0-44524  
polyacetylene, doped, p-n junction, elec. props., review (*Japanese*) 0-29410  
polyacetylene, doping with AsF<sub>5</sub>, mechanism, effect on elec. cond. and spectra 0-24473  
polyacetylene, dynamic nuclear polarisation of protons (*French*) 0-43217  
polyacetylene, electrical conducting, current status 0-44579  
trans-polyacetylene, electronic energy band struct., extended Hückel and MND0 studies 0-20065  
polyacetylene, nascent morphology obs. 0-24379  
polyacetylene, phototransport effects 0-44653  
polyacetylene, pure and heavily doped, optical and IR studies, electronic struct. calcs. 0-7347  
cis-polyacetylene, static lattice calcs. for crystals 0-10509  
polyacetylene, trans- and cis-isomer, electronic struct. calcs. 0-24788  
polyacetylene, undoped, thermally activated mobile defect, temp. EPR line broadening 0-43218  
polyacetylene and polyacetylene: AsF<sub>5</sub>, one-dimens. spin diffusion, NMR T<sub>1</sub> and dynamic nuclear polarisation meas. 0-44946  
polyacetylene film, partially oriented, anisotropic elec. cond., quasi-one-dimens. behaviour of fully oriented doped material 0-11112  
polyacetylene photoelectrochemical solar cell, fabrication and efficiency 0-50954  
polyacrylonitrile, AC conduction mechanism, freq. and temp. depend. (*Japanese*) 0-54706  
polyacrylonitrile, copolymerisation with poly-2-hydroxyethyl methacrylate rel. to crystallinity 0-38935  
polyacrylonitrile, elec. polarisation 0-7275  
polyacrylonitrile, pyrolyzed, pulsed photoconduction 0-24969  
polyacrylonitrile fibres, section cutting, technique (*Russian*) 0-7754  
polyacrylonitrile glassy polymer, energetics of gas sorption 0-29270  
polyalkaneimide, mech. and thermophys. props. at liq. He temps. 0-3117  
polyalkenamers, longitudinal accordion mode, low frequency Raman spectroscopy 0-25369  
polyamide, flashover behaviour at low temps. 0-25882  
polyamide, PA 66, rel. strain meas. during creep in liq. environments 0-30046  
polyamide 6 (polycapraamide), temp. depend. of complex permittivity rel. to moisture content 0-50251  
p-polyamide based organic fibres, effect of temp. and deform. time, on deform. strength props. 0-11720  
polyamide blends, formation by injection moulding, structs. (*Russian*) 0-44155  
polyamide fibre, sputter etching 0-21147  
polyamide mixtures, thermodynamically incompatible, composition-prop. relationship (*Russian*) 0-7872



## polymers continued

- polyamide-12 plasticized with sulphonamides, relaxation props. (*Russian*) 0-55031
- polyamide-polyoxirane copolymers, mechanical properties evaluated 0-11700
- polyamides, 1,3-cyclohexanebis(methylamine) based, thermal props. and glass transition temp. 0-39264
- polyaromatics, elec. cond. correl. with chem. struct. and synthesis, charge transfer complexes (*German*) 0-15514
- polyarylenealkyls, colour, EPR, electron density delocalisation degree determ. (*Russian*) 0-7152
- polyaryleneimides, oriented, elastic props. 0-40416
- polybrene, catalysis of  $\text{Co}(\text{NH}_3)_5\text{Br}^{2+}$  alkaline hydrolysis, high pressure, effect 0-55657
- polybutadiene, hydrogenation 0-26008
- polybutadiene, linear and star branched, rheology 0-23977
- polybutadiene, mol. motion in solid and soln.,  $^{13}\text{C}$  NMR relaxation meas. (*Japanese*) 0-2666
- 1,4-polybutadiene, oxidation stabilisation by singlet  $\text{O}_2$  quencher 4-(1-imidazolyl)-phenol 0-16677
- cis-1,4-polybutadiene, partially hydrogenated,  $^{13}\text{C}$  NMR 0-20472
- 1,4-cis-polybutadiene, stereoregular, recrystn. in partial melting temp. region (*Russian*) 0-6495
- polycapromide, crystn. effect on frictional props. 0-40551
- polycapromide, oriented, molecular rearrangements during deformation, IR spectra exam. 0-7644
- polycarbonate, brittle fracture of notched ductile polymers (*Japanese*) 0-16448
- polycarbonate, creep deform. caused by crazing 0-21133
- polycarbonate, effect of mol. weight on craze shape and fracture toughness 0-25858
- polycarbonate, fatigue crack propag., mol. wt. depend. 0-50700
- polycarbonate, glassy polymer, energetics of gas sorption 0-29270
- polycarbonate, insulators for superconducting magnets, effect of low temp. irradiation 0-25817
- polycarbonate, plastic insulation for cryogenic power cable, exam. of dielectric, tensile props. 0-25823
- polycarbonate, theoretical prediction of temp. rise at tip of running crack 0-2114
- polycarbonate, TSC anal. by activation energy spectra 0-20579
- polycarbonate, viscoelastic props. in plastic zone, cooling rate effect 0-40418
- polycarbonate notched beam, fracture due to central impact 0-16426
- polycarbonate of bisphenol A, neck form. and propag., strain anal. 0-16376
- polycarbonate resin-steel pair, temp. calc. under severe friction 0-40550
- polycarbonate track detector, electrochemically etched, meas. of low neutron fluences 0-32577
- polycarbonates unstretched and stretched, orientation relationships,  $^{13}\text{C}$  NMR meas. (*German*) 0-20474
- polydeoxyribonucleotides, poly(dA).poly(dT) and poly(dAT).poly(dAT), HF vibr. modes, Raman and IR spectra 0-32698
- polydiacetylenes, electronic struct., cyclic vs. linear models 0-54587
- polydiacetylenes, photocond. action spectrum of single crysts., charge transport obs. 0-15557
- polydimethyl siloxanes, cyclic and linear, neutron scatt. meas. of dimensions 0-18952
- polydimethylsiloxane, crystalline and amorphous, characterised by DTA, polarised light microscopy, dielectric relax. 0-25295
- polydimethylsiloxane, helical wormlike chain, dipole moment, elec. birefringence, elec. dichroism, statistical mech. calcs. 0-14262
- polyelectrolyte complexes, nonstoichiometric, solubility in water (*Russian*) 0-55674
- polyelectrolyte ion binding, Poisson-Boltzmann eqn. 0-45511
- all-trans polyene, ab initio studies 0-43222
- polyester, ion mobility from ionic injection current at strong diffusion 0-2210
- polyester (Mylar), plastic insulation for cryogenic power cable, exam. of dielectric, tensile props. 0-25823
- polyester fibre, sputter etching 0-21147
- polyester filmbase experience in motion picture industry, review 0-42278
- polyester-paper, flashover behaviour at low temps. 0-25882
- polyester-polyurethane interpenetrating polymeric network glues, props. 0-16640
- polyester-polyurethane semi-interpenetrating networks, mech. props., morphology 0-45362
- polyesteramide 6NT6 crystals, lamellar thickness invariance with crystallisation temp. 0-24380
- polyesters, corrosion-resistant, based on TMPD glycol, prep., phys. and corrosion props. 0-21136
- polyesters, linear,  $\text{H}_2\text{O}$  absorption and electric loss factor (*German*) 0-34849
- polyesters, photoreactive, synthesis and struct.-prop. relations 0-7826
- polyesters from bridged bicyclic lactones, struct. characterisation by NMR 0-20476
- polyethelene tubes and sheets, light resistance investigation under natural climatic conditions 0-21127
- polyether ester-PVC blends, annealed, dynamic mechanical and sonic velocity behaviour 0-25740
- polyether sulphone, evidence for crystallinity 0-28928
- polyethylacrylate, benzene penetrant diffusion, statistical mech. model 0-44352
- polyethylene: ( $\text{Dy}_2\text{O}_3$ ), mech. props. and transfer to steel surfaces 0-16496
- polyethylene: octadecanol, contact charging and donor impurity conc. relationship 0-20286
- polyethylene:NaCl, internal field strength, Raman spectra obs. 0-40061
- polyethylene,  $^{13}\text{C}$  NMR rotating frame relaxation 0-7182
- polyethylene, amorphous, struct. from NMR line shape analysis and MAR-NMR 0-28931
- polyethylene, annealed, crystallinity effect on mech. props. (*German*) 0-35230
- polyethylene, band struct. valence Hamiltonian minimal STO-3G basis calc., nonempirical model pot. 0-54596
- polyethylene, brittle fracture of notched ductile polymers (*Japanese*) 0-16448
- polyethylene, brominated, single cryst., IR analysis 0-25362
- polyethylene, carrier transport, expts. using hexatriacontane single cryst. as model polymer 0-6849
- polyethylene, carrier trap study by X-ray induced TSC and thermoluminescence (*Japanese*) 0-54713

## polymers continued

- polyethylene, chain defects influence on crystn., reference to cryst. size and perfection 0-38942
- polyethylene, comonomer unit partitioning, crystn. conditions effect 0-38943
- polyethylene, conform. stability, 1-electron levels, long-range effects calcs. 0-28123
- polyethylene, correlation between valence energies and low temp. flexibility 0-25815
- polyethylene: cryst., transverse deform. and transverse movement of defects 0-38958
- polyethylene, crystal, dielectric  $\alpha$ -relax., soliton as crystal defect 0-45004
- polyethylene, crystalline, steric struct. modelling of end defects 0-6371
- polyethylene, crystalline, twist disclination formation and longitudinal motion of defects 0-19810
- polyethylene, crystallisation of thick film from glassy state by annealing 0-54151
- polyethylene, crystn. under high pressure 0-38946
- polyethylene, deformation, Hartree-Fock SCF calcs. 0-18949
- polyethylene, dielec. props. rel. to mol. struct. 0-29681
- polyethylene, dielectric loss at very low temperatures (*Japanese*) 0-11331
- polyethylene, displacement of electronic spectrum during stretching, LCAO calc. 0-5481
- polyethylene, doubly oriented, low density, deformation and structure, exam. 0-11705
- polyethylene, drawn, ultrahigh modulus, linear, melting behaviour 0-19916
- polyethylene, dynamic modulus under high press., nature of high press. phase (*Japanese*) 0-3120
- polyethylene, effect of ketones, temp. depend., environmental stress relax. study 0-45336
- polyethylene, electrical capacitance under high DC elec. field 0-54705
- polyethylene, electrical tree growth anal. using simultaneous meas. of light intensity and partial discharges 0-45008
- polyethylene, environmental stress cracking, liq. efficiency criteria 0-21134
- polyethylene, fatigue, fractographic study 0-30101
- polyethylene, fatigue crack growth charact. 0-30100
- polyethylene, fibrillar, high mol. wt., oriented crystallisation, heat treatment effect (*Japanese*) 0-25738
- polyethylene, flashover behaviour at low temps. 0-25882
- polyethylene, glass filled solids, ultrasonic absorpt., scatt., velocity and attenuation 0-44262
- polyethylene, H bonding effects on skeletal optical and longitudinal acoustical modes 0-34914
- polyethylene, high density, hydrostatic extrusion behaviour 0-50649
- polyethylene, high density, influence of dimensions in mech. props. (*German*) 0-21039
- polyethylene, high density, oriented extended chain crystals, transparency (*Japanese*) 0-38955
- polyethylene, high mol. wt., deformability in physiological salt soln. 0-12305
- polyethylene, high- and low-density, crystallinity degree, comparative obs. (*Polish*) 0-1943
- polyethylene, high-density, damage accumulation kinetics under creep during prolonged loading 0-40447
- polyethylene, high-density, environmental stress crack growth 0-25895
- polyethylene, high-density, oriented crystalline, anisotropic thermal expansion 0-39324
- polyethylene, hip joint prosthetic component deformation meas. by holographic interferometry (*German*) 0-12302
- polyethylene, in toluene, pressure crystallised, swelling behaviour, rel. to densities 0-2167
- polyethylene, lamellar stacks, screw dislocations 0-19728
- polyethylene, laser-prod. plasma, space-resolved extreme UV emission 0-54015
- polyethylene, laser-produced plasma, momentum transfer and interaction phenomena of high power  $\text{CO}_2$  laser 0-48921
- polyethylene, linear,  $^{13}\text{C}$  spin-lattice relaxation 0-25235
- polyethylene, linear, crystallised from melt, effect of crystallisation time on density, mech. props., X-ray scattering 0-25680
- polyethylene, linear, glass transition temp. 0-15225
- polyethylene, linear, nuclear relaxation, mol. motion (*Russian*) 0-44949
- polyethylene, low density,  $\alpha$  mgch. dispersion in relation to spherulite deform. mech. 0-25781
- polyethylene, low density,  $\gamma$ -irrad., uniaxial elongation effect on elec. cond. 0-25812
- polyethylene, low density, isotropic, extensional deformation, and effects 0-7613
- polyethylene, low-density,  $\alpha$ -irrad., thermolum. mechanism biphenyl anions influence 0-2880
- polyethylene, low-density,  $\gamma$ -irrad., spin trapping reaction 0-39873
- polyethylene, low-density, fatigue fracture surfaces produced by monotonic and cyclic loading 0-40510
- polyethylene, low-density, in nonuniform AC fields, influence of temperature on breakdown obs. (*German*) 0-29685
- polyethylene, lubricant additive effect on operating performance of sintered materials 0-11785
- polyethylene, mag. susceptibility, constant mag. field effect 0-11154
- polyethylene, mech. and elec. low temp. props. 0-25814
- polyethylene, microfine powder prod. for dispersions (*German*) 0-29920
- polyethylene, microstruct. obs., variation during drawing and annealing, electron microscopy (*German*) 0-38944
- polyethylene, microwave dielec. losses variation rel. to different sample treatments 0-25881
- polyethylene, nascent, electron microscope study 0-38940
- polyethylene, neutron irradiation, radical distribution, ESR study (*Japanese*) 0-44920
- polyethylene, non-isothermal currents and space charge build-up 0-39590
- polyethylene, obtained from heterogeneous Ziegler-Natta catalysts, cryst. morphology and growth 0-38941
- polyethylene, of low density, determ. of avoiding of tensile cracks (*German*) 0-19874
- polyethylene, oriented, shear strain, effect on stuct., props. (*Russian*) 0-7656
- polyethylene, oriented chain-extended, Young's modulus, fracture and compression behavior 0-11747
- polyethylene, oxidised, charge carrier, transport phenomena 0-15515
- polyethylene, partial draining of low-molecular weight polymers with flexible chains 0-23592
- polyethylene, permanganic etchant for TEM obs. 0-21132



## polymers continued

- polyethylene, plastic insulation for cryogenic power cable, exam. of dielectric, tensile props. 0-25823
- polyethylene, polymer life eqn. appl. to dielec. strength 0-25304
- polyethylene, porous, tensile strength of interface with bone 0-30737
- polyethylene, radiation heating effect on creep 0-35285
- polyethylene, rapid crystn. from melt rel. to struct. 0-44152
- polyethylene, semi-crystn., neutron scattering study 0-38936
- polyethylene, semicrystallised chains, small-angle neutron scatt., mean dimension evaluation 0-43220
- polyethylene, shish-kebab crystals, core struct. 0-38945
- polyethylene, single crystal, estimation of fold surface densities using space filling models 0-10507
- polyethylene, single crystal, structural changes due to electron irradiation 0-29053
- polyethylene, solid, IR spectra, interference distortion of  $73\text{ cm}^{-1}$  absorpt. line 0-11375
- polyethylene, solid-state extruded, exam. of props. 0-11669
- polyethylene, space charge injected from electrode at low temps., luminesc. obs. 0-25464
- polyethylene, surface charge release, crossover phenomenon, thermally stimulated discharge current study 0-50255
- polyethylene, target impurity effect on laser produced expansion, ion spectrography 0-43945
- polyethylene, TSC study of deuteration 0-20581
- polyethylene, ultra high mol. wt., knee prosthesis, in vivo wear props. 0-17204
- polyethylene, ultra-high modulus, drawing behaviour, effect of drawing temp. 0-35232
- polyethylene, ultra-high-strength filaments, soln. spun/drawn, mech. and thermal props. 0-40440
- polyethylene, ultra-oriented high density, shrinkage as meas. of deformation efficiency 0-40398
- polyethylene, ultradrawn, electron microscope exam. of struct. after annealing 0-11662
- polyethylene, ultrahigh modulus, drawing temp. effect on void form. and modulus 0-35241
- polyethylene, voltage-induced charge transfer and its effects on tree initiation 0-25307
- polyethylene, X-ray emission spectra of  $\text{CO}_2$  laser-irradiated targets, nonlinear processes 0-33793
- polyethylene 2,6-naphthalate, AC conduction mechanism, freq. and temp. depend. (Japanese) 0-54706
- polyethylene 50 Hz tree propagation between needle electrodes 0-15968
- polyethylene and ethylene-vinyl acetate copolymer dielectric breakdown 0-15966
- polyethylene cables carrying DC current, TSC and space charge effects (French) 0-40042
- polyethylene catalyst,  $\text{TiCl}_4\text{-MgCl}_2$ , struct. and mechanism 0-11951
- polyethylene charge carrier injection, contactless electrode expt. 0-15540
- polyethylene chips on Cu-Ni mesh, surface, obs. at very low accel. voltage (200 V-1 kV) by SEM 0-10764
- polyethylene coating on galvanized steel, thermal oxidation affect on adhesion (German) 0-35419
- polyethylene cocrystals, partially and fully deuterated, chain folding,  $^1\text{H}$  NMR solid echo technique 0-20507
- polyethylene crystal, longitudinal growth in flowing soln., melting of continuous fibrillar crystal 0-19917
- polyethylene crystal, thermal creation of defects, dielec. evidence 0-44151
- polyethylene crystals, plastic deformation, molecular mech., TEM obs. 0-21022
- polyethylene electret, internal pot. topography, Raman and IR spectra 0-7362
- polyethylene electrets, charge trapping mechanism, TSC, DTA and optical meas. 0-11322
- polyethylene fibres, electron microscope investig. of internal struct. 0-28926
- polyethylene fibres, high density, ultra oriented, physical, mech. props. 0-25649
- polyethylene fibres, X-ray diffraction-profile Fourier analysis, determ. of microstruct. parameters 0-49042
- polyethylene fibres radiation initiated graft polymerisation of acrylonitrile, initiation rate rel. to props. (Russian) 0-7531
- polyethylene fibril, high mol. wt., high melting point crystal (Japanese) 0-38954
- polyethylene filaments, ultrahigh-strength, from soln. spinning and hot drawing 0-45268
- polyethylene insulation of HV cables, water-treeing, environmental stress cracking phenomenon of elec. origin 0-40575
- polyethylene life test needle electrode selection 0-15969
- polyethylene medium, embedded Ge particles, extinction cross section 0-9807
- polyethylene membrane, permeation of hydrocarbons 0-30281
- polyethylene molecule, fractured, local electron level calc. 0-14263
- polyethylene oxide, cryst., lowest laser Raman active accordion oscillations, elastic moduli effect 0-29734
- polyethylene oxide, drag-reducing, as corrosion inhibitor in Al tube 0-45445
- polyethylene photochemical aerosol, absorbance rel. to presence in Titan atmosphere 0-31249
- polyethylene surface field strength under DC stress 0-15967
- polyethylene terephthalate, crystn. effect on frictional props. 0-40551
- polyethylene terephthalate, exposed to aq. medium and  $\gamma$ -radiation, lifetime levels and fracture 0-40520
- polyethylene terephthalate, glassy, energetics of  $\text{CO}_2$  sorption 0-29270
- polyethylene terephthalate, polymer life eqn. appl. to dielec. strength 0-25304
- polyethylene terephthalate, tensile drawing behaviour 0-35279
- polyethylene terephthalate, TSC due to mobile ions and ionic conduction (Japanese) 0-54432
- polyethylene terephthalate, TSC meas., space charge and injected surface charge effects 0-11320
- polyethylene terephthalate charge transfer from metallic electrodes 0-15605
- polyethylene terephthalate-co-isophthalate, gelation and crystallization 0-24377
- polyethylene terephthalate-p-oxybenzoate, nematic-isotropic transition loss 0-44300
- polyethylene waveguide, O-type, loss characts. at  $337\text{ }\mu\text{m}$  0-33175
- polyethylene-2,6-naphthalate, pulsed photoconduction 0-24969

## polymers continued

- polyethylene-GaAs mixture, optical transmission spectra, IR filter prep. using computer appl. 0-2763
- polyethylene-glass pair, contact interaction under elastic strain, friction and  $\gamma$ -ray effects 0-40549
- polyethylene-isostatic polypropylene mixture, melting anal. 0-29150
- polyethylene-metal contact charging, electron transfer mechanism, PES characts. 0-35055
- polyethylene-steel pair, temp. calc. under severe friction 0-40550
- polyethylene-terephthalate track detector, electrochemically etched, meas. of low neutron fluences 0-32577
- polyethylene/Cu(Zn) adhesion, role of surface topography 0-35500
- polyethylenenaphthalate, elec. cond., appl. of model 0-24940
- polyethylenes, dielec. losses, for use in AC superconducting power transmission lines 0-25302
- polyglycine, IR spectra calc. for helix and  $\beta$  configs. 0-45853
- polyhexamethylene adipamide, calorimetric, X-ray and IR study 0-10512
- polyimide, adsorption modification of surface of macroporous  $\text{SiO}_2$  0-6624
- polyimide fibre reinforced polyamide-12 0-11754
- polyimides, cryst. lattices elasticity and mech. props. 0-20995
- polyimides, DFOF and DFOB, X-diff. exam. of structure and elasticity 0-6370
- polyimides, effect of orientational stretching on thermal aging 0-11721
- polyisobutane, relax. times, self diffusion, devel. and appl. of NMR data acquisition system 0-34807
- polyisobutylene, in simple extension, nonlinear stress relax., recovery after partial relax. 0-5949
- polyisobutylene, undiluted, mol. wt. influence on creep behaviour 0-45370
- polyisobutylene fibres, stretched, crystn. kinetic study using synchrotron radiation 0-33909
- polyisobutylenes, shear behaviour of Vistanex LMMH and L 100 0-1443
- polyisocyanurate foams, strength, cellular struct. effect 0-40518
- polyisoprene, from guayule rubber, TEM exam. of crystallisation 0-10508
- trans-1,4-polyisoprene, kinetics of thin film growth from melt 0-10505
- polyisoprenes, partly deuterated,  $^1\text{H}$ -NMR spectra, struct. 0-50202
- polymer materials, hysteresis flow model applicability for degree of inelasticity 0-28422
- polymer-metal friction pairs, triboelec. effects 0-11784
- polymer-semiconductor solar cells 0-16810
- polymeric, vibration-damping, for constructions, theory 0-10178
- polymeric systems, supported on inert substrates, dynamic thermomech. study 0-55623
- polymers, pyrolysis-mol. wt. chromatography-vapour phase IR spectrophotometry, on-line system, reviews 0-55768
- polymethacrylic acid:  $^{23}\text{Na}$ , nuclear relax. correl. times and counterion behaviour 0-50212
- polymethacrylic acid, benzene penetrant diffusion, statistical mech. model 0-44352
- polymethine-cyanine molecular aggregate, band struct. 0-53174
- polymethineimine, cryst. orbital studies by HF methods 0-44148
- polymethyl isopropenyl ketons, spectrally sensitized decomposition and Deep UV resists 0-40715
- polymethyl methacrylate, direct obs. of zero field surface 0-16133
- polymethyl methacrylate resist, electron depth distrib., expt. test of Bethe-Bloch model 0-16132
- polymethylmethacrylate, glass filled solids, ultrasonic absorpt., scatt., velocity and attenuation 0-44262
- polymethylsilosane resin MSN-7 additions to BN ceramic for increased strength and oxidation resistance 0-20880
- polymonochloro-p-xylylene,  $\gamma$ -ray-induced cond., hole injection effects 0-34452
- polyolefins, semi-crystn., neutron scattering study 0-38936
- polyorganosilasane impregnated BN composite 0-7526
- polyorganosiloxane impregnated BN composite 0-7526
- polyoxyethylene-glutaric acid eutectic, melting and crystn. 0-28924
- polyoxymethylene, drawn, extra meridional reflections 0-24376
- polyoxymethylene, irradi., thermoluminesc. above room temp. 0-2871
- polyoxymethylene, rapid crystn. from melt rel. to struct. 0-44153
- polyoxymethylene, ultrahigh modulus oriented, exam. of true crystal modulus, from -150 to  $20^\circ\text{C}$  0-11687
- polyoxymethylenes, determ. of crystalline fraction from X-ray diffraction 0-44150
- polyphenyl ether, glass transition temp., press. depend. 0-49135
- polyphenylquinoxaline-cellulose acetate, battery separator membrane, diffusion meas. 0-35574
- polypropene-alt-1,4-butadiene and hydrogenated derivative, mol. relaxations in glassy state 0-53177
- polypropylene, agitating type polymerizer, synthetic resins and fibres manufacturing process 0-3341
- polypropylene, crystalline spherulitic, shear bands formed under compression at low temp. 0-40507
- polypropylene, electron bombarded, radical formation, piezoelectric and pyroelectric effects, ESR study 0-7169
- polypropylene, electron bombarded electret, trapped charges ESR study 0-7170
- polypropylene, flashover behaviour at low temps. 0-25882
- polypropylene, Halen and Daplen, semicryst. melting and glass transitions 0-49346
- polypropylene, injection moulded, texture (Japanese) 0-25722
- polypropylene, insulators for superconducting magnets, effect of low temp. irradiation 0-25817
- polypropylene, isotactic, permanganic etchant for TEM obs. 0-21132
- polypropylene, lubricant additive, effect on operating performance of sintered materials 0-11785
- polypropylene, mag. polarisation, optical studies 0-55013
- polypropylene, oriented, compressive elastic modulus and yield strength 0-16385
- polypropylene, oriented crystalline, anisotropic thermal expansion 0-39324
- polypropylene, plastic insulation for cryogenic power cable, exam. of dielectric, tensile props. 0-25823
- polypropylene, semi-crystn., neutron scattering study 0-38936
- polypropylene, TSC meas. of relax. modes, apparent double glass transition 0-11323
- polypropylene chloride co-polymer powder, cold compaction, product strength, heat treatment effects 0-11621
- polypropylene fibre, with helical internal texture, SEM obs. of surface morphology 0-39394



## polymers continued

- polypropylene fibres,  $\gamma$ -irrad., microstruct. changes in glassy-high elastic state transition (*Rumanian*) 0-49347
- polypropylene fibres, high strength, elastic 0-20992
- polypropylene powder, cold compaction, product strength, heat treatment effects 0-11621
- polypropylene rods, prep. by die-drawing 0-45327
- polypropylene spherulites, refl. acoustic microscopy obs. 0-28922
- polypropylene-polyurethane laminates, meas. of dielectric losses at cryogenic temps. 0-25301
- polypropylenes, impact modified, testing by dynamic mech. anal. 0-16626
- polyquinones, ladder, partially-ladder, synthesis, struct., props., review (*Russian*) 0-7529
- polyriboxanthylic acid, spatial struct., H bonding 0-53086
- polysaccharide gel, anomalous behaviour of PMR line width of water (*Russian*) 0-11962
- polysiloxane dizwitterionomers, mech., dielec. relax., effect of H<sub>2</sub>O sorpt., thermal history 0-50261
- polysiloxane dizwitterionomers, mech. props., microstruct. 0-49131
- polysiloxane dizwitterionomers, morphology, ionic aggregation 0-49130
- polysiloxane dizwitterionomers, sorption of H<sub>2</sub>O, mechanism 0-49506
- polystyrene,  $\gamma$ -ray-induced cond., hole injection effects 0-34452
- polystyrene, and copolymers, optical fibre waveguides, spectral characts. 0-14461
- polystyrene, anionic, kinetic parameters assoc. with glass transition temp., calc. 0-49345
- polystyrene, annealed, enthalpic retardation times 0-19959
- polystyrene, atactic, bulk and surface elec. props., contact charging obs., dielec. const. 0-15615
- polystyrene, atactic, uniaxially oriented, Fourier transform IR spectroscopic exam. 0-25360
- polystyrene, chem. shift, conformational struct. (*Russian*) 0-5652
- polystyrene, crazed, orientation and struct., electron diff. meas. 0-30122
- polystyrene, crazed, orientation and struct., optical meas. 0-30121
- polystyrene, cryogenic foam insulators, low temp. props. 0-25818
- polystyrene, electron-beam-induced conduction 0-2397
- polystyrene, end group modified, chain dynamics studied by fluorescence depolarization 0-19724
- polystyrene, glass-transition temp., mol. wt. effect, thermodynamic theory 0-19920
- polystyrene, glassy, light scattering, quenching effect 0-20649
- polystyrene, glassy state, relax., free vol. fluctuations effect 0-19722
- polystyrene, isotactic, conformation in bulk crystallised state 0-43221
- polystyrene, isotactic, orientation of remaining amorphous chains during crystallisation 0-10506
- polystyrene, isotactic, semicrystallised chains, small-angle neutron scatt., mean dimension evaluation 0-43220
- polystyrene, isotactic and static cold-crystallised blends, thermal transitions 0-24381
- polystyrene, isotactic crystals, plastic deformation, molecular mech., TEM obs. 0-21022
- polystyrene, lamellar stacks, screw dislocations 0-19728
- polystyrene, monosubstituted, US relaxation, dynamics of mol. chains 0-29124
- polystyrene, O treated, interaction with vapour-deposited Cr and Ni atoms 0-3407
- polystyrene, partial draining of low-molecular weight polymers with flexible chains 0-23592
- polystyrene, polarised Rayleigh scatt. near glass-rubber relax., photon correl. spectroscopy 0-40124
- polystyrene, props. changes upon photooxidation 0-30123
- polystyrene, sorption of organic vapours, glassy-state relaxation induction and meas. 0-44415
- polystyrene, steric effects on excimer formation, fluorescence spectra exam. 0-25430
- polystyrene, stress cracking, pressure-induced, mechanism 0-35361
- polystyrene, unmodified and rubber modified, craze initiation in n-alcohols, kinetics 0-25894
- polystyrene aerosols, monodisperse, attachment of <sup>220</sup>Rn and <sup>222</sup>Rn delay products 0-41256
- polystyrene and model cpds., conformational struct. influence on normal modes of benzene ring, Raman study 0-14144
- polystyrene filament, melt spun, struct. and mech. props., effect of drawing, twisting, annealing, untwisting 0-45331
- polystyrene foils, breakdown-charged, surface charge densities and depths, TSC spectra 0-7260
- polystyrene latex, doublet particles, response of Knollenberg light scatt. counters 0-37152
- polystyrene latex monodisperse and peptized, structure determ. by neutron diff. and small angle scatt. 0-40748
- polystyrene latex particles, mixed sterically-stabilised dispersions, equilib. aspects of heteroflocculation 0-45570
- polystyrene lattice, emulsions-polymerised, particle size determ. by soap titration 0-40753
- polystyrene lattice cleaning, dialysis, steam stripping and ion exchange effectiveness 0-3414
- polystyrene microspheres, dye impregnated, fluoresc. spectra struct. resonances 0-50914
- polystyrene scintillators, extrusion prod. 0-37698
- polystyrene sphere crystals, in aqueous suspensions, solid-like phase transition 0-50893
- polystyrene-b-isoprene and hydrogenated derivative, mol. relaxations in glassy state 0-53177
- polystyrene-chloranil molecular complex, glass-rubber and liquid-liquid transitions 0-45002
- polystyrene-polyisoprene, block copolymers, association colloids 0-26064
- polystyrene-polyisoprene copolymers, macromol. chain conform. in lamellar phase (*French*) 0-2720
- polystyrol, ionizing radiation effect on life (*German*) 0-19853
- polysulphone, craze appearance effect on mech. props. 0-21135
- polysulphone, plastic insulation for cryogenic power cable, exam. of dielectric, tensile props. 0-25823
- polysulphone/S-glass adhesive failure, ISS and SIMS obs. 0-55626
- polysulphur nitride:Br mag. susceptibility, linear temp. depend. 0-25114
- polysulphur nitride:bromine, struct. and phase transition 0-24382
- polysulphur nitride, elec. cond. at microwave freq. 0-24922
- polysulphur nitride, Kohn anomalies in phonon dispersion 0-24555
- polysulphur nitride, low temp. thermal cond. 0-24689
- polysulphur nitride, pure and brominated, electronic model for high cond. 0-24923
- polysulphur nitride, temp. depend. and anisotropy of H<sub>c2</sub> 0-25054

## polymers continued

- polytetrafluoroethylene, degradation by electron or  $\gamma$ -ray bombardment in inert atmosphere (*German*) 0-19840
- polytetrahydrofuran, H bonding effects on skeletal optical and longitudinal acoustical modes 0-34914
- polytetramethylene glycol, short range order, amorphous and liquid, ideal peak method calcs. 0-28900
- polythene, ultraoriented, microhardness, extrusion conditions effect 0-50704
- polytrifluoroethylene, dielectric relax. processes above and below glass trans. (*Japanese*) 0-55028
- polytrimethylene terephthalate, struct. determ. 0-19727
- polyurethane, cryogenic foam insulators, low temp. props. 0-25818
- polyurethane foams, strength, cellular struct. effect 0-40518
- polyurethanes, crosslinked, thermoelastic props. 0-20991
- polyurethanes, linear, in vivo, degradation by ester hydrolysis (*Russian*) 0-40690
- polyurethanes, rigid foamed, cellular struct. effect on water absorpt. 0-39416
- polyvinyl acetate, partial draining of low-molecular weight polymers with flexible chains 0-23592
- polyvinyl acetate-polybutyl acetate crosslinked compositions, proton mag. relax., forced compatibility (*Russian*) 0-44950
- polyvinyl alcohol, bulk polarisation, thermally stimulated discharge current meas. 0-40039
- polyvinyl alcohol, ionic charge carriers, dielec. studies 0-25291
- polyvinyl alcohol-polyelectrolyte membranes, heterocharge electret form., divergence model 0-15943
- polyvinyl carbazole doped with trinitrofluorenone, thermoplastic-photocond., device for holographic recording 0-5707
- polyvinyl chloride, agitating type polymerizer, synthetic resins and fibres manufacturing process 0-3341
- polyvinyl-pyrrolidone/polyethylene glycol oligomers, elasticity theory, and compression meas. 0-44246
- polyvinylacetate and polyvinylacetate-microgels, light scatt. 0-20652
- polyvinylcarbazole-TCNQ complex, elec. cond. meas. 0-34456
- polyvinylcinnamate, crosslink form. by photoreaction 0-7823
- polyvinylidene electrets, IR and Raman spectra 0-7359
- polyvinylidene fluoride, dielec. props. and phase transitions (*French*) 0-55008
- polyvinylidene fluoride, equation of state, compression ratios, theory 0-10634
- polyvinylidene fluoride, piezoelec., pyroelec., and improper ferroelec. 0-7301
- polyvinylidene fluoride, piezoelectric effect formation due to injection process, TSC (*French*) 0-34856
- polyvinylidene fluoride, poling process effect on fine struct. 0-7285
- polyvinylidene fluoride, polycryst. ferroelec., microstruct., piezoelec. and pyroelec. props. 0-7303
- polyvinylidene fluoride, struct. study, piezoelec. and pyroelec. props. 0-7300
- polyvinylidene fluoride, structure, and its electret, review (*Japanese*) 0-10510
- polyvinylidene fluoride, thermodynamical model, applications (*French*) 0-39315
- polyvinylidene fluoride, TSC and thermoluminescence, reln. to molecular motion (*Japanese*) 0-55200
- polyvinylidene fluoride, US transducers, dielec. and acoustic losses 0-48541
- polyvinylidene fluoride, X-ray high press. study 0-6369
- polyvinylidene fluoride drift mobility meas., I<sub>2</sub> charge transfer from surface charge decay technique 0-49744
- polyvinylpyrrolidone, conformational states investig. by atom-atom function method (*Russian*) 0-53178
- polyvinyltoluene latex, doublet particles, response of Knollenberg light scatt. counters 0-37152
- polyvinyltrimethylsilane, diffusion, sorption, solubility, permeation of hydrocarbons, Xe (*Russian*) 0-6564
- polyvinyltrimethylsilane, sorption, diffusion, solubility of hydrocarbons, Xe rel. to temp. (*Russian*) 0-6565
- polyvinylpyridines, atactic, chem. shift, conformational struct. (*Russian*) 0-5652
- powders, corona-charging props. 0-6946
- perfluorinated polymer, DuPont Krytox 143-AB, viscoelastic and dielectric props. 0-1503
- propylene/butene-1 copolymers, coisotactic shift contribs. in <sup>13</sup>C NMR spectra 0-29635
- PTFE, annealing effect on melting and crystallisation (*Japanese*) 0-20980
- PTFE, Ne, Ar, Xe and He diffusion and solubility 0-6561
- PTFE, peroxy radical labelled, temp. dependent rots., EPR obs. 0-28125
- PTFE+metal, fluoride prod., DSC and XPS anal., rel. to polymer wear 0-11889
- PTFE-metal interaction, X-ray photoelectron spectroscopy obs. 0-11788
- PTFE-steel pair, temp. calc. under severe friction 0-40550
- pulsed photoconduction 0-24969
- PVA, swollen crystallinity determ. by laser Raman spectroscopy 0-38953
- PVA adsorbed on polystyrene latex particles, flocculation and stabilisation, concentration effects 0-45569
- PVA laser target, spherical-shell, energy absorpt., expt. determ. 0-54016
- PVAC dispersions, US method of determining plasticiser content (*German*) 0-21257
- PVC, brittle fracture of notched ductile polymers (*Japanese*) 0-16448
- PVC, chlorinated, fibres, radiation initiated graft polymerisation of acrylonitrile, initiation rate rel. to props. (*Russian*) 0-7531
- PVC, chlorinated, X-ray photoelectron spectra investig. 0-3469
- PVC, crystalline syndiotactic, exam. of chain folding, lattice energy 0-24373
- PVC, mechanochem. degradation 0-40371
- PVC, plasticised, fatigue, fractographic study 0-30101
- PVC, plasticised, fatigue crack growth charact. 0-30100
- PVC, plasticized, humidity depend. of ion mobility, polarity reversal of applied voltage method 0-49408
- PVC, reduced, dielec. props. rel. to mol. struct. 0-29681
- PVC, rigid, craze and yield zones in fracture 0-50701
- PVC, rigid, microdomains, small angle X-ray scattering study 0-28930
- PVC, rubbed, TSC meas. 0-55017
- PVC, sorption of organic vapours, glassy-state relaxation induction and meas. 0-44415
- PVC, stress relaxation in macrodeformation range 0-16370



## polymers continued

- PVC, unplasticized, evaluation method for chemical resistance (*Japanese*) 0-25893
- PVC plastisols, high resin level, rheological behaviour, discontinuous viscosity 0-23980
- PVC powder, cold compaction, product strength, heat treatment effects 0-11621
- PVC-chlorinated, piping for secondary criticality control of fissable solns. 0-13607
- PVF, charge injection from metallic electrode, obs. 0-15947
- PVDF, electret, polarisation process 0-7273
- radiation apps. (*Japanese*) 0-55413
- random coil polymer chain relax., lattice model with excluded vol., head movement rules 0-5642
- rectilinear on square lattice, series expansion 0-5646
- reinforced and isotropic high polymers, rubberelastic domain, thermodynamics 0-14579
- reinforcement, fracture mechanics 0-10207
- relaxation properties, photometric transducer method of meas. 0-3268
- rigid polymers, error estimation in viscoelastic problem soln., using method of approx. 0-19253
- rosin and carnauba wax thermal electret, elec. charge studied by TSC 0-7286
- saturated hydrocarbon polymers, conform. stability, 1-electron levels, long-range effects calcs. 0-28123
- self-diffusion detection, NMR matrix technique 0-15806
- self-interacting chains, Legendre transformation 0-15018
- semi-crystalline, diffusion mechanism and model, local conform. change 0-15288
- semiconducting biopolymers and their part in biochemical phenomena 0-12053
- semiconductive conjugated polymers, synthesis and elec. props., review 0-15513
- semicrystalline, partially and fully deuterated, chain folding,  $^1\text{H}$  NMR solid echo technique 0-20507
- short range order, amorphous and liquid, ideal peak method calcs. 0-28900
- single crystal, mosaic model for electron diff., bend distortion 0-44080
- sliding wear test apparatus, design and statistical evaluation, polymeric restoratives evaluation 0-21237
- sodium polyethylene sulphate, catalysis of  $\text{Co}(\text{NH}_3)_5\text{Br}^{2+}$  alkaline hydrolysis, high pressure, effect 0-55657
- sodium polyethylene sulphate, catalysis of  $\text{Co}(\text{NH}_3)_5\text{Fr}^{2+}$  aqution reactions, high pressure effect 0-55656
- sodium polystyrene sulphate, catalysis of  $\text{Co}(\text{NH}_3)_5\text{Fr}^{2+}$  aqution reactions, high pressure effect 0-55656
- solar water heater appl., low-cost unit development (*Afrikaans*) 0-7925
- solid state nuclear track detectors, review 0-37696
- solidification of low level radioactive waste, Dow process 0-37502
- solids, shock-induced electrical activity, mechanically induced bond scission model 0-50256
- sphere radii moments, size distrib. 0-21329
- sputtering, choice of type of electrostatic sputter (*Russian*) 0-50553
- square lattice, close packing of rectilinear polymers 0-48114
- stereochemical definitions, IUPAC nomenclature 0-23593
- stereoregularity distortions, local oscill. freqs., eqn. (*Russian*) 0-5653
- streamer breakdown in divergent field 0-25308
- structurally inhomogeneous, light scatt. by strains, theory and expt. 0-28162
- structure regularity, description and design 0-23591
- stycast 1266 epoxy, thermal contraction, 4-300K 0-4724
- styrene vinyltoluene, latex, doublet particles, response of Knollenberg light scatt. counters 0-37152
- styrene-acrylonitrile copolymer, amorphous, rubbery state, nonequil. tensile deform., effects of temp. and strain 0-40442
- styrene-isoprene triblock copolymer, mol. relax. in glassy state 0-53177
- styrene/MMA copolymers, struct. and rheology 0-1444
- surface, flame propagation velocity rel. to thermal props. (*Russian*) 0-7797
- synthetic, radiative degradation, chem., phys., environmental, technological effects, review 0-40948
- Teflon, flashover behaviour at low temps. 0-25882
- Teflon, non-destructive charge release 0-24946
- Teflon FEP, discharge area scaling and surface/subsurface damage due to electron beam irradi. 0-34853
- Teflon FEP, ethylene glycol, decane drops, effect of drop size on contact angle 0-2245
- Teflon FEP, negative streamer development, computational model for electron irradi. dielec. 0-34852
- Teflon spheres-nigrosin black dye-water dispersion, turbid laser backscatt. 0-1129
- Teflon-4, gamma irradi., wear resistance and antifirction props. 0-7691
- terephthalate copolyester, heat treatment effect on melting point (*Japanese*) 0-40400
- ternary polymer systems, diffusion controlled formation of porous structures 0-7539
- tetrafluoroethylene-vinylidene fluoride mixture, in epoxide-diphenylene propane resin, exam. of temp. depend. of stress relaxation, viscoelasticity 0-11688
- tetraglycidyl 4,4' diaminodiphenyl methane, diaminodiphenyl sulphone cured, failure and tensile mech. props., moisture effect 0-50735
- thermal diffusivity, Fourier theory 0-31456
- thermal expansion coefficient, determ. using optical dilatometer 0-45454
- thermomechanical and linear, dilatometric testing, automatic recording device 0-11858
- thermoplastic elastomers, crosslinked by secondary valence interactions, elasticity and processing, crosslinking behaviour 0-40320
- thermoset and coating technology, torsional braid and thermal anal. 0-55622
- thermosetting materials, formation and props., phase diagram and torsion pendulum anal. 0-55381
- three-dimensional cubic lattice, random walk of particle, polymer chain config. approach 0-22294
- tissue-equivalent plastic, A-150, thermal diffusivity, sp. ht., thermal cond. obs. 0-34258
- toluene sulphate diacetylene polymer, vibr. modes, strain depend. using Raman spectra 0-20626
- torsion pendulum dynamic mechanical testing, review 0-55620
- torsional braid analysis, conference, Anaheim, CA, USA, March 1978 0-51952
- total integrated light scatt. intensity 0-45092

## polymers continued

- treeing resistance assessment 0-15971
- US testing, using fast longitudinal and shear wave techniques 0-50793
- US velocity and damping coeff. meas. of polymers (*French*) 0-7723
- UV photoconduction expts. and electronic props. 0-15572
- Vespal SP-22 resin, thermal contraction, 4-300K 0-4724
- vinyl and related polymers, diffusion of simple penetrants, statistical mechanical model 0-10705
- vinylidene fluoride trifluoroethylene copolymer, ferroelec. behaviour 0-50284
- vinylidene fluoride-trifluoroethylene copolymers,  $^{19}\text{F}$  NMR (*Russian*) 0-7181
- viscoelastic, fatigue, fractographic study 0-30101
- viscoelastic, fatigue crack growth charact. 0-30100
- viscoelasticity and strength characterisation, advanced light scatt. techniques 0-11857
- vitreous, quasibrittle fracture 0-21094
- wear in thermally stressed state 0-3202
- $[\text{BH}_2]_n$ , energy band structure 0-5478
- $[\text{BeH}_2]_n$ , energy band structure 0-5478
- Al epoxy bonded joint, determ. and appl. of COD 0-30078
- Al-polyacrylonitrile-Al films, current-voltage characteristics 0-11125
- Al-polymer joint, meas. of temp. dependence of joint strength 0-50824
- $\text{Al}_2\text{O}_3$ -polymethylsiloxane composite, thermoreactive compaction 0-20879
- B fibre reinforced epoxy, dynamic Young's modulus and internal friction 0-27554
- C black-graft polymers crosslinked with epoxy resin, electrical props. (*Japanese*) 0-24920
- $(\text{CD})_n$ , polymer, heavily doped, IR spectra, vibronic intensity enhancement 0-28124
- $(\text{CH})_n$ , polymer, heavily doped, IR spectra, vibronic intensity enhancement 0-28124
- CrFeCN epoxy resin-based membrane studies, Ag sensitive electrode 0-16726
- Se, amorphous, vac. deposition on polymer substrates, use of temp. gradient vac. coating device 0-35099

## polymorphic transformations

see also displacive transformations; order-disorder transformations

- alkali metals, pressure influence on absolute zero isotherms, polymorphic transform., phonon spectra (*Russian*) 0-49363
- BBOA, polymorphism, radiothermoluminescence and differential scanning calorimetric study 0-24570
- t-butyl chloride- $d_0$  and - $d_9$ , polymorphism, Raman spectra 0-20617
- caesium propanoate, solid state transitions and melting process, diff. and conductometric meas. 0-10670
- critical isomorphous  $\gamma \rightarrow \alpha$  transition, phase equilibrium curve (*Russian*) 0-55397
- cubic-tetragonal transitions, symmetry anal. of deformable cryst. 0-10636
- deformable solids, fracture and hardening kinetics 0-35210
- 2,2-dinitropropane- $d_0$  ( $-d_9$ ), phase polymorphism, vibrational assignments, IR and Raman study 0-16031
- disordered crystals, 2H to 6H solid state transformation, deformation mechanism, X-ray diffraction study 0-33921
- disordered crystals, 2H to 6H solid state transformation, layer displacement, X-ray diffraction study 0-33920
- EBBA, polymorphism, radiothermoluminescence and differential scanning calorimetric study 0-24570
- highly dispersed systems, phase size effect 0-6488
- martensite formation, and lattice props. rel. to elastic constants 0-50630
- mechanochemical reactions, phase transformation and synthesis, review 0-3024
- metal-H, phase transitions 0-50631
- nematic liquid crystal, Merck 389, polymorphism, radiothermoluminescence and differential scanning calorimetric study 0-24570
- PAA, cryst. phase transitions, intermolecular motion, Raman and inelastic neutron scatt. spectra 0-2164
- PAP, cryst. phase transitions, intermolecular motion, Raman and inelastic neutron scatt. spectra 0-2164
- poly(tetramethylene terephthalate), IR obs. of reversible stress induced crystal-crystal phase transition 0-20627
- polymorphism at high press. and temp., thortveitite struct. stability (*French*) 0-10657
- quartz, natural and synthetic,  $\alpha$ - $\beta$  transition, impurities effect, refr. index meas. 0-20928
- quartz crystal, opalescence near  $\alpha$ - $\beta$  transition, static model rel. to domain wall form. 0-11420
- rubidium propanoate, solid state transitions and melting process, diff. and conductometric meas. 0-10670
- semiconductor-metal transition, struct. changes 0-34360
- shock wave induced transitions, review 0-15188
- simple order parameter, for reversible martensitic transformations 0-20932
- steel, austenitic, type En58B, martensite formation and reversion, effect on void swelling 0-11641
- steel, austenitic, type M316, martensite formation and reversion, effect on void swelling 0-11641
- steel, austenitic stainless, ferritic, single phase ferritic solidification in welds, exam. 0-7546
- steel, austenitic stainless, structure phase transitions due to high energy electron irradi. (*Russian*) 0-7553
- steel, C, pearlite grade ShKh15, struct. transformations, hot plastic strain influence (*Russian*) 0-20927
- steel, C, transform. kinetics, heat cond. and elastic-plastic stresses during quenching (*Japanese*) 0-25688
- steel, Cr-Mn, metastable constitution diagram and phase transforms. (*Russian*) 0-50590
- steel, Cr-Ni (18%, 12(8)%), martensite formation and reversion, effect on void swelling 0-11641
- steel, low C, ferrite grain nuclei form. during polymorphic transform. (*Russian*) 0-50626
- steel, low C-Si, LS1.2, LS1.5, phase transformation 0-45302
- steel, maraging, effect of thermal cycling ( $\gamma$  to and from  $\alpha$ ) on props. 0-20986
- steel, maraging, heated to high temperatures,  $\gamma$  to  $\delta$  transformations 0-20930
- steel, medium C, isothermally quenched, high-temp. deform. effects on struct. and props. (*Russian*) 0-25760
- steel, Ni and W, recrystallisation mech. during laser treatment 0-50658
- steel, phase conversion kinetics, exam. using ultrasonic method, apparatus design 0-21203



**polymorphic transformations continued**

- steel, stainless ferritic, drawability, mech. props., and grain boundaries in 08Kh16AMT and 08Kh18T1 0-35270
- steel, type 12Kh2N4A, belt grinding, struct. transformations 0-30169
- steels, high strength stainless, types 1Kh15N5AM3 and 1Kh16N4AB, phase transformations 0-20931
- 3,4,5-trichloroaniline, polymorphism,  $^{35}\text{Cl}$  NQR 0-54163
- weld metal, Type 316, transformation of  $\delta$ -ferrites, diffusion model 0-40347
- $\text{AgF}_3$ , high press. modification, cryst. and mag. props. 0-38988
- $\text{AgFeSe}_2$ , thermographic investigation of phase transitions (Russian) 0-10661
- $\text{AgFeTe}_2$ , thermographic investigation of phase transitions (Russian) 0-10661
- $\text{Ag}_3\text{GeTe}_6$ , optical props. and polymorphism 0-45082
- $\text{Ag}_3\text{Rb}(\text{PO}_4)_2$ , struct., density and elec. cond. 0-33952
- $\beta$ - $\text{AgSbS}_2$ , phase transitions, electrophysical props. 0-44316
- $\text{Ag}_3\text{SnSe}_6$ , cryst., Hall effect investigation of polymorphic transform. 0-39605
- Al alloys, liquid, kinematic viscosity temp. depend., porosity, H solubility, supercooling (Russian) 0-54425
- Al, kinematic viscosity temp. depend. porosity, H solubility, supercooling (Russian) 0-54425
- Al, liquid, kinematic viscosity temp. depend., porosity, H solubility, supercooling (Russian) 0-54425
- Al-Mg-Si, dil. alloy, Mn additions and heat treatment effect on  $\beta$ - $\alpha$  transformation 0-7566
- $\alpha$ - $\text{AlH}_3$ , prep., thermal decomposition, transform., struct. (French) 0-3326
- BN powder, wurtzite sphalerite struct. phase transition, effect on sub-struct. 0-25690
- BN, structural changes occurring during shock compression in presence of  $\text{H}_2\text{O}$  0-16301
- $\text{Ba}_2\text{K}_2\text{Nb}_2\text{O}_{15}$ , Raman scatt. experiments in tetragonal tungsten bronze compounds 0-40113
- $\text{Ba}_2\text{NaNb}_2\text{O}_{15}$ , Raman scatt. experiments in tetragonal tungsten bronze compounds 0-40113
- $\text{BiP}_2\text{O}_{14}$ , condensed, thermal behaviour and IR spectra 0-19912
- $\text{Bi}_2\text{Sn}_2\text{O}_7$ , polymorphic phase transition, X-ray, DSC, SHG, dielec. and optical obs. 0-44163
- $\text{CaCO}_3$ - $\text{NaAlSi}_3\text{O}_8$ , micromechanism for phase formation during sintering (Russian) 0-16253
- $\text{Ca}_2\text{SiO}_4$ - $\text{BaO}$ , conditions and mechanism in cryst.-chemical stabilisation of unstable phases 0-39302
- $\text{Ca}_2\text{SiO}_4$ - $\text{FeO}$ , conditions and mechanism in cryst.-chemical stabilisation of unstable phases 0-39302
- $\text{Ca}_2\text{SiO}_4$ - $\text{MgO}$ , conditions and mechanism in cryst.-chemical stabilisation of unstable phases 0-39302
- $\text{CdI}_2$ , hexagonal-rhombohedral polytypic transformation, electron diffr. and X-ray diffr. obs. 0-49163
- $\text{CdUO}_4$ , phase transforms., anomalous oxidation state change 0-54369
- Ce, Compton profile study of  $\gamma$ - $\alpha$  phase transition 0-11503
- Ce, electronic structure, Compton profile meas. rel. to  $\gamma$ - $\alpha$  transition 0-10867
- Ce, polymorphic  $\gamma$ - $\alpha$  transform. and volume anomalies under press. 0-34189
- Ce-Pr powder, DHCP=FCC transition, X-ray, DTA and resistivity studies 0-50629
- Co-Ni(Ti)(Cu)(Mn), cryst. struct. and stacking fault influence on mag. props. (Russian) 0-25164
- Cr bronze Sn, recrystn. props., hot rolling, annealing, polygonisation (Russian) 0-55419
- $\text{CsPbBr}_3$ , cubic-to-tetragonal phase transition, critical anomalies, phenomenological eqns. 0-39275
- $\text{CsPbCl}_3$ , cubic-to-tetragonal phase transition, critical anomalies, phenomenological eqns. 0-39275
- $\text{CsPbCl}_3$ , lattice thermal expansion, X-ray powder technique 0-19965
- Cu-Ni-Al, review 0-7564
- Cu-Zn-Al, memory alloy wire and ribbon reversible martensitic transformation, ageing effect, review 0-7564
- $\text{Cu}_2\text{S}$ , HP-FCC polymorphic transition stages 0-33924
- $\text{Cu}_2$ , S film, evaporated, ordering process, electron diffr. study 0-39477
- $\text{Cu}_2\text{SbS}_3$ , skinnerite, polymorphism, X-ray diffr. and NQR meas. 0-49165
- $\text{Cu}_2\text{Te}$ , HP-FCC polymorphic transition stages 0-33924
- Fe alloy type G18, martensitic  $\gamma$ - $\alpha$  transformation, dislocation pile-ups,  $\epsilon$  phase nucleation (Russian) 0-55396
- $\alpha$ -Fe, struct. after polymorphic transform. under press. (Russian) 0-29946
- Fe-Cr alloys and Fe, lattice parameters, 293 to 1273K,  $\alpha$  to  $\gamma$  phase transform., X-ray diffr. exam. (Russian) 0-50625
- Fe-Cr-Ni austenitic alloy, cold deformed,  $\alpha$ - $\gamma$  transition, calorimetric study (Russian) 0-55390
- Fe-Mn, Mossbauer spectroscopy of temp. hysteresis of phase transformations (Czech) 0-29949
- Fe-Mn (2 to 8 wt.%) alloys, phase transformations, tempering influence (Russian) 0-25735
- Fe-Mn alloys,  $\alpha$ ,  $\epsilon$  and  $\gamma$ , brittleness 0-35314
- $\alpha$ -Fe-Ni, struct. after polymorphic transform. under press. (Russian) 0-29946
- Fe-Ni (23 wt.%), struct., composition changes during  $\alpha$  to  $\gamma$  transform., martensite plastic deformation influence (Russian) 0-11642
- Fe-Ni alloy,  $\alpha$  to  $\gamma$  slow transformation mechanism, Ni content influence (Russian) 0-7569
- Fe-Ni-Cr-Mo superalloy, mech. props.,  $\eta$ -phase form. effect (Chinese) 0-20925
- Fe-Ni-Ti-Al-Nb, struct. mechanism for inverse  $\alpha$ - $\gamma$  transform. (Russian) 0-40351
- Fe-Pd, anomalous elec. cond. near mag. phase transition point,  $\alpha$  to  $\gamma$  phase transition 0-15722
- $\text{FeTiD}_x$  ( $0 \leq x \leq 1.9$ ), structural phase transitions, absorpt. and desorpt. isotherms 0-19948
- $\text{Ga}_2\text{O}_3$ ,  $\alpha$  to  $\beta$  monotropic transition heat determ. 0-54370
- $\text{GaSe}_{1-x}\text{S}_x$ , polytypes, exciton gap energies, luminesc. study 0-54611
- GeTe, interpretation of polymorphic transformations 0-15032
- GeTe-MnTe, heat treatment effect on struct., elec. props. 0-54725
- Hf electron field emitter, temp. drop meas., allotropic transform. temp. 0-2931
- $\text{HfO}_2$ : $\text{Er}_2\text{O}_3$ ( $\text{Y}_2\text{O}_3$ )( $\text{Eu}_2\text{O}_3$ ), elastic props., sonic reson. meas. 0-7612
- HgTe, pressure-induced polymorphic transition 0-10667
- $\text{InSbO}_4$ , monoclinic high-pressure modification, structural type 0-33925

**polymorphic transformations continued**

- $\text{K}_2\text{Cr}_2\text{O}_7$ , depend. on thermal and prep. history 0-34184
- $\text{KIO}_3$ ,  $\text{HIO}_3$ , structural modifications, NQR study 0-20487
- $\text{KMnF}_3$ , cubic-to-tetragonal phase transition, critical anomalies, phenomenological eqns. 0-39275
- $\text{K}_2\text{SO}_4$ , thermal phase transition 0-19738
- $\text{LaAlO}_3$ , Pm3m to R3c or R3c phase transitions, TEM method for domain identification 0-14980
- $\text{LaOF-LaF}_3$ , high pressure phase transitions 0-55368
- $\text{LiAlO}_2$ , matrix support material for molten carbonate fuel cell, thermal stability, effects of different environments 0-50952
- $\text{LiBO}_2$ - $\text{In}_2\text{O}_3$ , phase composition, mag. props. elec. cond. 0-55365
- $\text{LiNbO}_3$ , shock-wave compression, 2.4-44 GPa 0-34139
- Mn-Cu, alloying behaviour and high damping capacity 0-35160
- Mn-Y-Zn-Cd alloy, phase equilibria, plastic deformation, microhardness (Russian) 0-40334
- $\text{N}_2$ , solid, mol. libration and  $\alpha$ - $\gamma$  phase transition, Kihara pot. calcs. 0-44312
- $\text{NH}_4\text{Br}$ ,  $\beta$ - $\gamma$  phase transition, critical anomalies, phenomenological eqns. 0-39275
- $(\text{NH}_4)_2\text{H}(\text{SO}_4)_2$ , phase transitions, sp. ht. meas. 0-2157
- $(\text{NH}_4)_2\text{H}(\text{SO}_4)_2$ , successive phase transitions, dilatometric and X-ray expts. 0-11348
- $\text{NaClO}_4$ , metastable-stable phase transition mechanism (French) 0-15031
- $\alpha$ - $\text{NaSbS}_2$ , cryst. struct. and  $\beta$ - $\alpha$  phase transform. features 0-33961
- $\text{Na}_{1+x}\text{Si}_x\text{Zr}_2\text{P}_{3-x}\text{O}_{12}$ , monoclinic to rhombohedral phase transformation 0-29950
- $\text{Na}_3\text{Zr}_2\text{Si}_2\text{PO}_{12}$ , NASICON, phase transition, X-ray diffr., ionic cond. and sp. ht. meas. 0-19979
- Nb-Ge film, phase transformations due to annealing, electron diffr. study 0-54551
- Nb-Si diagram of state, melting temp., polymorphic transform. temp. (Russian) 0-50594
- $(\text{Ni}_{1-x}\text{Cu}_x)_2\text{Ti}$ , martensitic, shape memory effect kinetics and thermodynamics 0-3021
- $\text{NiTi}$ , martensitic, shape memory effect kinetics and thermodynamics 0-3021
- $\text{O}_2$ , solid, transformation charact. and orientation relations 0-33917
- Pb compounds, perovskites, polymorphic transformations possibility, mag. anal. elec. ordering effects 0-55389
- $\text{PbF}_2$ , polymorphic transition temps. under hydrostatic press., DTA study 0-2156
- $\text{Pb}_2\text{O}_4$ , tetragonal to orthorhombic transition, heat capacity meas. 0-20929
- Pd alloys, controllable hydrogen phase naklep, hardening and phase-strengthening 0-16323
- $\text{Pd}_3\text{AlCu-PdAl}$  system, interactions and solid-state transforms (Russian) 0-16272
- $\text{PdF}_2$ , high press. modification, cryst. and mag. props. 0-38988
- RbI, phase transition  $\text{NaCl}$ - $\text{CsCl}$  type, preferred orientation of  $\text{CsCl}$  type 0-49160
- $\text{RbIn}(\text{MoO}_4)_2$ : $\text{Fe}^{3+}$  monocrystals, EPR spectrum in the phase transition neighbourhood 0-2624
- $\text{RbLiSO}_4$ , successive struct. transitions, X-ray diffr. 0-10521
- $\text{Sc}_2\text{Si}_2\text{O}_7$ , polymorphism at high press. and temp., thortveitite struct. stability (French) 0-10657
- Se, monoclinic to trigonal conversion, thermodynamic stability and associated investigs. 0-24592
- SiC, epitaxial film, effect of impurities on polymorphism during growth 0-15414
- SiC, polytypic transform., interface struct. exam. by TEM 0-15033
- $\text{Si}_3\text{N}_4$ , N ion implantation synthesis, struct. and resonance mechanism of  $\alpha$ - $\beta$  transition during annealing 0-33981
- Sn polymorphic transformations ( $\beta$ - $\alpha$ ), effect of impurities, exam. 0-7557
- Sn-Bi, crystal struct. and superconductivity after appl. of high press. and quenching 0-10531
- SnTe, polymorphism, high press. and temp., X-ray diffr. study 0-54375
- $\text{Sr}_2\text{K}_2\text{Nb}_2\text{O}_{15}$ , Raman scatt. experiments in tetragonal tungsten bronze compounds 0-40113
- $\text{Sr}_2\text{NaNb}_2\text{O}_{15}$ , Raman scatt. experiments in tetragonal tungsten bronze compounds 0-40113
- $\text{SrSi}_2$ , phase diagram, 10 to 40 kbar, 600 to 1200°C, polymorphic transform. 0-29165
- $\text{TbSi}_2$ ,  $\gamma$ - $\gamma$  ang. correl. obs. of polymorphic transition, 200-900°C 0-29653
- Ti, diffusion of Be, temp. depend., radioactive tracer method (Russian) 0-10703
- Ti-Al, structural and phase changes due to annealing (Russian) 0-55440
- ( $\alpha$ + $\beta$ )-Ti-Al-Mo-Fe alloy VT-22, behaviour during creep testing, solid soln. dissoc. (Russian) 0-40346
- Ti-Al-V (4.7, 2 wt.%) pseudo alpha alloy, laminar struct. singularities,  $\beta$  to  $\alpha$  transformation (Russian) 0-7552
- Ti-Al-V (6.4 wt.%), phase transformation after hydrogenation 0-7560
- Ti-Cr, phase transformation, appl. of Philips STEM400 system 0-25689
- Ti-Fe, magnetic susceptibility depend. on phase composition (Russian) 0-54875
- Ti-Nb-Zr (35, 3 wt.%), martensitic  $\tau$  phase, X-ray diffr. obs. 0-16300
- Tl-Bi system, phase transitions near  $\text{Tl}_3\text{Bi}$ , elec. props. meas. 0-35181
- $\text{YFe}_2\text{O}_4$ , low temp. phase transitions and mag. props. 0-7106
- $\text{YOF-YF}_3$ , high pressure phase transitions 0-55368
- Zr based alloys,  $\beta$ - $\alpha$  phase transformation, cooling rate effects 0-7565
- Zr,  $\beta$ - $\alpha$  phase transformation, cooling rate effects 0-7565
- $\text{ZrO}_2$ , tetragonal to monoclinic phase transf. by ball-milling 0-25687

**polymorphism**

- see also crystal structure; isomorphism; polymorphic transformations
- n-alkane, long chain, syntactic coalescences between monoclinic and orthorhombic polymorphs 0-10520
- carbon tetrabromide, ordered phases, polymorphism obs. 0-54217
- carbon tetrachloride, ordered phases, polymorphism obs. 0-54217
- carbon tetraiodide, ordered phases, polymorphism obs. 0-54217
- ceramic characteristics (Japanese) 0-15075
- COOB, solid state dimorphism and cryst.-smectic transition, Raman study 0-45063
- n-hexatriacontane, cryst., orthorhombic modification, vibr. spectra 0-50314
- liquid crystals, solid state polymorphism, differential scanning calorimetry and IR and Raman spectra obs. 0-55094
- order-disorder groupoid family, parameters, stacking 0-38982
- order-disorder structures, desymmetrisation 0-38986



**polymorphism continued**

- order-disorder structures, layer stacking 0-38981  
 order-disorder structures, X-ray powder patterns features 0-38864  
 poly(vinylidene fluoride) orientation, solid state deformation by coextrusion 0-40394  
 PVDF, film, polymorphism induced by poling and annealing 0-24372  
 PVDF dielectric, piezoelec. and pyroelectric props. rel. to crystalline forms 0-15982  
 $\beta$ -AgI, luminesc. of 2H- and 4H-polytypes 0-2843  
 B, polymorphism rel. to CVD mechanics and deposit structs. 0-15403  
 $\delta$ -BaFe<sub>2</sub>O<sub>4</sub> room-temp. formation and polymorphism (*German*) 0-44192  
 Bi<sub>2</sub>Sn<sub>2</sub>O<sub>7</sub>, polymorphic phase transition, X-ray, DSC, SHG, dielec. and optical obs. 0-44163  
 C allotropes, diamond, graphite, gas-solid interface, electronic struct. HFR calc. 0-54745  
 (CO(NO)<sub>2</sub>CL)<sub>2</sub>, order-disorder struct., X-ray data 0-39037  
 CaBSi<sub>2</sub>O<sub>6</sub>, B=Mg, Fe<sup>3+</sup>, Al, pyroxenes, order-disorder interpretation 0-38987  
 CaNbF<sub>7</sub>, polymorphism, X-ray powder diffr. data (*French*) 0-19779  
 CdBr<sub>2</sub>, polytype 12R, cryst. struct. determ. 0-33937  
 CdI<sub>2</sub> crystals, growth conditions effect on polytypism, X-ray diffr. study 0-28942  
 Ce<sub>2</sub>Sn<sub>3</sub>, low temp. modification with tetragonal struct. 0-1963  
 Cs, structural energies, pseudopotential formalism 0-39519  
 CsNO<sub>3</sub>, high pressure phases III and IV, X-ray struct. determ. 0-28953  
 Fe<sup>2+</sup>BSi<sub>2</sub>O<sub>6</sub>, B=Mg, Fe<sup>3+</sup>, Al, pyroxenes, order-disorder interpretation 0-38987  
 $\delta$ -FeO(OH) and its solid solns. synthesis, X-ray diffr. and TEM studies 0-29891  
 Fe<sub>2</sub>S<sub>10</sub>, polytypism, Fe diffusion near antiferromag. to ferrimag. transition 0-44830  
 GeSe<sub>2</sub>, single crystals, 3 polymorphic forms, DTA, photolum., IR and Raman spectroscopy 0-33923  
 K<sub>2</sub>Zn(WO<sub>4</sub>)<sub>3</sub>, cryst. struct. and polymorphism 0-1996  
 La<sub>2</sub>Sn<sub>3</sub>, low temp. modification with tetragonal struct. 0-1963  
 LiR (WO<sub>4</sub>)<sub>2</sub>, R=La-Sm, triclinic modification, cryst. struct. 0-33976  
 Li<sub>2</sub>WO<sub>4</sub>, type II polymorph. cryst. struct. determ. 0-15073  
 MgBSi<sub>2</sub>O<sub>6</sub>, B=Mg, Fe<sup>3+</sup>, Al, pyroxenes, order-disorder interpretation 0-38987  
 MgNbF<sub>7</sub>, polymorphism, X-ray powder diffr. data (*French*) 0-19779  
 NaBSi<sub>2</sub>O<sub>6</sub>, B=Mg, Fe<sup>3+</sup>, Al, pyroxenes, order-disorder interpretation 0-38987  
 $\alpha$ -NaSbS<sub>2</sub>, cryst. struct. and  $\beta$ - $\alpha$  phase transform. features 0-33961  
 Nb<sub>0.87</sub>V<sub>0.13</sub>Se<sub>2</sub>(4Hb), stacking layer study, appl. of convergent beam electron diffr. 0-39116  
 P allotropic modifications, muonic X-ray intensities, computer analysis 0-23577  
 Pr<sub>2</sub>Sn<sub>3</sub>, low temp. modification with tetragonal struct. 0-1963  
 RbNO<sub>3</sub>, high pressure phase V, X-ray struct. determ. 0-28953  
 $\alpha$ -S, under hydrostatic press., deformable mol. lattice statics 0-49175  
 $\alpha$ -S, zone-centre lattice vibrs., including hydrostatic press. effects 0-49314  
 Se allotropic modifications, muonic X-ray intensities, computer analysis 0-23577  
 Si-Al-O-N ceramic systems, layer struct. 0-6382  
 Si-Al-O-N polytypes, hot-pressed, microstruct. 0-3023  
 SiC 147R<sub>(b)</sub>, polytype, crystal structure by X-ray diffraction method (*Chinese*) 0-54206  
 SiC, further polytypes discovered using Laue diffraction (*Chinese*) 0-10535  
 SiC, high period polytype at interface of two interacting spirals 0-20041  
 SiC polymorphs, widths of first minibands and effective masses, resist. anisotropy 0-20071  
 SiC polytype 6H, space group 0-1956  
 SiC polytypes, contribution of ionic bonding to thermal stability 0-28946  
 SiC polytypes, electrolum. in anodic oxidation, band model (*Russian*) 0-50429  
 SiC polytypes, localisation of cond. band minima in Brillouin zone 0-20082  
 SiC polytypes, stacking sequences by high resolution electron microscopy 0-15054  
 SiC polytypes deformed, resist. anisotropy in (0001) plane 0-20198  
 SiC, polytypic transform., interface struct. exam. by TEM 0-15033  
 $\alpha$ -SiC, single crystals. phase struct. rel. to heat treatment, nucleation 0-38991  
 SiO<sub>2</sub> polymorphs, CNDO/2 MO calc. 0-6386  
 SnS<sub>2</sub>, effect of powdering on polytypic cryst. struct. 0-1979  
 SnS<sub>2</sub> polytypes, electronic bandgap meas. 0-34358  
 TaSe<sub>2</sub>, 1T and 2H superstruct., cryst. struct. using X-ray diffr. 0-39044  
 TaSe<sub>2</sub>, 4Hb polytype, CWD induced atomic shifts 0-39045  
 TaSe<sub>2</sub>(6R), stacking layer study, appl. of convergent beam electron diffr. 0-39116  
 TbAl<sub>3</sub>, polytypism occurrence 0-44164  
 V<sub>13</sub>O<sub>24</sub> long-period Magneli phase as product of V<sub>6</sub>O<sub>11</sub>-V<sub>7</sub>O<sub>13</sub> periodic microsyntactic intergrowth 0-50618  
 ZnIn<sub>2</sub>S<sub>4</sub>, electronic props. of polytypic forms, pseudopot. calc. 0-38997  
 ZnS, Zn(S,Se), large single crystals, vapour growth and defect characterisation 0-25540  
 ZnS:Mn, dopant conc. effect on stacking fault energy 0-2041

**polynomials**

- see also splines (mathematics)*  
 associated Legendre polynomial P<sub>l</sub><sup>m</sup>(x), Chebyshev expansion 0-8774  
 Boltzmann eqn., Krook-Wu model solutions, distribution function (*French*) 0-17898  
 classical, dimensions of irreducible representations 0-18087  
 elasticity, appl. of orthogonal polynomials 0-36857  
 extended anisotropic body, equations of equilibrium, polynomial solutions (*Russian*) 0-42063  
 Gegenbauer, double angle sum formula 0-22  
 Hausdorff representation of positive polynomials and convex approx., aerodynamic shapes simulation 0-38430  
 Jacoby, tops and d-functions in even spaces (*Russian*) 0-4508  
 Laguerre, consistent approx. scheme for Schwinger function 0-336  
 multidimensional interpolation by polynomial roots 0-18778  
 neutron escape probability from absorbing body, polynomial expression 0-47523  
 operator polynomials, divisors, perturbation theory 0-36905  
 orthogonal polynomials, nonlinear eqns. for zeros 0-12888  
 smoothing, averaging method 0-31

**polynomials continued**

- topological resonance energy, new graphic polynomial, appl. to benzene and cyclobutadiene 0-5462  
 U(n) boson polynomials, appl. to physical problems 0-4890  
 Zernike-Tatani polynomials for interferogram reduction 0-37077  
 zeros of polynomial satisfying second order linear partial differential equation 0-12889
- polytypism** *see polymorphism*
- Pomeranchuk poles and trajectories**  
 cluster formulation in the dual topological unitarization scheme 0-13293  
 cut reggeon field theory, 4-pomeron couplings 0-42366  
 dual Pomeranchuk amplitude contrib. to multi-Regge limit and pomeron sister absence 0-13237  
 dual topological unitarization, glueball exchange effects, pomerons and reggeons 0-52482  
 hadronic matter, Pomeron and critical temp. 0-22566  
 Nambu string model, reggeon and pomeron interactions (*Russian*) 0-13294  
 Pomeron coupling diag. to order 1/N 0-47263  
 two component Pomeron,  $\pi$ N, kN, NN forward scatt. amplitudes 0-37245  
 pd scatt., intermediate inelastic states and triple-Regge couplings, Pomeron 0-4972  
 pp, high energy elastic scatt. cross sections, pomeron-nucleon coupling vertex, pomeron residue (*Russian*) 0-42492  
 pp $\rightarrow$ ( $\pi^+$ n)p,  $\pi$  energy and transverse momentum distrib., DHD model with nucleon exchange (*Russian*) 0-13327
- Pontyagin maximum principle** *see maximum principle*
- Poole-Frenkel effect**  
 chalcogenide glass films nonlinear current voltage characts., Poole-Frenkel effect 0-7007  
 hexatriacontane single cryst., elec. cond. and dielec. breakdown 0-6849  
 [p]-quinquaphenyl film between metal electrodes, memory switching 0-2484  
 poly(N-vinylcarbazole) layers, supermol. struct. effect on elec. props. 0-44606  
 polystyrene thin film, glow discharge formed, dark current and photocurrent obs. (*Japanese*) 0-15633  
 polytetrahydrofuran films, electrochemically prepared between metal electrodes, DC elec. props. 0-39695  
 shellac, electrical cond. mechanisms, Schottky and Poole-Frenkel processes and work function 0-29402  
 shielded point defect potential well calcs. using Poole-Frenkel effect 0-20122  
 TTT film, hopping cond. AC and DC meas. and EPR 0-11111  
 Al-CdSe-Ag dry air stabilised struct., elec. cond. mechanism, breakdown phenomena 0-34527  
 As<sub>2</sub>S<sub>3</sub>, vapour-deposited, pure and doped, hole mobility 0-49728  
 GeS film, between Al(Zn)(Sn) electrodes, Schottky and Poole-Frenkel cond. mechanisms 0-54799  
 Ge<sub>2</sub>Se<sub>2</sub>Te, amorphous layer, Poole-Frenkel controlled charge carrier transport, model of charged dangling bonds 0-49750  
 Ge<sub>2</sub>Se<sub>2</sub>Te, amorphous layers, charge carrier transport mechanism 0-54708  
 Si-P MOS devices, time dependence of depletion region formation at cryogenic temp. 0-34522  
 SiO<sub>2</sub>-Si, P ion implantation, electrical transport props. 0-39130  
 Ta<sub>2</sub>O<sub>5</sub> films, Poole-Frenkel effect and cond., effect of heat treatment in oxygen and in vacuum 0-39693  
 TeO<sub>2</sub> thin film, Al-TeO<sub>2</sub>-Al, field-assisted cond. mechanism 0-11105  
 WO<sub>3</sub> powders, hopping mechanism and Poole-Frenkel effect, elec. props. determ. 0-49734  
 ZnS-metal interface in MIM struct., photoexcitation level assignment (*French*) 0-15622
- popcorn noise** *see random noise*
- population inversion**  
*see also laser theory; lasers; stimulated emission*  
 alkali halides, coloured, light amplification at activator centres 0-2795  
 atom, resonant ionisation under adiabatic level inversion conditions (*Russian*) 0-32691  
 atomic excitation by self-induced resonance 0-28189  
 atomic transition, inverted, anomalous resonance-radiation press. 0-52946  
 catalysis, heterogeneous, vibr. excitation, classical trajectory calcs. 0-26045  
 chemical laser, electronic phototransition, with thermal initiation by shock wave 0-53283  
 collisional laser with energy exchange between excited levels of two systems 0-28188  
 gas waveguide laser, mode comp. of radiation 0-28192  
 homogeneously broadened three level atoms, intense standing wave saturated, spatial inhomogeneity, mode competition 0-23646  
 interstellar H II/OH masers, inversion and heating by ion streams 0-56912  
 interstellar masers,  $\Lambda$ -doublet population inversion in OH, OD, CH, CD and NH<sup>+</sup> collisions 0-22065  
 laser limiting characteristics in self-limiting transition 0-14311  
 lasers, kinetic processes 0-28190  
 molecular spontaneous symmetry breaking, induced representations 0-5464  
 molecular vibronic states population inversion during chemiluminesc. 0-3351  
 N two-level atoms, interaction with radiation field in restricted rotating wave approx. 0-5713  
 N-two level atoms, interaction with radiation field in restricted rotating wave approx., numerical anal. 0-5714  
 nozzle flows with boundary layer, CO<sub>2</sub>-N<sub>2</sub>-He, gain coefficients 0-14312  
 nuclear inversion coherent excitation by relativistic electron beam (*Russian*) 0-48206  
 photorecombination laser, shock wave triggered, waveguide mode optical gain 0-5730  
 ring laser, intensity fluctuations taking spatial population-inversion grating into account 0-14364  
 ruby, optically induced two-phonon processes connecting <sup>2</sup>E states 0-25443  
 solid-state lasers, influence of inversion depletion on ultrashort pulse evolution, mode-locking behaviour 0-5736  
 two-level molecular systems, optically pumped, increased inversion efficiency 0-23657  
 AgCl(Br), crossed elec. and mag. fields, hot electrons, streaming motion, population inversion 0-44649



**population inversion continued**

- Ar-He ion laser, population inversion radial distrib. and output charact., mag. field depend 0-19019  
 Bi pulsed laser, stimulated emission mechanism at 472.2 nm 0-19022  
 CH<sub>4</sub>+p-H<sub>2</sub>(He), collisional pumping of  $\Lambda$ -doublet transitions, pot. energy surface 0-23516  
 CO<sub>2</sub>, dissociation,  $\Sigma_g^+$  state, Wall Porter pot. surface, autodetachment and vibr. level population inversion 0-21275  
 CO<sub>2</sub>-N<sub>2</sub>-He mixture supersonic adiabatic expansion, population inversion and gain 0-19017  
 Cu vapour laser, population inversion kinetics, modified hook method meas. 0-53275  
 Cu+N<sub>2</sub>, Cu states population inversion by preferential energy transfer 0-43152  
 dye solution output conversion of Cu vapour laser to 5782 Å 0-48241  
 F+I<sub>2</sub>→IF+I, energy partitioning, vibr. populations and rot. temp., population inversion 0-50832  
 Fe<sup>3+</sup>:TiO<sub>2</sub>, low noise travelling wave maser, noise temp. 0-32945  
 Ge, far IR radiation amplification on hot hole population inversion (*Russian*) 0-16060  
 H<sub>2</sub>, recombining atomic plasmas, population inversion 0-32679  
 H<sup>+</sup> affinity radiation, theoretical study of negative absorption 0-38001  
 H<sub>2</sub>O-H<sub>2</sub>, cooling in supersonic nozzle, submillimetre wave generation 0-48229  
 H<sub>2</sub>O-H<sub>2</sub> mixtures, vibr. energy transfer in shock waves, population inversion 0-37996  
 He-Ne gas mixture plasma, role of charge exchange in form. of optical props. 0-28600  
 I flashlamp pumped photodissociation laser charact., local optical inhomogeneities 0-53284  
 N, recombining atomic plasmas, population inversion 0-32679  
 NH<sub>3</sub>, population inversion by adiabatic rapid passage 0-19073  
 Ne, population inversion mechanism between 4p-3d, laser generation conditions 0-1185  
 Ne, population of 5s[1/2]<sub>1</sub><sup>0</sup>, 4p[3/2]<sub>2</sub> levels interacting with laser radiation 0-23670  
 O I 6300 Å in type A aurora rays, emission intensification 0-4163  
 O, recombining atomic plasmas, population inversion 0-32679  
 OH main lines, IR pumping 0-46632  
 OH maser sources, interstellar, radiative transport effects on inversion 0-17681  
 OH+p-H<sub>2</sub>(He), collisional pumping of  $\Lambda$ -doublet transitions, pot. energy surface 0-23516  
 OH( $\Pi_{3/2}$ , v=1), population inversion of  $\Lambda$  doublets in microwave spectrum 0-974  
 Pb<sup>+</sup> high-gain laser populated by direct electron excitation, 1.159  $\mu$ m transition 0-37997  
 Si:Cr<sup>2+</sup> EPR spectra and spin state population inversion with unpolarised optical lighting (*Russian*) 0-44909  
 Tl, 6<sup>2</sup>P<sub>3/2</sub>-6<sup>2</sup>P<sub>1/2</sub> transition, population inversion 0-950

**porosity**

see also porous materials

- capillary phenomena in cylindrical pores, appl. to pore size anal. 0-15340  
 ceramics, polycrystn., porosity, twinning and grain-size depend. on spontaneous cracking 0-44253  
 ceramics acid-resistant, based on Artemov clay and obsidian 0-20852  
 dielectric film, electron beam produced pore form. mechanism, statistical model (*Russian*) 0-6667  
 fibre reinforced composites densification in free forging, exam. of specific work and kinetics 0-16218  
 film, microporosity described in terms of vacancies and voids 0-24769  
 glass sintered powder porous bodies, liq. penetration mechanism (*Japanese*) 0-53853  
 graphite, fusion reactor applications, mechanical constitutive laws for irradiation behaviour 0-32448  
 kyanite-sillimanite concentration, mullitisation and sintering, props. of refractory products 0-20867  
 measurement using soln. of luminescent material flowing around sorbent granules 0-53850  
 membrane selectivity, influence of particle/pore size ratio 0-11946  
 metal, welded joints, pore formation mechanism evaluation, rel. to solidification 0-3017  
 nuclear tracks, etched, statistical distrib. of quadratic holes on planar surface, computer simulation 0-37705  
 oxide coating, thermal sprayed, AE study of porosity 0-25927  
 oxide thermal-sprayed coating on steel, acoustic emission 0-21247  
 plasma sprayed materials, control of mech. props. 0-11560  
 polycrystals, models for constrained cavity growth 0-44251  
 polyvinyltrimethylsilane, sorption, diffusion, solubility of hydrocarbons, Xe rel. to temp. (*Russian*) 0-6565  
 powder, two component mixture, compact growth in liquid phase sintering 0-20835  
 quartz ceramic, physicochem. props., influence of surfactant incorporated during synthesis 0-20856  
 quartz ceramic, SiO<sub>2</sub>-Cr<sub>2</sub>O<sub>3</sub>-TiO<sub>2</sub>, creep and porosity, for ceramics with different structures 0-21011  
 random bed, area porosity profiles, stratified model 0-19495  
 refractories, multichamotte, sintering additives effect on props. 0-35147  
 rock pore aspect ratio spectrum determ., seismic velocities inversion 0-51387  
 rocks, fractures effect on compressibility, anal. using new model 0-8300  
 sintering and random structures, volume diffusion and creep effects 0-35125  
 solid gas layer, appl. to cryosorption pump (*Japanese*) 0-20031  
 steel, C, autectic, sintered, isothermal transformation behaviour, porosity effects 0-3031  
 steel, C, pore formation in surface layers, during As diffusion redistrib. 0-49421  
 steel, low alloy, sintered, isothermal transformations, porosity effects 0-3032  
 ternary polymer systems, diffusion controlled formation of porous structures 0-7539  
 thermal stress resistance, effect of spatially varying porosity during steady-state heat flow 0-1488  
 thin films, microporosity and absorptivity in vacuo meas. apparatus 0-9053  
 ZrC<sub>0.98</sub>, porosity influence on high temp. creep. (*Russian*) 0-25764  
 Al alloys, liquid, kinematic viscosity temp. depend., porosity, H solubility, supercooling (*Russian*) 0-54425

**porosity continued**

- Al coated steel, porosity evaluation, micro X-ray spectral anal. (*Russian*) 0-35389  
 Al, secondary H porosity, development and pore growth (*Russian*) 0-19946  
 Al sputtered coating development, porosity, durability temp. depend., electric arc metallisation regime (*Russian*) 0-39402  
 Al<sub>2</sub>O<sub>3</sub>-glass mixture, microstructural changes and shrinkage during sintering 0-25640  
 Al<sub>2</sub>O<sub>3</sub>-polymethylsiloxane composite, thermoreactive compaction 0-20879  
 Au film, ion plated, defect growth structs., SEM obs. 0-24768  
 Cu, ion plated, defect growth structs., SEM obs. 0-24768  
 Cu tripolyphosphate complexes, electrolyte development for direct deposition of Cu 0-45246  
 Cu vacuum coating on steel substrate, influence of precipitation conditions on porosity (*Russian*) 0-54578  
 Fe atomised powder, sintering effect on recrystn., mech. props. 0-40292  
 Fe, electrode, porous, discharge capacity, importance of physical struct. 0-26123  
 Fe powder, density distrib. in rolling deformation region 0-40288  
 Fe powder, sponge and atomized types, steam oxidation, pore closure and surface hardness 0-45441  
 Fe, sintered and pressed, props., effect of atomised Fe powder particle size distrib. 0-11601  
 Fe-Ni-C (0.15, 0.05 wt.%) pore formation kinetics during crystallisation, FORTRAN study (*Russian*) 0-54158  
 KCl, annealed in KBr vapour, crack and pore formation, diffusional induced stress relaxation (*Russian*) 0-40388  
 Li<sub>2</sub>O.2SiO<sub>2</sub>, directionally solidified, thermal and mech. props. (*Japanese*) 0-16295  
 100(Li<sub>2</sub>O.2SiO<sub>2</sub>).3B<sub>2</sub>O<sub>3</sub>(3Na<sub>2</sub>O)(3MgO)(3Al<sub>2</sub>O<sub>3</sub>)(3SiO<sub>2</sub>)(3P<sub>2</sub>O<sub>5</sub>), directionally solidified, thermal and mech. props. (*Japanese*) 0-16295  
 MgO-C in melts, corrosion resist., rel. to oxidation, porosity, content 0-40578  
 MnZn soft ferrites, commercial grade, microstruct. rel. to mag. props. 0-34009  
 Mo-Zr-B, porosity and mech. props. after neutron bombard., 780-1080°C (*Russian*) 0-24502  
 Mo-Zr-B alloy, neutron irradiat. at 780-1080°C, porosity, hardening and embrittlement (*Russian*) 0-29062  
 Ni, porosity depth distrib. of annealed samples following bombardment by 1 MeV Ar<sup>+</sup> ions 0-5333  
 Ni powders, stereological appl. in study of compacting process, elec. and mech. props. (*French*) 0-40286  
 Ni-Co-Cr-Al-Ti-Mo superalloy IN738, casting porosity removal using hydrostatic press. sintering 0-55322  
 Ni<sub>0.5-1.0</sub>Co<sub>0.5</sub>Zn<sub>0.5</sub>Fe<sub>2</sub>O<sub>4</sub> ferrosplinal solid solutions, cryst. lattice defects and props. 0-19796  
 Pb(Zr, Ti)O<sub>3</sub> internal struct., prep. effect, ionic shadowing obs. (*Polish*) 0-11612  
 Si and Si:H amorphous films, porosity and oxidation of evap., sputtered and plasma-deposited films 0-10838  
 Si<sub>3</sub>N<sub>4</sub>, reaction sintered, microstruct. charact. 0-35145  
 SiO<sub>2</sub>, adsorption of albumin 0-10777  
 SiO<sub>2</sub>, glass, monolithic, low temp. synthesis 0-40318  
 SiO<sub>2</sub>:Na<sup>+</sup>, heat treated, heat of immersion in H<sub>2</sub>O, organic compds. 0-3396  
 SiO<sub>2</sub>-base cores, for superalloys, high temp. characterisation 0-10640  
 SnO<sub>2</sub>, adsorption anomaly of water, effects of cryst. growth of solid 0-10779  
 Ti-Al system, compact growth in liquid phase sintering 0-20835  
 U core fuel elements, of A-1 reactor, volume growth (*Czech*) 0-27745  
 UO<sub>2</sub>-20CeO<sub>2</sub> mixed powder, X-ray and microprobe exam. of homogenisation 0-25609  
 W fibre reinforced Cu, interface porosity formation, on thermal cycling 0-30092  
 W-Ni-Fe (5(2), 5(2) wt.%) pore formation, effect on mech. props. 0-45396  
 Zn<sub>1-x</sub>Ni<sub>x</sub>Fe<sub>2</sub>O<sub>4</sub>, heat treatment and sintering effect on porosity 0-25610  
 ZrO<sub>2</sub> refractories, high-temp. induced porosity increase 0-35146

**porous materials**

see also flow through porous media

- atom-atom interaction law (*Russian*) 0-19861  
 Berea sandstone, effects of pore fluids on bulk and shear attenuation 0-51386  
 convective heat exchange in fibrous materials, at elevated press. in gaseous medium 0-19217  
 densification kinetics in hot pressing, under quasi-isostatic conditions 0-11585  
 densification kinetics in hot pressing under quasi-isostatic conditions 0-25592  
 directionally dependent lineal porosity materials, continuum theory from isothermal elasticity 0-48588  
 elastic deformation of porous body in rigid sheath, energy expenditure in the densification 0-16216  
 electrode, wetproofed, pore filling degree with electrolyte and liq. reactant 0-40702  
 ferromagnet, with Bloch walls and self-consistent magnetisation, energy and coercive field 0-15760  
 fibre reinforced porous matrix materials, densification kinetics in free hot pressing 0-25618  
 fluid effects on mechanical props. 0-23883  
 gas behaviour in closed porosity body, exam. 0-24642  
 gas diffusion technique for pore struct. investigation 0-30185  
 gel, electrical double layer on surface 0-11955  
 generalised thermorheologically simple porous materials, thermomechanical theory of viscoelasticity 0-33479  
 glass sintered powder porous bodies, liq. penetration mechanism (*Japanese*) 0-53853  
 gradient index lens fabrication by molecular stuffing 0-14499  
 graphite, heating in air atmosphere, spectral emissivity 0-19969  
 graphite ionisation chamber, ionisation error due to porosity 0-52829  
 haematite-magnetite two-phase system, internal stresses (*Russian*) 0-16319  
 heat conduction, thermodynamics of non-equilibrium processes (*Hungarian*) 0-178  
 metal, sintering of solids containing several dissolved gases 0-20836  
 metal, yield stress variation during cold deformation 0-16395  
 metal gauze, struct. and hydraulic characts. 0-11729



**porous materials continued**

metal porous strip, metal pressure in cold rolling in elastic aftereffect zone 0-40421  
 metal strip, elastic aftereffect in cold rolling 0-11689  
 metals porous, mean principal stress in rolling without lateral expansion 0-25803  
 Ni powder 2JJ, porous, effect of sintering conditions in struct. and strength 0-20823  
 nonlinear theory of elastic materials with voids 0-53623  
 permeability of conical shells deep drawn from porous sheet 0-11728  
 plastic deformation, anal. using plasticity theory 0-25802  
 poroelastic material dynamic characterisation, complex, modulus meas. 0-14640  
 porosity and pore size measurement using soln. of luminescent material flowing around sorbent granules 0-53850  
 production method using stainless steel gauzes, exam. of hydraulic characteristics 0-16243  
 rocks, dry and water-saturated, plane shock wave studies 0-21714  
 rocks, saturated, effective stress law for anisotropic elastic deform. 0-51385  
 rocks, self-consistent imbedding and ellipsoidal model 0-26503  
 sintered, mech. testing device for hydrostatic pressure conditions 0-40645  
 sintered battery material (*German*) 0-21394  
 sintered porous materials, effective thermal conductivities 0-19998  
 snow, volumetric constitutive law based on neck growth model 0-48595  
 softwoods, transverse Poisson's ratio and Young's modulus (*Japanese*) 0-2111  
 solar air heaters, use of porous flat plate solar collectors 0-35748  
 sorbent, biporous, internal diffusion 0-44414  
 sound attenuation in porous elastic solid containing compressible viscous fluid (*French*) 0-38149  
 sound pulse absorption, Fourier transform anal. 0-38170  
 specific surface, determ. using Hg porosimetry 0-29896  
 steel, Cr-Ni, rolled and sintered, to produce capillary structured filter material, exam. of mech. props., and production 0-16235  
 stresses induced by drying, elastoviscoplastic model, finite element anal. 0-23904  
 tensile strength, pore geometry effects 0-30048  
 Vycor glass, porous, adsorbed  $\text{NH}_3$  Raman scatt. 0-11948  
 $\text{Al}_2\text{O}_3$  porous refractories, production 0-35149  
 Au thin films, with nm-sized pores, prep. from Au-Ge eutectic films by etching 0-16227  
 Cu-Ga porous solid formed by shock compression 0-29905  
 Fe, carbonyl pore struct. orientation, shrinkage anisotropy effect 0-20845  
 Fe-glass porous material, wear resist. under dry friction 0-25876  
 $\text{Fe}_3\text{O}_4$ , sintered metallised compacts, pore struct. by Hg porosimetry 0-40280  
 Ni powder, porous, relationships between mech., physical, and microstructural chars. 0-20846  
 Ni powder, sintered, use of extruded porous materials as fuel cell electrodes 0-40853  
 Si, formation during anodic treatment in HF aq. soln., growth kinetics and density 0-20059  
 Si, porous, form. during anodic treatment in aq. HF 0-35369  
 $\text{SiO}_2$  gel, macroporous, modification of surface by adsorption of thin layer of polymer 0-6624  
 $\text{SiO}_2$  gel,  $\text{SiO}_2\text{Al}_2\text{O}_3$ ,  $\text{SiO}_2\text{MgO}$ , pore structure influence on X-ray intensity in EPMA (*Japanese*) 0-26046  
 $\text{Ta}_2\text{O}_5$ , hydrated, heat treatment effect on physicochem. props. 0-20966  
 Ti, anodic oxidation under high voltage, porous layers (*French*) 0-54574  
 Ti, porous structure, change in presence of liq. phase (*Russian*) 0-16223  
 Ti-Al (Sn), porous, effect of Al and Sn on sintering 0-20830  
 $\text{UO}_2$ , SiC coated, small surface area determ. by Kr adsorption 0-44429  
 W-Cu, porous material, skeletal type, produced by liquid phase sintering, exam. of mech. strength, determ. resistance 0-16245  
 Zn electrode, concentration changes during cycling 0-35666  
 $\text{ZrO}_2$ , stabilized porous refractory, mech. strength 0-35322

**porous media** see porous materials

**porphyrins** see organic compounds

**Portevin-Le Chatelier effect** see serrated yielding

**positors**

No entries

**position control**

capacitance-based micropositioning system for X-ray rocking curve measurements 0-205  
 displacement of mechanical guides in meas. systems, using speckle interferometry (*Czech*) 0-31852  
 elastic object in central force field, programmed motion control 0-17481  
 IR laser interferometer, length measuring, alignment using laser feedback 0-37075  
 micropositioning, piezoelectric transducer appl. (*German*) 0-8967  
 NC diamond turning system evolution 0-1369  
 tow system with depth control, hydrographic and current meas. 0-17403

**position finding** see navigation

**position measurement**

see also astrometry  
 analogue interpolation system for incremental transducers (*German*) 0-17929  
 astronomical photographs reduction by method of dependences 0-4237  
 eye position measurement from surface-recorded ERG 0-26400  
 geosynchronous satellite orbit determination using VLBI and computer program (*Japanese*) 0-21925  
 laser pulse, position determ. using ordinary paper 0-33046  
 magnetic suspension densimeter, differential capacitance sensor as position detector 0-196  
 mechanical component features comparative metrology, misalignment meas. using photocell 0-31716  
 Mini Range III positioning system, meas. range improvements, technical details and characts. (*Italian*) 0-56611  
 NAVSTAR Global Positioning System, sea trials results 0-12645  
 offshore surveys, accurate positioning at distances to 400 km 0-12328  
 photogram meas. system using optoelectronic convertor of linear coordinates 0-17917  
 speech production process, articulatory characteristics of tongue and jaw point movements in connected sounds of Japanese 0-26243  
 undersea platform location by acoustic signature processing 0-43519  
 VLBI, general considerations of international systems (*Japanese*) 0-17501  
 VLBI, Japanese domestic system, general aspects (*Japanese*) 0-17502  
 VLBI, Japanese domestic system, receiver and local oscillator (*Japanese*) 0-21923

**position measurement continued**

VLBI, Japanese domestic system, recording signal generator (*Japanese*) 0-21924  
 VLBI, Japanese domestic system, selection of radio sources and experimental procedure (*Japanese*) 0-21922  
 VLBI, principles of measurement (*Japanese*) 0-21921  
 VLBI, results of observations of radio source QSO 3C273 (*Japanese*) 0-17503  
 X-ray stereography, method of precision position determ. 0-56314

**position sensitive particle detectors**

angular distrib. meas. with positron sensitive detector 0-27899  
 Cherenkov, spot focusing detector 0-5440  
 data acquisition, CAMAC I/O module 0-47835  
 delay line for position readout in wire chambers 0-18757  
 digital scattering angle pre-processors 0-23268  
 drift chambers in high-energy gamma-ray telescope 0-41726  
 focal plane, large hybrid detectors, electric field uniformity improvements 0-37684  
 gas flow detector, back-scatter-type, conversion electron Mossbauer spectrometry 0-37680  
 ionisation chamber, liquid, pulse shape anal. of recoil electron signals 0-52823  
 LEED instrum. using pulse-counting electron detector 0-37133  
 low level activity meas. of  $^3\text{H}$  and  $^{14}\text{C}$  using multielement and cylindrical proportional counters, comparison (*Czech*) 0-52818  
 microchannel plates, low distortion resistive anodes 0-886  
 multianode cylindrical proportional counter for position sensing at high count rate 0-5446  
 multiwire and drift proportional chambers 0-47826  
 muscle contraction, time-resolved X-ray diff., data-collection system (*Japanese*) 0-46108  
 MWPC, compact low mass system of four cylindrical chambers 0-14046  
 MWPC, drift chambers and time projection chambers, development, operation and appl. (*Italian*) 0-879  
 MWPC, interwoven grid wires for second coordinate readout 0-27897  
 MWPC, large cylindrical dual coordinate 0-18759  
 MWPC, localisation of minimum ionising particles using cathode induced charge centre of gravity readout 0-32576  
 MWPC with high spatial resolution, construction and efficiency meas. (*Italian*) 0-9452  
 proportional counter, for X-ray residual stress meas. (*Japanese*) 0-11853  
 proportional single 1 m wire counter for low ionisation particles 0-5441  
 resistive unidimensional detectors employing rise time readout method, position resolution and linearity 0-14048  
 resonance neutron radiography using a position-sensitive proportional counter, appl. to meas. of nuclear fuel 0-13597  
 scintillation counter, energy resolution optimisation at high energies 0-37697  
 spark chamber digitisation using CCD 0-27902  
 time of flight telescope for high energy gamma-ray astronomy 0-31210  
 vidicon systems, time digitiser in CAMAC format 0-14062  
 X-ray position-sensitive scintillation detector for portable stress analyser 0-13190  
 X-ray stress anal. using position-sensitive proportional counter 0-1498  
 Ar, liquid, calorimeter, electron and proton response 0-47832  
 H scintillating gaseous drift chamber for use as positron sensitive target 0-9457  
 Pb single convertor photon detection efficiency below 500 MeV, semi-empirical formula 0-27866  
 Si, production using ion implantation methods 0-23247

**positioning** see position control

**positive column**

see also glow discharges

air, impulse breakdown processes at low press. 0-44021  
 arc in channel bearing turbulent gas flow, arc parameters calc. 0-6298  
 autocompression, influence of external mag. axial field, review (*Rumanian*) 0-24148  
 deflection of radiation intensity by transverse mag. field 0-28866  
 diffusion controlled circular positive column with one and two step ionisation, charact. eqn. 0-44033  
 diffusion controlled gas discharge, characts. rel. to diffusion and ionisation coeffs. 0-38333  
 electron energy distrib. function, Coulomb collision effects, in Xe plasma 0-38532  
 electron temperature with two- and three-body vol. recomb. 0-19645  
 glow discharge, ionisation waves, half subharmonic excitation 0-44006  
 glow discharge of electronegative gas, molecular excitation and ionisation by electron collisions 0-49031  
 inert gas, low-press. discharge, electron energy distrib., elec. field and electron wall loss effects 0-24294  
 metastable atom radial transport at various electron distrib., atom+atom collision effects 0-44037  
 metastable atom transport, excitation rate radial variation, flux to wall calc. 0-44038  
 nonstationary arc in channel with gas discharge (*Russian*) 0-14950  
 positive glow corona along a cylindrical rod between two parallel plates 0-38768  
 turbulent arc in channel with distributed gas flow, positive column anal. (*Russian*) 0-14949  
 Ar, contracted, balance equations anal. 0-6312  
 Ar, contracted, electron density, temp., elec. field, line emission 0-6311  
 Ar glow discharge, line radiation of plasma in early afterglow 0-38745  
 Ar, population processes of 4p levels, perturbation influence 0-38565  
 Ar-Br $_2$ , positive column at. state densities 0-44007  
 Ar-CO, glow discharge, ion cluster in positive column, ion mass spectra diagnostics 0-38752  
 Ar-hexamethyldisiloxane, glow discharge positive column ion mass spectra identification 0-38834  
 CO-He( $\text{O}_2$ ), glow discharge ion cluster in positive column, ion mass spectra diagnostics 0-38752  
 Cs plasma discharge, positive column constriction, ion conversion effect 0-44020  
 $\text{H}_2$  glow discharge with variable degrees of dissoc., diffusion theory of positive column 0-44018  
 He, composition at intermediate press. 0-19646  
 He, fast electron energy distrib. in positive column and negative glow 0-38764  
 He flow discharge, intermediate press., positive column conc. of ions and metastables 0-44017



**positive column continued**

- He glow discharge, low press., excitation transfer and quenching of  $n=3$  excited states 0-38743  
 He glow discharge plasma, ionis. waves in positive column 0-1876  
 He I, low-press., quenching of singlet states by  $N_2$  0-49030  
 He, magnetised, temps. of charged particles, nonlinear effect of ionis. waves 0-44023  
 He, medium press., contraction mechanism, inhomogeneous heating 0-44024  
 He-Ne gas discharge, positive column striations characts. 0-49032  
 Hg low-pressure arc, positive column, heat flow processes 0-24135  
 Hg, optically pumped positive column, E-I characts. 0-44035  
 Kr afterglow plasma, electron energy distrib. function 0-38748  
 Kr-Cl<sub>2</sub> mixture, glow discharge positive column, electron energy distrib. and rates of inelastic processes, negative Cl ions form. 0-19632  
 N<sub>2</sub> flowing, visible spectrum obs. 0-49026  
 N<sub>2</sub>, superelastic collisions and electron distrib. function 0-1858  
 N<sub>2</sub>-O<sub>2</sub> mixture, impulse breakdown processes at low press. 0-44021  
 Ne, low-press., atom densities of first excited state 0-38750  
 Ne, positive column contraction under diffusion-recombination conditions 0-24293  
 Ne-H-H<sub>2</sub> mixture, positive column characts. and comparison with approx. diffusion theory 0-44025  
 SF<sub>6</sub> plasma column, in Maecker type arc, diagnostics and model (French) 0-19652  
 Ti-Xe, electric discharge excitation of Ti in high-press. Xe 0-49025  
 Zn<sup>+</sup>-He, positive column laser discharge, upper and lower state densities, Penning collision 0-32964

**positive feedback** *see feedback***positive ray sources** *see ion sources***positive rays** *see ion beams***positive temperature coefficient thermistors** *see thermistors***positons** *see positrons***positron annihilation** *see electron positron interactions***positron annihilation in liquids and solids**

- alkali halides, positron annihilation, expt. techniques, positron states, book contrib. 0-2894  
 biomembrane phase transition studied by positron annihilation energy spectrometry 0-35854  
 core and valence electron enhancement factors from positron annihilation-correlation curves 0-25479  
 core annihilation enhancement in solid 0-2892  
 disordered alloy, positron annihilation, Fermi surface study, review 0-44480  
 electron gas, ang. correl. in positron annihilation 0-24821  
 electron liquid, collective description, positron annihilation 0-4632  
 epoxy resin, rubber modified, temp. depend. of o-positronium lifetime 0-29825  
 fusion reactor metals and alloys, microvoid form., gaseous impurity atom effects, positron annihilation study 0-49275  
 Inconel X750, positron annihilation study of ageing and creep 0-29824  
 ionic crystals, imperfect, positron stabilisation 0-40182  
 ionic crystals, positronic atom scatt. on optical phonons, positron thermalisation 0-50457  
 lunar regolith fine fraction, Luna-24 slow positron probe 0-26762  
 metal surface, positron-electron correlations, RPA calc. 0-40181  
 metals, positron annihilation, localised probe of lattice defects 0-55224  
 metals, positron annihilation expts., electronic struct. and Fermi surface studies 0-54594  
 metals, slow positron studies 0-55223  
 metals and alloys, NDT using positron meas. 0-55222  
 mylar, implantation of positrons from <sup>22</sup>Na 0-16118  
 negative ions, positronium formation, Doppler broadened positron annihilation line shapes 0-45164  
 nitrobenzene, quenching and inhibition of orthopositronium 0-35002  
 p-terphenyl, positronium and thermal defects 0-24496  
 photon energy spectroscopy, stability problems 0-29821  
 positron basic props., annihilation line shape, positronium formation, book contrib. 0-2893  
 positron trapping rate into vacancy clusters in metals 0-2890  
 positronium formation, in mixtures of competitive electron acceptors 0-28120  
 pyrene, positronium and thermal defects 0-24496  
 succinonitrile, defects in plastic phase, positron annihilation obs. 0-11504  
 thermalised positron annihilation, photon emission and spectator electron recoil, short range electron correl. determ. 0-50456  
 Al, positron annihilation, effects of quenching, annealing and neutron irradi. 0-20732  
 Al, positron annihilation, angular distrib., Umklapp effects (French) 0-50454  
 Al, positron annihilation studies using high-density proportional chambers 0-25478  
 Al, positron annihilation with high-momentum core electrons, vacancies study 0-25481  
 Al, quenched, muon<sup>+</sup> trapping at vacancies, compared with positron annihilation 0-15937  
 Al-Cu alloys, Cu precipitate detect. by positron annihilation, GP zone development 0-3051  
 Al-Cu samples (0.5, 2.0 and 4.0 wt.%) polycryst., precipitation, positron annihilation and TEM 0-50639  
 Al-Zn, age hardenable precipitation and dissolution, positron annihilation and X-ray scatt. 0-16314  
 B, electron structure study by positron annihilation 0-16117  
 CaF<sub>2</sub>, positron annihilation polarisation effects, electron momentum distribution 0-55225  
 CaF<sub>2</sub>:Sm, positron annihilation polarisation effects, electron momentum distribution 0-55225  
 Cd, positron annihilation lifetime spectra, low temp. trapping 0-29822  
 Co, phase transformations and vacancy form. by positron annihilation 0-2155  
 Co-Ni, deformed and isochronally annealed, positron lifetimes, annihilation at dislocation trapped monovacancy 0-55221  
 Co<sub>2</sub>:Fe, FCC, electronic struct., ang. correlation of positron annihilation  $\gamma$ -quanta, meas. 0-10864  
 Cu, deformed, defects, thermal relaxation, positron experiments (German) 0-50455  
 Cu, positron annihilation radiation, ang. correlation, APW calc. 0-7435  
 Cu, positron annihilation studies using high-density proportional chambers 0-25478

**positron annihilation in liquids and solids continued**

- Cu, positron annihilation with high-momentum core electrons, vacancies study 0-25481  
 Fe, deformed, defects, thermal relaxation, positron experiments (German) 0-50455  
 Fe, phase transformations and vacancy form. by positron annihilation 0-2155  
 Fe-Ni alloy, positron lifetime 0-2891  
 GaAs, electron-irrad., deep-level defect anal. using 2 $\gamma$  positron annihilation and IR absorption spectra 0-16120  
 GaAs:Si, positron lifetime temp. depend. 0-29826  
 Ge, neutron irradiated, positron annihilation, ESR and resist. meas. 0-15160  
 Ge:Be(Mg)(Ca)(Ba), positron annihilation ang. distrib. 0-45165  
 KBr, proton irradi., divacancies, positron capture, ionic cond. and TSC study 0-54289  
 KCl crystals, positron annihilation, Doppler broadening 0-40180  
 KCl, positronium states near defects in cationic sublattice 0-16121  
 Mo (100) clean surface electron struct., positron annihilation study 0-24988  
 Mo deformed single cryst., struct. state and dislocation splitting (Russian) 0-29029  
 Mo, positron annihilation and vacancy formation 0-16119  
 NaCl, positronic atom scatt. on optical phonons, positron thermalisation 0-50457  
 Nb, defect annealing in 7 MeV-irrad. samples, positron annihilation obs. 0-24497  
 Nb, positron annihilation and vacancy formation 0-16119  
 Nb, positron trapping and annihilation at vacancies 0-29823  
 Ni, phase transformations and vacancy form. by positron annihilation 0-2155  
 Pb-In, CPA interpretation of positron annihilation (Russian) 0-11507  
 Pb-Tl, vacancies, positron capture, function of Tl concentration (German) 0-49213  
 Pb-Tl alloys, positron trapping in vacancies, varying concentration effects (German) 0-25477  
 Pd, influence of adsorbed H on positron lifetime spectra 0-25480  
 Pd-Ag, influence of adsorbed H on positron lifetime spectra 0-25480  
 Pd-Cu, influence of adsorbed H on positron lifetime spectra 0-25480  
 RbBr crystals, positron annihilation, Doppler broadening 0-40180  
 Si, laser irradiated, positron annihilation crystal struct. imperfection monitoring 0-11506  
 n-Si:B, ion-implanted damage, positron annihilation and sheet resist. meas. 0-35003  
 Sm<sub>2</sub>Gd<sub>0.5</sub>S, valence transition, positron annihilation study 0-15454  
 SmS, valence transition, positron annihilation study 0-15454  
 $\beta$ -Sn, Fermi surface, electronic momentum densities, positron annihilation obs. 0-6696  
 Ta, positron annihilation and vacancy formation 0-16119  
 Ta, positron trapping and annihilation at vacancies 0-29823  
 Ti, pure (0.9998), positron annihilation study of defects 0-3281  
 Ti-Al-Mo-Sn alloy, elastically and plastically deformed, Doppler broadening meas. of positron annihilation 0-21038  
 U, vacancy formation and phase transformation by positron annihilation 0-49215  
 V, positron annihilation and vacancy formation 0-16119  
 V<sub>2</sub>Si, Fermi surface determ. by positron annihilation 0-2326  
<sup>48</sup>V positron source prep. for annihilation radiation lineshapes, positron lifetimes meas. 0-876  
 W, positron annihilation and vacancy formation 0-16119  
 W, positron trapping and annihilation at vacancies 0-29823  
 Zn, HCP struct., selection rule, electron momentum distrib. rel. to positron annihilation 0-39495  
 Zn-Al (22 wt.%), positron diffusion and trapping at grain boundaries 0-39157

**positron scattering** *see electron impact***positron states**

- alkali halides, positron annihilation, expt. techniques, positron states, book contrib. 0-2894  
 ionic cryst. positron-containing M-centre, struct. 0-49220  
 metals, positron-phonon interaction through cond. electrons (Russian) 0-29126  
 negative ions, positronium formation, Doppler broadened positron annihilation line shapes 0-45164  
 surface, positron-electron correlations, RPA calc. 0-40181  
 surface positron states, emission of positrons, positronium 0-54655  
 B, electron structure study by positron annihilation 0-16117  
 CaF<sub>2</sub>, positron annihilation polarisation effects, electron momentum distribution 0-55225  
 CaF<sub>2</sub>:Sm, positron annihilation polarisation effects, electron momentum distribution 0-55225  
 Cu (111) surface, negatively biased, positron impact, positronium form 0-35024  
 KCl, positronium states near defects in cationic sublattice 0-16121  
 Mg positron trapping and bound states 0-2367  
 Nb, positron trapping and annihilation at vacancies 0-29823  
 Ta, positron trapping and annihilation at vacancies 0-29823  
 W, positron trapping and annihilation at vacancies 0-29823

**positronium***see also electron pairs*

- annihilation in field of plane EM wave (Russian) 0-14259  
 energy levels, radiative corrections 0-32100  
 epoxy resin, rubber modified, positron annihilation 0-29825  
 formation, in mixtures of competitive electron acceptors 0-28120  
 formation cross sections in He, diluent gas effect 0-5640  
 magnetic quenching of substates, positronium capture model 0-1090  
 nitrobenzene, quenching and inhibition of orthopositronium 0-35002  
 positron annihilation, positron basic props., annihilation line shape, positronium formation, book contrib. 0-2893  
 relativistic positronium atom stimulated form. in high-intensity opposite EM wave 0-9766  
 succinonitrile, defects in plastic phase, positron annihilation obs. 0-11504  
 surface positron states, emission of positrons, positronium 0-54655  
 e<sup>+</sup>A<sup>-</sup>, positron-containing ground-state negative ions, self-consistent Fock field 0-47888  
 pp atoms, quasiatomic and very energetic  $\gamma$ -rays 0-42574  
 Cl<sup>-</sup> soln. inhibition of o-Ps formation 0-1089  
 Cu (111) surface, negatively biased, positron impact, positronium form 0-35024



## positronium continued

FeTi, positronium form. after hydrogenation-dehydrogenation cycling and annealing 0-18947  
KCl, positronium states near defects in cationic sublattice 0-16121  
No<sub>3</sub><sup>-</sup>-Cl<sup>-</sup> soln., inhibition of o-Ps formation 0-1089

## positrons

see also electron pairs; electrons

atomic anions positron complexes, ground and excited states theoretical studies 0-42934  
beam generation at low energy 0-5422  
bremsstrahlung, anomalous reduction in single cryst. 0-7433  
mobility in uniform elec. field 0-9793  
polarised positron, electron production by colliding photon beams in storage ring 0-5426  
relativistic positron channelling, radiation intensity and spectrum calcs. 0-2098  
superheavy collision systems, positron prod., internal conversion 0-5168  
ultrarelativistic collimated beam, emission spectra in Si 0-7434  
e<sup>-</sup>A<sup>+</sup>, positron-containing ground-state negative ions, self-consistent Fock field 0-47888  
e<sup>-</sup>Br<sup>-</sup>, positron-containing ground-state negative ions, self-consistent Fock field 0-47888  
e<sup>-</sup>I<sup>-</sup>, positron-containing ground-state negative ion, self-consistent Fock field 0-47888  
W crystal, EM showers produced by electrons, positron spectral distribution (Russian) 0-55218

## postal services

automated TLD processing and dose record keeping service 0-12267

## potassium

see also nuclei with .....

Ashcroft pseudopotential, unified study of props. 0-39239  
atom, 4<sup>2</sup>P<sub>1/2</sub> resonance substate, disorientation cross-section, Zeeman scanning obs. 0-42988  
atom, absolute optical electron-impact excitation functions 0-18933  
atom, D Rydberg state emission oscill. strength minima 0-32662  
atom, electron elastic and inelastic scatt., 54.4-217.7 eV, 2-145° 0-1067  
atom, generalised quantum defect, energy and radius depend. 0-14067  
atom, outer-shell photoelectron ang. distrib. 0-37797  
atom, s and d state radiative lifetimes, time and wavelength resolved fluoresc. spectra 0-14104  
atom, valence p-shell HeIIα photoelectron spectra, final state CI effects 0-14121  
atomic vapour quantum counter, Stark tuning 0-53242  
BCC crystal, elastic constants, thermal expansion and bulk modulus 0-6452  
cathode, liq., Ar arc, cathode erosion rate estimation (French) 0-44056  
CDW, detection attempt by neutron diff. 0-49634  
CDW vector orientation, positive ion lattice distortion 0-6759  
discharge plasma, K<sub>2</sub> excited mols. form. by K(4P) collisions 0-44013  
elastic scattering amplitudes, for high energy electron scattering, by ionised atoms, numerical calcs. 0-49057  
electrical resistivity, low-temp., electron-electron contrib., sample depend. 0-24875  
electron-dislocation scatt. anisotropy effect on electron-electron scatt. contrib. to elec. resist. 0-29398  
emission and fixation during pressurised fluidised bed combustion of coal 0-30352  
Fermi surface distortion 0-2325  
giant axon of the squid, gating current and K channels obs. 0-56012  
Hall coeff., 4.2 to 16K 0-44570  
helicon-phonon interaction for oblique propagation, dispersion relation 0-49315  
high field Righi-Leduc effect and lattice thermal conductivity, comment 0-10948  
high field Righi-Leduc effect and lattice thermal conductivity, reply to comment 0-10949  
inert gas+K, photon emission polarisation anal., coincidence studies 0-5614  
interatomic potentials from phonon spectra 0-19744  
intercalates with graphite, staging classical model variations, EXAFS results 0-45166  
intercalation compounds with graphite, interlayer screening and mag. susceptibility 0-44794  
isoelectronic series, hard-core pseudopotentials and struct. maps 0-44168  
liquid, shear waves, molecular dynamics 0-44096  
liquid, thermoelectric power, optimised model pot. calcs. 0-29391  
liquids, optimised cluster expansion, struct. function evaluation 0-49085  
metallic compressibilities, general pseudopotential approach 0-54631  
pair potentials calcs. elastic props. calc. 0-49176  
Pauli susceptibility and Knight shift meas., electron wave functions 0-44937  
phonon spectral density, pseudopotential calcs. 0-39234  
plasma, dense, in arc, elec. and heat conds., two-probe diagnostics 0-38560  
plasma, magnetic-mirror-trapped, heating with array of hot W wires 0-33789  
plasma in arc and capillary devices, optical props. 0-24244  
point contacts, current-voltage characts. at liq. He temps. 0-39663  
radiometric determ. in NPK and GVH fertilisers (Czech) 0-22427  
soft X-ray emission and absorpt. edges, self-absorpt. studies 0-40183  
structural energies, pseudopotential formalism 0-39519  
surface electron states and optical props. in IR spectral range (French) 0-54757  
thermodynamic and thermoelectric properties, phonon scatt. processes 0-29390  
US generation by EM radiation, surface scatt. effects 0-24973  
UV absorpt. spectra 0-2780  
vacancy formation energy calcs., electron density functional method 0-19801  
vapour, thermal cond., 800-1050K 0-19546  
vapour generator, heat transfer with drop motion in tube in supercrit. region 0-23880  
BaF<sub>2</sub>:K<sup>+</sup> ionic conductivity meas., computer analysis, point defect parameters 0-54429  
I<sub>2</sub>:K, doping effect on elec. cond., semicond. props. 0-49732  
K I, fine struct. splittings in some highly ionized n=3 doublets 0-43200  
K I 769.9 nm line obs. of solar 5-min. oscils. 0-26838  
K I to K XIX, energy levels, tabulated data 0-51966  
K<sup>+</sup> conductance in bullfrog, [Ca<sup>2+</sup>]<sub>i</sub>-linked, oscill. obs. 0-35867

## potassium continued

K<sup>+</sup>, direct excitation of levels, transition probs. and cross sections 0-37890  
K<sup>+</sup>, electrogenic transport obs. in rat soleus muscle 0-21456  
K<sup>+</sup> in molecular complexes, K-edge absorpt. spectra, Z+1 analogy, theory-expt. comparison 0-47935  
K<sup>+</sup>, reson. line regularities in plasma Stark widths and shifts 0-43881  
K+Cd(+N<sub>2</sub>), optical excitation, rate consts., collisional energy transfer kinetics 0-32801  
K+He(Ar)(Ne)(Xe), K 5<sup>2</sup>P level broadening and collisional relax., quantal, semiclassical and expt. comparison 0-18903  
K+He(Ne)(Ar), 0.7-80 keV, K excitation, reson.-line emission and polaris. 0-18911  
K+He(Ne)(Ar), K collision-induced alignment, reson.-line emission polaris. obs. 0-18912  
K+Hg, 15-1400 eV, electronic excitation, integral cross sections 0-43159  
K+HgBr<sub>2</sub>, laser irradi., HgBr form., chemiluminescence 0-55658  
K+N<sub>2</sub>(CO) atom electronic excitation, vibr. to electronic energy transfer, seeded mol. beam studies 0-47919  
K+N<sub>2</sub> collision, electronic excitation and energy transfer, time of flight spectra 0-43151  
K+N<sub>2</sub><sup>+</sup>, 50-1000 eV, crossed beams, electron transfer and excitation 0-14226  
K+N<sub>2</sub>(CO), rot. inelastic scatt., quantum effects, simple model surfaces 0-48064  
K+NO<sub>2</sub>, charge transfer reactions, energy and ang. differential cross-sections meas. 0-53125  
K+NaCl, three dims. collision, exponentiating trajectories and statistical behaviour 0-5595  
K+SF<sub>6</sub>, ion-pair form. reaction, energy loss spectra 0-55630  
K<sup>+</sup>+H<sub>2</sub>O, supermolecule calcs. with additive procedure, intermolecular interactions and binding energy 0-52880  
K<sub>2</sub>, optically pumped CW dimer lasers 0-14322  
K<sub>2</sub><sup>+</sup> ion formation in low press. K discharge plasma 0-43862  
39K pulsed NMR obs. of whole body live and dead newborn mice 0-40964  
39K/40K ratio for inclusions in Allende meteorite, normality confirmed 0-26820  
40K, natural content and internal radiation burden of Hungarian adult population 0-26355  
40K, pressure-induced changes in electron-capture decay const., theory 0-22771  
Na+H<sup>+</sup>, configuration interaction potentials and rainbow angle scatt. cross section 0-37745  
Si:K, amorphous, implantation effects on elec. props. 0-49716  
SrF<sub>2</sub>:Gd<sup>3+</sup>, K<sup>+</sup>, EPR of orthorhombic Gd<sup>3+</sup>-univalent metal ion complexes 0-11262  
TiO<sub>2</sub>, K<sup>+</sup> implantation, extended defects and precipitates 0-49251

## potassium alloys

Hg-K, liquid, structure factors, X-ray scatt. (Japanese) 0-54122  
K-Na(Cs), thermodynamic props. at high temps. 0-15262  
K-Rb, liq., form factors and transport coeffs., pseudopot. perturb. theory 0-44561  
Na-K, liq., form factors and transport coeffs., pseudopot. perturb. theory 0-44561  
Na-K, liquid, collective excitations, mol. dynamics calc. 0-28895  
Na-K liquid alloy, small angle X-ray scatt. study, conc.-fluctuation structure factors 0-54120  
Na-K-H system, H influence on component interactions (Russian) 0-54383  
NaK, liq., engineering handbook, purification, heaters, coolers, radiators 0-27045  
Nb-K melts, thermodynamic characts., elec. resistivity, single parameter rigid sphere calcs. (Russian) 0-34410

## potassium compounds

see also potassium alloys; Rochelle salt

1,1-cyclobutane dicarboxylic acids and K salts, IR and Raman vibr. spectra (French) 0-2758  
diffusion traps for divalent ions, dielectric loss and ionic thermocurrent techniques 0-6566  
graphite intercalation compounds, C<sub>n</sub>K, electronic struct. and elec. props. 0-44471  
graphite intercalation cpds., C<sub>n</sub>K, de Haas-van Alphen effect, cyclotron reson., and transport props. 0-44479  
graphite-K compounds, intercalates IR active lattice mode obs. 0-45072  
graphite-K intercalation compound, dielec. function, EELS study 0-45183  
graphite-K lamellar cpd., reversible intercalation of tetrahydrofuran 0-16211  
halides, lattice dynamics, bond-bending force model 0-54322  
hexahalogeno compounds: ReCl<sub>6</sub><sup>2-</sup>(ReBr<sub>6</sub><sup>2-</sup>), low symm. splittings in vibronic spectrum due to phase transitions 0-55161  
Hollandite, one-dimens. ionic conductor, modulation and incommensurability 0-19980  
intercalation lamellar graphite derivatives, KC<sub>24</sub>(tetrahydrofuran)<sub>m</sub>, (m=1 and 2), <sup>1</sup>H NMR study 0-44932  
K-TCNQ, high and low temp. phases, dielec. const. 0-34844  
K I, linear dichroism spectra, stress-induced, reorientation of O<sub>2</sub><sup>-</sup> and NO<sub>2</sub><sup>-</sup> impurity ions (Russian) 0-45127  
KOH solutions, effect on corrosion and electrochem. props. of Mo<sub>2</sub>C 0-11813  
lithium potassium tartrate monohydrate: Mn<sup>2+</sup>, isomorphism with lithium ammonium tartrate monohydrate, EPR obs. 0-29607  
oxalate, EPR of Mn<sup>2+</sup> and VO<sup>2+</sup> 0-39858  
oxalate monohydrate:VO<sup>2+</sup>, IR absorpt. study 0-55134  
potassium hydrogen malonate, deuterate, NQR data (I=1) from ENDOR expts. 0-54994  
potassium hydrogen oxalate, oriented single cryst., Raman spectra with very strong H-bonding 0-25359  
potassium oxalate, anhydrous, phase II, vibr. spectra and cryst. struct. 0-34901  
γ-quartz, reaction, with NaCl-KCl melt, exam. of struct., IR absorption spectra 0-55706  
rare earth double sulphates, K<sub>6+3n</sub>R<sub>4-n</sub>(SO<sub>4</sub>)<sub>9</sub>, (n≈0.4), cryst. struct. 0-28985  
trisoalatoferate complexes, Mossbauer studies of electronic relax. phenomena 0-44973  
β-Al<sub>2</sub>O<sub>3</sub>-K<sub>2</sub>O, ESR of paramag. defects in cond. planes 0-29617  
β<sup>-</sup>-Al<sub>2</sub>O<sub>3</sub>-K<sub>2</sub>O 0-11394



## potassium compounds continued

- Al<sub>2</sub>(SO<sub>4</sub>)<sub>3</sub>, K<sub>2</sub>SO<sub>4</sub>·24H<sub>2</sub>O, formation, survival and growth of nuclei from secondary nucleation 0-50540  
 Al<sub>2</sub>(SO<sub>4</sub>)<sub>3</sub>·K<sub>2</sub>SO<sub>4</sub>·24H<sub>2</sub>O, spirals, growth and dissolution from liq. state 0-15027  
 B<sub>2</sub>O<sub>3</sub>·K<sub>2</sub>O·Na<sub>2</sub>O·Rb<sub>2</sub>O·Cs<sub>2</sub>O glass, small angle X-ray scatt. exam. of struct. 0-38922  
 Ba<sub>2</sub>KNb<sub>6</sub>O<sub>15</sub>, Raman scatt. experiments in tetragonal tungsten bronze compounds 0-40113  
 BaO·K<sub>2</sub>O·Na<sub>2</sub>O·ZnO·SiO<sub>2</sub>, corrosion and microhardness, effect of detergents 0-16518  
 BaO·K<sub>2</sub>O·VO<sub>2</sub>·SiO<sub>2</sub>, glass, elec. cond. rel. to ion polarisability, polarons 0-49729  
 BeO·P<sub>2</sub>O<sub>5</sub>·K<sub>2</sub>O glass, gamma irradi., cation modifier effect on radiation centre formation 0-40720  
 C<sub>12n</sub>K, graphite intercalated, two-dimens. structurally disordered phases, X-ray diff. profiles 0-44181  
 C<sub>6</sub>K, graphite intercalated, phonon dispersion relations and Raman spectra 0-44272  
 C<sub>6</sub>K, intercalation cpd. with graphite, supercond. props. 0-44755  
 Cs<sub>2</sub>K<sub>2</sub>TmBr<sub>6</sub>(Cl<sub>6</sub>)(F<sub>6</sub>), mag. behaviour 2.9 to 251.3K, cryst. field levels, ang. overlap model (*German*) 0-29520  
 Cs<sub>2</sub>KYbF<sub>6</sub>, mag. behaviour, 3.5-251.3K (*German*) 0-50041  
 Cs<sub>2</sub>O·SiO<sub>2</sub> glass, low temp. heat capacity 0-49373  
 Cu<sub>2</sub>Cl<sub>2</sub>·2H<sub>2</sub>O, Heisenberg ferromag., mag. field effect on susceptibility near crit. point 0-39758  
 Cu<sub>2</sub>H<sub>2</sub>(PCrO<sub>3</sub>)<sub>2</sub>, cryst. struct. determ. 0-28989  
 n-GaAs/K<sub>2</sub>Se-K<sub>2</sub>Se<sub>2</sub>KOH/C solar cell, Ru (III) chemisorption on photoanode, effect on performance 0-3516  
 GeO<sub>2</sub>·K<sub>2</sub>O, glass composition effect on solubility in H<sub>2</sub>O 0-39303  
 HCl-KCl-H<sub>2</sub>O mixed electrolyte solns., elec. transport 0-3355  
 K·TCNQ, low temp. refl. spectra 0-25353  
 K<sub>2</sub>As<sub>4</sub>, superionic film, elec. ionic cond. and electron spectra 0-6543  
 KAlBr<sub>4</sub>, intramolecular configs., nucl. quadrupole double reson. obs. 0-34821  
 KAlF<sub>4</sub>, hydrothermal growth method in presence of hydrofluorhydric acid (*French*) 0-25543  
 KAl(SO<sub>4</sub>)<sub>2</sub>·12H<sub>2</sub>O·MnO<sub>4</sub><sup>-</sup>, visible and UV absorpt. spectra interpretation 0-45116  
 KAl[Fe(CN)<sub>6</sub>], isomer shift of Mossbauer spectra 0-29662  
 K<sub>2</sub>As<sup>III</sup>As<sup>V</sup><sub>4-x</sub>O<sub>11.5-x</sub>, solid-state synthesis, crystalline phase (*French*) 0-15079  
 K<sub>2</sub>As<sub>2</sub>O<sub>7</sub>, solid-state synthesis, X-ray powder data (*French*) 0-15079  
 K<sub>2</sub>BRCl<sub>6</sub>, B=Li, Ag, Na, systematic structs., X-ray Guinier-Simon method (*German*) 0-44186  
 K(B<sub>2</sub>W<sub>3-x</sub>)<sub>2</sub>O<sub>9</sub> (B=Na, Ca, Co, Ni, Cd, Ga, Bi, Nb, Ta) cryst. struct., temp. dielec. anomalies 0-1998  
 KBr, additively coloured, self-enhancement of amplitude hologram (*Russian*) 0-9828  
 KBr, additively dyed, amplitude-phase holograms (*Russian*) 0-1152  
 KBr, avalanche type crystal formation (*Hungarian*) 0-11552  
 KBr bicrystal, Ag<sup>+</sup> injection transport and grain boundary mobility, electrodecoration obs. 0-2214  
 KBr, diffusion-controlled defect recombination, quasi-steady radius, tunnelling and elastic interaction (*Russian*) 0-10908  
 KBr, doped with F-centres, Raman spectra meas. excitation in F and K bands 0-16027  
 KBr, efficiency of V<sub>L</sub>- and Ag<sup>0</sup>-centres generation (*Russian*) 0-39080  
 KBr, electron irradiated, defect accumulation kinetics of low temps. 0-10577  
 KBr, electron-spin memory and magnetic-circular-dichroic effects in F-centre luminesc. 0-29794  
 KBr, enthalpies of soln. in water 0-50880  
 KBr, excitation of thermolum. near liq. He temp. 0-40171  
 KBr, F-centre radiative lifetime meas. near 65K 0-25439  
 KBr, K<sup>+</sup> 3p core excitons, refl. spectra study, low temp. 0-29759  
 KBr, linear dichroism spectra, stress-induced, reorientation of O<sub>2</sub><sup>-</sup> and NO<sub>2</sub><sup>-</sup> impurity ions (*Russian*) 0-45127  
 KBr pellet, appl. to IR spectroscopy of inorganic species 0-22455  
 KBr photochromic materials, F→M transform., electrostatic field control of optical information recording (*Russian*) 0-48370  
 KBr, proton irradi., divacancies, positron capture, ionic cond. and TSC study 0-54289  
 KBr, pulse radiolysis of metastable interstitial centre of high temp. 0-20658  
 KBr, pulsed-laser-induced damage, role of avalanche multiplication and multiphoton absorpt. 0-48316  
 KBr, self-trapped exciton and F-centre form. by picosecond laser pulses 0-10546  
 KBr, single cryst., quenched, microstruct. around indentations 0-7628  
 KBr substrate, electron irradi., epitaxial growth and surface coverage of Te films 0-10825  
 KBr, thermally stimulated luminesc. accompanying recomb. of V<sub>F</sub> and F centres 0-55201  
 KBr, U<sub>2</sub> and U<sub>1</sub> centres, optical excitations 0-2803  
 KBr, V- and X-centres accumulation (*Russian*) 0-54228  
 KBr, whiskers, F-centre accumulation and track effects due to X-ray irradi. 0-39484  
 KBr, with alkali and halogen impurities, colour centre deformation induced nonradiative decay 0-7387  
 KBr, X-irrad., F-centre role in thermoluminescence 0-20720  
 KBr, X-irradiated cryst., luminesc. during press. release 0-20722  
 KBr, X-ray irradi., tunnelling recomb. luminesc. 0-2873  
 KBr:Ag, optical absorpt. spectra interpretation mol. orbital scheme 0-20671  
 KBr:BeF<sub>2</sub><sup>2-</sup>, IR absorption spectra of impurity anions (*Russian*) 0-2807  
 KBr:CN<sup>-</sup> 0-49316  
 KBr:Cl<sup>-</sup>, diffusion traps for divalent ions, dielectric loss and ionic thermocurrent techniques 0-6566  
 KBr:Eu<sup>2+</sup>, single cryst. optical absorpt. spectra 0-45117  
 KBr:In<sup>+</sup>, B-band, optical absorpt. and mag. circular dichroism calcs. 0-29765  
 KBr:In<sup>+</sup>, optical absorption and MCD spectra, Gaussian quadrature calc. 0-7367  
 KBr:Na, U-centres, HFS and g-factor, EPR spectra 0-39869  
 KBr:Na(Rb)(Cs), microcrystalline powders, isothermal decay of colour centres 0-2804  
 KBr:PO<sub>2</sub><sup>-</sup>, phosphorescence, triplet state sublevels, mixing 0-25446  
 KBr:Pb, A-luminesc., 8-80K 0-2836  
 KBr:Ti, Jahn-Teller system, negative mag. circular polarisation in emission spectrum 0-20694

## potassium compounds continued

- KBr:TI excitation in fund. absorpt. region, luminesc. and thermolum. 0-50433  
 KBr:TI<sup>+</sup>, quadratic Jahn-Teller effect, totally symm. vibr. mode effect, ang. overlap model 0-49680  
 KBr:TI<sup>2+</sup>, relation between bonding and g-shift 0-39492  
 KBr-Al<sub>2</sub>Br<sub>6</sub> soln. in toluene, conduction mechanism 0-6870  
 KBr-CaSO<sub>4</sub>:Dy thermolum. phosphor, thermal neutron detect. by activation 0-32581  
 KBr-KBrO<sub>3</sub>·H<sub>2</sub>SO<sub>4</sub>-Mn<sup>2+</sup> system, chem. automat with three steady states 0-7769  
 KBr-LiBr, liq. mixture, struct. and diffusion 0-24344  
 KBr-OH<sup>-</sup> electron irradi., F<sub>2</sub><sup>+</sup> centre stabilisation 0-54231  
 KBrO<sub>3</sub>, <sup>17</sup>O NQR, spin echo double reson. method, electronegativity 0-54970  
 KBrO<sub>3</sub>, hexagonal modification, temp. depend. of NQR freq., interpretation of long-wave spectra 0-25243  
 KBrO<sub>3</sub>·H<sub>2</sub>SO<sub>4</sub>-KBr-Mn<sup>2+</sup> system, chem. automat with three steady states 0-7769  
 KC<sub>24</sub>, intercalation compound, prep. by reduction of aromatic compounds 0-3306  
 KC<sub>8</sub>, graphite intercalation compound, band structure calc., charge transfer effect 0-6692  
 KC<sub>8</sub>, intercalated graphite, electronic and cryst. struct. 0-44472  
 KC<sub>8</sub>, lamellar cpds. with graphite, EPR studies 0-44902  
 KC<sub>8</sub>, lamellar cpds. with graphite, <sup>13</sup>C NMR studies 0-44936  
 KCN, cubic NaCl-type cryst., Debye temp. 0-54333  
 KCN, plastic phase, Raman scatt. spectra (*French*) 0-11379  
 KCN:HCN<sup>-</sup>, structural props. using ESR 0-25205  
 (KCN)<sub>0.5</sub>(KBr)<sub>0.5</sub>, lattice dynamics neutron scatt. obs., glass phase formation 0-15207  
 K<sub>2</sub>CO<sub>3</sub>·SiO<sub>2</sub>·As<sub>2</sub>O<sub>3</sub>, laser Raman spectrosc. study of ions in quenched reaction mixtures 0-25357  
 K<sub>2</sub>Ca(SO<sub>4</sub>)<sub>2</sub>·H<sub>2</sub>O, syngenite, thermal dehydration under nonisothermal conditions 0-3324  
 KCl, <sup>14</sup>N impurities, molecular point defects, EPR isotropic hyperfine triplets 0-2636  
 KCl, annealed in KBr vapour, crack and pore formation, diffusively induced stress relaxation (*Russian*) 0-40388  
 KCl, axial shift of self-trapped exciton, semiempirical calc. 0-2339  
 KCl, band struct. and charge densities, intersecting spheres model 0-49591  
 KCl, bulk and surface absorption comparison, 9.2 to 10.85 μm 0-33051  
 KCl, charge transfer and pair polarisability anisotropy 0-43173  
 KCl, colloidal suspension, radiowave dielec. dispersion 0-11311  
 KCl, colour centres laser spectra, induced F<sup>+</sup> band absorpt. 0-2779  
 KCl coloured crystal, susceptibility variation calculations 0-55055  
 KCl crystal, surface elementary steps interaction with Au particles 0-39400  
 KCl crystal, use of photoelectrons to investigate surface charges 0-2444  
 KCl crystal growth in fluidised bed, comparison to dissoln. (*French*) 0-16167  
 KCl crystals, positron annihilation, Doppler broadening 0-40180  
 KCl, ENDOR of F-centres, sign of <sup>41</sup>K elec. quadrupole moment 0-34820  
 KCl, electron-spin memory and magnetic-circular-dichroic effects in F-centre luminesc. 0-29794  
 KCl, etching, double poison role 0-54240  
 KCl, exp. valence charge density calc., accuracy of one-term Gaussian representation 0-28952  
 KCl, F-centre optical absorpt., estimate using symmetry-adapted wave functions 0-11448  
 KCl far IR complex permittivity meas. by dispersive Fourier transform spectroscopy, 7 to 300K 0-15940  
 KCl, γ-irrad., photoplastic effect and internal friction aftereffect 0-24529  
 KCl, influence of collisions on cryst. growth and secondary nucleation under conditions of meas. crystn. 0-50544  
 KCl, irradi. with intense nanosecond electron beam, super-Rayleigh vel. of brittle fracture front 0-6458  
 KCl, K<sup>+</sup> 3p core excitons, refl. spectra study, low temp. 0-29759  
 KCl laser-induced breakdown fields rel. to wavelength and focal spot radius 0-35019  
 KCl, linear dichroism spectra, stress-induced, reorientation of O<sub>2</sub><sup>-</sup> and NO<sub>2</sub><sup>-</sup> impurity ions (*Russian*) 0-45127  
 KCl long rod sample, calorimetric absorpt. coeff. meas. using pulsed CO<sub>2</sub> lasers 0-9918  
 KCl, melt, mol. dynamics simulation 0-54097  
 KCl, molten, vapour-liq. interface, mol. dynamics model 0-54362  
 KCl, optical breakdown from 0.53-10.6 μm 0-7292  
 KCl, photo-induced F-centres, hologram recording 0-28174  
 KCl, positronium states near defects in cationic sublattice 0-16121  
 KCl, pulsed-laser-induced damage, role of avalanche multiplication and multiphoton absorpt. 0-48316  
 KCl, radiative tunnel transitions in negatively charged colour centre systems 0-49655  
 KCl, single cryst., liq. inclusion movement in stress gradient field 0-44370  
 KCl, single cryst., quenched, microstruct. around indentations 0-7628  
 KCl, solution, apparent molar heat capacity and volume, at 298.15K 0-29179  
 KCl solution, in Ag-AgCl/KCl/AgCl-Ag thermocell, thermal liq. junction pot. at high temps. 0-16819  
 KCl solution, viscosity of nonfreezing thin interlayer between ice column and quartz capillary 0-54475  
 KCl, spirals, growth and dissolution from liq. state 0-15027  
 KCl, stress distrib., meas. by scattered light photoelasticity (*Russian*) 0-7326  
 KCl surface, TiH/KCl/TiH low absorpt. antireflection coatings 0-38078  
 KCl surface texture and optical props. after forging between polished dies 0-33102  
 KCl, temp. depend. of F-colouring efficiency 0-44204  
 KCl, thermal and photochemical conversion of colour centres, after high-dose electronic interaction (*Russian*) 0-39156  
 KCl, thermal annealing of F, V<sub>2</sub><sup>-</sup>, V<sub>3</sub><sup>-</sup> centres (*Russian*) 0-54229  
 KCl thermally stimulated luminesc. accompanying recomb. of V<sub>F</sub> and F centres 0-55201  
 KCl, thin film, crystal-vacuum (100) surface, mol. dynamics computer simulation 0-34288  
 KCl, U<sub>2</sub> and U<sub>1</sub> centres, optical excitations 0-2803  
 KCl, US plastic deform., dislocation struct. 0-19809  
 KCl, V- and X-centres accumulation (*Russian*) 0-54228



## potassium compounds continued

- KCl, vacancy complex formation and binding energies in zeroth approx. 0-24441  
 KCl, whiskers, F-centre accumulation and track effects due to X-ray irradi. 0-39484  
 KCl with  $\text{Al}_2\text{O}_3$  disperse spheres, dislocation mechanism for stress relaxation in cooling crystal (*Russian*) 0-54347  
 KCl, with alkali and halogen impurities, colour centre deformation induced nonradiative decay 0-7387  
 KCl, X-ray irradi., tunnelling recomb. luminesc. 0-2873  
 KCl:Ag, optical absorpt. spectra interpretation mol. orbital scheme 0-20671  
 KCl:Ag(In)(Tl), excitation in fund. absorpt. region, luminesc. and thermolum. 0-50433  
 KCl:Ba(Sr), Z-centre, luminesc. and absorpt. spectra obs. 0-49221  
 KCl:BeF<sub>4</sub><sup>2-</sup>, IR absorption spectra of impurity anions (*Russian*) 0-2807  
 KCl:CN<sup>-</sup>, paraelectric reson. study, tunnelling parameters and elec. dipole moment 0-25326  
 KCl:CN<sup>-</sup>, phonon-defect interaction, Brillouin scatt. obs. 0-34935  
 KCl:CN<sup>-</sup>, coherent admixtures of phonons with impurity librionic excitations, neutron scatt. study 0-49316  
 KCl:Ca, Z<sub>4</sub> centres, thermal and optical bleaching 0-19802  
 KCl:Ca<sup>2+</sup>, Cl<sup>-</sup>(Br<sup>-</sup>), diffusion traps for divalent ions, dielectric loss and ionic thermocurrent techniques 0-6566  
 KCl:Ca(Ba), effect of doping on dislocation distrib., in melt grown cryst. 0-6410  
 KCl:Ca(Ba)(Mg)(Sr), microcrystalline powders, role of Z-centres in stabilizing coloration 0-54227  
 KCl:Eu<sup>2+</sup>,  $\gamma$ -irrad., photostimulated low temp. recomb. luminesc. 0-11435  
 KCl:Eu<sup>2+</sup>, lattice defect equilib. optical absorpt. and cond. studies 0-29767  
 KCl:Eu<sup>2+</sup>, single cryst. optical absorpt. spectra 0-45117  
 KCl:F<sup>-</sup>(Br<sup>-</sup>)(I<sup>-</sup>), U-centres, local defect modes, Green's functions calcs. 0-44280  
 KCl:Fe(CN)<sub>6</sub><sup>4-</sup>, electron irradi., Mossbauer and ESR study 0-7238  
 KCl:H, dichroic H- and U-centres by polarised bleaching of interstitial H 0-29766  
 KCl:H, dynamical superhyperfine interaction 0-2663  
 KCl:I, luminesc. at low temp. 0-2818  
 KCl:In(Ga), ESR of impurity centres, impurity optical absorpt. bands 0-29618  
 KCl:KNO<sub>3</sub>(KNO<sub>3</sub>), anion exchange during tablet pressing, IR spectroscopy appl. 0-2764  
 KCl:KReO<sub>4</sub>, CO<sub>2</sub> pulse generation by free induction decay 0-53388  
 KCl:Li, F<sub>A</sub>-centre optical absorpt., estimate using symmetry-adapted wave functions 0-11448  
 KCl:Li<sup>+</sup>, phonon generation by EM excitation, mechanism 0-2129  
 KCl:Li<sup>+</sup>, Na<sup>+</sup>, F<sub>A</sub>(II) to F<sub>B</sub>(II) centre crystals, CW laser oscill. with extended tuning range 0-32997  
 KCl:Li<sup>+</sup> F<sub>A</sub>(II) colour-centre laser, mode locking and tunable picosecond IR pulse generation 0-43364  
 KCl:Na, electron trapping from  $\alpha$  and F<sub>A</sub>-centres, low temp. depend. 0-11444  
 KCl:Na, F<sub>A</sub> reorientation and F<sub>A</sub>  $\rightleftharpoons$  F'<sub>A</sub> conversions, laser induced, kinetic studies 0-10547  
 KCl:Na and pure, hologram recording through F $\rightarrow$ X conversion 0-48190  
 KCl:Na<sup>+</sup>, CW laser action of (F<sub>2</sub><sup>+</sup>)<sub>A</sub>-centres, tunable from 1.62 to 1.91  $\mu\text{m}$  0-32998  
 KCl:PO<sub>2</sub><sup>-</sup>, photo-orientation, spectrosc. and ODMR obs. 0-29772  
 KCl:PO<sub>2</sub><sup>-</sup>, triplet state, level anticrossing and pseudonuclear Zeeman effect, microwave ODMR 0-39896  
 KCl:Pb, geometrical parameters of impurity centres by scattered-light method 0-2043  
 KCl:Pb, ionic electret behaviour, ionic thermoconductivity technique 0-7274  
 KCl:Pb, lead aggregation effect on yield stress, incoherent precipitates, solubility determ. method 0-50645  
 KCl:Pb, light induced ionic polarisation 0-7264  
 KCl:Pb crystal surfaces, Au decoration, electron microscope study 0-15144  
 KCl:Pb crystals, development of mechanical stresses during growth 0-19735  
 KCl:Pb<sup>2+</sup>, low temp. sp. ht. 0-2178  
 KCl:Pb<sup>2+</sup>(Cu<sup>+</sup>) 0-34890  
 KCl:Pr<sup>3+</sup>(Sm<sup>3+</sup>), absorption spectra at 4.2 K, anal. 0-7378  
 KCl:SnCl<sub>2</sub>, X-ray irradi., polarised luminesc. and EPR study of Sn<sup>3+</sup> centres 0-39868  
 KCl:Sr, thermally pre-treated, glow curves 0-25470  
 KCl:Sr, triplet state of F<sub>2</sub>-centres, ESR spectra 0-29616  
 KCl:Ti, energy level scheme, mol. orbital model 0-10912  
 KCl:Ti, hole capture kinetics, influence of autolocalised and zone holes (*Russian*) 0-54714  
 KCl:Ti, Jahn-Teller system, negative mag. circular polarisation in emission spectrum 0-20694  
 KCl:Ti<sup>2+</sup>, quadratic Jahn-Teller effect, totally symm. vibr. mode effect, ang. overlap model 0-49680  
 KCl:Ti<sup>2+</sup> cryst., A band, mag. field effect 0-34897  
 KCl:Ti<sup>2+</sup>, optical absorpt. spectra interpretation mol. orbital scheme 0-20671  
 KCl:Ti<sup>2+</sup>, relation between bonding and g-shift 0-39492  
 KCl:TiCl<sub>3</sub>, lattice defects, X-ray line profile obs. 0-24455  
 KCl:V<sup>2+</sup>, EPR spectra above 300K 0-34765  
 KCl:Ba, X-ray irradi. cryst., thermoluminescence spectra 0-20719  
 KCl-CuCl solid solution supersaturated, precipitation, impurity aggregation 0-29174  
 KCl-KBr, solid soln., negative muon capture ratios 0-55007  
 KCl-KBr mixed crystals, thermolum. studies 0-11486  
 KCl-KBr mixed system, Gruneisen coefficient evaluation 0-39240  
 KCl-KF:Pb<sup>2+</sup>, point defects, ionic thermal currents and optical meas. 0-6403  
 KCl-KH, F- and U-centre redistrib. at end of proton tracks, microspectrophotometric anal. 0-10583  
 KCl-Mg, thermolum. of Z-centre, optical absorpt. 0-55203  
 KCl-NaCl, aq. solns., isopiestic studies, 383 to 474K 0-21320  
 KCl-OH<sup>-</sup>, electron irradi., F<sub>2</sub><sup>+</sup> centre stabilisation and tuneable laser operation 0-54231  
 KCl<sub>0.5</sub>Br<sub>0.5</sub>:Ca, X-ray irradi., Z<sub>1</sub>-centres, thermoluminesc. and optical absorpt. meas. 0-16108  
 KClO<sub>3</sub>, <sup>17</sup>O NQR, spin echo double reson. method, electronegativity 0-54970

## potassium compounds continued

- KClO<sub>3</sub>, NQR spectroscopy, parametric superregenerator with phase quantisation application 0-22398  
 KClO<sub>3</sub>, quadrupole spin echo envelope EFG tensor axisymmetry in mag. field 0-20497  
 KClO<sub>4</sub>, cryst. growth from gelatin gels, exam. of growth and morphology 0-7488  
 KClO<sub>4</sub>, X-irrad. induced paramag. defects, ESR study 0-24493  
 KClO<sub>4</sub>:MnO<sub>4</sub><sup>-</sup>, reson. Raman excitation profiles for totally symmetric mode, vibronic struct. 0-50309  
 KCl:Na, F<sub>A</sub>-centre optical absorpt., estimate using symmetry-adapted wave functions 0-11448  
 KCl:Pb<sup>3+</sup>, relation between bonding and g-shift 0-39492  
 KCl(aq.)-pyrex systems, electrokinetic coeff. determ. from sedimentation pot. 0-3365  
 K<sub>3</sub>Co(CN)<sub>6</sub>, <sup>59</sup>Co quadrupole coupling const., temp. depend. 0-44557  
 K<sub>3</sub>Co(CN)<sub>6</sub>, NMR spin lattice relax. of <sup>59</sup>Co rel. to Co(CN)<sub>6</sub> octahedra vibr. modes 0-39885  
 KCoF<sub>3</sub>, lattice parameter temp. depend., phase transitions and thermal expansion coeff. 0-1988  
 K<sub>2</sub>CoF<sub>4</sub>, pseudo Ising antiferromag., inelastic light scatt. by mag. excitons 0-11377  
 K<sub>2</sub>CoF<sub>4</sub>, specific heat capacity, critical amplitude, cross-over from 2-D Ising to Heisenberg behaviour 0-39791  
 K<sub>2</sub>CoF<sub>4</sub>:Mn<sup>2+</sup>, impurity induced mag. excitations, magnon gap mode, far IR spectra obs. 0-44821  
 KCrO<sub>2</sub>, two-dimens. mag. order, neutron powder diffr. obs. 0-44805  
 K<sub>2</sub>Cr<sub>2</sub>O<sub>7</sub>, growth and growth dispersion 0-49148  
 K<sub>2</sub>Cr<sub>2</sub>O<sub>7</sub>, polymorphic behavior, depend. on thermal and prep. history 0-34184  
 K<sub>2</sub>Cr<sub>2</sub>O<sub>7</sub>, single crystals, X-irrad., EPR spectra 0-2638  
 K<sub>2</sub>CuCl<sub>2</sub>.2H<sub>2</sub>O, ferromag., hyperfine and exchange interactions, NMR study 0-50208  
 K<sub>2</sub>CuCl<sub>4</sub>.2H<sub>2</sub>O, paramag. single cryst., PMR temp. depend., hyperfine const. and exchange interaction (*Korean*) 0-29630  
 KCuF<sub>3</sub>, <sup>63</sup>Cu NQR meas. 0-50219  
 KCuF<sub>3</sub>, nearly 1-D spin-1/2 antiferromagnet, spin wave energy dispersion 0-2551  
 K<sub>2</sub>CuF<sub>4</sub>, microwave excitation, optical detection of ferromagnetic reson. 0-50197  
 K<sub>2</sub>CuF<sub>4</sub>, two-dimensional planar ferromagnet, giant fluctuation of spins (*Japanese*) 0-54894  
 K<sub>2</sub>Cu<sub>2</sub>Zn<sub>1-x</sub>F<sub>4</sub>, two-dimens. ferromag., spin correl. near percolation limit 0-44840  
 KDP monocrystal, expansion and contraction coeffs., tricritical point, Landau theory explanation (*Russian*) 0-44340  
 KD<sub>2</sub>P<sub>4</sub>, nonlinear electrooptic effects 0-29721  
 KD<sub>2</sub>PO<sub>4</sub>, Brillouin spectrum and broad central component, depend. on scatt. wave vector direction 0-34931  
 KD<sub>2</sub>PO<sub>4</sub>, deuteron tunnelling, barrier height and energy level calc. 0-6482  
 KD<sub>2</sub>PO<sub>4</sub>, magnetoelectric susceptibilities, phenomenological rules for computation 0-55068  
 KD<sub>2</sub>PO<sub>4</sub>, microwave spectra, temp. depend. mode rel. to proton subsystem 0-24548  
 KD<sub>2</sub>PO<sub>4</sub> monocrystal, electrooptical props. in paraelectric phase (*Polish*) 0-11368  
 KD<sub>2</sub>PO<sub>4</sub>, nonlinear electrooptic coeffs. near Curie temp. 0-11366  
 KD<sub>2</sub>PO<sub>4</sub> photo-spatial light modulator, optical data processing appl. 0-9988  
 KD<sub>2</sub>PO<sub>4</sub> r<sub>63</sub> laser modulator (*Chinese*) 0-28260  
 KD<sub>2</sub>PO<sub>4</sub>, Rayleigh scatt. and narrow central component, depend. on scatt. wave vector direction 0-29747  
 KD<sub>3</sub>(SeO<sub>3</sub>)<sub>2</sub>, ferroelastic transition, EPR 0-7148  
 KD<sub>3</sub>(SeO<sub>3</sub>)<sub>2</sub>, phase transition, neutron diffr. 0-2158  
 KDy(WO<sub>4</sub>)<sub>2</sub>, Jahn-Teller transition, permittivity behaviour 0-55012  
 KDy(WO<sub>4</sub>)<sub>2</sub>, phase transition mechanism, absorpt. spectra, symmetry props. (*Russian*) 0-55130  
 KEr(WO<sub>4</sub>)<sub>2</sub>, crystallisation cond., stimulated emission in 2.8  $\mu\text{m}$  band 0-53301  
 KEuHP<sub>2</sub>O<sub>10</sub> acid, exam. of thermal decomposition 0-55638  
 $\alpha$ -KEu(PO<sub>3</sub>)<sub>3</sub>, vibr. spectra 0-34905  
 K<sub>2</sub>Eu(PO<sub>4</sub>)<sub>3</sub>, synthesis and IR spectra 0-16019  
 KF, ab initio SCF MO energy, dipole moment and polarisability 0-1085  
 KF, Compton profiles, anisotropies 0-20730  
 KF, F<sub>2</sub><sup>+</sup>-centre excited-state absorption spectrum, rel. to H<sub>2</sub><sup>+</sup> model 0-16066  
 KF, F-centre optical absorpt., estimate using symmetry-adapted wave functions 0-11448  
 KF, K<sup>+</sup> 3p core excitons, refl. spectra study, low temp. 0-29759  
 KF:Li, F<sub>A</sub>-centre optical absorpt., estimate using symmetry-adapted wave functions 0-11448  
 KF-LnF<sub>3</sub> (Ln=Y, La, Yb) binary liquid mixtures, thermochemistry 0-45538  
 (KF)<sub>n</sub>-FeF<sub>3</sub>, antiferromagnetic systems, dimensionality and spin reduction effects, Mossbauer study 0-39947  
 K<sub>3</sub>Fe(CN)<sub>6</sub>, electronic struct., elec. field gradient tensor 0-15483  
 K<sub>3</sub>Fe(CN)<sub>6</sub>.3H<sub>2</sub>O, C-N vibr., Raman study 0-40106  
 K<sub>2</sub>FeCl<sub>4</sub>(H<sub>2</sub>O), phase diagram, antiferromag., paramag. and spin flop phases 0-44831  
 KFeF<sub>4</sub>, amorphous, Mossbauer study 0-39970  
 K<sub>3</sub>FeF<sub>6</sub>, Mossbauer spectra, 1D antiferromag. 0-15886  
 K<sub>1+x</sub>Fe<sub>1-x</sub>Ga<sub>1-y</sub>O<sub>17</sub>, electron hopping and excitation at room temp., <sup>51</sup>Fe Mossbauer spectra 0-25257  
 KFeO<sub>2</sub>, overlap contribution to <sup>57</sup>Fe<sup>3+</sup> isomer shifts, nuclear size change 0-39903  
 KFe<sub>2</sub>O<sub>3</sub>,  $\beta''$  phase, mag. props., hyperfine interactions, Mossbauer study 0-20524  
 K<sub>2</sub>FeO<sub>4</sub>, antiferromag., critical fluctuations obs. using Mossbauer spectroscopy 0-39955  
 K<sub>2</sub>FeO<sub>4</sub>, XPS of hexavalent iron binding energies calcs. 0-43013  
 KFe(PO<sub>3</sub>)<sub>2</sub>F, crystal struct., interatomic distances, X-ray phase anal. 0-39053  
 KFeS<sub>2</sub>, cathodes for nonaqueous Li batteries 0-3506  
 KFeS<sub>2</sub>, cryst. struct. and mag. ordering, neutron diffr. and mag. susceptibility meas. 0-54867  
 KFeS<sub>2</sub>, crystal ligand field theory, band assignment, absorpt. spectra study 0-20657  
 KGaF<sub>4</sub> coating materials for IR laser components 0-33105  
 K<sub>2</sub>Ga<sub>2</sub>P<sub>8</sub>O<sub>24</sub>, cryst. struct., atomic coordinates, anisotropic temp. corrections 0-33974



## potassium compounds continued

- KH II states and  $KH^+$  ground state, pot. energy curves calc. 0-18812  
 $KH_2AsO_4$ , magnetoelectric susceptibilities, phenomenological rules for computation 0-55068  
 $KH_2AsO_4$ , transverse elec. susceptibilities 0-50273  
 $K(H_{1-x}D_x)_2PO_4$ , polarised impurity cluster effects in light scatt. expts. 0-29716  
 $KH_{1-x}D_{1-x}PO_4$ , domain struct. influence on switching processes 0-11355  
 $K(H_{1-x}D_x)_2(SeO_3)_2$ , Brillouin spectrum central peak, soft acoustic mode 0-2777  
 $KH_2PO_4$ , aq. soln., elec. conductance in saturation region, effect of light (Polish) 0-10983  
 $KH_2PO_4$  crystals, rel. between selective and total soln. 0-39103  
 $KH_2PO_4$ , dendritic growth in silica gel 0-35072  
 $KH_2PO_4$ , efficient high-energy SHG of triaxial flashlamp-pumped dye laser 0-38061  
 $KH_2PO_4$ , ferroelectric transition, neutron diffr. obs. 0-25324  
 $KH_2PO_4$ , growth from gel and aqueous soln., oriented inclusions 0-15023  
 $KH_2PO_4$ , light scatt. in elec. field, ferroelec.-paraelec. transition 0-2707  
 $KH_2PO_4$ , low temp. transition, thermal hysteresis, Cr impurity effect on transition temp. 0-2705  
 $KH_2PO_4$ , magnetoelectric susceptibilities, phenomenological rules for computation 0-55068  
 $KH_2PO_4$ , nonlinear electrooptic effects 0-29721  
 $KH_2PO_4$ , paraelectric phase, solns. of Bloch-type eqns. 0-7304  
 $KH_2PO_4$ , parametric generation of picosecond light pulses with an energy conversion greater than 50% 0-53377  
 $KH_2PO_4$ , press. and deuteration effects on static ferroelec. props., four-particle cluster approx. 0-34861  
 $KH_2PO_4$ , proton tunnelling, barrier height and energy level calc. 0-6482  
 $KH_2PO_4$ , spirals, growth and dissolution from liq. state 0-15027  
 $KH_2PO_4$ , transverse elec. susceptibilities 0-50273  
 $KH_2PO_4$ -type crystal, LF dynamics 0-10602  
 $KHSi_3O_8$ , cryst. struct., Patterson function anal., valency balance, hydrogen bonds 0-39051  
 $KHgC_8$  and  $KHgC_{10}$ , intercalation cpds., synthesis and struct. 0-44183  
 $KI$ ,  $^{14}N$  impurities, molecular point defects, EPR isotropic hyperfine triplets 0-2636  
 $KI$ , doped substrate for vac. deposition of Ag oriented films 0-2303  
 $KI$ , electron-spin memory and magnetic-circular-dichroic effects in F-centre luminesc. 0-29794  
 $KI$ , enthalpies of soln. in water 0-50880  
 $KI$  in acetone, press. effects on Walden products, ion-solvent interactions 0-3398  
 $KI$ ,  $K^+3p$  core excitons, refl. spectra study, low temp. 0-29759  
 $KI$ , luminesc. lines due to  $n=2$  free exciton state of Wannier series 0-29776  
 $KI$ , piezo-optical study of excitons 0-16055  
 $KI$ , quenched, absorpt. and emission spectra,  $\alpha$ -centres 0-11442  
 $KI$ , relationship between fourth moments in molten state and phonon freq. in solid phase 0-10477  
 $KI$ , self-trapped exciton and F-centre form. by picosecond laser pulses 0-10546  
 $KI$ , single cryst., quenched, microstruct. around indentations 0-7628  
 $KI$ ,  $U_1$  and  $U_2$  centres, optical excitations 0-2803  
 $KI$ , with alkali and halogen impurities, colour centre deformation induced nonradiative decay 0-7387  
 $KI$ , X-irradiated cryst., luminesc. during press. release 0-20722  
 $KI:Eu^{2+}$ , single cryst. optical absorpt. spectra 0-45117  
 $KI:Pb^{2+}$ , UV absorpt. and mag. circular dichroism spectra 0-25418  
 $KI:S^{2-}$ , vacancy dipoles, photo-induced polarisation and depolarisation 0-2690  
 $KI:Ti^{4+}$ ,  $A_T$  emission, mag. circular polarisation, WKB approx. for non-radiative transition rate 0-55180  
 $KI:Ti$ ,  $A_T$  emission, linear polarisation, appl. of semi-classical WKB formalism 0-45134  
 $KI:Ti$ , electron-hole and  $V_K$ - $Ti$  recomb., TSC and thermolum. study (French) 0-34461  
 $KI:Ti^{4+}$ , pre-resonant enhancement of Raman scatt. 0-7354  
 $KI$ -Hg interface, specific adsorption of I ions, electrical double layer, interface excess activity coeff. 0-49523  
 $KI$ - $Ti$ , Jahn-Teller system, negative mag. circular polarisation in emission spectrum 0-20694  
 $KIO_3$  and  $KIO_4$ , enthalpies of soln. in water 0-50880  
 $KIO_3 \cdot HIO_3$ , structural modifications, NQR study 0-20487  
 $KIn(SO_4)_2 \cdot 4H_2O$ , cryst. struct. 0-15082  
 $K_2IrCl_6$ , sp. ht. meas. at low temp. 0-7119  
 $KLa(PO_3)_4$  ( $\alpha$  and  $\beta$  forms), vibr. spectra 0-34905  
 $KLiSO_4$ , Li NMR, spin-lattice relax. (Chinese) 0-39884  
 $KLiSO_4(Cr)$ , uniaxial crystals, circular dichroism and optical activity 0-45029  
 $KMeF_3$  ( $Me=Cr, Mn, Fe, Co, Ni, Cu$ ), discrete variational  $\chi_\alpha$  cluster calcs. 0-15444  
 $KMg_2(AlSi_3O_{10})F_2 \cdot KMg_2Si_4O_{10}F_2$ , solid soln., melting and crystn., quenching and DTA study 0-39263  
 $KMgF_3$ , elastic moduli, press. and temp. depend., US technique 0-6453  
 $KMgF_3$ , F-centre, superhyperfine interaction, g-factor, symmetry, ENDOR obs. 0-39893  
 $KMgF_3:Ni$ , Ni-Ni pair optical spectra 0-45042  
 $KMnCl_3$ , magnetic spiral struct., neutron diffr. study 0-39748  
 $KMnCl_3$ , rare earth doped, energy transfer, emission spectra obs. 0-20684  
 $KMnF_3$ , cubic-to-tetragonal phase transition, critical anomalies, phenomenological eqns. 0-39275  
 $KMnF_3$ , dynamic scaling and US attenuation at structural phase transition 0-44260  
 $KMnF_3$ , exchange interaction of excited  $Mn^{2+}(^4A_1)$  ions, Anderson model 0-25124  
 $KMnF_3$ , exciton dynamics by time resolved emission spectroscopy 0-54615  
 $KMnF_3$ , IR-active phonons in tetragonal phases 0-2748  
 $KMnF_3$ , lattice parameter temp. depend., phase transitions and thermal expansion coeff. 0-1988  
 $KMnF_3$ , precursor order and Raman scatt. near displacive phase transitions 0-45061  
 $KMnF_3$ , soft phonons and mag. phase transitions 0-54889  
 $K_2MnF_4$ , nucl. spin-magnon relax. time, temp. depend., NMR study 0-25117  
 $K_2MnF_4$ , specific heat capacity, critical amplitude, cross-over from 2-D Ising to Heisenberg behaviour 0-39791

## potassium compounds continued

- $K_3Mn_2F_7$ , two magnon Raman scatt., magnon dispersion, susceptibility, Green's function methods 0-50340  
 $KMn_9Mo_{10}F_{32}$  ( $M=Co, Ni$ ), lattice parameter temp. depend., phase transitions and thermal expansion coeff. 0-1988  
 $K_2Mn_2(SO_4)_3$ , elastic props. using piezoelec. reson. and US vel. meas. 0-15180  
 $K_2MoO_4$ , hysteresis of phase transitions and modulated structures 0-29169  
 $KNO_2$ - $NaNO_2$ - $NaNO_3$  eutectic salt, use in indirect heating systems (German) 0-38233  
 $KNO_3$  melts, ion exchange reaction with Na silicate glasses 0-16673  
 $KNO_3$ , solns. coagulation of amphoteric latex sols, reversibility and specific ion effects 0-45567  
 $KNO_3$ , solution, apparent molar heat capacity and volume, at 298.15K 0-29179  
 $KNO_3$ - $Pb(NO_3)_2$  molten mixture, elec. cond., Tobolsky parameter (German) 0-15282  
 $KNO_3$ - $RbNO_3$ , liq., electromigration cation and mobility and isotope effect 0-10691  
 $K_2Na_2(Al_2Si_2O_{10}) \cdot 10H_2O$ , amacite, cryst. struct. determ. 0-28961  
 $KNbF_6$ , NMR, quadrupole effects and struct. distortion 0-15809  
 $KNbO_3$ , catalysts, ferroelectric, for reactions involving CO and NO, and adsorption of NO 0-30282  
 $KNbO_3$ , dielec. spectrum rel. to polarisation effects 0-15984  
 $KNbO_3$ , elec. and thermoelec. props., influence of O defects 0-29401  
 $KNbO_3$ , electronic props., SCF-MS- $X_\alpha$  calc. 0-54607  
 $KNbO_3$ , ferroelec. phase, phonon dispersion relations and lattice dynamics calcs., comparison with expt. 0-49319  
 $KNbO_3$ , ferroelectric transition, neutron diffr. obs. 0-25324  
 $KNbO_3$ , photovoltaic effect lux ampere characts., photoconductivity 0-15561  
 $KNbO_3$ , SHG with  $Ga_{1-x}Al_xAs$  lasers 0-5785  
 $KNbO_3$ , tetragonal phase, inelastic neutron scatt. 0-19676  
 $KNbO_3:Fe$ , orthorhombic, EPR of  $Fe^{3+}$  0-39861  
 $KNbO_3$ - $BaTiO_3$ , ferroelec. Curie temp., theory 0-7313  
 $KNbO_3$ - $PbTiO_3$ , ferroelec. Curie temp., theory 0-7313  
 $K_6Nb_4Si_4O_{26}$ , luminesc. bands, Stokes shift, rel. to crystal struct., stacking faults 0-34974  
 $K_6Nb_4Si_4O_{26}$ , luminesc. bands, Stokes shift, rel. to crystal struct., stacking faults 0-34974  
 $K:NdLi:F_{10}$  (KNLF), spectroscopy and lasing 0-5737  
 $\beta$ - $KNd(PO_3)_4$ , vibr. spectra 0-34905  
 $KNdP_4O_{12}$ , determ. of fluoresc. quantum efficiency and laser emission cross sections 0-48264  
 $KNdP_4O_{12}$ , laser emission cross sections, fluorescence spectra, radiative lifetimes, quantum efficiency 0-23694  
 $K_2Nd(PO_4)_2$ , synthesis and IR spectra 0-16019  
 $KNiCl_3$ , X-ray cryst. struct. determ. at room temp. 0-33938  
 $KNiF_3$ , lattice parameter temp. depend., phase transitions and thermal expansion coeff. 0-1988  
 $K_2NiF_4$ , nucl. spin-magnon relax. time, temp. depend., NMR study 0-25117  
 $K_2NiF_4$ , specific heat capacity, critical amplitude, cross-over from 2-D Ising to Heisenberg behaviour 0-39791  
 $K_2NiF_4$  structure, study by method of invariants, appl. to  $A_2BO_4$  oxides (French) 0-33959  
 $K_2NiF_4$ -type compounds, cationic radius ratio and formation 0-28992  
 $KNi_{1-x}Mn_xF_3$ , mixed antiferromagnet, light scatt. meas. 0-16025  
 $K_2Ni(MoO_4)_2$ , paramag. props., 90-800K (French) 0-39734  
 $K_2Ni_3(P_2O_7)_2 \cdot 10H_2O$ , formation from  $Ni_2P_2O_7$ - $K_4P_2O_7$ - $H_2O$  system 0-54381  
 $K_2NiP_2O_7 \cdot 4H_2O$  formation from  $Ni_2P_2O_7$ - $K_4P_2O_7$ - $H_2O$  system 0-54381  
 $K_2Ni_3(P_2O_7)_2 \cdot nH_2O$ , thermal dehydration 0-35513  
 $K_2O$ , non-isothermal decomp. kinetics 0-16649  
 $K_2O$ , thermal decomp. macrokinetics, differential thermal anal. 0-16650  
 $K_2O$ , effect on props. of  $PbO$  containing cryst. glass 0-24637  
 $K_2O$  glasses, partially leached, dehydrated surface reaction with water 0-3406  
 $K_2O$ - $Al_2O_3$ - $P_2O_5$  glass, low-temp. viscosity 0-39198  
 $K_2O$ - $B_2O_3$  glass,  $\gamma$ - and UV- irradi., thermodecolorisation and thermolum. 0-20721  
 $K_2O$ - $B_2O_3$ - $Mn^{2+}$  glass, fine struct. parameter distrib., EPR meas. 0-11256  
 $K_2O$ - $B_2O_3$ - $Fe_2O_3$  glasses, nonbridging O formation, Mossbauer spectroscopy 0-55001  
 $K_2O$ - $B_2O_3$ - $SiO_2$  glass, crystallisation range (German) 0-38934  
 $K_2O$ - $BaO$ - $B_2O_3$  glasses, ESR detection of immiscibility rel. to Cu II ions 0-20916  
 $K_2O$ - $BaO$ - $CaO$ - $SiO_2$  glass-Nichrome- $CaF_2$  multicomponent self-lubricating coating, prep. by plasma spraying, and props. 0-40604  
 $K_2O$ - $BaO$ - $SiO_2$ - $Nd^{3+}$  glasses, absorption and fluoresc. spectra, density 0-25417  
 $K_2O$ - $Fe_2O_3$ - $SiO_2$ , subsolidus sector of phase diagram, X-ray obs. 0-40335  
 $K_2O$ - $Ga_2O_3$ - $P_2O_5$ - $H_2O$ , reactions, 150-500°C 0-35514  
 $K_2O$ - $GeO_2$  glass, struct., Raman scatt. obs. 0-1936  
 $K_2O$ - $PbO$ - $ZnO$ - $B_2O_3$ - $SiO_2$ , corrosion and microhardness, effect of detergents 0-16518  
 $K_2O$ - $SiO_2$  glass, influence of electric charge phenomena on AES (French) 0-50478  
 $K_2O$ - $SiO_2$  glass, effect of high-dose X-rays and reactor radiation 0-19838  
 $K_2O$ - $SiO_2$  glass 0-33897  
 $K_2O$ - $SiO_2$  glass, structural analysis, using fluorescence excitation (German) 0-38923  
 $K_2O$ - $TiO_2$ - $SiO_2$  glass, Si-O bonding,  $SiK\beta$  X-ray fluorescence and IR spectra 0-10500  
 $K_2O$ - $V_2O_5$ - $Al_2O_3$  melts, soln. of  $Al_2O_3$  single crystals 0-20910  
 $K_2O$ , thermodynamic props. 0-29184  
 $K_2OCl_6$ , sp. ht. meas. at low temp. 0-7119  
 $KOH$ , beam, formed at 300-800°C, electron elastic scatt. obs., species identification 0-14231  
 $K_2O$ - $SiO_2$  glass, X-ray diffr. (Japanese) 0-19720  
 $(K_2O)_x$ - $TiO_2$  fibres, flux growth reactions 0-16171  
 $K_2O$ - $4TiO_2$ , new fibrous phase 0-20917  
 $KPF_6$ , temp. depend. hyperfine interactions of trapped pyramidal radicals 0-44918  
 $KPO_2$ , vitreous, microhardness 0-25864  
 $KPO_3$  crystal, P K-band X-ray emission spectra, state anal. 0-40190  
 $KPO_3$ - $Fe_2O_3$  glasses,  $\gamma$ -irrad., ESR 0-50182  
 $K_3PO_4$  crystal, P K-band X-ray emission spectra, state anal. 0-40190



## potassium compounds continued

- $K_2P_2O_7$  crystal, P K-band X-ray emission spectra, state anal. 0-40190  
 $KPO_3F$ , cryst. struct. (French) 0-19762  
 $K_2PbCu(NO_3)_6$ , phase transitions induced by Jahn-Teller effect, uniaxial stress effects 0-6512  
 $K_2PbCu(NO_3)_6$ , uniaxial stress, EPR meas. 0-20455  
 $K_2Pt(CN)_4$ , Peierls transition temp. and 0K energy gap, mean field theory calc. 0-24782  
 $K_2Pt(CN)_4$ , quasi-one-dimens. Peierls system, phonon dispersion and neutron scatt., calc. 0-24550  
 $K_2Pt(CN)_4Br_{0.3}3.2H_2O$ , linear cond.,  $^{195}Pt$  NMR evidence of low lying non-linear excitation 0-44933  
 $K_2Pt(CN)_4Br_{0.30}3H_2O$ , dynamic  $^{195}Pt$  NMR meas. below metal-insulator transition 0-34810  
 $K_2Pt(CN)_4Br_{0.3}3H_2O$ , spin-lattice model for elastic anomalies 0-15179  
 $K_2Pt(CN)_4Br_{0.3}3H_2O$ , quasi one-dimens. conductor, EPR linewidth 0-54938  
 $K_{1.75}Pt(CN)_41.5H_2O$ , Raman scatt. and luminesc. studies 0-25394  
 $K_2PtCl_6$ , diamag. sp. ht. meas. at low temp. 0-7119  
 $K_2PtCl_6$ ,  $K_2ReCl_6$ ,  $K_2SnCl_6$ , solid state phase transitions, lattice vibr., NMR and NQR obs. 0-34814  
 $K_2ReCl_6$ , sp. ht. meas. at low temp. 0-7119  
 $K_2ReCl_6$ , struct. props. and lattice dynamics, mag. struct. 0-44268  
 $K_2ReCl_6$ , thermodynamic relations at solid state phase transitions 0-29164  
 $KReO_4$ , matrix isolated, IR spectra 0-28012  
 $KReO_4$ , vibr. spectrum, Raman and IR spectra obs. 0-55104  
 $KSCN$ , molten, precipitation reaction of  $UO_2^{++}$  0-26040  
 $K_2SO_4$ ,  $\alpha$ - $\beta$  phase transition, Raman scatt. study (French) 0-55096  
 $K_2SO_4$ , displacive solid-state transformations meas., DTA method 0-218  
 $K_2SO_4$ , high temp. form, X-ray struct. redeterm. 0-54179  
 $K_2SO_4$ , mass spectrum obs. of vaporisation, vapour comp. and press., transition and form. heats 0-19933  
 $K_2SO_4$ , molten, struct. analysis using X-ray scatt., correl. with cryst. struct. 0-10486  
 $K_2SO_4$  powder, IR photothermal radiometry absorption spectra, 295-942K 0-26088  
 $K_2SO_4$ , thermal phase transition 0-19738  
 $K_2SO_4(NH_4)_2SO_4$ , X-irrad., EPR of  $NH_4^+$  0-11272  
 $K_2SO_4:MnO_4^{2-}$ , electronic struct. by ESR 0-44906  
 $K_2Sb$ , optical and dielectric props., energy spectra, density of states calcs. 0-20083  
 $K_2SeO_4$ , elastic compliance anomalies 0-45010  
 $K_2SeO_4$ , ferroelec., incommensurate struct., dynamic props. (Russian) 0-11373  
 $K_2SeO_4$ , lattice dynamics, displacive phase transform. 0-39248  
 $K_2SeO_4$ , non-zero wave vector incommensurate soft mode, light scatt. study 0-29754  
 $K_2SeO_4$ , Raman scatt. and dielec. props. 0-11313  
 $KSnBr_6:ReBr_6^{2-}$ , vibronic transition  $\Gamma_7(^2T_{2g}) \rightarrow \Gamma_8(^4A_{2g})$ , intensity distrib. 0-45142  
 $KSnCl_6:ReBr_6^{2-}$ , vibronic transition  $\Gamma_7(^2T_{2g}) \rightarrow \Gamma_8(^4A_{2g})$ , intensity distrib. 0-45142  
 $K_2SnCl_6$ , high-tem. phase, X-ray investigation 0-24409  
 $K(TCNQ)$ , Raman spectra from 30 to 2300  $cm^{-1}$  0-11392  
 $K(Ta,Nb)O_3$  ceramic, prep. and electro-optical props. 0-25620  
 $K_1Ta_{1-x}F_{18-5x}O_{35.5}$ , X-ray cryst. struct. determ. 0-15059  
 $K_1Ta_2F_{10}O_8$ , X-ray cryst. struct. determ. 0-39018  
 $KTaO_3$ , depletion region and donor levels determ., appl. in surface barrier volume wave transducer 0-33403  
 $KTaO_3$ , electronic props., SCF-MS-X $\alpha$  calc. 0-54607  
 $KTaO_3$ , Shubnikov-de Haas effect, cond. band struct. 0-10875  
 $KTaO_3:Fe^{3+}$  local phase transition, EPR line temp. broadening (Russian) 0-54944  
 $K_{1-x}Ta_{1-x}W_{1-x}O_6.nH_2O$ , composition, struct. and ionic conductivity 0-49410  
 $K_2(TeBr_6)$ , far IR and Raman spectra and phase transitions 0-11376  
 $KTh_2(VO_4)_3$ , X-ray cryst. struct. determ., Fourier and Patterson method 0-19757  
 $KTiMO_6$  ( $M=Ta, Nb$ ), ion exchange props., synthesis and crystallographic props. (French) 0-28997  
 $KTi(Fe(CN)_6)_2$ , isomer shift of Mossbauer spectra 0-29662  
 $K_2(UO_2)_2F_2 \cdot 2H_2O$ , single cryst., polarised Raman spectra, vibr. modes assignment (French) 0-29728  
 $K_2UO_2(HPO_4)_3$ , synthesis and comp. 0-35516  
 $KUO_2(NO_3)_3$ , fluoresc. decay rates, temp. depend. 0-25429  
 $K_2UO_2(NO_3)_4$ , fluoresc. decay rates, temp. depend. 0-25429  
 $K_1V_3O_{10}$ , hollandite-type struct., synthesis and cryst. struct. 0-29003  
 $K_2V_8O_{26}$ , hollandite-type struct., synthesis and cryst. struct. 0-29003  
 $K_{0.28}WO_3$ , single cryst. X-ray and powder neutron diffr. studies 0-29001  
 $K_{0.33}WO_3$ , supercond. and special phonons, neutron scatt. obs. 0-15643  
 $K_2WO_4$ , hysteresis of phase transitions and modulated structures 0-29169  
 $KXe$ , dye laser induced emission, excimer bands and uses 0-9650  
 $KY(WO_4)_2:Er^{3+}$ , stimulated emission at 300K 0-34951  
 $KY(WO_4)_2:Ho^{3+}$ , 3  $\mu$  stimulated emission at 300K 0-20667  
 $KZnF_3(Fe^{3+}O_2^{2-})$ , overlap and covalency contrib. to zero field splitting, LCAO-MO calc. 0-24850  
 $KZnF_3(Fe^{3+}-V(K)^+)$ , overlap and covalency contrib. to zero field splitting, LCAO-MO calc. 0-24850  
 $KZnF_3:Ni^{2+}$ ,  $Mn^{2+}$ , interference transition electric dipole mechanism 0-34896  
 $KZnF_3:V^{2+}$ , calc. of  $t_{2g}$  antibonding mol. orbital in  $|VF_6|^{1/2}$ , rel. to ESR 0-50174  
 $K_2Zn(WO_4)_3$ , cryst. struct. and polymorphism 0-1996  
 $K_2Zn_3[Fe(CN)_6]_2 \cdot xH_2O$ , X-ray cryst. struct. determ. and refinement (French) 0-28955  
 $K_2Zr_2O_{12}$ , cryst. struct., X-ray study 0-33957  
 $K[B(SO_3Cl)_4]$ , space group 0-33913  
 $K_2[ImO_6O_2] \cdot 5H_2O$ , X-ray cryst. struct. determ. 0-54183  
 $K[InBr_4(H_2O)_2]$ , X-ray cryst. struct. determ. 0-54186  
 $K_{1.75}[Pt(CN)_4]1.5H_2O$ , elec. cond. studies, Peierls transition 0-24901  
 $K_2[UF_6O_2(SO_4)] \cdot H_2O$ , X-ray cryst. struct. determ. 0-54194  
 $K_2[(UO_2)_2F_8 \cdot H_2O] \cdot 3H_2O$ , cryst. struct. (French) 0-49193  
 $KBr$   $^{14}N$  impurities, molecular point defects, EPR isotropic hyperfine triplets 0-2636  
 $KBr$  surface, residence times of Au atoms, time-of-flight meas. 0-10788  
 $K_4(\beta-SiMoW_{11}O_{40}) \cdot 9H_2O$ , X-ray cryst. struct. determ. and refinement 0-28973  
 $KCl$ , aqueous soln., high precision viscosity meas. 0-10695

## potassium compounds continued

- $KLiTi$ , excitation in fund. absorpt. region, luminesc. and thermolum. 0-50433  
 $KrF$ , excimer, electron impact deexcitation, low energy cross-sections and rate consts. 0-1071  
 $(Li,Na,K)(Nb,Ta)O_3$ , pseudo-binary and ternary systems quenched metastable glassy and cryst. phases 0-29935  
 $LiCl-KCl$  molten eutectic mixture,  $PbS$  solubility product and  $Li_2S$  solubility 0-54387  
 $LiF-NaF-KF-K_2GeF_6-GeO_2$  fused mixture, for electrodeposition of Ge powder 0-2979  
 $Li_2K(IO_3)_3$  in  $LiIO_3-KIO_3$  system, lattice parameter, equilib. and metastable phase diagram (Chinese) 0-7538  
 $LiKSO_4$ , thermal and dielec. props. 0-34860  
 $LiKSO_4$ , uniaxial crystal, pyroelectric, thermal expansion, phase transition 0-19966  
 $((NH_4)_xK_{1-x})_2SnCl_6$ , mixed cryst., NQR relax. and reson. 0-54990  
 $Na^+-K^+-F^-SO_4^{2-}$ , asymmetrical reciprocal molten salt system, excess enthalpies 0-30268  
 $NaCl:K_2IrCl_6$  electron irrad., ligand field anal., EPR obs. 0-29612  
 $NaCl-KCl$ , interdiffusion and demixing, electron microprobe anal. (French) 0-54444  
 $NaCl-KCl$  melt, reaction with  $LiO_2 \cdot 2SiO_2$  X-ray, IR exam. 0-55706  
 $NaCl-KCl-H_2O$  mixed electrolyte solns., elec. transport 0-3355  
 $NaNO_3-KNO_3-Ca(NO_3)_2 \cdot 4.09H_2O$  melt, mixed alkali effect 0-34219  
 $Na_2O-K_2O-SiO_2$  glass melt, interdiffusion coeffs. of  $Na^{2+}$ ,  $K^{2+}$ , temp. depend. 0-44348  
 $Na_2O-K_2O-SiO_2$  melts,  $Na^+$  and  $K^+$  diffusion and interdiffusion processes 0-34221  
 $NaVO_3-KVO_3-Al_2O_3$ , melts soln. of  $Al_2O_3$  single crystals 0-20910  
 $Ni_2P_2O_7-K_2P_2O_7-H_2O$  solubility at 25 degrees C, double phosphates formation 0-54381  
 $PbI_2:KI$ , trapped exciton states, absorption spectra 0-50383  
 $phase transition in transverse field with deform. depend., phonon anomaly separation  $KH_2PO_4$  0-39258$   
 $Rb,K_{1-x}H_2PO_4$ , 90° phase matching in freq. doubling, appl. to lasers 0-33088  
 $SiO_2-Al_2O_3-CaO-MgO-Na_2O-K_2O$  effect of partial substitution of  $Na_2O$  by  $K_2O$  on crystallisation 0-10499  
 $SiO_2-Al_2O_3-Fe_2O_3-Na_2O-K_2O-CaO-MgO$  glasses, Mossbauer spectra study 0-39967  
 $SiO_2-Al_2O_3-MgO-K_2O-F$ , glass ceramic, crystn., microstructures rel. to conditions 0-11638  
 $SiO_2-B_2O_3-Al_2O_3-k_2O$ , Ag interdiffusion, optical and NMR studies 0-24683  
 $SiO_2-Li_2O-Al_2O_3-K_2O:Ag_2O(-CeO_4)$  ( $-Sb_2O_3$ ), surface resist. meas. 0-44700  
 $SiO_2-Li_2O-K_2O-ZnO-P_2O_5$ , glass ceramic, phase changes and crystn. processes 0-7562  
 $SiO_2-Li_2O-K_2O-ZnO$  glass ceramic, prep., phase transformations and physical props. 0-45299  
 $SiO_2-M_2O$  ( $M=Na,K$ ) glasses, temp. depend. of elastic modulus 0-40410  
 $SiO_2-Na_2O-K_2O-CaO-MgO-Al_2O_3$  glass melt, anodic dissolution of Ti 0-19949  
 $SiO_2-ZrO_2-Al_2O_3-CaO-Na_2O-K_2O-Li_2O$ , chemical resistant glass for glass fibres 0-21128  
 $SiO_2B_2O_3-K_2O-Al_2O_3-As_2O_3$  glass fibres containing metallic granules, tensile strength, Young's modulus, DC conductivity 0-30023  
 $Sr_2KNb_2O_{15}$ , Raman scatt. experiments in tetragonal tungsten bronze compounds 0-40113  
 $TiO_2$ , solubility in KF aq. solns. 0-34197  
 $V_2O_5-BaO-K_2O-ZnO$  glasses, elect. props. and struct. 0-15547  
 $ZnCl_2-KCl$  melt, viscosity meas. by oscillating cylinder method (Japanese) 0-10696  
 $ZnS-Na_2O-K_2O-SiO_2$ , form. using electric furnace, furnace design 0-11620

## potential dividers see voltage dividers

## potential energy curves and surfaces of molecules

- for Morse curves see Morse potential  
 see also molecular vibration  
 ab initio CI pot. curves, mol. wavefunctions and vibr. freqs. comparison of methods 0-27956  
 ab initio effective core pot. method appl. to  $F_2$ ,  $Cl_2$  and  $LiCl$  0-32625  
 acetylene, core ionised, core-excited and shake-up states, ab initio MRD-CI methods 0-42950  
 adiabatic nuclear group transfer processes in condensed media, electronic energy hypersurfaces 0-25982  
 7-azaindole dimers, photoautomerisation by double proton transfer, double-well excited-state pot. surface 0-11880  
 benzene, noncrossing and degeneracy in Hubbard models 0-14096  
 p-benzoquinones, chlorinated, transferable force field for in-plane vibrs. 0-964  
 curve crossing systems, two-state, non-adiabatic transitions, semi classical Magnus approx. 0-37756  
 cyclobutadiene, noncrossing and degeneracy in Hubbard models 0-14096  
 cyclopentadienyl radical, pot. surface and vibronic states, ab initio CI calcs. 0-47897  
 diatomic molecule, overtone intensities in reson. Raman scatt. 0-48001  
 diatomic molecule, trigonometric pots., refinement 0-9676  
 diatomic molecules, empirical pot. curves, Pade approximant calcs. 0-14184  
 dihydrophenazine derivatives, in 3-methylpentane (ethanol) (PMMA), radiationless processes, temp. depend. 0-43087  
 dihydroxycarbene, singlet and triplet state rot. pot. surfaces 0-32627  
 dissociation, nonadiabatic interactions, conical and Jahn-Teller intersections, classical trajectory method 0-25997  
 B-DNA helix, sugar-phosphate backbone, molecular electrostatic pots. calc. 0-9679  
 electrostatic isopotential maps for large biomolecules, STO transferable bond calc. 0-3571  
 ethyl radical decomposition, mol. dynamics, trajectory studies 0-7780  
 ethylene, core ionised, core-excited and shake-up states, ab initio MRD-CI methods 0-42950  
 fluoroethyl radical, unimol. dissoc., pot. energy characts. and energy partitioning calcs. 0-45488  
 formaldehyde $^+$ , excited state dissoc., nonadiabatic interactions, conical and Jahn-Teller intersections, classical trajectory method 0-25997  
 formaldehyde, adiabatic CI pot. surface LCAO calc., gradient determ., mol. dynamics 0-48056



**potential energy curves and surfaces of molecules continued**

- formaldehyde, ground state, potential energy surface 0-42967  
 formyl radical, electronic struct., dissociation energy and potential energy surface  
 many body perturbation theory and couple cluster doubles calc. 0-23296  
 geometry optimisation with explicit inclusion of electron correlation 0-37748  
 ground state props., coupled cluster and MBPT methods appl. 0-47881  
 homonuclear molecular ions, adiabatic potential curves 0-929  
 inert gas complexes spectroscopic data, geometry, potential energy curve, dissociation energy, equilibrium internuclear distance, determination 0-53018  
 large molecular systems, local potential surface and charges, parametrisation scheme for quantum mechanical computation (*German*) 0-18793  
 methane, vibration-rotation energies of harmonic and combination levels 0-47962  
 methylene peroxide, multiconfig. SCF CI calcs. 0-18803  
 nitrosomethane, ground state and nonvertical  $n-\pi^*$  excitation energy calcs. 0-18804  
 nucleic acids, electronic absorption and emission spectra 0-55989  
 nucleotide bases, electronic absorption and emission spectra 0-55989  
 photochemical reactions, isomerisation, complexing, proton transfer, initiation of internal conversion processes 0-40713  
 polar mol. anion ab initio ground state potential energy surfaces calc. 0-47923  
 1-silabicyclo 2,2,2 octane, double-min. skeletal torsion, microwave spectroscopy 0-47972  
 spectroscopic data analysis, phenomenological and theoretical 0-52963  
 subtilisin charge-relay system, electrostatic potential map, STO transferable bond calc. 0-3571  
 transition metal nitrosyls, appl. of HF and CI calcs. 0-9513  
 triatomic molecular systems, unimol. decomp., exit-channel coupling effects 0-25984  
 triatomic molecules, motion, regular and irregular spectra, theory 0-9590  
 triatomic surface defined over orthogonal bond order coordinates 0-5492  
 tunnelling in double-well potentials, symmetric and asymmetric, periodic orbit theory 0-23488  
 unimolecular decay, nonadiabatic interactions, transition probability as function of Massey parameter 0-35503  
 valence-nonbonded H atoms interaction and two-centre contrib. to total energy of mol. 0-32624  
 van der Waals dimers, intramolecular vibr. dynamics, vibr. predissociation 0-28083  
 vibrational levels inversion splitting, generalised WKB method 0-9585  
 virial relations, for mols. in applied elec. field 0-53087  
 XY<sub>4</sub> molecules, tetrahedral, vibration-rotation energies of harmonic and combination levels 0-47962  
 Al<sub>2</sub>, repulsive region ground state potential curves, SCF with STO basis set calc. 0-14188  
 Al<sub>2</sub><sup>6+</sup>, repulsive region ground state potential curves, SCF with STO basis set calc. 0-14188  
 Al<sub>2</sub>H<sub>6</sub>, electron density distrib., reaction channels and bonding characts., electrostatic mol. potential CNDO/2 calc. 0-23309  
 AlO radical, ground state dissociation energy 0-53159  
 AlOH-HAlO system, intramol. rearrangement, ab initio calc. of potential surfaces and min. energy paths, geom. parameters 0-32623  
 ArBr, emission spectrum and chemiluminescence 0-45508  
 ArBr, potential curves, population distributions and chemiluminescence for B(1/2) and C(3/2) electronic states 0-45509  
 ArH<sup>+</sup>,  $\Sigma^+$  ground state, molecular constants calc. from potential curves 0-9680  
 ArN<sub>2</sub><sup>+</sup>, K<sup>+</sup> clusters, equilibrium configs. and binding energies 0-48115  
 ArO<sup>+</sup>, X<sup>2</sup> $\Sigma^+$  state, potential energy curves and correlation effects, elastic scattering cross sections 0-23502  
 Ar.HBr(DBr), van der Waals complexes, rot. spectra and struct. 0-48055  
 AsF, potential energy curves and dissociation energy, Hulbert-Hirschfelder calc. 0-30210  
 BH, potential energy curve, spectroscopic constants, perturbation theory appl. 0-23341  
 BOH-HBO system, heterovalent isomerism, ab initio calc. of potential surfaces and min. energy paths, geom. parameters 0-32622  
 BiBr, A<sup>2</sup>( $\sigma^+$ ) and X<sup>3</sup>Sigma( $\sigma^+$ ) states, potential energy functions comparison 0-43133  
 BrHe, potential energy curve in Br<sup>-</sup>+He electron detachment, SCF calc. 0-23503  
 BrHe<sup>-</sup>, potential energy curve, in Br<sup>-</sup>+He SCF calc. 0-23503  
 C<sub>2</sub>, potential curves, binding and ionisation energies and configuration. variational cellular method 0-32597  
 C<sub>2</sub>, Swan band system, vibr.-rot. interaction on potential energy curves 0-27965  
 CH, B<sup>2</sup> $\Sigma^-$  state predissociation, calcs. and time resolved spectrosc. 0-23576  
 CH<sup>+</sup>,  $\pi^*$   $\Sigma$  band systems, vibr.-rot. interaction on potential energy curves 0-27965  
 CN<sup>+</sup>, ground state, identity, ab initio CI calcs. 0-5468  
 CN<sup>+</sup>, lower states, potential energy curves, equilibrium distances SCF CI calcs. 0-27957  
 CO, potential curve by variational cellular method, electronic structure, calcs. 0-54591  
 CO, potential curves, binding and ionisation energies and configuration. variational cellular method 0-32597  
 CO+N<sub>2</sub>, electronically inelastic collision, distorted wave calc. and potential energy curve 0-9709  
 CO<sub>2</sub>, spectra, Fermi reson. and classical motion 0-28000  
 CO<sub>2</sub>, dissociation,  $\Sigma_u^+$  state, Wall Porter potential surface, autodetachment and vibr. level population inversion 0-21275  
 C<sub>3</sub>O<sub>2</sub>, bending potential function, vibr. depend. 0-48058  
 COS, mole. potential surface, evaluation from spectroscopic observations 0-43207  
 CaH, low lying electronic states, ab initio SCF-CI calcs. 0-52893  
 CrCl<sub>4</sub>, ligand field states, multiple scattering. Xalpha calcs. 0-47891  
 CrO molecule, B<sup>2</sup> $\pi$  and X<sup>3</sup> $\pi$  states, potential energy curves 0-42962  
<sup>63</sup>Cu<sub>2</sub>, B<sup>2</sup> $\Sigma_u^+$ -X<sup>3</sup> $\Sigma_u^+$  transition, Franck-Condon factors, r-centroids and potential curves 0-43114  
 D<sub>3</sub><sup>+</sup>, ab initio vibr. intervals and vibr. freq. refinement 0-47968  
 F<sub>2</sub>, potential energy curve, spectroscopic constants, perturbation theory appl. 0-23341  
 F<sub>2</sub>, potential curves, binding and ionisation energies and configuration. variational cellular method 0-32597  
 FHF<sup>-</sup>, H bonds, vibr. dynamics calcs. 0-23397  
 GaI, A<sup>0</sup>+X<sup>0</sup> and B<sup>1</sup>+X<sup>0</sup> transitions, isotope shifts, UV and visible spectra obs. 0-53005  
 H<sub>2</sub>, ground state, potential curves, MTX $\alpha_R$  method 0-5482  
 H<sub>2</sub>, potential curves, binding and ionisation energies and configuration. variational cellular method 0-32597  
 H<sub>2</sub><sup>+</sup>+H<sup>-</sup>→H<sub>2</sub><sup>+</sup>+H recombination react., calcs. (*Russian*) 0-55659  
 H<sub>3</sub><sup>+</sup>, ab initio vibr. intervals and vibr. freq. refinement 0-47968

**potential energy curves and surfaces of molecules continued**

- HCC→H+C=C dissociation, trajectory calcs., random vibr. excitation 0-45491  
 HCN<sup>+</sup>, A and B  $\Sigma^+$  states, potential surfaces, ab initio SCF calcs. 0-27959  
 HCOH, prediction, potential energy surface for ground state of formaldehyde 0-42967  
 HNO, low-lying states, potential energy curves 0-9533  
 H<sub>2</sub>O, energy levels, triat. large amplitude vibrs. model appl. 0-23392  
 H<sub>2</sub>O, molecule, shape as function of O-H separation 0-43203  
 HPO, 4-const. valence force potential, from IR(UV) matrix isolation spectra 0-47985  
 He<sub>2</sub><sup>2+</sup>, bound excited states, potential energy curves and rovibronic energy, dissociation 0-23327  
 He<sub>2</sub>, Van der Waals mol. vibr. predissoc. anharmonicity effects 0-52971  
 Hg<sub>2</sub>, electronic structure and photoabsorption calcs. 0-27932  
 I<sup>35</sup>Cl, predissociations in B<sup>1</sup> $\Pi_{0+}$  state 0-1033  
 I<sup>37</sup>Cl, predissociations in B<sup>1</sup> $\Pi_{0+}$  state 0-1033  
 KF, ab initio SCF MO energy, dipole moment and polarisability 0-1085  
 KrF, A state potential in Kr+F<sub>2</sub>(NF<sub>3</sub>)(CF<sub>3</sub>OF), emission spectra calc. 0-7799  
 KrO<sup>+</sup>, X<sup>4</sup> $\Sigma^-$  state, potential energy curves and correlation effects, elastic scattering cross sections 0-23502  
 LiAlF<sub>4</sub>, structure, potential energy surface, Li<sup>+</sup> migration, ab initio LCAO SCF calcs. 0-23305  
 LiAlH<sub>4</sub>, LiBH<sub>4</sub>, ab initio calc. of geom. structure, charge distribution, bonding and potential energy surfaces 0-18796  
 LiF, ab initio SCF MO energy, dipole moment and polarisability 0-1085  
 LiH, correlated potential energy curve, correlation hole concept, restricted Hartree-Fock solutions (*Spanish*) 0-14081  
 LiH, ground state, potential curves, MTX $\alpha_R$  method 0-5482  
 Mg<sub>2</sub>, empirical potential curves, Pade approximant calcs. 0-14184  
 MgH<sup>+</sup>, CI potential curves and cross sections for lowest singlet states 0-23343  
 N<sub>2</sub>, potential energy curve, spectroscopic constants, perturbation theory appl. 0-23341  
 N<sub>2</sub>, potential curves, binding and ionisation energies and configuration. variational cellular method 0-32597  
 NF, potential energy curves and dissociation energy, Hulbert-Hirschfelder calc. 0-30210  
 NH<sub>3</sub>, first triplet state, photodissociation and Rydbergisation investig. 0-53067  
 NH<sub>3</sub>, predissociation of A<sup>2</sup> state from UHF calcs. of potential energy surface 0-1034  
 N<sub>2</sub>H<sub>2</sub> radical, lowest two electronic states 0-925  
 NH<sub>2</sub>Cl, gas <sup>1</sup>A<sub>1</sub> ground state, potential surface 0-32626  
 NO<sup>+</sup>, potential energy curves calcs. 0-5602  
 NaAlH<sub>4</sub>, NaBH<sub>4</sub>, ab initio calc. of geom. structure, charge distribution, bonding and potential energy surfaces 0-18796  
 NaH, A<sup>1</sup> $\Sigma^+$ -X<sup>2</sup> $\Sigma^+$  electronic transition, spectroscopic anal. and potential energy curves 0-48102  
 NaH, ground state, potential curves, MTX $\alpha_R$  method 0-5482  
 NaH II states and NaH<sup>+</sup> ground state, potential energy curves calc. 0-18812  
 Ni, chemisorptive binding of O, CNDO calc. of potential energy curves (*German*) 0-44431  
 O<sub>2</sub>, microwave spectrum, pressure broadening 0-23412  
 OCS, motion, regular and irregular spectra, theory 0-9590  
 OCS, rot.-vibr. levels and semiclassical energy levels 0-37804  
 P<sub>2</sub><sup>+</sup>, electronic states potential energy curves, dissociation energy, ionisation potential, curve fitting 0-32796  
 PF, (PF<sup>+</sup>), potential energy curves and dissociation energy, Hulbert-Hirschfelder calc. 0-30210  
 PtH(D), potential energy curves, r-centroids, Franck Condon factors, rotational depend. 0-28082  
 SF<sub>6</sub>, multiphoton absorption, energy transfer, dissociation probability, laser field interaction, classical trajectory approx. 0-37730  
 SF<sub>6</sub>, photon-enhanced dissociative electron attachment, isotope selectivity 0-18939  
 S<sup>16</sup>O<sub>2</sub>(S<sup>16</sup>O<sub>2</sub>), <sup>1</sup>B<sub>2</sub>(A') state, force field for large amplitude motions 0-43023  
 SBF, potential energy curves and dissociation energy, Hulbert-Hirschfelder calc. 0-30210  
 SiH<sub>4</sub>, 1B<sub>1</sub>(1T<sub>2</sub>) potential energy surface calcs. 0-53085  
 XeF<sub>2</sub>, photodissociation yield in solid Xe and Kr, time-resolved photolum. excitation obs. 0-3372  
 XeO<sup>+</sup>, X<sup>2</sup> $\Sigma^+$  state, potential energy curves and correlation effects, elastic scattering cross sections 0-23502

**potential energy functions**

- see also Lennard-Jones potential; molecular vibration; Morse potential; muffin-tin potential  
 \*He, superfluid, one phonon excitation spectrum and interaction potential 0-54455  
 acetamide, IR spectra, amino group inversion transitions and potential functions 0-43041  
 acetonitrile, quadratic force fields, MOCIC potential functions calcs. 0-5475  
 alkali chlorides, thin film, crystal-vacuum (100) surfaces, molecular dynamics computer simulation 0-34288  
 alkali halide crystal, Gruneisen parameter, volume depend. anal. 0-2135  
 alkali halides, crystal, potential parameters, Hellman function calcs. 0-2181  
 alkali hydrides, Woodcock potential calcs. 0-43136  
 alkali metal, oscillator strengths, nonlocal Simons potential anal. 0-32795  
 alkali metal+inert gas, line profiles, width, shift and asymmetry, square well potential approx. 0-52936  
 alkali metal halides, crystal properties, cohesive energy, bulk modulus and pressure depend., interior force model 0-15035  
 amorphous solids, diffusion of nonspherical particles, correlation effects 0-39337  
 atom+triatom collisional energy transfer, ergodicity in molecular vibr., Henon-Heiles potential 0-18906  
 atom-diatom collinear collision, first order nonlinear matrix differential eqn. 0-37853  
 atomic collisions, rotationally induced transitions in two-state model 0-47945  
 atomic local potential, density functional formalism, linear response theory, appl. polarisability 0-42924  
 azabenzene dimers, C, N, H atom-atom parameters, dispersion energy calcs. 0-23489  
 B-DNA helix, guanine-cytosine base pair, electrostatic potential 0-8003  
 t-butyl cyanide-HF, hydrogen bonded heterodimer, spectroscopic constants from IR and microwave spectra 0-43039  
 chemisorbed atoms on transition metal surface, interaction energy calc. 0-54507



## potential energy functions continued

- chemisorption, pot. energy function of two H atoms around Pt atom protruding from metallic Pt surface 0-10781  
 complex potential energy surface systems, nonradiative processes, WKB calcs. 0-45133  
 computer modelling of matter, conf., Anaheim, USA (March 1978) 0-51954  
 condensed matter, SCF theory, orbital and pot. functions calc., eq. of state 0-44463  
 confining pot., eigenvalue problem for Schrodinger operator 0-27154  
 Coulomb Hamiltonian, one-dimensional, spectral props. 0-47859  
 crystal orbital calculations, deformation density method, transferable integrals 0-38992  
 crystal orbital calculations, deformation density method, transferable integrals, neutral atom pots. 0-38993  
 crystal-liquid phase boundary, pair distrib. functions and free energy functionals 0-24734  
 cyanomethane-HF, hydrogen bonded heterodimer, spectroscopic consts. from microwave spectrum 0-43038  
 cyclic voltammograms at spherical electrodes, switching pot., drop size effects, digital simulation technique 0-40766  
 cyclopentene, mol., pot. functions of bending modes 0-9753  
 diatomic mol. scatt., Schrodinger eqn. phase shift differences for some trigonometrical potentials 0-43132  
 diatomic mol. scatt., Tietz phase shift differences, semi-empirical relations, Varshni and Hulbert-Hirschfelder pots. 0-9673  
 diatomic molecule, pots. superposition, rel. to lattice dynamics, mol. consts. calcs. 0-5598  
 diatomic molecule, trigonometric pots., refinement 0-9676  
 diatomic molecules, homonuclear, molecular dynamics, translation-rotation coupling 0-44094  
 2,5-dihydrofuran, mol., pot. functions of bending modes 0-9753  
 dilute aqueous solutions, Monte Carlo studies of struct., review 0-54101  
 dilute gases, transport props., softness expansion for inverse power pot. 0-28589  
 dimethyl aluminium hydride dimer, electron density distrib., electrostatic mol. pot. anal. 0-52885  
 2,3-dimethylbuta-1,3-diene, IR, Raman spectra, torsional pot. function, thermodynamic function 0-43046  
 1,4-dioxadiene, mol., pot. functions of bending modes 0-9753  
 effective pair potentials, first order derivation of differential equations 0-1041  
 electron + molecule, scatt., polarisation pot. determ. 0-17721  
 empirical diatomic pot. functions comparison, BiBr  $A^3\Sigma^-(0^+)$  and  $X^3\Sigma^-(0^+)$  states calc. 0-43133  
 ethyl methyl sulphide, low freq. vibr. spectra, methyl torsional pot. functions and internal rot. 0-5543  
 ethylmethylamine, low freq., vibr. spectra, methyl torsional pot. functions, mol. struct. 0-43045  
 flexible double minimum potential, modified Gauss perturbed harmonic oscillator 0-1042  
 fluid, hard dumbbell mols., reference pot., perturbation theories, spherical reference systems 0-28898  
 fluid with nearly spherically symmetric molecules, thermodynamic perturbation theory 0-14985  
 fluids, hard core, distrib. functions and equation of state, zero-separation theorem 0-44089  
 fluoromethane, quadratic force fields, MOCIC pot. functions calcs. 0-5475  
 fluoromethane-HF, H-bonded complex, ab initio calcs. (French) 0-52866  
 formamide, IR spectra, amino group inversion transitions and pot. functions 0-43041  
 grain boundary segregation, computer simulation using Mie type interatomic pot. 0-54259  
 graphite surface interaction with He atom 0-34316  
 Hamiltonians, effective, appl. to atomic pot. transferability in hydrocarbons 0-42933  
 heavy metal diatomic halides, Wasastjerna pot. function, force consts. internuclear separations and binding energies 0-14187  
 high temperature electron diffraction, review 0-52237  
 hot matter, conductive opacities and free-free Gaunt factors 0-3361  
 inert gas atoms, pot. energy curves analysis 0-53083  
 inert gas diatomic molecule, excited state pots., fast calc. 0-9490  
 inert gas dimer ions, photofragment spectroscopy using fast ion beams 0-9755  
 inert gas systems, absolute total cross-section data anal. 0-53093  
 interacting particle systems, configuration with min. pot. energy per particle 0-4517  
 interatomic force calcs., zeroth-order exchange energy for optimised atomic basis set 0-43131  
 interatomic potential for atomic pairs, Thomas Fermi model with quantum corrections 0-32797  
 ion + polar molecule collision freq., thermodynamic model 0-43145  
 ion clusters, 3-body pots., SCF energy partitioning calcs. 0-18953  
 ionic crystal, thermodynamic props. calc., pot. energy function approach 0-54407  
 Kratzer molecular and general pot. superposed 0-9674  
 metallic glasses, structure and formation, thermodynamic props., cluster relaxation approx. 0-54143  
 metals, Gruneisen parameters, interatomic forces, pseudopot. calc. 0-44165  
 metals, interatomic potentials of Na, K, Al, Cu, Fe from phonon spectra 0-19744  
 methanol ( $d_3$ ), OH stretch fund., torsion-rot. levels, IR spectra obs. 0-32711  
 methyl groups in solids, tunnelling freq. for internal rotation in pot. function 0-49134  
 methylacetylene, quadratic force fields, MOCIC pot. functions calcs. 0-5475  
 microphysics to macrochemistry, discrete simulations, review 0-54102  
 molecular crystals, optimum packing in atom-atom approx., algorithm and computer program 0-1960  
 molecular fluids, coupling of rotation and translation 0-38892  
 molecular fluids, ref. system selection and average Mayer-function perturbation theory 0-38891  
 molecular homeomorphism, structural, between nuclear pot. and electronic charge density 0-42968  
 molecular liquid, mol. dynamics simulation, multiple time step methods and improved potential function 0-54098  
 molecular systems, saddle points and min. energy paths, constrained simplex optimisation procedure 0-42943  
 molecular vibrational energy transfer, potential well depths 0-43156

## potential energy functions continued

- molecules at equilibrium, nuclear-nuclear potential energy regularities 0-32793  
 non-spherical molecule ensemble, background correl. in statistical thermodynamic calcs. 0-36958  
 non-surface scattering, interatomic pot. functions (Japanese) 0-45192  
 nonadiabatic reactions, rate const. temp. depend., influence of charact. features of elastic scatt. 0-37852  
 nuclear matter, variational techniques, review 0-22748  
 one centre pot. energy functions and two electron integrals for STO's 0-14070  
 one-dimensional particle-in-the-box problem, perturbation theory illustration using champagne bottle situation 0-36816  
 organic compounds, low freq. anharmonic vibr., pot. function determ., Raman and IR spectra obs. 0-52997  
 ovalene, isolated ultra cold mol., intermediate level structure of  $S_2$  state 0-28048  
 perchlorohydrocarbons, crystn., intermol. potential-function models 0-49168  
 phospholipid inter- and intra-molecular interactions, PCIOCC and pot. function calc. 0-3570  
 polar molecule clusters, 3-body pots., SCF energy partitioning calcs. 0-18953  
 polyatomic mols., multiple photon IR processes, reviews 0-43125  
 polyatomic mols., nuclear charge model and valence force consts. prediction 0-43022  
 polynucleotides, double helical, conformation, pairwise pot. function calcs. 0-53173  
 porphyrins, reson. Raman spectra, selection rules, normal coord. treatment 0-53175  
 Poschl-Teller, symmetric, position-momentum uncertainty products for exactly solvable potentials 0-12939  
 isopropyl chloride, torsional pot. function, far IR and Raman obs. 0-28022  
 quasi-linear molecules, low frequency anharmonic vibrations, pot. function determ., Raman and IR spectra obs. 0-52997  
 rare gas solids, Debye Waller factors from unpaired elastic force model 0-19896  
 Rosen-Morse, symmetric, position-momentum uncertainty products for exactly solvable potentials 0-12939  
 simple fluid, mol. dynamics simulation, including three-body interactions 0-54100  
 solvated electrons, optical spectra and model potentials 0-30318  
 meso-tetraphenylporphine, potential parameters of H migration tunnel rates calcs. 0-5600  
 s-tetrazine, mol., pot. functions of bending modes 0-9753  
 thioacetamide, IR spectra, amino group inversion transitions and pot. functions 0-43041  
 third row element mols., general harmonic force field, SCF-MO-MNDO and freq. calc., MOCIC pot. 0-27948  
 transition metals, adatom surface diffusion characts., pair potential calcs. 0-39446  
 triatomic van der Waals complex, vibr. predissoc. and photodissoc. lifetimes 0-9661  
 valence-nonbonded H atoms interaction and two-centre contrib. to total energy of mol. 0-32624  
 water, liq., Monte Carlo studies of struct., review 0-54101  
 water, Monte Carlo simulation 0-54113  
 Al + Al, repulsive region ground state pot. curves, SCF with STO basis set calc. 0-14188  
 $Al^{3+} + Al^{3+}$ , repulsive region ground state pot. curves, SCF with STO basis set calc. 0-14188  
 AlOH-HAIO system, intramol. rearrangement, ab initio calc. of pot. surfaces and min. energy paths, geom. parameters 0-32623  
 Ar, aqueous soln., dil., energy and struct., pair pot. energy function, Monte Carlo calc. 0-54107  
 Ar, liquid, velocity autocorrelation from memory function, hard-sphere and square well pots. 0-28893  
 Ar-Ar pot. parameters, from CO in Ar matrix, empirical evaluation 0-48057  
 Ar-Kr, glory structure in total cross section, crossed supersonic atomic beam,  $n(x)-6$  potential 0-48060  
 Ar + Kr, elastic collision total cross-section, low energy 0-5603  
 Ar<sub>2</sub>, excited state pots., fast calc. 0-9490  
 Ar<sub>2</sub>, interatomic potential single parameter 0-48059  
 As<sub>2</sub>S<sub>3</sub>, chalcogenide glass, effect of press. on elastic props. 0-10590  
 BOH-HBO system, heterovalent isomerism, ab initio calc. of pot. surfaces and min. energy paths, geom. parameters 0-32622  
 Bi, spheres, mean inner pot., elec. biprism and interf. electron microscopy 0-49063  
 C-Ar pot. parameters, from CO in Ar matrix, empirical evaluation 0-48057  
 CO in Ar matrix, vibr. freq. shift and interaction pot., force-field calcs. 0-47958  
 CO + ZZ 0-9745  
 CO<sub>2</sub>, low energy electron (positron) collisions, ab initio adiabatic polarisation pots. 0-14240  
 CO<sub>2</sub> + ZZ 0-9745  
 C<sub>3</sub>O<sub>2</sub>, mol., pot. functions of bending modes 0-9753  
 Cu, pair potentials calcs., elastic props. calc. 0-49176  
 F<sup>-</sup>(H<sub>2</sub>O)<sub>2</sub>, 3-body pots., SCF energy partitioning calcs. 0-18953  
 F<sub>2</sub>O, absorpt. band freq. and intensities, electro-optical parameters, pot. energy, IR spectra 0-37812  
 GeO<sub>4</sub> compounds, vibr. pot. function, force consts., isotopic shifts, mean vibr. amplitudes 0-23395  
 H bonded  $\nu_{X-H}$  band, dynamic theories survey 0-52983  
 H, hyperfine shift and interatomic pots. in inert buffer gas 0-5491  
 H<sub>2</sub>, electron scatt., equivalent exchange pots., algebraic variational method, 2p-2p and 2s-2p transitions 0-18931  
 H<sub>2</sub>, interaction at jellium surface, adsorption curves, independent atom effective pot. study 0-29259  
 HCN...HF, hydrogen bonded heterodimer, spectroscopic consts. from microwave spectrum 0-43037  
 HF, nucl. mag. shielding and susceptibility, elec. field depend., SCF-Hartree Fock method 0-18791  
 (HF)<sub>3</sub>, 3-body pots., SCF energy partitioning calcs. 0-18953  
 H<sub>2</sub>O, complete quartic force field calc., algorithm 0-37736  
 H<sub>2</sub>O dimer, intermolecular pot. functions from ab initio calcs. 0-5473  
 H<sub>2</sub>S, complete quartic force field calc., algorithm complete quartic force field calc., algorithm 0-37736  
 H<sub>2</sub>Se, complete quartic force field calc., algorithm 0-37736



**potential energy functions continued**

- H<sub>2</sub>HF, H-bonded complex, ab initio calcs. (French) 0-52866  
 He+Ar, interatomic pot. well depth, SPFD pot., diffusion, viscosity and second virial coeff. 0-5599  
 He+H<sub>2</sub>, collinear collision, first order nonlinear matrix differential eqn. 0-37853  
 He+He, interatomic force calcs., zeroth-order exchange energy for optimised atomic basis set 0-43131  
 Hg vapour, absorpt. spectrum, 1849 Å line, self-broadening, interatomic interaction (French) 0-32661  
 K, pair potentials calcs., elastic props. calc. 0-49176  
 KI:Ti, A<sub>T</sub> emission, linear polarisation, appl. of semi-classical WKB formalism 0-45134  
 Kr-Kr(Ar)(Xe), glory structure in total cross section, crossed supersonic atomic beam, n(x)-6 potential 0-48060  
 Li<sup>+</sup>(OH)<sub>2</sub>, 3-body pots., SCF energy partitioning calcs. 0-18953  
 Mo, pair potentials calcs., elastic props. calc. 0-49176  
 N<sub>2</sub>, electron scattering, local-exchange approx. for intermediate-energy-differential cross sections 0-48094  
 N<sub>2</sub> gas, structure factor 0-43137  
 N<sub>2</sub>, liquid, mol. correl. functions, effective pair pot. evaluation 0-10476  
 N<sub>2</sub>, low energy electron (positron) collisions, ab initio adiabatic polarisation pots. 0-14240  
 NH<sub>3</sub>HF, H-bonded complex, ab initio calcs. (French) 0-52866  
 NO+Ne(Ar)(Kr)(Xe), angle depend. intermolecular pot., crossed beams study 0-9682  
 NO<sub>2</sub>, complete quartic force field calc., algorithm 0-37736  
 Na isoelectronic series, wave functions and effective pots. of valence electron 0-47873  
 Na, velocity autocorrelation from memory function, hard-sphere and square well pots. 0-28893  
 Na(3<sup>2</sup>P)<sub>1/2</sub>+Na(3<sup>2</sup>S)<sub>1/2</sub>, collisional excitation transfer, pot. symm. rules and cond. function 0-9690  
 Ne+Ne, pot. curve derived from gas and solid scatt. data, ESMSV pot. 0-1040  
 Ne<sub>2</sub>, excited state pots., fast calc. 0-9490  
 O-Ar pot. parameters, from CO in Ar matrix, empirical evaluation 0-48057  
 O<sub>2</sub>, liquid, mol. correl. functions, effective pair pot. evaluation 0-10476  
 O<sub>2</sub>, isotope effects, complete quartic force field calc., algorithm 0-37736  
 OH-HF, H-bonded complex, ab initio calcs. (French) 0-52866  
 Pd-Zn, L<sub>11</sub> type intermetallic phase, X-ray diff. study of lattice compression 0-49182  
 SF<sub>6</sub>, gas, thermodynamical and spectral props., effect of angle-dependent part of dispersion forces 0-43138  
 SO<sub>2</sub>, complete quartic force field calc., algorithm 0-37736  
 S<sup>16</sup>O(S<sup>18</sup>O)<sub>2</sub>, B<sub>2</sub>(A') state, force field for large amplitude motions 0-43023  
 SiO<sub>4</sub><sup>4-</sup> compounds, vibr. pot. function, force consts., isotopic shifts, mean vibr. amplitudes 0-23395  
 Xe-Xe(Kr), glory structure in total cross section, crossed supersonic atomic beam, n(x)-6 potential 0-48060

**potential energy surfaces for collision processes**

- acetic acid, ionised, pot. energy profiles for unimol. reactions 0-43210  
 acetic acid-pyridine, H-bonding, proton transfer, isolated system, solvent effect, MO calc. 0-55629  
 atom+atom, small angle differential cross section, semiclassical description 0-28086  
 atom+ion, electron capture, non relativistic theory and Coulomb pot. anal. 0-32804  
 bimolecular diffusion-controlled reversible reactions, detailed equilb. principle 0-7770  
 binary collisions, time correlation functions, influence of bounded trajectories 0-43143  
 classical small-angle anisotropic potential scattering, comparison with Li<sup>+</sup>+N<sub>2</sub>(CO) results 0-1043  
 curve crossing collisions, transition probabilities 0-32631  
 diatom-atom gas mixture, infrared line shape, rotational lines, influence of collision duration 0-43110  
 double well potential, transfer and tunnelling rates, density matrix calcs. 0-30209  
 electron+molecule, scatt., polarisation pot. determ. 0-17721  
 formaldehyde decomposing to H<sub>2</sub>+CO, reaction path Hamiltonian 0-45486  
 gaseous relax. phenomena, few-level approx. validity 0-53097  
 hypersurfaces, transition state location, energy minimisation method 0-52904  
 intermolecular interaction theory, modern state, rel. to large mols. 0-14186  
 intermolecular interactions and potential energy wave calcs., review 0-43140  
 internuclear parameters measurement method using total scatt. of fast electrons 0-32857  
 ion+permanent dipole, capture rate consts., transition state theory, summary of theories 0-28091  
 ion+polar molecule collision freq., thermodynamic model 0-43145  
 ion-Rydberg atom collision cross sections, classical trajectory Monte Carlo calcs. 0-43174  
 laser-controlled unimolecular and bimolecular processes, field-depend. rate const. 0-11906  
 model potential, phase shifts 0-927  
 molecular collision processes in presence of picosecond laser pulses, radiative transitions 0-23479  
 molecular systems, saddle points and min. energy paths, constrained simplex optimisation procedure 0-42943  
 nonadiabatic transitions, linear curve crossing problem, generalised Stueckelberg method 0-28085  
 nonempirical calculation methods, review 0-35505  
 organic ions, pot. energy profiles for unimol. reactions 0-43210  
 polyatomic mols., dissociation reaction path Hamiltonian 0-45486  
 symposium contrib., Florida, USA (March 1979) 0-51946  
 thermal chemistry as an exercise in photochem. 0-3379  
 transition state theory, absolute rate theory and variational formulations, Porter Karplus pot. surface 0-16642  
 Ar+H<sub>2</sub>, vibr. transition rates, thermally averaged, Monte Carlo trajectory calcs. 0-23519  
 CH+p-H<sub>2</sub>(He), collisional pumping of A-doublet transitions, pot. energy surface 0-23516  
 CO+N<sub>2</sub>, electronically inelastic collision, distorted wave calc. and pot. energy curve 0-9709

**potential energy surfaces for collision processes continued**

- Cs+Xe, Cs spectral line profile and absorpt. transitions 0-47944  
 Cs(5D<sub>5/2,m=1/2</sub>)+inert gas, dipole-induced transitions, pot. curves, oscillator strength 0-32816  
 D+F<sub>2</sub>, DF initial vibr. energy distrib., IR chemiluminesc. obs. 0-45497  
 F+H<sub>2</sub>, two electronic pot. energy surfaces, collinear quantum calcs. 0-16646  
 H+D<sub>2</sub>, pot. curve, thermal energy absolute integral cross-sections meas. 0-53096  
 H+F<sub>2</sub>→HF+F, vibr. adiabatic and static distorted wave Born approx. calcs. 0-7768  
 H+H<sub>2</sub>, reaction, quasi-classical trajectory calcs. using new pot. energy surface 0-7767  
 H+N<sup>3+</sup>, charge exchange, assoc. reaction, rel. to interstellar gas 0-7763  
 H+Zn<sup>2+</sup>(Cd<sup>2+</sup>)(B<sup>2+</sup>)(Mg<sup>2+</sup>)(C<sup>6+</sup>), electron capture by slow ions, pseudo-crossing 0-43176  
 H<sub>2</sub>, elastic electron scatt. at 1 keV, Glauber model 0-43178  
 H<sub>2</sub>+CO(N), pot. surfaces, HF calc. 0-16669  
 H<sub>2</sub>+D→HD+H, three dimens. ab initio pot. energy surface 0-55646  
 H<sub>2</sub>+CO excited products dissociation, proton transfer dynamics, correl. diagram anal., crossed beam obs. 0-48079  
 HCl+Ar(Xe), infrared line shape, rotational lines, influence of collision duration 0-43110  
 HN<sub>3</sub>+F, strong interactions in gas-phase reactions, arrested relax. IR chemilum. obs. 0-7773  
 He+H<sub>2</sub>(μH), interaction pots. and rot. scatt. calcs. 0-43158  
 He<sup>+</sup>+H<sub>2</sub>, DIM approx. pot. energy surfaces and nonadiabatic coupling 0-23330  
 He(2s<sup>2</sup>S,2<sup>3</sup>S)+Ne(Ar)(Kr)(Xe), Van der Waals forces, one-electron model pot. calcs. 0-14094  
 I+HCl, quenching of I(5<sup>2</sup>P<sub>1/2</sub>), temp. depend., time resolved at. absorpt. spectrophotometry 0-32655  
 K+N<sub>2</sub>(CO), rot. inelastic scatt., quantum effects, simple model surfaces 0-48064  
 Li+inert gas atom, low energy, excitation, emission cross sections and polarisation fractions 0-37867  
 N<sub>2</sub><sup>+</sup>+He, vibronic excitation, curve-crossing trajectories 0-23520  
 N<sub>2</sub><sup>+</sup>+Li(Na)(K), 50-1000 eV, crossed beams, electron transfer and excitation 0-14226  
 N<sub>2</sub><sup>2+</sup>(<sup>2</sup>P<sub>0</sub>)+H, charge transfer, ab initio CI pot. curves and coupling-matrix elements 0-37878  
 N<sub>3</sub><sup>+</sup>(<sup>1</sup>S)+H, charge transfer, ab initio CI pot. curves and coupling-matrix elements 0-37878  
 Na+Na, excited atoms, coupling terms, asymptotic pot., excitation energy transfer 0-23530  
 Na+Ne, differential cross section at thermal energy, expt. and theoretical results comparison 0-37851  
 Na+Ne, Na(3p) excitation 0-1056  
 Na+Xe, nonreson. two-photon absorpt., 4s excited states and pot. energy curves, close coupled eqns. 0-48068  
 Ne+HD, j=0 to 1 rot. excitation, differential cross sections, time of flight obs. 0-48104  
 Ne<sub>2</sub><sup>+</sup>+He, pot. energy surface, reaction cross sections, ab initio calcs. 0-11881  
 O<sup>+</sup>+H<sub>2</sub>, linear approach, pot. energy surface for H<sub>2</sub>O<sup>+</sup> 0-47922  
 O<sup>+</sup>+inert gas, potential energy curves from elastic scatt. cross sections 0-23502  
 O<sup>+</sup>+Ne, pot. energy curves, nonadiabatic coupling matrix elements 0-53110  
 O<sub>2</sub><sup>+</sup>, electron impact dissociation, recomb., pot. energy curves calcs. 0-53150  
 O(D)+Ar(Kr)(Xe), inelastic collisions, spin-orbit coupling 0-5605  
 OH+H<sub>2</sub>, pot. energy surface, barrier heights and transition state geometry, POL-CI calc. 0-55649  
 OH+p-H<sub>2</sub>(He), collisional pumping of A-doublet transitions, pot. energy surface 0-23516  
 O(<sup>1</sup>P,<sup>1</sup>D)+H<sub>2</sub>(<sup>1</sup>Σ<sup>+</sup>), H<sub>2</sub>O, potential energy surfaces, extended basis first-order CI study 0-7776  
 O(<sup>1</sup>P)+H<sub>2</sub>→OH+H, potential energy surface, theory 0-45492  
 U+U, K-shell ionis., classical relativistic trajectory method appl., 1, 10 GeV/n 0-43129  
 U<sup>+</sup>+U(U<sup>+</sup>)(U<sup>2+</sup>), elastic scatt. in plasma, interaction pots. and momentum transfer 0-38534

**potential scattering**

- 1/N perturbation theory, large orders by inverse scatt. in 1-dimens., anharmonic oscillators 0-22214  
 anisotropic, classical, small-ang., theory, comparison with Li<sup>+</sup>+N<sub>2</sub>(CO) results 0-1043  
 anisotropic, in classical mechanics (Russian) 0-27183  
 atom, neutral, scatt. by exponential corrugated pot. 0-25512  
 atom+atom/ion, total cross section, explicit bounds by geometric method 0-43130  
 atomic electron resonant potential scattering in a low-frequency laser field 0-23545  
 atomic resonances, S-wave pot. scatt., coord. rot. method 0-28104  
 atomic scattering amplitudes, two-cluster, partial-wave, analytic continuation 0-52045  
 Born series rearrangement in model space, resolvent operator expansion 0-13422  
 bound states for higher angular momenta, scatt. length 0-22209  
 boundedness of total cross-sections in potential scattering 0-79  
 charged particle scatt. in quantising mag. field 0-46853  
 composite Coulomb scatt., eikonal approx., short range interactions 0-31534  
 correspondence principle, rel. to potential step scattering, theory 0-46761  
 correspondence principle for potential x<sup>2N</sup> 0-42088  
 Coulomb off shell two body amplitudes, numerical computation 0-46858  
 curve crossing collisions, transition probabilities 0-32631  
 dilute gases, transport props., softness expansion for inverse power pot. 0-28589  
 eikonal approximation, analytic props. 0-32038  
 elastic scattering by central field, unified semiclassical description 0-31575  
 electron+atom potential scatt. in low freq. laser field, perturbation theory 0-43191  
 electron scatt. by any electrostatic multipole field, Born partial wave amplitude 0-53128  
 electron scattering by Coulomb potential in Born approx., bremsstrahlung statistics 0-5665  
 electron scattering in LF laser field, sum rule and classical limit 0-18978



**potential scattering** continued

- Faddeev eqn. soln. in adiabatic approx. with separable pots. (*Russian*) 0-52437
- Faddeev equations, two-potential formula, three-body scattering 0-4893
- finite-rank potential that reproduces the Pade approximant 0-42106
- heavy particle scatt. in solids, classical deflection ang. using Brinkman pot., numerical calc. 0-11525
- higher-order Levinson's theorems and the high-temperature expansion of the partition function 0-4558
- infrared radiation in potential scattering 0-42098
- interacting electron system, orthogonality catastrophe 0-6757
- Kratzer molecular and general pot. superposed 0-9674
- long range oscillating pots., scatt. theory and dispersion relations 0-22213
- multichannel wave eqns., explicit perturbative solns. 0-31577
- nonlinear Hamiltonian systems, integrability by inverse scatt. method 0-46864
- nonlinear Schrodinger eqn., inverse scatt. problem method 0-4577
- nonsingular potential, scatt. length by iterative-perturbation method 0-27160
- off energy two body t-matrix in the R-matrix theory (*Russian*) 0-22780
- off-shell scattering by Coulomb-like potentials 0-31560
- one dimensional wave function for the effective Hamiltonian of non-local potential 0-46847
- oscillating potentials, spectral and scatt. theory 0-52072
- oscillatory pots. of slow decay, moller wave operators and S operator unitarity 0-4559
- partial wave expansions summation in scatt. by short range pots. 0-31570
- particle scattering, low-energy, two-pot. formulation with  $r^{-4}$  interaction 0-31552
- path integral representation of pot. scatt. amplitudes 0-17820
- quantum scattering by external metrics and Yang-Mills potentials 0-31535
- quantum scattering theory, quasi-classical limit 0-4562
- refined Born approximation 0-77
- Saito potential, off-energy-shell unitarity 0-18207
- scattering amplitude for low energy, two sided estimates 0-46873
- spinless particle scattering by central pots., soln. 0-27156
- square-well potential, integral eqns. and scatt. solns. 0-31451
- static inhomogeneities, elastic low angle multiple scatt. (*Russian*) 0-46874
- transport theory integral eqn. soln. in Green's function formalism, scatt. amplitudes 0-4566
- unified formalism for quantum and classical scattering theories 0-100
- variable phase method for scatt. on non-local spheroidal pot. 0-95
- variational methods calcs., comparison of convergence 0-52043
- Wigner transform and the eikonal approximation for nonlocal potentials 0-13423
- Yukawa scatt. and impact parameter amplitudes using Legendre Pade approximants 0-22227
- $H+e^-(e^+)$ , elastic scatt., asymptotic effective pot. 0-14233

**potentials (bioelectric)** see *bioelectric potentials*

**potentials (electric)** see *electric potential*

**potentiometers**

see also *voltage measurement*

biopotentiostat of simplified design 0-35589

**powder diffraction cameras** see *cameras; X-ray crystallography apparatus*

**powder metallurgy**

- allows, two component, sintering 0-20847
- alloy manufacture for vacuum deposited resistive foils of low surface resistivity (*Polish*) 0-35124
- compact growth in liquid phase sintering 0-20835
- compaction, by impact of projectiles launched by compressed air 0-2973
- compaction equations, best description of expt. data 0-2974
- composite, metals and materials, powder metallurgical parts, development, and manufacture of semifinished products 0-50578
- composite materials (*German*) 0-20849
- conference on powder metallurgy, Bowness-on-Windermere, England (Oct.-Nov. (1978)) 0-17713
- densification on heating under high pressure, to 80 kbar 0-25602
- electric sintering (*German*) 0-25598
- electrical contacts based on powder metallurgy and powder composites 0-29902
- electrical discharge powder compaction 0-35135
- electronic industry appl. 0-29903
- Fe sintered material, operating performance, effect of polymer and graphite lubricant additives 0-11785
- magnetic materials technology developments, high-energy (*Italian*) 0-54914
- metallurgical-physical considerations rel. to metal powder prod. 0-11595
- metallic glasses props., development and appl. 0-19710
- micropowder, cyclic classification, using variable electric field, device design 0-36982
- mischmetal-Co-Cu-Fe-Mg, mag. props. 0-35353
- mischmetal-Co-Cu-Mg, mag. props. 0-35353
- Ni powder 2JJ, porous, effect of sintering conditions in struct. and strength 0-20823
- particles produced by gas evaporation, form., growth and interaction 0-16220
- Permalloy, pressing velocity effect on quality of compacts 0-20834
- Permalloy powders, electric pulse shaping and sintering 0-25605
- porous materials, production method using stainless steel gauzes, exam. of hydraulic characteristics 0-16243
- prealloyed powder blending, composite materials fatigue and tensile props. (*French*) 0-20850
- sintered materials, operating performance, effect of polymer and graphite lubricant additives 0-11785
- sintering, activated 0-25611
- sintering, rel. to definition powder metallurgy 0-20841
- sintering, surface oxide layer effects, oxide dissolution process, anal. 0-11588
- sintering at 1 to 10 MPa, melting mechanism (*German*) 0-35122
- sintering of solids containing several dissolved gases 0-20836
- solid state sintering, compact length change 0-11593
- steel, boriding in powdered mixture with high activity 0-30164
- steel, Cr (13 wt.%), sintered, organometallic complex addition effects on mech. props. 0-25595
- steel, high speed, W-Mo-Co-Cr-V, production from atomized powder 0-20837
- steel, Mn-Cr-Mo, Mn-V-Mo, high-strength heat-treatable sintered 0-50575
- powder metallurgy** continued
- steel, stainless, fibre reinforced porous coating, isostatically compressed for bone ingrowth 0-35134
- steel-Al bimetallic wire for overhead lines, manufacturing methods 0-16247
- vacuum treatment, method of calc. evacuation time and permeability 0-20827
- Ag, loosely packed powder, sintering SEM and dilatometry obs. 0-20843
- Ag, powder, sulphide coated, Fritt effect on appl. of DC voltage (*German*) 0-25599
- Ag, solid state sintering, compact length change 0-11593
- Ag, spherical powder, struct. of sintering necks in compacts 0-11594
- Ag<sub>3</sub>Sn-Hg, metallic powder-liquid system, correlation between hardness and evolution and sintering states 0-25614
- Al and Al alloy granules, hot rolling, angle parameters and forward slip 0-25601
- Al powder, resist.-sintability (*Japanese*) 0-16228
- Al powder thin foil, prep. for TEM study 0-42310
- Al sintering, low temp., form. of interparticle metallic contacts 0-20844
- Al-C, dispersion hardened, effect of processing parameters on mech. props. 0-20826
- Al-C alloys, dispersion hardened exam. of production method using pressed powders 0-16244
- Al-rare earth alloys, granules, rolling to form foil, exam. 0-20825
- Al-Zn-Mg-Cu-Co (6.5, 2.5, 1.5, 0.4 wt.%), fatigue crack propag. 0-55521
- Al<sub>2</sub>O<sub>3</sub> targets manufacture, for vacuum thin film deposition (*German*) 0-11586
- CC TaC based hard metal, non-stoichiometric sintering, mech. props. 0-25616
- CU-Zr-(Cr), powder metallurgical alloys, thermomech. treatment effect on props. 0-50660
- Co, powder, hot pressing on steel substrate, densification kinetics 0-40290
- Cr-C-Ni alloys, exam. of activated sintering 0-16241
- Cu, loosely packed powder, sintering SEM and dilatometry obs. 0-20843
- Cu powder, electrodeposition prep. conditions, statistical anal. 0-20828
- Cu powder, electrodeposition, mathematical model for current efficiency and electric power consumption 0-20831
- Cu, powder, exam. of consolidation process based on electronic structure of solid 0-20842
- Cu, powder, hot pressing on steel substrate, densification kinetics 0-40290
- Cu powder, two layered medium dynamic compaction 0-35138
- Cu powders, electroless tinning 0-25607
- Cu, solid state sintering, compact length change 0-11593
- Cu-Al-Ni (14, 8 wt.%),  $\gamma$ -martensitic, sintered high damping 0-50577
- Cu-Nb-Sn, multifilamentary supercond. composite wires, fabrication on laboratory scale and mech. props. 0-29897
- Cu-Ni, sintered, props. and degree of nonhomogeneity 0-20848
- Cu-Sn warm pressed compact prep. 0-35136
- Cu<sub>60</sub>Zr<sub>40</sub>, amorphous powder, production using gas-water atomisation unit 0-7518
- Fe alloy electrodes, rolled from powders, sintering problems 0-25608
- Fe and Fe-C, (0.8 wt.%), sintered, hot forging and chemothermal treatment, effect on wear resistance 0-25606
- Fe atomised powder, sintering effect on recrystn., mech. props. 0-40292
- Fe, carbonyl pore struct. orientation, shrinkage anisotropy effect 0-20845
- Fe, high dispersion ferromagnet, magnetic powder defectoscopy material 0-35137
- Fe powder, density distrib. in rolling deformation region 0-40288
- Fe, powder, exam. of consolidation process based on electronic structure of solid 0-20842
- Fe, powder, hot pressing on steel substrate, densification kinetics 0-40290
- Fe Powder, resist.-sintability (*Japanese*) 0-16228
- Fe powder, sponge and atomized types, steam oxidation, pore closure and surface hardness 0-45441
- Fe powder compacts, pressed under static or vibr. load, shrinkage anisotropy during sintering 0-50574
- Fe powders, Co- or Cu-plated, prep. by rad. and chem. plating, mag. props. 0-44867
- Fe, sintered and pressed, props., effect of atomised Fe powder particle size distrib. 0-11601
- Fe sintered compact, shrinkage and mech. props., admixed zinc stearate lubricant effect 0-45402
- Fe/Fe-Cr composite powder, X-ray diffr. exam. of densification during rolling 0-40289
- Fe-C (2. wt.%), sintering shrinkage kinetics 0-20829
- Fe-C-Mn (0.5, 0.6 wt.%), powder forged, mech. props. 0-21096
- Fe-Cu, liquid phase sintering 0-16232
- Fe-Cu-O-(Ni) powder, atomized, reduction and decarburizing annealing parameters 0-25603
- Fe-Mn powders, reactions with NH<sub>4</sub>Cl and (NH<sub>4</sub>)<sub>2</sub>CO<sub>3</sub> 0-11597
- Fe-Ni heterogeneous alloys, ferrite, martensite and austenite phase distrib., effect on mech. props. 0-45363
- Fe-Ni-C, atomized, O/C ratio effect, particle size on annealing kinetics, physicochemical props. 0-20832
- Fe-VC-WC(TiC), sintering, densification 0-25615
- Fe-WC-VC(TiC), sintering, densification 0-25615
- Ge<sub>30</sub>Si<sub>70</sub>, hot press sintering 0-50572
- Mn-V-Mo-C master alloys, development for low alloyed PM steel 0-50576
- Mo, powder, defective structure and activated sintering, exam. 0-16240
- Mo, prep. by powder metallurgy technique, appl. in lighting industry 0-29904
- Mo-Mn powder mixture, X-ray diffr. exam. of reaction between Mo and Mn, during sintering 0-16242
- Mu-Cr-Mo-C master alloys, development for low alloyed PM steel 0-50576
- Nb<sub>3</sub>Sn, composite supercond., powder metallurgical prep. 0-2981
- Nb<sub>3</sub>Sn, high-current A-15 microcomposite material 0-44781
- Nb<sub>3</sub>Sn-Cu, high-current A-15 microcomposite material 0-44781
- Ni alloy powders hot hydrostatic pressing of disk, capsule design 0-20839
- Ni base alloys, mathematical-physical considerations rel. to metal powder prod. 0-11595
- Ni, powder, hot pressing on steel substrate, densification kinetics 0-40290
- Ni powder, porous, relationships between mech., physical, and microstructural characts. 0-20846
- Ni powder, resist.-sintability (*Japanese*) 0-16228



**powder metallurgy continued**

- Ni powder, sintered, use of extruded porous materials as fuel cell electrodes 0-40853  
 Ni, powder, subjected to vibratory milling, exam. of plastic deformation, recrystallisation, sintering 0-16234  
 Ni-base superalloy, conventional and powder metallurgical,  $\sigma$ -phase precipitation 0-11646  
 Ni-Cr-Co-Ti, superalloy sintering thermochemical surface treatment 0-25617  
 Ni-Fe alloy, Ni base cathodes, powder metallurgy technique 0-29903  
 Ni-ZrB<sub>2</sub> powders, densification by hot pressing 0-25604  
 Ni<sub>3</sub>Al-Ti(Cr)(Fe)(Zr)(Mo)(W), powder, X-ray spectral analysis exam. 0-16239  
 Pb powder size and shape distribution via image anal. 0-16221  
 SmCo<sub>5</sub>, powder, comminution temp. effect on mag. props. 0-39819  
 SmCo<sub>5</sub>, sintered permanent magnet manufacture 0-20838  
 $\alpha$ -Sn, compact prep., from  $\beta$ -Sn containing 0.1 at.% Ge 0-55320  
 Sn fine powders, electrodeposition, effect of cathodic current density on structure 0-16238  
 Ta powder, cathodic electrodeposit, effect of electrolyte composition and process parameters, on particle size distribution 0-16233  
 Ti base alloys, mathematical-physical considerations rel. to metal powder prod. 0-11595  
 Ti, porous structure, change in presence of liq. phase (Russian) 0-16223  
 Ti powder, exam. of mechanochemical comminution, in the presence of epoxy resin or polysulphide rubber 0-16236  
 Ti powder, resist.-sinterability (Japanese) 0-16228  
 Ti-Al (Sn), porous, effect of Al and Sn on sintering 0-20830  
 Ti-Al (4 wt.%), sintered, long-time strength 0-40529  
 Ti-Al system, compact growth in liquid phase sintering 0-20835  
 TiC-Fe-Cr powder mixture, exam. of milling condition effects 0-16237  
 TiC-Ni powder compact, wetting problems in sintering 0-11596  
 V<sub>2</sub>Ga, high-current A-15 microcomposite material 0-44781  
 V<sub>2</sub>Ga-Cu, high-current A-15 microcomposite material 0-44781  
 W and W-Re alloy, prep., appl. in lighting industry 0-29904  
 W fibre reinforced, Co powder alloys, reactions and recryst. 0-11603  
 W, powder, subjected to vibratory milling, exam. of plastic deformation, recrystallisation, sintering 0-16234  
 W, powders, defective structure and activated sintering, exam. 0-16240  
 W production, H reduction of WO<sub>3</sub>, starting specific surface effect on kinetics 0-11599  
 W-Cr powder alloys, sintering in presence of Cu-Ni liq. phase 0-16246  
 W-Cu, porous material, skeletal type, produced by liquid phase sintering, exam. of mech. strength, determ. resistance 0-16245  
 W-Ni, liquid phase sintering 0-16232  
 W-Ni, liquid phase sintering 0-25613  
 W-Ni-Fe (5(2), 5(2) wt.%) pore formation, effect on mech. props. 0-45396  
 WC powder, chemical plating with Co and Co-P 0-25593  
 WC-Co from directionally carburized WO<sub>3</sub>-C-Co<sub>3</sub>O<sub>4</sub> mixtures, sinking (Japanese) 0-11589  
 WC-Co powder, prep. by direct carburisation of WO<sub>3</sub> in presence of Co<sub>3</sub>O<sub>4</sub> 0-50573  
 WC-Co powder form. from WO<sub>3</sub> and Co<sub>3</sub>O<sub>4</sub> carburization, C behaviour (Japanese) 0-7517

**powder sprayed coatings**

- adhesion, ASTM test 0-50812  
 detonation deposition, conducting powder temp. meas. 0-11559  
 detonation spraying, powder velocity, methods of meas. 0-16530  
 plasma deposited materials, control of mech. props. 0-11560  
 Cr<sub>2</sub>C<sub>3</sub> (Cr<sub>7</sub>C<sub>3</sub>) based coatings, detonation deposited, wear resist., 20-1000°C 0-11843  
 Ni-Al spraying powders, alumina and aluminide formation 0-25920  
 WC-Co (15 wt.%), alloy VK15 coating on Ti-Al, detonation sprayed, antifriction props. 0-21188

**powder spraying**

- detonation deposition, of coatings, conducting powder temp. meas. 0-11559  
 detonation spray deposition, metering devices 0-40256  
 detonation spraying, powder velocity, methods of meas. 0-16530  
 preferred orientation minimization by spray drying 0-3098  
 YIG, hot spraying to give fine, free flowing, sinterable powder 0-20865  
 ZrO<sub>2</sub> powders, stabilised, for plasma spray-coatings 0-20869  
 Al<sub>2</sub>O<sub>3</sub> coating on Ti, detonation deposition, impact interaction parameters 0-40602  
 MnZn, pressing powders, spray dried, pressing behaviour and props. 0-11617  
 WC-Co (15 wt.%) detonation spraying on to Cr-Ni steel with automatic powder feed 0-25558

**powder techniques** see powder technology**powder technology**

- see also densification; hot pressing; powder metallurgy; powder spraying; sintering  
 AGR fuel element design improvement 0-23112  
 ceramic, compaction during liq. phase sintering 0-55335  
 ceramic powder suspensions, sputter drying (Russian) 0-55324  
 ceramics, rate constants of wet and dry ball mill grinding (Japanese) 0-29895  
 compaction, of metal powders 0-40279  
 condensation powder, production by plasma jets, math. model (Russian) 0-7513  
 cryochemical techniques, prod. ultrafine ceramic powders 0-55336  
 diamond, synthesis and characterisation 0-50580  
 dustiness, determ. method 0-45455  
 electrostatic coating, charging characts. of some powders, deposition efficiency 0-50780  
 ferrites, hard and soft, conference on powder metallurgy, Bowness-on-Windermere, England (Oct.-Nov. (1978)) 0-17713  
 flame spraying process, of powders, intercrystn. corrosion of base material (Czech) 0-30158  
 freeze drying, prod. ultrafine ceramic powders 0-55336  
 G 0-25640  
 gas-water atomisation process unit, for producing amorphous powders 0-7518  
 glass, rate constants of wet and dry ball mill grinding (Japanese) 0-29895  
 high-speed shaping of free-flowing materials, computer investigation 0-25591  
 liquid phase sintering, elementary mechanisms, soln.-reprecipitation 0-50571

**powder technology continued**

- mixes, ordered, characterisation using X-ray microanal. 0-16215  
 mixing indices for multicomp. solid mixtures 0-39300  
 nonconducting powder, temp. determ. in detonation deposition 0-226  
 particle motion and segregation by density difference in V-type mixer 0-45250  
 particle size analysis by automatic sieves 0-52380  
 particles in nonisothermal plasma jet, trajectory and temp. calcs. (Russian) 0-7514  
 perlit, low temp., processes occurring during firing 0-11607  
 permanent magnet alloys manufacture, Co-mishmetal alloys (Polish) 0-35132  
 plasmochemical synthesis, powder dispersion control 0-55332  
 plasmochemical synthesis, powdered infusible compounds, props. 0-55330  
 polypropylene powder, cold compaction, product strength, heat treatment effects 0-11621  
 polyvinylidene chloride co-polymer powder, cold compaction, product strength, heat treatment effects 0-11621  
 pressing, role in producing zero defect parts (French) 0-40380  
 PVC powder, cold compaction, product strength, heat treatment effects 0-11621  
 refractory powders, wet decompaction and compaction 0-35150  
 Sialon, prep. and charact. of ultrafine powders 0-11604  
 sintering, study of phase contacts formation in porous disperse structs. (Russian) 0-20811  
 solution techniques, prod. ultrafine ceramic powders 0-55336  
 spherical particles production, equal-sized, controlled disintegration of free jets 0-7515  
 spray drying, prod. ultrafine ceramic powders 0-55336  
 stereological application, in study of compacting process, elec. and mech. props. (French) 0-40286  
 suspensions, dielectric separation of solid particles 0-16213  
 vibrated bed electrostatic separation 0-16641  
 Zircon ceramic, exam. of development and fabrication 0-11608  
 AlN, plasmochemical synthesis, powder dispersion control 0-55332  
 AlN powder, plasma-chem. and self-propag. high-temp. thermoplastic slips, synthesis 0-25633  
 AlN, prep. and charact. of ultrafine powders 0-2983  
 AlN, synthesis and impurities 0-55329  
 AlN, synthesis in low-temp. plasma 0-16257  
 Al<sub>2</sub>O<sub>3</sub> ceramics, with thermoplastic bond, prep. 0-45254  
 Al<sub>2</sub>O<sub>3</sub>, grinding material, grain shape optimization (Polish) 0-29916  
 Al<sub>2</sub>O<sub>3</sub>-AlN phase diagram and reaction sintering of transparent cubic ALON spinel 0-25669  
 $\beta''$ -Al<sub>2</sub>O<sub>3</sub>-Na<sub>2</sub>O-Li<sub>2</sub>O (8.85, 0.75 wt.%) pressing powders, prep. by spray drying 0-40294  
 Al<sub>2</sub>O<sub>3</sub>-Y<sub>2</sub>O<sub>3</sub> ceramics, corrosion protective W coating 0-35367  
 3Al<sub>2</sub>O<sub>3</sub>·2SiO<sub>2</sub>, mullite, synthesis by freeze drying 0-16252  
 Al<sub>4</sub>Si<sub>2</sub>C<sub>3</sub>, synthesis, X-ray diffraction pattern, lattice constants 0-50581  
 B C powders, effect of C on sintering 0-40312  
 B pellets preparation from powder, for X-ray materials testing under pressure 0-50569  
 BN, high-temp. plasmochem. synthesis, control of props. 0-55333  
 BaFe<sub>2</sub>O<sub>9</sub> powder, chemical plating with Co, Co-P, Ni-P and Cu 0-25593  
 CaO, produced from CaCO<sub>3</sub> powder decomp. in vac. and in CO<sub>2</sub> 0-45255  
 Ca<sub>10</sub>(PO<sub>4</sub>)<sub>6</sub>(OH)<sub>2-2x</sub>O<sub>x</sub>□<sub>x</sub> polycryst. sintered bodies, prep. and thermal props. 0-25624  
 Co powder, isostatic compression, elec. cond., densification models (French) 0-55321  
 Co-powder, isostatic compaction (French) 0-40285  
 Cu PM parts, improving cond. by pretreatment of green compact 0-20824  
 Cu-Ni-Co, alloy pre-form prep. through reduction of sintered oxides 0-40284  
 Cu-Ni-Fe, alloy pre-form prep. through reduction of sintered oxides 0-40284  
 Cu-Ni-Fe, spinodally decomposable, densification using four different powder methods 0-40283  
 Cu<sub>1-y</sub>Ag<sub>y</sub>InS<sub>2-x</sub>Se<sub>x</sub>, for solar photovoltaic cells 0-10982  
 Fe, water atomized powder, compaction, bending strength (French) 0-40287  
 Fe-SiO<sub>2</sub>-Al<sub>2</sub>O<sub>3</sub> Lisakovskii concentrate mixture, sintering process, temp. thermal treatment (Russian) 0-55317  
 Fe<sub>x</sub>O<sub>y</sub>, sintered metallised compacts, pore struct. by Hg porosimetry 0-40280  
 MgO powders, hot pressing, mechanisms 0-40300  
 MoS<sub>2</sub>, self-propag. high-temp. synthesis, wear props. 0-2975  
 MoSi<sub>2</sub>, ceramic additives effect on sintering, recrystallisation 0-40306  
 6NaCl.CdCl<sub>2</sub>, 60 wt.% powders, Suzuki phases prep. and stability 0-35123  
 NbB<sub>2</sub>, hot pressing 0-25635  
 Ni-Fe, alloy pre-form prep. through reduction of sintered oxides 0-40284  
 Pd sponge powder, sintering shrinkage kinetics 0-29900  
 Si-Al-O-N sintered ceramic, microstruct., phase composition and transformation mech., mech. props. 0-40309  
 SiAlON powder, prod. by reaction clay+C+N<sub>2</sub> 0-40295  
 SiC, form. by vapour phase method 0-25623  
 SiC, grinding material, grain shape optimization (Polish) 0-29916  
 Si<sub>3</sub>N<sub>4</sub>, prep. and charact. of ultrafine powders 0-2983  
 Si<sub>3</sub>N<sub>4</sub>, reaction sintered, microstruct. charact. 0-35145  
 Si<sub>3</sub>N<sub>4</sub>, sintering in powder bed with addition of MgO sintering aid 0-29910  
 Si<sub>3</sub>N<sub>4</sub>, slip casting from aqueous suspension, reactions with HCl and NaOH 0-16259  
 Si<sub>3</sub>N<sub>4</sub>/Al<sub>2</sub>O<sub>3</sub>, powder compact, electron microprobe investigation of reactions (French) 0-26009  
 Si<sub>3</sub>N<sub>4</sub>-MgO (2.5 wt.%) hot pressed, tensile creep testing 0-40423  
 Si<sub>3</sub>N<sub>4</sub>-Y<sub>2</sub>O<sub>3</sub>(CeO<sub>2</sub>), hot pressed, sintered, microstruct., flexural strength and fractographic anal. 0-40293  
 Si<sub>3</sub>N<sub>4</sub>-O-Al<sub>2</sub>O<sub>3</sub>, solid soln., prep., effect of Si<sub>3</sub>N<sub>4</sub> powder reactivity 0-45256  
 SiO<sub>2</sub> particles, movement and heating in air plasma jet (Russian) 0-7522  
 SiO<sub>2</sub>-Al<sub>2</sub>O<sub>3</sub> (36.6 wt.%) plasma prep. powder, metastable immiscibility and microstruct. during sintering 0-35143  
 SrFe<sub>12</sub>O<sub>19</sub>, powder, chemical plating with Co, Co-P, Ni-P and Cu 0-25593  
 SrO.nFe<sub>2</sub>O<sub>3</sub> isotropic ferrite magnets, manuf. process and mag. props. (Japanese) 0-29915  
 TiC, sintering and grain growth, metallographic anal. 0-25642



# powder technology continued

- TiC<sub>1-x</sub>N<sub>x</sub> formation in high temp. N flow, ultra disperse powder, thermodynamic anal. (*Russian*) 0-55325  
 TiN, from high-temp. reaction of NH<sub>3</sub> and TiCl<sub>4</sub>, physicochem. props. 0-55334  
 TiN powder, plasma-chem. and self-propag. high-temp. thermoplastic slips, synthesis 0-25633  
 TiO<sub>2</sub>-ZrO<sub>2</sub>; submicron powders, vapour phase production from TiCl<sub>4</sub>-ZrCl<sub>4</sub>-O<sub>2</sub> system 0-40301  
 TiS<sub>2</sub> synthesis 0-35141  
 (U,Pu)O<sub>2</sub> powder, FBR fuel prep. by Au/PuC coprecipitation process 0-814  
 U<sub>1-x</sub>alkali metal halide system, prep. 0-50568  
 UO<sub>2</sub> fuel fabrication by the AUC powder process 0-13744  
 UO<sub>2</sub>-20CeO<sub>2</sub> mixed powder, X-ray and microprobe exam. of homogenisation 0-25609  
 W powders, influence of geometrical props. on compaction (*Russian*) 0-20818  
 W/Cu powders, liq. phase sintering, particle rearrangement 0-45253  
 WS<sub>2</sub>, self-propag. high-temp. synthesis, wear props. 0-2975  
 YAG, production of densely sintered ceramic, exam. of recrystallisation during sintering 0-11609  
 ZrB<sub>3</sub>, synthesis and impurities 0-55329  
 ZrC powders produced by various methods, impurities 0-11615  
 ZrC, synthesis and impurities 0-55329  
 ZrO<sub>2</sub>, stabilized porous refractory, mech. strength 0-35322  
 ZrO<sub>2</sub>-Y<sub>2</sub>O<sub>3</sub> powder, prep. for plasma spheroidisation, sputter drying (*Russian*) 0-55324  
 ZrS<sub>2</sub> synthesis 0-35142  
 ZrSiO<sub>4</sub>-Al<sub>2</sub>O<sub>3</sub> system, particle rearrangement kinetics due to densification 0-25626

# powders

- see also densification; granular structure; particle size; powder sprayed coatings; powder spraying; sintering  
 aerosol, ultradisperse condensational, formation by plasma-jet powder evaporation (*Russian*) 0-55721  
 adhesive strength, meas. installation 0-40644  
 ceramic, ultrafine, prod. by cryochemical, freeze drying, spray drying or soln. techniques 0-55336  
 ceramic powder, thermal stresses during spheroidisation process (*Russian*) 0-40386  
 ceramic powders, equipment for sublimation drying, exam. 0-25733  
 compacted, stress relaxation pattern, moisture effect 0-20994  
 composition of finely dispersed powders, electrostatic device for determ., exam. 0-25588  
 compressed powder mixture electrical conductivity calc. (*German*) 0-10940  
 consolidation process, exam. of quasimelt in pressing, sintering stages 0-20816  
 dendritic particle characterisation of automatic methods 0-25590  
 diamond particles, finely dispersed, in active C shock wave produced powder, electron diff. identification 0-1903  
 diamond powder, explosion synthesized, impurity distrib. and thermal stability 0-15147  
 dimension and shape evaluation by SEM 0-40278  
 dynamic flow rates, meas. apparatus 0-14860  
 electrostatic behaviour, methods for study 0-52266  
 flow, gravity-induced particle, stochastic theories 0-14798  
 glass sintered powder porous bodies, liq. penetration mechanism (*Japanese*) 0-53853  
 glass theoretical aspect of sintering 0-20883  
 graphite, model for testing liq. cryst. method for detection of small objects in optical microscopy 0-9034  
 gypsum, powder Jeener-Broekaert three-pulse sequence, inhomogeneous lineshapes, second rank spin interactions 0-39891  
 laboratory techniques for powder handling 0-45475  
 magnetic particle inspection oxides, evaluation 0-40657  
 metal powders, packed, complex mag. permeability calcs. 0-29583  
 metallic, thermal diffusivity meas., constant rate heating method (*Japanese*) 0-6572  
 metallic fine particles, theory of melting in the Percus-Yevick limit, appl. to particles on SiO<sub>2</sub> and C substrates 0-20060  
 microscopic quantitative analysis 0-22475  
 mixture electric-discharge sintering mass transfer and homogenization 0-20817  
 morphological anal. of fine particles 0-20813  
 nonconducting powder, temp. determ. in detonation deposition 0-226  
 particle nonequaxiality effect on size distrib. meas. in pulse conductometric anal. 0-20833  
 particle profiles, morphological characterisation derived from Walsh coeffs. 0-50816  
 PMMA coated frit powder prep., corona-charging props. (*Japanese*) 0-25891  
 PMR spectra of powders with spin 1/2 nuclei arranged in isosceles triangular mag. config., shape function 0-2648  
 polyethylene, microfine powder prod. for dispersions (*German*) 0-29920  
 polymers, corona-charging props. 0-6946  
 polystyrene, sorption of organic vapours, glassy-state relaxation induction and meas. 0-44415  
 powder-water-oil system, cohesion of powder particles with water, rheological prop. (*Japanese*) 0-14647  
 PVC, sorption of organic vapours, glassy-state relaxation induction and meas. 0-44415  
 resistive alloy foils, manufacture and props. of multicomponent alloys (*Polish*) 0-35131  
 rolling bottle device, for measuring flow of liqs. and powders 0-6174  
 SAW interactions, for various directions of propagation 0-49486  
 semiconductor, prep., freeze drying of solid solutions, solvent choice 0-11583  
 β'-sialon compositions, reaction sintering obs. 0-55337  
 sintered bodies and powders, particle size distributions from chord and area distributions (*German, English*) 0-35126  
 sintering, electrical resistance, apparatus 0-16217  
 sintering and random structures, volume diffusion and creep effects 0-35125  
 sintering kinetics, powder kinetics, variation of mechanism dependent exponent, with coordination number and neck size 0-20815  
 specific heat, meas. apparatus for 4.3-300K 0-227  
 specific surface, determ. using Hg porosimetry 0-29896  
 specific surface, X-ray determ. method 0-47012

# powders continued

- superconductor MM range receiver for radio astronomy 0-21919  
 surface area, meas. by Monosorb surface-area analyser using Brunauer-Emmett-Teller eqn., reproducibility 0-36979  
 tetragonal powders, X-ray intensity corrections for preferred orientation 0-1880  
 ultra fine, prod. by rotating friction mill, mechanism in initial wear region (*Japanese*) 0-25589  
 X-ray powder patterns for tetragonal and hexagonal polycrystalline materials, improved indexing method 0-24312  
 Al powder, liq.-solid phase transforms. (*French*) 0-45294  
 AlN, ultradispersed powder, IR spectra 0-50312  
 Al<sub>2</sub>O<sub>3</sub>, tensile and compressive strengths of fine powder bed (*Japanese*) 0-25780  
 B, appl. in abrasive pastes 0-21114  
 B dispersed fractionated powder, struct. obs. 0-19703  
 BN, O content depend. on heat treatment temp., neutron activation analysis 0-16356  
 BN powder, wurtzite sphalerite struct. phase transition, effect on substruct. 0-25690  
 BaB<sub>2</sub> powder, surface struct. effects on thermionic emission characts. and vapour pressure (*Japanese*) 0-50506  
 Bi, fine, precipitation on passivated electrodes 0-2977  
 n-Bi<sub>2</sub>Te<sub>2.88</sub>Se<sub>0.12</sub>, extrusion deformed, powder dispersion degree influence on thermal and elec. props. (*Russian*) 0-39366  
 C blacks, powders, resistivity rel. to compression (*French*) 0-35349  
 CdS powder layers, surface pot. dark decay, moisture sorption and heat treatment effects 0-18038  
 Co powder, isostatic compression, elec. cond., densification models (*French*) 0-55321  
 Co-powder, isostatic compaction, mech. and elec. props. (*French*) 0-40285  
 Co<sub>2</sub>NiO<sub>4</sub> powder prep. by freeze drying of solid solutions, solvent choice 0-11583  
 Cu, compressed powder, thermoelectric effects 0-20155  
 Cu, electrolytic, particle profiles, morphological characts. derived from Walsh coeffs. 0-50816  
 Cu-Al powder compacts, elec. resist., temp. depend. 0-49690  
 Cu-Pb, gas-atomised, particle profiles, morphological characts. derived from Walsh coeffs. 0-50816  
 Fe, atomised powder, props. 0-25600  
 Fe, BH<sub>4</sub> reduced, coercive force and remanence ang. variation 0-44879  
 Fe, electrolytic, particle profiles, morphological characts. derived from Walsh coeffs. 0-50816  
 Fe powder, sponge and atomized types, steam oxidation, pore closure and surface hardness 0-45441  
 Fe powder compact, apparent density, mixing, and friction, zinc stearate lubricant effect 0-45403  
 Fe, prepared by BH<sub>4</sub> process, comp. and stability 0-44878  
 Fe pyrophoric powders, stabilising layer form. during passivation, saturation moment meas. 0-44865  
 Fe, sponge, particle profiles, morphological characts. derived from Walsh coeffs. 0-50816  
 Fe, water atomized powder, compaction, bending strength (*French*) 0-40287  
 GaP, powder, electroluminesc. excitation by SAW, nonlinear effects 0-16104  
 Ge, electrodeposition from fused salts 0-2979  
 Ge powder, diamag., strong mag. particle form., mag. props., EPR (*Russian*) 0-54863  
 Ge powder/Au electrode contact pot. difference, grain size depend. 0-44723  
 KCl:TiCl<sub>3</sub> lattice defects, X-ray line profile obs. 0-24455  
 KCl(Br)(I) with alkali and halogen impurities, colour centre deformation induced nonradiative decay 0-7387  
 K<sub>2</sub>SO<sub>4</sub> powder, IR photothermal radiometry absorption spectra, 295-942K 0-26088  
 MgO, tensile and compressive strengths of fine powder bed (*Japanese*) 0-25780  
 Mn<sub>2</sub>SiO<sub>3</sub>, effect of vibration during sintering, on electrical resistivity 0-16258  
 Mo, powder specimens, fatigue and threshold behaviour under high cycle fatigue 0-40487  
 Mo-W alloy, fatigue and threshold behaviour under high cycle fatigue 0-40487  
 NH<sub>4</sub>HSO<sub>4</sub>, ferroelectric powder dielectric behaviour particle size depend. 0-55046  
 NH<sub>4</sub>[TeO<sub>4</sub>], powder, Raman spectrum 0-39016  
 Nb<sub>3</sub>Al core wires and pressed powder compacts, supercond. transition 0-34541  
 NbC micropowder surface finishing of metals, surface struct. 0-11842  
 Ni alloy powder, crystallised by supercooling methods, struct. props. (*Russian*) 0-54483  
 Ni powder, neutron diff. study of Debye-Waller factor using reverse Fourier time-of-flight method 0-49050  
 Ni powders, stereological appl. in study of compacting process, elec. and mech. props. (*French*) 0-40286  
 Ni-Al thermally reactive powder, particle heating dynamics during plasma deposition 0-16179  
 Ni-W sintered powder pressings, intermetallic phases (*Russian*) 0-55349  
 NiF<sub>2</sub>, powder, preferred orientation, X-ray intensity corrections 0-1880  
 PbO, compressed powder magnetoresistance and apparent carrier mobility 0-35669  
 Pd, confined geometry, p-wave supercond. or itinerant ferromag. 0-11129  
 Sb, prod. by β-Sb<sub>2</sub>O<sub>3</sub> reduction, atomic H effect 0-2978  
 p-Sb<sub>48</sub>Bi<sub>0.52</sub>Te<sub>3</sub>, extrusion deformed, powder dispersion degree influence on thermal and elec. props. (*Russian*) 0-39366  
 α-SiC monocrystalline grains, mech. props. and grain separation (*Polish*) 0-40554  
 SiC, power, electroluminesc. excitation by SAW, nonlinear effects 0-16104  
 SiO<sub>2</sub> fused powder, difference between white and black silica, devitrification rates 0-28918  
 SiO<sub>2</sub>, tensile and compressive strengths of fine powder bed (*Japanese*) 0-25780  
 SiO<sub>x</sub> powder and vac. deposited, amorphous struct., X-ray diff. meas. 0-1931  
 Sm<sub>0.4</sub>R<sub>0.4-x</sub>M<sub>2</sub>Co<sub>3</sub> (R=Gd, Dy, M=Pr, Nd), temp. coeff. of magnetisation 0-34688  
 Sn, fine, electrodeposition from chloride-fluoride electrolytes 0-11598



**powders continued**

- Sn-Bi fine alloy powder, electrodeposition, electrolyte comp. effect 0-7519  
 SnO<sub>2</sub>, finely dispersed, Lamb-Mossbauer factor 0-39930  
 TZM powder alloys, fatigue and threshold behaviour under high cycle fatigue 0-40487  
 TiC micropowder surface finishing of metals, surface struct. 0-11842  
 TiC<sub>1-x</sub>N<sub>x</sub> formation in high temp. N flow, ultra disperse powder, thermodynamic anal. (*Russian*) 0-55325  
 TiCl powder, Debye-Waller parameter by neutron diffr. 0-29140  
 U, hydriding kinetics, 13.3 and 26.6 kPa, 50-250°C 0-16725  
 UO<sub>2</sub> powder, sintering effect of compaction 0-20874  
 UO<sub>2</sub> powder, temp. depend. of atomic thermal displacements, Rietveld profile-refinement procedure 0-49190  
 WC micropowder surface finishing of metals, surface struct. 0-11842  
 WO<sub>3</sub> powders, hopping mechanism and Poole-Frenkel effect, elec. props. determ. 0-49734  
 Zn-Cd liquid/Fe-Ni-Al mag. powder, effective viscosity of composites (*Russian*) 0-54424  
 Zn<sub>0.2</sub>Co(Ni)<sub>0.8</sub>O . 1.1Al<sub>2</sub>O<sub>3</sub> powders, ZnO vaporisation from 0-16675  
 ZnF<sub>2</sub> powder, preferred orientation, X-ray intensity corrections 0-1880  
 ZnO powders, electron-beam-induced desorption, phase-sensitive detection 0-54502  
 ZnO, UV luminesc. spectral distrib., comparison with single crystals., excitons role 0-55167  
 ZrO<sub>2</sub>-SiO<sub>2</sub> powder mixture for optical glass polishing 0-28367  
 ZrO<sub>2</sub>-Y<sub>2</sub>O<sub>3</sub> powder, prep. for plasma spheroidisation, sputter drying (*Russian*) 0-55324  
 ZrO<sub>2</sub>-SiO<sub>2</sub>-αAl<sub>2</sub>O<sub>3</sub> mixed powders, solid state reactions 0-40337

**power cables**

- see also *power overhead lines*; *superconducting cables*; *underground cables*  
 pipe-type, low-cycle fatigue tests 0-7731

**power control**

- see also *load regulation*  
 electro-optic modulator, servo controlled, for CW laser power stabilisation and control 0-19060  
 rechargeable fuel cell battery output power stabilisation theory 0-35674  
 InGaAsP InP DH lasers, optical power and wavelength stabilisation 0-38036

**power conversion**

- see also *direct energy conversion*  
 energy fluctuations power conversion, in diode circuit, thermodynamics 0-17911  
 solar cell arrays, DC to AC power conversion and utility interfacing, techniques, requirements and components used 0-45703  
 solar power satellite, appl. of solid state microwave technology 0-40870  
 solar power satellite, microwave power transmission technology 0-40868

**power converters**

- GaAs antenna mounted FET for DC-RF conversion in solar power satellite 0-40870

**power factor**

- Al-Al<sub>2</sub>O<sub>3</sub>-metal capacitor, capacitance and power factor rel. to voltage and temp. changes 0-54802

**power factor measurement**

- No entries

**power factor meters** see *power factor measurement***power factor Q** see *Q-factor***power generation, electric** see *electric power generation***power generators, electric** see *electric generators***power lines** see *power cables***power measurement**

- see also *wattmeters*

- defibrillator energy meters, traceable calibration methods 0-30928  
 digital, errors sources and suppression (*Rumanian*) 0-47078  
 FIR laser, optically pumped, nearly transparent power monitors 0-5773  
 heat receivers with moving heat carrier, freq. characts. 0-4733  
 laser beam energy distribution reconstruction using data from grid of bolometers 0-53350  
 laser power and energy meters, calorimeter system for calibration 0-38024  
 RF, method using sampling oscilloscope and LF multiplier, up to 1 GHz 0-37055  
 solar cells, photoelectrochem. and p-n junction, power conversion efficiency monitoring 0-50989  
 table top pulsed solar simulator, design and construction, for testing solar cell arrays powering artificial satellites 0-45696

**power overhead lines**

- see also *overhead line conductors*; *power cables*; *power transmission*  
 audible corona noise, assessment of human response using acoustic menu 0-19149  
 corona discharge from water drops, expt. 0-33851

**power overhead transmission lines** see *power overhead lines***power packs** see *power supplies to apparatus***power plants**

- see also *solar power*; *space vehicle power plants*; *wind power plants*  
 coal-fired, trace element anal. of radiological effluents 0-21426  
 environmental effect and protection measures (*German*) 0-26574  
 fuel cell power plant development and commercialisation program 0-16797  
 gas system entropy waves dissipation 0-19395  
 Labadie Power Plant plume, lidar obs. of particulate density distrib. and behavior 0-55956  
 MHD, environmental assessment of a coal-fired open-cycle MHD power plant 0-35795  
 MHD baseload power plant for intermediate and peaking duty 0-35702  
 operational danger levels, mathematical model determ. (*German*) 0-13633  
 site zone evaluation using computer-aided methods 0-861  
 thermal plant siting, regional policy and ecological aspect of landscape 0-862  
 ZnCl hydrate battery system, design fabrication and testing of 5 MWh system at BEST Facility 0-35763

**power station computer control**

- CANDU power plants, automated anal. system for control of secondary coolant chemistry 0-18446  
 direct chemical control of the WWR-SM research reactor 0-696  
 distributed microcomputer-based control system for a large scale solar total energy system 0-30396

**power station computer control continued**

- industrial management program for energy conservation 0-40849  
 MWR feedwater and recirculation flow, minicomputer-based digital control 0-23027  
 neutron instrumentation for protection and control of nuclear reactors (*French*) 0-32407  
 nuclear reactors, online, computer applications, information processing, control, monitoring, data acquisition and evaluation 0-47595  
 reactor protection computer systems, statistical verification of reliability 0-32417  
 solar total energy system, Fort Hood, control system 0-30397

**power station control**

- see also *power station computer control*  
 nuclear power plant licensing procedures in the UK 0-27708  
 solar central receiver plant, dynamic simulation of thermal-hydraulic characts. of Na-cooled plant 0-30400  
 wind turbine generator, control and stabilisation of DOE/NASA Mod-I 0-30370

**power stations**

- see also *energy resources*; *gas turbine power stations*; *geothermal power stations*; *hydroelectric power stations*; *nuclear power stations*; *power plants*; *solar power stations*; *steam power stations*; *tidal power stations*  
 290 MW compressed air storage power station, construction and commissioning 0-16842  
 atmospheric heat releases, effects 0-40942  
 atmospheric radioactivity, radiological impact from model coal-fired power plants and from nuclear systems 0-3557  
 coal fired power stations, review of conventional and advanced systems 0-35625  
 fossil plant maintainability, human factors engineering review of design, c.f. nuclear plant 0-22913  
 molten carbonate fuel cell based, coal fired power plants for electric power generation 0-30471  
 ocean thermal energy conversion, open cycle approach, plant design 0-30506  
 ocean thermal energy conversion, technology development program 0-30504  
 site zone evaluation using computer-aided methods 0-861  
 thermal, thermomagnetic gas analysers improvement (*Russian*) 0-3445  
 thermal plant siting, regional policy and ecological aspect of landscape 0-862  
 Tokamak power plants, impact of technology and maintainability on economic aspects 0-27807  
 waste heat utilisation for energy conservation 0-35655  
 SO<sub>2</sub> pollution electricity generation, policy options for control 0-51022

**power supplies to apparatus**

- see also *cells (electric)*; *power plants*; *prosthetic power supplies*  
 CAMAC diagnostic module for on-line monitoring of CAMAC integrity 0-5459  
 discharge lamps, metal halide, for film lighting, luminance fluctuations assessment 0-4796  
 electron and ion beam generation at high power, review 0-13988  
 electron-optical corrector (*German*) 0-42308  
 Helitron E, power supply and control systems 0-13897  
 large toroidal fusion expts., power supply situation 0-18635  
 low-noise power supply for electrical transient meas. 0-52273  
 mass spectrometer, programmable magnet power supply to allow rapid scanning with min. reset time 0-37121  
 neutral beam injector, 150 kV, 80 A solid state power supply 0-13888  
 quadrupole mass spectrometer with elliptical electrodes, 3-dim. 0-31931  
 telecommunication remote sites, solar cell power supply 0-26133  
 transformer-rectifier flux pump using inductive current transfer and thermally controlled Nb<sub>3</sub>Sn cryotrons 0-4727  
 Li batteries developments and appl. survey 0-50949

**power supply, emergency** see *emergency power supply***power supply industry** see *electricity supply industry***power supply systems** see *power systems***power system analysis computing**

- geothermal steam pipeline network, numerical simulation 0-40822  
 solar power satellite, computer modelling of power transmission system 0-40866

**power system CAD**

- solar heating and cooling systems, computer program validation methodology 0-35742  
 TRNSYS, solar energy systems design, computer simulation 0-35679

**power system computer aided analysis** see *power system analysis computing***power system computer aided design** see *power system CAD***power systems**

- see also *total energy systems*; *transmission networks*

- consumer electricity supply demands fulfilment and ensuring full employment (*German*) 0-36831  
 military space power program, development of 10 to 50 KWe solar power systems 0-30415  
 NASA space power technology program, power system distrib. and management 0-30494  
 nuclear power station electrical supply system performance, reliability of protection and control systems 0-52761  
 photovoltaic energy generation integrations into electric grid systems, general methodology 0-45647  
 photovoltaic space power systems, 25 kW power module evolution 0-30495  
 solar electrical system comprising DC separately excited motor and mechanical load driven by solar cell array, performance analysis 0-16801  
 stabilisation of electric power systems using superconducting mag. energy storage 0-30611  
 Tokamak fusion reactor power supply requirements 0-837  
 unloading charging voltages calc. using related maximum field strengths (*German*) 0-28130  
 Yugoslavia, system efficiency in the S.R. Croatia (*Croatian*) 0-3473

**power transformers**

- fault diagnosis, dissolved gas analysis of insulating oils 0-26097  
 leakage flux calc., use of integral transforms with non-standard kernels, teaching appl. 0-31466

**power transistors**

- VHF, UHF and microwave radiation effect on human body 0-8101

**power transmission**

- see also *transmission networks*  
 cryogenics role (*Rumanian*) 0-7933



**power transmission continued**

- electric connectors, Al/Cu bimetal, galvanic corrosion elimination 0-35387
- solar power satellite, computer modelling of power transmission system 0-40866
- solar power satellite, microwave power transmission technology 0-40868

**power transmission lines**

- corona discharges from water drops, obs. 0-33851
- pulsed HV measurement in vacuum using 2 MV resistive voltage divider 0-31803
- UHV, biological effects obs., on plants and animals 0-17003
- voltage wave propagation in mag. insulated line 0-5667

**power transmission networks** *see transmission networks***power utilisation**

- see also domestic appliances; drives; environmental engineering; heating; metering; refrigeration; transportation*
- buildings, residential and commercial, energy demand and conservation in USA, National Energy Plan impact 0-26121
- energy transfer by electric power generation and utilisation, economic case 0-16777
- residences, energy conservation and noise control measures comparison 0-35807
- space heating, energy utilisation improvements using new types of construction (*German*) 0-40903
- world distribution of commercial energy consumption (1950 to 1975) 0-26120

**PPP calculations**

- bipyridines, torsional isomerisation of biologically active bicyclic molecules 0-27996
- carbonyls, electric polarisability, in excited singlet and triplet states (*Bulgarian*) 0-52897
- dye laser materials, ground and excited states, triplet yields and efficiency 0-37743
- hydrocarbons, electric polarisability, in excited singlet and triplet states (*Bulgarian*) 0-52897
- molecular electronic absorption spectra, intramolecular hydrogen bond 0-42949
- organic molecules, quadrupole moments, dipole quadrupole A and C polarisabilities, perturbation theory anal. 0-27934
- organic solids, one-dimens. conductor, dimer level splitting, hopping integral calc. using PPP Hamiltonian 0-24890
- perturbation theory, many-body, arbitrary point group symmetry, wave operator matrix elements 0-23311
- stilbene, cis- and trans-, picosecond flash photolysis, intramol. charge-reson. transition obs. 0-7810
- TTT<sub>1</sub>, charge transfer salt, Coulomb effects, Madelung energy calcs. 0-19747

**praseodymium**

- see also nuclei with .....*
- antiferromagnetic ordering 0-15709
- de Haas-van Alphen effect, Fermi surface 0-15435
- DHCP, cryst. field effect in thermal expansion 0-49390
- doped La-Al(Ag)(Sn)(Pb) superconductors, cryst. field transitions linewidths 0-24854
- magnetic excitations, exchange, crystal field and magnetoelastic interactions 0-2563
- magnetic form factors, polarised neutron diff. meas. 0-50057
- magnetic ordering, stress induced 0-15776
- quasielastic mode damping, dynamic susceptibility 0-15705
- soft mode excitation behaviour under press., long range order 0-39838
- BaF<sub>2</sub>:Pr<sup>3+</sup>, wavelength and temp.-modulated UV absorpt. 0-2799
- BeF<sub>2</sub>:Pr<sup>3+</sup>, glass, optical homogeneous linewidths 0-7395
- CaF<sub>2</sub>:Pr<sup>3+</sup>, EPR data interpretation for octahedral Γ<sub>8</sub> state in cubic cryst. field 0-2634
- CaF<sub>2</sub>:Pr<sup>3+</sup>, wavelength and temp.-modulated UV absorpt. 0-2799
- GeO<sub>2</sub>:Pr<sup>3+</sup>, glass, optical homogeneous linewidths 0-7395
- H, and He, stopping powers meas. 0-42904
- LaCl<sub>3</sub>:Pr<sup>3+</sup>, dipole transition probabilities between states, electron correl. effects 0-23364
- LaCl<sub>3</sub>:Pr<sup>3+</sup>, Zeeman second-order effects, fluoresc. line narrowing technique 0-16103
- LaCl<sub>3</sub>(Br<sub>3</sub>):Pr<sup>3+</sup>, IR absorption, energy values for Stark manifolds 0-34955
- LaF<sub>3</sub>:Pr<sup>3+</sup>, cryst. field anal. of triply ionised ion spectra 0-2796
- LaF<sub>3</sub>:Pr<sup>3+</sup>, optical line narrowing by nuclear spin decoupling, photon echo meas. 0-48353
- LaF<sub>3</sub>:Pr<sup>3+</sup>, optical transition, spin decoupling and magic angle line narrowing 0-28286
- LaF<sub>3</sub>:Pr<sup>3+</sup>, spectroscopic and relaxation character of <sup>3</sup>P<sub>0</sub>-<sup>3</sup>H<sub>4</sub> transition, photon echo 0-39897
- LaF<sub>3</sub>:Pr<sup>3+</sup>, ultrahigh resolution photon echo spectroscopy 0-28285
- LiYF<sub>4</sub>:Pr<sup>3+</sup>, mag.-dipole transitions obs. in fluoresc. 0-11451
- LiYF<sub>4</sub>:Pr<sup>3+</sup>, spectroscopic determ. of ground config. energy levels 0-34969
- Pr<sup>3+</sup>, aquo ion spectra, MCD of <sup>3</sup>P<sub>0</sub>-<sup>3</sup>H<sub>4</sub> transition 0-7331
- Pr<sup>3+</sup>:NaCl(KCl), absorption spectra at 4.2 K, anal. 0-7378
- SrF<sub>2</sub>:Pr<sup>3+</sup>, wavelength and temp.-modulated UV absorpt. 0-2799
- YAlO<sub>3</sub>:Pr<sup>3+</sup>, ultrahigh resolution photon echo spectroscopy 0-28285

**praseodymium alloys**

- steel, austenitic, Cr-Ni-Pr(Ce,La,Na), nonmetallic inclusions modification using rare earth metals (*Russian*) 0-40369
- Al-Pr (16 wt.%), resist. depend. on temp. and hot rolling (*Polish*) 0-39555
- Ce-Pr powder, DHCP⇌FCC transition, X-ray, DTA and resistivity studies 0-50629
- Ce<sub>1-x</sub>Pr<sub>x</sub>Al<sub>2</sub>, mag. struct., comp. depend., neutron diff. and mag. susceptibility meas. 0-50054
- Nd-Pr, Kaufman approach to calc. of intra-rare earth phase diagrams 0-25657
- Nd<sub>2</sub>Pr<sub>2</sub>Sm<sub>2</sub>Co<sub>2</sub>, permanent magnets, coercive force, low-temp. annealing influence (*Russian*) 0-39812
- Pr-Al liquid alloys, atomic interactions, thermodynamic props. (*Russian*) 0-39307
- Pr-Ce, mag. order onset, elec. resistivity 0-20416
- Pr-Eu, dil., magnetisation, Mossbauer spectra 0-15928
- Pr-Ga (0 to 50 at.%), phase diagram and cryst. structs. of intermetallic cryst. 0-3002
- Pr-Nd (5 at.%), paramag. excitation spectrum, CPA calc. 0-50043
- Pr-Tm, mag. order onset, elec. resistivity 0-20416
- PrAl<sub>3</sub>, ferromagnetic, extraordinary Hall effect 0-39560

**praseodymium alloys continued**

- PrCo<sub>3</sub>-H<sub>2</sub>, phase equilibria, from dissociation isotherms 0-50591
- PrCo<sub>5</sub>, uniaxial ferromag. cryst., irreversible rotation processes 0-39768
- Pr(Co<sub>0.7</sub>Cu<sub>0.3</sub>)<sub>5</sub>, anomalous magnetisation curves 0-15757
- PrCu<sub>6</sub>, coolant for two stage nuclear demagnetisation refrigerator (*Japanese*) 0-47063
- PrEu(Gd), magnetic interactions, Mossbauer spectra quadrupole splitting, crystal field parameters 0-39907
- PrFe<sub>2</sub>, Curie temp., elec. quadrupole couplings, Mossbauer study 0-39538
- PrFe<sub>2</sub>, preparation and mag. props. 0-25259
- Pr<sub>2</sub>La<sub>1-x</sub>Al<sub>3</sub>, cryst. elec. field 0-24856
- PrNi<sub>5</sub>, crystal field investigation from inelastic slow neutron scatt. expts. 0-39538
- PrNi<sub>5</sub>, hexagonal, cryst. field effect in thermal expansion 0-49390
- PrNi<sub>5</sub>, metallic Van Vleck paramag., nucl. interactions, NMR meas. 0-44953
- PrNi<sub>5</sub>, nucl. cooling agent, relax. and exchange, EPR and NMR study 0-25237
- PrSb, neutron scatt., press. induced antiferromag. 0-15699
- PrSn<sub>3</sub>, magnetoresistance 0-24877
- PrSn<sub>3</sub>, Neel temp., hydrostatic press. depend. 0-29549
- PrSn<sub>3</sub>, low temp. modification with tetragonal struct. 0-1963
- Pr<sub>3</sub>Tl, critical fluctuations temp. depend. 0-25160
- Pr<sub>3</sub>Tl, transition temp. and magnetisation 0-25161
- Sm-Pr-Co, mag. props. and struct., comp. depend. (*Russian*) 0-20430
- Sm-Pr-Co, sintered, cryst. phases (*Russian*) 0-39004
- Sm<sub>0.6</sub>R<sub>0.4-1-x</sub>M<sub>x</sub>Co<sub>5</sub> (R=Gd, Dy, M=Pr, Nd), temp. coeff. of magnetisation 0-34688

**praseodymium compounds**

- see also praseodymium alloys*
- mixed valence compounds, charge dominated fluctuation props. comparison, mag. moments and ordering 0-54659
- praseodymium β-ketoesters, Pr<sup>3+</sup>, visible spectrum, interaction, intensity and bonding parameters 0-993
- prep. by electron beam evaporation, and optical and elec. props. 0-20793
- Van Vleck paramagnets, mag. props., anisotropy from NMR anal. 0-54862
- La<sub>1-x</sub>Pr<sub>x</sub>(Sn<sub>3</sub>), superconducting, cryst. field excitations, inelastic neutron scatt. obs. 0-15653
- Na<sub>2</sub>Pr(C<sub>4</sub>H<sub>9</sub>O<sub>2</sub>)<sub>3</sub>·2NaClO<sub>4</sub>·6H<sub>2</sub>O, single cryst., forbidden A<sub>1</sub>→A<sub>1</sub> transition, mag. field induced intensification 0-50302
- Pr-H, inelastic neutron scatt. exam. of lattice dynamics 0-29128
- PrB<sub>4</sub>, mag. and elec. props. 0-20386
- PrB<sub>6</sub>, plasma light reflection by free charge carriers 0-11403
- Pr(BH<sub>4</sub>)<sub>3</sub>, synthesis from chloride salts and NaBH<sub>4</sub> in tetrahydrofuran 0-20222
- Pr(BO<sub>2</sub>)<sub>3</sub>, single cryst., IR absorpt. spectra 0-34903
- PrCl<sub>3</sub>, rare earth ion overlap in crystal field theory, configuration interaction 0-44552
- Pr(ClO<sub>4</sub>)<sub>3</sub>, osmotic coeffs. 0-45556
- PrCl<sub>3</sub>·6H<sub>2</sub>O·TbCl<sub>3</sub>·6H<sub>2</sub>O, in DMSO soln., Tb<sup>3+</sup>→Pr<sup>3+</sup> energy transfer mechanism 0-5498
- PrF<sub>3</sub>, bomb calorimetric determ. of enthalpy of formation 0-50879
- PrF<sub>3</sub>, coating materials for IR laser components 0-33105
- PrF<sub>3</sub> crystals, shift tensors and F-diffusion, ion interactions, F<sup>-</sup> NMR study 0-20471
- PrH<sub>2.265</sub>, low-temp. sp. ht., mag., elec., and cryst. field splitting effects 0-49379
- Pr<sub>2</sub>(MoO<sub>4</sub>)<sub>3</sub>-Pr<sub>2</sub>(SO<sub>4</sub>)<sub>3</sub>, system, sulphatomolybdates and isomorphous substitution 0-19763
- Pr<sub>2</sub>MoO<sub>5</sub>, cryst. struct., IR spectra, elec. and mag. props. 0-33954
- PrNbO<sub>3</sub>-CaWO<sub>4</sub>, phase transitions of fergusonite-scheelite (*French*) 0-19942
- PrNiC<sub>2</sub>, struct. determ. using X-ray diffraction (*Ukrainian*) 0-33949
- PrO, 0-0 band in XVII system, hyperfine splitting, visible excitation spectra 0-28028
- PrO, high press. synthesis, struct. and lattice const. (*French*) 0-29913
- PrO, mag. props., lattice const., and X-ray absorpt. spectra 0-44798
- Pr(OH)<sub>3</sub>, cryst. struct. 0-24424
- Pr(OH)<sub>3</sub>, low temp. heat capacity, thermophys. props. optical spectra, anal. of Schottky contributions, review 0-24611
- Pr(OH)<sub>3</sub>, thermal decomposition, exam. 0-55640
- PrPb<sub>1-x</sub>Mo<sub>0.5+y</sub>S<sub>8</sub>, sputtered supercond. props. 0-50019
- PrS, plasma light reflection by free charge carriers 0-11403
- PrSb, forbidden band gap and electrotransfer parameters 0-39497
- PrSb, plasma light reflection by free charge carriers 0-11403
- PrSb, pressure-induced antiferromag., neutron scatt. study 0-39750
- PrSe, plasma light reflection by free charge carriers 0-11403
- Pr<sub>2</sub>Si<sub>2</sub>O<sub>7</sub>N<sub>2</sub>, lattice const., X-ray diff. anal. 0-28986
- SrPrFeO<sub>4</sub>, Mossbauer spectra 0-15880

**preamplifiers**

- bridge RF spectrometer, high freq. preamplifier 0-22380
- MESFET preamplifier in p-i-n/FET hybrid optical receiver for communication systems 0-33158
- spectrometric installation preamplifier modernisation by input FET operating regime control 0-32579
- GaAs FET, cooled (4.2K), for use in UHF SQUID magnetometer 0-52282
- HgI<sub>2</sub> thin sections with Peltier-cooled preamplification for X-ray spectrosc. 0-324

**precipitation**

- microstructural process and features only*
- see also Guinier-Preston zones; segregation; Widmanstatten structure*
- alloys, precipitated phases, size, shape, distrib., diffusion controlled changes 0-3072
- array model, stability concept 0-55411
- array model, stability criteria, reply 0-55412
- composites, planar, dissolution of precipitate plates, one-phase diffusion controlled 0-15244
- conference, phase transformations in metallurgy, York, England (Apr. 1979) 0-2994
- dielectric, dipolar point defects, studied by ITC 0-6405
- diffusional crystal growth mechanisms 0-3059
- discontinuous precipitation in binary metallic systems, review 0-3060
- FCC solid solutions, deformed, discontinuous precipitation 0-3053
- Fe-Cr-C (10.6, 0.22 wt.%), fibrous precipitation 0-16303
- Incoloy, alloy 800, M<sub>23</sub>C<sub>6</sub>/austenite phase boundary defect struct. resolution by weak beam microscopy 0-3046



## precipitation continued

- interface-controlled to diffusion-controlled coarsening kinetics, particle size distrib. 0-7579
- interphase boundary structure in solids, investig. 0-15112
- liquid phase sintering, elementary mechanisms, soln.-reprecipitation 0-50571
- metals, diffusion alloying conditions, deep chemical-heat treatment (*Russian*) 0-40393
- Nimonic, IN100,  $\gamma'$  precipitates, casting conditions effect on morphology 0-7548
- Nimonic 80A, struct., fracture characts. 0-3071
- Ostwald ripening, effect of precipitation vol. fraction 0-40356
- parallel plates, one-dimens. diffusion-controlled growth 0-55410
- particle size distribution, continuity eqn. 0-55406
- particle size distribution influence on exta-resist. of coherent precip. 0-49689
- peritectic structure formation criteria (*Ukrainian*) 0-11636
- peritectic systems with separate crystallisation of phases, number of phase constituents, calc. (*Ukrainian*) 0-25702
- platelet growth and stereological characterization of plates 0-55404
- quartz, defects growth, study by X-ray diff. topography (*French*) 0-39095
- refractory fusion reactor materials, neutron irradi., microstruct., voids, nucleation TEM study 0-29065
- solution reprecipitation during liq. phase sintering, grain growth, computer simulation 0-55427
- spherical precipitate, diffusion-limited growth, linearised gradient approx. 0-55400
- spherical precipitates in anisotropic matrix, elastic interaction energy 0-3049
- steel, alloy, forgings, H precipitation kinetics, diffusion to voids, effect on shattercrack formation 0-16344
- steel, alloy, type ST.5, structural and phase changes after high temp. heating (*Russian*) 0-55439
- steel, alloy 40Kh, sulphide cracking resistance, strengthening method influence 0-55577
- steel, austenite/ferrite interface, struct. and diff. effects, TEM exam. 0-16308
- steel, austenitic, Al-C, microstruct., Mossbauer obs. (*Russian*) 0-29655
- steel, austenitic, cold worked 10Kh11N23T3MR, structural transformations, aging effect, electron microscope obs. 0-40402
- steel, austenitic, Cr-Ni-Mn-V, X-ray anal. of carbide phases formed during ageing (*Russian*) 0-20936
- steel, austenitic Cr-Mn,  $M_{23}C_6$  carbide precipitates comp., heat and thermomech. treatment influence (*Russian*) 0-40361
- steel, austenitic stainless, 08Kh18N10T, hot-worked precipitation kinetics and struct. of dispersed phases, Ti effect 0-29964
- steel, austenitic stainless, 12Kh18N10T, deformed, phase comp. and props. after prolonged heating 0-30040
- steel, austenitic stainless, fatigue crack propag., stable and unstable, role of precipitation 0-40534
- steel, austenitic stainless, interaction of grain boundary dislocations with precipitates during high temperature creep 0-16384
- steel, austenitic stainless, Ni-alloyed,  $Cr_2N$  precipitation, interface struct. and morphology 0-11644
- steel, austenitic stainless, precipitates and grain orientation by non aqueous electrolyte potentiostatic etching method (*Japanese*) 0-15102
- steel, austenitic stainless, structure phase transitions due to high energy electron irradi. (*Russian*) 0-7553
- steel, austenitic stainless FV548, neutron irradiated, Si-rich phase occurrence of  $M_6C$  phase 0-15156
- steel, C, isofoming and warm rolling, effect of mech. props. 0-11673
- steel, carbide form. depend. on Mn, Cr, V additions, cementite stabilisation, microstruct. (*Russian*) 0-55399
- steel, Cr, exam. of surface layer after electrochemical treatment, effect on mech. props. (*Russian*) 0-7727
- steel, Cr-Mo, toughness of heat treated steels of equal tensile strength (*German*) 0-25727
- steel, CrMoV, carbide phases precipitation (*Czech*) 0-29961
- steel, Cu-Mo, tempered, cementite precipitation along twin boundaries 0-45309
- steel, deoxidised, AlN and V carbonitrides precip. effect on mech. props. (*French*) 0-45311
- steel, effect of  $\epsilon$ -Cu precipitates on H discharging phenomena (*Japanese*) 0-7583
- steel, ferritic, with interstitial N, continuous precipitation and clustering 0-7585
- steel, high-C, type U12, U15, U17, cementite precipitation cryst. geometry singularities during decomposition of martensite (*Russian*) 0-7577
- steel, hypereutectoid, austenite dissociation depend. on strain at intercritical temps., pearlite transform. (*Russian*) 0-40362
- steel, low alloy, low C grain boundary proeutectoid ferrite formation, direct obs. method 0-3074
- steel, low C, Mn effect on recrystallisation and texture (*French*) 0-3110
- steel, low C, quenched, interphase precipitates obs. (*Russian*) 0-29957
- steel, low C and alloy, serrated flow and thermomechanical treatment (*Korean*) 0-30026
- steel, maraging alloy, intermetallic compound solubility, thermodynamic calcs. (*Russian*) 0-40363
- steel, microalloyed, alloy carbide precipitation during isothermal ageing 0-3077
- steel, microalloyed, precipitation effect on microstruct. and mech. props. (*French*) 0-25708
- steel, multicomponent duplex stainless, high temp. precipitation of  $\alpha'$  0-20939
- steel, Ni-Co-Mo-Ti, microfractographical features, embrittlement and grain size influence on fracture behaviour (*German*) 0-30053
- steel, pearlitic, heat-resist., secondary phase precipitation, deform., and fracture during creep (*Russian*) 0-50669
- steel, stainless,  $\alpha$ -irradiated, He cavitation, rel. to TiC precipitation 0-45399
- steel, stainless, ferrite to austenite decomposition 0-3073
- steel, stainless, type 316, cold worked, precipitation response to neutron irradi. 0-34073
- steel, stainless type 304, AES of stoichiometric Cr carbides and carbide precipitates at grain boundaries 0-3055
- steel, stainless type 316,  $M_{23}C_6$  carbide precipitation, intermetallic phases, X-ray diff. study 0-7586
- steels, ferritic and martensitic, C and N migration at low temps., monograph 0-22149

## precipitation continued

- steels 2Kh13 and 20Kh1M1FTR, sulphide cracking resistance, strengthening method influence 0-55577
- stereological counting measurements, use in testing growth rate theories 0-16311
- thin films, segregation effects at surfaces and interfaces 0-39475
- Ag-CdO cermets, coprecipitated carbonates and hydroxides, physicomach. props. 0-25706
- Ag-Cu (8 wt.%), deformed, free energy changes in process of discontinuous precipitation 0-3054
- Ag-Cu (8 wt.%), plastic deform. effect on discontinuous precipitation 0-3053
- Al alloy 7075, serrated flow and thermomechanical treatment (*Korean*) 0-30026
- Al alloys, continuous precipitation, nucleation, spinodal decomposition 0-3061
- Al alloys, plate shaped precipitates, growth kinetics 0-3065
- Al film, vacuum evaporation growth, impurity presence, effects (*Hungarian*) 0-7495
- Al, superpure, anomalous primary creep behaviour, precipitate form. 0-7646
- Al-Ag (40 wt.%), deformed, free energy changes in process of discontinuous precipitation 0-3054
- Al-Ag (40 wt.%), plastic deform. effect on discontinuous precipitation 0-3053
- Al-Au (0.2 wt.%), precipitation mechanism and creep behaviour 0-3058
- Al-Cr(Zr), simultaneous recrystallisation and precipitation (*French*) 0-16313
- Al-Cu-Mg (2.6, 0.4 wt.%), Fe, Si, Mn and Ti addition effects on age-precipitation (*Japanese*) 0-20937
- Al-Cu(Zn, Ag, Mg, Si), intermediate precipitates, stability, X-ray, elec. resist. and hardness study 0-3063
- Al-Li (10 at.%), struct. changes on annealing, 25-500°C, Li atoms role 0-35183
- Al-Mg (2 wt.%), steady creep characts., precip. effect 0-35189
- Al-Mg-Si (1 wt.%), precipitation reactions 0-11652
- Al-Mg-Si, DTA exam. after small and medium deform. 0-21002
- Al-Mg-Si, heterogeneous precipitation studies using differential scanning calorimetry 0-3062
- Al-Mg-Si, nucleation and precipitation growth on dislocations, electron microscope studies 0-3064
- Al-Mn, direct chill-cast, struct. changes during heat treating (*German*) 0-40408
- Al-Si, dilute, anomalous primary creep behaviour, precipitate form. 0-7646
- Al-Zn, comparison between very-slow-neutron transmission and small-angle neutron scatt. expts. 0-19677
- Al-Zn, isothermal preprecipitation, small angle X-ray scatt. expts. 0-35186
- Al-Zn (15 at.%), supersaturated alloy, growth and decomposition kinetics 0-29965
- Al-Zn (40(50)(65) wt.%), deformed, free energy changes in process of discontinuous precipitation 0-3054
- Al-Zn (40(50)(65) wt.%), plastic deform. effect on discontinuous precipitation 0-3053
- Al-Zn-Mg (4.5, 2 to 3 at.%) solid state reactions by interrupted continuous heating 0-25737
- Al-Zn-Mg (5.9, 2.9 wt.%), ageing effects on microstruct. 0-16306
- Al<sub>3</sub>Ti, precipitate shape, and distribution in chill-cast Al-14 wt.% Ti alloy 0-16310
- BaF<sub>2</sub>, formation and growth of oxidation centres result of O<sup>2-</sup> diffusion 0-7706
- Be-bronze BrB2, struct. and phase transform. during mechano-thermal treatment (*Russian*) 0-11667
- Bi<sub>95</sub>Mn<sub>4</sub>, magnetisation of ferromag. precipitates, effect of ultrasonic pulses 0-2121
- CC Al-Zn-Mg (4.5,1(2)(3) at.%), decomposition during ageing, preageing and cooling rate influence 0-20938
- CaF<sub>2</sub>:CaO, optical scatt., absorpt. at 205 nm 0-20669
- CdF<sub>2</sub>:Eu, role of solution and precipitation phenomena on ITC spectra 0-7265
- CdTe:Cl, LPE from CdCl<sub>2</sub> soln., elec. props., defects 0-39689
- CdTe:P, annealing induced lattice defects, TEM obs. 0-2010
- Co-Ni-Cr-Nb, effect of Fe addition on precipitation behaviour 0-29962
- Co<sub>2</sub>Sm, magnetic domains, nucleation and pinning, magneto-optical Kerr effect 0-39811
- Cr-C, binary alloy formation of nonequilib. Cr<sub>7</sub>C in alloys quenched rapidly from melt 0-7581
- Cu alloys, continuous precipitation, nucleation, spinodal decomposition 0-3061
- Cu vacuum coating on steel substrate, influence of precipitation conditions on porosity (*Russian*) 0-54578
- Cu-Ag (8 wt.%), deformed, free energy changes in process of discontinuous precipitation 0-3054
- Cu-Ag (8 wt.%), plastic deform. effect on discontinuous precipitation 0-3053
- Cu-Be (2 wt.%), alloying addition effects on grain boundary reaction (*Japanese*) 0-49236
- Cu-Be alloys, CuBe precipitation 0-29966
- Cu-Be-Co, cuboid (Co, Cu, Ni, Fe)Be inclusions, metallography, ageing effects 0-11645
- Cu-Be(25 wt.%), discontinuous precipitation (*Japanese*) 0-55402
- Cu-Cd(2.7 wt.%), cellular precipitation kinetics and dissolution (*German*) 0-11651
- Cu-Cr, age hardened, fine precipitates struct., TEM study 0-3066
- Cu-Cr (0.55 wt.%), crystallography of precipitates, strain field study 0-25699
- Cu-Fe, dil., diffusion and ageing processes, Mossbauer study 0-7245
- Cu-Fe, dilute, low temp. heat capacity in mag. field, superparamagnetism 0-39804
- Cu-Fe, precipitation processes during aging, TEM, resistivity, hardness study (*Japanese*) 0-35221
- Cu-Fe (0.2 at.%), clustering, precipitation, and oxidation, 298 to 919K, Mossbauer study 0-7242
- Cu-Ga, high dislocation density alloys and oxide precipitated struct., NMR, spin echo 0-39892
- Cu-Ni alloys, artefacts in thin foil images 0-3056
- Cu-Ni-Be(Al) (30.0,5,(0.2-2) wt.%), Al addition effect on grain boundary reaction (*Japanese*) 0-54254
- Cu-Ni-Nb-Al, correlation of  $\gamma'$  and  $\gamma''$  precipitates phase stability 0-25704



# precipitation continued

- Cu-Si, high dislocation density alloys and oxide precipitated struct., NMR, spin echo 0-39892
- Cu-Ti, dil. alloy, cellular precipitates, nucleation, TEM study 0-3069
- $\beta$ -Cu-Ti, dil. alloy, growth phenomena associated with precipitation, TEM study 0-3070
- CuGaSe<sub>2</sub> crystals, electron probe microanal., correction procedure 0-2171
- CuInSe<sub>2</sub> crystals, electron probe microanal., correction procedure 0-2171
- Fe, (100) surface, S segregation and 2D compounds precipitation (Japanese) 0-35188
- Fe, Armco, inter- and intragranular sulphidation 0-55570
- $\alpha$ -Fe, irradiation induced void swelling, Cr additions effect 0-55408
- Fe-C, proeutectoid ferrite nucleation kinetics at austenite grain boundaries 0-55405
- Fe-CR (26 wt.%), role of C and N in brittle fracture 0-16456
- Fe-Cr, irradiation induced void swelling, Cr additions effect 0-55408
- Fe-Cr-C, austenite to ferrite+precipitate reaction, TEM/STEM study 0-3075
- Fe-Cr-C, isothermal transformations 0-16302
- Fe-Cr-C (10.0.2 wt.%), isothermally transformed, precipitate orientations 0-50640
- Fe-Cr-C (10.0.2 wt.%) isothermally transformed, carbide distrib., microstruct. development 0-3076
- Fe-Cr-Co, mechanism of coercive force 0-34674
- Fe-Cr-Ni melts, S solubility and solid soln. precipitation (Russian) 0-15251
- Fe-Cu alloy, effect of  $\epsilon$ -Cu phase on strain ageing (Japanese) 0-7582
- Fe-Cu alloys, transform. substruct., lath microstructure after quenching 0-16298
- Fe-Cu-Ni, austenite to ferrite+precipitate reaction, TEM/STEM study 0-3075
- Fe-Cu-Ni, Ni effect on austenite decomposition 0-3048
- Fe-Cu-Ni (2, 5 wt.%), interphase precipitation obs. in assoc. with Widmanstätten ferrite lateral growth 0-40365
- Fe-Cu-Ni (2.2 wt.%), isothermally transformed, precipitate orientations 0-50640
- Fe-Mn-V-C austenitic steel, discontinuous precipitation, morphological changes 0-3078
- Fe-N, nucleation and precipitation growth on dislocations, electron microscope studies 0-3064
- Fe-Nb creep resistant alloy, precipitate free zones elimination 0-16312
- Fe-Ni-Al, liq. alloys, N solubility and AlN precipitation 0-11648
- Fe-Ni-Al, magnetic anisotropy form. and struct. changes by annealing, Mossbauer obs. 0-39994
- Fe-Ni-Cr, Elinvar, struct. and mag. props., singularities during tempering (Russian) 0-50627
- Fe-Sb-Ti(V)(Cr)(Mn)(Co)(Ni), dil., interactions and precip., Mossbauer study 0-39997
- Fe-Si (3 wt.%), chemical comp. and hot rolling effect on brittleness (Czech) 0-50712
- $\alpha$ -Fe-Ti, ion-implanted and annealed, microstruct. evolution 0-15132
- Fe-V-C, austenite to ferrite+precipitate reaction, TEM/STEM study 0-3075
- Fe-V-C (0.3, 0.05 wt.%), interphase precipitation obs. in assoc. with Widmanstätten ferrite lateral growth 0-40365
- Fe<sub>1-x</sub>O, wustite decomposition, coherent magnetite precipitation, electron diffraction study (Russian) 0-16318
- Fe-Fe-Nb, cold-worked and aged, mag. props. and microstruct. 0-34690
- Ga-Cu-Sn solders, exam. of structural transformations due to hardening, heat treatment (Russian) 0-7578
- GaP crystal, structure defect formation due to annealing and stress, dendrites, slip, dislocations 0-29026
- Ge, As impurity precipitation from solid soln., neutron irradi. effect 0-29177
- Ge-As, supersaturated solid soln., dislocation form. during thermocyclic treatment (Russian) 0-3057
- HgCr<sub>2</sub>Se<sub>4</sub>Cd, precipitations during growth by chem. transport method 0-55409
- In film, vacuum evaporation growth, impurity presence, effects (Hungarian) 0-7495
- InSb:Se, exam. of defects in crystal 0-6423
- KCl-CuCl solid solution supersaturated, precipitation, impurity aggregation 0-29174
- Mg-Al-Zn (9wt.%Al), sand cast, preferred orientation and mechanical props. (Japanese) 0-20979
- Mg-Ce, workability, aging characts. and tensile strength 0-55416
- Mg-La, workability, aging characts. and tensile strength 0-55416
- Mg-Li-Al (31, 1 at.%), heat treated, precipitation 0-40364
- MgO, precipitate morphology, strain energy effects 0-40358
- Mn-Si (62.5 to 63.8 wt.%), phase anal. and cryst. struct. (Japanese) 0-15049
- Mo form MoF<sub>6</sub> by H<sub>2</sub> reduction, 500 to 1200°C (Russian) 0-7516
- Mo-Hf-C-Ni, electrochemical phase composition anal., precip. of HfC phase (Russian) 0-20901
- Mo-Zr, heavy ion irradiated, void swelling, phase instability 0-29084
- N<sub>2</sub>O<sub>4</sub>⇌2NO<sub>2</sub>⇌2NO+O<sub>2</sub>, precipitation of corrosion products in a fractionating column (Russian) 0-25707
- Na precipitation at Si-SiO<sub>2</sub> boundary, expt. (Russian) 0-49368
- NaCl:Eu<sup>2+</sup>, oriented growth and cryst. struct. of precipitated phases 0-24303
- Nb alloy SVMTs, high-temp. ageing, struct. and morphology of hardening phases (Russian) 0-40390
- Nb-H system, temp.-stimulated acoustic emission, hydride precip. 0-3044
- Nb-Hf (38 at.%) superconductor, peak effect, summation problem, mag. history flux pinning force 0-20362
- Nb<sub>3</sub>Sn, high-rate sputter-deposited, effect of oxygen on microstruct. 0-20343
- Ni base superalloy, directionally solidified, struct. and props. (Chinese) 0-20918
- Ni base superalloy,  $\gamma'$ -precipitation influence on recrystallisation 0-29955
- Ni, C precipitation 0-29958
- Ni, deformed, struct. form. during annealing, Ni<sub>3</sub>Al type ordered phase precipitation (Russian) 0-45325
- $\beta$ -Ni-Al, precipitation studies 0-3067
- Ni-Al-Ti ferromagnetic non-homogeneous alloy, composition determination by Curie temp. meas. 0-11196
- Ni-base superalloy, conventional and powder metallurgical,  $\sigma$ -phase precipitation 0-11646
- Ni-base superalloy, effects of grain boundary carbides on creep and back stress 0-3130

# precipitation continued

- Ni-based superalloys, TEM obs. of cellular transformation products 0-3045
- Ni-Co-Cr superalloy, powder produced, necklace struct. development 0-40395
- Ni-Cr, deformed, struct. form. during annealing, Ni<sub>3</sub>Al type ordered phase precipitation (Russian) 0-45325
- Ni-Cr-W-Mo-Al-Ti (15.6,3.2,2, wt.%), wrought, Si effect on transition brittleness (Chinese) 0-55491
- Ni-Fe-Nb (Mo), magnetic alloy, TEM and X-ray obs. (Chinese) 0-24401
- Ni-Ge, defect-solute interactions and radiation-induced segregation 0-25705
- Ni-Si, defect-solute interactions and radiation-induced segregation 0-25705
- Ni-Si, proton irradi.,  $\gamma'$  precipitation, early stages 0-34096
- Ni-Ti (3 wt.%), C precipitation 0-29958
- Ni<sub>1-x</sub>Au<sub>x</sub>-Co, dil., hyperfine field and isomer shift, precip. process, Mossbauer expts. 0-25267
- NiFe<sub>2</sub>O<sub>4</sub> precipitation process from silicate glass, ESR study, effective g value, transition temp. 0-25194
- NiFe<sub>2</sub>O<sub>4</sub> precipitation from silicate glass, Mossbauer study 0-54998
- Ni<sub>2/3</sub>Fe<sub>1/3</sub>O<sub>4</sub>, precipitation of  $\alpha$ -Fe<sub>2</sub>O<sub>3</sub>, optical microscopy, SEM and TEM studies (French) 0-11650
- Ni(H<sub>2</sub>V)<sub>2</sub>(H<sub>2</sub>O)<sub>2</sub>, synthesis and characterisation (French) 0-45225
- Pd<sub>77.5</sub>Cu<sub>6</sub>Si<sub>16.5</sub>, ternary miscibility gap, simulation, dispersed phase composite form. 0-54379
- Sb<sub>2</sub>O<sub>3</sub> hydrated, preseparation stage in dehydration, phase transformation 0-35524
- Si, Czochralski-grown, oxide precip. form. process 0-49364
- Si, Czochralski-grown crystals, thermally induced microdefects, annealing temp. and starting material effects 0-49141
- Si, dislocation-free, O<sub>2</sub> precip., IR and TEM obs. 0-29173
- Si, floating zone structural perfection changes by high temp. treatment, dendrites, dislocation interactions 0-29049
- Si MOS device, electron optical identification of precipitations 0-16309
- Si, O impurity precipitation from solid soln., neutron irradi. effect 0-29177
- Si, precipitation of O, 1000°C TEM, IR absorpt. and X-ray studies 0-34194
- Si, precipitation of O, annealing, IR spectra meas. 0-24606
- Si:<sup>57</sup>Co/<sup>57</sup>Fe, Mossbauer spectra, deep level Co impurity study 0-29666
- Si:Cu extinction of X-ray topographic images of Cu precipitates 0-45310
- Si:Fe, implanted, annealing and stripping, Mossbauer expts. 0-39141
- Si:O wafer, annealed, surface- and inner-microdefects, TEM obs. 0-54236
- Si-Au, solid soln., influence of precip. on relax. of <sup>29</sup>Si nucleus 0-11287
- Si-Ge, heavily doped, reversal of precip. 0-2409
- Sm-Pr-Co alloys, mag. props. and struct., comp. depend. (Russian) 0-20430
- Sn-Sb (10 wt.%), decomposition of supersaturated solid soln. 0-29960
- steel, Cr-Ni, ferrite precip. (Japanese) 0-35187
- Ta-Cr (15 wt.%), solid soln., discontinuous precipitation (German) 0-45314
- $\alpha$ + $\beta$ -Ti alloys, interfacial precipitation 0-3068
- Ti alloys, metallurgical characterisation using thermoelec. power meas. (French) 0-45462
- $\alpha$ -Ti, recrystallised commercial purity, Fe-rich precipitates obs. (French) 0-50637
- Ti-Al-V, (6.4 wt.%), single and dual ion irradi., microstruct. studies 0-29077
- Ti-Al-V (4.7, 2 wt.%) pseudo alpha alloy, laminar struct. singularities,  $\beta$  to  $\alpha$  transformation (Russian) 0-7552
- Ti-Al-V (6.4 wt.%), quenched, struct. and age hardening rel. to treatment temp. 0-11657
- TiO<sub>2</sub>, K<sup>+</sup> implantation, extended defects and precipitates 0-49251
- V-H rods, twisting effect, anelastic deviations on thermal cycling 0-21043
- V-Zr-C-Y alloy weld metal, hardening phase precipitates examination, TEM appl. 0-7576
- W-Cr solid solution, precipitation behaviour, reaction front motion, lattice parameters (German) 0-55401
- W-Ni, liquid phase sintering 0-25613
- ZnTe, TEM obs. of precipitates, shape of Te solidus line 0-25703
- ZnTe:Cu, precipitates, electron microscopic investigation 0-45312
- Zr, 10 keV deuteron irradiated, retention and precipitation 0-34099
- Zr-Al (14 wt.%), transformation sequence from Zr-Al martensite to Zr<sub>3</sub>Al phase 0-3027
- ZrO<sub>2</sub> ceramics, microstruct. and props., monoclinic to tetragonal transition 0-3035
- precipitation, electrostatic** see electrostatic precipitators; precipitation (physical chemistry)
- precipitation (atmospheric)** see atmospheric precipitation
- precipitation (meteorology)** see atmospheric precipitation
- precipitation (physical chemistry)** for precipitation within solid systems (microstructural changes) see precipitation
- see also coagulation; crystal growth from solution; flocculation
- acoustic particle agglomeration due to hydrodynamic collision between monodisperse aerosols 0-26191
- acoustic particle agglomeration of aerosols under standing-wave condition 0-30627
- cellulose, phase transitions, kinetics of precipitation from diluted cadoxen solns. 0-7845
- electrolyte, binary, cryst. growth kinetics during precipitation 0-49149
- formaldehyde, solid soln. in Xe, precipitation, IR spectra obs. 0-45059
- ionic crystals, precipitation from aq. solns., induction period 0-50882
- leisegang rings, calcs., nonlinear partial differential eqns. appls. 0-4510
- particle size analysis, of precipitation processes 0-50883
- silver thioamides, precip., electron microscope and potentiometric studies, growth of photosensitive crystals 0-33107
- soil, <sup>89</sup>Sr and <sup>90</sup>Sr determ. using total sample decomp. 0-35808
- Ag halides in thioamides, precip., electron microscope and potentiometric studies, growth of photosensitive crystals 0-33107
- Bi powders, fine, precipitation on passivated electrodes 0-2977
- C precipitates with preferred orientation [100], from dissoc. of n-xylene (Russian) 0-45484
- CaCO<sub>3</sub>, nucleation mechanism accompanying Ostwald ripening 0-50641
- CaO, single cryst. growth from molten CaCl<sub>2</sub> in wet atmosphere, habits 0-55287
- CsH, crystallisation in Cs+H<sub>2</sub> gas mixture, laser snow effect 0-40712



**precipitation (physical chemistry) continued**

- Cu-rare earth oxide-Y composite coatings, oxide and Y effect on coating precipitation 0-55554  
 $\text{Fe}_2\text{O}_3$ , magnetite, precip. with urea, prep. and props. 0-20854  
 $\text{FeOOH}$ , crystal growth in  $\text{FeSO}_4$  solution with NaOH or  $\text{NH}_4\text{OH}$  as precipitant, phase diagrams (*Chinese*) 0-44158  
 $\text{Ni}(\text{NH}_4)_2(\text{SO}_4)_2 \cdot 6\text{H}_2\text{O}$ , precipitation from equimolar aqueous solns., kinetics study 0-7848  
 $(\text{U,Pu})\text{O}_2$ , FBR fuel pellets, gel-supported precipitation conversion and prep. 0-813  
 $(\text{U,Pu})\text{O}_2$  powder, FBR fuel prep. by Au/PuC coprecipitation process 0-814  
 $\text{UO}_2^{++}$ , precipitation reaction in KSCN 0-26040  
 $\text{Y}_2\text{Ti}_2\text{O}_7$ , precipitation from oxalates, carbonates, exam. 0-55641  
 $\text{ZnCO}_3 \cdot 2\text{H}_2\text{O}$ , crystn. kinetics by precipitation 0-50884  
 $\text{ZrO}_2$  gels, calcination 0-11964

**precipitation ageing** *see precipitation hardening***precipitation annealing** *see precipitation hardening***precipitation hardening**

- alloys, Co effect on martensite ageing at 300-600°C (*Russian*) 0-20972  
 alloys, radiation effects on ageing and precipitation, review 0-29956  
 Elinvær,  $\gamma$  to  $\gamma'$  transformation and  $\gamma'$  phase form. kinetics, lattice consts. 0-35191  
 Lagneborg particle by-passing model, creep rate stress exponents and friction stress 0-55481  
 misfitting particles, precip. hardening, comparison with expts. 0-3086  
 Nimonic 90, creep rate stress exponents and friction stress, comparison with Lagneborg particle by-passing model 0-55481  
 Nimonic 90, dispersion hardened, friction stress rel. to initial and secondary creep 0-11711  
 precipitate hardened material, intergranular cavity growth inhibition 0-50677  
 sapphire: $\text{Ti}^{4+}$ , plastically deformed, precipitation hardening, TEM study 0-7592  
 steel, austenitic, age-hardening kinetics, study by resistivity, Young's modulus and internal friction (*Czech*) 0-29970  
 steel, austenitic, Cr-Ni, anomalous stress-depend. of creep rate 0-11712  
 steel, Co-Cr-Mo, maraging, age hardening, Mossbauer study 0-40002  
 steel, Co-Cr-Ni-Mo-Mn (39.65, 20.25, 15.33, 7.08, 1.9 wt.%) carbide formation during tempering after plastic deformation 0-16330  
 steel, Cr-Mo-Ni-Nb, Nb effect on mech. props. (*German*) 0-30012  
 steel, maraging, 18 Ni, welded joints ageing props. obs. (*Japanese*) 0-40401  
 steel, Ni-Co-Mo-Ti, maraging, electron diffr. obs. of second phase (*Chinese*) 0-11655  
 steel wire, drawn, mechanical and electrical props. relationship obs. 0-50662  
 texture influence on stress/strain curves, prestrain, solid soln. and particle hardening effect on inhomogeneous deform. (*German*) 0-30014  
 two phase alloy hardening by second phase particle coalescence 0-7591  
 Al-alloys, precipitation hardening, effect on dynamic strain ageing and jerky flow 0-20945  
 Al-Cu (4 wt.%) partially coherent precipitation hardened alloy, high temp. cyclic deform. 0-25710  
 Al-Cu full coherent precipitation hardened alloy, high temp. cyclic deform. 0-25711  
 Al-Cu single cryst., hardening due to oriented GP zones 0-55414  
 Al-Cu-Mn-Zr, type 2219, particle, coarsening of disk shaped  $\theta'$  particles 0-45315  
 Al-Cu-Ni, alloy RR 350,  $\theta'$ -hardened, deform. induced microstructural instability, high temps. 0-16321  
 Al-Li (2.8 wt.%), ageing in US field, precip. hardening (*Russian*) 0-29968  
 Al-Si (9 wt.%), precipitation hardening during isothermal ageing 0-29969  
 Al-Zn, age hardenable precipitation and dissolution, positron annihilation and X-ray scatt. 0-16314  
 Al-Zn-Mg-Cu-Co (6.5, 2.5, 1.5, 0.4 wt.%), fatigue crack propag. 0-55521  
 Cu-Zr-(Cr), powder metallurgical alloys, thermomech. treatment effect on props. 0-50660  
 Cu-Cr, age hardened, fine precipitates struct., TEM study 0-3066  
 Fe-Cu, precipitation hardening of  $\alpha$ -Fe containing weak and strong particles 0-20946  
 Fe-Mn-Ti alloys, austenitic, precipitation strengthened 0-25714  
 Fe-Ni austenitic, effect of Al and Ti on relaxation resist. 0-20993  
 Fe-Ti, precipitation hardening of  $\alpha$ -Fe containing weak and strong particles 0-20946  
 KCl:Pb, lead aggregation effect on yield stress, incoherent precipitates, solubility determ. method 0-50645  
 Mg-Ce, workability, aging characts. and tensile strength 0-55416  
 Mg-La, workability, aging characts. and tensile strength 0-55416  
 Mg-Sm, phase diagram and mech. props. (*Russian*) 0-20892  
 MgO, single cryst., order hardening by large precipitated vol. fraction of spinel particles 0-3085  
 NaCl:Ca, aggregation and precip. hardening in impurity vacancy, dipole decay 0-16322  
 NaCl+Pb, Pb aggregation effect on yield stress, incoherent precipitates, solubility determ. method 0-50645  
 Ni-Al-Ti ferromagnetic non-homogeneous alloy, composition determination by Curie temp. meas. 0-11196  
 Ni-alloys, precipitation hardening, effect on dynamic strain ageing and jerky flow 0-20945  
 Ta-O supersaturated solid solution, precipitation processes, hardness change meas. 0-25712  
 Ti-Al-V (6.4 wt.%), quenched, struct. and age hardening rel. to treatment temp. 0-11657

**prediction theory** *see filtering and prediction theory***predictor-corrector methods**

- see also Runge-Kutta methods*  
 elastic-plastic models, integration algorithms 0-5959  
 shock tube flows, unsteady non-equilibrium, discretisation of boundary layer terms 0-14742

**predissociation of molecules** *see molecular predissociation***prerotation** *see rotation***presentation, technical** *see technical presentation***presentation methods, radar** *see radar displays***presintering** *see sintering***pressing, hot** *see hot pressing***pressure**

- see also atmospheric pressure and density; high-pressure phenomena and effects; radiation pressure; vapour pressure*  
 W.Gulf of Maine, current and press. obs. rel. to winter circulation 0-51430  
 micelles, Laplace pressure 0-7865  
 pore fluid pressure in rocks, rel. to effective stress law for anisotropic elastic deform. 0-51385  
 PWR power plant flow pressure fluctuations as vibration source, relationships (*Hungarian*) 0-47685  
 skin temperature measurements using a disc sensor, effect of press. 0-56259  
 solar transition zone, energy balance and press. for network and active region features 0-21957  
 unit, optimum metric, for thermodynamic standard state 0-8950  
 $\text{N}_2$ - $\text{H}_2\text{O}$  mixtures, two-phase pressure drops in the low flowrate region 0-19480

**pressure, atmospheric** *see atmospheric pressure and density***pressure control**

- see also vacuum control*  
 nuclear power stations containment structures testing, for pressure tightness (*Spanish*) 0-13775

**pressure measurement**

- see also vacuum measurement; vapour pressure measurement*  
 arterial blood pressure noninvasive monitoring by US imaging and phonocuff-sphygmomanometry 0-36180  
 biomedical, pressure inside hollow organs, recording through tubes, nomograms for calc. of system parameters 0-3836  
 blood pressure measurement, noninvasive techniques 0-41298  
 blood pressure waves, forward and backward, total-occlusion method for anal. 0-56257  
 cardiac pressure noninvasive US measurement, scatt. from encapsulated bubbles 0-36048  
 equipment development, design and appls. 0-13091  
 ferrite sensors development, hydrostatic pressure effect on ferrite props. of pressure sensors (*Polish*) 0-31707  
 finger instantaneous arterial press. meas. method 0-56245  
 high dynamic, review of practical techniques 0-47070  
 high-pressure calibration scale based on Au, Ag and Cu melting curves, revision 0-39260  
 hydrophone, interferometric fibre optic, static press. sensitivity amplification 0-38094  
 hydrophone, multimode fibre optic, frustrated total internal reflection, testing 0-38096  
 intracranial pressure estimation, use of visually evoked pots. 0-26398  
 intracranial pressure measurement, some considerations 0-17155  
 intracranial pressure monitoring in neurotraumatology 0-17156  
 membrane pressure gauge with displacement sensor (*Hungarian*) 0-31733  
 ocular tonometry through sonic excitation and laser Doppler velocimetry 0-56152  
 piezoelectric transducer appl., for variable pressures up to  $6 \times 10^8 \text{ N/m}^2$  0-31785  
 pulmonary artery press. estimation using pulse wave velocity 0-12203  
 pulsed, using piezoelectric pick-up 0-31778  
 secondary standard gauges for measurement up to 1 GPa 0-27289  
 standards comparison, primary, mercury barometer vs. gas-operated pressure balance 0-13090  
 surfaces, sliding, lubricated (*German*) 0-14643  
 tonometer, applanation, for intraocular pressure meas. 0-30833  
 transdiaphragmatic pressure measurement using a single gastrooesophageal probe 0-56248  
 tube outlet section gas flow at supercritical pressure differentials 0-28569  
 turbulent structure determ. using thermoprobe unit in fluid stream (*Bulgarian*) 0-28584  
 U-shaped Hg manometer, 1300-2300 torr range 0-31784  
 venous system visualisation combined with press. meas., technique and equipment 0-36094  
 $\text{UF}_6$ , negative surface ionisation investigation using sensitive detector and pressure gauge 0-31781

**pressure sintering** *see sintering***pressure transducers**

- biomedical catheterisable sensors,  $\text{PO}_2$  probes, press. transducer and photometers 0-46080  
 biomedical transducer for intraluminal press. recording 0-17152  
 cylindrical tensoresistive pressure transducer 0-8978  
 differential, air-filled transducers, dynamic characts. 0-3879  
 epidural intracranial-pressure transducer with reduced tissue stress interference 0-41290  
 equipment development, design and appls. 0-13091  
 frequency response measurement technique for press., vol. and flow transducers 0-41344  
 gas-filled, effects of gas density on freq. response, medical appls. 0-56249  
 high resolution quartz transducer, high temperature electronics for geothermal energy 0-11997  
 high-pressure clamp cell for elec. conductivity measurements, 8 GPa, 77K 0-37047  
 jet-displacement transducer with sectional calibration, wide-band 0-4698  
 magnetic discharge manometric convertor 0-31779  
 manganin thin film microtransducers for elastohydrodynamic lubrication studies 0-37048  
 MOS structure, p-channel, effect of isotropic stress on Si valence band struct., press. transducer appl. 0-25011  
 MOSFET, piezoresistivity effects and use as press. transducers 0-4695  
 pick-up with Si column strain-gauge convertor 0-31732  
 pneumatic press. transducer for corrosive media, error and sensitivity 0-22345  
 polarisation and piezoelectric, high dynamic pressure measurements in solids 0-47070  
 pressure transducer measurements, thermal transient effects 0-31700  
 primary measuring transducers for fast-response gas analyzers, dynamic characts. 0-4697  
 secondary standard gauges for measurement up to 1 GPa 0-27289  
 semiconductor pressure sensors, thin Si diaphragm form., piezoresistive and capacitive structs. 0-13065  
 semiconductor pressure transducers, temp. compensation, strain gauge appls. (*Polish*) 0-31726  
 strain gauge semicond. transducers, Sapfir, development and appls. 0-13059



**pressure transducers continued**

- temperature coefficient sensitivity, compensated using positive feedback 0-17928
- tooth mobility measuring instrum. employing 24 V transducers 0-36187
- velocimeter for fluctuating temp. and vel. meas. in combustion field 0-14856
- zero offset change rel. to transducer performance 0-56255
- Si miniature biomedical piezoresistive pressure transducer (*German*) 0-37016

**pressure vessels**

- AGR pressure vessel, safeguards for man-access 0-27790
- AGR pressure vessels, radiation protection for shutdown man-access 0-5374
- axisymmetric, with structural discontinuities, computer aided elastic stress analysis (*Japanese*) 0-38265
- BWR, surface inspection methods, in-service inspection of reactor pressure vessel 0-27759
- BWR LOCA, containment dynamic loadings 0-763
- cell design for hydrostatic pressure up to 25 kbar 0-52260
- cladding, cracks under stainless steel cladding of pressure vessel, detection, causes, danger 0-52760
- composite spherical pressure vessels with hardening metal liners 0-7655
- concrete, fission reactor containment material, development of different types to overcome various problems 0-52738
- container for volatile inorganic hydrides of specially high purity 0-47043
- creep bounds and brittle damage estimates 0-23908
- fatigue design curves using modified Langer eqn. for pressure vessel alloys 0-30107
- fission reactor, safety anal. of cooling pipes 0-32370
- fission reactor pressure vessel and circuit development, conf. report 0-47541
- HTGR primary coolant system depressurisation accident, expt. and numerical anal. 0-775
- HTR-PRCV development of a removable closure for large cavities 0-5221
- hydraulic testing, leak detection using acoustic equipment (*French*) 0-789
- LMFBR, reactor closure assembly, rotating plug size 0-5227
- LMFBR reactor closure assembly, seals for rotating plugs 0-5226
- LMFBR vessel cavity and cell liners, elastic/plastic design 0-52728
- NMR probe for high-pressure and high-temp. expts. 0-22403
- nuclear power conf., Chicago, United States, July 1979 0-794
- nuclear reactor containment designs, value-impact assessment 0-797
- nuclear reactor containment structures, design and construction, ACI-ASME code of practice impact 0-798
- nuclear reactor pressure vessels, stress analysis program, STANSAS (*Japanese*) 0-22969
- plastic response of orthotropic spherical shells under blast loading 0-33477
- polycrystalline cubic BN plunger chamber for high-pressure Mossbauer meas. 0-31786
- PWR, control and effects of pressure vessel failure in steam-water cycle 0-770
- PWR pressure vessel reliability, simplified model extension and appl. 0-27786
- reinforced concrete containment model behaviour under thermal gradients and internal pressure 0-42837
- return to atm. press., desorption rate of H<sub>2</sub>O and H<sub>2</sub> (*French*) 0-42233
- steel, failure and radiation damage (*Czech*) 0-619
- stress intensity factor determ. 0-37455
- structural materials, pressure testing (*Spanish*) 0-52735
- structural representation in stress anal. 0-27703
- vent clearing analysis of a mark III pressure suppression containment 0-32371
- Ti-Al-Mo alloy VT-14, spherical pressure vessel, correlation between fracture stresses and mech. laboratory characts. 0-25838

**primary cells**

- cardiac pacemaker, neutron radiography investigation of electrolyte, USA National Bureau of Standards 0-56179
- cardiac pacemaker reliability technology workshop, Gaithersburg, USA (Oct. 1977) 0-27038
- galvanic cells using fluoride-conducting solid electrolytes 0-3501
- Li-I hermetically-sealed cells, long life expectancy, pacemaker power source 0-40850
- Li-metallic oxysalt organic electrolyte batteries 0-3502
- pacemaker battery characteristic meas. microcalorimeter 0-30936
- pacemaker battery internal loss characterisation calorimeter 0-30934
- pacemaker battery microcalorimetric testing 0-30933
- performance limits, technical and economic factors 0-45657
- polarity reversal, appl. of Evans' diagram 0-35664
- self-discharge process assessment by microcalorimetry 0-30935
- voltage delay in lithium non-aqueous battery systems 0-35662
- Ag/Ag<sub>2</sub>I<sub>2</sub>PO<sub>4</sub>/I<sub>2</sub> cell, cell voltage meas. 0-55315
- AgI-based solid electrolyte cell discharge mechanism 0-35663
- Li batteries, large energy content and long shelf life (*Danish*) 0-16794
- Li, developments and appl. survey 0-50949
- Li, future uses, production, and advantages 0-35659
- Li/SOCl<sub>2</sub>, cyclic voltammetric and coulometric obs. of SOCl<sub>2</sub> reduction 0-30440
- Li/SOCl<sub>2</sub> hermetic primary cells, effect of type of C on performance 0-35661
- Li-I<sub>2</sub> pacemaker battery electrolyte exam. by neutron radiography 0-30940
- Li-I<sub>2</sub> pacemaker cell end-of-life characteristic approximation 0-30937
- Li-I<sub>2</sub> power cell accelerated discharge test for battery longevity model 0-30938
- Li-SOCl<sub>2</sub> battery for implantable cardiac pacemakers 0-30939
- Li-SOCl<sub>2</sub> hermetic D cells, effect of Li<sub>2</sub>B<sub>10</sub>Cl<sub>10</sub> and Li<sub>2</sub>B<sub>12</sub>Cl<sub>12</sub> on performance 0-12000
- LiSOCl<sub>2</sub> battery undersea applications 0-45658
- Mg-MnO<sub>2</sub> dry batteries, impedance parameters and state-of-charge 0-21390
- Zn-air, comparison with conventional Leclanche cells 0-35660
- Zn-MnO<sub>2</sub> dry batteries, impedance parameters and state-of-charge 0-21390
- Zn-pore electrodes and cells, operation 0-26126

**primary cosmic radiation** *see primary cosmic rays***primary cosmic rays**

- hadron energy spectra produced by primary cosmic ray particles, E>10<sup>14</sup> eV 0-21880
- heavy nuclei diffusion in atmosphere, spectra and comp. 0-41680

**primary cosmic rays continued**

- low energy cosmic rays, Skylab meas. of heavy ions 0-56689
- nuclei composition effect on cosmic ray muons response function 0-41683
- nucleon spectrum calc. of atmospheric neutron/proton ratio and sea level neutron spectrum 0-8499
- sidereal variation of 10<sup>11</sup> eV particles and interplanetary mag. fields 0-17452

**printed circuits**

- PWB holes counting, wide-aperture telecentric laser scanning system design 0-1264
- space-quality solder joints, resistance to thermal fatigue 0-25831
- Sn-Pb composition anal. of PCBs using beta-backscatter gauge 0-16631

**printers**

- chromatography, data processor with thermal printer-plotter for GC and LC (*Japanese*) 0-50920
- ECG recorder and printer with fixed writing heads 0-3854
- electronic imaging hard copy methods and printing systems 0-47134
- laser alphanumeric character generator for line printer and COM 0-33067
- matrix, wire, high speed, wear resistivity obs. (*Japanese*) 0-55540
- modular contact printer for high speed automatic additive colour cinefilm printing 0-42276
- photofinishing printer response customisation 0-4793
- GaAs laser facsimile printer 0-30207

**printing**

- contact printing method utilising heated photoresist adhesive prop. for hologram copying 0-5704
- electronic imaging hard copy methods and printing systems 0-47134
- graveure and embossed papers, printability prediction by time series anal. 0-15345
- holographic printing of discrete stereograms of group portraiture (*Russian*) 0-23644
- laser printing, dry Ag material technology 0-13179

**printing industry**

- see also printing*
- laser printing, seminar, Los Angeles, USA (Jan. 1979) 0-12852

**prismatic dislocations**

- CdS, dislocation emission, photoluminesc. spectra 0-16084
- Si, oxidation-induced stacking faults, nucleation mechanism 0-15122
- Si-O<sub>2</sub> wafer, annealed, surface- and inner-microdefects, TEM obs. 0-54236
- Zn, basal dislocation-prismatic dislocation ring interactions by method of moments (*Russian*) 0-10550

**prisms (optical)** *see optical prisms***privacy of data** *see security of data***probability**

- see also game theory; Monte Carlo methods; queueing theory; random processes; statistics*
- additive and cancellative interacting particle systems, book 0-41960
- amplitude distributions, appl. in practical data assessment problems 0-27107
- atomic collisions, quasiclassical theory, transition between spatially degenerate levels 0-43150
- Bayesian prediction model for fire occurrences in nuclear power plants 0-18527
- cause-consequence chart to assess the availability of the containment spray system in a nuclear reactor 0-52756
- coarse riverbed material, probability density function of biased samples 0-12445
- colloidal systems, dynamical props., correlation and response functions 0-22286
- deterministic dynamics, relationship to probabilistic description 0-4646
- elastic neutron scattering, probability density function approach 0-13480
- fission, supercritical multiplying systems, extinction problem, point model approx., models for neutron multiplicity 0-22883
- fracture model, time dependent probabilistic, for strength of glass fibre reinforced plastics 0-40477
- hydrology, discharge probabilities, empirical formulae 0-26559
- Jeu de Rencontre, critical elaboration of de Moivre's resolution (*Italian*) 0-4499
- Jeu de Rencontre, work by Euler 1751 (*Italian*) 0-4500
- Jeu du Treize, demonstration of Nicolas Bernoulli's formula (*Italian*) 0-4498
- LWR nuclear reactor sabotage risk modelling 0-23001
- minor planets, orbital elements probability distrib. 0-46461
- nuclear plant specific risk studies, data specialisation, Bayes' theorem 0-47601
- nuclear power plant structure probable risk assessment, improved safety system research plan 0-797
- polymer, crosslinked, probabilistic theory of structural and physical characteristics 0-5649
- probability foundations, modal frequency interpretation 0-12885
- propensity theory, hidden variables, coin tossing appl. 0-42040
- PWR, selection of events for probabilistic safety assessment 0-742
- PWR LOCA, fuel rod behaviour, probabilistic anal. using response surface method 0-663
- PWR steam generator tube rupture, probability distrib. for releases of <sup>131</sup>I and <sup>133</sup>Xe 0-13668
- PWR steam line break, pipe rupture probability 0-18526
- quantitative risk evaluation, risk projection and human factors as related to nuclear systems 0-13722
- quantum and classical theories, probabilistic descriptions 0-36899
- quantum mech. foundations, conditional probability of a generalised probability theory 0-12949
- quantum probability in logical space 0-31579
- radioactivity and quantum mechanics unification, probabilistic conceptions, 0-12946
- risk analysis methods, practical applications 0-12894
- risk analysis of nuclear systems, anal. of human performance 0-18475
- river basin water resource, Pareto region, stochastic multicriterial problem in control 0-4055
- statistical mechanics, foundations 0-22271
- steady-state process, probability characts. error calcs. 0-42145
- teaching of probability and statistics, rel. to tennis 0-41997
- Weibull wind speed distrib. parameters, estimation using Weibull prob. paper and percentile estimators 0-50931

**probes**

- see also electron probes; muon probes; plasma probes*
- calorimeter probes for measuring high thermal flux 0-13080



**probes continued**

- conductivity, for dynamic measurements on non-metallic catalyst during adsorption and catalysis 0-13096
- electrodeless conductivity probe for high-temperature and pressure measurements 0-52272
- electron beam evaporation source with integrated rate control (*Hungarian*) 0-20798
- expendable bathythermograph digital recording and display system 0-46318
- fast breeder reactor boiler tubes, eddy current probe insertion for in service inspection, method development (*Japanese*) 0-822
- fission reactor, void fraction measurement, RF local probe development 0-568
- flow, four-wire, with output signal digital processing, appl. to cylinder wake characts. 0-19541
- foam insulation material thermal conductivity meas., unsteady probe method (*German*) 0-31740
- freely sinking probe horizontal velocity meas. interpretation 0-46321
- hot-wire, flow reversal detection in unsteady flow 0-10333
- hot-wire, used in subsonic airflow measurement, interpretation of signals 0-14857
- IR gas analyser, non-dispersive, for industrial processes and environment protection (*Hungarian*) 0-55735
- Kulite 2-probe synchronized sampling technique for measuring flows behind rotors, calibration 0-14865
- leak detector pickups, halide, optimal flow rate determ. 0-48825
- miniature probe microphone using optical fibre 0-48534
- nondestructive acoustic elec. field probe 0-47076
- nucleonic probe ccts with noise rejection, low-level activity meas. 0-52833
- open-ended waveguide probe/applicator combination (*French*) 0-3820
- oxygen monitoring in process gas streams, sensor 0-52181
- plasma impurity flux and differential wall changes, in Alcator-A Tokamak, surface probes 0-38664
- quartz tube orifice leaks for local, fast-response gas sampling to mass spectrometers 0-35609
- quick sample change probe for magic-angle-spinning NMR in a superconducting magnet 0-31834
- RF, for bubble size and vel. measurements 0-6177
- semiconductor domain instability and resistivity profile meas., universal capacitive probe 0-31796
- semiconductor temperature testing probes, accuracy and thermal characts. 0-52201
- spectrophotometer dip probe bubble formation prevention 0-13154
- thermoelastic expansion flexible acoustic probe 0-16618
- thin film growth measurement using galvanically separated quartz monitor probe (*German*) 0-11576
- two-dimensional space isothermal and nonisothermal turbulent flow (*German*) 0-28505
- velocity probes for non-uniform gas flow in large ducts 0-48829
- vibrating viscometer probe for measurement of viscosity of slurries, assessment 0-28586
- xerographic cascade flow, carrier bead velocity distribution meas. probe 0-47136
- Pt resistance temperature probes, constructional types and state of technique (*German*) 0-52213
- Xe, for radiation contamination monitoring 0-27826

**process computer control**

- electron beam evaporation rate automation by ion current meas. (*Hungarian*) 0-16198
- large laser control system, evolution from Shiva to Nova 0-9894
- machine tool for diamond-turned surface accuracy improvement 0-1367
- metrological support to computer-aided process control, design and upgrading 0-185
- multibeam microwave therapy with computer control 0-3766
- nuclear reactors, process monitoring and parameter estimation, multivariate signal analysis algorithms 0-47585
- photofinishing printer response customisation 0-4793
- polisher for small-tool fabrication of mirrors 0-14496
- VPE impurity profile computer-aided control 0-2962

**process control**

- see also process computer control*
- cold light production by high vacuum deposition of multilayer interference coatings (*German*) 0-53486
- crystal growth from solution in multisection continuous crystalliser 0-2935
- electronics in nuclear science and technology 0-9347
- electroplated coatings testing and control (*German*) 0-2967
- pellet fuels,  $\gamma$ -active, remotely operated plant for fabrication 0-32340
- production processes, nonstationary Doppler effect, freq.-phase methods of investig., control 0-45464
- recycle reactors for catalyst evaluation 0-3402
- rotary tube photographic processor design 0-4795
- sugar industry, measuring transducers for automation (*Polish*) 0-42212

**Procopiu effect**

No entries

**product control** *see quality control***production**

- this heading is restricted to industrial production*
- see also assembling; manufacture; quality control; reliability*
- artificial hand with sensory feedback 0-36191
- medical equipment production efficiency and quality improvement 0-3830
- Cd electrodes plastic bonded, for Ni-Cd accumulators, production methods 0-45659

**production control**

- see also process control; quality control*
- monitored parameters for quality control in instrument production 0-186
- Si substrates during sputtering and sputter etching, thermal history of substrates 0-25562

**production schedules** *see production control***production testing**

- diffraction pattern sampling, industrial appls. 0-9015
- laser interferometer application to length meas. in production (*German*) 0-18007
- microdensitometers for highly accurate metrology, industrial use 0-9017
- optical gauging, noncontact, by remote image tracking 0-8961
- optical glass fibres proof-tester 0-53412

**production testing continued**

- precision measurement, image analysis of precision components (*German*) 0-42193
  - steel, low alloy, welded joints, cracking during heat treatment, simple detection method 0-7724
- program and system documentation**
- pacemaker automated test system developments 0-30944
- program testing**
- reactor protection computer systems, statistical verification of reliability 0-32417
- programmed control**
- see also process control; production control*
  - aspherics precision manufacture with programmed microelectronic control 0-1368
  - lingual tactile sensory system, automated instrumentation for research 0-8205
  - NMR spectrometer, programming device for control of frequency synthesizers 0-22400
  - NQR spectrometer, programming device for a spin-echo installation 0-17972

**programmer training** *see training***programming, mathematical** *see mathematical programming***programs (computer listings)** *see complete computer programs***projectiles**

- see also ballistics; missiles; rockets*
- artillery shell, experimental determination of mass-property/trajectory-drift relationship 0-8779

**projectors (optical)** *see optical projectors***promethium**

*see also nuclei with .....*

No entries

**promethium alloys**

No entries

**promethium compounds**

*see also promethium alloys*

No entries

**prominences (solar)** *see solar prominences***propagation, wave** *see wave propagation***proportional + integral + differential control** *see three-term control***proportional control**

- solar battery, charging networks and stepping motors, microcomputer mechanical proportional control 0-50987

**proportional counters**

- see also position sensitive particle detectors*
- corona counter, determ. of U content in solid waste mats. by  $\alpha$ -detection (*Russian*) 0-27904
- cylindrical, operation at pressures up to 100 atm 0-23249
- data acquisition system 0-42913
- delay line for position readout in wire chambers 0-18757
- DePangher precision long counter and neutron dose-rate meters, calibration 0-47822
- drift chamber development 0-27879
- dual registration channel cct. based on hybrid IC 0-23266
- electron scattering experiments, detection system, Saclay linear accelerator facility 0-52809
- fast electron  $f(z)$  meas. using short accelerator pulses 0-12275
- gas scintillation counter, for high count rate X-ray detection 0-14052
- gas-filled electroluminescent detector for soft X-rays, constr. and characts. 0-32569
- high-pressure proportional counter at low temperatures 0-23250
- liquid H chamber Lyudmila, electronic apparatus for expanded diagnostic system 0-23265
- low level activity meas. of  $^3\text{H}$  and  $^{14}\text{C}$  using multielement and cylindrical proportional counters, comparison (*Czech*) 0-52818
- methane filled telescopes for fast neutron spectrometry 0-37683
- microdosimetric results from ionisation chamber and proportional counter compared 0-9429
- microdosimetric studies with low LET radiation using cylindrical walled and wall-less proportional counters 0-36140
- Mossbauer conversion electron spectroscopy at high temp., proportional 0-27886
- multianode cylindrical proportional counter for position sensing at high count rate 0-5446
- multielement, anticoincidence techniques for measuring low T activities 0-27874
- multiwire and drift proportional chambers 0-47826
- multiwire proportional chamber for identification of relativistic particles 0-23256
- multiwire proportional chamber with anode wire winding pitch of 1 mm 0-23257
- muscle contraction, time-resolved X-ray diff., data-collection system (*Japanese*) 0-46108
- MWPC, compact low mass system of four cylindrical chambers 0-14046
- MWPC, delay time distrib. meas. (*Chinese*) 0-23261
- MWPC, drift chambers and time projection chambers, development, operation and appl. (*Italian*) 0-879
- MWPC, IC tapped delay line readout 0-5455
- MWPC, interwoven grid wires for second coordinate readout 0-27897
- MWPC, large cylindrical dual coordinate 0-18759
- MWPC, localisation of minimum ionising particles using cathode induced charge centre of gravity readout 0-32576
- MWPC with high spatial resolution, construction and efficiency meas. (*Italian*) 0-9452
- neutron counter development, electron drift vel. simulation 0-48843
- neutron detectors, self-powered, sensitivity determ. on neutron flux density 0-52817
- neutron gas proportional  $\alpha$ -recoil spectrum 0-5433
- neutron primary beam and shielding radiation quality and absorbed dose obs. 0-12281
- position sensitive, for X-ray residual stress meas. (*Japanese*) 0-11853
- positron annihilation studies using high-density proportional chambers 0-25478
- proton spectrometer/polarimeter for photoreactions below 1 GeV 0-18751
- proton-recoil counter technique for measurement of fast neutron spectrum 0-9447
- resonance neutron radiography using a position-sensitive proportional counter, appl. to meas. of nuclear fuel 0-13597



# proportional counters continued

- simultaneous determ. of three elements by X-ray fluorescence 0-40786
- single 1 m wire position-sensitive counters for low ionisation particles 0-5441
- single atom detection in particle tracks 0-9475
- time-dependent properties of proportional counters SRPO-304 used with scintillation detectors 0-42894
- walled and wall-less proportional counter characteristics and microdosimetry 0-26371
- X-ray stress anal. using position-sensitive proportional counter 0-1498
- Ar, liquid, calorimeter, electron and proton response 0-47832
- BF<sub>3</sub>, response functions of spherically moderated neutron detectors 0-37687
- CH<sub>4</sub> filled, geom. effects on proton recoil spectra 0-14050
- D-D neutron meas. on 40 kV, 60 A neutral beam test facility 0-37710
- <sup>222</sup>Rn very low conc. meas. with proportional counter 0-27907
- Xe filled proportional scintillation detector for charged particles 0-32572
- Xe probe for radiation contamination monitoring 0-27826

# prospecting (geophysical) see geophysical prospecting

# prosthetic power supplies

- battery self-discharge process assessment by microcalorimetry 0-30935
- cardiac pacemaker batteries, neutron radiography investigation of electrolyte, USA National Bureau of Standards 0-56179
- pacemaker battery internal loss characterisation calorimeter 0-30934
- pacemaker battery microcalorimetric testing 0-30933
- pacemakers, Li-I hermetically-sealed cells, long life expectancy 0-40850
- Li-I<sub>2</sub> pacemaker battery electrolyte exam. by neutron radiography 0-30940
- Li-I<sub>2</sub> pacemaker cell end-of-life characteristic approximation 0-30937
- Li-I<sub>2</sub> power cell accelerated discharge test for battery longevity model 0-30938
- Li-SOCl<sub>2</sub> battery for implantable cardiac pacemakers 0-30939

# prosthetics

- see also *artificial limbs; artificial organs; orthotics; sensory aids*
- above-knee sockets, total surface bearing, self suspending 0-51294
- acoustic diagnostic technique for prosthetic fixation evaluation 0-21510
- arterial grafts, synthetic, mech. props. 0-17192
- biomaterials in dentistry and medicine, conf., Los Angeles, USA (Dec. 1978) 0-27028
- biomechanics conference, Ann Arbor, USA (Oct. 1978) 0-31408
- Bjork-Shiley aortic prosthesis, in vitro vel. meas. using laser-Doppler anemometer 0-17196
- blood substitutes, surface energetics anal. 0-41321
- cardiac disc mitral valve in left ventricle, computer model of motion 0-8214
- cardiac valves, role in artificial heart performance 0-21575
- circulatory device fluid mechanics and haemolysis, review 0-46101
- dental implant fixation by elec. mediated process, tissue ingrowth 0-8115
- dental implants, stress anal; effect of elastic parameters and geometry 0-30930
- dental implants, stress anal., effect of root-length and pseudo periodontal ligament incorporation 0-30931
- denture base acrylic tensile testing 0-16621
- diacrylate fissure sealants, film charact., dentistry appl. 0-12306
- elbow flexion-extension and forearm pronation-supination for elbow endoprosthesis design 0-3682
- extracorporeal circulation equipment, automatic control 0-3865
- femoral head replacement prosthetic, transmission of load actions 0-56284
- femoral implant, numerical simulation of acrylic grout curing 0-40968
- finite element analysis as an aid to implant design 0-30932
- heart valve, disk-type, numerical soln. for steady axisymmetric flow 0-35952
- heart valves, simple stress estimation method 0-8210
- hip joint prosthetic component deformation meas. by holographic interferometry (German) 0-12302
- hip prostheses, Charnley, expt. anal. of surface stresses 0-17191
- hip prostheses, expt. study of friction and lubrication 0-17189
- hip prostheses femoral component biomechanics, bone cement stress 0-56285
- intramedullary implants pre-coated with bone study, fixation study 0-7587
- joint replacements, mech. factors 0-56286
- knee joint design, assessment using electrogoniometric recording 0-56288
- knee joint simulator, development 0-17190
- knee prosthesis, sliding meniscus, design concepts, biomechanical techniques for movement study 0-41315
- laryngeal prosthesis, internally worn, design and construction 0-41318
- material mech. props., effects of physiological environment, cardiovascular appls. 0-8212
- medullary pin causing surface bone remodeling 0-3683
- myofeedback control system, design 0-51296
- myofeedback control system trainer 0-51297
- NDT by holographic interferometry and optical correl. 0-40659
- neural prostheses, review 0-21576
- phonetic defects caused by facial gaps, correction using prosthetics (French) 0-51298
- PMMA dental biomaterials, fracture toughness testing 0-50800
- poly (N,N'-terephthaloyl-L-lysine) membrane for artificial red blood cells, interaction with serum proteins (Japanese) 0-12061
- polyethylene, porous, tensile strength of interface with bone 0-30737
- polyethylene, ultra high mol. wt., knee prosthesis, in vivo wear props. 0-17204
- polymer biocompatibility evaluation by cell culture method (Japanese) 0-12301
- polymer endoprosthetic joint, fatigue life 0-40521
- polymers, adsorpt. of plasma proteins, Fourier transform IR spectrometry 0-16899
- polymers in medicine, review, book contrib. 0-12307
- rehabilitation engineering (Japanese) 0-12304
- scala tympani electrode for auditory prostheses, 8 channel 0-36194
- sensory feedback, human tracking performance with afferent elec. nerve stimulation 0-17195
- steel, austenitic stainless, stress corrosion cracking, mixed mode, fractographic evidence in surgical implant 0-30156
- steel, stainless, fibre reinforced porous coating, isostatically compressed for bone ingrowth 0-35134
- synovial fluid boundary lubrication model, structuring of boundary water 0-35950
- tetraplegics manipulator, microcomputer control 0-41314

# prosthetics continued

- thermoplastics, appl., deformability in physiological salt soln. 0-12305
- thromboresistance of biomaterial, influence of implantation techniques (German) 0-3861
- visual prosthetic implant, cortical electrical phosphene props. 0-12112
- wrist kinematic and kinetic analysis rel. to implant design 0-16999
- Au dental fillings, cause of dose perturbation in radiation therapy 0-12265
- Co-Cr-Mo alloy shoulder prosthesis, wear and fatigue tests 0-26415

# protactinium

- see also *nuclei with .....*
- lattice parameter variation at low temp., thermal expsn. 0-15046
- Mossbauer resonance, elec. field gradient 0-15927
- superconductivity, transition temp. and upper critical mag. field 0-44756
- <sup>231</sup>Pa dating of fossil corals and shells 0-12434
- <sup>231</sup>Pa Mossbauer resonance, elec. field grad. 0-7207
- <sup>233</sup>Pa importance in neutron economy Th-fuelled CANDU reactor 0-22980

# protactinium compounds

- Pa complex, protactinium tropolonate, synthesis, cryst. struct. parameters 0-33945
- PaAs<sub>2</sub>, Pa<sub>3</sub>As<sub>4</sub>, and PaAs, cryst. growth by chem. vapour transport, cryst. struct. 0-35066

# protection

- see also *alarm systems; corrosion protection; protective coatings; radiation protection; safety*
- photomultiplier protection against optical overloads, electromagnetic shutter control 0-23255

# protective coatings

- see also *corrosion protective coatings; wear resistant coatings*
- acrylic coating for optical fibres, surface tension effects 0-53487
- boride coatings, under elec. heating conditions, hydroabrasion wear resist. on Armco, Fe and steel 0-55543
- boride coatings on steel effect of Cu impurities in reaction mixture on brittleness, acoustic emission meas. 0-16581
- boride on W and Mo 0-21165
- ceramic self-cleaning catalyst for ovens and grills (Japanese) 0-55557
- contact fatigue limit testing machine, for metals, alloys under vibrating load 0-55617
- CrMoV, surface coating to prevent oxidation during high temp. AE 0-16539
- double-layer coating with double cone nozzle in-line with optical fibre drawing 0-53488
- fusion reactor environment, development of coatings 0-18618
- glass ceramic protective coatings for Ti, synthesis and props. 0-25900
- glass fibre protective coatings, using polymers, materials and techniques 0-33252
- glass-enamel coating on C steel tubes, prod. by induction fusion method, heating rate of steel effect 0-11825
- laser damage protective coating, electric field interference 0-33062
- lens, water soluble cryst., protective coating to aid polishing 0-33250
- nuclear facilities, surface protection materials, tests on 900 commercial products (German) 0-35356
- optical fibre primary coat using modified silicone, transmission characts 0-38098
- polyethylene resin coated paper formulation for photography 0-4794
- polymer film coating, electropolymerisation in aq. medium book contrib. 0-50778
- soft metallic films, role in reducing friction between metal surfaces 0-55592
- stainless steel, ferritic SUS 410 type, coated with organometallic complexes and Ti alkoxides 0-34078
- steel, boriding with B<sub>2</sub>C based paste 0-16583
- steel, C, wear of Cr, Zn protective coatings, exam. using nuclear radiation excited X-ray fluorescence 0-21206
- steel, type 08sp, vitreous enamel coatings effect on mech. props. of surface layers 0-35424
- Al, bulk and plasma-sprayed coating, D<sub>2</sub><sup>+</sup> trapping meas. 0-20754
- B coatings on graphite, fusion reactor appl. 0-23147
- B<sub>2</sub>C, first-wall coating for Tokamak, H retention and release 0-18620
- Be coated limiters, first wall protection 0-32483
- Be, plasma-sprayed coatings on Cu and stainless steel, fusion reactor appl. 0-18619
- C coatings for fusion applications 0-23146
- C fibre reinforced polyphenylsiloxane composites, long-time strength, and influence of protective coatings 0-3133
- CeF<sub>3</sub>, protective overcoating material for inhomogeneous interface laser mirror coatings 0-1252
- Cu-benzotriazole (benzimidazole) thin films, ellipsometric study 0-35114
- MoSi<sub>2</sub> coating for SiC heating elements 0-21137
- Ni-Al-Cr<sub>2</sub>C<sub>3</sub>, eutectic, Al<sub>2</sub>O<sub>3</sub> coatings for oxidation resist. 0-50776
- Pd, on stainless steel, interdiffusion at reactor wall temps., Rutherford backscatt. obs. 0-39361
- SiC coating on Mo, CVD and stability under thermal cycle conditions 0-7500
- SiC coatings for first-wall candidate materials by RF sputtering 0-25563
- Si<sub>3</sub>N<sub>4</sub>, C, protective coating for GaAs laser 0-5753
- TiB<sub>2</sub> coated limiters, first wall protection 0-32483
- TiB<sub>2</sub> coating on graphite by CVD 0-21131
- TiB<sub>2</sub>, first-wall coating for Tokamak, H retention and release 0-18620
- TiB<sub>2</sub>, plasma-sprayed coatings on Cu and stainless steel, fusion reactor appl. 0-18619
- TiC coated limiters, first wall protection 0-32483
- TiC, plasma-sprayed coatings on Cu and stainless steel, fusion reactor appl. 0-18619
- VBe<sub>2</sub>, coated limiters, first wall protection 0-32483
- VBe<sub>2</sub>, plasma-sprayed coatings on Cu and stainless steel, fusion reactor appl. 0-18619

# proteins

- see also *gelatin*
- acetylcholine receptor from Torpedo Californica, struct. anal., low-angle neutron scatt. obs. 0-30651
- acetylcholinesterase, membrane bound, activity rel. to struct. changes induced by cAMP 0-30674
- actomyosin kinetic anal., review 0-21441
- adsorbed, use of Si-SiO<sub>2</sub> as electrode for elec. and ellipsometric meas. 0-15366
- adsorbed at interfaces, fluoresc. spectroscopy study 0-12315
- albumin, adsorption on SiO<sub>2</sub> 0-10777
- albumin, human, labelling of microspheres with <sup>197</sup>Hg 0-51251



## proteins continued

- albumin and albumin microspheres,  $^{68}\text{Ga}$  labeling 0-17137  
 albumin denaturation, investigation by PMR 0-3582  
 amino acids, aromatic, solid, NMR, detection of individual C resonances, appls. 0-51042  
 amphiphilic-polymer liquid crystal, NaCl conc. influence on struct., X-ray diffr. study 0-44126  
 apoprotein of Folch-Lees lipoprotein, viscoelastic monolayer, dynamic surface potentials 0-3603  
 axoplasmic transport of proteins, review 0-21464  
 bacterial catalase,  $^{57}\text{Fe}$  enriched, active centre, Mossbauer spectra meas. 0-8024  
 bacteriorhodopsin, anomalous amide I IR absorpt. rel. to  $\alpha$  helices distorted struct. 0-12058  
 bacteriorhodopsin, in purple membrane, radial autocorrelation function, significance in X-ray diffr. patterns 0-51048  
 bacteriorhodopsin, purple membrane of *H. halobium*, effect of 560-570 transition and blue light on photochem. 0-30673  
 bacteriorhodopsin, reson. CARS spectrosc. 0-8014  
 bacteriorhodopsin, reson. Raman evidence for secondary protein-Schiff base interactions, primary excitation mechanism 0-55981  
 bacteriorhodopsin Br570, bathochromic shift of absorpt. band in external elec. field 0-35838  
 bacteriorhodopsin chromophore, bleaching by  $^{60}\text{Co}$   $\gamma$ -rays 0-30784  
 bacteriorhodopsin generated photocurrents on planar bilayer membranes 0-51050  
 bathoproducts of rhodopsin, isorhodopsin I, and isorhodopsin II 0-51088  
 bimolecular rate constant ionic strength dependence, effect of a molecular dipole 0-55977  
 biomembrane, phase changes and determination methods (Czech) 0-3599  
 biopolymer, electronic-conformation interactions 0-3588  
 biopolymer soln. heat capacity, conformational props. temp. depend. 0-8009  
 blood proteinpolymer interfacial behaviour, influence of hydrophilic-hydrophobic type of microphase separated struct. (Japanese) 0-12051  
 bovine trypsinogen, low-temp. study, effect on flexibility, temp. factor, mosaic spread, extinction and diffuse scattering 0-54214  
 C-reactive protein, interaction with artificial phosphatidylcholine bilayers 0-3579  
 calmodulin, stimulation of  $\text{Ca}^{2+}$  transport across red blood cell plasma membrane 0-12066  
 carbonmonoxymyoglobin, frozen soln., recoilless fraction, Mossbauer spectra meas. 0-8025  
 chloroquine-biopolymer binding interactions, PMR effects 0-55982  
 chorionic gonadotropin, human,  $\alpha$ -subunit, cDNA isolation, cloning and sequence anal. 0-3587  
 chromatin protein, increase kinetics for heated cells, possible role in cell killing 0-40980  
 chymotrypsin-like proteins,  $\gamma$ -irrad. rel. to UV irrad., unfolding obs. 0-35984  
 coiling and topology of the antiparallel  $\beta$ -struct. 0-40956  
 coiling and topology of the parallel  $\beta$ -struct. 0-40957  
 collagen fibrils, rat tail tendon, quasi-hexagonal mol. packing model 0-30660  
 conformations, quantitative approach 0-30652  
 $\beta$ -crystallin, lens protein, prep. 0-16921  
 cytochrome C, immobilised, investigs. using magnetic micromixer attachment for SPECORD UV VIS spectrophotometer 0-56302  
 cytochrome c-serotonin soln., UV effect on optical props. 0-30663  
 cytochrome oxidase reaction, semiconduction as mechanism 0-55983  
 cytochrome P-450, non-equilib. states formed by low-temp.-reduction, absorpt. spectra 0-35837  
 deoxy ferrous haemoglobin Fe atom distortion, pseudo-Jahn-Teller effect 0-55984  
 deoxyhaemoglobin, high mag. field Mossbauer spectra, electronic states 0-35845  
 deoxyhaemoglobin high spin ferrous ion, low lying electronic states, far IR mag. reson. 0-48110  
 deoxymyoglobin, frozen soln., recoilless fraction, Mossbauer spectra meas. 0-8025  
 deoxymyoglobin, high mag. field Mossbauer spectra, electronic states 0-35845  
 deoxymyoglobin high spin ferrous ion, low lying electronic states, far IR mag. reson. 0-48110  
 deoxymyoglobin single crystals, Mossbauer study with polarised  $\gamma$ -rays 0-40962  
 diamine oxidase solutions, proton mag. relax. dispersion obs. 0-51136  
 diffusion coefficient of plant protein using quasielastic light scatt. apparatus (German) 0-12314  
 dipalmitoylphosphatidylcholine/glucagon (cardiolipin/insulin) systems, Raman spectra study 0-16903  
*E. coli* cells, iron-storage protein, Mossbauer spectra obs. 0-8022  
 elastin ultrastruct., freeze-fracture electron microscopy 0-8036  
 electron-transport type, H-bonding, ab initio MO 0-51039  
 enzymatic active transport model 0-51049  
 enzyme dynamics, statistical phys. 0-21439  
 enzymes, membrane bound, influence of membrane fluidity on activity, book contrib. 0-30688  
 enzymes, membrane-bound, activity on exposure to 2450-MHz microwave radiation 0-56126  
 eye lens low molecular weight protein obs. and prep. 0-16921  
 Fc-fragment crystals, low-temp. study, effect on flexibility, temp. factor, mosaic spread, extinction and diffuse scattering 0-54214  
 ferredoxin, from *Clostridium pasteurianum*, Mossbauer effect, ESR, and mag. susceptibility meas. 0-40961  
 ferredoxin, soluble, investigation of 2 forms from pea leaves, EPR obs. 0-45851  
 ferredoxin synthetic analogues,  $[\text{Fe}_4\text{S}_4(\text{SR})_4]^{3-}$  clusters, Mossbauer effect, EPR, and mag. props. 0-41057  
 ferredoxin-like centres, membrane bound, in photosystem I of blue-green algae, Mossbauer and EPR study 0-40974  
 ferric haeme complex of low spin, Mossbauer spectra, crystal field parameters 0-26203  
 ferric myoglobin cpds., single cryst., Mossbauer studies 0-8016  
 fibres, natural, Brillouin scatt. shifts, comparison with synthetic polypeptide obs. 0-55991  
 Fourier refinement of structs. 0-51037  
 gamma globulin, effect on latex particles flocculation kinetics 0-11958  
 gel electrophoresis, 2-dimens., in study of somatic cell differentiation 0-46114

## proteins continued

- gel scanner for location of proteins separated by isoelec. focusing 0-30953  
 globin, human, isoelectric focusing method for chain separation 0-17219  
 globular, compressibility in water at 25°C 0-40951  
 globular, crystalline, intermol. interactions, denaturation, DSC and X-ray diffr. obs. 0-16897  
 gramicidin A in biomembrane channel, IR spectroscopic obs. 0-16901  
 haeme proteins and metalloporphyrins, redox chem. and oxygen binding 0-3573  
 haemoglobin, dielec. transient response following UV irrad. 0-51166  
 haemoglobin, dielectric props. under UV excitation 0-6912  
 haemoglobin, sickling deer type III, macromol. struct. refinement by restrained least-squares and interactive graphics 0-28870  
 haemoglobin aqueous solutions,  $\gamma$ -irrad. in air and Ar 0-41135  
 haemoglobins and chlorocruorins, extracellular respiratory, physico-chemical and functional props. 0-3581  
 haemoprotein, fine structure of Fe ions 0-30661  
 haemoproteins, Fe-ligand binding and electronic struct., Mossbauer studies 0-8021  
 HeLa cell nuclei protein content, effect of hyperthermia 0-40972  
 helical structure reconstruction from projections, phage tail appl. 0-8237  
 histones, H2a and H4, aggregation ionic strength effect (Russian) 0-55697  
 horseradish peroxidase cpd. II, high-field Mossbauer spectra, 4.2 to 120K 0-8026  
 human serum and erythrocyte microwave complex permittivity meas. 0-3889  
 hydrophilic side groups, linear H-bonded systems, proton conduction 0-40973  
 15-hydroxy prostaglandin dehydrogenase activity in tissues of mice, X-irrad. effects 0-51169  
 immunoglobulin (Ig)  $\kappa$  chain m RNAs, identical 3' non-coding sequences favour unique C, gene in mouse 0-8010  
 insulin, cryst. growth kinetics 0-35823  
 kinetic constants of association and dissociation, theoretical determ. 0-51033  
 $\beta$ -lactoglobulin, absorpt. spectra for complexes formed with vitamin-A 0-30664  
 leghemoglobin minimisation of functions of many variables appl. to X-ray struct. anal. 0-3589  
 lysozyme, binding to bacterial cell wall trisaccharide NAM-NAG-NAM, X-ray cryst. struct. anal. 0-35834  
 lysozyme, cryst., dynamic sp. ht. capacity meas. 0-21447  
 lysozyme, cryst. growth kinetics 0-35823  
 lysozyme, sorption and desorption of water, thermal-stimulated press. and thermogravimetric anal. 0-8008  
 lysozyme, tryptophan residues, H exchange for D, relax., proton NMR spectra 0-35846  
 lysozyme complex with substrate-inhibitors, photosensitised electron transfer, role of  $\text{Cu}^{2+}$  0-30638  
 membrane damage caused by light irradiation of fluorescent concanavalin A 0-56123  
 metalloenzymes and carriers, hydration effect on mobility of Mossbauer atoms 0-35819  
 methanol dehydrogenase, enzyme, electron spin echo, 35 GHz 0-13113  
 methionine sulfoxide in protein,  $^{13}\text{C}$  NMR anal., method and expt. obs. 0-56305  
 metmyoglobin, dynamics study using Rayleigh scatt. of Mossbauer radiation 0-40963  
 microwave effect observation prerequisite conditions 0-3592  
 mixed protein phospholipid films, viscoelastic behaviour and Marangoni effect 0-3602  
 model building procedure 0-51036  
 model chain, aperiodic, electronic spectra, hopping cond. 0-5641  
 multivalent binding to substrate, linear differential equations in chemical equilibrium calculations 0-30279  
 myoglobin, static and dynamic structure of biomolecules, Mossbauer effect 0-40952  
 myoglobin- $\text{H}_2\text{O}_2$ , high-field Mossbauer spectra, 4.2 to 120K 0-8026  
 myoglobin- $\text{O}_2(\text{CO})$ , elec. field gradient tensor, Mossbauer meas. 0-8017  
 myosin, interaction with adenosine 5'-diphosphate, intermolecular spin diffusion study 0-18951  
 myosin, interactions with HDO, intermolecular spin diffusion study 0-18951  
 myosin helical fragments, stepwise pattern of thermal denaturing 0-40966  
 myosin kinetic anal., review 0-21441  
 NADH coenzyme, two photon absorpt. cross section meas., reaction rate modification 0-51043  
 nitrogenase, cofactor centres, Mossbauer spectra obs. 0-8023  
 nitrogenase active site, Mossbauer spectra of Mo-Fe-S clusters 0-45852  
 nuclear Overhauser effect, truncated driven, in presence of spin diffusion 0-1095  
 nucleic-protein interactions in tobacco mosaic virus, spin label and fluorescence obs. 0-40949  
 ovalbumin aqueous soln., macromol. gel layer formed on ultrafiltration tubular membrane, charact. 0-14260  
 oxymetalloproteins, electronic spectroscopic data review 0-52977  
 oxymyoglobin, frozen soln., recoilless fraction, Mossbauer spectra meas. 0-8025  
 phospholipid membranes, orientational order and integral protein struct. 0-45862  
 photoinduced electron transport across protein-containing membranes 0-30768  
 pigment-protein complexes, oriented, of photosynthetic bacterium *Chromatium minutissimum*, linear dichroism 0-35841  
 plasma protein interaction with polyanion complex studied by circular dichroism and UV spectroscopy (Japanese) 0-12316  
 plasma proteins adsorbed on polymer surface, Fourier transform IR spectrometry 0-16899  
 polyacrylamide gel, automated scanning of  $^{14}\text{C}$  0-17221  
 precipitants and flocculants, dimensions of disperse forms of cross-linked polyelectrolytes 0-11957  
 radical limiting conc. on UV irrad. at 77K, effect of luminesc. quenchers 0-30662  
 red blood cells of thalassemia, sickle-cell anaemia, and haemoglobin Ham-mersmith, ferritin-like Fe, Mossbauer study 0-8018  
 redox enzyme, Fe-, Cu-, or Mo-containing, electron transfer peculiarities 0-16896



**proteins continued**

- rhodopsin, photo- and thermo-bleaching rel. to heterogeneity problem 0-41114  
 rhodopsin, picosecond spectroscopy obs. of primary events 0-56312  
 rhodopsin, red-absorbing visual pigment of butterflies 0-3646  
 rhodopsin, vertebrate, chromophore orientation obs. 0-40959  
 rhodopsin, visual pigment, mag. anisotropy estimation 0-51137  
 rhodopsin and its photoproducts, directional absorpt. props. obs. 0-51090  
 rhodopsin thermal stability in photoreceptor membrane, role of lipids, PMR spectroscopy 0-35874  
 rhodopsin-lipid interactions in photoreceptor membranes 0-12094  
 ribonuclease inactivation cross-sections for slow heavy ions 0-26286  
 ribonuclease-A, solid, PMR spin-lattice relax., mol. dynamics 0-51041  
 rigid assemblies of spheres, creeping flow translational resistance 0-54086  
 rubredoxin, frozen soln., recoilless fraction, Mossbauer spectra meas. 0-8025  
 secondary structure determ. by circular dichroism spectra 0-30653  
 secretion by pancreas, accounted for by diffusion-like process 0-21457  
 serum albumin, human,  $^{99m}\text{Tc}$  labelled kits, evaluation for cardiac blood pool imaging 0-17130  
 serum albumin, human, prep. of  $^{68}\text{Ga}$ -labelled microspheres 0-17131  
 serum albumin, permeability of vascular walls, physical theory 0-16908  
 serum interaction with poly( $\text{N}^{\epsilon}$ , $\text{N}^{\epsilon}$ -terephthylolyl-L-lysine) membrane for artificial red blood cells (*Japanese*) 0-12061  
 silk fibroin films, conformational changes induced by water immersion 0-10498  
 small molecules in protein solns., spin-lattice relax. times, inversion recovery spin-echo sequence 0-21446  
 solid, PMR spin-lattice relax., mol. dynamics 0-51041  
 solution, gel conc. and diffusivity at gelling determ. by ultrafiltration 0-21325  
 solutions, quasielastic light scatt. in small wave vector limit 0-45088  
 spectrin-actin monolayer, adsorbed at  $\text{Hg-H}_2\text{O}$  interface, ionic permeability 0-12064  
 synaptic proteins after electroconvulsive stimulation 0-56011  
 synthesis in human fibroblasts in vitro, US stimulation, role of cavitation 0-8100  
 transport across endothelial membrane 0-3601  
 $\alpha$ -tropomyosin, specific splitting at cysteine-190, physicochem. study of fragments 0-30647  
 tyrosinase in buffer soln., UV effect on biological activity 0-30791  
 tyrosine aminotransferase activity circadian rhythm, mouse liver, X-ray effects 0-41121  
 UV fluorescence spectra, resolution of components of complex spectra by Alentsev-Fok method 0-1097  
 UV fluorescence spectra, resolving of components, Alentsev-Fok method 0-1096  
 visual pigments, resonance Raman studies of the primary photochemical event 0-41020  
 $[\text{Fe}_2\text{S}_2(\text{SH})_4]^{2-}$ , HFS-LCAO calcs., 4-Fe active site model in high pot. Fe protein and ferredoxin 0-42929  
 $\text{Na}^+$ ,  $\text{K}^+$ -ATPase, brain, soluble, interaction with plane phospholipid membranes 0-35851  
 $^{21}\text{At}$  protein labelling technique using an acylation reaction 0-36130  
 $\text{H}^+$ -ATPase, soluble mitochondrial, thermal stability obs. 0-55992  
 H<sub>2</sub> exchange kinetics and internal motions 0-21440  
 $^3\text{H}$ -labelled, fluorography in immunoelectrophoresis 0-17220  
 NO-Fe(II) haemoproteins, orbit-orbit interaction, low temp. mag. circular dichroism obs. 0-30645

**proton absorption**

No entries

**proton accelerators***see also cosmotrons*

- intersecting storage accelerator ISABELLE, review 0-32545  
 neutrino target complex at Fermilab, operating experience 0-23230  
 radiation loading and heating of struct. 0-42883  
 RF field induced by a charged beam in a multipap resonator 0-52804  
 Saturn 2, 100 MeV-3 GeV proton accelerator (*French*) 0-32547  
 SPS, real-time control system, operating system principles 0-875  
 UNK project, 3 TeV accelerator, constructional problems (*Czech*) 0-869

**proton affinity**

- amino acid protonation ab initio Hartree-Fock-Roothaan SCF calcs. 0-9503

**proton angular distribution***see also proton spectra*

- $^{12}\text{C}(\text{Be},\text{p})$  at 11.4 MeV c.m. energy 0-9302  
 $^{20}\text{Ne}$ , levels,  $\text{J}^\pi$  and ang. distrib. from  $^{18}\text{O}(\text{t},\text{p})$  0-18204

**proton beam effects** *see proton effects***proton belt** *see radiation belts***proton detection and measurement**

- Melbourne proton microprobe 0-42302  
 photometric calorimeter for proton flux measurements 0-4718  
 polarisation meas. for  $^{12}\text{C}(\text{p},\text{p})$  at 40-75 MeV 0-52840  
 rem-dose measurement of mixed p-n radiation using solid state detectors of fission fragments 0-36137  
 p- $\gamma$  coincidence expt., use of Ge(Li) detector near 400 MeV intense proton beam 0-5452  
 Ar, liquid, calorimeter, electron and proton response 0-47832  
 C polarimeter, proton analysing power, 300-560 MeV 0-23279  
 D depth profiling with  $\text{D}^3(\text{He},\text{p})$ , proton detection at backward angles 0-30309  
 Si dosimeter, proton beam dosimetry in C, Al, Fe, mylar and  $\text{H}_2\text{O}$  0-47733

**proton-deuteron interactions***see also proton-deuteron scattering*

- charged-particle multiplicity distrib. at 400 GeV/c 0-13337  
 polarized proton-neutron total cross sections from proton-deuteron data 0-22633  
 rescattering effects in 19 GeV/c interactions,  $\Delta\Delta$  component of D 0-42500  
 pd, 350-1000 MeV, neutron prod. double differential cross section in meson generation reactions (*Russian*) 0-42490  
 pD annihilation, pion rescatt. effect at intermediate energies 0-5010  
 pd-pnp, 12.5 MeV, angular distrib. of p-n final state interaction in  $^2\text{H}(\text{p},\text{pn})^1\text{H}$  0-52672  
 pd-pnp, 1.67 GeV/c, secondary particle ang. distrib. and correlations (*Russian*) 0-27646  
 pd-p $\pi^+\pi^-$ d, interference phenomena in coherent production, nucleon diffractive amps., helicity-flip 0-47329

**proton-deuteron scattering***see also proton-deuteron interactions*

- intermediate inelastic states and triple-Regge couplings, Pomeron 0-4972  
 total cross sections in pure spin states, Coulomb interference and rescatt. corrections 0-432

**proton effects**

- accelerator, radiation loading and heating of struct. 0-42883  
 Artemia eggs, effects of 645 MeV and 9.2 GeV protons 0-45969  
 benzene in dilute cyclohexane solution, fluoresc. quenching on pulsed proton irradi., temp. depend. 0-21307  
 fast proton track energy deposition and ionisation calc. and obs. 0-12196  
 glass, multicomponent Schott, proton-induced colouring 0-9974  
 ice, monocrystalline, radiation damage, 100 keV proton channelling 0-34102  
 lunar regolite, Fe reduction on heating in vacuum, XPES spectra 0-41740  
 MgO, temp. depend. of int. angles for proton axial channelling 0-10586  
 Permalloy, proton radiation effects, Mossbauer obs. 0-40008  
 RBE of protons rel. to  $\gamma$ -rays for human cells 0-30798  
 solar system, early proton irradiation rel. to H and O isotope study in chondritic meteorites 0-36518  
 stainless steel, type 316, deuteron and proton bombarded, irradi. creep under stress 0-39209  
 Al, dislocation loops and pores due to 23 MeV proton irradi. (*Russian*) 0-54235  
 Al, proton flux depth-dose distrib., space-shielding appls. 0-39186  
 Al, vacancy distribution, interbonding atoms, heat peaks in scattered cascades (*Russian*) 0-39169  
 (AlGa)As DH, proton-stripped, proton-induced defects, photoluminesc. study 0-48251  
 (AlGa)As heterostruct., proton irradi., photoluminesc. 0-29808  
 $\text{Al}_2\text{O}_3\text{-BaO-SiO}_2$  glass coatings in fission and fusion reactors, permeation, elec. cond. and dielectric breakdown 0-18439  
 BeO, radiation induced detrapping of implanted D by  $^3\text{He}$  and proton irradiation 0-32482  
 Cu, proton irradiation, 10 to 16 MeV, isochronal annealing meas. 0-2083  
 Cu, proton irradiation, 10-16 MeV, neutron damage simulation 0-34089  
 Cu, proton irradiation, 10 to 16 MeV, resistivity changes 0-2082  
 Fe, proton irradi., 10-16 MeV, neutron damage simulation 0-34089  
 Fe, proton irradiation, 10 to 16 MeV, isochronal annealing meas. 0-2083  
 Fe, proton irradiation, 10 to 16 MeV, resistivity changes 0-2082  
 GaAs:Sn, proton implantation and annealing behaviour (*Chinese*) 0-44224  
 Ge, proton bombardment damage, irradi. energy depend., channelling meas. 0-24511  
 KBr, proton irradi., divacancies, positron capture, ionic cond. and TSC study 0-54289  
 KCl-KH, F- and U-centre redistrib. at end of proton tracks, microspectrophotometric anal. 0-10583  
 $^{15}\text{N}$  species formed by proton irradiation of water 0-45532  
 NaCl preirradiation effect on proton channelling, thermoluminescence study 0-19860  
 Ni-Si, proton irradi.,  $\gamma'$  precipitation, early stages 0-34096  
 Si, diffusion of self-interstitials and As, B and P, radn.-enhanced 0-29216  
 Si, divacancies due to proton irradi., IR absorpt., annealing effects 0-20673  
 Si, proton irradi., efficiency of form. and nature of defects, Hall meas. 0-6444  
 Si, Schottky barrier structs., proton bombarded, defect states 0-29356  
 Si:B, proton-irradi.-enhanced diffusion 0-29227  
 Si:B ion implantation, proton channelling effects, anal. using Promiss protonograph 0-19823  
 Si:B(P), proton enhanced diffusion, vacancies diffusion length 0-29226  
 SrO, neutron- or proton-irradi.,  $\text{F}^+$  centre fluoresc. yield and lifetime, 5 to 140K 0-55181  
 Zr, proton irradiation, 10 to 16 MeV, isochronal annealing meas. 0-2083  
 Zr, proton irradiation, 10 to 16 MeV, resistivity changes 0-2082

**proton excited X-ray emission** *see ion microprobe analysis*

**proton interactions** *see electron-proton interactions; kaon-proton interactions; lepton-nucleon interactions; photon-proton interactions; pion-proton interactions; proton-deuteron interactions; proton-nucleus reactions; proton-proton interactions*

**proton magnetic moment**

No entries

**proton magnetic resonance**

- albumin denaturation, investigation by PMR 0-3582  
 alkanes and cycloalkanes, saturated hydrocarbon chains characterisation (*Portuguese*) 0-5562  
 anilinium halides, and anilinium sulphate, proton mag. relax. obs. 0-34800  
 asbestos, dehydroxylation, PMR investigation 0-21269  
 biomolecules, conformation and struct., ESR, NMR and optical meas. 0-26201  
 2,2'-bipyrimidine, in nematic solvent, conformation, ab initio and PMR determ. 0-47869  
 blood plasma  $^1\text{H}$  NMR relax. rates, cancer-induced decrease obs. 0-56075  
 calcium formate, intermolecular shielding contributions, proton mag. shielding 0-34783  
 cancer diagnosis, FONAR scan of live human abdomen 0-8122  
 carboranes, small cage, antipodal H-H coupling 0-1003  
 cement pastes, setting at positive, subzero temps., PMR exam. 0-55625  
 chloroquine-biopolymer binding interactions, PMR effects 0-55982  
 diamine oxidase solutions, proton mag. relax. dispersion obs. 0-51136  
 dimethylammonium copper chloride bromide, mag. props., pulsed NMR expts. 0-11292  
 2,6-dimethylbenzoic acid,  $^1\text{H}$  chem. shift recovery from combined multiple pulse NMR and sample spinning 0-32738  
 EBBA, binary systems with non-nematic solutes, phase transition behaviour and  $^1\text{H}$  NMR anal. 0-34174  
 elastomer, segmented block, morphology, pulsed proton NMR study 0-33907  
 epoxy resin, mobility of sorbed water, low resolution PMR method 0-11276  
 ethyl-trimethyl phosphines,  $(\text{C}_2\text{H}_5)_3\text{-P}[\text{E}^{1\text{VB}}(\text{CH}_3)_3]_n$ , ( $\text{E}^{1\text{VB}}=\text{C};\text{Si};\text{Sn};\text{n}=0,1,2,3$ ), ( $^1\text{H}$ ,  $^{13}\text{C}$ ,  $^{29}\text{Si}$ ,  $^{31}\text{P}$ ,  $^{119}\text{Sn}$ ) NMR 0-32744  
 ethylene copolymers with acrylic monomers, NMR investig (*Russian*) 0-54959



## proton magnetic resonance continued

- ferrous porphyrin, intermediate ( $S=1$ ) spin state, PMR characterisation 0-48014  
 Fischer-Tropsch wax, NMR investigation 0-7186  
 graphite lamellar derivatives,  $KC_{24}$ (tetrahydrofuran)<sub>m</sub> ( $m=1$  and 2)  $^1H$  NMR study 0-44932  
 kidney, tissue water freezing study,  $^1H$  NMR obs. 0-8027  
 lecithin-deoxycholate mixed micelles, surface curvature and mobility, PMR study 0-21452  
 liquid crystal, thermotropic, diffusion and nucl. mag. relax. 0-24362  
 liquid crystals, protonated multiple quantum transitions, excitation detection, Fourier transform multiple quantum NMR 0-31819  
 lysozyme, tryptophan residues, H exchange for D, relax., proton NMR spectra 0-35846  
 magnetic shielding constants calc. by GIAO method using Gaussian functions 0-1001  
 manganese zinc formate dihydrate, two-dimens. antiferromag., anomalous crit. phenomena, neutron scatt. and PMR obs. 0-50104  
 medical imaging by NMR, book 0-31426  
 medical imaging by NMR, book contrib. 0-36064  
 medical imaging techniques, developments, review 0-26324  
 $^{13}C$ -methane- $d_2O$ , annealed, spin conversion and proton 2nd moment time-depend. 0-11283  
 methanols, labelled, proton  $T_1$  in presence of intramol. rots., intermol. relax. rate 0-2656  
 methylmercury nitrate, in nematic and lyotropic liq. crystals,  $r_a$ -struct. and anisotropy of Hg-C coupling const. 0-43071  
 molecular spectroscopic laboratory strategies, queueing theory and digital simulation use 0-30299  
 muscle, mouse, NMR multiwindow anal. and proton local fields and magnetisation distrib. 0-21444  
 muscle water, anal. in mouse above and below freezing 0-56073  
 muscle water, frog, varied mag. field, multiple-pulse and magic-angle spinning  $^1H$  NMR obs. 0-51135  
 neuroradiography by NMR imaging 0-51197  
 pentofuranosyl nucleosides, isomeric,  $^1H$  NMR coupling const., SCF FPT INDO approx. calc. 0-14156  
 phosphatidylcholine-cholesterol vesicles interacting with lucensomycin 0-40954  
 poly( $\alpha$ -methylvinyl alkyl ether)s,  $^1H$ ,  $^{13}C$ -NMR spectra, stereoregularity 0-48112  
 polybutyl acetate-polyvinyl acetate crosslinked compositions, proton mag. relax., forced compatibility (Russian) 0-44950  
 polyethylene, amorphous, struct. from NMR line shape analysis and MAR-NMR 0-28931  
 polyethylene cocrystals, partially and fully deuterated, chain folding,  $^1H$  NMR solid echo technique 0-20507  
 polyisocyanides, solns., struct. and acidification 0-19915  
 polyisoprenes, partly deuterated,  $^1H$ -NMR spectra, struct. 0-50202  
 polymer, cryst., broadline PMR spectra, math. separation procedure 0-2647  
 polymer gel, magic angle rot.  $^1H$  NMR spectra meas. by variable temp. probe 0-1830  
 polymers, semicrystalline, partially and fully deuterated, chain folding,  $^1H$  NMR solid echo technique 0-20507  
 polysaccharide gel, anomalous behaviour of PMR line width of water (Russian) 0-11962  
 powders with spin  $1/2$  nuclei arranged in isosceles triangular mag. config., shape function 0-2648  
 proteins, solid, PMR spin-lattice relax., mol. dynamics 0-51041  
 proton chemical shifts, combined pulse NMR and magic-angle spinning 0-44934  
 prymellitic and dianhydride, intermolecular shielding contributions, proton mag. shielding intermolecular shielding contributions, proton mag. shielding 0-34783  
 rhodopsin thermal stability in photoreceptor membrane, role of lipids, PMR spectroscopy 0-35874  
 ribonuclease-A, solid, PMR spin-lattice relax., mol. dynamics 0-51041  
 ring current theories, chem. shifts in conjugated systems 0-53020  
 skin, rat,  $^1H$  and  $^{13}C$  NMR obs. 0-40965  
 spectrometer for quantitative analysis, microprocessor-controlled digital integrator 0-11971  
 spin-lattice relaxation meas., variable nutation WEFT, biochemical appl. 0-20482  
 spin-lattice relaxation times from CW spectroscopy, phys. chem. lab. expt. 0-17775  
 steam, supercritical, compressed, proton spin-lattice relax. time meas. 0-22403  
 styrene, thermal polymerization, PMR obs. 0-3342  
 substituted benzoic acids, comparative study 0-39881  
 succinic acid, partially deuterated,  $^1H$  and  $^2H$  distant ENDOR obs. of mol. struct. parameters 0-23445  
 TCNQ salt, pyridinium (TCNQ)<sub>2</sub>, low temp. mag. phase transition, ESR study 0-25139  
 TCNQ salts, proton nucl. relax. meas. 0-20484  
 TCNQ-DIP  $\Phi_4$ , electronic diffusion coeffs. in chains, proton spin-lattice relax. and dynamic nucl. polarisation 0-25241  
 TCNQ-NMP, incomplete charge transfer, NMR relax. and line-shift meas. 0-20485  
 tetramethylammonium zinc tetrachloride,  $^{13}C$  NMR and PMR study of incommensurate phase transition 0-34863  
 1,2,3-trichlorobenzene, oriented mols.,  $^{13}C$  satellites use in proton spectra,  $r_a$ -structure 0-18872  
 triethylacetic acid, high resolution  $^1H$  and  $^{13}C$  NMR spectra at liquid-solid phase transition 0-11281  
 trimethyl ammonium cobalt chloride, magnetisation temp. depend. 0-7128  
 trimethylacetic acid, high resolution  $^1H$  and  $^{13}C$  NMR spectra at liquid-solid phase transition 0-11281  
 tunable notch filter for solvent elimination 0-22405  
 valinomycin conformation in a phospholipid bilayer 0-40958  
 vesicle membrane, large unilamellar,  $^1H$  NMR study of acetic acid permeation 0-8031  
 water, self-diffusion coeff., pressure and temp. depend. meas. by proton spin echo 0-39328  
 water, studies in biological systems 0-3886  
 water diffusion in wheat grain endosperm tissue,  $^1H$  NMR obs. 0-8001  
 water in biological systems, pulsed NMR obs. 0-35930  
 water molecules in biological systems, relax. rel. to vol., pulse NMR obs. 0-40960  
 yeast cell membrane, water transport study, pulse NMR obs. 0-40981

## proton magnetic resonance continued

- $CaF_2 \cdot H_2O$ , ionic conductivity study by NMR experiments (French) 0-29210  
 $CoCl_2 \cdot 2H_2O$ , magnetisation temp. depend. 0-7128  
 $CoCl_2 \cdot 2NC_2H_5$ , magnetisation temp. depend. 0-7128  
 $Co(II)$ -containing aq. electrolyte soln., nucl. mag. relax., hydration shell (Russian) 0-54966  
 $Cu$  complex,  $Cu(II)$  dimers, temp. depend. PMR relax., singlet-triplet separation determ. 0-43073  
 $H$  halides, spin-orbit coupling effect on proton mag. shielding 0-23440  
 $K_2CuCl_4 \cdot 2H_2O$ , paramag. single cryst., PMR temp. depend., hyperfine const. and exchange interaction (Korean) 0-29630  
 $LiH$ , solid, anion and neutron diffusion, NMR relax. and linewidth obs., Schottky disorder 0-15815  
 $NH_4 Br$  single cryst., low temp. PMR lineshapes of tunnelling  $NH_4^+$  ions 0-25223  
 $NH_3(D_3)$ , liq., longitudinal proton and deuteron relaxation rates, press. and temp. depend. 0-44941  
 $NH_3HF_2$ , powder, proton and fluorine 2nd moments meas., 77-395K 0-34803  
 $NOH$  polycryst. radicals, low temp. PMR 0-25220  
 $NaClO_4 \cdot H_2O$ ,  $^1H$  NMR second moment,  $H_2O$  dynamic disorder 0-25221  
 $Nb$ , proton diffusion, NMR obs., 120-480K 0-34812  
 $Ni(CN)_2$ -dodecylamine, lamellar paraffinic system, phase transitions, wide-line NMR obs. (French) 0-44929  
 $Si:H$ , plasma-deposited amorphous film, proton mag. reson. 0-44931  
 $SiO_2:Co(II)$ , adsorption of  $H_2O$ , coord. lifetime, surface effect, NMR obs. 0-34299  
 $TaH_x$ ,  $H$  diffusion and electronic struct., pulsed NMR obs. 0-54967  
 $TaS_2(NH_3)_x$ , NMR spectral densities and two-dimens. diffusion 0-50215  
 $TiH_x$ ,  $H$  diffusion, NMR obs. 0-34813  
 $TiS_2(NH_3)_{1.0}$ , NMR spectral densities and two-dimens. diffusion 0-50215  
 $Y-H$  system, solid soln. phase, wide-line PMR 0-25226  
 $ZrClH$ ,  $^1H$  NMR shielding anisotropy 0-20466

## proton-nucleus reactions

- for inelastic proton-nucleus scattering, see "proton-nucleus scattering"  
 see also neutron-proton interactions; proton-proton interactions; proton radiative capture  
 backward p,d,t production, p-p correlations 0-529  
 channelling, modulation of high energy interactions 0-37373  
 cluster cascade model, single particle distributions and two-particle correlations 0-18300  
 collective tube model of high energy proton scatt. on polarised nuclei 0-32273  
 conference on high energy physics and nuclear struct. Vancouver, Canada (Aug. 1979) 0-41936  
 inclusive production of neutral strange and charged particles, collective tube model 0-52538  
 leading proton spectrum at high energies in (p,X) reactions, intranuclear cascade model anal. 0-5139  
 linear acceleration reactors, anal. of neutron yield produced by high-energy protons 0-22895  
 nuclear size dependence of particle prod., hydrodynamical model 0-22593  
 photoemulsion nuclei, 70 and 250 GeV, hypernuclei formation (Russian) 0-9297  
 photon, electron and positron prod. from primary proton beams, Monte Carlo calcs. 0-32555  
 pseudorapidity distribution, energy and target depends., 24 and 70 GeV/c 0-5138  
 thermonuclear reaction rate data for intermediate mass nuclei 0-31427  
 (p,  $\alpha$ ) microscopic form factors, DWBA cluster form factor replacement 0-47478  
 (p,d), 52 MeV, deeply bound hole state transition strength giant resonance, DWBA anal. 0-47426  
 (p,d), intermediate energy study review 0-42653  
 (p,n), 1 GeV, quadrupole moment, isovector component, nuclear spin re-orientation effect 0-52573  
 (p, n), 22.2 MeV,  $A=27-197$ , neutron spectra, direct and equil. processes (Russian) 0-52648  
 (p,n), 2.5-5.8 MeV,  $A=89-130$ , cross sections, sub-Coulomb proton anomalous optical pot. 0-32278  
 (p,n) excitation functions for  $A=45$  to 80, proton optical pot. at sub-Coulomb energies 0-9292  
 (p, $\pi$ ), 4.2, 4.5 GeV/N, pion multiplicities and theoretical models, review 0-42657  
 (p, $\pi$ ), exclusive single nucleon transfer, theoretical status 0-42652  
 (p, $\pi^+$ ), 8-16 MeV, inclusive cross sections near threshold,  $A$  depend. 0-27644  
 (p, $\pi^+$ ), light nuclei, 0.5-10 MeV, total cross sections near pion Coulomb barrier 0-32280  
 (p, $\pi$ ) in emulsion, 70 GeV/c, Lorentz invariant kinematical anal. 0-47474  
 (p,t), even actinides, lowest  $0^+$  state excitation, collective phonon state, spectroscopic factors 0-13410  
 (p,t), pol. p, strong ground state transitions, anomalous anal. power, direct and sequential processes 0-5115  
 (p, t) ang. distrib., zero-range DWBA calc., volume absorptive optical pot. singular prop. 0-523  
 (p, t) ang. distrib. with deep minima, DWBA calcs. geometrical aspects 0-522  
 (p,X), 0.6-21 GeV,  $^{84}Rb$ ,  $A=83,84,86$  prod. cross sections and recoil props. 0-9295  
 (p,X), 5-9 GeV/c, total inelastic and knock-out cross sections, nuclear RMS radius (Russian) 0-32175  
 (p,X), 50-200 GeV/c, ang. distrib. of charged shower particles (Korean) 0-27641  
 (p,X), 70 GeV/c (Russian) 0-52681  
 (p,X), antiproton as nuclear probe 0-42704  
 (p,X), experimental information review, polarisation phenomena 0-42655  
 (p,x), few nucleon correlations in nuclei, cumulative particle production (Russian) 0-5145  
 (p,X) 90 MeV, inclusive spectra, 'quasi-two-body scaling' and 'hot spots' 0-5142  
 (p,X) emulsion, 400 GeV/c slow deuteron and proton prod. 0-52666  
 (p,X) in emulsion 24 GeV, clusters in rapidity interval method, multiperipheral model 0-5135  
 (p,xn) on heavy elements, K X-ray and nucl. satellites 0-27599  
 (p,xn $\gamma$ ), rare earth nuclei, complete fusion process n and  $\gamma$  multiplicity 0-18363



## proton-nucleus reactions continued

- $\pi^+$  prod. in 0.8-4.89 GeV collisions, energy depend. of  $180^\circ$  prod. 0-22834
- 6Li(p,n), 144 MeV, one pion exchange and PCAC expt. test 0-528
- Ag, emulsion nuclei, 28 GeV proton interactions (*Korean*) 0-18299
- Ag+p, role of pick-up processes in prod. of fast t and  $^3\text{He}$  0-27632
- $^A\text{Ag}(p,n)$ , A=107,109, 2.0-6.7 MeV, cross sections, Hauser-Feshbach optical calcs. for p absorption systematics 0-47483
- $^{107}\text{Ag}(p,\alpha X)$ , 20-45 MeV,  $\alpha$  spectra, exciton model anal. 0-18306
- Ag(p, $\alpha$ )X, direct knockout model for fragmentation, (p, $\alpha$ ) predictions 0-18275
- Ag(p,f), 600 MeV, fragment energies, cross sections level density and barrier heights 0-42723
- $^{27}\text{Al}(p,\alpha)$ , 6.44 MeV,  $^{28}\text{Si}$  resonance wave functions and differential cross sections 0-18261
- $^{27}\text{Al}(p,n)$ , 6.44 MeV,  $^{28}\text{Si}$  resonance wave functions and differential cross sections 0-18261
- $^{27}\text{Al}(p,\alpha)^{24}\text{Mg}$ , finite-range cluster-model description, DWBA approach 0-52667
- $^{27}\text{Al}(p,\alpha X)$ , direct knockout model for fragmentation, (p, $\alpha$ ) predictions 0-18275
- Al(p,X), 400 GeV/c, light ion backward prod., invariant cross section 0-32279
- Al(p,xpX), x=1, 2, 640 MeV, energetic backward p emission, inclusive differential cross section 0-9290
- $^{40}\text{Ar}(p,t)$ , 52 MeV,  $^{38}\text{Ar}$  levels,  $J^\pi$  and transition strengths, DWBA anal. 0-47378
- $^{75}\text{As}(p,2n\gamma)$ , 17-28 MeV,  $^{74}\text{Se}$  quasi- $\gamma$  bands and negative parity levels 0-456
- $^{75}\text{As}(p,3n)^{73}\text{Se}$ , production yields, excitation curves 0-36131
- $^{197}\text{Au}(p,X)$ , 11.5 GeV,  $^{24}\text{Na}$  fragment ang. and energy distrib., two-step model anal. 0-52678
- $^{197}\text{Au}(p,X)^{149}\text{Tb}$ , target fragmentation momentum transfer, collective tube model, collectivity effects 0-37359
- $^B(p,2\alpha)$ , possibility of thermonuclear fuel in relativistic plasma (*Russian*) 0-37573
- $^{10}\text{B}(p,\alpha\gamma)$ , 2.0-4.1 MeV,  $^{11}\text{C}$  levels and resonance,  $\gamma$ -ray excitation curves 0-9280
- $^{10}\text{B}(p,p,\gamma)$ , 2.0-4.1 MeV,  $^{11}\text{C}$  levels and resonance,  $\gamma$ -ray excitation curves 0-9280
- $^{10}\text{B}(p,\pi^+)$ , 320-605 MeV, cross sections, pion exchange model anal. 0-27676
- $^B(p,\alpha X)$ , direct knockout model for fragmentation, (p, $\alpha$ ) predictions 0-18275
- $^B(p,\pi^+)$ , 320-605 MeV, cross sections, pion exchange model anal. 0-27676
- Be(p,X), 200, 300 GeV/c direct photon prod.,  $\eta/\pi^0$  and  $\gamma/\pi^0$  prod. ratios 0-27618
- Be(p,X), 400 GeV/c, light ion backward prod., invariant cross section 0-32279
- Be(p,n), 35 and 46 MeV, neutron spectra 0-524
- Be(xpX), x=1, 2, 640 MeV, energetic backward p emission, inclusive differential cross section 0-9290
- $^{210}\text{Bi}^m(p,t)$ , 18.4 MeV,  $^{208}\text{Bi}$  two-particle, two-hole configuration, levels,  $J^\pi$  and excitation energies 0-32190
- Br, emulsion nuclei, 28 GeV proton interactions (*Korean*) 0-18299
- Br+p, role of pick-up processes in prod. of fast t and  $^3\text{He}$  0-27632
- Br(p,2n $\gamma$ ), 17-28 MeV,  $^{78,80}\text{Kr}$  quasi- $\gamma$  bands and negative parity levels 0-456
- $^{11}\text{Bu}(p,\alpha)\alpha$ , sputtering yield meas. (*Japanese*) 0-25513
- $^{12}\text{C}+p(d,\alpha)$ , transparency in composite particle-nucleus reactions 0-9273
- $^{12}\text{C}(p,X)$ , 50 MeV, effective cross sections for charged particles in outgoing channel 0-18294
- $^{12}\text{C}(p,2p)$ , 100 MeV,  $^{11}\text{B}$  states, spectroscopic factors from DWBA anal. 0-5057
- $^{12}\text{C}(p,n)$ , 144 MeV, one pion exchange and PCAC expt. test 0-528
- $^{12}\text{C}(p,n)$ , 62, 120 MeV, isobaric analogue states, differential cross sections 0-18202
- $^{12}\text{C}(p,n)^{12}\text{N}$ , test of Monte Carlo efficiency calcs. for scintillation counters 0-37713
- $^{12}\text{C}(p,p')$  proton polarisation and natural parity level excitations (*Russian*) 0-5144
- $^{12}\text{C}(p,n)$ , pol. nucleon quasi-elastic scatt., nuclear wave function and model tests 0-42656
- $^{13}\text{C}(p,\alpha)^{10}\text{B}_{gs}$ , 65 MeV, pol. p, DWBA form factor 0-52559
- $^{13}\text{C}(p,d)$ , 200, 500 MeV, differential cross section scaling, reaction mechanism 0-42625
- $^{13}\text{C}(p,d)$ , 800 MeV, cross sections, DWBA anal. 0-42667
- $^{14}\text{C}(p,n)$ , 35 MeV,  $^{14}\text{N}$   $1^+$  state cross sections, effective two nucleon interaction, isovector tensor component 0-18208
- $^{40}\text{Ca}+p(d,\alpha)$  transparency in composite particle-nucleus reactions 0-9273
- $^{40}\text{Ca}(p,^3\text{He})$ , 42.5 MeV,  $^{38}\text{K}$  low lying  $1^+$ , T=0 states, DWBA anal. 0-470
- Ca(p, $\alpha$ ), 40 MeV,  $^A\text{K}$ , A=37,39, levels, excitation and microscopic form factors, DWBA calcs. 0-32185
- C(p,X) (*Russian*) 0-52649
- C(p,X), 400 GeV/c, light ion backward prod., invariant cross section 0-32279
- C(p,X), 4.2 GeV/N, multiple  $\pi^-$  proc., mean multiplicity (*Russian*) 0-27647
- C(p,3p), 640 MeV, proton pair quasifree knock-out 0-22795
- C(p,xpX), x=1, 2, 640 MeV, energetic backward p emission, inclusive differential cross section 0-9290
- $^{54}\text{Cr}(p,\gamma)$ , 1.0-3.8 MeV,  $\gamma$ -yields, cross sections, predicted (p,n) cross section, Stat. anal. 0-5136
- $^{137}\text{Cs}$ , 10 GeV proton spallation for transmutation of radioactive waste, calc. of transmutation number 0-13470
- Cu(p,X), 400 GeV/c, light ion backward prod., invariant cross section 0-32279
- Cu(p,xpX), x=1, 2, 640 MeV, energetic backward p emission, inclusive differential cross section 0-9290
- $^{19}\text{F}(p,d)$ , 19.3 MeV,  $^{18}\text{F}$  levels,  $J^\pi$  and ang. distrib. DWBA anal. 0-42545
- Fe+p, 400 GeV, missing energy associated with  $\mu^+\mu^-$  prod. 0-22833
- $^{56}\text{Fe}(p,\alpha)^{51}\text{Mn}$ , 21 MeV analogue state, excitation 0-13471
- $^{56}\text{Fe}(p,\alpha)$ , 34 MeV,  $^{53}\text{Mn}$  low lying states, DWBA anal., shell model wave functions 0-32211
- F(p, $\alpha$ ), (p, $\alpha$ )  $\gamma$ , microanal. of F depth profile 0-45607
- $^{76}\text{Ge}(p,n\gamma)$ ,  $^{76}\text{As}$  level structure 0-47379

## proton-nucleus reactions continued

- Ge(p,n $\gamma$ ), 6.5-14 MeV,  $^A\text{As}$ , A=70, 72, level scheme, transitions,  $J^\pi$  and lifetimes 0-22695
- $^1\text{H}(^{15}\text{N},\alpha\gamma)$ , for H detection in metals 0-55767
- $^1\text{H}(p,\pi^+)^2\text{H}$ , SIS, 578 MeV, pol. beam and target, spin depend. parameters 0-42651
- $^2\text{H}(p,2p)n$ , 23, 39.5 MeV, noncoplanar reaction, breakup cross section 0-530
- $^2\text{H}(p,2p)n$ , 28.6 MeV, breakup cross sections in collinear geometry 0-9296
- $^2\text{H}(p,d\pi^+)$ , 800 MeV, pion prod. with spectator neutron, cross section 0-9294
- $^2\text{H}(p,n)2p$ , pol. n and p, 10.6-15.1 MeV, transverse polarisation transfer at  $0^\circ$  0-42630
- $^2\text{H}(p,pn)^1\text{H}$ , 12.5 MeV, angular distrib. of p-n final state interaction 0-52672
- $^2\text{H}(p,pn)$ , 1.67 GeV/c, secondary particle ang. distrib. and correlations (*Russian*) 0-27646
- $^2\text{H}(p,\pi^+)^3\text{H}$ , 400, 470, 600 MeV, differential cross section using isobar model 0-9291
- $^4\text{He}(p,^3\text{He})^2\text{H}$ , large momentum transfers,  $\pi$  exchange effects 0-5143
- $^4\text{He}(p,2p)$ , 250, 350, 500 MeV, cross section energy depend., DWIA calcs. 0-37375
- $^4\text{He}(p,2p)$ , pol. nucleon quasi-elastic scatt., nuclear wave function and model tests 0-42656
- $^4\text{He}(p,d)$ , intermediate energies, pion exchange currents in DWBA anal. 0-32199
- $^4\text{He}(p,d)$  pickup reaction, isobar configurations and short range correlations 0-22798
- $^4\text{He}(p,d)^3\text{He}$ , 770 MeV, multiple-scattering approach 0-27636
- $^4\text{He}(p,d)^3\text{He}$ , large momentum transfers,  $\pi$  exchange effects 0-5143
- $^4\text{He}(p,n\pi^+)$ , pion prod. operator non-relativistic approx. 0-27640
- $^{16}\text{O}(p,\alpha X)$ , 20-45 MeV,  $\alpha$  spectra, exciton model anal. 0-18306
- $^{11}\text{In}(p,n)$ , 2.0-6.7 MeV, cross sections, Hauser-Feshbach optical calcs. for p absorption systematics 0-47483
- $^{139}\text{La}(p,\alpha)^{135m}\text{Ba}$ ,  $^{135m}\text{Ba}$  yield depend. on energy of bombarding particle 0-5151
- $^{139}\text{La}(p,f)$ , 600 MeV, fragment energies, cross sections level density and barrier heights 0-42723
- $^6\text{Li}+p$  propagating fusion fuel cycle 0-37629
- $^6\text{Li}(p,^3\text{He})$ , 0.1-3.0 MeV, absolute differential and total cross sections, astrophysical S-factor 0-27642
- $^6\text{Li}(p,X)$ , 400 GeV/c, light ion backward prod., invariant cross section 0-32279
- $^6\text{Li}(p,pd)$ , 590 MeV,  $\alpha$ -d motion, impulse distrib., cluster momentum distrib. 0-52679
- $^7\text{Li}$ ,  $d\sigma(p,p,d)/d\sigma(p,nd)$ , 670 MeV, cross section ratio, cluster model estimate 0-22829
- $^7\text{Li}(p,\alpha)$ , 45 MeV, nuclear vertex constant in peripheral model for virtual decay  $^7\text{Li}\rightarrow\alpha+t$  0-18295
- $^7\text{Li}(p,d)$ , 800 MeV, cross sections, DWBA anal. 0-42667
- $^7\text{Li}(p,n)$  Be as therapy neutron source especially for small cyclotrons 0-26335
- $^{24}\text{Mg}(p,d)$ , 94.8 MeV,  $^{23}\text{Mg}$  hole states, transitions and spectroscopic factors, DWBA anal. 0-32161
- $^{26}\text{Mg}(p,\pi^+)$ , isobar configuration effects,  $p\rightarrow\Delta^0\pi$  model, ang. distrib. (*Chinese*) 0-47484
- $^A\text{Mo}(p,n)$ , A=94-96, 98, 1.7-6.7 MeV, total cross sections, p strength functions, optical model anal. 0-18301
- $^A\text{Mo}(p,p')$ , (A=92,94), 20 MeV, polarisation effects on nuclear excited states (*Russian*) 0-27645
- $^{95}\text{Mo}(p,n\gamma)^{95}\text{Tc}$ , energy levels of  $^{95}\text{Tc}$  0-37372
- $^{100}\text{Mo}(p,n\gamma)$ , 4-6.8 MeV,  $^{100}\text{Tc}$  low lying and isomeric levels, transitions and mean lines 0-42548
- $^{14}\text{N}(p,X)$ , 50 MeV, effective cross sections for charged particles in outgoing channel 0-18294
- $^{14}\text{N}(p,n)$ , 144 MeV, one pion exchange and PCAC expt. test 0-528
- $^{15}\text{N}(p,n)^{15}\text{O}$ , continuum random phase approx. 0-27635
- $^{20}\text{Ne}(p,\alpha)$ , 1-2.5 MeV,  $^{20}\text{Ne}$  non-isolated resonances, excitation functions and ang. distrib. (*Chinese*) 0-22788
- $^{93}\text{Nb}(p,\alpha X)$ , 20-45 MeV,  $\alpha$  spectra, exciton model anal. 0-18306
- $^{93}\text{Nb}(p,n)^{93}\text{Mo}$ , direct neutron decay of analogue resonances of  $^{94}\text{Mo}$  0-22824
- $^{150}\text{Nd}(p,2n\gamma)$ , 12.1-15.8 MeV,  $^{149}\text{Pm}$  high spin states and bands, rot. description and in-beam study 0-32153
- $^A\text{Ni}(p,\pi^+)$ , A=58, 64, 660 MeV, pion energy spectra, isotopic effects (*Russian*) 0-42669
- $^{58}\text{Ni}+p$ , 1 GeV, alpha-particle decay channels 0-22826
- $^{64}\text{Ni}(p,n\gamma)$ ,  $^{65}\text{Cu}$  analogue resonance direct n decay,  $^{64}\text{Cu}$  levels and transitions (*Russian*) 0-5104
- $^{57,61}\text{Ni}(p,d)$  50 MeV,  $^{57,61}\text{Ni}$ , ground hole-state analogues fine struct., isospin mixing 0-13401
- $^{57,61}\text{Ni}(p,X)$ , 340, 660 MeV, ang. distrib., proton quasi-elastic knockout (*Russian*) 0-52649
- $^{16}\text{O}+p(d,\alpha)$  transparency in composite particle reactions 0-9273
- $^{16}\text{O}(p,X)$ , 50 MeV, effective cross sections for charged particles in outgoing channel 0-18294
- $^{16}\text{O}(p,\alpha)^{13}\text{N}$ , in-cyclotron  $^{13}\text{N}$  prod., water loop target 0-23201
- $^{16}\text{O}(p,p')$ , proton polarisation and natural parity level excitations (*Russian*) 0-5144
- $^{17}\text{O}(p,\alpha)$ ,  $^{18}\text{F}$   $J^\pi=3^-$  doublet at 6241 keV, isospin mixing 0-511
- $^{18}\text{O}(p,\alpha)$ , 0.4-1.4 MeV,  $^{18}\text{F}$  levels and resonances, cross sections in R-matrix formalism 0-18267
- $^{18}\text{O}(p,t)$ , 20 MeV,  $^{16}\text{O}$  form factor effects, zero range, DWBA calcs. 0-491
- $^{340}\text{O}(p,X)$ , 340, 660 MeV, ang. distrib., proton quasi-elastic knockout (*Russian*) 0-52649
- $^{208}\text{Pb}(p,t)^{206}\text{Pb}(3^+)$ , pol. p, 22 MeV, anal. power and (p,d)(d,t) sequential transfer processes 0-5119
- Pb(p,xpX), x=1, 2, 640 MeV, energetic backward p emission, inclusive differential cross section 0-9290
- Pd(p,2n $\gamma$ ), 19, 25 MeV,  $^A\text{Ag}$ , A=99, 101, 103, levels, transitions and  $J^\pi$  0-47383
- Pd(p,n),  $^A\text{Ag}$ , A=104, 106, levels,  $J^\pi$ , and isobaric analogue resonances 0-32180
- Pt(p,t), 35 MeV,  $^{192,194,196}\text{Pt}$  states,  $J^\pi$ , ang. distrib. and transitions, DWBA anal. 0-468
- $^{88}\text{Rb}(p,2n\gamma)$ , 17-28 MeV,  $^{84}\text{Sr}$  quasi- $\gamma$  bands and negative parity levels 0-456
- Se(p,d), 33 MeV,  $^A\text{Se}$ , A=75, 77, 79, 81, levels and ang. distrib., spectroscopic factors 0-22696



## proton-nucleus reactions continued

- <sup>35</sup>Si(p,α), polarised proton, reaction struct. depend. 0-18296  
<sup>35</sup>Sn(p,π<sup>-</sup>), A=112, 124, 660 MeV, pion energy spectra, isotopic effects (Russian) 0-42669  
<sup>117</sup>Sn(p,d), polarised p, 12.9 MeV, anal. power 0-5114  
<sup>118</sup>Sn(p,αX), 20-45 MeV, α spectra, exciton model anal. 0-18306  
<sup>118</sup>Sn(p,t), ang. distrib. and cross sections full finite range CCBA anal. 0-5141  
<sup>119,122</sup>Sb level density, neutron spectra and ang. distrib. nonequib. processes (Russian) 0-37376  
<sup>181</sup>Ta(p,2nγ), 17 MeV, <sup>180</sup>W ground and K=2<sup>-</sup> octupole band ang. momenta coupling, lifetimes 0-9214  
<sup>181</sup>Ta(p,4n) <sup>178</sup>W radionuclide production and purification 0-12252  
<sup>181</sup>Ta(p,X), 400 GeV/c, light ion backward prod., invariant cross section 0-32279  
<sup>181</sup>Ta(p,X), 4.2 GeV/N, multiple π<sup>-</sup> prod., mean multiplicity (Russian) 0-27647  
<sup>181</sup>Ta(p,X), 8 GeV, β-active superdense nuclei search (Russian) 0-42535  
<sup>159</sup>Tb(p,f), 600 MeV, fragment energies, cross sections level density and barrier heights 0-42723  
<sup>232</sup>Th(p,f), 35-85 MeV, light mass nuclide charge dispersion curves for A=76-79 0-18349  
<sup>232</sup>Th(p,X), 10-100 MeV, spallation residue excitation functions, fissionability 0-18353  
<sup>232</sup>Th(p,f), 9.5-17 MeV, symmetric to asymmetric mass ratios for fragments 0-5178  
<sup>169</sup>Tm(p,αX), 20-45 MeV, α spectra, exciton model anal. 0-18306  
<sup>238</sup>U(p,X), 11.5 GeV, heavy fragment energies and masses, reaction mechanism 0-5140  
<sup>238</sup>U(p,X), 0.8-11.5 GeV, formation of A=131 isobaric nuclides 0-9293  
<sup>238</sup>U(p,X), 0.8-400 GeV, Sc fragment differential ranges and energy spectra 0-42666  
<sup>238</sup>U(p,X), 400 GeV/c, unusual backward enhancement in product ang. distrib. 0-514  
<sup>238</sup>U(p,f), 9.5-17 MeV, symmetric to asymmetric mass ratios for fragments 0-5178  
<sup>238</sup>U(p,f) 12 MeV, estimation of neutron yield from individual fragment in medium-excitation fission 0-542  
<sup>238</sup>U(p,f), 600 MeV, fragment energies, cross sections level density and barrier heights 0-42723  
<sup>51</sup>V(p,nγ), 3.95-4.65 MeV, <sup>51</sup>Cr bands, levels, EM transitions, J<sup>π</sup>, branching and mixing ratios 0-52606  
<sup>400</sup>W(p,X), 400 GeV, particle mean multiplicities 0-13473  
<sup>400</sup>W(p,X), 8 GeV, β-active superdense nuclei search (Russian) 0-42535  
<sup>400</sup>W(p,e<sup>+</sup>e<sup>-</sup>), 1.0-2.5 MeV, e<sup>+</sup>e<sup>-</sup> pair prod. search 0-27637  
<sup>320-590</sup>Xe prod. cross sections with protons of 320-590 MeV, nuclear medicine appl. 0-36133  
<sup>90,91,94</sup>Zr(p,4pxn)Rb, A=90, 91, 94, spallation reactions, nuclear structure influence on yields of product nuclei 0-22794  
<sup>90,91,94</sup>Zr(p,6pxn)Br, A=90, 91, 94, spallation reactions, nuclear structure influence on yields of product nuclei 0-22794  
<sup>92,94</sup>Zr(p,n), A=92, 94, 1.7-6.7 MeV, total cross sections, p strength functions, optical model anal. 0-18301  
<sup>92</sup>Zr(p,p<sup>+</sup>), (A=90,92), 20 MeV, polarisation effects on nuclear excited states (Russian) 0-27645  
<sup>89</sup>Zr(p,pol. A)<sup>89</sup>Y, finite-range cluster-model description, DWBA approach 0-52667  
<sup>94</sup>Zr(p,n), 6-9 MeV, <sup>94</sup>Nb level density, neutron spectra and ang. distrib. nonequib. processes (Russian) 0-37376

## proton-nucleus scattering

see also neutron-proton scattering; proton-proton scattering

- elastic scattering theory, multiple scatt. test review 0-42654  
 Ericson fluctuations in polarised (p,p) reactions (Rumanian) 0-5113  
 even-even spherical nuclei, 2<sup>+</sup> state deformation parameter from (p,p) and EM excitation 0-27549  
 gamma-ray line emission from nucleus de-excitation following energetic particle reactions 0-18219  
 multiple Coulomb scattering angle meas. 50 to 200 GeV/c 0-9315  
 neutron distribution in nuclei, elastic and inelastic proton scattering, review 0-22649  
 spline interpolation method appl. to optical potential 0-32272  
 (p,n), centre-of-mass spuriousity in continuum shell-model calculations 0-32210  
 (p, p), 1 GeV, polarisation data, Glauber anal. spin-orbit parameters, matter distrib. 0-52655  
 (p,p), 100-2200 MeV, total and reaction cross sections from optical pot. 0-18303  
 (p,p), 600, 750 MeV, polarisation and cross section, Glauber model calc., NN matrix test 0-47485  
 (p,p), A=9 to 70, differential cross sections, struct. effects, optical and coupled channel anal. 0-47482  
 (p,p), centre-of-mass spuriousity in continuum shell-model calculations 0-32210  
 (p,p), elastic, inelastic polarised and unpolarised, intermediate energy study review 0-42653  
 (p,p), pol. p, sd, fp shell nuclei, 65 MeV, effective two-body interaction range 0-32201  
 (p,p), single particle bound state, energy independ. optical model, asymmetry term 0-37316  
 (p,p<sup>+</sup>), A=6 to 208, 800 MeV, proton spectra, quasifree scatt., DWIA anal. 0-52677  
 (p,X), experimental information review, polarisation phenomena 0-42655  
<sup>107,109</sup>Ag(p,p), A=107,109, 2.0-6.7 MeV, cross sections, Hauser-Feshbach optical calcs. for p absorption systematics 0-47483  
<sup>28</sup>Al(p, p<sup>+</sup>), 6.44 MeV, <sup>28</sup>Si resonance wave functions and differential cross sections 0-18261  
<sup>40</sup>Ar(p,p), 18-44 MeV, differential cross sections, phase shift anal., energy depend. 0-47481  
<sup>13</sup>B(p,n)<sup>13</sup>C, shell model anal. of polarisation-analysing power differences 0-22804  
<sup>12</sup>C(p,p<sup>+</sup>), 1 GeV, proton polarisation in natural parity level excitation (Russian) 0-42634  
<sup>12</sup>C(p,p<sup>+</sup>), 62, 120 MeV, isobaric analogue states, differential cross sections 0-18202  
<sup>12</sup>C(p,p<sup>+</sup>), 800 MeV, multistep processes, ang. distrib., Glauber model anal. 0-47475  
<sup>12</sup>C(p,p<sup>+</sup>), non-eikonal effects in high energy inelastic scatt. 0-42608  
<sup>12</sup>C(p,p<sup>+</sup>)<sup>12</sup>C\*, pol. p., 19-23 MeV, giant resonances as doorway states, virtual excitation 0-5102  
<sup>12</sup>C(p,p<sup>+</sup>)<sup>12</sup>C\*, test of Monte Carlo efficiency calcs. for scintillation counters 0-37713  
<sup>12</sup>C(p,p), 144 MeV, elastic scatt. cross sections, optical pot. 0-42660  
<sup>12</sup>C(p,p), 40-75 MeV, polarisation meas., differential cross sections 0-52840  
<sup>12</sup>C(p,p), 50-160 MeV, energy depend. optical pot. 0-22830  
<sup>12</sup>C(p,p), optical potential, spin-orbit term 0-52668  
<sup>12</sup>C(p,p), pol. p, 450-600 keV, Mott-Schwinger interaction existence, anal. power 0-22805  
<sup>12</sup>C(p,p) spin 0-spin 1/2 phase shift anal. discrete ambiguities 0-18307  
<sup>12</sup>C(p,pγ), bremsstrahlung cross section near 1.7 MeV resonance, Feshbach-Yennie approx. 0-42662  
<sup>40</sup>Ca(p,p), spline interpolation method appl. to optical potential 0-32272  
<sup>48</sup>Ca(p,p), 1 GeV, elastic scatt. differential cross section calc. 0-47480  
<sup>48</sup>Ca(p,p), 5.55 to 8.4 MeV, <sup>48</sup>Sc isobaric analogue states and resonances, J<sup>π</sup> 0-13426  
<sup>106</sup>Cd(p,p<sup>+</sup>), 10, 12 MeV, compound nucleus lifetime by X-ray spectroscopy 0-22831  
<sup>106</sup>Cd(p,p<sup>+</sup>), 0.6-25 GeV, backward emitted proton inclusive spectra, short range correlation 0-32281  
<sup>106</sup>Cd(p,p<sup>+</sup>), 0.6-25 GeV, backward emitted proton inclusive spectra, short range correlation 0-32281  
<sup>154</sup>Eu(p,p<sup>+</sup>), 12 MeV, ground band rot. states, deformation parameters, coupled channels anal. 0-9195  
<sup>19</sup>F(p,p), 17.5 and 30 MeV, low lying level cross-sections, coupled-channel method 0-42649  
<sup>58</sup>Fe(p,p<sup>+</sup>), 39, 62 MeV, DWBA anal., collective spectra, direct process contrib. (Russian) 0-13408  
<sup>58</sup>Fe(p,p<sup>+</sup>γ), <sup>55</sup>Co f-wave resonances, inelastic p amplitudes, analogue state spectroscopic factors 0-47451  
<sup>2</sup>H(p,p<sup>+</sup>), 0.6-25 GeV, backward emitted proton inclusive spectra, short range correlation 0-32281  
<sup>2</sup>H(p,p), backscattering, large momentum transfers, π exchange effects 0-5143  
<sup>3</sup>He(p,p), generator coord. method study of <sup>4</sup>Li 0-27581  
<sup>3</sup>He(p,p), pol. p, 0.3-1.0 MeV, differential cross section, anal. power, and phase shifts 0-42629  
<sup>4</sup>He(p,p), 45-65 MeV, phase shift anal. 0-22832  
<sup>4</sup>He(p,p), A=3,4, backscattering, large momentum transfers, π exchange effects 0-5143  
<sup>15</sup>Li(p,p), 2.0-6.7 MeV, cross sections, Hauser-Feshbach optical calcs. for p absorption systematics 0-47483  
<sup>139</sup>La, level props., Coulomb excitation obs. 0-13378  
<sup>144</sup>Li(p,p), 144 MeV, elastic scatt. cross sections, optical pot. 0-42660  
<sup>7</sup>Li(p,p<sup>+</sup>), <sup>8</sup>Be lowest negative parity state, shell and cluster model calcs. 0-18205  
<sup>24</sup>Mg(p,p<sup>+</sup>), 0.8 GeV, rot., γ and β bands, ground state deformation, DWBA, coupled channels anal. 0-9198  
<sup>24</sup>Mg(p,p<sup>+</sup>), 20, 40, 800 MeV, γ-vibr. band, coupled channels anal. 0-9194  
<sup>24</sup>Mg(p,p<sup>+</sup>), 40 MeV, two step pickup-stripping process, negative parity states 0-32256  
<sup>24</sup>Mg(p,p), 15 MeV, excitation functions 0-22825  
<sup>24</sup>Mg(p,p), 18-44 MeV, differential cross sections, phase shift anal., energy depend. 0-47481  
<sup>14</sup>N(p,p), 144 MeV, elastic scatt. cross sections, optical pot. 0-42660  
<sup>15</sup>N(p,p), 18-44 MeV, differential cross sections, phase shift anal., energy depend. 0-47481  
<sup>58</sup>Ni(p,p), pol. p, 40 MeV, elastic and inelastic, asymmetries and differential cross sections (Russian) 0-27623  
<sup>16</sup>O(p,p<sup>+</sup>), 1 GeV, proton polarisation in natural parity level excitation (Russian) 0-42634  
<sup>16</sup>O(p,p<sup>+</sup>), 135 MeV, high spin particle-hole states, 4<sup>-</sup> states 0-9217  
<sup>16</sup>O(p,p<sup>+</sup>), 135 MeV, 4<sup>-</sup> particle-hole states, J<sup>π</sup> ambiguity removal 0-5036  
<sup>16</sup>O(p,p), 20-50 MeV differential cross section, polarisation ang. distrib., optical model exchange terms 0-27638  
<sup>16</sup>O(p,p), 50-160 MeV, energy depend. optical pot. 0-22830  
<sup>16</sup>O(p,p), spline interpolation method appl. to optical potential 0-32272  
<sup>18</sup>O(p,p), 18-44 MeV, differential cross sections, phase shift anal., energy depend. 0-47481  
<sup>208</sup>Pb(p,p<sup>+</sup>), pol. p, 9, 10 MeV, vol. integrals for optical pots., real symmetry pot. 0-42659  
<sup>208</sup>Pb(p,p<sup>+</sup>), 39, 62 MeV, DWBA anal., collective spectra, direct process contrib. (Russian) 0-13408  
<sup>208</sup>Pb(p,p), 20-50 MeV differential cross section, polarisation ang. distrib., optical model exchange terms 0-27638  
<sup>4</sup>Ru(p,p<sup>+</sup>γ), A=96, 98, 5-8 MeV, level schemes, transitions, vibr. state, mixing ratios 0-18199  
<sup>28</sup>Si(p,p), pol. p, 12-18 MeV, cross section, anal. power and states, <sup>29</sup>P resonance coherence widths 0-32258  
<sup>154</sup>Sm(p,p<sup>+</sup>), 35 MeV, ground state rot. band and multipole moment 0-32178  
<sup>4</sup>Sn(p,p<sup>+</sup>), A=115, 117, 119, 18 MeV, state spin assignment, particle-vibr. coupling 0-32160  
<sup>112</sup>Sn(p,p<sup>+</sup>), 20.51, 25.0 MeV, energy levels, excitation functions and ang. distrib. 0-32184  
<sup>112</sup>Sn(p,p<sup>+</sup>) 10, 12 MeV, <sup>113</sup>Sb mean nuclear lifetime from X-ray spectrum 0-9267  
<sup>117</sup>Sn(p,p), polarised p, 12.9 MeV, anal. power 0-5114  
<sup>106</sup>Ta(p,p<sup>+</sup>), 0.6-25 GeV, backward emitted proton inclusive spectra, short range correlation 0-32281  
<sup>232</sup>Th(p,p<sup>+</sup>), 35 MeV, ground state rot. band and multipole moment 0-32178  
<sup>48</sup>Ti(p,p), 1 GeV, elastic scatt. differential cross section calc. 0-47480  
<sup>238</sup>U(p,p<sup>+</sup>), 22 MeV, rot. band, multipole deformation parameters from coupled channel anal. 0-13369  
<sup>238</sup>U(p,p<sup>+</sup>), 35 MeV, ground state rot. band and multipole moment 0-32178  
<sup>176</sup>Yb(p,p<sup>+</sup>), 35 MeV, ground state rot. band and multipole moment 0-32178  
<sup>4</sup>Zn(p,p), A=66,68, 20-50 MeV differential cross section, polarisation ang. distrib., optical model exchange terms 0-27638  
<sup>4</sup>Zr(p,p), A=92, 94, 2-6.5 MeV, optical and Lane model anal. comparison 0-18302  
<sup>4</sup>Zr(p,p<sup>+</sup>), A=94,96, 11.2-13.4 MeV, anal. power and excitation function T<sup>+</sup> fluctuations 0-42626



**proton polarisation**

- display and calibration using automatically tuned NMR spectrometer 0-37669  
 low-energy protons, polarisation meas. using orientation effect in inner-shell atomic ionisation 0-9482  
 PANSI, polarisation anal. neutron scattering instrument, description and appls. 0-23280  
 synchrotron, spin flip by adiabatic passage of depolarisation resonances 0-5415  
 np→np, 6 GeV, spin-spin forces 0-433  
 pp→γγ annihilation, influence on sum rule proton polarisability 0-18143  
 pp→pX, high p<sub>T</sub>, spin-spin asymmetries, polarisation, hard scatt model with QCD 0-13339

**proton production**

- cumulative proton production in neutrino and antineutrino interactions with freon, 2 to 30 GeV (*Russian*) 0-4980  
 nuclear multi-particle rescatt. effects, cumulative π, p, K prod. (*Russian*) 0-52638  
 relativistic light ion collisions, two-fireball model improvements, p and π spectra 0-5158  
 (e, e'p), eN interaction in quasifree scatt., nonrelativistic Hamiltonian through 2nd order 0-52663  
 (e, e'p) quasi-free scatt., spectral function, sum rule discrepancy, shell model deviation 0-42641  
 e<sup>+</sup>e<sup>-</sup>→pp, 1925-2180 MeV total energy, form factors and cross sections 0-427  
 (γ, p), >100 MeV, using monochromatic photons, leading to final nuclear states 0-22814  
 γn→π<sup>-</sup>p reaction cross-section asymmetry in photon energy range 0.9 to 1.65 GeV (*Russian*) 0-32108  
 γp→ppp, threshold -4.8 GeV, elastic photoprod. cross section 0-52521 (p, X), 70 GeV/c (*Russian*) 0-52681  
 (p, X) emulsion, 400 GeV/c slow deuteron and proton prod. 0-52666  
 pn→pX, 100 to 400 GeV/c, slow-proton prod., Regge trajectory 0-22646  
 π<sup>-</sup>d→π<sup>-</sup>pn final state interactions and d breakup for 438 MeV/c π<sup>-</sup> impulse (*Russian*) 0-18145  
 π<sup>+</sup>n→pX, 100 to 400 GeV/c, slow-proton prod., Regge trajectory 0-22646  
 π<sup>-</sup>p, 200, 300 GeV, relative π<sup>+</sup>, K<sup>+</sup>, p, p̄ prod., charge ratios, high p<sub>T</sub> 0-47335  
 Π<sup>-</sup>ρ→p̄d, p̄ prod. obs. near 3.75 GeV/c threshold momentum 0-52533  
<sup>27</sup>Al(γ, p)<sup>26</sup>Mg, energy and angular distribution (*Korean*) 0-18289  
<sup>27</sup>Al(π, π<sup>+</sup>), 255 MeV, quasielastic knockout, proton yield, σ(π<sup>+</sup>)/σ(π<sup>-</sup>) cross section ratio 0-32305  
<sup>12</sup>C(e, e'p), eN interaction in quasifree scatt., nonrelativistic Hamiltonian through 4th order 0-47469  
<sup>12</sup>C(e, e'p), quasifree scatt., spin-orbit distortion of emerging nucleon 0-52664  
<sup>12</sup>C(e, e'p), cross sections from DWIA, optical, and shell model calcs. (*Russian*) 0-32270  
<sup>12</sup>C(γ, π<sup>-</sup> p), final state interaction, plane and distorted wave momentum distrib. 0-18286  
<sup>12</sup>C(γ, π<sup>-</sup>), (γ, π<sup>-</sup> p), knockout p interaction, optical model and quasifree π photoprod. mechanism (*Russian*) 0-42638  
<sup>12</sup>C(γ, π<sup>-</sup> p), 340-380 MeV, quasi-free photoprod., impulse and shell model anal. (*Russian*) 0-5124  
 C(p, X) (*Russian*) 0-52649  
<sup>3</sup>He(e, e'p) electrodisintegration by 1200 MeV electrons (*Russian*) 0-37370  
 N(p, X), 340, 660 MeV, ang. distrib., proton quasi-elastic knockout (*Russian*) 0-52649  
 O(p, X), 340, 660 MeV, ang. distrib., proton quasi-elastic knockout (*Russian*) 0-52649  
<sup>208</sup>Pb(π, π<sup>+</sup> p), 255 MeV, quasielastic knockout, proton yield, σ(π<sup>+</sup>)/σ(π<sup>-</sup>) cross section ratio 0-32305

**proton-proton inclusive interactions**

- Bose-Einstein statistics, wave packet formulation of multiparticle production at high energies 0-13338  
 cluster mass spectrum 0-37307  
 dihadron high mass continuum, phenomenological anal. of Fermilab data 0-42511  
 hadronic jets, possible intermediate bosons 0-18149  
 hadronic multiple prod. and average charged multiplicity, strato-gluon mechanism in pp, Kp, πp (*Chinese*) 0-22586  
 high p<sub>T</sub> direct single photon prod., 30-62 GeV 0-9189  
 jet thrust spectrum, 3-jet structure, QCD calc. 0-47333  
 pN collision, 200 GeV/c, production of long-lived hadrons and leptons, antinuclei production 0-13342  
 total cross-section asymptotics, stable approach, timelike and spacelike behaviour, vacuum polarisation 0-47332  
 vector meson production in pp interactions, constituent-interchange model 0-22579  
 η production, 30 to 50 GeV 0-5023  
 p(p̄)p→W<sup>±</sup>Z<sup>0</sup>(γ)X, high energy behaviour and hard photon prod. 0-5028  
 p(p̄)p→γX, large angle real photon prod. at large p<sub>T</sub>, QCD anal. 0-22644  
 pN, charm-pair production 0-22643  
 pp, 14.75 GeV/c, inclusive and semi-inclusive K<sup>±</sup>(890) and Σ<sup>±</sup>(1385) prod. 0-5027  
 pp, 200 GeV/c in Be, inclusive ω prod. at large p<sub>T</sub>, η' prod. upper limit 0-52547  
 pp, 22.4 GeV/c, azimuthal correlations and secondary transverse momentum alignment (*Russian*) 0-42509  
 pp, 28 GeV, in H, D, Be, inclusive Δ polarisation 0-47337  
 pp, 405 GeV/c, pion local number distrib. fluctuations, higher order correlations 0-18152  
 pp, 52.6 GeV, large transverse momentum charged hadron at 90°, jet like structs. 0-18150  
 pp, 62.4 GeV, e<sup>+</sup>e<sup>-</sup> massive pair prod., continuum and T resonance cross sections 0-18153  
 pp, 93 GeV, pp narrow enhancement at 1940 MeV, S(1936) mass 0-52542  
 pp, ISR energies, inclusive high p<sub>T</sub> ω<sup>0</sup> and η' prod. 0-42504  
 pp, pp, 540 GeV, T and ψ transverse momenta from QCD 2→3 processes, gluon subprocesses 0-52546  
 pp annihilation, low energy, prompt e<sup>+</sup>e<sup>-</sup>, ω<sup>0</sup> and η<sup>0</sup> prod., inclusive prod. rates 0-42506  
 pp collision inclusive spectra, fast pionisation at high energies, z-scaling (*Russian*) 0-47339

**proton-proton inclusive interactions continued**

- pp→hadrons, quark processes, interaction with hadronic sea, Lorentz transformation 0-37236  
 pp in W, 400 GeV, particle mean multiplicities 0-13473  
 pp jet prod., π<sup>0</sup> fragments, jet fragmentation function and momentum 0-443  
 pp→K<sub>s</sub><sup>0</sup>X, 147 GeV/c, cross-section, scaling 0-52539  
 pp→l<sup>+</sup>l<sup>-</sup>X, QCD corrections to Drell-Yan formula 0-22578  
 pp large p<sub>T</sub> reactions, jets, dual-string approach 0-32136  
 pp→Δ<sup>0</sup>X, small-angle production from nuclear and nucleon targets, collective tube model and triple-Regge picture 0-52538  
 pp→AK<sub>s</sub><sup>0</sup>X, 19 GeV/c, single particle props. 0-32139  
 pp→ΔX, 147 GeV/c, cross-section, scaling 0-52539  
 pp→Δ(K<sup>0</sup>)X, 12 GeV/c, beam polarisation induced asymmetries 0-42507  
 pp multiple hadron prod. up to 1500 GeV, hadronic matter eqn. of state (*Russian*) 0-32085  
 pp→pX, 50-400 GeV, differential cross sections, P diffractive dissociation (*Russian*) 0-5030  
 pp→pX, deep inelastic scatt. in nuclei, bare particles, multiple scatt. theory (*Russian*) 0-52549  
 pp→pX, diquark fragments, large transverse momentum baryon production 0-47330  
 pp→pX, high p<sub>T</sub>, spin-spin asymmetries, polarisation, hard scatt model with QCD 0-13339  
 pp→pX, leading proton spectrum, associated multiplicity distrib. in geometric bremsstrahlung model 0-37309  
 pp→p(slow)+X, 22.4 GeV/c, associative multiplicity (*Russian*) 0-5031  
 pp(p̄)→W<sup>±</sup>(Z<sup>0</sup>)X, QCD perturbation theory struct. function predictions 0-42505  
 pp→π<sup>+</sup>, large transverse momentum jets investig. at 52.4, 62.7 GeV 0-18151  
 pp→π<sup>0</sup>X, large p<sub>T</sub> processes, pion exchange model anal. (*Russian*) 0-27527  
 pp→π<sup>0</sup>X, scaling in the mean hypothesis and Feynman variable energy depend. 0-42501  
 pp→π<sup>0</sup>+X, secondary neutral pion-nucleon flux ratio at atm. top 0-8500  
 pp→π<sup>0</sup>π<sup>0</sup>X, ISR π<sup>0</sup>-π<sup>0</sup> azimuthal correlation data, comments 0-52543  
 pp→π<sup>0</sup>X reaction, quark-quark inelastic collision model (*Russian*) 0-32141  
 pp→π<sup>0</sup>X, √s=63 GeV, high momentum meson correlations 0-32138  
 pp→πX, QCD radiation and mean scaling, longitudinal and transverse momentum 0-42405  
 pp, polarised and unpolarised, jet cross sections vector boson signals, QCD-weak interference 0-5026  
 W-boson production, Weinberg-Salam model 0-9186  
 Z<sup>0</sup>-boson production, Weinberg-Salam model 0-9186  
 pp→D<sup>+</sup>X, 53 GeV, D<sup>+</sup>→K<sup>-</sup>π<sup>+</sup>π<sup>+</sup> (*Polish*) 0-9187

**proton-proton interactions**

- see also *proton-proton inclusive interactions; proton-proton scattering*  
 charged-particle multiplicity distrib. at 400 GeV/c 0-13337  
 cluster cascade model, single particle distributions and two-particle correlations 0-18300  
 dibaryon resonance behaviour, nonadiabatic rotational bands in light nuclei 0-13353  
 Drell-Yan lepton pair prod. processes, π structure function and scaling phenomena 0-405  
 explosive quark matter, hypothesis for Centauro event 0-22648  
 hydrodynamic theory of high energy interactions (*German*) 0-406  
 multiple particle generation, Monte Carlo model of proton high energy collisions (*Hungarian*) 0-13336  
 scalon production and detection (*Chinese*) 0-47324  
 spin dependence of products 0-434  
 t-flavoured meson production in photonicuclear and pp collision 0-22623  
 K<sup>-</sup>p→ΔX, 8.25 GeV/c, off shell KK and pp interactions, KNO scaling 0-52534  
 pp, 350-1000 MeV, neutron prod. double differential cross section in meson generation reactions (*Russian*) 0-42490  
 pp, 373-734 MeV/c, total cross section enhancement, 1936 MeV narrow resonance 0-13324  
 pp, x<sub>f</sub> P-wave charmonium states, hadronic prod. cross section 0-37292  
 pp, internal target expts., 1 TeV antiquark-heavy nucleus collisions 0-52536  
 pp, pp, beauty prod. total cross section from perturbative QCD 0-32080  
 pp, pp, Drell-Yan processes, scaling violation effects 0-382  
 pp, pp, integrated cross section compilation 0-32121  
 pp, pp, lepton pair prod., transverse momentum distrib., QCD calcs. to leading logarithms 0-42486  
 pp, pp, Z<sup>0</sup> high p<sub>T</sub> bremsstrahlung, Higgs versus quark or gluon jets 0-32063  
 pp→(π<sup>+</sup>n)p, π energy and transverse momentum distrib., DHD model with nucleon exchange (*Russian*) 0-13327  
 pp→dπ<sup>+</sup>, 0.8 GeV, differential cross section and polarisation asymmetries 0-27519  
 pp→dπ<sup>+</sup>, 750 MeV, T=1 NN phase shifts and total cross section 0-22630  
 pp→Δ<sup>++</sup>π<sup>-</sup>, 4 GeV/c, mass spectra, ang. distrib. and momentum transfer (*Russian*) 0-42489  
 pp→γγ annihilation, influence on sum rule proton polarisability 0-18143  
 pp→l<sup>+</sup>l<sup>-</sup>+hadrons, lepton pair prod. in hadronic collisions, review 0-5022  
 pp→meson+lepton pair, transverse momentum distrib. and branching ratios, proton gluon distribution 0-52537  
 pp→nn, 5-25 GeV/c, charge exchange scatt., πNN vertex function, one pion exchange 0-37291  
 pp→nn, charge exchange processes, baryonium trajectories, Regge pole description 0-9180  
 pp→π<sup>0</sup>π<sup>0</sup>, up to 10 GeV/c, correlation of momentum of π<sup>0</sup> pairs 0-5011  
 pp→π<sup>0</sup>d, 400-800 MeV, anal. by neutron exchange, ΔN intermediate states, diproton resonances 0-27518  
 pp→π<sup>0</sup>d, di-proton resonances 0-22631  
 pp→π<sup>0</sup>d, NΔ(1232) state contrib., K matrix theory anal. 0-5013  
 pp→π<sup>0</sup>d, SIS, 578 MeV, pol. beam and target, spin depend. parameters 0-42651  
 pp→π<sup>0</sup>π<sup>0</sup>π<sup>0</sup>π<sup>0</sup>, 1950 MeV/c<sup>2</sup>, experimental evidence 0-27516  
 pp→π<sup>0</sup>π<sup>0</sup>π<sup>0</sup>π<sup>0</sup>, 1950 MeV/c<sup>2</sup>, properties evidence for pp→ω<sup>0</sup>ρ<sup>0</sup> 0-27517  
 pp→πd, π<sup>+</sup> negative parity assignment 0-32117  
 pp reaction, exchange current corrections π and ρ exchange 0-26733



**proton-proton interactions continued**

pp, 5.7 GeV/c, nonannihilation channels  $\Delta^{++}$ ,  $\Delta^{+}$ ,  $\Delta^0$ ,  $\bar{\Delta}^0$  prod. cross sections 0-27515  
 pp  $\rightarrow \pi^+ \pi^-$ , 5.7 GeV/c, two-pion correls., interference effects 0-32116

**proton-proton scattering**

see also *proton-proton interactions*

exchange degeneracy violating  $A_1$ -Z Regge amplitude and dibaryon resonances 0-4971

Froissart bound saturation, logarithmic rise of total cross-section 0-47328  
 impact parameter representation (*Russian*) 0-5019

phase shifts at 4 GeV/c 0-22632

proton-proton potential models obtained from the Virginia phase-shift analysis 0-47401

scattering amplitudes, 6 GeV, phase shift anal. 0-37290

spin correlation parameters for 6 GeV elastic scatt., eikonal model anal. 0-5012

spin dependence at large  $P_T^2$  0-42493

spin dependent forces in 6 GeV polarised scatt. in eikonal model 0-37246

total cross sections in pure spin states, Coulomb interference and rescatt. corrections 0-432

urn model, modified, dimens. counting rule, pp elastic scatt. appl. 0-27485

pp, 406-922 MeV/c, backward elastic scatt. cross section, resonance search 0-32119

pp, 5.7 GeV/c, parton-cluster model, hadron struct. and non-diffractive collision impact parameters struct. 0-27454

pp, high energy elastic scatt. cross sections, pomeron-nucleon coupling vertex, pomeron residue (*Russian*) 0-42492

pp, pp high energy elastic scatt., cross section rise and polarisation, Regge model (*Russian*) 0-37301

pp elastic scatt., current-current interaction, spin depend. differential cross section 0-18147

pp elastic scatt., FESR constraint on baryonium resonances, S, T, U, contrib. 0-27520

pp high  $p_T$  polarised elastic scatt., QCD explanation of asymmetries 0-13323

**proton radiative capture**

direct and resonance capture, giant dipole and quadrupole resonances 0-37385

proton induced  $\gamma$ -ray yields, chemical anal. appl. 0-45608

sd shell nuclei, (p, $\gamma$ ) resonance strengths 0-22786

(p, $\gamma$ ), (p, $\gamma\gamma$ ), recent experiment review, future experiment suggestions 0-37382

(p, $\gamma$ ), exclusive single nucleon transfer, theoretical status 0-42652

(p, $\gamma$ ), isobaric analogue doorway states, excitation functions 0-47388

$^{208}\text{N}(\gamma)$ , pol. N, anal. power and giant multipole resonances, direct-semidirect model 0-18265

$^{10}\text{B}(\text{p},\gamma)$ , 1.11 MeV,  $^{12}\text{C}$  negative parity states lifetime limits and transition strengths 0-5092

$^{11}\text{B}(\text{p},\gamma)$ , pol. p,  $^{12}\text{C}$  p<sub>0</sub> channel E2 strength 0-22790

$^{12}\text{C}(\text{p},\gamma)\text{N}$ , pol. p, 10-17 MeV,  $^{13}\text{N}$  electric quadrupole strength semi-direct capture model calcs. 0-47370

$^{13}\text{C}(\text{p},\gamma)$ , pol. p, 6.25-17.0 MeV, anal. power and cross section ang. distrib., E1, E2 amplitudes 0-47461

$^{14}\text{C}(\text{p},\gamma)$   $^{14}\text{N}$  energy levels up to 11.05 MeV, transitions and resonance decay 0-47376

$^{54}\text{Cr}(\text{p},\gamma)$ , 1.0-3.8 MeV,  $\gamma$ -yields, cross sections, predicted (p,n) cross section, Stat. anal. 0-5136

$^{54}\text{Cr}(\text{p},\gamma)^{55}\text{Mn}$  energy levels, bound state mean lifetimes and spins 0-42586

$^{19}\text{F}(\text{p},\gamma)$ , 0.2-1.2 MeV,  $^{20}\text{Ne}$  resonances,  $J^\pi$ , excitation functions and branching ratio 0-22787

$^{19}\text{F}(\text{p},\gamma)$ , pd. p,  $^{20}\text{Ne}$  E1 resonance 0-22790

$^{54}\text{Fe}(\text{p},\gamma)$ , 1.1-1.75 MeV,  $^{55}\text{Co}$  resonance decay schemes branching ratios, analogue states 0-52643

$^3\text{H}(\text{p},\gamma)^3\text{He}$ , intermediate energy, ang. distrib., reaction amplitude and  $^3\text{He}$  vertices 0-22835

$^{40}\text{K}(\text{p},\gamma)$ ,  $^{41}\text{Ca}$  giant dipole resonance, isospin struct., direct-semidirect anal. 0-47449

$^6\text{Li}(\text{p},\gamma)$ , 200-1200 keV, cross section 0-13478

$^{27}\text{Mg}(\text{p},\gamma)$ , 80-350 keV,  $^{26}\text{Al}$  low energy resonances, decay and  $J^\pi$  assignments, branching ratios 0-42624

$^{15}\text{N}(\text{p},\gamma)$ , pol. p,  $^{16}\text{O}$  E1 and p<sub>0</sub> channel E2 strength 0-22790

$^{64}\text{Ni}(\text{p},\gamma)$ , 2.05-2.55 MeV,  $^{65}\text{Cu}$  levels and transitions,  $\gamma$ -strength function using average resonance capture 0-13411

$^{10}\text{O}(\text{p},\gamma)$ , 0.67 MeV,  $^{18}\text{F}$   $J^\pi=3^-$  doublet at 6241 keV, isospin mixing 0-511

$^{208}\text{Pb}(\text{p},\gamma)$ ,  $\gamma$ -ray ang. distrib. asymmetry effects through IAR, direct-semidirect model 0-42581

$\text{Sn}(\text{p},\gamma)$ , 3.4 MeV,  $^{121}\text{Sb}$ ,  $A=121,123$ , levels below 2 MeV, spins, transitions and mixing ratio 0-32191

$^{50}\text{Ti}(\text{p},\gamma)^{51}\text{V}$ , 2.1 to 3.1 MeV,  $^{51}\text{V}$ ,  $\gamma$ -strength function,  $\gamma$ -ray spectra, average resonance method 0-9257

**proton scattering** see *electron-proton scattering; kaon-proton scattering; lepton-nucleon scattering; photon-proton scattering; pion-proton scattering; proton-deuteron scattering; proton-nucleus scattering; proton-proton scattering*

**proton spectra**

(p,p'),  $A=6$  to 208, 800 MeV, proton spectra, quasifree scatt., DWIA anal. 0-52677

$^{27}\text{Al}(^3\text{He,p})$  9-14 MeV, stat. multistep compound emission, residual two-body interaction 0-47493

$^{74}\text{Kr}$ , charged particle evaporation following form. from  $^{58}\text{Ni}+^{16}\text{O}$  0-47453

**proton-surface impact** see *ion-surface impact*

**protonium** see *protons*

**protonosphere** see *upper atmosphere*

**protons**

see also *cosmic ray protons; delayed protons*

decay, confirmation of unification of forces, book contrib. 0-42383

decay, search techniques for lifetimes of order  $10^{34}$  years 0-47287

decay modes in SU(5) and SO(1) theories 0-13301

electron cooling of protons at CERN 0-9443

EM structure functions from electron scatt. data 0-13306

half life, Dirac approach to large number coincidences 0-27501

QCD perturbation theory for confined quarks and gluons, p glue content 0-52460

radiation belt, equatorial  $\alpha/p$  ratio near 1 MeV 0-4205

semileptonic decay in nuclei, pion attenuation 0-47286

size, lower limits in general relativity 0-22245

**protons continued**

spin, outcome of violent collisions 0-434

stopping power in  $\text{H}_2$ , He,  $\text{N}_2$ ,  $\text{O}_2$ ,  $\text{CO}_2$ , Ne, Ar, Kr, Xe 0-14057

SU(5) grand unified theories, proton decay, flavour mixing effects 0-377

pp atom, nucl. level shift and radiative transitions (*Russian*) 0-28121

**proximity effect**

bidimensional junction lattices, proximity effects (*French*) 0-49998

coupled superconducting weak links, voltage locking and other interactions 0-39719

normal-superconductor interface, boundary conditions, theory 0-39708

sandwich system, near transition temp., proximity effect and Josephson current 0-7039

superconductor-metal-insulator-metal-superconductor system, Josephson current, weak supercond. (*Russian*) 0-54842

Ag-In (Sn) multilayers, vapour quenched, supercond. transition temp. 0-20346

Ag-Sn proximity-effect bridges,  $T^*$  anomaly under phonon injection 0-34566

Ag-Sn proximity-effect bridges, phonon-injection-induced first-order transition obs. 0-39718

Al-oxide-Mg-Al, thin proximity effect sandwiches, spin-polarised tunnelling obs. 0-50007

Cu-Pb proximity sandwiches, tunnelling expt., barrier transmission effects 0-50002

In superconducting microbridge, voltage locking and other interactions 0-39720

Nb-Al proximity sandwiches, supercond. transition temp. and tunnelling meas. 0-7045

Pb/Bi-I-Al tunnel injected nonequilibrium supercond. struct., diffusive quasiparticle instability, multiple gap states 0-50005

Pb-Cd thin films, electron tunnelling study of supercond. proximity effect 0-2525

Pb-Cu contacts, proximity effect (*Russian*) 0-34558

**pseudobinary semiconductors** see *II-VI semiconductors; III-V semiconductors; III-VI semiconductors; IV-VI semiconductors; semiconductor materials*

**pseudopotential methods**

ab initio effective core pot. method appl. to  $\text{F}_2$ ,  $\text{Cl}_2$  and  $\text{LiCl}$  0-32625

alkali atom, in inert-gas solid, at level struct. calc. pseudopot. method 0-9532

alkali metal, Ashcroft pseudopotential, unified study of props. 0-39239

alkali metal atom, perturbed by rare gases, dipole moments of S-P transitions 0-27979

alkali metals, elastic and thermal props. by pseudopotential method 0-19899

alkali metals, Gruneisen parameter and temp. depend. of elastic consts. 0-39317

alkali metals, ideal thermal resist. and Lorenz number due to conduction electron-phonon scatt. 0-29377

alkali metals, pressure influence on absolute zero isotherms, polymorphic transform., phonon spectra (*Russian*) 0-49363

alloys, crystalline, liq., amorphous, stability and structure, pseudopotential calcs. (*German*) 0-38913

anisotropic normal metal, thermopower calc. 0-24879

atomic model potentials soluble in closed form 0-23287

binary alloy, determ. of distortion field 0-44536

binary alloy, of simple metals, with non-homovalent impurities 0-44464

binary compounds, structural stability, nonlocal density-functional atomic pseudopot. method 0-49174

$\beta$ -brass (40 to 50 at.% Zn), elastic shear consts., comp. depend., pseudopot. calc. (*Russian*) 0-24525

disordered simple metal, electronic and cohesive properties, review 0-44475

electron energy spectrum in crystals, use of atomic scatt. form factors 0-6688

electrons in disordered metals and at metallic surfaces, conf., Ghent, Belgium (Sept. 1978) 0-41946

elemental semiconductors, model pseudopotential, band struct. calcs., liquid semicond. resistivity calcs. 0-20075

exchange interaction and correlation effects on ion pseudopot. form factor 0-49639

formic acid, H bonding, electronic struct., geometries, moments, dimerisation energies, charge distrib., pseudopotential calcs. 0-27942

graphite intercalation compounds,  $\text{C}_6\text{K}$ , electronic struct. and elec. props. 0-44471

IV-VI semiconductors, transverse effective charge from one dimens. band struct. calc. 0-15038

IV-VI semiconductors, transverse effective charge from three dimens. band struct. calc. 0-15039

liquid metals, spin-orbit interactions effect on mag. susceptibility, effective pseudohamiltonian 0-29299

liquid polyvalent metals, struct. factors with shoulder 0-19686

metallic glasses, structure and formation, thermodynamic props., cluster relaxation approx. 0-54143

metals, compressibilities, general pseudopotential approach 0-54631

metals, cubic, monovacancy resist. using pseudopot. models 0-29378

metals, Gruneisen parameters, interatomic forces, pseudopot. calc. 0-44165

metals, pseudopotential study of electronic props. 0-20149

methanol, H bonding, electronic struct., geometries, moments, dimerisation energies, charge distrib., pseudopotential calcs. 0-27942

methyl halides, mol. force fields, IR intensities, and vibr. props. 0-47879

molecular models of condensed systems and interfaces (*German*) 0-20062

noble metals, Krasko-Gurskii model potential, test of validity for Cu 0-39485

norm-conserving pseudopotents. 0-14066

nucleic acid bases,  $\text{Zn}^{2+}$  binding, ab initio SCF (pseudopot.) calcs. 0-12052

one-dimensional conductors, Peierls instability, dynamics, structural energy, pseudopot. calc. 0-54676

polar semiconductor, conduction states, pseudopot. and tight-binding calcs. 0-24785

relativistic model pseudopot. yielding mag. model pseudopot. and effective Hamiltonian 0-29299

reliability criteria, for pseudopot. approaches to molecule, solid and surface electronic struct. 0-49563

semiconductors, amorphous, liquid, glassy, random field parameters and pseudopotential calc. 0-29316

simple metals, volume forces 0-15178

solids, total energy calcs., momentum space formalism 0-15468



**pseudopotential methods continued**

- superconductivity, pseudopotential, Bragg planes, effect on superconducting pairing and crit. temp. 0-15648  
 superconductivity theory, HF cut offs of Coulomb interaction, real freq. Coulomb pseudopotential derivation 0-49980  
 surface and interface calcs. 0-49853  
 transition metal, adsorption of CO, electronic struct., localised orbital pseudopot. method 0-39653  
 transition metal-carbonyl cluster molecules, electronic struct., localised orbital pseudopot. method 0-39653  
 vacancy, self-consistent electronic states 0-29354  
 Ag, phonon limited elec. resist., temp. depend. 0-24876  
 Ag, pseudopot. optimised form for phonon dispersion study 0-10611  
 Ag-Au(Cu), residual elec. resist., pseudopot. calc. 0-6813  
 Al, elastic consts., third order, pseudopotential calc. by method of homogeneous deformation 0-29106  
 Al, electronic Grüneisen parameter in shock Hugoniot eqn. of state 0-10635  
 Al, empirical pot. methods, use of Wedepohl pot., vacancy form energy 0-39230  
 Al, Fermi surface under homogeneous strain, local pseudopot. model 0-29308  
 Al, lattice thermal cond. at low temps., Ashcroft pseudopotential method 0-19897  
 Al-Mg, determ. of distortion field, induced by substitutional defect 0-44536  
 Al-Zn (10 at.%), short-range order parameter calc. in pseudopot. approx. (*Russian*) 0-49183  
 Ar, valence electron distrib., pseudopotential calcs. 0-2335  
 As, band structure on Jones zone boundary, pseudopot. calc. 0-54603  
 Au, phonon limited elec. resist., temp. depend. 0-24876  
 Au-Cu, residual elec. resist., pseudopot. calc. 0-6813  
 Be metal, electron distribution and momentum density, Compton scatt. 0-11502  
 Be, twin boundaries, computer simulation 0-39109  
 Cd, temp. depend. Knight shift 0-2655  
 Cd, twin boundaries, computer simulation 0-39109  
 CdSiP<sub>2</sub>, pseudodirect chalcopyrite semicond., electronic band struct. 0-20079  
 Cr-Ge liquid and amorphous alloys, struct. props., cond., viscosity, surface tension (*Russian*) 0-54119  
 Cs, phonon spectral density, pseudopotential calcs. 0-39234  
 Cs, structural energies, pseudopotential formalism 0-39519  
 CsI:Na, electronic struct. and luminesc. 0-16080  
 Cu isoelectronic series, hard-core pseudopotentials and struct. maps 0-44168  
 Cu, Krasko-Gurskii model potential, test of validity 0-39485  
 Cu, phonon limited elec. resist., temp. depend. 0-24876  
 Fe-Ni(Cu)(Al)(Si) liquid alloys, thermodynamic characts. calc. (*Russian*) 0-15264  
 GaAs (110), self-consistent pseudopotential calcs., electronic struct. and atomic co-ords. 0-49848  
 GaAs (110) surface, electronic struct., pseudopot. calc., surface relax. model 0-29456  
 Ge, electronic and struct. props., nonlocal pseudopot. calc. 0-34349  
 Ge:H, interstitial impurity levels, pseudopot. calc. 0-44533  
 H<sub>2</sub>O, H bonding, electronic struct., geometries, moments, dimerisation energies, charge distrib., pseudopotential calcs. 0-27942  
 HgGa<sub>2</sub>Se<sub>4</sub>, energy band struct. calc., empirical pseudopot. method 0-24793  
 InAs-GaSb (100) superlattice, electronic struct., self-consistent pseudopot. method 0-49884  
 InAs-GaSb superlattice, electronic struct., self-consistent pseudopot. calc. 0-29470  
 InSe, three-dimensional band structure 0-24799  
 K, Fermi surface distortion 0-2325  
 K isoelectronic series, hard-core pseudopotentials and struct. maps 0-44168  
 K, phonon spectral density, pseudopotential calcs. 0-39234  
 K, structural energies, pseudopotential formalism 0-39519  
 K-Rb, liq., form factors and transport coeffs., pseudopot. perturb. theory 0-44561  
 K<sub>2</sub>Sb, optical and dielectric props., energy spectra, density of states calcs. 0-20083  
 Li isoelectronic series, hard-core pseudopotentials and struct. maps 0-44168  
 Li isoelectronic series, relativistic pseudopot. appl. in HF calcs. 0-27960  
 Li, liq., elec. resistivity and thermoelec. power, orthogonalisation hole pseudopotential calc. 0-29376  
 Li, phonon spectral density, pseudopotential calcs. 0-39234  
 Li, twin boundaries, computer simulation 0-39109  
 Mg, twin boundaries, computer simulation 0-39109  
 MgO, valence electron distrib., pseudopotential calcs. 0-2335  
 Mo (001) surface with saturated H adsorption, band structure self-consistent calc. 0-15585  
 Mo, electronic and struct. props., nonlocal pseudopot. calc. 0-34349  
 Mo(001), H chemisorbed, self-consistent electron struct. 0-44693  
 Na, Fermi surface distortion 0-2325  
 Na isoelectronic series, hard-core pseudopotentials and struct. maps 0-44168  
 Na, phonon spectral density, pseudopotential calcs. 0-39234  
 Na-K(Cs), liq., form factors and transport coeffs., pseudopot. perturb. theory 0-44561  
 Na<sub>2</sub> (n≤8), equilibrium geometries and ionization energies calcs. 0-1099  
 NaCl, valence electron distrib., pseudopotential calcs. 0-2335  
 Ni-Pt, short-range order parameter calc. in pseudopot. approx. (*Russian*) 0-49183  
 β-NiAl, self consistent embedded cluster model for Fe, Co, Ni mag. impurities 0-2549  
 Ni<sub>2</sub>Fe, short-range order parameter calc. in pseudopot. approx. (*Russian*) 0-49183  
 O<sub>2</sub>, electronic struct., self-consistent pseudopot. calc. 0-9508  
 Pb, electronic thermal Grüneisen parameters 0-39242  
 Rb, phonon spectral density, pseudopotential calcs. 0-39234  
 Rb, structural energies, pseudopotential formalism 0-39519  
 Sb, electronic band struct. changes due to plane straining effects (*Russian*) 0-54602  
 Si, covalent semiconductor, electronic response to high symmetry lattice vibr. 0-10619  
 Si, electronic and struct. props., nonlocal pseudopot. calc. 0-34349  
 Si, electronic struct., non-spherical local pseudopotential calcs. 0-39496

**pseudopotential methods continued**

- Si, electronic structure at high press. near semicond.-metal transition 0-49586  
 Si, pseudopotential calculation of phonon dispersion curves 0-10620  
 p-Si, Raman spectra, pseudopot. calc. of discrete-continuum interference 0-2747  
 Si, structural props., self-consistent calc. 0-28947  
 Si, structurally related bulk and surface props., self-consistent pseudopot. method 0-54632  
 Si<sub>1-x</sub>Ge<sub>x</sub> system, lattice energy and consts., virtual cryst. approx., pseudopot. calc. 0-44166  
 W, electronic and struct. props., nonlocal pseudopot. calc. 0-34349  
 Zn, twin boundaries, computer simulation 0-39109  
 ZnIn<sub>2</sub>S<sub>4</sub>, electronic props. of polytypic forms, pseudopot. calc. 0-38997  
 ZnSiP<sub>2</sub>, pseudodirect chalcopyrite semicond., electronic band struct. 0-20079  
 Zr, BCC, phonon vibrs., pseudopot. method 0-15204

**pseudoternary semiconductors see ternary semiconductors****psi mesons**

- charmonium model and the  $\psi$  and T families 0-47253  
 charmonium psion states, confining pots. and inverse scatt. problem, T mass 0-4946  
 charmonium quark-antiquark pots., flavour independ.,  $\gamma$ ,  $\gamma'$ ,  $\psi$  and  $\psi'$  appls. 0-47254  
 EM transition rates, geometrodynamical quark model 0-47295  
 flavour independence of forces between quarks,  $\psi$  and T spectra 0-22569  
 hadronic prod., lepton pair ang. distribs., cross section  $\chi$  contribution 0-42487  
 mass spectra, quasipotential calcs. (*Russian*) 0-47268  
 masses and leptonic-decay widths, one-parameter potential 0-13279  
 pseudoscalar and vector meson decays, triangular quark diagram anomalies,  $\psi$ ,  $\eta$  and  $\eta'$  appl. (*Russian*) 0-42455  
 QCD, asymptotic freedom, energy levels J/ $\psi$  and T mass difference (*Chinese*) 0-52480  
 QCD, heavy-vector meson-nucleon scatt., cross section suppression, T and  $\psi$  0-22564  
 QCD and  $\psi$  parameters, charmed quark current in quark-gluon coupling (*Russian*) 0-13277  
 quark bag model with finite potential barrier, S-wave mass spectra of QQ and leptonic widths 0-47242  
 quarkonium, quantum mechanical applications, masses and leptonic widths of  $\psi$  and T 0-27484  
 radiative decay, gluonic bound state O<sup>-</sup> width 0-37272  
 Zweig rule in two-dimensional QCD,  $\psi$  and T decays 0-52479  
 B $\rightarrow$ J/ $\psi$ +hadrons, branching ratio, b quark decay calcs. 0-32095  
 b quark $\rightarrow\psi(\eta_c)+X$ , B branching ratios assuring colour suppression 0-37259  
 $\chi_1\rightarrow\gamma\psi$ , charmonium states radiative and hadronic widths, gluon spin 0-4998  
 e<sup>+</sup>e<sup>-</sup> annihilation, 3.1-5.2 GeV, DASP results 0-42483  
 e<sup>+</sup>e<sup>-</sup>, annihilation, production of new particles, J/ $\psi$ ,  $\psi'$  and  $\tau$  props. 0-5008  
 e<sup>+</sup>e<sup>-</sup> annihilation, gluon jets and heavy quarkonium prod., QCD test,  $\psi$  prod. 0-42479  
 $\eta$ - $\eta'$  mixing angle and relative radiative decay rates  $\Gamma(\psi\rightarrow\eta\gamma)/\Gamma(\psi\rightarrow\eta'\gamma)$  0-9173  
 $\gamma N\rightarrow\psi(3.1)+\text{anything}$ , cross section and N charmed quark composition 0-423  
 J/ $\psi$  decay, gluon source, search for scalar gluonium, QCD 0-47296  
 J/ $\psi\rightarrow\eta_c\gamma$ , radiational decays in charmonium (*Russian*) 0-13308  
 J/ $\psi\rightarrow\eta(\eta')\gamma$  decay rate, QCD sum rules 0-52497  
 $\mu^+\mu^-\rightarrow\psi X$ , diffractive and non-diffractive  $\psi$  leptoprod. in QCD 0-424  
 $\mu^+N$ , 280 GeV/c in Fe,  $\psi$  virtual photoprod. 0-37279  
 pp, pp, 540 GeV, T and  $\psi$  transverse momenta from QCD 2 $\rightarrow$ 3 processes, gluon subprocesses 0-52546  
 $\pi^+\pi^-\rightarrow\psi n$ , generalised Veneziano models,  $\psi$ /d production mechanism 0-22638  
 $\psi(3684)$  radiative decays, energy correlation 0-13307  
 $\psi(4.03)\rightarrow D\bar{D}$ , suppression problems, model-independent approach 0-52494  
 $\psi(4.42)\rightarrow D\bar{D}$ , suppression problems, model-independent approach 0-52494  
 $\psi(4.42)\rightarrow F\bar{F}$ , suppression problems, model-independent approach 0-52494  
 $\psi(3100)$  decay, inclusive  $\gamma$  and  $\pi^0$  momentum spectra, direct  $\gamma$  prod. at large x 0-42466  
 $\psi$  decay, high energy direct photons,  $\gamma$ ,  $\pi^0$  momentum distribs., QCD calcs. 0-32098  
 $\psi\rightarrow\eta(\eta')\gamma$ , SU<sub>3</sub> violation, symmetry breaking and decay amplitudes 0-52499  
 $\psi\rightarrow\eta(\eta')\gamma$ , Ward identity anal.,  $\eta$ ,  $\eta'$  quark-gluon struct. 0-42449  
 $\psi(3685)\rightarrow\gamma P/\chi\rightarrow\gamma\gamma J/\psi(\gamma\pi^+\pi^-)(\gamma K^+K^-)$ , investig. of  $\gamma\gamma\mu^+\mu^-$  final state 0-18132  
 $\psi\rightarrow J/\psi(\pi^0 J/\psi)$ , investig. of  $\gamma\gamma\mu^+\mu^-$  final state 0-18132  
 $\psi\rightarrow\psi\eta$ , Ward identity anal.,  $\eta$ ,  $\eta'$  quark-gluon struct. 0-42449  
 $\psi\rightarrow\psi\pi^0(\eta)$ , SU<sub>2</sub> violation, symmetry breaking and decay amplitudes 0-52499  
 $\psi''(4.42)\rightarrow D\bar{D}$ , FF, decay suppression, pseudo-dimension selection rule 0-9163  
 $\psi''(3772)$ , radiative decay nonoccurrence 0-4997  
 $\psi\rightarrow\chi_0\gamma$ , radiational decays in charmonium (*Russian*) 0-13308

**PSK see phase shift keying****psychological optics see vision****psychology**

- coloured surrounds, effects on colour naming and luminosity 0-56054  
 eye movement recorders, problems, use in laboratory 0-41331  
 eye movements, cognitive psychology, on-line computer applications 0-41329  
 frequency perception, colour as a pervading principle over pitch, rhythm, and form 0-56059  
 hearing aids, perceived sound quality obs. 0-41050  
 immersion in various liquids, anal. of dynamic cold sensation (*Japanese*) 0-21448  
 picture processing, eye tracking, computer raster graphics device 0-41330  
 psychophysical and VEP increment obs. of light adaption in a normal and a rod monochromat 0-16939  
 psychophysical evidence for sustained and transient channels in the monkey visual system 0-35896  
 psychophysical stress from long term ECG recording, hardware evaluation of parameters (*German*) 0-26388



**psychology continued**

- psychophysiological techniques applied to aircraft design and other operational problems 0-26384
- sleeping rhythm of mouse, classification using compact accelerator 0-56309
- spatial contrast sensitivity in albino and pigmented rats, behavioural obs. 0-41013
- spatial localisation during pursuit eye movements 0-51081
- spatial vision, psychophysical investigation, normal and reeler mutant mouse obs. 0-41032
- subjective noise annoyance by low level sound 0-35902
- trichromatic colour matching, high-level, rel. to pigment-bleaching hypothesis 0-35891
- vision, McCollough effect, role of test pattern background hue; 0-41036
- vision complex pattern discrimination, learning by young kittens, expt. obs. 0-56049
- visual acuity, infant, underestimation as near threshold gratings are not preferentially fixated, expt. obs. 0-56053
- visual stimuli generation, microprocessor based system 0-41328
- visually guided locomotion, psychophysical evidence for neural mechanism sensitive to flow patterns 0-51107

**PTC thermistors** *see thermistors***p.t.m.** *see pulse time modulation***pulp industry** *see paper industry***pulsars**

- see also neutron stars; radiofrequency cosmic radiation*
- atmospheres, numerical solns. of trans-relativistic shock relations 0-31202
- baryon star magnetospheres, inclined rotator case 0-26887
- coherent curvature radiation 0-56704
- coherent radio emission from pulsars, review 0-46596
- coherent radio emission in nature, theory, solar system and pulsars appl. 0-46393
- cosmic ray sources, evidence from Galaxy cosmic rays and mag. field distrib. 0-4207
- electron cap, electrons accel. in internal zone 0-46592
- elliptical cross section and linear polarization of pulsar radio beams 0-56865
- EM ion waves in cold relativistic plasmas, astrophys. appl. 0-21910
- EM vars. in curved space-times 0-56866
- emission geometry and pulse-width statistics 0-26893
- gamma-ray light curves, geometrical anal. 0-36653
- information sources for neutron star, dense matter and gravitational collapse physics 0-36657
- interpulse emission, structure 0-36652
- interstellar scintillation, analytic soln. of second-order moment eqn. 0-26726
- luminosities, upper bounds for narrowband and broadband emission processes 0-51797
- magnetosphere, magnetoactive plasma equilib. in gravit. field (*Russian*) 0-26895
- magnetosphere boundary layer phenomena 0-36776
- magnetosphere emission, mag. bremsstrahlung of ultrarelativistic particle beam in relativistic plasma 0-46390
- magnetosphere model, cylindrical, with particle inertia but no dissipative forces 0-51796
- magnetosphere models, interior and exterior struct., pair prod. 0-46594
- magnetosphere radio emission, plasma supply and elec. forces, review 0-46595
- magnetospheres, axisymmetric, self-consistent description 0-31318
- magnetospheres, relativistic MHD wind or plasma wave 0-31317
- magnetospheres, stellar-wind model for plasma-EM fields 0-22031
- magnetospheres and radio emissions, conf. Snowmass, Colorado, USA (Aug. 1978) 0-41939
- neutrino and cosmic ray source, energy spectra 0-31319
- NP 0531, distrib. model of press., density, ang. vel., matter rot., grav. field (*Ukrainian*) 0-12775
- NP 0532, Crab pulsar, mass and radius from supernova remnant physical theory 0-51834
- NP 0532, Crab pulsar, X-ray and gamma-ray radiation 0-41885
- NP 0532, Crab pulsar, gravitational radiation obs., energy flux upper limit 0-36655
- NP 0532 magnetosphere, cyclotron instability rel. to origin of radiation (*Russian*) 0-8645
- particle acceleration by DC electric fields 0-31316
- planetary systems, post supernova survival 0-56860
- plasma instabilities (*Russian*) 0-36656
- polar caps, particle acceleration and radio emission 0-51794
- polar caps as foil-less diodes, nonneutral relativistic beam accel. 0-17604
- positron production, galactic 511 keV gamma-ray line from positron annihilation 0-46590
- PSR 0329+54, binary motion to explain freq. variations 0-26894
- PSR 0525+21 occulted by solar corona, Faraday rot. at 1720 MHz 0-46526
- PSR 0531+21, Crab pulsar, optical light curve changes in 1970-7 period 0-36654
- PSR 0820+02, long-period binary pulsar, discovery from timing obs. 0-56867
- PSR 0833-45, Vela pulsar, optical pulse profile 0-46593
- PSR 0833-45, Vela pulsar, pulsed high energy gamma rays 0-41848
- PSR 0950+08, micropulses freq. struct. 0-22030
- PSR 1913+16, binary pulsar, components min. projected distance calc. 0-26904
- PSR 1913+16, binary pulsar, optical source and general relativistic effects 0-56868
- pulse polarisation patterns, rel. to quasi-transverse propag. theory 0-46591
- pulse timing measurements, appl. to search for gravit. waves 0-36743
- radio emission, mag. field, energisation, comparison with Jupiter 0-46466
- radio emission microstructure, propag. effects in shearing field-free plasma 0-17483
- radio flux density and pulse profile at 102.5 and 61 MHz, obs. 0-17601
- relativistic degenerate electron plasma, dielectric response in mag. field, plasma oscillations 0-54022
- relativistic spin-spin interaction theory for two concentric shells 0-46148
- rotation periods, long-term changes rel. to neutron star interior plasma 0-22029
- Ruderman-Sutherland model, emission zone limits 0-51795
- scintillations, cosmic ray streaming or mirror instability effects 0-51845
- scintillations, freq. cross-correl. and finite bandwidth effects 0-4392
- scintillations, interstellar density fluctuations effect 0-46649

**pulsars continued**

- scintillations, interstellar medium mirror instability growth effects 0-46648
- spectra, nature of low-freq. dropout 0-17602
- SS 433 as veiled pulsar 0-41842
- supernova off-centre explosions, rel. to high vel. pulsars form. 0-46587
- ultrarelativistic beam quasilinear relativistic plasma relax. in strong mag. field, magnetobremstrahlung (*Russian*) 0-38669
- Universe, high density matter, many body treatment, pulsars 0-26738

**pulsatile flow***see also peristaltic flow*

- air in heated channel, turbulent flow, velocity and temp. pulsation characteristics 0-14820
- arterial stenosis and stenotic atherosclerosis, dynamic press.-flow diagrams 0-3658
- arterial stenosis model, pulsatile flowfield downstream 0-17001
- binary boundary layer with press. pulsations, friction and heat and mass transfer 0-14653
- blood electric impedance, effects of pulsatile flow (*Japanese*) 0-21513
- blood flow in frog web arteriole 0-16964
- bubble motion in viscous liquid half-space near boundary with inviscid liquid 0-19494
- curved tube, axial velocity profile meas. 0-41088
- ducts, eddy motions induced by water waves and periodic flows 0-33679
- furrowed channels with pulsatile flow, Navier-Stokes soln. flow patterns, separation 0-33672
- furrowed channels with pulsatile flow, observed flow patterns, separation and vortices 0-33673
- gas phase catalytic reactions, periodic press. cycling, viscous flow effects 0-19521
- gas-liquid cocurrent downflow in fixed bed in pulsed regime, mass transfer fluctuations 0-19485
- Hartmann-Sprenger tube, air jet from convergent nozzle, air column oscillations generative mech. 0-14828
- hot-film probe, in reversing flow, forced convection, finite difference soln. 0-12177
- hydraulic lines, wave phenomena, coupled vibrations in bending and branching lines 0-14778
- incompressible liquid oscils. in variable cross section viscoelastic tube due to pulsating press. 0-31519
- jet, air, subsonic, fully pulsed, near field vel. meas. 0-19540
- laminar heat transfer between two parallel plates, pulsation effects (*German*) 0-33681
- n-incompressible and immiscible rarefied gases, pulsating flow between two plates 0-10306
- nonisothermal streams, turbulent velocity pulsations meas., procedure 0-19514
- post-stenotic turbulent wall pressure fluctuations, spectral and temporal characts. 0-16994
- propagation rate of pulse wave in arteries 0-41099
- pulmonary haemodynamics, quasi one-dimens. unsteady nonlinear fluid flow eqns. soln. 0-41104
- thermal convection in step wake with pulsating jet (*French*) 0-10240
- tube, oscillating and pulsating flow, critical Reynolds numbers (*German*) 0-1687
- unstaggered tube bank vibration induced by viscous liquid flow (*Russian*) 0-33677
- unsteady flow in a porous, elastic rectangular tube (*Japanese*) 0-6143
- unsteady viscous flow curved elastic tube model 0-16998
- vapour bubbles, analysis of oscillation 0-19487
- vapour bubbles, evaporation-condensation resonance frequency 0-19488
- viscous fluid in rotating channel 0-10311
- viscous sublayer and near wall turbulence struct., stroboscopic visualisation 0-19349
- wake structure of two-, three-dimensional flame holders 0-53786

**pulse amplitude analysers** *see pulse height analysers***pulse amplitude modulation**

- microwave field dosimetric device 0-3818

**pulse-code modulation**

- ADPCM, for speech waveform coding, developments in Japan 0-33353
- ADPCM coded speech, segmental SNR measure as indicator of quality 0-33359
- speech, sub-band coding with adaptive bit allocation 0-28386
- speech encoding, freq. domain techniques using APCM 0-33355

**pulse-code modulation links**

- digital transmission system for Deutsche Bundespost using fibre-optic link, PCM 480 system 0-38120

**pulse frequency modulation**

- fibre-optic video transmission to and from undersea vehicles 0-46310

**pulse generators***see also multivibrators*

- accelerator modulator charging system upgrade for 5 MeV electron accelerator 0-23182
- colour sensing optoelectronic device, neural mechanism modelling 0-12128
- HV pulser development for CS<sub>2</sub> laser cavity 0-23707
- injection diode modulated laser pulse generator and digital control cct. (*Russian*) 0-14372
- metal electroplastic deformation meas. pulse generator (*Russian*) 0-25931
- NMR pulse programmer, microprocessor-based 0-52289
- programmable pulse sequence generator for pulse NMR 0-17979
- square root of time mark generator using TTL digital ccts. for chronocoulometry 0-35588

**pulse height analysers**

- dead time corrections in coincidence measurements by time-to-pulse-height converters or standard coincidence systems 0-9472
- electron microprobe anal. using energy dispersive spectrometry 0-55765
- emission nebulae, first obs. with optical multichannel analysis of Sao Paulo University 0-26743
- high-speed single-input system for pulse identification 0-891
- MWPC, IC tapped delay line readout 0-5455
- nuclear laboratory instruction with multichannel analyser/microcomputer system 0-31471
- partial discharge spectra meas. by multichannel amplitude analyser system (*Italian*) 0-33847
- peak detector circuits, use with single-particle detectors and multichannel analysers 0-37707
- phoswich detectors in space borne hard X-ray expts. 0-36501



**pulse height analysers continued**

- photoelectronic spectrometer and coincidence instrum., use of AI-4096 analyzer 0-22473  
 pulse height store for A/D conversion 0-14054  
 recoil electron signals, pulse height anal., indication of low energy  $\gamma$  and  $\nu$  direction of incidence 0-52823  
 Royco aerosol particle counter 225, data processing system and modified system props. 0-37005  
 scintillation spectroscopy, organic, use of logarithmic pulse height and energy scales 0-37690  
 scintillator, NE 213, pulse, shape discrimination, appl. to neutron spectrometry 0-27862  
 time to amplitude converters, precision 1 GHz time calibration 0-27903

**pulse modulation**

- see also demodulators; modulators; pulse amplitude modulation; pulse-code modulation; pulse frequency modulation; pulse time modulation  
 NQR pulse spectrometer modulator 0-17971

**pulse motors** see stepping motors**pulse oscillators** see pulse generators**pulse repetition rate modulation** see pulse frequency modulation**pulse shaping circuits**

- HV pulser development for  $\text{CS}_2$  laser cavity 0-23707  
 power supply inductive pulse shaping for periodically pulsed  $\text{CO}_2$  laser 0-53311  
 quadrupole mass spectrometer with elliptical electrodes, 3-dim. 0-31931  
 scintillation beta spectrometer with compound detector 0-23243

**pulse time modulation**

- see also pulse width modulation  
 laser, passive mode locking, two laser amplifiers with slow saturable absorber 0-33041

**pulse transformers**

- high voltage impulse transformer for pulser-sustained laser appls. 0-1263

**pulse width modulation**

- acoustooptical modulators, computer controlled laser interferometer 0-56294  
 blood circulation apparatus, improved electromechanical drive regulator 0-3871  
 HPLC, two-pump gradient, accuracy and reproducibility 0-16742

**pulverised coal** see pulverised fuels**pulverised fuels**

- see also coal  
 gas flow distrib. in manifolds of uniformly variable section (Russian) 0-33666

**pumped-storage power stations**

- compressed air and underground pumped hydro storage, comparison 0-40910  
 geologic conditions 0-30577

**pumping** see pumps**pumping (optical)** see optical pumping**pumps****see also vacuum pumps**

- AC conduction pump with Na working fluid, performance characts., freq. depend. (Japanese) 0-13092  
 cavitating screw pump nonsteady-state press. component 0-19455  
 constant pitch inducer pumps, solidity effect limits 0-6108  
 d.c. electromagnetic pump, flow of conducting liquid (Rumanian) 0-28574  
 EHD, in attraction mode, efficiency 0-52187  
 fibre-optic glass manufacture using polypropylene sump pumps 0-14410  
 gas-lift pump design, <8 mm riser dia. 0-10324  
 induction MHD pump, active zones, effective forces, EHDA integrator study 0-43797  
 MHD, for Hg transfer in chlorine and caustic soda production 0-43787  
 MHD AC conduction pump for ferrous metal 0-33701  
 MHD conduction pump for filling casting mold 0-43798  
 PWR, reactor coolant pump failure investig. at Arkansas Nuclear One 0-9336  
 solar and wind powered, desalination plants appl., based on reverse osmosis (French) 0-55807  
 Toepler pump, all-metal automated, for laboratory use 0-52180  
 two channel DC EM pump, expt. study 0-43791  
 water pumping, by means of flat solar energy collectors (French) 0-55902  
 water pumping windmill, low-cost, using sail-type Savonius rotor 0-21367  
 wind pumps, development programme 0-55792  
 wind-operated, reciprocating water pump, stroke adjusting mechanism for rotor speed control 0-50930  
 windmill for use in irrigation, with horizontal axis sail 0-21368  
 windpump ITDG development program, for small-scale manufacture and use in under-developed arid regions 0-26106

**purification, crystal** see crystal purification**Purkinje effect** see vision**push pull amplifiers** see differential amplifiers**push pull microphones** see microphones**p.w.m.** see pulse width modulation**pyroelectric devices**

- detector, use in horizon sensors 0-37086  
 polymer film transducer, piezoelec. and pyroelec. response rel. to dipole polarisation 0-7267  
 solid state pyroelectric IR detector array 0-9036  
 TGS pyroelectric detector, compared with W-C point contact, appl. to temporal coherence meas. of HCN laser 0-31871  
 LiKSO<sub>4</sub>, thermal and dielec. props., use as pyroelectric detector 0-34860  
 PbZrO<sub>3</sub> pyroelectric detector, low temp. behaviour, expt. 0-31869

**pyroelectricity**

- adiabatic depolarization under cryogenic conditions 0-55045  
 charge storage, charge transport and electrostatics conference, Kyoto, Japan (Oct. 78) 0-7252  
 dielectrics, thermoelect. conversion using solid state heat engine 0-35707  
 dielectrets and dielectrics, conf., Sao Carlos, Brazil, Sept. (1975) 0-7251  
 ferroelectric films, pyroelectric response to step radiation signals 0-7302  
 insect, Periplaneta americana, pyroelectric coeff. and permittivity obs. 0-51315  
 insulator, pyroelec., role of surface ions in contact electrification 0-54762  
 leaves of rhododendron and encephalarts, pyroelectric coeff. and permittivity obs. 0-51315  
 nonlinear electroacoustics, fundamentals and appl. 0-34489

**pyroelectricity continued**

- PET, pyroelectric effects and depolarisation currents, illumination effects 0-34859  
 polar polymer, piezoelectricity and pyroelectricity 0-7267  
 polar polymer, pyroelectric response rel. to dipole polarisation 0-7267  
 polyacrylonitrile, elec. polarisation 0-7275  
 polymer film transducer, piezoelec. and pyroelec. response rel. to dipole polarisation 0-7267  
 polymers, electrical phenomena, nature and appl., book contrib. 0-50254  
 polypropylene, electron bombarded, radical formation, piezoelectric and pyroelectric effects, ESR study 0-7169  
 polyvinylidene fluoride, piezoelec., pyroelec., and improper ferroelec. 0-7301  
 polyvinylidene fluoride, polycryst. ferroelec., microstruct., piezoelec. and pyroelec. props. 0-7303  
 polyvinylidene fluoride, struct. study, piezoelec. and pyroelec. props. 0-7300  
 polyvinylidene fluoride, thermodynamical model, applications (French) 0-39315  
 PVDF dielectric, piezoelec. and pyroelectric props. rel. to crystalline forms 0-15982  
 rare earth molybdates, cryst. growth, cryst. chem., and phys. props., book contrib. 0-44194  
 TGS, pyroelec. single cryst., elec. field meas., thermally stimulated charges 0-45012  
 vinylidene fluoride-tetrafluoroethylene copolymer, two types of pyroelectricity 0-11346  
 vinylidene fluoride/tetrafluoroethylene copolymer, piezoelect. and pyroelect. response rel. to dipole polarisation 0-7267  
 Ag<sub>3</sub>AsS<sub>3</sub>, proustite, light effects on dielec. props., elec. resist. 0-49816  
 $\beta$ -AgSbS<sub>2</sub>, phase transitions, electrophysical props. 0-44316  
 BaTiO<sub>3</sub> and BaTi<sub>0.08</sub>Sn<sub>0.02</sub>O<sub>3</sub> films, pyroelectric response to step radiation signals 0-7302  
 LiCsSO<sub>4</sub>, thermal and dielec. props. 0-34860  
 LiKSO<sub>4</sub>, thermal and dielec. props. 0-34860  
 LiKSO<sub>4</sub>, uniaxial crystal, pyroelectric, thermal expansion, phase transition 0-19966  
 LiNbO<sub>3</sub>:Fe, unipolar Malter emission under pyroelectric effect conditions 0-29862  
 NH<sub>4</sub>NbF<sub>4</sub>, successive phase transitions, dielec. and optical props. obs. 0-50275  
 Pb<sub>3</sub>Ge<sub>2</sub>O<sub>7</sub>, dielectric thin film, obtained by sedimentation, exam. of dielectric props. and structure 0-2282  
 Pb<sub>3</sub>Ge<sub>2</sub>O<sub>11</sub> single crystals, switching behaviour and hysteresis 0-40077  
 3PbO.2GeO<sub>2</sub>, TSC in thermoelectret state during ceramic synthesis, pyroelec. currents and energy struct. of capture centres 0-55014  
 PbTiO<sub>3</sub>, anomalies in elec., photoelectric and mechanical props. 0-55051  
 SbNbO<sub>4</sub> single crystals, pure and doped, growth and pyroelec. and ferroelec. props 0-40248

**pyrolysis**

- AgBi(CrO<sub>4</sub>)<sub>2</sub>, synthesis, thermolysis, crystallography (French) 0-33946  
 asbestos, dehydroxylation, PMR investigation 0-21269  
 atactic polypropylene waste, pyrolytic conversion to fuel oil 0-35627  
 bioactive conversion systems, efficiency improvements 0-30511  
 coal gasification using COGAS pyrolysis process 0-30342  
 concrete, thermal decomposition in interaction with molten nuclear core materials 0-22946  
 copper molybdates, oxidation, reduction and thermal decomp. mechanisms 0-50847  
 H<sub>2</sub>O decomposition using S-I cycle, process eng. and bench-scale studies, for H prod. 0-35770  
 hexamethylcyclotrisilazane film, plasma-polymerised, TEM study 0-44456  
 hydrocarbons, coating nuclear fuel particles for HTR (German) 0-18585  
 hydrocarbons, gas phase oxidations and pyrolysis, wall-less reactor technique 0-45500  
 isotope compounds, conversion to metals by reduction-distillation methods 0-23223  
 laser specific and thermal reactions classifications 0-11919  
 plastic materials, waste, pyrolysis to produce organic raw materials (German) 0-3307  
 PMMA sheets, flame spread in laminar forced oxidising gas flow 0-35535  
 polyacetylene:AsF<sub>5</sub>, thermal decomp. kinetics, elec. cond., ESCA and mass spectra 0-50830  
 polymers, pyrolysis-mol. wt. chromatography-vapour phase IR spectrophotometry, on-line system, reviews 0-55768  
 pyrochemical process chemistry, appl. to nuclear fuel reprocessing 0-18578  
 pyrochemical processing for purification and recovery of spent reactor fuels 0-18577  
 pyrochemical reprocessing of nuclear fuels, process technology for Zn distillation, melt refining and salt transport 0-18579  
 pyrochemical reprocessing of spent nuclear fuels, evaluation of proliferation-resistant process 0-18580  
 radioactive liquid waste, thermal decomp. of Harvest feed slurries 0-52757  
 radioactive slagging pyrolysis incinerator, off gas treatment system 0-37514  
 rare earth oxyphosphates, x Ln<sub>2</sub>O<sub>3</sub>.y P<sub>2</sub>O<sub>5</sub>, synthesis, characterisation and thermal stability 0-16256  
 stainless steel, ferritic SUS 410 type, coated with organometallic complexes and Ti alkoxides 0-34078  
 Th-based nuclear fuels, pyrometallurgical reprocessing using Al alloys for proliferation resistance 0-18582  
 thermal decomposition reactions, H<sub>2</sub>O vapour evolution detection device 0-3440  
 trifluoroiodomethane, pyrolysis in Ar:O<sub>2</sub> matrix, forming trifluoromethylperoxy radical 0-50845  
 tyres, used, pyrolysis to produce organic raw materials (German) 0-3307  
 water, for H prod., development of two new thermochem. cycles at ORNL 0-35780  
 water, thermochem. H prod. using the Mark-13 process, status report 0-30606  
 AgN<sub>3</sub>, pyrolysis, 513 to 558K 0-7787  
 $\gamma$ -AlOOH, boehmite, dehydration to  $\gamma$ -Al<sub>2</sub>O<sub>3</sub> 0-21277  
 BBr<sub>3</sub>-SiBr<sub>4</sub> mixture, prep. of B-Si thermoelec. materials 0-20862  
 BaB<sub>2</sub>H<sub>11</sub>.10H<sub>2</sub>O, struct. dehydration, intermediate phases and thermooxidative degradation 0-33951  
 BiH(PO<sub>3</sub>)<sub>4</sub>, condensed, thermal behaviour and IR spectra 0-19912



## pyrolysis continued

- Bi<sub>2</sub>Mo<sub>2</sub>O<sub>9</sub>, thermal decomp. rel. to catalytic oxidation 0-35520  
 C-acetylene, production by methane pyrolysis and irradiation 0-36129  
 CaB<sub>2</sub>H<sub>11</sub>·10H<sub>2</sub>O, struct. dehydration, intermediate phases and thermooxidative degradation 0-33951  
 Cd<sub>3</sub>As<sub>2</sub>, thermal decomp., 550-850°C 0-35512  
 Cr complex, bis(ethylbenzene) chromium, thermal degradation, high purity Cr production (Russian) 0-35128  
 Cr pyrolytic coating, effect of support metal mech. props. on formation (Russian) 0-7713  
 Cs<sub>2</sub>Ni<sub>3</sub>(P<sub>2</sub>O<sub>7</sub>)<sub>2</sub>·nH<sub>2</sub>O, thermal dehydration 0-35513  
 Cu-H, evolution of gas during heating, mass spectroscopic exam. 0-30221  
 CuCr<sub>2</sub>O<sub>4</sub>, thermal decomp. mechanism (French) 0-50834  
 Dy<sub>2</sub>(SeO<sub>4</sub>)<sub>3</sub>·8H<sub>2</sub>O, thermal decomp. and IR spectra 0-3319  
 Er<sub>2</sub>(SeO<sub>4</sub>)<sub>3</sub>·8H<sub>2</sub>O, thermal decomp. and IR spectra 0-3319  
 GdCl<sub>3</sub>·6H<sub>2</sub>O, X-ray emission luminesc. (Japanese) 0-55763  
 H thermochemical prod. by H<sub>2</sub>O decomposition, review 0-45800  
 H, thermochemical prod. using General Atomic S-I cycle for H<sub>2</sub>O decomposition 0-55941  
 HBr decomposition using FeBr<sub>3</sub> and Fe<sub>3</sub>O<sub>4</sub> for H prod. 0-35778  
 HBr, pyrolysis for H prod. 0-35772  
 HI decomposition and H separation in S-I thermochem. prod. of H 0-35771  
 H<sub>2</sub>O, Br-Ca-Fe cycles for H production 0-35784  
 H<sub>2</sub>O, computer thermodynamic anal. and optimisation of thermochem. cycles for H prod. 0-45766  
 H<sub>2</sub>O decomposition by Ce-Cl cycle for H prod. 0-35783  
 H<sub>2</sub>O decomposition for H prod., equilibrium effects in high press. prod. 0-35775  
 H<sub>2</sub>O decomposition using S compounds, feasibility anal. for H prod. 0-35768  
 H<sub>2</sub>O decomposition using S-I cycle for H prod. 0-35769  
 H<sub>2</sub>O decomposition using S cycles, thermochem. anal. of energy balance for H prod. 0-35779  
 H<sub>2</sub>O decomposition using Mg-I cycle for thermochem. H prod. 0-35786  
 H<sub>2</sub>O dissociation using solar thermal energy for H prod. 0-45770  
 H<sub>2</sub>O, for H prod. optimum temp. conditions utilizing HTGR nuclear heat 0-35781  
 H<sub>2</sub>O, for thermochem. H<sub>2</sub> prod. 0-55928  
 H<sub>2</sub>O, high temp. H prod. using solar energy 0-45822  
 H<sub>2</sub>O, thermochemical water-splitting cycles based on Ce and alkaline earth phosphates for H<sub>2</sub> prod. 0-55945  
 H<sub>2</sub>Se decomposition 673 to 748K, appl. to thermochem. H prod. using ZnSe cycle 0-35782  
 Ho<sub>2</sub>(SeO<sub>4</sub>)<sub>3</sub>·SH<sub>2</sub>O, thermal decomp. and IR spectra 0-3319  
 InAs-InP, phase equilib. and decomp. 0-35170  
 K<sub>2</sub>Ca(SO<sub>4</sub>)<sub>2</sub>·H<sub>2</sub>O, syngenite, thermal dehydration under nonisothermal conditions 0-3324  
 KEuHP<sub>3</sub>O<sub>10</sub> acid, exam. of thermal decomposition 0-55638  
 K<sub>2</sub>Ni<sub>3</sub>(P<sub>2</sub>O<sub>7</sub>)<sub>2</sub>·nH<sub>2</sub>O, thermal dehydration 0-35513  
 KO<sub>2</sub>, non-isothermal decomp. kinetics 0-16649  
 LaI(r), thermodynamic stability, high-temp. mass spectra obs. 0-7781  
 Li<sub>2</sub>O<sub>2</sub>, thermal decomposition and heat capacity 301 to 566K, enthalpy 0-3322  
 LiOH(D)(T), thermal decomposition rates 530-690K, activation energy and enthalpy meas. 0-3321  
 Lu<sub>2</sub>(SeO<sub>4</sub>)<sub>3</sub>·8H<sub>2</sub>O, thermal decomp. and IR spectra 0-3319  
 Mg(AlH<sub>2</sub>)<sub>2</sub>, prep., thermal decomposition, molar heat capacity, heat of form. 0-3325  
 MgB<sub>2</sub>H<sub>12</sub>·10H<sub>2</sub>O, struct. dehydration, intermediate phases and thermooxidative degradation 0-33951  
 MnOOH, α- and γ-phase, thermal decomp., 20 to 670°C 0-35521  
 (NH<sub>4</sub>)<sub>2</sub>Ni<sub>3</sub>(P<sub>2</sub>O<sub>7</sub>)<sub>2</sub>·nH<sub>2</sub>O, thermal dehydration 0-35513  
 NO<sub>2</sub>, thermal decomposition kinetics (Russian) 0-3329  
 Na<sub>2</sub>Ni<sub>3</sub>(P<sub>2</sub>O<sub>7</sub>)<sub>2</sub>·nH<sub>2</sub>O, thermal dehydration 0-35513  
 NaO<sub>2</sub>, non-isothermal decomp. kinetics 0-16649  
 NaO<sub>2</sub>, thermal decomp. macrokinetics, differential thermal anal. 0-16650  
 NbO<sub>2</sub>, phase comp. on heating 2000-4000K 0-21267  
 O<sub>2</sub>, thermal decomposition, vibr.-rot. state depletion, Monte Carlo calc. 0-35506  
 PdH<sub>1.18</sub>, PdH<sub>1.20</sub>, prep., cryst. struct., chem. comp. determ. by thermal decomp. 0-34334  
 Pr(OH)<sub>3</sub>, thermal decomposition, exam. 0-55640  
 Rb<sub>2</sub>Ni<sub>3</sub>(P<sub>2</sub>O<sub>7</sub>)<sub>2</sub>·nH<sub>2</sub>O, thermal dehydration 0-35513  
 SiC fibres obtained from polycarbosilane fibre 0-50582  
 SiC powders, form. by vapour phase method 0-25623  
 SrB<sub>2</sub>H<sub>12</sub>·10H<sub>2</sub>O, struct. dehydration, intermediate phases and thermooxidative degradation 0-33951  
 Tb<sub>2</sub>(SeO<sub>4</sub>)<sub>3</sub>·8H<sub>2</sub>O, thermal decomp. and IR spectra 0-3319  
 Ti(OC<sub>4</sub>H<sub>9</sub>)<sub>4</sub>, pyrolysis, autocatalysis, TiO<sub>2</sub> film form. 0-55311  
 Tm<sub>2</sub>(SeO<sub>4</sub>)<sub>3</sub>·8H<sub>2</sub>O, thermal decomp. and IR spectra 0-3319  
 UO<sub>2</sub>, sintered, production by gel calcination and drying, thermal anal. (Czech) 0-45260  
 Y<sub>2</sub>(SeO<sub>4</sub>)<sub>3</sub>·8H<sub>2</sub>O, thermal decomp. and IR spectra 0-3319  
 Yb<sub>2</sub>(SeO<sub>4</sub>)<sub>3</sub>·8H<sub>2</sub>O, thermal decomp. and IR spectra 0-3319  
 Zn<sub>0.2</sub>Co(Ni)<sub>0.8</sub>O · 1.1Al<sub>2</sub>O<sub>3</sub> powders, ZnO vapourisation from 0-16675

## pyromagnetic effects see magnetocaloric effects

## pyrometers

see also temperature measurement

- high-temperature meas. and calibration, above 1000°C, based on Au melting point (Rumanian) 0-47061  
 IR, portable instrument for noncontact temp. meas. (German) 0-42229  
 IR pyrometry, calc. method for true temp. from expt. readings 0-13081  
 multiwavelength optical pyrometer for shock compression experiments 0-52229  
 multiwavelength radiation pyrometry where reflectance is measured to estimate emissivity 0-31757  
 optical, cylindrical cavity blackbody radiators, effect of surface roughness on quality of radiator 0-52228  
 optical, extension of use of UPO-6M2 equipment 0-8991  
 particles in flight, temp. meas. by monochromatic photographic pyrometry (French) 0-27312  
 photoelectric pyrometer 0-22364  
 photoelectric, using radiation invariant method, true temp. meas. of metals 0-52223  
 photon counting, 1400K to above 2200K within 0.5K and 1.0K 0-52232  
 radiation thermometry, applied precision, current status 0-52224  
 spectral ratio, scale correction by electric method (Russian) 0-37040

## pyrometers continued

- spectral ratio pyrometers, rated conversion characteristics (Russian) 0-42258  
 spectropyrometers, threshold sensitivity 0-8990  
 surface temperature meas. through radiance temp. and emissivity, algorithm for calc. 0-52209  
 Q see Q-factor  
 Q-factor  
 cylindrical TM<sub>010</sub>-mode cavity, meas. of dielectric parameters at microwave freq. 0-9002  
 driven magnetic fusion reactors, conf., Erice-Trapani, Italy (Sept. 1978) 0-41948  
 Earth crust beneath SW Honshu, Japan, Q-factor derived from explosion seismic waves 0-17242  
 Earth-ionosphere cavity, Q-factor and elec. cond. profiles from expt. Schumann reson. data 0-36360  
 flexensional transducer design trends 0-43588  
 fusion reactor, driven Tokamak, plasma parametric studies and appl. 0-42865  
 fusion reactor, using toroidally-linked mirrors 0-42858  
 mirror hybrid reactors 0-42860  
 mirror reactors, economic significance of Q 0-47722  
 peridotite, high-temp. anelasticity and elasticity 0-17256  
 phosphate glass laser, statistical props. and stabilisation 0-48266  
 tandem mirror reactors, fusion power reactor and fusion-fission hybrid reactor 0-42856  
 Q-factor measurement  
 quartz intrinsic Q estimation 0-43578  
 sediment classification by ocean subbottom acoustic Q meas. 0-46168  
 Q power factor see Q-factor  
 Q-switching  
 see also lasers  
 fluoromethane TEM<sub>00</sub> far IR laser with integrated pump laser 0-43348  
 intrasatellite, mirrors optimal reflection coeff. selection 0-48302  
 laser with nonlinear active medium, transient intracavity SHG, giant pulse generation 0-9948  
 plasma Q-switch in laser cavity 0-28259  
 ruby laser, spectroscopic props., operation modes, pulse amplification (Rumanian) 0-48265  
 ruby lasers, freq. synchronisation and locking by passive modulator 0-1249  
 solid laser, pulse train stability with periodic Q-switching 0-28239  
 solid laser, subnanosecond and picosecond operation 0-28262  
 solid-state ring laser, generation of microsecond pulses 0-9913  
 spherical cavities, Q-switching by rotating mirror in ruby and Nd:glass lasers 0-28261  
 transition-metal dithiophene complex dyes for 0.9 to 1.4 μ lasers 0-1200  
 CO laser passive Q-switching, intracavity Zeeman modulation detect. of NO 0-9597  
 CO<sub>2</sub> laser, 10 ns pulse generation, rotating mirror technique 0-33042  
 CO<sub>2</sub> laser, passive Q-switching by FIR laser gas CH<sub>3</sub>I 0-1246  
 Cr<sup>3+</sup>:BeAl<sub>2</sub>O<sub>4</sub> alexandrite laser, high gain performance 0-53299  
 Nd laser, with mirror plasma-optical Q-switch (Russian) 0-33028  
 Nd:glass laser with periodic Q-switching, mathematical model 0-33043  
 Nd:YAG oscillator, generation of high-power ns pulses 0-23730  
 Nd:YAG unstable-resonator oscillator, stable single-axial-mode operation by injection locking 0-53331  
 Nd<sup>3+</sup>:YAG continuously pumped pulse-periodic laser, stability 0-28241  
 Nd<sup>3+</sup>:YAG laser, contrast and configs. of LiNbO<sub>3</sub> electrooptic switches 0-33012  
 Nd:YAG laser, Q-switched, freq. doubled, 200 kW output 0-33026  
 Ni complex, BDN, saturable absorber, degenerate four-wave mixing, amplification and phase conjugation 0-43394  
 Ni complex, BDN II in tetrahydrothiophene-1,1-dioxide, saturation behaviour, Q-switching appl. 0-48354  
 QC see quality control  
 quadrupole crystal field interactions see crystal hyperfine field interactions  
 quadrupole lenses see electron lenses; electrostatic lenses; magnetic lenses  
 quadrupole mass analysers and filters see mass spectrometer components and accessories  
 quadrupole moments  
 see also atomic electric moment; molecular moments; nuclear electric moment; nuclear quadrupole resonance  
 molecular torsional oscills., NQR freq. temp. depend. electric field gradient asymmetry 0-18868  
 nuclear quadrupole moments and rms charge radii, shell model calcs. 0-47369  
 organic molecules, quadrupole moments, dipole quadrupole A and C polarisabilities, perturbation theory anal. 0-27934  
 As, np<sup>2</sup>(n+1)s excited-state config. quadrupole moments, Sternheimer shielding factor 0-37755  
 CO<sub>2</sub> IR Zeeman spectra utilizing copropag. wave reson., diamag. shift obs. 0-53055  
<sup>163</sup>Ho in HoVO<sub>4</sub>, NMR predictions of properties, dipolar interactions and antiferromagnetic exchange 0-50203  
<sup>Λ</sup>Mo, A=94, 96, 98, multiparticle states, method of generalised seniority 0-22759  
 N, np<sup>2</sup>(n+1)s excited-state config. quadrupole moments, Sternheimer shielding factor 0-37755  
 P, np<sup>2</sup>(n+1)s excited-state config. quadrupole moments, Sternheimer shielding factor 0-37755  
<sup>Λ</sup>Ru, A=96, 98, 100, multiparticle states, method of generalised seniority 0-22759  
 Sb, np<sup>2</sup>(n+1)s excited-state config. quadrupole moments, Sternheimer shielding factor 0-37755  
 ZnMn<sub>1-x</sub>Cr<sub>x</sub>FeO<sub>4</sub>, Mossbauer effect, quadrupole splitting 0-29664  
<sup>Λ</sup>Zr, A=92, 94, 96, multiparticle states, method of generalised seniority 0-22759  
 quality control  
 see also reliability  
 anemograph data 0-56642  
 automation of measuring equipment state-inspection results, USSR Krasnodar territory 0-52152  
 computed tomography scanner, fourth-generation, performance evaluation 0-46035  
 diesel nozzle sprayer castings, heat treatment quality inspection 0-35471  
 electromagnetic inspection review 0-35468  
 ferrous metallurgy, nondestructive inspection and quality control review 0-21201



**quality control continued**

- glossiness of curved surface, physical and psychological, meas. method 0-37074  
 manufacturing processes, industrial visual testing, photographic methods as technical aid (*German*) 0-31923  
 mass-produced camera objectives, effects of cosmetic defects 0-47135  
 materials testing machines, historical development of Instron Ltd. 0-35452  
 measuring equipment, state control in USSR 0-52150  
 measuring equipment, state control in USSR 0-52151  
 metal surface cleanliness control by photoemission recording (*Russian*) 0-49839  
 metrological support to quality-control management 0-184  
 monitored parameters choice for unification of measurements 0-186  
 NDT, data processing and acquisition for product quality control 0-11862  
 nuclear fuel pins, computer controlled meas. 0-5300  
 nuclear plant operations, quality assurance program 0-783  
 nuclear plant quality assurance criteria, international standardisation 0-780  
 nuclear plant quality assurance standards in USA, present status and appl. 0-781  
 optical fibres, measurement of refractive-index profiles in optical-fibre pre-forms by spatial-filtering technique 0-48403  
 optical surface quality standards based on total integrated scatt. 0-48391  
 photographic pulp quality control using He-Ne laser scanning system (*German*) 0-3272  
 precision measurement, image analysis of precision components (*German*) 0-42193  
 PWR, quality assurance by Framatome 0-782  
 refractory products, apparent density determination, using surface  $\gamma$  densimeter 0-35464  
 refractory slabs, radio wave phase method for quality control 0-40667  
 roughness of periodically shred surfaces, on-line meas. technique using He-Ne laser (*German*) 0-33014  
 Pt-Au, thick film, adherence meas. and evaluation 0-50813

**quality factor** *see* *Q-factor***quantale theory of chemical binding** *see* *bonds (chemical)***quantisation**

- action-angle variables in quantum mechanics, appl. to harmonic oscill., linear (triaxial) rotors 0-31543  
 antisymmetric tensor gauge fields, covariant quantisation, Faddeev Popov ghosts 0-27406  
 area preserving maps, quantisation 0-12924  
 canonical quantisation of gauge fields, gravitational field (*Chinese*) 0-22266  
 charged particle in mag. field, phase operator 0-8827  
 classical systems with non-integrable constraints, quantisation 0-36901  
 closed systems with nonconservative internal forces, Lie admissible quantisation, hadron struct. 0-37174  
 CM(3) collective model, geometric quantisation 0-5078  
 correspondence and opposition between quantum theory and classical physics, temporal logic 0-27176  
 damped harmonic oscillator, non-equilibrium quantum statistical mechanics, system quantisation 0-52070  
 Dirac quanta detection in Rindler and black hole space times,  $\xi$  quantisation scheme 0-31651  
 Dirac string Lagrangian in  $A^0_0$  gauge, path integral quantisation 0-32007  
 dissipative systems, canonical quantisation, von Neumann equation 0-52132  
 dynamic system, classical quantisation conditions with stochastic behaviour anal. 0-8922  
 EM field in dispersive medium, phenomenological quantisation 0-13240  
 EM wave, evanescent, quantisation, near dielectric surface, field momentum 0-43231  
 ergodicity, classical, quantum mech. implications 0-8898  
 Feynman path integral formulation using geometric quantisation techniques 0-31588  
 friction, stochastic quantisation, nonlinear Schrodinger equation 0-27164  
 Galilean and Lorentz particles, quantisation, a new approach 0-12951  
 geometric quantisation for multidimensional harmonic oscillators and Kepler problem, Maslov theory 0-17833  
 gravitational field, quantisation, Hilbert space of quantised system 0-52113  
 group actions on quantum bundles, geometric quantisation theory 0-17837  
 imprimitivity systems, quantisation and superselection rules 0-4592  
 Kepler problem, 1-D, invariant  $\ast$ -product quantisation 0-17831  
 light-cone quantisation of scalar field, current nonconservation 0-47220  
 magnetic monopoles with no strings, action principle and canonical quantisation 0-31990  
 mapping and deformation of polynomial observable classical algebra 0-27155  
 massless fields in asymptotically flat space-time, null surface quantisation and quantum theory 0-4625  
 massless fields with fixed arbitrary spin, quantisation 0-31992  
 Maxwell field, stochastic mechanics in Euclidean formulation 0-42081  
 Moyal quantum mechanics formulation and Weyl. quantisation generalisation, Lie algebras 0-17835  
 non-affine path algorithm in the functional integral calculus of Schrodinger kernels 0-31593  
 nonlinear problems, consistent quantisation procedure 0-4586  
 nonlinear super-Poincare fermion, quantisation in bag like formulation 0-4923  
 open system, new classical Hamiltonian-Lagrange mechanics 0-36900  
 phase space quantisation of interacting vortices in two dimensions 0-4634  
 Poisson Lie algebra deformation and quantisation 0-8854  
 polarons, Frohlich, mean field theory, phase transitions 0-34371  
 projective geometry for polarisations 0-52053  
 quantum spin systems, Fermi systems and group extensions in Weyl quantisation procedure 0-8905  
 relativistic Brownian motion, space-time approach to quantum mechanics 0-31567  
 Robertson-Walker cosmologies, Kostant-Souriau quantisation 0-12838  
 S-matrix for interaction of gravitational and Yang-Mills fields 0-42315  
 Schrodinger kernel as functional integral, non-uniqueness 0-31594  
 Schwinger boson representation, quantised rotator 0-18164  
 Segal-Weinless approach to linear Bose fields, uniqueness result 0-98

**quantisation continued**

- semiclassical, periodic orbit role for the quantal bound state 0-8831  
 soliton, non-topological, non-Abelian internal symmetry in 3+1 dimensional space-time, quantisation, collective coord. and Lorentz covariant methods 0-47199  
 space quantisation, classical explanation 0-42082  
 stochastic quantization and detailed balance in Fokker-Planck dynamics 0-4645  
 SU(2) harmonic analysis as basis for quantisation 0-9116  
 twistor theory, particle models 0-13278  
 unstable particle decay, second quantisation representation 0-4568  
 weak exchange interaction between atoms or ions orbitally degenerate ground states, atomic second quantisation method 0-32604  
 Weyl, classical limit 0-93  
 Weyl quantization of classical spin systems quantum spins and Fermi systems 0-31585  
 Yang-Mills fields, quantisation without fixing gauge 0-13207  
**quantisation (communications)** *see* *analogue-digital conversion*  
**quantitative analysis** *see* *chemical analysis*  
**quantum beat spectra**  
 aza-aromatic molecules, intersystem crossing, quantum interference effects 0-53037  
 polyatomic mols., quantum beats 0-37826  
 polymer solns. and gels, dynamics, photon heat expts. 0-55727  
 recoil-free  $\gamma$ -radiation, quantum beats 0-37142  
 resonance fluoresc., probe of intramolecular relax., density matrix formalism, lifetimes and quantum beats 0-32757  
 [ $^{15}\text{N}$ ], modulated coherent Raman beats 0-23464  
 Cs,  $7P_{3/2}-6S_{1/2}$  transition, photon-echo quantum beats obs. 0-23373  
 H, beam-foil excitation of 2P-state, alignment meas. 0-14215  
 H, beam-foil excited, zero-field quantum beats in  $H_\beta$  emission, polarisation energy depend. 0-14218  
 H, Stark-induced quantum beats in  $H_\beta$  0-9757  
 $\text{H}^+ + \text{He}(\text{Ar})$ ,  $\text{H}(n=4)$  s-d coherence, zero-field quantum beats obs. 0-32676  
 $^4\text{He}$ , beam foil and quantum beat spectra (*Chinese*) 0-32638  
 $^{191}\text{Hg}^m$ , and  $^{190m-185m}\text{Hg}$ , nucl. spins, on-line quantum beat spectrosc. determ. 0-9562  
 $^{215}\text{In}$ ,  $8P^{3/2}_{3/2}$ , HFS and lifetimes, fluoresc. decay and quantum heats, beam 0-32657  
 $^{15}\text{N}$ , beam foil and quantum beat spectra (*Chinese*) 0-32638  
 Na,  $^2\text{D}$  highly excited states, fine struct. splitting, field ionisation quantum interference 0-18835  
 Na, coherent ground state transients, beat meas. 0-948  
 Na, quantum beats of hyperfine levels observed in photoionisation 0-32690  
 Na, Rydberg states, high resolution spectroscopy 0-52901  
 Sm, coherent ground state transients, beat meas. 0-948  
**quantum beat spectroscopy**  
 atomic systems, beam-foil interaction process, quantum beats, alignment and orientation obs. 0-14252  
 light beating spectroscopic instrument for continuous meas. of tissue blood flow 0-41160  
 photoionisation, quantum beats, origin 0-52954  
 recoil-free  $\gamma$ -radiation, quantum beats 0-22498  
 review 0-22444  
 scanning technique and exptl. arrangement for quantum beat obs. 0-9757  
**quantum chemistry**  
*see also* *chemical reactions; orbital calculation methods; perturbation theory; potential energy surfaces for collision processes; pseudopotential methods; quantum statistical mechanics; quantum theory; reaction kinetics; wave functions*  
 symposium, Florida, USA (March 1979) 0-51946  
**quantum counters** *see* *photon counting*  
**quantum electrodynamics**  
*see also* *electromagnetism*  
 (1+1) dims. Todd chain and  $e^+e^-2\phi$  model, exact factorised S-matrices 0-18094  
 (1+1) dimensional model field, fermion-boson correspondence, Klein transformation 0-42379  
 (2+1) dimensional Georgi-Glashow model, critical Higgs mass, clustering, monopoles 0-52441  
 $\psi$  collapse and locality 0-372  
 't Hooft transformation, explicit solns. 0-345  
 Abelian and non-Abelian gauge theories, mass generation, renormalisation, chiral and unified theories 0-4871  
 Aharonov-Bohm effect, possible nonexistence 0-27434  
 Aharonov-Bohm effect, nonexistence condition, inaccessible fields 0-37194  
 Aharonov-Bohm effect revisited 0-32040  
 Aspect experiment, local and quantum theories 0-32051  
 axial currents, supercurrents and anomalies in supersymmetric QED 0-46933  
 axion- $e^+e^-$  after emission from  $^{12}\text{C}$  excited state 0-32235  
 bremsstrahlung of vector particle in nucl. field 0-37198  
 broken supersymmetry mass formula, quantum corrections 0-27424  
 charge-electric dipole interaction in 1 dimens. 0-42005  
 charged black hole, QED effects, Cauchy horizon (*Russian*) 0-51803  
 charged particle, stimulated radiation emission mechanism 0-42374  
 charged particle in mag. field, phase operator 0-8827  
 charged particle self-interaction 0-373  
 circuits at ultralow temp., QED verification 0-13247  
 coherent bremsstrahlung, energy and momentum spectral function 0-22546  
 coherent states of a nonrelativistic charged particle in a constant electric field 0-18103  
 conference, nonlinear problems in theoretical physics, Jaca, Gain 1978 0-4478  
 conference, quarks and leptons as fundamental particles, Schladming, Austria, (Feb.-Mar. 1978) 0-17709  
 confinement of compact QED for low couplings 0-18095  
 conformal field equations 0-46881  
 constant SU(2) non-Abelian gauge pot., vacuum polarisation by fermions, integral representation 0-22543  
 cosmology pair creation in presence of EM fields 0-41924  
 Coulomb off shell two body amplitudes, numerical computation 0-46858  
 current density and electric and magnetic multipole-moment operators in quantum mechanics 0-27433  
 DESY  $e^+e^-$  experiments, QED checks,  $\tau$  and T studies 0-18111  
 Dirac eqn., spinor field eqn. conformal covariance 0-52442



## quantum electrodynamics continued

Dirac fields in a curved space-time 0-18070  
 Dirac monopoles and the Hopf map  $S^3 \rightarrow S^2$  0-32042  
 Dirac particles, massless bound state, Coulomb potential 0-37189  
 Dyson spin and statistics, fibre bundle theory for interacting charges 0-32049  
 Dyson-Salam scheme subtractions, counterterm equivalence 0-13241  
 $e^+e^-$  spontaneous creation in inhomogeneous magnetic fields 0-22540  
 einstein dynamics compatible with Galilean kinematics 0-27437  
 electron gas interacting with radiation in mag. field, relaxation 0-17489  
 electron induced radiation in plane wave in mag. field 0-37196  
 electron internal dynamics, rel. to Lamb-Rutherford shift and microwave generation 0-13239  
 electron mass, truncated, gauge dependence 0-22542  
 electron mass operator in 2-D QED approx., radiative convections 0-4900  
 electron motion in standing wave fields 0-22539  
 electron self-energy, vacuum polarization, and vertex correction 0-47222  
 electron spin equations of motion in external field 0-18102  
 electron with anomalous moments in EM field 0-37197  
 EM field in dispersive medium, phenomenological quantisation 0-13240  
 EM field quantisation, canonical variables 0-32045  
 energy-momentum tensor vac. expectation values, depend. on manifold geom. and topology 0-355  
 Euclidean QED<sub>2</sub> on periodic lattice, continuum limit 0-18092  
 external EM fields, time-dependent, particle interpretation, Fock representations of Fermi field operators. 0-52439  
 external fields creating pairs, problems 0-42375  
 frequency-dependent electric and magnetic multipole moments and Siegert's theorem 0-27432  
 fundamental length hypothesis in a gauge theory context 0-9101  
 gauge and basis sets for EM interaction representation 0-42371  
 gauge dependence of spectral functions 0-37191  
 gauge invariance and pseudoperturbations 0-22545  
 generalized two-dimensional QED and functional determinants 0-42373  
 global characterisation on space time lattice (*Hungarian*) 0-37192  
 gravitational creation of odd numbers of fermions 0-32048  
 gyromagnetic ratios for muon and electron 0-22548  
 hard-soft renormalization of massless fields 0-13214  
 harmonic oscillator, EM field interaction, initial value problem 0-47223  
 heavy ion reactions, dynamical properties, field overview 0-18327  
 heavy particle effects through factorisation and renormalisation group, QED appl. 0-13243  
 how and why it works 0-18093  
 hydrogenic atoms, metastable 2S state in weak elec. field, radiative decay, bound state QED 0-42959  
 hypergeometric partial solutions in the problem of two Coulomb centers 0-4582  
 induced vacuum decay in scalar field theory 0-42372  
 intense field QED in continuous medium, appl. to Thomson scatt. and Cherenkov radiation 0-27435  
 Klein-Gordon particles, massless bound state, Coulomb potential 0-37188  
 Klein-Gordon particles in deep square wells 0-31982  
 Lamb shift in  $^{35}\text{Cl}$  XVI, precise meas. 0-9549  
 Lamb shift in  $\text{Cl}^{16+}$  meas. 0-9551  
 Lamb shift in hydrogenlike Ar meas. 0-9550  
 lattice gauge theory with fermions, renormalised phases, vacuum polarization 0-13198  
 leptonic mass generation model 0-375  
 Lippmann-Schwinger eqns. for three charged particles 0-4580  
 local structure of functional spaces and dynamical variables of gauge-invariant fields 0-9099  
 Lorentz group, IR problem and spontaneous breaking in QED 0-32047  
 magnetic monopole, relativistic classical eqns. of motion, electric dipole moment case 0-37195  
 magnetic monopoles with no strings, action principle and canonical quantisation 0-31990  
 mass formula of charged leptons 0-13244  
 massive vector boson field theory with spontaneous symmetry breaking 0-52443  
 massless boson, unified nonlinear theory 0-376  
 Maxwell theory, quantised, rosette of rosettes of Hilbert spaces 0-32043  
 Moller scatt., high intensity, scatt. energies 0-22541  
 multiphoton absorption by electrons 0-6224  
 multiphoton stimulated Compton scattering of relativistic electrons 0-48198  
 muonic He, hyperfine struct., relativistic, radiative and recoil corrections, QED test 0-14256  
 Nelsons stochastic mechanics, spinning particles and relativistic particles 0-31587  
 neutrino form factors in 2-D approx. of QED 0-9132  
 nonlinear approach, magnetic dipole moment, corrections to g-2 0-42370  
 nonlinear problems due to self-field of electron 0-4901  
 nonlocal stochastic equation of motion with damping in electrodynamics 0-17872  
 nonrelativistic, infrared problem 0-52440  
 $O(3) \otimes U(1) \otimes U(1)$  internal symmetry in massless vector field theory (*Russian*) 0-22531  
 orbit-orbit interaction, new tensor expansion, matrix and graphical forms 0-14064  
 pair production in slowly varying and constant fields, diagrammatic approach 0-374  
 pair production on photon scattering by intense EM wave in homogeneous mag. field (*Russian*) 0-47227  
 paramagnetic conjecture counter-example based on Bohm-Aharonov effect 0-32046  
 path group appl. to gauge theory and quarks 0-31985  
 phenomenological ideas toward a field theory of matter, unification of EM and gravity fields 0-378  
 photon splitting in the magnetised vacuum 0-4897  
 photon coalescence at an electron in plane wave approx. model 0-18100  
 photon fission, in intense laser fields and nuclear Coulomb field, QED test 0-4895  
 photon form factor, asymptotic behaviour in QED 0-18096  
 photon scattering, elastic large-angle, Delbruck and Rayleigh scattering below 5 MeV 0-13456  
 photon splitting cross sections in nucleus Coulomb field 0-32041  
 photon splitting into three components by electron in quantised plane EM field 0-18101  
 Planck's constant, origin of quantum theory 0-27179  
 Poincare self-stresses, model and field Lagrangian densities 0-52438  
 positronium annihilation in field of plane EM wave (*Russian*) 0-14259

## quantum electrodynamics continued

quantised electric charge as purely EM phenomena 0-37190  
 quantised lattice gauge field construction, mass generation and Abelian Higgs models 0-4831  
 quantum effects in systems with accelerated mirrors 0-22508  
 quarkonia, spectra, decays, levels, jets, sum rules 0-18112  
 radiation corrections to quantum processes in an intense electromagnetic field 0-4899  
 radiative corrections, exponential factor of soft photons 0-47225  
 relativistic charged particle, effect of multiple scattering on synchrotron radiation (*Russian*) 0-13245  
 relativistic classical and quantum dynamics 0-22192  
 relativistic electron wave diffraction by cylindrical capacitor 0-5671  
 relativistic electron-positron gas, polarisation in strong mag. field, EM wave propag. 0-4896  
 relativistic free-electron in uniform mag. field, Green's function of Dirac eqn. 0-18098  
 relativistic particle physics, book 0-41966  
 Robertson-Walker universes, particle creation, self-interacting quantised fields 0-17699  
 S-matrix electrodynamics, low-frequency photons in processes involving particles with spin 0-9131  
 scalar particle inverse bremsstrahlung in triple collision processes 0-47226  
 scale-invariant gauge theories, instanton role in QCD, QED and  $\text{CP}^{(N-1)}$  0-27400  
 Schrodinger electron-photon interaction, gauge and hybrid transforms. 0-22544  
 spin 1/2 particle, motion in field on mag. monopole 0-18097  
 spin motion eqn. in external field, Dirac particle quasiclassical theory 0-18099  
 $SU(2) \times U(1)$  gauge theories, successes and current issues 0-18064  
 superdense magnetised astrophysical objects, electron-positron pair prod. 0-17603  
 supersymmetric, absence of radiative corrections to axial current anomaly 0-13242  
 synchrotron radiation, quantum corrections 0-37193  
 Theiss' regularisation procedure appl. 0-9129  
 ultrarelativistic particle in homogeneous mag. field, trajectory, radiation damping 0-18104  
 vacuum decay, near superheavy atomic nucleus 0-32050  
 vacuum polarisation in intense EM fields, perturbation theory, renormalisation group calcs. (*Russian*) 0-52444  
 vacuum polarization and particle creation in a non-stationary homogeneous electromagnetic field (*Russian*) 0-13246  
 vacuum polarization connection to atomic spectrum in a strong magnetic field 0-42369  
 vacuum polarization in Delbruck scatt. 0-18288  
 vacuum polarization in uniform non-Abelian gauge fields 0-4898  
 vacuum quantum effects analogy in gravitational and EM fields 0-32044  
 vertex form factor radiative corrections in 2 dimensional QED approx. (*Russian*) 0-418  
 X-ray pulsars, vacuum polarisation effect rel. to radiative transfer and X-ray spectra 0-27015  
 X-Y model, gauge theory analogue, 4-D self-dual gauge model, phases and transitions 0-27399  
 Yang-Mills temporal gauge struct. by Feynman propagation kernel 0-37162  
 zero mass system, generalised EM field, reduction and second quantisation 0-27436  
 $e^+e^-$  calorimetric experiments,  $\gamma\gamma$  processes, tests of QCD 0-22628  
 $e^+e^- \rightarrow e^+e^- + \text{gluons}$ , gluon jet production, quark models 0-22576  
 $e^+e^- \rightarrow \mu^+\mu^-$ , early weak gauge boson restrictions from PETRA QED cut-off 0-52487  
 $e^+e^-$  pair creation in strong EM fields, gravitational effects 0-42376  
 $\mu\mu$  system in QED with internal fermion excitations 0-9130  
 $\mu^-$  to  $e^-$  conversion in nuclei, mediation by Majorana lepton 0-22547  
 $\mu^- N \rightarrow \mu^- \mu^- N$  in Pb, 10.5 GeV/c, short lived particle search, QED tridents 0-37275  
 $(n,\gamma)$ ,  $\gamma$ -rays, QED test review 0-37199  
 pp elastic scatt., total cross-section asymptotics, stable approach, timelike and spacelike behaviour, vacuum polarisation 0-47332  
 qq pair energy modification in Wilson loop formalism 0-18122

## quantum electronics see quantum optics

## quantum field theory

see also axiomatic field theory; Bethe-Salpeter equation; dispersion relations; gauge field theory; meson field theory; nonlinear field theory; quantisation; quantum field theory of elastic scattering; quantum field theory of interactions; Reggeon field theory; relativistic quantum field theory; renormalisation; scaling phenomena; Schwinger source theory; unified field theories  
 Bianchi IX model, spectral asymmetry and QFT in curved spacetime 0-56982  
 causal theory, removal of Einstein's objections to quantum theory, unification 0-31572  
 complex mass and field operator for unstable particle 0-9105  
 composite field theory, proof of two identities, order of integrations interchange (*Chinese*) 0-47196  
 critical exponents by quantum field theory methods (*Russian*) 0-4869  
 Deser-Gilbert-Sudarshan representation, existence 0-37167  
 Dirichlet forms, construction of stochastic processes 0-8921  
 effective potential anomalous behaviour 0-32023  
 fermions, micro- and macrocoherence relation (*German*) 0-31660  
 Feynman path integrals, conference, Marseille, France, 1978 0-31422  
 feynman path integrals and the corresponding method of stationary phase 0-31583  
 free vector field, canonical formulation, zero mass field connection 0-52388  
 magnetic charges, one pot. formulation 0-22512  
 massless fields with fixed arbitrary spin, quantisation 0-31992  
 modified renormalisation conditions, two-point Green functions 0-9089  
 n=0 models, reformulation using anticommuting scalar fields 0-52071  
 $O(3) \otimes U(1) \otimes U(1)$  internal symmetry in massless vector field theory (*Russian*) 0-22531  
 optical cavity with output coupling, one-dimens., quasimodes as field eigenvalue 0-9911  
 parafield theory and supergroup transformations 0-9124  
 perturbation theory at large orders 0-32022  
 scalar field theories, path integral derivation of the self-consistency condition 0-27408



**quantum field theory continued**

Segal-Weinless approach to linear Bose fields, uniqueness result 0-98  
 spin-2 field, free, canonical formulation 0-42316  
 symplectic framework for field theories, book 0-22130  
 time and space structures conference on quantum theory, Starnberg, W.Germany (July 1978) 0-27044  
 $\eta \rightarrow \pi^0 \gamma \gamma$  decay width and processes in chiral QFT (*Russian*) 0-32099

**quantum field theory of elastic scattering**

see also *elementary particle scattering; relativistic scattering theory*  
 $\sigma$  models, nonlinear, soft mass renormalisation of  $1/N$  expansion 0-47164  
 Abelian Higgs models, disorder parameter approach 0-27411  
 asymptotic conditions, field and Hamiltonian props. 0-13222  
 Ball-Zachariasen model of diffractive scattering, numerical soln. near singularity of Frechet derivative 0-9158  
 bilinear Bose Hamiltonian diagonalisation, Heisenberg field asymptotic behaviour 0-47201  
 binary qq system and local field 0-47244  
 cut-off potential, asymptotic energy behaviour of Green function 0-27165  
 Haag-Ruelle scattering theory as scattering theory in different state spaces 0-4593  
 local relativistic quantum field theory, additive conservation laws 0-22507  
 nuclear elastic scatt. with optical potential, complex angular momentum methods, poles and zeros of S-matrix, REGGE 0-47445  
 solitonlike fields, gauge phase factor operators, extended Higgs models and 't Hooft algebra 0-42324

**quantum field theory of gravitation**

see also *elementary particle gravitational interactions; gravitons; supergravity*  
 $\lambda \phi^4$ , momentum space renormalisation in curved space time 0-37158  
 $\lambda \phi^4$  field theory, renormalisation in curved space-time 0-42320  
 $\lambda \phi^4$  field theory renormalisation in curved space-time 0-42319  
 baryon number generation mechanism in expanding universe 0-51931  
 Belavin Yang-Mills pseudoparticle soln., metric representation, isotropic Universe relation 0-27404  
 Birkhoff's theorem and Dunn theory of gravitation 0-42132  
 canonical quantisation of gauge fields, gravitational field (*Chinese*) 0-22266  
 canonical quantisation of gravity, QFT in curved spacetime, Bianchi I cosmology 0-27202  
 coherent beam interference, phase shift in gauge and grav. fields 0-4627  
 collapsing shell, Schwarzschild-de Sitter space-time, thermodynamics and radiation 0-17607  
 commutation relations in vierbein formalism 0-27205  
 conformal and gauge spontaneous symm. breaking, cosmology quantum effects 0-37185  
 cosmological models and quantum effects (*Russian*) 0-27206  
 cosmology, effective Lagrangian and pair prod. 0-22123  
 cosmology pair creation in presence of EM fields 0-41924  
 development, book contrib. 0-22267  
 Dirac particle creation in Einstein-Cartan-Sciama-Kibble theory 0-4622  
 Dirac quanta detection in Rindler and black hole space times,  $\xi$  quantisation scheme 0-31651  
 discrete space structure dynamics 0-52392  
 Einstein's theories extended, book 0-22164  
 Einstein-Maxwell equations: gauge formulation and solutions for radiating bodies (*German*) 0-27194  
 Einstein-Yang-Mills system in six dimensions, static solution 0-8883  
 energy-momentum tensor vac. expectation values, depend. on manifold geom. and topology 0-355  
 expanding universes, positive frequency and Hamiltonians 0-4624  
 f-g fields, class relevant to quark confinement 0-125  
 Feynman diagrams, dimensionally regularised, symbolic evaluation, quantum gravity application 0-13259  
 gauge formulations, relationship to Riemannian holonomy struct. 0-42131  
 general relativity, vierbein formalism 0-22263  
 general relativity as a generalized Hamiltonian system 0-31650  
 general Taub-NUT-De Sitter metric, self-dual Yang-Mills soln. of gravity 0-46946  
 Gowdy universes, particle creation 0-56990  
 gravitational creation of odd numbers of fermions 0-32048  
 gravitational interaction, spin, rotation and quantum effects, review 0-37203  
 gravitational-field equation for quantum gravity 0-124  
 graviton loop calc. in general gauge 0-27204  
 graviton-graviton scatt., one loop scalar field contrib. and helicity nonconservation 0-52114  
 graviton-matter interaction, Zitterbewegung interpretation 0-122  
 gravity as a Goldstone field in the Lorentz gauge theory 0-31655  
 gravity as Hilbert space of quantised system 0-52113  
 H-spaces, gravitational instantons, spin coeff. method 0-31654  
 indefinite metric theory, supplementary remarks 0-42133  
 index theorem boundary terms for gravitational instantons 0-123  
 Kerr-Schild's gravitational fields, quantisation 0-31653  
 linear zero-spin fields in external gravit. and scalar fields, perturbation theory 0-31969  
 linearised gravitational pot., Euclidean and Minkowski space formulations 0-121  
 local structure of functional spaces and dynamical variables of gauge-invariant fields 0-9099  
 massive vector multiplet coupled to supergravity 0-17855  
 massless fields in asymptotically flat space-time, null surface quantisation and quantum theory 0-4625  
 monopole solutions for strong gravity coupled to SO(3) gauge fields 0-4621  
 moving mirror effects, back-reaction 0-46944  
 neutrino, Maxwell, and scalar fields in the cylindrical magnetic or plasma universe 0-120  
 non-inertial framed space-time configurations, gauge theory appl. 0-22262  
 nonlinear graviton unprimed spinor description 0-8892  
 nonlinear Heisenberg-Klein-Gordon equation, localised solns. in flat Schwarzschild space-time 0-4620  
 nonrenormalisability, one-loop divergences 0-4626  
 normal flat space-time, embedding hadronic microuniverses 0-9135  
 observability differences between classical EM and gravitational gauge fields 0-36925  
 particle creation by time depend. elec. and gravitational fields 0-4623

**quantum field theory of gravitation continued**

particle creation by time-depend. gravitational field, quantum equivalence principle 0-41925  
 Petrov's type III, N and O solutions, renormalisable theory, trapping of physical gravitons 0-31652  
 phenomenological ideas toward a field theory of matter, photons which satisfy Maxwell's eqns. for EM waves 0-378  
 phenomenological ideas toward a field theory of matter, unification of EM and gravity fields 0-378  
 post-Newtonian approximation of the Poincare gauge theory of gravitation 0-52115  
 probabilities of quantum processes in external gravit. fields 0-36932  
 projective geometry, Langrangian subspaces, and twistor theory 0-52112  
 projective geometry for polarisations 0-52053  
 quantum fluctuations near the classical space-time singularity 0-8893  
 quantum process probability in external gravitational fields, Green's function calcs. 0-36931  
 quaternionic multi  $S^4 \approx \text{HP}(1)$  gravitational and chiral instantons 0-31656  
 Robertson-Walker cosmologies, Kostant-Souriau quantisation 0-12838  
 Robertson-Walker universe, pair-creation of particles 0-22265  
 Robertson-Walker universes, field interaction effects on particle creation 0-42130  
 Robertson-Walker universes, particle creation, self-interacting quantised fields 0-17699  
 S-matrix for interaction of gravitational and Yang-Mills fields 0-42315  
 scalar quantum field in an external gravitational field 0-31974  
 Schwarzschild-de Sitter space-time vacuum energy-momentum tensor 0-52091  
 second order field equations for grav. field theory 0-27203  
 self-dual gauge fields and space-times 0-9108  
 semiclassical theory, appl. book contrib. 0-22268  
 spacetime structure theory at very short distances, nonlinear sigma model 0-12979  
 strong-gravity model, stability under perturbation, Hamiltonian formalism 0-52453  
 superunified theories in superspace 0-8886  
 thermal and nonthermal particle production without event horizons 0-4628  
 Thirring model coupled to gravity, classical solns. in generally covariant model with fermions 0-9091  
 torsion and gravitational Meissner effect 0-8894  
 translational gauge theory of gravity: post-Newtonian approximation and spin precession 0-46945  
 twistor theory, particle models 0-13278  
 unitary inequivalence of various theories 0-52111  
 vacuum quantum effects analogy in gravitational and EM fields 0-32044  
 Yang-Mills equations, Cauchy problem 0-13206  
 Yang-Mills higher-derivative theory, ghost problem 0-31970  
 Yang-Mills theory of gravity 0-42134  
 $e^+e^-$  pair creation in strong EM fields, gravitational effects 0-42376

**quantum field theory of interactions**

see also *elementary particle coupling constants; elementary particle interactions; Feynman diagrams; quantum electrodynamics; quantum field theory of gravitation; quantum field theory of strong interactions; quantum field theory of weak interactions; vertex functions*  
 axial vector meson model, quasi-renormalisation using BPHZ approach 0-13208  
 C\*-algebras of two body interactions, existence of scatt. theory of time automorphism groups 0-31972  
 correspondence and opposition between quantum theory and classical physics, temporal logic 0-27176  
 critical exponents, three dimensional system with short-range interaction, calc. 0-42348  
 crossing properties of scattering operators 0-32028  
 deep inelastic scatt., field theoretical description, QCD, quark-parton, and light cone algebra (*Russian*) 0-42388  
 gauge theories, quantised, large time behaviour, asymptotic anal. 0-27395  
 Hagedorn model, topological cross sections in multiplicity asymptotics (*Russian*) 0-9154  
 Lagrangian, effective, in path integral quantisation formalism 0-42325  
 multiparticle scatt. operators representation satisfying unitarity and crossing props. 0-32029  
 relativistic Hamiltonian theory, covariant formulation, on light cone, fields with spin (*Russian*) 0-9087  
 scaling of inclusive form factors with respect to a generalized scaled variable 0-417  
 spin-3 field theory, free massive Lagrangian, zero-mass limit of higher spin theories 0-52402  
 supersymmetric Sine-Gordon model, infinite set of local quantum conservation laws 0-47207

**quantum field theory of strong interactions**

see also *elementary particle strong interactions; Lee model*  
 $\sigma$  model,  $\text{SU}_2 \times \text{SU}_2$ , modified Goldberger-Treiman relation, pseudoscalar form factor 0-27421  
 $\sigma$  models, nonlinear, perturbative approach to symmetry restoration 0-37163  
 $\sigma$ -models, two-dimens. nonlinear, on Riemannian and Hermitian symmetric spaces 0-52404  
 $\phi^4$  model, strong-coupling expansion in the large-N limit 0-346  
 bi-local field on space-like surface 0-27403  
 charmonium spectroscopy, explicit soln. of wave eqn. for arbitrary power pots. 0-403  
 conformal-invariant field theory, anomalous dimensions, coupling const. 0-4870  
 covariant  $\sigma$  models, first order system of differential eqns. 0-31978  
 dimensional regulation,  $\text{SU}_2$  gauge theory, instantons 0-18066  
 eikonal pionisation graph summing in Lagrangian field theory 0-4973  
 elastic scattering between binary quark-antiquark system and local field 0-47244  
 four-dimensional  $\sigma$ -model on quaternionic projective space 0-9092  
 glueball singularity, flavour loops and the Harari-Freund picture 0-42433  
 hadrons, extended, second-quantisation of strongly interacting fields 0-13270  
 hard processes, parton model and QCD, review 0-47258  
 isotopic spin and coherent states 0-4843  
 lattice gauge theory with fermions, renormalised phases, vacuum polarization 0-13198



**quantum field theory of strong interactions continued**

- low energy light particle processes in spontaneously broken gauge theories, heavy particle effects 0-22521
- low equation, solns. in no-crossing approx. 0-32012
- MIT bag model, two-dimens., confined massive field vacuum fluctuations 0-4921
- modified renormalisation conditions, two-point Green functions 0-9089
- multilegged propagators in strong-coupling expansions 0-4861
- nontopological solitons, hadron appl. 0-47191
- O(N) nonlinear  $\sigma$ -model, two-dimens., fifth Painleve transcendent 0-32002
- path group appl. to gauge theory and quarks 0-31985
- perturbative field theory effects and Regge pole representation, QCD, dual topological unitarisation 0-42434
- pre-Schwinger model, Lorentz transforms. if operator solns. 0-47171
- QCD and heavy quarks (*German*) 0-37214
- quark field quantum fluctuation computation in arbitrary Yang-Mills instanton background 0-13268
- scalar U(N) QCD in the large-N limit, hamiltonian method 0-37212
- separable nucleon-nucleon potentials and minimal relativity 0-27495
- spacetime structure theory at very short distances, nonlinear sigma model 0-12979
- SU(2)×U(1) gauge theories, successes and current issues 0-18064
- $e^+e^-$  pair creation in strong EM fields, gravitational effects 0-42376
- pp interactions, cluster mass spectrum 0-37307
- $\pi$  form factor, expt. behaviour, influence of left-hand cut on second Ricmann sheet 0-13304

**quantum field theory of weak interactions**

- see also elementary particle weak interactions; Weinberg model
- CP violation and instantons 0-354
- Euclidean QFT, n-particle irreducible functions 0-13199
- lattice gauge theory with fermions, renormalised phases, vacuum polarization 0-13198
- SU(2)×U(1) gauge theories, successes and current issues 0-18064

**quantum fluids**

- see also boson systems; fermion systems; liquid helium
- Gross Pitaevskii eqn., generalised solns. 0-49437
- liquid, computer modelling 0-54472
- many body theory, appls. review of development 0-46968
- phase space quantisation of interacting vortices in two dimensions 0-4634
- quasiparticle kinetic eqn. construction 0-53905
- vortex formation and dynamics, Magnus force (*Russian*) 0-10719

**quantum generators (optical) see lasers****quantum mechanics see quantum theory****quantum numbers see quantum theory****quantum optics**

- see also photon counting
- absorptive optical bistability transient, analytical treatment 0-19077
- amplified spontaneous emission in spherical and disk-shaped laser media 0-1177
- atom, canonical dressing by intense radn. fields 0-1173
- atom, two- and three-level, transition in stochastic field, saturation and Stark splitting 0-9546
- atom in strong EM field, characts. calc. using quantum theory of Markovian processes 0-32943
- atomic cooperative system, light scatt. spectrum, coherent-state representation, numerical results 0-23650
- atomic motion in resonant fluctuating laser radiation 0-43310
- bistability equations for standing wave cavity, analytic solns. 0-48328
- bistable steady states in optical subharmonic generation, Wigner distrib. 0-53370
- broad band reson. light press., basic eqns. 0-28182
- cavity with outout coupling, one-dimens., quasimodes as field eigenvalue 0-9911
- charged dust grain, light scatt., quantum approach 0-48196
- charged particle self-interaction 0-373
- coherent and nonlinear optics, Conf., Leningrad, USSR (June 1978) 0-27027
- coherent multiphoton intense interactions, convergent perturbation anal. 0-1037
- collective radiation and the near-zone field 0-37977
- collective radiative phenomena in two level systems (*Russian*) 0-1174
- cooperative multiphoton ionisation, bistability effects, Bonifacio-Lugiato model 0-19010
- diatomic system, spontaneous emission, photon corrls. (*German*) 0-5711
- Dicke maser model, dynamical struct. 0-37985
- Dicke maser model, equilibrium states for mean field models 0-46961
- Dicke model, modification for long wave photons 0-1169
- Dicke model, spontaneous polarisability of two-level atoms 0-1167
- Dicke model phase transition, thermodynamic Green's function method 0-5715
- dispersive optical bistability with inhomogeneous broadening, exact soln. 0-53360
- dynamic behaviour of optical bistability, time depend. Fokker-Planck eqn. soln. 0-37980
- electric dipole interaction 0-19011
- Fabry-Perot cavity, instabilities for coherently driven absorber 0-53387
- free electron laser, coherent quasi-classical states 0-53251
- free electron laser, quantum theory 0-23656
- free-free transitions in quantum electronics 0-28183
- gas, spontaneous emission and absorpt. of weak wave, radn. capture effect 0-939
- Gaussian light, partially polarised, photon statistics 0-19012
- generating functions calc. 0-1168
- harmonic oscillators, charged, interaction with transverse EM field mode 0-5712
- homogeneously broadened three level atoms, intense standing wave saturated, spatial inhomogeneity, mode competition 0-23646
- injection laser quantum noise in optical fibre communication systems 0-48259
- Josephson junction, coherently driven, bistability model 0-15661
- laser cavity resonator, photon lifetime and reflectance meas., phase-shift method 0-38039
- laser fields, stochastically fluctuating, saturation and Stark splitting of resonant transitions 0-53245
- laser pump fluctuations, influence on resonance fluoresc. radiation intensity correlation 0-37981
- laser system qualitative change in threshold range, analogy with phase transition (*Czech*) 0-32949

**quantum optics continued**

- laserlike systems, stochastic master equation description 0-53243
- Lie algebra representations and coherent states, Trotter limits 0-22238
- mean field models, equilib. states 0-46961
- molecular rotational coherence, reson. collisional exchange, time-resolved microwave obs. 0-23525
- Moller scatt., high intensity, scatt. energies 0-22541
- multi-level atom with Raman reson., time-delayed laser scatt. 0-48343
- multilevel equidistant system, excitation by elec. field 0-37983
- multilevel relaxing systems, multitime corrl. in scatt. and fluoresc. 0-1166
- multiphoton stimulated Compton scattering of relativistic electrons 0-48198
- multiple coherent interaction in optical separated fields, superhigh resolution spectroscopy 0-52338
- N two-level atoms, interaction with radiation field in restricted rotating wave approx. 0-5713
- N two-level atoms, quantum theory of nonlinear optical phenomena 0-5790
- N-level atom (molecule), coherent dynamics, two- and three-level behaviour 0-23649
- N two level atoms, interaction with radiation field in restricted rotating wave approx., numerical anal. 0-5714
- nonlinear quantum systems, wave packet behaviour in pseudo-coherent state method (*Russian*) 0-1175
- nonresonant excitation, ensemble of two-level systems, rel. to multiphoton spectra, polyatomic mols. 0-5585
- optical bistability, nonlinear polarisability model 0-37976
- optical field quantisation from absorber theory 0-43309
- parametric interaction with reson. medium, EM field statistics 0-1171
- partially coherent light interpretation, optical theorems 0-53210
- photon antibunching, polaris. depend. 0-1170
- photon behaviour in high intensity coherent laser beams 0-28185
- photon existence testing by photoelectric counting and nonexistence of photons 0-9842
- photon stationary distribution in optical bistability 0-48197
- photon statistics, unsaturated k-photon absorption, exact soln. of master eqn. 0-37984
- photon statistics after destructive interf. of two-photon absorbed light 0-48199
- photon synchronisation effect on intensity interference (*Russian*) 0-48200
- photon-anticorrelation effect calc. in degenerate optical parametric amplifier 0-33079
- quantum meas. realisable with photoemissive detectors 0-53220
- resonant Raman scattering in laser fields of arbitrary strength, antibunching effects 0-23653
- ring cavity, dispersive bistability in homogeneously broadened systems 0-14306
- ring cavity, dressed mode dynamics of optical bistability 0-19013
- superfluorescence, phase-wave fluctuations 0-23652
- three two-level atoms system, continuously incoherently-pumped, radiation rate, spectrum 0-5716
- three-level atom, nonmonochromatic chaotic field, double optical reson. and reson. fluoresc., AC Stark splitting 0-9547
- three-level molecular system, populations, rate equations 0-37975
- three-level system, interacting with two strong EM fields, steady-state population distrib. and complex susceptibility 0-37978
- three-photon vector model, resonant coherent interaction (*Chinese*) 0-43306
- transition phenomena, review 0-32944
- two photon coherent states in degenerate four wave mixing 0-5717
- two-atom system, cooperative, reson. fluoresc. spectrum. sidebands 0-43000
- two-level atom, interatomic force depend. on intense radiation fields 0-53100
- two-level atom plane, one-dimens.  $\delta l=1$ ,  $\Delta m=0$  decay, soluble semiclassical model (*Portuguese*) 0-18809
- two-level atom system, reson. fluoresc., photon antibunching, propag. effect 0-9843
- two-level atomic system, superfluoresc. fluctuations 0-23651
- two-level atomic system, weak probe field absorption spectra in coherent laser field 0-23758
- two-level atoms, saturation in chaotic field 0-37982
- two-level system resonant processes in presence of nonresonant fields (*Russian*) 0-14308
- ultrashort light pulse propagation in resonant medium 0-43308
- $^{15}\text{NH}_3$ , modulated coherent Raman beats 0-23464

**quantum solids**

- see also solid helium
- crystal, computer modelling 0-54472
- crystals, appl. of method of quasiverages 0-10737
- discontinuous orientational phase transitions, thermodynamics, isotope effects 0-6590
- H<sub>2</sub>, short-range corre. and motional renormalisation of anisotropic interactions as function of density 0-34272
- O<sub>2</sub> solid,  $\alpha$ - $\beta$  transition, mag. susceptibility (*Russian*) 0-6592

**quantum statistical mechanics**

- see also jellium; many-body problems; quantum fluids; quantum solids; quantum theories of fluid structure
- $\phi^4$  system, metastable state, decay rate calc. 0-22301
- adatom interaction with solid substrate, effect of mechanical stress on chem. pot. 0-10784
- anharmonic crystals, Debye-Waller factor, specific heat thermal behaviour 0-54335
- Bose expansion for general spin, exact 0-31662
- Bose gas, ideal, virial series 0-42139
- Bose gas, weakly interacting in restricted geometries, low-temp. thermodynamics 0-34261
- Bose imperfect gas, condensed state, limit Gibbs state 0-52124
- Bose partition functions, functional integral representations and inequalities 0-31667
- Bose system, nonideal, condensation, momentum, correlation function 0-46966
- Bose-Einstein condensation, role of cosmology in elementary particle physics 0-27430
- Bose-Einstein condensation in Einstein universe 0-46959
- Bose-Einstein condensation of a relativistic gas in d dimensions 0-8902
- Bose-Einstein condensation of ideal gas 0-22272
- Bose-Einstein statistics, wave packet formulation of multiparticle production at high energies 0-13338



## quantum statistical mechanics continued

boson fluid, distribution functions within hypernetted-chain approx., appl. to liq. <sup>4</sup>He 0-24696  
 boson gas, interacting, approx. equilb. states 0-46962  
 boson magnetised ideal gas, effect of confinement, anal. 0-12987  
 boson system,  $\lambda$ -transition, renormalisation-group theory 0-143  
 Boson theory, quantum soliton and classical-soliton 0-12986  
 bures distance and relative entropy 0-84  
 canonical ensemble, appl. to equilb. between black hole and radiation field 0-52121  
 Casimir forces, appl. of analytic regularisation 0-36939  
 chemical potential, algebraic theory for usual gauge group 0-31661  
 coherence and randomness in quantum theory, uncertainty relations 0-22231  
 collective radiative phenomena in two level systems (*Russian*) 0-1174  
 constraints, flexible vs. rigid 0-31658  
 continuous dipole system in grand canonical ensemble, lack of screening 0-22273  
 correspondence and opposition between quantum theory and classical physics, temporal logic 0-27176  
 damped harmonic oscillator, non-equilibrium quantum statistical mechanics, system quantisation 0-52070  
 decay of unstable quantum system, survival probability 0-46965  
 density matrix for arbitrary spin, equations of motion for new SU(n) parameters 0-52592  
 density operators, equations of motion in external fields 0-36944  
 Dirac particles, interaction, and generalised phase factors 0-27168  
 Dirichlet's integral formula and the evaluation of the phase volume 0-17744  
 Dirichlet forms, construction of stochastic processes 0-8921  
 disordered system, divergence of partition function of attractive Frisch-Lloyd model 0-136  
 dominant partition method 0-47455  
 donor-acceptor transition kinetics, with allowance for vibr. struct. 0-144  
 Einstein, quantum mechanics, conceptual problems 0-46783  
 Einstein and the quantum theory, review 0-22237  
 electron gas, degenerate, static density response function calc. by QHNC 0-49633  
 electron gas, Tomonaga model, response function calc. method 0-22279  
 energy moments, analytic continuation of generalised zero function 0-36938  
 ergodic theory in von Neumann algebras 0-9104  
 ergodicity, classical, quantum mech. implications 0-8898  
 Fermi gas, one-dimensional theory, correlation functions 0-22278  
 fermion thermodynamic system, high-order perturbation expansion 0-4635  
 finite system, order parameter and sp. ht. for epitaxial ordering renormalisation-group calc. 0-17862  
 Gaussian quantum stochastic processes on the CCR algebra 0-12985  
 generating functionals in nonequilibrium statistical mechanics (*German*) 0-12981  
 Green's function for surface physics, partial differential eigenvalue eqn. 0-6929  
 harmonic oscillators, charged, interaction with transverse EM field mode 0-5712  
 HF approximations, thermodynamic Fermi systems 0-4642  
 hyper Raman effect, quantum statistics 0-23754  
 infinite chain, quantum mech. irreversible motion 0-4633  
 infinite macrosystems in standard representation, dynamical symmetries 0-4590  
 irreversible processes, time asymmetry 0-22215  
 irreversible processes and dissipative systems in quantum theory 0-8906  
 Ising transverse 1-D model, dynamics 0-29515  
 Keldysh's perturbation formalism 0-13217  
 Landau-Zener problem, random nature of motion role in intersecting terms problem 0-8937  
 laser with saturable absorber, stationary state, nondiffusive approx. 0-19076  
 laser- or black-body radiation, strong electron coupling, limitation of Fermi-Dirac statistics 0-29843  
 Lennard-Jones gas, second virial coeff. calc. using equilb. Wigner distrib. function variational principle 0-4685  
 linear hard core fluid as limit of lattice fluid 0-38882  
 linear quantum channel with thermal noise, quasiprobability distrib. 0-12984  
 linear response theory, master eqn. approach 0-31663  
 locally equilibrium correlation function calc. method 0-36943  
 macroscopic observables, treatment procedure 0-17864  
 many body theory, appls. review of development 0-46968  
 many fermion systems, energy lower bound 0-17860  
 many-boson model, spontaneous symmetry breakdown and restoration 0-52123  
 many-spin system, group approach in dynamics (*Russian*) 0-44900  
 Mayer cluster function and quantum two-body t matrix 0-17859  
 mean field models, equilb. states 0-46961  
 molecular relax. phenomena, quantum statistical mechanical approach, irreversible thermodynamic theory for radiationless decay 0-48028  
 Monte Carlo methods, quantum mechanical corrections to classical equilibrium statistical-mechanical results 0-135  
 multiparticle scattering operators, cluster decomp. 0-22592  
 n-component spin system, energy-energy correl. function calc. 0-31697  
 nonequilibrium systems, cluster expansions with contraction for homogeneous systems 0-46964  
 nonequilibrium systems, theory of irreversible processes 0-46963  
 nonlinear quantum oscillator ensemble excited by external periodic force, statistics (*Russian*) 0-27213  
 one particle reduced density matrix of impenetrable bosons in one dimension at zero temperature 0-17863  
 one-dimensional  $\phi^4$  and double quadratic systems, kinks 0-47197  
 one-dimensional Fermi gas with backscattering, coupling between charge and spin degrees of freedom 0-17861  
 one-dimensional sine-Gordon system, kinks 0-46969  
 one-dimensional system, Bose-Einstein condensation at const. press. 0-22276  
 one-particle quantum mechanics, duality between confining pots. and  $(R+L_\infty)$  pots. 0-31574  
 operator algebra and quantum statistical mechanics, book 0-41965  
 optics, generating functions calc. 0-1168  
 paragas thermodynamics at intermediate temps. 0-46970  
 partition functions, classical limit 0-52120  
 path integrals, distrib. definition 0-31595

## quantum statistical mechanics continued

path integrals and lower bounds for density matrices 0-138  
 phase space quantisation of interacting vortices in two dimensions 0-4634  
 photon statistics, unsaturated k-photon absorption, exact soln. of master eqn. 0-37984  
 process characterisation by method of local specifications (*French*) 0-31597  
 quadrupole phonon states, fifth label values, exact derivation 0-31664  
 quantum crystals, appl. of method of quasiaverages 0-10737  
 quantum mechanical addition, statistical distrib. 0-22274  
 relativistic paramagnetism, statistical mechanics in strong mag. field 0-17865  
 resonance transfer rate of electron excitation, model of convergent terms, effect of diffusional motion of particles 0-8936  
 Schwinger variational principle for dynamic susceptibilities 0-4639  
 sine-Gordon system, breathers, extended object QSM 0-42347  
 square-well fluid, nonclassical crit. behaviour 0-44291  
 thermal mechanics: a quantum mechanical analogue of nonequilibrium statistical thermodynamics, stochastic processes 0-52125  
 thermodynamics of quasi relativistic electron gas, pathway integral application (*Russian*) 0-22277  
 Toda, quantum mechanical lattice 0-46983  
 transport equation for electrons in nonmonochromatic EM field 0-10937  
 two-dimensional square Ising model in transverse magnetic field, renormalisation-group method 0-20428  
 virial theorem and scale transformations, for teaching 0-17763  
 Widom-Rowlinson lattice gas, grand partition function zeros 0-31681  
 H, condensed, spin-aligned, props. from variational calcs. 0-4637  
 H, spin-polarised, density, magnetisation, compression and thermal leakage 0-44391  
<sup>3</sup>He, superfluid A-phase, Cooper pairs vs. Bose condensed mols., ground-state current 0-49451  
<sup>4</sup>He, liquid, condensed phase, long-range order of one- and two-body density matrices 0-10726

**quantum statistics** see *quantum statistical mechanics*  
**quantum statistics of many-particle systems** see *quantum statistical mechanics*  
**quantum theories of fluid structure**  
 see also *liquid theory; quantum fluids*  
 dilute aqueous solutions, Monte Carlo studies of struct., review 0-54101  
 fluid with nearly spherically symmetric molecules, thermodynamic perturbation theory 0-14985  
 water, liq., Monte Carlo studies of struct., review 0-54101

**quantum theory**  
 see also *Clebsch-Gordan coefficients; complementarity; correspondence principle; indeterminacy; perturbation theory; quantisation; quantum field theory; spin hamiltonians; wave mechanics*  
 6) symbol calculation for compact groups 0-8856  
 action-angle variables in quantum mechanics, appl. to harmonic oscill., linear (triaxial) rotors 0-31543  
 adiabatic theorem 0-31546  
 Aharanov-Bohm effect, possible nonexistence 0-27434  
 Aharanov-Bohm effect 0-36893  
 Aharanov-Bohm effect, Feynman path integral approach 0-31578  
 Aharanov-Carmi thought expt., inertial and EM vector potentials 0-52051  
 Airy functions, asymptotic behaviour of derivatives 0-17830  
 ambiguity group for classical canonical transforms, role in quantum mechanics 0-8839  
 area preserving maps, quantisation 0-12924  
 atom scattering by corrugated potential wall, appl. to diffr. by cryst. surface 0-42104  
 atom-surface scatt., inelastic, eikonal approx. 0-50499  
 atom-surface scatt., inelastic, energy transfer and sticking coeff., classical and quantum treatments 0-40209  
 atomic RF spectroscopy, nonlinear and parametric effects, review 0-18816  
 axiomatic theory 0-76  
 Bell's inequality, joint measurability, real and imagined nonlocalities 0-46861  
 Bessel functions, asymptotic approx. 0-31562  
 Bloch electrons in mag. field, energy spectrum, struct. of Landau levels 0-54623  
 Blume-Emery-Griffiths model, renormalisation group centred, tricriticality 0-42165  
 Born series rearrangement in model space, resolvent operator expansion 0-13422  
 bound state decay in external field in semiclassical approx. 0-12941  
 bound state energy levels, quantum mechanical formalism, convergent perturbation theory (*Russian*) 0-4573  
 bound state wave function explicit normalisation, decay widths calc. 0-18116  
 bound states, semiclassical, in one-dimension, perturbation formalism 0-12937  
 bound states of bispherical and toroidal potentials (*French*) 0-75  
 bures distance and relative entropy 0-84  
 catastrophe and stochasticity in semiclassical quantum mechanics 0-8861  
 cavity of entropy 0-27158  
 Cayley quantum theory, new aspects in eight-dimens. Clifford algebra 0-8846  
 chemical bonding in inorganic complexes, quantum mech. ideas development and use 0-12878  
 chemical bonding in inorganic complexes, quantum mech. ideas development and use 0-12879  
 classical dynamics, quantum analogs, book 0-41969  
 coherent states,  $\hbar \rightarrow 0$  limit 0-31538  
 collapse postulate for observables with continuous spectra 0-36885  
 completely integrable field theory models, quantum-mech. approach 0-4574  
 completeness value for eigenfunctions of second order differential eqns. 0-31564  
 complex versus quaternionic quantum theory, note on Peres' proposed test 0-31576  
 conceptual anal. in microchannels theory, Hilbert space representation 0-22217  
 conditional probability of a generalised probability theory, quantum mech. foundations 0-12949  
 conference, group theoretical methods in physics, Austin, Texas, USA (Sep. 1978) 0-4474



## quantum theory continued

- conference, Starnberg, W.Germany (July 1978) 0-27044  
 conference on Lie admissible formulations, Cambridge, USA, (Aug. '79) 0-36765  
 confining potentials, peculiar prop. of wavefunctions 0-46863  
 contractions of expansions of fermion operators 0-17834  
 controllability, optimisation of quantum systems, pure states and mean values 0-22210  
 correspondence rules and path integrals 0-31590  
 coupled anharmonic oscillator energy levels, large quantum number behaviour, path integral method 0-91  
 covariance operators, reflection positivity using Dirichlet or Neumann boundary data 0-131  
 covariant observables and instruments 0-8842  
 damping, quantum mechanical 0-46862  
 decay processes and dynamical subgroups 0-8848  
 deformation of symplectic structure and quantization 0-8853  
 density functional theory, quantum mech. system, accurate pot. and energy functionals 0-52849  
 density matrices with continuous entropy for quantum mechanical system 0-13024  
 density matrix of scattered particles, comments on 0-22219  
 density matrix of scattered particles 0-22218  
 Deser-Gilbert-Sudarshan representation, existence 0-37167  
 differential inequalities, comparison theorem 0-31549  
 diffraction problem, non-homogeneous media, non-stationary problem 0-22211  
 diffusion coefficient of elementary particles, intrinsic 0-22222  
 dipole interaction of an oscillator with scalar field 0-94  
 Dirichlet's integral formula and the evaluation of the phase volume 0-17744  
 Dirichlet forms, construction of stochastic processes 0-8921  
 dissipative systems, dynamical description 0-17867  
 dissipative systems, time evolution of state vector 0-12935  
 dynamic system, classical quantisation conditions with stochastic behaviour anal. 0-8922  
 dynamic systems, deformation and quantification (*French*) 0-31598  
 education, relativistic quantum mechanics, free localised Dirac particle, Zitterbewegung 0-17739  
 education, Schrodinger eqn. for free particle, wave packet spreading in coord. representation 0-17736  
 eikonal approximation, analytic props. 0-32038  
 Einstein and the quantum theory, review 0-22237  
 Einstein-Podolsky-Rosen paradox, causal superluminal interpretation 0-45  
 Einstein-Podolsky-Rosen paradox, contradiction between classical quantum theory of meas. and total ang. momentum conservation (*French*) 0-52042  
 electron plasma with nonparabolic energy dispersion relation, EM fluctuations 0-2413  
 electronic wavefunctions in a space of constant curvature 0-5466  
 elementary length and elementary time interval, existence (*French*) 0-8815  
 EM potentials, effect on an internal degree of freedom 0-42101  
 entropy in operational statistics and quantum logic 0-17903  
 EPR paradox, quantum correlations and separability 0-31571  
 Euclidean semiclassical methods, use limitations 0-42102  
 event phase space structure, alternative to quantum logic 0-42093  
 extended relativity, T-violation and new particle 0-37182  
 Fenyves-Nelson stochastic model of quantum mechanics 0-86  
 Feynman diagrams, appls. in advanced quantum theory, book 0-22157  
 Feynman Lagrangian for short diffusion processes 0-31551  
 Feynman path integral, polygonal path formulation 0-31584  
 Feynman path integral and theory of forms 0-31586  
 Feynman path integral formulation using geometric quantisation techniques 0-31588  
 Feynman path integrals, conference, Marseille, France, 1978 0-31422  
 feynman path integrals and the corresponding method of stationary phase 0-31583  
 Feynman-type integrals defined in terms of general cylindrical approximations 0-31591  
 Fock, V., development of ideas in atomic phys. and quantum theory 0-22183  
 forced quantum oscillator equation, time-depend., soln. in coordinate representation 0-52044  
 formulation in geometric picture 0-36895  
 functional integration through inverse scattering variables 0-52065  
 Gamow state vectors as functionals over subspaces of the nuclear space 0-32227  
 Gel'fand-Levitan equations with comparison measures and comparison potentials 0-12931  
 generalised 6-j symbols 0-31557  
 generalised quantum defect, energy and radius depend. 0-14067  
 generalised quantum logics, geometry 0-42085  
 generalized deformations of nonassociative algebras. Definition and some simple examples 0-36887  
 generating functions for characters of group representations and their applications 0-8840  
 geometric quantization and internal symmetry 0-42089  
 Gleason's theorem generalisation 0-36889  
 group theoretical foundations of classical and quantum physics, kinematical symmetry groups and state spaces 0-52008  
 group theory applications to physical and chemical systems in relation to struct. and substructs. 0-42921  
 hadron microstructure, de Sitter microuniverse, relativistic Hooke group and nonrelativistic quark model 0-27480  
 Hamilton-Jacobi equation solns. in Coulomb pot. and quasiclassical approx. 0-46765  
 Hamilton-Jacobi generalised theory, phase space approach 0-36891  
 Hamiltonian operator, discrete spectrum calc. method (*Czech*) 0-17823  
 Hamiltonians, quadratic, classes of quadratic invariants, interrelations and symmetries 0-31565  
 Hamiltonians perturbed by pulses, quantum dynamics 0-17829  
 harmonic oscillator, extended Feynman path integral formula 0-36890  
 harmonic oscillator, quantum action angle variables 0-46842  
 harmonic oscillator, time-dependent 0-8826  
 Heisenberg's principle, distinguishing test from de Broglie's relation 0-42092  
 Hermitian matrix, disorder effect on spectrum 0-31547  
 heterodyning of elementary particles, radiation meas. method 0-42898  
 hidden symmetries in dynamical systems 0-37168  
 quantum theory continued  
 higher-order Levinson's theorems and the high-temperature expansion of the partition function 0-4558  
 hypergeometric partial solutions in the problem of two Coulomb centers 0-4582  
 hypervirial theorems and symmetry, optimal variational wave function 0-17841  
 implicate order, algebras, and the spinor 0-52047  
 infinite macrosystems in standard representation, dynamical symmetries 0-4590  
 inner-shell vacancy system, saddle point calcs. 0-23292  
 intramolecular dynamics, criteria for stochastic nonstochastic flow 0-53082  
 invariant phase space integral evaluation via Laplace transforms 0-31573  
 inverse Noether theorem, general formalism for symmetry and conservation 0-46850  
 IR radiation, interaction with molecular system, classical/semiclassical theory challenged 0-43117  
 irreversible processes, time asymmetry 0-22215  
 irreversible processes and dissipative systems in quantum theory 0-8906  
 ISO(n), explicit determ. of representation functions 0-31561  
 isotonic oscillator, coherent states for nonharmonic potentials 0-52061  
 isotopic spin and coherent states 0-4843  
 J<sup>2</sup> eigenvalues 0-17742  
 jarring of quantum system, theory of sudden perturbations 0-17839  
 jump processes, Cauchy problem for Schrodinger eqn. (*French*) 0-31596  
 Kepler stationary orbits of electron with velocity-depend. oscillatory perturbations 0-52062  
 Klein-Gordon particles in deep square wells 0-31982  
 KMS condition for Schrodinger dynamics 0-36896  
 Kramers rate theory, quantisation using Wigner representation 0-52054  
 ladder operators of group matrix elements 0-31555  
 lattice, orthocomplemented quasi modular, quantum logic interpretation 0-12950  
 Lippmann Schwinger eqns. for three charged particles 0-4580  
 logical problems of quantum mechanics 0-12883  
 macroscopic observables, treatment procedure 0-17864  
 mass formula of charged leptons 0-13244  
 mathematical foundations of dimensional analysis and the question of fundamental units 0-42086  
 matrix diagonalisations via involutorial transforms. 0-17827  
 matrix diagonalisations via reduced characteristic eqns., appl. to ang. mom. coupling 0-17828  
 matter stability despite catastrophic Coulomb forces 0-22212  
 measure theoretic ergodic theory in quantum mechanics 0-52069  
 measurement problem of quantum mechanics 0-12948  
 measurement techniques, interaction between classical and quantum systems 0-42099  
 measurement theory, argument against superluminal transmission 0-52055  
 measurement theory, ideal expts. appl. 0-42087  
 measurement theory, interaction between classical and quantum system 0-92  
 measurement theory, peculiarities and postulational excesses 0-27174  
 measurement theory 0-17824  
 measurements, simulation using programmable pocket calculator 0-41982  
 Melosh transformation, Eriksen like form, group theoretic interpretation 0-8859  
 mixed crystal or alloy, graded, effective Hamiltonian theory 0-34344  
 molecular charge distrib., quantum topology, bonding theory and molecular structure 0-5463  
 molecular struct. defn. in quantum mechanics 0-52843  
 molecule, diatomic, hyperfine struct. transitions, quantum theory, for undergraduate demonstration 0-17762  
 momentum operators for curvilinear coordinate systems 0-17743  
 Moyal quantum mechanics formulation and Weyl. quantisation generalisation, Lie algebras 0-17835  
 multiply connected spaces, quantisation in terms of Feynman path integrals 0-52060  
 multipole states, tensor struct., transition operator 0-36907  
 Muskhelishvili-Omnès equation and final state interactions 0-17821  
 Nelsons stochastic mechanics, spinning particles and relativistic particles 0-31587  
 Neother's theorem, time-dependent invariants and nonlinear equations of motion 0-12932  
 non relativistic quantum mechanics, quantum microsystem evolution, non-conservation effects 0-22515  
 nonassociative algebra, bibliography 0-36793  
 nonexistence of signal going backwards in time 0-42105  
 noninertial reference frame, laws of motion in invariant form (*German*) 0-36886  
 nonlinear functional theory of particles, general conservation formulae 0-46860  
 nonlinear systems mobility 0-31566  
 nonradiative transitions, solvent effects, dynamic coupling model, quantum mechanical theory 0-29787  
 nuclei, classification of states, unitary scheme 0-42550  
 observables, relation between quantum and classical 0-31537  
 octonions in quantum mechanics 0-27479  
 off-shell scattering by Coulomb-like potentials 0-31560  
 one dimens. symmetrical quantum systems, exact local states 0-46870  
 one-dimensional molecular chain, collective model for conformons 0-15456  
 one-dimensional particle-in-the-box problem, perturbation theory illustration using champagne bottle situation 0-36816  
 open system, new classical Hamiltonian-Lagrange mechanics 0-36900  
 operator equivalents, diagonal and off-diagonal, formula for derivation 0-22233  
 2 orthogonal time dimensions for concept reconciliation, speculation 0-31582  
 parameter-dependent system, energy soln. method 0-8828  
 parametric amplification, quantum-mechanical 0-42097  
 partial inner product spaces, compatibility relns. 0-46855  
 partial wave expansions summation in scatt. by short range pots. 0-31570  
 particle motion in potential channel, waveguide-optical analogy 0-12942  
 path integrals, distrib. definition 0-31595  
 path integrals in quantum theory, basic concepts, review 0-52066  
 path integrals in Riemannian spaces, smooth path spectral anal. 0-52059  
 path integrals on curved spaces, method of determination 0-31589  
 path sums for Brownian motion and quantum mechanics 0-36882  
 Pauli-Lenz vector, extension of SO(3) to SO(4) 0-31550



## quantum theory continued

- pendulum, representation of canonical relns. 0-42084
- percolation problems, quantal 0-31554
- perfect measurements in microchannel theory by conceptual anal. 0-17825
- perturbation theory, many-body, arbitrary point group symmetry, wave operator matrix elements 0-23311
- phase-space projection identities for diffraction catastrophes 0-27162
- photoelectron counting statistics, theory, fully quantum, review 0-52312
- physical foundations, stochastic formulation, proposed expt. test 0-52049
- physical nonexistence of signals going backwards in time 0-42094
- physical operations, diagram operations 0-46846
- physical symmetry groups, subgroups and invariant EM fields and potentials 0-8841
- Planck's constant, origin of quantum theory 0-27179
- Planck integral, non evaluation in terms of finite series of elementary functions 0-31563
- plethysms of finite and continuous groups, generating functions 0-31548
- Poisson summation formula, generalisations 0-4565
- position as only observational quantity, review 0-52048
- presymmetry in relativistic quantum mechanics, absence of kinematics 0-8843
- probability amplitudes of transitions between not necessarily stationary states, coupling const. 0-36902
- probability foundations, modal frequency interpretation 0-12885
- probability in logical space 0-31579
- probabilistic descriptions in classical and quantum theories 0-36899
- process characterisation by method of local specifications (*French*) 0-31597
- product operators, closed basic diagram generation program 0-8817
- projection-operator method, mathematical foundations 0-85
- projective limit of projective system of state operators 0-80
- propagator with friction 0-8821
- proton transfer reactions, kinetic isotope effects, quantum theory 0-3301
- pseudo-Hamiltonians, theory of minimal unitary dilations 0-27153
- QED, Aspect experiment, local and quantum theories 0-32051
- quantisation, semiclassical, periodic orbit role for the quantal bound state 0-8831
- quantum logics and orthomodular lattice embedding in Hilbert space 0-89
- quantum mechanical Brownian particle, tunnelling and transport problems 0-4644
- quantum mechanical particle in random potential, inverse participation ratio in  $2+\epsilon$  dims. 0-36908
- quantum mechanical system dynamic polarisability, van der Waals constants 0-46867
- quantum mechanics, description of operators 0-8820
- quantum mechanics, rel. to reality 0-27172
- quantum state entropy using covariant and contravariant symbols 0-52068
- quantum systems with elevated stability of stationary state, struct. and props. 0-4576
- quantum transition concept in undergrad. courses, explanation of photon creation and absorpt. 0-36807
- quarkonium, quantum mechanical applications, masses and leptonic widths of  $\psi$  and  $T$  0-27484
- quasiprobability distrib. in quantity operators correspondences 0-78
- quasiprobability distrib. in quantum mechanics, dynamic eqns. 0-27157
- radioactivity and quantum mechanics unification, probabilistic conceptions 0-12946
- relativistic  $\pi$ -mesic atom, eigenfunctions and eigenenergies, N-space dimensions calcs. 0-41988
- relativistic classical and quantum dynamics 0-22192
- relativistic particle physics, book 0-41966
- relativistic quantum mechanics, semigroup 0-27180
- relativity theory comparison 0-27175
- representation groups for semiunitary projective representations of finite groups 0-12933
- resolvent operator theory of sequential quantum processes 0-46849
- resonances in quantum mechanics over phase space, group theory aspects 0-8852
- resonant states, completeness props. 0-46857
- rigged Hilbert space and decaying states 0-4591
- scattering theory, nonsingular potential, scatt. length by iterative-perturbation method 0-27160
- Schlesinger systems, isomonodromy deformation, integrable Hamiltonian systems 0-22229
- Schrodinger equation, energy approximants and perturbation theory 0-22232
- Schrodinger equation, new type, evolution of wave function with respect to position 0-27178
- Schrodinger equation, perturbation problem, two-level atom interacting with EM field 0-52056
- Schrodinger equation, polynomial factor eigenfunctions, corresponding pots. (*Chinese*) 0-22236
- Schrodinger wave functions at pot. discontinuities, continuity conditions, for teaching 0-27077
- Schwinger equations, compact description 0-13204
- screened Coulomb pot., perturbation theory and hypervirial theorem, sixth order atom energy levels 0-14071
- semiclassical approximation to quantum dynamics 0-12927
- semiclassical path integrals in terms of catastrophes 0-8860
- solids, total energy calcs., momentum space formalism 0-15468
- soliton quantum mechanical mass in supersymmetric theories 0-22536
- space-time approach, relativistic Brownian motion 0-31567
- spin measurement on spin  $1/2$  particle, model of hidden variable 0-27167
- state props. in quantum logic, Hilbert-space formulation 0-12947
- stationary state, standing de Broglie wave, Aharonov-Bohm effect 0-22228
- Stern-Gerlach expts., observability of arbitrary spin operators 0-31568
- stochastic behaviour of quantum pendulum under periodic perturbations 0-8834
- stochastic formulation, quantum operator algebra origin 0-88
- stochastic Hamiltonian classical and quantum, systems, Volta Memorial Conf. 0-8738
- stochastic methods and techniques for quantum mechanics, book 0-4584
- stochastic parallel displacement of tensors, geodesic correction 0-8920
- structural stability in physics (conference, Tübingen, Germany, May and Dec. 1978) 0-8739
- Sturmian operator, four Euclidean conformal group struct. 0-87

## quantum theory continued

- superluminal communication through wave function collapse in quantum theory 0-27166
- superselection rules, subensemble selection 0-17826
- system influenced by time dependent electric field, fourth order variation perturbation theory 0-22230
- tensorial theory for higher order constants of motion 0-46852
- thermal mechanics: a quantum mechanical analogue of nonequilibrium statistical thermodynamics, stochastic processes 0-52125
- time asymmetries and classical and quantum physics 0-22216
- time operators, need for accurate derivation 0-27170
- time periodic perturbations, calc. of mean energy 0-46869
- time reversal in classical and quantum mechanics 0-42090
- transition probability, second order, time-independent perturbation asymptotic formalism 0-27159
- two photon reson. third harmonic generation, quantised field theory 0-43397
- $U(n)$ , multiplicity free Wigner and Racah coeff. 0-31556
- uniaxial spin systems, quasiclassical method appls. 0-8931
- unified formalism for quantum and classical scattering theories 0-100
- unitary quantum mechanics, nonlinear and relativistic invariant fields 0-4567
- unstable quantum states and rigged Hilbert spaces in nonrelativistic scatt. theory 0-8849
- variable phase method for scatt. on non-local spheroidal pot. 0-95
- wave diffraction, stationary problem in non-homogeneous media 0-68
- wave mechanics, origin, pedagogical approach (*Portuguese*) 0-22166
- weak coupled system, decay, general theory 0-36884
- Weierstrass-Mandelbrot fractal function 0-52063
- Wigner representation, semi-classical ergodicity of quantum eigenstates 0-8833
- work and energy in electrostatic and magnetic systems 0-52050
- $\Theta^4$  quantum field theory, numerical methods, anharmonic oscillator approx. 0-52390
- H atom, variations, quantum theory calcs., generator coord. calcs. 0-41987
- H atom in box, 2-D Schroedinger equation, influence of constant elec. field, finite-element method 0-31544
- H, eigenfunctions and eigenenergies, N-space dimensions calcs. 0-41988
- quantum theory of light *see quantum electrodynamics*
- quantum theory of many-body problems *see many-body problems*
- quark confinement
  - (2+1) dimensional Georgi-Glashow model, critical Higgs mass, clustering, monopoles 0-52441
  - $\Delta I = 1/2$  rule in QCD, higher order gluon corrections, diagrammatic anal. 0-4945
  - $\sigma$  models, nonlinear, perturbative approach to symmetry restoration 0-37163
  - Airy functions, asymptotic behaviour of derivatives 0-17830
  - algebraic approach to hadrons without seeing quarks 0-9143
  - asymptotic freedom, for teaching 0-17761
  - asymptotic freedom in the infinite-momentum frame,  $SU(N)$  Yang-Mills theory renormalisation 0-22519
  - asymptotically non-free Yang-Mills theory, IR divergences 0-37166
  - bag and multimeron solutions of the classical Yang-Mills equation 0-4853
  - bag model, analogy to bubbles in liquid 0-22587
  - bag model  $Q^2Q$  states, meson-nucleon low-energy S-wave scatt., P-matrix formalism 0-13271
  - bag model with finite potential barrier, S-wave mass spectra of  $QQ$  and leptonic widths 0-47242
  - baryon pionic transitions in MIT bag model using PCAC hypothesis 0-37228
  - baryon spectrum, second excited level in harmonic oscillator model, experimental situation 0-37233
  - baryons, with scalar raising pot., relativistic model 0-37231
  - bilocal gauge field theory 0-31986
  - binding energy in model classical field theories 0-4927
  - charmonium  $\psi$  states, confining pots. and inverse scatt. problem,  $T$  mass 0-4946
  - charmonium spectroscopy, explicit soln. of wave eqn. for arbitrary power pots. 0-403
  - chromelectric-flux-tube model, finite time corrections 0-32083
  - colour, confinement, ferroelectric mechanism analogue (*Russian*) 0-13274
  - conference, quarks and leptons as fundamental particles, Schladming, Austria, (Feb.-Mar. 1978) 0-17709
  - conference on hadron struct. and lepton-hadron interactions, Cargèse, France (July 1977) 0-4473
  - configuration space renormalisation to phase space, gauge coupling 0-18074
  - constituent particle scattering in the Regge region 0-37244
  - $CP^{N-1}$  model, QCD toy model, instantons  $\theta$  vacua and confinement 0-9138
  - DESY  $e^+e^-$  experiments, QED checks,  $\tau$  and  $T$  studies 0-18111
  - Dirac equation in a linear potential 0-27392
  - Dirac equation with quadratic scalar potential 0-27459
  - Dirac equation with relativistic linear potential, baryon properties,  $SU_6$  representations 0-47261
  - dual topological unitarization, glueball exchange effects, pomerons and reggeons 0-52482
  - dynamic confinement from vel. depend. interactions, appl. to quark-quark interactions 0-46800
  - Dyson equations, Ward identities, and the infrared behavior of Yang Mills theories 0-42353
  - electric and magnetic confinement schemes for mesons and baryons 0-4960
  - exchange degeneracy breaking, hadronic selection rules 0-37248
  - f-g fields, class relevant to quark confinement 0-125
  - fragmentation, trigger side momentum distrib. in large  $P_T$  processes 0-42422
  - free quarks 0-13289
  - free-spinor field on Regge trajectory as representation of strongly interacting quark field 0-32067
  - gauge fields, chiral fields on loop space, colour-electric flux rings 0-42327
  - glueball singularity, flavour loops and the Harari-Freund picture 0-42433
  - gluon distributions in QCD, definitions 0-37227
  - gluon jets,  $G \rightarrow GG$  and  $G \rightarrow q\bar{q}$  0-37209
  - gluon observation in P-wave quarkonium decay 0-32068
  - hadron high energy struct. models (*Hungarian*) 0-4924



## quark confinement continued

hadron matrix elements in relativistic quark model 0-37238  
 hadron spectroscopy, quark models and SU(5) grand unification scheme 0-4958  
 hadron spectroscopy with covariant Coulomb and confining interactions 0-32090  
 hadronic multiple prod. and average charged multiplicity, strato-gluon mechanism in pp,  $Kp$ ,  $\pi p$  (*Chinese*) 0-22586  
 hadrons and their constituents, wave-particle quality 0-9136  
 heavy quarks, EM shift of energy levels due to confinement, bag model 0-13287  
 heavy vector meson annihilation rate to lepton pairs, hadronic corrections 0-4943  
 Higgs lattice abelian model, finite temp. behaviour 0-13260  
 high  $p_T$  hadronic jet photoprod., QCD anal., quark and gluon jets 0-42474  
 instanton correction to vac. energy densities and bag const. 0-37211  
 instantons, dynamical role in quarkless chromodynamics, bag model test 0-47246  
 jet quantum number, identification model 0-42423  
 jet quantum number identification event by event, original parton and gluon jets 0-52466  
 Kuti-Weisskopf model, quark distrib. in mesons (*Russian*) 0-13291  
 ladder model of QCD, hadron struct. 0-37213  
 large  $p_T$  interactions, quark existence studies 0-37235  
 lattice gauge theory,  $Z_N$  Abelian group, phases, duality 0-42323  
 lattice models of quark confinement at high temperature 0-32082  
 lattice QED with low coupling confinement studies 0-18095  
 light quark spectroscopy, review 0-42424  
 local spin- $1/2$  wave equations and harmonic confinement 0-4926  
 long lived hyperstrange multi-quark droplets in MIT bag model 0-9137  
 low transverse momentum fragmentation processes, quark-gluon struct. of hadrons 0-22561  
 magnetic monopoles, non-Abelian, stability analysis, Yang-Mills equations 0-31987  
 massive gauge-invariant QCD, quark confinement and vortices 0-384  
 massive Schwinger model, saturation, fermion confinement and instantons 0-47175  
 massless non-abelian gluon confinement and rising total cross sections 0-13264  
 meson mass spectrum, planar bootstrap, and Regge approach 0-22581  
 meson weak and EM decays, relativistic confined quarks, MIT bag model 0-47277  
 mesons, deformations and spectral props. 0-13203  
 mesons, heavy, one-parameter potential 0-13279  
 MIT bag model, coloured quark and gluon constituents of mesons 0-4929  
 MIT bag model,  $G_2$  struct. function 0-4947  
 MIT bag model, two-dimens., confined massive field vacuum fluctuations 0-4921  
 mixing of gluon bound states and quark-antiquark states,  $\eta$  and  $\eta'$  appl. 0-47255  
 multi-quark meson states, struct. 0-9146  
 multi-quark states, obs. in  $pp$  formation and prod. expts. 0-9153  
 naive model, pre-flavour states, quark searches 0-18110  
 non-Abelian gauge theories, coupling constant IR props., glue propagator 0-31999  
 non-Abelian gauge theories, local covariant operator formation, quark confinement 0-47190  
 non-Abelian gauge theories, Faddeev-Popov ghost decoupling, QCD gauges and gluons 0-52406  
 nonlinear super-Poincare fermion, quantisation in bag like formulation 0-4923  
 nonlinear superfields and quark confinement (*Chinese*) 0-42346  
 nonlocal quark model in  $SU(3) \times SU^c(3) \times U(1)$ , meson decay and mass correction (*German*) 0-27456  
 nucleon form factors, asymptotic relations from quark-gluon model, scaling violation 0-42463  
 orthoquarkonium decay, Dalitz plot population and thrust ang. distrib., scalar gluon nonexistence 0-27470  
 particle struct. studies, book 0-41952  
 pathological lattice field theory for interacting strings 0-47186  
 Pati-Salam neutral vector gluons, possible expt. search in  $e^+e^-$  collisions 0-37202  
 perturbative QCD, hard hadronic processes,  $e^+e^-$  annihilation, lepton-hadron deep inelastic scatt. 0-52477  
 phase transitions in two dimensions, and quantum field theory, analogies, review 0-52149  
 pole-dipole relativistic string model 0-386  
 power law confinement potentials, bound states 0-18123  
 QCD, 2-dimens., Bose form,  $SU(N)$  confining phase 0-52463  
 QCD, baryons in  $1/N$  expansion, mesons and glue states 0-13267  
 QCD, hadron interaction effective string lagrangian, Regge slope, charmonium pot. model 0-4939  
 QCD, higher order, charge conjugation asymmetries from two gluon exchange 0-4935  
 QCD, quark and gluon propagators 0-52469  
 QCD, quark confinement, background theory 0-18113  
 QCD, weak coupling approx. Schwinger-Dyson eqn. (*Chinese*) 0-52476  
 QCD and dual resonance model vertices, string prod. operators, singlet colour states (*Russian*) 0-42410  
 QCD and hadronic structure 0-42416  
 QCD perturbation theory for confined quarks and gluons,  $p$  glue content 0-52460  
 QCD perturbation theory for confined quarks and gluons 0-401  
 QCD phenomenology, quarks and gluons in medium energy nuclear physics 0-42563  
 QCD theory for the strong interaction 0-4962  
 QCD transverse lattice theory, confinement and hadron bound states 0-4961  
 QCD vacuum nonperturbative fluctuations, bag effect in low  $p_T$  hadronic spectra 0-37218  
 quantised dual string theory, string functional and propagators 0-32088  
 quantum mechanical applications to quarkonium 0-27484  
 quantum-chromodynamic phenomenology of gluon jets 0-4941  
 quark and gluon jet longitudinal momenta, QCD anal. 0-22571  
 quark recombination mechanism in multi-hadron production 0-18114  
 quark-gluon phase transition 0-27475  
 quarkonia, S- and P-wave, gluon jets, perturbative QCD anal. 0-32070  
 quarkonia, spectra, decays, levels, jets, sum rules 0-18112  
 quarkonium, observed dynamical groups 0-9149

## quark confinement continued

quarkonium mass spectra, one gluon exchange corrections, gauge invariance and choice 0-52483  
 quarkonium systems, binding energy effect on mass spectra 0-37229  
 quaternionic Hilbert space and colour confinement, admissible symmetry groups 0-27458  
 quaternionic Hilbert space and colour confinement 0-27457  
 relativistic string model generalisation in geometrical approach, Yang-Mills approx. 0-383  
 Roper resonance photocoupling in relativistic quark model with scalar confining pot. 0-4936  
 Schrodinger wave equation soln. for logarithmic pot. 0-32065  
 solitons in some geometrical field theories 0-27390  
 space-like fields for quark confinement 0-42426  
 static confinement conditions, two-dimens. anal.,  $SO_2$  mesons 0-13262  
 static Euclidean  $SU(2)$  solns., global struct. 0-4862  
 string operator eqns. of motion in QCD 0-4953  
 string reconstructions and quark matter 0-37226  
 string representation of gauge fields, chiral field topological props. 0-52410  
 strings in non-Abelian gauge theories 0-52403  
 $SU(2)$  colour Yang-Mills theory, quark source charge screening, confinement 0-22565  
 $SU(5)$  grand unification, nucleon lifetime, bag model calc. 0-52450  
 superrenormalisable abelian gauge model with confinement in four dimensions 0-31998  
 time space structure and quark confinement 0-4964  
 two photon processes, manifestation strength of colour below and above colour threshold 0-381  
 $U(N)$  lattice gauge theories with quarks, string eqns., Dyson-Schwinger eqns. 0-4857  
 $U(N)$  lattice gauge theory, string representation, Wilson loop amplitudes 0-4856  
 $U(N)$  lattice Yang-Mills theory, Schwinger-Dyson eqns., string model equivalence 0-4855  
 vector gluon-quark theories, Nambu-Goldstone realisation proof 0-22563  
 vortex condensation mechanism for static quark confinement, Abelian gauge theories 0-52457  
 Wilson loop expectation value, area law and loop wave eqn., quark confinement 0-47185  
 Yang-Mills instanton gas, bag-to-vacuum phase transition, mean field approx. 0-9097  
 Yang-Mills lattice gauge theories, comparison with gauge groups  $SU(2)$  and  $Z_2$  0-31966  
 $\chi_c \rightarrow \gamma\psi$ , charmonium states radiative and hadronic widths, gluon spin 0-4998  
 $D^0 \rightarrow K^0 \pi^0$ , branching ratio from final state soft gluon exchange 0-52498  
 $e^+e^-$ , annihilation, polarised gluon bremsstrahlung as QCD test 0-32077  
 $e^+e^-$ , weak corrections to three-jet angular distributions 0-22629  
 $e^+e^-$  annihilation, gg and qg coupling equality on resonance, QCD calcs., expt. tests 0-389  
 $e^+e^-$  annihilation, gluon jets and heavy quarkonium prod., QCD test,  $\psi$  prod. 0-42479  
 $e^+e^-$  annihilation, hadronic final state charge current asymmetry, QCD test, neutral gluons 0-37289  
 $e^+e^-$  annihilation, hard gluon bremsstrahlung from heavy quarks, jet cross section 0-32078  
 $e^+e^-$  annihilation, two and three gluonic jet prod., perturbation theory (*Russian*) 0-52525  
 $e^+e^-$  annihilation, vector or scalar gluon jets 0-27474  
 $e^+e^- \rightarrow e^+e^- + 2$  gluon jets from  $\gamma\gamma$  interactions cross section, gluon role in QCD 0-4976  
 $e^+e^- \rightarrow e^+e^- gg$ , gluon jet polarisation in photon-photon scatt., QCD test 0-52550  
 $e^+e^- \rightarrow hX$ , high energy predictions from perturbative QCD 0-42417  
 $e^+e^- \rightarrow$  hadrons, 13-31.6 GeV, gluon bremsstrahlung evidence, seagull effect, one sided jet broadening 0-430  
 $e^+e^- \rightarrow$  hadrons, planar events, gluon jet identification 0-47317  
 $\eta'$ , QCD sum rules for mass, possible pseudoscalar gluonium, instanton effects 0-388  
 $\gamma^* \rightarrow \psi N$ , gluon momentum, spin, parity and coupling 0-42395  
 $J/\psi$  decay, gluon source, search for scalar gluonium, QCD 0-47296  
 $\Lambda_b^0$  octet baryon mag. moment, MIT bag model 0-47290  
 $\Lambda_c^+$  lifetime, semileptonic branching fractions, nonspectator quark interactions 0-37260  
 $\mu N \rightarrow \mu X$ , broken colour gauge theory of integer charge quarks 0-13313  
 $N^*$  resonances, radiative decays, static quark bag model (*Russian*) 0-47299  
 $nd \rightarrow p\pi d$ , interference phenomena in coherent production, nucleon diffractive amps., helicity-flip 0-47329  
 NN short range interaction, six quark symmetry props., nucleon colour mag. attraction (*Russian*) 0-42411  
 $\nu N$ , quark properties and existence studies, book contrib. 0-42441  
 $\nu$  nonleptonic decay branching ratios from Weinberg-Salam and MIT bag models 0-37261  
 $pd \rightarrow p\pi^+ \pi^- d$ , interference phenomena in coherent production, nucleon diffractive amps., helicity-flip 0-47329  
 $pp$ , pp, 540 GeV, T and  $\psi$  transverse momenta from QCD 2 $\rightarrow$ 3 processes, gluon subprocesses 0-52546  
 $pp$  large  $p_T$  reactions, jets, dual-string approach 0-32136  
 $\psi$ , radiative decay, gluonic bound state  $O^-$  width 0-37272  
 $\psi \rightarrow \eta(\eta')\gamma$ , Ward identity anal.,  $\eta, \eta'$  quark-gluon struct. 0-42449  
 $\psi \rightarrow \psi\eta$ , Ward identity anal.,  $\eta, \eta'$  quark-gluon struct. 0-42449  
 $qg \rightarrow 1\gamma$ , high  $p_T$  photon polarisation as QCD test 0-4934  
 QQ mass, approx. scheme is QCD 0-42398  
 qq pair energy modification in Wilson loop formalism 0-18122  
 $\Sigma^+$  octet baryon mag. moment, MIT bag model 0-47290  
 t-quark, properties and signatures 0-37223  
 $\theta$  vector particles, calibration interaction macroscopic confinement radius (*Russian*) 0-47257  
 T, heavy quark bound states in potential model with relativistic corrections 0-37247  
 $\Xi^0$  octet baryon mag. moment, MIT bag model 0-47290

## quark models

see also colour model

$O^-$  meson, EM form factor in straton model (*Chinese*) 0-22616  
 $\Delta S=1$  nonleptonic weak decays,  $\Delta I=1/2$  rule, quark models and current algebra 0-47282  
 $\eta_c$  prod. cross section ratio in quark parton model (*Korean*) 0-27466  
 additive quark model with six flavours 0-27455



## quark models continued

algebraic approach to hadrons without seeing quarks 0-9143  
 antiquark sea role in determ. of  $\sin^2\theta_W$  from total neutron cross sections (Russian) 0-4910  
 bag model, lightest state mass determ. 0-42414  
 bag model of confinement, analogy to bubbles in liquid 0-22587  
 bag model  $Q\bar{Q}$  states, meson-nucleon low-energy S-wave scatt., P-matrix formalism 0-13271  
 bag model with finite potential barrier, S-wave mass spectra of  $Q\bar{Q}$  and leptonic widths 0-47242  
 baryon magnetic moment, incorrect value from static compound quark models 0-9169  
 baryon magnetic moments, implications for quark model 0-13290  
 baryon pionic transitions in MIT bag model using PCAC hypothesis 0-37228  
 baryon spectrum, second excited level in harmonic oscillator model, experimental situation 0-37233  
 baryonium, empirical evidence and theoretical interpretation review 0-42394  
 baryonium, molecular model, quark-diquark picture of baryon 0-27462  
 baryonium, S-matrix representation 0-399  
 baryonium masses in a quark model 0-37241  
 baryons, mag. moment calcs. in quark models 0-27505  
 baryons, with scalar raising pot., relativistic model 0-37231  
 beautyonium bound states, T, T', T'', dispersion sum rules (Russian) 0-13235  
 Bjorken scaling law violation, mass dependent, quark-quark interactions 0-9160  
 bound and rebound states, relativistic eikonal approximations 0-27491  
 bound state wave function explicit normalisation, decay widths calc. 0-18116  
 Cabibbo-suppressed nonleptonic D decays,  $\Delta I=1/2$  rule 0-52501  
 Callan-Gross relation, instanton violation, nonperturbation correction asymptotic behaviour 0-27409  
 centauro, Geminion and multipion events, quark matter hadronisation, prod. cross sections 0-47331  
 Chao-Yang statistics, particle ratios and quarks 0-27486  
 charmed baryons, elec. and mag. quarks rel. to Dirac mag. monopoles 0-402  
 charmed hadron masses, from effective quark masses, sum rules 0-4965  
 charmed meson mass splitting in universal confining potential model 0-4967  
 charmonium model and the  $\psi$  and T families 0-47253  
 charmonium pison states, confining pots. and inverse scatt. problem, T mass 0-4946  
 charmonium quark-antiquark pots., flavour independ.,  $\gamma$ ,  $\gamma'$ ,  $\psi$  and  $\psi'$  appls. 0-47254  
 charmonium spectroscopy, explicit soln. of wave eqn. for arbitrary power pots. 0-403  
 coherent state model for electron-positron annihilation 0-13321  
 composite models, mag. moments of quarks, leptons and hadrons 0-32081  
 composite quark and lepton model 0-27473  
 conference, quarks and leptons as fundamental particles, Schladming, Austria, (Feb.-Mar. 1978) 0-17709  
 conference, trends in physics, York, England (Sep. 1978) 0-31416  
 conference on hadron struct. and lepton-hadron interactions, Cargese, France (July 1977) 0-4473  
 constituent quark model and production of particles from nuclear targets 0-380  
 constituent quarks in SU(3) and SU(6), current algebra., hadron decays, review, book contrib. 0-47259  
 coupling  $S^*$  and  $\epsilon$  to  $\pi\pi$  and KK 0-22580  
 current quark masses and symmetry-breaking effects 0-4952  
 deep inelastic scatt., hadron secondary average transverse momentum, comparison with  $e^+e^-$  annihilation 0-37281  
 deep inelastic struct. functions 0-42461  
 dense quark matter, thermodynamic functions, instanton contrib. 0-52464  
 DESY  $e^+e^-$  experiments, QED checks,  $\tau$  and T studies 0-18111  
 dilepton production in  $\nu(\bar{\nu})$  reactions, bottom quark excitation contrib. 0-42439  
 diquark contribs. to scaling violation and deep inelastic  $\sigma_L/\sigma_T$ , structure functions, QCD 0-22573  
 discrete mass eigenstates and hadron-hadron low energy scatt. 0-42415  
 Drell-Yan scaling, absorptive corrections, for initial and final hadronic state interaction 0-4950  
 dynamical Higgs mechanism, weak  $\Delta I=1/2$  rule, sum rules, heavy quarks and leptons 0-27442  
 elastic scattering between binary quark-antiquark system and local field 0-47244  
 explosive quark matter, hypothesis for Centauro event 0-22648  
 flavour and colour quark groups, unitary symmetry links 0-9151  
 flavour independence of forces between quarks,  $\psi$  and T spectra 0-22569  
 flavour number determination using Higgs scalar particle 0-13288  
 fragmentation function, low transverse momentum hadron fragmentation 0-13261  
 free quarks 0-13289  
 gauge theories, box diagrams with nonvanishing external four-momenta, massive-external-quark 0-22525  
 Gelfand pattern, charmed hadrons and magnetic moment 0-398  
 Gross-Neveu model, mass generation, renormalisation 0-27393  
 ground-state baryons in a quark model with hyperfine interactions, masses 0-4944  
 hadron+hadron, jet production, large transverse momentum 0-42503  
 hadron EM interactions, review 0-412  
 hadron EM mass differences and struct. 0-27502  
 hadron high energy struct. models (Hungarian) 0-4924  
 hadron interactions, local thermodynamic equilibrium (Russian) 0-9155  
 hadron lepton model interpretation of particle resonance states 0-4957  
 hadron matrix elements in relativistic quark model 0-37238  
 hadron microstructure, de Sitter microuniverse, relativistic Hooke group and nonrelativistic quark model 0-27480  
 hadron spectroscopy, quark models and SU(5) grand unification scheme 0-4958  
 hadron-lepton deep inelastic scatt., review, book contrib. 0-47260  
 hadronic coupling constants and the nonrelativistic quark model with charmonium potential 0-37207  
 hadronic matter, phase transition of second band, anal. in one-loop theory in renormalisable field theory 0-4930  
 hadronic matter exponential mass spectrum, incompatibility with weakly interacting quark phase 0-37219

## quark models continued

hadrons with charm, beauty and taste, mass sum rules and SU<sub>3</sub> subalgebras of SU<sub>6</sub> 0-9152  
 hamiltonian for the nonrelativistic two-fermion bound state 0-13273  
 heavy quark (b,t) bound states, phenomenological estimates 0-47262  
 heavy quarks, possible exotic charge or baryon number 0-47245  
 heavy triply charmed spin  $3/2^+$  baryon, radial excitation spectrum 0-27482  
 heavy vector meson annihilation rate to lepton pairs, hadronic corrections 0-4943  
 Higgs induced neutral currents, natural flavour conservation and quark mixing angles 0-42392  
 high energy neutrino physics, recent expt. results 0-4982  
 high mass dilepton prod., comparison with Drell-Yan formula in asymptotically free theories 0-4942  
 horizontal-quantum-flavour-dynamics approach to the fermion mass spectrum in  $[SU(2) \times U(1)]_{WS} \times U'(1)$  gauge 0-52474  
 hypercharge-exchange reactions,  $K^-p$  and  $\pi^+p$  at 10 and 16 GeV/c, comparison with additive quark model prediction 0-13335  
 integral and fractional charged quark model test using  $\eta$  and  $\eta'$  props. 0-32074  
 interquark potential, instanton contrib. in dilute gas approx. 0-37220  
 isospin-violating mixing in meson nonets, dd-uu(ss) mass differences 0-32096  
 jet cross sections and quark current-photon pointlike coupling, sum rules 0-32104  
 Kobayashi-Maskawa model, Cabibbo-like parameter and quark mass relation (Chinese) 0-42408  
 Kobayashi-Maskawa six quark model, mixing angles, mass matrix and CP violation 0-13284  
 Kuti-Weisskopf model, quark distrib. in mesons (Russian) 0-13291  
 lepton and quark spectra difference eqns.,  $\tau$  and toponium mass 0-22589  
 long lived hyperstrange multi-quark droplets in MIT bag model 0-9137  
 Lorentz groups, homogeneous and inhomogeneous, teaching method to illustrate difference 0-17766  
 Lorentz transformation for quark processes, interaction with hadronic sea 0-37236  
 low transverse momentum fragmentation processes, quark-gluon struct. of hadrons 0-22561  
 meson and baryon prod. sum rules in quark recombination model 0-4922  
 meson isosinglets, mixing angles, non-relativistic quark model, Schwinger-type mass relations for SU<sub>4</sub> and SU<sub>3</sub> 0-18125  
 meson isosinglets, mixing angles, non-relativistic quark model, SU<sub>3</sub> and SU<sub>n</sub> 0-22591  
 meson mass spectrum, planar bootstrap, and Regge approach 0-22581  
 meson mass spectrum and unitarity in quark model 0-18115  
 meson P-wave radial mixing, effect on E1 radiative decays, charmonium mass 0-37271  
 meson strong decay, 2 quark-antiquark pair model 0-52496  
 mesons, heavy, one-parameter potential, linear confinement 0-13279  
 mixing of gluon bound states and quark-antiquark states,  $\eta$  and  $\eta'$  appl. 0-47255  
 modern atomic and nuclear physics (book) 0-11  
 modified Han-Nambu and SUB models 0-22562  
 multigeneration SU(2)<sub>L</sub>  $\times$  U(1)-based model, quark-lepton correspondence 0-22584  
 multi-lepton configurations in b and t decays from  $\bar{t}t$  and  $b\bar{b}$  0-18130  
 multilocal field theory description of hadron struct. 0-9148  
 multi-quark meson states, struct. 0-9146  
 muon scattering at Fermilab, inclusive scatt., quark models, scaling violation 0-5001  
 naive model, pre-flavour states, quark searches 0-18110  
 neutral currents, flavour-changing, Weinberg-Salam model 0-22553  
 neutrino flux from quark matter at core of collapsed stars 0-22028  
 nonlocal quark model in SU(3)  $\times$  SU<sup>2</sup>(3)  $\times$  U(1), meson decay and mass correction (German) 0-27456  
 nontopological solitons, hadron appl. 0-47191  
 nuclear force, parity violating, unified treatment 0-47400  
 nuclear forces, nonrelativistic quark model study, resonating group method 0-47403  
 nucleon internal structure, expt. evidence from IN collisions, book contrib. 0-42413  
 nucleon weak interaction pots. in the Weinberg-Salam model (Russian) 0-13258  
 O(10) theory of strong, weak and EM interactions, masses and mixing 0-13248  
 one boson exchange model, OZI rule, nucleon-nucleon-boson coupling 0-32066  
 particle struct. studies, book 0-41952  
 pion EM props., dressed quark model (Russian) 0-52508  
 pionisation influence on beam hardness, beam evolution eqns. for hadronic processes (Russian) 0-42407  
 point like spin-3/2 quarks, contrib. to deep inelastic struct. functions 0-47250  
 Pomeron and critical temp. 0-22566  
 pseudoscalar and vector meson decays, triangular quark diagram anomalies,  $\psi$ ,  $\eta$  and  $\eta'$  appl. (Russian) 0-42455  
 pseudoscalar mesons, EM mass shifts, quark-parton model, SU<sub>3</sub> quark triplet 0-42459  
 quantum field theory of extended hadrons 0-13270  
 quantum flavour dynamics, renormalisability conditions 0-42404  
 quantum fluctuations of quark fields, in arbitrary Yang-Mills instanton background 0-13268  
 quantum mechanical applications to quarkonium 0-27484  
 quark attenuation and recombination in nuclear matter, hadron-nucleus reactions 0-52601  
 quark lattice and QCD in nuclei 0-5101  
 quark mass ratio, chiral perturbation in new key 0-37208  
 quark parton model with large parton  $k_T$  0-42412  
 quark recombination mechanism in multi-hadron production 0-18114  
 quark strong interactions as weak interaction symmetry breaking mechanism 0-18117  
 quark-gluon phase transition 0-27475  
 quark-lepton correspondence in neutral current interactions 0-27450  
 quarkonia, spectra, decays, levels, jets, sum rules 0-18112  
 quarkonium leptonic decay rates for 1S and 2S states, constraints 0-37252  
 quarkonium mass spectra, one gluon exchange corrections, gauge invariance and choice 0-52483  
 quarks and leptons, high energy and nuclear physics interface 0-41974  
 Regge cuts, not applicable to multigraph and baryon models 0-27464



## quark models continued

Regge pole exchange amplitudes 0-404  
 relativistic covariant formulation, meson form factors (*Russian*) 0-9140  
 relativistic harmonic oscillator model, hadron EM interactions and props. 0-37225  
 relativistic oscillator formalism for hadron struct. and props. 0-9144  
 relativistic quark models,  $c\bar{c}$  and  $b\bar{b}$  singlet triplet splitting, mass formulae (*Russian*) 0-37232  
 Roper resonance photocoupling in relativistic quark model with scalar confining pot. 0-4936  
 sea quarks, null plane current anticommutators, sum rules and appls. 0-52436  
 six flavour model, mixing at small angles 0-27453  
 six quark model, CP nonconservation upper bounds in neutral theory meson systems 0-42397  
 six quark models, group theoretic anal. 0-9150  
 six-quark model, mixing angles, mass depend. on  $q^2$  0-37224  
 space-like fields for quark confinement 0-42426  
 spontaneous CP nonconservation in theories with more than four quarks 0-47212  
 standard weak-EM gauge model, six-quark phenomenology and Grand Unification 0-37204  
 Sterman-Weinberg formula for quark jets and gluon jets, leading log version, master equation 0-22552  
 string reconections and quark matter 0-37226  
 string-junction model, hair pin line rule and baryonium decay 0-27487  
 $(SU_2 \times U_1) \times S_n$  flavour dynamics, flavour number bound,  $n$  quark and  $n$  lepton generations unification 0-4907  
 $SU_1(3) \otimes U(1)$  gauge model, exact Cabibbo universality,  $\tau^-$  and  $X^-$  0-4852  
 $SU(2)_L \times SU(2)_R \times U(1)$  gauge with permutation symmetry, quark mass and Cabibbo angles 0-47232  
 $SU(2)_L \times SU(2)_R \times U(1)$  six quark gauge models, flavour violation 0-4951  
 $SU(2)_L \times U(1)$ , natural flavour conservation of Higgs couplings and Cabibbo mixing conflict 0-37200  
 $SU(2)_L \otimes U(1)$  theory, CP violation and Cabibbo angle 0-52447  
 $SU(2) \times U(1) \times U(1)$  model, Cabibbo angle and Higgs coupling strangeness conservation 0-47233  
 $SU(2) \times U(1)$  scheme, CP violation parametrization, quark  $n$ -doublet weak interaction (*Russian*) 0-13231  
 $SU(3)$  gauge model of weak and EM interactions, Weinberg angle, Han-Nambu quarks 0-52452  
 $SU(4) \times SU(4)$  symmetry breaking, Cabibbo angle, nonlinear hadronic Lagrangian, PCAC (*Russian*) 0-42360  
 $SU(4)$  16-plet boson mass formulas, flavour symmetry breaking 0-37250  
 $SU(5)$ , Clebsch-Gordan series, quark model appl. 0-47256  
 $SU(5)$  grand unification embedding in  $SU(N)$ ,  $SU(9)$  theory, flavour unification 0-32059  
 $SU(5)$  grand unified theory, flavour number limit from fermion mass higher order corrections 0-4904  
 $SU(6) \times O(3)_1$  multiplets, semilocal duality, quark-orbital Regge trajectories 0-27490  
 $SU(9)$  grand unification of flavor with three generations 0-13251  
 superconformal group and quark-like fermionic coordinates 0-9145  
 $T^+(10040)$  as an  $I=1$  vector meson resonance 0-47241  
 $t$ -flavoured meson production in photonuclear and  $pp$  collision 0-22623  
 Thomas-Fermi type picture of EM structure of  $\pi$  and  $N$  0-9170  
 three quark operators, anomalous dimensions, baryon form factors and quantum numbers 0-22568  
 three-quark systems, dynamics, linear mass spectra baryon models 0-42390  
 topped and bottomed hadrons, mag. moments in additive quark model 0-52478  
 vacuum polarization effects in lattice gauge theories 0-13211  
 vector gluon-quark theories, Nambu-Goldstone realisation proof 0-22563  
 vector meson production in  $pp$  interactions, constituent-interchange model 0-22579  
 vector mesons, leptonic decays, six-quark sequential model 0-52490  
 weak and EM interaction unification with strong interactions following  $\tau$  and  $T$ , book contrib. 0-47235  
 $B \rightarrow J/\psi$  + hadrons, branching ratio,  $b$  quark decay calcs. 0-32095  
 $B \rightarrow \psi K^*$ , search for  $b$  flavoured baryons 0-42450  
 $b$  quark  $\rightarrow \psi(\eta_c) + X$ ,  $B$  branching ratios assuring colour suppression 0-37259  
 $B^0\bar{B}^0$  mixing in six quark model, decay, mass mixing and CP nonconservation 0-42406  
 $c\bar{c}$  and  $b\bar{b}$  states, spectra and strong decays 0-52502  
 $\chi_c$  radiative decay,  $\psi$  and  $\psi'$  prod., straton coupling constants (*Chinese*) 0-42467  
 $\chi_L$  P-wave charmonium states, hadronic prod. cross section in  $K^-p$ ,  $\bar{p}p$ , and  $\pi^-p$  0-37292  
 D mesons, anomalous Cabibbo suppressed decay ratios, simple model 0-42452  
 D two body nonleptonic decays, quark model predictions 0-9164  
 $D^0 \rightarrow K^+K^-$ , Cabibbo suppressed decays, Penguin diagram contribution, mixing angles 0-22604  
 $D^0 \rightarrow \pi^+\pi^-$ , Cabibbo suppressed decays, Penguin diagram contribution, mixing angles 0-22604  
 $D^+$  decay, Cabibbo suppression, strong 20-plet dominance and W exchange 0-42453  
 $D^0 - D^+$  lifetime difference, possible mechanism  $D^0 \rightarrow s + \bar{d} + \text{gluon}$  0-37255  
 ed scatt., P-violation calc. in weak interaction theory 0-42469  
 $e^+e^-$ , jet cross sections and quark current-photon pointlike coupling, sum rules 0-32104  
 $e^+e^- \rightarrow$  hadrons, quark existence and theory 0-37234  
 $e^+e^- \rightarrow$  hadrons, scaling and quark struct. 0-425  
 $e^+e^-$  annihilation, hadron secondary average transverse momentum, comparison with deep inelastic scatt. 0-37281  
 $e^+e^- \rightarrow$  hadron jets, quark helicities, neutral current vector and axial couplings 0-32114  
 $e^+e^- \rightarrow$  hadrons, new flavour search at PETRA 0-37282  
 $e^+e^- \rightarrow$  jets, high energy,  $q\bar{q}$  pair conversion model, seagull effect 0-5007  
 $e^+e^- \rightarrow$  quarkonium state, D, F, T mesons, importance as experimental tool in new particle searches 0-42425  
 ep deep inelastic scatt., pol. p and e, straton model, sum rule (*Chinese*) 0-42475  
 $\eta(958)$ , three triplets of fractionally charged quarks 0-9172  
 $F^+$  decay widths and branching ratios, quark recombination widths, free quark model 0-27500

## quark models continued

$\gamma(10.0)$ , two-body hadronic and radiative decays, pseudo-dimension rule,  $\pi\pi$  and  $K\bar{K}$  suppression,  $SV_3$  singlet 0-52495  
 $\gamma\gamma$ , jet cross sections and quark current-photon pointlike coupling, sum rules 0-32104  
 $\gamma\gamma$  collision, deep inelastic, helicity method 0-22606  
 $\gamma N \rightarrow \psi(3.1) + \text{anything}$ , cross section and N charmed quark composition 0-423  
 $J/\psi$ , EM transition rates, geometrodynamical quark model 0-47295  
 $J/\psi \rightarrow \eta_c \gamma$ , radiational decays in charmonium (*Russian*) 0-13308  
 $K \rightarrow 3\pi$ , CP violation, current algebra anal., six quark Weinberg-Salam model 0-47281  
 $K_L \rightarrow \mu\bar{\mu}$ , quark mixing angle upper bounds in standard 6 quark model 0-18131  
 $\bar{K}N$ , below 1 GeV/c,  $Y^*$  states,  $SU(6) \otimes O(3)$  quark model classification 0-27523  
 $K^-p \rightarrow K^*(890) \Delta(1236)$ , 10 GeV/c, multidimens. anal., reaction sub-channel separation 0-32127  
 $K^+p$ , 32 GeV/c,  $\rho$ ,  $K^*$ ,  $\phi$  inclusive prod., quark fusion model 0-32135  
 $K_L^0 p \rightarrow K_S^0 \pi^+ + \pi^-$ , p, up to 17 GeV/c,  $Q^0-Q^0$  prod., cross sections 0-32129  
 $\mu N$  scatt., deep-inelastic, EM production of trimuons 0-22619  
 $\mu^- N \rightarrow \mu^- X$ , six-quarks model, upper bounds for  $t$ -quark production 0-13297  
 n electric dipole moment, quark and gluon corrections 0-4994  
 $N^*(1470)$ , Roper resonance, quark pair creation model soln. 0-47252  
 NN narrow meson resonances near threshold, theoretical approaches 0-9157  
 NN potential short range behaviour with the quark model 0-47409  
 $\nu$ , massless, left-right symmetric gauge models,  $SU_{2L} \times SU_{2R} \times U_1$  0-27461  
 $\bar{\nu} p \rightarrow \mu^+ X$ , deep inelastic scatt., MQM description 0-47305  
 $\bar{\nu} p \rightarrow \mu^+ + X$ , 4.5 GeV<sup>2</sup>, p struct. functions x depend., quark distrib. 0-32097  
 $\omega\phi$ -baryonium mixing model 0-32072  
 $\pi\gamma$ , one-gluon exchange, quark loop contrib. to photon total cross sections 0-4999  
 $pN$ , 300 GeV, quark fragmentation functions in additive model 0-37222  
 $pN$ , charm-pair production 0-22643  
 $pN$ ,  $\bar{p}N$ , 200 GeV/c, dimuon prod. cross section, Drell-Yan predictions, struct. functions 0-37300  
 $\bar{p}n \rightarrow \bar{p}p\pi^-$ , 2.98 GeV/c,  $\bar{\Delta}^{--}$  prod. in additive quark model framework 0-52529  
 $\bar{p}p$ ,  $\bar{p}p$ , Drell-Yan processes, scaling violation effects 0-382  
 $\bar{p}p, \bar{p}p$ ,  $Z^0$  high  $p_T$  bremsstrahlung, Higgs versus quark or gluon jets 0-32063  
 $\bar{p}p$  elastic scatt., FESR constraint on baryonium resonances, S, T, U, contrib. 0-27520  
 $pp$  multiple hadron prod. up to 1500 GeV, hadronic matter eqn. of state (*Russian*) 0-32085  
 $pp \rightarrow \pi^+ X$  reaction, quark-quark inelastic collision model (*Russian*) 0-32141  
 $\pi N$  in Al, quark jet multiple production 0-9188  
 $\pi^+ N$ , 200 GeV/c, dimuon prod. cross section, Drell-Yan predictions, struct. functions 0-37300  
 $\pi^- p \rightarrow \phi n$ , quark line rule, violations 0-52530  
 $\pi^+ p \rightarrow (\pi^+ \bar{p}) p$  50 GeV/c, narrow baryonium states, diffractive prod. cross sections 0-442  
 $\pi^+ p \rightarrow \Lambda X$ , 32 GeV/c, cross section, quark recombination model 0-52541  
 $\pi^+ p \rightarrow \pi^+ \pi^+ \pi^-$ , 16 GeV/c, clustering, multidimens. study using Yang variables 0-5020  
 $\tau$  and  $b$ -quark spin value, implications for quark and lepton theories 0-32076  
 T family, EM transition rates, geometrodynamical quark model 0-47295  
 $v$  p-wave ground state, mass scaling inequalities for quarkonium levels 0-32071  
 $D^0$ ,  $D^+$  decay widths and branching ratios, quark recombination widths, free quark model 0-27500  
 $\Delta(1236)-N(939)$  mass difference from deep inelastic scatt. quark wave functions, hyperon masses 0-47289  
 $\psi \rightarrow \chi_0 \gamma$ , radiational decays in charmonium (*Russian*) 0-13308  
 $S^*-\delta^0$  scalar meson mixing as threshold phenomenon from coupling constants 0-27477

## quarks

see also quark confinement; quark models

affinity to water molecule, centre expansion SCF calcs. 0-43213  
 $b$ -quark,  $SU(5)$ , broken, meson mass formulae 0-47267  
 character, possibility of simple constituents 0-42437  
 Clifford algebra based unified theory for quarks and leptons 0-47228  
 colour magnetic moment 0-42400  
 composite models, mag. moments of quarks, leptons and hadrons 0-32081  
 composite quark and lepton model 0-27473  
 cosmology, quark era in primeval Universe 0-36746  
 current quark masses and symmetry-breaking effects 0-4952  
 deep inelastic lepton scatt. in nuclei, energetic quark beam prod. 0-47304  
 dyonic models of hadrons, quark mag. charge allowed values (*Russian*) 0-13275  
 electron-hadron interactions, P-invariance, lepton, quark anapolar moments with pol. e (*Russian*) 0-52518  
 elementary particle physics, information from astronomical observations 0-51935  
 Fermi-Bose couple of coloured preons, primordial QCD, leptons and quarks 0-52461  
 fractionally charged in matter, existence searches 0-42513  
 fractionally charged ions, search in He gas 0-8954  
 free quarks, production in early universe 0-393  
 hadronic charmed particle decays, quark and particle helicities, charm changing current chirality 0-37256  
 hadronic decays of quark-antiquark resonances, suppression 0-9163  
 heavy quarks, EM shift of energy levels due to confinement, bag model 0-13287  
 heavy quarks, possible exotic charge or baryon number 0-47245  
 infrared properties of quark gas 0-395  
 isospin violating mass differences and mixing angles, quark mass and QCD 0-52505  
 Kobayashi-Maskawa model, Cabibbo-like parameter and quark mass relation (*Chinese*) 0-42408  
 lepton and quark spectra difference eqns.,  $\tau$  and toponium mass 0-22589  
 leptoproduction,  $\mu N \rightarrow \mu X$ , broken colour gauge theory of integer charge quarks 0-13313



## quarks continued

- low lying baryons, anomalous mag. moment contrib. from quarks 0-42462  
 magnetism in neutron star superdense core 0-8646  
 mass, chiral charge space, statistical analysis 0-42428  
 mass, symmetry-breaking in hadron spectra 0-42436  
 mass of third and fourth generation quarks, prediction 0-18133  
 mass of u and d quarks from weak and EM interaction model 0-13254  
 masses from Weinberg-Salam model renormalisation group eqns. 0-42377  
 mesonic processes and quarks in nuclei 0-42564  
 nucleon Fermi motion in deuteron, smearing effects, (West  $\beta$  correction), on expt. results. 0-32107  
 O(10) theory of strong, weak and EM interactions, masses and mixing 0-13248  
 physical pion low energy photo- and electroprod., photoprod. phenomenology, quark mass 0-5004  
 QCD, perturbative contributions to quark masses 0-47249  
 spin, relation to isospin, strangeness and charm 0-37183  
 SU(2)<sub>c</sub> × SU(2)<sub>R</sub> × U(1) gauge with permutation symmetry, quark mass and Cabibbo angles 0-47232  
 SU(3) quark-meson  $\sigma$ -model, quark masses 0-47178  
 SU(5) combined quark-lepton decuplets, particle families (*Russian*) 0-47217  
 SU(5) grand unification, strong CP violation, quark-lepton mass ratio 0-32057  
 SU(n) decomposition theorem, appl. to CP violation through quark mass diagonalisation 0-47216  
 SU(N) grand unification with several quark-lepton generations 0-27443  
 t-quark production by  $\nu$  and  $\bar{\nu}$  semileptonic decay 0-13297  
 top quark production, deep inelastic  $\nu$ N scatt., Bjorken scaling law violation 0-9160  
 unified description of quarks and leptons using colour and flavour degrees of freedom 0-27445  
 unified theory of weak interactions of leptons and quarks, gauge model 0-22556  
 weak quark and lepton chiral symmetries, dynamical breaking gauge interaction 0-47215  
 Yang-Mills theory, magnetic monopoles in the presence of quark sources 0-13213  
 c-u mass difference, baryon mag. moments 0-37240  
 $e^+e^-$  annihilation, heavy quark jet ang. distrib., quark mass, QCD anal. 0-42481  
 $\nu_e(\bar{\nu}_e)$ N, c arm meson prod. and decay, lepton inclusive distrib., c-quark fragmentation function (*Russian*) 0-52493  
 t-quark, mass in SU(3) horizontal symmetry 0-37230  
 t-quark, properties and signatures 0-37223  
 U +  $^{20}\text{Ne}$ , quark matter, signature in nuclear fireball model 0-37395

## quartz

- $\alpha$ -phase, constitutive eqns. by group theoretic methods 0-1954  
 acoustic resonance vibrations, Berg-Barrett X-ray diffr. method 0-40063  
 adsorbed multilayers of water, surface forces 0-6597  
 alpha particle induced radiation defects, EPR and thermoluminescence study 0-20461  
 amorphous layer on mech. treated single crysts. electron microscope and RHEED obs. 0-24721  
 anthracene-quartz interface exciton luminescence, Frenkel exciton metallic quenching (*Russian*) 0-50421  
 bent perfect crystal, diffractive focusing, X-ray spectroscopy (*Russian*) 0-54076  
 birefringence measurement using photoelastic modulator 0-31838  
 c-axis orientation in Saxony Granulites, petrofabric anal. by optical and X-ray diffr. studies 0-21740  
 ceramic, physicomach. props., influence of surfactant incorporated during synthesis 0-20856  
 ceramic, quartz glass based, organosilicon binder, spalling-resistant, prod. 0-40313  
 ceramics, thermal and temp. cond. in range 500-1900K 0-39370  
 CNDO/2 MO calc. of SiO<sub>2</sub> polymorphs 0-6386  
 complex dielec. const. at audio freqs., 5.5 to 380K 0-25272  
 crystal, AT-cut, ion plating of Ag film, crystallographic structure obs. 0-2280  
 crystal flexure bars and tuning forks, frequency-temp. characts. 0-5971  
 crystal growth in fluoride environment, growth features and props. 0-6373  
 crystal lattices of SiO<sub>2</sub> system, spatial symmetry laws 0-19784  
 crystal microbalance with coatings of finite viscosity, transmission line analogy 0-17933  
 crystal units, vacuum system for cleaning and cold welding (*Polish*) 0-31776  
 Dauphine twinning, stress-induced, acoustic emissions 0-6414  
 defects growth, study by X-ray diffr. topography (*French*) 0-39095  
 delay line second harmonic generation in SAW (*French*) 0-34285  
 density of states, bulk electronic struct., tight binding calcs. 0-44502  
 distribution in Atlantic sediments relation to climate, last glaciation 0-8308  
 doubly rotated  $\alpha$ -quartz plates vibrating in thickness, zero polarizing effect 0-55038  
 electron beam irradi., defect form., annealing and migration effects, ESR obs. 0-50180  
 electron pulse irradiation effect on defect formation 0-15155  
 erosion of windblown quartz sand on Mars 0-17525  
 far IR ordinary-ray optical constants 0-45025  
 ferroelastoelectricity, expt. 0-40078  
 fibre, torsion balance, sat up by welding fused quartz rods and fibres (*Japanese*) 0-31738  
 glass, IR emissivity, 673-1673K 0-24623  
 glass, spectral absorpt., 3000-4000K 0-25401  
 glass, spectral absorpt. coeff., 0.25 to 1.25  $\mu$  and 1300 to 1700K 0-20622  
 glass, surface energy evaluation, by a microindentation method 0-16473  
 glassy quartz, thermal expansion coeffs., represented by Gaussian spline polynomials 0-44341  
 Gruneisen parameter, meas. at high press. 0-8299  
 HF acoustic losses, measurement using Fabry-Perot acoustic interferometer 0-5887  
 high purity, impurity distrib., neutron activation anal. 0-24485  
 hydrogenic trapped hole species in  $\alpha$ -phase, EPR studies 0-44915  
 hydrothermal crystallisation, role of soln. density 0-10516  
 impurity C determ. by isotopic spectral method 0-26093  
 intrinsic luminescence 0-16098

## quartz continued

- intrinsic Q estimation 0-43578  
 irradiated, fused, crystalline, absorpt. spectra, colour centres 0-7384  
 lattice constants, impurity effects 0-39034  
 microtopographical obs. of 2nd order prism faces, hydrothermally-grown crysts. 0-54481  
 muonium EPR transitions by muon-spin rot. 0-29668  
 muonium hyperfine splitting meas., muon spin rot. technique 0-50246  
 natural, gamma-irradiated, stress effect on thermolum. sensitivity 0-11482  
 natural, virgin ( $\gamma$ -irradiated), polarisation effect on thermolum. sensitivity 0-11483  
 opalescence near  $\alpha$ - $\beta$  transition, static model rel. to domain wall form. 0-11420  
 optical fibres, acoustic modulation of light propagation 0-33209  
 particle, EM wave irradiated, evaporation, diffusion approx. 0-44308  
 phase transition,  $\alpha$ - $\beta$ , in natural and synthetic quartz crystals, effect of impurities 0-20928  
 phase transition, high-low, effect on compressional and shear wave velocities in rocks under high press. 0-12380  
 photochromic fused quartz, LITMO, optical props. 0-1287  
 quartz:Fe absorption spectra and structural state of Fe<sup>3+</sup> ion 0-16071  
 $\alpha$ -quartz, ferroelastic hysteresis 0-19869  
 quartz, grinding and surface treatment by ball mill in cetyl alcohol (*Japanese*) 0-25890  
 quartz, nonlinear polarisation plane rotation due to ruby laser irradi. (*Russian*) 0-53390  
 $\gamma$ -quartz, reaction, with NaCl-KCl melt, exam. of struct., IR absorption spectra 0-55706  
 resonator, nonlinear thermoelastic couplings (*French*) 0-34118  
 resonators, thickness-mode, thermal stress effects on reson. freq., theory 0-50272  
 SAW cut with orthogonal temp. compensated propag. directions 0-10770  
 SAW diffraction 0-38160  
 SAW dispersive delay lines, new cut of quartz for temperature stability 0-19185  
 SAW GHz quartz transversal filters, fabrication limits and characteristics 0-43562  
 smoky,  $\gamma$ -irrad., electric dipolar echoes 0-20604  
 smoky quartz, thermal props. at very low temp. 0-24610  
 spectral excitation in inert gas medium, detection limits of contaminants 0-55746  
 substrate, adherence of Ti and Cr films 0-7496  
 substrate, chemical vapour deposition of TaB<sub>2</sub> 0-29880  
 surface, action of glow discharge (*Russian*) 0-25886  
 surface, polymolecular adsorbed layers of water, IR absorption spectra 0-9595  
 surface, seasoned, cyclobutene decomp., variable encounter method calcs. 0-50885  
 surface, viscosity of nonfreezing thin interlayer between ice column and quartz capillary 0-54475  
 surface skimming bulk waves, excitation and detection on rotated Y-cut quartz 0-43492  
 surface space-charge layer form. on  $\gamma$ -irrad. 0-10575  
 synthetic, as-grown and etched cobbled Z-surfaces, SEM obs. (*French*) 0-24719  
 synthetic, dislocations obs. by light scatt. tomography 0-49229  
 synthetic, electron beam irradi.-induced interstitial ion mobility, ESR centres and IR spectra meas. 0-39153  
 FTIR diagnostic windows, radiation damage 0-34063  
 transducer for shear US meas. of aqueous liquids 0-53599  
 tube orifice leaks for local, fast-response gas sampling to mass spectrometers 0-35609  
 twinned crystals, after Japan Law, investigation of regrowth 0-54162  
 US absorption, influence of plastic deform. and electrostatic field (*Russian*) 0-39226  
 wedge, refl., transmission and conversion of normally incident SAW 0-2257  
 Z-cut crystal with Ge additive, radiation attenuator appl., 0.25 to 1  $\mu$ m, with attenuation coeff. up to 10<sup>3</sup> 0-48415  
 Al<sub>2</sub>O<sub>3</sub>-B<sub>2</sub>O<sub>3</sub>-SiO<sub>2</sub> system, liq. phase calc. for commercial quartzite powders 0-25671  
 SiO<sub>2</sub>-Cr<sub>2</sub>O<sub>3</sub>-TiO<sub>2</sub>, ceramics, creep and porosity, for ceramics with different structures 0-21011  
 WC-Co cemented composites, abrasion by quartz 0-16495

## quartz resonators see crystal resonators

## quasars

- see also BL Lacertae-type objects; cosmology; galaxies; radiofrequency cosmic radiation; stars  
 0043+389, strong emission line quasar with redshift  $z=0.189$ , spectrum and photometry 0-8710  
 0241+622, possibly associated with CG 135+1, low-energy  $\gamma$ -ray obs. 0-31392  
 0957+561 A, B, twin QSOs, spectroscopic obs. with multiple-mirror telescope 0-12827  
 0957+561 A and B, twin QSOs, direct imaging rel. to gravit. lens interpretation 0-17686  
 1400 Å emission feature, rest wavelength and identification 0-12825  
 absolute magnitude-volume diagrams, appl. to cosmology (*French*) 0-8705  
 absorption lines, rel. to galactic coronae and intracluster medium origin 0-31355  
 absorption lines in QSOs of small and intermediate emission redshift, homogeneous survey results 0-31218  
 accretion disks in quasars and active galactic nuclei, theoretical review (*Polish*) 0-26739  
 accretion from gas-rich dwarf galaxies, rel. to quasars cosmological evolution 0-31349  
 annihilation model of quasi-stellar objects 0-22109  
 atmosphere instability rel. to cool regions in relativistic plasma 0-17486  
 B2 1225+31, abundances in  $z=1.7941$  absorpt. line system 0-12826  
 black hole model (*Japanese*) 0-22114  
 black hole supercritical disc accretion model 0-41850  
 5C3 sources, optical ident., spectroscopic results 0-46689  
 3C 147, 3C 380, milli-arcsecond struct. determined by hybrid mapping with five-station array 0-46694  
 3C 273, gamma-ray emission from Penrose powered black hole 0-56925  
 3C 273, quasar, second-order Compton interpretation of X-rays and  $\gamma$ -radiation 0-22106  
 3C 273, quasar containing dust, IR spectra obs. 0-56970



## quasars continued

- 3C 273, X-ray spectrum, 2-60 keV 0-12824  
 3C 273 (3U 1224+02), weak X-ray source, ANS meas. 0-46701  
 3C 286 spectrum, optical absorpt. lines obs. 0-4454  
 3C 345, optical spectrum variability 0-8709  
 3C 395, compact radio source, high resolution obs. at 1671 MHz 0-56960  
 coherent curvature radiation 0-56704  
 compact group of QSOs in Leo 0-27006  
 compact radio sources, relativistic jets model 0-4448  
 complete samples, volumes analysis 0-51899  
 diffuse gamma-ray emission from active galaxies 0-12806  
 distance determination, from correl. anal. of radio luminosity features and optical light curve (*Russian*) 0-51880  
 double radio sources, collimation 0-22098  
 dust opacity and photoionization in far UV 0-46696  
 emission lines, photoionisation models, dust in or near quasars 0-27009  
 energy loss by resonance line photons in an absorbing medium 0-56699  
 energy mechanism, Penrose photoproduction processes 0-31365  
 energy source models and cosmological evolution 0-27002  
 evolution with resolved components, deceleration parameter determ. 0-31386  
 extended radio sources, VLBI obs. of compact components 0-17680  
 extended sources, radiatively driven winds 0-51901  
 faint blue objects in high galactic latits., candidate QSOs catalogue near South Galactic Pole 0-46415  
 G-varying cosmology, galaxy and QSO magnitude/red shift relations 0-56980  
 gas clouds, radiatively driven, dynamics and stability of plane parallel slabs 0-22107  
 gravitational and Doppler redshifts, interpreted as massive black holes ejected from galaxies 0-46695  
 gravitational screens and superluminal separation 0-51896  
 gravitational-inertial field of Universe, crit. systems struct. 0-8720  
 hard X-ray spectra, models of unsaturated Compton accretion discs around supermassive black holes 0-22033  
 high redshift quasars, search for 21 cm absorpt. 0-4453  
 high-redshift QSOs, optically-selected, Image Dissector Scanner (IDS) spectrometry 0-22111  
 Hoyle-Fowler model, photon emission critical angle 0-31383  
 image doubling, assoc. with absorpt. systems 0-22112  
 information sources for neutron star, dense matter and gravitational collapse physics 0-36657  
 line identifications, red shifted UV lines or violet shifted IR lines 0-8707  
 low-red shift quasars fields, photoelectric UVB stellar sequences (*French*) 0-51904  
 luminosity function evolution ion Friedman model with zero pressure solns. (*Chinese*) 0-51905  
 luminosity functions for complete samples, observational magnitude cutoff bias elimination 0-56940  
 magnetic flare model, magnetised accretion disc around massive black hole 0-22113  
 magnitude estimation from Palomar Sky Survey prints 0-36510  
 Markarian 813, photoelectric UBVR photometry (*Russian*) 0-36721  
 Michigan-Tololo quasars, spectrophotometry 0-22105  
 NAB 0137-01, UVB photometry and brightness vars. 0-56967  
 narrow line region physical conditions 0-31364  
 NGC 1073 field, obs. of three QSOs lying in galaxy spiral arms 0-22110  
 OQ 172, H<sub>2</sub> lines in absorpt. spectrum 0-36734  
 OV-236 (1921-29), radio outburst obs. 0-51906  
 PHL 957, upper limits on Lyman  $\alpha$  halo 0-51907  
 PKS 0736+01, optical spectrum variability 0-8709  
 PKS 1157+014, spectral obs., of QSO with no L $\alpha$  emission 0-31384  
 pregalactic black holes as power source 0-56978  
 Q 0932+501, bright quasar with broad absorption features 0-46697  
 Q 0957+561, double quasar, intervening galaxy obs. rel. to gravit. lens hypothesis 0-27005  
 Q 2240.9-3702, Q 2238.9-4115, optically selected QSOs with broad-lined absorpt. systems spectra 0-4456  
 QSO 0241+622, nearby X-ray quasar, extended radio emission search 0-31382  
 QSO 0752+258 and 1049+616, new redshifts 0-46661  
 QSO 0957+561, H I 21 cm radio absorpt. line redshifted to 594 MHz 0-36735  
 QSO 0957+561 A, B, 1.666 GHz VLBI meas. and gravitational lens hypothesis 0-27007  
 QSO 0957+561 AB, flux var. and image splitting by stars 0-27008  
 QSO 1038+528 A,D, close pair of radio-emitting quasi-stellar objects, radio and optical obs. 0-51902  
 QSO candidates, spectroscopic obs., identifications 0-31385  
 QSO candidates and radio galaxies, optical spectroscopy 0-56966  
 QSO emission lines, hard X-ray effects 0-26974  
 QSO emission-line, radiatively accelerated clouds, structure, shape and evolution 0-17685  
 QSO radio emission, Faraday rotation and cosmological magnetic fields 0-22087  
 QSO/galaxy associations, redshifts and distances 0-31369  
 QSOs, new type, identified through IR meas. 0-8708  
 QSOs, relativistic jets and continuum emission 0-51898  
 radiation field, spectral shape effect on ionisation equilb., thermal equilb. and radiative accel. 0-41909  
 radio emission, from quasar group selected for optical brightness 0-41910  
 radio sources, ang. size-redshift diagram interpretation 0-22101  
 radio sources, double, separation depend. on redshift 0-22096  
 radio sources, extended, MHD instabilities and electron accel. 0-27000  
 radio sources, extended, relation between radio luminosity and spectrum 0-51894  
 radio sources, jets configuration and propag. 0-31374  
 radio-quiet quasars, Hubble diagram, luminosity function and density evolution 0-51903  
 radioastronomy, Z (*French*) 0-46411  
 red shift parameter  $\ln(1+z)$ , periodicity 0-17687  
 red shift-magnitude link for strong interplanetary scintillation (*Chinese*) 0-12828  
 relativistic blast waves in two dimensions, adiabatic case solns. 0-22108  
 Seyfert 1 galaxy nuclei, luminosity function and implications for X-ray background 0-8682  
 southern quasars, optical monitoring 0-56969  
 spectral characts. of three high redshift objects 0-4455  
 spectral props. of 85 quasars from spectrophotometry 0-51897  
 steep spectrum radiosources, spectral index dependent props. 0-36730

## quasars continued

- supercritical accretion discs winds struct. and appearance, numerical models 0-21984  
 surface density of QSOs 0-8706  
 surface distribution, intergalactic dust effects in visible, extinction 0-17651  
 synchrotron radiation model for IR emission 0-31387  
 Tautenburg objective prism survey quasars, high-resolution spectra and redshifts 0-4436  
 theory of H line emission from dense plasmas 0-51900  
 UV photoelectric photometry, of low-red shift quasars (*French*) 0-51904  
 UV excess objects, ubvi photometry 0-46698  
 UV excess objects in region of NGC 2639 companion galaxy, discovery and redshifts 0-56965  
 variable quasars as pulsating accretion discs 0-46693  
 X-ray properties from Einstein Observatory obs. 0-27004  
 H emission line ratios, implications 0-56968  
 H, line and continuum emission calcs. 0-27003  
 Mg II 2798 Å and H $\beta$  emission, line profiles 0-12807

## quasi-particles

- see also excitons; helicons; magnons; phonons; plasmons; polaritons; polarons; ripples; rotons; solitons  
 amorphous solids, low-energy excitations of phonons, magnons, electrons rel. to struct. factor 0-44488  
 Anderson model, quasiparticle lifetimes 0-44532  
 Bose gas, two-dimens., charged, in zero mag. field, quasiparticle energy spectrum and damping 0-142  
 boson-soliton scatt., sine-Gordon model 0-9109  
 Brownian quasiparticle model 0-46976  
 de Haas-van Alphen effect, quasiparticle approach 0-10897  
 dense gas, quasiparticle kinetic eqn. construction 0-53905  
 disordered systems, phonon-like excitations, dispersion and damping 0-49331  
 ferromagnetic metals, dislocation drag by conduction electrons 0-24451  
 hadron microstructure, de Sitter microuniverse, relativistic Hooke group and nonrelativistic quark model 0-27480  
 Josephson tunnel junction, interference current component, Riedel peak width (*Russian*) 0-11137  
 magnetic semiconductors, excitation spectrum, temp. and band occupation depend. 0-49588  
 magnetic soliton, in one-dimensional mag. systems, obs. (*Japanese*) 0-2555  
 nuclei in 2p-1f shell, quasi-particle-phonon interaction 0-22770  
 pairing rotations and quadrupole modes, many-quasiparticle excitations 0-18165  
 para-Bose states, generalised Bogoliubov transform. coeff. 0-27211  
 paramagnet, electron state density for narrow-band model with Coulomb interaction 0-10852  
 sine-Gordon equation, two soliton solutions, breather solution 0-12945  
 solid solution theory, quasi-particles method 0-24560  
 spin wave damping, magnetic materials with canted mag. struct., thermodynamic and high freq. props. 0-11184  
 superconducting film, photoexcited, phonon spectrum 0-11132  
 superconducting film, surface impedance, effects of quasiparticle redistrib. 0-44764  
 superconducting films, optically irradi., quasiparticle energy distrib. function 0-2527  
 superconducting phase slip centre, charge imbalance waves and nonequilb. dynamics 0-54830  
 superconducting states out of thermal equilb. stability 0-2526  
 superconducting weak link, short, with distinct chem. potentials at boundary 0-2528  
 superconducting-normal interface, boundary resist. 0-50006  
 superconductor, formation of nonequilibrium distribution, electron-electron collisions effect (*Russian*) 0-7033  
 superconductor, kinetic eqns. for electron excitations and phonons 0-7032  
 superconductor, quasiparticle charge imbalance induced by supercurrent with thermal gradient 0-34546  
 superconductor-insulator junction, quasiparticle nonlinear relax. to nonequilb. state (*Russian*) 0-7040  
 superconductors, kinetic eqns., nature and decay rate of new mode 0-49978  
 superconductors, nonequilibrium,  $T^*$  model of quasiparticle and phonon distrib. 0-25039  
 yrast-band of odd nuclei, quasi-particle-phonon interaction 0-22651  
 Al, superconducting, energy gap enhancement by tunnelling extraction 0-34564  
 Al, superconducting, quasiparticle charge distrib. due to tunnel injection 0-44771  
 He, dense gas, transport eqns., shear viscosity and acoustic vel., quasiparticle kinetic eqn. calcs. 0-53906  
<sup>3</sup>He quasiparticle excitation spectrum and second sound vel. meas., dil. soln. of <sup>3</sup>He in superfluid <sup>4</sup>He 0-24708  
<sup>3</sup>He, superfluid, sound propag. and kinetic coeffs., book contrib. 0-2237  
<sup>3</sup>He, superfluid A-phase, orbital dynamics 0-2232  
<sup>3</sup>He-<sup>4</sup>He, solid soln., struct. of vacancies 0-2242  
<sup>3</sup>He-<sup>4</sup>He, superfluid, osmotic and mag. props., review (*French*) 0-10733  
<sup>3</sup>He-<sup>4</sup>He quantum solns., spatial separation of opposite charges and dipole complex form. (*Russian*) 0-6588  
<sup>4</sup>He superfluidity, macroscopic quantum waves, bound quasi-particles 0-39378  
 Nb<sub>3</sub>Ge, superconducting thin films, energy gaps from tunnelling meas. 0-25050  
 Nb<sub>3</sub>Sn, superconducting thin films, energy gaps from tunnelling meas. 0-25050  
 Pb<sub>0.99</sub>Bi<sub>0.02</sub>-Cd, superconductor-normal-metal boundary resist., mag. field depend. 0-44772  
 Si, inversion layer, temp. depend. of subband energies, exchange and correlation effects 0-20281  
 Sn, superconducting current carrying film, resistive region boundary movement, ambient media depend. 0-44763  
 Sn, superconducting film, energy gap suppression and instability under strong quasiparticle injection 0-7042  
 Sn superconducting thin-film bridge, IV curves oscill. instability and quasi-particle recomb. (*Russian*) 0-44769  
 V<sub>3</sub>Si, superconducting thin films, energy gaps from tunnelling meas. 0-25050



quasi-stellar objects *see quasars*quasi-stellar sources *see quasars***quasimolecules**

- inert gas complexes spectroscopic data, geometry, pot. energy curve, dissoc. energy, equil. internuclear distance, determ. 0-53018  
 inert gas dimer+atom, IQSA calc. for total integral cross sections for excitation, exchange and dissoc. 0-1044  
 molecular X-rays from heavy-ion collisions, superheavy quasi-molecule spectroscopy 0-23509  
 superheavy quasimolecules, inner-shell vacancy formation, coupled channel anal. 0-48116  
 triatomic van der Waals complex, vibr. predissoc. and photodissoc. lifetimes 0-9661  
 van der Waals complex, formation, role of entropy 0-7840  
 van der Waals complex, prod. and rot. spectra assignments 0-5532  
 van der Waals complexes, IR continuum spectrum at low temps. 0-980  
 van der Waals dimers, intramolecular vibr. dynamics, vibr. predissociation 0-28083  
 van der Waals molecules, vibrationally excited, lifetimes, momentum gap 0-5601  
 Ar-O<sub>3</sub> Van der Waals complex, struct. and props., RF and microwave obs. 0-32704  
 CO<sub>2</sub><sup>-</sup>, hydrated anion stable gas phase heteronuclear clusters, mass spectra, autodetachment rates 0-14266  
 He pair, dispersion interaction, independent particle model, polarisabilities 0-37732  
 He<sub>2</sub>, 600 Å emission continuum 0-1012  
 He<sub>2</sub><sup>+</sup>, Van der Waals mol. vibr. predissoc. anharmonicity effects 0-52971  
 HeSr<sup>+</sup> states population probability in He(2s<sup>2</sup>S<sub>1/2</sub>)+Sr Penning collision 0-23533  
 KrF<sup>+</sup>, oscillatory bound-free emission spectra, semiclassical anal. method 0-7799  
 KrHCl, van der Waals complex, prod. and rot. spectra assignments 0-5532  
 N<sub>2</sub><sup>2+</sup>(<sup>3</sup>P<sub>0</sub>)+H, charge transfer, ab initio CI pot. curves and coupling-matrix elements 0-37878  
 Na+Ne, Na(3p) excitation 0-1056  
 Nb+Nb, selected MO X-ray coincidence with separated at. K X-rays 0-43148  
 Ne<sub>2</sub>, vibr. spectra, calc. from pot. curve 0-1040  
 Ne<sub>2</sub>+Ar, total integral cross sections for excitation, exchange and dissoc. 0-1044  
 Ne<sub>2</sub>+Kr total integral cross sections for excitation, exchange and dissoc. 0-1044  
 O<sup>+</sup>+Ne(Ar)(Kr), 0.2-1 keV, elastic and inelastic reduced differential cross-sections 0-32829  
 XeF, ground state dissoc. vibr. equilibrium 0-9652

**quench hardening**

- Elinvar,  $\gamma$  to  $\gamma'$  transformation and  $\gamma'$  phase form. kinetics, lattice consts. 0-35191  
 steel, low-alloy, case carburised, retained austenite effect on contact fatigue strength 0-30096  
 steel dies, durability improvement using isothermal hardening in salt bath 0-35198  
 Al, quenched, irradiated, and quenched plus irradiated, grain boundary hardening 0-3162  
 $\alpha+\beta$  Ti alloy VT3-1, drop forgings, grain orientation and props., combined mech. working, hardening and high-temp. heat treatment influence (*Russian*) 0-20973

**quenching (optical) *see radiation quenching*****quenching (thermal)***see also quench hardening*

- alloy, austenitic, mechanical changes after electrolytic quenching (*Russian*) 0-50653  
 amorphous alloy ribbons manufacturing, chill-block metal spinning process 0-29898  
 butadiene nitrile, soot filled, thermal treatment influence on mech. props. (*German*) 0-30000  
 composite superconductors, triple-phase phenomena, during quenching by pressurised superfluid <sup>4</sup>He 0-20364  
 filament reinforced hypoeutectoid C steel, strength characts. after deform. and quenching 0-35271  
 glass, coloured, toughening process, spectral characts. 0-43416  
 glass, flat, dependence of creep, viscosity on cooling intensity, during quenching 0-20964  
 glass, horizontal quenching, technological parameters rel. to optical properties 0-45264  
 glass thermopulishing, by use of low temp. plasma radiation (*Russian*) 0-45406  
 graphite nucleation, role of pre-heat treatments (*Japanese*) 0-35220  
 heat treated, stresses and cracks form. (*Czech*) 0-20977  
 isoprene rubber elastomers, thermal treatment influence on mech. props. (*German*) 0-30000  
 magnetic amorphous alloys, props. improvement and appl. 0-7693  
 metallic glass ribbons, quenching stabiliser to improve geometrical uniformity and cross-section 0-55343  
 metallic glasses, polymer model 0-6361  
 metallic glasses, structure, stability and prod., elec., mag. and mech. props., review 0-44134  
 polycarbonate, TSC anal. by activation energy spectra 0-20579  
 polyester-organic solvent mixtures, phase diagrams, eutectic props., devitrification, crystn. (*French*) 0-3015  
 polyethylene, annealed, crystallinity effect on mech. props. (*German*) 0-35230  
 polyethylene, linear, crystallised from melt, effect of crystallisation time on density, mech. props., X-ray scattering 0-25680  
 polyethylene, linear, glass transition temp. 0-15225  
 polyethylene, linear, quenching of thin films to amorphous state 0-28929  
 polyethylene, rapid crystn. from melt rel. to struct. 0-44152  
 polyoxymethylene, rapid crystn. from melt rel. to struct. 0-44153  
 polystyrene, glassy, light scattering, quenching effect 0-20649  
 real liquids, quenched to glassy state, struct., one dimens. Ising model appl. 0-54134  
 splat cooling process, using piston and anvil technique, mathematical model 0-11679  
 steel, 0Kh12G14N4Yu2, struct. after deformation under conditions of superplasticity 0-21031  
 steel, alloy, austenitic, grain size, tempering effect on brittle fracture susceptibility 0-55534  
 steel, alloy, high speed rapid stepless cyclic method 0-16352  
 steel, alloy, nonsteady temp. fields during cooling, calc. 0-16346  
 steel, austenitic Mn-Ni ageing, alloying element influence on struct. and mechanical props. (*Russian*) 0-35256  
 steel, austenitic stainless, type 00Kh18N20S3M3D3B, anticorrosion props., heat treatment effects 0-30168  
 steel, austenitic stainless, type 316, hydrogen embrittlement, tensile testing 0-7671  
 steel, C1020, dual phase, mech. behaviours and structs. (*Korean*) 0-25779  
 steel, C, martensitic by quenching 0-3038  
 steel, C, transform. kinetics, heat cond. and elastic-plastic stresses during quenching (*Japanese*) 0-25688  
 steel, cast, high tensile strength, heat treatment 0-16358  
 steel, Co-Cr-Ni-Mo-Mn (39.65, 20.25, 15.33, 7.08, 1.9 wt.%) carbide formation during tempering after plastic deformation 0-16330  
 steel, Cr, corrosion resist., tempering after air-hardening in rolling heat (*German*) 0-45324  
 steel, Cr-Al (12, 6 wt.%), ferritic stainless, high temp. treated, strengthening mechanisms 0-3106  
 steel, Cr-Mo-V, heat treated, mech. props. (*German*) 0-25724  
 steel, Cr-Ni, effect of tempering under load on mech. props. 0-16354  
 steel, cylinder, quenched without transform., residual stresses (*German*) 0-25725  
 steel, ferritic, with interstitial N, continuous precipitation and clustering 0-7585  
 steel, high C, high alloy, M<sub>23</sub>C<sub>6</sub> type carbides, effect of alloying elements on defect struct. and hardness 0-16481  
 steel, high purity, low S content, for tough semi-finished products in nuclear power plant (*German*) 0-45393  
 steel, high speed, type R6M5K5, secondary and red hardness of marquenching 0-16350  
 steel, high strength HP 9-4-20, retained austenite influence on fatigue crack propag. 0-21106  
 steel, Kh18N9T, strengthening by vibrational stirring effect 0-40405  
 steel, low alloy, brittle fracture, quenched and tempered 0-11677  
 steel, low C, effect of heat treatment on resistance to fatigue crack propag. 0-11675  
 steel, low C, Mn effect on recrystallisation and texture (*French*) 0-3110  
 steel, low C, packet martensite struct. and localisation of residual austenite, electron microscope obs. (*Russian*) 0-25695  
 steel, low C, quenched, interphase precipitates obs. (*Russian*) 0-29957  
 steel, low or medium alloy, work hardening effect on martensitic transform. cond. (*French*) 0-16329  
 steel, low-C, gas nitrocarburised, aged, fatigue behaviour 0-40514  
 steel, maraging, effect of deformation on props. 0-21032  
 steel, medium C, isothermally quenched, high-temp. deform. effects on struct. and props. (*Russian*) 0-25760  
 steel, medium C 0-11752  
 steel, microalloyed, alloy carbide precipitation during isothermal ageing 0-3077  
 steel, Mn-Cr-V, tool, quenched and tempered, fracture toughness (*German*) 0-25726  
 steel, Mn-Mo-Ni-Cr, bainitic, microstruct. and mech. props. (*French*) 0-16362  
 steel, Ni(9 wt.%), isothermal bainitic transform., thermomechanical effects on mech. props. (*German*) 0-40383  
 steel, Ni and W, recrystallisation mech. during laser treatment 0-50658  
 steel, Ni-Cr-Mo, quenched and tempered, notched bar tensile tests (*German*) 0-35247  
 steel, quenched, adsorption of P on austenite grain boundaries rel. to tendency to delayed fracture of type 18Kh2N4VA (*Russian*) 0-45378  
 steel, quenched, local H distrib. and internal microstresses (*Russian*) 0-50654  
 steel, quenched surface layer hardness rel. to adsorption contact fatigue (*Ukrainian*) 0-40478  
 steel, residual quenching stress determ. in cylinder, consideration of transform. (*German*) 0-35213  
 steel, Si-Cr-Mo-W-V (2.4,1.3,2 wt.%), heat treatment and props. 0-16349  
 steel, stainless, fusion reactor He embrittlement simulation, splat cooling in development of B doping 0-30072  
 steel, stainless, XM19, stress corrosion resistance 0-16558  
 steel, tool, quenching procedure effect on distortion, tool life 0-50657  
 steel, tool, type KhBG, carburising and quenching, effect on fracture toughness 0-29997  
 steel, tool, W-Mo, heat treatment effect on props. 0-50656  
 steel, type 28Kh3SNMVFA, strain hardened martensite, resist. to tempering, exam. 0-16348  
 steel, type 52100, heat treatment effect on microstruct. and mech. props. 0-29993  
 steel, ultrahigh C, superplastic struct. development by heat treatment 0-11703  
 steel, W-Mo, sintered high-speed, naphthalenelike grain form., quenching effect on fracture toughness 0-30103  
 steel 30KhGSNA, low alloy, quenched, grain refinement influence on impact strength (*Russian*) 0-20974  
 steel forgings, expt.-calc. model of quenching, temp. meas. across cross section 0-16345  
 steel tubes, square section, collapse in bending 0-25792  
 steels, C, quenched and tempered, struct.-prop. relationships 0-7599  
 Ticonal, two- and one-dimens. modulated struct. after thermomag. treatment and water quenching (*Russian*) 0-29983  
 transition metal amorphous alloys, mag. props. 0-29576  
 water-isobutyric acid (2,6-lutidine) mixtures, critically quenched, phase separation and coalescence 0-24581  
 Zircaloy-4,  $\beta$ -transformed, flow stress and dynamic strain ageing 0-3101  
 Ag-Sn (68.2)(11 wt.%), splat-quenched, X-ray line broadening 0-40397  
 AgAu, quenched, short range order effects on specific heat 0-29181  
 Al alloys, dil., quenched, foreign element effects on dislocation loop form. 0-54239  
 Al, interaction between <sup>57</sup>Co atoms and quenched-in vacancies, Mossbauer meas. 0-7234  
 Al, positron annihilation, effects of quenching, annealing and neutron irradi. 0-20732  
 Al, quenched, muon<sup>+</sup> trapping at vacancies, compared with positron annihilation 0-15937  
 Al, splat-cooled, grain-size distrib. function, TEM study 0-40396  
 Al, superpure, anomalous primary creep behaviour, precipitate form. 0-7646



**quenching (thermal) continued**

- Al wire, hot and cold deformation drawing strengthened, thermal EMF study (*Russian*) 0-54674
- Al-alloy plates, type VAD23, thermomech. parameters effect on struct. and props. 0-20988
- Al-Cu samples (0.5, 2.0 and 4.0 wt.%) polycryst., precipitation, positron annihilation and TEM 0-50639
- Al-Cu(Zn, Ag, Mg<sub>2</sub>Si), intermediate precipitates, stability, X-ray, elec. resist. and hardness study 0-3063
- Al-Ge (6.8 at.%), quenching from mushy state for production of metastable phases 0-35223
- Al-Mg<sub>2</sub>Si (1 wt.%), precipitation reactions 0-11652
- Al-Mg<sub>2</sub>Si (1.42 wt.%), aged, dislocation structs. caused by plastic deformation 0-25786
- Al-Mg-Zn alloys, liq./solid phase equilibria determ. (*German*) 0-50601
- Al-Mn(Cr), quenched, thermal stability (*Russian*) 0-20976
- Al-Si, dilute, anomalous primary creep behaviour, precipitate form. 0-7646
- Al-Zn, G.P. zone form., temp. limit 0-16317
- Al-Zn-Mg, plastic deform. influence on structural transform. and mechanical props. (*Russian*) 0-7623
- Al-Zn-Mg, polygonized struct. in extrusions, thermal stability and mech. props. 0-50659
- Al<sub>2</sub>O<sub>3</sub>-Dy<sub>2</sub>O<sub>3</sub>, phase diagram at high temps. (*Japanese*) 0-50619
- As<sub>2</sub>S<sub>3</sub>, secondary electron emission, fluctuation state effect 0-40193
- Au, hardening mechanisms, grain size effect 0-35302
- Au quenched single crystals, vacancies, diffuse scatt. and resist. obs. 0-33994
- Au, thin foil, growth of stacking fault tetrahedra 0-19815
- Au-Ni-Cu-Zn, white gold, metallographic struct., heat treatment and plastic working effect 0-40403
- B<sub>2</sub>O<sub>3</sub>-BaO, liquid immiscibility region, equilibration and quenching expts. 0-45288
- BaO-Fe<sub>2</sub>O<sub>3</sub>-B<sub>2</sub>O<sub>3</sub> glass, splat cooled, low temp. micromagnetism 0-34660
- BaTiO<sub>3</sub>-CeO<sub>2</sub> liquid immiscibility region, X-ray diffr. anal. 0-50611
- Be-bronze BrB2, struct. and phase transform. during mechano-thermal treatment (*Russian*) 0-11667
- Bi foil, splat quenched, preferred orientation 0-40381
- Bi<sub>2</sub>Te<sub>3</sub>-SbTe<sub>3</sub>, ordered structure formation, heat treatment effect on thermal cond. 0-54448
- C, noncrystalline conversion to diamond, diffusion conversion enhanced rate due to shock compression 0-39221
- CaO:Li, thermally quenched, generation of Li<sup>0</sup> centres 0-50382
- Cd foil, splat quenched, preferred orientation 0-40381
- CdGeAs<sub>2</sub>, amorphous, thermal gradient expts., recrystn. 0-55438
- Co-Ga β' quenched single crystals, annealing-out of point defects 0-55426
- Cr-C, binary alloy formation of nonequilib. Cr<sub>3</sub>C in alloys quenched rapidly from melt 0-7581
- Cr-Co-Fe permanent magnet anisotropic alloys, plastic deform., ageing, particle alignment temp. 0-35254
- Cu-Al (21 at.%) transition state (*French*) 0-55392
- Cu-Al alloy UA10, heat treatment (*French*) 0-35225
- Cu-Al-Fe, mech. props. rel. to heat treatment 0-50682
- Cu-Al-Ni (14.3, 4 wt.%), ω-phase form. during quenching and ageing (*Russian*) 0-25686
- Cu-Au, vacancies and divacancies, quenching effects and elec. resist. meas. 0-39072
- Cu-Be (2 wt.%), alloying addition effects on grain boundary reaction (*Japanese*) 0-49236
- Cu-Fe, precipitation processes during aging, TEM, resistivity, hardness study (*Japanese*) 0-35221
- Cu-Fe (0.2 at.%), quenched, Fe dimers and defects 0-40007
- Cu-Fe (2.46 wt.%), reversion phenomena and cold-working effect (*Japanese*) 0-35204
- Cu-Sn(-Al), quenched and aged, struct. of phases (*Russian*) 0-49184
- Cu-Zn (30 wt.%), slip band growth, thermally activated 0-40457
- CuCrS<sub>2</sub> single cryst., spectral study and phys. props. (*French*) 0-29002
- Cu<sub>0.9</sub>Fe<sub>0.1</sub>O<sub>4</sub>, ferrite, determination of specific heat at 298-800K 0-2579
- Cu<sub>3</sub>Ga, transition state between long range order and short range order, model, computer simulation (*French*) 0-49371
- Fe, pure, splat-quenched, martensite morphology, SEM study 0-7547
- Fe, quenched-in hydrogen, yield stress decrease of prestrained specimens 0-16454
- Fe-Al alloys, rapidly quenched, mag. props. 0-29579
- Fe-C, martensite, struct., Mossbauer meas. 0-40000
- Fe-C (0.001 to 0.44 wt.%), C effect on low temp. brittleness (*Japanese*) 0-50711
- Fe-Co-Si-B alloy, amorphous, mag. heads appl. (*Japanese*) 0-54922
- Fe-Cu alloys, transform. substruct., lath microstructure after quenching 0-16298
- Fe-Mn (2 to 8 wt.%) alloys, phase transformations, tempering influence (*Russian*) 0-25735
- Fe-Si (6.5 wt.%) ribbon, prep. by rapid quenching and mag. props. 0-45251
- Fe-Zn, crystallographic relations by X-ray diffr. 0-24408
- Fe<sub>40</sub>Ni<sub>20</sub>B<sub>30</sub>, metallic glassy ribbon, casting conditions (*Japanese*) 0-55386
- Fe<sub>40</sub>Ni<sub>40</sub>B<sub>20</sub>, amorphous, casting conditions effect on mag. props. (*Japanese*) 0-34698
- Fe<sub>1-x</sub>O, surface struct., XPS study 0-20759
- Ga-As-Sb system, two- and three-phase fields obs. 0-55373
- Ga<sub>2</sub>S<sub>3</sub>-PbS system, phase diagram and crystallographic study (*French*) 0-29937
- GeSe<sub>2</sub>-As<sub>2</sub>Se<sub>3</sub>-Sb<sub>2</sub>Se<sub>3</sub>, quenched glass system, elec. cond., low temp. heat treatment effect 0-39586
- H<sub>2</sub>, quenching method (*Japanese*) 0-7604
- He quenching method (*Japanese*) 0-7604
- Hf-V foil, rapidly quenched and heat treated, supercond. props. 0-54852
- Ir-Cr, yield stress and saturation magnetisation 0-16389
- KCl:Pb, lead aggregation effect on yield stress, incoherent precipitates, solubility determ. method 0-50645
- KCl:Sr, thermally pre-treated, glow curves 0-25470
- KCl(Br)(I), single cryst., quenched, microstruct. around indentations 0-7628
- KI, quenched, absorpt. and emission spectra, α-centres 0-11442
- KMg<sub>2</sub>(AlSi<sub>3</sub>O<sub>10</sub>)F<sub>2</sub>·KMg<sub>2</sub>Si<sub>4</sub>O<sub>16</sub>F<sub>2</sub>, solid soln., melting and crystn., quenching and DTA study 0-39263
- (Li,Nb,K) (Nb,Ta)O<sub>3</sub>, pseudo-binary and ternary systems quenched metastable glassy and cryst. phases 0-29935
- quenching (thermal) continued**
- LiF-AlF<sub>3</sub>-Na<sub>3</sub>AlF<sub>6</sub>-Al<sub>2</sub>O<sub>3</sub> system, phase equilibrium, X-ray diffr., DTA, quenching, optical microscopy study 0-50610
- LiNbO<sub>3</sub>:Cr<sup>3+</sup> glass, roller quenched, crystn. kinetics 0-44143
- Li<sub>2</sub>O-Al<sub>2</sub>O<sub>3</sub>(Ga<sub>2</sub>O<sub>3</sub>)(Bi<sub>2</sub>O<sub>3</sub>), quenched glasses, crystn. and ionic cond. 0-33899
- Li<sub>2</sub>TiO<sub>3</sub> growth by Bridgman-Stockbarger technique 0-25548
- Mg-Li-Al (31, 1 at.%), heat treated, precipitation 0-40364
- MgO:S, cathodoluminesc. spectrum (*Russian*) 0-55197
- Mn-Al-C, ferromag., transform. kinetics 0-34627
- Mn-Cu, alloying behaviour and high damping capacity 0-35160
- Mo-Re, σ phase alloy, critical mag. field, elec. resistance 0-54850
- NaCl, dislocation rosettes around Vickers diamond pyramid indents, quenching effect 0-11740
- NaCl, rock salt, quenched, residual stresses, optical study 0-55061
- NaCl, X-ray irradi., vacancy conc., thermal expansion meas. 0-6431
- NaCl+Pb, Pb aggregation effect on yield stress, incoherent precipitates, solubility determ. method 0-50645
- 6NaCl.CdCl<sub>2</sub>, 60 wt.% powders, Suzuki phases prep. and stability 0-35123
- Nb<sub>20</sub>Zr<sub>80</sub>, supercond., US attenuation 0-44766
- Ni, C precipitation 0-29958
- β<sub>2</sub>-Ni-Al, elastic consts., supersaturated thermal vacancy effects 0-54298
- Ni-C-W-Cr(-Mo), Vickers hardness and crystallisation temp. 0-16361
- Ni-Fe-Nb-Al(-Mo), wear resisting mag. head material, mag. props. and struct. 0-35350
- Ni-Mo (20.8 wt.%), order, heat treatment effects 0-40406
- Ni-Mo-C(-Cr)(W), Vickers hardness and crystallisation temp. 0-16361
- Pb<sub>1-x</sub>Al<sub>x</sub>F<sub>2+x</sub>, ionic cond. of quenched and annealed specimens, interstitial cond. mechanism 0-2199
- PbF<sub>2</sub>-AlF<sub>3</sub> glass, optical props., crystn. and thermal expansion 0-48367
- PbF<sub>2</sub>-AlF<sub>3</sub> glass, prep. and props. 0-49120
- Pd-Cu-Si, laser melting and splat quenching to form foils for TEM obs. 0-29986
- Pt, interstitial thermal conversion study by elec. cond. meas. 0-15096
- Sb, liquid-quenched, stabilisation and transformation kinetics of metastable phases 0-3022
- Sb<sub>2</sub>Te<sub>3</sub>-Sb<sub>2</sub>Se<sub>3</sub>, ordered structure formation, heat treatment effect on thermal cond. 0-54448
- Si, EPR of quenched-in defects 0-29620
- Si ribbons, roller quenching method of prep., grain sizes and carrier conc. 0-40275
- Si with defects produced in quenching, photocond. and elec. props. 0-6837
- Si-Au films, quenched condensed, elec. resist. and supercond. 0-54669
- SiO<sub>2</sub> glass, strengthened by ion exchange and quenching brittle destruction theory 0-45398
- SiO<sub>2</sub>, vitreous, Raman active defects, thermal equilibration 0-55092
- SiO<sub>2</sub>-Al<sub>2</sub>O<sub>3</sub>-CaO-MgO-Na<sub>2</sub>O-K<sub>2</sub>O effect of partial substitution of Na<sub>2</sub>O by K<sub>2</sub>O, on crystallisation 0-10499
- Sm(Co<sub>0.84</sub>Cu<sub>0.16</sub>)<sub>6.9</sub>, microstruct. and domain struct., mag. reversal (*Russian*) 0-20429
- Sm(Co<sub>0.81</sub>Cu<sub>0.15</sub>Fe<sub>0.04</sub>)<sub>6.9</sub> and Sm(Co<sub>0.84</sub>Cu<sub>0.16</sub>)<sub>6.9</sub> powders, mag. props. (*Russian*) 0-20434
- Sn droplets, on Bi, Zn and Al, heterogeneous nucleation 0-44294
- Sn-Bi, crystal struct. and superconductivity after appl. of high press. and quenching 0-10531
- Sn-Sb (10 wt.%), decomposition of supersaturated solid soln. 0-29960
- Sn-Sb-Ag, splat cooled foils, TEM study 0-40344
- Ta, low temp., diffusion of H and D from quenching and annealing study 0-6555
- Ta, low temp. diffusion of H and D from quenching and annealing study 0-6555
- Ti-Al-Mo-Sn-Si (2.25, 4, 11, 0.25 wt.%), type IMI 680, internal friction study of martensitic transformations 0-7573
- Ti-Al-Mo-Sn-Si (2.25, 4, 11, 0.25 wt.%), type IMI 680, stability of martensitic phases 0-7574
- Ti-Al-Mo-Sn-Si (4, 4, 4, 1/2 wt.%), type IMI 551, internal friction study of martensitic transformations 0-7573
- Ti-Al-Mo-Sn-Si (4, 4, 4, 1/2 wt.%), type IMI 551, stability of martensitic phases 0-7574
- Ti-Al-V (6, 4 wt.%), type IMI 318, internal friction study of martensitic transformations 0-7573
- Ti-Al-V (6, 4 wt.%), type IMI 318, stability of martensitic phases 0-7574
- Ti-Al-V (6, 4 wt.%) cylinders, residual stresses introduced by quenching elastoplastic anal. (*French*) 0-45355
- Ti-Al-V (6, 4 wt.%), quenched, struct. and age hardening rel. to treatment temp. 0-11657
- Ti-Al(Fe) microprobe anal. of alloying addition distrib. 0-55358
- Ti-Be, metallic glass form. and props. 0-16219
- Ti-Nb-Zr (35, 3 wt.%), martensitic τ phase, X-ray diffr. obs. 0-16300
- Ti-Ni, laser melting and splat quenching to form foils for TEM obs. 0-29986
- TiO<sub>2-x</sub>, reduced, cond. between elec. props. in equil. at 1100°C and after quenching, defects role (*French*) 0-44582
- Tl<sub>2</sub>S-SnS<sub>2</sub> phase equilibria exam. 0-55369
- Tl<sub>2</sub>SeAs<sub>2</sub>Te<sub>3</sub>, secondary electron emission, fluctuation state effect 0-40193
- W, vacancies, quenching and recovery invest., resist. and TEM study 0-39074
- Zn foil, splat quenched, preferred orientation 0-40381
- ZnTe, dominant acceptors, annealing and quenching 0-24463
- ZnTe, TEM obs. of precipitates, shape of Te solidus line 0-25703
- ZnTe:Li, impurity segregation during short annealing and quenching, SEM, TEM and elec. meas. 0-10676
- Zr-Be, metallic glass form. and props. 0-16219
- Zr-Cu (1.6 wt.%), near eutectoid, active eutectoid decomposition ageing and quenching effects 0-2993
- Zr-V foil, rapidly quenched and heat treated, supercond. props. 0-54852
- ZrO<sub>2</sub>-SiO<sub>2</sub> (11 to 13 wt.%), X-ray phase anal. 0-35195
- queueing theory**
- molecular spectroscopic laboratory strategies, queueing theory and digital simulation use 0-30299
- queueing theory** see queueing theory
- R and D management** see research and development management
- R-centres**
- CdS laser irradi. native defect formation, influence on photoelectric props., IR luminescence (*Russian*) 0-11039
- NaCl:Ca, hologram recording on R-centres 0-1157



**R waves** *see Rayleigh waves*

**Racah coefficients** *see angular momentum theory*

## radar

*see also Doppler effect; optical radar*

Doppler radar data analysis in meteorological obs. 0-41564

Doppler weather radar, development of weather echo props. 0-26645

ocean wave synthetic aperture radar imagery rel. to surface structure 0-46197

random media causing pulse spreading and wandering 0-37942

**radar altimeters** *see radioaltimeters*

## radar antennas

Mills' cross array antenna, digital baseband processing 0-36500

## radar applications

atmosphere, precipitating clouds observed by RONSARD radars 0-51568

atmospheric measurement by VHF pulsed Doppler method, lower atmos. 0-46277

atmospheric research, high power VHF radar appl. (*German*) 0-46294

atmosphere winds and turbulence continuous meas. using VHF Doppler radar, preliminary results 0-8444

backscattering coefficient and wind speed meas., determ. of winds at sea 0-26644

cloud and clutter targets observed by radar, broad-band noise technique 0-51454

cloud and precipitation particle observation, vertical X- and K<sub>a</sub>-band system 0-46273

clouds and precipitation study form correl. and spectral anal. of radar signals 0-12529

correlation function and averaged power of radar signals reflected from sea waviness 0-46190

crop types monitored by side-looking radar 0-46280

geological interpretation, from composited radar and Landsat imagery 0-56647

geophysical reflection factor data, cartesian interpolation and display 0-31136

hail detection technique, quasilinear discriminant function 0-21861

ice sounding, studies by Arctic and Antarctic Research Institute, Leningrad 0-4504

iceberg detection and characterisation, using synthetic aperture radar 0-26622

mesosphere remote sensing, VHF signal detection 0-46274

meteorological radar network optimal positions, multiple-Doppler system 0-31140

nightglow, 6300 Å emission profiles from incoherent scatt. radar and photometry (*Portuguese*) 0-41591

oceanography, SEASAT synthetic aperture microwave-imaging radar expt., overview 0-46267

precipitation forecasting 0-6 hours ahead, radar and satellite imagery, FRONTIERS plan 0-12509

rain cell monitoring, algorithms for automatic detection and tracking 0-51544

remote sensing and telecommunication, book 0-36431

remote sensing by stereo side-looking radar, accuracy anal. 0-56646

RONSARD atmospheric radar, calibration techniques 0-46278

sea state radar, long-range sensing using HF sky wave, minimisation of ionospheric disturbance 0-21857

sea-state parameter extraction from sample-averaged data, accuracy 0-51561

SHF signal attenuation by rain, monitored by radar 0-51567

short pulse radar ocean wave sensing, preliminary results 0-46315

surface current mapping by Coastal Ocean Dynamics Radar 0-46316

surveillance, large sea areas, using side looking airborne radar system (*Dutch*) 0-12560

thunderstorm observed by two-channel polarisation diversity radar 0-51453

tropopause detection, by partial specular refl. with VHF radar 0-8411

troposphere and stratosphere sounding by pulsed VHF radar 0-51566

Venus atmospheric precipitation detect., remote sensing radar and radio techniques 0-56741

weather radar, Doppler, estimation of echo spectral moment 0-51563

weather radar, signal anal. (*French*) 0-36418

weather radar, storm precipitation estimated with dual-wavelength radar 0-46220

weather radar detection of area precipitation (*German*) 0-46227

weather surveillance near airports using Doppler radar 0-46272

wind shear detection radar, for airport use 0-51565

## radar clutter

cloud noise reduction, broad-band noise technique for fast-scanning radar 0-51454

weather clutter, Weibull-distributed, observations using L-band long range ARSR 0-36353

## radar cross-sections

infinitely long circular cylinder, backscatter of arbitrarily polarised EM wave 0-9778

rain, drop-size and temp. effects on forward and backward scattering on microwaves 0-17317

## radar displays

*see also cathode ray tube displays; fluorescent screens*

geophysical reflection factor data, cartesian interpolation and display 0-31136

**radar echo areas** *see radar cross-sections*

## radar equipment

fibre-optic delay line signal processing devices 0-48443

meteorology radar signal recording on video machine, coherent Doppler radar 0-46275

RONSARD atmospheric radar, for precipitation obs. 0-51568

SAW filter design for TV, CATV and radar appls. 0-53579

SAW slanted device technology for radar system appl. 0-19181

SEASAT radar altimeter 0-56613

Ni-Fe polycrystalline film cross-tie memory for shipborne radar/sonar 0-42204

## radar interference

*see also radar clutter*

HF sky wave radar remote sensing of sea state, minimisation of ionospheric disturbance 0-21857

parallel-polarised and cross-polarised radar returns from rough sea surface 0-51408

## radar measurement

altimeter height and timing bias report 0-46326

## radar measurement continued

atmosphere winds and turbulence continuous meas. using VHF Doppler radar, preliminary results 0-8444

aurora, Doppler vel. meas., radio aural spectral characts. and incident incoherent scatter meas. 0-56663

equatorial counter-electrojet, two-stream instability, HF radar meas. 0-26671

Gulf of Alaska SeaSat Experiment synthetic aperture radar wave imagery 0-46199

iceberg underwater shape determ., impulse radar appl. 0-26621

meteor echo rates, correl. with zonal winds at 95 km altitude 0-56775

meteor trail, maximum ionization height detect. method 0-8487

Moon, Earth-based radar mapping, review 0-12694

ocean surface wind obs., SeaSat scatterometer/scanning radiometer/altimeter comparison 0-46249

peat bog and sapropel bed thickness meas. by radar 0-21860

remote sensing and profiling of lower atmosphere using radiowaves, ground-based 0-56628

sea ice, anisotropic props. in 50-150 MHz range 0-17274

SEASAT altimeter wave height comparisons 0-46201

thermosphere temperatures over Malvern, incoherent scatter data comparison with two global thermospheric models 0-8467

tropopause, detect. by partial specular refl. with VHF radar 0-8411

Venus, astrometric radar meas. in 1977, results 0-17522

## radar receivers

RONSARD atmospheric radar, calibration techniques 0-46278

## radar stations

meteorological radar, vertical precipitation structure recording appl. (*German*) 0-17358

## radar systems

BASORA secondary radar, sounding balloon tracking appl. 0-17357

fast-scanning radar, cloud and clutter targets noise, reduced by broad-band method 0-51454

Geos 3 tracking systems, intercomparison 0-4227

L-band air-route surveillance radar for observations of Weibull-distributed weather clutter 0-36353

meteorological and ATC radar system development 0-26651

sea surface contour airborne radar as remote sensing instrument 0-51562

SEASAT synthetic aperture microwave-imaging radar expt., overview 0-46267

surveillance, large sea areas, using side looking airborne radar system (*Dutch*) 0-12560

synthetic aperture radar, satellite borne, terrestrial surface mapping appl. 0-12572

synthetic-aperture, Spacelab expts., for active remote sensing from space 0-36409

VHF Doppler radar, appl. to atmospheric winds and turbulence continuous meas. 0-8444

**radar telescopes** *see radiotelesopes*

## radar theory

correlation function and averaged power of radar signals reflected from sea waviness 0-46190

ground cover remotely sensed by radar, backscatter cross-section 0-46279

resistive strips scattering E- and H-polarised waves 0-37941

sea ice, radar wave reflected power intensity reduction with range (*Japanese*) 0-36329

weather radar, Doppler, estimation of echo spectral moment 0-51563

**radarscopes** *see radar displays*

**radiance** *see brightness*

## radiation

*see also atmospheric radiation; beta-rays; cathode rays; electromagnetic waves; heat radiation; radiation effects; radiative transfer; stellar radiation*

gas flows, selfgravitating, thermodynamic processes and radiation, numerical method 0-14848

interstellar polarisation rel. to grain size, polarimetric obs. of four deviating stars 0-12792

PWR containment building, design and anal. of cavity shield system 0-18713

risk to health assessment 0-41124

## radiation belts

*see also atmospheric electron precipitation; atmospheric proton precipitation*

cosmic rays, element ions, interval  $6 \leq Z \leq 28$ , energies composition, Skylab study 0-8501

electron pitch angle distrib. determ. using Molniya 1 omnidirectional detectors 0-8437

electron-coherent whistler wave interaction, rel. to precipitation 0-46349

outer trapped electron belt, self-modulated VLF wave-electron interactions 0-41658

protons and He ions, equatorial  $\alpha/p$  ratio near 1 MeV 0-4205

stability of invariant tori 0-31177

trapping boundary at midnight, sharply defined L depend. energy threshold for anisotropy 0-41649

trapping region, quasiperiodic electron density pulsations, satellite detection 0-4198

Van Allen, mapping technique, student computing exercise 0-27076

**radiation biology** *see biological effects of radiation*

## radiation chemistry

*see also chemical effects of nuclear reactions and scattering; photolysis; radiochemistry; radiolysis*

alkaline frozen solutions, polycryst. and glassy, photocond. and radiometric obs. 0-45531

alkaline glassy state, aq., density determ., radiation chem. 0-42197

amino acid radioreaction, geochem. and cosmochem. implications 0-45975

benzene in dilute cyclohexane solution, fluoresc. quenching on pulsed proton irr., temp. depend. 0-21307

biologically active compounds, MM-wave interactions 0-16707

biphenyl single crystals,  $\gamma$ -ray induced radicals, EPR and optical absorpt. studies 0-44921

carcinogenesis, redox model 0-26298

cellulose acetate-g-polyacrylamide membranes, radiation grafted, appl. in water desalination by reverse osmosis 0-45548

cyclohexane, neutron irradiation, radical distribution, ESR study (*Japanese*) 0-44920

diacetylenes, urethane substituted, polymer conversions in  $\gamma$ -ray polymerisation 0-26014



**radiation chemistry continued**

- 5,6-dihydro-6-methyluracil, X-ray irradi., free radical form; ESR spectra obs. 0-50189  
 1,3-dimethyluracil, non-hydrogen bonding crystal, radical formation 0-35552  
 dodecane-tributyl phosphate solns., radiolysis, liquid products 0-40723  
 electron linac chemistry facility, 140 MeV 0-37640  
 electron track end effects in water 0-11932  
 heavy-particle track structure rel. to radical physical distrib. and chemical effects 0-11933  
 imidazole, Z-irrad., EPR study of H exchange 0-40718  
 methanol-2-methyltetrahydrofuran mixed glasses, annealed,  $\gamma$ -ray produced electrons transfer from IR to bisible traps 0-11440  
 $\alpha$ -methyl-D-glucopyranoside, X-irrad., ESR and ENDOR study of free radicals 0-45526  
 N-acetyl-L-leucine, single crystals, X-ray induced free radicals 0-45525  
 organic reactions in solid state 0-21309  
 particle stopping power dependence on physical and chemical states 0-9480  
 photochromic polymer, thermal effect in photomech. conversion 0-16706  
 PMMA, neutron irradiation, radical distribution, ESR study (Japanese) 0-44920  
 polar liquids, MM-wave interactions 0-16707  
 polyethylene, low-density,  $\gamma$ -irrad., spin trapping reaction 0-39873  
 polyethylene, neutron irradiation, radical distribution, ESR study (Japanese) 0-44920  
 polymer materials, appls. (Japanese) 0-55413  
 polymer network, crystn. and form. through crystn., crystallinity influence on radiation induced form. 0-38964  
 polypropylene, electron bombarded, radical formation, piezoelectric and pyroelectric effects, ESR study 0-7169  
 polypropylene, electron bombarded electret, trapped charges ESR study 0-7170  
 protein, radical limiting conc. on UV irradi. at 77K, effect of luminesc. quenchers 0-30662  
 radiation processing, conf., Miami, FL, USA (Oct. 1978) 0-36772  
 dl-tartaric acid, radiation products, ESR-ENDOR OBS. 0-55682  
 tartaric acid salts, and deuterated forms, irradi.-crysts., primary reactions, EPR obs. 0-3370  
 2,2,3,3-tetramethylbutane,  $\gamma$ -irrad., EPR spectrum assignment 0-15800  
 l-thioproline single cryst., X-irrad., ESR and ENDOR study of radicals 0-45528  
 trapped electrons in glassy hydrocarbons, gamma ray irradi., relax., spectral obs. 0-23416  
 uridine 5'-phosphate (Na salt), NO<sub>2</sub> species in an irradi. single crystal, EPR obs. 0-40719  
 n-vinyl carbazole, radiation induced polymerization ESH study 0-7817  
 n-vinyl carbazole-acrylamide, post radiation induced polymerisation 0-7818  
 n-vinyl carbazole-acrylamide, radiation induced polymerization, monomer crystallinity effects 0-7819  
 BeO-P<sub>2</sub>O<sub>5</sub>-RO(R<sub>2</sub>O) (R=Li,Na,K,Mg,Ca,Sr,Ba) glasses, gamma irradi., cation modifier effect on radiation centre formation 0-40720  
 C-bearing gases, K-shell X-ray yields, proton-induced, chem. effects 0-37820  
 CoFeCN.xH<sub>2</sub>O, electron irradi., Mossbauer spectra 0-29652  
 MgO, dissoci. under heat and electron bombardment 0-7834  
<sup>13</sup>N species formed by proton irradiation of water 0-45532  
 Na (111) surface, epitaxial film, electron induced dissociation 0-6646  
 NaClO<sub>4</sub>, aq. glass, formation of trapped H-atoms and electrons on X-irrad. 0-35559  
 O<sub>2</sub> radiobiological effect, molecular and cellular basis 0-26211  
 l-proline monohydrate single cryst., X-irrad., ESR and ENDOR study of radicals 0-45528

**radiation counters** *see counters***radiation damage** *see radiation effects***radiation detection and measurement**

- see also alpha-particle detection and measurement; beta-ray detection and measurement; electron detection and measurement; gamma-ray detection and measurement; hyperon detection and measurement; meson detection and measurement; muon detection and measurement; neutrino detection and measurement; neutron detection and measurement; particle detectors; proton detection and measurement; radioactivity measurement*  
 $\Delta E$ -E sample particle identification with wide dynamic range 0-14058  
 A/D converters, cyclic scale compensated 0-14039  
 angular distrib. meas. with positron sensitive detector 0-27899  
 Cicoli personal RF radiation hazard detector, evaluation 0-5337  
 cloud chambers, factors affecting registration efficiency in low level activity counting (Russian) 0-27875  
 dead time corrections in coincidence measurements by time-to-pulse-height converters or standard coincidence systems 0-9472  
 dead time meas. of individual detecting system 0-9470  
 dead time of detection systems, determination method (Slovenian) 0-47815  
 delayed coincidence expts., precision of half life estimation 0-27908  
 deuteron beam polarimeter, <sup>3</sup>He(d,p) 0-47834  
 digital data processing using integer arithmetic 0-27917  
 dosimetry, fluence of secondary photons generated by attenuation in thin walls 0-18699  
 dosimetry, primary standards for industrial radiation processing 0-5356  
 dosimetry standardisation in Japan, review 0-5359  
 dosimetry standardisation in UK, review 0-5358  
 efficiency calc. for extended flat sources 0-9469  
 electronic measurement apparatus development at ATOMKI (Hungarian) 0-18768  
 electronics in nuclear science and technology 0-9347  
 fission fragment atomic number identification using gas ionisation chamber 0-27863  
 fission fragments, kinetic energies and fly-off angles, ionisation method of meas., online numerical processing (Russian) 0-52838  
 fringing field effects in a cylindrical condenser 0-52821  
 gamma spectrometry, secondary standard prep. 0-18701  
 heterodyning of elementary particles, radiation meas. method 0-42898  
 international radiation standards, role of ICRU 0-9414  
 international standard reference radiations and their application to the type testing of dosimetric apparatus 0-9416  
 ionising gases, meas. of m-values 0-18694  
 ionising particle beam interactions with liquids, acoustic effect, laser beam simulations 0-23262

**radiation detection and measurement continued**

- ionising radiation, metrology and calibration, French system (French) 0-5351  
 ionising radiation, primary standards and transfer methods in France, review (French) 0-5352  
 ionising radiation, traceability in meas. systems 0-5355  
 linear radiation-flux functionals, estimation of local perturbations using Monte Carlo method 0-5457  
 medical dosimetry standards programme of the National Bureau of Standards, USA, review 0-8187  
 modern atomic and nuclear physics (book) 0-11  
 MWPC, localisation of minimum ionising particles using cathode induced charge centre of gravity readout 0-32576  
 neutron collimated fast beam, radiation quality local distrib. 0-12247  
 non-polar liquids, elec. charges, appl. to high energy radiation detectors 0-20217  
 nuclear counting, method to reduce cosmic background 0-897  
 nuclear gauge, with digital response, statistical method for stability testing (Rumanian) 0-9459  
 nuclear medicine and metrology of ionising radiations (French) 0-17057  
 nuclear radiation detection lab., desk top calculators 0-36821  
 particle motion through matter, fluctuations in cascade processes 0-5456  
 particle passage through medium, cascade process fluctuation 0-18769  
 personal monitor for uranium and thorium in uranium mine dust 0-52792  
 polarisation meas., set of efficient estimators 0-27909  
 proton spectrometer/polarimeter for photoreactions below 1 GeV 0-18751  
 radiation calorimetry of single electron pulses from a LINAC 0-42872  
 random search algorithm for 2-D data fitting 0-27915  
 random summing in multi-detector counting system meas. radionuclide mixtures 0-36097  
 reactor core radiation transport code, comparison of electron transport models 0-23030  
 resistive unidimensional detectors employing rise time readout method, position resolution and linearity 0-14048  
 semiconductor detectors of nuclear radiation, effect of trapping on response 0-5447  
 small angle scattering, axially symmetric geometry, main features 0-52836  
 solid angle integrals for rad. detectors, Monte Carlo solns. 0-9468  
 spatial noise reduction in detector arrays, controlled lateral shifts 0-53436  
 thickness measurement by backscattered radiation 0-47829  
 threshold detection equivalence with and without dead time 0-32580  
 transceiver, inexpensive, use in cosmic ray time coincidence expts. with long baselines 0-52837  
<sup>60</sup>Co radiation therapy, eval. of dosimetric accuracy and uniformity 0-12269  
 Fe calorimeter, hadronic cascade curves between 20 and 8000 GeV 0-36464  
 Ge detector, charge collection characteristics, influence on timing performance 0-47820  
 He backscattered ions, electrostatic anal., electronic reduction of charge state energy doublets 0-27870  
 He beam, magnetic spectrom. meas. using automatic tracking NMR system 0-27869  
<sup>235</sup>U decay heat meas. and calcs., review 0-13732  
 Xe probe for contamination monitoring 0-27826
- radiation detectors** *see particle detectors*  
**radiation dosimetry** *see dosimetry*  
**radiation effects**  
*see also acoustic wave effects; alpha-particle effects; beta-ray effects; biological effects of radiation; deuteron effects; electron beam effects; gamma-ray effects; hyperon effects; ion beam effects; laser beam effects; meson effects; neutron effects; proton effects; radiation chemistry; radiation hardening; voids (solid); X-ray effects*  
 acrylic scintillator and wavelength shifter material, radiation induced degradation 0-5442  
 alkali halide, Frenkel defect pairs formation mechanism (Russian) 0-10542  
 alkali halide, irradiated crystal, recombination of radiation defects (Russian) 0-39151  
 alkali halides, interstitial motion during radiation damage and sputtering processes 0-54230  
 alkaline earth phosphate (MO-Al<sub>2</sub>O<sub>3</sub>-P<sub>2</sub>O<sub>5</sub>) irradiated electret glasses, relax. of external field intensity on heating 0-25282  
 alloys, radiation effects on ageing and precipitation, review 0-29956  
 blistering, interpretation based on radiation stimulated vacancy migration 0-49265  
 coatings for nuclear fuel particles, irradiation performance, additives effects (German) 0-27748  
 conference on fusion reactor materials [Miami Beach, Florida, Jan. 1979] 0-31407  
 damage cascades, stochastic theory of particle transport 0-54291  
 defect clusters, nucleation and growth due to energetic particle radiation, chemical rate reaction theory, computer program 0-49263  
 defect processes, theory, rate eqns., chemical rules 0-33990  
 defect theory and processes, review 0-2009  
 defects, X-ray diffraction study, review (Japanese) 0-15152  
 defects and surfaces in bulk metallic, covalent and ionic systems, review 0-34049  
 diamond, defects and impurities 0-29017  
 diatomic materials, displacement function calc. 0-34047  
 energetic heavy particles, radiation damage, cascade formation (Japanese) 0-29094  
 FBR carbide fuels, comparative irradiation tests of pellet and sphere-pac fuels 0-643  
 FBR fuel element structural materials, consequences of improved behaviour under irradiation 0-640  
 FCC crystal, interstitial and solute concentration gradients, flux expression derivation (French) 0-54219  
 fission reactor oxide fuel, irradiated, physical processes (Japanese) 0-27742  
 Frenkel pairs, unstable, mechanism for radiation stimulated processes in solids 0-34050  
 fusion reactor materials, appl. of dynamical computer models to high energy cascades 0-34046  
 fusion reactor materials, microstructure evolution under irradiation 0-34041



## radiation effects continued

fusion reactor materials, range calculations using multigroup transport methods 0-34070  
 gas bubbles in solids, simultaneous hetero- and homogeneous nucleation model 0-2066  
 GCFR pressure-equalised fuel irradiation program 0-648  
 glass, light effects, history of development of photosensitive and polychromatic glasses 0-40080  
 graphite, fusion reactor applications, mechanical constitutive laws for irradiation behaviour 0-32448  
 high-level liquid waste, damage to organic extractant in positioning process 0-9345  
 ICF reactor, first wall protection schemes 0-32437  
 II-VI semiconductors, radiation effects, optoelectric props. control 0-25458  
 infrared multiphoton processes, apparent step cross-sections, pulse spatial structure, irradiation techniques 0-32792  
 interaction with matter, review and bibliography (*Japanese*) 0-39149  
 ionic crystals, radiation defect accumulation temp. depend. 0-19803  
 Kapron fibres, elongation and tensile strength rel. to UV irradiation 0-25796  
 LMFBR MX-type highly rated advanced fuels, fission gas release and correl. with fuel restructuring 0-642  
 materials science, phys. and mech. props. 0-25538  
 metals, irradiation induced swelling, bias factor 0-2062  
 metals, radiation-induced creep and swelling, radiation dose depend. (*Russian*) 0-29050  
 metals radiation damaged long term strength curve forecasting (*Russian*) 0-34040  
 Mossbauer effect appl., conference, Kyoto, Japan (Aug.-Sept. 78) 0-7199  
 nuclear reactor driver fuel, irradiation behaviour 0-32346  
 Oklo fossil nuclear reactors, radiation damage of minerals 0-21751  
 Oklo natural fission reactor materials, thermoluminesc. props., effect of radiation damage 0-21750  
 optical fibre waveguide, low loss, ionizing radiation effect on attenuation 0-38112  
 optical fibre waveguide, low loss, radiation induced transmission loss behaviour 0-38111  
 optical fibres, nuclear pulsed thermal radiation effects, hardening techniques 0-33170  
 optical glass fibre development, large-core, for military appls. 0-48451  
 PAC method appl. (*German*) 0-2679  
 phase stability, radiation disorder model 0-16297  
 phosphors, halophosphate, recombination processes effect (*Russian*) 0-7424  
 planetary spacecraft, Jovian environment simulation, materials hardening and mass shielding 0-36472  
 point defect production in irradiation, swelling, cascade diffusion theory 0-34044  
 polyatomic materials, damage energy functions 0-49264  
 polyethylene tubes and sheets, light resistance investigation under natural climatic conditions 0-21127  
 pulsed radiation effect on void growth and swelling 0-34043  
 quartz, irradiated, fused, crystalline, absorpt. spectra, colour centres 0-7384  
 refractory multiphase systems, infusible, some novel effects, rel. to practical appls. 0-55460  
 ring laser gyroscope, nuclear radiation vulnerability 0-9935  
 risk evaluation model, on-site meteorological data, environmental consequences 0-36155  
 semiconductor crystals, role of nonequilibrium state in radiation treatments 0-39152  
 semiconductors, defect processes, electronic stimulation 0-24665  
 semiconductors, defects and radiation effects, conf., Nice, France (Sept. 1978) 0-22140  
 semiconductors, fast particle irradi., Frenkel defect formation threshold energy 0-6404  
 semiconductors, Watkins-type radiation defects, low temp. form. mechanism 0-15153  
 semiconductors, elemental and binary, under subthreshold irradi. conditions, defect formation ionisation mechanism possibility 0-6430  
 silk, natural, elongation and tensile strength rel. to UV irradiation 0-25796  
 steel,  $I_2$  adsorption on steel in HTGR He environment 0-44233  
 steel, non-irradiated and irradiated specimens, autoclaves for fatigue crack growth tests (*German*) 0-45467  
 steel, stainless, constitution changes due to radiation effects 0-34048  
 steel, stainless, dilation and bowing in EBR II ducts and cladding 0-625  
 steel, stainless, GCFR ribbed cladding, post-irradiation creep rupture tests 0-18430  
 steel, stainless, laser fusion reactor first wall, void growth charact. 0-34042  
 steel, stainless, nucl. reactor driver fuel, irradiation behaviour 0-32346  
 steel, stainless type 316, temp. effects on swelling 0-32347  
 structural materials, review 0-49267  
 superconductor critical temp. depend. on radiation defects, electron density of states calcs. 0-44758  
 Tokamaks, lifetime of reactor components 0-32445  
 TTF-TCNQ, Matthiessen's rule, effective defect resistivity 0-6821  
 type II superconductors, radiation-induced changes in crit. props., radiation defects (*Russian*) 0-25027  
 void arrays in crystals, TEM contrast 0-14975  
 void sink strength depend. on mutual recombination, point defect loss to fixed sinks 0-33995  
 voids, sink strength of random array, steady-state diffusion problem, variational technique 0-49266  
 Zircaloy clad  $UO_2$  fuel elements, irradi. effects 0-666  
 Zircaloy-2, effect of simulated fission products on elongation fractography and metallography 0-649  
 $Al_2O_3$ , displacement function calc. 0-34047  
 Au-Ag, radiation damage and diffusion 0-24645  
 C, structure change, during thermal ordering, radiation disordering 0-54283  
 $CO_2$  laser range finder, performance in radiation environments 0-38054  
 $CaF_2:Mn^{3+}$ , fluorite, radiation and thermal redox processes 0-55678  
 $CaO$ , displacement function calc. 0-34047  
 Cu, radiation damage and diffusion 0-24645  
 $Cu_3Au$ , under irradiation, microstructural-based estimate of disordering 0-2067  
 Fe, amorphous, radiation damage simulation 0-34045  
 $\alpha$ -Fe, point defects, short term annealing, computer simulation 0-54282

## radiation effects continued

Fe-Cr-Ni austenitic alloys, environment sensitive cracking, metallurgical variables effect 0-35391  
 $Ga_{1-x}Al_xAs$ -GaAs solar cell, radiation resist., theoretical evaluation and optimisation 0-35681  
 Ge- $GeO_2$  MIS structure, growth of  $GeO_2$  from liq. phase, appl. of UV irradiation (*Russian*) 0-40273  
 HgCdTe short-wavelength IR photovoltaic detectors, radiation testing 0-37084  
 HgTe, VPE growth control by EM irradi. (*Russian*) 0-34338  
 KBr, V- and X-centres accumulation (*Russian*) 0-54228  
 KCl, temp. depend. of F-colouring efficiency 0-44204  
 KCl, V- and X-centres accumulation (*Russian*) 0-54228  
 KCl:H, dichroic H- and U-centres by polarised bleaching of interstitial H 0-29766  
 $K_2O-B_2O_3$  glass,  $\gamma$ - and UV- irradi., thermodecolorisation and thermolum. 0-20721  
 MgO, displacement function calc. 0-34047  
 NaCl, V- and X-centres accumulation (*Russian*) 0-54228  
 Nd:YAG laser range finder, performance in radiation environments 0-38054  
 Ni alloys, constitution changes due to radiation effects 0-34048  
 Ni, radiation damage and diffusion 0-24645  
 PbSnTe long-wavelength IR photovoltaic detectors, radiation testing 0-37084  
 PbTe, and  $Pb_{1-x}Sn_xTe$ , VPE growth control by EM irradi. (*Russian*) 0-34338  
 Pu radioactive waste, oxidation by radiation, effect on migration rate 0-13714  
 Si, radiation induced defects, IR absorpt. bands 0-25424  
 $Si-Al_2O_3$  MIS structure, with dielectric film, from UV irradiation converted metalorganic compounds (*Russian*) 0-45245  
 $SiO_2$ , vitreous, intrinsic radiation defects, nonbridging O 0-19837  
 TaO, displacement function calc. 0-34047

## radiation hardening

radiation processing, conf., Miami, FL, USA (Oct. 1978) 0-36772  
 steel, ferritic, impurity defect interaction influence on radiation hardening and embrittlement 0-35199  
 steel, ionic nitriding, procedure and equipment, nitrided layer hardness obs. 0-45414  
 steel, reactor pressure vessel failure and radiation damage (*Czech*) 0-619  
 steel, type 1Kh18N9T, neutron irradiated, microstruct. and mech. props. (*Russian*) 0-24503  
 Al, quenched, irradiated, and quenched plus irradiated, grain boundary hardening 0-3162  
 Al, US hardening kinetics rel. to dislocations 0-50644  
 Cu, electron irradi. at 100K, dislocation vel. meas. etch pit technique 0-49271  
 Cu, electron irradi. at 100K, comparison of irradi. hardening with dislocation vel. 0-54284  
 Cu, US hardening kinetics rel. to dislocations 0-50644  
 Fe, nitrogen, impurity defect interaction influence on radiation hardening and embrittlement 0-35199  
 Fe, US hardening kinetics rel. to dislocations 0-50644  
 Mg, US hardening kinetics rel. to dislocations 0-50644  
 Mo, neutron irradiated, radiation softening and hardening 0-34083  
 Mo-Zr-B alloy, neutron irradi. at 780-1080°C, porosity, hardening and embrittlement (*Russian*) 0-29062  
 Ni, acoustic hardening, influence of US treatment temps. and material purity (*Russian*) 0-11656  
 Ni-Ti(Fe), neutron irradiated, thermally activated deform. 0-6438  
 V, oxygen impurity defect interaction influence on radiation hardening and embrittlement 0-35199  
 Zn, US hardening kinetics rel. to dislocations 0-50644

## radiation hardening (electronics)

MOS capacitor structs. radiation hardness eval. using elec. meas. technique 0-34516  
 MOS structures, irradiated  $SiO_2$  film, electron and hole trapping 0-11098

## radiation injuries see biological effects of radiation

## radiation monitoring

## see also dosimetry

AGR fuel plug maintenance facility, corrosion product contamination control 0-5388  
 airborne  $\gamma$ -ray spectrometer calibration, altitude effects 0-18754  
 airborne radioactivity meas. in HFEF/N 0-18687  
 alpha-in-air monitoring system, real-time 0-23155  
 area monitoring, problems associated with the placement of fixed area monitors around irradiated fuel storage pools 0-18711  
 BWR, control blade worth depletion meas. 0-719  
 chromatography radioactive source leak testing under dynamic flow conditions 0-3432  
 Cicoil personal RF radiation hazard detector, evaluation 0-5337  
 computerised digital count-rate estimation using adaptive exponentially weighted moving averages [for radiation monitoring] 0-18689  
 decommissioned nuclear facilities, radiation exposure pathways 0-13957  
 DePangher precision long counter and neutron dose-rate meters, calibration 0-47822  
 dose limitation system, application problems 0-47767  
 Dungeness A, radiation and contamination control 0-5386  
 fast reactor burnup, correlation of  $^{134}Cs/^{137}Cs$  0-677  
 fast reactors, track detector determ. of fuel contamination of primary Na coolant 0-32394  
 FBR fuel reprocessing, radiological protection problems 0-5376  
 film dosimetry, endurance of film in personnel monitoring 0-23171  
 FIR laser, optically pumped, nearly transparent power monitors 0-5773  
 free air chamber for X-ray exposure standardisation at high quantum energies 0-14053  
 inhaled heavy elements deposited in vivo, external counting, review 0-36152  
 linear accelerator calibration monitor with a memory 0-3821  
 liquid waste, control of hospital waste using NaI(Tl) detectors (*Italian*) 0-56224  
 low level radiation monitors, calibration accuracy and precision 0-9428  
 LWR, chemical factors controlling  $\gamma$  radiation fields around coolant circuits 0-5371  
 LWR, fuel reprocessing plant, NDT control methods 0-5314  
 LWR plant, plume exposure monitoring system 0-42875  
 LWR power plant, radioisotope activity meas. in secondary loop coolant 0-5345



**radiation monitoring continued**

microwave radiation hazard monitors, measurement standards for calibration 0-26374  
 milk radioactive fallout monitoring in Britain 0-12283  
 natural soil radioactivity monitoring with portable gamma ray spectum. 0-31148  
 neutron dosimeter and monitoring instrumentation calibration using  $^{252}\text{Cf}$  and  $^{238}\text{PuBe}$  sources 0-13946  
 neutron radiation damage simulation, effect of He preinjection on swelling of stainless steel 0-44236  
 neutron spherical survey meter response 0-18679  
 nonionising RF and microwave radiation hazards (*French*) 0-3824  
 NRPB TLD and dose record keeping service 0-5344  
 nuclear failed fuel element detection by delayed neutrons using solid state track-etch technique 0-5249  
 nuclear fuel reprocessing plant, neutron monitors for process and safety control 0-5458  
 nuclear power plants and the fuel cycle, conf., Bristol, England (Nov. 1978) 0-4471  
 nuclear power plants secondary system radioactivity monitoring 0-18445  
 nuclear power station, decentralised system using microprocessors (*Spanish*) 0-47727  
 nuclear power stations, radiation dosage determination, monitoring and control for personnel safety (*German*) 0-842  
 nuclear reactor accident risk calcs., models and data 0-47613  
 occupational exposure at Millstone 2 PWR, long-term man-rem meas. program 0-5383  
 occupational radiation exposure, evaluation and control, US research program 0-5370  
 on-line computer application to radiological protection programme of Tokai-II nuclear power station 0-5391  
 Oregon, meas. of natural radioactivity 0-37638  
 Parker, H.M., biographical note on medical physics contribs. 0-12  
 particle accelerators, radiation exposure, design of cooling and ventilation systems 0-5350  
 PWR, radionuclide surface activities meas. 0-13941  
 PWR, T sources, releases, monitoring, management and environmental impact 0-18690  
 PWR steam generator,  $\gamma$ -dose rate distrib. meas. 0-5382  
 radiation protection progress report, EEC, 1978, book 0-22148  
 radioactive aerosols, atmos. conc. monitoring, radionuclide anal. 0-21427  
 radioactive waste storage, integrated biological dose evaluation 0-5379  
 random summing in multi-detector counting system meas. radionuclide mixtures 0-36097  
 reactor coolant activity monitoring, automatic on-line system 0-684  
 reactor integrated safeguards system, fuel labelling and perimeter monitors 0-37536  
 research reactor, self-protection criteria for reactor fuel elements 0-9361  
 RF fields below 300 MC/s, legislation proposals for workers' protection 0-56223  
 Serpukhov proton synchrotron shield, mixed radiation dose equivalent outside 0-32530  
 Sizewell power station 0-5387  
 surface contamination monitors for hospital use, calibration 0-36153  
 synchrotron, alternating gradient, efficient slow extraction, nonlinear growth of betatron oscillations, magnetic septum 0-47793  
 thermoluminescence dosimeter, personal monitoring, judgement of uncleanness in elements by residual value method (*Japanese*) 0-21546  
 Three Mile Island, environmental radiation monitoring using pressurised ionisation chambers 0-37637  
 TLD cards based on  $\text{CaSO}_4:\text{Dy}$  Teflon discs, annealing and repeated readout 0-3812  
 TLD element, precise calibrator (*Japanese*) 0-23159  
 TLD personnel monitoring, occupational radiation exposure in Austria (*German*) 0-26352  
 total radiation monitoring using liquid crystals and thermoluminescence 0-3819  
 tritium distribution in technological systems of Novovoronezh nuclear power station 0-32533  
 virtual impactor aerosol separators, analytical study 0-42874  
 water cooled, water moderated reactor, coolant tritium content in first loop 0-32334  
 water pool spent fuel storage units, neutron anal., criticality state (*Spanish*) 0-32517  
 Westinghouse PWR, radiation levels 0-5296  
 $\text{B}_4\text{C-Al(silicone)}$ (graphite), neutron shielding materials, long term radiation effects 0-9413  
 $\text{CaSO}_4:\text{Dy}$  Teflon TLD discs, metal filters for compensation of photon energy depend. 0-30901  
 $^{60}\text{Co}$  gamma ray sources, exposure efficiency dependence on distance, theoretical interpretation (*Czech*) 0-850  
 $^{60}\text{Co}$  long-lived  $\gamma$ -emitting aerosols, max. allowable emission rate from nuclear power station 0-32532  
 $\text{Ge(Li)}$  in situ spectrometry, exposure rates due to rainfall 0-42873  
 HT-HTO in air meas. system 0-21433  
 $^{125}\text{I}$  airborne vapour detection 0-51027  
 $^{125}\text{I}$  worker thyroid meas. 0-36151  
 Pu air monitor with background compensation system 0-27824  
 Pu handling, radiation protection and monitoring of personnel 0-5389  
 Pu-island element, B304, gamma scanning of power and burnup distrib. 0-721  
 Rn, at active U mines and mills, emission and control 0-41264  
 Rn continuous monitor response to transient Rn concs. 0-32519  
 Rn daughter airborne conc. meas. in atmosphere 0-37636  
 Rn emanation from ground, statistical anal. 0-41259  
 Rn release from geothermal resources 0-41263  
 Rn releases from nucl. power phosphate mining and coal burning 0-46072  
 $^{222}\text{Rn}$  conc. in energy efficient buildings 0-41261  
 $^{222}\text{Rn}$ , environmental sources in contiguous United States 0-41258  
 $^{222}\text{Rn}$ , human exposure due to Ra bearing residues 0-41260  
 $^{222}\text{Rn}$ , sources, distrib., exposure in residential buildings 0-41262  
 T monitoring at nuclear power stations 0-18691  
 T monitoring methodology using  $\text{SiO}_2$  desiccant, appl. to research reactor facility 0-21434  
 T species, sources and reactions 0-21432  
 T storage and monitoring, CANDU heavy water reactors 0-5291  
 U mines, radiological evaluation 0-42806

radiation monitors *see radiation monitoring*radiation patterns, antenna *see antenna radiation patterns***radiation pressure**

*see also acoustic streaming*  
 atmospheres, wave propag. with high radiation pressure 0-26729  
 atomic beam separation by light press. in isotope-separation setup 0-52943  
 atomic motion in resonant fluctuating laser radiation 0-43310  
 atomic transition, inverted, anomalous resonance-radiation press. 0-52946  
 atomic velocities, phasing in field of moving EM wave (*Russian*) 0-14253  
 binary stars, equipotential surfaces, modification due to pressure of radiation of component (*French*) 0-56880  
 broad band reson. light press., basic eqns. 0-28182  
 drag and levitation forces on moving resistive sheet 0-18989  
 Earth radiation budget, accelerometer direct meas. (*French*) 0-46287  
 gas cooling to broad band reson. light press. 0-48835  
 interplanetary small particles in solar system, radiation forces 0-17461  
 Io Na cloud, solar radiation press. as cause of east-west asymmetries 0-36560  
 laser, radiation in plasma, nonlinear press. forces 0-28682  
 meteor stream disintegration, solar radiation and planetary perturbation effects (*Russian*) 0-46495  
 Na atomic beam focusing and defocusing using reson. radiation press. 0-47143  
 optical motion control applied to Atmospheric Cloud Physics Laboratory on Shuttle/Spacelab 0-12634  
 plasma flow, radiation press. effects 0-1763  
 QSOs, ionisation equilib., thermal equilib. and radiative accel. near radiation sources with different spectral shapes 0-41909  
 quasars, radiatively driven gas clouds dynamics and stability, plane-parallel slabs theory 0-22107  
 solar, for maximization of spacecraft orbital momentum and energy 0-12640  
 solar radiation pressure, orbital perturbations of spheroidal satellite 0-4219  
 solar radiation pressure induced coupled librations of gravity stabilized artificial satellite 0-21888  
 SS 433, radiation press. rel. to mass accel. and collimation mechanisms 0-4368  
 Ge, radiation pressure, photon drag effect in far-IR 0-50452  
 Mg atoms, cooling to broad band reson. light press. 0-48835  
 Na beam deflection by reson. standing wave radiation 0-52945  
 Na neutral atom beam, focusing and defocusing forces, radiation press. from CW dye laser 0-52944  
 Na vapour, laser induced diffusion (*Russian*) 0-6195  
 Si, radiation pressure, photon drag effect in far-IR 0-50452

**radiation protection**

*see also radiation monitoring*  
 advanced fuel reprocessing, remote operation and maintenance demonstration facility 0-18568  
 AGR, internal radiation shields, design and performance evaluation 0-5373  
 AGR, radiation protection during operation and maintenance of irradiated fuel route 0-5375  
 AGR fuel plug maintenance facility, corrosion product contamination control 0-5388  
 AGR pressure vessel, safeguards for man-access 0-27790  
 AGR pressure vessels, radiation protection for shutdown man-access 0-5374  
 airborne radioactivity in reactor containment building,  $^{133}\text{Xe}$  and  $^{131}\text{I}$  activity following shutdown 0-47749  
 ALARA, effectiveness of design modifications 0-18546  
 ALARA, reactor implant design, a regulatory viewpoint 0-23016  
 ALARA implant design for occupational radiation exposure, cost-benefit anal. 0-18547  
 ALARA objectives, reactor design for occupational exposure 0-23017  
 ALARA occupational radiation exposure, utility design viewpoint 0-18548  
 barytes concrete, gamma ray buildup factors 0-27823  
 basic safety standards, status 0-47774  
 benchmark problems by CSEWG 0-47736  
 benchmark shielding problems, American Nuclear Society Standards Committee, documentation of computational methods 0-47737  
 benchmark shielding problems obtained from integral tests of neutron cross sections 0-47740  
 biological shield removal, associated radiological protection problems 0-9431  
 BWR, anal. of occupational radiation exposure, design implications 0-5380  
 BWR, control of Fe feed rate into feedwater system to reduce shutdown radiation level 0-5384  
 BWR, shield design against neutron streaming in pressure vessel vicinity 0-13678  
 BWR power plant shielding concept 0-18712  
 BWR shield wall penetrations, radiation shielding 0-13679  
 chemical carcinogenesis, redox model 0-26298  
 chromosome aberration of human lymphocytes, microdosimetric expts. 0-26289  
 collective dose commitment, evaluation problems (*French*) 0-47760  
 collective dose equivalent, cost anal. 0-47761  
 collective dose exposures during radiotherapy, optimisation, man-rem monetary value 0-51274  
 community shelters for protection from radioactive fallout 0-5338  
 concrete, albedo for low energy  $\gamma$ -radiation 0-32534  
 concrete buildup factors based on the American National Standard for flux-to-dose-rate conversion 0-47732  
 conference, dose limitation systems, Vienna, Austria (Mar. 1979) 0-46736  
 decommissioning of nuclear facilities, deform. of acceptable residual radioactive contamination levels 0-13973  
 decommissioning of nuclear facilities, establishment of activity limits for items to be released for unrestricted use 0-13972  
 decontamination of radioactive isotopes 0-13950  
 deep penetration problems, rebalance methods, effectiveness 0-47533  
 devices for protection at urological fluoroscopy working stations 0-41254  
 dose equivalent index, practical implications 0-47778  
 dose equivalent index, practicality for regulations 0-47777  
 dose limitation system, application problems 0-47767  
 dosimetry calibration problems in connection with radiation protection around nuclear facilities 0-9422



## radiation protection continued

Dungeness A, radiation and contamination control 0-5386  
 electron transport by the method of condensed collisions 0-47000  
 electrons, diffusion of pencil beam, ang. distrib. model 0-23273  
 EM fields, range 3-30 MHz, exposure, maximum permissible intensity and duration, physiological effects (*German*) 0-12179  
 ENDF/B-V cross section data for shielding appls., Monte Carlo MCNP integral calcs. 0-47744  
 ENDF/B-V nuclear data for shielding appls., energy balance anal. 0-47745  
 environmental dispersion models, evaluation of uncertainties 0-46074  
 eye, human, holographic diagnosis, fail-safe shutter system 0-12209  
 eye irradiation, limitations in international recommendations 0-51278  
 fast neutron transport through laminated Fe-H<sub>2</sub>O shield 0-13931  
 FBR, commercial demonstration reactor, radiation damage shielding 0-23178  
 FBR fuel reprocessing, radiological protection problems 0-5376  
 FBR fuel reprocessing plant, radiation protection, containment and shielding 0-23179  
 fibrosis in the rat gut, protective effect of hypoxia 0-30772  
 fission reactor fuel, mixed oxide, suitability of spent fuel shipping casks 0-27757  
 fusion power, radiological protection review 0-9411  
 fusion reactor irradiation test facility, higher energy neutrons, shielding calcs. 0-13786  
 fusion reactor safety, radiation exposure and maintainability 0-13828  
 fusion reactor shield integral expts. at ORNL 0-47709  
 fusion reactor shielding concretes, neutron activation props. 0-13787  
 fusion reactor shielding experiment, cross-section sensitivity calcs., one- and two-dimensional models 0-27799  
 gamma buildup factors for photons in air, water, iron, moments method code 0-27828  
 gamma exposure rate, real time simulation by puff model 0-47618  
 gamma ray spectral penetration through radiation shields, review 0-5343  
 gamma-ray buildup factors for mats. with very low atomic numbers 0-27822  
 gamma-ray streaming through ducts, spectral meas. 0-32523  
 GCFR, design of deep penetration integral expt. for ThO<sub>2</sub> blanket and radial shield mockup 0-23167  
 GCFR grid plate shield design, anal. of confirmation expt. 0-23166  
 GCFR shielding expts. at Tower Shielding Facility, ORNL 0-47739  
 geologic waste repositories, long term safety assessment methodology 0-37487  
 glass fibre materials for radiation filtration 0-5341  
 glove box for sealed manipulator maintenance 0-18684  
 glove boxes, Pu-contaminated, size reduction and waste packaging 0-18469  
 graphite, neutron penetration, Monte Carlo calculations for 30, 45 MeV (*Japanese*) 0-18677  
 graphite, proton bombardment at 52 MeV, neutrons and photons penetration 0-27821  
 health aspects of low-level radiation, radiation protection standards 0-26375  
 health physics quantities and units 0-8193  
 Hinkley Point B, AGR radiation protection, design criteria and operating experience 0-27832  
 hot cell complex for post irradiation exam. in Japan, O-arai Engng. Centre (*Japanese*) 0-47536  
 hot cell laboratory, refurbishing  $\beta$ - $\gamma$  cell line, upgrading operational routines 0-23160  
 hot cell liners, removable, design 0-18685  
 hot fuel examination facility, auxiliary equipment for remote handling systems 0-18686  
 HTR, direct cycle, radiation exposure during maintenance and repair of He turbine 0-18563  
 HY LIFE converter concept, remote systems requirements 0-18614  
 ICRP (1977) recommendations, implementation problems in Korea 0-47779  
 ICRP dose limitation system (*French*) 0-47753  
 ICRP recommendation implication in Israel 0-47773  
 ICRP recommendations, applications in practice 0-47771  
 instrumentation, reliability and availability 0-18709  
 instrumentation reliability, non-instrumental constraints upon the performance of systems for radiological protection 0-18710  
 integrated approach for protection from ionising rad. and other mutagens 0-51276  
 intense neutron source facility, skyshine anal. methods comparison 0-5349  
 International Commission on Radiological Protection, dose limits (1934-77) 0-12266  
 International Commission on Radiological Protection, recommendations 0-47752  
 ionising radiation, mortality of radiation workers 0-8108  
 irradiated fuel rods, in-cell welding techniques 0-22956  
 isotope induction at LAMPF, fabrication, cladding, handling of irradiated targets 0-23231  
 laser radiation hazards and protection standards 0-46069  
 laser safe operation control measures 0-9928  
 leaktight remote handling equipment for operations in an irradiating and contaminating environment 0-13951  
 LMFBFR fuel elements, remote exam. of shroud tubes 0-18470  
 low-level radiation during development studies, implications for ICRP-26 0-51281  
 LWR, chemical factors controlling  $\gamma$  radiation fields around coolant circuits 0-5371  
 LWR, rem reduction plan for standard 1100MW(e) plant designs 0-745  
 LWR containment vessel, I removal by spray after LOCA, MIRA-PB code 0-47593  
 LWR irradiated fuel transport flasks, shielding and engineering aspects 0-27831  
 LWR power plants, protection of maintenance personnel 0-5368  
 LWR radiation dose minimization during operation, maintenance and inspection 0-5294  
 LWR shielding, neutron transport anal. comparison of several multigroup libraries 0-23168  
 Magnox power station, decommissioned, rad. levels, neutron activation, waste disposal 0-13976  
 Magnox reactors, influence of design and operation on personnel radiation dose meas. 0-5385  
 manipulation unit equipment for radiotherapy depts. 0-30903

## radiation protection continued

materials, benchmark radiation transport data, air-over-ground neutron and gamma spectroscopy 0-23161  
 medical accelerators, international standards 0-51272  
 medical findings for GDR works, documentation to meet ICRP-26 0-51280  
 medical radiation practice, ICRP recommendations in worker medical monitoring (*French*) 0-51275  
 meteorological information system for response to nuclear power station accidental release of radioactivity 0-16888  
 methyl iodide desorption kinetics from impregnated charcoal 0-52791  
 microdosimetry, conf., Brussels, Belgium (May 1978) 0-4472  
 microwave, standards and need for field measurements 0-26377  
 minicomputer-based radiation protection networks for nuclear plants 0-855  
 mixed oxide fuel fabrication plant decommissioning, public radiation exposure 0-42800  
 multi-attribute approach to the rationalization of radiation protection options (*French*) 0-47765  
 multigroup electron transfer cross-section method 0-46999  
 multigroup transfer coeffs., efficient eval. for shielding appls. 0-47747  
 N-reactor, radiation source control, chemical decontamination 0-23058  
 natural background approach to setting radiation standards 0-47782  
 natural radiation dose, variability as comparison point for acceptable radiation risk 0-51282  
 neutron and gamma transport, expt. and theoretic results comparison 0-47750  
 neutron bomb radiation protection, calc. of rad. penetration in air and shielded human tissue dose equiv. 0-47743  
 neutron dosimetry for radiation protection, European workshop 0-23177  
 neutron shield material tests 0-37543  
 new waste calcining facility, radiation shield integrity testing 0-13940  
 non-ionising radiation exposure control in Canada 0-36150  
 nonionising radiation hazard definition problems 0-3823  
 nonionising radiation protection, international programme 0-3822  
 nuclear facilities, cost-benefit anal. problems 0-47770  
 nuclear fuel reprocessing plant ventilation control 0-5318  
 nuclear power plant operation, radiation exposure ALARA concept 0-32388  
 nuclear power plants and the fuel cycle, conf., Bristol, England (Nov. 1978) 0-4471  
 nuclear power station safety, regulatory control in UK 0-18707  
 nuclear power stations, radiation dosage determination, monitoring and control for personnel safety (*German*) 0-842  
 nuclear safety, radiation protection estimation of individual and collective equivalent dose (*Spanish*) 0-5336  
 nuclear waste management, radiological protection criteria 0-47780  
 occupational exposure, averaging, weighting, ICRP-2G recommendations 0-47781  
 occupational radiation exposure, evaluation and control, US research program 0-5370  
 occupational radiological exposure at nuclear fuel prep. plants, UK regulatory control 0-18708  
 optimisation at nuclear research centre using ICRP recommendations 0-47759  
 optimisation methodologies (*French*) 0-47758  
 optimisation recommendations, implementation methodology 0-47766  
 optimization of radiation protection 0-47757  
 Parker, H.M., biographical note on medical physics contris. 0-12  
 particle accelerator decommissioning, radioactive waste management 0-18720  
 particle accelerators, radiation exposure, design of cooling and ventilation systems 0-5350  
 PDX Tokamak, neutron skyshine Monte Carlo calcs. 0-47711  
 perturbation theory, higher order generalised 0-47731  
 PFR Dounreay, radiation and contamination control 0-27834  
 PFR Dounreay, utilisation of neutrons meas. for shielding calcs. 0-32538  
 photon calibration of radiation protection instruments in an authorized metrology service 0-9423  
 Pilgrim power station, radiation source control activities 0-23059  
 polyethylene, neutron penetration, Monte Carlo calculations for 30, 45 MeV (*Japanese*) 0-18677  
 portable instrumentation test and calibration 0-9420  
 present trends, impact of ICRP-26 0-47783  
 progress report, EEC, 1978, book 0-22148  
 public radiation exposure, optimisation, problems 0-47768  
 PWR, anal. of occupational radiation exposure, design implications 0-5381  
 PWR, cavity streaming problem, shield config. optimisation 0-9352  
 PWR, control of fission products activity in primary coolant, computer code 0-32537  
 PWR, low-pressure drop reactor cavity shield system 0-13677  
 PWR coolant pH effect on radiation field buildup 0-23060  
 PWR decommissioning, public radiation exposure 0-42800  
 PWR radiation shielding design 0-5372  
 PWR refuelling shutdown, control of <sup>58</sup>Co dissolution in coolant using H<sub>2</sub>O<sub>2</sub> 0-23066  
 quality factor, lineal energy correction for saturation effects 0-26376  
 quality factor recommendations and dose limits 0-26369  
 quantities used in radiological protection—an explanation 0-46070  
 radiation calorimetry of single electron pulses from a LINAC 0-42872  
 radiation risk assessment, importance 0-47754  
 radiation risks in nuclear industry, comparison to other jobs 0-18680  
 radiation shield integrity testing 0-5390  
 radiation source reduction, potential benefits of occupational radiation exposure reduction 0-23057  
 radioactive solid wastes disposal, benefit-cost anal. 0-18556  
 radioactive solution sampling, vacuum-bottle system 0-18688  
 radioactive waste calcining facility, radiation protection features 0-5377  
 radioactive waste solidification facility, radiological aspects of design 0-5378  
 radiography, foetal vs. parenteral radiosensitivity 0-51271  
 radiological safety rules at CEGB 0-5369  
 radionuclide intakes by workers, limits, recommendation from ICRP 0-47762  
 radionuclide migration from repository sites, stochastic anal. 0-37486  
 radionuclides incorporated into stem cell DNA, biological damage, radiation protection implications 0-12187  
 radiotherapy, organ shielding using Pb-Sn-Bi-Cd low melting point alloy block (*Korean*) 0-36154



## radiation protection continued

- radiotherapy electron accelerator neutron production, conf., Gaithersburg, USA (Apr. 1979) 0-46730  
 radiotherapy neutron leakage characts. rel. to room shielding 0-51273  
 reactor, radiation source control programs at EPRI 0-23056  
 reactor cavity neutron shield design at Millstone Unit No.2 0-47748  
 reactor decommissioning, radioactivity limits for release of liquid radwaste, math. model 0-13737  
 reactor shielding, 6 MeV gamma photons penetration through Al, concrete and graphite determ. 0-5256  
 reactor spent fuel storage vault, criticality safety determ. (Korean) 0-37478  
 regulatory control, implications of ICRP publication 26 0-18706  
 residual activity levels allowing radioactive waste to be considered inactive 0-13735  
 RF and microwave exposure, USA occupational safety and health standards 0-3727  
 RF fields below 300 MC/s, legislation proposals for workers' protection 0-56223  
 risk justification, theory and appl. 0-47755  
 safety glasses, physical factors determining the utility 0-46067  
 safety regulation impact on nuclear medicine (French) 0-47764  
 scattering expansion truncation error correction program 0-47001  
 scintillation counter, for gamma radiation, design calibration and construction (Spanish) 0-5437  
 secondary neutron polarization via penetration through a ferromagnetic shielding wall 0-47742  
 Serpukhov proton synchrotron shield, mixed radiation dose equivalent outside 0-32530  
 SGHWR, radiation protection and plant maintenance 0-27789  
 SHIELD computational system, nucl. fuel cycle appl. 0-37517  
 shielding, radiation transport theory, tracklength biasing in Monte Carlo methods 0-5335  
 shielding of structures against initial nuclear radiation: Monte Carlo methodology 0-47741  
 Sizewell power station, radiation and contamination control 0-5387  
 skin contamination, difficulties in applying ICRP-26 0-51279  
 skin irradiation, limitations in international recommendations 0-51278  
 sodium reactor experiment decommissioning, radiation protection 0-9432  
 SOLASE laser fusion reactor, Monte Carlo shielding calc. for mirror-laser beam duct system 0-23174  
 solid neutron shield development, materials eval. for spent fuel shipping cask 0-13939  
 source definition for head shielding requirements in linear accelerators, effect on room shielding design 0-46068  
 Soviet radiation safety standards (Russian) 0-47756  
 spacecraft thermionic reactors, neutron leakage control using boronated reflector drums leading to lower shielding mass 0-47663  
 standards for people involved in more than one source of hazard (French) 0-47772  
 storage ring, SRS, shielding design 0-37659  
 surface coating materials in nuclear generating stations, ionising radiation protection (German) 0-18681  
 synergism of radiation and other DNA damaging agents 0-26299  
 temporary confinement structures, design criteria and guidelines 0-18683  
 TFTR neutral beam injectors, concrete shielding calcs. 0-47734  
 TFTR neutral-beam injectors, shielding calcs. 0-23172  
 TFTR vacuum pump system, radiation exposures during maintenance 0-13788  
 Thoramat automatic thoracic radiography unit experience 0-12212  
 Tokamak fusion test reactor, in-vessel maintenance remote manipulator system 0-18611  
 Tokamak reactor blankets, effects of neutral beam injection tubes, shielding calcs. 0-23173  
 tritium distribution in technological systems of Novovoronezh nuclear power station 0-32533  
 Tsuruga power station anal. of corrosion products 0-23062  
 UK legislation embodying ICRP-26 and IAEA safety standards 0-47763  
 UK population, sources of radiation exposure, review 0-36156  
 US Nuclear Regulatory Commission practices for assuring worker protection 0-5367  
 USA NRC reactions to ICRP (1977) recommendations, practical implications 0-47776  
 Windscale nuclear fuel reprocessing, shielding and radiation protection 0-18714  
 workers and the ICRP recommendations (French) 0-47775  
 X-ray attenuation, effect on dose distrib. and choice of quantities for protection standards 0-51277  
 X-ray shielding arrangement, for diff. equipment 0-849  
 $\beta$ -ray point source dosimetry using variable cavity chamber, appl. to protection instrument response 0-13942  
 B<sub>4</sub>C-Al(silicone)(graphite), neutron shielding materials, long term radiation effects 0-9413  
<sup>14</sup>C, formation, distrib. in nuclear fuel cycle (Russian) 0-5316  
<sup>60</sup>Co long-lived  $\gamma$ -emitting aerosols, max. allowable emission rate from nuclear power station 0-32532  
 Fe radiation shielding, computational benchmark for deep penetration 0-47738  
 Fe radiation shielding, TLD meas. of neutron and gamma-ray energy deposition 0-23163  
 Fe shield, meas. of neutron and gamma ray penetration 0-47730  
 I, radioisotopes, environmental and biological effects from nuclear fuel cycle (Russian) 0-52768  
<sup>125</sup>I labelling hazards, recommended code of practice 0-51270  
<sup>131</sup>I filters, design against weathering 0-32524  
<sup>85</sup>Kr, pressurised cylinder storage tests 0-5269  
 MgO, GCFR shielding material, anal. of shielding effectiveness 0-47746  
 Pu handling, radiation protection and monitoring of personnel 0-5389  
 Pu, high burnup fuels, shielding and handling problems 0-27833  
 PuO<sub>2</sub> powder, leak rate determ. 0-42808  
<sup>222</sup>Rn A=220, 222, decay products attachment to polystyrene aerosols 0-41256  
<sup>222</sup>Rn conc. in energy efficient buildings 0-41261  
<sup>222</sup>Rn diffusion in soil, moisture effects 0-37491  
<sup>222</sup>Rn, sources, distrib., exposure in residential buildings 0-41262  
 T concentration reduction for aquifer 0-21423  
 T, role in radiation safety in nucl. fuel cycle (Russian) 0-56227  
 U mines, dose limitations, ICRP recommendations, implementation problems 0-47769  
 W, radiation shielding material, integral tests of ENDF/B-IV high-energy neutron cross-section data 0-23162

## radiation quenching

- acetylenic hydrocarbons, cyclohexane soln., structureless fluoresc. 0-5575  
 alkali halides, luminescence quenching of F-centres 0-50417  
 anthracene, vapour, fluoresc. spectra, mol. vibr. freq. reson. laser IR irradiation, quenching 0-18883  
 anthracene film, effect of struct. on luminesc. quenching (Russian) 0-7411  
 benzaldehyde-biacetyl system, self-quenching and electronic energy transfer obs. 0-5571  
 benzene in dilute cyclohexane solution, fluoresc. quenching on pulsed proton irradiat., temp. depend. 0-21307  
 chlorophyll-a, conc. quenching rel. to functional charge transfer 0-30666  
 complex molecules, photoinstability and quenching effect on laser generation kinetics 0-3390  
 1,5-dimethylnaphthalene, fluoresc. quenching by cyclic azoalkanes, micelle system probe 0-35578  
 dioxane solutions, radioluminescence quenching in mixtures of solvents (Russian) 0-55192  
 1,6-diphenylhexatriene, lower excited states fluoresc. quenching 0-1016  
 electron irradiat. effect on electrolum., defects form. and quenching obs. 0-55194  
 high temperature metallic species, absorpt. and fluoresc., high temp. fast flow reactor technique 0-42231  
 indole soln. containing histidine, fluoresc. rel. to soln. pH 0-2826  
 liquid scintillation counters, external standard quench correct. capability, inexpensive method for acquisition 0-47810  
 luminescence quenching, hopping mechanism, kinetics 0-7406  
 methacrylate polymer, carbazoyl substituted, excimer and charge transfer complex trapping of excitons 0-34367  
 methylated benzene+tetracyanobenzene, fluorescent exciplex form., electronic relax. 0-5573  
 1-methylpyrene, fluoresc. quenching by Cu<sup>2+</sup> in micellar system, general kinetic model 0-32753  
 micelle-confined molecules reaction, diffusion-controlled, luminesc. quenching, excimer form. 0-50890  
 molecular vibrational energy transfer, potential well depths 0-43156  
 $\alpha$ -NPO, fluoresc. spectrum light quenching factor wavelength depend. 0-18882  
 organic photoconductor, electric field-induced fluoresc. quenching 0-34967  
 phase fluorometry as a probe of diffusion-controlled molecular encounters in dense fluids 0-32799  
 phosphate glass: Nd<sup>3+</sup>, highly conc., electron energy deactivation and transfer (Russian) 0-29802  
 photoluminescence concentrational depolarisation by excitation energy transfer 0-2821  
 phthalimide acetyl derivatives in polar solvents, luminesc. kinetics and phosphoresc. quenching 0-18885  
 POPOP, fluoresc. spectrum light quenching factor wavelength depend. 0-18882  
 POPOP laser, bleaching of vapour 0-19027  
 protein, radical limiting conc. on UV irradiat. at 77K, effect of luminesc. quenchers 0-30662  
 proteins, adsorbed at interfaces, fluoresc. spectroscopy study 0-12315  
 retinals, prod. and quenching of singlet oxidation 0-35840  
 rhodamine 101, quenching of emission in methanol and latex particle suspensions 0-3374  
 rhodamine 6G, aqueous soln., absorpt. spectra, ground and triplet state photoprotonation pH depend. 0-42961  
 $\beta$ -SiC, optical quenching of luminesc., acceptor ionisation energy 0-55178  
 solid, luminesc. quenching parameters, donor-acceptor exchange mechanism 0-2840  
 TOPOT, 1,4-bi[2-(5-p-tolyloxazoly)]benzene laser, bleaching of vapour 0-19027  
 TOPOT, fluoresc. spectrum light quenching factor wavelength depend. 0-18882  
 tryptophan soln. containing histidine, fluoresc. rel. to soln. pH 0-2826  
 Ar, hydrogenlike, Lamb shift meas. by motional elec. field quenching time-of-flight expt. 0-9550  
 ArCl\*, excimer formation rate consts., B state radiative lifetimes, quenching, VUV excitation 0-55631  
 ArF, electron quenching rate consts. meas. by fluoresc. anal., laser implications 0-32969  
 Ar\*, quenching by O(2p<sup>4</sup> 3P), population and depopulation of O(3p<sup>3</sup> P) 0-42958  
 Ar\*+Kr, flowing afterglow, energy transfer reaction and quenching rates 0-23529  
 As<sub>2</sub>S<sub>3</sub>:Fe glass, photolum. and ESR, Fe impurities as non-radiative recomb. centres 0-29788  
 Ba, (5d<sup>3</sup>D<sub>3</sub>) state, quenching obs. 0-52926  
 BaO-P<sub>2</sub>O<sub>5</sub>(SiO<sub>2</sub>) glasses, quenching of Nd<sup>3+</sup> luminesc. by transition metal and rare earth ions 0-25449  
 Br+O<sub>2</sub>(NO), quencher paramagnetism, deactivation rate const., spin-orbit relax. study 0-21263  
 C<sub>2</sub>, low lying a<sup>1</sup> $\Pi_u$  state produced in intense IR field, fluoresc. and quenching obs. 0-11931  
 CO, b<sup>1</sup> $\Sigma^+$  state excitation, low-energy electron impact,  $\nu'$ =3 level lifetime 0-1072  
 CO+CO<sub>2</sub>, vibr. level depend. quenching of CO( $\nu$ =1-16) 0-32808  
 CS(A<sup>1</sup> $\Pi$ ) vibr. relax. in He 0-53106  
 Ca(4p<sup>3</sup> P<sub>1</sub>) + Ba, collisional deactivation and optical lifetime 0-48070  
 Cd+K(+N<sub>2</sub>), optical excitation, rate consts., collisional energy transfer kinetics 0-32801  
 Cd<sub>2</sub>, quenching and predissociation, possible excimer laser 0-32770  
 CdS(Se)(Te):Co<sup>2+</sup>, IR luminesc. quenching, Co<sup>2+</sup> level position, ionisation energy 0-16079  
 Cd(5P<sub>0</sub>) + methane (H<sub>2</sub>)(D<sub>2</sub>)(N<sub>2</sub>), absolute quenching cross sections 0-5604  
 ClFCS, second excited singlet state photophysics, laser excitation obs. 0-32758  
 Cs, resonant 6P state, quenching by CO<sub>2</sub> mols. in He-CO<sub>2</sub>-Cs discharge 0-43860  
 EuCl<sub>3</sub>·6H<sub>2</sub>O-NdCl<sub>3</sub>·6H<sub>2</sub>O(HoCl<sub>3</sub>·6H<sub>2</sub>O), in DMSO soln., Eu<sup>3+</sup>→Nd<sup>3+</sup>(Ho<sup>3+</sup>) radiationless energy transfer 0-5499  
 F VIII, 1s2p<sup>3</sup> P<sub>0</sub> and <sup>3</sup>P<sub>1</sub> levels, lifetimes, hyperfine quenching effects, UV beam foil spectra 0-47931  
 GaAs-Au, quenching of exciton luminesc. by surface elec. field 0-29801  
 (Gd<sub>1-x</sub>Tb<sub>x</sub>)<sub>2</sub>O<sub>3</sub> phosphor, concentration quenching of Tb<sup>3+</sup> luminesc. 0-29785  
 H+He, H Balmer- $\alpha$  fine-struct. line shift and broadening 0-37783



## radiation quenching continued

- H<sub>2</sub> 3s, 3d:  $^3\Sigma$ ,  $^1\Pi$ ,  $^1\Delta$  complex, fine struct., Doppler-free laser spectroscopy 0-1087
- HCN (001)+HCN(Ar)(N<sub>2</sub>)(CO<sub>2</sub>)(CO), relax. rate consts., using Cs vap. IR source 0-9696
- He and He<sup>+</sup>,  $^3P$  and  $^4F$  levels excitation with electron beams, radiation decay obs. 0-43188
- He glow discharge, low press., excitation transfer and quenching of n=3 excited states 0-38743
- He glow discharge, n=3 sublevel quenching and energy transfer, laser perturbation method 0-44060
- He I glow discharge, low-pressure, quenching of singlet states by N<sub>2</sub> 0-49030
- He, metastable states, props., energy transfer mechanisms, exptl. techniques 0-27921
- He<sup>+</sup> Lamb-shift measurement by the quenching-radiation anisotropy method 0-18824
- Hg+halomethane,  $^3P_1$ -state total quenching 0-52927
- Hg<sub>2</sub> excimers, photoassoc., spectroscopy and kinetic processes of high-lying vibronic states, laser applics. 0-9649
- Hg<sub>2</sub>, quenching and predissociation, possible excimer laser 0-32770
- HgBr, laser photolysis prep., laser induced fluoresc., collisional quenching processes 0-38014
- HgBr\*, collisional quenching by inert gas (molecule) 0-42986
- HgBr\*, collisional quenching by inert gas (molecules) 0-43091
- HgCl\*, collisional quenching by inert gas (N<sub>2</sub>) 0-42986
- HgI\*, collisional quenching by inert gas (N<sub>2</sub>) 0-43091
- I+HCl, quenching of I( $^5P_{1/2}$ ), temp. depend., time resolved at. absorpt. spectrophotometry 0-32655
- I+methane d<sub>0</sub>(d<sub>3</sub>), d<sub>4</sub>, excited atoms, quenching, isotope effects, time resolved reson. fluoresc. 0-32656
- I<sub>2</sub>+CO<sub>2</sub>, collisional energy transfer, quenching effects 0-14193
- K<sub>8</sub>Nb<sub>4</sub>Si<sub>4</sub>O<sub>26</sub>, luminesc. bands, Stokes shift, rel. to crystal struct., stacking faults 0-34974
- K<sub>8</sub>Nb<sub>4</sub>Si<sub>4</sub>O<sub>47</sub>, luminesc. bands, Stokes shift, rel. to crystal struct., stacking faults 0-34974
- KrCl\*, excimer formation rate consts., B state radiative lifetimes, quenching, VUV excitation 0-55631
- KrF, electron quenching rate consts. meas. by fluoresc. anal., laser implications 0-32969
- La<sub>1-x</sub>Tb<sub>x</sub>OBr phosphor, concentration quenching of Tb<sup>3+</sup> luminesc. 0-29785
- N,  $3p^2S^2$ -state quenching in low-pressure glow discharge 0-23355
- N<sub>2</sub>, solid and matrix isolated mol., triplet state spectra (Russian) 0-5574
- NH<sub>2</sub> (A<sup>2</sup>A<sub>1</sub>), excited state dynamics and bimol. quenching processes 0-9681
- NO, Rydberg states quenching rate consts., two photon excitation method 0-5581
- NO<sub>2</sub>, laser-induced fluoresc. quenching rate const. and lifetimes 0-11930
- Na-fluorescein, glycerol-alcohol soln., luminesc. decay time, conc. depend. 0-34960
- Na(3p<sup>2</sup>P<sub>3/2</sub>)+N<sub>2</sub>(O<sub>2</sub>)(CO)(NO), electronic energy quenching dynamics, crossed beam expt. 0-9683
- O+O<sub>2</sub>, quenching of O( $^1S$ ) state, rate coeff. 0-41581
- O<sub>2</sub> in chloroform and carbon tetrachloride solns., sensitized luminesc. 0-32762
- O<sub>2</sub>, singlet states, quenching by O<sub>2</sub>(N<sub>2</sub>), shock tube study 0-23511
- OCS, high-intensity laser photolysis at 157 nm, S( $^1S$ ) prod., photoionisation, and loss, laser appl. 0-21306
- O( $^1D$ ) quenching in Earth atmosphere, translationally hot O( $^3P$ ) energy distrib. 0-21811
- O( $^1D$ )+Ar(Kr)(Xe), inelastic collisions, spin-orbit coupling 0-5605
- O( $^1D$ )+CO( $^1\Sigma^+$ ), collisional quenching, energy transfer processes 0-23501
- OH(A<sup>2</sup> $\Sigma^+$ )+N<sub>2</sub>(O<sub>2</sub>)(H<sub>2</sub>O)(air), quenching rates and fluoresc. efficiency, rel. to atmosphere 0-14199
- O(2D<sub>5/2</sub>)+N<sub>2</sub>(O<sub>2</sub>)(N<sub>2</sub>O)(CO<sub>2</sub>)(H<sub>2</sub>O)(methane), collisional deactivation meas., 295K, rel. to atmospheric processes 0-16663
- Rb(nS, nD<sub>3/2</sub>)+Rb(ground state), collisional quenching cross sections 0-43146
- Se<sub>2</sub>, photolysis by UV lasers, appl. to kinetics of group VI laser systems 0-7807
- Se<sub>2</sub>, photolytic dissociation obs. using inert gas halide lasers 0-11935
- Si, amorphous, spin depend. recomb., luminesc. and light induced ESR 0-50393
- Si amorphous film, dangling bond ESR, light-induced quenching 0-50162
- SiS\*, collisional quenching from Si+OCS 0-45505
- Sn+N<sub>2</sub>O→SnO(a<sup>2</sup> $\Sigma$ )+N<sub>2</sub>, chemiluminesc. high temp. fast flow reactor obs. 0-45493
- SrO, luminesc. band edge, 4-6.5 eV, optical absorpt., photoluminesc., cathodoluminescence, photocond. obs. 0-50411
- TbCl<sub>3</sub>·6H<sub>2</sub>O-PrCl<sub>3</sub>·6H<sub>2</sub>O(ERCl<sub>3</sub>·6H<sub>2</sub>O), in DMSO soln., Tb<sup>3+</sup>→Pr<sup>3+</sup>(Er<sup>3+</sup>) energy transfer mechanism 0-5498
- UF<sub>6</sub>, photophysical props., laser study 0-28040
- UF<sub>6</sub>, UV photophysics, energy balance through quantum efficiency meas. 0-9634
- Xe afterglow, radiative and collisional deexcitation of reson. states, absorpt. and emission obs. 0-38742
- XeCl, relax. and quenching rate consts., emission spectra modelling 0-28211
- XeF, electron quenching rate consts. meas. by fluoresc. anal., laser implications 0-32969
- XeF, relax. and quenching rate consts., emission spectra modelling 0-28211
- Zn, excited states, collisional quenching cross sections and exit channels, fluoresc. quenching obs. 0-18919
- Zn<sub>2</sub>, quenching and predissociation, possible excimer laser 0-32770
- Zn<sub>2</sub>-Cd<sub>1-x</sub>S, resonance Raman scatt. involving exciton complexes 0-16039
- ZnS, excited phosphor, IR stimulation and quenching of luminesc., review (Russian) 0-11455
- ZnS(Se)(Te):Co<sup>2+</sup>, IR luminesc. quenching, Co<sup>2+</sup> level position, ionisation energy 0-16079

## radiation therapy

- accelerator neutron leakage survey 0-51269
- accelerator primary beam neutron contamination 0-51268
- accelerators, international standards 0-51272
- adenocarcinoma of colon and rectum, current place of radiation therapy (French) 0-17075
- anatomy, 3D display for radiotherapy treatment planning 0-3773

## radiation therapy continued

- autoimmune reactions, non-organ specific, absence of after treatment 0-12185
- beam characteristics of a 22 MeV microtron 0-51260
- benign thyroid disease treatment, <sup>131</sup>I appl., review 0-36107
- beta particle emitters used in therapy, figure of merit 0-36083
- bone and joint disease, radioisotope therapy 0-36111
- bone metastases of prostatic gland carcinoma, <sup>89</sup>Sr therapy 0-36076
- brachytherapy source, dose rate meas., fundamental accuracy limitation 0-3815
- breast and chest wall, comparison of radiation techniques 0-30837
- breast cancer, conservative treatment method (French) 0-17076
- breast carcinoma, cosmetic results anal. after primary therapy 0-3782
- breast carcinoma, efficiency of postoperative radiation 0-46008
- breast carcinoma, radiation therapy as primary treatment, review (Dutch) 0-17078
- calibration and meas. standards in USA 0-8188
- cancer, using microwaves, economical and safety aspects 0-3754
- cancer therapy, microwave hyperthermia, design of implantable radiators 0-41164
- cancer therapy, physical hyperthermic techniques, EM coupling-modalities 0-41163
- cancer treatment by microwave hyperthermia (French) 0-3764
- cell kinetic quantitative models for tumour response, equivalence 0-30770
- cervical cancer, self-adjusting applicator 0-51208
- cervix carcinoma, transvaginal cone electron beam technique 0-21531
- chromosome aberration of human lymphocytes, microdosimetric expts. 0-26289
- clinical trials for radiation therapy (Japanese) 0-51179
- collective dose exposures during radiotherapy, optimisation, man-rem monetary value 0-51274
- computed tomography, spectral artefact correction and determ. of electron density and at. no. 0-51231
- computer interface for a linear accelerator 0-51226
- computer program for negative pion beam calcs. 0-46061
- computerised internal mammary lymphoscintigraphy in radiation treatment planning 0-12223
- computerised tomography, use in treatment planning (German) 0-17090
- computerised tomography in childhood craniofacial sarcoma management 0-12221
- conference, New Orleans, USA (Oct. 1979) 0-41931
- continuous external irradiation 0-3781
- contrast enhancement of high-energy radiotherapy films 0-8126
- deep tissue temp. monitoring by ultraminiature thermistors 0-3761
- depth dose function concept, definition and values 0-3814
- diathermy, shortwave and microwave, for deep-tissue heating 0-17050
- diathermy, temp. distrib. obtained with a phantom 0-17051
- dosage selectivity by planning 3-D radiation treatment using computer 0-41178
- dose calculation, based on computed tomography images use of scatt. radiation meas. 0-51265
- dose compensation filter design using megavoltage radiography 0-3785
- dose perturbation from Au dental fillings 0-12265
- dose/cure relationships of irradiated tumours, statistical anal. 0-46052
- dose/cure relationships study 0-56218
- dosimetry study of split beam technique 0-12264
- electron accelerator neutron prod. 0-51240
- electron accelerator neutron production, conf., Gaithersburg, USA (Apr. 1979) 0-46730
- electron accelerator photoneutron prod., survey of European meas. 0-51241
- electron beam collimation in SL 75 linear accelerator, design, appl. and performance 0-41204
- electron beam dosimetry for treatment planning 0-3817
- electron beam therapy of lateralised lesions of oral cavity and oropharynx 0-12215
- electron beam therapy with medium energy electrons, review 0-36069
- electron beams, 50 MeV, in treating deeply situated tumors (Chinese) 0-56209
- electron depth dose distrib., central axis, analytic expression 0-3813
- elementary particles from 1 GeV range accelerators, medicine appl. (German) 0-41210
- EMI scanner picture automatic outlining, for radio therapy treatment planning 0-41206
- energetic heavy ion beam model for radiobiology 0-26293
- external beam radiotherapy, isodose planning, new suite of programs 0-41243
- fast neutron therapy, radiobiological bases 0-35995
- fast neutron therapy facility at the cyclotron 'Cyclone', Louvain-la-Neuve 0-41192
- feto-placental tissues, irradiated effects after treatment of material genital carcinoma 0-45964
- fibrosarcoma, hamster, absence of metastases following US treatment 0-35960
- fundus oculi tissue, thermal effects on exposure to laser radiation 0-26261
- Gaussian-beam launcher for microwave exposure studies, dielectric hemisphere-loaded scalar horn 0-12206
- glottic cancer, early, review 0-12217
- glottic cancer, early, review 0-12218
- gustatory function, radiation-induced changes, neutrons rel. to photons 0-12184
- haematologic disorders, radionuclide therapy 0-36109
- head and neck tumours, unorthodox fractionation 0-3780
- high energy photon beams, advantages and props. 0-51238
- high energy X-ray machines, effect on tumour cure rate 0-36067
- high LET radiation therapy beams, expt. microdosimetry 0-12280
- high-energy accelerators, mixed photon-neutron field meas. 0-51267
- high-energy linear accelerator photon beam exit design for neutron prod. minimisation 0-51242
- high-energy X-ray beams, scatt. radiation rel. to leakage radiation 0-51266
- hyperthermia combined with radiotherapy, normal and cancer cell effects obs. 0-45972
- hyperthermia research with dual-beam microwave applicator 0-17052
- hyperthyroidism, childhood, role of radioiodine treatment 0-41182
- hyperthyroidism, use of <sup>131</sup>I in treating children and adolescents 0-46013
- interstitial, dosimetric localisation, use of computerised tomography scanner 0-21540
- intracavitary uses of colloids 0-36110
- intracavity radiotherapy, interactive treatment planning using CT 0-8145



## radiation therapy continued

- ionization-chamber-dependent factors for calibration of megavoltage X-ray and electron beam therapy machines 0-18704  
 isocentric fast neutron therapy facility at Edinburgh 0-30842  
 larynx carcinoma, primary therapy, review 0-12216  
 laser, CO<sub>2</sub>, appls. and results 0-56155  
 laser applications in clinical medicine (*Japanese*) 0-12211  
 laser applications in medical research, biophysical aspects 0-51201  
 linear accelerator, Varian Clinac 18/10, use of polystyrene filters for electron energy modification 0-56168  
 linear accelerator calibration monitor with a memory 0-3821  
 linear accelerator neutron sources and characts. 0-51239  
 liver, appl. of <sup>90</sup>Y for cancer therapy 0-17098  
 lymphatic metastasis from primary tumour growing in foot, localised preirradiation X-irrad. influence 0-45976  
 lymphocytic leukemia, chronic, total body irradiation 0-3778  
 lymphoma, non-Hodgkin's, total body irradiation 0-3779  
 magnetic modification of electron beam dose distributions 0-30893  
 malignant thyroid disease treatment, <sup>131</sup>I appl. 0-36108  
 mammary carcinoma conservative radiotherapy, computer assisted dosimetric soln. (*Dutch*) 0-36139  
 manipulation unit equipment 0-30903  
 maternal cancer, internal irradiation technique, dose calcs. (*Dutch*) 0-3816  
 meson factory, therapeutic use (*Japanese*) 0-26351  
 metastatic thyroid cancer, use of <sup>131</sup>I 0-36084  
 Mevatron 60, X-ray linear accelerator 0-21530  
 microdosimetry, conf., Brussels, Belgium (May 1978) 0-4472  
 microwave, for cancer treatment 0-26320  
 microwave applicator, broad band, for heating tumours 0-30830  
 microwave hyperthermia simulation (*French*) 0-3770  
 microwave irradiated breast tumour thermal pattern calc. (*French*) 0-3759  
 microwave power appls., conf., London, England (Nov. 1979) 0-21520  
 microwave tissue heating system for hyperthermia research 0-30829  
 microwaves in cancer therapy, review of 4 years 0-56162  
 missing tissue compensator 0-3784  
 Moire topography camera, simulator mounted, for constructing compensating filters 0-46024  
 multibeam microwave therapy with computer control 0-3766  
 neutron collimated beam RBE for cell survival rel. to lineal energy spectral differences 0-12200  
 neutron collimated fast beam, radiation quality local distrib. 0-12247  
 neutron irradiation facility, TRIGA Mk.II reactor, remodelling and dosimetry 0-56200  
 neutron leakage characts. rel. to room shielding 0-51273  
 neutron radiotherapy planning and radiation quality definition 0-12246  
 neutron RBE, rel. to leakage from HV electron accelerators 0-51177  
 neutron secondary spectra prod. by high energy bremsstrahlung in C, N, O and tissue 0-41239  
 neutron source using <sup>7</sup>Li(p,n)<sup>7</sup>Be, especially for smaller cyclotrons 0-26335  
 neutron teletherapy, effects of filters and wedges on skin sparing and  $\gamma$ /neutron dose ratios 0-46029  
 neutron-irradiated tissue and equivalent material recoil spectra 0-17022  
 oral tongue, postoperative split course treatment of carcinoma 0-12220  
 organ shielding using Pb-Sn-Bi-Cd low melting point alloy block (*Korean*) 0-36154  
 oropharyngeal epithelioma treatment, role of radiation therapy (*French*) 0-41190  
 orthovoltage X-ray therapy, TLD dose intercomparison 0-12272  
 osteogenic sarcoma treatment, role of radiation therapy (*French*) 0-17077  
 pelvis, optimisation of box technique to reduce femur dose 0-12263  
 photodermatological uses of dye lasers, erythema production, psoriasis treatment, tumour destruction (*German*) 0-56164  
 photogrammetry use in absorbed dose determ. 0-12222  
 photon activation anal. for high energy radiation therapy 0-21534  
 photon and electron transport simulation, deceleration photons prod. using linear accelerator (*French*) 0-12282  
 photon beam characts. of 20 MV accelerator for radiation therapy appls. 0-26430  
 pion region tumours, treatment results 0-12219  
 pion<sup>+</sup>, biological effect prediction, star distrib. for high LET dose determ. 0-12248  
 pion<sup>+</sup>, biomedical experiences, conf., Brugg-Windisch, Switzerland (Dec. 1978) 0-22138  
 pion<sup>+</sup>, energy deposition spectra and radiation therapy appl. 0-26363  
 pion<sup>+</sup>, in vivo dosimetry using Al activation 0-46060  
 pion<sup>+</sup>, pre-clinical studies at TRIUMF 0-26264  
 pion<sup>+</sup>, suitability for use, radiobiological obs. 0-26338  
 pion<sup>+</sup> and pion<sup>0</sup>, stopping density distrib. in 1 and 2 dimensions 0-26340  
 pion<sup>+</sup> broad therapeutic beams, microdosimetric characterisation 0-12277  
 pion<sup>+</sup> cancer radiotherapy, RBE in and near large beam 0-12245  
 pion<sup>+</sup> radiation, uniform depth-dose distrib. technique and cell survival obs. 0-17139  
 pion applicator, meas. at  $\pi E^3$  single beam correl. to dosimetry and therapy-planning 0-26361  
 pion beam, appl. of thermolum. dosimetry 0-26362  
 pion beam treatment planning, deep seated tumours, computerised tomographic scans 0-41180  
 planning and dosimetry for pion applicator 0-26360  
 planning programs development for SIN pion applicator 0-26339  
 primary dosimetric standards at the Memorial Sloan-Kettering Cancer Center, NY, USA 0-8190  
 prostatic carcinoma treatment planning, US imaging rel. to computerized tomography 0-3786  
 proton beam absorbed dose determ. 0-46062  
 radiation biology conf., Sapporo, Japan (Sept. 1978) 0-8105  
 Radiation Oncology Research Program, recommended research proposals 0-3787  
 radiobiological data for clinical dosimetry in pion tumour therapy 0-26266  
 radionuclide therapy, pot. future appl. 0-36031  
 radiotherapeutic agents, props., dosimetry and radiobiologic considerations 0-36106  
 safety regulation impact on nuclear medicine (*French*) 0-47764  
 scattered radiation to fetus for partial treatment of Hodgkin's disease 0-21533  
 skin melanoma therapy by laser irradiation (*German*) 0-12208

## radiation therapy continued

- source definition for head shielding requirements in linear accelerators, effect on room shielding design 0-46068  
 Space Radiation Effects Laboratory 710-MeV He ion beam, biophysical aspects 0-30871  
 spleen radiotherapy and computed tomography in treatment planning 0-56180  
 techniques and modes of action, review (*French*) 0-21523  
 temperature distrib. in microwave-irradiated cylinders simulating living tissues 0-3760  
 tissue equivalent bolus, 1 to 10 GHz electrical prop. characterisation 0-3763  
 toxic diffuse goiter, simultaneous treatment with <sup>131</sup>I and antithyroid drugs 0-56193  
 transskull transmission of axisymm. focused US beams, 0.5 to 1 MHz 0-51184  
 treatment planning, accuracy of a 2-sensor sonic digitizer 0-30806  
 treatment planning, depth dose scaling using computerised tomography scans 0-30899  
 treatment planning, inter-hospital interactive computerised system 0-36068  
 treatment planning, three dimensional model for CT radiotherapy 0-8192  
 treatment planning appl. of computed tomographic imaging 0-51232  
 treatment planning using microcomputer 0-8191  
 treatment time and sub-lethal repair, CHO cell obs. 0-30773  
 tumour, feasibility of focused microwave antenna array system 0-21521  
 tumour location by computerised tomography, use of masking lattice (*German*) 0-41213  
 uterine adenocarcinoma, Paul Cogniaux Centre results, 1960-1970 (*French*) 0-41191  
 uterus, mouse, US irradiation at therapeutic intensities in standing wave fields 0-41112  
 UV light therapy for skin diseases 0-36057  
 vertical couch extender 0-3783  
 X-ray beam, 4 MeV linear accelerator, dosimetric aspects 0-17140  
<sup>198</sup>Au, use in ovarian carcinoma treatment 0-36087  
 Co teletherapy, T3-carcinoma in Bilharzial bladder, hyperfractionation and conventional fractionation comparison 0-41179  
<sup>60</sup>Co radiation therapy, eval. of dosimetric accuracy and uniformity 0-12269  
<sup>60</sup>Co teletherapy unit dose calibration, comparison of methods 0-30900  
<sup>60</sup>Co total body irradiation, dose distrib. meas. using thermoluminescent dosimeters 0-41245  
<sup>131</sup>I, radioisotopes, history of use 0-42032  
<sup>131</sup>I therapy, review of contamination and exposure hazards 0-41257  
<sup>131</sup>I-therapy of cancer or hyperthyroidism, absorbed dose to ovaries or uterus 0-36138  
<sup>188</sup>Re labelled EHDP preparation and possible use in osseous neoplasms treatment 0-56215  
<sup>222</sup>Rn curved plesiotherapy applicators, dosimetry 0-51261  
<sup>222</sup>Rn external plesiotherapy, dosimetry obs. 0-36135
- radiationless transitions** see nonradiative transitions
- radiative corrections**  
 "radiative corrections" is distinguished in use from "electromagnetic corrections" by application to atomic and molecular spectra  
 see also electromagnetic corrections; radiative shifts  
 atom, bound state quantum fluctuations and variational method, relativistic HF calc. with radiative effects 0-42918  
 electron mass operator in 2-D QED approx. 0-4900  
 molecular crystal, surface exciton levels, radiation corrections 0-34962  
 muonic He, hyperfine struct., relativistic, radiative and recoil corrections, QED test 0-14256  
 unstable atoms, in time-depend. EM field, radiative corrections 0-23321  
 H, n=2 levels, Lamb shift and fine struct. reson. meas. 0-23321  
 S compounds, one-electron binding and Auger energies 0-52872  
 S, one-electron binding and Auger energies 0-52872
- radiative lifetimes**  
 alkali halide:Ti<sup>3+</sup>-like ions, triplet state lifetime, hyperfine interaction 0-2844  
 atmospheric thermal plasma, continuous emission, ionisation potential lowering and total excitation cross section 0-38705  
 atom, multielectron, correlated transitions in decay of two inner-shell vacancies 0-37799  
 atom, rel. oscillator strengths determ. by combined absorption/emission meas., Ti appl. 0-37784  
 atomic collisions, rotationally induced transitions in two-state model 0-47945  
 atomic metastable states, props., energy transfer mechanisms, exptl. techniques 0-27921  
 trans-azobenzene, S<sub>2</sub>→S<sub>0</sub> fluoresc. 0-28044  
 beam-foil lifetime measurement, cascading problem, ANDC method use and error limits 0-14249  
 beam-foil spectroscopy uses in atomic lifetime meas., review 0-14248  
 bound states, beam-foil excitation and decay near ionis. limit 0-9552  
 charged particle scatt. in quantising mag. field 0-46853  
 chlorofluoromethylene radical, gas phase laser-induced fluoresc. spectroscopy 0-14173  
 chlorophylls a and b and pheophytins, fluoresc. and phosphoresc. 0-12057  
 cofacial diporphyrins, electron transfer reactions following picosecond excitation, CT state lifetimes, optical difference spectra 0-25995  
 curve crossing systems, two-state, non-adiabatic transitions, semi classical Magnus approx. 0-37756  
 diamagnetic band structure, second order calc. using Landau functions, optical transition probability determ. 0-24784  
 difluorocarbene, A'<sup>1</sup>B<sub>1</sub>-X'<sup>1</sup>A<sub>1</sub> system spectrosc. and photophysics 0-5577  
 4-diphenylphosphorylstilbenes, fluoresc., photodimerisation 0-1015  
 discharge, running striation excitation, metastable atoms lifetime influence 0-38760  
 energy transfer dye lasers and laser induced intermol. and intramol. energy transfer processes 0-9647  
 fluorescence quantum efficiencies and lifetimes, environmental effects, semiclassical approach 0-7393  
 formaldehyde-d<sub>1</sub> (-d<sub>2</sub>), single vibronic levels, fluoresc. emission, radiative lifetimes and vibr. relax 0-23521  
 haloacetylene cations, electron impact excitation A→X band system assignment 0-32766  
 heavy ion, beam-foil spectra from 20 to 238 MeV energy, 5 to 60 nm, lifetime meas. problems 0-9722



## radiative lifetimes continued

- heavy ions, beam-foil decay curves for reson. transitions, simulation 0-9721
- hydrogen-like ions, beam-foil excitation, relative initial populations, lifetime curves 0-14210
- induced electronic transitions, radiative lifetimes, non-Condon effects 0-53051
- 9-iodoanthracene, picosecond fluoresc. lifetimes, thermally activated  $S_1 \rightarrow T_1$  intersystem crossing 0-28045
- ions, multiply charged, highly excited states, parity nonconservation effects 0-52898
- ions, multiply charged, level lifetimes relativistic calc., S-matrix approach 0-47942
- K-shell Auger rates, level widths and fluoresc. yields, relativistic Dirac Hartree Slater calc. 0-52957
- laser-based methods for transient chem. events meas. 0-40801
- mesoatoms in static electromagnetic fields, excited state lifetimes and population, nuclear moments (*Russian*) 0-53170
- metal surface, fast ion scatt. by plasmons, theory 0-45190
- molecular, calc. methods 0-23462
- molecular collision, quasi-classical and quantum moments of distrib. of states, semiclassical comparison 0-23480
- molecular collision processes in presence of picosecond laser pulses, radiative transitions 0-23479
- molecular metastable states, props., energy transfer mechanisms, exptl. techniques 0-27921
- molecule, electron impact, K-shell electrons excitation with high energy resolution, review 0-37899
- pentacene films, luminesc., struct. 0-11461
- plasma, Jeffries' level population ratios and Seaton's cascade matrix 0-52934
- poly-2-vinylnaphthalene, soln., lowest triplet props., flash photolysis and radiolysis obs. 0-32861
- polyatomic molecule, ultrafast vibr. using laser light pulses 0-9699
- resonance fluoresc., probe of intramolecular relax., density matrix formalism, lifetimes and quantum beats 0-32757
- thiophosgene,  $B^1A_1$ -state, photophys., fluoresc. lifetime meas. 0-53033
- three two-level atoms system, continuously incoherently-pumped, radiation rate, spectrum 0-5716
- time-correlated picosecond laser pulses generation, rapid sampling of optical relax. phenomena 0-9969
- 1,3,5-trichloro-2,4,6-trifluorobenzene radical cation,  $B^2A_2' \rightarrow X^2E''$  laser-induced fluoresc. spectra 0-14172
- two electron systems, coupling schemes, transition energies and probabilities of autoionising states 0-18828
- ( $\mu p$ )<sub>15</sub> muonic atoms in gaseous H, triplet state lifetime 0-23579
- Al II to Al VI, beam-foil obs. from 1100 to 1900 Å, lifetimes and oscillator strengths 0-14108
- Al II to Al VI, beam-foil obs. from 300 to 2000 Å, mean lives and oscillator strengths 0-14109
- Al IV, lifetimes of  $n=3$  and 4 levels meas. and calc. (*French*) 0-9554
- Al IX to Al XI, beam-foil obs. of lifetimes and oscillator strengths, 300 to 1000 Å 0-14110
- AlGaAs-GaAs heterostructures, luminescent characts., efficiency and radiative lifetime conc. depend. 0-55151
- AlO,  $B^2\Sigma^-X^2\Sigma$ , Einstein A coeffs., band strength and band oscillator strength 0-43113
- Ar, condensed electron beam excited, exciton radiative lifetimes 0-6727
- Ar high density plasma, highly excited atomic levels, spectral-line-blending study 0-48969
- Ar, hydrogenlike, Lamb shift meas. by motional elec. field quenching time-of-flight expt. 0-9550
- Ar IV to Ar XII, beam-foil obs. of lifetimes and oscillator strengths, spectral identifications, 400-2000 Å (*French*) 0-9555
- Ar, photoionisation, Auger processes, decay lifetime, line shift, profile, X-ray photoelectron spectra 0-37798
- Ar<sup>15+</sup> and Ar<sup>16+</sup>, beam-foil obs. of lifetimes of metastable states 0-14116
- ArCl\*, excimer formation rate consts., B state radiative lifetimes, quenching, VUV excitation 0-55631
- ArH<sup>+</sup>,  $\Sigma^+$  ground state, molecular consts. calc. from pot. curves 0-9680
- ArI, transition probabilities calc. 0-32666
- ArS, photoluminesc. in rare gas matrices 0-5568
- As,  $4p^3 \rightarrow 4p^25s$ , transition probabilities 0-47943
- B-like ions, autoionisation states calcs. 0-43006
- Be isoelectronic sequence, highly ionised, beam-foil obs. of oscillator strengths for E1 transitions 0-14112
- Be like ion, radiative decay of  $2^3P_0^o$  level 0-27984
- Be sequence,  $2s3p^3P_1-2s^2^1S_0$  intercombination line transition probabilities 0-18823
- Bi<sub>2</sub>Ge<sub>2</sub>O<sub>12</sub> crystals, doped with Dy<sup>3+</sup>, Ho<sup>3+</sup>, Er<sup>3+</sup>, Tm<sup>3+</sup>, Yb<sup>3+</sup>, growth, spectral and laser props. 0-45115
- C foil, ion irradi., graphitisation rel. to lifetime, relevance to beam-foil spectroscopy 0-15166
- CBr<sub>2</sub> emission in solid Ar, laser excitation spectra and lifetimes 0-48034
- CBrCl emission in solid Ar, laser excitation spectra and lifetimes 0-48034
- CF<sub>2</sub>, fluoresc. and radiative lifetime obs. in dibromodifluoromethane UV laser photolysis 0-16703
- CO,  $b^2\Sigma^+$  state excitation, low-energy electron impact,  $\nu'=3$  level lifetime 0-1072
- Ca II, lifetime extraction from beam-foil decay curves 0-14107
- Ca+He,  $^1P_1$  level lifetime, Hanle measurement 0-23365
- Ca( $4p^3P_1$ )+Ba, collisional deactivation and optical lifetime 0-48070
- Cd,  $5s, 6^3D_3 \rightarrow 5^1P_1$  transition probabilities meas. by US pulverisation/flame emission (*French*) 0-42995
- Cd I, excited states radiative lifetimes 0-942
- Cd<sub>2</sub>(Cd<sub>3</sub>), fluoresc. kinetics, optical excitation, energy spacings and equilib. consts. 0-43090
- CdHg, fluoresc. kinetics, optical excitation, energy spacings and equilib. consts. 0-43090
- Cl ions, multiply-charged, beam-foil obs. of allowed L-shell transitions 0-14113
- Cl<sup>16+</sup>, Lamb shift meas. using beam-foil excitation, QED test 0-9551
- Cl<sub>2</sub>, and isotopic forms,  $B^1\Pi(0_u^+)$  state, laser-induced fluoresc., collisional energy transfer rates 0-53038
- ClFCS, second excited singlet state photophysics, laser excitation obs. 0-32758
- Co I and Co II, beam-foil obs. of lifetimes 0-14111
- Cs II, radiative lifetimes of excited states 0-9558

## radiative lifetimes continued

- CsI, self-trapped exciton electronic struct., semi-empirical mol. orbital method 0-49605
- Cu, isoelectronic series, semi-empirical oscillator strengths, lifetime, transition probability 0-32672
- Cu-like ions, E1 transitions, wavelengths, oscillator strengths and transition probabilities, data tables 0-37780
- Eu chelate, fluoresc. lifetime, depend. on optical environment 0-9630
- Eu(III) complexes, f-f transition probabilities, ligand polarisation model, anisotropic contribs. 0-53049
- Fe XXII, allowed transition Cl wave functions, oscill. strengths and transition probabilities 0-32664
- Fe XXII, intercomb. transitions, oscill. strengths, transition probs., rel. to solar spectra 0-52935
- FeV and VI, beam-foil lifetime meas., 1100-1900 Å 0-23532
- GaAs, acceptor bound exciton Auger and radiative transition rates, radiative recomb. 0-6733
- GaAs, doped, radiative lifetimes, quantum mechanical model 0-55151
- H, beam foil excitation,  $n=2$  density operator and prod. probability meas., transition probabilities 0-14219
- H like, metastable 2S state in weak elec. field, radiative decay, bound state QED 0-42959
- H<sub>2</sub>, electron impact excited singlet-g states, optical and time resolved spectra, radiative lifetimes, quenching rates for rovibronic levels 0-23564
- H<sub>2</sub>, predissociation probabilities of  $4p\pi^1\Pi_u + \nu' \geq 1$  levels, dissociation channels interference 0-28074
- HCl, transition probabilities, IR chemilum. obs. of form. channels in H+ClF reaction 0-26017
- HF, transition probabilities, IR chemilum. obs. of form. channels in H+ClF reaction 0-26017
- He and He<sup>+</sup>,  $3^3P$  and  $4^2F$  levels excitation with electron beams, radiation decay obs. 0-43188
- He-N<sub>2</sub> plasma, N<sub>2</sub>  $B^1\Pi_g$  state excitation, role of long lived states, luminesc. 0-37829
- He+Ne<sup>+</sup>, impact excitation, cascade-fluorescence spectroscopy, level-crossing techniques 0-23357
- Hg, 6D levels excited by dye laser, lifetimes 0-42996
- Hg<sub>1-x</sub>Cd<sub>x</sub>Te, acceptor bound exciton Auger and radiative transition rates, radiative recomb. 0-6733
- I VI and I VII, beam-foil obs. of lifetimes, spectral assignments, 400 to 1300 Å 0-9556
- I VII, beam-foil lifetime meas., cascading problem 0-14249
- <sup>215</sup>In,  $8P^3P_{3/2,1/2}$ , HFS and lifetimes, fluoresc. decay and quantum heats, beam 0-32657
- K, s and d state radiative lifetimes, time and wavelength resolved fluoresc. spectra 0-14104
- K<sup>+</sup>, direct excitation of levels, transition probs. and cross sections 0-37890
- KBr, F-centre radiative lifetime meas. near 65K 0-25439
- K<sub>2</sub>NdLi<sub>2</sub>F<sub>10</sub> (KNLF), spectroscopy and lasing 0-5737
- KXe, dye laser induced emission, excimer bands and uses 0-9650
- Kr I, transition probabilities in transition arrays 0-32667
- Kr I atom,  $4p^3$  nd ( $n=4,5,6,7$ ) configurations, experimental lifetimes 0-27981
- Kr I electric dipole lines, absolute transition probabilities 0-9560
- Kr VIII, beam-foil decay curves for reson. transitions simulation 0-9721
- Kr XXXIII and Kr XXXIV, beam-foil obs. of transition wavelengths and oscillator strengths 0-14115
- Kr<sub>2</sub>, prod. and decay of  $0_u^+$  and  $1_u$  states, synchrotron excited 0-43109
- KrCl\*, excimer formation rate consts., B state radiative lifetimes, quenching, VUV excitation 0-55631
- KrS, photoluminesc. in rare gas matrices 0-5568
- Li, excited-state lifetime meas. using disc-shaped heat-pipe oven 0-52941
- Li<sup>+</sup>,  $2^2S_1$  metastable state radiative lifetime, fluoresc. meas. 0-42999
- Mg<sub>9+1</sub>,  $^3p$  triplet system, lifetime meas. 0-47946
- Mg<sub>9+1</sub>, beam-foil excited, spin orbit-forbidden X-ray transition obs. 0-23537
- Mo<sup>32+</sup>, dielectronic recomb. rate coeffs. in plasma 0-43853
- Mo<sup>38+</sup>, dielectronic recomb. rate coeffs. in plasma 0-43852
- N I plasma jet, spectroscopic diagnostics, Stark broadening and shift, study 0-38727
- N V, beam-foil decay curves, mean lives determ. 0-9553
- NH<sub>2</sub> ( $A^2A_1$ ), excited state dynamics and bimol. quenching processes 0-9681
- NO<sub>2</sub>, laser-induced fluoresc. quenching rate const. and lifetimes 0-11930
- Na like ions, dielectronic recombination rate, scaling props. 0-32668
- Na<sub>2</sub>, laser excited, atomic and molecular fluorescence with long radiative decay times 0-27976
- Ne, beam-foil excited  $^3P$  state, delayed coincidence Auger electron lifetime meas. 0-14117
- Ne I, transition probabilities in const. elec. field 0-37785
- Ne, Townsend discharge afterglow, decay rate of metastable ats. 0-44011
- O, beam-foil excited  $^4P$  state, delayed coincidence Auger electron lifetime meas. 0-14117
- O, beam-foil spectra, multiply ionised O 0-42977
- O<sub>2</sub> in chloroform and carbon tetrachloride solns., sensitized luminesc. 0-32762
- OH, A-X system, rot. transition probabilities 0-43027
- O(S), prod. and props. in liq. Ar and N<sub>2</sub>, by N<sub>2</sub>O photodissociation 0-43063
- P, highly ionised, beam foil radiative lifetimes and EUV spectrum 0-32671
- Pb I and II, transition probabilities, Stark broadening parameters 0-23367
- Rb, radiative lifetime, time resolved laser induced fluorescence 0-37781
- Rb, radiatively excited states, ionis. rate coeffs. in two atom collisions 0-43160
- Rb<sup>+</sup>, levels direct excitation, cross sections and transition probabilities determ. 0-52899
- Ru complexes, Ru(bipy)<sub>3</sub>Cl<sub>2</sub>·6H<sub>2</sub>O and Ru(bipy-d<sub>3</sub>)<sub>3</sub> Cl<sub>2</sub>·6H<sub>2</sub>O, soln. electronic excitation energy, deactivation determ. 0-55173
- S(S), prod. and props. by OCS photodissociation in liq. Ar and N<sub>2</sub> 0-43064
- Se<sub>2</sub>, photolysis by UV lasers, appl. to kinetics of group VI laser systems 0-7807
- Se<sub>2</sub>, photolytic dissociation obs. using inert gas halide lasers 0-11935
- Si, highly ionised, beam-foil lifetime obs. 0-32670
- Si ions, multiply-charged, beam-foil obs. of  $1s2p^3P_1$  lifetime 0-14114
- SiC<sub>2</sub> (6H), radiation damaged, luminesc. 0-25462
- Sn<sup>+</sup> ( $5s5p^2$ )  $^4P_{1/2}$  level, lifetime and Lande g-factor (*French*) 0-52938



**radiative lifetimes continued**

- Sr+He,  $^1P_1$  level lifetime, Hanle measurement 0-23365  
 Sr $^2(P_{3/2})$ , Penning ion, polarised emission, Hanle effect obs., radiative decay rate meas. 0-5520  
 Tb complexes, intermol. energy transfer to Eu complexes in aq. soln. 0-25426  
 Tb complexes, intermol. energy transfer to Eu complexes in aq. soln. 0-25427  
 Ti( $^3D_2$ ) lifetime, in rel. oscill. strengths determ. by combined absorption/emission meas. 0-37784  
 UF $_6$ , UV photophysics, energy balance through quantum efficiency meas. 0-9634  
 Xe, condensed electron beam excited, exciton radiative lifetimes 0-6727  
 Xe II, beam-foil spectroscopy 0-18825  
 Xe, in gas discharge, collisional excitation, radiation lifetimes, macroscopic alignment obs. 0-33734  
 Xe VIII, beam-foil lifetime meas., cascading problem 0-14249  
 Xe $^{2+}$ , energy level radiative lifetimes using 1-5 MeV ions 0-47947  
 XeS, photoluminesc. in rare gas matrices 0-5568  
 Zn I isoelectronic series, 4s4p $^1P$  lifetimes meas. 0-42998  
 Zn II, lifetime extraction from beam-foil decay curves 0-14107  
 ZnI, II, excited states, radiative lifetimes, multi-channel delayed-coincidence method 0-32669  
 ZrO, B $^{II}$  state radiative lifetimes, transition rates and oscillator strengths, reson. fluoresc. decay 0-28053

**radiative shifts**

- collective radiative phenomena in two level systems (*Russian*) 0-1174

**radiative transfer**

- albedo problem in inhomogeneous isotropically scatt. atmospheres, appl. of max. variational principle 0-36398  
 anisotropic scatt. in one-dimens. system, radiative transfer parametric anal. 0-5920  
 aqueous media, radiation transfer prediction techniques, assessment 0-33428  
 atmosphere, IR cooling rate in standard atmosphere 0-26609  
 atmosphere, IR radiative transfer rel. to zonal radiation balance perturbation by stratospheric aerosol layer 0-56602  
 atmosphere, longwave radiative transfer model rel. to CO $_2$  effect on heating rates 0-17376  
 atmosphere, perturbed, photochemical radiative convective model for thermal struct. and relaxation rates 0-8408  
 atmosphere, radiation under cumulus cloud conditions, Monte Carlo method (*Russian*) 0-21793  
 atmosphere, static radiative flux model rel. to anthropogenic CO $_2$  influence on temp. 0-51486  
 atmosphere, thermal sensing from Earth orbit, spatial temp. and geopot. fields 0-36429  
 atmosphere boundary layer, temperature inversion, characts. of stable nighttime layer 0-41533  
 atmosphere heat and radiation budget during solar eclipse, above pine forest (*German*) 0-46226  
 atmosphere-ocean system, matrix operator approach 0-8330  
 atmospheres, spherical symmetry, radiative transfer, non-conservative problem 0-36492  
 Be stars, electron scatt. effects on Balmer emission lines 0-17589  
 black hole accretion discs, radiative transfer rel. to Lightman-Eardley instabilities and disc thickening 0-31324  
 Boltzmann linear eqn., Pade approximants 0-551  
 channel, annular, long, free-mol. and radiative transport, approx. analytical soln. 0-6165  
 cloud droplet growth effects 0-8404  
 clouds, radiative properties parameterisation 0-56601  
 cloudy atmosphere, thermal radiation fluxes calc. (*Russian*) 0-4103  
 cloudy sky, theoretical scheme for IR radiative transfer 0-51540  
 Crab Nebula, ionising radiation transfer rel. to emission line spectrum 0-22068  
 cylinder, infinite isothermal, fitted with scatt. medium, radiation problem soln. 0-4676  
 diatomic gas, vibr. nonequil., probabilistic modelling 0-33434  
 differential approx. for linear-anisotropic scattering 0-33429  
 diffuse radiation view factors from differential plane sources to spheres 0-5921  
 Earth-atmosphere radiative heating effects on climate, NOAA radiometer meas. 0-8425  
 energy balance model, climate sensitivity to radiation flux calcs. 0-8421  
 energy loss by resonance line photons in an absorbing medium 0-56699  
 evaporating droplets, radiative absorption 0-33426  
 finite medium freezing (melting), variational anal., radiation and convection effects 0-38244  
 flat layer of selective medium with semitransparent boundaries, radiative-conductive heat transfer 0-19227  
 fluidised bed, radiative contribution to total heat transfer 0-19384  
 Fourier analysis limitations for radiative transfer soln. in small angle scatt. approx. 0-37952  
 gray, planar, absorbing-emitting-scatt. medium bounded by nonisothermal walls, radiative heat transfer 0-1413  
 H-function for anisotropic scattering, approx. form 0-36491  
 Hartmann MHD flow, radiative transfer 0-6161  
 Hercules X-1, reson. Compton cyclotron scatt. rel. to cyclotron line form. 0-8711  
 homogeneous atmosphere of finite optical thickness, standard problem 0-51646  
 hot matter, conductive opacities and free-free Gaunt factors 0-3361  
 hypersonic flow around blunt body, similarity law for radiant heat transfer coeff. 0-33705  
 inhomogeneous gas layer, transmission calc. for model with exponential distrib. of line intensities 0-17899  
 inhomogeneous molecular gas radiation calc. using spectral comp. modelling 0-32697  
 integration over frequency method for radiative transfer calc. in real spectrum 0-33430  
 interstellar clouds, diffuse UV radiation penetration 0-56901  
 interstellar polarisation in irregularly fluctuating medium, statistical anal. 0-26926  
 inverse Compton reflection, time-depend. theory, X-ray sources appl. 0-12652  
 inverse problem, for 3-term phase function 0-13007  
 irreversible processes (*French*) 0-13002  
 Lambertian cavity with dielectric window, effective absorptivity 0-38237  
 layered random media, remote sensing, radiative-transfer theory 0-36413

**radiative transfer continued**

- light scattering by dielectric particles, statistical theory 0-32913  
 linear Boltzmann eqn., Pade approximants, appl. to spherical geometry, luminosity and albedo problem 0-52143  
 Markov chain formalism, adding algorithm 0-21902  
 Mars, lower atmosphere modelling, multilayer radiative transfer 0-46451  
 Mars atmosphere, thermal radiative transfer, numerical modelling 0-8574  
 microwave passive remote sensing of snowpacks, theory and expt. 0-26632  
 multidimensional inverse problem in transport theory 0-174  
 multidimensional radiative transfer in stratified atmosphere, grey radiative equilb. 0-26845  
 multiple scattering, two-dimens., in absorbing medium 0-10126  
 non-gray gases, radiative transfer, simple differential approx. 0-38240  
 nonplane geometry media, approx. and num. methods of eqns. soln. 0-33431  
 organic liquids, radiant heat exchange effect 0-19996  
 parabolic reflectors, diffuse-specular axisymmetric surfaces, radiative anal. 0-33438  
 planetary spherical shell atmospheres, appl. to Venus, line form. level 0-17487  
 plasma, multicomponent multiply ionised, mean radiation paths calc. 0-33754  
 plasma, radiative, with anisotropic permittivity, developing wavefronts 0-43896  
 point source in finite sphere, radiation field calcs. 0-13006  
 polarised radiation propag. in shearing field-free plasma, rel. to pulsar microstruct. 0-17483  
 polarized radiation field, asymptotic characts. for low absorpt., appl. to nonconservative Rayleigh scatt. 0-5686  
 protostellar envelopes of masses 3 M $\odot$  and 10 M $\odot$ , coupled radiative transfer/hydrodynamics eqns. and IR appearance 0-36616  
 pulsar magnetosphere, electron absorpt. rel. to spectra low-freq. dropoff 0-17602  
 PWR rod bundles, radiative heat transfer calc. method 0-33602  
 quasars, radiative transfer theory for H line emission from dense plasmas 0-51900  
 quasars, radiatively driven gas clouds dynamics and stability, plane-parallel slabs theory 0-22107  
 quasi-stellar objects, fully interlocked transfer calcs. for H emission line ratios, implications 0-56968  
 radiant-convective heat exchange problems, nonstationary, analytical soln. method 0-33432  
 radiation problems transport eqns., using Wigner distribution 0-168  
 random velocity fields, radiative transfer and line form., intensity moment transfer eqn. derivation 0-52967  
 rectangular enclosure, six-flux model evaluation 0-1415  
 resonance radiation transport with varying Doppler width, thermosphere appl. 0-26737  
 resonance scattering with absorpt. or differential expansion, Monte Carlo calcs. 0-21901  
 scattering indicatrix, expansion coefficient through Mie coeff., anal. 0-18993  
 Schuster-Schwarzschild approx. for media with spherical and cylindrical symmetry 0-23875  
 scintillations in astrophysics, analytic soln. of second-order moment eqn. 0-26726  
 seawater, optical transfer function meas. in Sargasso Sea 0-8328  
 semi-infinite atmosphere containing energy sources, radiation field calc. 0-21907  
 slab, anisotropic radiative transfer, iterative soln. 0-33439  
 slab, planar radiative transfer with isotropic scatt. 0-23876  
 soil, surface roughness effect on microwave emission 0-17264  
 solar atmosphere, spectral line profiles, acoustic wave effects 0-46517  
 solar flares, Fe K $\alpha$  fluoresc. radiative transfer problem 0-17569  
 solar prominences, radiation diffusion integral eqns. rel. to H early Balmer lines emission (*Russian*) 0-12718  
 solar resonance radiation, multiple scatt. in nearby interstellar medium 0-41874  
 spectral line formation in axisymmetric moving envelopes, numerical method and appl. to YY Orionis stars 0-41813  
 spherical harmonic approximations 0-173  
 stellar atmosphere in statistical equilb., effects of deviations from LTE 0-31290  
 stellar atmospheres, line formation in microturbulent magnetic fields 0-31201  
 stellar atmospheres, radiation scatt., approx. soln. (*Russian*) 0-36621  
 stellar magnetic atmospheres, analytical soln. 0-36494  
 sunlight under fractional cloud cover, two-stream approx. 0-51534  
 sunspot model, radiation transfer theory 0-21964  
 sunspots, magneto-optical effects rel. to linearly polarised intensity distrib. obs. with vector magnetograph 0-21965  
 supernovae, type II, nonequilb. processes in evolution 0-46586  
 surface heat flux, nonisothermal grey gas, complex grey walls 0-10125  
 surfaces in diathermal medium, radiation anisotropy modelling 0-33435  
 temperature jumps in a transient radiative transfer problem 0-33427  
 thermal emission, doubling and superposition methods 0-1414  
 thermotechnical equipment, radiant heat exchange modelling in rectangular chamber with attenuating medium 0-33433  
 troposphere, IR transfer in partial cloud cover, model 0-12544  
 troposphere, O $_3$  effects on Earth-atmosphere system radiative energy budget and climate 0-36365  
 turbid water 0-8331  
 turbulent plasma, wave scintillations, fourth-order moment eqn., astrophys. appl. 0-46381  
 Unno-Kondo generalized Eddington approx. in extended atmospheres 0-21997  
 Venus atmosphere, model based on Venera 10 data (*Russian*) 0-12698  
 Venus atmosphere, thermal radiative transfer, numerical modelling 0-8574  
 Venus clouds, absorpt. lines curve of growth rel. to spectropolarimetric equivalent widths information content 0-31215  
 water mass, inherent optical props. of Lake Ontario coastal waters 0-36337  
 water suspensions, radiative property measurements 0-9811  
 X-ray pulsars, vacuum polarisation effect rel. to radiative transfer and X-ray spectra 0-27015  
 X-ray radiation emitted near black holes, relativistic radiative transfer and polarisation features 0-46700  
 X-ray sources, compact, optically thick radiative transfer rel. to X-ray spectra form. 0-22115



**radiative transfer continued**

- X-ray sources, high-freq. EM waves propag. through magnetised plasma in curved space time 0-48894  
 X-rays Comptonization by low-temp. electrons, Monte Carlo calc. 0-12653  
 Au plasma, high-density, high-temp., radiative opacity, particle beam fusion system 0-10365  
 CO<sub>2</sub> plasma, atm. press. opt. props., 400-1200 nm spectral range and 10<sup>2</sup>-2×10<sup>4</sup>K temp. 0-33753  
 CO<sub>2</sub>, rot.-vibr. bands, absorpt. coeff. calc. method, Fermi reson. effect on spectral lines 0-32696  
 CO<sub>2</sub>-N<sub>2</sub> nonequib. mixture convective and radiational heat exchange during flow past body 0-14850  
 H plasma plane and cylindrical layer emission field calc. (*Russian*) 0-33755  
 OH maser sources, interstellar, radiative transport effects on inversion 0-17681  
 SiO film on Al, radiative cooling surface 0-50439

**radicals, free** *see free radicals***radio applications**

- see also radioastronomy; radiocommunication; radionavigation*  
 aurora, Doppler vel. meas., radio aural spectral characts. and incident incoherent scatter meas. 0-56663  
 dielectric medium, strongly absorbing, local defect detect. 0-35481  
 synoptic meteorology, shipboard sounding system for GWE 0-17394  
 synoptic windfinding technique, Loran and VLF nav aids used with radio-sondes 0-17392  
 synoptic windfinding using Omega VLF nav aid, atmos. radiowave propag. 0-17309  
 synoptic windfinding using radiotheodolite system, of USA National Weather Service 0-17379

**radio broadcasting**

- F-layer ionisation through a solar cycle, SW communications appl. 0-41626  
 SW transmission, proportional effect of ionospheric damping, solar activity (*Hungarian*) 0-56675

**radio equipment**

- see also antennas; loudspeakers; transceivers*  
 digital frequency-to-temp. converter for use in radio telemetry systems 0-8119

**radio links**

- see also microwave links; radiocommunication*  
 ELF/VLF goniometer receiver, remote, unmanned, in Antarctica, UHF telemetry link 0-21854  
 precise time dissemination via OMA-50 kHz 0-47032  
 radiosonde meas. and spectral anal. of LOS fading 0-56568  
 satellite transmission, distribution of sound, graphical pictures 0-31463  
 SHF signal attenuation by rain, monitored by radar 0-51567  
 standard long-range operating stations in shelters with integrated thermal-syphon system 0-53616

**radio receivers**

- ELF/VLF goniometer receiver, remote, unmanned, in Antarctica, UHF telemetry link 0-21854  
 marine radiofacsimile weather chart receiver and recorder 0-46297  
 powered superconductor MM range receiver for radio astronomy 0-21919  
 VLBI, Japanese domestic system, receiver and local oscillator (*Japanese*) 0-21923

**radio reception**

- see also atmospherics*  
 SHF signal attenuation by rain, monitored by radar 0-51567

**radio reception quality** *see radio reception***radio relay systems** *see radio links***radio transceivers** *see transceivers***radioactive age determination** *see radioactive dating***radioactive chemical analysis**

- see also radiochemistry*  
<sup>14</sup>C determination, chemical anal., in HTGR spent fuel elements 0-42745  
 aluminosilicate glass, diffusion of Sn(IV) 0-49417  
 biomedical radioassays, historical development 0-42034  
 biomedical radioimmunoassay for bioprotein 0-36101  
 niacin, biologically active forms, radiometric microbiologic assay 0-17208  
 nuclear reactor irradiated fuel, anal. of α-emitting isotopes through laser micro-boring 0-37444  
 progesterone in crude serum extracts, radioimmunoassay using <sup>3</sup>H and <sup>125</sup>I labelled tracers 0-56185  
 radioimmunoassay, plasma renin activity estimation, microprocessor controlled 0-46023  
 radioimmunoassay appls. of Philips gamma counter PW 4800 and scintillation counter PW 4700 0-56173  
 radioimmunoassay as aid to diagnosis, review (*French*) 0-21522  
 radioimmunoassay of acute myocardial infarction markers 0-3809  
 silicate glaze, diffusion of Sn(IV) 0-49417  
 thyroxine, free, radioimmunoassay with prebound anti-T<sub>4</sub> microcapsules 0-46014  
 water samples, U conc. determ. by fission track registration technique 0-12565  
 X-ray diffr. studies of radioactive materials 0-3450  
 β-Al<sub>2</sub>O<sub>3</sub>, <sup>22</sup>Na labelled monocrystals, radiochemical anal. by isotope dilution method 0-11976  
<sup>14</sup>C low level liq. scintillation counting using small vol. teflon-Cu vial 0-16887  
 Es compounds, X-ray powder diffr. 0-2002  
<sup>59</sup>Fe/<sup>55</sup>Fe activity ratio of blood, meas. using semicond. detector 0-17062  
 Pu isotopes, in soil, determination using alpha-spectrometry 0-45601  
 U isotopes, in soil, determination using alpha-spectrometry 0-45601

**radioactive dating**

- see also geochronology*  
 Antarctic igneous rocks, palaeomag. and K-Ar age 0-12332  
 apatite, fission track retention as function of heating time during isothermal expts. 0-36420  
 Archean gneiss dating using zircon data in Labrador 0-3959  
 Azores, K-Ar age of oldest volcanics, volcanic history 0-46158  
 Binda howardite, <sup>87</sup>Rb-<sup>87</sup>Sr meteorite chronology 0-26819  
 chondrite Kirin H, inert gas content interpretation (*German*) 0-46505  
 chondrite Yamato-74191, inert gas composition and neutron capture effects 0-46504  
 Coast-Plutonic Complex, British Columbia, geochronology and thermal history 0-12351

**radioactive dating continued**

- Coast Plutonic Complex, British Columbia, Rb-Sr geochronometry 0-12350  
 corals and shells, <sup>230</sup>Th, <sup>231</sup>Pa and open system dating 0-12434  
 cosmochronology, implications of Allende meteorite isotopic anomalies 0-4462  
 cyclospetry, <sup>10</sup>Be conc. criterion for dating geochemical remains (*French*) 0-21859  
 Deccan Traps volcanic rocks, India, <sup>40</sup>Ar/<sup>39</sup>Ar date and volcanic history 0-46178  
 EPR method of dating minerals 0-36415  
 Farmington chondrite, U-Pb abundances and Pb isotopic studies 0-56778  
 fission track data reports standardisation 0-31436  
 fission track dating method, standard error estimation 0-36419  
 fission track dating technique 0-36417  
 fission track retention as function of heating time during isothermal expts. 0-36420  
 Franciscan series, K-Ar radiochronology (*French*) 0-21692  
 igneous rocks from Gulquac Lake area, New Brunswick, Rb-Sr ages 0-31006  
 S.Indian Craton, Archean gneiss Rb-Sr date of 3360 Myr old 0-46155  
 Kapoeta howardite, <sup>40</sup>Ar/<sup>39</sup>Ar chronology of lithic clasts 0-46501  
 KBS Tuff, E.Turkana, Kenya, K-Ar age estimate 0-56433  
 meteorite, Unter-Massing iron, cosmic-ray exposure age and preatmospheric size (*German*) 0-46507  
 meteorites, <sup>87</sup>Rb-<sup>87</sup>Sr chronology of enstatite chondrites 0-8596  
 meteorites, <sup>87</sup>Rb-<sup>87</sup>Sr dating, shock and brecciation effects in L chondrites 0-51705  
 minerals, fission fragment range and closing temp. for track retention 0-41566  
 Oklo natural fission reactor, dating from U-Pb isotopic data 0-21763  
 Oklo natural fission reactor, radioactive dating from Pb and Th meas. (*French*) 0-21762  
 Oklo natural fission reactors, U and rare earth migration in core sample, appl. to dating of reactions (*French*) 0-21760  
 painting and artist identity, autoradiography and gamma-ray spectroscopy appl. 0-26073  
 polar ice cap, low-level beta counting with an automatic sample changer 0-31147  
 Richardton chondrite, U-Pb abundances and Pb isotopic studies 0-56778  
 Roberts Arm Group, Newfoundland, age rel. to phases of volcanism 0-12354  
 Saglek area, Labrador, Uivak II gneiss, zircon age meas. 0-3958  
 Shergotty achondrite, <sup>40</sup>Ar/<sup>39</sup>Ar age and post-shock thermal history 0-46502  
 Shergotty achondrite, Rb-Sr age and isochron age resetting 0-41774  
 Stillwater complex, USA gabbro Sm/Nd age and mantle evolution curve of Nd 0-41410  
 tektites, fission-track plateau dating evidence of australites older than indochinites 0-56780  
 thermoluminescence dating, radiation dose-rate data 0-31964  
 Umfraville Gabbro, Ontario, palaeomag. study and K-Ar age 0-12330  
 volcanic rocks in Lesser Antilles island arc, palaeomagnetic survey 0-8265  
 Whitehorse map area, Yukon, plutonic rock dates 0-31005  
<sup>26</sup>Al dating, separation of <sup>26</sup>Al and <sup>26</sup>Mg isobars, via negative ion mass spectroscopy 0-31146  
<sup>40</sup>Ar/<sup>39</sup>Ar dating, felsic and mafic mineral separates from an Abitibi dike 0-17237  
<sup>40</sup>Ar/<sup>39</sup>Ar dating by step-heating method, appl. to E.Iceland lava 0-36273  
<sup>40</sup>Ar-<sup>39</sup>Ar dating of magnetizations in Archean Shelley Lake granite 0-30982  
<sup>13</sup>C record in tree rings, industrial CO<sub>2</sub> affecting <sup>13</sup>C assimilation 0-51586  
<sup>13</sup>C/<sup>12</sup>C dating of New Zealand kauri cellulose for last millennium 0-21819  
<sup>14</sup>C dating method using 20 keV Kr ion beam for objects <65000 yrs. (*Danish*) 0-8440  
<sup>14</sup>C dating technique using cyclotrons, or Van de Graaff as mass spectrometer 0-5414  
<sup>14</sup>C, dissolved in groundwater initial activity determ., new model and review 0-8458  
<sup>14</sup>C of lake bottom core rel. to ice-free corridor in Late Pleistocene Alberta 0-26552  
 I-Xe dating of silicate and troilite in Fe meteorites, group IAB 0-17554  
 K-Ar dating of volcanic rocks from Morocco (*French*) 0-51322  
 K-Ar isochron method for age of North Mountain Basalt, Nova Scotia 0-3960  
<sup>40</sup>K-<sup>40</sup>Ar mineral ages for rocks in SW.Brooks Range, Alaska 0-26469  
 Po haloes in rocks and geochronology 0-56468  
 Rb-Sr dating, deformation in Hellroaring Plateau area, Beartooth Mountains, Montana 0-17238  
 Rb-Sr dating, geologically meaningless total rock isochron determ. 0-31014  
<sup>187</sup>Re-<sup>187</sup>Os systematics in meteorites, rel. to solar system early chronology and Galaxy age 0-41778  
 U ore dating from meas. of <sup>238</sup>U and Ru conc. 0-21863  
 U-Pb age method, calc. of uncertainties of U-Pb isotope data 0-46269  
 U-Pb age of uraniferous opals, Spor Mountain, Utah, USA 0-46149

**radioactive decay periods**

- A=79-145, β-delayed neutron emission probabilities, half-life 0-52634  
 alpha-decay, liq. drop model (*Russian*) 0-32246  
 constant, effect of chem. surroundings, electron capture 0-42601  
 cyclic activation method of determining short half-lives 0-47421  
<sup>15</sup>C beta decay transition rates and half life, <sup>15</sup>N excited states and transitions 0-18248  
<sup>114</sup>Cs β-decay, half life and branching ratio, <sup>114</sup>Xe excited states and γ-rays 0-47436  
<sup>67</sup>Ga γ- and X-ray emission probabilities and half-life obs. 0-32242  
<sup>153</sup>Ho-<sup>153</sup>Dy, decay scheme, lifetimes 0-22765  
<sup>138</sup>La, radioactive decay meas., half life, γ energies 0-13418  
<sup>140</sup>La, beta decay half life 0-47435  
<sup>144</sup>La, radioactive decay meas., half life, <sup>144</sup>Ce levels 0-13417  
<sup>6</sup>Li β-decay half life from <sup>7</sup>Li(d,p) 0-13483  
<sup>157</sup>Lu, short lived α emitter, α energy, T<sub>1/2</sub> and branching ratio 0-501  
<sup>176</sup>Lu β-decay half life 0-52633  
<sup>102</sup>Mo, β-decay, T<sub>1/2</sub>, <sup>102</sup>Tc deduced levels, tentative J<sup>π</sup> and transitions 0-52630



**radioactive decay periods continued**

- <sup>32</sup>P, half-life and mean beta disintegration energy determ by low-temp calorimetry 0-5094  
<sup>238,239</sup>Pu,  $\alpha$ -activity and atom ratios 0-5100  
<sup>187</sup>Re, decay const. determ. from <sup>187</sup>Re, <sup>187</sup>Os systematics in meteorites 0-41778  
<sup>94</sup>Rh decay,  $T_{1/2}$ , <sup>94</sup>Ru levels and  $\gamma$ -transitions 0-18244  
<sup>39</sup>S decay, half life, <sup>39</sup>Cl excited states and transitions 0-42595  
<sup>46</sup>Sc, beta decay half life 0-47435  
<sup>A</sup>T, A=212, 213, 214, decay energies and half lives from <sup>176</sup>Hf(<sup>40</sup>Ar,X) 0-47440  
<sup>201</sup>Tl  $\gamma$ - and X-ray emission probabilities and half-life obs. 0-32242  
<sup>153</sup>Tm, short lived  $\alpha$  emitter,  $\alpha$  energy,  $T_{1/2}$  and branching ratio 0-501  
<sup>232</sup>U half-life from specific and relative activity methods 0-9270

**radioactive decay schemes**

- see also nuclear energy levels  
 charact., natural occurrences, technological enhancement and health effects 0-46071  
 gamma emission, math. modelling 0-32236  
 impulse approx. with nuclear current conservation, off-shell form factors 0-52632  
<sup>131</sup>Ba, decay, electric monopole transitions 0-22752  
<sup>152</sup>Eu, decay, gamma transitions and probabilities of beta transitions 0-22768  
<sup>153</sup>Ho-<sup>153</sup>Dy, decay scheme, lifetimes 0-22765  
<sup>169</sup>Lu, radioactive decay, gamma ray and conversion electron spectra 0-22766  
<sup>169</sup>Lu, radioactive decay scheme 0-22767  
<sup>185</sup>Pt<sup>m</sup> decay, population of <sup>185</sup>Ir levels 0-9269  
<sup>75</sup>Se, decay, electric monopole transitions 0-22752  
 U mining, U refining and decay processes, radioactive mining waste disposal (Dutch) 0-21418  
<sup>235</sup>U, thermal neutron irradi., fission product decay power calc. 0-22868

**radioactive lifetimes** see radioactive decay periods**radioactive sources**

- see also radioisotopes  
 alpha-particle sources, thin, prep. from solns. at low temps. 0-27843  
 automatic radioisotope production devices adapted to a medical cyclotron 0-12260  
 beta particle emitters used in therapy, figure of merit 0-36083  
 chromatography radioactive source leak testing under dynamic flow conditions 0-3432  
 cyclotron irradiated gaseous targets, optimum flow rate (French) 0-14025  
 cyclotron production of radiodiagnostic isotopes 0-51255  
 cyclotron production of radionuclides for medical appl., UC-Davis program 0-51257  
 gamma ray sources for exposure rate meas. instrument calibration 0-32562  
 gamma-ray source properties, electron momentum density studies 0-14028  
 isotope induction at LAMPF, fabrication, cladding, handling of irradiated targets 0-23231  
 isotope production at LAMPF, hot cell chemistry 0-18674  
 manipulation unit equipment for radiotherapy depts. 0-30903  
 receptor binding radiotracer preparation 0-51258  
 sealed radioactive sources, US leak and surface contamination tests (Czech) 0-27846  
<sup>106m</sup>Ag,  $\gamma$ -ray energies meas. for Ge(Li) detector calibration 0-27865  
<sup>241</sup>Am thin source preparation 0-18730  
<sup>241</sup>Am, absolute yields of 43.5, 74.7 and 117.8 keV photons 0-32568  
<sup>131</sup>Ba, decay, electric monopole transitions 0-22752  
<sup>109</sup>Cd, production in nuclear reactors by neutron irradi. of <sup>107</sup>Ag 0-52798  
<sup>60</sup>Co gamma ray sources, exposure efficiency dependence on distance, theoretical interpretation (Czech) 0-850  
<sup>60</sup>Co teletherapy unit dose calibration, comparison of methods 0-30900  
<sup>62</sup>Cu generator for medical and biological uses 0-30890  
<sup>152</sup>Eu gamma source, uncertainties in peak area determ. for Ge detector calibration 0-5436  
<sup>152</sup>Eu, X-ray emission probabilities per decay 0-14027  
<sup>125</sup>I, encapsulated, and other photon sources, microdosimetric props. 0-36146  
<sup>192</sup>Ir radioactive sources, field determ. of output and effective size 0-30193  
<sup>40</sup>K,  $\gamma$ -ray energies meas. for Ge(Li) detector calibration 0-27865  
<sup>226</sup>Ra decay chain,  $\gamma$ -ray energies meas. for Ge(Li) detector calibration 0-27865  
<sup>A</sup>Re, A=181, 182, 187, magnetic moments meas. by PAC 0-22688  
<sup>75</sup>Se, decay, electric monopole transitions 0-22752  
<sup>82</sup>Sr-<sup>82</sup>Rb generator improvement using inorganic exchangers 0-17135  
<sup>177</sup>Ta, magnetic moments meas. by PAC 0-22688  
<sup>99</sup>Tc<sup>m</sup> generator of higher activity 0-17136

**radioactive tracers**

- <sup>55</sup>Co for nuclear medicine, production by <sup>3</sup>He bombardment of <sup>55</sup>Mn 0-36132  
 applications in industry and science (Czech) 0-32554  
 cerebral blood flow meas. in animals using <sup>14</sup>C-ethanol 0-41205  
 corrosion monitoring in chem. equipment, distant-reading radiometric method 0-50795  
 hydrological pollution control, tracers appl. (French) 0-7995  
 ion exchange, Zn<sup>2+</sup>-Cl<sup>-</sup> system, complex form. studied using radiotracer, effect of macroelectrolyte cation 0-16659  
 lake studies, isotope techniques appl., advisory group meeting, Vienna (1977 August 29 to September 2) 0-41950  
 neurophysiology, transmitter-specific retrograde labelling in the striato- and raphe-nigral pathways 0-51309  
 nuclear medicine, trends (French) 0-26327  
 nuclear medicine conference, Karlovy Vary, Czechoslovakia (May, 1979) 0-12840  
 nuclear medicine imaging principles, concepts and equipment 0-17113  
 positron active tracer for liquid-flow measurement system, microcomputer-controlled 0-24113  
 production for biomedical uses, review (French) 0-17056  
 radiopharmaceuticals preparation by Szilard-Chalmers labelling and radioprotection in ice lattice 0-51259  
 receptor binding radiotracer preparation 0-51258  
 red blood cells, <sup>99m</sup>Tc labelling 0-41236  
 red blood cells, in vivo labelling with <sup>99m</sup>Tc with stannous pyridoxylideneamines 0-46049  
 water pollution, silt double-labelling technique for radioactive tracing (French) 0-7994

**radioactive tracers continued**

- <sup>211</sup>At protein labelling technique using an acylation reaction 0-36130  
<sup>7</sup>Be, atmospheric, distrib. within high-press. systems in E. United States 0-4072  
<sup>77</sup>Br-labelled 5 $\alpha$ -dihydrotestosterone, synthesis and distrib. in rats rel. to <sup>77</sup>Br-bromide 0-51247  
<sup>80m</sup>Br labelling of tyrosine, uracil and cytosine 0-51248  
<sup>11</sup>C methionine positron emission computerised tomography, pancreatic scanning obs. 0-30861  
<sup>11</sup>C, production by cyclotron, biomedical appls. (French) 0-56216  
<sup>11</sup>C-acetylene, production by methane pyrolysis and irradi. 0-36129  
<sup>11</sup>C-labelled amino acids for rectilinear and positron tomographic imaging of human pancreas 0-12258  
<sup>14</sup>C, autoradiography of thin laminars (French) 0-35438  
<sup>18</sup>F labelled compounds, rat prostate imaging expts. 0-51215  
<sup>18</sup>F, skeletal tracer kinetics in rats, evaluation of model 0-56188  
<sup>52</sup>Fe, production for use in a radionuclide generator system 0-51253  
<sup>67</sup>Ga citrate, use in detect. and follow-up of extrapulmonary tuberculosis 0-46012  
<sup>67</sup>Ga, metallic, prep. and appl. to tracer diffusion studies in liq. Ga 0-24629  
<sup>68</sup>Ga, ionic, pot. column chromatography generators 0-46050  
<sup>68</sup>Ga labelling of albumin and albumin microspheres 0-17137  
<sup>68</sup>Ga-labelled human serum albumin microspheres, prep. 0-17131  
<sup>3</sup>H labelled biologically active compounds obtained using at. <sup>3</sup>H bundles, appls. 0-30888  
<sup>3</sup>H labelled retinal, inadequacy for visual pigment regeneration studies 0-41357  
<sup>193</sup>Hg, labelling of human albumin microspheres 0-51251  
<sup>203</sup>Hg, tracer for Hg conc. in seawater expts., <sup>75</sup>Se tracer 0-21420  
<sup>125</sup>I labelled compounds, rat prostate imaging expts. 0-51215  
<sup>125</sup>I labelled DNA, pot. tumour imaging agent 0-30892  
<sup>125</sup>I labelled DNA, prep. method and in vivo studies of tumour localisation 0-51249  
<sup>125</sup>I, labelling facilities for biomedical appls. 0-41235  
<sup>125</sup>I microelectrolytic labelling of polypeptide hormones 0-12255  
<sup>125</sup>I, rel. to <sup>99m</sup>Tc in thyroid imaging 0-36077  
<sup>125</sup>I-7-iodo-6-demethyl-6-deoxytetracycline HCl use for bone mineralisation obs. 0-12214  
<sup>131</sup>I labelled chorionic gonadotropin, use in ovarian imaging, rat expts. 0-41186  
<sup>131</sup>I labelled Hippuran, evaluation of renal grafts 0-46017  
<sup>131</sup>I labelled ioglycamide acid, evaluation in hepatobiliary disorder scintiscanning 0-36072  
<sup>131</sup>I labelled o-iodohippurate, in vitro stability 0-16668  
<sup>131</sup>I-4-iodoantipyrine preparation from <sup>131</sup>I-iodide 0-12256  
<sup>111</sup>In 8-hydroxyquinoline labelling of human platelets 0-12259  
<sup>111</sup>In oxine, radiolabelled liposomes as metabolic and scanning tracers in mice 0-17073  
<sup>111</sup>In oxine cell damage resulting from labelling rat lymphocytes and HeLa S3 cells 0-56145  
<sup>115</sup>In aerosol generation technique for atm. tracer obs. 0-26190  
<sup>113m</sup>In-labelled transferrin, use in meas. of blood vols. in rat, rabbit 0-3878  
<sup>13</sup>N, production by cyclotron, biomedical appls. (French) 0-56216  
<sup>13</sup>N-labelled NH<sub>3</sub> and NO<sub>3</sub> ions, prod. for biol. expts. using 3 MV Van de Graaff accelerator 0-26349  
<sup>63</sup>Ni applications in biological research 0-12321  
<sup>60</sup>Co, production by cyclotron, biomedical appls. (French) 0-56216  
<sup>81</sup>Rb/<sup>81m</sup>Kr ratio as radioactive tracer study of organic bleeding (Dutch) 0-3807  
<sup>82</sup>Rb generators, alumina-based, medical evaluation and appl. 0-41237  
 Rn decay products, stability index measurement by natural radioactive tracers (Spanish) 0-51448  
<sup>97</sup>Ru preparation investigation 0-30891  
<sup>103</sup>Ru in determination of rate of passage of food through gut of captive wild birds 0-26425  
<sup>73</sup>Se, yield for various reactions and chem. processing 0-36131  
<sup>75</sup>Se labelled adenosyl selenomethionine, distrib. in rat and prostate scanning appl. 0-17132  
<sup>75</sup>Se, tracer for Se conc. in seawater expts., <sup>203</sup>Hg tracer 0-21420  
<sup>178</sup>Ta radiopharmaceuticals for lung and liver imaging, rat expts. 0-51254  
<sup>178</sup>Ta, scintigraphic imaging with the Anger scintillation camera 0-12231  
<sup>99m</sup>Tc DTPA, radiolabelled liposomes as metabolic and scanning tracers in mice 0-17073  
<sup>99m</sup>Tc, gamma camera array of <sup>99</sup>Mo impurities 0-36100  
<sup>99m</sup>Tc glucoheptonate, prep. using formamide sulfonic acid 0-51252  
<sup>99m</sup>Tc labelled 2,3-dimercaptopropylsulfonate, prep. and distrib. in the rat 0-51244  
<sup>99m</sup>Tc labelled bovine thrombin and streptokinase-activated human plasmin, in vitro assessment 0-41238  
<sup>99m</sup>Tc labelled human serum albumin kits, evaluation for cardiac blood pool imaging 0-17130  
<sup>99m</sup>Tc labelled pertechnetate, evaluation of renal grafts 0-46017  
<sup>99m</sup>Tc labelled radiopharmaceuticals, comparison of 2 types for lymphoscintigraphy 0-41185  
<sup>99m</sup>Tc labelled red blood cells, ultrafiltration labelling technique 0-51243  
<sup>99m</sup>Tc labelled stannous pyrophosphate, mouse myocardial uptake obs. 0-46019  
<sup>99m</sup>Tc pyrophosphate rel. to <sup>99m</sup>Tc methylene diphosphonate in acute myocardial infarction 0-17070  
<sup>99m</sup>Tc radiopharmaceuticals, As for P substitution, bone-seeking agent analogues 0-51250  
<sup>99m</sup>Tc, rel. to <sup>125</sup>I in thyroid imaging 0-36077  
<sup>99m</sup>Tc-Ti-DTPA, prep., control and biological distrib. 0-51246  
<sup>99m</sup>Tc-fibrinogen, usefulness of phlebography for pulmonary embolism patients 0-36093  
<sup>99m</sup>Tc-radiopharmaceuticals, ligand determ., electrophoretic method 0-40699  
<sup>99m</sup>TcS colloid, bone marrow scanning in pediatric oncology 0-17067  
<sup>99m</sup>TcS colloid, mucociliary transport monitoring method, bronchiectatic patient appl. 0-30840  
<sup>99m</sup>TcS colloid lymphoscintigraphy 0-36114  
<sup>99m</sup>Tc(Sn)methylendiphosphonate uptake in canine tibia rel. to blood flow 0-56192  
 Th, stability index measurement by natural radioactive tracers (Spanish) 0-51448  
<sup>199</sup>Tl, production by <sup>197</sup>Au( $\alpha$ , 2n) reaction 0-51245  
<sup>201</sup>Tl, use in thyroid 'cold' areas scintigraphic evaluation 0-36078



## radioactive waste

see also *fission reactor materials; fusion reactor materials; materials handling; radioactivity; waste disposal*

active spent fuel storage, replacement of underwater storage racks 0-23035

ANS leachability standard, figure of merit determ. 0-47623

aqueous tritiated waste management from fuel reprocessing 0-5272

area skyline from radioactive waste, gamma-ray backscatt. photon spectra 0-31119

atmospheric dispersion models, comparison between critical sector and overall-site techniques 0-16873

atmospheric pollutant dispersion 0-47621

atmospheric pollution, concentration time integral (*German*) 0-26378

atmospheric transport from large area sources, finite element method 0-16874

basic electrolyte for low-level decontamination 0-37528

bitumen solidification for low/medium level wastes 0-23094

bituminization program for PWR waste in Korea 0-23096

boric acid solutions, extractive purification from radioactive corrosion and fission products 0-18458

breeder reactor security and environmental impact (*French*) 0-47614

build-up minimisation, design, construction and operation aspects 0-23074

BWR, off-gas explosions, minimisation procedures 0-9369

BWR, vol. reduction and bitumen solidification of low level waste 0-9380

BWR spent fuel storage and refueling La Crosse 0-23034

BWR steam turbine, blast cleaning to remove radioactive deposits 0-18554

Canadian program for nuclear fuel waste disposal 0-37483

Canadian radioactive waste management, bibliography of published literature 0-36796

CANDU irradiat. fuel bundles, sheathed in Zircaloy-4, long term stability investig. 0-13774

CANDU irradiated fuel, disposal in dry storage 0-27788

CANDU-PHW decommissioning, costs, environmental impact, radioactive waste management 0-13964

CANDU-PHW reactors, preparation and storage and solid radwaste 0-5262

cask concepts for spent-fuel storage 0-5284

cement solidification at Ringhals, Sweden 0-23086

centrifugal clarifier, appl. in BWR crud removal 0-23082

cermet approach to nucl. waste management 0-37516

characts., natural occurrences, technological enhancement and health effects 0-46071

chemical migration of radionuclides in soil 0-17144

chemical toxicity issues in high-level waste disposal 0-42798

chronic radioactive release assessment, models and computer codes 0-13710

Commonwealth Edison's Zion Generating station, decontamination of radwaste evaporation 0-9376

conference, on-site management, Zurich, Switzerland (Mar. 1979) 0-22143

contact-handled transuranic waste transportation 0-37538

containers, struct. dynamic response anal., appl. of endochronic plasticity 0-16407

COPRECAL conversion of (Pu,U)NO<sub>3</sub> to mixed oxide 0-37570

corrosion and fission products, ion exchange separation 0-18460

corrosion and fission products, liquid-liquid extractions with metal diethyldithiocarbamates 0-18459

Cosmos 954 crash in Canada, air pollution, obs. of lichens 0-55960

decommissioned structural materials, long-lived activity and implications for containment 0-13739

decommissioning of nuclear facilities, quantitative anal. of radioactive waste development 0-13974

decommissioning of the surface facilities associated with repositories for the deep geological disposal of high-level nuclear waste 0-13734

decommissioning of U ore processing facilities, engineering eval. 0-13977

decontamination facility for large reactor components 0-13740

deep ocean sediment thermal conductivity meas. platform rel. to nuclear waste storage 0-46175

defense waste processing facility, anal. of radionuclides 0-37518

denitration of aqueous waste solns. from fuel reprocessing 0-5313

development of techniques for radwaste systems in CANDU power stations 0-37547

disposal, decision anal. 0-18488

disposal, operation of a pilot solid waste incinerator 0-22990

disposal, thermomech. impact around rock salt borehole 0-5278

disposal by imbedding in glass blocks 0-18462

disposal by incineration in shaft furnaces (*German*) 0-47584

disposal by Julich incineration process (*German*) 0-47583

disposal criteria proposals by EPA and NRDC, review 0-18484

disposal following decommissioning of nuclear facilities (*French*) 0-13736

disposal in mines, Dutch policy (*Dutch*) 0-671

disposal in sea 0-37472

disposal operations Peach Bottom power station system backfit considerations 0-5261

dodecane-tributyl phosphate solns., radiolysis, liquid products 0-40723

dry spent fuel storage installation, design and operation 0-23036

educational module on nuclear reactor safeguards and waste management 0-36802

EM filtration of crud in PWR primary circuits 0-23081

environmental dispersion models, evaluation of uncertainties 0-46074

environmental impact assessment, of oceanic and geological disposal, use of box model method (*Japanese*) 0-9346

evaporator concentrates, pretreatment before solidification 0-23079

fission product waste solidification, high-level, for final storage (*German*) 0-22958

fission reactor fuel, mixed oxide, suitability of spent fuel shipping casks 0-27757

fluid, processing plant for long-term storage rel. to ocean dumping 0-5279

fuel reprocessing, safety problems re environment and operating staff 0-816

fusion reactor transmutation waste management system 0-37482

gamma-emitting activation products, plant uptake of <sup>59</sup>Fe, <sup>58</sup>Co, <sup>54</sup>Mn and <sup>65</sup>Zn 0-30614

geochemical aspects of radionuclide migration from waste repositories 0-13711

geologic disposal, in situ expts. 0-5276

geologic media, radionuclide migration model 0-37499

## radioactive waste continued

geologic repositories, characteristics for radioactive waste acceptance criteria 0-18486

geologic repositories, computer anal. of long-term radiation hazards 0-18483

geologic repositories, feasibility study of granite formations, Stripa, Sweden 0-18481

geologic repositories, survey methods for assessment of radiological release 0-18489

geologic repositories, US Earth Science Technical Plan 0-18482

geologic repositories, US Geological Survey Program [for nuclear waste geologic repositories] 0-22989

geologic repositories for commercial nuclear waste, feasibility study of basalt formations 0-18479

geologic repositories for nuclear waste isolation 0-18584

geologic repository, site search and qualification process 0-18474

geologic repository, status report on Waste Isolation Pilot Plant 0-18478

geologic repository for nuclear waste at Nevada Test Site 0-18480

geologic waste repositories, long term safety assessment methodology 0-37487

geological disposal, chemical factors controlling environmental actinide sorption 0-13713

geological disposal of spent fuel, criticality considerations 0-37533

geological long-term disposal of high-level waste, Sweden 0-13712

geological storage, experience gained at Oklo natural fission reactors 0-21773

geological storage, natural retention experience at Oklo natural reactor 0-18561

geosphere transport model for WIPP site 0-16854

German reactor safety study, consequence model 0-18524

glass leaching, <sup>90</sup>Sr diffusion modelling 0-37519

glove box for sealed manipulator maintenance 0-18684

glove boxes, Pu-contaminated, size reduction and waste packaging 0-18469

groundwater flow models, mass transport models, dose models 0-16853

groundwater modelling, hydrogeologic conditions at radioactive waste burial sites 0-21550

groundwater system, transport of chain decaying radionuclides 0-51019

Hanford site, transuranic distrib. beneath retired underground disposal facility 0-42802

health hazards of waste disposal, EEC-JRC research 0-42786

high level, conversion to glass, exptl. joule-heated ceramic melter 0-18471

high level, long term integrity of deep geologic repositories 0-37498

high level waste form props. 0-37520

high-level liquid waste, damage to organic extractant in positioning process 0-9345

high-level radioactive waste management 0-37470

high-level waste, hot cell facility and equipment for tests of radionuclide removal process 0-18675

high-level waste disposal in salt formation, far-field temp. calcs. 0-5277

HLLW, safety analysis of tank storage 0-740

HLW repository, water intrusion scenario studies 0-52765

hot cell liners, removable, design 0-18685

HTGR spent carbide fuel storage, water-cooled storage concepts 0-22996

hydrodynamic dispersion in transport models 0-17146

immobilisation of highlevel nuclear wastes, US program 0-13708

immobilisation using glass 0-42812

immobilised nuclear waste, disposal centre conceptual design 0-52774

incineration at reactor site 0-23093

inert-carrier radwaste volume reduction and solidification system 0-23046

inventory report for reactor and fuel fabrication facility wastes 0-37532

isotope concentration and precipitation via ion exchange methods (*Hungarian*) 0-18450

leach rates, effect of temp. and leaching media 0-22991

leach rates determ. by activation anal. 0-37523

leach tests interpretation 0-42810

leach-migration experiments to determine the mobility of radionuclides in geologic media 0-18487

light-water waste management systems, vol. reduction and economics 0-9367

liquid, low level, treatment by precipitation and centrifugation 0-23084

liquid, solidification techniques by mobile units 0-23087

liquid, zero release, and treatment using ACEREN evaporator (*French*) 0-23083

liquid high level waste, vitrification (*Japanese*) 0-22971

liquid waste, control of hospital waste using NaI(Tl) detectors (*Italian*) 0-56224

LMFBR, borosilicate glass and glass ceramics with highly radioactive waste 0-5271

LMFBR coolant, decontamination by low-pressure distillation 0-13694

LMFBR waste management, USA 0-23073

long-term entrapment, asphalt props. relevant to safe immobilization 0-9355

loop disposal system of sodium loop safety facility 0-18467

low and intermediate levels, current Canadian development programs, review 0-13733

low level, solid/liquid waste, volume reduction, solidification technique 0-23092

low level, solidification in Dow processes 0-23090

low level radwaste, on-site management options 0-13692

low level solid waste, vol. reduction in Ontario Hydro 0-9379

low level waste leachability, ANS standard 0-47622

low level waste leaching, material parameter defined by ANS standard 0-47624

low-level radioactive solid wastes disposal, benefit-cost anal. 0-18556

low-level solid radwaste, regulations and guides 0-5263

low-level volume reduction, fluidised bed dryer/incinerator 0-9378

low-level waste, industrial processes for treatment and storage 0-5280

low-level waste, inert-carrier process for vol. reduction and solidification 0-9370

low-level waste, vol. reduction policy 0-9366

low-level waste burial grounds, nonradiological hazards 0-42797

low-level waste disposal alternatives 0-37527

low-level waste transport and disposal, logical 0-23044

LWR, accidents, effects and damages 0-22961

LWR, borosilicate glass and glass ceramics with highly radioactive waste 0-5271

LWR, liquid effluent treatment 0-18444

LWR, low-level liq. and solid waste, vol. reduction and solidification 0-9368



**radioactive waste continued**

LWR, radwaste solidification processes, safety aspects 0-13673  
 LWR fuel, population dose calc. 0-46073  
 LWR irradiated fuel transport flasks, shielding and engineering aspects 0-27831  
 LWR power station decommissioning, radioactive waste decay behaviour 0-13738  
 LWR reprocessed fuel, EPMA 0-5306  
 LWR spent fuel assemblies, interim and long range storage 0-5286  
 LWR spent-fuel processing and packaging options, for disposal in geologic repository 0-18485  
 Magnox power station, decommissioned, rad. levels, neutron activation, waste disposal 0-13976  
 management, mathematical modelling 0-701  
 management and storage, review 0-5315  
 management in (U,Pu)O<sub>2</sub> FBR fuel cycle 0-47682  
 management of irradiated fuel pond at Trawsfynydd power station 0-23072  
 management practices in Federal Republic of Germany 0-23068  
 management practices in selected European countries 0-37471  
 membrane filter appl. for crud separation in LWR waste water 0-23080  
 metal surface chemical decontamination 0-37530  
 metallic surfaces, radioactive waste electrodecontamination using a basic electrolyte 0-37529  
 metallic waste, decontamination by smelting 0-13741  
 microbial prod. of tritiated and <sup>14</sup>C methane from radioactive waste 0-45868  
 migration velocities determ. from partitions coeffs. 0-37525  
 mobile radwaste processing systems, logistical advantages 0-18555  
 neutron dosimetry characterization of spent thermal reactor fuel assemblies, using nondestructive methods 0-23164  
 neutron shield material tests 0-37543  
 Nevada Nuclear Waste Storage Investigations, site evaluation activity 0-37489  
 new waste calcining facility, radiation shield integrity testing 0-13940  
 nondestructive analysis applications in the nuclear industry 0-13706  
 NRC high-level waste management program 0-13709  
 nuclear fuel reprocessing, radioactive waste elimination by nuclear transmutation (*Spanish*) 0-5298  
 nuclear fuel reprocessing in West Germany, case against suspension (*German*) 0-32418  
 nuclear installations, ambient radioactivity, standards rel. to dose and radioactive waste limits (*Spanish*) 0-52789  
 nuclear power plant licensing procedures in the UK 0-27708  
 nuclear power station accidental activity release, effect of meteorological parameters 0-17142  
 nuclear power stations, fuel circuit review, radioactive conditioned waste final storage (*German*) 0-799  
 nuclear power stations prospects, w.r.t. environmental problems (*Hungarian*) 0-13742  
 nuclear reactors, decommissioning, main problems 0-676  
 nuclear spent fuel shipping cask licensing 0-37545  
 nuclear spent fuel valuation, procedure appls. and analysis 0-738  
 nuclear waste constituents, stabilisation in Portland cement 0-13630  
 ocean dumping of high level waste 0-32376  
 Oklo phenomenon, isotopic abundances, long-term radioactive waste storage information 0-52769  
 on-site facilities for processing and disposal 0-23095  
 on-site management, Canada 0-23069  
 on-site management at power reactors, India 0-23070  
 organic alpha waste, vol. reduction by pyrohydrolysis 0-5273  
 origin in power plants, average yearly quantities for LWRs 0-23067  
 ORNL interface and logistics studies 0-37540  
 packaging containers, a survey 0-23097  
 packaging techniques, evolution in France (*French*) 0-23098  
 particle accelerator decommissioning, radioactive waste management 0-18720  
 Peach Bottom power station radwaste system backfit considerations 0-9351  
 Perch Lake Basin, Ontario, hydrological and geochemical studies conference, Chalk River, 1978 April 25 to 26 0-51955  
 poisoned fuel rods, treatment on-site, France (*French*) 0-47674  
 polymeric solidification of low level radioactive waste, Dow process 0-37502  
 pool systems for spent-fuel interim storage facilities 0-5283  
 portable vol. reduction and solidification system 0-37515  
 processing, management and storage, INFCE report summary (*Dutch*) 0-52750  
 processing and encapsulation techniques, France (*French*) 0-47675  
 processing of high-level waste, consequences of separation of long-lived  $\alpha$ -emitters (*Czech*) 0-5251  
 protective clothing, dry cleaning versus water wash 0-13691  
 public radiation exposure, optimisation, problems 0-47768  
 Purex solvent extracting system, monitoring and control instrumentation 0-37566  
 PWR, startup, secondary-side corrosion product transport 0-9377  
 PWR coolant pH effect on radiation field buildup 0-23060  
 PWR decommissioning, public radiation exposure 0-42800  
 PWR dismantling, management of radioactive waste 0-27756  
 PWR liquid waste management 0-52758  
 radiation protection features of waste calcining facility 0-5377  
 radioactive reprocessing, comprehensive system of major hazard control 0-818  
 radioactive waste storage, integrated biological dose evaluation 0-5379  
 radiological aspects of the design of a facility to solidify radioactive sludge 0-5378  
 radiological protection criteria for disposal 0-47780  
 radionuclide geospheric transport eqn., boundary conditions 0-47611  
 radionuclide migration from repository sites, stochastic anal. 0-37486  
 radionuclide migration resulting from site intrusion 0-13701  
 radionuclide transport through heterogeneous media 0-32382  
 radwaste concentrator at Millstone Unit 1, decontamination and repair experience 0-13693  
 rare gas separation by membrane permeation, improvement in separation factor 0-18559  
 reactor decommissioning, radioactivity limits for release of liquid radwaste, math. model 0-13737  
 reactor fuel element storage and transportation 0-13707  
 reactor spent fuel storage vault, criticality safety determ. (*Korean*) 0-37478

**radioactive waste continued**

reprocessing of irradiated fuels, French and European policies (*French*) 0-809  
 reprocessing solvents, decontamination and clean-up process 0-5254  
 residual activity levels allowing radioactive waste to be considered inactive 0-13735  
 resuspension models, chronic releases of radionuclides to atmosphere 0-16871  
 resuspension models, factors determining amount of material resuspended 0-16872  
 risk evaluation model, on-site meteorological data, environmental consequences 0-36155  
 safety criteria for LWRs 0-18472  
 seismic design considerations for deep geologic repositories 0-23019  
 shale investigation as radioactive waste repository, vermiculite role 0-32354  
 shallow land disposal of low-level radioactive waste, radionuclide sorption 0-16851  
 SHIELD computational system, nucl. fuel cycle appl. 0-37517  
 simulation of high level liquid waste evaporation and storage 0-37476  
 site selection criteria development and appl. 0-37484  
 siting, geologic studies of Paradox Basin 0-37485  
 slagging pyrolysis incinerator, off gas treatment system 0-37514  
 society effects of nuclear power developments 0-47590  
 sodium reactor experiment decommissioning, radiation protection 0-9432  
 soil interactions, radionuclide migration 0-42801  
 solid, impact resistance test program 0-37521  
 solid combustible waste, Pu recovery 0-5274  
 solid neutron shield development, materials eval. for spent fuel shipping cask 0-13939  
 solid radwaste, current concerns, treatment system design changes 0-5258  
 solid radwaste system utilizing cement 0-5260  
 solidification of evaporator concentrates by hydraulic binding agents (*French*) 0-23088  
 solidification of highly active liquid wastes (*Korean*) 0-52759  
 solidification of waste water concentrates using a roller drier 0-23089  
 solidification system, Dow, state-of-the-art 0-5259  
 solidified, leach testing, background 0-42809  
 solution concentrator equipment for criticality safety 0-18432  
 Soviet disaster 1957-8, explosion of stored nucl. waste, causes 0-22974  
 Soviet nuclear disaster, 1957-8, radioactive waste origin 0-45823  
 space disposal of nucl. waste, waste mixes and forms 0-37534  
 spent fuel, bremsstrahlung spectra and average energies, analytic calc. method 0-22985  
 spent fuel, neutron interrogation 0-5307  
 spent fuel storage, away-from-reactor facilities, Tennessee Valley Authority studies 0-18496  
 spent fuel storage, away-from-reactor storage basin design 0-22994  
 spent fuel storage, requirements for away-from-reactor facility 0-22993  
 spent fuel storage, US licensing and regulation 0-23039  
 spent fuel storage, use of poisoned racks at Point Beach 0-23038  
 spent fuel storage and transportation, operators experience 0-23037  
 spent fuel storage at independent installations, comparative risk assessment of external source damage 0-23041  
 spent fuel storage at independent installations, licensing considerations 0-23042  
 spent fuel storage pool racking, licensing experience at Trojan 0-23040  
 spent fuel storage pools, behaviour of B<sub>4</sub>C reactor materials 0-42771  
 spent fuel transportation, effect of AFR storage location 0-18497  
 spent LWR fuel storage in Pacific Basin at Palmyra Island, decision making methods 0-27763  
 spent nuclear fuel shipment, appl. of ALARA principles 0-37541  
 spent nuclear fuel transportation by barge and rail, risk anal. 0-18498  
 spent-fuel assembly inspection plant 0-5285  
 spent-fuel transportation required to implement the DOE spent-fuel policy 0-22995  
 steel waste form containers, corrosion 0-18493  
 storage, Am sorption on major rock-forming minerals 0-13716  
 storage, interaction of actinides and humic acid 0-13715  
 storage, migration of <sup>137</sup>Cs in Magenta dolomite by aquifer 0-13718  
 storage, mineral-contributed anion effects on the retention of trivalent actinides in the environment 0-13717  
 storage, Pu oxidation by radiation, effect on migration rate 0-13714  
 storage, thermodynamics of free-convection air-cooled storages 0-5282  
 storage of fissile materials, use of neutron absorber for enhanced criticality safety 0-13609  
 storage time evaluation for active solid waste produced in hospitals 0-26333  
 subsurface migration studies at Radioactive Waste Management Complex, Idaho 0-42805  
 subsurface nuclear waste disposal, groundwater modelling 0-16852  
 synthetic mineral nuclear waste ceramics 0-42813  
 T immobilisation, possible solid mats. 0-27755  
 temporary confinement structures, design criteria and guidelines 0-18683  
 thermal analysis of irradiated nuclear fuel transport flasks 0-5281  
 trace element analysis of radiological effluents from coal-burning power plants 0-21426  
 transmutation of fission product waste using DT neutrons 0-32383  
 transmutation of waste actinides in thermal reactors 0-18491  
 transport model for radionuclides through geologic media 0-786  
 transportation, DOE transportation technology centre 0-37537  
 transportation, ORNL Nuclear Legislative Data Base program 0-37539  
 transportation in urban areas, radiological, nonradiological and economic environmental impact 0-18473  
 transportation SABRE II combat simulation model 0-37542  
 transuranic nuclear waste management, evaluation of alternatives 0-18490  
 transuranic nuclide migration in earthen burial trenches at Savannah River Plant 0-42804  
 transuranic waste degradation under WIPP conditions 0-37526  
 treatment, handling, characterisation at Winfrith SGHWR 0-23076  
 treatment at Czechoslovak nuclear power station 0-23077  
 treatment experience at Atucha, Argentina 0-23075  
 treatment experiences, Tarapur, India 0-23078  
 treatment prospects for ENEL's reference power station 0-23071  
 treatment techniques for CANDU power stations 0-23085  
 trench leachates, low-level radioactive waste disposal sites, organic carbon content 0-17145  
 tritiated, gas generation by autoradiolysis 0-32384  
 Tsuruga power station anal. of corrosion products 0-23062



**radioactive waste continued**

- US Nucl. Regulatory Commission high level waste management repository assessment methods and anal. 0-37497  
 Vermont Yankee management system zero-liquid-release 0-13695  
 vitrification, slurry feeding to an electric glass melter 0-18492  
 vitrification of fission product solutions at Marcoule [description and hot operation results] 0-5270  
 vitrification of highly active liquid waste, thermal decomp. of Harvest feed slurries 0-52757  
 volume reduction and solidification of low level radioactive wastes 0-42794  
 volume reduction techniques for radwaste management 0-23091  
 volumetric reduction techniques for low level waste 0-23045  
 WAK reprocessing plant, a design basis for large-scale reprocessing plant 0-5310  
 WAK reprocessing plant, chemical decontamination of highly active process cell 0-5312  
 Waste Isolation Performance Assessment Program 0-37496  
 waste isolation Pilot Plant, deep geological nuclear waste disposal 0-5275  
 Waste Isolation Pilot Plant, siting status 0-37488  
 waste isolation safety assessment methods, overview 0-37495  
 water pollution, computer anal. of relative potential hazards 0-21422  
 water pool spent fuel storage units, neutron anal., criticality state (*Spanish*) 0-32517  
<sup>108</sup>Ag<sup>m</sup>, prod. in nuclear reactors by thermal neutron capture in stainless-steel structure 0-42747  
 AmO<sub>2</sub>-UO<sub>2</sub>, target possibilities for waste incineration, simulation study 0-32419  
 CO, radioactive and stable, determ. in marine biological materials 0-36157  
 Cs in basalt, migration velocities determ. from partitions coeffs. 0-37525  
 CsAlSiO<sub>3</sub>, and CsAlSi<sub>2</sub>O<sub>12</sub>, cryst. evap., mass spectral investig. 0-49353  
<sup>137</sup>Cs, 10 GeV proton spallation for transmutation of radioactive waste, calc. of transmutation number 0-13470  
<sup>137</sup>Cs, diffusion in bitumen block coating, radioactive waste treatment (*Russian*) 0-52771  
<sup>137</sup>Cs, separation from nucl. waste using sodium zirconate 0-27760  
<sup>137</sup>Cs, study of absorpt. by Lemna minor 0-30677  
<sup>137</sup>CsCl, use of Cs<sub>2</sub>O·Al<sub>2</sub>O<sub>3</sub>·4SiO<sub>2</sub> (pollucite) for long term-storage 0-37467  
 H production from radioactive waste heat and utilisation in gas turbines 0-30326  
 I absorpt. on ion exchange resins in aqueous solns. 0-47610  
 I radioactive isotopes, nuclear fuel cycle radiation safety problem, (*Russian*) 0-18560  
 I, radioisotopes, environmental and biological effects from nuclear fuel cycle (*Russian*) 0-52768  
<sup>129</sup>I, dose to world population from nucl. power industry 0-47619  
<sup>129</sup>I storage, IO<sub>3</sub><sup>-</sup> adsorption by hematite 0-22992  
<sup>131</sup>I in milk, rapid method of detect. 0-46106  
<sup>85</sup>Kr entrapment in continuous-biased sputter-deposited glassy metals 0-24603  
<sup>85</sup>Kr, pressurised cylinder storage tests 0-5269  
<sup>85</sup>Kr waste encapsulation, in amorphous alloy 0-47589  
<sup>85</sup>Kr waste management, strategy anal. 0-37531  
<sup>54</sup>Mg, removal from waste water by oxine-impregnated activated charcoal 0-9344  
 Na, contaminated, packaging and storage 0-18468  
 Na<sub>2</sub>O·B<sub>2</sub>O<sub>3</sub>·SiO<sub>2</sub>·MoO<sub>3</sub> glass containing high level radioactive waste, phase separation 0-25683  
<sup>237</sup>Np migration potential 0-3537  
<sup>238,239,240</sup>Pu, concs. in arthropods at a nuclear facility 0-30905  
 Pu compounds 18B packaging for transportation 0-37544  
 Pu contaminated incinerator facility, decontamination and decommissioning 0-13987  
 Pu contaminated incinerator ash incorporated in cement, leach studies 0-37522  
 Pu contamination of soil near Rocky Flats plant 0-42803  
 Pu in lungs of pronghorn antelope near a nuclear fuel reprocessing plant 0-30906  
 Pu in situ array for electropolishing bath, Monte Carlo calcs. 0-37524  
 Pu in waste, anal. of enhanced variance and twin gate methods 0-5454  
 Pu migration through soil 0-37490  
 Pu, neutron analysis in solid waste 0-42840  
 Pu processing for fast reactor fuel cycle 0-27793  
 Pu recovery from nitric acid waste, comparison of anion exchange resins 0-681  
 Pu transport, environmental impact 0-779  
 Pu(NO<sub>3</sub>)<sub>4</sub>-nitric acid soln., direct denitration in screw calciner 0-37567  
 PuO<sub>2</sub> powder, leak rate determ. 0-42808  
<sup>238</sup>Pu<sup>4+</sup>, <sup>238</sup>Pu<sup>6+</sup>, <sup>239</sup>Pu<sup>4+</sup>, <sup>239</sup>Pu<sup>6+</sup>, alga uptake rel. to isotope and oxidation state 0-30692  
<sup>239</sup>Pu, <sup>240</sup>Pu, concs. in fish and seawater from Kwajalein Atoll 0-26380  
<sup>239</sup>Pu citrate, internally deposited, pot. genetic dose, influence of testicular microanatomy 0-36147  
<sup>226</sup>Ra, assessment of quantities in North Carolina drinking water supplies 0-45826  
<sup>226</sup>Ra, conc. in water near a phosphate facility 0-45827  
 Rn diffusion consts. for soil covers of U mill tailings 0-42807  
<sup>222</sup>Rn, conc. in water near a phosphate facility 0-45827  
<sup>222</sup>Rn diffusion in soil, moisture effects 0-37491  
<sup>222</sup>Rn releases associated with cultivation of agricultural land 0-16850  
 Ru, processing from nuclear fuel by aluminosilicate gels (*Japanese*) 0-22973  
<sup>90</sup>Sr, diffusion in bitumen block coating, radioactive waste treatment (*Russian*) 0-52771  
 T leaching behaviour from hardened cement paste 0-18443  
 T storage and monitoring, CANDU heavy water reactors 0-5291  
<sup>99</sup>Tc migration potential 0-3537  
 (U,Pu)C, controlled oxidation for head-end step reprocessing 0-5308  
 U content in solid waste mats. using  $\alpha$ -particle detectors, two layer proportional counter (*Russian*) 0-27904  
 U mines, radiological evaluation 0-42806  
 U mining, U refining and decay processes, radioactive mining waste disposal (*Dutch*) 0-21418  
 U tailings management, economic impact on nuclear fuel cycle 0-18494  
<sup>234</sup>U, <sup>235</sup>Th, <sup>226</sup>Ra, superposition soln. of transport of decay chain through sorbing medium 0-37500  
<sup>234</sup>U, <sup>235</sup>Th, <sup>226</sup>Ra decay chain, hydrogeological migration anal. 0-37501

**radioactivity**

- see also *alpha decay; atmospheric radioactivity; beta-decay; radioactive decay periods; radioactive decay schemes; radioactive sources; radioactive tracers; radioactivity measurement; radiochemistry; spontaneous fission*  
 aerosol particles, hot  $\beta$  active emission electrification in varying force fields 0-7868  
 AVR reactor steam generator leakage, meas. of activities and their origin in leakage water 0-693  
 biosphere contamination, explosion and power plant influence (*Hungarian*) 0-21548  
 bone and muscle radioactivity separation by dermestid ingestion 0-30949  
 Canon City meteorite, <sup>37</sup>Ar and <sup>39</sup>Ar radioactivities 0-36582  
 Dhajala meteorite, <sup>37</sup>Ar and <sup>39</sup>Ar radioactivities 0-36582  
 education, stochastic model, radioactive decay, difference-differential eqns. 0-51992  
 enriched heavy minerals in sand grains, enhanced natural radiation exposure (*German*) 0-51018  
 gamma-ray spectrometry, correction for dead-time losses, mixture of short-lived radionuclides 0-42312  
 quantum mechanics and radio activity unification, probabilistic conceptions 0-12946  
 radiation dosimetry, standardised radioactive decay data sets 0-13945  
 seawater of Narragansett Bay, USA coast, radionuclide content 0-12399  
 secondary education, learning of radioactivity (*Japanese*) 0-4484  
 soil, U and Ac series nuclides radioactive disequilibrium 0-4014  
 UK population, sources of radiation exposure, review 0-36156
- radioactivity measurement**  
 see also *radioactivity measuring apparatus*  
 atmospheric radioactive gas monitoring by silicone oil absorbent scintillation counter 0-12044  
 chromatography radioactive source leak testing under dynamic flow conditions 0-3432  
 curve fitting to data with low statistics 0-9471  
 cutting fluids testing rel. to tool wear, thin layer activation technique 0-55619  
 electronic measurement apparatus development at ATOMKI (*Hungarian*) 0-18768  
 gamma-radiating radionuclide activity, comparison of standards within COMECON framework 0-42899  
 geological samples, large volume, absolute activity determs. independ. of self-absorpt. effects 0-56643  
 inhaled heavy elements deposited. in vivo, external counting, review 0-36152  
 ionising radiation, traceability in meas. systems 0-5355  
 liquid column chromatography, scintillation counters, review (*Czech*) 0-27885  
 natural soil radioactivity monitoring with portable gamma ray spectrum 0-31148  
 Oregon, meas. of natural radioactivity 0-37638  
 photon irradiator calibration, compensation for geometry induced errors 0-18702  
 PWR, T sources, releases, monitoring, management and environmental impact 0-18690  
 random summing in multi-detector counting system meas. radionuclide mixtures 0-36097  
 standards program of the NBS, USA 0-18700  
 units, definitions and interrelations 0-17914  
 $\alpha$ -particle detectors, two layer proportional counter for measuring U content in solid-waste mats. (*Russian*) 0-27904  
<sup>14</sup>C, low level activity measurement, comparison of proportional counters (*Czech*) 0-52818  
<sup>59</sup>Fe/<sup>55</sup>Fe activity ratio of blood, meas. using semicond. detector 0-17062  
 HT-HTO in air meas. system 0-21433  
<sup>3</sup>H, low level activity measurement, comparison of proportional counters (*Czech*) 0-52818  
<sup>125</sup>I airborne vapour detection 0-51027  
<sup>125</sup>I worker thyroid meas. 0-36151  
 Pu dosimetry, calibration of whole-body counters 0-21547  
 Pu in waste, anal. of enhanced variance and twin gate methods 0-5454  
<sup>226</sup>Ra, alpha scintillation counter for determ. of low natural conc. 0-9456  
 Rn daughter airborne conc. meas. in atmosphere 0-37636  
<sup>222</sup>Rn, alpha scintillation counter for determ. of low natural conc. 0-9456  
<sup>222</sup>Rn very low conc. meas. with proportional counter 0-27907  
 T monitoring at nuclear power stations 0-18691  
 T monitoring methodology using SiO<sub>2</sub> desiccant, appl. to research reactor facility 0-21434  
 T monitoring with proportional counters 0-27874  
 T species, sources and reactions 0-21432  
 U activity, liquid scintillation counting 0-27873
- radioactivity measuring apparatus**  
 gas radiometer, portable, for noble gases and gaseous tritium meas., by ionisation method 0-32570
- radioactivity protection** see *radiation protection*
- radioaltimeters**  
 see also *aircraft instrumentation; radionavigation*  
 Geos 3 altimeter, biases from comparison with other tracking systems 0-4227  
 ocean surface wind obs., SeaSat : scatterometer/scanning radiometer/altimeter comparison 0-46249  
 radar altimeter height and timing bias report 0-46326  
 SEASAT altimeter wave height comparisons 0-46201  
 SEASAT radar altimeter 0-56613
- radioastronomical observations**  
 see also *radiosources (astronomical)*  
 5 GHz galactic plane sources, catalogue 0-4269  
 Abell 2256, X-ray cluster of galaxies, radio props. 0-36726  
 Abell clusters of galaxies, Westerbork 610 MHz survey of extended radio emission 0-36727  
 Abell clusters of galaxies containing tailed radio galaxies, Westerbork synthesis obs. 0-56957  
 AFGL IR sources, mol. line obs. 0-51856  
 AO 0235+164, BL Lacertae-type object, VBLI obs. of redshifted H I absorpt. 0-46658  
 B2 1502+28, head-tail galaxy in Abell 2022, Westerbork obs. of spectral index and polarisation distrib. 0-36727  
 B 0844+31, extended radio galaxy, multifreq. obs. 0-56963  
 B-type stars embedded in R-associations, free-free emission obs. 0-26851  
 1580 Betulia, radar obs. and radius of Amor-type object 0-36544  
 3C 111, 3C 236, radio galaxies, 150 GHz obs. 0-41908



## radioastronomical observations continued

- 3C 129 and 129.1, in situ particle accel. and energy supply 0-46691  
 3C 147, 3C 380, quasars, milli-arcsecond struct. determined by hybrid mapping with five-station array 0-46694  
 3C 27 area sources, 2695 MHz continuum obs. 0-46688  
 3C 310, extended radio galaxy, multifreq. obs. 0-51890  
 3C 319, radio struct. and optical identification with elliptical galaxy 0-31377  
 3C 345, 418, 371, compact radio sources, arcsecond struct. 0-4450  
 3C 345 and NRAO 512, relative position to submilliarcsecond accuracy via VLBI 0-22097  
 4C 39.04, powerful giant radio galaxy, multifreq. obs. 0-17682  
 3C 391, supernova remnant, obs. at 1.4 and 10.7 GHz 0-4417  
 3C 395, compact radio source, high resolution obs. at 1671 MHz 0-56960  
 3C 449, radio jet structure at 1465 and 4885 MHz 0-12823  
 4C sources in Zwicky galaxy clusters, detailed interferometer obs. and anal. 0-22099  
 VY Canis Majoris, OH/IR star, 1612 MHz OH maser multibaseline VLBI obs. 0-12766  
 Cassiopeia A,  $^{14}\text{N}$  radioemission at 26 MHz 0-41886  
 Cassiopeia A, intensity and polarisation at 9 mm wavelength 0-36732  
 Cassiopeia A, secular decrease in radio emission flux density at 437 and 510 MHz (*Russian*) 0-8702  
 Centaurus A (NGC 5128), slowly varying flux component, 22 GHz confirmation 0-56939  
 Cepheus A mol. cloud, OH maser lines obs., star form. region 0-36691  
 Cepheus OB3 association molecular cloud, mol. obs. rel. to star form. 0-12798  
 Ceres, radar obs. at 12.6 cm wavelength, surface roughness 0-36545  
 o Ceti, SiO maser variability at 86 GHz 0-41839  
 Circinus X-1, radio flare phenomena Dec. 1979 and Jan. 1980 obs. 0-36731  
 circumsolar plasma, d.m. propag., Venera 10 meas. 0-21886  
 CIT 6 (IRC+30219), IR C star, CO obs. of mass outflow 0-12761  
 clusters of galaxies, H I broad band emission search 0-46667  
 Coma cluster, H I emission search, gas content determ. of elliptical galaxies 0-46657  
 Cone nebula, formaldehyde kinematics and distrib. 0-4418  
 cosmic microwave background, no anisotropies at 31 GHz 0-51922  
 cosmic microwave background radiation, anisotropy meas. 0-41918  
 couple galaxies, H I 21 cm. line obs. 0-51886  
 Crab Nebula, lunar occultation obs. at 114 and 26.3 MHz, small-scale struct. 0-46627  
 Crab Nebula, radio emission from compact source, HF meas. with URAN-1 interferometer 0-31343  
 CTB 80, peculiar supernova remnant, central radio source optical and H I obs. 0-56896  
 CTD 93, compact radio source, high resolution obs. at 1671 MHz 0-56960  
 cyanoacetylene, cyanodiacetylene in interstellar clouds, obs. 0-46634  
 cyanodiacetylene ( $\text{HC}_3\text{N}$ ), obs. in (Heiles's cloud 2) 0-22054  
 V1057 Cygni, OH obs. 0-36629  
 NML=V1489 Cygni, OH/IR star, 1612 MHz OH maser multibaseline VLBI obs. 0-12766  
 V1500 Cygni (Nova 1975), radio emission from expanding shell 0-26868  
 Cygnus A, radio galaxy, 150 GHz obs. 0-41908  
 Cygnus X, H I 21 cm line emission maps of field containing G78.2+2.1 SNR 0-56917  
 DA 267, compact radio source, arcsecond struct. 0-4450  
 dark and molecular clouds, 30 GHz obs. in  $\text{I}_0\text{-O}_1$  transition of SO 0-46639  
 HR Delphini (Nova 1967), radio emission from expanding shell 0-26868  
 double galaxies, observational data on well-defined sample 0-17674  
 elliptical galaxies, H I emission search, gas content determ. 0-46657  
 extended radio sources, VLBI obs. of compact components 0-17680  
 extragalactic radio sources, mag. field orientation evidence 0-46690  
 faint radio sources, statistical study of mean ang. size and sky density at 81.5 MHz 0-51893  
 FJM 6, molecular cloud, far IR, near IR radio mol. line studies 0-26929  
 formaldehyde- $\text{d}_1$ , detect. in interstellar clouds 0-8670  
 G126.2+1.6 SNR near 4U 0115+63 X-ray transient 0-8668  
 G309.81+0.07, point radio source and possible stellar remnant of supernova, obs. 0-51849  
 G339.2-0.4, radio recombination line obs. of low-excitation H II region 0-46650  
 G339.2-0.4, supernova remnant or planetary nebula, radio and optical obs. 0-22104  
 G78.2+2.1 in Cygnus X region, H I 21 cm line emission maps 0-56917  
 G 109.7+2.2, type I OH maser source near Herbig-Haro object (*Russian*) 0-17684  
 galactic centre, OH absorpt. struct. determ. using regularisation method 0-17505  
 galactic centre direction, 327 MHz obs. upper limit for D/H ratio 0-26949  
 galactic H I absorption, obs. of struct. on small ang. scales 0-22051  
 galactic non-thermal radio radiation from polar regions, spectra 0-22082  
 galaxies, 21 cm line obs. of H I large-scale distrib. in early type objects 0-8685  
 galaxies, bright, distrib. and density of neighbouring background radio sources 0-56964  
 galaxies, nearby, H I profiles obs. 0-41895  
 galaxy clusters, radio halos, 610 MHz obs. 0-17673  
 galaxy clusters, Sunyaev-Zeldovich effect at 9 mm wavelength 0-41919  
 giant molecular clouds,  $\text{H}_2$  densities and  $^{12}\text{C}/^{13}\text{C}$  ratio 0-51837  
 giant molecular clouds, turbulent cores, CS obs. 0-51822  
 giant radio galaxies, 26-100 MHz obs. of four objects 0-56961  
 globular clusters, search of OH and  $\text{H}_2\text{O}$  lines for extraterrestrial intelligence 0-56725  
 globular clusters, southern, gas content upper limits 0-22047  
 head-tail radio galaxies, intrinsic parameters distrib. 0-17653  
 Heiles 2 dust cloud,  $\text{NH}_3$ , and cyanobutadiene emission relative distrib. 0-17641  
 Herbig-Haro objects, radio obs. and nearby compact H II regions 0-51756  
 Hercules supercluster, evidence for intracluster medium 0-22092  
 HFE 2.3, molecular cloud, for IR radio mol. line studies 0-26929  
 high-velocity H I cloud near M33, obs. rel. to M33 H I tail 0-12815  
 high-velocity H I clouds, map 0-26923

## radioastronomical observations continued

- W Hydrae, long-period variable, suspected Zeeman splitting in OH masers 0-36632  
 IC 1805, 1848, giant H II regions, physical anal. from radio obs. 0-36695  
 IC 342, Scl galaxy, discovery of companion 0-36712  
 IC 443, supernova remnant, shocked CO discovery 0-8669  
 interplanetary scintillations spectra, influence of source sizes, obs. 0-46361  
 interstellar (*Russian*) 0-36698  
 interstellar excited H, decametric range radio lines search (*Russian*) 0-12822  
 interstellar molecular clouds containing Herbig-Haro objects, mol. obs. and physical props. 0-36689  
 interstellar molecules, RF emission spectra obs. towards  $\zeta$  Ophiuchi 0-26958  
 Io, SHF radioemission and radiation belts (*Russian*) 0-36565  
 IRC+10216, butadiynyl  $\text{N}=\text{12}-11$  doublet study 0-51829  
 IRC-10442 (GL5268S), near IR and radio obs. 0-4412  
 isothiocyanic acid, interstellar detect. in Sagittarius B2, mm wave spectrum 0-41878  
 Jupiter, decametric obs. using facility at Mt. Zao, Japan 0-51656  
 Jupiter, decametric radio bursts, modulation lanes in dynamic spectra 0-17535  
 Jupiter, EM noise and radiowave propag. below 100 kHz in atm., equatorial region 0-26782  
 Jupiter, kilometric radiation, 10-56 kHz, Voyager obs. 0-26781  
 Jupiter, MF radio emissions latitudinal beaming 0-31246  
 Jupiter, radio S-bursts, source of 2.5-35 MHz radiation 0-36562  
 Jupiter, rotation period, decametric radio meas. 0-17541  
 Jupiter, S-burst drift rates from 26-33 MHz obs. 0-12705  
 Jupiter, Voyager 1 planetary radio astronomy obs. 0-26796  
 Jupiter atmosphere and ionosphere, Voyager 1 preliminary radio profiles 0-26791  
 Jupiter bursts, obs. with student-designed radiotelescope, multidisciplinary teaching exercise 0-17759  
 L1544, L1521B, interstellar clouds in Taurus,  $\text{HC}_3\text{N}$  detect. 0-26957  
 BL Lacertae objects, radio structure and spectral index, reviews 0-46672  
 R Leonis, SiO maser variability at 86 GHz 0-41839  
 LMC X-1 region (MC76 and 77), 2 cm obs. 0-51875  
 lunar total eclipse, 1978 March 24, 3.4 mm obs. 0-31220  
 Lynds 134, OH emission obs. in dark nebula 0-22062  
 Lynds 1778/1780, H I and OH emission obs. in dark nebula 0-17628  
 M31, H I emission in SW region 0-51873  
 M31, polarised radio emission distrib. rel. to large-scale mag. field 0-41899  
 M33, H I distrib. obs. and spiral struct. 0-56948  
 M33 H I tail, obs. rel. to adjacent high-vel. H I cloud 0-12815  
 M82, M104, VLBI obs. of galactic nuclei at 18 centimetres 0-22078  
 M87 jet, radiation from knots rel. to model (*Russian*) 0-36719  
 Markarian galaxies, radio continuum obs. at 1410, 2380 and 5000 MHz 0-46668  
 Mars, radio brightness longit. depend. confirmation 0-21937  
 meteors, radio echo characteristics rel. to deionisation processes and meteoroid props. 0-17550  
 methyl formate, microwave spectra, rot. const., moments and struct., radio astronomy appl., review 0-17637  
 methyl mercaptan, interstellar detect. in Sagittarius B2, mm wave spectrum 0-41877  
 microwave background radiation large-scale anisotropy meas. 0-8718  
 Milky Way sources, obs. at 8.87 GHz near ( $l=333^\circ$ ) 0-22102  
 Monoceros R1 molecular clouds ring struct., CO obs. 0-12784  
 Moon, Earth-based radar mapping, review 0-12694  
 Moon, plasma near surface, radio source occultation obs. 0-8559  
 Moon, surface radio reflection, Luna 23 meas. at 3.1 cm wavelength 0-8560  
 MXB 1730-335, 4100 MHz obs. of microwave bursting pattern 0-46705  
 NGC 1052, 4278, VLBI obs. of galactic nuclei at 18 centimetres 0-22078  
 NGC 1265, 1275, in Perseus cluster, low-resolution aperture synthesis map at 408 MHz 0-56958  
 NGC 1275 nucleus, structural changes at 2.8 cm wavelength 0-31359  
 NGC 2024, search for linear polarisation in radio recomb. lines of H II region 0-41872  
 NGC 253, radio recombination line obs. of galaxy 0-56941  
 NGC 2685, H I 21 cm line survey of galaxy 0-56943  
 NGC 4258, high resolution 21 cm, line obs. of active galaxy 0-56946  
 NGC 4725/47 interacting galaxy pair, 21 cm line obs. of H I distrib. 0-46662  
 NGC 5128 (Centaurus A), formaldehyde absorpt. obs. at 14 GHz 0-17657  
 NGC 5383, H I 21 cm line obs. of barred spiral galaxy 0-8687  
 NGC 5474, peculiar Scl galaxy, H I distrib. and kinematics 0-8683  
 NGC 6240, unusual radio galaxy, radio and optical, obs. 0-4440  
 NGC 6251, radio galaxy, radio jets misalignment, VLBI obs. 0-27001  
 North Polar Spur, radio continuum obs. at 1420 MHz 0-22100  
 nova shells, radio emission obs. 0-26868  
 OMC-1, methane- $\text{d}_1$  abundance upper limits from rot. spectrum obs. 0-56705  
 Orion A, 22 GHz water line giant outburst 0-8703  
 Orion A, confirmation of  $\text{H}_2\text{O}$  22 GHz line outburst 0-8704  
 Orion A, SiO maser variability at 86 GHz 0-41839  
 Orion Molecular cloud, CO vel. features rel. to shock fronts and expansion of Orion H II region 0-41880  
 Orion Molecular Cloud,  $\text{NH}_3$  emission obs. 0-36687  
 Orion Molecular Cloud, SO obs. rel. to rotational explanation of high-vel. mol. emission 0-36688  
 Orion Nebula, SO 36 GHz emission line detect., rel. to mag. fields 0-46642  
 Orionid meteor shower 1975, radar echo rates, long-baseline obs. 0-36576  
 V380 Orionis, B8-A2e star, assoc. interstellar CH emission obs. 0-51856  
 OV-236 (1921-29), radio outburst obs. of quasar 0-51906  
 Perseus galaxy cluster, low-resolution aperture synthesis map at 408 MHz 0-56958  
 Perseus OB2 association molecular cloud, mol. obs. rel. to star form. 0-12798  
 planetary nebulae, stellar, VLA obs. 0-22056  
 PSR 0525+21 occulted by solar corona, Faraday rot. at 1720 MHz 0-46526



## radioastronomical observations continued

- PSR 0820+02, long-period binary pulsar, discovery from timing obs. 0-56867
- PSR 0950+08, pulsar, micropulses freq. struct. 0-22030
- pulsars, interpulse emission struct. 0-36652
- pulsars, radio flux density and pulse profile at 102.5 and 61 MHz 0-17601
- QSO 0241+622, nearby X-ray quasar, extended radio emission search 0-31382
- QSO 0957+561, H I 21 cm radio absorpt. line redshifted to 594 MHz 0-36735
- QSO 0957+561 A, B, 1.666 GHz VLBI meas. and gravitational lens hypothesis 0-27007
- QSO 1038+528 A,D, close pair of radio-emitting quasi-stellar objects, radio and optical obs. 0-51902
- QSO 3C273, using VLBI (*Japanese*) 0-17503
- quasar radio emission, from quasar group selected for optical brightness 0-41910
- quasars of high redshift, search for 21 cm absorpt. 0-4453
- quiet Sun, high-resolution obs. at 6 cm using Westerbork Synthesis Radio Telescope 0-36601
- radar meteor echo rates, correl. with zonal winds at 95 km altitude 0-56775
- radio galaxy 1159+583, wide-angle tailed, radio obs. and models 0-31352
- radio sources in North Polar Spur region, 1420 MHz obs. and catalogue 0-22100
- radiometers characts. assessment, statistical analysis of time-dependent series (*Russian*) 0-56777
- ring galaxy discovery in Bootes on Palomar Sky Survey prints, radio flux meas. 0-26985
- Rosette Nebula (NGC 2237/2246), new physical parameters from 6.5 GHz obs. 0-4414
- S232, H II region, mag. field strength meas. 0-51840
- S252 (NGC 2175), mol. line obs. of star-forming complex 0-4411
- S255, H II region, CO emission small-scale struct. from lunar occultation obs. 0-46637
- Saturn, decimetric radio obs., brightness temp. 0-46474
- Saturn rings, 3 mm obs. and props. 0-46470
- FH Serpens (Nova 1970), radio emission from expanding shell 0-26868
- Sharpless 235A, optical, radio and IR obs. of H II region 0-4415
- solar coronal hole, obs. with  $\lambda$  8-cm radioheliograph 0-4326
- solar flares, microwave and optical emissions comparison 0-31284
- solar flares and type I sources, evolutionary relation from 146 MHz obs. (*Chinese*) 0-8609
- solar metre-wave emission, source positions determ. rel. to wave ducting 0-21978
- solar moving type IV bursts, gyro-synchrotron modulation obs. 0-26833
- solar multiply impulsive bursts, hard X-ray and microwave spectral evolution 0-26828
- solar noise storms and radio bursts during cycle 20, statistical anal. 0-56794
- solar radio bursts at 3.7 and 11.1 cm wavelength, interferometric obs. 0-31285
- solar radio emission, S-component spectrum fine struct. in 5.0 to 7.0 GHz freq. range 0-21977
- solar radioflux, 1970 absolute calibration at 2800 MHz 0-17570
- solar type II radio burst with reverse freq. drift against noise storm background, obs. 0-17567
- solar type U radio bursts, polarisation evolution 0-26834
- solar type V radio bursts, dynamic spectra distinctive struct. 0-46527
- southern extragalactic radio sources of large ang. extent, emission spectrum vars. 0-17683
- southern open clusters, search for interstellar H I 0-46619
- spiral galaxies, 21 cm line studies rel. to local mass-to-light ratio 0-31361
- SS 433, 1979 May-June radio flare, 3.24 GHz obs. 0-46567
- SS 433, H I absorption obs. and distance 0-56848
- SS 433, radio and optical positions coincidence 0-56840
- SS 433, radio jet discovery 0-31381
- SS 433, VLBI detect. and ang. struct. 0-31304
- stars, OH maser emission from late-type objects, UHF obs. 0-56826
- steep spectrum radiosources, spectral index dependent props. 0-36730
- stellar SiO masers,  $J=1\rightarrow 0$   $\nu=1$  and 2 masers relative intensity and vel. 0-4339
- Sun, 1978 May 7 events, radio, optical and geophysical manifestations (*French*) 0-8611
- Sun, 2800 MHz radio minimum (1976 February) 0-4324
- Sun, active region coronal loops, gyroresonance absorption evidence 0-56792
- Sun, brightness distrib. at 8.6 mm, interferometer obs. 0-56800
- Sun, coronal holes, EUV and radio spectrum 0-56802
- Sun, decametric obs. of corona at high resolution 0-31288
- Sun, emission pulsations in 1.9-3.5 cm wavelengths (*Russian*) 0-17563
- Sun, H $\alpha$ -flares rel. to radio bursts and sunspots 0-41803
- sun, quiet, obs. with student-designed radiotelescope, multidisciplinary teaching exercise 0-17759
- Sun, radius at centimetre wavelengths and brightness distrib. across disc 0-21968
- Sun, type II radiobursts and shock waves in interplanetary medium 0-56690
- Sun, type III bursts, fundamental emission in 25-200 kHz range 0-56789
- Sun, type III-like bursts, UHF obs. 0-56793
- Sun total microwave flux, search at Toyokawa for five minute oscillations 0-4327
- supernova remnants, southern, high resolution radio obs. 0-51849
- sybiotic stars, survey at 1612 MHz 0-12774
- T Tauri stars, props. of assoc. ionized regions 0-36624
- Taurus A, intensity and polarisation at 9 mm wavelength 0-36732
- Taurus Molecular Cloud 2 (TMC-2), HC $_3$ N and NH $_3$  obs. 0-26957
- Tycho's supernova remnant, radio flux density meas. separated by 15-year interval 0-26955
- Tycho supernova remnant, radio struct. 0-56919
- ultracold molecular gas toward galactic centre, CO isotopic rotational transitions 0-51826
- Uranus, decimetric radio obs., brightness temp. 0-46474
- Uranus, microwave radiometry and interferometry 0-56766
- Vela supernova remnant, rot. measure and turbulent struct. 0-51836
- Vela X supernova remnant, radio polarisation maps 0-56909
- Venus, astrometric radar meas. in 1977, results 0-17522

## radioastronomical observations continued

- Venus, atmosphere, turbulence from Pioneer multiprobe radio scintillations 0-46437
- Venus, impact cratering and tectonic activity, evidence from radar obs. 0-46426
- Venus, lightning discharges, frequency of occurrence 0-56743
- Venus, nightside ionosphere, Pioneer orbiter radio occultations 0-46441
- Venus, radar obs. of atmos., soil and relief 0-36537
- Venus, radio interferometric meas. of retrograde zonal winds below clouds 0-46436
- Venus, surface features, Pioneer orbiter topographic and surface imaging 0-46438
- Venus atmosphere, model from radio, radar and occultation obs. 0-46420
- Venus daytime ionosphere, two-freq. radio transillumination data using Venera-9, 10 probes 0-21936
- Viking relativity experiment: verification of signal retardation by solar gravity 0-36933
- Viking spacecraft, Doppler and range data rel. to geocentric gravit. const. evaluation 0-3891
- VLBI expt. with mobile equipment, 5 GHz operation 0-31217
- Voyager 2, obs. of solar coronal occultation, 1979 August 0-51639
- W28 A, H II region, RATAN-600 2-13 cm wavelength obs. (*Russian*) 0-17642
- W48, OH emission and absorption, spatial distrib. in H II region (*Russian*) 0-36733
- W49A, high sensitivity H $\alpha$  radio recomb. line obs. 0-26998
- W51 Main, H $_2$ O maser emission 0-8701
- young stars, high-freq. radio continuum obs. 0-51766
- Zw 1400+0949 cluster (NGC 5416 group), 21 cm obs. 0-22090
- C stars, search for HCN and CH maser emissions 0-51856
- CH, detect. in NGC 4945, NGC 5128 and LMC 0-46673
- CO in interstellar dark clouds, evidence for isotopic fractionation 0-46638
- CO, interstellar, distrib. around ( $l=30^\circ$ ,  $b=0^\circ$ ) 0-41868
- CO, interstellar, isotope fractionation in Lynds 134 dust cloud 0-26924
- (CO) $_2$ , RF lab. meas. and interstellar search 0-43035
- $^{13}\text{CO}$  in external galaxies,  $^{12}\text{CO}/^{13}\text{CO}$  intensity ratios 0-4416
- CO emission in Markarian and Seyfert galaxies, unsuccessful search 0-26975
- Cygnus A, intensity and polarisation at 9 mm wavelength 0-36732
- H I, column density as function of position in southern sky 0-4420
- H I, galactic subsystem, 21 cm line profile rel. to galactic rot. curve (*Russian*) 0-36724
- H I 21 cm line radial vel. contour maps 0-17626
- H I at high galactic latitudes, time variable 21 cm line profiles correction 0-51844
- H I regions, new feature discovery in Vulpecula-Delphinus (*Russian*) 0-46654
- H $_2$ O, interstellar, 183 GHz line emission obs. 0-41869
- H $_2$ O maser features, high-velocity, in W3(OH), obs. 0-31339
- H $_2$ O maser sources in different stages of evolution, new VLBI maps 0-26954
- $^{14}\text{N}$  interstellar neutral gas, search for radioemission 0-41886
- O/H abundance ratio determ. in Galaxy from H II regions radio obs. 0-36692
- OH 1612 MHz survey at high declinations 0-4452
- OH in interstellar dust clouds, nonthermal main lines obs. and OH abundance 0-36683
- OH, interstellar, new main line maser obs. with probable Zeeman pattern 0-56908
- OH maser sources, accurate position meas. 0-46646
- rho Ophiuchi dark cloud, o-formaldehyde excitation temp. and optical depths 0-51846
- SiO 86.2 GHz maser sources, polarisation props. 0-4449

## radioastronomical techniques

- acousto-optical spectrometer for processing of MM-wave signals 0-4253
- aperture synthesis radioastronomy (*French*) 0-46410
- Arecibo Observatory, radiotelescope and instrumentation description 0-4249
- astrometry, using interferometers, principles and accuracy (*French*) 0-46411
- background deflection analysis, appl. to faint radio sources statistical study at 81.5 MHz 0-51893
- baseline ripple reduction by quasi-optical phase modulation, mm radio spectra 0-56710
- CETI call signals, mutual search strategy 0-56723
- ETI signals search, obs. program using existing facilities 0-4266
- geodynamic monitoring and earthquake research, radiointerferometry appl. 0-31151
- image reconstruction 0-56718
- interferometer signal processing by acoustooptic correlation devices, radio astronomy applications 0-8543
- interferometric meas., atm. turbulence effects (*French*) 0-46402
- interferometry, theoretical review 0-12676
- interplanetary scintillation meas. in conditions of strong radio interference 0-46413
- interplanetary scintillation method, appl. to faint radio sources statistical study at 81.5 MHz 0-51893
- mm radioheliograph, design (*Chinese*) 0-12661
- multielement radio interferometer, baseline coordinate vector measurement, maximum-likelihood method 0-26753
- pencil beam formation by fan beam rotation 0-4262
- planetary nebulae radio search near galactic centre, implications of flux density distrib. 0-56913
- power spectrum estimation using maximum entropy method, data analysis appl. 0-37006
- quantum amplifiers and their application in space research, review 0-36503
- radiometers characts. assessment, statistical analysis of time-dependent series (*Russian*) 0-56777
- regularisation method, appl. to radio telescope resolving power increase 0-17505
- search for radio emissions from extraterrestrial civilizations 0-4273
- SETI strategy in microwaves 0-4265
- solar corona, magnetic field determ. using type II burst obs. and theory 0-41785
- solar flux calibration in 1970, at 2800 MHz 0-17570
- source mapping by fixed base interferometry (*Russian*) 0-17499
- sources Faraday rotation measures, computation method 0-4263



**radioastronomical techniques continued**

- submillimetresecond astrometry via VLBI, relative position of radio sources 3C 345 and (NRAO 512) 0-22097  
 synchronous dispersion reception method for detecting signals from ETI 0-4264  
 UHF, antenna direction patterns recovering, improved optical simulator appl. 0-26742  
 velocity meas. rel. to microwave background for clusters of galaxies 0-46686  
 Venus atmospheric precipitation detect., remote sensing radar and radio techniques 0-56741  
 VLBI, appl. to astrometry (*Japanese*) 0-21930  
 VLBI, correction for effects of troposphere, ionosphere and Earth crustal tide (*Japanese*) 0-21926  
 VLBI, first expt. in Japan during 1977 0-4268  
 VLBI, general considerations of international systems (*Japanese*) 0-17501  
 VLBI, improvement of freq. stability of local oscillators (*Japanese*) 0-17504  
 VLBI, Japanese domestic system, general aspects (*Japanese*) 0-17502  
 VLBI, Japanese domestic system, receiver and local oscillator (*Japanese*) 0-21923  
 VLBI, Japanese domestic system, recording signal generator (*Japanese*) 0-21924  
 VLBI, Japanese domestic system, selection of radio sources and experimental procedure (*Japanese*) 0-21922  
 VLBI, mapping of planetary radio sources (*Japanese*) 0-21927  
 VLBI, orbit determ. of geostationary satellites 0-4238  
 VLBI, orbit determination of geosynchronous satellites using computer program (*Japanese*) 0-21925  
 VLBI, principles of measurement (*Japanese*) 0-21921  
 VLBI, resolution of celestial radio sources (*Japanese*) 0-26754  
 VLBI, results of observations of radio source QSO 3C273 (*Japanese*) 0-17503  
 VLBI, time synchronization (*Japanese*) 0-26755  
 VLBI between geostationary satellites for hectometric observations of radio stars (*Japanese*) 0-21928  
 OH maser sources, accurate position meas. 0-46646

**radioastronomy**

- see also pulsars; quasars; radiofrequency cosmic radiation; radiosources (astronomical); radiotelescopes; solar radiofrequency radiation  
 Canadian developments, review 0-8542  
 CETI from Earth satellite orbit 0-4275  
 extraterrestrial intelligence, search of OH and H<sub>2</sub>O lines 0-56725  
 image restoration appls., conf., Bordeaux, France (Mar. 1979) 0-41935  
 intergalactic graphite whiskers, RF adsorp. props. rel. to microwave background radiation 0-31357  
 interstellar communication, review of theory 0-4271  
 interstellar molecules, microwave astronomy, modern aspects, book contrib. 0-56921  
 inverse problem, regularisation method appl. to radio telescope resolving power increase 0-17505  
 millimetre-wave astronomy, advances and prospects (*French*) 0-36502  
 planetary atmosphere HF radio occultation meas., phase screen concept 0-56735  
 planetary nebulae radio search near galactic centre, implications of flux density distrib. 0-56913  
 pulsars radio emission, mag. field, energisation, comparison with Jupiter 0-46466  
 scattering cross section of radiowaves reflected from planet with spherically symmetrical atmosphere 0-21935  
 SETI, systems analysis 0-4274  
 SETI strategies 0-4270  
 sources of EM radiation and terrestrial effects (*Japanese*) 0-51600  
 stray radiation problem and time variable 21 cm lines 0-56708  
 VLBI expt. with mobile equipment, 5 GHz operation 0-32127  
 water hole (1400-1700 MHz), rationale for SETI 0-4272

**radiocarbon dating** see radioactive dating**radiochemistry**

- see also radioactive chemical analysis; radioactive tracers  
 alpha-particle sources, thin, prep. from solns. at low temps. 0-27843  
 astatotyrone and astatotryptophan, prep. and stability 0-55687  
 cyclobutane-t, chem. activated by nucl. recoil reaction, energy transfer interpret. 0-25985  
 DNA costacking nucleotides,  $\gamma$ -irrad., charge-migration phenomena, EPR obs. 0-36015  
 hot atom chemistry, general variational principles 0-11941  
 intermolecular energy transfer following kinetically controlled chem. activation, multistep deactivation processes 0-25985  
 isotope production at LAMPF, hot cell chemistry 0-18674  
 layers, intermediate thickness, radionuclides activity calc. 0-21311  
 Miller-Urey reaction, N isotope fractionations, appl. to carbonaceous chondrites 0-46496  
 nuclear reactor irradiated fuel, anal. of  $\alpha$ -emitting isotopes through laser micro-boring 0-37444  
 $\alpha$ -phthalocyanine target, reactor-irrad., extraction rate and mechanism of  $^{64}\text{Cu}$  0-35563  
 radiopharmaceuticals preparation by Szilard-Chalmers labelling and radioprotection in ice lattice 0-51259  
 symmetrical implosion system, charged reaction products, electrostatic field effects 0-32499  
 teaching, undergraduate, courses, facilities 0-27086  
 $^{32}\text{P}$  incorporated in DNA, transmutation effects 0-26283  
 Ag/CN, coverage meas. using surface enhanced Raman scatt. and radioisotope meas., electrochemical treatments 0-29260  
 $^{211}\text{At}$  protein labelling technique using an acylation reaction 0-36130  
 $^{80\text{m}}\text{Br}$  labelling of tyrosine, uracil and cytosine 0-51248  
 $\text{CF}_3\text{Cl}$ ,  $^{18}\text{F}$ -recoil labelling 0-23203  
 $^{13}\text{C}$ -acetylene, production by methane pyrolysis and irrad. 0-36129  
 $^{121}\text{I}$  labelling of radiographic contrast media 0-26350  
 $^{123}\text{I}$  labelling of radiographic contrast media 0-26350  
 $^{63}\text{Ni}$  applications in biological research 0-12321  
 $^{228}\text{Ra}$ , separation from thorium oxalate 0-45600  
 $^{186}\text{Re}$  labelled EHDP preparation and possible use in osseous neoplasms treatment 0-56215  
 $^{97}\text{Ru}$  preparation investigation 0-30891  
 T+HD hot atom exchange reactions, trajectory calcs. 0-26037  
 $^{99\text{m}}\text{Tc}^{\text{m}}$  decay constant, chemical state effect 0-42591  
 $^{99\text{m}}\text{Tc}$  glucoheptonate, prep. using formamidic sulfonic acid 0-51252  
 $^{99\text{m}}\text{Tc}$  labelled 2,3-dimercaptopropansulphonate, prep. and distrib. in the rat 0-51244

**radiocommunication**

- see also mobile radio systems; radio links; radio reception; radiotelegraphy  
 CETI call signals, mutual search strategy 0-56723  
 CETI from Earth satellite orbit 0-4275  
 electrodynamics and electrostatic problems, solns. 0-1105  
 interstellar communication, theory 0-4271  
 ionosphere, UHF and VHF scintillation, signals from geostationary satellite 0-56674  
 ionosphere transmission of L-band signals coded by phase reversal, signal degradation 0-41632  
 ionospheric propagation forecast chart, high solar activity period appl. 0-26664  
 propagation aspects in planning of services 0-12613  
 radiowave propagation above 30 MHz, role of sporadic-E layer and troposphere 0-41636  
 SHF signal attenuation by rain, monitored by radar 0-51567

**radiocrystallography** see X-ray crystallography**radiofrequency amplifiers**

- see also preamplifiers  
 Tokamak plasma power coupling by 500 KW RF amplifier 0-13877  
 VHF, UHF and microwave radiation effect on human body 0-8101

**radiofrequency and microwave spectra of diatomic inorganic molecules**

- see also nuclear magnetic resonance; paramagnetic resonance  
 diatomic mol., hyperfine struct. transitions, quantum theory for undergraduate demonstration 0-17762  
 OH main lines, IR pumping in Mira variable stars and OH-IR sources 0-46632  
 $^{79}\text{BrF}$ , ( $^{81}\text{BrF}$ ), hyperfine struct., elec. dipole moment, rot. transitions, microwave spectral obs. 0-32695  
 CO isotopic rotational transitions in ultracold molecular gas 0-51826  
 CS, vibr. states in RF discharge plasma, microwave spectrosc. obs. 0-14133  
 ClO, aircraft search for 3 mm emission in stratosphere 0-41510  
 CuBr, rot. spectrum hyperfine struct., coupling consts., microwave spectroscopy study 0-18844  
 I<sub>2</sub> vapour, absorpt. lines meas. using FM spectrosc. 0-42262  
 NO<sup>+</sup>, interstellar transitions in mm and IR wavelengths 0-56906  
 N<sub>2</sub><sup>+</sup>+OCS 0-48063  
 O<sub>2</sub>, microwave spectrum, press. broadening 0-23412  
 OH, nonthermal main lines in interstellar dust clouds and OH abundance 0-36683  
 OH, prod. by photolysis, A-doublets, population, rot. states, hyperfine struct., microwave spectra 0-32694  
 OH+H<sub>2</sub>O(NO<sub>2</sub>)(CH<sub>3</sub>Cl)(N<sub>2</sub>)(H<sub>2</sub>)(He), mean collision cross sections from microwave spectroscopy 0-1046  
 OH( $^2\Pi_{3/2}$ , v=1), population inversion of A doublets in microwave spectrum 0-974  
 PbCl, rot. analysis of A-X<sub>1</sub> system 0-32703  
 SO  $_{10-0}$  transition in dark and molecular clouds, 30 GHz obs. 0-46639  
 SO in Orion Molecular Cloud, line profile rel. to rotational explanation of high-vel. mol. emission 0-36688

**radiofrequency and microwave spectra of organic molecules and substances**

- see also nuclear magnetic resonance; paramagnetic resonance  
 1,3-butadiene-1-one, spectroscopic consts., IR and microwave spectra, prep. 0-18859  
 absorption by water in heterogeneous organic materials 0-15998  
 $\Delta^6$ -bicyclo[3.2.0]heptene, microwave spectrum and dipole moment 0-9591  
 bromomethyl methyl ether, microwave spectra, quadrupole computing effect 0-18848  
 bromomethyl methyl ether, microwave spectra, quadrupole coupling effect 0-14135  
 bromomethylsilane, microwave spectra, quadrupole computing effect 0-18848  
 bromomethylsilane, microwave spectra, quadrupole coupling effect 0-14135  
 butadiynyl in IRC+10216, N=12 $\rightarrow$ 11 doublet study 0-51829  
 t-butyl cyanide-HF, hydrogen bonded heterodimer, spectroscopic consts. from IR and microwave spectra 0-43039  
 2-chloro-2-nitropropane, far IR-microwave estimation of binary collision approx. 0-55095  
 chloromethyl oxirane, microwave spectra and conformations of cis and gauche-2 forms 0-5534  
 N-cyanomorphimide-d<sub>2</sub>, struct., microwave transitions 0-973  
 cyanomethane-HF, hydrogen bonded heterodimer, spectroscopic consts. from microwave spectrum 0-43038  
 p,p'-di-n-alkoxyazobenzene series, C<sub>1</sub>-C<sub>7</sub>, submillimetre wave absorpt. investig. 0-34910  
 difluoromethylborane, microwave spectra and struct. obs. 0-43036  
 dimethyl ether, review of microwave spectrum, tabulated data 0-51965  
 ethyl formate, microwave rot. spectrum, centrifugal distortion effects 0-52979  
 ethylene oxide,  $^{13}\text{C}$  and D variants, T<sub>2</sub>-relax., 2<sub>20</sub>-2<sub>11</sub> rot. transition by microwave pulse spectrometer 0-47976  
 formaldehyde, interstellar, excitation, effects of microwave background radiation observed spectrum 0-36681  
 formaldehyde, microwave-microwave double resonance 0-53029  
 formaldehyde, T<sub>2</sub>-relax., rot. transitions, time resolved spectra, microwave pulsed spectrometer study 0-18846  
 formaldehyde in giant molecular clouds, H<sub>2</sub> densities and  $^{12}\text{C}/^{13}\text{C}$  ratio 0-51837  
 o-formaldehyde in rho Ophiuchi dark cloud, excitation temp. and optical depths 0-51846  
 formyl fluoride, and isotopic forms, mol. struct., from electron diffr. and microwave data 0-23570  
 isocyanic acid, molecular structure and centrifugal distortion constants 0-47974  
 isothiocyanic acid, H<sup>15</sup>NCS, HN<sup>13</sup>CS and HNC<sup>34</sup>S, ground state spect. constants and molecular struct. 0-47973  
 methane,  $\nu_3=1$  state, dipole moment and IR-radiofrequency double reson. spectra 0-14161  
 methane-d<sub>1</sub>, laboratory rotational spectrum and upper limits on abundance in (OMC-1) 0-56705  
 methyl formate, microwave spectra, rot. consts., moments and struct., radio astronomy appl., review 0-17637  
 methyl vinyl sulphide, syn-gauche equilib., force field and ab initio calcs., microwave and Raman spectra 0-23573  
 7-methylbicyclo[2.2.1]-hept-2-ene-5-one, config., microwave spectrosc. obs. 0-9593



**radiofrequency and microwave spectra of organic molecules and substances continued**

- methylchlorosilane, Stark effect and microwave-microwave double reson., struct. (German) 0-47975  
 methylidyne, search for maser emission in C stars 0-51856  
 morpholine, centrifugal distortion consts., microwave spectrum 0-5531  
 natural rubber latex <sup>13</sup>C NMR spectra 0-15816  
 polyatomic mol. gas phase spectra, struct., review and tabulation 0-14136  
 1-silabicyclo 2,2,2 octane, double-min. skeletal torsion, microwave spectroscopy 0-47972  
 tertiarybutylisocyanide-borane, vibr., rot. consts., moment of inertia, microwave spectra obs. 0-32706  
 thioketen, microwave spectrum, substitution structure and dipole moment 0-975  
 o(m)-toluidine + o-chlorophenol, H-bonded mol. complex, microwave absorpt., dipole moment and relax. times 0-14134  
 vinyl bromide, mol. struct., from gas-phase electron diff. and microwave data 0-23571  
 vinyl mercaptan -d<sub>0</sub>, -d<sub>1</sub>, anti rotamer, conform., microwave spectrum 0-9592  
 vinyl mercaptan -d<sub>0</sub>, -d<sub>1</sub>, synrotamer, conform., microwave spectrum 0-5535  
 C<sub>3</sub>O<sub>2</sub>, vibr.-rot. band, microwave, spectrum obs. 0-5536  
 OCS + nonpolar perturbation, J=1-2 microwave line press. broadening 0-9644

**radiofrequency and microwave spectra of polyatomic inorganic molecules**

*see also nuclear magnetic resonance; paramagnetic resonance*

- OCS, submillimetre rot. lines, press. shifts 0-23463  
 polyatomic mol. gas phase spectra, struct., review and tabulation 0-14136  
 Ar-O<sub>2</sub> Van der Waals complex, struct. and props., RF and microwave obs. 0-32704  
 Ar.HBr(DBr), van der Waals complexes, rot. spectra and struct. 0-48055  
 BF(OH)<sub>2</sub>, identification, rot. and centrifugal consts., mol. struct., microwave spectra obs. 0-32705  
 (CO)<sub>2</sub>, RF lab. meas. and interstellar search 0-43035  
 COCl<sub>2</sub>, phosgene, Cl<sub>2</sub> nuclear quadrupole coupling tensor, microwave spectra 0-52982  
 HCN, microwave-microwave double resonance 0-53029  
 HCN, search for maser emission in C stars 0-51856  
 HCN...HF, hydrogen bonded heterodimer, spectroscopic consts. from microwave spectrum 0-43037  
 HCO<sup>+</sup> + H<sub>2</sub>, J=0-1 transition press. broadening, microwave absorpt. 0-52981  
 HNCS, ground state spectroscopic const., microwave, millimeter and IR spectra 0-28010  
 H<sub>2</sub>O maser emission from W51 Main 0-8701  
 KrHCl, van der Waals complex, prod. and rot. spectra assignments 0-5532  
 KrHCl, van der Waals complexes, struct., RF and microwave spectra, isotope effects 0-37806  
 KrHCl, weak complex, rot. spectra 0-52980  
 NH<sub>3</sub>, magnetic relaxation rates for microwave spectrum and contributions to linewidth 0-5564  
 NH<sub>3</sub>, microwave-microwave double resonance 0-53029  
 NH<sub>3</sub>, mol. beam state selection and focusing, hyperfine spectrum 0-28119  
 N<sub>2</sub>O, submillimetre rot. lines, press. shifts 0-23463  
 OCS, microwave-microwave double resonance 0-53029  
 OCS + H<sub>2</sub>(CO<sub>2</sub>)(fluoromethane) rot. relax. parameters, microwave spectra linewidth parameters 0-28009  
 OCS + N<sub>2</sub>\* 0-48063  
 OSC, N<sub>2</sub>O, submillimetre rot. lines, press. shifts 0-23463  
 SF<sub>5</sub>Cl, pure rot. spectra, 300 GHz, isotope effects 0-5533  
 SO<sub>2</sub>, T<sub>2</sub>-relax., rot. transitions, time resolved spectra, microwave pulsed spectrometer study 0-18846

**radiofrequency cosmic radiation**

*see also pulsars; quasars; radioastronomy*

- absolute motion of Earth rel. to relic radiation (Czech) 0-31394  
 background microwave radiation, cosmological explanation (Polish) 0-41920  
 background radiation nonequilib. distrib., radiation flux spectrum source 0-46710  
 cosmic background radiation, isotropy and Planck spectrum rel. to generalised cosmological principle, in Newtonian and relativistic theories (Polish) 0-27025  
 cosmic microwave background, pregalactic fluctuations visibility and upper limit on q<sub>0</sub> 0-8717  
 cosmic microwave background isotropy, role of asymptotic freedom in early big bang 0-46712  
 cosmic microwave background spectrum, distortion by intercluster medium 0-4426  
 G-varying cosmology, thermodynamic relations and 3K background radiation 0-56979  
 galactic non-thermal radio radiation from polar regions, spectra 0-22082  
 galactic radiation belts, trapped electrons as radiowave source 0-26982  
 galactic synchrotron radio emission, rel. to Galaxy cosmic rays and mag. field distrib. 0-4207  
 intergalactic graphite whiskers, RF adsorpt. props. rel. to microwave background radiation 0-31357  
 microwave 3K background, in Hoyle-Narlikar conformal gravitation theory 0-56698  
 microwave background, no anisotropies at 31 GHz 0-51922  
 microwave background intensity and velocity meas. of clusters of galaxies 0-46686  
 microwave background radiation, anisotropy meas. 0-41918  
 microwave background radiation, influence of observed spectrum on interstellar formaldehyde excitation 0-36681  
 microwave background radiation density, accreting blackholes contrib. 0-4461  
 microwave background radiation large-scale anisotropy meas. 0-8718  
 microwave background radiation spectrum, effect of interstellar dust and molecules (Russian) 0-8719  
 microwave background spectrum distortion by dust 0-27022  
 photon-tachyon interactions and the isotropic photon flux 0-446  
 Sunyaev-Zeldovich effect at 9 mm wavelength 0-41919  
 universal microwave radiation and extragalactic  $\gamma$  radiation 0-22121

**radiofrequency filters**

- frequency to voltage convertor using SAW linear FM chirp filter 0-19182

**radiofrequency filters continued**

- SAW filters, low insertion loss, using multiphased unidirectional transducers 0-28397  
 SAW TV IF filter, temp. stable ZnO/Pyrex glass substrate 0-43566  
 VHF SAW delay line filters, wideband, low insertion loss 0-28398

**radiofrequency heaters *see radiofrequency heating*****radiofrequency heating**

- calorimetric measurements of microwave energy absorption. of mice, equipment and obs. 0-55996  
 cancer therapy, review of 4 years use of microwaves 0-56162  
 diathermy, shortwave and microwave, for deep-tissue heating 0-17050  
 geophysical research appl. of microwaves, oil composition analysis by means of cracking, permittivity thermal dependences obs. (Czech) 0-46289  
 hyperthermia research with dual-beam microwave applicator 0-17052  
 immune system, RF induced alterations due to hyperthermia, mouse obs. 0-35975  
 industrial and food processing appls., conf., London, England (Nov. 1979) 0-21520  
 microwave applicator, broad band, for heating tumours 0-30830  
 microwave irradiated breast tumour thermal pattern calc. (French) 0-3759  
 microwave power symposium, Monaco (1979) 0-3758  
 mouse foetal body weight effects of 148 MHz irradiation 0-3726  
 multibeam microwave therapy with computer control 0-3766  
 open-ended waveguide probe/appliator combination (French) 0-3820  
 plasma, magnetized rarefied 0-24195  
 rat embryo acute viral infection inhibition by whole-body microwave heating 0-3769  
 rat embryo localised microwave heating effect 0-3728  
 semiconductor, UHF heating of charge carriers using lumped-capacitance resonators 0-20203  
 tissue heating system for hyperthermia research 0-30829  
 UO<sub>2</sub>, UO<sub>3</sub>, U<sub>3</sub>O<sub>8</sub>, microwave heating in nuclear fuel preparation 0-37556

**radiofrequency interference**

- see also atmospherics; radar interference; whistlers*  
 industrial RF heaters, measurements of elec. and mag. field strengths 0-52175  
 interplanetary scintillation meas. in conditions of strong radio interference 0-46413  
 magnetic field strength meter calibration system (Polish) 0-51311

**radiofrequency oscillators**

- NMR detector, transistorised marginal oscillator, for student lab. 0-27078

**radiofrequency spectra of diatomic inorganic molecules *see radiofrequency and microwave spectra of diatomic inorganic molecules*****radiofrequency spectra of inorganic solids**

- see also nuclear magnetic resonance; paramagnetic resonance*  
 B-C system, struct. of paramag. centres 0-20460

**radiofrequency spectra of organic molecules and substances *see radiofrequency and microwave spectra of organic molecules and substances*****radiofrequency spectra of polyatomic inorganic molecules *see radiofrequency and microwave spectra of polyatomic inorganic molecules*****radiofrequency spectrometers**

- see also magnetic resonance spectrometers*  
 acousto-optical spectral analyser at RATAN-600 radio telescope, first test (Russian) 0-51668  
 deep level transient spectrometer, automatic calibration cct 0-37067  
 magnetic field modulator, EPR radiospectrometer having discrete set of modulation frequencies 0-52285  
 magnetic flux stabiliser, resonance conditions stabilisation 0-52286  
 pulsed NQR-FFT radiofrequency spectrometer for <sup>14</sup>N, description and operation 0-17982  
 radioastronomy, RATAN-600 radiotelescope, acousto-optic spectrograph 0-46398  
 resonator uniaxial crystal deformation unit 0-31822

**radiofrequency spectroscopy**

- see also magnetic resonance spectroscopy; nuclear magnetic resonance; radiofrequency spectrometers*  
 air lubricated sample turbine for applications in solid body multipulse spectroscopy (German) 0-52284  
 dielectric relaxation spectroscopy, liquids, frequency and time domain expt. methods 0-40044  
 subMM laser spectroscopy of solids 0-31895  
 time-domain, methods, appl. to dielectrics 0-52310

**radiofrequency sputtering**

- electrodeless discharge sputtering system (Japanese) 0-16183  
 glow discharge, Langmuir probe study at various freqs. 0-55294  
 impedance matching networks, experimental and design information 0-50555  
 magnetron sputtering, appl. to sputtered thin compound films, review (Japanese) 0-25561  
 Permalloy RF sputtered films, struct.-sensitive mag. props. 0-34705  
 Al magnetron sputtering target, oxidation in Ar/O<sub>2</sub> mixtures 0-55291  
 Au-TiC, multilayer struct., microhardness and elec. resist. 0-2950  
 CdO-SnO<sub>2</sub> film, prep. by RF sputtering, elec. cond. and transparency 0-7492  
 Cr<sub>2</sub>O<sub>3</sub>, RF sputtered coating for wear appls., on Inconel X-750 foil, prep. and props. 0-40605  
 Fe-Co-Cr film RF sputtering for magnetic recording 0-2947  
 n-GaAs-Au-Mo, RF sputtering, elec. props. of contacts, compensating damage centres form. 0-34507  
 GaP films, RF sputtering on glass and Au film substrates, struct. and elec. props. 0-2311  
 Gd<sub>0.27</sub>Co<sub>0.64</sub>Kr<sub>0.09</sub>, amorphous film, thermal release of Kr and H, meas. using UHV mass spectrometric technique 0-3439  
 Ge<sub>1.5</sub>Te<sub>0.1</sub>X<sub>1.4</sub> amorphous semicond. switches, fabrication technology (German) 0-7493  
 Hf, RF sputter deposition, ion bombardment and ion implantation 0-25564  
 HfN, RF sputter deposition, ion bombardment and ion implantation 0-25564  
 In<sub>2</sub>O<sub>3</sub>-SnO<sub>2</sub>/GaAs, solar cell, fabrication, characts. and interfacial chemistry 0-21401  
 In<sub>2</sub>O<sub>3</sub>-SnO<sub>2</sub>/InP, solar cell, fabrication, characts. and interfacial chemistry 0-21401  
 Mo sputtering for laser mirror refurbishment 0-14498  
 MoS<sub>2</sub>, RF sputtered layers with variable stoichiometry, lubrication props. 0-40557



**radiofrequency sputtering continued**

- MoS<sub>2</sub>, RF sputtered lubricant, wear life, sputtering parameter effects 0-40558  
 Pb, Josephson junction, oxide formation process, ellipsometric meas. (Japanese) 0-11561  
 Pb/Au/Pb, Josephson junction, oxide formation process, ellipsometric meas. (Japanese) 0-11561  
 Pb-In and Pb-In/Au, Josephson junction, oxide formation process, ellipsometric meas. (Japanese) 0-11561  
 PbTiO<sub>3</sub>, ferroelectric thin films, characts. 0-40261  
 Pb(Zr,Ti)O<sub>3</sub> thin film, ferroelec., fabrication by RF sputtering (Japanese) 0-25560  
 Pd-Au-Si amorphous films, composition and thermal behaviour 0-55292  
 Pd-Si amorphous films, compositions and thermal behaviour 0-55292  
 Si, amorphous, control of dihydride bond density using RF sputtering 0-34327  
 Si, amorphous, Schottky barrier solar cell, large-area RF sputtered, contact form, scaling and optimisation 0-45679  
 Si, amorphous, sputtered, Auger surface spectroscopy 0-50472  
 Si, amorphous film, RF-sputtered, influence of O<sub>2</sub> and deposition conditions, elec. cond., IR absorpt. and ESR 0-2949  
 Si, minority carrier lifetime, effect of SiO<sub>2</sub> coating deposited by RF diode sputtering 0-11003  
 Si:H, amorphous, RF sputtered, suitability as solar cell material 0-40864  
 Si:H, amorphous, RF sputtered, Schottky barrier solar cells, photovoltaic props. and capacitance-voltage charact. 0-45678  
 Si:N, amorphous, prep. by RF sputtering and props. 0-44229  
 SiC coatings for first-wall candidate materials by RF sputtering 0-25563  
 SiC thin film, RF-sputtered, highly reliable temp. sensor 0-224  
 Si<sub>3</sub>N<sub>4</sub> film production, by HF plasma (German) 0-7507  
 SiO<sub>2</sub>, RF magnetron sputtered coatings for laser fusion targets 0-35089  
 SnO<sub>2</sub> thin films, solid state gas sensor 0-40790  
 Sr<sub>2</sub>Nb<sub>2</sub>O<sub>7</sub>, sputtered films, amorphous, dielec. props. 0-54573  
 Ti, RF sputter deposition, ion bombardment and ion implantation 0-25564  
 Ti-W, bias-sputtered, resist. and comp. 0-25023  
 Ti-W magnetron sputtered films metallisation 0-45231  
 TiN, RF sputter deposition, ion bombardment and ion implantation 0-25564  
 TiO<sub>2</sub>-SiO<sub>2</sub> multilayered film striped optical filters, optical props. and fabrication of RF sputtering 0-10030  
 Zr, RF sputter deposition, ion bombardment and ion implantation 0-25564  
 ZrN, RF sputter deposition, ion bombardment and ion implantation 0-25564

**radiogalaxies** *see galaxies; radiosources (astronomical)*

**radiogoniometers** *see goniometers*

**radiographs (x-ray photography)** *see radiography*

**radiography**

- see also electrophotography; neutron radiography; nondestructive testing; radioisotope scanning and imaging; scanning radiography*  
 abdominal arteriography, super selective, technics and indications in children (French) 0-36092  
 absorption-edge transmission technique using <sup>139</sup>Ce for stable I conc. meas. 0-56194  
 analytical X-ray photogrammetry, use for patellar tracking patterns meas. 0-30864  
 angiocardigraphic image computer quantitation 0-36118  
 angiograms, augmentation of computed tomograms 0-8150  
 angiographic I imaging using spectral anal. 0-36122  
 angiographic methods for the diagnosis and therapy of liver diseases (German) 0-56211  
 angiography, computerised, anal. and visualisation of blood dynamics and motion of organs 0-8170  
 angiography installation, first experiences 0-17080  
 apparatus optimal operating conditions 0-30847  
 arthrotomographic diagnosis of meniscus perforations in the temporomandibular joint 0-56170  
 atherosclerosis detection, computerised electronic radiographs appl. 0-8169  
 bone, disease diagnosis, automatic texture anal. methods 0-8156  
 bone and bone marrow involvement in malignant lymphoma, detect. obs. 0-36086  
 bone density and irregularity meas. in normal hands 0-30839  
 bone density measurement by <sup>125</sup>I photon absorptiometric anal., dialysis patients 0-36075  
 breast parenchymal patterns meas. 0-8155  
 bremsstrahlung, filtered spectra, equivalent half-value thicknesses and mean energies 0-46011  
 bronchial angiography in the staging of bronchogenic carcinoma 0-46007  
 cardiovascular measurements, conf., Bellingham, USA (Sept. '78) 0-31419  
 CaWO<sub>4</sub> intensifying screen, meas. of X-ray induced light photons emitted 0-41218  
 cellular logic techniques in radiological image analysis 0-8171  
 chest film, pre-operative, rel. to post-operative management 0-51207  
 chest radiograph nodule detection system 0-8140  
 chest radiographs, computed detection of nodules 0-8172  
 chest radiographs, processing of large numbers, problems 0-8138  
 chest radiography screening for employees in nuclear industry 0-26342  
 chest X-ray automated screening, texture anal. of lung fields 0-41228  
 compton scatter densitometry determ. of bone density in living patients 0-17102  
 computed radiography, contrast-detail-dose evaluation 0-41221  
 computerised electronic radiography 0-8162  
 computerised fluoroscopy for non-invasive cardiovascular imaging 0-17121  
 contrast enhancement of high-energy radiotherapy films 0-8126  
 contrast improvement using fore-and-aft rotating aperture wheel device 0-41227  
 contrast media labelling with <sup>121</sup>I and <sup>123</sup>I 0-26350  
 convergent wide-angle beam, for polycrystals 0-40634  
 coronary angiogram computer quantitation 0-41233  
 crack detection, effect of stress 0-40653  
 detection of bars and discs in quantum noise [radiography] 0-41042  
 diagnostic, anal. of making, reading and reporting films, rel. to equipment design 0-17123  
 diagnostic, foetal vs. parenteral radiosensitivity 0-51271  
 diagnostic, X-ray spectra determ., high intensity 0-41217

**radiography continued**

- diagnostic imaging systems, non-silver halide, recent developments and pot. 0-41223  
 diagnostic radiological digital image processing facility 0-36127  
 diazotype radiographic duplicating system as diagnostic aid 0-8137  
 dose compensation filter design using megavoltage radiography 0-3785  
 dose distribution description by X-ray quality monitoring (German) 0-41251  
 ECG-ZZ 0-26344  
 electronic radiography, computerised, for early detect. of vascular disease 0-41226  
 electronic scanning of X-ray images 0-8161  
 electrophoretic radiographic device 0-22501  
 electrophotetic X-ray imager, self-contained instant display erasable 0-22491  
 electroradiographic image laser readout 0-41225  
 electrostatic X-ray imaging, book 0-31426  
 electrostatic X-ray imaging, book contrib. 0-36112  
 equipment, idealised, for routine chest exams., specifications and requirements 0-46034  
 equipment, method and algorithm for adjusting 0-30852  
 fetal exposure in diagnostic radiology 0-8133  
 film quality, CAA 0-8158  
 fine puncture and biopsy, efficiency and technique in tumour diagnosis (German) 0-41212  
 fluorescent X-ray intensifying screen, efficiency determ., standard method 0-37140  
 fluoro-arteriography and -phlebography by the middle format technique (German) 0-56212  
 fluoroscopic cardiac imaging, real-time computerised system 0-36123  
 fluoroscopic image recording using multiformat camera 0-51234  
 fluoroscopy, automatic brightness control operating protocols and effect on image quality 0-17120  
 fluoroscopy without the grid, dose reduction method 0-41240  
 hand radiographs, congenital abnormalities classification 0-30870  
 heavy ion radiography 0-17122  
 hysterosalpingography, appraisal of current indications 0-56169  
 IEEE statement on technology development 0-41199  
 image anal. 0-8163  
 image formation, perceptual eval. of phys. parameters, computer-simulated images 0-41222  
 image intensifier closed circuit TV system 0-3775  
 image intensifier fluorography, image quality rel. to patient dose 0-17081  
 image intensifier fluorography in paediatric radiology 0-41201  
 image performance, comparison with computed radiography 0-12250  
 imaging system, new, in computed radiography 0-8147  
 imaging techniques, developments, review 0-26324  
 intravenous angiography, digital video subtraction system 0-41234  
 kidney, conf., Brussels, Belgium (Oct. 1978) 0-31409  
 kidney, intra-operative X-ray diagnostics in detection and localization of residual concretions 0-41202  
 knee ligament disorder diagnosis, radiological meas. of laxity (French) 0-8136  
 laser fusion targets, X-ray meas. using least squares fitting 0-32425  
 magnification angiography, routine 0-21527  
 magnification mammography evaluation 0-17124  
 mammographic dose reduction, Kodak Definium Medical rel. to Kodak Min R film (German) 0-12243  
 mammographic imaging, historical review in terms of image quality and reduced radiation dose 0-41229  
 mammographs, high quality low-radiation, tone reproduction system 0-41198  
 mammography, breast cancer determinants rel. to radiographic features 0-41170  
 mammography, detective quantum efficiency anal. of electrostatic imaging and screen-film imaging 0-41232  
 mammography, experience with 153 breast carcinoma cases (German) 0-12244  
 mammography, exposure timing by use of film/screen systems 0-17059  
 mammography, most reliable method for early breast cancer detect. 0-21528  
 mammography, test object for assessing image quality 0-56171  
 mammography reliability for early breast cancer detection 0-8127  
 mammography techniques, appl. to bird skull struct. anal. 0-36209  
 mammography techniques comparison, in vitro studies of breast microcalcification detectability 0-41230  
 mammography with magnification and grids: detail visibility and dose measurements 0-41231  
 mamography, risks, radiation dosage and picture quality, review (German) 0-36103  
 medical imaging, conf., San Diego, USA, (Aug 1978) 0-17025  
 megavoltage imaging, influence of metal screens on contrast 0-30866  
 metabolic bone diseases in childhood (German) 0-17091  
 metal screen-film detector MTF at megavoltage X-ray energies 0-30868  
 micro-dose system 0-51233  
 microcoded, aperture imaging, appl. to laser plasma diagnosis 0-24251  
 microdosimetry, conf., Brussels, Belgium (May 1978) 0-4472  
 microprocessor-based teleradiology system 0-26343  
 neoroscope, 0D-10N, for scanning radiograph 0-35494  
 neuroradiology, radiation dose to critical organs of staff and patients 0-8184  
 optical centreing systems, operation 0-30831  
 optical density variation, characterisation of radiographic edge-blurring effect 0-13176  
 optical instrumentation in medicine, conf., Toronto, Canada, (Mar. '79) 0-36777  
 OTF as means of evaluation of image characts. (German) 0-35450  
 OTF of radiographic imaging systems 0-17085  
 paediatric patient, radiation exposure from cardiac catheterisation and angiography 0-41241  
 patient exposure 0-46066  
 pediatric cardiac catheterisation, absorbed dose in presence of contrast agents 0-30897  
 pelvimetry, low radiation dose gridless method 0-46010  
 penetrometer for measuring peak kilovoltage of dental X-ray sets 0-41171  
 phantoms for testing X-ray imaging performance 0-51229  
 photofluorographic camera with electro-optical image intensifier 0-36128  
 photogrammetry use in absorbed dose determ. in radiation therapy 0-12222



**radiography continued**

- photographic film response to 25 MV X-rays, sensitometric curves, relative dosimetry 0-52376  
 photography of medical X-ray plates, audio-visual presentations for physicians 0-37103  
 pinhole camera, hole size required for no distortion 0-46028  
 plasmas, laser produced, as X-ray source for microradiography 0-320  
 pneumoconiosis, small lesions, computer aided identification 0-30887  
 processing radiographs, computer appl. 0-3259  
 projection microradiography, historical development and applications 0-37138  
 pulmonary arterial occlusion, comparison of methods in detect., dog expts. 0-56191  
 pulmonary radiograph interpretation, review of models used 0-36089  
 pulmonary vascularity computerised texture features rel. to catheterisation parameters 0-8154  
 radiology conference, London, England (Apr. 1979) 0-30838  
 radiopaque marker clinical usefulness in left ventricular function 0-36119  
 rare-earth screens, effect of P X-rays 0-30867  
 reduced scatter, effect on information content and patient exposure 0-51225  
 review of X-ray imaging, image intensification systems and techniques 0-51236  
 roentgen stereophotogrammetric methods for human knee joint evaluation 0-30952  
 rotating aperture wheel device for radiographic contrast improvement 0-56202  
 RUM-20 apparatus, obs. on improving roentgenogram quality 0-30850  
 safety training program for radiographers 0-17141  
 screen-film combination selection 0-46047  
 screen-film system evaluation, intensity vs. time scale sensitometry 0-41219  
 screen-film system evaluation, sensitometric method 0-41220  
 shape descriptors, Fourier-Walsh, radiographic image processing appls. 0-8153  
 skeletal maturity determination system (*French*) 0-41209  
 skull, frontal diagnostics of injuries (*German*) 0-36104  
 small-grain development of emulsion monofilms for electron-microscope autoradiography (*Russian*) 0-297  
 steel, austenitic stainless, mottling on radiographs of weldments and castings 0-16614  
 steel, pressing die X45 CrNiWMoVCo 9.9, test results (*German*) 0-50785  
 stereography, method of precision position determ. 0-56314  
 subtraction device for daily practice and vascular procedures 0-36090  
 technological and philosophical changes over a decade of X-ray tubes 0-37136  
 test objects for systems performance evaluation 0-46022  
 TEXAC image processing computer for radiographic feature enhancement 0-12251  
 Thoramat automatic thoracic radiography unit experience 0-12212  
 three dimensional image recording and reconstruction 0-31953  
 traumatised patient diagnostic radiology requirements 0-8128  
 tube current fall-off during an exposure, investigation and explanation 0-56203  
 upper airways in newborn and infants, X-ray physiological exam. using Orbiskop 0-8130  
 urodynamic combination EMG and functional X-ray exam. technique 0-8131  
 urography, double-dose, image clarity and contrast range obs. (*German*) 0-30875  
 uterine venography, value in diagnosis of pelvic pain in women (*French*) 0-17079  
 venous system visualisation combined with press. meas., technique and equipment 0-36094  
 ventricle, left, boundary detection from cineangiograms 0-8168  
 ventricle, left, human, geometric modelling, using biplane cineangiograms 0-35955  
 X-ray beam characteristic time vars. meas. using solid state devices 0-46048  
 X-ray focal spot, MTF, modified meas. method 0-37149  
 X-ray generators, acceptable latitudes in the specifications 0-37137  
 X-ray image converter with video signal output 0-36125  
 X-ray image intensifier performance, image quality, and development trends 0-36124  
 X-ray image intensifiers, quantum noise meas. 0-46033  
 X-ray image magnification technique 0-18054  
 X-ray installation, for rapid process frame-by-frame registration 0-47159  
 X-ray tube performance characteristic rel. to radiologic image quality 0-17125  
 X-ray TV chain MTF and image quality determ. factors 0-36126  
 xerography and mammary microcalcifications (*French*) 0-51224  
 xeromammography, absorbed dose obs. 0-41242  
 xeromammography, Monte Carlo calc. of integral radiation dose 0-41248  
 xeroradiographic imaging linearity and MTF applicability 0-4825  
 xeroradiography, negative development, doses and clinical indications in breast exams. 0-56217  
 xeroradiography of frontal skull and nasopharynx (*German*) 0-30873  
 xeroradiomammography, positive rel. to negative mode considerations (*French*) 0-51223  
 Fe, pure, Sn and Cr diffusion, effect of boundary struct., autoradiography study (*Japanese*) 0-49419  
<sup>192</sup>Ir radioactive sources, field determ. of output and effective size 0-30193  
 Se, electroradiographic layer, radiographic contrast 0-12241  
 Se, X-ray sensitivity, induced photocurrents, xeroradiographic meas., pair creation energy 0-22490  
 Si:P, neutron irradi. crysts., qualitative distrib. of P using autoradiography 0-24486

**radioisotope scanning and imaging**

- see also computerised tomography; scanning radiography*  
 abdominal abscesses detection, role of <sup>67</sup>Ga-scintigraphy, ultrasonography and computerised tomography 0-17096  
 Anger, Hal O., work at the Donner Lab. 0-42027  
 Anger scintillation camera, development since 1958 0-12234  
 angiocardigram anal. program for radiology trainees 0-8143  
 Auger camera performance, effects of a reduction in crystal thickness 0-41187  
 automated interpretation of nuclear medicine studies 0-8164  
 basic radionuclide imaging techniques, book contrib. 0-36113

**radioisotope scanning and imaging continued**

- biliary tract disorders, evaluation by cholecintigraphy, ultrasonography and computerised tomography 0-17093  
 blood flow and tracer uptake in normal and abnormal canine bone 0-17072  
 blood-pool imaging in <sup>99m</sup>Tc myocardial scintigraphy 0-12228  
 bolus-injection system for dynamic time-function studies 0-41194  
 bone diseases, benign, the particular usefulness of radioisotope methods 0-51209  
 bone marrow haemopoietic activity assessment in normal subjects 0-36073  
 bone marrow scanning in pediatric oncology, evaluation of <sup>99m</sup>TcS colloid 0-17067  
 bone scan, whole body, value in breast carcinoma pre-operative assessment 0-51210  
 bone scanning, historical survey 0-42029  
 bone scans, appearance following fractures 0-56189  
 bone scintigraphy, importance in pretherapeutic development of mammary neoplasms (*French*) 0-8135  
 bone scintigraphy, use in uremic pulmonary calcification detect., <sup>99m</sup>Tc HEDP obs. 0-3788  
 bone scintigraphy as detect. method for bone and bone marrow involvement in malignant lymphoma 0-36086  
 book, basic radionuclide imaging techniques 0-31426  
 brain, combined static and circulation imaging 0-51211  
 brain activity concentration after administration of <sup>11</sup>C- $\alpha$ -p-iodoanilino phenylacetone nitrile 0-3776  
 brain autoradiographs, rapid semiautomatic quantification, microprocessor appl. 0-41332  
 brain imager, transverse-section, for single-gamma emitters 0-3794  
 brain isotope distribution reconstruction, error anal. for instrument design 0-3772  
 brain scintigraphy, early and delayed image evaluation using <sup>99m</sup>Tc glucoheptonate 0-3790  
 bronchial epithelium tissue, technique for high sensitivity  $\alpha$  autoradiography 0-17210  
 cardiac blood pool imaging, evaluation of <sup>99m</sup>Tc labelled human serum albumin kits 0-17130  
 cardiac output determination, automated computer program 0-56196  
 cardiac shunts, left-to-right, deconvolution anal. in radionuclide quantitation 0-12229  
 cardiology, conf., London, England (June 1979) 0-36759  
 cardiomyopathy scintigraphic diagnosis by <sup>99m</sup>Tc-labelled pyrophosphate, method sensitivity 0-17061  
 cardiovascular measurements, conf., Bellingham, USA (Sept. '78) 0-31419  
 cerebral blood flow noninvasive meas., analytical problems 0-41208  
 cerebral blood volume meas. by <sup>11</sup>C-labelled carboxyhaemoglobin 0-8134  
 cerebral tissue perfusion rate determ. from <sup>15</sup>O activity decay after photon activation 0-26341  
 collimator optimal design parameters for dynamic spatial resolution 0-17087  
 colour scintiphotographic radionuclide angiography, aide to isotope ventriculography 0-12239  
 comparison at rest and during isometric exercise 0-30857  
 computed tomography, review 0-56213  
 computer applications 0-3801  
 computer applications in nuclear medicine, history 0-42037  
 computer applications in nuclear medicine, review (*German*) 0-41214  
 computer processing of static gamma camera images 0-36095  
 computer reconstruction of scintigraphic images 0-30846  
 computerised internal mammary lymphoscintigraphy in radiation treatment planning 0-12223  
 computerised positron emission tomography for assessment of myocardial integrity 0-36120  
 computerised rotating laminar radionuclide camera 0-3796  
 computerised tomography, fundamental limitations in radionuclide imaging 0-30882  
 computerised tomography, longitudinal reconstruct. using calligraphic CRT graphics system 0-8173  
 computerised tomography system, expt. meas. of impulse response and noise 0-56182  
 conference, Karlovy Vary, Czechoslovakia (May, 1979) 0-12840  
 constant infusion of short-lived isotopes, theoretical study of quantitative flow meas. 0-17088  
 coronary artery disease, significance of abnormal rest <sup>201</sup>Tl myocardial image 0-17060  
 coronary artery disease extent prediction by <sup>201</sup>Tl myocardial images 0-26336  
 cranial scintigraphy, value of adding emission CT sections to conventional pertechnetate images 0-56187  
 digital data collection system, portable, cost-effective 0-41195  
 digitised images display, minimisation of data transfer losses 0-56206  
 display algorithms evaluations 0-8144  
 dynamic phantom for radionuclide cardiology 0-12232  
 emission computerised tomography using positron-emitting isotope, review 0-17083  
 encephalic exploration, clinical value of single photon emission CT 0-51216  
 exercise-radionuclide ventriculograms, methods for eliminating motion 0-41193  
 external counting procedures, history 0-42033  
 extrapulmonary tuberculosis, use of <sup>67</sup>Ga citrate in detect. and follow-up 0-46012  
 Fourier multiaperture emission tomography 0-41188  
 fourier reconstruction with a distortion function 0-8174  
 gamma camera dynamic studies, use of principal components in quantitative anal. 0-56207  
 gamma camera imaging, recent advances 0-17127  
 gamma cameras, state of art 0-3802  
 gamma detector, gaseous, good low-energy resolution for  $\leq 50$  keV imaging 0-3795  
 gamma scintillation chamber, operating model 0-30848  
 gamma tomograph, GSG-2 twin-sensor, functional and clinical qualities 0-56172  
 gastrointestinal bleeding, evaluation by <sup>99m</sup>Tc labelled red blood cells 0-51219  
 Grigg, Emanuel Radu Newman, (1916-1976) radiologist and historian, biography 0-42026  
 heart, computerised tomography of normal and infarcted patients 0-30859



- radioisotope scanning and imaging continued**  
heart wall motion cine display using  $^{99m}\text{Tc}$ -labelled red blood cells 0-17129  
hepatic mass evaluation, relationship of ultrasonography, nuclear medicine and computerised tomography 0-17092  
hepatic steatosis,  $^{133}\text{Xe}$  retention rel. to biopsy 0-17069  
hepatobiliary disorder scintiscanning, evaluation of  $^{131}\text{I}$  labelled ioglycamide acid 0-36072  
hepatobiliary functional scintillation recording, review (*German*) 0-30874  
hepatobiliary study of liver-transplant patients,  $^{99m}\text{Tc}$  diethyl-iminodiacetic acid rel. to  $^{131}\text{I}$  rose bengal 0-3793  
image linear filtering, optimal compromise 0-36071  
image processing system for display and anal., computerised 0-41174  
imaging principles, concepts and equipment 0-17113  
imaging techniques, book 0-12861  
imaging techniques, developments, review 0-26324  
incremental deconvolution, possible method 0-56208  
Indian nuclear medicine, review 0-36082  
instruments and radiopharmaceutical production, review (*French*) 0-17056  
joint imaging, technical aspects 0-56197  
left ventricular ejection fraction meas. in equilib. radionuclide angiography 0-46009  
left ventricular ejection fraction determ. by equilib. radionuclide angiography 0-12227  
left ventricular equilib. radionuclide angiography, arrhythmia effects correction method 0-17089  
left-ventricular aneurysm, reliability of gated scintigrams in detect. 0-30856  
left-ventricular ejection fractions meas. by equilib. radionuclide angiography 0-12226  
leukocyte migratory patterns, use of  $^{99m}\text{Tc}$  as radioactive label for study 0-51222  
liposomes labelled with  $^{111}\text{In}$  oxine or  $^{99m}\text{Tc}$  DTPA, metabolic and scanning tracers, mouse 0-17073  
liquid scintillation counting, apparent and actual  $^{14}\text{C}$  retention 0-36080  
liquid scintillation vial system, new container geometry for better sensitivity 0-46021  
liver, comparison of scintigraphy, US and computerised tomography scanning 0-17105  
liver, dynamic studies with  $^{99m}\text{Tc}$  labelled S colloid, processing 0-41169  
liver, nuclear imaging, comparison of conventional rectilinear and multi-plane tomographic scanning 0-17106  
liver, respiratory motion in supine and upright positions 0-30858  
liver cirrhosis, evaluation of 1D profile scans with a whole body counter 0-51213  
liver hepatoma, dog, evaluation of 3 imaging instruments 0-17074  
liver imaging,  $^{178}\text{Ta}$  radiopharmaceuticals rat expts. 0-51254  
liver scintigraphy, pattern recognition 0-8157  
liver volume measurement by emission computerised tomography 0-12230  
lung, gated and cinematic perfusion imaging, dogs with expt. pulmonary embolism 0-17071  
lung imaging,  $^{178}\text{Ta}$  radiopharmaceuticals rat expts. 0-51254  
lung imaging, history 0-42035  
lung imaging, technique for contralateral subtraction 0-41207  
lung phantom, dynamic, use as educational tool 0-8757  
lung scanning and radionuclide venography 0-3791  
lung ventilation model, radioactive tracer tidal breathing 0-56095  
lymphography in prostatic carcinoma, implications for metastases diagnosis 0-41168  
lymphoscintigraphy, comparison of 2  $^{99m}\text{Tc}$  labelled radiopharmaceuticals 0-41185  
lymphoscintigraphy, radiocolloid optimal uptake in rabbit parasternal nodes 0-46018  
lymphoscintigraphy using  $^{99m}\text{Tc}$  colloid 0-36114  
mandibular bone graft fate determ., quantitative radionuclide imaging 0-3792  
MDS computer systems, improvement of pulse-mode photographic images 0-30862  
medical gamma-ray cameras of Anger type, optimisation (*French*) 0-26328  
medical imaging, conf., San Diego, USA, (Aug 1978) 0-17025  
metrology of ionising radiations and nuclear medicine (*French*) 0-17057  
muco-ciliary transport monitoring method using  $^{99m}\text{Tc}$  colloid, bronchiectatic patient appl. 0-30840  
multiplane tomographic scanner, simulated, correct. for out-of-focal-plane blurring 0-51221  
myocardial  $^{201}\text{Tl}$  imaging, redistrib. rel. to rest images 0-12225  
myocardial  $^{201}\text{Tl}$  perfusion images, computer anal. method 0-30860  
myocardial  $^{201}\text{Tl}$  perfusion scintigrams in the evaluation of aortocoronary saphenous bypass surgery 0-12235  
myocardial  $^{201}\text{Tl}$  scintigraphy, effect of gate width 0-41172  
myocardial infarction, acute,  $^{99m}\text{Tc}$  pyrophosphate rel. to  $^{99m}\text{Tc}$  methylene diphosphonate 0-17070  
myocardial infarction, perioperative, comparison of ECG, scintigraphy and enzyme diagnosis 0-30855  
myocardial perfusion evaluation by coded aperture tomographic technique 0-21537  
myocardial perfusion imaging using  $^{201}\text{Tl}$ , algorithm for background activity calc. 0-56195  
myocardial uptake of  $^{99m}\text{Tc}$  stannous pyrophosphate in expt. viral myopericarditis, mouse obs. 0-46019  
neuroradiology, radiation dose to critical organs of staff and patients 0-8184  
nMTCB task analysis of nuclear medicine technology 0-8753  
nuclear counting, method to reduce cosmic background 0-897  
nuclear medicine, trends (*French*) 0-26327  
organ radionuclide uptake, quantitative meas. by a  $\gamma$ -camera 0-51212  
OTF in evaluation of  $\gamma$ -camera data in moving organ exam. 0-30845  
ovarian imaging, use of  $^{131}\text{I}$  labelled chorionic gonadotropin, rat expts. 0-41186  
pancreas,  $^{11}\text{C}$ -labelled amino acids for rectilinear and positron tomographic imaging 0-12258  
pancreatic disease, study by multiple imaging modalities 0-17094  
pancreatic scanning with  $^{11}\text{C}$  methionine positron emission computerised tomography 0-30861  
pericardial effusion, malignant, myocardial accumulation of labelled phosphate 0-17068  
peritoneum and retroperitoneum, anatomic correls. in  $^{67}\text{Ga}$  imaging 0-17097
- radioisotope scanning and imaging continued**  
phantom for clinical evaluation of total system resolution 0-41197  
photomultiplier tube balance assessment 0-41196  
polyacrylamide gel, automated scanning of  $^{14}\text{C}$  0-17221  
positron camera using ring detector system, for emission tomography of brain 0-30880  
positron emission computer-assisted tomographic scanner 0-36116  
positron emission computerised tomography, optimisation of system design parameters 0-26347  
positron emission tomography, appl. to meas. of cerebral metabolic rate 0-3799  
positron emission tomography, fully 3D considerations 0-36098  
positron tomographic system, single slice, physical performances and preliminary clinical results 0-56181  
positron-emitting blood pool imaging agents compared 0-12213  
prostate scanning with  $^{75}\text{Se}$  labelled adenosyl selenomethionine, rat distrib. obs. 0-17132  
prostrate, rat, rel. to  $^{77}\text{Br}$ -bromide 0-51247  
prostrate imaging, comparison of  $^{18}\text{F}$  and  $^{125}\text{I}$  labelled compounds in the rat 0-51215  
pulmonary arterial occlusion, comparison of methods in detect., dog expts. 0-56191  
pulmonary arterial pressure, noninvasive estimation in dogs using  $^{133}\text{Xe}$  images 0-41184  
pulmonary embolism patients, usefulness of  $^{99m}\text{Tc}$ -fibrinogen phlebography 0-36093  
pulmonary embolism resolution rates assessed by serial positron imaging 0-3789  
radioassays, historical development 0-42034  
radioisotope angiocardigraphic image, left ventricular contour extraction and vol. computation (*Japanese*) 0-3798  
radiology conference, London, England (Apr. 1979) 0-30838  
random summing in multi-detector counting system meas. radionuclide mixtures 0-36097  
refractory products, apparent density determination, using surface  $\gamma$  densimeter 0-35464  
regional left-ventricular dyskinesia, paradox nuclear image as noninvasive index 0-56190  
regional ventilatory clearance, estimation by  $\text{Xe}$  scintigraphy 0-30854  
renal cortical imaging and renal mass lesion detect. 0-46016  
renal graft evaluation with pertechnetate and  $^{131}\text{I}$  Hippuran 0-46017  
renal imaging with radionuclides, US and computerised tomography 0-17095  
renal scintigraphy, value of additional lateral scans 0-36074  
review of apparatus, techniques and performance 0-51237  
RI image processing with a microprocess 0-8175  
scintigraphic imaging with  $^{178}\text{Ta}$  and the Anger scintillation camera 0-12231  
scintigraphic investigations in neuroradiology (*German*) 0-12242  
scintillation camera dead time with and without computer 0-3777  
scintillation camera upgrading, comparative study 0-12236  
scintillation camera whole-body single-photon emission computerized tomography system 0-17086  
scintillation camera/high energy collimator system, misleading results with a bar phantom image 0-12237  
scintillation cameras, automatic field uniformity corrections 0-17128  
scintillation probe detector in assessment of cardiovascular disease 0-3800  
sigma scan, method for enhancement of statistically significant differences 0-36096  
skeletal disease, profile scanning,  $^{47}\text{Ca}$  rel. to  $^{32}\text{P}$  0-51218  
skeletal tracer kinetics,  $^{99m}\text{Tc}(\text{Sn})$  methylenediphosphonate uptake in canine tibia rel. to blood flow 0-56192  
spleen and liver colloid take up ratio in diagnosis and treatment of diffuse hepatic disease 0-41203  
statistics, understanding and using 0-12233  
technology conference, Louisville, USA (Feb. 1980) 0-51949  
testicular perfusion imaging, [ $^{99m}\text{Tc}$ ] sodium pertechnetate study, method and obs. 0-12238  
thyroid 'cold' areas scintigraphic evaluation using  $^{201}\text{Tl}$  0-36078  
thyroid imaging,  $^{125}\text{I}$  rel. to  $^{99m}\text{Tc}$  0-36077  
thyroid scan with  $^{99m}\text{Tc}$ -bleomycin, evaluation of cold areas 0-56183  
thyroid scintigraphy with time-coded aperture 0-3797  
tomographic imaging, historical review 0-42038  
transmission densitometry, modified method 0-36091  
transverse-sectional imaging with  $\text{Na}^{18}\text{F}$  in myocardial infarction 0-46015  
tumour localisation studies and method for labelling DNA with  $^{125}\text{I}$  0-51249  
tumour-localising radionuclides in retrospect and prospect 0-42036  
ventilation abnormalities detection using  $^{133}\text{Xe}$ , washout rel. to single-breath imaging 0-41183  
ventilation-perfusion scintigraphy on pulmonary disease, artefact suppression 0-17082  
 $\text{Bi}_2\text{Ge}_2\text{O}_{12}$ , low-temp. scintillation props. and appl. to high-energy  $\gamma$ -imaging devices 0-55191  
 $^{113m}\text{In}$ -labelled transferrin, use in meas. of blood vols. in rat, rabbit 0-3878  
 $^{63}\text{Ni}$  applications in biological research 0-12321
- radioisotope separation** see isotope separation
- radioisotopes**  
see also radioisotope scanning and imaging  
 $^{222}\text{Rn}$  concentration distribution under ground, effect on natural  $\gamma$ -ray flux density and exposure rate 0-36300  
application to solid phase synthesis mechanism in  $\text{LaMnO}_3$  and  $\text{YMnO}_3$  0-21268  
applications in industry and science (*Czech*) 0-32554  
automatic radioisotope production devices adapted to a medical cyclotron 0-12260  
charact., natural occurrences, technological enhancement and health effects 0-46071  
collective dose commitments from the release of radioactive nuclides to the atmosphere 0-3556  
cyclotron production of radiodiagnostic isotopes 0-51255  
cyclotron production of radioisotopes for medical appl. 0-51256  
cyclotron production of radionuclides for medical appl., UC-Davis program 0-51257  
decontamination of radioactive isotopes 0-13950  
dose calculations for inhaled natural radioactive nuclides 0-26354  
haematologic disorders, radionuclide therapy 0-36109



## radioisotopes continued

- internal radionuclide point source microdosimetry, specific energy density calc. 0-26373
- laser spectroscopy of unstable isotopes, nucl. props. determ. from atomic spectra using fast beams 0-9720
- lung histological sections, techniques for studying radionuclides 0-56315
- malignant thyroid disease treatment 0-36108
- material location technique, rat small intestine 0-8226
- production using 14 MeV neutron generators 0-3811
- pulmonary effects of radionuclide and chemical pollutants (*French*) 0-8102
- radiation therapy, pot. future appl. of radioisotopes 0-36031
- radioactive material migration in soil, hydrologic transport model 0-16848
- radioactive waste, geochemical aspects of radionuclide migration from waste repositories 0-13711
- radioactive waste, leach-migration experiments to determine the mobility of radionuclides in geologic media 0-18487
- radionuclide migration from repository sites, stochastic anal. 0-37486
- radionuclide transport through heterogeneous media 0-32382
- receptor binding radiotracer preparation 0-51258
- soluble radioisotopes, meas. of activities and their origin in reactor steam generator leakage water 0-693
- thermoelectric generator cooling in spacecraft 0-40881
- thermoelectric generator shock and vibration test program for MB-M75(A) 0-35711
- thermoelectric generators, design optimisation for Solar-Polar Mission 0-40880
- thermoelectric generators, power degradation predictions 0-40879
- thermoelectric generators, SNAP 19 performance update for Pioneer and Viking missions 0-40883
- trace element analysis of radiological effluents from coal-burning power plants 0-21426
- waste disposal in geologic media, radionuclide migration model 0-37499
- <sup>133</sup>Xe custom trapping and holding system for animal research, design and evaluation 0-30950
- <sup>222</sup>Rn daughters exposure, electronic dosimeter 0-46054
- <sup>108</sup>Ag<sup>m</sup>, prod. in nuclear reactors by thermal neutron capture in stainless-steel structure 0-42747
- <sup>A</sup>Ar, A=37,39, simultaneous activity meas. 0-23270
- <sup>A</sup>At, A=209, 210, production by photospallation of <sup>232</sup>Th and <sup>238</sup>U 0-52797
- <sup>198</sup>Au, use in ovarian carcinoma treatment 0-36087
- <sup>10</sup>Be conc., vars. search in marine sediment core during geomag. reversal 0-26511
- <sup>10</sup>Be survival and cosmic ray age distribs. in galactic convective halo 0-51625
- <sup>76</sup>Br, <sup>77</sup>Br, production from decay of cyclotron produced <sup>76</sup>Kr and <sup>77</sup>Kr 0-52799
- <sup>11</sup>C, production by cyclotron, biomedical appls. (*French*) 0-56216
- <sup>11</sup>C production for nuclear medicine use 0-30889
- <sup>11</sup>C-labelled radiopharmaceuticals, automated synthesis 0-17133
- <sup>14</sup>C dating method using 20 keV Kr ion beam for objects <65000 yrs. (*Danish*) 0-8440
- <sup>14</sup>C dating technique using cyclotrons, or Van de Graaff as mass spectrometer 0-5414
- <sup>14</sup>C, dissolved in groundwater initial activity determ., new model and review 0-8458
- <sup>14</sup>C, formation, distrib. in nuclear fuel cycle (*Russian*) 0-5316
- <sup>14</sup>C labelled amino acids, optimisation factors in liquid scintillation counting 0-30951
- <sup>14</sup>C low level liq. scintillation counting using small vol. teflon-Cu vial 0-16887
- <sup>45</sup>Ca, effect on spleen and thymus of Indian desert gerbil 0-8106
- <sup>45</sup>Ca, effects on bone marrow of Indian desert gerbil 0-45971
- <sup>109</sup>Cd, production in nuclear reactors by neutron irradiation of <sup>107</sup>Ag 0-52798
- <sup>144</sup>Ce absorption through damaged and undamaged skins of guinea pigs 0-26383
- <sup>144</sup>Ce, removal rate in lower stratosphere, seasonal vars. 0-55957
- <sup>252</sup>Cf fission-neutron spectrum unfolding experiment 0-13514
- <sup>252</sup>Cf, measured neutron and  $\gamma$  spectra in a tissue equivalent medium 0-3805
- <sup>36</sup>Cl in meteorites from Antarctic, cosmic irradiation histories 0-21950
- <sup>34m</sup>Cl<sup>-</sup> production, inorganic yields 0-23202
- <sup>244</sup>Cm, inhalation carcinogenesis of high-fired <sup>244</sup>CmO<sub>2</sub> in rats 0-21502
- <sup>244</sup>Cm, mobility in bronchially intubated rat 0-30967
- <sup>60</sup>Co absorption through damaged and undamaged skins of guinea pigs 0-26383
- <sup>60</sup>Co radiation therapy, eval. of dosimetric accuracy and uniformity 0-12269
- <sup>60</sup>Co source irradiation of 2 media, absorbed dose in vicinity of an interface 0-30894
- <sup>134</sup>Cs and <sup>137</sup>Cs in Clyde Sea Area 0-3541
- <sup>137</sup>Cs absorption through damaged and undamaged skins of guinea pigs 0-26383
- <sup>137</sup>Cs, migration in Magenta dolomite, effect on radioactive waste storage 0-13718
- <sup>137</sup>Cs radiation effect on Chinese hamster cells, marker phenotype rescue 0-17005
- <sup>137</sup>Cs radioactive fallout and lacustrine sedimentation rates 0-4048
- <sup>137</sup>Cs, study of absorpt. by Lemna minor 0-30677
- <sup>137</sup>Cs whole-body content in a normal New Mexico population 1956-1977 0-26382
- <sup>18</sup>F recoil labelling of CF<sub>3</sub>Cl 0-23203
- <sup>18</sup>F-5-fluorouracil, synthesis and purification by fractional sublimation 0-17134
- <sup>59</sup>Fe/<sup>57</sup>Fe activity ratio of blood, meas. using semicond. detector 0-17062
- HT-HTO in air meas. system 0-21433
- <sup>3</sup>H labelled amino acids, optimisation factors in liquid scintillation counting 0-30951
- <sup>203</sup>Hg, tracer for Hg conc. in seawater expts., <sup>75</sup>Se tracer 0-21420
- I, adsorption in soils, concentration depend. obs. (*Czech*) 0-12031
- I isotopes, history of use in medicine 0-42032
- I, radioisotopes, environmental and biological effects from nuclear fuel cycle (*Russian*) 0-52768
- I, adsorption on steel in HTGR He environment 0-44233
- <sup>121</sup>I labelling of radiographic contrast media 0-26350
- <sup>121</sup>I, production on Heidelberg compact cyclotron, dosimetry studies 0-21539
- <sup>123</sup>I labelling of radiographic contrast media 0-26350
- <sup>125</sup>I airborne vapour detection 0-51027

## radioisotopes continued

- <sup>125</sup>I, counting device with automatic efficiency correction 0-42897
- <sup>125</sup>I labelling hazards, recommended code of practice 0-51270
- <sup>125</sup>I microelectrolytic labelling of polypeptide hormones 0-12255
- <sup>125</sup>I worker thyroid meas. 0-36151
- <sup>129</sup>I, dose to world population from nucl. power industry 0-47619
- <sup>129</sup>I storage, IO<sub>3</sub><sup>-</sup> adsorption by hematite 0-22992
- <sup>131</sup>I, airborne release from operating BWRs 0-23033
- <sup>131</sup>I airborne release from PWR, determ. of sources 0-17138
- <sup>131</sup>I and antithyroid drugs, simultaneous treatment of toxic diffuse goiter 0-56193
- <sup>131</sup>I dosimetry of the rat thyroid, accurate method 0-46063
- <sup>131</sup>I therapy, review of contamination and exposure hazards 0-41257
- <sup>131</sup>I therapy, role in childhood hyperthyroidism treatment 0-41182
- <sup>131</sup>I, thyroid dose eval. following accidental release from reactor spent fuel 0-26366
- <sup>131</sup>I, treatment of benign thyroid disease, review 0-36107
- <sup>131</sup>I, use in hyperthyroidism treatment of children and adolescents 0-46013
- <sup>131</sup>I, use in the treatment of metastatic thyroid cancer 0-36084
- <sup>131</sup>I-4-iodoantipyrine preparation from <sup>131</sup>I-iodide 0-12256
- <sup>40</sup>K, natural content and internal radiation burden of Hungarian adult population 0-26355
- <sup>40</sup>K, pressure-induced changes in electron-capture decay const., theory 0-22771
- <sup>85</sup>Kr radioisotope, estimation of radiation safety 0-5346
- <sup>28</sup>Mg, intestinal absorpt. obs. in man 0-36217
- <sup>28</sup>Mg radionuclide yield from <sup>27</sup>Al( $\alpha$ ,p) and <sup>26</sup>Mg( $\alpha$ ,2p) 0-32290
- <sup>54</sup>Mg, removal from waste water by oxine-impregnated activated charcoal 0-9344
- <sup>99</sup>Tc separation in <sup>99</sup>Tc<sup>m</sup> generator of higher activity 0-17136
- <sup>13</sup>N, production by cyclotron, biomedical appls. (*French*) 0-56216
- <sup>13</sup>N production for nuclear medicine use 0-30889
- <sup>13</sup>N production in cyclotron by <sup>16</sup>O(p, $\alpha$ )<sup>13</sup>N, water loop target 0-23201
- <sup>13</sup>N species formed by proton irradiation of water 0-45532
- <sup>15</sup>N-NH<sub>3</sub>, absorpt. and transfer to amino-N, rat small intestinal sac 0-16909
- <sup>63</sup>Ni applications in biological research 0-12321
- <sup>237</sup>Np migration potential in radioactive waste 0-3537
- <sup>15</sup>O, production by cyclotron, biomedical appls. (*French*) 0-56216
- <sup>15</sup>O production for nuclear medicine use 0-30889
- <sup>210</sup>Pb and <sup>210</sup>Po concs. in liver and kidneys of cattle 0-30904
- <sup>210</sup>Pb, external  $\gamma$ -counting and bioassay meas. on retired U miners 0-26332
- <sup>210</sup>Pb/<sup>210</sup>Po atmospheric ratio, modification by volcanic emissions 0-41507
- <sup>238,239,240</sup>Pu, concs. in arthropods at a nuclear facility 0-30905
- Pu air monitor with background compensation system 0-27824
- Pu in lungs of pronghorn antelope near a nuclear fuel reprocessing plant 0-30906
- Pu, Manhattan project workers, 32-year medical follow-up 0-26379
- <sup>239</sup>Pu, effect on mouse haemopoietic stem cells 0-51174
- <sup>239</sup>Pu, polymeric, effects on erythrocyte survival in mice 0-45973
- <sup>228</sup>Ra, <sup>228</sup>Ra, dose-response relationships for female dial painters 0-21545
- <sup>226</sup>Ra, conc. in Florida phosphate materials 0-30615
- <sup>226</sup>Ra, radioactivity of thermal and mineral springs in Slovenia 0-7963
- <sup>81</sup>Rb/<sup>81m</sup>Kr ratio as radioactive tracer study of organic bleeding (*Dutch*) 0-3807
- <sup>81</sup>Rb-<sup>81m</sup>Kr, production in ( $\alpha$ ,2n) and (<sup>3</sup>He,3n) reactions on KBr 0-12253
- <sup>82</sup>Rb generator with alumina column, radioactive Sr adsorption 0-12257
- <sup>186</sup>Re labelled EHDP preparation and possible use in osseous neoplasms treatment 0-56215
- Rn decay products, influence of elec. charge and humidity on diffusion coeff. 0-6192
- Rn, diffusion coefficient and exhalation rate from building materials, meas. technique 0-4694
- Rn, evolution in neutral atmospheres (*Spanish*) 0-4058
- <sup>21</sup>Rn, production by photospallation of <sup>232</sup>Th and <sup>238</sup>U 0-52797
- <sup>222</sup>Rn, conc. over intertropical convergence zone of Atlantic 0-26648
- <sup>222</sup>Rn exhalation meas., soil and meteorological effects (*Spanish*) 0-31082
- <sup>222</sup>Rn, radioactivity of thermal and mineral springs in Slovenia 0-7963
- <sup>75</sup>Se, yield for various reactions and chem. processing 0-36131
- <sup>75</sup>Se, tracer for Se conc. in seawater expts., <sup>203</sup>Hg tracer 0-21420
- <sup>82</sup>Sr-<sup>82</sup>Rb generator improvement using inorganic exchangers 0-17135
- <sup>89</sup>Sr therapy of bone metastases of prostatic gland carcinoma 0-36076
- <sup>90</sup>Sr, effect on fetal mouse ovary rel. to time administered during pregnancy 0-51163
- <sup>90</sup>Sr, pollution in N. Pacific surface water during 1974, conc. meas. 0-26181
- T concentration reduction for aquifer 0-21423
- T, in PWR, sources, releases, monitoring, management and environmental impact 0-18690
- T monitoring at nuclear power stations 0-18691
- T monitoring methodology using SiO<sub>2</sub> desiccant, appl. to research reactor facility 0-21434
- T release from nuclear power stations 0-23032
- T species, sources and reactions 0-21432
- <sup>99m</sup>Tc migration potential in radioactive waste 0-3537
- <sup>99m</sup>Tc-EDTA complex production method and renal retention obs. 0-12254
- Th, stability index measurement by natural radioactive tracers (*Spanish*) 0-51448
- <sup>232</sup>Th, reevaluation of dose unit per unit intake 0-26356
- <sup>201</sup>Tl, myocardial perfusion evaluation by coded aperture tomographic technique 0-21537
- U, radioactivity of thermal and mineral springs in Slovenia 0-7963
- U, urine analysis by delayed neutrons 0-26331
- <sup>234</sup>U-<sup>230</sup>Th-<sup>226</sup>Ra, superposition soln. of transport of decay chain through sorbing medium 0-37500
- <sup>234</sup>U-<sup>230</sup>Th-<sup>226</sup>Ra decay chain, hydrogeological migration anal. 0-37501
- <sup>235</sup>U, conc. in UO<sub>2</sub>(NO<sub>3</sub>)<sub>2</sub> aq. soln., pulsed NMR determination 0-2658
- <sup>238</sup>U, conc. in Florida phosphate materials 0-30615
- <sup>178</sup>W, productions in <sup>181</sup>Ta(p,4n), purification procedure 0-12252
- Xe prod. cross sections with protons of 320-590 MeV, nuclear medicine appl. 0-36133
- <sup>135</sup>Xe air contamination, meas. technique 0-41255
- <sup>135</sup>Xe solubility coefficients in water, saline, dog blood and organs 0-56331
- <sup>90</sup>Y, appl. to cancer therapy of liver 0-17098
- <sup>91</sup>Y, removal rate in lower stratosphere, seasonal vars. 0-55957



**radiology**

- see also patient diagnosis; patient treatment; radiation therapy; radioisotope scanning and imaging  
calibration of radiological instrumentation by British Calibration Service 0-8186  
computer appls., conf. Newport Beach, CA, USA (June 1979) 0-8141  
computer use 0-8142  
conference, London, England (Apr 1979) 0-51938  
diagnostic radiology efficacy study 0-8167  
diagnostic techniques (*Slovenian*) 0-30863  
education program in medical radiological physics based on nucl. engineering 0-31448  
functional imaging, appls. in three radiological modalities 0-8139  
imaging at Bureau of Radiological Health 0-8160  
left ventricular images digital processing (*Japanese*) 0-12224  
medical engineering, review of present state 0-17023

**radiolysis**

- acetaldehyde formation on radiolysis of ethanol formaldehyde systems (*Russian*) 0-55684  
alcohols, glass, electron trapping, pulse radiolysis obs. 0-30264  
alkaline frozen solutions, polycryst. and glassy, photocond. and radiometric obs. 0-45531  
ascorbic acid, action with perhydroxyl radicals 0-35523  
Cherenkov radiation light source in pulse radiolysis 0-42267  
chloroform-paraffin system chem. changes after  $^{60}\text{Co}$   $\gamma$ -irradiation, dosimetry appl. 0-30258  
cholesteric esters, effect of nature of organic solvent on gamma radiolysis 0-7835  
cyclohexane+toluene, energy transfer, pulse radiolysis obs. 0-16714  
dodecane-tributyl phosphate solns., radiolysis, liquid products 0-40723  
dulcitol, X-irrad., 4.2K, electron traps, alkoxy hyperfine coupling, ENDOR obs. 0-50863  
electro-optical multichannel spectrometer for transient resonance Raman and absorption spectroscopy 0-31890  
EPR, ns time-resolved, in pulse radiolysis, via spin echo method 0-43075  
ethylene-butane matrix, D atom bombardment, ethyl radical proton exchange reaction, indirect ESR obs. 0-16700  
frozen media, electron transfer reactions and multiphonon transition theory 0-7812  
graphite moderator structure design and manufacturing specification 0-23110  
high-level liquid waste, damage to organic extractant in positioning process 0-9345  
ion beam pulse radiolysis, LET dependence of transient yields 0-30260  
methane adsorbed on  $\gamma\text{-Al}_2\text{O}_3$ ,  $\gamma$ -radiolysis 0-3375  
molecular solid, electron tunnelling, long-range electron transfer processes, orbital overlap model 0-7813  
monophenyl phosphate in aq. soln., pulse radiolysis obs. 0-30261  
perfluorocarbons,  $\gamma$ -irrad. solns., mag. field effect on fluoresc. 0-55677  
poly-2-vinylnaphthalene, soln., lowest triplet props., flash photolysis and radiolysis obs. 0-32861  
poly-N-vinylcarbazole, soln., picosecond time-resolved fluoresc. by pulse radiolysis 0-28122  
polychlorinated biphenyls, pollutants, radiation degradation in organic solvents,  $\text{H}_2\text{O}$  0-30262  
polymers, synthetic, radiative degradation, chem., phys., environmental, technological effects, review 0-40948  
product detection by Pt electrode rest potential 0-11973  
1-propanol, glassy, electron trapping, pulse radiolysis obs. 0-30264  
pyrimidine  $\text{N}_2\text{O}$  aq. solns., dimer formation in  $\gamma$ -radiolysis, chromatographic obs. 0-7785  
sorbitol, X-irrad., 4.2K, electron traps, alkoxy hyperfine coupling, ENDOR obs. 0-50863  
2,2,3,3-tetramethylbutane, radiolysis, radical prods., EPR obs. 0-32747  
thymine aq., and  $\text{N}_2\text{O}$  solns., radiolysis products anal. 0-30257  
toluene-9,10-diphenylanthracene, soln., electron beam pulse radiolysis, energy transfer 0-7808  
tritiated radioactive waste, gas generation by autoradiolysis 0-32384  
waste water of sulphate cellulose prod., radiation treatment (*Russian*) 0-55688  
xylytol, X-irrad., 4.2K, electron traps, alkoxy hyperfine coupling, ENDOR obs. 0-50863  
Ag, and  $\text{Ag}^+$ , solvation in deuterated-ice matrices, electron spin echo obs. 0-15780  
 $\text{CO}_2$ , Febetron radiolysis in the presence of  $\text{O}_2$  and  $\text{CO}$  0-35557  
 $\text{CoSeO}_4$ , electron capture and  $\gamma$ -radiolysis, radn. damage 0-16705  
 $\text{Cu(II)}$  iminodiacetates in aqueous solution, gamma-ray radiolysis 0-35560  
 $\text{Fe(H}_2\text{PO}_4)_2$ ,  $\gamma$ -ray and electron radiolysis, Mossbauer study 0-7816  
 $\text{FeSeO}_4$ , electron capture and  $\gamma$ -radiolysis, radn. damage 0-16705  
H, radiolytic/thermal cycles 0-51011  
 $\text{H}_2\text{SO}_4$ , frozen soln., EPR of trapped H-atoms produced by UV and X-irrad. 0-3369  
 $\text{He-N}_2$ , de excitation rate consts., energy transfer, pulse radiolysis obs. 0-30303  
KBr, pulse radiolysis of metastable interstitial centre of high temp. 0-20658  
KBr, V- and X-centres accumulation (*Russian*) 0-54228  
KCl, V- and X-centres accumulation (*Russian*) 0-54228  
 $\text{LiBrO}_3$ , radiation damage, XPS obs. 0-29844  
 $\text{LiClO}_4$ , radiation damage, XPS obs. 0-29844  
 $\text{LiIO}_4$ , radiation damage, XPS obs. 0-29844  
 $^{54}\text{Mg}$ , removal from waste water by oxine-impregnated activated charcoal 0-9344  
N+alkene (1,3-butadiene)(acetylene), reaction rate consts., pulse radiolysis obs. 0-35508  
 $\text{N}_2\text{O}$ , pure and in mixtures, electron attachment near 1 atm., microeave cond. meas. 0-1063  
 $\text{NaCl}$ , V- and X-centres accumulation (*Russian*) 0-54228  
 $\text{NaCl-O}_2^-$  X-ray irrad., defect generation during radiolysis 0-7831  
 $\text{NaClO}_3$ , radiation damage, XPS obs. 0-29844  
 $\text{NaClO}_4$ , frozen soln., EPR of trapped H-atoms produced by UV and X-irrad. 0-3369  
 $\text{NaOH}$ , frozen soln., EPR of trapped H-atoms produced by UV and X-irrad. 0-3369  
 $\text{Ne+SF}_6(\text{N}_2)$ , metastable state de-excitation, rate consts., radiolysis obs. 0-40709  
 $\text{O}_2\text{-CO}_2$  (ethylene)(neopentane), thermal electron attachment meas., microwave cond., pulse radiolysis 0-28592  
 $\text{O}^{(3)}\text{P}$  atom yield in radiolysis of water by  $^1\text{H}^+$  and  $^4\text{He}^{2+}$  0-35556

**radiometers**

- see also infrared detectors; microwave detectors  
absolute radiometer with uniform response, fabrication, characts. and anal. 0-268  
atmosphere precipitable water, dual-channel microwave method 0-51564  
automatic nulling radiometer for the 3-4-mm band 0-18016  
IR, thermopiles appl. 0-47104  
low-temperature, with conical light pipe, IC manufacture appl. 0-47105  
microwave radiometer blackbody calibration standard for MM wavelengths 0-269  
microwave radiometers, ice movement measurement (*Danish*) 0-26624  
MM wavelength band, Josephson superconducting point contact as detector 0-21918  
multichannel scanning, for spatially-resolved radiance measurements of short-duration rocket plumes 0-13164  
multipurpose, large thermal vacuum chambers, Johnson Space Centre 0-31875  
ocean surface wind obs., SeaSat scatterometer/scanning radiometer/altimeter comparison 0-46249  
pyranometer, inclination depend. of sensitivity 0-8465  
SeaSat scanning multichannel microwave radiometer 0-46248  
spectroradiometer for reflectance measurements 0-56658  
thermal radiation detector design with uniform surface response 0-27345  
thermal radiation sources, high-temp., for calibrating radiometers 0-17946  
UV radiation meas. using ferrioxalate actinometer 0-41731  
Visible and Infrared Radiometer evaluation from SeaSat-A surface temp. obs. 0-46325  
GaAs single-cell, for artificial satellite measurement system 0-13147

**radiometry**

- see also radiometers  
9 GHz radiometry of tumours (*French*) 0-3767  
22.75 GHz microwave attenuation characts. at high elevation (*Japanese*) 0-27346  
atmospheric water vapour and liquid monitoring using radiometry at 21 and 32 GHz 0-26628  
automatic radiometric flaw detection with X-rays on series production parts (*German*) 0-21240  
cloud microwave radiation emission meas. 0-17351  
cylindrical gradient index lens and array radiometric props. 0-14421  
density of materials on supply line, neutron radiometric inspection 0-21205  
Earth resources survey sensor, calibration linear photodiode array, satellite appl. 0-56693  
433 Eros, thermal props. from radiometric and refl. light obs. 0-31231  
forest fire sources, microwave radiation spectra 0-52314  
isotope radiometry, nonlinear information processing in random signal detection (*Russian*) 0-22428  
Jupiter and satellites, IR obs. from (Voyager 1) 0-26790  
medical appls., radiation balance microwave thermograph 0-26315  
microwave brightness temperature measurements (*Danish*) 0-26625  
microwave radiometric methods and the problem of forest and peat fires 0-31877  
microwave thermography, principle and biomedical appls. (*French*) 0-30957  
ocean passive radiometry, radio meteorology colloquium, Victoria, British Columbia, Canada (1978 June 14 to 21) 0-46724  
ocean surface, microwave radiometry remote sensing 0-36428  
open-ended waveguide probe/appliator combination (*French*) 0-3820  
optical coherence, review 0-48140  
optical system aperture, effect on measurements in thermophysical research 0-17992  
photothermal radiometry, contact-free condensed matter anal.,  $\text{K}_2\text{SO}_4$  powder appl. 0-26088  
remote sensing and profiling of lower atmosphere using radiowaves, ground-based 0-56628  
remote sensing of cloudy atmospheres by microwave radiometry (*Chinese*) 0-51549  
remote sensing using solid-state linear array technology 0-4150  
slot method, radiometric determ. of concentration profile during zone melting (*Czech*) 0-55289  
soil moisture content measurement by microwave radiometry, review 0-17425  
solar cell spectral response characterisation, 400 to 1000 nm 0-35675  
statistical image anal., 3 parameter probability distrib. density function 0-43266  
suspensions, colloidal, radiometric method for particulate processes characterisation, theory 0-45578  
total luminous flux meas. on radiometric base, goniophotometer 0-42250  
tritium water, small samples, radiometry with gas-flow counter 0-17989  
UV radiation meas. using ferrioxalate actinometer 0-41731  
yeast cells in suspension, vacuole detect. by transmittance radiometry 0-26418  
K determ. in NPK and GVM fertilisers (*Czech*) 0-22427  
U at Oklo natural fission reactors, radiometric meas. and isotopic anal. (*French*) 0-21754

**radiometry, ultraviolet** see photometry**radionavigation**

- inertial navigation system, error analysis using spatial Gauss-Markov models of ocean currents 0-36411  
marine and hydrographic surveys appl., available systems survey, modes and accuracy 0-36408  
Mini Range III positioning system, meas. range improvements, technical details and characts. (*Italian*) 0-56611  
Navstar global positioning system, meteorological appl. 0-17396  
NAVSTAR Global Positioning System, sea trials results 0-12645  
oceanographic research problems (*Russian*) 0-17286  
offshore surveys, accurate positioning at distances to 400 km 0-12328  
Omega system, hydrophysical research appls. (*Russian*) 0-17418

**radios** see radio receivers**radiosondes**

- see also meteorological instruments  
atmospheric turbulence, radiosonde meas. and spectral anal. of LOS fading 0-56568  
BASORA secondary radar, sounding balloon tracking appl. 0-17357  
tropical constant-level balloon system 0-17395  
windfinding, NCAR aircraft dropwindsonde system 0-17393

**radiosources (astronomical)**

- see also BL Lacertae-type objects; pulsars; quasars  
5 GHz galactic plane sources, catalogue 0-4269



# radiosources (astronomical) continued

- 0406+121, optical spectra 4950-7950 Å, of possible BL Lacertae object 0-51895
- 1159+583, wide-angle tailed radio galaxy, radio obs. and models 0-31352
- 2 A 1052+606, X-ray and optical variability of RS CVn star 0-31331
- Abell 2256, X-ray cluster of galaxies, radio props. 0-36726
- Abell clusters of galaxies, Westerbork 610 MHz survey of extended radio emission 0-36727
- AFGL IR sources, mol. line obs. 0-51856
- AO 0235+164, BL Lacertae object, possible correlated optical-radio outburst 0-56924
- astometric determinations using VLBI (*Japanese*) 0-21930
- B2 1308+326, optical and IR variability during 1978 outburst 0-51888
- B2 1502+28, head-tail galaxy in Abell 2022, Westerbork obs. of spectral index and polarisation distrib. 0-36727
- B 0844+31, extended radio galaxy, multifreq. obs. 0-56963
- B-type stars embedded in R-associations, free-free emission obs. 0-26851
- bursting sources, search for 2-60 keV emission 0-17679
- 5C3 sources, optical ident., spectroscopic results 0-46689
- 4C+36.11, extragalactic source, Faraday rot. in S232 rel. to mag. field strength 0-51840
- 3C 111, 3C 236, radio galaxies, 150 GHz obs. 0-41908
- 3C 129 and 129.1, in situ particle accel. and energy supply 0-46691
- 3C 273, quasar containing dust, IR spectra obs. 0-56970
- 3C 27 area sources, 2695 MHz continuum obs. 0-46688
- 3C 310, 326, relaxed double radio sources, implications of fine scale struct. 0-51891
- 3C 310, extended radio galaxy, multifreq. obs. 0-51890
- 3C 318.1 (NGC 5920), poor cluster cD galaxy, extended X-ray emission obs. 0-51884
- 3C 319, radio struct. and optical identification with elliptical galaxy 0-31377
- 3C 33, 98, 184.1 and 218, rotation axes 0-26997
- 3C 33, optical line emission rel. to physical conditions in compact head 0-51892
- 3C 345, 418, 371, compact radio sources, arcsecond struct. 0-4450
- 3C 345 and NRAO 512, relative position to submilliarcsecond accuracy via VLBI 0-22097
- 4C 39.04, powerful giant radio galaxy, multifreq. obs. 0-17682
- 3C 391, supernova remnant, obs. at 1.4 and 10.7 GHz 0-4417
- 3C 395, compact radio source, high resolution obs. at 1671 MHz 0-56960
- 3C 449, radio jet structure at 1465 and 4885 MHz 0-12823
- 3C 58, supernova remnant, soft X-ray flux upper limits 0-56915
- 3C 58 (SN 1181), plerionic supernova remnant, supernova absolute magnitude and type classification 0-56862
- 4C sources in Zwicky galaxy clusters, detailed interferometer obs. and anal. 0-22099
- VY Canis Majoris, OH/IR star, 1612 MHz OH maser multibaseline VLBI obs. 0-12766
- RS Canum Venaticorum systems, candidate list for southern HD stars 0-4395
- RS Canum Venaticorum systems, X-ray obs. and coronal model development 0-56873
- Cassiopeia A, weak X-ray source, ANS meas. 0-46701
- Cassiopeia A, <sup>14</sup>N radioemission at 26 MHz 0-41886
- Cassiopeia A, intensity and polarisation at 9 mm wavelength 0-36732
- Cassiopeia A, numerical model of SNR 0-12790
- Cassiopeia A, possible binary pulsar 0-56868
- Cassiopeia A, secular decrease in radio emission flux density at 437 and 510 MHz (*Russian*) 0-8702
- Cassiopeia A, supernova remnant, anal. of motion of details in thin shell model (*Russian*) 0-56920
- Cassiopeia A supernova remnant, abundance inhomogeneities 0-12797
- Cassiopeid A used to study ionosphere inhomogeneities 0-36454
- celestial, resolution using VLBI (*Japanese*) 0-26754
- Centaurus A, gamma-ray emission from Penrose powered black hole 0-56925
- Centaurus A, nuclear gamma-ray lines, origin in relativistic plasma 0-41890
- Centaurus A, X-ray struct., radio-lobe energy source evidence 0-26978
- Centaurus A (NGC 5128), high-resolution spectroscopy and tubelike model of dust band 0-56945
- Centaurus A (NGC 5128), slowly varying flux component, 22 GHz confirmation 0-56939
- Cepheus OB3 association molecular cloud, mol. obs. rel. to star form. 0-12798
- Circinus X-1, radio flare phenomena Dec. 1979 and Jan. 1980 obs. 0-36731
- CIT 6 (IRC+30219), IR C star, CO obs. of mass outflow 0-12761
- clusters of galaxies, H I broad band emission search 0-46667
- compact extragalactic radio sources, relativistic jets model 0-4448
- cosmological evolution, free-form analysis, self-consistent luminosity function 0-46716
- coube galaxies, H I 21 cm. line obs. 0-51886
- CTB 80, peculiar supernova remnant, central radio source optical and H I obs. 0-56896
- CTB 80, supernova remnant, optical emission and historical evidence 0-51853
- CTD 93, compact radio source, high resolution obs. at 1671 MHz 0-56960
- V1057 Cygni, OH obs. 0-36629
- NML=V1489 Cygni, OH/IR star, 1612 MHz OH maser multibaseline VLBI obs. 0-12766
- V1500 Cygni (Nova 1975), radio emission from expanding shell 0-26868
- Cygnus A, radio galaxy, 150 GHz obs. 0-41908
- Cygnus X, H I 21 cm line emission maps of field containing G78.2+2.1 SNR 0-56917
- Cygnus X-3, efficient particle acceleration 0-31391
- DA 267, compact radio source, arcsecond struct. 0-4450
- HR Delphini (Nova 1967), radio emission from expanding shell 0-26868
- dense radio H II regions distrib. in inner Galaxy, kinematic models 0-12813
- double extragalactic radio sources, collimation 0-22098
- expanding synchrotron sources theory, relativistic corrections 0-12821
- extended, particle accel. and radiative losses effects on source dynamics 0-46687
- extended extragalactic radio sources, MHD instabilities and electron accel. 0-27000

# radiosources (astronomical) continued

- extended extragalactic radio sources, relation between radio luminosity and spectrum 0-51894
- extended radio galaxies, multiple explosion model 0-41894
- extended radio sources, VLBI obs. of compact components 0-17680
- extragalactic, optically violent variables, monitoring of long-term vars. optically violent variables, monitoring of long-term vars. 0-31376
- extragalactic double radio sources separation, depend. on redshift 0-22096
- extragalactic objects with active nuclei, distance determ. method (*Russian*) 0-51880
- extragalactic radio sources, ang. size-redshift diagram interpretation 0-22101
- extragalactic radio sources, jets configuration and propag. 0-31374
- extragalactic radio sources, obs. of galactic H I absorpt. struct. on small ang. scales 0-22051
- extragalactic radio sources in vicinity of bright galaxies, distrib. and density 0-56964
- faint radio sources, statistical study of mean ang. size and sky density at 81.5 MHz 0-51893
- Faraday rotation measures, computation method 0-4263
- Faraday rotation of extragalactic sources and intergalactic magnetic fields 0-22086
- FJM 6, molecular cloud, far IR, near IR radio mol. line studies 0-26929
- formaldehyde near Cone nebulae and NGC 2264 IR source, kinematics and distrib. 0-4418
- G126.2+1.6 SNR near 4U 0115+63 X-ray transient 0-8668
- G127.11+0.54, optical spectroscopy and photometry of assoc. luminous obscured galaxy 0-31371
- G292.0+1.8, young supernova remnant, high vel. material obs. 0-22064
- G309.81+0.07, point radio source and possible stellar remnant of supernova, obs. 0-51849
- G339.2-0.4, radio recombination line obs. of low-excitation H II region 0-46650
- G339.2-0.4, supernova remnant or planetary nebula, radio and optical obs. 0-22104
- G 109.7+2.2, type I OH maser source near Herbig-Haro object (*Russian*) 0-17684
- G-varying cosmology, radio source counts and models 0-56981
- galactic centre, OH absorpt. struct. determ. using regularisation method 0-17505
- galactic masers, role of plasma effects in generating high-vel. and symmetric spectral features 0-31378
- galactic polar regions, non-thermal radio radiation spectra 0-22082
- galactic radiation belts, trapped electrons as radiowave source 0-26982
- galactic synchrotron radio emission, rel. to Galaxy cosmic rays and mag. field distrib. 0-4207
- galaxies, early-type accretion from gas-rich dwarf galaxies 0-31349
- galaxies, Markarian and Seyfert types, search for CO emission 0-26975
- galaxies, nearby, H I profiles obs. 0-41895
- galaxies clustering about extragalactic radio sources, cross-correl. anal. 0-22103
- galaxies with radio jets, H $\alpha$  and 450 nm obs. 0-51889
- Galaxy H I subsystem, rot. curve (*Russian*) 0-36724
- giant radio galaxies, 26-100 MHz obs. of four objects 0-56961
- HB 3, supernova remnant, soft X-ray obs. 0-56915
- HB 9, soft X-ray emission obs. from old SNR 0-36697
- head-tail radio galaxies, intrinsic parameters distrib. 0-17653
- head-tail radio sources formation, role of hot gas in elliptical galaxies 0-36703
- Heiles's cloud 2, cyanodiacetylene (HC<sub>3</sub>N) obs. 0-22054
- Heiles 2 dust cloud, NH<sub>3</sub>, and cyanobutadiyne emission relative distrib. 0-17641
- HFE 2.3, molecular cloud, for IR radio mol. line studies 0-26929
- high-velocity H I clouds, map 0-26923
- HR 1099, RS Canum Venaticorum binary, February 1978 radio flare obs. 0-26911
- W Hydrae, long-period variable, suspected Zeeman splitting in OH masers 0-36632
- hydrodynamical acceleration of particles in supernovae and extragalactic radio sources 0-31313
- IC 1805, 1848, giant H II regions, physical anal. from radio obs. 0-36695
- IC 342, Sed galaxy, discovery of companion 0-36712
- interplanetary scintillations spectra, influence of source sizes, obs. 0-46361
- interstellar (*Russian*) 0-36698
- interstellar clouds, cyanoacetylene and cyanodiacetylene obs. 0-46634
- interstellar excited H, decametric range radio lines search (*Russian*) 0-12822
- interstellar H II/OH maser regions, heating by ion streams 0-56912
- interstellar masers, A-doublet population inversion in OH, OD, CH, CD and NH<sup>+</sup> collisions 0-22065
- interstellar masers membership in star form. regions rel. to population categories 0-17645
- interstellar molecular clouds containing Herbig-Haro objects, mol. obs. and physical props. 0-36689
- interstellar molecules, RF emission spectra obs. towards  $\zeta$  Ophiuchi 0-26958
- IRC-10442 (GL5268S), near IR and radio obs. 0-4412
- jets inextragalactic radio sources, particle acceleration 0-31379
- L1544, L1521B, interstellar clouds in Taurus, HC<sub>3</sub>N detect. 0-26957
- linear polarisation, catalogue 0-51671
- Loop I, X-ray features, SNR model 0-22066
- LS I +61°303, radio variable Be star, UV spectrum, stellar models 0-26879
- M31, polarised radio emission distrib. rel. to large-scale mag. field 0-41899
- M33, H I distrib. obs. and spiral struct. 0-56948
- M33 H I tail, obs. rel. to adjacent high-vel. H I cloud 0-12815
- M82, M104, VLBI obs. of galactic nuclei at 18 centimetres 0-22078
- M87 galaxy, jet, nonlinear Poynting flux for radio emission 0-26736
- M87 jet, synchrotron optical and radio emission origin (*Russian*) 0-8694
- M87 jet knots, polarisation, spectroscopic and radio props. 0-12817
- magnetic field orientation evidence 0-46690
- magnetogasdynamics of double sources 0-26999
- Markarian 501, UV and X-ray obs. of BL Lacertae-type object 0-36717
- Markarian galaxies, radio continuum obs. at 1410, 2380 and 5000 MHz 0-46668
- MC2(3) radio sources, optical positions from Palomar Sky Survey 0-31375



**radiosources (astronomical) continued**

- MC76, MC77 (LMC X-1 region), 2 cm obs. 0-51875  
 Milky Way sources, obs. at 8.87 GHz near ( $l=333^\circ$ ) 0-22102  
 morphology of extended extragalactic sources rel. to gaseous halos 0-17675  
 NGC 1052, 4278, VLBI obs. of galactic nuclei at 18 centimetres 0-22078  
 NGC 1265, 1275, in Perseus cluster, low-resolution aperture synthesis map at 408 MHz 0-56958  
 NGC 1275 nucleus, structural changes at 2.8 cm wavelength 0-31359  
 NGC 2110, Seyfert 2 X-ray galaxy, optical studies 0-22071  
 NGC 2264, continuum source 6 cm map and formaldehyde kinematics and distrib. 0-4418  
 NGC 5128 (Centaurus A), formaldehyde absorpt. obs. at 14 GHz 0-17657  
 NGC 5128 (Centaurus A), struct. and evolution from photographic and spectroscopic obs. 0-4429  
 NGC 5474, peculiar Sd galaxy, H I distrib. and kinematics 0-8683  
 NGC 612, rotation of lenticular radio galaxy 0-51874  
 NGC 6240, unusual radio galaxy, radio and optical, obs. 0-4440  
 NGC 6251, radio galaxy, CCD photometry rel. to central supermassive object 0-26966  
 NGC 6251, radio galaxy, radio jets misalignment, VLBI obs. 0-27001  
 North Polar Spur, radio continuum obs. at 1420 MHz 0-22100  
 nova shells, radio emission obs. 0-26868  
 OH 0739-14, M-type giant in reflection nebula, IR obs. 0-46692  
 OJ 287, BL Lacertae object, case for synchronous optical-radio outbursts 0-8679  
 OMC-1, methane- $d_1$  abundance upper limits from rot. spectrum obs. 0-56705  
 Orion A, 22 GHz water line giant outburst 0-8703  
 Orion A, confirmation of H<sub>2</sub>O 22 GHz line outburst 0-8704  
 Orion A, SiO maser variability at 86 GHz 0-41839  
 Orion Molecular Cloud, NH<sub>3</sub> emission obs. 0-36687  
 Orion Molecular Cloud, rotational explanation of high-vel. mol. emission 0-36688  
 Orion Nebula, H<sub>2</sub>O 183 GHz line emission obs. 0-41869  
 U Orionis, Mira variable, relation between 1612 MHz flare and light curve 0-56844  
 OV-236 (1921-29), radio outburst obs. of quasar 0-51906  
 particle acceleration and radio emission above pulsar polar caps 0-51794  
 particle acceleration in double sources 0-31380  
 $\beta$  Persei (Algol), radio outbursts and possible period change 0-26907  
 Perseus galaxy cluster, low-resolution aperture synthesis map at 408 MHz 0-56958  
 Perseus OB2 association molecular cloud, mol. obs. rel. to star form. 0-12798  
 PKS 1144-379 BL Lacertae object, radio, IR and optical obs. 0-4451  
 PKS 2155-304 (H2155-304), newly discovered BL Lacertae object, optical and X-ray props. 0-36702  
 planetary, mapping using VLBI (*Japanese*) 0-21927  
 planetary and stellar magnetospheres, conf., Snowmass, Colorado, USA (Aug. 1978) 0-41939  
 planetary nebulae, radio emission flux density distrib. rel. to radio search near galactic 0-56913  
 planetary nebulae, stellar, VLA obs. 0-22056  
 plasma turbulent reactors, effect of Compton scattering of transverse waves by relativistic electrons 0-51644  
 QSO 0241+622, nearby X-ray quasar, extended radio emission search 0-31382  
 QSO 1038+528 A,D, close pair of radio-emitting quasi-stellar objects, radio and optical obs. 0-51902  
 QSOs, new type, identified through IR meas. 0-8708  
 quasar radio emission, from quasar group selected for optical brightness 0-41910  
 radio galaxies, optical catalogue 0-21931  
 radiogalaxies, faint southern objects, identification and spectrophotometry 0-56935  
 radiogalaxies, optical spectroscopy and redshifts for 18 objects 0-56966  
 radiogalaxy models, relativistic channel flow, soliton soln. stability 0-56962  
 relativistic blast waves in two dimensions, adiabatic case solns. 0-22108  
 Rosette Nebula (NGC 2237/2246), new physical parameters from 6.5 GHz obs. 0-4414  
 S252 (NGC 2175), H II region, mol. line obs. of star-forming complex 0-4411  
 S255, H II region, CO emission small-scale struct. from lunar occultation obs. 0-46637  
 Sagittarius B2, mm wave detect. of isothiocyanic acid 0-41878  
 Sagittarius B2, mm wave detect. of methyl mercaptan 0-41877  
 FH Serpens (Nova 1970), radio emission from expanding shell 0-26868  
 southern extragalactic radio sources of large ang. extent, emission spectrum vars. 0-17683  
 spatial distribution, statistical method of multiple binning 0-8698  
 spiral galaxies, local mass-to-light ratio radial var. 0-31361  
 SS 433, 10 GHz variability and thermal radio emission hypothesis 0-31307  
 SS 433, 1979 May-June radio flare, 3.24 GHz obs. 0-46567  
 SS 433, 6.55 day periodicity in emission line wavelengths 0-51784  
 SS 433, binary star model including mag. white dwarf 0-4385  
 SS 433, discrepancy between optical and radio positions 0-31303  
 SS 433, early-type binary model 0-56843  
 SS 433, enormous periodic Doppler shifts obs. 0-17593  
 SS 433, evidence for association with supernova remnant (W50) 0-51851  
 SS 433, H I absorption obs. and distance 0-56848  
 SS 433, IR and visible obs., IR excess and emission processes 0-4387  
 SS 433, IR energy distrib. obs. 0-31312  
 SS 433, IR light curves from BV1JHK photometry, period and ephemeris 0-8642  
 SS 433, IR spectral obs., reddening and emission 0-4388  
 SS 433, light minimum epoch and period 0-26886  
 SS 433, mass accel. and collimation mechanisms 0-4368  
 SS 433, mass loss rates and lifetime from W50 optical filaments 0-12804  
 SS 433, nature and evolutionary state (*Russian*) 0-36647  
 SS 433, Of star orbited by neutron star, model 0-22025  
 SS 433, photometry, 1979 July to October, and 6.5 day period identification 0-8643  
 SS 433, radio and optical positions coincidence 0-56840  
 SS 433, radio jet discovery 0-31381  
 SS 433, short term H $\alpha$  central intensity increases 0-4375  
 SS 433, spectroscopic obs. and probable binary nature 0-51780

**radiosources (astronomical) continued**

- SS 433, VLBI detect. and ang. struct. 0-31304  
 SS 433 (W50), assoc. optical supernova remnant discovery 0-56916  
 SS 433 as veiled pulsar 0-41842  
 SS 433 model, precessing jets in ultra-close binary system 0-4384  
 steep spectrum radiosources, spectral index dependent props. 0-36730  
 stellar SiO masers,  $J=1\rightarrow 0$   $\nu=1$  and 2 masers relative intensity and vel. 0-4339  
 Stephenson-Sanduleak 433, 1.2-2.5  $\mu$ m spectroscopy, photometry and polarimetry 0-41838  
 Stephenson-Sanduleak 433, Thomson scatt. lines in spectrum, relativistic gas motions 0-22019  
 superluminal radio sources, cosmological proper motion-redshift relation 0-22095  
 superluminal radio sources, mag. dipole model 0-56959  
 supernova remnants, galactic, new optical obs. 0-17636  
 supernova remnants, southern, high resolution radio obs. 0-51849  
 V711 Tauri (HR 1099), Lyman  $\alpha$  H I and D I interstellar absorption 0-8658  
 Taurus A, intensity and polarisation at 9 mm wavelength 0-36732  
 Taurus Molecular Cloud 2 (TMC-2), HC<sub>3</sub>N and NH<sub>3</sub> obs. 0-26957  
 Turner-Gott galaxy groups, virial mass/galaxy mass ratio from galaxy H I profiles 0-56937  
 Tycho's supernova remnant, radio flux density meas. separated by 15-year interval 0-26955  
 Tycho supernova remnant, radio struct. 0-56919  
 Vela supernova remnant, rot. measure and turbulent struct. 0-51836  
 Vela supernova remnant, X-ray maps comparison with radio and optical features 0-51838  
 Vela X supernova remnant, radio polarisation maps 0-56909  
 W28 A, H II region, RATAN-600 2-13 cm wavelength obs. (*Russian*) 0-17642  
 W3(OH), high vel. water maser features obs. 0-31339  
 W3 region, near IR obs. of far IR sources G133.8+1.4 (W3N) and G133.982+1.14 (BS4) 0-22058  
 W48, OH emission and absorption, spatial distrib. in H II region (*Russian*) 0-36733  
 W49A, high sensitivity Hna radio recomb. line obs. 0-26998  
 W50, supernova remnant, optical filaments spectra rel. to SS 433 mass loss rates and lifetime 0-12804  
 W50, supernova remnant, spectrum of optical nebulosity 0-51851  
 W50 (SS 433), supernova remnant, optical filamentary nebulosity discovery 0-56916  
 W51, W49, airborne for IR spectroscopic obs. rel. to dust cloud model 0-36684  
 W51 Main, H<sub>2</sub>O maser emission 0-8701  
 young stars, high-freq. radio continuum obs. 0-51766  
 Zw 1400+0949 cluster (NGC 5416 group), 21 cm obs. 0-22090  
 CO in interstellar dark clouds, evidence for isotopic fractionation 0-46638  
 CO, interstellar, distrib. around ( $l=30^\circ$ ,  $b=0^\circ$ ) 0-41868  
 CO, interstellar, isotope fractionation in Lynds 134 dust cloud 0-26924  
 CO, interstellar, radio emission rel. to cold mol. clouds in inner Milky Way 0-4425  
<sup>13</sup>CO in external galaxies, <sup>12</sup>CO/<sup>13</sup>CO intensity ratios 0-4416  
 Cygnus A, intensity and polarisation at 9 mm wavelength 0-36732  
 H I, column density as function of position in southern sky 0-4420  
 H I at high galactic latitudes, time variable 21 cm line profiles correction 0-51844  
 H I regions, new feature discovery in Vulpecula-Delphinus (*Russian*) 0-46654  
 H II regions, H137 $\beta$ /109 $\alpha$  intensity ratio interpretation 0-31344  
 H II regions, multiple-component, radio recomb. lines press. broadening 0-4419  
 H<sub>2</sub>O maser sources in different stages of evolution, new VLBI maps 0-26954  
 OH 1612 MHz survey at high declinations 0-4452  
 OH in interstellar dust clouds, nonthermal main lines obs. and OH abundance 0-36683  
 OH, interstellar, new main line maser obs. with probable Zeeman pattern 0-56908  
 OH maser sources, accurate position meas. 0-46646  
 OH maser sources, interstellar, radiative transport effects on inversion 0-17681  
 SiO 86.2 GHz maser sources, polarisation props. 0-4449
- radiostars** see *radiosources (astronomical)*
- radiotelemetry**  
 INMARSAT marine system, satellite radio teletype communication 0-26614
- radiotelescopes**  
 see also *radioastronomy*  
 N.American observatories, VLBI meas. rel. to intra-plate crustal deformation 0-51379  
 aperture synthesis using very long baseline interferometry 0-46414  
 Arecibo Observatory, radiotelescope and instrumentation description 0-4249  
 compound spherical mirror for space telescope 0-41720  
 correlator interferometer antenna arrays, theory 0-12670  
 cost-scaling laws applicable to very large optical telescopes and radiotelescopes 0-41722  
 decametre radiotelescope facility at Mt. Zao Observatory, Japan 0-51656  
 decametric range radio telescope, for interstellar excited H lines searching (*Russian*) 0-12822  
 design, multidisciplinary teaching exercise, Jupiter bursts and quiet Sun obs. 0-17759  
 development survey (*Japanese*) 0-12664  
 feeds, compact dual-hybrid-mode feeds with low crosspolar radiation 0-12662  
 hectametric cross-shaped radiotelescope for 2.8 to 10 MHz obs., design (*Russian*) 0-12660  
 interferometer signal processing by acoustooptic correlation devices, radio astronomy applications 0-8543  
 Jodrell Bank, Multi Telescope Radio Linked Interferometer (MTRLI) system 0-12676  
 millimetre-wave astronomy, advances and prospects (*French*) 0-36502  
 Mills' cross array antenna, digital baseband processing 0-36500  
 MM range receiver using powdered superconductor 0-21919  
 MM wavelength band radiometer, Josephson superconducting point contact as detector 0-21918  
 phase switched interferometer for amateurs, construction details 0-12663



**radiotelescopes continued**

- RATAN-600 radio telescope, acousto-optical spectral analyser first test (Russian) 0-51668  
 RATAN-600 radiotelescope, acousto-optic spectrograph 0-46398  
 resolving power, increase using regularisation method 0-17505  
 space radiotelescope, modular design proposal 0-51655  
 spherical wide angle mirror under oblique illumination, diffraction in focal region 0-1108  
 stray radiation problem and time variable 21 cm lines 0-56708  
 Table Mountain 8 mm wavelength interferometer 0-26741

**radiotherapy** *see radiation therapy***radiowave propagation**

*see also electromagnetic wave propagation*

- 22.75 GHz microwave attenuation characts. at high elevation (Japanese) 0-27346  
 accelerating atomic clock synchronisation by radiowave propag., one-way Doppler effects 0-13044  
 amplitude distributions, appl. in practical data assessment problems 0-27107  
 atmosphere, refraction of MM-wave radio noise from cosmic sources near horizon, meas. 0-21813  
 atmospheric absorpt. by water vapour in 0.8-20 mm range 0-4086  
 atmospheric boundary layer, ultrashort wave refr. index derivation 0-36380  
 auroral radio absorption, spike events 0-12589  
 axisymmetric scattering by conical bodies 0-18971  
 bistatic radar signals, scattering by planetary surfaces 0-41743  
 circumsolar plasma, d.m. propag., Venera 10 meas. 0-21886  
 Comstar beacon cumulative slant path rain attenuation statistics, 28.56 GHz 0-26582  
 correlation bandwidth, empirical evaluation over troposcatter paths (French) 0-41527  
 crosspolarisation and attenuation meas. at 11.6 GHz using theoretical rain model, canting angle distrib. 0-4070  
 D-region, irregularities responsible for partial reflection 0-41629  
 D-region, radiowave absorption during solar minimum, 2.5-4.1 MHz 0-41628  
 ELF propagation in Earth-ionosphere waveguide 0-41634  
 F<sub>2</sub>-layer ionisation through a solar cycle, SW communications appl. 0-41626  
 fluctuating component of scattered field in far-field zone 0-36456  
 guiding properties of a smoothly inhomogeneous layer and diffraction excitation of ionospheric waveguides 0-36449  
 HF signals, magnetospheric propag. mechanism 0-4196  
 HF signals magnetospheric propag. on Earth-Earth path, exptl. investigations 0-4195  
 HF sky wave radar remote sensing of sea state, minimisation of ionospheric disturbance 0-21857  
 HF waves reflected from ionosphere, freq. var. (Chinese) 0-56665  
 ionosphere, backscatter inversion is spherically asymm. ionosphere 0-36446  
 ionosphere, forecast chart for periods of high solar activity, amateur radio appl. 0-26664  
 ionosphere, HF Doppler observations at Chubu Inst. Tech. (Japan) (Japanese) 0-31165  
 ionosphere, HF signal, group path variations from modulation envelope measurements 0-51597  
 ionosphere, HF signals transmitted along high-latitude radio path 0-41609  
 ionosphere, inhomogeneous isotropic, propag. parameters of VLF radio waves during sunrise period 0-31166  
 ionosphere, L-band signals coded by phase reversal, signal degradation 0-41632  
 ionosphere, mid-latit. absorpt. rel. to zero and maximal vel. contours in equatorial ionosphere 0-12597  
 ionosphere, midlatitude, VLF radio waves anomalies assoc. with geomag. disturbances 0-56671  
 ionosphere, physical model and profile reconstruction, for inhomogeneous ionised regions 0-1109  
 ionosphere, ray path eqns., multisegment quasi-parabolic ionosphere 0-41633  
 ionosphere, spatial dependencies of props. of wavelike inhomogeneities, anal. of diffraction patterns 0-36448  
 ionosphere, spread-F parameters, related to geomag. disturbance index 0-8471  
 ionosphere, topside sounding and determination of electron profiles 0-56669  
 ionosphere, VHF system for spaced-receiver meas. of scintillation irregularities 0-56639  
 ionosphere ducts, trapping of radio waves scattered by meteor trails 0-4172  
 ionosphere EM wave absorpt. rel. to wind and temp. struct., winter 1975/6 obs. 0-36438  
 ionosphere equatorial region, UHF and VHF signal scintillation 0-56674  
 ionosphere radiowave scintillation, nighttime equatorial F-region 0-26681  
 ionospheric ducting at high-frequency, review 0-21872  
 ionospheric effects on radio communication and ranging pulses 0-26667  
 ionospheric irregularities and associated VHF/UHF scintillations 0-46345  
 ionospheric plasma, hysteresis effect on artificial excitation of inhomogeneities 0-36450  
 ionospheric plasma, radiowave scattering by superexcited atoms, quantum model 0-32677  
 ionospheric reflections, meas. of fluctuations in angle of arrival and amplitude 0-17439  
 LF sky wave, atm. refr. effects (Chinese) 0-4165  
 long-delay echoes generation, models 0-26670  
 long-distance, relationship with processes in Earth's crust 0-26682  
 lower atmosphere, remote sensing and profiling using ground-based measurements 0-56628  
 lower atmosphere remotely sensed by two satellites, radio illumination method 0-51550  
 magnetosphere, ELF emissions, geographic control search 0-12615  
 magnetosphere, HF and VLF propag. between mag. conjugate pts. on Earth surface 0-41639  
 magnetosphere, VLF pulse propagation and distortion, fast Fourier transform investig. 0-56679  
 microwave absorption coefficient and refractive index, optimal orthogonal functions 0-36379  
 microwave attenuation under adverse dust-storm conditions 0-46247

**radiowave propagation continued**

- microwave cross polarization discrimination statistics for spatially non-uniform rain 0-12534  
 microwave crosspolarization, effects of sizes of nonspherical raindrops 0-21790  
 microwave crosspolarization on satellite to Earth path, effect of rain 0-21789  
 microwave dielectric constant logging, EM wave propag. method 0-12558  
 microwave remote sensing, radiative transfer eqns. 0-21855  
 MM-wave, Earth's sphericity and radiowave refraction influence on atmospheric radio emission 0-56589  
 nonlinear refl. from inhomogeneous plasma bodies 0-1806  
 over-the-sea propag. hops in Republic of Indonesia 0-46245  
 periodically nonstationary process, envelope distrib. functions and phase 0-4173  
 phase fluctuations in anisotropic turbulent atmosphere when emitted by moving source 0-17352  
 planetary atm., refraction attenuation of radio waves 0-4280  
 planetary atmosphere HF radio occultation meas., phase screen concept 0-56735  
 plasmopause, sounder design using ray tracing studies from geostationary satellite 0-4191  
 pulse-long distance propagation measurements in HF region, results (German) 0-41637  
 radar impulse reflection from nonlinear random sea 0-12416  
 radar reflection from lunar surface, Luna 23 meas. at 3.1 cm wavelength 0-8560  
 radiocommunication services, propagation aspects in planning 0-12613  
 rain attenuation in microwave and MM wavebands, estimation of duration time distribution (Japanese) 0-21788  
 rain attenuation meas., microwave radio link projected design appls. (Slovenian) 0-46217  
 rain scattering of microwaves, drop-size and temp. effects on forward and backward scattering 0-17317  
 rain-cell modelling for earth-space links using SIRIO satellite radiowave propagation data 0-36352  
 random media causing pulse spreading and wandering 0-37942  
 refraction in atmospheric boundary layers 0-36400  
 refraction values in troposphere in air temp. inversion 0-4087  
 refractivity gradient variation in atmosphere, statistical distrib. and max. critical value 0-12522  
 satellite communications above 10 GHz, rain effects 0-8410  
 scattering cross section of radiowaves reflected from planet with spherically symmetrical atmosphere 0-21935  
 SHF radar altimetry from Geos 3, backscatter characts. 0-3915  
 SHF signal attenuation by rain, monitored by radar 0-51567  
 SHF waves for satellite broadcasting, rainfall attenuation characts. (Japanese) 0-12501  
 SIRIO, fade statistics for 11.6 and 17.8 GHz (Italian) 0-4095  
 SIRIO-1 satellite link, analysis of oblique propag. measurements made at Gometz-la-Ville Earth station (French) 0-56504  
 solar EM radiation and terrestrial effects (Japanese) 0-51600  
 solar radio bursts at 26 MHz, obs. brightness distrib., possible ionospheric effects 0-41806  
 sporadic-E and troposphere effects on radiowave propag. above 30 MHz 0-41636  
 SW transmission, proportional effect of ionospheric damping, solar activity (Hungarian) 0-56675  
 synoptic windfinding using Omega VLF navaid, atmos. radiowave propag. 0-17309  
 TM mode-conversion at terminator for anisotropic ionosphere, param. study (German) 0-46333  
 troposcatter developments in North Sea 0-46246  
 troposphere, angular depend. of rain scatt. at freqs. below 30 GHz 0-8416  
 troposphere, ducting of HF radiowaves, numerical study 0-36378  
 troposphere, radio refractive index, calc. from temp., press. and humidity data (Czech) 0-36351  
 troposphere and ionosphere, propag. errors during geomag. storms 0-4077  
 tropospheric ducts used for line-of-sight links, protection against signal cancellations (French) 0-17303  
 tropospheric transhorizon propag. at freqs. >1 GHz on transmission paths set up in CSSR and GDR (German) 0-17364  
 tropospheric waveguide, numerical comparison of ray method and normal wave method 0-21858  
 VHF propagation through ionosphere equatorial plasma bubbles, transequatorially 0-41635  
 VLF direction-finding techniques comparison for determ. whistlers exit point at ionosphere 0-26631  
 VLF plane wave airborne survey of ground resistivity, resolution studies 0-12333  
 VLF subionospheric propag., whistler-induced anomalies 0-26668  
 whistlers, effect of Earth-ionosphere waveguide propagation on polarisation and arrival angles 0-36457

**radium**

*see also nuclei with .....*

- atom, Rydberg series, ionisation limit derivation from multichannel quantum defect theory, UV absorpt. spectra 0-52918  
 separation from thorium oxalate of <sup>226</sup>Ra 0-45600  
<sup>226</sup>Ra, <sup>226</sup>Ra, dose-response relationships for female dial painters 0-21545  
<sup>226</sup>Ra, alpha scintillation counter for determ. of low natural conc. 0-9456  
<sup>226</sup>Ra, assessment of quantities in North Carolina drinking water supplies 0-45826  
<sup>226</sup>Ra, conc. in Florida phosphate materials 0-30615  
<sup>226</sup>Ra, conc. in water near a phosphate facility 0-45827  
<sup>226</sup>Ra, radioactivity of thermal and mineral springs in Slovenia 0-7963  
<sup>234</sup>U, <sup>230</sup>Th, <sup>226</sup>Ra, superposition soln. of transport of decay chain through sorbing medium 0-37500  
<sup>234</sup>U, <sup>230</sup>Th, <sup>226</sup>Ra decay chain, hydrogeological migration anal. 0-37501

**radium compounds**

No entries

**radium emanation** *see radon***radius measurement** *see diameter measurement***radius of curvature measurement** *see curvature measurement***radon**

*see also nuclei with .....*

- <sup>222</sup>Rn concentration distribution under ground, effect on natural  $\gamma$ -ray flux density and exposure rate 0-36300



**radon continued**

- adsorption, on surface of elastically deformed body 0-10775
- carcinogenic effects of low level exposure 0-41142
- daughters in mine air, equilib. factor rel. to relative conc. 0-7977
- decay products, influence of elec. charge and humidity on diffusion coeff. 0-6192
- decay products as tracers for atmospheric stability (*Spanish*) 0-51448
- diffusion coefficient and exhalation rate from building materials, meas. technique 0-4694
- diffusion in soil, moisture effects 0-37491
- disequilibrium ratio in the atmosphere, Rn decay products/Rn (*Spanish*) 0-31083
- emanation from ground, statistical anal. 0-41259
- environmental sources in contiguous United States 0-41258
- evolution in neutral atmospheres (*Spanish*) 0-4058
- exposure standards for U mining 0-46055
- flow in porous medium, temporal (spatial) conc. variation, rel. to Earth crust 0-33671
- gamma spectrometry of Ra daughters in air 0-30628
- geothermal resources, Rn release 0-41263
- human exposure due to Ra bearing residues 0-41260
- monitor, continuous, response to transient Rn concs. 0-32519
- pollution and human disease, impact of energy conservation in residential buildings 0-56225
- radiation exposure in energy efficient buildings 0-41261
- radioactivity releases from nucl. power phosphate mining and coal burning 0-46072
- short lived daughters, detection method (*Chinese*) 0-42889
- sources, distrib., exposure in residential buildings 0-41262
- <sup>222</sup>Rn daughters exposure, electronic dosimeter 0-46054
- <sup>222</sup>Rn A=220, 222, decay products attachment to polystyrene aerosols 0-41256
- <sup>222</sup>Rn, alpha scintillation counter for determ. of low natural conc. 0-9456
- <sup>222</sup>Rn characts., natural occurrences, technological enhancement and health effects, review 0-46071
- <sup>222</sup>Rn, conc. in water near a phosphate facility 0-45827
- <sup>222</sup>Rn conc. over intertropical convergence zone of Atlantic 0-26648
- <sup>222</sup>Rn curved plesiotherapy applicators, dosimetry 0-51261
- <sup>222</sup>Rn exhalation meas., soil and meteorological effects (*Spanish*) 0-31082
- <sup>222</sup>Rn external plesiotherapy, dosimetry obs. 0-36135
- <sup>222</sup>Rn, radioactivity of thermal and mineral springs in Slovenia 0-7963
- <sup>222</sup>Rn releases associated with cultivation of agricultural land 0-16850
- <sup>222</sup>Rn very low conc. meas. with proportional counter 0-27907
- <sup>222</sup>Rn-CO<sub>2</sub>, thermal diffusion, expt. method for study 0-5922
- U mill tailings, diffusion consts. for soil covers 0-42807
- U mines, radiological evaluation 0-42806
- U mines and mills, Rn emission and control 0-41264

**radon compounds**

No entries

**rail traffic**

see also railways; traffic control

- acoustic noise, conf. Oct. 1978, Lyon, France 0-48495
- acoustic noise propagation models 0-48500
- aerodynamic noise generated by high-speed trains 0-48512
- coaches, noise generation expts. 0-48498
- environmental railway noise impact assessment, high speed trains in AMTRAK Northeast corridor 0-48507
- ground noise, underground systems 0-48490
- ground vibration, propagation pathway modelling 0-48491
- ground vibration measurement 0-48494
- noise, annoyance in residential areas 0-48503
- noise, attenuation by tree belts, pilot study 0-48501
- noise, Dutch study 0-48511
- noise, effect on sleeping subjects 0-48509
- noise, environmental controls for new housing sites 0-48505
- noise, environmental impact in Britain 0-48508
- noise, importance in France 0-48510
- noise, service evaluation tests on locomotives, AMTRAK Northeast corridor 0-48506
- noise, wheel/rail mechanisms 0-48496
- subway trains, retrofit noise control of rapid transit cars 0-48502
- train generated ground vibrations, propagation and wayside effects 0-48489
- wayside noise, high-speed trains 0-48497

railroads see railways

**railways**

see also locomotives; traction

- acoustic noise, conf. Oct. 1978, Lyon, France 0-48495
- acoustic noise propagation models 0-48500
- coaches, noise generation expts. 0-48498
- environmental noise impact assessment, high speed trains in AMTRAK Northeast corridor 0-48507
- ground noise, underground systems 0-48490
- ground vibration, propagation pathway modelling 0-48491
- noise, annoyance and activity interference patterns 0-48504
- noise, Dutch study 0-48511
- noise, effect on sleeping subjects 0-48509
- noise, environmental controls for new housing sites 0-48505
- noise, environmental impact in Britain 0-48508
- noise, importance in France 0-48510
- noise, service evaluation tests on locomotives, AMTRAK Northeast corridor 0-48506
- noise and vibration, annoyance in residential areas 0-48503
- sound meas. standards 0-14531
- subway trains, retrofit noise control of rapid transit cars 0-48502
- train generated ground vibrations, propagation and wayside effects 0-48489
- train noise, attenuation by tree belts, pilot study 0-48501
- underground, tunnel structure-borne sound levels and spectra 0-48499
- wayside noise, high-speed trains 0-48497
- wheel/rail noise research 0-48496
- H-fuelled railway motive power systems 0-40923

**rain**

- acidic rain interacting with rock partially covered by lichen 0-17302
- acidity, release of S and nitrogen oxides by burning fossil fuels 0-26590
- Africa, southern east coast rainfall rel. to southern oscill. and subtropical high press. belt 0-12518
- annual rainfall records, comparison methods for climatology 0-51587
- attenuation characts. of SHF waves for satellite broadcasting (*Japanese*) 0-12501

**rain continued**

- cloud seeding with AgI and metaldehyde, Fujian province, China (*Chinese*) 0-46235
- cold-frontal rainband, cellular struct. obs. 0-51512
- Comstar beacon cumulative slant path rain attenuation statistics, 28.56 GHz 0-26582
- dipole scattering of EM waves 0-36388
- Diyaal catchment, Iraq, water balance between Derbendikhan and Himrin dams 0-12462
- drizzle drop collision coalescence in presence of elec. field 0-51516
- drop size spectra and growth in cumulus cells, model 0-21800
- droplet collisions, satellite drop production expts. 0-12492
- EM sensor window materials, particulate erosion 0-38080
- evaporation from nimbostratus, effect on mesoscale unsaturated down-draughts, numerical anal. 0-8400
- evaporation rate of large water drops falling at terminal vel. in air, wind tunnel investig. 0-56541
- flash floods, synoptic and mesoscale mechanisms for heavy rainfalls 0-8385
- forecast accuracy for rain, limit due to spatial variability of rainfall 0-56510
- forecasting quantitative precipitation, prediction formula using Spanish data (*Spanish*) 0-36374
- frequency relationships study for Karnataka region, India 0-31094
- frontal rainband, conditional symm. instability explanation 0-56584
- gamma ray exposure rates due to rainfall, in situ Ge(Li) spectrum 0-42873
- halestone nuclei formation, role of giant aerosols (*Russian*) 0-56530
- Hawaiian rainfall normals, ridge regression-time extrapolation 0-51489
- long-period rainfall records in England and Wales, spectral and filter anal. 0-4080
- central Mali, rainfall comparison between Kabara and Tombouctou 0-4092
- maximum possible in Great Britain—time limited, determ. methods 0-4091
- measurement of rain rate and drops size distribution, with fast-response optical sensor 0-31135
- mesoscale structure of line convection at surface cold fronts 0-12514
- microwave attenuation for SIRIO link, fade statistics for 11.6 and 17.8 GHz (*Italian*) 0-4095
- microwave cross polarization discrimination statistics for spatially non-uniform rain 0-12534
- microwave crosspolarization, effects of sizes of nonspherical raindrops 0-21790
- microwave crosspolarization on satellite to Earth path 0-21789
- microwave radiometry by Nimbus 6 for rainfall over land 0-56635
- microwaves scattering, drop-size and temp. effects on forward and backward scattering 0-17317
- Middle East, monthly temps./rainfall relation appl. to palaeoclimates evaluation 0-31091
- monsoon circulations numerical simulation 0-21812
- Monsoon Experiment, Monex, GARP subprogram 0-8428
- monsoon over India during Aug. 1977, tropospheric structure 0-56570
- monsoon rainwater, India, halogen and sea-salt conc. 0-51517
- monthly rainfall in NW Georgia, spatial correls. rel. to climatology and weather modification expts. 0-51479
- Negev rainfall diurnal variation, climatological and meteorological implications 0-17344
- Oxford, 1682 May 31, point deluge and tornado 0-51521
- radar measurement of clouds and precipitation, correl. and spectral anal. 0-12529
- radar observation of rainfall, differential refl. method 0-46221
- radiowave attenuation in microwave and MM wavebands, estimation of duration time distribution (*Japanese*) 0-21788
- radiowave attenuation meas., microwave radio link projected design appls. (*Slovenian*) 0-46217
- radiowave attenuation on SIRIO-1 Earth-satellite link (*French*) 0-56504
- radiowave propag., angular depend. of rain scatt. at freqs. below 30 GHz 0-8416
- radiowave propag., crosspolarisation and attenuation meas. at 11.6 GHz using theoretical rain model, canting angle distrib. 0-4070
- radiowave propagation data from SIRIO satellite for earth-space rain-cell modelling 0-36352
- raindrop sizes and related parameters for GATE 0-41521
- rainfall variation in historical and contemporary epochs 0-36390
- satellite communications above 10 GHz, rain effects 0-8410
- scavenging of urban pollutants, inorganic nonmetallic species, convective storm systems 0-12039
- SHF signal attenuation by rain, monitored by radar 0-51567
- spatial distrib. in small catchment, influence on storm runoff 0-8357
- storm and tornado watches compared to observed tornadoes, rel. to weather modifications 0-12505
- storm type effect on precipitation in small mountain watershed, theoretical study 0-8355
- Tasmania, rainfall increase accompanying cloud-seeding expt. 0-51485
- Transcaucasia rainless periods, 1966-75 obs. 0-26603
- United Kingdom, regional units, wet and dry periods defined 0-51522
- urban influence on rainfall, obs. at St. Louis, USA 0-51513
- urban storm water management, flood vol. distrib. 0-8361
- vertical precipitation structure recording, meteorological radar appl. (*German*) 0-17358
- Ag cloud seeding of Florida cumuli, rainwater conc. obs. 0-56563
- Hg in S.New England coastal rain 0-41508
- SO<sub>2</sub> and sulphates in rain, urban and rural Norfolk, England 0-55955

rainfall see rain

Raman effect see Raman spectra

**Raman lasers**

- external-resonator controlled, pumped by CW CO laser, mol. spectroscopy uses 0-9624
- fibre Raman and Brillouin laser gains, polarisation effects 0-9887
- fibre Raman laser, CW, bandwidth reduction using prisms, gratings and etalons 0-53366
- fibre Raman oscillator, pulse synchronisation for fibre dispersion meas. 0-48410
- gain enhancement in Raman amplifiers with broadband pumping 0-43398
- IR and far IR source, powerful and tunable 0-5787
- methyl fluoride Raman FIR laser, high-intensity CO<sub>2</sub> laser pumping, new emission lines 0-23675



**Raman lasers continued**

- molecular spectroscopy and atmospheric constituents detection uses, review 0-55762  
 multiple-pass Raman gain cell 0-48334  
 $H_2$ , efficient tunable Raman laser 0-28245  
 $H_2$ , for efficient coherent summation of Nd laser nanosecond pulses 0-23718  
 $H_2$  gas, efficient higher-Stokes-order Raman conversion 0-33082  
 $H_2$  high power tunable IR compressed laser, for spectroscopy 0-48277  
 $Hg_{1-x}Cd_xTe$ , nonlinear optical effects 0-14389  
 n-InSb Raman spin-flip laser, hot electron effect distrib. calc. 0-23743  
 InSb, spin-flip Raman laser, charact. and phys. props., review (*Japanese*) 0-39576  
 $N_2$  high power tunable liq. Raman laser, for spectroscopy 0-48277  
 $N_2$ , liq., possible active media in high-power Raman lasers 0-19028  
 $O_2$ , liq., possible active media in high-power Raman lasers 0-19028

**Raman scattering** *see* Raman spectra**Raman spectra**

- see also* molecular rotation; molecular vibration; Raman spectra of diatomic inorganic molecules; Raman spectra of inorganic liquids and solutions; Raman spectra of inorganic solids; Raman spectra of organic molecules and substances; Raman spectra of polyatomic inorganic molecules; Raman spectroscopy; stimulated Raman scattering  
 adsorbed molecules, surface induced reson. Raman scatt., theory 0-54518  
 atoms, laser cooling, Raman mechanism 0-23371  
 combinational scatt. of light, discovery and history 0-27101  
 combinational scatt. of light, history 0-27100  
 crystals, book 0-2774  
 cubic crystals, Raman scatt. from tunnelling of substitutional molecules 0-40107  
 cyclohexane, plastic and liquid crystal phase, rot. correl. func. by Raman spectroscopy 0-23403  
 diatomic molecule, overtone intensities in reson. Raman scatt. 0-48001  
 dielectric cylinder embedded mols., Raman and fluoresc. scatt. 0-37949  
 disordered media, LF spectrum study from Raman scattering cross section 0-25363  
 disordered system, reson. Raman scatt. 0-2772  
 Doppler-free Raman spectroscopy and suppression of laser-induced mol. Doppler broadened transitions 0-9638  
 electron-phonon interaction effects on polarisation 0-55088  
 electron-phonon system, weakly coupled, resonant light scatt. and luminescence 0-40100  
 ferromagnetic film, shift of ant. temp. as result of Raman scatt. 0-54909  
 fluid, of isotropic mols., DID Rayleigh and Raman depolarised scatt., lattice-gas model 0-10356  
 Franck-Condon effects in resonance Raman spectra and excitation profiles, appl. to  $CrO_4^{2-}$  and  $\beta$ -carotene 0-14129  
 gaseous mixtures, equilib. at high temp., Raman scatt. obs. 0-45619  
 gases, high resolution rotational Raman spectra, review 0-23425  
 gases, rot.-vibr. Raman spectrosc., high resolution, review 0-22442  
 gases and vapours, degree of depolarisation of scattered light, meas. accuracy, Raman-lines effect 0-1737  
 hydrogenic atoms, metastable, Raman-like two-photon scatt., calc. 0-47953  
 hyper Raman effect, quantum statistics 0-23754  
 inhomogeneous Airy function,  $Gi(3)$  and  $Hi(3)$  0-43259  
 intermolecular forces Raman scatt. obs., review 0-23427  
 ionic solvation, spectroscopic data comparison for methanolic and aqueous solns. 0-26099  
 Jahn-Teller multimode effect for E-term with strong vibronic coupling, IR and Raman spectra band shapes 0-20139  
 liquid droplets, forced vibr., Raman scatt. obs. 0-34929  
 liquid structure and dynamics from light scatt. spectra 0-55105  
 living cells, laser Raman spectra, review 0-56113  
 molecular Raman scatt. theory, vibr. state summation, polarisability tensor upper and lower bounds 0-48000  
 molecules, chemisorbed on metal surface, spectrosc., electron gas effects 0-54504  
 nuclear-gamma ray scatt. using  $(n,\gamma)$  photons 0-18288  
 PAA, light scatt. near cryst. to nematic transition 0-16046  
 partially orientated symmetrical molecules, polarised Raman scatt. expressions 0-988  
 plasma, laser amplitude calibration from Raman spectra, for diagnostics (*Russian*) 0-38702  
 plasma laser pulse amplifier using induced Raman or Brillouin processes 0-1279  
 polarisation reduced Raman light scatt., review 0-34928  
 polariton Fermi resonance, Raman spectra in band of many-particle states 0-25374  
 premixed  $H_2$ - $O_2$ - $N_2$  laminar flames, temp. profiles, Raman, absorpt. and line reversal obs. 0-42227  
 resonance interactions of atomic and molecular systems driven by strong laser field, theory 0-14097  
 resonance Raman cross-section, theory 0-5551  
 resonance Raman effect, theory and appls. 0-23428  
 resonance Raman profile with consideration for quadratic vibronic coupling 0-55099  
 resonance Raman scatt. from mols., temp. effect, displaced harmonic oscillator model 0-23424  
 resonance Raman scattering, appl. to ultrafast dephasing and relax. obs., phonon scatt. effects 0-7337  
 resonance Raman scattering and luminescence of excitons in self-trapping process 0-20689  
 resonance Raman scattering in systems with localised carriers 0-7356  
 resonance Raman spectra lineshapes, first order, rel. to optical absorpt. lineshapes 0-5548  
 resonance Raman spectroscopy, inorg. chem. appls., book contrib. 0-972  
 resonant Raman scattering in laser fields of arbitrary strength, antibunching effects 0-23653  
 resonant scattering of light by slowly fluctuating localized electrons 0-7365  
 scattering cross-sections in gases and liquids 0-23426  
 semiconductor, Raman scatt., one-phonon final states and many-body effects 0-34913  
 small volume flames, temp., temporal meas., two line at. fluoresc. technique, Raman scatt. 0-42226  
 solid, disordered, IR and Raman spectra, analytic models 0-7336  
 solvated electrons, Raman spectrum modification, polarisation CARS obs. 0-5549  
 spin system, optical-acoustic two-phonon relax. 0-11244

**Raman spectra continued**

- time dependent theory, vibr. Raman scatt. in weak field limit 0-28023  
 transition quasilinear spectra of resonant secondary emission (*Russian*) 0-16102  
 two-photon saturation effect on ordinary Raman scatt. 0-9967  
 very thin films, improvement in Raman spectrometry 0-31911  
 vibrational intensity changes due to long-range interactions 0-53084  
 Ar, Raman scatt., single particle HF approx. and RPA many-electron correlations calcs. 0-23374  
 CN monolayer on Ag, picosecond Raman gain spectroscopy 0-25351  
 $D_2$ + $D_2$ , collision effect on depolarised light scatt. linewidths 0-53059  
 $F_2$ , Raman scatt. cross section for transitions between ground fine-struct. electronic states 0-23349  
 $H_2$ + $H_2$ , collision effect on depolarised light scatt. linewidths 0-53059  
 $InX(X_2)(X_3)$ ,  $InAlX_4$ ,  $X=Cl, Br$ , Raman spectra, up to 1200K 0-48003  
 $LiNO_3$  in N,N-dimethylacetamide, Raman, IR and US relaxation studies 0-50315  
 LISCN in N,N-dimethylacetamide, Raman, IR and US relaxation studies 0-50315  
 $NaNO_3$  in N,N-dimethylacetamide, Raman, IR and US relaxation studies 0-50315  
 $NaSCN$  in N,N-dimethylacetamide, Raman, IR and US relaxation studies 0-50315  
 $Sm^{3+}$  in cubic environment, importance of  $T^{-5}$  and  $T^{-7}$  terms in spin-lattice relax. time 0-25192

**Raman spectra of diatomic inorganic molecules**

- $Br_2$ , adsorbed layer on zeolites, Raman spectra, aromatic bromination catalysis 0-3408  
 $CN^-$ , chemisorbed on AG (110), Raman scatt. 0-45075  
 $Cl_2$ , near Ag electrode, intense Raman spectra, free radical form. 0-55076  
 H bonding molecules, self assoc., intermolecular interactions, matrix isolation vibr. spectra obs. Raman and IR spectra 0-52995  
 $H_2$ ,  $D_2$  and HD, intermol. collision process obs. using light scatt. expts. 0-53001  
 $H_2$  isotope mols. in laser fusion microsphere targets, nondestructive anal. using rot. Raman spectroscopy 0-50896  
 $H_2$ , Raman scattering, cooperative effect observations (*Russian*) 0-5553  
 $^1H^1H$  and  $^2H^1H$ , pure rot. and vibr.-rot. Raman spectra 0-14145  
 $He_2$ , polarisability and collision induced Raman spectra 0-48005  
 $I_2$  in  $CCl_4$  (cyclohexane) soln., ps dye laser excitation, fluoresc. and resonance Raman emission 0-28021  
 $InX(X_2)(X_3)$ ,  $InAlX_4$ ,  $X=Cl, Br$ , Raman spectra, up to 1200K 0-48003  
 $N_2$  dissolved in Ar, mol. orientation, Raman spectrosc. obs. 0-52994  
 $N_2$ , light polarisability parameters, Raman scatt. ang. meas. 0-37814  
 $N_2$ , matrix isolated, fundamental vibr. Raman spectra 0-272  
 $N_2$ , polarisability tensor anisotropy, Raman spectra differential scatt. cross section 0-18860  
 $N_2$ , Raman intensities calcs., ab initio method 0-52993  
 $N_2$ , Raman intensity, ab initio calc. 0-1028  
 $N_2$ , Raman spectra, intermol. torques and orientational correlation times 0-48006  
 $N_2$ , rot. Raman scatt. of Thomson scatt. 0-1844  
 $N_2$ , single and multiple free jets, CW laser Raman spectroscopy 0-32727  
 NO, press. broadening coeffs., spin-flip Raman laser spectrosc. 0-43147  
 $O_2$  dissolved in Ar, mol. orientation, Raman spectrosc. obs. 0-52994  
 $O_2$ , light polarisability parameters, Raman scatt. ang. meas. 0-37814  
 $O_2$ , polarisability tensor anisotropy, Raman spectra differential scatt. cross section 0-18860

**Raman spectra of inorganic liquids and solutions**

- metal-electrolyte interface, optical methods of study (*French*) 0-7318  
 molecular rotation, model for IR and Raman studies in liqs. and gases 0-11390  
 polyatomic fluid, local dynamics, spectroscopic studies, summer school lecture series 0-6343  
 solid-liquid interface, optical methods of study (*French*) 0-7318  
 succinic acid and its alkaline salts in aqueous soln., Raman and IR spectra (*French*) 0-32723  
 $B_2O_3$ , molten,  $BO_3$  triangles in boroxyl rings and random networks, Raman intensity investig. 0-45058  
 Bi complexes,  $Bi(III)$  halide complexes, Raman spectra in aq. soln. 0-25354  
 $CoCl_2$ , saturated soln., jet flow Raman spectroscopy for highly absorbing liq. systems 0-52323  
 $CuCl_2$ , saturated soln., jet flow Raman spectroscopy for highly absorbing liq. systems 0-52323  
 DCl, liquid, on coexistence line, light scatt., orientational correlation function 0-20632  
 $FeBr_4^-$  in various solvents,  $^4A_1$   $E$  d-d band reson. Raman spectra, solvent depend. 0-55085  
 $GaCl_3$ , Raman spectral differences from liquid to glassy state, ionic equilib. interpretation 0-20619  
 HBr, liquid, on coexistence line, light scatt., orientational correlation function 0-20632  
 HCl, liq., IR spectral intensity and Raman cross-section meas. 0-2742  
 HCl, liquid, on coexistence line, light scatt., orientational correlation function 0-20632  
 $^4He$ , liquid, integrated polarised Raman scatt. intensity calcs., Jastrow ground state 0-50342  
 $K_2CO_3$ - $SiO_2$ - $As_2O_3$ , laser Raman spectrosc. study of ions in quenched reaction mixtures 0-25357  
 $N_2$  dissolved in Ar, mol. orientation, Raman spectrosc. obs. 0-52994  
 $N_2$ , Raman lineshape 0-11384  
 $N_2O$ , pure liq., mol. motion, anisotropic interaction 0-24345  
 $NbCl_5$  in chloroaluminate melts, Raman spectral study 0-34915  
 $O_2$  dissolved in Ar, mol. orientation, Raman spectrosc. obs. 0-52994  
 $O_2$ , phase equilibria near 298K, Raman spectral study of solid and fluid 0-19937  
 $PHD_3$ , vibr. dephasing in liq. and solid  $PD_3$ , calcs. 0-19884  
 $Se$ , liquid, short range orientation effects, vibr. Raman spectra 0-2759  
 Se, Raman scatt. meas., comparison with amorphous Se spectra 0-50328
- Raman spectra of inorganic solids**  
 adamantane, plastic cryst. lattice vibr. study of phase transition 0-7355  
 alkali germanate glasses, struct., Raman scatt. obs. 0-1936  
 alkali metal tetrafluoroborates, intramol. force fields and mean vibr. amplitudes 0-2743  
 boroxyl ring breakdown in vitreous  $B_2O_3$ , Raman intensity investig. 0-45058  
 chalcogenide magnetic semiconductors, spinal-type, closed tube vapour transport method (*Japanese*) 0-25539



**Raman spectra of inorganic solids continued**

- ferromagnetic semiconductors, Raman scattering of light on plasmon excitations 0-2738  
 graphite intercalated with  $\text{AsF}_5$ ,  $\text{HNO}_3$  and  $\text{SbCl}_5$ , Raman scatt. in low stage cpds. 0-20638  
 graphite intercalation compounds,  $\text{C}_6\text{M}$ , ( $\text{M}=\text{K}, \text{Rb}, \text{Cs}$ ), Breit-Wigner line shape anal., Raman spectra 0-50336  
 graphite intercalation cpds., Raman scatt. and IR refl., review 0-45066  
 graphite- $\text{AlCl}_3$ , well-staged, Raman and IR spectra 0-50339  
 ice VI, OH stretching peak freq. press. depend., Raman spectra using diamond anvil cell 0-16023  
 non-crystalline materials of low atomic number, X-ray Raman edge extended modulation for struct. study 0-49111  
 optical glass, Raman scatt. and nonlinear refl. index 0-2749  
 phosphate glasses, cation-site interactions 0-2744  
 polysulphur nitride:bromine, struct. and phase transition 0-24382  
 rare earth orthophosphates,  $\text{RPO}_4$  ( $\text{R}=\text{Tb}, \text{Dy}, \text{Ho}, \text{Er}, \text{Tm}, \text{Yb}, \text{Lu}$ ), IR and Raman spectra 0-34904  
 rare earth zirconate,  $\text{R}_2\text{Zr}_2\text{O}_7$ , Raman spectra, anion disorder characterization 0-25358  
 ruby, Raman  $^2\text{E}$  and phosphorescence transitions, line widths, time correl. study 0-20621  
 semiconducting crystal, opaque, inelastic dynamical light diffraction 0-25399  
 semiconductor, excitons, exciton-phonon interaction, review, book contrib. 0-49624  
 semiconductors, resonant Raman scatt. from exciton-polaritons (*Japanese*) 0-50349  
 steel, stainless, surface oxide characterisation by Raman spectroscopy 0-50308  
 superionic conductors, light scatt. and IR absorpt. book contrib. 0-25382  
 tetramethylammonium hexabromotellurate, far IR and Raman spectra and phase transitions 0-11376  
 Ag electrode, adsorbed cyanide, enhanced Raman effect 0-50348  
 Ag, surface roughness induced electronic Raman scatt. 0-50347  
 Ag/CN, coverage meas. using surface enhanced Raman scatt. and radioisotope meas., electrochemical treatments 0-29260  
 AgBr, exciton relaxation by intervalley scattering 0-20644  
 AgBr:Cl, exciton-phonon interaction, reson. Raman scatt. vs photolum. 0-29798  
 $\beta\text{-AgI}$ , polariton dispersion curves, Raman spectra 0-29338  
 $\alpha\text{-AgI}$ , superionic, continuous order-disorder transition, Raman spectroscopic evidence 0-45070  
 $\text{AgNa}(\text{NO}_3)_2$ , ferroelectric transitions, group theoretic comparison with  $\text{NaNO}_3$  0-7311  
 $\text{AlGa}_{1-x}\text{Sb}$ , vibr. spectra, Raman light scatt. study 0-45080  
 $\beta\text{-Al}_2\text{O}_3$ , stoichiometric, Raman and IR spectra, Frenkel defects, order-disorder transition and cation cond. 0-55086  
 $\alpha\text{-Al}_2\text{O}_3\text{:Cr}^{3+}$ , Raman effect to probe dynamical processes of  $\text{Cr}^{3+}$  photoexcited states 0-2740  
 $\beta^*\text{-Al}_2\text{O}_3\text{-Ag}_2\text{O}$ , Raman scatt. from mobile cations 0-11394  
 $\beta^*\text{-Al}_2\text{O}_3\text{-K}_2\text{O}$  0-11394  
 $\beta\text{-Al}_2\text{O}_3\text{-Na}_2\text{O}$ , cation vibrations, disorder and hydration, IR and Raman spectra (*French*) 0-7343  
 $\beta^*\text{-Al}_2\text{O}_3\text{-Na}_2\text{O}$ , Raman scatt. from mobile cations 0-11394  
 $\alpha\text{-AlPO}_4$ , IR and Raman spectra, optical phonons 0-2767  
 $\text{Al}_2\text{SiO}_5$ , andalusite, phonon spectra and rigid-ion model calcs. 0-11391  
 As, amorphous, intermediate range order from polarised features of Raman spectrum 0-49113  
 As, amorphous, vibr. excitations at defect sites, IR and Raman spectra calc. 0-49329  
 As, amorphous, vibrational excitations of defect sites 0-49332  
 As amorphous films, interference enhanced Raman scatt. 0-50326  
 As, black phosphorous struct., Raman vibr. spectra and bonding 0-11411  
 As-S glasses, resonance Raman scatt. 0-50325  
 $\text{As}_2\text{O}_3$ , glassy, intermediate range order from polarised features of Raman spectrum 0-49113  
 $\text{As}_2\text{O}_3$ , vitreous, local struct. and vibrational spectra 0-55091  
 $\text{As}_2\text{S}_3$  glass, press. effect on optical props. 0-50363  
 $\text{As}_2\text{S}_4$ , effects of pressure and temp. on phonons, Raman scattering study 0-7360  
 $\text{As}_2\text{Se}_3$ , photodarkening and photostructural effects, Raman, IR and NQR studies 0-16036  
 B, amorphous, X-ray Raman edge extended modulation for struct. study 0-49111  
 B amorphous film, interference enhanced Raman scatt. 0-50326  
 $\text{B}_2\text{O}_3$  glass, struct. and phonon spectra 0-50324  
 $\text{BaCl}_2$  film, non-cryst., very-low-freq. inelastic light scatt. 0-25367  
 $\text{BaCl}_2$ , non-crystalline film, disorder-induced Raman scatt. 0-11387  
 $\text{BaFCl}$  film, non-cryst., very-low-freq. inelastic light scatt. 0-25367  
 $\text{BaFCl}$ , non-crystalline film, disorder-induced Raman scatt. 0-11387  
 $\text{Ba}_2\text{KNb}_2\text{O}_{15}$ , Raman scatt. experiments in tetragonal tungsten bronze compounds 0-40113  
 $\text{Ba}_2\text{NaNb}_2\text{O}_{15}$ , Raman scatt. experiments in tetragonal tungsten bronze compounds 0-40113  
 $\text{Ba}_2\text{TiSi}_2\text{O}_8$ , luminescence of  $\text{TiO}_3$  group, decay time, IR and Raman spectrosc. 0-2819  
 $\text{Be}_2\text{Al}_2(\text{SiO}_3)_6\text{:Cr}^{3+}$ , Raman effect to probe dynamical processes of  $\text{Cr}^{3+}$  photoexcited states 0-2740  
 $\text{BeCl}_2\cdot 4\text{H}_2\text{O}$ , IR and Raman spectra (*French*) 0-20618  
 $\text{BeSO}_4\cdot 4\text{H}_2\text{O}$ , IR and Raman spectra (*French*) 0-20618  
 C, amorphous, diamond-like 3-fold coord. 0-50323  
 C, amorphous film, struct. props., Raman scatt. study 0-11417  
 $\text{C}_8\text{K}(\text{Rb})$ , graphite intercalated, phonon dispersion relations and Raman spectra 0-44272  
 $\text{CaCO}_3$ , aragonite, split  $\nu_4$  mode of  $\text{CO}_3^{2-}$  ions 0-45077  
 $\text{CaF}_2\text{:Dy}^{3+}$ , cubic cryst. field effects 0-2368  
 $\text{CaHPO}_4\cdot 2\text{H}_2\text{O}$  powder and crystals, vibrational spectra, factor group anal. 0-45076  
 $\beta$ - and  $\gamma\text{-Ca}_2\text{P}_2\text{O}_7$ , IR and Raman vibr. spectra 0-25355  
 $\text{CaSO}_4$ , anhydrite and gypsum, phonon spectroscopy, lattice dynamical calc. 0-19889  
 $\text{Cd}(\text{ClO}_4)_2$ , single crystals, Raman scatt. 0-55106  
 $\text{CdCr}_2\text{S}_4$ , magnetic semicond., resonance Raman scatt., mag. circular polarisation props. 0-50341  
 $\text{CdI}_2\text{:Fe}^{2+}$ , polarised electronic Raman scatt. 0-29733  
 $\text{Cd}(\text{NH}_4)_2\text{X}_2$ ,  $\text{X}=\text{Br}, \text{Cl}, \text{I}$ , orientational phase transitions 0-11382  
 CdS, Raman shift dispersion near exciton reson., two-phonon cascade processes 0-11405  
 CdS, two photon Raman scatt. at high excitation levels (*Russian*) 0-16032

**Raman spectra of inorganic solids continued**

- CdS, virtually excited biexcitons polaritons dispersion, two photon Raman scatt. 0-45067  
 $\text{CdS:F}(\text{Cl})$ , shallow donors electronic Raman scatt., reson. enhancement 0-45068  
 $\text{CdSe}$ , polarisation correl. of resonant Raman scatt. or hot luminesc. 0-25384  
 $\text{CdTe}$ , reson. Raman scatt. by excitonic polaritons 0-11396  
 $\text{CoCl}_2\cdot 2\text{H}_2\text{O}$ , antiferromag., light scatt. from phonons and magnons 0-40104  
 $\text{CoCl}_2\cdot 2\text{H}_2\text{O}$ , magnon-phonon interactions and two-magnon Raman scatt., magnetoelastic waves and selection rules 0-34917  
 Cr, antiferromagnetic, surface Raman scatt., calc. 0-45069  
 Cs-Graphite, interaction ordered and disordered cpd., Raman spectra 0-11393  
 $\text{CsCoBr}_3$ , quasi one dimensional antiferromag., magnon Raman scatt. 0-11395  
 $\text{CsH}_2\text{PO}_4$ , Raman scatt. and high temp. props. 0-16024  
 $\text{CsMgCl}_3$ ,  $\text{Cs}_2\text{MgCl}_5$ , Raman spectrosc. investigation of struct. 0-49202  
 $\text{CsSbF}_6(\text{OH})_2$ , solid, IR and Raman spectra 0-40114  
 $\text{CsSbF}_6(\text{OH})$ , solid, IR and Raman spectra 0-40114  
 $\text{Cs}_2(\text{TeBr}_6)$ , far IR and Raman spectra and phase transitions 0-11376  
 Cu halides, phonon anomalies for  $\text{Cu}^+$  at off-centre sites, dynamical model and Raman meas. 0-10618  
 CuBr, dispersion of multicomponent exciton polaritons, hyper-Raman emission spectra 0-20096  
 $\text{CuCl}$ , fission of relaxed excitonic mols. into upper and lower branch polaritons induced by  $\text{M}_1$  emission 0-11380  
 $\text{CuCl}$ , phonon interaction of excitonic molecule 0-50316  
 $\text{CuCl}(\text{Br})(\text{I})$ , Raman spectra, Cu ions vibr. and diffractive motions 0-11412  
 $\text{Cu}_2\text{O}$ , exciton-phonon dynamics, reson. Raman scatt. 0-11406  
 $\text{Cu}_2\text{VS}_4$ , Raman active modes 0-11414  
 $\text{o-D}_2$ , solid, up to 150 kbar, 5K, Raman spectrum 0-50332  
 DF, cryst., Raman spectra 0-55075  
 DI, crystalline, Raman and IR spectra, mol. vibr., libration and translation 0-2757  
 $\text{EuO}(\text{S})(\text{Se})(\text{Te})$ , cryst. and electronic struct., mag., elec., and optical props., book contrib. 0-39760  
 EuTe, antiferromagnet, phonon Raman scatt. from spin superstructures 0-16030  
 $\text{Eu}_{1-x}\text{X}_x\text{S}$  ( $\text{X}=\text{Sr}, \text{Gd}$ ), spin-disorder-induced Raman scatt. from phonons, expt. investigation 0-20635  
 $\text{Eu}_{1-x}\text{X}_x\text{S}$  ( $\text{X}=\text{Sr}, \text{Gd}$ ), spin-disorder-induced Raman scatt. from phonons, theory 0-20636  
 $\text{EuX}$  ( $\text{X}=\text{O}, \text{S}, \text{Se}$ ) 0-20635  
 $\text{EuX}$  ( $\text{X}=\text{O}, \text{S}, \text{Se}$ ), spin-disorder-induced Raman scatt. from phonons, theory 0-20636  
 $\text{FeCl}_2\cdot 2\text{H}_2\text{O}$ , magnon-phonon interactions and two-magnon Raman scatt., magnetoelastic waves and selection rules 0-34917  
 $\text{FeF}_3$ , one-magnon Raman scatt., anomalous behaviour of anti-Stokes-Stokes intensity ratio 0-40115  
 $\text{Ga}_{1-x}\text{Al}_x\text{As}$ , IR refl. spectra and Raman spectra 0-20623  
 $\text{Ga}_{1-x}\text{Al}_x\text{Sb}$ , second order Raman spectra, photon combinations (*French*) 0-34912  
 GaAs, anodised, interfacial reactions, Raman scatt. obs. 0-49544  
 GaAs, effective mass, Raman spectrum determ. 0-24797  
 GaAs, excited, LO phonon effective temp., Raman meas. 0-20639  
 p-GaAs, heavily doped, self energy of phonons 0-44277  
 GaAs, ion implanted, laser induced recrystn. and damage, ion backscatt. and Raman scatt. obs. 0-49248  
 GaAs, Raman scattering absolute cross section band struct. model calcs. 0-7349  
 p-GaAs:Zn, Raman scatt. by LO phonon-plasmon coupled modes, wave vector non-conservation 0-16033  
 $\text{GaAs-Ga}_{1-x}\text{Al}_x\text{As}$  superlattice, Raman scatt., polar phonon anisotropy 0-45052  
 $\text{GaAs}_{1-x}\text{H}_x$ , amorphous, vib. props., Raman and IR meas. 0-50322  
 $\text{GaCl}_3$ , Raman spectral differences from liquid to glassy state, ionic equilibrium interpretation 0-20619  
 $\text{Ga}_{1-x}\text{In}_x\text{As}_2\text{P}_{1-x}$ , conduction band and phonons, Shubnikov-de Haas effect, magnetophonon resonance, Raman scattering 0-24795  
 $\text{Ga}_{1-x}\text{In}_x\text{Se}$ , Raman scatt. spectra, optical phonon freq., cryst. vibr. freq. types 0-29744  
 GaP, surface polaritons, light scattering studies, effect of surface roughness 0-6753  
 $\text{GaP:Cu}$ , Raman scatt. from acceptor state 0-11408  
 n-GaSb, coupled LO-phonon-plasmon modes, Raman spectrum 0-11409  
 p-GaSb, hot exciton luminesc., LO phonon Raman scatt. 0-11474  
 GaSe, cascade resonant Raman processes 0-25385  
 Ge, amorphous, growth rate of crystallisation, Raman spectroscopy study 0-44227  
 p-Ge, heavily doped, self energy of phonons 0-44277  
 Ge-Si alloys, defect modes and optical spectra 0-11413  
 $\text{GeO}_2$ , glassy high freq. vibr. bands, central force model 0-49330  
 $\text{Ge}(\text{S}, \text{Se})_2$  glasses, comparison  $\text{A}_1$  Raman line, microscopic origin 0-29740  
 $\text{GeS}_2$ , glassy, high freq. vibr. bands, central force model 0-49330  
 $\text{GeSe}_2$ , single crystals, 3 polymorphic forms, DTA, photolum., IR and Raman spectroscopy 0-33923  
 $\text{GeSe}_2\text{S}_{1-x}$  solid solutions, long-wavelength optical phonons, Raman spectra 0-25378  
 $\text{HEu}(\text{PO}_3)_4$ , vibr. spectra 0-34905  
 HF, cryst., Raman spectra 0-55075  
 HI, crystalline, Raman and IR spectra, mol. vibr., libration and translation 0-2757  
 $\text{HIO}_3$  crystals, anharmonicity effects in Raman spectra 0-25379  
 $\text{HIO}_3$ , polariton Fermi-resonance and dissociated phonon states (*Russian*) 0-20634  
 $\text{HSO}_4\text{F}$  crystal, indication of molecules existing as infinite chains (*French*) 0-989  
 $\text{HfS}_3$ , one-dimensional semicond., Raman spectra meas. 0-50345  
 $\text{HfS}_3(\text{Se})_3$ , phonon study of chemical bonding 0-20645  
 $\alpha\text{-HgI}_2$ , Raman scatt. at room temp., improved polarisation spectra 0-25368  
 $\alpha\text{-HgS}$ , cinnabar, reson. Raman effect and luminesc. meas. 0-50338  
 $\text{In}_{1-x}\text{Ga}_x\text{P}$ , phonon density of states, cluster Bethe lattice treatment 0-6475  
 InP, surface space charge layers and Schottky barrier form., Raman scatt. study 0-50319



## Raman spectra of inorganic solids continued

- $\text{InP}_{1-x}\text{As}_x$ , long wave and short wave phonons, Raman spectra obs. 0-50317  
 $\text{InSb}$ , electronic interband Raman scatt. 0-11407  
 $\text{InSe}$ , Raman scatt. spectra, optical phonon freq., cryst. vibr. freq. types 0-29744  
 $\text{InTe}$ , Raman spectra, phonon modes 0-40109  
 $\text{KBr}$ , doped with F-centres, Raman spectra meas. excitation in F and K bands 0-16027  
 $\text{KCN}$ , plastic phase, Raman scatt. spectra (*French*) 0-11379  
 $\text{K}_2\text{CO}_3\text{-SiO}_2\text{-As}_2\text{O}_3$ , laser Raman spectrosc. study of ions in quenched reaction mixtures 0-25357  
 $\text{KClO}_4\text{-MnO}_4^-$ , reson. Raman excitation profiles for totally symmetric mode, vibronic struct. 0-50309  
 $\text{K}_2\text{CoF}_4$ , pseudo Ising antiferromag., inelastic light scatt. by mag. excitons 0-11377  
 $\alpha\text{-KFe(PO}_3)_4$ , vibr. spectra 0-34905  
 $\text{K}_2\text{Fe(CN)}_6\cdot 3\text{H}_2\text{O}$ , C-N vibrs., Raman study 0-40106  
 $\text{KLiTi}^{4+}$ , pre-resonant enhancement of Raman scatt. 0-7354  
 $\text{KLa(PO}_3)_4$  ( $\alpha$  and  $\beta$  forms), vibr. spectra 0-34905  
 $\text{KMnF}_3$ , precursor order and Raman scatt. near displacive phase transitions 0-45061  
 $\text{K}_3\text{Mn}_2\text{F}_7$ , two magnon Raman scatt., magnon dispersion, susceptibility, Green's function methods 0-50340  
 $\beta\text{-KNd(PO}_3)_4$ , vibr. spectra 0-34905  
 $\text{KNi}_2\text{Mn}_{1-x}\text{F}_3$ , mixed antiferromagnet, light scatt. meas. 0-16025  
 $\text{K}_{1.75}\text{Pt(CN)}_4\cdot 1.5\text{H}_2\text{O}$ , Raman scatt. and luminesc. studies 0-25394  
 $\text{KReO}_4$ , vibr. spectrum, Raman and IR spectra obs. 0-55104  
 $\text{K}_2\text{SO}_4$ ,  $\alpha$ - $\beta$  phase transition, Raman scatt. study (*French*) 0-55096  
 $\text{K}_2\text{SeO}_4$ , ferroelec., incommensurate struct., dynamic props. (*Russian*) 0-11373  
 $\text{K}_2\text{SeO}_4$ , Raman scatt. and dielec. props. 0-11313  
 $\text{K(TCNQ)}$ , Raman spectra from 30 to  $2300\text{ cm}^{-1}$  0-11392  
 $\text{K}_2(\text{TeBr}_6)$ , far IR and Raman spectra and phase transitions 0-11376  
 $\text{K}_3(\text{UO}_2)_2\text{F}_7\cdot 2\text{H}_2\text{O}$ , single cryst., polarised Raman spectra, vibr. modes assignment (*French*) 0-29728  
 $\text{LaB}_6$ , synthesis and props. (*Japanese*) 0-40255  
 $\text{LaNbO}_4$ , Raman scatt. and fluorec. spectra 0-20625  
 $\text{LaP}_2\text{O}_{14}$ , ferroelastic transition, polarised Raman study 0-16035  
 $\text{LiEu(PO}_3)_4$ , vibr. spectra 0-34905  
 $\text{LiH(D)}$ , resonant Raman scattering in crystals with self-trapping excitons 0-7344  
 $\alpha\text{-LiIO}_3$ , Raman spectra behaviour in electrostatic field (*Chinese*) 0-7333  
 $\text{LiNbO}_3$ , spontaneous parametric scatt. line profile, IR absorpt. coeffs. 0-25377  
 $\text{Li}_2\text{O-Li}_2\text{SO}_4\text{-B}_2\text{O}_3$ , vitreous electrolytes, ionic cond. and Raman spectra (*French*) 0-24656  
 $\text{Li}_2\text{Si}_2\text{O}_5\text{-TiO}_2$  glasses, struct. and crystn. investigation using Raman spectra 0-38918  
 $\text{MgO}$  film, graphitic C detected by surface Raman spectra 0-2297  
 $\text{Mn}^{2+}$ , in nearly tetrahedral clusters,  $^4\text{E}$  levels, orbit-lattice interaction and Jahn-Teller effect, spectra obs. 0-24860  
 $\text{MoS}_2(2\text{H})$ , Raman spectra, phonon modes, high press. effects 0-40111  
 $\text{MoSe}_2(\text{Te}_2)$ , IR and Raman spectra, lattice vibrs. interlayer bonding 0-40110  
 $\text{N}_2$ , solid,  $\alpha$ - and  $\gamma$ -forms, Raman spectra, vibron and lattice freq. shifts, libration 0-16020  
 $\text{N}_2$ , solid, Raman spectroscopy up to 374 kbar 0-7353  
 $(\text{ND}_4)(\text{SO}_4)_3$ , ferroelec. langbeinites, Raman scattering 0-34926  
 $\text{NH}_3$ , IR and Raman intensity of lattice vibrs., theory 0-11381  
 $(\text{NH}_4)_3\text{BeF}_6$ , ferroelec., incommensurate struct., dynamic props. (*Russian*) 0-11373  
 $\text{NH}_4\text{Br}$  and  $\text{NH}_4\text{I}$ , Raman scatt., 1 bar-7 kbar, 86-295 K 0-34909  
 $(\text{NH}_4)_2\text{Cd}_2(\text{SO}_4)_3$ , ferroelec. langbeinites, Raman scattering 0-34926  
 $\text{NH}_4\text{Cl}$ , Raman scatt. of light on limiting and nonlimiting dipole vibr. 0-11402  
 $(\text{NH}_4)_2\text{CuCl}_4\cdot 2\text{H}_2\text{O}$ , lattice dynamics, anal. of Raman scatt. measurements 0-34149  
 $\alpha\text{-NH}_4\text{HgCl}_3$ , Raman study of phase transition (*French*) 0-11378  
 $(\text{NH}_4)_2\text{SnCl}_6$ ,  $^{35,37}\text{Cl}$  NQR, Raman spectra and spin lattice relax., hindered rot. 0-54974  
 $(\text{NH}_4)_2(\text{TeBr}_6)$ , far IR and Raman spectra and phase transitions 0-11376  
 $\text{NH}_4[\text{TeO}_4]$ , powder, Raman spectrum 0-39016  
 $\text{Na}_2\text{-S-GeS}_2$  system, glass formation, struct. and ionic conduction 0-54138  
 $\text{NaCN}$ , plastic phase, Raman scatt. spectra (*French*) 0-11379  
 $\text{NaCl(Br)}$  (F) (I), lattice dynamics and statics, three-body-force shell model 0-49323  
 $\text{NaI}$ , resonant Raman scattering in crystals with self-trapping excitons 0-7344  
 $\text{NaNO}_2$ , ferroelectric transitions, group theoretic comparison with  $\text{AgNaNO}_2$  0-7311  
 $\text{NaNO}_3$ , fine structure changes on interaction with weak shock waves (*Russian*) 0-54313  
 $\text{Na}_2\text{W}_2\text{O}_7$ , Raman and IR spectra 0-25356  
 $\text{Na}_2\text{WO}_3$ , metallic, light-scatt. studies 0-45071  
 $\text{NbSe}_3$ , phonon study of chemical bonding 0-20645  
 $\text{Ni}$ , with chemisorbed CO 0-2755  
 $\text{Ni-Cr}$ , surface oxide characterisation by Raman spectroscopy 0-50308  
 $\text{NiBr}_2(\text{Cl}_2)$  two-phonon vibronic progressions, Raman obs. 0-29742  
 $\text{O}_2$ , phase equilibria near 298K, Raman spectral study of solid and fluid 0-19937  
 $\text{P}$ , amorphous, vibrational excitations of defect sites 0-49332  
 $\text{P}$ , amorphous red, Raman scattering 0-11416  
 $\text{P}$ , black phosphorous struct., Raman vibr. spectra and bonding 0-11411  
 $\text{PCL}_3\text{-HCl}_2$ , Raman spectra, solid and melt, species identification (*German*) 0-45083  
 $\text{PF}_3(\text{H}_2\text{O})$ , Raman and IR spectra 0-14147  
 $\text{PHD}_2$ , vibr. dephasing in liq. and solid  $\text{PD}_3$ , calcs. 0-19884  
 $\text{P}_2\text{O}_5$ , glassy, high freq. vibr. bands, central force model 0-49330  
 $\text{Pb}$ , aq. corrosion film, IR and Raman spectroscopy 0-55567  
 $\text{PbCl}_2$ , Raman spectra, phonon modes 0-2754  
 $\text{Pb}_2\text{Ge}_2\text{O}_{11}$ , ferroelectric, anharmonic effects in low freq. symm. modes, Raman study 0-25365  
 $\text{Pb}_2\text{Ge}_2\text{O}_{11}$ , paraelectric and ferroelectric, Raman spectra near ferroelectric transition 0-55090  
 $\text{Pb}_3(\text{PO}_4)_2$ , ferroelastic, Raman scatt. by soft vibr. involved in ferroelastic phase transition 0-16040  
 $\text{Pb}_3(\text{P}_{1-x}\text{-V}_x\text{O}_4)_2$ ,  $x=0.1, 0.2$ , Raman scatt. by low freq. vibrs. 0-55111  
 $\text{Pb}_2\text{SiO}_4\text{-PbSiO}_3$ , Raman and IR spectra of crystalline phases 0-3013

## Raman spectra of inorganic solids continued

- $\text{Pd}$  complex, linear ionic mixed valence cpd., IR and resonance Raman spectra rel. to lattice modes 0-25393  
 $\text{Pd}$  mixed valence-mixed metal compounds, ionic crystals, longitudinal lattice modes, Raman spectroscopy 0-40099  
 $\text{Pt}$  complex,  $[\text{Pt}(\text{en})_2][\text{Pt}(\text{en})_2\text{Cl}_2](\text{ClO}_4)_4$ , reson. Raman spectra 0-2760  
 $\text{Pt}$  complex, linear ionic mixed valence cpd., IR and resonance Raman spectra rel. to lattice modes 0-25393  
 $\text{Pt}$ , mixed valence-mixed metal compounds, ionic crystals, longitudinal lattice modes, Raman spectroscopy 0-40099  
 $\text{RbCaF}_3$ , precursor order and Raman scatt. near displacive phase transitions 0-45061  
 $\text{Rb}_2\text{CoF}_4$ , pseudo Ising antiferromag., inelastic light scatt. by mag. excitons 0-11377  
 $\text{RbEu(PO}_3)_4$ , vibr. spectra 0-34905  
 $\text{RbMnCl}_3$  crystal, structural phase transition, birefringence, elastic moduli and Raman spectra 0-15243  
 $\text{Rb}_2(\text{TeBr}_6)$ , far IR and Raman spectra and phase transitions 0-11376  
 $\text{Rb}_2\text{ZnBr}_4$ , Raman scatt., normal-incommensurate-commensurate phase transitions, soft modes 0-40071  
 $\text{Rb}_2\text{ZnCl}_4$ , phase transition, Raman scatt. evidence 0-40116  
 $\text{Rb}_2\text{ZnCl}_4$  single crystals, Raman scatt. spectra, temp. range covering two phase transitions 0-7340  
 $\text{Re}$ , Raman scattering spectrum at room temp. 0-25373  
 $\text{ReO}_3$  type lattice, group-theoretical symmetry anal. of vibr. (*Russian*) 0-10610  
 $\text{Si}_3\text{N}_4$ , effects of pressure and temp. on phonons, Raman scattering study 0-7360  
 $\text{Sb}$ , amorphous, vibrational excitations of defect sites 0-49332  
 $\text{SbBr}_3$ ,  $^{121}\text{Sb}$ , low freq. Raman and IR spectra, force consts. 0-55097  
 $\text{Se}$ , amorphous, Raman scatt. meas., comparison with liq. spectra 0-50328  
 $\text{Se}$  amorphous film, interference enhanced Raman scatt. 0-50326  
 $\text{Se-Ge}$ , amorphous, Raman spectra and average band gap 0-50327  
 $\text{Si}$  films, polycryst., glow discharge deposited below  $250^\circ\text{C}$ , struct. and morphology 0-49535  
 $\text{Si}$ , photoexcited, highly stressed, electronic Raman scatt. and antireson. 0-29737  
 $\text{Si}$ , Raman scattering absolute cross-section 0-11410  
 $\text{p-Si}$ , Raman spectra, pseudopot. calc. of discrete-continuum interference 0-2747  
 $\text{Si:F}$ , amorphous, pure and doped, vibr. excitations at defect sites, IR and Raman spectra calc. 0-49329  
 $\text{Si:H}$  amorphous films, interference enhanced Raman scatt. 0-50326  
 $\text{SiO}_2$ , amorphous, intrinsic surface phonons, Raman scatt. and IR refl. 0-24728  
 $\text{SiO}_2$  and  $\text{SiO}_2\text{-B}_2\text{O}_3$  glasses, struct. and phonon spectra 0-50324  
 $\text{SiO}_2$ , vitreous, Raman active defects, thermal equilibration 0-55092  
 $\text{SiO}_2$ , amorphous and recrystallised layer, optical props. 0-25474  
 $\text{Sn}_2\text{P}_2(\text{S}_{1-x}\text{Se}_x)_6$ , solid solutions, ferroelectric soft mode freq., displacive transformations 0-29701  
 $(\text{Sn}_{1-x}\text{Pb}_x)_2\text{P}_2\text{S}_6$ , solid solutions, ferroelectric soft mode freq., displacive transformations 0-29701  
 $\text{SrCl}_2$  film, non-cryst., very-low-freq. inelastic light scatt. 0-25367  
 $\text{SrCl}_2$ , non-crystalline film, disorder-induced Raman scatt. 0-11387  
 $\text{SrCl}_2\cdot 2(\text{H}_2\text{O})_2\text{O}$ , IR and Raman spectra, force fields 0-2753  
 $\text{SrCl}_2\cdot 2\text{H}_2\text{O}$ , IR and Raman spectra, force fields 0-2753  
 $\text{Sr}_2\text{KNb}_2\text{O}_{15}$ , Raman scatt. experiments in tetragonal tungsten bronze compounds 0-40113  
 $\text{Sr}_2\text{NaNb}_2\text{O}_{15}$ , Raman scatt. experiments in tetragonal tungsten bronze compounds 0-40113  
 $\text{Sr}_2\text{Nb}_2\text{O}_7$ , optical mode softening in incommensurate phase 0-7352  
 $\text{SrTiO}_3$ , hyper Raman scatt. on polaritons, polariton branches (*Russian*) 0-50334  
 $\text{SrTiO}_3$ , hyper-Raman scatt. spectra due to lattice vibr. 0-29732  
 $\text{SrTiO}_3$ , tetragonal, effect of impurities on Raman spectrum 0-2770  
 $\text{TaS}_3$ , Raman spectra, CDW induced metal-semicond. transition 0-11404  
 $\text{Te}$  film, interference enhanced Raman scatt. 0-42273  
 $\text{Ti}$  film, interference enhanced Raman scatt. 0-40105  
 $\text{Ti}_2\text{O}_3$  film, interference enhanced Raman scatt. 0-40105  
 $\text{TiAsS}_4$ , optical phonons, Raman and refl. spectra 0-11400  
 $\text{TlBr}$ , reson. Raman scatt., forbidden one phonon and intervalley scatt. at direct exciton 0-45073  
 $\text{TlBr}$ , second order Raman scatt., reson. behaviour rel. to phonon bands 0-40101  
 $\text{Ti}_2\text{Cd}_2(\text{SO}_4)_3$ , ferroelec. langbeinites, Raman scattering 0-34926  
 $\text{TiCl}_2$ , second order Raman scatt., reson. behaviour rel. to phonon bands 0-40101  
 $\text{TiGaS}_2(\text{Se}_2)$ , phase transforms. under hydrostatic press., Raman scatt. study 0-25366  
 $\text{TiGaTe}_2$ , IR refl. and Raman scatt. spectra, lattice vibrs. 0-40108  
 $\text{TiGaTe}_2$ , multilayer cryst., lattice vibr. symm., IR absorpt. and Raman scatt. selection rules 0-39231  
 $\text{TlInSe}_2(\text{Te}_2)$ , multilayer cryst., lattice vibr. symm., IR absorpt. and Raman scatt. selection rules 0-39231  
 $\text{TlInTe}_2(\text{Se}_2)$ , IR refl. and Raman scatt. spectra, lattice vibrs. 0-40108  
 $\text{TlSe}$ , Raman spectra, phonon modes 0-40109  
 $\text{TmSe}$ , intermediate valent, Raman scatt. 0-16038  
 $\text{V}_1$ , antiferromag., zone-boundary phonon Raman scattering, modulation of exchange interaction 0-11386  
 $\text{V}_1$ , antiferromagnet, phonon Raman scatt. from spin superstructures 0-16030  
 $\text{YAG:Cr}^{3+}$  0-2740  
 $\text{ZnAl}_2\text{O}_4\text{-Cr}^{3+}$ , Raman effect to probe dynamical processes of  $\text{Cr}^{3+}$  photoexcited states 0-2740  
 $\text{ZnCd}_{1-x}\text{S}_x$ , resonance Raman scatt. involving exciton complexes 0-16039  
 $\text{ZnP}_2$ , second-order vibr. spectra and dispersion of phonon branches 0-25376  
 $\text{ZnP}_2\text{As}$ , local vibrs. of impurity ions, Raman study 0-29745  
 $\text{ZnS(Se)(Te)}$ , second order Raman scatt., lattice dynamical calc. and expt. 0-25370  
 $\text{ZnSe}$ , relaxation processes in Raman scattering and exciton luminescence under resonant excitation 0-25386  
 $\text{ZnTe}$ , relaxation processes in Raman scattering and exciton luminescence under resonant excitation 0-25386  
 $\text{ZnTe}$  crystals, secondary radiation polarization and relaxation of optical excitation 0-11399  
 $\text{ZnTe}$ , resonance Raman scatt. at high excitation levels (*Russian*) 0-55109  
 $\text{ZnTeSe}_{1-x}$ , Raman phonon spectra, resonance interaction effect 0-25375



**Raman spectra of inorganic solids continued**

- ZrS<sub>3</sub>, Raman spectra and cryst. symm. 0-34922  
 ZrS<sub>3</sub>(Se<sub>2</sub>)(Te<sub>2</sub>), phonon study of chemical bonding 0-20645  
 ZrSe<sub>3</sub>, long wavelength optical phonons, Raman scatt. and IR refl. 0-34921  
 ZrSiO<sub>4</sub>, zircon, resonance splitting of internal vibr. freq. of complex anion 0-55080

**Raman spectra of organic molecules and substances**

- 3,3,3-trifluoropropene, struct. and vibr. spectra, IR, Raman polarisation study 0-18845  
 acetone, liq., C-C stretching mode relax., Fermi reson. influence 0-25352  
 acetonitrile, in liq. phase, Raman band profiles, calc. using IR intensities 0-2741  
 n-alkanes, longitudinal acoustic modes, Raman intensities 0-32718  
 γ-aminobutyric acid, aq. soln., low freq. vibrs. Raman spectra obs. 0-987  
 anthracene, isotopically mixed cryst., exciton dynamics 0-29329  
 anthracene crystal, resonance secondary emission, Raman scatt. in exciton absorpt. region (*Russian*) 0-40120  
 anthracene-pyromellitic dianhydride, mol. charge transfer cryst., Raman scatt. meas. 0-29743  
 bacteriorhodopsin, reson. CARS spectrosc. 0-8014  
 bacteriorhodopsin, reson. Raman evidence for secondary protein-Schiff base interactions, primary excitation mechanism 0-55981  
 BBOA, smectic B phase, fluidlike mol. dynamics, Raman scatt. study 0-20630  
 benzaldehydes, para-halogenated, IR and Raman spectra, vibr. assignments, thermodynamic functions 0-14139  
 benzene, bromination on zeolite adsorption complex, Raman spectroscopic anal. 0-16670  
 benzene, cryst., IR and Raman intensity of lattice vibrs., theory 0-11381  
 benzene, molecule translational mobility in depolarised Raman spectra 0-14150  
 benzene, stimulated Raman scatt., anti-Stokes components, class II radiation cones 0-28276  
 benzene, ultrahigh sensitivity stimulated Raman gain spectroscopy 0-48337  
 benzene adsorbed on metal surface, obs. of vibrational modes 0-6649  
 benzene in solution, rotational motion, Raman study 0-44104  
 benzene-p-dioxan, mixtures, mol. reorientation and assoc., depolarised Raman scatt. obs. 0-7341  
 p-bromochlorobenzene, vibr. relax., Raman active phonons temp. depend. 0-29139  
 t-butyl chloride-d<sub>0</sub> and -d<sub>9</sub>, polymorphism, Raman spectra 0-20617  
 carbon tetrachloride, solid, Raman study of phase transition and dynamic struct. 0-34916  
 β-carotene, Franck-Condon effects in resonance Raman spectra and excitation profiles 0-14129  
 1-chloro-2-methylbutane, conformer depend. C-Cl stretching vibrs., Raman optical activity spectrum simulation 0-14146  
 p-chlorobenzylidene-p-n-pentylaniline, metastable phases formed by rapid cooling of mesophase, IR and Raman spectra and DSC obs. 0-34919  
 chloroform-d<sub>0</sub>(-d<sub>1</sub>), Raman and IR intensity anal. 0-18857  
 chloroform-He(Ar)(N<sub>2</sub>) gaseous compressed mixture, mol. reorientation, Raman spectra 0-23422  
 chloroform-p-dioxan and chloroform-benzene mixtures, mol. reorientation and assoc., depolarised Raman scatt. obs. 0-7341  
 m-chloronitrobenzene, cryst., low freq. vibrs., polarised Raman and IR spectra study (*French*) 0-16029  
 m-chloronitrobenzene, molecular crystals, translational and orientational vibr. determ. 0-55103  
 COOB, solid state dimorphism and cryst.-smectic transition, Raman study 0-45063  
 crystal violet, prereson. Raman spectra 0-32721  
 1,1-cyclobutane dicarboxylic acids and K salts, IR and Raman vibr. spectra (*French*) 0-2758  
 cyclobutane-d<sub>0</sub>(d<sub>8</sub>), cryst. modifications, low. freq. Raman and IR spectra 0-7342  
 cyclohexane-d<sub>0</sub>(d<sub>6</sub>), plastic crystal phase transition, mol. reorientation, Raman scatt. phonon spectra 0-20631  
 cyclopropyl bromide, IR absorption, Raman scatt., assignments, thermodynamic functions 0-984  
 meso-2,3-dibromo-1,4-dichlorobutane, rot. isomerism, IR and Raman spectra 0-981  
 dichloroanilines, vibr. assignments, Raman spectra obs., thermodynamic functions 0-52992  
 p-dichlorobenzene, vibr. relax., Raman active phonons temp. depend. 0-29139  
 4,4'-dichlorobenzophenone, phase changes, Raman spectra (*French*) 0-2756  
 3,4-dichlorobromobenzene, liq., laser Raman spectrum, LF band assignments 0-48002  
 N,N-dimethyl acrylamide (-d<sub>3</sub>,d<sub>6</sub>,d<sub>9</sub>), force field, IR and Raman spectra obs. 0-47979  
 dimethyl di(trifluoromethyl) germanium, and perdeuterated analogues, vibr. spectra, normal coord. anal. (*German*) 0-5547  
 2,3-dimethylbuta-1,3-diene, IR, Raman spectra, torsional pot. function, thermodynamic function 0-43046  
 dimethylsulphoxide, effects on water struct., Raman and IR spectral study 0-14143  
 2,2-dinitropropane-d<sub>0</sub>(d<sub>6</sub>), phase polymorphism, vibrational assignments, IR and Raman study 0-16031  
 dipalmitoylphosphatidylcholine/glucagon (cardiolipin/insulin) systems, Raman spectra study 0-16903  
 2,5-distyrylpyrazine, absorpt., Raman and fluoresc. spectrosc. 0-28049  
 EBBA, metastable phases formed by rapid cooling of mesophase, IR and Raman spectra and DSC obs. 0-34919  
 ethane, liq., correl. function modelling, third order memory function method 0-7339  
 ethoxyhexyltolan, Raman spectra, molecular conformational instability, internal field effects 0-54127  
 ethoxyoctyltolan, Raman spectra, molecular conformational instability, internal field effects 0-54127  
 ethyl methyl sulphide, low freq. vibr. spectra, methyl torsional pot. functions and internal rot. 0-5543  
 ethylmethylamine, low freq., vibr. spectra, methyl torsional pot. functions, mol. struct. 0-43045  
 fluorescent molecules, stimulated spectra, excited state intramol. vibrs. 0-32717  
 hexafluorobenzene-benzene, liq., mol. interactions, IR and Raman line-shape obs. 0-28907

**Raman spectra of organic molecules and substances continued**

- hexafluorobutene, vibrational broadening, dense fluid region, Raman and NMR study 0-43056  
 hexafluoropropene, struct. and vibr. spectra, IR, Raman polarisation study 0-18845  
 n-hexatriacontane, cryst., orthorhombic modification, vibr. spectra 0-50314  
 hydrocarbons, mol. Raman intensities calcs. 0-52993  
 liquid crystals, solid state polymorphism, differential scanning calorimetry and IR and Raman spectra obs. 0-55094  
 lithium ammonium tartrate monohydrate, Raman spectra, anomalous low-lying response 0-2746  
 malononitrile, displacive phase transition, 294.7K, Raman and Brillouin-Rayleigh scatt. obs. 0-16047  
 MBBA, metastable phases formed by rapid cooling of mesophase, IR and Raman spectra and DSC obs. 0-34919  
 metallo-octaethyl porphyrins, I oxidation products, metallic cond., EPR and reson. Raman spectra 0-29610  
 metalloporphyrins, reson. Raman spectra, intra- and inter-manifold couplings interference 0-28020  
<sup>13</sup>C-methane, ν<sub>1</sub> fund., quasi-CW inverse Raman spectra 0-48004  
 methane, intradoppler CARS saturation spectroscopy 0-43057  
 methane, pulsed photoacoustic Raman spectrosc., gaseous trace anal. 0-40769  
 methane, solid, Raman spectra and II-III phase transition 0-2745  
 methane, stimulated Raman scatt. obs. 0-53003  
 methane, vibration-rotation energies, 2ν<sub>2</sub> and ν<sub>2</sub>+ν<sub>4</sub> bands 0-47963  
 methane-air flame, stimulated Raman scatt. obs. 0-53003  
 α,ω-methoxy-poly(ethylene oxide) effect of swelling on longitudinal acoustic mode 0-29739  
 methyl ammonium chloride, Raman spectra, 70 to 300K, H stretching vibrs. 0-20628  
 methyl iodide, liq., A<sub>1</sub> modes, vibr. relax., temp. depend. Raman spectra obs. 0-32806  
 methyl thionine chloride, intramol. vibr. spectra 0-977  
 methyl torsion modes, vibrational optical activity, inertial contrib. 0-5524  
 methyl tri(trifluoromethyl) germanium, and perdeuterated analogues, vibr. spectra, normal coord. anal. (*German*) 0-5547  
 methyl vinyl sulphide, syn-gauche equilib., force field and ab initio calcs., microwave and Raman spectra 0-23573  
 N-methylacetamide, structure (*French*) 0-7343  
 molecular rotation, model for IR and Raman studies in liqs. and gases 0-11390  
 molecular shape determination, of high temp. species 0-52233  
 naphthalene, melting of rotational degrees of freedom near cryst.-liq. transition 0-54352  
 naphthalene, vibr. dephasing and Raman active localised internal mode temp. depend. 0-45060  
 naphthalene in nonpolar solvent, vibr. and reorientational relax., correl. function 0-45065  
 nearly tetrahedral cpds., Mn<sup>2+</sup>, <sup>4</sup>E levels, orbit-lattice interaction and Jahn Teller effect 0-24860  
 N-nitrodimethylamine-do(-d<sub>6</sub>), structural phase transition, Raman study 0-34911  
 octafluoronaphthalene, phase transitions at elevated press., Raman and mid-IR spectroscopy obs. 0-45062  
 organic compounds, low freq. anharmonic vibr., pot. function determ., Raman and IR spectra obs. 0-52997  
 organo-arsenic compounds, (CF<sub>3</sub>)<sub>3</sub>AsSCH<sub>3</sub> and (CF<sub>3</sub>)<sub>3</sub>AsSeCH<sub>3</sub>, gas phase IR and liq. Raman spectra, normal coord. anal. (*German*) 0-32725  
 organophosphorus compounds, (CF<sub>3</sub>)<sub>2</sub>PSCl<sub>3</sub> and (CF<sub>3</sub>)<sub>2</sub>PSeCl<sub>3</sub>, gas phase IR and liq. Raman spectra, normal coord. anal. (*German*) 0-32725  
 organosilane coupling agent interphase of glass-fibre reinforced plastics, molecular organisation 0-44195  
 PAA, cryst. phase transitions, intermolecular motion, Raman and inelastic neutron scatt. spectra 0-2164  
 PAP, cryst. phase transitions, intermolecular motion, Raman and inelastic neutron scatt. spectra 0-2164  
 phenol, cryst., mol. vibrs., factor group splittings 0-16021  
 poly-1,6-di-p-toluenesulphonyloxy-2,4-hexadiyne, thermal polymerisation, Raman spectra 0-35531  
 polyacetylene, doped and neutral, resonance Raman scatt. 0-55107  
 polyacetylene, doping with AsF<sub>5</sub>, mechanism, effect on elec. cond. and spectra 0-24473  
 polyalkenamers, longitudinal accordion mode, low frequency Raman spectroscopy 0-25369  
 polyatomic fluid, local dynamics, spectroscopic studies, summer school lecture series 0-6343  
 polydeoxyribonucleotides, poly(dA).poly(dT) and poly(dAT).poly(dAT), HF vibr. modes, Raman and IR spectra 0-32698  
 polyethylene:NaCl, internal field strength, Raman spectra obs. 0-40061  
 polyethylene, crystn. under high pressure 0-38946  
 polyethylene, H bonding effects on skeletal optical and longitudinal acoustic modes 0-34914  
 polyethylene, linear, glass transition temp. 0-15225  
 polyethylene, rapid crystn. from melt rel. to struct. 0-44152  
 polyethylene electret, internal pot. topography, Raman and IR spectra 0-7362  
 polyethylene oxide, cryst., lowest laser Raman active accordion oscillations, elastic moduli effect 0-29734  
 polymer, light and Raman scattering obs. of high press. phases (*Japanese*) 0-2773  
 polymer viscoelasticity and strength characterisation, advanced light scatt. techniques 0-11857  
 polymethylene, extended chain, C-H stretching band struct., Fermi reson., Raman spectrum 0-5552  
 polyoxymethylene, rapid crystn. from melt rel. to struct. 0-44153  
 polystyrene and model cpds., conformational struct. influence on normal modes of benzene ring, Raman study 0-14144  
 polytetrahydrofuran, H bonding effects on skeletal optical and longitudinal acoustic modes 0-34914  
 polyvinylidene electrets, IR and Raman spectra 0-7359  
 porphyrins, reson. Raman spectra, selection rules, normal coord. treatment 0-53175  
 potassium hydrogen oxalate, oriented single cryst., Raman spectra with very strong H-bonding 0-25359  
 potassium oxalate, anhydrous, phase II, vibr. spectra and cryst. struct. 0-34901



**Raman spectra of organic molecules and substances continued**

- isopropyl chloride, torsional pot. function, far IR and Raman obs. 0-28022
- 1,3-propylenediammonium manganese tetrachloride, vibr. study of phase transitions, IR and Raman spectra 0-40103
- PVA, swollen crystallinity determ. by laser Raman spectroscopy 0-38953
- pyrazine adsorbed on electrode, surface enhanced Raman spectra, symmetry and polarisability changes 0-50310
- pyridine, adsorbed on Ag, Raman intensity enhancement using surface plasmons 0-7334
- pyridine, adsorbed on Ag electrodes, ang. resolved Raman spectra 0-16017
- pyridine, adsorbed on Cu(Au) electrode, angle-resolved Raman spectroscopy 0-52991
- pyridine, near Ag electrode, intense Raman spectra, free radical form. 0-55076
- pyridine adsorbed on Ag, reson. Raman scatt. 0-25380
- pyridine iodine complexes, charge transfer complexes, vibr. spectra, laser Raman obs. 0-52990
- pyridine-d<sub>5</sub>, physisorbed thin film on Ag surface, enhanced Raman scatt. study 0-20620
- pyridine-I<sub>2</sub>(Br<sub>2</sub>) charge transfer complexes, vibr. spectra, vibronic contrib., intensity enhancement 0-53048
- resorcin, Raman line intensity as function of mol. orientation 0-11383
- rhodamine B, 6G, resonance CARS line shape, scatt. processes in ground or excited states 0-48043
- sodium hydrogen oxalate monohydrate, oriented single cryst., Raman spectra with very strong H-bonding 0-25359
- stearyl alcohol, H bonding effects on skeletal optical and longitudinal acoustical modes 0-34914
- succinic acid and its alkaline salts in aqueous soln., Raman and IR spectra (*French*) 0-32723
- TCNQ salts, conducting, Raman spectra, estimation of degree of charge transfer from vibrational frequencies 0-50344
- meso-1,2,3,4-tetrabromobutane, IR and Raman spectral studies 0-32722
- tetrabromomethane, in disordered phases, IR active mode Raman line shape, dipole-dipole interaction 0-9603
- meso-1,2,3,4-tetrachlorobutane, IR and Raman spectral studies 0-32722
- tetrafluoromethane, in disordered phases, IR active mode Raman line shape, dipole-dipole interaction 0-9603
- thiocyanate complexes at Ag electrode surface, Raman spectroscopic study 0-37813
- thiourea, phonon modes near order-disorder transforms., hard-core modes due to pseudospin-phonon coupling 0-44285
- thiourea, phonon modes near phase transitions, IR and Raman spectra 0-45084
- thymine monoanions in soln., tautomer identification by laser Raman spectroscopy 0-14148
- toluene, molecule translational mobility in depolarised Raman spectra 0-14150
- toluene sulphonate diacetylene polymer, vibr. modes, strain depend. using Raman spectra 0-20626
- toxic organic substances detection in water using matrix isolation Raman spectroscopy 0-30616
- tri-*i*-propylgermylamine, and isotopomers, IR and Raman spectra, normal coord. anal. (*German*) 0-32716
- tri-*t*-butylstannylamine, and isotopomers, IR and Raman spectra, normal coord. anal., Mossbauer spectrum (*German*) 0-32716
- tribromotrifluoroethane, IR and Raman spectra, normal coord. anal. (*German*) 0-32726
- trichlorotrifluoroethane, IR and Raman spectra, normal coord. anal. (*German*) 0-32726
- triethylsilylamine, and isotopomers, IR and Raman spectra, normal coord. anal. (*German*) 0-32716
- trifluoroethane(-d<sub>3</sub>), IR and Raman spectra, normal coord. anal. (*German*) 0-32726
- trifluoromethyl trimethyl germanium (tin)(lead), and perdeuterated analogues, vibr. spectra, normal coord. anal. (*German*) 0-5547
- trifluorotriiodoethane, IR and Raman spectra, normal coord. anal. (*German*) 0-32726
- TTF and derived cpds., intramolecular vibr. and vibronic effects, IR and Raman spectra 0-25387
- TTF halides, charge transfer effect on internal modes, Raman scatt. 0-25392
- TTF-TCNQ, charge transfer determ. from spectral line shift using Raman scatt. 0-25392
- uracil monoanions in soln., tautomer identification by laser Raman spectroscopy 0-14148
- trans-Ni(S<sub>2</sub>N<sub>2</sub>CH<sub>3</sub>)<sub>2</sub>, IR and Raman spectra, normal coord. anal. 0-28019

**Raman spectra of polyatomic inorganic molecules**

- high temperature, review 0-52234
- inorganic species, vibr. and electronic props., reson. Raman spectra appl. 0-52996
- molecular shape determination, of high temp. species 0-52233
- quasi-linear molecules, low frequency anharmonic vibrations, pot. function determ., Raman and IR spectra obs. 0-52997
- rare earth oxalates, struct., IR absorpt. and Raman spectra (*French*) 0-32714
- [<sup>15</sup>N]NH<sub>3</sub>, modulated coherent Raman beats 0-23464
- B<sub>2</sub>H<sub>6</sub> gas (liq.) phase, vibr. dephasing and Raman spectra 0-48101
- Ba(ClO<sub>4</sub>)<sub>2</sub>, solutions in amides and esters, structure (*French*) 0-7343
- CO<sub>2</sub>, conc. and temp. in flames, Raman spectroscopy 0-32720
- CO<sub>2</sub>, pulsed photoacoustic Raman spectrosc., gaseous trace anal. 0-40769
- CO<sub>2</sub>, pure rotational stimulated Raman photoacoustic spectroscopy 0-32724
- CO<sub>2</sub>, rarefied jet beam, Raman scatt., for rot. temp. and density 0-6185
- CO<sub>2</sub>, single and multiple free jets, CW laser Raman spectroscopy 0-32727
- CS<sub>2</sub>, liq., props. from allowed light scatt. spectra 0-25364
- CrO<sub>4</sub><sup>2-</sup>, Franck-Condon effects in resonance Raman spectra and excitation profiles 0-14129
- CuBr<sub>4</sub><sup>2-</sup>, ground state Zeeman splittings, reson. Raman spectra and mag.-optical activity 0-5579
- FeBr<sub>4</sub><sup>2-</sup>, ground state Zeeman splittings, reson. Raman spectra and mag.-optical activity 0-5579
- HClO<sub>4</sub>-H<sub>2</sub>O, aq. soln., IR and Raman spectra, conc. depend. (*Russian*) 0-53002
- H<sub>2</sub>O, in D<sub>2</sub>O ice I<sub>c</sub>, decoupled vibr. spectra 0-52984

**Raman spectra of polyatomic inorganic molecules continued**

- HSO<sub>3</sub>F, gas, indication of molecules existing as cyclic dimers (*French*) 0-989
- HSO<sub>3</sub>F, liquid, indication of molecules existing as mixture of cyclic dimers and infinite chains (*French*) 0-989
- InX(X<sub>2</sub>)(X<sub>3</sub>), InAlX<sub>4</sub>, X=Cl,Br, Raman spectra, up to 1200K 0-48003
- IrCl<sub>6</sub><sup>3-</sup>, ground state Zeeman splittings, reson. Raman spectra and mag.-optical activity 0-5579
- LiClO<sub>4</sub>, solutions in amides and esters, structure (*French*) 0-7343
- NH<sub>3</sub>, adsorbed on amorphous silica 0-11948
- NH<sub>3</sub> in benzene(CCl<sub>4</sub>)(pentane) Fermi resonance, solvent and phase depend. 0-47960
- NH<sub>3</sub>, rot.-inversion Raman spectra, K-splitting 0-9611
- NO<sub>3</sub><sup>-</sup>, aq. soln., vibr. width and dephasing, conc. depend. 0-43029
- N<sub>2</sub>O, pulsed photoacoustic Raman spectrosc., gaseous trace anal. 0-40769
- N<sub>2</sub>O, pure rotational stimulated Raman photoacoustic spectroscopy 0-32724
- O<sub>2</sub><sup>+</sup>AsF<sub>6</sub><sup>-</sup>, thermal decomposition, Raman spectra study, free radical mechanism 0-55652
- OCS in *n*-alkane, rot. relax., solvent hydrodynamic props., Raman and IR spectra 0-45055
- PF<sub>6</sub>H(D), vibr. spectra and normal coordinate anal., Raman and IR spectra 0-14147
- Pd complex, Pd<sup>II</sup>Pt<sup>II</sup>(CNCH<sub>3</sub>)<sub>6</sub>(PF<sub>6</sub>)<sub>2</sub>, vibr. spectra, M-M bonds. (*French*) 0-47997
- Pd(S<sub>2</sub>N<sub>2</sub>)<sub>2</sub>, IR and Raman spectra, normal coord. anal. 0-28019
- Pt complex, Pt<sup>II</sup>(CNCH<sub>3</sub>)<sub>4</sub>(PF<sub>6</sub>)<sub>2</sub>, Pt<sup>II</sup>(CNCH<sub>3</sub>)<sub>6</sub>(PF<sub>6</sub>)<sub>2</sub>, and Pt<sup>II</sup>Pd(CNCH<sub>3</sub>)<sub>6</sub>(PF<sub>6</sub>)<sub>2</sub>, vibr. spectra, M-M bonds. (*French*) 0-47997
- SF<sub>6</sub>, vibr. spectra, rot. const., IR spectra, Raman spectra obs. 0-32719

**Raman spectroscopy**

- see also Raman lasers; Raman spectra
- active Raman spectroscopy, high resolution molecular methods 0-52998
- anti-Stokes spectrometer, microcomputer-controlled 0-24111
- atmosphere, minor constituents detection using tunable spin flip Raman laser, review 0-55762
- augmented CARS spectroscopy linewidth parameter from laser mode structure 0-33083
- book 0-22155
- chromatograph, liquid, coupled with Raman spectroscopy for anal. of mixtures (*French*) 0-45595
- coherent, molecular shape determination, of high temp. species 0-52233
- coherent Raman spectroscopy techniques, review 0-22440
- combustion, coherent Raman spectrosc. obs. 0-16691
- combustion diagnostics, laser appls. 0-16688
- computer acquisition, simultaneous, of IR, microwave and Raman spectral data (*Japanese*) 0-4776
- crystals, book 0-2774
- Doppler broadening at electronic resonance 0-38065
- electro-optical multichannel spectrometer for transient resonance Raman and absorption spectroscopy 0-31890
- electrocrystallisation, recent progress in electrochem. and physical methods (*French*) 0-7510
- evanescent waves in total reflection, Raman scatt. direct recording, boundary layer obs. 0-52317
- films, very thin absorbing, interference enhanced Raman scatt. 0-42273
- flame diagnostics using multichannel pulsed Raman spectroscopy 0-30237
- gas, angularly resolved CARS config. 0-22453
- high pressure cell for matrix isolation Raman spectroscopy 0-272
- high temperature chemistry, review 0-52234
- high-resolution, using tunable spin flip Raman laser, review 0-55762
- industrial atmospheric pollutant remote analysis by Raman lidar 0-12047
- interference enhanced Raman scatt., app. to amorphous semicond. thin films 0-50326
- internal combustion engine, CARS noninvasive temp. and species meas. 0-30293
- intradoppler CARS saturation spectroscopy 0-43057
- inverse Raman scattering spectroscopy and chem. appls. 0-37094
- jet flow technique for highly absorbing liq. systems 0-52323
- laser, implications of 5062Å Ar ion laser line CW oscillation 0-1186
- laser Raman spectrometer, 180° microscope sampling and viewing attachment 0-13150
- matrix isolation, toxic organic substances detection in water 0-30616
- microcomputer-controlled Raman spectrometer 0-27352
- molecular spectroscopy book 0-27051
- molecular spectroscopy book 0-27052
- molecular structure and properties from high-resolution spectra of gases 0-53000
- molecules, stimulated Raman and two-photon absorpt. 0-52999
- molecules and crystals, recent applications (*French*) 0-7343
- photoionisation, quantum beats, origin 0-52954
- picosecond laser techniques for obs. of vibr. modes in liqs. 0-5800
- picosecond Raman techniques, vibr. dynamics in liqs. 0-52325
- polymers, Raman, spectroscopy of thin films, integrated optical techniques 0-22432
- pulse-sequenced CARS spectroscopy, method for nonreson. background suppression 0-53375
- pulsed photoacoustic Raman spectrosc., gaseous trace anal. 0-40769
- remote detection of CARS employing fibre optic guides 0-9984
- resonance four-wave mixing spectroscopy, recent developments 0-53383
- resonance Raman cross-section, theory 0-5551
- resonance scattering methods in atomic spectroscopy 0-53167
- sample heating apparatus, for laser Raman spectroscopy 0-22439
- stimulated Raman gain spectroscopy, ultrahigh sensitivity, S/N ratio meas. 0-48337
- stimulated Raman scattering, sensitivity enhancement by quasi CW laser scheme 0-53003
- surface picosecond Raman gain spectroscopy 0-25351
- surface vibrational spectroscopy using stimulated Raman scatt. 0-38062
- time-resolved resonance Raman spectroscopy and vidicon Raman spectrography, vibr. spectra on nsec scale 0-37095
- vibrational spectroscopy, high pressure, and conformational analysis 0-9758
- Nd:YAG laser multipass cell for Raman scatt. diagnostics 0-1231

**Ramsauer effect see collision processes****random-access storage**

- Josephson nondestructive readout RAM cells, design criteria 0-50000
- RAM, use as  $\alpha$ -particle detector 0-37701



**random functions**

see also *random processes*  
No entries

**random noise**

see also *thermal noise*

- astronomical data, effect of noise on accuracy of max. entropy method 0-56712  
catastrophe and fractal regimes in random waves 0-8811  
coherent Raman spectroscopy techniques, review 0-22440  
computerised tomography, noise factor of a polyenergetic X-ray beam 0-56204  
current fluctuations in strong elec. field, interelectron collisions, drifted Maxwellian distrib. (*Russian*) 0-2436  
Cygnus X-1, X-ray flux time variability struct. (*Russian*) 0-51921  
diffusion noise, VHF extension of Einstein relation 0-17901  
digital fibre optical communication system, average error probability calc. 0-53228  
electrodes, ellipsoidal, embedded in conductor, spreading resist. and 1/f cond. fluctuations 0-2435  
EM radiation, noncoherent polarimetry anal. 0-1111  
fission reactors, coupled core system, noise sources in coupling medium, stochastic study 0-22962  
K-distributed noise, statistics 0-27220  
laser radar system, mobile computerised meteorological phenomena observation 0-56644  
MBBA, nematic, EHD transitions, white noise effects 0-6159  
MOSFET, flicker noise theory 0-11100  
multiturn fibre Sagnac interferometer, shot-noise-limited inertial rotation meas. 0-1349  
nonequilibrium phase transitions in presence of external non-white noise 0-42182  
nonlinear noisy sine wave oscillator, optimal control 0-27218  
optical fibre communication systems, computer design aids 0-28350  
optical fibre magnetostrictive perturbation for possible mag. field detect., shot noise 0-53450  
optical fibre system, timing error tolerant waveforms 0-14293  
optical fibres, modal noise, dependence on source coherence and fibre length 0-48402  
probability density, time dependent, for nonlinear non-Markovian stochastic process, coloured noise effect 0-22281  
respiratory impedance and derived parameters in young children by forced random noise 0-30745  
retarding field energy analyser in electron spectrometry, noise meas. 0-27377  
satellite Fourier spectroscopy methods and problems (*German*) 0-36477  
semiconductor, 1/f noise origin 0-11060  
semiconductor, current and voltage fluctuation determ. by noise spectral density meas. 0-15577  
semiconductor, theory of carrier multiplication and noise due to avalanche processes 0-6865  
semiconductors, lightly doped, 1/f noise for hopping conduction, theory 0-44683  
sound Gaussian noise and its transformation by moving boundary condition effect 0-33281  
spin wave parametric excitation by noise pumping (*Russian*) 0-34617  
superfluorescence, phase-wave fluctuations 0-23652  
transport noise, Green's function procedures 0-17902  
tunnel-effects in junctions generating burst-noise (*Rumanian*) 0-6960  
Bi film, carrier conc., mobility and 1/f noise 0-44748  
Bi, thin film, 1/f noise, boundary scatt. effect 0-49836  
n-Cd,Hg<sub>1-x</sub>Te, single crystal, scattering mechanism on intensity of 1/f noise 0-39642  
PbTe, semiconductor polycrystalline thin films, low-frequency 1/f noise meas. 0-15629  
Si p-n diode, 1/f noise calc., free carrier mobility interpretation 0-54774

**random phase approximation** see *RPA calculations*

**random processes**

see also *Brownian motion; fluctuations; Markov processes; probability; queueing theory; stochastic processes*

- anisotropic system, random field conjugate to non-crit. variable, effect on phase transition 0-13022  
arbitrary random noise and vibration waves, statistical consideration of peak distribution 0-23836  
atmospheric boundary layer and upper ocean layer, fluctuations, linear filtration errors 0-12425  
atomic migration on disordered surfaces, theory 0-54516  
chaos, reinjection principle, folded and cut chaotic flows 0-12996  
chaotic states of anharmonic systems in periodic fields 0-22288  
chemical reactions, diffusion-controlled, continuous-time random walk modelling 0-3297  
chloroplast conformational vars., auto-correl. anal. 0-30680  
coherence and randomness in quantum theory, uncertainty relations 0-22231  
correlated walks theory, exact results 0-27214  
coupled random walk process specified by Hamiltonian in pot. field 0-42169  
crack propagation considered as random walk process 0-43666  
Cygnus X-1 shot-noise variability, extended-bandwidth X-ray obs. vel. to energy depend. 0-17689  
diffusion in presence of high diffusivity paths, random walk model 0-24640  
diffusion in solids, random walk model with correlated jumps, appl. to H in metals 0-24639  
diffusion processes with two-point boundary conditions, probability distrib. 0-42144  
diffusion product (*French*) 0-8909  
direct renormalisation soln. 1D random walk problem 0-4512  
dissipative structures, non-equilibrium systems, self organisation (*Chinese*) 0-42168  
European air temperature band-pass filtered series, random phase displacements 0-26579  
Fokker-Planck eqn. eigenfunction expansion soln. extension, first order system 0-31668  
frequency meas., using automatic electronic meter (*Bulgarian*) 0-27283  
grains in random arrays, spectral properties 0-12727  
Hajek-Renyi type inequalities for random elements in Hilbert space 0-17784  
homogeneous random fields, modelling realisations 0-8911  
interstellar clouds, turbulence effects on collapse, three-dimensional numerical models 0-56910

**random processes continued**

- interstellar polarisation in irregularly fluctuating medium, statistical anal. 0-26926  
Ising model, thermodynamic limit 0-17885  
Ising systems of different spin values, random system 0-11144  
laminated composites, mechanics of homogenisation and random evolutions 0-28423  
Landau-Zener problem, random nature of motion role in intersecting terms problem 0-8937  
laser beam scatt. by diffusing surfaces (*Chinese*) 0-1128  
lattice random walks, occupation times 0-42162  
lattices, finite, with traps, random walks, Monte Carlo simulations 0-52131  
linear dynamic mol. system, correlated radiation impulse sequence interaction 0-38058  
localization of eigenstates in one-dimensional infinite disordered systems with off-diagonal randomness 0-17876  
Lorenz model, intermittency, first limit cycle-second strange attractor transition 0-31674  
Markovian nature of the two-dimensional self-avoiding random walk problem 0-4648  
martingales, set function processes, vector lattices, Riesz decomposition and characts. (*French*) 0-8908  
memory effects in random walk process 0-27232  
metastable chaos, transition to sustained chaotic behavior in Lorentz turbulent convection model 0-4643  
metastable state relaxation, critical point region nucleation in thermodynamic systems (*Russian*) 0-13026  
neural networks with random topology randomness of generated eigenvalues 0-22291  
ocean random gravity wave mathematical representation 0-46198  
oceanic crust random magnetisation, effect on coherence of short-wavelength marine mag. anomalies 0-36225  
organic compounds, complex, nuclear relaxation influence on stimulated emission 0-48019  
oscillator, linear, excitation by stationary random force (*Russian*) 0-27116  
oscillator with dry friction, forced vibr., response random process treatment (*Russian*) 0-36841  
oscillators, nonlinear stochastic, triangular wave, optimally controlled, Weiner process and Poisson process, numerical studies 0-52128  
palaeoclimatology, abrupt events time scales and causes 0-51531  
point defects short term annealing, in  $\alpha$ -Fe, computer simulation 0-54282  
polymer network, Riemann's metric degeneration to graph metric demonstration, chain entanglement problems 0-38963  
polymer network formation, struct. and mech. props., computer simulation 0-38965  
PSR 0950+08, pulsar, micropulses freq. struct. 0-22030  
pulsar microstructure shot-noise model, propag. effects in shearing field-free plasma 0-17483  
radio sources distribution in vicinity of bright galaxies, evidence for random population 0-56964  
random walk properties on periodic and random lattices via generating function 0-42157  
resonance transfer rate of electron excitation, model of convergent terms, effect of diffusional motion of particles 0-8936  
saltating solid particles in turbulent flow, accel. and forces (*Russian*) 0-1675  
self-avoiding random walk, renormalisation group eqn. 0-36947  
self-avoiding random walks on lattice strips 0-17875  
signal processing method for circular arrays 0-4123  
stationary, correlation between level-crossing time interval lengths 0-22292  
statistics, use of stochastic occupation densities and local times (*French*) 0-46972  
steady-state process, probability characts. error calcs. 0-42145  
three-dimensional cubic lattice, random walk of particle, polymer chain config. approach 0-22294  
three-dimensional lattices with coord. number 4, random walk calcs., tracer diffusion 0-13001  
tight-binding Green's functions for surfaces, thin films, and solid interfaces using random-walk theory 0-54753  
time ordered operator cumulants, statistical independence and noncommutativity 0-31670  
two-layer plate, random temp. fields and heat conduction, Monte Carlo method 0-33417  
universal time, random function determ. 0-46120  
viscoelasticity, stress/strain relationships, fluctuations 0-17802  
walks with Markovian steps (*French*) 0-17868  
weak spherical shock waves, propagation from arbitrary piston motions 0-22204
- range finding** see *distance measurement*
- range of particles** see *energy loss of particles*
- ranging (sonar)** see *sonar*
- rare earth alloys**  
see also *cerium alloys; dysprosium alloys; erbium alloys; europium alloys; gadolinium alloys; holmium alloys; lanthanum alloys; lutetium alloys; neodymium alloys; praseodymium alloys; promethium alloys; rare earth compounds; samarium alloys; terbium alloys; thulium alloys; ytterbium alloys*  
amorphous, cryst. field, nonaxial elec. field gradient 0-20138  
amorphous, mag. props., Mossbauer spectra 0-7225  
amorphous, random anisotropy antiferromag. model 0-20399  
amorphous, random mag. anisotropy 0-20398  
amorphous, transport props. 0-20152  
conference, St. Pierre-de-Chartreuse, France (Sept. 1978) 0-12844  
crystal field interactions, book contrib. 0-39540  
crystal field splitting in alloys with Cu<sub>3</sub>Au struct. 0-54663  
cubic intermetallics, self polarisation field at rare earth nuclei 0-15487  
Curie temperature, high press. effects (*Japanese*) 0-20444  
germanides, X-ray emission, absorption and photoelectron spectra (*Russian*) 0-11509  
high-energy magnetic materials, development, props., treatment procedures and testing (*Italian*) 0-54914  
intermediate valence systems, neutron scatt., review 0-49674  
intermetallic compounds, containing d-transition metal, hydrogenated, magnetism 0-34609  
intermetallic compounds, RM<sub>2</sub>, low temp. sp. ht. 0-15259  
intermetallic cpds., cryst. chemistry, book contrib. 0-39010  
intermetallics, mag. struct. 0-15698



**rare earth alloys continued**

- intermetallics, neutron scatt., induced moment magnetism, high press. 0-15699  
 intermetallics, quadrupole interactions, magnetoelasticity 0-15489  
 ion exchange chromatography for Co and rare earth determ. in alloys for high energy magnets (*Polish*) 0-35606  
 Laves phase compounds,  $R_xR_{1-x}Fe_2$ , magnetostriction, anisotropy energy 0-25177  
 magnetic properties, impurity effects, CPA calc. 0-44784  
 magnetic props., book contrib. 0-39759  
 magnetostrictive underwater sound transducers 0-19204  
 magnets, cylindrical, dynamic characts. of repelling force system, forced vibrations of one-degree-of-freedom system (*Japanese*) 0-4744  
 misch metal, improvement of Al alloy 51S, for space appl. 0-55466  
 mischmetal-Co-Cu-Fe-Mg, mag. props. 0-35353  
 mischmetal-Co-Cu-Mg, mag. props. 0-35353  
 Mischmetal-Ni,  $MMNi_5$  substituted hydrides for H storage appls. 0-45791  
 NMR, EPR, and Mossbauer effect, book contribs. 0-39883  
 permanent magnets, physics and technology 0-20433  
 permanent magnets flux stability enhancement by thermomechanical treatments, gyroscope-based guidance systems performance improvement 0-50144  
 phase diagram, infra-rare earth systems, Kaufman approach 0-25657  
 photoemission, rel. to electronic struct., book contrib. 0-16157  
 rare earth cobalt oriented materials as permanent multipole magnets 0-37925  
 rare earth-3d transition metal amorphous alloys, crystallisation behaviour 0-49116  
 rare earth-transition metal (4f-3d) intermetallic cpds., mag. moment and mag. anisotropy 0-25107  
 rare earth-transition metal amorphous thin films, mag. potential distribution and wall velocity meas. 0-34725  
 rare earth-transition metal amorphous thin films for thermomag. recording 0-20403  
 spin glasses, bulk mag. props. in amorphous and cryst. systems 0-20415  
 structural, electronic, and mag. props., book 0-36785  
 structural instabilities in alloys with CsCl struct. 0-24587  
 transition metal alloys, amorphous, struct. and mag. props., book contrib. 0-39818  
 transition metal alloys, binary system constitution diagram interrelations (*Russian*) 0-7535  
 transition metal alloys, magnetic amorphous films for mag. bubble memories, materials review (*Polish*) 0-34715  
 transition metal intermetallics, H absorpt., Mossbauer studies 0-39987  
 transition metal-rare earth intermetallics, two sublattice system with high competing single ion anisotropies, model 0-39767  
 US attenuation, temp. and mag. field depend. 0-15195  
 valence, coordination no., polyhedral at. vols. 0-19742  
 Ag-rare earth alloys, Ag-rich, phase equilib. 0-45276  
 Al-rare earth alloys, granules, rolling to form foil, exam. 0-20825  
 Co-mischmetal-rare earth alloys for high energy permanent magnets, manufacture technology (*Polish*) 0-35132  
 Cr-rare earth alloys, liquid phase, topology in diagrams of state (*Russian*) 0-54121  
 Fe, cast, cast Fe, spheroidal graphite, rare earth treated, nodularizing element distrib. (*Chinese*) 0-11653  
 $GaNiR$ , ( $R=Ce, Pr, Nd, Sm, Gd, Tb, Dy, Ho, Er, Tm, Yb, Lu, Y$ ), struct. by X-ray powder method (*Ukrainian*) 0-10529  
 $(Gd_{1-x}R_x)(Co_{1-y}Mn_y)_2$ ,  $R=rare\ earth, M=Cu, Ni, Pt$ , origin of hyperfine fields acting on Gd, Mossbauer study 0-44967  
 Ge-rare earth alloys, nature of chemical interaction, X-ray emission, absorpt. and photoelectron study (*Russian*) 0-55261  
 H storage props. and characts. 0-21416  
 Mg-R, dil., mag. susceptibility and magnetisation 0-15689  
 Ni-Cr-Co-R, oxidation depend. on alloying element, cohesion strength (*Russian*) 0-40587  
 $R-Al$ , ( $R=Gd, Dy, Tb, Ho$ ), cubic Laves phase compounds, exchange striction determ. 0-44895  
 $R-Au$ , amorphous, mag. and transport props. 0-34605  
 $R-Co$ , ferromagnet, first and second order transitions 0-34631  
 $R-Cu$ , amorphous, mag. and transport props. 0-34605  
 $R-Fe$  rod, US resonance with large eddy currents 0-54933  
 $R-Ga$  ( $R=rare\ earth$ ), cryst. struct. investigation 0-33930  
 $RAI_2$ , anisotropic magnetostriction, temp. depend. 0-39841  
 $R_4Au$  heavy-rare-earth based alloys, anisotropy versus exchange 0-34624  
 $RCO_2$ , elec. resistivity, thermopower, X-ray struct. meas. 0-24874  
 $RCO_3$ , X-ray absorpt. spectra, electronic struct. 0-16122  
 $RCO_3-H(D)$  system, mag. orientation aftereffect 0-50148  
 $RCu_2$  intermetallic compds., single crystals, mag. props. 0-54892  
 $RCu_4Al_8$ , mag. struct. and interactions 0-25092  
 $RFe_2$ , electronic heat capacity coeffs. 0-39787  
 $RFe_2$ , Laves phase intermetallics, ordered and paramagnetic phases, mean field exchange consts. 0-50084  
 $RFe_2$ , magnetostriction studies, book contrib. 0-39846  
 $R(Fe, Rh_{1-x})_2$ , mag. props., Mossbauer spectra 0-25108  
 $RGa_2$ , magnetic ordering and exchange interactions 0-39779  
 $RM_2$ , ( $M=Fe, Co, Ni$ ), magnetism, review 0-20365  
 $RM_4Al_8$  ( $M=Cr, Mn, Fe, Cu$ ), magnetism and hyperfine interactions 0-25256  
 $RM_2X_2$ , ( $M=Rh, Pd, Ag, Ir, Pt, Au$ ;  $X=Si, Ge$ ), cryst. struct. 0-1964  
 $RPT$ , ( $R=Gd, Tb, Dy, Ho, Er, Tm$ ), structs. and mag. props. 0-50069  
 $R_3Ru$  and  $R_3Ru_2$ , cryst. struct. 0-1965  
 $RZn_{12}$ , mag. struct. and interactions 0-25092

**rare earth compounds**

- see also under the individual compounds e.g. cerium compounds  
 see also rare earth alloys  
 alkali metal rare earth double metaphosphates, vibr. spectra, rel. to struct. 0-34905  
 amorphous films for mag. bubble memories, materials review (*Polish*) 0-34715  
 binary, regression eqns., for calc. props. from electron struct. 0-39498  
 borides, higher types, phys. props. and electronic struct., group orbitals-LCAO calcs. 0-20077  
 carbonates, determ. by mass spectrometric complexometric method 0-3442  
 chalcogenides, cryst. field splitting, press. depend. 0-24852  
 conference, St. Pierre-de-Chartreuse, France (Sept. 1978) 0-12844  
 crystal field interactions, book contrib. 0-39540  
 dihydrides and dideuterides, electronic and mag. props. 0-25260

**rare earth compounds continued**

- dodecaborides, magnetic susceptibility temp. depend., 90-1200K 0-20374  
 ethyl sulphates:  $Ce^{3+}$ , Kramers ions, virtual phonon exchange, field theoretic formalism 0-20137  
 formates, second optical harmonic generation 0-43403  
 garnet thin films, macroscopic mag. props., magneto-optical expts. 0-46764  
 garnets, Debye charact. temp. and reciprocal lattice consts. 0-29144  
 garnets, prep. and props. book contrib. 0-44193  
 geochemistry and mineralogy, book contrib. 0-46157  
 germanides, X-ray emission, absorption and photoelectron spectra (*Russian*) 0-11509  
 halides, prep. and props., book contrib. 0-54211  
 handbook 0-41957  
 hexaboride single crystals, microhardness meas. 0-21087  
 hexaborides, obtained by melting, micromech. props., rel. to bonding 0-21082  
 hexagonal, cryst. field effect in thermal expansion 0-49390  
 hydride films, prep., struct. and props., general review 0-54556  
 hydrides, props., book contrib. 0-45291  
 hydrides, rare earth and intermetallic, electronic and mag. props., Mossbauer study 0-34830  
 hydroxides, heat capacity from near 5 to 350K, lattice and Schottky contribs. 0-49374  
 intermediate valence systems, neutron scatt., review 0-49674  
 lanthanide(III) complexes, f-f transition intensities, general theory of solvent effect 0-18811  
 ligand fields calcs., strong and intermediate fields, tensor algebra 0-42922  
 magnetic superconductor, appl. of reformulated boson theory to mixed state 0-7050  
 Mischmetal-Ni,  $MMNi_5$  substituted hydrides for H storage appls. 0-45791  
 mixed valence compounds, charge dominated fluctuation props. comparison, mag. moments and ordering 0-54659  
 mixed valence compounds, spin dynamics, mag. neutron scatt., Mossbauer effect, XPS studies 0-39786  
 molybdates, cryst. growth, cryst. chem., and phys. props., book contrib. 0-44194  
 molybdenum chalcogenides, Chevrel phase correlation between struct. and supercond. transition temp. 0-7023  
 monazites, search for superheavy elements 0-36297  
 monochalcogenides, 4f-6s excitation energy, metallic and insulating elec. props. 0-44603  
 nickelates, form. conditions and props. 0-21270  
 niobate based ceramics, synthesis, struct., elec. cond., mag. props. (*Czech*) 0-45259  
 NMR, EPR, and Mossbauer effect, book contribs. 0-39883  
 non-metallic compounds, handbook 0-51972  
 oxalates, struct., IR absorpt. and Raman spectra (*French*) 0-32714  
 oxides, binary, struct. and props., book contrib. 0-45292  
 oxides, determ. by mass spectrometric complexometric method 0-3442  
 oxides, electronic structure rel. to valence, chem. bonding 0-54601  
 oxides, mixed, phase relations and struct., book contrib. 0-45293  
 oxides, thin films, in MOS struct., elec. props. and band struct. 0-7013  
 oxyphosphates,  $x\text{Ln}_2\text{O}_3 \cdot y\text{P}_2\text{O}_5$ , synthesis, characterisation and thermal stability 0-16256  
 perovskites, prep. and props. book contrib. 0-44193  
 photoemission, rel. to electronic struct., book contrib. 0-16157  
 pnictides, cryst. field splitting, press. depend. 0-24852  
 pnictides, prep. and props., book contrib. 0-54212  
 rare earth complexes, paramag., and shift reagents, NMR, book contrib. 0-53023  
 selenides, cryst. struct., book contrib. 0-54210  
 sesquioxide films, prep., struct. and props., general review 0-54556  
 Slater-Koster tables for f electrons 0-44461  
 solutions, absorpt. and fluoresc. spectra, book contrib. 0-45112  
 spin glasses 0-50132  
 structural, electronic, and mag. props., book 0-36785  
 sulphides, cryst. struct., book contrib. 0-54210  
 superconducting pairing, mag. ordering effect 0-15641  
 tellurides, cryst. struct., book contrib. 0-54210  
 ternary compounds, supercond. and antiferromag. coexistence 0-25030  
 theoretical chemistry, book contrib. 0-42919  
 trifluorides, bomb calorimetric determ. of enthalpy of formation 0-50879  
 tungstates, elec. cond. and thermoelec. power meas., band theory 0-20191  
 valence changes, book contrib. 0-39533  
 valence fluctuation type, replicate core level XPS probe 0-25521  
 valence fluctuations, electron-phonon coupling effect 0-20134  
 valence instabilities, rel. to electronic structure of  $GaMn_3(C_{1-x}N_x)$  (*French*) 0-34596  
 Cu-rare earth oxide-Y composite coatings, oxide and Y effect on coating precipitation 0-55554  
 $K_{6+3n}R_{4-n}(SO_4)_9$ , ( $n \approx 0.4$ ), cryst. struct. 0-28985  
 $Lu_2O_3-K_2O_3$  ( $K=Ho, Er, Tm, Yb, Y$ ), crystn. by Verneuil method 0-40254  
 $Na_3RSi_2O_{12}$  ( $R=Sm\text{ to }Lu, Y, Sc$ ), solid electrolytes, struct. characts. 0-1997  
 R (III) complex, octahedral, f-f transitions, mag. dipole intensities, vibronic coupling model 0-25404  
 R complex, formation and props., book contrib. 0-43204  
 R-M-B systems ( $M=transition\ metal$ ), phase diagrams and struct. considerations 0-16286  
 $RB_4$ , mag. and elec. props., metallic character 0-20386  
 $RCl_3 \cdot 6H_2O$ ,  $Gd^{3+}$  EPR, linear point charge model predictions 0-25200  
 $RCu_2Si_2$ , interconfiguration fluctuation system, NMR meas. 0-15817  
 $RFeO_3$ , cubic anisotropy consts. 0-11190  
 $RFeO_3$ , linear dichroism influence on Faraday effect 0-2737  
 $R_3Fe_2O_7-H$ , TGA-DTA meas., H absorption characts. 0-24600  
 $R_2FeSi_2$ , superconductivity 0-49968  
 $RGa_3(BO_3)_4$ , high temperature crystallisation, composition, struct., props. 0-40253  
 $RIr_4B_4$ ,  $NdCo_4B_4$  type struct., mag. behaviour 0-20375  
 $RIr_4B_4$ , supercond., magnetism and metastability 0-29501  
 $RMo_8S_8$  ( $Se$ ), supercond. and long range mag. order coexistence 0-15642  
 $RMo_8S_8$ , supercond. and magnetism coexistence (*Japanese*) 0-7025  
 $RNaMTa_2O_{15}$  ( $R=rare\ earth, M=K, Rb, Tl, Cs$ ), relative stability of struct. types, and piezoelec. props. (*French*) 0-49206



**rare earth compounds continued**

- RNbO<sub>4</sub>-CaWO<sub>4</sub>, phase transitions of fergusonite-scheelite (*French*) 0-19942  
 R(OH)<sub>3</sub>, R=La, Ce, Pr, Nd, Pm, Sm, Eu, Gd, Tb, Dy, Ho, Er, Tm, Y, Am, Cm, single cryst. X-ray lattice constants determ. 0-19766  
 RO<sub>3</sub>B<sub>4</sub>, NdCo<sub>3</sub>B<sub>4</sub> type struct., mag. behaviour 0-20375  
 RRh<sub>2</sub>B<sub>4</sub> and RMo<sub>2</sub>X<sub>8</sub> (X=S, Se), mag. order and supercond., neutron scatt. studies 0-44807  
 RRh<sub>2</sub>B<sub>4</sub>, NMR and sp. ht. in supercond. and mag. ordered phases 0-7037  
 RRh<sub>2</sub>B<sub>4</sub>, supercond. and long range mag. order coexistence 0-15642  
 R<sub>2</sub>S<sub>3</sub> condensates, struct. and optical transmittance 0-20727  
 R<sub>2</sub>(SO<sub>4</sub>)<sub>3</sub>·8H<sub>2</sub>O:Gd<sup>3+</sup>, EPR 0-20458  
 R<sub>2</sub>(SiO<sub>3</sub>)<sub>3</sub>, mag. susceptibility, temp. depend., 77-800K 0-20372  
 R<sub>1-x</sub>Sr<sub>x</sub>CoO<sub>3</sub>, R=La, Pr, Sm, Nd, Gd, ferromag. reson., Lande g-factor 0-25215  
 RTiO<sub>3</sub>, R=La, Nd, Sm, Gd, Y, cryst. struct. and cryst. chem. 0-1984  
 R<sub>2</sub>Ti<sub>2</sub>O<sub>7</sub>, pseudoperoxskite struct., nonlinear spectral and luminesc. charact. 0-29771  
 R<sub>2</sub>(V<sub>4/3</sub>W<sub>3/3</sub>)O<sub>7</sub>, (R=Gd, Tb, Dy, Ho, Er, Tm, Xb, Lu), synthesis and elec. props. 0-29914  
 R<sub>2</sub>Zr<sub>2</sub>O<sub>7</sub> (R=Nd, Sm, Gd, Dy, Er, Yb), Raman spectra, anion disorder characterization 0-25358  
 SiO<sub>2</sub>-RO-Na<sub>2</sub>O-Li<sub>2</sub>O (RO=MgO, CaO, SrO) glass-ceramic coating, optimisation of props. by selective oxide action 0-55552  
 Sr<sub>2</sub>RAiO<sub>5</sub> (R=La, Pr, Nd, Sm, Eu, Ga, Tb), monocrystals growth by flux method 0-20776  
 Sr<sub>2</sub>RFeO<sub>5</sub> (R=Nd, Sm, Eu, Gd), monocrystal growth by flux method 0-20776  
 YIG-RIG solid solns., magnetisation temp. depend. calcs. 0-20388

**rare earth elements** *see rare earth metals***rare earth metals**

- see also the individual metals e.g. cerium*  
 4f, electron impact excited soft X-ray spectra, resonances and many body effects 0-50468  
 APS, position of unoccupied 4f levels 0-16125  
 Archæan granite composition in Yellowknife, Northwest Territories, Canada 0-4007  
 band structure calcs. 0-15441  
 basalt isotopic and element composition, Reykjanes Peninsula, Iceland 0-21725  
 basaltic achondrite meteorites, rare earth element abundance patterns rel. to origin 0-36581  
 bone uptake, Mossbauer study 0-8019  
 chemical analysis by selective excitation of probe ion luminesc. 0-40797  
 conduction electron interactions, anisotropic 0-15492  
 conference, St. Pierre-de-Chartreuse, France (Sept. 1978) 0-12844  
 elastic properties, connection with electron struct. (*Russian*) 0-19895  
 electrical resistivity, high temp., scatt. mechanisms 0-39553  
 electronic excitation energies calcs. 0-54592  
 electronic structure rel. to valence, chem. bonding 0-54601  
 energy transfer and two-centre optical transitions in OH<sup>-</sup> and rare earth double-doped solid 0-7398  
 excitation energies, 3d electrons, relativistic calcs. 0-20109  
 4f level energy position relative to Fermi energy 0-6764  
 films, prep., struct. and props., general review 0-54556  
 fission product isotopes, separation in thin-layer chromatography (*German*) 0-37635  
 geochemistry and mineralogy, book contrib. 0-46157  
 Hall effect, 80-1000K 0-15504  
 heat capacity near melting pt., vacancy mechanism of melting 0-15221  
 impurities in Ba silicate and phosphate glasses, quenching of Nd<sup>3+</sup> luminesc. 0-25449  
 impurities in s-p metals, isomer shifts 0-15839  
 industry review 0-25537  
 ion energy separation, 4f<sup>N</sup>-4f<sup>N-1</sup> nl, host depend. 0-49676  
 ionic crystal:R, intra- and inter-ionic multiphonon transitions 0-34973  
 ions, ligand-induced pseudoquadrupole absorpt., vibronic contribs. 0-52978  
 ions in aq. solns., optoacoustic spectroscopy using pulsed dye laser for micron thick film 0-42265  
 ions in cubic field, anal. of absorption spectra 4f<sup>N+1</sup>→4f<sup>N</sup>5d-6s 0-7382  
 ions in soln., absorpt. and fluoresc. spectra, book contrib. 0-45112  
 isotopic analysis, Oklo natural fission reactor fluence distrib. meas. (*French*) 0-21759  
 isotopic analysis at Oklo natural fission reactor (*French*) 0-21761  
 lasers, solid, gas and liq., book contrib. 0-53306  
 liquid, resistivity 0-24865  
 magnetic properties, nonlinear s-f exchange interaction effect 0-15711  
 metal:rare earth, effective exchange interaction model 0-25127  
 neutron activation anal., geochem. of genesis of ore deposits (*German*) 0-30301  
 p-nitrobenzoic acid:rare earth laser materials, vibr. spectra, wavelength 125 to 500 nm 0-2769  
 NMR, EPR, and Mossbauer effect, book contribs. 0-39883  
 Oklo natural reactors, data on stability and remobilisation, summary (*French*) 0-21771  
 oxidation potential 0-5495  
 paramagnetic metals, polarised neutron studies of field induced magnetisation 0-25084  
 photoemission, rel. to electronic struct., book contrib. 0-16157  
 purification, laser methods 0-16712  
 RKKY interactions, anisotropic effects from spin-split bands 0-15712  
 semi-infinite surface with magnetic structure, density of states calc. 0-10851  
 separation from clays, complexation method 0-3442  
 structural, electronic, and mag. props., book 0-36785  
 submonolayer films, electronic phase transitions, heat of absorption 0-24736  
 valency, ionicity and electronic config. 0-18775  
 XPS and bremsstrahlung isochromat spectra of f<sup>N+1</sup>, f<sup>N-1</sup> states 0-40220  
 CaF<sub>2</sub>:Eu,R, thermolum. meas. 0-2870  
 CaF<sub>2</sub>:rare earth ion, hydrogenated, local lattice modes, spectroscopy 0-50375  
 CdF<sub>2</sub>:rare earth, electronic props., compared to CaF<sub>2</sub> (*French*) 0-49662  
 CsMnCl<sub>3</sub>(Br):R<sup>3+</sup>, rare earth doped, energy transfer, emission spectra obs. 0-20684  
 H, and He, stopping powers meas. 0-42904  
 KMnCl<sub>3</sub>:R<sup>3+</sup>, rare earth doped, energy transfer, emission spectra obs. 0-20684

**rare earth metals continued**

- R doped crystals, nonradiative processes, book contrib. 0-55188  
 R-activated phosphors, chemistry and physics, book contrib. 0-55187  
 Rb<sub>2</sub>MnCl<sub>4</sub>:R<sup>3+</sup>, rare earth doped, energy transfer, emission spectra obs. 0-20684  
 YAG:rare earth metal, US absorpt. meas., relax. model 0-24539

**rare gases** *see inert gases***rarefied fluid dynamics**

- see also atomic beams; Knudsen flow; molecular beams*  
 aerosol beam instruments, nozzle inlet design 0-6183  
 atomic beam, produced by laser-metal surface impact 0-5637  
 atomic beam, produced from He nozzle flow, high speed ratio 0-5636  
 atomic beam production, He skimmed from freejet zone of silence 0-5635  
 centrifuged flow with recirculation, book contrib. 0-1604  
 channel, annular, long, free-mol. and radiative transport, approx. analytical soln. 0-6165  
 cluster formation, in rarefied nozzle flowfield 0-5639  
 compressible and incompressible flows, recent theoretical and expt. developments, book 0-1620  
 diffusophoresis of nonspherical aerosol particles in a free molecular flow 0-43765  
 discrete kinetic theory, maths. and numerical aspects, Couette flow appls. 0-19413  
 electrically conducting rarefied gas near accelerated porous plate, MHD flow 0-14836  
 evaporation, quasisteady half-space problem, gas kinetics theory and expt. 0-6106  
 evaporation, quasisteady one-dimens. problem, entropy-balance relation 0-6168  
 evaporation-condensation two-surface problem, in presence of noncondensable gas 0-6169  
 evaporation-effusion problem, rarefied regime, nonlinear numerical soln. 0-6167  
 finite length plate in supersonic low density flow, surface pressures and corrections 0-14741  
 flat plate trailing edge in rarefied supersonic airflow, boundary layer 0-24046  
 free jet, N<sub>2</sub><sup>+</sup> UV spectra for rot. temp. 0-6184  
 free molecule heating of micron size particles at hypersonic speeds 0-19442  
 gas, nonisothermal flow in cylindrical capillary, calc. of vel. profile and flux 0-6098  
 gas clouds released at satellite orbital velocity, dynamics expts. 0-14748  
 gas flow over a flat plate, influence of internal degrees of freedom 0-6099  
 H-matrix for time depend. problems in rarefied gas dynamics 0-43739  
 heat transfer in rarefied MHD laminar channel flow 0-48687  
 hypersonic cavitation of high and low gas mixtures at low density (*German*) 0-1651  
 initial shock parameters for explosion in rarefied gas 0-53815  
 ionospheric rocket-borne mass spectrometer, Monte Carlo prediction of +ve ion collection 0-8459  
 isotope separation techniques based on vel. slip in freejet expansions 0-19441  
 mass transfer in cylindrical channel with evaporation and condensation at walls 0-6101  
 MHD channel flow, effects of external cct. 0-33630  
 molecular gas radiation in the thermal entrance region of a duct 0-6051  
 n-incompressible and immiscible rarefied gases, pulsating flow between two plates 0-10306  
 nozzle flow formation of cluster beam, high energy beam 0-5638  
 plasma, nonisothermal, transport processes and Lenard-Balescu eqn. 0-6222  
 shock wave structure close to wall, book contrib. 0-1650  
 shock waves in monatomic gas, ionising large Mach numbers 0-6096  
 Shuttle/Spacelab platform in near Earth ionospheric plasma, aerodynamics 0-8517  
 sphere, drag in low velocity rarefied gas flow 0-48752  
 surface flow of dilute gas in model pores, free mol. flow calc. in adsorbent force field 0-6100  
 transition flow, macroscopic theory (*Japanese*) 0-1647  
 two-dimensional long slots, rarefied gas transition flow 0-43738  
 Ar, clusters in supersonic beam, electron diffr. study 0-5655  
 CO<sub>2</sub>, free jet, homogeneous condensation scaling law 0-6121  
 CO<sub>2</sub>, rarefied jet beam, Raman scatt., for rot. temp. and density 0-6185  
 H<sub>2</sub>, cluster beam formation, from nozzle flow, isotope effect 0-6127  
 N<sub>2</sub>, flow meas. by electron beam-body interactions 0-6186  
 Na vapour jet target, gating and pumping action 0-10281

**rarefied gas dynamics** *see rarefied fluid dynamics***rarefied gas flow** *see rarefied fluid dynamics***Rayleigh-Benard instability** *see flow instability***Rayleigh law** *see Rayleigh scattering***Rayleigh limit** *see Rayleigh scattering***Rayleigh scattering**

- acetonitrile, soln., high press., mol. reorientation, correl. times, depolarised Rayleigh scatt. obs. 0-29748  
 agglomerates of small spheres, scatt. efficiency factors 0-1131  
 atmosphere, aerosol effects on polarisation of scatt. light from point source (*Russian*) 0-4106  
 atmosphere, sunlight scattering, Rayleigh and Mie theory 0-56605  
 atomic Rayleigh scattering, 0-10 mc 0-9536  
 CBOOA, isotropic, nematic, smectic-A phases, Brillouin scatt. 0-11421  
 collision-induced spectrum, intermediate density, second freq. moment, appl. to Ar 0-24125  
 colloidal dispersions, birefringence in Rayleigh and anomalous diff. approximations 0-29710  
 crystals, book 0-2774  
 Delbruck and Rayleigh scattering below 5 MeV 0-13456  
 disperse systems, light scatt., decay in orientationally induced var., Rayleigh approx. 0-45576  
 electron-phonon system, weakly coupled, resonant light scatt. and luminescence 0-40100  
 fluid, of isotropic mols., DID Rayleigh and Raman depolarised scatt., lattice-gas model 0-10356  
 fluids, polarisation state of light scatt. in elec. and mag. fields, symmetry indications 0-29751  
 forced, for anal. of light-induced grating structs., review 0-20646  
 forced scattering, principle techniques and expts., review 0-34938



**Rayleigh scattering continued**

- gases and vapours, degree of depolarisation of scattered light, meas. accuracy, Raman-lines effect 0-1737  
 Gaussian light, partially polarised, photon statistics 0-19012  
 inverse scattering problem in Rayleigh-Debye approx., diameter distrib. functions of helical structs. 0-27182  
 liquid binary mixtures of optically anisotropic molecules, depolarized Rayleigh scatt. 0-40122  
 liquid structure and dynamics from light scatt. spectra 0-55105  
 liquids, depolarised Rayleigh scatt., nonlorentzian behaviour, 3-variable theories (*French*) 0-25395  
 liquids, molecular, depolarised light scatt., flow birefringence and local order 0-45094  
 localised electron nonequilibrium vibration interaction secondary radiation spectrum 0-2778  
 low temp. plasma diagnostics by reson. Rayleigh scatt. 0-48980  
 malononitrile, dispersive phase transition, 294.7K, Raman and Brillouin-Rayleigh scatt. obs. 0-16047  
 metmyoglobin, dynamics study using Rayleigh scatt. of Mossbauer radiation 0-40963  
 molecular spectroscopy book 0-27052  
 nitrobenzene, in acetone-isopropanol soln., Rayleigh scatt. and viscosity 0-5550  
 nitroethane-isooctane mixture, depolarised Rayleigh scatt. near crit. point 0-45089  
 nuclear-gamma ray scatt. using (n, $\gamma$ ) photons 0-18288  
 PMMA, amorphous polymer, Rayleigh scattering of Mossbauer  $\gamma$ -rays 0-39926  
 polyatomic fluid, local dynamics, spectroscopic studies, summer school lecture series 0-6343  
 polycrystalline materials, freq. and grain size dependency of US attenuation 0-50783  
 polymer, total integrated light scatt. intensity 0-45092  
 polystyrene, polarised Rayleigh scatt. near glass-rubber relax., photon correl. spectroscopy 0-40124  
 quartz crystal, opalescence near  $\alpha$ - $\beta$  transition, static model rel. to domain wall form. 0-11420  
 radiation field polarized, asymptotic characts. for low absorpt., appl. to nonconservative Rayleigh scatt. 0-5686  
 resonant scattering of light by slowly fluctuating localized electrons 0-7365  
 stratified fluid layer, propagative thermal excitations, Rayleigh scatt. meas. (*French*) 0-33590  
 transition quasilinear spectra of resonant secondary emission (*Russian*) 0-16102  
 two component reacting fluid, density fluctuations, light scatt. spectrum 0-25397  
 water dodecane potassium oleate hexanol, micro emulsion, Rayleigh scatt., micellisation (*French*) 0-43055  
 water toluene sodium dodecylsulfate butanol, micro emulsion, Rayleigh scatt., micellisation (*French*) 0-43055  
 Ar, depolarised Rayleigh scatt., mol. dynamics calcs., fluid density effects 0-24123  
 Ba<sub>0.54</sub>Sr<sub>0.46</sub>Nb<sub>2</sub>O<sub>6</sub>, line broadening effect in Rayleigh scatt. of Mossbauer radiation 0-50238  
 BaTiO<sub>3</sub>, line broadening effect in Rayleigh scatt. of Mossbauer radiation 0-50238  
 CS<sub>2</sub>, liq., props. from allowed light scatt. spectra 0-25364  
 Co<sup>+</sup>, Rayleigh and Compton scatt., differential cross section determ. 0-52912  
 D<sub>2</sub>+D<sub>2</sub>, collision effect on depolarised light scatt. linewidths 0-53059  
 Fe, 3d<sup>6</sup>4s<sup>2</sup> and 3d<sup>7</sup>4s configs., Rayleigh and Compton scatt., differential cross sections 0-52912  
 Fe<sup>+</sup>(Fe<sup>2+</sup>), Rayleigh and Compton scatt., differential cross section determ. 0-52912  
 H atoms, Rayleigh scatt. from n=2 states, fusion plasma diagnostics appls. 0-43002  
 H<sub>2</sub>, D<sub>2</sub> and HD, intermol. collision process obs. using light scatt. expts. 0-53001  
 H<sub>2</sub>, diffusion flame, Rayleigh temp. profiles meas. 0-16692  
 H<sub>2</sub>+H<sub>2</sub>, collision effect on depolarised light scatt. linewidths 0-53059  
 KD<sub>2</sub>PO<sub>4</sub>, Brillouin spectrum and broad central component, depend. on scatt. wave vector direction 0-34931  
 KD<sub>2</sub>PO<sub>4</sub>, Rayleigh scatt. and narrow central component, depend. on scatt. wave vector direction 0-29747  
 $\alpha$ -LiO<sub>3</sub>, Raman spectra behaviour in electrostatic field (*Chinese*) 0-7333  
 Na, reson. line, laser excitation, combustion Rayleigh scatt., at. flame fluoresc. spectroscopy 0-42972  
 Ni<sup>2+</sup>, Rayleigh and Compton scatt., differential cross section determ. 0-52912  
 O (O<sup>+</sup>) (O<sup>2+</sup>), Rayleigh and Compton X-ray scatt. cross sections in plasma 0-43884  
 Sb, Mossbauer radiation, Rayleigh scatt., Debye-Waller factor determ., annealing effect 0-39963  
 Sb<sub>2</sub>Te<sub>3</sub>, Mossbauer radiation, Rayleigh scatt., Debye-Waller factor determ., annealing effect 0-39963  
 Te, amorphous, Rayleigh scatt. of Mossbauer radn., lattice dynamics 0-15845

**Rayleigh-Taylor instability** *see flow instability*

**Rayleigh waves**

*see also surface acoustic waves*

- acoustic microscope, ray interpretation of material signature 0-1386  
 dispersion, rel. to mantle structure under north central Italy 0-3977  
 dispersion function computations for unlimited freq. values 0-21837  
 elastic surface waves propag., characts. for SAW filters, book contrib. 0-1378  
 energy flux for trains of inhomogeneous plane waves 0-46817  
 ferrous material, wave vel. and attenuation 0-2258  
 isotropic materials, third-order elastic moduli meas. using Rayleigh waves (*Russian*) 0-50786  
 magnetothermoelastic Rayleigh waves with thermal relaxation in uniform magnetostatic field 0-2617  
 microcracks, Rayleigh waves interaction, and extension 0-39214  
 microseisms obs. at New York Rayleigh and Love wave characts., geologic control 0-26462  
 seismic, fundamental mode and harmonic waves, appl. to distant earthquakes focal depths determ. 0-21654  
 seismic study of crustal and upper mantle structure beneath Apennines 0-46153  
 seismic wave dispersion and rifting in Tyrrhenian Sea 0-56445

**Rayleigh waves continued**

- seismic waves under Pacific Ocean, group vels. and response 0-41398  
 semi-infinite isotropic elastic medium, reson. scatt. of Rayleigh waves by mass defect 0-20025  
 shell, cylindrical, Rayleigh wave propag. using elasticity theory (*Russian*) 0-38307  
 surface-tension dispersion of Rayleigh waves 0-14513  
 transmission coeffs. through vertical interface 0-46144  
 transmission prevention, trench performance, seismic model experiments 0-24727  
 Walvis Ridge, lithospheric struct. from Rayleigh wave dispersion 0-41412  
 Al, plastic deform. effect on third-order elastic moduli, dislocation anharmonism (*Russian*) 0-50786  
 KCl, irradi. with intense nanosecond electron beam, super-Rayleigh vel. of brittle fracture front 0-6458  
 LiNbO<sub>3</sub>-CdS, layered structure, transverse acousto-electric current 0-44669

**reactance, electric** *see electric reactance*

**reaction kinetics**

- see also catalysis; chemical exchanges; chemical reactions; explosions; potential energy surfaces for collision processes; reaction kinetics theory; reaction rate constants*  
 actomyosin kinetic anal., review 0-21441  
 alkali silicate glasses in aqueous solutions, leaching kinetics rel. to surface pot. 0-11803  
 aqueous soln. reaction kinetics meas. microwave apparatus 0-3470  
 7-azaindole dimers, photoautomerisation by double proton transfer, fluoresc. kinetics 0-11880  
 Belousov-Zhabotinskii reaction, existence of solitary travelling wave solns. 0-35525  
 Bray reaction, kinetics obs. (*French*) 0-7788  
 carbonaceous chondrites, reduction kinetics, Mossbauer obs. 0-41777  
 corrosion pit, convective diffusion 0-40601  
 cyclobutane-1, chem. activated by nucl. recoil reaction, energy transfer interpret. 0-25985  
 DC plasma jet, NO synthesis, chem. kinetics obs. 0-38728  
 electrochemistry, double-layer capacity and kinetic parameters, simultaneous meas. instrument 0-40704  
 electron attachment to O<sub>2</sub> and H<sub>2</sub>O in flames, kinetics 0-3349  
 electron transfer, in rigid medium, exothermic rate restrictions 0-30224  
 epoxy resin, curing investigation by polarisation current method 0-3345  
 esterification kinetic study by monitoring pitch changes in cholesteric liq. cryst. solvent 0-7786  
 ethyl radical decomposition, mol. dynamics, trajectory studies 0-7780  
 fast kinetics studied by NMR, review 0-55662  
 fast reaction kinetics meas. by ESR of free radicals 0-21286  
 flame, counterflow diffusion, struct. in elec. field, interferometric obs. 0-16685  
 flames, effects of finite reaction rate and molecular transport on premixed turbulent combustion 0-3348  
 Fourier transform ion reson. spectroscopy of ions undergoing collisions with mols. 0-35598  
 groundwater, confined, form. rate of chem. composition 0-46207  
 high temperature metallic species, absorpt. and fluoresc., high temp. fast flow reactor technique 0-42231  
 high temperature system characterisation, models, phys. and chem. reference data sources 0-41958  
 high-pressure stopped-flow apparatus up to 3 kbar 0-3350  
 interstellar dust condensation in clouds, importance of reaction kinetics 0-26939  
 ion+molecule, electronic states, kinetic energy, molecular beams obs. 0-20230  
 ion+molecule reactions, kinetics, conf., La Baule, France (1978) 0-27043  
 ion-molecule equilibria in solvolysis, secondary  $\beta$  <sup>2</sup>H isotope effects, hyperconjugation 0-50874  
 IR laser chemistry research using mol. beam (*German*) 0-55683  
 labile species, electron photoejection, reaction kinetics characterisation 0-26089  
 Lagrange-Hamilton formalism, concept of chemical inertia 0-7756  
 Landau-Zener problem, random nature of motion role in intersecting terms problem 0-8937  
 masked antifogging, hydrolysis stability, photographic process depend. (*German*) 0-45530  
 metal, H<sub>2</sub>-diffusion-rate-limited hydriding and dehydriding kinetics 0-35764  
 metal-gas reactions, surface chemiluminesc. study 0-55708  
 metal-slag interface, interaction under diffusion conditions, impurity oxidation (*Russian*) 0-35390  
 metals and alloys, chemicothermal treatment, process kinetics 0-35415  
 methane gas-C(dissolved)+2H<sub>2</sub> (gas), kinetics on Fe and Fe-Ni surface 0-55712  
 micelle dissociation-recombination kinetics, stochastic model 0-30291  
 multistep reaction rate eqn. integration, interactive computer program system 0-31469  
 myosin kinetic anal., review 0-21441  
 nonequilibrium molecular system, time-depend. kinetic-thermodynamic description 0-9877  
 organic reactions in solid state 0-21309  
 oscillating chemical reaction, entrainment by periodic light pulses of variable freq. (*French*) 0-35551  
 2'-oxindan (dihydroisobenzofuran) spiropyran, photochromic transforms, spectrokinetic study 0-30259  
 photosynthesis, redox conversion kinetics in the electron transport chain 0-40950  
 plasma, nonideal, elem. excitations and macroscopic props., review 0-43842  
 polyether-urethane elastomers, crosslinked, three dimensional polymerisation, kinetics, gel. form., mech. props. (*Russian*) 0-7792  
 shock initiation, vol. of activation determ. 0-16683  
 silicate+Ca(OH)<sub>2</sub>, reaction rates 0-26006  
 silicate+Portland cement, reaction rates 0-26006  
 solids, reactivity control, review 0-50853  
 solvent effects, semiempirical model 0-25986  
 steel, Cr-Mo (2.25,1 wt.%), exposed to H<sub>2</sub>-H<sub>2</sub>O-H<sub>2</sub>S environment, fatigue crack growth 0-40623  
 stirred tank reactor, homogeneous p-order reactions, mixing effects, two parameters model 0-14843  
 superconducting composites, bronze process, metallurgy 0-3004



## reaction kinetics continued

thermal fluctuation of self oscillating reaction system under periodic external force 0-50828  
 thionine coated electrode for photogalvanic cells, kinetics 0-35696  
 transition metal complexes, reaction mechanisms and solvent effects 0-26012  
 turbulent diffusion, flames, high Reynolds number, rocket exhaust appl., chem. processes theory 0-45504  
 unimolecular dissociation, master eqns., analytic theory of extrema 0-50841  
 Al dissolution in HCl soln., inhibition by hydrazine derivatives 0-50759  
 Al magnetron sputtering target, oxidation in Ar/O<sub>2</sub> mixtures 0-55291  
 Al<sub>2</sub>Ge<sub>2</sub>O<sub>7</sub>, reduction processes by C, kinetic analysis, reaction products (Russian) 0-55644  
 Ar+NO<sup>+</sup>, reaction product ratios, 300K 0-7783  
 Ar<sup>+</sup>+NO, reaction product ratios, 300K 0-7783  
 BCl<sub>3</sub>+methane reaction, laser-induced, vibr. excitation influence on reactivity, isotope selectivity 0-11921  
 Ba(PO<sub>3</sub>)<sub>2</sub>, hydrolytic decomp. 0-21271  
 CO, oxidation over Ir, tracer studies on reaction path and kinetics of CO oxidation 0-7857  
 CS<sub>2</sub>, aerosol form. by laser, kinetics study and photoreaction products chem. nature study 0-21324  
 CaF<sub>2</sub>:Eu, oxidation and reduction of Eu, EPR and optical studies 0-25199  
 CaGeO<sub>3</sub>, reduction processes by C, kinetic analysis, reaction products (Russian) 0-55644  
 Cl<sub>2</sub>+H<sub>2</sub>(H<sub>2</sub>S)(methanethiol), laser-initiated chain reactions, rates, mechanisms, chemiluminesc. obs. 0-55651  
 F<sub>2</sub>+Mg(Ca)(Sr)(Ba), crossed beam chemilum., kinetics and mechanisms 0-21264  
 Fe surface, adsorbed O<sub>2</sub> effect on chem. reaction kinetics 0-55572  
 Fe/Cu<sub>2</sub>O displacement reaction kinetics at temps. between 800 and 1050°C 0-21278  
 Fe-Cr (24 wt.%), low temperature oxidation, kinetics, oxide morphology 0-11838  
 (Fe<sup>2+</sup>+Fe<sub>1-x</sub><sup>3+</sup>+M<sub>x</sub><sup>3+</sup>)O<sub>4</sub><sup>2-</sup> (M<sup>3+</sup>=Al<sup>3+</sup>, Cr<sup>3+</sup>), oxidation to  $\gamma$  lacunar spinels, rate law vs. O<sub>2</sub> press. 0-50849  
 FeO surface, water-gas shift reaction kinetics 0-11949  
 Fe<sub>2</sub>O<sub>3</sub>, direct reduction by H<sub>2</sub> reaction kinetics 0-40689  
 GaAs hydrothermal oxidation kinetics, exam. 0-40566  
 Ge+Br<sub>2</sub>, surface reaction, rate-limiting step, ellipsometric and photochem. meas. 0-16730  
 GeO formation from Ge-GeO<sub>2</sub> mixtures, gasification kinetics (Russian) 0-21273  
 GeO<sub>2</sub>, reduction processes by C, kinetic analysis, reaction products (Russian) 0-55644  
 H, thermochemical prod. by H<sub>2</sub>O decomposition, impact of thermal burdens and kinetics 0-35787  
 H, thermochemical production by steam reforming of methane, kinetic anal. 0-35788  
 H<sub>2</sub> sorption/desorption by ternary LaNi<sub>5</sub> type alloys, reaction kinetics 0-45813  
 HBr, laser emission at 4  $\mu$ m based on chem. generation of Br atoms 0-9878  
 HCl, in nonequib. plasma, electron energy distrib. function and dissociation kinetics 0-11882  
 HF chemical laser, time-depend. kinetic-thermodynamic description 0-9877  
 H<sub>16</sub>MoO<sub>3</sub> bronze, form., kinetic, thermodynamic investig. (French) 0-45247  
 H<sub>2</sub>SO<sub>4</sub>-KBrO<sub>3</sub>-KBr-Mn<sup>2+</sup> system, chem. automat with three steady states 0-7769  
 I laser, photolytically pumped, chem. kinetics 0-48235  
 InCl disproportionation under influence of high pressure 0-16660  
 InP hydrothermal oxidation kinetics, exam. 0-40566  
 Ir (110), adsorption of CO and reaction with O<sub>2</sub>, transient study 0-30284  
 KO<sub>2</sub>, non-isothermal decomp. kinetics 0-16649  
 KO<sub>2</sub>, thermal decomp. macrokinetics, differential thermal anal. 0-16650  
 LiOH(D)(T), thermal decomposition rates 530-690K, activation energy and enthalpy meas. 0-3321  
 Mg nitridation in HF discharge, temp. effect 0-3399  
 Mg/Mg<sub>2</sub>Cu eutectic, hydriding and dehydriding kinetics obs. by press. sweep method 0-35765  
 Mg+O<sub>2</sub>=MgO+O, shock-tube study of evap. and oxidation kinetics 0-16651  
 Mg<sub>2</sub>GeO<sub>4</sub>, reduction processes by C, kinetic analysis, reaction products (Russian) 0-55644  
 Mo, nitriding kinetics 0-35415  
 Mo<sub>2</sub>C, corrosion and electrochem. props. in aq. H<sub>2</sub>SO<sub>4</sub>, HCl, HNO<sub>3</sub> and KOH solns. 0-11813  
 MoF<sub>6</sub> reduction by H, chemical kinetics eqn., adsorbed component interactions (Russian) 0-35569  
 MoO<sub>2</sub> powder bed, H<sub>2</sub> reduction kinetics 0-16230  
 N heterogeneous atom recomb. on glass, Langmuir-Rideal mechanism 0-7853  
 NaO<sub>2</sub>, non-isothermal decomp. kinetics 0-16649  
 NaO<sub>2</sub>, thermal decomp. macrokinetics, differential thermal anal. 0-16650  
 Na<sub>2</sub>O-SiO<sub>2</sub>-Ga<sub>2</sub>O<sub>3</sub>-Al<sub>2</sub>O<sub>3</sub> glasses in mixed AgNO<sub>3</sub>-NaNO<sub>3</sub> melts, ion exchange 0-21282  
 Nb, corrosion kinetics in sulphidizing atm. 0-35396  
 Nb, nitriding kinetics 0-35415  
 Nd<sub>2</sub>O<sub>3</sub>-HfO<sub>2</sub> system, phase relationships 0-35169  
 Ni-Mn, hydrogenation kinetics, magnetisation, interstitial H influence 0-35528  
 NiO-ZnO, solid solution, exam. of mechanism and kinetics of reaction with Fe<sub>2</sub>O<sub>3</sub> ferrite formation 0-3309  
 O(P), translationally hot, in Earth atmosphere, energy distrib. function 0-21811  
 PtO<sub>2</sub>, sputtered film, optical props. under H<sub>2</sub> reduction 0-20728  
 $\beta$ -Sb<sub>2</sub>O<sub>3</sub> reduction to Sb powder, atomic H effect 0-2978  
 Si:P(As)(B)-SiO<sub>2</sub> interface oxidation kinetics, high doping levels, experiment 0-11828  
 Si-H, amorphous, thermal stability and decomp. kinetics 0-24758  
 Si-SiO<sub>2</sub>, bonding at (111) interface, stoichiometry and kinetics, synchrotron radiation photoemission spectroscopy 0-24744  
 Si-SiO<sub>2</sub> interface oxidation kinetics, high doping levels, theory 0-11827  
 SiC-fission product reaction kinetics in HTGR TRISO UC<sub>2</sub> and UC<sub>2</sub>O<sub>2</sub> fuel in thermal gradient 0-47570

## reaction kinetics continued

SiO<sub>2</sub> polymerisation and deposition from dil. solns., kinetics, 5-180°C 0-7790  
 SiO<sub>2</sub>, vaporisation in steam atmosphere 0-44306  
 SiO<sub>2</sub>, deposition by reactive sputtering of Si in magnetron sputtering system, reaction kinetics 0-49553  
 SmCo<sub>5</sub> hydriding kinetics, inverse over pressure effect 0-55944  
 SmCo<sub>5</sub>, thin film, hydride form., kinetics, mag. monitoring 0-35571  
 T+HD hot atom exchange reactions, trajectory calcs. 0-26037  
 Ta<sub>2</sub>N film, high temp. nitriding kinetics depend. on press. (Russian) 0-50838  
 UO<sub>2</sub>-zircaloy-4, reaction kinetics at high temps., O<sub>2</sub> diffusion 0-16667  
 WF<sub>6</sub>, mechanism of heterogeneous reduction by H<sub>2</sub> (Russian) 0-21265  
 WO<sub>3</sub> reduction with H, starting specific surface effect on kinetics 0-11599  
 ZnS-CdS, equimolar solid soln. formation kinetics 0-39289

## reaction kinetics models and mechanisms see reaction kinetics theory

## reaction kinetics theory

A+A<sub>n</sub>=A<sub>n+1</sub><sup>\*</sup>, cluster dynamics, classical trajectory study 0-3316  
 absolute rate theory, ab initio calcs., elementary gas phase reaction 0-7757  
 acetic acid-formic acid, 'dimer', tritium  $\beta$ -decay causing H<sup>+</sup> transfer, ab initio MO calc. 0-3391  
 adiabatic nuclear group transfer processes in condensed media, electronic energy hypersurfaces 0-25982  
 aromatic compounds, oxidative bromination, chem. oscills. 0-3335  
 atom+diamon, microcanonical reaction probability, classical transition state theory 0-50842  
 atom+diamon reactive collision, three dimens., exact classical formulation in natural coords. 0-50835  
 Belousov-Zhabotinski reaction, chem. oscill. mechanisms 0-3304  
 Belousov-Zhabotinski reaction, oscill., thermal props. 0-7762  
 Belousov-Zhabotinski reaction, nonlinear effects 0-3302  
 bifurcation diagram of model chemical reactions 0-3303  
 bistable reaction system, stochastic dynamics investig. of discrete trimolecular chemical model 0-16645  
 Briggs-Rauscher reaction, chem. oscill. obs. 0-3336  
 Brusselator, dynamic correl. functions, Mori-Zwanzig formalism 0-25988  
 catalysis, heterogeneous, vibr. excitation, classical trajectory calcs. 0-26045  
 catalytic pellet, isothermal n-order decomposition reaction, steady state stability anal., topological degree and Lyapunov method 0-30280  
 chaos and strange attractors 0-7760  
 chemical evolution far from equilibrium, concepts (French) 0-7761  
 chemiluminescence reactions, electron exchange initiated, kinetics correl. with free energy changes 0-50856  
 competitive decomposition and stabilisation models for collisional efficiency in external activation systems 0-25989  
 decomposition, reaction rate calc. by differential quotient 0-25990  
 diamon+atom, cross section, translational excitation features, dynamical model 0-16655  
 diffusion controlled reactions, correlated and uncorrelated particle pairs 0-45477  
 diffusion-controlled chemical reactions modeled by continuous-time random walks 0-3297  
 diffusion-controlled reaction kinetics 0-16643  
 dissipative structures in chemical systems, nonlinear effects 0-3302  
 double well potential, transfer and tunnelling rates, density matrix calcs. 0-30209  
 Eckart barrier tunnelling, Arrhenius plot curvature 0-3298  
 electrochemical reaction, metal surface adsorbed surfactant effect 0-40703  
 Faddeev equations and Franck-Condon models for chemical reactions, appl. to H+Cl<sub>2</sub> 0-35507  
 formamide dimer, tritium  $\beta$ -decay causing H<sup>+</sup> transfer, ab initio MO calc. 0-3391  
 formic acid dimer, tritium  $\beta$ -decay causing H<sup>+</sup> transfer, ab initio MO calc. 0-3391  
 gas mixtures, kinetic eqn. 0-25983  
 Hafke-Gilles reaction, oscill., thermal props. 0-7762  
 intermolecular energy transfer following kinetically controlled chem. activation, multistep deactivation processes 0-25985  
 interstellar molecules, collision-induced dissociation 0-17632  
 intrinsic field theory, intrinsic reaction coordinate approach 0-11877  
 ion-molecule association reacs., gas phase, statistical phase space theory approach 0-50839  
 ion-molecule reaction, exothermic, rate coefficient, transition state method 0-40688  
 isomerisation, model reaction, SCF-SI theory calcs. 0-23399  
 Kramers' theory, accuracy anal. 0-7758  
 Kramers theory of friction and vel. in chemical kinetics 0-50826  
 Langevin theory, generalised, for many-body problems, formulation and equiv. harmonic chain representation 0-35504  
 metals, electrocrystallisation and passivation kinetics, multiple stationary states and dissipative structs. theory (French) 0-7804  
 metastable and unstable states relax., analytical theory of extrema 0-50829  
 micellar diffusion-controlled reaction kinetics 0-30213  
 micellar interface, reaction kinetics, rotamer population, fast proton transfer 0-26050  
 micellar phase dissoc.-recombination kinetics, stochastic model 0-55628  
 molecular dynamics simulation of chemical reactions in solution 0-40673  
 molecular models of condensed systems and interfaces (German) 0-20062  
 monotonic time laws, kinetic process anal. (German) 0-11875  
 multi-component one dimensional chemical kinetics calculations, new algorithm development 0-45479  
 multiple stationary states systems, meas. of stability and relative stability 0-3338  
 non-ionic reactions, temp. and press. effect on kinetic and thermodynamic parameters 0-3300  
 nonlinear reaction-diffusion equations, pattern selection at the bifurcation point 0-50827  
 oil-water interface, chem. and hydrodynamic instabilities (French) 0-7789  
 open chemical reaction system with exactly evaluable limit cycle oscillations 0-21260  
 open chemical system, noise-induced transitions 0-3337  
 oscillating reactions, thermal props. 0-7762  
 polymer network formation, relaxational props. variation 0-38961  
 proton transfer reactions, kinetic isotope effects, quantum theory 0-3301



## reaction kinetics theory continued

- pumped chemical system, stationary states, relative dynamic stability, model calc. 0-30211  
 quantum reactive scatt. theory, 3-dimens. 0-55637  
 reaction-diffusion phenomena, singularity theory, calcs., nonlinear partial differential eqns. appls. 0-4510  
 solid-gas reactions, existence of instabilities 0-7861  
 spherical reaction diffusion systems, steady state spatial patterns, mitosis secondary bifurcation theory 0-40672  
 surfactant inhibition of electrochem. reaction rate, random error effect on characteristic parameters 0-40705  
 synergetics, chemical processes far from equilb., conf. Bordeaux, France (Sept. 78) 0-3334  
 system far from equilibrium, stochastic simulation 0-3339  
 teaching, complex chem. reacts., kinetics, Markov chain appl. 0-27085  
 transition state theory, absolute rate theory and variational formulations, Porter Karplus pot. surface 0-16642  
 transition state theory generalisations, classical mech. theory, applcs. to collinear reactions of  $H_2$  0-26002  
 transition state theory generalisations, quantum effects for collinear reactions of  $H_2$  0-26003  
 translationally driven reactions, transition state theory, cross section curve 0-26000  
 triatomic molecular systems, unimol. decomp., exit-channel coupling effects 0-25984  
 unimolecular decay dynamics, pole approx. calcs. 0-35501  
 unimolecular reaction theory, transition probabilities, relax. matrix, commutative properties 0-25991  
 unimolecular reactions, nonequil. time-depend., model calc., single collision approx. 0-25987  
 $H_2 + F$ , collinear trajectories, statistical behaviour and detailed dynamics 0-16664  
 $O_3$ , UV photodissoc. rate, expt. and theory 0-40722

## reaction rate coefficients see reaction rate constants

## reaction rate constants

- absolute rate theory, ab initio calcs., elementary gas phase reaction 0-7757  
 acetone- $d_6$ , multiphoton dissociation, recomb. to ethane 0-3371  
 1-alkynes +  $O(^3P)$ , CO prod., vibr. population distrib., rate consts., laser reson. absorpt. technique 0-40676  
 allyl isocyanide, state-selected, visible absorption spectra and photolysis kinetics 0-11879  
 ascorbic acid, action with perhydroxyl radicals, radiolytic study 0-35523  
 atom + molecule reaction rate meas. 0-16676  
 bimolecular rate constant ionic strength dependence, effect of a molecular dipole 0-55977  
 butyl radical +  $O_2$ , reaction rate consts. meas. 0-45490  
 carbohydrates, reactions with hydrated electrons and hydroxyl radicals, rate constants obs. 0-50825  
 catalyst surface mag. field effect on mol. dissociation rate 0-16721  
 charge transfer reactions, empirical rate coeffs. status and astrophysical appls. 0-56701  
 chlorodifluoroethane, CW laser-induced reaction, vibr. rate enhancement obs. 0-11922  
 chloropentafluoroethane, multiphoton dissociation, crossed laser and mol. beam obs. 0-11908  
 coumarin 102, excited state protonation kinetics, laser pH jump and picosecond spectroscopy 0-25992  
 cycloheptatriene, and substituted forms, vibr. highly excited, steady-state photoisomerisation 0-16704  
 cyclopropane, thermal unimol. isomerisation, vibr. energy transfer, diffusion cloud method 0-26001  
 cyclopropane + inert gas, reactant decomp., rot.-vibr. energy transfer, relax. analytic soln. 0-55650  
 decomposition, reaction rate calc. by differential quotient 0-25990  
 dimethylamino radical +  $O_2(NO)(NO_2)$ , reaction rate constants, FTIR obs. 0-16652  
 direct chemical reactions in fast molecule collisions, eikonal approx. calcs. (Russian) 0-3332  
 DNA-Au (III) interaction, rate consts., activation energies, pH, spectro-photometric obs. 0-30228  
 ethyl acetate, CW laser induced reactions, activation energies, temps. and rate consts. 0-40710  
 ethylacetate, CW laser induced reactions, activation energies, temps. and rate consts. 0-40710  
 ethylperoxy radical +  $NO_2$ , reaction rate const. meas. 0-21262  
 formaldehyde +  $O$ , absolute rate consts., discharge flow and flash photolysis reson. fluoresc. meas. 0-55648  
 gas phase reaction consts. for electronically excited species, relax. processes, data tables 0-16644  
 hot atom chemistry, general variational principles 0-11941  
 hydrocarbons, reactions, rate consts., temp. depend., photolysis, high temp. fast flow reactor technique 0-42231  
 inert gas excited molecules formation, rate const. determ. 0-9859  
 inert gas afterglow, excimer form., VUV emission obs. at low press. 0-38755  
 ion + molecule, association, temp. depend., rate coeffs. calc. 0-16661  
 ion + molecule, slow reactions, carbonyl addition rate consts. rel. to struct. 0-30232  
 ion + molecule, slow reactions, nucleophilic displacement, rate consts. rel. to struct. 0-30232  
 ion + molecule, slow reactions, proton transfer, rate consts. rel. to struct. 0-30232  
 ion + molecule, slow reactions, three body assoc., rate consts. rel. to struct. 0-30232  
 ion + neutral atom, reactant internal energy, rate constants, drift tube 0-30231  
 ion + neutral molecule, reactant internal energy, rate constants, drift tube 0-30231  
 ion-molecule association reacts., gas phase, statistical phase space theory approach 0-50839  
 ion-molecule thermochemistry, flames and diagnostic techniques 0-55664  
 Kramers theory of friction and vel. in chemical kinetics 0-50826  
 laser induced reactions, activation energies, temps. and rate consts. 0-40710  
 laser specific and thermal reactions classifications 0-11919  
 laser studies of relaxation and reaction of species in defined quantum states 0-11918  
 laser system, trimer form. rates 0-50831  
 laser-based methods for transient chem. events meas. 0-40801

## reaction rate constants continued

- laser-controlled unimolecular and bimolecular processes, field-depend. rate const. 0-11906  
 laser-induced predissociation, diatomic and polyatomic mols., photocatalytic effect 0-11907  
 3-methoxybenzanthrone in ethanol, photoprolytic reactions, spectra, rate consts. and lasing thresholds 0-43327  
 molecular dynamics simulation of chemical reactions in solution 0-40673  
 non-ionic reactions, temp. and press. effect on kinetic and thermodynamic parameters 0-3300  
 organic ion, excited electronic state correlation with mass-spectral fragmentation pattern 0-45482  
 photoelectrochemical cells, metal, electrodes in contact with fluorescent dye solns., photovoltage generation, comprehensive model 0-40871  
 plasma, chemical reactions, rate coeffs., database creation, DATSTOR 0-48846  
 plasma, nonequilb., diat. mols. vibr. excited state population, rel. to plasma chem. 0-19553  
 plasma of given chemical content, chemical reactions, computer generation, REACS 0-48844  
 polyatomic molecule under nonequilibrium conditions, dissociation kinetics, unimol. decomp. rates 0-11886  
 proteins, kinetic constants of association and dissociation, theoretical determ. 0-51033  
 resistivity relaxation measuring system, for surface reaction meas. 0-55718  
 semiconductors, multiply doped, donor-acceptor complexes and interactions, physicochem. nature 0-15472  
 shock tube measurements of elem. gas reaction rate coeffs., review 0-3299  
 stilbene, cis→trans photoisomerisation rate const., direct meas. 0-30250  
 styrene, thermal polymerization, PMR obs. 0-3342  
 toluene + OH, rate constant under simulated atmospheric conditions 0-50846  
 trichloroethane + OH→ $H_2O + CH_2CCl_3$ , rate const. and tropospheric chem. 0-16658  
 trifluoromethyl radical reactions, prod. and meas. by IR multiphoton dissociation of iodotrifluoromethane 0-26036  
 unimolecular reactions induced by monochromatic IR radiation, intensity and laser energy fluence influence 0-11903  
 Zircaloy-4, oxidation in steam, 900-1500°C, kinetics 0-3241  
 Al +  $SO_2$ , high temp. fast flow reactor obs. of kinetics 0-30226  
 Ar, stationary afterglow obs. of singly charged atomic ions, three-body rate coeffs. 0-38757  
 Ar<sup>+</sup> + Ar, quasi-resonant charge transfer at thermal energies 0-48082  
 ArCl<sup>+</sup>, excimer formation rate consts., B state radiative lifetimes, quenching, VUV excitation 0-55631  
 Br, recomb., in presence of inert gas atoms and mols. 0-45496  
 Br + Br + Ar→Br<sub>2</sub> + Ar recombinations rate const. calcs. 0-40685  
 Br +  $H_2O_2$ , rate constant upper limit 0-30216  
 Br + NOBr, primary and secondary photochemistry, vibrationally excited NO, IR fluoresc. obs. 0-48030  
 C oxidation kinetics, in Fe-C melts by  $CO_2$  (Russian) 0-40680  
 C<sup>2+</sup> +  $H_2(N_2)(O_2)$  (inert gas), charge transfer reaction rate consts. 0-7779  
 CO<sub>2</sub> + inert gas, reactant decomp., rot.-vibr. energy transfer, relax. analytic soln. 0-55650  
 (CO<sub>2</sub>)<sub>2</sub><sup>+</sup>, ion-mol. reaction product distrib. and rate coeffs. 0-50852  
 CO<sub>2</sub>, CO<sub>2</sub><sup>+</sup> + SO<sub>2</sub>, reaction rate coeff. and product distrib. 0-3305  
 CaO + CO<sub>2</sub>→CaCO<sub>3</sub>, reaction kinetics, effect of temp. and CO<sub>2</sub> press. 0-45552  
 Cl, recomb., in presence of inert gas atoms and mols. 0-45496  
 Cl + NOCl, primary and secondary photochemistry, vibrationally excited NO, IR fluoresc. obs. 0-48030  
 Cl<sub>2</sub> absorption in acetic acid, kinetics in presence of homogeneous catalysts 0-11876  
 Cl<sub>2</sub>-O<sub>2</sub>-H<sub>2</sub> dilute mixtures, photolysis products, Fourier Transform IR kinetic obs. 0-26033  
 Cl<sup>2</sup>(P) + CH<sub>4</sub>→CH<sub>3</sub> + HCl, reaction rate const., laser flash photolysis-resonance fluoresc. kinetic study 0-45485  
 Cr<sub>2</sub>O<sub>3</sub>, reduction by H<sub>2</sub>, reaction kinetics 0-11950  
 DO<sub>2</sub> + NO, reaction kinetics, near IR chemiluminesc. determ. 0-21261  
 F + O<sub>2</sub>, quantum reactive scatt. theory, 3-dimens. 0-55637  
 Fe, sponge, oxidation kinetics by nuclear γ-resonance method (Russian) 0-40681  
 GeCl<sub>4</sub> hydrolysis and oxidation kinetics for graded-index fibre vapour phase axial deposition 0-48477  
 H + BrF(IF)→HF + Br(I), reaction product energy distrib. 0-30219  
 H + H<sub>2</sub>(O<sub>2</sub>), quantum reactive scatt. theory, 3-dimens. 0-55637  
 H + N<sup>3+</sup>, charge exchange, assoc. reaction, rel. to interstellar gas 0-7763  
 HNO<sub>3</sub>-HNO<sub>2</sub>, aq. soln., N isotope exchange in presence of NO 0-16662  
 HO<sub>2</sub> radical, atmospheric reactions studied by laser mag. reson. spectroscopy 0-12511  
 HO<sub>2</sub> + HO<sub>2</sub>, reaction rate, press. depend. 0-7766  
 HO<sub>2</sub> + NO, reaction kinetics, near IR chemiluminesc. determ. 0-21261  
 HO<sub>2</sub> + NO<sub>2</sub>→OH + NO<sub>2</sub>, kinetics temp. depend. 0-3313  
 H<sub>2</sub>O + Ar<sup>+</sup>, thermal-energy charge transfer, H<sub>2</sub>O<sup>+</sup> product internal and kinetic energy 0-16654  
 H<sub>2</sub>O<sub>2</sub> 0-34826  
 I<sub>2</sub>, hydrolysis, reaction rate const. 0-11883  
 Kr, stationary afterglow obs. of singly charged atomic ions, three-body rate coeffs. 0-38757  
 Kr<sup>+</sup> + Kr, quasi-resonant charge transfer at thermal energies 0-48082  
 Kr<sup>2+</sup> + H<sub>2</sub>(N<sub>2</sub>)(O<sub>2</sub>) (inert gas), charge transfer reaction rate consts. 0-7779  
 KrCl<sup>+</sup>, excimer formation rate consts., B state radiative lifetimes, quenching, VUV excitation 0-55631  
 KrF<sup>+</sup> + inert gas, three body collision rate consts., trimer form. rates 0-50831  
 N + alkene (1,3-butadiene)(acetylene), reaction rate consts., pulse radiolysis obs. 0-35508  
 N<sup>+</sup>, dissociative recombination in ionosphere, rate cont. 0-17435  
 NH<sub>2</sub> + NO<sub>2</sub>, reaction rate const. meas. 0-7772  
 NH<sub>4</sub><sup>+</sup> + molecule (n=0 to 4), reactions, selected ion flow tube obs. 0-45489  
 NO<sup>+</sup> + molecule, reaction rate consts. meas. 0-7782  
 NO + BrO, temp. depend. kinetic study, stratospheric Br photochemistry implication 0-50866  
 NO + O, chemiluminesc., O<sub>2</sub> effect 0-45507  
 NO<sub>2</sub>, thermal decomposition kinetics (Russian) 0-3329



**reaction rate constants continued**

- $\text{NO}_2 + \text{OH} + \text{M} \rightarrow \text{HNO}_3 + \text{M}$ , rate constant under simulated atmospheric conditions 0-50846  
 $\text{N}_2\text{O}$  photodissociation, CC O(S), prod. and props. in liq. Ar and  $\text{N}_2$  0-43063  
 $\text{N}_2\text{O} + \text{inert gas}$ , reactant decomp., rot.-vibr. energy transfer, relax. analytic soln. 0-55650  
 $\text{Ne}^+ + 2\text{Ne} \rightarrow \text{Ne}_2^+ + \text{Ne}$  processes in Townsend discharges 0-38747  
 $\text{Ne}^+ + \text{Ne}$ , quasi-resonant charge transfer at thermal energies 0-48082  
 Ni-Cr alloy, phosphidation in P vapour, 700°C, phosphide layer struct. and kinetics 0-25906  
 $\text{Ni}, \text{Zn}, \text{Fe}_2\text{O}_3$ , catalytic oxidation of CO, mag. props., kinetic parameters and composition depend. 0-16723  
 $\text{O}^{2+}$  reactions with atoms or molecules of ionospheric importance, lab. meas. 0-26004  
 $\text{O} + \text{methane}$ , photochem. reaction, high temp., rate coeff. meas. 0-16699  
 $\text{O}_2 + \text{CH}_3 \rightarrow \text{OH} + \text{H}_2\text{CO}$ , 368K, rate const. upper limit 0-7771  
 $\text{O}_2 + \text{inert gas}$ , reactant decomp., rot.-vibr. energy transfer, relax. analytic soln. 0-55650  
 $\text{O}_3$ , laser flash photolysis, O(<sup>1</sup>D) quantum yields in fall-off region 0-45524  
 $\text{O}_3$ , laser-induced photolysis, reactions of O(<sup>3</sup>P), O(<sup>1</sup>D) and O(<sup>1</sup>Δ) 0-11928  
 $\text{O}_3$ , UV photodissoc. rate, expt. and theory 0-40722  
 $\text{O}_3 + \text{O}_2(\Delta_g)(\text{O}_2^*)$ , UV photolysis, O(<sup>3</sup>P) prod., rate consts. determ. 0-55636  
 $\text{O}_3 + \text{O}(\text{D})$ , UV photolysis, O(<sup>3</sup>P) prod., rate consts. determ. 0-55636  
 OCS photodissociation, S(<sup>1</sup>S) prod. and props. in liq. Ar and  $\text{N}_2$  0-43064  
 $\text{OH} + \text{H}_2 \rightarrow \text{H}_2\text{O} + \text{H}$ , rate constant, ab initio calc. 0-45478  
 $\text{OH} + \text{trichloroethane}$ , 1,1,1- and 1,1,2-isomers, reaction kinetics, 298-460K, lower atmos. chem. 0-16657  
 $\text{ON} + \text{azomethane}$ , rate const. meas. 0-7771  
 $\text{O}(^2\text{D}) + \text{N}_2(\text{O}_2)(\text{N}_2\text{O})(\text{CO}_2)(\text{H}_2\text{O})(\text{methane})$ , collisional deactivation meas., 295K, rel. to atmospheric processes 0-16663  
 Rb, radiatively excited states, ionis. rate coeffs. in two atom collisions 0-43160  
 $\text{S}^+ + \text{NO} \rightarrow \text{NO}^+ + \text{S} + 1.1 \text{ eV}$ , rate consts. kinetic energy depend., drift tube meas. 0-7778  
 $\text{S}^+ + \text{O}_2 \rightarrow \text{SO}^+ + \text{O} + 0.26 \text{ eV}$ , rate consts. kinetic energy depend., drift tube meas. 0-7778  
 Si, thermal oxidation in  $\text{O}_2$ -trichloroethylene mixture, 900, 1000 and 1100°C 0-3221  
 $\text{SiCl}_4$  hydrolysis and oxidation kinetics for graded-index fibre vapour phase axial deposition 0-48477  
 U powder, hydriding kinetics, 13.3 and 26.6 kPa, 50-250°C 0-16725  
 $\text{Xe}^+ + \text{Xe}$ , quasi-resonant charge transfer at thermal energies 0-48082  
 $\text{Xe}^{2+} + \text{H}_2(\text{N}_2)(\text{O}_2)$  (inert gas), charge transfer reaction rate consts. 0-7779  
 $\text{XeF}_2$  photolysis with VUV radiation, XeF (B,C) state prod. and kinetics 0-32975  
 $\text{XeF}^+ + \text{inert gas}$ , three body collision rate consts., trimer form. rates 0-50831  
 Zn, phosphidation in P vapour, kinetics and associated diffusion coeffs. 0-3405

**reactions (chemical) see chemical reactions****reactions (nuclear) see nuclear reactions and scattering****reactive sputtering**

- cathode, ion generation by O low pressure reactive sputtering (*Japanese*) 0-50494  
 ceramics coating by physical vapour deposition processes (*Japanese*) 0-55306  
 dielectric films, low temp. epitaxy in laser sputtering 0-34335  
 $\text{Fe-SiO}_2$  cermet film, solar absorbing, production by dual cathode DC magnetron sputtering 0-16186  
 magnetron-plasmatron processing and instrumentation, review 0-35090  
 metal-semiconductor system, interfacial reaction, dynamical obs. at room temp. using AES 0-10798  
 Al magnetron sputtering target, oxidation in  $\text{Ar}/\text{O}_2$  mixtures 0-55291  
 Al-Cu, film, prep. by planar magnetron sputtering (*Japanese*) 0-16184  
 $\text{Al}_2\text{O}_3$  optical waveguide, fabrication by reactive Al sputtering in  $\text{O}_2$ -Ar atm. 0-33262  
 $\text{Cu-Al}_2\text{O}_3$  cermet film, solar absorbing, production by dual cathode DC magnetron sputtering 0-16186  
 $\text{In}_2\text{O}_3$  film reactive sputtering gas composition and film growth rate (*Russian*) 0-50554  
 $\text{IrO}_2$ , electrochromic film, prep. by reactive sputtering 0-29876  
 Mo, product identification by absorpt. spectra 0-28027  
 $\text{MoO}_3$ -Si photodiode, fabrication as function of  $\text{O}_2$  partial press. 0-29464  
 $\text{MoS}_2$ , RF sputtered layers with variable stoichiometry, lubrication props. 0-40557  
 Ni-Pd-H, film, struct. and phases formed, when Ni, Pd are sputtered in H 0-29289  
 Si-H, amorphous, control and anal. of deposition, using plasma spectroscopy 0-45230  
 SiC, coating on graphite, by reactive magnetron sputter deposition (*Japanese*) 0-16185  
 $\text{SiO}_2$ , deposition by reactive sputtering of Si in magnetron sputtering system, reaction kinetics 0-49553  
 TiN thin films, elec. props. 0-15638  
 $\text{TiO}_2$ , reactively sputtered optical coating for inertial confinement fusion laser components 0-23705

**reactively sputtered coatings**

- borosilicate glass films, phys. and chem. props., B diffusion into Si,  $\text{SiO}_2$  0-29040  
 Al-Cu, film, prep. by planar magnetron sputtering (*Japanese*) 0-16184  
 AlN, formation and characterisation 0-44452  
 $\text{AlO}_x$ , obtained by oxidation of Al magnetron sputtering target in  $\text{Ar}/\text{O}_2$  mixtures 0-55291  
 $\text{Al}_2\text{O}_3$ , form. and behaviour under particle bombard. 0-35029  
 $\text{Al}_2\text{O}_3$  optical waveguide, fabrication by reactive Al sputtering in  $\text{O}_2$ -Ar atm. 0-33262  
 $\text{CdO-SnO}_2$ , transparent electrode props., optimum sputtering conditions 0-11116  
 $\text{Cu}_2\text{S}$ , Hall effect meas., 90-300K 0-15541  
 Ge-H, amorphous, H content determ. by IR absorpt., gas evolution and nuclear reaction methods 0-44130  
 $\text{IrO}$  reactively sputtered electrochromic films, electrocatalytic  $\text{O}_2$  evolution 0-26125  
 $\text{MnCo}_2\text{O}_4$  DC sputtered films, struct. and elec. props. 0-54812

**reactively sputtered coatings continued**

- $\text{MoS}_2$ , RF sputtered layers with variable stoichiometry, lubrication props. 0-40557  
 Nb-Ta-N films and their anodic-oxides, elec. props. of resist. and dielec. films 0-11126  
 Ni-Pd-H, film, struct. and phases formed, when Ni, Pd are sputtered in H 0-29289  
 Si-H, amorphous, H content determ. by IR absorpt., gas evolution and nuclear reaction methods 0-44130  
 Si-H, amorphous, H content effect on props. 0-49714  
 Si-H, amorphous, sputter deposited,  $\text{O}_2$  incorporation during and after fabrication 0-49541  
 Si-H, Li, amorphous, DC electrical conductivity, absorption edge and IR meas., role of H 0-54694  
 Si-H amorphous film, sputtered IR vibr. spectra and photolum., effects of partial evolution of H 0-44413  
 Si-H amorphous films, role of Ar in deposition process, IR absorpt. and photocond. meas. 0-50321  
 Si-H, amorphous, on Nb or W, spectrally selective absorber, IR spectra 0-26164  
 Si-H, amorphous, thermal stability and decomp. kinetics 0-24758  
 SiC, comp. and struct. props., effect of target materials 0-54549  
 SiC, on graphite, by reactive magnetron sputter deposition (*Japanese*) 0-16185  
 SiH, amorphous reactively sputtered films, optical props. 0-50444  
 $\text{Si}_3\text{N}_4$ , formation and characterisation 0-44452  
 Sn, discharge produce evaluation, mass spectrometer obs. 0-6668  
 $\text{Ta}_2\text{O}_5$ , reactive DC sputtering deposited films with magnetron-plasmatron, mechanical elec., optical props. 0-25566  
 TiC reactively sputtered coatings on Ni-Cr-Mo-Ti (19,11,3 wt.%), adherence, XPES and wear study 0-25565  
 TiC sputtered coatings on Ti-Al-V (6,4 wt.%), adherence, XPES and wear study 0-25565  
 TiN thin films, elec. props. 0-15638  
 TiN, sputtered in  $\text{Ar-N}_2$  atm., elec. and struct. props. 0-15636  
 $\text{TiO}_2$ , reactive DC sputtering deposited films with magnetron-plasmatron, mechanical elec., optical props. 0-25566  
 $\text{TiO}_2$ , reactively sputtered optical coating for inertial confinement fusion laser components 0-23705

**reactors (nuclear) see fission reactors****read-only storage**

- holographic storage system, laser apparatus for recording transparencies of ROM 0-28177  
 microscopically rough substrate local smoothing for optical storage 0-14288  
 modular arithmetic inner product processor optical implementation 0-48170

**readout, digital see digital readout****real time computer systems see real-time systems****real-time systems****see also online operation**

- acoustic holography system, Sonoscan using microprocessor 0-38184  
 data buoy wideband wave directional spectra, real-time telemetry 0-46305  
 distribution function parameters determ. in real time, instrument description 0-202  
 ECG real-time analyser with digital readout, portable device 0-56234  
 ECG slow wave real-time anal., hardware implementation of selective Bouilland transform 0-56233  
 eye movement research, data collection using on-line computers 0-41329  
 fluoroscopic cardiac imaging, real-time computerised system 0-36123  
 geophysical data, real-time processing using DGU-2 curve plotter 0-36422  
 image edge enhancement 0-43273  
 ionosphere, Dynasonde software, real-time data acquisition and display 0-36405  
 ionosphere soundings using small spaced receiving system 0-36406  
 minicomputer, portable, for dynamic ocean data acquisition and display 0-12552  
 oceanography, data anal. by Naval Coastal Systems Center (NCSC) environmental measuring system 0-12570  
 optical data processing operations achievable, real-time devices, systems and applications 0-9816  
 sea surface contour airborne radar as remote sensing instrument 0-51562  
 side-entry surface acousto-optic interaction signal processor 0-48174  
 signal processing activities of United States Army 0-48172  
 solar spectrometric research, automation system for on-line signal processing (*Russian*) 0-12659  
 SPS, real-time control system, operating system principles 0-875  
 US real-time diagnostic system 0-30819

**reboilers see boilers****receivers**

- see also acoustic receivers; radar receivers; radio receivers; telephone receivers; transceivers**  
 acousto-optic parallel channel wideband receiver 0-48447  
 heat receivers with moving heat carrier, freq. characts. 0-4733  
 ionosphere soundings using small spaced receiving system 0-36406  
 sound production receiver for radiomicrophones, film, TV studios, theatres appl. (*German*) 0-4787

**recombination, electron-hole see electron-hole recombination****recombination, ion see ion recombination****reconnaissance satellites see artificial satellites****record players see gramophones****recorders****see also recording; tape recorders**

- AC electrical load information recorder utilising standard multi-point chart recorder 0-42238  
 automatic device for thermomechanical and linear dilatometric testing of polymers 0-11858  
 Biomation 8100, DMA interface for Intel MDS-800 microcomputer system 0-203  
 boxcar integrator/US recording unit using sample-and-hold circ., for student lab. 0-27083  
 digital temperature recorders, advantages over analogue instruments 0-210  
 ECG recorder and printer with fixed writing heads 0-3854  
 high-speed physical process parameter measurement by means of time-scale conversion 0-8968  
 lightning counter, multichannel, with digital display 0-51570



**recorders continued**

- lightning peak current meas. and recording device results (*Japanese*) 0-46288
- muscle isometrical contraction maximum and standby tension, additional equipment (*Hungarian*) 0-41342
- photoelectric spectrographic detection, direct reading attachment 0-275
- photographic immunogram recording apparatus, self-contained, modified version using Polaroid film 0-17209
- spectra registration system for spectrophotometers, graphical and digital forms 0-47113
- transient, for natural and induced phenomena 0-27284
- transient recorder for signal averaging, microcomputer-controlled 0-31723
- X-ray tube for recording rapid processes, type RTR-1 0-9080

**recording**

- see also *audio recording; magnetic recording; video recording*
- contactless electropneumatic transducer parameter determ. (*Bulgarian*) 0-47045
- optical, on disc using diode laser 0-19001

**recording instruments** see *recorders***recovering** see *recovery***recovery**

- see also *recovery-creep*
- cellulose acetate films, light scatt., tensile creep, desalination 0-16050
- FCC metals, props. of vacancies and divacancies 0-10545
- oxides, interaction between point defects and dislocations, cryst. plasticity 0-15149
- steel, low C, instability obs. by large strain compression 0-35253
- steel, Si-P-C, low C, varying Si content, cold rolled annealing 0-3090
- steel, stainless 316, recovery by annealing of creep produced dislocations 0-11702
- Al cell structures produced by cycling and monotonic creep 0-55452
- Al, deformed, thermal recovery, microstruct. and stress-strain relations 0-16325
- Al, recovery annealing, exam. using in situ high voltage electron microscopy 0-7596
- CdO, influence of initial compacting press. on elec. resist. Hall coeff. 0-20872
- $\alpha$ -Fe, internal friction for low temp. deform. 0-40420
- Fe-Al, deformed, low temp. recovery of elec. resist. (*Russian*) 0-7697
- Fe-Al alloys, cold-worked, Mossbauer study of recovery 0-7593
- Mo, dislocation structure inhomogeneity in electromachining crater zone, rel. to plastic deform., dynamic recovery (*Russian*) 0-16326
- Ta, rolled single crystal, recovery and recrystallization 0-3093
- Te, electron irradi., mobility increase due to defect prod. 0-24501
- Ti-Mo-Zr-Sn (11.5, 6, 4.5 wt.%), metastable beta III phase, recrystallization and grain growth 0-3091
- Ti-Ni, effect of alloying on crit. points and martensitic transform. hysteresis 0-20935
- W and W alloys, ion-irradiated, recovery behaviour studied by field ion microscope 0-29074
- W, thermal neutron irradiated, recovery processes 0-19848
- Zn, neutron irradiated, recovery of c-axis spacing and elec. resist. 0-34081
- Zr-Al (8.6 wt.%), neutron irradiated, irradiation growth and recovery, annealing 0-15162

**recovery-creep**

- polythene, ultraoriented, microhardness, extrusion conditions effect 0-50704
- Pb, work hardening, and recovery rates during steady state deformation, temp. and stress effect 0-45319
- Si<sub>3</sub>N<sub>4</sub>-MgO, compressive creep, source of viscoelastic effect 0-50675

**recrystallisation**

- microstructural processes and features only
- see also *recrystallisation annealing; recrystallisation texture*
- alloy, austenitic, mechanical changes after electrolytic quenching (*Russian*) 0-50653
- biotite, deform. and recrystallisation in Woodroffe Thrust mylonite zone 0-21739
- $\alpha$ -brass, texture, recrystallised orientation distrib. function comparison with 40°(111) rolling texture 0-25723
- dynamic recrystallisation diagrams (*German*) 0-25729
- mylonites, grainsize reduction and grain boundary sliding rel. to flow strength 0-21721
- 1,4-cis-polybutadiene, stereoregular, recrystn. in partial melting temp. region (*Russian*) 0-6495
- quartz, twinned crystals, after Japan Law, investigation of regrowth 0-54162
- steel, alloy, high speed, type R18, hot deformation and recrystn. 0-16391
- steel, alloy type 25KhN3MFA, tempering of bainitic structure 0-20983
- steel, austenite hot deformation influence on phase transformations 0-7606
- steel, austenitic, Cr-Ni (25, 20 wt.%) recrystallisation and sigma phase formation 0-35211
- steel, austenitic stainless, 08Kh18N10T, hot-worked precipitation kinetics and struct. of dispersed phases, Ti effect 0-29964
- steel, low C, Mn effect on recrystallisation and texture (*French*) 0-3110
- steel, mild, plastic deform. around fatigue cracks, X-ray microbeam and recrystn. studies 0-35258
- steel, Ni and W, recrystallisation mech. during laser treatment 0-50658
- steel, Si-P-C, low C, varying Si content, cold rolled annealing 0-3090
- steel, tempering effect on struct. and mech. props. of types 70, U8, and U12 (*Russian*) 0-50655
- steels, hot forming property and struct. (*German*) 0-25730
- supercooled, struct. refinement mech. (*Russian*) 0-20975
- TCNQ complex formed from cation (methyl-l-N-ethyl benzimidazolium)<sup>+</sup> conductivity transition 0-10954
- TGS:Cr single cryst., lattice defect influence on critical behaviour 0-25315
- Ag epitaxial films, grain boundary struct. evolution during recrystn., interface energy effect (*Russian*) 0-15387
- Al epitaxial films, grain boundary struct. evolution during recrystn., interface energy effect (*Russian*) 0-15387
- Al sheet, recrystallization, DSC eval. 0-3105
- Al, subgrain coalescence, grain boundary recrystallisation nucleation 0-3094
- Al substitutional solid solution alloys, volumetric effect and props. (*Russian*) 0-39293
- Al wire, hot and cold deformation drawing strengthened, thermal EMF study (*Russian*) 0-54674

**recrystallisation continued**

- Al-Cr(Zr), simultaneous recrystallisation and precipitation (*French*) 0-16313
- Al-Cu-Zr, superplastic alloy Supral, solidification and recrystallisation 0-7550
- Al-Mn(Cr), quenched, thermal stability (*Russian*) 0-20976
- Al-Pb alloys, with isolated liq. phase inclusions, recrystn. (*Russian*) 0-20970
- Al-Zn alloys, recrystallisation and superplasticity, HVEM straining 0-39207
- Al-Zn-Mg, polygonized struct. in extrusions, thermal stability and mech. props. 0-50659
- As<sub>2</sub>(S<sub>2</sub>Se)<sub>2</sub>, chalcogenide, covalent non crystalline topology, short range order 0-15009
- Au epitaxial films, grain boundary struct. evolution during recrystn., interface energy effect (*Russian*) 0-15387
- CdGeAs<sub>2</sub>, amorphous, thermal gradient expts., recrystn. 0-55438
- CdGeAsMn, glass, recrystallisation 0-44133
- CdS:Ag, vacuum deposited film, recrystn. by H<sub>2</sub>S heat treatment 0-34328
- CdS:Cu(Cl), thin layer, electron pulse induced cond. relax. 0-2501
- Cu, cold rolling, mechanical props., ageing, annealing, recrystallisation, plastic strain (*Russian*) 0-35202
- Cu, grain growth rate, 520-970°C (*Russian*) 0-29972
- Cu, polycryst., grain size and high-temp. yield strength 0-7641
- Cu-Sb, dil., grain growth rate, 520-970°C (*Russian*) 0-29972
- Fe atomised powder, sintering effect on recrystn., mech. props. 0-40292
- Fe-Ni-Co, texture form. after cold working and annealing (*German*) 0-3089
- Fe-V(Cr)(Mn)(Ni), unlimited component solubility, intercrystallite inter-nal adsorption (*Russian*) 0-39294
- GaAs:Cr pulsed electron beam induced recrystallisation and damage, amorphous layer formation 0-34052
- Ge, regrowth under laser irradi. 0-24481
- Ge-Sb glasses, microgravity effect on recrystn., optical and elec. props. 0-49127
- Ge<sub>2</sub>(S<sub>2</sub>Se)<sub>2</sub>, chalcogenide covalent non crystalline topology, short range order 0-15009
- KCl:TiCl, lattice defects, X-ray line profile obs. 0-24455
- MoSi<sub>2</sub>, ceramic additives effect on sintering, recrystallisation 0-40306
- NaCl, halite, dynamic recrystn. during compression creep, geophys. appl. 0-25772
- Nb alloy SVMTs, high-temp. ageing, struct. and morphology of hardening phases (*Russian*) 0-40390
- Nb-Zr-C alloys, plastic deform. and annealing, dislocation struct. (*Russian*) 0-20951
- Ni alloy, recryst. after hot deform. (*German*) 0-25716
- Ni base superalloy,  $\gamma$ -precipitation influence on recrystallisation 0-29955
- Ni, deformed, struct. form. during annealing, Ni<sub>3</sub>Al type ordered phase precipitation (*Russian*) 0-45325
- Ni, powder, subjected to vibratory milling, exam. of plastic deformation, recrystallisation, sintering 0-16234
- Ni, supercooled, struct. refinement mech. (*Russian*) 0-20975
- Ni-based superalloys, TEM obs. of cellular transformation products 0-3045
- Ni-Co-Cr superalloy, powder produced, necklace struct. development 0-40395
- Ni-Cr, deformed, struct. form. during annealing, Ni<sub>3</sub>Al type ordered phase precipitation (*Russian*) 0-45325
- Si, amorphous, ion implanted, laser annealing, reflectivity meas. 0-29039
- Si, photoacoustic signal changes assoc. with crystallinity, recrystallisation after laser annealing 0-16127
- Si, polycryst., CVD, electron beam recrystn. 0-24759
- Si, polycrystalline, recrystn. after plastic deform. and annealing 0-3145
- Si, pulsed laser annealing, nonthermal, plasma annealing 0-25498
- Si, recrystallisation of CVD-grown polycryst. Si and influence of B, Al dopants on grain growth 0-54575
- Si, regrowth under laser irradi. 0-24481
- Si:Ne(Ar)(Kr), amorphous, implanted and sputtered, epitaxial regrowth, influence of noble gas atoms 0-2289
- Si-Al system, Si regrowth minimisation methods in Al films 0-15384
- Si<sub>3</sub>N<sub>4</sub>, consolidation by hot isostatic pressing 0-11605
- SiO<sub>x</sub>, amorphous and recrystallised layer, optical props. 0-25474
- Ta, rolled single crystal, recovery and recrystallization 0-3093
- Te film condensed on mica, struct. and electrophysical props. 0-39688
- Ti-Al, structural and phase changes due to annealing (*Russian*) 0-55440
- Ti-Al-V (6.4 wt.%) alloy foil, substrate temp. effect on struct. 0-7497
- Ti-Al(Mo), swaged and recrystallized, grain growth 0-3092
- Ti-Mo-Zr-Sn (11.5, 6, 4.5 wt.%), metastable beta III phase, recrystallization and grain growth 0-3091
- W fibre reinforced, Co powder alloys, reactions and recryst. 0-11603
- W, powder, subjected to vibratory milling, exam. of plastic deformation, recrystallisation, sintering 0-16234
- YAG, production of densely sintered ceramic, exam. of recrystallisation during sintering 0-11609

**recrystallisation annealing**

- annealing twins density, photoemission microscopy 0-35208
- Fe, Armco, electron microscope object prep. method 0-50789
- laser annealing, optical constants, ellipsometry observation 0-34024
- semiconductor epitaxial regrowth, ion implantation induced defects, annealing 0-24479
- semiconductor laser annealing, review and anal. 0-25741
- semiconductor laser annealing to round edges of Si structures 0-25742
- steel, Cr (17 wt.%), stainless, hot-rolled texture, effect on cold-rolled and annealed textures 0-55425
- steel, unrolled deep drawing sheets, influence of N content on recrystn. (*German*) 0-40376
- B<sub>2</sub>C<sub>3</sub>, sintering and subsequent high temp. annealing, struct. and props. 0-20858
- Bi film, surface defects and struct., electron microscopy and elec. props. (*French*) 0-15415
- CdS, polycrystn. films, recrystn. accompanying annealing (*Russian*) 0-20948
- Cr bronze Sn, recrystn. props., hot rolling, annealing, polygonisation (*Russian*) 0-55419
- Cu film, on Ni, recrystallisation and interdiffusion, electron microscope obs., 450-600°C 0-39363
- Cu-Al (3 wt.%), annealing twins density, photoemission microscopy 0-35208
- Fe-Si-B, melt C content effect on grain growth and induction 0-35351



**recrystallisation annealing continued**

- GaAs, ion implanted, laser induced recrystn. and damage, ion backscatt. and Raman scatt. obs. 0-49248  
 GaAs, ion implanted, mode-locked Nd:YAG laser annealing, recrystn. 0-19817  
 GaAs, ion implanted and laser-annealed, photoacoustic meas. 0-47117  
 GaAs, ion-implanted, laser pulse annealing of amorphous surface layer, TEM 0-55436  
 GaP, ion implanted, mode-locked Nd:YAG laser annealing, recrystn. 0-19817  
 Mo, powder, defective structure and activated sintering, exam. 0-16240  
 Mo-Ti-Zr, alloy TZM, polycrystalline, anal. of elastic anisotropy and microyielding 0-30050  
 Ni, (99 wt.%), annealing twins density, photoemission microscopy 0-35208  
 Ni, pure, anomalous grain growth 0-20984  
 Si amorphous layer, solar furnace annealing to induce solid-phase epitaxy 0-2277  
 Si, deep amorphous layer implantation, laser effects, channelling diff. study 0-25494  
 Si, defect annihilation depth by pulse laser annealing 0-16128  
 Si, ion implantation and pulsed laser annealing of group III and group V dopants, supersat. alloy form. 0-54267  
 Si, ion implanted, mode-locked Nd:YAG laser annealing, recrystn. 0-19817  
 Si, ion implanted, scanning electron beam annealing 0-6420  
 Si p-n homoeptitaxial junctions, elec. and struct. characts. 0-6662  
 SiC(6H), ion-implanted, laser-induced recrystallization and defects 0-44221  
 $\alpha$ -Ti, recrystallised commercial purity, Fe-rich precipitates obs. (French) 0-50637  
 W, powders, defective structure and activated sintering, exam. 0-16240

**recrystallisation texture**

- $\alpha$ -brass, rel. to rolling temp. 0-11664  
 Ag, rel. to rolling temp. 0-11664  
 Cu, rel. to rolling temp. 0-11664  
 Fe, pure, initial grain boundaries effect on cold-rolling and annealing textures (Japanese) 0-35205  
 Fe-Co-Si (4.1.5 wt.%), textured, mag. props. 0-35200  
 Mo-Ti-Zr, alloy TZM, polycrystalline, anal. of elastic anisotropy and microyielding 0-30050  
 Ni-Cr-Al-Y<sub>2</sub>O<sub>3</sub> superalloy, recrystn. and texture development 0-16328  
 Ni<sub>65</sub>Mo<sub>2</sub>Fe, O<sub>2</sub> effect on secondary recrystallisation and mag. props. 0-35201

**rectangular waveguides**

- H<sub>10</sub> mode scatt., in rectangular waveguide, by cylinder with longitudinal slot 0-43238  
 liquid and solid complex permittivity meas., rectangular waveguide method 0-15941  
 optical, propagation losses at 10.6  $\mu$ m for distributed feedback appl. 0-38101  
 subMM and MM detection by Josephson junctions mounted in a waveguide 0-4767  
 total reflection by small slotted capacitive cylinder 0-5662  
 Ge waveguide, nonlinear third harmonic generation of submillimetre waves 0-44632  
 n-InSb, optical SHG in rectang. waveguide 0-43401  
 InSb waveguide, nonlinear third harmonic generation of submillimetre waves 0-44632  
 LiNbO<sub>3</sub> microwave laser beam electro-optic modulators using rectangular waveguides, 1.0 to 10 GHz 0-43381  
 LiNdP<sub>2</sub>O<sub>12</sub> glass-clad rectangular waveguide, laser performance 0-32996  
 n-Si, rod, in rectangular waveguide, microwave field distribution 0-39622

**rectification**

- metal whisker point contact junctions, tunnelling and rectification characts. 0-6955  
 GaAs-Ga<sub>0.7</sub>Al<sub>0.3</sub>As n-n heterojunction, LPE, rectification 0-49888  
 Ni-Nichrome, MOM diode, breakdown effect in visible and near-IR regions 0-6999  
 PbTe surfaces, Te coating, struct. and junction characts. 0-50743  
 SnO<sub>2</sub>-Si heterojunction solar cell, elec. props. (Korean) 0-45665  
 W-Ni, MOM diode, breakdown effect in visible and near-IR regions 0-6999

**rectifier tubes**

No entries

**rectifier valves** *see rectifier tubes***recursive functions**

- Anderson localisation problem, cond. numerical studies 0-49673  
 education, Fibonacci numbers, recurrence relation soln., combinatorics function anal. 0-51988  
 Gaussian integrals, evaluation by backwards recursion or Taylor expansion 0-31488  
 octahedral group, symmetry-adapted functions, calc. of rotation matrices using recursion relation 0-31482

**red giants** *see stars***red shift**

- see also cosmology; Doppler effect; gravitational red shift*  
 0957+561 A, B, twin QSOs, absorpt.-line redshifts from multiple-mirror telescope obs. 0-12827  
 AO 0235+164, BL Lacertae-type object, VBLI obs. of redshifted H I absorpt. 0-46658  
 bacteriorhodopsin, reson. Raman evidence for secondary protein-Schiff base interactions, primary excitation mechanism 0-55981  
 3C 286, quasar, optical absorpt. lines detect., redshift 0-4454  
 cluster of galaxies 0122-688, spectrographic obs., redshift 0-41906  
 cosmological constant and data reduction 0-41923  
 ESO 012-G21, Seyfert 1 galaxy, spectrum, redshift, UVB photometry and X-ray identification 0-8695  
 extragalactic objects, redshift distrib. and luminosity function (Chinese) 0-4437  
 extragalactic redshifts, interpretation 0-4427  
 G-varying cosmology, galaxy and QSO magnitude/red shift relations 0-56980  
 galaxies, bright, nearby, vel. field and Local Group peculiar motion rel. to Virgo cluster 0-36699  
 galaxies, double, redshift intervals periodicity 0-56923  
 galaxies, early-type, in NGC 7331 field, distances rel. to red shifts 0-4435

**red shift continued**

- galaxies, early-type, redshift distance moduli rel. to distances from relative luminosities 0-31363  
 galaxies, interacting, radial vels. rel. to luminosities and diameters 0-17677  
 galaxies, nearby, H I profiles and redshifts 0-41895  
 galaxies, optical redshifts 0-56936  
 galaxies, redshifts for 196 bright objects 0-46661  
 galaxies, redshift-distance relation and evidence for linearly expanding Universe 0-31354  
 galaxies in Yerkis poor clusters 0-51858  
 galaxies red shifts, evolution free test for non-zero cosmological const. 0-4465  
 galaxies redshift-magnitude bands, internal struct. and galaxies morphological evolution 0-22070  
 galaxy redshifts survey, data reduction techniques 0-22074  
 galaxy vel.-distance relations and Local Supercluster Hubble ratio 0-17698  
 Hercules supercluster, basic redshift data 0-36725  
 Hercules supercluster, cosmography 0-51883  
 Hubble's law, appl. to inverse square law deduction from Newtonian cosmology (Italian) 0-8722  
 Hubble Law, rel. to Newtonian mechanics and gravitational theory (Italian) 0-12835  
 IC 342, Scd galaxy, companion galaxy discovery and systemic velocity difference 0-36712  
 IC 5152, low-luminosity barred galaxy, struct., rot. curve and redshift 0-56950  
 M83 and Centaurus galaxy group, redshifts rel. to distance 0-4434  
 MKW 3s, poor galaxy cluster, redshifts obs. rel. to cD galaxy extended X-ray emission 0-51884  
 NGC 2639 companion galaxy, redshift and assoc. UV excess objects 0-56965  
 NGC 5128 (Centaurus A), heliocentric rel., struct. and evolution 0-4429  
 NGC 6240 unusual radio galaxy, optical redshifts 0-4440  
 NGC 6872, remarkable barred spiral, redshift distance and linear extent 0-31358  
 OQ 172, quasar, H<sub>2</sub> absorpt. lines identifications and redshifts 0-36734  
 PKS 1157+014, spectral obs., of QSO with no L $\alpha$  emission 0-31384  
 primeval galaxies, investigation of red shift 0-31372  
 profile of lines emitted by massive body or bodies behind it (French) 0-46670  
 Q 0957+561, double quasar, red shift of galaxy component of spectrum 0-27005  
 Q 2240.9-3702, Q 2238.9-4115, optically selected QSOs with broad-lined absorpt. systems, redshifts 0-4456  
 QSO 1038+528 A,D, close pair of radio-emitting quasi-stellar objects, optical redshifts 0-51902  
 QSO candidates, redshifts for 38 objects 0-56966  
 QSO candidates, spectroscopic obs., indentifications 0-31385  
 QSO/galaxy associations, redshifts and distances 0-31369  
 QSOs, high-redshift, Image Dissector Scanner (IDS) spectrometry and redshifts 0-22111  
 QSOs lying in spiral arms of NGC 1073, spectrophotometric obs. and redshifts 0-22110  
 QSOs of small and intermediate emission redshift, absorpt. lines homogeneous survey results 0-31218  
 quasar, strong emission line, with redshift  $z=0.189$ , spectrum and photometry 0-8710  
 quasars, gravit. and Doppler redshifts, interpreted as massive black holes ejected from galaxies 0-46695  
 quasars, line identifications, red shifted UV lines or violet shifted IR lines 0-8707  
 quasars, spectral characts. of three high redshift objects 0-4455  
 quasars in region of NGC 1629 companion galaxy, spectra and redshifts 0-56965  
 quasars of Michigan-Tololo survey, spectrophotometry and redshift distrib. 0-22105  
 quasars with strong interplanetary scintillation, magnitude-red shift link (Chinese) 0-12828  
 quasar red shift parameter  $\ln(1+z)$ , periodicity 0-17687  
 radio galaxies, optical catalogue 0-21931  
 radio sources, double, separation depend. on redshift 0-22096  
 radio sources, extragalactic, ang. size-redshift diagram interpretation 0-22101  
 radio-quiet quasars, Hubble diagram, luminosity function and density evolution 0-51903  
 radiogalaxies, optical spectroscopy and redshifts for 18 objects 0-56966  
 radiosources cosmological evolution, free-form analysis, self-consistent luminosity function 0-46716  
 spherically symmetric self-similar universe, redshifts and blueshifts 0-8727  
 steep spectrum radiosources, spectral index dependent props. 0-36730  
 superluminal radio sources, cosmological proper motion-redshift relation 0-22095  
 Tautenburg objective prism survey objects, high-resolution spectra and redshifts 0-4436  
 velocity-distance relation, history 0-12880  
 Zw 1400+0949 cluster (NGC 5416 group), radial vels. rel. to group dynamics 0-22090  
 H, line spectrum, relativistic red shift phenomenon 0-32675

**reduction (chemical)**

- see also oxidation*  
 , 0-55642  
 actinide oxides, preparation of metals and refractory cpds. 0-16229  
 aromatic compounds, by KC<sub>24</sub> intercalation compound 0-3306  
 bacteriorhodophyll-800, implication in picosec. electron transfer to bacteriopheophytin in R. rubrum reaction centres 0-35844  
 Bering Sea shelf sediments, denitrification estimates 0-12433  
 carbonaceous chondrites, reduction kinetics, Mossbauer obs. 0-41777  
 carbothermic process for production of pure highly reactive metals from oxides 0-3311  
 coal, new catalysts for CO-H<sub>2</sub>O induced liquefaction 0-30335  
 copper molybdates, oxidation, reduction and thermal decomp. mechanisms 0-50847  
 cytochrome C, immobilised, investigs. using magnetic micromixer attachment for SPECORD UV VIS spectrophotometer 0-56302  
 cytochrome P-450, non-equilib. states formed by low-temp-reduction, absorpt. spectra 0-35837  
 ferrite reduction using plasma methods (Russian) 0-7700



**reduction (chemical)** continued

- haeme proteins and metalloporphyrins, redox chem. and oxygen binding 0-3573  
 isotope compounds, conversion to metals by reduction-distillation methods 0-23223  
 lunar regolite, Fe reduction on heating in vacuum, XPS spectra 0-41740  
 magnetite nodules, from superconcentrates, strengthening annealing and reduction (*Russian*) 0-16333  
 metal ion electroreduction, ion-induced adsorpt. 0-21297  
 metal oxide reduction using plasma methods (*Russian*) 0-7700  
 photoelectrochemical cells, semiconductor based, interaction of light and transport control 0-12020  
 polymeric reducing agent design 0-26050  
 rare earths, purification, laser methods 0-16712  
 semiconductor-electrolyte solar cells for photochemical reduction of CO<sub>2</sub> to organic fuel 0-55880  
 steel, deoxidation by Ca-Si alloy, thermodynamics (*Russian*) 0-16268  
 steel, stainless, reduction of oxide layer by H atoms 0-40738  
 TCNQ salts with heterocyclic amines and hydroquinone form. via redox reaction 0-26013  
 thermal energy, electrochem. conversion using cells with reversal of pot. with temp. 0-26124  
 thermochemical H prod. from water based on mordenite-hosted redox reactions 0-55939  
 Zn-salt, molten system, separation of Hf and Zr 0-11884  
 Al<sub>2</sub>Ge<sub>2</sub>O<sub>7</sub> reduction by C, gaseous and metallic Ge yields (*Russian*) 0-40737  
 Al<sub>2</sub>Ge<sub>2</sub>O<sub>7</sub>, reduction processes by C, kinetic analysis, reaction products (*Russian*) 0-55644  
 B films, prep. by H reduction of BCl<sub>3</sub>, struct. and hardness 0-54543  
 BBr<sub>3</sub>-PCl<sub>5</sub>-H<sub>2</sub>, gas phase equil. comp. 0-35166  
 CO<sub>2</sub> electrochemical reduction for H storage 0-7934  
 CaF<sub>2</sub>·Mn<sup>2+</sup>, fluorite, radiation and thermal redox processes 0-55678  
 CaGeO<sub>3</sub>, reduction processes by C, kinetic analysis, reaction products (*Russian*) 0-55644  
 CdUO<sub>4</sub>, phase transforms., anomalous oxidation state change 0-54369  
 CeO<sub>2</sub> doped electrolyte cell, polarisation phenomena associated with CeO<sub>2</sub> reduction 0-55827  
 Cr<sub>2</sub>O<sub>3</sub>, by C, mechanism 7573-2073K (*Russian*) 0-45483  
 Cr<sub>2</sub>O<sub>3</sub> dissociation in presence of C in Ar, CO and vac. atm., Cr<sub>2</sub>C<sub>2</sub> form. (*Russian*) 0-35570  
 Cr<sub>2</sub>O<sub>3</sub>, reduction by H<sub>2</sub>, reaction kinetics 0-11950  
 Dy<sub>2</sub>O<sub>3</sub> reduction by B, DyB<sub>3</sub> form. mechanism, DTA appl 0-55643  
 EsCl<sub>3</sub>(Br<sub>3</sub>)(I<sub>3</sub>), prep., characterisation and decay of Es(II) 0-16727  
 α-F<sub>2</sub>O<sub>3</sub>, alkali metal hydroxides, reduction, Mossbauer spectra 0-16672  
 Fe, deoxidation by V, phase equilibrium with V<sub>2</sub>O<sub>3</sub> (*Russian*) 0-16275  
 Fe whisker growth, on wustite, Wagner's mechanism 0-10847  
 Fe-C-O alloys, deoxidation when cooled and frozen, appl. of quasiequil. two-phase zone model (*Russian*) 0-16222  
 Fe-Ni-C, atomized, O/C ratio effect, particle size on annealing kinetics, physicochemical props. 0-20832  
 Fe(H<sub>2</sub>PO<sub>4</sub>)<sub>2</sub>, γ-ray and electron radiolysis, Mossbauer study 0-7816  
 FeO surface, water-gas shift reaction kinetics 0-11949  
 Fe<sub>2</sub>O<sub>3</sub>, direct reduction by H<sub>2</sub> reaction kinetics 0-40689  
 GeO<sub>2</sub>, reduction processes by C, kinetic analysis, reaction products (*Russian*) 0-55644  
 H production by thermochemical cycles using fusion energy source 0-51010  
 H production from coal using steam-Fe process, development status 0-55942  
 H<sub>2</sub>, production by solar energy, homogeneous photoredox system 0-3387  
 H<sub>2</sub>O<sub>2</sub>, vac. thermal reduction with Th, for Ho prod. (*Russian*) 0-16226  
 HfO<sub>2</sub> reduction by Ca 0-18746  
 La<sub>0.9</sub>Ca<sub>0.1</sub>CrO<sub>3</sub> polar semiconductor, elec. props., slight reduction effect 0-20183  
 La<sub>2</sub>O<sub>3</sub>, reduction by Si in solar furnace (*French*) 0-16784  
 Mg<sub>2</sub>GeO<sub>4</sub>, reduction processes by C, kinetic analysis, reaction products (*Russian*) 0-55644  
 Mo-RE-O system, Mo-Re alloys prep. (*Russian*) 0-16225  
 MoF<sub>6</sub> reduction by H, chemical kinetics eqn., adsorbed component interactions (*Russian*) 0-35569  
 MoF<sub>6</sub>, reduction by H<sub>2</sub> at 500-1200°C to Mo, exam. of Mo props. and MoF<sub>6</sub> props. (*Russian*) 0-7516  
 MoO<sub>3</sub> powder bed, H<sub>2</sub> reduction kinetics 0-16230  
 Mo(ZrO<sub>2</sub>·La<sub>2</sub>O<sub>3</sub>) structural changes during reduction and sintering 0-25636  
 Nb-Mo, prod. by simultaneous carbothermic reduction of oxides/electron beam melting method (*Japanese*) 0-11590  
 Pt(IV), reduction to Pt(II), X-ray irradi., Ar ion bombardment, XPS obs. 0-35573  
 PtO<sub>2</sub>, sputtered film, optical props. under H<sub>2</sub> reduction 0-20728  
 SOCl<sub>2</sub>, in Li/SOCl<sub>2</sub> cell discharge reaction, cyclic voltammetric and coulometric obs. 0-30440  
 β-Sb<sub>2</sub>O<sub>3</sub> reduction to Sb powder, atomic H effect 0-2978  
 SiCl<sub>4</sub>, conversion to SiCl<sub>3</sub> in unipolar HF discharge 0-1855  
 SiO<sub>2</sub> decomposition and reduction, in low temp. plasma jet (*German*) 0-45499  
 SiO<sub>2</sub>, on Si, reduction by heating in Ga mol. beam at 800°C 0-50730  
 TiCl<sub>4</sub>, electrochemical behaviour in alkali chloride baths 0-30243  
 TiO<sub>2</sub>, reduction with CaH<sub>2</sub>, preparation of rolled Ti foils 0-18744  
 W surface wetting by liquid Cu depend. on preliminary surface treatment (*Russian*) 0-35388  
 WF<sub>6</sub>, mechanism of heterogeneous reduction by H<sub>2</sub> (*Russian*) 0-21265  
 WO<sub>3</sub>, with H, starting specific surface effect on kinetics 0-11599  
 W(ZrO<sub>2</sub>·La<sub>2</sub>O<sub>3</sub>), structural changes during reduction and sintering 0-25636

**reed relays**

- optical multimode fibre routing reed switch improvement 0-53463

**reeling** see winding (process)**references (standards)** see standards**refining, oil** see oil refining**reflectance** see reflectivity**reflection**

- see also acoustic wave reflection; electromagnetic wave reflection; neutron reflection; reflectivity  
 magnetohydroviscoelastic waves reflection at semi-infinite solid boundary 0-48633  
 ocean propagating inertial and internal waves, refl. at rigid boundary rel. to induced drift currents 0-51403

**reflection** continued

- P-wave reflection at non-vertical incidence, synthetic seismograms 0-56401  
 plane obstacles, weak shock wave reflection in air 0-48751  
 Schottky barrier, excitonic refl. of light 0-10885  
 seismic waves, multiple reflections and head waves in Gulf of Suez 0-56400  
 shock waves diffraction and reflection from shock tube, numerical computation (*Chinese*) 0-43735  
 tsunami simulation, Hawaii, open boundary reflection interference 0-17232

**reflection high energy electron diffraction**

- quartz, amorphous layer on mech. treated single crystals, electron microscope and RHEED obs. 0-24721  
 semiconductor, electron spectroscopy techniques, review (*Japanese*) 0-49061  
 ternary semiconductors, measurement of lattice parameters of thin heteroepitaxial layers, RHEED technique 0-15406  
 Ag, epitaxial growth on electron bombard. NaCl(111) surfaces, RHEED and AES 0-15419  
 AlN, epitaxial film growth by MBE, physical and optical props. 0-2293  
 CdIn<sub>2</sub>S<sub>4</sub> film, vac. deposited, growth, struct., optical and photoelectronic props. 0-10831  
 Cu deposition on Au electrode in underpotential region, RHEED investig. 0-54539  
 InSb (110), clean, O<sub>2</sub> adsorption, AES, LEED, RHEED and field effect meas. 0-49501  
 InSb (110), ion bombard. effect on surface struct. and electronic props. 0-6923  
 InSb (110) surface, struct. and electronic props., RHEED and field effect meas. 0-11068  
 Na (111) surface, epitaxial film, electron induced dissociation 0-6646  
 Ni, epitaxial growth, on NiO(100), by low pressure hydrogen reduction (*French*) 0-11578  
 NiSi<sub>2</sub>, epitaxial film on Si, <sup>4</sup>He ion channelling meas. and RHEED anal. 0-10834  
 PbTe (111), lattice vibr. amplitude anisotropy, RHEED study 0-39408  
 PtTe, VPE, on LiNbO<sub>3</sub>, struct. and morphology obs. 0-54561  
 Pd<sub>2</sub>Si, epitaxial film on Si, <sup>4</sup>He ion channelling meas. and RHEED anal. 0-10834  
 PtSi, epitaxial film on Si, <sup>4</sup>He ion channelling meas. and RHEED anal. 0-10834  
 Si (111) 7×7 surface, structure model from anal. of RHEED patterns 0-49471  
 Si, epitaxial film growth on Si(111) and sapphire (1̄102), simultaneous RHEED/AES study 0-10833  
 Si, glow discharge film decomposed from silane, on amorphous substrate, elec. cond., RHEED study 0-20044  
 Si, ion bombard. effect on surface struct., RHEED and Au decoration 0-2096  
 Si, MBE growth and surface struct. 0-10816  
 ZnSe:In films, MBE growth, doping effect on photoluminesc. 0-10818

**reflection nebulae** see nebulae**reflection spectra** see reflectivity; spectra**reflectivity**

- see also electroreflectance; magnetorelectance; piezorelectance; thermorelectance  
 actinide compounds, spectroscopic techniques for electronic props. meas. 0-11427  
 adsorbed molecules, surface plasmon enhanced light absorption 0-40176  
 adsorbed species, IR ellipsometric spectroscopy 0-39434  
 airborne laser scanner, modulation techniques 0-5770  
 anthracene single cryst., Frenkel exciton spectra at dielectric and conducting layer interfaces 0-44510  
 beam incidence angle determ. from refl. meas. (*French*) 0-37072  
 black chrome solar selective absorber, microstruct., chemical comp. and reflective props. 0-7959  
 coal, considerations involved in automation of reflectance microscopy 0-18001  
 p-CuInTe<sub>2</sub>, single cryst., IR study of lattice and free carrier effects 0-45074  
 cylindrical dielectric array, multiple scatt. effects in photon diffraction 0-1905  
 p-dibromodiphenylether surface, normal and ultra-Brewster refl. spectra 0-25400  
 dielectric thin films, refractive index variation for given reflectivity, analytic soln. to synthesis problem 0-34996  
 diffuse reflectance meas. for buildings 0-27334  
 EM waves, parallel polarised, equal reflectance at normal and oblique incidence, dielec. const. meas. 0-1119  
 N-p-ethoxybenzylidene-p'-cyanoaniline, nematic, mol. reorientation in DC elec. field, IR ATR spectra study 0-45064  
 excitons internal structure, review, book contrib. 0-44518  
 film, optical consts. determ. 0-2883  
 film pulsed laser damage determ., optical techniques 0-33060  
 fluorescence spectrometry, beam splitter and cell window errors 0-31897  
 formamide, liq., vac. UV optical and dielec. meas. 0-25329  
 Fresnel formula for dielectric multilayer mirrors 0-33118  
 glossiness of curved surface, physical and psychological, meas. method 0-37074  
 graphite intercalation compounds, alkali and halogen, electronic props., conductivity and optical reflect. (*German*) 0-49837  
 graphite intercalation compounds, band struct. model, dynamical dielec. function, reflectivity 0-34348  
 graphite intercalation cpds., Raman scatt. and IR refl., review 0-45066  
 graphite-alkali metal intercalation cpds., electronic props. 0-45202  
 inhomogeneous diffuse media, reflectances and transmittances, charact. matrices 0-32915  
 interference filters, multilayer, design method 0-48396  
 IR reflection spectrum, dispersion formula fitting, Kramers-Kronig anal. 0-50311  
 laser cavity resonator, photon lifetime and reflectance meas., phase-shift method 0-38039  
 layer surfaces, reflectivity at 3.39 μm, meas. method, relevance to pipelines 0-52340  
 liquid semiconductors, data and model densities of states 0-50364  
 MBBA, nematic liq. cryst. isotropic phase, phase-conjugate refl. by degenerate four-wave mixing 0-43389  
 measurement of reflectance and transmittance, arrangement for integrating sphere (*German*) 0-31844



## reflectivity continued

- metal surface, perturbative calc. of elec. field 0-45108  
 metal-electrolyte boundary, electrodynamics in visible and near UV range, microscopic effects 0-45521  
 metallic glass, bulk and surface properties, review 0-44147  
 metallic thin films, free-electron, optical props., theory including electron surface scatt. 0-29817  
 microscope photometry in studies of molecular struct. of carbonized bitumens and pyrobitumens 0-18011  
 molecular crystal, surface exciton levels, radiation corrections 0-34962  
 multilayer nonabsorbent coating reflectivity computation program 0-28293  
 multiwavelength radiation pyrometry where reflectance is measured to estimate emissivity 0-31757  
 normal reflectance of conductors and insulators, dispersion relations and sum rules 0-29706  
 optical apparatus for reflectivity meas. by changing incident angle 0-18000  
 optical system, cryogenic and contamination effects 0-38113  
 petrographic characterization of coal using automatic image analysis 0-18002  
 planetary reflectance meas. in thermal emission region, thermal component removal 0-17497  
 plant canopies reflectance meas. using spectroradiometer 0-56658  
 plasma target, underdense, Brillouin backscatt. saturation 0-14886  
 polar semiconductor, electron-hole liquid, electron-phonon interactions 0-6739  
 polyacetylene, pure and heavily doped, optical and IR studies, electronic struct. calcs. 0-7347  
 radiative transfer between surfaces in diathermal medium, radiation anisotropy modelling 0-33435  
 refractory metal films, evaporated, optical props., rel. to struct. 0-55211  
 rocks from Cr-rich areas, visible and near IR spectra, remote sensing appls. 0-4000  
 roughness measurement using laser scanning analyser 0-36992  
 selective solar absorbers, reflectance calcs. for inhomogeneous surfaces 0-12029  
 semiconductor, surface electronic props., optical spectroscopic techniques, review 0-11070  
 semiconductor dopant surface concentration determ. by IR reflectance 0-34036  
 solar photothermal non-selective and energy control films coatings 0-26157  
 solar reflectivity of common building materials, effect on roof heat gain 0-55810  
 solar selective absorber coatings, reflectance, emittance, and thermal stability 0-12027  
 solid dielectric complex and power reflectivity determ., 100 GHz to 3 THz 0-15999  
 solid-liquid transition, optical reflectance spectra 0-24569  
 solids, effect of angular aperture and radiation polarisation of instrument on reflection coeff. 0-9020  
 spectral reflectance and transmittance measuring apparatus for variable angle of incidence 0-250  
 structural colours of beetles, analysis using reflectance measurements from macro- and microspectrophotometers 0-18023  
 surface contaminant generation and bidirectional reflectance distrib. function meas. 0-14493  
 surface ripples, role of reflectivity in light scatt. 0-20653  
 TCNQ salt, (NMe<sub>2</sub>H)(I)(TCNQ), one-dimens. semicond. with metal-like cond. 0-24909  
 TCNQ salt, K-TCNQ, single crystal, charge transfer band interpretation, refl. spectrum obs. 0-25353  
 TCNQ salt, MTPA (TCNQ)<sub>2</sub>, IR refl., dielec. function and cond. 0-34924  
 TCNQ salts, anomalous infra-red activity and the determination of electron-molecular vibration coupling constants 0-25389  
 tetracene surface states, electric field effects, exciton-charge carrier interactions (*Russian*) 0-24989  
 thiourea, phonon modes near phase transitions, IR and Raman spectra 0-45084  
 tissue model, two-layer, theoretical anal. of diffuse reflectance 0-35956  
 TTF-TCNQ, electron-molecular distortion coupling near Peierls transition, IR spectra obs. 0-25390  
 TTF-TCNQ, IR reflectance in conducting phase 0-25388  
 TTT-(I)<sub>2</sub>, physical props., elec., mag. and optical meas. 0-24908  
 Ag film, evaporated, chemisorption effects on reflectance and elec. resist. 0-11495  
 Ag surfaces, Cs and Cs-O covered, surface plasma waves, ATR study 0-39451  
 Ag<sub>2</sub>GeTe<sub>3</sub>, optical props. and polymorphism 0-45082  
 β-AgI (4H), visible spectra, reflected light phase and amplitude, exciton resonance 0-45110  
 Al, diamond-turned, surface reflectivity meas. 1 to 12 μm 0-1298  
 Al, IR laser reflectance, anomalous absorpt., plasma ignition 0-7439  
 Al reflective coating, reflectance in UV and visible 0-28307  
 Al-Cu alloy, deposition from RF induction source, onto laminated polyimide substrates and characterisation 0-16535  
 Al<sub>2</sub>O<sub>3</sub> anodic films, formed on Al, optical reflectance method anal. 0-37073  
 Al<sub>2</sub>O<sub>3</sub>:Ni anodised films, electrolytically coloured, spectrally selective surface 0-11490  
 As<sub>2</sub>O<sub>3</sub>, vitreous, local struct. and vibrational spectra 0-55091  
 Au, films, optical props. meas. rel. to electron surface scatt. theory 0-29818  
 Au<sub>2</sub>Si<sub>9</sub>, optical refl., 0.5 to 6 eV, hall coeff. and elec. resist. 0-29755  
 B, β-rhombohedral, optical absorption band in 8 μm region, anomaly of temp. dependence 0-29735  
 B<sub>12</sub>C<sub>2</sub>, phonon energies and electronic props., x depend., refl. spectra and thermolec. power meas. 0-16052  
 BaO, logarithmic derivative reflectance spectra 0-11429  
 (Be, Al)B<sub>12</sub>, wide-gap semicond., elec. cond., refl. and absorpt. spectra 0-20188  
 Be substrate for lightweight mirror, surface quality and thermal props. 0-23762  
 BiI<sub>3</sub>, layered compound, exciton spectra, surface and stacking fault effects 0-40134  
 Bi<sub>2</sub>Se<sub>3</sub>:Hg point defects in crystal lattice, Hall coefficient and IR spectra determ. 0-55129  
 CaSO<sub>4</sub>, anhydrite, resonance splitting of complex anion internal vibrs. 0-55081

## reflectivity continued

- CaSO<sub>4</sub>, anhydrite and gypsum, phonon spectroscopy, lattice dynamical calc. 0-19889  
 Cd films, nucleation and growth, props. 0-29878  
 CdCr<sub>2</sub>Se<sub>4</sub>, magnetic red shift origin, specular reflectivity, band struct. 0-40127  
 CdGa<sub>2</sub>Se<sub>4</sub>, IR refl. spectra, optical phonon dispersion 0-29746  
 CdGa<sub>2</sub>Se<sub>4</sub>, struct. of valence band, photocond. and reflection spectra meas. 0-6719  
 Cd<sub>1-x</sub>Hg<sub>x</sub>Te, band struct. and optical props. 0-15450  
 n-Cd<sub>1-x</sub>Hg<sub>x</sub>Te, conduction band struct., IR refl. spectra obs. 0-39502  
 CdS, A<sub>n-1</sub>-exciton, reflectance and thermoreflectance spectra, spatial dispersion and angle of incidence effects 0-25409  
 CdS active surface, exciton stimulated emission and superradiance refl. spectra, props. 0-25411  
 CdS, excitonic polariton reflectance, B-exciton and k-linear term 0-7369  
 CdS, high intensity excited, exciton reflection spectra, reflection struct. 0-20692  
 CdS, influence of Lamb US waves on exciton spectra (*Russian*) 0-7374  
 CdS<sub>1-x</sub>Se<sub>x</sub> film, resonance between Se atom dipole vibr. and interference modes, IR spectra obs. (*Russian*) 0-2888  
 CdSe, high intensity excited, exciton reflection spectra, reflection struct. 0-20692  
 CdSiP<sub>2</sub>, reflectance spectra at 300K 0-25407  
 CdTe, spatial dispersion rel. to exciton reflection spectra (*Russian*) 0-40126  
 CdTe:Fe(Ni), luminesc. and refl. spectra, high temp. annealing effects 0-24472  
 CeSb, forbidden band gap and electrotransfer parameters 0-39497  
 Co film, optical props. by self-consistent photometric technique 0-55217  
 Co<sub>1-x</sub>Fe<sub>x</sub>Si, elec. and optical props. 0-49740  
 CoO-MgO-Cr<sub>2</sub>O<sub>3</sub>-Fe<sub>2</sub>O<sub>3</sub>-TiO<sub>2</sub>, form. and colour of spinel solid soln. (*Japanese*) 0-16059  
 Cr<sub>2</sub>O<sub>3</sub>-Cr black, selective coating, optical and topographical props. 0-26165  
 CsPbBr<sub>3</sub>, electronic and optical props. 0-25414  
 CsPbCl<sub>3</sub>, electronic and optical props. 0-25414  
 CsPbCl<sub>3</sub>Br<sub>1-x</sub>, optical meas., LCAO band scheme 0-25437  
 Cu film, EXAFS meas. by total refl. 0-55228  
 Cu, fine interaction of surface electrons, IR spectra 0-16041  
 Cu-Al, optical composition modulation spectra, dielec. const. var., Fermi surface and electronic level shifts 0-6707  
 Cu-Zn, optical composition modulation spectra, dielec. const. var., Fermi surface and electronic level shifts 0-6707  
 CuFeS<sub>2</sub>, single crystal, optical reflectivity spectrum 0-40129  
 Cu<sub>2</sub>S, optical and calorimetric meas. of thin films for Cu<sub>2</sub>S-CdS solar cells 0-55863  
 EuS films, ferromag., optical spectra and light scatt. from spin waves 0-16116  
 Eu<sub>1-x</sub>Sr<sub>x</sub>S, exciton refl. spectra 0-2782  
 Fe-Cr alloys, passivation films, modulation spectroscopy study 0-3244  
 Fe<sub>2</sub>O<sub>3</sub>, haematite, anal. of refl. spectrum by Kramers-Kronig relations 0-16058  
 Ga<sub>1-x</sub>Al<sub>x</sub>As, IR refl. spectra and Raman spectra 0-20623  
 GaAs (110), surface states, optical techniques 0-6939  
 GaAs anodic oxide film, ellipsometric and IR spectroscopic studies 0-11493  
 GaAs, anodisation obs. by in situ differential refl. 0-50732  
 GaAs, CC Ga-3d-excitation, high resolution reflectivity down to 15K 0-25415  
 n-GaAs, conduction band nonparabolicity and coupled plasmon-phonon modes, IR refl. spectra 0-55110  
 GaAs, ion implanted, mode-locked Nd:YAG laser annealing, recrystn., optical reflectivity meas. 0-19817  
 GaP, ion implanted, mode-locked Nd:YAG laser annealing, recrystn., optical reflectivity meas. 0-19817  
 GaP, polariton dispersion, IR reflection spectroscopy 0-11415  
 GaS, reflectivity from 4 to 32 eV, Kramers-Kronig anal. 0-34943  
 GaS(Se), polar optical phonon ang. behaviour, IR refl. meas. 0-20633  
 GaSe excitonic spectra fine struct., reflection and transmission spectra (*Russian*) 0-55126  
 GaSe, reflectivity from 4 to 32 eV, Kramers-Kronig anal. 0-34943  
 GaTe, exciton polariton effect on absorpt. edge, absorpt. and refl. spectra, 4.2 to 300K 0-20664  
 GaTe, excitonic absorpt. edge, transmission and refl. meas. 0-40133  
 GeO<sub>2</sub>, ultrathin layers on Ge substrate, ATR spectra, thickness depend., struct. obs. 0-55214  
 GeSe, amorphous film, laser induced light absorpt. oscillation, exciton model 0-50446  
 Ge(111)2×1, oxide layer, surface states detect optical reflectivity obs. 0-50368  
 H<sub>2</sub>O, liquid, far IR optical const. meas. with optically pumped laser 0-40082  
 H<sub>3</sub>PO<sub>4</sub>(MoO<sub>3</sub>)<sub>12</sub>.29H<sub>2</sub>O, electrochromic solid-state cells 0-2724  
 (H<sub>3</sub>PO<sub>4</sub>)(WO<sub>3</sub>)<sub>12</sub>.29H<sub>2</sub>O, electrochromic solid-state cells 0-2724  
 HfS<sub>2</sub>, quasi one-dimens., optical phonon anisotropy, IR spectra study 0-40112  
 Hg<sub>2</sub> vapour, high-press., selective refl. meas. up to 700 bar 0-28031  
 Hg<sub>0.75</sub>Cd<sub>0.25</sub>Te, single crystal, reflection spectra 0-40140  
 n-HgCr<sub>2</sub>Se<sub>4</sub>, ferromagnetic semiconductor, plasmon refl., 86 to 320K 0-50346  
 InN film, specular reflection spectra, lattice parameters 0-7428  
 InP, free carriers, freq. depend. relax. time 0-2385  
 InP, reflection spectra, optical functions, exciton peaks (*Russian*) 0-50372  
 InS, IR reflection spectra 0-11389  
 InSe, energy band structure, chem. bond polarity, photoemission, semiempirical tight binding method 0-44504  
 InSe, optical props. from 2-25 eV 0-29760  
 InSe, polar optical phonon ang. behaviour, IR refl. meas. 0-20633  
 InSe, reflectivity and low energy absorption 0-34944  
 InSe, reflectivity from 4 to 32 eV, Kramers-Kronig anal. 0-34943  
 KBr:Na(Rb)(Cs), microcrystalline powders, isothermal decay of colour centres 0-2804  
 KCl:Ca(Ba)(Mg)(Sr), microcrystalline powders role of Z centres in stabilizing coloration, optical absorption 0-54227  
 KCl(Br)(I) with alkali and halogen impurities, colour centre deformation induced nonradiative decay 0-7387  
 KF(Br)(Cl)(I), K<sup>+</sup>3p core excitons, refl. spectra study, low temp. 0-29759  
 La compounds, plasma light reflection by free charge carriers 0-11403



## reflectivity continued

- Li<sub>0.5</sub>Fe<sub>2.5</sub>O<sub>4</sub>, magneto-optical spectra, polar Kerr rotation, dielectric tensor elements spectra 0-40091  
 MnAs<sub>0.88</sub>P<sub>0.12</sub>, excitonic absorpt., derivative refl. spectra 0-25406  
 Mn<sub>2</sub>Fe<sub>1-x</sub>O<sub>4</sub>, optical props. 0-20606  
 Mo film, CVD, with high IR refl. and large solar absorpt., prep. and props. 0-26163  
 Mo film, polycryst., energy loss function, Kramers-Kronig anal., reflectivity, optical props., EELS 0-40194  
 MoSe<sub>2</sub>(Te<sub>2</sub>), IR and Raman spectra, lattice vibrs. interlayer bonding 0-40110  
 NaCl, single cryst., for IR dispersive refl. meas., low temp., rel. to anharmonicity calcs. 0-11371  
 NaClO<sub>4</sub>, Brewster type surface mode dispersion, IR refl. meas. 0-11415  
 NdSb, forbidden band gap and electrotransfer parameters 0-39497  
 Ni (110), chemisorption of N<sub>2</sub>, mol. and dissociative mechanisms 0-39431  
 Pb<sub>1-x</sub>Ge<sub>x</sub>Te, ferroelec. phase transition, IR refl. and resist. meas. 0-11353  
 PbHPO<sub>4</sub>, microwave permitt. and far IR refl. spectra in paraelec. and ferroelec. phases 0-40033  
 Pbl<sub>2</sub>, film, reflectance meas., optical const., humidity effects 0-34994  
 Pbl<sub>2</sub>, layered compound, exciton spectra, surface and stacking fault effects 0-40134  
 PbS film, vac. deposited, optical and phys. props. 0-2315  
 PbTe very thin epitaxial films, transmission and refl. spectra, 1 to 5 eV 0-7430  
 Pdl<sub>n</sub>, refractive index, reflectivity and band struct., APW calcs. 0-40139  
 Pr compounds, plasma light reflection by free charge carriers 0-11403  
 PrSb, forbidden band gap and electrotransfer parameters 0-39497  
 Pt evaporated film, optical props. meas. in VUV, 220 to 150 Å 0-45159  
 Sbl<sub>3</sub>, layered compound, exciton spectra, surface and stacking fault effects 0-40134  
 Si, amorphous, ion implanted, laser annealing, reflectivity meas. 0-29039  
 Si amorphous film, film, glow discharge deposited, refl. spectra and dielec. function 0-50360  
 Si amorphous film, optical props., electronic states 0-25475  
 Si, free carrier and interband absorpt. at 1.06 μm, temp. depend. 0-2783  
 Si, glow discharge amorphous film, reflectance and transmittance (Japanese) 0-34995  
 Si, glow discharge deposited, optical spectra, reflectance, dielectric function and oscillator strength 0-11492  
 Si, ion implanted, mode-locked Nd:YAG laser annealing, recrystn., optical reflectivity meas. 0-19817  
 Si, ion irradi., temp. and dose depend. of defect profiles 0-29097  
 Si on sapphire, laser annealing dynamics epitaxial regrowth, optical reflectivity 0-29285  
 Si, surface roughness evaluation by UV refl. 0-39393  
 Si<sub>3</sub>N<sub>4</sub> thin film, multiple internal refl. IR spectroscopy 0-11499  
 SiNH films, thickness and refractive index meas., comparison of techniques 0-8957  
 SiO film on Al, radiative cooling surface 0-50439  
 SiO<sub>2</sub> films, thickness and refractive index meas., comparison of techniques 0-8957  
 SiO<sub>2</sub>, ion implanted, fused, refr. index profiles 0-54272  
 SiO<sub>2</sub>, ultrathin layers on Ge substrate, ATR spectra, thickness depend., struct. obs. 0-55214  
 Si(111)2×1, oxide layer, surface states detec., optical reflectivity obs. 0-50368  
 SmSb, forbidden band gap and electrotransfer parameters 0-39497  
 SnS<sub>2</sub>(Se<sub>2</sub>), optical transitions from d core levels 0-45105  
 SrO, logarithmic derivative reflectance spectra 0-11429  
 TeO<sub>2</sub>, paratellurite, optical absorpt. and refl. spectra, 80-500K, optical const. determ. 0-50359  
 Th, optical reflectivity 0-16054  
 Ti, clean and oxidised surfaces, refl., 2-25 eV 0-55123  
 TiO<sub>2</sub>, antireflection coatings for solar cells, optical, struct., and compositional characts. 0-55852  
 Ti<sub>2</sub>O<sub>3</sub>, metal-semicond. transition, refl. spectra study 0-10880  
 TiS<sub>2</sub>, evidence for semicond. props., Hall coeff., refl., cond., thermolec. power 0-20220  
 TiS<sub>2</sub>, transport props. and semicond. nature 0-44598  
 TiSe<sub>2</sub>(S<sub>2</sub>) (1T), electronic and vibronic struct. 0-44500  
 Tl<sub>2</sub>As<sub>2</sub>, optical phonons, Raman and refl. spectra 0-11400  
 TiGaS<sub>2</sub>Se<sub>2(1-x)</sub>, layer solid soln., long wave lattice vibrs., IR reflection spectra 0-11388  
 TiGaTe<sub>2</sub>, IR refl. and Raman scatt. spectra, lattice vibrs. 0-40108  
 TlInS<sub>2</sub>Se<sub>2(1-x)</sub>, layer solid soln., long wave lattice vibrs., IR reflection spectra 0-11388  
 TlInTe<sub>2</sub>(Se<sub>2</sub>), IR refl. and Raman scatt. spectra, lattice vibrs. 0-40108  
 US, ferromagnet, electronic structure, reflectivity (German) 0-49567  
 US, optical props. and electronic struct. 0-25410  
 USb, reflectivity spectrum, band struct. 0-7368  
 Use (s) 0-16053  
 VO<sub>2</sub>, nonstoichiometry influence on electron struct. and metal-insulator phase transition 0-44507  
 VO<sub>2</sub> single cryst. film, ion-irrad., 'splitting' of semicond.-metal transition 0-11053  
 VO<sub>2</sub> variable-reflectance mirror for CO<sub>2</sub>-N<sub>2</sub>-He 10.6 μm scan laser 0-38026  
 V<sub>2</sub>O<sub>5</sub> film, amorphous, thickness, density and refr. index determ. from reflectance interference spectra 0-55206  
 V<sub>2</sub>O<sub>5</sub>, optical props. in metallic and semicond. phase 0-40135  
 W (110) surface, adsorption of H, band struct. and adsorbate geometry, surface-reflectance-spectroscopy 0-44416  
 W, chemisorbed H, surface cond. and intrinsic surface states, surface refl. spectra 0-15378  
 W-Fe spin glass, optical props. and electronic states 0-20412  
 Xe, crystalline, polariton effects, reflectivity, absorpt., and resonant luminesc. spectra calcs. 0-20095  
 YIG, magneto-optical spectra, polar Kerr rotation, dielectric tensor elements spectra 0-40091  
 YbSb, forbidden band gap and electrotransfer parameters 0-39497  
 ZnO, polariton dispersion, IR reflection spectroscopy 0-11415  
 Zn<sub>3</sub>P<sub>2</sub> bulk and thin film, UV reflectivity spectra, photovoltaic effects, optical const. 0-25472  
 ZnSe crystal, exciton reflection spectra, control of exciton-free surface layer thickness 0-7373  
 ZnSiP<sub>2</sub>, reflectance spectra at 300K 0-25407  
 ZnTe, reflectivity meas., double beam wavelength modulated technique (Korean) 0-50365

## reflectivity continued

- ZrS<sub>2</sub>(Se<sub>2</sub>), quasi one-dimens., optical phonon anisotropy, IR spectra study 0-40112  
 ZrSiO<sub>4</sub>, zircon, resonance splitting of internal vibr. freq. of complex anion 0-55080
- reflector antennas**  
 Cassegrain, double knife-edge diffraction for curved screens 0-14273  
 feeds, compact dual-hybrid-mode feeds with low crosspolar radiation 0-12662
- reflex klystrons**  
 No entries
- refraction**  
*see also acoustic wave refraction; electromagnetic wave refraction; refractive index*  
 metallic surface state, influence of refr. of p-polarised light on photoemission 0-20772  
 ocean wave refraction by circular island, model 0-36316  
 seismic waves, nature of errors in refractor vel. determ. 0-56621  
 tetragonal media, elliptical conical refraction of elastic waves 0-5976
- refractive index**  
*see also photorefractive effect; refractometers*  
 acetic acid-acetone mixture, physical parameters 0-2716  
 alkali halide, optoelectronic props. 0-25330  
 alkali metal halide, laser damage morphology simulation 0-35015  
 alkaline earth silicate glasses, morphology effects on props. 0-49118  
 anilines, substituted, in benzene soln., dielectric relax. time, dipole moment 0-50259  
 antireflection coating, three-layer, refractive index optimum combination 0-28306  
 asymmetric three-layer optical waveguide, radiation losses due to discontinuities 0-53446  
 benzene, magneto-optic rotatory dispersion curves 0-45040  
 tert-butyl alcohol in nonpolar solvents, liq. struct. from dielectric studies 0-38894  
 CdS film, polycryst, optical spectra, 0.5-6.5 eV 0-55212  
 cellulose acetate, conc. soln., light scatt. studies 0-16050  
 chalcopyrites, refr. index dispersion 0-55057  
 Cherenkov radiation, variation of colour attenuation due to refr. index modifications (Spanish) 0-7432  
 cholesteric liquid crystal, molecular polarisability, arrangement order calc. (Polish) 0-10495  
 complex, for Lorentzian-type absorption band 0-50291  
 crystal optics, spectral expansions of refr. index tensors 0-34873  
 curved graded index medium, aberration analysis 0-14295  
 cylindrical gradient index lens and array radiometric props. 0-14421  
 degenerate four-wave mixing, refr. index changes 0-9936  
 DH diode lasers, appl. of equivalent-index method 0-23772  
 dielectric interference film, with equal optical thicknesses of layers, theoretical design (Russian) 0-43471  
 dielectric liquid, charge generation and transport from contacting surface, Mach-Zehnder and Schlieren obs. 0-20589  
 dielectric thin films, refractive index variation for given reflectivity, analytic soln. to synthesis problem 0-34996  
 diffused waveguide, refractive index profile determ. by inverse scatt. theory 0-5838  
 double Gauss basic lenses, design (German) 0-53398  
 elastooptical constants and refractive index, thermo-optical method for meas. 0-7327  
 electromagnetic wave scattering, physical model and profile reconstruction, for inhomogeneous ionised regions 0-1109  
 EM wave propagation in stochastically stratified medium, transmission coeff. 0-32887  
 ferromagnetic semiconductor, refr. index variation in strong alternating mag. field 0-23741  
 film, optical const. determ. 0-2883  
 film pulsed laser damage determ., optical techniques 0-33060  
 formamide, liq., vac. UV optical and dielec. meas. 0-25329  
 gases, compressed, refractive index meas. using Fabry-Perot interferometer (French) 0-14878  
 geodesic aspherical perfect lens, general sol. for integrated optics 0-10049  
 geodesic lenses, aberration-corrected rounded edge, profile calcs. 0-10048  
 glass, chem. tempered, surface stress meas. using opt. waveguide effect (Japanese) 0-45473  
 glass, refractive index freq. depend., dispersion enq. calc. 0-40083  
 glass, thermally tempered sheet and plate, surface stress meas. using optical waveguide effect 0-25967  
 glass cylinder refractive index variation by field-assisted ion exchange 0-14500  
 glass optical waveguide fabrication by effusion 0-5850  
 glass planar optical waveguide fabricated by ion exchange, refr. index profile 0-14460  
 graded fibres with non-circular index contours, core fields 0-14455  
 graded glass fibre, effect of shape of refractive index profile, on distortion 0-33197  
 graded index fibre, low-loss, produced by double crucible technique 0-48449  
 graded index fibres made by vapour phase axial deposition, refr. index profile 0-48477  
 graded index rod lens applications in optical fibre communications 0-14485  
 graded-index fibre transmission characteristic computation 0-1321  
 gradient index fibre array, illumination intensity unevenness, theory and expt. 0-14480  
 gradient index fibre array, transmittance analysis 0-14478  
 gradient index fibre array development and imaging props. 0-14483  
 gradient index fibre array for photocopying machine 0-14492  
 gradient index fibre image intensifier system 0-14484  
 gradient index imaging lens and system status 0-14420  
 gradient index imaging system theory 0-14294  
 gradient index lens array fabrication for office photocopier 0-13178  
 gradient index lens fabrication by molecular stuffing 0-14499  
 gradient index material models and exptl. verification 0-16002  
 gradient index optical imaging systems, topical meeting, Rochester, USA (May 1979) 0-12851  
 gradient index SELFOC lens, aberration improvement 0-14425  
 gradient index spherical lens design for selfcoupled optical pickup system 0-14427  
 heavy water, piezo- and elasto-optic props. under high press. 0-50296



## refractive index continued

- p-heptyl-p'-cyanobiphenyl, refractive index, dielec. const., mag. susceptibility, orientational ordering (*Dutch*) 0-33884  
 II-VI semiconductors, mag. susceptibility, effect of physical parameters 0-44793  
 inhomogeneous and randomly distributed media, diffracted amplitude and intensity, statistical models (*Spanish*) 0-48151  
 interference coating, with narrow reflection bands, design (*Russian*) 0-43472  
 interpolation of data, collection of program library 0-55056  
 isotropic medium, nonlinear refr. index, self-induced polarisation rot. 0-5802  
 laser with inhomogeneous active medium, emission asymmetry 0-28191  
 liquid, of chiral mols., magnetorefractive effect, linear 0-25343  
 liquid crystal, refractive index near smectic-A/smectic-C transition, orientational order 0-24572  
 liquid with absorbing particles, laser beam illum., refr. index change, bubbles form. 0-25334  
 liquids for cooling and index matching of Nd:glass laser systems 0-33015  
 MBAB, liq. cryst., Brillouin-Mandelstam light scatt. and refr. index 0-55119  
 MBBA, nematic liq. crys., refractive index distrib. and mol. alignment in electro-optical effect (*Japanese*) 0-20613  
 MBBA, refractive index, dielec. const., mag. susceptibility, orientational ordering (*Dutch*) 0-33884  
 medium-particle correlation effects in single scattering from particles in fluctuating medium 0-32917  
 metal oxide layers, obtained by cathode and HF sputtering, light scatt. and refr. index reduction 0-29877  
 microwave absorption coefficient and refractive index, optimal orthogonal functions 0-36379  
 multimode fibre bandwidth, calc. from refr. index profile meas. 0-5817  
 multimode fibre bandwidth spectrum, depend. on refr. index profile 0-9985  
 nitrobenzene, oscill. optically induced Kerr kinetics 0-1286  
 nitromethane-isooctane, liq. mixture, coexistence curve, refr. index meas. 0-10655  
 nonlinear optical crystals, SHG, absorpt. coeffs. and temp. variation of refr. index difference 0-14390  
 nonlinear refractive index  $n_2$  of transparent dielectric crystals (*Chinese*) 0-45028  
 ocean refractive index microstruct. from diffusive and turbulent ocean mixing 0-56486  
 optical fibre, arbitrary index profile, formula for  $TE_{01}$  cutoff freq. 0-48418  
 optical fibre, gamma irradiated, radii and refr. index changes 0-1338  
 optical fibre, graded index, intermodal dispersion meas. 0-38115  
 optical fibre, high bandwidth graded-index, propag. consts. meas. related to material props. 0-38103  
 optical fibre, low V-number, secondary maxima in far-field radiation pattern 0-33182  
 optical fibre, power-law graded-index, core/cladding power distrib., propag. const. and group delay 0-48420  
 optical fibre, power-law refractive index profile, scalar modal eigenvalues and group delays 0-28322  
 optical fibre, quasiparabolic index profile, propag. characts., perturbation anal. (*French*) 0-33189  
 optical fibre refractive index profile models 0-14453  
 optical fibre single mode characterisation by  $LP_{11}$  mode radiation pattern 0-23790  
 optical fibre with profile distortion, multimode delay compensation 0-33143  
 optical fibres, graded-index, propag. consts. and group delays 0-23770  
 optical fibres, profile synthesis using algorithm for inverse Sturm-Liouville problem 0-28351  
 optical fibres, refractive index profile, effect on fibre bandwidth 0-23773  
 optical fibres and preforms, modified CVD, axial refr. index depression, interf. microscopy obs. 0-1319  
 optical glass, Raman scatt. and nonlinear refr. index 0-2749  
 optical glasses, development and manufacturing processes 0-53393  
 optical system, cryogenic and contamination effects 0-38113  
 optical waveguide, asymmetric dielectric-slab, beam mode scatt. characts. 0-38114  
 organic molecular crystals, optical anisotropies 0-50287  
 organic thin film refractive index adjustment by absorbing dyes 0-43413  
 PAA, refractive index, dielec. const., mag. susceptibility, orientational ordering (*Dutch*) 0-33884  
 parabolic gradient index lens, SELFOC, chromatic aberration in imaging system 0-14422  
 photocopier lens array design, Wood lens and gradient index fibre comparison 0-14479  
 photographic gradient singlet, total aberrations 0-13177  
 plano-cylindrical Fresnel plastic lens, design and performance analysis as solar collector 0-53403  
 plastic gradient index lens fabrication and image evaluation 0-14426  
 PMMA, piezobirefringence, optical and mech. relaxations, temp. depend. 0-34885  
 polymer, total integrated light scatt. intensity 0-45092  
 polymeric films, solvent cast, optical anisotropy origin 0-20610  
 polystyrene, crazed, orientation and struct., optical meas. 0-30121  
 quartz, natural and synthetic,  $\alpha$ - $\beta$  transition, impurities effect, refr. index meas. 0-20928  
 radial refractive index gradient optical element, off-axis aberrations 0-14423  
 rare earth molybdates, cryst. growth, cryst. chem., and phys. props., book contrib. 0-44194  
 ray tracing in general index distributions 0-14279  
 sapphire, shock compressed, refractive index, density, and polarisability behaviour 0-50295  
 schlieren method for the determination of electric field distributions in dielectrics 0-31720  
 self-filtering multilayer S-waveguides with absorption and radiation losses 0-38102  
 semiconductors, Moss relation between refr. index and energy gap 0-11357  
 single mode optical fibres, microbending loss evaluation, core index profile effects 0-48412  
 smoke aerosol microstruct. and refr. index, optical determ., inversion method 0-36399  
 soda lime glass gradient index variation by ion exchange and migration 0-14412

## refractive index continued

- step-index fibres, multimode silicone-clad, mode dispersion 0-33142  
 structural phase transition induced refractive index changes in crystals. 0-16000  
 structure const., height depend., turbulent atmosphere 0-36397  
 tapered gradient index rod, geometrical optics and imaging props. 0-14280  
 trichloroacetonitrile, IR dispersion, complex refractive index and permittivity, time correl. function 0-45057  
 waveguide, clad parabolic-index square-law dielectric, perturbation anal. 0-33190  
 waveguide, curved, with parabolic refr. index profile over cross section, light propag. 0-19104  
 waveguide, with refr. index varying over cross section, curved, light propag. 0-19103  
 waveguides, diffused glass, graded refractive index, anisotropy 0-33210  
 zero Petzval curvature radial gradient index lens, third-order aberrations 0-14424  
 $Ag_8GeTe_6$ , optical props. and polymorphism 0-45082  
 AgI large single crystals, gel and soln. growth and props. 0-35071  
 $Al_2O_3$  optical waveguide, fabrication by reactive Al sputtering in  $O_2$ -Ar atm. 0-33262  
 $Al(PO_3)_3$ -NaF-LiF glasses, mixed-alkali effect 0-19715  
 As-S-Se-Ge semiconducting glasses, IR characts. (*Czech*) 0-25332  
 As-Se and  $As_2S_3$  films, electron-stimulated changes in optical props. and dissolution rate 0-29709  
 As-Se chalcogenide glass, optical const. photoinduced changes mechanism 0-7321  
 $As_2S_3$  glass, press. effect on optical props. 0-50363  
 $As_{100-x}$  amorphous film, photoinduced changes in optical props. 0-50445  
 B:H amorphous CVD films, IR, visible, and near UV optical props. 0-50442  
 BN film, undoped and P-doped, effect of CVD parameters on props. 0-25571  
 $BaF_2$  crystal, refr. index temp. increments meas. 0-33098  
 $BaGeO_3$ -(0.25MgF $_2$ -0.75YF $_3$ )- $Ga_2O_3$  glass, synthesis and props. 0-25648  
 $BaO-Al_2O_3-GeO_2-MF_2$  ( $M=0.45CaF_2+0.55MgF_2$ ),  $MgF_2$  and  $CaF_2$  effect on physicochem. props. 0-34876  
 $BaO-PbO-GeO_2-MF_2$  ( $M=0.45CaF_2+0.55MgF_2$ ),  $MgF_2$  and  $CaF_2$  effect on physicochem. props. 0-34876  
 Bi film, refractive index determ. using Rayleigh-Lowe refractometer 0-7427  
 $Bi_2Si_2O_7$  films on Si, form. kinetics and props. 0-35358  
 $Bi_2(Te_{1-x}S_x)_3$  film, optical consts. meas., Shamir-Graff method evaluation 0-11489  
 C, vapour-deposited, transparent and hard insulating layer, struct. and props. 0-10830  
 $CO_2$  refractive index meas., intermolecular interaction effects 0-33728  
 $CO_2$ , density and refractive index, volumetric meas. by Burnett method 0-29707  
 $CS_2$ , liq., struct. and equil. optical props. 0-45026  
 $CS_2$ -glass boundary, optical bistability at nonlinear interface 0-33094  
 $Ca-SiO_4-MgO$ , conditions and mechanism in cryst.-chemical stabilisation of unstable phases 0-39302  
 $CdCr_2Se_4$ , refr. index variation in strong alternating mag. field 0-23741  
 $CdS:Li$  film, optical props. 0-2886  
 $CdTe$ , cryogenic refractive indices and temp. coeffs. meas. 0-7319  
 $CeSb$ , forbidden band gap and electrotransfer parameters 0-39497  
 $CsBr$ , cryogenic temp. IR refractive index obs. 0-7320  
 $CsCaCl_3$ , optical characts. over wide spectral range 0-34875  
 $CsI$ , cryogenic temp. IR refractive index obs. 0-7320  
 $Cu_2NaBiCl_6$ , optical, photoelastic, acoustooptic props. 0-55064  
 $Cu_2S$ , polycryst. thin films, struct., optical and elect. props. for solar energy appl. 0-10837  
 $DyAsO_4$ , cooperative Jahn-Teller transition, optical study 0-15240  
 $DyVO_4$ , cooperative Jahn-Teller transition, optical study 0-15240  
 Eu complex, benzoyltrifluoro-acetone-chelate, refr. index determ. of fluorescent films 0-40175  
 GaAs amorphous film, EXAFS, optical and elec. props. 0-49547  
 GaAs anodic oxide film growth obs. by in situ differential refl. 0-50732  
 GaAs, refr. index and induced birefringence dispersion 0-2717  
 GaP amorphous film, EXAFS, optical and elec. props. 0-49547  
 GaP, refr. index meas., temp. variation 300 to 75K 0-25328  
 Ge-S-Se system, glass-forming, struct. and props. 0-19713  
 GeO film, optical props., rel. to possible appl. in holography 0-29816  
 $H_2O$ , liquid, far IR optical consts. meas. with optically pumped laser 0-40082  
 He, liq. and vapour phases, thermodynamic and thermophysical props. calc. using HEPROP computer program 0-6529  
 $Hg_{1-x}Cd_xSe$ , IR absorpt. spectra, band struct., refr. index 0-50337  
 $Hg_{1-x}Cd_xTe$ , anodic oxide films, formation and props. 0-3212  
 $HgGa_2S_4$ , melt growth, optical props. and SHG,  $HgS-HgGa_2S_4$  phase diagram 0-50548  
 I flashlamp pumped photodissociation laser characts., local optical inhomogeneities 0-53284  
 I, iodoseptofluoropropane photodissoc. laser, refr. index distrib. fields, double exposure holography 0-9873  
 InGaAsP-InP DH laser with self-aligned struct., oscillation characts. 0-38017  
 InSb, anode oxide film coated, ellipsometric and interferential study, optical parameters (*Russian*) 0-50449  
 InSb, low-power nonlinear refraction effect on laser beam propagation 0-5801  
 InSb, optical bistability, signal amplification, low power nonlinear effect applications 0-19066  
 KBr, additively dyed, amplitude-phase holograms (*Russian*) 0-1152  
 $K_2O-SiO_2$  glass 0-33897  
 $K_2Sb$ , optical and dielectric props., energy spectra, density of states calcs. 0-20083  
 $LaF_3-BaF_2-ZrF_4(-MF)$ ,  $M=Na, Li$ , glassy transition, refr. index, density and molar refr. 0-1937  
 $LiBiNd_{1-x}P_3O_{12}$  waveguide laser layer epitaxially grown on  $LiNdP_4O_{12}$  substrate 0-23709  
 $\alpha-LiIO_3$ , single crystals, light diff. under DC field 0-11367  
 $LiNbO_3$ , SHG, refr. index induced optical inhomogeneity effect 0-9951  
 $LiNbO_3$ , waveguide and modulator form. by ion implantation 0-48469  
 $LiNbO_3:Fe$ , photorefraction,  $\gamma$ -irrad. influence, polarisation-optic and holographic obs. 0-11359  
 $LiNbO_3:Ti$  waveguide, in-plane scatt. obs. and countermeasures 0-33215



## refractive index continued

- Mn film, refractive index determ. using Rayleigh-Lowe refractometer 0-7427
- MnF<sub>2</sub>, magnetic, thermal, elastic refraction of light, mag. order influence on refractive index (*Russian*) 0-34880
- Mn<sub>2</sub>Fe<sub>3</sub>O<sub>4</sub>, optical props. 0-20606
- NaO-SiO<sub>2</sub>, glass, distrib. of different O ions, molar refractivity meas. 0-33897
- Nd<sup>3+</sup>, glass, nonlinear refractive index, two-photon resonant absorption by Nd<sup>3+</sup> (*Chinese*) 0-43387
- NdSb, forbidden band gap and electrotransfer parameters 0-39497
- P-Se-Te system glasses, mag. susceptibility and opt. props. 0-25079
- P-Se-Tl system glasses, polarisation, refr. index and dielec. const. meas. 0-20608
- PbF<sub>2</sub>-AlF<sub>3</sub> glass, optical props., crystn. and thermal expansion 0-48367
- PbI<sub>2</sub>, film, reflectance meas., optical const., humidity effects 0-34994
- PbO-SiO<sub>2</sub>, glass, distrib. of different O ions, molar refractivity meas. 0-33897
- Pb<sub>2</sub>Si<sub>2</sub>O<sub>7</sub>, films on Si, form. kinetics and props. 0-35358
- Pd<sub>0.77</sub>Cu<sub>0.06</sub>Si<sub>0.165</sub> glass, optical props. in energy range 0.67 to 5.6 eV 0-34872
- PdIn, refractive index, reflectivity and band struct., APW calcs. 0-40139
- PrSb, forbidden band gap and electrotransfer parameters 0-39497
- SF<sub>6</sub>, refractive index meas., intermolecular interaction effects 0-33728
- Sb<sub>2</sub>Si<sub>2</sub>O<sub>7</sub>, films on Si, form. kinetics and props. 0-35358
- Si, CVD, amorphous and polycryst., solar thermal absorber, temp. variation of absorpt. edge 0-12028
- Si rubber as electro-optic material for optical hydrophones 0-43412
- Si:H, amorphous, refr. index, temp. depend., implications for thermoreflectance and electoreflectance 0-50290
- Si:H, amorphous film, prep. by plasma decomp. of SiH<sub>4</sub> under mag. field, and characterisation 0-45239
- Si:H amorphous film, prep. by RF glow discharge decomp. of SiH<sub>4</sub>, optical props. and H conc. 0-15416
- Si:H amorphous film, prop. by glow discharge deposition, and plasma parameter effects on props. 0-45240
- Si:H amorphous films for solar cells, optical and elec. props. of RF glow discharge deposited films 0-54576
- Si:N, ion implantation, refractive index, IR spectra, ion range and straggling meas. 0-34020
- Si-SiO<sub>2</sub> interface, props. variation in SiO<sub>x</sub> region 0-49548
- SiH<sub>0.16</sub> amorphous films, optical props. and photocond. near optical gap 0-50443
- SiH<sub>x</sub> amorphous reactively sputtered films, optical props. 0-50444
- SiN<sub>x</sub> film, plasma deposited, comp. and characterisation, optical and elec. props. 0-15401
- Si<sub>3</sub>N<sub>4</sub> film, CVD, high-field dark currents 0-54791
- SiO, film, effect of ion implanted O<sub>2</sub> on optical props. 0-45027
- SiO<sub>2</sub> films, CVD at reduced press., optical props. 0-2957
- SiO<sub>2</sub>, fused, refractive index dispersion, thermal history depend. 0-25331
- SiO<sub>2</sub>, fused, shock compressed, refractive index, density, and polarisability behaviour 0-50295
- SiO<sub>2</sub>, ion implanted, fused, refr. index profiles 0-54272
- SiO<sub>2</sub> thin films, comparison of RI and IR spectra 0-11497
- SiO<sub>x</sub>, amorphous and recrystallised layer, optical props. 0-25474
- SiO<sub>x</sub> amorphous film, dispersion of refr. index and chem. comp. 0-7429
- SiO<sub>x</sub> film, durable optical, ion plating onto plastics, optical and mech. props. 0-38141
- SmSb, forbidden band gap and electrotransfer parameters 0-39497
- SrF<sub>2</sub> fusion-cast prism refractive index obs., 0.2138 to 11.475  $\mu$ m 0-34882
- Ta<sub>2</sub>O<sub>5</sub>, reactive DC sputtering deposited films with magnetron-plasmatron, mechanical elec., optical props. 0-25566
- TiO<sub>2</sub>, reactive DC sputtering deposited films with magnetron-plasmatron, mechanical elec., optical props. 0-25566
- TiO<sub>x</sub> antireflection coatings for solar cells, optical, struct., and compositional characts. 0-55852
- TiO<sub>x</sub> film, durable optical, ion plating onto plastics, optical and mech. props. 0-38141
- TiBr-TiI, TiCl-TiBr, KRS-5 and KRS-6 crystals, refr. index temp. increments meas. 0-33098
- Ti-PbF<sub>2</sub> graded-index film coating technique and results 0-33265
- V<sub>2</sub>O<sub>5</sub> film, amorphous, thickness, density and refr. index determ. from reflectance interference spectra 0-55206
- YbSb, forbidden band gap and electrotransfer parameters 0-39497
- ZnB<sub>2</sub>O<sub>4</sub>-MF<sub>2</sub> (M=Mg, Ca, Sr, Ba) glass system, physicochem. props. 0-34877
- Zn<sub>3</sub>P<sub>2</sub>, bulk and thin film, UV reflectivity spectra, photovoltaic effects, optical const. 0-25472
- ZnS antireflection coatings on solar cells 0-43414
- ZnSe crystal, refr. index temp. increments meas. 0-33098

## refractive index measurement

- see also refractometers
- absorbing media using frustrated total internal reflection refractometer 0-9021
- atmospheric, microwaves non-conventional appl. survey (*Italian*) 0-13093
- coating technique and refractive index meas. 0-43488
- computer-controlled heterodyne interferometer for index gradient meas. 0-13131
- continuous wavelength interferometry for measuring dispersion of complex refractive index 0-22423
- dielectric film refractive index meas., synchronous angle integrated optical method 0-15976
- dielectric thin film refractive index and thickness, algorithm for determ. on basis of ellipsometric meas. 0-34881
- dielectric thin films, accurate meas. by symmetric prism wave couplers (*Chinese*) 0-2885
- dispersed system, simultaneous determ. of refr. index and particle size from scattered radiation characts. 0-27335
- film optical const. meas., Shamir-Graff method evaluation 0-11489
- fluorescent film, method for refr. index and thickness determ. 0-40175
- gases, compressed, refractive index meas. using Fabry-Perot interferometer (*French*) 0-14878
- glass disc, laser beam path 0-46779
- glass surface, ellipsometric study of zone of optical contact 0-4754
- graded index fibre profile determ., interferometric method 0-14481
- gradient index material profiles and chromatic props. 0-14409
- image-moire method 0-22420
- isotropic and anisotropic media, meas. at 35 GHz 0-256
- liquid crystals refractive index meas. by cylindrical cell method 0-11358

## refractive index measurement continued

- liquid group refractive index meas. using synchronously pumped stimulated Raman oscillator 0-55059
- multimode fibre waveguides, optical characts. meas. by backscatt. 0-23801
- optical fibre, mech. deform. meas. by light scatt. method 0-14452
- optical fibre, single mode, refractive index profile meas., focusing method 0-33144
- optical fibre preform, nondestructive profile determ. 0-1312
- optical fibres (*Japanese*) 0-10020
- optical fibres 0-43458
- perspex prism, crit. angle method, student expt. 0-12873
- schlieren probe method for measurement of refractive index profile of shock wave in fluid 0-23785
- single mode fibre transmission characts. and refr. index profile meas. from exit radiation pattern 0-9986
- solids, Fabry-Perot interferometer 0-52297
- transmission technique for planar film index-profile measurements 0-33230
- transparent solids, multiple-beam interferometers 0-52299
- SiNH films, thickness and refractive index meas., comparison of techniques 0-8957
- SiO<sub>2</sub> films, thickness and refractive index meas., comparison of techniques 0-8957
- refractivity see refractive index
- refractometers
- differential refractometer for continuous liq. phase residence time distrib. studies 0-17999
- Fabry-Perot interferometer as refractometer 0-264
- frustrated total internal reflection refractometer, optical const. of absorbing media 0-9021
- opticophysical and physicochemical meas. instrum. 0-13121
- UV region SP-129 refractometer 0-31846
- refractometry see refractive index measurement
- refractories
- see also ceramics; cermets; clay
- actinide compounds, synthesis from oxides and single cryst. growth 0-16229
- Al<sub>2</sub>O<sub>3</sub>-SiO<sub>2</sub> refractories, using neutron-2 equipment 0-45612
- alloy composites, refractory fibre reinforced, diffusional reaction, effect of alloying calc. 0-20851
- apparent density determination, using surface  $\gamma$  densimeter 0-35464
- borides, manufacture and appl. in electronic and electrotechnic field (*French*) 0-40311
- borides, proposed classification 0-19741
- carbides, manufacture and appl. in electronic and electrotechnic field (*French*) 0-40311
- corundum refractories, dense production and performance 0-20866
- crystal growth, use of Xe-lamp imaging furnace (*Japanese*) 0-50547
- electron structure, and phys. props. of infusible compounds 0-54585
- erosion resistance during action of highly concentrated energy fluxes 0-55562
- fatigue, effect of texture/crack relationship (*German*) 0-25829
- fatigue behavior, effect of texture and crack kinetics, AE anal. (*German*) 0-21061
- fracture under thermal shock, AE study 0-25865
- fusion reactor materials, neutron irradi., microstruct., voids, nucleation TEM study 0-29065
- gas cooled reactors, internal insulation 0-47537
- glass-making, progress, review 0-40303
- graphite, CVD of TiB<sub>2</sub> coating 0-21131
- hardness, methods of increasing by prod. method 0-25643
- heat conduction, contrib. of segregation and diffusion 0-20001
- heat of formation determ. using self-propagating high-temp. synthesis 0-3392
- high temp.-high flux material testing, solar power station appls. 0-40668
- high temperature metallic species, absorpt. and fluoresc., high temp. fast flow reactor technique 0-42231
- high-temperature materials, technological requirements, R and D, report 0-45222
- hydrogen embrittling effects from acoustic emission meas. 0-11742
- kyanite-sillimanite concentration, multilutisation and sintering, props. of refractory products 0-20867
- metal, refractory, water vapour attack, immersion heater appl. in vacuum radiation furnace (*German*) 0-21184
- metal compounds, diffusive creep, theory (*Russian*) 0-40437
- metals, enhanced diffusion model for activated sintering 0-25612
- metals, mech. props. and diffusion figures (*Russian*) 0-40436
- metals, nitriding reactions and processing conditions, thermodynamic approach (*Russian*) 0-21169
- metals, work function, ionising radiation effects meas. method 0-6951
- MgO:Cr<sup>3+</sup>, single cryst., ESR linewidth 0-29605
- molybdenum ternary sulfides, Chevrel phase, synthesis and superconductivity (*German*) 0-25038
- multichamotte, sintering additives effect on props. 0-35147
- multiphase systems, some novel effects, rel. to practical appls. 0-55460
- nitrides, manufacture and appl. in electronic and electrotechnic field (*French*) 0-40311
- oxide, thermal shock resist. mechanisms 0-25860
- oxides surface mass transport mechanisms obs. (*Japanese*) 0-54479
- periclase-spinel refractories, phase conversions up to 1720°C 0-25670
- plasmachemical synthesis, powder dispersion control 0-55332
- plasmachemical synthesis, powdered infusible compounds, props. 0-55330
- powders, wet decompaction and compaction 0-35150
- Sialon, prep. and charact. of ultrafine powders 0-11604
- SiC fibre-reinforced Ti-alloy, component interaction kinetics (*Russian*) 0-55364
- silicides, oxidation and hot corrosion resistance kinetics 0-25896
- slabs, radio wave phase method for quality control 0-40667
- thermal conductivity, hot wire meas. techniques 0-37038
- thermal conductivity, hot-wire meas. method, 20-900°C 0-31759
- thermal conductivity, microcracks contrib. 0-19999
- thermal expansion, and strain, filler content and temp. influence (*Russian*) 0-19964
- thermal stresses produced by temp. gradient, finite element anal. (*Japanese*) 0-33538
- transition metal borides, refractory carbides, borides and nitrides, wetting by and interactions with liq. metals 0-54473
- transition metal borides, silicides and germanides, binding energies from X-ray photoelectron spectra 0-49170



## refractories continued

- transition metal carbides, refractory carbides, borides and nitrides, wetting by and interactions with liq. metals 0-54473  
 transition metal carbonitrides, physicochem. props., comp. depend. 0-55370  
 transition metal compounds, electron and phonon behaviour 0-54624  
 transition metal nitrides, refractory carbides, borides and nitrides, wetting by and interactions with liq. metals 0-54473  
 transition metal silicides, self-propag. high-temp. synthesis 0-2988  
 transitional metal sulphides, enthalpy and specific heat, temp. depend. 0-54406  
 X-ray powder diff. meas. of phase composition, and flexural strength 0-3449  
 ZrO<sub>2</sub> powders, stabilised, for plasma spray-coatings 0-20869  
 $\alpha$ -AlB<sub>12</sub>, prep. and electrothermal props. 0-20863  
 AlC<sub>2</sub>N<sub>3</sub>, refractory deposit, prep. by thermal decomp. of Al dialkylamides and characterisation 0-11572  
 AlMgB<sub>14</sub>, prep. and electrothermal props. 0-20863  
 AlN, plasmochemical synthesis, powder dispersion control 0-55332  
 AlN powder, synthesis, in low-temp. plasma 0-16257  
 AlN powders, synthesis and impurities 0-55329  
 AlN, prep. and charact. of ultrafine powders 0-2983  
 AlN, ultradispersed powder, IR spectra 0-50312  
 Al<sub>2</sub>O<sub>3</sub>, crack detection caused by thermal shock, AE technique (*Japanese*) 0-21248  
 Al<sub>2</sub>O<sub>3</sub> films, amorphous, self-supporting, vac.-tight, from electrochem. oxidation of Al in (NH<sub>4</sub>)<sub>2</sub>CO<sub>3</sub> solns. 0-16177  
 Al<sub>2</sub>O<sub>3</sub> porous refractories, production 0-35149  
 Al<sub>2</sub>O<sub>3</sub>, reactions with Ti-Al-Cr-Mo alloy VT3-1 0-16585  
 Al<sub>2</sub>O<sub>3</sub>-Na<sub>2</sub>O,  $\beta$  and  $\beta'$  phases, formation by solid state reaction between NaAlO<sub>2</sub> and  $\gamma$ -Al<sub>2</sub>O<sub>3</sub> 0-29912  
 Al<sub>2</sub>O<sub>3</sub>-SiO<sub>2</sub>-Fe<sub>2</sub>O<sub>3</sub>-CaO-MgO-TiO<sub>2</sub>, refractory, corrosion and mech. behaviour correlations 0-40563  
 B C powders, effect of C on sintering 0-40312  
 B<sub>2</sub> C, mech. and thermal props. 0-21083  
 B<sub>2</sub>C<sub>3</sub>, sintering and subsequent high temp. annealing, struct. and props. 0-20858  
 B<sub>2</sub>C, FBR control rod elements, neutron damage and post-irrad. annealing 0-13581  
 B<sub>2</sub>C, synthesis in HF EM field 0-20864  
 B<sub>2</sub>C-Ti(V)(Cr), contact reaction with liq. Ni 0-55707  
 BN, cubic, high pressure synthesis, solvent effects 0-40310  
 BN, high-temp. plasmochem. synthesis, control of props. 0-55333  
 BN, polycryst. cubic, props. 0-21013  
 BN powder, wurtzite sphalerite struct. phase transition, effect on sub-struct. 0-25690  
 BN, shock synthesis (*Japanese*) 0-29918  
 BN, wurtzite, chem. comp. and processing props. in prep. of Geksanit-R sinterings 0-25632  
 B<sub>2</sub>O<sub>3</sub>, mech. and thermal props. 0-21083  
 B<sub>12</sub>Si,  $\beta$  rhombohedral, conduction mechanism, thermoelectric props. 0-24932  
 BaO-Al<sub>2</sub>O<sub>3</sub>-SiO<sub>2</sub>-Ta<sub>2</sub>O<sub>5</sub>-Mo glass ceramic metal composites, cermet prep. 0-11618  
 C refractories, alkali attack as catalyst for oxidation 0-40562  
 CaAl<sub>2</sub>O<sub>4</sub> compounds and cements, quantitative thermogravimetry after hydrothermal treatment 0-16737  
 CaO-MgO-ZrO<sub>2</sub>-SiO<sub>2</sub> refractories, phase diagram 0-11634  
 CeO<sub>2</sub>, plasma deposition of crystals and their characterisation 0-20800  
 Cr-Mo-N system, at high-pressure, temp., X-ray anal., phase diagram 0-50607  
 Cr<sub>2</sub> C<sub>3</sub>, reactions with Ti-Al-Cr-Mo alloy VT3-1 0-16585  
 CrB<sub>2</sub>, reactions with Ti-Al-Cr-Mo alloy VT3-1 0-16585  
 Cr<sub>2</sub>C<sub>2</sub> (Cr<sub>7</sub>C<sub>3</sub>) based coatings, detonation deposited, wear resist., 20-1000°C 0-11843  
 Cr<sub>2</sub>C<sub>2</sub>, reactions with Ti-Al-Cr-Mo alloy VT3-1 0-16585  
 Cr<sub>2</sub>C<sub>2</sub>-(Ni-Cr) sprayed coatings, for gas cooled reactor heat exchangers, factors affecting performance 0-40609  
 Cr<sub>2</sub>O<sub>3</sub>, RF sputtered coating for wear appls., on Inconel X-750 foil, prep. and props. 0-40605  
 Dy B<sub>2</sub>, prep. and props., DTA study 0-20859  
 HfC-HfB<sub>2</sub> alloys, wear in vacuum, role of boride phase 0-21113  
 HfO<sub>2</sub>, plasma deposition of crystals and their characterisation 0-20800  
 La compounds, plasma light reflection by free charge carriers 0-11403  
 MgO and MgO-dolomite, crack detection caused by thermal shock, AE technique (*Japanese*) 0-21248  
 MgO single crystals, crack formation process, micro-deformation and fracture (*Japanese*) 0-24530  
 MgO, sintering, effect of Ca compound additions (*Japanese*) 0-55340  
 MgO-C in melts, corrosion resist., rel. to oxidation, porosity, content 0-40578  
 MgO-CaMgSiO<sub>4</sub>-(Al<sub>0.5</sub>Cr<sub>0.5</sub>)<sub>2</sub>O<sub>3</sub>(Al<sub>2</sub>O<sub>3</sub>)(Cr<sub>2</sub>O<sub>3</sub>), spinel phase, phase equilibrium relations and spinel bonding 0-55376  
 MgO-Al<sub>2</sub>O<sub>3</sub>-Fe<sub>2</sub>O<sub>3</sub>-Al<sub>2</sub>O<sub>3</sub>-SiO<sub>2</sub>, clinker production from dolomite and magnesite 0-55339  
 MgO-MgAl<sub>2</sub>O<sub>4</sub>(FeCr<sub>2</sub>O<sub>4</sub>), thermoplastic and thermophys. props. for steel vacuuming installations 0-35281  
 MgO-spinel concrete, cast, hardening by elec. heating 0-21258  
 Mo, candidate refractory for Tokamak, thermal fatigue failure testing 0-32454  
 Mo, powder, defective structure and activated sintering, exam. 0-16240  
 Mo<sub>2</sub>B<sub>3</sub>, monocryst., grain size, abrasive and strength props. 0-11787  
 Mo<sub>2</sub>B<sub>3</sub>-based alloys, mech. props., rel. to appl. as electrodes in electros-park machining 0-21174  
 Mo<sub>2</sub>C, free energy of form. and thermodynamic props. of C in solid Mo 0-15266  
 MoSi<sub>2</sub>, reaction VT3-1 0-16585  
 MoSi<sub>2</sub>, self-propag. high-temp. synthesised, sintering and props. 0-11616  
 Nb, fusion reactor first wall material, cyclic deform. tests 0-30074  
 Nb, H<sub>2</sub> isotope release 0-37580  
 NbB<sub>2</sub>, hot pressing 0-25635  
 NbC crystals, electron energy spectra 0-49568  
 NbC, deformation behaviour during rubbing in wide temp. range 0-16486  
 NbC micropowder surface finishing of metals, surface struct. 0-11842  
 NbC single crystals, synthesis and impurities 0-55329  
 NbN preparation, by precip. from gaseous NgF<sub>2</sub>-N<sub>2</sub>-H<sub>2</sub> mixture 0-20857  
 Nd<sub>2</sub>O<sub>3</sub>-HfO<sub>2</sub> system, phase relationships 0-35169  
 Nd<sub>2</sub>Zr<sub>2</sub>O<sub>7</sub>-Nd<sub>2</sub>Hf<sub>2</sub>O<sub>7</sub>, struct., elec. cond. and melting point 0-54197  
 Pr compounds, plasma light reflection by free charge carriers 0-11403  
 Si-Al-B-O-N, calc. of phase diagrams from data set 0-55362

## refractories continued

- Si-Al-Zr-O-N, calc. of phase diagrams from data set 0-55362  
 SiB<sub>4</sub>, mech. and thermal props. 0-21083  
 SiC, chem. stability, mech. and thermal props. rel. to appls. 0-21103  
 SiC fibres obtained from polycarbosilane fibre 0-50582  
 SiC, grinding material, grain shape optimization (*Polish*) 0-29916  
 SiC, oxidation and corrosion behaviour, formation of protective SiO<sub>2</sub> coatings (*German*) 0-25885  
 SiC, oxidation and hot corrosion resistance kinetics 0-25896  
 SiC powders, form. by vapour phase method 0-25623  
 SiC, reactions with oxidising atms. 0-11812  
 SiC, resist. to oxidation and corrosion at high temps. (*German*) 0-35357  
 SiC, self-bonded polycryst., electrophys. props. 0-10980  
 $\alpha$ -SiC, single cryst. phase struct. rel. to heat treatment, nucleation 0-38991  
 SiC, specimen preparation for TEM by ion beam thinning (*German, English*) 0-11861  
 $\beta$ -SiC, twinned crystals, fracture characts. 0-3193  
 $\beta$ -SiC, undoped compact, microstruct. development during heating 0-25746  
 $\beta$ -SiC/Si abrasive resistant material, prep. and props. 0-20878  
 Si<sub>3</sub>N<sub>4</sub> films, plasma etching, MOS processing appl. 0-40577  
 Si<sub>3</sub>N<sub>4</sub>, finely dispersed, high-temp. synthesis 0-55331  
 $\alpha/\beta$ -Si<sub>3</sub>N<sub>4</sub>, formation during nitridation of Si 0-50609  
 Si<sub>3</sub>N<sub>4</sub>, fracture toughness meas. using Knoop indentation method (*German*) 0-25830  
 Si<sub>3</sub>N<sub>4</sub>, hot pressed, strength and life prediction 0-3173  
 Si<sub>3</sub>N<sub>4</sub>, hot pressed, surface wave scatt. from elliptical cracks for failure prediction 0-55608  
 Si<sub>3</sub>N<sub>4</sub>, oxidation and hot corrosion resistance kinetics 0-25896  
 Si<sub>3</sub>N<sub>4</sub>, prep. and charact. of ultrafine powders 0-2983  
 Si<sub>3</sub>N<sub>4</sub>, reaction sintered, microstruct. charact. 0-35145  
 Si<sub>3</sub>N<sub>4</sub>, sintering in powder bed with addition of MgO sintering aid 0-29910  
 Si<sub>3</sub>N<sub>4</sub>-(MgO+Al<sub>2</sub>O<sub>3</sub>)(Y<sub>2</sub>O<sub>3</sub>), hot-pressed and sintered, microstruct. and impurity distrib. 0-49261  
 Si<sub>3</sub>N<sub>4</sub>-MgO, (5 wt.%), hot pressed, fracture toughness as function of initial  $\alpha$ -phase content, SEM 0-3174  
 Si<sub>3</sub>N<sub>4</sub>-Si<sub>3</sub>N<sub>2</sub>O-Mg<sub>2</sub>SiO<sub>4</sub>, melting and eutectic studies 0-45285  
 Si<sub>3</sub>N<sub>4</sub>-Y<sub>2</sub>O<sub>3</sub>, hot-pressed, oxidation kinetics 0-16520  
 Si<sub>3</sub>N<sub>4</sub>-AlN-Al<sub>2</sub>O<sub>3</sub> system, reaction sintering forming  $\beta$ -Si<sub>3</sub>N<sub>4</sub> solid solns. 0-50585  
 Si<sub>3</sub>N<sub>4</sub>, hot pressed, subcritical crack growth boundaries at internal fracture origins 0-11748  
 SiO<sub>2</sub> concrete, elastic moduli meas. during heating and cooling 0-55451  
 SiO<sub>2</sub> fused powder, difference between white and black silica, devitrification rates 0-28918  
 SiO<sub>2</sub>-Al<sub>2</sub>O<sub>3</sub>-Cr<sub>2</sub>O<sub>3</sub> system, KT-11 type, chromia-containing material production based on high-silica glass fabric 0-45266  
 SiO<sub>2</sub>-base cores, for superalloys, high temp. characterisation 0-10640  
 (Ta,Ti)B<sub>2</sub> on graphite, CVD coating, hardness meas., SEM study 0-24760  
 TaC, reactions with Ti-Al-Cr-Mo alloy CT3-1 0-16585  
 ThO<sub>2</sub>, plasma deposition of crystals and their characterisation 0-20800  
 (Ti,V)C, activated reactive evaporation deposited films, annealing study, microstructure 0-24762  
 (Ti,Zr)B<sub>2</sub> on graphite, CVD coatings, hardness meas., SEM study 0-24760  
 Ti, H<sub>2</sub> isotope release 0-37580  
 Ti-Cr-B system, self-propagating high temp. synthesis, crystallochemical and mech. props. 0-20861  
 TiB<sub>2</sub> coating, on WC-Co alloy cutting plates, hardness and struct. 0-21175  
 TiB<sub>2</sub>, electric arc melting prep. and oxidation props. 0-20860  
 TiB<sub>2</sub>, preparation method rel. to compressive strength 0-55327  
 TiB<sub>2</sub>, reactions with Ti-Al-Cr-Mo alloy VT3-1 0-16585  
 TiC, activated reactive evaporation deposited films, annealing study, microstructure 0-24762  
 TiC, deformation behaviour during rubbing in wide temp. range 0-16486  
 TiC micropowder surface finishing of metals, surface struct. 0-11842  
 TiC, production from tetrachloride and hydrocarbon, thermodynamic analysis (*Russian*) 0-7523  
 TiC, reactions with Ti-Al-Cr-Mo alloy VT3-1 0-16585  
 TiC reactively sputtered coatings on Ni-Cr-Mo-Ti (19,11,3 wt.%), adherence, XPES and wear study 0-25565  
 TiC single crystals, synthesis and impurities 0-55329  
 TiC, sintering and grain growth, metallographic anal. 0-25642  
 TiC sputtered coatings on Ti-Al-V (6,4 wt.%), adherence, XPES and wear study 0-25565  
 TiC-B, struct. and mech. props. 0-55461  
 TiC-TiB<sub>2</sub>, friction characts., comp. depend., 20-1000°C 0-3203  
 TiC-TiB<sub>2</sub>, strength and antifriction props. over wider range of concs. 0-50673  
 TiC-TiB<sub>2</sub> alloys, wear in vacuum, role of boride phase 0-21113  
 TiC-TiN, hardness var. charact. in homogeneity field 0-3192  
 TiC-TiN system, electro- and thermo-phys. props. 0-34210  
 TiC-VC, mag. susceptibility, elec. cond. and thermoelec. props. 0-50033  
 TiC-ZrC, mag. susceptibility, elec. cond. and thermoelec. props. 0-50033  
 TiC<sub>2</sub> refractory layers on steel surfaces, ESCA obs. 0-39471  
 TiC<sub>2</sub>-N<sub>2</sub>, formation in high temp. N flow, ultra disperse powder, thermodynamic anal. (*Russian*) 0-55325  
 TiC<sub>2</sub>N<sub>2</sub>, thermal cond., elec. cond., and thermal expansion 0-10714  
 TiC<sub>2</sub>O, thermal cond., elec. cond., and thermal expansion 0-10714  
 TiN film as protective coating for vacuum deposition chamber, Auger electron spectroscopy study 0-25922  
 TiN, from high-temp. reaction of NH<sub>3</sub> and TiCl<sub>4</sub>, physicochem. props. 0-55334  
 TiN, reactive ion plating with auxiliary discharge deposition conditions influence on film props. 0-20801  
 TiN, self-propag. high-temp. synthesis under high N<sub>2</sub> pressures 0-25630  
 TiSi<sub>3</sub> synthesis 0-35141  
 Ti(Zr,Hf)-Gd-B system, phase equilib. 0-11629  
 V, and V-H, fusion reactor first wall material, cyclic deform. tests 0-30074  
 W, candidate refractory for Tokamak, thermal fatigue failure testing 0-32454  
 W, powders, defective structure and activated sintering, exam. 0-16240  
 W-ThO<sub>2</sub>, candidate refractory for Tokamak, thermal fatigue failure testing 0-32454  
 W-Ti, Ti addition effect on heat resistance and radiative props. (*Russian*) 0-25515



**refractories continued**

- W-Zr, Zr addition effect on heat resistance and radiative props. (*Russian*) 0-25515  
 W-Zr-C, Zr and C addition effect on heat resistance and radiative props. (*Russian*) 0-25515  
 W<sub>2</sub>B<sub>3</sub>, monocryst., grain size, abrasive and strength props. 0-11787  
 W<sub>2</sub>B<sub>3</sub>, reactions with Ti-Al-Cr-Mo alloy VT3-1 0-16585  
 W<sub>2</sub>B<sub>3</sub>-based alloys, mech. props., rel. to appl. as electrodes in electrosark machining 0-21174  
 WC, deformation behaviour during rubbing in wide temp. range 0-16486  
 WC micropowder surface finishing of metals, surface struct. 0-11842  
 WC powder, sintering processing conditions 0-11614  
 WC, reactions with Ti-Al-Cr-Mo alloy VT3-1 0-16585  
 Y<sub>2</sub>O<sub>3</sub> fused single crystals, struct. 0-19804  
 Y<sub>2</sub>O<sub>3</sub>-2Y<sub>2</sub>O<sub>3</sub>-Al<sub>2</sub>O<sub>3</sub> two-phase refractory, fracture 0-21080  
 Y<sub>6</sub>WO<sub>12</sub>-ZrO<sub>2</sub>(MgO)(CeO)(SrO)(BaO), polycryst., elec. cond., 800-7400°C 0-15517  
 Zr-based thermal barrier coating evaluation 0-40619  
 Zr-Cr-B system, self-propagating high temp. synthesis, crystallochemical and mech. props. 0-20861  
 ZrB<sub>2</sub>, electric arc melting prep. and oxidation props. 0-20860  
 ZrB<sub>2</sub>, powders, synthesis and impurities 0-55329  
 ZrB<sub>2</sub>, reactions with Ti-Al-Cr-Mo alloy VT3-1 0-16585  
 ZrB<sub>2</sub>-SiC-C(V)-(Nb), refractory cermet, hot pressing and oxidation resist. 0-3231  
 ZrC crystals, electron energy spectra 0-49568  
 ZrC powders, synthesis and impurities 0-55329  
 ZrC powders produced by various methods, impurities 0-11615  
 ZrC, reactions with Ti-Al-Cr-Mo alloy VT3-1 0-16585  
 ZrC single crystals, synthesis and impurities 0-55329  
 ZrC-W (75 wt.%) eutectic refractory alloys, smelting in suspended states, components distrib. (*Russian*) 0-19913  
 ZrC-ZrB<sub>2</sub>, friction characts., comp. depend., 20-1400°C 0-3203  
 ZrC-ZrB<sub>2</sub>, strength and antifriction props. over wider range of concs. 0-50673  
 ZrC-ZrB<sub>2</sub> alloys, wear in vacuum, role of boride phase 0-21113  
 ZrC<sub>0.91</sub>, sintered, strength charact. effect of struct. and substruct. 0-16260  
 ZrN-Al<sub>2</sub>O<sub>3</sub>, sintering reaction thermodynamics 0-2989  
 ZrO<sub>2</sub>, elec. cond. variation, gas flow effect 0-39581  
 ZrO<sub>2</sub>, high-temp. induced porosity increase 0-35146  
 ZrO<sub>2</sub>, plasma deposition of crystals and their characterisation 0-20800  
 ZrO<sub>2</sub>, stabilized porous refractory, mech. strength 0-35322  
 ZrO<sub>2</sub>, substoichiometric, thermodynamic props. at lower phase boundary 0-29185  
 ZrO<sub>2</sub>, Y<sub>2</sub>O<sub>3</sub> stabilized, heat-resistant granular artifacts, procedure for making 0-35148  
 ZrO<sub>2</sub>-Nd<sub>2</sub>O<sub>3</sub>(Sm<sub>2</sub>O<sub>3</sub>)(Dy<sub>2</sub>O<sub>3</sub>) eutectic, unidirectional solidification, microstruct. and crystallographic characterization 0-35176  
 ZrSi<sub>3</sub>, synthesis 0-35142  
 ZrSiO<sub>4</sub>, synthesis, influence of rare-earth additives on props. 0-20868

**refractory materials** *see refractories***refrigeration**

- see also cryogenics; freezing; low-temperature production*  
 counterflow gas-liquid helium heat exchanger with copper grid 0-17947  
 dilution refrigerator, anomalous cooling power, heat transport of <sup>3</sup>He-<sup>4</sup>He solutions 0-37045  
 high vacuum cryopumps optimisation using thermal design criteria 0-22377  
 nuclear demagnetisation refrigerator, double range, microkelvin range 0-31769  
 phonon-drag low temperature thermoelectric refrigeration, use of Bi 0-22366  
 portable self-contained refrigerants transfer system, for use with supercond. magnet dewars 0-8993  
 regenerative, generalised ideal reference cycle, isothermal systems 0-38228  
 saltwater drop falling in organic phase, ice growth 0-15218  
 solar energy driven absorption refrigeration system, theoretical model 0-30413  
 solar energy transition and materials problems 0-26115  
 solar powered refrigeration units, absorption systems with intermittent or continuous cycles 0-45729  
 solar zeolite collector for solid-gas absorpt. refrigeration system 0-35754  
 storage of thermal energy, annual cycle, ice storage and three-coil heat pump 0-55917  
 thermoelectric coolers with high current pulse and finite cold junction, fast transient behaviour 0-27290  
 thermoelectric refrigerators, performance optimisation using asymptotic temp. distrib. 0-230  
 He cryorefrigerator, exergy method of anal. 0-4723  
 He refrigerated and liquefiers, optimisation for larger superconducting systems 0-8994  
 He refrigerator for temp. varying Mossbauer meas., 20-300K 0-4726  
<sup>3</sup>He refrigerator for studying Ge below 1K 0-8997

**refrigerators**

- energy conservation estimates by second law anal. 0-45723  
 free piston Stirling refrigerator performance characts. determ. 0-35722  
 noise, subjective annoyance by low level sound, sound character as a physical attribute 0-35902  
 nuclear demagnetisation refrigerator, microprocessor controller 0-37043  
 photovoltaic/thermoelectric refrigerator for medicine storage for developing countries 0-35712  
 reciprocating magnetic refrigerator for 2-4K operation 0-2577  
 solar open cycle absorption refrigeration system, anal. and simulation 0-16788  
 solar-powered solid-state heat transfer device based on photovolt. and Peltier effects 0-217  
 SQUID appls. portable refrigerator 0-27313  
 thermochemical heat pump/refrigerator thermodynamic analysis 0-35716  
 He, closed-cycle, containing laser diode, measurement of wave-number stability 0-31906

**regenerative receivers** *see radio receivers***Regge poles and trajectories**

- $\pi^+$  theories, Regge-pole behaviour 0-18081  
 absorption model approx. for particles with spin, Regge cuts, crossing symmetry violation (*Russian*) 0-42435  
 baryonium and nonexotic hadron trajectories from a color-dependent potential 0-13286

**Regge poles and trajectories continued**

- broken global symmetries, nondegeneracy of vector meson mass, non-trivial mixing 0-13236  
 cluster formulation in the dual topological unitarization scheme 0-13293  
 constituent particle scattering in the Regge region 0-37244  
 Dirac's large-number hypothesis, angular momentum for Regge trajectory with  $n=2$  0-18091  
 dual Pomeranchuk amplitude contrib. to multi-Regge limit and pomeron sister absence 0-13237  
 dual topological unitarisation, higher rank cylinder kernel 0-27492  
 dual topological unitarisation, singular cylinder kernel 0-27493  
 dual topological unitarization, glueball exchange effects, pomerons and reggeons 0-52482  
 free-spinor field on Regge trajectory as representation of strongly interacting quark field 0-32067  
 giant multipole resonances, Regge poles and collective model 0-13436  
 hadron spectrum, planar amplitudes without Regge cuts 0-27464  
 hadronic reactions, trajectory slopes in gauge-dual-topological approach 0-18142  
 hypercharge-exchange reactions,  $K^-p$  and  $\pi^+p$ , exchange-degenerate Regge pole prediction 0-13335  
 $I=1$  bosonic reggeon-particle scatt., dispersion sum rules (*Russian*) 0-32089  
 $I=1$  reggeon-baryon scatt., superconvergent dispersion sum rules and vertices struct. (*Russian*) 0-27494  
 KNO scaling and scaling in the mean for semi-inclusive processes (*Chinese*) 0-22538  
 meson mass spectrum, planar bootstrap, and Regge approach 0-22581  
 multiperipheral parton model, Reggeisation and dual unitarisation 0-37249  
 Nambu string model, reggeon and pomeron interactions (*Russian*) 0-13294  
 nuclear elastic scatt. with optical potential, complex angular momentum methods, poles and zeros of S-matrix, REGGE 0-47445  
 nucleonic form factor, pion exchange, model 0-22608  
 perturbative field theory effects and Regge pole representation, QCD, dual topological unitarisation 0-42434  
 proton-neutron multiplets, odd-odd nuclei, parabolic Regge trajectories, exchange of quadrupole phonon 0-52590  
 QCD, hadron interaction effective string lagrangian, Regge slope, charmonium pot. model 0-4939  
 QCD, slope of leading Regge trajectory 0-42391  
 quark model, determ. of Regge pole exchange amplitudes 0-404  
 SU(6)×O(3), multiplets, semilocal duality, quark-orbital Regge trajectories 0-27490  
 two-Reggeon cut in the ordered phase of Reggeon field theory 0-52422  
 $K_{1p} \rightarrow K_{sp}$ , 5 to 10 GeV, differential cross-section,  $\omega$  Regge trajectory 0-22637  
 NN→N(N $\pi$ ) diffractive dissociation process, one pion Regge-pole exchange amplitude (*Russian*) 0-42491  
 $p^+$ nucleus, inclusive production of neutral strange and charged particles, collective tube model 0-52538  
 $pd$  scatt., intermediate inelastic states and triple-Regge couplings, Pomeron 0-4972  
 $pn \rightarrow np$ , charge exchange processes, baryonium trajectories, Regge pole description 0-9180  
 $pn \rightarrow pX$ , 100 to 400 GeV/c, slow-proton prod., Regge trajectory 0-22646  
 $pp$ ,  $pp$  high energy elastic scatt., cross section rise and polarisation, Regge model (*Russian*) 0-37301  
 $pp \rightarrow$ charged particle+X, small-angle production from nuclear and nucleon targets, collective tube model and triple-Regge picture 0-52538  
 $pp \rightarrow \Delta^+X$ , small-angle production from nuclear and nucleon targets, collective tube model and triple-Regge picture 0-52538  
 $pp \rightarrow \bar{n}n$ , charge exchange processes, baryonium trajectories, Regge pole description 0-9180  
 $pp$  scatt., exchange degeneracy violating  $A_1$ -Z Regge amplitude and dibaryon resonances 0-4971  
 $\pi^+n \rightarrow pX$ , 100 to 400 GeV/c, slow-proton prod., Regge trajectory 0-22646  
 $\pi^-p \rightarrow \eta n$ , Reggeon field theory, behaviour of  $A_2$  trajectory 0-22594  
 $\pi^-p \rightarrow \phi n$ , quark line rule, violations 0-52530  
 $\pi^-p \rightarrow \psi n$ , generalised Veneziano models 0-22638  
 QQ mass, approx. scheme is QCD 0-42398

**Reggeon field theory**

- bound and rebound states, relativistic eikonal approximations 0-27491  
 broken global symmetries, nondegeneracy of vector meson mass, non-trivial mixing 0-13236  
 cut theory, 4-pomeron couplings 0-42366  
 finite mass sum rule and Reggeon vertices, unitarity constraint equations 0-13292  
 lattice model, critical behaviour, Monte Carlo calc. 0-18126  
 massless non-abelian gluon confinement and rising total cross sections 0-13264  
 quark masses and structure functions 0-22585  
 two-Reggeon cut in the ordered phase of Reggeon field theory 0-52422  
 $\pi^-p \rightarrow \eta n$ , Reggeon field theory, behaviour of  $A_2$  trajectory 0-22594

**region of escape** *see exosphere***regulators** *see controllers***Rehbinder effect** *see mechanical properties of substances; surface phenomena***relative density** *see density***relative humidity** *see humidity***relativistic band structure calculations**

- actinide dioxides, electronic struct. and ionicity 0-10872  
 actinides, electronic excitation energies calcs. 0-54592  
 density functional formalism 0-10848  
 one-dimensional monatomic cryst., relativistic electronic state 0-54590  
 rare earths, electronic excitation energies calcs. 0-54592  
 Au, photoelectron spectra, bulk and surface, rel. to band struct. 0-20770  
 Ce, density functional theory 0-15442  
 CuBr(Cl)(I), energy bands, relativistic KKR method, UV absorpt. spectra 0-39501  
 Eu, relativistic band struct. calcs., unoccupied 4f level calc., Fermi level, atomic configuration 0-49584  
 HfN, electronic struct., relativistic energy band struct. calc. 0-34354  
 InSe, reflectivity and low energy absorption 0-34944  
 La, density functional theory 0-15442  
 SnTe, self-consistent relativistic energy bands 0-10870  
 TaN, electronic struct., relativistic energy band struct. calc. 0-34354  
 Th, density functional theory 0-15442



**relativistic band structure calculations continued**

- TiCl<sub>3</sub>, self-consistent electronic struct. and ground state props. 0-15451  
 UF<sub>6</sub>, electronic struct. calc. 0-6716  
 UN, electronic struct., relativistic energy band struct. calc. 0-34354

**relativistic corrections**

see also *Lamb shift*

- 6d metal superheavy hexafluorides, relativistic mol. calcs. 0-5484  
 atom, bound state quantum fluctuations and variational method, relativistic HF calc. with radiative effects 0-42918  
 atom, estimation method, relativistic corrections 0-14091  
 atom+ion slow collisions, K-shell excitation of relativistic atoms 0-48073  
 atom with partially-filled shell, relativistic theory, secular operator renormalisation (*Russian*) 0-52896  
 atom with two electrons in open shell, level shifts (*Russian*) 0-14092  
 atomic systems, many-electron autoionisation states, transition probability and autoionisation rate, perturbation theory Z-expansion 0-52863  
 atoms, photoionisation, multichannel relativistic RPA calcs. 0-9570  
 atoms, review of relativistic corrections 0-47914  
 Bose-Einstein condensation in Einstein universe 0-46959  
 central field approximation, RELAC method and use 0-9520  
 Dirac operator, essential self adjointness anal. 0-18794  
 hydrides, MH<sup>+</sup>, MH<sub>2</sub>, M=alkaline earths: Zn, Cd, Hg, Yb, No, relativistic (non-relativistic) HF one-centre expansion calcs. 0-52908  
 hydrocarbons, normal, mass-spectrometric fragmentation processes, quantum field theory 0-40782  
 inert gases, outer shell photoionisation, relativistic RPA calcs. 0-9571  
 inert gases, photoelectron spin polarisation, ab initio calcs. 0-18833  
 K-LL Auger spectra in intermediate-coupling scheme with CI, relativistic Dirac Hartree Slater calc. 0-52958  
 K-shell Auger rates, level widths and fluorenc. yields, relativistic Dirac Hartree Slater calc. 0-52957  
 K-shell ionis. by charged particle impact, electronic relativistic effects 0-28099  
 Lamb shift, anomalous mag. moment, relativistic Dirac eqn. 0-42954  
 light muonic atoms, nuclear size effects, energy levels, Lamb shift 0-14254  
 M-shell radiationless transitions, subshell fluorenc., Coster Kronig yields and X-ray linewidths, relativistic Dirac Hartree Slater calcs. 0-52959  
 methylene, singlet-triplet separation, relativistic corrections 0-32618  
 molecule, estimation method, relativistic corrections 0-14091  
 molecules, review of relativistic corrections 0-47914  
 multiconfiguration Dirac-Fock program, appl. to Ba X-ray levels and 5p excited spectra 0-47865  
 multiply charged ions, relativistic perturbation theory appls. 0-23323  
 multiply charged ions, superposition of quasidegenerate configurations 0-42956  
 muonic He, hyperfine struct., relativistic, radiative and recoil corrections, QED test 0-14256  
 nucleus+hydrogenic atom electron capture, ultrarelativistic limit relativistic corrections 0-14230  
 one electron atom, relativistic corrections to nonrelativistic hamiltonian 0-42955  
 orbit-orbit interaction, new tensor expansion, matrix and graphical forms 0-14064  
 oscillator strength calculations, ab initio methods for relativistic effects introduction 0-9519  
 RPA, relativistic, development from linearised time-depend. HF theory 0-47925  
 RPA appls. to He-like ions energy levels and Mo<sup>30+</sup>, 12+ photoionis. 0-47913  
 spherical Gaussian basis sets, for relativistic Hartree-Fock calcs. 0-32595  
 two-electron atom, relativistic corrections to nonrelativistic hamiltonian 0-42955  
 [Re<sub>2</sub>Cl<sub>8</sub>]<sup>2-</sup>, spectral assignment, metal-metal bonds, SCF X $\alpha$  SW calcs., relativistic corrections 0-53006  
 Ag, ionisation energies and oscill. strengths calcs. 0-5488  
 Ar, inner electron energy characteristics, validity of Hartree-Fock-Pauli approx. 0-42957  
 Au, relativistic 1s wavefunctions test, using exptl. Compton profiles 0-32600  
 B-like ions, autoionisation states calcs. 0-43006  
 Bi II ion, relativistic effects in hyperfine splitting of second spectrum 0-23344  
 CdCl<sub>2</sub>, deformation densities, relativistic effect 0-42928  
<sup>35</sup>Cl XVI, beam-foil excitation, Lamb shift and fine struct., QED test 0-9549  
 Cr XVIII, XIX, spectral energy levels, relativistic corrections, config. superposition method 0-32616  
 Cs, isostructural transition and lattice vibrs., relativistic LMTO calc. 0-20074  
 Cu-like ions, E1 transitions, wavelengths, oscillator strengths and transition probabilities, data tables 0-37780  
 Fe XIX, XXI, spectral energy levels, relativistic corrections, config. superposition method 0-32616  
 Fe XXI, relativistic energy levels, Dirac-Fock multiconfig. calc., triplet state fine struct. and Lamb shift 0-23315  
 H atom, energy level calcs. in superstrong mag. field 0-37737  
 H atom in superstrong magnetic field 0-23320  
 H, line spectrum, relativistic red shift phenomenon 0-32675  
 H, relativistic, in strong mag. field 0-9518  
 H-like atom, fine struct. and HFS levels, Zeeman effect, relativistic corrections 0-37776  
 H-like ions, ground-state, elastic electron (positron) scatt., relativistic Glauber amplitudes 0-23550  
 H<sup>+</sup>+Au(Bi) (U), L X-ray production cross sections, 0.3-1.8 MeV, expt. rel. to PWBA prediction 0-53115  
 H<sup>+</sup>+H(1s) $\rightarrow$ H(1s)+H<sup>+</sup>, electron capture at relativistic energies, scatt. amplitude 0-1061  
 Hg<sub>2</sub><sup>+</sup>, electronic struct. and photoabsorpt. calcs. 0-27932  
 Hg<sub>2</sub>-Pt, <sup>199</sup>Hg Mossbauer meas., isomer shift and quadrupole splitting calcs. 0-28039  
 HgCl<sub>2</sub>, deformation densities, relativistic effect 0-42928  
 Hg<sub>2</sub>F<sub>2</sub>, <sup>199</sup>Hg Mossbauer meas., isomer shift and quadrupole splitting calcs. 0-28039  
 HgI<sub>2</sub>, relativistic effects, photoelectron spectra, Hartree-Fock-Slater method, perturbation theory approach 0-27962  
 I<sub>2</sub>, relativistic effects, photoelectron spectra, Hartree-Fock-Slater method, perturbation theory approach 0-27962  
 Kr, inner electron energy characteristics, validity of Hartree-Fock-Pauli approx. 0-42957

**relativistic corrections continued**

- Li isoelectronic series, relativistic pseudopot. appl. in HF calcs. 0-27960  
<sup>14</sup>N, spherical ground state nuclear quadrupole interaction, Breit interaction, relativistic perturbation theory 0-42939  
 Na isoelectronic series, oscill. strengths, effective orbital quantum no. method 0-9521  
 Ne, isoelectronic sequence, excitation energy and oscillator strength, level crossing anomaly, relativistic RPA calc. 0-14077  
 Ne, isoelectronic series, ionisation pots., Ritz law and Edlen formula 0-32854  
 Ni XXI, XXIII, spectral energy levels, relativistic corrections, config. superposition method 0-32616  
 Pb, relativistic 1s wavefunctions test, using exptl. Compton profiles 0-32600  
 Pb+Pb<sup>+</sup>,  $\delta$ -electrons from K- and L-shell ionisation in adiabatic collisions 0-23541  
 Rb, ground state, hyperfine struct., relativistic many-body calcs. 0-23322  
 Rb, ionisation energies and oscill. strengths calcs. 0-5488  
 S compounds, one-electron binding and Auger energies 0-52872  
 S, one-electron binding and Auger energies 0-52872  
 Si IV radial wave functions of discrete spectrum calcs., dipole and quadrupole polarisation 0-5476  
 Si isoelectronic sequence, CI calcs. of oscillator strengths, L-S framework 0-14089  
 ThH<sub>4</sub>, Dirac-Fock one-centre expsn. calc. 0-5485  
 TlF, electric dipole hyperfine struct. calc. 0-53162  
 UF<sub>6</sub>, electronic struct. and geometry, ab initio calcs. using relativistic ECP 0-32606  
 UH<sub>6</sub>, Dirac-Fock one-centre expsn. calc. 0-5485  
 V, atom and ions, shell energy struct., SCF calc. by Dirac-Fock-Slater method 0-52877  
 Xe, inner electron energy characteristics, validity of Hartree-Fock-Pauli approx. 0-42957  
 Xe, relativistic Hartree-Fock calcs. using spherical Gaussian basis sets 0-32595  
 ZnCl<sub>2</sub>, deformation densities, relativistic effect 0-42928

**relativistic electron beam tubes**

- circular waveguide, microwave generation by relativistic electron beam 0-48128  
 injection into drift cavity, pot. profile finite size particle calc. 0-18987  
 intense microwave radiation, generation by relativistic electron beam introde 0-14887  
 low atomic number foil target, anomalous energy dissipation of tightly pinched relativistic electron beam 0-29833  
 O-type relativistic electron devices, linear theory 0-43242  
 O-type relativistic electron devices, nonlinear theory 0-43243

**relativistic fluid dynamics**

- anisotropic spheres, adiabatic contraction in general relativity 0-36489  
 compact extragalactic radio sources, relativistic jets model 0-4448  
 EM fluid flows 0-52094  
 equilibrium of slowly rotating relativistic fluids 0-46898  
 gravitational compression of a body within the approximation of the special theory of relativity 0-4611  
 heat conduction in relativistic extended thermodynamics 0-43803  
 incompressible heat-conducting relativistic fluid, four-vector form 0-33707  
 magnetofluid flows, geometry 0-46895  
 MHD eqns. with radiative reaction and relativistic Boltzmann eqn. 0-36956  
 MHD of heat conducting, charged relativistic fluid, Cauchy problem solutions, existence and uniqueness (*Italian*) 0-48821  
 perfect magnetofluid, matter tensor, convective deformations 0-36922  
 plane wave growth eqn. in polytropic heat cond. relativistic fluid (*French*) 0-28580  
 quasars, two-dimensional relativistic blast waves, solns. for adiabatic case 0-22108  
 radio sources, relativistic corrections in expanding synchrotron sources theory 0-12821  
 radiogalaxy models, relativistic channel flow, soliton soln. stability 0-56962  
 rotating fluids, central behaviour, tetrad formalism 0-53888  
 Schwarzschild black hole stationary spherical accretion, stability 0-51800  
 singular hypersurfaces, asymptotic regularisation as alternative to distrib. 0-36923  
 thermal waves and growth eqn. (*French*) 0-28579  
 thermo-viscous fluid dynamics, heat conduction and wave propag. 0-24107  
 trans-relativistic shock relations, numerical solns. 0-31202  
 transonic flow on axially symmetric torus 0-28527  
 vorticity streets stability on curved surfaces with reflection symmetry 0-46810  
 weak discontinuities in high temp. phenomena, relativistic theory 0-53889

**relativistic mechanics**

see also *relativistic fluid dynamics*

- Alfven wave accelerated particles, distrib. function self-similar soln. 0-56702  
 Brownian motion, space-time approach to quantum mechanics 0-31567  
 charges in EM field, generalised covariant Hamiltonian formulation 0-46794  
 classical and quantum dynamics 0-22192  
 continuum in generic motion, action of volume and surface forces, second cardinal equation of dynamics 0-31501  
 dynamics of right angled lever 0-12900  
 electron beams, collective relativistic interactions in faster than light media (*Russian*) 0-46803  
 elementary bodies, relativistic dynamics in seven-dimens. space 0-32015  
 energy-momentum tensor of extended relativistic systems 0-46798  
 free particle, relativistic, in thermal radiation within classical electrodynamics, equilib. distrib. 0-8935  
 Hamiltonian dynamics, constraints origin 0-17797  
 heat flow in relativistic equilibrium thermodynamics 0-52017  
 magnetic monopole, relativistic classical eqns. of motion, electric dipole moment case 0-37195  
 mass variations obs., periodic, using electromechanical vibrating system 0-47020  
 Maxwell-Boltzmann statistical distrib. function, Hsu's space-light transformations, agreement with Lorentz results 0-17858  
 Minkowski force from Frenet-Serret eqns. for curve in Riemann space 0-22208



**relativistic mechanics continued.**

- nonequilibrium relativistic strain tensor, rigid disc relativistic rotation (Russian) 0-22195
- nonlinear wave propagation in relativistic continuum mechanics 0-22203
- paramagnetism, statistical mechanics in strong mag. field 0-17865
- path integrals on curved spaces, method of determination 0-31589
- Poincare group, phase space representation, relativistic particle mechanics appl. 0-8784
- point charge free fall motion under weak gravitational field 0-42057
- point charge moving in arbitrary way, superposition of two fields (Russian) 0-22251
- position variables in classical Hamiltonian mechanics 0-27123
- presymmetry in relativistic quantum mechanics, absence of kinematics 0-8843
- ray theory in relativistic anisotropic elasticity (French) 0-36846
- relativistic string dynamics, geometrical approach 0-9100
- rotating frames and continuum mechanics, relativistic appraisal 0-17795
- rotating plane-fronted waves and their Poincare-invariant differential geometry 0-332
- shock formation in elastic solids in relativity (French) 0-31496
- special relativity, principle of covariance and basic inertial frame, non-invariance of rest mass 0-22194
- special relativity space-time test theory, dynamical aspects 0-17798
- three point particle system, spin-mass relation 0-36845
- two body problem, appl. of dynamic confinement from vel. depend. interactions 0-46800
- ultrarelativistic particle in homogeneous mag. field, trajectory, radiation damping 0-18104
- weak plane gravitational wave action on two connected masses 0-17851
- world line conditions for spinning particles, spin orbit forces 0-36844
- world-line invariance in predictive mechanics 0-31498

**relativistic plasmas**

- Alfvenic particle streaming in astrophysical plasmas 0-31206
- Centaurus A, nuclear gamma-ray lines, origin in relativistic plasma 0-41890
- charged particle drift motion under resonance conditions 0-38611
- collective ion acceleration by relativistic electron cloud (Russian) 0-48961
- Compton scattering of transverse waves by relativistic electrons 0-51644
- cool regions in relativistic plasmas: thermal instabilities 0-17486
- degenerate electron plasma, dielectric response in mag. field, plasma oscillations 0-54022
- dense relativistic electron gas, EM response in strong mag. fields, particle polarisation, mode struct. 0-43963
- dispersion in warm and hot plasmas 0-48960
- echo oscillations (Russian) 0-53990
- electron beam, with inhomogeneous ion density, self-consistent model 0-43247
- electron beam injection into drift cavity, pot. profile finite size particle calc. 0-18987
- electron cyclotron waves in plasma, relativistic nonlinear 0-10377
- electron power law spectra in random mag. field 0-24240
- EM cyclotron instability 0-21912
- EM ion waves in cold relativistic plasmas, astrophys. appl. 0-21910
- energy loss due to binary collisions in a relativistic plasma 0-24127
- general relativistic plasma sphere with central gravitating mass, MHD eqns. 0-6276
- Hamiltonian to order  $v^2/c^2$  of slightly relativistic plasma 0-54024
- kinetic equation, fully convergent, for homogeneous isotropic slightly relativistic plasma 0-54025
- Langmuir turbulence of relativistic plasma in strong mag. field (Russian) 0-28678
- laser-irradiated solid target, nonlinear dynamics 0-28767
- longitudinal waves (Russian) 0-54023
- modulational instability of nonlinear waves with nonlinear Landau damping (Russian, English) 0-53955
- moving magnetoplasma slab, space charge waves propag. 0-38700
- oscillations, EM and electrostatic, in isotropic relativistic plasma 0-54026
- pulsar magnetospheres, relativistic MHD wind or plasma wave 0-31317
- radiation scattering by high-temp. relativistic plasma, polarising props. calcs. (Russian) 0-53937
- radiative collapse of a relativistic electron-positron plasma to ultrahigh densities 0-14929
- radiosources, extended, particle accel. and radiative losses effects on source dynamics 0-46687
- runaway relativistic electron scatt. on oscills. in Tokamak (Russian) 0-48849
- self-pinch beam, radial expansion with distrib. energy, anal. 0-19609
- shearing field-free plasma, EM wave propag. effects rel. to pulsar microstruct. 0-17483
- trans-relativistic shock relations, numerical solns. 0-31202
- transverse Cherenkov mode nonlinear stabilisation by external mag. field 0-38642
- ultrarelativistic beam quasilinear relativistic plasma relax. in strong mag. field, magnetobremstrahlung (Russian) 0-38669
- ultrarelativistic particle beam in relativistic plasma, emission due to mag. bremsstrahlung 0-46390
- B-H, possibility of thermonuclear fuel in relativistic plasma (Russian) 0-37573

**relativistic quantum field theory**

- $\lambda\phi^4$  momentum space renormalisation in curved space time 0-37158
- $\lambda\phi^4$  field theory, renormalisation in curved space-time 0-42320
- $\lambda\phi^4$  field theory renormalisation in curved space-time 0-42319
- additive conservation laws for local relativistic quantum field theory 0-22507
- automorphic fields on flat space-times, vacuum stress tensor 0-22510
- automorphic theory, mathematical issues 0-22509
- bi-local field on space-like surface 0-27403
- black hole evaporation, inevitability of associated naked singularity 0-36924
- bound-state equation, relativistic single-particle, numerical solutions 0-52389
- Breit equation, discontinuous solns. for spin  $1/2$  particle 0-4834
- C\*-algebras of two body interactions, existence of scatt. theory of time automorphism groups 0-31972
- Casimir effect in quantum field theory 0-42330
- causal A-statistics 0-22504
- conformal conservation laws in action-at-a-distance theory 0-42335
- conformal relativity, bare mass theory 0-27417
- cosmology, effective Lagrangian and pair prod. 0-22123

**relativistic quantum field theory continued**

- covariant  $\sigma$  models, first order system of differential eqns. 0-31978
- curved space-time quantum stochastic processes, covariant Kolmogorov-Klein-Fock eqn. 0-18083
- Dirac fields in a curved space-time 0-18070
- Dirac model of extended particles, physical aspect of interactions 0-9142
- Dirac particle propagator, supersymmetric methods 0-342
- Dirac string Lagrangian in  $A^0=0$  gauge, path integral quantisation 0-32007
- discrete space structure dynamics 0-52392
- dynamical groups for the motion of relativistic composite systems 0-9115
- Dyson-Salam scheme subtractions, counterterm equivalence 0-13241
- elastic scattering between binary quark-antiquark system and local field 0-47244
- elementary bodies, relativistic dynamics in seven-dimens. space 0-32015
- elementary domain theory 0-42318
- energy-momentum tensor vac. expectation values, depend. on manifold geom. and topology 0-355
- Euclidean approach in curved spacetime, functional anal. 0-27181
- Euclidean light cone gauge,  $1/N$  expansions with non-isoscalar gluons 0-47169
- expanding universes, positive frequency and Hamiltonians 0-4624
- extended hadrons in geometrically formulated gauge dynamics with fibre bundles 0-9141
- Fermifield bosonisation in 1+1 dimensions 0-47172
- fermion interactions, convergence difficulties, soln. 0-4836
- Feynman diagrams, appls. in advanced quantum theory, book 0-22157
- Feynman propagator in curved spacetime, momentum space representation 0-32004
- finite-band solutions to the duality equation on  $S^4$  and two-dimensional relativistically invariant systems 0-42349
- five dimensional QFT, generalised free fields conformal group 0-4837
- free scalar massless field in 2-dimens. space time 0-52426
- frequency decompositions in curved space-time 0-31973
- Friedmann model, spontaneous symmetry breakdown 0-51929
- gauge field construction, lattice approx. convergence 0-37156
- gauge field theory, space-time symmetry, Higgs model 0-52385
- geometric quantization and internal symmetry 0-42089
- Green's function method for many-body problem for relativistic meson field theory, book contrib. 0-357
- Haag's theorem and dimensional regularization 0-52409
- Hamiltonian form for massless higher-spin fermions 0-52412
- Hamiltonian theory, covariant formulation, on light cone, fields with spin (Russian) 0-9087
- Heisenberg equations of motion in a nonabelian gauge theory (German) 0-27387
- Kaluza-Klein bundle, unified theory 0-37153
- Klein-Gordon charged particles, perturbation theory for non-equilibrium stat. Green's functions 0-31994
- Klein-Gordon charged particles, quantum distrib. function 0-31993
- ladder approximation with effective propag. and vacuum stability, Bethe-Salpeter bound state 0-47168
- Laplace transform, inversion, non-unitary representations of MH(2) and group  $ax+b$  0-4866
- Lee model in EM field, mag. moment calc. using Schwinger source theory 0-42350
- Lie algebra representations and coherent states, Trotter limits 0-22238
- light-cone quantisation of scalar field, current nonconservation 0-47220
- linear field equations on self-dual spaces 0-42328
- linear zero-spin fields in external gravit. and scalar fields, perturbation theory 0-31969
- lorentz-invariant spin-1/2 equation for the representation  $(1,1/2) \oplus (1/2,0) \oplus (0,1/2) \oplus (1/2,1)$  0-42334
- magnetic monopoles with no strings, action principle and canonical quantisation 0-31990
- massive Thirring model, multisoliton solns. in Pohlmeier-Lund-Regge system 0-47195
- massive Thirring model, repulsive case, new effects 0-27415
- massive Thirring model, two-dimens., inverse scatt. method 0-4840
- massive vector boson field theory with spontaneous symmetry breaking 0-52443
- massless fields in asymptotically flat space-time, null surface quantisation and quantum theory 0-4625
- massless scalar particle prod. by cosmological torsion field 0-51936
- mesons, deformations and spectral props. 0-13203
- Nelsons stochastic mechanics, spinning particles and relativistic particles 0-31587
- non-linear coupling of quantum theory and classical gravity 0-27389
- nonlinear super-Poincare fermion, quantisation in bag like formulation 0-4923
- nuclear matter equation of state, relativistic quantum field theory of neutron stars 0-5088
- nuclei, description in relativistic field theory, book contrib. 0-358
- null plane fields and automodel random processes 0-32018
- $O(n)$   $\sigma$  model, nonlocal charges in two dimensions 0-18075
- $O(n)$  nonlinear  $\sigma$ -model, field eqn. reduction 0-31979
- oscillator formalism for hadron struct. and props. 0-9144
- particle creation by time depend. elec. and gravitational fields 0-4623
- phonon splitting in the magnetised vacuum 0-4897
- Poincare covariant particle model with mass and spin mixing 0-32016
- pole-dipole relativistic string model 0-386
- pre-Schwinger model, Lorentz transforms. if operator solns. 0-47171
- quantum effects in systems with accelerated mirrors 0-22508
- quantum microsystem evolution, nonconservation effects 0-22515
- relativistic string dynamics, geometrical approach 0-9100
- renormalon singularities, contribution to Borel transform. 0-4848
- Salpeter equations, integral transform and relativistic radial eqns. 0-4835
- scalar field vacuum fluctuations in curved space-time localised region 0-42116
- scalar meson field and many-body forces, book contrib. 0-359
- scalar quantum field in an external gravitational field 0-31974
- self-dual gauge fields and space-times 0-9108
- self-dual Yang Mills fields in Minkowski space 0-18078
- sine-Gordon eqns., Lax pairs for certain generalisations 0-31997
- $SO(2,R)$  non-compact group for Dirac eqn. 0-22503
- $SO(4,2)$  infinite component fields, model of composite relativistic defects 0-18071
- solitons in some geometrical field theories 0-27390
- space-like fields for quark confinement 0-42426
- spin 1 field in flat Clifford Klein space times 0-27391
- spin 1/2, gauge invariant antisymmetric tensor spinor field 0-47184



**relativistic quantum field theory continued**

- spin-1 particles, multispinor eqn. 0-4865
- spin-1/2 quantised Dirac theory, field representation 0-4845
- spinning and charged particles, conformally covariant description in  $O(2,4)$  symmetry 0-22524
- spinor fields, conformal, dimensions, scale invariance 0-27394
- spontaneous symmetry violations 0-52411
- SU(2), Yang-Mills field eqn. configurations in curved spacetimes 0-18076
- SU(2) gauge field configuration in curved spacetimes 0-18077
- tachyons and quantum field theory 0-18069
- Thirring model, phase transitions 0-18067
- Thirring model coupled to gravity, classical solns. in generally covariant model with fermions 0-9091
- Thirring model massive phase, dynamic mass generation 0-4851
- Thirring model of massless scalar field, conformal transformations 0-52428
- unitarity restrictions on semi-classical approximations to certain functional integrals 0-32026
- unitary quantum mechanics, nonlinear and relativistic invariant fields 0-4567
- unitary relativistic wave equation exhibiting extended particle structure 0-9102
- vector field, general type, group of internal symm. of quantum theory 0-47198
- zero energy fermions in U(1) pointwise monopole field (*Chinese*) 0-42345
- $e^+e^-$  pair creation in strong EM fields, gravitational effects 0-42376
- $\pi$  form factor, expt. behaviour, influence of left-hand cut on second Riemann sheet 0-13304
- $^{40}\text{Ca}$ , finite nuclear props. in relativistic quantum field theory, mass and p densities 0-9219
- $^{208}\text{Pb}$ , finite nuclear props. in relativistic quantum field theory, mass and p densities 0-9219

**relativistic scattering theory**

- see also elementary particle scattering; quantum field theory of elastic scattering
- AKNS-ZS inverse method, canonical struct. and generalised Marchenko eqn. calcs. 0-47192
- analytic extrapolations towards interior points from a cut, applic. to elementary particle scatt. theory 0-12952
- eikonal approximation, analytic props. 0-32038
- elastic scatt., impact parameter representation (*Russian*) 0-5019
- elastic scattering amplitude, singularities in  $\cos \theta$  plane 0-37186
- EM wave scatt. by relativistic uniformly accel. interface 0-4891
- Faddeev eqn. soln. in adiabatic approx. with separable pots. (*Russian*) 0-52437
- Faddeev equations, two-potential formula, three-body scattering 0-4893
- Friedrichs model unitary regularisation for many particle system 0-32039
- gauge invariance, Lorentz covariance and EM props. of elementary systems 0-32037
- gravitational scattering, post-linear approx. 0-27190
- inelastic, high energy, non-eikonal effects 0-42608
- infinite momentum limit of relativistic elementary systems 0-32036
- internal Lorentz basis for two-particle states 0-31499
- inverse problem in abstract relativistic scatt. theory 0-4894
- large angle scattering amplitude corrections 0-37187
- multiparticle scattering operators, cluster decomp. 0-22592
- nonlinear field equations 0-4882
- plasma medium, relativistic electron beam, Vlasov eqn. 0-14910
- position variables in classical Hamiltonian mechanics 0-27123
- quark confinement, Dirac equation with relativistic linear potential, baryon properties, SU<sub>6</sub> representations 0-47261
- separable nucleon-nucleon potentials and minimal relativity 0-27495
- spin 1/2 particles, relativistic scatt., continuous cut-off method 0-4892
- two body correlations through tachyon exchange 0-42367
- two- and three-body scatt. operators using light front dynamics 0-13238
- $\gamma d \rightarrow \pi^0 d$ , meson-exchange currents in photomesic reactions, relativistic many-body theory 0-422
- $K^- d \rightarrow \pi^- \Lambda p$ , three body Faddeev formalism, unstable dibaryon bound state search 0-32130
- $K^- p \rightarrow (K^+ \pi^-) p$ , 4.2 GeV/c, partial wave anal. in Q region 0-13330
- $k^- p \rightarrow \Lambda \pi^+ \pi^-$ , partial wave anal. in  $\Lambda(1520)$  region,  $\Lambda$  partial decay widths (*Russian*) 0-32131
- $\pi N$  dynamics, medium energy, dispersion relations, isobar expansion for  $\pi N$  0-4917
- $\pi N$  medium energy dynamics from  $\pi N$ , isobar model rescatt. corrections 0-4918
- $pp \rightarrow pX$ , deep inelastic scatt. in nuclei, bare particles, multiple scatt. theory (*Russian*) 0-52549
- $\pi d$  elastic scatt., 142-256 MeV, dibaryon resonance interference with Faddeev amplitudes 0-32123
- $\pi^- d$ , 552 MeV/c, elastic differential cross section Glauber theory anal. (*Russian*) 0-52700
- $\pi N$  low energy partial wave anal., cross sections,  $\Delta^0$  and  $\Delta^{++}$  0-52531
- $\pi N$  scatt., isospin violation from  $\pi^0 \eta$  mixing, partial wave anal.,  $N^*(1540)$  struct. 0-27426
- $\pi p$ , quasi-potential reconstruction, scatt. theory inverse problem (*Russian*) 0-5016
- $\pi^- p \rightarrow K^0 \Lambda^0$  up to 2.375 GeV/c, resonance parameters, partial wave anal. 0-32133
- $\pi^- p \rightarrow p \bar{p} n$ , 18 GeV,  $p \bar{p}$  resonant state partial wave anal. 0-32134
- $\pi^- p \rightarrow \pi^- \pi^+ p$ , 63, 94 GeV/c,  $A_2$  meson prod. from partial wave anal. 0-37303
- $\pi^- p \rightarrow \pi^- \pi^- \pi^+ p$ , 63, 94 GeV/c,  $A_1$  meson existence from partial wave anal. 0-37304
- $\pi^- p \rightarrow \pi^- \pi^- \pi^+ p$ , 63, 94 MeV/c,  $A_3$  meson,  $3\pi$  resonances in  $2^-$  partial waves 0-37305
- $\pi^- p \rightarrow \pi^- \pi^+ \pi^- n$ ,  $\pi\pi$  scatt. partial wave anal. f, g and h mesons 0-5015
- H-like ions, ground-state, elastic electron (positron) scatt., relativistic Glauber amplitudes 0-23550
- $H^+H^-$ , relativistic classical theory of electron capture 0-18920
- U+U, K-shell ionis., classical relativistic trajectory method appl., 1, 10 GeV/n 0-43129

**relativity**

- see also general relativity; light cones; relativistic mechanics; relativistic quantum field theory; relativistic scattering theory; special relativity
- Einstein's contribution to twentieth century physics (*Chinese*) 0-17
- quantum theory comparison 0-27175

**relaxation**

- for dislocation relaxation see dislocation damping
- see also anelastic relaxation; chemical relaxation; dielectric relaxation; magnetic relaxation; stress relaxation; ultrasonic relaxation; viscoelasticity
- cellulose blotter/torsion pendulum technique, for relax. determ. 0-54357
- ionic crystals, elastic relax. associated with formation and motion of Schottky defects 0-49216
- minerals release-adiabat measurements, effect of viscosity 0-51388
- organic compounds, complex, nuclear relaxation influence on stimulated emission 0-48019
- polystyrene, glassy state, relax., free vol. fluctuations effect 0-19722
- thunderstorms air relaxation time, influence of cloud and precip. particles contrib. to elec. cond. 0-17332

**relaxation oscillators**

- Van der Pol oscillator, renormalised perturbation theory 0-27225
- Van der Pol oscillators, diffusion-coupled active medium, nonlinear waves 0-4546

**relaxation time, carrier** see carrier relaxation time**relay systems (radio)** see radio links**relay systems (satellite)** see satellite relay systems**relays**

- see also reed relays; switches
- inductance measurement to TGL 24961 specification methods for Fe-cored coils (*German*) 0-4736
- piezoelectric, multilayer plates bending, anal. 0-40064
- Cu-Ni (20 wt.%) alloy appl., contour plate for spring, creep characts. obs., use of Larson-Miller method (*Japanese*) 0-55454

**relays (repeaters)** see repeaters**reliability**

- see also circuit reliability; quality control; standards; testing
- biomedical equipment, reliability and safety aspects 0-36172
- Brunswick plant post-startup optimization 0-23048
- cardiac pacemaker reliability technology workshop, Gaithersburg, USA (Oct. 1977) 0-27038
- dial gauges quality obs., manufactured in Rumania (*Rumanian*) 0-47049
- dissolved  $O_2$  in rivers, reliability parameter in probabilistic programming models 0-26179
- fission reactor fuel element sheathing, reliability, including hydration process, probabilistic model (*Russian*) 0-52742
- fission reactor materials theft, fault tree and reliability relationships for analyzing noncoherent two-state systems 0-47600
- fission reactors, CRBR shutdown system, Markovian reliability anal. 0-27761
- hydro-photovoltaic plants, peak power generation economics and reliability 0-45706
- instrument reliability assessment using mathematical models 0-22348
- irradiated fuels reprocessing, French and European policies (*French*) 0-809
- laminated cylindrical shells, prepared by continuous filament winding calc. of strength and reliability 0-10194
- LEED crystallography and reliability indices 0-54081
- LWR, deterministic criteria vs. probabilistic analyses 0-32377
- measurement reliability, statistical approach (*Russian*) 0-22317
- MIS solar cells, stability and degradation mechanisms 0-16806
- MNOS P-channel switch, accelerated reliability testing (*German*) 0-6988
- nuclear engineering risk estimates, communication techniques 0-18514
- nuclear power plants secondary system radioactivity monitoring 0-18445
- nuclear power statups, aseismic design and testing of equipment and components, Japan 0-52763
- nuclear power stations, electrical supply system performance, reliability of protection and control systems 0-52761
- nuclear reactor instrumentation, reliability improvements 0-32416
- nuclear reactor redundancy systems, common mode failures 0-13641
- nuclear stations, maintenance optimization through trend monitoring 0-18552
- plastics, for transmission media, thermomech. reliability 0-40666
- PWR neutron flux detectors, reliability tests (*French*) 0-32403
- reactor protection computer systems, statistical verification of reliability 0-32417
- reactor safety equipment, reliability in design 0-37555
- semiconductor junction lasers (*German*) 0-19034
- solar power systems availability and reliability analysis 0-35687
- Westinghouse plant availability anal. with operating data base 0-23050
- $Al_0Ga_{1-x}As$  buried heterostruct. laser, fabrication, optical props. and reliability 0-53322
- $Al_0Ga_{1-x}As$  laser diode, reliability 0-53320
- $Ga_{1-x}Al_x$  junction-up TJS laser electron injection efficiency improvement 0-48300
- $GaAs-(GaAl)As$  DH lasers, automated LPE growth, CW reliability tests 0-20804
- Na valves for advanced reactors, reliability data collection at CREDO 0-22897
- Ni-Cd 6.0 Ah cells, accelerated testing of cell failure for life prediction 0-35670
- U isotope separation processes (*French*) 0-806

**remnance**

- see also coercive force
- achondrite meteorites, brecciation and shock effects on mag. susceptibility and NRM 0-8603
- biological materials, remanent magnetization as evidence for room temp. superconduction 0-35926
- chondritic meteorite, remanent magnetisation rel. to shock and metamorphic history 0-36598
- chondritic meteorite magnetisation 0-36599
- clay thermoremanent magnetisation, cooling-rate depend. 0-46174
- $\gamma\text{-Fe}_2\text{O}_3$  acicular particles, remanent coercive force 0-44872
- gyromagnetic magnetisation in anisotropic mag. material 0-50142
- IRM of Yellowstone Group comparison with DRM of Pearllette ash beds 0-21624
- Lake Tahoe, California-Nevada, remanence, props. and palaeomagnetism 0-41371
- magnetic tapes, static and antihysteretic mag. props. 0-44868
- magnetite, partial thermal remanent magnetisation additivity 0-26498
- meteorite impact site, Slate Islands, Canada, shock remanent magnetisation 0-30986
- rock magnetism, rotational remanent magnetisation, explanation 0-51390
- rock magnetism, self-reversal of remanent magnetisation of lava 0-56462



remenance continued  
 rocks, NRM stress sensitivity meas. using cryogenic magnetometer 0-26506  
 rocks, Ziederfeld vector diagrams use in multicomponent, palaeomag. studies 0-17420  
 rocks remanent magnetisation, uniaxial stress effects, stress cycling and domain state depend. 0-26505  
 sediments, oblique anhysteretic remanent magnetisation 0-21717  
 shock-diminished remanence at Charlevoix impact structure, Quebec 0-26441  
 spin glass, EPR frequency and mag. transverse susceptibility with remanent magnetisation (*French*) 0-7145  
 spin glass, slow decay of remanence magnetisation, theory 0-11211  
 spin-glass, two-dimensional-Ising model, low temp. dynamic props. 0-20425  
 Thunder Bay Late Quaternary sediments, palaeomagnetic record from remanent mag. meas. 0-17230  
 titanomagnetite, TRM acquired by multi-domain single cryst. 0-36293  
 Au-Fe spin glass, energy flux associated with remanent magnetization relaxation (*French*) 0-7110  
 Co-Ni-P, film, props. independent of mag. hysteretic and anhysteretic remanences (*French*) 0-2604  
 Co-Ni-P electrolytic layers, partial anhysteretic remanent magnetisation, additivity prop. (*French*) 0-44882  
 Cu-Mn spin glass, hysteresis loops, temp. and field depend. 0-15742  
 Cu-Ni-Fe, permanent magnet, temp. effect 0-34701  
 CuMn, spin glass, remanence, new approach from zero field NMR 0-34785  
 Eu, $\text{Sr}_{1-x}\text{S}$ , insulating spin glass, mag. props. 0-2589  
 Fe powder,  $\text{BH}_4$  reduced, coercive force and remanence ang. variation 0-44879  
 Fe powders, prep. by  $\text{BH}_4$  process, comp. and stability 0-44878  
 Fe-B-Si amorphous ribbon, strain induced anisotropy, and toroid diam. effect on mag. props. 0-34623  
 Fe-Cr-Co, permanent magnet, temp. effect 0-34701  
 Fe-Cr-Co(-Mo), mag. props. after isothermal thermomag. treatment (*Russian*) 0-25159  
 Fe-Ni-Al-Cu (25, 14, 4 wt.%), alloy YuND4, effect of Ti addition on structure, mag. props. 0-15714  
 $\text{Fe}_{40}\text{Ni}_{40}\text{B}_{20}$ , amorphous, casting conditions effect on mag. props. (*Japanese*) 0-34698  
 $\text{Fe}_{40}\text{Ni}_{40}\text{P}_{14}\text{B}_6$ , amorphous ribbon, influence of torsion on mag. props. 0-7138  
 $\gamma\text{-Fe}_2\text{O}_3$ , densified, rheological and mag. props. 0-44873  
 $\text{Fe}_3\text{O}_4$ , magnetite, grain size limits for pseudosingle domain behaviour, rel. to palaeomagnetism 0-11215  
 $\text{Fe}_3\text{O}_4$ , magnetite particles, interaction fields effect on hysteretic props. 0-54921  
 Gd alloys, amorphous, mag. props. and ferromag. reson. 0-54952  
 $(\text{Ni}_{1-x}\text{Fe}_x)_{1-y}\text{S}$ , anisotropic spin glass, mag. props. 0-39793  
 Ni<sub>3</sub>Mn, thermoremanent magnetisation and blocking temp. 0-34601  
 NiS film, electrolytically deposited, S content influence 0-44884  
 $\text{Sm}(\text{Co}_{0.86-x}\text{Cu}_{0.14}\text{Fe}_x)_2$ , permanent magnet, sintering and heat treatment effects 0-39817  
 W-Fe alloys, spin glass props., DC susceptibility and remanence meas., 1.6 to 295K 0-29560

#### remanent magnetism see remanence

remote consoles  
 disabled persons employment using traffic operator position system 0-36197

remote control see telecontrol

remote control equipment see telecontrol equipment

remote metering see telemetering

#### remote sensing

see also infrared imaging; remote sensing by laser beam  
 aerospace photographic image information, atmospheric effect evaluation 0-4101  
 agriculture applications 0-56329  
 air pollution, population exposure in USA, evaluated by satellite 0-40936  
 American Society of Photogrammetry Annual Convention, Washington, USA (March 1978) 0-4149  
 central Asia, active faulting and Cenozoic tectonics of Tien Shan, Mongolia and Baykal 0-8278  
 atmosphere, conf. (Innsbruck, 1978 May 29-June 10) 0-31415  
 atmosphere sounding by interferogram measurement technique, temp. profile 0-17413  
 atmosphere spatial temp. and geopot. fields, thermal sensing from Earth orbit 0-36429  
 atmosphere temperature, by microwave radiometry 0-46293  
 atmosphere turbidity monitored by satellite, obs. of reflected sunlight 0-51471  
 atmosphere water vap. and liq., and wind vel. at ocean surface, satellite microwave technique 0-41573  
 atmospheric remote sensing by aerosol lidar backscatter (*Dutch*) 0-4110  
 atmospheric temperature-pressure profile meas. by microwave remote sensing (*Chinese*) 0-4116  
 atmospheric water vapour, passive microwave profiling technique 0-21856  
 atmospheric water vapour and liquid monitoring using radiometry at 21 and 32 GHz 0-26628  
 auroral data from DMSP, calibration 0-8443  
 cartography, point transfer error determ. 0-17227  
 cartography by Mapsat (Automated Mapping Satellite System), proposed parameters 0-17468  
 chlorophyll, gradient map from high-altitude ocean colour scanner data 0-26551  
 clay soil sand content, determ. from percent reflectance 0-56475  
 cloud determination, SMS IR data appl. during GATE 0-31113  
 cloud microwave radiation emission meas. 0-17351  
 cloudy atmospheres, ground based microwave radiometry (*Chinese*) 0-51549  
 continental ice sheet, thickness changes from Geos 3 altimetry 0-4051  
 crop types monitored by side-looking radar 0-46280  
 diffuse reflectance models for aquatic suspended solids measurement, test 0-8453  
 digital image processing developments 0-14287  
 Earth's surface obs. contrast attenuation factors calc., using atmospheric models 0-4135  
 Earth resources survey sensor, calibration linear photodiode array in push-broom scan mode, satellite appl. 0-56693

#### remote sensing continued

earth surface, electron system for image transformation and coding in conventional colours 0-4117  
 Earth-atmosphere radiative heating effects on climate, NOAA radiometer meas. 0-8425  
 energy conservation for reflectivity and transmissivity at a very rough surface 0-53188  
 environmental pollution monitoring, most promising trends 0-35811  
 feature identification and location experiment FILE, sensors 0-56657  
 forest fire sources, microwave radiation spectra 0-52314  
 gaseous atmospheric pollutants, teledetect. (*French*) 0-7988  
 gaseous pollutants, mobile Fourier transform interferometer 0-12043  
 geological interpretation, from composited radar and Landsat imagery 0-56647  
 geology, Washington, DC, Landsat reconnaissance 0-41444  
 Geostationary Operational Environmental Satellite data acquisition analysis and display 0-17382  
 Gironde inlet and Pertuis of Maumusson, estuarine waters seaward dispersion, remote sensing study (*French*) 0-8324  
 ground cover remotely sensed by radar, backscatter cross-section 0-46279  
 ground reflectances, atmospheric effects in space meas. 0-17373  
 ground resistivity, airborne survey using VLF plane waves, resolution studies 0-12333  
 Gulf stream, surface boundaries measured by Geos 3 radar altimetry and IR data 0-4021  
 hail, radar detection technique, quasilinear discriminant function 0-21861  
 HF sky wave radar remote sensing of sea state, minimisation of ionospheric disturbance 0-21857  
 high altitude low contrast imaging, sensor requirements 0-4152  
 hurricane sea surface wind speed, L-band radar backscatt. obs. 0-56561  
 ionosphere, topside sounding and determination of electron profiles, review 0-56669  
 Kelvin waves in mesosphere and stratosphere, struct. and behaviour from Nimbus 5 IR meas. 0-8394  
 lake identification by closed planar curve analysis using LANDSAT (*Japanese*) 0-26635  
 lake quality monitoring, multirate Landsat data extraction program 0-17299  
 land use mapping by radar imagery, techniques 0-8449  
 land-use map accuracy testing, sampling designs 0-17226  
 LANDSAT digital data for detect. of moisture stress by Green Index Number method 0-17423  
 Landsat imagery, planimetric restitution using Zeiss Stereotop 0-56648  
 Landsat images, digital differential rectification 0-41570  
 landscape multispectral data, Karhunen-Loove analysis 0-48164  
 large format camera for Space Shuttle, cartography appl. 0-4232  
 layered random media, radiative-transfer theory 0-36413  
 light diffusion in atmosphere, estimation using const. transmission function 0-4100  
 lower atmosphere remotely sensed by two satellites, radio illumination method 0-51550  
 lower atmosphere using radiowaves, ground-based measurements 0-56628  
 marine boundary layer aerosol, optical thickness 0-17326  
 meteorology, satellite data uses, ESA conf. (Lannion, France, 17-21 September 1979) 0-36783  
 meteorology, satellite imagery appl. appl. to numerical forecasting model initial conditions assessment 0-31084  
 microwave, from space, synthetic-aperture radar systems and Spacelab expts. 0-36409  
 microwave monitoring Earth, from satellite, advantages 0-17409  
 microwave remote sensing of Earth, radiative transfer eqns. 0-21855  
 multiple-Doppler system 0-31140  
 multispectral information vol. optimisation of natural formations 0-4118  
 multispectral linear arrays, alternative to LANDSAT D thematic mapper 0-4153  
 multispectral scanner imagery, two-dimensional digital filters appl. 0-31152  
 ocean, synoptic eddies (*Russian*) 0-12420  
 ocean acid waste dump, particulate Fe mapping 0-56497  
 ocean colour 0-8460  
 ocean internal waves, acoustic reverberation data 0-41562  
 ocean passive radiometry, radio meteorology colloquium, Victoria, British Columbia, Canada (1978 June 14 to 21) 0-46724  
 ocean surface, microwave radiometry remote sensing 0-36428  
 ocean surface circulation, remote sensing with radar altimetry 0-46189  
 ocean surface layer temp. sounding (*Russian*) 0-4138  
 ocean surface microwave emissivity, model of wind roughening 0-46184  
 ocean surface waves, acoustic meas., theory 0-12564  
 upper ocean velocity field, nonlinear motion. obs. using range-gated Doppler sonar 0-51422  
 ocean wave heights, GEOS 3 radar altimeter data anal. 0-8452  
 ocean wave imaging and wavelength meas. by aerial photography 0-46323  
 ocean wave model, summary of verification results using wave height study 0-4027  
 ocean waves, height and dominant wavelength obtained from Geos-3 altimeter study 0-4024  
 ocean waves, high sea state, wave height measurements from Geos-3 radar altimeter data, aircraft and shipdata—a comparison 0-4025  
 oceanographic microwave remote sensing 0-56612  
 oceanography, Naval Coastal Systems Center (NCSC) environmental measuring system 0-12570  
 particle size distrib., anomalous diffraction approx. solns. 0-17386  
 photogrammetry, high intensity dot grids appl. to accurate area determ. 0-17225  
 photometric interpretation process for colour film 0-42251  
 planetary atmospheres, new inversion method 0-12677  
 plant canopies reflectance meas. using spectroradiometer 0-56658  
 radar reflection factor data, cartesian interpolation and display 0-31136  
 radio echo sounding of ice sheets, internal props. var. with depth 0-26633  
 radiometer measurements, microwave brightness temperature (*Danish*) 0-26625  
 rainfall over land, microwave radiometry by Nimbus 6 ESMR 0-56635  
 random media, active remote sensing, theory 0-51571  
 rock type discrimination using enhanced Landsat imagery 0-41568  
 RPV, high-altitude, for environmental appls. 0-17470  
 saline seep detection and mapping, IR remote sensing techniques 0-4154  
 SAMIR microwave radiometric system, Bhaskara satellite, geophysical data acquisition 0-56638



## remote sensing continued

- satellite altimetry measurements for oceanic geoid determination, short arc adjustment model technique 0-21830
- satellite mapping, by synthetic aperture radar 0-12572
- satellite photograph production using laser beam recorder (*German*) 0-5777
- sea foam produced by storms, microwave remote sensing of storm intensity 0-41528
- sea ice, anisotropic props. in 50-150 MHz range 0-17274
- sea state, significant wave height extracted by algorithms 0-4023
- sea state, surface roughness slope density calcs. from Geos-3 data 0-4022
- sea surface contour airborne radar as remote sensing instrument 0-51562
- sea-surface temperatures in tropical Pacific, satellite determ. and climatological usefulness 0-31044
- sediments below turbid water 0-8331
- short pulse radar ocean wave sensing, preliminary results 0-46315
- significant wave height, comments on airborne profilometer problems 0-4026
- snow albedo following dustfall, satellite remote sensing 0-17385
- snow cover parameters, microwave radiometry determination 0-56652
- snowpacks, microwave passive remote sensing, theory and expt. 0-26632
- soil, surface roughness effect on microwave emission 0-17264
- soil moisture, by visible and IR false colour photography 0-56653
- soil moisture and geology mapping, thermal inertia method 0-8344
- soil moisture content measurement by microwave radiometry, review 0-17425
- solid-state linear array appls., user-oriented data processing 0-4151
- solid-state linear array technology appls. 0-4150
- staring IR sensor, acoustooptic tunable filter performance 0-36407
- stereo side-looking radar, accuracy anal. 0-56646
- stratosphere, artificial satellite instrums. description 0-26713
- surface based remote sensors, coding technique for boundary layer echoes 0-17400
- surface wind, algorithm for wind speeds using Geos 3 measurements 0-4078
- system specification using computer image simulation 0-48439
- telecommunication and remote sensing, book 0-36431
- teledetection of gaseous atmos. pollutants, data acquisition and anal., pollution mapping (*French*) 0-7989
- thermal spectrozonal aerial photography, capabilities and future prospects 0-18036
- thunderstorm intensity from satellite data 0-41518
- trichlorofluoromethane, 8-12  $\mu\text{m}$  bands intensities, temp. depend. 0-43048
- tropopause, detect. by partial specular refl. with VHF radar 0-8411
- troposphere moisture, temp., IR soundings anal. by statistical struct. and correl. functions 0-8398
- ultramafic rocks from Cr-rich areas, visible and near IR spectra, remote sensing appls. 0-4000
- Venus atmospheric precipitation detect., remote sensing radar and radio techniques 0-56741
- Visible and Infrared Radiometer evaluation from SeaSat-A surface temp. obs. 0-46325
- visible range spectrometric investigation from Salyut 4, radiation characteristics of environment 0-51638
- water quality from Landsat imagery of Wisconsin lakes 0-41469
- water vapour images from Meteosat, comparison to tropical streamline analyses 0-8384
- wave heights and wind speeds from Geos 3 data 0-4079
- wind determination by acoustic radar (*Chinese*) 0-46290
- wind velocity, remote meas. using video equipment for pollution monitoring (*French*) 0-7990
- wing and struct. const., MM wave and optical line-of-sight probing 0-36426
- U exploration, LANDSAT data merged with geol. and geophysics data 0-56651

## remote sensing by laser beam

- aerosol pattern recognition (*Japanese*) 0-51028
- air pollutants, laser spectroscopic detection 0-17366
- airborne fluorescence system for OH and trace gas meas. 0-36425
- airport environs, air pollution, remote monitoring by laser systems 0-17368
- atmosphere,  $\text{O}_3$  vertical distrib., shortened version of Umkehr ob. method 0-8430
- atmospheric remote sensing (*Chinese*) 0-46292
- atmospheric gaseous pollutants meas., mobile lidar system 0-35814
- atmospheric pollutants, real time monitoring using laser two photon ionisation spectroscopy 0-7996
- atmospheric propagation of optical signals, statistical characts. analysis 0-36412
- atmospheric sounding, lidar characts., optical system parameters effect 0-33065
- atmospheric visibility using lidar 0-31141
- cloud, vertical laser beam heating causing convection (*Russian*) 0-56529
- cross-wind velocity meas., interference fringe visibility and spacing, atmospheric turbulence effects 0-51572
- crosswind profiles, remote sensing using correlation slope method 0-31131
- dye laser, efficient forced oscillator, to meas. upper atmospheric Na layer 0-41563
- Earth's crust, tidal displacement, Geos-3 laser ranging obs. 0-3913
- fluoresensor systems using  $\text{N}_2$  and KrF lasers 0-21428
- industrial atmospheric pollutant remote analysis by Raman lidar 0-12047
- lidar, laser rangefinder, characteristics of atmospheric aerosols 0-51580
- lidar method for half width and intensity of gas absorption lines (*Russian*) 0-21844
- LIDAR teledetection and measurement of minority atmospheric constituents for pollution control (*French*) 0-7992
- meteorological phenomena observation, mobile computerised laser radar system 0-56644
- optical radar, logarithmic fast-response photodetector for atm. sounding, photometric properties 0-51585
- polar position, motion due to Earth's rot. Gen-3 laser ranging study 0-3912
- radiation effect on laser system performance 0-38054
- range resolved Brillouin scattering using pulsed laser 0-38055
- surface pressure, remote meas. by multicolour laser ranging system 0-8429
- Teflon spheres-nigrosin black dye-water dispersion, turbid laser backscatt. 0-1129

## remote sensing by laser beam continued

- teledetection of atmospheric pollutants by differential absorption of a  $\text{CO}_2$  laser at two frequencies (*French*) 0-7991
- toxic gas monitor based on laser photoacoustic spectrometer (*German*) 0-12046
- trace gas monitoring system, with tunable diode laser, improvements 0-16882
- wave height profiling, depth sounding, laser beam reflection method, sea surface wavenumber effects 0-31121
- wind speed, meas. from orbit using lidar system 0-4114
- wind transverse vel., remote meas. using laser Doppler velocimeter 0-4115
- $\text{CO}$  absorption meas. using long-path laser, system improvements 0-3563
- $\text{HNO}_3$ , high resolution spectral meas. of 5.9  $\mu\text{m}$  band using tunable diode laser 0-32707
- $\text{O}_3$  in troposphere, differential absorption lidar appl. 0-12554
- $\text{O}_3$  stratospheric layer, laser-radar obs. using excimer lasers 0-17410
- $\text{SO}_2$  plume in atmosphere, remote sensing mask correl. spectrosc. method 0-55966

## renormalisation

- $\lambda\phi^4$  momentum space renormalisation in curved space time 0-37158
- $\lambda\phi^4$  field theory, renormalisation in curved space-time 0-42320
- $\lambda\phi^4$  field theory renormalisation in curved space-time 0-42319
- $\sigma$  models, nonlinear, perturbative approach to symmetry restoration 0-37163
- $\sigma$  models, nonlinear, soft mass renormalisation of  $1/N$  expansion 0-47164
- $\sigma$  SU(N) model, spontaneous symmetry breaking, renormalisation 0-42340
- $\phi^4$  renormalisable field theory, virtual heavy particle effects 0-22513
- $\phi^4$  theory, renormalisation groups transformation explicit construction 0-4832
- $\phi^4$ -model in two and three dimensions, real-space renormalisation for arbitrary single-site pot. 0-22307
- $(\bar{\psi}\psi)^2$  model, spontaneous symmetry breaking, renormalisation 0-42340
- 't Hooft transformation, explicit solns. 0-345
- A-15 space group struct., phase transitions, renormalisation group theory comparison with Landau theory 0-6489
- Abelian and non-Abelian gauge theories, mass generation, renormalisation, chiral and unified theories 0-4871
- adsorbed monolayer of orientable molecules, lattice fluid model, real-space renormalisation group method 0-17882
- alloys, binary, BCC, order-disorder transform., three-body interaction effects 0-39257
- Anderson localisation, real-space renormalisation approach 0-2364
- Anderson localisation in random system, renormalisation group study 0-39530
- Anderson model, asymmetric, t-matrix approx., ground state 0-20061
- antiferromagnets,  $n=4$  type II, phase transitions, Landau Ginzburg Wilson Hamiltonian 0-15735
- asymptotic freedom in the infinite-momentum frame, SU(N) Yang-Mills theory renormalisation 0-22519
- atom with partially-filled shell, relativistic theory, secular operator renormalisation (*Russian*) 0-52896
- axial vector meson model, quasi-renormalisation using BPHZL approach 0-13208
- baryon decay effective lagrangian flavour struct. and renormalisation, grand unification 0-27447
- BCC Ising model with competing interactions, fluctuation-induced first-order transition 0-20424
- Bethe-Salpeter model, scaling reconstruction using renormalisation group, Callan-Symanzik eqn.,  $\phi_6$  theory (*Russian*) 0-42351
- block-cluster approach to percolation 0-161
- Blume-Emery-Griffiths model, renormalisation group centred, tricriticality 0-42165
- bond percolation in anisotropic square lattice 0-46989
- bond percolation in square, cubic, hypercubic lattice, probability renormalisation group method 0-31680
- Borel transform, contribution of renormalons 0-4848
- boson system,  $\lambda$ -transition, renormalisation-group theory 0-143
- boundary effects in quantum field theory 0-42331
- Callan-Symanzik and Weinberg equations: frame dependence of fixed points 0-4838
- Casimir effect in quantum field theory 0-42330
- chiral field, BPHZL renormalisation and  $1/N$  expansion and critical behaviour 0-52383
- colour spin and path ordered phase factor, path integrals 0-4932
- conference on dynamical critical phenomena, Geneva (Apr. 1979) 0-27040
- configuration space renormalisation to phase space, gauge coupling 0-18074
- conformal relativity, bare mass theory 0-27417
- coupling constant relationships 0-353
- $\text{CP}_{n-1}$  models and non-Abelian  $\text{HP}_{n-1}$ , quantum props.,  $\sigma$  relation, renormalisation 0-13210
- $\text{CP}^{N-1}$  model ( $D=2,3$ ), UV renormalisation and phase transition 0-31989
- critical dynamics, field theoretic method 0-27255
- critical dynamics, real-space renormalisation group approach, Migdal approx., review 0-27257
- critical dynamics, real-space renormalisation group approach 0-31699
- critical exponents by quantum field theory methods (*Russian*) 0-4869
- critical phenomena, renormalisation group theory, critical props. of generalised 2D Ising model 0-4665
- critical phenomena, renormalisation group theory, numerical method for calc. of free energy and correl. length of generalised Ising model 0-4664
- diamond lattice, Gaussian model in three dimensions, differential real-space renormalisation 0-17896
- dilute magnetic alloys, asymmetric Anderson model, renormalisation-group approach, static props. 0-44802
- dilute magnetic alloys, symm. Anderson model, renormalisation-group approach, static props. 0-44801
- dynamic renormalisation group in the large- $n$  limit 0-4842
- dynamical renormalisation group method, mode coupling theory 0-27254
- Dyson-Salam scheme subtractions, counterterm equivalence 0-13241
- E(6) grand unified theories, one loop renormalisation effects, stepwise symmetry breaking 0-32058
- effective potential for non-Abelian gauge theories and spontaneous symmetry breaking 0-4863
- elastic phase transitions, crit. dynamics 0-2146



## renormalisation continued

FCC lattice, Gaussian model in three dimensions, differential real-space renormalisation 0-17896  
 Fermi gas, one dimensional with backward scatt., gap renormalisation 0-24818  
 Fermi one dimensional gas with long range potential, renormalisation group, exchange, Umklapp interactions 0-2351  
 ferromagnet, random uniaxial, dipolar interactions, crossover behaviour, renormalisation group equations numerical soln. 0-50136  
 ferromagnetic, anisotropic, in random longitudinal field, multicrit. point, theory 0-54903  
 ferromagnetic metal, anomalous magneto-optic effects near Curie temp., s-f exchange model 0-2736  
 ferromagnets, exchange and dipolar coupled, spin wave renormalisation, Damon-Eshbach surface spin waves 0-2564  
 finite system, order parameter and sp. ht. for epitaxial ordering renormalisation-group calc. 0-17862  
 fragmentation functions beyond leading order in QCD 0-13282  
 G-convolution of n-point functions in quantum field theory 0-18065  
 gapless semiconductor valence band in mag. field 0-49600  
 gauge fields, chiral fields on loop space, colour-electric flux rings 0-42327  
 gauge theories, high temperature behaviour, symmetry restoration, renormalisation group methods 0-31996  
 gauge theory, anomalies, unitarity and renormalization, book contrib. 0-42352  
 gauge theory,  $Z(2)$ , renormalisation group calc. 0-22514  
 grand unification  $E_8$  theory, Weinberg-Salam model reproduction (*Russian*) 0-4909  
 graphical solutions of renormalization group equations 0-4560  
 Green functions, two-point, quantum field theory 0-9089  
 Gross-Neveu model, renormalisation, mass generation 0-27393  
 hard-soft renormalization of massless fields 0-13214  
 heavy particle effects through factorisation and renormalisation group, QED appl. 0-13243  
 Heisenberg antiferromagnetic chain, random, low temp. thermodynamic props. in zero mag. field 0-34657  
 Heisenberg magnet, classical, with layer structure, mag. phase transitions, anisotropic lattice, theory 0-29557  
 Heisenberg spin systems, two-dimensional, phase diag. 0-4847  
 hierarchical model, renormalisation group approach 0-34580  
 high temperature series renormalization group method 0-4660  
 Hubbard model, one-dimens., extended,  $2k_F$  and  $4k_F$  correl. functions, computer renormalisation group calcs., appl. to one-dimens. conductors 0-54625  
 instanton correction to vac. energy densities and bag const. 0-37211  
 instantons as link between weak and strong coupling in QCD 0-42403  
 intense field QED in continuous medium, appl. to Thomson scatt. and Cherenkov radiation 0-27435  
 Ising, 2- and 3-dimens. antiferromag. lattices, appl. of Kadanoff's variational approx. 0-2583  
 Ising ferromagnet and spin glass systems, random, crit. dynamics 0-34666  
 Ising lattice model with directional bonding, renormalisation group study 0-28894  
 Ising model, 1-D, energy conserving relax. 0-20420  
 Ising model, bond-diluted, percolation-thermal crossover index calc. 0-11145  
 Ising model, free energy, variational calc. for 3 dimens. system 0-42167  
 Ising model, renormalisation group calcs. on critical phenomena 0-42171  
 Ising model, square lattice bond dilute, renormalisation group attempts to obtain transition line 0-44836  
 Ising model, Yang-Lee edge singularity, real-space renormalisation group method 0-34643  
 Ising model in 1-D with random transverse field at  $T=0$ , real space renormalisation group method 0-4656  
 Ising spin  $1/2$  model, renormalisation group approach 0-2582  
 Ising systems, finite thickness, renormalization-group transformation, real-space 0-15749  
 Ising type model, elastically coupled, effects of dipolar forces on crit. sound attenuation in uniaxial systems 0-50158  
 Ising universality class, structural phase transform., real-space renormalisation calc. 0-39255  
 Kerr-Schild's gravitational fields, quantisation 0-31653  
 kinetic Ising chain, renormalisation group transform. for master eqn. 0-11214  
 kinetic Ising model, real space renormalisation group for arbitrary dimension 0-4666  
 Kondo Hamiltonians, s-d exchange, ground states, renormalisation group calcs. 0-50046  
 Kondo lattice Hamiltonian, ground state props., real-space renormalisation study 0-34590  
 ladder model of QCD, hadron struct. 0-37213  
 large-cell Monte Carlo renormalization group for percolation 0-46994  
 lattice gauge theories, extrapolation to continuum limit 0-349  
 lattice gauge theory with fermions, renormalised phases, vacuum polarization 0-13198  
 lattice spin systems, matching conditions for crit. props., group struct. of block transforms 0-22305  
 magnets, mixed, competing spin glass and mag. order, phase diagrams, crit. points 0-39802  
 massless  $(\phi^3)_6$  theory, exponentiation of IR logarithms 0-31965  
 master eqn., dynamical renormalisation group transform., Ginzburg-Landau model, kinetic Ising model 0-42170  
 Migdal transformation, renormalisation group, recursion relations 0-34647  
 n-component spin system, energy-energy correl. function calc. 0-31697  
 nematic to smectic C phase transition, renormalisation group anal. 0-34173  
 nematic-smectic A phase transition, renormalisation group approach to crit. dynamics 0-10646  
 non-perturbative quantum field theory, lattice renormalisation construction 0-9098  
 nonrandom Ising system, random-field singularities in position-space renormalization-group transformations 0-13000  
 $O(N)$   $\sigma$ -model, two-dimens., mag. susceptibility, phase transitions and high temp. expansion 0-47177  
 one-dimensional  $\phi^4$  and double quadratic systems, kinks, quantum statistical mechanics 0-47197  
 one-dimensional superconductivity, response functions, from renormalisation group theory 0-54829

## renormalisation continued

operator-product expansion in dimensional renormalization 0-42100  
 optical percolation in 3-D, renormalisation group approach 0-22299  
 Padé approximation method as renormalisation group method 0-17909  
 percolation conduction crit. exponent, large cell renormalisation group calc. 0-12998  
 perturbative QCD, chiral symmetry using dimensionless regularisation 0-27476  
 phase separation dynamics, renormalised time-depend. Ginzburg-Landau model 0-29175  
 phase transition in 2D Coulomb gas, sine-Gordon theory and XY model, renormalisation group anal. 0-36950  
 phenomenological renormalisation group theory, general principles 0-4663  
 physical systems, renormalisation group anal. 0-17838  
 plasma, ion-acoustic solitary wave, third-order corrections, reductive perturbation method 0-43898  
 plasma, Langmuir turbulence, large-scale, renormalisation group method 0-38650  
 plasma, renormalised Vlasov turbulence 0-19579  
 plasma simulation of turbulence, phase space granulation due to mode-mode coupling 0-38651  
 $Pm3n$  space group struct., phase transitions, renormalisation group theory comparison with Landau theory 0-6489  
 Potts model, first order phase transitions, Monte Carlo renormalisation group method 0-34645  
 Potts q-state model, variational renormalisation group approach 0-31679  
 QCD, infrared behaviour of effective coupling 0-42393  
 QCD, perturbative contributions to quark masses 0-47249  
 QCD, six-quark model,  $\Delta S=1$  weak nonleptonic decays 0-22582  
 QCD, slope of leading Regge trajectory 0-42391  
 QCD calc. of structure function moments, renormalisation prescription depend. 0-4948  
 QCD coupling const., renormalisation prescription depend. 0-4954  
 quantum flavour dynamics, renormalisability conditions 0-42404  
 quantum gravity, dynamics, trapping of physical gravitons 0-31652  
 quantum gravity, nonrenormalisability, one-loop divergences 0-4626  
 quark form factor and jet cross sections, high energy asymptotics 0-32112  
 quark mass, current, induced isospin violations 0-32069  
 quark masses from Weinberg-Salam model renormalisation group eqns. 0-42377  
 random conductors, position-space renormalisation and exponent theory 0-153  
 real fluids, static and dynamic crit. phenomena, theory, summer school lecture series 0-6344  
 real space renormalization and the honeycomb lattice, ferromag. (antiferromag.) appls. 0-11200  
 real-space renormalization-group scheme for spin and gauge systems 0-32008  
 relaxational dynamics in systems with many-component order parameter, renormalisation group anal. 0-42181  
 renormalized operator form of quantum action principle 0-42314  
 semiclassical QCD, regularisation and renormalisation 0-4925  
 singular solutions of renormalisation group eqns. 0-17840  
 $SO(10)$  grand unified theories, one loop renormalisation effects, stepwise symmetry breaking 0-32058  
 solitonlike fields, gauge phase factor operators, extended Higgs models and 't Hooft algebra 0-42324  
 solitons, static form factor, quantum correction in 2-D field theory with classical lump, asymptotic behaviour 0-52395  
 spacetime structure theory at very short distances, nonlinear sigma model 0-12979  
 spin systems, model, Monte Carlo simulation appl. 0-20421  
 spontaneously broken symmetry and heavy scalar particle decoupling, renormalisation group eqn. 0-47189  
 statistical equality connecting zero Fourier harmonics with average quantities 0-133  
 structural stability in statistical mechanics 0-8932  
 structure functions, deep inelastic renormalisation group sum rules 0-22611  
 $SU(2) \times U(1)$  unified theory, symmetry and renormalisation 0-22551  
 $SU(6)$  grand unified theories, one loop renormalisation effects, stepwise symmetry breaking 0-32058  
 superconductors, ferromagnetic, phase transitions, renormalisation group treatment 0-29505  
 supergravity,  $OSp(1,4)$  renormalisable theory with higher derivatives 0-36930  
 surface magnetisation profile, in crit. region by  $\epsilon$ -expansion, Wilson perturbation theory calc. 0-50100  
 thermodynamic anomalies near tricritical point, renormalisation group anal. (*Russian*) 0-13027  
 Thirring model of massless scalar field, conformal transformations 0-52428  
 three-dimensional Ising model, crit. behaviour 0-4672  
 triangular and honeycomb lattice gases, order-disorder transitions to  $2 \times 2$  struct. 0-4674  
 triangular Ising lattice, anal. of Kadanoff lower-bound renormalisation-group, approx. 0-8930  
 turbulence, fully-developed, renormalisation group 0-28495  
 two-dimensional Ising model, Monte Carlo renormalisation-group method 0-4673  
 two-dimensional spin system on square lattice, exact duality-decimation transform. 0-17890  
 two-point correl. function near coexistence surface 0-44847  
 unitarity and renormalized 't Hooft identities 0-13205  
 vacuum polarisation in intense EM fields, perturbation theory, renormalisation group calcs. (*Russian*) 0-52444  
 Van der Pol oscillator, renormalised perturbation theory 0-27225  
 Wess-Zumino model, massive, dimensional regularisation, supersymmetry 0-27398  
 Yang-Mills theory developed around instanton, renormalisation 0-32027  
 $\epsilon_\mu$  system in QED with internal fermion excitations 0-9130  
 N elastic form factor, exclusive and almost exclusive process asymptotic behaviour, renormalisation group 0-42464  
 $\pi$  longitudinal struct. function, exclusive and almost exclusive process asymptotic behaviour, renormalisation group 0-42464  
 $\pi^- \rightarrow \eta\pi$ , Reggeon field theory, behaviour of  $A_2$  trajectory 0-22594  
 $\pi\pi$  elastic scatt., exclusive and almost exclusive process asymptotic behaviour, renormalisation group 0-42464  
 $H+H^+$ , nuclear repulsion, contrib. to charge transfer 0-18922



**renormalisation continued**

- H<sub>2</sub>, quantum cryst., short-range corre. and motional renormalisation of anisotropic interactions as function of density 0-34272  
 He film, jump in superfluid density, real-space renormalisation group anal. 0-44387  
 He, liq., critical and tricritical dynamics, renormalisation group calc. 0-29239  
<sup>3</sup>He-<sup>4</sup>He mixture, critical and tricritical dynamics, renormalisation group calc. 0-29239  
<sup>4</sup>He, superfluid, near transition, second sound damping, rel. to renormalisation gp. predictions 0-10725  
 Pb<sub>1-x</sub>Sn<sub>x</sub>Te, narrow gap, many-body interaction effects, Bloch electron scatt. lifetimes, energy renormalisation 0-49637

**repackaging** *see packaging***repeaters**

- monolithically integrated optical repeater, fabrication and characts. 0-28353  
 optical fibre PCM repeaters with low power requirements, design and operation (*German*) 0-28315  
 single-mode fibre cabling for low-loss communication 0-53467

**replica techniques**

- extraction replica evaluation, Ashby-Ebeling model analysis (*Czech*) 0-49062  
 silicate glass, low voltage electron microscopy of heated surfaces using C replica technique 0-25974  
 surface measurement replicas, comparative study 0-36987  
 SiO<sub>2</sub>-TiO<sub>2</sub> antireflection coating, 1.064  $\mu$ m laser damage, barrier 0-33059

**replicas**

- film type, surface reproduction characteristics 0-36988  
 surface measurement replicas, comparative study 0-36987

**reproduction (copying)**

- see also photocopying; printing*  
 colour transparency projector/scanner and printer 0-52343  
 diazotype photographic duplicating system as diagnostic aid 0-8137  
 electronic imaging hard copy methods and printing systems 0-47134  
 photography, copying process for colour reversal films (*German*) 0-30254

**research and development management**

- American Society of Heating, Refrigerating, and Air-Conditioning Engineers, thermal energy storage activities overview 0-16844  
 controlled fusion research and the Joint European Torus project 0-18593  
 fission and fusion reactors in Japan 0-47701  
 signal processing research programme of United States Air Force 0-48171  
 solar, geothermal, hydrogen energy, and coal gasification and liquefaction, Japan's energy programme 0-3478  
 technological innovation, autobiographical notes R.N. Noyce 0-51997  
 H<sub>2</sub> energy economy, R&D programmes 0-26171

**residual stresses** *see internal stresses***resins** *see polymers***resistance, electric** *see electric resistance***resistance furnaces**

- temperature control 0-27307

**resistance noise** *see thermal noise***resistance thermometers**

- atmospheric temperature measurement in range, 253-318K 0-46291  
 automatic contact, for liquid streams temperature meas. 0-47055  
 compound carbon thermometer using Speer and Allen-Bradley resistors 0-225  
 computerised, TI calculator program (*Czech*) 0-13078  
 electronic thermometer, microprocessor based linearisation of thermocouple temp. charact. 0-221  
 frequency response of cold-wire thermometers used for atmospheric turbulence meas. in marine environment 0-56650  
 high-pressure temperature meas. in liquid He region 0-31748  
 industrial appl., advantages 0-42221  
 platinum resistance thermometers, state of the art review (*Spanish*) 0-52212  
 review of resistance thermometry, error sources 0-52206  
 temperature meas. devices developments (*German*) 0-8986  
 C-glass, stability characts. 0-31751  
 Cu, heat shock influence on elec. cond. and thermophysical props. (*Russian*) 0-52210  
 determination of magnetoresistance in liquid He temp. range 0-31752  
 p-GaAs, 4.2 to 100K range, thermometric characts. approx. 0-31746  
 Ge, for measurements between 0.5 and 30K 0-42225  
 Ge, interpolation method 0-22357  
 n-Ge resistance thermometer material for 14 to 300K (*Russian*) 0-49731  
 Ge resistive sensing devices, temp. calibration and reproducibility, high mag. field effect (*Czech*) 0-37029  
 Pt, determination of dynamic behaviour (*German*) 0-17940  
 Pt, heat shock influence on elec. cond. and thermophysical props. (*Russian*) 0-52210  
 Pt, linearisation technique (*German*) 0-42224  
 Pt resistance elements, temperature detectors 0-27296  
 Pt resistance temperature probes, constructional types and state of technique (*German*) 0-52213  
 Pt resistance thermometer, oxidation problems 0-52206  
 Pt-alloy thermocouples, reference-standard testing apparatus 0-13077  
 Rh-Fe for measurements between 0.5 and 30K 0-42225

**resistivity** *see electrical conductivity***resistors**

- see also photoresistors; posistors; thermistors; thin film resistors; varistors*  
 manufacture, Cr-Si coatings deposition, by flash evaporation, residual gas atmosphere analysis (*German*) 0-6681  
 precision variable, rotation-angle pickup appl., for goniometer 0-47047  
 spiralling resistors with laser beam (*Polish*) 0-28242  
 vacuum deposited resistive foils, manufacture and props. of multicomponent alloys (*Polish*) 0-35131  
 C black-graft polymers crosslinked with epoxy resin, electrical props. (*Japanese*) 0-24920  
 ZnO:<sup>31</sup>P<sup>+</sup> implanted nonlinear resistor production and characteristics (*Russian*) 0-49252  
 ZnO-based ceramic microstructure and nonlinear props., B diffusion effects (*Russian*) 0-49423

**resolving power (optical)** *see optical resolving power***resonance**

- see also atomic beam electric resonance; circuit resonance; cyclotron resonance; dielectric resonance; Fermi resonance; magnetic resonance; magnetoacoustic resonance; molecular beam electric resonance; optical double resonance; vibrations*  
 air column resonance spectra, meas. using basic lab. apparatus 0-41998  
 analytic continuation in decay-scattering systems, singularities as model basis 0-8850  
 asteroid orbits in vicinity of 1:3 commensurability with Jupiter, reson. motion and orbital evolution (*Russian*) 0-36486  
 atmosphere, linear reson. of flow equil. rel. to blocking weather systems 0-56536  
 cantilevered fibre-optic scanner 0-53428  
 celestial mechanics, props. of Delaunay-Zeipel transformation in reson. problems 0-46378  
 circular disk resonators in vicinity of thickness resonance, vibration mode anal. 0-48634  
 cylindrical shell with liquid, resonance frequencies determ. 0-43661  
 decay-scattering systems, resonances and their eigenfunctionals in Friedrich's model 0-8847  
 disorienting collisions, nonlinear resonance induction 0-37900  
 elastic cylinder, end resonance under axisymmetric vibr. (*Ukrainian*) 0-23932  
 flowmeter, float-area-type, jumping instabilities of float 0-14855  
 fluid-loaded cylindrical shell, resonant component isolation in acoustic scatt. 0-5864  
 galaxy particle resonance, nearby stellar orbits theoretical study 0-26914  
 homoclinic points and resonance in dynamical systems 0-4240  
 impact vibrations, steady, of body having hysteresis collision characteristics 0-14602  
 multi-degree of freedom mechanical systems, antiresonances (*Chinese*) 0-42049  
 nonlinear two-degree-of-freedom system, internally resonanced, forced vibrs. 0-36838  
 quantum mechanical over phase space, group theory aspects 0-8852  
 sound scattering from water droplets in air 0-33306  
 stellar dynamics, reson. orbits comparison 0-56889  
 stretched wires as standards of straightness (*German*) 0-36976  
 tensioned bar with initial curvature, parametric excitation 0-43654  
 Trojan asteroids, long-period effects in motion and problems of 1/1 resonance 0-41755  
 US backscattered wave minima for solid metal cylinder immersed in water (*French*) 0-53510  
 violin G-string, resonant response and excitation of wolf-note 0-53540  
 Co<sub>2</sub>Ga<sub>4</sub>, superparamag. response to low DC fields 0-44860  
 Fe-Ni(Cr), Invar, exchange interactions between ferromag. and antiferromag. components 0-29545

**resonance reactions and scattering, nuclear** *see nuclear resonance reactions and scattering***resonances, baryon** *see baryon resonances***resonances, meson** *see meson resonances***resonant absorption of gamma-rays** *see Mossbauer effect***resonant cavities** *see cavity resonators***resonant cavity wavemeters** *see wavemeters***resonant gamma-ray interactions in crystals** *see Mossbauer effect***resonators**

- see also cavity resonators; crystal resonators; resonance*  
 circular disk resonators in vicinity of thickness resonance, vibration mode anal. 0-48634  
 coupled resonator chain, transverse beam instability, multimode approx. 0-52803  
 microwave absorption by water in heterogeneous organic materials 0-15998  
 mode distribution, diffractals 0-8782  
 open resonator methods for microwave permittivity meas. 0-15942  
 radiospectrometer resonator uniaxial crystal deformation unit 0-31822  
 SAW metallic gratings, equivalent circuit of step discontinuity, rel. to SAW devices 0-33389  
 stabilizing resonator of high-power klystron self-oscillator for microwave supply system of linear accelerator 0-42878  
 toroidal resonator excitation by uniformly moving charge 0-18726  
 torsion, liq. viscoelastic props. meas., 20-1200 KHz (*Russian*) 0-52196

**retrieval, information** *see information retrieval***revaporisation** *see vaporisation***reverberation**

- see also anechoic chambers; architectural acoustics; echo*  
 acoustic absorption, classroom experiment 0-42016  
 bat's sonar system simulation in anechoic chamber (*French*) 0-56072  
 city streets and tunnels, expressions for stationary sound pressure level 0-19159  
 interior spaces, impulse response and lack of reverberance in certain freq. bands 0-28383  
 musical acoustics, room reverberation time meas. 0-42000  
 power series for the reverberation time 0-43546  
 rectangular rooms, prediction of reverberation using geometrical acoustics 0-23837  
 room resonance measurement techniques (*German*) 0-53586  
 sonar, incoherent and coherent processing against echo fading in shallow water 0-19142  
 urban built-up environments, room acoustical model of external reverberation 0-53563  
 US absorpt. in liquids at 500 KHz, determination using reverberation technique 0-38197

**reversible shape memory effect** *see shape memory effects***reviews**

- see also Bibliography Index (special index bound with Author index)*  
 A15 type compound, props. and one-dimensionality 0-2530  
 abdominal abscesses detection, role of <sup>67</sup>Ga-scintigraphy, ultrasonography and computerised tomography 0-17096  
 abrasion and erosion, superficial plastic deformations by particles (*French*) 0-40540  
 accretion disks, theoretical review (*Polish*) 0-26739  
 acoustic emission detection for small components production testing, review 0-16632  
 acoustic noise measurement 0-33381  
 acoustical holography and imaging 0-23841  
 acoustical holography in the UK (*German*) 0-53567  
 actinide compounds, specific heat meas., review 0-6524



## reviews continued

- actinide compounds, structure, mag. and related props., review 0-6389  
 actinide metallic systems, magnetism 0-7076  
 adaptive optics technology status and prospects 0-33132  
 additional heating in Tokamaks, specific diagnostics review 0-28753  
 adenocarcinoma of colon and rectum, current place of radiation therapy (French) 0-17075  
 adhesion measurement, problems and prospects 0-50817  
 adhesion measurement 0-50819  
 adhesive failure, and thin film adhesion, a prospective 0-50820  
 adiabatic plastic deformation, shearing phenomena 0-50692  
 adsorbate layer, phase transition theory 0-44433  
 adsorbed layers, two-dimensional phase transitions 0-39419  
 advances in basic magnetism during past twenty-five years 0-36791  
 aerosol, size meas. by optical methods, review 0-40746  
 air flow and sound generation in musical wind instruments, book contrib. 0-19174  
 air pollution, gaseous, aerosol and particulate methods of chemical anal. 0-7876  
 alkali halides, sputtering, thermal effects 0-35033  
 alloy electrodeposition theories 0-11581  
 alloys, radiation effects on ageing and precipitation 0-29956  
 alternative energy strategies, development of solar-based renewable resources 0-30417  
 amorphous alloys and metastable phases, crystallisation (Japanese) 0-38912  
 amorphous ferromagnetic alloys, domain struct. and mag. microstruct. 0-15751  
 amorphous magnetic thin films for magnetic bubble memories, materials (Polish) 0-34715  
 amorphous semiconductors, tetrahedrally bonded, electronic struct., far infrared absorption 0-45051  
 amorphous solids, inorganic, struct. 0-15004  
 analytical atomic spectrometry (Japanese) 0-11990  
 analytical electrophoresis, book contrib. 0-12322  
 Anderson transition, electron localisation in disordered systems 0-29361  
 Anger scintillation camera, development since 1958 0-12234  
 angle-resolved photoemission 0-45214  
 animal joints, mechanics, book contrib. 0-21488  
 annular film thickness measurement 0-31439  
 anodic activation of passive metals, theory 0-25918  
 anomalous X-ray scattering 0-54075  
 antibody binding and complement interactions at the cell surface, dynamics, book contrib. 0-30689  
 antiferromagnets, low anisotropy, nuclear spin waves spectra, relaxation, parametric excitation, NMR dynamic shift (Russian) 0-11180  
 antiferromagnets, spin waves, microwave and optical expts., review 0-50081  
 aquatic sediment lipids, Recent and ancient 0-51583  
 arterial stenoses, fluid mechanics 0-35948  
 aspherical surfaces, holographic methods of testing, review 0-33257  
 astronomical IR interferometry, high spatial resolution methods, speckle and aperture synthesis (French) 0-46405  
 astronomy, far IR, detectors and sources 0-56726  
 astronomy and astrophysics, annual review, 17th volume 0-12646  
 atmosphere, mol. complexes presence and role in residual absorpt., light scatt. obs. 0-56607  
 atmosphere natural organic aerosols of terrestrial origin, review 0-36381  
 atmospheric boundary layer simulation 0-51469  
 atmospheric gravity wave sources 0-26572  
 atomic absorption bibliography (Jan.-June 1979) 0-31441  
 atomic and molecular structure and collision data rel. to Tokamak impurity problem 0-43959  
 atomic collisions, in solids, rel. to vacuum system 0-54290  
 atomic double vacancy states, correl. photon and electron transition, perturbation theory 0-27968  
 atomic excited state collisional relax., line broadening, interat. interactions 0-43149  
 atomic processes for mag. fusion research 0-42851  
 atomic resonances, S-wave pot. scatt., coord. rot. method 0-28104  
 atomic RF spectroscopy, nonlinear and parametric effects 0-18816  
 atoms, collective dynamics, hydrodynamic approach and many body approach based on RPA calcs. 0-47855  
 auditory-evoked response methodology in animals 0-46103  
 Auger microanalysis, high resolution 0-40792  
 Auger spectroscopy, directional effects (French) 0-47153  
 aurora-generated gravity waves dynamic effects on midlatit. ionosphere 0-17438  
 N.Australia Precambrian shields and platforms, struct. and tectonic style 0-3982  
 Auto-Resonant acceleration of ions, theoretical research program 0-5411  
 Auto-Resonant accelerator experimental program 0-5412  
 autocompression of plasma column, influence of external mag. axial field (Rumanian) 0-24148  
 automobile propulsion using H<sub>2</sub> and electric power, comparative evaluation 0-16769  
 axoplasmic transport of proteins 0-21464  
 balsa wood, cryogenic insulation, exam. of strength specifications, props. 0-25819  
 baroclinic finite amplitude instabilities, book contrib. 0-19328  
 baryon-antibaryon nuclei 0-22709  
 baryonium, empirical evidence and theoretical interpretation review 0-42394  
 Bauschinger effect, in metals, review 0-21025  
 beam-foil spectroscopy advances 0-9756  
 beam-foil spectroscopy uses in atomic lifetime meas. 0-14248  
 benign thyroid disease treatment, <sup>131</sup>I appl. 0-36107  
 Bianchi cosmologies, singularities, Einstein eqn. solns. 0-12837  
 biliary tract disorders, evaluation by cholescintigraphy, ultrasonography and computerised tomography 0-17093  
 binary stars, freqs. on main sequence 0-26901  
 bioelectrochemistry and bioenergetics (book) 0-8749  
 biological effects of EM radiation expt. techniques 0-8239  
 biological macromolecules, 3D struct., electron microscopical anal. 0-35836  
 biological systems, network anal., review 0-30635  
 biological X-ray microanalysis 0-41349  
 biomass system studies (Japanese) 0-26436  
 biomechanics, scope and recent trends (Japanese) 0-16984  
 biomechanics of human major articulating joints 0-56105  
 biomechanics of the human body, book contrib. 0-12176

## reviews continued

- biomedical engineering, emerging field 0-36167  
 biomedical engineering textbook for undergraduates 0-8750  
 biomedical image processing, state of art (Japanese) 0-56251  
 biomedical instrumentation elements, electrophysiology appl., book contrib. 0-12293  
 biomedical tomography, equipment and reconstructive methods 0-30849  
 biomembrane active transport of ions, elec. events 0-12068  
 biomembrane mechanics and thermodynamics 0-45863  
 biomembrane mechanics and thermodynamics 0-51052  
 biophysics and bioengineering, book 0-17723  
 biopolymer chains, intramol. reacts., enzyme catalysis appl., review 0-40953  
 Bloch electrons in mag. field, energy spectrum, struct. of Landau levels 0-54623  
 blood volume regulation, effects of space flight, review 0-3826  
 bodies with initial stresses, elastic wave propag., review 0-38323  
 Bose system, Jastrow wavefunction, hypernetted chain method 0-17866  
 bound excitons in semiconductors, book contrib. 0-44519  
 bow shock ion acceleration, upstream region obs. 0-31168  
 breast carcinoma, radiation therapy as primary treatment (Dutch) 0-17078  
 brittle fracture 0-29116  
 brontides, natural atmospheric explosive noise 0-12523  
 Canada contemporary crustal movements 0-8273  
 Canadian continental margins, evolution and geophys. features 0-8274  
 cancer treatment by hyperthermia (French) 0-17024  
 carbide fuels, vibro-compacted, initial stages of sintering and hot-pressing 0-16254  
 carbonaceous chondrite origin and classification 0-56781  
 cardiac arrhythmias in ambulatory persons, review of 1000 ECG recordings 0-36184  
 cardiac valves, role in artificial heart performance 0-21575  
 catalysis and surface science 0-40740  
 cathode spot of a vacuum arc 0-24290  
 cavitation inception in liquids 0-38465  
 cell membrane organisation dynamics, book contrib. 0-30687  
 ceramic fuels, vibro-compacted, initial stages of sintering and hot-pressing 0-16254  
 ceramic material fracture mechanics 0-45373  
 ceramics, applications in fusion system, neutron effects 0-32473  
 ceramics utilization in nuclear industry 0-32350  
 CERN ISR, facility and hadron physics program 0-873  
 chemical analysis by activation methods, medical appls., book contrib. 0-11995  
 chemical fast kinetics studied by NMR 0-55662  
 chemistry, computers, and microelectronics: present and future prospects 0-55627  
 Chevrel phase compounds, bonding and phys. props. rel. to struct., book contrib. 0-49209  
 children who wear individual hearing aids in British Columbia, Canada 0-41326  
 chiral symmetry and pion condensation, review book contrib. 0-437  
 classical eqns. exact cylindrically symmetric solns. from compact Lie groups (Russian) 0-42317  
 clinical engineering, USA nationwide survey of present use in hospitals 0-36177  
 cloud and bubble tube detectors (Chinese) 0-52830  
 coal fired power stations, review of conventional and advanced systems 0-35625  
 coal hydrogasification by nuclear steam reforming of methane 0-30325  
 coatings for fusion reactor environment 0-18618  
 coherent antiStokes Raman spectroscopy 0-22443  
 coherent optical correlation techniques 0-43277  
 coherent radio emission from pulsars 0-46596  
 coherent radio emission in nature, theory, solar system and pulsars appl. 0-46393  
 coherent Raman spectroscopy techniques 0-22440  
 collective acceleration of heavy ions, problems and prospects 0-14013  
 collective accelerators, review of current status 0-5394  
 collective radio-emission from plasmas 0-46392  
 collisional activation mass spectra 0-48106  
 colour vision recent studies (Japanese) 0-12127  
 community shelters for protection from radioactive fallout 0-5338  
 compact galaxy, review 0-17668  
 compaction, of metal powders 0-40279  
 compartmental system analysis: state of the art 0-35815  
 composite materials, reliability, exam. of mech. strengths and fatigue char-acts., review 0-11762  
 computer applications in biomedical engineering (Japanese) 0-12289  
 computer development 0-4503  
 computer generated holography 0-9827  
 computerised tomography, definition and scientific basis, health care needs, appls. and costs 0-36115  
 computerised tomography scanning evaluation, cost containment 0-36117  
 constituent quarks in SU(3) and SU(6), current algebra., hadron decays, book contrib. 0-47259  
 contactless resistivity measurements 0-37054  
 corona discharge applications 0-33849  
 corpuscular diagnostic method of metastable atoms in glow discharge plasma (Czech) 0-24241  
 corrosion science, surface analytic techniques 0-31929  
 corrosion science and control (Japanese) 0-45408  
 corrosion studies, electrochemical methods, appl. and limitations (Japanese) 0-45465  
 corundum, grinding material, review (Polish) 0-29917  
 cosmic dust grains, observed IR props. 0-26943  
 cosmic rays, low energy, Skylab meas. review 0-56689  
 Cosmology, astrophysics and elementary particle physics 0-51935  
 Coulomb systems, statistical mechanics 0-52119  
 covalent semiconductors, electronic struct. of localised defects 0-44535  
 crack resistance in materials under long term static loading, evaluation methods 0-45461  
 cranial CT, valve and limitations in spreading process diagnosis (German) 0-36105  
 critical dynamics, real-space renormalisation group approach, Migdal approx. 0-27257  
 crystal growth, from soln., implication for industrial crystn. 0-49147  
 crystal growth, in pure and impure systems 0-49145  
 crystal growth, instabilities and pattern formation 0-35064



## reviews continued

- crystal growth, of sparingly soluble single crystals from soluble complexes 0-29868  
 crystal growth from soln., hydrodynamic environment effects (*French*) 0-29872  
 crystal habit, modifications control in growth 0-49150  
 crystal-size distribution, population models, review 0-49153  
 current algebra and electromagnetic hadron interactions, book contrib. 0-47240  
 CVD films for interlayer dielectrics 0-45235  
 cyclotron radiation from magnetically confined plasmas 0-38722  
 V1500 Cygni (Nova 1975), review of development (*French*) 0-17598  
 D-region winter anomaly, recent advances 0-17437  
 data acquisition system assembly for pulsed fusion experiments 0-49011  
 deep inelastic scatt., field theoretical description, QCD, quark-parton, and light cone algebra (*Russian*) 0-42388  
 defect theory and processes, review 0-2009  
 density functional theory of metallic surfaces 0-44698  
 diagnostic imaging systems, non-silver halide, recent developments and pot. 0-41223  
 diagnostic uses of US in medicine and biology 0-4481  
 diamond, optical absorption and luminesc. spectra 0-2848  
 dichalcogenides, CDWs and phys. props. (*Japanese*) 0-49635  
 die wear during wire drawing 0-30113  
 dielectric, dipolar point defects, studied by ITC 0-6405  
 dielectric permittivity in X- and  $\gamma$ -ray regions 0-44998  
 dielectric relaxational polarisation, theory development and applicability 0-11334  
 dielectric response of molecular interactions in liquids 0-25298  
 dielectrics, transfer processes, theoretical model review 0-15529  
 dielectronic recombination, appls. in astronomy 0-46391  
 difference polarography, review of method, instrumentation 0-26078  
 diffraction gratings, review of Japanese research 0-10018  
 diffusely reflecting object, deformation meas. by lasers (*Japanese*) 0-9832  
 diffusion in macromolecular solutions 0-15273  
 diffusional crystal growth mechanisms 0-3059  
 digital image processing research, Osaka University 0-9820  
 digital voltmeters, used for true effective voltage meas. (*French*) 0-42213  
 dimethyl ether, review of microwave spectrum, tabulated data 0-51965  
 diogenesis, plate tectonic controls 0-12387  
 discontinuous precipitation in binary metallic systems 0-3060  
 dislocation theory, nonlinear elastic problems, book contrib. 0-39093  
 dislocations, elasticity theory, book contrib. 0-39090  
 dislocations, state of art review, book contrib. 0-39089  
 dispersion hardening, of metallic materials (*German*) 0-45316  
 dispersion hardening, of metallic materials (*German*) 0-50646  
 DNA, conformation of native molecule, influence of solvent struct. 0-30655  
 Doppler-free spectroscopy feats and fancies 0-43001  
 dosimetric primary and secondary standardization within the European Communities 0-9415  
 dosimetry, calibration and meas. standards at Austrian Dosimetry Laboratory 0-5362  
 dosimetry, secondary standard laboratory organisation in India 0-5366  
 dosimetry, secondary standards laboratory, role in a nuclear power utility 0-5365  
 dosimetry of electrons and photons, standardisation in Germany 0-5353  
 dosimetry standardisation in Japan 0-5359  
 dosimetry standardisation in UK 0-5358  
 dressing effect on grinding performance 0-16502  
 drop formation in a circular liquid jet, book contrib. 0-19467  
 drop size measurement methods 0-17916  
 dye indicators of membrane pot. 0-21594  
 dynamic nuclear polarisation in solid dielectrics 0-29649  
 dynamic plasticity experiments 0-35288  
 Earth global dynamics, Canadian contribs., 1971-79 period 0-8262  
 ECG, computer assisted interpretation, critical appraisal 0-17151  
 echography, real time, contrib. to diagnosis and management of palpable breast lumps 0-17027  
 echomammography: indications and limitations in tumours with or without calcification (*French*) 0-36039  
 EEG and head trauma 0-46076  
 Einstein and the quantum theory, review 0-22237  
 Einstein centenary 0-46782  
 elastic electron scattering at large momentum transfer, review 0-22820  
 elastomer, role of particulate fillers, review 0-29921  
 electric vehicle secondary cell development program of US Dept. of Energy, review 0-30442  
 electrical phenomena in polymers, nature and appl. 0-50254  
 electrodialysis and its applications 0-55702  
 electrodynamics, Ritz's theory based on particle interactions, review of original paper of 1908 0-47  
 electroinitiated polymerisation on electrodes 0-50854  
 electrokinetic phenomena in biology, book contrib. 0-12326  
 electromagnetic inspection review 0-35468  
 electromechanical transducers in hostile environments 0-37019  
 electron and ion beam generation at high power 0-13988  
 electron beam therapy of lateralised lesions of oral cavity and oropharynx 0-12215  
 electron beam therapy with medium energy electrons 0-36069  
 electron beams as virtual electrodes 0-6861  
 electron bombardment ion thruster efflux, interaction with spacecraft 0-31440  
 electron cyclotron heating in Elmo bumpy torus 0-28750  
 electron energy loss spectrometry, local characterisation of solids 0-31948  
 electron energy-loss spectroscopy in context of TEM 0-31945  
 electron flow, photosynthetic and respiratory, in dual functional bacterial membrane 0-16914  
 electron holography progress (*Japanese*) 0-52369  
 electron microdiffraction, book contrib. 0-10464  
 electron microscope image analysis 0-31947  
 electron microscope image contrast and localized signal selection techniques 0-37126  
 electron microscope resolution, prospects for extending limit 0-37128  
 electron microscopy, high resolution, mol. struct. determ. 0-21595  
 electron microscopy, phase problem, review 0-33862  
 electron microscopy, recent applications to biology 0-41347  
 electron optics, coherence, review 0-32900  
 electron scattering, resonances in atoms and molecules 0-9734  
 electron scattering by crystals 0-14969

## reviews continued

- electron spectroscopy techniques for semicond. investig. (*Japanese*) 0-49061  
 electron-molecule collision theory 0-32847  
 electronic and cohesive properties of disordered simple metals 0-44475  
 electrostatic X-ray imaging, book contrib. 0-36112  
 elementary particle strong interactions at very high energies 0-440  
 elementary processes and chemical reactions in plasma (*Czech*) 0-24126  
 ellipsometry work at Gakushuin University from 1955, review 0-9019  
 EM methods for determining dielec. const. and resistivity of ground 0-22382  
 EM scattering and radiation problems soln. by spectral domain approach 0-5663  
 emission computed tomography 0-56213  
 energy conservation through recycling 0-21388  
 energy dispersive X-ray diffraction method, annotated bibliography (1968-78) 0-36794  
 energy supply and demand, United States government analyses 0-30320  
 environmental actinides, pot. carcinogenic effects 0-30780  
 environmental conditions at 18000 yr BP, continental record initial evaluation 0-51529  
 enzyme dynamics, statistical phys. 0-21439  
 enzymes, membrane bound, influence of membrane fluidity on activity, book contrib. 0-30688  
 epitaxy, growth modes, exp. techniques, book contrib. 0-49558  
 epoxy resin systems, synthesis review, phys. and mech. props. at low temps. 0-25650  
 EPR of transition metal, lanthanide and actinide ions, 1974 literature 0-11253  
 EPR spectra of stable radicals, slow molecular motion study, review 0-25212  
 excimer laser application to laser-radar obs. of stratospheric O<sub>3</sub> 0-17410  
 excimer lasers, excitation mechanisms, review 0-9865  
 excimer lasers, optically pumped CW 0-14322  
 excited semiconductor, extended phase diagram 0-44521  
 exciton physics, book contrib. 0-44517  
 excitons, internal struct., book contrib. 0-44518  
 excitons and exciton-phonon interactions, resonant Raman and Brillouin spectroscopy, book contrib. 0-49624  
 extracorporeal processing devices, book contrib. 0-12308  
 extractive metallurgy, developments in basic principles and phys. chem., review 0-20819  
 extractive metallurgy of Pb, Zn, and Sn, developments 0-20820  
 fatigue testing techniques and life prediction 0-21251  
 Fermi surface study of disordered alloys, positron annihilation experiments 0-44480  
 Fermi system, Jastrow wavefunction, hypernetted chain method 0-17866  
 ferroelectric and ferroelastic phase transition, dynamics, Brillouin spectra 0-55115  
 ferroelectric theory and dynamics, optical, acoustic electro-optical props., Brillouin zone struct. 0-11347  
 ferromagnetic semiconductor, theory review 0-20369  
 ferromagnetic transition metal alloys, mag. props. 0-44823  
 ferromagnetism, itinerant electron theory, local moment approach (*Japanese*) 0-25071  
 ferromagnetism of disordered systems 0-29513  
 ferromagnets, domain struct. effects on dynamic props. 0-34678  
 ferrous metallurgy, nondestructive inspection and quality control review 0-21201  
 fertility in man, influence of radiation 0-56137  
 fibre optic communication cable development 0-1331  
 fibre optic transmission technology, single mode systems in 1.0 to 1.8  $\mu$ m region 0-38105  
 fibre optics, developments in theory 0-43457  
 field desorption mass spectrometry, appl. to biochemistry, medicine, and environmental science 0-35592  
 films and foils, mechanical testing methods, review 0-40637  
 fish, problem of sound perception (*Russian*) 0-41043  
 fission reactor LOFT program, recent results (*Japanese*) 0-673  
 fission reactor multiphase systems, expt. and theoretical review of density-wave oscillations 0-18369  
 fission reactor oxide fuel, irradiated, physical processes (*Japanese*) 0-27742  
 fission reactor safety, aspects of the historical, philosophical and mathematical background to the statutory management of nuclear plant risks in the United Kingdom 0-5293  
 fixed charge membrane modules, pot. controlled transient gating mechanism, book contrib. 0-12067  
 fluid interfaces, isothermal and deformable, mass transfer and surface tension 0-33564  
 fluid mechanics, annual review, book 0-17722  
 forced Rayleigh scattering, principle techniques and expts. 0-34938  
 forced Rayleigh scattering, principles and techniques 0-20646  
 four-wave mixing spectroscopy, recent developments 0-53383  
 fracture, use in engineering, industry and crafts 0-50702  
 fracture and plasticity, lattice-statics approach 0-39212  
 fracture mechanisms review 0-35296  
 freeze-fracture techniques and appls. in struct. anal. of mammalian plasma membranes, book contrib. 0-30960  
 French Tokamak research (*Russian*) 0-38690  
 frontiers of time 0-12886  
 fuel cycles, bibliography of AECL publications 0-5  
 fusion possibilities and plasma confinement and interactions in mag. conf. Tokamak, review (*French*) 0-54017  
 fusion power, radiological protection review 0-9411  
 gait analysis of bipedal locomotion 0-56104  
 galaxies, origin and early evolution 0-17669  
 gamma ray spectral penetration through radiation shields 0-5343  
 gas chromatography techniques, mistakes made by non-specialists 0-55730  
 gas chromatography-mass spectrometry, integrated analytical systems, appls. in biomed. and related sciences, review 0-36200  
 gas chromatography/Fourier transform IR spectroscopy, review 0-55729  
 gas phase reaction consts. for electronically excited species, relax. processes, data tables 0-16644  
 gas sorption and transport in glassy polymers 0-15360  
 gaseous nebulae, riddle of spectra, history 0-8676  
 gases, high resolution rotational Raman spectra, review 0-23425  
 gases, rot.-vibr. Raman spectrosc., high resolution 0-22442  
 gases in metals, trends in modern anal. (*Russian*) 0-15123



## reviews continued

- generalized vector dominance, photon-hadron interaction anal. book contrib. 0-47265  
 geomagnetic influences on man-made systems 0-12887  
 geomagnetism, secular variations on historical time scale 0-36236  
 Geos 3 project, review 0-4224  
 geoscience information services, review, conf., April 1978, London 0-46183  
 geostrophic turbulence, book contrib. 0-19336  
 geothermal energy, environmental problems, air and water pollution, subsidence, induced seismicity, blowouts, noise 0-55797  
 geothermal resources for elect. generation or direct heat utilisation, review 0-35636  
 giant planet atmospheres, IR radiation 0-8568  
 glass ceramics, phase transformations 0-3025  
 glass fibre production methods for optical communications (*German*) 0-23813  
 glass making refractories, progress 0-40303  
 global nuclear power is alternate source of energy, prospects and issues 0-7897  
 glottic cancer, early, radiotherapy 0-12217  
 glottic cancer, early, radiotherapy 0-12218  
 graphite, electron-phonon interactions, rel. to elec. transport 0-34156  
 graphite, pyrolytic, galvanomag. effects, effect of fast neutron irradiation 0-34465  
 graphite compound, metallic electronic props. and correl. with chemistry 0-44567  
 graphite intercalation cpds., Raman scatt. and IR refl. 0-45066  
 gravitation, gauge group deformations, generalised Gupta program 0-12957  
 gravitational interaction, spin, rotation and quantum effects 0-37203  
 hadron+hadron high energy collisions, variables and optical concepts 0-444  
 hadron EM interactions 0-412  
 hadron photoproduction, high energy diffractive processes, book contrib. 0-47309  
 hadron photoproduction nondiffractive processes, review, book contrib. 0-47313  
 hadron resonance, EM decay and excitation, review, book contrib. 0-47300  
 hadron-lepton deep inelastic scatt., book contrib. 0-47260  
 haematologic disorders, radionuclide therapy 0-36109  
 haemoglobins and chlorocruorins, extracellular respiratory, physico-chemical and functional props. 0-3581  
 Hall effect, discovery and applications 0-31477  
 hand prostheses, ideas on sensory feedback 0-51295  
 harmonic generation, state of art 0-33090  
 heart rate and blood pressure biofeedback, literature review 0-21484  
 heart rate and blood pressure biofeedback theoretical models review 0-16974  
 heat exchangers, R and D in Japan 0-35737  
 heat transfer, review of 1978 literature 0-23860  
 heat transfer bibliography, Japanese works 0-31442  
 heat transfer bibliography 0-51978  
 heavy ion accelerator facilities in Europe 0-42880  
 heavy ion dissipative collisions, ang. momentum transfer 0-13501  
 heavy ion elastic and inelastic scatt., book contrib. 0-27668  
 heavy ion fusion, expt. data comparison with classical trajectory models 0-9324  
 heavy ion reactions, dynamical properties, field overview 0-18327  
 heavy ion reactions, energy depend. struct., book contrib. 0-27671  
 heavy ion transfer reactions, book contrib. 0-27669  
 hepatic mass evaluation, relationship of ultrasonography, nuclear medicine and computerised tomography 0-17092  
 hepatobiliary functional scintillation recording (*German*) 0-30874  
 HF heating in Tokamaks and stellarators 0-28736  
 high dynamic pressure measurements in solids 0-47070  
 high energy collisions, theoretical overview 0-42682  
 high energy particle interactions on nuclei, review 0-42658  
 high energy resolution X-ray spectroscopy 0-14959  
 high impact strength materials, laser beam effects 0-21073  
 high magnetic field generation in Grenoble and appls. 0-13110  
 high power neutral injectors 0-18656  
 high pressure molecular beam mass spectrometric sampling 0-52355  
 high temperature vapours, phase transitions, equations of state, appl. of laser pulse heating 0-52230  
 high-power lasers 0-32950  
 high-temperature electron diffraction, by gases 0-52237  
 high-temperature materials, technological requirements, R and D, report 0-45222  
 highly excited atoms, review of recent expts. 0-23325  
 hot electron physics (*Japanese*) 0-49754  
 HTR LEU oxide fuels, performance data review 0-42780  
 hydrodynamic interfacial instability, mechanical, chem. and elec. constraints, review 0-34278  
 hydrodynamic stability problems with time-depend. boundary conditions, numerical simulation methods 0-19411  
 hydrometallurgy, developments 0-45252  
 hypernuclear physics, beginnings 0-47418  
 hyperthyroidism, childhood, role of radioiodine treatment 0-41182  
 hysteresispingography, appraisal of current indications 0-56169  
 II-VI semiconductors, impurity and defect centre energy states, luminesc. meas. 0-55150  
 II-VI semiconductors, radiation effects, optoelectric props. control 0-25458  
 III-V compounds and alloys, MBE process and problem areas 0-10815  
 III-V quaternary alloys, melt and soln. growth of bulk single crystals. 0-35079  
 III-V semiconductors, deep level defects, review 0-24841  
 III-V semiconductors, p-n heterostructures, epitaxial growth techniques, appl. to optoelectronics 0-54770  
 image reconstruction formulae, computer implementation 0-52179  
 impinging free shear layers, self sustained oscillations, book contrib. 0-19466  
 implanted atoms, Mossbauer studies 0-39913  
 impurity conduction phenomena, review of exptl. work (*Japanese*) 0-49737  
 impurity defect interaction influence on radiation hardening and embrittlement 0-35199  
 incommensurably distorted structures, rel. to structural phase transition 0-10665

## reviews continued

- Indian nuclear medicine 0-36082  
 inductively coupled plasma-AES, present and future position in analytical chem. 0-7887  
 inert gas crystals with imbedded impurities, struct. and diffusion props. 0-10563  
 infrared multiphoton dissociation of molecules (*Japanese*) 0-11885  
 inhaled heavy elements deposited in vivo, external counting, review 0-36152  
 injection lasers, mode comp., control with selective cavities 0-19037  
 inner shell excitation in molecules by electron impact 0-37899  
 inner shell excitation processes in heavy ion-atom collisions 0-37874  
 inorganic crystals, vibr. spectroscopy 0-55093  
 inorganic photochemistry, review 0-3382  
 intensity fluctuation spectroscopy studies of Brownian motion 0-52129  
 intercalation properties (*Japanese*) 0-49838  
 intermolecular forces, Raman scatt. obs. 0-23427  
 intermolecular interaction theory, modern state, rel. to large mols. 0-14186  
 intermolecular interactions and potential energy wave calcs. 0-43140  
 internal ocean waves, book contrib. 0-21781  
 International Magnetosphere Research programme, review (*Russian*) 0-17467  
 international radiation standards, role of ICRU 0-9414  
 international standard reference radiations and their application to the type testing of dosimetric apparatus 0-9416  
 interstellar communication, theory 0-4271  
 intracranial pressure measurement, some considerations 0-17155  
 intraocular pressure survey, pediatric patient emphasis 0-30712  
 inverse scattering problem and instanton construction by algebraic geometry 0-47203  
 ion beam deposition, thin film formation technique (*Japanese*) 0-35107  
 ion bombardment, electron microscopical anal. of surface effects and volume defects (*Rumanian*) 0-29093  
 ion implantation, dosimetry techniques 0-32527  
 ion implantation, metastable phases in metals 0-49254  
 ion-surface scattering, low-energy elastic case 0-40211  
 ion-surface scattering, low-energy inelastic case 0-40212  
 ionic crystal, intrinsic electronic excitations and defects (*Russian*) 0-10881  
 ionic crystals, dielectric loss and relaxation theory and kinetics 0-11335  
 ionic crystals, spectroscopy, lattice localised modes 0-50375  
 ionic mechanisms of excitation in Paramecium 0-21458  
 ionising radiation, primary standards and transfer methods in France (*French*) 0-5352  
 ionising radiation calibration, meas. standards, CNEN, Italy 0-12273  
 ionosphere and plasmasphere studies using ATS-6 satellite 0-56677  
 ionosphere radiowave scintillation, nighttime equatorial F-region 0-26681  
 ionospheric EM wave propag., ducting at high-freq. 0-21872  
 ionospheric topside sounding and determination of electron profiles 0-56669  
 IR and sub-MM astronomy with balloon-borne telescopes 0-8547  
 IR ellipsometric spectroscopy, appl. to study of adsorbed species 0-39434  
 IR spectroscopy, ultra-high resolution (*Japanese*) 0-31912  
 IR spectroscopy observations of solid/liquid interface interactions 0-40733  
 IR stimulation and quenching of luminescence (*Russian*) 0-11455  
 island films, diffusive mass transfer 0-20054  
 ISR projects situation (1979) (*Czech*) 0-870  
 Japanese medical technology, development and future problems (*Japanese*) 0-12287  
 jets, turbulent, structure 0-48760  
 Jupiter magnetosphere-satellite interactions, aspects of energetic charged particle loss 0-36566  
 Jupiter upper atmosphere, photochemical models 0-36567  
 kimberlite and kimberlitic intrusives of SE Australia 0-51392  
 Knudsen effusion cell, interactions with systems, high-temp. mass spectrometry 0-52354  
 Kondo alloy, low temp. props. 0-2569  
 lamellar intercalation compounds, NMR studies 0-39882  
 larynx carcinoma, primary radiotherapy 0-12216  
 laser annealing, review and anal. 0-25741  
 laser beam propagation through atmospheric turbulence 0-41550  
 laser gyro, tutorial review 0-1266  
 laser isotope separation 0-32851  
 laser radiation, selective action on matter 0-7832  
 laser radiation interaction with plasma 0-43953  
 laser spectroscopy in mol. beams 0-22446  
 laser wavelength measurements 0-48320  
 laser-excited luminescence spectrometry in chem. analysis 0-40800  
 laser-ZZ 0-48975  
 lasers, influence in biological and medical research, review 0-26318  
 lasers, organic cpds. as active media (*Russian*) 0-38015  
 lasers, research in International Business Machines Corp., USA 0-23696  
 lasers and masers, fluctuating intensity regimes 0-19015  
 latent-image formation: the contribution of the Research Division, Kodak Limited, Harrow 0-22458  
 lattice dynamics of trigonal Se and Te 0-54327  
 lattice energy, calcs., problems and solns. (*French*) 0-19746  
 lattice gauge theory and spin systems 0-22528  
 light quark spectroscopy 0-42424  
 light reflection by rough surface 0-18996  
 light scattering by liquid He 0-54454  
 lightning characts. 0-51470  
 linear isotropic elasticity, boundary problems, book contrib. 0-39092  
 linear-chain conductors 0-24887  
 liquid, simple, equilib. theories 0-38887  
 liquid column chromatography, scintillation counters (*Czech*) 0-27885  
 liquid crystals, symmetry and thermodynamic states 0-10493  
 liquid dielectrics, electrical conductivity and breakdown, liquid impurity effects 0-11340  
 liquid metal embrittlement of metals 0-3257  
 liquid spreading on solid surfaces, static and dynamic contact lines, book contrib. 0-20015  
 living cells, laser Raman spectra 0-56113  
 local atomic arrangements, associated with ordering 0-50632  
 long-wavelength IR spectroscopy, obs. of intermol. interactions in condensed medium 0-34927  
 Lorentz transformations derivation by Ives (1945) 0-4523  
 low temp. dense plasma electrode phenomena 0-33743  
 low-dimensional mag. systems, neutron scatt., review 0-50103



## reviews continued

- lower hybrid heating in toroids, US experimental program 0-28748  
 lunar magnetism origin, theories 0-36522  
 lunar materials, KREEP origin 0-4279  
 lunar radar mapping 0-12694  
 LWR in-core fuel management techniques (*Italian*) 0-18447  
 LWR safety research programs by US NRC 0-42796  
 lymphocyte plasma membrane components, distrib. and mobility, book contrib. 0-36090  
 macroscopic metal catalysts, morphology and etching processes 0-7856  
 magnetic anisotropy, book contrib. 0-11191  
 magnetic bubble materials 0-50153  
 magnetic chains in solids 0-15737  
 magnetic densities and magnetic excitations, neutron studies, book contrib. 0-11170  
 magnetic field measurement in toroidal plasma systems 0-49004  
 magnetic materials, elastic props. 0-7142  
 magnetic resonance, book contrib. 0-11242  
 magnetics research, materials development and appl. during past 25 years 0-36792  
 magnetocrystalline anisotropy (*Rumanian*) 0-25125  
 magnetoelctrets 0-25289  
 magnetolectric dipole gas as explanation of biocosmic phenomena, summary of phenomena 0-8241  
 magnetolectric effects in magnetic materials, review (*Japanese*) 0-50159  
 magnetosphere, double layers and electrostatic shocks review 0-36460  
 magnetosphere, quantitative models of 0 to 100 keV near Earth plasma 0-36459  
 magnetospheric simulation expts. 0-46347  
 magnetostriction, book contrib. 0-11241  
 magnetostriction, temperature dependence, origin, elastic and magnetoelastic energies (*Rumanian*) 0-34747  
 magnetron sputtering, appl. to sputtered thin compound films (*Japanese*) 0-25561  
 major solar energy research programs 0-40843  
 malignant thyroid disease treatment, <sup>131</sup>I appl. 0-36108  
 mammography, experience with 153 breast carcinoma cases (*German*) 0-12244  
 mammography, risks, radiation dosage and picture quality (*German*) 0-36103  
 many body theory, appls. review of development 0-46968  
 Mars, surface morphology review 0-56748  
 martensite formation, and lattice props. rel. to elastic constants 0-50630  
 martensitic transformations 0-3037  
 mass spectrometry applications in study of porphyrins and related tetrapyrroles 0-51306  
 mass spectrometry by Wien-Thompson method 0-45613  
 mass spectrometry instrumentation for chemists and biologists 0-42297  
 material science, current topics, book 0-46747  
 mechanochemical reactions, phase transformation and synthesis, review 0-3024  
 medical diagnosis, EM techniques 0-36063  
 medical dosimetry standards programme of the National Bureau of Standards, USA 0-8187  
 medical engineering, review of developments and facilities 0-12292  
 medical engineering, review of present state 0-17023  
 medical imaging by NMR, book contrib. 0-36064  
 medical imaging techniques, developments 0-26324  
 medical research, laser applications, biophysical aspects 0-51201  
 membrane excitability mechanisms, book contrib. 0-12062  
 Mercury, post-Mariner 10 assessment 0-12697  
 mesic atomic and molecular processes in H<sub>3</sub> isotope mixtures 0-23580  
 meson exchange currents, configuration mixing, role in nucl. mag. moment, beta decay, review, book contrib. 0-478  
 meson theory of nuclear vector and axial vector exchange currents, review, book contrib. 0-474  
 mesonic processes and quarks in nuclei 0-42564  
 metal, diffusion of H(D), slow neutron scatt. obs. 0-34248  
 metal films, on alkali halide substrates, nucleation and growth, surface study techniques 0-10809  
 metal hydrides use as energy conversion media (*Japanese*) 0-55934  
 metal structures, thin walled, crack growth problems 0-55527  
 metal surface, atomic and mol. beam scatt. 0-40203  
 metal surfaces, clean polycrystalline, ion-induced electron emission 0-35032  
 metal-H, phase transitions 0-50631  
 metal-H system, electro- and thermotransport of H, book contrib. 0-24644  
 metal-H system study by neutron scattering, review (*French*) 0-34226  
 metal-H systems, anelastic and plastic props., review 0-49298  
 metal/air batteries, status and potential, review 0-55828  
 metallic alloy, random, first principles band theory, review 0-44473  
 metallic glass, bulk and surface properties, review 0-44147  
 metallic glasses, struct., stability and prod., elec., mag. and mech. props. 0-44134  
 metallography, quantitative methodology (*French*) 0-30205  
 metals, 3d and 4f, electron impact excited soft X-ray spectra, resonances and many body effects 0-50468  
 metals, friction and wear rel. to comp., struct. and props., review 0-25872  
 metals, H effect on mech. props., review 0-50718  
 metals, H trapping, book contrib. 0-24491  
 metals, ion-implanted, friction and wear, review 0-40555  
 metals, positron annihilation, localised probe of lattice defects 0-55224  
 metals, positron annihilation expts., electronic struct. and Fermi surface studies 0-54594  
 metals, slow positron studies 0-55223  
 metals and alloys, fatigue behaviour, vacuum effect 0-35309  
 metals and alloys, sulphidation mechanism, review (*Polish*) 0-45413  
 metastatic thyroid cancer, use of <sup>131</sup>I 0-36084  
 methane-ethane liq. mixture, phase equilb., heat of mixing, vol. change, data evaluation 0-15233  
 methyl formate, microwave spectra, rot. consts., moments and struct., radio astronomy appl. 0-17637  
 MHD materials 0-40240  
 micelles, reversed, solubilisation and catalysis 0-45545  
 microelectronics revolution, appl. in telecommunications, medicine, education 0-31446  
 microkymography, and related techniques 0-36215  
 microphysics to macrochemistry, discrete simulations 0-54102  
 microprocessor, in industry (*French*) 0-17729

## reviews continued

- microprocessors in bioscience 0-21557  
 microwave biological effects, research in Soviet Union and Eastern Europe since 1976 0-35971  
 microwave effects on blood-brain barrier 0-56121  
 microwave holographic imaging 0-23645  
 microwave power for fusion machines 0-23151  
 microwaves in cancer therapy, review of 4 years 0-56162  
 middle atmosphere dynamics 0-17338  
 middle atmosphere processes revealed by satellite observations 0-21803  
 mirror machine, fusion reactors, survey 0-47721  
 modern electrometer techniques 0-37052  
 moire topography, historical review 0-9024  
 molecular dynamics method in statistical physics 0-18895  
 molten salt, thermal cond., heat storage (*Japanese*) 0-6573  
 Monte Carlo methods, struct. of liq. water and dil. aq. solns. 0-54101  
 multibarrier kinetics, subcritical crack velocity stress depend., review 0-23958  
 muon capture progress, weak interaction form factors 0-42643  
 muonic X-rays, formation and expts. 0-43215  
 musical acoustics 0-10096  
 myopia, Prentice Memorial Lecture [optometry] 0-27089  
 myosin and actomyosin kinetic anal. 0-21441  
 NDT, use of accelerated electrons 0-35480  
 nearly closed shell atoms, binding energy and isotope shift correl. 0-27980  
 negative ion lifetimes, book contrib. 0-9529  
 negative ions, form. processes and props. (*Japanese*) 0-53127  
 neural prostheses 0-21576  
 neurosurgery, laser appls. 0-26317  
 neutral beam injection heating in Tokamaks, review 0-28729  
 neutrinos, review of discovery, production, meas. and appls. (*Russian*) 0-13344  
 neutron activation anal., appl. using <sup>252</sup>Cf neutrons 0-18728  
 neutron diffraction, struct. investigations of melts and amorphous substances (*German*) 0-44108  
 neutron diffraction studies of mag. materials, book contrib. 0-11169  
 neutron distribution in nuclei, elastic and inelastic proton scattering 0-22649  
 neutron star, thermal X-ray emission 0-41849  
 neutron stars thermal properties and detectability, cooling and heating processes 0-31323  
 neutron transport theory, collision probability method 0-27706  
 Newman-Penrose method in general relativity, book contrib. 0-46905  
 Newtonian cosmology for unbounded Universe (*Italian*) 0-12836  
 nitrides, structs. and cryst. growth 0-29865  
 NMR, ring current theories 0-53020  
 NMR spectroscopy, appl. to organic compounds anal. 0-16756  
 NMR studies of water in biological systems 0-3886  
 NMR-NQR double resonance, two-freq. methods, resonance spectrometers 0-20512  
 nMTCB task analysis of nuclear medicine technology 0-8753  
 non-linear optics, recent advances 0-33075  
 non-Newtonian fluids 0-33637  
 non-oxide ceramics, hot pressing 0-25641  
 nonequilibrium phenomena in superconductors 0-49982  
 nonlinear acoustics, model eqns., book contrib. 0-19126  
 nonlinear crystals for frequency conversion of optical radiation (*Russian*) 0-38068  
 nonlinear wave theory 0-36874  
 nonmathematical review of gravitational capture 0-26734  
 NQR, NMR and EPR, spectral parameters, influence of mol. motion dynamics, review 0-20486  
 nuclear and atomic research review 0-43216  
 nuclear applications for low-temperature heat 0-7903  
 nuclear cluster correlation in heavy ion-nucleus collisions, book contrib. 0-27670  
 nuclear clustering, microscopic description 0-487  
 nuclear fuel cycle, uncertainties rel. to reprocessing and waste management 0-5315  
 nuclear fuel cycle materials, neutron and photon assay techniques and instrumentation 0-18426  
 nuclear fusion power, state-of-the-art and problems to be overcome (*Dutch*) 0-37574  
 nuclear heat for urban district heating, costs and technology 0-26118  
 nuclear imaging, apparatus, techniques and performance 0-51237  
 nuclear ion microprobe at MeV energies production and use 0-7883  
 nuclear magnetism of liquid systems in the Earth field range 0-50206  
 nuclear matter, variational techniques 0-22748  
 nuclear medicine, appl. of computers (*German*) 0-41214  
 nuclear medicine, trends (*French*) 0-26327  
 nuclear medicine, tumour-localising radionuclides in retrospect and prospect 0-42036  
 nuclear medicine, understanding and using statistics 0-12233  
 nuclear medicine and metrology of ionising radiations (*French*) 0-17057  
 nuclear medicine instruments and radiopharmaceutical production (*French*) 0-17056  
 nuclear muon capture, developments in theory and expts. 0-42642  
 nuclear orientation and NMR of oriented nuclei, appl. to solid state magnetism 0-44928  
 nuclear shadowing of electromagnetic processes, vector dominance model anal., book contrib. 0-47266  
 nucleation, theory for high and low supersaturations, review 0-49142  
 nucleation 0-49143  
 nucleic acids, H<sub>2</sub> exchange kinetics and internal motions 0-21440  
 nucleic acids functions, interactions with metal ions 0-3577  
 nucleus shapes and motions in even-even and odd A nuclei 0-5054  
 occupational radiation exposure, evaluation and control, US research program 0-5370  
 ocean eddies and the general circulation of model gyres 0-56490  
 ocean surface, microwave radiometry remote sensing 0-36428  
 ocean thermal energy conversion, review of engng. problems for technical and economic development 0-3486  
 oceanic and atmospheric fields, linear prediction models 0-56590  
 ocular physiology review 0-56023  
 oil demand projections to 1985 0-3482  
 oil shale, in situ technological developments 0-30354  
 Oklo natural fission reactors, formation, propagation and control (*French*) 0-21774  
 Oklo natural fission reactors, geophysical eval. of U distrib., topography, sedimentology and structure (*French*) 0-21755



## reviews continued

Oklo natural fission reactors, review of French geological research (*French*) 0-21744  
 Oklo natural reactors, data on stability and remobilisation, summary (*French*) 0-21771  
 Oklo natural reactors, review of mineralogical and petrographic studies at Strasbourg (*French*) 0-21745  
 oligomers, polymer-derived, mass spectral charact. 0-37916  
 oscillatory radiation sources, theory and appl. 0-37947  
 one dimensional conductors, electron-electron interactions and Kohn anomaly 0-24895  
 one dimensional Fermi gas model in relation to spin and field theoretical models 0-24816  
 one-dimensional inverse scattering problem for stratified inhomogeneous media 0-46346  
 optical coherence, review 0-48140  
 optical design, contemporary, aspects 0-23766  
 optical fibre as a transmission medium 0-14456  
 optical fibre communication, progress review of fibre design, low-loss and low-dispersion (*German*) 0-28325  
 optical fibre waveguide, low loss, radiation induced transmission loss behaviour 0-38111  
 optical fibres, measurements of characts. 0-43458  
 optical properties of small inorganic and organic metal particles 0-45106  
 optical storage medium specification and performance trends 0-43415  
 optical stress analysis using moiré fringe and laser speckles 0-10217  
 optical system, evaluation criteria and problems (*German*) 0-43268  
 optical waveguide lenses (*Japanese*) 0-10019  
 optical waveguide process and materials, review of progress 0-23768  
 optics, recent advances 0-28155  
 optoelectronic devices, digital data processing, review 0-19106  
 orbital disease, appl. obs. computerised tomography scanning 0-56174  
 organic molecular crystals, photoemission, book contrib. 0-16158  
 organic molecules, UV photoelectron spectroscopy, systematic review 0-28057  
 origin of life 0-4111  
 oropharyngeal epithelioma treatment, role of radiation therapy (*French*) 0-41190  
 orthopaedic engineering in Oxford 0-17187  
 orthopaedic load meas. using strain gauges 0-56262  
 osteogenic sarcoma treatment, role of radiation therapy (*French*) 0-17077  
 OTF of radiographic imaging systems 0-17085  
 oxides, sputtering, thermal effects 0-35033  
 palaeoclimatic research, status and opportunities 0-51527  
 palliative treatments for fretting fatigue, review 0-21126  
 pancreatic disease, study by multiple imaging modalities 0-17094  
 Papua New Guinea, Late Cainozoic geotectonics and volcanism 0-51372  
 parity non-conservation in nuclei 0-32207  
 parity-nonconserving nuclear forces, theoretical and phenomenological approach review 0-42556  
 particle accelerators, historical review, impact on scientific culture 0-868  
 parton model, QCD and hard processes 0-47258  
 passivity, in metals and alloys 0-50750  
 path integrals in quantum theory, basic concepts 0-52066  
 peripheral circulation evaluation, noninvasive techniques 0-56163  
 personnel dosimetry performance, testing standard 0-9421  
 phase ordering (*Japanese*) 0-2352  
 phase transformations in metals and alloys, thermodynamic and mechanistic classification 0-2995  
 phonons, high-frequency, spectroscopy, transport phenomena 0-49325  
 phosphate laser glasses 0-9888  
 phospholipids, exchange between membranes, book contrib. 0-30695  
 photoacoustic spectroscopy, of solids (*Japanese*) 0-31887  
 photoacoustic spectroscopy, theory, techniques and appls., book contrib. 0-9050  
 photoactive catalyst used in light induced photocuring of coating systems 0-7820  
 photochromic glass, with Ag halides:Cu, formation and theoretical models 0-43418  
 photodetectors, thermal detectors and photodetectors, operating conditions and applications 0-47110  
 photoelectrochemical solar energy conversion principles, review 0-35695  
 photoelectron counting statistics, theory, fully quantum 0-52312  
 photoelectron spectroscopy, charact. of vapours oven heated inorganic solids 0-52239  
 photoelectron spectroscopy, synchrotron radiation appls., book contrib. 0-14035  
 photoemission, theoretical aspects 0-45213  
 photolytic generation of transient radicals for EPR spectroscopy 0-11271  
 photopolymer industry in Japan 0-4800  
 photoselective bimetallic aggregation, new route to bimetallic clusters 0-53182  
 photosynthesis, electronic structural props. of relevant mols. 0-16902  
 photovoltaic power systems, US DOE R and D program 0-55874  
 physics and its methods in medicine (*Polish*) 0-12048  
 piano acoustics (*Japanese*) 0-33375  
 picosecond Raman techniques, vibr. dynamics in liqs. 0-52325  
 pion excitations and phase transitions in nuclear matter, review, book contrib. 0-483  
 pionic atoms, nuclear and atomic research review 0-43216  
 planar optics, goals, methods, potential appl., principles and trends 0-33231  
 planetary and solar system origin, model comparisons 0-17508  
 plant condition monitoring in nuclear power generating industry 0-47612  
 plasma, H line Stark broadening, role of ion dynamics simulation 0-24144  
 plasma, nonideal, excitations and macroscopic props. 0-43842  
 plasma, reflection coeffs. for light ion-surface interaction (*Russian*) 0-38663  
 plasma deposition, of inorganic thin films 0-50564  
 plasma diagnostics in Tokamak, far IR lasers development for Thomson scatt. 0-24242  
 plasma heating using negative ion based neutral beams 0-42852  
 plasma ionic-covalent nonadiabatic coupling 0-38535  
 plasma spectroscopy techniques development 0-43991  
 plasmas, optical scattering of light by atoms, techniques theory 0-54044  
 plastic surgery, biomechanical aspects 0-56103  
 plate tectonics, driving force models for plate stress 0-56450  
 PNP project, prototype HTR and coal gasification plant 0-5393  
 polar polymer, piezoelectricity and pyroelectricity 0-7267  
 polarisation model, appl. to hydrated Li<sup>+</sup> 0-54115

## reviews continued

polarization phenomena in hadronic reactions 0-52527  
 polyacetylene, doped, p-n junction, elec. props. (*Japanese*) 0-29410  
 polyatomic mol. gas phase spectra, struct., review and tabulation 0-14136  
 polyatomic mols., multiple photon IR processes 0-43125  
 polyethylene, lightly crosslinked, processed under mol. orient., struct., props., review 0-38957  
 polymer membranes transport from liq. phase 0-16720  
 polymer self-diffusion 0-29193  
 polymer solns., cooperative phase transitions 0-45850  
 polymer solns. and gels dynamic behaviour by light scatt. 0-55727  
 polymer testing by dynamic mech. anal. 0-16626  
 polymeric systems, fluid, rheology, characterised by mol. int. distrib., review 0-1504  
 polymeric systems, supported on inert substrates, dynamic thermomech. study 0-55623  
 polymers, broadline NMR 0-11277  
 polymers, multiple dielectric relax. processes, mol. aspects, book contrib. 0-50264  
 polymers, pyrolysis-mol. wt. chromatography-vapour phase IR spectro-photometry, on-line system, reviews 0-55768  
 polymers, synthetic, radiative degradation, chem., phys., environmental, technological effects, review 0-40948  
 polymers, torsion pendulum dynamic mechanical testing 0-55620  
 polymers in medicine, book contrib. 0-12307  
 polymorphic phase transitions induced by shock waves 0-15188  
 polyquinones, ladder, partially-ladder, synthesis, struct., props., review (*Russian*) 0-7529  
 polystyrene-polyisoprene two-block copolymer soln., conformation, small angle neutron scattering, X-ray diffraction (*Rumanian*) 0-6348  
 polyvinylidene fluoride, structure, and its electret (*Japanese*) 0-10510  
 POPOP dye vapour lasers, optical and electron beam pumping 0-48237  
 positron annihilation, positron basic props., annihilation line shape, positronium formation, book contrib. 0-2893  
 positron annihilation investigation apparatus 0-23240  
 positron emission computer-assisted tomographic scanner 0-36116  
 potential energy surfaces of chemical reactions, nonempirical calcs. 0-35505  
 powder metallurgical parts, development, and manufacture of semifinished products 0-50578  
 premartensitic phenomena, nucleation, shape memory effect, review 0-3041  
 primary dosimetric standards at the Memorial Sloan-Kettering Cancer Center, NY, USA 0-8190  
 prosthetic circulatory device fluid mechanics and haemolysis 0-46101  
 prosthetic joint replacements, mech. factors 0-56286  
 prosthetic material mech. props., effects of physiological environment, cardiovascular appls. 0-8212  
 proteins, H<sub>2</sub> exchange kinetics and internal motions 0-21440  
 pulmonary radiograph interpretation, review of models used 0-36089  
 pulsar magnetosphere radio emission, plasma supply and elec. forces 0-46595  
 pulse discharges in gases under conditions of strong ionization by electrons 0-44064  
 pulsed laser fluorescence for atomic and mol. excited states obs., book contrib. 0-9760  
 PWR steam generator blowdown review of international handling procedures 0-690  
 pyrocarbon coatings, deposition in fluidized bed, TEM, changes by irradiation 0-34084  
 pyrometallurgy, process developments 0-25596  
 QCD, inclusive deep-inelastic scatt., asymptotic freedom 0-32084  
 QCD phenomenology, quarks and gluons in medium energy nuclear physics 0-42563  
 QSO/galaxy associations, redshifts and distances 0-31369  
 quantum amplifiers and their application in space research 0-36503  
 quantum beats 0-22444  
 quantum mechanics based on position 0-52048  
 quantum optics, transition phenomena 0-32944  
 quantum-chemical  $\pi$ -electron system, molecules-in-molecule model (*German*) 0-5490  
 quasis resonant atomic collisions, asymptotic calcs. 0-23512  
 radar observation of lower atmos., VHF pulsed Doppler method 0-46277  
 radiation blistering 0-44239  
 radiation damage, defects and surfaces in bulk metallic, covalent and ionic systems 0-34049  
 radiation induced creep, fundamental mechanisms (*Italian*) 0-55457  
 radiation induced defects, X-ray diffraction study (*Japanese*) 0-15152  
 Radiation Oncology Research Program, recommended research proposals 0-3787  
 radiation physics, interaction with matter (*Japanese*) 0-39149  
 radiation therapy, calibration and meas. standards in USA 0-8188  
 radiation therapy, history of the use of radioactive iodine 0-42032  
 radiation therapy, intracavitary uses of colloids 0-36110  
 radiation thermometry, applied precision, current status 0-52224  
 radiative transfer, irreversible processes (*French*) 0-13002  
 radio signal transmission, long-delay echoes generation, models 0-26670  
 radioactive waste, low and intermediate level, current development program 0-13733  
 radioactive waste disposal criteria proposals by EPA and NRDC 0-18484  
 radioactive waste processing, consequences of separation of long-lived  $\alpha$ -emitters (*Czech*) 0-5251  
 radioastronomy, interferometry theory and appl. 0-12676  
 radioastronomy image reconstruction 0-56718  
 radioimmunoassay as aid to diagnosis (*French*) 0-21522  
 radioisotope scanning of bone, historical survey 0-42029  
 radioisotope therapy in bone and joint disease 0-36111  
 radioisotope tomographic imaging, historical review 0-42038  
 radiological fine puncture and biopsy, efficiency and technique in tumour diagnosis (*German*) 0-41212  
 radionuclide imaging techniques, book contrib. 0-36113  
 radionuclide therapy, pot. future appl. 0-36031  
 radiotherapeutic agents, props., dosimetry and radiobiologic considerations 0-36106  
 radiotherapy (*French*) 0-21523  
 radiotherapy accelerator neutron leakage survey 0-51269  
 radiotherapy electron accelerator photoneutron prod., survey of European meas. 0-51241  
 rail/wheel noise research 0-48496  
 railway tunnels, structure-borne sound levels 0-48499



## reviews continued

- Raman laser uses in molecular spectroscopy and atmospheric constituents detection 0-55762  
 Raman lasers, high-power, liquid, N<sub>2</sub> and O<sub>2</sub> as possible active media 0-19028  
 Raman scattering cross-sections in gases and liquids 0-23426  
 Raman scattering of light by polaritons 0-34928  
 Raman spectroscopy, in high temp. chem. 0-52234  
 rare earth alloys, RFe<sub>2</sub>, magnetostriction studies, book contrib. 0-39846  
 rare earth alloys, RM<sub>2</sub>, (M=Fe, Co, Ni), magnetism, review 0-20365  
 rare earth complexes, formation and props., book contrib. 0-43204  
 rare earth compounds, valence changes, book contrib. 0-39533  
 rare earth hydrides, props., book contrib. 0-45291  
 rare earth intermediate valence systems, neutron scatt. 0-49674  
 rare earth intermetallic cpds., cryst. chemistry, book contrib. 0-39010  
 rare earth intermetallic cpds., mag. props., book contrib. 0-39759  
 rare earth ions in soln., absorpt. and fluoresc. spectra, book contrib. 0-45112  
 rare earth metals, hydrides and oxides, film prep., struct. and props., general review 0-54556  
 rare earth molybdates, cryst. growth, cryst. chem., and phys. props., book contrib. 0-44194  
 rare earth oxides, binary, struct. and props., book contrib. 0-45292  
 rare earth oxides, mixed, phase relations and struct., book contrib. 0-45293  
 rare earth perovskites and garnets, prep. and props. book contrib. 0-44193  
 rare earth systems, cryst. field interactions, book contrib. 0-39540  
 rare earth systems, NMR, EPR, and Mossbauer effect, book contribs. 0-39883  
 rare earth-transition metal alloys, amorphous, struct. and mag. props., book contrib. 0-39818  
 rare earths, and their alloys and cpds., photoemission, rel. to electronic struct., book contrib. 0-16157  
 rare earths industry 0-25537  
 reactive DC sputtering, magnetron-plasmatron processing and instrumentation 0-35090  
 refractory borides, carbides, nitrides, manufacture and appl. in electronic and electrotechnic field (*French*) 0-40311  
 relativistic electron beam induced turbulence and heating 0-38672  
 relativistic experiments in gravitational fields 0-42135  
 relativistic heavily ionising particles, energy loss 0-32583  
 relativistic heavy ion collisions, reaction mechanism and recent topics, review 0-42683  
 relativistic heavy ion-nucleus reactions, book contrib. 0-27672  
 relativistic theory of the classical electron 0-12923  
 renal imaging with radionuclides, US and computerised tomography 0-17095  
 reproductive epitaxy, exam. 0-55303  
 residual stress, X-ray evaluation, treatments for nonlinear distribs. 0-25966  
 residual stresses, review 0-44245  
 residual waste treatment technology 0-40932  
 resistance thermometry 0-52206  
 resonance ionization spectroscopy and one-atom detection 0-22441  
 resonance scattering methods in atomic spectroscopy 0-53167  
 retina, current research and study, selected review 0-30710  
 Rosenstiel School of Marine and Atmospheric Science, University of Miami, review 0-8755  
 Salyut, international spaceport, review 0-31196  
 Salyut space stations, review 0-31195  
 satellite time transfer technology 0-47029  
 Saturn's satellites, surfaces and interiors present knowledge 0-4297  
 SAW devices, signal processing appls., review 0-38204  
 scanning electron probe microanalyser, development of x-ray microanalysis 0-37139  
 scintillation pickups with plateau in counting characteristic 0-47811  
 search for interplanetary quantity controlling development of magnetospheric storms 0-17447  
 Secondary Standards Dosimetry Laboratory, review of role 0-5361  
 secondary-ion emission, ionisation process 0-35040  
 sedimentation of flocculent suspensions 0-35577  
 self-gravitating rotating masses, book contrib. 0-21915  
 semiconducting biopolymers and their part in biochemical phenomena 0-12053  
 semiconductive conjugated polymers, synthesis and elec. props. 0-15513  
 semiconductor, strong electron-lattice interaction (*Japanese*) 0-49664  
 semiconductor, surface electronic props., optical spectroscopic techniques 0-11070  
 semiconductor, zero-gap props. correlated to  $\Gamma_8$  symmetry, review 0-6717  
 semiconductor gas sensors (*German*) 0-55974  
 semiconductor interface and overlay electronic struct. 0-49841  
 semiconductor materials for junction lasers (*Polish*) 0-19029  
 semiconductor physics in high mag. fields (*Japanese*) 0-50192  
 semiconductor superlattices, optical and transport props. (*Slovak*) 0-20288  
 semiconductor surface structure and properties (*Japanese*) 0-49483  
 semiconductors, chemical thermodynamics 0-55692  
 semiconductors, exciton condensation and electron hole liquids, state-of-the-art 0-49625  
 semiconductors, interface and surface physics 0-49872  
 semiconductors, intervalley electron transfer, drift velocity and diffusion coefficient 0-39594  
 semiconductors, photoelectron spectra and band struct., book contrib. 0-16155  
 semiconductors, thermoelectric and thermomagnetic effects, heat transfer due to quasi-particle subsystems (*Russian*) 0-24959  
 semiconductors and insulators, role of electron-hole interaction in optical spectra, review 0-45113  
 semimagnetic semiconductors 0-49702  
 semimetals, group V, low temp. transport props. 0-49708  
 sensory substitution systems—current status and future trends (*Japanese*) 0-36195  
 SHG in laser plasma 0-53993  
 ship boundary layers, book contrib. 0-19346  
 shock compression of solids 0-24534  
 shock tube measurements of elem. gas reaction rate coeffs. 0-3299  
 simple metals, photoemission theory, book contrib. 0-16159  
 SIMS, appl. to surface anal. 0-40204

## reviews continued

- sintered permanent magnets, development history, magnetic and physical props., appl. 0-29901  
 sintering, rel. to definition powder metallurgy 0-20841  
 skeletal demineralisation osteopathy, quantitative diagnosis (*German*) 0-30872  
 skull, frontal diagnostics of injuries (*German*) 0-36104  
 sliding anvil device for high press. and large volumes (*French*) 0-47067  
 small superconductor in magnetic field, first and second order phase transitions 0-2519  
 soft connective tissues, biomechanical behaviour 0-56102  
 softwoods, flow paths (*Japanese*) 0-3288  
 soil moisture content measurement by microwave radiometry 0-17425  
 solar, air heating/cooling systems for buildings 0-45754  
 solar cell developments and appls. for large scale electricity prod. 0-40861  
 solar cells, developments, appls., and economics of solar photovoltaic conversion (*German*) 0-26132  
 solar cells, heterojunction thin films, survey or semi-conductor combinations 0-50974  
 solar cells, materials aspect, review 0-50971  
 solar collectors, design, thermal performance and economic anal. 0-51001  
 solar constant, Smithsonian Astrophysical Observatory program, (1902 to 1962) 0-36606  
 solar cooling systems for buildings 0-45756  
 solar cosmic rays, relativistic 0-56798  
 solar electricity production by direct and indirect conversion schemes, review 0-50981  
 solar energy, review using rational units 0-30389  
 solar energy R and D in Thailand 0-26113  
 solar energy storage 0-55916  
 solar flares, observational and theoretical status 0-51728  
 solar heating and cooling systems design, operation, feasibility 0-45755  
 solar neutrino problem, theory versus obs. 0-17566  
 solar photovoltaic research and development in Japan, review 0-12012  
 solar photovoltaic systems, design for intermediate-sized appls. 0-30490  
 solar ponds for thermal conversion/storage 0-30550  
 solar power utilisation 0-16790  
 solar selective surfaces for thermal absorbers, review of basic physics and requirements 0-45752  
 solar system origin, relation to supernova explosions 0-17509  
 solar thermal conversion, collectors, storage systems, energy transport and economics 0-51003  
 solar thermal technology 0-30555  
 solid, near phase transition, light scatt. 0-29752  
 solid dielectrics, electric breakdown mechanism, discharge development, electron impact ionisation 0-15961  
 solid soln. spectroscopy, investigs. by F. Klement (*Russian*) 0-8767  
 solid solution hardening in metals, review of theories (*Czech*) 0-3084  
 solid state nuclear track detectors 0-37696  
 solid state phase transformation, detection techniques 0-2996  
 solid state physics rel. to solar cells 0-49601  
 solid-solid reactions, analysis and reaction development 0-16648  
 solids, reactivity control 0-50853  
 soliton theory 0-47204  
 somatosensory evoked potentials, in man, cerebral, subcortical, spinal and peripheral nerve pots. 0-16961  
 Soviet physics, review articles, book 0-46742  
 space vehicle nuclear propulsion, historical review of advanced consent 0-36475  
 special relativity, ether drift, historical review 0-49  
 special relativity, neo-Lorentzian relativity of G. Builder 0-46  
 spectral analysis, review of methods biomedical appls. 0-21560  
 spectroscopic effects in dense and ultradense plasmas 0-43990  
 speech waveform coding technique developments in Japan 0-33353  
 spin echo spectroscopy, two-freq. 0-20506  
 spinodal alloys characterisation techniques, props. and appls. 0-50588  
 sputtering mechanisms 0-40213  
 sputtering process and sputtered ion emission 0-35044  
 sputtering use in depth profiling 0-40214  
 steam generators of water cooled nuclear power plants, corrosion phenomena 0-558  
 steel, C and HSLA, grain size and substruct. control by alloying and thermomech. treatment 0-3082  
 steel, H effect on weldability 0-50720  
 steel, low alloy, creep crack growth, microstruct., fatigue effects 0-7672  
 steel, ultra high strength, historical 0-7609  
 steel casting, meas. and significance of residual stresses 0-21253  
 steels, ferritic and martensitic, C and N migration at low temps., monograph 0-22149  
 steels, secondary hardened, microstruct. rel. to mech. props. 0-25851  
 stellar chromospheres, observational indicators, empirical models 0-12755  
 stellar coronae, evidence for existence from X-ray and UV obs. 0-12756  
 stereoscopic microscopes, domestic, review 0-27342  
 steroid research using mass spectrometry 0-51308  
 Stirling cycle machine anal. using nodal anal. techniques 0-30532  
 stochastic cooling of particle beams 0-37675  
 stochastic instability theory applies. to nonlinear plasma systems, review (*Czech*) 0-38580  
 stochastic self-oscillations and turbulence 0-4537  
 storage cell impedance theory and experimental data review 0-55667  
 stripe-geometry heterojunction lasers 0-53288  
 structural materials, radiation effects 0-49267  
 structural phase transition, intrinsic and extrinsic central peak properties 0-34168  
 structural phase transition induced refractive index changes in crystals. 0-16000  
 sub-picosecond optical pulses, generation and meas. 0-23731  
 Sun, prominence-corona interface 0-4333  
 Sun, quiescent prominence formation, support and stability 0-4334  
 superconducting magnet conductors, props. and fabrication techniques (*Japanese*) 0-25042  
 superconductivity and elementary particle theory 0-4911  
 superconductors, thermoelectric effects 0-11133  
 superconductors, tilted vortices, mixed state features in surface layers (*Russian*) 0-29512  
 superheavy element research 0-37411  
 superionic conducting oxides 0-49414  
 superionic conductors, light scatt. and IR absorpt. book contrib. 0-25382  
 superionic conductors, mag. reson., book contrib. 0-25240  
 superplastic materials, flow and failure 0-50690



## reviews continued

superplasticity, deformation mechanisms 0-50691  
 surface analysis, appl. to lubrication problems (*French*) 0-45616  
 surface analysis, probing and imaging techniques 0-54487  
 surface characterisation, physical methods (*French*) 0-7889  
 surface chemical bonding, electron spectroscopy, book contrib. 0-24992  
 surface damage, plastic deformation cause in fatigue, wear, fretting and rolling fatigue 0-40537  
 surface exciton polaritons, book contrib. 0-49623  
 surface science, survey of recent research 0-39384  
 surface treatment processes in France (*French*) 0-16528  
 surface vibrational spectroscopy using stimulated Raman scatt. 0-38062  
 surfactant-water liquid crystal phases 0-28913  
 suspension concentrates, physical stability criteria 0-45562  
 swirl defects in single crystals. 0-44200  
 synoptic windfinding technique, Loran and VLF nav aids used with radio-sondes 0-17392  
 synthesis, structure and electrical properties of doped polyacetylene 0-15623  
 TCNQ salt, (TSeF)<sub>x</sub>(TTF)<sub>1-x</sub>-TCNQ, struct., elec. and mag. props., review 0-20158  
 TEM, experience at Univ. of California (Berkeley) 0-37130  
 TEM observation of cavities 0-14974  
 temperature measurement, high-speed pyrometry in laser-pulse heating expts. 0-52225  
 theory of defects in solids 0-6400  
 thermal analysis applications 0-26083  
 thermoconvective instabilities of confined fluids 0-38399  
 thermocouple thermometry 0-52207  
 thermodynamic temperature, meas. techniques and concept. 0-52204  
 thermodynamics of irreversible processes 0-13020  
 thermophysical properties, standardisation of meas. methods 0-52197  
 thermophysical properties, temp. measurement methods at high temp. 0-52208  
 thermophysical properties dynamic meas. techniques 0-52219  
 thermoset and coating technology, torsional braid and thermal anal. 0-55622  
 thermosphere and ionosphere, chemical processes 0-17431  
 thermospheric dynamics 0-21866  
 thick film conductor, adhesion meas. 0-50808  
 thin film, and surface anal., modern methods 0-54486  
 thin film growth due to crystallite surface migration 0-10810  
 tissue, mammalian, survey of US vel. and attenuation data 0-46744  
 TLD characteristics and recent trends (*Korean*) 0-41253  
 Tokamak, recycling and surface erosion processes 0-33805  
 Tokamak demonstration power reactors, engineering problems rel. to system components 0-32511  
 topology and physics, historical review (*Russian*) 0-8770  
 total current spectroscopy 0-45185  
 total pressure meas., ultrahigh vacuum 0-31782  
 tracking microscope, design and operation 0-36214  
 5d-transition metal antiferroelectric crystal, struct. props. and lattice dynamics, mag. struct. 0-44268  
 transition metal compounds, localisation of electrons 0-49650  
 transition metal dichalcogenides, physical props., (*Japanese*) 0-33969  
 transition metal hydrides (binary ternary systems with metallic cond.) review of research on catalytic props. 0-30273  
 transition metal magnetic clusters, neutron inelastic scatt. 0-50083  
 transition metal-H systems under high H pressure, phase diagrams., electrical cond., mag. props. 0-29923  
 transition metals, and their alloys and cpds., photoelectron energy distrib. curves, rel. to band struct., book contrib. 0-16156  
 transition metals, H diffusion 0-29219  
 transition oscillator strengths of alkali metal atoms 0-52937  
 transition state theory generalisations 0-26002  
 transition state theory generalisations 0-26003  
 transuranic nuclear waste management, evaluation of alternatives 0-18490  
 TTF-TCNQ, physical properties (*Japanese*) 0-24883  
 tunable laser progress 0-43344  
 turbulence, fully-developed, renormalisation group 0-28495  
 turbulence measurement by laser Doppler anemometers, book contrib. 0-19538  
 turbulence theory 0-4536  
 turbulent flow separation 0-1543  
 turbulent wall flows, constant press. and press. gradient flows, book contrib. 0-19347  
 twin composition plane as extended defect, structure-building entity 0-44218  
 two dimensional systems, phase transition, review 0-52149  
 two-dimensional system, phase transitions and metal-insulator transitions 0-2143  
 two-phase flow characterisation using neutron techniques (*Italian*) 0-19479  
 ultrasonography of the kidney in 1979 (*French*) 0-56149  
 ultrasonography rel. to computerised tomography in upper abdomen and retroperitoneum exam. 0-21506  
 underwater explosions, surface effects 0-14745  
 underwater sound, deep ocean LF attenuation data 0-33318  
 undulators and 'free-electron lasers' 0-9794  
 unification of fundamental forces in nature, elementary particle constituents, SU(3), gauge symmetry 0-27448  
 Universe long-term future, review 0-41927  
 US imaging of abdomen, book contrib. 0-36046  
 US imaging of carotid arteries, book contrib. 0-36047  
 US imaging over view, appls. and future trends 0-48536  
 US inspection of coarse grained metals, struct. reverberation interference 0-45456  
 US phased array sector scanning, medical diagnosis 0-36038  
 US tomography techniques survey 0-30823  
 uterine venography, value in diagnosis of pelvic pain in women (*French*) 0-17079  
 UV radiometric standards, gas discharges, plasma diagnostics appls. 0-47088  
 vapour pressure measurement, effusion method, review 0-51995  
 variable stars, physical and eclipsing, surveys and obs. 0-12772  
 venous occlusion plethysmography for the detection of venous thrombosis 0-56268  
 vibration isolation, survey of use and characterization 0-19144  
 vinyl alcohol-vinyl acetate copolymers, mol. architecture and physico-chem. props. 0-44103

## reviews continued

viscous compressible flows at high Reynolds number, book contrib. 0-19424  
 vision, photopigment and receptor props. in *Drosophila* compound eye and ocellar receptors 0-8063  
 vision, photostable pigments, function in fly photoreceptors 0-8058  
 visual pigment chromophores, models, spectroscopic and photochemical studies 0-30723  
 Visual pigment systems, implications of bistability 0-8059  
 visual stress, functional consequences, annotated bibliography 0-26222  
 VLF heating methods, thermonuclear prospects 0-28738  
 voltammetry, phase selective anodic stripping type 0-40788  
 vortex interactions, book contrib. 0-19410  
 wakes in stratified flow, book contrib. 0-19473  
 Wannier excitons, fine structure, lineshape and dispersion 0-44520  
 water, chemical analysis 0-7877  
 Western Australian Shield, struct. and tectonic style 0-3983  
 whistlers, nature, types and observations 0-36458  
 whistlers, present state of research and history 0-46348  
 wildlife biotelemetry 0-30966  
 wind energy conversion, fluid dynamic aspects 0-7909  
 wind energy conversion, review of the US Wind Energy Programme 0-50929  
 wing section theory of Kutta and Zhukovski, book contrib. 0-1514  
 X-ray computed tomography, annotated bibliography 0-30876  
 X-ray diffractometry handling problems, survey 0-1898  
 X-ray fluorescence matrix correction methods using scattered radiation 0-3456  
 X-ray imaging, image intensification systems and techniques 0-51236  
 X-ray planigraphic examination of the abdomen 0-21529  
 X-ray spectrometry, empirical influence coefficient methods 0-3455  
 X-ray tube technological and philosophical changes over a decade 0-37136  
 xerography and mammary microcalcifications (*French*) 0-51224  
 Yang-Mills type gauge fields, geometrical setting 0-32014  
 e<sup>+</sup>e<sup>-</sup> annihilation, radiative corrections, review, book contrib. 0-47320  
 e<sup>+</sup>e<sup>-</sup> annihilation by one-photon processes, book contrib. 0-47272  
 e<sup>+</sup>e<sup>-</sup> hadron jet, 3 to 17 GeV, including charm threshold and upslon resonances 0-47321  
 e<sup>+</sup>e<sup>-</sup> hadrons, jet behaviour 0-52524  
 eN→eX, form factors and structure functions, book contrib. 0-47294  
 eN→e+hadrons, E<2 GeV, formalism, book contrib. 0-47312  
 γ sources, properties, produced by neutron capture 0-14029  
 γN, many body processes, book contrib. 0-47303  
 γp→X, strong interaction model anal., review, book contrib. 0-47310  
 Λ- and Σ-hypernuclei, γ-transitions, spin-orbit components of single particle pots. 0-42574  
 Λ- and Σ-hypernuclei and hyperon-nucleus interactions, review 0-42575  
 μ<sup>±</sup> spin rotation, μ relaxation and repolarisation, muonic X-rays 0-42644  
 NN interaction in pion exchange, nuclear matter and pion condensation, review 0-42557  
 NN resonances and total cross sections, expt. evidence review 0-42558  
 (p,d), intermediate energy study review 0-42653  
 (p,γ), exclusive single nucleon transfer, theoretical status 0-42652  
 (p,p), elastic, inelastic, polarised and unpolarised, intermediate energy study review 0-42653  
 (p,p), elastic scattering theory, multiple scatt. test review 0-42654  
 (p,π), exclusive single nucleon transfer, theoretical status 0-42652  
 (p,X), experimental information review, polarisation phenomena 0-42655  
 pp atoms, quasiautomatic and very energetic γ-rays 0-42574  
 (π,π) elastic scattering, microscopic theory 0-47511  
 (π,X), reaction mechanisms, nuclear environment and models 0-42700  
 π, photoproduction in E<450 MeV region, dispersion relations, CT invariance, book contrib. 0-47311  
 πd elastic scattering, microscopic theory 0-47511  
 Al I to XIII, energy levels and ionisation energies, data compilation 0-14100  
 Al<sub>2</sub>O<sub>3</sub>-Ni cermets, prep. and props. (*French*) 0-20877  
 C fibre and glass fibre hybrid reinforced plastics, review of physical properties 0-55496  
 C stars, spectroscopic problems 0-56832  
<sup>13</sup>C-<sup>13</sup>C spin-spin coupling consts., data compilation, meas. and appls. review 0-17725  
 Ca I to XX, energy levels and ionisation energies, data compilation 0-14101  
 Ca<sub>2</sub>SiO<sub>4</sub>-CaMgSiO<sub>4</sub>, T phase, review 0-50612  
 Cu, production and extractive metallurgy, developments 0-20821  
 Cu-Ni-Al, memory alloy wire and ribbon reversible martensitic transformation, ageing effect 0-7564  
 Cu-Zn-Al, memory alloy wire and ribbon reversible martensitic transformation, ageing effect 0-7564  
 EuO(S)(Se)(Te), cryst. and electronic struct., mag., elec., and optical props., book contrib. 0-39760  
 Fe electrodes, semicond. model of passive layer 0-26022  
 Fe<sup>+</sup>, isoionic study, excited config. position and level struct., review 0-32621  
 Fe-C, martensitic transformation, thermodynamical study (*Chinese*) 0-55395  
 Fe-Cr-Ni austenitic alloys, environment sensitive cracking, metallurgical variables effect 0-35391  
 Fe-Si-B-N-S, B, S, N effects on grain boundary segregation and grain growth inhibition, review 0-3047  
 GaAs ohmic contacts fabrication, review 0-49901  
<sup>67</sup>Ga imaging of peritoneum and retroperitoneum, anatomic correls. 0-17097  
 H assisted cracking, mechanisms, review 0-50721  
 H biological photoprod. using sunlight 0-45777  
 H diffusion, and solubility in solid metals 0-49422  
 H energy, industrial appls. of liquid and gaseous H 0-45801  
 H energy, R and D programs 0-45802  
 H photoelectrolytic production by H<sub>2</sub>O decomposition using sunlight 0-45774  
 H production, EPRI R and D program for electric utility industry 0-30610  
 H production and utilisation, EEC R and D program review 0-45821  
 H production by H<sub>2</sub>O electrolytic dissociation 0-30429  
 H, storage, transmission and distribution 0-30596  
 H storage electrolysis-based technology R and D at BNL 0-40920  
 H storage in metals, book contrib. 0-26175  
 H thermochemical prod. by H<sub>2</sub>O decomposition 0-45800  
 H<sub>2</sub> energy bibliography 0-12863



## reviews continued

- H<sub>2</sub> production and utilisation, EEC R&D program progress and results 0-16767
- H<sub>3</sub>PO<sub>4</sub>, technology development for commercial systems 0-30464
- <sup>3</sup>H( $\pi,\pi$ ), expt. and theoretical work, present status, model testing,  $\pi$ N interaction 0-42699
- He, condensed phases, neutron scatt. techniques and results, book contrib. 0-2230
- <sup>3</sup>He superfluid, hydrodynamics and inhomogeneous states 0-49453
- <sup>3</sup>He-<sup>4</sup>He, superfluid, osmotic and mag. props. (*French*) 0-10733
- <sup>131</sup>I therapy, review of contamination and exposure hazards 0-41257
- InSb, charact. and phys. props. (*Japanese*) 0-39576
- LaB<sub>6</sub>, synthesis and props. (*Japanese*) 0-40255
- NH<sub>4</sub>IO<sub>4</sub>, high order phase transition, quadrupole coupling temp. depend. 0-54371
- NH<sub>4</sub>ReO<sub>4</sub>, high order phase transition, quadrupole coupling temp. depend. 0-54371
- NbH(D), struct. phase diagrams, morphologies, prep. methods, book contrib. 0-25675
- <sup>17</sup>O, NQR at natural isotope abundance, double reson. new techniques 0-53013
- <sup>31</sup>P NMR analysis of intact tissue 0-26432
- Pb chalcogenide diode lasers, recent advances 0-5732
- Pd-H and Pd alloy-H systems, review of props., book contrib. 0-24605
- PdH, supercond., book contrib. 0-25037
- Pr(OH)<sub>3</sub>, low temp. heat capacity, thermophys. props. optical spectra, anal. of Schottky contributions, review 0-24611
- RbMnF<sub>3</sub>, nuclear spin waves spectra, relaxation, parametric excitation, NMR dynamic shift (*Russian*) 0-11180
- S cycle of NE United States, role of man-made S sources 0-26178
- Si, reconstructed surface physics, review 0-10766
- Si, technology and physics 0-34353
- Si, vertical etching, at very high aspect ratios 0-50744
- Si/metal system, silicide form. by thin film interactions 0-49429
- Si<sub>3</sub>, resist. to oxidation and corrosion at high temps. (*German*) 0-35357
- <sup>153</sup>Sm, gamma spectra, energy levels (*Dutch*) 0-47430
- Sn polymorphic transformations ( $\beta \rightarrow \alpha$ ), effect of impurities, exam. 0-7557
- TaH(D), struct. phase diagrams, morphologies, prep. methods, book contrib. 0-25675
- Ta<sub>2</sub>(IT) pure and doped, Mott and Anderson localisation, commensurate phase transition 0-39641
- <sup>99m</sup>Tc-fibrinogen, usefulness of phlebography for pulmonary embolism patients 0-36093
- Th-H system, supercond., book contrib. 0-25037
- (U,Pu)O<sub>2</sub>, FBR fuel cycle 0-47682
- UF<sub>6</sub>, conversion to UO<sub>2</sub> 0-23099
- <sup>235</sup>U decay heat meas. and calcs. 0-13732
- VH(D), struct. phase diagrams, morphologies, prep. methods, book contrib. 0-25675
- VO<sup>2+</sup> EPR in solids, review 0-11254
- XeCl, excimers and excimer lasers 0-48217
- ZnS, epitaxial growth, appl. to electronic devices (*Japanese*) 0-55281
- revolution** see rotation
- revolving** see rotation
- rewinding** see winding (process)
- Reynolds number** see flow
- r.f. amplifiers** see radiofrequency amplifiers
- r.f. filters** see radiofrequency filters
- r.f. heating** see radiofrequency heating
- r.f. oscillators** see radiofrequency oscillators
- r.f. sputtering** see radiofrequency sputtering
- r.f.i.** see radiofrequency interference
- RHEED** see reflection high energy electron diffraction
- rhodium**
- see also nuclei with .....
- adsorption of H within wide temp. range 0-10778
- adsorption of O<sub>2</sub>, effect of struct. defects, steps and kinks 0-29269
- atom, nuclear K-X-ray satellites, Z<sub>f</sub>=50-83, by  $\alpha$ -bombard., 17.5-22.5 MeV 0-42984
- atomic vibr. and fermion behaviour of HCP metals 0-6474
- chemisorption of CO on (0001) surface, role of d-orbitals, angular resolved UPS and thermal desorption meas. 0-40232
- Fermi surface hydrostatic press. depend., de Haas-van Alphen phase shift meas. 0-54593
- metal oxides, high temperature interactions with Re 0-16665
- Raman scattering spectrum at room temp. 0-25373
- surface, supported, CO chemisorption, activated surface processes, IR spectra 0-16724
- surface dopant in Mo, effect on fatigue (*Russian*) 0-7660
- thermionic work function of low index planes 0-55255
- films, plasma deposited, from Re<sub>2</sub>(CO)<sub>10</sub> vapour decomp. 0-20799
- Mo alloy:Re, effect of Re on mechanical props. 0-35196
- Re XLVIII X-ray spectra from laser produced plasmas 0-42981
- Re/Os cosmochronology, nuclear correction factor 0-17485
- <sup>186</sup>Re labelled EHPD preparation and possible use in osseous neoplasms treatment 0-56215
- <sup>187</sup>Re-<sup>187</sup>Os systematics in meteorites, rel. to solar system early chronology and Galaxy age 0-41778
- W:Re, polygonisation in diffusion process, glide dislocation interactions 0-38998
- rhodium alloys**
- see also rhodium compounds
- rare earth alloys, R(Fe,Rh<sub>1-x</sub>)<sub>2</sub>, mag. props., Mossbauer spectra 0-25108
- Cr-Re, mag. excitations in commensurate antiferromag. phase 0-50079
- Mo-Re, prep. from reduction in Mo-Re-O system (*Russian*) 0-16225
- Mo-Re,  $\sigma$  phase alloy, critical mag. field, elec. resistance 0-54850
- Mo-Re-C (0.3, 0.2 at.%) time-of-flight atom-probe expts. 0-55741
- Re-Cu-Al phase diagram, X-ray structural and microscopic anal. (*Russian*) 0-20895
- Sc<sub>1-x</sub>Re<sub>x</sub>Si<sub>3</sub>, X-ray cryst. struct. determ. 0-39009
- W-Re, amorphous wire, elec. resist., 2-20K, dimens. and mag. field depend., quantum localisation 0-39547
- W-Re, ion irradiated, recovery behaviour studied by field ion microscope 0-29074
- W-Re, thin wires, fatigue limit and tensile strength 0-25834
- W-Re alloy, prep. by powder metallurgy technique, appl. in lighting industry 0-29904
- rhodium compounds**
- see also rhodium alloys
- alkali hexahalogeno compounds: ReCl<sub>6</sub><sup>2-</sup>(ReBr<sub>6</sub><sup>2-</sup>), low symm. splittings in vibronic spectrum due to phase transitions 0-55161
- alkali metal hexahalogenostannate: ReBr<sub>6</sub><sup>2-</sup>, vibronic transition  $\Gamma_7(T_{2g}) \rightarrow \Gamma_8(A_{2g})$ , intensity distrib. 0-45142
- [ReCl<sub>6</sub>]<sup>2-</sup>, spectral assignment, metal-metal bonds, SCF X $\alpha$  SW calcs., relativistic corrections 0-53006
- K<sub>2</sub>ReCl<sub>6</sub>, struct. props. and lattice dynamics, mag. struct. 0-44268
- ReBr<sub>2</sub>, electron struct., Fermi energy and surface, bonding 0-20076
- ReBr<sub>2</sub><sup>2-</sup> doped K<sub>2</sub>PtCl<sub>6</sub> type crystals, vibronic side band intensity distrib.,  $\Gamma_7(T_{2g}) \rightarrow \Gamma_8(A_{2g})$  transition 0-10609
- Re<sub>2</sub>(CO)<sub>10</sub> vapour decomposition, for plasma deposited Re films 0-20799
- ReCl<sub>6</sub><sup>2-</sup> doped K<sub>2</sub>PtCl<sub>6</sub> type crystals, vibronic side band intensity distrib.,  $\Gamma_7(T_{2g}) \rightarrow \Gamma_8(A_{2g})$  transition 0-10609
- ReCl<sub>6</sub> metal cluster complexes, He(I) photoelectron spectrum, SCC DV X $\alpha$  calcs., Re<sub>2</sub>Cl<sub>6</sub><sup>2-</sup> comparison 0-28063
- ReO<sub>3</sub>, compressibility collapse phase transition, NQR study 0-39282
- ReO<sub>3</sub> type lattice, group-theoretical symmetry anal. of vibr. (*Russian*) 0-10610
- ReO<sub>4</sub><sup>-</sup> doped alkali halide, saturable absorber at 10.6  $\mu$ m 0-53384
- Re<sub>2</sub>P<sub>26</sub>, binary crystals containing plane Re<sub>4</sub> clusters (*French*) 0-19774
- ReSe<sub>2</sub>, layer cryst., dislocations and domain struct. 0-39102
- ReSe<sub>2</sub>, layer cryst., dislocations and domain struct. 0-39102
- rheology**
- see also biorheology; plasticity; viscoelasticity
- anisotropic micropolar fluid theory 0-31515
- aqueous polymer solns., shear stress and normal stress meas. using cone-and-plate rheogoniometer 0-1496
- bituminous pitch oils, flow curves, mag. field effect 0-33553
- ceramic suspensions, effect of grainy filler 0-43685
- chromorheology, exptl. verification of numerical solns. of elastic-plastic problems 0-48659
- chromorheology, new exptl. method 0-48658
- circular plates, thermoviscoelastic anal. of a thermorheologically simple material 0-10161
- colloids, rheological props., terminology and symbols 0-26065
- continuous models of suspensions, nonequilib. thermodynamic approach 0-28479
- crosslinked polymer systems, probabilistic theory 0-19314
- cyclic loading, elementary and classical rheological models, global behaviour (*French*) 0-22197
- dipolar dumbbells in a viscoelastic Oldroyd liquid, dilute soln., electric field effect on rheological behaviour 0-6009
- elastohydrodynamic contact, rheological model 0-33544
- electrorheological suspension flow, vibr. effect (*Russian*) 0-53877
- extensional rheometer, elongation props. meas. of polymer melts 0-6004
- ferromagnetic suspension, magnetorheological characts. meas., errors 0-33550
- flow regulating system operating with Newtonian and non-Newtonian fluids (*German*) 0-1535
- glass workability rel. to melting history, microstruct., apparent liquidus temp., mechanical props. 0-11633
- hydrodynamic stability of structurally viscous medium, effect of elastic factor 0-19303
- journal bearing rheometer, experimental investigations (*German*) 0-6014
- LPDE melt, tensile stress overshoot in uniaxial extension, single integral constitutive eqn. 0-1507
- lubricant, shear rheological behaviour at high press. 0-35342
- mantle return flow and non-linear rheology 0-46152
- metals and alloys, yield criterion, rheological interpretation (*Russian*) 0-21014
- multiphase non-Newtonian systems, rheological props. variation in barotreatment 0-19304
- non-Newtonian fluids, capillary and slit methods of normal stress measurements 0-43807
- non-Newtonian fluids, rheological props., pressure induced change of yield stress 0-53736
- nonisothermal flow of anomalous systems in pipes, rheological aspects (*Russian*) 0-43775
- nonisothermal flow of anomalously viscous liquids in channels of screw extruders 0-19305
- nonlinear rheological media, variational criterion of material stability 0-28480
- orthogonal stagnation flow, a framework for steady extensional flow experiments 0-1653
- pitch and coke-pitch disperse system, viscoelastic props. 0-1500
- Poiseuille flow of viscoelastic fluid between eccentric cylinders 0-1652
- poly-p-aminobenzhydryde terephthalamide in dimethyl sulphoxide soln., rheological study 0-43683
- poly-p-phenyleneterephthalamide solns., rheological props. comparison with nylon 6,6 soln. 0-6007
- polybutadiene, hydrogenated, linear and star branched, melt rheology 0-23978
- polybutadiene, linear and star branched, rheology 0-23977
- polyethylene, high-density, polymer melt, shear stress at wall 0-19450
- polyethylene, linear, melt rheology 0-23976
- polyethylene, low density melts, temp. depend. of the elongational behaviour 0-6012
- polyisobutylene solution in cetane, hyperelasticity, filler effect 0-10223
- polyisobutylenes, shear behaviour of Vistanex LMMH and L 100 0-1443
- polymer, filled, solution, normal stresses and hyperelasticity under simple shear flow 0-1506
- polymer melt, particulate mixing, fluid dynamics, rheological and energetic considerations 0-43686
- polymer melt, polydispersity, estimation from rheological data 0-6535
- polymer melts, elastic, uniform extension by const. force, rheology 0-43682
- polymer melts, elongational behaviour in const. elongation rate, tensile stress and tensile force expts. 0-38372
- polymer melts, elongational properties, microscopic stretch history 0-23981
- polymer melts, meas. of elongation props. with universal extensional rheometer 0-6004
- polymer melts, rheological props., effects of hydrostatic press. 0-48663
- polymer solns., rheological props. in flow through porous media 0-53819
- polymer solutions, concentrated, viscous function, hyperelasticity and viscoelasticity 0-48662
- polymeric systems, fluid, rheology, characterised, by mol. int. distrib., review 0-1504



**rheology continued**

- polymers, conc. solns. in volatile solvents, high temps., method for viscosity meas. 0-19535  
 polyoxymethylene-copolyamide mixtures, melt rheological props., extrudate microstruct. (*Russian*) 0-7530  
 polystyrene in chlorinated biphenyl, flow birefringence on appl. of step-shear strain 0-25335  
 polytrifluorochloroethylene, rheological props. (*Russian*) 0-6015  
 pore geometry effects on pressure loss, model channels with varying diameter (*German*) 0-1677  
 powder-water-oil system, cohesion of powder particles with water, rheological prop. (*Japanese*) 0-14647  
 primary macromolecules, mol. wt. distrib. influence on crosslinked polymer systems 0-19313  
 PVC compositions, influence of formulation on the compounding and rheological props. 0-40321  
 rectilinear flow, pressure error upper and lower bounds with pressure gradient 0-6010  
 Reiner-Rivlin fluids, rheological props. 0-14646  
 rigid ellipsoidal particles in external field, dil. suspension, rheological eqns. (*Ukrainian*) 0-48661  
 rotational rheometry, edge effects and related error sources 0-19536  
 solid-liquid mixtures, rheological characts., shear stress/strain rate relationships 0-10287  
 spectrophasemeter, for polymer systems meas. 0-33547  
 spherical particle, free-fall rate in immobile liq. 0-19302  
 styrene/MMA copolymers, struct. and rheology 0-1444  
 surface chemistry, rheological props., terminology and symbols 0-26065  
 suspension concentrates, physical stability criteria, review 0-45562  
 suspension in nonstationary flow, rheological behaviour 0-6130  
 technical fabrics, viscoelastic compliance, appl. of stress-time analogy method 0-1497  
 thermotropic liquid crystals, anomalous rheological responses, spectrometer study 0-6358  
 triblock copolymer, model for rheology 0-23979  
 upsetting tests developments for better stress/strain curve results (*German*) 0-38368  
 viscoelastic fluid flow, heat transfer at low Deborah numbers, rheological effects 0-19445  
 viscoelastic material, stress-strain behaviour, mathematical simulation (*German*) 0-1442  
 viscoelastic materials, under prolonged loading, failure hypothesis 0-3180  
 viscous fluid, squeezing between elliptic plates 0-28478  
 water in single capillary, electrokinetic and rheological parameters 0-10220  
 C black conc. suspensions in low mol. wt. vehicles, rheology anal. 0-19312  
 $\gamma$ -Fe<sub>2</sub>O<sub>3</sub>, densified, rheological and mag. props. 0-44873  
 Fe<sub>2</sub>O<sub>3</sub>, flocculated suspension in ethylene glycol, intrinsic viscosity rel. to shear rate 0-1502

**rho mesons**

- chiral SU(3)×SU(3),  $\rho$ -meson as dormant Goldstone boson 0-368  
 $e^+e^- \rightarrow \pi^+\pi^-(\pi^0\omega)$ ,  $\rho$ (1250) description, EM form factors, bound states, N/D method (*Russian*) 0-42465  
 electroproduction, parity-violating effects 0-9178  
 interaction cross sections in QCD (*Russian*) 0-4968  
 masses in QCD lattice gauge theory 0-4928  
 meson strong decay, 2 quark-antiquark pair model 0-52496  
 QCD exclusive processes,  $\pi$ , K,  $\rho$  form factors, hadronic wavefunction evolution eqns. 0-18135  
 $e^+e^- \rightarrow e^+e^-\rho$ , bremsstrahlung production of neutral vector mesons 0-5006  
 $\eta \rightarrow \rho\gamma$ , radiative widths,  $\delta$  and S\* background, SU(3) and VDM anal. 0-419  
 $K_L^0 K_S^0$  transmission regeneration on deuterons and neutrons, 10 to 50 GeV/c 0-4985  
 $K^\pm p$ , 32 GeV/c,  $\rho$ , K\*,  $\phi$  inclusive prod., quark fusion model 0-32135  
 $\pi N \rightarrow \pi^+\pi^- N$ , 4-17 GeV/c,  $\rho^0$  and f prod. mech. 0-436  
 $\pi\omega \rightarrow \pi\omega$ ,  $\rho$ (1250) meson and two channel  $\pi\pi$ ,  $\pi\omega$  problem, N/D method (*Russian*) 0-37297  
 $\pi^+\pi^-\pi^+\pi^-$ , narrow epsilon resonance under rho 0-5021  
 $\pi^+\pi^-\pi^+\pi^- \Delta^{++}$ , narrow epsilon resonance under rho 0-5021  
 $\pi\pi \rightarrow \pi\omega$ ,  $\rho$ (1250) meson and two channel  $\pi\pi$ ,  $\pi\omega$  problem, N/D method (*Russian*) 0-37297  
 $\pi\pi \rightarrow \pi\pi$ ,  $\rho$ (1250) meson and two channel  $\pi\pi$ ,  $\pi\omega$  problem, N/D method (*Russian*) 0-37297  
 $\rho$ - $\omega$  mixing, quark mass differences 0-37243  
 $\rho$ (1600) diffractive photoprod. in two pion final state 0-22624  
 $\tau \rightarrow \mu\rho$  decay parameters from PCAC and current algebra, A<sub>1</sub> characts. 0-37314  
 $\tau^- \rightarrow \rho^- \nu$ , branching fraction meas. 0-13296

**rhodium**

- see also nuclei with .....*  
 adsorbed S on (110), surface struct. anal. using hybridisation model 0-44423  
 atom, K $\beta$ /K $\alpha$  rel. intensity obs. 0-32665  
 band structure and photoemission from low index surfaces 0-24790  
 chemisorbed CO on (111), dissociation probability, isotopic exchange and AES meas. 0-40743  
 chemisorption, of CO, <sup>13</sup>C NMR obs. 0-1000  
 chemisorption of CO and CO<sub>2</sub> on (111), high resolution EELS, thermal desorption, and LEED study 0-44419  
 coadsorption of O<sub>2</sub> and H<sub>2</sub> below 140K on (111) surface 0-29276  
 dissociative chemisorption of CO<sub>2</sub> on (111) surface, EELS and thermal desorption spectra meas. 0-6656  
 electrode, evaporation rate from cathode spot in vac. arcs. 0-49024  
 film, deposited by cylindrical magnetron sputtering, internal stresses 0-24773  
 surface, (110), S-adsorbed, LEED crystallographic determ. of struct. 0-44422  
 surface (111), LEED crystallography and reliability indices 0-54081  
 surface atoms, Debye temps. determ. during field evaporation and LEED 0-39406  
 Rh<sup>+</sup>, Rh<sup>2+</sup>, field evaporation, field ion mass spectra and field ion appearance spectra study 0-7479  
 Rh-Si thin film interaction, interdiffusion, temp. depend. 0-54443

**rhodium alloys**

- see also rhodium compounds*  
 ferromagnetic Heusler alloys, peaks in low field AC susceptibility 0-50071

**rhodium alloys continued**

- Permalloy-Rh, film, influence of Rh on corrosion resist. and mag. props. 0-3235  
 rare earth alloys, RRh<sub>2</sub>X<sub>2</sub> (X=Si,Ge), cryst. struct. 0-1964  
 Au-Rh, dil., Friedel d-reson. scatt. and elec. resists. 0-44566  
 Gd(Rh<sub>1-x</sub>Fe<sub>x</sub>)<sub>2</sub>, x≤0.15, magnetisation and EPR studies 0-34767  
 Nb-Rh, radiation disorder model of phase stability 0-16297  
 Ni-Fe-Rh films, mag. and corrosion props. 0-34702  
 (Ni<sub>1-x</sub>Rh<sub>x</sub>)<sub>99</sub>Mn, ferromagnetic, NMR study of local environment effect 0-7192  
 (Ni<sub>1-x</sub>Rh<sub>x</sub>)<sub>99</sub>Mn, ferromagnetic, NMR study of local environment effect, relaxation mechanism 0-7193  
 PdFeRh, ferromag., Curie temp. depend. on susceptibility, non-mean field theory 0-44829  
 Pd<sub>0.9</sub>Rh<sub>0.1</sub>, lattice dynamics, inelastic neutron scatt. meas. at 296K 0-29135  
 Pt-Rh, elec. cond., temp. influence (*Russian*) 0-39549  
 Pt-Rh, surface comp. determ. by ion scatt. spectroscopy 0-6602  
 Pt-Rh-W (30, 8 wt.%), intergranular embrittlement by Se vapour 0-3185  
 PtRh5 alloy, phosphate glass addition effect on high temp. strength (*German*) 0-25807  
 Rh-Al, transition metal group VIII aluminide, NMR near equiatomic composition (*Russian*) 0-20479  
 Rh-C (graphite), adhesion and wettability of graphite (*Russian*) 0-20008  
 Rh-Si thin film interaction, interdiffusion, temp. depend. 0-54443  
 Rh<sub>2</sub>MnGe(Pb), hyperfine mag. field at Cd impurity, TDPAC study 0-39905  
 Rh<sub>2</sub>Si-n-Sn Schottky diodes, rectifying barrier height meas. 0-49896  
 Sc-Rh-Si system, partial phase diagram, X-ray diffr. and microprobe anal. 0-25659  
 (Zr<sub>1-x</sub>Er<sub>x</sub>)<sub>3</sub>Rh, amorphous, influence of mag. ordering on supercond. props. 0-29511

**rhodium compounds**

*see also rhodium alloys*

- double oxides, elec. cond. 0-34438  
 rare earth borides, ternary, superconducting, phase diagrams and upper crit. fields 0-2531  
 rare earth compounds, RRh<sub>2</sub>B<sub>4</sub>, supercond. and long range mag. order coexistence 0-15642  
 rare earth rhodium borides, RRh<sub>2</sub>B<sub>4</sub>, NMR and sp. ht. in supercond. and mag. ordered phases 0-7037  
 Cr<sub>1-x</sub>Rh<sub>x</sub>O<sub>2</sub>, oxidative prep. method, mag. props. 0-44863  
 (Er<sub>0.6</sub>Ho<sub>0.4</sub>)Rh<sub>2</sub>B<sub>4</sub>, reentrant supercond., magnetisation meas. near lower crit. temp. 0-25043  
 (Er<sub>1-x</sub>Ho<sub>x</sub>)Rh<sub>2</sub>B<sub>4</sub>, superconductive and mag. interactions, hydrostatic press. effect 0-49973  
 Er<sub>x</sub>Y<sub>1-x</sub>Rh<sub>2</sub>B<sub>4</sub>, supercond. phase transitions, recentering temp. to normal ferromag. state 0-7024  
 Hf-Rh-B systems, phase equilb. and cryst. structs. 0-15072  
 Rh(III) complexes, luminesc. rise time meas. by wavelength shifter 0-50390  
 Rh<sub>2</sub>Si-n-Sn Schottky diodes, rectifying barrier height meas. 0-49896  
 Sc-Rh-B system, phase equilb. and cryst. structs. 0-15072  
 SmRh<sub>2</sub>B<sub>4</sub>, coexistence of supercond. and antiferromag. order 0-11140  
 SmRh<sub>2</sub>B<sub>4</sub>, mag. ordered, persistence of supercond. 0-54834  
 YRh<sub>2</sub>B<sub>4</sub>, supercond., anomalous cond.-electron polaris. 0-25047  
 Zr-Rh-B system, phase equilb. and cryst. structs. 0-15072

**Richardson effect** *see thermionic emission***ridge waveguides** *see rectangular waveguides***Riemann-Cristoffel tensors** *see general relativity; tensors***Righi-Leduc effect** *see thermomagnetic effects***rigidity** *see shear modulus***ring lasers**

- anisotropic resonator, polarisation and freq. splitting of opposite waves 0-33037  
 beam divergence, mode competition effect 0-48303  
 cavity, dispersive bistability in homogeneously broadened systems 0-14306  
 detuning, generation of high-frequency pulsations 0-48304  
 diffraction biased unstable ring resonators, appl. in laser gyroscopes 0-1238  
 diffraction theory, Gaussian approx. 0-53338  
 drift splitting of opposite wave frequencies, effect of elastic collisions 0-14370  
 dye CW laser, ring resonator, mode selection 0-14371  
 dye laser, CW, technology developments and appl. 0-43383  
 dye laser, injection-locked pumped by Xe ion laser, 4-mirror ring-cavity 0-48280  
 dye laser, tunable, flashlamp pumped, ultra-narrow bandwidth 0-9897  
 dye laser, unstable ring resonator, N<sub>2</sub> laser pumped 0-53326  
 dye ring laser, flashlamp pumped, injection of N<sub>2</sub> laser excited oscillator beam 0-5754  
 dye ring laser characts. (*German*) 0-14365  
 dye travelling-wave CW laser, mode locking 0-43354  
 frequency noninteraction of oppositely travelling waves in gas ring laser 0-38043  
 frequency response of ring laser with reversible pedestal 0-48308  
 gas, limiting characts. of power resonances 0-19058  
 gas laser, scale factor for saturating oppositely travelling waves 0-9910  
 gas laser interaction of elliptically polarised opposing waves 0-38044  
 general relativity test, precision ring laser interferometry technique 0-52117  
 gyro, dispersion and gas flow effects 0-1267  
 gyro, integrated 3 axis design 0-1268  
 gyro, low-scatter low-loss mirror prod. 0-1272  
 gyro, Rockwell programme 0-1271  
 gyro, tutorial review 0-1266  
 gyro, two-mode, four-mode soln. to locking problem 0-1270  
 gyro, Zeeman laser, beat-note sensitivity 0-53340  
 gyro evaluation plan and test results 0-9934  
 gyro performance analysis using fast Fourier transforms 0-9933  
 gyroscope, accuracy limit, model calc. 0-1241  
 gyroscope, nuclear radiation vulnerability 0-9935  
 gyroscope, Raytheon four freq., mag. mirror, Faraday and Zeeman biasing 0-1269  
 gyroscope application (*German*) 0-53337  
 homogeneously broadened, mode competition, intensity fluctuations 0-43375  
 inertial rotation sensors, conf., San Diego USA (Aug. 1978) 0-1265



**ring lasers continued**

- intensity fluctuations taking spatial population-inversion grating into account 0-14364
- misalignment sensitivity of ring resonator with focusing elements 0-1242
- nonlinear nonreciprocity effects, laser placed in longit. mag. field 0-43377
- nonlinear polarisability of two-isotope active medium 0-14369
- nonreciprocal effects on appl. of transverse mag. field to active medium 0-53341
- optical cavity, nearly confocal, with spatially inhomogeneous medium, threshold gain 0-43373
- plasma, laser gas discharge, Faraday rot. diagnostics 0-43981
- PT asymmetry and four-fold EM degeneracy lifting, appl. to ring laser mode splitting 0-23606
- resonator with diaphragmed spherical mirror and inhomogeneous amplifying media (*Russian*) 0-28256
- rotation rate sensors, Air Force appls. 0-9932
- semiclassical equations of motion for system with spontaneous emission in generation channel 0-1240
- solid state, with intracavity bleachable filter, conditions for CW stimulated emission 0-14368
- solid-state laser, travelling-wave, linear stage of field development 0-23724
- solid-state ring laser, generation of microsecond pulses 0-9913
- travelling wave cross-saturation asymmetry 0-43371
- travelling-wave Zeeman gas laser operating at high radiation intensities, theory 0-9912
- tunable laser progress 0-43344
- two-mode, intensity fluctuations 0-33038
- Zeeman, four-mode operation 0-19053
- Zeeman laser, interaction of modes characterized by orthogonal circular polarizations 0-48306
- He-Ne, operating well above lasing threshold Zeeman effect 0-33039
- He-Ne laser placed in longit. mag. field, nonlinear nonreciprocity effects 0-43377
- He-Ne ring laser, absorbing medium press. influence on power resonance characts. (*Russian*) 0-23725
- He-Ne ring laser, influence of pressure on Zeeman effect 0-19056
- He-Ne ring laser with methane absorpt. cell, power reson. characts. 0-28255
- He-Ne-methane ring laser, frequency stabilized, operating charact. 0-14366
- I photodissoc. ring laser, lasing regimes, emission and polarization characts. 0-48236
- Nd<sup>3+</sup>:YAG CW ring laser, fluctuation spectrum 0-9914

**ringers** see *bells***riometers** see *ionospheric measuring apparatus***ripples**

- He, liquid, charged surface, current instability theory (*Russian*) 0-29243
- He, liquid, short-wave surface excitation study using electron gas nonlinear I-V characts. (*Russian*) 0-10717
- He, liquid surface, electron-ripple spectrum in mag. field normal to surface (*Russian*) 0-49444
- <sup>3</sup>He-<sup>4</sup>He, charged interface, ripple softening 0-34269
- <sup>4</sup>He, liquid, surface electron interaction with EM radiation (*Russian*) 0-54449
- <sup>4</sup>He, superfluid, free surface, book contrib. 0-2231
- <sup>4</sup>He, superfluid, surface, ripples, adsorbed <sup>3</sup>He and heat conduction meas. 0-49459

**rivers**see also *lakes*

- Alberta bankfull discharge, effects of channel enlargement by river ice 0-8369
- Amazon suspended sediment reaction with seawater, cation exchange characts. 0-8337
- basin study simulation model 0-31079
- basin water resource, Pareto region, stochastic multicriterial problem in control 0-4055
- bed load transport, Bagnold's granular fluid model 0-51442
- bedload dynamics, grain-grain interactions in water flows 0-31069
- bedload transport measurement, calibration of acoustic device 0-56620
- Bhagirathi River, West Bengal, unidirectional alluvial channels, metamorphosis philosophy 0-31075
- Breg in W.Germany, uranine tracer for karstified aquifer 0-26564
- Bulgarian river flow prediction, methods 0-26562
- Caniapiscaw River, Canada, shaping by ice during the last 6000 years (*French*) 0-12439
- Caspian Sea feeders, continental runoff contrib. to biogenous elements balance 0-31073
- coarse riverbed material, probability density function of biased samples 0-12445
- Cochin backwater, India, estuarine water, particulate heavy metal content 0-7964
- Cochin Harbour mouth, India, hydrographic characts. and tidal prism 0-41452
- discharge forecasting using hydrologic model of Mahanadi basin 0-31130
- discharge gauging using weirs and flumes, Soviet rules 0-26561
- discharge volume after marsh reclamation, theory including groundwater 0-36349
- dissolved Fe, Mn organic matter, estuarine mixing implications 0-17296
- dissolved O<sub>2</sub> reliability parameter in probabilistic programming models 0-26179
- Diyala catchment, Iraq, water balance between Derbendikhan and Himrin dams 0-12462
- drainage density prediction techniques, evaluation of surrogate methods 0-8365
- drainage history of karstic limestone terrain, Texas 0-56501
- FLUCOMP numerical river flow model 0-26653
- fluid dynamics conference, Aug. 1978, Strasbourg, France 0-36764
- free-surface sediment conveying river bed flow, flowrate and momentum correction factors 0-36339
- Garonne-Gironde river estuary system, radioactive tracing of physico-chemical behaviour of Zn (OH)<sub>2</sub> (*French*) 0-7994
- Gironde inlet and Pertuis of Maumusson, estuarine waters seaward dispersion, remote sensing study (*French*) 0-8324

**rivers continued**

- groundwater recharge mechanism, Los Naranjos area, Mexico, using environmental isotope methods 0-12458
- N.Gulf of Alaska, river runoff rel. to coastal flow meas. by drogued drift buoys 0-51431
- Gulf of Taganrog salinity, after restriction of exchange with Sea of Azov 0-36335
- hybrid river models software support 0-56499
- ice processes, radiohydroacoustic monitoring method 0-26649
- Iowa, wind-aided drainage in loess 0-41467
- Krishnapatnam coastal inlet, stability rel. to wave conditions and longshore currents 0-41449
- Louisiana canals hydrologic simulation model 0-31080
- old Mangalore Port, India, sediment transport and siltation of navigational channel 0-56488
- old Mangalore port, seasonal vars. in estuarine and oceanic waters hydrographic conditions 0-41451
- meander of small stream with sand bed, flow and sediment transport 0-41466
- Nile, Kalman forecasting model 0-31081
- nonuniform suspended load, non-equilibrium transportation (*Chinese*) 0-8339
- Passaic River, New Jersey, nitrification, historical and expt. investigation 0-7968
- pollutants, radioactive tracers appl. (*French*) 0-7995
- pollution, dynamic behaviour of distributed systems (*Dutch*) 0-3542
- Pomme de Terre River, Missouri, USA, Holocene erosion and climate 0-51446
- riverine lake inflow and lake temperatures, effect on spring circulation 0-26555
- sandwave bottom river, turbulent flow expts. 0-36350
- sediment source identification, mag. meas. techniques 0-8348
- sediment yields of Western Southern Alr rivers, New Zealand 0-21787
- shallow flows, turbulence in depth-limited boundary layer 0-12406
- Siberia, river diversions to south, effect on Arctic ice cover, climate 0-41541
- St. Lawrence, E.Canada temp. and salinity changes rel. to magnetotelluric fields time depend. 0-26451
- St. Lawrence Estuary turbidity maximum, sediment, salinity, suspended matter study 0-4015
- stages digital simulation model 0-31078
- storm runoff, flow component separation, solute conc. and contact time study 0-8358
- storm runoff effected by rainfall spatial distribution in small catchment 0-8357
- stream water solute conc. rel. to throughflow 0-31070
- streambank erosion, stereometric meas. 0-17421
- streams, chem., hydrological, thermal characts., Haney, British Columbia 0-8350
- streams draining granite terrain, S.Carolina, dissolved Fe as groundwater component indicator 0-12444
- Suwannee River sill, effect on Okefenokee Swamp water level 0-8356
- tidal waves in channel, energy dissipation due to bottom friction and eddy losses 0-31058
- Tomaki River, New Zealand, bed material transport 0-4054
- tributary diameter, topologically random channel networks anal. 0-8372
- turbulent flow over sand wave field 0-51441
- water quality models, Monte-Carlo anal. 0-8367
- As conc. meas., column chromatography versus flameless atomic absorption spectrophotometry 0-55969

**RKKY interaction**

- dilute local moment local magnetisation, Kondo-like deviations from free spin behaviour 0-44800
- random Heisenberg model for mag. alloys, RKKY type interaction 0-44788
- rare earth dodecaborides, mag. susceptibility temp. depend., 90-1200K 0-20374
- rare earth intermetallics, RGe<sub>2</sub>, ordering and exchange interactions 0-39779
- rare earth metal, RKKY interactions, anisotropic effects from spin-split bands 0-15712
- semiconductors, magnetic, static magnetic properties, mean field approach 0-7090
- spin glasses, Ising, sp. ht. 1/T behaviour 0-11210
- spin glasses, phase transition, fluctuations of local spins, mean-field theory 0-34661
- superconducting amorphous metals, mag. impurity interactions 0-44777
- Ag-Mn, spin glass, mag. susceptibility hydrostatic press. depend., RKKY interaction 0-44845
- Cd<sub>1-x</sub>Mn<sub>x</sub>Te, spin-orbit coupled bands, indirect exchange interaction via electrons 0-34407
- Ce<sub>0.72</sub>Ho<sub>0.27</sub>Ru<sub>2</sub>, superconductors, mag. correlations and crystal-field levels 0-34547
- EuB<sub>6</sub>, exchange interaction, EPR obs. in Sr<sub>x</sub>Eu<sub>1-x</sub>B<sub>6</sub> and La<sub>x</sub>Eu<sub>1-x</sub>B<sub>6</sub> 0-20457
- Gd, RKKY interactions, anisotropic effects from spin-split bands 0-15712
- Gd(Al<sub>1-x</sub>Cu<sub>x</sub>)<sub>2</sub>, thermolec. power, exchange interactions 0-24881
- (Ge,Pb)<sub>1-x</sub>Mn<sub>x</sub>Te, mag. and elec. props. meas. 0-29534
- Hg<sub>1-x</sub>Mn<sub>x</sub>Se, spin-orbit coupled bands, indirect exchange interaction via electrons 0-34407
- Hg<sub>1-x</sub>Mn<sub>x</sub>Te, spin-orbit coupled bands, indirect exchange interaction via electrons 0-34407
- La<sub>x</sub>Eu<sub>1-x</sub>B<sub>6</sub>, EPR linewidth conc. depend., Sr<sub>x</sub>Eu<sub>1-x</sub>B<sub>6</sub> comparison, exchange interaction in EuB<sub>6</sub> 0-20457
- Pd-H-Gd, dil., ESR exam. of low temp. region of phase diagram, and electronic props. 0-29930
- PdGdH, diagram of state elec. props., indirect exchange interaction, EPR study (*Russian*) 0-50179
- PdH<sub>2</sub>-Fe, dil., Kondo system, local moment hyperfine studies, Mossbauer expt. 0-39908
- Sr<sub>x</sub>Eu<sub>1-x</sub>B<sub>6</sub>, EPR linewidth conc. depend., La<sub>x</sub>Eu<sub>1-x</sub>B<sub>6</sub> comparison, exchange interaction in EuB<sub>6</sub> 0-20457
- YIG-rare earth garnet solid solutions, magnetisation temp. depend. calcs. 0-20388

**road traffic**

- air pollution, statistical models with reference to Los Angeles Catalyst Study (LACS) data 0-30620
- microtremor measurement, by He-Ne laser interferometer (*Japanese*) 0-9025



**road traffic continued**

- noise, analysis of sequence of sound level readings (*Japanese*) 0-35806
- noise, annoyance and activity interference patterns 0-48504
- noise, effect of skewness and standard deviation on sampling errors 0-35803
- noise, effect of structure-borne tunnel vibrations on buildings 0-48492
- noise, effect on sleeping subjects 0-48509
- noise, environmental impact in Britain 0-48508
- noise, human response in residential areas 0-55962
- noise, importance in France 0-48510
- noise, improvements to the equally-spaced vehicles model, grouping effect (*Japanese*) 0-55963
- noise, model investigation on acoustical performance of courtyard houses 0-10077
- noise, prediction of time pattern of fluctuating sound levels (*Japanese*) 0-55965
- noise, prediction using a scale model 0-45838
- noise, sound immission mapping in urban areas 0-48533
- noise, traffic control effect on evaluation index 0-51024
- noise annoyance measurement, simulated 0-28379
- noise data, appl. of multivariate joint probability function of state variables with quantized levels 0-36836
- noise levels, relationship with traffic volume (*Japanese*) 0-33335
- noise measurements in Antwerp and Brussels and their relation with annoyance 0-33332
- noise pollution, new road traffic noise model (*Japanese*) 0-35804
- noise prediction calc. on straight road in suburbs (*Japanese*) 0-19147
- noise propag. in city area, investigation using scale models and field measurements (*Japanese*) 0-19152
- noise reduction by multiple finite barriers, prediction method 0-38171
- noise screening effect by buildings (*German*) 0-10076
- pollutant dispersion over highways, wind and temp. study of turbulence 0-12038
- urban noise level variation and attenuation with height 0-10078
- vehicle noise attenuation over short grass 0-19146

**road vehicles**

- electric vehicles, energy economy aspects (*German*) 0-30427
- solar powered automotive transport utilising stirling heat engine 0-55824
- sound meas. standards 0-14531
- thermal energy storage system for a Stirling engine powered highway vehicle 0-30584

**robots**

- adaptive industrial, orientation angle calc. method (*Russian*) 0-42192
- retinal hue signal generation, optoelectronic robot model 0-3647
- voice command of a six-degree-of-freedom manipulator, robotic arm appl. 0-12313

**Rochelle salt**

- deuterated, complex dielec. const., 5 MHz-24GHz, -45 to +45°, relax. mechanism 0-15983
- ferroelectric phase transition, external field induced 0-29700
- ferroelectric surface creep discharge plasma channel and domain interactions 0-15996
- heat capacity, meas. by adiabatic low temp. calorimeter (*Japanese*) 0-52218
- irradiated crystal, and deuterated form, primary reactions, EPR obs. 0-3370
- VO<sup>2+</sup> doped Rochelle salt, EPR study 0-34762

**rock magnetism**

- see also palaeomagnetism*
- alkaline rocks and magnetic anomalies (*Rumanian*) 0-12338
- ancient oceanic lithosphere, mag. props. as alteration indicators, Othris ophiolite example 0-8297
- Caerfai Bay Shales, S.Wales, diagenetic magnetisation of Lower Cambrian rocks 0-36227
- clay thermoremanent magnetisation, cooling-rate depend. 0-46174
- Devonian Onondaga limestone (New York), palaeomagnetism re-examination 0-3928
- dyke rocks of Permian S.W. Sweden 0-36228
- gyromagnetic magnetisation in anisotropic mag. material 0-50142
- igneous rock, mag. props. rel. to composition and Fe-oxide grains 0-36294
- Lake Tahoe, California-Nevada, remanence, props. and palaeomagnetism 0-41371
- lava flows of Mt. Etna, partial self-reversal and NRM 0-46126
- magnetic vector determination of rock specimen, statistical method 0-51556
- magnetite, grain size limits for pseudosingle domain behaviour, rel. to palaeomagnetism 0-11215
- magnetite, partial thermal remanent magnetisation additivity 0-26498
- magnetite (Fe<sub>3</sub>O<sub>4</sub>), mag. susceptibility under hydrostatic press. and implications for tectonomagnetism 0-26504
- magnetite (Fe<sub>3</sub>O<sub>4</sub>), piezomag. response depth depend. rel. to tectonomagnetism as earthquake precursor 0-26465
- measurement of magnetisation of laboratory sample, combination of individual vectors 0-46271
- metalliferous sediments of E.Pacific Rise, three-dimensional distrib. and mag. props. 0-21705
- NRM, stress sensitivity meas. using cryogenic magnetometer 0-26506
- oblique anhysteretic remanent magnetisation 0-21717
- oceanic basalts, titanomagnetites low-temp. oxidation rel. to mag. anomalies statistical anal. 0-36233
- oceanic crust random magnetisation, effect on coherence of short-wavelength marine mag. anomalies 0-36225
- Pliocene rhyolite from San Vincenzo, Tuscany 0-56357
- red sandstone from N.Calcareous Alps, Permo-Triassic palaeomagnetism 0-56358
- remanent magnetisation, uniaxial stress effects, stress cycling and domain state depend. 0-26505
- rotational remanent magnetisation, explanation 0-51390
- rotational remanent magnetisation acquired during alternating field demagnetisation 0-36295
- sediment magnetisation studies, high-press. cell for chem. demagnetisation 0-31126
- self-reversal of remanent magnetisation of lava 0-56462
- submarine pillow basalts, seafloor weathering effects on geomag. palaeointensities determ. 0-3927
- tectonomagnetics and small scale secular variation, symposium, Seattle, Washington (1977 August 22) 0-22133
- Tertiary volcanics from Sardinia 0-56343
- titanomagnetite, TRM acquired by multi-domain single cryst. 0-36293

**rock magnetism continued**

- Yerington mine, Nevada, in situ induced polarisation and mag. susceptibility meas. 0-51323
- Fe ore deposits, magnetic prospecting, 3-D anisotropic body mag. field calcs. and algorithm 0-4141

**rocket vehicles *see rockets*****rockets**

- see also missiles; space vehicles*
- ballistic, intercontinental, Keplerian paths, pencil with two common points, nongravitational foci 0-52005
- China 2 rocket (1971-18B), orbit determ. and geophysical interpretations 0-4231
- European space technology developments, Swiss role (*German*) 0-4234
- exhaust plumes, short-duration, rapid-scan instrumentation for spectrally and spatially resolved radiance measurements 0-13164
- intermediate thrust arcs in rotating potential force fields 0-52007
- multiple propulsion concept, theory and performance 0-4229
- potential and charge neutralisation, electron beam injection in Araks expt. (*Russian*) 0-17472
- wind meas. by meteorological rocket sounding methods, since World War II 0-17398
- Zarnitsa.2 electron injection expt., circumrocket glow spectral obs. (*Russian*) 0-12596
- H<sub>2</sub>, laser-heated, analysis of nozzle flow 0-10283

**rocks**

- see also geology; minerals; rock magnetism*
- Z (*Chinese*) 0-56615
- acoustic anisotropy of sedimentary rocks, due to overburden press. 0-56455
- andesites, Andean region, petrogenetic composition variations 0-8313
- anisotropic elastic deformation, effective stress law, appl. to saturated porous rocks 0-51385
- Antarctic Peninsula igneous rocks, transverse geochemical vars. rel. to calc-alkaline magmas genesis 0-56466
- apparent resistivity changes under uniaxial compression (*Chinese*) 0-3995
- Archaean granite in Yellowknife, Northwest Territories, Canada, rare earth and trace element data 0-4007
- Archaean metamorphic rocks, Zijderfeld vector diagrams use in multicomponent palaeomag. studies 0-17420
- Arendal orthogneiss, geologically meaningless Rb-Sr total rock isochron 0-31014
- artificially fractured rock, heat transfer agents flow patterns 0-17239
- Mid Atlantic Ridge crest, geological and geophys. investigations 0-8284
- avalanches and landslides, mechanism based on law of dry friction 0-8314
- banding phenomena, calcs., nonlinear partial differential eqns. appls. 0-4510
- basalt, feasibility of geologic repository for nuclear waste 0-18479
- basalt, measurement of magnetic torque acting on rotating sample using air sample 0-31811
- basalt glasses from FAMOUS area, Mid-Atlantic Ridge, regional var. and petrogenesis 0-31041
- basalt-seawater interaction, trace element and Sr isotopic vars. in glassy basalt 0-8286
- basaltic pillars, in collapsed lava pools on deep ocean floor 0-3991
- basalts, oceanic, elec. resistivity meas. 0-21713
- basalts geochemistry from back-arc spreading centre, East Scotia Sea 0-3989
- basalts with xenoliths from S.E. Arizona, petrogenesis 0-8303
- bedrock freeze-thaw weathering in Colorado front range alpine zone 0-31039
- Berea sandstone, effects of pore fluids on bulk and shear attenuation 0-51386
- carbonate rock, interrelation of flow or fracture and phase transition during deform. 0-51389
- Carboniferous Limestone, in-situ seismic methods for crack anisotropy in NW.England 0-17240
- cleavage, morphological classification 0-21736
- complex resistivity meas. by freq. domain method (*German*) 0-4001
- composite dike geochemistry, magmas commingling model for coexisting acidic and basic melts 0-12391
- compressional and shear wave velocities under high press., effect of high-low quartz transition 0-12380
- compressional and shear waves in saturated rock during water-steam transition 0-30995
- compressional wave velocities at high temps. and press., rel. to crustal low-vel. zones 0-41435
- compressional wave velocity and damping, minerals and rocks at high-press. (*German*) 0-31031
- conglomerates of flat pebbles, stone rosettes, as indicators of ancient shorelines 0-26489
- crack growth and thermoelastic behaviour 0-26502
- crenulation cleavage, mechanical significance investigations 0-21737
- deep-sea basalts, clinopyroxenes chemistry statistical anal. 0-41437
- deep-sea basalts, He and Xe as measure of magmatic differentiation 0-31040
- deformability, determ. by in situ methods 0-17411
- deformation, fault slips, processes 0-8263
- deformation in brittle rock masses preceding earthquake rupture, failure models 0-8255
- deformation of foliated medium due to plane strain, theory 0-21720
- deformation under pressure, failure precursors, laboratory study 0-8298
- Denchai Basalt, N.Thailand, palaeomagnetism, age and geochemistry 0-41421
- diabase, dilatancy anisotropy and response to large cyclic loads 0-21715
- diabase, thermal expansion at high-press. 0-21719
- dilatancy anisotropy and response to large cyclic loads 0-21715
- dilatancy-magnetic effect to explain earthquake assoc. mag. variation (*Chinese*) 0-56374
- dunite, thermal expansion at high-press. 0-21719
- dyke strain relief meas. near mine working in Boksburg, S.Africa 0-17263
- elastic wave vel. before earthquakes 0-8256
- elastic wave velocity, brittle rocks undergoing deformation at high-press. (*German*) 0-36296
- Eltanin fault zone, Pacific Ocean, crustal struct. from petrographic data 0-12376
- fibrous dissemination, flat. characts. and models 0-4002
- fluid distrib. in partial melt, mech. and thermodynamic constraints 0-21685



## rocks continued

- Fohnsdorf tertiary basin, Styria, in situ tension measurements (*German*) 0-21665  
 folding of sedimentary rocks, Malaguide Complex, Spain 0-8312  
 folding stress outside buckled layers, theory 0-4003  
 fracture intensity, expressed as fracture surface area per vol. 0-8301  
 fracture measurement in laboratory, under geological conditions 0-46171  
 gabbro, compression expts., microcrack development and seismic vel. anal. 0-17250  
 Galesville sandstone, for compressed air energy storage appls. 0-30576  
 gas-oil-source rock masses, lithogenesis (*Russian*) 0-4006  
 geothermal saturated strata maintained by linear, ring batteries of wells, heat exchange 0-45630  
 grain orientation in sheared dispersion, appl. to sedimentary and igneous rocks 0-3420  
 granite, dilatancy anisotropy and response to large cyclic loads 0-21715  
 granite, feasibility for radioactive waste repository 0-18481  
 granite, thermal expansion at high-pressure 0-21719  
 granites from British Late Caledonian, O and Sr isotope ratios 0-36276  
 granites from Mt. Rokko, electron probe X-ray microanalysis 0-31038  
 granites microcracking and heating, new evidence from cathodoluminescence 0-51391  
 granites of Great Britain, Caledonian suture zone, geophys. correl. 0-17259  
 grandiorite, naturally deformed stress corrosion cracking of mica and feldspar 0-36299  
 granulitic outcropping, trace elements determination by thermal and epithermal neutron activation (*Portuguese*) 0-7874  
 hydrogen embrittling effects from acoustic emission meas. 0-11742  
 hysteresis effects under loading 0-21712  
 Icelandic igneous rocks, Mossbauer anal. 0-17253  
 ignimbrites with low aspect ratio, characters 0-41423  
 joints, mapping via photogrammetry and EDP appl. 0-56470  
 joints filled with wet clay, shearing at high-pressure 0-41438  
 Jurassic evaporites of Gulf of Mexico-Caribbean area, distrib. rel. to Permian-Triassic continental reconstruction 0-56431  
 Kiglapait intrusion, Labrador, influence of augite on plagioclase fractionation 0-12390  
 kimberlite and kimberlitic intrusives of SE Australia, review 0-51392  
 landslides following 1946 June 23 central Vancouver Island earthquake 0-21637  
 lavas from Archaean volcanism in Malartic Group, Abitibi, petrography and geochemistry 0-17258  
 limestone, thermal expansion at high-pressure 0-21719  
 lower mantle rocks Gruneisen parameter, evidence for approximation  $\gamma_p = \text{const.}$  0-3970  
 magmas, influence of volatile components 0-41418  
 magmatic, anchizone comp. 0-12381  
 mantle hydrous nodules 0-56420  
 mantle peridotite, high-temp. anelasticity and elasticity 0-17256  
 marble, diametral compressive testing method 0-35495  
 marble thermal expansion at high-pressure 0-21719  
 mechanical properties rel. to cooling (*Japanese*) 0-31036  
 lower metadiabase from Michigan Basin basement, preliminary petrological study 0-4009  
 metasedimentary sequence of N.Hill End Trough, NSW, metamorphism and deform. time relations 0-26510  
 mid-ocean ridge basalts, density var. rel. to magma mixing and primitive lavas scarcity 0-56460  
 migmatite rise, numerical expts. based on continuum dynamics 0-51381  
 migmatite tectonics, Hidaka metamorphic belt, Japan 0-8310  
 late Miocene shallow marine sediments, New Zealand, C isotope stratigraphy appl. 0-26479  
 Murnaghan constants evaluation as function of pressure 0-31037  
 mylonites, grainsize reduction and grain boundary sliding rel. to flow strength 0-21721  
 North Mountain Basalt, Nova Scotia, K-Ar isochron method for age determ. 0-3960  
 ocean basalt, seawater reactions, chemical exchange, Fe, Mn, and S species results 0-17294  
 oceanic crust basalt, U abundance, heat flow implications, fission track anal. 0-8287  
 oceanic tholeiites siderophile contents compared with lunar highland rocks 0-8562  
 oceanic upper mantle seismic anisotropy, evidence from ophiolite complex 0-21677  
 oil shale from Piceance Creek Basin, Colorado, permittivity by microwave radiation method 0-12378  
 Oklo natural fission reactors, temp. of mineral phase assemblages and rock textures 0-21722  
 Oklo natural reactors, fluid phases contemporaneous with sandstone diagenesis, and tectonic movements (*French*) 0-21746  
 ophiolite rocks of Samail, Oman, study of petrogenesis and hydrothermal alteration 0-46177  
 ophiolite suite, dynamothermal aureole of Bay of Islands 0-51355  
 ophiolitic peridotites structures, role of young lithosphere thrusting in subduction zones 0-56446  
 E.Pacific Rise, igneous rocks of young cratered volcanoes pair 0-12374  
 Parece Vela Basin, E.Philippine Sea, petrology rel. to evolution 0-41431  
 pebble abrasion studies 0-4004  
 picrite calculation of Gruneisen parameter and specific heat from measurements of US vel. 0-41436  
 piezo-magnetic effect to explain earthquake assoc. mag. variation (*Chinese*) 0-56374  
 piezomagnetic effect, lake ground loading, during filling 0-8346  
 Late Pleistocene tephra in South Island, New Zealand, identification and significance 0-8306  
 plutonic rocks from Whitehorse map area, Yukon, ages 0-31005  
 pore aspect ratio spectrum determ., seismic velocities inversion 0-51387  
 porous, dry and water-saturated, plane shock wave studies 0-21714  
 porous, self-consistent imbedding and ellipsoidal model 0-26503  
 potassic igneous rocks from Roccamonfina volcano, Roman comagmatic region, Italy., O isotope geochemistry 0-41420  
 pyroclastic flow deposits, utilisation 0-12365  
 quartzite, grain boundary and struct., analogue expts. using ice 0-21718  
 quartzite, Gruneisen parameter at high pressure 0-8299  
 quartzite, thermal expansion at high-pressure 0-21719  
 radioactive waste storage, Am sorption on major rock-forming minerals 0-13716  
 radioactivity of large volume geological samples, absolute activity determs. 0-56643

## rocks continued

- radiochemical neutron activation anal. of environmental matrices for Hg and noble metals 0-16889  
 reconnaissance using enhanced Landsat imagery 0-41568  
 rhyodacitic pillow lava and isolated-pillow breccia from Fishguard Volcanic Group, SW.Wales 0-12389  
 Sambagawa schist, Central Shikoku, Japan, relationship between albite porphyroblasts growth and deform. 0-26509  
 sandstone elastic wave velocity, function of moisture content 0-56459  
 Saxony Granulites, petrofabric anal. by optical and X-ray diff. studies 0-21740  
 Seal Group, Quebec, magnetisation study of igneous rocks 0-3918  
 seismic classification of rock mass qualities, vel. data 0-17248  
 seismic velocity of rocks, expts. on two-phase aggregates 0-56463  
 seismic wave attenuation in dry and saturated rocks, lab. meas. 0-3998  
 seismic wave attenuation in partially saturated rocks 0-3997  
 seismic wave attenuation mechanisms in dry and saturated rocks 0-3999  
 serpentinites, Glenrock, New South Wales, foliation development 0-21738  
 shatter cones, geometry and description procedure 0-51398  
 single-layer folds, shape at small but finite amplitude 0-56473  
 stressed rocks, crack induced anisotropy, effective elastic moduli and attenuation 0-56461  
 submarine lithosphere, geophys., geochem. and petrological model 0-3994  
 Swedish rapakivi suite, palaeomag. study rel. to Proterozoic tectonics of Baltic Shield 0-56346  
 tektites and natural glasses, N concs. 0-41446  
 Tertiary submarine gabbros and peridotites, Zijderfeld vector diagrams use in multicomponent palaeomag. studies 0-17420  
 texture goniometer for analysis of rocks 0-26630  
 thermal conductivity and thermal expansion, conference, Chicago, USA (Nov. 79) 0-31425  
 Tokyo, base rock, seismic explosion obs. (*Japanese*) 0-41403  
 transversely layered isotropic media, seismic wave vel. calcs. 0-12344  
 Uivak II gneiss from Saglek area, Labrador, zircon age meas. 0-3958  
 Ukrainian Shield, rock mag. props. map rel. to composition and metamorphism 0-17229  
 ultramafic, from Cr-rich areas, visible and near IR spectra, remote sensing appls. 0-4000  
 ultramafic partial melt fluid distrib. under hydrostatic stress, expts. 0-21716  
 uniaxially compressed rock cylinders, longitudinal splitting anal. 0-17249  
 vaporisation to elements, meteorite impact study 0-36583  
 volcanic, in Eiffel fields, pliocene and quaternary volcanic phases, K/Ar age determ. 0-46160  
 volcanic, Lesser Antilles island arc, palaeomagnetic and geochronological survey 0-8265  
 volcanic material alteration in marine sediments, SE.Pacific Ocean 0-3990  
 volcanic rocks of Marcus-Necker Ridge, comp. and stages of development 0-36282  
 wave propagation, frictional attenuation, amplitude depend. 0-31034  
 Westerly granite, stress-strain hysteresis loops shapes 0-26499  
<sup>13</sup>C/<sup>12</sup>C ratio in magmatic gases of Afar ridge volcanism 0-21732  
 Nd-Sr isotopic patterns rel. to petrogenetic mixing models 0-3965  
 Rb-Sr dating, deformation in Hellroaring Plateau area, Beartooth Mountains, Montana 0-17238  
<sup>34</sup>S/<sup>32</sup>S ratio in magmatic gases of Afar ridge volcanism 0-21732

## Roentgen ray see X-rays

## rolling

see also cold rolling

- bimetal rolling, calc. of strains by variational method (*Polish*) 0-45323  
 $\alpha$ -brass, recrystallisation texture, rel. to rolling temp. 0-11664  
 $\alpha$ -brass, texture, recrystallised orientation distrib. function comparison with 40°(111) rolling texture 0-25723  
 critical line nature in multiple-roll passes (*Russian*) 0-38347  
 cross-rolling and compression textures, numerical prediction 0-40382  
 deformation by lamination, hydrodynamic analogy, utilisation of current function (*French*) 0-19292  
 elastohydrodynamic film thickness, meas. of artificially produced dents and grooves 0-36975  
 elastoplastically deformed strengthened material, stress deformed state during rolling (*Russian*) 0-54299  
 Fe, cast, high Cr, hardfacing of roll, wear resistance and thermal durability 0-7686  
 inhomogeneous deformation model 0-48650  
 metal electroplastic deformation meas. pulse generator (*Russian*) 0-25931  
 metals, complex sections, unified anal. function of surface of strain focus (*Russian*) 0-21017  
 metals porous, mean principal stress in rolling without lateral expansion 0-25803  
 plasticity problem soln. by symbolic computer processing of formulae 0-17803  
 $\beta$ -poly(vinylidene fluoride) films, single cryst. orientation, piezoelec. 0-20591  
 polyethylene, lightly crosslinked, processed under mol. orient., transparent film prep. 0-38957  
 polymer solutions, high mol. wt., birefringence lines in elongational flow (*French*) 0-25337  
 porous metal gauze materials, struct. and hydraulic characts. 0-11729  
 profile measurement of hot rolled strip during hot rolling (*German*) 0-25929  
 shear band formation models, in rolling and extrusion 0-3152  
 square blank, rolling process, math. model based on plasticity theory (*Russian*) 0-16335  
 steel, 0.2 to 0.8% C, ferrite-pearlite transformation, tensile strength, cooling rate effect 0-7549  
 steel, 3Kh2V8F, brittleness depend. on high temp. deform. at high stress. temp. (*Russian*) 0-50698  
 steel, alloy, high speed, type R18, hot deformation and recrystn. 0-16391  
 steel, austenitic stainless, 08Kh18N10T, hot-worked precipitation kinetics and struct. of dispersed phases, Ti effect 0-29964  
 steel, C, isoforming and warm rolling, effect of mech. props. 0-11673  
 steel, C, naval, corrosion in harbour anaerobic sediments, rolling direction and tensile stress effects 0-30135  
 steel, C, naval, corrosion in natural seawater, rolling direction and tensile stress effects 0-30134  
 steel, C, pearlite grade ShKh15, struct. transformations, hot plastic strain influence (*Russian*) 0-20927



**rolling continued**

- steel, C and Ni-Cr surface hardened, rolling contact fatigue failure 0-16608  
 steel, correlation links between mech. props. 0-35234  
 steel, Cr (17 wt.%), stainless, hot-rolled texture, effect on cold-rolled and annealed textures 0-55425  
 steel, Cr-Ni, rolled and sintered, to produce capillary structured filter material, exam. of mech. props., and production 0-16235  
 steel, die, thermal fatigue resistance, high temp. thermomech. treatment effect 0-50715  
 steel, hollow cylinder, thick walled, effect of thermomech. treatment 0-11674  
 steel, hot rolled strip and plate shape meas. device 0-35498  
 steel, low C, effect of heat treatment on resistance to fatigue crack propag. 0-11675  
 steel, low C, Mn effect on recrystallisation and texture (*French*) 0-3110  
 steel, maraging, effect of deformation on props. 0-21032  
 steel, medium C 0-11752  
 steel, microalloyed, precipitation effect on microstruct. and mech. props. (*French*) 0-25708  
 steel, Mn-Mo-Ni-Cr, bainitic, microstructures and mechanical properties (*French*) 0-16362  
 steel, Nb, controlled-rolled into ferrite temp. range, soln. temp. and rolling effects 0-11678  
 steel, nonmetallic inclusion, effect on hot ductility 0-29999  
 steel, plastic deform. resist. during continuous hot rolling (*Russian*) 0-55462  
 steel, plastically deformed, force and speed criteria interactions during hot rolling (*Russian*) 0-55463  
 steel, plate, thickness and rolling ratio influence on inclusion behaviour 0-16340  
 steel, stainless, gas liberation in vac., effect of different methods of surface treatment (*Russian*) 0-45429  
 steel, V, high C, faceted Mn sulphide formation on crystn., thermomech. treatment effect on dendritic struct. (*Russian*) 0-50621  
 steel alloy, austenite transformation in hot rolled strips 0-55407  
 steel-Al bimetallic wire for overhead lines, manufacturing methods 0-16247  
 steels 45, 17G2AF, 55S2, 60S2, faceted Mn sulphide formation on crystn., dendrites (*Russian*) 0-50621  
 stress distrib. in rolled material 0-48651  
 strip rolling, kinetostatics (*Russian*) 0-38348  
 surface damage, plastic deformation cause in fatigue, wear, fretting and rolling fatigue 0-40537  
 surface damage eval. by X-ray diffr. technique (*Japanese*) 0-25892  
 Ag, recrystallisation texture, rel. to rolling temp. 0-11664  
 Al and Al alloy granules, hot rolling, angle parameters and forward slip 0-25601  
 Al-Cu-Mg, rolled plate fatigue charact. (*Russian*) 0-16437  
 Al-rare earth alloys, granules, rolling to form foil, exam. 0-20825  
 B fibre reinforced Al-Zn-Mg, packet rolling, thermodeform. process parameters (*Russian*) 0-55433  
 Be foil, nucl. target fabrication 0-23225  
 Cr bronze Sn, recrystn. props., hot rolling, annealing, polygonisation (*Russian*) 0-55419  
 Cu, recrystallisation texture, rel. to rolling temp. 0-11664  
 Cu+Fe+Cd, nucl. target preparation by evaporation and rolling 0-23224  
 Cu+Fe+Sn, nuclear target preparation by evaporation and rolling 0-23224  
 Fe powder, density distrib. in rolling deformation region 0-40288  
 Fe/Fe-Cr composite powder, X-ray diffr. exam. of densification during rolling 0-40289  
 Fe-Si (3 wt.%), chemical comp. and hot rolling effect on brittleness (*Czech*) 0-50712  
 Fe-Si-B, melt C content effect on grain growth and induction 0-35351  
 LiNbO<sub>3</sub>:Cr<sup>3+</sup> glass, roller quenched, crystn. kinetics 0-44143  
 Ni, high-purity, softening of strained single crystals (*Russian*) 0-40499  
 $\alpha$ -Ti alloy, rolled, elastic stiffness and Bauschinger effect accompanying anisotropic hardening (*Russian*) 0-40435  
 Ti-Al-V, rolled, elastic stiffness and Bauschinger effect accompanying anisotropic hardening (*Russian*) 0-40435  
 Ti-Nb-Zr (35, 3 wt.%), martensitic  $\tau$  phase, X-ray diffr. obs. 0-16300  
 V foil, nucl. target fabrication 0-23225  
 W, foil, nucl. target fabrication 0-23225  
 W wire from rolled rods, mech. props. and struct. 0-25743

**rolling mills**

- cold rolling mills, roll service life, rehardening by heat treatment 0-16347  
 steel, hot rolled strip and plate shape meas. device 0-35498

**roots of polynomials** *see polynomials***rotamers** *see rotational isomerism***rotating bodies**

- see also angular velocity measurement; centrifuges; gyroscopes; rotation*  
 1979 VA, precise posns., and rotation period from UVB photometry 0-17534  
 accretion disc in soft potential well, excess surface density ring form. 0-8532  
 387 Aquitania, slow spinning asteroid with rot. period of nearly one day, photometric evidence 0-17529  
 artificial satellite, spinning, symmetric, in planar periodic orbit, attitude stability 0-4220  
 asteroid, 1980 AA, rot. period observed photometrically 0-36558  
 asteroids, rotation rates, collisional evolution theory 0-17532  
 asteroids, rotation rates, pole positions and shapes 0-17531  
 asymmetric top rotational Brownian motion and electric polarisation calc. 0-15949  
 bar, gravitational field, and forced oscill. of resonant antenna 0-52090  
 776 Berbericia, slow spinning asteroid with rot. period of nearly one day, photometric evidence 0-17529  
 black hole, light propag. and sky appearance from accretion disc 0-17605  
 black hole and accretion disc seen by non rotating observers, light propag. 0-17606  
 black holes, nonsymmetric disc accretion (*Russian*) 0-36661  
 brittle disk, probability theory appl. to rupture strength 0-43662  
 3C 33, 98, 184.1 and 218, rotation axes 0-26997  
 952 Caia, rot. period and light curve from photoelectric obs. 0-46454  
 cantilever, stability and instability conditions, Lyapunov function method (*Russian*) 0-36840  
 circular cylindrical elastic membranes bifurcation 0-33494

**rotating bodies continued**

- creep analysis of rotating orthotropic disks 0-33476  
 dynamic balancing, influence coefficient method, balancing of rigid rotors 0-53724  
 elliptical galaxies, three-dimens. shapes 0-51868  
 elliptical galaxy rotation curve determ. 0-46675  
 182 Elsa, photoelec. light curve and rot. period of asteroid 0-56750  
 247 Eukrate, UVB photometry, light curve and rot. period 0-21942  
 galactic bar, isolating integrals of motion for stellar orbits 0-4404  
 galaxies, dissipation and merging rel. to rotation 0-4444  
 galaxies, extent of bars rel. to inner Lindblad Resonance and corotation radius 0-46666  
 galaxies, flat, with double-peaked rot. curves, spiral struct. generation 0-46679  
 galaxies, mass and ang. momentum, statistical relations 0-8689  
 galaxies, N-body simulation 0-17670  
 galaxies, nonlinear stability theory for rotating gravitating disc 0-17488  
 galaxies, rot. curves rel. to stellar disc central density min. 0-17663  
 gas-dust clouds, mass transport processes rel. to solar system origin 0-8556  
 gyrostat, reorientation 0-8780  
 gyrostats, kinetic energy bounds 0-46793  
 heavy gyrostat, steady motion stability for free and restrained dynamical systems 0-46791  
 IC 5152, low-luminosity barred galaxy, struct., rot. curve and redshift 0-56950  
 ionized medium, technique for rot. freq. meas. 0-41730  
 isothermal disc, heat transfer meas. using Mach Zehnder interferometer 0-38223  
 Jupiter, natural vibration spectrum, rot. effects, calc. 0-8583  
 22 Kalliope, pole coordinates from photoelectric photometry 0-31230  
 Kelvin, background, teaching motivation, demonstrations 0-42025  
 Mars, rot. model, including precession and nutation 0-21938  
 Mars, rotation theory in Euler angles 0-51684  
 mechanical resonance,  $J_0(x)$  obs. on reson. rot. vertical chain 0-42006  
 9 Metis, pole coordinates from photoelectric photometry 0-31230  
 9 Metis, UVB photometry, light curve and rot. period 0-21942  
 NGC 612, rotation of lenticular radio galaxy 0-51874  
 nonholonomic systems under external influences, sledge on incline, gyroscope in cup (*Russian*) 0-52011  
 44 Nysa, pole coordinates from photoelectric photometry 0-31230  
 orthotropic rotating discs, flexure, stresses and deflection 0-5927  
 118 Peitho, rot. period and light curve from photoelectric obs. 0-46454  
 Periodic Comet Encke, spin axis precession, nongravitational motion and sublimation 0-46483  
 Periodic Comet Halley, rotation period from halo diameter meas. 0-51694  
 planets, rotation resulting from accumulation process, numerical expts. (*Russian*) 0-8557  
 308 Polyxo, photoelectric lightcurves and rotation period 0-46455  
 790 Pretoria, C-type asteroid, light vars. obs. and rot. period 0-21941  
 protostellar clouds, ring form. during dynamic collapse 0-56820  
 protostellar gas clouds, fragmentation 0-51827  
 pulse phenomena produced by a flat mass on one of its supports (*Italian*) 0-4514  
 rectangular prismatic bodies, free motion, translatory and auto-rotating modes 0-43605  
 rotor dynamics analysis using tapered beam finite element 0-38316  
 Saturn, natural vibration spectrum, rot. effects, calc. 0-8583  
 shell subjected to centrifugal force, stress anal. (*German*) 0-23900  
 140 Siwa, C-type asteroid, light vars. obs. 0-21941  
 solid body dynamics with one fixed point, inverse problems (*Russian*) 0-52010  
 spacecraft, eigenvalue problems solution, with real symmetric matrix of same dimension 0-12895  
 spin 1/2 plane waves interacting with rot. body, gravitational scatt. helicity depend. (*German*) 0-52088  
 spindle unit on test stand, wheel failure 0-19277  
 spiral galaxies, max. rot. vel. rel. to morphological type in stochastic star form. model 0-12818  
 87 Sylvia, UVB photometry, light curve and rot. period 0-21942  
 symmetric gyroscope motion, differential eqns. stabilisation procedure including perturbing torques 0-4244  
 88 Thisbe, photoelectric light curves and rotation 0-17528  
 variational principle for spinning liquid-filled solid bodies 0-43609  
 Venus, free wobble damping time 0-17516  
 Venus, spin evolution 0-46423  
 Venus, tidal theory and torque balance 0-46422  
 viscous liquid filled cavity in solid, free rotational motion 0-38420  
 wind turbines, rotational dynamics, eval. of turbine response to wind speed changes 0-55785  
 He, cryostat, rotating, centrifugal field rel. to residual press. in vac. cavity 0-42232

**rotation**

- see also angular velocity measurement; Earth rotation; molecular rotation; optical rotation; rotating bodies; rotational flow; stellar rotation*  
 asteroids shape and spin axis orientation determination, photometric method (*Russian*) 0-8581  
 astronomical systems, ang. momenta mass depend. rel. to self-similarity 0-36490  
 fluid, binary mixture, in centrifugal field, crit. dynamics 0-44310  
 galactic halo, rot. from subdwarf kinematics 0-22003  
 galaxies, bright, elliptical, effect of form. by merging on rot. 0-56922  
 galaxies, spiral, rot. direction determ. by means of edge-on systems (*Russian*) 0-36722  
 galaxies rotation, contrib. from galaxy merging 0-4439  
 Galaxy H I subsystem, rot. curve (*Russian*) 0-36724  
 Galaxy rotational spiral struct. parameters, derivation from stellar kinematics 0-17665  
 Galilean satellites volcanism and rotation, influence of Jupiter mag. field 0-31247  
 gases, rot.-vibr. Raman spectrosc., high resolution, review 0-22442  
 hadrons, uncharmed, rotational states 0-22596  
 infinitesimal operators of translation and rot., dynamic eqns. lineage 0-17788  
 interplanetary magnetic field, imperfect corotation as source of cosmic ray semidiurnal var. 0-8497  
 Jupiter atmosphere, origin of differential rot. 0-46467  
 Liapunov's periodic motions at heavy rigid body with fixed point (*Russian*) 0-22190



**rotation continued**

- M31 nuclear bulge, rotational vels. meas. 0-41888  
 M33 rotation curve, influence of warped optical phase 0-56944  
 Neptune rotation period, effects of seeing on reflected spectrum 0-46479  
 NGC 5128 (Centaurus A), disc rot. curve rel. to galaxy struct. and evolution 0-4429  
 NGC 520, Irr II galaxy, new photographic and spectroscopic obs. 0-41889  
 Orion Molecular Cloud, rotational explanation of high-vel. mol. emission 0-36688  
 rigid body translational-rotational motion in gravit. field of sphere, Poincaré periodic solns. of third kind 0-46377  
 rotor, linear (triaxial) (asymmetric), action-angle variables in quantum mechanics 0-31543  
 sample rotation, biaxial, in supercond. solenoid (*Czech*) 0-37010  
 Saturn atmosphere, origin of differential rot. 0-46467  
 steady motions of complex rotating systems, computational anal. 0-53618  
 Uranus, rot. period spectroscopic determ. 0-51691  
 Uranus rotation period, effects of seeing on reflected spectrum 0-46479  
 Venus rotation, possible dynamical evolution since formation 0-56742  
 KCN:HCN<sup>+</sup>, structural props. using ESR 0-25205

**rotation by magnetisation** *see Einstein-de Haas effect***rotational flow***see also vortices*

- abruptly rotated cylinder, turbulent boundary layers, numerical anal. 0-43716  
 air flow, turbulent, in infinite medium spatial speed distrib. (*Rumanian*) 0-53826  
 air-water surfaces, turbulence characts., mass transfer and eddies 0-14665  
 annular diffuses with conical walls, swirling flow and separation 0-43715  
 annular flow, vel. distrib., expt. determ. 0-38510  
 asymmetric Stokes flow from closed torus in quiescent viscous flow 0-43719  
 asymptotic drag formulas for rapidly rotating radial channels of rectangular cross section 0-6065  
 atmosphere, effects of Earth rot. rate vars. rel. to climate 0-4097  
 baroclinic fluid, rapidly rotating, sine-Gordon eqn. model 0-46820  
 Bodewadt flow, spin-up, angular momentum adjustment 0-28511  
 body-propeller combination, numerical soln. including swirl and data comparisons 0-19407  
 centrifuged flow with recirculation, book contrib. 0-1604  
 coaxial circular discs, hydrodynamical problem 0-24032  
 coaxial cyclone flow, heat transfer from a cylinder 0-48698  
 compressible atmosphere, vertically rotating, critical levels 0-6073  
 compressible finitely conducting rotating fluid in mag. field, Rayleigh-Taylor instability 0-10228  
 conducting fluids, dynamics under rotational mag. forces 0-48820  
 convective flows in spherical shell, bifurcation and stability 0-28507  
 cryostat, rot. vap. column flow anal. 0-4722  
 cyclone flow, boundary layer on cylindrical insert surface 0-10251  
 Czochralski bulk flow in the growth of garnet crystals 0-38979  
 diffusive instabilities in rotating elec. conducting compressible layers 0-38379  
 disc, inviscid cell chain with viscous interlayers 0-53794  
 disc, rotating, convective mass transfer 0-43707  
 disc in viscous fluid, deceleration 0-28515  
 disc rotating in fluid with surfactant surface layer 0-10284  
 ducts, eddy motions induced by water waves and periodic flows 0-33679  
 dynamo action associated with random waves in a rotating stratified fluid 0-33687  
 Ekman layer, mechanically induced unsteady compressible, theory 0-24033  
 energy stability for the flow between rotating, coaxial disks 0-14712  
 ferrofluid constitution examination by rotating test tube method 0-33693  
 ferrofluid devices, magnetostatic and centrifugal, nonmagnetic body motion 0-33700  
 ferrosuspensions, internal rotations and the other transport phenomena 0-28573  
 finite shrouded disc, laminar boundary layer in rot. compressible isothermal flow 0-43727  
 flow past porous plate, rotation effects 0-10256  
 fluid, perfect, 3-dimens. rot. flow, Lagrangian invariants appl. 0-43720  
 free oscillation in a rotating spherical shell 0-19409  
 free shear layer behavior in rotating systems 0-1545  
 fully developed turbulent channel flow, perturbation propag. in viscous sublayer and wall region 0-19513  
 gas centrifuge, numerical anal. of weakly compressible rotating flows 0-47726  
 generalised Benard problem for stratified fluid, rotation effects 0-24031  
 geostrophic flows in rapidly rot. gases, thermally insulating boundaries, Ekman and Stewartson layers 0-14711  
 heat and mass transfer from rotating disk with sink flow 0-19402  
 horizontal rotating fluid layer, heated from below, convection rolls nonlinear props. 0-6066  
 hydrodynamic resistance and heat exchange from flow past rotating cylinder (*Russian*) 0-1586  
 hydromagnetic convection, thermally driven, in rapidly rotating sphere 0-14548  
 hydromagnetic penetration in a rotating fluid, fluid fluctuations 0-14839  
 inclinable pipe, suspension in turbulent flow, Markovian model, eddies 0-48790  
 incompressible turbulence, statistical investigation of eddy viscosity 0-14675  
 internal flows with initial swirl, generated heat and mass transfer law 0-24025  
 jet, axisymmetric free shear flow with Reynolds stress closure 0-19469  
 laminar swirling flow, integral method of anal. (*Japanese*) 0-28512  
 large eddies in wake and turbulent boundary layer, vel. fluctuations 0-24036  
 laser heated nozzle flow with swirl, axisymmetric comp. boundary layer 0-14775  
 liquid filled spinning spheroids, stability via Liapunov's second method 0-48677  
 magnetic fluid in rotating vessel, flow in homogeneous mag. field 0-33691  
 magnetisable fluid, motion in rotating homogeneous mag. field 0-28572  
 magnetohydrodynamic flow between rotating and stationary porous coaxial discs 0-43799

**rotational flow continued**

- MHD, gas boundary layer swirling nozzle and diffuser flows with mag. field 0-1693  
 MHD, heat transfer between porous discs, one rotating one at rest 0-28561  
 MHD Ekman layer on free convection past infinite porous flat plate 0-14830  
 MHD shift flow, in strong field, of viscous fluid 0-28576  
 MHD stratified flow between oscillating disks, boundary layers 0-28570  
 MHD turbulent boundary layers in rot. circ. vessel, drag 0-33697  
 micropolar liquid between two infinite slowly rotating discs 0-53796  
 non-isothermal disc rot. in quiescent compressible gas, heat transfer 0-14704  
 noninertial particle transfer to rotating in laminar flow under external force field 0-10250  
 nonlinear axisymmetric flow between concentric rot. spheres, numerical anal. 0-19412  
 nonstationary convection in a rotating system, book contrib. 0-1593  
 nonstationary eqns. soln., appl. to flow between discs 0-28516  
 ocean, wind-driven flow in zonal channel on rotating Earth 0-51402  
 plates, eddy motions induced by water waves and periodic flows 0-33679  
 polymers, unsteady flow in rotary devices 0-24061  
 quasiperiodic flow between rot. cylinders, second charact. mode visualisation 0-28519  
 radial turbomachine, meridian plane characts. for subsonic and transonic flow, finite element calcs. (*French*) 0-38418  
 radially progressive surface waves from rot. circular cylinder 0-14722  
 Rayleigh-Taylor instability in presence of rotation 0-53749  
 recirculating flow behind backward-facing step, mean vel. and Reynolds stresses meas. 0-19355  
 rectangular channels, heat transfer, press. drop calcs. (*German*) 0-1594  
 relativistic case, centre of stationary rotating star, tetrad formalism 0-53888  
 Rossby wave interactions and stability in rot. two-layer fluid on  $\beta$ -plane 0-10257  
 Rossby waves in rotating annulus, laboratory and theoretical study (*Russian*) 0-19509  
 rotating disc in polymer solutions under a turbulent regime 0-33634  
 rotating spheres, heat transfer coeffs. for gas-solid two-phase flow 0-19369  
 shock and detonation wave anal. 0-53792  
 slow viscous flow due to motion of sphere on axis of circular cone 0-14654  
 slowly rotating sphere submerged in fluid with surfactant surface layer 0-48717  
 sound wave, effect of rotation on flow past flat plate due to standing sound field 0-24028  
 sphere, nonconducting, slowly rotating in steady MHD flow, exact soln. 0-33695  
 spherical annulus flow, torque characts., secondary flow effects 0-43718  
 spherical Couette flows, loss of stability between two rotating spheres 0-1527  
 spheroid, slow motion in rotating fluid 0-14710  
 spinning yawed axisymmetric body, three-dimens. flow 0-38422  
 spiral flow between coaxial cylinders, branching and stability loss 0-19406  
 stability problems with time-depend. boundary conditions, numerical simulation methods, review 0-19411  
 stationary disc in rotating cylinder, laminar compressible flow 0-43728  
 steady and unsteady, fluid in finite cylindrical container 0-14708  
 steady flow between a rotating circular cylinder and fixed square cylinder 0-24035  
 steady streaming induced between oscillating circular cylinders 0-1602  
 stratified Boussinesq fluid, in rotating spherical annuli, small Reynolds number convection 0-6047  
 stratified rotating fluid, mass transfer between layers causing vortex 0-12401  
 streamline patterns and eddies in low-Reynolds-number flow 0-33612  
 subsonic turbulent jet, entry zone flow wave struct., eddies 0-14773  
 superfluid, gauge wheel of superfluid <sup>3</sup>He, two fluid model 0-44379  
 swirling turbulent flow in cylindrical channels, heat and momentum transport, local props. 0-14819  
 swirling or axisymmetric flow, meas. using press. difference meter 0-10330  
 symmetric flow between concentric spheres (*German*) 0-1609  
 Taylor column irregularity in rapidly rotating MHD fluid, mag. field effects 0-43786  
 Taylor instability, transition to turbulence 0-28491  
 throughflow between rotating and stationary disk calc., laminar, finite difference method appl. (*Japanese*) 0-6064  
 torsionally oscillating impermeable disc and stationary naturally permeable disc, flow streamlines 0-24030  
 turbulence, non isotropic homogeneous, pure rotation influence (*French*) 0-33568  
 turbulent flow, annular, with inner cylinder rot., computation 0-1544  
 turbulent thermal convection in presence of rot. and mag. field, stellar and planetary dynamos appl. 0-6042  
 turbulent two-dimens. recirculating flow, numerical model calcs. 0-19358  
 turbulent wake of axial flow turbomachinery rotor blades, numerical anal. 0-1596  
 two coaxial cylinders, fluctuating flow and heat transfer for incompressible fluid 0-24013  
 two-phase flow, annular, crit. heat flux, swirl effect 0-10113  
 unsteady flow arising from rotating fluid above a fixed plane 0-24029  
 unsteady MHD flow in rotating system, Hall current effects 0-33704  
 velocity distrib., wall friction in rotational turbulent laminar boundary flow (*German*) 0-1526  
 viscoelastic flow past stationary and rotating cylinders 0-43744  
 viscoelastic fluid, steady flow and heat transfer between two coaxial rot. discs 0-14755  
 viscoelastic liquid, heat transfer in rot. flow, suction and injection effects 0-33596  
 viscous flow between rotating discs with injection on the porous disc 0-14713  
 viscous fluid flow due to rotating torus 0-43713  
 viscous fluid in rotating channel pulsatile flow 0-10311  
 viscous liquid filled cavity in solid, free rotational motion 0-38420  
 viscous toroidal eddy generation in cylinder, Stokeslet streamlines 0-19404



**rotational flow continued**

- vortices formation near reson. for elastoid-inertia waves 0-12473  
<sup>4</sup>He, superfluid rot. film, melting of two-dimensional vortex lattices 0-2539

**rotational isomerism**

- 1,3-butadiene-1-one, spectroscopic consts., IR and microwave spectra, prep. 0-18859  
 S,S'-dimethyldithiocarbonate, pot. for rot. about C(sp<sup>2</sup>)-S bonds, electron diff. obs. 0-23572  
 acetaldehyde, first triplet state geometry, fragmentation into free radicals 0-47915  
 anilines, substituted, in benzene soln., dielectric relax. time, dipole moment 0-50259  
 anilines, substituted, in nonpolar solvent, dielec. relax. obs. 0-55022  
 benzaldehydes, o- and m-substituted fluoro- and chloro- forms, rot. isomerism, n<sub>r</sub>\* spectra obs. 0-5631  
 benzyl fluoride, mol. struct., NMR and gas electron diffraction obs., ab initio and mol. mechanics calcs. 0-23574  
 chloromethyl formate(-d<sub>1</sub>,d<sub>2</sub>,d<sub>3</sub>), gas, solid. and liq., IR spectra assignments and struct. 0-32715  
 meso-2,3-dibromo-1,4-dichlorobutane, rot. isomerism, IR and Raman spectra 0-981  
 dibutyl-phenyl-benzoyloxy-benzoate, nematic liq. cryst., rot. barrier, PCiLO and CNDO/2 calcs. 0-33874  
 1,2-dichloroethane, conformer equilibrium by effusive beam-matrix IR spectroscopy 0-48100  
 1,2-difluoroethane, internal rotation temp. frozen in supersonic jet, matrix IR spectroscopy 0-9594  
 dihydroxycarbene, singlet and triplet state rot. pot. surfaces 0-32627  
 2,3-dimethylbuta-1,3-diene, IR, Raman spectra, torsional pot. function, thermodynamic function 0-43046  
 dithioformic acid, pot. for rot. about C(sp<sup>2</sup>)-S bonds, ab initio calc. 0-23572  
 ethyl methyl sulphide, low freq. vibr. spectra, methyl torsional pot. functions and internal rot. 0-5543  
 ethylene(-d<sub>4</sub>), Rydberg states assignments, electron energy loss spectra 0-53153  
 ethylmethanamine, low freq., vibr. spectra, methyl torsional pot. functions, mol. struct. 0-43045  
 Hamiltonian of a molecular type system with internal rotation 0-18842  
 methanol-d<sub>1</sub>(-d<sub>4</sub>), far-IR internal rotation spectrum 0-47989  
 methyl group hinderance barrier, spin-rot. relax. times 0-53011  
 methyl groups in solids, tunnelling freq. for internal rotation in pot. function 0-49134  
 methyl nitrate, internal rotation temp. frozen in supersonic jet, matrix IR spectroscopy 0-9594  
 methyl vinyl sulphide, syn-gauche equilb., force field and ab initio calcs., microwave and Raman spectra 0-23573  
 N-methylformamide, cis-isomer rot. struct., IR absorpt. spectrosc. obs. 0-14138  
 micellar interface, reaction kinetics, rotamer population, fast proton transfer 0-26050  
 monothioformic acid, pot. for rot. about C(sp<sup>2</sup>)-S bonds, ab initio calc. 0-23572  
 PAA, nematic liq. cryst., rot. barrier, PCiLO and CNDO/2 calcs. 0-33874  
 phospholipids, <sup>31</sup>P NMR, slow-motional lineshapes for very anisotropic rot. diffusion 0-5644  
 polymer chain dynamics, ang. correl. function decay by multiple rot. pot. diffusion 0-3569  
 transition metal complexes, mol. dissymmetry, book 0-27057  
 tri-i-propylgermylamine, and isotopomers, IR and Raman spectra, normal coord. anal. (German) 0-32716  
 tri-t-butylstannylamine, and isotopomers, IR and Raman spectra, normal coord. anal., Mossbauer spectrum (German) 0-32716  
 triethylsilylamine, and isotopomers, IR and Raman spectra, normal coord. anal. (German) 0-32716  
 trifluoroacetates, methyl and ethyl, intramol. relax. at microwave freqs. 0-55020  
 vibrational level classification by Longuet-Higgins group 0-43030  
 vinyl isocyanate, and vinylcyano ether, geometry and conform., ab initio minimal STO-3G MO calcs. 0-23337  
 vinyl mercaptan -d<sub>0</sub>, -d<sub>1</sub>, anti rotamer, conform., microwave spectrum 0-9592  
 vinyl mercaptan -d<sub>0</sub>, -d<sub>1</sub>, synrotamer, conform., microwave spectrum 0-5535  
 2-vinylanthracene, conform. conversion kinetics, fluoresc. 0-9631  
 vinylcyano ether, and vinyl isocyanate, geometry and conform., ab initio minimal STO-3G MO calcs. 0-23337  
 N<sub>3</sub>H<sub>3</sub> radical, lowest two electronic states 0-925  
 PtCl<sub>2</sub>(NH<sub>3</sub>)<sub>2</sub>, cis- and trans-isomers, electronic struct., SCF-X $\alpha$  study 0-18795  
 SH<sub>3</sub><sup>+</sup> geometry and inversion barrier, basis set depend. 0-921

**rotator phase in solids** see nuclear magnetic resonance; plastic crystals

**rotatory dispersion power** see optical rotation

**rotors**

- <sup>4</sup>He, superfluid, one phonon excitation spectrum and interaction pot. 0-54455  
 superfluidity, model Hamiltonian 0-44377  
 o-D<sub>2</sub>, solid, up to 150 kbar, 5K, Raman spectrum 0-50332  
 H<sub>2</sub>, solid, rotational excitations, higher order effects 0-6591  
 He, film, superfluid props. 0-34270  
 He II, superfluid, single atom neutron scatt. and two roton connected state branches (Russian) 0-44381  
 He, liquid, short-wave surface excitation study using electron gas non-linear I-V characts. (Russian) 0-10717  
<sup>3</sup>He-<sup>4</sup>He, liquid mixture, second sound, quantised vortex creation at constrictions, excitation model 0-44383  
<sup>3</sup>He-<sup>4</sup>He, superfluid soln., dil., low temp. props., book contrib. 0-15330  
<sup>4</sup>He film, adsorbed, few atomic layers, excitations, two-dimensional roton. 0-39381  
<sup>4</sup>He, liq., neutron scatt., book contrib. 0-2230  
<sup>4</sup>He, superfluid, excitation energy spectrum, roton contrib. 0-24699  
<sup>4</sup>He, superfluid, pressurised, vortex nucleation by neg. ions, thermal roton influence 0-10721  
<sup>4</sup>He, superfluid, two-dimens., microscopic theory, excitation spectrum and thermodynamics props. 0-24709  
<sup>4</sup>He, superfluid, viscosity and thermal conductivity (Russian) 0-10720

**rotors**

- bicycle rotors for vertical axis wind turbines, design and performance 0-30367  
 coil planetary motion, angular velocity control method 0-42202  
 Coriolis ocean turbine energy system status 0-45628  
 cryoturbogenerator transition process simulation, cryostat damping casings electrical characteristics determination (Russian) 0-8996  
 dynamics analysis using tapered beam finite element 0-38316  
 flywheel energy storage interface unit for photovoltaic applications 0-30571  
 flywheel energy storage system, rotating flywheel in an evacuated casing 0-30570  
 flywheel energy storage system 0-30569  
 flywheel rotor design utilising natural cellulosic materials for energy storage appls. 0-30568  
 flywheel rotor with high energy density for energy storage 0-30565  
 flywheels, development of low loss magnetic bearings, for energy storage appls. 0-30566  
 flywheels, performance of retainerless bearings for vehicular energy storage appls. 0-30567  
 gas turbine, vibration contactless meas. system (Russian) 0-8982  
 gyroscope, scanning laser based vibration detector (Russian) 0-22351  
 steel, Ni (3.5 wt.%), heavy rotor forgings, temper embrittlement, metallurgical investigations (German) 0-16471  
 transonic compressor, single-stage, flow measurement using 2-probe synchronised sampling technique, calibration 0-14865  
 wind-operated, reciprocating water pump, stroke adjusting mechanism for rotor speed control 0-50930

**roughness measurement** see surface topography measurement

**vibronic levels** see molecular rotation-vibration

**RPA calculations**

- anisotropic paramagnet, statistical mechanics using second order Green's function theory 0-25074  
 atom, open-shell, 1st order transition matrices calc., graphical method in RPA 0-47846  
 atoms, collective dynamics, hydrodynamic approach and many body approach based on RPA calcs. 0-47855  
 atoms, photoionisation, multichannel relativistic RPA calcs. 0-9570  
 borazine, triplet instability, RPA calculations 0-27938  
 Bose gas, two-dimens., charged, in zero mag. field, dielec. response 0-142  
 CDW dynamics in presence of free carriers 0-6760  
 chemical bond energy, ground state correlation energy 0-47847  
 collective excitations from high-q electron scatt., RPA AND ATDMF calcs. 0-22673  
 cooperative Jahn-Teller T-systems dynamics vibronic excitation branches 0-10934  
 coupled bands in even-even nuclei in RPA approach 0-32143  
 degenerate electron liquid, compression modulus, perturbative calc. 0-36942  
 electron correlations in solids, local approach 0-29344  
 electron gas, semi-infinite, nonlocal cond. tensor calc., effective optical surface region 0-20283  
 excited nuclei, self-consistent theory of giant dipole resonance, thermodynamic RPA (Russian) 0-5106  
 formaldehyde, triplet instability, RPA calculations triplet instability, RPA calculations 0-27938  
 Heisenberg ferromagnet, isotropic, second-order Green's function theory 0-2578  
 Heisenberg-Mattis model, long-wavelength dynamic response 0-20409  
 high spin states and band coupling, theory and heavy ion expts. (Russian) 0-18160  
 inert gases, outer shell photoionisation, relativistic RPA calcs. 0-9571  
 inert gases, photoabsorption to bound state and photoabsorption to continuum state (ionisation), comparison, HF calcs. 0-47910  
 inert gases, photoelectron spin polarisation, ab initio calcs. 0-18833  
 Ising, quenched dil. random-bond model, CPA difference eqn. and crit. curves 0-2584  
 isoscalar effective charge in large A limit Tamm-Dancoff and RPA calcs. 0-42534  
 isoscalar giant quadrupole resonances, RPA calcs., E2 strength fragmentation, spectroscopic factors 0-13437  
 linear aggregates, small, polarisability determ., CNDO method and analytical models (French) 0-29298  
 linear response and Hartree-Fock, coordinate space representation and gradient iteration 0-18216  
 liquid, simple, equilb. theories, review 0-38887  
 liquid structure function evaluation, using optimised cluster expansion 0-49085  
 molecules, chemisorbed on metal surface, spectrosc., electron gas effects 0-54504  
 multicomponent electron-hole plasma correlation energy by RPA and mean component approx. calc. 0-24824  
 nuclear form factors of 0<sup>+</sup>-0<sup>-</sup> transition in A=16 system, nuclear struct. effects 0-18246  
 nuclei, transitional, pairing rotations and quadrupole modes 0-18165  
 open shell nuclei by seniority and reduced isospin projections 0-47415  
 open shell RPA unitary group formulation, Hartree Fock stability eqns. 0-52860  
 plasma, complex dielectric function long wave limit, Coulomb systems with bound states, elec. cond. 0-33738  
 plasmon dispersion, correlation correction 0-43917  
 quasi-one-dimensional solid, CDW distorted, macroscopic dielec. function 0-39515  
 relativistic, appls. to He-like ions energy levels and Mo<sup>30+,12+</sup> photoionis. 0-47913  
 relativistic effects in oscillator strength calculations, ab initio methods 0-9519  
 relativistic RPA development from linearised time-depend. HF theory 0-47925  
 Rochelle salt, ferroelectric phase transition, external field induced 0-29700  
 semiconductors, electron-hole liquid 0-6743  
 spin systems, coupled itinerant localised systems, dynamic magnetic response 0-34583  
 surface, positron-electron correlations, RPA calc. 0-40181  
 s-triazine, triplet instability, RPA calculations 0-27938  
 TTFcCuBDT, spin-Peierls transition in spin 1/2 Heisenberg chains, RPA calcs. 0-25150  
 Ar, ns- $\rightarrow$ ep photoelectrons, spin polarisation 0-37792



**RPA calculations continued**

- Ar, Raman scatt., single particle HF approx. and RPA many-electron correlations calcs. 0-23374  
 Ge, electron-hole droplets, luminesc. and absorpt. lineshapes, RPA theory 0-49613  
 He( $2^1S$ ), inelastic scatt., RPA and 1st Born approx. calcs. 0-53148  
 HeCo<sub>2</sub>, ground state spin excitations, inelastic neutron scatt. study 0-50077  
 K, Pauli susceptibility and Knight shift meas., electron wave functions 0-44937  
 Kr, ns- $\epsilon p$  photoelectrons, spin polarisation 0-37792  
 N<sub>2</sub>, Raman intensity, ab initio calc. 0-1028  
<sup>15</sup>N( $n,n'$ )<sup>15</sup>N, continuum random phase approx. 0-27635  
 Nb-Mo system, electron-phonon coupling const. and supercond. transition temp., average T-matrix approx. 0-39707  
 Ne, autoionising resons. near 575 Å, ab initio relativistic RPA calc. 0-32681  
 Ne, isoelectronic sequence, excitation energy and oscillator strength, level crossing anomaly, relativistic RPA calc. 0-14077  
<sup>16</sup>O collective and giant multipole states, Brueckner RPA particle-hole state description 0-32169  
<sup>16</sup>O, pion condensation effects, RPA calcs. (Chinese) 0-47407  
 Se, trigonal, dielec. matrix calcs. 0-54630  
 Si, continuum-exciton effect in optical spectrum 0-25416  
 TbP, singlet-groundstate magnetism, static mag. props. 0-7109  
 TbY<sub>1-x</sub>Sb<sub>x</sub>, elec. resist., cryst. field and exchange interaction contribs. 0-39556  
 Te, trigonal, dielec. matrix calcs. 0-54630  
 Xe, ns- $\epsilon p$  photoelectrons, spin polarisation 0-37792  
 Xe, photoelectron studies of 5p branching ratio 0-37793

**rubber**

- see also rubber industry*  
 balloon bursting under biaxial strain, tear behaviour 0-19287  
 biaxial deformation of rubber-like solids 0-1431  
 binary polymeric mixtures, soln. viscosities meas. 0-54423  
 butyl rubber, resin cured, filled, relaxation study (German) 0-35243  
 composites with asbestos, classification 0-7484  
 cylinder, effect of stretch on wave speed 0-1467  
 elasticity, network entanglement contrib. 0-39203  
 elasticity, props. prediction on basis of microscopic structure, small angle neutron scattering appl. 0-3113  
 filled, light scatt. by strains, theory and expt. 0-28162  
 filled epoxy polymers, dense-woven, fracture characts. 0-11757  
 filled rubber, stress/strain behaviour at moderate strains 0-38293  
 friction of rubber containing CuSO<sub>4</sub> paired with steel, selective transfer mechanism 0-55544  
 gasket inspection, US system, gas pipe appl. 0-30178  
 graphite filled, performance assessed against steel structures under water lubrication conditions 0-21123  
 latex+free polymer, dispersion flocculation, equilib. anal. 0-45574  
 latex sphere aggregates, dynamic shape factors determ. by sedimentation vel. meas. in capacitor 0-26063  
 mixture, wear determ. device 0-21226  
 natural rubber latex <sup>13</sup>C NMR spectra 0-15816  
 network, crosslinks and trapped entanglements, two-network model 0-38962  
 network, elasticity, mol. theory 0-38290  
 network, finite linear viscoelastic theory, time-depend. deform. behaviour 0-38292  
 network, highly swollen, long time dynamics 0-38291  
 nitrite, heat ageing, light scatt. method study (Russian) 0-40407  
 nonGaussian theory, under biaxial strain, mech. props. 0-16366  
 nonGaussian theory, under biaxial strain, optical props. 0-16367  
 partially hydrogenated, <sup>13</sup>C NMR 0-20472  
 penetrant diffusion, statistical mech. model 0-44352  
 polybutadiene rubber, modified with oligoester acrylate, plastic-elastic and rheological props. (German) 0-19871  
 polybutadienes, use of high modulus inclusion gauge, in stress analysis 0-21254  
 polybutadiene rubber-styrene copolymers, control of morphology and props. (Bulgarian) 0-35153  
 polyisoprene, from guayule rubber, TEM exam. of crystallisation 0-10508  
 polystyrene, polarised Rayleigh scatt. near glass-rubber relax., photon correl. spectroscopy 0-40124  
 polystyrene, rubber-filled, mech. props. (German) 0-35320  
 prestrain effect on dynamic modulus of elasticity and attenuation coeff. in nonconducting materials 0-29110  
 radiation heating effect on creep 0-35285  
 radiation processing, conf., Miami, FL, USA (Oct. 1978) 0-36772  
 rigidity and loss factor, meas. under steady vibr. 0-55602  
 rubber-brass interface, adhesion failure, XPS study 0-40671  
 shell, spherical, mode of loading effect on stability 0-24528  
 steric hindrance, rubber-elastic networks, stress-deformation behaviour (German) 0-35277  
 strain-energy density function for rubber-like materials 0-25773  
 styrene butadiene, dielectric const. and loss, lignin content depend. 0-29670  
 swollen, low-freq. dynamics, optical and mech. props. 0-43626  
 synthetic, network fracture mechanism, particle reinforcement 0-41928  
 teacher resource paper on entropy an rubbery elasticity 0-17777  
 thermoplastic elastomers, crosslinked by secondary valence interactions, elasticity and processing, crosslinking behaviour 0-40320  
 Si rubber as electro-optic material for optical hydrophobes 0-43412

**rubber industry**

- microwave appl., w.r.t. economics and safety 0-3754

**rubbing (abrasion) *see abrasion*****rubidium**

- see also nuclei with .....*  
 Ashcroft pseudopotential, unified study of props. 0-39239  
 atom, 4p level He II photoelectron spectra, energies and intensities 0-5511  
 atom,  $5^2S$ - $n^2S$  transitions, Rydberg levels, high resolution two photon spectra obs. 0-52923  
 atom, Doppler-free two-photon absorpt. spectrum 0-42975  
 atom, ground state, hyperfine struct., relativistic many-body calcs. 0-23322  
 atom, ionisation energies and oscill. strengths calcs. 0-5488  
 atom, K $\beta$ /K $\alpha$  rel. intensity obs. 0-32665  
 atom, L-shell soft X-ray emission spectra, oscillator strengths 0-32651

**rubidium continued**

- atom, outer-shell photoelectron ang. distrib. 0-37797  
 atom, photoionis. cross section, elec. field depend. 0-37796  
 atom, radiative lifetime, time resolved laser induced fluorescence 0-37781  
 atom, radiatively excited states, ionis. rate coeffs. in two atom collisions 0-43160  
 atom, self-broadened first reson. lines, near-wing asymmetries 0-9535  
 atom, valence p-shell HeII $\alpha$  photoelectron spectra, final state CI effects 0-14121  
 BCC crystal, elastic constants, thermal expansion and bulk modulus 0-6452  
 crystal nucleation and symmetry, interaction pots. effect 0-34169  
 elastic scattering amplitudes, for high energy electron scattering, by ionised atoms, numerical calcs. 0-49057  
 equation of state meas. 0-19905  
 equations of state determ. 0-24564  
 fluid, simulated, atom pairs, dynamic behaviour 0-44098  
 graphite, Rb-intercalated, theory of order-disorder phase transitions 0-19908  
 interatomic pair potential, phonon spectra 0-33927  
 lattice vibrations, seven parameter non-central force model 0-44270  
 liquid, classical, long-time anomalies suppression 0-24339  
 liquid, expanded, eqn. of state, transport up to 1700°C, 400 bar 0-2136  
 liquid, kinetic theory of self motion, memory function of vel. autocorrel. function calc. 0-14986  
 liquid, vel. correl. function, memory function calcs. 0-49081  
 metallic compressibilities, general pseudopotential approach 0-54631  
 MHD generation appl., owing to low ionisation potentials (Hungarian) 0-3526  
 phonon spectral density, pseudopotential calcs. 0-39234  
 specific heat at high temp., Monte Carlo calc. 0-29182  
 Stark shift of  $6^2P_{1/2}$  to  $5^2S_{1/2}$  line, mag. scanning meas. 0-27977  
 structural energies, pseudopotential formalism 0-39519  
 two photon spectrum, Doppler free, self-broadening and shift meas. 0-5506  
 UV absorpt. spectra 0-2780  
 vacancy formation energy calcs., electron density functional method 0-19801  
 vapour, thermal cond. meas. 0-14870  
 KBr:Rb, microcrystalline powders, isothermal decay of colour centres 0-2804  
 Rb<sup>+</sup>, levels direct excitation, cross sections and transition probabilities determ. 0-52899  
 Rb<sup>2+</sup>, crossed beam electron impact excitation, cross sections 0-43190  
 Rb<sup>2+</sup> formation during electron-ion collisions, ultrasoft X-ray spectroscopic study (Russian) 0-43193  
 Rb<sup>35+</sup>, <sup>1</sup>P and <sup>3</sup>P energy levels relativistic RPA calc. 0-47913  
<sup>85,87</sup>Rb, high Rydberg levels, press. broadening and shifts 0-52902  
 Rb+<sup>131</sup>Xe, spin-exchange cross section, <sup>131</sup>Xe nucl. spin relax. obs. 0-37868  
 Rb+atom, Rb Rydberg states, collisional ionisation, rate consts. 0-32817  
 Rb+Hg, 15-1400 eV, electronic excitation, integral cross sections 0-43159  
 Rb+Rb(Cs), continuum- and bound-state pair absorption, 2300-3100 Å, 410-540°C 0-42970  
<sup>81</sup>Rb/<sup>81m</sup>Kr ratio as radioactive tracer study of organic bleeding (Dutch) 0-3807  
<sup>82</sup>Rb generator with alumina column, radioactive Sr adsorption 0-12257  
<sup>82</sup>Rb generators, alumina-based, medical evaluation and appl. 0-41237  
<sup>82</sup>Rb+inert gas, D<sub>1</sub>-line hyperfine components perturbation, interferometer obs. 0-32635  
 Rb( $nS$ ,  $nD_{3/2}$ )+Rb(ground state), collisional quenching cross sections 0-43146  
 Ru<sup>3+</sup> isoelectronic series, radial charge distrib. calc. 0-9507  
 SrF<sub>2</sub>Gd<sup>3+</sup>, Rb<sup>+</sup>, EPR of orthorhombic Gd<sup>3+</sup>-univalent metal ion complexes 0-11262  
<sup>82</sup>Sr-<sup>82</sup>Rb generator improvement using inorganic exchangers 0-17135

**rubidium alloys**

- Au-Rb, charge transfer, Mossbauer effect <sup>197</sup>Au isomer shifts, XPS valence-band spectra 0-2676  
 K-Rb, liq., form factors and transport coeffs., pseudopot. perturb. theory 0-44561

**rubidium compounds**

- see also rubidium alloys*  
 graphite-Rb compounds, intercalates IR active lattice mode obs. 0-45072  
 graphite-Rb lamellar cpd., reversible intercalation of tetrahydrofuran 0-16211  
 platino-oxalate, one-dimens. conductors, prep., struct. and elec. cond. 0-24900  
 rubidium propanoate, solid state transitions and melting process, diffr. and conductometric meas. 0-10670  
 rubidium uranyl propionate, low temp. absorpt., luminesc. spectra, intermol. interactions 0-2830  
 trisoxalatoferrate complexes, Mossbauer studies of electronic relax. phenomena 0-44973  
 Ag<sub>2</sub>Rb(PO<sub>3</sub>)<sub>2</sub>, struct., density and elec. cond. 0-33952  
 B<sub>2</sub>O<sub>3</sub>-K<sub>2</sub>O-Na<sub>2</sub>O-Rb<sub>2</sub>O-Cs<sub>2</sub>O glass, small angle X-ray scatt. exam. of struct. 0-38922  
 C<sub>24</sub>Rb, graphite intercalated, de Haas-van Alphen effect, cyclotron reson., and transport props. 0-44479  
 C<sub>8</sub>Rb, graphite intercalated, phonon dispersion relations and Raman spectra 0-44272  
 Cs<sub>1-x</sub>Rb<sub>x</sub>MF<sub>3</sub> (M=Mg, Co, Ni, Zn), hexagonal fluoride perovskite structural evolution by cationic substitution (French) 0-24430  
 Cs<sub>2</sub>RbTmF<sub>6</sub>, mag. behaviour 2.9 to 251.3K, cryst. field levels, ang. overlap model (German) 0-29520  
 Cs<sub>2</sub>RbYbF<sub>6</sub>, mag. behaviour, 3.5-251.3K (German) 0-50041  
 (NH<sub>4</sub>)<sub>x</sub>Rb<sub>1-x</sub>Al(SO<sub>4</sub>)<sub>2</sub>·12H<sub>2</sub>O·Cr<sup>3+</sup> EPR study, effect of monovalent ions on trigonal distortion 0-11255  
 (NH<sub>4</sub>)<sub>1-x</sub>(Rb)<sub>x</sub>SO<sub>4</sub> mixed cryst., EPR of NH<sub>3</sub><sup>+</sup> and SeO<sub>3</sub><sup>-</sup> radicals 0-50190  
 (NH<sub>4</sub>)<sub>2(1-x)</sub>Rb<sub>2x</sub>SO<sub>4</sub>, mixed crystal, dielectric and US meas. of ferroelec. phase transition (Japanese) 0-7305  
 (NH<sub>4</sub>)<sub>2(1-x)</sub>Rb<sub>2x</sub>SO<sub>4</sub>, stoichiometry defects, electron probe microanal. 0-39143  
 NbSe<sub>2</sub>Rb, intercalation cpd., EXAFS study 0-2897  
 Rb-TCNQ-II, two-carrier cond. 0-44625  
 RbAg<sub>4</sub>I<sub>5</sub>, phase transition, statics and local dynamics, mean field and Mori theory 0-39347



**rubidium compounds continued**

- RbAg<sub>4</sub>I<sub>5</sub> solid electrolyte, interface with metal, photocurrent obs. on illumination 0-34513  
 RbAlF<sub>4</sub>, hydrothermal growth method in presence of hydrofluorhydric acid (*French*) 0-25543  
 Rb<sub>4</sub>As<sub>2</sub>O<sub>7</sub>, solid-state synthesis, X-ray powder data (*French*) 0-15079  
 Rb<sub>2</sub>BRCl<sub>6</sub>, B=Li, Ag, Na, systematic structs., X-ray Guinier-Simon method (*German*) 0-44186  
 Rb(B, W<sub>1-x</sub>)<sub>2</sub>O<sub>3</sub> (B=Na, Ca, Co, Ni, Cd, Ga, Bi, Nb, Ta) cryst. struct., temp. dielec. anomalies 0-1998  
 RbBr crystals, positron annihilation, Doppler broadening 0-40180  
 RbBr, evaluation of photoelastic consts. 0-50297  
 RbBr, harmonic and anharmonic props. from phonon dispersion at three temps. 0-39235  
 RbBr, optical absorpt. centre formation time meas. 0-40081  
 RbBr, self-trapped exciton and F-centre form. by picosecond laser pulses 0-10546  
 RbBr, sputtering of atoms by 540 eV electrons, delay times 0-35025  
 RbBr, suprapure, thermolum. glow and emission studies at room temp. 0-7423  
 RbBr:Cu<sup>+</sup>, off-centre ion position, ionic thermocurrent study 0-7271  
 RbBr:Eu<sup>2+</sup>, single cryst. optical absorpt. spectra 0-45117  
 RbBrO<sub>3</sub>, <sup>17</sup>O NQR, spin echo double reson. method, electronegativity 0-54970  
 RbBrO<sub>3</sub>, hexagonal modification, temp. depend. of NQR freq., interpretation of long-wave spectra 0-25243  
 RbC<sub>8</sub>, intercalated graphite, band struct. determ. by angle-resolved photoemission 0-45203  
 RbC<sub>8</sub>, lamellar cpds. with graphite, EPR studies 0-44902  
 RbC<sub>8</sub>, lamellar cpds. with graphite, <sup>13</sup>C NMR studies 0-44936  
 RbCN, cubic, temp. and press. derivatives of elastic consts. 0-6456  
 RbCaF<sub>3</sub>, critical scatt. at struct. phase transition, Mossbauer diff. 0-20546  
 RbCaF<sub>3</sub>, cubic to tetragonal phase transition, <sup>87</sup>NMR meas. 0-7187  
 RbCaF<sub>3</sub>, cubic to tetragonal phase transform., X-ray, neutron, Mossbauer diff. study 0-49360  
 RbCaF<sub>3</sub>, precursor order and Raman scatt. near displacive phase transitions 0-45061  
 RbCaF<sub>3</sub>, struct., phase transitions, neutron diff. study 0-33918  
 RbCaF<sub>3</sub>, structural phase transition, superlattice points, neutron diff. obs. 0-19944  
 RbCaF<sub>3</sub>:Gd<sup>3+</sup>, O<sub>h</sub>-D<sub>4h</sub> struct. transition, ESR obs. 0-50178  
 RbCaF<sub>3</sub>:Mn<sup>2+</sup>, overlap and covalency contrib. to zero field splitting, LCAO-MO calc. 0-24850  
 RbCdF<sub>3</sub>:Gd<sup>3+</sup>, O<sub>h</sub>-D<sub>4h</sub> struct. transition, ESR obs. 0-50178  
 RbCl, aqueous soln., high precision viscosity meas. 0-10695  
 RbCl, evaluation of photoelastic consts. 0-50297  
 RbCl, F-centre optical absorpt., estimate using symmetry-adapted wave functions 0-11448  
 RbCl, sp. ht. at low temps., Debye temp. determ. 0-2177  
 RbCl, thin film, crystal-vacuum (100) surface, mol. dynamics computer simulation 0-34288  
 RbCl:Cu<sup>+</sup>, off-centre ion position, ionic thermocurrent study 0-7271  
 RbCl:Eu<sup>2+</sup>, EPR of <sup>153</sup>Eu<sup>2+</sup> and <sup>151</sup>Eu<sup>2+</sup> 0-11259  
 RbCl:Eu<sup>2+</sup>, single cryst. optical absorpt. spectra 0-45117  
 RbCl:Eu<sup>2+</sup>, tetragonal sites, spin Hamiltonian parameters, EPR and UV absorpt. spectra obs. 0-50177  
 RbCl:H, dynamical superhyperfine interaction 0-2663  
 RbCl:Li<sup>+</sup>, Na<sup>+</sup>, F<sub>A</sub>(II) to F<sub>B</sub>(II) centre crystals, CW laser oscill. with extended tuning range 0-32997  
 RbCl:Na, F<sub>A</sub>-centre optical absorpt., estimate using symmetry-adapted wave functions 0-11448  
 RbCl:Na, U-centres, HFS consts., g-factors, EPR spectra 0-39869  
 RbCl:Ti, origin of 3.55 eV emission band 0-7401  
 2RbCl.CuCl, and 2RbCl.3CuCl, phase transform. heats, DTA obs. (*Russian*) 0-55698  
 RbCoCl<sub>3</sub>.2D<sub>2</sub>O, metamagnetic phase transition, crystallographic and mag. struct., neutron diff. meas. 0-44174  
 Rb<sub>2</sub>CoF<sub>4</sub>, pseudo Ising antiferromag., inelastic light scatt. by mag. excitons 0-11377  
 Rb<sub>2</sub>CoF<sub>4</sub>:<sup>57</sup>Fe, Ising antiferromag., Mossbauer spectra, critical dynamics 0-15884  
 Rb<sub>2</sub>CoF<sub>4</sub>:<sup>57</sup>Fe, Mossbauer spectra, critical region anal. 0-15888  
 Rb<sub>2</sub>Co<sub>0.95</sub>Mg<sub>0.05</sub>F<sub>4</sub>:<sup>57</sup>Fe, Mossbauer spectra, critical region anal. 0-15888  
 Rb<sub>2</sub>Co<sub>2</sub>Mg<sub>1-x</sub>F<sub>4</sub>, random two-dimens. Ising antiferromag., unstable mag. long-range order, neutron scatt. obs. 0-44839  
 Rb<sub>2</sub>Co<sub>2</sub>Mg<sub>1-x</sub>F<sub>4</sub>, dilute antiferromag. two dimens. Ising system, phase boundary effective medium theory 0-50130  
 Rb<sub>2</sub>Cr<sub>2</sub>O<sub>10</sub>, hexagonal form, cryst. data (*French*) 0-28979  
 Rb<sub>2</sub>CuBr<sub>4</sub>.2H<sub>2</sub>O, ferromag., static and dynamic mag. props. 0-50074  
 Rb<sub>2</sub>CuBr<sub>4</sub>.2H<sub>2</sub>O, ferromag., hyperfine and exchange interactions, NMR study 0-50208  
 RbCuCl<sub>3</sub>, quasi-1-dimens., NQR obs. 0-54987  
 Rb<sub>2</sub>CuCl<sub>4</sub>.2H<sub>2</sub>O, ferromag., hyperfine and exchange interactions, NMR study 0-50208  
 RbCuF<sub>3</sub>, <sup>63</sup>Cu NQR meas. 0-50219  
 Rb<sub>2</sub>Cu<sub>16</sub>I<sub>13</sub> in CuCl-CuI-RbCl system, high Cu ion cond. solid electrolyte, elec. props. and powder X-ray diff. anal. 0-15295  
 RbD<sub>3</sub>PO<sub>4</sub>, struct. at room temp., diffractometer study 0-1994  
 RbD<sub>3</sub>(SeO<sub>3</sub>)<sub>2</sub>, <sup>2</sup>D NMR struct. anal. 0-2661  
 RbD<sub>3</sub>(SeO<sub>3</sub>)<sub>2</sub>, incommensurate nature of intermediate phase, neutron diff. obs. 0-50276  
 RbDy(MoO<sub>4</sub>)<sub>2</sub>, Dy<sup>3+</sup> doublets, temp. anomaly in splitting separation due to structural phase transformation (*Russian*) 0-39274  
 RbEu<sub>2</sub>F<sub>10</sub>, crystal struct., X-ray studies (*French*) 0-33955  
 RbEu(PO<sub>3</sub>)<sub>3</sub>, vibr. spectra 0-34905  
 Rb<sub>2</sub>Eu(PO<sub>4</sub>)<sub>2</sub>, synthesis and IR spectra 0-16019  
 (RbF)<sub>n</sub>-FeF<sub>3</sub>, antiferromagnetic systems, dimensionality and spin reduction effects, Mossbauer study 0-39947  
 RbFeCl<sub>3</sub>.2H<sub>2</sub>O, 2D Ising system, crit. fluctuations, Mossbauer spectra study 0-44842  
 RbFeF<sub>3</sub>, Mossbauer spectra, mag. phases 0-15878  
 Rb<sub>2</sub>FeF<sub>5</sub>, Mossbauer spectra, 1D antiferromag. 0-15886  
 RbFeS<sub>2</sub>, crystal ligand field theory, band assignment, absorpt. spectra study 0-20657  
 RbH<sub>2</sub>PO<sub>4</sub>, for tunable frequency-doubled CW dye laser 0-53372  
 RbH<sub>2</sub>PO<sub>4</sub>, transverse elec. susceptibilities 0-50273  
 Rb<sub>2</sub>HPO<sub>4</sub>.RbH<sub>2</sub>PO<sub>4</sub>.Te(OH)<sub>6</sub>, monoclinic, cryst. struct. (*French*) 0-33964  
 RbHSO<sub>4</sub>, acoustic and dielectric props. near phase transition 0-55053  
 RbHSO<sub>4</sub>, dielec. dispersion near ferroelec. phase transition 0-2684

**rubidium compounds continued**

- RbHSO<sub>4</sub>, isotope effect, dielec. const. and spin polarisation investigation 0-20574  
 RbHSeO<sub>4</sub>, ferroelec. phase transition, X-ray study 0-7309  
 RbHSeO<sub>4</sub>, successive phase transitions 0-15985  
 RbH<sub>3</sub>(SeO<sub>3</sub>)<sub>2</sub>, ferroelec. domain struct., obs. using dew method 0-50283  
 RbHgC<sub>8</sub>, and RbHgC<sub>8</sub>, intercalation cpds., synthesis and struct. 0-44183  
 RbI, evaluation of photoelastic consts. 0-50297  
 RbI, NaCl to CsCl phase transition by elastic diffuse and inelastic neutron scatt. 0-2162  
 RbI, optical absorpt. centre formation time meas. 0-40081  
 RbI, phase transition NaCl-CsCl type, preferred orientation of CsCl type 0-49160  
 RbI, self-trapped exciton and F-centre form. by picosecond laser pulses 0-10546  
 RbI, sputtering of atoms by 540 eV electrons, delay times 0-35025  
 RbI<sub>2</sub>Cl<sub>4</sub>, <sup>35</sup>Cl NQR spectra, press. cond. temp. depend 0-20501  
 RbI<sub>2</sub>Cl<sub>4</sub>, NQR of <sup>35</sup>Cl, press. and temp. depend., phase transform. obs. 0-15820  
 RbIO<sub>3</sub>, hexagonal modification, temp. depend. of NQR freq., interpretation of long-wave spectra 0-25243  
 RbIn(MoO<sub>4</sub>)<sub>2</sub>:Fe<sup>3+</sup> monocystals, EPR spectrum in the phase transition neighbourhood 0-2624  
 Rb<sub>2</sub>K<sub>1-x</sub>H<sub>2</sub>PO<sub>4</sub>, 90° phase matching in freq. doubling, appl. to lasers 0-33088  
 RbLiSO<sub>4</sub>, successive struct. transitions, X-ray diff. 0-10521  
 RbMgF<sub>3</sub>:Mn<sup>2+</sup>, EPR obs. and struct. interpret. (*French*) 0-50167  
 RbMnBr<sub>3</sub>, X-ray cryst. struct. determ. 0-54187  
 RbMnCl<sub>3</sub>, crystal, structural phase transition 0-15243  
 Rb<sub>2</sub>MnCl<sub>4</sub>, layer antiferromag., optical absorpt., temp. and mag. field depend. 0-20661  
 Rb<sub>2</sub>MnCl<sub>4</sub>, 2D Heisenberg antiferromag. spin wave analysis 0-54879  
 Rb<sub>2</sub>MnCl<sub>4</sub>, rare earth doped, energy transfer, emission spectra obs. 0-20684  
 RbMnF<sub>3</sub>, antiferromagnetic resonance, optical detection, luminescence 0-7174  
 RbMnF<sub>3</sub>, nuclear spin waves spectra, relaxation, parametric excitation, NMR dynamic shift (*Russian*) 0-11180  
 Rb<sub>2</sub>Mn<sub>2</sub>Mg<sub>1-x</sub>F<sub>4</sub>, two-dimens. antiferromag., spin fluctuations, neutron diff. study 0-44846  
 Rb<sub>2</sub>Mn<sub>2</sub>Mg<sub>1-x</sub>F<sub>4</sub>, spin dynamics near percolation threshold, EPR study 0-39859  
 RbNO<sub>3</sub>, high pressure phase V, X-ray struct. determ. 0-28953  
 RbNO<sub>3</sub>, phase transition, IR spectra 0-7350  
 RbNO<sub>3</sub>.KNO<sub>3</sub>, liq., electromigration cation and mobility and isotope effect 0-10691  
 Rb<sub>2</sub>Nd(PO<sub>4</sub>)<sub>2</sub>, synthesis and IR spectra 0-16019  
 RbNiF<sub>3</sub>, neutron scatt., automatic data processing (*Russian*) 0-54079  
 Rb<sub>2</sub>NiF<sub>4</sub>, planar antiferromagnet, cluster-Bethe-lattice method 0-22306  
 Rb<sub>2</sub>NiF<sub>4</sub>, specific heat capacity, critical amplitude, cross-over from 2-D Ising to Heisenberg behaviour 0-39791  
 RbNi<sub>2</sub>Mn<sub>1-x</sub>F<sub>3</sub>, powder, mag. props. 0-2560  
 Rb<sub>2</sub>Ni<sub>3</sub>(P<sub>2</sub>O<sub>7</sub>)<sub>2</sub>.nH<sub>2</sub>O, thermal dehydration 0-35513  
 RbPO<sub>3</sub>, vitreous, microhardness 0-25864  
 RbPbCl<sub>6</sub>(Br<sub>6</sub>):ReCl<sub>6</sub><sup>2-</sup>(ReBr<sub>6</sub><sup>2-</sup>), vibronic side bands 0-10609  
 Rb<sub>2</sub>PbCu(NO<sub>3</sub>)<sub>6</sub>, uniaxial stress, EPR meas. 0-20455  
 Rb<sub>2</sub>SO<sub>4</sub>, solid-to-solid transition temperature under hydrostatic pressures to 0.6 GPa 0-24586  
 RbSnCl<sub>6</sub>:ReBr<sub>6</sub><sup>2-</sup>, vibronic transition  $\Gamma_7(^2T_{2g}) \rightarrow \Gamma_8(^4A_{2g})$ , intensity distrib. 0-45142  
 RbSnCl<sub>6</sub>(Br<sub>6</sub>):ReCl<sub>6</sub><sup>2-</sup>(ReBr<sub>6</sub><sup>2-</sup>), vibronic side bands 0-10609  
 RbSnX<sub>3</sub>(X=Cl, Br, I), single cryst. gel growth, X-ray diff. study 0-29870  
 Rb<sub>2</sub>(TeBr<sub>6</sub>), far IR and Raman spectra and phase transitions 0-11376  
 RbTeCl<sub>6</sub>(Br<sub>6</sub>):ReCl<sub>6</sub><sup>2-</sup>(ReBr<sub>6</sub><sup>2-</sup>), vibronic side bands 0-10609  
 RbTiMo<sub>5</sub> (M=Ta, Nb), ion exchange props., synthesis and crystallographic props. (*French*) 0-28997  
 RbUO<sub>2</sub>(NO<sub>3</sub>)<sub>3</sub>, fluoresc. decay rates, temp. depend. 0-25429  
 Rb<sub>33</sub>WO<sub>3</sub>, supercond. and special phonons, neutron scatt. obs. 0-15643  
 Rb<sub>2</sub>WO<sub>4</sub>, resistivity, Hall effect and Seebeck coeff. from 1.5 to 300K 0-6879  
 Rb<sub>2</sub>ZnBr<sub>4</sub>, Raman scatt., normal-incommensurate-commensurate phase transitions, soft modes 0-40071  
 Rb<sub>2</sub>ZnCl<sub>4</sub>, phase transition, Raman scatt. evidence 0-40116  
 Rb<sub>2</sub>ZnCl<sub>4</sub> single crystals, Raman scatt. spectra, temp. range covering two phase transitions 0-7340  
 Rb<sub>2</sub>ZnCl<sub>4</sub>, spin-lattice relax. in incommensurate phase, phason and amplitudon excitations 0-50213  
 Rb<sub>2</sub>ZnCl<sub>4</sub>, US velocity and attenuation, around normal-incommensurate phase transition 0-40072  
 Ru<sub>2</sub>B<sub>3</sub>, stella quadrangula as struct. building unit 0-15055  
 Te(OH)<sub>6</sub>.Rb<sub>2</sub>HAsO<sub>4</sub>.Rb<sub>2</sub>H<sub>2</sub>AsO<sub>4</sub>, synthesis and cryst. data (*French*) 0-33948

**ruby**

- Cr<sup>3+</sup> ion doped, R-line region, absorpt. spectrum, dispersion rel. to mag. field 0-2732  
 double electron-nuclear resonance at Cr<sup>3+</sup> B1, B2 absorpt. lines, optical detection (*Russian*) 0-7194  
 energy diffusion distance, upper limit within fluoresc. lifetime 0-29789  
 ESR and NMR correl. line broadening effect assoc. with external mag. field inhomogeneities 0-50227  
 laser, generation, amplification of high power picosecond pulses depend. on superluminescence 0-53305  
 laser, graphical method for pumping coeff. estimation 0-14343  
 laser, negative feedback, cavity Q insertion effect on parameters of modulated pulses 0-43376  
 laser, power enhancement by intracavity plasma 0-53330  
 laser, Q-switched, spectroscopic props., operation modes, pulse amplification (*Rumanian*) 0-48265  
 laser, rotating beam generation 0-1258  
 laser, single-pulse, controllable phototropic shutter design 0-23699  
 laser and LiNbO<sub>3</sub> cryst. in difference freq. laser, tunable MM range emission 0-5764  
 laser generating ultrashort light pulses, saturating absorber efficiency increase 0-23700  
 lasers, freq. synchronisation and locking by passive modulator 0-1249  
 maser, research and development 0-27094  
 maser with wide tuning band 0-53247  
 NMR laser, <sup>27</sup>Al nucl. spin system, collective ordering phenomena, instabilities 0-11278



**ruby continued**

- NMR laser, dynamic props. from point of view of synergetics 0-43341  
 optical free induction decay modulation and absorpt. line struct. due to superhyperfine interaction 0-33091  
 optical hole burning, Stark and pump-probe studies 0-48356  
 optically excited, diffusion of bottlenecked  $29\text{ cm}^{-1}$  phonons 0-6472  
 optically induced two-phonon processes connecting  ${}^2E$  states 0-25443  
 phonon bottleneck of direct decay within  $E({}^2E)$  state, optical detection 0-10608  
 phonons, at  $29\text{ cm}^{-1}$ , stimulated emission 0-45114  
 Raman  ${}^2E$  and phosphorescence transitions, line widths, time correl. study 0-20621  
 Raman effect to probe dynamical processes of  $\text{Cr}^{3+}$  photoexcited states 0-2740  
 raser, instabilities and first order phase changes (*German*) 0-48263  
 resonance interaction of electronic two-level states and short-wave phonon radiation 0-24551  
 ruby, anisotropic  $29\text{ cm}^{-1}$  phonon capture (*Russian*) 0-6471  
 spin-strain coupling tensor meas. US modulated EPR obs. 0-50170  
 stimulated photon echo modulation 0-38074  
 $\text{Al}_2\text{O}_3:\text{Cr}^{3+}$ , shock compression, absorpt. spectra 0-20675  
 ${}^{27}\text{Al}$ , distant ENDOR and dynamic nucl. polarisation 0-2664

**Rudermann-Kittel-Kasuya-Yosida interaction** see *RKKY interaction***Runge-Kutta methods**

- electron mass, truncated, gauge dependence 0-22542  
 ray tracing in general index distributions 0-14279  
 viscous liquid emerging from slot, nonlinear differential equation, Runge-Kutta numerical integration 0-52030

**Russell-Saunders coupling**

- transformation matrices,  $jj$ -LS, for  $p^n$  and  $d^n$  configurations 0-47862  
 transition metal complexes, vibronic coupling and spin relax. NMR decay rate study 0-18870  
 two electron systems, coupling schemes, transition energies and probabilities of autoionising states 0-18828  
 C, optical oscillator strengths, independent particle model, excited state wave functions, LS coupling and Born approx. 0-32674  
 ${}^{57}\text{Fe}$ , configuration interaction, SL-dependent, effect on hyperfine structure 0-37749  
 He, K and LS coupling between states, transition probs., depend. on elec. field 0-37782  
 He-like ions, highly charged, electron impact, intermediate-coupling strengths for fine struct. transitions 0-32837  
 Na like ions, dielectronic recombination rate, scaling props. 0-32668  
 Ne,  $2p^6({}^1S_0)$  ground state electron impact excitation cross sections 0-23558  
 Si isoelectronic sequence, CI calcs. of oscillator strengths, L-S framework 0-14089

**rust prevention** see *corrosion protection***ruthenium**

- see also *nuclei with .....*  
 adsorption and desorption kinetics of CO from clean and S covered Ru 0-6643  
 adsorption and desorption kinetics of  $\text{H}_2$  from clean and S covered Ru 0-6644  
 adsorption of NO on (001) surface, EELS obs. 0-20741  
 adsorption of NO on (001) surface, KPS, UPS, and X-ray AES meas. 0-6655  
 atomic vibr. and fermion behaviour of HCP metals 0-6474  
 chemisorption by GaAs, surface recombination rate reduction 0-49866  
 chemisorption effects on grain boundaries in n-GaAs solar cells 0-55879  
 coadsorption of  $\text{O}_2$  and CO on (001), uptake and flash desorption meas. 0-39450  
 desorption, associative from mixed adlayers of O and N 0-54512  
 electrical contact material, environmental interactions and prep. 0-29463  
 impurity in Cu-Ni sulphidised alloys, behaviour during carbonylation (*Russian*) 0-40584  
 isotopic analysis of U ore 0-21764  
 isotopic composition of Oklo reactor and other samples (*French*) 0-21765  
 nuclear fuel reprocessing by fluoride volatility process, distrib. of Ru contaminants 0-13743  
 radioactive, processing from nuclear fuel by aluminosilicate gels (*Japanese*) 0-22973  
 surface, (0001), adsorbed Xe layer, 5p photoemission, local surface struct. influence 0-2920  
 surface, (1010), interactions with  $\text{N}_2\text{O}$  0-55713  
 surface, stepped ( $\sim 001$ ) cryst.,  $\text{O}_2$  chemisorption, LEED and AES obs. 0-11947  
 surface CO adsorbed particle interactions, lattice gas quasi-chem. approx. 0-49529  
 thermo-EMF and Nernst effect under mag. breakdown conditions (*Russian*) 0-24878  
 Ru (III) chemisorption on photoanode of n-GaAs/ $\text{K}_2\text{Se}-\text{K}_2\text{Se}_2\text{-KOH/C}$  solar cell, effect on performance 0-3516  
 ${}^{97}\text{Ru}$  preparation investigation 0-30891  
 ${}^{103}\text{Ru}$  in determination of rate of passage of food through gut of captive wild birds 0-26425  
 U ore dating from meas. of  ${}^{238}\text{U}$  and Ru conc. 0-21863

**ruthenium alloys**see also *ruthenium compounds*

- ferromagnetic Heusler alloys, peaks in low field AC susceptibility 0-50071  
 rare earth alloys,  $\text{R}_3\text{Ru}$  and  $\text{R}_5\text{Ru}_2$ , cryst. struct. 0-1965  
 $\text{Ce}_{0.73}\text{Ho}_{0.27}\text{Ru}_2$ , spontaneous mag. order below superconducting transition temp., Mossbauer study 0-39701  
 $\text{Ce}_{0.73}\text{Ho}_{0.27}\text{Ru}_2$ , superconductors, mag. correlations and crystal-field levels 0-34547  
 $(\text{Ce}_{1-x}\text{Ho}_x)\text{Ru}_2$ , superconducting, mag. props., neutron scatt. study 0-44808  
 $\text{CeRu}_2$ , H absorption induced Ce valence change, mag. and supercond. props. 0-50042  
 $\text{Cr-Ru}$ , dil. absence of mag. hyperfine field, TDPAC meas. 0-50237  
 $\text{Fe-Ru}$ , antiferromag. ordering, hyperfine fields 0-15867  
 $\text{Fe-Ru-SiO}_2$  supported catalysts, Mossbauer spectra 0-11296  
 $\text{LaRu}_2$ , H absorption induced Ce valence change, mag. and supercond. props. 0-50042  
 $(\text{Mo}_{0.6}\text{Ru}_{0.4})_{82}\text{B}_{18}$ , supercond. metallic glass, neutron irradiat. effects 0-29060  
 Nb-Ru, impurity diffusion and vacancy-impurity binding energy 0-15307  
 Ni-Ru peritectic alloys, rapidly cooled, crystn. peculiarities (*Russian*) 0-20922

**ruthenium alloys continued**

- $(\text{Ni}_{1-x}\text{Ru}_x)_{99}\text{Mn}$ , ferromagnetic, NMR study of local environment effect 0-7192  
 Ru-Al, transition metal group VIII aluminide, NMR near equiatomic composition (*Russian*) 0-20479  
 Ru-Hf, dil.,  ${}^{178}\text{Hf}$  Mossbauer transition, electric quadrupole interaction 0-39928  
 Ru-FeSn, hyperfine mag. field, Mossbauer spectra 0-15865  
 Ti-Ru, radiation disorder model of phase stability 0-16297  
 W-Ru based refractory transition metal-metalloid glass, struct. 0-1938

**ruthenium compounds**see also *ruthenium alloys*

- double oxides, elec. cond. 0-34438  
 $\text{Ba}_4\text{Ru}_2\text{Mo}_{12}$ , ( $\text{M}=\text{Ta}, \text{Nb}$ ), Ru oxidation state, Mossbauer study 0-44965  
 Ru complex, ruthenium(II) tris(2,2'-bipyridine), absorption spectrum and quantum yield of formation (*French*) 0-5554  
 Ru complex, tris-(2,2'-bipyridyl)-Ru(II) complex, photoelectrochemical systems, solar energy utilisation (*German*) 0-45713  
 Ru complexes,  $\text{Ru}(\text{bipy})_3\text{Cl}_2 \cdot 6\text{H}_2\text{O}$  and  $\text{Ru}(\text{bipy-d}_4)_3\text{Cl}_2 \cdot 6\text{H}_2\text{O}$ , soln. electronic excitation energy, deactivation determ. 0-55173  
 $\text{RuF}_5$ , mag. props. 0-15707  
 $\text{RuO}_2$ , as elec. contact material, environmental interactions and prep. 0-29463  
 $\text{RuO}_2$ , porous powder electrodes, proton diffusion meas. 0-54436  
 $\text{RuO}_2\text{-TiO}_2$  anode, wear-resistant, use in applied electrochem. 0-40701  
 $\text{RuO}_2$ , confinement of oxides volatilised during nucl. fuel reprocessing 0-47680  
 $\text{RuS}_2$  amorphous, preparation at ambient temp., magnetic susceptibility meas. 0-35119

**rutile** see *titanium compounds***S-matrix theory**see also *dispersion relations*

- $(1+1)$  dimens. Todd chain and  $e^{\phi}+e^{-2\phi}$  model, exact factorised S-matrices 0-18094  
 $\lambda\phi^4$ , momentum space renormalisation in curved space time 0-37158  
 atom surface scatt., reflection and sticking coeffs., short range forces, low energy limit 0-40208  
 atomic excited state collisional relax., line broadening, interat. interactions, review 0-43149  
 baryonium, S-matrix representation 0-399  
 baryonium dual S-matrix approach 0-52526  
 black hole evaporation, predictability, CPT invariant superscatt. operator and S-matrix 0-46600  
 boson-soliton scatt., sine-Gordon model 0-9109  
 charged particle scatt. in quantising mag. field 0-46853  
 chiral SU(N) Thirring model, S-matrix bound state poles fixing 0-360  
 conserved currents and symmetries of the S-matrix 0-9110  
 coupling strength of particle production, Ball-Zachariasen model of diffractive scattering 0-9158  
 crossing properties of scattering operators 0-32028  
 cut-off potential, asymptotic energy behaviour of Green function 0-27165  
 elastic scattering, semiclassical time-independ. formulation in three-dimens with complex trajectories 0-27605  
 electron scattering from ats.(mols.), partial resonance widths, Siegert eigenvalues, basis-set calc. 0-37880  
 fine-structure transition probability, semiclassical multichannel scatt. matrix 0-37854  
 gauge dependence in the Yang-Mills S matrix 0-351  
 gauge invariance, Lorentz covariance and EM props. of elementary systems 0-32037  
 gauge invariant S-matrix elements with Yang-Mills SU(2) instantons and antiinstanton 0-22511  
 glueball singularity, flavour loops and the Harari-Freund picture 0-42433  
 gravitational and Yang-Mills fields interaction 0-42315  
 Gross-Neveu chiral model, scatt. theory,  $1/N$  expansion 0-348  
 Hamilton-Jacobi equation solns. in Coulomb pot. and quasiclassical approx. 0-45765  
 heavy ion large-angle scatt., elastic cross-section, excitation functions 0-52689  
 heavy ion large-angle scatt., inelastic cross-section and collective state excitation 0-52690  
 intense field QED in continuous medium, appl. to Thomson scatt. and Cherenkov radiation 0-27435  
 ions, multiply charged, level lifetimes relativistic calc., S-matrix approach 0-47942  
 Kugo-Ojima formalism for gauge theories, unitary proof validity 0-37164  
 low-frequency photons in processes involving particles with spin 0-9131  
 many channel scattering model, exactly soluble 0-43127  
 mass generation for fermion field in absence of chiral symmetry breaking 0-347  
 massive Thirring model, S-matrix calcs., required number of conserved currents 0-42329  
 massless fields in asymptotically flat space-time, null surface quantisation and quantum theory 0-4625  
 molecular collinear scattering, information content, dynamical approach 0-23500  
 multiparticle scatt. operators representation satisfying unitarity and crossing props. 0-32029  
 multiparticle scattering operators, cluster decomp. 0-22592  
 nuclear deep inelastic collisions, parametrised S-matrix approach 0-32249  
 nuclear elastic scatt. with optical potential, complex angular momentum methods, poles and zeros of S-matrix, REGGE 0-47445  
 on-shell counterterms and nonlinear invariances 0-22522  
 optical fibres, mode-coupled multimode, baseband transmission theory based on scattering matrix 0-14468  
 ordered hadronic amplitude graphs, mathematical props. 0-42354  
 Pade approximants and  $\pi\text{N}$  scattering 0-22634  
 quantum collision theory, generalised sensitivity anal. 0-31542  
 relativistic Fermi-Bose system quantisation, by compensated functional method (*Russian*) 0-42142  
 scaling of energy and quantum no. for nonreactive collisions 0-9695  
 Schrodinger eqn., radial, general pot. props. for soln. by hypergeometric functions 0-4581  
 Schrodinger eqn. with Hardy pot. 0-96  
 supergraph anal., gauge supersymmetry, S-matrix 0-27422  
 supergravity, covariant canonical formulation, subsidiary conditions and physical S-matrix unitarity 0-12974  
 tachyons and quantum field theory 0-18069  
 unitarity and renormalized 't Hooft identities 0-13205



**S-matrix theory continued**

- unstable quantum states and rigged Hilbert spaces in nonrelativistic scatt. theory 0-8849
- wave-spreading effects in nuclear scattering at intermediate energies 0-18252
- Yang-Mills theory, massive, appl. of path integrals to non-perturbative study 0-32020
- $Z_2$ -symmetric factorized S-matrix in two space-time dimensions 0-4883
- $\pi$ NN form factor,  $\Delta(1236)$  contrib., calc. 0-22609
- $^{10}\text{B}(t, \alpha)^9\text{Be}^*(2s_{1/2})$ , resonant spectra 0-22691
- $\text{H}+\text{H}^+$ , nuclear repulsion, contrib. to charge transfer 0-18922
- He I plasma lines, Stark broadening, quantum mechanical calcs. 0-43880
- Li+He,  $P_{1/2-3/2}$ , fine-structure transition probability, semiclassical multi-channel scatt. matrix 0-37854
- $^{15}\text{N}(n, n')^{15}\text{N}$ , continuum random phase approx. 0-27635

**safety**

- see also accidents; alarm systems; fission reactor safety; health hazards; protection
- air filters, portable electrostatic devices 0-36158
- antennas, 10MHz to 1GHz, ANSI and EPA recommendations 0-30765
- balloon pump counterpulsation, increasing operational safety 0-3869
- biomedical equipment, reliability and safety aspects 0-36172
- breeder reactor security and environmental impact (French) 0-47614
- CANDU irrads. fuel bundles, sheathed in Zircaloy-4, long term stability investig. 0-13774
- chemical laboratory, airborne contaminants monitoring, USA regulations 0-12869
- coal mining, deep-level seams, bed rocks instability obs., by monitoring acoustic emission activity (Japanese) 0-10071
- decommissioned nuclear facilities, radiation exposure pathways 0-13957
- decommissioning, activation and dose rate calcs. 0-13958
- design safety principles and safety assessment techniques for nuclear chemical plants 0-820
- electrical measuring instruments, new CEI standards (Italian) 0-31789
- electrical stimulation parameters, cortical response to callosal stimulation 0-3614
- electron accelerator, linear highfrequency, hazard factors and conditions for safe operation (Czech) 0-52794
- EM absorption in multilayer cylindrical models of man 0-30767
- EM fields, range 3-30 MHz, exposure, maximum permissible intensity and duration, physiological effects (German) 0-12179
- energy systems, comparative risk anal. 0-30423
- eye injury potential of propelled objects, assessment system 0-21591
- flash point meas. of liquid wastes for safe disposal 0-47051
- flowmeters, turbine-type, made in Bulgaria, survey (Bulgarian) 0-6173
- fuel cycle optimization with nonproliferation objectives 0-730
- fusion-fission hybrid reactor blanket design accidental criticality 0-32497
- highly enriched U plates, assay in random driver, absorption modified multiplication effects 0-32399
- HLLW, safety analysis of tank storage 0-740
- industrial radiography radiation exposures, causes, safety training program 0-17141
- irradiated nuclear fuels, passive neutron assay, burnup determination 0-32398
- laser, beam diameter meas. methods survey 0-53348
- laser medicine development trends 0-51198
- laser safe operation control measures 0-9928
- liquefied natural gas, safe handling, measurement system, prediction of roll-over 0-27269
- LNG, transport and storage hazards 0-45620
- low-level solid radwaste, regulations and guides 0-5263
- LWR, radwaste solidification processes, safety aspects 0-13673
- LWRs at Harrisburg and Mulheim-Karlich, safety systems comparison (German) 0-22966
- magnetic safety valve 0-8966
- medical electrical equipment, safety problems 0-56228
- methane, stored energy needed to ignite by discharger from charged person 0-54063
- microwave appl., in industry, science and medicine 0-3754
- microwave power symposium, Monaco (1979) 0-3758
- microwave radiometric methods and the problem of forest and peat fires 0-31877
- MM-wave interaction with biologically active compounds and polar liquids 0-16707
- nonionising RF and microwave radiation hazards (French) 0-3824
- nuclear fuel cycle plants, accident anal., special completeness proof for licensing 0-817
- nuclear installations, seismotectonic map of France for antiseismic design 0-860
- nuclear materials, supervision in West Germany, by Euratom and IAEA (German) 0-18415
- nuclear plant, aircraft crash probabilities for selected plant parts 0-859
- nuclear power plant, intrusion detection system 0-47787
- nuclear power plant security system, American experience 0-47786
- nuclear power plants, safeguards network anal. procedure, SNAP, appl. 0-47672
- nuclear power plants, security in America 0-47785
- nuclear power station accident prevention, 1300 MW nuclear reactor steam isolating valve blowdown tests (German) 0-22967
- nuclear power station protection against seism-aseismic bearings 0-857
- nuclear power stations, leakage tests, Spanish policies (Spanish) 0-5247
- nuclear power stations, nuclear materials, safeguarding experiences (German) 0-611
- nuclear power stations, radiation dosage determination, monitoring and control for personnel safety (German) 0-842
- nuclear power stations, seismic category I building design, structural anal. 0-858
- nuclear reactor, multigoal fuel cycle optimization including nonproliferation objectives 0-52764
- nuclear reactor redundancy systems, common mode failures 0-13641
- nuclear reactor spent fuel storage vault, criticality safety determ. (Korean) 0-37478
- particle accelerator decommissioning, radioactive waste management 0-18720
- permit-to-work certification scheme, for use in health building laboratories 0-22338
- power plants, operational danger levels, mathematical model determ. (German) 0-13633
- proliferation-resistant reprocessing methods 0-27792
- PWR assemblies, pool-s.te fuel inspection and exam. techniques 0-18567

**safety continued**

- radiation, risk to health assessment 0-41124
- radiation protection, US Nuclear Regulatory Commission practices for assuring worker protection 0-5367
- radiation safety glasses, physical factors determining the utility 0-46067
- radioactive fuel, nonproliferation characts. 0-5304
- radioactive reprocessing, comprehensive system of major hazard control 0-818
- radiological safety rules at CEBG 0-5369
- radionuclide movement from hypothetical nuclear waste repository, Waste Isolation Safety Analysis Program 0-16853
- reflection holographic portraits, diffraction efficiency and safety 0-37968
- research reactor Caramel  $\text{UO}_2$  fuel, proliferation resistant fuel service 0-27746
- research reactors, safeguards requirements for highly enriched uranium and reduced enrichments 0-22952
- RF and microwave exposure, USA occupational safety and health standards 0-3727
- RF industrial heaters, elec. and mag. field strengths meas. 0-52175
- risk analysis methods, practical applications 0-12894
- sodium reactor experiment decommissioning, radiation protection 0-9432
- solar concentration system health hazards 0-3492
- spent fuel assembly storage racks, dynamic anal. 0-13639
- spent fuel measurements using high resolution gamma systems 0-32400
- static electricity generation, dangers and safety precautions (Italian) 0-28131
- suppression of industrial explosions 0-31725
- water pool spent fuel storage units, neutron anal., criticality state (Spanish) 0-32517
- H production and distrib., US safety regulations and standards, bibliography 0-41976
- LiAl/FeS batteries, principles and construction, load levelling of nuclear stations 0-21392
- Pu recycle and nuclear proliferation, economic analysis 0-5302
- U isotope separation processes (French) 0-806
- safety systems**
  - see also alarm systems
  - anti-collision, for cars, microwaves and non-conventional appl. survey (Italian) 0-13093
  - flame sensor-trigger device for explosion barrier in underground mines 0-52313
  - nuclear power, human factors, safety system problems and risk assessment 0-22968
  - nuclear power stations, electricity supplies for safety system, German Regulation KTA 3701.1 (German) 0-37466
  - safety closure with deflector 0-53425
- salt water conversion** see desalination
- samarium**
  - see also nuclei with .....
  - atom, coherent ground state transients, beat meas. 0-948
  - atoms, Hanle effect expt. on  $4f^6 6s^2 \text{F}_1$  level 0-43004
  - electrical resistivity, Neel temp., 15 to 300K 0-54672
  - film, ion plating deposition system using electron beam evaporation (French) 0-20802
  - Oklo natural fission reactors, migration in core sample, appl. to dating of reactions (French) 0-21760
  - poisoning transient anal. in fission reactors using XESAMO code (Spanish) 0-52749
  - surface, electron spectroscopy of 4f energy shift 0-2925
  - surface, X-ray prod. by 5 MeV/amu deuterons (oxygen ions), projectile Z depend. 0-42982
  - surface electronic structure, XPS study 0-55259
  - XPS, electronic struct. determ. for surface 0-20765
  - $\text{CaF}_2/\text{Sm}$ , positron annihilation polarisation effects, electron momentum distribution 0-55225
  - $\text{CaSO}_4/\text{Sm}$  phosphors, X-ray induced fluorescence and phosphorescence 0-55179
  - Dy-Sm, magnetic moment growth due to Sm addition (Russian) 0-34608
  - $\text{LaF}_3/\text{Sm}$ , cryst. field anal. of triply ionised ion spectra 0-2796
  - $\text{La}_2\text{O}_3/\text{Al}_2\text{O}_3/\text{SiO}_2/\text{Sm}^{3+}$ , luminesc. selective laser excitation line narrowing 0-25434
  - $\text{POCl}_3/\text{MCl}_4/\text{Sm}^{3+}$  ( $\text{M}=\text{Sn}, \text{Zr}, \text{Ti}$ ), splitting of  $\text{Sm}^{3+}$  near IR absorpt. bands 0-2750
  - Si-Sm, implanted impurity location, Mossbauer and channelling expts. 0-39128
  - $\text{Sm}^{3+}$  in cubic environment, importance of  $T^{-5}$  and  $T^{-7}$  terms in spin-lattice relax. time 0-25192
  - $\text{Sm}^{3+}:\text{NaCl}(\text{KCl})$ , absorption spectra at 4.2 K, anal. 0-7378
  - $\text{Sm}+\text{H}^+(\text{He}^+)$ , X-ray intensity ratios, projectile energy depend. 0-23535
- samarium alloys**
  - misch metal, improvement of Al alloy 51S, for space appl. 0-55466
  - $\text{Co}_2\text{Sm}$ , magnetic domains, nucleation and pinning, magneto-optical Kerr effect 0-39811
  - Ho-Dy-Sm, magnetic moment growth due to Sm addition (Russian) 0-34608
  - Ho-Sm, Hall effect, field and temp. depend., 4.2-150K, singularities (Russian) 0-29387
  - Ho-Sm, magnetic moment growth due to Sm addition (Russian) 0-34608
  - Ho-Sm, magnetic phase diagrams, helicoid-ferromag. transform. (Russian) 0-50089
  - Mg-Sm, phase diagram and mech. props. (Russian) 0-20892
  - Nd, Pr, Sm,  $\text{Co}_5$  permanent magnets, coercive force, low-temp. annealing influence (Russian) 0-39812
  - $(\text{Nd}, \text{Sm}_{1-x})_2(\text{Co}_{0.7}\text{Fe}_{0.3})_{17}$ , mag. anisotropy 0-34622
  - Sm-Co-Cu-Fe-Zr, reversible changes in coercive force and struct. state during heat treatment 400-800°C (Russian) 0-29574
  - Sm-Cu system, phase struct. investigation by X-ray diff. (Russian) 0-49185
  - Sm-Dy (3 wt.%), electrical resistivity, Neel temp., 15 to 300K 0-54672
  - Sm-Fe-B ternary systems, phase equilibria and cryst. struct. (Ukrainian) 0-11626
  - Sm-Pr-Co, mag. props. and struct., comp. depend. (Russian) 0-20430
  - Sm-(Pr)-Co, sintered, cryst. phases (Russian) 0-39004
  - $\text{SmAl}_3$ , exchange and cryst. field effects 0-24857
  - $\text{SmAl}_3$ , hyperfine fields, ferromagnetic coupling between rare earth spins, NMR study 0-39880
  - $\text{SmCO}_5$ , based permanent magnets, props. and cryst. orientation (Russian) 0-20431
  - Sm(Co, Cu) alloys, coercivity mech. 0-44862



**samarium alloys continued**

- SmCo<sub>5</sub>, exchange and cryst. field effects 0-24857  
 SmCo<sub>5</sub> films, struct. transformations effect on coercive force and mag. reversal (*Russian*) 0-20436  
 SmCo<sub>5</sub>, hard mag. props., book contrib. 0-39759  
 SmCo<sub>5</sub> hydriding kinetics, inverse over pressure effect 0-55944  
 SmCo<sub>5</sub> magnets, ageing at high temp. 0-7129  
 SmCo<sub>5</sub>, permanent magnet stability, during long-term ageing (*Chinese*) 0-55428  
 SmCo<sub>5</sub>, powder, comminution temp. effect on mag. props. 0-39819  
 SmCo<sub>5</sub>, sintered, anisotropic thermal expansion and fracture of radially oriented toroids (*Chinese*) 0-10686  
 SmCo<sub>5</sub>, sintered permanent magnet manufacture 0-20838  
 SmCo<sub>5</sub> thin film, hydride form., kinetics, mag. monitoring 0-35571  
 Sm(Co<sub>0.65</sub>Cu<sub>0.35</sub>)<sub>5.6</sub>, cryst. struct. and coercive force, heat treatment effects (*Russian*) 0-44170  
 Sm(Co<sub>0.84</sub>Cu<sub>0.16</sub>)<sub>6.9</sub>, microstruct. and domain struct., mag. reversal (*Russian*) 0-20429  
 Sm(Co<sub>0.81</sub>Cu<sub>0.19</sub>Fe<sub>0.04</sub>)<sub>6.9</sub> and Sm(Co<sub>0.84</sub>Cu<sub>0.16</sub>)<sub>6.9</sub> powders, mag. props. (*Russian*) 0-20434  
 Sm(Co<sub>0.86-x</sub>Cu<sub>0.14</sub>Fe<sub>x</sub>)<sub>7</sub>, permanent magnet, sintering and heat treatment effects 0-39817  
 SmFe<sub>2</sub>, ferromagnetic-ferrimag. cpds., mean field exchange const., Stoner itinerant model calcs. 0-50084  
 Sm<sub>1-x</sub>Gd<sub>x</sub>Al<sub>2</sub>, hyperfine fields, ferromagnetic coupling between rare earth spins, NMR study 0-39880  
 Sm<sub>0.4</sub>R<sub>0.4-x</sub>M<sub>0.2</sub>Co<sub>5</sub> (R=Gd, Dy, M=Pr, Nd), temp. coeff. of magnetisation 0-34688  
 Tb-Sm (*Russian*) 0-34608

**samarium compounds**

see also *samarium alloys*

- mixed valence, metals or small gap insulators, two-band Hubbard Hamiltonian 0-34399  
 Ba<sub>1-x</sub>Sm<sub>x</sub>B<sub>2</sub>, prep., elec. cond. and thermoelec. props. 0-49697  
 CaB<sub>6</sub>-SmB<sub>6</sub>, mag. props., comp. depend. 0-50034  
 Ca<sub>2</sub>Nb<sub>2</sub>O<sub>7</sub>-Sm<sub>2</sub>NbO<sub>7</sub> system, phase equilb. 0-20907  
 La-Sm-Lu iron garnet film grown as NdGaG substrates, mag. props. 0-44888  
 LaB<sub>6</sub>, surface (100), atomic struct., angle-resolved XPS, LEED and ISS investigation 0-10765  
 SmB<sub>6</sub>, mag. and elec. props., metallic character 0-20386  
 SmB<sub>6</sub>, <sup>11</sup>B nucl. quadrupole interaction, NMR meas. 0-2660  
 SmB<sub>6</sub> film, prep. by electron beam evaporation, and optical and elec. props. 0-20793  
 SmB<sub>6</sub>, mixed valence cpd., EPR and heat capacity obs., metal-semicond. behaviour 0-20456  
 SmB<sub>6</sub>, mixed valent, large low-temp. Hall effect and resist. 0-39611  
 SmB<sub>6</sub>, specific heat anomalies 0-34199  
 SmB<sub>6</sub>, valence fluctuating state, sp. ht. 0-20127  
 SmB<sub>6</sub>, valence fluctuation system, ground state and elementary excitations, Anderson lattice model Hamiltonian, dense Kondo problem 0-54656  
 SmB<sub>6</sub>(B<sub>2</sub>), growth by soln. method, struct. and mech. props. 0-16168  
 Sm(BH<sub>2</sub>)<sub>3</sub>, synthesis from chloride salts and NaBH<sub>4</sub> in tetrahydrofuran 0-30222  
 Sm(BO<sub>2</sub>)<sub>3</sub>, single cryst., IR absorpt. spectra 0-34903  
 Sm<sub>2</sub>Bi<sub>3</sub>, press.-induced valence instability 0-20261  
 Sm(ClO<sub>4</sub>)<sub>3</sub>, osmotic coeffs. 0-45556  
 SmCl<sub>3</sub>·6H<sub>2</sub>O:Gd<sup>3+</sup>, X-ray band EPR lines, exact anal. using intensity operator 0-20448  
 SmF, vaporisation, sublimation, Knudsen effusion method 0-6508  
 Sm<sub>2</sub>Ga<sub>2</sub>O<sub>12</sub>, garnet-perovskite transform 0-15239  
 Sm<sub>2</sub>Gd<sub>0.2</sub>S, valence transition, positron annihilation study 0-15454  
 Sm<sub>1-x</sub>Gd<sub>x</sub>S system, semicond. to metallic isomorphous phase transition mechanism 0-2338  
 SmH<sub>2.2-2.4</sub>, low-temp. sp. ht., mag., elec., and cryst. field splitting effects 0-49379  
 SmH<sub>4</sub> [x=2.78, 2.85, 2.91], electrical resistance anomalies at high pressures 0-29381  
 Sm<sub>2</sub>La<sub>1-x</sub>B<sub>2</sub>, solid solns., exam. of structure, elec. props. 0-39290  
 Sm<sub>1-x</sub>M<sub>x</sub>S, M=transition metal, valence charges, band struct. 0-20131  
 Sm<sub>2</sub>MoO<sub>4</sub>, cryst. struct., IR spectra, elec. and mag. props. 0-33954  
 SmN, magnetic props., neutron diff. and mag. susceptibility meas. 0-50036  
 Sm(NO<sub>3</sub>)<sub>3</sub>, osmotic coeffs. 0-45556  
 SmNbO<sub>4</sub>-CaWO<sub>4</sub>, phase transitions of fergusonite-scheelite (*French*) 0-19942  
 SmO, intermediate valence state (*French*) 0-20132  
 SmO, mag. props., lattice const., and X-ray absorpt. spectra 0-44798  
 Sm<sub>2</sub>O<sub>3</sub>, isotopically enriched target preparation using electron gun 0-23226  
 SmRh<sub>2</sub>B<sub>4</sub>, coexistence of supercond. and antiferromag. order 0-11140  
 SmRh<sub>2</sub>B<sub>4</sub>, mag. ordered, persistence of supercond. 0-54834  
 SmS (001) surface, mixed valency and phase transitions 0-39658  
 SmS, and Sm<sub>0.8</sub>Tb<sub>0.2</sub>S, resistivity and thermopower 0-20260  
 SmS, defect struct., precipitate colonies, dislocation loops, TEM obs. 0-44214  
 SmS, electronic phase transition, mechanism, trivalent metal impurity effects 0-49604  
 SmS, induced magnetic form factor, polarised neutron studies 0-25078  
 SmS, metallic phase, compressibility anomalous behaviour 0-29114  
 SmS, phonon anomalies and electron-lattice coupling 0-39490  
 SmS type cpd., fd mixing effect on impurity levels, local valence transition 0-24831  
 SmS, valence fluctuation phenomena 0-24800  
 SmS, valence fluctuation system, ground state and elementary excitations, Anderson lattice model Hamiltonian, dense Kondo problem 0-54656  
 SmS, valence transition, positron annihilation study 0-15454  
 SmS:P, neutron irradi., semiconductor-metal transition 0-24975  
 Sm<sub>2</sub>S<sub>4</sub>, mag. susceptibility meas., valence state of Sm 0-15684  
 SmS<sub>1-x</sub>P<sub>x</sub>, intermediate valence cpd., lattice parameter and mag. susceptibility 0-7091  
 SmSb, forbidden band gap and electrotransfer parameters 0-39497  
 Sm<sub>2</sub>SnS<sub>4</sub>, X-ray cryst. struct. determ. (*French*) 0-19760  
 Sm<sub>2</sub>Tb<sub>1-x</sub>FeO<sub>3</sub>, gyrotropic props. and birefringence, in spin reorientation range 0-7324  
 Sm<sub>2</sub>WO<sub>6</sub> and Sm<sub>14</sub>W<sub>4</sub>O<sub>33</sub>, high-temp. enthalpy and specific heat 0-34205  
 (SmYCa)<sub>3</sub>(FeGe)<sub>5</sub>O<sub>12</sub> epitaxial layer, growth kinetics and struct. as functions of cryst. lattice parameter mismatch 0-6677  
 Sm<sub>0.25</sub>Y<sub>0.75</sub>S, phonon anomalies and electron-lattice coupling 0-39490

**samarium compounds continued**

- Sm<sub>0.75</sub>Y<sub>0.25</sub>S, intermediate valence compound, phonon investigation by neutron scatt. 0-6476  
 Sm<sub>0.75</sub>Y<sub>0.25</sub>S, mixed valence, phonon dispersion theory 0-34153  
 Sm<sub>0.76</sub>Y<sub>0.24</sub>S, induced magnetic form factor, polarised neutron studies 0-25078  
 Sm<sub>2</sub>Zr<sub>2</sub>O<sub>7</sub> pyrochlore phase, O ion conduction 0-24654  
 (Y,Sm,Lu,Ca)<sub>3</sub>(Fe,Ge)<sub>5</sub>O<sub>12</sub> bubble magnetic garnet film, LPE grown, props., CaCO<sub>3</sub>/GeO<sub>2</sub> molar ratio influence 0-50152  
 (Y,Sm,Lu,Cu)<sub>3</sub>(Fe,Ge)<sub>5</sub>O<sub>12</sub>, ion implanted, hard bubble suppression 0-11238  
 (Y,Sm,Lu,Tm,Ca)<sub>3</sub>(Fe,Ge)<sub>5</sub>O<sub>12</sub>, epitaxial garnet film, temp. depend. mag. props. 0-39825  
 (Y,Sm)<sub>3</sub>(Fe,Ga)<sub>5</sub>O<sub>12</sub>, garnet LPE films, growth rate anisotropy 0-54558  
 (Y,Sm)<sub>3</sub>(Ga,Fe)<sub>5</sub>O<sub>12</sub>/(Eu,Er)<sub>3</sub>(Ga,Fe)<sub>5</sub>O<sub>12</sub>, double-layer self-biasing garnet films, dynamic behaviour of domain walls 0-34722  
 (YBiSmCa)<sub>3</sub>(FeGe)<sub>5</sub>O<sub>12</sub> epitaxial layer, growth kinetics and struct. as functions of cryst. lattice parameter mismatch 0-6677  
 Y<sub>1.62</sub>Sm<sub>0.21</sub>Lu<sub>0.27</sub>Cu<sub>0.9</sub>Ge<sub>0.9</sub>Fe<sub>4.1</sub>O<sub>12</sub>, implanted bubble garnet, anisotropy profile, FMR study 0-7103  
 (YSmCaLu)<sub>3</sub>(FeGe)<sub>5</sub>O<sub>12</sub>, bubble film inhomogeneity, spin wave reson. meas. 0-44439  
 (YSm)<sub>3</sub>(FeGa)<sub>5</sub>O<sub>12</sub> film, LPE on Gd<sub>3</sub>Ga<sub>5</sub>O<sub>12</sub>, interface processes, horizontal dipping obs. 0-49552  
 (YSmLuCa)<sub>3</sub>(FeGe)<sub>5</sub>O<sub>12</sub>, double layer struct., LPE growth from molybdate and Pb borate fluxes 0-39827  
 (YSmLuCa)<sub>3</sub>(FeGe)<sub>5</sub>O<sub>12</sub>, bubble material, dynamic characterisation, comparison between transport and FMR methods 0-39833  
 YSmLuCaGe garnets, 7 μm-period bubble devices 0-44887  
 (YSmLu)<sub>3</sub>(FeGaSc)<sub>5</sub>O<sub>12</sub>, submicron mag. bubble garnet 0-54929  
 YSmTmCaGe garnets, 7 μm-period bubble devices 0-44887  
 ZrO<sub>2</sub>-Sm<sub>2</sub>O<sub>3</sub> eutectic, unidirectional solidification, microstruct. and crystallographic characterization 0-35176

**sample and hold circuits**

- boxcar integrator/US recording unit using sample-and-hold circ., for student lab. 0-27083  
 luminous flux meas., automatic null method (*French*) 0-27331

**sand**

- aeolian sedimentation on Earth and Mars, comparisons 0-31042  
 Athabasca oil sands, electrical props. 0-31030  
 Baltic beach scouring and detritus accumulation in short-term disturbance (*Russian*) 0-36288  
 barrier beach shoreline accumulative section, protective dune ridge morphodynamics (*Russian*) 0-36287  
 barrier beach shoreline transit section, protective dune ridge morphodynamics (*Russian*) 0-36286  
 bedload dynamics, grain-grain interactions in water flows 0-31069  
 clay soil/sand mixtures, reflectance 0-56475  
 clock, historical development 0-22185  
 cyclic liquefaction strength 0-3996  
 dune formations in Canada 0-12386  
 dynamic properties w.r.t. seismic risk prediction, stress condition effect (*Japanese*) 0-17235  
 enriched heavy minerals in sand grains, enhanced natural radiation exposure (*German*) 0-51018  
 erosion of windblown quartz and basaltic sand on Mars 0-17525  
 surface texture rel. to wind vel. conditions 0-41443  
 thermal diffusivity measurement, constant rate heating method (*Japanese*) 0-6572  
 tracer dispersion under progressive water waves, laboratory and field obs. 0-46170  
 US attenuation in fluid-saturated sand 0-33307  
 Waipipi ironsands in New Zealand, mag. assessment technique for titanomagnetite 0-17254  
 Al-C-siliceous sand mixture in N<sub>2</sub> atmos., weight loss during heating, compaction (*Japanese*) 0-35151  
 Hg pollution of Mediterranean sediments around Alexandria, Egypt 0-3538

**sapphire**

- chemical analysis, O conc. determ. using non Coulomb H ion backscatt. 0-55753  
 complex dielec. const. at audio freqs., 5.5 to 380K 0-25272  
 crystal defects from X-ray irradiation, F-centres, X-ray luminesc. obs. 0-55176  
 etching, HF ion-plasma, cryst. surface layers treatment and study (*Russian*) 0-16517  
 etching of arrays of orifices using Pt-Cr composite layer mask 0-3216  
 fibres, meas. of bending strength 0-25964  
 interface with vac., phonon refl. 0-15358  
 internal friction, low temp. peak 0-2033  
 leucosapphire, crystal growth by Kyropoulos method, temp. effect on structural and optical quality 0-20784  
 leucosapphire fibres, multicapillary growth 0-44459  
 leucosapphire large crystals, anomalies in block struct. formation 0-9972  
 metal-sapphire interface, effect on shear strength of adsorbed species 0-49485  
 neutron damaged 14.8 MeV, optical vibronic absorption spectra 0-50384  
 sapphire filaments in Al<sub>2</sub>O<sub>3</sub>:MgO matrix, single cryst. boundary migration 0-44369  
 shock compressed, refractive index, density, and polarisability behaviour 0-50295  
 SOS films, cryst. quality improvement by Si ion channelling, annealing 0-44222  
 SOS wafer for beam profile monitoring in high-current ion implantation systems 0-13182  
 substrate for directed crystallisation of GaSb thin layers 0-35111  
 substrate for directed crystallisation of InSb thin layers 0-35112  
 substrate for Si film, laser annealing dynamics epitaxial regrowth, optical reflectivity 0-29285  
 substrate for vacuum deposited heteroepitaxial Si films, struct. and elec. props. 0-15390  
 synthetic and natural, optical spectra comparison and identification 0-40138  
 TFR diagnostic windows, radiation damage 0-34063  
 thermophysical props., temp. wave methods 0-24624  
 white, brittle fracture, microstruct. depend. 0-16469  
 α-Al<sub>2</sub>O<sub>3</sub>:Co,H, Co and proton ENDOR, IR and optical spectra charge compensator nature and defect struct. 0-44956  
 Si-sapphire interface in SOS ICs, elec. investigation 0-11097



**sapphire continued**

- $\text{Ti}^{4+}$  doped, plastically deformed, precipitation hardening, TEM study 0-7592
- $\text{W}/\alpha\text{-Al}_2\text{O}_3$ , heteroepitaxial structs., refined formulation of relative orientation criterias 0-44448

**satellite atmospheres** *see extraterrestrial atmospheres; planetary satellites***satellite links**

- see also artificial satellites*
- 22.75 GHz microwave attenuation characts. at high elevation (*Japanese*) 0-27346
- ATS 6/Geos 3, satellite to satellite range-rate obs. for  $5^\circ$  mean gravity anomalies recovery 0-41366
- Canadian government research, role and development in communications 0-43481
- Comstar beacon cumulative slant path rain attenuation statistics, 28.56 GHz 0-26582
- crosspolarization of microwaves due to rain on satellite to Earth path 0-21789
- educational broadcasting for developing countries, case for use of satellites 0-4485
- European Space Agency activities (*German*) 0-8516
- geosynchronous satellite orbit determination using VLBI and computer program (*Japanese*) 0-21925
- Global Weather Expt., roles played by METEOSAT and TIROS-N 0-26714
- intercontinental clock synchronisation, ramp method 0-47034
- international time synchronisation, precision tracking package TEMPUS, NAVSTAR satellite network appl. 0-22332
- ionosphere, UHF and VHF scintillation, signals from geostationary satellite 0-56674
- lake identification by closed planar curve analysis using LANDSAT (*Japanese*) 0-26635
- meteorological information provision for weather sensitive economic activities 0-46244
- National Bureau of Standards time code relay to western hemisphere by satellite 0-47039
- orbital antenna farm, concept 0-8514
- precise time recovery from Transit satellites 0-47037
- rain attenuation in microwave and MM wavebands, estimation of duration time distribution (*Japanese*) 0-21788
- rain effects above 10 GHz 0-8410
- SHF signal attenuation by rain, monitored by radar 0-51567
- SHF waves for satellite broadcasting, rainfall attenuation characts. (*Japanese*) 0-12501
- SIRIO, microwave attenuation, fade statistics for 11.6 and 17.8 GHz (*Italian*) 0-4095
- SIRIO radiowave propag. data for earth-space rain-cell modelling 0-36352
- SIRIO-1, analysis of oblique propag. measurements made at Gometz-la-Ville Earth station (*French*) 0-56504
- solar activity and effects on satellite performance 0-56812
- sound, graphical picture transmission, distrib. via domestic satellite, education appl. 0-31463
- Symphonie geostationary satellite, time transfer link for atomic clock synchronisation 0-47038
- synthetic aperture radar, satellite borne, terrestrial surface mapping appl. 0-12572
- time and frequency, conf., Helsinki, Finland (Aug. 1978) 0-46728
- time transfer experiment using Nova satellite time signals 0-47036
- time transfer technology, review 0-47029
- TV broadcasting satellite, use for precise real-time signal dissemination 0-47033
- VLBI, general considerations of international systems (*Japanese*) 0-17501
- VLBI, Japanese domestic system, general aspects (*Japanese*) 0-17502
- VLBI, Japanese domestic system, receiver and local oscillator (*Japanese*) 0-21923
- VLBI, Japanese domestic system, recording signal generator (*Japanese*) 0-21924
- VLBI, Japanese domestic system, selection of radio sources and experimental procedure (*Japanese*) 0-21922
- VLBI, principles of measurement (*Japanese*) 0-21921
- VLBI between geostationary satellites for hectometric observations of radio stars (*Japanese*) 0-21928

**satellite relay systems**

- CETI from Earth satellite orbit 0-4275
- direct broadcasting in Europe and associated European Space Agency programme 0-12638
- environmental telemetering service, geostationary, polar orbiting satellites 0-56592
- geostationary, effect of solar eclipses by the Moon on broadcast satellites, prediction of occurrence 0-31199
- geosynchronous orbiting, interference from solar power satellites 0-45634
- meteorological data relay, aircraft-to-satellite 0-17380
- TDRSS, Ni-Cd secondary battery system design 0-30460

**satellite vehicles** *see artificial satellites***satellites, artificial** *see artificial satellites***satellites, planetary** *see planetary satellites***saturable absorption, optical** *see optical saturable absorption***saturation control** *see chemical variables control***saturation effects, optical** *see optical saturation***saturation measurement** *see chemical variables measurement***Saturn**

- 1979 S 3, discovery of possible satellite 0-26802
- 1979 S 3 to 6, 1980 S 1, possible new satellites, discovery 0-46472
- 1980 S 2, new Saturnian satellite, discovery and possible orbital periods 0-46473
- atmosphere, IR radiation, review 0-8568
- atmosphere, seasonal phenomena from  $3\mu$ , methane band obs. 0-26803
- atmosphere differential rotation, origin 0-46467
- B-ring, optical reflectance polarimetry interpretation 0-31248
- decimetric radio obs., brightness temp. 0-46474
- Enceladus, near IR spectra and JHK photometry 0-56761
- F-ring and new satellite, Pioneer II discoveries 0-8585
- Hyperion, near IR spectra and JHK photometry 0-56761
- Iapetus, near IR reflectivity of dark and light faces 0-26800
- innermost satellites, separations and times of elongation, (1980 February 29 to March 18) 0-56762
- ionosphere, chem. and phys. props., model calcs. 0-26801
- magnetic dipole axisymmetry 0-56361

**Saturn continued**

- magnetic field origin 0-36564
- magnetic moment, prediction from scaling law test 0-21934
- magnetopause, affected by Jupiter's mag. tail 0-12706
- Mimas and Tethys, orbital theory including perturb. 0-36568
- natural vibration spectrum, rot. effects, calc. 0-8583
- near IR spectral albedo, obs 0-31242
- outer ring, discovery and extent 0-46472
- outer ring search, 1979 November obs. 0-17543
- Phoebe, near IR spectra and JHK photometry 0-56761
- Pioneer 11 investig. 0-46476
- Rhea, icy satellite, mass-radius relationship 0-31222
- ring brightness, model for azimuthal brightness variation 0-31251
- ring E, inferences from obs. of radiation belt particles 0-41762
- ring system, origin and location of narrow rings 0-56764
- ring system, polarimetry of light scatt. during 1979 opposition 0-36570
- rings, 3 mm obs. and props. 0-46470
- rings, four colour phase curves, analysis 0-4295
- rings, International Planetary Patrol obs. and data reduction 0-4294
- rings, IR brightness and eclipse cooling obs. 0-56763
- rings, thickness caused by satellite and solar perturb. and planetary precession 0-36569
- rings, vertical struct. and thickness 0-4296
- rings and regular satellite system formation 0-41746
- satellites, light curve, surface meteoroid bombardment effects 0-26786
- satellites, surfaces and interiors, review 0-4297
- satellites and exterior ring obs. (1980 Feb.-March) 0-51690
- Titan, 16-30  $\mu$ m spectroscopy 0-56760
- Titan, icy satellite, mass-radius relationship 0-31222
- Titan, IR spectrum from 0.8 to 2.5 microns 0-21946
- Titan, optical props. and vertical distrib. of aerosols in atmosphere 0-46471
- Titan, suspected near IR variability 0-46469
- Titan (Saturn VI) eclipse, 1979 December 20, photometric obs. 0-31250
- Titan atmosphere, photochemical aerosols identification 0-31249
- Titan atmosphere, photochemical models 0-36567
- H atom cloud, generated by photo-sputtering of ice in rings 0-46475

**SAW** *see surface acoustic waves***SC (sudden commencement)** *see magnetic storms***scale invariance** *see scaling phenomena***scales (circuits)** *see scaling circuits***scales** *see balances***scaling circuits**

- X-ray diffractometer scanning block modernisation by scaler adjustment 0-31958

**scaling phenomena**

- see also elementary particle theory; renormalisation*
- $\phi^4$  Euclidean field theory, scale limit of  $\phi^2$  0-333
- Bethe-Salpeter model, scaling reconstruction using renormalisation group, Callan-Symanzik eqn.,  $\phi^3$  theory (*Russian*) 0-42351
- Bjorken scaling law violation, mass dependent, quark-quark interactions 0-9160
- Callan-Gross relation, instanton violation, nonperturbation correction asymptotic behaviour 0-27409
- critical exponents, three dimensional system with short-range interaction, calc. 0-42348
- diffusion in bistable potential, systematic WKB treatment 0-46975
- diquark contribs. to scaling violation and deep inelastic  $\sigma_L/\sigma_T$ , structure functions, QCD 0-22573
- Drell-Yan scaling, absorptive corrections, for initial and final hadronic state interaction 0-4950
- elastic form factors, asymptotic behaviour, Callan-Symanzik eqns. (*Portuguese*) 0-18137
- elastic phase transitions, crit. dynamics 0-2146
- emulsion nuclei, 28 GeV proton interactions (*Korean*) 0-18299
- hadron+hadron, high-energy, inclusive spectra of secondary pions, Feynman scaling and statistical model 0-42502
- hadron interactions, local thermodynamic equilibrium (*Russian*) 0-9155
- hadron-nucleus reactions, 20-400 GeV, multiplicity of relativistic charged particles (*Russian*) 0-5191
- hadronic muon pair prod. QCD radiation and mean scaling, longitudinal and transverse momentum 0-42405
- hadronic reactions, universal scaling law 0-18082
- heavy meson hadroproduction, QCD effect on scale breaking 0-37239
- high mass dilepton prod., comparison with Drell-Yan formula in asymptotically free theories 0-4942
- inclusive form factor scaling w.r.t. generalised scaled variable 0-417
- Ising model with free surface, series anal. 0-25062
- Ising spin  $1/2$  model, renormalisation group approach 0-2582
- Jost-Lehmann-Dyson representation, scale invariance breaking and spectral function 0-13316
- kinematical scale breaking in high  $p_T$  interactions, parton fragmentation function 0-367
- KNO scaling and scaling in the mean for semi-inclusive processes (*Chinese*) 0-22538
- lattice gauge theories, extrapolation to continuum limit 0-349
- muon scattering at Fermilab, inclusive scatt., quark models, scaling violation 0-5001
- non-linear transport equations: Properties deduced through transformation groups 0-4680
- nucleon form factors, asymptotic relations from quark-gluon model, scaling violation 0-42463
- one particle reduced density matrix of impenetrable bosons in one dimension at zero temperature 0-17863
- perturbative QCD, jets, inelastic distribs., colourless clusters, scaling, multiplicity and tree evolution 0-52459
- point like spin-3/2 quarks, contrib. to deep inelastic struct. functions 0-47250
- QCD, quark and gluon propagators 0-52469
- QCD, scaling violation pattern, higher order terms 0-27468
- QCD, slope of leading Regge trajectory 0-42391
- QCD extended leading logarithm approx. for inclusive distribs. and lepton pair prod. 0-379
- quarkonium, quantum mechanical applications, masses and leptonic widths of  $\psi$  and  $T$  0-27484
- Reggeon field theory on a lattice, critical behaviour, Monte Carlo calc. 0-18126
- spacetime structure theory at very short distances, nonlinear sigma model 0-12979
- spinor fields, conformal, dimensions, scale invariance 0-27394



**scaling phenomena continued**

- t-flavoured meson production in photonuclear and pp collision, parton distribution functions with scale breaking 0-22623  
 Thomas-Fermi type picture of EM structure of  $\pi$  and N 0-9170  
 Tokamaks with shear, scaling law for trapped ion anomalous diffusion 0-32492  
 (c,e), A=2, 3, 4, scaling laws in relativistic impulse approx. model, spin effects 0-52662  
 ed deep inelastic scatt. cross sections, quark-parton model with broken scaling (*Russian*) 0-32109  
 e<sup>+</sup>e<sup>-</sup> → hadrons, scaling and quark struct. 0-425  
 ep, deep inelastic scatt. cross sections, quark-parton model with broken scaling (*Russian*) 0-32109  
 ep deep inelastic scatt., scaling violations and QCD parametrisations, struct. functions (*Russian*) 0-37277  
 K<sup>-</sup>p →  $\Delta X$ , 8.25 GeV/c, off shell KK and pp interactions, KNO scaling 0-52534  
 K<sup>+</sup>p, K<sub>S</sub><sup>0</sup> and  $\Lambda$  inclusive production at 147 GeV/c 0-52539  
 N, EM form factors, dipole fit and scaling law, electroproduction in  $\Delta_{33}$  energy region 0-22625  
 np inelastic interactions, scaling deviations in secondary hadron energy distrib. 0-9161  
 p+nucleus, inclusive production of neutral strange and charged particles, collective tube model 0-52538  
 pp, K<sub>S</sub><sup>0</sup> and  $\Lambda$  inclusive production at 147 GeV/c 0-52539  
 pp, pp, Drell-Yan processes, scaling violation effects 0-382  
 pp-charged particle+X, small-angle production from nuclear and nucleon targets, collective tube model and triple-Regge picture 0-52538  
 pp collision inclusive spectra, fast pionisation at high energies, z-scaling (*Russian*) 0-47339  
 pp Drell-Yan lepton pair prod. processes,  $\pi$  structure function and scaling phenomena 0-405  
 pp →  $\Lambda^0 X$ , small-angle production from nuclear and nucleon targets, collective tube model and triple-Regge picture 0-52538  
 pp → p(slow)+X, 22.4 GeV/c, associative multiplicity (*Russian*) 0-5031  
 pp →  $\pi^0 X$ , scaling in the mean hypothesis and Feynman variable energy depend. 0-42501  
 pp →  $\pi^+ X$ , QCD radiation and mean scaling, longitudinal and transverse momentum 0-42405  
 $\pi^-$  p, 147 GeV/c, neutral particle prod., K<sub>S</sub>,  $\Lambda$ ,  $\bar{\Lambda}$ ,  $\gamma$ , multiplicity scaling form 0-22645  
 $\pi^-$  p Drell-Yan lepton pair prod. processes,  $\pi$  structure function and scaling phenomena 0-405  
 $\pi^+$  p, K<sub>S</sub><sup>0</sup> and  $\Lambda$  inclusive production at 147 GeV/c 0-52539

**scaling tubes** see counting tubes**scandium**

- see also nuclei with .....  
 crystal surface, N and O adsorption, refl. electron energy loss spectra obs. 0-20742  
 electron and positron multiple scatt. 0-15171  
 Sc<sup>+</sup>, excited config. position and level struct., review 0-32621

**scandium alloys**

- see also scandium compounds  
 Al-Sc foil, alloying effect on strength characts. and weldability 0-55475  
 Ce<sub>1-x</sub>Sc<sub>x</sub>Al<sub>2</sub>, fluctuating valence system, quadrupole interaction temp. depend. 0-54972  
 Dy<sub>0.9</sub>Sc<sub>0.1</sub>Al<sub>2</sub>, hyperfine field, NMR spectra 0-15811  
 Gd<sub>1-x</sub>Sc<sub>x</sub>, Mossbauer spectra, hyperfine interactions 0-15923  
 Sc-[Co,Ni,Cu]-Ga, phase equilibria, diagrams of state, X-ray, microstructural study (*Russian*) 0-53356  
 Sc-Gd spin glass, sp. ht., 0.3-10K 0-25145  
 Sc-H, conc.-temp. depend. at room temp. of elec. resist. thermo-EMF, mag. susceptibility, and Hall coeff. 0-29382  
 Sc-Rh-Si system, partial phase diagram, X-ray diff. and microprobe anal. 0-25659  
 Sc-Tb, induced-moment spin glass, simple mean-field theory 0-29553  
 ScAl<sub>2</sub>Er(Dy)(Nd), dil., EPR and mag. susceptibility 0-15797  
 Sc<sub>0.1</sub>Re<sub>0.9</sub>Si<sub>3</sub>, X-ray cryst. struct. determ. 0-39009  
 Tb-Sc, mag. ordering temps., susceptibility meas. 0-25136  
 Zr-Sc-Ga, phase equilibria 800°C (*Ukrainian*) 0-35157

**scandium compounds**

- see also scandium alloys  
 scandium octaethylporphyrin,  $\mu$ -oxo bridged dimer, triplet states and geometrys, ODMR obs. 0-9625  
 scandium octaethylporphyrin, triplet states and geometrys, ODMR obs. 0-9625  
 Eu<sub>2</sub>O<sub>3</sub>-Sc<sub>2</sub>O<sub>3</sub>-Ta<sub>2</sub>O<sub>5</sub> system, orthotantalate section, X-ray diff. and luminesc. obs., conc. depend. 0-54205  
 (La, Y, Sc)B<sub>6</sub> solid solns. electron work function, thermal emission technique 0-20755  
 Sc-H, conc.-temp. depend. at room temp. of elec. resist. thermo-EMF, mag. susceptibility, and Hall coeff. 0-29382  
 Sc-H, p-T phase diagram and influence of H pressure, on decomposition temp., DTA exam. 0-29929  
 Sc-M-B systems (M=Rh,Ir), phase equil. and cryst. structs. 0-15072  
 ScCl<sub>3</sub>, electronic struct., self-consistent and non-self-consistent band calcs. 0-44499  
 ScCl<sub>3</sub>, phonon dispersion curves 0-2130  
 ScH<sub>2</sub>,  $\Sigma$  state, Dirac-Fock one-centre calcs. 0-23301  
 ScH<sub>2</sub>, electronic struct., photoelectron spectra study 0-50527  
 ScH<sub>2</sub>, self-consistent bond struct., charge transfer 0-49590  
 ScH<sub>2</sub>, self-consistent energy bands, KKR method with Hedin-Lundqvist approx. 0-49593  
 ScH<sub>2</sub>, synchrotron XPS obs., rel. to theory for metal dihydrides 0-55275  
 ScH<sub>2</sub>:Er, ESP determ. of proton locations 0-34768  
 ScI<sub>3</sub>, vaporisation thermodynamics, sublimation and formation 0-54366  
 Sc<sub>2</sub>Ir<sub>4</sub>(Os<sub>2</sub>)(Ru<sub>4</sub>), cubic struct. type described by cluster concept, X-ray determ. 0-33933  
 (Sc<sub>2</sub>Lu<sub>1-x</sub>)<sub>2</sub>V<sub>2</sub>O<sub>7</sub> 0-29547  
 ScO molecule, B<sup>2</sup> $\Sigma^-$ -X<sup>2</sup> $\Sigma^-$  system, Franck-Condon factors and r-centroids 0-1025  
 Sc<sub>2</sub>O<sub>3</sub>, solid solubility in MgO 0-15247  
 Sc<sub>2</sub>O<sub>4</sub>, polycryst., form. conditions of anion vacancies, phase comp. 0-54220  
 ScP, electronic struct., self-consistent Hedin-Lundqvist and X $\alpha$  APW calcs. 0-29322  
 ScP, energy band struct., exchange-correl. pot. effects, APW calcs. 0-29321  
 ScRu<sub>4</sub>B<sub>4</sub>, superconducting and crystallographic data 0-33968

**scandium compounds continued**

- ScS, B<sup>2</sup> $\Sigma^-$ -X<sup>2</sup> $\Sigma^-$  system, rot. struct. and hyperfine effects near IR spectrum 0-5544  
 ScSi, paramag. susceptibility 0-50035  
 Sc<sub>2</sub>(SiO<sub>3</sub>)<sub>3</sub>, mag. susceptibility, temp. depend., 77-800K 0-20372  
 Sc<sub>2</sub>Si<sub>2</sub>O<sub>7</sub>, polymorphism at high press. and temp., thortveitite struct. stability (*French*) 0-10657  
 U<sub>3</sub>O<sub>8</sub>-Sc<sub>2</sub>O<sub>3</sub>, solid soln. electrode, high temp. electrochem. appl. 0-6828
- scanning electron microscope applications**  
 adhesion measurement, locus of failure, bond failure in adhesive joints 0-50801  
 adhesive energy, meas. techniques for metal/ceramic system 0-50803  
 Aspergillus niger dying spores, electron refl. and transmission SEM expts. after irradi. 0-56111  
 electron beam particulate analysis of air samples 0-40785  
 planar diode, heavily doped, collection efficiency and surface recomb. vel. modulation 0-20291  
 scanning laser microscope, electron beam excited 0-52303  
 semiconductor materials and devices, SEM characterisation methods 0-49064  
 Si p-n junction local temp. meas. using pulsed SEM, induced-current mode 0-54775
- scanning electron microscope examination of materials**  
 see also scanning electron microscopy  
 , 0-24456  
 acrylonitrile-butadiene-styrene copolymers, micromechanism of deform. and rupture (*German*) 0-35276  
 p-alkoxy-phenyl-p-acryloyloxy benzoate polymers, mesomorphic struct. 0-38905  
 $\alpha$ -brass, stress corrosion cracking in 15N ammonia solns., fractographic aspects 0-16547  
 CANDU irradi. fuel bundles, sheathed in Zircaloy-4, long term stability investig. 0-13774  
 cartilage, articular, meas. of surface microgeometry 0-3880  
 cast iron, white, high Cr-Mo, fracture toughness 0-50726  
 ceramic, brittle, specimen prep. for optical and SEM obs. (*German, English*) 0-35457  
 coloured coatings on Al, prod. in AC electrolysis, thick coatings case 0-25908  
 coloured coatings on Al, prod. in AC electrolysis, thin coatings case 0-21176  
 diamond, synthetic grits, crystal morphology of cyclic twins 0-2037  
 diffusion welded joints, creep deformation effect on characts. 0-25806  
 elastin ultrastruct., freeze-fracture electron microscopy 0-8036  
 epoxy resin, filled, wear props., SEM obs. 0-16500  
 epoxy resins, struct. changes under mag. field action 0-40516  
 ferromagnets, domain structure image obtained by SEM (*Polish*) 0-34682  
 fracture, surfaces (*Chinese*) 0-11849  
 glass, laser irradi. effects, SEM meas. (*German*) 0-24492  
 glass fibre reinforced polyester, fatigue behaviour 0-25856  
 graphite, D<sup>+</sup> bombardment, surface damage, sputtering, SEM study 0-32459  
 graphitic materials deformation, crack and fracture behaviour, SEM exam 0-11706  
 Hastelloy X, grain size effect. creep and creep-rupture (*Japanese*) 0-16382  
 Inconel 600, PWR primary corrosion products 0-13578  
 Inconel 625, nitriding in N<sub>2</sub>-H<sub>2</sub> glow discharge 0-16590  
 Inconel 625, plasma nitriding, surface topography obs. by SEM 0-45442  
 insulating films, on Si, struct. stability 0-54564  
 macroscopic metal catalysts, morphology and etching processes, review 0-7856  
 metal layered contacts, low temp. diffusion (*German*) 0-6538  
 metals, mechanical props., testing and modelling 0-25811  
 Metglas 2826 ribbons, ferromagnetic resonance and SEM obs. 0-15804  
 Ni powder 21J, porous, effect of sintering conditions in struct. and strength 0-20823  
 nylon 66, fatigue crack propagation, effect of moisture 0-3166  
 nylon 66 films, superstructural ordering 0-15344  
 optical fibre, mechanical strength, fractographical analysis, review (*Japanese*) 0-35319  
 p-n junction, short circuit, SEM investigation 0-6957  
 poly-1,6-dip-toluenesulphonyloxy-2,4-hexadiyne single cryst., twinning 0-33906  
 polyacetylene, nascent morphology obs. 0-24379  
 polyethylene, fibrillar, high mol. wt., oriented crystallisation, heat treatment effect (*Japanese*) 0-25738  
 polyethylene, obtained from heterogeneous Ziegler-Natta catalysts, cryst. morphology and growth 0-38941  
 polyethylene, ultra-high-strength filaments, soln. spun/drawn, mech. and thermal props. 0-40440  
 polyethylene electrets, charge trapping mechanism, TSC, DTA and optical meas. 0-11322  
 polypropylene fibre, with helical internal texture, SEM obs. of surface morphology 0-39394  
 polystyrene filament, melt spun, struct. and mech. props., effect of drawing, twisting, annealing, untwisting 0-45331  
 powder and sintered material particles, dimension and shape evaluation by SEM 0-40278  
 PVC, rigid, craze and yield zones in fracture 0-50701  
 PZT/polymer composites, simplified fabrication 0-40323  
 quartz, grinding and surface treatment by ball mill in cetyl alcohol (*Japanese*) 0-25890  
 quartz, synthetic, as-grown and etched cobbled Z-surfaces (*French*) 0-24719  
 Rene 95, as hot isostatically pressed (HIP) and HIP+forged, low cycle fatigue 0-25854  
 semiconductors, surface potentials using electron energy anal., SEM study 0-15582  
 stainless steel:C, surface, obs. at very low accel. voltage (200 V-1 kV) by SEM 0-10764  
 stainless steel, coated with C, surface damage by D<sup>+</sup> and He<sup>+</sup> ions irradi. 0-23146  
 steel, austenitic stainless, 18-8, effect of H on martensitic transformation (*Chinese*) 0-55394  
 steel, austenitic stainless, precipitates and grain orientation by non aqueous electrolyte potentiostatic etching method (*Japanese*) 0-15102  
 steel, C1020, dual phase, mech. behaviours and structs. (*Korean*) 0-25779



## scanning electron microscope examination of materials continued

- steel, C, failure mechanisms in impact fatigue 0-40493  
 steel, C, fatigue subsurface crack initiation, result of residual stresses 0-25833  
 steel, C and stainless, ductile fracture, in situ obs. of microprocess of failure (*Chinese*) 0-55492  
 steel, cast structural, heat treatment and mech. working influence on mech. props. (*Russian*) 0-40392  
 steel, composition effect on carburizing 0-35432  
 steel, Cr-Mo, toughness of heat treated steels of equal tensile strength (*German*) 0-25727  
 steel, Cr-Mo (2.25, 1 wt.%), damage accumulation and microstruct. changes during creep 0-3129  
 steel, Cr-Mo (2.25, 1. wt.%), small changes effect in impurity elements, creep life 0-25790  
 steel, ductile fracture in presence of elongated sulphides (*French*) 0-45394  
 steel, high speed type M-50 and 18-4-1, fracture and fatigue 0-16457  
 steel, high strength, H<sub>2</sub> embrittlement due to cathodic charging during specimen prep. for SEM (*German, English*) 0-11760  
 steel, maraging 300 grade, serrated flow in austenitic state 0-30041  
 steel, martensitic, age hardening with Cu, Nb additions, exam. of hardness 0-7681  
 steel, medium C, shell-shaped fracture due to B embrittlement (*Chinese*) 0-55493  
 steel, mild, AISI 1009 and 1018, corrosion incipient processes in hypersaline geothermal brine at 90°C 0-50753  
 steel, stainless, blistering owing to He<sup>+</sup> bombard., 2 MeV 0-49279  
 steel, stainless, He ion irradi., fracture behaviour, in-situ HV electron microscopy 0-29089  
 steel, stainless, PWR primary corrosion products 0-13578  
 steel, struct. type 05KhGM, crack initiation and propagation during H<sub>2</sub> embrittlement 0-35313  
 steel gas nitrosulphurising, S25C, wear property 0-50729  
 steels, austenitic stainless, crack propag. rates under high-temp. low cycle fatigue conditions 0-21088  
 steels, free-machining, fractography and X-ray photoelectron spectroscopy 0-7673  
 steels, structural St 37-2, cleavage fracture, report 0-25868  
 steels, welded, types D36, D50, secondary ion anal. of segregation 0-7580  
 Teflon foils, cryst. struct. and texture changes due to polarisation process (*Polish*) 0-35209  
 thermoplastic, partially crystalline, microscopic methods of struct. anal. (*German, English*) 0-30198  
 untreated insulating materials, direct viewing without charging, modification to Cambridge SEM 0-47150  
 X-ray dispersive crystal spectrometers, geometric accuracy (*Chinese*) 0-22495  
 Zircaloy, PWR primary corrosion products 0-13578  
 Zircaloy-2, effect of simulated fission products on elongation fractography and metallography 0-649  
 Zircaloy-4 cladding rubes, burst strain and stress corrosion cracking, I influence 0-3248  
 Ag film, sputtered, hillock growth and agglomeration by annealing, SEM obs. 0-2309  
 Ag, film, sputtering mechanism, SEM 0-29839  
 Ag films, hillock form. hole growth and agglomeration 0-44455  
 Ag, loosely packed powder, sintering SEM and dilatometry obs. 0-20843  
 Al alloy 7075-T7351, fretting fatigue crack form. 0-35344  
 Al lithographic sheet, AC etching, surface study 0-35547  
 Al, plasma-sprayed, effect of Si substrate surface conditions and impact velocity of sprayed particles 0-21145  
 Al, surface exfoliation and blistering induced by He ion bombard. in energy range 10-80 keV 0-39173  
 Al-Cu-Mg (4.1 wt.%), behaviour during ductile fracture, SEM (*Rumanian*) 0-21062  
 Al-Mg (1 wt.%), behaviour during ductile fracture, SEM (*Rumanian*) 0-21062  
 Al-Mg<sub>2</sub>Si (1.42 wt.%), aged, dislocation structs. caused by plastic deformation 0-25786  
 Al-Pd eutectic, microstruct. morphology 0-3018  
 Al-silicide-Si systems with CoSi<sub>2</sub>, Pt<sub>3</sub>Ni<sub>1-x</sub>Si, and MoSi<sub>2</sub> as silicide, diffusion, compound form., and microstructure 0-34253  
 Al-Zn-Mg, stress conversion cracking based on micromech. surface reactions 0-7716  
 Al-Zn-Mg-Cu, age hardened, effect of strain rate, temp. and environment on ductility 0-45368  
 Al<sub>2</sub>xO<sub>3</sub>, sintered, elec. cond. temp. and comp. depend., thermoelec. power 0-2438  
 Al<sub>2</sub>O<sub>3</sub>, defect microstructure due to ion bombardment, TEM study 0-34100  
 Al<sub>2</sub>O<sub>3</sub>, grinding and polishing, quantitative control and optimization (*German, English*) 0-35460  
 Al<sub>2</sub>O<sub>3</sub>, hot pressing, microstruct., texture 0-40299  
 Al<sub>2</sub>O<sub>3</sub> substrate, notched, grain struct., SEM study (*German*) 0-33860  
 Al<sub>2</sub>O<sub>3</sub> substrates, grain growth during sintering 0-40302  
 Al<sub>2</sub>O<sub>3</sub>:Ni anodised films, electrolytically coloured, spectrally selective surface 0-11490  
 Al<sub>2</sub>O<sub>3</sub>-glass mixture, microstructural changes and shrinkage during sintering 0-25640  
 Au film, interface reaction with n-type Ga<sub>0.7</sub>Al<sub>0.3</sub>As and GaAs 0-39482  
 Au film, ion plated, defect growth structs., SEM obs. 0-24768  
 Au, hardening mechanisms, grain size effect 0-35302  
 BaTiO<sub>3</sub>, surface microrief revealed by ion irradiation 0-54485  
 BaTiO<sub>3</sub> powder, US dispersed, SEM study (*German*) 0-33860  
 Be, implanted D and He, interaction and radiation enhanced oxidation 0-39120  
 Be-Cu strip surface quality and preparation 0-50779  
 C CVD coating, surface damage and erosion under energetic D<sup>+</sup> and <sup>4</sup>He<sup>+</sup> irradi. 0-39174  
 C fibre reinforced plastic, SEM obs. of fatigue 0-11737  
 C fibre reinforced plastic, fractography of fracture surface under three-point bending (*Japanese*) 0-55506  
 CaO, produced from CaCO<sub>3</sub> powder decomp. in vac. and in CO<sub>2</sub> 0-45255  
 Ca<sub>3</sub>(PO<sub>4</sub>)<sub>2</sub>, soln., coagulation effects on light scatt. obs., TEM, SEM 0-45090  
 Cd films, nucleation and growth, props. 0-29878  
 Cd,Hg<sub>1-x</sub>Te, correlation between structural and chemical inhomogeneity (*Russian*) 0-49484

## scanning electron microscope examination of materials continued

- CdIn<sub>2</sub>S<sub>4</sub> film, vac. deposited, growth, struct., optical and photoelectronic props. 0-10831  
 CdS, Au deposition, Schottky diodes and MIS devices, surface treatment effects, SEM obs. 0-54794  
 CdS solar photovoltaic panels, deposited by spray pyrolysis, film and junction structure studies 0-45689  
 CdSe film, vac. deposited, elec. resist. and surface changes by laser annealing 0-2491  
 CdSe, grown from melt, SEM exam. of dislocation boundaries 0-24456  
 CdTe sputtered films, struct., photocond., and trap distrib. 0-29489  
 Co-Cr superalloy, type MAR M509, high temp. fatigue behaviour 0-40485  
 Cr whisker cryst., growth incorporated with field electron emission 0-44458  
 Cr-V-B-Y system, fatigue strength and fatigue fracture at 20 and 1100°C, SEM study 0-3194  
 Cr<sub>2</sub>O<sub>3</sub>, grain growth during sintering (*Japanese*) 0-16261  
 Cr<sub>2</sub>O<sub>3</sub>, reduction by H<sub>2</sub>, reaction kinetics 0-11950  
 Cr<sub>2</sub>O<sub>3</sub>-Cr black, solar collector coating, microstruct., FIM and SEM obs. 0-26166  
 Cu, corrosion protection by benzotriazole pretreatment 0-16555  
 Cu, film, sputtering mechanism, SEM 0-29839  
 Cu, ion plated, defect growth structs., SEM obs. 0-24768  
 Cu, loosely packed powder, sintering SEM and dilatometry obs. 0-20843  
 Cu mirror, surface defect layer form. on mech. polishing 0-33122  
 Cu:Au:C, surface, obs. at very low accel. voltage (200 V-1 kV) by SEM 0-10764  
 Cu-Al-Ni-Fe system, corrosion behaviour in sea water 0-45421  
 Cu-Au thin films after accelerated ageing, failure by Kirkendall porosity, SEM study 0-6675  
 Cu-Ni alloys 706 and 715, corrosion in flowing sea water, dissolved sulfide effect 0-35379  
 Cu-Ni:polyethylene, surface, obs. at very low accel. voltage (200 V-1 kV) by SEM 0-10764  
 Cu-Sn-P (5, 1-5 wt.%), effect of P on friction and wear characts. 0-16494  
 Cu<sub>2</sub>S-CdS, SEM meas. of diffusion lengths, recombination vel. and junction collection efficiency 0-16808  
 Cu<sub>46</sub>Zr<sub>54</sub>, devitrification effect on mech. props. 0-30082  
 ErRh<sub>2</sub>Bi, film, sputter deposition and low temp. props. 0-2948  
 Fe, Armco, borided surface layers, Mossbauer and metallographic anal. 0-50769  
 Fe, ductile, with different secondary struct., abrasive wear (*German*) 0-25871  
 Fe, nitriding by ion beam 0-2095  
 Fe, pure, splat-quenched, martensite morphology, SEM study 0-7547  
 Fe whisker growth, on wustite, Wagner's mechanism 0-10847  
 Fe/ZrB<sub>2</sub>, metal-like cpd. form. in diffusion layer during solid phase saturation 0-19994  
 Fe-Cr-Al (0.3 wt.%), oxidation behaviour at high temps. (*Japanese*) 0-35404  
 Fe-Cr-Al-(Y), isothermal oxidation behaviour at 1200°C, SEM 0-50755  
 Fe-Cr-Al-(Y), thermal cycling influence on oxidation behaviour at 1200°C, SEM 0-50756  
 Fe-Mn-Ti alloys, austenitic, precipitation strengthened 0-25714  
 Fe-Ni superstructure in metal particles in chondrites 0-12713  
 Fe-Ni-Al system, multiphase diffusion at 1000°C, diffusion structs. and props. 0-19995  
 Fe-Ni-C (23, 0.39 wt.%), austenitic or martensitic structs., corrosion faces anal. (*French*) 0-21181  
 Fe-Ni-Cr, high Ni content, intergranular corrosion, effect of Cr (*French*) 0-7708  
 Fe<sub>2</sub>N, hard coating preparation by ion beam methods 0-25579  
 GaAlAs DH laser, In solder deterioration, Au diffusion in In 0-33019  
 GaAs, electron-beam induced conductivity 0-10922  
 GaAs, VPE layer growth with abrupt doping profile 0-24746  
 GaAs:Al, back surface gettering 0-10758  
 GaAs-Al<sub>x</sub>Ga<sub>1-x</sub>As current injection multi-quantum-well heterostructure lasers, MBE grown 0-19042  
 GaN:Al, VPE grown, luminesc. and elec. props. depend. on doping conc., bound excitons 0-20688  
 GaSb, CVD using organometallics, epitaxial growth 0-29879  
 Hf, RF sputter deposition, ion bombardment and ion implantation 0-25564  
 HfN on stainless steel, activated reactive evaporated coatings, high rate deposition, microhardness 0-25580  
 HfN, RF sputter deposition, ion bombardment and ion implantation 0-25564  
 Hg-Ag-Sn, dental amalgams, corrosion penetration in crevices 0-3238  
 HgCr<sub>2</sub>Se<sub>4</sub>:Cd, precipitations during growth by chem. transport method 0-55409  
 InGaAsP, epitaxial layer, defect evaluation by cathodoluminescence 0-2866  
 InP substrate, LEC-grown, defect evaluation by cathodoluminescence 0-2866  
 LaB<sub>6</sub>, high temp. interaction with O<sub>2</sub>, AES and mass desorption expts. 0-7698  
 LaB<sub>6</sub> single crystal needles, thermal field emitted electron total energy distribution spread 0-45218  
 Li electrode, in lithium perchlorate-propylene carbonate solution, surface anal. (*French*) 0-50859  
 Li electrode, passivation layer, in LiClO<sub>4</sub>-propylene carbonate solution, composition (*French*) 0-11899  
 Li-SOCl<sub>2</sub> hermetic D cells, effect of Li<sub>2</sub>B<sub>10</sub>Cl<sub>10</sub> and Li<sub>2</sub>B<sub>12</sub>Cl<sub>12</sub> on performance 0-12000  
 LiF, single crystal, neutron and gamma irradiation, SEM and Bragg profile anal. 0-15158  
 Li<sub>2</sub>O-SiO<sub>2</sub> glass, bulk crystn., SEM and optical microscope studies 0-44142  
 Mg-Ni-S, electroforming, mech. props. rel. to heat treatment 0-35133  
 MgO, hot-pressed, elasticity props. of polycrystals and single crystals 0-54301  
 MgO, precipitate morphology, strain energy effects 0-40358  
 MgO, solid solubility of Se<sub>2</sub>O<sub>3</sub>, Al<sub>2</sub>O<sub>3</sub>, Cr<sub>2</sub>O<sub>3</sub>, SiO<sub>2</sub> and ZrO<sub>2</sub> 0-15247  
 MnCO<sub>3</sub> crystals, gel. grown, Ca<sup>2+</sup>, Ni<sup>2+</sup> impurity influence, SEM study 0-20778  
 MnCo<sub>2</sub>O<sub>4</sub> DC sputtered films, struct. and elec. props. 0-54812  
 Mo flame sprayed coatings, comp., microstruct. and mech. props. 0-16598



## scanning electron microscope examination of materials continued

- Mo, fracture and crack propag. tested in tension along [001] axis (*Russian*) 0-50697  
 Mo laser mirror, optical and metallurgical characterisation 0-33129  
 Mo whisker cryst., growth incorporated with field electron emission 0-44458  
 Mo-Mn alloy, plasticity, fracture, strength depend. on C content (*Russian*) 0-35257  
 $\text{NH}_4\text{Fe}_3(\text{SO}_4)(\text{OH})_5$ , jarosite, decomposition 0-11624  
 $\text{NaO-CaO-SiO}_2$  glasses, fluorinating agents effect on comp. and surface struct. 0-35364  
 $\text{Na}_2\text{O-CaO-SiO}_2$  glass, fractographic anal. of delayed failure 0-45387  
 $\text{Na}_2\text{O-Al}_2\text{O}_3\cdot 10\text{TiO}_2$ , crystallized bronze, chem. comp., morphology, optical and thermal props. (*Japanese*) 0-16172  
 Nb, CVD, kinetics and microstruct., pressure and temp. depend. 0-11569  
 Nb CVD coatings on graphite, grain struct. depend. on temp. 0-25574  
 Nb, flaking and blistering due to He and Ne ion bombardment 0-29092  
 Nb, local heating during abrupt strain, catastrophic slip band formation 0-7652  
 Nb, superconducting bridges by electron beam lithography and ion implantation Josephson effect 0-20355  
 Nb/Cu-Sn-Mg, superconductor, effect of Mg addition to Cu-Sn matrix 0-25028  
 Nb-Ge-Si film, CVD, struct., comp., stability and homogeneity 0-15421  
 Nd:YAG, solid-state formation 0-35121  
 Ni, grain boundary cavities growth under applied stress and internal pressure 0-29032  
 Ni, plasma-sprayed, effect of Si substrate surface conditions and impact velocity of sprayed particles 0-21145  
 Ni, single crystals, H and liq.-Hg embrittlement 0-25862  
 Ni solar collector coating, microstruct., FIM and SEM obs. 0-26166  
 Ni, solar selective black coatings, electrochem. deposition on Zn surfaces 0-29885  
 Ni-Pd surfaces, electrochem. passive film form. and comp. determ. by SEM, SIMS, XPS 0-39401  
 Ni-pigmented anodic  $\text{Al}_2\text{O}_3$ , for selective absorpt. of solar energy, optical and struct. props. 0-55892  
 Ni-Si-B powder, oxidation at 850°C, SEM, ESCA, and elec. cond. meas. 0-7717  
 Ni-Ti (1.6, 7.64 wt.%), monophasic high temp. scaling, metallography study 0-21159  
 Ni-W surfaces in contact, deform. and adhesion at very low loads 0-39457  
 $\text{Ni}_{1-x}\text{Fe}_x\text{O}_4$ , precipitation of  $\alpha\text{-Fe}_2\text{O}_3$ , optical microscopy, SEM and TEM studies (*French*) 0-11650  
 Pb, electrode, potential effect on surface struct. in  $\text{H}_2\text{SO}_4$  in anodic region 0-16592  
 Pb, film, sputtering mechanism, SEM 0-29839  
 Pb superconducting microbridges, two-dimens. imaging of resist. voltage changes caused by electron irradi. 0-15659  
 Pb-In (40 wt.%), solid soln., single phase, superplastic behaviour 0-21048  
 PbS film, soln. grown on Si, struct. and comp. of heterojunction 0-54530  
 Pd sponge powder, sintering shrinkage kinetics 0-29900  
 PtRh5 alloy, phosphate glass addition effect on high temp. strength (*German*) 0-25807  
 Si, amorphous, hydrogenated film, struct. determ. using electron microscopy 0-10806  
 Si, CVD on  $\text{SiO}_2$  and  $\text{Si}_3\text{N}_4$ , SEM study (*Dutch*) 0-2960  
 n-Si, edge dislocation and stacking fault defect electrical recombination efficiency 0-15106  
 Si, electron-channelling imaging, defect obs. 0-10471  
 Si films, polycryst., glow discharge deposited below 250°C, struct. and morphology 0-49535  
 Si, fluorocarbon ion beam etching characts. 0-35363  
 Si, implanted annealed layers, amorphised structure formation mechanism and crystallographic nature 0-29091  
 Si, ion implanted, scanning electron beam annealing 0-6420  
 Si oxides, grown in Cl-containing ambients, correl. between elec. and material props. 0-39479  
 Si p-n junction, charge carrier recomb. at dislocations, combined SEM and TEM study 0-15105  
 Si:H plasma deposited film, amorphous, microstruct., TEM and SEM obs. 0-10801  
 Si-Al interface in semiconductors, electronic parts, electromigration aspects 0-39355  
 Si-Al-O-N, high-temp. fracture and diffusional deform. mechanisms 0-40509  
 Si-Al-O-N, oxidation mechanisms 0-40570  
 SiC coating on Mo, CVD and stability under thermal cycle conditions 0-7500  
 SiC, impurity redistrib. and anomalous grain growth effects during polycrystalline transform. 0-15033  
 SiC, single cryst., friction and wear behaviour in sliding contact with various metals 0-21112  
 $\beta\text{-SiC}$ , undoped compact, microstruct. development during heating 0-25746  
 SiC-Ni based superalloy reaction, at elevated temps., interface obs. 0-3287  
 $\text{Si}_3\text{N}_4$ , hard coating preparation by ion beam methods 0-25579  
 $\text{Si}_3\text{N}_4\text{-CeO}_2$ , surface stress development during oxidation 0-50736  
 $\text{Si}_3\text{N}_4\text{-MgO}$  (5 wt.%), hot pressed, fracture toughness as function of initial  $\alpha$ -phase content, SEM 0-3174  
 $\text{Si}_3\text{N}_4\text{-Y}_2\text{O}_3$ , hot-pressed, oxidation kinetics 0-16520  
 $\text{SiO}_2$ , fluorocarbon ion beam etching characts. 0-35363  
 Sn droplets, on Bi, Zn and Al, heterogeneous nucleation 0-44294  
 $\text{SrTiO}_3$ , surface microrelief revealed by ion irradiation 0-54485  
 (Ta,Ti)B<sub>2</sub> on graphite, CVD coating, hardness meas., SEM study 0-24760  
 Ta, CVD, kinetics and microstruct., pressure and temp. depend. 0-11569  
 Te, evaporated deposition, absorptivity and emissivity 0-25473  
 (Ti,Zr)B<sub>2</sub> on graphite, CVD coatings, hardness meas., SEM study 0-24760  
 $\alpha\text{-}\beta\text{Ti}$  alloys, high strength, heat-treated weldments, intergranular fracture 0-21097  
 Ti, RF sputter deposition, ion bombardment and ion implantation 0-25564  
 $\alpha\text{-Ti}$ , recrystallised commercial purity, Fe-rich precipitates obs. (*French*) 0-50637  
 Ti-Al-V (6.4 wt.%), fretting fatigue behaviour of temps. up to 600°C 0-21104  
 Ti-Al-V (6.4 wt.%), phase transformation after hydrogenation 0-7560

## scanning electron microscope examination of materials continued

- Ti-Al-V-Sn (6.6, 2 wt.%), depend. of  $K_{\text{ISCC}}$  on loading rate and crack orientation 0-45427  
 Ti-Al-Zr-Mo alloy 685, phase at  $\alpha/\beta$  interface (*French*) 0-25661  
 TiB<sub>2</sub> CVD coating, surface damage and erosion under energetic D<sup>+</sup> and <sup>4</sup>He<sup>+</sup> irradi. 0-39174  
 TiB<sub>2</sub> coating, D<sup>+</sup> and <sup>4</sup>He<sup>+</sup> irradi. effects 0-20753  
 TiN, RF sputter deposition, ion bombardment and ion implantation 0-25564  
 TiN-Ti<sub>3</sub>N<sub>2</sub>, activated reactive evaporation formed deposits, microstructure, transformation depend. on depositing conditions 0-24761  
 $\text{UO}_2\text{-20CeO}_2$  mixed powder, X-ray and microprobe exam. of homogenisation 0-25609  
 V<sub>3</sub>Ga superconducting tape, stress effect on critical current (*Japanese*) 0-50020  
 V<sub>2</sub>O<sub>5</sub>, (001) surface modification, during catalytic oxidation of propene (*French*) 0-45557  
 W, drawn wire, microstruct. effect on fracture 0-3177  
 W fibre reinforced Cu, interface porosity formation, on thermal cycling 0-30092  
 W, plasma-sprayed, effect of Si substrate surface conditions and impact velocity of sprayed particles 0-21145  
 W spheres, in liq. Ni, sintered, coalescing, crystallographic orientation, SEM study 0-45249  
 W whisker cryst., growth incorporated with field electron emission 0-44458  
 W, with different microstructs., temp. depend. of yield strength 0-16404  
 W/Cu powders, liq. phase sintering, particle rearrangement 0-45253  
 W-Al<sub>2</sub>O<sub>3</sub> cermet films, oxide evaporation deposited on Mo, Ti, Al<sub>2</sub>O<sub>3</sub> substrates, struct., props. 0-25581  
 W-Cr solid solution, precipitation behaviour, reaction front motion, lattice parameters (*German*) 0-55401  
 WC-Co carbide, crack paths, SEM study (*Japanese*) 0-50710  
 WC-Co cemented composites, abrasion by quartz 0-16495  
 Zircaloy-4, heat treated in  $\text{SiO}_2$  capsules, Zr and Si vapour transport surface struct. anal. of deposits 0-55437  
 Zn, film, sputtering mechanism, SEM 0-29839  
 $\text{Zn}_{1-x}\text{Ni}_x\text{Fe}_x\text{O}_4$ , heat treatment and sintering effect on porosity 0-25610  
 ZnO crystals, SEM study (*German*) 0-33860  
 ZnSe:In films, MBE growth, doping effect on photoluminesc. 0-10818  
 ZnTe, elec., SEM and TEM studies of impurity segregation during long annealing 0-30001  
 ZnTe:Li, diffusion investigation by SEM and TEM 0-10706  
 ZnTe:Li, impurity segregation during short annealing and quenching, SEM, TEM and elec. meas. 0-10676  
 Zr, RF sputter deposition, ion bombardment and ion implantation 0-25564  
 ZrN, RF sputter deposition, ion bombardment and ion implantation 0-25564
- scanning electron microscopes**  
 see also scanning electron microscopy  
 Cambridge, modification for viewing untreated insulating materials 0-47150  
 development and appls. 0-13187  
 energy dispersive spectrometer 0-27378  
 filter for removing backscattered electrons in energy-dispersive analysis 0-13189  
 liquid He state 0-9073  
 magnification standard reissue 0-27375  
 microprocessor controlled vector scan pattern generator 0-13188  
 principle and degrees of sophistication 0-37124  
 sample preparation for X-ray microanalysis, cryogenic stage 0-42306  
 semiconductor detector for testing SEM quality parameters 0-22484  
 vacuum improvement technique 0-27381
- scanning electron microscopy**  
 see also scanning electron microscope applications; scanning electron microscope examination of materials; scanning electron microscopes  
 Auger, instruments and appl. 0-52370  
 Auger SEM using digital integrator 0-37131  
 cell organelles, ultrastructure from SEM of thick sections etched by O plasma 0-21584  
 cross-section preparation and handling, chick embryo appls. 0-21588  
 development and appls. 0-13187  
 direct grounding tool for uncoated specimens examination 0-4821  
 electrocrystallisation, recent progress in electrochem. and physical methods (*French*) 0-7510  
 electron-channelling imaging, defect obs. 0-10471  
 elemental analysis, X-ray, energy dispersive vs. wavelength dispersive concepts 0-16739  
 energy dispersive spectroscopy 0-27378  
 fatigue crack propagation, new measurement and observation techniques 0-45463  
 filter for removing backscattered electrons in energy-dispersive analysis 0-13189  
 freeze fractured chicken erythrocyte nuclei, 3D view of chromatin 0-8229  
 freeze-drying of articular cartilage for investigation of rat femoral heads 0-26433  
 high specimen chamber pressure techniques 0-22483  
 intercellular junctions in FANFT-induced carcinomas of rat urinary bladder in tissue culture 0-8230  
 ion etching, SEM dynamic study 0-50734  
 magnetic contrast, type-2, isolation by lock-in technique 0-13184  
 mass analyzer using electron-beam-guiding type ion source 0-31933  
 module for continuous rotation of cylindrical specimens 0-22486  
 powder scintillators, type P-47 0-22487  
 principles and examples of SEM photographs (*German*) 0-33860  
 resolution degradation, effect of collector field 0-52372  
 sample holder for critical point drying 0-22485  
 sample preparation, for materials microanal. with SEM 0-37129  
 scintillation detector, electro-optical props. 0-52819  
 signal treatment, backscattered electron spectral distrib. (*French*) 0-42305  
 solar cell interaction with SEM electron beam anal. 0-7943  
 spatial resolution of SEM electron beam induced conductivity images 0-6327  
 stereological analysis in SEM 0-22482  
 stress-strain, recording attachment 0-25961  
 surface analysis, AES and ESCA combined with SEM (*French*) 0-47154  
 surface associated microorganisms, effects of specimen preparation on preservation 0-21582



**scanning electron microscopy continued**

thin film, and surface anal., modern methods 0-54486  
voids in sintered materials, qualitative and quantitative investig. 0-16212  
Au decoration technique, TEM and SEM study of localisation of decorating crystallites (*French*) 0-10470

**scanning radiography**

see also *computerised tomography; radioisotope scanning and imaging*  
abdominal examination by X-ray planigraphy 0-21529  
Arnold-Chiari malformation: diagnosis by iodo-myelo-tonsiollography with tomography 0-36088  
colour TV system with soft X-ray preferred display 0-56186  
computerised tomography, X-ray, Rotate/Rotate type whole body scanner using direct magnification 0-21565  
flashing tomosynthesis, pre-folded Fourier-filter reconstruction of coded-aperture images 0-53222  
grid-coded flashing tomosynthesis, heart phantom radiographs 0-51206  
image reconstruction from parallel projections (*French*) 0-3808  
kymography, motion picture apparatus 0-30851  
kymography, theoretical aspects 0-30844  
pulmonary hila, 55° posterior oblique tomography 0-41189  
X-ray tomography, non-computed, using coherent light reconstruction 0-17116

**scanning-transmission electron microscope examination of materials**

see also *scanning-transmission electron microscopy*  
acetylene, catalytic decomposition, STEM of catalyst particles 0-24328  
aluminosilicate glass, phase separated, phase characterization by STEM and X-ray microanal. 0-50643  
amorphous materials, small area struct. studies 0-44087  
asbestos, elemental intensity ratio variation used to identify fibres 0-3462  
FCC metal, microdeform. at low temp. 0-47155  
II-VI semiconductors, lattice defects, X-ray diffr. and electron microscopic study 0-15088  
image resolution and penetration in amorphous and polycrystalline materials, comparison with conventional TEM 0-14976  
polyacetylene, nascent morphology obs. 0-24379  
small particles, characterisation and microanal. by STEM combined with other techniques 0-50901  
steel, carbide particles, EM400 electron microscope 0-24328  
steel, commercial alloy ferritic, meas. of alloy and impurity elemental distrib. using STEM 0-35601  
steel, Cr ferritic stainless, meas. of alloy and impurity elemental distrib. using STEM 0-35601  
steel, Cr-Mo (2.25, 1 wt.%), small changes effect in impurity elements, creep life 0-25790  
steel, Cr-Mo low alloy ferritic, meas. of alloy and impurity elemental distrib. using STEM 0-35601  
stress induced martensitic transformations 0-47155  
Al-water vapour reaction, stress corrosion susceptibility STEM study, Mg addition effect 0-3247  
C amorphous film, adsorpt., atomic imaging using the dark-field annular detector in the STEM 0-6331  
Fe-Cr-C, austenite to ferrite+precipitate reaction, TEM/STEM study 0-3075  
Fe-Cu-Ni, austenite to ferrite+precipitate reaction, TEM/STEM study 0-3075  
Fe-V-C, austenite to ferrite+precipitate reaction, TEM/STEM study 0-3075  
Pb, supercooled liquid thin films, liq. struct. factor determ. by STEM 0-10487  
Si<sub>3</sub>N<sub>4</sub>-(MgO+Al<sub>2</sub>O<sub>3</sub>)(Y<sub>2</sub>O<sub>3</sub>), hot-pressed and sintered, microstruct. and impurity distrib. 0-49261  
Ti-Cr, phase transformation, appl. of Philips STEM400 system 0-25689

**scanning-transmission electron microscopes**

see also *scanning-transmission electron microscopy*  
double focus electron probe, lens for STEM 0-9074  
filtered diffr. patterns and images, direct prod. 0-31950  
fine microstructural details, characterisation 0-24328  
image accumulation, storage and display system 0-37132  
specimen stage, low temp. in-situ deform. of metals 0-47155

**scanning-transmission electron microscopy**

see also *scanning-transmission electron microscope examination of materials; scanning-transmission electron microscopes*  
atomic imaging using the dark-field annular detector in the STEM 0-6331  
diffraction patterns and bent contours visibility in thick composite amorphous-crystalline specimens 0-1906  
fine microstructural details, characterisation 0-24328  
image resolution and penetration in amorphous and polycrystalline materials, comparison with conventional TEM 0-14976  
in-situ deform. of metals, room temp. to 16K 0-47155

**scattering**

see also *acoustic wave scattering; backscatter; electromagnetic wave scattering; potential scattering*  
analytic continuation in decay-scattering systems, singularities as model basis 0-8850  
analytic extrapolations towards interior points from a cut, applic. to elementary particle scatt. theory 0-12952  
Bessel functions, asymptotic approx. 0-31562  
Boltzmann equation, exactly soluble, with persistent scatt. 0-46997  
classical limit for scattering in liquids 0-17842  
completeness value for eigenfunctions of second order differential eqns. 0-31564  
Coulomb problem, symmetry and invariance, canonical transformations 0-41989  
decay-scattering systems, resonances and their eigenfunctionals in Friedrich's model 0-8847  
density matrix of scattered particles, comments on 0-22219  
density matrix of scattered particles 0-22218  
Faddeev integral eqns. for three charged particles (*Russian*) 0-8830  
Fokker-Planck eqn., kinetic effects due to detailed equilibrium violation, elastic scatt. (*Russian*) 0-31687  
gravitational radiation, long-wave, primordial, induced scatt. by galaxies 0-17661  
Haag-Ruelle scattering theory as scattering theory in different state spaces 0-4593  
hidden symmetries in dynamical systems 0-37168  
internal waves with finite fluid depth, inverse scatt. problem, Backlund transformation 0-31517  
inverse scattering and solitons, geometric considerations 0-4550

**scattering continued**

inverse scattering problem in Rayleigh-Debye approx., diameter distrib. functions of helical structs. 0-27182  
3×3 inverse scattering transform, soliton perturb. scheme 0-27151  
longitudinal wave scattering by sphere-like bodies of revolution (*Ukrainian*) 0-22202  
ocean continental shelf waves, scatt. by isolated topographic irregularities 0-51423  
Painleve transcendents, geometric struct. and inverse scatt. problems 0-31600  
Poisson summation formula, generalisations 0-4565  
quantum field systems, scattering theory asymptotic conditions, field and Hamiltonian props. 0-13222  
resonance transfer rate of electron excitation, model of convergent terms, effect of diffusional motion of particles 0-8936  
rigged Hilbert space and decaying states 0-4591  
small angle scattering, by ellipsoid of rev. or sphere distrib., equivalence 0-99  
solid layers, conversion electron scatt. processes anal. 0-45181  
two-particle scattering systems, general, sum rules 0-8862  
unstable quantum states and rigged Hilbert spaces in nonrelativistic scatt. theory 0-8849  
wave scattering, second order approx. in planar linear sheet 0-17812

**scattering matrix** see *S-matrix theory***SCF calculations**

for *MS SCF (MS Xalpha) calculations* see *Xalpha method*  
see also *HF calculations; Xalpha calculations*  
acetaldehyde, first triplet state geometry, fragmentation into free radicals 0-47915  
acetonitrile, quadratic force fields, MOCIC pot. functions calcs. 0-5475  
acetylene, mol. and cluster Auger spectrum calc., SCF core-valence-valence spectra 0-48045  
acetylene, multipole moments and polarisabilities, SCF calcs. 0-5471  
acrolein, excitation, ionisation and electron affinity, expts., HAM/3 calcs. 0-18790  
adenine tautomers, relative stabilities, nonempirical MO calcs. 0-21442  
amides, geometry from ab initio calcs. 0-23338  
amino acid protonation ab initio Hartree-Fock-Roothaan SCF calcs. 0-9503  
atom, bound state quantum fluctuations and variational method, relativistic HF calc. with radiative effects 0-42918  
atom, SCF electron-gas local-spin-density model including correlation, appl. to He through Ar 0-9488  
atom-pair interactions in molecules, semi-empirical MO calc. 0-915  
atomic anions positron complexes, ground and excited states theoretical studies 0-42934  
atoms, complete active space method, comparison of super C I and Newton Raphson scheme 0-47904  
atoms, nucl. vol. isotope shift theory, many electron effects 0-47851  
benzene,  $\pi$  electron system, excitation energy, appl. of MBPT 0-52876  
benzene, SCF-EHT polarisability calc. 0-47895  
bond orbital model, atomic charges calcs., fully localised SCF method 0-42923  
carbonic anhydrase, active site substrate binding, environmental effects, CNDO and SCF LCAO calcs. 0-8002  
carbonyls, core ionisation phenomena, nonempirical LCAO MO SCF investigation. 0-37906  
chromium formate, mol., Hartree-Fock instability of SCF wavefunctions 0-9492  
condensed matter, orbital and pot. functions calcs., eq. of state 0-44463  
coronene, excited state Faraday values mag. circular dichroism spectra and MO CI calcs. 0-18877  
coupled vibration systems, eigenvalues, semi-classical SCF calcs. 0-27929  
cubic lattices, dipole moments of point polarisable atoms, uniform applied electric field, SCF equations 0-50257  
dihydroxycarbene, singlet and triplet state rot. pot. surfaces 0-32627  
dynamical damping in ab initio MO SCF calcs., energy minimisation method 0-18777  
effective convergence to complete orbital bases and at HF limit through systematic Gaussian primitive sequences 0-14065  
EM wave transient scattering, time domain method 0-38655  
ethane, multipole moments and polarisabilities, SCF calcs. 0-5471  
ethylene, mol. and cluster Auger spectrum calc., SCF core-valence-valence spectra 0-48045  
ethylene, multipole moments and polarisabilities, SCF calcs. 0-5471  
ethylene, planar dissociation, electronic rearrangement, states, bonds, ab initio multiconfigurational SCF calcs. 0-27937  
ethylene, quasidegeneracy and effective Hamiltonians, canonical transformation cluster expansion formalism 0-52888  
exponential transformation, quadratically convergent SCF procedure, appl. to closed shell ground states 0-47875  
ferrocene, metal to ring distance, ab initio MO SCF calcs. 0-47870  
fluoroethyl radical, unimol. dissoc., pot. energy characts. and energy partitioning calcs. 0-45488  
fluoroform, quadratic force fields, MOCIC pot. functions calcs. 0-5475  
formaldehyde H<sub>2</sub>S(H<sub>2</sub>O) complexes, ab initio SCF MO calcs., binding energy dispersion contrib. 0-27967  
formic acid, conform. hypersurface determ. and analysis 0-1078  
geometry optimisation with explicit inclusion of electron correl. 0-37748  
guanine tautomers, relative stabilities, nonempirical MO calcs. 0-21442  
HAM/3 formalism, semiempirical, energy expression derivation 0-903  
Hartree, anal. of dilute polymer solns. 0-5648  
Heisenberg antiferromagnet, AFMR freq. temp. depend., integral peak intensities (*Russian*) 0-54951  
hydrocarbons, small, electron momentum distrib. in  $\pi$  orbitals from (e,2e) expts. 0-14239  
inorganic binary ionic-covalent compounds, cryst., inorganic static effective charge calcs. (*French*) 0-2331  
intermolecular energies calculation from delocalised pictures, artifacts and elimination 0-18899  
intermolecular forces, ab initio calcs. applicability and accuracy 0-18898  
internal conversion calc., Hartree-Fock-Slater and Hartree-Fock models 0-18238  
ion clusters, 3-body pots., SCF energy partitioning calcs. 0-18953  
isomerisation, model reaction, SCF-SI theory calcs. 0-23399  
light atom molecules, general quadratic force fields, semiempirical MOCIC calcs. 0-5474  
liquid crystals, mesomorphic state formation mechanism and molecular struct. correlation 0-54128  
MCSCF method improvement 0-52857



## SCF calculations continued

metals, compressibilities, general pseudopotential approach 0-54631  
 methane, mol. and cluster Auger spectrum calc., SCF core-valence-valence spectra 0-48045  
 methyl halides, mol. force fields, IR intensities, and vibr. props. 0-47879  
 methylacetylene, quadratic force fields, MOCIC pot. functions calcs. 0-5475  
 methylene peroxide, multiconfig. SCF CI calcs. 0-18803  
 MNDO semiempirical calcs. accuracy rel. to current MO methods 0-47893  
 mol. and cluster Auger spectrum calc., SCF core-valence-valence spectra 0-48045  
 molecular crystal, action of external forces on mesogenic struct. form. 0-2147  
 molecular electronic structure, solid state approach 0-9508  
 molecular systems, saddle points and min. energy paths, constrained simplex optimisation procedure 0-42943  
 molecules, complete active space method comparison of super C I and Newton Raphson scheme 0-47904  
 molecules, natural orbitals, Brillouin-Levy-Berthier theorem, multiconfigurational SCF optimisation 0-27936  
 molybdenum formate, mol., Hartree-Fock instability of SCF wavefunctions 0-9492  
 Mott transition in the presence of impurities, Hubbard model and SCF anal. 0-10878  
 multiconfiguration Dirac-Fock program, appl. to Ba X-ray levels and 5p excited spectra 0-47865  
 nitrosomethane, ground state and nonvertical  $n-\pi^*$  excitation energy calcs. 0-18804  
 nucleic acid bases,  $Zn^{2+}$  binding, ab initio SCF (pseudopot.) calcs. 0-12052  
 one-dimensional molecular crystals, electronic struct., mol. orbital theory 0-54588  
 one-electron Hamiltonian method applied in SCF theory to states with open shell 0-23302  
 open-shell SCF secular eqn., iterative algorithm soln. 0-52868  
 organic molecules, quadrupole moments, dipole quadrupole A and C polarisabilities, perturbation theory anal. 0-27934  
 organic system, nonlinear second-order optical susceptibility 0-9947  
 ozone,  $^1A_1$  ground state, dipole moment function, ab initio SCF and CI calcs. 0-32628  
 pentofuranosyl nucleosides, isomeric,  $^1H$  NMR coupling consts., SCF FPT INDO approx. calc. 0-14156  
 photosynthetically relevant molcs., electronic structural props. 0-16902  
 pinacyanol dye, adsorbed on CdS substrate, aggregation effect on mol. electronic states 0-37757  
 polar molecule, excited state MCSCF wave functions, BeO appl. 0-47916  
 polar molecule clusters, 3-body pots., SCF energy partitioning calcs. 0-18953  
 polarization Green's function with multiconfiguration self-consistent-field reference states 0-37724  
 polyatomic molecule, SCF-SI theory applic. to coupled vibr. motion 0-23399  
 polycrystals, single phase, stress strain relations by X-ray diffraction (*Russian*) 0-5999  
 polydiacetylenes, electronic struct., cyclic vs. linear models 0-54587  
 polyethylene, deformation, Hartree-Fock SCF calcs. 0-18949  
 polymer chains, Coulombic contributions, LCAO-SCF-CO method, Fourier representations 0-32862  
 pseudopotential form factor determ., exchange interaction and correlation effects 0-49639  
 pyrazine, excited and  $N_{1s}$  ionised states, ab initio calcs. broken orbital symm. 0-27931  
 quark affinity to water molecule, centre expansion SCF calcs. 0-43213  
 radical, small, isotropic hyperfine coupling consts., MINDO/3 calcs. 0-52894  
 SCF-LCAO-MO calculation, semi-empirical, correct orthogonalisation of basis set 0-32613  
 semiconductors, deep levels, self consistent LCAO MO calcs. 0-29353  
 single-particle density matrix, perturbation expansion 0-54635  
 sparse s and p type Gaussian basis set LCAO MO SCF calc., mol. props. 0-23306  
 supermolecule calcs. with additive procedure, intermolecular interactions and binding energy 0-52880  
 TCNQ salt, NMP-TCNQ, electronic struct., SCF calc., total energy polarisation effects 0-15469  
 thiocarbonates, mol. struct., S-substitution effect (*French*) 0-23335  
 thionitrates, mol. struct., S-substitution effect (*French*) 0-23335  
 third row element molcs., general harmonic force field, SCF-MO-MNDO and freq. calc., MOCIC pot. 0-27948  
 three-dimensional crystal, Hartree-Fock theory of surface states 0-44468  
 transition metal atom, many-config. approx. in X-ray and electronic spectra interpret. 0-32615  
 transition metal dihydrides, gas phase geometrical struct. calcs. 0-42951  
 triphenylene, excited state Faraday values mag. circular dichroism spectra and MO CI calcs. 0-18877  
 $e^+A^-$ , positron-containing ground-state negative ions, self-consistent Fock field 0-47888  
 $e^+Br^-$ , positron-containing ground-state negative ions, self-consistent Fock field 0-47888  
 $e^+I^-$ , positron-containing ground-state negative ion, self-consistent Fock field 0-47888  
 $[Re_2Cl_2]^{2+}$ , spectral assignment, metal-metal bonds, SCF X $\alpha$  SW calcs., relativistic corrections 0-53006  
 Al, single vacancy formation energy calc., SCF-LCGO modified solid state scatt. theory 0-54637  
 Al $_2$ , repulsive region ground state pot. curves, SCF with STO basis set calc. 0-14188  
 Al $_2^{6+}$ , repulsive region ground state pot. curves, SCF with STO basis set calc. 0-14188  
 AlH $^+$  radical cation, EPR matrix isolation obs., hyperfine components calcs. 0-14158  
 Ar, aqueous soln., dil., energy and struct., pair pot. energy function, Monte Carlo calc. 0-54107  
 Ar, solid, self consistent field calcs. of isotherms and thermodynamic props. (*Russian*) 0-10633  
 Ar, solid, thermodynamic props. under press., multiparametric pairwise and Lennard Jones potential calcs. 0-39316  
 Ar $_2$ , interatomic potential single parameter 0-48059  
 Be cluster, multibody expansions, convergence 0-23594

## SCF calculations continued

$Br^- + He$ , electron detachment, SCF calcs.,  $BrHe^-$  and  $BrHe$  pots. 0-23503  
 $Br^-(H_2O)_n$ , hydration energies, orientation, ab initio-LCAO SCF MO calcs. 0-27944  
 $CF_3$ ,  $CF_3^-$ , and  $CF_3^+$ , optimised struct. and bonding, ab initio SCF MO calc. 0-23334  
 $CN^+$ , ground state, identity, ab initio CI calcs. 0-5468  
 $CN^+$ , lower states, pot. energy curves, equilib. distances SCF CI calcs. 0-27957  
 $CO$ , electronic struct., binding energy and interatomic distance, SCF variational cellular calc. 0-9498  
 $CO$ , one-electron props., SCF and CI calcs. 0-27951  
 $CO_2$ , low energy electron (positron) collisions, ab initio adiabatic polarisation pots. 0-14240  
 $CO_2$ , nonbonding, vibr. motion calc. using SCF-SI theory 0-23399  
 $CS_2$ , symmetric stretch mode, moments and polarisability derivatives, SCF calcs. 0-901  
 $CdH$ , low lying electronic states, ab initio SCF-CI calcs. 0-52893  
 $Cd$ , as 470 nm absorber, multiconfig. SCF calcs. 0-32731  
 $Cd^{2+}$ , 470 nm absorber, multiconfiguration SCF calcs. 0-27963  
 $CoCl_n$ , electronic struct., INDO theory 0-42948  
 $Cu$  (100) monolayer, self consistent electronic struct. 0-6926  
 $CuCl_n$ , electronic struct., INDO theory 0-42948  
 $CuO$ , ab initio HF-MC-SCF with GTO basis set, dissoci. energy and bond length 0-47890  
 $FCIO^+$ , radical cation, struct. and electronic props., ab initio RHF SCF MO calc. 0-52883  
 $FH-OH_2$  (dimethyl ether), H-bonded complexes, cubic force consts. calcs. 0-47868  
 $F^-(H_2O)_2$ , 3-body pots., SCF energy partitioning calcs. 0-18953  
 $FeCl_n$ , electronic struct., INDO theory 0-42948  
 $n-GaAs-Ga_{1-x}Al_xAs$ , superlattice, subband struct. and optical spectra, self-consistent calc. 0-15443  
 $H$ , bond energy, chem. substitution influence 0-37718  
 $H_2$ , nucl. mag. shielding and susceptibility, elec. field depend., SCF-Hartree Fock method 0-18791  
 $H_2$ , polarisability, finite field MC SCF calcs. 0-14075  
 $H_2$ , repulsive intermol. pot. 0-32794  
 $H_2 + H_2$ , interaction polarisability comparison with the He diatom, ab initio SCF calcs. 0-27943  
 $HCCN$ , a cyanocarbene, geom. struct., electron correl. effects 0-1077  
 $HCN^+$ , A and B  $^2\Sigma^+$  states, pot. surfaces, ab initio SCF calcs. 0-27959  
 $HCS^+-CSH^+$ , struct. and stability, ab initio SCF calcs., CNDO calcs. 0-32608  
 $HF$ , nucl. mag. shielding and susceptibility, elec. field depend., SCF-Hartree Fock method 0-18791  
 $(HF)_3$ , 3-body pots., SCF energy partitioning calcs. 0-18953  
 $HN_3$ , ground  $A'$  state, SCF and CI calcs., conform., geom., vibr. freqs. and dissoci. 0-18806  
 $H_2O$ , ground state ionis. pots., generalized Mo theory 0-52907  
 $H_2O + H_2O(F^-)(CH_4)$ , interaction energy calc. using minimal basis sets 0-9678  
 $(H_2O)_n$ ,  $n=2$  to 8, correlation energies, ab initio and SCF calcs. semiempirically corrected 0-43223  
 $Hg_2^{2+}$ , electronic struct. and photoabsorpt. calcs. 0-27932  
 $H_n^+$  ( $n=7, 9, 11, 13$ ), geometry optimisation, ab initio SCF calcs. 0-53180  
 $K^+$  in molecular complexes, K-edge absorpt. spectra, Z+1 analogy, theory-expt. comparison 0-47935  
 $KF$ , ab initio SCF MO energy, dipole moment and polarisability 0-1085  
 $Li$ -like ions, partial photoionis. cross-sections and radiative recomb. rate coeffs. 0-52951  
 $Li_2$ , second virial coeffs., Konowalow MCSCF potential calcs. 0-23312  
 $Li_2^n$  ( $n=1, 2, 3$ ), stable cluster configs., ionisation pots., binding energies, vibr. freqs., ab initio SCF and CEPA calcs. 0-14265  
 $LiAlF_4$ , struct. pot. energy surface,  $Li^+$  migration, ab initio LCAO SCF calcs. 0-23305  
 $LiF$ , ab initio SCF MO energy, dipole moment and polarisability 0-1085  
 $LiF$ , F centre study by mol. SCF calcs. 0-44530  
 $LiF^+$ , ground and excited states, ab initio calcs. single config. and multiconfig. SCF calcs. 0-52873  
 $Li^+(OH_2)_3$ , 3-body pots., SCF energy partitioning calcs. 0-18953  
 $Mg$  cluster, multibody expansions, convergence 0-23594  
 $N_2$ , 50 eV elastic electron scatt., centrifugal-dominant channel decoupling 0-32831  
 $N_2$ , electron-mol. adiabatic polarisation pots. and ab initio SCF polarisabilities 0-9499  
 $N_2$ , electronic struct., binding energy and interatomic distance, SCF variational cellular calc. 0-9498  
 $N_2$ , ground state ionis. pots., generalized Mo theory 0-52907  
 $N_2$ , low energy electron (positron) collisions, ab initio adiabatic polarisation pots. 0-14240  
 $N_2$ , multiple moments, polarisabilities and anisotropic long range interaction coeffs. 0-43206  
 $N_2$ , one-electron props., polarisabilities and polarisability derivatives, SCF and CI calcs. 0-37746  
 $NF_3$ ,  $NF_3^-$ , and  $NF_3^+$ , optimised struct. and bonding, ab initio SCF MO calc. 0-23334  
 $NH_3$ , HF geometry calcs. and SCF calcs. 0-47877  
 $NH_3$ , lowest triplet state geometry, SCF and CEPA-PNO calc. 0-914  
 $NH_3 + 2H_2$ , triplet  $n3S$  Rydberg state, ab initio UHF CI SCF calc. 0-53095  
 $N_2H_2$ , model rearrangement system, electron correlation and basis set effects 0-3317  
 $N_3H_3$  radical, lowest two electronic states 0-925  
 $NH_4Cl$ , gas  $A_1$  ground state, pot. surface 0-32626  
 $^{15}N-^{13}C$  spin-spin coupling constants calc. using SCF and INDO method 0-32609  
 $NbC$ , electronic struct. of vacancies, effect on supercond. transition temp. 0-29347  
 $NiNO$ , ground and core hole states, config. depend. HF LCAO SCF calc., relax. and binding energy 0-29453  
 $O_2$ , electronic struct., self-consistent pseudopot. calc. 0-9508  
 $O_2^+$ , electron impact dissoci. recomb., pot. energy curves calcs. 0-53150  
 $O_2$ , open-shell SCF secular eqn., iterative algorithm soln. 0-52868  
 $OCl_2^+$ , radical cation, struct. and electronic props., ab initio RHF SCF MO calc. 0-52883  
 $PbS$ , first-principles calc. of eqn. of states 0-49649  
 $Re_2Cl_6$  metal cluster complexes,  $He(I)$  photoelectron spectrum, SCC DV X $\alpha$  calcs.,  $Re_2Cl_6^{2-}$  comparison 0-28063



**SCF calculations continued**

- $\text{Si}_2^{2+}$ , electronic struct. and localised MOs, bonding nature and geom. struct. 0-18798  
 $\text{SO}_2$ , low lying bound mol. electronic states, SCF CI calc. 0-23314  
 $\text{Se}_n^{+}$ , electronic struct. and localised MOs, bonding nature and geom. struct. 0-18798  
 $\text{Si}$ , Jahn-Teller distorted vacancy, electronic struct. 0-10869  
 $\text{Si}$ , vacancy, self-consistent electronic states 0-29354  
 $\text{SiF}_3$ , XUV spectra, overlapping core-valence and core-Rydberg transitions and resons. 0-32735  
 $\text{Si}_2\text{H}_4$  ground state struct., ab initio SCF calcs., singlet silylsilylene 0-27945  
 $\text{SiX}_4$  ( $\text{X}=\text{Cl}, \text{H}, \text{F}$ ), chemical shifts, relax., X-ray spectra, SCF Xalpha calcs. 0-27928  
 $\text{Ti}_5$ , electronic structure of five and ten atom chains SCF-X $\alpha$ -SW calcs. 0-5483  
 $\text{TiF}_3$ ,  $\text{TiF}_4$ , X-ray emission, core level chem. shift calcs. 0-53010  
 $\text{TiH}$ , electronic structure of five and ten atom chains SCF-X $\alpha$ -SW calcs. 0-5483  
 $\text{TiH}_4$ , X-ray emission, core level chem. shift calcs. 0-53010  
 $\text{TiH}_3\text{F}$ , X-ray emission, core level chem. shift calcs. 0-53010  
 $\text{V}$ , atom and ions, shell energy struct., SCF calc. by Dirac-Fock-Slater method 0-52877  
 $\text{VN}$ , electronic struct. of vacancies, effect on supercond. transition temp. 0-29347

**scheduling**

- nuclear power plant startup scheduling 0-13687

**schizons** see elementary particle weak interactions**schlieren systems**

- amplitude transfer charact., Monte Carlo method 0-28336  
 arc, high current, rotating, hot wake investigation by streak photography and schlieren systems 0-1862  
 current disruption, in Tokamak plasmas, schlieren signal meas. from millimetre waves 0-48998  
 electric field distrib. in dielectrics, schlieren method for determ. 0-31720  
 flowing gas conc. fluctuation meas., laser schlieren technique 0-3444  
 gas trace anal. by laser-induced Schlieren technique 0-9929  
 gradient index material profiles and chromatic props. 0-14409  
 high speed interferometry to measure effects of neutral gas density reduction on negative pulseless glow-spark transition 0-33850  
 hologram production using shearing interferometers with a wide light source 0-43293  
 irregular phase objects, dynamic interferometry, differential holography using phase conjugate refl. 0-37969  
 laser beam probe method for measurement of refractive index profile of shock wave in fluid 0-23785  
 laser thermonuclear fusion, shell target parameters meas. using X-ray schlieren method 0-14942  
 light optical imaging, of focused US field (*German*) 0-3275  
 negative DC corona study in atmospheric air using Schlieren and interferometric techniques 0-49023  
 spatial filtering techniques represented by phase contrast function 0-9813  
 temperature measurement of laser irradiated transparent materials, Moire-Schlieren technique 0-53392  
 trace analysis in gases by laser-induced schlieren technique 0-3436  
 transfer function of optical systems with small residual aberrations, schlieren effects (*German*) 0-32923  
 US pulse scattering observations, elastic cylinder appl. (*French*) 0-53500  
 US visualisation for NDT of solids 0-22424  
 $\text{O}_2$ , liq., stimulated Raman scatt., vibr.-translational relax. rate, schlieren technique meas. 0-9955

**Schottky anomaly**

- rare earth hydroxides, heat capacity from near 5 to 350K, lattice and Schottky contribs. 0-49374  
 $\text{CaF}_2\text{:Dy}^{3+}$ , cubic cryst. field effects 0-2368  
 $\text{Pr}(\text{OH})_3$ , low temp. heat capacity, thermophys. props. optical spectra, anal. of Schottky contributions, review 0-24611  
 $\text{Smb}_6$ , mixed valence cpd., EPR and heat capacity obs., metal-semicond. behaviour 0-20456

**Schottky-barrier diodes**

## see also semiconductor-metal boundaries

- BARITT devices, boundary conditions, RF performance 0-49955  
 barrier height variation techniques 0-20284  
 capacitance, inverse square, for p-type Schottky diodes with deep acceptor impurities 0-2468  
 deep level properties measurement, capacitance spectrometer (*German*) 0-15471  
 grid devices, preparation on  $\text{Zn}_3\text{P}_2$ , performance evaluation 0-44708  
 IR C-CD staring sensors, operation and performance 0-10029  
 IR detector, nomographs for parameter evaluation, 77K 0-31870  
 magnetic surface levels in presence of depletion-type band bending 0-20285  
 metal-GaAs(GaP), elec. props. under mech. stress 0-11087  
 metal-Ge Schottky barrier quantum detectors, optoelectronic props. 0-13146  
 MM-wave and sub MM-wave receiver elements 0-11558  
 photodiode, quantitative meas. of body motion using laser beam 0-12207  
 photovoltaic IR detector, Schottky barrier 0-9040  
 solar cells appl., props. obs. by electron beam induced currents 0-3518  
 thermographic diagnosis, high resolution dynamic method, detector system 0-41167  
 tunnel junction mixers, quantum limited detection 0-18015  
 Al-GaAs-Al,  $\text{Ga}_{1-x}\text{As}$  Schottky barrier diodes, prep., characts. 0-6948  
 Al-InP Schottky barrier, increase 0-15603  
 Al-Si, with Ti contact, voltage-current characts., appl. to ignition circuits 0-11088  
 Au-CdS junction diodes, chemically etched CdS cryst. surfaces effect on barrier layer 0-44722  
 Au-Cr-GaAs Schottky-barrier diodes, effect of  $\gamma$ -radiation on current-voltage charact. (*Russian*) 0-2459  
 Au-GaAs, photosensitivity losses, field and spectral depend. 0-2452  
 CdS, Au deposition, Schottky diodes and MIS devices, surface treatment effects, SEM obs. 0-54794  
 CdTe/Langmuir film photovoltaic structures for solar cells 0-49918  
 GaAs epitaxial layers, structural defect and conc. inhomogeneities influence on barrier diode I-V characts. 0-15602  
 GaAs fast light detector, beat freq. generation between visible lasers 0-1253  
 GaAs, gamma and electron irradi. defect formation depend. on interface, luminescence study 0-34057

**Schottky-barrier diodes continued**

- GaAs MOS diodes, interface states, deep-level transient spectroscopy 0-44727  
 GaAs, polycryst. Schottky barrier solar cells, effect of grain size on efficiency 0-50968  
 n-GaAs Schottky diode, impurity photoluminesc. 0-29781  
 GaAs thin layers, MBE, growth conditions and phys. props. (*German*) 0-55307  
 n-GaAs vapour phase epitaxial film electrophysical props. rel. to growth temp. (*Russian*) 0-49961  
 GaP-Ag(Au), Schottky barrier, stress effects on elec. props. 0-34512  
 HgCdTe Schottky barrier diode and n-p diffused junction IR detectors, comparison 0-9039  
 $\text{Hg}_{1-x}\text{Cd}_x\text{Te}$  photodiodes, for IR detection 0-13144  
 $\text{PbSnTe}(\text{Se})$  Schottky barrier diode and n-p diffused junction IR detectors, comparison 0-9039  
 Pd-TiO, Schottky barrier, work function depend. on adsorbed species 0-54782  
 Pd-ZnO,  $\text{H}_2$  sensitivity 0-11085  
 $\text{Rh}_3\text{Si}$ , n-Sn Schottky diodes, rectifying barrier height meas. 0-49896  
 Si, amorphous, hydrogenated, electronic density of states determ. from Schottky diode meas. 0-49907  
 Si, amorphous, photovoltaic diodes, influence of mag. field on charge transport 0-49891  
 Si, amorphous, Schottky barrier solar cell, large-area RF sputtered, contact form, scaling and optimisation 0-45679  
 Si, Schottky diodes on sputtered amorphous Si:H, light induced ageing effects, interpretation of photovoltaic stability 0-54780  
 Si:F:H, amorphous, glow discharge deposited elec. props. and device aspects 0-44744  
 Si:H, amorphous, RF sputtered, Schottky barrier solar cells, photovoltaic props. and capacitance-voltage charact. 0-45678  
 Si:H, amorphous, Schottky diode, spectral response and hole drift mobility 0-39673  
 Si:H, amorphous, Schottky barrier solar cell, degradation mechanisms affecting stability and operation 0-45680  
 Si:H, amorphous, Schottky barrier solar cell, deposition parameter effects on elec. props. 0-45681  
 a-Si:H Schottky barrier diodes, capacitance studies 0-49908  
 n-Si:Pd Schottky diodes photocapacitance meas., photon and carrier capture cross sections 0-20309  
 Si-Au Schottky barrier solar cell fabrication, doping of a-Si 0-50969  
 a-Si-H sputtered solar cells, temp. depend. of Schottky barrier characts. 0-45669  
 Si-IRSi interface microstructure and Schottky barrier height 0-34508  
 $\text{Zn}_3\text{P}_2$ , single crystal, growth, electronic and device props. 0-25551  
 $\text{ZnS:Mn}$  Schottky diodes, reverse-biased, electroluminescence, hot electron impact excitations 0-25005  
 $\text{ZnSiP}_2$ -In Schottky diode, photovoltaic spectra 0-2423  
 $\text{ZnTe:Cu}$ , red centre, electric and optical props. 0-20239

**Schottky barriers** see Schottky effect**Schottky defects**

- enthalpy, possibility of decrease with increasing temp. 0-2012  
 ionic crystals, elastic relax. associated with formation and motion of Schottky defects 0-49216  
 $\text{AlH}_3$ , dark electrical cond., exam. 0-39624  
 $\text{CsCl-TlCl}$  solid soln., point defect parameters 0-54224  
 $\text{LiH}$ , solid, anion and neutron diffusion, NMR relax. and linewidth obs., Schottky disorder 0-15815  
 $\text{MgO}$ , lattice defects., calcination temp. effect 0-15091

**Schottky effect**

## see also work function

- amorphous barrier, capacitance-voltage meas., localised density of states determ. 0-49900  
 barriers, Bardeen and Schottky limits of interface index 0-49868  
 contacts, submicron, high-field pulsed electroplating technique 0-49899  
 epitaxial film, dopant profile and Schottky barrier height determ. by second differential method (*Chinese*) 0-49257  
 excitonic reflection of light 0-10885  
 hexatriacotane single cryst., elec. cond. and dielec. breakdown 0-6849  
 homogeneous random fields, modelling realisations 0-8911  
 III-V oxide interface state and Schottky barrier form., unified mechanism 0-44724  
 inert gas, liq., electron mobility, role of shallow traps 0-34440  
 metal-InP contacts, intermediate adsorbed layer effect on electronic props. 0-39674  
 MOS structs., Schottky barrier characterisation by scanned internal photoemission 0-49915  
 photocurrent, recomb. losses in Schottky barriers (*Russian*) 0-2470  
 photoelectrochemical solar cells, semiconductor/redox electrolyte junctions, functions examples and problems 0-45714  
 photoemission and Auger spectroscopy for anal. of semiconductor-oxide interface and Schottky barriers 0-50536  
 photosensitivity losses 0-2452  
 polytetrahydrofuran films, electrochemically prepared between metal electrodes, DC elec. props. 0-39695  
 Schottky barrier grid devices, preparation on  $\text{Zn}_3\text{P}_2$ , performance evaluation 0-44708  
 semiconductor, spatial resolution of SEM electron beam induced conductivity images 0-6327  
 semiconductor materials, shallow and deep level evaluation using Schottky contacts, conc. and distrib. 0-49669  
 semiconductor on insulator substrate, capacitance meas. for Schottky barrier 0-39678  
 semiconductor-metal boundary, Schottky barrier form., chem. mechanisms 0-49869  
 shellac, electrical cond. mechanisms, Schottky and Poole-Frenkel processes and work function 0-29402  
 n-Si-electrolyte junction, Schottky barrier height and reverse current 0-6979  
 solar cells, electrochem. liquid-junction, Schottky barrier height, photovoltage and photocurrent 0-26162  
 solar cells n-type Schottky barrier, theoretical anal. of band edges, Fermi levels 0-50975  
 surface barrier current instability in Schottky-barrier structs., uniaxial crystal compression 0-20310  
 zinc blende type ionic semiconductors, vacancies, bound state energy level calcs., tight binding approx. 0-44694  
 Al-polyacrylonitrile-Al films, current-voltage characteristics 0-11125



**Schottky effect continued**

- Al-silicide-n-Si systems with  $\text{CoSi}_2$ ,  $\text{MoSi}_2$ , and  $\text{Pt}_x\text{Ni}_{1-x}\text{Si}$  as silicide, Schottky-barrier height 0-34520  
 Au-CdS, Schottky junction, surface defects, photovoltaic, piezoelectric and V-I characteristics (*French*) 0-49898  
 Au-GaAs Schottky barrier, photocurrent, recomb. losses (*Russian*) 0-2470  
 Au-n-Al<sub>0.1</sub>Ga<sub>0.9</sub>As-n-GaAs Schottky barrier solar cells, prep. and props. 0-26140  
 Au-SiO<sub>2</sub>-Au structure AC conductivity, bulk and interface effects 0-54798  
 Bi-NbO<sub>3</sub>-Bi system, Schottky barrier effects in transport and dielec. props. 0-29486  
 CdS Schottky barrier solar cells, spectral distrib. and photocapacitance 0-55864  
 Cu-CdS, Schottky barrier, Cu diffusion and photovolt. mechanism 0-6980  
 Cu-CdS, Schottky barrier, reverse differential capacitance, diffusion of Cu (*French*) 0-15424  
 Ga<sub>1-x</sub>Al<sub>x</sub>As:Sn, layer Schottky barrier, deep level spectroscopy 0-49666  
 GaAs (110)-Al(Ga)(In), Schottky barrier form., defect mechanism 0-49902  
 GaAs structures, charge accumulation and transmission, physical modelling (*Bulgarian*) 0-6947  
 GaAs, surface, vacancies, bound state energy level calcs., tight binding approx. 0-44694  
 GaAs:Ag, diffusion of Ag at 1000°C, profiles, Schottky barrier and Hall effect meas. 0-54435  
 GaAs-metal interface, metal-induced chem. reactions and surface states 0-20311  
 GaAs-metal Schottky barrier height rel. to chem. reactivity 0-25008  
 GaAs(Sb), Schottky barrier and semicond./insulator interface states formation 0-49906  
 n-GaP, deep state controlled minority carrier lifetime 0-20211  
 GaP Schottky barriers, voltage fluctuations, meas. 0-15604  
 GaP-metal Schottky barrier height rel. to chem. reactivity 0-25008  
 p-GaP-NaOH interface, Schottky barrier model of photoelectrochemical effect 0-55673  
 GeS film, between Al(Zn)(Sn) electrodes, Schottky and Poole-Frenkel cond. mechanisms 0-54799  
 HgSe/CdSe lattice-matched heterostructs. as Schottky barriers, CVD epitaxial growth and elec. props. 0-49877  
 In-SrTiO<sub>3-x</sub> contacts, differential capacitance, elec. field depend. permittivity effect 0-54779  
 In<sub>1-x</sub>Ga<sub>x</sub>Sb-Au, photovoltaic effect and Schottky barriers 0-49897  
 InP, cleaved surface, metal contact props. and influence of intermediate adsorbed layers 0-49905  
 InP, deep level trap interaction with lowest and upper cond. minima 0-49654  
 InP, Schottky barrier and semicond./insulator interface states formation 0-49906  
 InP surface preparation for Schottky barrier and ohmic contact formation 0-39671  
 InP, surface space charge layers and Schottky barrier form., Raman scatt. study 0-50319  
 InP-Ag Schottky barrier, hot electron attenuation length 0-49904  
 n-InP-Al(Hg), Schottky barrier height and stability characterisation 0-54786  
 In<sub>2-x</sub>Sn<sub>x</sub>O<sub>3-y</sub>-CdTe(InP) photovoltaic heterojunctions, surface and interface studies, efficiency 0-45691  
 Pb-Si:Sb Schottky tunnel junction, variable range hopping assisted tunnelling 0-39670  
 Pb<sub>0.8</sub>Sn<sub>0.2</sub>Te-Pb, Schottky barrier form., Auger depth profiling and I-V meas. 0-49903  
 PbTe-Au Schottky barrier junctions, Landau level oscills. in tunnelling data 0-49945  
 Si, amorphous, Schottky barrier solar cells, deep hole traps, spectral response and TSC meas. 0-50962  
 Si, cleaved surface, metal contact props. and influence of intermediate adsorbed layers 0-49905  
 Si, Schottky barrier struct., proton bombarded, defect states 0-29356  
 Si:H, amorphous, RF sputtered, suitability as solar cell material 0-40864  
 Si:H, amorphous, RF sputtered, Schottky barrier solar cells, photovoltaic props. and capacitance-voltage charact. 0-45678  
 Si:H, amorphous Schottky barrier solar cells, depletion region, capacitance study 0-50963  
 Si:H(F), amorphous, Schottky barrier profiles, depletion region width 0-49871  
 Si/metal system, silicide form. by thin film interactions, review 0-49429  
 Si/Pd-W, contact reactions, backscattering, X-ray diffr. meas. 0-20040  
 Si-*IrSi* interface microstructure and Schottky barrier height 0-34508  
 Si-metal systems, interfacial reaction and Schottky barrier 0-39672  
 SiH<sub>x</sub> amorphous reactively sputtered films, in Pd Schottky barrier devices, photovoltaic props. 0-49910  
 Si<sub>1-x</sub>H<sub>x</sub>, amorphous, gap states, DLTS 0-49656  
 WO<sub>3</sub> films on Si, sapphire, glass and metal substrates, colour intensity dependence obs. (*Russian*) 0-2430  
 ZnO ceramic, nonohmic, drift phenomena of capacitance and current 0-39587  
 ZnS-metal interface, metal-induced chem. reactions and surface states 0-20311  
 ZnS-metal Schottky barrier height rel. to chem. reactivity 0-25008  
 ZnS-metal Schottky barrier height rel. to chem. reactivity 0-25008

**Schottky gate field effect transistors**

- GaAs LPE buffer layers for MESFET appls. 0-29887  
 GaAs MESFET, optical detector appl., sensitive high-speed device 0-13143  
 GaAs, MESFET structure, buffered, LPE growth 0-40271  
 GaAs MESFET struct., high-resolution deep level meas., photo-FET method 0-44531  
 GaAs, possible use of anodic Al<sub>2</sub>O<sub>3</sub> for passivation, elec. props. of GaAs-Al<sub>2</sub>O<sub>3</sub> interface 0-49934  
 GaAs Schottky-gate FET, monolithic integration with GaAlAs injection laser 0-48275  
 GaAs:Sn films, MBE power MESFETs 0-50563

**Schottky noise** *see random noise***Schrodinger equation**

- 3-body problem with one infinite mass particle, integral and Schrodinger eqn. equivalence 0-18255

**Schrodinger equation continued**

- Alfven waves, circularly polarised, spiky soliton soln. to nonlinear evolution eqn. 0-38590  
 anharmonic oscillator pot., eigenvalues and eigenfunctions 0-27163  
 atom, bound state decay in external field in semiclassical approx. 0-12941  
 atom, multiphoton ionisation, resonant, with intense monochromatic laser, appl. to H(Na)(Cs) 0-32689  
 atom models, ionisation time depend. under intense EM fields 0-32683  
 atomic collisions, rotationally induced transitions in two-state model 0-47945  
 atomic model potentials soluble in closed form 0-23287  
 atoms, many body problem, Schrodinger eqn. standard solns. 0-47863  
 band struck. in 1-D, continued fraction approach 0-6694  
 boson, nonrelativistic, potentials, attractive discreteness of ground state 0-46957  
 boson quantum thermodynamical system in one space dimension, high-order perturbation expansion 0-4636  
 bound states for higher angular momenta, scatt. length 0-22209  
 bound states of bispherical and toroidal potentials (*French*) 0-75  
 Cauchy problem, jump process in quantum theory (*French*) 0-31596  
 charmonium spectroscopy, explicit soln. of wave eqn. for arbitrary power pots. 0-403  
 coherent states of a nonrelativistic charged particle in a constant electric field 0-18103  
 confining pot., eigenvalue problem for Schrodinger operator 0-27154  
 correspondence rules and path integrals 0-31590  
 damped oscillator approach to nuclear structure 0-27569  
 diatomic mol. scatt., phase shift differences for some trigonometrical potentials 0-43132  
 diffraction problem, non-homogeneous media, non-stationary problem 0-22211  
 education, Schrodinger eqn. for free particle, wave packet spreading in coord. representation 0-17736  
 education, two-electron atom, 1snl excited levels, ionisation energy calc., perturbation, Schrodinger eqn. methods 0-17728  
 eigenvalue problem soln. with long range pots. 0-83  
 electron-photon interaction, gauge and hybrid transforms. 0-22544  
 energy approximants and perturbation theory 0-22232  
 envelope wave stability 0-43410  
 evolution equations, completely integrable, natural generalisation (*French*) 0-27152  
 exciton-neutral donor complexes, dissociation energy 0-34364  
 friction, stochastic quantisation, nonlinear Schrodinger equation 0-27164  
 Friedrich extension for differential operators with strongly singular potentials 0-27150  
 Gel'fand-Levitan equations with comparison measures and comparison potentials 0-12931  
 Gel'fand-Levitan kernel for 3-D Schrodinger eqn. 0-36892  
 Green functions for discrete-time Schrodinger equation 0-46859  
 Hardy pt., S-matrix formalism 0-96  
 harmonic oscillator, general time depend., quantal fluctuations and invariant operators 0-36898  
 harmonic oscillator with  $\lambda x^M$  perturbation 0-27161  
 harmonic time depend. oscillator with damping and perturbative force 0-82  
 heavy ion scattering cross-sections, WKB calcs., unphysical reflection phenomena 0-27656  
 hypergeometric partial solutions in the problem of two Coulomb centers 0-4582  
 integral transform groups for differential operators from Lie algebras 0-4887  
 Jost solutions for general Gaussian potentials 0-46854  
 JWKB phase integrals, to high-order 0-5632  
 Kepler stationary orbits of electron with velocity-depend. oscillatory perturbations 0-52062  
 kink Schrodinger equation and one dimensional non-linear solitons, general method for soln. 0-46871  
 KMS condition for Schrodinger dynamics 0-36896  
 linear dynamic mol. system, correlated radiation impulse sequence interaction 0-38058  
 local bound states, existence conditions in weak fields, stationary Schrodinger eqn. calcs. 0-36904  
 localised wave field evolution, nonlinear Schrodinger equation exact soln. 0-53191  
 logarithmic, nonlinear gaussian solns. 0-46865  
 logarithmic pot., soln. for quark model particle spectroscopy 0-32065  
 metallic alloy, random, first principles band theory, review 0-44473  
 minimal operator self adjointness 0-17836  
 molecular multicentre potential,  $X_n$ , scattered waves method and Schrodinger eqn. soln. 0-37740  
 moving electron in field of two Coulombic ions fixed in space, rel. to H<sub>2</sub><sup>+</sup> line spectrum 0-42083  
 non-affine path algorithm in the functional integral calculus of Schrodinger kernels 0-31593  
 non-linear coupling of quantum theory and classical gravity 0-27389  
 nonlinear, appl. of variation of action method of one field solitons 0-331  
 nonlinear, discrete version with variable coefficient 0-8819  
 nonlinear, inverse scatt. problem method 0-4577  
 nonlinear, Lie theory calc. of invariants 0-22234  
 nonlinear eqn., slowly varying solitary wave solns. 0-73  
 nonlinear field equations, scattering theory 0-4882  
 nonlinear Schrodinger eqn., soliton solns. 0-27173  
 nonlinear Schrodinger equation, appl. to deep water waves,  $O(\epsilon^4)$  perturb. anal. 0-4569  
 nonlinear Schrodinger equation solns., recurrent motion in continuum dynamical systems 0-22235  
 nonlinear stationary operator equations, evolution (*French*) 0-46845  
 nonlinear variant search using neutron interferometry 0-52064  
 nonseparable potentials, vibr. energy level semiclassical calc. 0-8832  
 nuclear elastic scatt. with optical potential, complex angular momentum methods, poles and zeros of S-matrix, REGGE 0-47445  
 Numerov scheme for Schrodinger eqn. soln. 0-52046  
 one dimensional systems with resonance interaction, collective particle like excitations, Schrodinger eqn. 0-46868  
 one-dimensional band calculations using perturbation theory 0-44460  
 one-dimensional systems, with reson. interaction, soliton-like solns. 0-46831  
 one-particle quantum mechanics, duality between confining pots. and  $(R+L^\infty)$  pots. 0-31574  
 open system, new classical Hamiltonian-Lagrange mechanics 0-36900



# Schrodinger equation continued

- operator evolution equations, completely integrable, nonlinear Schrodinger eqn. 0-12938
- particle motion in potential channel, waveguide-optical analogy 0-12942
- pendulum, representation of canonical relns. 0-42084
- perturbation problem, two-level atom interacting with EM field 0-52056
- perturbation theory applications to numerical integration methods 0-12926
- plasma, laser-irradiated, Langmuir soliton generation at crit. density 0-6267
- polynomial factor eigenfunctions, corresponding pots. (*Chinese*) 0-22236
- position evolution of wave function, new type of Schrodinger eqn. 0-27178
- proper functions and absence of bound states for Schrodinger operator 0-4563
- QED external EM fields, time-dependent, particle interpretation, Fock representations of Fermi field operators. 0-52439
- quantum collision theory, generalised sensitivity anal. 0-31542
- quantum damped oscillator, master equation and pure state representations 0-8823
- quantum theory, physical foundations, stochastic formulation, proposed expt. test 0-52049
- quarkonium, quantum mechanical applications, masses and leptonic widths of  $\psi$  and  $T$  0-27484
- radial, general pot. props. for soln. by hypergeometric functions 0-4581
- radial, propag. method, appl. to close coupled eqns. 0-42096
- radial, propagation method 0-8816
- radial one-dimens., second order perturbative numerical calcs. 0-31580
- radial reduced Coulomb Green's function 0-31559
- relativistic Bethe-Salpeter harmonic oscillator 0-32006
- Schrodinger's route to wave mechanics 0-17783
- Schrodinger kernel as functional integral, non-uniqueness 0-31594
- SL(2,R) approach to Schrodinger spectral problem with pseudosingular potential 0-8845
- solids, Bloch waves, Lane eqn. interpretation 0-39489
- soliton stability, 3-D nonrelativistic (*Russian*) 0-4583
- solution by hand-held calculator 0-52052
- solution method for special class of potentials 0-36897
- spectrum of  $p^2 + V(x) + ex$ , periodic  $V$ , complex  $e$  0-22225
- spin-orbit coupling origin in Schrodinger representation 0-42914
- spinless particle scattering by central pots., soln. 0-27156
- square-well potential, integral eqns. and scatt. solns. 0-31451
- stochastic origins, model 0-81
- stochastic solution, asymptotic behaviour (*French*) 0-46844
- SU<sub>n</sub> Heisenberg spin chain derivation 0-37184
- time depend., two-dimens. finite difference schemes 0-97
- time dependent Schrodinger eqn., alternative approx. soln. for heavy ion reactions 0-32296
- translation invariant N-body harmonic oscillator problem 0-31558
- transport theory integral eqn. soln. in Green's function formalism, scatt. amplitudes 0-4566
- two component derivative nonlinear Schrodinger equations, Alfvén waves appls. 0-48883
- vacuum polarization connection to atomic spectrum in a strong magnetic field 0-42369
- wave diffraction, stationary problem in non-homogeneous media 0-68
- wave functions at pot. discontinuities, continuity conditions for teaching 0-27077
- wave-packet motion in Eckart and quadratic pots., appl. to H interstitials in transition metals 0-52067
- weakly bound particle ionisation, perturbation theory series convergence in alternating field 0-4575
- weakly coupled one-dimensional Schrodinger operators, asymptotic behaviour of ground state 0-22220
- WKB five term approx. 0-31569
- Yukawa potential bound states, Sturmian group theoretical approach 0-8825
- $\Theta^4$  quantum field theory, numerical methods, anharmonic oscillator approx. 0-52390
- H atom in box, 2-D Schroedinger equation, influence of constant elec. field, finite-element method 0-31544
- H atom in mag. field, Schrodinger eqn., Monte Carlo soln. 0-31545
- H, Schrodinger eqn. in two-dimens., for teaching 0-31457
- N<sub>2</sub>, Raman intensity, ab initio calc. 0-1028
- U (M,f), muon excitation probabilities, muonic atoms, Schrodinger eqn. 0-47515

**Schrodinger equation** see *Schrodinger equation*

## Schwarz-Hora effect

No entries

## Schwarzschild metric

see also *cosmology*

- black hole in external mag. field, relativistic particle radiation 0-22035
- black-hole space-times, mass positivity 0-8880
- bundle boundary for the Schwarzschild and Friedmann solutions 0-31603
- celestial mechanics, astron. meas. and coord. systems 0-36481
- collapsing shell, Schwarzschild-de Sitter space-time, thermodynamics and radiation 0-17607
- EM radiation, partial polarisation in Schwarzschild gravitational field (*Russian*) 0-51801
- gravitation, relativistic theory, static solutions and Poincaré press. 0-31648
- Kruskal extension from vacuum field eqns. 0-42112
- Kruskal metric, nominal source 0-12956
- local relative motion in general relativity 0-42123
- Lorentz-covariant model of the system of two gravitating particles 0-8865
- point mass alternative space-time 0-31638
- spherical symmetric field, spin ang. momentum tensor calc. 0-42107
- symmetry constraints in general relativity and the Schwarzschild interior metric 0-4605
- vacuum energy-momentum tensor in Schwarzschild de Sitter space time 0-52091
- world function of Schwarzschild field, power series representation 0-12954

**Schwarzschild space** see *Schwarzschild metric*

## Schwinger source theory

- (1+1) dims. Todd chain and  $e^+e^-2\phi$  model, exact factorised S-matrices 0-18094
- (1+1) dimensional model field, fermion-boson correspondence, Klein transformation 0-42379

## Schwinger source theory continued

- consistent approx. scheme based as Laguerre polynomials 0-336
- covariance problems in two-dimens. QCD 0-22575
- EM field, minimal coupling, relativistic wave equations for particles of unique mass, constraints 0-22526
- Fermi field bosonisation in 1+1 dimensions 0-47172
- Keldysh's perturbation formalism 0-13217
- Lagrangian formulation generalisation 0-42332
- Lee model in EM field, mag. moment calc. 0-42350
- massive Schwinger model, saturation, fermion confinement and instantons 0-47175
- pre-Schwinger model, Lorentz transforms. if operator solns. 0-47171
- QCD, weak coupling approx. Schwinger-Dyson eqn. (*Chinese*) 0-52476
- QCD lattice gauge theory, matrix Padé approximants, ratio of hadron to nucleon mass 0-4928
- quantised rotator, Schwinger boson representation, derivation of canonical variables 0-18164
- Reggeon field theory on a lattice, critical behaviour, Monte Carlo calc. 0-18126
- Schwinger equations, compact description 0-13204
- static ultralocal solutions, 1/N expansion of O(N) symmetric theories 0-52401
- superradiance from vacuum persistence amplitude 0-48195
- synchrotron radiation, quantum corrections 0-37193

**science education** see *education*

**scientific societies** see *societies*

## scintillation

see also *phosphorescence; phosphors*

- anthracene crystals,  $\alpha$ -particle induced scintillation, mag. field effects 0-40161
- biomedical liquid scintillation counting, apparent and actual <sup>14</sup>C retention 0-36080
- cosmic ray interplanetary scintillations at 250 GV, statistical props. 0-8496
- EM or optical pulse arrival time statistics in turbulent media 0-48154
- interplanetary scintillation meas. in conditions of strong radio interference 0-46413
- interplanetary scintillation of quasars, red shift-magnitude link (*Chinese*) 0-12828
- interplanetary scintillations spectra, influence of source sizes, obs. 0-46361
- ionosphere, scintillation probability distrib. function 0-41598
- irradiance enhanced variance from target glint 0-5691
- liquid scintillation counting of <sup>3</sup>H or <sup>14</sup>C amino acids, optimisation factors 0-30951
- liquid scintillation vial system, new container geometry for better sensitivity 0-46021
- oxazole scintillator solns., two- and three-component, laser emission spectra 0-32980
- plastic scintillator excited by <sup>60</sup>Co  $\gamma$ -rays, absolute radioluminesc. yield meas. 0-2829
- powder scintillators, type P-47, for SEM 0-22487
- pulsar scintillations, freq. cross-correl. and finite bandwidth effects 0-4392
- pulsar signals, cosmic ray streaming or mirror instability effects 0-51845
- pulsar signals, interstellar density fluctuations effect 0-46649
- pulsar signals, interstellar medium mirror instability growth effects 0-46648
- pulsar signals interstellar scintillation, analytic soln. of second-order moment eqn. 0-26726
- radio source scintillation from artificial ionosphere inhomogeneities at 25, 240 and 290 MHz 0-36454
- radio sources, faint, interplanetary scintillation statistical study at 81.5 MHz 0-51893
- radiowave scintillation in ionosphere, UHF and VHF radiocommunication 0-56674
- turbulent plasma, wave scintillations, fourth-order moment eqn., astrophys. appl. 0-46381
- Venus atmosphere, turbulence from Pioneer multiprobe radio scintillations 0-46437
- VHF/UHF, ionospheric irregularities 0-46345
- Bi<sub>2</sub>Ge<sub>2</sub>O<sub>12</sub>, low-temp. scintillation props. and appl. to high-energy  $\gamma$ -imaging devices 0-55191
- CsI:Ti, gamma-scintillation growth front, external elec. field effect 0-34984
- NaI:Ti, scintillation excitation mechanism 0-2857
- Na<sub>2</sub>ZrSiO<sub>5</sub>, scintillation props., excited by  $\alpha$  particles 0-29809

## scintillation chambers

see also *scintillation counters*

- alpha-in-air monitoring system, real-time 0-23155
- biomedical  $\gamma$ -chamber, operating model 0-30848
- high-speed single-input system for pulse identification 0-891

## scintillation counters

see also *photomultipliers; position sensitive particle detectors*

- acrylic low cost scintillators 0-37699
- acrylic scintillator and wavelength shifter material, radiation induced degradation 0-5442
- air showers for 10<sup>4</sup> to 10<sup>6</sup> particles, lateral distrib. of EM component, detection 0-17459
- alpha scintillation counter for determ. of low natural conc. of <sup>222</sup>Rn and <sup>226</sup>Ra 0-9456
- atmospheric radioactive gas monitoring by silicone oil absorbent scintillation counter 0-12044
- beta detector with ring-type conical phosphor 0-27881
- beta ray plastic scintillator survey meter for directly absorbed dose meas. (*Japanese*) 0-848
- capture gamma-ray detector, neutron sensitivity 0-18767
- dead time of detection systems, determination method (*Slovenian*) 0-47815
- dioxane based gel, scintillation yield and mechanisms involved study (*French*) 0-52816
- dosimeter for gamma radiation, design calibration and construction (*Spanish*) 0-5437
- efficiency meas. for fluxes of 5-100 keV photons 0-14044
- electro-optical properties, in SEM 0-52819
- electron scattering experiments, detection system, Saclay linear accelerator facility 0-52809
- energy resolution optimisation at high energies 0-37697
- fluorescence decay times determ. in nanosec. and subnanosec. range 0-5443



**scintillation counters continued**

- gamma camera imaging, recent advances 0-17127
- gas counter with selective level population for high-intensity neutron fluxes detection 0-23253
- gas scintillation counter, for high count rate X-ray detection 0-14052
- gas scintillation drift counter for fast X-ray detection 0-888
- gas scintillation spectrometer for X-ray astronomy, performance characteristics 0-56709
- gas-filled electroluminescent detector for soft X-rays, constr. and characts. 0-32569
- hodoscope for meas. of ionisation losses of relativistic particles 0-42892
- hodoscopes, with hodoscope photomultipliers 0-47817
- liquid, colorimetric analysis appl., use of miniature  $^{14}\text{C}$  and  $^3\text{H}$  standards 0-21346
- liquid column chromatography, scintillation counters, review (Czech) 0-27885
- liquid counters, external standard quench correct. capability, inexpensive method for acquisition 0-47810
- low-efficiency counter, for meas. of average number of charged particles 0-23252
- multiplicative core selector for EAS axis determ. 0-41682
- NE213, detection efficiency meas. for 130 MeV neutrons 0-27888
- NE213 liquid cylindrical neutron spectrom., anisotropy of response 0-5434
- NE213 liquid scintillator, light output for electrons and protons, coincidence spectrometer 0-32564
- NE213 neutron counter, efficiency calibration 0-27877
- NE 213, pulse shape discrimination, appl. to neutron spectrometry 0-27862
- NE 213 scintillator, neutron response functions, energy range to 40 MeV (Japanese) 0-18756
- neutron, calibration of threshold 0-23258
- neutron detection, test of Monte Carlo calcs. by  $^{12}\text{C}(\text{p},\text{n})$  and  $^{12}\text{C}(\text{p},\text{p})$  cross section meas. 0-37713
- neutron detection from short-lived plasma 0-23263
- neutron detector for TOF meas. with very fast burst source (French) 0-14040
- neutron spectrometers, with LED and PIN photodiode, stabilising system 0-47821
- optronic converters with  $\text{Cu}_2\text{S}(\text{Se})$ - $\text{CdS}(\text{Se})$  p-n heterophotoclements, props. on X-irrad. of scintillator 0-34505
- organic, neutron response functions, Monte Carlo program 0-14047
- organic, use of logarithmic pulse height and energy scales 0-37690
- organic scintillator efficiency using Monte Carlo code 0-889
- pickups with plateau in counting characteristic, gamma and neutron radiation, review 0-47811
- Pilot U scintillator for 55-225 MeV neutrons 0-18762
- plastic scintillator,  $Q_\beta$  value determ. from endpoint energies of  $\beta$ -spectra 0-27864
- polystyrene scintillators, extrusion prod. 0-37698
- probe detector in assessment of cardiovascular disease 0-3800
- pulse shape analysers for phoswich detectors in space borne hard X-ray expts. 0-36501
- pulse-width discriminator for multilayer scintillators 0-27883
- radioimmunoassay appls. of Philips gamma counter PW 4800 and scintillation counter PW 4700 0-56173
- scintigraphic image adaptive restoration 0-27914
- scintillation cameras, automatic field uniformity corrections 0-17128
- solutes in liquids, conc. determ. by  $(\text{n},\alpha)$  and  $(\text{n},\gamma)$  reacts., scintillation counting 0-35602
- thin film waveshifter coatings for fluorescent radiation converters 0-32574
- time-dependent properties of proportional counters SRPO-304 used with scintillation detectors 0-42894
- timing errors evaluation 0-5445
- X-ray crystal spectrograph with active readout 0-4826
- X-ray position-sensitive scintillation detector for portable stress analyser 0-13190
- $\pi^-$  discrimination and absolute counting for nucl. capture at rest expts. 0-5432
- Ar, liquid, scintillating target, fast neutron polarisation analyser 0-47833
- $\text{Bi}_4\text{Ge}_3\text{O}_{12}$ , low-temp. scintillation props. and appl. to high-energy  $\gamma$ -imaging devices 0-55191
- $\text{Bi}_4\text{Ge}_3\text{O}_{12}$  scintillators, appl. as high energy gamma detectors 0-47827
- $^{14}\text{C}$  low level liq. scintillation counting using small vol. teflon-Cu vial 0-16887
- CsI crystal, growth time of scintillation pulse activator concentration and ionisation density 0-23251
- CsI:TL, gamma-scintillation growth front, external elec. field effect 0-34984
- Fe calorimeter, hadronic cascade curves between 20 and 8000 GeV 0-36464
- H scintillating gaseous drift chamber for use as positron sensitive target 0-9457
- $^3\text{H}$  counting efficiencies and sample time stabilities in a Triton X-100/toluene scintillant 0-52813
- He high press. gas counter, neutron polarisation meas., Monte Carlo convolutions 0-14061
- $^{125}\text{I}$  airborne vapour detection 0-51027
- Li glass NE-912, neutron detection efficiency (Russian) 0-27901
- Li(I), response functions of spherically moderated neutron detectors 0-37687
- $^6\text{Li}$  sandwich counter, meas. of neutron spectra in fast neutron systems 0-27884
- NaI scintillation spectrometer, gamma-ray energy released from fission products, response matrix (Japanese) 0-42888
- NaI(Tl), anomalous intensity variation of backscattered gamma ray peaks 0-37691
- NaI(Tl), plume exposure monitoring system for LWR plant 0-42875
- NaI(Tl), portable, natural soil radioactivity monitoring 0-31148
- Pb spectrom. for fast reactor fuel pins 0-37461
- Rn continuous monitor response to transient Rn concs. 0-32519
- U activity, liquid scintillation counting 0-27873
- Xe filled proportional scintillation detector for charged particles 0-32572
- YAG: $\text{Ce}^{3+}$ , scintillation detector, in SEM, electro-optical props. 0-52819

**scintillation detectors** *see* **scintillation counters****scintillation spectrometers** *see* **particle spectrometers; scintillation counters****scintillators** *see* **scintillation; scintillation counters****scintillometers** *see* **scintillation counters****scorching** *see* **combustion****Scott effect**

No entries

**s.c.r.** *see* **thyristors****screening** *see* **shielding****screening, nuclear** *see* **nuclear screening****screens, fluorescent** *see* **fluorescent screens****screens, phosphorescent** *see* **fluorescent screens****screens (display)***see also* **fluorescent screens**

holographic screens for colour flat image projection (Russian) 0-9066

liquid crystal translucent screens, resolution 0-28335

 $\text{CdS}$ ,  $\text{CdS}_x\text{Se}_{1-x}$ , scanning semiconductor laser with transverse electron-beam pumping 0-9904**screw dislocations**

amorphous Lennard-Jones solid, edge and screw dislocation, stability, elasticity, simulation 0-15099

anisotropic crystals, infinite rectilinear dislocation, vibr. 0-44210

antiferromagnet, magnetic dislocation domains, mag. moment distribution 0-2601

crack tips, yielding on inclined planes 0-33525

crystallite with screw dislocation, determination of particle size and distortion 0-15098

cubic crystal edge and screw dislocation—point defect elastic interactions 0-15151

deformation potential operator, electron dislocation interaction (Russian) 0-2021

diamond lattice, dynamic symmetry and plastic deform. 0-24527

dislocation-phonon interaction in cryst. with anisotropic slip system 0-29137

displacement field when moving in elastic nonlinear medium (Russian) 0-44206

electrolytic crystal growth, role of screw dislocations 0-54540

electron-microscope image of dislocations, in anticlassical scattering region, dislocation axis contrast 0-38877

ferromagnet, rectilinear screw dislocation, magnetisation distrib. 0-44897

finite-two phase bodies, response to internal and external stresses, numerical considerations 0-24742

Invar, dislocation motion anomaly 0-10554

metal, FCC or BCC, dislocation annihilation during tensile and cyclic deform. and limits of dislocation densities 0-34007

metals, BCC, dislocation processes, straining expts., electron microscope obs. 0-29025

metals, Snoek-Koster relaxation, theory 0-16369

polyethylene, lamellar stacks, screw dislocations 0-19728

polystyrene, lamellar stacks, screw dislocations 0-19728

roughening transitions of finite order 0-38975

steel, stainless, single crystals, shear cracks, electron microscope study 0-40522

surface dislocation model, Z-phase interface boundary problem 0-39085

surface-dynamics of growing crystals 0-44160

Al, cold-worked, plastically deformed, internal friction spectrum, Hasiguti peaks associated with dislocations 0-7618

 $\text{CdS}$ , deformed, dislocation struct., TEM obs. 0-54250

Cu, fatigued single crystals., temp. depend. of saturation stress and dislocation substruct. 0-44211

Cu plates, thin, dislocation-dislocation interaction inducing cross-slip, X-ray topographic anal. 0-49233

 $\alpha$ -Fe, internal friction for low temp. deform. 0-40420

Fe, quenched-in hydrogen, yield stress decrease of prestrained specimens 0-16454

Fe, softening and hardening by  $\text{H}_2$  charging during tensile deformation 0-16453 $\text{GaAlAs-GaAs}$  DH lasers, degradation caused by growth of dislocation networks 0-53289

Ge chalcogenides, screw dislocations in layer crystal growth from vapour (Russian) 0-1953

Ge, cross-slip of single dissociated screw dislocations, double etching and X-ray topography studies 0-15104

 $\text{LiF}$ , plastic strain accompanying local rise in surface temp., of natural shear (Russian) 0-6411 $\text{LiF}$ , radiation induced voids, formation on dislocations 0-15159 $\text{MgO}$ , crack propagation during in-situ deform., plastic zone formation 0-16468

Mo, mechanical props. and dislocation struct., mag. field effect 0-54935

Mo, single crystals., work hardening and softening in cyclic strain 0-20957

 $\text{Na}_2\text{Al}_2\text{Si}_2\text{O}_{10}\cdot 2\text{H}_2\text{O}$ , natrolite, cleavage etching in acidic and neutral media 0-6407 $\text{NaCl}$  single crystals, screw dislocations, influence of interionic potentials on core configs. 0-34000 $\text{NaCl}$ , spiral dislocation mobility depend. on elec. field, relaxation time 0-39105Nb, deformed,  $\alpha'$ -peak in internal friction spectra 0-16368

Nb, mechanical props. and dislocation struct., mag. field effect 0-54935

Ni, rectilinear screw dislocation, magnetisation distrib., mag. moment anal. 0-44897

Si, cross-slip of single dissociated screw dislocations, double etching and X-ray topography studies 0-15104

Si, dislocation growth during laser melting and solidification 0-2022

Si, stacking fault energies, intrinsic and extrinsic, by TEM 0-10562

 $\text{Si:P(B)}$ , high temp. impurity diffusion via vacancies and self-interstitials 0-24667 $\text{SiC}$ , high period polytype at interface of two interacting spirals 0-20041

Sn chalcogenides, screw dislocations in layer crystal growth from vapour (Russian) 0-1953

Te, piezoelectrical free-carrier scatt. by screw dislocations, Hall effect and cond. meas. 0-24926

 $\text{TiO}_2$ , rutile single crystals, stoichiometric, dynamic strain ageing 0-50661

V, strain hardening, screw dislocations and microtwinning (Russian) 0-29971

V-Ta (5 wt.%), strain hardening, screw dislocations and microtwinning (Russian) 0-29971

Zn, basal dislocation—prismatic dislocation ring interactions by method of moments (Russian) 0-10550

Zn polycrystals, deformation, grain sizes effect at room temp. (Czech) 0-45359

ZnTe:Ag, doped during growth and by diffusion, defect form. 0-15129



scrubbing (abrasion) *see abrasion*scuffing *see abrasion*sealing *see seals (stoppers)***seals (stoppers)***see also glass-metal seals*

breeder reactor cover gas seals, design approach 0-47562

elastomer seal for large toroidal vacuum chamber 0-27315

glass-ceramic, annealing effect on internal stresses 0-40389

laser technology, parallel plate, polarisation problems obs. and solution 0-1225

LMFBR, 1000 MW(e), selection of reactor cover seals and bearings 0-5219

magnetic safety valve 0-8966

magnetofluid seals appl. to rot. cryostats 0-4721

metal hollow O-ring seal, for UHV and cryogenic use (*Japanese*) 0-22374

metal-seal valve for high radiation use in high vacuum 0-233

noble-metal tubes, cold-weld sealing 0-41556

pressure-mode soft-metal vacuum seal, for glass and ceramics 0-17952

UHV bakeable vacuum chamber, use of Al alloy (*Japanese*) 0-52248

vacuum, axial-rotation, for independent rotation of objects on common axis 0-31772

vacuum feedthroughs, coaxial and multipin, cryogenic performance 0-8995

vacuum grease, for analytical electron microscopy, reduction of contamination (*Japanese*) 0-11978

vacuum pressure, with thermomechanical drive of Ti-Ni 0-31773

vacuum seals, Cu-ceramic, metalisation process 0-37046

As<sub>2</sub>S<sub>3</sub> thin films, vacuum deposited on Ge and PbS, sealing props. and TEM 0-35097**seawater**acoustic wave scattering by sea surface, props. (*French*) 0-53502

Adriatic Sea, chem. parameters, spring and winter time obs. 0-41447

Antarctic Intermediate Water in SE.Pacific and S.Atlantic 0-36306

Arabian Sea, trace metal content obs. and marine chem. 0-56495

N.Atlantic deep water, production since Miocene, sediment evidence 0-46186

Baltic Sea, salt transports determ. from conservation calculations in natural coordinates 0-51433

basalt-seawater interaction, trace element and Sr isotopic vars. in glassy basalt 0-8286

Black Sea, H<sub>2</sub>S and O<sub>2</sub> zone boundaries rel. to water mass dynamics (*Russian*) 0-12435

brass, admiralty, dezincification conditions in fresh or seawater, thermogalvanic method 0-16548

chlorophyll concentration, estimation from outgoing radiation spectrum meas. from helicopter 0-36333

Cochin backwater, India, estuarine water, particulate heavy metal content 0-7964

Cochin Harbour mouth, India, hydrographic characts. and tidal prism 0-41452

concrete, cracking in seawater due to embedded metal corrosion 0-30116

convection of fluid cooling from surface (*Russian*) 0-1582

coral reef water, O isotope composition rel. to evaporation and precipitation 0-46202

crystal unusual growth 0-26516

Cs accumulation in muscle tissue of marine fishes 0-35797

Dead Sea rift valley, Sr behaviour in subsurface CaCl<sub>2</sub> brines 0-17295

deep Sargasso Sea, organic carbon flux at 3.2 km, annual variation 0-41460

density, vertical structure meas. using optical interferometry (*Russian*) 0-51569

dissolved trace gases in tropical Pacific 0-41509

electrochemical potential of pure metals (*Chinese*) 0-31062electrolysis, for H<sub>2</sub> and O<sub>2</sub> prod. 0-30435

electrolytic dissociation, utilisation of ocean hydropower systems for H prod. 0-30374

Galapagos Rift, submarine thermal springs 0-8295

NE Gulf of Alaska, processes affecting suspended matter distrib. and transport 0-12398

W.Gulf of Maine, current, temp. and press. obs. rel. to winter circulation 0-51430

Gulf of Taganrog salinity, after restriction of exchange with Sea of Azov 0-36335

hydrochemical structure in NE tropical Atlantic (*Russian*) 0-17284

hydrographic data, appl. to current flow vel. determ. 0-17415

ice melting model, appl. to Antarctic ice shelf and icebergs 0-4036

ignimbrite/sea water explosions, volcanic ash generation 0-26480

light field rel. to hydro-optical characts. (*Russian*) 0-17279

low-temperature interaction with basalt, effect on S distrib. in oceanic crust layer 2 0-41432

Mangalore coast, India, 1976-7 nearshore water conditions 0-8315

old Mangalore port, seasonal vars. in estuarine and oceanic waters hydrographic conditions 0-41451

marine boundary layer, optical beam propag., analytical model 0-8329

marine sediments interstitial solns. comp. and diagenesis, seawater-sediment interface fluxes 0-3988

E.Mediterranean Sea, T and O<sub>2</sub> profiles 0-17298multilayered stratified flow investigation (*Russian*) 0-1703

Naragansett Bay, USA coast, natural radionuclide content 0-12399

ocean basalt reactions, chemical exchange, Fe, Mn and S species results 0-17294

ocean optics, conf. proceedings (San Diego, 30-31 August 1978) 0-8325

ocean thermal energy conversion to electricity (*French*) 0-21389

oceanic fronts, optical and particulate matter properties 0-51418

oil conc., continuous meas. by towed fluorometer 0-45846

oil migration, mixed Lagrangian-Eulerian model 0-45830

optical coherence loss meas. in Atlantic coastal waters 0-8333

optical props. in region of large variability 0-8327

optical transfer function meas. in Sargasso Sea 0-8328

N.Pacific, size distrib. of suspended particles in surface water 0-4047

Pacific Ocean, Mn distrib. 0-56494

N.Pacific Ocean, west, depth, var. of temp., salinity and sound vel. meridional gradients 0-51429

Pacific Ocean waters, nitrate N distrib. 0-31065

E.Pacific Rise, hydrothermal vents on seabed issuing H<sub>2</sub> and methane 0-41422

pollution by dinitrotoluene isomers, occurrence and determ. in seawater 0-7966

**seawater continued**

radiative transfer in atmosphere-ocean system, matrix operator approach 0-8330

radiative transfer in turbid water 0-8331

rain-formed mixed layer 0-36323

reaction with Amazon suspended sediments, cation exchange characts. 0-8337

refractive index microstruct. from diffusive and turbulent ocean mixing 0-56486

refractive microstructure from diffusive and turbulent mixing 0-8326

side convection characteristics (*Russian*) 0-1580

silicates dissolved in deep water of Bering Sea 0-31061

sound absorption contour chart for Atlantic, Indian and Pacific Oceans 0-36303

sound absorption in seawater, borate-complex relaxation 0-36304

surface charge 0-36331

surface microlayer, <sup>210</sup>Pb and <sup>210</sup>Po enrichment obs. 0-56496

surface temperature, appl. in climate change predictions 0-8377

surface water, remotely sensed by microwave radiometry 0-36428

suspended material concentration, estimation from outgoing radiation spectrum meas. from helicopter 0-36333

temperature gradient meas., anal. of two methods 0-31149

temperature vertical gradients, meas. via moored vector averaging current meters 0-12561

transmission props. for underwater laser communication 0-33069

transparency, rel. to hydrochemical characts. distrib. 0-31057

transparency meter, Se photocell device, for biological activity 0-8442

underwater irradiance in Norwegian and Barents Sea, relation to water temp. 0-31055

vertical buoyancy flux, atmospherically induced 0-4039

vertical eddy viscosity, effects on Rossby and Eady waves 0-51404

water, fluorometric dye meas. background variation expts. 0-45844

Al-air, seawater activated secondary cell 0-26128

CO<sub>2</sub> solution in ocean surface waters, role of homogeneous buffer factor 0-21783Ca<sup>2+</sup>, total activity coeff. determ. 0-31064CaCO<sub>3</sub> and scale formation on OTEC heat exchangers 0-41461

Cu-Al-Ni-Fe system, corrosion behaviour in sea water 0-45421

Cu-Ni(10 (30) wt.%), seawater corrosion rate meas., electrochem. method validity 0-45426

Fe, conc. determ. by graphite furnace atomic absorpt. spectroscopy 0-40768

Fe(ni), influence of Ni content on seawater corrosion props. (*German*) 0-35370<sup>203</sup>Hg, tracer for Hg conc. in seawater expts., <sup>75</sup>Se tracer 0-21420

Mn, conc. determ. by graphite furnace atomic absorpt. spectroscopy 0-40768

N<sub>2</sub>O composition of Pacific surface water 0-51519

Nd isotopic composition of sediments of different oceans 0-21704

<sup>75</sup>Se, tracer for Se conc. in seawater expts., <sup>203</sup>Hg tracer 0-21420SiO<sub>2</sub>, dissolved silica content over opaline sediments 0-51419

U extraction from seawater using composite absorbents 0-24730

Zn, conc. determ. by graphite furnace atomic absorpt. spectroscopy 0-40768

**second-order optical susceptibility** *see nonlinear optical susceptibility***second sound***see also liquid helium sound propagation*

CBOOA, isotropic, nematic, smectic-A phases, Brillouin scatt. 0-11421

vortices pinning in nucleopores, effect on second sound resonators 0-49439

He, liquid, first and second sound generation by immersed Ge cryst. optical pumping 0-6581

<sup>3</sup>He, A<sub>1</sub> phase, broken relative symmetry and dynamics 0-24705<sup>3</sup>He-<sup>4</sup>He, liquid mixture, second sound, quantised vortex creation at constrictions, excitation model 0-44383<sup>3</sup>He-<sup>4</sup>He, superfluid solns., nonlinear sound interaction 0-34267He, liq., dynamic scaling near T<sub>λ</sub> 0-34264<sup>4</sup>He, liq., second sound, quantised vortex creation at constrictions, excitation model 0-44383<sup>4</sup>He, superfluid, continuum theory based on classical theory of irreversible processes 0-29236<sup>4</sup>He, superfluid, near transition, second sound damping, rel. to renormalisation gp. predictions 0-10725<sup>4</sup>He, superfluid, second sound damping, hydrodynamic regime below T<sub>λ</sub> 0-10727<sup>4</sup>He, superfluid, sound pulse amplitude meas. method sound transform. at free surface 0-54451<sup>4</sup>He, superfluid, stationary flow, combined meas. 0-49446<sup>4</sup>He superfluidity, macroscopic quantum waves, bound quasi-particles 0-39378<sup>4</sup>He-<sup>3</sup>He, dil. soln., <sup>3</sup>He quasiparticle excitation spectrum and second sound vel. meas. 0-24708**secondary cells**

alkali and alkaline earth metal electrodes, in nonaqueous secondary cells, electrochem. behaviour 0-35665

Battery Energy Storage Test facility, test programs and data processing 0-30449

electric vehicle secondary cell development program of US Dept. of Energy, review 0-30442

electrode materials for solid state, high energy batteries 0-55836

high performance batteries, materials requirements 0-12002

metal-air batteries for electric vehicle propulsion, comparison of Li, Al, Zn, Fe systems 0-30444

metal/air batteries, status and potential, review 0-55828

Pb/acid, design and performance characteristics for remote photovoltaic applications 0-55833

performance limits, technical and economic factors 0-45657

polyphenylquinoxaline-cellulose acetate, battery separator membrane, diffusion meas. 0-35574

solar electricity battery storage Systems optimisation of solar cell/ battery 0-51007

solid solution cathodes for electrochem. power sources, dynamic aspects 0-3508

superionic conduction accumulator with high energy density (*French*) 0-26131

thermal management of battery systems for electric vehicles and utility load leveling 0-30458

Al-air, seawater activated cell 0-26128

β-Al<sub>2</sub>O<sub>3</sub>-Na<sub>2</sub>CaO, microstruct. and ionic resistivity 0-44357β-Al<sub>2</sub>O<sub>3</sub>-Na<sub>2</sub>O, solid electrolyte, battery appl. (*Polish*) 0-12005



## secondary cells continued

- $\beta$ - $\text{Al}_2\text{O}_3$ - $\text{Na}_2\text{O}$ - $\text{Li}_2\text{O}$  (8.85, 0.75 wt.%) pressing powders, prep. by spray drying 0-40294  
 $\text{Ba}_0\text{FeS}_2$  cathodes for nonaqueous Li batteries 0-3506  
 $\text{H}_2$ - $\text{Cl}_2$  cell, electrochemically regenerative, mass and heat balances 0-3503  
 $\text{KFeS}_2$  cathodes for nonaqueous Li batteries 0-3506  
 Li battery, use of  $\text{MoS}_2$  as cathode 0-29892  
 Li, electrochem. props. of amorphous  $\text{MoS}_2$  cathodes 0-40851  
 Li/ $\text{SO}_2$ , safety studies, DTA of constituents 0-16795  
 Li-Al/ $\text{FeS}$  cells for electric vehicle propulsion 0-30446  
 Li- $\text{FeS}$  battery eng. problems for elec. load levelling plant design 0-30457  
 Li-TiS<sub>2</sub> storage batteries (German) 0-12001  
 LiAl/ $\text{FeS}$  batteries, principles and construction, load levelling of nuclear stations 0-21392  
 LiAl/ $\text{FeS}$  electric vehicle battery, charging system developments 0-30447  
 LiAl/ $\text{FeS}$  cell with negative electrode prep. by powder metallurgy, performance 0-26130  
 LiAl/metal sulphide high temp. battery with multi-foil insulation container for electric vehicle appls. 0-30448  
 Li<sub>2</sub>V<sub>2</sub>O<sub>5</sub> (0.1 < x < 1.0), phase relationship in ambient temperature system 0-20912  
 Na/S, recharging characts. in two liquid phase region 0-26127  
 Na/S batteries, load levelling and traction 0-21391  
 Na/S cells, evaluation of sintered SiC as electrode 0-35355  
 Na/S sintered battery material (German) 0-21394  
 Na-S accumulator, electrical energy storage (French) 0-55835  
 Na-S batteries, current development trends and characts. 0-55830  
 Na-S batteries, energy storage for peak power generation 0-30455  
 Na-S batteries, reproducibility and performance of large prototype cells 0-30454  
 Na-S battery, improved capacity (French, German) 0-30441  
 Na-S battery for energy storage 0-30453  
 Na-S cells, failure anal. of  $\beta$ - $\text{Al}_2\text{O}_3$ - $\text{Na}_2\text{O}$ - $\text{Li}_2\text{O}$  membranes 0-12003  
 Na-S cells, S electrode resistance calc. 0-35667  
 Ni-Cd, Nimbus-Landsat spacecraft power subsystems, flight performance 0-30459  
 Ni-Cd, plastic bonded Cd electrodes, production methods 0-45659  
 Ni-Cd, sealed aerospace cells,  $\text{H}_2$  recombination during over discharge 0-30461  
 Ni-Cd, with plastic bonded Ni oxide electrodes, basic electrochemical parameters 0-50951  
 Ni-Cd 6.0 Ah cells, accelerated testing of cell failure for life prediction 0-35670  
 Ni-Cd accumulators, plastic bonded electrodes, active layer composition influence on galvanostatic and potentiostatic discharge curves 0-55834  
 Ni-Cd battery system design for tracking and data relay satellite system 0-30460  
 Ni-Cd cell lifetime prediction, computerised pattern recognition 0-3504  
 Ni-Cd spacecraft batteries, power system perform. anal. using computer modelling 0-30497  
 Ni-Cd system, characteristics and new developments for telephone industry applications 0-55829  
 Ni-H<sub>2</sub> 50 Ahr battery for low earth orbit satellite appls. 0-30463  
 Ni-H<sub>2</sub> cells for space appls., characterisation and simulated low earth orbit cycling 0-30462  
 Ni-Zn cells, heat transfer anal. 0-30458  
 Ni-Zn electric vehicle battery, performance characts. 0-30443  
 Ni-Zn sealed cylindrical dry-cell batteries, high working voltage 0-40852  
 Pb battery anode reverse polarisation corrosion test method (Bulgarian) 0-50950  
 Pb-acid, cell design analysis computing for optimal electrical performance characteristics 0-55832  
 Pb-acid, cylindrical, pure lead, design features and performance experiences in float service applications 0-55831  
 Pb-acid batteries, DSA type positive grids, characts. improvement, soln. 0-35668  
 Pb-acid batteries, for elec. vehicle propulsion, heat transfer, math. anal. 0-3509  
 Pb-acid batteries for electric vehicles 0-30445  
 Pb-acid battery, effect of  $\text{H}_3\text{PO}_4$  on positive electrode, mechanism 0-26129  
 Pb-acid battery, grid corrosion, effect of addition agents 0-3505  
 Pb-acid battery, thermopassivation of  $\text{PbO}_2$  plate 0-3507  
 Pb-acid cells, heat transfer anal. 0-30458  
 Pb-acid system, characteristics and new developments for telephone industry applications 0-55829  
 Pb-Ca batteries, float current 0-12004  
 Pb-H<sub>2</sub>SO<sub>4</sub> cells, Sb alloying effect on solid Pb electrochemical properties 0-55668  
 PbO<sub>2</sub>, compressed powder magnetoresistance and apparent carrier mobility 0-35669  
 $\text{Sr}_0\text{FeS}_2$  cathodes for nonaqueous Li batteries 0-3506  
 Zn-Ag<sub>2</sub>O, concentration changes in porous Zn electrodes during cycling 0-35666  
 Zn-Br<sub>2</sub> battery for utility energy storage appls. 0-30450  
 Zn-Br<sub>2</sub> non-circulating storage batteries 0-30451  
 Zn-Cl<sub>2</sub> batteries for electric vehicles, battery design modelling 0-30452  
 Zn-Cl<sub>2</sub> battery, half-cell overpotential measurements 0-21393

## secondary electron emission

- air, weakly-ionised, secondary electron distrib., produced by electron source distrib. 0-6211  
 amorphous semiconductors, universal yield curve verification 0-45179  
 atmospheric positive streamer corona, primary wave emission, secondary electron emission 0-44008  
 Boltzmann equation, appl. (French) 0-20740  
 conference on inelastic ion surface collisions, Hamilton, Ontario, Canada (Aug. 1978) 0-31402  
 dielectric, irradi. by electron beams, effect of bulk and surface cond. on pot. 0-2446  
 discharge, RF, gamma regime, ionis. balance and plasma characts., model 0-44022  
 discharge in heterogeneous medium 0-38858  
 discharge tube wall, secondary electron emission in cathode fall region of tube wall 0-44001  
 gas, weakly-ionised, electron stopping model and secondary-electron distrib. 0-6263  
 glow discharge breakdown, temporal development of electrode pot. 0-44003

## secondary electron emission continued

- graphite film, secondary electron emission and EELS rel. to plasmons 0-50481  
 ion-bombarded solid, direct and recoil-induced electron emission 0-11526  
 laser channel with secondary emitter, transverse microwave discharge He-Ne laser 0-9899  
 lunar regolith, secondary electron emission characts. determ. method 0-12687  
 metal surfaces, clean polycrystalline, ion-induced electron emission, review 0-35032  
 microdosimetry, secondary electron emission and two-target theory 0-12274  
 polyethylene film, soln.-cast, low energy electron scatt. obs. of band struct. 0-16131  
 reflection and transmission secondary emission (Japanese) 0-45180  
 saturated liquid polydielectrics, secondary electron emission and energy loss spectra 0-55239  
 semiconducting channel ion source, secondary emission and ion feedback 0-31936  
 solid, heavy ion bombard., Mach shock electron distrib. 0-45194  
 spectroscopy, total current, study of surface regions and bulk physics 0-31952  
 stainless steel:C, surface, obs. at very low accel. voltage (200 V-1 kV) by SEM 0-10764  
 steel, stainless, secondary electron emission, ion-induced for cluster ions  $\text{V}_n^+$ ,  $\text{Nb}_n^+$ , and  $\text{V}_n\text{Nb}_n^+$  0-35035  
 surface analysis, AES and ESCA combined with SEM (French) 0-47154  
 Ag film, on Au substrate, monolayer overgrowth, quantitative AES method 0-10813  
 Al, appl. of Boltzmann equation (French) 0-20740  
 Al, clean and oxidised surfaces, secondary electron spectrum, EELS, and AES, comparison 0-55237  
 Al, secondary electron emission by reflection, Boltzmann eqn. resolution method 0-45178  
 As<sub>2</sub>S<sub>3</sub>, secondary electron emission, fluctuation state effect 0-40193  
 Au, Boltzmann eqn. appl. (French) 0-55238  
 Be film, on Cu substrate, monolayer overgrowth, quantitative AES method 0-10813  
 CaO, optimum composition of dielectric materials for AC-operated plasma display panels 0-14945  
 Cu, Boltzmann eqn. appl. (French) 0-55238  
 Cu, surface contaminant anal. by ion-electron spectroscopy 0-54490  
 Cu:Au:C, surface, obs. at very low accel. voltage (200 V-1 kV) by SEM 0-10764  
 Cu-Ni:polyethylene, surface, obs. at very low accel. voltage (200 V-1 kV) by SEM 0-10764  
 GaAs, excitation: by 2-4 KeV  $\text{Ar}^+$  ions, electron energy spectra 0-11529  
 InP, excitation by 2-4 KeV  $\text{Ar}^+$  ions, electron energy spectra 0-11529  
 K<sub>2</sub>O-SiO<sub>2</sub>, glass, influence of electric charge phenomena on AES (French) 0-50478  
 LiF(Cl)(Br) film, electron emission under metastable He and Ne atom impact 0-20747  
 MgO, adsorption of Cs and Li, AES, LEED, work function, and secondary electron emission meas. 0-44407  
 Mo, adsorption of CO, O<sub>2</sub>, metastable He de-excitation spectroscopy and UPS study 0-34314  
 Mo surface, metastable He atom beam contamination by fast neutral atoms, effect on secondary emission 0-55253  
 Na<sub>2</sub>AlF<sub>6</sub> film, evaporated, electron bombard. effect on secondary electron emission, Auger peak shifts 0-2903  
 NaF(Cl) film, electron emission under metastable He and Ne atom impact 0-20747  
 Ni, (100) surface, secondary electron spectra, adsorbed elements effects 0-50480  
 Ni, secondary electron emission under  $\text{Ar}^+$  ion bombard. near Curie point 0-29838  
 SrO, optimum composition of dielectric materials for AC-operated plasma display panels 0-14945  
 Ti<sub>2</sub>SeAs<sub>2</sub>Te<sub>3</sub>, secondary electron emission, fluctuation state effect 0-40193  
 W, ion induced secondary electron emission, probe for adsorbed O 0-55251  
 W, secondary emission and photoemission props., effect of one-electron density of states 0-16152

## secondary emission

- see also secondary electron emission; secondary ion emission  
 Cu (001) surface, with adsorbed O,  $\text{Ar}^+$  bombarded, particle ejection ang. depend. 0-50489  
 Cu surface, secondary charge emission coeffs., low energy  $\text{H}^0$  flux meas. 0-25509

## secondary ion emission

- see also secondary ion mass spectra; secondary ion mass spectroscopy  
 alloy surfaces, sputtering process and sputtered ion emission models 0-35044  
 elements, sputtering process and sputtered ion emission models 0-35044  
 ion-surface impact, surface atomic struct., effect on recoil atom energy distrib. 0-35050  
 ionisation process, review 0-35040  
 metal, with adsorbed Cs effects on photon and secondary ion emission during sputtering 0-35038  
 oxidised surfaces, sputtering process and sputtered ion emission models 0-35044  
 silicates, ion bombardment, secondary positive mono-atomic ion emission, cation conc. depend and matrix effects (French) 0-50487  
 solid surface, energetic particle irradi., collision cascade 0-45186  
 steel, austenitic, non-oxidising, B and by secondary ion emission and X-ray microanal. (French) 0-11985  
 tissuelike medium a trajectory heavy secondary ion ejection 0-9466  
 Tokamak fusion devices, secondary ion emission, appl. to impurity control 0-37584  
 Be, clean and O covered, secondary-ion emission energy depend. 0-50502  
 Be surfaces, O and H covered, secondary ion emission, coverage dependence 0-35043  
 Cu (110), O adsorption, low-energy ion bombardment investigation 0-34302  
 GaAs thin film, effect of O on thin film compositions obtained by secondary ion emission 0-26079  
 Si bombardment with atomic and molecular noble-gas ions, secondary ion emission 0-35042



# secondary ion emission continued

- Si thin film, effect of O on thin film compositions obtained by secondary ion emission 0-26079  
 SiC, thin film, effect of O on thin film compositions obtained by secondary ion emission 0-26079  
 Ta, secondary ion emission, normalised energy spectra from Hg<sup>+</sup> impact 0-45193  
 TiO<sub>2</sub>, (100) surfaces, ionisation of sputtered-atomic particles 0-20750  
 V, anomalous secondary ion emission, normalised energy spectra from Hg<sup>+</sup> impact 0-45193

# secondary ion mass spectra

- amino acid valine, heavy ion induced desorption, time-of-flight mass spectra anal. 0-54509  
 chromel and alumel thermocouples, decalibration, quantitative SIMS anal. 0-4705  
 electron microprobes and scanning electron microscopy, conf., Orsay, France, Dec. (1978) 0-11979  
 ferrite spinel films, LPE growth and props., SIMS, X-ray diffr., and spin wave reson. obs. 0-34323  
 graphite fibres, HM, surface comp. and energetics 0-54480  
 lubrication, spectroscopic methods for surface anal. (French) 0-26095  
 semiconductors, characterisation of thin epitaxial layers and bulk material (French) 0-50904  
 sputtering, preferred, phenomenological model for SIMS and Auger profiling 0-55254  
 steel, C, friction faces, S, O content, secondary ion-ion emission obs. 0-55545  
 steels, welded, types D36, D50, secondary ion anal. of segregation 0-7580  
 surface analysis, appl. of SIMS, review 0-40204  
 surface problems, in materials science and technology, conference, Gothenburg, Sweden, June 1979 0-51950  
 thin film, and surface anal., modern methods 0-54486  
 Ag-Au, surface layer, effect of Ar<sup>+</sup> bombardment, AES and SIMS 0-25504  
 Al-Mg-Zn, O<sub>2</sub><sup>+</sup> ion bombard., SIMS and photon emission spectra, local thermodynamic equilib. model 0-20751  
 Au-Cu-Cr, thin layer, deposited on glass or Si substrate, X-ray microanalysis (French) 0-50902  
 BN, chem. bonding and electronic struct., AES and SIMS meas. 0-50512  
 B<sub>2</sub>O<sub>3</sub>, chem. bonding, electronic struct., ESCA, Auger, and SIMS spectra 0-50512  
 CdTe, trace anal. by heavy ion induced X-ray emission and SIMS 0-55755  
 Cu-Ni, clean surface, surface segregation and growth process of altered layer (Japanese) 0-24720  
 Cu-Ni, surface layer, effect of Ar<sup>+</sup> bombardment, AES and SIMS 0-25504  
 CuBe, Be distrib. in vicinity of oxidation boundary (French) 0-11984  
 Fe-TiB<sub>2</sub>, phase composition, secondary ion-ion emission study (Russian) 0-20896  
 Fe<sub>40</sub>Ni<sub>60</sub>B<sub>20</sub> glass, <sup>10</sup>B self-diffusion, meas. by SIMS 0-49406  
 GaAs:<sup>11</sup>B, physicochem. and resistivity meas. 0-24933  
 GaAs:Cr, bulk and epitaxial, ion implanted, Cr conc., depth distrib. and diffusion coeff. 0-49243  
 GaAs:Cr substrates and LPE layers, Au film deposition, Cr redistrib., TEM and SIMS 0-15312  
 GaAs:Se, ion implanted, Cr redistrib. during annealing, SIMS anal. 0-10570  
 GaN:Al, VPE grown, luminesc. and elec. props. depend. on doping conc., bound excitons 0-20688  
 Ge amorphous film, O depth profiling by SIMS 0-39480  
 H<sub>2</sub>BO<sub>3</sub>, chem. bonding, electronic struct., ESCA, Auger, and SIMS spectra 0-50512  
 In film, oxidized polycrystalline, spectra obtained from combined XPES and SIMS investigation of surface 0-52377  
 InP (110), low coverage adsorption, SIMS study 0-49500  
 MgO-Al<sub>2</sub>O<sub>3</sub>-SiO<sub>2</sub> glass/polysulphone adhesive failure, ISS and SIMS obs. 0-55626  
 N<sub>2</sub> adsorbed on W, effect of SIMS sputtering induced recomb. anal. 0-55243  
 Nb (110) and (750), interaction with O<sub>2</sub>, LEED, AES, SIMS, and EELS obs. 0-44408  
 Ni (100) and polycrystalline surfaces, CO chemisorption, low energy SIMS and AES 0-34309  
 Ni, reaction of H<sub>2</sub> and O<sub>2</sub> on polycryst. surface, SIMS and thermal desorption meas. 0-40742  
 Ni-Pd surfaces, electrochem. passive film form. and comp. determ. by SEM, SIMS, XPS 0-39401  
 Pb-Sb alloy, Sb distrib. profile as function of depth in corrosion films 0-21177  
 Pd-Ag, thin layer, deposited on glass or Si substrate, X-ray microanalysis (French) 0-50902  
 Si, dry etching induced surface contamination, SIMS, AES, and XPS obs. 0-11810  
 Si:Cr, ion implanted, Cr conc., depth distrib. and diffusion coeff. 0-49243  
 Si:D, ion implanted, D depth distrib., SIMS meas. 0-54279  
 Si:P, diffusion-doped laser irradiation effects, electrical reactivation of P 0-39124  
 Si-SiO<sub>2</sub> interfacial region on TCE/O<sub>2</sub> and CCl<sub>4</sub>/O<sub>2</sub> oxidised Si, struct. and comp. 0-50741  
 Si-SiO<sub>2</sub> transition region width, SIMS depth profiling 0-39454  
 SiC, sputtering processes by energetic ions, combined SIMS-AES study 0-40201  
 SiO<sub>2</sub>, dry etching induced surface contamination, SIMS, AES, and XPS obs. 0-11810  
 SnTe, <sup>119</sup>Sn diffusion coeff. meas., stoichiometric deviation, SIMS 0-34236  
 β-Ta sputtered film, stabilisation by Ta-Si interlayer, SIMS depth profiling 0-54568  
 TiN film as protective coating for vacuum deposition chamber, Auger electron spectroscopy study 0-25922  
 TiO<sub>2</sub>-(Cr<sub>2</sub>O<sub>3</sub>), rutile, Cr<sub>2</sub>O<sub>3</sub> effects on O<sub>2</sub> tracer diffusivity, depth profile meas. by SIMS 0-24651  
 W (100), coadsorption of Zr and O<sub>2</sub> at high temp. 0-6653

# secondary ion mass spectroscopy

- adhesion measurement, locus of failure, bond failure in adhesive joints 0-50801

# secondary ion mass spectroscopy continued

- computerised system for energy spectra determ. 0-3423  
 corrosion science, surface analytic techniques 0-31929  
 depth profiles obtained by ion-beam sputtering, edge-effects correction 0-55757  
 film surface analysis techniques survey, for development and production (Hungarian) 0-54537  
 instrument combining XPES and SIMS for surface studies 0-52377  
 metal and oxide surfaces, and interfaces, slow exchange processes study using SIMS 0-55653  
 p-n junction potential step meas. 0-34503  
 solid surface investig. applications (Rumanian) 0-49510  
 sputtering use in depth profiling, review 0-40214  
 surface analysis, appl. of SIMS, review 0-40204  
 surface analysis, appl. to lubrication problems, review (French) 0-45616  
 surface analysis, probing and imaging techniques 0-54487  
 surface characterisation, physical methods, review (French) 0-7889  
 surface reactions, appl. of SIMS (French) 0-45603  
 Be-Cu dynode, depth profiling anal. of surface layer 0-2253  
 Cu, sputtered, ionisation probability, energy dependence 0-35041  
 Ni, sputtered, ionisation probability, energy dependence 0-35041  
 Si:As sputter rate meas. SIMS combination with Rutherford backscatter 0-21334

# security of data

- see also data handling  
 computer trends, effects on society 0-47590

# security of information see security of data

# sedimentation

- see also disperse systems; sediments; water treatment  
 aeolian sedimentation on Earth and Mars, comparisons 0-31042  
 NE Atlantic continental margin, sediments differential deposition and distrib. by bottom currents 0-12372  
 binary fluid mixture, in centrifugal field, crit. dynamics 0-44310  
 binary particle mixtures 0-40757  
 Caspian Sea, lake bottom sedimentation contrib. to biogenous elements balance 0-31073  
 clay minerals in estuarine and coastal waters, role of suspended particles surface charge 0-36331  
 colloids, sedimentation hydrodynamic interaction between spherical particles, effect of repulsive interparticle forces 0-45577  
 disperse suspension of solid particles in viscous fluid, Markov model 0-28551  
 disaggregation effects, porous solid matrix stresses, aggregate max. size 0-16732  
 DNA, high mol. wt., sedimentation data, radiation-induced single-strand breakage, additives effect 0-30667  
 DNA, sedimentation constants, direct meas. by analytical ultracentrifugation (French) 0-8004  
 estuarine sedimentation, measurement techniques, book 0-36788  
 flocculent suspensions, review 0-35577  
 central Gulf of California, sedimentation rate effects on heat flow 0-3968  
 histones H<sub>2</sub>A and H<sub>4</sub>, mixed solns., oligomer structs. 0-30648  
 latex sphere aggregates, dynamic shape factors determ. by sedimentation vel. meas. in capacitor 0-26063  
 lymphocytes, living and dead, mag. props. and mag. sedimentation 0-35925  
 old Mangalore Port, India, sediment transport and siltation of navigational channel 0-56488  
 old Mangalore port siltation, meas. of seasonal vars. in seawater hydrographic conditions 0-41451  
 oceanic phosphorites, Fe, Ti and Al behaviour during initial form. stages 0-31029  
 polymer, absolute mol. wt. and mol. heterogeneity determ. from sedimentation vel. in ultracentrifugation (German) 0-14261  
 polymer solutions and gels, dynamic behaviour obs. using light scatt. 0-55727  
 pyrex-H<sub>2</sub>O(aq. KCl) systems, electrokinetic coeff. determ. from sedimentation pot. 0-3365  
 quartz, grinding and surface treatment by ball mill in cetyl alcohol (Japanese) 0-25890  
 solar nebula, fine dust grains clustering and sedimentation time 0-26937  
 suspensions, creeping flow, hindered settling, particle shape effect 0-14797  
 suspensions, fluid dynamical aspects of operating conditions of suspension stirrers (German) 0-26058  
 suspensions of equal spheres, cluster settling, appl. of distrib. of kth nearest neighbours 0-40758  
 thick clay suspensions, electroenforced sedimentation in consolidation region 0-26057  
 thick water film in turbulent flow over impermeable slope, erosion and sedimentation (French) 0-43692  
 velocity-voidage relations for sedimentation and fluidisation 0-24076

# sediments

- see also rocks; sedimentation  
 abyssal clay containing meteoroid ablation spheres 0-46500  
 aeolian sedimentation on Earth and Mars, comparisons 0-31042  
 alluvial ground surface dislocation due to buried fault movements (Japanese) 0-21723  
 Amazon suspended sediment reaction with seawater, cation exchange characts. 0-8337  
 aquatic sediment lipids, Recent and ancient 0-51583  
 Atlantic coast barrier islands, shoreline periodicities and edge waves 0-12375  
 N. Atlantic Foraminifera sediment, ocean deep water production since Miocene 0-46186  
 Atlantic Ocean, quartz distrib. relation to climate in last glaciation 0-8308  
 Baltic Sea, continuous underwater gamma-survey 0-12377  
 Barents Sea sediments, continuous seismic profiling with two receiver systems 0-31150  
 barite, deposits at deep-sea hydrothermal site on strike-slip fault 0-21710  
 barrier island breach morphology and dynamics, study in stability 0-12371  
 beach deposits sedimentary material differentiation and bedding form. dynamico 0-26496  
 Bering Sea shelf sediments, denitrification estimates 0-12433  
 Bhagirathi River, West Bengal, unidirectional alluvial channels, metamorphosis philosophy 0-31075



## sediments continued

- Blake Plateau, Late Cenozoic sedimentary record rel. to Gulf Stream vel. fluctuations 0-12432  
 Bulgarian continental shelf, morpholithodynamic study 0-26495  
 E.China Sea sediments, mineral comp. and distrib. (*Chinese*) 0-8293  
 classification by ocean subbottom acoustic Q meas. 0-46168  
 coarse riverbed material, probability density function of biased samples 0-12445  
 deep ocean sediment thermal conductivity meas. platform rel. to nuclear waste storage 0-46175  
 deep sea benthic mixing, radioactive tracer study 0-8294  
 deep sea sediment cores, Au, Pd, Ir, Mn sources, neutron activation anal. 0-17247  
 deep-sea, O<sub>2</sub> uptake and nutrient exchange meas. 0-3564  
 deep-sea Mn nodules, quant. distrib. and metal content (*Japanese*) 0-8292  
 dredger spoil, dumping ground obs., motion of fine particles with current 0-17287  
 dredging from Gulf of La Napoule in France, pollution abatement attempt results 0-16857  
 NE.France, forest borealisation rel. to last (Eemian) interglacial abrupt end 0-21818  
 free-surface sediment conveying river bed flow, flowrate and momentum correction factors 0-36339  
 Galapagos Rift hydrothermal mounds, obs. with DSRV Alvin and detailed heat flow studies 0-51383  
 Galapagos sea floor sediments, hydrothermal mounds, stratigraphy and chem. 0-26497  
 geoelectrical prospecting in marine areas, dipole and unipole resistivity methods 0-56641  
 geophone and hydrophone recordings in Californian offshore sediment 0-46192  
 Georges Bank, NW.Atlantic, seismic vel. of sediments to 1.4 km depth 0-21644  
 Gironde inlet and Pertuis de Maumusson, suspended sediment seaward dispersion, remote sensing study (*French*) 0-8324  
 glacial deposits, wind action on sub-Antarctic Marion Island 0-31093  
 W.Gulf of Oman, Mahran deformed sediment prism rel. to tectonics 0-8279  
 Gulf of Sidra (Mediterranean Sea), platform upper sediment mantle geological struct. 0-36290  
 Gulf of Suez, sediment layers rel. to multiple seismic refls. and head waves 0-56400  
 Hepworth carboniferous sediment geochemistry, Fe minerals and concretions origin 0-17262  
 Holocene lake sediments, N.Poland, palaeomag. 0-21616  
 India, W. continental shelf, CaCO<sub>3</sub>, Mg<sup>2+</sup>, and Ca<sup>2+</sup> content 0-8289  
 India, W. continental shelf, marine sediment P<sub>2</sub>O<sub>5</sub> content 0-8288  
 W.India continental shelf, topography and sediments 0-56454  
 Indian Ocean, palaeotemps. during Brunhes epoch from sediment core study 0-12429  
 Lake Tahoe, California-Nevada, sediments, palaeomag. and sedimentological studies 0-41371  
 Late Pleistocene and Holocene dry lake deposits, Mexico, palaeomag. record 0-21618  
 loess, in Iowa, wind-aligned drainage 0-41467  
 Los Angeles Basin SW block, sedimentary record rel. to thermal subsidence and petroleum generation 0-3967  
 magnetic spherules in Arctic Ocean sediments 0-26488  
 magnetisation studies, high-pressure cell for chem. demagnetisation 0-31126  
 marine, acoustic wave penetration as function of physico-mech. characts. (*French*) 0-33324  
 marine, interstitial water extraction using pneumopress 0-26643  
 marine, ratio of compressional wave vel. to shear wave vel. and Poisson's ratios 0-12404  
 marine, saturated, acoustic nonlinearity 0-19132  
 marine sediments, acoustic anisotropy due to overburden press. 0-56455  
 marine sediments, interstitial methane profiles 0-12373  
 marine sediments interstitial solns. comp. and diagenesis, seawater-sediment interface fluxes 0-3988  
 E.Mediterranean, during glacial max., surface temp. and salinity from foraminifera in sediments 0-41456  
 metal-rich deposits at ocean ridge crests, form. 0-41430  
 minerals diagenesis, plate tectonic controls 0-12387  
 Miocene-glaciomarine, southern Ross Ice Shelf 0-36292  
 mirex in lake Ontario sediments, circulation simulation 0-26556  
 multilayered media, layer-indexed acoustic reflection model 0-43517  
 neutron activation anal., geochem. of genesis of ore deposits (*German*) 0-30301  
 Newfoundland, depositional environments and benthos of the continental slope and rise 0-3987  
 nonuniform suspended load, non-equilibrium transportation (*Chinese*) 0-8339  
 North Sea floor, lunar type features explanation 0-31028  
 oblique anhyetretic remanent magnetisation 0-21717  
 ocean bed carbonate sediments, acoustic stratigraphy 0-21709  
 ocean sediment free-fall penetrometer with Doppler telemetry 0-46320  
 ocean sediments, experimental studies of acoustic wave attenuation 0-10067  
 oceanic phosphorites, Fe, Ti and Al behaviour during initial form. stages 0-31029  
 Oneida Lake, New York, Mn nodule growth rate 0-46208  
 opaline pelagic sediment, dissolution of silica into seawater 0-51419  
 SW.Pacific basin, reverberant subbottom layers distrib. 0-8290  
 N.Pacific Cenozoic sedimentation history 0-31027  
 Pacific Ocean bottom sediments, interstitial waters B content 0-36289  
 Pacific Pliocene benthonic foraminifera, O isotopes for deep ocean temp. 0-56492  
 E.Pacific Rise, metalliferous sediments three-dimensional distrib. 0-21705  
 palaeocurrent indicators in deep-sea sediments 0-3992  
 penetration of highly directional acoustic beams 0-14511  
 Pitt Lake, BC, sedimentation rates from <sup>137</sup>Cs measurements 0-4048  
 pollen and spore concentration from fine grained sediments by sieving method 0-17402  
 pollution by Hg and As, instrumental neutron activation and atomic abs. spectrometric anal. 0-16890  
 reservoir supplying major mining centre, water and sediments heavy metals content 0-30617  
 reservoirs of Uttar Pradesh, sedimentation 0-31076  
 Rio Grande Rise, marine sediments and erosional canyons of late Cainozoic 0-56456

## sediments continued

- river sediment transport meander of sand bedded stream 0-41466  
 rivers, sediment yield of New Zealand S. Alps 0-21787  
 sand tracer dispersion under progressive water waves, laboratory and field obs. 0-46170  
 source identification, mag. meas. techniques 0-8348  
 South China Sea basin, sediments thickness from profiler-sonobuoy meas. 0-8291  
 St. Lawrence Estuary turbidity maximum, sediment, salinity, suspended matter study 0-4015  
 standard reference materials, based on river sediment and urban particulate matter (SRM 1645 and SRM 1648) 0-21831  
 supernova created sediment,  $\gamma$ -ray ablation of Moon 0-56731  
 surface charge 0-36331  
 suspended sediment load of estuarine and oceanic waters of old Mangalore port, seasonal vars. 0-41451  
 suspended sediment sources identified by magnetic measurements 0-4052  
 Thunder Bay Late Quaternary sediments, palaeomagnetic record from remanent mag. meas. 0-17230  
 tidal power schemes of West Bengal, siltation estimation 0-31059  
 transport near breakwater, physical and numerical modelling 0-51401  
 Vancouver Island, Wisconsin stratigraphy, climate reconstruction 0-8267  
 volcanic material alteration in marine sediments, SE.Pacific Ocean 0-3990  
 Y-5 ash layer in E.Mediterranean, age, origin and volcanology 0-56444  
<sup>10</sup>Be conc. vars. search in marine sediment core during geomag. reversal 0-26511  
 H<sub>2</sub>S contaminated sediments composition, stagnation coeff. and appl. in palaeogeographic reconstruction 0-36291  
 Hg pollution of Mediterranean sediments around Alexandria, Egypt 0-3538  
 Mn nodulus and micronodules of NW.Atlantic, rare earth element study 0-46167  
 Nd isotope composition of ocean bed 0-21704  
<sup>18</sup>O in equatorial Pacific core, glacial time scales and climate 0-21817

## Seebeck effect

- amorphous semiconductors, appl. to thermoelec. generators 0-35704  
 metals, diffusion thermopower, boundary scatt. effect 0-6817  
 rare earth compounds, R<sub>2</sub>MoO<sub>5</sub>, cryst. struct., IR spectra, elec. and mag. props. 0-33954  
 rare earth pyrochlores, R<sub>2</sub>(V<sub>4/3</sub>W<sub>3/3</sub>)O<sub>7</sub>, (R=Gd, Tb, Dy, Ho, Er, Tm, Xb, Lu), synthesis and elec. props. 0-29914  
 volume component determination 0-49788  
 Al-TeO<sub>2</sub>-Al, field-assisted cond. mechanism 0-11105  
 AlH<sub>3</sub>, thermo-EMF meas. 0-39617  
 BaTiO<sub>3</sub>, H<sub>2</sub>-reduced, elec. cond. mechanism, EPR, resist. and Seebeck coeff. meas. 0-10976  
 BaTiO<sub>3</sub>, semiconducting ceramic, AC thermopower measurement 0-44624  
 n-Bi<sub>2</sub>Se<sub>3</sub>, single cryst., new aspect of carrier scatt. 0-49707  
 Cd<sub>3</sub>As<sub>2</sub>, band structure, pressure dependence of galvanomagnetic effects 0-6722  
 Cr<sub>2</sub>S<sub>3</sub>-Se<sub>3</sub>, elec. resist., thermal cond. and Seebeck coeff. meas. 0-24958  
 CrSe<sub>2</sub>, layered, phys. and elec. props. 0-44594  
 Cs<sub>2</sub>WO<sub>3</sub>, normal phase and supercond. props 0-25035  
 Fe<sub>3</sub>O<sub>4</sub>-xF<sub>2</sub>, substituted magnetite, low temp. resistivity, Seebeck coeff., thermopower 0-20234  
 GeBi<sub>2</sub>Te<sub>4</sub>, Hall const., thermoelec. power, and elec. cond. 0-29407  
 HgTe, magnetophonon oscils. of thermoelec. power 0-49789  
 La<sub>1-x</sub>Sr<sub>x</sub>CoO<sub>3-y</sub>, Seebeck coeff. meas., small polaron hole conduction model 0-20233  
 La<sub>1-x</sub>Sr<sub>x</sub>CrO<sub>3</sub> (0≤x≤0.4), localised level hopping transport 0-10974  
 NdTiO<sub>3</sub>, physicochem. props. 0-25625  
 PbS:Ti, Hall and Seebeck coeffs., Hall mobility, impurity states 0-15545  
 Rb<sub>2</sub>WO<sub>3</sub>, resistivity, Hall effect and Seebeck coeff. from 1.5 to 300K 0-6879  
 Si Seebeck effect position sensor for CO<sub>2</sub> laser beam alignment 0-5772  
 TiO<sub>2</sub>-Ti<sub>2</sub>O<sub>3</sub>-P<sub>2</sub>O<sub>5</sub>, glass form., struct. and elec. props. 0-44592  
 V<sub>2</sub>O<sub>5</sub>-BaO-K<sub>2</sub>O-ZnO glasses, elect. props. and struct. 0-15547  
 V<sub>2</sub>O<sub>5</sub>-MoO<sub>3</sub> solid solns., small polaron cond., elec. resist. and thermoelec. power meas. 0-34447  
 V<sub>2</sub>O<sub>5</sub>-P<sub>2</sub>O<sub>5</sub> (70-30), electrical cond. and thermoelectric meas., Au-glass-Au sandwich 0-29403  
 Y<sub>2</sub>(V<sub>4/3</sub>W<sub>3/3</sub>)O<sub>7</sub> pyrochlore, synthesis and elec. props. 0-29914

## segregation

- microstructural processes and features only*  
 see also Guinier-Preston zones; spinodal decomposition  
 , 0-55642  
 alloy surface, free energy of segregation 0-29256  
 alloy with two ferromagnetic components, surface excitations 0-25179  
 binary metal alloys, surface segregation correlation with bulk diffusion 0-54388  
 crystal growth, macroscopic equilib. and transport concepts, book 0-27054  
 Cunial MNA13-3, Mn addition effect on props. 0-21035  
 Czochralski growth, fluctuating growth rates effect on segregation, no backmelting 0-54161  
 diffusion phenomena, vacancy-impurity complexes effect, appl. to nonequilibrium segregation near grain boundaries (*Russian*) 0-44350  
 dopant segregation during liq. phase electrocrystallization, theory and expt. 0-54384  
 extractive metallurgical processes, thermodynamic evaluations 0-11591  
 FCC crystal, interstitial and solute concentration gradients, flux expression derivation (*French*) 0-54219  
 fission reactor materials, defect trapping and solute segregation in irradiated alloys 0-13603  
 glass fibre reinforced plastic, failure due to deform., optical investigation method (*Russian*) 0-35437  
 grain boundary, X-ray spectral analysis method, for element distrib. determination 0-21337  
 grain boundary decohesion, exchange type soft solute segregation in hard hosts 0-54258  
 grain boundary segregation, computer simulation using Mie type interatomic pot. 0-54259  
 hydrocarbons decomposition reaction, with Ta and  $\alpha$ -Hf, surface segregation influence of O<sub>2</sub> or N<sub>2</sub> 0-55654  
 impurity atoms diffusion and impurity-vacancy interactions (*Russian*) 0-19985  
 paramagnets, diluted solid, clustering of mag. ions, study method 0-11155



## segregation continued

- refractory materials, contrib. of segregation and diffusion to heat cond. 0-20001
- solidification, directional, processor-operated segregation of minority atoms 0-29941
- steel, austenitic-pearlitic transformation, partitioning, atom probe microanal. 0-3079
- steel, C, cementite formation and properties 0-45313
- steel, C martensitic, tempering induced decomposition and segregation, atom probe study 0-3112
- steel, Cr-Mn eutectoid, pearlite growth kinetics and partitioning 0-29963
- steel, Cr-Mo (2.25, 1 wt.%), SCC and temper brittleness, P grain boundary segregation effect 0-55571
- steel, ferritic, with interstitial N, continuous precipitation and clustering 0-7585
- steel, grain boundary segregation of C, atom probe FIM study 0-37134
- steel, low alloy, macrosegregation 0-11647
- steel, Mo-Cr (3 wt.%), CrC formation in isochronal tempering, electron microscope study 0-7584
- steel, NC6, cementite network separation, kinetics (Polish) 0-25698
- steel, Ni-Cr, cast, tempering embrittlement due to impurities, Auger spectroscopy exam. 0-11683
- steel, Ni-Cr, P doped, tempered martensite embrittlement 0-30089
- steel, quenched, adsorption of P on austenite grain boundaries rel. to tendency to delayed fracture of type 18Kh2N4VA (Russian) 0-45378
- steel, rimming, teeming and solidification (French) 0-16296
- steel, Si, electron irradi. in HVEM, void swelling, Si role 0-54285
- steel, stainless, He effects on microstruct. in ion-irrad. 0-29078
- steel, temper embrittled, grain boundary failure model for intergranular fracture modes 0-25825
- steel, W-Cr (3 wt.%), CrC formation in isochronal tempering, electron microscope study 0-7584
- steel alloy, austenite transformation in hot rolled strips 0-55407
- steels, hot forming property and struct. (German) 0-25730
- steels, welded, types D36, D50, secondary ion anal. of segregation 0-7580
- surface segregation and bond strength-atomic size representation 0-20940
- surface segregation kinetics, theory 0-11649
- thin films, segregation effects at surfaces and interfaces 0-39475
- water-isobutyric acid (2,6-lutidine) mixtures, critically quenched, phase separation and coalescence 0-24581
- ZnO-based varistor, grain-boundary segregation, thin film X-ray spectroscopy obs. 0-35185
- Ag-Au, surface layer, effect of Ar<sup>+</sup> bombardment, AES and SIMS 0-25504
- Ag-Cu, surface segregation, electronic theory, density of states, cluster-Bethe-lattice approx. 0-49369
- Ag-S solid solution, grain boundary segregation and S diffusion in Ag 0-25700
- Al, quenched, irradiated, and quenched plus irradiated, grain boundary hardening 0-3162
- Al, vacancy distribution, interbonding atoms, heat peaks in scattered cascades (Russian) 0-39169
- Al-Cu alloy, cast, chilled zone composition and thickness obs. (Japanese) 0-7541
- Al-Mg alloy, cast, chilled zone composition and thickness obs. (Japanese) 0-7541
- Al<sub>2</sub>O<sub>3</sub>, dense, exposed to steam, influence of Ca migration on strength reduction 0-11797
- Al<sub>2</sub>O<sub>3</sub>, sintered, electron microprobe anal. of impurity and additive distrib. 0-40359
- Al<sub>2</sub>O<sub>3</sub>-Ca (0.6 to 1.6 at.%), fracture behaviour, Ca segregation effect 0-40504
- Au, electron irradiated, interstitials and their clusters, diffuse X-ray scatt. study 0-33997
- Au/Ti thin films, effect of Cl<sub>2</sub> on elec. resistance, Ti atom migration and preferred orientation 0-34530
- Au-Ag(Cu), surface segregation, electronic theory, density of states, cluster-Bethe-lattice approx. 0-49369
- Au-Cu, dil., electron irradiated, interstitials and their clusters, diffuse X-ray scatt. study 0-33997
- Au-Ni-Cu-Zn, white gold, metallographic struct., heat treatment and plastic working effect 0-40403
- Au(111) and polycrystalline surfaces, O<sub>2</sub> adsorption, LEED, AES and energy loss spectra 0-34310
- B, preparation and purification, physical characterisation (French) 0-16189
- Co-C, dil., C segregation to single cryst. surfaces 0-39301
- Cu-Au system, grain boundary adsorption thermodynamics (Russian) 0-44317
- Cu-Fe (0.2 at.%), clustering, precipitation, and oxidation, 298 to 919K, Mossbauer study 0-7242
- Cu-Mn-S, Mn surface segregation and Mn/S cosegregation 0-40367
- Cu-Ni, clean surface, surface segregation and growth process of altered layer (Japanese) 0-24720
- Cu-Ni, sputter-induced subsurface segregation, Auger electrons obs. 0-10757
- Cu-Ni, surface layer, effect of Ar<sup>+</sup> bombardment, AES and SIMS 0-25504
- Cu-Ni (50 wt.%) alloys, estimation of sublimation energy of Cu atoms, evaporation rate and surface composition, AES meas. (Japanese) 0-49352
- Fe, (100) surface, S segregation and 2D compounds precipitation (Japanese) 0-35188
- Fe, Armco, inter- and intragranular sulphidation 0-55570
- α-Fe, irradiation induced void swelling, Cr additions effect 0-55408
- Fe surfaces, adhesion, effect of adsorbed atoms, AES study 0-39456
- Fe-Co, surface comp. and surface segregation 0-34280
- Fe-Cr, irradiation induced void swelling, Cr additions effect 0-55408
- Fe-Cr(55 wt.%), phase decomp. early stages and clustering (Japanese) 0-55403
- Fe-Mo-P, P-induced temper embrittlement, Mo role 0-35316
- Fe-Ni (30 wt.%), Ni segregation singularities during dendrito-cellular solidification (Russian) 0-7542
- Fe-Ni-Cr, high Ni content, intergranular corrosion, effect of Cr (French) 0-7708
- Fe-Ni-P, segregation kinetics, theory, and temper brittleness 0-11649
- Fe-Ni-Sb-S, S/Sb surface site competition in segregation 0-40366
- Fe-Si-B-N-S, B, S, N effects on grain boundary segregation and grain growth inhibition, review 0-3047

## segregation continued

- Fe-Sn, grain boundary embrittlement by Sn segregation, Mossbauer study 0-7239
- Fe-Sn, segregation of Sn, kinetics, theory 0-11649
- α-Fe-Sn alloy, grain boundary hardening and segregation 0-55417
- Fe-Sn system, Sn binding state, using segregated <sup>119m</sup>Sn, Mossbauer anal. (Japanese) 0-20525
- GaAs layers, Cu segregation along grain boundaries, spectroscopy study 0-49234
- GaAs:Sn, dopant segregation during liq. phase electroepitaxy 0-54384
- Ge, ion bombarded, radiation defect formation, atom-atom collision cascades modelling 0-10582
- Ge-S-Cu, phase separation in melt centrifugal quenching 0-25701
- KCl:Pb, lead aggregation effect on yield stress, incoherent precipitates, solubility determ. method 0-50645
- KCl-CuCl solid solution supersaturated, precipitation, impurity aggregation 0-29174
- LaNi<sub>5</sub>, surface segregation, influence of O<sub>2</sub>, H<sub>2</sub>, H<sub>2</sub>O, SO<sub>2</sub> (German) 0-51008
- MgO:Mn<sup>2+</sup>, clustering of mag. ions, study method 0-11155
- Mo, doped, surface tension driven flow in electron beam floating zone expts. 0-19731
- Mo, grain boundary segregation of O, atom probe FIM study 0-37134
- Mo-Fe metalceramic alloy, brittle fracture investigation, segregation, morphology, struct. (Russian) 0-55503
- Mo-Mn metalceramic alloy, brittle fracture investigation, segregation, morphology, struct. (Russian) 0-55503
- Mo-O system, grain boundary segregation and intergranular fracture 0-55516
- Mo-O-C system, grain boundary segregation and intergranular fracture 0-55516
- NaCl:Sr, dimer and trimer aggregate formation by NMR, ionic cond. and dielectric losses 0-15094
- NaCl+Pb, Pb aggregation effect on yield stress, incoherent precipitates, solubility determ. method 0-50645
- Na<sub>2</sub>O-B<sub>2</sub>O<sub>3</sub>-SiO<sub>2</sub>-Yb(Tb), luminesc. cooperative processes, glass struct. and comp. effect 0-16101
- Na<sub>2</sub>WO<sub>3</sub> bronzes (0.4<x<1), domain, surface and substrate structs. 0-34281
- Nb (110) and (750), interaction with O<sub>2</sub>, LEED, AES, SIMS, and EELS obs. 0-44408
- Nb thin foils, surface segregation during sputtering at elevated temps., Auger study 0-54386
- Ni, binary alloy, irradi. with heavy ions, non-equilib. segregation phenomena 0-19950
- Ni, intergranular corrosion in dil. H<sub>2</sub>SO<sub>4</sub> solns., S segregation effects 0-30152
- Ni-Cr-Fe, Inconel, effects of heat treatment on surface segregation, Auger spectroscopic exam. 0-7602
- Ni-Cu, sputtering rate, radiation-induced segregation and preferential sputtering effects, kinetic model 0-40199
- Ni-Ge, defect-solute interactions and radiation-induced segregation 0-25705
- Ni-Mo, sputtering rate, radiation-induced segregation and preferential sputtering effects, kinetic model 0-40199
- Ni-Si, defect-solute interactions and radiation-induced segregation 0-25705
- Ni-Si, proton irradi., γ' precipitation, early stages 0-34096
- Ni<sub>3</sub>Al-B, L1<sub>2</sub> type intermetallic cpd. room temp. ductility improvement by B addition (Japanese) 0-35263
- Ni<sub>3</sub>Si coatings, form. and stability during high temp. irradi. 0-35088
- Pb-Se-As-Ge, phase separation in melt centrifugal quenching 0-25701
- Pd-C, dil., C segregation to single cryst. surfaces 0-39301
- Pt-C, dil., C segregation to single cryst. surfaces 0-39301
- S segregation on Fe(111) surface, LEED, AES and work-function change 0-15350
- S-metal interactions 0-55710
- Si, Czochralski cryst. growth, faceted and nonfaceted, Sb microsegregation 0-45227
- Si, Czochralski crystals, O microsegregation, swirl defect distrib., growth rate depend. meas. 0-39295
- Si, ion bombarded, radiation defect formation, atom-atom collision cascades modelling 0-10582
- Si:Co, implanted or diffused, and annealed, localisation of Co. atoms, Mossbauer obs. 0-39140
- Si-Al-O-N, high-temp. fracture and diffusional deform. mechanisms 0-40509
- Sn, binding state of atoms segregated at boundary of Fe and Fe alloys, Mossbauer study 0-7232
- α-Ti, recrystallised commercial purity, Fe-rich precipitates obs. (French) 0-50637
- UO<sub>2</sub>, desintering of unstructured UO<sub>2</sub> fuel during film boiling testing, grain boundary separation 0-22997
- V-Cr (15 wt.%), radiation-induced solute segregation 0-29086
- YSmCaFeGe, mag. garnet films, segregation of Ca and Ge in LPE growth 0-29959
- ZnTe, elec., SEM and TEM studies of impurity segregation during long annealing 0-30001
- ZnTe:Li, impurity segregation during short annealing and quenching, SEM, TEM and elec. meas. 0-10676
- Zr-Al (14 wt.%), transformation sequence from Zr-Al martensite to Zr<sub>3</sub>Al phase 0-3027
- Zr-Ni, surface layer, segregation of ferromag. Ni, magnetooptic investigation 0-2256
- Zr-Ni-H, surface segregation of Ni, influence on catalytic activity 0-30275
- Zr-Ni-H<sub>2</sub>(x=2.8 to 3), surface layer, segregation of ferromag. Ni, magnetooptic investigation 0-2256
- ZrNi, surface segregation of Ni, influence on catalytic activity 0-30275
- Seidel theory see aberrations
- Seignette salt see Rochelle salt
- Seignetteelectric materials see ferroelectric materials
- seismic waves see also seismology
- absorption of longitudinal waves in upper mantle 0-46145
- alluvial valley, ground motion due to plane SH waves 0-56383
- S.America, seismic wave propag. in Nazca plate, Altiplano and continental margin 0-36264
- anisotropy in isotropic media-horizontally layered, isotropy assumption anal. 0-12343



## seismic waves continued

- anomalous propag. through shearing contact zone in New Hebrides Island Arc 0-3948  
 Appalachian Mountain topography and ground motions 0-56382  
 attenuation in dry and saturated rocks, lab. meas. 0-3998  
 attenuation in partially saturated rocks 0-3997  
 attenuation mechanisms in dry and saturated rocks 0-3999  
 Berea sandstone, effects of pore fluids on bulk and shear attenuation 0-51386  
 body wave propagation through anisotropic ground, seismic station problem (*Russian*) 0-31128  
 body wave theory, moment tensor representation of seismic source 0-36262  
 body waves from intermediate and deep focus earthquakes, magnitude scale rel. to activity temporal var. 0-3943  
 body-wave magnitude, rel. to modified Mercalli intensity 0-36259  
 collocation formulation of wave equation migration 0-4126  
 compressional and shear waves in saturated rock during water-steam transition 0-30995  
 compressional wave velocities in rocks at high temps. and press., rel. to crustal low-vel. zones 0-41435  
 constant Q-wave propagation and attenuation 0-30996  
 continents and oceans, wave field assoc. with fine structured Moho 0-12361  
 converted waves of nearby earthquakes, appl. to deep crustal struct. determ. 0-30999  
 core phases, Bangui obs. (*French*) 0-56396  
 crack anisotropy in NW.England Carboniferous Limestone, in-situ methods 0-17240  
 crack propagation theory, Lamb's problem for a point source 0-56375  
 diffracted wave travel times determ. method 0-8432  
 dispersion, continuous representation technique 0-51334  
 displacement potentials for motion in homogeneous isotropic elastic medium 0-21649  
 effective velocities, determ. in continuous seismic profiling with two receiver systems 0-31150  
 elastic wave fields, discrete wave number representation in three space dimensions 0-3945  
 elastic wave propagation, point pulse source in anisotropic media 0-3939  
 elastic wave radiation expts. from fault models 0-3938  
 elastic wave vel. before earthquakes 0-8256  
 explosion seismic waves, appl. to Earth crust Q-factor beneath SW.Honshu, Japan 0-17242  
 free oscillations attenuation in viscoelastic Earth, theoretical contrib. 0-21652  
 frictional attenuation, amplitude depend. 0-31034  
 Friuli earthquake, 1976, seismic response of different recording sites 0-41379  
 Friuli focal area, Italy, seismic body-wave dispersion 0-36267  
 Hawaii tsunami simulation, open boundary reflection interference 0-17232  
 Iberian Peninsula crustal structure from seismic wave dispersion (*Spanish*) 0-36269  
 Izu Peninsula, Japan, shear waves used to construct underground struct. (*Japanese*) 0-41387  
 Izu-Oshima-kinkai earthquake, Japan, 14 Jan. 1978, seismic waves anal. (*Japanese*) 0-41385  
 Izu-Oshima-kinkai earthquake, Japan, Jan. 1978, aftershocks and main shock ground accel. (*Japanese*) 0-41386  
 L<sub>g</sub>-phase propagation in E British Columbia, evidence from 1918 February 4 earthquake 0-3932  
 Love waves, propag. in 3-dimens. structures, finite element techniques 0-21631  
 Love-type surface wave props. in frictionally bonded layer 0-21630  
 magneto-thermo-elastic surface waves in stressed conducting media, theoretical study 0-8253  
 mantle base lateral heterogeneity from PKP phases amplitudes 0-21675  
 mantle base shear-wave velocity, by diff. SH wave data 0-56380  
 mantle velocity variations below E.Australia and SW.Pacific 0-36279  
 microseisms obs. at New York Rayleigh and Love wave characts., geologic control 0-26462  
 Mid-Atlantic Ridge, fault mechanisms and sub-crustal seismic vel. 0-36265  
 modified Merco Mercalli intensity scale, modification 0-36260  
 Mount Rainier, Washington, underlying struct. from teleseismic body waves 0-31011  
 multilayered elastic medium, reflection seismograms for explosive source, theory 0-17233  
 multiple reflections and head waves in Gulf of Suez, obs. 0-56400  
 multiple seismic wave suppression on seismograms 0-46281  
 nuclear explosion generated body waves, time functions 0-56376  
 oceanic crust, vel. in high-vel. layer indicating garnet comp. 0-17251  
 oceanic upper mantle seismic anisotropy, evidence from ophiolite complex 0-21677  
 of R-waves from great earthquakes, initial phase anal. 0-41405  
 P wave/S wave ratios in foreshocks, rel. to faults premonitory slip and earthquake prediction 0-3944  
 P- and S-waves decoupling in inhomogeneous elastic media 0-21650  
 P-residuals azimuthal var. in southern California, mantle structure 0-3954  
 P-wave amplitude anomalies, interpretation 0-56386  
 P-wave codas, spectral composition of earthquakes and explosions 0-21640  
 P-wave reflection at non-vertical incidence, synthetic seismograms 0-56401  
 P-wave time residuals, three-dimens. inversion 0-21849  
 P-wave travel time stability in La Malbaie, Quebec region 0-21639  
 P-waves, earthquake focus orientation effects 0-3940  
 P-waves records complexity appl. for discrimination of artificial and natural seismic sources 0-12340  
 parabolic wave theories and applications 0-51436  
 PKKP scattering, core-mantle boundary roughness 0-56437  
 Pn waves, high freq., propag. in Central and South Pacific, rel. to lower lithosphere struct. 0-26459  
 prestressed Earth model, P- and S-wave radiation patterns 0-56404  
 propagation in non-ideal elastic medium, spherical sources 0-3941  
 PV waves station corrections for Cracow, Homogeneous Magnitude System 0-8254  
 Q<sub>SS</sub> frequency dependence 0-56381  
 Q-frequency depend. of coda, surface-body wave hypothesis 0-21660  
 quasi P-SV waves in transversely isotropic media 0-36266

## seismic waves continued

- ray amplitudes of compressional, shear, and converted body waves in laterally inhomogeneous media 0-56408  
 Rayleigh dispersion function computations for unlimited freq. values 0-21837  
 Rayleigh wave dispersion and rifting in Tyrrhenian Sea 0-56445  
 Rayleigh wave dispersion rel. to mantle structure under north central Italy 0-3977  
 Rayleigh wave scatt. from uneven topography or inclusion, theory 0-36263  
 Rayleigh wave study of crustal and upper mantle structure beneath Apennines 0-46153  
 Rayleigh wave transmission coeffs. through vertical interface 0-46144  
 Rayleigh waves, dispersion in Walvis Ridge rel. to lithospheric struct. 0-41412  
 Rayleigh waves, fundamental mode and harmonics, appl. to distant earthquakes focal depths determ. 0-21654  
 Rayleigh waves transmission prevention, trench performance, seismic model experiments 0-24727  
 Rayleigh waves under Pacific Ocean, group vels. and response 0-41398  
 refractor velocity determ., cause and nature of errors 0-56621  
 rock elastic props., expts. on two-phase aggregates 0-56463  
 S<sub>g</sub> waves, propag. through Bering Sea and NW.Pacific Ocean 0-51346  
 SH wave scattered by cavity of arbitrary shape 0-51341  
 SH waves due to shearing-stress discontinuity in viscoelastic half-space, displacement 0-56405  
 SH waves in layered transversely isotropic media, wave approach 0-30991  
 SH waves propagating in layered transversely isotropic media 0-36250  
 SH waves refl. and refr. at plane boundary 0-12339  
 SH waves scattering, linearised inverse problem, density perturbation soln. (*French*) 0-51333  
 shallow crustal vels., phase time inversions for Galway Lake earthquake aftershocks 0-21634  
 shear-wave attenuation in crust and upper mantle, 0.05-25 Hz 0-36268  
 sP and P amplitudes for fault plane soln. of shallow quake 0-51335  
 spectral analysis, total field structure anal., autocorrelation functions 0-4142  
 structural foundations, excitation by seismic surface wave 0-10182  
 subduction beneath W.South America, evidence from converted phases 0-26484  
 submarine lithosphere, geophys., geochem. and petrological model 0-3994  
 surface displacement, extended asymmetric surface source in elastic half-space 0-36251  
 surface displacements of stratified half space, theory 0-56403  
 surface wave phase vel., partial derivatives calc. algorithm 0-4140  
 surface waves, dispersion across Iceland Plateau rel. to deep struct. 0-41413  
 surface waves from E.North American earthquakes, rel. to focal mechanisms and tectonics 0-3942  
 surface waves influenced by gravity, effects of anisotropy 0-8252  
 threefold seismic or acoustic holographic interferograms for improved reconstructed-image definition and contrast 0-23844  
 Tibet earthquake, 14 July 1973, source mechanism and seismic wave attenuation 0-36252  
 transfer function for horizontally stratified media, unification of seismic and magnetotelluric problems 0-56622  
 transversely layered isotropic media, seismic wave vel. calcs. 0-12344  
 travel time inversion, for 3-D vel. struct., Backus-Gilbert method 0-21838  
 travel time inversion, geometrical approach 0-3946  
 traveltime data nonlinear least-squares inversion 0-4124  
 tsunami, 1978 June '12, Miyagi Prefecture, Japan (*Japanese*) 0-41401  
 tsunami, damping in stratified ocean with rough bottom (*Russian*) 0-21651  
 tsunami, due to Izu-Oshima-kinkai earthquake, Jan. 1978, source mechanism 0-41393  
 tsunami, generation and propag., simulation using shallow water eqns. 0-41407  
 tsunami, response of bay water (*Japanese*) 0-41399  
 tsunami along Mie coast, central Japan, 1707 and 1854 records (*Japanese*) 0-41402  
 tsunami caused by Izu-Oshima-kinkai earthquake, Jan. 1978, source mechanism (*Japanese*) 0-41392  
 tsunami from Sanriku earthquake, 1933 March 2, initial motion rel. to dislocation model 0-31000  
 tsunami with Miyagiken-oki 1978 June 12 earthquake (*Japanese*) 0-41400  
 tsunamis propagation, finite difference simulation, book contrib. 0-3956  
 S.Tyrrhenian Sea region, seismic wave study of crustal struct. 0-41380  
 E. United States, Rayleigh and Love wave velocities 0-56385  
 velocities, inaccurate data r.m.s. cubic spline approx. 0-17406  
 velocities inversion, for rock pore aspect ratio determ. 0-51387  
 velocity anomalies rel. to local seismicity 0-3953  
 velocity data used for rock mass quality classification 0-17248  
 velocity-density law, rel. to deep seismic sounding and gravimetry data combined interpretations 0-21845  
 wave groups arrival times and azimuth, minimum data technique for earthquakes global location (*German*) 0-56627  
 wave-equation datuming technique, appls. and computations 0-51553

## seismographs see seismometers

## seismology

- see also earthquakes; lunar seismology; seismic waves; seismometers  
 acoustic holography applied to seismic data processing 0-46268  
 acoustic impedance logs computed from seismic traces 0-56398  
 Afar region plate tectonics, seismic and volcanic evidence 0-21700  
 air gun array, high resolution or deep penetration survey, characts. 0-12557  
 Alaska, earthquake, 1964, March 28, static displacement data inversion anal. 0-30998  
 Aleutian subduction zone seismicity, volcano-trench separation, rel. to great thrust-type earthquakes 0-21655  
 Andaman Sea crust, seismotectonics and tectonic history 0-8283  
 anelasticity of Earth interior, stress/strain relation 0-26471  
 anomalies associated with hydrocarbon bearing anticlines, location tool and theory 0-17234  
 AR method for seismic moment calcs. WWSSN instrument appl. 0-21828  
 Asal-Ghoubbet rift zone, Afar, 1978-9 geodetic survey after seismo-volcanic activity 0-46164



# seismology continued

central Asia, active faulting and Cenozoic tectonics of Tien Shan, Mongolia and Baykal 0-8278  
Middle Asia, geomag. investigations rel. to seismic activity 0-26464  
Atlantic Ocean south of Bermuda, geophys. survey within Mesozoic mag. anomaly sequence 0-26492  
Atlantic S.E. of Azores, crustal struct. rel. to mag. anomalies and bathymetry 0-51384  
NW.Australia, crustal profile across Archaean cratons 0-51352  
SE.Australia, explosion seismic profiles and crustal evolution 0-51332  
Avalon zone, Atlantic Canada, extent determ. from mag., seismic and gravity data 0-12384  
axisymmetric seismic response of thick circular plate supporting many rods, nuclear power plant appl. 0-1458  
Badra area, Iraq, microseismicity 0-56413  
Baikal rift zone, seismic activity rel. to continental rift form. (*Russian*) 0-12364  
Baltic Shield, lithospheric thickness from S-wave anal. 0-3978  
Bay of Islands ophiolite complex, Newfoundland, seismic vel. struct 0-21688  
Beaufort Sea area, earthquake data, tectonic setting and stress study 0-3931  
blind zone problem with multiple refraction layer overburden, soln. 0-17241  
book 0-27055  
borehole acoustic velocity measurement system, within or between boreholes 0-51557  
British Columbia, crustal structure from seismic refr. profile 0-17236  
brittle rocks undergoing non-elastic deformation at high-press., elastic wave vel. (*German*) 0-36296  
brontides associated with seismicity 0-12523  
Caledonides of N.Britain, struct. contrast, seismic wave interpretation 0-3975  
S.California, teleseismic P-residuals rel. to mantle structure 0-3954  
S.California, downwarping, tectonomagnetic anomaly and seismicity 0-21626  
E.Canada tectonically active region, magnetotelluric fields time depend. 0-26451  
Central Asia seismicity, historical and modern data 0-36254  
Chandler wobble, seismic excitation 0-26437  
China, geophysical methods of seismology and earthquake prediction (*Rumanian*) 0-8257  
Chinese earthquake catalogue for evaluation of seismic risk 0-36258  
classification of rock mass qualities, vel. data 0-17248  
coal prospecting by seismic profiling, new technique testing 0-17404  
complex trace analysis and colour encoded data display 0-21646  
compression experiments on Gabbro, microcrack development and seismic vel. anal. 0-17250  
compressional wave velocity and damping, minerals and rocks at high-press. (*German*) 0-31031  
continuous seismic profiling with two receiver systems, effective vels. determ. 0-31150  
crack anisotropy in NW.England Carboniferous Limestone, in-situ methods 0-17240  
crack propagation theory, Lamb's problem for a point source 0-56375  
crust deep structure, determ. via nearby earthquakes converted seismic waves 0-30999  
crustal low-velocity zones, compressional wave vels. meas. in rocks at high temps. and press. 0-41435  
Cuvier Basin, off W.Australia, crust form. by rifting, seismic study 0-12368  
data filtering and smoothing, least-squared error, stationary and nonstationary 0-4158  
deep crustal structure beneath Wind River Range, Wyoming, USA 0-46141  
deep seismic sounding and gravimetry, combined data interpretation 0-21845  
depositional facies interpretation from seismic data 0-4122  
direct inversion procedure for Claibout's eqns. 0-21645  
dispersion in seismic data, continuous representation technique 0-51334  
double seismic zone in downgoing slabs and mesosphere viscosity 0-26472  
Earth free oscillations, finite element modelling 0-51338  
earthquake fault mapping in Japan (*Japanese*) 0-51348  
earthquake focal depth determination method 0-56389  
earthquake mechanisms, Izu Peninsula, Japan 0-12345  
earthquake precursors, conf., Jan. 1977, Tokyo, Japan 0-46146  
earthquake prediction, bursts of aftershocks as strong earthquakes long-term precursors 0-41406  
earthquake prediction, from micro-earthquake obs. near Wakayama city, Kii Peninsula, Central Japan 0-31001  
earthquake prediction, implications of tectonomagnetic studies in Tajikistan 0-26446  
earthquakes, intermediate and deep focus, temporal var. of activity 0-3943  
distant earthquakes focal depths, determ. from fundamental mode and harmonic Rayleigh surface waves 0-21654  
earthquakes global location using minimum information (*German*) 0-56627  
elastic wave fields, discrete wave number representation in three space dimensions 0-3945  
epicentre location procedure for RESMAC seismic array 0-56616  
N.Europe, Benelux region, upper mantle struct. from seismic data 0-21691  
E. and central Europe, velocity-depth distribution in upper mantle 0-3980  
exact and asymptotic synthetic multiplet spectra on ellipsoidal Earth 0-21673  
explosion seismology, data processing, predictive dynamic deconvolution (*Rumanian*) 0-8454  
explosion seismology data analysis (*Hungarian*) 0-21841  
explosion seismology in boreholes, multiple wave intensity at large explosion-seismometer distance (*Russian*) 0-30994  
fast Walsh transform configuration program derivation, appl. to seismic data processing (*Chinese*) 0-21853  
fault model, frictional, earthquake sequence 0-30992  
Fennoscandia seismic risk, by recurrence periods 0-21664  
foreshocks, characts. rel. to earthquake prediction and premonitory slip on faults 0-3944  
free oscillations, eigenspectral estimates from decaying time series, uncertainty estimation 0-30993

# seismology continued

Gabilan Range, central California, pressure-induced seismic vel. gradient 0-21635  
Garm region, weak earthquakes space-time sequence 0-21653  
Georges Bank, NW.Atlantic, seismic vel. of sediments to 1.4 km depth 0-21644  
geothermal gradient at 1000 km depth 0-8260  
Geysers geothermal field, California, explosions and microearthquakes study 0-3964  
global geodynamics, Canadian contris., 1971-79 period. 0-8262  
Grass Valley, Nevada, USA, microseisms in geothermal exploration 0-21647  
ground motion simulation and spectral representation using non-stationary amplitude modulated mathematical model (*Spanish*) 0-56397  
W.Gulf of Oman, multichannel seismic refl. profiles rel. to tectonics 0-8279  
Gulf of Sidra (Mediterranean Sea), seismic profiling rel. to sediment mantle geological struct. 0-36290  
Gulf of Suez, multiple refts. and head waves obs. 0-56400  
Hellenic arc earthquakes, fault plane mechanisms rel. to E.Mediterranean area neotectonic evolution 0-56451  
Himalayas, epicentre distrib. rel. to south-central Asia large-scale Cenozoic tectonics 0-17246  
Hokkaido and Tohoku, Japan, intraplate seismicity and large quakes 0-51337  
SW.Honshu, Japan, crust Q-factor derived from explosion seismic waves 0-17242  
Honshu, Japan, deep seismic zone and upper mantle struct. 0-8269  
horizontally stratified media sounding, geophysical problems unification 0-56622  
HTGR core, seismic anal. 0-32327  
Iberian Peninsula, 1977 earthquakes and seismicity (*Spanish*) 0-36270  
Iceland Plateau, deep crust and mantle struct. from surface waves dispersion 0-41413  
imaging expt. 0-46130  
Indian Shield, deep seismic study 0-12358  
initial phase analysis, of R-waves from great earthquakes 0-41405  
intraplate seismicity on bathymetric features, 1968 Emperor Trough earthquake 0-30997  
inverse problem for SH wave scattering (*French*) 0-51333  
inverse problem for two-dimensional velocity variations 0-21833  
Italy, crustal structure from deep seismic soundings 0-56417  
Italy, earthquake prone areas, pattern recognition 0-56411  
N.-central Italy, upper mantle structure from Rayleigh wave dispersion 0-3977  
Izu Peninsula, Japan, tidal effects on swarm activity, 1975-8 period (*Japanese*) 0-41389  
Izu-Oshima kinkai earthquake, 1978, fore- and aftershock distrib. (*Japanese*) 0-41383  
Izu-Oshima-kinkai earthquake, 14 Jan. 1978, aftershocks and crust struct. (*Japanese*) 0-41384  
Izu-Oshima-Kinkai earthquake, 1978, foreshock and aftershock activity (*Japanese*) 0-51349  
Izu-Oshima-kinkai earthquake, Jan. 1978, foreshocks of Oshima Volcano (*Japanese*) 0-46138  
Izu-Oshima-kinkai earthquake, Jan. 1978, precursory mag. field changes (*Japanese*) 0-41395  
Izu-Oshima-kinkai earthquake, Japan, 14 Jan. 1978, seismic waves anal. (*Japanese*) 0-41385  
Izu-Oshima-kinkai earthquake, Japan, Jan. 1978, aftershocks and main shock ground accel. (*Japanese*) 0-41386  
Izu-Oshima-kinkai earthquake of Jan. 1978, pre- and post-event seismicity (*Japanese*) 0-41382  
Japan, deep seismic zone cross-section beneath NE Honshu 0-3951  
Jordan-Dead Sea Rift, crust and upper mantle struct. from seismic refr. data 0-26474  
kaersutite, sound vels. and anisotropy, rel. to upper mantle seismic struct. 0-26501  
Kangshuang-Dachang region near Peking, deep struct. and earthquake foci (*Chinese*) 0-56415  
S.Kanto and Tokai districts, Japan, crustal plate dynamics (*Japanese*) 0-51382  
S.Kanto district, Japan, crustal struct. by explosion seismology (*Japanese*) 0-51368  
Lachlan Fold Belt, SE.Australia, deep crust. struct. 0-56436  
Lake Jocassee area, S.Carolina, seismicity, earthquake prediction algorithms 0-51345  
Lake Keowee, S.Carolina, USA, 1978 earthquake swarm 0-36255  
Laramide Wind River uplift, Wyoming, USA, gravity and seismic refl. data 0-21679  
Lassen Volcanic National Park, California, 1976-8 seismic events 0-36257  
lateral inhomogeneities affecting propag., computational approach 0-21661  
layer pressures inferred from wave velocity (*Hungarian*) 0-21840  
Lehmann discontinuity, mantle props. beneath continents 0-56425  
local magnitude, determination method from seismoscope records 0-56393  
local seismicity rel. to vel. anomalies 0-3953  
low-vel. zone inversion, Weichert-Herglotz integral 0-21829  
lower mantle Gruneisen parameter, seismic evidence for approximation  $\gamma_p = \text{const}$  0-3970  
magnitude of seismic event, statistical models 0-51343  
mantle, density inhomogeneities beneath oceanic trenches, island areas and marginal seas from DSS data 0-21676  
mantle, peridotite high-temp. anelasticity and elasticity at seismic freqs. 0-17256  
mantle, velocity-depth structure, Central Europe 0-3976  
upper mantle seismic discontinuities, implications of monticellite (CaMg-SiO<sub>4</sub>) high-press. phase transforms 0-17255  
marine sediments, acoustic anisotropy due to overburden press. 0-56455  
Markansu Valley earthquake, Tadjikistan, USSR, 1974 August 11, seismotectonics 0-21659  
Mediterranean earthquake catastrophes, statistics 0-3955  
trans-Mexican volcanic belt, seismic refl. and geomag., leg 17 of project CICAR (*Spanish*) 0-36280  
microearthquakes preceding Hollister, California, 1974 November 28 earthquake, fault-plane solns. 0-3936  
Middle America Trench offshore Guatemala, seismic refr. and refl. meas. 0-26493



## seismology continued

- Mogod, 1967 January 5, earthquake, focal mechanism and parameter determ. 0-3937
- Moho dip beneath Scotland, by PS reflections 0-41409
- motion from seismic sources 0-36248
- Mozambique Channel, crustal struct., seismology study 0-51362
- New Hebrides Island Arc, anomalous propag. through shearing contact zone 0-3948
- E.North American earthquakes, surface wave focal mechanisms with tectonic implications 0-3942
- North Sea, Buchan and Witchground Grabens, seismology study 0-51364
- nuclear explosion generated body waves, time functions 0-56376
- ocean crust layer 2, oblique seismic expt. on DSDP leg 52 0-36275
- oceanic crust, structure from refraction expts. 0-3952
- oceanic crust seismological methods, expanded spread and const. offset profile 0-56632
- oceanic trench earthquakes, props. rel. to plates bending at trenches 0-41426
- Okhotsk Sea and Kuril Islands, earthquake magnitude determination, body wave anal. 0-4139
- Ontong Java and Manihiki Pacific oceanic plateaus, seismic struct. 0-21680
- Oroville earthquake, USA, foreshock identification 0-56379
- NW.Pacific attenuation from intensity data 0-21642
- SW.Pacific basin, reverberant subbottom layers distrib. 0-8290
- Pacific plate subduction beneath Japan Islands, 3-D seismic struct. 0-51376
- parabolic wave theories and applications 0-51436
- Parece Vela Basin, E.Philippine Sea, seismic refr. data rel. to evolution 0-41431
- Parkfield earthquake, USA, foreshock identification 0-56379
- Parkfield earthquakes, California, comparison of 1966 and 1934 sequences 0-56412
- Pasadena magnitude scale of earthquakes, based on vertical ground accel. 0-51344
- pipng systems under seismic excitation, modal anal. 0-33512
- plate boundary quakes, magnitude-freq. relation 0-56390
- polarisation state of waves, theory 0-56525
- power spectrum estimation using maximum entropy method, data analysis appl. 0-37006
- quality factor and effective viscosity relationship 0-12360
- W.Quebec zone, focal depth changes 0-26453
- quiescence duration in seismic gap, empirical determ. method 0-26627
- radioactive waste deep geological repositories, seismic design considerations 0-23019
- Raft River geothermal area, Idaho, seismic refr. study 0-3963
- recording station situated on anisotropic ground, body wave propagation (*Russian*) 0-31128
- reflection seismograms for explosive source in multilayered elastic medium, theory 0-17233
- reflection seismology, synthetic seismograms at non-vertical incidence 0-56401
- reflectivity method extensions 0-56640
- refraction method, velocity inversion errors, computation and recognition 0-4132
- refractor velocity determ., cause and nature of errors 0-56621
- reversed reflection traveltimes data, computerised method for effective vel. 0-21832
- Reykjanes Ridge, mid-Atlantic 59°N, seismic crustal struct. 0-56423
- risk in S.Europe through to India, using Gumbel's third distrib. of extreme values 0-21648
- rock pore aspect ratio spectrum determ., seismic velocities inversion 0-51387
- Rockall Bank, N.Atlantic, seismic struct., synthetic reconstruction 0-21670
- Roosevelt hot springs, Utah, seismic noise study 0-56399
- San Andreas fault (central California), mag. field local vars., creep rate changes and local earthquakes 0-26450
- San Andreas fault aftershocks 0-36249
- sand seismic response, effect of stress condition on dynamic props. (*Japanese*) 0-17235
- N.Scandinavia, compressional and shear wave anal. of lower lithosphere fine structure 0-3979
- sedimentary rocks, anisotropy due to overburden press. 0-56455
- seismic exploration, technique and processing, book 0-51975
- seismic hazard mapping, Bayesian model 0-56391
- seismic moment tensor estimated by linear inversion method 0-31125
- seismic prospecting techniques for oil resources (*French, English*) 0-21362
- seismicity 1897-1906, reevaluation 0-21656
- seismograms, synthetic, lossless layered media, time-domain state space models 0-12342
- seismomagnetic earthquake precursors, uniaxial stress effects upon rocks remanent magnetisation 0-26505
- seismomagnetic effect during Gazly, 1976 May 17, earthquake, unsuccessful search 0-26463
- seismotectonic map of France for appl. to antiseismic design of nuclear installations 0-860
- shallow earthquake source characts., Sanriku-Oki region, Japan 0-12346
- Shizuoka district, Japan, crustal struct., explosion seismology data 0-12359
- signal processing method for circular arrays 0-4123
- Snake Bay-Kakagi Lake greenstone belt, NW.Ontario, expanding spread seismic refl. survey 0-12356
- Snyder, Texas, USA, 16th June 1978, seismic activity 0-56395
- South China Sea basin, crustal struct. from profiler-sonobuoys meas. 0-8291
- station correction for Cracow, Homogeneous Magnitude System for PV waves 0-8254
- stick slip earthquake, rupture propag. and energy focusing in foam rubber model 0-3947
- strike-slip faulting, in crust of horizontally variable rigidity, model 0-56377
- strong-motion duration, definition using r.m.s. accel. as parameter 0-56392
- subcrustal lithosphere structural variation, explosion seismic profiles 0-3974
- surface multiple reflections, suppression on seismic records 0-56402
- central Sverdrup Basin, crustal struct. from seismic refr. data 0-12355
- Taiwan velocity risk mapping for seismic resistant building design 0-31002

## seismology continued

- Tamayo transform fault, E.Pacific Rise, deep tow study 0-51361
- Tarbela reservoir, Pakistan Himalayas, seismicity during initial filling 0-56388
- tectonics conference on passive margins, Jun. 1978, Nova Scotia, Canada 0-36774
- tectonometrics and small scale secular variation, symposium, Seattle, Washington (1977 August 22) 0-22133
- tectonometism, implications of magnetite mag. susceptibility under hydrostatic press. 0-26504
- tectonometism as earthquake precursor, piezomagnetism response depth depend. 0-26465
- Texas-New Mexico Permian Basin seismicity rel. to hydrocarbon recovery operations 0-36256
- theoretical introduction, book 0-41962
- theoretical problems, conf., Aug. 1978, Caracas, Venezuela 0-51400
- Tokyo, base rock, seismic explosion obs. (*Japanese*) 0-41403
- Tonga-Kermadec region, deep and intermediate earthquakes energy release rel. to mantle flow depth 0-41404
- toplogy of ray surfaces in low-velocity zones 0-21633
- travel time inversion, computational methods 0-51340
- travel time inversion, geometrical approach 0-3946
- travel-time inversion problem, new approach 0-51339
- two-dimensional strike-slip fault, static deform. of laterally inhomogeneous half-space 0-31012
- Ukrainian Shield, deep seismic sounding profile reinterpretation 0-56407
- NE United States, crust and mantle struct. by seismic vel. 0-56429
- E.United States, seismic struct., shear wave vel. 0-56385
- United States, western region, strain accumulation rates, 1970-78 period 0-21607
- E.United States of America, seismicity, 1754-1972 data 0-36253
- Utah seismic refr. profile DELTA-W, crustal phases 0-56384
- S.Wales, deep geologic struct. by explosion seismology 0-36261
- wave-equation datuming technique, appls. and computations 0-51553
- Yellowstone National Park, USA, teleseismic delay anal. mantle struct. 0-3981
- Yoshioka-Shikano Fault, Japan Sea SW coast, geomag. induction study rel. to seismic activity 0-26475

## seismometers

- see also seismology
- beamforming array, linear adaptive algorithm 0-21834
- borehole acoustic velocity measurement system, within or between boreholes 0-51557
- bubble tiltmeter use as horizontal seismometer, comment 0-21839
- geophone sensitivity in Chebyshev optimised arrays 0-21835
- gravimeter of Gs-11/12 type adapted to seismometer operation (*German*) 0-31127
- laser interferometer, NBS system, for earthquake prediction 0-13125
- Milne seismograph, reconstructed to assess effective magnification 0-21656
- ocean bed seismic station, self-contained system with mag. recorder (*Russian*) 0-36410
- ocean bottom hydrophone system 0-51582
- RESMAC seismic array, epicentre location procedure 0-56616
- seismic moment tensor estimated by linear inversion method 0-31125
- signal enhancement seismograph linked with graphics computing system description and application 0-4131

## selenium

- see also nuclei with .....
- adsorbed on Ni, photoelectron diff. data 0-29851
- adsorbed on Ni (001), photoelectron diff. obs. 0-40223
- adsorption on Ni (111), angle-resolved photoemission 0-40230
- allotropic modifications, muonic X-ray intensities, computer analysis 0-23577
- amorphous, effect of doping on mol. struct. and valence alternation states 0-49249
- amorphous, electronic props., xerographic use 0-20242
- amorphous, monostable switching, current noise 0-44682
- amorphous, photoconductivity quantum yield, experimental validation of fund. theory 0-6909
- amorphous, theoretical calc. of defect states 0-49657
- amorphous and liq. states, Raman scatt. meas. 0-50328
- amorphous film, interference enhanced Raman scatt. 0-50326
- amorphous film, vac. evaporated, density meas., microcrystalline model of struct. 0-2313
- amorphous thin film, elec. noise, monostable switching 0-44684
- atom, chemisorption on Cu, cluster theory 0-29264
- atom, chemisorption on Ni, cluster theory 0-29264
- atom, electron impact ionisation, characteristic X-radiation ang. distrib. obs. 0-1069
- atom, photoionisation cross sections and ang. distrib., outer p subshell 0-9572
- carrier mean transit time superlinear depend. on material thickness 0-6894
- chemical bonding in group V and VI elements and compounds with tetradymite structure 0-15036
- coating, on Al thin film, effect on supercond. 0-7026
- Compton profile, charge and momentum density 0-55220
- dark current relax., barrier cond. mech. 0-6904
- differential dosimetric characts. w.r.t.  $\gamma$ -radiation 0-32529
- electroconductivity, X-ray effects (*Russian*) 0-15519
- electrophotographic layers, amorphous, resolution parameters 0-31926
- electroradiographic layer, radiographic contrast 0-12241
- film, gas-evaporated, selective absorpt. characts. and emissivity 0-50998
- film, laser beam hole machining 0-30207
- film, noncryst., ageing and crystn. obs., tentative struct. model 0-2295
- film, obliquely deposited, elec. resist. anisotropy 0-2486
- glassy, pure and K-doped, photolum. and optically induced ESR 0-50398
- lin prod. in 2 MV Van de Graaff 0-14031
- liquid, eqn. of state determ., crit. props. and mol. comp. 0-49336
- molecular photolytic dissociation, obs. using inert gas halide lasers 0-11935
- muonic allotropes, muonic Roentgen intensities (*German*) 0-53168
- nanosecond switching investigation 0-20263
- neutron activation analysis determ. of Se in human urine 0-36079
- nonoclinic to trigonal conversion, thermodynamic stability and associated investigs. 0-24592
- phonon dispersion curves, scaling formalism 0-54326
- photoconductor for  $KD_2PO_4$  spatial light modulator, optical data processing appl. 0-9988



**selenium continued**

- photographic migration images, liquid developed, fixing and abrasion resistance 0-4792  
 photoreceptors, phthalocyanine sensitized, elec. cond., charge decay characts. 0-15630  
 physics, conf., Königstein, Germany (May 1979) 0-51958  
 poly(N-vinyl carbazole) sensitisation with Se, purification effect on electrophotographic characts. 0-49825  
 spectrochemical analysis, atomic absorption using vapour generation method 0-16745  
 steel, maraging, Se microalloying, machinability improvement 0-21116  
 trigonal, dielec. matrix calcs. 0-54630  
 trigonal, force field calc. of phonon dispersion relations 0-54328  
 trigonal, luminesc. identification of indirect transition 0-55189  
 trigonal, state-of-the-art review of model calcs. 0-54327  
 trigonal, surface lattice dynamics, mean square displacement spectra in long wavelength limit 0-54498  
 trigonal, vitreous and red amorphous, phonon density of states comparison 0-54329  
 trigonal single crystal, peak in temp. dependence of elec. cond. 0-44663  
 vapour, photolysis by UV lasers, appl. to kinetics of group VI laser systems 0-7807  
 vitreous, darkened films, thermal and optical bleaching, light transmission obs. 0-50447  
 vitreous, elastic coeffs. about glass transition temp. US study (French) 0-19865  
 X-ray K-emission satellites, HF and LF, origin 0-50465  
 X-ray sensitivity, induced photocurrents, xeroradiographic meas., pair creation energy 0-22490  
 As-Se film, amorphous, chemical modification of props. 0-49250  
 Cs-Se thermionic converter, output power, vap. source depend. 0-44000  
 GaAs:Cr, Se, shallow impurity implantation, elec. props. after annealing 0-24465  
 GaAs:Se, implantation and laser annealing 0-24476  
 GaAs:Se, ion implanted, Cr redistrib. during annealing, SIMS anal. 0-10570  
 GaAs:Se, ion implanted, laser annealing 0-24482  
 n-GaAs:Se, nonalloyed ohmic contacts of TiPtAu by pulse-electron-beam annealed Se implants 0-2466  
 GaAs:Se, pulsed electron beam annealing, doping profiles 0-6421  
 GaAs:Se<sup>+</sup>, TEM structural study, surface and interior damage 0-34025  
 He-Se<sup>+</sup> white light laser 0-1226  
 InAs:Te(Se)(S), intrinsic pt. struct. defects 0-33998  
 InAs:Zn, Se, solubility and donor-acceptor interaction 0-54263  
 InP:Se, implantation and laser annealing 0-24476  
 InSb:Se, exam. of defects in crystal 0-6423  
 InSb:Se, reson. states and reson. scatt. 0-49738  
 Se, amorphous, vac. deposition on polymer substrates, use of temp. gradient vac. coating device 0-35099  
 Se, trigonal, low temp. sp. ht. and elastic const., piezoelec. effect influence on phonons 0-54404  
 Se-Ag<sub>2</sub>Se, heterojunction with memory, transient switching characteristics 0-44718  
 Se-Ag<sub>2</sub>Se, heterojunction, electrically controlled negative differential conductance, mechanism 0-44720  
 Se-binding agent electrophotographic film characteristics and sensitivity (German) 0-4789  
 Se + H<sup>+</sup>, K-shell ionisation cross-section determ. 0-48077  
 Se + Zn,  $\pi^-$  capture, radioactivity meas. 0-47831  
 Se<sub>8</sub><sup>+</sup>, electronic struct. and localised MOs, bonding nature and geom. struct. 0-18798  
 (Se)<sub>n</sub>, crystn. and melting 0-40241  
<sup>75</sup>Se, yield for various reactions and chem. processing 0-36131  
<sup>75</sup>Se labelled adenosyl selenomethionine, distrib. in rat and prostate scanning appl. 0-17132  
<sup>75</sup>Se, tracer for Se conc. in seawater expts., <sup>203</sup>Hg tracer 0-21420

**selenium alloys**

- see also *selenium compounds*  
 Na-Se system, liq., thermodynamic props. 0-21319  
 Se-Te liquid alloy, effect of branched chain polymers on bond equilib. 0-24348  
 Te<sub>1-x</sub>Se<sub>x</sub>, liquid semiconductor, diamagnetism and paramagnetism, dangling bond paramag. centres, mag. susceptibility obs. 0-44797

**selenium compounds**

- see also *selenium alloys*  
 chemical bonding in group V and VI elements and compounds with tetradymite structure 0-15036  
 As-Se, amorphous, glass transition and specific heat, intermolecular bond saturation 0-15011  
 As-Se amorphous film, density of upper valence band states, annealing effects, UPS obs. 0-29845  
 As-Se and As<sub>2</sub>S<sub>3</sub> films, electron-stimulated changes in optical props. and dissolution rate 0-29709  
 As-Se chalcogenide glass, optical const. photoinduced changes mechanism 0-7321  
 As-Se glasses, low temp. photocond. 0-49808  
 As-Se-Te, amorphous, electron and hole drift mobilities 0-34442  
 As-Se(Ge) chalcogenide glasses, mode-guiding layer in IR waveguides 0-28329  
 As<sub>2</sub>S<sub>3-x</sub> chalcogenide, covalent non crystalline topology, short range order 0-15009  
 As<sub>2</sub>(Se,Te), glasses, X-ray absorption and photoelectron spectroscopy study 0-7463  
 AsSe<sub>1-x</sub>Bi<sub>0.05</sub> glasses, soln. rate in alkali solns. 0-16531  
 GaSe<sub>1-x</sub>S<sub>x</sub>, magnetic susceptibility anisotropy, chemical bonds, electron density distribution (Russian) 0-50073  
 Ge-Se-Ga thin film, elec. cond., switching phenomena (Polish) 0-11120  
 Ge<sub>20</sub>Bi<sub>10</sub>Se<sub>70-x</sub>Te<sub>10</sub>, n-type semiconducting glasses, resistivity and thermoelectric power meas. 0-54695  
 Ge<sub>2</sub>Se<sub>1-x</sub>, amorphous, excitation spectra of photolum. fatigue and creation of paramag. centres 0-50402  
 Ge<sub>2</sub>Se<sub>1-x</sub>, amorphous, X-ray diffr. and local order modelling 0-49125  
 Ge<sub>2</sub>Se<sub>1-x</sub> chalcogenide, covalent non crystalline topology, short range order 0-15009  
 (Ge<sub>1/3</sub>Se<sub>2/3</sub>)<sub>100-x</sub>Ni<sub>x</sub>, ESR, rel. to elec. cond. 0-7155  
 (Ge<sub>0.32</sub>Se<sub>0.32</sub>Te<sub>0.32</sub>As<sub>0.4</sub>)<sub>100-x</sub>Ni<sub>x</sub>, ESR, rel. to elec. cond. 0-7155  
 NbSe<sub>2</sub>Cu<sub>x</sub>, ordering study using electron diffr. and microscopy 0-39043  
 P-Se, amorphous, glass transition and specific heat, intermolecular bond saturation 0-15011  
 P-Se-Te system glasses, mag. susceptibility and opt. props. 0-25079

**selenium compounds continued**

- P-Se-Tl glasses, NMR of <sup>31</sup>P and <sup>205</sup>Tl 0-15812  
 S-Se, liquid semicond., bonding energies and entropies, mag. susceptibility meas. 0-49082  
 Sb<sub>3</sub>Se<sub>8</sub>, polycrystalline, elec. cond. mech. 0-49705  
 Se-Ge, amorphous, Raman spectra and average band gap 0-50327  
 Se-Ge, amorphous thin film, photocontraction rel. to surface struct. 0-49551  
 Se-Ge amorphous system, AC elec. cond., near T<sub>g</sub>, temp. depend. 0-49791  
 Se-Ge glasses, extreme far IR absorpt. meas. 0-50318  
 Se-Si system glasses, vibr. IR spectra 0-20643  
 Se-Te crystallised glasses, struct. transforms. and IR spectra 0-19712  
 Se + H<sup>+</sup>, K-shell ionisation cross-sections calcs. 0-43165  
 SeBr<sub>2</sub>, photoelectron spectra, visual assessment stripping program anal. 0-28062  
 SeS gas, thermodynamic props., quadrupole mass filter study 0-16716  
 Se<sub>1-x</sub>Te<sub>x</sub> systems, amorphous and liq. states, short range order, neutron scatt. study 0-49124  
 Se<sub>2</sub>Te<sub>1-x</sub>, liq., thermoelec. transport at mobility edge 0-49787  
 Te-Se mixtures, liquid, electrical conductivity and thermoelectric power, high temps. and pressures 0-39639  
 Te-Se liquid binary mixtures, phase separation under press. 0-34183  
 Tm, Se, Te<sub>1-x</sub>, magnetic ordering studies (German) 0-54882

**self-adjusting systems**

- pH-neutralisation process, self-tuning control 0-30242

**self-consistent field calculations** see *SCF calculations***self-diffusion**

- see also *self-diffusion in gases; self-diffusion in liquids; self-diffusion in solids*  
 electron gas, classical and two-dimens., self-diffusion theory 0-141  
 multicomponent self-diffusion measurement using spin echo expts. on standard Fourier transform NMR spectrometers 0-22401

**self-diffusion in gases**

- binary mixture, moderate density diffusive creep along flat surface 0-43822  
 n-butane-N<sub>2</sub>(CO<sub>2</sub>) mixtures, viscosity, diffusion coeffs. 0-1722  
 ethane-CO<sub>2</sub>(N<sub>2</sub>)(SF<sub>6</sub>)(tetrafluoromethane) mixtures, viscosity, diffusion coeffs. 0-1722  
 gas discharge with travelling mag. field, isotope separation by mass diffusion 0-44050  
 isotope separation, HF stationary discharge, travelling mag. field, barodiffusion separation 0-44049  
 propane-N<sub>2</sub>(CO<sub>2</sub>) mixtures, viscosity, diffusion coeffs. 0-1722  
 Ar + Kr, binary diffusion coeff. pressure depend. meas. 0-43826  
 CO<sub>2</sub> gas, electron mobility to lateral diffusion coeff. ratio 0-43836  
 N<sub>2</sub> + Ar, binary diffusion coeff. pressure depend. meas. 0-43826  
 N<sub>2</sub> + O<sub>2</sub>, binary diffusion coeff. pressure depend. meas. 0-43826  
 O<sub>2</sub> gas, electron mobility to lateral diffusion coeff. ratio 0-43836  
 O<sub>2</sub> + Ar, binary diffusion coeff. pressure depend. meas. 0-43826  
 Si-Ge-Br system, diffusion mass transfer 0-33911

**self-diffusion in liquids**

- 2-chloro-2-nitropropane, far IR-microwave estimation of binary collision approx. 0-55095  
 electrolyte transport, irreversible thermodynamics calcs. 0-3364  
 hard sphere fluid in small pores, mol. dynamics simulation 0-24333  
 IBPBAC, smectic phases, self-diffusion coeffs., radiotracer meas. 0-49394  
 liquid metals, diffusion mechanisms, and coeff. determ. (Russian) 0-34215  
 macromolecular solutions, review 0-15273  
 metals, liq., self diffusion coeff. determ. using radial distrib. function 0-15280  
 methylcyclohexane, dense liq., self-diffusion and viscosity 0-15278  
 PAA, homologous series, isotropic phase, mol. self diffusion by spin echo method 0-44109  
 polyelectrolyte soln., small ion self-diffusion, Manning's limiting law derivation 0-54416  
 polymer self-diffusion, review 0-29193  
 sodium cholate-decanol, soln., aggregate form., comp. and dynamics 0-45575  
 TBBA liquid crystal, self diffusion coeffs., neutron diffr. and NMR study 0-19689  
 Van Hove self-correlation function, intermediate incoherent scatt. function, beyond Ficks law 0-6532  
 water, diffusion const. in presence of large background gradients, modified pulsed gradient technique 0-31831  
 water, self-diffusion coeff., pressure and temp. depend. meas. by proton spin echo 0-39328  
 CaO-SiO<sub>2</sub> melt, <sup>31</sup>Si tracer diffusivity at 1600°C 0-54418  
 DCl, liq., self-diffusion coeffs., NMR spin-echo meas. 0-50223  
 Ga, self-diffusion coeffs. by radioactive tracer technique 0-49392  
 Ga, tracer diffusion studies using metallic <sup>67</sup>Ga 0-24629  
 HCl aqueous solutions, diffusion coeffs. at 298K, conductimetric obs. 0-24628  
 HCl, liq., self-diffusion coeffs., NMR spin-echo meas. 0-50223  
 HCl, liq. struct. simulated by a Lennard-Jones pot. 0-1917  
 Hg, liq., self-diffusion coeffs. by radioactive tracer technique 0-49392  
 KBr-LiBr, liq. mixture, struct. and diffusion 0-24344  
 KCl, molten, vapour-liq. interface, mol. dynamics model 0-54362  
 LiBeF<sub>3</sub>, LiBeF<sub>4</sub>, molten, self-diffusion of Li 0-54417  
 Na<sub>2</sub>O-K<sub>2</sub>O-SiO<sub>2</sub> glass melt, interdiffusion coeffs. of Na<sup>2+</sup>, K<sup>2+</sup>, temp. depend. 0-44348  
 Sn<sup>113,117m,125</sup>, Sn diffusion coeff. meas. (Ukrainian) 0-10690  
 Tl<sub>2</sub>Se, fused, diffusion of <sup>204</sup>Tl, <sup>110</sup>Ag, <sup>112</sup>Sn impurities 0-54415

**self-diffusion in solids**

- see also *diffusion creep*  
 $\beta$ -Al<sub>2</sub>O<sub>3</sub>-Na<sub>2</sub>O, diffusion and ionic cond. meas. 0-6542  
 $\beta$ -Al<sub>2</sub>O<sub>3</sub>-Na<sub>2</sub>O, mechanism of diffusion 0-2202  
 binary alloys, ordered, self-diffusion kinetics 0-10698  
 $\alpha$ -brasses, cold worked, atomic diffusion kinetics to stacking faults, Laplace transformation method 0-19977  
 classical model single particle Hamiltonian 0-39340  
 defective solids, chemical diffusion, steady-state computer simulation method for lattice gas 0-49401  
 FCC crystal, interstitial and solute concentration gradients, flux expression derivation (French) 0-54219  
 FCC metals, props. of vacancies and divacancies 0-10545  
 fluorite lattices, <sup>19</sup>F<sup>-</sup>, self-diffusion, spin lattice relax., NMR techniques 0-34801



**self-diffusion in solids continued**

- interstitial solid solutions, self-diffusion activation energy rel. to partial molar energy 0-15291  
 liquid crystal, thermotropic, diffusion and nucl. mag. relax. 0-24362  
 metal layered contacts at low-temps. (*German*) 0-6538  
 metal-H system, electro- and thermotransport of H, book contrib. 0-24644  
 metal-H systems at high H press., physicochemical props., book contrib. 0-24535  
 metals, diffusion alloying conditions, deep chemical-heat treatment (*Russian*) 0-40393  
 metals, pure and alloyed, grain boundary relaxation model, (*Russian*) 0-39107  
 nuclear fuel, transport phenomena under severe temp. gradient 0-615  
 oxides, point defects diffusion coeffs. calc. (*Japanese*) 0-15302  
 polyisobutane, relax. times, self diffusion, devel. and appl. of NMR data acquisition system 0-34807  
 polymer, NMR matrix technique 0-15806  
 polymer self-diffusion, review 0-29193  
 refractory metals, mech. props. and diffusion figures (*Russian*) 0-40436  
 simple solid family of phase states (*Russian*) 0-15216  
 steel, austenitic stainless, Cr-Ni (18, 10 wt.%),  $^{59}\text{Fe}$  self-diffusion in ferrite/austenite interface (*French*) 0-19975  
 steel, austenitic stainless AISI 321, Cr tracer diffusion coeffs. 0-2193  
 steel, austenitic stainless Cr-Ni,  $^{51}\text{Cr}$  tracer diffusion coeffs. 0-34225  
 superionic conductors, continuous stochastic models, book contrib. 0-24663  
 superionic conductors, lattice gas models, book contrib. 0-24661  
 transition metal-H system, exam. of excitation spectra and diffusion mobility of H using neutrons 0-29203  
 vacancy migration vol. 0-10701  
 vacancy nonlinear diffusion in crystal 0-39338  
 Ag, surface self-diffusion coeff.,  $\text{O}_2$  potential effect 0-15354  
 AgBr, activation parameters of mass transfer processes. (*German*) 0-38974  
 AgCl, activation parameter of mass transfer processes (*German*) 0-38974  
 Al-Zn (15 at.%), supersaturated alloy, growth and decomposition kinetics 0-29965  
 Au-Ag, radiation damage and diffusion 0-24645  
 Co, FCC, self-diffusion and isotope effect, influence of mag. order-disorder transition 0-29205  
 Cr, thermal vacancies, energy of form. and conc. 0-29014  
 Cu, elastoresistivity of Frenkel pairs, defect migration (*French*) 0-2073  
 Cu, radiation damage and diffusion 0-24645  
 Cu-Al, vacuum condensate, struct. and mech. props. depend. on deposition conditions 0-15417  
 Cu-Fe, dil., diffusion and ageing processes, Mossbauer study 0-7245  
 Cu-Ni, diffusion of Ni, resistometric meas. 0-29222  
 Cu-Ni, neutron irradiation, enhanced diffusion, elec. resist. meas. 0-6440  
 Cu-Ni, sintered, props. and degree of nonhomogeneity 0-20848  
 CuBe, SIMS quantitative anal. of Be distrib. in vicinity of oxidation boundary (*French*) 0-11984  
 CuCl(Br)(I), Raman spectra, Cu ions vibr. and diffractive motions 0-11412  
 $\text{Er}_2\text{O}_3$ , pure and  $\text{HfO}_2$ -doped polycryst., Er self-diffusion 0-29207  
 Fe alloys, ion-implanted, depth profile and diffusion coeff. 0-54277  
 $\alpha$ -Fe,  $\text{O}_2$  potential effect on surface self-diffusion coeff. 0-15353  
 Fe-Al-C, gamma irr., crystal lattice parameter reversible changes (*Russian*) 0-10576  
 Fe-C interstitial solid solutions, self-diffusion activation energy rel. to partial molar energy 0-15291  
 Fe-Co(Cr), compositional diffusionally bonded alloy, mass transfer investigation (*Russian*) 0-39342  
 Fe-Cr-Ni, austenitic, self-diffusion and swelling under irradiation 0-39343  
 $\text{Fe}_{40}\text{Ni}_{40}\text{B}_{20}$  glass,  $^{10}\text{B}$  self-diffusion, meas. by SIMS 0-49406  
 $\text{Fe}_3\text{Si}_{10}$ , polytypism, Fe diffusion near antiferromag. to ferrimag. transition 0-44830  
 $\text{Gd}_2\text{O}_3$ , polycryst. monoclinic, Gd self-diffusion 0-24655  
 Ge, self- and impurity diffusion 0-29213  
 Ge, self-diffusion, dynamical recovery 0-29215  
 $\text{H}_2\text{WO}_4$  films, proton diffusion coeffs. 0-6548  
 In, vacancy formation and activation volume, macroscopic model 0-54221  
 $\text{LaMnO}_3$ , solid phase synthesis mechanism 0-21268  
 $\beta$ - $\text{LaNi}_{1-x}\text{Al}_x$  hydrides, H diffusion, NMR studies 0-15298  
 $\text{LaNi}_2\text{H}_6$ , diffusion const. in presence of large background gradients, modified pulsed gradient technique 0-31831  
 $\text{LaNi}_2\text{H}_{3.0}$ , H diffusion coeff., neutron scatt. obs. 0-24643  
 Li wire, NMR line shape, eddy current effect in presence of self-diffusion 0-54955  
 LiAl,  $\beta$  phase thermodynamic props., chem. diffusion coeff., electrochem. meas. 0-39308  
 LiH, anion and neutron diffusion, NMR relax. and linewidth obs., Schottky disorder 0-15815  
 $\text{Li}_2\text{O}$ ,  $\text{Li}^+$  ion self-diffusion coeff., sectioning technique 0-15296  
 Na, self-diffusion mech., NMR meas. 0-44356  
 Nb CVD coatings on graphite, grain struct. depend. on temp. 0-25574  
 Nb/Cu-Sn-Mg, superconductor, effect of Mg addition to Cu-Sn matrix 0-25028  
 $\text{NbC}_x$ ,  $x=0.868, 0.834, 0.766$ , self-diffusion of  $^{14}\text{C}$  0-29206  
 $\alpha$ - $\text{NbH}_2\text{D}_2$ , H diffusion, NMR spin echo obs. 0-34228  
 Ni, mass transfer parameters, lattice defect effects under laser pulse action (*Ukrainian*) 0-6537  
 Ni, radiation damage and diffusion 0-24645  
 Ni, surface self-diffusion in presence of adsorbed halogens (*French*) 0-24723  
 Ni-Co-Cr-Al-Ti-Mo superalloy IN738, caking porosity removal using hydrostatic press. sintering 0-55322  
 Ni-ZrB<sub>2</sub> powders, densification by hot pressing 0-25604  
 NiO, grain boundary thermal grooving, mass transport, self-diffusion coeffs. 0-44217  
 Pb, impurity diffusion and self-diffusion activation volumes 0-2209  
 Si, (p,  $\gamma$ ) resonance broadening method 0-24646  
 Si, diffusion of self-interstitials and As, B and P, radn.-enhanced 0-29216  
 Si, intrinsic, self-diffusion, 885-1175°C 0-10700  
 Si, self diffusion entropy 0-29211  
 Si, self- and impurity diffusion 0-29213  
 Si, self-diffusion, dynamical recovery 0-29215

**self-diffusion in solids continued**

- Si, stacking fault growth, oxidation-induced, HCl and interstitial effects 0-49241  
 Si, tracer diffusion of  $^{71}\text{Ge}$  and  $^{31}\text{Si}$  in intrinsic and doped samples 0-29214  
 Si-SiO<sub>2</sub> interface, oxidation stacking faults, growth rel. to self-diffusion 0-49239  
 $\beta$ -SiC, polycrystn.,  $\text{C}^{14}$  self diffusion 0-2200  
 Sn, vacancy formation and activation volume, macroscopic model 0-54221  
 SnTe,  $^{117}\text{Sn}$  diffusion coeff. meas., stoichiometric deviation, SIMS 0-34236  
 SrCl<sub>2</sub>, anion diffusion mechanism 0-2201  
 SrF<sub>2</sub>:Er, activation vol. for interstitial motion, dielec. const. meas. 0-49412  
 TaH<sub>x</sub>, H diffusion and electronic struct., pulsed NMR obs. 0-54967  
 Ti-H, diffusion in hydride phase, exam. 0-29204  
 TiH<sub>x</sub>, H diffusion, NMR obs. 0-34813  
 TiO<sub>2</sub>(-Cr<sub>2</sub>O<sub>3</sub>), rutile, Cr<sub>2</sub>O<sub>3</sub> effects on O<sub>2</sub> tracer diffusivity, depth profile meas. by SIMS 0-24651  
 TiO<sub>2</sub> electrodes, room temp. diffusions, capacitance, spectral response and volt-ampere characts. 0-15294  
 (U,Pu)C, self-diffusion meas. 0-6544  
 (U,Pu)N, self-diffusion meas. 0-6544  
 V-Fe,  $^{57}\text{Co}$  Mossbauer spectra, diffusion mechanism of Fe 0-15292  
 W, vacancies, quenching and recovery invest., resist. and TEM study 0-39074  
 YMnO<sub>3</sub>, solid phase synthesis mechanism 0-21268  
 ZnTe:Ag, real structure effect on luminescence and absorption spectra, dislocations 0-16085  
 ZrH<sub>x</sub>, of T, autoradiographic study, energy of soln. in H sublattice (*Russian*) 0-2194
- self-focusing**  
 see also electrostriction; Kerr electro-optical effect; optical Kerr effect; optical self-focusing  
 coaxial atomic and light beams, simultaneous self-focusing and self channeling (*Russian*) 0-28292  
 electron beam, pulsed high-intensity, low-press. gas obs. 0-32899  
 electron beam, relativistic, high-current, self-focused, energy dissipation at focus 0-5674  
 EM wave self-action during thermal modulation instability of high hybrid oscills. (*Russian*) 0-53980  
 liquid crystal, nematic, orientational acoustic nonlinearity 0-34143  
 semiconductor injection laser, intensity pulsation enhancement by self focusing 0-48253
- self-induced transparency**  
 aerosol, plasma production by CO<sub>2</sub> laser beam, brightening channel 0-6272  
 coherent pulse propagation,  $0\pi$  pulse generation from zero-area pulse 0-48352  
 diphenylpyrene, self induced transparency under nonreson. excitation, luminesc. and stimulated emission 0-11436  
 diphenyl with pyrene cryst., self induced transparency self stimulated excitation (*Russian*) 0-14403  
 EM wave self-action during thermal modulation instability of high hybrid oscills. (*Russian*) 0-53980  
 initial-value problem for zero-area pulses, anal. props. 0-23756  
 resonant propagation of two concomitant optical pulses interacting with three-level atomic system, num. modelling 0-9942  
 retarding interaction allowance, dipole moment of transformation (*Russian*) 0-14402  
 solitons, laser physics appls. 0-48333  
 three-level system, double-reson. self-induced transparency, numerical integration 0-28288  
 CO<sub>2</sub> laser nanosecond pulse coherent interactions with amplifying media (*Russian*) 0-14314
- self inductance** see inductance
- self-optimising systems** see self-adjusting systems
- self-organising systems** see self-adjusting systems
- self-trapping**  
 anisotropic resonance medium, radiation trapping 0-9970  
 envelope wave stability 0-43410  
 exciton motion depend. on lattice vibr., inner potential energy, ground state, effective mass (*Chinese*) 0-54610  
 inert gas discharge, reson. radiation imprisonment model 0-38756  
 magnetoplasma, collisionless, self-trapping and self-focusing of elliptical laser beam 0-53991  
 molecular rotational coherence, reson. collisional exchange, time resolved microwave obs. 0-23525
- SEM** see scanning electron microscopy
- semi-insulating materials** see semiconductor materials
- semiconductor alloys** see semiconductor materials; semiconductors
- semiconductor counters**  
 see also position sensitive particle detectors  
 C-CD Si substrate ionisation trails prod. by cosmic ray background 0-51669  
 charged particle spectrometer telescope 0-42895  
 cosmic ray charge meas., minimum pulse selection method, energy levels 0-37712  
 ion implantation, isotope separator, prep. of p-n junction particle detectors 0-34034  
 IR radiation pulses meas. response characts. of AuSi detectors 0-52308  
 magnetic plus Si(Li)-Si(Li) sum coinc. technique for internal pair transitions 0-18752  
 MOS thin film dielectric breakdown counters, heavy-ion detection props. 0-52827  
 nuclear radiation detectors, effect of trapping on response 0-5447  
 peak identification in spectral analysis program 0-37706  
 RAM, use as  $\alpha$ -particle detector 0-37701  
 spectrometers, Fano factor determ. in semiconductors 0-47813  
 state of art and future prospects for  $\gamma$ -ray detectors (*Hungarian*) 0-42890  
 X-ray beam characteristic time vars. meas. using solid state devices 0-46048  
 CdTe, detector grade semi-insulating crystals, determ. of product of mobility and carrier lifetime 0-39601  
 CdTe detectors, use in spectrometers, physical and electronic factors (*Czech*) 0-23259  
 CdTe detectors, X-ray fluorescence escape peaks in X-ray spectra 0-9448



# semiconductor counters continued

- CdTe, irradiation-induced damage on  $\gamma$ -detector performance 0-23264
- Ce(Li), fast neutron leakage spectrum determ. 0-32565
- Ge camera, high purity, for nucl. medicine imaging 0-17113
- Ge detector, charge collection characteristics, influence on timing performance 0-47820
- Ge detectors, calibration using  $^{152}\text{Eu}$  source uncertainties in peak area determ. 0-5436
- Ge, efficiency calibration in range 122-412 keV 0-37682
- Ge(Li) balloon borne spectrom. for obs. of neutron star cyclotron line emissions 0-41721
- Ge(Li) coincidence detector system, meas. on  $^{144}\text{Ce}$  decay 0-52605
- Ge(Li) detector, use near 400 MeV proton beam in p- $\gamma$  coincidence expt. 0-5452
- Ge(Li), gamma spectra calibration problems in automatic processing (Romanian) 0-5431
- Ge(Li),  $\gamma$ -ray energies of  $^{40}\text{K}$ ,  $^{108m}\text{Ag}$  and  $^{226}\text{Ra}$  decay chain 0-27865
- Ge(Li) planar detector efficiency curve obtained using  $K_{\beta}/K_{\alpha}$  X-ray intensity ratio 0-880
- HgI<sub>2</sub>, charge collection efficiency 0-32575
- HgI<sub>2</sub>, cryst. growth by multiple vacuum sublimation 0-7485
- Hg<sub>2</sub>I<sub>2</sub>, cryst. growth by multiple vacuum sublimation 0-7485
- Rn, short lived daughters, detection method (Chinese) 0-42889
- Si barrier layer counter, reduction of noise level (German) 0-47809
- Si dosimeter, proton beam dosimetry in C, Al, Fe, mylar and H<sub>2</sub>O 0-47733
- Si junction detectors, low noise, fabrication 0-52820
- Si particle detection, use of dislocation-free Si 0-42893
- Si, surface-barrier detector, impurity distrib., influence on characts. 0-18766
- n-Si- $^{119}\text{Sn}$  resonant detector for Mossbauer spectroscopy 0-883
- Si-Li surface-barrier detectors for electron and soft X-ray spectrometry 0-882
- Si(Li) detector response function approach in least squares anal. of X-ray fluorescence spectra 0-11989
- Si(Li) detector system, discrepancies in X-ray excitation efficiencies 0-9450
- Si(Li) detector window of aluminised mylar for X-ray fluorescence meas. 0-27894
- Si(Li) photopeak efficiency meas., 0.52-8.04 keV 0-27889
- Si(Li) X-ray detector, efficiency calibration in 1.5 to 60 keV energy range 0-47823
- Si(Li) X-ray spectrometer, development, and interdisciplinary appl. (Hungarian) 0-18056

# semiconductor defects see crystal defects

# semiconductor device manufacture

- Used for commercial manufacture only
- diode laser manufacture and test procedures 0-9895
- oxidation with trichloroethylene additive to eliminate oxidation induced stacking faults 0-39118
- production equipment, high vacuum cryopumps optimisation using thermal design criteria 0-22377
- solar cells, polycrystalline Si, amorphous Si and CdS/CuS, function and construction (Swedish) 0-7940
- VPE, reduced pressure, advances 0-40242
- Si junction detectors, low noise, fabrication 0-52820
- Si<sub>3</sub>N<sub>4</sub> passivation planar plasma deposition system, productivity increase 0-40269

# semiconductor device models

- C-CD, surface channel, interface trapping noise calc. 0-11058
- heterojunction theory, Anderson model review 0-6961
- hyperabrupt varactors, fabrication from vapour phase epitaxial GaAs 0-29288
- metal-insulator-Si(n)-Si(p<sup>+</sup>) device, switching voltage criteria 0-15610
- MIS transistor, mobility in inversion channel calc. (German) 0-6996
- MNOS structure, model for degradation mechanisms 0-29477
- MOS transistor, Au-doped, Au surface-state energy levels 0-11092
- MOSFET, flicker noise theory 0-11100
- solar cell, Si, p<sup>+</sup>-n-n<sup>+</sup>, edge-illuminated, analytical model 0-12018
- GaAs LED modulation bandwidth, influence of inhomogeneous current density distrib. 0-9993
- Si solar cell, device model for tandem junction cell 0-16813
- Si solar cells, edge-illuminated p<sup>+</sup>-nn<sup>+</sup>, analytical model under concentrated sunlight 0-7942
- Si:Zn p-n junction diode, computer-aided study of carrier lifetimes 0-24999

# semiconductor device testing

- see also integrated circuit testing
- acoustic microscopes, nondestructive testing appls. 0-48537
- deep-level transient spectroscopy appl., using HP-IB instruments and desk-top computer 0-37091
- diode laser manufacture and test procedures 0-9895
- EM monitoring methods for thin film devices (Russian) 0-214
- MIS structures mobile charges determ., using triangular voltage sweep methods (German) 0-4740
- MNOS P-channel switch, accelerated reliability testing (German) 0-6988
- p-n junction potential step meas. by SIMS 0-34503
- pacemaker electrostatic discharge sensitivity grouping 0-30941
- resistivity profile meas. using two-probe spreading resistance techniques 0-49742
- SEM characterisation of semiconductor materials and devices 0-49064
- solar cells, electron beam induced currents appl. 0-3518
- temperature testing probes, accuracy and thermal characts. 0-52201
- Ga<sub>1-x</sub>Al<sub>x</sub>As junction-up TJS laser electron injection efficiency improvement 0-48300

# semiconductor devices

- see also field effect devices; Gunn devices; integrated circuits; semiconductor counters; semiconductor diodes; semiconductor junction lasers; space-charge limited devices; thermistors; thyristors; transistors; transit time devices; varactors
- detector for testing SEM quality parameters 0-22484
- detectors, determination of thickness of sensitive layer with aid of  $\beta$  and  $\gamma$  sources 0-22323
- elementary semiconductor physics, book 0-6824
- gas sensors (Japanese) 0-31736
- InSb subMM detector, fast response, for use in measuring electron cyclotron emission 0-27347
- photoanodes, corrosion stability 0-21130
- pressure sensors, thin Si diaphragm form., piezoresistive and capacitive structs. 0-13065

# semiconductor devices continued

- reradiation effects in negative electron affinity photocathodes 0-55274
- sensors development trends and appl. (German) 0-52186
- superlattice microwave/infrared detectors 0-13138
- temperature meas. devices developments (German) 0-8986
- thermomagnetic recording using semiconductor optical image transducers (Russian) 0-44833
- PbS-Si heterojunction detector, direct injection readout 0-4765

# semiconductor diode light emitters see light emitting diodes

# semiconductor diodes

- see also avalanche diodes; BARITT diodes; charge storage diodes; light emitting diodes; photodiodes; Schottky-barrier diodes; solid-state rectifiers; tunnel diodes; varactors; Zener diodes
- DLTS for diodes with large leakage currents 0-34504
- electric field effect on thermal emission of traps 0-11073
- heavily doped planar diode, collection efficiency and surface recomb. vel. modulation 0-20291
- ion controlled chemically sensitive diodes 0-13066
- leak detector appl., sparking 0-31774
- p-i-n, analytical expressions for duration of initial step recovery phase 0-25000
- p-n diode, 1/f noise calc., free carrier mobility interpretation 0-54774
- p-n junction, electrical parameters, optical derivative meas. 0-2455
- point contact, subMM wave mixing in metal-metal and metal-semiconductor diodes 0-4769
- radiation effects, damage coeffs. for fission neutron and gamma-ray irradi. 0-34058
- semiconductor-insulator-semiconductor solar cells, basic principles of operation theoretical characts. 0-50986
- semiconductor-insulator-semiconductor solar cells, fabrication and performance characts. 0-45707
- transient process calcs., minority nonequilibrium carriers, potinjection EMF 0-6971
- GaAs diode temperature sensors, characts. obs. at 4.2 to 393K 0-47054
- GaAs, p<sup>+</sup>-v-n, nonlinear transport phenomena (Japanese) 0-6850
- GaAs-Ge<sub>1-x</sub>(GaAs)<sub>x</sub> n-p heterojunctions, hydrostatic press. effect on elect. and photoelectric props. 0-20304
- p-GaP electrode, photoelectrochemical effect 0-55673
- GaP, high temperature electronics for geothermal energy 0-11997
- Ge:Hg, S-type diode, elec. props. 0-20299
- Si diodes as low temperature sensors (German) 0-31744
- Si, minority-charge-carrier lifetime, rel. to abrasion of surface (Russian) 0-11805
- Si, n-n<sup>+</sup> point junctions 0-44719
- Si:Au, p<sup>+</sup>-n junction, quantitative study of Au atoms by TSC method 0-2458
- Si:BF<sub>2</sub><sup>+</sup>, ion implanted, arc annealing by flash lamp 0-44223
- Si:Zn, p-n junction diode, computer-aided study of carrier lifetimes 0-24999

# semiconductor doping

- see also doping profiles; ion implantation
- amorphous tetrahedrally bonded cpds. 0-2361
- borosilicate glass sputtered film, phys. and chem. props., B diffusion into Si, SiO<sub>2</sub> 0-29040
- computer controlled neutron irradi. system 0-19851
- developments, late 1970s innovations 0-6666
- diamond: Li, ion implantation doped, IR photocond. 0-20249
- diamond: Li, ion implantation, Hall effect and elec. cond. meas. 0-15526
- diamond:Sb, ion implanted under channelling conditions, depth profile, distribution tail 0-2057
- dopant surface concentration determ. by IR reflectance 0-34036
- epitaxial layers and bulk material, SIMS characterisation (French) 0-50904
- n-GaAs:Cr(Si), deep-level extrinsic photocond. response, decay at 4.2K 0-2420
- Gunn diode, anode domain disappearance dynamics, computer simulation calcs. 0-6859
- hyperabrupt junction, C-V index, junction parameters depend. 0-49876
- II-V compounds, indirect doping method (Czech) 0-24468
- II-VI compounds, indirect doping method (Czech) 0-24468
- III-V compounds and alloys, MBE process and problem areas, review 0-10815
- impurity conduction, at very low temp. (Japanese) 0-20200
- ion implantation, ion imaging for micromachining (French) 0-34027
- ion implantation, semiconductor device processing 0-34031
- ion implantation systems, high throughput 0-34029
- ion implanted layers, annealing by laser beam 0-24469
- ion implanter, semiconductor device processing 0-31944
- laser annealing of ion implanted semiconductors (Japanese) 0-19821
- neutron transmutation doping, conf., Columbia, USA (April 1978) 0-12849
- neutron transmutation doping, damage-energy distrib. 0-15137
- neutron transmutation doping 0-15133
- nonuniformly doped MOS devices with lateral symmetry 0-15606
- polyacetylene:I, electric props. in semicond. and metallic regions 0-29432
- polyacetylene, doping with AsF<sub>5</sub>, mechanism, effect on elec. cond. and spectra 0-24473
- polyacetylene, p-n junction, elec. props., review (Japanese) 0-29410
- polyacetylene, pristine and acceptor doped isomers, EPR, DC cond., evidence against solitons 0-15782
- polyacetylene film, (CH)<sub>x</sub>, synthesis, struct. and elec. props., doped materials, review 0-15623
- polyacetylene film, partially oriented, anisotropic elec. cond., quasi-one-dimens. behaviour of fully oriented doped material 0-11112
- Schottky barrier, real and ideal, photosensitivity losses 0-2452
- solar cells, photovoltage source in photocond. materials due to comp. and doping var. 0-7938
- $\alpha$ TTF:Br, transport and mag. props., effect of doping 0-24934
- VPE impurity profile computer-aided control 0-2962
- [n-]GaAs:Fe, diffusion doped compensated layers 0-15125
- Al<sub>1-x</sub>Ga<sub>x</sub>As DH laser, rake-line form. in LPE growth, doping effects 0-2287
- Al<sub>1-x</sub>Ga<sub>x</sub>As:Zn epitaxial layers, composition and Zn carrier conc. 0-25585
- Al<sub>1-x</sub>Ga<sub>x</sub>Sb:Zn, impurity diffusion, p-n junction depth 0-24678
- As:Ni(Ge)(S)(Se)(Te) film, amorphous, chemical modification of props. 0-49250
- As<sub>2</sub>S<sub>3</sub>(Se<sub>3</sub>):Ag glassy films, doped by photodiffusion and thermodiffusion, photocond. 0-29441



## semiconductor doping continued

CdCr<sub>2</sub>Se<sub>4</sub>:Ag, magneto-electrical props. temp. behaviour depend. on dopant conc. (*Russian*) 0-11006  
 CdCr<sub>2</sub>Se<sub>4</sub>:In (Ga)(Ag), and undoped, elec. prop., vac. heat treatment effect 0-15518  
 (CdGeAs<sub>2</sub>)<sub>1-x</sub>D<sub>x</sub> amorphous films, property control in common target spudding, elec. cond. 0-7494  
 Cd<sub>1-x</sub>Hg<sub>x</sub>Te, dopants behaviour and p-n junction formation 0-44225  
 CdS, indirect doping method (*Czech*) 0-24468  
 CdS:Cu(Cl), thin layer, electron pulse induced cond. relax. 0-2501  
 CdS:In film, flash evaporated, prep. and elec. props. 0-20792  
 CdS:Li lattice, location of implanted Li atoms 0-6428  
 CdS:Se<sub>1-x</sub>In film, flash evaporated, prep. and elec. props. 0-20792  
 CdSi<sub>2</sub>:Na(Bi), single crystal, photocond. under laser excitation 0-44661  
 CdTe:Fe(Ni), luminesc. and refl. spectra, high temp. annealing effects 0-24472  
 CdTe-Au system, phase diagram rel. to doping 0-16282  
 CoO<sub>2</sub>S<sub>2</sub> acceptor properties of S, free electron concentrations 0-34395  
 Co<sub>3</sub>O<sub>4</sub>:Li(Cr)(Al)(S), and pure Co<sub>3</sub>O<sub>4</sub>, elec. cond. and thermo-EMF 0-20231  
 GaAs autoepitaxial structure on heavily Te-doped GaAs substrate (*Russian*) 0-49556  
 GaAs deposition by molecular epitaxy, uncontrolled doping obs. (*Russian*) 0-2276  
 GaAs, diffusion of Cr and Ag, radiotracer profiles 0-24680  
 GaAs, electron and neutron irradi., defect clusters, carrier lifetime changes, doping level depend. 0-2077  
 GaAs, epitaxial, Si and Ge doping 0-24470  
 GaAs epitaxial layers, transient processes during doping for large conc. jumps. 0-39134  
 GaAs, ion implanted, diffusion of Zn and Ag, profiles 0-24681  
 GaAs, ion implanted, laser pulse annealing 0-19825  
 GaAs, neutron transmutation doping, shallow donors magneto-optical effects 0-20255  
 GaAs, site selective doping by ion implantation of radioactive nuclei 0-34023  
 GaAs structures produced by laser doping, recombination radiation, anomalous temp. depend. 0-2847  
 GaAs thin layers, MBE, growth conditions and phys. props. (*German*) 0-55307  
 GaAs, transmutation doping by thermal neutrons 0-10581  
 GaAs, VPE, hole diffusion lengths, effect of transition metal diffusional doping 0-15628  
 GaAs, VPE, incorporation of deep levels, effects of growth conditions 0-20111  
 GaAs, VPE in CVD systems, anisotropic phenomena 0-54563  
 GaAs:Cu, back surface gettering 0-10758  
 GaAs:Cr, gettering by back surface mech. damage 0-10759  
 GaAs:Si encapsulated with AlN, Si<sub>3</sub>N<sub>4</sub> layers, photolum., annealing effects 0-20681  
 GaAs:Sn, effect of ambient As vapour press. on surface stability 0-2208  
 GaAs:Sn films, MBE power MESFETs 0-50563  
 GaAs:Te, superdilatation and defects, lattice parameter meas. and carrier mobility 0-10569  
 GaAs:Zn epitaxial layers, composition and Zn carrier conc. 0-25585  
 GaAs<sub>1-x</sub>Al<sub>x</sub>As variable gap p-n junction, variable gap and photo EMFs 0-15596  
 GaAs<sub>0.4</sub>P<sub>0.6</sub>, VPE, hole diffusion lengths, effect of transition metal diffusional doping 0-15628  
 GaAs<sub>1-x</sub>P<sub>x</sub>, n implantation, characterisation by photolum. and channelling 0-54262  
 GaAs<sub>1-x</sub>P<sub>x</sub>, structural defects, optical props. effect 0-55208  
 GaN, indirect doping method (*Czech*) 0-24468  
 GaN:Al, VPE grown, luminesc. and elec. props. depend. on doping conc., bound excitons 0-20688  
 GaN:Zn, VPE growth, photoluminesc. rel. to doping conditions 0-55159  
 GaP, site selective doping by ion implantation of radioactive nuclei 0-34023  
 GaP:Cu, elec. and optical props., rel. to doping and heat treatment 0-16056  
 GaP:N, epitaxial layers, N concentration determination by two independent methods 0-39142  
 GaP:Zn, doping from gas phase during LPE 0-55312  
 GaP:Zn, Sn doped epitaxial layers, Hall const., hole mobility and conc. 0-15143  
 GaSb, effect of n-doping on Debye temp. 0-2175  
 GaSb, site selective doping by ion implantation of radioactive nuclei 0-34023  
 Ge, hopping cond. at intermediate impurity concs. 0-6840  
 Ge:Al, limiting solubility, rel. to charge carrier conc. 0-24596  
 Ge:Mg, diffusion and p-type cond. 0-6419  
 Ge:P(Sb), growth atm. effect on struct. microdefect form. 0-20779  
 Ge:Sb, limiting solubility, rel. to charge carrier conc. 0-24596  
 Ge-Si:Sb, energy spectrum of Sb 0-34382  
 Ge-Si, elec. cond. and thermally stimulated currents 0-20194  
 Ge<sub>30</sub>S<sub>70</sub> glass film, Ag photodoping sensitivity 0-39121  
 HgSe:In, enrichment of doping substances at pseudo phase boundaries (*German*) 0-29036  
 HgTe:In, enrichment of doping substances at pseudo phase boundaries (*German*) 0-29036  
 n-In Ar:Te(Sn), heavily doped, cathodoluminescence, doping effect on luminesc. band position and spectral profile 0-45153  
 n-InAs, edge luminescence band, shape depend. on degree of doping, band gap 0-7405  
 InAs, site selective doping by ion implantation of radioactive nuclei 0-34023  
 InAs:CdTe interaction between impurities, effect on elec. props., Hall effect. 0-19832  
 InAs:Zn,S(Se), solubility and donor-acceptor interaction 0-54263  
 InGaAsP, LPE grown, impurity effect on surface morphology 0-29291  
 In<sub>2</sub>O<sub>3</sub>, electro-conducting transparent film, props. rel. to production method (*Japanese*) 0-25557  
 InP, LPE grown, impurity effect on surface morphology 0-29291  
 InP, site selective doping by ion implantation of radioactive nuclei 0-34023  
 InP, terracing of LPE growth, doping effects 0-10846  
 InP:Fe, deep acceptor levels, photocond. meas. 0-20116  
 p-InP:Zn, vapour grown, prep. and props. 0-54268  
 InSb, low defect crystal growth by InN doping, IR detector appl. 0-20780

## semiconductor doping continued

InSb, site selective doping by ion implantation of radioactive nuclei 0-34023  
 In<sub>2</sub>Te<sub>3</sub>-type semiconductor, mechanism of electrically inactive impurities 0-24834  
 Mn<sub>3</sub>O<sub>4</sub>:Li(Cr)(Al)(S), and pure Mn<sub>3</sub>O<sub>4</sub>, elec. cond. and thermo-EMF 0-20231  
 Ni-n-GaP:Si(Ge) contacts, doping effect in elec. props. 0-6983  
 n-PbSe, heterodiffusion of Sn 0-34245  
 PbTe, ion implantation induced damage and reson. levels 0-49255  
 Se, amorphous, effect of doping on mol. struct. and valence alternation states 0-49249  
 Si amorphous film, heavy doping by alkali ion implantation 0-2045  
 Si, by thermal neutron irradi., annealing characts. of bulk electron traps obs. 0-49244  
 Si, Czochralski cryst. growth, faceted and nonfaceted, Sb microsegregation 0-45227  
 Si, Czochralski growth from heavily Sb doped melt, interface morphological instability 0-2939  
 Si, diffusion of P from spin-on SiO<sub>2</sub>:P film 0-2050  
 Si, diffusion of self-interstitials and As, B and P, radn.-enhanced 0-29216  
 Si, diffusion of transition elements, anomalous behaviour 0-29044  
 Si, ESR in neutron transmutation doped samples 0-20462  
 Si, epitaxial, minority carrier lifetime and impurity conc. meas. (*Japanese*) 0-25025  
 Si, epitaxial growth, adsorbed layer model for autodoping mech. 0-7505  
 Si, epitaxial layer, incorporation conc. depend. of P from silane-phosphine-H<sub>2</sub> mixture 0-2053  
 Si epitaxial layer growth in vacuum, Ar, Xe ion bombardment effect 0-39463  
 Si, Ga diffusion open-tube system 0-19822  
 Si, homogeneous n-type doping by thermal neutrons 0-2051  
 Si, laser annealing, nonequilib. incorporation of impurities during rapid solidification 0-55286  
 Si MOSFET, conductance oscills., source-drain limited cond. 0-20316  
 Si, minority carrier lifetime in neutron doped samples 0-20218  
 Si, neutron irradi., residual radioactivity meas. 0-19829  
 n-Si, neutron irradiated, annealing behaviour characterisation by electrochem. meas., transmutation doping 0-19847  
 Si, neutron transmutation doping, photoluminesc. characterisation 0-11453  
 Si, neutron transmutation doping, impurities 0-15134  
 Si, neutron transmutation doping, radioactivity form. 0-15135  
 Si, neutron transmutation doping for IR detector material 0-15136  
 Si, neutron transmutation doping in Harwell reactors 0-15138  
 Si, neutron transmutation doping, irradi. facilities 0-15139  
 Si, neutron transmutation doping, General Electric test reactor 0-15140  
 Si, neutron transmutation doping, automated irradi. facility 0-15141  
 Si, neutron transmutation doping, annealing, lattice damage 0-15163  
 Si, neutron transmutation doped, highly compensated, resistivity fluctuations 0-15531  
 Si, neutron transmutation doped, elec. props. 0-15532  
 Si, neutron transmutation doping, irradi. techniques 0-19827  
 Si, neutron transmutation doped, isochronal annealing of resistivity 0-19828  
 Si, neutron transmutation doping, <sup>31</sup>P conc. meas. 0-19833  
 Si, neutron transmutation doping, at. displacement effects 0-19852  
 Si, neutron transmutation doping, annealing, deep defect levels 0-20123  
 Si, neutron transmutation doping using nuclear reactor thermal neutron irradi., review 0-39161  
 Si, P<sup>+</sup> implantation, induced disorders. 0-6422  
 Si, p-n junctions, neutron transmutation doping, breakdown process 0-15600  
 Si solar cells, diffusion fabrication process, low cost, highly automated 0-30487  
 Si solar cells, implanted layers characteristics, laser irradiation effects 0-35692  
 Si solar cells, ion implanted, from EFG Si ribbons 0-30485  
 Si surface layers, impurities, elec. and photoelec. props. 0-2298  
 Si, technology and physics, review 0-34353  
 Si, tracer diffusion of <sup>71</sup>Ge and <sup>31</sup>Si in intrinsic and doped samples 0-29214  
 Si:Al effect of dopants on grain growth 0-54575  
 Si:As, solid solubility of As determ. by ion implantation, CW laser annealing 0-6517  
 Si:As(Sb), MBE, n-type doping techniques 0-15126  
 Si:Au, p<sup>-</sup>n junction, quantitative study of Au atoms by TSC method 0-2458  
 Si:B, conc. depend. of B diffusion coeff. 0-39353  
 Si:B, diffusion from BN source with H<sub>2</sub> injection, AES study 0-19986  
 Si:B, implanted, effectiveness of charged vacancies in diffusion 0-34239  
 Si:B, ion implantation, anal. of disordered regions in crystal with Promiss protonograph 0-19823  
 Si:B, lateral effect of oxidation on B diffusion 0-29217  
 Si:B, proton-irrad.-enhanced diffusion 0-29227  
 Si:B,As selective area simultaneous doping 0-34015  
 Si:B,P, anomalous diffusion 0-29229  
 Si:B effect of dopants on grain growth 0-54575  
 Si:B(Al), (P)(As)(In), ion implanted film, elec. prop. impurity depend. 0-24467  
 Si:B(P), proton enhanced diffusion, vacancies diffusion length 0-29226  
 Si:B(P) polycrystalline thin film, plasma annealing, effect on elec. props. 0-7005  
 Si:D, ion implanted, D depth distrib., SIMS meas. 0-54279  
 Si:Ga, neutron irradi., Hall effect meas. of shallow donor levels 0-20124  
 Si:Ga(As) 0-19824  
 Si:Ge B, strain compensation, X-ray Bragg reflexion 0-39137  
 Si:H, amorphous, Brillouin scattering from acoustic bulk and surface waves 0-11425  
 Si:H, amorphous, model for variable gap intrinsic semiconductor 0-10988  
 Si:H, amorphous and crystalline, hydrogenation and dehydrogenation, luminesc. spectra 0-11477  
 Si:H, amorphous films, absorption edge and doping 0-29042  
 Si:H,Li, amorphous, DC electrical conductivity, absorption edge and IR meas., role of H 0-54694  
 Si:H(Li)(Ni), amorphous, vac. evaporated, doping, transport and optical props. 0-49715  
 Si:N, amorphous, prep. by RF sputtering and props. 0-44229  
 Si:Na ion implanted, Hall effect temp. depend., electron surface density and mobility 0-11018



# semiconductor doping continued

- Si:O, evaporated amorphous film, effect of O<sub>2</sub> on props., ESR spectra 0-11265  
 Si:P, amorphous, CVD, defect compensation 0-54644  
 Si:P, BF<sub>3</sub><sup>+</sup> ion implantation, anomalous carrier profiles 0-2048  
 Si:P, diffusion of P impurities stimulated by gas discharge Ar plasma, low temp. 0-6560  
 Si:P, diffusivity, strain-induced band gap narrowing, E-centres 0-29228  
 Si:P, doped by neutron transmutation, lattice defects 0-34018  
 Si:P, impurity cond., hopping conduction and the Coulomb gap 0-44605  
 Si:P film, polycryst. pulsed electron beam annealing 0-10566  
 Si:P non-Fickian diffusion, parameter depend. on doping level and impurity gradient (*German*) 0-54440  
 Si:P<sup>+</sup> ion implanted single crystals, secondary defects development during annealing 0-44228  
 Si:P(As)(B)-SiO<sub>2</sub> interface oxidation kinetics, high doping levels, experiment 0-11828  
 Si:P(B), high temp. impurity diffusion via vacancies and self-interstitials 0-24667  
 Si:P(B) effect of impurities on solar cell performance 0-55848  
 Si:Sb, diffusional doping by doped oxide method 0-15127  
 Si:Sb, dopant implantation, activation analysis errors due to isotope comp. (*German*) 0-34037  
 Si:Sb, epitaxial film, growth by mol. beam technique 0-2292  
 Si:Sb, ion implanted doping, isotopic composition shifts on neutron activation determination 0-24487  
 Si-Au Schottky barrier solar cell fabrication, doping of a-Si 0-50969  
 Si-SiO<sub>2</sub> interface, Au traps 0-20319  
 Si-SiO<sub>2</sub> interface oxidation kinetics, high doping levels, theory 0-11827  
 SiC:Al epitaxial layers, growth, Al distrib. and solubility 0-15391  
 SiC:Al<sup>+</sup> p-n junctions, elec. props., defect effects 0-15594  
 SiTe:Ge(Sn), substitution of Si, thermoelectric props. (*Russian*) 0-11023  
 SnO<sub>2</sub>, electro-conducting transparent film, props. rel. to production method (*Japanese*) 0-25557  
 SnO<sub>2</sub>:As film, prep. and elec. cond. 0-2959  
 TiO<sub>2</sub>:S, acceptor properties of S, free electron concentrations 0-34395  
 Zn<sub>0.3</sub>Cd<sub>0.7</sub>:S-Cu, photoluminescence 0-29783  
 ZnO:P<sup>+</sup> implanted nonlinear resistor production and characteristics (*Russian*) 0-49252  
 ZnO-based ceramic microstructure and nonlinear props., B diffusion effects (*Russian*) 0-49423  
 Zn<sub>3</sub>P<sub>2</sub>, single crystal, growth, electronic and device props. 0-25551  
 ZnS:Mn, dopant conc. effect on stacking fault energy 0-2041  
 ZnS:Ne, implanted single crystals, photolum. and bombardment effect, thermolum. curve obs. 0-55166  
 ZnSe:Ga,As, characts. of simultaneous incorporation, by Mn<sup>2+</sup> ESR and X-ray fluoresc. anal. 0-34017  
 ZnSe:Ga(As), edge luminesc. 0-20699  
 ZnSe:In films, MBE growth, doping effect on photoluminesc. 0-10818  
 ZnTe:Ag, doped during growth and by diffusion, defect form. 0-15129  
 ZnTe:Cr(Mn)(Fe), exciton refl. spectra 0-2806  
 ZnTe:Li, diffusion investigation by SEM and TEM 0-10706  
 ZnTe:Li, impurity segregation during short annealing and quenching, SEM, TEM and elec. meas. 0-10676

# semiconductor-electrolyte boundaries

- conduction noise (*French*) 0-20306  
 electrode, interpretation of selective etching, electrochem. props 0-7703  
 electron injections from semicond electrodes liq. NH<sub>3</sub> 0-6977  
 n-type semiconductor anode, illum., charge transfer modes, digital simulation 0-2464  
 photoelectrochemical cells, semiconductor based, interaction of light and transport control 0-12020  
 photoelectrochemical solar cells, semiconductor/redox electrolyte junctions, functions examples and problems 0-45714  
 photoelectrochemical solar energy conversion principles, review 0-35695  
 photoelectrode, appl. in reproducible photoelectrochem. imaging 0-14446  
 photoelectrolysis cells, props. of oxide-based heterostruct. photoelectrodes 0-12023  
 photovoltaic effect, phenomenological theory and expt. confirmation 0-15601  
 n-Si-electrolyte junction, Schottky barrier height and reverse current 0-6979  
 solar cells, electrochem. liquid-junction, Schottky barrier height, photovoltage and photocurrent 0-26162  
 TCNQ salt in aqueous media, electrochem. behavior 0-6976  
 transfer of electrons and ions in and on semiconductors (*French*) 0-6935  
 CdS polycrystalline thin-film liq. junction photovolt. cell 0-50988  
 CdS, single cryst. surfaces, diff. gratings, electrochem. recording of holograms 0-32934  
 CdS-NiCl<sub>2</sub> interface, transverse acoustoelec. voltage spectroscopy 0-49828  
 CdS(Se) photoanodes, effect of S(Se) substitution, photoelectron spectroscopy obs. 0-2463  
 CdSe electrochem. photovoltaic cells, effect of thin film electrode prep. and conc. on efficiency 0-55847  
 n-Fe<sub>2</sub>O<sub>3</sub> electrodes, characterisation and behaviour in acetonitrile solns. 0-25004  
 n-Fe<sub>2</sub>O<sub>3</sub> electrodes, enhanced photoeffects by electrocatalysis and peroxide effects 0-16815  
 Fe<sub>2</sub>O<sub>3</sub> film, semicond. model for electronic struct., high electronic cond. 0-2493  
 Fe<sub>2</sub>O<sub>3</sub> thermal oxide film on Fe, capacitance, temp. and freq. depend., in aq. electrolyte soln. 0-54776  
 GaAs photoanode, using n/n<sup>+</sup> struct., power conversion efficiency 0-50990  
 n-GaAs, VPE, hi-lo, carrier conc. profiling by electrochem. methods 0-49958  
 n-GaAs/K<sub>2</sub>Se-K<sub>2</sub>Se<sub>2</sub>-KOH/C solar cell, Ru (III) chemisorption on photoanode, effect on performance 0-3516  
 n-GaAs/K<sub>2</sub>Se-K<sub>2</sub>Se<sub>2</sub>-KOH/C liq. junction cell, effect of Ru ion chemisorption on grain boundaries 0-55879  
 n-GaAs-electrolyte interface, surface pretreatment rel. to photocurrent, spectral response 0-3204  
 GaAs-electrolyte interface, surface barrier electroreflection anisotropy (*Russian*) 0-34895  
 GaAs-NaOH interface, inversion layer form. and surface states 0-2465  
 Ga<sub>0.9</sub>In<sub>0.1</sub>-P, flat band pot., impedance meas. and photoelectrochemistry (*French*) 0-49894  
 p-GaP electrodes with metal adatoms, surface states form. due to impregnated H 0-54778

# semiconductor-electrolyte boundaries continued

- p-GaP semiconductor-electrolyte solar cells for photochemical reduction of CO<sub>2</sub> to organic fuel 0-55880  
 GaP-liq. NH<sub>3</sub> soln. junctions, elec. characts. (*French*) 0-2460  
 p-GaP-NaOH interface, Schottky barrier model of photoelectrochemical effect 0-55673  
 Ge surface states, recombination centre formation (*Russian*) 0-29459  
 MoSe<sub>2</sub>-I<sup>-</sup>, photoelectrode, time resolved photocurrent, nanosecond excitation 0-45708  
 Nb<sub>2</sub>O<sub>5</sub> electrodes, in aq. and acetonitrile solns., electrochromism 0-50298  
 NiO and lithiated NiO, thermally grown, electrochemical capacitance variations 0-29475  
 NiO electrode for photolysis 0-40696  
 Si, electrochemical carrier conc. profiling 0-2461  
 Si/SiO<sub>2</sub>-electrolyte interface, electron exchange at surface of thermally grown SiO<sub>2</sub> 0-16696  
 SrTiO<sub>3</sub> semicond. electrode, electrochem., photoelectrochem. props. 0-3352  
 TiO<sub>2</sub> electrode, doping density dependent attachment of rhodamine B 0-54777  
 TiO<sub>2</sub> electrodes, in aq. electrolytes, surface states, photocurrent obs. 0-49895  
 TiO<sub>2</sub> electrodes in photoelectrochem. cell, photothermal effect 0-7947  
 n-TiO<sub>2</sub> photoanodes, corrosion suppression mechanism 0-2462  
 n-TiO<sub>2</sub>:Be electrodes, photoassisted oxidation of water 0-30502  
 TiO<sub>2</sub>:Cu, anodic, effect of Cu on optical props., rel. to possible appl. in solar energy conversion 0-16115  
 TiO<sub>2</sub>-aqueous electrolyte interface, pot. distrib., Mott-Schottky plots 0-11084  
 n-TiO<sub>2</sub>-electrolyte interface, equivalent circuit elements from impedance meas. 0-39669  
 n-TiO<sub>2</sub>-electrolyte interface, charge-transfer-controlled photocurrent 0-50992  
 TiO<sub>2</sub> electrodes, effect of processing variables on photoelectrochem. props 0-6975  
 TiO<sub>2</sub> electrodes, room temp. diffusions, capacitance, spectral response and volt-ampere characts. 0-15294  
 ZnO, sintered, for dye-sensitised solar photocell 0-16816  
 ZnSe:I/aqueous electrolyte junction, electrochem. behaviour in dark and under illum. 0-25003
- semiconductor electron states** see band structure of crystalline semiconductors and insulators; electron energy states of amorphous solids; electron energy states of liquid semiconductors
- semiconductor epitaxial layers**  
 coeff. and surface conc. 0-39122  
 deep level studies, growth by time difference method at controlled vapour pressure 0-39522  
 dopant profile and Schottky barrier height determ. by second differential method (*Chinese*) 0-49257  
 film-substrate boundary, epitaxial interface form. and transition regions 0-10821  
 GaAs MBE growth, deep levels effect on electron and hole trap densities 0-49652  
 groove and tunnel growth mechanism 0-10804  
 heteroepitaxial film deformation, causes and countermeasures (*Russian*) 0-49561  
 heteroepitaxial surface morphologies and misalignments (*Japanese*) 0-15411  
 heterojunction, band-edge discontinuities and interface pot. step, two-band narrow-gap approach 0-39665  
 III-V compounds and alloys, MBE process and problem areas, review 0-10815  
 ion implantation induced defects, annealing 0-24479  
 laser annealing, optical constants, ellipsometry observation 0-34024  
 reduced pressure, advances 0-40242  
 resistivity and thickness monitoring, use of spreading-resistance method 0-47075  
 Si, stacking faults, development, structure and props. (*Russian*) 0-24461  
 SIMS characterisation (*French*) 0-50904  
 ternary semiconductors, measurement of lattice parameters of thin heteroepitaxial layers, RHEED technique 0-15406  
 Al-GaAs-Al<sub>0.5</sub>Ga<sub>0.5</sub>As Schottky barrier diodes, prep., characts. 0-6948  
 (Al+Si)-Si thin films, struct. transitions and phase comp. 0-49537  
 AlGaAs-GaAs transverse mode stabilised plano-convex waveguide laser made by single step LPE 0-48274  
 Al<sub>0.5</sub>Ga<sub>0.5</sub>As thin graded band-gap layers, isothermal LPE growth 0-34325  
 Al<sub>0.5</sub>Ga<sub>0.5</sub>As:Sn(Te), persistent photocond., due to donor-related centres, symmetry 0-15558  
 p-Al<sub>0.5</sub>Ga<sub>0.5</sub>As:Ge layer on GaAs substrate, Hall and elec. cond. meas., Hall mobility 0-2402  
 Al<sub>0.5</sub>Ga<sub>0.5</sub>As:Zn epitaxial layers, composition and Zn carrier conc. 0-25585  
 Al<sub>0.5</sub>Ga<sub>0.5</sub>As-GaAs n-n heterojunction, interface width determ. 0-49887  
 AlGaAsP(Sb), compositional grading by LPE 0-10844  
 Cd chalcogenides, film, on NaCl, preferential epitaxy induced by electron bombard. or elec. field 0-10824  
 Cd<sub>0.5</sub>Hg<sub>0.5</sub>Te, variable-gap structures, galvanomagnetic effects 0-11014  
 CdS, grown by vac. evaporation on Si 0-25567  
 CdS-CdTe double layers on various GaAs surfaces, morphology and crystallography 0-34326  
 CdS(Se)(Te), condensation from gas phase of controlled comp., and props. 0-54562  
 CdSe epitaxial layers, on GaP-CdS substrates, absorption and electroabsorption 0-40178  
 CdTe epitaxial films, surface morphology, layer and spiral growth 0-10823  
 CdTe, on CdS substrate, closed-tube vapour growth 0-55302  
 CdTe-PbTe(InSb) superlattices, laser deposition of multilayer heteroepitaxial structs. 0-44450  
 Cd<sub>1-x</sub>Zn<sub>x</sub>S-p-GaAs heterojunctions, elec. and photovolt. props. rel. to growth technique 0-29466  
 CuGaTe<sub>2</sub> films deposited on GaAs substrates by flash evaporation, struct. and elec. cond. 0-24755  
 CuInS<sub>2</sub>, epitaxial thin film on GaAs, exam. of growth, electrical props. 0-24754  
 GaAl<sub>0.25</sub>Ga<sub>0.75</sub>As DH lasers grown by MBE, growth conditions influence on threshold current density 0-32984  
 Ga<sub>1-x</sub>Al<sub>x</sub>As epitaxial layer, absorpt. and transmission coeffs. (*French*) 0-2887



## semiconductor epitaxial layers continued

Ga<sub>1-x</sub>Al<sub>x</sub>As epitaxial layer, elec. cond., Hall effect, band struct. 0-49964  
 Ga<sub>1-x</sub>Al<sub>x</sub>As, LPE growth and characterisation 0-50566  
 Ga<sub>1-x</sub>Al<sub>x</sub>As, photoluminescence, deep level trap emission capture 0-29805  
 Ga<sub>1-x</sub>Al<sub>x</sub>As transverse mode DH laser with inbuilt plano-convex waveguide 0-48296  
 Ga<sub>1-x</sub>Al<sub>x</sub>As VPE layers, X-ray diffr. 0-29296  
 Ga<sub>1-x</sub>Al<sub>x</sub>As<sub>1-y</sub>P<sub>y</sub> epitaxial film, nonradiative recomb. at dislocations 0-44213  
 GaAs, (100) surfaces, reconstructed, ang. resolved photoemission from surface states, adsorption and annealing effects 0-16143  
 GaAs (111) epitaxial film, adsorption of Cs, Cs+O ellipsometric study 0-29282  
 GaAs autoepitaxial structure on heavily Te-doped GaAs substrate (*Russian*) 0-49556  
 GaAs, back etching and growth by liq. phase epitaxy, surface morphology obs. 0-29287  
 n-GaAs, defect clusters, charge-carrier mobility temp. depend. anal. 0-54701  
 p-GaAs, electron minority carrier diffusion lengths 0-29807  
 n-GaAs, epilayer, on semi-insulating substrate, elec. field distrib. (*French*) 0-20333  
 GaAs, epitaxial, Si and Ge doping 0-24470  
 GaAs, epitaxial deposition, growth kinetics (*French*) 0-2961  
 GaAs, epitaxial film, amorphous and polycrystalline, vol. plasmon energy and linewidth, electron scatt. obs. 0-50482  
 n-GaAs epitaxial film, pure and Cr doped, heavy electron trapping, Gunn oscils. 0-6857  
 GaAs epitaxial film recombination props. (*Russian*) 0-49812  
 GaAs epitaxial films, deep levels, impurity photocond. 0-20247  
 n-GaAs epitaxial films, residual cond. meas., struct. perfection rel. to photomemory 0-7010  
 GaAs epitaxial layer, Be, O, Si, S, Zn and Sn impurity concentrations 0-49260  
 GaAs epitaxial layer, photoluminesc. defect complex 0-29804  
 GaAs epitaxial layer high power Gunn diode development and fabrication 0-16199  
 GaAs epitaxial layers, from mixed Ga solns., C solubility 0-15392  
 GaAs epitaxial layers, structural defect and conc. inhomogeneities influence on barrier diode I-V characts. 0-15602  
 GaAs, epitaxial layers, MBE grown, Hall mobilities, substrate temps. 0-20335  
 GaAs, epitaxial layers, grain boundaries, deep level transient spectroscopy study 0-49234  
 GaAs, etching by water vapour, rate 0-16519  
 GaAs film optical components, prep. by MBE using Si shadow masking technique 0-28358  
 GaAs, gamma and electron irradi. defect formation depend. on interface, luminescence study 0-34057  
 GaAs grown by VPE using organometallic method, deep trap levels 0-10923  
 n-GaAs, hot electron magnetophonon resonance, Fourier anal. 0-54718  
 GaAs LPE buffer layers for MESFET appls. 0-29887  
 GaAs, LPE growth from supercooled soln., thickness uniformity 0-54547  
 GaAs, LPE layers, outdiffusion of recomb. centres from substrate during growth 0-39466  
 GaAs layers, electroepitaxy and thermal LPE growth, defect struct. and electronic characts. 0-2290  
 GaAs, MBE, undoped, growth and characterisation 0-10836  
 GaAs, MBE (001) layers, work function meas. 0-49870  
 GaAs MBE epilayers, photoluminesc. and elec. characterisation 0-11500  
 GaAs MOS diodes, interface states, deep-level transient spectroscopy 0-44727  
 GaAs, nonequilibrium carrier relax., recombination radn. 0-7416  
 GaAs, photoluminescence, deep level trap emission capture 0-29805  
 GaAs, polariton wave packet propag. in exciton reson. 0-2345  
 GaAs ribbons from Ga-AsCl<sub>3</sub>-H<sub>2</sub> epitaxy 0-7498  
 GaAs, selective in situ vapour etch of substrate and growth 0-2958  
 GaAs, self-compensation due to shallow and deep levels 0-24837  
 GaAs structures produced by epitaxy, recombination radiation, anomalous temp. depend. 0-2847  
 GaAs thin layers, MBE, growth conditions and phys. props. (*German*) 0-55307  
 GaAs, time-resolved spectra, carrier relax. time, phonon lifetime 0-11433  
 GaAs, transient processes during doping for large conc. jumps. 0-39134  
 n-GaAs, undoped, correl. incorporation of donors, photocond. meas. at 4.2K 0-6898  
 n-GaAs, VPE, hi-lo, carrier conc. profiling by electrochem. methods 0-49958  
 GaAs, VPE, hole diffusion lengths, surface prep. and heat treatment effects, etchant evaluation 0-15627  
 GaAs, VPE, hole diffusion lengths, effect of transition metal diffusional doping 0-15628  
 GaAs, VPE, incorporation of deep levels, effects of growth conditions 0-20111  
 p-GaAs, VPE growth and characterisation, doping levels 0-10841  
 GaAs, VPE growth on {110} cryst. plane 0-10840  
 GaAs, VPE layer growth with abrupt doping profile 0-24746  
 GaAs, VPE layer props. control using boundary layer characts. 0-50561  
 GaAs VPE layers, back surface gettering, Cr out diffusion 0-10802  
 GaAs VPE layers, elec. props., semi-insulating substrates effect 0-11123  
 GaAs VPE layers, electron irradi., electron traps 0-25026  
 n-GaAs VPE layers, Hall mobility, effect of Cu contamination, photolum. expts. 0-54810  
 GaAs VPE layers for FET devices, impurity characterisation 0-29491  
 n-GaAs vapour phase epitaxial film electrophysical props. rel. to growth temp. (*Russian*) 0-49961  
 GaAs:Be, deep levels 0-29358  
 GaAs:Be(C)(Ge)(Sn), MBE layers, photoluminesc. 0-29803  
 GaAs:Cr, epitaxial layers, MBE grown, Hall mobilities, substrate temps. 0-20335  
 GaAs:Cr, ion implanted, Cr conc., depth distrib. and diffusion coeff. 0-49243  
 GaAs:Cr substrates and LPE layers, Au film deposition and annealing, Cr redistrib. 0-15312  
 GaAs:Ge, MBE layers, complex free-carrier profile synthesis 0-54266  
 GaAs:Ge, mol. beam epitaxy of n- and p-types 0-10839  
 n-GaAs:Ni(Zn), VPE, deep-level transient spectroscopy 0-34383  
 GaAs:Si epitaxial films, elec. and photoelec. props., impurity distrib. 0-7006

## semiconductor epitaxial layers continued

GaAs:Si LPE layers, surface morphology, substrate misorientation, initial supercooling effects 0-34329  
 GaAs:Si layers, MBE growth, elec. and optical props., doping characts. 0-10819  
 GaAs:Si p-n structs., effect of growing conditions on distrib. of recomb. parameters 0-39668  
 GaAs:Sn diode, LPE grown, electron irradi. effect on characts. 0-39667  
 GaAs:Sn films, MBE 0-50563  
 GaAs:Te diffused LED, electron irradi. effect on characts. 0-39667  
 p-GaAs:Zn, luminescent, ion doped MBE growth 0-44436  
 GaAs:Zn epitaxial layers, composition and Zn carrier conc. 0-25585  
 GaAs-Al, X-ray total-external-refl.-Bragg diffr. study 0-34321  
 GaAs-AlGa<sub>1-x</sub>As current injection multi-quantum-well heterostructure lasers, MBE grown 0-19042  
 GaAs-AlGa<sub>1-x</sub>As DH lasers, MBE grown, substrate temp. effect on current threshold 0-48243  
 GaAs-AlGaAs photoelectroluminescent diodes, characts., radiant power 0-6972  
 GaAs-GaAlAs laser, degraded, characterisation by selective etching and photoetching 0-48252  
 GaAs-Ge<sub>1-x</sub>(GaAs)<sub>x</sub> n-p heterojunctions, hydrostatic press. effect on elect. and photoelectric props. 0-20304  
 GaAsP epitaxial film, composition self modulation, defect struct. 0-34331  
 GaAsP, VPE, lattice forbidden band composition depend. (*Hungarian*) 0-6669  
 GaAs<sub>0.6</sub>P<sub>0.4</sub>, VPE, hole diffusion lengths, surface prep. and heat treatment effects, etchant evaluation 0-15627  
 GaAs<sub>0.6</sub>P<sub>0.4</sub>, VPE, hole diffusion lengths, effect of transition metal diffusional doping 0-15628  
 GaAs<sub>1-x</sub>P<sub>x</sub>, structural defects, optical props. effect 0-55208  
 GaAs<sub>1-x</sub>Sb<sub>x</sub>, undoped epitaxial layers, photoluminesc. meas. 0-20703  
 Ga<sub>0.47</sub>In<sub>0.53</sub>As, LPE growth and characterisation 0-10845  
 Ga<sub>1-x</sub>In<sub>x</sub>As-GaAs epitaxial interface with small misfits, TEM image contrast 0-2275  
 Ga<sub>1-x</sub>In<sub>x</sub>As, substrate orientation effect on liq.-solid distrib. coeffs., 600-700°C 0-2278  
 GaInAsP, VPE growth and props. 0-16194  
 Ga<sub>1-x</sub>In<sub>x</sub>As<sub>1-y</sub>P<sub>y</sub>, conduction band and phonons, Shubnikov-de Haas effect, magnetophonon resonance, Raman scattering 0-24795  
 n-Ga<sub>1-x</sub>In<sub>x</sub>As<sub>1-y</sub>P<sub>y</sub>, photoluminesc. of epitaxial films, isovalent substitution 0-16097  
 Ga<sub>1-y</sub>In<sub>y</sub>As<sub>1-x</sub>Sb<sub>x</sub>, LPE on GaSb, miscibility gap in liq. phase and lattice mismatch 0-15404  
 Ga<sub>1-x</sub>In<sub>x</sub>P<sub>1-y</sub>As<sub>y</sub>, carrier compensation and alloy scatt. 0-29490  
 GaN:Al, VPE grown, luminesc. and elec. props. depend. on doping conc., bound excitons 0-20688  
 GaP, birefringence observations of strain and plastic deform. 0-50678  
 GaP, current controlled LPE from finite volume melt 0-20805  
 GaP epitaxial growth from solution in melt, crystn. theory 0-16204  
 GaP:Fe n-i-n epitaxial struct., photoconductivity, recombination scheme (*Russian*) 0-15569  
 GaP:N, epitaxial layers, N concentration determination by two independent methods 0-39142  
 GaP:N(N,O) epitaxial struct., luminesc. study of degradation during heat treatment 0-45139  
 GaP:Zn, doping from gas phase during LPE 0-55312  
 GaP:Zn, Sn doped epitaxial layers, Hall const., hole mobility and conc. 0-15143  
 GaP<sub>0.9</sub>As<sub>0.1</sub>/GaP, heteroepitaxial structs., refined formulation of relative orientation criterias 0-44448  
 Ge, amorphous, growth rate of crystallisation, Raman spectroscopy study 0-44227  
 Ge, epitaxial-diffusion p-n junction, inductive props. in secondary breakdown 0-15598  
 Ge-GaAs heteroepitaxial system, dislocation struct. in stress measurements 0-29030  
 Ge-Si, solid phase heteroepitaxy 0-6670  
 Hg<sub>1-x</sub>Cd<sub>x</sub>Te, LPE growth and characterisation 0-50565  
 InAs, epilayer, MBE growth parameters, relationship with elec. props. 0-2296  
 InAs, heteroepitaxial, far IR refl. and transmission meas., surface and interface effects 0-16044  
 InAs, heteroepitaxial layers, AsCl<sub>3</sub> mole. fraction and substrate orientation effects on elec. parameters 0-39690  
 InAs, laser action mechanisms with electron beam excitation 0-28240  
 InAs, organometallic VPE growth on InAs and GaSb 0-16193  
 InAs<sub>1-x</sub>Sb<sub>x</sub> on GaSb, LPE growth 0-29293  
 In<sub>1-x</sub>Ga<sub>x</sub>As, epitaxial solid soln. film, spectral depend. of transparency, absorpt. spectra calcs. 0-45161  
 In<sub>1-x</sub>Ga<sub>x</sub>As layers, on GaAs substrate, MBE fabrication and laser operation 0-10820  
 InGaAsP, epitaxial layer, defect evaluation by cathodoluminescence 0-2866  
 InGaAsP, LPE growth, impurity depend. of distrib. coeff. 0-10843  
 InGaAsP, LPE grown, impurity effect on surface morphology 0-29291  
 In<sub>1-x</sub>Ga<sub>x</sub>As<sub>1-y</sub>P<sub>y</sub> DH laser, low threshold current density, near equilibrium LPE growth 0-19040  
 In<sub>1-x</sub>Ga<sub>x</sub>As<sub>1-y</sub>P<sub>y</sub>, traps in device quality n- and p-type LPE material 0-10999  
 InGaAsSb, LPE growth, and appl. in GaSb/AlGaAsSb/InGaAsSb/AlGaAsSb/GaSb DH 0-16205  
 In<sub>1-x</sub>Ga<sub>x</sub>P, epitaxial growth on GaAs substrate, formation of intermediate layers 0-2304  
 In<sub>1-x</sub>Ga<sub>1-y</sub>P<sub>1-y</sub>As<sub>y</sub>-InP, LPE, lattice matching, phase 0-54350  
 InP, (100)-orientated, vapour phase deposited in closed-tube system, surface comp. variation 0-24752  
 InP, LPE grown, impurity effect on surface morphology 0-29291  
 InP layer growth method, model validity evaluation (*Slovak*) 0-54535  
 InP layers, LPE growth from undercooled melts, numerical method 0-6665  
 InP, organometallic growth by cracking of In(C<sub>2</sub>H<sub>5</sub>)<sub>3</sub> and PH<sub>3</sub> 0-11575  
 InP, photoluminesc. of epitaxial films, isovalent substitution 0-16097  
 InP, terracing of LPE growth, doping effects 0-10846  
 InP, VPE layer props. control using boundary layer characts. 0-50561  
 p-InP:Zn, vapour grown, prep. and props. 0-54268  
 InP/InGaAsP/InP double heterostructure, grown on InP(111)B substrate, threading dislocation multiplication 0-54237  
 InP(100) undoped homoepitaxial films grown by MBE, photoluminesc. props. 0-2809



## semiconductor epitaxial layers continued

- InSb, epitaxial film, amorphous and polycrystalline, vol. plasmon energy and linewidth, electron scatt. obs. 0-50482  
 n-InSb film, low energy electron irradi. effect on elec. props. 0-7009  
 InSb, LPE growth characteristics, substrate surface contamination dependence 0-39470  
 InSb-PbTe(CdTe) superlattices, laser deposition of multilayer heteroepitaxial struct. 0-44450  
 InSb, heteroepitaxial, MBE growth and elec. props. 0-2301  
 PbSe, X-ray diffr. exam. of struct., and luminescence props. 0-55209  
 Pb<sub>0.7</sub>Sn<sub>0.22</sub>Te:In epitaxial layers, dislocation density, Hall effect, conductivity, photoeffects 0-25024  
 Pb<sub>0.8</sub>Sn<sub>0.2</sub>Te, far IR refl. spectra, carrier density, Hall const., and plasma freq. 0-20629  
 Pb<sub>1-x</sub>Sn<sub>x</sub>Te heterojunction lasers, instantaneous vacuum evaporation grown, threshold current density 0-5759  
 Pb<sub>1-x</sub>Sn<sub>x</sub>Te LPE grown heterostructures, dislocation etch pitch, interfaces 0-2023  
 Pb<sub>1-x</sub>Sn<sub>x</sub>Te layers, LPE growth on metal-etched substrates 0-55313  
 Pb<sub>1-x</sub>Sn<sub>x</sub>Te:In epitaxial layers, growth, elec. props., and luminesc. 0-54542  
 PbTe (111) epitaxial films, localised electron irradi. effects on elec. props. and O<sub>2</sub> sorption 0-49472  
 PbTe, crystallite size in epitaxial layers by X-ray diffraction rocking curves 0-20052  
 PbTe epitaxial films, quantum size effect, optical meas. 0-11121  
 PbTe, VPE, on LiNbO<sub>3</sub>, struct. and morphology obs. 0-54561  
 PbTe very thin epitaxial films, transmission and refl. spectra, 1 to 5 eV 0-7430  
 PbTe-CdTe(InSb) superlattices, laser deposition of multilayer heteroepitaxial struct. 0-44450  
 PbTe-ZrO<sub>2</sub> (SiO<sub>2</sub>), epitaxial MIS struct., fabrication and elec. props. 0-2472  
 Sb<sub>2</sub>Te<sub>3</sub> epitaxial films, growing conditions effect on elec. cond., thermoelectric 0-39687  
 Si amorphous layer, solar furnace annealing to induce solid-phase epitaxy 0-2277  
 Si, autoepitaxy, displacement of microrelief 0-2307  
 Si beam epitaxy for epitaxial film growth and p-n junction formation in high vacuum 0-16187  
 Si, epitaxial growth, adsorbed layer model for autodoping mech. 0-7505  
 Si epitaxial interface migration, theory and expt. test 0-29290  
 Si, epitaxial layer, growth mechanism from ion-molecular beams 0-2299  
 Si, epitaxial layer, incorporation conc. depend. of P from silane-phosphine-H<sub>2</sub> mixture 0-2053  
 Si epitaxial layer, minority carrier lifetime obs. (Russian) 0-49765  
 Si epitaxial layer growth in vacuum, Ar, Xe ion bombardment effect 0-39463  
 Si epitaxial structures, junction layer width and impurity conc. estimates (Russian) 0-49893  
 Si, growth in Si-P-H system, depend. of doping element incorporation on temp. in CVD 0-45234  
 Si, growth on Si(111) and sapphire (1102), simultaneous RHEED/AES study 0-10833  
 Si heteroepitaxial films on sapphire, vac. deposited, struct. and elec. props. 0-15390  
 Si, heteroepitaxial growth using SiH<sub>4</sub> in H<sub>2</sub>-He atm. 0-20049  
 Si layer growth by CVD on Sn-coated background (Dutch) 0-7502  
 Si, MBE growth and surface struct. 0-10816  
 Si MBE layer resistivity and carrier mobility obs. (Russian) 0-49962  
 Si, minority carrier lifetime and impurity conc. meas. (Japanese) 0-25025  
 Si on sapphire, laser annealing dynamics epitaxial regrowth, optical reflectivity 0-29285  
 Si p-n homoepitaxial junctions, elec. and struct. characts. 0-6662  
 Si, solid-state epitaxial growth of amorphous layer 0-10803  
 Si surface layers, impurities, elec. and photoelec. props. 0-2298  
 Si thin autoepitaxial layers low temp. growth mechanism in SiCl<sub>4</sub>-H<sub>2</sub> system 0-20795  
 Si, VPE layer props. control using boundary layer characts. 0-50561  
 Si:As(Sb), MBE, n-type doping techniques 0-15126  
 Si:Ge, regrowth behaviour from backscatt. and channelling meas. 0-2300  
 Si:Sb, epitaxial film, growth by mol. beam technique 0-2292  
 Si:Sb, epitaxial layers, doping profile techniques 0-44231  
 Si-Al interface, solid phase epitaxial growth of Si 0-34324  
 SiC, epitaxial growth by sublimation sandwich method, effect of impurities 0-25568  
 SiC epitaxial layer growth from sublimation in vac., kinetics 0-20791  
 SiC, exam. of N solubility, in epitaxial layers 0-6520  
 SiC:Al epitaxial layers, growth, Al distrib. and solubility 0-15391  
 Te, on electron irradi. KBr, epitaxial growth and surface coverage 0-10825  
 Zn chalcogenides, film, on NaCl, preferential epitaxy induced by electron bombard. or elec. field 0-10824  
 ZnO epitaxial film on Al<sub>2</sub>O<sub>3</sub> substrate, recombination radiation in intense single photon excitation 0-7410  
 ZnO film, prep. by reactive ionized cluster beam deposition, and characterisation 0-10829  
 ZnO, ionized-cluster beam and reactive ionized-cluster beam deposition, cathodolum. characterisation 0-16202  
 ZnO, piezoelec. films produced by gas transport reaction, US excitation efficiency 0-2700  
 ZnS, epitaxial growth, appl. to electronic devices, review (Japanese) 0-55281  
 ZnS(Se), growth kinetics on CaF<sub>2</sub> by vapour phase transport (French) 0-54572  
 ZnS,Se<sub>1-x</sub>, on CaF<sub>2</sub>, comp. and temp. depend. of fund. band gap 0-11115  
 ZnS,Se<sub>1-x</sub>, VPE, characterisation of defect centres by photoelectronic meas. 0-10914  
 ZnSb, epitaxial films, growing conditions effect on elec. cond., thermoelectric 0-39687  
 ZnSe epitaxial layers, prep. by chem. transport reactions 0-16192  
 ZnSe:In films, MBE growth, doping effect on photoluminesc. 0-10818  
 ZnSe:Li(Na)(Ga) doped and pure cryst., donor-acceptor bands 0-11465  
 ZnTe film, prepared by single-source vacuum deposition method (Japanese) 0-6664

## semiconductor growth

- alloy semiconductor, for appl. in IR detector arrays, comp. control 0-31872

## semiconductor growth continued

- CdSe whiskers, growth in H<sub>2</sub> 0-15425  
 chalcogenide magnetic semiconductors, spinal-type, closed tube vapour transport method (Japanese) 0-25539  
 crucible shape effect on crystallisation front 0-16173  
 developments, late 1970s innovations 0-6666  
 epitaxial groove and tunnel growth mechanism 0-10804  
 FeS<sub>2</sub>, thin films, prep. and charact. 0-16178  
 GaAs MBE growth, deep levels effect on electron and hole trap densities 0-49652  
 α-HgS, cryst. growth from soln. at low temps. 0-7487  
 II-VI semiconductors, from melt, dependence of mass losses upon press. 0-25547  
 III-V compounds, vapour growth, using organometallic sources (Japanese) 0-16195  
 III-V compounds and alloys, MBE process and problem areas, review 0-10815  
 III-V quaternary alloys, melt and soln. growth of bulk single crystals 0-35079  
 III-V semiconductor heterostructures, growth and dissolution kinetics by LPE 0-49543  
 III-V semiconductors, VPE by metalorganic CVD (Japanese) 0-50562  
 MBE, device appls. 0-25570  
 MBE (Japanese) 0-55305  
 microscopic mechanism of film growth from non-condensed phases, kinetic anal. 0-54565  
 molecular beam epitaxy for superlattices control 0-2283  
 reactive closed-space vapour transport, simplified theory 0-15396  
 reproductive epitaxy, exam. 0-55303  
 VPE impurity profile computer-aided control 0-2962  
 zone melting, process parameters influence on radial scatter of resist. 0-16174  
 Al-Ga-Sb ternary phase diagram, calc., DTA and LPE expts. 0-29931  
 AlGaAs-GaAs transverse mode stabilised plano-convex waveguide laser made by single step LPE 0-48274  
 Al<sub>0.9</sub>Ga<sub>0.1</sub>As thin graded band-gap layers, isothermal LPE growth 0-34325  
 Al<sub>0.9</sub>Ga<sub>0.1</sub>As:Zn epitaxial layers, composition and Zn carrier conc. 0-25585  
 Al<sub>0.9</sub>Ga<sub>0.1</sub>As-GaAs heterostruct. lasers, metalorganic CVD 0-23692  
 Al<sub>0.9</sub>Ga<sub>0.1</sub>As-GaAs multiple-quantum-well injection lasers grown by metalorganic CVD, room temp. continuous operation 0-1218  
 AlSb film, laser-induced metal-semicond. transition in Al-Sb mixed film 0-6661  
 Cd chalcogenides, film, on NaCl, preferential epitaxy induced by electron bombard. or elec. field 0-10824  
 Cd<sub>3</sub>As<sub>2</sub> platelet, single vap.-grown cryst., passive annealing, Fermi energy variation 0-45223  
 CdCr<sub>2</sub>Se<sub>4</sub>, single cryst. growth by chem. transport reactions 0-16163  
 (CdGeAs<sub>2</sub>)<sub>1-x</sub>D<sub>x</sub> amorphous films, property control in common target sputtering, elec. cond. 0-7494  
 CdGeP<sub>2</sub>, crystals, prep. by chem. vapour transport 0-55280  
 CdIn<sub>2</sub>S<sub>4</sub> film, vac. deposited, growth, struct., optical and photoelectronic props. 0-10831  
 CdP, single crystal growth 0-35065  
 CdS, CdSe, growth rate, sublimation rate and etching behaviour along polar axis 0-24387  
 CdS, grown by vac. evaporation on Si 0-25567  
 CdS photosensitive film production from chelated metallo-organic compounds (Russian) 0-49813  
 CdS-CdTe double layers on various GaAs surfaces, morphology and crystallography 0-34326  
 CdS,Se<sub>1-x</sub> photosensitive films, prep., props., and use for photodetectors 0-55298  
 CdS(Se)(Te), epitaxial, condensation from gas phase of controlled comp., and props. 0-54562  
 CdSe films, growth kinetics and cryst. struct. during vacuum condensation 0-2305  
 CdSe photosensitive film production from chelated metallo-organic compounds (Russian) 0-49813  
 CdSnP<sub>2</sub> crystal growth, DTA obs. of Cd-Sn-CdSnP<sub>2</sub> phase diagram 0-24394  
 CdTe epitaxial films, on CdS substrate, closed-tube vapour growth 0-55302  
 CdTe epitaxial films, surface morphology, layer and spiral growth 0-10823  
 CdTe film, low-resist., prep. by multi-source evaporation method, and characterisation 0-25582  
 CdTe reactive close-spaced vapour transport, simplified theory 0-15396  
 CdTe, single cryst. sublimation growth, X-ray topographic characterisation 0-29866  
 CdTe-Te film, prep. by combined hot-wall-flash evaporation method, and characterisation 0-55296  
 Cd<sub>1-x</sub>Zn<sub>x</sub>S-p-GaAs heterojunctions, elec. and photovolt. props. rel. to growth technique 0-29466  
 CuGaS<sub>2</sub>, crystal growth by solid phase crystallisation 0-25556  
 CuGaTe<sub>2</sub> films deposited on GaAs substrates by flash evaporation, struct. and elec. cond. 0-24755  
 (CuInTe<sub>2</sub>)<sub>1-x</sub>(2ZnTe)<sub>x</sub> phase diagram and cryst. growth of CuZn<sub>2</sub>InTe from ZnCl<sub>2</sub> flux 0-16287  
 Cu<sub>2</sub>S evaporated thin films, composition, prep. and characts. 0-25569  
 Ga-Al-Al<sub>0.27</sub>Ga<sub>0.73</sub>As DH lasers grown by MBE, growth conditions influence on threshold current density 0-32984  
 GaAlAs based heterojunctions, integrated optics appl., technology advancements (Slovak) 0-33226  
 Ga<sub>1-x</sub>Al<sub>x</sub>As, LPE growth and characterisation 0-50566  
 Ga<sub>1-x</sub>Al<sub>x</sub>As layer form. on GaAs during dissolution in Ga-Al-As soln. 0-10799  
 GaAlAsSb/GaSb alloys, prep. and optoelectronic device appl. 0-25587  
 GaAs and related cpds., conference, St. Louis, MO, USA (Sept. 1978) 0-8737  
 GaAs, back etching and growth by liq. phase epitaxy, surface morphology obs. 0-29287  
 GaAs, epitaxial, Si and Ge doping 0-24470  
 GaAs, epitaxial layer, micron and submicron vap. phase growth, for FET 0-11577  
 GaAs epitaxial layer high power Gunn diode development and fabrication 0-16199  
 GaAs epitaxial layers, from mixed Ga solns., C solubility 0-15392  
 GaAs film optical components, prep. by MBE using Si shadow masking technique 0-28358



## semiconductor growth continued

- GaAs grown by VPE using organometallic method, deep trap levels 0-10923
- GaAs LPE buffer layers for MESFET appls. 0-29887
- GaAs, LPE layers, outdiffusion of recomb. centres from substrate during growth 0-39466
- GaAs layers, electroepitaxy and thermal LPE growth, defect struct. and electronic characts. 0-2290
- GaAs layers, from gas phase, impurity influence on growth micromechanism 0-45237
- GaAs, MBE, undoped, growth and characterisation 0-10836
- GaAs, MESFET structure, buffered, LPE growth 0-40271
- GaAs MM-wave and sub MM-wave receiver elements, Schottky-barrier resistive mixer devices LPE 0-11558
- GaAs, prep. of thin films by ionised-cluster beam deposition (*Japanese*) 0-25576
- GaAs ribbons from Ga-AsCl<sub>3</sub>-H<sub>2</sub> epitaxy 0-7498
- GaAs, selective in situ vapour etch of substrate and growth 0-2958
- GaAs thin layers, MBE, growth conditions and phys. props. (*German*) 0-55307
- GaAs, VPE, incorporation of deep levels, effects of growth conditions 0-20111
- GaAs VPE, influence of growth parameters, AsCl<sub>3</sub> transport method 0-29881
- p-GaAs, VPE growth and characterisation, doping levels 0-10841
- GaAs, VPE growth on {110} cryst. plane 0-10840
- GaAs, VPE in CVD systems, anisotropic phenomena 0-54563
- GaAs, VPE layer growth with abrupt doping profile 0-24746
- GaAs, VPE layer props. control using boundary layer characts. 0-50561
- GaAs:Ge, mol. beam epitaxy of n- and p-types 0-10839
- GaAs:Si LPE layers, surface morphology, substrate misorientation, initial supercooling effects 0-34329
- GaAs:Si layers, MBE growth, elec. and optical props., doping characts. 0-10819
- GaAs:Si p-n structs., effect of growing conditions on distrib. of recomb. parameters 0-39668
- n-GaAs:Sn, VPE growth, reactor design 0-2956
- GaAs:Sn films, MBE 0-50563
- GaAs:Zn, diffusion during LPE, impurity gradients and annealing effects 0-29882
- p-GaAs:Zn, luminescent, ion doped MBE growth 0-44436
- GaAs:Zn epitaxial layers, composition and Zn carrier conc. 0-25585
- GaAs-Al<sub>0.5</sub>Ga<sub>0.5</sub>As DH lasers, very low current threshold, MBE grown 0-43353
- GaAs-Al<sub>0.5</sub>Ga<sub>0.5</sub>As DH lasers, MBE grown, substrate temp. effect on current threshold 0-48243
- n-GaAs-n<sup>+</sup>-Al<sub>0.5</sub>Ga<sub>0.5</sub>As heterostructure production, by MBE (*German*) 0-44711
- GaAsP, VPE, lattice forbidden band composition depend. (*Hungarian*) 0-6669
- Ga<sub>0.4</sub>In<sub>0.5</sub>As, LPE growth and characterisation 0-10845
- Ga<sub>0.1</sub>In<sub>0.9</sub>As, substrate orientation effect on liq.-solid distrib. coeffs., 600-700°C 0-2278
- Ga<sub>0.1</sub>In<sub>0.9</sub>As, VPE growth, thermodynamic anal. 0-2933
- GaInAsP, diffusion-limited growth in LPE 0-10842
- GaInAsP, VPE growth and props. 0-16194
- GaInAsP-InP DH lasers made by melt-back method, operating characteristics 0-48287
- GaInAsP-InP DH injection lasers prep. by LPE, 1.11-1.67 µm operation 0-53321
- Ga<sub>1-x</sub>In<sub>x</sub>As<sub>1-y</sub>Sb<sub>1-y</sub>, LPE on GaSb, miscibility gap in liq. phase and lattice mismatch 0-15404
- Ga<sub>0.1</sub>In<sub>0.9</sub>P solid solutions, single cryst. prep. and props. 0-16162
- Ga<sub>0.1</sub>In<sub>0.9</sub>Sb, temp. gradient zone melting 0-50550
- Ga<sub>0.1</sub>In<sub>0.9</sub>Sb p-n junction photodiode fabrication, sensitivity as 1 to 2.5 µm detectors (*Japanese*) 0-52311
- GaN, deposition from plasma reactor, organo-metallic and donor-acceptor complex exchange in HF plasma 0-38839
- GaN, growth and morphology of crystals (*Japanese*) 0-11548
- GaP, current controlled LPE from finite volume melt 0-20805
- GaP epitaxial growth from solution in melt, crystn. theory 0-16204
- GaP ribbon waveguide, vapour-grown, phase-matched SHG 0-48339
- GaP:Zn, doping from gas phase during LPE 0-55312
- GaSb, CVD using organometallics, epitaxial growth 0-29879
- GaSb, sputtered films, on GaAs, growth, Hall effect, impurity levels 0-20334
- GaSb thin layers, directed crystn. on sapphire, props. 0-35111
- Ge, crystal growth, O equilib. between Ge and gas over melt 0-2938
- Ge, polycrystalline epitaxial film, exam. of growth kinetics and props. 0-55304
- Ge:P(Sb), growth atm. effect on struct. microdefect form. 0-20779
- Hg<sub>0.60</sub>Cd<sub>0.40</sub>Te, LPE growth from Te-rich soln. 0-7508
- Hg<sub>1-x</sub>Cd<sub>x</sub>Te, for appl. in IR detector arrays, comp. control 0-31872
- Hg<sub>1-x</sub>Cd<sub>x</sub>Te, LPE current controlled 0-40272
- Hg<sub>1-x</sub>Cd<sub>x</sub>Te, LPE growth and characterisation 0-50565
- α-HgI<sub>2</sub>, single cryst. growth from iodomercure complexes 0-35069
- HgSe/CdSe lattice-matched heterostructs. as Schottky barriers, CVD epitaxial growth and elec. props. 0-49877
- HgTe, VPE growth control by EM irradi. (*Russian*) 0-34338
- InAs, epilayer, MBE growth parameters, relationship with elec. props. 0-2296
- InAs, organometallic VPE growth on InAs and GaSb 0-16193
- InAs:Cd,Te interaction between impurities, effect on elec. props., Hall effect. 0-19832
- InAs<sub>1-x</sub>Sb<sub>x</sub> on GaSb, LPE growth 0-29293
- InAs<sub>1-x</sub>Sb<sub>x</sub>, organometallic VPE growth on InAs 0-45233
- InGaAs, lattice-matched VPE on (100) InP, photodiode appl. 0-35102
- InGaAs on (100) InP substrate, VPE 0-40267
- In<sub>0.53</sub>Ga<sub>0.47</sub>As-InP heterostructure, LPE growth 0-11582
- In<sub>0.5</sub>Ga<sub>0.5</sub>As, VPE on (100), (111)A, and (111)B InP substrates 0-15382
- InGaAsP, LPE growth, impurity depend. of distrib. coeff. 0-10843
- InGaAsP/InP DH, vapour phase growth by dual-growth-chamber method 0-50559
- In<sub>0.8</sub>Ga<sub>0.2</sub>As<sub>0.5</sub>P<sub>0.5</sub>, LPE growth 0-11557
- In<sub>1-x</sub>Ga<sub>x</sub>As<sub>1-y</sub>P<sub>y</sub> DH laser, low threshold current density, near equilibrium LPE growth 0-19040
- InGaAsSb, LPE growth, and appl. in GaSb/AlGaAsSb/InGaAsSb/AlGaAsSb/GaSb DH 0-16205
- In<sub>1-x</sub>Ga<sub>x</sub>P, epitaxial growth on GaAs substrate, formation of intermediate layers 0-2304
- semiconductor growth continued
- InGaSb, LPE growth characteristics, substrate surface contamination dependence 0-39470
- In<sub>2</sub>O<sub>3</sub>, electro-conducting transparent film, props. rel. to production method (*Japanese*) 0-25557
- In<sub>2</sub>O<sub>3</sub>:Sn, glass like thin film, electron evaporated, conductive transport (*Chinese*) 0-49960
- InP, LPE growth 0-11557
- InP layer growth method, model validity evaluation (*Slovak*) 0-54535
- InP layers, LPE growth from undercooled melts, numerical method 0-6665
- InP, MBE from In and P<sub>2</sub> beams, substrate temp. limits 0-15385
- InP, organometallic growth by cracking of In(C<sub>2</sub>H<sub>5</sub>)<sub>3</sub> and PH<sub>3</sub> 0-11575
- InP, terracing of LPE growth, doping effects 0-10846
- InP VPE, In-H<sub>2</sub>-PCl<sub>3</sub> chemistry 0-11549
- InP, VPE layer props. control using boundary layer characts. 0-50561
- InP VPE with new metallorganic compound 0-55278
- p-InP:Zn, vapour grown, prep. and props. 0-54268
- InP-Ga<sub>1-x</sub>In<sub>x</sub>P<sub>1-y</sub>As<sub>1-y</sub> heterostruct. lasers, growth and characterisation 0-23691
- InP-In<sub>1-x</sub>Ga<sub>x</sub>P<sub>1-y</sub>As<sub>2-y</sub> heterostructure laser, single and multiple quantum-well, liquid-phase epitaxial growth 0-38031
- InSb, charact. and phys. props., review (*Japanese*) 0-39576
- InSb film, heteroepitaxial, MBE growth and elec. props. 0-2301
- InSb films on LiNbO<sub>3</sub>, prep. and props. 0-35093
- InSb, LPE growth characteristics, substrate surface contamination dependence 0-39470
- InSb, low defect crystal growth by InN doping, IR detector appl. 0-20780
- InSb, prep. of thin films by ionised-cluster beam deposition (*Japanese*) 0-25576
- InSb thin layers, directed crystn. on sapphire, struct. 0-35112
- In<sub>2</sub>Te<sub>3</sub> film thermal deposition, transmission spectra and elec. cond. (*Russian*) 0-49555
- MoS<sub>2</sub>, synthetic molybdenite single crystals, growth from vapour, elec. props. 0-34446
- PbSe films, synthesis characts. 0-35094
- Pb<sub>1-x</sub>Sn<sub>x</sub>Te layers, LPE growth on metal-etched substrates 0-55313
- Pb<sub>1-x</sub>Sn<sub>x</sub>Te single crystals, selection using travelling solvent method (*German*) 0-2936
- Pb<sub>1-x</sub>Sn<sub>x</sub>Te:In epitaxial layers, growth, elec. props., and luminesc. 0-54542
- Pb<sub>0.5</sub>Sn<sub>0.5</sub>Te, for appl. in IR detector arrays, comp. control 0-31872
- PbTe, and Pb<sub>1-x</sub>Sn<sub>x</sub>Te, VPE growth control by EM irradi. (*Russian*) 0-34338
- PbTe-ZrO<sub>2</sub> (SiO<sub>2</sub>), epitaxial MIS struct., fabrication and elec. props. 0-2472
- Si, amorphous CVD films for high temp. solar photothermal conversion 0-26161
- Si amorphous layer, solar furnace annealing to induce solid-phase epitaxy 0-2277
- Si, amorphous whisker growth characts. by SiH<sub>4</sub> thermal decomposition 0-34342
- Si beam epitaxy for epitaxial film growth and p-n junction formation in high vacuum 0-16187
- Si bridging epitaxy from Si windows onto SiO<sub>2</sub>, ruby laser pulse annealing 0-44441
- Si, CVD, underlying oxide layer thickness effect on in-process thickness monitoring 0-6679
- Si, CVD on SiO<sub>2</sub> and Si<sub>3</sub>N<sub>4</sub>, SEM study (*Dutch*) 0-2960
- Si, CVD on SiO<sub>2</sub> and Si<sub>3</sub>N<sub>4</sub> substrates, nucleation in SiH<sub>4</sub>-HCl-H<sub>2</sub> system at high temp. 0-49538
- Si, crystal growth conditions effect, on microdefect distrib. 0-50549
- Si, crystal growth from melt in vac., origin of SiC impurities 0-2940
- Si, crystalline sheets production, low cost, crystal growth techniques comparison 0-35083
- Si, Czochralski crystal growth, low O content 0-40251
- Si, Czochralski growth, equilib. of dissolved C and O with CO in ambient atm. 0-1949
- Si, Czochralski growth from heavily Sb doped melt, interface morphological instability 0-2939
- Si, Czochralski-grown, oxide precip. form. process 0-49364
- Si, Czochralski-grown crystals, thermally induced microdefects, annealing temp. and starting material effects 0-49141
- Si devices, application of epitaxy technology, deposition techniques 0-7501
- n-Si, dislocation free, process induced cryst. defects 0-24392
- Si, epitaxial film growth on Si(111) and sapphire (1102), simultaneous RHEED/AES study 0-10833
- Si, epitaxial growth, adsorbed layer model for autodoping mech. 0-7505
- Si epitaxial interface migration, theory and expt. test 0-29290
- Si, epitaxial layer, growth mechanism from ion-molecular beams 0-2299
- Si epitaxial layer growth in vacuum, Ar, Xe ion bombardment effect 0-39463
- Si, filamentary, grown by chem. transport reaction method, banded struct. 0-38978
- Si film, glow discharge deposition, SiH<sub>4</sub> discharge parameters obs. 0-44030
- Si film deposition by CO<sub>2</sub> laser irradi. of SiH<sub>4</sub> 0-16190
- Si, growth conditions rel. to cryst. struct. perfection (*Russian*) 0-38971
- Si, growth processes, in-situ obs. (*Japanese*) 0-35104
- Si, heteroepitaxial growth using SiH<sub>4</sub> in H<sub>2</sub>-He atm. 0-20049
- Si layer growth by CVD on Sn-coated background (*Dutch*) 0-7502
- Si, local mechanical defects, annealing and effect on autoepitaxial growth (*Russian*) 0-7701
- Si, MBE growth and surface struct. 0-10816
- Si, reactive close-spaced vapour transport, simplified theory 0-15396
- Si ribbon growth, ribbon-to-ribbon process, thermal environment control 0-35116
- Si ribbon growth by capillary action shaping technique 0-29888
- Si ribbon growth from melt, monitoring device for width and thickness uniformity 0-35077
- Si solar cells, crystal growth, heat exchanger method, fixed abrasive slicing technique 0-35082
- Si solar cells, growth of large grain polycryst. layers on graphite substrates by CVD on liquid layers 0-55849
- Si, solar-grade, directional solidification in carbon crucibles 0-45663
- Si, solid-state epitaxial growth of amorphous layer 0-10803
- Si thin autoepitaxial layers low temp. growth mechanism in SiCl<sub>4</sub>-H<sub>2</sub> system 0-20795
- Si VPE, reduced pressure, advances 0-40242



**semiconductor growth continued**

Si, VPE layer props. control using boundary layer characts. 0-50561  
 Si wafer prod., diffusion furnace temp. profile meas. systematic errors, theoretical model (*German*) 0-8989  
 Si, zone melting, swirl defects A-type as source of dislocation generation on macroscopic scale 0-25554  
 Si:H, amorphous, control and anal. of deposition, using plasma spectroscopy 0-45230  
 Si:H, amorphous film, prep. by plasma decomp. of SiH<sub>4</sub> under mag. field, and characterisation 0-45239  
 Si:N, amorphous, prep. by RF sputtering and props. 0-44229  
 Si:Ne(Ar)(Kr), amorphous, implanted and sputtered, epitaxial regrowth, influence of noble gas atoms 0-2289  
 Si:P, doping element incorporation, temp. depend. in CVD epitaxy 0-45234  
 Si:Sb, epitaxial film, growth by mol. beam technique 0-2292  
 Si-Al interface, solid phase epitaxial growth of Si 0-34324  
 SiC, epitaxial growth by sublimation sandwich method, effect of impurities 0-25568  
 SiC, epitaxial growth by direct synthesis in vacuum 0-40262  
 SiC epitaxial layer growth from sublimation in vac., kinetics 0-20791  
 SnO<sub>2</sub>, electro-conducting transparent film, props. rel. to production method (*Japanese*) 0-25557  
 SnO<sub>2</sub>:As film, prep. and elec. cond. 0-2959  
 Sn<sub>1-x</sub>Pb<sub>x</sub>Te, film, production under quasi-equilibrium conditions 0-45241  
 Te film, on electron irradi. KBr, epitaxial growth and surface coverage 0-10825  
 V<sub>2</sub>O<sub>5</sub> film, amorphous, CVD prep. method 0-55299  
 V<sub>2</sub>O<sub>5</sub> film, amorphous, thickness, density and refr. index determ. from reflectance interference spectra 0-55206  
 Zn chalcogenides, film, on NaCl, preferential epitaxy induced by electron bombard. or elec. field 0-10824  
 Zn<sub>1-x</sub>Mg<sub>x</sub>Te alloys, high purity, metallurgical and analytical methods of prep. 0-40247  
 ZnO, ZnS, growth rate, sublimation rate and etching behaviour along polar axis 0-24387  
 Zn<sub>1-x</sub>P<sub>x</sub>, single crystal, growth, electronic and device props. 0-25551  
 ZnS, Bridgeman growth under pressure, macroscopic inclusions and defects 0-45226  
 ZnS, epitaxial growth, appl. to electronic devices, review (*Japanese*) 0-55281  
 ZnS-CdS films, prep. by atomisation 0-16176  
 ZnS(Se), growth kinetics on CaF<sub>2</sub> by vapour phase transport (*French*) 0-54572  
 ZnSe, Bridgeman growth under pressure, macroscopic inclusions and defects 0-45226  
 ZnSe epitaxial layers, prep. by chem. transport reactions 0-16192  
 ZnSe:In films, MBE growth, doping effect on photoluminesc. 0-10818  
 ZnSiP<sub>2</sub> crystal growth, DTA obs. of Sn-Zn-ZnSiP<sub>2</sub> phase diagram 0-24394  
 ZnTe film preparation and props., by single-source vacuum deposition method (*Japanese*) 0-6664

**semiconductor-insulator boundaries**

capacitance meas. for Schottky barrier 0-39678  
 electrostatic interaction of charges with semiconductor-insulator interface 0-24996  
 ferrite-semiconductor structure, EM wave excitation and amplification 0-6891  
 ferrite-semiconductor structure with volume magnetostatic waves, effect of convolution 0-54761  
 III-V oxide interface state and Schottky barrier form., unified mechanism 0-44724  
 interfacial polarisation effect on dielectric props., sandwich capacitor model 0-15614  
 ionic semiconductor-oxide interface, plasmon-phonon interactions 0-44730  
 MIS transistor, mobility in inversion channel calc. (*German*) 0-6996  
 photoemission and Auger spectroscopy for anal. of semiconductor-oxide interface and Schottky barriers 0-50536  
 richardson-Schottky type photoinjection current from photoconductor into insulating liquid 0-15608  
 SOS films, cryst. quality improvement by Si ion channelling, annealing 0-44222  
 surface magnetoplasma wave spectrum in HF mag. field 0-24995  
 CdSe-SiO<sub>2</sub> thin film transistors, slow states, trapping state densities and cross sections 0-15613  
 GaAs, film and solar cell on graphite, struct. and elec. props. 0-2286  
 GaAs, GaO<sub>x</sub>N<sub>y</sub>-passivated, surface state density 0-11809  
 GaAs MIS diodes, interface states determ., by deep-level transient spectroscopy (*Japanese*) 0-49917  
 GaAs, oxidation, initial process and oxide/semicond. interface formation 0-50739  
 GaAs substrate, plasma polymerised polysiloxane film growth, dry etching process 0-25575  
 GaAs/SiON substrate/film system, interface formation during CVD, modelling 0-24764  
 GaAs-Al<sub>2</sub>O<sub>3</sub> interface, fabricated by interactive oxidation, props. 0-49935  
 GaAs-GaAs oxide interface layer characterisation by spectroscopic ellipsometry 0-50738  
 n-GaAs-oxide, plasma-grown, surface states, modified DLTS meas. 0-11094  
 GaAs-oxide interfaces, local atomic and electronic struct., high resolution XPS 0-49927  
 GaAs-Ta<sub>2</sub>O<sub>5</sub> interface, fabricated by interactive oxidation, props. 0-49935  
 GaAs(Sb), Schottky barrier and semicond./insulator interface states formation 0-49906  
 Ge (111)-amorphous SiO<sub>2</sub> or Si<sub>3</sub>N<sub>4</sub> film, dislocation interactions, substrate bending and edge effects 0-39472  
 Ge-dielectric layer interface discrete levels in Ge-metal contacts, surface treatment effects (*Russian*) 0-34497  
 Ge-metal oxide, elec. props., molecular deposition method 0-34525  
 Hg<sub>1-x</sub>Cd<sub>x</sub>Te interface with native oxide, elec. props. 0-20318  
 Hg<sub>1-x</sub>Cd<sub>x</sub>Te-oxide interfaces, MIS capacitance characts. 0-49926  
 In<sub>2</sub>O<sub>3</sub>-SnO<sub>2</sub>/Si diode solar cells, loss mechanisms, characts., band struct. 0-26135  
 InP, Schottky barrier and semicond./insulator interface states formation 0-49906  
 InP/SiO<sub>2</sub> substrate/film system, interface formation during CVD, modelling 0-24764

**semiconductor-insulator boundaries continued**

n-PbTe-oxide interface, quantized surface states in accumulation layer 0-20279  
 Si (111)-SiO<sub>2</sub> interfaces, sixth-valley state stability a priori calc. 0-49859  
 Si, CVD on SiO<sub>2</sub> and Si<sub>3</sub>N<sub>4</sub> substrates, nucleation in SiH<sub>4</sub>-HCl-H<sub>2</sub> system at high temp. 0-49538  
 Si, diffusion of P from spin-on SiO<sub>2</sub>:P film 0-2050  
 Si disc semiconductor-insulator structure, for liq. cryst. incoherent-coherent image converter 0-28342  
 p-Si film, on sapphire, elastoresist. coeffs., room temp. 0-34532  
 Si heteroepitaxial films on sapphire, vac. deposited, struct. and elec. props. 0-15390  
 Si substrate, struct. stability of dielec. film 0-54564  
 Si, thin single crystal, MeV ion scatt. and channelling obs. of interfaces 0-50492  
 Si:B, with insulating coating, mechanical stress influence on B diffusion, strained surface layers 0-29224  
 Si:P(As)(B)-SiO<sub>2</sub> interface oxidation kinetics, high doping levels, experiment 0-11828  
 Si/Si<sub>3</sub>N<sub>4</sub>, charges at laser recrystallised poly Si/insulator interface 0-54789  
 Si/SiO<sub>2</sub>, charges at laser recrystallised poly Si/insulator interface 0-54789  
 Si-Al<sub>2</sub>O<sub>3</sub> interface, charge injection from surface depletion region 0-54797  
 Si-rare earth oxide interface in MOS struct., charge density 0-7013  
 Si-sapphire interface in SOS ICs, elec. investigation 0-11097  
 Si-SiO<sub>2</sub>, anodic polarisation in electrolyte containing fluoride ions, effect on oxide props. 0-39679  
 Si-SiO<sub>2</sub>, bonding at (111) interface, stoichiometry and kinetics, synchrotron radiation photoemission spectroscopy 0-24744  
 Si-SiO<sub>2</sub>, ESR centres, interface states and oxide fixed charge 0-2474  
 Si-SiO<sub>2</sub>, H<sub>2</sub> and D<sub>2</sub> ion bombardment effects 0-34086  
 Si-SiO<sub>2</sub>, impurity redistrib. during oxidation, numerical soln. including interfacial fluxes 0-25888  
 Si-SiO<sub>2</sub>, interface, reconstructing states 0-49925  
 Si-SiO<sub>2</sub>, interface defect states obs. by constant capacitance DLTS 0-49924  
 p-Si-SiO<sub>2</sub>, inversion-channel photoelectric cell characteristic (*Russian*) 0-49941  
 Si-SiO<sub>2</sub>, oxide defect density depend. on appl. elec. field and thickness 0-19791  
 Si-SiO<sub>2</sub>, (111) interfaces, sixfold valley degeneracy in electron inversion layers 0-49936  
 Si-SiO<sub>2</sub> boundary, precipitation of Na (*Russian*) 0-49368  
 Si-SiO<sub>2</sub> interface, Au doping, trapping states 0-20319  
 Si-SiO<sub>2</sub> interface, backscattering-channelling study 0-34320  
 Si-SiO<sub>2</sub> interface, cluster Bethe-lattice method appl. 0-49852  
 Si-SiO<sub>2</sub> interface, effect of oxidation time and temp. using AES 0-35359  
 Si-SiO<sub>2</sub> interface, electrically active paramag. centres detect., photocond. reson. obs. 0-50185  
 n-Si-SiO<sub>2</sub> interface, hot carrier surface thermo EMF depend. on surface band bending 0-44734  
 Si-SiO<sub>2</sub> interface, light induced reson. centres, photocond. reson., EPR obs. 0-50184  
 Si-SiO<sub>2</sub> interface, oxidation stacking faults, growth rel. to self-diffusion 0-49239  
 Si-SiO<sub>2</sub> interface, props. variation in SiO<sub>x</sub> region 0-49548  
 Si-SiO<sub>2</sub> interface, radiation damage coeffs. for fission neutron and gamma-ray irradi. 0-34058  
 Si-SiO<sub>2</sub> interface, surface generation velocity study, gate-controlled diode structure application 0-6986  
 Si-SiO<sub>2</sub> interface, surface states characterization, expt. techniques review 0-49949  
 Si-SiO<sub>2</sub> interface, thermally grown, inhomogeneities of surface potential 0-34524  
 Si-SiO<sub>2</sub> interface layer characterisation by spectroscopic ellipsometry 0-50738  
 Si-SiO<sub>2</sub> interface oxidation kinetics, high doping levels, theory 0-11827  
 Si-SiO<sub>2</sub> interface state distribution, Br incorporation effects 0-11091  
 Si-SiO<sub>2</sub> interface state density, dependence on thermal oxidation process variables 0-15607  
 Si-SiO<sub>2</sub> interface study by XPS 0-50507  
 Si-SiO<sub>2</sub> interfaces, local atomic and electronic struct., high resolution XPS 0-49927  
 Si-SiO<sub>2</sub> interfacial region on TCE/O<sub>2</sub> and CCl<sub>4</sub>/O<sub>2</sub> oxidised Si, struct. and comp. 0-50741  
 Si-SiO<sub>2</sub> interfacial transition layer thickness, XPS obs. 0-11540  
 p-Si-SiO<sub>2</sub> system, C-V meas. using Au/Hg probe, work function difference between probe and Si 0-2450  
 Si-SiO<sub>2</sub> transition region width, SIMS depth profiling 0-39454  
 SiO<sub>2</sub>-Si, low-energy neutral particle bombardment of SiO<sub>2</sub> film, degradation 0-54790  
 SiO<sub>2</sub>-Si, P ion implantation, electrical transport props. 0-39130  
 SiO<sub>2</sub>-Si MOS capacitor, two-stage process for building up of radiation induced interface states 0-20313  
 SiO<sub>2</sub>-Si stratified system surface charges, adsorption and desorption effects (*Russian*) 0-49942  
 Si(100), inversion layer, interface induced transition at low density 0-15581

**semiconductor integrated circuits** see *monolithic integrated circuits*

**semiconductor junction lasers**

acoustic distributed feedback, resonant acousto-optic interaction in degenerate semicond. 0-19036  
 active mode locking, effect of noise 0-19030  
 communication sources, 1 μm range, LED and laser diodes 0-48448  
 composite waveguide laser with end-fire excitation, output characts. 0-23738  
 consumer's guide to laser diodes 0-14356  
 coupled multiple stripe diode lasers, exptl. and analytic studies 0-5752  
 coupling efficiency of semicond. laser beam into fibre, matching element misalignment influence 0-48432  
 defect-forming resonance electron capture, theory 0-14341  
 degradation (*Japanese*) 0-19032  
 DH diode lasers, appl. of equivalent-index method 0-23772  
 DH laser diodes, impedance characts. 0-23690  
 DH stripe laser light source to meas. Faraday effect in single-mode optical fibre 0-48245  
 dielectric optical waveguide characts. determ., far-field radiation patterns, semiconductor laser structure appl. 0-48407



## semiconductor junction lasers continued

dielectric transverse mode confinement semiconductor laser intensity fluctuation limits 0-48258  
 diffusion and rooftop etching technique 0-1227  
 diode, modulated, with short external cavity, single mode operation 0-5756  
 diode laser, optical isolator struct. simplification 0-1209  
 diode laser, principle of operation (*Polish*) 0-53294  
 electron-beam-induced stripe waveguide laser 0-28237  
 fibre communication, elimination of polarisation in optical isolators 0-5844  
 fibre optic communication systems, utilisation of optoelectronic devices 0-1328  
 GaAs laser diodes for optical communication transmission (*German*) 0-28252  
 guided-wave optical signal processing, diode laser sources and photodetectors 0-48465  
 guided-wave optical systems and devices, seminar, Washington, USA (April 1979) 0-31418  
 holographic memory devices, optoelectronic ROM memory, injection laser appls. in construction (*Polish*) 0-19007  
 III-V semiconductors, p-n heterostructures, epitaxial growth techniques, appl. to optoelectronics, review 0-54770  
 III-V semiconductors, radiative recomb. and related phenomena, conference, Prague, Czechoslovakia (Sept. 1979) 0-51940  
 injection laser, intensity pulsation enhancement by self focusing 0-48253  
 injection laser, output instabilities related to optical gain and lasing conditions 0-1203  
 injection laser diode coupling to planar waveguide 0-33245  
 injection laser output regulation by NTC resistor cct. 0-14353  
 injection lasers and appls., fundamental aspects (*German*) 0-23688  
 IR analytical instrumentation using tunable diode lasers 0-16762  
 IR spectra, intermode calibration using tandem etalons 0-32982  
 laser diodes for optical fibre transmission systems, reliability tests 0-43464  
 long lived diode laser manufacture and test procedures 0-9895  
 materials technology, review (*Polish*) 0-19029  
 MBE, device appls. 0-25570  
 near and far field characterization 0-48242  
 meas. generators of optical pulses appl. 0-23711  
 mode composition of injection laser, control with selective cavities 0-19037  
 mode selection and control, radiation freq. modulation, self-focusing (*Polish*) 0-19035  
 multilayered structures containing optically active medium, absorption and amplification of light (*Japanese*) 0-19052  
 multiple-quantum-well laser, optical analysis, three-region waveguide model 0-14337  
 narrow band gap semiconductor IR devices, advances 0-48464  
 optical fibre communication equipment 0-43459  
 optical fibre couple, lasing spectra 0-1202  
 optical fibre-laser transverse coupling and front-mirror monitoring for feedback control of laser transmitters 0-33151  
 optical isolators for semiconductor laser, in laser-to-fibre coupling module 0-48267  
 optical mode spectra, photodetector scanning and IR photography 0-48257  
 optical radiation generators, for power pulse meas. 0-23710  
 optoelectronic devices and optical imaging techniques, book 0-27059  
 pattern effect minimization at high-rate pulse modulation 0-19059  
 photon spectrum and distribution function, analogy with nonideal Bose gas 0-23689  
 planar stripe laser with deep Zn diffusion, stable transverse mode oscill. 0-14338  
 planar stripe-geometry injection laser, SWAN, mode control 0-48281  
 properties and appls., reliability (*German*) 0-19034  
 pulsed Pb salt tunable diode laser appl. to micrometer IR detect. 0-13148  
 quantum noise of injection lasers in optical fibre communication systems 0-48259  
 radiation coherence, interferometric analysis methods (*Polish*) 0-19065  
 radiation sources for 1.1 to 1.6  $\mu\text{m}$  range, p-n heterojunctions based on III-V and II-VI semiconductors (*Czech*) 0-32983  
 scanning optical microscope using semiconductor laser with longitudinal electron pumping 0-18012  
 simultaneous feedback control of bias and modulation currents for injection lasers 0-43332  
 single frequency injection laser diodes for integrated optics and fibre optic appls. 0-1237  
 single mode semiconductor laser (*Japanese*) 0-14339  
 single-mode, fabrication and oscillation characts. (*Japanese*) 0-28231  
 spatial coherence studied with reversing front interferometer 0-32993  
 stabilisation of radiated power, electronic 0-23702  
 state-of-the-art injection lasers 0-1236  
 stimulated emission, principle of operation (*Polish*) 0-53293  
 stripe contact injection lasers, heterostructure model, lateral mode control 0-14342  
 stripe-contact heterolasers, watt-ampere characts. 0-14340  
 stripe-geometry heterojunction lasers, review 0-53288  
 temperature compensated semicond. junction laser module for optical fibre communications 0-5757  
 threshold current temperature dependence potential barrier height influence 0-53296  
 TJS, single mode oscill. with low threshold currents, for optical communication 0-14355  
 TJS single-mode junction-up lasers, accelerated life tests 0-19045  
 transverse junction stripe injection laser structural improvement 0-23687  
 tunable diode laser for IR-spectroscopy (*German*) 0-43361  
 tunable diode laser spectrometry, noise reduction in appl. to hot gases 0-31909  
 wave-number stability of laser diode mounted in closed-cycle He refrigerator 0-31906  
 wavelength extension, difference freq. generation in nonlinear optical waveguide using IR generator 0-33084  
 (Al,Ga)As, ageing-induced self-pulsation stabilisation and initial degradation elimination by facet coatings 0-43347  
 (AlGa)As CW narrow stripe injection laser with induced waveguide, expt. props. 0-32988  
 AlGaAs constricted DH laser with large optical cavity, CW high-power single-mode operation 0-48276

## semiconductor junction lasers continued

(AlGa)As DH, proton-stripped, proton-induced defects, photoluminesc. study 0-48251  
 AlGaAs DH diode laser, ps optical pulse generation with RF modulated 0-9882  
 AlGaAs DH laser mirror degradation mechanism and lasing characts. changes 0-9919  
 AlGaAs DH laser preamplifier to improve optical receiver sensitivity 0-53316  
 AlGaAs DH laser with external grating oscillation properties 0-48247  
 (AlGa)As DH narrow stripe injection laser with rigid waveguide, expt. props. 0-32987  
 AlGaAs DH stripe laser, side lobe suppression by Te facet coating 0-5744  
 (AlGa)As heterostruct., proton irradi., photoluminesc. 0-29808  
 AlGaAs high-power constricted DH diode laser, for optical recording 0-43351  
 AlGaAs injection lasers, undoped, estimation of intra-band relax. time 0-43335  
 AlGaAs lasers, relaxation oscillation rel. to carrier diffusion length, spontaneous emission 0-32986  
 (AlGa)As oxide-defined strip lasers, self-sustained oscillations, ageing effects 0-32991  
 AlGaAs, principle of operation (*Hungarian*) 0-53295  
 AlGaAs resonant laser amplifier, gain and saturation power 0-53315  
 AlGaAs-GaAs CW injection heterolaser, single freq., tunable by external dispersive resonator 0-28236  
 AlGaAs-GaAs double heterostructure laser lifetime, point defect generation model calcs. 0-32992  
 AlGaAs-GaAs transverse mode stabilised plano-convex waveguide laser made by single step LPE 0-48274  
 Al<sub>1-x</sub>Ga<sub>x</sub>As buried heterostruct. laser, fabrication, optical props. and reliability 0-53322  
 Al<sub>1-x</sub>Ga<sub>x</sub>As DH laser, rake-line form. in LPE growth, doping effects 0-2287  
 Al<sub>1-x</sub>Ga<sub>1-x</sub>As laser diode, reliability 0-53320  
 Al<sub>1-x</sub>Ga<sub>1-x</sub>As laser-alloyed stripe-geometry lasers 0-5745  
 Al<sub>1-x</sub>Ga<sub>1-x</sub>As pulsating DH laser, spectral broadening 0-23686  
 Al<sub>1-x</sub>Ga<sub>1-x</sub>As-Al<sub>1-x</sub>Ga<sub>1-x</sub>As DH laser, threshold current temp. depend., potential barrier height influence 0-53296  
 Al<sub>1-x</sub>Ga<sub>1-x</sub>As-GaAs, CW 300k quantum-well heterojunction laser, optical and injection pumping operation 0-5735  
 Al<sub>1-x</sub>Ga<sub>1-x</sub>As-GaAs, DH integrated optics development 0-33240  
 Al<sub>1-x</sub>Ga<sub>1-x</sub>As-GaAs, p-n heterojunction laser, low temp. operation 0-1204  
 Al<sub>1-x</sub>Ga<sub>1-x</sub>As-GaAs, p-n heterostruct. laser, tunnel injection and phonon-assisted recomb. 0-5733  
 Al<sub>1-x</sub>Ga<sub>1-x</sub>As-GaAs DH lasers, metalorganic CVD growth and performance characts. 0-53312  
 Al<sub>1-x</sub>Ga<sub>1-x</sub>As-GaAs heterostructures, MO-CVD, phonon assisted recomb. and stimulated emission 0-1205  
 Al<sub>1-x</sub>Ga<sub>1-x</sub>As-GaAs heterostruct. lasers, metalorganic CVD 0-23692  
 Al<sub>1-x</sub>Ga<sub>1-x</sub>As-GaAs laser, made by organometallic CVD, continuous room temp. operation 0-1201  
 Al<sub>1-x</sub>Ga<sub>1-x</sub>As-GaAs multiple-quantum-well injection lasers grown by metal-organic CVD, room temp. continuous operation 0-1218  
 Al<sub>1-x</sub>Ga<sub>1-x</sub>As-GaAs quantum-well heterostructure laser diode, threshold current temp. depend. 0-43331  
 Al<sub>1-x</sub>Ga<sub>1-x</sub>As-GaAs quantum well heterostructure lasers, operation 0-53292  
 (Ga,In)(As,P) DH lasers, 1.55  $\mu\text{m}$ , low-threshold current densities 0-1221  
 Ga-Al<sub>0.27</sub>Ga<sub>0.73</sub>As DH lasers grown by MBE, growth conditions influence on threshold current density 0-32984  
 GaAlAs based heterojunctions, integrated optics appl., technology advancements (*Slovak*) 0-33226  
 (GaAl)As buried-heterostructure laser with buried optical guide, highly efficient operation 0-1219  
 (GaAl)As DH laser, gradual degradation accel. as exponent of driving current value 0-32990  
 GaAlAs DH laser, In solder deterioration, Au diffusion in In 0-33019  
 (GaAl)As DH stripe contact injection lasers, local attached data fibre link appls. 0-19044  
 GaAlAs DH stripe geometry lasers, degradation phenomena 0-53290  
 (GaAl)As heterojunction laser with distributed Bragg refl., mode switching 0-43336  
 GaAlAs heterostructure lasers, fine-structure in spectra 0-19033  
 GaAlAs injection lasers, stability in single transverse mode operation 0-38027  
 GaAlAs injection laser, monolithic integration with Schottky-gate FET 0-48275  
 GaAlAs lasers, return-beam-induced noise generation model 0-48244  
 GaAlAs-GaAs DH laser diodes, long-life diodes for optical fibre communication 0-48246  
 GaAlAs-GaAs DH lasers, degradation caused by growth of dislocation networks 0-53289  
 Ga<sub>1-x</sub>Al<sub>x</sub>As buried heterostructure lasers for analogue communication 0-48297  
 Ga<sub>1-x</sub>Al<sub>x</sub>As DH catastrophically degraded laser, TEM obs. of defects 0-32989  
 Ga<sub>1-x</sub>Al<sub>x</sub>As, deep level-dislocation interactions, DLTS meas. 0-29357  
 Ga<sub>1-x</sub>Al<sub>x</sub>As junction-up TJS laser electron injection efficiency improvement 0-48300  
 Ga<sub>1-x</sub>Al<sub>x</sub>As pulsed injection laser, SHG in KNbO<sub>3</sub> 0-5785  
 Ga<sub>1-x</sub>Al<sub>x</sub>As stripe laser with stable transverse mode structure 0-48298  
 Ga<sub>1-x</sub>Al<sub>x</sub>As symmetrised epitaxial variable-gap waveguide, coherent radiation generation 0-38018  
 Ga<sub>1-x</sub>Al<sub>x</sub>As transverse mode DH laser with inbuilt plano-convex waveguide 0-48296  
 Ga<sub>1-x</sub>Al<sub>x</sub>As visible diode lasers, degradation 0-43330  
 Ga<sub>1-x</sub>Al<sub>x</sub>As-GaAs narrow stripe laser for improved communication performance 0-48299  
 Ga<sub>1-x</sub>Al<sub>1-x</sub>As injection heterojunction distributed output laser, exptl. study 0-43369  
 Ga<sub>1-x</sub>Al<sub>1-x</sub>As-GaAs double heterostructure laser diode, temp. depend. of photolum. 0-5734  
 GaAlAsSb/GaSb, for LW optical communication systems 0-10043  
 GaAlAsSb/GaSb alloys, prep. and optoelectronic device appl. 0-25587  
 GaAs CW injection laser diode specification for integrated optical circuits 0-33034  
 GaAs DH, for data recording on optical disc 0-19001



**semiconductor junction lasers continued**

- GaAs DH laser, alloying of ohmic contacts, Nd:YAG laser irradiation 0-43357
- GaAs DH laser, self-induced modulation, noise, instability 0-48250
- GaAs distributed Bragg reflection lasers, large optical cavity, optimal design 0-38028
- GaAs electrooptically tuned external-cavity CW injection laser, FM optical communication appl. 0-14351
- GaAs injection laser, active region effect on single-freq. stimulated emission conditions 0-9884
- GaAs injection laser, output instabilities related to optical gain and lasing conditions 0-1203
- GaAs injection laser, single heterostruct., mode competition effects, tuning characts. 0-48255
- GaAs injection lasers, amplified luminesc. 0-2824
- GaAs laser facsimile printer 0-30207
- GaAs,  $\text{Si}_{1-x}\text{C}_x$  protective coating 0-5753
- GaAs single-channel injection laser, polarisation characts. 0-48256
- GaAs stripe-geometry laser, nonlinear temp. characteristics (*Chinese*) 0-43337
- GaAs-(GaAl)As DH lasers, automated LPE growth, CW reliability tests 0-20804
- GaAs-Al<sub>1-x</sub>Ga<sub>x</sub>As current injection multi-quantum-well heterostructure lasers, MBE grown 0-19042
- GaAs-Al<sub>1-x</sub>Ga<sub>x</sub>As DH broad contact pulse lasers, second-order coherence props. 0-23685
- GaAs-Al<sub>1-x</sub>Ga<sub>x</sub>As DH lasers, very low current threshold, MBE grown 0-43353
- GaAs-Al<sub>1-x</sub>Ga<sub>x</sub>As DH lasers, MBE grown, substrate temp. effect on current threshold 0-48243
- GaAs-Al<sub>1-x</sub>Ga<sub>x</sub>As strip buried heterostructure laser with passive DBR 0-14352
- GaAs-AlAs multilayer heterostructure laser, power and photoelectroluminescence characts. 0-53297
- GaAs-AlGaAs DH injection laser, emission energy, wavelength depend. in strong mag. fields 0-48248
- GaAs-AlGaAs DH laser, degradation rate rel. to photocurrent 0-28233
- GaAs-Ga<sub>1-x</sub>In<sub>x</sub>P heterostruct., MBE layers, photolum. props., assessment as laser struct. 0-20705
- GaAs-GaAlAs, heterostructure laser diode, lasing threshold calc. 0-28232
- GaAs-GaAlAs CW diode laser, lateral mode stabilization using apertured facet reflectors 0-23708
- GaAs-GaAlAs CW injection laser, stripe geometry DH, temporal coherence 0-38016
- GaAs-GaAlAs channelled-substrate narrow-stripe lasers, low threshold currents 0-23706
- GaAs-GaAlAs DH injection laser, integrated optics techniques 0-33033
- GaAs-GaAlAs laser, degraded, characterisation by selective etching and photoetching 0-48252
- GaAs-GaAlAs laser, practical appls. 0-1212
- GaAs-GaAlAs nonplanar large optical cavity laser, pulsed room temp. operation 0-28244
- GaAsAl<sub>1-x</sub>Ga<sub>x</sub>As heterostruct., anomalous elec. and optical characts. 0-2865
- GaAsP/InP diodes for 1.56  $\mu\text{m}$  CW operation 0-48254
- GaInAsP/InP DH lasers, direct modulation charact. meas. by sharp pulse method 0-1245
- (GaIn)(AsP)/InP DH 1.27 micron lasers, nonradiative carrier loss and temperature sensitivity of threshold 0-43333
- GaInAsP/InP system, chemical etching, fabricating laser diodes and integrated optical circuits 0-38030
- GaInAsP/InP DH lasers, 1.1 to 1.3  $\mu\text{m}$ , fibre optics communications 0-14360
- GaInAsP/InP DH laser, room temp. CW laser 0-28235
- GaInAsP/InP DH lasers made by melt-back method, operating characteristics 0-48287
- GaInAsP/InP DH lasers, LPE growth and operational characts. 0-53313
- GaInAsP/InP DH injection lasers prep. by LPE, 1.11-1.67  $\mu\text{m}$  operation 0-53321
- GaInAsP/InP facet lasers with chemically etched end mirrors 0-1228
- GaInAsP/InP mesa substrate buried heterostruct. injection laser, fabrication and lasing props. 0-53319
- GaInAsP/InP planar stripe lasers, sputtered  $\text{SiO}_2$  film as Zn-diffusion mask 0-48249
- GaInAsP/InP surface emitting injection laser, fabrication and lasing props. 0-28234
- Ga<sub>1-x</sub>In<sub>x</sub>As<sub>1-y</sub>P<sub>y</sub> laser, room temp. electron-beam-pumped laser with dielec. waveguide, output characts. 0-5761
- GaInAsSb/GaSb DH lasers, 2 micron CW operation at 80K 0-53291
- Ga<sub>1-x</sub>In<sub>x</sub>P<sub>y</sub>As<sub>1-y</sub> laser, DH integrated optics development 0-33240
- In<sub>1-x</sub>Ga<sub>x</sub>As layers, on GaAs substrate, MBE fabrication and laser operation 0-10820
- InGaAsP DH laser characts., temp. depend. 0-1223
- InGaAsP InP DH lasers, optical power and wavelength stabilisation 0-38036
- InGaAsP single-mode CW ridge waveguide laser emitting at 1.55 micron for optical fibre links 0-9883
- InGaAsP/InP, for LW optical fibre communication 0-9885
- InGaAsP/InP, for graded-index fibre cables, transmission meas. in 1.2 to 1.6  $\mu\text{m}$  range 0-10037
- InGaAsP/InP, for LW optical communication systems 0-10043
- InGaAsP/InP DFB injection lasers 0-5746
- InGaAsP/InP DH laser, self-aligned struct. 0-9893
- InGaAsP/InP heterostruct. lasers as optical source, CW operation at room temp. 0-1220
- InGaAsP/InP, double heterostructure laser lifetime, point defect generation model calcs. 0-32992
- InGaAsP/InP, LPE, 1.5  $\mu\text{m}$  range, effects of double cladding struct. 0-48290
- InGaAsP/InP DH laser with self-aligned struct., oscillation characts. 0-38017
- InGaAsP/InP embedded mesa strip lasers 0-14350
- In<sub>1-x</sub>Ga<sub>x</sub>As<sub>1-y</sub>P<sub>y</sub> DH laser, low threshold current density, near equilibrium LPE growth 0-19040
- InGaAsSb, LPE growth, and appl. in GaSb/AlGaAsSb/InGaAsSb/AlGaAsSb/GaSb DH 0-16205
- InGaAsSb-AlGaAsSb DH laser, room temp. operation at 1.8  $\mu\text{m}$  wavelength 0-43358
- In<sub>1-x</sub>Ga<sub>x</sub>As<sub>1-y</sub>Sb<sub>1-y</sub> laser, nonequilibrium carrier recombination, luminesc. study 0-50431
- In<sub>1-x</sub>Ga<sub>x</sub>P electron-beam-pumped, LPE and VPE growth 0-2281

**semiconductor junction lasers continued**

- InGaPAs-InP DH laser, threshold current temp. depend., potential barrier height influence 0-53296
- In<sub>1-x</sub>Ga<sub>x</sub>P<sub>1-y</sub>As<sub>y</sub> electron-beam-pumped, LPE and VPE growth 0-2281
- InP-Ga<sub>1-x</sub>In<sub>x</sub>P<sub>1-y</sub>As<sub>y</sub> heterostruct. lasers, growth and characterisation 0-23691
- InP-In<sub>1-x</sub>Ga<sub>x</sub>P<sub>1-y</sub>As<sub>y</sub> heterostructure laser, single and multiple quantum-well, liquid-phase epitaxial growth 0-38031
- InP-InGaAsP-InP DH diode lasers, room temp. CW operation 0-1222
- Pb chalcogenide diode lasers, recent advances 0-5732
- PbS current tunable p-n junction laser (*Polish*) 0-32985
- Pb<sub>1-x</sub>Sn<sub>x</sub>Se laser, optical feedback effects on performance, external cavity modes 0-32981
- Pb<sub>1-x</sub>Sn<sub>x</sub>Te DH laser, minority carrier lifetimes and lasing thresholds 0-19031
- Pb<sub>1-x</sub>Sn<sub>x</sub>Te heterojunction lasers, instantaneous vacuum evaporation grown, threshold current density 0-5759
- ZnSe-GaAs narrow junction lasers 0-43334

**semiconductor junctions**

- see also p-n junctions
- electric field effect on thermal emission of traps 0-11073
- electron-phonon scatt. 0-24997
- heterojunction, band-edge discontinuities and interface pot. step, two-band narrow-gap approach 0-39665
- heterojunction interfaces energy band discontinuities nontransitivity 0-44714
- interface and surface phenomena, conference, Pacific Grove, USA (Jan.-Feb. 1979) 0-46725
- multilayer heterojunction struct., impurity and phonon scatt. 0-2456
- multilayer semiconductor structures, plasma-wave beams 0-49795
- p<sup>+</sup>-n-n<sup>+</sup> heterostructure, variable gap base, carrier injection, quasioelectric field, transient process anal. 0-44716
- superlattices, optical and transport props., review (*Slovak*) 0-20288
- tunnel-effects in junctions generating burst-noise (*Rumanian*) 0-6960
- Al<sub>1-x</sub>Ga<sub>x</sub>As-GaAs, heterojunction, interface width, AES obs. 0-20290
- Al<sub>1-x</sub>Ga<sub>x</sub>As-GaAs n-n heterojunction, interface width determ. 0-49887
- As<sub>50</sub>Te<sub>50</sub>, amorphous films, metal and semicond. contacts, threshold switching, IR emission 0-49831
- C, amorphous, struct. and semicond. props. and heterojunction form. with single cryst. Si 0-25002
- CdTe-HgTe ideal superlattice, electronic props. calc. 0-49885
- Ga<sub>1-x</sub>Al<sub>x</sub>As n-p<sub>1</sub>-p<sub>2</sub>-p<sub>1</sub>-p<sub>0</sub> struct., degradation electrochem. 0-50428
- GaAs epitaxial layers, structural defect and conc. inhomogeneities influence on barrier diode I-V characts. 0-15602
- GaAs, intrinsic, on degenerate n-Ge, surface polaritons, hydrodynamical model 0-6752
- GaAs-Ga<sub>0.7</sub>Al<sub>0.3</sub>As n-n heterojunction, LPE, rectification 0-49888
- GaAs-Ga<sub>1-x</sub>Al<sub>x</sub>As, variable band gap, photo-EMF 0-20296
- GaAs-Ge interface, photoemission 0-25530
- n-GaAs-n-GaN, diffusion growth kinetics, morphology and electrical properties 0-20294
- n-GaAs-n<sup>+</sup>-Al<sub>1-x</sub>Ga<sub>x</sub>As production, by MBE (*German*) 0-44711
- GaP:Fe n-i-n epitaxial struct., photoconductivity, recombination scheme (*Russian*) 0-15569
- InAs-GaSb (001) superlattices, two-dimens. effects and effective masses 0-49883
- InAs-GaSb (100) superlattice, electronic struct., self-consistent pseudopot. method 0-49884
- InAs-GaSb superlattice, electronic struct., self-consistent pseudopot. calc. 0-29470
- InAs-GaSb superlattice, semiconductor-semimetal transition obs. 0-44710
- InAs-GaSb superlattices, crystallography, Rutherford backscatt. and channelling obs. 0-49533
- InAs-GaSb superlattices, semicond.-semimetal transition obs. 0-49882
- In<sub>1-x</sub>Ga<sub>x</sub>P<sub>1-y</sub>As<sub>y</sub> laser, LPE, lattice matching, phase 0-54350
- In<sub>1-x</sub>Sn<sub>x</sub>O<sub>3-y</sub>(SnO<sub>2</sub>)-CdSe-CdS:Cd,Cl sandwich photoconductor injection obs. (*Russian*) 0-54773
- Si, n-n<sup>+</sup> point junctions 0-44719
- Si:Cd n<sup>+</sup>-n-n<sup>+</sup> struct., photoresist. props. under exclusion conditions 0-39666
- Si:Zn, p-n-n<sup>+</sup> and p-n-p struct., reson. characts. of impedance near excitation threshold of recomb. waves 0-20301
- Si/Si-Ge alloy, amorphous, solar cell, multijunction structure, increased conversion efficiencies, low cost 0-45677
- Si-CdSe n-n heterojunction, photovoltage sign reversal, energy band profile (*Korean*) 0-29469
- n-Si-SiC film junction device, elec. props. 0-15591
- SnO<sub>2</sub>-InSe n-n heterostructures, photoelec. props., 80 to 300K 0-20297
- SnO<sub>2</sub>-Si heterojunction solar cell, elec. props. (*Korean*) 0-45665
- SnO<sub>2</sub>-Si heterojunctions, elec. and photovoltaic props. 0-26141
- ZnSe-Ge (100) interface, electronic struct. calc., scattering theoretic approach 0-6940

**semiconductor materials**

- see also amorphous semiconductors; degenerate semiconductors; elemental semiconductors; heavily doped semiconductors; II-VI semiconductors; III-V semiconductors; III-VI semiconductors; IV-VI semiconductors; liquid semiconductors; magnetic semiconductors; many-valley semiconductors; narrow band gap semiconductors; organic semiconductors; polar semiconductors; semiconductors; ternary semiconductors
- n-(Bi<sub>1-x</sub>Sb<sub>x</sub>)<sub>2</sub>Te<sub>3</sub>, magnetoresist. in quantising mag. field 0-24953
- Cu<sub>2</sub>S-CdS solar cell, interface recombination and junction field studies, exptl. technique 0-45683
- FeS<sub>2</sub>, thin films, prep. and charact. 0-16178
- rare earth compounds, R<sub>2</sub>MoO<sub>5</sub>, cryst. struct., IR spectra, elec. and mag. props. 0-33954
- rare earth pyrochlores, R<sub>2</sub>(V<sub>4/3</sub>W<sub>3/3</sub>)O<sub>7</sub>, (R=Gd, Tb, Dy, Ho, Er, Tm, Yb, Lu), synthesis and elec. props. 0-29914
- $\beta$ -SiC, optical quenching of luminesc., acceptor ionisation energy 0-55178
- (2CdTe)<sub>1-x</sub>(In<sub>1-x</sub>Sn<sub>1-x</sub>)<sub>1-x</sub>, x=0.25, 0.5, 0.75, tetrahedral semiconductor, chem. interaction of Sn atoms, Mossbauer study 0-39977
- AgBr, electron-hole liquid, RPA calcs. 0-6743
- AlH<sub>3</sub>, dark electrical cond., exam. 0-39624
- AlH<sub>3</sub>, polycrystalline, photoconductivity and photochemical decomp. 0-44638
- As<sub>2</sub>O<sub>3</sub>, crystalline and amorphous, EXAFS study of struct. 0-19776
- As<sub>2</sub>S<sub>3</sub> film, vacuum deposited, selective etching characts. obs. (*Russian*) 0-3207
- As<sub>2</sub>Se<sub>3</sub>, photosensitive layer, in metal-photoconductor-insulator multilayered struct., optical image recording 0-42286



## semiconductor materials continued

- B-Si compounds, thermoelec. material, prep. by pyrolysis of  $\text{BBr}_3\text{-SiBr}_4$  mixture 0-20862  
 $\text{Bi}_2\text{C}_3$ , phonon energies and electronic props.,  $x$  depend., refl. spectra and thermoelec. power meas. 0-16052  
 $\text{Bi}_4\text{S}_3$ ,  $\beta$  rhombohedral, conduction mechanism, thermoelectric props. 0-24932  
 $\text{Bi}_4\text{S}_3$  elec. props., medium range disorder model 0-15522  
 $\text{BaF}_2$  solid electrolyte, n-type electronic cond., 700-900°C 0-29448  
 $(\text{Be, Al})\text{Bi}_{12}$ , elec. cond., refl. and absorpt. spectra 0-20188  
 $(\text{Bi, Sb})\text{Te}_3$  solid soln., semiconductor film, oxidation, electrophysical props. 0-45407  
 $\text{Bi-Sb}$  alloys, lattice dielec. const., comp. depend. 0-39516  
 $\text{Bi}_2\text{O}_3$ , thermoelec. props., 500-1500K 0-29423  
 $\text{Bi}_{1-x}\text{Sb}_x\text{Te}_{1-x}\text{Se}_x$  solid solution, density-of-states effective mass, carrier mobility temp. depend. 0-24931  
 $\text{Bi}_2\text{Se}_3$ , mechano-caloric energy conversion 0-10962  
 $\text{Bi}_{12}\text{SiO}_{20}$ , visible and UV refl. and absorpt. spectra 0-34950  
 $\text{Bi}_2\text{Te}_3$ , anodic oxide films, two-dimens. nucleation and growth 0-11807  
 $\text{Bi}_2\text{Te}_3$ , constant current anodisation, representation of layer periodicity 0-3218  
 $\text{Bi}_2\text{Te}_3$ , mechano-caloric energy conversion 0-10962  
 $\text{Bi}_2\text{Te}_3$  single crystals, melt grown, structural perfection 0-15101  
 $\text{Bi}_2\text{Te}_3\text{-Bi}_2\text{Se}_3$  thermoelectric alloys, diffusion and evaporation of volatile component during prep. 0-35118  
 $\text{Bi}_2\text{Te}_3\text{-SbTe}_3$ , ordered structure formation, heat treatment effect on thermal cond. 0-54448  
 $\text{Bi}_2\text{Te}_3\text{Se}_{0.12}$  magnetoresistance and Hall EMF meas., using AM method 0-52278  
 $n\text{-Bi}_2\text{Te}_{3.8}\text{Se}_{0.12}$ , extrusion deformed, powder dispersion degree influence on thermal and elec. props. (Russian) 0-39366  
 $\text{Bi}_2\text{Te}_3\text{-Se}_x$  films, surface band struct. and scatt. mechanism 0-34535  
 $\text{Cd}_{1-x}\text{Mn}_x\text{Te}$ , exchange interaction, magneto-optical spectra 0-25348  
 $\text{CdAs}_2$ , thermoelec. props., anisotropy 0-34470  
 $\text{Cd}_3\text{As}_2$ , anisotropy of electronic  $g^*$ -factor 0-44483  
 $\text{Cd}_3\text{As}_2$ , electron effective mass. temp. depend., Hall effect and thermoelec. power meas. 0-39613  
 $\text{Cd}_3\text{As}_2$  platelet, single vap.-grown cryst., passive annealing, Fermi energy variation 0-45223  
 $\text{Cd}_3\text{As}_2$ , Shubnikov-de Haas effect 0-11020  
 $\text{Cd}_3\text{As}_2$ , thermal dissoc., 550-850°C 0-35512  
 $\text{Cd}_3\text{As}_2$  type crystals, symmetry props. of energy bands 0-39500  
 $\text{CdF}_2$ , conversion into semicond. by heating in  $\text{H}_2$  atm., resist. meas. 0-20978  
 $\text{Cd}_2\text{GeO}_4$ , n-type, prep. and photoelectronic props. 0-39628  
 $\text{CdMnTe}$ , exciton ground state, magnetic field influence 0-54616  
 $\text{Cd}_0.6\text{Mn}_{0.4}\text{Te}$  crystals,  $\text{Mn}(3d^5)$  band, photoemission evidence 0-11535  
 $\text{CdP}_4$  single crystal growth 0-35065  
 $\text{CdP}_4$ , thermodynamic functions, 55-300K 0-34203  
 $\text{Cd}_2\text{P}_2$ , band struct.,  $D_{4h}^{15}$  space group symmetry props. 0-34357  
 $\text{CdSb}$ , energy spectrum, influence of chem. bonds, LCAO calc. 0-34356  
 $\text{CeO}_2\text{S}$ , acceptor properties of S, free electron concentrations 0-34395  
 $\text{CeO}_2$ , in  $\text{O}_2 + \text{CO}_2 + \text{SO}_2$  atmosphere, elec. cond. study 0-39583  
 $\text{Co}_2\text{NiO}_4$ , powder prep. by freeze drying of solid solutions, solvent choice 0-11583  
 $\text{Co}_3\text{O}_4\text{-Li}(\text{Cr})(\text{Al})(\text{S})$ , and pure  $\text{Co}_3\text{O}_4$ , elec. cond. and thermo-EMF 0-20231  
 $\text{Co}_3\text{O}_4\text{S}$ , defect struct. and elec. props., electron, hole conc. 0-44601  
 $\text{Cr}_2\text{S}_3\text{-Se}_x$ , elec. resist., thermal cond. and Seebeck coeff. meas. 0-24958  
 $\text{CuBr}$ , IS exciton triplet state, magneto-optical props. 0-25345  
 $\text{CuBr}$ , exciton absorpt. band shape, dielectric const. real part derivatives (Russian) 0-25413  
 $\text{CuBr}$ , P exciton fine struct. 0-20091  
 $\text{CuBr}(\text{Cl})(\text{I})$ , energy bands, relativistic KKR method, UV absorpt. spectra 0-39501  
 $\text{CuCl}$ , donor-acceptor recomb. spectra 0-45131  
 $\text{CuCl}$ , energy bands and effective mass 0-10859  
 $\text{CuCl}$ , excitonic polariton, picosecond time of flight meas. 0-29337  
 $\text{CuCl}$ , propagation process of polaritons (Japanese) 0-24809  
 $\text{CuCl}$ , two-photon absorpt. and luminesc., biexcitons 0-11434  
 $\text{CuCl}$ , XPS and Auger spectroscopy, elec. struct. 0-29852  
 $\text{Cu}(\text{Mo}_2\text{Re}_2)\text{S}_8$ , synthesis and electrical props. of mixed tetrahedral cluster phases 0-2971  
 $\text{Cu}_2\text{O}$ , energy band interactions under uniaxial compression 0-25412  
 $\text{Cu}_2\text{O}$ , resonant Raman and Brillouin spectroscopy, review, book contrib. 0-49624  
 $\text{Cu}_2\text{O}$ , sample thickness depend. of exciton polariton absorption coeff. 0-34941  
 $\text{Cu}_2\text{S}$ , optical and calorimetric meas. of thin films for  $\text{Cu}_2\text{S-CdS}$  solar cells 0-55863  
 $\text{Cu}_2\text{S}$ , polycryst. thin films, struct., optical and elec. props. for solar energy appl. 0-10837  
 $\text{Cu}_2\text{S}$ , thermoelectric props. 0-54726  
 $\text{Cu}_2\text{S/CdS}$  solar cell, design and fabrication 0-30481  
 $\text{Cu}_2\text{S-CdS}$  heterojunction solar cell, interface recomb. vel. determ. by capacitance/collection efficiency variation 0-50959  
 $\text{Cu}_2\text{S-CdS}$  solar cells, EBIC and capacitance measurements, stability problems 0-45684  
 $\text{Cu}_{2-x}\text{S/CdS}$  heterostructures, heat treated, capacitance voltage meas. anal. 0-20292  
 $\text{Cu}_2\text{S}$  evaporated thin films, composition, prep. and characs. 0-25569  
 $\text{Cu}_2\text{S-CdS}$  solar cells, screen printed, prep. and photovoltaic props. 0-40863  
 $\text{Cu}_{2-x}\text{Se}$ , electrical activity of Cu vacancies 0-39606  
 $\text{Cu}_{2-x}\text{Te}$ , electrical activity of Cu vacancies 0-39606  
 $\text{Cu}_3\text{VS}_4$ , conducting ions as mobile donors 0-11055  
 $\text{Cu}_3\text{VS}_4$ , Raman active modes 0-11414  
 $\text{Eu}_2\text{Sb}_3$ , cryst. struct., elec. and mag. props. 0-33958  
 $\text{Fe}(\text{Mo}_2\text{Re}_2)\text{S}_8$ , synthesis and electrical props. of mixed tetrahedral cluster phases 0-2971  
 $n\text{-Fe}_2\text{O}_3$  electrodes, characterisation and behaviour in acetonitrile solns. 0-25004  
 $\text{Fe}_x\text{O}_y$  thermal oxide film on Fe, capacitance, temp. and freq. depend., in aq. electrolyte soln. 0-54776  
 $\alpha\text{-FeP}_4$ , diamag., semicond., Mossbauer study 0-50243  
 $\text{FeS}_3$ , ionisation loss spectra, density of unoccupied states 0-55241  
 $\text{FeS}_2$ , pyrite, semiconducting props., energy gap press. and lattice parameter depend., Mossbauer obs. 0-44494  
 $(\text{GaAs})_x(\text{ZnSe})_{1-x}$  single crystal, visible cathodoluminesc. spectra 0-20716

## semiconductor materials continued

- $\text{Ga}(\text{Mo}_2\text{Re}_2)\text{S}_8$ , synthesis and electrical props. of mixed tetrahedral cluster phases 0-2971  
 $\text{GaSb-GaAs-Ge}$  system, props. and struct. 0-20232  
 $\text{Ga}_2\text{Se}_3$ , evaporation, thermodynamic props. 0-54365  
 $\text{Ga}_2\text{Te}_3$  single crystals, switching effect., carrier trapping 0-6919  
 $\text{Gd}_2\text{S}_3$ , resonance excitation of  $\text{Gd}^{3+}$ , luminescence, absorption spectra (Russian) 0-50381  
 $\alpha\text{-Gd}_2\text{S}_3\text{-Nd}^{3+}$ , spectroscopic props. from absorpt., photoluminesc. and excitation spectra 0-34968  
 $(\text{Ge,Pb})_{1-x}\text{Mn}_x\text{Te}$ , Te, mag. and elec. props. meas. 0-29534  
 $\text{Ge-GaAs}$ , crystallisation at superhigh cooling rates 0-54349  
 $\text{Ge-metal}$  films codeposited, amorphous and polycryst., struct. and elec. props. 0-24766  
 $\text{Ge-Se-Ga}$  thin film, elec. cond., switching phenomena (Polish) 0-11120  
 $\text{Ge-Si}$  alloys, defect modes and optical spectra 0-11413  
 $\text{Ge-Si:Sb}$ , energy spectrum of Sb 0-34382  
 $\text{GeO}_2$ , band struct., tight-binding calc. 0-24796  
 $\text{GeSe}_3$ , single crystals, 3 polymorphic forms, DTA, photolum., IR and Raman spectroscopy 0-33923  
 $\text{GeTe-MnTe}$ , heat treatment effect on struct., elec. props. 0-54725  
 $\text{HfS}_3$ , one-dimensional semicond., Raman spectra meas. 0-50345  
 $\text{HfSe}_2\text{-Te}_x$ , elec. resist. and mag. suscept. studies 0-44599  
 $\alpha\text{-HgI}_2$ , Raman scatt. at room temp., improved polarisation spectra 0-25368  
 $\text{HgI}_2$ , red anisotropic polariton dispersion, reson. Brillouin scatt. 0-7366  
 $\alpha\text{-HgI}_2$ , single cryst. growth from iodomercurate complexes 0-35069  
 $\text{Hg}_{1-x}\text{Mn}_x\text{Te}$ , energy levels at  $\Gamma$ -point in intense mag. fields, Shubnikov-de Haas effect meas. 0-24951  
 $\text{Hg}_{1-x}\text{Mn}_x\text{Te}$ , magneto-optical and impurity effects 0-6721  
 $\text{I}_2\text{Li}(\text{Na})(\text{K})(\text{Cs})(\text{Be})(\text{Mn})(\text{Fe})(\text{Cr})$ , doping effect on elec. cond., semicond. props. 0-49732  
 $\text{In}_2\text{O}_3$  thin film on polyester substrate, struct. determ. by TEM 0-6674  
 $\text{In}_2\text{O}_3$ , transparent heat mirror formation by ion plating on ambient temp. substrates and props. 0-25578  
 $\text{In}_2\text{O}_3\text{-Sn}$  films, pure and doped, prod. by ion plating, elec. and optical props. 0-2488  
 $\text{In}_2\text{O}_3\text{-Sn-Si}$  heterojunctions, current mechanisms and barrier height 0-11083  
 $\text{In}_2\text{S}_7$ , TSC at various cooling rates (Russian) 0-11000  
 $\text{InSb-NiSb}$  eutectic, struct. and optical props., IR polariser appl. 0-45078  
 $\alpha\text{-In}_2\text{Se}_3$ , X-ray diffr. line broadening 0-49047  
 $\text{In}_2\text{Se}_3\text{-Cu}_2\text{S}$  system, electrophys. props., influence of 1-4%  $\text{Cu}_2\text{S}$  0-20219  
 $(\text{In}_{1-x}\text{Sn}_x)_2\text{O}_3\text{-Si-N}$  solar cell efficiency and elec. props. 0-35676  
 $\text{In}_{2-x}\text{Sn}_x\text{O}_{3-y}\text{-CdTe}(\text{InP})$  photovoltaic heterojunctions, surface and interface studies, efficiency 0-45691  
 $\text{In}_2\text{Te}_3$  defect semicond., photoconductivity kinetics 0-11035  
 $\text{In}_2\text{Te}_3$  film thermal deposition, transmission spectra and elec. cond. (Russian) 0-49555  
 $\text{In}_2\text{Te}_3$ -type semiconductor, mechanism of electrically inactive impurities 0-24834  
 $\text{In}_2\text{Te}_3$ , photocond. and absorption spectra, polarisation dependences 0-20642  
 $\text{La}_{1-x}\text{Sr}_x\text{CoO}_{3-y}$ , Seebeck coeff. meas., small polaron hole conduction model 0-20233  
 $\text{MnCo}_2\text{O}_4$  DC sputtered films, struct. and elec. props. 0-54812  
 $\text{Mn}_3\text{O}_4\text{-Li}(\text{Cr})(\text{Al})(\text{S})$ , and pure  $\text{Mn}_3\text{O}_4$ , elec. cond. and thermo-EMF 0-20231  
 $\text{Mn}_3\text{O}_4\text{S}$ , defect struct. and elec. props., electron, hole conc. 0-44601  
 $\text{MnSe}$ , and  $\text{MnSe}_2$ , thermodynamic props. 0-19958  
 $(\text{MnTe})_{1-x}(\text{Bi}_2\text{Te}_3)_x$  ( $x \leq 0.05$ ) solid solution, electrophys. props. 0-24925  
 $\text{MoS}_2$ , clean surface, AES and LEED exam. 0-10762  
 $\text{MoS}_2$ , surface electronic struct., slow electron reflection, total current spectroscopy (Russian) 0-54759  
 $\text{MoS}_2$ , synthetic molybdenite single crystals, growth from vapour, elec. props. 0-34446  
 $\text{MoSe}_2\text{-I}$ , photoelectrode, time resolved photocurrent, nanosecond excitation 0-45708  
 $\text{NbO}_2$ , semicond., thermal expansivity 0-34213  
 $\text{NbO}_2$ , threshold switching recovery curve, distribution trapped carrier lifetime 0-20258  
 $\text{Nb}_2\text{O}_5$  electrodes, in aq. and acetonitrile solns., electrochromism 0-50298  
 $\text{NbS}_3$ , phase transitions and elec. props. 0-20178  
 $\text{NbS}_3$ , transport props. 0-20175  
 $\text{Ni}(\text{Mo}_2\text{Re}_2)\text{S}_8$ , synthesis and electrical props. of mixed tetrahedral cluster phases 0-2971  
 $\text{NiO}$  and lithiated  $\text{NiO}$ , thermally grown, electrochemical capacitance variations 0-29475  
 $\text{NiO-Li}_2\text{O-ZnO}$  p-n heterojunction, contact resist., effects of water vapour 0-34506  
 $\text{PbI}_2$  crystals, exciton condensation, excitation and luminesc. study 0-55182  
 $\text{PbI}_2$ , direct gap semiconductor, exciton lifetime and condensation threshold, luminescence spectra 0-34981  
 $\text{PbI}_2$ , exciton absorpt. band shape, dielectric const. real part derivatives (Russian) 0-25413  
 $\text{PbI}_2$ , exciton magneto-optical spectra 0-25347  
 $\text{PbI}_2$ , film, reflectance meas., optical consts., humidity effects 0-34994  
 $\text{PbI}_2$ , layered cryst. under uniaxial compression, low temp. thermal cond. (Russian) 0-44374  
 $\text{PbI}_2$ , thin cryst. barrier, reson. and inelastic tunnelling 0-44739  
 $\text{PbI}_2$ , three-photon absorpt. coeff. determ. by nonlinear luminesc. expt. 0-14384  
 $\text{PbI}_2$ , visible exciton spectrum, exciton-phonon interactions, dielectric const. and oscill. strengths 0-25405  
 $p\text{-Sb}_{1.48}\text{Bi}_{0.52}\text{Te}_3$ , extrusion deformed, powder dispersion degree influence on thermal and elec. props. (Russian) 0-39366  
 $\text{Sb}_2\text{O}_3$ , thermoelec. props., 500-1500K 0-29423  
 $\text{Sb}_2\text{Se}_3$ , photocond., photo-EMF and photodielectric effect, expts. 0-20245  
 $\text{Sb}_3\text{Se}_{6.5}$ , polycrystalline, elec. cond. mech. 0-49705  
 $\text{Sb}_2\text{Te}_3$  epitaxial films, growing conditions effect on elec. cond., thermo-EMF 0-39687  
 $\text{Sb}_2\text{Te}_3$ , mechano-caloric energy conversion 0-10962  
 $\text{Sb}_2\text{Te}_3\text{-Sb}_2\text{Se}_3$ , ordered structure formation, heat treatment effect on thermal cond. 0-54448  
 $\text{Sb}_2\text{Te}_3\text{-Sb}_2\text{Se}_3$  thin layers, struct., phase comp., and elec. cond. 0-15389  
 $\text{Si-Ge}$ , heavily doped, reversal of precip. 0-2409  
 $\text{Si-Ge}$  solid solution, thermal neutron monochromators 0-49053  
 $\text{SiC}$ , 6H polytype, elec. and thermal cond., carrier concentrations 0-2223



**semiconductor materials continued**

- $\alpha$ -SiC (6H), dynamic hologram high-speed recording and erasure mechanism 0-5710
- $\alpha$ -SiC (6H) laser excited thermostimulated luminescence light sum dose depend. (*Russian*) 0-16111
- SiC, electron-hole liquid, RPA calcs. 0-6743
- SiC, epitaxial growth by sublimation sandwich method, effect of impurities 0-25568
- SiC, epitaxial growth by direct synthesis in vacuum 0-40262
- SiC film electron beam preparation technique, diffraction pattern anal. (*German*) 0-55297
- SiC luminophor powders, SAW nonlinear acoustoelectro-luminescence 0-45143
- $\beta$ -SiC, n-type, thermoelectric efficiency at high temps. 0-35706
- SiC polymorphs, widths of first minibands and effective masses, resist. anisotropy 0-20071
- SiC polytypes deformed, resist. anisotropy in (0001) plane 0-20198
- SiC reverse biased p-n junctions, prebreakdown violet luminesc. 0-7420
- SiC, self-bonded polycryst., electrophys. props. 0-10980
- SiC, sputtered, comp. and struct. props., effect of target materials 0-54549
- SiC:Al epitaxial layers, growth, Al distrib. and solubility 0-15391
- SiC:Al<sup>+</sup> p-n junctions, elec. props., defect effects 0-15594
- SiC:Al(Ga)(B) (6H) LEDs, fabrication by rotation dipping technique, electrolum. mechanisms 0-50426
- SiC-n-Si junction device, elec. props. 0-15591
- $\alpha$ -SiC(6H), electron bombardment, formation of defects on (0001) surface 0-19844
- $\alpha$ -SiC(6H), two stage transitions, nonlinear absorpt., thermoluminesc. method 0-7425
- SiGe, matrix isolated cluster, optical absorpt. 0-16045
- Si<sub>1-x</sub>Ge<sub>x</sub> system, lattice energy and consts., virtual cryst. approx., pseudopot. calc. 0-44166
- Sm<sub>1-x</sub>Gd<sub>x</sub>S system, semicond. to metallic isomorphous phase transition mechanism 0-2338
- SmS, defect struct., precipitate colonies, dislocation loops, TEM obs. 0-44214
- SmS type cpd., fd mixing effect on impurity levels, local valence transition 0-24831
- SmS:P, neutron irradi., semiconductor-metal transition 0-24975
- SnI<sub>2</sub> band struct., layer model 0-44501
- SnO<sub>2</sub>, band struct., tight-binding calc. 0-24796
- SnO<sub>2</sub> coated glass, surface elec. breakdown 0-25303
- SnO<sub>2</sub>, semiconductor, photoluminescence, depend. on lattice temp. and excitation intensity 0-45137
- SnO<sub>2</sub> surface, interactions with O<sub>2</sub>, H<sub>2</sub>O and H<sub>2</sub>, desorpt., ESR and cond. meas 0-10790
- SnO<sub>2</sub>:As film, prep. and elec. cond. 0-2959
- SnO<sub>2</sub>-GaSe heterojunction photocell, fine struct. of photo-EMF spectra 0-6967
- SnO<sub>2</sub>-InSe n-n heterostructures, photoelec. props., 80 to 300K 0-20297
- SnO<sub>2</sub>-Sb<sub>2</sub>S<sub>3</sub>-Sn structures, photovoltaic effects (*Korean*) 0-44647
- SnO<sub>2</sub>-Si heterojunctions, elec. and photovoltaic props. 0-26141
- SnO<sub>2</sub>-Si solar cells, electron-beam deposited, struct., photovolt. props. 0-50956
- SnS, polytypes, electronic bandgap meas. 0-34358
- SnS<sub>2</sub>(Se<sub>2</sub>), optical transitions from d core levels 0-45105
- TeO<sub>2</sub>, band struct., tight-binding calc. 0-24796
- TeO<sub>2</sub> thin film, Al-TeO<sub>2</sub>-Al, field-assisted cond. mechanism 0-11105
- Th<sub>3</sub>As<sub>2</sub>-U<sub>3</sub>As<sub>4</sub> solid soln., electronic props. 0-34469
- TiO<sub>2</sub> (rutile), (001) and (110) faces, UPS and LEED obs. 0-45206
- TiO<sub>2</sub> (rutile), (001) and (110) surfaces, surface and bulk density of states calcs. 0-49858
- TiO<sub>2</sub>, elec. cond., temp. depend. resistivity meas. at 77 to 600K, unswitched samples 0-20262
- TiO<sub>2</sub> electrode, doping density dependent attachment of rhodamine B 0-54777
- TiO<sub>2</sub> electrodes, in aq. electrolytes, surface states, photocurrent obs. 0-49895
- TiO<sub>2</sub> electrodes in photoelectrochem. cell, photothermal effect 0-7947
- TiO<sub>2</sub>, indirect forbidden transitions, band struct. enhancement 0-44503
- n-TiO<sub>2</sub> photoanodes, corrosion suppression mechanism 0-2462
- TiO<sub>2</sub>, photodesorption of H<sub>2</sub>O, pulsed-laser-dynamic-mass-spectrometer study 0-35568
- TiO<sub>2</sub>, rutile ceramics, space charge effects 0-24945
- TiO<sub>2</sub> sputtered film, photocond. and TSC meas. 0-15560
- TiO<sub>2</sub>, stoichiometric single crystals, anisotropy of ion transport 0-2206
- TiO<sub>2</sub>, two photon spectra, quantitative investigation, temp. depend. 0-50373
- n-TiO<sub>2</sub>:Be electrodes, photoassisted oxidation of water 0-30502
- TiO<sub>2</sub>:Cu, anodic, effect of Cu on optical props., rel. to possible appl. in solar energy conversion 0-16115
- TiO<sub>2</sub>:S, acceptor properties of S, free electron concentrations 0-34395
- TiO<sub>2</sub>:S, in O<sub>2</sub>+CO<sub>2</sub>+SO<sub>2</sub> atmosphere, elec. cond. study 0-39583
- TiO<sub>2</sub>-aqueous electrolyte interface, pot. distrib., Mott-Schottky plots 0-11084
- n-TiO<sub>2</sub>-electrolyte interface, charge-transfer-controlled photocurrent 0-50992
- TiO<sub>2</sub>-Pd Schottky barrier, work function depend. on adsorbed species 0-54782
- TiO<sub>2</sub>-Si solar cell hybrid electrodes for photoelectrochem. H prod. 0-45775
- TiO<sub>2-x</sub>, reduced, cond. between elec. props. in equil. at 1100°C and after quenching, defects role (*French*) 0-44582
- Ti<sub>2</sub>O<sub>7</sub> and (Ti<sub>1-x</sub>V<sub>x</sub>)<sub>4</sub>O<sub>7</sub>, metal-insulator transitions, EPR, elec. and mag. props. 0-2336
- TiS<sub>2</sub> (1T), electronic and vibronic struct. 0-44500
- TiS<sub>2</sub>, evidence for semicond. props., Hall coeff., refl., cond., thermoelec. power 0-20220
- TiS<sub>2</sub>, LEED, single-reflection layer scatt. theory 0-49059
- TiO<sub>2</sub> electrodes, effect of processing variables on photoelectrochem. props 0-6975
- TiO<sub>2</sub> electrodes, room temp. diffusions, capacitance, spectral response and volt-ampere characts. 0-15294
- TiCl<sub>3</sub> band structure and optical spectra, local field and exchange effects 0-24798
- TiCl<sub>3</sub>, self-consistent electronic struct. and ground state props. 0-15451
- TiCl(Br), electron-hole liquid, RPA calcs. 0-6743
- Tl<sub>2</sub>Te<sub>3</sub>, exam. of electrical props., in solid, liquid state 0-54686
- V<sub>1-x</sub>Fe<sub>x</sub>O<sub>2-x</sub>F<sub>x</sub>, 0<x<0.20, magnetic susceptibility and electron cond. (*German*) 0-39754

**semiconductor materials continued**

- VO<sub>2</sub>, cylindrical specimen, thermal switching 0-44679
- VO<sub>2</sub>, nonstoichiometry influence on electron struct. and metal-insulator phase transition 0-44507
- VO<sub>2</sub> single cryst. film, ion-irradi., 'splitting' of semicond.-metal transition 0-11053
- VO<sub>2</sub>, single crystal and polycrystalline, synthesis and resist. near metal-semicond. phase-transition 0-44680
- VO<sub>2</sub>, switching effect, temp. depend. 0-20259
- V<sub>2</sub>O<sub>5</sub> crystal, photoinduced threshold switching in VO<sub>2</sub> channel 0-29450
- V<sub>2</sub>O<sub>5</sub>, thermoelec. props., 500-1500K 0-29423
- V<sub>2</sub>O<sub>5</sub>:Na(Li), pure and doped, elec. cond. and thermoelec. power meas. 0-10987
- V<sub>2</sub>O<sub>5</sub>-BaO-K<sub>2</sub>O-ZnO glasses, elect. props. and struct. 0-15547
- WO<sub>3</sub> layers, semiconductor electrodes, electrochromism and photoelectrochemistry 0-35544
- $\delta$ -Y<sub>2</sub>S<sub>3</sub>:Nd<sup>3+</sup>, spectroscopic props. from absorpt., photoluminesc. and excitation spectra 0-34968
- Y<sub>2</sub>(V<sub>4/3</sub>W<sub>2/3</sub>)O<sub>7</sub> pyrochlore, synthesis and elec. props. 0-29914
- Zn<sub>3</sub>As<sub>2</sub>, optical band-gap, absorption meas. 0-25372
- Zn<sub>3</sub>As<sub>2</sub>-ZnSe(ZnTe) solid solutions, single cryst., phase equilb. and props. 0-16283
- ZnF<sub>2</sub>:Mn, thin films, electroluminescence, brightness voltage characts. hysteresis 0-20709
- Zn<sub>1-x</sub>Mg<sub>x</sub>Te alloys, high purity, metallurgical and analytical methods of prep. 0-40247
- Zn<sub>1-x</sub>Mg<sub>x</sub>Te alloys, luminesc. and elec. props. 0-2813
- Zn(Mo<sub>2</sub>Re<sub>2</sub>)S<sub>8</sub>, synthesis and electrical props. of mixed tetrahedral cluster phases 0-2971
- ZnP<sub>2</sub>, second-order vibr. spectra and dispersion of phonon branches 0-25376
- ZnP<sub>2</sub>, sublimation 0-34181
- ZnP<sub>2</sub> tetragonal crystals, light scatt. by optic phonons 0-55116
- ZnP<sub>2</sub>:As, local vibrs. of impurity ions, Raman study 0-29745
- Zn<sub>3</sub>P<sub>2</sub> bulk and thin film, UV reflectivity spectra, photovoltaic effects, optical consts. 0-25472
- Zn<sub>3</sub>P<sub>2</sub>, direct and indirect optical transitions, metal-Zn<sub>3</sub>P<sub>2</sub> contact photovoltage response 0-25402
- Zn<sub>3</sub>P<sub>2</sub>, single crystal, growth, electronic and device props. 0-25551
- Zn<sub>3</sub>P<sub>2</sub>, stoichiometry deviation from phase diagram 0-35164
- ZnSb, epitaxial films, growing conditions effect on elec. cond., thermo-EMF 0-39687

**semiconductor-metal boundaries**

see also Schottky-barrier diodes

- bulk states in semiconductors and insulators in contact with metals, charging 0-54781
- contact barrier inhomogeneities, characterisation by scanned internal photoemission 0-49915
- contact resistance, method for analysing influence of extrinsic parameters 0-25007
- double injection structure, V-I characteristics and contact effects (*Russian*) 0-49911
- III-V oxide interface state and Schottky barrier form., unified mechanism 0-44724
- interfacial reaction, dynamical obs. at room temp. using AES 0-10798
- junction layer charge migration with localised state participation (*Russian*) 0-49913
- metal-amorphous Si barrier, electronic props. 0-11089
- metal-InP contacts, intermediate adsorbed layer effect on electronic props. 0-39674
- photoelectron emission from metal into semiconductor 0-6984
- phthalocyanine-metal interfaces, surface photovoltage 0-20308
- Schottky barrier form., chem. mechanisms 0-49869
- Schottky barrier height variation techniques 0-20284
- Schottky barriers, Bardeen and Schottky limits of interface index 0-49868
- Schottky barriers, photocurrent, recomb. losses (*Russian*) 0-2470
- Schottky contacts, submicron, high-field pulsed electroplating technique 0-49899
- Schottky-barrier structs., surface barrier current instability, uniaxial crystal compression 0-20310
- silicide formation in thin layers of W or Mo (*German*) 0-7859
- SIMS characterisation (*French*) 0-50904
- solid surface, theory, book 0-36787
- space charge effects of semicond. coatings on metal substrate, on triboelec. charge exchange 0-54763
- superconductivity at disordered interface 0-20347
- surface barrier volume wave transducer 0-33403
- variable-gap surface-barrier structs., photoelec. effect, theoretical anal. 0-15564
- volume and contact parameter determ. from V-I characteristic (*Russian*) 0-49912
- Ag-InP contact in InP Gunn device, relationship between microwave efficiency and metallurgical state of cathode contact 0-6981
- Al/III-V interfaces, photoemission 0-25526
- Al-Ge (100) interfaces, MBE prep. and geometrical struct., total refl. X-ray diffr. study 0-49531
- Al-InP Schottky barrier, increase 0-15603
- Al-TiSi<sub>2</sub>-n-Si struct., elec. props., charge transfer mechanism across TiSi<sub>2</sub>-Si interface (*Russian*) 0-34515
- (Al+Si)-Si thin films, struct. transitions and phase comp. 0-49537
- As<sub>2</sub>S<sub>3</sub>-Ag system, photosensitivity depend. on As<sub>2</sub>S<sub>3</sub> thickness (*Russian*) 0-54784
- As<sub>2</sub>S<sub>3</sub>-Ag system, photosensitivity depend. on metallic layer thickness (*Russian*) 0-54785
- Au-CdS junction diodes, chemically etched CdS cryst. surfaces effect on barrier layer 0-44722
- Au-GaAs, photosensitivity losses, field and spectral depend. 0-2452
- Au-n-AlGa<sub>1-x</sub>As-n-GaAs Schottky barrier solar cells, prep. and props. 0-26140
- Au-Si interface, valence band and core levels, Si diffusion, alloy form., photoelectron spectra obs. 0-45205
- Au-Si system, transition layer struct. form. and heat treatment influence, amorphisation obs. 0-54529
- CdS, Au deposition, Schottky diodes and MIS devices, surface treatment effects, SEM obs. 0-54794
- CdS-Au, Schottky junction, surface defects, photovoltaic, piezoelectric and V-I characteristics (*French*) 0-49898
- Cu-CdS, Schottky barrier, Cu diffusion and photovolt. mechanism 0-6980



## semiconductor-metal boundaries continued

- Cu-CdS, Schottky barrier, reverse differential capacitance, diffusion of Cu, solar cell appl. (*French*) 0-15424
- Cu<sub>2</sub>-S/CdS heterostructures, heat treated, capacitance voltage meas. anal. 0-20292
- Ga<sub>1-x</sub>Al<sub>x</sub>As-Au variable-gap surface-barrier struct., photoelec. effect 0-39634
- GaAs (110), chemisorption of Al, electronic struct., tight binding calc. 0-49842
- GaAs (110), chemisorption site geometry and interface electronic struct. of Al and Ga, photoelectron spectra 0-49843
- GaAs (110)-Al(Ga)(In), Schottky barrier form., defect mechanism 0-49902
- GaAs MESFET struct., high-resolution deep level meas., photo-FET method 0-44531
- n-GaAs Schottky diode, impurity photoluminesc. 0-29781
- GaAs Schottky-contact, influence of surface states and hole traps (*Bulgarian*) 0-25006
- n-GaAs, ultra low resistance ohmic contacts 0-20307
- GaAs:Cr substrates and LPE layers, Au film deposition and annealing, Cr redistrib. 0-15312
- GaAs/Au-Ge/Ni contact system, alloying behaviour, microprobe AES and X-ray diffr. 0-54548
- GaAs-Al (Ni-AuGe) contacts, elec. characts. 0-29476
- GaAs-Al interface, ellipsometric anal. methods, correl. between optical props., thickness and surface roughness meas. (*German*) 0-55215
- GaAs-Al interface, struct. study by X-ray total-external-refl.-Bragg diffr. 0-34321
- GaAs-Al(Ga)(Ge), surface reactions and interdiffusion, photoemission study 0-49532
- GaAs-Au, quenching of exciton luminesc. by surface elec. field 0-29801
- GaAs-Au interface, atomic modulation of interdiffusion, effect of reactive Al monolayers 0-49432
- GaAs-Au Schottky barrier, photocurrent, recomb. losses (*Russian*) 0-2470
- n-GaAs-Au-Mo, RF sputtering, elec. props. of contacts, compensating damage centres form. 0-34507
- GaAs-metal interface, metal-induced chem. reactions and surface states 0-20311
- GaAs-metal interface form., chem. and electronic struct. 0-25009
- GaAs-metal Schottky barrier height rel. to chem. reactivity 0-25008
- GaAs(Sb), Schottky barrier and semicond./insulator interface states formation 0-49906
- GaP, electron traps around dislocations in p-n junction and metal-semicond. structs. 0-34388
- GaP Schottky barriers, voltage fluctuations, meas. 0-15604
- GaP-Ag(Au), Schottky barrier, stress effects on elec. props. 0-34512
- GaP-metal Schottky barrier height rel. to chem. reactivity 0-25008
- GaSb-Pb junction, Ar ion bombard. effect on tunnelling props. 0-54783
- Ge, amorphous, -metal junction, current-voltage charact., contact material effect 0-44725
- Ge powder/Au electrode contact pot. difference, grain size depend. 0-44723
- Ge/Al thin film couples, accel. ageing 0-44726
- Ge-metal contacts, surface electron state spectrum surface treatment effects (*Russian*) 0-34497
- In<sub>1-x</sub>Ga<sub>x</sub>Sb-Au, photovoltaic effect and Schottky barriers 0-49897
- InP, cleaved surface, metal contact props. and influence of intermediate adsorbed layers 0-49905
- InP, Schottky barrier and semicond./insulator interface states formation 0-49906
- InP surface preparation for Schottky barrier and ohmic contact formation 0-39671
- InP-Ag Schottky barrier, hot electron attenuation length 0-49904
- n-InP-Al(Hg), Schottky barrier height and stability characterisation 0-54786
- InP-metal ohmic contacts, elec. and metallurgical props., heat treatment effects 0-34514
- Mo-Si, non-volatile memory switching 0-54814
- Nb-Si, bridge, crit. current 0-20359
- Ni-n-GaP:Si(Ge) contacts, doping effect in elec. props. 0-6983
- Pb-Si:Sb Schottky tunnel junction, variable range hopping assisted tunnelling 0-39670
- Pb<sub>0.9</sub>Sn<sub>0.1</sub>Te-Pb, Schottky barrier form., Auger depth profiling and I-V meas. 0-49903
- PbTe-Au Schottky barrier junctions, Landau level oscills. in tunnelling data 0-49945
- Pd/Si interface, chem. and struct. props. during silicide form., AES and TEM obs. 0-49430
- Pd-Si (111) interface, microscopic Pd<sub>2</sub>Si form., UPS obs. 0-24743
- Pt-SrTiO<sub>3</sub> (100) interface, struct. and electronic props., AES, LEED, EELS, and UPS study 0-24986
- Pt-SrTiO<sub>3</sub> (100) interface, Auger and photoemission studies, relax. and chem. shift effects 0-54749
- Si (111)-Au interface, chemically driven intermixing, UPS study 0-50533
- Si, amorphous, interface with V, V silicide formation, backscattering, diffraction meas. 0-2285
- Si, amorphous, Schottky barrier solar cell, large-area RF sputtered, contact form, scaling and optimisation 0-45679
- Si, amorphous, thin film reaction with Pd, metal-rich silicide formation 0-2284
- Si amorphous film, crystn. on annealing at low temps. in contact with Al 0-24765
- Si, cleaved surface, metal contact props. and influence of intermediate adsorbed layers 0-49905
- Si solar cells, semiconductor thick film cell contacts, all metal 0-30489
- Si, thin single crystal, MeV ion scatt. and channelling obs. of interfaces 0-50492
- Si/Al interfaces, chemical bonding states, low energy AES 0-6985
- Si/Al thin film couples, accel. ageing 0-44726
- a-Si/Au barrier, capacitance and cond. 0-2469
- a-Si/metal barrier, capacitance and cond. meas. interpretation 0-49909
- Si/Pd-W, contact reactions, backscattering, X-ray diffr. meas. 0-20040
- Si-Al, solid phase epitaxial growth of Si 0-34324
- Si-Al devices, thickness meter for Al contacting layers (*Russian*) 0-36980
- Si-Al interface, ellipsometric anal. methods, correl. between optical props., thickness and surface roughness meas. (*German*) 0-55215
- Si-Al interface in semiconductors, electronic parts, electromigration aspects 0-39355
- Si-Al system, Si regrowth minimisation methods in Al films 0-15384

## semiconductor-metal boundaries continued

- Si-Co interface metal-semiconductor transition, rel. to first compound nucleation 0-24771
- Si-*Ir*Si interface microstructure and Schottky barrier height 0-34508
- Si-metal systems, interfacial reaction and Schottky barrier 0-39672
- Si-Mg, laser induced formation of MgSi<sub>2</sub> 0-35011
- p-Si-Mn contact, barrier height 0-34510
- Si-Pd(Pt), substrate-film system, ion-induced intermixing 0-15420
- SiH<sub>4</sub>, amorphous reactively sputtered films, in Pd Schottky barrier devices, photovoltaic props. 0-49910
- Si<sub>1-x</sub>H<sub>x</sub>, amorphous, gap states, DLTS 0-49656
- SrTiO<sub>3-x</sub>In contacts, differential capacitance, elec. field depend. permittivity effect 0-54779
- Te-Au thin film interface, evolution, switching effects (*French*) 0-6660
- TiO<sub>2</sub>-Pd Schottky barrier, work function depend. on adsorbed species 0-54782
- Zn<sub>3</sub>P<sub>2</sub>-Au(In) photovoltage response, optical transitions in Zn<sub>3</sub>P<sub>2</sub> 0-25402
- ZnS-metal interface, metal-induced chem. reactions and surface states 0-20311
- ZnS-metal Schottky barrier height rel. to chem. reactivity 0-25008
- ZnSe-metal Schottky barrier height rel. to chem. reactivity 0-25008
- semiconductor-metal transition** see *electrical conductivity transitions; metal-insulator transition*
- semiconductor processing** see *semiconductor technology*
- semiconductor storage devices**  
see also *integrated memory circuits*  
graded and stepped energy band-gap MIS structures 0-2473  
linear accelerator calibration monitor with a memory 0-3821  
MIS memories, tunnelling and photoionisation of states 0-11099  
MIS structure, radiation induced charge storage 0-6997  
BaTiO<sub>3</sub>/SiO<sub>2</sub> charge storage memory films for IGFETs 0-11566  
Si<sub>3</sub>N<sub>4</sub>-SiO<sub>2</sub>-As, graded and stepped energy band-gap MIS struct. 0-2473  
TiO<sub>2</sub>/SiO<sub>2</sub> charge storage memory films for IGFETs 0-11566
- semiconductor switches**  
chalcogenide glass-GaAs(InP) p-n junction, fabrication, characterization, switching 0-49892  
MNOS P-channel switch, accelerated reliability testing (*German*) 0-6988  
pn-p switching transistors, anomalous breakdown regions, laser scanning obs. 0-34854  
switch, laser-activated, high-power switching with ps. precision 0-2416  
As<sub>40</sub>Te<sub>60</sub>, amorphous films, metal and semicond. contacts, threshold switching, IR emission 0-49831  
Cd<sub>22</sub>Ge<sub>12</sub>As<sub>65</sub>, amorphous, threshold switching, expt. 0-49830  
CdS<sub>0.5</sub>Se<sub>0.5</sub>, picosecond optoelectronic switching 0-54734  
GaAs, control of fast Pockel cell for active pulse shaping in ps domain 0-28257  
GaAs switch, laser-activated, high-power switching with ps. precision 0-2416  
Ge<sub>1-x</sub>Te<sub>x</sub>X<sub>4</sub> amorphous semicond. switches, fabrication technology (*German*) 0-7493  
Si laser activated switch, synchronisation jitter reduction in streak cameras 0-53440  
Si MIS switch diode, charge storage effects, threshold depend. on driving voltage pulse freq. 0-49939  
Te<sub>40</sub>As<sub>30</sub>Ge<sub>30</sub>Si<sub>10</sub>, amorphous, threshold switching, expt. 0-49830  
TeO<sub>2</sub>-V<sub>2</sub>O<sub>5</sub> glass threshold devices, reversible monopolar switching 0-2434  
VO<sub>2</sub> thin film semiconductor-metal transition applications 0-49835
- semiconductor technology**  
see also *under specific device headings*  
see also *semiconductor doping; semiconductor growth*  
anodic oxidation for Si film removal and determination of active impurity distrib. 0-40583  
conference, ion implantation equipment, Povo-Trento, Italy (Aug., 1978) 0-31413  
dielectric thin films, accurate meas. by symmetric prism wave couplers (*Chinese*) 0-2885  
integrated circuit, plasma-removal of polymeric layers 0-1851  
interleaved glass layer prism for semiconductor mask testing 0-43425  
ion implantation, semiconductor device processing 0-34031  
ion implanter, semiconductor device processing 0-31944  
laser annealing, review and anal. 0-25741  
laser annealing of ion-implanted defects, and other processing 0-55431  
microwave plasma etching of Si wafers, role of ions and neutral active species 0-3217  
MOSFETs, short channel, fabrication by ion implantation and laser annealing 0-20312  
oxidation with trichloroethylene additive to eliminate oxidation induced stacking faults 0-39118  
plasma etching methods for semicond. struct. and devices (*Slovak*) 0-40564  
sapphire, etching of arrays of orifices using Pt-Cr composite layer mask 0-3216  
solar cell fabrication, preliminary 'test case' manufacturing sequence for 50 cent/watt solar photovoltaic modules in 1986 0-55858  
VLSI multilayer metallisation interlayer dielectrics, CVD films 0-45235  
wafer C impurity IR absorption spectrometry, thickness fringe elimination 0-55132  
wafer O interstitial IR absorption spectrometry, multiple reflection correction 0-55131  
wafers, scribing and subsequent fracture 0-11743  
Cu<sub>1-x</sub>Ag<sub>x</sub>InS<sub>2-x</sub>Se<sub>2x</sub>, for solar photovoltaic cells 0-10982  
Cu<sub>2</sub>S-CdS integrated thin film solar cell generators, fabrication techniques 0-55857  
GaAs, ion implantation, trends 0-39132  
GaAs<sub>1-x</sub>Sb<sub>x</sub> organometallic VPE, use of trimethyl As and trimethyl Sb 0-45238  
Ga<sub>1-x</sub>In<sub>x</sub>As organometallic VPE, use of trimethyl As and trimethyl Sb 0-45238  
Hg<sub>1-x</sub>Cd<sub>x</sub>Te photodiodes, implanted n<sup>+</sup>-p, improved performance using insulated field plates 0-52309  
InP substrates, chem. etching by H<sub>2</sub>O<sub>2</sub>-H<sub>2</sub>SO<sub>4</sub>-H<sub>2</sub>O soln. 0-35360  
Si 0-44200  
Si etch rate uniformity in CF<sub>4</sub>+4% O<sub>2</sub> plasma 0-40568  
Si, microwave O<sup>+</sup> plasma, magnetoactive, for oxidation of Si 0-38831  
Si, plasma etching in Freon plasma, for microelectronics apps. 0-3080  
Si, polycryst., charges at laser recrystallised poly Si/insulator interface 0-54789  
Si, process-induced in-plane distortion, correl. with wafer bowing 0-54579



**semiconductor technology continued**

- Si, purification technology for the development of low cost solar cells 0-50976  
 Si solar cell production, Union Carbide Corporation Silane Process, cost analysis 0-21403  
 Si, surface cleaning by pulsed laser irradiation 0-45173  
 Si, technology and physics, review 0-34353  
 $\text{Si}_3\text{N}_4/\text{Ge}$  films, intrinsic stress rel. to deposition conditions, use as Si oxidation mask 0-39467  
 $\text{SiO}_2$  MOS structures, removal of electron traps by RF annealing 0-44728  
 $\text{SiO}_2$  nonporous film, plasma deposition method, appl. to semicond. device manufacture (Russian) 0-16197  
 $\text{SiO}_2/\text{B}$  implanted, thin films, props. (Polish) 0-39692

**semiconductor thin films**

- for electronic conduction in crystalline and amorphous films, see "electronic conduction in crystalline semiconductor thin films" and "electrical conductivity of amorphous semiconductors and insulators", respectively see also amorphous semiconductors; semiconductor epitaxial layers  
 amorphous, effect of ion bombardment on cond. (Russian) 0-49969  
 amorphous, vac. evaporated, doping, transport and optical props. 0-49715  
 anthracene derivative, Langmuir-Blodgett multilayer film, semiconducting props., optical and elec. meas. 0-11122  
 anthracene film, effect of struct. on luminesc. quenching (Russian) 0-7411  
 anthracene film, electroabsorption spectra obs. 0-50301  
 carrier temperature and density self-oscill. near instability threshold 0-11118  
 chalcogenide glass films, high field, short pulse cond. expt. 0-49751  
 chalcogenide glass films, photostructural changes, photodarkening 0-49121  
 chalcogenide glass films nonlinear current voltage characts., Poole-Frenkel effect 0-7007  
 coated Mo tips characterised by atom probe FIM, atomic clusters, voids 0-33863  
 copper phthalocyanine, photoelectrochem. behaviour on  $\text{SnO}_2$  electrodes 0-15626  
 exciton polariton attenuation, spatial dispersion effect 0-20097  
 ferrite-semiconductor film struct., cyclotron resonance in static elec. mag. fields 0-29624  
 $\text{FeS}_2$  thin films, prep. and charact. 0-16178  
 glassy-crystalline, with switching channel, electrothermal instability 0-15576  
 heterojunction thin film solar cells, survey or semiconductor combinations 0-50974  
 laminated systems, two dimensional and surface plasmon mixing (Russian) 0-15466  
 multilayer semiconductor structure, current noise 0-20302  
 multilayer semiconductor structures, plasma-wave beams 0-49795  
 optical characterization 0-50352  
 organic films, heating, electrode barrier presence, polarisation and depolarisation currents obs. 0-49764  
 photogalvanic effect calcs., electron mean free path, size effect 0-34487  
 phthalocyanine films, metal-free, adsorbed o-chloranil effect on surface photovoltage 0-34485  
 semiconductor film, size-quantised, EM wave absorpt. coeff. in coherent hypersonic wave field 0-29819  
 sheet resistance meas. by four point probe technique (Chinese) 0-52262  
 $\text{a-Si:H}_x$  structure, effect of H-Ar plasma contact on elec. props., and optical gap 0-34533  
 solar cells, low cost fabrication utilising polycryst. and amorphous thin films 0-50972  
 solar cells, thin film, performance analysis employing loss minimisation of essential characteristics 0-45682  
 sound propagation, in strong EM wave field (Russian) 0-39483  
 space charge effects of semicond. coatings on metal substrate, on triboelec. charge exchange 0-54763  
 sputtered layers, EPMA of inert gas content 0-3443  
 tetracene, amorphous film, TSC meas., carrier traps 0-2496  
 TTT film, hopping cond. AC and DC meas. and EPR 0-11111  
 two-photon absorption, exciton effects (Russian) 0-40174  
 $\text{Al-CdSe-Ag}$  dry air stabilised struct., elec. cond. mechanism, breakdown phenomena 0-34527  
 As, amorphous, photoluminescence, bulk and sputtered thin films 0-25457  
 As amorphous films, interference enhanced Raman scatt. 0-50326  
 $\text{As:Ni(Ge)(S)(Se)(Te)}$  film, amorphous, chemical modification of props. 0-49250  
 As-S glassy film, photobrightening effect 0-11498  
 As-Se amorphous film, density of upper valence band states, annealing effects, UPS obs. 0-29845  
 As-Se and  $\text{As}_2\text{S}_3$  films, electron-stimulated changes in optical props. and dissolution rate 0-29709  
 As-Se system, chalcogenide vitreous semiconductors, darkened films, thermal and optical bleaching, light transmission obs. 0-50447  
 As-Se(Te), laser-beam recordings by thermal creation of holes 0-35010  
 As-Te-metal amorphous film, switching, memory effects 0-44677  
 $\text{As}_{2-x}\text{S}_{3+x}$  hydrogenated chalcogenide glasses, prep. by plasma decomposition 0-49735  
 $\text{As}_2\text{S}_3$  evaporated, elec. cond. mech. obs. (Japanese) 0-11028  
 $\text{As}_2\text{S}_3$  film, amorphous, deposited at different temps., IR spectra 0-40102  
 $\text{As}_2\text{S}_3$  thin glassy films, hole drift mobility, interaction with deep localised levels 0-11117  
 $\text{As}_{100-x}$  amorphous film, photoinduced changes in optical props. 0-50445  
 $\text{As}_{100-x}$  chalcogenide glass, absorption in range of large optical densities (Russian) 0-11428  
 $\text{As}_2\text{S}_3(\text{Se}_2)\text{Ag}$  glassy films, doped by photodiffusion and thermodiffusion, photocond. 0-29441  
 $\text{As}_{2-x}\text{Se}_{3+x}$  hydrogenated chalcogenide glasses, prep. by plasma decomposition 0-49735  
 $\text{As}_2\text{Se}_3$  amorphous, hole emission defect states 0-49759  
 $\text{As}_2\text{Se}_3$  amorphous thin films, illumination-induced change in contact pot. 0-20251  
 $\text{a-As}_2\text{Se}_3$  film, metallic impurity effect on transport props. 0-49963  
 $\text{As}_2\text{Se}_3$ , photodarkening and photostructural effects, Raman, IR and NQR studies 0-16036  
 $\text{As}_2\text{Se}_3$  amorphous film, photocond., TSC, light-induced changes 0-49810  
 $\text{As}_2\text{Se}_2$  chalcogenide semicond. film, thermophysical transitions with photostructural transformations (Russian) 0-16016

**semiconductor thin films continued**

- $\text{As}_2\text{Se}_2(\text{S}_2)$ , glassy film, photostructural effects, NQR study 0-49549  
 $\text{As}_2\text{Te}_3$ , amorphous, defect and impurity states, hopping cond. obs. 0-54650  
 B amorphous film, interference enhanced Raman scatt. 0-50326  
 B:H amorphous CVD films, IR, visible, and near UV optical props. 0-50442  
 $(\text{Bi}, \text{Sb})_2\text{Te}_3$  solid soln., semiconductor film, oxidation, electrophysical props. 0-45407  
 $\text{Bi}_2\text{Te}_3$ -Se, films, surface band struct. and scatt. mechanism 0-34535  
 C, amorphous, struct. and semicond. props. and heterojunction form. with single cryst. Si 0-25002  
 C, film, amorphous, two-dimensional variable range hopping cond. 0-10977  
 C:H amorphous films, elec. cond. and optical absorpt. 0-49723  
 $\text{CdAs}_2$  film, optical absorption edge 0-50450  
 $\text{CdCr}_2\text{Se}_4$  films, mag. hysteresis, domain struct., mag. viscosity 0-25169  
 $\text{Cd}_{32}\text{Ge}_{12}\text{As}_{65}$  amorphous, threshold switching, expt. 0-49830  
 $(\text{CdGeAs}_2)_{1-x}\text{D}_x$  amorphous films, property control in common target sputtering, elec. cond. 0-7494  
 $\text{CdIn}_2\text{S}_4$ , vacuum deposited, growth, struct., optical and photoelectronic props. 0-10831  
 $\text{CdO-SnO}_2$  film, prep. by RF sputtering, elec. cond. and transparency 0-7492  
 $\text{CdS}$ , diffusion of Cu, 20 to 200°C (French) 0-15424  
 $\text{CdS}$ , electrolessly deposited, annealing effect on optical spectra 0-2884  
 $\text{CdS}$  film, surface struct. and elec. props. 0-34531  
 $\text{CdS}$  films, precip. from soln., phase comp. change during annealing in air at 200-600°C 0-15393  
 $\text{CdS}$  optical waveguide polariser 0-33180  
 $\text{CdS}$  photosensitive film production from chelated metallo-organic compounds (Russian) 0-49813  
 $\text{CdS}$ , polycryst., optical spectra, 0.5-6.5 eV 0-55212  
 $\text{CdS}$  polycrystalline thin-film liq. junction photovolt. cell 0-50988  
 $\text{CdS}$ , polycrystn. films, recrystn. accompanying annealing (Russian) 0-20948  
 $\text{CdS}$  solar photovoltaic panels, deposited by spray pyrolysis, film and junction structure studies 0-45689  
 $\text{CdS:Ag}$ , vacuum deposited, recrystn. by  $\text{H}_2\text{S}$  heat treatment 0-34328  
 $\text{CdS:Cu,Cl}$ , photocond., applied voltage freq. effect on props. 0-39635  
 $\text{CdS:Cu(Cl)}$ , thin layer, electron pulse induced cond. relax. 0-2501  
 $\text{CdS:In}$ , flash evaporated, prep. and elec. props. 0-20792  
 $\text{CdS:Li}$ , chemical bath deposited, photocond. and optical props. 0-2426  
 $\text{CdS:Li}$  film, optical props. 0-2886  
 $\text{CdS-Cu}_2\text{S}$  solar cells, screen printed, prep. and photovoltaic props. 0-40863  
 $\text{CdS}_{1-x}\text{Se}_x$  film, resonance between Se atom dipole vibr. and interference modes, IR spectra obs. (Russian) 0-2888  
 $\text{CdS,Se}_{1-x}$ , flash evaporated, prep. and elec. props. 0-20792  
 $\text{CdS,Se}_{1-x}$  photosensitive films, prep., props., and use for photodetectors 0-55298  
 $\text{CdS(Se)(Te)}$ , vacuum condensed, growth and struct., HEED obs. 0-29292  
 $\text{CdSe}$  electrochem. photovoltaic cells, effect of thin film electrode prep. and conc. on efficiency 0-55847  
 $\text{CdSe}$  films, growth kinetics and cryst. struct. during vacuum condensation 0-2305  
 $\text{CdSe}$  photocond. film, plasma reson., IR refl. obs. 0-11037  
 $\text{CdSe}$  photosensitive film production from chelated metallo-organic compounds (Russian) 0-49813  
 $\text{CdSe-LiNbO}_3$  structure, electroacoustic effects and signal convolution 0-10098  
 $\text{CdTe}$  film, photopolarisation 0-25286  
 $\text{CdTe}$ , hexagonal film, effective birefringence 0-16004  
 $\text{CdTe}$ , low resist., prep. by multi-source evaporation method, and characterisation 0-25582  
 $\text{CdTe}$  sputtered films, struct., photocond., and trap distrib. 0-29489  
 $\text{CdTe-Te}$  film, prep. by combined hot-wall-flash evaporation method, and characterisation 0-55296  
 $\text{CdTe}_{1-x}\text{Se}_x$  solid solution films, prep., struct., and photocond. 0-54541  
 $\text{CuBr}$ , exciton absorpt. band shape, dielectric const. real part derivatives (Russian) 0-25413  
 $\text{CuInSe}_2$ , evaporation source temp. effect, on comp. 0-39478  
 $\text{Cu}_2\text{S}$ , optical and calorimetric meas. of thin films for  $\text{Cu}_2\text{S-CdS}$  solar cells 0-55863  
 $\text{Cu}_2\text{S}$ , polycryst. thin films, struct., optical and elect. props. for solar energy appl. 0-10837  
 $\text{Cu}_2\text{S-CdS}$  integrated thin film solar cell generators, fabrication techniques 0-55857  
 $\text{Cu}_2\text{S-CdS}$  thin film solar cell fabrication by electrophoresis 0-55862  
 $\text{Cu}_{2-x}\text{S/CdS}$  heterostructures, heat treated, capacitance voltage meas. anal. 0-20292  
 $\text{Cu}_2\text{S}$  evaporated thin films, composition, prep. and characts. 0-25569  
 $\text{EuO}_{1-x}$  films, Faraday effect dispersion rel. to electronic struct., visible and IR spectra 0-45162  
 $\text{EuS}$  films, ferromag., optical spectra and light scatt. from spin waves 0-16116  
 $\text{Fe}_2\text{O}_3$  thermal oxide film on Fe, capacitance, temp. and freq. depend., in aq. electrolyte soln. 0-54776  
 $\text{Ga}_{1-x}\text{Al}_x\text{As}$  layer form. on GaAs during dissolution in Ga-Al-As soln. 0-10799  
 GaAs amorphous film, EXAFS, optical and elec. props. 0-49547  
 GaAs, amorphous sputtered films, hydrogenated, photoinduced optical absorpt. 0-50362  
 GaAs, effect of O on thin film compositions obtained by secondary ion emission 0-26079  
 GaAs, film and solar cell on graphite, struct. and elec. props. 0-2286  
 GaAs layers, from gas phase, impurity influence on growth micromechanism 0-45237  
 GaAs, prep. of thin films by ionised-cluster beam deposition (Japanese) 0-25576  
 GaAs, RF sputtered, ESCA, surface chemistry suitability for photovolt. appl. 0-7476  
 GaAs solar cells on Ge substrates, thin film shallow homojunction struct., quantum efficiencies 0-35677  
 $\text{GaAs:H}$  amorphous sputtered films, high field cond. props. 0-44607  
 $\text{GaP}$  amorphous film, EXAFS, optical and elec. props. 0-49547  
 $\text{GaSb}$ , sputtered films, on GaAs, growth, Hall effect, impurity levels 0-20334  
 $\text{Ga}_{0.25}\text{Te}_{0.75}$ , amorphous, off-state recovery after nanosecond switching 0-44681



## semiconductor thin films continued

- $\text{Ga}_{0.25}\text{Te}_{0.75}$  amorphous film, nanosecond switching, resist. fluctuations in low-resist. state 0-44676  
 $\text{Ga}_{0.25}\text{Te}_{0.75}$  time evolution of nanosecond switching 0-6921  
 Ge, amorphous, crystallisation study 0-3389  
 Ge, amorphous, laser pulse annealing 0-15006  
 Ge, amorphous, vac. evaporated, density meas., microcrystalline model of struct. 0-2313  
 Ge amorphous film, effects of alloying chalcogen atoms 0-49670  
 Ge amorphous film, high freq. phonon scatt. 0-49328  
 Ge, amorphous film, high freq. cond., AC loss 0-49792  
 Ge, amorphous film, large aligned grain solid-phase growth during scanned laser crystallisation 0-49100  
 Ge amorphous film, O depth profiling by SIMS 0-39480  
 Ge amorphous film, ultra high vac. prep., DC elec. cond. 0-49721  
 Ge amorphous films, high elec. field cond. and magnetoresist. at 4.2K 0-49748  
 Ge, amorphous sputtered films, hydrogenated, photoinduced optical absorpt. 0-50362  
 Ge film, amorphous, two-dimensional variable range hopping cond. 0-10977  
 Ge:H, amorphous, H content determ. by IR absorpt., gas evolution and nuclear reaction methods 0-44130  
 Ge:H amorphous films, photoemission spectra 0-50517  
 Ge:Sb, amorphous, electronic transport props. 0-44589  
 Ge-S amorphous film, defect states, ESR 0-49670  
 Ge-Se(Te), laser-beam recordings by thermal creation of holes 0-35010  
 $\text{Ge}_2\text{S}_3$ -Ag contact, photoinduced diffusion of Ag in amorphous semicond. film 0-49418  
 $\text{Ge}_{10}\text{S}_{70}$  glass film, Ag photodoping sensitivity 0-39121  
 $\text{GeS}(\text{S}_2)$  amorphous films, photostructural changes, UPS study 0-49550  
 $\text{GeSe}_2$  amorphous film, laser induced light absorpt. oscillation, exciton model 0-50446  
 $\text{GeSe}_2$  amorphous film, photocond., photo-induced ESR, optical edge shift 0-49809  
 $\text{GeSe}(\text{Se}_2)$  amorphous films, photostructural changes, UPS study 0-49550  
 GeTe films, elec. props. and struct., influence of annealing and condensation conditions 0-15388  
 $\text{Ge}_{15}\text{Te}_{85}\text{X}_2$  amorphous semicond. switches, fabrication technology (*German*) 0-7493  
 HgTe thin film Hall sensor fabrication 0-2951  
 $\text{In}_{0.53}\text{Ga}_{0.47}\text{As}$ , interband magnetoabsorption study, quasi-Ge model application 0-50304  
 $\text{In}_{\text{Ga}_{1-x}\text{As}}$  ( $x=0.03$  and  $0.05$ ), grown as GaAs substrate, with InGaAsP buffer layer, exam. of dislocation density 0-44447  
 InN film, specular reflection spectra, lattice parameters 0-7428  
 $\text{In}_2\text{O}_3$ , electro-conducting transparent film, props. rel. to production method (*Japanese*) 0-25557  
 $\text{In}_2\text{O}_3$  thin film on polyester substrate, struct. determ. by TEM 0-6674  
 $\text{In}_2\text{O}_3/\text{Sn}$ , glass like thin film, electron evaporated, conductive transport (*Chinese*) 0-49960  
 InSb, charact. and phys. props., review (*Japanese*) 0-39576  
 InSb, film,  $E_0$ ,  $E_1$  absorption edge size quantisation, optical and electroreflectance spectra 0-34998  
 InSb films on  $\text{LiNbO}_3$ , prep. and props. 0-35093  
 InSb, prep. of thin films by ionised-cluster beam deposition (*Japanese*) 0-25576  
 InSb thin film element having non-linear galvanomagnetic effect 0-34534  
 $\text{In}_{0.53}\text{Te}_{0.75}$ , amorphous, off-state recovery after nanosecond switching 0-44681  
 $\text{In}_{0.25}\text{Te}_{0.75}$  amorphous film, nanosecond switching, resist. fluctuations in low-resist. state 0-44676  
 $\text{In}_{0.25}\text{Te}_{0.75}$  time evolution of nanosecond switching 0-6921  
 $\text{PbCl}_2/\text{NaCl}$ , trapped exciton states, absorption spectra 0-50383  
 $\text{Pb}_{1-x}\text{Hg}_x\text{S}$  electroless-deposited films, optical and elec. props. 0-7011  
 $\text{PbI}_2$ , exciton absorpt. band shape, dielectric const. real part derivatives (*Russian*) 0-25413  
 $\text{PbI}_2$ , film, reflectance meas., optical consts., humidity effects 0-34994  
 $\text{PbI}_2/\text{KI}$ , trapped exciton states, absorption spectra 0-50383  
 $\text{PbS}$ , soln.-grown on Si, struct. and comp. of heterojunction 0-54530  
 $\text{PbSe}$  films, synthesis characts. 0-35094  
 $\text{Pb}_{1-x}\text{Sn}_x\text{Te}$  films, size quantisation, optical orientation of free carriers 0-20725  
 $\text{Pb}_{1-x}\text{Sn}_x\text{Te}$ , sputtered, for IR detector appl. elec. and optical props. 0-35084  
 $\text{Pb}_2\text{Sn}_{1-x}\text{Te}$ , oxidation, appl. of Mossbauer method 0-45410  
 $\text{PbTe}$  film, optical consts., support roughness effect 0-2882  
 $\text{PbTe}$ , ion implantation induced damage and reson. levels 0-49255  
 $\text{PbTe}$ , semiconductor polycrystalline thin films, low-frequency  $1/f$  noise meas. 0-15629  
 $\text{SB-S}$ , laser-beam recordings by thermal creation of holes 0-35010  
 $(\text{Sb}_2\text{S}_3)_{0.95}(\text{Na}_2\text{S})_{0.05}$ , condensate, local states and switching effect 0-20336  
 $\text{Sb}_2\text{Te}_3$ - $\text{Sb}_2\text{Se}_3$  thin layers, struct., phase comp., and elec. cond. 0-15389  
 Se, amorphous, vac. evaporated, density meas., microcrystalline model of struct. 0-2313  
 Se, amorphous electrophotographic layers, resolution parameters 0-31926  
 Se amorphous film, interference enhanced Raman scatt. 0-50326  
 Se, amorphous thin film, elec. noise, monostable switching 0-44684  
 Se, gas-evaporated, selective absorpt. characts. and emissivity 0-50998  
 Se, noncryst., ageing and crystn. obs., tentative struct. model 0-2295  
 Se, vitreous, darkened films, thermal and optical bleaching, light transmission obs. 0-50447  
 Se-Ge, amorphous thin film, photocontraction rel. to surface struct. 0-49551  
 Si, amorphous, as photo-receptor for electrophotography 0-47126  
 Si, amorphous, control of dihydride bond density using RF sputtering, dark anal. and photocond. 0-34327  
 Si amorphous, crystallisation study 0-33890  
 Si, amorphous, crystn. on annealing at low temps. in contact with Al 0-24765  
 Si, amorphous, doped, density of states determ. from transport meas. 0-49720  
 Si, amorphous, film, hydrogenation by H diffusion, effect on elec. cond., band gap (*Korean*) 0-45326  
 Si, amorphous, glow-discharge, optically detected mag. reson., annealing and substrate temp. effects 0-20519  
 Si, amorphous, hydrogenated film, struct. determ. using electron microscopy 0-10806

## semiconductor thin films continued

- Si, amorphous, hydrogenated, soft H plasma effect, IR absorpt. (*French*) 0-45054  
 Si, amorphous, photostructural changes, photodarkening 0-49121  
 Si, amorphous, RF-sputtered, influence of  $\text{O}_2$  and deposition conditions, elec. cond., IR absorpt. and ESR 0-2949  
 Si, amorphous CVD film photodetector for picosecond pulses 0-47101  
 Si, amorphous CVD films for high temp. solar photothermal conversion 0-26161  
 Si amorphous film, dangling bond ESR, light-induced quenching 0-50162  
 Si amorphous film, glow discharge deposited, refl. spectra and dielec. function 0-50360  
 Si, amorphous film, heavily doped, glow discharge, AC cond. 0-49718  
 Si amorphous film, heavy doping by alkali ion implantation 0-2045  
 Si amorphous film, hole carrier transport 0-2500  
 Si amorphous film, optical props., electronic states 0-25475  
 Si amorphous film, vacuum deposited, microscopic voids, gas absorpt., crystn. study 0-49534  
 Si, amorphous films, characterisation by Rutherford backscatt. spectrometry 0-50498  
 Si, amorphous films, ion implanted, elec. and photocond. props. 0-49717  
 Si, amorphous glow discharge films,  $\text{H}_2$  content, elec. props., and photostability 0-25577  
 Si amorphous layers, laser annealing, photoluminesc. study 0-2049  
 Si, amorphous sputtered films, hydrogenated, photoinduced optical absorpt. 0-50362  
 Si, amorphous sputtered thin film, US anomalies, 0.5-300K 0-34145  
 Si, and Si:H, amorphous, sputter deposited,  $\text{O}_2$  incorporation during and after fabrication 0-49541  
 Si and Si:H amorphous films, porosity and oxidation of evap., sputtered and plasma-deposited films 0-10838  
 Si, CVD, amorphous and polycryst., microscopic surface roughness, effective-medium models, ellipsometric expts. 0-24756  
 Si, CVD, underlying oxide layer thickness effect on in-process thickness monitoring 0-6679  
 Si, CVD on  $\text{SiO}_2$  and  $\text{Si}_3\text{N}_4$  substrates, nucleation in  $\text{SiH}_4$ -HCl- $\text{H}_2$  system at high temp. 0-49538  
 Si, dopant distrib. in mono- and polycryst. samples, C-V technique 0-6425  
 Si, effect of O on thin film compositions obtained by secondary ion emission 0-26079  
 Si, film, amorphous, two-dimensional variable range hopping cond. 0-10977  
 Si, glow discharge amorphous film, reflectance and transmittance (*Japanese*) 0-34995  
 Si, glow discharge deposited, optical spectra, reflectance, dielectric function and oscillator strength 0-11492  
 Si, glow discharge deposition,  $\text{SiH}_4$  discharge parameters obs. 0-44030  
 Si, glow discharge film decomposed from silane, on amorphous substrate, elec. cond., RHEED study 0-20044  
 Si, growth of large grain polycryst. layers on graphite substrates by CVD on liquid layers 0-55849  
 Si, ion-implanted polycrystalline film, defect build-up efficiency 0-2054  
 Si, polycryst. CVD, electron beam recrystn. 0-24759  
 Si, polycryst., thinning using plasma etching (*Slovak*) 0-45405  
 Si, polycryst. films, transport props. and grain boundary charact. by TEM 0-50980  
 Si, polycrystalline, glow discharge deposited below 250°C, struct. and morphology 0-49535  
 Si polycrystalline CVD films, non-volatile memory switching 0-54814  
 Si, recrystallisation of CVD-grown polycryst. Si and influence of B, Al dopants on grain growth 0-54575  
 Si scattering surface layer, optical props. (*Russian*) 0-11419  
 Si, semi-insulating polycrystalline CVD layers, AES and XPS characterisation 0-16129  
 Si solar cell fabrication, R and D on low-cost processes, effect of impurities on cell performance 0-50978  
 Si, thin sub-monolayer film, Auger emission coeffs. meas. 0-55236  
 Si:B(Al), (P)(As)(In), ion implanted film, elec. prop. impurity depend. 0-24467  
 Si:B(P) polycrystalline thin film, plasma annealing, effect on elec. props. 0-7005  
 Si:F, amorphous film, effect of F on elec. cond. 0-34444  
 Si:H, amorphous, control and anal. of deposition, using plasma spectroscopy 0-45230  
 Si:H, amorphous, dopant conc., glow discharge optical spectroscopy 0-49546  
 Si:H, amorphous, glow discharge deposited, laser annealing 0-49104  
 Si:H, amorphous, H content determ. by IR absorpt., gas evolution and nuclear reaction methods 0-44130  
 Si:H, amorphous, plasma deposited, cond. adsorbate and insulating layer effects 0-49749  
 Si:H, amorphous, plasma-deposited, effect of DC elec. field superimposed during deposition 0-44643  
 Si:H, amorphous, prep. by RF glow discharge decomp. of  $\text{SiH}_4$ , optical props. and H conc. 0-15416  
 Si:H, amorphous, RF sputtered, suitability as solar cell material 0-40864  
 Si:H, amorphous, reactively sputtered, H content effect on props. 0-49714  
 Si:H, amorphous, refr. index, temp. depend., implications for thermoreflectance and electroreflectance 0-50290  
 n-Si:H, amorphous, thickness depend. cond. 0-49724  
 Si:H, amorphous film, prep. by plasma decomp. of  $\text{SiH}_4$  under mag. field, and characterisation 0-45239  
 Si:H, amorphous sputtered, excitation spectra and photoluminesc. 0-50396  
 Si:H, Cl(F), amorphous, photocond., dark cond. and photoluminesc. 0-49802  
 Si:H, plasma-deposited amorphous film, proton mag. reson. 0-44931  
 Si:H,F,O amorphous, plasma deposited, comp. and optical props. 0-50441  
 Si:H,P, amorphous, heavily hydrogenated, high gap state densities 0-49803  
 Si:H amorphous film, plasma-deposited, growth morphology and defects 0-44128  
 Si:H amorphous film, plasma-deposited, elec. and comp. heterogeneity 0-44745  
 Si:H amorphous film, prop. by glow discharge deposition, and plasma parameter effects on props. 0-45240  
 Si:H amorphous film, sputtered IR vibr. spectra and photolum., effects of partial evolution of H 0-44413



## semiconductor thin films continued

- Si:H amorphous films, interference enhanced Raman scatt. 0-50326  
 Si:H amorphous films, optoelectronic behaviour depend. on impurity incorporation during plasma deposition 0-49804  
 Si:H amorphous films, photovoltaic and photocond. spectra, photoluminesc. 0-44645  
 Si:H amorphous films, photoinduced optical absorpt. and photocond. 0-50361  
 Si:H amorphous films, role of Ar in deposition process, IR absorpt. and photocond. meas. 0-50321  
 Si:H amorphous films for solar cells, optical and elec. props. of RF glow discharge deposited films 0-54576  
 Si:H amorphous sputtered film, photoluminesc., photocond. 0-20729  
 Si:H amorphous sputtered films, optical gap, IR absorpt. meas. 0-50320  
 Si:H film, amorphous, bombarded, defects, luminesc. and ESR meas. 0-34977  
 Si:H film, amorphous, photocond. imaging 0-1300  
 Si:H plasma deposited film, amorphous, microstruct., TEM and SEM obs. 0-10801  
 Si:H sputtered amorphous film, luminesc. and non-radiative decay 0-50395  
 Si:H(B)(P), amorphous, UV absorpt. spectra 0-25420  
 Si:H(D), amorphous films, CVD, post-hydrogenation 0-54552  
 Si:In amorphous films, EPR, elec. cond., and magnetoresist. 0-50160  
 Si:Li(Na)(K)(F)(Cl), amorphous, implantation effects on elec. props. 0-49716  
 Si:Mn(Fe)(Ni) amorphous films, ESR and elec. cond. 0-50171  
 Si:O, amorphous, sputtered, influence of O and deposition conditions 0-54693  
 Si:O, evaporated amorphous film, effect of O<sub>2</sub> on props., ESR spectra 0-11265  
 Si:O,H amorphous, plasma-deposited, electronic and struct. props. 0-50391  
 Si:P, amorphous, CVD, defect compensation 0-54644  
 Si:P, heavily doped, glow-discharge-produced, elec. and optical props 0-2497  
 Si:P film, CVD polycrystalline, low press. and atmos. press., oxidation 0-3214  
 Si:P film, polycryst. pulsed electron beam annealing 0-10566  
 Si:Sb, amorphous, electronic transport props. 0-44589  
 Si/Au films, laser-irrad., phase transform. study 0-49536  
 Si/Si-Ge alloy, amorphous, solar cell, multijunction structure, increased conversion efficiencies, low cost 0-54677  
 Si-H, amorphous, on Nb or W, spectrally selective absorber, IR spectra 0-26164  
 Si-H, amorphous, thermal stability and decomp. kinetics 0-24758  
 a-Si-H sputtered solar cells, temp. depend. of Schottky barrier characts. 0-45669  
 Si<sub>1-x</sub>As<sub>x</sub>-H, amorphous system, struct. and defects, Raman and EPR meas. 0-49103  
 Si<sub>1-x</sub>Au<sub>x</sub> amorphous films, IR absorpt. spectra 0-16034  
 SiC film electron beam preparation technique, diffraction pattern anal. (German) 0-55297  
 SiC, sputtered, comp. and struct. props., effect of target materials 0-54549  
 SiH<sub>0.16</sub> amorphous films, optical props. and photocond. near optical gap 0-50443  
 SiH, amorphous reactively sputtered films, optical props. 0-50444  
 SnO<sub>2</sub>, electro-conducting transparent film, props. rel. to production method (Japanese) 0-25557  
 SnO<sub>2</sub> film, orientating action of solid substrates, on liq. cryst. layer exam. 0-44111  
 SnO<sub>2</sub>, gas sensor, prep. 0-39691  
 SnO<sub>2</sub> thin films, solid state gas sensor 0-40790  
 Sn<sub>1-x</sub>Pb<sub>x</sub>Se(Te) thin films, resistance to oxidation, Mossbauer study 0-39986  
 Sn<sub>1-x</sub>Pb<sub>x</sub>Te, production under quasiequilibrium conditions 0-45241  
 SnS(Se), electron diffr. struct. anal. 0-44449  
 Te, evaporated deposition, absorptivity and emissivity 0-25473  
 Te film condensed on mica, struct. and electrophysical props. 0-39688  
 Te, gas-evaporated, selective absorpt. characts. and emissivity 0-50998  
 Te, interference enhanced Raman scatt. 0-42273  
 Te textured thin films, prep., high solar absorptivity by multiples refl. 0-11568  
 Te-Au thin film interface, evolution, switching effects (French) 0-6660  
 Te<sub>40</sub>As<sub>35</sub>Ge<sub>7</sub>Si<sub>8</sub>, amorphous, threshold switching, expt. 0-49830  
 TiO<sub>2</sub> semicond. films for water photoelectrolysis 0-26146  
 TiO<sub>2</sub> sputtered film, photocond. and TSC meas. 0-15560  
 VO<sub>2</sub> film, visualisation of microwave and IR radiation 0-5839  
 VO<sub>2</sub>, nonstoichiometry influence on electron struct. and metal-insulator phase transition 0-44507  
 VO<sub>2</sub> single cryst. film, ion-irrad., 'splitting' of semicond.-metal transition 0-11053  
 VO<sub>2</sub> thin film semiconductor-metal transition applications 0-49835  
 V<sub>2</sub>O<sub>5</sub>, amorphous, CVD prep. method 0-55299  
 V<sub>2</sub>O<sub>5</sub>, amorphous, thickness, density and refr. index determ. from reflectance interference spectra 0-55206  
 Zn,Cd<sub>1-x</sub>S, film, single-thermal-source form. 0-2492  
 ZnF<sub>2</sub>:Mn, thin films, electroluminescence, brightness voltage characts. hysteresis 0-20709  
 ZnO film, prep. by reactive ionized cluster beam deposition, and characterisation 0-10829  
 ZnO, film for solar cell appl. structural, optical and elec. props. 0-2294  
 ZnO, piezoelec. films produced by gas transport reaction, US excitation efficiency 0-2700  
 Zn<sub>1-x</sub>P<sub>x</sub> bulk and thin film, UV reflectivity spectra, photovoltaic effects, optical consts. 0-25472  
 ZnS:Mn AC electrolum. device, filament behaviour 0-20712  
 ZnS:Mn co-deposited electrolum. device, phys. and elec. characterisation 0-20713  
 ZnS:Tb<sup>3+</sup>, NdF<sub>3</sub>, vac. deposited, electrolum. energy transfer 0-2861  
 ZnS:TbF<sub>3</sub>, between semicond. Y<sub>2</sub>O<sub>3</sub> layers, bright green electrolum. 0-2859  
 ZnS-CdS films, prep. by atomisation 0-16176  
 ZnS-metal interface in MIM struct., photoexcitation level assignment (French) 0-15622  
 ZnSe, film, hopping cond. 0-2499  
 ZnTe film, prepared by single-source vacuum deposition method (Japanese) 0-6664  
 ZnTe films, grown on glass using atomic layer evaporation 0-44453  
 ZnTe thin film, model for off-on transition 0-54742

## semiconductors

- Generalities and properties of unspecified materials only. For specific materials see semiconductor materials.  
 see also amorphous semiconductors; degenerate semiconductors; heavily doped semiconductors; magnetic semiconductors; many-valley semiconductors; narrow band gap semiconductors; polar semiconductors; thermoelectric effects in semiconductors and insulators  
 1/f noise origin 0-11060  
 AC thermopower measurement 0-44624  
 acoustic studies progress (Japanese) 0-49310  
 acoustoelectric current at moderate US freq. 0-29444  
 acoustoelectric effects, electron absorption and amplification of sound at intermediate freqs. 0-54740  
 atomic displacement threshold energy determ. from defect creation by electron irradi. 0-19799  
 Auger recombination in semiconductors involving traps 0-49763  
 avalanche breakdown field, approx. formula 0-11025  
 bound excitons, review, book contrib. 0-44519  
 Bragg X-ray diffr. in elastically bent cryst. 0-24310  
 Burstein-Moss effect, photostimulated absorption of light 0-29757  
 capacitive profilometry, accuracy 0-9005  
 carrier collisions with impurity ions 0-34434  
 carrier multiplication, noise due to avalanche processes, theory 0-6865  
 charge carrier UHF heating using lumped-capacitance resonators 0-20203  
 charged impurity diffusion 0-6563  
 chemical thermodynamics, review 0-55692  
 chemiluminescence heterogeneous excitation, ionisational mechanism 0-40173  
 coated semiconductor spheres, surface modes, plasmon oscils. 0-54730  
 compensated, electron capture probability by Coulomb centre in case of optical phonon emission 0-20214  
 compensated, photoresponse, spectral depend. 0-15562  
 compensated semiconductor, theory of transient processes 0-24930  
 compound semiconductor, electronic polarisability rel. to energy gap 0-10524  
 core excitons, binding energy in effective mass approx. 0-24808  
 covalent, non-orthogonal tight-binding approach 0-2442  
 covalent semiconductor, heating of charge carriers, energy dissipation 0-49755  
 covalent semiconductors, substitutional deep traps, theory 0-54651  
 covalent semiconductors, vacancy screening, dielec. const., exchange correl. pot., Thomas-Fermi description 0-44528  
 critical points for electron-hole system 0-44511  
 crystal surfaces props., structural, chemical and electronic, use of LEED methods (Italian) 0-49467  
 cubic, Debye temp., elastic consts. averaging 0-54332  
 cubic, in mag. field, exciton states 0-24807  
 cubic, Seitz coefficients calc. for resistivity 0-6880  
 current and voltage fluctuation determ. by noise spectral density meas. 0-15577  
 cyclotron resonance linewidth, quantum-limit 0-7171  
 dangling-bond states theory 0-24840  
 deep impurities, exptl. techniques (Japanese) 0-15476  
 deep impurity state characterisation 0-6776  
 deep levels, self consistent LCAO MO calcs. 0-29353  
 deep levels associated with 60° dislocations (French) 0-29352  
 deep trap activation energy, effect of non-exponential transients, DLTs method 0-20115  
 defect processes, electronic stimulation 0-24665  
 defects and radiation effects, conf., Nice, France (Sept. 1978) 0-22140  
 degenerate electrons, relax. of spin and energy 0-10965  
 degenerate four-wave mixing near band gap 0-5782  
 diamagnetic susceptibility of excitonic molecules (Russian) 0-7074  
 diamond-structure semiconductor, Compton profile interpretation 0-29820  
 dielectric screening, Thomas-Fermi model 0-49648  
 differential conductivity with inelastic electron scatt. (Russian) 0-2399  
 direct-gap, two-photon absorpt. 0-50292  
 direct-gap crystals, one-photon absorpt., Keldysh and perturbation formulas 0-20607  
 dislocation structure, optical microscopy obs. techniques 0-24458  
 disorder effects on electronic props. of pseudobinary system (Japanese) 0-49709  
 disordered, electroabsorption, contact excitons influence 0-10882  
 disordered, light induced stationary non-equilibrium distribution of electrons, balance equation 0-39528  
 disordered, optical magnetabsorption coeff. calc. in strong mag. field 0-16011  
 disordered, photon-phonon-assisted hopping, theory 0-44642  
 donor van der Waals interactions, spectral line shapes 0-11450  
 donor-acceptor complexes and interactions, physicochem. nature 0-15472  
 doped, cluster model of impurity states 0-20117  
 doped, insulator-metal transition, dielec. const. enhancement on insulating side 0-20087  
 doped, insulator-metal transition, dielec. constant enhancement on insulating side 0-20088  
 doped, variable range hopping, computer simulation 0-24929  
 doped with magnetic impurity, ordering mechanism 0-2572  
 electric field induced nonequib. phase transitions 0-10879  
 electric resistance, temp. depend., qualitative anal. by audible demonstration 0-46775  
 electrical conduction in strong elec. fields, percolation mechanism 0-20206  
 electrical conductivity and Hall mobility in disordered systems, theory 0-54697  
 electrical conductivity and magnetoresistance of semiconductor with charged defects 0-20225  
 electrical properties, mag. field effect determ., method 0-44623  
 electron drift vel. and phonon multiplication 0-6848  
 electron multiplication, phonon scatt., ionisation rate calcs., Markov processes 0-50267  
 electron scattering by deep level impurities 0-10968  
 electron spectroscopy techniques, review (Japanese) 0-49061  
 electron states of point defects 0-39526  
 electron-hole drop, shape change during motion 0-20093  
 electron-hole drop nucleation, Fokker-Planck treatment 0-6732  
 electron-hole droplet cloud, role of thermalisation phonons 0-49617  
 electron-hole liquid, RPA calcs. 0-6743  
 electron-hole liquid droplets, theory 0-44689



## semiconductors continued

electron-hole plasma current layering, electron cooling length, momentum scatt. 0-6890  
 electron-hole plasma phase transition in direct and indirect gap semiconductors 0-24803  
 electron-hole-plasma, instability in heating elec. field 0-15552  
 electron-phonon interactions, phonons and localisation at impurities 0-24812  
 electronic polarizability as function of Penn gap 0-49638  
 electronic properties, rel. to chem. bonding and lattice dynamics 0-44169  
 elementary semiconductor physics, book 0-6824  
 EM radiation gain, semicond. subjected to mag. and US fields 0-48201  
 EM wave propagation in semiconductor plasma, hot carriers, Hall effect, calc. 0-39620  
 energy spectrum of discrete centre in high inhomogeneous electric field of space charge region 0-10873  
 evanescent states and complex bound structure 0-34387  
 evaporation, injection of nonequilibrium vacancies 0-39273  
 excited, extended phase diagrams, review 0-44521  
 exciton and impurity states, unified theory, for arbitrary mag. field 0-39511  
 exciton condensation, microwave cond., book contrib. 0-11043  
 exciton condensation and electron hole liquids, state-of-the-art 0-49625  
 exciton light absorpt. band formation, linear and quadratic exciton acoustic photon interactions (*Russian*) 0-34368  
 exciton light absorpt. spectra depend. on crystal anisotropy (*Russian*) 0-50386  
 exciton physics, review, book contrib. 0-44517  
 exciton-polaritons, resonant Raman scattering (*Japanese*) 0-50349  
 excitons, book 0-41951  
 excitons, exciton-phonon interaction, resonant Raman and Brillouin spectroscopy, review, book contrib. 0-49624  
 extrinsic, resonance transitions between ground states of donor and acceptor impurities 0-45126  
 extrinsic semiconductors, impurity interaction and metal-nonmetal transition 0-29325  
 Fano factor determ. 0-47813  
 far IR spectroscopy, appl. of far IR lasers 0-31914  
 Faraday rotation in the presence of deep repulsive traps 0-29724  
 fast particle irradi., Frenkel defect formation threshold energy 0-6404  
 ferrite-semiconductor hybrid struct., magnetoelastic wave interaction with drifting carriers 0-54934  
 ferrite-semiconductor layer struct., with negative differential cond., spin wave instability 0-25118  
 ferrite-semiconductor layer structure, EMF created by spin-wave, effect of current 0-11072  
 Fourier transformed X-ray Compton profiles 0-35004  
 galvanomagnetic effects in high mag. fields, for electron scatt. by optical phonons 0-2405  
 Hall current method generalisation to arbitrary magnitude mag. fields (*Russian*) 0-29421  
 Hall effect in semiconductor with superlattice 0-39612  
 high density excitons and biexcitons, recomb. radiation bands profiles, time depend. 0-45140  
 high magnetic field semiconductor physics, review (*Japanese*) 0-50192  
 highly excited photomagnetoelc. effect under Auger recomb. 0-44664  
 hologram recording on semiconductor, photochem. etching control 0-28179  
 hot electron fluctuations with displaced Maxwellian distribution 0-29418  
 hot electron physics, review (*Japanese*) 0-49754  
 hot electron recombination at impurity centres 0-10995  
 hot electrons in longitudinal quantising mag. fields 0-39593  
 hydrogen embrittling effects from acoustic emission meas. 0-11742  
 impact ionisation theory 0-49752  
 impurity conduction phenomena, review of exptl. work (*Japanese*) 0-49737  
 impurity interaction and donor-acceptor recombination 0-16094  
 impurity ion pot., nonlinear Poisson eqn. soln., var. principles 0-29350  
 impurity optical spectra, p-phonon processes 0-16061  
 influence on Auger transitions depend. of impact ionisation on electron energy impact ionisation, influence of scatt. on Auger transitions 0-44608  
 inhomogeneous, anomalous elec. props. in mag. field 0-44621  
 inhomogeneous, EM waves under elec. and mag. fields 0-20237  
 inhomogeneous electric fields in oscillatory photoconductivity 0-2421  
 inhomogeneous struct., transverse acoustoelectric effect 0-39638  
 interband absorption in strong parallel mag. and elec. fields 0-6799  
 interface and overlayer electronic struct., review 0-49841  
 interface and surface phenomena, conference, Pacific Grove, USA (Jan.-Feb. 1979) 0-46725  
 interface and surface physics, review 0-49872  
 interface formation, initial steps, surface states and thermodynamics 0-49503  
 interimpurity radiative recombination, intermediate exciton state (*Russian*) 0-49621  
 ion irradiation produced amorphisation, disorder-ion fluence functions, disorder mechanisms 0-29090  
 ionised impurity scattering, theory 0-20181  
 IR thermometry, semiconductor material temperature measurement (*Spanish*) 0-47062  
 isovalent impurity long range potential, role in electron scatt. 0-10966  
 laser annealing after ion implantation, temp. distrib. 0-54265  
 layered, constant current anodisation, representation of layer periodicity 0-3218  
 light absorption, two-photon, by excitons in static elec. field 0-11364  
 light pulse propagation, high-power, transitions between bands with different effective masses 0-34871  
 lightly doped, 1/f noise for hopping conduction, theory 0-44683  
 local centre parameter determ. from thermally stimulated excitation curve derivative singularities 0-11004  
 local fields, nonuniform charge distrib. 0-24826  
 local level parameters from thermally stimulated excitation curves, influence of variations of rate of heating 0-6769  
 luminescence, PH band profile, exciton-electron interactions 0-20702  
 magnetic oscillation of momentum distribution of hot photoexcited electrons (*Russian*) 0-2854  
 magnetic phase transitions in impurity band (*Russian*) 0-50097  
 magneto-microwave Kerr effect, K-band interferometer 0-52263  
 magneto-optical effects and cyclotron reson. in high mag. fields 0-27321  
 magneto-optical spectra, relax. and reson. struct. 0-29723  
 magnetoresistance, superoperator theory 0-49776

## semiconductors continued

minority carrier lifetime meas. for crystals with high quantum efficiency (*Japanese*) 0-54711  
 Moss relation between refr. index and energy gap of semiconductors 0-11357  
 Mossbauer spectra of implanted  $^{83}\text{Kr}$ , line widths, isomer shifts 0-39899  
 multicomponent exciton gas, composition calc. 0-49618  
 multiple bound excitons, density functional calc. 0-10889  
 natural EM oscillations excitation by stream of electrons or EM field 0-34378  
 non-linear transport theory, field depend. of carrier screening 0-29415  
 non-polar cpd. semiconductor surfaces, chemisorption of O,  $\pi$ -bonding contrib. 0-6631  
 nondegenerate, band electrons at arbitrary electron-phonon coupling, transport props. 0-39592  
 nondegenerate, free carrier absorpt. in quantising mag. fields 0-45044  
 nonlinear equation, asymptotics of spectral boundary-value problem 0-6851  
 nonlinear intense EM wave absorpt. theory (*Russian*) 0-29425  
 nonlinear optical properties 0-25333  
 nonradiative multiphonon carrier capture by deep neutral traps 0-6871  
 opaque, inelastic dynamical light scatt. 0-25399  
 optical nonuniformity, spatial distrib. determ. 0-13116  
 optical properties, review 0-45106  
 optical properties with electron temp. superlattice (*Russian*) 0-34879  
 optical thermal breakdown, fluctuations and wave processes 0-20587  
 optically anisotropic, effect of modulation of mag. field on absorption 0-34898  
 paramagnetic phonon resonance, theory 0-50187  
 parametric conversion of acoustic/optical phonons, ultrasonic pumping 0-15209  
 partially disordered, density of states calcs., forbidden gap energy depth (*Russian*) 0-34347  
 partly disordered, with mobility threshold, transport props. and thermoelec. parameters 0-34449  
 permittivity of crystal in strong EM field, light absorpt. and emission effect 0-15938  
 phonon assisted electron impact ionisation and Auger recombination, theory 0-39591  
 photoconductor-air gap-semiconductor system, calc. of surface charges under voltage in darkness 0-6905  
 photoelectric conductance submicrosecond relaxations meas. (*Czech*) 0-31804  
 photoelectron spectra and band struct., book contrib. 0-16155  
 photoemission in solids, book 0-12860  
 photoemission meas. of surface and bulk states 0-25527  
 photoionisation of deep impurity levels 0-34386  
 photosemiconductor-dielectric systems, two-component, photoelectret state 0-25287  
 plasma, solitons in radiophysics 0-48124  
 plate, light irradiation, heating and thermoelastic stress 0-25499  
 Poisson's equation, linear and nonlinear numerical solution including spatially variable dielectric const. 0-6825  
 polaritons, two-phonon Brillouin scattering 0-20656  
 polaron transport eqn. soln. in strong alternating elec. field 0-39596  
 polycrystalline, with low angle grain boundaries, residual cond. 0-15525  
 powder, prep., freeze drying of solid solutions, solvent choice 0-11583  
 pure, carrier mobility and electron state damping at low temps. (*Russian*) 0-15530  
 quasi elastic hot electron impurity scatt. in quantising mag. field 0-24938  
 radiation effects, role of nonequilibrium state 0-39152  
 radiative and nonradiative recombination, spontaneous and stimulated emission (*Polish*) 0-53293  
 radiative recombination at donors and acceptors, majority impurity config. average calcs. 0-40154  
 Raman scattering, one-phonon final states and many-body effects 0-34913  
 recombination wave modes in case of several trap levels 0-39602  
 resistivity and Hall effect meas., nondestructive four-electrode characterization 0-49743  
 resonance two-photon absorption, theory 0-28268  
 runaway electron-heating dynamics 0-39597  
 SEM characterisation of semiconductor materials and devices 0-49064  
 semiconductor-transition metal, Anderson model localised impurity states (*Russian*) 0-6788  
 semiconductors, elementary excitations in disordered systems with localised electrons, polarons (*Russian*) 0-49632  
 semiconductors, free carrier density in strong electric and quantised mag. fields 0-6860  
 shallow and deep level evaluation using Schottky contacts, conc. and distrib. 0-49669  
 shallow impurity levels, effective mass approx. 0-6781  
 solid films and surfaces, conference, Tokyo, Japan (Jul. 78) 0-10739  
 solid state physics, conf. Munster, Germany (March 1979) 0-41941  
 specific heat rel. to energy gap temp. depend. 0-54403  
 spreading resistances, multilayer analysis, errors in resistivities 0-10964  
 stationary recombination equations, analytical solutions in source limiting cases 0-44662  
 strong electron-lattice interaction, review (*Japanese*) 0-49664  
 strong EM wave interaction 0-6852  
 substrate, work function rel. to AES (*French*) 0-50479  
 superlattice, optical phonon excitation by light absorpt., impurity photoionisation 0-44275  
 superlattice, phonon spectrum, effect of strong elec. field, parametric reson. 0-44273  
 superlattice, plasma oscills. in strong elec. field 0-44637  
 superlattice impurity photoconductivity electron spectrum reconstruction 0-24966  
 superlattices, electroplasma parametric resonance 0-34475  
 superlattices, optical and transport props., review (*Slovak*) 0-20288  
 surface, macroscopic recomb. centres 0-6933  
 surface, reson. inelastic light scatt. by charge carriers 0-20655  
 surface, theory, book 0-36787  
 surface and interface electronic structure, scattering theoretic approach 0-6940  
 surface and interface states, meas. (*Japanese*) 0-20269  
 surface Brillouin scattering from acoustic phonons 0-55113  
 surface characterisation using SAW 0-11069  
 surface electron states, empirical tight-binding method, critique 0-49854  
 surface electronic props., optical spectroscopic techniques, review 0-11070



**semiconductors continued**

- surface helicon waves in Faraday geometry, existence 0-44703  
 surface magnetoplasma wave spectrum in HF mag. field 0-24995  
 surface potentials using electron energy anal., SEM study 0-15582  
 surface reconstruction, dynamical theory 0-10773  
 surface spectroscopy, exciton effects, theory 0-49856  
 surface structure and properties, review (*Japanese*) 0-49483  
 temperature dependence of energy gap 0-2321  
 temperature dependences meas., of electric conductivity, Hall coeff. and magnetoresistance, automated installation 0-31792  
 temperature superlattice with hot electrons 0-20202  
 tetrahedrally coordinated covalent semiconductor point defects, multiple scatt. X $\alpha$  model 0-54636  
 thermal conductivity, calc. using numerical soln. of Boltzmann eqn. 0-44373  
 thermoelectric amplification of sound 0-2427  
 thermoelectric and thermomagnetic effects, heat transfer due to quasi-particle subsystems (*Russian*) 0-24959  
 thermoelectromagnetic waves in conductors in a mag. field (*Russian*) 0-49695  
 thermophysical props. determ. from Ettingshausen effect meas. method 0-44376  
 transient donor recombination, adiabatic approx. 0-49761  
 transverse conductivity in quantising mag. fields, finite radius scatterer neutral impurities (*Russian*) 0-29400  
 two-dimensional electron-hole systems in high mag. fields, phase transitions 0-49608  
 two-photon interband optical transitions involving deep impurity centres, photon drag 0-16069  
 unijunction transistor transition critical exponents, negative resistance phenomena 0-44713  
 unipolar, n-type, field-effect mobility, energy spectrum of surface states 0-39657  
 valence band calc. using many-electron theory 0-15434  
 Van der Pauw structure with finite contacts, anal. of Greek cross, sheet resistance meas. 0-22387  
 variable-gap, photoluminesc. under transient excitation conditions 0-20698  
 variable-gap semiconductors, anal. of drift of recombination radiation 0-16096  
 Wannier excitons, fine structure, lineshape and dispersion, review 0-44520  
 Watkins-type radiation defects, low temp. form. mechanism 0-15153  
 wide gap monocrytalline semiconductor, determ. of bulk and surface absorption coeffs., photoacoustic spectroscopy 0-4781  
 zero gap semiconductors, electron scatt., thermoelec. power and Hall effect at low temp. 0-44628  
 zero-gap semiconductor, reson. scatt. of electrons 0-10938  
 zinc blende type ionic semiconductors, vacancies, bound state energy level calcs., tight binding approx. 0-44694  
<sup>129</sup>I impurities implanted in semiconductors, isomer shift 0-20522  
 Si, solar-grade, directional solidification in carbon crucibles 0-45663

**semileptonic decays**

- baryon octets, SU<sub>3</sub> theorems 0-32030  
 flavour-changing meson semileptonic decays 0-22553  
 hyperon semileptonic decay, SU(3) spectrum generation, Cabibbo angle 0-9119  
 neutrons, ultracold, use for lifetime meas., collision loss calcs. (*Russian*) 0-52504  
 proton semileptonic decay in nuclei, pion attenuation 0-47286  
 B-meson decay, partial unification of strong, weak and EM interactions 0-18106  
 D $\rightarrow$ K $\pi$  $\nu$ , current algebra calcs., form factors and decay distrib. 0-42447  
 D semileptonic branching ratio and lifetime from  $e^+e^- \rightarrow e^+X$  0-4983  
 K $\rightarrow\pi e(\mu)\nu$ , form factors, SU(3)  $\sigma$ -model one loop calc., chiral symmetry breaking 0-52506  
 K $\rightarrow\pi^+\pi^-e^+e^-$ , decay amplitude using simple model with PCAC 0-9162  
 $\Lambda_c^+$  lifetime, semileptonic branching fractions, nonspectator quark interactions 0-37260  
 $\mu$  production by decay of hadronic shower, EM production of trimuons in deep inelastic muon scatt. 0-22619  
 n $\rightarrow e\bar{\nu}$ , H atom spectra and metastable state (*Russian*) 0-37262  
 $\nu_e(\bar{\nu}_e)N$ , charm meson prod. and decay, lepton inclusive distrib., c-quark fragmentation function (*Russian*) 0-52493  
 $\nu N$ , high energy, dilepton events, D meson semileptonic decay 0-42446  
 p, decay, confirmation of unification of forces, book contrib. 0-42383  
 p, decay, search techniques for lifetimes of order 10<sup>14</sup> years 0-47287  
 p decay modes in SU(5) and SO(10) theories 0-13301  
 $\Sigma^- \rightarrow \Delta e^- \nu$ ,  $\mu$  0-42458  
 t-quark, obs. in  $\nu N \rightarrow \mu^+ X$  0-13297  
 $\tau$  decay,  $\nu_e(\bar{\nu}_e)N \rightarrow \tau^+ X$ , beam-dump experiment, observation of  $\nu_\tau$  interactions 0-22601  
 $\tau \rightarrow \nu \pi \omega$ , decay width and form factor calc. using vector dominance hypothesis (*Russian*) 0-47271  
 $\tau \rightarrow \nu \rho \pi$  decay parameters from PCAC and current algebra, A<sub>1</sub> characts. 0-37314  
 $\tau^- \rightarrow \rho^- \nu$ , branching fraction meas. 0-13296  
 $\Xi^- \rightarrow \Delta e^- \nu$ ,  $\mu$  0-42458

**semimetallic thin films**

- As, condensed layers, low temp. allotropic phase transition (*Russian*) 0-54553  
 Bi epitaxial films, size effect in elec. props. 0-54813  
 Bi film, carrier conc., mobility and 1/f noise 0-44748  
 Bi film, evaporated, lattice distortion spectrum, elec. resistance temp. variation 0-54806  
 Bi film, quantum size effect and band struct. Bi-dielec.-metal system obs. 0-54811  
 Bi film deposition by vacuum evaporation on NaNO<sub>3</sub> single cryst. cleavage 0-35091  
 Bi, on Si(111) substrate, MBE deposition kinetics 0-10817  
 Bi, spheres, mean inner pot., elec. biprism and interf. electron microscopy 0-49063  
 Bi, surface defects and struct., electron microscopy and elec. props. (*French*) 0-15415  
 Bi, thin film, 1/f noise, boundary scatt. effect 0-49836  
 Bi thin wire, resist. anomaly, possibility of one-dimensional quantum size effect 0-54809  
 Bi-Sb alloy, amorphous nature, AC and DC cond. and Hall coeff. obs. 0-11114

**semimetallic thin films continued**

- Bi<sub>1-x</sub>Sb<sub>x</sub> alloy films, quantum resistance oscils. at low temps., surface band distortion (*Russian*) 0-11110  
 Sb, amorphous film on glass substrate, effect of substrate temp. on crystallisation 0-39468  
 Sb, thin films, IR absorpt. and intraband transitions 0-16114

**semimetals**

- see also antimony; arsenic; bismuth; semimetallic thin films*  
 electron heating due to acoustic phonon scatt. in Bi type semimetals (*Russian*) 0-10991  
 metal-semimetal system, local and total density of states determ. (*Russian*) 0-54586  
 mixed superconducting-excitonic insulator phase, diamagnetism, virtual intraband transitions 0-2520  
 thermoelectromagnetic waves in conductors in a mag. field (*Russian*) 0-49695  
 Bi-Sb, magnetoplasma effects at 300 GHz in Voigt configuration 0-39619  
 Hg<sub>1-x</sub>Cd<sub>x</sub>Se, zinc blende structure, optical and electronic properties 0-6723  
 Hg<sub>1-x</sub>Cd<sub>x</sub>Te, (x<0.16), semimetallic phase, acceptor states and galvanomagnetic effects 0-6882  
 TiSe<sub>2</sub> (1T), electronic and vibronic struct. 0-44500

**Senftleben-Beenakker effect**

- linear mol. gas thermal cond. Senftleben-Beenakker effect, effective collision cross section 0-24117  
 shear viscosity SBE collision integrals, linear mol. gas, Liouville algebra 0-10353  
 CO<sub>2</sub>+O<sub>2</sub>(NO), Senftleben-Beenakker effect, saturation field, Kohler-Raum theory and obs. 0-28596

**sensing devices see detectors****sensing devices, electric see electric sensing devices****sensing devices, nonelectric see nonelectric sensing devices****sensitivity**

- acousto-optic parallel channel wideband receiver 0-48447  
 EM distance measurement (EDM), single-wavelength, data ratios rel. to line length changes resolution 0-4143  
 fluorometric techniques and instrumentation 0-45845  
 geomagnetic field local changes determ., narrow line <sup>87</sup>Rb, magnetometers accuracy and noise reduction 0-26636  
 gravitational-wave resonant antennas, optimum filtering and sensitivity 0-8545  
 hydrophone, interferometric fibre optic, static press. sensitivity amplification 0-38094  
 hydrophone, multimode fibre optic, frustrated total internal reflection, testing 0-38096  
 image isocn, threshold and contrast sensitivities rel. to appl. in astrophysical obs. (*Russian*) 0-12671  
 magnetic sensor, high permeability metal core solenoid absolute sensitivity calibration 0-31133  
 mouse sensitivity to curariform drug. 2.45 GHz irradiation effect (*French*) 0-3717  
 quantitative IR spectral analysis, background and overlapping of absorpt. bands influence on accuracy 0-55748  
 space applications of LF supercond. sensors inc. SQUID devices 0-56691  
 spatial light modulator with CCD address 0-48445  
 spectrometers, threshold sensitivity 0-8990  
 underwater sound transducers, parabolic reflector as nearfield calibration device 0-48528  
 Zn-In-S ultraviolet detector (*Russian*) 0-18014

**sensitivity analysis**

- see also control system analysis; dynamic response; frequency response; transient response*  
 fission reactor thermal hydraulics analysis, differential sensitivity theory for nonlinear equations with nonlinear responses 0-47551  
 quantum collision theory, generalised sensitivity anal. 0-31542

**sensors, nonelectric see nonelectric sensing devices****sensory aids**

- see also contact lenses; hearing aids*  
 acoustic seeing aid for blind (*Polish*) 0-8215  
 deaf speech and hearing aids, vocoders, frequency lowering and lipreading cues 0-12309  
 eikonic lens design for minus prescriptions 0-46095  
 hearing and seeing aids, electronic developments 0-51285  
 lenses of TiO glass, and astigmatism of oblique rays (*Italian*) 0-56278  
 nonvocal communication aid improvement by microprocessor technology 0-8217  
 ophthalmic lenses, thin, chemtempered, static load strength testing 0-5812  
 ophthalmic lenses, thin, chemtempered, strength meas. by drop-ball testing 0-5811  
 optical-to-tactile converter of wide images, blind aid 0-26414  
 prosthetic hand pinch force, sensory-feedback system compatible with myoelectric control 0-41324  
 rehabilitation engineering (*Japanese*) 0-12304  
 rehabilitation of severely disabled, microcomputer environmental control and communication system 0-8216  
 semantically accessible communication aid development trends 0-8218  
 tactual vocoder, max. information transmission, time-invariant stimulation (*Japanese*) 0-41317  
 telephone handling aids for handicapped people 0-36196  
 US, mobility aid for blind people 0-56290

**separation**

- see also desalination; distillation; drying; filtration; isotope separation; magnetic separation*  
 boric acid solutions, extractive purification from radioactive corrosion and fission products 0-18458  
 dialysis device, high-speed 0-17205  
 element mass separation mechanism in plasma discharge in intersecting fields (*Russian*) 0-14943  
 flotation, noninertial, effect of particle aggregation 0-55719  
 fluidised bed, continuous gas-solid, min. carrying vel. of particles prediction 0-33670  
 ion exchange membrane selectivity w.r.t. dialysis prospects 0-45560  
 isocyanate polymers, partitioning between isotropic and anisotropic phases 0-24343  
 liquid mixture, shallow, laser separation, thermal mechanism 0-5925  
 particulate materials, vibrated bed electrostatic separation 0-16641



**separation continued**

- plasma centrifuges, fluid flow analysis, third-order differential equation solution (*Japanese*) 0-53949
- powder particle motion and segregation by density difference in V-type mixer 0-45250
- radionuclide corrosion and fission products, ion exchange separation 0-18460
- radionuclide corrosion and fission products, liquid-liquid extractions with metal diethyldithiocarbamates 0-18459
- rare earth element separation from clay, complexation method 0-3442
- rare earths, purification, laser methods 0-16712
- suspensions, dielectric separation of solid particles 0-16213
- virtual impactor for particle classif. and generation of test aerosols with narrow size distrib. 0-30626
- volatile trace organics, aqueous environmental samples, head space anal. 0-40763
- Ar purification system and electronegative impurity conc. meas. instrument 0-32571
- Be, determ. in biological materials, flameless atomic absorption spectrometry (*Japanese*) 0-26428
- Cu electrorefining process, quantitative evaluation of Ag transfer 0-30246
- <sup>64</sup>Cu, extraction from reactor-irrad.  $\alpha$ -phthalocyanine target 0-35563
- H, thermochemical production, irreversibility anal. of separation schemes from binary gas mixtures 0-35767
- He-Ar mixture, mass separation during molecular beam sampling process 0-31937
- Xe-He(Ne), gas mixture, element and isotope separation in impulse plasma centrifuge (*Russian*) 0-38725

**series (mathematics)**

- binary lattice gas, crit. phenomena, series anal. 0-4671
- Born series rearrangement in model space, resolvent operator expansion 0-13422
- charge density functions, Bertaut series, convergence props. study 0-27104
- critical exponents in three dimensions, derivation from  $\phi^4$  field theory with Gaussian propagator 0-4686
- Debye lattice, thermal props., WINIMAX approx. appl. 0-49333
- diffusion, linear eqn., improved series soln. method 0-8939
- electrical engineering dimensional unification (*Italian*) 0-27266
- ferromagnetic classical vector model, extension of high temp. free energy series 0-7062
- flow between concentric rot. spheres, nonlinear, axisymmetric 0-19412
- Fourier series, concept of basic number 0-4513
- Fourier series in celestial mechanics, fast evaluation 0-56711
- Fourier-Bessel series soln. of exterior Dirichlet boundary-value problem with rot. symm. 0-1103
- Gaussian integrals, evaluation by backwards recursion or Taylor expansion 0-31488
- Ising model with free surface, series anal. 0-25062
- Lagrange's inversion formula, soln. 0-31484
- Legendre series summation, recursive procedure, gravit. potential evaluation 0-31486
- linear systems, response to square wave force, transients, teaching appl. 0-31467
- Percus-Yevick eqn., orthonormal series expansion soln. 0-49065
- Planck integral, non evaluation in terms of finite series of elementary functions 0-31563
- polymers, rectilinear on square lattice, series expansion 0-5646
- Stark effect, perturbation and variation treatments, appl. to H(1s) reson. 0-14105
- Taylor series method for two-body shell model matrix elements 0-32212
- Taylor series method for two-nucleon reduced widths in symmetric two-centre shell model 0-32213

**serrated yielding**

- $\alpha$ -brass, Portevin-LeChatelier effect (*Japanese*) 0-11724
- steel, low C and alloy, serrated flow and thermomechanical treatment (*Korean*) 0-30026
- steel, maraging 300 grade, serrated flow in austenitic state 0-30041
- Al alloy 7075, serrated flow and thermomechanical treatment (*Korean*) 0-30026
- Fe, cast, ductile, strain rate and temp., influence on strength, elongation and deformation (*Japanese*) 0-45356
- TiO<sub>2</sub> rutile single crystals, stoichiometric, dynamic strain ageing 0-50661

**service programs see utility programs****services, information see information services****servo systems see servomechanisms****servomechanisms**

- arterial O tension servocontrol in preterm infants 0-17183
- electro-optic modulator, servo controlled, for CW laser power stabilisation and control 0-19060
- metrology, Cs beam freq. standard, servo-control system anal. 0-42201
- moving material fault test rig (*German*) 0-11855
- HF chemical laser phase control servo system 0-33063

**set theory**

- crystals, cubic-tetragonal transitions, symmetry anal. 0-10636
- function processes, vector lattices, Riesz decomposition and characts. (*French*) 0-8908
- lattice, orthocomplemented quasi modular, quantum logic interpretation 0-12950
- lattices, regular, isoperimetric problems, convex-set theory and lattice symmetry 0-46988
- nilpotent Lie algebra, prime spectra of an enveloping algebra (*French*) 0-8777
- partial inner product spaces, compatibility relns. 0-46855
- quantum logic, props. of states 0-12947
- shock waves, global structure anal. 0-8800
- supersonic plane flow, past a curved wedge, quasi-linear hyperbolic systems (*French*) 0-10261

**sets (mathematics) see set theory****sferics see atmospheric****shadow universe see cosmology****shape memory effects**

- alloy, props. and appl. 0-30049
- alloy connector for optical fibres 0-53475
- criteria for efficiency assessment (*Russian*) 0-21015
- practical apps. of shape-memory alloys 0-45307
- premartensitic phenomena, nucleation, shape memory effect, review 0-3041

**shape memory effects continued**

- Ti-Ni, electron emission and shape memory effect 0-50687
- Ag-Cd (45 at.%) martensite, shape memory mech. and related phenomena 0-30009
- Cu-Al-Ni(Mn), duplex shape memory effect after nonuniform plastic deform. (*Russian*) 0-25759
- Cu-Zn-Ga(Al), martensites, internally faulted, shape memory mechanism 0-30010
- Fe-Ni-Co-Ti, shape memory effect after appl. of bending moment (*Russian*) 0-45305
- NaCl, plastic deformation influence on shape recovery effects 0-6684
- Ni-Ti, Nitinol memory material heat engine, comment on efficiency 0-3529
- Ni-Ti, Nitinol memory material heat engine, reply to comments on efficiency 0-3530
- Ni-Ti alloys, criteria for efficiency assessment (*Russian*) 0-21015
- Ni-Ti shape memory alloy processing and medical applications (*German*) 0-17203
- Ni-Ti shape memory alloy trigger for space satellite boom latch and release mechanism 0-7575
- (Ni<sub>1-x</sub>Cu<sub>x</sub>)Ti, martensitic, shape memory effect kinetics and thermodynamics 0-3021
- NiTi, martensitic, shape memory effect kinetics and thermodynamics 0-3021

**shear see crystallographic shear****shear flow****see also shear turbulence**

- aniline-cyclohexane, crit. mixture with shear flow, light scatt. obs. 0-6521
- anisotropic micropolar fluid theory 0-31515
- approximations of unidirectional flow, unification using stress tensor 0-27139
- atmosphere shearing instability mechanism model, effect of horizontal diffracting 0-26578
- average flow model, appl. to lubrication between rough sliding surfaces 0-16497
- Brownian motion in shear flow, exact solution by operator formalism 0-17874
- Brownian particle diffusion in shear induced convection, Poiseuille flow 0-33591
- buoyant surface jet, 2-D flow props. (*Japanese*) 0-48762
- bursting phenomenon in bounded turbulent shear flow, streamwise vortices 0-1600
- cholesterics, shear flow induced propagating domains 0-54131
- compressible atmosphere, vertically rotating, critical levels 0-6073
- counter gradient flow downstream of two different diameter cylinders (*French*) 0-43693
- critical fluids, non-Newtonian effect and normal stress effect 0-49396
- critical fluids under shear flow, nonequilib. steady state, renormalisation group approach 0-6026
- cyclohexane-aniline mixture, shear induced transition to mean-field crit. behaviour 0-7364
- cylinder with elliptic limaçon cross-section, stagnation points 0-23984
- dilatant liquids, propag. of shear perturbations 0-6103
- directed fluid sheets and gravity waves in compressible and incompressible fluids 0-14714
- EHD with asymmetric stress tensor fluid 0-19520
- entangled monodisperse polymers kinetic network model for nonlinear viscoelastic flow props. 0-28538
- flow fields in plate and cone viscometers with small gap angles 0-19516
- fluctuating free convection flow on horizontally magnetised plate 0-33683
- fluid fluctuations about hydrodynamic nonequilibrium steady states, Langevin method calcs. 0-53761
- fluidised, open channel flow 0-14826
- forming limit curve for bending processes 0-7627
- free shear layer, compressibility effect on stability 0-33562
- free shear layer in viscous critical layer regime, nonlinear stability 0-33576
- fully developed turbulent pipe flow, low Mach number wall turbulence-sound interaction 0-6148
- gas, nonlinear shear viscosity in steady Couette flow 0-28588
- glass-fibre reinforced PET, order-disorder transitions during extrusion 0-50633
- hurricanes, shearing environmental steering current rel. to spiral bands excitation 0-56538
- impinging free shear layers, self sustained oscillations, book contrib., review 0-19466
- inviscid shear flow over flexible membranes, stability 0-14658
- jet, axisymmetric free shear flow with Reynolds stress closure 0-19469
- Lennard-Jones fluid, nonlinear viscous flow 0-24060
- liquid crystal, reentrant nematic, oriented, capillary shear flow 0-49344
- liquid thin film, evaporation and breakdown driven by shear stresses 0-38410
- MHD shear inviscid flow, vortex sheet stability 0-28571
- near-field jet entrainment, overlaid viscous/inviscid model, BOAT computational model 0-19457
- nematic liquid crystals, shearing flow solns., stability and dissipation 0-49288
- non-linear model, constitutive equation testing with free. vol. relax. spectrum 0-6011
- nonsteady plane stagnation point flow with hard blowing 0-33579
- plane Couette flow, finite amplitude, instability shear layer parallel flow, cellular motion 0-1601
- Poiseuille channel flow, finite amplitude, instability shear layer parallel flow, cellular motion 0-1601
- polyacrylamides-water-glycerol, streaming birefringence in extensional flow 0-6013
- polyethylene, high-density, polymer melt, shear stress at wall 0-19450
- polyethylene, low density melts, temp. depend. of the elongational behaviour 0-6012
- polyethylene melts, low-density, viscosity and viscoelasticity, filler effect 0-10222
- polyethylene oxide, aq. soln., mech. props. in parallel superposed flows, geometric effects 0-19448
- polyisobutylenes, shear behaviour of Vistanex LMMH and L 100 0-1443
- polymer, filled, solution, normal stresses and hyperelasticity under simple shear flow 0-1506
- polymer crystallisation from solns. and melts, deform. effects 0-10504
- polymer solns., dilute, Hartree self-consistent field analysis 0-5648



## shear flow continued

- polymeric, liq., spike-strain test relevance for network connectivity destruction by deformation 0-6001  
 polymers, conc. solns. in volatile solvents, high temps., method for viscosity meas. 0-19535  
 polymers, unsteady flow in rotary devices 0-24061  
 polymers solutions, zero-shear viscosity estimates from falling sphere data 0-19306  
 polystyrene-Aroclor 1254, streaming birefringence in extensional flow 0-6013  
 polystyrene-decalin solns., flow irregularity obs. in theta conditions 0-38453  
 polystyrene-mineral oil mixture, viscosity and normal stress coeff. 0-44349  
 polystyrene melts, stresses and birefringence in intermittent shear flows 0-19308  
 PVC plastisols, high resin level, rheological behaviour, discontinuous viscosity 0-23980  
 Reynolds stress transport eqns. 0-19320  
 rotation effects on flow past porous plate 0-10256  
 rotational rheometry, edge effects and related error sources 0-19536  
 second moment turbulence closure to heat and mass transport in two-dimens. thin shear flow 0-24010  
 shear stress determination, in laminar and Taylor vortex flows using flush-mounted hot film probe 0-28486  
 shock wave structure close to wall, book contrib. 0-1650  
 spherical Couette flows, loss of stability between two rotating spheres 0-1527  
 Stokes flow, attached and free eddies 0-48679  
 stratified, Stewartson vertical layers 0-48772  
 streamline patterns and eddies in low-Reynolds-number flow 0-33612  
 symmetrical wake calc., two-dimens. laminar and turbulent flows 0-14707  
 transient viscosity determination method 0-43746  
 two layer system with baroclinic mean shear flow, solitary Rossby waves theory 0-17293  
 viscometric data from Brookfield RVT viscometer, conversion to shear stress-shear rate relationship 0-1495  
 viscous electrically cond. fluid, laminar free shear flow, transverse mag. field effect 0-48811  
 viscous fluid in rotating channel pulsatile flow 0-10311  
 vortex-edge interaction, low frequency component generation mechanisms 0-53795  
 wall shear stress meas. in shock wave-boundary layer interaction, comments 0-14670  
 Al, numerical smoothing of flow patterns 0-7625  
 Al plastic flow in plain strain extrusion, photographic appl. 0-7626  
 Fe<sub>2</sub>O<sub>3</sub>, flocculated suspension in ethylene glycol, intrinsic viscosity rel. to shear rate 0-1502

## shear modulus

- $\beta$ -brass (40 to 50 at.% Zn), elastic shear consts., comp. depend., pseudo-pot. calc. (Russian) 0-24525  
 cap, cracked, transverse shear and material orthotropy effects 0-10144  
 carotid artery, human, shear modulus determ. 0-26253  
 chain networks, static and dynamic entanglements, contrib. to equilib. shear modulus 0-28126  
 composite material models, three phase sphere and cylinder models soln. for effective shear props. 0-25749  
 composites, circular specimens, shear modulus determ. 0-25752  
 composites, three-dimensional structure, mech. characts. 0-38266  
 curved structural members, large displacement theory, applic. to lateral-torsional buckling anal. of circular arches 0-23924  
 cylindrical shell, circumferentially cracked, transverse shear effect 0-28472  
 elastohydrodynamic contact, rheological model 0-33544  
 elastomeric network, finite linear viscoelastic theory, time-depend. deform. behaviour 0-38292  
 electron solid, two-dimens., shear modulus and melting, temp. depends. 0-158  
 fibre reinforced composites, weakened by periodic system of cracks, longitudinal shear 0-35323  
 gelatin gels, coloured component addition, struct. form., dynamic shear modulus, viscosity meas. (Russian) 0-7871  
 glass, C and glass/C hybrid reinforced plastics, fatigue props. and flexural rigidity (Japanese) 0-55510  
 glass fibre reinforced plastic, dynamic stress conc. around defects, discrete model 0-30024  
 glass fibre reinforced polyester resin laminate cantilever, bending fatigue strength, cyclic freq. effect (Japanese) 0-55507  
 glass with frozen structure, viscous flow, valence configuration flow theory 0-39335  
 graphite, irradiated, stored at room temp., neutron damage annealing and C<sub>44</sub> shear modulus 0-2080  
 liquids, complex shear modulus meas. by Ni-tube resonator in kHz range 0-17936  
 liquids, relation between viscoelasticity and shear-thinning behaviour 0-19307  
 lung, shear modulus and pleural membrane tension, improved meas. 0-30746  
 measurement by fully automated torsional pendulum, in range -180 to 250°C (German) 0-17935  
 metals, radiation effects on elasticity and elastic moduli, yield stress 0-2078  
 mixtures and suspensions, flow rate meas., ultrasound propagation and scatt. approach 0-43806  
 multilayer cylindrical shell, theory in inhomogeneous temp. field 0-1434  
 photoemulsions, gels, coloured component addition, struct. form., dynamic shear modulus, viscosity meas. (Russian) 0-7871  
 plastic, glass-reinforced bottoms with a filler, rigidity 0-15183  
 poly-4-methylpentene-1, elastic parameters, US velocity meas. at 2.1-240K 0-40415  
 polymer network formation, pre-gel intramol. reaction and gelation, shear moduli and glass transition 0-45501  
 polymer network formation, relaxational props. variation 0-38961  
 polymers solutions, zero-shear viscosity estimates from falling sphere data 0-19306  
 polymers with periodic deform., longitudinal flow 0-6008  
 rubber, rigidity and loss factor, meas. under steady vibr. 0-55602  
 sand, dynamic properties w.r.t. seismic risk prediction, stress condition effect (Japanese) 0-17235

## shear modulus continued

- steel, stainless AISI 316, neutron irradiated, rel. between irradiation induced swelling and shear modulus 0-15157  
 steel, stainless type 304, elastic const. variability, US vel. meas. 0-55446  
 thin shell, 9-node Lagrangian element 0-23888  
 TORUS II Tokamak, toroidal field coil, fatigue test results 0-13928  
 Al<sub>2</sub>O<sub>3</sub> ceramics, elastic props. meas. in 100 to 300°C range 0-55445  
 C fibre reinforced plastic, moduli meas. (Russian) 0-39199  
 Cu, electron-irradiation internal friction behaviour, shear modulus and damping meas. 0-55444  
 Fe-Cr-Ni, neutron irradiated, rel. between irradiation induced swelling and shear modulus 0-15157  
 Fe-Ni solid solution, deformation mechanism, softening phenomena, dislocation-solute atom interactions (French) 0-45344  
 Fe-Ni-Mn-C (5.9, 4.4, 0.48 wt.%) alloy, elastic moduli near martensitic transform. 0-7619  
 MnBi, mictomag. alloys, elastic props. (Russian) 0-7141  
 Ni-Al, neutron irradiated, rel. between irradiation induced swelling and shear modulus 0-15157  
 Nichrome, plasma spray coatings, relaxation phenomena 0-19876  
 Pd, elastic consts. 4 to 300K 0-6455  
 $\beta$ -PdH<sub>0.66</sub>, elastic consts. 4 to 300K, Debye temp. 0-6455  
 Se, vitreous, elastic coeffs. about glass transition temp. US study (French) 0-19865  
 SiO<sub>2</sub> vitreous fibres, relax. props. near glass transition interval 0-34137  
 Tb<sub>0.3</sub>Dy<sub>0.7</sub>Fe<sub>2</sub>, sound velocity mag. field and temp. depend. elastic moduli calcs. 0-39839  
 W, plasma spray coatings, relaxation phenomena 0-19876

## shear strength

- adhesives, thermosetting acrylic, electron beam curing 0-16634  
 adiabatic plastic deformation, shearing phenomena, review 0-50692  
 arches stability analysis, flat, sandwich-type 0-48570  
 composite material, in-plane shear charact. 0-35251  
 epoxy based structural adhesives, time-temp. cure behaviour, torsional braid anal. 0-55621  
 epoxy resin based composites, superconducting magnet insulators, gamma-ray radiation effects 0-24495  
 fibre reinforced composites, Monte Carlo study of strength 0-25844  
 glass fibre reinforced epoxy, deterioration in water, hydraulic press. effect (Japanese) 0-55470  
 glass fibre reinforced epoxy, deterioration in water, immersion time effect (Japanese) 0-55471  
 glass fibre reinforced epoxy, struts for superconductive storage magnets, mech. props. 0-25824  
 glass fibre reinforced epoxy, wound, strength in twisting, stretching and transverse bending 0-11622  
 glass fibre reinforced plastic, dynamic stress conc. around defects, discrete model 0-30024  
 glass fibre reinforced plastic, punching shear tests under static and impact loadings (Japanese) 0-55512  
 glass fibre reinforced plastics, cyclic strength in complex stressed state 0-3181  
 glass fibre reinforced poly- and vinyl ester thermoset moulding, cure cycle effect on mech. props. 0-45369  
 glass fibre reinforced polyester, struts for superconductive storage magnets, mech. props. 0-25824  
 glass-epoxy laminate, superconducting magnet insulators, gamma-ray radiation effects 0-24495  
 granular materials deformation, microscopic and macroscopic exam., stress/strain characts. calc. (Japanese) 0-11691  
 ice, shear strength temperature depend. 0-24523  
 joints, double adhesive bonded, loaded in shear tension (French) 0-23968  
 laminated plates, optimum design under shear 0-23925  
 lubricant, shear rheological behaviour at high press. 0-35342  
 meas. installation for solids meas., at 120 to 300K and up to 100 kbar 0-50787  
 metal-sapphire interface, effect on shear strength of adsorbed species 0-49485  
 ocean sediment free-fall penetrometer with Doppler telemetry 0-46320  
 organotextolite, in plane state of stress, temp. depend. variant of strength 0-40449  
 plastic, fibre-glass reinforced, flat stressed state, strength and deformation props. function of reinforcement struct. 0-19866  
 plastic laminates, glass- and fibre-reinforced, strength anisotropy comparative anal. 0-19872  
 polyethylene/Cu(Zn) adhesion, role of surface topography 0-35500  
 polymer films, superconducting magnet insulators, gamma-ray radiation effects 0-24495  
 polystyrene, cryogenic foam insulators, low temp. props. 0-25818  
 polyurethane, cryogenic foam insulators, low temp. props. 0-25818  
 prefluorinated polymer, DuPont Krytox 143-AB, viscoelastic and dielectric props. 0-1503  
 prosthetic intramedullary implants pre-coated with bone study, fixation study 0-7587  
 sand, cyclic liquefaction strength 0-3996  
 steel, stainless, with Ni base filler metals, brazed joint strength (Japanese) 0-16636  
 steel granular model material, equipment for shear deform. investigation (German) 0-35449  
 struct. changes, through simulated multiple layer welding, micro-tensile and shearing tests (German) 0-35215  
 Tresca type plastic material, simple shear deform. with combined work hardening (Japanese) 0-35206  
 Al-Ag alloys, critical resolved shear stress 0-49296  
 B fibre reinforced Al composite, strength of fibre-matrix interface and tensile strength (Russian) 0-21005  
 C fibre reinforced C, processing, room temp. mech. props., and low temp. expansion 0-25820  
 C fibre reinforced epoxy, epoxy matrix, strength in twisting, stretching and transverse bending 0-11622  
 C fibre reinforced epoxy, deterioration in water, hydraulic press. effect (Japanese) 0-55470  
 C fibre reinforced epoxy, deterioration in water, immersion time effect (Japanese) 0-55471  
 C-C composite, structure model, Rosen model with fractional matrix 0-11719  
 C-fibre reinforced epoxy resin, laminated structs. mech. props. 0-50672  
 Ni<sub>49</sub>Fe<sub>29</sub>P<sub>14</sub>B<sub>6</sub>Si<sub>2</sub> glass, flow and failure 0-40438



**shear strength continued**

(U,Th)O<sub>2</sub> fuel rods, analytical stressing in hot cell 0-18566  
 Zn single crystals, temp. and strain rate effects on strength, slip and twinning 0-16373

**shear turbulence**

aerosol particles, turbulent migration phenomenon 0-53836  
 bottom settling of solid particles in turbulent shear flow, distribution statistical properties (*Japanese*) 0-19344  
 boundary layer, compressible, Reynolds number effects on turbulence field 0-19434  
 boundary layer, struct. and development in oscill. external flow 0-19353  
 buoyant plumes behaviour on release at ground level, lab. wind tunnel obs. 0-30624  
 chemically reacting turbulent shear layer between two streams obs. 0-6163  
 counter gradient flow downstream of two different diameter cylinders (*French*) 0-43693  
 critical points in unsteady flow, functional anal. 0-33571  
 cylinders placed in turbulent plane mixing layer, time-averaged aerodynamic forces 0-28524  
 duct, square, developing turbulent flow computation 0-1554  
 duct with rough walls, turbulent shear flow, stability anal. 0-38496  
 electrodiffusive flow and shear transducer electrical anal. 0-48824  
 finite difference techniques accuracy in complex geometries 0-19357  
 flow in plane channel, least energy dissipation rate principle 0-33577  
 fluctuations in shear stress of turbulent flow near wall (*German*) 0-19345  
 forward facing step, neutrally stable atmospheric flow, shear layer, separation, vortices 0-48685  
 free flows, turbulent stress modelling using turbulence distortion linear statement 0-1538  
 free shear layer, Reynolds stress closures systematic modelling rules 0-1552  
 free shear layer behavior in rotating systems 0-1545  
 free turbulent shear flow, acoustic pressure fluctuations due to large scale coherent struts. 0-14677  
 free turbulent shear flows with strong density fluctuations 0-19342  
 gas-solid turbulent shear channel flow, particulate motion, numerical simulation 0-53863  
 incompressible turbulence, statistical investigation of eddy viscosity 0-14675  
 intermittency in free turbulent shear flows 0-19348  
 jet, axisymmetric free shear flow with Reynolds stress closure 0-19469  
 laminar separation bubbles, airfoil performance effects, turbulent shear layer reattachment 0-48774  
 large eddy simulation 0-38390  
 large scale structure and fine grained turbulence interactions 0-33575  
 molecular Prandtl number, influence on turbulence in shear flow, book contrib. 0-1541  
 near-wake phenomena, with and without external compression, axial and radial air injection effects 0-10273  
 pipe flow, turbulent, past rectangular roughness element 0-1555  
 pipe flow, turbulent, perturbed by sudden enlargement 0-19354  
 plane mixing layer, two-point LDV meas., vorticity distrib. 0-38506  
 polymer solution, dil., turbulent flow behaviour in annulus 0-33633  
 recirculating flow behind backward-facing step, mean vel. and Reynolds stresses meas. 0-19355  
 separating boundary layer, subsonic, integral prediction method 0-1623  
 shear stress generation models, three-dimens. boundary layers 0-19360  
 stress transport closures, overview 0-19359  
 subsonic turbulent flow past a downstream facing annular step, flow separation 0-43696  
 suction-induced asymptotic boundary layers, exptl. and predicted props. 0-1553  
 surface jets, heated, three-dimens., modelling 0-24065  
 symposium, University Park, PA, USA (April 1977) 0-17720  
 turbulent boundary layer with separated flow, integral method 0-1547  
 turbulent shear stresses in compressible boundary layers 0-14736  
 two-dimensional free shear flow, modified one-equation model 0-6034  
 velocity distrib., wall friction in rotational turbulent laminar boundary flow (*German*) 0-1526  
 wall jet, algebraic Reynolds stress model calc. 0-1668

**shear turbulent flow** *see shear turbulence***sheathing, cable** *see cable sheathing***sheaths, plasma** *see plasma sheaths***shell model (nuclear)** *see nuclear shell model***shielding**

*see also magnetic shielding; radiation protection*

AGR, internal radiation shields, design and performance evaluation 0-5373  
 AGR pressure vessels, radiation protection for shutdown man-access 0-5374  
 air-over-ground neutron and gamma spectroscopy 0-23161  
 analyses crystal of neutron spectrometer 0-42887  
 benchmark problems by CSEWG 0-47736  
 benchmark shielding problems, American Nuclear Society Standards Committee, documentation of computational methods 0-47737  
 benchmark shielding problems obtained from integral tests of neutron cross sections 0-47740  
 biological shield removal, associated radiological protection problems 0-9431  
 boron shielding material, neutron transmission calc. 0-854  
 BWR, shield design against neutron streaming in pressure vessel vicinity 0-13678  
 BWR power plant shielding concept 0-18712  
 BWR shield wall penetrations, radiation shielding 0-13679  
 concrete, albedo for low energy  $\gamma$ -radiation 0-32534  
 concrete buildup factors based on the American National Standard for flux-to-dose-rate conversion 0-47732  
 ENDF/B-V cross section data for shielding appls., Monte Carlo MCNP integral calcs. 0-47744  
 ENDF/B-V nuclear data for shielding appls., energy balance anal. 0-47745  
 fast neutron transport through laminated Fe-H<sub>2</sub>O shield 0-13931  
 FBR, commercial demonstration reactor, radiation damage shielding 0-23178  
 FBR fuel reprocessing plant, radiation protection, containment and shielding 0-23179  
 fission reactor fuel, mixed oxide, suitability of spent fuel shipping casks 0-27757

**shielding continued**

fusion reactor irradiation test facility, higher energy neutrons, shielding calcs. 0-13786  
 fusion reactor materials, neutronics analysis using ENDF/B-V cross-section covariance data 0-47710  
 fusion reactor shielding concretes, neutron activation props. 0-13787  
 gamma ray spectral penetration through radiation shields, review 0-5343  
 gamma-ray albedo data, removal of negative albedo terms 0-5347  
 GCFR, design of deep penetration integral expt. for ThO<sub>2</sub> blanket and radial shield mockup 0-23167  
 GCFR grid plate shield design, anal. of confirmation expt. 0-23166  
 GCFR shielding expts. at Tower Shielding Facility, ORNL 0-47739  
 graphite, neutron penetration, Monte Carlo calculations for 30, 45 MeV (*Japanese*) 0-18677  
 graphite, proton bombardment at 52 MeV, neutrons and photons penetration 0-27821  
 HTGR refuelling, equipment safety, gamma dose meas. 0-47668  
 LWR irradiated fuel transport flasks, shielding and engineering aspects 0-27831  
 LWR shielding, neutron transport anal. comparison of several multigroup libraries 0-23168  
 Monte Carlo methodology for shielding of structures against initial nuclear radiation 0-47741  
 multigroup transfer coeffs., efficient eval. for shielding appls. 0-47747  
 neutron bomb radiation protection, calc. of rad. penetration in air and shielded human tissue dose equiv. 0-47743  
 neutron primary beam and shielding radiation quality and absorbed dose obs. 0-12281  
 new waste calcining facility, radiation shield integrity testing 0-13940  
 PDX Tokamak, neutron skyshine Monte Carlo calcs. 0-47711  
 perturbation theory, higher order generalised 0-47731  
 PFR Dounreay, radiation and contamination control 0-27834  
 PFR Dounreay, utilisation of neutrons meas. for shielding calcs. 0-32538  
 polyethylene, neutron penetration, Monte Carlo calculations for 30, 45 MeV (*Japanese*) 0-18677  
 PWR, cavity streaming problem, shield config. optimisation 0-9352  
 PWR, low-pressure drop reactor cavity shield system 0-13677  
 PWR containment building, design and anal. of cavity shield system 0-18713  
 PWR radiation shielding design 0-5372  
 radiation protection and monitoring of personnel handling Pu reactor fuels 0-5389  
 radiation shield integrity testing 0-5390  
 radiation transport theory, tracklength biasing in Monte Carlo methods 0-5335  
 radiotherapy, organ shielding using Pb-Sn-Bi-Cd low melting point alloy block (*Korean*) 0-36154  
 radiotherapy neutron leakage characts. rel. to room shielding 0-51273  
 reactor, 6 MeV gamma photons penetration through Al, concrete and graphite determ. 0-5256  
 reactor cavity neutron shield design at Millstone Unit No.2 0-47748  
 secondary neutron polarization via penetration through a ferromagnetic shielding wall 0-47742  
 Serpukhov proton synchrotron shield, mixed radiation dose equivalent outside 0-32530  
 shield integral expts. at ORNL 0-47709  
 SOLASE laser fusion reactor, Monte Carlo shielding calc. for mirror-laser beam duct system 0-23174  
 solid neutron shield development, materials eval. for spent fuel shipping cask 0-13939  
 source definition for head shielding requirements in linear accelerators, effect on room shielding design 0-46068  
 spacecraft thermionic reactors, neutron leakage control using boronated reflector drums leading to lower shielding mass 0-47663  
 TFR neutral-beam injectors, shielding calcs. 0-23172  
 Tokamak reactor blankets, effects of neutral beam injection tubes, shielding calcs. 0-23173  
 Windscale nuclear fuel reprocessing, shielding and radiation protection 0-18714  
 X-ray shielding arrangement, for diff. equipment 0-849  
 Fe radiation shielding, computational benchmark for deep penetration 0-47738  
 Fe radiation shielding, TLD meas. of neutron and gamma-ray energy deposition 0-23163  
 Fe shield, meas. of neutron and gamma ray penetration 0-47730  
 MgO, GCFR shielding material, anal. of shielding effectiveness 0-47746  
 Pu, high burnup fuels, shielding and handling problems 0-27833  
 W, radiation shielding material, integral tests of ENDF/B-IV high-energy neutron cross-section data 0-23162

**shielding, magnetic** *see magnetic shielding*

**shift register sequences** *see binary sequences*

**ships**

*see also navigation*

course speed and lateral drift, acoustical determination 0-5892  
 ocean ambient noise, source level model for propeller blade radiation 0-43513  
 shipboard meteorological data system 0-46299  
 submersible data acquisition system SCRIBE 0-46266

**shock, thermal** *see thermal shock*

**shock control**

gyroscope, forced vibrations shock absorber selection parameters 0-43659

**shock measurement**

piezoelectric transducer systems, noise suppression and prevention for shock and vibration meas. 0-22353

**shock tubes**

*see also shock waves*

airfoils, transonic testing at high Reynolds number in shock tube 0-14852  
 aqueous fog form. 0-19531  
 chemical kinetics, elem. gas reaction rate coeffs. meas., review 0-3299  
 diffraction and reflection from open end, shock waves, numerical computation (*Chinese*) 0-43735  
 flows, unsteady non-equilibrium, discretisation of boundary layer terms ionisation relaxation as example 0-14742  
 gases, characterisation, reactive flow in shock tubes, laser absorpt. spectroscopy 0-45618  
 Ludwig tube, steady flow duration extension 0-1700  
 piston structure and gas distrib. in strong shock wave 0-10265  
 valves, fast-acting, formation of shock waves 0-24052



**shock tubes continued**

- Mg+O<sub>2</sub>=MgO+O, shock-tube study of evap. and oxidation kinetics 0-16651  
 O<sub>2</sub>, singlet states, quenching by O<sub>2</sub>(N<sub>2</sub>), shock tube study 0-23511  
 Pb I and II, transition probabilities, Stark broadening parameters 0-23367  
 Xe, s-p transitions, Stark consts. and oscill. strengths, shock tube meas. 0-18822

**shock wave effects**

- acceleration of energetic charged particles by interplanetary and supernova shock waves 0-31189  
 achondrite meteorites, mag. effects of brecciation and shock 0-8603  
 andalusite, shock-loaded, deform. 0-19873  
 astrophysical plasmas, particle acceleration in collisionless shocks 0-31208  
 3C 310, 326, relaxed double radio sources, in situ shock wave accel. model 0-51891  
 chemical laser, electronic phototransition, with thermal initiation by shock wave 0-53283  
 compression expts. on materials, measurement of spectral radiance using multiwavelength optical pyrometer 0-52229  
 cosmic ray acceleration by supernova shocks in interstellar medium 0-31179  
 Cygnus Loop, H I shock excitation rel. to high-rel. gas H $\alpha$  emission 0-41873  
 diamond, mechanical strength depend. on thermal working parameters, microcracks (*Russian*) 0-55501  
 diamond, shock synthesis (*Japanese*) 0-29918  
 diamond, synthesis and characterisation 0-50580  
 dispersed media, shock compressibility, brittle destruction 0-49303  
 Fermi acceleration of charged particles in astrophysical plasmas 0-31207  
 foamed plastics, shock absorbing capacity determ. (*German*) 0-19877  
 graphite, self focusing high current relativistic electron beam for structural and chemical transformations (*Russian*) 0-15190  
 hydrocarbons, shock compression, dynamic high press. eqns. of state 0-6450  
 hydrodynamical acceleration of particles in supernovae and extragalactic radio sources 0-31313  
 IC 443, supernova remnant, H I shock excitation rel. to high-rel. gas H $\alpha$  emission 0-41873  
 interstellar medium, mechanical heating rate by supernova blast waves 0-36682  
 interstellar molecules, collision-induced dissociation 0-17632  
 interstellar shock waves, CH<sup>+</sup> prod. in diffuse clouds 0-56898  
 liquid drop aggregate breakup in shock waves 0-24084  
 magnetic field generation by detonation waves 0-24533  
 metals, fracture due to laser irradi. and shock compressed plasma (*Russian*) 0-55500  
 metals, shock wave compression, reduced Hugoniot curve and eqn. of state (*Chinese*) 0-44259  
 minerals pressure-density path, effect of viscosity on release adiabat meas. 0-51388  
 particle acceleration by propagating interplanetary shocks 0-31188  
 photorecombination laser, shock wave triggered, waveguide mode optical gain 0-5730  
 photorecombination reactions initiated by shock wave, light amplification (*Russian*) 0-38011  
 plasma heating and radiation due to gas layer impact against obstacle at very high vel. 0-19602  
 point defect formation in weak shock wave front (*Russian*) 0-6401  
 poly(pyromellitimide), shock-induced electrical activity, mechanically induced bond scission model 0-50256  
 polymeric solids, shock-induced electrical activity, mechanically induced bond scission model 0-50256  
 retrograde vapour, shock wave induced condensation 0-34177  
 sapphire, shock compressed, refractive index, density, and polarisability behaviour 0-50295  
 shock compression-pulse heating working process, apparatus design 0-16357  
 solar flares, proton and electron accel. by shock waves 0-21974  
 solid, shock compression, review 0-24534  
 star formation through accretion shock, model for H II blisters 0-21994  
 steel, low C, surface shot blasting, prep. for plasma deposition 0-16586  
 stellar coronae, shock wave heating rel. to two-parameter models 0-8619  
 Tunguska catastrophe, computational modelling 0-41779  
 ureilite meteorites, mag. effects of brecciation and shock rel. to strong nebular mag. fields 0-8602  
 viscoelastic rod, shock rel. to hard obstacle (*Russian*) 0-23911  
 Al alloys, surface shot blasting, prep. for plasma deposition 0-16586  
 Al<sub>2</sub>O<sub>3</sub>, dynamic deform., stress-wave response 0-21020  
 Al<sub>2</sub>O<sub>3</sub> phase transformations,  $\gamma$  to  $\alpha$ , produced by shock wave working 0-16305  
 Al<sub>2</sub>O<sub>3</sub>:Cr<sup>3+</sup>, shock compression, absorpt. spectra 0-20675  
 Al<sub>2</sub>O<sub>3</sub>-SiO<sub>2</sub> system, andalusite and kyanite powders, shock induced transformations 0-45301  
 Ar, liq., shock wave compression, 400 to 910 kbar 0-29101  
 Ar liquid, shock compression temp., detonation front glow 0-43737  
 BN, self focusing high current relativistic electron beam for structural and chemical transformations (*Russian*) 0-15190  
 BN, shock synthesis (*Japanese*) 0-29918  
 BN, structural changes occurring during shock compression in presence of H<sub>2</sub>O 0-16301  
 BN structure after high temp. shock compression 0-39220  
 BN wurtzite-sphalerite phase transition, stacking fault role 0-6418  
 C, glassy, migration into steel during shock compression 0-24679  
 C, noncrystalline conversion to diamond, diffusion conversion enhanced rate due to shock compression 0-39221  
 Cu powder, two layered medium dynamic compaction 0-35138  
 Cu, shock compressed, release isentropes, eqn. of state at high energy density (*Russian*) 0-54340  
 Cu, shock wave compression, reduced Hugoniot curve and eqn. of state (*Chinese*) 0-44259  
 Cu surface shot blasting, prep. for plasma deposition 0-16586  
 Cu-Ga porous solid formed by shock compression 0-29905  
 Fe, cast, structural changes, due to pulsed action of high temps. and pressures (*Russian*) 0-7554  
 Fe, shock wave compression, reduced Hugoniot curve and eqn. of state (*Chinese*) 0-44259  
 LiNbO<sub>3</sub>, shock-wave compression, 2.4-44 GPa 0-34139

**shock wave effects continued**

- Mg, shock wave compression, reduced Hugoniot curve and eqn. of state (*Chinese*) 0-44259  
 N liquid, shock compression temp., detonation front glow 0-43737  
 NaNO<sub>3</sub>, fine structure changes on interaction with weak shock waves (*Russian*) 0-54313  
 Pb, shock compressed, release isentropes, eqn. of state at high energy density (*Russian*) 0-54340  
 S, shock wave method observation of transition to highly conducting state 0-4738  
 SiO<sub>2</sub> film, amorphous, shock crystn. obs. 0-10828  
 SiO<sub>2</sub>, fused, shock compressed, refractive index, density, and polarisability behaviour 0-50295  
 Si<sub>3</sub>O<sub>4</sub>N<sub>2</sub> film, amorphous, shock crystn. obs. 0-10828  
 U, liquid, electronic density of states, shock vaporization technique 0-29300  
 Xe, electrical conductivity beyond critical point, intermediate density between gas plasma and solid (*Russian*) 0-20265

**shock waves**

- see also *detonation; explosions; plasma shock waves; shock tubes; shock wave effects; supersonic flow*  
 1-dimensional shock wave propagation after explosion, calculation using BKWAVE 0-38448  
 absorption, fluid-saturated porous solids 0-53726  
 acceleration waves in radiating gases, local and global behaviour 0-1618  
 adiabatic perturbations of solitons and shock waves 0-46830  
 airscorps, vortex filament-shock front interference, vortex dissipation 0-10253  
 asymmetric double exponential waveform, weak-shock soln. for nonlinear propag. 0-10061  
 atmosphere, influence of aqueous fog on shock wave propag. 0-19531  
 Baneberry nucl. explosion, numerical simulation 0-841  
 blunt body in supersonic flow, Navier-Stokes eqns. numerical computation 0-10263  
 Burgers equation, sawtooth soln. decay 0-31529  
 3C 310, 326, relaxed double radio sources, shock waves prod. by fine scale struct. 0-51891  
 cascade shock loss location and magnitude by high speed smoke visualisation 0-24051  
 chemically frozen multicomponent boundary layer, thermal diffusion effects behind strong shock 0-53772  
 combined bodies, supersonic inviscid flow, shock interactions (*Chinese*) 0-6084  
 compression shock stability in streams of spontaneously condensing vapour 0-28563  
 cones, axisymmetric impingement of supersonic air jets, shock pattern 0-48741  
 converging cylindrical shock wave prod. 0-48748  
 cosmic ray acceleration in shock waves, energy loss effects (*Russian*) 0-17449  
 cosmology, shock form. and shock struct. in radiative era 0-4463  
 curved shock waves in ideal fluid mixtures with multiple temps., theory of singular surfaces 0-28533  
 delta wings in supersonic flow, crossflow shocks 0-48749  
 density distribution in a non-stationary bow wave in a transonic flow, book contrib. 0-1631  
 detached bow waves around bodies at slightly greater than sonic speed, book contrib. 0-1630  
 detonation sputtering, interaction between detonation waves and gas and powder flows (*Russian*) 0-16182  
 diatomic radiating low density gas, shock wave struct., vibrational energy 0-38504  
 diffraction and reflection from shock-tube, numerical computation (*Chinese*) 0-43735  
 diffraction on plane with semicircular cylindrical roughness, numerical integration (*Ukrainian*) 0-22201  
 diffraction over concave corners, von Neumann paradox, Mach reflection 0-28535  
 diffusion flame in turbulent boundary layer on liq. propellant surface behind shock wave 0-53763  
 dilatant (nondilatant) media, shock wave propagation 0-14608  
 discontinuity formation, phase velocities role 0-19440  
 dispersion on plane layer (*Russian*) 0-33628  
 droplet motion induced by weak shock waves 0-33627  
 dust entrainment in shock-induced turbulent air flow, dust entrainment 0-43763  
 elastic wave propagation in isotropic space 0-28448  
 expansion corner effect on shock-wave and boundary layer interactions 0-14737  
 explosion due to inertial plate drive by pressure pulse 0-53811  
 explosion shock wave propagation in hollow circular cylinder (*Japanese*) 0-10175  
 explosive instability upon interaction of localized and nonlocalized waves 0-31530  
 explosives, volume of activation, shock initiation 0-16683  
 flux-corrected transport algorithm, rezoning technique 0-31516  
 freon gas flow around blunt object, bow shock instability 0-10266  
 galactic shocks in barred spiral galaxies, steady-state gas-dynamical study 0-12819  
 gas, laser absorpt. wave propag., shock waves 0-28597  
 gas blown from cylinder end in hypersonic flow, shocks and blowing parameter 0-33624  
 gas motion near symmetry centre for energy release on the periphery, shocks 0-33626  
 gas-radiating particle mixture, shock wave struct. numerical investigation 0-10298  
 global structure anal. 0-8800  
 gravitational compression of a body within the approximation of the special theory of relativity 0-4611  
 Hartmann-Sprenger tube, thermal effects, finite difference method for analysis 0-14771  
 high Reynolds number supersonic flow, compression corner flowfields, turbulent boundary layer separation 0-14735  
 hydraulic shock during tube filling by liquid (*Russian*) 0-24053  
 hypersonic conical nozzle, boundary layer separation from compression shock 0-48766  
 hypersonic flow, shock layer separation, asymptotic soln. (*Russian*) 0-33625  
 hypersonic flow through body wall 0-38447  
 hypersonic wedge flow, dusty gas effect 0-6083



**shock waves continued**

ideal electrically conducting gas, weak discontinuities in singular surface theory 0-43736  
 ideal gas flow, arrival of a shock wave at the expanding part of a channel 0-6088  
 ideal radiating gas, sonic discontinuities, shock development 0-43802  
 industrial explosions, causes, propagation, and suppression methods 0-31725  
 initial shock parameters for explosion in rarefied gas 0-53815  
 insulator, transparent, laser breakdown, acoustic characts. 0-50269  
 interplanetary shock waves in turbulent medium, energetic particles interaction 0-4210  
 interplanetary shock waves interaction with bow shock-magnetopause system 0-26712  
 interplanetary two-fluid shock waves propag., model 0-26711  
 interstellar shocks, analytical results for post-shock gas temp., density, vel. and comp. 0-56911  
 interstellar shocks, mol. diagnostics 0-56899  
 ionising shock waves, in monatomic gas, large Mach numbers 0-6096  
 isothermal blast waves, one-dimens. in mag. field, mathematical theory 0-28532  
 isotropic elastic medium, finite deformation shock waves, centric cumulation 0-53673  
 Kortweg de Vries (Burgers) nonlinear long waves, mathematical modelling 0-8791  
 Lennard-Jones 6-12 crystal, shock wave mol. dynamics, nonsteady to steady wave transition 0-15189  
 lightning channels radial expansion and shock wave form. 0-12530  
 liquefaction shock waves, shock tube expt. study 0-19439  
 liquid containing gas bubbles, struct. of supersonic waves and cavitation development 0-33643  
 Mach reflexion transition for strong shocks 0-6091  
 Mach waves, kinematics inside and outside supersonic jets, book contrib. 0-1640  
 magnetosphere, double layers and electrostatic shocks review 0-36460  
 metagalactic shock waves, thermal processes 0-46678  
 metals under contact explosion loading, shock damping process 0-54309  
 monatomic gas, non-stationary oblique shock wave reflexions, domains and boundaries 0-48750  
 nebulae ionisation-shock fronts hydrodynamic linear theory 0-17625  
 non-asymptotic shock-detachment distance of slender cones in transonic flow, book contrib. 0-1632  
 nonequilibrium gas flow, growth of discontinuities 0-48734  
 nonlinear elastic media 0-48629  
 nonlinear hydrodynamic shock propagation, finite element anal. and method of weighted residuals 0-53813  
 nonsteady two-dimens. transonic flow, numerical solns., shock waves 0-53808  
 numerical shock structure, nonlinear corrections for difference schemes in conservation form 0-36878  
 one-dimensional quiescent lattices, shock profiles, end condition effects 0-34138  
 one-dimensional unsteady flow, numerical solution of hyperbolic initial-boundary value problem (*German*) 0-6095  
 panels, cylindrical, failure under gasdynamic periodic shock waves 0-14611  
 piston structure and gas distrib. in strong shock wave 0-10265  
 planar detonation waves, diffraction at an abrupt area change 0-14744  
 plane converging duct, separation zone for turbulent boundary layer and oblique shock interaction 0-14759  
 plane obstacles, weak shock wave reflection in air 0-48751  
 plane shock impinging on wavy contact surface, results (*German*) 0-14747  
 polymorphic phase transitions induced by shock waves, review 0-15188  
 polytropic medium, shock compression using absorbing layer 0-6092  
 polytropic plastic gas, nonstationary shock wave propag., closed form soln., thermonuclear microfusion 0-28534  
 porous rocks, dry and water-saturated, plane shock wave studies 0-21714  
 post shock expansion behind normal shock on curved wall, flow separation, book contrib. (*German*) 0-1628  
 potential theory model for separation regions behind shock waves (*German*) 0-1636  
 propagation of strong plane waves in optically thin grey atmosphere 0-53810  
 pulse wave propagation in arteries 0-41099  
 quasars, two-dimensional relativistic blast waves, solns. for adiabatic case 0-22108  
 quasars and active galactic nuclei, magnetic flare model, magnetised accretion disc around massive black hole 0-22113  
 quasilinear hyperbolic system of gas dynamics (*Russian*) 0-33629  
 radiative boundary shock wave struct. 0-10264  
 radio sources, compact, emission from moving shock wave in relativistic jet 0-4448  
 radiosources, extended, particle accel. and radiative losses effects on source dynamics 0-46687  
 reflected shock wave at wall, press. change meas. 0-53812  
 reflection of detonation waves from a wall 0-53885  
 relaxing gas, sonic discontinuities 0-28531  
 relaxing gas flow, discontinuity growth 0-28525  
 resonance tube, jet flow and heating, unsteady complex shock struct. 0-6115  
 rods, simple orthotropic elastic, shock waves and wave-type instability 0-48622  
 rotating shock and detonation wave anal. 0-53792  
 schlieren probe method for measurement of refractive index profile of shock wave in fluid 0-23785  
 shell, shallow spherical, plastic deformation under explosive loading 0-14589  
 shock separated boundary layer, suction effects, compressible Navier-Stokes eqn. solns. 0-24050  
 shock tubes, use of fast-acting valves, shock wave formation 0-24052  
 shock-boundary layer interaction flows, multieqn. turbulence modes for duct and channel 0-24093  
 simple gases, relativistic shock wave struct., Boltzmann eqn. soln. 0-1644  
 singular hypersurfaces, asymptotic regularisation as alternative to distrib. 0-36923  
 solar corona, shock wave propag. rel. to type II radio burst with reverse freq. drift 0-17567  
 solar wind, magnetoacoustic solitons ahead of near Earth shock wave front 0-4217  
 solid, heavy ion bombard., Mach shock electron distrib. 0-45194

**shock waves continued**

sonic boom, infrasound generated by Concorde used to monitor stratospheric winds 0-51492  
 sonic boom propag. in thermosphere 0-33305  
 spark channel, high-conducting, shock wave degeneration to sound waves 0-38428  
 spark channel, highly-conducting, shock wave degeneration to sound waves 0-38429  
 spherical blast waves generated by spherical flames, anal. 0-16686  
 spherical shock, interaction with plate 0-38446  
 spherically blunted cone with massive surface blowing, laminar and turbulent flows, shocks 0-38445  
 stability in gas-dynamic context (*Russian*) 0-6093  
 stability of an ionizing shock wave in an electromagnetic field 0-6076  
 stellar collapse, adiabatic hydrodynamics and shock wave propag. 0-56861  
 stellar explosion models, new solns. 0-12751  
 stress measurements in severe shock-wave environments using low-impedance Mn gauges 0-38367  
 structure close to wall, book contrib. 0-1650  
 sub and transonic flow over wing, flow separation, vortex struct., shock wave shape (*French*) 0-14733  
 supernova blast waves, propag. rel. to interstellar medium mechanical heating 0-36682  
 supernova remnants, fast shock wave optical emission 0-46631  
 supernovae, MHD shock wave model 0-46588  
 supernovae, type II, nonequilibrium processes in evolution 0-46586  
 supersonic, flow through body wall 0-38447  
 supersonic gas particle flows over wedge (*German*) 0-43731  
 supersonic inviscid conical corner flowfields, complex shock interactions 0-48739  
 supersonic jet, nonsteady interaction with barrier, math. model of oscillatory cycle 0-19462  
 symmetrical airfoil, transonic flow, inviscid and turbulent flow props., wake 0-48736  
 thermoelastic fluids, stability of motion anal. 0-10221  
 thin walled sphere in contact with elastic or acoustic media, interior dynamics 0-5981  
 thread, nonlinear elastic, cone-induced shock, self-similar problem soln. (*Russian*) 0-53677  
 three dimensional interactions with obstacles 0-53814  
 three dimensional separated turbulent flows at supersonic speeds 0-19435  
 torus, axially symmetric, transonic flow 0-28527  
 transonic diffuser flow, shock wave oscillations 0-14729  
 transonic flow with shocks, finite element method appl., shock-fitting 0-14730  
 transonic shock/boundary-layer interaction subject to large pressure fluctuations 0-38433  
 trapped nonlinear waves near sonic type singularity 0-24041  
 two dimensional shockwave-turbulent boundary layer interaction, flow separation 0-14758  
 two-dimensional turbulent blunt body flows with impinging shock 0-38444  
 Tycho supernova remnant, shock front rel. to radio remnant struct. 0-56919  
 underwater explosion generation of sound wave pulse, nonlinear region 0-56493  
 underwater explosions, shock wave interactions 0-14746  
 underwater explosions, surface effects, review 0-14745  
 underwater explosive shock waves, formulation of weak shock soln. 0-10070  
 unsteady transonic shock motions in two-dimens. flow 0-14731  
 Venus bow shock, Pioneer magnetometer obs. 0-36535  
 vibration relaxation time in nozzle and shocktube expansion flows, physical model 0-24067  
 viscous compressible flow at high Reynolds number, global approach and coupling approach 0-48742  
 viscous heat-conducting gas, numerical simulation methods 0-38449  
 viscous supersonic flow over external axial corners, shock and bubble generation computation 0-14734  
 wall shear stress meas. in shock wave-boundary layer interaction, comments 0-14670  
 wave fronts of nonlinear waves in vibr. relaxing gas, comments and reply 0-1645  
 weak discontinuities in high temp. phenomena, relativistic theory 0-53889  
 weak spherical shock waves, propagation from arbitrary piston motions 0-22204  
 weakly dissipative system, higher order approx. in reductive perturbation method, shock wave appl. 0-14743  
 wing, oscillating, in transonic flow, unsteady airloads and flow linearisation 0-19426  
 Zemplen's studies on shock waves (*Hungarian*) 0-31476  
 Al foil, with Au overlay, impedance-match expts. using laser-driven shock waves 0-29119  
 Al foil in quartz dust, electrical explosion for accelerator application 0-6314  
 Ar, gas in planar nozzle, shock-wave propag., effect of transverse mag. field 0-6094  
 CO<sub>2</sub>-He-N<sub>2</sub>, gas dynamic laser, gain coeff. numerical estimates, book contrib. 0-1183  
 Fe, thermal props. at high-press. (150 GPa), from shock-wave expts., Earth core struct. 0-21683  
 H<sub>2</sub>O-H<sub>2</sub> mixtures, vibr. energy transfer in shock waves, population inversion 0-37996  
 LiF(Mg), shock waves in (111) direction, elastic precursor amplitudes 0-54314

**shocks, electric** *see electric shocks*

**short-circuit currents**

p-n junction minority carrier diffusion length meas. 0-31849

**short-range order**

*see also order-disorder transformations*

alloy, disordered, energy band struct. and elec. cond., effect of short-range order 0-10860  
 alloys, DO<sub>22</sub> and L1<sub>0</sub> superstructures, atomic ordering, multicluster approx., order-disorder transition 0-38990  
 antiferromagnetic heavily doped semiconductors, Faraday light depolarisation in mixed mag. states 0-29726  
 binary alloys, diagrams of state, component interaction parameters (*Russian*) 0-55354



**short-range order continued**

- disordered multicomponent solid solutions conc. fluctuation waves, microscopic theory 0-44327
- Elivnar,  $\gamma$  to  $\gamma'$  transformation and  $\gamma'$  phase form. kinetics, lattice consts. 0-35191
- ferromagnetic alloys, disordered crystalline and amorphous, dipole field distribution 0-25101
- ferromagnetism, itinerant electron model, spin quantization direction fluctuations, short range order. 0-34582
- fluid, classical, short-range struct. universality, bridge functions 0-10478
- fluid, of isotropic mols., DID Rayleigh and Raman depolarised scatt., lattice-gas model 0-10356
- Ising square lattice, phase transitions, next nearest neighbour interactions 0-50128
- liquid metals, atomic radial distrib. curve anal. (Russian) 0-14996
- liquid metals, structure factor modelling using quasi-crystallised model (Russian) 0-54118
- metallic glass, short-range order, hyperfine field distrib. determ. by Mossbauer spectroscopy 0-39962
- mixed valence systems, Falicov-Kimball model, mag. short- and long-range order 0-15480
- nematic liquid crystals, continuum theory of disorder, comparison with lattice models 0-54126
- nematic mesophase, statistical model, orientational order parameters 0-28910
- one-dimens. ionic conductor, modulation and incommensurability 0-19980
- one-dimensional disordered systems, electron transmission and wave propag. 0-24907
- solid solutions, AC-BD, X-ray diffr. determ. of short-range order parameters 0-38875
- steel, austenitic, Al-C, microstruct., Mossbauer obs. (Russian) 0-29655
- steel transformer, Mossbauer atomic struct. anal., decarburising annealing, cold rolling (Russian) 0-11294
- ternary oxides, short-range order and superstructures 0-49159
- thin disordered film, electronic energy spectrum calcs. extended Halpern Green's function technique 0-20066
- Ag-Al, short-range order, X-ray and electron diffr. study 0-54173
- Ag-Al,  $\delta$ -phase (Japanese) 0-15256
- AgAu, quenched, short range order effects on specific heat 0-29181
- Al-Zn (10 at.%), short-range order parameter calc. in pseudopot. approx. (Russian) 0-49183
- Al<sub>2</sub>O<sub>3</sub> amorphous films, struct., electron diffr. investigation 0-20046
- As, amorphous, intermediate range order from polarised features of Raman spectrum 0-49113
- As<sub>2</sub>O<sub>3</sub>, glassy, intermediate range order from polarised features of Raman spectrum 0-49113
- As<sub>2</sub>(S<sub>2</sub>Se)<sub>1-x</sub>, chalcogenide, covalent non crystalline topology, short range order 0-15009
- Ce<sub>0.73</sub>Hf<sub>0.27</sub>Ru<sub>2</sub>:Co, spontaneous mag. order below superconducting transition temp., Mossbauer study 0-39701
- Co<sub>2</sub>ZrS<sub>2</sub>, (0< $x$ ≤0.50), intercalation compounds, ordered phases obs. 0-33962
- Cr-Ge liquid and amorphous alloys, struct. props., cond., viscosity, surface tension (Russian) 0-54119
- Cu-Al (21 at.%) transition state, tempered and quenched alloy (French) 0-55392
- Cu-Mn (15 at.%), mictomagnetic, short-range ordering, neutron scatt. polarisation anal. 0-50110
- Cu<sub>3</sub>Ga, transition state between long range order and short range order, model, computer simulation (French) 0-49371
- Cu<sub>2</sub>MS<sub>2</sub>, (0< $x$ ≤0.50) (M=Zr, Hf), intercalation compounds, ordered phases obs. 0-33962
- $\gamma$ -Cu<sub>15</sub>Mn<sub>85</sub>, antiferromag., neutron diffr. 0-2550
- Cu(NO<sub>3</sub>)<sub>2</sub>·2H<sub>2</sub>O, singlet ground state system, mag. props. 0-44850
- Fe, liq., short-range order struct., O impurity influence (Russian) 0-38901
- Fe-B, amorphous, short-range order, Mossbauer meas. 0-44986
- Fe-B(Si) amorphous alloys, Mossbauer spectra, struct. 0-15840
- Fe-C, liquid, C content effect on short-range order struct., X-ray diffr. obs. 0-6351
- Fe-C system, mixing variables, activities and entropies calc., short range order model (German) 0-25655
- Fe-Ni alloys, ordering on annealing and electron irradi., mech. props. change (Russian) 0-29981
- Fe-P-B, amorphous alloy, Mossbauer effect and short-range order 0-2675
- Fe-P-C, amorphous alloy, Mossbauer effect and short-range order 0-2675
- Fe-P-C amorphous alloys, Mossbauer spectra, struct. 0-15840
- Fe<sub>84</sub>B<sub>16- $x$</sub> C <sub>$x$</sub> , amorphous alloys, short range order, Mossbauer and DSC study 0-39960
- Fe<sub>2</sub>, first order mag. phase transition, neutron scatt. study 0-50090
- (Fe<sub>1-x</sub>Ni<sub>x</sub>)<sub>75</sub>B<sub>25</sub>, amorphous and cryst., short range order, Mossbauer study 0-39961
- Fe<sub>77</sub>Ni<sub>23</sub>P<sub>14</sub>B<sub>6</sub>, amorphous, Hall resist. and mag. props., short range order effects 0-34422
- FeO-FeS, mag. susceptibility, eutectic phase diagram (Russian) 0-15682
- FeP(Ga)(As)(Sb), dil., short-range order, neutron diffuse scatt. and spin echo NMR 0-50106
- Fe<sub>2</sub>ZrS<sub>2</sub>, (0< $x$ ≤0.50), intercalation compounds, ordered phases obs. 0-33962
- Ga<sub>0.67</sub>Cr<sub>2</sub>S<sub>4</sub>, semiconducting thiospinelide, spin glass type mag. ordering (Russian) 0-50123
- Gd-Co amorphous films, annealed, short-range order and perpendicular mag. anisotropy 0-15765
- Ge<sub>2</sub>(S<sub>2</sub>Se)<sub>1-x</sub>, chalcogenide covalent non crystalline topology, short range order 0-15009
- H<sub>2</sub>, quantum cryst. short-range corre. and motional renormalisation of anisotropic interactions as function of density 0-34272
- HoP, floside mag. struct. to ferromag. transition, elastic neutron scatt. obs. 0-50058
- KReO<sub>4</sub>, vibr. spectrum, Raman and IR spectra obs. 0-55104
- Mn-Ge amorphous films, short-range order, electron diffr. obs. 0-39473
- MnF<sub>2</sub>, magnetic, thermal, elastic refraction of light, mag. order influence on refractive index (Russian) 0-34880
- Ni-Cr-Mn-Fe-Nb (20,3,3,2.5 wt.%), short-range order effects on tensile behaviour 0-25793
- Ni-Cu alloys, short-range atomic clustering, residual resist. meas. 0-29386
- Ni-Mo (10.7 wt.%) alloy, ordering energy calc. 0-10522
- Ni-Pt, short-range order parameter calc. in pseudopot. approx. (Russian) 0-49183
- Ni<sub>3</sub>Fe, short-range order, diffusive elastic neutron scattering 0-24400

**short-range order continued**

- Ni<sub>3</sub>Fe, short-range order parameter calc. in pseudopot. approx. (Russian) 0-49183
- Ni<sub>3</sub>Fe-Sn, dil., atomic order detection by <sup>119</sup>Sn spectroscopy 0-39993
- NiFe<sub>2</sub>O<sub>4</sub> precipitation process from silicate glass, ESR study, effective g value, transition temp. 0-25194
- NiPt, short-range order, effect of plastic deform., electron diffr. anal. (Russian) 0-24403
- Ni<sub>2</sub>ZrS<sub>2</sub>, (0< $x$ ≤0.50), intercalation compounds, ordered phases obs. 0-33962
- O, solid, magnetic props. theory for Heisenberg system (Russian) 0-54900
- Pb-Tl-Cd(Sn) melt, short-range order struct. 0-49088
- PbMg<sub>1/3</sub>Nb<sub>2/3</sub>O<sub>3</sub>, short-range ordering, electron microscope and diffr. study 0-10469
- Se, amorphous, effect of doping on mol. struct. and valence alternation states 0-49249
- Se<sub>1-x</sub>Te<sub>x</sub> systems, amorphous and liq. states, short range order, neutron scatt. study 0-49124
- Si<sub>3</sub>N<sub>4</sub> films, struct. 0-54545
- SrTiO<sub>3</sub>, structural phase transition, intrinsic and extrinsic central peak properties 0-34168
- Tb(OH)<sub>3</sub>, powder and single crystal, mag. props. 0-2558
- V<sub>n</sub>O<sub>2n-1</sub> (3≤ $n$ ≤9), Magneli phases, mag. susceptibilities at low temp. 0-20389
- V<sub>n</sub>O<sub>2n-1</sub>, insulating Magneli phases, mag. susceptibility and sp. ht. meas. 0-34604
- Y-Si melts, enthalpy of formation and dissolution, microinhomogeneous struct., interatomic interactions (Russian) 0-34206
- shot noise** see random noise
- showers, cosmic ray** see cosmic ray showers and bursts
- Shpolskii spectra**
- 2,5-distyrylpyrazine, absorpt., Raman and fluoresc. spectrosc. 0-28049
- haloaceneaphthenes in n-heptane, quasi-line phosphoresc. spectra, vibronic spin-orbit interaction 0-43096
- naphthalene, and deuterio derivatives, fluoresc., absorpt. spectra under Shpolskii conditions 0-2825
- porphyrins orientation in n-alkane Shpolskii hosts, spectra 0-48035
- shrinkage**
- alloy powder, two component, sintering 0-20847
- brittle elastic body, stability and post-critical growth of system of cooling or shrinkage cracks 0-1486
- fibre reinforced composites, viscoelastic thermal shrinkage stresses 0-38287
- graphite, neutron effects on shrinkage 0-37456
- polyethylene, ultra-oriented high density, shrinkage as meas. of deformation efficiency 0-40398
- polystyrene melt, carbon-black filled, rheological study 0-48665
- thermoplastic elastomers, crosslinked by secondary valence interactions, elasticity and processing, crosslinking behaviour 0-40320
- Ag, loosely packed powder, sintering SEM and dilatometry obs. 0-20843
- Al<sub>2</sub>O<sub>3</sub>-glass mixture, microstructural changes and shrinkage during sintering 0-25640
- CrC-Ni alloys, exam. of activated sintering 0-16241
- Cu, loosely packed powder, sintering SEM and dilatometry obs. 0-20843
- Fe, carbonyl pore struct. orientation, shrinkage anisotropy effect 0-20845
- Fe ore, sintering, agglomeration charge layer shrinkage (Russian) 0-16224
- Fe powder compacts, pressed under static or vibr. load, shrinkage anisotropy during sintering 0-50574
- Fe sintered compact, shrinkage and mech. props., admixed zinc stearate lubricant effect 0-45402
- Fe, vacancy mobility determ., HVEM expts. 0-33993
- Fe-C (2. wt.%), sintering shrinkage kinetics 0-20829
- Si, oxidation-induced stacking faults, influence of annealing ambient on shrinkage kinetics 0-29035
- Ti-Al (Sn), porous, effect of Al and Sn on sintering 0-20830
- W-Ni, liquid phase sintering 0-25613
- Shubnikov-de Haas effect** see magnetoresistance
- Si-Ge alloys** see Ge-Si alloys
- SIC** see monolithic integrated circuits
- signal acquisition** see signal detection
- signal coding** see encoding
- signal delay lines** see delay lines
- signal detection**
- coherent detection of partially coherent sources 0-47109
- computerised tomography, detectability in CT images 0-3806
- destabilising factors, evolution of influence 0-9825
- digital moving target indicator system for detection of intracranial arterial echoes 0-17035
- hearing, detection of signals with identical energy spectra but different waveforms under conditions of signal uncertainty 0-51125
- IR heterodyne detect. 10.6  $\mu$ m, using (Hg,Cd)Te photodiodes in CO<sub>2</sub> laser system 0-9042
- isotope radiometry, nonlinear information processing in random signal detection (Russian) 0-22428
- P wave detection and identification using statistical signal analysis 0-8202
- photoelectric pulse signals, precision loss meas. using microcomputer 0-13142
- radar signals refl. from mesosphere, VHF signal detection 0-46274
- sampled/raster displays, assessment of information visibility using signal detection model 0-19002
- SonoChromascope, US B-scan image acquisition, display and recording 0-30818
- threshold detection equivalence with and without dead time 0-32580
- time-varying signal coherent detection using multiple obs. 0-43553
- signal generators**
- see also function generators; noise generators; swept-frequency oscillators
- LMFBR safety testing, scram signal generator for fluid motion monitoring 0-18551
- VLBI, Japanese domestic system, recording signal generator (Japanese) 0-21924
- signal processing**
- see also bandwidth compression; correlation theory; data compression; filtering and prediction theory; picture processing; signal detection; signal synthesis; Walsh functions
- acoustic, analysis of fill time effects on cylindrical hydrophone arrays 0-19163



- signal processing continued**  
 acoustic, energy processing technique for stress wave emission signals, comments 0-48520  
 acoustic, estimation of differential Doppler shifts 0-19162  
 acoustic, Fourier efficiency using analytic translation and Hilbert samples 0-48519  
 acoustic array gain for signals and noise having amplitude and phase fluctuations 0-43548  
 acoustic array processing, comments on errors 0-19164  
 acoustic diffraction field, B-scan viewing using backward wave propagation 0-33352  
 acoustic holography system, Sonoscan using microprocessor 0-38184  
 acoustic signal, pulsed, mathematical models (*Russian*) 0-38180  
 acoustic signal coherence limits in random ocean environment 0-46193  
 acoustical holography, digital reconstruction and computer graphics display 0-23842  
 acousto-optic planar guided-wave Bragg modulators, RF signal processing appls. 0-38131  
 audio, compensating circuit for audio system functions (*Japanese*) 0-53566  
 audio spectrum analyser HP3582A using digital signal processing 0-43567  
 audition, signal anal. by Hopf bifurcation in cochlear fluid 0-26241  
 bioelectric signals, time-connectivity patterns quantification of point processes 0-21564  
 biomedical recording system, TDM multiplexing system for multichannel signal averaging of visually evoked responses 0-36165  
 C-CD appls. in sonar systems 0-53535  
 cardiac arrhythmias, automatic detection in long term ECG monitoring 0-3850  
 channel vocoder based on CCD discrete Fourier transform processors 0-53568  
 chirp transform processors using US strip dispersive delay lines, implementation 0-53577  
 convolution effect in volume magnetostatic waves in ferrite-semiconductor structure 0-54761  
 delay line signal processors using acousto-optic interactions, real time system 0-28384  
 discrete integration, optimum filter design, geophys. appl. 0-200  
 ECG, digital filter for the QRS complex detection 0-36166  
 ECG, QRS detection accuracy rel. to anal. of HF components 0-17158  
 echotomograph, ultrafast, using optical processing of US signals 0-51180  
 EEG signals, analyser-integrator model ANIEG-8 for frequency analysis 0-41295  
 geomagnetic  $D_{st}$  variations analyses, comparison using distortion free filter 0-17419  
 geomagnetic fluctuations, spectral stacking and smoothing rel. to Earth global elec. cond. character 0-17231  
 hydrophone arrays, optimum turbulent boundary layer induced noise suppression with suboptimum realizations 0-19161  
 interferometer signal processing by acousto-optic correlation devices, radio astronomy applications 0-8543  
 isotope radiometry, nonlinear information processing in random signal detection (*Russian*) 0-22428  
 laser beam interferometric wavelength measurements through post-detection signal processing 0-42254  
 linear sonar array processor finite impulse response digital filter design 0-43549  
 Mills' cross array antenna, digital baseband processing 0-36500  
 MM wave signals in radio astronomy using acousto-optical spectrometer 0-4253  
 NDT probe array using 4 transducers 0-35499  
 nonlinear acoustoelectro-luminescence excited by SAW poss. processing appl. 0-45143  
 numerical digital filter for on-line processing of wind tunnel data (*French*) 0-19537  
 ocean acoustic background noise, detection of sinusoids 0-33347  
 passive coherence processing sonars, near-field performance 0-33346  
 prosthesis, multifunctional upper extremity, control signal generation using EMG signal processing 0-8219  
 real 1D signal convolution and correlation by freq. plane filtering 0-32919  
 real time phaseless filter with delay circuit, ECG appl. (*Japanese*) 0-56253  
 response function relaxational frequency spectra, simultaneous meas. by digital signal processing 0-15959  
 rotating machinery diagnostics, signal extraction and filtering 0-23840  
 SAW, physical props. and communication signals processing applications and devices 0-38162  
 SAW convolver, convolution voltage enhancement due to carrier transverse drift 0-1381  
 SAW devices, review 0-38204  
 SAW filter design for TV, CATV and radar appls. 0-53579  
 SAW filters, design, construction, appl., book 0-1393  
 SAW metallic gratings, equivalent circuit of step discontinuity, rel. to SAW devices 0-33389  
 scanning background-limited IR sensor with adaptive threshold signal processing logic, performance 0-37082  
 sediment classification by ocean subbottom acoustic Q meas. 0-46168  
 seismic exploration, signal processing method for circular arrays 0-4123  
 seismic exploration, technique and processing, book 0-51975  
 seismic records, surface multiples suppression 0-56402  
 SEM, signal treatment, backscattered electron spectral distrib. (*French*) 0-42305  
 solar flares, principal component anal. in soft X-ray flux 0-41781  
 sonar ranging systems, pulse compression techniques 0-33350  
 sonar system design, beamforming and signal processing systems 0-33325  
 SPAC, speech processing using the autocorrelation function, noise reduction in speech communication (*Japanese*) 0-33371  
 spectrum width estimates for weather echoes 0-12477  
 speech, equalizer in spectral domain for speech processing by autocorrelation function 0-1383  
 speech samples of deaf children, effect of timing errors on intelligibility 0-19167  
 surface texture assessment, Walsh function method 0-36995  
 tagging flowmeter, signal processing 0-10328  
 Three Array Processor beamforming system 0-43550  
 ultrasonics, signal processing, conf., London, England, Jan. 1980 0-33351  
 undersea platform location by acoustic signature processing 0-43519  
 underwater acoustic pulse compression system, source and receiver methods 0-56630
- signal processing continued**  
 underwater sound, source location in random dispersive media using generalised reduction methods 0-43509  
 US digitiser/processor for extraction of clinical parameters from Doppler-shift waveforms 0-36042  
 US in patient diagnosis 0-36049  
 US testing, axial resolution by signal processing (*German*) 0-7736  
 US tissue characterisation, clinical spectrum anal. techniques 0-45998  
 $\text{LiNbO}_3$  SAW plate convolvers at 1 GHz 0-1382  
 Ni-Fe polycrystalline film cross-tie memory for shipborne radar/sonar 0-42204
- signal processing, computerised** *see computerised signal processing*  
**signal synthesis**  
 computer-synthesized noise, signal detection 0-21476  
 harmonic waves, introduced through Fourier synthesis, for teaching 0-27080
- signal transformers** *see pulse transformers*  
**silica minerals** *see minerals*  
**silicate glasses** *see glass*  
**silicate minerals** *see minerals*  
**silicon**  
*see also nuclei with .....*  
 100 kW peak photovoltaic power system, design, construction and capabilities 0-45705  
 accumulation layer, intersubband-cyclotron combined resonance, theory 0-20278  
 additive to fluoride-oxide slags, influence on elec. cond. (*Russian*) 0-39572  
 AES, backscattering factor, Monte Carlo method calc. 0-7449  
 amorphised by ion implant., localised states and cond., irradi. and heat treatment, doping 0-39529  
 amorphous, anomalous magnetoresistance 0-6877  
 amorphous, as photo-receptor for electrophotography 0-47126  
 amorphous, control of dihydride bond density using RF sputtering 0-34327  
 amorphous, Coulomb gap and hopping cond. 0-44583  
 amorphous, crystallisation study 0-33890  
 amorphous, CVD, retarding crystn. by alloying with C,N,B or Ge 0-44129  
 amorphous, doped, density of states determ. from transport meas. 0-49720  
 amorphous, doped, non-polaronic, cond. and thermopower near band edge 0-49719  
 amorphous, doping and absorption edge 0-29042  
 amorphous, electronic density of states, mol. liq. model 0-49581  
 amorphous, electronic struct., far infrared absorption 0-45051  
 amorphous, electronic structure and molecular liquid model 0-54133  
 amorphous, film, hydrogenation by H diffusion, effect on elec. cond., band gap (*Korean*) 0-45326  
 amorphous, glow discharge, fatigue effect in luminesc., recovery by annealing 0-50416  
 amorphous, glow-discharge deposited, ODMR spectrum, deposition temp. and annealing effects 0-50229  
 amorphous, hydrogenated, electronic density of states determ. from Schottky diode meas. 0-49907  
 amorphous, hydrogenated, electronic struct., SCF  $X\alpha$  calc. 0-49580  
 amorphous, hydrogenated, small angle X-ray scatt., void distrib. 0-15087  
 amorphous, hydrogenated, soft H plasma effect, IR absorpt. (*French*) 0-45054  
 amorphous, hydrogenated, stacked solar cells 0-55842  
 amorphous, hydrogenated film, struct. determ. using electron microscopy 0-10806  
 amorphous, ideal network struct., electronic struct., tight-binding model 0-44485  
 amorphous, interface with V, V silicide formation, backscattering, diffraction meas. 0-2285  
 amorphous, ion implanted, laser annealing, reflectivity meas. 0-29039  
 amorphous, monolithic solar cell appl. 0-45666  
 amorphous, p-n junction devices, barrier profile effect on elec. props. 0-49890  
 amorphous, photostructural changes, photodarkening 0-49121  
 amorphous, photovoltaic cell, plasma deposited, horizontally multilayered struct. 0-50964  
 amorphous, photovoltaic diodes, influence of mag. field on charge transport 0-49891  
 amorphous, position of Fermi level, spectroscopic and transport determ. 0-6706  
 amorphous, possible ABB-type excitonic superconductor (*Chinese*) 0-7029  
 amorphous, ps. relax., optically induced absorpt. 0-48325  
 amorphous, recomb. centre study by spin-depend. photocond. 0-49805  
 amorphous, Schottky barrier solar cell, large-area RF sputtered, contact form, scaling and optimisation 0-45679  
 amorphous, solar cell appl. (*Chinese*) 0-45671  
 amorphous, solar cells, and photovoltaic devices (*Japanese*) 0-50965  
 amorphous, solar cells, efficiency, transport props. 0-50961  
 amorphous, spin depend. recomb., luminesc. and light induced ESR 0-50393  
 amorphous, sputter deposited,  $\text{O}_2$  incorporation during and after fabrication 0-49541  
 amorphous, sputtered, Auger surface spectroscopy 0-50472  
 amorphous, struct. and growth kinetics, topological principles 0-49123  
 amorphous, structural defects EPR 0-25208  
 amorphous, time resolved photoluminesc. near band gap 0-25445  
 amorphous, time-resolved ODMR and luminesc. 0-25254  
 amorphous, transport results interpretation 0-44590  
 amorphous, undoped and B doped, ESR-linewidth temp. depend. meas. 0-20459  
 amorphous barrier with metal, capacitance and cond. meas. interpretation 0-49909  
 amorphous CVD fabrication for solar photothermal conversion appl. 0-7504  
 amorphous CVD film photodetector for picosecond pulses 0-47101  
 amorphous film, dangling bond ESR, light-induced quenching 0-50162  
 amorphous film, glow discharge deposited, refl. spectra and dielec. function 0-50360  
 amorphous film, glow-discharge, optically detected mag. reson., annealing and substrate temp. effects 0-20519  
 amorphous film, heavily doped, glow discharge, AC cond. 0-49718  
 amorphous film, heavy doping by alkali ion implantation 0-2045  
 amorphous film, hole carrier transport 0-2500



## silicon continued

- amorphous film, optical props., electronic states 0-25475  
 amorphous film, reflectance and transmittance (*Japanese*) 0-34995  
 amorphous film, RF-sputtered, influence of  $O_2$  and deposition conditions, elec. cond., IR absorpt. and ESR 0-2949  
 amorphous film, vacuum deposited, microscopic voids, gas absorpt., crystn. study 0-49534  
 amorphous films, characterisation by Rutherford backscatt. spectrometry 0-50498  
 amorphous films, ion implanted, elec. and photocond. props. 0-49717  
 amorphous films, porosity and oxidation of evap., sputtered and plasma-deposited films 0-10838  
 amorphous glow discharge films,  $H_2$  content, elec. props., and photostability 0-25577  
 amorphous layer, solar furnace annealing to induce solid-phase epitaxy 0-2277  
 amorphous Schottky barrier solar cells, deep hole traps, spectral response and TSC meas. 0-50962  
 amorphous sputtered films, hydrogenated, photoinduced optical absorpt. 0-50362  
 amorphous sputtered thin film, US anomalies, 0.5-300K 0-34145  
 amorphous/cryst. interface, supercond. mechanism 0-44783  
 anodic oxide superficial layer, X-ray emission spectrometry and ion back-scattering (*French*) 0-49482  
 antireflection coating, 100 ns pulsed laser damage at 2.7 and 3.8  $\mu m$  0-33057  
 atom, highly ionised, beam-foil lifetime obs. 0-32670  
 atom, SCF electron-gas local-spin-density model including correlation 0-9488  
 Auger band-to-band recomb. temp. depend. 0-29416  
 Auger electron prod. by  $Ne^+$  bombard. 0-7460  
 Auger recombination coefficient, temp. depend. 0-24942  
 autoepitaxial growth, low temp., using  $SiCl_4-H_2$  system 0-20795  
 autoepitaxy, displacement of microrelief 0-2307  
 band structure of diamond like crystals, cluster-Bethe lattice model calc. 0-6713  
 bandgap narrowing in heavily doped material 0-15479  
 bent single crystal, proton beam trajectory control (*Russian*) 0-19859  
 bicrystals, grain boundary states and varistor characts. 0-24829  
 bound multiexciton complexes, luminesc. 0-10888  
 Bragg diffraction from crystals,  $Mo K_\alpha$  radiation polarisation 0-1893  
 bridging epitaxy from Si windows onto  $SiO_2$ , ruby laser pulse annealing 0-44441  
 Brillouin scattering from surface waves, appl. of surface Green's function mapping method 0-40125  
 C-CD Si substrate ionisation trails prod. by cosmic ray background 0-51669  
 cell for precise measurement of thermal expansion, at low temps., results for Cu, NaF 0-37027  
 channelling of fast electrons, flux redistrib. meas. 0-19856  
 channelling spectra of relativistic electrons, 28 and 56 MeV 0-24516  
 charge carrier UHF heating using lumped-capacitance resonators 0-20203  
 chemisorbed H on surface, relation of Si-H vibr. freq. to surface bonding geometry 0-49502  
 chemisorbed  $O_2$  on (111) surface, bonding geometry, electron yield EXAFS meas. 0-50461  
 chemisorbed  $O_2$  on (111) surface, electronic struct. tight-binding calc., XPS and UPS meas. 0-49845  
 chemisorption of H on (111) surface, localised model, ab initio HF-LCAO calc. 0-6930  
 cleaved surface, metal contact props. and influence of intermediate adsorbed layers 0-49905  
 Compton profiles, directional, X-ray scattering factors and 1-electron density matrix 0-10458  
 conductivity, study with supercond. metal contacts 0-15621  
 continuum-exciton effect in optical spectrum 0-25416  
 controlled etching in catalysed ethylenediamine-pyrocatechol-water solns. 0-3223  
 core and valence electron excitations, AES, chemical shift and line shape 0-2365  
 core level spectra, electronic polarisation effects 0-6765  
 core levels, chem. shift and relaxation energy, temp. dependence 0-39520  
 core levels, temp. depend. of conduction band and core exciton energies 0-24828  
 covalent semiconductor, electronic response to high symmetry lattice vibr. 0-10619  
 cross-slip of single dissociated screw dislocations, double etching and X-ray topography studies 0-15104  
 crystal growing technology (*Korean*) 0-50538  
 crystal growth conditions effect, on microdefect distrib. 0-50549  
 crystal growth from melt in vac., origin of SiC impurities 0-2940  
 crystal structure and lattice imperfections 0-24398  
 CVD, amorphous and polycryst., solar thermal absorber, temp. variation of absorpt. edge 0-12028  
 CVD, underlying oxide layer thickness effect on in-process thickness monitoring 0-6679  
 CVD amorphous films, for high temp. solar photothermal conversion 0-26161  
 CVD films, polycryst., non-volatile memory switching 0-54814  
 CVD on  $SiO_2$  and  $Si_3N_4$ , SEM study (*Dutch*) 0-2960  
 CVD on  $SiO_2$  and  $Si_3N_4$  substrates, nucleation in  $SiH_4-HCl-H_2$  system at high temp. 0-49538  
 Czochralski cryst. growth, faceted and nonfaceted, Sb microsegregation 0-45227  
 Czochralski crystal growth, low O content 0-40251  
 Czochralski crystals, O microsegregation, swirl defect distrib., growth rate depend. meas. 0-39295  
 Czochralski growth, equilib. of dissolved C and O with CO in ambient atm. 0-1949  
 Czochralski growth from heavily Sb doped melt, interface morphological instability 0-2939  
 Czochralski wafers, thermally oxidized, stacking fault distrib., O conc. depend. 0-2042  
 Czochralski-grown, oxide precip. form. process 0-49364  
 Czochralski-grown crystals, thermally induced microdefects, annealing temp. and starting material effects 0-49141  
 deep amorphous layer implantation, laser effects, channelling diffr. study 0-25494  
 deep dislocation states 0-24836  
 deep donor character of muons and protons 0-10911

## silicon continued

- defect annihilation depth by pulse laser annealing 0-16128  
 defect form. under radiation-accelerated diffusion conditions 0-19854  
 defect formation kinetics during charged particle irradiation 0-29096  
 defect storage kinetics during neutron irradiation 0-24505  
 degenerate four wave mixing of 1.06  $\mu m$  laser radiation 0-5794  
 diamagnetism of excitons and biexcitons, recomb. spectra (*Russian*) 0-7412  
 diamond-Si heterostructure, Auger spectra electron microscopy study 0-34340  
 dielectric polarisation calcs., microscopic local fields 0-20582  
 diffraction grating, rectangular profile, fabricated from single cryst. 0-38093  
 diffusion of Ga, using open-tube system 0-19822  
 diffusion of P from spin-on  $SiO_2:P$  film 0-2050  
 diffusion of self-interstitials and As, B and P, radn.-enhanced 0-29216  
 diffusion of transition elements, anomalous behaviour 0-29044  
 diodes as low temperature sensors (*German*) 0-31744  
 dip-coated on graphite substrate, photovoltaic effects 0-29442  
 dislocation ensembles motion in neutron irradiated covalent crystals (*Ukrainian*) 0-10579  
 dislocation free, C and O impurity clouds, heat treatment influence on light scatt. 0-6427  
 dislocation growth during laser melting and solidification 0-2022  
 dislocation observation by electron channelling imaging in SEM 0-10471  
 dislocation-free,  $O_2$  precip., IR and TEM obs. 0-29173  
 dislocationless plates, microdefect dissolving due to high temp. annealing (*Russian*) 0-54378  
 dislocations, extended glide, motion obs. by high voltage electron microscopy 0-10555  
 dispersion law of indirect excitons 0-24805  
 divacancies due to proton irradiation, IR absorpt., annealing effects 0-20673  
 divacancies orientation induced by IR light, EPR spectra 0-25209  
 divacancy photoionisation cross section, photocapacitance meas. 0-6901  
 donor ion pot., small r behaviour of nonlinear Poisson eqns. 0-54652  
 dopant distrib. in mono- and polycryst. samples, C-V technique 0-6425  
 dopant segregation by pulsed-laser annealing, test case for thermal melting concept 0-24489  
 doping by thermal neutron irradiation, annealing characts. of bulk electron traps obs. 0-49244  
 double polycrystalline VLSI devices, low temp. differential oxidation 0-16521  
 dry etching induced surface contamination, SIMS, AES, and XPS obs. 0-11810  
 edge dislocation, crystal surface interception, X-ray diffr. obs. in Bragg case 0-49228  
 edge-type dislocations, energy spectrum 0-24842  
 effective supersystem cryst. simulation method, geometrical parameters, bulk moduli, impurity levels calcs. (*French*) 0-15430  
 elastically bent crystal, with large strain gradient, X-ray diffraction study 0-44073  
 electrochemical carrier conc. profiling 0-2461  
 electron beam irradiation at 31 GeV, polarised photon emission (*Russian*) 0-29811  
 electron density distribution, 0-49189  
 electron inversion layer, minigaps 0-20282  
 electron irradiation, resistivity-fluence relation 0-54700  
 electron irradiation, rod-shaped defects, electron microscopy and IR spectra obs. 0-39159  
 electron irradiation, two-vacancy defect EPR 0-29619  
 electron irradiation, damage, capacitance meas. 0-24935  
 electron irradiation, induced defects, bulk photo-EMF meas. 0-39160  
 electron trapping, donor state generation, photo I-V study 0-20210  
 electron-hole droplet condensation, crit. point 0-49612  
 electron-hole droplet condensation model, phase diagram and surface tension 0-6734  
 electron-hole droplet spatial distrib., luminesc. obs. 0-49615  
 electron-hole drops, nonequilib. paramagnetism 0-6749  
 electron-hole drops, thermodynamical parameter determ. from luminescence data 0-2845  
 electron-hole drops radius, luminesc. meas. 0-50415  
 electron-hole liquid, free excitons, biexciton gas, luminesc. 0-6750  
 electron-hole liquid, RPA calcs. 0-6743  
 electronic and struct. props., nonlocal pseudopot. calc. 0-34349  
 electronic properties, rel. to chem. bonding and lattice dynamics 0-44169  
 electronic structure, non-spherical local pseudopotential calcs. 0-39496  
 electronic structure, self consistent local description 0-20067  
 electronic structure at high press. near semicond.-metal transition 0-49586  
 emission spectra of ultrarelativistic collimated positrons 0-7434  
 energy deposition in heavy-ion path using Monte Carlo transport anal. of delta rays in track 0-39185  
 epitaxial, minority carrier lifetime and impurity conc. meas. (*Japanese*) 0-25025  
 epitaxial film growth and p-n junction formation by Si beam epitaxy in high vacuum 0-16187  
 epitaxial film growth on Si(111) and sapphire (1 $\bar{1}$ 02), simultaneous RHEED/AES study 0-10833  
 epitaxial growth, adsorbed layer model for autodoping mech. 0-7505  
 epitaxial growth in Si-P-H system, depend. of doping element incorporation on temp. in CVD 0-45234  
 epitaxial growth of amorphous layer 0-10803  
 epitaxial interface migration, theory and expt. test 0-29290  
 epitaxial layer, growth mechanism from ion-molecular beams 0-2299  
 epitaxial layer, incorporation conc. depend. of P from silane-phosphine- $H_2$  mixture 0-2053  
 epitaxial layer, minority carrier lifetime obs. (*Russian*) 0-49765  
 epitaxial layer growth in vacuum, Ar, Xe ion bombardment effect 0-39463  
 epitaxial layers, development, structure and props. of stacking faults (*Russian*) 0-24461  
 epitaxial structures, junction layer width and impurity conc. estimates (*Russian*) 0-49893  
 epitaxy technology, application to Si devices, deposition techniques 0-7501  
 EPR and cyclotron resonance of laser annealed Si 0-34773  
 EPR of quenched-in defects 0-29620  
 etch rate uniformity in  $CF_4+4\% O_2$  plasma 0-40568  
 etching, HF ion-plasma, cryst. surface layers treatment and study (*Russian*) 0-16517  
 exciton ground state splitting 0-6736



## silicon continued

exciton lifetime, temp. depend., photoluminesc. meas. in high-purity Si 0-44508  
 exciton-plasma transitions, dense electron-hole system portrait composition (Russian) 0-49622  
 excitonic molecules, thermodynamics, luminesc. 0-25442  
 excitons and electron-hole liquid, luminesc. 0-6746  
 extrinsic IR detectors, As doped, low-level  $\gamma$ -ray irradi. effects 0-37085  
 fast particle irradi., Frenkel defect formation threshold energy 0-6404  
 filamentary, grown by chem. transport reaction method, banded struct. 0-38978  
 film, amorphous, crystn. on annealing at low temps. in contact with Al 0-24765  
 film, amorphous, two-dimensional variable range hopping cond. 0-10977  
 film, CVD, amorphous and polycryst., microscopic surface roughness, effective-medium models, ellipsometric expts. 0-24756  
 film, epitaxial growth from noncondensed phases, kinetic anal. 0-54565  
 film, glow discharge deposition, SiH<sub>4</sub> discharge parameters obs. 0-44030  
 film, on sapphire, laser annealing dynamics epitaxial regrowth, optical reflectivity 0-29285  
 film, polycryst., thinning using plasma etching (Slovak) 0-45405  
 film, polycrystalline, glow discharge deposited below 250°C, struct. and morphology 0-49535  
 film, polycrystalline, low press. CVD, resist. meas. 0-2494  
 film, removal using anodic oxidation, determination of active impurity distrib. 0-40583  
 film deposition by CO<sub>2</sub> laser irradi. of SiH<sub>4</sub> 0-16190  
 films, polycrystalline elec. props., grain size and dopant conc. influence 0-29492  
 floating zone structural perfection changes by high temp. treatment, dendrites, dislocation interactions 0-29049  
 fluorocarbon ion beam etching characts. 0-35363  
 foreign interstitial atoms rel. to thermal intrinsic defects 0-29018  
 free carrier and interband absorpt. at 1.06  $\mu$ m, temp. depend. 0-2783  
 n-GaAs:Cr(Si), deep-level extrinsic photocond. response, decay at 4.2K 0-2420  
 galactic cosmic rays, Ne, Mg and Si isotopes high resolution meas. 0-51631  
 gamma radiation angular distribution of channelled 900 MeV electrons (Russian) 0-19858  
 gas-sensitive microtransducer, cond. variation with pulsed ethanol adsorption (Russian) 0-50915  
 glow discharge deposited, optical spectra, reflectance, dielectric function and oscillator strength 0-11492  
 glow discharge film decomposed from silane, on amorphous substrate, elec. cond., RHEED study 0-20044  
 grain boundaries, TEM obs. 0-15118  
 growth conditions rel. to cryst. struct. perfection (Russian) 0-38971  
 heavily doped, carrier recomb. through shallow donor and acceptor states 0-15535  
 heavy ion ranges, 120 keV Pb ions backscatt. obs. 0-19855  
 heteroepitaxial films on sapphire, vac. deposited, struct. and elec. props. 0-15390  
 heteroepitaxial growth using SiH<sub>4</sub> in H<sub>2</sub>-He atm. 0-20049  
 high resistivity, specific resistance depend. determ. using impedance freq. depend. (Czech) 0-15536  
 hole localisation, solid solubility, excitonic Auger lifetime of acceptors 0-20216  
 hot electron distrib. function, response to step changes in elec. field 0-24937  
 hydrogenated, amorphous, theoretical calc. of defect states 0-49657  
 implanted, annealed layers, amorphised structure formation mechanism and crystallographic nature 0-29091  
 implanted layers, interaction of defects and impurities stimulated by induced ionisation, ESR 0-11270  
 impurity interstitials, EHT calcs. 0-24845  
 impurity penetration depth, chemical-spectral determ. 0-19830  
 impurity precipitation from solid soln., neutron irradi. effect 0-29177  
 impurity redistribution during single oxidation step, computer program calc. 0-2060  
 impurity states and core excitons, binding energies, perturb. theory 0-49659  
 internal photoelectric effect, quantum efficiency 0-20254  
 intrinsic, self-diffusion, 885-1175°C 0-10700  
 inversion layer, cyclotron resonance in extreme quantum limit, collective ground state 0-50191  
 inversion layer, on vicinal plane, band structure 0-24994  
 inversion layer, polaron model for localisation 0-20280  
 inversion layer, temp. depend. of subband energies, exchange and correlation effects 0-20281  
 inversion layer, theory of impurity-shifted intersubband transitions 0-20324  
 inversion layer, transient response of hot electrons, calc. 0-49747  
 inversion layer, voltage tunable far IR emission 0-25018  
 inversion layer in MOS struct., carrier-phonon interaction, nonohmic transport 0-49943  
 inversion layers, effects of uniaxial stress on cyclotron reson. 0-20322  
 inversion layers, first order intervalley scatt. 0-29484  
 inversion layers, prep. domain studies of intersubband optical transitions 0-20637  
 inversion layers, resolution of Shubnikov-de Haas paradoxes 0-39648  
 inversion layers under stress, density functional calc. of subband struct. 0-20321  
 ion backscattering, H<sup>+</sup>, H<sub>2</sub><sup>+</sup>, and He<sup>+</sup>, energy spectra and charge fractions 0-35046  
 ion bombarded, projectile energy depend. and line shape of Ar-L AEs 0-16139  
 ion bombarded, radiation defect formation, atom-atom collision cascades modelling 0-10582  
 ion bombardment effect on surface struct., RHEED and Au decoration 0-2096  
 ion implantation, semiconductor device processing 0-34031  
 ion implantation, target heating, temp. measurement 0-34032  
 ion implantation and pulsed laser annealing of group III and group V dopants, supersat. alloy form. 0-54267  
 ion implantation systems, high throughput, appl. to Si 0-34029  
 ion implanted, mode-locked Nd:YAG laser annealing, recrystn. 0-19817  
 ion implanted, scanning electron beam annealing 0-6420  
 ion implanted, SiO<sub>2</sub> antireflection coating effect on CW laser annealing 0-49242  
 ion implanted, spin density effect on laser annealing 0-11517

## silicon continued

ion implanted and laser annealed, characterisation 0-29043  
 ion irradi., temp. and dose depend. of defect profiles 0-29097  
 ion-implanted, lapping and staining techniques, junction depth determ. 0-29468  
 ion-implanted, low-fluence, primary defects, transient capacitance spectroscopy 0-44238  
 ion-implanted, period surface struct. in laser annealing, new expt. evidence 0-29836  
 ion-implanted polycrystalline film, defect build-up efficiency 0-2054  
 ion-implanted structure annealing, defect behaviour obs. (Russian) 0-49281  
 ions, multiply-charged, beam-foil obs. of 1s2p<sup>3</sup>P<sub>1</sub> lifetime 0-14114  
 IR absorption spectra, Si-H bonds, crystal defects (Chinese) 0-55073  
 isoelectronic sequence, CI calcs. of oscillator strengths, L-S framework 0-14089  
 isomer shift values of implanted <sup>133</sup>Xe/<sup>133</sup>Cs, Mossbauer spectra 0-7240  
 Jahn-Teller distorted vacancy, electronic struct. 0-10869  
 Jahn-Teller Mn<sup>0</sup> centre ESR spectrum, depend. on axial press. 0-44911  
 Kikuchi diagrams, by electron diff., temp. depend. 0-1904  
 Kikuchi electron diffraction lines, forbidden, formation mechanism 0-44081  
 Kikuchi structures, phonon scatt. and thermal diffuse scatt., transmission electron diffraction study (German) 0-44082  
 laser, atomic, pulsed microwave discharge of SiH<sub>4</sub> source gas 0-48233  
 laser annealed, defect luminesc. 0-50388  
 laser annealed ion implanted, elec. props., melting threshold 0-10969  
 laser annealing, nonequib. incorporation of impurities during rapid solidification 0-55286  
 laser annealing, optical constants, ellipsometry observation 0-34024  
 laser annealing after ion implantation, temp. distrib. 0-54265  
 laser annealing at 1.06  $\mu$ m, free carrier absorpt. role 0-24964  
 laser annealing of ion bombardment damage 0-25502  
 laser irradiation effect on cohesion 0-50470  
 laser pulsed annealing, carrier diffusion role in lattice heating 0-45172  
 laser-induced bulk breakdown and free carrier generation, photocond. meas. 0-35018  
 lattice parameter determ. by X-ray multiple diff. study (Russian) 0-10460  
 layer growth by CVD on Sn-coated background (Dutch) 0-7502  
 local electron irradi., Frankel pair separation, influence on photo EMF 0-44203  
 local field, microscopic electronic polarisation 0-25283  
 localised defect, self consistent Green's function calc. 0-10919  
 low angle boundary formation, in single crystals, effect of impurities on cryst. growth conditions 0-11555  
 matrix isolated cluster, optical absorpt. extended Huckel calcs., electron energy levels 0-16045  
 MBE growth and surface struct. 0-10816  
 MBE layer resistivity and carrier mobility obs. (Russian) 0-49962  
 mechanical defects, local, annealing and effect on autoepitaxial growth (Russian) 0-7701  
 mechanical strength, origin of difference in Czochralski grown and float-zone-grown cryst. 0-44212  
 mechanically treated surface, chem. state (Russian) 0-11805  
 melt, structural factors, at. distrib. curves, thermodynamic and neutron diff. study (German) 0-19687  
 melt, structural factors, tetrahedral concs., neutron diff. study (German) 0-19688  
 metal-amorphous Si barrier, electronic props. 0-11089  
 metal-TiO<sub>2</sub>-SiO<sub>2</sub>-Si structure, SiO<sub>2</sub> growth under TiO<sub>2</sub> film during postdeposition high temp. annealing 0-15400  
 metal-ZnO-SiO<sub>2</sub>-Si structures, charge injection 0-49919  
 microdefects, diffuse X-ray scatt. obs. 0-34014  
 miniature biomedical piezoresistive pressure transducer (German) 0-37016  
 minority carrier lifetime, effect of low dose ion implantation (Japanese) 0-54715  
 minority carrier lifetime, effect of SiO<sub>2</sub> coating deposited by sputtering 0-11003  
 minority carrier lifetime in neutron doped samples 0-20218  
 MIS switch diode, charge storage effects, threshold depend. on driving voltage pulse freq. 0-49939  
 model pseudopotential, band struct. calcs., liquid semicond. resistivity calcs. 0-20075  
 monocrystalline plates, purification by thermal diffusion impurity migration anal. 0-25553  
 MOS capacitor, nondestructive of P<sup>+</sup> and He<sup>+</sup> induced damage, doping profiles 0-34087  
 MOS device, electron optical identification of precipitations 0-16309  
 MOS diodes interface trap states obs., due to electron beam lithography using DLTS (Japanese) 0-54787  
 MOS inversion layer, magnetoconductance oscillations 0-20325  
 MOS inversion layers, negative magnetoresist. 0-49922  
 MOS structure, p-channel, effect of isotropic stress on Si valence band struct., press. transducer appl. 0-25011  
 MOS structure, space-charge generation props. of Au 0-2475  
 MOSFET, conductance oscills., source-drain limited cond. 0-20316  
 MOSFET, n-channel, Hall meas. on trap states at 77K 0-44732  
 MOST, comparison of Shubnikov-de Haas effect and cyclotron reson. under uniaxial stress 0-20320  
 n<sup>+</sup>-p-p<sup>+</sup> avalanche photodiodes, carrier multiplication and noise in avalanche devices 0-15579  
 n-n<sup>+</sup> point junctions, elec. props. in microwave electric fields 0-44719  
 n-p-n heterojunction transistor 0-6959  
 n-type, carrier relax. time, mag. field effects, rel. to Hall effect 0-39608  
 n-type, degenerate, density of states from elastic consts. 0-6690  
 n-type, dislocation free, process induced cryst. defects 0-24392  
 n-type, drag thermoelec. power, anisotropy parameter determ. 0-20235  
 n-type, edge dislocation and stacking fault defect electrical recombination efficiency 0-15106  
 n-type, EPR linewidth, Orbach relax. process, conc. depend. 0-44901  
 n-type, exoelectron emission, effect of surface polishing rel. to defect distrib. in surface layer 0-40239  
 n-type, field and current domains, at low temp. 0-6868  
 n-type, heavily doped, meas. of minority carrier transport parameters 0-15537  
 n-type, HF plasma oscills. in external mag. field 0-54731  
 n-type, impurity-assoc. magnetophonon reson. 0-20221  
 n-type, inverted MOSFET surface, evidence for Lande factor g=2, finite valley splitting 0-6989



## silicon continued

- n-type, irradiated with large-neutron doses, defect annealing 0-19849  
n-type, magnetoresistance, growth layer influence, effect of randomly distributed inhomogeneities 0-20229  
n-type, neutron irradiated, annealing behaviour characterisation by electrochem. meas. 0-19847  
n-type, new small donors, energy spectra, photoionisation energy (Russian) 0-34391  
n-type, rod, placed in rectangular waveguide, microwave field distrib. 0-39622  
n-type, surface polaritons in DC current 0-34369  
n-type 0-11010  
n-type doping, homogeneous, by thermal neutrons 0-2051  
n-type gamma ray irradi., impurity composition influence on recombination centre formation 0-6872  
n-type neutron and electron irradi., isochronous annealing influence on edge absorpt. 0-11449  
neutron doped,  $\gamma$ -irradi. influence on elec. props. 0-6845  
neutron irradi., point defects photopopulation and photoion., IR spectra meas. 0-25423  
neutron irradi., residual radioactivity meas. 0-19829  
neutron irradi., small angle neutron scatt. meas. 0-29073  
neutron irradiated, Hall effect and magnetoresist. meas. 0-6883  
neutron transmutation doped, elec. props. 0-15532  
neutron transmutation doped, ESR 0-20462  
neutron transmutation doped, highly compensated, resistivity fluctuations 0-15531  
neutron transmutation doped, isochronal annealing of resistivity 0-19828  
neutron transmutation doping,  $^{31}\text{P}$  conc. meas. 0-19833  
neutron transmutation doping, annealing, deep defect levels 0-20123  
neutron transmutation doping, annealing, lattice damage 0-15163  
neutron transmutation doping, at. displacement effects 0-19852  
neutron transmutation doping, automated irradi. facility 0-15141  
neutron transmutation doping, General Electric test reactor 0-15140  
neutron transmutation doping, impurities 0-15134  
neutron transmutation doping, irradi. facilities 0-15139  
neutron transmutation doping, irradi. techniques 0-19827  
neutron transmutation doping, photoluminesc. characterisation 0-11453  
neutron transmutation doping, radioactivity form. 0-15135  
neutron transmutation doping for IR detector material 0-15136  
neutron transmutation doping in Harwell reactors 0-15138  
neutron transmutation doping using nuclear reactor thermal neutron irradi., review 0-39161  
nitridation, fluoride accelerated 0-7705  
nitridation to form  $\alpha$ - or  $\beta$ - $\text{Si}_3\text{N}_4$  0-50609  
noble-gas ion bombardment, secondary ion emission 0-35042  
nonlinear optical susceptibility, tight binding bonding orbital model 0-5784  
nuclear radiation detectors, effect of trapping on response 0-5447  
optical demultiplexer using Si echelette grating 0-53422  
optical properties, scatt. surface layer (Russian) 0-11419  
oxidation in  $\text{HCl}/\text{O}_2$  ambients, phase separation and Na passivation in thermal oxides 0-3219  
oxidation in  $\text{O}_2$ - $\text{H}_2$ - $\text{HCl}$  mixture, kinetics, and  $\text{SiO}_2$  film elec. props. 0-40569  
oxidation of Si, magnetoactive  $\text{O}^+$  plasma 0-38831  
oxidation of surface, in wet  $\text{O}_2$  environment 0-3410  
oxidation-induced stacking faults, influence of annealing ambient on shrinkage kinetics 0-29035  
oxidation-induced stacking faults, nucleation mechanism 0-15122  
oxide layer, vibration of adsorbed molecules, effect on electron capture by deep centres 0-29458  
 $\text{p}^+$ -n junction 0-24509  
 $\text{p}^+$ -n junction diodes, flow fluence S implanted unequal defect densities, dynamical obs. 0-20293  
 $\text{p}$ -i-n laser detector, wavelength and temp. depend. characts. 0-13134  
 $\text{p}$ -n diode,  $1/f$  noise calc., free carrier mobility interpretation 0-54774  
 $\text{p}$ -n junction local temp. meas. using pulsed SEM, induced-current mode 0-54775  
 $\text{p}$ -n homoepitaxial junctions, elec. and struct. characts. 0-6662  
 $\text{p}$ -n homojunction, radiation detector appl., for integrated optics (Czech) 0-33227  
 $\text{p}$ -n junction, charge carrier recomb. at dislocations, combined SEM and TEM study 0-15105  
 $\text{p}$ -n junction, ellipsometric method of temp. meas. rel. to secondary breakdown (Russian) 0-11074  
 $\text{p}$ -n junction, polycryst.-single cryst., elec. characts. 0-11077  
 $\text{p}$ -n junctions, high-voltage, elec. props. by optical scanning 0-6969  
 $\text{p}$ -n junctions, neutron transmutation doping, breakdown process 0-15600  
 $\text{p}$ -type, interband transitions, contrib. to conductivity at submillimetre wavelengths 0-34473  
 $\text{p}$ -type, millimetric and far-IR cond., freq.-depend. carrier relax time 0-34460  
 $\text{p}$ -type, Raman spectra, pseudopot. calc. of discrete-continuum interference 0-2747  
 $\text{p}$ -type, surface elec. behaviour after chem. treatment 0-20185  
 $\text{p}$ -type film, on sapphire, elastoresist. coeffs., room temp. 0-34532  
 $\text{p}$ -type inversion-channel photoelectric cell characteristic (Russian) 0-49941  
packing defects, change in size during heat treatment 0-39079  
particle detection, use of dislocation-free Si 0-42893  
periodic stepped structure, on vicinal planes, LEED obs. 0-24725  
phonon dispersion curves, pseudopotential calc. 0-10620  
photo-EPR of dislocations in deformed sample 0-11267  
photoacoustic signal changes assoc. with crystallinity, recrystallisation after laser annealing 0-16127  
photocathode, negative electron affinity process obs. by laser beam scanning (Japanese) 0-55262  
photoconductivity, influence of surface recombination rate and carrier diffusion 0-44660  
photoconductivity, temp. dependence, excitation with laser pulses (Russian) 0-11031  
photoconductivity and electrical resistivity of Si with thermal defects 0-6837  
photoconductivity kinetics, effect of exciting illumination (Russian) 0-11032  
photodetector, for improved short-wavelength quantum efficiency 0-31874  
photodetector, shallow junction type, internal quantum efficiency meas. model fits, visible quantum yield 0-267  
photodetectors, surface-barrier 0-4771

## silicon continued

- photodiode array for integrated optical spectrum analyser 0-33241  
photodiode array for position-sensitive X-ray detector 0-52831  
photodiode array for radiation detection in AES and analytical appl. (German) 0-11992  
photoelectric converters, bilateral sensitivity, optical characts. anal. 0-40858  
photoelectric converters, photoelectric parameters under illumination 0-40857  
photoemission, primary and secondary yields using low-energy monochromatic X-rays 0-35053  
photoexcited, highly stressed, electronic Raman scatt. and antireson. 0-29737  
photovoltaic concentrator cells development project, developments, performances and future trends 0-45699  
photovoltaic generators using optical concentration, current status and development trends review 0-45697  
photovoltaic solar energy conversion [conf. Berlin, West Germany, April 79] 0-30482  
piezoresistive accelerometer power transfer factor (German) 0-37017  
piezoresistive coefficient calc. and meas. (German) 0-39571  
piezospectroscopic effect on zero-phonon luminescence lines 0-50406  
plasma, of laser-irradiated glass shell, electron temp. and density X-ray emission diagnostics (Chinese) 0-38718  
plasma etching in Freon plasma, for microelectronics appls. 0-3080  
plasmon dispersion relation, local microscopic field effects 0-20103  
plastic properties, internal friction, dislocation motion (Russian) 0-54305  
plastically deformed, spin-depend. charge transport 0-6895  
point charge impurity screening 0-6783  
point defect aggregates, high resolution diffuse X-ray scattering study 0-49211  
point defect trapping in stainless steel, anal. from interstitial loop growth rate temp. depend. obs. 0-49270  
point defects, multiple scatt.  $\chi_\alpha$  model 0-54636  
point defects, negative-U props. 0-49660  
polycrystalline, CVD, electron beam recrystn. 0-24759  
polycrystalline, elec. and photovolt. props., grain size effects 0-49800  
polycrystalline, end point detection in plasma etching by optical emission spectroscopy 0-50733  
polycrystalline, for efficient low cost solar cells 0-21405  
polycrystalline, laser recrystallised poly Si/insulator interface, charges at interface 0-54789  
polycrystalline, recrystn. after plastic deform. and annealing 0-3145  
polycrystalline films 0-50980  
polycrystalline solar cell base material characterisation, defect states 0-50979  
porous, form. during anodic treatment in aq. HF 0-35369  
porous, formation during anodic treatment in HF aq. soln., growth kinetics and density 0-20059  
porous layer, oxidation, and oxide film props. 0-55556  
precipitation of O, 1000°C TEM, IR absorpt. and X-ray studies 0-34194  
precipitation of O, annealing, IR spectra meas. 0-24606  
proton energy loss, 0.1-1.0 MeV 0-42909  
proton irradiated, efficiency of form. and nature of defects, Hall meas. 0-6444  
pulsed laser annealing, mechanism 0-25739  
pulsed laser annealing, nonthermal, plasma annealing 0-25498  
purification technology for the development of low cost solar cells 0-50976  
radiation induced defects, IR absorpt. bands 0-25424  
radiation pressure, photon drag effect in far-IR 0-50452  
Raman scattering absolute cross-section 0-11410  
reactive close-spaced vapour transport, simplified theory 0-15396  
reactive plasma etching with  $\text{CF}_4$ , mag. field control 0-11796  
reconstructed surface physics, review 0-10766  
recrystallisation of CVD-grown polycryst. Si and influence of B, Al dopants on grain growth 0-54575  
regrowth under laser irradi. 0-24481  
resistivity depth profiles calcs. from spreading resist. meas. using math. algorithm 0-2393  
ribbon growth, ribbon-to-ribbon process, thermal environment control 0-35116  
ribbon growth by capillary action shaping technique 0-29888  
ribbon growth from melt, monitoring device for width and thickness uniformity 0-35077  
ribbons, roller quenching method of prep., grain sizes and carrier conc. 0-40275  
Schottky barrier photovoltaic IR detector 0-9040  
Schottky barrier struts., proton bombarded, defect states 0-29356  
Schottky diodes on sputtered amorphous Si:H, light induced ageing effects, interpretation of photovoltaic stability 0-54780  
Seebeck effect position sensor for  $\text{CO}_2$  laser beam alignment 0-5772  
self diffusion entropy 0-29211  
self- and impurity diffusion 0-29213  
self-diffusion, dynamical recovery 0-29215  
self-diffusion, probed by (p, $\gamma$ ) resonance broadening method 0-24646  
self-ion implanted, laser annealing, channelling and TEM meas. 0-24466  
semi-insulating polycrystalline CVD layers, AES and XPS characterisation 0-16129  
semiconductors, defect processes, electronic stimulation 0-24665  
shear deformed, Smith-Herring and mobility change piezoresistance 0-6842  
sheets production, low cost, crystal growth techniques comparison 0-35083  
a-Si:H, structure, effect of H-Ar plasma contact on elec. props., and optical gap 0-34533  
Si:P(As)(Sb)(Bi), high resolution study of group V impurities absorption 0-7388  
n-Si-electrolyte junction, Schottky barrier height and reverse current 0-6979  
slice resistivity var. meas. using automated photovoltaic systems 0-52274  
snowflake defect due to annealing in H at 1000°C X-ray topography study (Chinese) 0-49227  
solar cell, amorphous, technological development trends for low cost energy requirements 0-26136  
solar cell, device model for tandem junction cell 0-16813  
solar cell array with concentration, design and development 0-45700  
solar cell fabrication, R and D on low-cost processes, effect of impurities on cell performance 0-50978  
solar cell fabrication developments using Si on ceramics and minute spherical cells 0-55839



## silicon continued

solar cell production, Union Carbide Corporation Silane Process, cost analysis 0-21403  
 solar cells, Al-thin oxide-Si, Schottky barrier, degradation effects, ion beam induced nuclear reactions 0-30488  
 solar cells, amorphous, glow discharge produced 0-12013  
 solar cells, calculations of absorption coefficient 0-7944  
 solar cells, crystal growth, heat exchanger method, fixed abrasive slicing technique 0-35082  
 solar cells, design, fabrication and evaluation of a 2" high efficiency cell for concentrator systems 0-55854  
 solar cells, developments, appls., and economics of solar photovoltaic conversion (*German*) 0-26132  
 solar cells, developments (*French*) 0-55845  
 solar cells, diffused horizontal homojunction, effects of junction depth and impurity conc. 0-55877  
 solar cells, diffused junction,  $n^+pp^+$  or  $p^+nn^+$ , prep. using solid diffusion sources 0-35689  
 solar cells, diffusion fabrication process, low cost, highly automated 0-30487  
 solar cells, edge-illuminated  $p^+nn^+$ , analytical model under concentrated sunlight 0-7942  
 solar cells, efficiency limits, comprehensive explanation 0-35688  
 solar cells, experimental efficiency optimisation of  $n^+pp^+$  and  $p^+nn^+$  cells 0-30486  
 solar cells, for satellite solar power systems, developments and future trends 0-45694  
 solar cells, growth of large grain polycryst. layers on graphite substrates by CVD on liquid layers 0-55849  
 solar cells, implanted layers characteristics, laser irradiation effects 0-35692  
 solar cells, ion implanted, from EFG Si ribbons 0-30485  
 solar cells, low mass space blanket using 50  $\mu$ m cells 0-30498  
 solar cells, low-cost, starting materials technology and economics 0-30483  
 solar cells, low-cost sheet fabrication 0-50977  
 solar cells, multi-bandgap concentrator cells, Si and  $Al_xGa_{1-x}As$  systems, operation with spectrum splitting filter 0-45698  
 solar cells, photoelectric effect and principles of operation and efficiency 0-50983  
 solar cells, polycrystalline  $n^+/p$ , computer model of spectral response and photocurrent 0-55853  
 solar cells, production problems of polycryst. Si cells (*Rumanian*) 0-21398  
 solar cells, RAD polysilicon sheets, photovoltaic potentialities, conversion efficiencies, limitations 0-30484  
 solar cells, screen printed, effect of double exponential on efficiency and yield 0-55851  
 solar cells, semiconductor thick film cell contacts, all metal 0-30489  
 solar cells, technological developments of single crystal cells and cost-effective cells 0-50984  
 solar cells, technology development of 50  $\mu$ m cells for space power systems 0-30499  
 solar cells, terrestrial photovoltaic systems, historical developments and current research and development trends 0-45702  
 solar cells, thin cell with back surface reflector, and controlled optical absorbance 0-35691  
 solar cells effects of B and P impurities on cell performance 0-55848  
 solar cells for cathode protection of submerged marine structures 0-40859  
 solar cells with concentrating collectors and integrated heat use system 0-45701  
 solar concentration cells, concentrated sunlight effects, experimental results, interpretation 0-35690  
 solar grade Si prod., using Dow Corning process 0-29894  
 solar-grade, directional solidification in carbon crucibles 0-45663  
 SOS films, cryst. quality improvement by Si ion channelling, annealing 0-44222  
 SOS wafer for beam profile monitoring in high-current ion implantation systems 0-13182  
 sputter-machined surface,  $Ar^+$  ion, lattice disordering obs. (*Japanese*) 0-3228  
 sputtered amorphous film, photocond. and electronic props., effects of annealing in plasma gas 0-44644  
 sputtered layers, EPMA of Ar content 0-3443  
 sputtering rate on Ar ion bombard. 0-55245  
 stacking fault energies, intrinsic and extrinsic, by TEM 0-10562  
 stacking fault growth, oxidation-induced, HCl and interstitial effects 0-49241  
 steam oxidation, low temp., high press., oxide growth kinetics and props. 0-16523  
 steel:Si alloy formation kinetics at solid cathodes, metal electrodeposition from molten salt electrolytes 0-26028  
 stress measurement, appl. of photoelastic technique 0-48656  
 structural properties, self-consistent calc. 0-28947  
 structurally related bulk and surface props., self-consistent pseudopot. method 0-54632  
 structure factors, determ. by intersecting-Kikuchi-line method 0-14971  
 substrate, effect of surface conditions on plasma sprayed metal coatings 0-21145  
 substrate, ion induced intermixing of Pd or Pt film 0-15420  
 substrate, Nb thin film intermixing with substrate, ion induced silicide formation 0-34101  
 substrate, nucleation controlled interaction with metal film, silicide form. 0-10711  
 substrate, process-induced in-plane distortion, correl. with wafer bowing 0-54579  
 substrate, solid state reaction with Ti film, backscatt. anal. 0-34257  
 substrate, struct. stability of dielec. film 0-54564  
 substrate, thermally oxidised, interface props., sputter deposition parameters effects (*German*) 0-40257  
 substrate, vitreous  $SiO_2$  film defect struct. comparison with crystalline  $SiO_2$  and Si-O bond nature 0-54557  
 substrate (111), MBE deposition kinetics of Bi film 0-10817  
 substrate for Pb, Sb, and Bi silicate films, form. kinetics and props. 0-35358  
 surface, (001)-(2 $\times$ 1), reconstruction-induced mean-square displacements 0-15343  
 surface, (100), inversion layer, interaction induced transition at low density 0-15581  
 surface, (111)2 $\times$ 1, surface states, reflectivity obs. 0-50368  
 surface, (111)7 $\times$ 7, electronic struct. calc. 0-24993

## silicon continued

surface, (111), atomic and electronic struct. 0-54746  
 surface, (111), clean and  $O_2$ -chemisorbed, electron states by AES 0-54747  
 surface, (111), low energy  $H^+$  and  $He^{++}$  ion refl., computer simulation 0-11524  
 surface, (111), low press. baked, dominant interactions and average distances between paramag. centres 0-15783  
 surface, (111), non-orthogonal tight-binding approach to surface states 0-2442  
 surface, (111),  $O_2$  adsorption, atomic steps and residual gas effects 0-54517  
 surface, (111), oxide formation, AES and EELS meas. 0-3232  
 surface, (111), with and without H chemisorption, Auger surface spectroscopy 0-50472  
 surface, adatom indirect interaction, theory 0-44696  
 surface, clean and gas ( $O_2$  and  $H_2O$ ) covered, appl. of UPS ultrahigh vacuum apparatus (*Japanese*) 0-37125  
 surface, decontamination of Au impurities by etching 0-55559  
 surface, electron states, surface photovoltage spectroscopy study, doping effects 0-49860  
 surface, etched and heat-treated, optically stimulated ESR investigation 0-11245  
 surface,  $He^+$  bombardment, damage production, defect diffusion 0-39181  
 surface, high index, theory of inversion layers 0-44697  
 surface, KLL Auger peaks, bremsstrahlung-induced 0-45199  
 surface, near (111), dislocation movement at annealed scratches, X-ray topography obs. 0-2029  
 surface, stacking fault generation due to mech. damage, preoxidation annealing influence 0-54261  
 surface (100), atomic and electronic structs., energy minimisation calc. 0-49480  
 surface (110), intrinsic surface states, photoemission study 0-50514  
 surface (111)7 $\times$ 7, electronic struct., angle-resolved UPS study 0-40226  
 surface (111), chemisorpt. of Cl, electronic states tight-binding method appl. 0-49564  
 surface (111), density of states from soft X-ray absorpt. spectra 0-40187  
 surface (111), geometric struct., LEED obs. 0-49479  
 surface (111), with Al overlayers, electronic states 0-11061  
 surface (111) 7 $\times$ 7, chemisorption of  $H_2O$  0-10792  
 surface (111) 7 $\times$ 7, electronic struct., angle-resolved UPS study 0-50513  
 surface (111) 7 $\times$ 7, structure model from anal. of RHEED patterns 0-49471  
 surface (111) (7 $\times$ 7) structs., LEED anal. and energy minimisation calcs. 0-49478  
 surface (111) reconstruction, milk-stool model, quantum chem. ab initio calc. 0-49477  
 surface Brillouin scatt. from acoustic phonons 0-55113  
 surface characterisation using SAW 0-11069  
 surface cleaning by pulsed laser irradi. 0-45173  
 surface energy evaluation, by a microindentation method 0-16473  
 surface interacting with adsorbed gases, paramag. props., EPR study 0-34772  
 surface inversion layers, intersubband optical absorpt., Auger-type transition 0-29741  
 surface layers, impurities, elec. and photoelec. props. 0-2298  
 surface peak anal. by 100-350 keV protons 0-55247  
 surface radiation damage cross sections, influence of distortions 0-6442  
 surface roughness evaluation by UV refl. 0-39393  
 surface structures after pulsed laser annealing, LEED obs. 0-54494  
 surface-barrier detector, impurity distrib., influence on characts. 0-18766  
 surfaces, amorphous, hydrogenated, and monocryst., AES and LEED, comparative study (*French*) 0-44398  
 surfaces, electronic struct., tight-binding calc. 0-54755  
 swirl defects in single crystals. 0-44200  
 switch, laser-activated, high-power switching with ps. precision 0-2416  
 technology and physics, review 0-34353  
 temperature field determ. under laser irradiation (*German*) 0-25496  
 temporary trap characteristic after heat treatment (*German*) 0-34459  
 textured wafer, selective absorber for solar thermal conversion 0-30544  
 thermal conductivity, calc. using numerical soln. of Boltzmann eqn. 0-44373  
 thermal neutron cross sections, in single crystals. 0-19672  
 thermal oxidation in  $O_2$ -trichloroethylene mixture, 900, 1000 and 1100°C 0-3221  
 thermal oxidation in wet  $O_2$ /trichloroethylene mixtures at 1200°C 0-16522  
 thermally induced microdefect form., C and O role 0-11439  
 thermally induced microdefects, effect of C, TEM obs. (*Japanese*) 0-54244  
 thin film, effect of O on thin film compositions obtained by secondary ion emission 0-26079  
 thin foil cells, technology developments 0-35693  
 thin single crystal, MeV ion scatt. and channelling obs. of interfaces 0-50492  
 thin sub-monolayer film, Auger emission coeffs. meas. 0-55236  
 thyristors, high-output, air cooling intensification design method (*Chinese*) 0-19229  
 tracer diffusion of  $^{71}Ge$  and  $^{31}Si$  in intrinsic and doped samples 0-29214  
 transformation, order-disorder, repeatable, using intense laser beam 0-39150  
 transistor, microwave Stark effect spectrometer, with electric molecular modulation (*Russian*) 0-9003  
 transmutation-produced in Al, by neutron irradi., effects on positron annihilation 0-20732  
 two-dimensional inversion layer on surface, minigap and conductivities 0-20267  
 vacancies and interstitials 0-29015  
 vacancy, possible Anderson negative-U system 0-2358  
 vacancy, self consistent Green's function method 0-24843  
 vacancy, self-consistent electronic states 0-29354  
 vacancy, tight-binding calc. 0-24844  
 vacancy electronic struct., self-consistent Koster-Slater method 0-10920  
 vacancy screening, dielec. const., exchange correl. pot., Thomas-Fermi description 0-44528  
 valence band Auger spectrum, cluster approach, comparison with experimental spectrum 0-40191  
 valence bands, XPS excited by Zr  $M\zeta$  radiation 0-40236  
 vertical etching, at very high aspect ratios, review 0-50744  
 VPE, growth processes, in-situ obs. (*Japanese*) 0-35104  
 VPE, reduced pressure, advances 0-40242



## silicon continued

- VPE layer props. control using boundary layer characts. 0-50561  
wafer, automatic meas. system for resist. profiles 0-39574  
wafer, chemically etched, surface roughness by gas adsorption techniques 0-15398  
wafer, nondestructive method for meas. of spatial distrib. of minority carrier lifetime 0-13098  
wafer, thermal characts. of  $\text{H}_2\text{SO}_4\text{-H}_2\text{O}_2$  cleaning soln. 0-3225  
wafer C impurity IR absorption spectrometry, thickness fringe elimination 0-55132  
wafer O interstitial IR absorption spectrometry, multiple reflection correction 0-55131  
wafer prod., diffusion furnace temp. profile meas. systematic errors, theoretical model (*German*) 0-8989  
wafers, Au contamination during plasma etching 0-19831  
wafers, Czochralski-grown, lifetime improvement by two-step annealing 0-49916  
wafers, microwave plasma etching, role of ions and neutral active species 0-3217  
wafers, scribing and subsequent fracture 0-11743  
whisker, (111) oriented, FIM and atom-probe FIM obs. 0-10473  
whisker for field desorption ion source for isotope abundance ratios 0-11975  
whisker growth characts. by  $\text{SiH}_4$  thermal decomposition 0-34342  
zone melting, swirl defects A-type as source of dislocation generation on macroscopic scale 0-25554  
Al-Si interface in semiconductors, electronic parts, electromigration aspects 0-39355  
Al-Si<sub>3</sub>N<sub>4</sub>-Si struct., surface energy bands under step function illumination 0-49840  
Al-Si-Al contact current response to 100 keV neutron irradi. (*Russian*) 0-49956  
Al-SiO<sub>2</sub>-Si, void form. in Al interconnection lines at Si-SiO<sub>2</sub> boundaries 0-2476  
Al-SiO<sub>2</sub>-Si structure, positive interface charge, exciton and H diffusion models 0-2471  
Al-SiO<sub>2</sub>-Si system with reactively sputtered SiO<sub>2</sub>, work functions difference 0-6987  
Al-SiO<sub>2</sub>-Si MIS solar cells, I-V characts. temp. depend. 0-7935  
Al-SiO<sub>2</sub>-p-Si MIS solar cells with back surface fields 0-12006  
Al-TiSi<sub>2</sub>-n-Si struct., elec. props., charge transfer mechanism across TiSi<sub>2</sub>-Si interface (*Russian*) 0-34515  
(Al+Si)-Si thin films, struct. transitions and phase comp. 0-49537  
Al<sub>2</sub>O<sub>3</sub>-Si-Te-Al<sub>2</sub>O<sub>3</sub> layered apertured facet reflector, for lateral mode stabilisation of diode lasers 0-23708  
Au-Si interface, valence band and core levels, Si diffusion, alloy form., photoelectron spectra obs. 0-45205  
Au-Si system, transition layer struct. form. and heat treatment influence, amorphisation obs. 0-54529  
Bi implanted, elimination of He<sup>+</sup> beam effect on channelling dips 0-54292  
Cr-SiO<sub>2</sub>-Si MIS solar cell, current cond. 0-7936  
Ga<sub>1-x</sub>Al<sub>x</sub>As:Si photoelectric converters, broadband varizone creation 0-40856  
GaAs:Si, donor-acceptor pair defects absorpt. bands 0-16064  
GaAs:Si, ion-implanted, capless anneal, effect of As partial press. 0-29038  
GaAs:Si, positron lifetime temp. depend. 0-29826  
n-GaAs:Si, radiative transitions induced by modest annealing, photoluminesc. spectra 0-55158  
GaAs:Si encapsulated with AlN, Si<sub>3</sub>N<sub>4</sub> layers, photolum., annealing effects 0-20681  
GaAs:Si epitaxial films, elec. and photoelec. props., impurity distrib. 0-7006  
GaAs:Si LPE layers, surface morphology, substrate misorientation, initial supercooling effects 0-34329  
GaAs:Si layers, MBE growth, elec. and optical props., doping characts. 0-10819  
GaAs:Si p-n light-emitting structs., soln. of general minority carrier transport eqn. 0-15597  
GaAs:Si p-n structs., effect of growing conditions on distrib. of recomb. parameters 0-39668  
GaAs:Si substrate, VPE growth, photoluminesc. and emission spectra 0-29774  
Ge-Si, solid phase heteroepitaxy 0-6670  
Ge-Si, solid soln., local IR transmission 0-7357  
GeSi:Si, elec. cond. and thermally stimulated currents 0-20194  
<sup>1</sup>H ion implantation at 0.5 to 300 keV, range parameter meas. 0-44242  
He-like ion, spectral broadening in plasma, theory 0-6223  
In<sub>2</sub>O<sub>3</sub>-SnO<sub>2</sub>/Si solar cells, antireflection props. of oxide film 0-3513  
InP:Si, pulse electron annealing, carrier activation and mobility 0-15124  
(In<sub>1-x</sub>Sn<sub>x</sub>)<sub>2</sub>O<sub>3</sub>-Si-N solar cell efficiency and elec. props. 0-35676  
MnSi, amorphous, sputtered, mag., elec., struct. and thermal props., spin glass behaviour 0-50124  
Nb-Si, bridge, crit. current 0-20359  
Ni-Cr-W-Mo-Al-Ti (15,6,3,2,2, wt.%), wrought, Si effect on transition brittleness (*Chinese*) 0-55491  
Ni-n-GaP:Si contact, doping effect in elec. props. 0-6983  
O depth profiling, comparison of techniques 0-29048  
Pb-Si:Sb Schottky tunnel junction, variable range hopping assisted tunnelling 0-39670  
PbS-Si heterojunction detector, direct injection readout 0-4765  
Pd-amorphous Si thin film interaction, metal rich Pd-silicide formation 0-2284  
Rh-Si thin film interaction, interdiffusion, temp. depend. 0-54443  
Si (001)-SiO<sub>2</sub>, n-inversion layer, valley splitting without effect mass approx. 0-15586  
Si (111)-Au interface, chemically driven intermixing, UPS study 0-50533  
Si (111)-Pd interface, microscopic Pd<sub>2</sub>Si form., UPS obs. 0-24743  
Si (111)-SiO<sub>2</sub> interfaces, sixth-valley state stability a priori calc. 0-49859  
n-Si, current carrier-dislocation interactions, resistance in UHF range (*Russian*) 0-54732  
p-Si, high ohmic material, deep level investigation, vacuum growth (*Russian*) 0-54654  
Si I CI calcs. of oscillator strengths, L-S framework 0-14089  
Si I lines in far UV spectra of G-type dwarf stars 0-56829  
Si II, oscillator strength meas. and trends in group IV homologous ions 0-42991  
Si II lines in A-type star  $\alpha$  Lyrae (Vega), Copernicus UV obs. 0-8627  
Si III, <sup>3</sup>F<sup>0</sup> Rydberg series, energy levels, multiconfigurational HF procedure 0-47882

## silicon continued

- Si III, EUV spectra in solar transition zone rel. to energy balance and press. 0-21957  
Si III 1892 Å emission line obs. of solar atmosphere 0-31277  
Si III 1892 Å emissivity in solar spectrum, effect of charge transfer rel. to spectral diagnostics 0-41717  
Si III and IV, electron impact width of plasma lines, approximative semi-classical formula 0-43972  
Si IV, V, VI, beam-foil level populations, charge state fractions 0-52913  
Si IV radial wave functions of discrete spectrum calcs., dipole and quadrupole polarisation 0-5476  
Si, laser irradiated, positron annihilation crystal struct. imperfection monitoring 0-11506  
n-Si MOS inversion layers, Hall cond. meas. 0-39676  
a-Si, resonant and non-resonant photoconductivity changes 0-49814  
a-Si, resonant and non-resonant luminesc. changes theory 0-50410  
Si VII, excited level populations, line intensity ratios, solar corona appl. 0-32637  
Si wafer, heat treatment behaviour of microdefects and residual impurities, X-ray diffr. and IR absorpt. study 0-49214  
Si XI, beam-foil obs. of oscillator strengths for E1 transitions 0-14112  
Si XI, wavefunctions and oscill. strengths, CI calcs. 0-23317  
Si XII, in plasma, ion electron collisional radiative recomb. coeffs., bottleneck calc. 0-53942  
Si XIII, 1s<sub>2s</sub><sup>3</sup>S-1s2p<sup>3</sup>P transitions, Lamb shift, VUV beam foil spectra obs. 0-52919  
Si XIII, ground-state electron impact excitation strengths, close-coupling calcs. 0-23561  
Si<sup>+</sup> reson. line regularities in plasma Stark widths and shifts 0-43881  
Si<sup>12+</sup>, 1s<sub>2s</sub><sup>3</sup>S<sub>1</sub>-1s2p<sup>3</sup>P<sub>0,2</sub> transition wavelengths, by beam-foil 0-32649  
Si<sup>19+</sup>, excited state population density in p and p<sup>2</sup> configs., temp. depend. 0-31273  
Si:<sup>57</sup>Co, ion-implanted, Mossbauer study, annealing effects 0-7231  
Si:<sup>57</sup>Co/<sup>57</sup>Fe, Mossbauer spectra, deep level Co impurity study 0-29666  
Si:<sup>85</sup>Kr, ion-implanted, impurity distrib. 0-15145  
Si:O, electrical activity due to heat treatment, Hall effect meas. 0-15543  
Si:Al ribbon, edge-defined film-fed growth, Al redistr. 0-29873  
Si:As, anomalous tail generation, As ion channelling 0-49246  
Si:As, displacement effect beam energy depend., vacancy trapping 0-33996  
Si:As, electron induced displacement, channelling study 0-29058  
Si:As, H, amorphous system, struct. and defects, Raman and EPR meas. 0-49103  
Si:As, high-dose implanted, irradi. time and subsequent heat treatment effects on laser annealing 0-29041  
Si:As, implanted, thermal diffusion of As 0-39352  
Si:As, implanted through SiO<sub>2</sub> films, elec. props., defect struct. 0-54264  
Si:As, ion implantation system, high current, design of end station 0-34030  
Si:As, ion implanted, beam techniques 0-24474  
Si:As, ion-implanted, CW IR laser annealing 0-34022  
Si:As, p-n junction form. by laser annealing, space charge region, effects on reverse current 0-54772  
Si:As, solid solubility of As determ. by ion implantation, CW laser annealing 0-6517  
Si:As implanted emitters, oxidizing drive-in ambient deleterious effect 0-2044  
Si:As ion implanted, laser induced diffusion modelling 0-24672  
Si:As ion implanter system, high current, architecture and control 0-31942  
Si:As photoconductive detector for IR astronomy, responsivity and system noise 0-51665  
Si:As sputter rate meas. SIMS combination with Rutherford backscatter 0-21334  
Si:As(B), implanted CW laser annealing, elec. props., cryst. struct. and limitations 0-39131  
Si:As(Sb), MBE, n-type doping techniques 0-15126  
Si:Au, method of determining content of impurities with deep levels 0-2056  
Si:Au, p<sup>+</sup>-n junction, quantitative study of Au atoms by TSC method 0-2458  
Si:Au Ar ion implant gettering obs. by MOS and Rutherford backscatter techniques 0-39119  
Si:Au donor and acceptor centre obs. using IR absorpt. and dynamic nucl. polarisation with optical pumping 0-54639  
Si:Au(P)(B) whiskers, impurity inhomogeneity 0-39145  
Si:Au(Pt), electron and hole capture, DLTS obs. 0-49661  
Si:Au(Pt), heavily doped, gradual p<sup>+</sup>-n junctions, trap levels (*French*) 0-34392  
Si:B, antiferromagnetic ordering of holes, recombination radiation polarisation (*Russian*) 0-45121  
Si:B, conc. depend. of B diffusion coeff. 0-39353  
Si:B, diffusion from BN source with H<sub>2</sub> injection, AES study 0-19986  
Si:B, heat treatment centres changes, EPR obs. 0-29601  
Si:B, heavily doped, paramagnetic props., anomalous hole spin susceptibility (*Russian*) 0-54861  
Si:B, hole mobility calc. for dopant density and temp. var., resistivity meas., effective mass calcs. 0-54703  
Si:B, IR spectra of acceptor levels 0-34953  
Si:B, implantation distribution determ. using ion bombardment 0-44230  
Si:B, implanted, effectiveness of charged vacancies in diffusion 0-34239  
Si:B, inhomogeneous surface layer, diffusion and implanted, X-ray rocking curves 0-6603  
Si:B, ion implantation, anal. of disordered regions in crystal with Promiss protonograph 0-19823  
n-Si:B, ion-implanted damage, positron annihilation and sheet resist. meas. 0-35003  
Si:B, lateral effect of oxidation on B diffusion 0-29217  
Si:B, P, deep diffusion of B and P, expt. results 0-54437  
Si:B, photolum. of heavily doped p- and n-type 0-20708  
Si:B, proton-irrad.-enhanced diffusion 0-29227  
Si:B, redistr. of B during thermal oxidation, numerical and analytical calcs. 0-49259  
Si:B, self-interstitials location by Rutherford backscatter. of channelled ions 0-2101  
Si:B, with insulating coating, mechanical stress influence on B diffusion, strained surface layers 0-29224  
Si:B,As selective area simultaneous doping 0-34015  
Si:B,In, sharp line series in near-band-edge photolum. 0-16092  
Si:B,P, anomalous diffusion 0-29229



## silicon continued

- Si:B,P, double implanted layer, n-p-n struct., single pulse laser annealing 0-49247  
 Si:B ion implanted, X-ray topographical images at different absorption conditions 0-2052  
 Si:B sputtering by Ar<sup>+</sup>, computer simulation of sputter broadening in impurity depth profiling 0-2908  
 Si:BF<sub>3</sub><sup>+</sup> ion implanted, arc annealing by flash lamp 0-44223  
 Si:B(Al), (P)(As)(In), ion implanted film, elec. prop. impurity depend. 0-24467  
 Si:B(Al)(Ga)(In)(Tl), binding energy, excited state spectra, photolum., semi-empirical short range pot. 0-44534  
 Si:B(Li)(P), piezospectroscopic studies of bound multiexciton complexes 0-16006  
 Si:B(P), proton enhanced diffusion, vacancies diffusion length 0-29226  
 Si:B(P), uniaxially stressed, impurity-assisted intervalley scatt., photoluminesc. obs. 0-34979  
 Si:B(P) polycrystalline thin film, plasma annealing, effect on elec. props. 0-7005  
 Si:Bf<sub>3</sub><sup>+</sup> layers, ion-implanted, anomalous carrier tail generation mechanism 0-19819  
 Si:Bi(As), optical polarisation of <sup>29</sup>Si nuclei, nucl. relax. due to optical pumping 0-2665  
 Si:C(O)(Sb), striated impurity distrib. calc. in melt-grown crystals 0-24488  
 Si:Cd n<sup>+</sup>-n-n<sup>+</sup> structs., photoresist. props. under exclusion conditions 0-39666  
 Si:Co, implanted or diffused, and annealed, localisation of Co atoms, Mossbauer obs. 0-39140  
 Si:Cr, ion implanted, Cr conc., depth distrib. and diffusion coeff. 0-49243  
 Si:Cr<sup>+</sup> EPR spectra and spin state population inversion with unpolarised optical lighting (*Russian*) 0-44909  
 Si:Cu extinction of X-ray topographic images of Cu precipitates 0-45310  
 Si:D, amorphous, thermal stability, comparison with Si:F 0-49542  
 Si:D, ion implanted, D depth distrib., SIMS meas. 0-54279  
 Si:F, amorphous, pure and doped, vibr. excitations at defect sites, IR and Raman spectra calc. 0-49329  
 Si:F, amorphous, thermal stability, comparison with Si:D 0-49542  
 Si:F, amorphous film, effect of F on elec. cond. 0-34444  
 Si:F, H amorphous films, optical props., photoconductivity, photostructural changes 0-11034  
 Si:F,H, amorphous, glow discharge deposited elec. props. and device aspects 0-44744  
 Si:F(H), amorphous, electronic struct., orthogonalised LCAO calc. 0-44486  
 Si:Fe, B thermally activated Fe interstitial, elec. and kinetics props. (*German*) 0-34035  
 Si:Fe, implanted, annealing and stripping, Mossbauer expts. 0-39141  
 Si:Fe, implanted, Mossbauer spectra, conversion electron, temp. dependence 0-40025  
 Si:Fe, interstitial form., Au dopant effect 0-29611  
 Si:Fe, laser annealing of implanted <sup>57</sup>Co sources, Mossbauer obs. 0-39139  
 Si:Fe, laser implantation, Mossbauer obs. 0-39125  
 Si:Ga, electron irradiation-induced defects, DLTS meas. 0-24499  
 Si:Ga, IR spectra of acceptor levels 0-34953  
 Si:Ga, neutron irradiation, Hall effect meas. of shallow donor levels 0-20124  
 Si:Ga(As) 0-19824  
 n-Si:Ge, electron induced defects, room temp. instability 0-29052  
 Si:Ge, regrowth behaviour from backscatt. and channelling meas. 0-2300  
 Si:Ge B, strain compensation, X-ray Bragg reflexion 0-39137  
 Si:H, amorphous, Brillouin scattering from acoustic bulk and surface waves 0-11425  
 Si:H, amorphous, control and anal. of deposition, using plasma spectroscopy 0-45230  
 Si:H, amorphous, defect creation and H evolution 0-50392  
 Si:H, amorphous, density of states determ. using field effect 0-49937  
 Si:H, amorphous, dopant conc., glow discharge optical spectroscopy 0-49546  
 Si:H, amorphous, electronic struct. calc., rel. to UPS data 0-39527  
 Si:H, amorphous, excess carrier thermalisation and recomb., luminesc. decay and photocond. 0-50397  
 Si:H, amorphous, exodiffusion of H, EPR expts. 0-49102  
 Si:H, amorphous, glow discharge deposited, thermal dehydrogenation, IR spectra 0-44442  
 Si:H, amorphous, glow discharge deposited, laser annealing 0-49104  
 Si:H, amorphous, H content determ. by IR absorpt., gas evolution and nuclear reaction methods 0-44130  
 Si:H, amorphous, in p<sup>+</sup>-i-n<sup>+</sup> struct., hole diffusion length meas. 0-44712  
 Si:H, amorphous, light-induced ESR and photoluminesc., dangling bonds with positive correl. energy 0-50161  
 Si:H, amorphous, luminesc., band tail states and thermalization 0-25455  
 Si:H, amorphous, mobility edge position using continuous random network model for struct. 0-44544  
 Si:H, amorphous, model for variable gap intrinsic semiconductor 0-10988  
 Si:H, amorphous, p<sup>+</sup>-i-n<sup>+</sup> struct. solar cells, material parameters and deposition condition optimisation study for higher efficiencies 0-45676  
 Si:H, amorphous, plasma deposited, cond. adsorbate and insulating layer effects 0-49749  
 Si:H, amorphous, plasma-deposited, effect of DC elec. field superimposed during deposition 0-44643  
 Si:H, amorphous, ps. relax., optically induced absorpt. 0-48325  
 Si:H, amorphous, RF sputtered, suitability as solar cell material 0-40864  
 Si:H, amorphous, RF sputtered, Schottky barrier solar cells, photovoltaic props. and capacitance-voltage charact. 0-45678  
 Si:H, amorphous, radiative recomb. by diffusion and tunnelling, photocond. quantum efficiency 0-50394  
 Si:H, amorphous, radiative recomb. and luminescent processes 0-55152  
 Si:H, amorphous, refr. index, temp. depend., implications for thermorefectance and electorefectance 0-50290  
 Si:H, amorphous, Schottky diode, spectral response and hole drift mobility 0-39673  
 Si:H, amorphous, Schottky barrier solar cell, degradation mechanisms affecting stability and operation 0-45680  
 Si:H, amorphous, Schottky barrier solar cell, deposition parameter effects on elec. props. 0-45681  
 Si:H, amorphous, solar cell struct., photocurrent meas., absorpt. coeff. 0-50960  
 Si:H, amorphous, solar cells, carrier generation, recombination, and transport 0-55844

## silicon continued

- Si:H, amorphous, sputter deposited, O<sub>2</sub> incorporation during and after fabrication 0-49541  
 Si:H, amorphous, sputtered, Auger surface spectroscopy 0-50472  
 Si:H, amorphous, structural model 0-49105  
 Si:H, amorphous, surface activated, photoemission spectra, minority carrier diffusion length 0-40235  
 n-Si:H, amorphous, thickness depend. cond. 0-49724  
 Si:H, amorphous and crystalline, hydrogenation and dehydrogenation, luminesc. spectra 0-11477  
 Si:H, amorphous defect model 0-24363  
 Si:H, amorphous field induced and quenched-in excess cond. 0-24968  
 Si:H, amorphous film, prep. by plasma decomp. of SiH<sub>4</sub> under mag. field, and characterisation 0-45239  
 Si:H, amorphous Schottky barrier solar cells, depletion region, capacitance study 0-50963  
 Si:H, amorphous sputtered, excitation spectra and photoluminesc. 0-50396  
 Si:H, Cl(F), amorphous, photocond., dark cond. and photoluminesc. 0-49802  
 Si:H, electron states 0-29355  
 Si:H, ion-implanted, photoluminesc. spectrum 0-45129  
 Si:H, plasma-deposited amorphous film, proton mag. reson. 0-44931  
 a-Si:H, spin defect and recombination influence on electronic transport 0-50409  
 Si:H,F,O amorphous, plasma deposited, comp. and optical props. 0-50441  
 Si:H,Li, amorphous, DC electrical conductivity, absorption edge and IR meas., role of H 0-54694  
 Si:H,P, amorphous, heavily hydrogenated, high gap state densities 0-49803  
 Si:H amorphous, cooperative charge disproportionation of defects, rel. to photolum. 0-54649  
 Si:H amorphous film, plasma-deposited, growth morphology and defects 0-44128  
 Si:H amorphous film, plasma-deposited, elec. and comp. heterogeneity 0-44745  
 Si:H amorphous film, prep. by RF glow discharge decomp. of SiH<sub>4</sub>, optical props. and H conc. 0-15416  
 Si:H amorphous film, prop. by glow discharge deposition, and plasma parameter effects on props. 0-45240  
 Si:H amorphous film, sputtered IR vibr. spectra and photolum., effects of partial evolution of H 0-44413  
 Si:H amorphous films, interference enhanced Raman scatt. 0-50326  
 Si:H amorphous films, optoelectronic behaviour depend. on impurity incorporation during plasma deposition 0-49804  
 Si:H amorphous films, photoinduced optical absorpt. and photocond. 0-50361  
 Si:H amorphous films, role of Ar in deposition process, IR absorpt. and photocond. meas. 0-50321  
 Si:H amorphous films for solar cells, optical and elec. props. of RF glow discharge deposited films 0-54576  
 Si:H amorphous sputtered film, photoluminesc., photocond. 0-20729  
 Si:H amorphous sputtered films, optical gap, IR absorpt. meas. 0-50320  
 Si:H film, amorphous, bombarded, defects, luminesc. and ESR meas. 0-34977  
 Si:H film, amorphous, photocond. imaging 0-1300  
 Si:H film, amorphous, reactively sputtered, H content effect on props. 0-49714  
 a-Si:H MIS junction, electronic struct. study by tunnelling 0-44729  
 Si:H plasma deposited film, amorphous, microstruct., TEM and SEM obs. 0-10801  
 a-Si:H Schottky barrier diodes, capacitance studies 0-49908  
 Si:H solar cells, photovoltage source in photocond. materials due to comp. and doping var. 0-7938  
 Si:H sputtered amorphous film, luminesc. and non-radiative decay 0-50395  
 a-Si:H sputtered films, ohmic contacts by H depletion, H diffusion 0-34511  
 Si:H(B)(P), amorphous, UV absorpt. spectra 0-25420  
 Si:H(D), amorphous films, CVD, post-hydrogenation 0-54552  
 Si:H(D), H-related defects, channelling and IR meas. 0-25422  
 Si:H(F), amorphous, Schottky barrier profiles, depletion region width 0-49871  
 Si:H(Li)(Ni), amorphous, vac. evaporated, doping, transport and optical props. 0-49715  
 Si:In, backward wave phonon spectroscopy 0-2357  
 Si:In, electron irradiation, Hall effect meas. 0-2401  
 Si:In, MIS structure, determ. of deep level parameters in surface layer of semiconductor 0-15612  
 Si:In amorphous films, EPR, elec. cond., and magnetoresist. 0-50160  
 Si:Li(Na)(K)(F)(Cl), amorphous, implantation effects on elec. props. 0-49716  
 p-Si:Mn, giant residual cond. 0-20250  
 Si:Mn(Fe)(Ni) amorphous films, ESR and elec. cond. 0-50171  
 Si:N, amorphous, prep. by RF sputtering and props. 0-44229  
 Si:N, ion implantation, refractive index, IR spectra, ion range and straggling meas. 0-34020  
 Si:N<sup>+</sup> ion, implantation, disorder profiles meas. by Rutherford backscatt. and channelling 0-54270  
 Si:Na ion implanted, Hall effect temp. depend., electron surface density and mobility 0-11018  
 Si:Na<sup>+</sup>, inversion layer, far IR optical spectroscopy 0-20680  
 Si:Ne(Ar)(Kr), amorphous, implanted and sputtered, epitaxial regrowth, influence of noble gas atoms 0-2289  
 Si:Ni, capture probabilities of two deep impurity levels by photocond. decay 0-49799  
 Si:O, amorphous, sputtered, influence of O and deposition conditions 0-54693  
 n-Si:O, charge carrier scattering on neutral centres 0-49762  
 Si:O, cryst., donor form. during annealing, elec. resist. study 0-49653  
 Si:O, electrical and infrared spectroscopic investigations 0-34389  
 Si:O, evaporated amorphous film, effect of O<sub>2</sub> on props., ESR spectra 0-11265  
 Si:O, impurity conc. profiles, scanning IR absorpt. using semicond. laser 0-50376  
 Si:O, ion-implanted between 2 and 20 MeV, range and range straggling 0-44241  
 Si:O,H, amorphous plasma-deposited, electronic and struct. props. 0-50391



## silicon continued

- Si:O wafer, annealed, surface- and inner-microdefects, TEM obs. 0-54236
- Si:P, amorphous, CVD, defect compensation 0-54644
- Si:P, BF<sub>3</sub><sup>+</sup> ion implantation, anomalous carrier profiles 0-2048
- Si:P, defect annealing, ionisation effects, DLTS meas. 0-24483
- Si:P, determ. of P content in high-purity Si using meas. of Mo in 12-molybdophosphoric acid by NAA and AAS 0-15148
- Si:P, diffusion of P impurities stimulated by gas discharge Ar plasma, low temp. 0-6560
- Si:P, diffusion-doped laser irradiation effects, electrical reactivation of P 0-39124
- Si:P, diffusivity, strain-induced band gap narrowing, E-centres 0-29228
- Si:P, disorders produced during high-current and high-dose P ion implantation 0-6422
- Si:P, doped by neutron transmutation, lattice defects 0-34018
- Si:P, heavily doped, glow-discharge-produced, elec. and optical props 0-2497
- Si:P, heavily doped, mag.-field depend. of sp. ht. 0-29183
- Si:P, implanted, pulsed electron beam annealing, Hall effect and sheet resist. meas. 0-34467
- Si:P, ion implanted and unimplanted, laser annealing, photoluminesc. study 0-2049
- Si:P, ion-implanted, carrier conc. reduction caused by wet O<sub>2</sub> oxidation 0-10565
- Si:P, ion-implanted, laser annealing 0-10564
- Si:P, neutron irradi. crystals, qualitative distrib. of P using autoradiography 0-24486
- Si:P, polycryst., CVD, elec. activation of impurities, EPR obs. 0-34774
- Si:P, satellite of bound excitons, transient decay 0-11466
- Si:P, variable range hopping at very low temp. 0-49736
- Si:P CVD films, ion-implanted, doping effect on elec. props. 0-2495
- Si:P diffused solar cells, laser treatment to dissolve diffused P precipitates 0-45667
- Si:P dislocation p-n junctions, capacitive props. 0-20300
- Si:P film, CVD polycrystalline, low press. and atmos. press., oxidation 0-3214
- Si:P film, polycryst. pulsed electron beam annealing 0-10566
- Si:P non-Fickian diffusion, parameter depend. on doping level and impurity gradient (*German*) 0-54440
- Si:P solar cells, improved P diffusion using laser treatment 0-55850
- Si:P<sup>+</sup>, Zeeman energy transfer at surface layer 0-11247
- Si:P<sup>+</sup> ion implanted single crystals, secondary defects development during annealing 0-44228
- Si:P(As)(B)-SiO<sub>2</sub> interface oxidation kinetics, high doping levels, experiment 0-11828
- Si:P(B), high temp. impurity diffusion via vacancies and self-interstitials 0-24667
- n-Si:Pd Schottky diodes photocapacitance meas., photon and carrier capture cross sections 0-20309
- Si:Pt, depth depend. of atomic mixing by ion beams 0-29837
- Si:S,  $\gamma$ -irrad. influence on elec. props. 0-6845
- Si:Sb, amorphous, electronic transport props. 0-44589
- Si:Sb, diffusional doping by doped oxide method 0-15127
- Si:Sb, dopant implantation, activation analysis errors due to isotope comp. (*German*) 0-34037
- Si:Sb, epitaxial film, growth by mol. beam technique 0-2292
- Si:Sb, epitaxial layers, doping profile techniques 0-44231
- Si:Sb, ion implanted doping, isotopic composition shifts on neutron activation determination 0-24487
- Si:Sm, implanted impurity location, Mossbauer and channelling expts. 0-39128
- Si:Sn, Mossbauer spectra of <sup>119</sup>Sn impurity atoms 0-15935
- Si:Sn, thermal conductivity, Hall mobility depend. on Sn conc., phonon-defect scatt. 0-29232
- Si:Te, implanted impurity location, Mossbauer and channelling expts. 0-39128
- Si:Te implanted, laser annealing, Mossbauer obs. 0-39127
- Si:Ti, deep level impurity, Hall meas. 0-6768
- Si:Tl, ion implantation, indirect doping method 0-10568
- Si:Zn, photoionisation of deep impurity levels 0-34386
- Si:Zn, reson. characts. of impedance near excitation threshold of recomb. waves 0-20301
- Si:Zn (Mn) (In), surface characterised by negative electrochemical pot., electronic props. 0-44695
- Si:Zn p-n junction diode, computer-aided study of carrier lifetimes 0-24999
- Si/Al interfaces, chemical bonding states, low energy AES 0-6985
- Si/Al thin film couples, accel. ageing 0-44726
- a-Si/Au barrier, capacitance and cond. 0-2469
- Si/Au films, laser-irrad., phase transform. study 0-49536
- Si/metal system, silicide form. by thin film interactions, review 0-49429
- Si/Pd interface, chem. and struct. props. during silicide form., AES and TEM obs. 0-49430
- Si/Pd-W, contact reactions, backscattering, X-ray diffr. meas. 0-20040
- Si/Si-Ge alloy, amorphous, solar cell, multijunction structure, increased conversion efficiencies, low cost 0-45677
- Si/SiO<sub>2</sub>-electrolyte interface, electron exchange at surface of thermally grown SiO<sub>2</sub> 0-16696
- Si/SiO<sub>2</sub>/In<sub>2</sub>O<sub>3</sub>-SnO<sub>2</sub> diode solar cells, loss mechanisms, characts., band struct. 0-26135
- n-Si-<sup>119</sup>Sn resonant detector for Mossbauer spectroscopy 0-883
- Si-Al devices, thickness meter for Al contacting layers (*Russian*) 0-36980
- Si-Al interface, ellipsometric anal. methods, correl. between optical props., thickness and surface roughness meas. (*German*) 0-55215
- Si-Al interface, solid phase epitaxial growth of Si 0-34324
- Si-Al Schottky diodes, with Ti contact, voltage-current characts., appl. to ignition circuits 0-11088
- Si-Al system, Si regrowth minimisation methods in Al films 0-15384
- Si-Al<sub>2</sub>O<sub>3</sub>, MIS structure, with dielectric film, from UV irradiation converted metalorganic compounds (*Russian*) 0-45245
- Si-Al<sub>2</sub>O<sub>3</sub> interface, charge injection from surface depletion region 0-54797
- Si-Au Schottky barrier solar cell fabrication, doping of a-Si 0-50969
- Si-B crystal, Bond method, of meas. lattice parameters, asymmetric Bragg reflections appl. 0-38861
- Si-borosilicate glass, B diffusion from sputtered glass film into Si 0-29040
- Si-C interface on polycryst. Si ribbon, effect on solar cell efficiency (*French*) 0-54531

## silicon continued

- Si-CdSe n-n heterojunction, photovoltage sign reversal, energy band profile (*Korean*) 0-29469
- Si-Co interface metal-semiconductor transition, rel. to first compound nucleation 0-24771
- Si-H, amorphous, H three-dimens. distrib., ion-induced AES and Rutherford backscattering 0-44132
- Si-H, amorphous, plasma-deposited, H evolution and defect creation 0-44914
- Si-H, amorphous, random network model 0-1932
- Si-H, amorphous, struct. and press. induced transition 0-44131
- Si-H, amorphous film, in situ prepared, photoemission studies 0-35060
- a-Si-H sputtered solar cells, temp. depend. of Schottky barrier characts. 0-45669
- p-Si-In<sub>2</sub>-Sn<sub>2</sub>O<sub>3</sub>- $\gamma$  solar cells, thermal degradation mechanisms 0-55841
- Si-In<sub>2</sub>O<sub>3</sub>-Sn heterojunctions, current mechanisms and barrier height 0-11083
- Si-Li(Au)(Cu), diffusion-induced defects, X-ray triple cryst. diffractometry 0-2213
- Si-metal systems, interfacial reaction and Schottky barrier 0-39672
- p-Si-Mn contact, barrier height 0-34510
- Si-MoO<sub>3</sub> photodiode, fabrication as function of O<sub>2</sub> partial press. 0-29464
- Si-P MOS devices, time dependence of depletion region formation at cryogenic temp. 0-34522
- Si-PbS heterojunction, struct. and comp. 0-54530
- Si-sapphire interface in SOS ICs, elec. investigation 0-11097
- n-Si-SiC film junction device, elec. props. 0-15591
- Si-SiO<sub>2</sub>, anodic polarisation in electrolyte containing fluoride ions, effect on oxide props. 0-39679
- Si-SiO<sub>2</sub>, bonding at (111) interface, stoichiometry and kinetics, synchrotron radiation photoemission spectroscopy 0-24744
- Si-SiO<sub>2</sub>, ESR centres, interface states and oxide fixed charge 0-2474
- Si-SiO<sub>2</sub>, impurity redistrib. during oxidation, numerical soln. including interfacial fluxes 0-25888
- Si-SiO<sub>2</sub>, interface, reconstructing states 0-49925
- Si-SiO<sub>2</sub>, interface defect states obs. by constant capacitance DLTS 0-49924
- Si-SiO<sub>2</sub>, interface states, new model 0-29478
- Si-SiO<sub>2</sub>, oxide defect density depend. on appl. elec. field and thickness 0-19791
- Si-SiO<sub>2</sub>, P ion implantation, elec. transport props. 0-39130
- Si-SiO<sub>2</sub>, SiO<sub>2</sub> layer charging in UV irradi. of MISS struct., photoinjection currents (*Russian*) 0-39680
- Si-SiO<sub>2</sub> (111) interfaces, sixfold valley degeneracy in electron inversion layers 0-49936
- Si-SiO<sub>2</sub> boundary, precipitation of Na (*Russian*) 0-49368
- Si-SiO<sub>2</sub> interface, Au doping, trap distribution 0-20319
- Si-SiO<sub>2</sub> interface, backscattering-channelling study 0-34320
- Si-SiO<sub>2</sub> interface, cluster Bethe-lattice method appl. 0-49852
- Si-SiO<sub>2</sub> interface, defects, intimate valence attenuation pairs 0-54132
- Si-SiO<sub>2</sub> interface, effect of oxidation time and temp. using AES 0-35359
- Si-SiO<sub>2</sub> interface, effect of hot electron injection on interface charge density 0-49921
- Si-SiO<sub>2</sub> interface, electrically active paramag. centres detect., photocond. reson. obs. 0-50185
- n-Si-SiO<sub>2</sub> interface, hot carrier surface thermo EMF depend. on surface band bending 0-44734
- Si-SiO<sub>2</sub> interface, light induced reson. centres, photocond. reson., EPR obs. 0-50184
- Si-SiO<sub>2</sub> interface, local at. struct., XPS obs. 0-20042
- Si-SiO<sub>2</sub> interface, oxidation stacking faults, growth rel. to self-diffusion 0-49239
- Si-SiO<sub>2</sub> interface, props. variation in SiO<sub>2</sub> region 0-49548
- Si-SiO<sub>2</sub> interface, radiation damage coeffs. for fission neutron and gamma-ray irradi. 0-34058
- Si-SiO<sub>2</sub> interface, radiation hardness eval. using elec. meas. technique 0-34516
- Si-SiO<sub>2</sub> interface, surface generation velocity study, gate-controlled diode structure application 0-6986
- Si-SiO<sub>2</sub> interface, surface states characterization, expt. techniques review 0-49949
- Si-SiO<sub>2</sub> interface, thermally grown, inhomogeneities of surface potential 0-34524
- Si-SiO<sub>2</sub> interface as electrode for electrical and ellipsometric meas. of adsorbed organic molecules 0-15366
- Si-SiO<sub>2</sub> interface layer characterisation by spectroscopic ellipsometry 0-50738
- Si-SiO<sub>2</sub> interface oxidation kinetics, high doping levels, theory 0-11827
- Si-SiO<sub>2</sub> interface state spectroscopy using MOS tunnelling structures 0-6991
- Si-SiO<sub>2</sub> interface state distribution, Br incorporation effects 0-11091
- Si-SiO<sub>2</sub> interface state density, dependence on thermal oxidation process variables 0-15607
- Si-SiO<sub>2</sub> interface study by XPS 0-50507
- Si-SiO<sub>2</sub> interfaces, local atomic and electronic struct., high resolution XPS 0-49927
- Si-SiO<sub>2</sub> interfacial region on TCE/O<sub>2</sub> and CCl<sub>4</sub>/O<sub>2</sub> oxidised Si, struct. and comp. 0-50741
- Si-SiO<sub>2</sub> interfacial transition layer thickness, XPS obs. 0-11540
- Si-SiO<sub>2</sub> MOS capacitor, two-stage process for building up radiation induced interface states 0-20313
- p-Si-SiO<sub>2</sub> system, C-V meas. using Au/Hg probe, work function difference between probe and Si 0-2450
- Si-SiO<sub>2</sub> transition region width, SIMS depth profiling 0-39454
- Si-SiO<sub>2</sub>-Si<sub>3</sub>N<sub>4</sub>, internal photoemission 0-7475
- Si-SiO<sub>2</sub>-Al photodiode experimental verification of theoretical predictions 0-29485
- Si-silicide-Al systems with CoSi<sub>2</sub>, Pt<sub>x</sub>Ni<sub>1-x</sub>-Si, and MoSi<sub>2</sub> as silicide, diffusion, compound form., and microstructure 0-34253
- n-Si-silicide-Al systems with CoSi<sub>2</sub>, MoSi<sub>2</sub>, and Pt<sub>x</sub>Ni<sub>1-x</sub>-Si as silicide, Schottky-barrier height 0-34520
- Si-SnO<sub>2</sub> heterojunctions, elec. and photovoltaic props. 0-26141
- Si-undoped poly Si interface, in oxidation process, defects generation 0-40571
- Si+F<sub>2</sub>, chemilum., at. absorption, and laser-induced fluoresc. obs. 0-3315
- Si+Ga<sup>+</sup> ion implantation at high current density, lattice disorder, proton backscattering 0-34085
- Si+La<sub>2</sub>O<sub>3</sub>, reduction in solar furnace (*French*) 0-16784
- Si+NH<sub>3</sub>, surface nitride form., XPS excited by Zr M<sub>1</sub> radiation 0-40236



## silicon continued

- Si+OCS, SiS multiple collision chemiluminesc., intercombination systems and SiS\* collisional quenching 0-45505  
 $\text{Si}^{4+} + \text{H}$ , charge transfer, total and partial cross-sections calcs. 0-23542  
 $\beta$ -SiC/Si abrasive resistant material, prep. and props. 0-20878  
 $\text{Si}_{1-x}\text{H}_x$ , amorphous, atomic struct., X-ray study 0-49106  
 $\text{Si}_{1-x}\text{H}_x$ , amorphous, gap states, DLTS 0-49656  
 $\text{SiLx}$ , solar emission lines, density dependence 0-21963  
 $\text{Si}(\text{Li})$  detectors, escape peak losses 0-27383  
 $\text{Si}(\text{Li})$  electron spectrometer with superconducting transporting magnets 0-27376  
 $\text{SiO}_2$ -Si, low-energy neutral particle bombardment of  $\text{SiO}_2$  film, degradation 0-54790  
 $\text{SnO}_2/\text{n-Si}$  spray-deposited solar cells 0-12007  
 $\text{SnO}_2$ -Si, heterojunction solar cells, anomalous photocurrent 0-3515  
 $\text{SnO}_2$ -Si heterojunction solar cell, elec. props. (Korean) 0-45665  
 $\text{SnO}_2$ -Si solar cells, electron-beam deposited, struct., photovolt. props. 0-50956  
Ti-Si film thin film interaction, metallisation, X-ray diffr. and sheet resist. 0-54442  
 $\text{YIG:Si, Fe}^{2+}$  spectroscopic props., nontrigonal cryst. field effects 0-44553

## silicon alloys

- see also Ge-Si alloys  
Al-Si (2.4 wt.%), liq. fluidity, solid-liq. coexisting zone (Japanese) 0-15175  
binary alloys, detection of compositional homogeneities using ion-induced Auger electron spectroscopy 0-25514  
coatings, for high temp. alloys, process development and props. 0-40614  
rare earth alloys,  $\text{RM}_2\text{Si}$  (M=Rh, Pd, Ag, Ir, Pt, Au), cryst. struct. 0-1964  
Sendust alloy, magnetic head wear resistance and surface characts. against mag. tape (Japanese) 0-35335  
steel, Cr-Mn-C-Si (20, 14, 0.2, 0 to 3 wt.%), high-temp. oxidation (Russian) 0-25904  
steel, highly-oriented, domain and grain patterns obs., using ferromagnetic colloid technique 0-11856  
steel, Mn-Si, St 52-3, cleavage fracture toughness, temperature and notch sharpness influence (German) 0-35291  
steel, Mn-Si, St 52-3, fracture toughness determ. from yield strength and cleavage fracture strength (German) 0-35292  
steel, Si, commercial, ordering after heat treatment, Mossbauer meas. 0-7556  
steel, Si, electron irradi. in HVEM, void swelling, Si role 0-54285  
steel, Si-Cr-Mo-W-V (2.4, 1.3, 2 wt.%), heat treatment and props. 0-16349  
supercooled, struct. refinement mech. (Russian) 0-20975  
transition metal silicides,  $\text{V}(\text{Nb})(\text{Ta})(\text{Cr})(\text{Mo})(\text{W})\text{-Si-Cu}$ , struct. and supercond., Cu influence 0-50592  
Al-Cu-Mg-Mn-Si-Fe, endurance with cyclic bending, effect of loading conditions 0-50724  
Al-Cu-Mg-Mn-Si-Fe, subcritical crack growth under static plane stress 0-55528  
Al-Cu-Mn-Mg-Si-Fe, corrosive environment effect on fatigue crack growth rate 0-55584  
Al-Cu-Si, effect of sample conditions on sputtering and intensities, emission spectrochem. anal. using glow discharge (Japanese) 0-21349  
Al-Mg-Si (1 wt.%), precipitation reactions 0-11652  
Al-Mg-Si (1.42 wt.%), aged, dislocation structs. caused by plastic deformation 0-25786  
Al-Mg-Si, DTA exam. after small and medium deform. 0-21002  
Al-Mg-Si, dil. alloy, Mn additions and heat treatment effect on  $\beta \rightarrow \alpha$  transformation 0-7566  
Al-Mg-Si, heterogeneous precipitation studies using differential scanning calorimetry 0-3062  
Al-Mg-Si, nucleation and precipitation growth on dislocations, electron microscope studies 0-3064  
Al-Mg-Si core, deformation behaviour contrib. in rod drawing (German) 0-11684  
Al-Ni-Si, directionally solidified eutectic, morphological and mech. props. (Russian) 0-30057  
Al-Si, deformed, local lattice rotations at second phase particles 0-25709  
Al-Si, dilute, anomalous primary creep behaviour, precipitate form. 0-7646  
Al-Si, liq., dissoln. and diffusion of alloying components, 700-1000°C (Russian) 0-15275  
Al-Si, three dimensional dry cutting, with sintered diamond tool (Japanese) 0-25917  
Al-Si (16 wt.%) melt, fivefold twinned Si cryst. growth, crystallographic study 0-2942  
Al-Si (9 wt.%), precipitation hardening during isothermal ageing 0-29969  
Al-Si coatings, form. and behaviour under particle bombard. 0-35029  
Al-Si crystals, work hardened, softening and creep rates on annealing 0-11663  
Al-Si eutectic, depend. between min. creep rate and time of beginning of secondary creep (Czech) 0-35267  
Al-Si eutectic, pressure effect on metal-die heat transfer coeffs. during solidification 0-7544  
Al-Si eutectic alloys, superplasticity 0-11710  
Al-Si foil, alloying effect on strength characts. and weldability 0-55475  
Al-Si melts, struct. factors, at. distrib. curves, thermodynamic and neutron diffr. study (German) 0-19687  
Al-Si-Cu, LM30, crack propag. rates in air and salt soln. 0-21063  
Al-Si-Cu-Mg-Ni, piston, depend. between min. creep rate and time of beginning of secondary creep (Czech) 0-35267  
Al-Si-P (19, 0.02 wt.%), primary Si crystals in Al melt, Ostwald ripening and solidification growth 0-35179  
Au-Si, liq. alloy, thermodynamic activity meas. by Knudsen-cell mass spectrometry (French) 0-10684  
Au-Si interface, valence band and core levels, Si diffusion, alloy form., photoelectron spectra obs. 0-45205  
 $\text{Au}_8\text{Si}_{19}$ , optical refl., 0.5 to 6 eV, hall coeff. and elec. resist. 0-29755  
 $\text{Au}_{1.4}\text{Si}_{18.6}$ , glass forming alloy, Gibbs free energy change on crystallisation 0-25676  
 $\text{Au}_{1-x}\text{Sn}_x$  liq./solid alloy, resist. and percolation 0-6804  
B fibre reinforced Al-Si, calc. of thermodynamic interaction potential between B fibre and matrix 0-11627  
Ca-Si, deoxidation of steel, thermodynamics (Russian) 0-16268  
Ce-Co-Si, thermoelectromotive force and electrocond. (Ukrainian) 0-54670

## silicon alloys continued

- Ce-Fe-Si, thermoelectromotive force and electrocond. (Ukrainian) 0-54670  
Ce-Ni-Si, thermoelectromotive force and electrocond. (Ukrainian) 0-54670  
CeCoSi<sub>2</sub> film, Hall effect and magnetoresist. (Russian) 0-11109  
CeCu<sub>2</sub>Si<sub>2</sub>, strong Pauli paramagnetism, superconductivity obs. 0-29499  
CeCu<sub>2</sub>Si<sub>2</sub>, transport anomalies 0-20148  
CeMn<sub>2</sub>(Si, Ge<sub>1-x</sub>)<sub>2</sub>, Ce(Mn<sub>1-x</sub>B<sub>x</sub>)<sub>2</sub>Si<sub>2</sub>, (B=Fe, Cu) mag. props. 0-25134  
(Co, Fe, M)<sub>78</sub>Si<sub>18</sub>B<sub>4</sub> amorphous alloys (M=V, Nb, Ta, Cr, Mo, W, Mn or Ni), zero magnetostriction and low field mag. props. 0-34741  
Co-Ni-Fe-Si, amorphous ribbon, magnetostriction meas. 0-15778  
(Co<sub>1-x</sub>Fe<sub>x</sub>Ni)<sub>80</sub>(Si<sub>1-x</sub>B<sub>x</sub>)<sub>20</sub>, amorphous films, spin wave spectra 0-34777  
Co<sub>75-x</sub>Fe<sub>25</sub>Si<sub>10</sub>B<sub>10</sub>, quenched ferromag. ribbon, Brillouin spectra 0-2776  
Co<sub>1-x</sub>M<sub>x</sub>Si<sub>2</sub> (M=Fe, Ni), elec. field gradient, quadrupole splitting of <sup>59</sup>Co 0-29641  
Co<sub>30</sub>Ni<sub>20</sub>Fe<sub>5</sub>Si<sub>12</sub>B<sub>12</sub>, amorphous, mag. props., effects mech. deform. 0-39840  
Cr-Si, thin films, deposition method, for controllable comp. with given elec. props. 0-35087  
Cu-Si, dil., oxide film form. in ammoniacal Cu(II) solns., AES obs. 0-45415  
Cu-Si, high dislocation density alloys and oxide precipitated struct., NMR, spin echo 0-39892  
Cu-Si, melt, enthalpy of formation at 1370K 0-26042  
Cu-V-Si, two-step supercond. transition 0-34539  
DyM<sub>2</sub>Si<sub>2</sub>, (M=Mn, Fe, Co, Ni, Cu), Mossbauer spectra 0-20558  
EuCu<sub>2</sub>Si<sub>2</sub>, fluctuating valence system, quadrupole interaction temp. depend. 0-54972  
EuCu<sub>2</sub>Si<sub>2</sub>, valence fluctuation and temp. depend. of Cu nuclear quadrupole interaction 0-15818  
Fe, cast, grey Al-Si, eutectoid decomp. of austenite 0-29951  
Fe-As-Si, Si additions to Fe-As melts, influence on surface tension and density (Russian) 0-15337  
Fe-As-Sn-Si, melts, As and Sn distrib., Si, Cr, and Mn influence (Russian) 0-16274  
Fe-B-Si, amorphous ferromag. alloys, mag. struct., Mossbauer study 0-39746  
Fe-B-Si amorphous ribbon, strain induced anisotropy, and toroid diam. effect on mag. props. 0-34623  
Fe-B-Si amorphous ribbons, effect of annealing conditions on magneto-mechanical props. 0-34740  
Fe-C-Mn-Si (4, 2, 1.5 wt.%), cast wire, influence of B addition on struct. and elec. cond. (Russian) 0-55391  
Fe-C-Si, graphitisation during heat treatment (Russian) 0-20971  
Fe-Ci, high permeability, mag. props., applied stress effects 0-34726  
Fe-Ci (3 wt.%), commercially produced, grain-oriented, mag. props., stress coating effects 0-34727  
Fe-Co-Si, BCC solid soln. interchange energies, high temp. neutron diffr. 0-29166  
Fe-Co-Si (4, 1.5 wt.%), textured, mag. props. 0-35200  
Fe-Co-Si solid solutions, BCC, atomic configs., Mossbauer study 0-39006  
Fe-Co-Si-B, amorphous, rapidly quenched, mag. heads appl. (Japanese) 0-54922  
Fe-Co-Si-B sputtered amorphous thin film, coercivity, galvanomagnetic props., resistivity 0-29578  
Fe-Hf (Si) (Ti) (V), molten, gaseous O<sub>2</sub> absorption 0-11836  
Fe-Mn-Si, mag. contribs. to  $\gamma \rightarrow \epsilon$  phase transforms 0-25694  
Fe-Ni-Si-B, amorphous paramag. alloys, hyperfine field distrib., Mossbauer study 0-39958  
Fe-Ni-Si-Mn-Cr(Co-Mo), effect of prolonged aging on mag. props. 0-16513  
Fe-Si, BCC, cyclic cleavage crack growth model for fatigue 0-55519  
Fe-Si, coated, effective domain and grain obs. methods and Fe losses 0-34675  
Fe-Si, etch figure method appl. (Chinese) 0-21194  
Fe-Si, fatigue crack propag., low temp. 0-35311  
Fe-Si, hyperfine fields, Mossbauer meas. 0-40024  
Fe-Si, liq., thermodynamic characts. calc. (Russian) 0-15264  
Fe-Si, maze domains upon appl. of horizontal mag. field or mech. tension 0-11218  
Fe-Si, microplastic deform. and amplitude depend. of internal friction (Russian) 0-45349  
Fe-Si, oxide layer form. during annealing, AES in-depth anal. (German) 0-16576  
Fe-Si (0-6 wt.%) melts, viscosity (Russian) 0-15285  
Fe-Si (2.5%), mag. stray fields above stripe domains, electron optic meas. 0-15755  
Fe-Si (3 wt.%), chemical comp. and hot rolling effect on brittleness (Czech) 0-50712  
Fe-Si (3 wt.%), domain struct. rel. to cryst. size (Russian) 0-29568  
Fe-Si (3 wt.%), fatigue crack propag. work coeff. 0-16422  
Fe-Si (3 wt.%), grain growth inhibition by MnS spherical particles with size distrib. 0-35218  
Fe-Si (3 wt.%), mag. props., stress coating effects 0-34728  
Fe-Si (3 wt.%), polycrystal in mag. field, stress induced magnetisation, synchrotron Bragg refl. topography obs. 0-50139  
Fe-Si (3 wt.%), single crystals, and polycrystals, strain rate influence on low cycle fatigue props. 0-3126  
Fe-Si (3 wt.%), US oscillatory stress superimposition effects on deformation 0-35287  
Fe-Si (3 wt.%) laminations, isotropic and cube-on-face, magnetostriction behaviour 0-39843  
Fe-Si (3 wt.%) locally deformed, EM loss depend. on cryst. struct. and orientation (Russian) 0-7694  
Fe-Si (3 wt.%) steel, high permeability, magnetostriction, stress inducing coating effects 0-34730  
Fe-Si (3 wt.%) steel, oriented, stress depend. mag. props., coating effects 0-34729  
Fe-Si (3.25 wt.%), Burgers vector identification from electron microscope images 0-2030  
Fe-Si (3.25 wt.%), dislocations in twin boundaries, electron microscopic images 0-34006  
Fe-Si (4 at. %), Bloch wall thickness determ. by neutron small-angle scatt. 0-15754  
Fe-Si amorphous alloys, Mossbauer spectra, struct. 0-15840  
Fe-Si amorphous film, crystallisation, Mossbauer studies 0-33900  
Fe-Si amorphous film, struct. and crystallisation, Mossbauer study 0-11300  
Fe-Si crystal, neutron depolarisation studies of ferromagnetic domain structures 0-25155



silicon alloys continued

- Fe-Si melts, high Si, O solubility (*Russian*) 0-15252  
 Fe-Si protective oxide film form. 0-11818  
 Fe-Si single crystals with cube-on-edge orientation, iron-loss-domain-struct. correls. (*Japanese*) 0-7534  
 Fe-Si single crystals, interaction of  $\{110\}$   $90^\circ$  walls with lattice imperfections 0-39807  
 Fe-Si-B, melt C content effect on grain growth and induction 0-35351  
 Fe-Si-B, surface tension, density, and oxidation kinetics 0-20028  
 Fe-Si-B amorphous films, mag. props. 0-34710  
 Fe-Si-B-N-S, B, S, N effects on grain boundary segregation and grain growth inhibition, review 0-3047  
 Fe-Si(3 wt.%), ferromag. alloy, mag. anisotropy induced by cold rolling 0-30114  
 Fe-Si(4 wt.%), (110) and  $\{100\}$ [001] oriented, simulation of domain wall bowing 0-44854  
 Fe-Si(6.5 wt.%) ribbon, prep. by rapid quenching and mag. props. 0-45251  
 Fe<sub>80</sub>B<sub>10</sub>Si<sub>10</sub>, amorphous, Mossbauer study of hyperfine interaction and mag. anisotropy 0-40027  
 Fe<sub>80</sub>B<sub>15</sub>Si<sub>5</sub> metallic glass, large uniaxial magnetostrictive anisotropy, magnetisation reversal 0-34736  
 Fe<sub>80</sub>(B<sub>10</sub>Si<sub>1-y</sub>)<sub>20</sub>, amorphous, saturation magnetostriction, comp. effects 0-34735  
 Fe<sub>81</sub>B<sub>14</sub>Si<sub>5</sub>, amorphous metal ribbon, stresses, magnetoelastic anisotropy and zero-field mag. domain struct. 0-44896  
 Fe<sub>82</sub>B<sub>15</sub>Si<sub>3</sub>, metallic glass, low temp. specific heat, metalloid effects 0-34654  
 (Fe<sub>1-x</sub>Co<sub>x</sub>)<sub>77</sub>Si<sub>10</sub>B<sub>13</sub>, amorphous magnetic alloys, density meas. 0-1934  
 (Fe<sub>1-x</sub>Co<sub>x</sub>)<sub>78</sub>Si<sub>10</sub>B<sub>12</sub>, amorphous alloys, magnetic anisotropy meas. 0-2570  
 Fe<sub>70</sub>Co<sub>10</sub>Si<sub>10</sub>B<sub>10</sub>, amorphous magnetic alloy, decrease of permeability after demagnetisation, disaccommodation 0-39814  
 Fe<sub>70</sub>Co<sub>10</sub>Si<sub>10</sub>B<sub>10</sub>, amorphous, crystn. effect on mag. props. (*Russian*) 0-44858  
 Fe<sub>2.45</sub>Mn<sub>0.05</sub>Si, slow neutron polariser, by single cryst. (111) refl. 0-49052  
 (Fe<sub>1-x</sub>Ni<sub>x</sub>)<sub>77</sub>Si<sub>10</sub>B<sub>13</sub>, amorphous magnetic alloys, density meas. 0-1934  
 (Fe<sub>1-x</sub>Ni<sub>x</sub>)<sub>77</sub>Si<sub>10</sub>B<sub>13</sub>, amorphous alloy system, saturation mag. moment, Curie temp., mag. susceptibility 0-39753  
 Fe<sub>2</sub>Pd<sub>2-x</sub>Si<sub>18</sub>, amorphous, magnetisation, magnetoresist., spin glass and ferromag. phases 0-34697  
 FeSi, domain struct. and magnetisation reversal, time depend. neutron depolarisation 0-50138  
 $\alpha$ -Fe<sub>1-x</sub>Si<sub>x</sub>, many-body atomic correlations, Mossbauer spectroscopy study 0-15934  
 Fe<sub>2</sub>Si<sub>2</sub>Al<sub>1-x</sub>Co, dil., site preference of <sup>57</sup>Co impurities, Mossbauer study 0-39999  
 Fe<sub>2</sub>Si<sub>15</sub>B<sub>10</sub>, mag. behaviour rel. to magnetostatic interactions 0-11224  
 HfFe<sub>2-x</sub>Si<sub>x</sub>, Mossbauer spectra, hyperfine interactions 0-15862  
 MgSi<sub>2</sub>, laser irradi. induced form., cryst. microstruct. 0-35011  
 Mn-Fe-Si-C, melts, activities of Mn at 1673K 0-50597  
 Mn-Si, liq. alloys, equilibria between MnO-SiO<sub>2</sub>-CaO-MgO slags 0-10639  
 Mn-Si, melt, activation determ. by vapour press. meas. 0-16279  
 Mn-Si (62.5 to 63.8 wt.%), phase anal. and cryst. struct. (*Japanese*) 0-15049  
 Mn-Si-C, melts, activities of Mn at 1673K 0-50597  
 MnCoSi, effect of press on mag. transition temp. (*Russian*) 0-25137  
 MnSi, amorphous magnetisation meas. 0-34599  
 Mn<sub>3</sub>Si-Mn<sub>3</sub>Ge<sub>3</sub>, electrical resistivity meas., order-disorder transition 0-10945  
 Monel, Norton-Bailey parameters, from creep rupture data 0-30098  
 Nb-Ge-Si, A15 struct. superconductor, high field transport props. TEM study 0-34574  
 Nb-Ge-Si film, CVD, struct., comp., stability and homogeneity 0-15421  
 Nb-Si diagram of state, melting temp., polymorphic transform. temp. (*Russian*) 0-50594  
 Nb-Si liquid quenched alloy, metastable A-15 and amorphous phases, interstitials 0-54394  
 Nb-Si-C, phase equilib. and supercond. 0-50593  
 NbFe<sub>2-x</sub>Si<sub>x</sub>, crystalline struct., electron microscopy determ. (*French*) 0-54174  
 Nb<sub>78</sub>Fe<sub>40</sub>Si<sub>80</sub>, X-ray cryst. struct. determ. (*French*) 0-15048  
 NbSi<sub>3</sub>, superconducting transition temp. meas. of sputtered films and bulk 0-7019  
 Nb<sub>3</sub>Si, A-15 diffusion layers, influence of additions of growth and supercond. props. (*German*) 0-11130  
 Nb<sub>3</sub>Si, high T<sub>c</sub> supercond. props. from extrapolation of sp. ht. meas. on A-15 Nb-Si 0-25045  
 Nb<sub>3</sub>Si, metastable A-15 struct. synthesis by ion implantation, supercond. transition temp. 0-55319  
 Nb<sub>3</sub>Si, structural and supercond. props. press. effects 0-39700  
 Nb<sub>3</sub>Si, supercond., A15 film, electron beam evaporation 0-29284  
 Nb<sub>3</sub>Si, superconducting A-15 type compounds, transition temp., radii ratio and structure (*Chinese*) 0-44752  
 Ni-Cr-Fe-Si-B wear-resist. and corrosion-resist. coatings by furnace melting 0-35428  
 Ni-Mn-Al-Si-Co, Al<sub>2</sub>Si<sub>3</sub>, Ettingshausen-Nernst coeff. and transport props. from 200 to 473K 0-44573  
 Ni-Si, defect-solute interactions and radiation-induced segregation 0-25705  
 Ni-Si, proton irradi.,  $\gamma$  precipitation, early stages 0-34096  
 Ni-Si liquid alloys, thermodynamic props., enthalpy of mixing (*Russian*) 0-34207  
 Ni-Si-B powder, oxidation at 850°C, SEM, ESCA, and elec. cond. meas. 0-7717  
 Ni-SiC coating, heat treated, as plated, electrochemical study of corrosive wear 0-16536  
 (Ni<sub>0.75</sub>Mn<sub>0.25</sub>)<sub>85</sub>Si<sub>10</sub>B<sub>5</sub>, amorphous, exchange anisotropy, mag. susceptibility meas., 4.2K to room temp. 0-11186  
 NiSi<sub>3</sub>, epitaxial film on Si, <sup>4</sup>He ion channelling meas. and RHEED anal. 0-10834  
 Ni<sub>1-x</sub>Si<sub>x</sub>, electronic states of Si NMR study 0-50216  
 Ni<sub>3</sub>Si coatings, form. and stability during high temp. irradi. 0-35088  
 NpCo<sub>2</sub>Si<sub>2</sub>, mag. props., high press. studies with <sup>237</sup>Np(60)-resonance 0-39924  
 NpFe<sub>2-x</sub>Co<sub>x</sub>Si<sub>2</sub>, mag. and hyperfine props. 0-7247  
 Pd-Ag-Si alloys, amorphous, crystn. kinetics, DSC meas. 0-1933  
 Pd-Au-Si, amorphous films, RF sputter deposition, composition and thermal behaviour 0-55292

silicon alloys continued

- Pd-Cu-Si, laser melting and splat quenching to form foils for TEM obs. 0-29986  
 Pd-Si amorphous films, RF and DC sputter deposition, composition and thermal behaviour 0-55292  
 Pd-Si glasses, changes in density of states with alloys comp., UPS obs. 0-50531  
 Pd-Si-Fe amorphous alloy, Mossbauer spectra, struct. and bonding 0-7224  
 Pd<sub>0.775</sub>Cu<sub>0.06</sub>Si<sub>0.165</sub> glass, optical props. in energy range 0.67 to 5.6 eV 0-34872  
 Pd<sub>77.5</sub>Cu<sub>6</sub>Si<sub>16.5</sub>, metallic glass, composition, mech. props., simulation 0-49117  
 Pd<sub>77.5</sub>Cu<sub>6</sub>Si<sub>16.5</sub> metallic glass wire, cold drawing 0-50650  
 Pd<sub>77.5</sub>Cu<sub>6</sub>Si<sub>16.5</sub>, ternary miscibility gap, simulation, dispersed phase composition form. 0-54379  
 Pd<sub>60</sub>Ni<sub>20</sub>Si<sub>20</sub>, amorphous, struct., high resolution electron microscopy 0-1969  
 PdSi, amorphous, structural relaxation enhancement following stress reduction 0-3118  
 PdSi, formation by Xe ion beam bombard. of Pd film on Si substrate 0-10800  
 Pd<sub>2</sub>Si, epitaxial film on Si, <sup>4</sup>He ion channelling meas. and RHEED anal. 0-10834  
 Pd<sub>2</sub>Si, formation at Pd-Si (111) interface, UPS obs. 0-24743  
 Pd<sub>2</sub>Si, on Si substrate, thermally induced Si accumulation, AES study 0-24718  
 Pd<sub>80</sub>Si<sub>20</sub>, amorphous, elec. resist. and magnetoresist. 0-49693  
 Pd<sub>80</sub>Si<sub>20</sub>, amorphous, structural changes with neutron irradi., X-ray scatt. obs. 0-33898  
 Pd<sub>80</sub>Si<sub>20</sub> metallic glass, high-resolution XPS study, electronic state struct. 0-29846  
 Pd<sub>80</sub>Si<sub>20</sub>, metallic glass, composition, mech. props., simulation 0-49117  
 PdSiCu, amorphous, US attenuation and vel. studies 0-19881  
 Pd<sub>3</sub>Si<sub>4</sub>Cu<sub>6</sub>, glass, changes in density of states with alloys comp. UPS obs. 0-50531  
 Pd<sub>30</sub>Si<sub>70</sub>Cu<sub>30</sub>, glass, changes in density of states with alloys comp., UPS obs. 0-50531  
 Pd<sub>82-x</sub>V<sub>x</sub>Si<sub>18</sub>, metallic glasses, effect of press. on elec. resist. 0-6805  
 Pt-Si melts, surface tension and density (*Russian*) 0-39388  
 PtSi, epitaxial film on Si, <sup>4</sup>He ion channelling meas. and RHEED anal. 0-10834  
 Rh-Si thin film interaction, interdiffusion, temp. depend. 0-54443  
 Rh<sub>2</sub>Si<sub>3</sub>-n-Sn Schottky diodes, rectifying barrier height meas. 0-49896  
 Sc-Rh-Si system, partial phase diagram, X-ray diff. and microprobe anal. 0-25659  
 Sc<sub>31</sub>Re<sub>2</sub>Si<sub>3</sub>, X-ray cryst. struct. determ. 0-39009  
 Si-Al, silumin, crystn. of eutectic phases (*Russian*) 0-29942  
 Si-Au, solid soln., influence of precip. on relax. of <sup>29</sup>Si nucleus 0-11287  
 Si-Au films, quenched condensed, elec. resist. and supercond. 0-54669  
 Si-B based CVD coating for gas turbine blading, props. 0-40615  
 Si-Fe, domain and grain obs. using ferromag. colloid technique 0-11219  
 Si-Ge, solid soln., vol. effect on bulk modulus 0-24526  
 Si-H, amorphous, struct. and press. induced transition 0-44131  
 Si<sub>100-x</sub>Al<sub>x</sub>, RF sputtered, amorphous, props. 0-34754  
 Si<sub>1-x</sub>Au<sub>x</sub>, amorphous films, IR absorpt. spectra 0-16034  
 Si<sub>1-x</sub>B<sub>x</sub>H<sub>1-x</sub>, amorphous films, thermopower and cond. for mixed band and broad tail state cond. 0-49786  
 Si<sub>1-x</sub>H<sub>x</sub>, amorphous, gap states, DLTS 0-49656  
 TaSi<sub>3</sub>, superconducting transition temp. meas. of sputtered films and bulk 0-7019  
 TbSi<sub>2</sub>,  $\gamma$ - $\gamma$  ang. correl. obs. of polymorphic transition, 200-900°C 0-29653  
 Ti-Al-Mo-Zr-Si (6.6, 3.3, 1.8, 0.3 wt.%)SiC fibrous composite, component interaction kinetics (*Russian*) 0-55364  
 Ti-Al-Sn-Zr-Mo-Si (6, 2, 4, 2, 0.1 wt.%) effect of elevated temperature and environment on fatigue crack growth 0-40486  
 Ti-Si computered films, silicide form., X-ray diff. and resist. study 0-54546  
 Ti-Si film thin film interaction, metallisation, X-ray diff. and sheet resist. 0-54442  
 UIr<sub>2</sub>Si<sub>2</sub>, cryst. struct. 0-1964  
 U<sub>3</sub>Ni<sub>4</sub>Si<sub>4</sub>, X-ray cryst. struct. determ. 0-33931  
 U<sub>3</sub>Si, crystalline elec. field studies using neutron inelastic scatt. at NRCN 0-10931  
 V-Si, strengthening by internal oxidation 0-55424  
 V<sub>2</sub>Si-C, phase equilib. and supercond. 0-50593  
 (V<sub>1-x</sub>Cr<sub>x</sub>)<sub>3</sub>Si, mag. susceptibility, 4.2 to 320K, density of states model 0-7035  
 V<sub>3-x</sub>Cr<sub>x</sub>Si, x=0 to 3, struct., supercond. and mag. props. 0-1962  
 V<sub>1-x</sub>Si<sub>x</sub>, A-15 cpds., nucl. mag. relax. in normal and supercond. state 0-49993  
 V<sub>2</sub>Si, d-spacing fluctuations above Martensitic phase transition 0-7570  
 V<sub>2</sub>Si, electrical resistivity, saturating contrib. from electron-phonon interactions 0-2376  
 V<sub>2</sub>Si, Fermi surface determ. by positron annihilation 0-2326  
 V<sub>2</sub>Si, ion irradiated, influence on struct., resist., and supercond. transition temp. 0-54823  
 V<sub>2</sub>Si, NMR meas. near struct. transform. (*Russian*) 0-44942  
 V<sub>2</sub>Si, NMR of <sup>51</sup>V above and below 21K struct. transition (*Russian*) 0-34796  
 V<sub>2</sub>Si, normal, mixed and supercond. state, specific heat meas., thermodynamic and superconducting props. 0-49987  
 V<sub>2</sub>Si, plastic deform. effect on supercond. props. 0-29500  
 V<sub>2</sub>Si, single crystals, supercond. tunnel characts. 0-7044  
 V<sub>2</sub>Si, superconducting, optical props. and electron-phonon interactions 0-2510  
 V<sub>2</sub>Si, superconducting thin films, energy gaps from tunnelling meas. 0-25050  
 V<sub>2</sub>Si, thermal expansion, 20-300°C, using differential push-rod dilatometer 0-39320  
 V<sub>2</sub>Si, US anomaly when cooled below martensitic and supercond. transition temps. 0-20354  
 V<sub>3</sub>(Si<sub>1-x</sub>C<sub>x</sub>), bulk, effect of C on supercond. transition temps. and microstructure 0-54824  
 W-Ru-Si-B glass, struct. obs. 0-1938  
 Y-Si melts, enthalpy of formation and dissolution, microinhomogeneous struct., interatomic interactions (*Russian*) 0-34206  
 YbCu<sub>2</sub>Si<sub>3</sub>, valence fluctuation and temp. depend. of Cu nuclear quadrupole interaction 0-15818



## silicon compounds

- see also quartz; silicon alloys; silicones
- 21.2 km graded-index VAD fibre with low loss and wide bandwidth 0-53414
- $\text{Al}_2\text{O}_3\text{-SiO}_2$  refractories, using neutron-2 equipment 0-45612
- corundum refractories, dense production and performance 0-20866
- electron trapping, donor state generation, photo I-V study 0-20210
- glass, tunnelling systems, intrinsic elec. dipole moment, coherent elec. echo obs. 0-29705
- Jupiter, atmosphere coloration due to Si compounds 0-51689
- metal-ZnO-SiO<sub>2</sub>-Si structures, charge injection 0-49919
- neutron radiation damage of graphite rods and vitreous silica blocks 0-29070
- opals, crystal struct. and IR spectra 0-40117
- organic and inorganic free mol. chemical shift, binding energy and Auger spectra 0-32782
- oxide melts, specific weight, electrical conductivity, viscosity and surface tension meas. methods survey (Slovak) 0-47079
- oxides, grown in Cl-containing ambients, correl. between elec. and material props. 0-39479
- Permalloy-SiO<sub>2</sub>-Schott glass, bubble propagation struct. 0-34719
- plasma etching in Freon plasma, for microelectronics appls. 0-3080
- protosilicate particles, IR laboratory spectra rel. to interstellar silicate absorption bands 0-56907
- quasi-linear molecules, low frequency anharmonic vibrations, pot. function determ., Raman and IR spectra obs. 0-52997
- $\beta$ -Sialon, high strength, reaction sintering 0-7525
- Sialon, prep. and charact. of ultrafine powders 0-11604
- $\beta$ -sialon compositions, reaction sintering obs. 0-55337
- SiAlON X-phase, X-ray diffr. data 0-49198
- sialons, ceramic material fracture mechanics, review 0-45373
- $\beta$ -SiC, optical quenching of luminesc., acceptor ionisation energy 0-55178
- SiC-ZZ 0-42744
- silica hard coating for magnetic surfaces 0-7715
- silica surface, amorphous, with adsorbed ammonia, Raman scatt. 0-11948
- silica-alumina hard coating for magnetic surfaces 0-7715
- silicate+Ca(OH)<sub>2</sub>, reaction rates 0-26006
- silicate+Portland cement, reaction rates 0-26006
- silicate glaze, diffusion of Sn(IV) 0-49417
- silicate minerals, Mossbauer anal. of Fe chem. state 0-20547
- silicates, core-level XPS peak intensity ratio ang. variations rel. to surface anal. and chemisorption 0-40225
- silicates, elec. field gradient at Fe<sup>2+</sup> sites, Mossbauer spectra 0-15484
- silicates, ion bombardment, secondary positive mono-atomic ion emission, cation conc. depend and matrix effects (French) 0-50487
- silicates, layered, cylindrical crystallite layer disorder, X-ray diffr. intensity effect 0-39113
- silicates, molten, struct. and stat. interpret. of Masson theory (French) 0-49078
- silicates, molten, with high and medium Si contents, stat. theory (French) 0-49079
- silicates dissolved in deep water of Bering Sea 0-31061
- silicides, oxidation and hot corrosion resistance kinetics 0-25896
- silicone, B<sub>2</sub>C filled, neutron shielding materials, long term radiation effects 0-9413
- SiN, hot-pressed, creep 0-16380
- steel, structural, addition of solid SiO, effect on ductile fracture 0-16465
- systems Ni ions anal. by ESCA (Japanese) 0-40787
- tetrahalides of Gp.IV elements, M-X bond flexibility, by compliance scheme 0-37805
- tris(trimethylsilyl)phosphine, gamma irr., free radicals, struct. and EPR spectra 0-29623
- Zircon ceramic, exam. of development and fabrication 0-11608
- Al/SiO<sub>2</sub>-B<sub>2</sub>O<sub>3</sub>/Au (French) 0-39681
- Al-Si<sub>3</sub>N<sub>4</sub>-Si struct., surface energy bands under step function illumination 0-49840
- Al-SiO<sub>2</sub>, surface reactions and interdiffusion, photoemission study 0-49532
- Al-SiO<sub>2</sub> (2wt.%), dispersion hardened particulate composite, prep. 0-7588
- Al-SiO<sub>2</sub> interface, internal photoemission and photon-assisted tunnelling 0-6982
- Al-SiO<sub>2</sub>-Si, void form. in Al interconnection lines at Si-SiO<sub>2</sub> boundaries 0-2476
- Al-SiO<sub>2</sub>-Si structure, positive interface charge, exciton and H diffusion models 0-2471
- Al-SiO<sub>2</sub>-Si system with reactively sputtered SiO<sub>2</sub>, work functions difference 0-6987
- Al-SiO<sub>2</sub>-Si MIS solar cells, I-V characts. temp. depend. 0-7935
- Al-SiO<sub>2</sub>-p-Si MIS solar cells with back surface fields 0-12006
- Al<sub>4</sub>C<sub>3</sub>-Be<sub>2</sub>C-SiC system, phase equilibria 0-45284
- Al<sub>2</sub>O<sub>3</sub>-B<sub>2</sub>O<sub>3</sub>-SiO<sub>2</sub> system, liq. phase calc. for commercial quartzite powders 0-25671
- Al<sub>2</sub>O<sub>3</sub>-Si<sub>3</sub>N<sub>4</sub> preparation, compressive strength 0-25634
- Al<sub>2</sub>O<sub>3</sub>-SiO<sub>2</sub> system, solid state transform. of andalusite to mullite 0-16281
- Al<sub>2</sub>O<sub>3</sub>-SiO<sub>2</sub>-Fe<sub>2</sub>O<sub>3</sub>-CaO-MgO-TiO<sub>2</sub>, refractory, corrosion and mech. behaviour correlations 0-40563
- 3Al<sub>2</sub>O<sub>3</sub>.2SiO<sub>2</sub> as intermediate cubic phase in kaolinite-mullite thermal sequence 0-25652
- 3Al<sub>2</sub>O<sub>3</sub>.2SiO<sub>2</sub>, mullite, synthesis by freeze drying 0-16252
- As<sub>2</sub>Te<sub>3</sub>Ge<sub>16</sub>S<sub>21</sub>, chalcogenide semiconductor study of electric properties (French) 0-29414
- Au-SiO<sub>2</sub>-Au evaporated thin film sandwich, circulating and emission currents 0-11102
- Au-SiO<sub>2</sub>-Au structure AC conductivity, bulk and interface effects 0-54798
- B<sub>2</sub>O<sub>3</sub>-Na<sub>2</sub>O-SiO<sub>2</sub>-Al<sub>2</sub>O<sub>3</sub>, effect of alumina dispersions on the thermal cond./diffusivity/stress resist. 0-39368
- BAO-K<sub>2</sub>O-VO<sub>2</sub>-SiO<sub>2</sub>, glass, elec. cond. rel. to ion polarisability, polarons 0-49729
- BaO-La<sub>2</sub>O<sub>3</sub>-VO<sub>2</sub>-SiO<sub>2</sub>, glass, elec. cond. rel. to ion polarisability, polarons 0-49729
- BaSi<sub>2</sub>-Ge<sub>2</sub>, solid solution with type SrSi<sub>2</sub> struct., lattice parameters at high press. 0-54203
- Ba<sub>2</sub>SiO<sub>4</sub>Cl<sub>2</sub>-Eu, blue-emitting phosphor high quenching temp. 0-16076
- Bi<sub>2</sub>O<sub>3</sub>-SiO<sub>2</sub>, melt struct. model 0-33870
- Bi<sub>2</sub>O<sub>3</sub>-SiO<sub>2</sub>, metastable phases form., crystn. conditions, melt viscosity and density effects 0-35167
- CaO-MgO-ZrO<sub>2</sub>-SiO<sub>2</sub> refractories, phase diagram 0-11634

## silicon compounds continued

- CaO-SiO<sub>2</sub> melt, <sup>31</sup>Si tracer diffusivity at 1600°C 0-54418
- CaO-SiO<sub>2</sub> slags, containing CaF<sub>2</sub> and B<sub>2</sub>O<sub>3</sub>, SO<sub>2</sub> capacity determ. by encapsulation method 0-11944
- CaO-SiO<sub>2</sub>-Al<sub>2</sub>O<sub>3</sub>, wollastonite, low dielec. loss factors, fabrication (Japanese) 0-55032
- CaO-SiO<sub>2</sub>-MnO molten mixtures, struct. and phys. props. (French) 0-24635
- $\beta$ -CaO.SiO<sub>2</sub>, parawollastonite, rel. between structs. proposed 0-15056
- $\beta$ -Ca<sub>2</sub>SiO<sub>4</sub>-CaO-SiO<sub>2</sub> paste, hydration, compression strength and composition 0-50584
- CdSiP<sub>2</sub>, birefringence, effects on hydrostatic pressure and temp. 0-45033
- CdSiP<sub>2</sub>, pseudodirect chalcopyrite semicond., electronic band struct. 0-20079
- Ce<sub>2</sub>O<sub>3</sub>.2Si<sub>3</sub>N<sub>4</sub>, preferred unit cell for indexing powder diffr. pattern 0-49200
- Cr-SiO films, sputtered, elec. and struct. props. 0-39694
- Cr-SiO<sub>2</sub>-Si MIS solar cell, current cond. 0-7936
- Cs<sub>2</sub>O.Al<sub>2</sub>O<sub>3</sub>.4SiO<sub>2</sub> (pollucite) for long term-storage of <sup>137</sup>CsCl 0-37467
- Cu-SiO<sub>2</sub>/B<sub>2</sub>O<sub>3</sub>-Cu thin film, amorphous, conductance and capacitance, effect of electroforming 0-34537
- Cu-SiO<sub>2</sub>, deformed, lattice rotations at second phase particles 0-25709
- Fe-M-SiO<sub>2</sub> (M=Ru,Pt), supported catalysts, Mossbauer spectra 0-11296
- Fe-SiO<sub>2</sub> multilayer film, interface magnetisation 0-7135
- Fe-SiO<sub>2</sub> cermet film, solar absorbing, production by dual cathode DC magnetron sputtering 0-16186
- Fe-SiO<sub>2</sub> granular film, interface props., Mossbauer spectroscopy 0-34336
- Fe-SiO<sub>2</sub> granular films, superparamag., Mossbauer effect 0-7131
- Fe-SiO<sub>2</sub> supported catalysts, Mossbauer spectra 0-11296
- Fe-SiO<sub>2</sub>-Al<sub>2</sub>O<sub>3</sub> Lisakovskii concentrate mixture, sintering process, temp. thermal treatment (Russian) 0-55317
- Fe(H<sub>2</sub>O)<sub>6</sub>.SiF<sub>6</sub>, pressure-induced orbital ground state inversion, Mossbauer study 0-39979
- FeO-Fe<sub>2</sub>O<sub>3</sub>-SiO<sub>2</sub> system, molten, struct. using high temp. X-ray method (Japanese) 0-14992
- FeO-Fe<sub>2</sub>O<sub>3</sub>-SiO<sub>2</sub> system, molten, struct. by high temp. X-ray diffr. 0-49084
- In<sub>2</sub>O<sub>3</sub>-SnO<sub>2</sub>/SiO<sub>2</sub>/Si diode solar cells, loss mechanisms, characts., band struct. 0-26135
- K<sub>2</sub>O-B<sub>2</sub>O<sub>3</sub>-SiO<sub>2</sub>, glass, crystallisation range (German) 0-38934
- K<sub>2</sub>O-Fe<sub>2</sub>O<sub>3</sub>-SiO<sub>2</sub>, subsolidus sector of phase diagram, X-ray obs. 0-40335
- K<sub>2</sub>O-SiO<sub>2</sub>, glass, influence of electric charge phenomena on AES (French) 0-50478
- La-SiO-N, comments on new apatite phase 0-15255
- Li<sub>2</sub>O-SiO<sub>2</sub>, glass ceramics, phase transformation processes 0-3025
- Li<sub>2</sub>O.2SiO<sub>2</sub>, directionally solidified, thermal and mech. props. (Japanese) 0-16295
- 100(Li<sub>2</sub>O.2SiO<sub>2</sub>).3B<sub>2</sub>O<sub>3</sub>(3Na<sub>2</sub>O)(3MgO)(3Al<sub>2</sub>O<sub>3</sub>)(3SiO<sub>2</sub>)(3P<sub>2</sub>O<sub>5</sub>), directionally solidified, thermal and mech. props. (Japanese) 0-16295
- 100(Li<sub>2</sub>O.2SiO<sub>2</sub>).3SiO<sub>2</sub>, directionally solidified, thermal and mech. props. (Japanese) 0-16295
- MgO-CaO(SiO<sub>2</sub>)(B<sub>2</sub>O<sub>3</sub>)(Cr<sub>2</sub>O<sub>3</sub>), effective of impurities on high temp. creep 0-40455
- MgO-CaO-Fe<sub>2</sub>O<sub>3</sub>-Al<sub>2</sub>O<sub>3</sub>-SiO<sub>2</sub>, clinker production from dolomite and magnesite 0-55339
- Mn-Si, liq. alloys, equilibria between MnO-SiO<sub>2</sub>-CaO-MgO slags 0-10639
- Mn-SiO cermet films, DC and AC resist. 0-54804
- Mn-SiO cermet films, elec. resist., annealing behaviour 0-54803
- Na<sub>2</sub>O-CaO-SiO<sub>2</sub> glass, electronic struct. and optical props. 0-2790
- Na<sub>2</sub>O-NaF-CaO<sub>2</sub>ZnO<sub>1-x</sub>-Al<sub>2</sub>O<sub>3</sub>-SiO<sub>2</sub>, opal glasses, strength, surface composition 0-30066
- Na<sub>2</sub>O-Si<sub>2</sub>O glass, high-temp. peak of internal friction 0-39218
- Na<sub>2</sub>O-SiO<sub>2</sub>, melt, EMF meas., partial molar enthalpy and entropy 0-6525
- Na<sub>2</sub>O-SiO<sub>2</sub> glass, electronic struct. and optical props. 0-2790
- Na<sub>2</sub>O-SiO<sub>2</sub>-NiO systems Ni ions anal. by ESCA (Japanese) 0-40787
- Ni/SiO<sub>2</sub>, adsorption of CO, scavenging effect of H<sub>2</sub>, in situ Fourier transform IR spectra obs. 0-39410
- Ni-SiO<sub>2</sub> multilayer film, interface magnetisation 0-7135
- Ni-SiO<sub>2</sub>, high temp. plasticity, oxide inclusion effect 0-50681
- Ni-SiO<sub>2</sub> supported catalysts, particle size, H<sub>2</sub> chemisorption, Mossbauer study 0-7219
- P<sub>2</sub>O<sub>5</sub>-SiO<sub>2</sub> clad low-loss monomode fibres for 1.2 to 1.6  $\mu$ m, modified CVD prep. 0-48479
- Pb-SiO<sub>2</sub>-Pb<sub>1-x</sub>Ge<sub>x</sub>Te, semicond. band struct., tunnelling obs. 0-54795
- PbO-SiO<sub>2</sub> glass, electronic struct. and optical props. 0-2791
- PbO-SiO<sub>2</sub> glasses, elec. cond. and dielec. behaviour 0-44361
- PbTe-ZrO<sub>2</sub> (SiO<sub>2</sub>), epitaxial MIS struct., fabrication and elec. props. 0-2472
- Se-Si system glasses, vibr. IR spectra 0-20643
- Si (001)-SiO<sub>2</sub>, n-inversion layer, valley splitting without effect mass approx. 0-15586
- Si (111)-SiO<sub>2</sub> interfaces, sixth-valley state stability a priori calc. 0-49859
- Si rubber as electro-optic material for optical hydrophones 0-43412
- Si:P(As)(B)-SiO<sub>2</sub> interface oxidation kinetics, high doping levels, experiment 0-11828
- Si/SiO<sub>2</sub>-electrolyte interface, electron exchange at surface of thermally grown SiO<sub>2</sub> 0-16696
- Si-Al-B-O-N, calc. of phase diagrams from data set 0-55362
- $\beta$ -Si-Al-O-N, Mg-containing phases, crystn. 0-39297
- Si-Al-O-N, mullite like cpd. comp., EPMA, X-ray and chem. anal. obs. (Japanese) 0-35175
- Si-Al-O-N, oxidation mechanisms 0-40570
- Si-Al-O-N ceramic systems, layer struct. 0-6382
- Si-Al-O-N polytypes, hot-pressed, microstruct. 0-3023
- Si-Al-O-N sintered ceramic, microstruct., phase composition and transformation mech., mech. props. 0-40309
- Si-Al-O-N system, ionic cond. from 850 to 1400°C 0-2203
- Si-Al-Zr-O-N, calc. of phase diagrams from data set 0-55362
- Si-Al(Ti)C, sintered, exam. of props. 0-25644
- Si-B system, liq., surface tension, density, and oxidation kinetics, 1410-1700°C 0-20011
- Si-Ge-Br system, diffusion mass transfer 0-33911
- Si-H, amorphous, on Nb or W, spectrally selective absorber, IR spectra 0-26164
- Si-H, amorphous, random network model 0-1932
- Si-H, amorphous, thermal stability and decomp. kinetics 0-24758
- Si-SiO<sub>2</sub>, anodic polarisation in electrolyte containing fluoride ions, effect on oxide props. 0-39679



## silicon compounds continued

- Si-SiO<sub>2</sub>, bonding at (111) interface, stoichiometry and kinetics, synchrotron radiation photoemission spectroscopy 0-24744  
 Si-SiO<sub>2</sub>, ESR centres, interface states and oxide fixed charge 0-2474  
 Si-SiO<sub>2</sub>, interface, reconstructing states 0-49925  
 Si-SiO<sub>2</sub>, interface defect states obs. by constant capacitance DLTS 0-49924  
 Si-SiO<sub>2</sub>, interface states, new model 0-29478  
 Si-SiO<sub>2</sub>, oxide defect density depend. on appl. elec. field and thickness 0-19791  
 Si-SiO<sub>2</sub>, SiO<sub>2</sub> layer charging in UV irradi. of MISS struct., photoinjection currents (Russian) 0-39680  
 Si-SiO<sub>2</sub> (111) interfaces, sixfold valley degeneracy in electron inversion layers 0-49936  
 Si-SiO<sub>2</sub> boundary, precipitation of Na (Russian) 0-49368  
 Si-SiO<sub>2</sub> interface, Au doping, trapping states 0-20319  
 Si-SiO<sub>2</sub> interface, backscattering-channelling study 0-34320  
 Si-SiO<sub>2</sub> interface, cluster Bethe-lattice method appl. 0-49852  
 Si-SiO<sub>2</sub> interface, defects, intimate valence attenuation pairs 0-54132  
 Si-SiO<sub>2</sub> interface, effect of oxidation time and temp. using AES 0-35359  
 Si-SiO<sub>2</sub> interface, effect of hot electron injection on interface charge density 0-49921  
 Si-SiO<sub>2</sub> interface, electrically active paramag. centres detect., photocond. reson. obs. 0-50185  
 Si-SiO<sub>2</sub> interface, light induced reson. centres, photocond. reson., EPR obs. 0-50184  
 Si-SiO<sub>2</sub> interface, local at. struct., XPS obs. 0-20042  
 Si-SiO<sub>2</sub> interface, oxidation stacking faults, growth rel. to self-diffusion 0-49239  
 Si-SiO<sub>2</sub> interface, props. variation in SiO<sub>2</sub> region 0-49548  
 Si-SiO<sub>2</sub> interface, surface generation velocity study, gate-controlled diode structure application 0-6986  
 Si-SiO<sub>2</sub> interface, surface states characterization, expt. techniques review 0-49949  
 Si-SiO<sub>2</sub> interface, thermally grown, inhomogeneities of surface potential 0-34524  
 Si-SiO<sub>2</sub> interface as electrode for electrical and ellipsometric meas. of adsorbed organic molecules 0-15366  
 Si-SiO<sub>2</sub> interface layer characterisation by spectroscopic ellipsometry 0-50738  
 Si-SiO<sub>2</sub> interface oxidation kinetics, high doping levels, theory 0-11827  
 Si-SiO<sub>2</sub> interface state spectroscopy using MOS tunnelling structures 0-6991  
 Si-SiO<sub>2</sub> interface state distribution, Br incorporation effects 0-11091  
 Si-SiO<sub>2</sub> interface state density, dependence on thermal oxidation process variables 0-15607  
 Si-SiO<sub>2</sub> interface study by XPS 0-50507  
 Si-SiO<sub>2</sub> interfaces, local atomic and electronic struct., high resolution XPS 0-49927  
 Si-SiO<sub>2</sub> interfacial region on TCE/O<sub>2</sub> and CCl<sub>4</sub>/O<sub>2</sub> oxidised Si, struct. and comp. 0-50741  
 Si-SiO<sub>2</sub> interfacial transition layer thickness, XPS obs. 0-11540  
 p-Si-SiO<sub>2</sub> system, C-V meas. using Au/Hg probe, work function difference between probe and Si 0-2450  
 Si-SiO<sub>2</sub> transition region width, SIMS depth profiling 0-39454  
 Si-SiO<sub>2</sub>-Si<sub>3</sub>N<sub>4</sub>, internal photoemission 0-7475  
 Si-SiO<sub>2</sub>-Al photodiode experimental verification of theoretical predictions 0-29485  
 SiAlON powder, prod. by reaction clay+C+N<sub>2</sub> 0-40295  
 Si<sub>3</sub>-Al<sub>2</sub>O<sub>3</sub>N<sub>8-22</sub>, β-Sialon, form. from Si<sub>3</sub>N<sub>4</sub>-SiO<sub>2</sub>-AlN system (Japanese) 0-45261  
 Si<sub>3</sub>As<sub>1-x</sub>H<sub>x</sub>, amorphous system, struct. and defects, Raman and EPR meas. 0-49103  
 SiB<sub>4</sub>, mech. and thermal props. 0-21083  
 SiBr<sub>4</sub>, X-ray absorpt. spectra struct. 0-37819  
 SiC 147R<sub>(b)</sub> polytype, crystal structure by X-ray diffraction method (Chinese) 0-54206  
 SiC, 6H polytype, elec. and thermal cond., carrier concentrations 0-2223  
 SiC (1 OH), phonon spectrum, dispersion curves energy discontinuity and vibr. modes, IR spectra obs. 0-44274  
 α-SiC (6H), dynamic hologram high-speed recording and erasure mechanism 0-5710  
 SiC, (6H), radiation damaged, luminesc. 0-25462  
 α-SiC (6H) laser excited thermostimulated luminescence light sum dose depend. (Russian) 0-16111  
 SiC brittle coating for B fibres, critical thickness effect on strength (Russian) 0-40426  
 SiC CVD substrate, Cu mirror vapour deposition, pulsed laser damage characts. 0-48314  
 SiC, ceramic material fracture mechanics, review 0-45373  
 SiC, chem. stability, mech. and thermal props. rel. to appls. 0-21103  
 SiC, coating on graphite, by reactive magnetron sputter deposition (Japanese) 0-16185  
 SiC coating on Mo, CVD and stability under thermal cycle conditions 0-7500  
 SiC coatings for first-wall candidate materials by RF sputtering 0-25563  
 SiC coatings for HTR nuclear fuels, characterisation by small-angle X-ray scatt. 0-44451  
 SiC continuous fibres, mech. props. depend. on testing conditions (Russian) 0-35297  
 SiC crystals, 2H to 6H solid-state transformation, X-ray diffraction study 0-28943  
 SiC, cubic, atomic displacement energy determ. by bracketing technique 0-49272  
 SiC distribution profiles of 30 keV Al ions using Lindhard-Scharff-Schiott model (German) 0-15172  
 SiC, electron-hole liquid, RPA calcs. 0-6743  
 SiC, epitaxial film, effect of impurities on polymorphism during growth 0-15414  
 SiC, epitaxial growth, appl. for solid state devices (Japanese) 0-11579  
 SiC, epitaxial growth by sublimation sandwich method, effect of impurities 0-25568  
 SiC, epitaxial growth by direct synthesis in vacuum 0-40262  
 SiC epitaxial layer growth from sublimation in vac., kinetics 0-20791  
 SiC, exam. of N solubility, in epitaxial layers 0-6520  
 SiC fibre reinforced Al interaction between components and compatibility, mech. props. effect 0-11761  
 SiC fibre reinforced Al-Mg, heat treatment effect on struct., tensile strength 0-55487  
 SiC fibre reinforced Ti, effect of Al, Zr and Mo alloying additions on reaction rate of Ti with fibres 0-16249

## silicon compounds continued

- SiC fibre reinforced Ti-Al-Mo-Zr composites, matrix selection (Russian) 0-35192  
 SiC fibre reinforced Ti-Al-Mo-Zr-Si (6.6, 3.3, 1.8, 0.3 wt.%) composite, component interaction kinetics (Russian) 0-55364  
 SiC fibres obtained from polycarbosilane fibre 0-50582  
 SiC filament reinforced phosphate foam ceramics, bending strength 0-11716  
 SiC formation on polycryst. Si ribbon, effect on solar cell efficiency (French) 0-54531  
 SiC, further polytypes discovered using Laue diffraction (Chinese) 0-10535  
 SiC, grinding material, grain shape optimization (Polish) 0-29916  
 SiC, HF, ion-plasma etching, cryst. surface layers treatment and study (Russian) 0-16517  
 SiC heating element, MoSi<sub>2</sub> protective coating 0-21137  
 SiC, high period polytype at interface of two interacting spirals 0-20041  
 SiC luminescent powders, SAW nonlinear acoustoelectro-luminescence 0-45143  
 α-SiC monocrystalline grains, mech. props. and grain separation (Polish) 0-40554  
 β-SiC, n-type, thermoelectric efficiency at high temps. 0-35706  
 SiC, oxidation and corrosion behaviour, formation of protective SiO<sub>2</sub> coatings (German) 0-25885  
 SiC, oxidation and hot corrosion resistance kinetics 0-25896  
 SiC, permeability and solubility of H<sub>2</sub>, 1200-1450°C 0-39351  
 SiC, polar semiconductor, electron-hole liquid, electron-phonon interactions 0-6739  
 β-SiC, polycrystn., C<sup>14</sup> self diffusion 0-2200  
 SiC polymorphs, widths of first minibands and effective masses, resist. anisotropy 0-20071  
 SiC polytype 6H, space group 0-1956  
 SiC polytypes, contribution of ionic bonding to thermal stability 0-28946  
 SiC polytypes, electrolum. in anodic oxidation, band model (Russian) 0-50429  
 SiC polytypes, localisation of cond. band minima in Brillouin zone 0-20082  
 SiC polytypes, stacking sequences by high resolution electron microscopy 0-15054  
 SiC polytypes deformed, resist. anisotropy in (0001) plane 0-20198  
 SiC, polytypic transform., interface struct. exam. by TEM 0-15033  
 SiC powders, form. by vapour phase method 0-25623  
 SiC, power, electroluminesc. excitation by SAW, nonlinear effects 0-16104  
 SiC, reactions with oxidising atms. 0-11812  
 SiC reinforced Al, thermal stresses in unit cell 0-10160  
 SiC, resist. to oxidation and corrosion at high temps. (German) 0-35357  
 SiC reverse biased p-n junctions, prebreakdown violet luminesc. 0-7420  
 SiC, self-bonded polycryst., electrophys. props. 0-10980  
 SiC, single cryst., friction and wear behaviour in sliding contact with various metals 0-21112  
 SiC single crystal, friction and fracture in contact with itself and Ti 0-11780  
 α-SiC, single crystals, phase struct. rel. to heat treatment, nucleation 0-38991  
 SiC, sintered, electrode and container material in Na/S cell 0-35355  
 SiC, specimen preparation for TEM by ion beam thinning (German, English) 0-11861  
 SiC, sputtered, comp. and struct. props., effect of target materials 0-54549  
 SiC, sputtering processes by energetic ions, combined SIMS-AES study 0-40201  
 SiC surface, roughness factor measurement, energetic D<sup>+</sup>, He<sup>+</sup>, Ar<sup>+</sup> irradiation 0-39172  
 SiC, surface defect annealing, following Ar ion and electron irradi. 0-7603  
 SiC, surface defects due to Ar ion bombardment, 100-1000 eV 0-6445  
 SiC, tensile strength distrib. 0-40471  
 SiC, thermal diffusivity measurement, constant rate heating method (Japanese) 0-6572  
 SiC, thin film, effect of O on thin film compositions obtained by secondary ion emission 0-26079  
 SiC thin film, RF-sputtered, highly reliable temp. sensor 0-224  
 β-SiC, twinned crystals, fracture characts. 0-3193  
 β-SiC, undoped compact, microstruct. development during heating 0-25746  
 SiC, X-ray diffuse scattering 0-14964  
 SiC:Al epitaxial layers, growth, Al distrib. and solubility 0-15391  
 SiC:Al<sup>+</sup> p-n junctions, elec. props., defect effects 0-15594  
 SiC:Al(Ga)(B) (6H) LEDs, fabrication by rotation dipping technique, electrolum. mechanisms 0-50426  
 β-SiC/Si abrasive resistant material, prep. and props. 0-20878  
 SiC-2H, structure parameters and polarity, X-ray diff. meas. 0-19781  
 α-SiC-Al<sub>2</sub>O<sub>3</sub>, sintering 0-11611  
 SiC-fibre reinforced glass, fabrication, thermal expansion, flexural and fracture toughness 0-40319  
 SiC-fission product reaction kinetics in HTGR TRISO UC<sub>2</sub> and UC<sub>2</sub>O<sub>2</sub> fuel in thermal gradient 0-47570  
 SiC-n-Si junction device, elec. props. 0-15591  
 Si<sub>1-x</sub>C<sub>x</sub> protective coating for GaAs laser 0-5753  
 α-SiC(6H), electron bombardment, formation of defects on (0001) surface 0-19844  
 SiC(6H), ion-implanted, laser-induced recrystallization and defects 0-44221  
 α-SiC(6H), two stage transitions, nonlinear absorpt., thermoluminesc. method 0-7425  
 SiCl<sub>4</sub>, conversion to SiCl<sub>3</sub> in unipolar HF discharge 0-1855  
 SiCl<sub>4</sub> hydrolysis and oxidation kinetics for graded-index fibre vapour phase axial deposition 0-48477  
 SiCl<sub>4</sub>, X-ray absorpt. spectra struct. 0-37819  
 SiCl<sub>4</sub>-TiCl<sub>4</sub> liq., beat effects, neutron diff. studies 0-38897  
 SiF<sub>4</sub>, (SiCl<sub>4</sub>), (SiBr<sub>4</sub>), X-ray absorpt. spectra struct. 0-37819  
 SiF<sub>4</sub>-CO<sub>2</sub> laser-irrad., dissoc. product fluoresc., wavelength depend. 0-11900  
 SiF<sub>4</sub> molecule, saturated absorpt. of CO<sub>2</sub> laser radiation 0-37811  
 SiF<sub>4</sub>, stella quadrangula as struct. building unit 0-15055  
 SiF<sub>4</sub>, X-ray absorpt. spectra struct. 0-37819  
 SiF<sub>4</sub>, XUV spectra, overlapping core-valence and core-Rydberg transitions and resons. 0-32735  
 Si<sub>2</sub>F<sub>6</sub>, normal coord. analysis, vibr. freqs. and amplitudes, shrinkage and distortion const., force const. 0-27989



## silicon compounds continued

- Si<sub>3</sub>Ge<sub>1-x</sub>O<sub>2</sub>, amorphous, electronic struct. in Bethe lattice approx. 0-44487
- SiH, ground state, A-type doubling 0-23431
- SiH<sub>0.16</sub>, amorphous films, optical props. and photocond. near optical gap 0-50443
- SiH<sub>2</sub>, 1B<sub>1</sub>-state, geometry calcs., avoided crossings 0-53085
- SiH<sub>3</sub>-group containing mols., normal coord. anal. 0-9579
- SiH<sub>4</sub>, 1B<sub>1</sub>(1T<sub>2</sub>) pot. energy surface calcs. 0-53085
- SiH<sub>4</sub> discharge, low pressure, plasma parameters, relevance to Si film deposition 0-44030
- SiH<sub>4</sub>, irradi. by CO<sub>2</sub> laser, Si film deposition 0-16190
- SiH<sub>4</sub>, low temp. oxidation, film growth rates, IR absorption spectra 0-15399
- SiH<sub>4</sub>, magnetisation relax., appl. of theory of spin-lattice relax. 0-50214
- SiH<sub>4</sub>+UF<sub>6</sub>, photoinduced reaction in low temp. SiH<sub>4</sub> matrix 0-30256
- SiH<sub>4</sub>, amorphous reactively sputtered films, in Pd Schottky barrier devices, photovoltaic props. 0-49910
- SiH, amorphous reactively sputtered films, optical props. 0-50444
- SiH<sub>4</sub> ground state struct., ab initio SCF calcs., singlet silylsilylene 0-27945
- Si<sub>2</sub>H<sub>2</sub> cluster, Si valence band Auger spectrum, cluster approach, comparison with experimental spectrum 0-40191
- Si<sub>2</sub>H<sub>2+2</sub>, silane, SCF X $\alpha$  MO calc., appl. to amorphous hydrogenated Si 0-49580
- Si<sub>2</sub>H<sub>4-n</sub>, enthalpies of formation, effusion mass spectrometric meas. 0-26043
- SiH<sub>4</sub>(Si<sub>2</sub>)<sub>2</sub>+F<sub>2</sub>, chemilum., at. absorption, and laser-induced fluoresc. obs. 0-3315
- SiN, interatomic interactions from XPS 0-49171
- SiN, film, plasma deposited, comp. and characterisation, optical and elec. props. 0-15401
- Si<sub>3</sub>N<sub>4</sub>, amorphous, CVD prep., struct. characts. by pulsed neutron diffr. 0-33891
- Si<sub>3</sub>N<sub>4</sub> amorphous film, CVD, core and valence electron excitations, low energy electron loss spectroscopy and AES 0-2365
- Si<sub>3</sub>N<sub>4</sub>, CVD, chem. bond nature, Compton scatt. expts. 0-49539
- Si<sub>3</sub>N<sub>4</sub> CVD thin film, multiple internal refl. IR spectroscopy 0-11499
- Si<sub>3</sub>N<sub>4</sub>, ceramic material fracture mechanics, review 0-45373
- Si<sub>3</sub>N<sub>4</sub>, consolidation by hot isostatic pressing 0-11605
- Si<sub>3</sub>N<sub>4</sub> dielectric film on Ge, dislocation interactions 0-39472
- Si<sub>3</sub>N<sub>4</sub>, effect of oxide impurities on physicochemical props. 0-16396
- Si<sub>3</sub>N<sub>4</sub>, end point detection in plasma etching by optical emission spectroscopy 0-50733
- Si<sub>3</sub>N<sub>4</sub> film, CVD, high-field dark currents 0-54791
- Si<sub>3</sub>N<sub>4</sub> film, HF plasma deposition (*German*) 0-7507
- Si<sub>3</sub>N<sub>4</sub> film, on Si, influence of induced stresses on B diffusion in Si 0-29224
- Si<sub>3</sub>N<sub>4</sub> film, on Si, struct. stability 0-54564
- Si<sub>3</sub>N<sub>4</sub> film, reactive ion beam sputtering deposition, form. and characterisation 0-44452
- Si<sub>3</sub>N<sub>4</sub> film on Si substrate, dislocation generation at film edge, suppression effect of SiO<sub>2</sub> 0-2025
- Si<sub>3</sub>N<sub>4</sub> film on Si substrate, electrical properties (*Korean*) 0-55300
- Si<sub>3</sub>N<sub>4</sub> films, plasma etching, MOS processing appl. 0-40577
- Si<sub>3</sub>N<sub>4</sub> films, prep., characterisation and appl. 0-40268
- Si<sub>3</sub>N<sub>4</sub> films, prep. by thermal nitridation of Si in NH<sub>3</sub>, comp. and oxidation resist. 0-3215
- Si<sub>3</sub>N<sub>4</sub> films, struct. 0-54545
- Si<sub>3</sub>N<sub>4</sub>, finely dispersed, high-temp. synthesis 0-55331
- $\alpha/\beta$ -Si<sub>3</sub>N<sub>4</sub>, formation during nitridation of Si 0-50609
- Si<sub>3</sub>N<sub>4</sub>, fracture toughness meas. using Knoop indentation method (*German*) 0-25830
- Si<sub>3</sub>N<sub>4</sub>, hard coating preparation by ion beam methods 0-25579
- Si<sub>3</sub>N<sub>4</sub>, hot pressed, strength and life prediction 0-3173
- Si<sub>3</sub>N<sub>4</sub>, hot pressed, surface wave scatt. from elliptical cracks for failure prediction 0-55608
- $\beta$ -Si<sub>3</sub>N<sub>4</sub>, hot-pressed, containing small amounts of Be and O in solid soln. 0-2985
- Si<sub>3</sub>N<sub>4</sub>, low press CVD film, steady-state electron and hole space charge distrib. 0-29493
- Si<sub>3</sub>N<sub>4</sub>, N ion implantation synthesis, struct. and resonance mechanism of  $\alpha$ - $\beta$  transition during annealing 0-33981
- Si<sub>3</sub>N<sub>4</sub>, oxidation and hot corrosion resistance kinetics 0-25896
- Si<sub>3</sub>N<sub>4</sub>, prep. and charact. of ultrafine powders 0-2983
- Si<sub>3</sub>N<sub>4</sub>, reaction sintered, microstruct. charact. 0-35145
- Si<sub>3</sub>N<sub>4</sub>, rolling bearing materials, effects of high temp. operation 0-21124
- Si<sub>3</sub>N<sub>4</sub>, sintering in powder bed with addition of MgO sintering aid 0-29910
- Si<sub>3</sub>N<sub>4</sub>, slip casting from aqueous suspension, reactions with HCl and NaOH 0-16259
- $\beta$ -Si<sub>3</sub>N<sub>4</sub> solid soln. prod. by reaction sintering SiO<sub>2</sub>-AlN mixture 0-25645
- Si<sub>3</sub>N<sub>4</sub> sputtered layer, GaAs:Si encapsulation, photolum., annealing effects 0-20681
- Si<sub>3</sub>N<sub>4</sub> substrate, nucleation of CVD Si in SiH<sub>4</sub>-HCl-H<sub>2</sub> system at high temp. 0-49538
- Si<sub>3</sub>N<sub>4</sub>, synthesis in Cl<sub>2</sub> system 0-40308
- Si<sub>3</sub>N<sub>4</sub>, tensile strength distrib. 0-40471
- Si<sub>3</sub>N<sub>4</sub>(MgO+Al<sub>2</sub>O<sub>3</sub>)(Y<sub>2</sub>O<sub>3</sub>), hot-pressed and sintered, microstruct. and impurity distrib. 0-49261
- Si<sub>3</sub>N<sub>4</sub>:Ge films, intrinsic stress rel. to deposition conditions 0-39467
- Si<sub>3</sub>N<sub>4</sub>:H, film, impurity profile determ. by 1.2 MeV proton-proton scatt. 0-49256
- Si<sub>3</sub>N<sub>4</sub>/Al<sub>2</sub>O<sub>3</sub>, powder compact, electron microprobe investigation of reactions (*French*) 0-26009
- Si<sub>3</sub>N<sub>4</sub>/Zr laminates, metal to ceramic joints, adherence props. 0-45386
- Si<sub>3</sub>N<sub>4</sub>-Al<sub>2</sub>O<sub>3</sub>-AlN, isothermal sections, free energy of formation 0-55363
- Si<sub>3</sub>N<sub>4</sub>-AlN-Al<sub>2</sub>O<sub>3</sub>-SiO<sub>2</sub>-Y<sub>2</sub>O<sub>3</sub>, phase equilibrium study by X-ray diffr. and optical microscopy 0-50614
- Si<sub>3</sub>N<sub>4</sub>-CeO<sub>2</sub>, surface stress development during oxidation 0-50736
- Si<sub>3</sub>N<sub>4</sub>-Mg<sub>2</sub>SiO<sub>4</sub>-Si<sub>2</sub>N<sub>2</sub>O, compressive creep, composition effect 0-50674
- Si<sub>3</sub>N<sub>4</sub>-MgO, (5 wt.%), hot pressed, fracture toughness as function of initial  $\alpha$ -phase content, SEM 0-3174
- Si<sub>3</sub>N<sub>4</sub>-MgO, compressive creep, source of viscoelastic effect 0-50675
- Si<sub>3</sub>N<sub>4</sub>-MgO, compressive creep, oxidation induced compositional change 0-50676
- Si<sub>3</sub>N<sub>4</sub>-MgO (2-5 wt.%) hot pressed, tensile creep testing 0-40423
- Si<sub>3</sub>N<sub>4</sub>-Si<sub>2</sub>N<sub>2</sub>O-Mg<sub>2</sub>SiO<sub>4</sub>, melting and eutectic studies 0-45285
- Si<sub>3</sub>N<sub>4</sub>-SiC-Y<sub>2</sub>O<sub>3</sub> (La<sub>2</sub>O<sub>3</sub>)(Ce<sub>2</sub>O<sub>3</sub>)(Eu<sub>2</sub>O<sub>3</sub>)(Gd<sub>2</sub>O<sub>3</sub>), reactively sintered, microstruct. and strength 0-25631

## silicon compounds continued

- Si<sub>3</sub>N<sub>4</sub>-SiO<sub>2</sub>:As, graded and stepped energy band-gap MIS struct. 0-2473
- Si<sub>3</sub>N<sub>4</sub>-SiO<sub>2</sub>-AlN system,  $\beta$ -Sialon form. (*Japanese*) 0-45261
- Si<sub>3</sub>N<sub>4</sub>-SiO<sub>2</sub>-ZrN-ZrO<sub>2</sub>, X-ray diffr. phase anal. and reactions Si<sub>3</sub>N<sub>4</sub>+ZrO<sub>2</sub>, SiO<sub>2</sub>+ZrN 0-50613
- Si<sub>3</sub>N<sub>4</sub>-Y<sub>2</sub>O<sub>3</sub>, hot-pressed, oxidation kinetics 0-16520
- Si<sub>3</sub>N<sub>4</sub>-Y<sub>2</sub>O<sub>3</sub> ceramic, thermal degradation, C impurity effect 0-50708
- Si<sub>3</sub>N<sub>4</sub>-Y<sub>2</sub>O<sub>3</sub>(CeO<sub>2</sub>), hot pressed, sintered, microstruct., flexural strength and fractographic anal. 0-40293
- Si<sub>3</sub>N<sub>4</sub>+ZrO<sub>2</sub>, X-ray diffr. phase anal. of reaction products 0-50613
- Si<sub>3</sub>N<sub>4</sub>/AlN-Al<sub>2</sub>O<sub>3</sub> system, reaction sintering forming  $\beta$ -Si<sub>3</sub>N<sub>4</sub> solid solns. 0-50585
- SINH films, thickness and refractive index meas., comparison of techniques 0-8957
- Si<sub>2</sub>N<sub>2</sub>O, fast neutron irradiation, variation of lattice parameters 0-24504
- Si<sub>2</sub>N<sub>2</sub>O-Al<sub>2</sub>O<sub>3</sub>, solid soln., prep., effect of Si<sub>3</sub>N<sub>4</sub> powder reactivity 0-45256
- Si<sub>3</sub>N<sub>4</sub>-Y<sub>2</sub>O<sub>3</sub> prepared by hot press, cryst. struct. 0-10534
- Si<sub>3</sub>N<sub>4</sub>-15Y<sub>2</sub>O<sub>3</sub>, sintering under high N<sub>2</sub> pressure 0-29907
- Si<sub>3</sub>N<sub>4</sub>, hot pressed, subcritical crack growth boundaries at internal fracture origins 0-11748
- SiO 86.2 GHz maser, astronomical sources polarisation props. 0-4449
- SiO amorphous film, high freq. phonon scatt. 0-49328
- SiO, amorphous film, vac. evaporated, density meas., microcrystalline model of struct. 0-2313
- SiO, evaporated film, AC cond meas. 0-20236
- SiO, film, effect of ion implanted O<sub>2</sub> on optical props. 0-45027
- SiO film, vacuum evaporation on NaCl single cryst., IR absorption spectra 0-35098
- SiO film on Al, radiative cooling surface 0-50439
- SiO in Ar matrix, vac. UV spectrum, vibr. progression 0-23432
- SiO, interstellar abundances rel. to interstellar shocks mol. diagnostics 0-56899
- SiO maser variability at 86 GHz of R Leonis,  $\alpha$  Ceti and Orion A 0-41839
- SiO, single-layer vac. antirefl. coatings for near IR spectral region 0-33099
- SiO-B<sub>2</sub>O<sub>3</sub> composite dielec. films, EPR, dangling bonds and dielec. loss 0-11246
- SiO-CO gas phase, Si and C transfer to Fe-C liquid alloys 0-55655
- SiO<sub>2</sub>, amorphous, intrinsic surface phonons, Raman scatt. and IR refl. 0-24728
- SiO<sub>2</sub>, amorphous, local at. struct., XPS obs. 0-20042
- SiO<sub>2</sub>, amorphous, phonon scatt. by density fluctuations and thermal cond. 0-10626
- SiO<sub>2</sub>, amorphous, temp. below 1K, props., tunnelling 0-49576
- SiO<sub>2</sub>, amorphous and  $\alpha$ -cristobalite cryst., band struct., photoelectron and X-ray spectra interpret. 0-24787
- SiO<sub>2</sub>, amorphous and cryst., neutron irradi. and unirrad., intrinsic defect photolum. 0-50401
- SiO<sub>2</sub>, amorphous charge transport and storage 0-6864
- SiO<sub>2</sub>, amorphous estimate valence alternation pairs 0-54132
- SiO<sub>2</sub> amorphous film, thermal, core and valence electron excitations, low energy electron loss spectroscopy and AES 0-2365
- SiO<sub>2</sub>, and SiO<sub>0.7</sub>, amorphous sputtered thin film, US anomalies, 0.5-300K 0-34145
- SiO<sub>2</sub> antireflection coating effect on CW laser annealing of ion implanted Si 0-49242
- SiO<sub>2</sub>, B<sub>2</sub>O<sub>3</sub> glasses, struct. and phonon spectra 0-50324
- SiO<sub>2</sub> CVD thin film, multiple internal refl. IR spectroscopy 0-11499
- SiO<sub>2</sub> capsule, contamination effects on heat treatment of Zircaloy, vapour transport of Zr and Si 0-55437
- SiO<sub>2</sub> charge transfer from metallic electrodes 0-15605
- SiO<sub>2</sub> concrete, elastic moduli meas. during heating and cooling 0-55451
- SiO<sub>2</sub>, core levels, chem. shift and relaxation energy, temp. dependence 0-39520
- SiO<sub>2</sub>, core levels, temp. depend. of conduction band and core exciton energies 0-24828
- SiO<sub>2</sub> crystal and amorphous modifications, structural defect model 0-38915
- SiO<sub>2</sub>, crystalline and amorphous density of states, bulk electronic struct., tight binding calcs. 0-44502
- SiO<sub>2</sub>, dangling bond states 0-24846
- SiO<sub>2</sub> decomposition and reduction, in low temp. plasma jet (*German*) 0-45499
- SiO<sub>2</sub> dielectric film on Ge, dislocation interactions 0-39472
- SiO<sub>2</sub>, diffusion of As, diffusivity and masking oxide thickness 0-39350
- SiO<sub>2</sub>, dry etching induced surface contamination, SIMS, AES, and XPS obs. 0-11810
- SiO<sub>2</sub> film, amorphous, shock crystn. obs. 0-10828
- SiO<sub>2</sub> film, electron-beam-induced cond. 0-20337
- SiO<sub>2</sub> film, migration parameters of alkali ions, elec. meas. 0-39359
- SiO<sub>2</sub> film, on Si, influence of induced stresses on B diffusion in Si 0-29224
- SiO<sub>2</sub> film, on Si, struct. stability 0-54564
- SiO<sub>2</sub> film, on Si wafer, surface roughness by gas adsorption techniques 0-15398
- SiO<sub>2</sub> film, thermally grown, thickness, XPS obs. 0-11540
- SiO<sub>2</sub> film electron beam induced conductivity theory and expts. 0-15640
- SiO<sub>2</sub> film grown by Si oxidation in O<sub>2</sub>-H<sub>2</sub>-HCl mixture, elec. props. 0-40569
- SiO<sub>2</sub>, film on Si, electron beam damage, obs. using scanning AES 0-2070
- SiO<sub>2</sub> film on Si substrate, Na transport caused by ion and atom impact 0-6682
- SiO<sub>2</sub> film on thermally oxidised Si substrate, interface props., sputter deposition parameters effects (*German*) 0-40257
- SiO<sub>2</sub> films, CVD at reduced press., optical props. 0-2957
- SiO<sub>2</sub> films, plasma etching, MOS processing appl. 0-40577
- SiO<sub>2</sub> films, spin-on diffusion sources, debris-induced effects 0-39465
- SiO<sub>2</sub> films, thickness and refractive index meas., comparison of techniques 0-8957
- SiO<sub>2</sub>, finite amplitude SAW distorted rippling profiles, optical probing obs. 0-34287
- SiO<sub>2</sub>, fluorocarbon ion beam etching characts. 0-35363
- SiO<sub>2</sub>, fused, ion beam induced luminescence 0-40166
- SiO<sub>2</sub>, fused, isothermal compressibility to 20 kbar, inductance coil method 0-49302
- SiO<sub>2</sub>, fused, refractive index dispersion, thermal history depend. 0-25331
- SiO<sub>2</sub>, fused, shock compressed, refractive index, density, and polarisability behaviour 0-50295



## silicon compounds continued

- SiO<sub>2</sub>, fused, single particle impact damage 0-40508  
 SiO<sub>2</sub>, fused, structural analysis, using fluorescence excitation (*German*) 0-38923  
 SiO<sub>2</sub>, fused fibres, radii determ. by multiwavelength laser light scatt. 0-22321  
 SiO<sub>2</sub>, fused powder, difference between white and black silica, devitrification rates 0-28918  
 SiO<sub>2</sub> gel, macroporous, modification of surface by adsorption of thin layer of polymer 0-6624  
 SiO<sub>2</sub> gel, SiO<sub>2</sub>-Al<sub>2</sub>O<sub>3</sub>, SiO<sub>2</sub>-MgO, pore structure influence on X-ray intensity in EPMA (*Japanese*) 0-26046  
 SiO<sub>2</sub> gel, steam treatment, struct. changes 0-35579  
 SiO<sub>2</sub>, glass, <sup>29</sup>Si hyperfine struct. of E' centre, microwave saturation props. 0-7165  
 SiO<sub>2</sub> glass, electronic struct. and optical props. 0-2790  
 SiO<sub>2</sub> glass, IR spectral emissivity and absorpt. coeff. at 600 to 1700K 0-16018  
 SiO<sub>2</sub>, glass, irradi., EPR of Al E' centres 0-11268  
 SiO<sub>2</sub> glass, monolithic, low temp. synthesis 0-40318  
 SiO<sub>2</sub> glass, phonon scatt., >10<sup>2</sup> GHz, by supercond. junction spectrosc. 0-10625  
 SiO<sub>2</sub> glasses, radial distrib. functions 0-44136  
 SiO<sub>2</sub>, growth under deposited TiO<sub>2</sub> film on Si during postdeposition high temp. annealing 0-15400  
 SiO<sub>2</sub>, impurity redistrib. in Si-SiO<sub>2</sub> during oxidation, numerical soln. including interfacial fluxes 0-25888  
 SiO<sub>2</sub>, in MIS structures, polarisation hysteresis, ion motion (*Russian*) 0-54793  
 SiO<sub>2</sub>, interfacial chemistry with deposited Ba, AES obs. 0-44434  
 SiO<sub>2</sub>, intrinsic luminescence 0-16098  
 SiO<sub>2</sub>, ion implanted, fused, refr. index profiles 0-54272  
 SiO<sub>2</sub> irradiated film, electron and hole trapping 0-11098  
 SiO<sub>2</sub>, isotopically enriched target preparation using electron gun 0-23226  
 SiO<sub>2</sub>, laser coating, UV damage obs. 0-33056  
 SiO<sub>2</sub>, laser irradiated, in-depth and surface temp. meas. by Moire-Schlieren technique 0-53392  
 SiO<sub>2</sub> layers, in MOS struct., hole trapping induced by ion implantation and annealing at room temp. 0-54792  
 SiO<sub>2</sub>, low temp. CVD on n-InSb, surface quality improvement and characterisation 0-49932  
 SiO<sub>2</sub>, MIS devices, radiation induced charge storage 0-6997  
 SiO<sub>2</sub> MOS structures, removal of electron traps by RF annealing 0-44728  
 SiO<sub>2</sub> MOST-transistor struct., breakdown-initiated negative resist. device 0-20314  
 SiO<sub>2</sub>, magnetron sputtered film, oblique deposition effect on growth rate, etching rate, and struct. (*Japanese*) 0-54555  
 SiO<sub>2</sub> monolayer, core excitons and inner well resonances in surface soft X-ray absorpt. spectra 0-40187  
 SiO<sub>2</sub>, new catalyst for CO-H<sub>2</sub>O induced coal liquefaction 0-30335  
 SiO<sub>2</sub> nonporous film, plasma deposition method, appl. to semicond. device manufacture (*Russian*) 0-16197  
 SiO<sub>2</sub>, of albumin 0-10777  
 SiO<sub>2</sub>, on Si, H<sub>2</sub> and D<sub>2</sub> ion bombardment effects 0-34086  
 SiO<sub>2</sub>, on Si, reduction by heating in Ga mol. beam at 800°C 0-50730  
 SiO<sub>2</sub> particles, movement and heating in air plasma jet (*Russian*) 0-7522  
 SiO<sub>2</sub>, polymerisation and deposition from dil. solns., kinetics, 5-180°C 0-7790  
 SiO<sub>2</sub> polymorphs, CNDO/2 MO calc. 0-6386  
 SiO<sub>2</sub> protective coating formation on SiC (*German*) 0-25885  
 SiO<sub>2</sub> RF magnetron sputtered coatings for laser fusion targets 0-35089  
 SiO<sub>2</sub>, RF sputtered films, anomalous etching phenomenon 0-3226  
 SiO<sub>2</sub>, RF sputtered films, AC conductivity and conduction mechanisms 0-20338  
 SiO<sub>2</sub>, seawater composition over opaline sediments 0-51419  
 SiO<sub>2</sub>, selective etching, using reactive ion etching with CF<sub>4</sub>-H<sub>2</sub> 0-3224  
 SiO<sub>2</sub> single-mode optical fibre, wavelength dispersion characs. in low-loss region 0-53423  
 SiO<sub>2</sub>, solid solubility in MgO 0-15247  
 SiO<sub>2</sub>, solid state reaction with Ti film, backscatt. anal. 0-34257  
 SiO<sub>2</sub> sputtered film as Zn-diffusion mask for GaInAsP-InP planar stripe lasers 0-48249  
 SiO<sub>2</sub> sputtered films in thin film transistors, trapping centres 0-7014  
 SiO<sub>2</sub> substrate, for interdigital transducer (*Czech*) 0-19201  
 SiO<sub>2</sub> substrate, nucleation of CVD Si in SiH<sub>4</sub>-HCl-H<sub>2</sub> system at high temp. 0-49538  
 SiO<sub>2</sub> surface defects, influence of adsorbed O<sub>2</sub> EPR spectra 0-7163  
 SiO<sub>2</sub>, surface electronic struct., electron irradi. effects, EELS study 0-24985  
 SiO<sub>2</sub>, surface pot. during ion implantation 0-19826  
 SiO<sub>2</sub>, surfaces, electronic struct. calc., scattering theoretic approach 0-6940  
 SiO<sub>2</sub> system, spatial-symmetry laws of cryst. lattices 0-19784  
 SiO<sub>2</sub>, tensile and compressive strengths of fine powder bed (*Japanese*) 0-25780  
 SiO<sub>2</sub> thermal films, hole and electron trapping density reduction 0-2400  
 SiO<sub>2</sub>, thin film coated sample, absorptive laser damage analysis by Weibull distrib. 0-33061  
 SiO<sub>2</sub> thin films, comparison of RI and IR spectra 0-11497  
 SiO<sub>2</sub> thin films, plasma deposition in prod. planar reactor 0-2966  
 a-SiO<sub>2</sub>, transient photocond. simulations using multiple-trap model 0-49801  
 SiO<sub>2</sub>, transport of electrons at high electric fields 0-20208  
 α-SiO<sub>2</sub>, trigonal crystals, anisotropy of linear electrooptic effect 0-34894  
 SiO<sub>2</sub>, ultrathin layers on Ge substrate, ATR spectra, thickness depend., struct. obs. 0-55214  
 SiO<sub>2</sub> undoped film, cathodoluminescence (*Russian*) 0-40164  
 SiO<sub>2</sub>, vapourisation in steam atmosphere 0-44306  
 SiO<sub>2</sub>, vitreous, effect of high-dose X-rays and reactor radiation 0-19838  
 SiO<sub>2</sub>, vitreous, heat treatment effect on viscosity and struct. 0-19714  
 SiO<sub>2</sub>, vitreous, hypersound velocity meas. from Brillouin scatt. freq. 0-27349  
 SiO<sub>2</sub>, vitreous, impurity C determ. by isotopic spectral method 0-26093  
 SiO<sub>2</sub>, vitreous, intrinsic radiation defects, nonbridging O 0-19837  
 SiO<sub>2</sub>, vitreous, low temp. thermal props. and intrinsic defects 0-29057  
 SiO<sub>2</sub>, vitreous, multiphonon IR absorpt. 0-25381  
 SiO<sub>2</sub>, vitreous, non-bridging O centre, optical props. and energetic struct. 0-34976  
 SiO<sub>2</sub>, vitreous, Raman active defects, thermal equilibration 0-55092  
 SiO<sub>2</sub>, vitreous, resist. to NaOH 0-21143

## silicon compounds continued

- SiO<sub>2</sub>, vitreous, spin-lattice relaxation times of paramag. hole and E' centres 0-39871  
 SiO<sub>2</sub>, vitreous, struct. and phonon spectra 0-50324  
 SiO<sub>2</sub>, vitreous film on Si, defect struct. comparison with crystalline SiO<sub>2</sub> and Si-O bond nature 0-54557  
 SiO<sub>2</sub>, vitreous films on Si, channel and network defects 0-54142  
 SiO<sub>2</sub> wafers, Au contamination during plasma etching 0-19831  
 SiO<sub>2</sub>, <sup>85</sup>Kr, ion-implanted, impurity distrib. 0-15145  
 SiO<sub>2</sub>:B implanted, thin films, props. (*Polish*) 0-39692  
 SiO<sub>2</sub>:Co(II), adsorption of H<sub>2</sub>O, coord. lifetime, surface effect, NMR obs. 0-34299  
 SiO<sub>2</sub>:Fe<sup>3+</sup>, vitreous silica, absorpt. spectra and structural state 0-16071  
 SiO<sub>2</sub>:Ga film, impurity distrib. after annealing, neutron activation anal. 0-24484  
 SiO<sub>2</sub>:Ge single-mode fibres, dispersion meas., pulse synchronisation technique 0-48410  
 SiO<sub>2</sub>:Na<sup>+</sup>, heat treated, heat of immersion in H<sub>2</sub>O, organic compds. 0-3396  
 SiO<sub>2</sub>:Nd<sup>3+</sup> films, cathodoluminesc. 0-20717  
 SiO<sub>2</sub>:P, diffusion from spin-on source 0-44367  
 SiO<sub>2</sub>:P film, spin-on, diffusion of P into Si 0-2050  
 SiO<sub>2</sub>/InP film/substrate system, interface formation during CVD, modelling 0-24764  
 SiO<sub>2</sub>-Al<sub>2</sub>O<sub>3</sub>, mullite, sintering behaviour and microstruct. 0-20876  
 SiO<sub>2</sub>-Al<sub>2</sub>O<sub>3</sub> (36.6 wt.%) plasma prep. powder, metastable immiscibility and microstruct. during sintering 0-35143  
 SiO<sub>2</sub>-Al<sub>2</sub>O<sub>3</sub>-Si<sub>3</sub>N<sub>4</sub>, isothermal sections, free energy of formation 0-55363  
 SiO<sub>2</sub>-based glassy layers, passivating Cu at 500°C 0-3246  
 SiO<sub>2</sub>-basic oxide system, struct. model 0-54109  
 SiO<sub>2</sub>-borosilicate glass, B diffusion from sputtered glass film into SiO<sub>2</sub> 0-29040  
 SiO<sub>2</sub>-CdSe thin film transistors, slow states, trapping state densities and cross sections 0-15613  
 SiO<sub>2</sub>-FeO<sub>2</sub> particulate mass transfer mechanism in modified CVD, thermophoresis 0-2955  
 SiO<sub>2</sub>-GeO<sub>2</sub> particles, deposition props. in flame hydrolysis reaction for optical fibre fabrication 0-48470  
 SiO<sub>2</sub>-InP capacitor, carrier generation and trapping 0-49929  
 SiO<sub>2</sub>-InP system, interface and dielec. props. 0-49930  
 SiO<sub>2</sub>-M<sub>2</sub>O (M=Na,K) glasses, temp. depend. of elastic modulus 0-40410  
 SiO<sub>2</sub>-Na<sub>2</sub>O-CaO (13, 11 wt.%) glass, phase separation, SiO<sub>2</sub> purity effect 0-44144  
 SiO<sub>2</sub>-PbO, interdiffusion layer optical waveguide, prep. and props. 0-43489  
 SiO<sub>2</sub>-RO-Na<sub>2</sub>O-Li<sub>2</sub>O (RO=MgO, CaO, SrO) glass-ceramic coating, optimisation of props. by selective oxide action 0-55552  
 SiO<sub>2</sub>-Si, low-energy neutral particle bombardment of SiO<sub>2</sub> film, degradation 0-54790  
 SiO<sub>2</sub>-Si, P ion implantation, electrical transport props. 0-39130  
 SiO<sub>2</sub>-Si MOS capacitor, two-stage process for building up of radiation induced interface states 0-20313  
 SiO<sub>2</sub>-Si MOS system, ion irradi. effects on struct. and electrophysical props. 0-6995  
 SiO<sub>2</sub>-Si stratified system surface charges, adsorption and desorption effects (*Russian*) 0-49942  
 SiO<sub>2</sub>-TiO<sub>2</sub> antireflection coating, 1.064 μm laser damage, barrier 0-33059  
 SiO<sub>2</sub>-ZnO-Na<sub>2</sub>O-Li<sub>2</sub>O, glass-ceramic coating, optimisation of props. by selective oxide action 0-55552  
 SiO<sub>2</sub>-ZrO<sub>2</sub>-Li<sub>2</sub>O-Na<sub>2</sub>O based crystallisable glasses composition and properties 0-50731  
 SiO<sub>2</sub>+F, heterogeneous reaction, discharge-flow tube meas. 0-21274  
 SiO<sub>2</sub>+ZrN, X-ray diffr. phase anal. of reaction products 0-50613  
 SiO<sub>2-x</sub>, paramagnetic E centre, reply to comment on new concept of model 0-24445  
 SiO<sub>2-x</sub>, paramagnetic E'-centre, comment on new concept of model 0-24444  
 SiO<sub>4</sub><sup>4-</sup> compounds, vibr. pot. function, force consts., isotopic shifts, mean vibr. amplitudes 0-23395  
 SiO<sub>x</sub>, amorphous and recrystallised layer, optical props. 0-25474  
 SiO<sub>x</sub> amorphous film, dispersion of refr. index and chem. comp. 0-7429  
 SiO<sub>x</sub> amorphous films, high energy electron diffr. study 0-38911  
 SiO<sub>x</sub>, antireflection coating, 100 ns pulsed laser damage at 2.7 and 3.8 μm 0-33057  
 SiO<sub>x</sub> film, durable optical, ion plating onto plastics, optical and mech. props. 0-38141  
 SiO<sub>x</sub>, grown in HCl/O<sub>2</sub> ambients, phase separation and Na passivation 0-3219  
 SiO<sub>x</sub>, powder and vac. deposited, amorphous struct., X-ray diffr. meas. 0-1931  
 SiO<sub>2</sub>-(Ag), CW CO<sub>2</sub> laser deposited dielect. thin film, optical and struct. props. 0-7506  
 Si(OH)<sub>4</sub>, NO<sub>3</sub><sup>-</sup>, PO<sub>4</sub><sup>3-</sup>, ratios in Moroccan upwelling region 0-4045  
 SiON/GaAs film/substrate system, interface formation during CVD, modelling 0-24764  
 SiO<sub>2</sub>N<sub>2</sub> CVD thin film, multiple internal refl. IR spectroscopy 0-11499  
 SiO<sub>2</sub>N<sub>2</sub> film, on Si, struct. stability 0-54564  
 Si<sub>3</sub>O<sub>2</sub>N<sub>4</sub> film, amorphous, shock crystn. obs. 0-10828  
 SiS multiple collision chemiluminesc., intercombination systems from Si+OCS 0-45505  
 SiS\*, collisional quenching from Si+OCS 0-45505  
 SiTe:Ge(Sn), substitution of Si, thermoelectric props. (*Russian*) 0-11023  
 SiX<sub>4</sub> (X=Cl,H,F), chemical shifts, relax., X-ray spectra, SCF Xalpha calcs. 0-27928  
 SiX<sub>n</sub> radical, (X=H,D; n=1,2,3), thermodynamic function in ideal gas state 0-14871  
 SiO<sub>2</sub> blazed holographic gratings, fabrication by reactive ion etching 0-53484  
 SiO<sub>2</sub> deposition by reactive sputtering of Si in magnetron sputtering system, reaction kinetics 0-49553  
 SnO<sub>2</sub>-SiO<sub>2</sub>-n-Si heterojunction, cheap solar elements for ground-based appls. 0-40860  
 Te<sub>40</sub>As<sub>35</sub>Ge<sub>25</sub>Si<sub>18</sub>, amorphous, threshold switching, expt. 0-49830  
 TiO<sub>2</sub>-SiO<sub>2</sub> multilayered film striped optical filters, optical props. and fabrication of RF sputtering 0-10030  
 ZnO-SiO<sub>2</sub> system, struct. and phase comp. of luminescent Zn orthosilicate 0-19951  
 ZnSiAs<sub>2</sub>, birefringence, effects on hydrostatic pressure and temp. 0-45033



## silicon compounds continued

- ZnSiP<sub>2</sub>, birefringence, effects on hydrostatic pressure and temp. 0-45033  
 ZnSiP<sub>2</sub>, pseudodirect chalcopyrite semicond., electronic band struct. 0-20079  
 ZnSiP<sub>2</sub>-In Schottky diode, photovoltaic spectra 0-2423  
 ZrB<sub>2</sub>-SiC-C(-V)(-Nb), refractory cermet, hot pressing and oxidation resist. 0-3231  
 ZrO<sub>2</sub>-Al<sub>2</sub>O<sub>3</sub>-SiO<sub>2</sub> fusion cast ceramics, crystn., microstructures rel. to conditions 0-11638  
 ZrO<sub>2</sub>-SiO<sub>2</sub> (11 to 13 wt.%), X-ray phase anal. 0-35195  
 ZrO<sub>2</sub>-SiO<sub>2</sub> powder mixture for optical glass polishing 0-28367  
 ZrO<sub>2</sub>-SiO<sub>2</sub>-Al<sub>2</sub>O<sub>3</sub> mixed powders, solid state reactions 0-40337

silicon controlled rectifiers *see thyristors*silicon integrated circuits *see monolithic integrated circuits*silicon-on-sapphire integrated circuits *see field effect integrated circuits*silicon reference diodes *see avalanche diodes; Zener diodes*

## silicones

- atmospheric radioactive gas monitoring by silicone oil absorbent scintillation counter 0-12044  
 double-layer coating with double cone nozzle in-line with optical fibre drawing 0-53488  
 fluid conductivity meas. under DC field 0-15533  
 liquid, electrification during laminar flow in metal pipe 0-6954  
 oil drop spreading on horizontal surfaces 0-2250  
 optical fibre primary coat using modified silicone, transmission characts 0-38098  
 poly(vinyl pyrrolidone), silicone grafted, for contact lenses, surface props. and stability of thin tear film 0-17194  
 polyorganosiloxane fluids, temp. determ. in friction zone accompanying breakdown, using TV (*Russian*) 0-7688  
 resin clad fibre technology, optical and mech. props. 0-28349

## silver

*see also nuclei with .....*

- adsorbed Cs and Cs-O, surface plasma waves, ATR study 0-39451  
 adsorbed ethylene, photon-induced field ionisation mass spectroscopy 0-6639  
 adsorbed I<sub>2</sub> on (111) surface, surface EXAFS study 0-40186  
 adsorbed layer of Xe, lateral compression effects calc. 0-6641  
 adsorption, O<sub>2</sub>-induced, and reaction of H<sub>2</sub>, water, CO, and CO<sub>2</sub> on (110) surface 0-55714  
 adsorption and surface reaction of formic acid 0-40741  
 adsorption of organic dye, excited mol. decay near metal surface, energy transfer to plasmon surface polaritons 0-50440  
 adsorption of Xe on Ag(111), structural and thermodynamic studies 0-6640  
 adsorption on W, substrate temp. effect on relation between work function and coverage, FEM obs. 0-2272  
 atom, 4d level He II photoelectron spectra, energies and intensities 0-5511  
 atom, ionisation energies and oscill. strengths calcs. 0-5488  
 atom, K $\beta$ /K $\alpha$  rel. intensity obs. 0-32665  
 atom, XPS and XES, dynamical effects 0-52924  
 catalysts, multiply-twinned particles 0-15114  
 chemisorbed CN<sup>-</sup> on (110), Raman scatt. 0-45075  
 clusters on Si substrates, opt. spectra investig. of struct. (*German*) 0-25492  
 coating, vapour deposited on Cu, defects and their effect on props. 0-39474  
 crystal structure stability, collinear three-ion interaction theory 0-49173  
 Debye temperature correlations at high temp. 0-15210  
 deformed, exoelectron emission and electron energy distrib. 0-7481  
 deposited on InP surfaces, Schottky barrier formation 0-39671  
 determ. in water and organic materials, flameless atomic absorpt. spectrometry with wire loop atomiser 0-45586  
 diffusion in GaAs substrates, radiotracer profiles 0-24680  
 diffusion in ion implanted GaAs, profiles 0-24681  
 diffusion of Ti, V, Cr and Mn in Ag, 1051 to 1220K 0-15308  
 diffusion transfer systems, graphic arts appl. 0-37106  
 electrical resistivity, low temp., T<sup>4</sup> behaviour rel. to electron scatt. mechanisms 0-39552  
 electrical resistivity, pseudoharmonic effect of phonons 0-34414  
 electrical resistivity, temp. depend. data 0-51967  
 electrode, enhanced Raman effect from adsorbed cyanide 0-50348  
 electrode, evaporation rate from cathode spot in vac. arcs. 0-49024  
 electrode, intense Raman spectra in presence of Cl<sup>-</sup> and pyridine 0-55076  
 electrodes, adsorbed pyridine, ang. resolved Raman spectra 0-16017  
 electron beam plasma sputtered coatings on KCl substrate, islet struct. (*Russian*) 0-39460  
 electron range, low-energies continuous-slowing-down approx. and range straggling calcs. 0-39183  
 electroreflectance of single cryst. electrodes, obs. in aqueous solns. 0-25342  
 electroreflectance spectroscopy, longitudinal surface plasmons 0-40137  
 epitaxial films, ang. depend. UPS 0-55270  
 epitaxial films, grain boundary struct. evolution during recrystn., interface energy effect (*Russian*) 0-15387  
 epitaxial growth, cluster mobilities, in-situ electron microscopes obs. 0-15407  
 epitaxial growth on electron bombard. NaCl(111) surfaces, RHEED and AES 0-15419  
 etching by graphite suspension method in 0.5 H<sub>2</sub>SO<sub>4</sub> soln. (*Japanese*) 0-35406  
 fatigued, relationship between stress and point defect cluster density 0-10592  
 FCC, props. of vacancies and divacancies 0-10545  
 film, condensate obtained in electric field, anisotropy of elec. props. 0-44743  
 film, damping and vel. of longit. elastic waves at 9.4 GHz 0-10596  
 film, deposited by cathodic sputtering using high-resolution electron microscopy, voids obs. 0-49557  
 film, discontinuous, adsorption of alkali halide mols., effect on elec. cond. 0-2487  
 film, electroplated, stress meas. using holographic interferometry 0-20806  
 film, evaporated, adhesion meas. 0-50822  
 film, evaporated, chemisorption effects on reflectance and elec. resist. 0-11495  
 film, granular, adhesion measurement 0-50807  
 film, in situ struct. determ. by internal stress meas. 0-54569  
 film, Maxwell stresses at charged surface from elastoresistance 0-49957

## silver continued

- film, on Au substrate, monolayer overgrowth, quantitative AES method 0-10813  
 film, on Cu, ion-induced intermixing 0-15420  
 film, spike effects of heavy ion sputtering 0-35034  
 film, sputtered, hillock growth and agglomeration by annealing, SEM obs. 0-2309  
 film, surface and volume plasmon light emission due to low energy electron scatt. 0-40177  
 film, vacuum deposited, defect density and activation energy depend. on deposition rate 0-29294  
 film, vacuum deposited, internal stress and its depend. on gas adsorption 0-6683  
 film deposition by ion plating, on AT-cut quartz crystal, crystallographic structure obs. 0-2280  
 foil, foils, polycryst. and bicrystals, grain boundaries, <sup>119</sup>Sn Mossbauer anal. 0-7229  
 frictional behaviour, effect of mechanical properties 0-55548  
 grain boundary energy misorientation, hydrostatic press. effect, press. induced struct. phase transformations 0-54257  
 granules and colloidal particles on Cs<sub>2</sub>O film in Ag-O-Cs photocathode (*Chinese*) 0-2279  
 heat pipe meas. of corrosion and vapour press. 0-23878  
 p-InSb:Cu, Ag, deep impurity centres, acceptor conc. effect on conduction type 0-44602  
 interatomic pair potential, phonon spectra 0-33927  
 interdiffusion in SiO<sub>2</sub>-B<sub>2</sub>O<sub>3</sub>-Al<sub>2</sub>O<sub>3</sub>-Na<sub>2</sub>O(K<sub>2</sub>O), optical and NMR studies 0-24683  
 ion bombardment, sputtering, re-emitted kinetic energy ang. distrib. 0-2910  
 ion injection transport and grain boundary mobility in KBr bicryst. 0-2214  
 kinetic friction re-examination using modified pin and disc machine 0-55547  
 lattice dynamics, energy wave number charact., by reson. model 0-10612  
 lattice dynamics, ion-ion and ion-electron interactions 0-49321  
 layers, thickness determ. by laser microprobe and flame atomic absorpt. 0-27355  
 light ion (H, D, He, Li) irradi., defect prod. and electronic stopping power 0-34088  
 liquid metals, structure factor modelling using quasi-crystallised model (*Russian*) 0-54118  
 loosely packed powder, sintering SEM and dilatometry obs. 0-20843  
 melting curve to 60 kbar press., reinvestigation 0-39260  
 microcrystals on C foil, size distrib. from electron micrograph obs., UV absorpt. spectra obs. 0-55121  
 microwave transmission, time-of-flight effects in Fermi vel. determ., calc. 0-20238  
 Mossbauer resonance at 88 keV, temp. depend. 0-7213  
 pair potentials calc., appl. to point defect props. 0-19798  
 particles, ultrafine, effect of truncation of size distrib. 0-49562  
 phonon dispersion 0-10611  
 phonon dispersion relation in resonant model potential 0-6473  
 phonon limited electrical resistivity, temp. depend. 0-24876  
 photoemission, primary and secondary yields using low-energy monochromatic X-rays 0-35053  
 photoemission spectra and total primary yields for exploding wire radiator source 0-32773  
 photoneutron yields released by incident electrons, improved calc. 0-27630  
 photoreactive diffusion in glassy As<sub>2</sub>S<sub>3</sub> 0-19991  
 powder, sulphide coated, Fritt effect on appl. of DC voltage (*German*) 0-25599  
 recrystallisation texture, rel. to rolling temp. 0-11664  
 shear band effects on rolling deformation, of (211)[ $\bar{1}11$ ] single crystals. 0-50651  
 size effect, ballistic-type field penetration at 45 GHz, 3 MHz 0-44634  
 solid metal embrittlement of Ti-Al-V-Sn (6.6, 2 wt.%) 0-16551  
 solid state sintering, compact length change 0-11593  
 specific entropy, and surface heat determ. as function of temp. (*German*) 0-6619  
 spherical powder, struct. of sintering necks in compacts 0-11594  
 sputtering, temp. depend. 0-2914  
 sputtering rate on Ar ion bombard. 0-55245  
 stopping ratios of 50-300 keV H<sup>+</sup>, He<sup>+</sup>, <sup>7</sup>Li<sup>+</sup>, and <sup>8</sup>Be<sup>+</sup> 0-42903  
 surface, adsorbed pyridine Raman intensity enhancement using surface plasmons 0-7334  
 surface, CN monolayer, picosecond Raman gain spectroscopy 0-25351  
 surface, diffusion of labelled adsorbed Cl<sup>-</sup>, I<sup>-</sup> ions 0-39413  
 surface, enhanced Raman scatt. by physisorbed pyridine-d<sub>5</sub> thin film 0-20620  
 surface, X-ray prod. by 5 MeV/amu deuterons (oxygen ions), projectile Z depend. 0-42982  
 surface (111) surface Au decoration by chemical polishing and electrodeposits (*French*) 0-44445  
 surface roughness induced electronic Raman scatt. 0-50347  
 surface self-diffusion coeff., O<sub>2</sub> potential effect 0-15354  
 thin sub-monolayer film, Auger emission coeffs. meas. 0-55236  
 transverse electron focusing and specular refl. from cryst. faces 0-6823  
 two-parameter dynamical model appl., sp. ht. and Debye-Waller factor calc. 0-10597  
 vacuum deposition of oriented coating on doped alkali halide substrates 0-2303  
 vacuum deposition on evaporated AgBr layers, growth mechanism 0-35095  
 yield point, temp. depend., 2 to 300K (*Russian*) 0-45346  
 Ag, and Ag<sup>+</sup>, solvation in deuterated-ice matrices, electron spin echo obs. 0-15780  
 Ag film, epitaxial growth on isolated Au patches covered with amorphous C layer 0-40270  
 Ag films, hillock form. hole growth and agglomeration 0-44455  
 Ag surfaces, temp. depend. of sputtering based on thermal spike effect 0-50491  
 Ag vacuum deposited coating on glass, strength 0-55505  
 Ag<sup>+</sup>, generation by laser ionis. source for ICR spectroscopy, chem. appls. 0-45597  
 Ag/Al thin film couples, diffusional alloying, Kiessig X-ray interf. obs. 0-10713  
 Ag/CN, coverage meas. using surface enhanced Raman scatt. and radiolabel meas., electrochemical treatments 0-29260



## silver continued

- Ag/Si (111), metastable 2D condensations, epitaxy, growth modes, exp. techniques, book contrib. 0-49558  
 Ag-<sup>4</sup>He interface, Kapitza conductance, proof of surface superfluidity in enhanced power anomaly 0-15359  
 Ag-AgCl/KCl/AgCl-Ag thermocell, and thermal liq. junction pot. for KCl solns. at high temp. 0-16819  
 Ag-Al<sub>2</sub>O<sub>3</sub>-Au structure, electrorefl. meas. (*French*) 0-50366  
 Ag-Au, pseudoballoy behaviour at interfaces, grain boundary diffusion 0-6567  
 Ag-CdO cermets, coprecipitated carbonates and hydroxides, physicomech. props. 0-25706  
 Ag-Cs<sub>2</sub>O photocathode, light absorption and photoemission 0-50510  
 Ag-Cu couple, grain boundary diffusion of Ag through Cu film, Rutherford backscattering obs. 0-34252  
 Ag-Ge, amorphous, junction, current-voltage charact. 0-44725  
 Ag-He CW mW-level laser source at 224 nm 0-43352  
 Ag-In (Sn) multilayers, vapour quenched, supercond. transition temp. 0-20346  
 Ag-InP contact in InP Gunn device, relationship between microwave efficiency and metallurgical state of cathode contact 0-6981  
 Ag-InP Schottky barrier, hot electron attenuation length 0-49904  
 Ag-metals thin film couples, room temp. interactions 0-2220  
 Ag-O-Cs photocathode, Ag colloidal particles and long wavelength response (*Chinese*) 0-45195  
 Ag-O-Cs photocathode, role of Ag colloidal particles in photoemission (*Chinese*) 0-40215  
 Ag-SiO<sub>2</sub>, CW CO<sub>2</sub> laser deposited dielect. thin film, optical and struct. props. 0-7506  
 Ag-Sn proximity-effect bridges, T\* anomaly under phonon injection 0-34566  
 Ag-Sn proximity-effect bridges, phonon-injection-induced first-order transition obs. 0-39718  
 Ag<sup>+</sup>-Na<sup>+</sup> ion-exchanged optical waveguide repeatability improved by melt dilution 0-53493  
 Ag+H<sup>+</sup>, K-shell ionisation cross-section determ. 0-48077  
 AgCl<sub>2</sub>Br<sub>1-x</sub>, binary melt, Ag solubility, temp. and conc. depend. 0-10677  
 Ag(T<sub>1</sub>)/AgI/Ag(T<sub>2</sub>) cell, thermo-EMF of highly conducting solid electrolytes 0-24659  
 Al-CdSe-Ag dry air stabilised struct., elec. cond. mechanism, breakdown phenomena 0-34527  
 As<sub>2</sub>S<sub>3</sub>-Ag system, photosensitivity depend. on As<sub>2</sub>S<sub>3</sub> thickness (*Russian*) 0-54784  
 As<sub>2</sub>S<sub>3</sub>-Ag system, photosensitivity depend. on metallic layer thickness (*Russian*) 0-54785  
 As<sub>2</sub>S<sub>3</sub>(Se<sub>2</sub>)<sub>x</sub>Ag glassy films, doped by photodiffusion and thermodiffusion, photocond. 0-29441  
 As<sub>2</sub>Se<sub>3</sub>X (X=Cu, Ag, Tl, I, Ge), effect of doping, NMR meas. 0-11282  
 Au/Si films, laser-irrad., phase transform. study 0-49536  
 BaO-Al<sub>2</sub>O<sub>3</sub>-B<sub>2</sub>O<sub>3</sub>-Ag, X-ray irrad., atomic centre interactions, EPR spectra 0-25207  
 Bi-Ag, microhardness anisotropy 0-21079  
 CaO-Ag, electroluminesc. meas. 0-40162  
 CdCr<sub>2</sub>Se<sub>4</sub>-Ag, elec. props., vac. heat treatment effect 0-15518  
 p-CdCr<sub>2</sub>Se<sub>4</sub>-Ag, electrical props., 100-300K 0-54692  
 CdCr<sub>2</sub>Se<sub>4</sub>-Ag, magneto-electrical props. temp. behaviour depend. on dopant conc. (*Russian*) 0-11006  
 Cd,Hg<sub>1-x</sub>Te-Ag, impurity diffusion, gamma-ray effects 0-54441  
 CdS-Ag, vacuum deposited film, recrystn. by H<sub>2</sub>S heat treatment 0-34328  
 CdS-Ag crystals, spectral shifts of induced impurity photocond. bands 0-39633  
 CdTi<sub>2</sub>Se<sub>4</sub>-Ag, doping effect on surface tension of melt and cryst. microhardness 0-49464  
 CrFeCN epoxy resin-based membrane studies, Ag sensitive electrode 0-16726  
 Cu electrorefining process, quantitative evaluation of Ag transfer 0-30246  
 Ga-Ag tunnel junction, evidence for existence of anisotropy of supercond. energy gap 0-20357  
 GaAs-Ag, diffusion of Ag at 1000°C, profiles, Schottky barrier and Hall effect meas. 0-54435  
 GaP-Ag, Schottky barrier, stress effects on elec. props. 0-34512  
 p-Ge-Ag, Sb, electron beam irradiation cond. characts. 0-19842  
 Ge<sub>2</sub>S<sub>3</sub>-Ag contact, photoinduced diffusion of Ag in amorphous semicond. film 0-49418  
 Ge<sub>30</sub>S<sub>70</sub> glass film, Ag photodoping sensitivity 0-39121  
 HgTe-Ag, impurity diffusion, gamma-ray effects 0-54441  
 KBr-Ag, optical absorpt. spectra interpretation mol. orbital scheme 0-20671  
 KCl-Ag, excitation in fund. absorpt. region, luminesc. and thermolum. 0-50433  
 KCl-Ag, optical absorpt. spectra interpretation mol. orbital scheme 0-20671  
 Li ions stopping power and straggling 0-42908  
 MgF<sub>2</sub>-Ag film substrate tunable external-reflector retarder, computer based anal. 0-53407  
 NaBr-Ag<sup>+</sup>, UV absorption bands, temp. depend. 0-20672  
 NaCl-Ag, absorpt. spectra, influence of elec. field 0-2794  
 NaCl-Ag, excitation in fund. absorpt. region, luminesc. and thermolum. 0-50433  
 Pb-In, containing Ag particles, flux pinning in superconducting matrix 0-2534  
 SrF<sub>2</sub>Gd<sup>3+</sup>, Ag<sup>+</sup>, EPR of orthorhombic Gd<sup>3+</sup>-univalent metal ion complexes 0-11262  
 ZnCdS-Ag, phosphor screen, electron beam excited, light ang. distrib., modulation transfer function 0-45150  
 ZnCdS-Ag screen, electron beam excited, light emission spectra 0-25466  
 ZnS-Ag, luminesc. efficiency deterioration due to surface oxidation by (NH<sub>4</sub>)<sub>2</sub>Cr<sub>2</sub>O<sub>7</sub> thermal decomp. 0-29810  
 ZnS-Ag, phosphor, luminesc. of surface glow centres 0-29782  
 ZnS-Ag, single crystal, ionisation mechanism of field trapping centres 0-45156  
 ZnS-Ag, TSC and induced impurity photoconductivity, existence of two electron trapping centres 0-44655  
 ZnS-Ag,Al phosphors, luminesc. excitation spectra and exciton struct. 0-55164  
 ZnS-Ag,Cl, embedded in HBO<sub>3</sub>-glass matrix, blue electrolum. 0-55195  
 ZnTe-Ag, doped during growth and by diffusion, defect form. 0-15129  
 ZnTe-Ag, real structure effect on luminescence and absorption spectra, dislocations 0-16085

## silver alloys

- Ag-Pd, surface comp. changes under ion bombardment, AES study 0-55250  
 chemical analysis by low energy  $\gamma$ -rays and neutron transmission meas. 0-35591  
 rare earth alloys, RAg<sub>2</sub>X<sub>2</sub> (X=Si,Ge), cryst. struct. 0-1964  
 Ag-Al, short-range order, X-ray and electron diffr. study 0-54173  
 Ag-Al,  $\delta$ -phase, short range order (*Japanese*) 0-15256  
 Ag-Au, surface layer, effect of Ar<sup>+</sup> bombardment, AES and SIMS 0-25504  
 Ag-Au-Cu, sputtering and AES 0-50503  
 Ag-Au(Cu), residual elec. resist., pseudopot. calc. 0-6813  
 Ag-Cd (45 at.%) martensite, shape memory mech. and related phenomena 0-30009  
 Ag-Cd (50 at.%), BCC  $\beta$  phase, high temp. creep, existence of master curve 0-55473  
 Ag-Cu, surface segregation, electronic theory, density of states, cluster-Bethe-lattice approx. 0-49369  
 Ag-Cu (10 wt.%), contact material, contamination layer thickness, resist., ESCA study (*German*) 0-55561  
 Ag-Cu (8 wt.%), deformed, free energy changes in process of discontinuous precipitation 0-3054  
 Ag-Cu (8 wt.%), plastic deform. effect on discontinuous precipitation 0-3053  
 Ag-Dy, dil., thin films, ESR spectra, stress effects 0-39866  
 Ag-Dy(Ho)(Tm), dil., high field magnetoresist. 0-15503  
 Ag-Fe, dil., ion implanted, phase comp., Mossbauer study 0-7244  
 Ag-Mn, dil. alloy, transverse magnetoresist. in spin glass regime 0-34417  
 Ag-Mn, spin glass, mag. susceptibility hydrostatic press depend., RKKY interaction 0-44845  
 Ag-Pb (30 wt.%), contact material, contamination layer thickness, resist., ESCA study (*German*) 0-55561  
 Ag-Pd, H mobility and solubility, appearance pot. spectra obs. 0-55231  
 Ag-Pu (0.5 wt.%) deposited profiles, homogeneity, from hexagonal point source array 0-25559  
 Ag-rare earth alloys, Ag-rich, phase equilib. 0-45276  
 Ag-Sn (6(8.2)(11) wt.%), splat-quenched, X-ray line broadening 0-40397  
 Ag-Te, liq., struct. and elec. props. 0-49083  
 Ag-Zn, negative muon capture ratios 0-55007  
 Ag-Zn, vacancy prod. rate by displacement cascades, anelastic meas. during neutron irrad. 0-19794  
 Ag-Zn (2 to 12 wt.%) containing several metals, internal oxidation (*Japanese*) 0-16570  
 Ag-Zn (50 at.%), BCC  $\beta$  phase, high temp. creep, existence of master curve 0-55473  
 AgAu, quenched, short range order effects on specific heat 0-29181  
 AgCd, charge transfer, core-electron binding-energy shift 0-2676  
 Ag<sub>2</sub>Mg, structure of ordered alloy, electron diffraction, kinematical vs. dynamical diffraction calc. 0-10530  
 Ag<sub>2</sub>Mg, two different types of long-period ordered alloys, characterisation by high resolu. electron microscopy 0-49181  
 Ag<sub>2</sub>Sn-Hg, metallic powder-liquid system, correlation between hardness and evolution and sintering states 0-25614  
 Al-Ag, dil., Hall coeff. by OPW Fermi surface model 0-6816  
 Al-Ag, precipitation study by internal friction (*French*) 0-35190  
 Al-Ag (40 wt.%), deformed, free energy changes in process of discontinuous precipitation 0-3054  
 Al-Ag (40 wt.%), plastic deform. effect on discontinuous precipitation 0-3053  
 Al-Ag alloys, critical resolved shear stress 0-49296  
 Al-Ag liquid alloys, diffusion of Ge, mechanism (*Russian*) 0-15276  
 Al-Ag mirror for use as solar reflector, co-sputtering 0-20789  
 Al-Cu-Mg-(Ag), effect of addition on fatigue microstructure relationships 0-40483  
 Al-Cu(Zn, Ag, Mg<sub>2</sub>Si), intermediate precipitates, stability, X-ray, elec. resist. and hardness study 0-3063  
 Al-Mg-(Ag), effect of addition on fatigue microstructure relationships 0-40483  
 Au-Ag, appl. of self-consistent cluster Bethe lattice study of two-band alloy model 0-29303  
 Au-Ag, cold worked, impurity conc. rel. to internal friction Bordoni peak, solid soln. hardening mech. 0-16363  
 Au-Ag, radiation damage and diffusion 0-24645  
 Au-Ag, surface segregation, electronic theory, density of states, cluster-Bethe-lattice approx. 0-49369  
 Au-Ag, thin film struct., Rutherford backscattering spectrometry, signal overlap subtraction 0-50486  
 Au-Ag-Cu, optical props. study using automatic nulling spectroellipsometer 0-55058  
 Au<sub>x</sub>Ag<sub>1-x</sub>, density of states and resist., CPA calc. 0-24780  
 Au<sub>2.5</sub>Ag<sub>2.5</sub>Cd<sub>47.5</sub>, pseudoelastic behaviour associated with thermoelastic martensitic transform. 0-16304  
 Cs-Ag, dil., electronic struct., density functional approach 0-44492  
 Cu-Ag (8 wt.%), plastic deform. effect on discontinuous precipitation 0-3053  
 Ge-Ag film, codeposited, amorphous and polycryst., struct. and elec. props. 0-24766  
 Hg-Ag-Sn, dental amalgams, corrosion penetration in crevices 0-3238  
 LaAg, Tb and Pr substituted, superconductors, cryst. field transitions linewidths 0-24854  
 LaAg,In<sub>1-x</sub>, crystal struct., neutron diffr. obs. 0-49187  
 La<sub>1-x</sub>Gd<sub>x</sub>Ag, antiferromagnet, spin echo NMR anal. 0-15821  
 La<sub>1-x</sub>Tb<sub>x</sub>Ag, paramag. anisotropy of Tb<sup>3+</sup> in cubic cryst. field 0-15687  
 Mg-Ag-Cu, phase comp. in Mg-rich region (*Russian*) 0-40331  
 Ni-Ag alloy, metallographic struct. and formability (*German, English*) 0-30201  
 Ni-Cu alloy, surface comp. and catalysis 0-54489  
 Pb-Ag, diffusion of Au, de-enhancement by Ag impurities 0-19990  
 Pb-In-Ag, transport current distribution in longitudinal mag. field 0-25057  
 Pd-Ag, Fermi energy influence on soln. behaviour of H, B and C (*German*) 0-44323  
 Pd-Ag, influence of adsorbed H on positron lifetime spectra 0-25480  
 Pd-Ag, thin layer, deposited on glass or Si substrate, X-ray microanalysis (*French*) 0-50902  
 Pd-Ag electrical resistivity, thermo-EMF and thermal diffusivity at high temps. (*Russian*) 0-6808  
 Pd-Ag microwires, electrical resistance, influence of gaseous environment in heat treatment (*Russian*) 0-20146  
 Pd-Ag-Si alloys, amorphous, crystn. kinetics, DSC meas. 0-1933  
 Pd<sub>0.96</sub>Ag<sub>0.04</sub>, phonon dispersion curves at 296K 0-24546



## silver alloys continued

- PdAg<sub>1-x</sub>, possibility of superconductivity 0-10862.  
 PdAgFe, ferromag., Curie temp. depend. on susceptibility, non-mean field theory 0-44829  
 Sn-Sb-Ag, splat cooled foils, TEM study 0-40344  
 Tb<sub>2</sub>Ag<sub>18</sub>, amorphous, mag. aftereffect 0-20435  
 YbPd-YbAg system, valency state, Yb behaviour (*French*) 0-45277

## silver compounds

- AgBi(CrO<sub>4</sub>)<sub>2</sub>, synthesis, thermolysis, crystallography (*French*) 0-33946  
 $\beta$ -Al<sub>2</sub>O<sub>3</sub>-Ag<sub>2</sub>O, antiferroelectric transformation, Potts' model universality class 0-50277  
 chalcopyrites, refr. index dispersion 0-55057  
 glycine silver nitrate, dielec. relax. in paraelec. and ferroelec. phases 0-29678  
 halide dry materials for laser printing appls. 0-13179  
 halide emulsion colouring, k-value and sensitivity relationship (*German*) 0-7815  
 halide photochromic centres in glass, isothermal relax. kinetics 0-16072  
 halide photochromic glass, optically induced anisotropy 0-1282  
 halides:Cu, in photochromic glass, formation and theoretical models, review 0-43418  
 halides, anal. of cryst. binding and Anderson-Gruneisen parameters 0-15040  
 halides calc. of heat of fusion using quantum mechanical relations 0-6491  
 thioamides, precip., electron microscope and potentiometric studies, growth of photosensitive crystals. 0-33107  
 (Ag, Tl, Ca)NO<sub>3</sub>, aqueous solutions, vapour press. meas. 0-6504  
 Ag complexes, Ag(II) porphyrins, picosec. flash photolysis, transient absorpt. 0-52976  
 Ag halide emulsions, induced sensitized photodichroism 0-9061  
 Ag halides in thioamides, precip., electron microscope and potentiometric studies, growth of photosensitive crystals. 0-33107  
 Ag photographic films, thermal development (*Russian*) 0-303  
 Ag-AgCl reference electrode, construction and thermodynamic props., high temp. aq. environment appl. 0-21288  
 Ag-AgCl/KCl/AgCl-Ag thermocell, and thermal liq. junction pot. for KCl solns. at high temp. 0-16819  
 Ag-Ge-S glasses, X-ray determ. of struct. (*Japanese*) 0-10501  
 Ag-S solid solution, grain boundary segregation and S diffusion in Ag 0-25700  
 Ag<sub>3</sub>AsS<sub>3</sub>, proustite, light effects on dielec. props., elec. resist. 0-49816  
 Ag<sub>3</sub>AsS<sub>3</sub>, proustite, structural changes in low temp. phase transition, NQR study 0-19935  
 Ag<sub>3</sub>AsS<sub>3</sub>, proustite upconverter, effect of temp. on phase match angle characts. 0-5799  
 Ag<sub>3</sub>AsS<sub>3</sub>, SHG, absorpt. coeffs. and temp. variation of refr. index difference 0-14390  
 Ag<sub>7</sub>As<sub>6</sub>, thermal, crystallographic and elec. props. (*French*) 0-40338  
 Ag<sub>7</sub>Se<sub>6</sub>, thermal, crystallographic and elec. props. (*French*) 0-40338  
 AgBi(CrO<sub>4</sub>)<sub>2</sub>, cryst. struct., neutron diffr. time-of-flight study (*French*) 0-15057  
 AgBr, activation parameters of mass transfer process by radiochemical meas. (*German*) 0-38974  
 AgBr, crossed elec. and mag. fields, hot electrons, streaming motion and population inversion 0-44649  
 AgBr, electron-hole liquid, RPA calcs. 0-6743  
 AgBr, evaporated layer, influence of sublayer on stability and photographic characteristics (*Bulgarian*) 0-42281  
 AgBr evaporated layers, spectral sensitization using cyanine dyes 0-26035  
 AgBr, evaporated layers, use as registering system (*Bulgarian*) 0-52344  
 AgBr, exciton absorpt. at high excitation rates 0-2343  
 AgBr, exciton relaxation by intervalley scattering 0-20644  
 AgBr grains, photographic emulsion, sensitivity centre variation with grain size 0-9055  
 AgBr grains, photographic emulsion, grain diameter dependent development probability 0-9056  
 AgBr luminescence/wavelength relationship visible and near IR spectra (*Russian*) 0-50422  
 AgBr melts, surface energy and surface tension coeffs., effect on photographic emulsion microcryst. growth rate (*Russian*) 0-47132  
 AgBr, microcrystals, activation energy for ionic cond. 0-34237  
 AgBr, new shoulder in luminesc. spectra, triplet excitons 0-20706  
 AgBr, nucl. emulsion, latent image form., grain diameter depend. 0-9453  
 AgBr, polar semiconductor, electron-hole liquid, electron-phonon interactions 0-6739  
 AgBr, quadrupolar deformability theory by tight binding method 0-10614  
 AgBr single-crystal IR optical fibres, growth from melt 0-53449  
 AgBr, streaming cyclotron motion of hot electrons, at intense microwave fields 0-6703  
 AgBr, vacuum deposition of Ag, growth mechanism 0-35095  
 AgBr:Cl, exciton-phonon interaction, reson. Raman scatt. vs photolum. 0-29798  
 AgBr:Li<sup>+</sup> (Na<sup>+</sup>), impurity induced IR absorpt. 0-7386  
 AgBr:Pd(II), photolysis-induced trapping behaviour, EPR study 0-54949  
 AgBr-AgCl, mixed crystals, pure and I doped, lattice defect parameters, Frenkel defect form. energy, ionic cond. 0-44359  
 AgBr-Li<sup>+</sup> (Na<sup>+</sup>), local mode freqs., Green's function calc. 0-39237  
 (AgBr)<sub>3</sub>, gas, He(I) photoelectron spectra 0-43103  
 AgBr(I) crystals, luminesc. of individual microcrystals (*Russian*) 0-301  
 AgCl, activation parameters of mass transfer process by radiochemical meas. (*German*) 0-38974  
 AgCl, crossed elec. and mag. fields, hot electrons, streaming motion and population inversion 0-44649  
 AgCl, luminescence/wavelength relationship visible and near IR spectra (*Russian*) 0-50422  
 AgCl melts, surface energy and surface tension coeffs., effect on photographic emulsion microcryst. growth rate (*Russian*) 0-47132  
 AgCl, paramagnetic S-centres, saturation props., ESR meas. 0-50181  
 AgCl photochromic glass, additional absorpt. spectrum, ellipsoidal model of colour centres 0-40142  
 AgCl, quadrupolar deformability theory by tight binding method 0-10614  
 AgCl, surface crystallisation, due to colloid adsorption 0-54544  
 AgCl:CdCl<sub>2</sub>, point defect model, free energy and radial distrib. functions 0-44201  
 AgCl:Ni, double quantum EPR transition, superhyperfine struct. 0-7154

## silver compounds continued

- AgCl:Ni, optically detected double resonance, radiative recombination electron traps 0-20518  
 AgCl-AgNO<sub>3</sub>, eutectic mixture, estimation of impurity distrib. coeffs. 0-55290  
 AgCl-NaCl molten solns., activities and surface tension 0-10748  
 (AgCl)<sub>3</sub>, gas, He(I) photoelectron spectra 0-43103  
 AgCl:Br<sub>1-x</sub>, binary melt, Ag solubility, temp. and conc. depend. 0-10677  
 AgClO<sub>3</sub>, <sup>35</sup>Cl NQR spectrum under press. at 311 K 0-11291  
 AgClO<sub>3</sub>, mol. torsional oscils., cooperative study by NQR 0-25244  
 AgClO<sub>3</sub>, structural phase transition, <sup>35</sup>Cl NQR meas. 0-15819  
 AgCrS<sub>2</sub>, mixed conductor props. 0-44675  
 AgF<sub>2</sub>, high press. modification, cryst. and mag. props. 0-38988  
 AgFeSe<sub>2</sub>, thermographic investigation of phase transitions (*Russian*) 0-10661  
 AgFeTe<sub>2</sub>, Mossbauer parameters in phase-transition region 0-11308  
 AgFeTe<sub>2</sub>, thermographic investigation of phase transitions (*Russian*) 0-10661  
 AgGaS<sub>2</sub>, iso-index coupled-wave electrooptic filter 0-1324  
 AgGaSe<sub>2</sub>, SHG, absorpt. coeffs. and temp. variation of refr. index difference 0-14390  
 $\beta$ -Ag<sub>2</sub>GeSe<sub>6</sub>, X-ray cryst. struct. determ. (*French*) 0-39020  
 Ag<sub>2</sub>GeTe<sub>4</sub>, optical props. and polymorphism 0-45082  
 AgH, relativistic (non-relativistic) HF one-centre expansion calcs. 0-52908  
 Ag<sub>2</sub>HgI<sub>4</sub>, disordered multicomponent solid solutions conc. fluctuation waves, microscopic theory 0-44327  
 $\beta$ -AgI (4H), visible spectra, reflected light phase and amplitude, exciton resonance 0-45110  
 AgI aerosols, particle size influence on cryst. struct. 0-2000  
 AgI, B1 phase, high press. elastic props., thermally activated rel. anomaly 0-44261  
 AgI, colloid seeding expts., Fujian province, China (*Chinese*) 0-46235  
 AgI, conductivity, hopping system, master equation 0-39348  
 AgI hydrosols, appl. of radiometric method for particulate processes characterisation 0-45579  
 $\alpha$ -AgI, ionic cond. in 8-40 GHz range 0-44358  
 AgI large single crystals, gel and soln. growth and props. 0-35071  
 $\beta$ -AgI, luminesc. of 2H- and 4H-polytypes 0-2843  
 $\alpha$ -AgI, neutron powder diffr. meas. interpretation 0-10533  
 $\alpha$ -AgI, neutron scatt. expts., Ag<sup>+</sup> ion motion 0-6552  
 AgI, phase transition, statics and local dynamics, mean field and Mori theory 0-39347  
 $\beta$ -AgI, polariton dispersion curves, Raman spectra 0-29338  
 AgI, quadrupolar deformability theory by tight binding model 0-10614  
 $\alpha$ -AgI, single particle and collective aspects of Ag<sup>+</sup> ion motion 0-6553  
 AgI solid electrolyte  $\alpha$ -phase stabilisation 0-29209  
 $\alpha$ -AgI, state of order, config. model 0-6390  
 $\alpha$ -AgI, superionic, continuous order-disorder transition, Raman spectroscopic evidence 0-45070  
 $\alpha$ -AgI, superionic conductor, microwave absorption spectrum 0-11515  
 AgI, superionic conductor, density of valence states, photoelectron spectra meas. 0-25523  
 $\alpha$ -AgI, superionic conductor, struct. and dynamics, two-dimens. mol. dynamics model 0-49413  
 $\alpha$ -AgI, superionic conductor, soft-core model, Monte Carlo study 0-54430  
 $\alpha$ -AgI, superionic phase, struct., X-ray scatt. anal. 0-28983  
 AgI, surfactant adsorpt., electrokinetic investig. 0-3363  
 $\beta$ -AgI thin film, exciton spectrum 0-55216  
 B-AgI, X-ray diffuse scattering 0-14964  
 AgI/polyamine iodide solid electrolytes, conc. depend. of elec. cond. 0-24647  
 AgI-AgCl, eutectic mixture, estimation of impurity distrib. coeffs. 0-55290  
 AgI-AgNO<sub>3</sub>, eutectic mixture, estimation of impurity distrib. coeffs. 0-55290  
 AgI-based solid electrolyte cell discharge mechanism 0-35663  
 AgI-type solid electrolytes, introductory survey 0-6549  
 (AgI)<sub>3</sub>, gas, He(I) photoelectron spectra 0-43103  
 (AgI)<sub>3</sub>(Ag<sub>2</sub>O.B<sub>2</sub>O<sub>3</sub>)<sub>1-x</sub> glass, ionic cond. and disorder modes 0-39344  
 AgIO<sub>4</sub>, chem. shift, NMR obs. 0-48015  
 Ag<sub>2</sub>I<sub>2</sub>PO<sub>4</sub> film formation from electrolysis of HI-H<sub>3</sub>PO<sub>4</sub> soln., electrocodepositional method 0-55315  
 Ag<sub>2</sub>I<sub>2</sub>PO<sub>4</sub>, solid electrolyte, ionic cond. meas., 4-79°C 0-54433  
 AgInS<sub>2</sub>-SnS<sub>2</sub>, spinel phase Ag<sub>x</sub>In<sub>1-x</sub>Sn<sub>1-x</sub>S<sub>2</sub> obs., stoichiometry (*French*) 0-44326  
 Ag<sub>2</sub>MoO<sub>4</sub>, cathodic props. in Li primary batteries 0-3502  
 AgN<sub>3</sub>, dielec. breakdown by elec. induced chem. decomposition 0-20586  
 AgN<sub>3</sub> pyrolysis, 513 to 558 K 0-7787  
 AgNO<sub>3</sub> melt, contact with glass, conc. changes in surface layer 0-44372  
 AgNO<sub>3</sub> melt, diffusion of silver into Na<sub>2</sub>O.2SiO<sub>2</sub> glass 0-44371  
 AgNO<sub>3</sub>-NaNO<sub>3</sub> mixed melts containing Na<sub>2</sub>O-SiO<sub>2</sub>-Ga<sub>2</sub>O<sub>3</sub>-Al<sub>2</sub>O<sub>3</sub> glasses, ion exchange 0-21282  
 AgNO<sub>3</sub>-NaNO<sub>3</sub> mixture, contact with glass, conc. changes surface layer 0-44372  
 AgNa mordenite, chemisorpt. of CO and H<sub>2</sub> 0-2752  
 AgNaNO<sub>3</sub>, ferroelectric transitions, one-mode model 0-29702  
 AgNa(NO<sub>3</sub>)<sub>2</sub>, ferroelectric transitions, group theoretic comparison with NaNO<sub>3</sub> 0-7311  
 AgNbO<sub>3</sub>, cryst. growth and phase transitions 0-40243  
 AgNbO<sub>3</sub>, single crystals, flux growth, space group determ. 0-55282  
 Ag<sub>2</sub>O-B<sub>2</sub>O<sub>3</sub> glasses, electrical props. and dielectric relaxation (*Japanese*) 0-20199  
 Ag<sub>2</sub>Rb(PO<sub>4</sub>)<sub>2</sub>, struct., density and elec. cond. 0-33952  
 $\beta$ -Ag<sub>2</sub>S, fast-ion conductor, Ag ion density, neutron diffr. study 0-34234  
 Ag<sub>2</sub>S, liquid, ionic and electronic cond., thermoelec. power 0-39329  
 Ag<sub>2</sub>S-As<sub>2</sub>S<sub>3</sub>-AgI glasses, temp. and comp. depend. of ionic cond. (*French*) 0-34229  
 Ag<sub>2</sub>SI, superionic cond., phase transition and cryst. structs., sp. ht., neutron and X-ray diffr. obs. 0-10662  
 Ag<sub>2</sub>SbS<sub>4</sub>, electron absorption and dispersion of ultrasound velocity 0-15197  
 Ag<sub>2</sub>Se, liquid, ionic and electronic cond., thermoelec. power 0-39329  
 Ag<sub>8</sub>SnSe<sub>6</sub>, cryst., Hall effect investigation of polymorphic transform. 0-39605  
 Ag(Tl)/AgI/Ag(Tl) cell, thermo-EMF of highly conducting solid electrolytes 0-24659  
 AgTaO<sub>3</sub>, single crystals, flux growth, space group determ. 0-55282  
 Ag<sub>2</sub>Te, liquid, ionic and electronic cond., thermoelec. power 0-39329  
 Ag<sub>2</sub>TeO<sub>4</sub>, cathodic props. in Li primary batteries 0-3502



## silver compounds continued

- Ag<sub>2</sub>UO<sub>2</sub>(NO<sub>3</sub>)<sub>3</sub>, fluoresc. decay rates, temp. depend. 0-25429  
 Ag<sub>2</sub>WO<sub>4</sub>, cathodic props. in Li primary batteries 0-3502  
 AgX, XX (*Russian*) 0-293  
 AgZr<sub>2</sub>(PO<sub>4</sub>)<sub>3</sub> system, phase charact. at different temps. 0-29936  
 β-Al<sub>2</sub>O<sub>3</sub>-Ag<sub>2</sub>O, cryst. structs. of stoichiometric and non-stoichiometric phases by X-ray diffr. (*French*) 0-28987  
 β<sup>+</sup>-Al<sub>2</sub>O<sub>3</sub>-Ag<sub>2</sub>O, Raman scatt. from mobile cations 0-11394  
 β-Al<sub>2</sub>O<sub>3</sub>-Ag<sub>2</sub>O, superionic conductor, microwave absorption spectrum 0-11515  
 Cd<sub>1-x</sub>Ag<sub>x</sub>Cr<sub>2</sub>Se<sub>4</sub>, Ag acceptor states effect on exchange interaction 0-20397  
 CuAg<sub>3</sub>I<sub>4</sub>, co-ionic cond. obs. 0-34231  
 Cu<sub>1-y</sub>Ag<sub>y</sub>InS<sub>2-x</sub>Se<sub>2x</sub>, for solar photovoltaic cells 0-10982  
 Cu<sub>1-y</sub>Ag<sub>y</sub>InS<sub>2(1-x)</sub>Se<sub>2x</sub> pentenary alloy system, appl. to photovoltaic solar-energy conversion 0-35680  
 CuBr-AgI system, ionic cond. and phase diagram 0-2198  
 RbAg<sub>4</sub>I<sub>6</sub>, phase transition, statics and local dynamics, mean field and Mori theory 0-39347  
 Se-Ag<sub>2</sub>Se, heterojunction with memory, transient switching characteristics 0-44718  
 Se-Ag<sub>2</sub>Se, heterojunction, electrically controlled negative differential conductance, mechanism 0-44720

## SIMS see secondary ion mass spectra; secondary ion mass spectroscopy

## simulation

- see also aerospace simulation; analogue simulation; brain models; digital simulation; hybrid simulation; modelling; physiological models; plasma simulation; semiconductor device models  
 air-based solar heating systems with phase-change energy storage, performance anal. using computer simulation 0-35762  
 atmosphere O<sub>3</sub> production transport and distribution, numerical simulations with global general circulation model 0-56544  
 Baneberry nucl. explosion, numerical simulation 0-841  
 bond graph fluid line models for inclusion with dynamic systems simulations 0-27136  
 cardiac activity signal simulator 0-56230  
 ceramics, ion beam irradiation techniques for simulation of 14 MeV neutron irradiation 0-10584  
 chemical system far from equilibrium, stochastic simulation 0-3339  
 clusters of galaxies, velocity dispersion profiles of N-body simulations 0-21908  
 clusters of galaxies compared with N-body simulations, masses and mass segregation 0-22091  
 coil, AC loss meas. in superconducting wires 0-37050  
 composite fracture with bonding strength defects between components, computer simulation 0-11771  
 cosmic rays, scatt. in simulated interplanetary mag. field fluctuations 0-51626  
 Coulomb friction in mechanical systems, overview 0-53723  
 dielectric charge carrier drift simulation using stochastic graphs 0-15539  
 diffusion, chemical, highly defective solids, steady-state computer simulation method for lattice gas 0-49401  
 dilute aqueous solutions, Monte Carlo studies of struct., review 0-54101  
 disturbed cell renewal systems, simulation by microprocessor system 0-35859  
 electron interactions, low-energy, single and twin biological targets 0-12195  
 FBR blanket, integral neutron reaction rate meas., in FBBF facility 0-22887  
 galaxy clustering N-point simulations, covariance function 0-31373  
 galaxy merging, cosmological N-body simulations 0-56922  
 geothermal reservoir simulation, math. models 0-12446  
 geothermal reservoir simulation, numerical soln. techniques 0-12447  
 geothermal steam pipeline network, numerical simulation 0-40822  
 heat storage in porous medium with circulating heat transfer fluid, solar system appl. (*French*) 0-40916  
 high current density magnet, thermal stability 0-37057  
 hourly global radiation sequences, stochastic simulation 0-36382  
 Keplerian systems, computer simulations 0-26720  
 knee joint simulator, development 0-17190  
 light source coherence meas. and fibre modal noise simulation by Michelson interferometer 0-48324  
 linac injection system beam dynamics 0-13989  
 LMFBR fuel assembly, 19 pin, simulation of flow blockage 0-582  
 LMFBRs, mixed Na convection problems, digital model simulation (*French*) 0-42737  
 magnetospheric simulation expts. 0-46347  
 membrane potentials, meas. in ionic environment, biological membrane simulation 0-3412  
 merging galaxies, numerical simulations 0-36716  
 microwave hyperthermia simulation (*French*) 0-3770  
 Monte-Carlo simulation of photon transport in a heterogeneous phantom 0-26257  
 Morishita neurons, modelling networks, cerebellum appl. 0-30703  
 nucleation in finite systems, theory and computer simulation 0-26038  
 optical simulator, for UHF antennas 0-26742  
 pattern generation in lobster stomatogastric ganglion, pyloric network simulation 0-12076  
 polymer, molecular dynamics simulation of struct. 0-28923  
 random coil polymer chain relax., lattice model with excluded vol., head movement rules 0-5642  
 random vibrations, wide-band, automatic system 0-53730  
 reactor fuel pin simulators for thermodynamic expts. with nucl. fuel elements 0-37420  
 rotation, contrib. from galaxy merging 0-4439  
 scintillation-camera simulator for remote-data acquisition testing 0-46020  
 solar central receiver plant, dynamic simulation of thermal-hydraulic characts. of Na-cooled plant 0-30400  
 solar collectors, tubular, computerised performance simulation 0-55903  
 solar power, heating systems, performance mathematical simulation for optimal dimensioning (*German*) 0-26110  
 solid-liquid interface, optical methods of study (*French*) 0-7318  
 star clusters containing massive central black holes, dynamical simulations with self-consistent potentials 0-26915  
 star formation process simulation, hydrostatic models evolution (*Polish*) 0-21998  
 strong ground motions along principal axes, simulation, 1971 February 9 San Fernando earthquake appl. 0-3935  
 tissue substitute materials formulation, effective atomic numbers 0-17169  
 transonic flow simulation by tracking and blowing (*German*) 0-6081

## simulation continued

- turbulence, laboratory-generated, simulating atm. turbulence effects on optical propag. 0-9803  
 vibration simulating system optimisation 0-53729  
 vibration-simulating systems optimisation, rel. to efficiency and cost 0-53728  
 vibrations, random, wide-band, simulators design optimisation 0-53731  
 Cl<sub>2</sub>, liquid-vapour surface, computer simulation 0-54478  
 N<sub>2</sub>, liquid-vapour surface, computer simulation 0-54478  
 O and O<sub>2</sub>, distrib. in lower thermosphere assuming tidal effects, one dimens. nonstationary diffusion-photochemical model 0-4160  
 O I 6300 Å nightglow, simulation rel. to neutral atmosphere parameters var. (*Portuguese*) 0-41584  
 UO<sub>2</sub> pellet compliance model based on out-of-pile simulation 0-42753

## simulation, digital see digital simulation

## simulators see simulation

## Sinanoglu's theory see atomic structure

## sinks, heat see heat sinks

## sintering

## see also densification

- α-Al<sub>2</sub>O<sub>3</sub>, production rel. to props. of dense corundum refractories 0-25627  
 alloy powder, two component, sintering 0-20847  
 carbide fuels, vibro-compacted, initial stages of sintering and hot-pressing 0-16254  
 ceramic, sintering kinetic laws with involvement of a liq. phase 0-55335  
 ceramic fuels, vibro-compacted, initial stages of sintering and hot-pressing 0-16254  
 ceramics, technique for studying internal and external gas pressure within pores 0-11606  
 ceramics acid-resistant, based on Artemov clay and obsidian 0-20852  
 coke, effect of addition of borides on hot-pressing 0-40282  
 conf., Dubrovnik, Yugoslavia, (Sep. 1977) 0-17719  
 diffusion controlled sphere-sphere sintering, simulation 0-20814  
 electrical contact materials, sintered materials based on powder metallurgy and powder composites 0-29902  
 ferrite spinel, DC resistivity depend. on substitutions 0-44565  
 glass powders, theoretical aspect of sintering 0-20883  
 grain growth, chem. driven, during liq. phase sintering, computer simulation 0-55427  
 kyanite-sillimanite concentration, multistage and sintering, props. of refractory products 0-20867  
 liquid phase 0-16232  
 liquid phase sintering, elementary mechanisms, soln.-reprecipitation 0-50571  
 liquid phase sintering, expt. obs. of densification by sintering 0-11584  
 magnetic materials, sintering, structure and props., external mag. and elec. field influence 0-50570  
 metal, sintering of solids containing several dissolved gases 0-20836  
 metal, solid state sintering, compact length change 0-11593  
 metal powders, at 1 to 10 MPa, melting mechanism (*German*) 0-35122  
 metal supported crystallites, wetting in sintering and redispersion 0-24751  
 metals, surface oxide layer effects, oxide dissolution process, anal. 0-11588  
 mischmetal-Co-Cu-Fe-Mg, mag. props. 0-35353  
 mischmetal-Co-Cu-Mg, mag. props. 0-35353  
 Na<sub>2</sub>O-CaO sintering process, removal of S compounds for Al<sub>2</sub>O<sub>3</sub> production (*Chinese*) 0-55323  
 Ni powder 2JJ, porous, effect of sintering conditions in struct. and strength 0-20823  
 optical waveguides, inhomogeneous glass sintering, self stresses producing bulk flow 0-14448  
 particle dimension and shape evaluation by SEM 0-40278  
 perlite, low temp., processes occurring during firing 0-11607  
 Permalloy, pressing velocity effect on quality of compacts 0-20834  
 Permalloy powders, electric pulse shaping and sintering 0-25605  
 permanent magnet alloys manufacture, Co-mischmetal alloys (*Polish*) 0-35132  
 permanent magnets, development history, magnetic and physical props., appl. 0-29901  
 piezoelectric ceramics, bimorph element for loudspeakers manufacture (*Japanese*) 0-53597  
 porous materials, gas diffusion through pore during sintering 0-40281  
 porous materials, production method using stainless steel gauzes, exam. of hydraulic characteristics 0-16243  
 porous materials, sintered, mech. testing device for hydrostatic pressure conditions 0-40645  
 powder, apparatus for exam. sintering, electrical resistance 0-16217  
 powder, two component mixture, compact growth in liquid phase sintering 0-20835  
 powder consolidation process, exam. of quasimelt in pressing, sintering stages 0-20816  
 powder kinetics, variation of mechanism dependent exponent, with coordination number and neck size 0-20815  
 powder mixture electric-discharge sintering mass transfer and homogenization 0-20817  
 powdered metals, electric (*German*) 0-25598  
 powders, sintering, study of phase contacts formation in porous disperse structs. (*Russian*) 0-20811  
 powders and sintered bodies, particle size distributions from chord and area distributions (*German, English*) 0-35126  
 random structures, volume diffusion and creep effects 0-35125  
 rare earth magnetic materials, in controlled atmosphere, permanent magnets flux stability enhancement, gyroscope-based guidance systems performance improvement 0-50144  
 refractories, multichamotte, sintering additives effect on props. 0-35147  
 refractory metals, enhanced diffusion model for activated sintering 0-25612  
 rel. to powder metallurgy 0-20841  
 rel. to powder metallurgy 0-25611  
 SEM, qualitative and quantitative evaluation of void structures 0-16212  
 β-Sialon, high strength, reaction sintering 0-7525  
 β-Sialon compositions, reaction sintering obs. 0-55337  
 skinned sintering kinetics, cryst. surface calcs. (*Russian*) 0-40276  
 steel, C, autectic, sintered, isothermal transformation behaviour, porosity effects 0-3031  
 steel, Cr (13 wt.%), sintered, organometallic complex addition effects on mech. props. 0-25595



## sintering continued

steel, Cr-Ni, rolled and sintered, to produce capillary structured filter material, exam. of mech. props., and production 0-16235  
 steel, high speed, sintered, and wrought, type T6 strength and toughness 0-30102  
 steel, high speed, W-Mo-Co-Cr-V, production from atomized powder 0-20837  
 steel, low alloy, sintered, isothermal transformations, porosity effects 0-3032  
 steel, Mn-Cr-Mo, Mn-V-Mo, high-strength heat-treatable sintered 0-50575  
 steel, stainless, fibre reinforced porous coating, isostatically compressed for bone ingrowth 0-35134  
 texture anal. of sinter struct., appl. to Ca ferrites in sinters of rich Fe ores 0-18009  
 YIG, hot spraying to give fine, free flowing, sinterable powder 0-20865  
 Zircon ceramic, exam. of development and fabrication 0-11608  
 Ag, loosely packed powder, sintering SEM and dilatometry obs. 0-20843  
 Ag, solid state sintering, compact length change 0-11593  
 Ag, spherical powder, struct. of sintering necks in compacts 0-11594  
 Ag<sub>3</sub>Sn-Hg, metallic powder-liquid system, correlation between hardness and evolution and sintering states 0-25614  
 Al contacts sintering in vacuum and O<sub>2</sub>, room temp. 0-7512  
 Al powder, resist.-sintability (*Japanese*) 0-16228  
 Al sintering, low temp., form. of interparticle metallic contacts 0-20844  
 AlN, activating sintering process 0-25639  
 Al<sub>2</sub>xO<sub>3</sub>, sintered, elec. cond. temp. and comp. depend., thermoelec. power 0-2438  
 Al<sub>2</sub>O<sub>3</sub>, sintering, rate controlled 0-20871  
 Al<sub>2</sub>O<sub>3</sub>, derived from gels, sintering behaviour, microstruct. 0-20875  
 Al<sub>2</sub>O<sub>3</sub> powder, active, sintering 0-20870  
 Al<sub>2</sub>O<sub>3</sub>, sintered, electron microprobe anal. of impurity and additive distrib. 0-40359  
 Al<sub>2</sub>O<sub>3</sub>, sintering, calcination cond. effect (*German*) 0-16251  
 Al<sub>2</sub>O<sub>3</sub>, sintering behaviour, effect of calcination with mineralisers (*German*) 0-25622  
 Al<sub>2</sub>O<sub>3</sub> substrates, grain growth during sintering 0-40302  
 Al<sub>2</sub>O<sub>3</sub> targets manufacture, for vacuum thin film deposition (*German*) 0-11586  
 Al<sub>2</sub>O<sub>3</sub>-AlN phase diagram and reaction sintering of transparent cubic ALON spinel 0-25669  
 Al<sub>2</sub>O<sub>3</sub>-glass mixture, microstructural changes and shrinkage during sintering 0-25640  
 $\beta$ -Al<sub>2</sub>O<sub>3</sub>-Na<sub>2</sub>O-Li<sub>2</sub>O (8.85, 0.75 wt.%) pressing powders, prep. by spray drying 0-40294  
 Al<sub>2</sub>O<sub>3</sub>-Si<sub>3</sub>N<sub>4</sub> preparation, compressive strength 0-25634  
 Al<sub>2</sub>O<sub>3</sub>-ZrSiO<sub>4</sub> mixture, reaction sintering, correlation between densification and reaction 0-29911  
 $\beta$ -Al<sub>2</sub>O<sub>3</sub>(Na<sub>2</sub>O.11Al<sub>2</sub>O<sub>3</sub>), prep. by diffusional transform. during sintering of Al<sub>2</sub>O<sub>3</sub> in presence of NaAlO<sub>2</sub> 0-25637  
 B C powders, effect of C on sintering 0-40312  
 Bi<sub>2</sub>C<sub>3</sub>, sintering and subsequent high temp. annealing, struct. and props. 0-20858  
 BN ceramic with organosilicon polymer additions, strength and oxidation resistance 0-20880  
 BN, cubic, sintering technology and cutting performance of tools 0-29919  
 BN, wurtzite, chem. comp. and processing props. in prep. of Geksanit-R sinters 0-25632  
 Ba<sub>2</sub>Co<sub>2</sub>Zn<sub>2-2</sub>Fe<sub>2</sub>O<sub>22</sub>, mechanically oriented, topotactic prod. technique, mag. props. 0-35140  
 BaTiO<sub>3</sub>-Mn, polycryst., annealing effect on transition temps. 0-3100  
 Bi<sub>2</sub>GeO<sub>20</sub>, X-ray sensitive ceramic, sintering 0-25621  
 CC TaC based hard metal, non-stoichiometric sintering, mech. props. 0-25616  
 CaCO<sub>3</sub>-NaAlSiO<sub>4</sub>, micromechanism for phase formation during sintering (*Russian*) 0-16253  
 CaO sintering, Cr<sub>2</sub>O<sub>3</sub> addition effect (*Czech*) 0-45258  
 Ca<sub>10</sub>(PO<sub>4</sub>)<sub>6</sub>(OH)<sub>2-2</sub>O<sub>x</sub>□<sub>x</sub> polycryst. sintered bodies, prep. and thermal props. 0-25624  
 CaTiO<sub>3</sub>-CaTiSiO<sub>3</sub>, sintering and dielectric props. 0-40307  
 CdTe thick films, prep. by sintering and elec. props. 0-29451  
 Cr-C-Ni alloys, exam. of activated sintering 0-16241  
 Cr<sub>2</sub>O<sub>3</sub>, grain growth during sintering (*Japanese*) 0-16261  
 Cu alloys, reduction processes in sintering (*German*) 0-25597  
 Cu, in contact with <sup>3</sup>He, thermal conductance, rel. to elec. resist., heat flow model calc. 0-10728  
 Cu, loosely packed powder, sintering SEM and dilatometry obs. 0-20843  
 Cu, single crystal sintering model evaluation, Kossel interference and digital graphic simulation appl. (*German*) 0-2980  
 Cu, solid state sintering, compact length change 0-11593  
 Cu-Al, sintering, reduction processes, resist. meas. (*German*) 0-25597  
 Cu-Al-Ni, mixed powder compacts, Ni content influence in sintering behaviour (*Japanese*) 0-35130  
 Cu-Al-Ni (14, 8 wt.%),  $\gamma$ -martensitic, sintered high damping 0-50577  
 Cu-Ni, sintered, props. and degree of nonhomogeneity 0-20848  
 Fe alloy electrodes, rolled from powders, sintering problems 0-25608  
 Fe and Fe-C, (0.8 wt.%), sintered, hot forging and chemothermal treatment, effect on wear resistance 0-25606  
 Fe atomized powder, sintering effect on recryst., mech. props. 0-40292  
 Fe, carbonyl pore struct. orientation, shrinkage anisotropy effect 0-20845  
 Fe, operating performance, effect of polymer and graphite lubricant additives 0-11785  
 Fe ore, agglomeration charge layer shrinkage (*Russian*) 0-16224  
 Fe ore concentrates, two-layer charge, sintering conditions (*Russian*) 0-45248  
 Fe Powder, resist.-sintability (*Japanese*) 0-16228  
 Fe powder, sponge and atomized types, steam oxidation, pore closure and surface hardness 0-45441  
 Fe powder compacts, pressed under static or vibr. load, shrinkage anisotropy during sintering 0-50574  
 Fe, sintered, strength and elongation, rel. to density 0-30047  
 Fe, sintered and pressed, props., effect of atomized Fe powder particle size distrib. 0-11601  
 Fe sintered compact, shrinkage and mech. props., admixed zinc stearate lubricant effect 0-45402  
 Fe-C (2, wt.%), sintering shrinkage kinetics 0-20829  
 Fe-Cu, liquid phase sintering 0-16232  
 Fe-Cu-Ni-Cr<sub>2</sub>C<sub>3</sub>-C based sintered friction material, wear, surface geometry and struct. effects 0-25875

## sintering continued

Fe-Ni heterogeneous alloys, ferrite, martensite and austenite phase distrib., effect on mech. props. 0-45363  
 Fe-SiO<sub>2</sub>-Al<sub>2</sub>O<sub>3</sub> Lisakovskii concentrate mixture, sintering process, temp. thermal treatment (*Russian*) 0-55317  
 Fe-VC-WC(TiC), sintering, densification 0-25615  
 Fe-WC-VC(TiC), sintering, densification 0-25615  
 Fe<sub>2</sub>O<sub>3</sub>, sintered metallised compacts, pore struct. by Hg porosimetry 0-40280  
 Ge<sub>2</sub>Si<sub>70</sub>, hot press sintering 0-50572  
 Li<sub>2</sub>K(IO<sub>3</sub>) in LiIO<sub>3</sub>-KIO<sub>3</sub> system, lattice parameter, equilb. and metastable phase diagram (*Chinese*) 0-7538  
 Li<sub>x</sub>Ni<sub>1-x</sub>O (x=0 to 0.03), solid soln. effect of Li on densification during sintering 0-25638  
 MgO, lattice defects, calcination temp. effect 0-15091  
 MgO powder, active, sintering 0-20870  
 MgO, sintering, effect of Ca compound additions (*Japanese*) 0-55340  
 MgO/Ni-Cr (80, 20 wt.%) cermet, sintered, elec. resist. temp. effect 0-3206  
 MgO-CaO-Fe<sub>2</sub>O<sub>3</sub>-Al<sub>2</sub>O<sub>3</sub>-SiO<sub>2</sub>, clinker production from dolomite and magnesite 0-55339  
 Mn<sub>2</sub>SiO<sub>3</sub>, effect of vibration during sintering, on electrical resistivity 0-16258  
 MnZn ferrite fabricated by hot isostatic pressing, recording head appl. 0-35139  
 Mo, powder, defective structure and activated sintering, exam. 0-16240  
 Mo, sintered, fusion reactor blanket struct. material, low cycle fatigue behaviour 0-30073  
 Mo sintered composite, MoS<sub>2</sub> containing, friction and wear props. 0-11786  
 Mo-Mn powder mixture, X-ray diffr. exam. of reaction between Mo and Mn, during sintering 0-16242  
 MoSi<sub>2</sub>, ceramic additives effect on sintering, recrystallisation 0-40306  
 MoSi<sub>2</sub>, self-propag. high-temp. synthesised, sintering and props. 0-11616  
 Mo(ZrO<sub>2</sub>-La<sub>2</sub>O<sub>3</sub>) structural changes during reduction and sintering 0-25636  
 Na- $\beta$ -Al<sub>2</sub>O<sub>3</sub> ceramics, synthesis 0-40305  
 Ni dispersions, semi-amorphous, on Al<sub>2</sub>O<sub>3</sub>-graphite, mag. characterisation 0-44876  
 Ni, high temp. plasticity, oxide inclusion effect 0-50681  
 Ni powder, porous, relationships between mech., physical, and microstructural characts. 0-20846  
 Ni powder, resist.-sintability (*Japanese*) 0-16228  
 Ni powder, sintered, use of extruded porous materials as fuel cell electrodes 0-40853  
 Ni, powder, subjected to vibratory milling, exam. of plastic deformation, recrystallisation, sintering 0-16234  
 Ni-Co-Cr-Al-Ti-Mo superalloy IN738, casking porosity removal using hydrostatic press. sintering 0-55322  
 Ni-Cr-Co-Ti, superalloy sintering thermochemical surface treatment 0-25617  
 Ni-W sintered powder pressings, intermetallic phases (*Russian*) 0-55349  
 PbTiO<sub>3</sub>-Pb(Fe<sub>1/2</sub>Nb<sub>1/2</sub>)O<sub>3</sub>-PbZrO<sub>3</sub>, with additions, exam. of electrical characteristics 0-2698  
 Pb(Zr,Ti<sub>1-x</sub>)O<sub>3</sub>, high density, sol-gel technique prep., piezoelec. props. 0-20596  
 Pd sponge powder, sintering shrinkage kinetics 0-29900  
 Si-Al-O-N sintered ceramic, microstruct., phase composition and transformation mech., mech. props. 0-40309  
 Si-Al(Ti)C, sintered, exam. of props. 0-25644  
 Si<sub>6-7</sub>-Al<sub>2</sub>O<sub>3</sub>-N<sub>8-9</sub>,  $\beta$ -Sialon, form. from Si<sub>3</sub>N<sub>4</sub>-SiO<sub>2</sub>-AlN system (*Japanese*) 0-45261  
 SiC, electrode and container material in Na/S cell 0-35355  
 SiC, self-bonded polycryst., electrophys. props. 0-10980  
 $\beta$ -SiC/Si abrasive resistant material, prep. and props. 0-20878  
 $\alpha$ -SiC-Al<sub>2</sub>O<sub>3</sub>, sintering 0-11611  
 Si<sub>3</sub>N<sub>4</sub>, reaction sintered, microstruct. charact. 0-35145  
 Si<sub>3</sub>N<sub>4</sub>, sintering in powder bed with addition of MgO sintering aid 0-29910  
 $\beta$ -Si<sub>3</sub>N<sub>4</sub> solid soln. prod. by reaction sintering SiO<sub>2</sub>-AlN mixture 0-25645  
 Si<sub>3</sub>N<sub>4</sub>/Al<sub>2</sub>O<sub>3</sub>, powder compact, electron microprobe investigation of reactions (*French*) 0-26009  
 Si<sub>3</sub>N<sub>4</sub>-SiC-Y<sub>2</sub>O<sub>3</sub> (La<sub>2</sub>O<sub>3</sub>)(Ce<sub>2</sub>O<sub>3</sub>)(Eu<sub>2</sub>O<sub>3</sub>)(Gd<sub>2</sub>O<sub>3</sub>), reactively sintered, microstruct. and strength 0-25631  
 Si<sub>3</sub>N<sub>4</sub>-Y<sub>2</sub>O<sub>3</sub>(Ce<sub>2</sub>O<sub>3</sub>), hot pressed, sintered, microstruct., flexural strength and fractographic anal. 0-40293  
 Si<sub>3</sub>N<sub>4</sub>-AlN-Al<sub>2</sub>O<sub>3</sub> system, reaction sintering forming  $\beta$ -Si<sub>3</sub>N<sub>4</sub> solid solns. 0-50585  
 Si<sub>3</sub>N<sub>4</sub>-15Y<sub>2</sub>O<sub>3</sub>, sintering under high N<sub>2</sub> pressure 0-29907  
 SiO<sub>2</sub>-Al<sub>2</sub>O<sub>3</sub>, mullite, sintering behaviour and microstruct. 0-20876  
 SiO<sub>2</sub>-Al<sub>2</sub>O<sub>3</sub> (36.6 wt.%) plasma prep. powder, metastable immiscibility and microstruct. during sintering 0-35143  
 SiO<sub>2</sub>-Al<sub>2</sub>O<sub>3</sub>-Cr<sub>2</sub>O<sub>3</sub> system, KT-11 type, chromia-containing material production based on high-silica glass fabric 0-45266  
 SiO<sub>2</sub>-Al<sub>2</sub>O<sub>3</sub>-RO-R<sub>2</sub>O type glass additions, sintering of porcelain bodies 0-45265  
 Sm(-Pr)-Co, sintered, cryst. phases (*Russian*) 0-39004  
 SmCo<sub>5</sub>, sintered permanent magnet manufacture 0-20838  
 Sm(Co<sub>0.86-x</sub>Cu<sub>0.14</sub>Fe<sub>x</sub>)<sub>7</sub>, permanent magnet, sintering and heat treatment effects 0-39817  
 SrO.nFe<sub>2</sub>O<sub>3</sub> isotropic ferrite magnets, manuf. process and mag. props. (*Japanese*) 0-29915  
 Ti, porous structure, change in presence of liq. phase (*Russian*) 0-16223  
 Ti powder, resist.-sintability (*Japanese*) 0-16228  
 Ti-Al (Sn), porous, effect of Al and Sn on sintering 0-20830  
 Ti-Al (4 wt.%), sintered, long-time strength 0-40529  
 Ti-Al system, compact growth in liquid phase sintering 0-20835  
 Ti-Si cosputtered films, silicide form., X-ray diffr. and resist. study 0-54546  
 TiC, sintering and grain growth, metallographic anal. 0-25642  
 TiC-Fe-Cr powder mixture, exam. of milling condition effects 0-16237  
 TiC-Ni powder compact, wetting problems in sintering 0-11596  
 TiC-Ni-Mo sintered hard alloy TN-20, fracture surfaces 0-7684  
 TiO<sub>2</sub>, sintering, struct., pressing, atm., and doping effects 0-20873  
 UC FBR fuel fabrication by reaction sintering of UO<sub>2</sub> and UC<sub>2</sub> 0-812  
 UO<sub>2</sub> micropore sintering, irradiated below 1100°C, in Winfrith SGHWR 0-5255  
 UO<sub>2</sub>, powder, sintering effect of compaction 0-20874  
 UO<sub>2</sub>, sintered, production by gel calcination and drying, thermal anal. (*Czech*) 0-45260



## sintering continued

- $\text{UO}_2$ , sintering, initial stage kinetics, diffusion coeff. 0-2987  
 $\text{UO}_2 + \text{Nd}_2\text{O}_3$ , sintering, initial stage kinetics, diffusion coeff. 0-2987  
W, powder, subjected to vibratory milling, exam. of plastic deformation, recrystallisation, sintering 0-16234  
W, powders, defective structure and activated sintering, exam. 0-16240  
W/Cu powders, liq. phase sintering, particle rearrangement 0-45253  
W-Cr powder alloys, sintering in presence of Cu-Ni liq. phase 0-16246  
W-Cu, porous material, skeletal type, produced by liquid phase sintering, exam. of mech. strength, determ. resistance 0-16245  
W-Fe-Co, sintering and mechanical props. (*Japanese*) 0-21086  
W-Ni, liquid phase sintering 0-16232  
W-Ni, liquid phase sintering 0-25613  
W-Ni compact, sintering behaviour and workability (*Japanese*) 0-20822  
W-Ni-Fe, W-Ni-Fe-Mo (Mn), sintering and mechanical props. (*Japanese*) 0-21086  
W-Ni-Fe 5(2), 5(2) wt.% pore formation, effect on mech. props. 0-45396  
WC powder, processing conditions 0-11614  
WC-Co and WC-Co-TaC-TiC-NbC cemented carbides, microstructure, high temp. deformation, uniaxial plastic compression 0-40451  
WC-Co from directionally carburized  $\text{WO}_3\text{-C-Co}_3\text{O}_4$  mixtures, sinking (*Japanese*) 0-11589  
WC-Co particles electrophoretic deposition, on metal surfaces, wear resistant coatings preparation (*German*) 0-2969  
WC-Co powder, prep. by direct carburisation of  $\text{WO}_3$  in presence of  $\text{Co}_3\text{O}_4$  0-50573  
WC-Co-C based hard alloy VK6, densification kinetics in hot pressing 0-11600  
W( $\text{ZrO}_2\text{-La}_2\text{O}_3$ ), structural changes during reduction and sintering 0-25636  
YAG, production of densely sintered ceramic, exam. of recrystallisation during sintering 0-11609  
 $\text{YCrO}_3\text{-MgCr}_2\text{O}_4$  sintered ceramics, elec. cond. 0-24927  
 $\text{Y}_2\text{O}_3$  powder, active, sintering 0-20870  
 $\text{Zn}_{1-x}\text{Ni}_x\text{Fe}_2\text{O}_4$ , heat treatment and sintering effect on porosity 0-25610  
ZnO electrode, for dye-sensitized solar photocell 0-16816  
ZnO-based ceramic microstructure and nonlinear props., B diffusion effects (*Russian*) 0-49423  
 $\text{ZrO}_{0.91}$ , sintered, strength charact. effect of struct. and substruct. 0-16260  
 $\text{ZrN-Al}_2\text{O}_3$ , sintering reaction thermodynamics 0-2989  
 $\text{ZrN-Mo}$ , cermet, sintering reaction thermodynamics 0-2989  
 $\text{ZrO}_2$  products from granules, props., prep. method effect 0-25628  
 $\text{ZrO}_2$ , stabilised, fabrication by hot petroleum drying method, X-ray diff. and thermal anal. study 0-40297  
 $\text{ZrO}_2$ , stabilized porous refractory, mech. strength 0-35322  
 $\text{ZrO}_2\text{-HfO}_2$ , monoclinic solid soln., ceramic prep. and use 0-55338

size, particle see particle size

## size effect

- field-emission cathode peak current, size effect 0-29863  
interactions due to static lattice displacements, continuum and lattice theory approach 0-39082  
many-valley semicond., size-induced changes in valley populations in strong elec. fields 0-6855  
metals, diffusion thermopower, boundary scatt. effect 0-6817  
metallic granules, electron work function interrelation with granule size 0-39660  
point defect interactions due to static lattice displacements, continuum and lattice theory approach 0-39082  
semiconductor film, size-quantised, EM wave absorpt. coeff. in coherent hypersonic wave field 0-29819  
semiconductor thin films, degenerate one-valley and many-valley, photogalvanic effect calcs. 0-34487  
small particles, cause of reduction in lattice spacing (*Russian*) 0-38967  
small superconductor in magnetic field, first and second order phase transitions 0-2519  
superconductor, intermediate state, magnetoacoustic size effect (*Russian*) 0-7047  
Ag, size effect, ballistic-type field penetration at 45 GHz, 3 MHz 0-44634  
Al, bicrystalline, RF size effect at intercryst. boundary (*Russian*) 0-29431  
Al, Sondheimer size effect, phonon-limited mean path, 1.8-12K 0-49698  
Al-Pb(Sn), liquid, surface tension, size effect (*French*) 0-15341  
 $\text{AlGa}_{1-x}\text{As-GaAs}$ , CW 300k quantum-well heterojunction laser, optical and injection pumping operation 0-5735  
Be wires and strips, elec. resist. at 77K, size factor (*Russian*) 0-24867  
Bi epitaxial films, size effect in elec. props. 0-54813  
Bi film, quantum size effect and band struct. Bi-dielec-metal system obs. 0-54811  
Bi thin wire, resist. anomaly, possibility of one-dimensional quantum size effect 0-54809  
CdS, acoustoelectronic current SHG 0-6916  
CdS, size effect of dense electron hole systems 0-7413  
Cu-Pb, liquid, surface tension, size effect (*French*) 0-15341  
Fe single crystals, size effect on slip deformation ability at very low temps. 0-21049  
 $\text{GaAs-Ga}_{1-x}\text{Al}_x\text{As}$  heterostructures, quantum size effect in superlattices, electronic props. 0-29471  
Ge, nonuniformly deformed, electron-hole drop density depend. on size (*Russian*) 0-20092  
InSb, film,  $E_0$ ,  $E_1$  absorption edge size quantisation, optical and electroreflectance spectra 0-34998  
 $\text{NaNO}_2$ , size effect and spin-lattice relax. of  $^{14}\text{N}$  0-20480  
 $\text{Ni}_{65}\text{Mo}_5\text{Fe}$ ,  $\text{O}_2$  effect on secondary recrystallisation and mag. props. 0-35201  
PbTe epitaxial films, quantum size effect, optical meas. 0-11121  
 $\text{SrCl}_2\text{-Gd}^{3+}$ , small dielec. particles, cryst. field size effects 0-44913  
W, RF size effect, surface electron scatt. influence (*Russian*) 0-2414  
Zn-Pb(Bi), liquid, surface tension, size effect (*French*) 0-15341

## skin

- auditory impedance changes elicited by tactile and electrocutaneous stimulation 0-56066  
biofeedback control of skin potential level 0-21572  
cancer induction by UV, evidence 0-35962  
cell survival derivation method using tissue damage obs. after fractionated irradiation 0-36016  
cellular survival kinetic parameters in rats after fractionated irradiation 0-21496

## skin continued

- collagenous tissues, flat, struct. theory for homogeneous biaxial stress-strain rels. 0-3695  
cumulative radiation effect, cell survival description 0-30771  
depth-dose relationships near the skin resulting from parallel beams of fast neutrons 0-30902  
elasticity of living dolphins (*Russian*) 0-45926  
electrical quantities, frog, method for in situ meas. 0-36208  
electrocuteaneous stimulation, information transmission characts. (*Japanese*) 0-35872  
epidemiologic monitoring, neutron activation anal. of trace elements in human skin lesions 0-17100  
epidermis, ultrastruct. stereology after X-irrad., rat tail expts. 0-36003  
epithelial stem cell survival parameters, considerations in use of mouse foot system 0-36017  
evaporimeter, anal. of performance 0-56256  
guinea pig keratinocytes and melanocytes in tissue culture, influence of electron microscope obs. on results 0-21583  
hand temperature self-regulation, assessment technique 0-16906  
immersion in various liquids, anal. of dynamic cold sensation (*Japanese*) 0-21448  
lesion Mn, Cu and Zn conc. meas. by neutron activation 0-17063  
melanoma therapy by laser irradiation (*German*) 0-12208  
neutron teletherapy, effects of filters and wedges on skin sparing and  $\gamma$ /neutron dose ratios 0-46029  
NMR of rat skin,  $^1\text{H}$  and  $^{13}\text{C}$  obs. 0-40965  
planarian, regeneration of epidermis and basement membrane after total-body X-irrad. 0-36022  
plastic surgery, biomechanical aspects 0-56103  
radionuclide absorption through damaged and undamaged skins of guinea pigs 0-26383  
RBE of mouse skin damage, pions<sup>-</sup> rel. to X-rays 0-26272  
reconstructive surgery, in-plane compressive strain limits prediction 0-41069  
rheological behaviour, expt. results and struct. model 0-16968  
rheological properties of skin components under compressive load 0-35945  
strain measurement in elastic thin membranes moire interferometry method, appl. to human skin 0-30828  
stratum corneum, human, linear meas. of water content using microwave probe 0-21518  
subcutaneous tissue gas space pressure during superficial isobaric counter-diffusion 0-30968  
T content in organs, and DNA of rat liver cells, after doses of tritiated food, protein or water 0-56226  
tactile sensation, mechanoreception physiology and psychophysics (*Japanese*) 0-16962  
temperature change rate effect on local sweating rate 0-35848  
temperature measurements using a disc sensor, effect of press. 0-56259  
temperature probe design, exptl. calibration results and numerical model predictions 0-56258  
tissue pH electrodes for clinical applications 0-36175  
transcutaneous  $\text{O}_2$  and skin blood flow, laser system for simultaneous meas. 0-26321  
undulation propagation rate, dolphin expts. (*Russian*) 0-45927  
UV irradiated human strain cells, herpes virus production as repair marker 0-30783  
UV light therapy for skin diseases 0-36057  
veins temperature increase due to subcutaneous perpendicular to surface 0-40970  
wheelchair sent evaluation by time-lapse and quantitative thermography of skin after sitting 0-51205  
X-irradiation, mech. and struct. response 0-35994  
X-irradiation combined with hyperthermia, fractionation studies 0-56138  
X-irradiation response of mouse tumour and skin, effect of heating order 0-3738  
X-ray and fast neutron damage, relationship between OER, RBE and no. of fractions 0-35978  
xeromammography, absorbed dose obs. 0-41242  
 $^{137}\text{Cs}$ -irradiation, fractionated high dose-rate and continuous low dose-rate effect on pig skin 0-41127  
T radiation dose absorbed in rat organs, after feeding with organically bound T 0-51262

## skin effect

- see also anomalous skin effect  
electroplasticity, skin effect 0-21046  
exploding foils, current distribution in LC circuit (*Russian*) 0-19628  
graphite, EPR, effect of motional averaging, anisotropy, skin effect rel. to heat treatment and neutron irradiation (*French*) 0-34752  
metals, with open Fermi surfaces, galvanomag. effects, static skin effect (*Russian*) 0-29389  
nuclear spin system, in spherical conductor, free induction decay and skin effect 0-2649  
polarity changes, skin effect of electrically conducting spherical shell 0-46389  
pyrocarbons, EPR, effect of motional averaging, anisotropy, skin effect rel. to heat treatment and neutron irradiation (*French*) 0-34752  
transients on hollow sphere in plane field of system of conductors (*German*) 0-37927  
Al wires, eddy current effects on NMR 0-2645  
Bi, static skin effect (*Japanese*) 0-15555  
Mo, skin effect, Gantmakher-Kaner effect peculiarities (*Russian*) 0-49796

## sky

- see also night sky; sky brightness  
clear daytime skies near Kitt Peak National Observatory, probability 0-12512  
cloudless, diffuse solar irradiance 0-51505

## sky brightness

- see also airglow; twilight  
background brightness meas., 4500-10600 Å (*Chinese*) 0-12540  
daytime sky, brightness oscills. rel. to stellar extinction oscills. 0-56606  
diffuse cosmic UV background, spectrum 0-17696  
dust loading of atmos., 1923-54, pyrheliometric and circumsolar sky radiation obs. 0-46240  
galactic 2 μm radiation, mean intensity in solar neighbourhood 0-36744  
light pollution over Jena, night sky brightening at Karl-Schwarzschild Observatory 0-51533  
phase problem in astronomy, sky brightness distrib. 0-46258  
Sacramento Peak Observatory, night sky brightness conditions 0-12545



- sky brightness** continued  
solar resonance radiation multiply scattered by nearby interstellar medium, backscattered intensity 0-41874  
UV, aerosol scattering albedo determ. using sky brightness meas. (*Russian*) 0-21822
- sky surveys** see *astronomical catalogues*
- Slater-type orbital calculations** see *STO calculations*
- sliderules** see *calculating apparatus*
- sliding contacts, electrical** see *electrical contacts*
- slip**  
see also *kink bands; plastic flow*  
BCC crystals in tension and compression, theoretical latent hardening 0-24459  
BCC metals, plastic deform., computer simulation 0-40456  
 $\alpha$ - $\beta$  brass, two phase bicrystal, deform. and fracture at 450K 0-16409  
 $\alpha$ - $\beta$ -brass, two phase bicrystals, deform. and fracture at 150K 0-16388  
cross slip dislocation self-interaction, Orowan loops 0-24453  
cross-rolling and compression textures, numerical prediction 0-40382  
cubic crystal edge and screw dislocation-point defect elastic interactions 0-15151  
discrete obstacle model, dislocation pile-up kinetics dislocation mobility activation parameters 0-29022  
dislocation behaviour, in fatigue, friction and back stress from hysteresis loops 0-3176  
dislocation ensembles, local heating at low temps., parallel glide planes, temp. distribution (*Russian*) 0-29020  
dislocation gliding, by-passing of hardened particles, coplanar Orowan loops form., stress-strain curves 0-49226  
dislocation interaction, in intersecting slip planes 0-39087  
dislocation interaction with point obstacle in non-uniform stress field, localised force approx. 0-15150  
dislocation multiplication, statistical approach 0-49230  
dislocation segment oscillations, internal props., point obstacle collisions, glide plane motion (*Russian*) 0-39088  
dislocation-phonon interaction in cryst. with anisotropic slip system 0-29137  
dynamic waves along dislocations overcoming local obstacles 0-29021  
epitaxial island mobility, one-dimens. model sinusoidal pot. 0-44457  
eutectoid thermomechanically treated, textural studies 0-29978  
free boundaries, slip-line field solutions, matrix technique 0-53640  
granular mats., stress-strain relations, intergrain slip 0-16374  
interface slip, caused by plane horizontally polarised SH stress pulse 0-53648  
kinematic hardening rule in single crystals 0-10551  
metal, BCC, polycrystalline aggregate, prediction of plastic props., deformation by {111} pencil glide 0-11731  
metal, FCC, deformation mechanism under high hydrostatic pressure (*Ukrainian*) 0-25758  
metal, FCC or BCC, dislocation annihilation during tensile and cyclic deform. and limits of dislocation densities 0-34007  
metallic polycrystals, deform. during cooling, revealed by deposited graphite layer (*Polish*) 0-25755  
misfit dislocations, Volterra-type model and relax. of nonequilibrium arrangements 0-2020  
naphthalene single crystals, surface active substances effect on plastic flow 0-44248  
non-crystallographic slip, in cubic cryst., algebraic determ. (*French*) 0-2112  
olivine, hardness var. with temp., rel. to polycryst. yield stress 0-26500  
oxides, interaction between point defects and dislocations, cryst. plasticity 0-15149  
piecewise homogeneous elastic medium, crack with finite branch, slip lines 0-38342  
plastic failure, effect of deep wedge shaped notches of small flank angle 0-48593  
plastic yielding, modelling at a crack tip by inclined slip planes 0-33472  
polyethylene, oriented, shear strain, effect on struct., props. (*Russian*) 0-7656  
shear band formation models, in rolling and extrusion 0-3152  
shear band formation models, in rolling and extrusion 0-11666  
sheet drawing, slip line field for mid-plane cracking or splitting 0-50648  
stainless steel, type 316, irradi. in simulated environment, tensile props. 0-34076  
steel, austenitic stainless, interaction of grain boundary dislocations with precipitates during high temperature creep 0-16384  
steel, Cr-Ni (1.47, 1.48 wt.%), lath martensite microstruct. and props., cold rolling effect 0-55422  
steel, CrNi, etchability of austenite (*German, English*) 0-11860  
steel, low C, plastic deformation by pencil glide,  $r$ -values and yield loci 0-7654  
steel, low C, slip band expt. studies during fatigue process 0-45374  
steel, low-alloy 12GN2MFAYu, heat treated, testing temp. influence on fatigue strength (*Russian*) 0-40501  
steel, mild, orientation distribution function, representation of texture and slip directions 0-11665  
steel, Mn-Cr-B (1.46, 1.03, 0.003 wt.%) 0-55422  
steel, Ni-Co-Mo (17.55, 8.02, 4.92 wt.%) maraging, lath martensite microstruct. and props., cold rolling effect 0-55422  
steel, plastic deformation and cryst. texture in equibiaxial expts. 0-7653  
steel, stainless, neutron irradiation effect on low cycle fatigue and tensile props. at 298K 0-30059  
steel, stainless, single crystals, shear cracks, electron microscope study 0-40522  
steels, structural St 37-2, cleavage fracture, report 0-25868  
steels, ultrahigh C, superplastic, mech. behaviour at elevated temps 0-21028  
tilt grain boundaries, stress-induced migration in cubic crystals. 0-44252  
two phase alloy hardening by second phase particle coalescence 0-7591  
wedge shaped object, elasticity theory 0-38294  
Ag, (211)[111] single crystals, shear band effects on rolling deformation 0-50651  
Ag, yield point, temp. depend., 2 to 300K (*Russian*) 0-45346  
Al alloy, type 2024-T3, fatigue deformation and crack growth, holographic study 0-25836  
Al bicrystals, fatigue crack initiation, cryst. boundary effect 0-55537  
Al, crit. resolved shear stress, orientation depend. 0-2f001  
Al crystal, lattice rotation during tensile deform., X-ray diff. meas. 0-49231  
Al, deformed in tension, elec. cond. changes at 78 and 283K, grain boundary effect (*Japanese*) 0-30029
- slip** continued  
Al-Ag alloys, critical resolved shear stress 0-49296  
Al-Cu, single and two phase, superplastic behaviour 0-11709  
Al-Cu-Mg-(Ag), effect of addition on fatigue microstructure relationships 0-40483  
Al-Mg, creep behaviour in broad stress interval at 623K 0-30044  
Al-Mg-(Ag), effect of addition on fatigue microstructure relationships 0-40483  
Al-Zn-Mg-Cu, age hardened, effect of strain rate, temp. and environment on ductility 0-45368  
Al-Zn-Mg-(Zr) alloy, microstruct. effect on fatigue crack growth 0-3164  
CdS, deformed, dislocation struct., TEM obs. 0-54250  
CdS, exciton optical and luminescence spectra characts. near dislocation slip bands 0-45111  
CdS, plastically deformed cryst. with dislocation slip band, residual cond. 0-6839  
Co-Ni alloy, slip charact., and fatigue, FCC twinning and FCC to HCP martensite transform. effect 0-35182  
Cu free electrolytic films, tensile creep for various film thicknesses calcs. (*Russian*) 0-11697  
Cu plates, thin, dislocation-dislocation interaction inducing cross-slip, X-ray topographic anal. 0-49233  
Cu-Zn (30 wt.%), slip band growth, thermally activated 0-40457  
Cu<sub>3</sub>Au, dislocation slip band mobility, critical stress 0-2032  
Cu<sub>2</sub>O, thermal activation of plastic deform. (*French*) 0-16394  
Fe, high purity single crystals, thermally activated slip deformation between 4.2 and 300K 0-25801  
Fe single crystals, size effect on slip deformation ability at very low temps. 0-21049  
Fe, slip-initiation phenomenon by fatigue, appl. to stress meas. 0-45342  
GaAs, during deformation, acoustic emission rel. to cracks, dislocations 0-35441  
GaP, birefringence observations of strain and plastic deform. 0-50678  
GaP crystal, structure defect formation due to annealing and stress, dendrites, slip, dislocations 0-29026  
Ge, cross-slip of single dissociated screw dislocations, double etching and X-ray topography studies 0-15104  
InP, damage induced during handling for TEM obs. 0-2024  
LiF, plastic strain accompanying local rise in surface temp., of natural shear (*Russian*) 0-6411  
LiF single crystals, glide band sources, work hardening 0-34126  
LiF(Mg), shock waves in {111} direction, elastic precursor amplitudes 0-54314  
Mg, dislocation struct. after US deform. (*Russian*) 0-29027  
Mg-Al spinel, non-stoichiometric, climb dissociation of network dislocations 0-2031  
Mg-Cd, single crystals, temp. depend. of crit. resolved shear stress (*Czech*) 0-29112  
MgAl<sub>2</sub>O<sub>4</sub>, microplasticity at room temp., dislocations, TEM study 0-19805  
MgO, compressive stress-strain behaviour at high temps. 0-25774  
MgO, crack propagation during in-situ deform., plastic zone formation 0-16468  
MgO(Al<sub>2</sub>O<sub>3</sub>)<sub>n</sub> spinel, plastic deformation at 400°C 0-40453  
Mg<sub>2</sub>SiO<sub>4</sub>, forsterite, decorated dislocations 0-54245  
Mo, powder specimens, fatigue and threshold behaviour under high cycle fatigue 0-40487  
Mo, slip geometry, HVEM straining 0-39207  
Mo, strain localisation and fatigue, glide plane shearing stress 0-7683  
Mo-W alloy, fatigue and threshold behaviour under high cycle fatigue 0-40487  
Mo, single crystals, surface orientation effect as high temp. creep and fracture type 0-16403  
NaCl, dislocation struct. of slip bands, hydrostatic press. effect 0-54249  
NaCl, hydrostatically compressed crystals, in easy glide stage, plastic deformation 0-7630  
NaCl, rock salt, quenched, residual stresses, optical study 0-55061  
Nb, local heating during abrupt strain, catastrophic slip band formation 0-7652  
Nb, neutron bombarded, defect size distrib. influence on hardening (*Russian*) 0-10580  
NbB<sub>2</sub>, single crystals, hardness anisotropy and slip 0-21085  
NbC<sub>x</sub> ( $x=0.868, 0.834, 0.766$ ), single crystals, thermomech. behaviour during annealing 0-3104  
Ni, lattice defects, formation kinetics, work hardening and resistivity study (*Russian*) 0-10557  
Ni, single crystals, strengthening, tested under compression at 293 and 77K (*German*) 0-50689  
Ni<sub>2</sub> (Al, Nb) single crystals, orientation and temp. depend. of yield stress 0-25791  
(Ni,Co)<sub>1-x</sub>Ge single crystals, L<sub>1</sub>2 struct., cross-slip 0-40459  
Ni<sub>3</sub>Fe, single crystals, long range order degree influence on strain hardening (*Russian*) 0-11660  
Si, cross-slip of single dissociated screw dislocations, double etching and X-ray topography studies 0-15104  
Si, extended glide dislocations, motion obs. by high voltage electron microscopy 0-10555  
Si, near {111} surface, dislocation movement at annealed scratches, X-ray topography obs. 0-2029  
Si:B, with insulating coating, mechanical stress influence on B diffusion, strained surface layers 0-29224  
Sn crystal, white, time-dependent internal friction 0-7610  
Sn-Bi, eutectic, superplastic anisotropy (*German*) 0-25808  
TZM powder alloys, fatigue and threshold behaviour under high cycle fatigue 0-40487  
Ti, pure plate, silver band formation in ductile fracture process (*Japanese*) 0-16445  
Ti-Al-V-Sn (6, 6, 2 wt.%) weldments, heat treated, transangular fracture 0-40524  
V, purification and plastic props. 0-25810  
V, strain hardening, screw dislocations and microtwinning (*Russian*) 0-29971  
V-Ta (5 wt.%), strain hardening, screw dislocations and microtwinning (*Russian*) 0-29971  
W-Re, polygonisation in diffusion process, glide dislocation interactions 0-38998  
W-Mo, vapour deposited, long-term strength and thermocyclic creep 0-16405  
WC-Co, elastic and plastic charact. 0-35280  
Zn, basal dislocation-prismatic dislocation ring interactions by method of moments (*Russian*) 0-10550



- slip** continued  
 Zn bicrystals, (10 $\bar{1}$ 0) tilt, misorientation depend. of grain boundary sliding 0-15119  
 Zn bicrystals, grain boundary slip in deform. 0-34008  
 Zn, density of basal dislocations, rel. to deforming stress, 1.5-300K (*Russian*) 0-29028  
 Zn single crystals, temp. and strain rate effects on strength, slip and twinning 0-16373  
 Zn-Al (10,22,50wt.%), low temp. mech. props. plastic deformation, glissile dislocation nucleation (*Russian*) 0-11695
- small polaron conduction**  
 disordered solids, electron-electron interaction effects on low temp. hopping 0-44584  
 tunnelling, thermally assisted, computer anal. 0-2391  
 As<sub>2</sub>Se<sub>3</sub>-As<sub>2</sub>Te<sub>3</sub> glass thermoelec. power, and transport mechanism 0-2408  
 BaO-K<sub>2</sub>O-VO<sub>2</sub>-SiO<sub>2</sub>, glass, elec. cond. rel. to ion polarisability, polarons 0-49729  
 BaO-La<sub>2</sub>O<sub>3</sub>-VO<sub>2</sub>-SiO<sub>2</sub>, glass, elec. cond. rel. to ion polarisability, polarons 0-49729  
 Fe<sub>3</sub>O<sub>4</sub>, magnetite, charge carriers, optical props. 0-34874  
 La<sub>0.9</sub>Ca<sub>0.1</sub>CrO<sub>3</sub> polar semiconductor, elec. props., slight reduction effect 0-20183  
 La<sub>1-x</sub>Sr<sub>x</sub>CoO<sub>3-y</sub>, Seebeck coeff. meas., small polaron hole conduction model 0-20233  
 La<sub>1-x</sub>Sr<sub>x</sub>CrO<sub>3</sub> (0 ≤ x ≤ 0.4), localised level hopping transport 0-10974  
 Mn ferrites, Fe-excess, charge carriers, optical props. 0-34874  
 NbCl<sub>4</sub>, high press. elec. resistivity 0-29404  
 NbO<sub>2</sub>, high press. elec. resistivity, phase transition 0-29404  
 V<sub>2</sub>O<sub>5</sub>-MoO<sub>3</sub> solid solns., small polaron cond., elec. resist. and thermoelec. power meas. 0-34447
- smectic liquid crystals**  
 aliphatic compounds, trans, trans-cyclohexyl cyclohexanoates, synthesis, mesomorphic phases 0-44121  
 alkyl cyanobiphenyls, pretransitional behaviour, alkyl chain length depend., light scatt. in isotropic phase 0-44301  
 alkylcyano-cyclohexyl-cyclohexanoates, nematic and smectic mesophases 0-19692  
 alkylcyclohexyl-cyclohexyl-cyclohexanoates, nematic and smectic mesophases 0-19692  
 trans-4-n-alkylcyclohexylbenzylamines, synthesis and mesomorphic props. 0-44116  
 BBOA, smectic B phase, fluidlike mol. dynamics, Raman scatt. study 0-20630  
 BBOA, smectic liq. cryst. glass-supercooled transition and Debye temp., <sup>57</sup>Fe Mossbauer effect 0-54999  
 biphenylbenzoates, synthesis, mesomorphic, and thermodynamic props. 0-44117  
 N-n-butoxybenzylidene-n-butylaniline, US propag. near nematic-smectic A transition, mag. field effect 0-39266  
 N-p-butoxybenzylidene-p-n-octylaniline, smectic A-B transition, birefringence pretransitional behaviour 0-15226  
 C phase, mol. director behaviour at domain EHD instability 0-15000  
 C-phase, biaxial mol. order, NMR meas. 0-25227  
 CBOOA, isotropic, nematic, smectic-A phases, Brillouin scatt. 0-11421  
 chiral ferroelectric, flexoelectric effects, dielectric const. 0-33877  
 chiral smectic C phase, mol. theory 0-19695  
 chiral smectic critical behaviour near phase transformation point between two ferroelectric phases (*Russian*) 0-44124  
 COOB, solid state dimorphism and cryst.-smectic transition, Raman study 0-45063  
 critical dynamics near nematic-smectic A phase transition, renormalisation group approach 0-10646  
 p-cyano-p'-pentylbiphenyl/p-pentylbenzoic acid, mixture, induced smectic phase, dielec. props. 0-6498  
 diakyl-cyclohexyl-cyclohexanoates, nematic and smectic mesophases 0-19692  
 DOBAMBC, chiral smectic, flexoelectric effect and polarisation props. (*Russian*) 0-15002  
 DOBAMBC, chiral smectic C-phase ferroelectric liq. crystal film, classical X-Y system, props. 0-44123  
 DOBAMBC, dielec. props. near ferroelec. smectic A to C transition 0-45015  
 DOMBAMBC, ferroelectric, colour switching in elec. field 0-29719  
 dyes, field-induced colour changes 0-25340  
 ferroelectric, linear electrooptic effect 0-11365  
 ferroelectric phenomena, symmetry and thermodynamic states, review 0-10493  
 ferroelectric smectic single C liquid cryst., electric field induced bend undulation instability 0-24351  
 HBPA, smectic liq. cryst. glass-supercooled transition and Debye temp., <sup>57</sup>Fe Mossbauer effect 0-54999  
 4-n-heptyl-4'-β-cyanovinylbiphenyl, isotropic mechanism of mol. rot., dielec. permitt. meas. 0-10491  
 n-hexyl 4'-n-decyloxybiphenyl-4-carboxylate, smectic C phase, tilt angle using electron reson. spectroscopy 0-33886  
 4-n-hexyloxybenzylidene-4'-n-hexylaniline, liquid crystal, exam. of orientation order of dissolved molecules 0-44112  
 IBPBAC, smectic phases, self-diffusion coeffs., radiotracer meas. 0-49394  
 induced helical struct., ferroelectric props. and spontaneous polarisation, C→A transition 0-54123  
 nematic bend-splay elasticity near the nematic-smectic-A transition 0-24360  
 nematic to smectic C phase transition, renormalisation group anal. 0-34173  
 nematic-smectic A transition, orientational fluctuation effect 0-6496  
 4-nitrophenyl-4'-alkoxybenzoates, incommensurate smectic A phase 0-10647  
 4-n-octyl-4'-cyano-diphenyl, appl. in detection of graphite powder particles by optical microscopy 0-9034  
 p-n-octyl-p'-cyanobiphenyl, thermally addressed liq. cryst. display, light scatt. and contrast 0-34892  
 4-n-octyloxybenzoyloxy-4'-cyanostilbene, re-entrant polymorphism, nematic-smectic A-nematic-smectic A, X-ray study 0-34172  
 oxyloxycyanobiphenyl, nematic-smectic-A transition, high-resolution 0-10649  
 p-pentoxyl-benzylidene-alkylaniline series, smectic phases, dielec. anisotropy 0-55010  
 4-n-pentyl-phenylthiol-4'-alkoxybenzoate, homologous series, specific heat meas., nematic-smectic-A tricritical point 0-15227
- smectic liquid crystals** continued  
 4-pentylphenyl-4'-benzoyloxybenzoate/TBBA system, smectic A<sub>1</sub>-smectic A<sub>2</sub> transition, X-ray diffr. obs. 0-44303  
 phenylcyclohexanes, alkylamino substituted, synthesis and mesomorphic props. 0-44120  
 PNAOBA, type C smectic liq. crystals, electrohydrodynamic instability 0-1927  
 refractive index near smectic-A/smectic-C transition, orientational order 0-24572  
 Schiff's base compounds, double axis, Siamese Twin type liq. crystals, thermal and X-ray obs. 0-39312  
 smectic A to smectic C transition, separate order parameter for layer thickness and optical tilt angle 0-19923  
 TBBA, self diffusion coeffs., neutron diffr. and NMR study 0-19689  
 TBPA, liq. cryst., smectic F phase, X-ray diffr. obs. 0-44122  
 thermotropic, anomalous rheological responses, spectrometer study 0-6358  
 thermotropic liquid crystal, diffusion and nucl. mag. relax. 0-24362  
 TTF derivatives, smectic and nematic, for liq. cryst. device appl. 0-54124
- smell (physiological)** *see* chemioception
- smoke**  
*see also air pollution; dust*  
 acetylene, optoacoustic meas. of absorpt. at 0.5145, 10.6 μm 0-43060  
 acetylene smoke particles, agglomerated, optical extinction meas. at 0.5145 and 10.6 μm 0-48155  
 acetylene smoke particles, optoacoustic meas. 0-50895  
 aerosol microstruct. and refr. index, optical determ., inversion method 0-36399  
 atmospheric particulate concentration, rise of smoke plumes, application of lidar 0-51026  
 diesel smoke particles, optoacoustic meas. 0-50895  
 dispersion modelling, meteorological methods appls. (*German*) 0-51496  
 Na smoke particles, nucleation and growth, light scatt. study 0-35580
- snap off varactors** *see* varactors
- Snoek effect**  
 steels, ferritic and martensitic, C and N migration at low temps., monograph 0-22149  
 Be, internal friction, temperature spectrum and dislocation damping, anelastic relaxation (*Russian*) 0-2118  
 NaCl:Ca, aggregation and precip. hardening in impurity vacancy, dipole decay 0-16322
- Snoek-Koster relaxation** *see* anelastic relaxation; dislocation damping
- snow**  
 ablation hollows on melting snow surface (*Japanese*) 0-36345  
 accumulation, distrib., melt and runoff 0-36338  
 acidity, release of S and nitrogen oxides by burning fossil fuels 0-26590  
 aggregation of falling flakes, theory 0-12491  
 albedo following dustfall, satellite remote sensing 0-17385  
 Arctic Ocean sea ice, snow and ice cover conditions 0-26547  
 avalanche release explosions, ionospheric effects 0-36451  
 blizzard, 1978 February 18 to 19, in SW.England and S.Wales 0-12507  
 cohesion strength and compression resistance in snow cover 0-26560  
 crystal growth by droplet accretion 0-41495  
 Devon Island ice cap, NWT, Canada, δ<sup>18</sup>O vars. in snow 0-4050  
 dry slab avalanche release mechanism, shear fracture precipitated by strain softening 0-8338  
 falling crystals, attached aerosols direct obs. 0-17362  
 ground cover remotely sensed by radar, backscatter cross-section 0-46279  
 hailstone nuclei formation, role of giant aerosols (*Russian*) 0-56530  
 Lake Ontario induced snowfall systems, objective forecast method 0-51484  
 laser beam attenuation by snowfall, characts. 0-26611  
 melting on slopes of Mt. Asahidake, Hokkaido (*Japanese*) 0-36343  
 melting rate, urban/rural area comparison in Sapporo, Hokkaido (*Japanese*) 0-36342  
 microwave passive remote sensing, theory and expt. 0-26632  
 microwave radiometry determination of snow cover parameters 0-56652  
 Mt. Asahidake, Hokkaido, snow accumulation and ablation (*Japanese*) 0-36344  
 Mt. Teine, Hokkaido, deposition and melting of snow with altitude (*Japanese*) 0-36346  
 New England, 1816, snow and frost in year without summer rel. to Tambora volcano eruption 0-4089  
 radiowave attenuation on SIRIO-1 Earth-satellite link (*French*) 0-56504  
 snowpack, model of planetary boundary layer above surface 0-41477  
 volumetric constitutive law based on neck growth model 0-48595  
 water content meas., calorimetric method (*Japanese*) 0-31142  
 wet, grain clusters obs. 0-26553  
 winter accumulation in Sapporo, Hokkaido (*Japanese*) 0-31071  
 T fallout at South Pole in 1954-1978 snow samples 0-16867
- SNR** *see* supernova remnants
- social and behavioural sciences**  
*see also economic and sociological effects; psychology; teaching*  
 animals unusual behaviour before earthquakes, positive and negative reports 0-26455  
 associated movement study, portable micro-system 0-51299
- societies**  
 American Association of Physics Teachers, 1979 winter meeting 0-42042  
 role of scientific and engineering societies in development 0-31480  
 Webb Society handbook of double stars 0-8744  
 Webb Society handbook of planetary and gaseous nebulae 0-8743
- sociological effects** *see* economic and sociological effects
- sociology** *see* social and behavioural sciences
- sockets (electrical)** *see* electric connectors
- sodar** *see* sonar
- sodium**  
*see also nuclei with .....*  
 adsorbed c(2×2) overlayer on Ni (001), core level excitation effects, synchrotron radiation UPS study 0-40234  
 adsorbed on Ni, hybridisation between s and p reson., jellium model 0-6932  
 adsorbed on W (100), binding props. calc. 0-49522  
 Ashcroft pseudopotential, unified study of props. 0-39239  
 atom, <sup>2</sup>D highly excited states, fine struct. splitting, field ionisation quantum interference 0-18835  
 atom, coherent ground state transients, beat meas. 0-948  
 atom, Compton profiles using Gaussian expansion of at. orbitals 0-945  
 atom, D<sub>1</sub> line profile, Zeeman scanning 0-47928  
 atom, D line broadening by inert gases, fluoresc. obs. 0-32663



## sodium continued

atom, D-line saturation, under high power laser illumination 0-32653  
 atom, depolarisation obs. of near-resonant scattered light 0-52921  
 atom, diabatic field ionisation of highly excited at. states 0-43202  
 atom, ground state,  $\text{Li}^+$  electron capture cross sections 10-60 keV 0-48084  
 atom, in flames, laser-induced fluoresc. temp. meas. 0-11893  
 atom, laser oriented, refl. by non-disorienting surfaces, optical activity detect. 0-55252  
 atom, laser temporal coherence effects in two-photon resonant three-photon ionisation 0-32686  
 atom, multiphoton ionisation, resonant, with intense monochromatic laser 0-32689  
 atom, oscillator strength measurement using reson. Faraday effect in monochromatic light 0-23363  
 atom, outer-shell photoelectron ang. distrib. 0-37797  
 atom, photoionis. cross section resons., time-dependent HF theory 0-32684  
 atom, quantum beats of hyperfine levels observed in photoionisation 0-32690  
 atom, reson. absorpt. transitions, laser saturation spectroscopy with optical pumping 0-47121  
 atom, reson. transition, laser saturation spectroscopy with optical pumping 0-52334  
 atom, reson. two-photon ionisation via  $3p^2P_{3/2}$  state, photoelectron ang. distrib. 0-43016  
 atom, Rydberg states, high resolution spectroscopy 0-52901  
 atom, Rydberg states, high resolution two-photon mm spectroscopy, metrology appl. 0-43018  
 atom, SCF electron-gas local-spin-density model including correlation 0-9488  
 atom, seeded flames, excitation, laser radiation absorpt., sound vel., opto-acoustic effects obs. 0-43345  
 atom, single, detection by laser fluoresc. (Russian) 0-35620  
 atom, Stark shifts, absolute and differential, coherent optical transient meas. 0-37773  
 atom, three-photon ionisation, laser bandwidth and intensity effects 0-52956  
 atom, two-photon absorpt. processes, polarisation selection rules 0-9574  
 atom, two-photon transition, distinction of competing processes in non-linear resonant freq. mixing 0-33080  
 atom beam, focusing and defocusing forces, radiation press. from CW dye laser 0-52944  
 atomic beam focusing and defocusing using reson. radiation press. 0-47143  
 atomic gas, polarisation spectroscopy and forward scatt. 0-52336  
 atomic Rydberg transitions to detect far IR radn. 0-4763  
 atomic spectra, quantum defects and ionis. pots., graphical procedure for students 0-7  
 atomic vapour, Doppler-broadened system, degenerate four-wave mixing, line shape and strength angular depend. 0-43391  
 atomic vapour doublet, dispersion free point, cooperative phased-array radiation 0-53352  
 atoms, spectroscopy, masers and superradiance study 0-53248  
 BCC crystal, elastic constants, thermal expansion and bulk modulus 0-6452  
 beam, deflection by reson. standing wave radiation 0-52945  
 biomembrane channels, inactivation delay 0-45872  
 boiling in tubes, heat transfer and pressure drop 0-28408  
 catalytic cycle, origin for luminosity of meteor trains, lifetimes 0-12711  
 charge-exchange continuous-action nuclear bombardment target 0-23205  
 combustion of large pools in LMFBFR, determ. of burning rate and flame struct. 0-47644  
 D<sub>2</sub> resonance line broadening in atom and molecule collisions (Russian) 0-14119  
 distribution in Io Na cloud around Jupiter 0-46464  
 dynamical structure factor calc., High temp. 0-15047  
 elastic scattering amplitudes, for high energy electron scattering, by ionised atoms, numerical calcs. 0-49057  
 electrical resistivity, low-temp., electron-electron contrib., sample depend. 0-24875  
 emission and fixation during pressurised fluidised bed combustion of coal 0-30352  
 equation of state meas. 0-19905  
 equations of state determ. 0-24564  
 estimation in cotton clothing for use in neutron activation dosimetry 0-47729  
 evaporative removal from LMFBFR components 0-32348  
 fast reactors, track detector determ. of fuel contamination of primary Na coolant 0-32394  
 Fermi surface distortion 0-2325  
 film, slow electron bombarded, light radiation 0-40168  
 film for expendable filter in VUV, use and preparation technique 0-33193  
 first excited states, non-resonant emission spectra (Chinese) 0-42971  
 gas diffusion induced by resonance light field 0-53918  
 hyperthermal atoms, ionisation on W (110), temp. depend. 0-50504  
 interatomic potentials from phonon spectra 0-19744  
 Io Na cloud, solar radiation press. as cause of east-west asymmetries 0-36560  
 ions in liquid, Born-Oppenheimer pot. derivative, Monte Carlo calcs. 0-54117  
 isoelectronic sequence, dielectronic recombination rate coeffs.,  $2 \cdot 10^3$  eV 0-10357  
 isoelectronic series, dipole polarisability, numerical Coulomb approx. 0-43199  
 isoelectronic series, hard-core pseudopotentials and struct. maps 0-44168  
 jellium model, appl. to X-ray spectra 0-39523  
 $K\alpha_1$  and  $K\alpha_2$  wavelengths 0-50464  
 liquid, contaminated, packaging and storage 0-18468  
 liquid, coordination numbers, calc. in microinhomogeneous struct. model (Russian) 0-38902  
 liquid, engineering handbook, purification, heaters, coolers, radiators 0-27045  
 liquid, entropy calc. using phonon theory of liquids 0-39310  
 liquid, loop disposal system of sodium loop safety facility 0-18467  
 liquid, molten chlinak extraction of  $\text{I}_2$  in Na cooled fast reactor 0-27702  
 liquid, natural convection from plane surfaces, LMFBFR design, review 0-37417  
 liquid, shear waves, molecular dynamics 0-44096  
 liquid, thermoelectric power, optimised model pot. calcs. 0-29391

## sodium continued

liquid, velocity autocorrelation from memory function, hard-sphere and square well pots. 0-28893  
 liquid, working fluid in AC cond. pump, performance characts., freq. depend. (Japanese) 0-13092  
 liquid metals, structure factor modelling using quasi-crystallised model (Russian) 0-54118  
 liquid reactor coolant, effect of  $\text{O}_2$  on  $\text{H}_2$  permeability, partial pressure 0-614  
 liquids, optimised cluster expansion, struct. function evaluation 0-49085  
 LMFBFR, core-disruptive accidents, neutronic and fuel element behaviour 0-32357  
 LMFBFR, long-term in-reactor corrosion of stainless steel cladding by liquid Na 0-16593  
 LMFBFR, Na flow meas. in main pipes, application aspects 0-22884  
 LMFBFR, Na flow transient anal. using NATOF-2D code 0-47633  
 LMFBFR, Na loop temp. control using 100 kW elect. heater (Czech) 0-5203  
 LMFBFR coolant, SAS-3D analysis of natural-convection boiling behavior in the sodium boiling test facility 0-47635  
 LMFBFR coolant boiling under low heat flux condition during loss-of-heat sink accident 0-47636  
 LMFBFR HCDA, Na interaction with basalt concrete and silaceous firebrick 0-47638  
 LMFBFR Na/basalt concrete interactions following accident, chemical phenomenology 0-47639  
 LMFBFR rot. shield plug annulus, Na vapour, deposition rate, controlling factors 0-47591  
 metallic compressibilities, general pseudopotential approach 0-54631  
 microelectrodes, Na-selective liquid ion-exchanger, for intracellular meas. 0-3888  
 $\text{Na}_2$ , laser-excited, emission bands obs. in visible and IR 0-48036  
 normal atom conc. determ. by resonance line broadening with Hg press. 0-43883  
 optical properties in generalised HF approximation 0-24825  
 phonon spectra, self-consistency condition for force const. models 0-44264  
 phonon spectral density, pseudopotential calcs. 0-39234  
 photoemission theory, book contrib. 0-16159  
 plasma, dense, in arc, elec. and heat conds., two-probe diagnostics 0-38560  
 point contacts, current-voltage characts. at liq. He temps. 0-39663  
 precipitation at Si-SiO<sub>2</sub> boundary, expt. (Russian) 0-49368  
 radiation-induced changes in Na preference and fluid intake in the rat 0-35986  
 resonance line, laser excitation, combustion Rayleigh scatt., at. flame fluoresc. spectroscopy 0-42972  
 smoke particles, nucleation and growth, light scatt. study 0-35580  
 solid, self-diffusion mech., NMR meas. 0-44356  
 steel, austenitic stainless type 316, corrosion mechanism in hot flowing Na, computer simulation 0-3251  
 surface, Cl<sub>2</sub> reaction, surface chemiluminesc. study 0-55708  
 surfaces, (100) and (111), electron energy states (French) 0-34496  
 thermal energy storage in a packed bed of iron spheres with liquid sodium coolant, thermocline broadening 0-45762  
 tissue exchange, incorporating diffusion effects into multicompartment models using digital simulation 0-3611  
 upper atmospheric layer, meas. by efficient forced oscillator dye laser 0-41563  
 UV absorpt. spectra 0-2780  
 vacancy formation energy calcs., electron density functional method 0-19801  
 vapour, assoc. ionis. by CW dye laser and applics. (Japanese) 0-5515  
 vapour, diffusion coeff. of oriented atoms in buffer gases 0-53908  
 vapour, effective freq. conversion of radiation 0-28278  
 vapour, induced optical anisotropy (Russian) 0-38526  
 vapour, laser induced diffusion (Russian) 0-6195  
 vapour, magnetically induced SHG, intensity saturation 0-1273  
 vapour, particle size meas. using anemometer 0-13195  
 vapour, reson. freq. conversion by two-photon reson. pumping 0-28277  
 vapour, saturation holes meas. using FM spectrosc. 0-42262  
 vapour, spontaneous field induced optical SHG, multiphoton ionisation 0-14395  
 vapour, two-photon resonant fifth harmonic generation 0-53374  
 vapour, viscosity meas., 1101-1186K, 0.2-0.8 bar 0-1723  
 vapour in inert gas, effect of oxidant on optical props. 0-1736  
 vapour jet target, gating and pumping action 0-10281  
 variational cellular method, electronic struct. calcs. 0-54591  
 wetting studies, heat pipe meas. with gas plug containment up to 720°C 0-23878  
 X-ray absorption and emission edges, one-electron and many-body effects 0-25484  
 X-ray emission spectra, double plasmon high energy satellites 0-29829  
 X-ray emission spectra,  $L_{2,3}$  satellite, interpretation 0-20737  
 $\text{Ag}^+ \cdot \text{Na}^+$  ion-exchanged optical waveguide repeatability improved by melt dilution 0-53493  
 $\text{AgBr}:\text{Na}^+$ , impurity induced IR absorpt. 0-7386  
 $\text{AgBr}:\text{Na}^+$ , local mode freqs., Green's function calc. 0-39237  
 a-As<sub>2</sub>Se<sub>3</sub>:Na, doped film, photoluminescence intensity and lineshape study 0-50448  
 $\text{BaF}_2:\text{Na}^+$ , ionic conductivity meas., computer analysis, point defect parameters 0-54429  
 $\text{CaF}_2:\text{Na}$ , single cryst., X-irrad., optical absorpt. and thermoluminesc. 0-34952  
 $\text{CaF}_2:\text{Na}$ , vacancy motion activation vol., complex dielec. const. meas. 0-39356  
 $\text{CaS}:\text{Bi}^{3+}, \text{Na}^+$  phosphor, luminescence of associated centres (French) 0-40155  
 $\text{CdS}:\text{Na}$  film, chemical bath deposited, photothermoelectric effect 0-6906  
 $\text{CdS}:\text{Na}$  thin film, photoconducting props. 0-39623  
 $\text{CsI}:\text{Na}$ , electronic struct. and luminesc. 0-16080  
 $\text{CsI}:\text{Na}$ , self-trapped exciton emission polarisation 0-49607  
 Ge-Na interfaces, interdiffusion, electron states, EELS study 0-50484  
 $\text{I}_2:\text{Na}$ , doping effect on elec. cond., semicond. props. 0-49732  
 $\text{KBr}:\text{Na}$ , microcrystalline powders, isothermal decay of colour centres 0-2804  
 $\text{KBr}:\text{Na}$ , U-centres, HFS and g-factor, EPR spectra 0-39869  
 $\text{KCl}:\text{Na}$ , electron trapping from  $\alpha_A$  and  $F_A$ -centres, low temp. depend. 0-11444  
 $\text{KCl}:\text{Na}$ ,  $F_A$  reorientation and  $F_A \rightleftharpoons F'_A$  conversions, laser induced, kinetic studies 0-10547



## sodium continued

- KCl:Na and pure, hologram-recording through F $\rightarrow$ X conversion 0-48190  
 KCl:Na, F $\lambda$ -centre optical absorpt., estimate using symmetry-adapted wave functions 0-11448  
 Li $^{+}$ , Na $^{+}$ :KCl(RbCl), F $\lambda$ (II) to F $\beta$ (II) centre crystals, CW laser oscill. with extended tuning range 0-32997  
 LiNbO $_3$ :Na $^{+}$  films, LPE growth from Li $_2$ O-V $_2$ O $_5$  flux, X-ray and acoustic characterisation 0-15383  
 Na I, fine struct. splittings in some highly ionized n=3 doublets 0-43200  
 Na I, interstellar, obs. in 30 Doradus nebula in LMC 0-46643  
 Na I 8190 Å absorption feature in M31 and M32, equivalent widths 0-51862  
 Na I D $_2$ -line at 5890 Å, laser obs. of ground-state hyperfine structure 0-931  
 Na I D-line, nightglow spectra correl. to atmos. Na density 0-41585  
 Na I D-line obs., Doppler width from intensity integral 0-41782  
 Na I interstellar absorption in NGC 4321 galaxy 0-51847  
 Na I reson. line broadening by collisions with dipolar mols. 0-941  
 Na isoelectronic series, oscill. strengths, effective orbital quantum no. method 0-9521  
 Na positron complex, ground and excited states theoretical studies 0-42934  
 Na $^{+}$ , autoionising 2s2p $^6$ ns, np states, electron reson. scatt. calc. 0-53142  
 Na $^{+}$ , electrogenic transport obs. in rat soleus muscle 0-21456  
 Na $^{+}$ , reson. line regularities in plasma Stark widths and shifts 0-43881  
 Na $^{+}$ :KCl, CW laser action of (F $_2^{+}$ ) $_A$ -centres, tunable from 1.62 to 1.91  $\mu$ m 0-32998  
 Na/S batteries, load levelling and traction 0-21391  
 Na-S accumulator, electrical energy storage (French) 0-55835  
 Na+Ar, Na spectral lineshape, orientation and vel. relax. contribs., low press. region 0-5503  
 Na+Ar $^{2+}$ , Ar $^{+}$  form, electron capture Ar $^{+}$  excited states relative population distrib. 0-23544  
 Na+Ar $^{2+}$  collision, single electron capture into Ar $^{+}$  excited states, 0.2-12 eV, emission cross section 0-48071  
 Na+Ar $^{2+}$  collision, single electron capture into Ar $^{+}$  excited states, relative population distrib. 0-48072  
 Na+H $^{+}$ , charge transfer cross section and equilibrium fractions, 1-25 keV 0-5616  
 Na+H $^{+}$ , configuration interaction potentials and rainbow angle scatt. cross section 0-37745  
 Na+H $^{+}$ (He $^{+}$ ), Na 2p $^3$ 3s $^2$  2P $_{3/2}$  state alignment by 5-30 keV excitation 0-14200  
 Na+He, Na (3S $_{1/2}$ -3P $_{1/2}$ ) photon echo, collision vel. changes and dissimilar electronic states superposition 0-32803  
 Na+He(Ne)(Ar), Na collision-induced alignment, reson.-line emission polaris. obs. 0-18912  
 Na+Hg, 15-1400 eV, electronic excitation, integral cross sections 0-43159  
 Na+inert gas, collisional redistrib., two-photon absorpt. with near-reson. intermediate state 0-23505  
 Na+N $_2$ , atom electronic excitation, vibr. to electronic energy transfer, seeded mol. beam studies 0-47919  
 Na+N $_2^{+}$ , 50-1000 eV, crossed beams, electron transfer and excitation 0-14226  
 Na+Na, excited atoms, coupling terms, asymptotic pot., excitation energy transfer 0-23530  
 Na+Ne, differential cross section at thermal energy, expt. and theoretical results comparison 0-37851  
 Na+Ne, Na(3p) excitation 0-1056  
 Na+Xe, nonreson. two-photon absorpt., 4s excited states and pot. energy curves, close coupled eqns. 0-48068  
 Na $^{+}$ +Cd, Cd(5 $^2$ P $_1$ ) and (5 $^1$ P $_1$ ) and mag. sublevels, excitation cross-sections 0-9710  
 Na $^{+}$ +HeI, anisotropic collisions, direct meas. method 0-23498  
 Na $^{+}$ +H $^{+}$ , 3P $_1$  fine structure transitions 0-37864  
 Na $_2$ , ground state, vibr.-rot. relax., optical pumping transients obs. 0-28067  
 Na $_2$ , laser excited, atomic and molecular fluorescence with long radiative decay times 0-27976  
 Na $_2$ , optically pumped CW dimer lasers 0-14322  
 Na $_2$ , spectroscopy and structure, triplet excimer continuum emission 0-32769  
 Na $_2$  supersonic beam rovibronic level population, anal. by laser spectroscopy 0-43118  
 Na $_2$ +He, optically pumped state to state differential cross sections for rot. transitions, rainbow phenomena 0-5609  
 Na $_2$ +He, rot. excitation, rainbow oscils., coupled states and IOS approx. calcs. 0-23518  
 Na $_n$  (n $\leq$ 8), equilibrium geometries and ionization energies calcs. 0-1099  
 Na $^{+}$ H $_2$ O, supermolecule calcs. with additive procedure, intermolecular interactions and binding energy 0-52880  
 $^{23}$ Na spin- $3/2$  nuclei, double quadrupole resonance 0-32634  
 Na $_2^{*}$ , fluoresc. red continuum emission, atom-mol. energy transfer 0-43086  
 Na(3 $^2$ P $_1$ )+Na(3 $^2$ S $_{1/2}$ ), collisional excitation transfer, pot. symm. rules and cond. function 0-9690  
 Na(3 $^2$ P $_1$ )+N $_2$ (O $_2$ )(CO)(NO), electronic energy quenching dynamics, crossed beam expt. 0-9683  
 RbCl:Na, F $\lambda$ -centre optical absorpt., estimate using symmetry-adapted wave functions 0-11448  
 RbCl:Na, U-centres, HFS const., g-factors, EPR spectra 0-39869  
 Si:Na, amorphous, implantation effects on elec. props. 0-49716  
 Si:Na ion implanted, Hall effect temp. depend., electron surface density and mobility 0-11018  
 Si:Na $^{+}$ , inversion layer, far IR optical spectroscopy 0-20680  
 SiO $_2$ :Na $^{+}$ , heat treated, heat of immersion in H $_2$ O, organic compds. 0-3396  
 SrF $_2$ :Gd $^{3+}$ , Na $^{+}$ , EPR of orthorhombic Gd $^{3+}$ -univalent metal ion complexes 0-11262  
 V $_2$ O $_5$ :Na, elec. cond. and thermoelec. power meas. 0-10987  
 ZnSe:Li(Na)(Ga) doped and pure cryst., donor-acceptor bands 0-11465

## sodium alloys

- Cs-Na, liq., thermodynamic props. at high temps. 0-15262  
 Hg-Na, liquid, structure factors, X-ray scatt. (Japanese) 0-54122  
 Li-Na liquid binary mixtures, phase separation under press. 0-34183  
 Na-Ga, solid and liq., mag. susceptibility and elec. cond. (Russian) 0-29522  
 Na-Ga liquid alloy, thermodynamic props. of mixing derivation method 0-54385

## sodium alloys continued

- Na-K, liquid, collective excitations, mol. dynamics calc. 0-28895  
 Na-K liquid alloy, small angle X-ray scatt. study, conc.-fluctuation structure factors 0-54120  
 Na-K-H system, H influence on component interactions (Russian) 0-54383  
 Na-K(Cs), liq., form factors and transport coeffs., pseudopot. perturb. theory 0-44561  
 Na-Li, liq., Knight shift calc. by multiple scatt. X $\alpha$  method 0-54961  
 Na-Se system, liq., thermodynamic props. 0-21319  
 NaK, liq., engineering handbook, purification, heaters, coolers, radiators 0-27045  
 Nb-K melts, thermodynamic characts., elec. resistivity, single parameter rigid sphere calcs. (Russian) 0-34410

## sodium compounds

see also Rochelle salt; sodium alloys

- $\beta$ -Al $_2$ O $_3$ -Na $_2$ O, diffusion and ionic cond. meas. 0-6542  
 $\beta$ -Al $_2$ O $_3$ -Na $_2$ O, mechanism of diffusion 0-2202  
 amphiphilic-polymer liquid crystal, NaCl conc. influence on struct., X-ray diff. study 0-44126  
 dodecylsulphate, micellar system, 1-methylpyrene quenching by Cu $^{2+}$ , general kinetic model 0-32753  
 furan, adsorbed on NaCl, evidence of new condensed phase, IR spectra (French) 0-16028  
 hexahalogeno compounds: ReCl $_6^{2-}$ (ReBr $_6^{2-}$ ), low symm. splittings in vibronic spectrum due to phase transitions 0-55161  
 Na $_2$ V $_2$ Ti $_6$ O $_{16}$ , characterisation and mag. props., 90-800K, Na $_x$ Ti $_4$ O $_8$  bronze isotypes (French) 0-39735  
 oxalate, cryst. struct. rel. to those of Na $_2$ Sn(C $_2$ O $_4$ ) $_2$ , SnC $_2$ O $_4$  (French) 0-2004  
 polyethylene:NaCl, internal field strength, Raman spectra obs. 0-40061  
 $\gamma$ -quartz, reaction, with NaCl-KCl melt, exam. of struct., IR absorption spectra 0-55706  
 salt solutions, freezing in cells, heat and mass transfer with phase change 0-6493  
 sodium cholate-decanol, soln., aggregate form., comp. and dynamics 0-45575  
 sodium decanoate-n-decanol-water system, lamellar G-phase, orientational-order, EPR investigation 0-24355  
 sodium decyl sulphate/water/decanol/Na $_2$ SO $_4$ , lyotropic mesophase, mag.-oriented, X-ray diff. obs. 0-1921  
 sodium dodecylsulphate-H $_2$ O system, X-ray anal. 0-1926  
 sodium dodecylsulphate micelle, intramolecular fluorescence quenching of [1-pyrenyl-(CH $_2$ ) $_n$ -N(CH $_3$ ) $_3$ ] $^{+}$ Cl $^{-}$  by cationic surfactant nitroxyl radical 0-9627  
 sodium hydrogen oxalate monohydrate, oriented single cryst., Raman spectra with very strong H-bonding 0-25359  
 sodium iron fluorophosphate glasses, EPR and Mossbauer resonance study 0-39968  
 sodium lauryl sulphate micelles, chlorophyll-a, soln., dilution expts., solubilisation anal. 0-35587  
 sodium lauryl sulphate-3,3'-diethylthiacarbocyanine iodide-rhodamine-6G, soln., premicellar region, energy transfer 0-20685  
 sodium salicylate-toluene, singlet-singlet energy transfer in Manoxol OT-cyclohexane-water 0-9531  
 sodium tetraborate glass, melt, temp. depend. of high viscosity property (Russian) 0-39336  
 sodium tin oxalate, cryst. struct. rel. to those of Na $_2$ C $_2$ O $_4$ , SnC $_2$ O $_4$  (French) 0-2004  
 sodium uranyl acetate (deuteroacetate) 0-2830  
 steel, mild, in Na $_2$ SO $_4$  soln., anodic polarisation study of corrosion by AC 0-40582  
 steel, stainless, type 304, corrosion fatigue and stress corrosion cracking, in boiling NaOH 0-7719  
 thermal expansion measurement using X-ray powder diffractometer with polythermal attachment 0-311  
 tourmaline, elastic const. by US phase-comparison method 0-2108  
 trisoxalatoferate complexes, Mossbauer studies of electronic relax. phenomena 0-44973  
 zeolite-S layers, high-temp. activated dipole moments in S clusters (Russian) 0-20575  
 [B $^{3+}$ -Al $_2$ O $_3$ -H $^{+}$ (H $_2$ O)] $_n$ , IR study 0-16037  
 AgNO $_3$ -NaNO $_3$  mixed melts containing Na $_2$ O-SiO $_2$ -Ga $_2$ O $_3$ -Al $_2$ O $_3$  glasses, ion exchange 0-21282  
 AgNa mordenite, chemisorpt. of CO and H $_2$  0-2752  
 AgNa(NO $_3$ ) $_2$ , ferroelectric transitions, group theoretic comparison with NaNO $_2$  0-7311  
 $\beta$ -Al $_2$ O $_3$ ,  $^{22}$ Na labelled monocrystals, radiochemical anal. by isotope dilution method 0-11976  
 $\beta$ -Al $_2$ O $_3$ -Na $_2$ -CaO, microstruct. and ionic resistivity 0-44357  
 B $^{3+}$ -Al $_2$ O $_3$ -Na $_2$ O, bulk and grain boundary ionic cond. from conductance and capacitance meas. 0-2204  
 Al $_2$ O $_3$ -Na $_2$ O,  $\beta$  and  $\beta'$  phases, formation by solid state reaction between NaAlO $_2$  and  $\gamma$ -Al $_2$ O $_3$  0-29912  
 Al $_2$ O $_3$ -Na $_2$ O,  $\beta'$  and  $\beta''$  phases, engineering props. data compilation, rel. to energy storage 0-49415  
 $\beta$ -Al $_2$ O $_3$ -Na $_2$ O, ESR of paramag. defects in cond. planes 0-29617  
 $\beta$ -Al $_2$ O $_3$ -Na $_2$ O, layered material, contact free conductivity 0-2195  
 $\beta''$ -Al $_2$ O $_3$ -Na $_2$ O, Li $_2$ O stabilised, electrolyte polarisation anal. by complex admittance method 0-2689  
 $\beta$ -Al $_2$ O $_3$ -Na $_2$ O, non-stoichiometric, amorphous, US attenuation and velocity 0-39228  
 $\beta$ -Al $_2$ O $_3$ -Na $_2$ O, preferable orientation for Na $^{+}$  cond. 0-35144  
 $\beta''$ -Al $_2$ O $_3$ -Na $_2$ O, Raman scatt. from mobile cations 0-11394  
 $\beta''$ -Al $_2$ O $_3$ -Na $_2$ O, rapid ion conductor, Na penetration 0-24653  
 $\beta$ -Al $_2$ O $_3$ -Na $_2$ O, solid electrolyte, battery appl. (Polish) 0-12005  
 $\beta$ -Al $_2$ O $_3$ -Na $_2$ O, superionic conductor, microwave absorption spectrum 0-11515  
 $\beta$ -Al $_2$ O $_3$ -Na $_2$ O  $^{23}$ Na asymmetry parameter, temp. variations 0-6540  
 Al $_2$ O $_3$ -Na $_2$ O-Li $_2$ O, phase transformations during firing 0-3036  
 $\beta''$ -Al $_2$ O $_3$ -Na $_2$ O-Li $_2$ O (8.85, 0.75 wt.%) pressing powders, prep. by spray drying 0-40294  
 $\beta$ -Al $_2$ O $_3$ -Na $_2$ O-Li $_2$ O membranes from Na-S cells, failure anal. 0-12003  
 $\beta$ -Al $_2$ O $_3$ (Na $_2$ O.11Al $_2$ O $_3$ ), prep. by diffusional transform. during sintering of Al $_2$ O $_3$  in presence of NaAlO $_2$  0-25637  
 Al(PO $_3$ ) $_3$ -NaF-LiF glasses, mixed-alkali effect 0-19715  
 B $_2$ O $_3$ -K $_2$ O-Na $_2$ O-Rb $_2$ O-C $_2$ O glass, small angle X-ray scatt. exam. of struct. 0-38922  
 B $_2$ O $_3$ -Na $_2$ O-SiO $_2$ -Al $_2$ O $_3$ , effect of alumina dispersions on the thermal cond./diffusivity/stress resist. 0-39368



## sodium compounds continued

$\text{Ba}_2\text{NaNb}_2\text{O}_{15}$ , electrooptical diff. by periodic domain struct. 0-40090  
 $\text{Ba}_2\text{NaNb}_2\text{O}_{15}$ , Raman scatt. experiments in tetragonal tungsten bronze compounds 0-40113  
 $\text{BaO-K}_2\text{O-Na}_2\text{O-ZnO-SiO}_2$ , corrosion and microhardness, effect of detergents 0-16518  
 $\text{BeO-P}_2\text{O}_5\text{-Na}_2\text{O}$  glass, gamma irr., cation modifier effect on radiation centre formation 0-40720  
 $\text{CaAl}_2\text{Si}_2\text{O}_8\text{-NaAlSi}_3\text{O}_8$  (anorthite-albite) system, crystal growth rates and processes 0-4010  
 $\text{CaCO}_3\text{-NaAlSiO}_4$ , micromechanism for phase formation during sintering (Russian) 0-16253  
 $\text{Cs}_2\text{NaRCl}_6$ ,  $\text{R}=\text{Pr}^{3+}$ ,  $\text{Eu}^{3+}$ ,  $\text{Tb}^{3+}$ , crystal field, ligand polarisability contributions 0-39536  
 $\text{Cs}_2\text{NaTmF}_6$ , mag. behaviour 2.9 to 251.3K, cryst. field levels, ang. overlap model (German) 0-29520  
 $\text{Cs}_2\text{NaYbF}_6(\text{Br})_6$ , mag. behaviour, 3.5-251.3K (German) 0-50041  
 $\text{Cs}_2\text{O-SiO}_2$  glass, low temp. heat capacity 0-49373  
 $\text{D NaCl-Fe}$ , defect struct., Mossbauer spectra and X-ray diff. obs. 0-7237  
 $\text{EuCl}_3\text{-NaPO}_3\text{-H}_2\text{O}$  system, Eu polyphosphates form. at  $0^\circ\text{C}$  0-35515  
 $\text{Fe}$ , influence of acid  $\text{Na}_2\text{PO}_4$  soln. in tap water as a corrosion inhibitor 0-45424  
 $\text{Fe}_2\text{O}_3\text{-Na}_2\text{O-BaO}$  glass, mag. props. 4.2-295K, micromagnetism (French) 0-39782  
 $\text{GaAs-NaOH}$  interface, inversion layer form. and surface states 0-2465  
 $\text{GeO}_2\text{-Na}_2\text{O}$ , glass composition effect on solubility in  $\text{H}_2\text{O}$  0-39303  
 $\text{KH II}$  states and  $\text{KH}^+$  ground state, pot. energy curves calc. 0-18812  
 $\text{KNO}_3\text{-NaNO}_2\text{-NaNO}_3$  eutectic salt, use in indirect heating systems (German) 0-38233  
 $\text{LaF}_3\text{-BaF}_2\text{-ZrF}_4\text{-NaF}$ , glassy transition, refr. index, density and molar refr. 0-1937  
 $\text{La}_2\text{O}_3\text{-Na}_2\text{SiO}_3$  molten glasses, surface tension and density, 900-1500 $^\circ\text{C}$  0-15334  
 $(\text{Li},\text{Na},\text{K}) (\text{Nb},\text{Ta})\text{O}_3$ , pseudo-binary and ternary systems quenched metastable glassy and cryst. phases 0-29935  
 $\text{LiCl-NaCl-AlCl}_3$  melt, elec. cond., 800 to 1200K (Japanese) 0-24633  
 $\text{LiF-AlF}_3\text{-Na}_3\text{AlF}_6\text{-Al}_2\text{O}_3$  system, phase equilibrium, X-ray diff., DTA, quenching, optical microscopy study 0-50610  
 $\text{LiF-NaF-KF-K-GeF}_6\text{-GeO}_2$  fused mixture, for electrodeposition of Ge powder 0-2979  
 $\text{LiF-NaPO}_3\text{-MeF}_x$  ( $\text{Me}=\text{Mg}, \text{Ca}, \text{Al}$ ) glasses, IR spectroscopy study 0-16042  
 $100(\text{Li}_2\text{O}.2\text{SiO}_2)\text{-Na}_2\text{O}$ , directionally solidified, thermal and mech. props. (Japanese) 0-16295  
 $(\text{Na},\text{Cs})(\text{F},\text{Cl},\text{I})$  quaternary reciprocal system, calc. of phase diagrams 0-25666  
 $\text{Na}$  (111) surface, epitaxial film, electron induced dissociation 0-6646  
 $\text{Na}$  diethyldithiocarbamates, use in liquid-liquid extraction of corrosion and fission products 0-18459  
 $\text{Na-}\beta\text{Al}_2\text{O}_3$  ceramics, synthesis 0-40305  
 $\text{Na-Fe}$  fluorophosphate glass, EPR and Mossbauer resonance study 0-15838  
 $\text{Na-Fe}$  fluorophosphate glass, Mossbauer study, mag. and optical props. 0-16065  
 $\text{Na}^+\text{-K}^+\text{F}^-\text{SO}_4^{2-}$ , asymmetrical reciprocal molten salt system, excess enthalpies 0-30268  
 $\text{Na}_2\text{-S-GeS}_2$  system, glass formation, struct. and ionic conduction 0-54138  
 $\text{NaAlCl}_4$ , relative enthalpy to 573K and standard enthalpy of form., molar enthalpy of fusion 0-50878  
 $\text{Na}_3\text{AlF}_6$  film, evaporated, electron bombard. effect on secondary electron emission, Auger peak shifts 0-2903  
 $\text{NaAlH}_4$ , ab initio calc. of geom. struct., charge distrib., bonding and pot. energy surfaces 0-18796  
 $\text{NaAlSi}_3\text{O}_8$ , radial distribution functions, quasi-crystalline model 0-1879  
 $\text{Na}_8(\text{Al}_6\text{Si}_2\text{O}_{24})\text{Cl}_2$ , sodalite, electronic struct. of F-centre 0-2356  
 $(\text{NaAl})\text{Si}_2\text{O}_7\text{-H}_2\text{O}$ , analcite, polyhedral tilt transitions obs. at high press. 0-6515  
 $\text{Na}_2\text{Al}_2\text{Si}_2\text{O}_{10}\text{-H}_2\text{O}$ , natrolite, cleavage etching in acidic and neutral media 0-6407  
 $\text{NaBH}_4$ , ab initio calc. of geom. struct., charge distrib., bonding and pot. energy surfaces 0-18796  
 $\text{NaBSi}_3\text{O}_8$ ,  $\text{B}=\text{Mg}, \text{Fe}^{3+}$ , Al, pyroxenes, order-disorder interpretation 0-38987  
 $\text{Na}_0.\text{Bi}_{0.5}\text{TiO}_{1.5}$ , dielectric const. thermal hysteresis, ferroelectric-antiferroelectric transitions 0-50281  
 $\text{NaBr}$ ,  $^{14}\text{N}$  impurities, molecular point defects, EPR isotropic hyperfine triplets 0-2636  
 $\text{NaBr}$ , heat capacity, Gruneisen parameters, 2 to 20K 0-29180  
 $\text{NaBr}$ , lattice dynamics and statics, three-body-force shell model 0-49323  
 $\text{NaBr}$ , muonic X-ray intensities, Lyman series 0-23578  
 $\text{NaBr}$ , self-trapped exciton and F-centre form. by picosecond laser pulses 0-10546  
 $\text{NaBr}$ ,  $\text{U}_2$  and  $\text{U}_1$  centres, optical excitations 0-2803  
 $\text{NaBr-Ag}^+$ , UV absorption bands, temp. depend. 0-20672  
 $\text{NaBr-U}$ -centre containing cryst., X-ray radiation induced cation vacancy generation 0-39078  
 $\text{NaBrO}_3$ ,  $^{17}\text{O}$  NQR, spin echo double reson. method, electronegativity 0-54970  
 $\text{NaBrO}_3$ , dispersion of Faraday effect 0-2731  
 $\text{NaBrO}_3$ , surface polariton spectroscopy, frustrated total reflection method (Russian) 0-49628  
 $\text{NaBr.2H}_2\text{O}$ , polycryst. hydrates, librational motion of  $\text{H}_2\text{O}$  mols., neutron diff. exam. 0-10604  
 $\text{NaCN}$ , diffuse scatt., hard-core correl., weak-graph method 0-49137  
 $\text{NaCN}$ , plastic phase, Raman scatt. spectra (French) 0-11379  
 $\text{NaCN}$ , struct. domains, NMR determ. 0-50204  
 $\text{Na}_2\text{CO}_3$ , new catalyst for  $\text{CO-H}_2\text{O}$  induced coal liquefaction 0-30335  
 $\text{NaCl}$ ,  $^{15}\text{N}$  impurities, molecular point defects, EPR isotropic hyperfine triplets 0-2636  
 $\text{NaCl}$  (001) substrate, preferential epitaxy of evaporated films induced by electron bombard. or elec. field 0-10824  
 $\text{NaCl}$  (111) surfaces, electron bombard. effects and subsequent Ag epitaxial growth, RHEED and AES 0-15419  
 $\text{NaCl}$ , absorpt. spectra, influence of elec. field 0-2794  
 $\text{NaCl}$ , additively coloured, SHG 0-1274  
 $\text{NaCl}$ , adsorption of  $\text{CO}_2$ , atomic interaction pot. on (100) face (German) 0-15380  
 $\text{NaCl}$ , adsorption of  $\text{CO}_2$ , gas-solid interaction potential, adsorption sites and surface migration 0-24738

## sodium compounds continued

$\text{NaCl}$ , adsorption of methane, adsorpt. pot., localised and mobile phases, hopping adsorbates 0-24739  
 $\text{NaCl}$ , aq. soln., pulsed limiter discharge, nonideal plasma chem. composition 0-19657  
 $\text{NaCl}$  aqueous aerosols, fixation and microscopic sizing 0-16734  
 $\text{NaCl}$ , aqueous soln., high precision viscosity meas. 0-10695  
 $\text{NaCl}$  aqueous soln., mol. dynamics simulation, central force model 0-49077  
 $\text{NaCl}$ , automated scan of X-ray powder diffraction pattern 0-22492  
 $\text{NaCl}$ , bi-exciton luminescence possibility 0-40167  
 $\text{NaCl}$ , bulk and surface absorption comparison, 9.2 to 10.85  $\mu\text{m}$  0-33051  
 $\text{NaCl}$ , crystal, electron emission under uniaxial compression 0-7483  
 $\text{NaCl}$  crystal surface struct., effect of ionic bombardment (German) 0-24507  
 $\text{NaCl}$  crystals irr. by high electron doses, annealing, colour centre prod. 0-2074  
 $\text{NaCl}$  crystals with dipole O colour centres, radiation colouring and holographic recording 0-48187  
 $\text{NaCl}$  cubical 4  $\mu\text{m}$  particles, 0.627  $\mu\text{m}$  light scatt. meas. 0-9804  
 $\text{NaCl}$ , dielectric polarisation calcs., microscopic local fields 0-20582  
 $\text{NaCl}$  dimer, electron diff. study of mol. struct. 0-28951  
 $\text{NaCl}$ , dipole polarisation, depend. on AC and DC voltage superposition 0-20577  
 $\text{NaCl}$ , dislocation rosettes around Vickers diamond pyramid indents, quenching effect 0-11740  
 $\text{NaCl}$ , dislocation struct. of slip bands, hydrostatic press. effect 0-54249  
 $\text{NaCl}$ , doped substrate for vac. deposition of Ag oriented films 0-2303  
 $\text{NaCl}$ , effect of annealing and neutron irr. on block struct. 0-29061  
 $\text{NaCl}$ , electric field induced by homogeneous stresses 0-11343  
 $\text{NaCl}$  electron excited luminescence yield orientational depend. 0-40169  
 $\text{NaCl}$ , electronic struct., SCF cryst. cluster model 0-24792  
 $\text{NaCl}$ , electronic structure calculation, CNDO semi-empirical methods (Russian) 0-10909  
 $\text{NaCl}$ , emission of Cl atoms during  $\text{V}_k$  centre decomposition 0-10578  
 $\text{NaCl}$  etalon used to control modelocked multiline TEA  $\text{CO}_2$  laser 0-23713  
 $\text{NaCl}$ , evaporating cryst. surfaces, successive monatomic step trains with different density 0-29254  
 $\text{NaCl}$  film, electron emission under metastable He and Ne atom impact 0-20747  
 $\text{NaCl}$ , for thermoelectrochemical prod. of  $\text{H}_2$  0-55946  
 $\text{NaCl}$ ,  $\gamma$ -irr., photoplastic effect and internal friction aftereffect 0-24529  
 $\text{NaCl}$ ,  $\gamma$ -irradiated, F $\rightarrow$ M phototransformation, effect on aquoluminescence 0-7418  
 $\text{NaCl}$ , halite, dynamic recrystn. during compression creep, geophys. appl. 0-25772  
 $\text{NaCl}$ , hydrostatically compressed crystals. in easy glide stage, plastic deformation 0-7630  
 $\text{NaCl}$ , interfaced polarisation and losses, superimposed AC and DC voltage study 0-25276  
 $\text{NaCl}$ , interpolational eqn. of state with allowance for melting, vaporis., dissoc. and ionis. processes 0-24566  
 $\text{NaCl}$ , ionic mobilities in cellulose acetate membranes 0-45550  
 $\text{NaCl}$ , irradiated, at 80K, thermolum. processes 0-34990  
 $\text{NaCl}$ , laser damage, phenomenological theory 0-19836  
 $\text{NaCl}$  laser-induced breakdown fields rel. to wavelength and focal spot radius 0-35019  
 $\text{NaCl}$ , laser-induced damage threshold variations 0-14380  
 $\text{NaCl}$ , lattice dynamics and statics, three-body-force shell model 0-49323  
 $\text{NaCl}$ , local field, microscopic electronic polarisation 0-25283  
 $\text{NaCl}$ , M-centre statistical prod. meas. 0-15097  
 $\text{NaCl}$ , moving dislocations, interaction with defects, elec. effects meas. in plastic deformation (Hungarian) 0-10572  
 $\text{NaCl}$ , muonic X-ray intensities, Lyman series 0-23578  
 $\text{NaCl}$ , optical breakdown from 0.53-10.6  $\mu\text{m}$  0-7292  
 $\text{NaCl}$  particle, luminesc. duration rel. to time in  $\text{CO}_2$  laser beam focal zone 0-34983  
 $\text{NaCl}$ , plastic deformation influence on shape recovery effects 0-6684  
 $\text{NaCl}$ , positronic atom scatt. on optical phonons, positron thermalisation 0-50457  
 $\text{NaCl}$  preirradiation effect on proton channelling, thermoluminescence study 0-19860  
 $\text{NaCl}$ , pulsed-laser-induced damage, role of avalanche multiplication and multiphoton absorpt. 0-48316  
 $\text{NaCl}$ , quantum-chem. calcs. of electronic and hole centres and surface 0-20118  
 $\text{NaCl}$ , rock salt, quenched, residual stresses, optical study 0-55061  
 $\text{NaCl}$ , single cryst., for IR dispersive refl. meas., low temp., rel. to anharmonicity calcs. 0-11371  
 $\text{NaCl}$ , single cryst. expt. on distension of gas-filled cavity 0-49286  
 $\text{NaCl}$  single crystals, screw dislocations, influence of interionic potentials on core configs. 0-34000  
 $\text{NaCl}$ , solution, apparent molar heat capacity and volume, at 298.15K 0-29179  
 $\text{NaCl}$ , spiral dislocation mobility depend. on elec. field, relaxation time 0-39105  
 $\text{NaCl}$ , sputtering of atoms by 540 eV electrons, delay times 0-35025  
 $\text{NaCl}$  structure ionic cryst., high temp. dynamics, var. approach 0-29130  
 $\text{NaCl}$  substrate for condensed Au film, ion bombarded, thermally stimulated exoelectron emission 0-50537  
 $\text{NaCl}$  surface, residence times of Au atoms, time-of-flight meas. 0-10788  
 $\text{NaCl}$ , surface charge meas. in ultra high vac. 0-20287  
 $\text{NaCl}$  surface conditions of step decoration 0-15349  
 $\text{NaCl}$  surface with adsorbed water layer, absorpt. and thickness meas. 0-16001  
 $\text{NaCl}$ , thermal expansion meas. after X-ray irr., F-centre bleaching 0-44338  
 $\text{NaCl}$ , thermodynamic equil. vapourisation, transpiration mass spectrometry 0-52356  
 $\text{NaCl}$ , thin film, crystal-vacuum (100) surface, mol. dynamics computer simulation 0-34288  
 $\text{NaCl}$  type ionic crystals, statistical theory calcs. of surface energy and surface tension 0-17894  
 $\text{NaCl}$ ,  $\text{U}_2$  and  $\text{U}_1$  centres, optical excitations 0-2803  
 $\text{NaCl}$ , V- and X-centres accumulation (Russian) 0-54228  
 $\text{NaCl}$ , vacancy complex formation and binding energies in zeroth approx. 0-24441  
 $\text{NaCl}$ , valence electron distrib., pseudopotential calcs. 0-2335  
 $\text{NaCl}$  whiskers, plastification in elec. field (Russian) 0-21010



## sodium compounds continued

- NaCl, X-ray irradi., vacancy conc., thermal expansion meas. 0-6431  
 NaCl:Ag, absorpt. spectra, influence of elec. field 0-2794  
 NaCl:Ag, excitation in fund. absorpt. region, luminesc. and thermolum. 0-50433  
 NaCl:Ca, aggregation and precip. hardening in impurity vacancy, dipole decay 0-16322  
 NaCl:Ca, hologram recording on R-centres 0-1157  
 NaCl:Ca, microhardness and thermoluminescence, hardness-quenching temp. variation 0-29813  
 NaCl:Ca,  $Z_1$  centre thermoluminescence study 0-16109  
 NaCl:Ca crystals, optimum temp. for holographic recording (*Russian*) 0-1163  
 NaCl:Ca<sup>2+</sup> crystals, influence of dipoles and dipole complexes on yield point 0-39208  
 NaCl:Eu<sup>2+</sup>, oriented growth and cryst. struct. of precipitated phases 0-24303  
 NaCl:Eu<sup>2+</sup>, single cryst. optical absorpt. spectra 0-45117  
 NaCl:Ga(In), ESR of impurity centres, impurity optical absorpt. bands 0-29618  
 NaCl:K<sub>3</sub>IrCl<sub>6</sub>, electron irradi., ligand field anal., EPR obs. 0-29612  
 NaCl:Li, U-centres, HFS consts., g-factor, EPR spectra 0-39869  
 NaCl:Mn<sup>2+</sup>, CN<sup>-</sup>, EPR spectrum rel. to Mn<sup>2+</sup>-vacancy-CN<sup>-</sup> complex 0-54942  
 NaCl:O, hologram recording, colloidal type centre transformation (*Russian*) 0-55147  
 NaCl:Pb<sup>2+</sup> crystals, grown from aq. soln., flotation study 0-39144  
 NaCl:Pr<sup>3+</sup> (Sm<sup>3+</sup>), absorption spectra at 4.2 K, anal. 0-7378  
 NaCl:S<sup>2-</sup>, enthalpy of anion vacancy migration 0-15309  
 NaCl:Sr, dimer and trimer aggregate formation by NMR, ionic cond. and dielectric losses 0-15094  
 NaCl:Ti<sup>3+</sup>,  $\gamma$ -irradi., aquoluminesc. obs. 0-2856  
 NaCl:V<sup>2+</sup>, EPR spectra above 300K 0-34765  
 NaCl:V<sup>2+</sup>, elec. field effect on Z-like centres spectrum 0-2802  
 NaCl-AgCl molten solns., activities and surface tension 0-10748  
 NaCl-CsCl-MnCl<sub>2</sub>, molten salt system, molar volume and elec. cond. meas. 0-34217  
 NaCl-CsCl-MnCl<sub>2</sub>, molten salt system, molar volume and elec. cond. meas. 0-34218  
 NaCl-KCl, aq. solns., isopiestic studies, 383 to 474K 0-21320  
 NaCl-KCl, interdiffusion and demixing, electron microprobe anal. (*French*) 0-54444  
 NaCl-KCl melt, reaction with LiO<sub>2</sub>·2SiO<sub>2</sub>, X-ray, IR exam. 0-55706  
 NaCl-KCl(MgCl<sub>2</sub>)·H<sub>2</sub>O mixed electrolyte solns., elec. transport 0-3355  
 NaCl-LiCl mixed crystals, Au decoration study of solid-melt interface, phase separation 0-15026  
 NaCl-MgO mixture, high pressure uniaxial stress component effect on eqns. of state, opposed anvil X-ray determ. 0-49301  
 NaCl-NaBr, solid soln., negative muon capture ratios 0-55007  
 NaCl-NaBr-TeO<sub>2</sub>, condition diagram, thermographic obs. (*Russian*) 0-55377  
 NaCl-NaF:Pb<sup>2+</sup>, point defects, ionic thermal current and optical meas. 0-6403  
 NaCl-O<sup>2-</sup>, X-ray irradi., defect generation during radiolysis 0-7831  
 NaCl-OH<sup>-</sup>, electron irradi., F<sub>2</sub><sup>+</sup> centre stabilisation and tuneable laser operation 0-54231  
 NaCl+K, three dimens. collision, exponentiating trajectories and statistical behaviour 0-5595  
 NaCl+Pb, Pb aggregation effect on yield stress, incoherent precipitates, solubility determ. method 0-50645  
 NaCl:(Ca), irradi. at room temp., stored energy rel. to thermolum. 0-10574  
 NaCl<sub>1-x</sub>Br<sub>x</sub>, mixed cryst., vibr. and optical props. 0-29133  
 NaClO<sub>3</sub>, <sup>17</sup>O NQR, spin echo double reson. method, electronegativity 0-54970  
 NaClO<sub>3</sub>, dispersion of Faraday effect 0-2731  
 NaClO<sub>3</sub>, magnetoelectric susceptibilities, phenomenological rules for computation 0-55068  
 NaClO<sub>3</sub>, metastable-stable phase transition mechanism (*French*) 0-15031  
 NaClO<sub>3</sub>, mol. torsional oscils., cooperative study by NQR 0-25244  
 NaClO<sub>3</sub>, radiation damage, XPS obs. 0-29844  
 NaClO<sub>3</sub>, Zeeman NQR powder spectra 0-20502  
 NaClO<sub>4</sub>, aq. glass, formation of trapped H-atoms and electrons on X-irradi. 0-35559  
 NaClO<sub>4</sub>, Brewster type surface mode dispersion, IR refl. meas. 0-11415  
 NaClO<sub>4</sub>, frozen soln., EPR of trapped H-atoms produced by UV and X-irradi. 0-3369  
 NaClO<sub>4</sub>·H<sub>2</sub>O, <sup>1</sup>H NMR second moment, H<sub>2</sub>O dynamic disorder 0-25221  
 6NaCl.CdCl<sub>2</sub>, 60 wt.% powders, Suzuki phases prep. and stability 0-35123  
 Na<sub>2</sub>Co<sub>2</sub>Ti<sub>6</sub>O<sub>14</sub>F<sub>2</sub>, characterisation and mag. props., 90-800K, Na<sub>x</sub>Ti<sub>4</sub>O<sub>8</sub> bronze isotypes (*French*) 0-39735  
 NaCrO<sub>2</sub>, two-dimens. mag. order, neutron powder diffr. obs. 0-44805  
 Na<sub>2</sub>Cr<sub>2</sub>Ti<sub>2</sub>O<sub>10</sub>, characterisation and mag. props., 90-800K, Na<sub>x</sub>Ti<sub>4</sub>O<sub>8</sub> bronze isotypes (*French*) 0-39735  
 Na(D<sub>2</sub>H<sub>1-x</sub>)<sub>3</sub>(Se<sub>3</sub>)<sub>2</sub>, ferroelec. dispersion 0-40069  
 Na<sub>2</sub>Eu(PO<sub>4</sub>)<sub>2</sub>, synthesis and IR spectra 0-16019  
 Na<sub>2</sub>Eu(PO<sub>3</sub>)<sub>7</sub>·12H<sub>2</sub>O and Na<sub>2</sub>Eu(PO<sub>3</sub>)<sub>6</sub>·6H<sub>2</sub>O, form. in EuCl<sub>3</sub>-NaPO<sub>3</sub>-H<sub>2</sub>O system at 0°C 0-35515  
 NaF, antireflection coating, 100 ns pulsed laser damage at 2.7 and 3.8  $\mu$ m 0-33057  
 NaF antireflection coating, multithreshold damage meas. at HF and DF laser wavelengths 0-33058  
 NaF, band struct. and charge densities, intersecting spheres model 0-49591  
 NaF, Compton profiles, anisotropies 0-20730  
 NaF film, electron emission under metastable He and Ne atom impact 0-20747  
 NaF film on CaF<sub>2</sub>, interface and bulk absorption meas. 0-35001  
 NaF film on ZnSe plate, absorption coeff. ATR spectroscopy 0-35000  
 NaF, heat capacity, Gruneisen parameters, 2 to 20K 0-29180  
 NaF laser coating, UV damage obs. 0-33056  
 NaF, lattice dynamics and statics, three-body-force shell model 0-49323  
 NaF, measurement of thermal expansivity at low temp. using Si cell 0-37027  
 NaF, phonon conductivity correction due to three phonon normal processes in presence of dislocations 0-15318  
 NaF, pulsed-laser-induced damage, role of avalanche multiplication and multiphoton absorpt. 0-48316  
 NaF: Mn<sup>2+</sup>, VUV absorpt. spectrum and EPR 0-55142  
 NaF:Ca, migration enthalpy and entropy, TSC obs. 0-54716

## sodium compounds continued

- NaF:OH<sup>-</sup>, electron irradi., F<sub>2</sub><sup>+</sup> centre stabilisation 0-54231  
 NaF/GeSe, IR multilayer partial mirrors effective from 1.3 to 16  $\mu$ m 0-9978  
 NaF-LnF<sub>3</sub> (Ln=Y, La, Yb) binary liquid mixtures, thermochemistry 0-45538  
 NaF-YF<sub>3</sub> system, fusibility diagram, quasibinary section of NaF-YF<sub>3</sub>-YOF system characts. 0-55371  
 Na<sub>2</sub>(Fe,Mn)<sub>2</sub>(PO<sub>4</sub>)<sub>4</sub>, arrojadite, X-ray cryst. struct. determ. 0-39058  
 NaFeF<sub>4</sub>, amorphous, Mossbauer study 0-39970  
 Na<sub>2</sub>FeTi<sub>2</sub>O<sub>16</sub>, characterisation and mag. props., 90-800K, Na<sub>x</sub>Ti<sub>4</sub>O<sub>8</sub> bronze isotypes (*French*) 0-39735  
 NaH, A<sup>1</sup> $\Sigma^+$ -X<sup>1</sup> $\Sigma^+$  electronic transition, spectroscopic anal. and potential energy curves 0-48102  
 NaH, ground state, pot. curves, MTX<sub>R</sub> method 0-5482  
 NaH II states and NaH<sup>+</sup> ground state, pot. energy curves calc. 0-18812  
 NaHSeO<sub>3</sub>, and NaDSeO<sub>3</sub>, NMR of <sup>23</sup>Na and <sup>2</sup>D, hydrogen bonding 0-44190  
 NaH<sub>2</sub>(SeO<sub>3</sub>)<sub>2</sub>, ferroelectric, electromechanical props. near Curie point 0-29690  
 NaI, continuous slowing down approx., range difference for 0.2 to 10 MeV electrons 0-39187  
 NaI, impurity in AC metal halide discharge, atomic plasma characts., a priori method 0-44034  
 NaI in acetone, press. effects on Walden products, ion-solvent interactions 0-3398  
 NaI, lattice dynamics and statics, three-body-force shell model 0-49323  
 NaI, motion of free excitons and their self-localisation 0-2342  
 NaI, resonant Raman scattering in crystals with self-trapping excitons 0-7344  
 NaI scintillation spectrometer, gamma-ray energy released from fission products, response matrix (*Japanese*) 0-42888  
 NaI, self-trapped exciton and F-centre form. by picosecond laser pulses 0-10546  
 NaI, temp. varying Mossbauer spectra, isomer shift 0-4726  
 NaI, thermal dissoc. of photoproduced excitons at UV band edge, recomb. luminesc. obs. 0-50412  
 NaI, U<sub>2</sub> and U<sub>1</sub> centres, optical excitations 0-2803  
 NaI:Ti, scintillation excitation mechanism 0-2857  
 NaInO<sub>2</sub>, prep., props. and struct. 0-35517  
 NaInS<sub>2</sub>, prep., props. and struct. 0-35517  
 Na<sub>2</sub>In(SO<sub>4</sub>)<sub>3</sub>·3H<sub>2</sub>O, cryst. struct. by X-ray methods 0-6393  
 Na<sub>2</sub>In<sub>2</sub>S<sub>2</sub>, intercalation-substitution compounds, NMR study 0-44952  
 NaK, detailed spectroscopic study, sub-Doppler spectroscopic techniques 0-52339  
 NaK dimer formed in supersonic beam, laser-induced emission 0-9636  
 NaK, sub-Doppler laser spectrosc., high resolution 0-52320  
 NaMgF<sub>3</sub>, orthorhombic perovskite, contribution to crystal chem. 0-19777  
 Na<sub>2</sub>Mg<sub>2</sub>SiO<sub>4</sub>, ionic cond. meas. 0-6545  
 Na<sub>2</sub>Mg<sub>2</sub>Si<sub>2</sub>O<sub>10</sub>, ionic cond. meas. 0-6545  
 Na<sub>2</sub>Mg<sub>2</sub>Si<sub>2</sub>O<sub>10</sub>, powder diffr. cryst. data 0-19765  
 NaMnCl<sub>3</sub>, antiferromagnet, exciton self-localisation luminesc. and excitation spectra (*Russian*) 0-11456  
 Na<sub>2</sub>Mn(Ti(Si<sub>2</sub>O<sub>7</sub>))<sub>2</sub>, Kazakovite, cryst. struct. determ. 0-19782  
 Na<sub>2</sub>MoO<sub>4</sub> based melt, crystn. from Cl<sub>2</sub>(MoO<sub>4</sub>)<sub>3</sub> and La<sub>2</sub>(MoO<sub>4</sub>)<sub>3</sub> 0-20920  
 Na<sub>2</sub>MoO<sub>4</sub>(S<sub>4</sub>)(Se<sub>4</sub>) crystals, charge transfer spectra of MoX<sub>4</sub><sup>2-</sup> complexes 0-54658  
 NaNO<sub>2</sub> and NaNO<sub>3</sub>, muonic X-ray intensities, Lyman series 0-23578  
 NaNO<sub>2</sub>, antiferroelec. phase, struct. anal. by neutron diffraction 0-24410  
 NaNO<sub>2</sub>, ferroelec., electron distrib., X-ray and neutron diffraction study 0-24411  
 NaNO<sub>2</sub>, ferroelectric transitions, group theoretic comparison with AgNaNO<sub>2</sub> 0-7311  
 NaNO<sub>2</sub>, ferroelectric transitions, one-mode model 0-29702  
 NaNO<sub>2</sub>, incommensurate phase transition, Bethe-Peierls and mol. field approx. 0-20599  
 NaNO<sub>2</sub>, incommensurate-and-antiferroelectric phase transition, amplitude mode, ultrasonic study 0-39227  
 NaNO<sub>2</sub>, linear compressibility to 27 kbar, X-ray diffr. obs. 0-34125  
 NaNO<sub>2</sub>, size effect and spin-lattice relax. of <sup>14</sup>N 0-20480  
 NaNO<sub>3</sub>, aq. soln., pulsed limiter discharge, nonideal plasma chem. composition 0-19657  
 NaNO<sub>3</sub>, dielec. loss anal., Debye type loss peaks 0-50260  
 NaNO<sub>3</sub> in N,N-dimethylacetamide, Raman, IR and US relaxation studies 0-50315  
 NaNO<sub>3</sub>, linear compressibility to 27 kbar, X-ray diffr. obs. 0-34125  
 NaNO<sub>3</sub> melts, ion exchange reaction with Na silicate glasses 0-16673  
 NaNO<sub>3</sub>, single cryst. cleavage, Bi film deposition by vacuum evaporation 0-35091  
 NaNO<sub>3</sub> solution cathodic gas evolution rate rel. to electrode material (*Russian*) 0-26020  
 NaNO<sub>3</sub>-AgNO<sub>3</sub> mixture, contact with glass, conc. changes in surface layer 0-44372  
 NaNO<sub>3</sub>-KNO<sub>3</sub>-Ca(NO<sub>3</sub>)<sub>2</sub>·4.09H<sub>2</sub>O melt, mixed alkali effect 0-34219  
 NaNO<sub>3</sub>-TiNO<sub>3</sub>-Ca(NO<sub>3</sub>)<sub>2</sub>·4.09H<sub>2</sub>O melt, mixed alkali effect 0-34219  
 NaNO<sub>3</sub>, fine structure changes on interaction with weak shock waves (*Russian*) 0-54313  
 Na<sub>3</sub>Na(PO<sub>4</sub>)<sub>2</sub>, synthesis and IR spectra 0-16019  
 NaNbF<sub>6</sub>, NMR, quadrupole effects and struct. distortion 0-15809  
 NaNbO<sub>3</sub>, elec. and photoelec. props. near ferroelec.-antiferroelec. phase transition 0-15989  
 NaNbO<sub>3</sub>, elec. and thermoelec. props., influence of O defects 0-29401  
 NaNbO<sub>3</sub>-BaTiO<sub>3</sub>, ferroelec. Curie temp., theory 0-7313  
 NaNbO<sub>3</sub>-BaTiO<sub>3</sub>, unidirectionally solidified transparent ceramics 0-25677  
 NaNbO<sub>3</sub>-based ferroelec. solid solns., morphotropic transitions and elec. props., enhanced vacancy conc. 0-55048  
 NaNbO<sub>3</sub>-PbTiO<sub>3</sub>, ferroelec. Curie temp., theory 0-7313  
 NaNdP<sub>4</sub>O<sub>12</sub>, laser emission cross sections, fluorescence spectra, radiative lifetimes, quantum efficiency 0-23694  
 NaNdX, zeolite hydrated, ion exchange of Na for Nd, cryst. structs. 0-33979  
 Na<sub>2</sub>Ni<sub>10</sub>X(MoO<sub>4</sub>)<sub>2</sub>, paramag. props., 90-800K (*French*) 0-39734  
 Na<sub>2</sub>Ni<sub>2</sub>(P<sub>2</sub>O<sub>7</sub>)<sub>2</sub>·nH<sub>2</sub>O, thermal dehydration 0-35513  
 Na<sub>2</sub>Ni<sub>2</sub>Ti<sub>6</sub>O<sub>14</sub>F<sub>2</sub>, characterisation and mag. props., 90-800K, Na<sub>x</sub>Ti<sub>4</sub>O<sub>8</sub> bronze isotypes (*French*) 0-39735  
 NaO-CaO-SiO<sub>2</sub> glasses, fluorinating agents effect on comp. and surface struct. 0-35364



## sodium compounds continued

- NaO-SiO<sub>2</sub> glass, distrib. of different O ions, molar refractivity meas. 0-33897
- NaO<sub>2</sub>, elastic interaction, role in disordered-pyrite to ordered-pyrite phase transition 0-19739
- NaO<sub>2</sub>, non-isothermal decomp. kinetics 0-16649
- NaO<sub>2</sub>, physical mechanisms of phase transitions 0-6381
- NaO<sub>2</sub>, thermal decomp. macrokinetics, differential thermal anal. 0-16650
- Na<sub>2</sub>O aerosol gravitational fallout rate, validation of computer code for fast reactor accident anal. 0-18535
- Na<sub>2</sub>O aerosols, aerodynamic props. 0-23011
- Na<sub>2</sub>O, effect on props. of PbO containing cryst. glass 0-24637
- Na<sub>2</sub>O glasses, partially leached, dehydrated surface reaction with water 0-3406
- Na<sub>2</sub>O particles, effect on optical props. of Na vapour 0-1736
- Na<sub>2</sub>O-SiO<sub>2</sub> glass, high-temp. thermolum., colour centre absorpt. 0-16110
- Na<sub>2</sub>O-Al<sub>2</sub>O<sub>3</sub>-P<sub>2</sub>O<sub>5</sub> glass, low-temp. viscosity 0-39198
- Na<sub>2</sub>O-Al<sub>2</sub>O<sub>3</sub>-P<sub>2</sub>O<sub>5</sub>-Eu glasses, fluorescence line narrowing meas. (French) 0-34975
- Na<sub>2</sub>O-Al<sub>2</sub>O<sub>3</sub>-SiO<sub>2</sub> glass, leaching in HCl solns., Na conc. distrib. in surface layers 0-21141
- Na<sub>2</sub>O-Al<sub>2</sub>O<sub>3</sub>-SiO<sub>2</sub> glass, interaction with aq. salt solns., alkali ions distrib. in surface layers 0-21142
- Na<sub>2</sub>O-Al<sub>2</sub>O<sub>3</sub>-SiO<sub>2</sub>-xH<sub>2</sub>O, fibrous crystal growth in silica gel, X-ray, electron probe and IR spectra obs. 0-25541
- Na<sub>2</sub>O-Al<sub>2</sub>O<sub>3</sub>-SnO<sub>2</sub>-SiO<sub>2</sub> glass, chemical stability in NaOH and Na<sub>2</sub>CO<sub>3</sub> solns. 0-16532
- Na<sub>2</sub>O-Al<sub>2</sub>O<sub>3</sub>-ZrO<sub>2</sub>-SiO<sub>2</sub> glass, chemical stability in NaOH and Na<sub>2</sub>CO<sub>3</sub> solns. 0-16532
- Na<sub>2</sub>O-B<sub>2</sub>O<sub>3</sub> glass, wetting and adherence on Au 0-24714
- Na<sub>2</sub>O-B<sub>2</sub>O<sub>3</sub> glass-forming melts, thermodynamic functions 0-25673
- Na<sub>2</sub>O-B<sub>2</sub>O<sub>3</sub> glasses, electrical props. and dielectric relaxation (Japanese) 0-20199
- Na<sub>2</sub>O-B<sub>2</sub>O<sub>3</sub>-Au glasses, Au solubility, oxidation state and opt. absorpt. 0-44321
- Na<sub>2</sub>O-B<sub>2</sub>O<sub>3</sub>-Cu<sup>2+</sup>-ZZ 0-34760
- Na<sub>2</sub>O-B<sub>2</sub>O<sub>3</sub>-Fe<sub>2</sub>O<sub>3</sub> glass, Fe<sup>2+</sup>(<sup>3</sup>) impurity ions struct.-chem. state, Mossbauer data 0-40028
- Na<sub>2</sub>O-B<sub>2</sub>O<sub>3</sub>-Mn<sup>2+</sup> glass, fine struct. parameter distrib., EPR meas. 0-11256
- Na<sub>2</sub>O-B<sub>2</sub>O<sub>3</sub>-SiO<sub>2</sub>-Yb(Tb), luminesc. cooperative processes, glass struct. and comp. effect 0-16101
- Na<sub>2</sub>O-B<sub>2</sub>O<sub>3</sub>-SiO<sub>2</sub>-MoO<sub>3</sub> glass containing high level radioactive waste, phase separation 0-25683
- Na<sub>2</sub>O-BaO-SiO<sub>2</sub> based oxide glasses, ion-bombarded, optical line intensities 0-35037
- Na<sub>2</sub>O-BaO-SiO<sub>2</sub>-Nd<sup>3+</sup> glasses, absorption and fluoresc. spectra, density 0-25417
- Na<sub>2</sub>O-CaO glass, crack nucleation during indentation, micromechanics 0-30069
- Na<sub>2</sub>O-CaO-MgO-Al<sub>2</sub>O<sub>3</sub>-SiO<sub>2</sub>, corrosion and microhardness, effect of detergents 0-16518
- Na<sub>2</sub>O-CaO-SiO<sub>2</sub> glass, electronic struct. and optical props. 0-2790
- Na<sub>2</sub>O-CaO-SiO<sub>2</sub> glass, microprobe anal. of corroded surface 0-7704
- Na<sub>2</sub>O-CaO-SiO<sub>2</sub> glass, effect of phase on liquids and gas diffusion (German) 0-38931
- Na<sub>2</sub>O-GeO<sub>2</sub> glass, struct., Raman scatt. obs. 0-1936
- Na<sub>2</sub>O-GeO<sub>2</sub> glass, X-ray diff. study of Ge coordination number 0-10503
- Na<sub>2</sub>O-GeO<sub>2</sub> glasses, neutronographic study of Ge<sup>4+</sup> struct. state 0-19711
- Na<sub>2</sub>O-GeO<sub>2</sub>-Fe<sub>2</sub>O<sub>3</sub> glass, Fe<sup>2+</sup>(<sup>3</sup>) impurity ions struct.-chem. state, Mossbauer data 0-40028
- Na<sub>2</sub>O-K<sub>2</sub>O-SiO<sub>2</sub> glass melt, interdiffusion coeffs. of Na<sup>2+</sup>, K<sup>2+</sup>, temp. depend. 0-44348
- Na<sub>2</sub>O-K<sub>2</sub>O-SiO<sub>2</sub> melts, Na<sup>+</sup> and K<sup>+</sup> diffusion and interdiffusion processes 0-34221
- Na<sub>2</sub>O-MoO<sub>3</sub>, melt, EMF meas., rel. partial molar thermodynamic props. 0-6526
- Na<sub>2</sub>O-NaF-CaO-ZnO<sub>1-x</sub>-Al<sub>2</sub>O<sub>3</sub>-SiO<sub>2</sub>, opal glasses, strength, surface composition 0-30066
- Na<sub>2</sub>O-P<sub>2</sub>O<sub>5</sub> glass, XPS quantitative struct. anal. 0-2917
- Na<sub>2</sub>O-SiO<sub>2</sub> glass, high-temp. peak of internal friction 0-39218
- Na<sub>2</sub>O-SiO<sub>2</sub>, (5.3, 94.7 wt.%) glass, liq.-phase separated, struct., heat treatment effect 0-16359
- Na<sub>2</sub>O-SiO<sub>2</sub>, melt, EMF meas., partial molar enthalpy and entropy 0-6525
- Na<sub>2</sub>O-SiO<sub>2</sub>, Na<sub>2</sub>O-CaO-SiO<sub>2</sub> glasses, thermal capacity meas. at low temps. 0-44334
- Na<sub>2</sub>O-SiO<sub>2</sub> glass, effect of high-dose X-rays and reactor radiation 0-19838
- Na<sub>2</sub>O-SiO<sub>2</sub> glass, electronic struct. and optical props. 0-2790
- Na<sub>2</sub>O-SiO<sub>2</sub> glass, influence of p(O<sub>2</sub>) on Na vaporisation at 1345°C 0-6502
- Na<sub>2</sub>O-SiO<sub>2</sub> glass, tunnelling recomb. luminesc. 0-2875
- Na<sub>2</sub>O-SiO<sub>2</sub> melts, cryoscopic struct. study 0-14994
- Na<sub>2</sub>O-SiO<sub>2</sub>-Fe<sub>2</sub>O<sub>3</sub> glass, Fe<sup>2+</sup>(<sup>3</sup>) impurity ions struct.-chem. state, Mossbauer data 0-40028
- Na<sub>2</sub>O-SiO<sub>2</sub>-Ga<sub>2</sub>O<sub>3</sub>-Al<sub>2</sub>O<sub>3</sub>-B<sub>2</sub>O<sub>3</sub>-SnO<sub>2</sub> glasses, ion exchange reactions with NaNO<sub>3</sub> and KNO<sub>3</sub> melts 0-16673
- Na<sub>2</sub>O-SiO<sub>2</sub>-Ga<sub>2</sub>O<sub>3</sub>-Al<sub>2</sub>O<sub>3</sub> glasses in mixed AgNO<sub>3</sub>-NaNO<sub>3</sub> melts, ion exchange 0-21282
- Na<sub>2</sub>O-SiO<sub>2</sub>-NiO systems Ni ions anal. by ESCA (Japanese) 0-40787
- Na<sub>2</sub>O-SiO<sub>2</sub>-(B<sub>2</sub>O<sub>3</sub>) glass, torsional deform. above T<sub>g</sub> under low stresses 0-25804
- Na<sub>2</sub>O-SnO<sub>2</sub>-ZrO<sub>2</sub>-SiO<sub>2</sub> glass, chemical stability in NaOH and Na<sub>2</sub>CO<sub>3</sub> solns. 0-16532
- Na<sub>2</sub>O-TiO<sub>2</sub>-SiO<sub>2</sub> glass, Si-O bonding, SiK $\beta$  X-ray fluorescence and IR spectra 0-10500
- Na<sub>2</sub>O-V<sub>2</sub>O<sub>5</sub>-Al<sub>2</sub>O<sub>3</sub> melts, soln. of Al<sub>2</sub>O<sub>3</sub> single crystals 0-20910
- Na<sub>2</sub>O-V<sub>2</sub>O<sub>5</sub>-(VO<sub>2</sub>)<sub>2</sub>-V<sub>2</sub>O<sub>3</sub>, phase comp. and equil. 0-35172
- Na<sub>2</sub>O-ZrO<sub>2</sub>-SiO<sub>2</sub> glass, treated with 2 N solns. of NaCO<sub>3</sub> and NaOH, surface layer comp. 0-35366
- NaOH, frozen soln., EPR of trapped H-atoms produced by UV and X-irrad. 0-3369
- NaOH fusion for heat storage, heat utilisation for turbo-alternator unit (French) 0-40915
- NaOH, liq., thermal storage, steel corrosion, appl. in accumulation type steam generator (French) 0-40914
- Na<sub>2</sub>O(K<sub>2</sub>O)-P<sub>2</sub>O<sub>5</sub> glasses, P K-band X-ray emission spectra, state anal. 0-40190

## sodium compounds continued

- Na<sub>2</sub>O<sub>2</sub>Al<sub>2</sub>O<sub>3</sub>·10TiO<sub>2</sub>, crystallized bronze, chem. comp., morphology, optical and thermal props. (Japanese) 0-16172
- Na<sub>2</sub>O<sub>2</sub>SiO<sub>2</sub> glass, diffusion of Ag into surface layer from AgNO<sub>3</sub> melt 0-44371
- Na<sub>2</sub>O<sub>2</sub>y(Al<sub>1-x</sub>Fe<sub>x</sub>)<sub>2</sub>O<sub>3-m</sub>,  $\beta''$ -Al<sub>2</sub>O<sub>3</sub> phase stability, lattice constants 0-45283
- NaPO<sub>3</sub> crystal, P K-band X-ray emission spectra, state anal. 0-40190
- NaPO<sub>3</sub>, heat content between 300.05 and T (T from 400 to 1000K) drop calorimetry (French) 0-10682
- NaPO<sub>3</sub>, vitreous, microhardness 0-25864
- Na<sub>3</sub>PO<sub>4</sub> crystal, P K-band X-ray emission spectra, state anal. 0-40190
- Na<sub>2</sub>P<sub>2</sub>O<sub>7</sub> crystal, P K-band X-ray emission spectra, state anal. 0-40190
- Na<sub>2</sub>Pr(C<sub>2</sub>H<sub>4</sub>O<sub>3</sub>)<sub>2</sub>·2NaClO<sub>4</sub>·6H<sub>2</sub>O, single cryst., forbidden A<sub>1</sub>→A<sub>1</sub> transition, mag. field induced intensification 0-50302
- Na<sub>3</sub>RSi<sub>4</sub>O<sub>12</sub> (R=Sm to Lu, Y, Sc), solid electrolytes, struct. characts. 0-1997
- NaReO<sub>4</sub>, <sup>23</sup>Na and <sup>187</sup>Re NMR and NQR temp. depend. 0-54973
- NaReO<sub>4</sub>, matrix isolated, IR spectra 0-28012
- Na<sub>2</sub>RuO<sub>4</sub>, <sup>99</sup>Ru Mossbauer spectra, antiferromag. order, mag. relax. 0-50234
- Na<sub>2</sub>S, muonic X-ray intensities, Lyman series 0-23578
- NaSCN, and similar salts, Na atomic charge determ. by numerical integration 0-28944
- NaSCN in N,N-dimethylacetamide, Raman, IR and US relaxation studies 0-50315
- Na<sub>2</sub>SO<sub>3</sub> and Na<sub>2</sub>SO<sub>4</sub>, muonic X-ray intensities, Lyman series 0-23578
- Na<sub>2</sub>SO<sub>4</sub> in aqueous soln., diffusion coeffs. and Onsager-Fuoss theory disagreement 0-40729
- Na<sub>2</sub>SO<sub>4</sub>, melting point determ., DTA method 0-218
- Na<sub>2</sub>SO<sub>4</sub>, thermodynamic equil. vapourisation, transpiration mass spectrometry 0-52356
- Na<sub>2</sub>SeO<sub>3</sub>·2D<sub>2</sub>O, bonding in [S<sub>2</sub>O<sub>6</sub>]<sup>2-</sup>, X-ray diff. refinement and pictorial representation 0-54177
- Na<sub>2</sub>SeO<sub>3</sub>·2D<sub>2</sub>O, X-ray diff. cryst. struct. redeterm. 0-39014
- Na<sub>2</sub>SeO<sub>3</sub>·2H<sub>2</sub>O, bonding in [S<sub>2</sub>O<sub>6</sub>]<sup>2-</sup>, X-ray diff. refinement and pictorial representation 0-54177
- Na<sub>2</sub>SeO<sub>3</sub>·2H<sub>2</sub>O, X-ray diff. cryst. struct. redeterm. 0-39014
- Na<sub>2</sub>SeO<sub>3</sub>·5H<sub>2</sub>O, solidification, heat transfer processes (Japanese) 0-6372
- Na<sub>2</sub>SeO<sub>3</sub>·5H<sub>2</sub>O, use in polishing of lead glass 0-33258
- $\alpha$ -Na<sub>2</sub>Se<sub>2</sub>, cryst. struct. and  $\beta$ - $\alpha$  phase transform. features 0-33961
- NaSeS<sub>2</sub>, crystal struct. determ. by X-ray powder diff. 0-49205
- Na<sub>2</sub>Se<sub>2</sub>V<sub>3</sub>O<sub>12</sub>·Yb<sup>3+</sup>, EPR of Yb<sup>3+</sup> in octahedral sites 0-54948
- Na<sub>2</sub>Se, muonic X-ray intensities, Lyman series 0-23578
- Na<sub>2</sub>SeO<sub>3</sub> and Na<sub>2</sub>SeO<sub>4</sub>, muonic X-ray intensities, Lyman series 0-23578
- Na<sub>1+x</sub>Si<sub>1-x</sub>Zr<sub>2</sub>P<sub>3-x</sub>O<sub>12</sub>, monoclinic to rhombohedral phase transformation 0-29950
- Na<sub>2</sub>SiO<sub>2</sub>-CaO glass, thermostimulated and tunnel luminesc. 0-45157
- Na<sub>2</sub>SiO<sub>3</sub> glass pH meter electrode performance (German) 0-40695
- Na<sub>2</sub>TiS<sub>2</sub>, electrochemically intercalated, ion ordering, X-ray diff. meas. 0-44177
- NaVO<sub>3</sub>-KVO<sub>3</sub>-Al<sub>2</sub>O<sub>3</sub>, melts soln. of Al<sub>2</sub>O<sub>3</sub> single crystals 0-20910
- Na<sub>2</sub>V<sub>10</sub>O<sub>28</sub>·18H<sub>2</sub>O, X-ray cryst. struct. determ. (French) 0-54191
- Na<sub>2</sub>VS<sub>2</sub>(Se<sub>2</sub>), intercalation compounds, phys. props. 0-44179
- Na<sub>2</sub>W<sub>2</sub>O<sub>7</sub>, Raman and IR spectra 0-25356
- Na<sub>2</sub>WO<sub>3</sub> bronzes (0.4<x<1), domain, surface and substrate structs. 0-34281
- Na<sub>2</sub>WO<sub>3</sub>, core level photoelectron spectra, final state effects 0-50509
- Na<sub>2</sub>WO<sub>3</sub> films, chem. pot. variation of Na, free electron gas model 0-16698
- Na<sub>2</sub>WO<sub>3</sub>, Knight shift, spin-lattice and spin-spin relax., high press. NMR obs. 0-50211
- Na<sub>2</sub>WO<sub>3</sub>, metallic, light-scatt. studies 0-45071
- Na<sub>2</sub>WO<sub>3</sub>, metallic, optical and electronic props. 0-24398
- Na<sub>2</sub>WO<sub>3</sub>, x=0.6 and 0.8, surface characts. 0-39392
- Na<sub>2</sub>W<sub>2</sub>O<sub>7</sub>, phase transitions obs. (French) 0-6516
- Na<sub>2</sub>W<sub>2</sub>O<sub>7</sub>F<sub>6</sub>, single cryst., prep., optical and dielec. studies (French) 0-15994
- NaX zeolite, hydrated, cryst. struct. at t=20 and -165°C 0-33978
- NaZn<sub>3</sub>, stella quadrangula as struct. building unit 0-15055
- Na<sub>2</sub>ZnTh<sub>6</sub>F<sub>29</sub>, X-ray cryst. struct. determ. (French) 0-19761
- Na<sub>1+x</sub>Zr<sub>2-x</sub>In<sub>2</sub>(PO<sub>4</sub>)<sub>3</sub>, three-dimens. solid soln., comp. depend. of ionic cond. (French) 0-34230
- Na<sub>2</sub>Zr(MoO<sub>4</sub>)<sub>3</sub>, synthesis and cryst. struct. 0-39059
- Na<sub>4</sub>Zr(MoO<sub>4</sub>)<sub>4</sub>, synthesis and cryst. struct. 0-39059
- NaZr<sub>2</sub>O<sub>7</sub>, H ion exchange material, use in <sup>137</sup>Cs separation from nucl. waste 0-27760
- Na<sub>2</sub>ZrSiO<sub>5</sub>, scintillation props., excited by  $\alpha$  particles 0-29809
- Na<sub>2</sub>Zr<sub>2</sub>Si<sub>2</sub>PO<sub>12</sub>, NASICON, phase transition, X-ray diff., ionic cond. and sp. ht. meas. 0-19979
- Na<sub>2</sub>O<sub>3</sub>B<sub>2</sub>O<sub>3</sub>xFe<sub>2</sub>O<sub>3</sub>, borate glass, Fe<sup>3+</sup> spin state and distrib. meas. 0-39966
- Na<sub>8</sub>[B<sub>12</sub>O<sub>20</sub>(OH)<sub>4</sub>], X-ray cryst. struct. determ. and refinement 0-19753
- P<sub>2</sub>O<sub>5</sub>-Al<sub>2</sub>O<sub>3</sub>-Na<sub>2</sub>O-K<sub>2</sub>O-Li<sub>2</sub>O-(CaO+MgO) glass system, ion exchange effect on mech. props. 0-30229
- PbCl<sub>2</sub>:NaCl, trapped exciton states, absorption spectra 0-50383
- Sb<sub>2</sub>O<sub>3</sub>-Na<sub>2</sub>O-B<sub>2</sub>O<sub>3</sub>-SiO<sub>2</sub> glass, elec. cond. meas., -160 to 200°C 0-20190
- (Sb<sub>2</sub>S<sub>3</sub>)<sub>0.95</sub>(Na<sub>2</sub>S)<sub>0.05</sub>, condensate, local states and switching effect 0-20336
- SiO<sub>2</sub>-Al<sub>2</sub>O<sub>3</sub>-CaO-MgO-Na<sub>2</sub>O-K<sub>2</sub>O effect of partial substitution of Na<sub>2</sub>O by K<sub>2</sub>O, on crystallisation 0-10499
- SiO<sub>2</sub>-Al<sub>2</sub>O<sub>3</sub>-Fe<sub>2</sub>O<sub>3</sub>-Na<sub>2</sub>O-K<sub>2</sub>O-CaO-MgO glasses, Mossbauer spectra study 0-39967
- SiO<sub>2</sub>-B<sub>2</sub>O<sub>3</sub>-Al<sub>2</sub>O<sub>3</sub>-NaO, Ag interdiffusion, optical and NMR studies 0-24683
- SiO<sub>2</sub>-B<sub>2</sub>O<sub>3</sub>-Na<sub>2</sub>O glass, high silica, conductivity behaviour, Na ion dependence 0-24652
- SiO<sub>2</sub>-CaO-ZnO-B<sub>2</sub>O<sub>3</sub>-Na<sub>2</sub>O-S, SrO effect on crystallisation 0-54135
- SiO<sub>2</sub>-M<sub>2</sub>O (M=Na,K) glasses, temp. depend. of elastic modulus 0-40410
- SiO<sub>2</sub>-Na<sub>2</sub>O-CaCO<sub>3</sub> sheet glass, rupture upon local contact loading 0-50725
- SiO<sub>2</sub>-Na<sub>2</sub>O-CaO (13, 11 wt.%) glass, phase separation, SiO<sub>2</sub> purity effect 0-44144
- SiO<sub>2</sub>-Na<sub>2</sub>O-CaO glass, phase separation characts., melting atmosphere effect 0-44141
- SiO<sub>2</sub>-Na<sub>2</sub>O-CaO-MgO-Al<sub>2</sub>O<sub>3</sub>, toughening by electrochemical treatment in Sn melt 0-11800
- SiO<sub>2</sub>-Na<sub>2</sub>O-CaO-MgO-Fe<sub>2</sub>O<sub>3</sub>-Al<sub>2</sub>O<sub>3</sub>-SO<sub>3</sub>-Sn thermally polished, exam. of strength of surfaces 0-25887



**sodium compounds continued**

- SiO<sub>2</sub>-Na<sub>2</sub>O-K<sub>2</sub>O-CaO-MgO-Al<sub>2</sub>O<sub>3</sub> glass melt, anodic dissolution of Ti 0-19949  
 SiO<sub>2</sub>-RO-Na<sub>2</sub>O-Li<sub>2</sub>O (RO=MgO, CaO, SrO) glass-ceramic coating, optimisation of props. by selective oxide action 0-55552  
 SiO<sub>2</sub>-TiO<sub>2</sub>-Na<sub>2</sub>O(-CaO), thermal diffusivity in range 0-600°C, influence of TiO<sub>2</sub> 0-29233  
 SiO<sub>2</sub>-ZnO-Na<sub>2</sub>O-Li<sub>2</sub>O, glass-ceramic coating, optimisation of props. by selective oxide action 0-55552  
 SiO<sub>2</sub>-ZrO<sub>2</sub>-Al<sub>2</sub>O<sub>3</sub>-CaO-Na<sub>2</sub>O-K<sub>2</sub>O-Li<sub>2</sub>O, chemical resistant glass for glass fibres 0-21128  
 SiO<sub>2</sub>-ZrO<sub>2</sub>-Li<sub>2</sub>O-Na<sub>2</sub>O based crystallisable glasses composition and properties 0-50731  
 SiO<sub>2</sub>-Na<sub>2</sub>O-CaO-MgO-Al<sub>2</sub>O<sub>3</sub> charge, silicate formation during heating 0-55342  
 Sr<sub>2</sub>NaNb<sub>6</sub>O<sub>15</sub>, Raman scatt. experiments in tetragonal tungsten bronze compounds 0-40113  
 Te(OH)<sub>6</sub>-Na<sub>2</sub>HAsO<sub>4</sub>·H<sub>2</sub>O, synthesis and cryst. data (*French*) 0-33948  
 Zn-Ti, environmental factors affecting pitting corrosion potential in NaOH solns. 0-45423  
 ZnCl<sub>2</sub>-NaCl, melt, viscosity meas. by oscillating cylinder method (*Japanese*) 0-10696  
 ZnS-Na<sub>2</sub>O-K<sub>2</sub>O-SiO<sub>2</sub>, form. using electric furnace, furnace design 0-11620

**sodium potassium tartrate tetrahydrate** see *Rochelle salt*

**sofar** see *sonar*

**soft modes**

see also *displacive transformations; lattice phonons*

- aniline-HBr, ferroelasticity, orthorhombic to monoclinic phase transition, X-ray scatt. 0-39276  
 benzil, structural transition model, cryst. symm. spontaneous strain components 0-2161  
 bis(p-toluene sulphonate)diacetylene, monomer and polymer, solid state phase transformation, far IR transmission spectra obs. 0-55077  
 chaotic states of anharmonic systems in periodic fields 0-22288  
 cluster phenomena, displacive to order disorder crossover 0-10629  
 coated semiconductor spheres, surface modes, plasmon oscils. 0-54730  
 DOBAMBC, dielec. props. near ferroelec. smectic A to C transition 0-45015  
 elastic phase transitions, crit. dynamics 0-2146  
 ferroelectric, uniaxial, electrostrictive interaction, mode damping 0-34862  
 ferroelectric ferromagnet, soft modes and ferromag. reson. 0-11275  
 ferroelectric semiconductor, magnetic field influence, ferroelectric transitions 0-55049  
 ferromagnetic ferroelectric, soft mode damping, temp. anomalies (*Russian*) 0-44284  
 hydrogen-bonded ferroelectric, Ising model in transverse tunnelling field and proton-lattice interaction 0-7307  
 IV-VI compounds, mag.-field-induced displacive phase transition 0-50278  
 IV-VI compounds, phase transitions induced by electron-phonon interaction 0-10656  
 Lindemann's criterion and necessary condition for melting curve maximum 0-2145  
 locally distorted impurity dynamics in host lattice with displacive phase transition 0-34159  
 magnetic phase transitions 0-54889  
 one-dimensional conductors, Peierls instability, dynamics, structural energy, pseudopot. calc. 0-54676  
 structural phase transition induced refractive index changes in crystals. 0-16000  
 structural phase transitions in crystals of D<sub>2d</sub> symm. 0-15986  
 TCNQ, lattice softening mechanism 0-6481  
 thiourea, phonon modes near phase transitions, IR and Raman spectra 0-45084  
 5d-transition metal antiferroelectric cryst., struct. props. and lattice dynamics, mag. struct. 0-44268  
 TTfCuBDT, spin-Peierls transition in spin 1/2 Heisenberg chains, RPA calcs. 0-25150  
 two-dimensional Wigner-crystal-liquid-surface system, eigenmodes and instability of charged liq. surface 0-10896  
 two-electron level with quasidegenerate levels, local phase transitions and temp. effects in lattice dynamics 0-10666  
 uniaxial ferroelectric, acoustic attenuation near transition point 0-11350  
 AgI, phase transition, statics and local dynamics, mean field and Mori theory 0-39347  
 AgNaNO<sub>2</sub>, ferroelectric transitions, one-mode model 0-29702  
 Al<sub>2</sub>SiO<sub>5</sub>, andalusite, phonon spectra and rigid-ion model calcs. 0-11391  
 Ba I-Ba II phase boundary, Ba I fusion curve peak at high press. (*Russian*) 0-2165  
 Cd(NH<sub>4</sub>)<sub>2</sub>X<sub>2</sub>, X=Br, Cl, I, orientational phase transitions, Raman spectra 0-11382  
 CsPbBr<sub>3</sub>, cubic-to-tetragonal phase transition, critical anomalies, phenomenological eqns. 0-39275  
 CsPbCl<sub>3</sub>, cubic-to-tetragonal phase transition, critical anomalies, phenomenological eqns. 0-39275  
 CsVF<sub>4</sub>, structural phase transitions above room temp. 0-29167  
 In-Pb alloys, elastic consts. of three phases, acoustic mode softening 0-30006  
 KBr, doped with F-centres, Raman spectra meas. excitation in F and K bands 0-16027  
 KD<sub>2</sub>PO<sub>4</sub>, Brillouin spectrum and broad central component, depend. on scatt. wave vector direction 0-34931  
 KD<sub>2</sub>PO<sub>4</sub>, deuteron tunnelling, barrier height and energy level calc. 0-6482  
 KD<sub>3</sub>(SeO<sub>3</sub>)<sub>2</sub>, ferroelastic transition, EPR 0-7148  
 K(H<sub>1-x</sub>D<sub>x</sub>)<sub>2</sub>(SeO<sub>3</sub>)<sub>2</sub>, Brillouin spectrum central peak, soft acoustic mode 0-2777  
 KH<sub>2</sub>PO<sub>4</sub>, light scatt. in elec. field, ferroelec.-paraelec. transition 0-2707  
 KH<sub>2</sub>PO<sub>4</sub>, paraelectric phase, solns. of Bloch-type eqns., soft mode freq. fluctuations 0-7304  
 KH<sub>2</sub>PO<sub>4</sub>, proton tunnelling, barrier height and energy level calc. 0-6482  
 KH<sub>2</sub>PO<sub>4</sub>-type crystal, LF dynamics 0-10602  
 KMnF<sub>3</sub>, cubic-to-tetragonal phase transition, critical anomalies, phenomenological eqns. 0-39275  
 KMnF<sub>3</sub>, precursor order and Raman scatt. near displacive phase transitions 0-45061  
 KMnF<sub>3</sub>, soft phonons and mag. phase transitions 0-54889  
 KNbO<sub>3</sub>, ferroelec. phase, phonon dispersion relations and lattice dynamics calcs., comparison with expt. 0-49319  
 KNbO<sub>3</sub>, tetragonal phase, inelastic neutron scatt. 0-19676

**soft modes continued**

- K<sub>2</sub>PtCl<sub>6</sub>, K<sub>2</sub>ReCl<sub>6</sub>, K<sub>2</sub>SnCl<sub>6</sub>, solid state phase transitions, lattice vibr., NMR and NQR obs. 0-34814  
 K<sub>2</sub>SeO<sub>4</sub>, lattice dynamics, displacive phase transform. 0-39248  
 K<sub>2</sub>SeO<sub>4</sub>, non-zero wave vector incommensurate soft mode, light scatt. study 0-29754  
 K<sub>2</sub>SeO<sub>4</sub>, Raman scatt. and dielec. props. 0-11313  
 KTaO<sub>3</sub>:Fe<sup>3+</sup>, local phase transition, EPR line temp. broadening (*Russian*) 0-54944  
 LaP<sub>2</sub>O<sub>4</sub>, ferroelastic transition, polarised Raman study 0-16035  
 LiNbO<sub>3</sub>, ferroelec. phase, phonon dispersion relations and lattice dynamics calcs., comparison with expt. 0-49319  
 NH<sub>4</sub>Br, β-γ phase transition, critical anomalies, phenomenological eqns. 0-39275  
 NH<sub>4</sub>IO<sub>3</sub>, ferroelec., structural phase transition 0-7308  
 (NH<sub>4</sub>)<sub>2</sub>(1-x)Rb<sub>2x</sub>SO<sub>4</sub>, mixed crystal, dielectric and US meas. of ferroelec. phase transition (*Japanese*) 0-7305  
 NaNbO<sub>3</sub>, ferroelectric transitions, one-mode model 0-29702  
 Na<sub>2</sub>WO<sub>4</sub>, metallic, light-scatt. studies 0-45071  
 Nb<sub>0.75</sub>Zr<sub>0.25</sub>, effect of force constant, disorder on Eliashberg function 0-29504  
 Ni<sub>1-x</sub>S, metal-semimetal transition, lattice dynamics and thermodynamic props. 0-29324  
 (Pb, Sn)Te-type semiconductors, displacive ferroelec. phase transitions, vibronic theory 0-11354  
 Pb<sub>2</sub>Ge<sub>2</sub>O<sub>11</sub>, ferroelectric, anharmonic effects in low freq. symm. modes, Raman study 0-25365  
 Pb<sub>2</sub>Ge<sub>2</sub>O<sub>11</sub>, paraelectric and ferroelectric, Raman spectra near ferroelectric transition 0-55090  
 Pb<sub>1-x</sub>Ge<sub>x</sub>Te, degenerate semiconducting ferroelectric, structural phase transition temp., mag. field effects 0-45017  
 Pb<sub>1-x</sub>Ge<sub>x</sub>Te, ferroelec. phase transition, IR refl. and resist. meas. 0-11353  
 Pb<sub>3</sub>(PO<sub>4</sub>)<sub>2</sub>, ferroelastic, Raman scatt. by soft vibr. involved in ferroelastic phase transition 0-16040  
 Pb<sub>3</sub>(PO<sub>4</sub>)<sub>2</sub>, ferroelastic phase transition, inelastic neutron scatt. (*French*) 0-24584  
 Pb<sub>1-x</sub>Sn<sub>x</sub>Te, (x<0.35), permittivity and soft modes, carrier density and comp. effects 0-7256  
 Pb<sub>1-x</sub>Sn<sub>x</sub>Te, mag. and kinetic props. near ferroelec. transition 0-11160  
 PbTe-SnTe compound semiconductors, lattice instability by mm-wave magnetoplasma refl. 0-54336  
 PbTiO<sub>3</sub>, soft mode decay mechanism, damping parameter freq. depend. 0-54324  
 Pr, magnetic ordering, stress induced 0-15776  
 Pr, soft mode excitation behaviour under press., long range order 0-39838  
 RbAg<sub>4</sub>I<sub>5</sub>, phase transition, statics and local dynamics, mean field and Mori theory 0-39347  
 RbCaF<sub>3</sub>, cubic to tetragonal phase transition, <sup>87</sup>NMR meas. 0-7187  
 RbCaF<sub>3</sub>, precursor order and Raman scatt. near displacive phase transitions 0-45061  
 RbCaF<sub>3</sub>, structural phase transition, superlattice points, neutron diffr. obs. 0-19944  
 Rb<sub>2</sub>ZnBr<sub>4</sub>, Raman scatt., normal-incommensurate-commensurate phase transitions, soft modes 0-40071  
 Rb<sub>2</sub>ZnCl<sub>4</sub>, phase transition, Raman scatt. evidence 0-40116  
 SbSI, ferroelectric, anharmonic at. pot. and temp. depend. of thermal vibrs. 0-39246  
 Sm<sub>0.75</sub>Y<sub>0.25</sub>S, intermediate valence compound, phonon investigation by neutron scatt. 0-6476  
 Sn<sub>0.5</sub>Ge<sub>0.5</sub>Te, Mossbauer spectra, soft modes 0-20550  
 Sn<sub>2</sub>P<sub>2</sub>Se<sub>6</sub>, illumination effect on soft mode and dielectric props., luminesc. study (*Russian*) 0-50420  
 Sn<sub>2</sub>P<sub>2</sub>(S<sub>1-x</sub>Se<sub>x</sub>)<sub>6</sub>, solid solutions, ferroelectric soft mode freq., displacive transformations 0-29701  
 (Sn<sub>1-x</sub>Pb<sub>x</sub>)<sub>2</sub>P<sub>2</sub>Se<sub>6</sub>, solid solutions, ferroelectric soft mode freq., displacive transformations 0-29701  
 SnTe, bond gap, phase transform., optical dielec. const. meas. 0-10630  
 SnTe, displacive phase transition at 22K, Mossbauer spectra and elec. resist. meas. 0-6514  
 SnTe film, polycrystalline, anomalous resist. at struct. phase transition 0-29488  
 Sr<sub>2</sub>Nb<sub>2</sub>O<sub>7</sub>, optical mode softening in incommensurate phase 0-7352  
 SrTiO<sub>3</sub>, structural phase transition, intrinsic and extrinsic central peak properties 0-34168  
 SrTiO<sub>3</sub>:Cr<sup>3+</sup>, nonlinear Jahn-Teller coupling, local dynamics, near struct. transition 0-2625  
 TaS<sub>2</sub> (1T) and (2H), bonding and charge density wave phase transitions 0-44282  
 TbP, mag. excitations above antiferromag. ordering temp., inelastic neutron scatt. obs. 0-50112  
 TiSe<sub>2</sub>(S<sub>2</sub>) (1T), electronic and vibronic struct. 0-44500  
 TmSe, intermediate valent, Raman scatt. 0-16038  
 WO<sub>3</sub>, triclinic, condensed modes 0-15211  
 YS, electronic instability and phonon softening, APW calc. 0-29323

**software (computers)** see *computer software*

**software engineering**

- solar heating and cooling systems, computer program validation methodology 0-35742  
 Spar Buoy Oceanographic Telemetry System software engineering 0-46308

**sogicons** see *semiconductor devices*

**soil**

- atmosphere soil particles in Nagoya area, characterisation via urban aerosol Si and Al concs. 0-26581  
 chemical migration of radionuclides in soil 0-17144  
 clay soil/sand mixtures, reflectance 0-56475  
 Cumberland Peninsula, Baffin Island, hornblende grain etching, age and palaeoclimate indicator 0-8307  
 drying, evaporation, solar radiation and atm. temp. effect 0-8373  
 elastoplastic deformation, volumetric constitutive equation 0-53655  
 electrical conductivity measurement, via HF EM induction profiling (*Polish*) 0-51547  
 electrical parameter measurement in SW range 0-22388  
 Everglades Agricultural Area, USA, soil temp. obs. in winter nighttime 0-56559  
 hysteresis effects under loading 0-21712  
 infiltration, spatial var. of hydrological effects, Monte Carlo anal. 0-8363



**soil continued**

- interblock hydraulic conductivity values for transient unsaturated flow problems, finite difference soln. 0-12460
- irrigation, connection between soil and groundwater 0-26554
- microwave emission, surface roughness effect 0-17264
- moist, thermodynamic state functions (*German*) 0-4056
- moistening, one-dimensional, surface water effects (*Russian*) 0-46209
- moisture, heat and salt transport, math. model 0-26563
- moisture and geology mapping, thermal inertia method 0-8344
- moisture content measurement by microwave radiometry 0-17425
- moisture of surface, remote sensing by visible and false colour IR photography 0-56653
- pathogenic fungus population reduction by 2.45 GHz irradiation 0-3719
- physics, book 0-27056
- pore size distrib. estimation from moisture charact. 0-12454
- radioactive disequilibrium, of U and AC series nuclides 0-4014
- radionuclide contamination, <sup>89</sup>Sr and <sup>90</sup>Sr determ. using total sample decomp. 0-35808
- sands, poorly graded, moisture distrib. in capillary crack (*German*) 0-31066
- seepage, free water surface behaviour in porous media 0-8349
- soil-water system,  $\gamma$ -ray transmission studies, calibration 0-26629
- solar energy accumulation by soil in shed hothouse 0-21373
- solar energy storage, pebble layer heat exchange investigation 0-21374
- solute conc. rel. to throughflow 0-31070
- tree root potential meas. electrode earthing method (*Russian*) 0-26420
- trench leachates, low-level radioactive waste disposal sites, organic carbon content 0-17145
- tundra, CO from arctic surfaces during spring thaw 0-41511
- water diffusivity, scaling using universal consts. 0-8371
- AI leaching response to acid precip., effects on high-elevation watersheds in NE. United States 0-12442
- I, radioactive, adsorption concentration depend. obs. (*Czech*) 0-12031
- Pu isotopes, in soil, determination using alpha-spectrometry 0-45601
- Rn concentration variation, temporal (spatial), simple model 0-33671
- <sup>222</sup>Rn concentration distribution under ground, effect on natural  $\gamma$ -ray flux density and exposure rate 0-36300
- <sup>222</sup>Rn exhalation meas., soil and meteorological effects (*Spanish*) 0-31082
- <sup>222</sup>Rn releases associated with cultivation of agricultural land 0-16850
- U isotopes, in soil, determination using alpha-spectrometry 0-45601

**solar absorber-convertors**

- active collectors, design features and performance definition 0-51000
- air collectors with porous absorber to reduce radiative heat transfer losses (*French*) 0-55900
- air heaters, single and double exposure, heat balance anal. 0-45734
- air heating/cooling systems for buildings, review 0-45754
- air-cooled solar receiver, analytical and expt. determ. of rad. and temp. distrib. 0-55894
- austenitic stainless steel thermal treatment for spectrally selective surface fabrication 0-35752
- axial conduction effects on heat removal factor 0-7955
- biological solar radiation utilisation, optical model for polar animal pelts 0-51045
- black chrome solar selective absorber, microstruct., chemical comp. and reflective props. 0-7959
- black Cr coatings, optical props., using inhomogeneous medium theories 0-12026
- Brayton cycle solar electric plant receiver, 1 MW, bench model design and testing 0-55896
- Cassegrainian solar concentrator, optical and thermal analysis 0-40906
- cavity solar collectors with selective radiation-absorption properties, optimal geometric parameters 0-21410
- cavity-type solar receivers, HEAP computer simulation program for heat energy anal. 0-30548
- central receiver solar power stations, solar receiver tube thermal stresses, fatigue aspects 0-40908
- central receiver systems for thermoelectric conversion 0-45760
- ceramic solar cavity receivers for thermal electric systems 0-30549
- chemical, using SO<sub>2</sub> gas, 'Solchem' project 0-50994
- coating, on to pipe (*Japanese*) 0-16834
- collector, evacuated cylindrical, analysis 0-21415
- collector array performances calc., using Hottel-Whillier-Bliss equation and field-derived data 0-45724
- collector arrays, calc. of performance for N collectors in series from single collector test data 0-45740
- collector efficiency equation for corrugated steel sheet solar water heater 0-16839
- collector system for thermal power generation, with tracking cylindrical parabolic reflector (*Korean*) 0-45735
- collector transmittance-absorbance, calc. of monthly averages 0-45742
- collector-heat storage systems for solar heating and ventilating by natural means 0-45758
- collectors, design, thermal performance and economic anal., review 0-51001
- collectors, free convective heat transfer 0-45748
- collectors, high temp., flat plate, cover system effects 0-26156
- collectors, monthly mean radiation calcs. for vertical and inclined surfaces 0-45746
- collectors for hot water supply system, heat collection characts. and energy conservation 0-45743
- collectors for solar heating systems for use in Britain 0-35637
- combined photovoltaic/thermal flat plate collectors, extended Hottel-Whillier model 0-3520
- comparative ranking of 0.1 to 10 MWe solar thermal power systems 0-30559
- compound parabolic concentrator collectors, prediction of thermal performance 0-55905
- compound parabolic concentrator solar collector design 0-3532
- concentrating collector design, economics and optical loss anal. 0-45751
- concentrating collectors, single axis, orientation, economic criterion 0-40907
- concentrating solar collectors, concentration/acceptance relationships 0-21414
- cooling, heating and hot water supply for hospital, evacuated glass tube solar collector system appl. 0-26155
- cooling systems for buildings, review 0-45756
- cylindrical absorbers for solar energy collecting system, thermal power (*Korean*) 0-21380
- domestic space heating in Ireland, computer simulation model of thermal performance 0-45732

**solar absorber-convertors continued**

- double-exposure flat plate solar collectors, mirror configurations 0-50999
- electrodeposited chrome black solar absorber surfaces, characterisation using <sup>54</sup>Cr(p, $\gamma$ ) 0-7878
- electroplating appl., 1979 prospects w.r.t. economics 0-3490
- energy gain analysis of flat plate and evacuated tube collectors 0-55904
- evacuated heat pipe solar collector, rectangular performance characts., trap mechanism 0-3531
- evacuated tubular solar collector integration with LiBr absorption cooling systems 0-3493
- Fe-SiO<sub>2</sub> cermet film, solar absorbing, production by dual cathode DC magnetron sputtering 0-16186
- figure of merit for solar collectors with several separate absorber segments 0-55908
- fixed collector, optimised design, radiation collection study 0-40839
- flat plate collector, transient plate temp. rise for coolant blockage 0-26154
- flat plate collector technology 0-45747
- flat plate collectors, advanced non-concentrating designs 0-45749
- flat plate collectors, appl. to space heating (*German*) 0-26152
- flat plate collectors, effect of a self consistent effective ambient temp. of efficiency parameters 0-45741
- flat plate collectors, for water pumping (*French*) 0-55902
- flat plate collectors, use of porous construction for solar air heaters 0-35748
- flat plate multiple pass solar collector using aqueous optical properties 0-7957
- flat plate solar collector performance with fluid phase change 0-35750
- flat plate solar collectors, insulation damage if fluid flow stops 0-3519
- flat plate solar collectors, optical props. of selective surfaces, effect on collector efficiency (*French*) 0-55897
- flat plate solar collectors for water heating system, collection temp. and efficiency 0-45744
- flat-plate collector, below atmospheric pressure, distributed-flow, modules integration into arrays 0-26153
- flat-plate collector loops with on-off control, anal. of dynamic behaviour (*French*) 0-55901
- flat-plate collectors, absorption chillers for cooling and hot water system 0-50941
- flat-plate solar collector test facility to determine thermal performance characts. 0-45730
- flat-plate solar collectors, thermal performance testing of air and liquid solar water heaters 0-55911
- fluorescent collectors for thermal energy conversion, evaluation 0-16836
- fluorescent planar collector-concentrators for solar energy conversion 0-45745
- heat mirrors, spectral selectivity of conducting micromeshes 0-26160
- heat pump evaporator using solar collector, thermal performance 0-30520
- heating and cooling of buildings, Shenandoah Solar Recreational Center 0-45757
- heating and cooling systems, computer program validation methodology 0-35742
- heating and cooling systems design, operation, feasibility, review 0-45755
- heating systems, collector and storage efficiencies 0-45736
- heating systems, economic anal. of passive and active residential designs 0-35746
- heating systems, instrumentation principles for performance meas. 0-35743
- high temp.-high flux material testing, solar power station appls. 0-40668
- high temperature solar collector with optimal concentration: Non-focusing Fresnel lens with secondary concentrator 0-35753
- hot water supply using solar collectors (*Dutch*) 0-7954
- hot water systems, marginal cost of electricity used for backup 0-35747
- ideal selective absorbing surface, absorp. and radiation coefficients calc. 0-40900
- industrial solar inclined-step distiller, test results 0-40901
- integrated collector-heat storage systems for heating and ventilation 0-51002
- non-selective and energy control films for enhanced photothermal solar energy collection 0-26157
- open solar regenerator, heat and mass transfer coefficients, moisture evaporation 0-38238
- optical simulation for a fixed spherical solar collector 0-7912
- optics applied to solar energy, [Conf. San Diego, CA, USA Aug. 1978] 0-7926
- optimal feedback controller for collector flow rate, optimal control law 0-45739
- optimal insulation of solar heating system pipes and tanks 0-35745
- passive solar heating systems design, microeconomic anal. methodology 0-35744
- PCM wall thermal storage, design criteria 0-35759
- PCM wall thermal storage, modelling 0-35758
- photoelectrolysis cells, props. of oxide-based heterostruct. photoelectrodes 0-12023
- planar solar convertor based on uranyl Hd and Ho glasses 0-40904
- plastic modular solar energy collector with reticulated foam 0-16833
- ponds, heat transfer model to predict temp. rise 0-55912
- ponds, non-convective, operating characts. 0-45750
- PULSONAR polymer thick film hybrid convertor 0-55878
- quantum utilizing solar energy convertor efficiency in absence of intraband thermalisation 0-26144
- R and D program at the Inst. of Engng. of the Nat. Univ. of Mexico 0-40845
- reflector and absorber design, spherical stationary mirror, and automatic tracking absorber 0-50997
- refrigeration units, absorption systems with intermittent or continuous cycles 0-45729
- sandwich-type collector panels, weight minimisation 0-30547
- selective absorber coatings, reflectance, emittance, and thermal stability 0-12027
- selective solar absorbers, reflectance calcs. for inhomogeneous surfaces 0-12029
- selective surface, thermal emissivity 0-7953
- selective surface absorber coatings, technique for comparing effectiveness 0-30545
- selective surface for thermal absorbers, review of basic physics and requirements 0-45752
- selective surfaces instrumentation for high temp. and hemispherical meas. 0-4756



# solar absorber-convertors continued

semiconductors, Moss relation between refr. index and energy gap, rel. to solar heat absorbers 0-11357  
shadow effect of adjacent solar collectors in large scale systems 0-45738  
simulator design for testing solar collectors 0-50996  
solar greenhouse with soil heat accumulator, temp. conditions anal. 0-40898  
space heating, energy utilisation improvements using new types of construction (*German*) 0-40903  
space heating, experimental installation, using solar absorbers, heat pumps, heat exchangers and measurement and control gear (*German*) 0-35741  
space heating, photovoltaic and thermal collector system design and testing 0-45675  
space heating, solar air heaters, aerodynamic drag investigation 0-40899  
spectral characteristics for improving solar collector performance 0-35650  
spectrally selective surfaces in photothermal solar energy conversion 0-45753  
spherical solar still, design, operation, and appls. 0-55913  
stainless steel, coloured, reflectance meas. 0-7958  
standards for heating and cooling appl. 0-7915  
stationary solar collector design to make most of diffuse radiation 0-30517  
steady state salt gradient solar pond 0-35749  
stills, basin-type, periodic anal. for estimating distillate output 0-45733  
stills, design and thermodynamic parameters, numerical anal. 0-55914  
storage of heat, solar collector performance analysis 0-30390  
systems analysis of solar-electric facilities 0-35685  
thermal balance, role of selectivity and concentration (*French*) 0-55895  
thermal collector, fixed, design optimisation 0-40905  
thermal collectors, prediction of long term average energy delivery 0-3553  
thermal collectors, prediction of long term average performance for concentrating and non-conc. systems 0-7956  
thermal conversion, collectors, storage systems, energy transport and economics, review 0-51003  
thermal emittance, optical technique for meas. (*Spanish*) 0-16835  
thermal receiver utilising a small particle heat exchanger 0-30557  
thin film thermal convertors 0-12011  
transwall for passive solar heating of buildings, thermal performance comparison 0-40840  
tri-mode solar conversion system, design and operation 0-55907  
Trombe wall control strategies for passive solar heating systems 0-45737  
Trombe-Michel wall using phase change materials, solar energy collection and thermal storage 0-55909  
tubular solar collectors, non-tracking, low-conc., steady state thermal anal. 0-55903  
underground constant flow solar collector/storage system 0-21412  
underground thermal storage in the operation of solar ponds 0-40911  
utilisation in human settlements, inexpensive systems, appls., function and techniques 0-51004  
water heating systems, test procedure for performance rating 0-55910  
water system for photographic processing laboratory, solar heated 0-40837  
zeolite collector for solid-gas absorpt. refrigeration system 0-35754  
Al film colour anodised, selective surfaces preparation and characts. obs. (*Japanese*) 0-55893  
Al-PbS selective surfaces for solar photothermal conversion, prep., emissivity, absorptivity 0-12030  
Au film on Al, reflectance and absorpt. obs. 0-7426  
CoO as a spectrally selective material for solar collector appls. 0-26159  
Cr black solar absorber surfaces, determ. of O<sub>2</sub> content using <sup>16</sup>O(<sup>3</sup>He, p) 0-45610  
Cr, fine particle solar absorber, effective medium theory 0-21396  
Cr-Cr<sub>2</sub>O<sub>3</sub>, black, electrolytic deposited, characterisation and thermal stability (*French*) 0-55898  
Cr-Cr<sub>2</sub>O<sub>3</sub>, black, solar selectivity at average temps. (100 to 250°C) (*French*) 0-55899  
Cr<sub>2</sub>O<sub>3</sub>-Cr black, selective coating, optical and topographical props. 0-26165  
Cr<sub>2</sub>O<sub>3</sub>-Cr black, solar collector coating, microstruct., FIM and SEM obs. 0-26166  
Cu-Al<sub>2</sub>O<sub>3</sub> cermet film, solar absorbing, production by dual cathode DC magnetron sputtering 0-16186  
CuO selective black coatings for large area appls., prep. and props. 0-21411  
CuS selective black coatings for large area appls., prep. and props. 0-21411  
Mo film, CVD, with high IR refl. and large solar absorpt., prep. and props. 0-26163  
Mo thin film fabrication for photothermal solar convertors using CVD 0-11573  
Mo thin films for solar photothermal conversion, CVD fabrication 0-7503  
Ni solar collector coating, microstruct., FIM and SEM obs. 0-26166  
Ni solar selective black coatings, electrochem. deposition on Zn surfaces 0-29885  
Ni-pigmented anodic Al<sub>2</sub>O<sub>3</sub>, for selective absorpt. of solar energy, optical and struct. props. 0-55892  
PbS+CuS selective black coatings for large area appls., prep. and props. 0-21411  
Se film, gas-evaporated, selective absorpt. characts. and emissivity 0-50998  
Si, amorphous, CVD, retarding crystn. by alloying with C,N,B or Ge, absorber life expectancy 0-44129  
Si, amorphous CVD fabrication for solar photothermal conversion appl. 0-7504  
Si, amorphous stabilised CVD films for high temp. solar photothermal conversion 0-26161  
Si, CVD prepared amorphous and polycryst., solar thermal absorber, temp. variation of absorpt. edge 0-12028  
Si solar cells with concentrating collectors and integrated heat use system 0-45701  
Si thin textured film prep. for selective absorption 0-30544  
Si-H, amorphous, on Nb or W, spectrally selective absorber, IR spectra 0-26164  
Te film, gas-evaporated, selective absorpt. characts. and emissivity 0-50998  
Te textured thin films, prep., high solar absorptivity by multiples refl. 0-11568  
Zn<sub>1-x</sub>Cd<sub>x</sub>S solid solution based devices 0-21409

# solar absorbers see solar absorber-convertors

## solar activity

see also solar flares; solar prominences; solar-terrestrial relationships; sunspots  
1978 May 7 events, radio, optical and geophysical manifestations (*French*) 0-8611  
active regions and X-ray bright points, birthplaces 0-12739  
active regions development, rel. to radio emission S-component spectrum fine struct. 0-21977  
active regions height struct., X-ray obs., OSO-8 limb crossing obs. 0-31280  
clock mechanism of interior driving sunspot cycle 0-17562  
corona, high-temp. regions rel. to solar wind flows associated with hot heavy ions 0-51635  
coronal index of activity, for 1971-76 period 0-4322  
coronal interconnecting loops transient brightenings, sudden brightenings morphology 0-21972  
coronal loops, thermal instabilities in magnetically confined plasmas 0-36600  
coronal X-ray bright point and small active region fine struct. rapid vars. 0-12741  
cosmic rays, high-energy, modulation, anisotropy spectrum var. with solar activity cycle 0-51628  
cycle 20, statistical anal. of noise storms on 260 MHz and radio bursts on 29.5 MHz 0-56794  
cycle dependence of F-region equatorial vertical drifts 0-31159  
cycle variation of interplanetary mag. field config. 0-12632  
cycle variations of interplanetary mag. field intensity 0-26809  
ephemeral active regions during solar minimum 0-31279  
F<sub>2</sub>-layer ionisation through a solar cycle, SW radiocommunication appl. 0-41626  
faculae and sunspots, mag. field effects on solar luminosity 0-46515  
flares and type I sources, evolutionary relation, 146 MHz obs. (*Chinese*) 0-8609  
fluctuations, and deviations of light rays during eclipses (*French*) 0-56795  
fluctuations, reln. to variation in O<sub>3</sub> conc. and layer temp. 0-31110  
forecast for Cycle 21, comparison with previous cycles (*Chinese*) 0-8608  
high-temperature plasma, anal. using dielectronic recomb. spectra 0-46391  
ionosphere, electron temp. var. with solar activity satellite meas. 0-26678  
magnetic flux emergence, ephemeral active regions and X-ray bright spots, flux-rope theory 0-46519  
magnetic flux emergence, evidence for globally coherent variability 0-51716  
Mauder Minimum, catalogues of auroral obs. 0-51722  
McMath 12686, type III burst producing McMath 12686, type III burst producing active region, overlying coronal struct. Skylab obs. 0-21976  
microwaves total flux, fluctuations power spectra correl. with solar activity 0-4327  
neutrino flux correls. 0-46522  
ozonosphere-solar cycle relationships 0-17342  
photosphere faculae intensity, centre to limb var. 0-21967  
photospheric faculae, models 0-12716  
plasma frequency bursts, implications of Voyager 2 coronal occultation obs., 1979 August 0-51639  
polar faculae, rel. to Sun high-latit. mag. field and Earth rot. nonuniformity 0-46119  
sectorial struct. of interplanetary mag. field, large scale spiral waves in solar wind 0-12633  
soft X-ray bursts, statistical distrib. 0-26839  
soft X-ray polychromator for Solar Maximum Mission 0-51660  
sunspot cycle morphology, theory (*Chinese*) 0-12722  
sunspot cycles, relation to polar coronal holes 0-21979  
sunspot cycles and effects on satellite performance 0-56812  
sunspot minimum, correl. with afternoon counter-electrojet events occurrence in Indian region 0-56672  
sunspot turning points and aurorae since (AD 1510) 0-21980  
surge, EUV limb spectra obs. from Skylab 0-17560  
surges, flare-assoc. ejection mechanism 0-21975  
transition zone, energy balance and press. for network and active region features 0-21957  
type II radio burst with reverse freq. drift against noise storm background, obs. 0-17567  
type III radio bursts, EM radiation direct generation from beam-plasma system 0-54007  
type III radio bursts, fundamental emission and polarisation 0-36603  
type III radio bursts, nonlinear stability theory 0-26826  
type U radio bursts, polarisation evolution 0-26834  
type V radio bursts, dynamic spectra distinctive struct. 0-46527  
X-ray active regions temp. and emission measure rel. to coronal mag. fields 0-12745  
X-ray bright points, short-term temporal vars. 0-12740  
X-ray bright points correl. with sunspot intensity, cycle var. 0-41783  
X-ray corona, slowly moving disturbances 0-21971  
X-ray temperature-emission measure modelling of corona 0-12746  
N IV and Ne VII emission line ratios, electron density and temp. determ. 0-17559

## solar atmosphere

see also chromosphere; photosphere  
axisymmetric convection in presence of mag. field, solar granulation and sunspots appl. 0-12724  
centimetre wave emission, Sun radio radius and brightness distrib. across disc 0-21968  
coronal hole, atmosphere model rel. to brightness temp. obs. by  $\lambda$  8-cm radioheliograph 0-4326  
five minute oscillation (*Japanese*) 0-21981  
flare model atmospheres, reverse current effects on electron beam dynamics and X-ray bremsstrahlung 0-51711  
flare particle streams, collective plasma effects associated with continuous injection model 0-21954  
flares, Fe XXIV-XXV X-ray lines wavelengths rel. to hot plasma motions 0-21973  
frequency response of magnetic flux sheaths 0-12743  
granulation, convection models, book contrib. 0-4329  
high-temperature plasma, anal. using dielectronic recomb. spectra 0-46391  
laboratory and space plasmas, conference, Nagoya, Japan (1977 December 8 to 9) 0-4470  
Langmuir waves, upconversion of ion-sound impossible 0-41716



**solar atmosphere continued**

- magnetic flux ropes, equilib. and stability (*Russian*) 0-8617
- magnetostatic equilib. in stratified atmosphere 0-51652
- photoabsorption cross sections for positive atomic ions with  $Z \leq 30$  0-26727
- plasma, highly ionized, ionization equilib. validity 0-21906
- plasma density determination, N III and O IV intersystem multiplets appl. 0-31264
- radiative transfer in magnetic atmospheres, analytical soln. 0-36494
- spectral line intensity, electron impact excitation 0-36605
- supergranulation on quiet Sun, high-resolution obs. at 6 cm using Westerbork Synthesis Radio Telescope 0-36601
- supergranulation structure in coronal holes 0-51729
- surges, flare-associ. ejection mechanism 0-21975
- temperature minimum region heating during solar flares, implications of Al I autoionisation lines obs. 0-26829
- thin magnetic tube instability rel. to network struct. 0-12725
- velocity field, estimation by measuring solar spectrum integral characts. 0-46530
- velocity fields, large-scale, from Doppler line shift obs. 0-12730
- wave propagation in nonisothermal atmosphere, rel. to solar five minute oscills. 0-31276
- Fe, K $\alpha$  fluoresc. due to solar flares 0-17569
- O abundance, influence of diffusion on line intensities 0-4318
- Si III 1892 Å emissivity, charge transfer effect on appl. of line as spectral diagnostic 0-41717

**solar batteries** *see solar cells***solar cell arrays***see also solar power*

- 5 kW photovoltaic generator system, analysis, design and realisation 0-45704
- 100 kW peak photovoltaic power system, design, construction and capabilities 0-45705
- 900 mW solar battery construction and characteristics (*German*) 0-12008
- battery installation and performance in mid-European latitudes (*German*) 0-21399
- combined photovoltaic/thermal flat plate collectors, extended Hottel-Whillier model 0-3520
- DC to AC power conversion and utility interfacing, techniques, requirements and components used 0-45703
- design of high concentration solar cell arrays, components, technology and performance 0-50955
- developments and new appls., cost effectiveness 0-16800
- digital consumer products appl., light-power conversion problem 0-3517
- direct photovoltaic conversion, future development prospects, research projects and new appls. 0-16798
- distributed photovoltaic systems for electricity generation, economic and technologic feasibility 0-55906
- economics modelling of photovoltaic module manufacturing, SAMICS methodology developments 0-55860
- electrical system comprising DC separately excited motor and mechanical load driven by solar cell array, performance analysis 0-16801
- heating and cooling of buildings, Shenandoah Solar Recreational Center 0-45757
- microcomputer controlled solar battery, charging networks and stepping motors for cell control 0-50987
- monolithic solar cell panel of amorphous Si 0-45666
- p-n homojunction integrated tandem solar cell performance 0-3521
- photovoltaic cells production technology, future systems efficiency and cost effectiveness 0-16799
- photovoltaic concentrator cells development project, developments, performances and future trends 0-45699
- photovoltaic energy system, 25 kWp, for agricultural appl., performance anal. 0-30491
- photovoltaic modules, physical and electrical degradation in terrestrial environment 0-30492
- photovoltaic solar arrays and DC motors, direct coupling theory 0-3523
- photovoltaic solar cell array used for supplemental power generation 0-35686
- photovoltaic systems, design for intermediate-sized appls. 0-30490
- photovoltaic/thermoelectric refrigerator for medicine storage for developing countries 0-35712
- power loss in photovoltaic arrays due to mismatch in cell characteristics 0-16802
- review of US DOE R and D program 0-55874
- satellite photoelectric power stations, alternate favourable option 0-16791
- satellite power system technology, environmental and societal impact 0-30386
- satellite solar power stations using solar cell arrays and microwave transmission 0-50982
- space power generators, past developments and future trends 0-45693
- space vehicle power extension package for Shuttle Orbiter fuel cell system 0-30496
- spacecraft, flight perform. of Nimbus-Landsat power systems 0-30459
- spacecraft, power system perform. anal. using computer modelling 0-30497
- spacecraft appls., concentrator enhanced arrays utilising thin film Kapton mirror 0-30501
- spacecraft solar electric propulsion, 25 kW solar array development testing 0-30500
- table top pulsed solar simulator, design and construction, for testing solar cell arrays powering artificial satellites 0-45696
- terrestrial flat plate photovoltaic modules, environmental testing 0-30560
- terrestrial solar generators, design, fabrication, testing and economic power generation 0-45672
- terrestrial solar modules, sandwich type glass encapsulation, climatic parameters effect, economic anal. 0-45673
- Al<sub>0.93</sub>Ga<sub>0.07</sub>As-GaAs monolithic series-connected solar cell array 0-7939
- Cu<sub>2</sub>S-CdS integrated thin film solar cell generators, fabrication techniques 0-55857
- GaAs photovoltaic solar system for utility substation appls. 0-30493
- Si solar cell array with concentration, design and development 0-45700
- Si solar cell fabrication, R and D on low-cost processes, effect of impurities on cell performance 0-50978
- Si solar cells with concentrating collectors and integrated heat use system 0-45701

**solar cells**

- antireflection coatings applied from metal-organic derived liquid precursors 0-5847

**solar cells continued**

- batteries for solar electricity storage, Systems optimisation of solar cell/battery 0-51007
- bifacial, theoretical anal. of efficiency and spectral response, fabrication and appls. 0-55856
- binary alloys, detection of compositional homogeneities using ion-induced Auger electron spectroscopy 0-25514
- book, current topics in material science 0-46747
- costs in 1985, economic forecast (*Swedish*) 0-7919
- desalination plant coupling to solar conversion system, technical and economic evaluation 0-55804
- developments and appls. for large scale electricity prod., review 0-40861
- developments and new appls., cost effectiveness 0-16800
- direct photovoltaic conversion, future development prospects, research projects and new appls. 0-16798
- distributed photovoltaic systems for electricity generation, economic and technologic feasibility 0-55906
- economic power generation, photovoltaic modules fabrication cost analysis 0-45674
- electron beam interaction, spatial variations effect of number density of recomb. centres on SEM meas. 0-7943
- electrochemical liquid-junction solar cells, Schottky barrier height, photovoltage and photocurrent 0-26162
- electrochemical solar cells, design and operation, underlying theoretical principles 0-40872
- electron beam induced currents appl., topotaxiality and dead region determ. 0-3518
- fabrication, preliminary 'test case' manufacturing sequence for 500 cent/watt solar photovoltaic modules in 1986 0-55858
- fluorescent planar collector-concentrators for solar energy conversion 0-45745
- grid lines, optimal design to reduce conductive losses 0-7945
- grid patterns, optimisation of multilayer front-contact patterns 0-16803
- heterojunction thin film solar cells, survey or semiconductor combinations 0-50974
- high efficiency Transcells and vertical multijunction cells for double-sided concentrated illumination 0-55855
- hydride concentration cells for solar conversion 0-35698
- III-V semiconductors, p-n heterostructures, epitaxial growth techniques, appl. to optoelectronics, review 0-54770
- introduction to the use of solar cells 0-35678
- irradiation distribution and concentration and output power conversion (*Spanish*) 0-35683
- isotype heterojunction, I-V characts. anal. 0-26138
- liquid junction cells, fill factor and stabilisation of photoanodes 0-2464
- low cost photovoltaic cells utilizing semiconducting thin films and advanced concentrator concepts 0-50972
- low-cost encapsulation materials for terrestrial solar cell modules 0-3522
- materials, fabrication and research for low cost photovoltaic solar cells 0-55838
- MIS, optimal interface design using computer simulation and expt. meas. 0-16805
- MIS, spectral response characts. and meas. of effective diffusion lengths 0-16804
- MIS Si solar cells, low-temp. CVD of SiO<sub>2</sub> to form inversion layer 0-12019
- MIS solar cells, basic principles of operation theoretical characts. 0-50986
- MIS solar cells, fabrication and performance characts. 0-45707
- monolithic solar cell panel of amorphous Si 0-45666
- Moss relation between refr. index and energy gap of semiconductors rel. to photovoltaic solar cells 0-11357
- multi-bandgap concentrator cells, Si and Al<sub>x</sub>Ga<sub>1-x</sub>As systems, operation with spectrum splitting filter 0-45698
- n<sup>+</sup>-n-p high-low-emitter junction solar cell, open-circuit voltage in conc. sunlight 0-50957
- numerical analysis of comb-shaped cells in 3-D 0-50973
- optoelectronic devices and optical imaging techniques, book 0-27059
- p-n heterojunction solar cells, band structure and photocurrent collection 0-21402
- p-n junction, photoinjected carrier lifetime meas. by reverse voltage pulse response 0-45664
- photoconverter, bilateral sensitivity, n<sup>+</sup>-p-p<sup>+</sup> structure, volt-ampere characts. under illumination 0-40855
- photoelectrochemical, enhanced photoeffects by electrocatalysis and peroxide effects 0-16815
- photoelectrochemical, function and construction of regenerative cell 0-26147
- photoelectrochemical, semiconductor/redox electrolyte junctions, functions examples and problems 0-45714
- photoelectrochemical solar energy conversion principles, review 0-35695
- photoelectrochemical systems (*German*) 0-45713
- photoelectrolytic production of H<sub>2</sub> and electricity, LaCrO<sub>3</sub>-TiO<sub>2</sub> photoactive anode 0-12024
- photoemissive solar-cells, efficiency calc., use of negative affinity photoemitters 0-55876
- photovoltage source in photocond. materials due to comp. and doping var. 0-7938
- photovoltaic cell efficiency calc., using irradiance-transmittance solar spectrum 0-26137
- photovoltaic cells production technology, future systems efficiency and cost effectiveness 0-16799
- photovoltaic conversion, Canadian R and D program 0-55872
- photovoltaic conversion, EEC R and D program 0-55873
- photovoltaic conversion, French R and D program 1976-79 0-55871
- photovoltaic conversion, Italian R and D program 0-55870
- photovoltaic converters, two junction, appl. of multijunction solar cells to photovoltaic systems 0-16812
- photovoltaic electricity generation in India 0-21381
- photovoltaic generators using optical concentration, current status and development trends review 0-45697
- photovoltaic power systems, equipment performance and manufacturing techniques improvements and system design problems for telecommunication applications 0-55843
- photovoltaic power systems for rural areas of developing countries 0-50967
- photovoltaic R and D in US, National Photovoltaic Program plan 0-55868
- photovoltaic R and D program in US, National Photovoltaic Program, status report 0-55867
- photovoltaic research and development in Japan, review 0-12012



## solar cells continued

- photovoltaic research and development projects in the Federal Republic of Germany 0-55869
- photovoltaic solar energy conversion [conf. Berlin, West Germany, April 79] 0-30482
- photovoltaic solar generators, ampere-hour efficiency, charging and discharge power 0-29434
- photovoltaic systems, design for intermediate-sized appls. 0-30490
- photovoltaics commercialization readiness assessment by US DOE 0-55859
- polyacetylene photoelectrochemical solar cell, fabrication and efficiency 0-50954
- polycrystalline, physics, operation and parameters of cryst. heterojunctions 0-50985
- polycrystalline Si, amorphous Si and CdS/CuS, function and construction (Swedish) 0-7940
- power conversion efficiency monitoring in photoelectrochem. and p-n junction cells 0-50989
- power supplies for remote telecommunication sites 0-26133
- principle, construction and operation, 1979 state and world-wide research survey 0-40862
- RAD polysilicon sheets, photovoltaic potentialities, conversion efficiencies, limitations 0-30484
- recombination velocity at III-V compound heterojunctions,  $\text{Al}_x\text{Ga}_{1-x}\text{As}$ -GaAs<sub>1-x</sub>Sb solar cells 0-12010
- review of US DOE R and D program 0-55874
- review using rational units 0-30389
- satellite solar power systems, developments and future trends 0-45694
- Schottky barrier, n-type, theoretical anal. of band edges, Fermi levels 0-50975
- semiconductor-insulator-semiconductor solar cells, basic principles of operation theoretical characts. 0-50986
- semiconductor-insulator-semiconductor solar cells, fabrication and performance characts. 0-45707
- solar cells, materials aspect, review 0-50971
- solid state physics rel. to solar cells, review 0-49601
- space heating, photovoltaic and thermal collector system design and testing 0-45675
- space power generators, past developments and future trends 0-45693
- spectral response, enhancement by fluorescent wavelength shifting 0-26139
- spectral response, pulsed measurement, test set-up and apparatus, shortcomings and planned improvements 0-45695
- spectral response characterisation, 400 to 1000 nm 0-35675
- student laboratory experiment on solar energy 0-17776
- temperature dependence of the maximum theoretical efficiency in solar cells 0-45670
- terrestrial solar generators, design, fabrication, testing and economic power generation 0-45672
- test facility using plane mirror heliostat 0-45668
- thermophotovoltaics, conc. ratio and efficiency 0-7946
- thin film, performance analysis employing loss minimisation of essential characteristics 0-45682
- thin film photovolt. convertors 0-12011
- transparent electrode photo-galvano-voltaic cell, using Mg-meso-tetraphenylporphine-coated glass (Chinese) 0-40865
- two-sided photovoltaic solar cell static concentrators 0-35684
- two-stage, fraction of radiation usefully converted, power prod. efficiency 0-30477
- V-I characteristics; AMO efficiency, rel. to spectral composition 0-3514
- varizone photoelectric convertor efficiency anal. 0-21397
- water desalting by solar powered electrodialysis 0-55805
- Ag/AgCl photogalvanic cells for solar energy conversion, basic electrochemistry 0-45715
- Ag-Si Schottky barrier cells, characts. of ZnS antireflection coatings 0-43414
- Al-SiO<sub>2</sub>-Si MIS solar cells, I-V characts. temp. depend. 0-7935
- Al-SiO<sub>2</sub>-p-Si MIS solar cells with back surface fields 0-12006
- Al-thin oxide-Si, Schottky barrier, degradation effects, ion beam induced nuclear reactions 0-30488
- AlGaAs tunnel diode, fabrication and appl. in cascade solar cell struct. 0-35682
- (AlGa)As-GaAs solar cells, theoretical perform. of multi-layer grid patterns 0-55846
- Al<sub>0.5</sub>Ga<sub>0.5</sub>As heterostructures, photoelectric convertors of conc. solar radiation 0-12015
- Al<sub>0.5</sub>Ga<sub>0.5</sub>As-GaAs<sub>1-x</sub>Sb<sub>x</sub> solar cells, appl. of recomb. vel. at III-V cpd. heterojunctions (Korean) 0-54771
- Au-n-Al<sub>0.5</sub>Ga<sub>0.5</sub>As-n-GaAs Schottky barrier solar cells, prep. and props. 0-26140
- CC Si diffused junction, n<sup>+</sup>pp<sup>+</sup> or p<sup>+</sup>nn<sup>+</sup>, prep. using solid diffusion sources 0-35689
- CdS heterojunction solar cells by CVD method 0-45685
- CdS photovoltaic panels, deposited by spray pyrolysis, film and junction structure studies 0-45689
- CdS Schottky barrier solar cells, spectral distrib. and photocapacitance 0-55864
- CdS:Cu<sub>2</sub>S sputtered solar cells, energy anal. of cell fabrication techniques 0-50966
- CdS/Cu<sub>2</sub>S, design and fabrication 0-30481
- CdS/Cu<sub>2</sub>S heterojunction solar cells, optimal material props. theory and experimental verification 0-45686
- CdS-Cu<sub>2</sub>S solar cells, conversion efficiency improvement 0-16807
- CdS-Cu<sub>2</sub>S solar cells, screen printed, prep. and photovoltaic props. 0-40863
- CdSe electrochem. photovoltaic cells, effect of thin film electrode prep. and conc. on efficiency 0-55847
- CdSe MIS thin film solar cell 0-45688
- CdTe, shallow homojunctions, characteristics and surface resistance influences 0-45690
- CdTe/Langmuir film photovoltaic structures 0-49918
- Cd<sub>1-x</sub>Zn<sub>x</sub>S/Cu<sub>2</sub>S thin film heterojunction solar cells, operational charact. 0-45687
- Cr-SiO<sub>2</sub>-Si MIS solar cell, current cond. 0-7936
- Cu-CdS, Schottky barrier, reverse differential capacitance, diffusion of Cu, solar cell appl. (French) 0-15424
- Cu<sub>1-x</sub>Ag<sub>x</sub>InS<sub>2-2x</sub> for solar photovoltaic cells 0-10982
- Cu<sub>1-x</sub>Ag<sub>x</sub>InS<sub>2(1-x)</sub>Se<sub>2x</sub> pentenary alloy system, appl. to photovoltaic solar-energy conversion 0-35680
- Cu<sub>2</sub>O thin film solar cells, fabrication and anal. 0-55865

## solar cells continued

- Cu<sub>2</sub>S/CdS, developments, appls., and economics of solar photovoltaic conversion (German) 0-26132
- Cu<sub>2</sub>S/CdS solar cells, performance, obs. 0-30480
- Cu<sub>2</sub>S-CdS, optical and calorimetric meas. of Cu<sub>2</sub>S semiconductor thin films 0-55863
- Cu<sub>2</sub>S-CdS heterojunction, photoelectric props. 0-29467
- Cu<sub>2</sub>S-CdS heterojunction solar cell, interface recomb. vel. determ. by capacitance/collection efficiency variation 0-50959
- Cu<sub>2</sub>S-CdS solar cell, interface recombination and junction field studies, exptl. technique 0-45683
- Cu<sub>2</sub>S-CdS solar cells, EBIC and capacitance measurements, stability problems 0-45684
- Cu<sub>2</sub>S-CdS solar cells in backwall configuration, model of photovoltaic effect 0-55861
- Cu<sub>2</sub>S-CdS thin film solar cell fabrication by electrophoresis 0-55862
- Cu<sub>2</sub>S-Zn<sub>1-x</sub>Cd<sub>x</sub> heterojunction, composition meas. near interface using aqueous ion-exchange 0-29465
- Cu<sub>2-x</sub>S-CdS p-n heterojunction solar cells, props., Burstein-Moss effects 0-21404
- Cu<sub>2</sub>S evaporated thin films, composition, prep. and characts. 0-25569
- Cu<sub>2</sub>S-CdS, SEM meas. of diffusion lengths, recombination vel. and junction collection efficiency 0-16808
- Cu<sub>2</sub>S-CdS heterojunction solar cells, time evolution of spectral characts. 0-30478
- Cu<sub>2</sub>S-CdS heterojunction solar cells spectral distrib. and photocapacitance 0-55864
- GaAlAs solar cells, appl. for navigational satellite power systems 0-35694
- Ga<sub>1-x</sub>Al<sub>x</sub>As:Si photoelectric convertors, broadband varizone creation 0-40856
- Ga<sub>1-x</sub>Al<sub>x</sub>As-GaAs, radiation resist., theoretical evaluation and optimisation 0-35681
- Ga<sub>1-x</sub>Al<sub>x</sub>As-GaAs solar cells, photoluminesc. characterisation 0-3512
- Ga<sub>1-x</sub>Al<sub>x</sub>As-GaAs solar cells, computer anal. of cell characts. incl. band gap variation 0-55866
- GaAl<sub>1-x</sub>P high-temp. solar cell with 0.3 eV band gap 0-21400
- GaAs, developments, appls., and economics of solar photovoltaic conversion (German) 0-26132
- GaAs, film and solar cell on graphite, struct. and elec. props. 0-2286
- GaAs, minority carrier lifetime at high temp., solar cell performance appl. 0-24947
- GaAs n-p solar cells, theoretical perform. of multi-layer grid patterns 0-55846
- GaAs photovoltaic solar system, appl. in electric utility system 0-55875
- GaAs, polycryst. Schottky barrier solar cells, effect of grain size on efficiency 0-50968
- GaAs polycryst. tunnel MIS solar cells, grain boundary problem 0-16809
- GaAs, polycrystalline, carrier transport at grain boundaries, rel. to solar cell performance 0-29411
- GaAs, shallow homojunction solar cell, resist. to 1 MeV electron radiation 0-50953
- GaAs, shallow-homojunction solar cell by MBE, conversion efficiency 0-30476
- GaAs solar cell structs., photolum. props. 0-50958
- GaAs, solar cells, electron-irrad., annealing kinetics 0-7937
- GaAs solar cells on Ge substrates, thin film shallow homojunction struct., quantum efficiencies 0-35677
- GaAs solar cells with shallow homojunction on Ge substrates 0-26142
- n-GaAs/K<sub>2</sub>Se-K<sub>2</sub>Se<sub>2</sub>-KOH/C solar cell, Ru (III) chemisorption on photoanode, effect on performance 0-3516
- n-GaAs/K<sub>2</sub>Se-K<sub>2</sub>Se<sub>2</sub>-KOH/C liq. junction cell, effect of Ru ion chemisorption on grain boundaries 0-55879
- GaAs-(SN)<sub>x</sub> solar cell fabrication and efficiency 0-26143
- GaAs-AlGaAs two-junction stacked solar cell, growth and characterisation 0-16811
- p-GaAs-Cd<sub>1-x</sub>Zn<sub>x</sub>S heterojunctions, elec. and photovolt. props. rel. to growth technique 0-29466
- GaAs-Ga<sub>1-x</sub>Al<sub>x</sub>As, variable band gap, photo-EMF, appl. to solar cells 0-20296
- GaAs-GaAlAs LPE grown, parameters dependence upon impurity concentration and temp. performances for series resistance reduction 0-45692
- p-GaP semiconductor-electrolyte solar cells for photochemical reduction of CO<sub>2</sub> to organic fuel 0-55880
- InGaP-InGaAs solar cell, high internal collection efficiency, low bandgap 0-26134
- n-In<sub>2</sub>O<sub>3</sub>/p-InP heterojunction, photovolt. effects 0-12014
- In<sub>2</sub>O<sub>3</sub>-SnO<sub>2</sub>/GaAs, solar cell, fabrication, characts. and interfacial chemistry 0-21401
- In<sub>2</sub>O<sub>3</sub>-SnO<sub>2</sub>/InP, solar cell, fabrication, characts. and interfacial chemistry 0-21401
- In<sub>2</sub>O<sub>3</sub>-SnO<sub>2</sub>/Si, antireflection props. of oxide film 0-3513
- In<sub>2</sub>O<sub>3</sub>-SnO<sub>2</sub>/SiO<sub>2</sub>/Si diode solar cells, loss mechanisms, characts., band struct. 0-26135
- In<sub>2-x</sub>Sn<sub>x</sub>O<sub>3-y</sub>-CdTe(InP) photovoltaic heterojunctions, surface and interface studies, efficiency 0-45691
- (SbBr<sub>0.4</sub>)<sub>x</sub>GaAs, single crystal and polycrystalline 0-16810
- Si, 50  $\mu\text{m}$  cell technology developments for low mass space blanket 0-30498
- Si, 50  $\mu\text{m}$  cells for space power systems, technology development 0-30499
- Si, amorphous, affect of transport props. on cell efficiency 0-50961
- Si, amorphous, glow discharge produced 0-12013
- Si, amorphous, hydrogenated, stacked solar cells 0-55842
- Si, amorphous, plasma deposited, horizontally multilayered struct. 0-50964
- Si, amorphous, solar cell appl. (Chinese) 0-45671
- Si, amorphous, solar cells, and photovoltaic devices (Japanese) 0-50965
- Si, amorphous, technological development trends for low cost energy requirements 0-26136
- Si, amorphous glow discharge films, H<sub>2</sub> content, elec. props., and photostability 0-25577
- Si, amorphous Schottky barrier solar cells, deep hole traps, spectral response and TSC meas. 0-50962
- Si, calculations of absorption coefficient 0-7944
- Si cell fabrication, recrystallisation of CVD-grown polycryst. Si and influence of B, Al dopants on grain growth 0-54575
- Si crystal growth, heat exchanger method, fixed abrasive slicing technique 0-35082
- Si, crystalline sheets production, low cost, crystal growth techniques comparison 0-35083



## solar cells continued

- Si, design, fabrication and evaluation of a 2" high efficiency cell for concentrator systems 0-55854  
 Si, developments, appls., and economics of solar photovoltaic conversion (German) 0-26132  
 Si, device model for tandem junction solar cell 0-16813  
 Si, diffused horizontal homojunction solar cells, effects of junction depth and impurity conc. 0-55877  
 Si, diffusion fabrication process, low cost, highly automated 0-30487  
 Si, directional solidification in carbon crucibles 0-45663  
 Si, edge-illuminated  $p^+nn^+$ , analytical model under concentrated sunlight 0-7942  
 Si, effects of B and P impurities on cell performance 0-55848  
 Si, efficiency limits, comprehensive explanation 0-35688  
 Si, experimental efficiency optimisation of  $n^+pp^+$  and  $p^+nn^+$  cells 0-30486  
 Si, for cathode protection of submerged marine structures 0-40859  
 Si, for improved short-wavelength quantum efficiency 0-31874  
 Si, growth of large grain polycryst. layers on graphite substrates by CVD on liquid layers 0-55849  
 Si, implanted layers characteristics, laser irradiation effects 0-35692  
 Si, Interdigitated Back Contact solar cells, surface recombination minimisation 0-12017  
 Si, ion implanted, from EFG Si ribbons 0-30485  
 Si, light trigger for slave flashguns 0-47125  
 Si, low-cost, starting materials technology and economics 0-30483  
 Si, low-cost photovoltaic solar cell fabrication developments using Si on ceramics and minute spherical cells 0-55839  
 Si, low-cost sheet fabrication, structural defects, effect on electronic props. and cell performance 0-50977  
 Si modules, photovoltaic units combined with storage batteries (German) 0-55840  
 Si  $p^+n-n^+$  edge-illuminated cell, analytical model 0-12018  
 Si photoelectric convertors, photoelectric parameters under illumination 0-40857  
 Si photoelectric convertors, bilateral sensitivity, optical characts. anal. 0-40858  
 Si, polycryst., elec. and photovolt. props., grain size effects 0-49800  
 Si, polycryst. films, transport props. and grain boundary charact. by TEM 0-50980  
 Si, polycryst. solar cells, production problems (Rumanian) 0-21398  
 Si, polycrystalline, for efficient low cost solar cells 0-21405  
 Si, polycrystalline  $n^+/p$ , computer model of spectral response and photocurrent 0-55853  
 Si, polycrystalline solar cell base material characterisation, defect states 0-50979  
 Si, production, Union Carbide Corporation Silane Process, cost analysis 0-21403  
 Si, purification technology for the development of low cost solar cells 0-50976  
 Si ribbon growth, ribbon-to-ribbon process, thermal environment control 0-35116  
 Si ribbon growth by capillary action shaping technique 0-29888  
 a-Si Schottky barrier, large-area RF sputtered, effect of hydrogenation, optimum barrier performance and bulk props. 0-45679  
 Si, screen printed solar cells, effect of double exponential on efficiency and yield 0-55851  
 Si, semiconductor thick film cell contacts, all metal 0-30489  
 Si solar cells, developments (French) 0-55845  
 Si solar cells, photoelectric effect and principles of operation and efficiency 0-50983  
 Si solar concentration cells, concentrated sunlight effects, experimental results, interpretation 0-35690  
 Si, solar grade, prod., using Dow Corning process 0-29894  
 Si solar photovoltaic cells, large scale production, materials, efficiency and economics 0-50970  
 Si, technological developments of single crystal cells and cost-effective cells 0-50984  
 Si terrestrial photovoltaic systems, historical developments and current research and development trends 0-45702  
 Si, thin cell with back surface reflector and controlled optical absorbance 0-35691  
 Si, thin foil cells, technology developments 0-35693  
 Si:H, amorphous,  $p^+n$  struct. solar cells, material parameters and deposition condition optimisation study for higher efficiencies 0-45676  
 Si:H, amorphous, RF sputtered, suitability as solar cell material 0-40864  
 Si:H, amorphous, RF sputtered, Schottky barrier solar cells, photovoltaic props. and capacitance-voltage charact. 0-45678  
 Si:H, amorphous, Schottky barrier, degradation mechanisms affecting stability and operation 0-45680  
 Si:H, amorphous, Schottky barrier diode, deposition parameter effects on elec. props. 0-45681  
 Si:H, amorphous, solar cell struct., photocurrent meas., absorpt. coeff. 0-50960  
 Si:H, amorphous, solar cells, carrier generation, recombination, and transport 0-55844  
 Si:H, amorphous Schottky barrier solar cells, depletion region, capacitance study 0-50963  
 Si:H amorphous films for solar cells, optical and elec. props. of RF glow discharge deposited films 0-54576  
 Si:P diffused solar cells, laser treatment to dissolve diffused P precipitates 0-45667  
 Si:P solar cells, improved P diffusion using laser treatment 0-55850  
 Si/Si-Ge alloy, amorphous multijunction structure, increased conversion efficiencies, low cost 0-45677  
 Si-Au Schottky barrier solar cell fabrication, doping of a-Si 0-50969  
 Si-C interface on polycryst. Si ribbon, effect on solar cell efficiency (French) 0-54531  
 a-Si-H sputtered solar cells, temp. depend. of Schottky barrier characts. 0-45669  
 p-Si-In<sub>2</sub>-Sn<sub>2</sub>O<sub>3</sub> solar cells, thermal degradation mechanisms 0-55841  
 SnO<sub>2</sub>/n-Si spray-deposited solar cells 0-12007  
 SnO<sub>2</sub>-Si, heterojunction solar cells, anomalous photocurrent 0-3515  
 SnO<sub>2</sub>-Si heterojunction solar cell, elec. props. (Korean) 0-45665  
 SnO<sub>2</sub>-Si heterojunctions, elec. and photovoltaic props. 0-26141  
 SnO<sub>2</sub>-Si solar cells, electron-beam deposited, struct., photovolt. props. 0-50956  
 SnO<sub>2</sub>-Si solar cells, stability and degradation mechanisms 0-16806  
 SnO<sub>2</sub>-SiO<sub>2</sub>-n-Si heterojunction, cheap solar elements for ground-based appls. 0-40860

## solar cells continued

- TiO<sub>2</sub>-Si solar cell hybrid electrodes for photoelectrochem. H prod. 0-45775  
 Zn<sub>2</sub>Cd<sub>1-x</sub>S, film, single-thermal-source form. 0-2492  
 Zn<sub>2</sub>Cd<sub>1-x</sub>S/GaAs heterojunction solar cells, meas. of minority carrier diffusion length 0-26158  
 ZnO, film for solar cell appl. structural, optical and elec. props. 0-2294  
 ZnO sintered electrode, for dye-sensitised solar photocell 0-16816  
 ZnO-Ti transparent type MIS solar cells 0-45662  
 Zn<sub>3</sub>P<sub>2</sub>, single crystal, growth, electronic and device props. 0-25551
- solar chromosphere** *see* **chromosphere**
- solar composition**  
 chromosphere-corona transition region, diffusion effects on comp. 0-46525  
 Be abundance calcs., effect of misidentification of Be I 2650 Å line 0-32636  
 CNO, abundances rel. to Si in different solar regions 0-46518  
 Fe abundance determ., Fe II oscillator strengths and choice of model atmosphere 0-56791  
 Fe abundance in photosphere, determ. from weak Fe I Fraunhofer lines (Russian) 0-12720  
 He abundance inferred from global oscills. obs. in spectra cosmology implications 0-51724  
 He content of solar models, implications for convective mixing length 0-26835  
 O, diffusion effects on photospheric and outer atmosphere abundances 0-4318
- solar constant** *see* **solar radiation**
- solar corona**  
 acoustic wave refl. in transition region 0-36607  
 active region loops, gyroresonance absorption evidence 0-56792  
 active regions height struct., X-ray obs., OSO-8 limb crossing obs. 0-31280  
 activity, coronal index, for 1971-76 period 0-4322  
 adiabatic flow in coronal loops 0-56803  
 chemical abundances, relative, in coronal hole and other solar regions 0-46518  
 chromosphere-corona transition region, diffusion effects on comp. 0-46525  
 colours during solar eclipse and dust composition 0-51730  
 cosmic rays with relativistic energy, review 0-56798  
 decametric obs. at high resolution 0-31288  
 electrostatic ion-cyclotron heating, in coronal mag. loops 0-51708  
 eruptive prominences, assoc. coronal brightness and structure changes 0-4337  
 eruptive prominences, coronal manifestations, theory 0-4338  
 eruptive prominences and coronal transients 0-56809  
 Faraday rotation during PSR 0525+21 occultation 0-46526  
 fast electrons stream, free dispersal in solar corona with nonsteady injection 0-17568  
 flare models, high-temp. and low-temp. comparison 0-12714  
 flare/surge events, hydrodynamic simulation 0-12748  
 global-scale 3-D reconstruction 0-56719  
 H $\alpha$  post-flare loops dynamics, 1973 July 29 flare 0-31286  
 hole, obs. with  $\lambda$  8-cm radioheliograph 0-4326  
 hole model 0-8606  
 holes, EUV and radio spectrum 0-56802  
 holes physical structure, influence of mag. fields and coronal heating 0-46520  
 horizontal temperature gradient in prominence/corona transition zone, meas. rel. to prominence condensation 0-26832  
 hot coronal regions, rel. to solar wind flows associated with hot heavy ions 0-51635  
 hydromagnetic surface waves, dissipation 0-21904  
 interconnecting loops transient brightenings, sudden brightenings morphology 0-21972  
 interplanetary dust and electrons spatial distrib. round Sun, contrib. to corona 0-46514  
 ion dynamics and abundance in coronal holes 0-41807  
 kink instability of loops and solar flares 0-41802  
 loop heating by fast mode MHD waves 0-41801  
 loops, thermal instabilities in magnetically confined plasmas 0-36600  
 magnetic arcades and prominence formation 0-41800  
 magnetic field determ. using type II burst obs. and theory 0-41785  
 magnetic field models, validity of Green's function solns. 0-21970  
 magnetic fields, Laplace's eqn. direct soln. using line-of-sight boundary conditions 0-12742  
 magnetic traps, plasma instability periodical regimes (Russian) 0-8616  
 mass flow and ionization equilb. 0-36608  
 metre-wave emission, wave ducting rel. to fundamental/harmonic source coincidence 0-21978  
 oscillations above active region, Fe XIV spectra obs. 0-41794  
 plasma, low-density, autoionisation contrib. to total ionisation rates 0-9738  
 polar coronal holes, rel. to solar cycles 0-21979  
 polar holes, evolution from He I 1083 nm synoptic maps 0-56801  
 prominence interface, review 0-4333  
 prominences as corona condensing along mag. field lines 0-46524  
 quasi-static loops, numerical modelling with uniform energy input 0-21958  
 quiescent prominences, heating and cooling, calc. 0-12738  
 radio emission, S-component local sources struct. 0-46528  
 shock waves during large solar flares, proton and electron accel. 0-21974  
 stability analysis of min. flux corona theory rel. to spicules 0-41795  
 supergranulation structure in coronal holes 0-51729  
 surge, EUV limb spectra obs. from Skylab 0-17560  
 temperature constraints in open mag. field regions 0-12744  
 transition region, EUV line emission weakening short of 912 Å wavelength 0-21962  
 transition region, line intensities from Si VI, VIII and XII excitation calcs. 0-31273  
 transition region, OSO 8 UV obs. of optically thick region 0-56788  
 transition-zone plasmas, electron densities and mass motions in flares 0-56804  
 turbulent heating role 0-12715  
 type II radio burst with reverse freq. drift against noise storm background, obs. 0-17567  
 type III burst producing active region, Skylab obs. of overlying coronal struct. 0-21976  
 type U radio bursts, polarisation evolution 0-26834



**solar corona continued**

- Voyager 2 occultation, 1979 August, radio signals ang. and spectral broadening 0-51639  
 X-ray active regions temp. and emission measure rel. to coronal mag. fields 0-12745  
 X-ray bright point and small active region fine struct. rapid vars. 0-12741  
 X-ray bright points, obs. rel. to globally variability in solar mag. flux emergence 0-51716  
 X-ray burst, impulsive, from coronal source, obs. 0-26836  
 X-ray corona, slowly moving disturbances 0-21971  
 X-ray observations, using rocket-borne real-time imaging system 0-41725  
 X-ray temperature-emission measure modelling of corona 0-12746  
 C-like ions emission lines, density depend. 0-21963  
 Fe XV EUV line intensities 0-51731  
 N IV and Ne VII emission line ratios, electron density and temp. determ. 0-17559  
 N isoelectronic sequence ions, level populations and EUV line intensities for solar coronal conditions 0-51649  
 Ni XVII EUV line intensities 0-51731  
 O I isoelectronic sequence, excited level populations, line intensity ratios, solar corona appl. 0-32637  
 O III, electron impact excitation of semi-forbidden transitions in coronal holes 0-48092

**solar corpuscular radiation** *see solar wind***solar corpuscular streams** *see solar wind***solar cosmic ray particles**

- acceleration in flares, X-ray and gamma-ray obs. 0-31265  
 electron nonthermal props. rel. to solar wind kinetic instabilities 0-41691  
 electrons stream, free dispersal in solar corona with nonsteady injection 0-17568  
 energetic particles in solar flares 0-31266  
 energetic particles in stream-structured solar wind 0-41674  
 first phase acceleration mechanisms in solar flares 0-31267  
 flare accelerated particles, charge spectrum and comp. form. 0-46529  
 flare electron events, Oct. 1972 to Dec. 1974 obs. 0-56796  
 flare protons, quantitative estimation from characts. of microwave radio bursts at 9 GHz 0-4323  
 flare protons, radiation danger during manned space flights 0-41788  
 flare protons, stochastic accel. 0-21953  
 flare protons and electrons, accel. by shock waves 0-21974  
 gamma-rays, hard intensity radiation pulsations in the atmosphere (*Russian*) 0-17454  
 hard X-ray burst, 1972 August 4, trap-plus-precipitation model 0-12747  
 intensity enhancement, diurnal var., 1973 May 22-June 4 event 0-56685  
 interplanetary diffusion, Monte Carlo method 0-12623  
 Jupiter magnetosphere, Voyager 1 obs. of solar cosmic ray particles 0-26798  
 long-lived sources, collapsing magnetic regions 0-31268  
 MeV protons associated with solar flare, May 1979 obs. 0-51627  
 neutrino detection, new expts. proposal 0-31181  
 neutrino flux correls. with solar activity 0-46522  
 neutrino puzzle, explanations for missing neutrinos 0-51723  
 propagation, anisotropic diffusion-convection eqn., dimensional soln. 0-17453  
 proton events forecasting rel. to microwave bursts (*Chinese*) 0-12723  
 proton flux, calc. using microwave burst parameters 0-41789  
 proton flux, energy and temporal spectra, influenced by interplanetary mag. field 0-41672  
 protons, radiation hazard in shielded spacecraft 0-8194  
 relativistic cosmic rays, review 0-56798  
 spectrum formation near Earth, propagation and acceleration (*Russian*) 0-4211  
 X-rays and gamma-rays, obs. by Signe II MP satellite expt. 0-41696  
<sup>26</sup>Al, from <sup>3</sup>He-rich solar flares 0-36461  
<sup>10</sup>Be, from <sup>3</sup>He-rich solar flares 0-36461  
 He ions superheating and superacceleration 0-12631  
<sup>22</sup>Na, from <sup>3</sup>He-rich solar flares 0-36461

**solar cosmic ray photons**

No entries

**solar disturbances** *see solar activity***solar eclipses**

- 1966 November 12, ionization rates in South Atlantic geomagnetic anomaly 0-12608  
 1970 March 7, corona, colours during eclipse and dust composition 0-51730  
 1972 July 10, corona, colours during eclipse and dust composition 0-51730  
 1973, June 30, Dutch expedition for solar spectra exam. 0-8614  
 1973, June 30, report of Dutch expedition 0-8615  
 1976, October 23rd, upper atmos. wind obs. 0-46327  
 1978 April 29, limb darkening obs. during partial eclipse (*French*) 0-8612  
 1979, February 26, an illustrated record from N.American obs. 0-4328  
 1979 February 26, shadow band obs. 0-17372  
 1981 July 31, obs. of gravit. deflection of light (Einstein effect), prospects (*Russian*) 0-51651  
 ancient events as record of lunar motion 0-46182  
 effect on geostationary broadcast satellites and prediction of occurrence 0-31199  
 light bending by Sun, vars. caused by solar activity (*French*) 0-56795  
 terrestrial heat and radiation budget during solar eclipse, above pine forest (*German*) 0-46226

**solar-electric power stations** *see solar power stations***solar energy concentrators**

- cassegain solar collector with thermoelectric module, concentration efficiency 0-35709  
 Cassegain solar furnace, determ. of concentration 0-7932  
 Cassegainian solar concentrator, optical and thermal analysis 0-40906  
 cells irradiation distribution and concentration (*Spanish*) 0-35683  
 central receiver program, heliostat, receiver and storage subsystems 0-30404  
 central receiver solar power systems, terminal concentrator concept analysis 0-26116  
 circular film concentrator with a concentric seam of constant curvature, effect of seam on shape of reflecting surface 0-40827  
 composite focusing parabola and compound parabolic concentrator, sequential use 0-45638

**solar energy concentrators continued**

- compound elliptical concentrator, geometrical vector flux field 0-33119  
 compound parabolic concentrator collectors, prediction of thermal performance 0-55905  
 compound parabolic concentrator solar collector design 0-3532  
 concentrating collectors, single axis, orientation, economic criterion 0-40907  
 concentrating solar collectors, concentration/acceptance relationships 0-21414  
 concentration system health hazards 0-3492  
 cylinder-parabolic, with envelope pipe, steam generation efficiency calculation model (*German*) 0-33112  
 cylindrical absorbers, sun following reflectors, semi-parabolic reflector, thermal power and efficiency (*Korean*) 0-21380  
 cylindrical parabolic mirror utilisation as solar receiver (*Rumanian*) 0-7914  
 design, economics and optical loss anal. of concentrating solar collectors 0-45751  
 design of high concentration solar cell arrays, components, technology and performance 0-50955  
 design variables, optical efficiency, heat loss coefficient and heat removal factor 0-7927  
 fixed mirror, appl. to H solar-thermochemical prod. of H<sub>2</sub>O 0-45767  
 fixed mirror solar concentrator for application to a 100 MW(e) electric generating plant 0-30393  
 fluorescent planar collector-concentrators for solar energy conversion 0-45745  
 fluorescent planar concentrators—performance and experimental results 0-45646  
 FMDF solar-thermal-electric system, optical concentration profiles and receiver perform. anal. 0-30392  
 foam-film parabolic-cylindrical concentrator surface fabrication 0-21372  
 focusing collectors, cylindro-parabolic mirrors (*Rumanian*) 0-50934  
 Fresnel lens, colour-corrected linear convex, for solar concentration 0-45640  
 furnace, focal spot thermal analysis 0-21383  
 glass components, specularly meas. using Fourier transform anal. 0-5804  
 heliostat facets, optical characterisation 0-53485  
 hydride concentration cells 0-35698  
 ideal concentrators for distant radiation sources 0-35751  
 image characteristics, non-uniform intensity distrib. 0-55816  
 linear echelon refractor/reflector solar concentrators 0-7929  
 linear focusing solar reflector, production by elastic deformation of flat sheet 0-30391  
 linear Fresnel solar reflector concentrator, geometrical design 0-45636  
 low cost photovoltaic cells utilizing semiconducting thin films and advanced concentrator concepts 0-50972  
 luminescent concentrators, operation theory and performance evaluation techniques 0-7913  
 maximal concentration from new class of radiation concentrators 0-45639  
 mirror arrays, large Earth orbit structures reflecting sunlight for power generation, lighting, and agriculture 0-45632  
 mirrors design, American and Australian practices (*Italian*) 0-50935  
 nonimaging concentrator design as second stages with image-forming first-stage concentrators 0-50933  
 nonimaging solar concentrator design, cavity enhancement by controlled directional scattering 0-45631  
 optical simulation for a fixed spherical solar collector 0-7912  
 Optics applied to solar energy, [Conf. San Diego, CA, USA Aug. 1978] 0-7926  
 parabolic concentrator, use of fin receiver 0-21379  
 parabolic dish thermal power systems, technology and appl. 0-30558  
 parabolic solar reflector for accurate and economic producibility 0-7930  
 paraboloid concentrator fabrication, simplified method 0-16837  
 photovoltaic, electrodialysis desalting plant appl. 0-55805  
 photovoltaic concentrator cells development project, developments, performances and future trends 0-45699  
 photovoltaic concentrator system for Roxborough Park 0-30408  
 photovoltaic generators using optical concentration, current status and development trends review 0-45697  
 plano-cylindrical Fresnel plastic lens, design and performance analysis as solar collector 0-53403  
 pond potentialities as solar collector 0-30388  
 reflector and absorber design, spherical stationary mirror, and automatic tracking absorber 0-50997  
 reflector shapes for truncation of nonimaging cusp concentrators 0-21385  
 self-contained solar power installation concentrating system design and optical/energy characts. testing 0-40828  
 spacecraft appls., concentrator enhanced arrays utilising thin film Kapton mirror 0-30501  
 spectral characteristics for improving solar collector performance 0-35650  
 spectral emissivity measurement device, high-temp. materials 0-37039  
 stationary solar collector design to make most of diffuse radiation 0-30517  
 system designs for low cost-low ratio solar concentrators 0-7928  
 thermal conversion, collectors, storage systems, energy transport and economics, review 0-51003  
 thermal energy collection, comparative eval. of fixed and tracking collectors 0-7931  
 thermal generating station design, engineering problems (*German*) 0-30381  
 thermodynamics of solar-thermal processes, second-law anal. 0-21378  
 thermoelectric conversion, concentrators and central receiver systems 0-45760  
 thermogravimetric method for recording mass transport of materials under action of radiant fluxes 0-17944  
 tower-type solar furnaces, two mirror, high power, optical characts., calc. for design 0-40824  
 tracking parabolic reflecting concentrators, solar-heated water for photographic processing laboratory 0-40837  
 tri-mode solar conversion system, design and operation 0-55907  
 two-sided photovoltaic solar cell static concentrators 0-35684  
 Al-Ag alloy mirror for use as solar reflector, co-sputtering 0-20789  
 Si solar cell array with concentration, design and development 0-45700  
 Si solar cells with concentrating collectors and integrated heat use system 0-45701  
 Si solar concentration cells, concentrated sunlight effects, experimental results, interpretation 0-35690



**solar energy conversion**

- see also solar absorber-convertors; solar cells
- air-based solar heating systems with phase-change energy storage, performance anal. using computer simulation 0-35762
- alcohol fuel production from biomass 0-55773
- alternative resources and technologies, Conf., Chicago, IL, USA, Nov. (1978) 0-23123
- automotive transport utilising stirling heat engine 0-55824
- bacterial biomass production, efficiency bypasses that of photosynthesis 0-21408
- bioconversion of solar energy, review 0-45720
- bioenergy conversion systems, efficiency improvements 0-30511
- biomass conversion to fuels and chemicals, Purdue Process 0-26149
- biomass energy conversion, energy sources for rural development 0-30509
- central receiver program, heliostat, receiver and storage subsystems 0-30404
- chemical, by  $\text{NH}_3$  dissociation 0-30513
- chemical energetics in solar energy conversion, storage and transport (French) 0-7917
- chemical heat pump/energy storage system 0-30512
- chemical reactor theory and designs (French) 0-7916
- chemical storage, long-term efficiency of iterative cyclic reactions 0-45764
- chemistry research and developments (French) 0-11999
- climate impact of thermal electric, biomass, photovoltaic and ocean thermal conversion systems 0-30612
- cold water pipe designs for ocean thermal energy conversion plants 0-45725
- computer simulation for systems design 0-35679
- conference, Ontario, Canada (Aug. 1978) 0-41949
- desalination appl., combination with greenhouse installation (French) 0-55806
- desalination plant coupling to solar collector systems, low-temperature multiple-effect type, technical and economic evaluation 0-55804
- desalting plant appl. based on solar powered electrodialysis 0-55805
- direct solar irradiance, indirect meas. 0-45644
- economics, component cost of solar energy systems 0-45651
- electric generating systems, resource requirements 0-7923
- electric solar pumps for water pumping 0-50942
- electricity production by direct and indirect conversion schemes, review 0-50981
- electrochemical heat engine for direct solar energy conversion 0-30519
- electromagnetics and environment, book 0-36431
- fluidyne pump, design and operating characts., expt. test results 0-55890
- flywheel energy storage interface unit for photovoltaic applications 0-30571
- heat generation for multipurpose utilization systems by heat of dilution converted from solar energy 0-55915
- heat storage in porous medium with circulating heat transfer fluid, solar system appl. (French) 0-40916
- heating system economic evaluation and optimisation 0-35644
- hydride concentration cells 0-35698
- Iranian solar town conceptual development 0-35645
- liquid thermal storage tanks, thermal stratification enhancement 0-40918
- major solar energy research programs, review 0-40843
- metal hydride solar heat pump and power system, design and costs for space heating appls. 0-30521
- microwave power transmission technology 0-40868
- MINI-OTEC ocean thermal energy conversion plant test 0-45727
- molybdenite ore treatment using 2 kW solar furnace 0-3107
- NASA space power technology program, photovoltaic energy conversion 0-30494
- ocean swell and wave energy conversion system, feasibility 0-55795
- ocean thermal energy conversion for electrolytic H prod. 0-30546
- Ocean Thermal Energy Conversion platform environmental impact assessment 0-45726
- OTEC; analysis of a heat exchanger-thermoelectric generator system 0-35710
- OTEC, design of seacoast test facility, Hawaii 0-55888
- OTEC, evaluation of bottom-fixed OTEC platforms on the edge of a continental shelf 0-55887
- OTEC plant development, an unfavourable analysis 0-55889
- OTEC R and D in Japan 0-35738
- parabolic dish thermal power systems, technology and appl. 0-30558
- passive solar building thermal performance modelling by passive solar test boxes, expt. 0-3494
- passive solar building thermal performance modelling by passive solar test boxes, theory 0-7921
- passive solar buildings, thermal heat flow modelling using model expansion methods 0-45645
- phase-change, energy storage unit sizing for air-based solar heating systems 0-7922
- photo-electrochemical production of C-C bonds from carbon dioxide 0-21407
- photoelectric conversion cost reduction (Italian) 0-30479
- photoelectrochemical cells, chlorophyll sensitised reactions 0-7948
- photoelectrochemical cells, surface aspects 0-12021
- photoelectrochemical systems, material aspects, charge transport, energy output 0-12022
- photoelectrochemistry, laser sources use for solar energy conversion 0-40873
- photoelectrolytic production of  $\text{H}_2$  and electricity,  $\text{LaCrO}_3\text{-TiO}_2$  photoactive anode 0-12024
- photogalvanic, EDTA-methylene blue cells props. and appl. 0-21406
- photovoltaic research and development in Japan, review 0-12012
- photovoltaic space power systems, 25 kW power module evolution 0-30495
- photovoltaic-wind hybrid alternative energy system 0-30409
- photovoltaic/thermoelectric refrigerator for medicine storage for developing countries 0-35712
- polymer films, solar energy materials, transparent, optical characts. investigation 0-20724
- ponds, daily performance characts. of shallow solar ponds 0-30554
- ponds, economics and performance characts. of salty and saltless ponds 0-30553
- power systems availability and reliability analysis 0-35687
- quantum utilizing solar energy convertor efficiency in absence of intraband thermalisation 0-26144
- radiation enhancement using surface polaritons 0-7941
- salt-gradient solar ponds, performance characts. 0-30551
- salty solar ponds, stability criteria for saturated ponds 0-30552

**solar energy conversion continued**

- satellite, appl. of solid state microwave technology 0-40870
- satellite, assessment for European appl. 0-40867
- satellite, computer modelling of power transmission system 0-40866
- satellite, microwave system perform. during startup/shutdown 0-40869
- satellite photoelectric power stations, alternate favourable option 0-16791
- satellite solar power stations using solar cell arrays and microwave transmission 0-50982
- solar energy transition and materials problems 0-26115
- solar power satellite, construction in space, fabrication methods, materials, tools 0-21377
- Solar Power Satellites, energy anal. 0-50937
- solar-electric heat pump for houses, design and tests (German) 0-7951
- solid films and surfaces, conference, Tokyo, Japan (Jul. 78) 0-10739
- space vehicle thermionic generators for solar energy conversion 0-35714
- Stirling engine power conversion for MWe solar power system with parabolic concentrators 0-30561
- student laboratory experiment 0-17776
- synthetic chloroplasts for H prod. 0-30508
- terrestrial utilisation of solar energy, scope and experience (German) 0-40829
- thermal, advanced solar thermal technology, review 0-30555
- thermal, review of solar pond concepts 0-30550
- thermal, Stirling heat engine, solar powered, for reverse osmosis desalination plant 0-55891
- thermal power system, open cycle air turbine (French) 0-45641
- thermal solar pumps for water pumping 0-50942
- thermal systems, long-term perform. characts. using closed-form solns. 0-30556
- thermal systems, technology status 0-40842
- thermochemical receiver for solar thermal power, design 0-7950
- thermodynamic conversion for solar water pumping 0-45728
- thermoelectric, appls. to OTEC and agricultural irrigation 0-35708
- thermoelectric conversion, collector systems and thermal storage 0-45759
- thermophotovoltaics, conc. ratio and efficiency 0-7946
- utilisation, conf., Cairo, Egypt (June 1978) 0-46734
- utilisation, direct and indirect (German) 0-3489
- utilisation via plant photosynthesis 0-3491
- water and space heating systems; economic feasibility 0-7920
- water heating, polyethylene low-cost unit development (Afrikaans) 0-7925
- water heating by system of solar collectors and central hot water tank 0-55809
- water heating system, solar, technical and economic anal. 0-50936
- water solar photodecomposition, redox reaction thermodynamics 0-35697
- $\text{CaCl}_2$ -methanol thermochem. cycle for solar thermal energy storage 0-30587
- $\text{CuGaSe}_2$  single crystals, elect. and optical props. for solar cell appl. 0-10981
- $\text{Cu}_2\text{S}$ , polycryst. thin films, struct., optical and elect. props. for solar energy appl. 0-10837
- Fe-thionine photogalvanic, cells 0-35696
- H as the solar energy translator 0-30608
- H biological photoprod. using sunlight, review 0-45777
- H biological prod. by solar energy conversion, coupling of hydrogenase and chloroplast photosystems 0-45778
- H photochemical prod. by  $\text{H}_2\text{O}$  photolysis using sunlight 0-45776
- H photoelectrolytic production by  $\text{H}_2\text{O}$  decomposition using sunlight, review 0-45774
- H prod. by  $\text{H}_2\text{O}$  pyrolysis using solar thermal energy 0-45770
- H prod. by  $\text{H}_2\text{O}$  solar photolysis by engineering methods using biological materials (Japanese) 0-45765
- H production by  $\text{H}_2\text{O}$  dissociation using solar energy 0-30597
- H production by  $\text{H}_2\text{O}$  photocatalysis on  $\text{TiO}_2$  using solid C 0-26150
- H production for solar energy utilisation, solar-H energy system 0-51014
- H, thermochemical prod. by high temp.  $\text{H}_2\text{O}$  decomposition using solar energy 0-45822
- H-rich synthetic fuel prod. and transportation for solar energy utilisation 0-51015
- $\text{H}_2$  gas, photosynthesis prod. by green algae, turnover times and pool sizes 0-16821
- $\text{H}_2$  generation by water solar photolysis, large-scale impracticability 0-26172
- $\text{H}_2$  photoelectrochemical production using solar energy and  $\text{Zn}(\text{Mg})(\text{Cr})(\text{Ni})$  phthalocyanine dyes (French) 0-55936
- $\text{H}_2$  production by solar photochemical decomposition of  $\text{H}_2\text{O}$  0-16822
- $\text{H}_2$  production using  $\text{Mg}(\text{Al})(\text{Fe})(\text{Co})(\text{Ni})(\text{Cu})(\text{Zn})$  sulphates for solar energy storage (French) 0-55935
- $\text{H}_2/\text{O}_2$  thermochemical prod. by  $\text{H}_2\text{O}$  decomposition using solar energy 0-40919
- $\text{H}_2\text{SO}_4\text{-H}_2\text{O}$  chemical heat pump energy storage system 0-30515
- $\text{TiO}_2\text{-LaCrO}_3\text{-GaP}$  photoelectrochem. reactor for materials synthesis using solar energy 0-45712

**solar energy power stations** see solar power stations**solar flares**

- 1973 September 5, two-temp. model 0-56805
- 1977 April 12, gyro-synchrotron modulation in assoc. moving type IV bursts 0-26833
- blue continuum flares and D3 preflare shell obs. 0-51709
- chromosphere flares, H Lyman  $\alpha$  direct collisional excitation rel. to profile and polarisation 0-41780
- corona, flares correl. with interconnecting loops transient brightenings 0-21972
- coronal turbulent heating rel. to flares 0-12715
- cosmic ray protons,  $\geq 130$  MeV, April and May 1979 obs. 0-51627
- cosmic ray solar modulation, semi-diurnal anisotropy on flare days 0-46356
- current buildup prior to flares, obs. test to distinguish between slow and transient 0-31281
- current sheet in compressible plasma, self-similar resistive decay 0-1755
- dynamics of flare sprays 0-56808
- electron beams, diagnostic using chromospheric spectrum 0-26827
- electron density and temp. from Ca II/Fe I emission line ratios (Russian) 0-51717
- electron events, Oct. 1972 to Dec. 1974 obs. 0-56796
- elementary flare bursts, model, kernels excitation 0-31283
- energetic particles, acceleration 0-31266
- EUV and hard X-ray sources relationship 0-46512
- EUV radiation, detect. using ionosphere sudden freq. deviations (SFD) 0-8484



**solar flares continued**

- evolutionary relation to type I sources, 146 MHz obs. (*Chinese*) 0-8609  
 fast electrons stream, free dispersal in solar corona with nonsteady injection 0-17568  
 first phase acceleration mechanisms 0-31267  
 Forbush decreases in 1973-1974, unusual characts. 0-12624  
 gamma-ray spectroscopy 0-31271  
 H $\alpha$  post-flare loops dynamics, 1973 July 29 flare 0-31286  
 hard X-ray burst, 1972 August 4, trap-plus-precipitation model 0-12747  
 Hard X-Ray Burst Spectrometer on Solar Maximum Mission 0-51658  
 Hard X-ray Imaging Spectrometer on Solar Maximum Mission 0-51659  
 hard X-ray polarization 0-41787  
 hydrodynamic simulations of flare/surge events 0-12748  
 interplanetary manifestations, solar wind flows associated with hot heavy ions 0-51635  
 kink instability of coronal loops 0-41802  
 Langmuir waves, upconversion of ion-sound impossible 0-41716  
 magnetic energy conversion 0-56682  
 magnetic fields, role in disarptions brusques of solar filaments (*Russian*) 0-51726  
 magnetic structures, models and predictions of flux rope theory 0-21955  
 microwave and optical emissions comparison 0-31284  
 microwave spectrum, appl. of quasi-thermal electrons gyrosynchrotron emission theory 0-36602  
 models, high-temp. and low-temp. comparison 0-12714  
 multiply impulsive solar bursts, spectral evolution 0-26828  
 nonthermal electron beams, effect of reverse currents on beam dynamics and X-ray bremsstrahlung 0-51711  
 observational and theoretical status, review 0-51728  
 particle acceleration, charge spectrum and comp. form. 0-46529  
 particle acceleration, X-ray and gamma-ray obs. 0-31265  
 particle streams, collective plasma effects associated with continuous injection model 0-21954  
 plasma, compressible magnetic-field reconnection 0-6226  
 plasma column merging, simulation expt. (*Japanese*) 0-31269  
 plasma processes, magnetospheric substorm similarities 0-41671  
 plasma stream from flare, struct. rel. to flare location on Sun 0-41790  
 proton events forecasting rel. to microwave bursts (*Chinese*) 0-12723  
 proton flares, quantitative identification from characts. of microwave radio bursts at 9 GHz 0-4323  
 protons, radiation hazard in shielded spacecraft 0-8194  
 protons, stochastic accel. by Alfvén wave turbulence 0-21953  
 radiation danger during manned space flights 0-41788  
 second-stage X-ray emission, spectrum beyond 200 keV 0-51710  
 shock waves, coronal, during large solar flares, proton and electron accel. 0-21974  
 soft X-ray flux, principal component anal. 0-41781  
 soft X-ray polychromator for Solar Maximum Mission 0-51660  
 spectra, high dielectronic satellite lines analysis for plasma props. calc. 0-12728  
 surges, flare-assoc. ejection mechanism 0-21975  
 temperature minimum region, heating mechanisms, theory 0-31282  
 third phase flare acceleration, collapsing magnetic regions as cosmic ray sources 0-31268  
 transition-zone plasmas, electron densities and mass motions in flares 0-56804  
 two-ribbon flare, assoc. umbral brightening 0-41804  
 two-ribbon flares, force-free magnetic arcades 0-56806  
 type III bursts and flare occurrence in spotless regions 0-56810  
 X-ray burst, impulsive, from coronal source, obs. 0-26836  
 X-ray flares, selected, physical parameter profiles 0-17561  
 X-ray spectra, Fe XXIV-XXV lines wavelengths in 1.85-1.87 Å region 0-21973  
 X-ray spectra, high-resolution obs. 0-26837  
 X-ray spectra, laboratory reproduction in region of Fe XXV-XXVI reson. lines 0-18819  
 X-ray temperature-emission measure modelling of corona 0-12746  
 Al I, 1932 and 1936 Å autoionisation lines in solar flare, Skylab obs. 0-26829  
 Fe, K $\alpha$  fluoresc. due to solar flares 0-17569  
 Fe XXI 1354 Å line width, obs. from Skylab rel. to ionisation equilb. calcs. 0-21956  
 Fe XXIV, dielectronic satellite spectra, solar flares appl. 0-32646  
 Fe XXIV, oscillator strengths, electron impact excitation collision strengths, solar flare spectra appl. 0-32647  
 Fe XXV, dielectronic satellite line spectra as measure of nonthermal electron energy distrib. 0-21911  
 H $\alpha$ -flares rel. to radio bursts and sunspots 0-41803  
<sup>3</sup>He-rich flares producing <sup>26</sup>Al and <sup>10</sup>Be cosmic ray particles 0-36461  
 Mg XII, resonance line, atomic parameters calc. for dielectronic satellite lines 0-42983

**solar furnaces** *see* **furnaces****solar interior**

- clock mechanism of interior driving sunspot cycle 0-17562  
 connection, random fluctuations rel. to stochastic evolution and oscill. props. 0-31293  
 convection efficiency of Opik's cellular convection theory 0-12732  
 convection zone, convective overstability in mag. field in downdraft in sunspot 0-21960  
 convection zone dynamics, effect of rot. on turbulent viscosity and cond. 0-36612  
 global oscillations affecting spectra, He abundance implications 0-51724  
 models, H-R diagram fits rel. to He content and convective mixing length 0-26835  
 neutrino capture rate problem, role of pion in composite neutron mode 0-41808  
 neutrino problem, theory versus obs. 0-17566  
 neutrino puzzle, explanations for missing neutrinos 0-51723  
 pp reaction, exchange current corrections  $\pi$  and  $\rho$  exchange 0-26733

**solar magnetic fields** *see* **solar magnetism****solar magnetism**

- active region, 1978 April to May, mag. field morphology (*Chinese*) 0-8613  
 active regions, asymmetric mag. loop rel. to type U radio bursts polarisation evolution 0-26834  
 active regions, magnetosensitive line contours (*Russian*) 0-51718  
 active regions and X-ray bright points, birthplaces 0-12739  
 axisymmetric convection in presence of mag. field, solar granulation and sunspots appl. 0-12724

**solar magnetism continued**

- collapsing magnetic regions as long-lived sources of solar cosmic rays 0-31268  
 corona, field determ. using type II burst obs. and theory 0-41785  
 corona, global-scale 3-D reconstruction 0-56719  
 corona, influence of mag. fields on coronal holes physical struct. 0-46520  
 corona, mag. flux tubes ducting of metre-wave radio emission 0-21978  
 corona, metre-wave emission ducting rel. to fundamental/harmonic source coincidence 0-21978  
 corona magnetic traps, plasma instability periodical regimes (*Russian*) 0-8616  
 coronal interconnecting loops, mag. flux emergence rel. to sudden brightenings morphology 0-21972  
 coronal loops, thermal instabilities in magnetically confined plasmas 0-36600  
 coronal magnetic field models, validity of Green's function solns. 0-21970  
 coronal magnetic fields, Laplace's eqn. direct soln. using line-of-sight boundary conditions 0-12742  
 coronal magnetic loops, electrostatic ion-cyclotron heating 0-51708  
 coronal temperature constraints in open mag. field regions 0-12744  
 ephemeral active regions and X-ray bright spots, flux-rope theory 0-46519  
 equatorial, plane, large-scale spiral waves in solar wind rel. to interplanetary mag. field sector struct. 0-12633  
 faculae and sunspots, mag. field effects on solar luminosity 0-46515  
 filament formation dynamics, thermal instability in sheared magnetic field 0-4319  
 filaments disarptions brusques, evidence for role of mag. field (*Russian*) 0-51726  
 flares, Alfvén wave turbulence in mag. trap rel. to protons stochastic accel. 0-21953  
 flares, compressible mag. field reconnection theory 0-6226  
 flares, mag. field determ. from theory of gyrosynchrotron emission from quasi-thermal electrons 0-36602  
 flares, mag. structs. models and predictions of flux rope theory 0-21955  
 flares, observational and theoretical status, review 0-51728  
 flares multiply impulsive bursts, spectral evolution rel. to mag. field strengths 0-26828  
 flux emergence, evidence for globally coherent variability 0-51716  
 flux ropes, equilb. and stability (*Russian*) 0-8617  
 frequency response of magnetic flux sheaths 0-12743  
 high-latitude magnetic field, possible connection with Earth rot. nonuniformity 0-46119  
 interplanetary three-dimens. struct. of solar mag. field 0-31191  
 moving type IV radio bursts, expanding mag. arch MHD rel. to gyrosynchrotron modulation 0-26833  
 network features, structure and evolution 0-41793  
 photosphere, surface (capillary) waves in mag. field, props. (*Russian*) 0-12726  
 photospheric mag. field affecting solar proton flux 0-41672  
 photospheric faculae, models 0-12716  
 photospheric vertical motion in intense mag. flux tube, slender tube approx. 0-31278  
 polarity changes, skin effect of electrically conducting spherical shell 0-46389  
 prominences, polarimetric obs. and magnetic field determ. 0-4332  
 radiative transfer in magnetic atmospheres, analytical soln. 0-36494  
 sunspot cycle morphology, theory (*Chinese*) 0-12722  
 sunspot group for August 1972, force-free magnetic field 0-46521  
 sunspot magnetic fields higher rot. rate at photosphere, Doppler meas. 0-46516  
 sunspot moats, lifetimes from magnetograph obs. 0-21966  
 sunspots, convective propulsion of magnetic flux tubes 0-4313  
 sunspots, coronal mag. field struct. rel. to local sources of solar radio emission S-component 0-46528  
 sunspots, heat flow in convective downdraft 0-4314  
 sunspots, magneto-optical effects rel. to linearly polarised intensity distrib. obs. with vector magnetograph 0-21965  
 sunspots, twisted magnetic fields 0-41799  
 sunspots and mag. flux tube physics, connective overstability in mag. field in downdraft 0-21960  
 sunspots and magnetic flux tubes physics, umbral dots and longitudinal overstability 0-26825  
 surges, flare-assoc. current disruption mechanism 0-21975  
 thin magnetic tube instability in atmosphere rel. to network struct. 0-12725  
 two-ribbon flares, force-free magnetic arcades 0-56806  
 X-ray active regions temp. and emission measure rel. to coronal mag. fields 0-12745  
 X-ray bright points, short-term temporal vars. 0-12740

**solar noise** *see* **noise**; **solar radiofrequency radiation****solar power**

- see also* **solar energy concentrators**  
 absorption refrigeration system, theoretical model 0-30413  
 active energy systems for cooling and heating, thermal and economic anal. 0-50940  
 air conditioning, solar cooling with air collectors by desiccant/r bed method 0-30412  
 alternative energy sources, feasibility and cost anal. of solar systems 0-50939  
 alternative energy strategies, development of solar-based renewable resources, review 0-30417  
 automotive transport utilising stirling heat engine 0-55824  
 building solar-climate control systems, control options evaluation by simulation 0-40844  
 buildings, heating and cooling, solar augmented and assisted systems 0-7918  
 chemical heat pump/storage system for air conditioning 0-55886  
 chemical reactors, solar thermochemistry at high temps., appls. to chemical and thermal storage (*French*) 0-55815  
 climatic solar heating performance, calc. of solar fraction for building heat 0-16786  
 cooling, heating and hot water supply for hospital, evacuated glass tube solar collector system appl. 0-26155  
 cooling, thermodynamic anal. of sorption machines, coeff. of performance calcs. (*French*) 0-55814  
 cooling and hot water system, design and operation 0-50941  
 daily irradiation, ARIMA modelling with constant and seasonal parameters 0-55821



**solar power continued**

- desalination, solar-assisted reverse osmosis plant using Stirling heat engine 0-55891
- desalination appl. reverse osmosis, expt. installations (*French*) 0-55807
- desiccant dehumidifier development 0-30411
- design optimisation of solar energy district, systems anal. of external energy supply 0-30398
- development possibilities of energy resources (*German*) 0-21355
- diffuse and beam radiation, correl. with hours of bright sunshine 0-40841
- dispersed solar power and energy conservation 0-55811
- distributed photovoltaic systems for electricity generation, economic and technologic feasibility 0-55906
- domestic space heating in Ireland, computer simulation model of thermal performance 0-45732
- domestic water heating methods (*German*) 0-40833
- domestic water heating systems, in Great Britain, design and economic aspects 0-40835
- economics, component cost of solar energy systems 0-45651
- electric generating systems, resource requirements 0-7923
- electroplating appl., 1979 prospects w.r.t. economics 0-3490
- energy conversion, conference, Ontario, Canada (Aug. 1978) 0-41949
- energy flux prediction in polluted urban areas 0-30394
- energy resources, overall view (*French*) 0-40804
- energy storage using chemical potential changes associated with drying of zeolites 0-51006
- energy system control, 16 channel data logger and serial data link 0-50947
- energy systems, electrical analogue simulator development 0-30382
- European Community Italian Centre activities (*Italian*) 0-785
- flat plate solar photovoltaic power system with 100 kW peak power 0-35653
- global and net radiation distribution over Greece 0-21382
- global aspects of sunlight as a major energy source 0-30385
- global solar radiation at Lyon and at Macon, France, for (1978) (*French*) 0-55812
- Hawaii, wind and insolation as alternative energy resources 0-45623
- heat pump house, Dunham-Bush development 0-40830
- heat pumps, solar-powered absorption cycle with energy storage, theoretical anal. 0-55885
- heat storage in passive solar heated building using concrete block under concrete slab 0-55922
- heating, microclimate of solar greenhouses 0-40902
- heating, periodic heat flux through a three layered slab exposed to solar radiation 0-43598
- heating and cooling of buildings, Shenandoah Solar Recreational Center 0-45757
- heating and cooling systems, status and prospects 0-30384
- heating and ventilation using integrated collector-heat storage systems 0-51002
- heating system, heat accumulator utilisation, calc. procedure 0-40825
- heating system perform. estimation using sinusoidal inputs 0-35648
- heating systems, collector and storage efficiencies 0-45736
- heating systems, energy conservation characteristics and resource requirements 0-45731
- heating systems, performance mathematical simulation for optimal dimensioning (*German*) 0-26110
- heating systems for use in Britain, collector design aspects 0-35637
- heating systems performance over range of storage capacities, prediction 0-45642
- high temperature solar furnace for chemical appl. (*French*) 0-16784
- hourly global radiation sequences, stochastic simulation 0-36382
- hybrid passive/active solar system: performance and cost 0-45635
- hybrid solar/H fuel system producing high energy 0-45809
- industry, economic considerations and feasibility in Britain 0-26111
- insolation modelling, review of solar radiation resource assessments 0-35640
- intensity, atmospheric transmission data rehabilitation, SOLMET-2 procedures criticised 0-4071
- irradiation above thermal collector critical levels for 10-min and 1-hr integrals 0-16789
- Japanese energy programme 0-3478
- laminar free convection in 1-D solar induced flows, theory 0-3495
- leak-proof heat exchanger for solar water heating systems 0-30524
- light water fission reactor, solar-assisted hybrid power plant 0-13561
- Lisbon solar radiation climate, direct, diffuse and global intensities 0-36383
- longwave radiation incident upon inclined surfaces 0-16785
- LWR nuclear reactors with solar collectors, SOAR power system concept 0-55820
- major solar energy research programs, review 0-40843
- materials problems rel. to transition to solar energy 0-26115
- measurement, microcomputer-controlled photodiode light meter and thermistors 0-50946
- microcomputer control for solar energy applications 0-50945
- microwave power transmission technology 0-40868
- mirror arrays, large Earth orbit structures reflecting sunlight for power generation, lighting, and agriculture 0-45632
- monthly mean solar radiation calc. using daily time intervals 0-17353
- natural gas/solar energy transition strategy 0-30414
- Ocean Thermal Energy Conversion [OTEC], the Florida Current, thermal 0-26117
- ocean thermal energy conversion, electricity to shore schemes 0-16783
- ocean thermal energy conversion for electrolytic H prod. 0-30546
- office complex design, with up to 70% energy savings 0-40831
- optics applied to solar energy, [Conf. San Diego, CA, USA Aug. 1978] 0-7926
- optimal solar investment decision criteria, appl. to space and water heating systems 0-35643
- orbital power systems, waste heat rejection development requirements for thermal control 0-30416
- parabolic concentrator, use of fin receiver 0-21379
- passive solar heating systems, Trombe wall control strategies 0-45737
- passive solar space heating, sensitivity anal. of direct gain systems 0-35647
- photovoltaic electricity generation in India 0-21381
- photovoltaic energy generation integrations into electric grid systems, general methodology 0-45647
- photovoltaic power systems for rural areas of developing countries 0-50967
- photovoltaic-wind hybrid alternative energy system 0-30409

**solar power continued**

- practical uses of solar energy in Switzerland (*French*) 0-55808
- pumping of water using thermal or electric solar pumps 0-50942
- Quebec, hourly radiation values for horizontal surface 0-17354
- R and D program at the Inst. of Engng. of the Nat. Univ. of Mexico 0-40845
- radiation characts. and intensity calc. 0-45649
- radiation levels on tilted surfaces, computer model validation 0-35641
- radiation on vertical and inclined surfaces, monthly mean calcs. 0-45746
- rational use of energy in houses (*Dutch*) 0-40836
- reflectivity of common building materials, effect on roof heat gain 0-55810
- renewable energy resources utilisation for the development of rural areas 0-45650
- renewable energy sources, Rumania (*Rumanian*) 0-35639
- renewable solar-based energy resources for future energy strategy 0-30383
- residential utilisation, conceptual development of a solar town in Iran 0-50944
- review using rational units 0-30389
- satellite, appl. of solid state microwave technology 0-40870
- satellite, assessment for European appl. 0-40867
- satellite, computer modelling of power transmission system 0-40866
- satellite, energy anal. 0-50937
- satellite, microwave system perform. during startup/shutdown 0-40869
- satellite applications to solar energy monitoring 0-50982
- satellite power system technology, environmental and societal impact 0-30386
- secondary cells, Pb/acid, design and performance characteristics for remote photovoltaic applications 0-55833
- shaded vertical receivers, monthly average radiation estimates 0-35646
- shadow effect of adjacent solar collectors in large scale systems 0-45738
- solar declination and the length of the solar day 0-45648
- solar enhanced oil recovery; an assessment of economic feasibility 0-40832
- solar heating, appl. of flat plate collectors and thermal stores (*German*) 0-26152
- Solar One, a 10 MW solar thermal central receiver pilot plant 0-35651
- solar open cycle absorption refrigeration system, anal. and simulation 0-16788
- solar-electric heat pump for houses, design and tests (*German*) 0-7951
- space heating, correspondence between solar load ratio method for passive water wall systems and f-Chart performance estimates 0-16787
- space heating, heat-pump assisted systems, perform anal. 0-35649
- space heating systems, load optimisation algorithms 0-45643
- space power generators, past developments and future trends 0-45693
- spectral characteristics for improving solar collector performance 0-35650
- steam production by solar power for industrial appl. 0-30401
- stochastic weather algorithms for predictions of solar cooling performance 0-35642
- storage, review of methods 0-55916
- sun loading on fixed, tracking surfaces, solar energy availability investig. 0-40838
- swimming pool outdoor, heating indirect, heat pump appl. (*German*) 0-16781
- synergetic aspects of solar energy and the fast breeder reactor 0-7907
- terrestrial utilisation of solar energy, scope and experience (*German*) 0-40829
- test facilities and meas. standards in developed and developing countries 0-55819
- test systems, elec. utility demonstration projects 0-3488
- Thailand, research and development in solar energy, review 0-26113
- thermal storage cell for high temperature solar systems 0-55923
- thermal storage of solar energy 0-51005
- thermal systems, technology status 0-40842
- Third World rural development prospects 0-30399
- timber dryer, forced-air, for tropical latitudes, solar heating appl. 0-21384
- total radiation intensity, universal formula using climatological data 0-31108
- tracking system, heliotropic fluid-mech. drive system, dynamic response anal. 0-55823
- tracking systems for photovoltaic collector control (*Spanish*) 0-45637
- United Nations energy program for solar and wind energy appls. 0-3496
- utilisation, conf., Cairo, Egypt (June 1978) 0-46734
- utilisation, energy model anal. to 2010 cf. nuclear power (*German*) 0-26109
- utilisation, review 0-16790
- utilisation, solar energy planning for developing countries 0-50943
- utilisation in developing countries, conf. report, Varese, Italy (March 1979) 0-40834
- utilisation in Egypt for water heating and distillation, power generation and air conditioning 0-50938
- utilisation in human settlements, inexpensive systems, appls., function and techniques 0-51004
- water distillation using basin-type solar stills, use of wood charcoal beds 0-7924
- water heating, State of Nebraska Solar Heat Pilot Project 0-55817
- water heating models comparison 0-30387
- water heating system, materials corrosion 0-30131
- zeolite collector for solid-gas absorpt. refrigeration system 0-35754
- ZnCl<sub>2</sub>·6H<sub>2</sub>O heat of fusion system for solar energy storage 0-16846
- H prod. by H<sub>2</sub>O pyrolysis using solar thermal energy 0-45770
- W-halogen quartz lamps with optical filters, solar simulator appls. 0-16838

**solar power stations**

- 10 MWe pilot Central Receiver Solar Thermal Power System, design concept 0-16792
- 100 kW peak photovoltaic power system, design, construction and capabilities 0-45705
- 150 kW plant, Dead Sea, solar pond details 0-35638
- Brayton cycle solar electric plant receiver, 1 MW<sub>e</sub> bench model design and testing 0-55896
- central receiver plant, dynamic simulation of thermal-hydraulic characts. of Na-cooled plant 0-30400
- central receiver power plant, 10-MW pilot plant project 0-30405
- central receiver program, heliostat, receiver and storage subsystems 0-30404
- central receiver solar power systems, terminal concentrator concept analysis 0-26116



**solar power stations continued**

- central receiver type, solar receiver tube thermal stresses, fatigue aspects 0-40908  
 comparative ranking of 0.1 to 10 MWe solar thermal power systems 0-30559  
 design, global yield and economics, current projects (*French*) 0-55803  
 distributed microcomputer-based control system for a large scale solar total energy system 0-30396  
 Earth orbiting, economic, political, and environmental problems 0-45633  
 Earth orbiting, interference with space communications systems 0-45634  
 economic impact analysis of solar thermal plants in small utilities 0-30407  
 electric power generation in remote locations, costs comparison with diesel generators 0-55813  
 electrical system comprising DC separately excited motor and mechanical load driven by solar cell array, performance analysis 0-16801  
 fixed mirror solar concentrator for application to a 100 MW(e) electric generating plant 0-30393  
 flat plate solar photovoltaic power system with 100 kW peak power 0-35653  
 high temp.-high flux material testing, solar power station appls. 0-40668  
 high temperature solar power tower plants concept considerations and operational criteria 0-55822  
 hybrid solar-fossil power generation, combined cycle system 0-30406  
 hydro-photovoltaic plants, peak power generation economics and reliability 0-45706  
 large scale electricity production, solar cell developments and appls., review 0-40861  
 Large Solar Power System Programme, in United States, progress since 1972 0-26114  
 meteorological effects of solar thermal electric conversion plant, numerical modelling 0-35794  
 microwave power transmission technology 0-40868  
 military space power program, development of 10 to 50 KWe solar power systems 0-30415  
 ocean thermal energy conversion (OTEC), 100 to 400 MW, developments survey (*Dutch*) 0-12025  
 photovoltaic power systems, equipment performance and manufacturing techniques improvements and system design problems for telecommunication applications 0-55843  
 photovoltaic power systems for rural areas of developing countries 0-50967  
 photovoltaic/thermal electric central solar power station 0-30410  
 power systems availability and reliability analysis 0-35687  
 Rankine cycle solar thermal power plants, operating experience 0-30523  
 satellite, appl. of solid state microwave technology 0-40870  
 satellite, assessment for European appl. 0-40867  
 satellite, computer modelling of power transmission system 0-40866  
 satellite, energy anal. 0-50937  
 satellite, in Earth orbit, survey 0-21376  
 satellite, microwave system perform. during startup/shutdown 0-40869  
 satellite, solid-state solar-power station spherical solar collector, enhanced power generation 0-12009  
 satellite ground station rectifying antenna, basic design concepts 0-16782  
 satellite photoelectric power stations, alternate favourable option 0-16791  
 self-contained solar power installation concentrating system design and optical/energy characts. testing 0-40828  
 Solar One, a 10 MW solar thermal central receiver pilot plant 0-35651  
 solar power satellite, construction in space, fabrication methods, materials, tools 0-21377  
 steam generation system for industrial appls. 0-55825  
 Stirling engine power conversion for MWe solar power system with parabolic concentrators 0-30561  
 techno-economic development of advanced plants 0-30395  
 thermal electric generation, dynamics and control of Stirling engines 0-30522  
 thermal electric power systems, comparative economics of small systems 0-55818  
 thermal energy storage in aquifers for a solar power plant 0-55925  
 thermal generating station design, engineering problems (*German*) 0-30381  
 thermal power system, open cycle air turbine (*French*) 0-45641  
 thermoelectric conversion, collector systems and thermal storage 0-45759  
 total energy system, Fort Hood, control system 0-30397  
 total energy system at Georgia, USA 0-35652  
 total energy system evaluation program 0-30402  
 tower-type solar furnaces, two mirror, high power, optical characts., calc. for design 0-40824  
 turbine sizing of a solar thermal power plant, performance and economic anal. 0-30403  
 undersea hot water storage system 0-45763  
 utilisation efficiency and feasibility criteria 0-40826  
 GaAs photovoltaic solar system for utility substation appls. 0-30493  
 GaAs photovoltaic solar system, appl. in electric utility system 0-55875

**solar prominences**

- 1973 August 14 loop prominence, XUV emission and density 0-56807  
 active loop prominences, numerical model 0-56787  
 active structures and total current 0-4336  
 chemical abundances, relative, in prominences and other solar regions 0-46518  
 coronal condensation forming prominences, condensation along mag. field lines 0-46524  
 coronal interface, review 0-4333  
 electron density and temp. from Ca II/Fe I emission line ratios (*Russian*) 0-51717  
 eruptive prominence, gyrosynchrotron modulation in assoc. moving type IV bursts 0-26833  
 eruptive prominences, assoc. coronal brightness and structure changes 0-4337  
 eruptive prominences, coronal manifestations, theory 0-4338  
 eruptive prominences and coronal transients 0-56809  
 EUV limb spectra of prominence, Skylab obs. 0-12717  
 filament formation dynamics, thermal instability in sheared magnetic field 0-4319  
 filaments disparitions brusques, evidence for role of mag. field (*Russian*) 0-51726  
 formation and coronal arcade structure 0-41800  
 horizontal temperature gradient in prominence/corona transition zone, meas. rel. to prominence condensation 0-26832  
 IAU Colloquium 44 (Oslo, 14-18 August 1978) 0-4330

**solar prominences continued**

- magnetic field boundary relations 0-4335  
 model for quiescent prominences 0-4316  
 polarimetric obs. and magnetic field determ. 0-4332  
 quiescent, heating and cooling, calc. 0-12738  
 quiescent, middle Balmer decrement meas. 0-12737  
 quiescent prominence formation, support and stability 0-4334  
 spectra, interpretation 0-4331  
 spectral observations, prominence model 0-31287  
 H early Balmer lines emission, theory (*Russian*) 0-12718  
 H I spectra, Balmer line form. in bright prominences, theory (*Russian*) 0-36609

**solar radiation**

- see also *solar cosmic ray photons; solar radiofrequency radiation; solar spectra; solar wind; sunlight*  
 atmosphere, solar heating annual var. rel. to large-scale eddy transports linear parameterisation 0-17361  
 atmosphere scattering, arrival angle statistics rel. to turbulence around solar telescope 0-26740  
 corona X-ray emission, slowly moving disturbances obs. 0-21971  
 coronal interconnecting loops transient brightenings, sudden brightenings morphology 0-21972  
 coronal quasi-static loops, EUV and X-ray emission numerical modelling with uniform energy input 0-21958  
 coronal X-ray observations, using rocket-borne real-time imaging system 0-41725  
 cylinders, perfectly conducting arrays, transport prop. investig. 0-13011  
 daily and monthly averages of solar radiation data, statistical correl. 0-8409  
 dielectronic recombination spectra, appl. to high-temp. plasma diagnostics 0-46391  
 electromagnetics and environment, book 0-36431  
 EM radiation measurement using CdS photoresistor 0-31092  
 EUV and H Lyman-alpha, AEROS and TAIYO satellite results 0-46340  
 EUV line emission, contrib. of spicules 0-4325  
 flare second-stage X-ray emission, spectrum beyond 200 keV 0-51710  
 flares, EUV and hard X-ray sources relationship 0-46512  
 flares, EUV radiation, detect. using ionosphere sudden freq. deviations (SFD) 0-8484  
 flares, high-resolution X-ray spectra obs. 0-26837  
 flares, principal component anal. in soft X-ray flux 0-41781  
 flares, radiation props. of particle streams continuous radiation model 0-21954  
 flares, X-ray emission rel. to physical parameter profiles 0-17561  
 flares microwave and optical emissions comparison 0-31284  
 flares multiply impulsive bursts, spectral evolution 0-26828  
 flares nonthermal electron beams, reverse currents effects on dynamics and X-ray bremsstrahlung 0-51711  
 H-R diagram fits of solar models, rel. to He content and convective mixing length 0-26835  
 hard X-ray burst, 1972 August 4, trap-plus-precipitation model 0-12747  
 hard X-ray polarization from flares 0-41787  
 luminosity long-term variations, correl. with sunspot struct. and Earth climate 0-31272  
 luminosity variations caused by mag. field 0-46515  
 measurement, inclination dependence of pyranometer sensitivity 0-8465  
 neutrino problem, theory versus obs. 0-17566  
 neutrino puzzle, explanations for missing neutrinos 0-51723  
 photosphere faculae intensity, centre to limb var. 0-21967  
 radiation forces on small particles in solar system 0-17461  
 radiation pressure induced coupled librations of gravity stabilized artificial satellite 0-21888  
 resonance radiation, multiple scatt. in nearby interstellar medium 0-41874  
 soft X-ray bursts, statistical distrib. 0-26839  
 solar constant, rel. to energy-balance climate models stability theorem 0-56594  
 solar constant, Smithsonian Astrophysical Observatory program, (1902 to 1962) 0-36606  
 solar constant standard data and spectral irradiance outside Earth atm. (*Chinese*) 0-4320  
 spheroidal satellite, orbital perturbations due to direct solar radiation press. 0-4219  
 sunspot model, radiation transfer theory 0-21964  
 sunspots, magneto-optical effects rel. to linearly polarised intensity distrib. obs. with vector magnetograph 0-21965  
 UV meas. and physics 0-41784  
 X-ray bright points, obs. rel. to globally variability in solar mag. flux emergence 0-51716  
 X-ray bright points, short-term temporal vars. 0-12740  
 X-ray bright points correl. with sunspot intensity, cycle var. 0-41783  
 X-ray burst, impulsive, from coronal source, obs. 0-26836  
 X-ray temperature-emission measure modelling of corona 0-12746  
 H Lyman  $\alpha$  in chromospheric flares, direct collisional excitation rel. to profile and polarisation 0-41780

**solar radio emission** see *solar radiofrequency radiation***solar radiobursts** see *solar radiofrequency radiation***solar radiofrequency radiation**

- 146 MHz C-type bursts correl. with mag. storms (*Chinese*) 0-4321  
 2800 MHz radio minimum (1976 February) 0-4324  
 bursts at 26 MHz, obs. brightness distrib., possible ionospheric effects 0-41806  
 bursts at 29.5 MHz during solar cycle 20, statistical anal. and comparison with noise storms 0-56794  
 bursts at 3.7 and 11.1 cm wavelength, interferometric obs. 0-31285  
 bursts rel. to Ha-flare visual features 0-41803  
 centimetre radio waves emission, brightness var. at extreme solar limb 0-21969  
 centimetre wave emission, Sun radio radius and brightness distrib. across disc 0-21968  
 collective radio-emission from plasmas 0-46392  
 corona, decametric obs. at high resolution 0-31288  
 coronal hole, obs. with  $\lambda$  8-cm radioheliograph 0-4326  
 decimetric emission quasiperiodic fluctuations 0-41791  
 emission at 6 cm wavelength, sunspot assoc. model 0-51712  
 emission pulsations in 1.9-3.5 cm wavelengths (*Russian*) 0-17563  
 flares microwave and optical emissions comparison 0-31284  
 flares microwave spectrum, appl. of quasi-thermal electrons gyrosynchrotron emission theory 0-36602  
 flux calibration in 1970, at 2800 MHz 0-17570



**solar radiofrequency radiation continued**

- McMath 12686, type III burst producing McMath 12686, type III burst producing active region, overlying coronal struct. Skylab obs. 0-21976  
 metre-wave emission, wave ducting rel. to fundamental/harmonic source coincidence 0-21978  
 microwave burst spectra, source inhomogeneities, statistical analysis 0-41805  
 microwave bursts, characts. at 9 GHz freq. appl. to proton flares identification 0-4323  
 microwave bursts rel. to proton events forecasting (*Chinese*) 0-12723  
 microwave bursts used to calc. solar proton flux 0-41789  
 moving type IV bursts, gyro-synchrotron modulation obs. 0-26833  
 noise storms and terrestrial EM wave propag. (*Japanese*) 0-51600  
 noise storms during solar cycle 20, statistical anal. and comparison with radio bursts 0-56794  
 plasma frequency bursts, implications of Voyager 2 coronal occultation obs., 1979 August 0-51639  
 pulsations, role of plasma instabilities periodical regimes in coronal mag. traps (*Russian*) 0-8616  
 quasiperiodic microwave bursts and adiabatic heating 0-51713  
 quiet Sun, high-resolution obs. at 6 cm using Westerbork Synthesis Radio Telescope 0-36601  
 S-component emission, local sources struct. 0-46528  
 S-component spectrum, fine struct. in 5.0 to 7.0 GHz freq. range 0-21977  
 total microwave flux, search at Toyokawa for five minute oscillations 0-4327  
 type I sources, 146 MHz obs. (*Chinese*) 0-8609  
 type II burst obs. and theory for coronal magnetic field determ. 0-41785  
 type II radio burst with reverse freq. drift against noise storm background, obs. 0-17567  
 type II radiobursts and shock waves in interplanetary medium 0-56690  
 type III bursts, fast electrons stream free dispersal in solar corona with nonsteady injection 0-17568  
 type III bursts, fundamental emission in 25-200 kHz range 0-56789  
 type III bursts, nonlinear stability, electron exciters obs. near 1 AU 0-46513  
 type III bursts and flare occurrence in spotless regions 0-56810  
 type III radio bursts, EM radiation direct generation from beam-plasma system 0-54007  
 type III radio bursts, fundamental emission and polarisation 0-36603  
 type III radio bursts, nonlinear stability theory 0-26826  
 type III solar radio burst sources, plasma wave clumping origin 0-21959  
 type III-like bursts, UHF obs. 0-56793  
 type U radio bursts, polarisation evolution 0-26834  
 type V radio bursts, dynamic spectra distinctive struct. 0-46527

**solar radiowaves** *see solar radiofrequency radiation***solar rotation**

- chromosphere, rot. depend. on size of tracer features 0-12731  
 differential rotation, generation by rot. effect on convection zone turbulent viscosity and cond. 0-36612  
 interplanetary sector boundaries config. rel. to certain days of solar rot. 0-41764  
 sunspot groups, rotation rates 0-41797  
 velocity, comparison with other lower main-sequence stars 0-51767  
 velocity fields, large-scale, from Doppler line shift obs. 0-12730

**solar spectra**

*see also solar activity; solar corona; solar radiation*

- atmosphere, spectral line intensity, electron impact excitation 0-36605  
 blue continuum flares and D3 preflare shell obs. 0-51709  
 chromosphere flare spectrum, electron beam diagnostics 0-26827  
 chromosphere-corona transition region, OSO 8 UV obs. of optically thick region 0-56788  
 corona, oscillations above active region, Fe XIV spectra obs. 0-41794  
 coronal holes, EUV and radio spectrum 0-56802  
 eclipse, 1973 June 30, spectroscopic obs. by Dutch expedition 0-8615  
 emission lines of NeV, MgVII, SiIX, SXI, population levels as function of electron density and temp. 0-21963  
 EUV emission lines in different solar regions, relative chemical abundances determ. 0-46518  
 EUV line emission, contrib. of spicules 0-4325  
 EUV line emission weakening short of 912 Å wavelength 0-21962  
 EUV spectra, appl. to transition zone energy balance and press. 0-21957  
 faculae, 5000 Å continuum diagnostics 0-4315  
 far IR emission spectrum, meas. rel. to chromosphere/photosphere boundary temp. (*German*) 0-51721  
 flare second-stage X-ray emission, spectrum beyond 200 keV 0-51710  
 flare spectra, high dielectronic satellite lines analysis for plasma props. calc. 0-12728  
 flares, Fe XXI 1354 Å line obs. from Skylab rel. to ionisation equilib. calcs. 0-21956  
 flares, Fe XXV dielectronic satellite line spectra as measure of nonthermal electron energy distrib. 0-21911  
 flares, high-resolution X-ray spectra obs. 0-26837  
 flares microwave spectrum, appl. of quasi-thermal electrons gyrosynchrotron emission theory 0-36602  
 flares multiply impulsive bursts, spectral evolution 0-26828  
 flares X-ray spectra, Fe XXIV-XXV lines wavelengths in 1.85-1.87 Å region 0-21973  
 flares X-ray spectra, laboratory reproduction in region of Fe XXV-XXVI reson. lines 0-18819  
 Gamma Ray Experiment on Solar Maximum Mission, spectrometer 0-51657  
 global oscillations affecting spectra, He abundance implications 0-51724  
 Hard X-Ray Burst Spectrometer on Solar Maximum Mission 0-51658  
 Hard X-ray Imaging Spectrometer on Solar Maximum Mission 0-51659  
 limb emission lines near Ca II H and K, spatial intensity vars. obs. 0-51720  
 line asymmetries, radial movement effects 0-41792  
 line asymmetry meas. rel. to  $\alpha$  Bootis (Arcturus) 0-51753  
 line profiles, acoustic wave effects 0-46517  
 line shift obs. interpretation 0-51714  
 line shifts and asymmetries in sunspot penumbrae 0-51715  
 line shifts and asymmetry, appl. to solar atmosphere vel. field estimation 0-46530  
 magnetosensitive line contours in active regions (*Russian*) 0-51718  
 microwave burst spectra, source inhomogeneities, statistical analysis 0-41805  
 oscillator strengths of astrophysical interest 0-12656  
 photosphere Fraunhofer lines formation, effects of 'microturbulent' vel. and damping const. (*Russian*) 0-12719  
 photosphere line profiles for Na I and O I, acoustic wave effects 0-17558  
 photosphere-chromosphere transition region, spectra during eclipse June 30 1973 0-8614  
 photospheric oscillations depth depend. 0-31275  
 prominence, EUV limb spectra, Skylab obs. 0-12717  
 prominence H I spectra, theory of Balmer line form. (*Russian*) 0-36609  
 prominence model based on spectral obs. 0-31287  
 prominences, early H Balmer lines (*Russian*) 0-12718  
 prominences, interpretation 0-4331  
 quiescent prominences, middle Balmer decrement meas. 0-12737  
 quiet-time near-IR variability 0-12729  
 radio emission, S-component spectrum fine struct. in 5.0 to 7.0 GHz freq. range 0-21977  
 resonance radiation, multiple scatt. in nearby interstellar medium 0-41874  
 solar prominence, EUV spectrum rel. to horizontal temp. gradient meas. and prominence condensation 0-26832  
 sunspot, radiation transfer rel. to spectral lines polarisation 0-21964  
 sunspot chromosphere, spectroscopic obs. rel. to radial vel. and brightness oscils. regimes (*Russian*) 0-51727  
 sunspot magnetic fields higher rot. rate at photosphere, Doppler meas. 0-46516  
 sunspots, IR opacity due to molecular vibration rotation bands 0-41798  
 sunspots, MgO red and near UV bands calc. rel. to umbral spectrum 0-12736  
 sunspots, O<sub>2</sub> Schumann-Runge band system in umbral UV spectrum 0-12735  
 surge, EUV limb spectra obs. from Skylab 0-17560  
 type V radio bursts, dynamic spectra distinctive struct. 0-46527  
 UV line blending and wavelengths, spectral resolution influence 0-56811  
 UV spectra, N III and O IV intersystem multiplets as plasma density indicators 0-31264  
 UV vars. rel. to terrestrial climatic change 0-26607  
 velocity fields, large-scale, from Doppler line shift obs. 0-12730  
 X-ray burst, impulsive, from coronal source, spectral struct. 0-26836  
 X-ray imaging spectrometer polychromator, solar obs. from Space Shuttle 0-17495  
 X-ray meas. by photometer on Prognostic satellites, description and meas. method 0-17462  
 Al I, 1932 and 1936 Å autoionisation lines in solar flare, Skylab obs. 0-26829  
 Be lines formation, non-LTE calc., rel. to solar Be I 2650 Å line misidentification 0-32636  
 C III 1909 Å and Si III 1892 Å emission lines, echelle obs. 0-31277  
 Ca I 6102, 6122, 6162 Å multiplet, collisional broadening 0-37777  
 Ca II 3737 Å emission line studies of prominences and flares (*Russian*) 0-51717  
 Ca ions, dielectronic recombination excitation in solar X-ray lines 0-51725  
 Fe I 3737 Å emission line studies of prominences and flares (*Russian*) 0-51717  
 Fe I lines, equivalent widths and microturbulent vels. determ. (*Russian*) 0-51719  
 Fe I low excitation lines, collisional broadening 0-37778  
 Fe I weak lines, 'microturbulent' vel. and damping const. rel. to photosphere Fe abundance (*Russian*) 0-12720  
 Fe II spectrum, oscillator strengths and choice of solar model atmosphere rel. to Fe abundance 0-56791  
 Fe, K $\alpha$  fluoresc. due to solar flares 0-17569  
 Fe lines, wing shapes anal. 0-4317  
 Fe X, 3p<sup>4</sup>s levels, population processes 0-47926  
 Fe XV coronal EUV line intensities 0-51731  
 Fe XXII, intercomb. transitions, oscill. strengths, transition probs., rel. to solar spectra 0-52935  
 Fe XXIV, dielectronic satellite spectra, solar flares appl. 0-32646  
 Fe XXIV, oscillator strengths, electron impact excitation collision strengths, solar flare spectra appl. 0-32647  
 Fe<sup>+</sup>, gf values determ. in laboratory, for solar studies 0-42994  
 H I Lyman  $\alpha$  profile and interstellar wind dynamics 0-8610  
 H Lyman  $\alpha$  emission, absorpt. by hot interstellar H between Sun and Earth 0-31185  
 H Lyman  $\alpha$  in chromospheric flares, direct collisional excitation rel. to profile and polarisation 0-41780  
 He I 10830 Å triplet in umbral spectrum (*Russian*) 0-36604  
 K I 769.9 nm line obs. of solar 5-min. oscils. 0-26838  
 Mg XII, resonance line, atomic parameters calc. for dielectronic satellite lines 0-42983  
 N IV and Ne VII emission line ratios, electron density and temp. determ. 0-17559  
 N isoelectronic sequence ions, level populations and EUV line intensities for solar coronal conditions 0-51649  
 Na I D-line obs., Doppler width from intensity integral 0-41782  
 Ni XVII coronal EUV line intensities 0-51731  
 Ni(IX), resonance transitions, classification 0-42985  
 O I isoelectronic sequence, excited level populations, line intensity ratios, solar corona appl. 0-32637  
 O III, <sup>3</sup>P<sup>o</sup>-<sup>5</sup>S<sup>o</sup>, diagnostic studies of quiet Sun and coronal holes 0-48092  
 O IV, O VI line intensities, diffusion effects rel. to solar O abundance 0-4318  
 Si III 1892 Å emissivity, charge transfer effect on appl. of line as spectral diagnostic 0-41717  
 Si VI, VIII and XII, line intensities in transition region 0-31273

**solar system**

*see also celestial mechanics; planets; Sun*

- apex of motion, correl. with long-period comets perihelion points distrib. 0-4304  
 asteroids in vicinity of 1:3 commensurability with Jupiter, orbital evolution, model calcs. results (*Russian*) 0-36486  
 celestial mechanics, perturbed potentials effects on libration points stability in restricted problem 0-4241  
 coherent radio emission in nature, theory, solar system and pulsars appl. 0-46393  
 cosmogony 0-41736  
 early chronology, determ. from <sup>187</sup>Re-<sup>187</sup>Os systematics in meteorites 0-41778



# solar system continued

- early solar system, minor planets EM heating 0-36555
- Earth and Moon origin, book 0-17266
- extrplanetary mission possibilities 0-17466
- formation of Jupiter, evidence from atmospheric comp. deduced from absorpt. bands in refl. sunlight 0-56758
- interplanetary dust, symmetry plane in inner solar system 0-56767
- interstellar grain streaming 0-26810
- isotopic anomalies from neutron reactions during stellar explosive C burning 0-12651
- Kirkwood gap 1:3, width (*Russian*) 0-36559
- magnetic field of solar nebula, Allende meteorite chondrule record 0-36520
- meteorite components primordial condensation, expt. evidence of source medium state 0-26816
- meteorite condensation from solar nebula, enstatite chondrite petrology 0-51699
- meteorite magnetism as probe of early solar system 0-36597
- nebula, chondrules origin 0-4310
- nebula, condensation temps. rel. to Trojan asteroids comp. 0-56751
- nebula, evidence for strong mag. fields from ureilites mag. props. 0-8602
- nebula, fine dust grains clustering and sedimentation time 0-26937
- nebula, Ga, Ge and Sb condensation rel. to Fe meteorites chemical classification 0-36594
- nebula, N isotopic comp. vars. rel. to  $^{15}\text{N}/^{14}\text{N}$  ratios in carbonaceous chondrites 0-46496
- nebula, primitive, interaction with giant gaseous protoplanets, computer anal. 0-56727
- nebula, role of grains as isotopic anomalies carriers 0-26757
- nebula differentiation into planets,  $^{15}\text{N}/^{14}\text{N}$  ratio 0-36519
- noble gases isotopic anomalies in Murchison meteorite, evidence for stellar condensates 0-41772
- origin, protosolar OB association supernovae rel. to Allende isotopic anomalies and cosmochronology 0-4462
- origin, relation to supernova explosions 0-17509
- origin, supernova trigger, Allende meteorite evidence 0-12683
- osculating elements reduction to proper elements for entire solar system 0-21897
- planetary formation as adiabatic phase transition, isentropic model 0-26763
- planetary system accumulation model, numerical expts. results (*Russian*) 0-8557
- planetary system origin, model comparisons 0-17508
- planetesimal population, equilib. vels. 0-31219
- planets spin angular momentum distrib. explanation 0-41741
- presolar nebula birth, condensation sequence revealed in Allende meteorite 0-26758
- protoplanetary disc nebula disruption by T Tauri-like solar wind 0-36516
- radiation forces on small particles in solar system 0-17461
- refractory lithophile elements, condensation and fractionation 0-36517
- relativistic celestial mechanics, astron. meas. and coord. systems 0-36481
- solar motion constants, determ. for AGK3 proper motion system in polar region (*Russian*) 0-12647
- solar nebulae, mass transport processes in rotating dust cloud 0-8556
- D/H ratio in early Solar Systems, H and O isotope study in chondritic meteorites 0-36518
- $^{22}\text{Ne}$  anomalous abundance in Orgueil meteorite, evidence for presolar grains 0-41773

# solar-terrestrial relationships

- 1978 May 7 events, radio, optical and geophysical manifestations (*French*) 0-8611
- air temp. in Tbilisi rel. to solar activity (1848-1970) 0-26595
- atmospheric circulation changes correl. with solar and interplanetary mag. sector struct. 0-17340
- atmospheric electricity supply current, solar modulation 0-17329
- climate over last 250 million years, global heat balance 0-46252
- D-region, radiowave absorption during solar minimum, 2.5-4.1 MHz 0-41628
- Earth rotation modulated by solar cycle 0-56336
- Earth rotation nonuniformity, possible connection with Sun high-latit. mag. field 0-46119
- equatorial counter-electrojet, afternoon events occurrence correl. with sunspot minimum 0-56672
- F<sub>2</sub>-layer, electron density long-period variation  $f_0$  evidence 0-56667
- F<sub>2</sub>-layer, geometrical parameters and critical frequencies, solar activity dependence study 0-4182
- F-region, equatorial anomaly, solar cycle and seasonal variation of electron content 0-41622
- F-region, solar activity rel. to temp. and electron density 0-46337
- gamma-rays, hard intensity radiation pulsations in the atmosphere rel. to 5-min. solar oscills. (*Russian*) 0-17454
- geomagnetic activity, rel. to Sun polar coronal holes and sunspot cycles 0-21979
- geomagnetism secular variation and solar cycle, Rumanian data 0-56366
- HF signals magnetospheric propag. on Earth-Earth path, depend. on solar activity 0-4195
- ionosphere, electron temp. var. with solar activity satellite meas. 0-26678
- ionosphere hot electron layer, electron heating near Sq focus anomaly 0-51599
- ionosphere sudden frequency deviations (SFD), appl. as detectors of solar flares EUV radiation 0-8484
- magnetic storms correl. with solar 146 MHz C-type bursts (*Chinese*) 0-4321
- magnetic storms prediction by multivariate statistical anal. (*Chinese*) 0-12614
- meteorological variability mechanisms 0-51467
- ozonosphere temp. and O<sub>3</sub> conc. rel. to solar activity fluctuations 0-31110
- ozonosphere-solar cycle relationships 0-17342
- Sq at low latitude, hourly study of secondary effect 0-56362
- stratosphere cosmic rays, eleven-year cycle 0-4212
- sunspot structure, vars. correl. with Earth climate 0-31272
- thermosphere circulation 0-56661
- thermosphere ionisation and variable solar UV flux, 1974-9 obs. 0-17430
- thermosphere temperatures depend. on solar activity, incoherent scatter data comparison with global models 0-8467
- upper atmosphere and solar-terrestrial relations, introduction to aerospace environment, book 0-8466
- UV vars. rel. to climatic changes 0-26607

# solar-terrestrial relationships continued

- weather and climate, solar-terrestrial influences, symposium/workshop proceedings (Columbus, Ohio, 1978 August 24-28) 0-27037
- weather relation, vorticity area index to interplanetary mag. sector struct. 0-46222
- weather-solar activity relationships, possible mechanisms 0-17341
- Zurich annual sunspot number link with temp. and precipitation for USA 0-17328
- O<sub>3</sub> content of atmos. rel. to solar activity 0-41488

# solar visible radiation see sunlight

# solar wind

see also solar cosmic ray particles

- Alfven waves, exact, nonlinear, existence of solitons 0-24159
- Alfven waves, large amplitude, propag. direction rel. to average interplanetary mag. field 0-26709
- antenna in plasma, detect. of natural noises 0-24181
- charged particle fluxes, electron calibration of Mariner 10 instrumentation 0-12628
- coherent radio emission in nature, theory, solar system and pulsars appl. 0-46393
- cometary plasma tail disconnection events, rel. to sector boundary crossings and high-speed stream encounters 0-46482
- coronal holes, influence of mag. fields and coronal heating on solar wind props. 0-46520
- coronal temperature constraints in open mag. field regions 0-12744
- cosmic ray propagation in solar wind, latitude variation 0-12622
- cosmic ray solar modulation, theory 0-51629
- current sheet in compressible plasma, self-similar resistive decay 0-1755
- current sheets, resistive instabilities 0-4218
- decimetre radiowaves propagation in circumsolar plasma during flight of Venera-10 spacecraft 0-21886
- early solar system, minor planets EM heating by dense solar wind 0-36555
- effect on high latitude tropospheric pressure 0-56515
- electromagnetic instabilities near Earth orbit, theory (*Russian*) 0-31190
- electron exciters of type III radio bursts, obs. near 1 AU 0-46513
- electron of solar wind plasma, subthermal, thermal and extrathermal populations 0-41688
- energetic particle acceleration mechanisms 0-31187
- flare streams, struct. rel. to flare location on Sun 0-41790
- flows associated with hot heavy ions, obs. rel. to props. and origin 0-51635
- geomagnetic micropulsations, solar wind vel. and Pc 3, 4, 5 activity 0-41665
- heat transport in solar wind, closure relation 0-41689
- heliosphere, props. of dust in plasma environment 0-26930
- high speed streams and galactic cosmic ray modulation 0-41673
- high-speed stream, parametric decay of ion cyclotron pump wave 0-41690
- high-speed streams, correl. with unusual cosmic ray Forbush decreases 0-12624
- inert gas abundance, 500 Myr ago from lunar dust anal. (*German*) 0-51637
- interaction with Venus 0-41687
- interplanetary dust and electrons spatial distrib. round Sun, contrib. to corona 0-46514
- interplanetary mag. field, sectoral struct. due to large scale spiral waves 0-12633
- interplanetary magnetic field between 0.3 and 1 AU, Helios 1 and 2 obs. 0-21887
- interplanetary plasma inhomogeneities, anisotropy (*Russian*) 0-36468
- interplanetary two-fluid shock waves propag., model 0-26711
- interstellar gas interaction (*Russian*) 0-36467
- interstellar medium interaction region struct., rel. to H atoms penetrating solar wind 0-41686
- ion frequencies and velocities,  $^3\text{He}^{++}$ ,  $^4\text{He}^{++}$ ,  $\text{O}^{6+}$ ,  $\text{O}^{7+}$ , multiply charged Fe (*German*) 0-51636
- Jupiter magnetosphere interaction, Voyager 1 studies preliminary results 0-26793
- kinetic instability due to electron nonthermal props. 0-41691
- lunar dust, inert gas conc., separation methods and methods of treatment (*French*) 0-51674
- magnetic fluctuations, directional anisotropy and Landau damping of Alfven waves 0-21885
- magnetosphere, high-energy protons produced by substorms, interplanetary conditions 0-51615
- magnetosphere interaction, magnetopause configuration in two dims. (*German*) 0-31167
- magnetosphere model, particle (electric current) approach 0-17442
- magnetosphere substorms, prediction of occurrence by solar wind and IMF obs. 0-41648
- magnetosphere-solar wind interaction, Chapman-Ferraro image method graphs correction 0-12620
- Mars, heavy ions in solar wind plasma flow 0-8576
- Mars, solar wind interaction region, ion flux meas. interpretation 0-8575
- mass loss from Sun, implications of models He content and convective mixing length 0-26835
- MHD solitons in solar wind, nonlinear dispersion eqn. qualitative anal. 0-4217
- origin in polar coronal holes, rel. to geomag. activity and solar cycles 0-21979
- particle acceleration by propagating interplanetary shocks 0-31188
- plasma electron temperature, 0.5-1 AU, satellite obs. 0-12630
- plasma wave propagation, magnetoacoustic wave transverse to mag. field 0-12629
- plasmas with arbitrary orientation of mag. field, two-stream instability 0-41715
- protoplanetary disc nebula disruption by T Tauri-like solar wind 0-36516
- shock wave acceleration of energetic charged particles 0-31189
- stream structure, energetic solar particle events 0-41674
- streams magnetic classification 0-41692
- type III solar radio burst sources, plasma wave clumping origin 0-21959
- velocity, determ. from Voyager 2 coronal occultation, 1979 August 0-51639
- Venus bow shock, Pioneer magnetometer obs. 0-36535
- Venus magnetic tail, formed by solar wind interaction 0-51679
- viscous boundary layer between the solar wind and cometary plasmas 0-56769
- He ions superheating and superacceleration 0-12631



- soldering**  
laser material processing, IR holographic elements appl. 0-37964  
space-quality solder joints, resistance to thermal fatigue 0-25831  
superconducting wire to cryogenic leads, simple repeatable method 0-4728  
thick-film conductor, adhesion meas. technique 0-50811  
Cd, spreadability on Cu and brass plates (*Japanese*) 0-29252  
Pt-Au, thick film, adherence meas. and evaluation 0-50813  
Sn-Pb solder on Cu plate, spreadability, effect of fluoride and iodide addition to  $\text{ZnCl}_2$  flux (*Japanese*) 0-29251
- solenoids**  
*see also coils; electromagnets*  
homogeneous magnetic field synthesis in internal region of cylindrical solenoid (*German*) 0-37923  
impedance of solenoid surrounding cylindrical conductor with surface crack, eddy currents, calc. 0-23601  
magnetic sensor, high permeability metal core solenoid absolute sensitivity calibration 0-31133  
magnetisation meas. using field gradient of high-field solenoid 0-31813  
pulsed 70-T system with long operational life, Faraday effect meas. 0-42243  
solid state physics, high mag. fields, generation and application 0-27321  
superconducting, biaxial sample rot. use (*Czech*) 0-37010  
superconducting, magnetic field inhomogeneity measurement method, Hall probe appl. (*Czech*) 0-13107  
superconducting magnet system, development for physical experiments 0-9008  
superconducting solenoid, optimisation of aperture solenoid with rectangular windings 0-4747  
transient response of solenoid driven conducting cylinder 0-23599  
Cu-steel composites for intense pulsed mag. field generation 0-42245  
Nb-Ti superconducting magnet system, for short sample test on Tokamak superconductor 0-9010
- solid effect**  
phonon bottleneck, influence on dynamic nucl. polarisation by solid effect 0-20511
- solid electrolytes** *see superionic conducting materials*
- solid helium**  
<sup>3</sup>He, solid, two parameter model of mag. and thermal props., spin exchange 0-49461  
adsorbed layers, porosity of solid gas layers, appl. to cryosorption pump (*Japanese*) 0-20031  
coherent diffusion of isotropic impurities 0-54468  
melting curve shifts due to pore condensation 0-54469  
neutron scattering, book contrib. 0-2230  
<sup>3</sup>He, low temp. thermal cond., structural crystalline defects 0-2240  
<sup>3</sup>He, mag. ordering, NMR study 0-54470  
<sup>3</sup>He, nuclear antiferromagnet. reson. 0-54471  
<sup>3</sup>He, possible explanation for recently obs. phase transition in high mag. fields 0-20006  
<sup>3</sup>He, two-dimens. solid, melting mechanism 0-10643  
<sup>3</sup>He-<sup>4</sup>He, solid soln., struct. of vacancies 0-2242  
<sup>4</sup>He, boundary limited thermal cond., Poiseuille phonon flow 0-2241  
<sup>4</sup>He, extension of HCP-FCC phase diagram to about 9 kbar 0-39383  
<sup>4</sup>He, HCP, ground-state props. 0-44389  
<sup>4</sup>He HCP crystals, US attenuation, dislocation damping 0-24711  
<sup>4</sup>He, phase transition 0-15333
- solid hydrogen**  
adsorbed layers, porosity of solid gas layers, appl. to cryosorption pump (*Japanese*) 0-20031  
discontinuous orientational phase transition, thermodynamics, isotope effects 0-6590  
electronic stopping power calcs. 0-2104  
p-H<sub>2</sub>, NMR study of dilute o-H<sub>2</sub> impurity 0-25228  
HCP, density depend. of elastic consts. 0-6589  
inhomogeneous many-body system integral equations 0-22732  
metallic, electron-lattice interaction effect on equilib. struct. form. (*Russian*) 0-34380  
metallic, transition press. and physical props. (*Chinese*) 0-54467  
pellet ablation in plasma 0-19589  
phonon absorption line shape as function of density 0-50329  
quadrupolar glass, relax. time and low temp. sp.ht., computer simulations 0-49377  
quadrupolar glass, press. meas. 0-34271  
quantum crystal, short-range corre. and motional renormalisation of anisotropic interactions as function of density 0-34272  
rotation-libration transition under press., Monte Carlo study 0-49460  
rotational excitations, higher order effects 0-6591  
solubility in high press. He 0-10674  
substrate for liquid <sup>4</sup>He film, film transfer velocity, Van der Waals interaction (*Russian*) 0-54465  
thermonuclear plasma, H<sub>2</sub> fuel pellet ablation, atomic processes effect 0-18596  
p-H<sub>2</sub>, crystal field energy for o-H<sub>2</sub> impurities, NMR studies 0-15331  
p-H<sub>2</sub>, NMR spectrum of isolated o-H<sub>2</sub> pairs 0-15332  
HD-T<sub>2</sub>, liq. and solid, vibr.-rot. IR spectra 0-50313  
HT-T<sub>2</sub>, liq. and solid, vibr.-rot. IR spectra 0-50313
- solid lasers**  
*see also gamma-ray lasers; Raman lasers; semiconductor junction lasers*  
alkali halides, coloured, light amplification at activator centres 0-2795  
amplifier with spatial filters, graphoanalytic determ. of energy parameters 0-48322  
amplifier with spatial filters, optimal length and operating conditions 0-48323  
colour centre laser, progress in tunable lasers 0-43344  
colour centre laser with superfluid He cooling 0-48282  
conference, laser engineering and appls., Washington, USA (May-June 1979) 0-1216  
dye ultrafast saturable absorbers for Nd lasers 0-53386  
F-centre, laser, continuously tunable near IR (*German*) 0-1207  
fibre laser high-power stimulated emission pulses, substruct. 0-9890  
fibre Raman and Brillouin laser gains, polarisation effects 0-9887  
fluorophosphate laser glass, highly homogeneous, production 0-14411  
interlocked solid-state lasers, radiation intensity modulation for precision meas. 0-1250  
inversion depletion on ultrashort pulse evolution, mode-locking behaviour 0-5736  
IR source, tunable, efficient 0-5789  
lenses focal distances meas., in active elements, using Zernike interferometer 0-48268
- solid lasers continued**  
measurement, radiation pulse width determ. using Fabry-Perot interferometer 0-23736  
measurement, radiation pulses formation and stabilisation 0-23735  
measurement, single-pulse, with uniform distribution of energy density, correction equipment 0-23703  
Mikron high-power multichannel laser pulse system, Nd:glass rods 0-28249  
multimode laser, mode interaction and radiation fluctuations 0-43338  
nonlinear active medium laser, transient intracavity SHG, giant pulse generation 0-9948  
nonlinear stratified system, plane wave propagation 0-43343  
Nova 200 TW glass laser system for thermonuclear fusion, large laser control system, evolution from Shiva to Nova 0-9894  
periodic mode loss, use of grating mirrors in IR laser resonators 0-28254  
phosphate glass laser, statistical props. and stabilisation 0-48266  
phosphate laser glasses, review 0-9888  
plasma Q-switch in laser cavity 0-28259  
pulse train stability with periodic Q-switching 0-28239  
rare earth doped  $\text{Bi}_4\text{Ge}_3\text{O}_{12}$ , cryst. growth, spectral and laser props. 0-45115  
rare earth lasers, book contrib. 0-53306  
ring laser, generation of microsecond pulses 0-9913  
ring laser, solid state, with intracavity bleachable filter, conditions for CW stimulated emission 0-14368  
ring laser, travelling-wave, linear stage of field development 0-23724  
rods, with negative lenses, distributed aperture effect 0-38046  
ruby, freq. synchronisation and locking by passive modulator 0-1249  
ruby, graphical method for pumping coeff. estimation 0-14343  
ruby, power enhancement by intracavity plasma 0-53330  
ruby, pulsed, laser annealing to round edges of Si structures 0-25742  
ruby, Q-switched, semicond. wafer laser annealing, review and anal. 0-25741  
ruby, Q-switched, spectroscopic props., operation modes, pulse amplification (*Rumanian*) 0-48265  
ruby, rotating, beam generation 0-1258  
ruby, single-pulse laser, controllable phototropic shutter design 0-23699  
ruby, spatial coherence meas. with holographic coherence meter 0-9837  
ruby laser, generation, amplification of high power picosecond pulses depend. on superluminescence 0-53305  
ruby laser, negative feedback, cavity Q insertion effect on parameters of modulated pulses 0-43376  
ruby laser, spherical cavities, Q-switching by rotating mirror 0-28261  
ruby laser generating ultrashort light pulses, saturating absorber efficiency increase 0-23700  
ruby laser third harmonic generation in Ti vapour, focusing degree influence 0-48348  
ruby lasers and  $\text{LiNbO}_3$  cryst. in difference freq. laser, tunable MM range emission 0-5764  
ruby NMR laser, <sup>27</sup>Al nucl. spin system, collective ordering phenomena, instabilities 0-11278  
ruby NMR laser, dynamic props. from point of view of synergetics 0-43341  
ruby pulsed laser radiation action on polydisperse water aerosols 0-14378  
ruby raser, instabilities and first order phase changes (*German*) 0-48263  
scanning laser microscope, electron beam excited 0-52303  
short pulse generation, subnanosecond and picosecond operation 0-28262  
stability, using resonator without external mirrors 0-33024  
CdS, CdS,  $\text{Se}_{1-x}$ , scanning semiconductor laser with transverse electron-beam pumping 0-9904  
CdS, doped laser mechanism and output study 0-43340  
CdS, electron-beam-pumped laser, basis of scanning optical microscope 0-31864  
CdS semiconductor laser, longitudinally pumped, electron beam scanning vel. rel. to output parameters 0-9889  
CdS, stimulated and spontaneous emission from degenerate electron-hole plasma at 300K 0-29762  
CdS streamer laser, generation of ps. light pulses 0-9908  
CdS, two-photon-excitation, tunable laser emission, luminesc. processes 0-55127  
CdS,  $\text{Se}_{1-x}$ , strongly excited by electron beam, determ. of nonequilibrium carrier lifetime 0-39603  
Ce:LiYF<sub>4</sub>, tunable UV laser at 325, 309 nm, KrF laser excitation 0-38022  
Co:MgF<sub>2</sub>, laser, broadly tunable CW operation, output powers, optical pumping 0-32995  
Cr<sup>3+</sup>:Al<sub>2</sub>BeO<sub>4</sub>, Alexandrite, tunable laser sources development and appl. 0-48262  
Cr<sup>3+</sup>:BeAl<sub>2</sub>O<sub>4</sub> alexandrite laser, high gain performance 0-53299  
Cr<sup>3+</sup>:BeAl<sub>2</sub>O<sub>4</sub> alexandrite laser, wavelength-tunable CW laser action 0-53300  
Er<sup>3+</sup>:Lu<sub>2</sub>Al<sub>2</sub>O<sub>12</sub>, 3- $\mu\text{m}$  crystal laser functional scheme, stimulated emission 0-43339  
GaAs electron-pumped uncooled laser, degradation rel. to dislocation density 0-14344  
GaAs, stimulated and spontaneous emission from degenerate electron-hole plasma at 300K 0-29762  
Ho<sup>3+</sup>:LiYF<sub>4</sub>, 1.392, 1.673 and 3.914  $\mu\text{m}$  stimulated emission, laser cascades 0-9886  
InAs, epitaxial, laser action mechanisms with electron beam excitation 0-28240  
InAs, Sb, P<sub>1-x-y</sub>, efficient electron-beam-pumped laser at 3.1-3.7  $\mu\text{m}$  0-5738  
KCl-OH<sup>-</sup>, electron irr., F<sub>2</sub><sup>+</sup> centre stabilisation and tuneable laser operation 0-54231  
KEr(WO<sub>4</sub>)<sub>2</sub>, crystallisation cond., stimulated emission in 2.8  $\mu\text{m}$  band 0-53301  
K<sub>2</sub>NdLi<sub>2</sub>F<sub>10</sub> (KNLF), spectroscopy and lasing 0-5737  
KNdP<sub>4</sub>O<sub>12</sub>, determ. of fluoresc. quantum efficiency and laser emission cross sections 0-48264  
KNdP<sub>4</sub>O<sub>12</sub>, laser emission cross sections, fluorescence spectra, radiative lifetimes, quantum efficiency 0-23694  
Li<sup>+</sup>, Na<sup>+</sup>:KCl(RbCl), F<sub>A</sub>(II) to F<sub>B</sub>(II) centre crystals, CW laser oscill. with extended tuning range 0-32997  
Li<sup>+</sup>:KCl, F<sub>A</sub>(II) colour-centre laser, mode locking and tunable picosecond IR pulse generation 0-43364  
Li-Nd-La phosphate glass active elements, laser characts., comparison with Nd:YAG 0-33002  
LiBi<sub>2</sub>Nd<sub>1-x</sub>P<sub>4</sub>O<sub>12</sub>, waveguide laser layer epitaxially grown on LiNdP<sub>4</sub>O<sub>12</sub> substrate 0-23709



## solid lasers continued

LiF crystal with  $F_2^+$  centres, periodic pulsed tunable laser, Nd laser second harmonic excited 0-38021  
 LiF OH-stabilised  $F_2^+$ -centre laser, appl. to intracavity laser spectroscopy 0-32999  
 LiF tunable laser production,  $F_2^+$  centre accumulation and generation (Russian) 0-28238  
 LiF-OH,  $\gamma$ -irrad., colour centre lasing at 0.84-1.13  $\mu$  at 300K 0-5739  
 LiNd(PO<sub>3</sub>)<sub>4</sub> laser with external and Fabry-Perot resonators, 1.05, 1.32  $\mu$ m CW oscill. 0-23693  
 LiNdP<sub>4</sub>O<sub>12</sub> efficient miniature laser pumped with GaAlAs laser diode 0-32994  
 LiNdP<sub>4</sub>O<sub>12</sub> glass-clad rectangular waveguide, laser performance 0-32996  
 LiNdP<sub>4</sub>O<sub>12</sub>, grown by top seeded pulling technique, possible laser material 0-25542  
 LiNdP<sub>4</sub>O<sub>12</sub>, laser emission cross sections, fluorescence spectra, radiative lifetimes, quantum efficiency 0-23694  
 LiNdP<sub>4</sub>O<sub>12</sub> single crystal growth, study of Li<sub>2</sub>O-Nd<sub>2</sub>O<sub>3</sub>-P<sub>2</sub>O<sub>5</sub> phase diagram 0-25668  
 Lu<sub>3</sub>Al<sub>5</sub>O<sub>12</sub>:Ho<sup>3+</sup>(Er<sup>3+</sup>), sensitized stimulated emission at 3 microns 0-53302  
 Ni:MgF<sub>2</sub>, laser, broadly tunable CW operation, output powers, optical pumping 0-32995  
 Na<sup>+</sup>:KCl, CW laser action of ( $F_2^+$ )<sub>A</sub>-centres, tunable from 1.62 to 1.91  $\mu$ m 0-32998  
 NaCl-OH<sup>-</sup>, electron irrad.,  $F_2^+$  centre stabilisation and tuneable laser operation 0-54231  
 NaNdP<sub>4</sub>O<sub>12</sub>, laser emission cross sections, fluorescence spectra, radiative lifetimes, quantum efficiency 0-23694  
 Nd<sup>3+</sup>,Cr<sup>3+</sup>:glass, nonradiative energy transfer from Cr to Nd, optical pumping efficiency improvement 0-33001  
 Nd crystals, determ. of fluoresc. quantum efficiency and laser emission cross sections 0-48264  
 Nd doped (fluoro) phosphate laser glass piezo-optic coeffs. meas. at 0.6328 and 1.15  $\mu$ m 0-34888  
 Nd, emission freq. conversion by method of reson. pumping of active media 0-1206  
 Nd laser plasma diagnostics, probing radiation Raman scatt. (Russian) 0-19618  
 Nd, lasers, efficiency enhancement by pump radiation conversion in luminesc. liq. 0-48293  
 Nd, multifreq. laser, coherence time meas. using bleaching dyes 0-23739  
 Nd pulsed garnet lasers, pulse repetition frequency, optimal operating regime 0-53303  
 Nd, with mirror plasma-optical Q-switch (Russian) 0-33028  
 Nd<sup>3+</sup> ion miniature phosphate glass lasers with high ion concentration 0-19038  
 Nd<sup>3+</sup> miniature laser principles, materials and integrated optical design 0-33004  
 Nd:glass, optical inhomogeneity cancellation using LiIO<sub>3</sub> parametric converter 0-33049  
 Nd:glass, silicate and phosphate glass, comparison of gains 0-19039  
 Nd:glass 2 TW laser for fusion expts. 0-33035  
 Nd:glass disc amplifiers, possibility for efficiency improvement 0-33000  
 Nd:glass laser, generation of picosecond light continua depending on various nonlinear processes 0-33095  
 Nd:glass laser, luminesc. filters efficiency 0-1213  
 Nd:glass laser, spherical cavities, Q-switching by rotating mirror 0-28261  
 Nd:glass laser amplifiers, self-focusing and suppression by spatial filtering 0-14406  
 Nd:glass laser cooling and index-matching liquid props. 0-33015  
 Nd:glass laser system with parametric freq. conversion 0-1277  
 Nd:glass laser with periodic Q-switching, mathematical model 0-33043  
 Nd:glass laser with US modulated emission 0-48309  
 Nd:glass laser with unstable resonator and additional feedback, angular divergence 0-48307  
 Nd:glass passively mode-locked laser, obs. of external feedback influence 0-23729  
 Nd:phosphate glass, high-power laser, design and performance 0-48270  
 Nd:YAG, grown from melt, in Mo crucibles, laser props. 0-48261  
 Nd:YAG, heat capacity and thermal diffusivity meas. 0-19956  
 Nd:YAG, mode locked oscillator, operation at 1.052  $\mu$ m 0-33017  
 Nd:YAG, pulse exchanges with plasma (German) 0-48918  
 Nd:YAG, semicond. wafer laser annealing, review and anal. 0-25741  
 Nd:YAG, thermal lens effect on emission stability 0-19064  
 Nd:YAG CW laser, active stabilisation, laser noise 0-48295  
 Nd:YAG laser, CW, with high output coupling modulation 0-9917  
 Nd:YAG laser, coherence time meas. of picosecond pulser by light-induced grating method 0-53347  
 Nd:YAG laser multipass cell for Raman scatt. diagnostics 0-1231  
 Nd:YAG laser range finder, performance in radiation environments 0-38054  
 Nd:YAG mode-locked laser pulse, quadratic phase evolution direct meas., time resolved interferometry 0-48318  
 Nd:YAG oscillator, Q-switched, generation of high-power ns pulses 0-23730  
 Nd:YAG Q-switched oscillator for underwater appls. 0-8461  
 Nd:YAG unstable-resonator oscillator, stable single-axial-mode operation by injection locking 0-53331  
 Nd<sup>3+</sup>:Ca<sub>3</sub>Ga<sub>2</sub>Ge<sub>2</sub>O<sub>12</sub>, stimulated emission at 300K 0-38019  
 Nd<sup>3+</sup>:La<sub>2</sub>Mg<sub>3</sub>(NO<sub>3</sub>)<sub>12</sub>·24H<sub>2</sub>O, proton raser, self-radiating nuclear spin system (German) 0-53298  
 Nd<sup>3+</sup>:phosphate glass laser, brightness enhancement by spatial filtering in amplifying channel 0-48321  
 Nd<sup>3+</sup>:YAG, contrast and configs. of LiNbO<sub>3</sub> electrooptic switches 0-33012  
 Nd<sup>3+</sup>:YAG, laser characts., comparison with Li-Nd-La phosphate glass active elements 0-33002  
 Nd<sup>3+</sup>:YAG CW ring laser, fluctuation spectrum 0-9914  
 Nd<sup>3+</sup>:YAG continuously pumped pulse-periodic laser, stability 0-28241  
 Nd<sup>3+</sup>:YAG laser, conc. determ. of <sup>137</sup>Cs fission product in coated-particle fuel 0-18416  
 Nd-YAG laser, Q-switched, freq. doubled, 200 kW output 0-33026  
 Nd(Ga,Cr)<sub>3</sub>(BO<sub>3</sub>)<sub>4</sub>, cryst. growth by LPE, Nd<sup>3+</sup> fluorescence, lattice constants 0-29883  
 NdLa<sub>1-x</sub>P<sub>3</sub>O<sub>14</sub>, crystal growth, laser generation characts. 0-38020  
 Ni<sup>2+</sup>:MgO laser system, optical parameters 0-48260  
 Tm:LiYF<sub>4</sub>, XeF pumped, excimer excited storage laser 0-33003  
 YAG stable resonator, yielding high output energy and very low divergence beam 0-23721  
 ZnO single cryst., UV laser, electron beam excited 0-53304

## solid lasers continued

ZnO, two-photon-excitation, tunable laser emission, luminesc. processes 0-55127  
 ZnS single cryst., UV laser, electron beam excited 0-53304

## solid-liquid transformations

see also crystallisation; freezing; melting; solidification  
 acoustic levitation technique, for phase transition studies and props. of liqs. 0-43565  
 asymmetrical Ising model, phase transitions 0-17891  
 binary metallic system, conc. profiles across solid-liq. interfaces 0-55382  
 t-butyl bromide, elec cond., temp. depend. in liq. and plastic phases 0-1944  
 t-butyl chloride, elec cond., temp. depend. in liq. and plastic phases 0-1944  
 chlorobenzene-cis-decalin mixtures, phase transitions and dielec. behaviour study in 77-330K 0-29680  
 crystal nucleation and symmetry, interaction pots. effect 0-34169  
 dynamic Ginzburg-Landau theory 0-44292  
 furan, adsorbed on NaCl, evidence of new condensed phase, IR spectra (French) 0-16028  
 hard-sphere system, liquid-solid transition, chem. pot. calcs. 0-54088  
 heat transfer and interface motion 0-53609  
 interphase mass flux and mass fluxes within phases 0-48561  
 lubricant, shear rheological behaviour at high press. 0-35342  
 metal-H, phase transitions 0-50631  
 stability limit of liquid and crystal phase, three-parameter law of corresponding matter 0-49340  
 triethylacetic acid, high resolution <sup>1</sup>H and <sup>13</sup>C NMR spectra at liquid-solid phase transition 0-11281  
 trimethylacetic acid, high resolution <sup>1</sup>H and <sup>13</sup>C NMR spectra at liquid-solid phase transition 0-11281  
 vacancy cell model and BGY integral eqn. 0-38887  
 Al-Sn alloy, conc. profiles across solid-liq. interfaces 0-55382  
 Ar monolayer adsorbed on graphite basal planes, heat capacity anomaly rel. to phase transition 0-6636  
 Fe, cast, grey eutectic transform. mechanism (Russian) 0-20924  
 Ga, transition from ordered solid to disordered liquid, viewed by photoemission 0-45217  
 Hg, transition from ordered solid to disordered liquid, viewed by photoemission 0-45217  
 In, transition from ordered solid to disordered liquid, viewed by photoemission 0-45217  
 Kr absorption on graphite, monolayer regime phase diagram 0-49507  
 Kr adsorbed monolayer, on graphite basal face, fluid-registered solid transition 0-49491  
 Li soaps, n.C<sub>13</sub>-n.C<sub>20</sub>, phase transition temps. and enthalpies, DSC obs. 0-45544  
 Ni-Pb alloy, conc. profiles across solid-liq. interfaces 0-55382  
 SbCl<sub>5</sub>, phase diagram to 43 kbar 0-2144  
 SiO<sub>2</sub>-Al<sub>2</sub>O<sub>3</sub>-FeO-CaO-MgO pyroxene glasses, phase changes 0-15013  
 SiO<sub>2</sub>-base cores, for superalloys, high temp. characterisation 0-10640  
 Ti, transition from ordered solid to disordered liquid, viewed by photoemission 0-45217

## solid mechanics see mechanics

## solid solubility

alkaline earth silicate glasses, morphology effects on props. 0-49118  
 metallic system, compound formation rel. to heat of mixing 0-55689  
 refractory compound fibre reinforced cpd. materials, diffusional reaction, effect of alloying calc. 0-20851  
 steel, carbide and nitride phases dissolution (Russian) 0-20888  
 steel, Cr-C and C, carbide coating by CVD, interlayer form. 0-11574  
 steel, maraging alloy, intermetallic compound solubility, thermodynamic calcs. (Russian) 0-40363  
 (Ba<sub>x</sub>Sr<sub>1-x</sub>)SO<sub>4</sub>:Eu mixed crystal series, X-ray diffr. study of miscibility 0-2168  
 CaAl<sub>2</sub>O<sub>4</sub>-SrAl<sub>2</sub>O<sub>4</sub>-BaAl<sub>2</sub>O<sub>4</sub>, binary and ternary systems, solid solubility (Japanese) 0-35174  
 (Ca<sub>x</sub>Cd<sub>1-x</sub>)CO<sub>3</sub>, cryst. struct. and cation isomorphous miscibility 0-33972  
 CaO-MnO system, solid soln. form. and analysis 0-28996  
 Ca<sub>2</sub>SiO<sub>4</sub>-BaO, conditions and mechanism in cryst.-chemical stabilisation of unstable phases 0-39302  
 Ca<sub>2</sub>SiO<sub>4</sub>-FeO, conditions and mechanism in cryst.-chemical stabilisation of unstable phases 0-39302  
 Ca<sub>2</sub>SiO<sub>4</sub>-MgO, conditions and mechanism in cryst.-chemical stabilisation of unstable phases 0-39302  
 CaX-MnX, X=S, Se, Te, solubility limits 0-44320  
 CdTe-ZnS system, phase diagram and solid solubility 0-20909  
 CeMg<sub>11</sub>V(Cr)(Mn)(Fe)(Co), hydriding and appl. in H<sub>2</sub> storage 0-51009  
 Cr-C, binary alloy formation of nonequilib. Cr<sub>7</sub>C in alloys quenched rapidly from melt 0-7581  
 Cr-Si-Cu, structure and supercond., Cu influence 0-50592  
 Cu-Cd, structure, electrolytic deposition on monocrystalline Cu cathodes (Polish) 0-44435  
 Cu-Fe (0.2 at.%), clustering, precipitation, and oxidation, 298 to 919K, Mossbauer study 0-7242  
 Cu-Ga porous solid formed by shock compression 0-29905  
 Cu-Mn-P alloys, phase diagram (Russian) 0-20891  
 Cu-Ti, solubility of Ti, exam. using NMR of <sup>63</sup>Cu (French) 0-7179  
 $\alpha$ -Fe, Armco, determ. of H solubility 0-54390  
 Fe-Sb-Ti(V)(Cr)(Mn)(Co)(Ni), dil., interactions and precip., Mossbauer study 0-39997  
 GaAs:Cr diffusion profile meas. 0-6554  
 Ge:Al, limiting solubility, rel. to charge carrier conc. 0-24596  
 Ge:Sb, limiting solubility, rel. to charge carrier conc. 0-24596  
 H<sub>2</sub>, solubility in high press. He 0-10674  
 Hf-M-B systems (M=Rh,Ir), phase equilib. and cryst. structs. 0-15072  
 In<sub>2</sub>Se<sub>3</sub>-Cu<sub>2</sub>S system, electrophys. props., influence of 1-4% Cu<sub>2</sub>S 0-20219  
 Ir, diffusion of C from surface into bulk, theory 0-6562  
 Mg-Ag-Cu, phase comp. in Mg-rich region (Russian) 0-40331  
 Mg-Ga-In(Tl) and Mg-In-Tl, phase diagrams and electrochem. props. (Russian) 0-40330  
 Mg-Tb, (up to 45 wt.%), phase diagram, and mech. preps. 0-16277  
 Mg-Y-Zn alloys, phase equilib. (Russian) 0-16271  
 MgO, solid solubility of Sc<sub>2</sub>O<sub>3</sub>, Al<sub>2</sub>O<sub>3</sub>, Cr<sub>2</sub>O<sub>3</sub>, SiO<sub>2</sub> and ZrO<sub>2</sub> 0-15247  
 (MnTe)<sub>1-x</sub>(Bi<sub>2</sub>Te<sub>3</sub>)<sub>x</sub> (x $\leq$ 0.05) solid solution, electrophys. props. 0-24925  
 Mo-Si-Cu, struct. and supercond., Cu influence 0-50592  
 Mo<sub>2</sub>C, free energy of form. and thermodynamic props. of C in solid Mo 0-15266



**solid solubility continued**

- NaCl-KCl, interdiffusion and demixing, electron microprobe anal. (French) 0-54444  
 NaCl+Pb, Pb aggregation effect on yield stress, incoherent precipitates, solubility determ. method 0-50645  
 Na<sub>2</sub>O-B<sub>2</sub>O<sub>3</sub>:Au glasses, Au solubility, oxidation state and opt. absorpt. 0-44321  
 Na<sub>2</sub>O-CaO-SiO<sub>2</sub> glass, effect of phase on liquids and gas diffusion (German) 0-38931  
 Nb-Ge-Cu, phase equilib. and supercond. props. (Russian) 0-40332  
 Nb-Si-Cu, struct. and supercond., Cu influence 0-50592  
 Ne solid, solubility in high press. He 0-10674  
 Pb, of Au, elec. resist. meas. 0-39298  
 Pd-H, low temp. transport props., heterogeneous-mixture model 0-24871  
 PdAl-Fe(Ni), phase diagrams, eutectic points and solubility (Russian) 0-40333  
 Pd<sub>75</sub>Cu<sub>25</sub>Si<sub>16.5</sub>, ternary miscibility gap, simulation, dispersed phase composite form. 0-54379  
 Pr-Ga (0 to 50 at.%), phase diagram and cryst. structs. of intermetallic cryst. 0-3002  
 Sc-M-B systems (M=Rh,Ir), phase equilib. and cryst. structs. 0-15072  
 Si, hole localisation, solid solubility, excitonic Auger lifetime of acceptors 0-20216  
 Si:As, high-dose implanted, irradi. time and subsequent heat treatment effects on laser annealing 0-29041  
 Si:As, solid solubility of As determ. by ion implantation, CW laser annealing 0-6517  
 SiC, exam. of N solubility, in epitaxial layers 0-6520  
 SiC:Al epitaxial layers, growth, Al distrib. and solubility 0-15391  
 Ta-Si-Cu, struct. and supercond., Cu influence 0-50592  
 V, H solubility and diffusivity around room temp. 0-29225  
 V-Nb(Ti)(Zr)(Cr)(Mo)(Fe)(Cu), H solubility and diffusivity around room temp. 0-29225  
 V-Si-Cu, struct. and supercond., Cu influence 0-50592  
 W-Si-Cu, struct. and supercond., Cu influence 0-50592  
 ZnS, wurtzite, ZnO solubility, 1444-1240°C 0-15248  
 ZnSe:Ga,As, characts. of simultaneous incorporation, by Mn<sup>2+</sup> ESR and X-ray fluoresc. anal. 0-34017  
 α-Zr, H terminal solid solubility, optical metallographic study 0-34195  
 Zr-M-B systems (M=Rh,Ir), phase equilib. and cryst. structs. 0-15072

**solid solution hardening**

- chemically hardening material cast in elastic cylindrical mold, transient thermal stresses 0-7589  
 metal, review of theories (Czech) 0-3084  
 metals, BCC, crystal resolved shear stress depend. on dislocations 0-40373  
 statistical behaviour analysis, with aid of computer (Japanese) 0-11658  
 steel, low-alloy, props. with nitride and Cu hardening at low temps. (Russian) 0-40372  
 steel, Si-P-C, low C, varying Si content, cold rolled annealing 0-3090  
 texture influence on stress/strain curves, prestrain, solid soln. and particle hardening effect on inhomogeneous deform. (German) 0-30014  
 Al-CuAl, eutectic, heat treatment and interlamellar spacing effect on tensile deformation 0-29979  
 Au-Cu(Ag)(Pt), cold worked, impurity conc. rel. to internal friction Bordoni peak, solid soln. hardening mech. 0-16363  
 Cu-Ni-Sn (10, 6 wt.%), temp. depend. of yield stress and work hardening 0-21026  
 Fe-Ni solid solution, deformation mechanism, softening phenomena, dislocation-solute atom interactions (French) 0-45344  
 Mg-Cd, single crystals, temp. depend. of crit. resolved shear stress (Czech) 0-29112  
 Mo alloy:Re, effect of Re on mechanical props. 0-35196  
 Nb alloys, solid solution hardening, crystal resolved shear stress depend. on dislocations 0-40373  
 Ni alloys EhP539L, heat-resist., heat treatment effect on props. and hardening phase morphology 0-29995  
 Ni, dislocation intersection and solution strengthening, effect of solute on obstacle profiles 0-7590  
 Ni/Cr-Fe-C, Inconel, dislocation intersection and solution strengthening, effect of solute on obstacle profiles 0-7590  
 Ni-Co, dislocation intersection and solution strengthening, effect of solute on obstacle profiles 0-7590  
 Pd alloys, controllable hydrogen phase naklep, hardening and phase-strengthening 0-16323  
 Ti-Zr-W-(Al) alloys, phase struct. and props. (Russian) 0-16270

**solid solutions**

- solid solutions such as Au-Cu are indexed under alloys of the named elements i.e. 'gold alloys' and 'copper alloys' in this example see also alloys; solid solubility 0-55642  
 alkali earth halides, spectroscopy, investigations by F. Klement (Russian) 0-8767  
 alkali halides, spectroscopy investigations by F. Klement (Russian) 0-8767  
 alloys, interstitial solid solns., HCP, ordering type transitions within thermodynamics theory framework 0-49162  
 azeotropic and two terminal solid solution type binary diagrams, synthesis 0-19901  
 binary, order-disorder transition, long range order parameter and chemical potential 0-6487  
 binary alloys, diagrams of state, component interaction parameters (Russian) 0-55354  
 binary alloys, diagrams of state, component interaction parameters, computer calcs. (Russian) 0-55355  
 carbide, decomposition temp. expression 0-55398  
 dichalcogenides, pyrite-type, <sup>57</sup>Fe isomer shift, quadrupole splitting, Mossbauer study 0-15832  
 diffusion, chemical, highly defective solids, steady-state computer simulation method for lattice gas 0-49401  
 diffusive creep, theory (Russian) 0-40437  
 disordered multicomponent solid solutions conc. fluctuation waves, micro-spectroscopy theory 0-44327  
 Elinvär, γ to γ' transformation and γ' phase form. kinetics, lattice consts. 0-35191  
 FCC crystal, interstitial and solute concentration gradients, flux expression derivation (French) 0-54219  
 2-fluoronaphthalene-2-naphthol system, phase relations, X-ray diffr. and DTA study 0-45287

**solid solutions continued**

- freeze drying of solid solutions, solvent choice in semiconducting powder prep. 0-11583  
 glass-ceramics and photosensitive glass, microstructure rel. to properties (German) 0-38926  
 heterovalent, use of expt. data to estimate energy of soln. 0-54380  
 homogeneous solid solution crystallisation crucible 0-45224  
 impurity atoms diffusion and impurity-vacancy interactions (Russian) 0-19985  
 inhomogeneous, with conc. expansion, thermodynamics, energy defect diffusion calcs. 0-24618  
 interstitial solid solutions, self-diffusion activation energy rel. to partial molar energy 0-15291  
 ionic compounds, monovalent, surface comp. calc. using monolayer model 0-6607  
 l (French) 0-11984  
 liquid phase sintering, elementary mechanisms, soln.-reprecipitation 0-50571  
 metallic system, compound formation rel. to heat of mixing 0-55689  
 metals, FCC, under H<sub>2</sub> press., crit. phenomena and isomorphic transitions 0-49367  
 nondiagonal disordered system, excitation spectrum 0-15429  
 paradibromobenzene-paradichlorobenzene solid solutions, mol. cryst., NQR study 0-25242  
 polyhedrization of quinary metallic systems with isomorphic intermediate phases (Russian) 0-45270  
 quasi-particles method in solid solution theory 0-24560  
 refractory carbides, borides and nitrides, wetting by and interactions with liq. metals, solid soln. form 0-54473  
 short-range order parameters, AC-BD, X-ray diffr. determ. 0-38875  
 spectroscopy investigations by F. Klement (Russian) 0-8767  
 substitutional impurities in solids, entropy and volume of solution 0-15253  
 superionic-electronic solid solution electrodes, partial cond. meas. technique 0-44360  
 TCNQ salt, TTF<sub>1-x</sub>TSeF<sub>x</sub>-TCNQ, mol. substitutional disorder 0-24438  
 o-terphenyl, dipolar solutes, reorientational motions, dielectric relax. below glass transition 0-19706  
 thermodynamic functions calc., ternary alloy of quasi-binary cross sections 0-16265  
 transition metal carbonitrides, physicochem. props., comp. depend. 0-55370  
 Al substitutional solid solution alloys, volumetric effect and props. (Russian) 0-39293  
 Al-Mg solid solns., decomposition studied by ultrasonic meas. of elastic props. 0-35184  
 Al-Mg<sub>2</sub>Si (1 wt.%), precipitation reactions 0-11652  
 Al-Mn, direct chill-cast, struct. changes during heat treating (German) 0-40408  
 Al-Mn(Cr), quenched, thermal stability (Russian) 0-20976  
 Al-Zn (20 (30) (35) (40) (60) at.%), effect of UTS on cyclic creep strength (Korean) 0-25778  
 Al-Zn-Mg, polygonized struct. in extrusions, thermal stability and mech. props. 0-50659  
 Al-Zn-Mg (4.8, 1.2 wt.%), quenched, Guinier Preston zones formation 0-45273  
 Al<sub>12-4x</sub>Be<sub>2</sub>C<sub>10-3x</sub> (-1≤x≤1), solid soln., comp. vs lattice constants 0-45284  
 Al<sub>4</sub>C<sub>3</sub>3Be<sub>2</sub>C, X-ray diffr. and TEM study 0-14973  
 Al<sub>3</sub>Ga<sub>1-x</sub>Sb solid solns., freq. dependences of form of luminesc. spectra 0-40160  
 Al<sub>2</sub>O<sub>3</sub>-Cr<sub>2</sub>O<sub>3</sub>, solid soln., thermal expansion anisotropy, lattice consts. 0-54411  
 (Al<sub>2</sub>O<sub>3</sub>-Fe<sub>2</sub>O<sub>3</sub>):Cr<sup>3+</sup>, (0.04 mol.% Fe<sub>2</sub>O<sub>3</sub>), paramag., cross relax., annealing temp. effect from Mossbauer meas. 0-44983  
 AsSe-GeSe<sub>2</sub>-PbSe, glass form., struct. defects, elec. cond., assoc. (Russian) 0-54144  
 Au-Ni-Cu-Zn, white gold, metallographic struct., heat treatment and plastic working effect 0-40403  
 BaO-MoO<sub>3</sub>, solid phase reaction, thermal analysis 0-55639  
 BaO-WO<sub>3</sub>, solid phase reaction, thermal anal. 0-55639  
 BaS-CaS:Cu phosphors, X-ray diffr. and fluoresc. spectra 0-40148  
 BaSi<sub>2-x</sub>Ge<sub>x</sub>, solid solution with type SrSi<sub>2</sub> struct., lattice parameters at high press. 0-54203  
 (Bi, Sb)<sub>2</sub>Te<sub>3</sub> solid soln., semiconductor film, oxidation, electrophysical props. 0-45407  
 Bi-MnBi, directionally solidified composite, processing parameter role on mag. props. 0-35352  
 Bi<sub>2</sub>Te<sub>3</sub>-SbTe<sub>3</sub>, ordered structure formation, heat treatment effect on thermal cond. 0-54448  
 (Ca<sub>x</sub>Cd<sub>1-x</sub>)CO<sub>3</sub>, cryst. struct. and cation isomorphous miscibility 0-33972  
 Ca<sub>2</sub>Nb<sub>2</sub>O<sub>7</sub>-Sm<sub>2</sub>NbO<sub>7</sub> system, phase equilib. 0-20907  
 CaO-Fe<sub>2</sub>O<sub>3</sub>-Al<sub>2</sub>O<sub>3</sub> system, solid soln. of Ca<sub>2</sub>Fe<sub>2(1-x)</sub>Al<sub>2x</sub>O<sub>5</sub> (Russian) 0-16284  
 CaO-MnO system, solid soln. form. and analysis 0-28996  
 CaS-Y<sub>2</sub>S<sub>3</sub> (1 wt.%), solid electrolyte, elec. cond. under low partial pressures of S (Japanese) 0-49409  
 Ca<sub>2</sub>SiO<sub>4</sub>-CaO, conditions and mechanism in cryst.-chemical stabilisation of unstable phases 0-39302  
 Ca<sub>2</sub>SiO<sub>4</sub>-FeO, conditions and mechanism in cryst.-chemical stabilisation of unstable phases 0-39302  
 Ca<sub>2</sub>SiO<sub>4</sub>-MgO, conditions and mechanism in cryst.-chemical stabilisation of unstable phases 0-39302  
 CaX-MnX, X=S, Se, Te, solubility limits 0-44320  
 Cd,Hg<sub>1-x</sub>Te, vacancy mech. of resorption of Hg droplets 0-39070  
 Cd<sub>1-x</sub>M<sub>x</sub>S (M=Sr, Ca, Mg, Pb, Sn), solid soln., prep. and semicond. props. 0-2383  
 CdTe-ZnS ternary mutual system, phase diagram 0-20904  
 CdTe<sub>1-x</sub>Se<sub>x</sub> solid solution films, prep., struct., and photocond. 0-54541  
 Co<sub>2</sub>Mg<sub>1-x</sub>O, EPR of Co<sup>2+</sup> (Russian) 0-11251  
 Co<sub>2</sub>NiO<sub>4</sub>, powder prep. by freeze drying of solid solutions, solvent choice 0-11583  
 CoO-MgO-Cr<sub>2</sub>O<sub>3</sub>-Fe<sub>2</sub>O<sub>3</sub>-TiO<sub>2</sub>, form. and colour of spinel solid soln. (Japanese) 0-16059  
 Co<sub>1-x</sub>Zn<sub>x</sub>Fe<sub>2(1-y)}</sub>Cr<sub>2y</sub>O<sub>4</sub> spinels, solid solns., struct. 0-19764  
 Cr binary substitutional solutions, thermodynamics 0-54410  
 Cr-Mo-N system, at high-pressure, temp., X-ray anal., phase diagram 0-50607  
 Cr-N, interaction with dense stream of N ions, metallography, microhardness, specific volume (Russian) 0-15169



**solid solutions continued**

Cr-Os, magnetic transition T-P-C diagram, triple points (*Russian*) 0-54895  
 CrS-FeS, sulphur spinel, struct. and elec. props. 0-49834  
 Cr<sub>2</sub>S<sub>3</sub>-Se<sub>2</sub>, elec. resist., thermal cond. and Seebeck coeff. meas. 0-24958  
 CsCl-TlCl, determ. and computation of phase diagram 0-55379  
 CsCl-TlCl solid soln., point defect parameters 0-54224  
 Cu alloy solid solution condensed films, influence of alloying components on phase composition and lattice spacing (*Russian*) 0-20047  
 Cu-Ga porous solid formed by shock compression 0-29905  
 Cu-Ti (3.5 wt.%), aged by US strain, struct. and props. (*Russian*) 0-21003  
 CuBr-AgI system, ionic cond. and phase diagram 0-2198  
 (CuCr<sub>2</sub>S<sub>4</sub>)<sub>x</sub>-(Cu<sub>0.5</sub>In<sub>0.5</sub>Cr<sub>2</sub>S<sub>4</sub>)<sub>1-x</sub>, piezoelectric effect, X-ray struct. anal. (*Russian*) 0-15978  
 CuCr<sub>2</sub>Se<sub>4</sub>(S<sub>4</sub>)(Te<sub>4</sub>), binary and ternary solid solns., mag. and elec. props. 0-2407  
 CuInSe<sub>2</sub>-CuInS<sub>2</sub>, solid soln., photo-EMF spectra 0-20248  
 Fe solid solution, substitution strengthening by Cr and Mo (*Czech*) 0-30080  
 Fe-bearing binary, substitutional liq. and solid solns., statistical thermodynamics 0-11630  
 Fe-C interstitial solid solutions, self-diffusion activation energy rel. to partial molar energy 0-15291  
 α-Fe-C(N), C and N migration at low temps., monograph 0-22149  
 Fe-Co-Si, BCC solid soln. interchange energies, high temp. neutron diffr. 0-29166  
 Fe-Co-Si solid solutions, BCC, atomic configs., Mossbauer study 0-39006  
 α-Fe-Me-C(N), C and N migration at low temps., monograph 0-22149  
 Fe-N, interaction with dense stream of N ions, metallography, microhardness, specific volume (*Russian*) 0-15169  
 Fe-Ni solid solution, deformation mechanism, softening phenomena, dislocation-solute atom interactions (*French*) 0-45344  
 α-Fe<sub>2</sub>O<sub>3</sub>-Li<sub>2</sub>O, structural and thermal phase behaviour from mag., spectral and thermal studies 0-2673  
 FeSb solid solution, supersaturated, mag. hyperfine field, Mossbauer study 0-44961  
 α-FeTiD<sub>0.057</sub>, solid soln., interstitial D, neutron diffr. study 0-39071  
 Fe<sub>2</sub>V<sub>2-x</sub>O<sub>8</sub>, specific heat near semiconductor-metal transition 0-24612  
<sup>57</sup>Fe interstitial cpds. and solid solns., Mossbauer spectra 0-20557  
 Ga<sub>2</sub>In<sub>1-x</sub>P solid solutions, single cryst. prep. and props. 0-16162  
 Ga<sub>2</sub>In<sub>1-x</sub>Se, fabrication, struct., elec. and optical props. 0-44180  
 GaSb-GaAs-Ge system, props. and struct. 0-20232  
 GdCrO<sub>3</sub>-GdAlO<sub>3</sub>, solid solutions 0-20887  
 Ge, As impurity precipitation from solid soln., neutron irradi. effect 0-29177  
 Ge:Al, solid solns. decomp. 0-15249  
 Ge:Sb, solid solns. decomp. 0-15249  
 Ge-GaAs, crystallisation at superhigh cooling rates 0-54349  
 Ge-Si, solid soln., local IR transmission 0-7357  
 Ge-Si:Sb, prepared in Universal Furnace expt. in Soyuz-Apollo programme, melting and crystn. 0-19737  
 GeSe<sub>2</sub>S<sub>1-x</sub>, long-wavelength optical phonons, Raman spectra 0-25378  
<sup>3</sup>He-<sup>4</sup>He, solid soln., struct. of vacancies 0-2242  
 Hf-C-N-O-H, solid solns. of H, exam. of props. 0-29172  
 InAs-InP, phase equilib. and dissoc. 0-35170  
 InSb-CdTe solid solns., electroreflectance spectra, Brillouin zone transitions 0-7330  
 In<sub>2</sub>Se<sub>3</sub>-Cu<sub>2</sub>S system, electrophys. props., influence of 1-4% Cu<sub>2</sub>S 0-20219  
 KCl-CuCl solid solution supersaturated, precipitation, impurity aggregation 0-29174  
 KCl-KBr, solid soln., negative muon capture ratios 0-55007  
 KMg<sub>2</sub>(AlSi<sub>3</sub>O<sub>10</sub>)F<sub>2</sub>-KMg<sub>2</sub>Si<sub>4</sub>O<sub>10</sub>F<sub>2</sub>, solid soln., melting and crystn., quenching and DTA study 0-39263  
 (La, Y, Sc)B<sub>6</sub>, electron work function, thermal emission technique 0-20755  
 La<sub>1-x</sub>Eu<sub>x</sub>B<sub>6</sub> solid solutions, cryst. lattice defectiveness, mag. susceptibility and elec. conductivity 0-15083  
 Li<sub>2</sub>Ni<sub>1-x</sub>O (x=0 to 0.03), solid soln. effect of Li on densification during sintering 0-25638  
 Li<sub>2</sub>O-Al<sub>2</sub>O<sub>3</sub>-SiO<sub>2</sub>, anal. of composition by IR reflection spectra 0-40783  
 M<sub>1-x</sub>Sr<sub>x</sub>Si<sub>2</sub> (M=Ca, Eu, Ba), solid solution with type SrSi<sub>2</sub> struct., lattice parameters at high press. 0-54203  
 (MgAl<sub>2</sub>O<sub>4</sub>)<sub>x</sub>(AMn<sub>2</sub>O<sub>4</sub>)<sub>1-x</sub>, A=Mg,Mn,Zn,Cd, 0<x<1, mixed oxide spinels, chemical shifts of Mn K-absorpt. edge 0-29828  
 MgCu<sub>2-x</sub>Ni<sub>x</sub>, X-ray and neutron diffr. investigation of Laves phases of MgCu<sub>2</sub>-type (*German*) 0-15050  
 MgCu<sub>2-x</sub>Zn<sub>x</sub>, X-ray and neutron diffr. investigation of Laves phases of MgCu<sub>2</sub>-type (*German*) 0-15050  
 MgNi<sub>2-x</sub>Zn<sub>x</sub>, X-ray and neutron diffr. investigation of Laves phases of MgCu<sub>2</sub>-type (*German*) 0-15050  
 Mn-Y-Zn-Cd alloy phase equilibria, plastic deformation, microhardness (*Russian*) 0-40334  
 Mn<sub>2</sub>Mg<sub>1-x</sub>O, EPR, mag. interactions (*Russian*) 0-44908  
 (MnTe)<sub>1-x</sub>(Bi<sub>2</sub>Te<sub>3</sub>)<sub>x</sub> (x≤0.05) solid solution, electrophys. props. 0-24925  
 Mo-low alloys, C enrichment mechanism of intercrystallite zones (*Russian*) 0-20963  
 Mo-Nb solid solutions, enthalpy of soln. of H meas. 0-2166  
 NaCl-NaBr, solid soln., negative muon capture ratios 0-55007  
 Na<sub>2</sub>(MoO<sub>4</sub>)<sub>2</sub>-Nd<sub>2</sub>(SO<sub>4</sub>)<sub>3</sub> system, sulphatomolybdates and isomorphous substitution 0-19763  
 Na<sub>2</sub>O-SiO<sub>2</sub>-Ga<sub>2</sub>O<sub>3</sub>-Al<sub>2</sub>O<sub>3</sub> glasses in mixed AgNO<sub>3</sub>-NaNO<sub>3</sub> melts, ion exchange 0-21282  
 Nb-C-N-O-H, solid solns. of H, exam. of props. 0-29172  
 Nd<sub>2</sub>Eu<sub>1-x</sub>B<sub>6</sub> solid solution, mag. susceptibility, lattice parameters, Weiss temp. 0-29535  
 Nd<sub>2</sub>Zr<sub>2</sub>O<sub>7</sub>-Nd<sub>2</sub>Hf<sub>2</sub>O<sub>7</sub>, struct., elec. cond. and melting point 0-54197  
 Ni-bearing substitutional binary solutions, thermodynamics 0-44336  
 Ni-Cr, solid soln., lattice parameter meas. rel. to conc. and temp. depend. (*Czech*) 0-28949  
 Ni-Ti (1.6, 7.64 wt.%), monophasic high temp. scaling, metallography study 0-21159  
 α-Ni-Zn, solid soln. diffusion annealing effect (*Japanese*) 0-34255  
 Ni<sub>0.5-x</sub>Co<sub>x</sub>Ni<sub>0.5</sub>Fe<sub>2</sub>O<sub>4</sub> ferrosil spinel solid solutions, cryst. lattice defects and props. 0-19796  
 Ni<sub>1-3x</sub>Fe<sub>2+2x</sub><sup>3+</sup> Vac<sub>0.4</sub><sup>2-</sup> (Vac=cation vacancy), solid solns., cryst. lattice imperfections 0-39069  
 Ni<sub>2</sub>Mg<sub>1-x</sub>O, EPR in magnetocentrated solid solution (*Russian*) 0-39856  
 NiO:Cr, effect of Cr additives on structure parameters (*Bulgarian*) 0-44319

**solid solutions continued**

NiO-ZnO, solid solution, exam. of mechanism and kinetics of reaction with Fe<sub>2</sub>O<sub>3</sub> ferrite formation 0-3309  
 PCl<sub>3</sub>-HCl<sub>3</sub>, Raman spectra, solid and melt, species identification (*German*) 0-45083  
 Pb-In (40 wt.%), solid soln., single phase, superplastic behaviour 0-21048  
 2PbFe<sub>1/2</sub>Nb<sub>1/2</sub>O<sub>3</sub>-Pb<sub>2</sub>FeReO<sub>6</sub>, comp., struct., dielec. and mag. props. 0-2704  
 2PbFe<sub>1/2</sub>Ta<sub>1/2</sub>O<sub>3</sub>-Ba<sub>2</sub>FeReO<sub>6</sub>, comp., struct., dielec. and mag. props. 0-2704  
 2PbFe<sub>1/2</sub>Ta<sub>1/2</sub>O<sub>3</sub>-Pb<sub>2</sub>FeReO<sub>6</sub>, comp., struct., dielec. and mag. props. 0-2704  
 Pb<sub>3</sub>(Ge<sub>1-x</sub>Si<sub>x</sub>)<sub>2</sub>O<sub>11</sub> solid solutions, dielec. props., ferroelec. phase transitions 0-15988  
 Pb<sub>3</sub>(P<sub>1-x</sub>V<sub>x</sub>O<sub>4</sub>)<sub>2</sub>, x=0.1, 0.2, Raman scatt. by low freq. vibrs. 0-55111  
 Pb<sub>1-x</sub>Sn<sub>x</sub>Te: Mn, Mn mag. and elec. active states, mag. impurity behaviour 0-44627  
 Pb<sub>1-x</sub>Sn<sub>x</sub>Te:In epitaxial layers, growth, elec. props., and luminesc. 0-54542  
 PbTe-PbSe system, thermodynamic props. 0-11635  
 Pb(Zr, Ti)O<sub>3</sub> internal struct., prep. effect, ionic shadowing obs. (*Polish*) 0-11612  
 1-xPbZrO<sub>3</sub>-xPbScO<sub>3</sub>-Nb<sub>2</sub>O<sub>5</sub>, 0≤x≤1, phase transitions, X-ray, dielec., and thermal anal. 0-45020  
 Pr<sub>2</sub>(MoO<sub>4</sub>)<sub>3</sub>-Pr<sub>2</sub>(SO<sub>4</sub>)<sub>3</sub> system, sulphatomolybdates and isomorphous substitution 0-19763  
 RbNi<sub>2</sub>Mn<sub>1-x</sub>F<sub>3</sub>, powder, mag. props. 0-2560  
 Sb<sub>2</sub>Te<sub>3</sub>-Sb<sub>2</sub>Se<sub>3</sub>, ordered structure formation, heat treatment effect on thermal cond. 0-54448  
 Se-Te crystallised glasses, struct. transforms. and IR spectra 0-19712  
 Si, O impurity precipitation from solid soln., neutron irradi. effect 0-29177  
 Si-Au, solid soln., influence of precip. on relax. of <sup>29</sup>Si nucleus 0-11287  
 Si-Ge, solid soln., vol. effect on bulk modulus 0-24526  
 β-Si<sub>3</sub>N<sub>4</sub> solid soln. prod. by reaction sintering SiO<sub>2</sub>-AlN mixture 0-25645  
 Si<sub>3</sub>N<sub>4</sub>/Al<sub>2</sub>O<sub>3</sub>, powder compact, electron microprobe investigation of reactions (*French*) 0-26009  
 Si<sub>3</sub>N<sub>2</sub>O-Al<sub>2</sub>O<sub>3</sub>, solid soln., prep., effect of Si<sub>3</sub>N<sub>4</sub> powder reactivity 0-45256  
 Sm<sub>2</sub>La<sub>1-x</sub>B<sub>6</sub>, solid solns., exam. of structure, elec. props. 0-39290  
 Sn-Sb (10 wt.%), decomposition of supersaturated solid soln. 0-29960  
 Sn<sub>1-x</sub>Ge<sub>x</sub>Te, solid soln. series, Mossbauer study 0-39985  
 Sn<sub>2</sub>P<sub>2</sub>(Se<sub>2</sub>S<sub>1-x</sub>)<sub>6</sub>, ferroelec. props. (*Russian*) 0-25313  
 Sn<sub>1-x</sub>Pb<sub>x</sub>Te, film, production under quasi-equilibrium conditions 0-45241  
 Sn<sub>2</sub>(I<sub>1-x</sub>O<sub>2</sub>)<sub>2</sub>, solid soln., thermal reaction with V(V), Cr(III), Cr(VI), Mn(II), Fe(III), Co(II), Ni(II), Cu(II), Sb(III) 0-16674  
 Sr<sub>2</sub>Fe<sub>2</sub>Ru<sub>1-x</sub>O<sub>4</sub> solid soln., Mossbauer spectrosc. study 0-50235  
 Ta-Cr (15 wt.%), solid soln., discontinuous precipitation (*German*) 0-45314  
 TaH<sub>2</sub>, H diffusion and electronic struct., pulsed NMR obs. 0-54967  
 TeO<sub>2</sub>-NaCl-(NaBr), condition diagram, thermographic obs. (*Russian*) 0-55377  
 Ti alloy in Al alloy melt, reaction zone formation, component interaction (*Russian*) 0-54377  
 Ti fibres, high-temp. nitriding kinetics (*Russian*) 0-21166  
 Ti-C-N-O-H, solid solns. of H, exam. of props. 0-29172  
 α-Ti-Zr-W, effect of W impurity on mech. props. 0-16392  
 TiAl<sub>3</sub> crystals dissolution in pure Al liq., grain refinement of α-Al solid-solution by Ti addition 0-35178  
 TiC-ZrC, solid soln., conc. and temp. dependence of props. 0-39736  
 TiGa<sub>2</sub>Se<sub>2</sub>(1-x), solid soln., fundamental optical absorpt. edge 0-25408  
 U<sub>3</sub>O<sub>8</sub>-Y<sub>2</sub>O<sub>3</sub>(Sc<sub>2</sub>O<sub>3</sub>), solid soln. electrode, high temp. electrochem. appl. 0-6828  
 V-based ternary solutions, containing H, thermodynamics 0-19961  
 V-O system β phase BCT, X-ray diffr. study of additional scatt. effect (*Russian*) 0-10537  
 VO<sub>2</sub>-CrNbO<sub>4</sub>, solid solns., synthesis and phase diagram 0-35171  
 V<sub>2</sub>O<sub>5</sub>-MoO<sub>3</sub>, small polaron cond., elec. resist. and thermoelec. power meas. 0-34447  
 W-Cr solid solution, precipitation behaviour, reaction front motion, lattice parameters (*German*) 0-55401  
 W-ThO<sub>2</sub>-B, thermocathodes diffusion mobility, based on deboronation kinetics 0-39349  
 Y-H system, solid soln. phase, wide-line PMR 0-25226  
 YCrO<sub>3</sub>-MgCr<sub>2</sub>O<sub>4</sub> sintered ceramics, elec. cond. 0-24927  
 Y<sub>3-x</sub>Gd<sub>x</sub>Fe<sub>2-x</sub>Al<sub>2</sub>O<sub>12</sub>, solid solns., IR absorpt. spectra, physical props. 0-55082  
 Y<sub>3-x</sub>Gd<sub>x</sub>Fe<sub>2</sub>O<sub>12</sub>, solid solns., IR absorpt. spectra, physical props. 0-55082  
 YIG-rare earth garnet solid solutions, magnetisation temp. depend. calcs. 0-20388  
 YbCr<sub>1-x</sub>Al<sub>x</sub>O<sub>3</sub> solid solutions 0-20887  
 YbNi<sub>2</sub>-YbCu<sub>2</sub>ZZ (*French*) 0-45277  
 YbPd-YbAg-ZZ (*French*) 0-45277  
 YbPt-YbAg system, valency state, Yb behaviour (*French*) 0-45277  
 Zn<sub>3</sub>As<sub>2</sub>-ZnSe(ZnTe) solid solutions, single cryst., phase equilib. and props. 0-16283  
 ZnFe<sub>2</sub>O<sub>4</sub>-Fe<sub>3</sub>O<sub>4</sub> solid solns., form. of α-Fe<sub>2</sub>O<sub>3</sub> during oxidation 0-25889  
 Zn<sub>2</sub>Hg<sub>1-x</sub>Te, vacancy mech. of resorption of Hg droplets 0-39070  
 ZnS-CdS, equimolar solid soln. formation kinetics 0-39289  
 ZnS-CdS films, prep. by atomisation 0-16176  
 ZnS-MnS-CuInS<sub>2</sub>, subsolidus equilb., phase diagrams 0-3016  
 (ZnSe)<sub>1-x</sub>(GaAs)<sub>x</sub>, solid solns., photoluminescence spectra 0-40159  
 Zr fibres, high-temp. nitriding kinetics (*Russian*) 0-21166  
 Zr-C-N-O-H, solid solns. of H, exam. of props. 0-29172  
 ZrO<sub>2</sub>-HfO<sub>2</sub>, monoclinic solid soln., ceramic prep. and use 0-55338

**solid-state microwave circuits**

see also Gunn oscillators  
 solar power satellite, appl. of solid state microwave technology 0-40870  
 subMM wave mixing in metal-metal and metal semiconductor point contact diodes 0-4769

**solid-state microwave devices**

see also BARITT diodes  
 hyperabrupt varactors, fabrication from vapour phase epitaxial GaAs 0-29288  
 MM-wave and sub MM-wave receiver elements 0-11558  
 GaAs devices and their use for generation and freq. conversion of microwave oscillations 0-15534  
 GaAs FET, ion implantation, trends 0-39132



## solid-state microwave devices continued

- GaAs:Sn films, MBE power MESFETs 0-50563  
InP, transferred electron device, relationship between microwave efficiency and metallurgical state of cathode contact 0-6981

## solid-state phase transformations

see also ageing; decomposition; ferroelasticity; ferroelectric transitions; glass transition; high-pressure solid-state phase transformations; martensitic transformations; order-disorder transformations; polymorphic transformations; precipitation; segregation; spinodal decomposition

- A-15 space group struct., phase transitions, renormalisation group theory comparison with Landau theory 0-6489  
absorption edge anomalies, phenomenological anal. 0-2718  
actinide, compounds, f-electron systems with fluctuating valence, phase transitions 0-6789  
alkali fluoantimonates, dielectric props. and structural phase transitions (German) 0-25274  
alkali hexahaloeno compounds:  $\text{ReCl}_6^{2-}$  ( $\text{ReBr}_6^{2-}$ ), low symm. splittings in vibronic spectrum due to phase transitions 0-55161  
alkali metal fluo-perovskites, weakly discontinuous phase transition, linear birefringence obs. 0-11362  
di-alkylammonium copper tetrachloride, weakly discontinuous phase transition, linear birefringence obs. 0-11362  
alloys, precipitated phases, size, shape, distrib., diffusion controlled changes 0-3072  
aniline-HBr, ferroelasticity, orthorhombic to monoclinic phase transition, X-ray scatt. 0-39276  
anthracene-tetracyanobenzene crystals, deuteration effect on phase transition, triplet state EPR study 0-50163  
asymmetrical Ising model, phase transitions 0-17891  
atom probe techniques for phase transformation studies 0-3000  
austenite transformation in hot rolled strips 0-55407  
benzil, structural transition model, cryst. symm. spontaneous strain components 0-2161  
bis(p-toluene sulphonate)diacetylene, monomer and polymer, solid state phase transformation, far IR transmission spectra obs. 0-55077  
bromofom, solid, phase transform., dielec. dispersion and differential scanning calorimetric obs. 0-24582  
caesium propanoate, solid state transitions and melting process, diff. and conductometric meas. 0-10670  
carbazole, birefr. meas., 20 to 190°C, crystal-to-crystal phase transform. 0-45031  
carbon tetrachloride, solid, Raman study of phase transition and dynamic struct. 0-34916  
cellular phase separation rate, extremum condition 0-2137  
central peak phenomena and incommensurate structures, non-linear physics in crystals 0-10631  
ceramics, microstructural consequences of phase transformation 0-3034  
chloral hydrate, phase transform. rate,  $^{35}\text{Cl}$  NQR rate 0-54983  
2-chloro-1,3,2-dioxo-arsolane, temp. depend. of NQR spectra parameters of  $^{75}\text{As}$  and  $^{35}\text{Cl}$  0-20494  
coherent phase form. at stress concentrators, effect of dislocation splitting, dislocation pile-ups, and phase elastic moduli (Russian) 0-49356  
conference, phase transformations in metallurgy, York, England (Apr. 1979) 0-2994  
cooperative Jahn-Teller T-systems dynamics vibronic excitation branches 0-10934  
cyclobutane- $\text{d}_0(\text{d}_8)$ , cryst. modifications, low. freq. Raman and IR spectra 0-7342  
cyclohexane- $\text{d}_0(\text{d}_8)$ , plastic crystal phase transition, mol. reorientation, Raman scatt. phonon spectra 0-20631  
DL-cysteine, phase transition obs. at 10°C (French) 0-49355  
detection techniques, review 0-2996  
4,4'-dichlorobenzophenone, phase changes, Raman spectra (French) 0-2756  
Dicke model, modification for long wave photons 0-1169  
p-dihalobenzenes, apparent NQR spin-spin relax. times obs. 0-54991  
dimethyl tin difluoride, solid, methyl group motion, neutron scatt. study 0-10607  
dimethylammonium cadmium tetrachloride-type compounds, theory struct. phase transitions 0-10668  
dimethylammonium iron tetrachloride, Mossbauer study of struct. phase transition 0-39278  
dimethylammonium manganese tetrachloride- $\text{d}_6$ , structural and mag. phase transitions, neutron scatt. and AC susceptibility meas. 0-44825  
direct observation using TEM 0-2997  
Earth mantle, phase transitions and gravit. differentiation effects on convection 0-51371  
elastic phase transitions, crit. dynamics 0-2146  
electron microscopy, quantitative analytic studies 0-2998  
ethylammonium tetrachloromanganate, dielec. props. in phase transition region 0-55011  
FCC to BCC transition, under [100] tensile loading, theory 0-39279  
ferrocene, cryst., stable low-temp. phase 0-34185  
Fischer-Tropsch wax, NMR investigation 0-7186  
fission reactor materials, constitution changes due to radiation effects 0-34048  
furan, adsorbed on NaCl, evidence of new condensed phase, IR spectra (French) 0-16028  
gamma-ray diffractometry, phase transitions, domain structures, twinned texture studies 0-19678  
glasses, inorganic, thermal expansion coeff. rel. to phys. props. 0-49389  
graphite, self focusing high current relativistic electron beam for structural and chemical transformations (Russian) 0-15190  
graphite intercalation compounds, two-dimensionality, structural phase transitions 0-19938  
impurity centres and phase transitions (Russian) 0-10907  
incommensurably distorted structures, review 0-10665  
interstitial solutions, impurity subsystem free energy, impurity distrib., temp. depend. 0-44232  
Ising universality class, structural phase transform., real-space renormalisation calc. 0-39255  
IV-VI compounds, phase transitions induced by electron-phonon interaction 0-10656  
IV-VI mixed compounds, structural phase transition 0-15242  
Johnson-Mehl and cellular microstructure, comparative analysis, computer simulation 0-54392  
kaolinite-mullite thermal sequence, intermediate cubic phase 0-25652  
light scattering studies, in book 0-2774  
malonic acid, phase transition at 360K, IR study 0-44311

## solid-state phase transformations continued

- metal, Fermi surface topological transition, electron-phonon interaction contrib. calc. 0-6697  
metals and alloys, thermodynamic and mechanistic classification review 0-2995  
methane- $\text{d}_4$ , solid, thermodynamic props. calc. using significant structures method, 6 to 87K 0-24616  
microcline, maximum, room temp. phase transition, heat capacity meas. 0-54373  
microcline, maximum room temp. phase transition, unit cell parameters, thermal expansion 0-54208  
modulated ordered phases, superspace group description (Chinese) 0-8942  
naphthalene, single crystal, anomaly in permittivity, Costa Ribeiro effect 0-7258  
N-nitrodimethylamine- $\text{d}_0$ -( $\text{d}_6$ ), structural phase transition, Raman study 0-34911  
nonlinear elastic media, second order phase transitions (Russian) 0-24583  
NQR studies, elec. field effects 0-20488  
nuclear quadrupole splittings in phase transitions 0-20489  
octaphenylcyclotetrasiloxane, phase behaviour and nucleation kinetics 0-29168  
organic charge transfer crystals, transport props., phase transitions, mol. dynamic (German) 0-39507  
organic crystal, appl. of TEM 0-24327  
organic reactions in solid state 0-21309  
PAC method appl. (German) 0-2679  
n-paraffin, crystals, phase transitions, statistical theory 0-44290  
perovskites, instability and phase transition splitting at non-ferroelec. structural phase transitions 0-44314  
photoemission electron microscopy, use in phase transformation continuous obs. 0-2999  
pivalic acid,  $^{13}\text{C}$  NMR chem. shift, plastic-brittle transition 0-2652  
Pm3n space group struct., phase transitions, renormalisation group theory comparison with Landau theory 0-6489  
poly(vinylidene fluoride) films, poled, piezoelec. activity and field-induced cryst. struct. transitions 0-20592  
polyhedrization of quinary metallic systems with isomorphic intermediate phases (Russian) 0-45270  
polysulphur nitride-bromine, struct. and phase transition 0-24382  
1,3-propylenediammonium manganese tetrachloride, vibr. study of phase transitions, IR and Raman spectra 0-40103  
proteins, globular, crystalline, intermol. interactions, denaturation, DSC and X-ray diff. obs. 0-16897  
pyrazine, cryst. phases, entropy changes and struct. implications 0-54397  
PZT, polycrystn., thermal expansions, elasticity and internal friction 0-35238  
rare earth alloys,  $\text{RCO}_2$ , elec. resistivity, thermopower, X-ray struct. meas. 0-24874  
rare earth intermetallics, structural instabilities 0-24587  
rare earth perovskites, prep. and props. book contrib. 0-44193  
rare-earth  $\text{CaWO}_4$ , phase transitions of fergusonite-scheelite (French) 0-19942  
rubidium propanoate, solid state transitions and melting process, diff. and conductometric meas. 0-10670  
solid electrolyte dielectric permeability, phase transition to superionic state (Russian) 0-49403  
steel, 0.2 to 0.8% C, ferrite-pearlite transformation, tensile strength, cooling rate effect 0-7549  
steel, alloy, type ST.5, structural and phase changes after high temp. heating (Russian) 0-55439  
steel, alloy, V-W-Mo-Cr, exam. of carbide transformation 0-16299  
steel, austenite hot deformation influence on phase transformations 0-7606  
steel, austenitic-pearlitic transformation, partitioning, atom probe microanal. 0-3079  
steel, bainitic, invariant plane strain theory, determ. of habit planes and orientation relationships 0-55388  
steel, C, autectic, sintered, isothermal transformation behaviour, porosity effects 0-3031  
steel, C content influence on brittle and tough fracture, heat treatment (Russian) 0-40500  
steel, carbide form. depend. on Mn, Cr, V additions, cementite stabilisation, microstruct. (Russian) 0-55399  
steel, eutectoid, anisothermal strain with phase transform., effect on tensile strength (Russian) 0-40431  
steel,  $\text{Fe}_2\text{O}_3$ , transformation to  $\text{Fe}_3\text{O}_4$  in oxide scales conversion kinetics 0-7561  
steel, ferritic containing N, continuous transformations 0-7585  
steel, high alloy, strain induced martensite and austenite influence on crack formation (Russian) 0-21007  
steel, hypereutectoid, austenite dissociation depend. on strain at intercritical temps., pearlite transform. (Russian) 0-40362  
steel,  $\text{Kh}_2\text{G}_2\text{P}$ , high-temp. plastic strain influence on austenite transformation kinetics (Russian) 0-21004  
steel, low alloy, sintered, isothermal transformations, porosity effects 0-3032  
steel, low alloyed (Mo,Cr,B), structural and mech. props., report (French) 0-25691  
steel, low C (0.01-0.05 wt.%), structural and mech. props., report (French) 0-25691  
steel, medium C, Nb addition, effect on transformation and strength 0-7607  
steel, Ni(9 wt.%), isothermal bainitic transform., thermomechanical effects on mech. props. (German) 0-40383  
steel, pearlitic and bainitic transformations in austenite, processes during incubation period 0-40348  
steel, stainless, austenitic,  $\text{H}_2$  induced transformation obs. (Japanese) 0-11640  
steel, stainless, constitution changes due to radiation effects 0-34048  
steel, stainless, ferrite to austenite decomposition 0-3073  
steel, stainless 316, ion implantation produced crystalline phase transitions 0-7558  
structural phase transitions, applicability of thermodynamic theory 0-2139  
structurally incommensurate systems, transition and excitations 0-44293  
succinonitrile, defects in plastic phase, positron annihilation obs. 0-11504  
TCNQ alkali salt spin-Peierls transition 0-29395  
TCNQ salt, MEM(TCNQ) $_2$ , phase transition electronic struct. interpretation 0-24781  
TCNQ salt, MEM(TCNQ) $_2$ , phase transitions, elec. cond., ESR, mag. susceptibility study 0-24981



## solid-state phase transformations continued

- TCNQ salt, N-propyl-quinolinium(TCNQ)<sub>2</sub>, defect conc. depend. phase transition 0-44577
- tetramethylammonium hexabromotellurate, far IR and Raman spectra and phase transitions 0-11376
- thermodynamic relations, appl. to K<sub>2</sub>ReCl<sub>6</sub> 0-29164
- thiourea, lock-in phase transform. 0-29698
- tilted perovskites, influence of ionic radii on transition temp. 0-24590
- tool steel transformation hardening by CO<sub>2</sub> laser 0-16483
- transition metal, dichalcogenide layer cpds., bonding and phase transitions 0-34186
- 5d-transition metal antiferromagnetic crystal, struct. props. and lattice dynamics, mag. struct. 0-44268
- TTF(MBDT) spin-Peierls transition, mag. exchange interactions, mag. props. 0-25138
- TTF-halides, conductors with chain struct., lattice phonons and distortions, incommensurability transitions 0-24549
- TTF-TCNQ, divergent mag. responses at 2k<sub>F</sub> and structural phase transitions 0-20376
- two-electron level with quasidegenerate levels, local phase transitions and temp. effects in lattice dynamics 0-10666
- unijunction transistor, negative resistance as phase transition, critical exponents (*French*) 0-49746
- xylyleneaniline-p'-benzonitril 0-44328
- Ag-Ga(In)(Sn)(Te) thin film couples, room temp. interactions, struct. transformations 0-2220
- Ag<sub>3</sub>AsS<sub>3</sub>, proustite, structural changes in low temp. phase transition, NQR study 0-19935
- Ag<sub>3</sub>AsS<sub>6</sub>, thermal, crystallographic and elec. props. (*French*) 0-40338
- Ag<sub>3</sub>AsSe<sub>6</sub>, thermal, crystallographic and elec. props. (*French*) 0-40338
- AgClO<sub>3</sub>, structural phase transition, <sup>35</sup>Cl NQR meas. 0-15819
- AgFeTe<sub>2</sub>, Mossbauer parameters in phase-transition region 0-11308
- AgI solid electrolyte α-phase stabilisation 0-29209
- α-AgI, superionic conductor, soft-core model, Monte Carlo study 0-54430
- AgNbO<sub>3</sub>, cryst. growth and phase transitions 0-40243
- Al-Mg-Si, heterogeneous precipitation studies using differential scanning calorimetry 0-3062
- Al-Zn-Mg, plastic deform. influence on structural transform. and mechanical props. (*Russian*) 0-7623
- Al<sub>2</sub>O<sub>3</sub>-Na<sub>2</sub>O-Li<sub>2</sub>O, phase transformations during firing 0-3036
- Al<sub>2</sub>O<sub>3</sub>-SiO<sub>2</sub> system, solid state transform. of andalusite to mullite 0-16281
- Au-Cu (50% at.), pretransitional fluctuations (*French*) 0-2160
- BN, self focusing high current relativistic electron beam for structural and chemical transformations (*Russian*) 0-15190
- BaTiO<sub>3</sub>, piezoceramic, elastic normal wave propagation, phase transitions (*Russian*) 0-40067
- BaVSe<sub>3</sub>, one-dimensional, struct. and mag. props. 0-28993
- Be-bronze BrB<sub>2</sub>, struct. and phase transform. during mechano-thermal treatment (*Russian*) 0-11667
- BiVO<sub>4</sub>, struct. and ferroelastic phase transition 0-29004
- C foil, ion irradi., graphitisation rel. to lifetime, relevance to beam-foil spectroscopy 0-15166
- C foil, ion irradiation, correlation of energy loss and crystallographic transform. 0-23215
- C shock compression, diamond production 0-11613
- Ca<sub>2</sub>Nb<sub>2</sub>O<sub>7</sub>, crystal struct. rel. to isomorphous crystals (*Japanese*) 0-49208
- CaSnCl<sub>6</sub>, Cl NQR anomalous temp. depend., crystal struct. and phase transitions 0-54977
- Cd(NH<sub>3</sub>)<sub>6</sub>X<sub>2</sub>, X=Br, Cl, I, orientational phase transitions, Raman spectra 0-11382
- Co, deformed, microstruct. singularities in pre-transform. temp. range (*Russian*) 0-45347
- Co, phase transformations and vacancy form. by positron annihilation 0-2155
- Cr-Mo-V rotor steel, austenite to bainite transformation under cooling conditions, effect on creep 0-3033
- CrSe<sub>2</sub>, layered, phys. and elec. props. 0-44594
- Cs, isostructural transition and lattice vibrs., relativistic LMTO calc. 0-20074
- CsCaCl<sub>3</sub> crystal, cubic-tetragonal phase transition 0-10681
- CsCl, twin form. by compressive stress during phase transform. 0-49358
- CsCrI<sub>3</sub>, Mossbauer spectra, struct., electronic and mag. props. 0-15908
- CsCuCl<sub>3</sub>, piezoelectricity, Jahn-Teller type phase transform. 0-40065
- CsCuCl<sub>3</sub> submillimetre spectra phasons, low freq. modes, phase fluctuations (*Russian*) 0-50333
- CsFeF<sub>4</sub>, struct. phase transition at 250K 0-10663
- CsH<sub>2</sub>PO<sub>4</sub>, Raman scatt. and high temp. props. 0-16024
- Cs<sub>2</sub>HgBr<sub>4</sub>, phase transitions and singularities of cryst. struct., NQR study 0-19936
- CsNO<sub>3</sub>, phase transition, IR spectra 0-7350
- Cs<sub>2</sub>(TeBr<sub>6</sub>), far IR and Raman spectra and phase transitions 0-11376
- CsVF<sub>4</sub>, structural phase transitions above room temp. 0-29167
- Cu-Al-Ni (14.3, 4 wt.%), ω-phase form. during quenching and ageing (*Russian*) 0-25686
- CuI solid electrolyte α-phase stabilisation 0-29209
- Cu(NH<sub>3</sub>)<sub>5</sub>(ClO<sub>4</sub>), EPR parameters and dilatometry 0-39850
- Cu<sub>1-x</sub>S-Cu<sub>2</sub>S thin films, phase transforms kinematic electron diff. study 0-29295
- Cu<sub>2</sub>S, optical and calorimetric meas. of thin films for Cu<sub>2</sub>S-CdS solar cells 0-55863
- Cu<sub>2</sub>Zn<sub>1-x</sub>SiF<sub>6</sub>·6H<sub>2</sub>O, heat capacities and thermodynamic props., 14 to 300K, cooperative Jahn-Teller transition 0-21314
- Dy, hexagonal-orthorhombic transition temp., effects of press. and crystallinity 0-24585
- DyAsO<sub>4</sub>, cooperative Jahn-Teller transition, optical study 0-15240
- DyAsO<sub>4</sub>, first-order cooperative Jahn-Teller phase transition, dielec. suscept. studies 0-19940
- DyVO<sub>4</sub>, cooperative Jahn-Teller transition, optical study 0-15240
- Fe, phase transformations and vacancy form. by positron annihilation 0-2155
- Fe-Cr-C (10.0, 2 wt.%) isothermally transformed, carbide distrib., microstruct. development 0-3076
- Fe-Cr-Ni, cold-rolled foils, dilatometric study 0-21033
- Fe-Cu alloys, transform. substruct., lath microstructure after quenching 0-16298
- Fe-Mn (9 to 20 wt.%), <sup>57</sup>Fe Mossbauer spectroscopy in phase transformations 0-29948

## solid-state phase transformations continued

- Fe-Ni-Cr, Elinvar, struct. and mag. props., singularities during tempering (*Russian*) 0-50627
- Fe<sub>80</sub>B<sub>20</sub>, amorphous to cryst. transform. 0-34188
- FeCr<sub>2</sub>S<sub>4</sub>, Mossbauer spectra, second order phase transition 0-20539
- Fe<sup>2+</sup>Fe<sub>0.2</sub><sup>3+</sup>Cr<sub>1.8</sub><sup>3+</sup>O<sub>4</sub>, acoustic props. rel. to cooperative Jahn Teller effect and structural phase transform 0-24538
- Fe<sub>3-x</sub>Mg<sub>x</sub>O<sub>4</sub>, Verwey transition, Mossbauer study 0-39942
- (Fe<sub>100-x</sub>Ni<sub>x</sub>)<sub>100-y</sub>B<sub>y</sub>, metallic glass, embrittlement and crystn. transformation products 0-7685
- Fe<sub>2</sub>O<sub>3</sub> based γ defective spinels, elec. cond. behaviour during transform. to α rhombohedral phases (*French*) 0-49354
- Fe<sub>3</sub>O<sub>4</sub> magnetite, low temp. phase transition, diffuse electron scattering (*Japanese*) 0-24591
- Fe<sub>3</sub>O<sub>4</sub>, magnetite, phase transition, X-ray diff. meas. 0-15238
- Fe<sub>3</sub>O<sub>4</sub>, typical spontaneous symmetry breakdown in solid state 0-34737
- Fe<sub>3</sub>O<sub>4</sub>, Verwey transition, electron-phonon versus Coulomb interaction effects 0-39280
- Fe<sub>3</sub>O<sub>4</sub>:Cd<sup>2+</sup>(Zn<sup>2+</sup>), Verwey transition 0-6513
- δ-FeOOH, structure and phase transform., Mossbauer, X-ray, DTA study (*Chinese*) 0-54368
- GaMn<sub>3</sub>(C<sub>1-x</sub>N<sub>x</sub>), mag. struct., phase transition, rel. to valence instabilities in rare earth compounds (*French*) 0-34596
- GaSe, layer compounds, lattice instability, deformation dipole model 0-39249
- Gd<sub>2</sub>Ga<sub>2</sub>O<sub>12</sub>, garnet-perovskite transform 0-15239
- H bond lattice with diamond struct., 3D statistical model of phase transition (*Chinese*) 0-8924
- <sup>3</sup>He, solid, possible explanation for recently obs. phase transition in high mag. fields 0-20006
- <sup>4</sup>He, phase transition 0-15333
- HfV<sub>2</sub>, C-15 struct., phase transitions, elec. cond., crystal lattice parameters (*Russian*) 0-54826
- HfV<sub>2</sub>, latent heat of structural transform. 0-24589
- Hg<sub>3-2</sub>AsF<sub>6</sub>, one dimensional phonons and chain ordering 0-24544
- Hg<sub>3-2</sub>AsF<sub>6</sub>, theory of phase transitions 0-6486
- InSe, layer compounds, lattice instability, deformation dipole model 0-39249
- KCoF<sub>3</sub>, lattice parameter temp. depend., phase transitions and thermal expansion coeff. 0-1988
- KD<sub>3</sub>(SeO<sub>3</sub>)<sub>2</sub>, phase transition, neutron diff. 0-2158
- KDy(WO<sub>4</sub>)<sub>2</sub>, Jahn-Teller transition, permittivity behaviour 0-55012
- KDy(WO<sub>4</sub>)<sub>2</sub>, phase transition mechanism, absorpt. spectra, symmetry props. (*Russian*) 0-55130
- KMnF<sub>3</sub>, dynamic scaling and US attenuation at structural phase transition 0-44260
- KMnF<sub>3</sub>, lattice parameter temp. depend., phase transitions and thermal expansion coeff. 0-1988
- KMn<sub>0.9</sub>M<sub>0.1</sub>F<sub>3</sub>, (M=Co,Ni), lattice parameter temp. depend., phase transitions and thermal expansion coeff. 0-1988
- K<sub>2</sub>MoO<sub>4</sub>, hysteresis of phase transitions and modulated structures 0-29169
- KNbF<sub>6</sub>, NMR, quadrupole effects and struct. distortion 0-15809
- KNiF<sub>3</sub>, lattice parameter temp. depend., phase transitions and thermal expansion coeff. 0-1988
- K<sub>2</sub>PtCl<sub>6</sub>, K<sub>2</sub>ReCl<sub>6</sub>, K<sub>2</sub>SnCl<sub>6</sub>, solid state phase transitions, lattice vibr., NMR and NQR obs. 0-34814
- K<sub>2</sub>SO<sub>4</sub>, α-β phase transition, Raman scatt. study (*French*) 0-55096
- K<sub>2</sub>SeO<sub>4</sub>, non-zero wave vector incommensurate soft mode, light scatt. study 0-29754
- K<sub>2</sub>(TeBr<sub>6</sub>), far IR and Raman spectra and phase transitions 0-11376
- K<sub>2</sub>WO<sub>4</sub>, hysteresis of phase transitions and modulated structures 0-29169
- LaP<sub>2</sub>O<sub>7</sub>, ferroelastic transition, polarised Raman study 0-16035
- La<sub>1-x</sub>Sr<sub>x</sub>CoO<sub>3</sub>, specific heat meas., using laser-flash method, high-order and ferromagnetic transitions obs. (*Japanese*) 0-54898
- La<sub>2</sub>Ti<sub>2</sub>O<sub>7</sub>, crystal struct. rel. to isomorphous crystals (*Japanese*) 0-49208
- β-LiAlSiO<sub>4</sub>, eucryptite, one-dimensional ionic conductor, neutron scatt. study 0-49361
- LiKSO<sub>4</sub>, uniaxial crystal, pyroelectric, thermal expansion, phase transition 0-19966
- LiNbO<sub>3</sub>, piezoceramic, elastic normal wave propagation, phase transitions (*Russian*) 0-40067
- Li<sub>2</sub>O-SiO<sub>2</sub>, glass ceramics, phase transformation processes 0-3025
- Mg-Li-Al (31, 1 at.%), heat treated, precipitation 0-40364
- MgO-Al<sub>2</sub>O<sub>3</sub>-SiO<sub>2</sub>, glass ceramics, phase transformation processes 0-3025
- N<sub>2</sub>, α-β transition obs., thermometric fixed point applicability 0-13076
- NH<sub>4</sub>Cl, thermal cond. and heat capacity of solid phases under press. 0-2225
- NH<sub>4</sub>HgCl<sub>3</sub>, high resolution heat capacity meas. (*Japanese*) 0-52218
- αNH<sub>4</sub>HgCl<sub>3</sub> quassone dimensional type cryst., phase transition statistics, molecular field approx. calcs. 0-34190
- NH<sub>4</sub>IO<sub>4</sub>, high order phase transition, quadrupole coupling temp. depend. 0-54371
- NH<sub>4</sub>IO<sub>3</sub>·2HIO<sub>3</sub>, dielec. constant, elec. cond. phase transition and cryst. struct. 0-1999
- ((NH<sub>4</sub>)<sub>2</sub>K<sub>1-x</sub>SnCl<sub>6</sub>), mixed cryst., NQR relax. and reson. 0-54990
- NH<sub>4</sub>NbF<sub>6</sub>, successive phase transitions, dielec. and optical props. obs. 0-50275
- NH<sub>4</sub>NO<sub>3</sub>, phase transition, IR spectra 0-7350
- (NH<sub>4</sub>)<sub>2</sub>PtCl<sub>6</sub>, crystal symm., struct. phase transition, <sup>127</sup>I NQR freq. 0-34815
- NH<sub>4</sub>ReO<sub>4</sub>, high order phase transition, quadrupole coupling temp. depend. 0-54371
- NH<sub>4</sub>SbF<sub>6</sub>, dielectric props. and structural phase transitions (*German*) 0-25274
- (NH<sub>4</sub>)<sub>2</sub>(TeBr<sub>6</sub>), far IR and Raman spectra and phase transitions 0-11376
- Na<sub>2</sub>Mg<sub>2</sub>Si<sub>2</sub>O<sub>10</sub>, orthorhombic to cubic phase transformation at 198K 0-19765
- Na<sub>2</sub>W<sub>2</sub>O<sub>6</sub>F<sub>5</sub>, phase transitions obs. (*French*) 0-6516
- NbH<sub>3</sub>, HF phonons, neutron spectral obs. 0-49317
- Nd<sub>2</sub>Ti<sub>2</sub>O<sub>7</sub>, crystal struct. rel. to isomorphous crystals (*Japanese*) 0-49208
- Ni (111) surface, C interaction, monolayer form. and struct. stability 0-10756
- Ni alloys, constitution changes due to radiation effects 0-34048
- Ni based superalloys, sigma phase prediction techniques 0-7567
- Ni, ion implantation produced crystalline phase transitions 0-7558
- Ni, phase transformations and vacancy form. by positron annihilation 0-2155



## solid-state phase transformations continued

- Ni<sub>3</sub>B<sub>2</sub>O<sub>7</sub>, unit cell parameters and struct. transitions, 20 to 293K, X-ray diffr. study 0-24431  
 Ni(CN)<sub>2</sub>-dodecylamine, lamellar paraffinic system, phase transitions, wide-line NMR obs. (French) 0-44929  
 NiCr<sub>2</sub>O<sub>4</sub>, acoustic props. rel. to cooperative Jahn Teller effect and structural phase transform 0-24538  
 NiCr<sub>2</sub>O<sub>4</sub>:Fe, Mossbauer effect 0-15874  
 Ni<sup>2+</sup>Fe<sub>0.75</sub><sup>3+</sup>V<sub>1.25</sub><sup>3+</sup>O<sub>4</sub>, acoustic props. rel. to cooperative Jahn Teller effect and structural phase transform 0-24538  
 Ni<sub>4</sub>Mo, coherent phase form. at stress concentrators (Russian) 0-49356  
 Ni(NH<sub>3</sub>)<sub>2</sub>I<sub>2</sub>, EPR of Ni<sup>2+</sup> ion near structural phase transformation 0-11248  
 O<sub>2</sub> solid,  $\alpha$ - $\beta$  transition, mag. susceptibility (Russian) 0-6592  
 PLZT ceramics, diffuse phase transitions and thermodynamics 0-29694  
 PLZT ceramics, ferroelectric and struct. transitions, crystallographic, thermal, and dielec. anal. 0-29693  
 PLZT ceramics, phase transitions induced by elec. fields 0-29695  
 Pb<sub>3</sub>GaTaO<sub>6</sub>, transition from pyrochlore to imperfect fluorite struct. 0-19939  
 Pb<sub>1-x</sub>Ge<sub>x</sub>Te, n- and p-type, effective masses 0-44481  
 Pb<sub>3</sub>(PO<sub>4</sub>)<sub>2</sub>, ferroelastic, Raman scatt. by soft vibr. involved in ferroelastic phase transition 0-16040  
 Pb<sub>3</sub>(PO<sub>4</sub>)<sub>2</sub>, ferroelastic phase transition, inelastic neutron scatt. (French) 0-24584  
 Pb<sub>3</sub>(PO<sub>4</sub>)<sub>2</sub>, temp. depend. of lattice parameters and spontaneous strain 0-29170  
 Pb<sub>3</sub>(PO<sub>4</sub>)<sub>2</sub>:Gd<sup>3+</sup>(Eu<sup>2+</sup>), EPR spectra of  $\alpha$ - and  $\beta$ -phases 0-11261  
 PbTiO<sub>3</sub>, phase transition study by X-ray powder structural refinement 0-40075  
 PbTiO<sub>3</sub>, soft mode decay mechanism, damping parameter freq. depend. 0-54324  
 PdGdH, diagram of state elec. props., indirect exchange interaction, EPR study (Russian) 0-50179  
 PdH<sub>x</sub>, incoherent phase transition, lattice gas model 0-29171  
 RbCaF<sub>3</sub>, critical scatt. at struct. phase transition, Mossbauer diffr. 0-20546  
 RbCaF<sub>3</sub>, cubic to tetragonal phase transition, <sup>87</sup>NMR meas. 0-7187  
 RbCaF<sub>3</sub>, structural phase transition, superlattice points, neutron diffr. obs. 0-19944  
 RbCaF<sub>3</sub>:Gd<sup>3+</sup>, O<sub>h</sub><sup>1</sup>-D<sub>4h</sub><sup>18</sup> struct. transition, ESR obs. 0-50178  
 RbCdF<sub>3</sub>:Gd<sup>3+</sup>, O<sub>h</sub><sup>1</sup>-D<sub>4h</sub><sup>18</sup> struct. transition, ESR obs. 0-50178  
 RbDy(MoO<sub>4</sub>)<sub>2</sub>, Dy<sup>3+</sup> doublets, temp. anomaly in splitting separation due to structural phase transformation (Russian) 0-39274  
 RbMnCl<sub>3</sub>, crystal, structural phase transition 0-15243  
 RbNO<sub>3</sub>, phase transition, IR spectra 0-7350  
 Rb<sub>2</sub>(TeBr<sub>6</sub>), far IR and Raman spectra and phase transitions 0-11376  
 Rb<sub>2</sub>WO<sub>3</sub>, resistivity, Hall effect and Seebeck coeff. from 1.5 to 300K 0-6879  
 Rb<sub>2</sub>ZnCl<sub>4</sub>, single crystals, Raman scatt. spectra, temp. range covering two phase transitions 0-7340  
 Sb, liquid-quenched, stabilisation and transformation kinetics of metastable phases 0-3022  
 Sb<sub>2</sub>O<sub>3</sub>, hydrated, preseparation stage in dehydration, phase transformation 0-35524  
 SiC crystals, 2H to 6H solid-state transformation, X-ray diffraction study 0-28943  
 SiO<sub>2</sub>-Li<sub>2</sub>O-K<sub>2</sub>O-ZnO-P<sub>2</sub>O<sub>5</sub>, glass ceramic, phase changes and crystn. processes 0-7562  
 SmCo<sub>5</sub> films, struct. transformations effect on coercive force and mag. reversal (Russian) 0-20436  
 Sm<sub>2</sub>Ga<sub>2</sub>O<sub>12</sub>, garnet-perovskite transform 0-15239  
 $\alpha$ -Sn, compact prep., from  $\beta$ -Sn containing 0.1 at.% Ge 0-55320  
 SnCl<sub>2</sub>(H<sub>2</sub>O)<sub>x</sub>(D<sub>2</sub>O)<sub>2-x</sub>, high resolution heat capacity meas. (Japanese) 0-52218  
 Sr<sub>1-x</sub>Ba<sub>x</sub>ZrO<sub>3</sub>, struct., X-ray powder diffr. study for different phases 0-1989  
 Sr<sub>2</sub>Nb<sub>2</sub>O<sub>7</sub>, crystal struct. rel. to isomorphous crystals (Japanese) 0-49208  
 Sr<sub>2</sub>Nb<sub>2</sub>O<sub>7</sub>, normal-incommensurate phase transition, electron microscopy and diffraction study 0-39277  
 Sr<sub>2</sub>Ta<sub>2</sub>O<sub>7</sub>, crystal struct. rel. to isomorphous crystals (Japanese) 0-49208  
 Sr<sub>2</sub>Ta<sub>2</sub>O<sub>7</sub>, structural phase transition to superlattice, electron microscopy and diffraction study 0-39277  
 TbPO<sub>4</sub>, phase transitions at low temp. 0-15237  
 TbZn, ferromag. transition, transport coeffs. critical behaviour 0-15498  
 Ti alloys, metallurgical characterisation using thermolec. power meas. (French) 0-45462  
 Ti-Al-Zr alloy, TA6Zr5D, structural evolution during continuous cooling at different rates (French) 0-45300  
 TiCl<sub>3</sub>, phase transition, phonon dispersion curves 0-2130  
 TiCo-H system, thermodynamic rels. and struct. transformations 0-49385  
 Ti<sub>1-x</sub>Hf<sub>x</sub>Se<sub>2</sub> mixed cryst., elec. resist. and phase transition temp. 0-24928  
 TiNi-H system, thermodynamic rels. and struct. transformations 0-49385  
 Ti<sub>1-x</sub>V<sub>x</sub>Se<sub>2</sub> (0  $\leq$  x  $\leq$  0.1), elec. resist. and Hall effect 0-2386  
 Ti, photoemission studies 0-45217  
 TiCdF<sub>3</sub>, third and fourth order elastic consts., press. depend. near phase transition (French) 0-34116  
 TiCdF<sub>3</sub>, weakly discontinuous phase transition, linear birefringence obs. 0-11362  
 TiH<sub>2</sub>PO<sub>4</sub>, high resolution heat capacity meas. (Japanese) 0-52218  
 TiI, XPS and UPS study of phase transforms. 0-45210  
 TmCd(Zn), quadrupolar phase transitions, magnetoelastic and quadrupolar coupling consts. 0-15744  
 $\alpha$ -U, charge density wave, first order transition 0-10664  
 U, vacancy formation and phase transformation by positron annihilation 0-49215  
 UO<sub>2</sub>, mag. ordering lattice internal rearrangement transition, theory 0-20402  
 V<sub>1-x</sub>Fe<sub>x</sub>O<sub>2-x</sub>F<sub>x</sub>, 0 < x < 0.2, phase diagrams, <sup>57</sup>Fe-Mossbauer spectra, X-ray diffr. studies (German) 0-29663  
 V<sub>2</sub>O<sub>5</sub>, high-temp. phase transition, resistivity, valence photoelectron spectra 0-49357  
 V<sub>2</sub>Si, NMR meas. near struct. transform. (Russian) 0-44942  
 V<sub>2</sub>Si, NMR of <sup>51</sup>V above and below 21K struct. transition (Russian) 0-34796  
 V<sub>2</sub>Zr(Hf), struct. transform. at low temp., X-ray diffr. anal. (Russian) 0-45298  
 W (001), surface phase transition, electronic contribs., surface susceptibility, ab initio self-consistent thin-film energy band calc. 0-29255  
 W, field cathode with (001) orientation preparation technique 0-15241

## solid-state phase transformations continued

- WO<sub>3</sub>, triclinic, condensed modes 0-15211  
 Zr-Al (14 wt.%), transformation sequence from Zr-Al martensite to Zr<sub>3</sub>Al phase 0-3027  
 Zr-Nb (20 wt.%),  $\omega$ -phase form., diffuse Mossbauer scatt. 0-25324  
 ZrO<sub>2</sub> ceramics, microstruct. and props., monoclinic to tetragonal transition 0-3035  
 ZrV<sub>2</sub>, C-15 struct., phase transitions, elec. cond., crystal lattice parameters (Russian) 0-54826  
 ZrV<sub>2</sub>, latent heat of structural transform. 0-24589

## solid-state plasma

- see also helicons; plasmons  
 complex dielectric function long wave limit, Coulomb systems with bound states, elec. cond. 0-33738  
 conductor, MHD kink instability 0-6307  
 dichalcogenide layer compounds, interface plasmon-phonon interactions, transverse cond. 0-49641  
 electron plasma in presence of EM wave, DC mag. field, Coulomb screening, dielec. const. 0-15464  
 electron plasma with nonparabolic energy dispersion relation, EM fluctuations 0-2413  
 electron-hole plasma, striation form. during homogeneous heating 0-6889  
 electron-hole plasma, strongly degenerate, helical density waves 0-15550  
 electron-hole plasma current layering, electron cooling length, momentum scatt. 0-6890  
 free electron Compton scatt. of spectrally narrow radiation flux 0-20731  
 highly degenerate multicomponent plasma thermodynamic props. 0-33739  
 inelastic light scattering, single particle excitations in many valley semiconductors 0-29749  
 metals, collective modes of void-surface coupled systems, surface plasmons 0-49642  
 metals, proper EM radiation on inelastic electron tunnelling with photon emission, cond. (Russian) 0-54765  
 molecular crystal, stimulated Mandelstam-Brillouin scatt., dipole-plasma oscils. 0-1278  
 multicomponent electron-hole plasma correlation energy by RPA and mean component approx. calc. 0-24824  
 multilayer semiconductor structures, plasma-wave beams 0-49795  
 narrow-gap semiconductor, recomb. instability of electron-hole plasma 0-39621  
 one dimensional Fermi gas model in relation to spin and field theoretical models 0-24816  
 piezoelectric, magnetised heavily doped semicond., hybrid mode parametric excitation 0-29427  
 plasmon-acoustic wave interactions due to deformation potential (Russian) 0-15356  
 randomly inhomogeneous cond. medium in mag. field 0-19558  
 semiconductor, crit. points for electron-hole system 0-44511  
 semiconductor electron-hole-plasma, instability in heating elec. field 0-15552  
 semiconductor plasma, magnetised, stimulated Brillouin scatt. 0-33085  
 semiconductor plasma, solitons in radiophysics 0-48124  
 semiconductor plasma, unstable EM wave propagation, hot carriers, Hall effect, calc. 0-39620  
 semiconductor surface, resonance inelastic light scattering by carriers 0-20655  
 semiconductor-plasma with two-hole species, parametric instability 0-2410  
 semiconductors, surface magnetoplasma wave spectrum in HF mag. field 0-24995  
 shear waves, rotary activity under helicon-phonon interaction 0-2412  
 small overdense plasma particle Thomson-like RF scatt., linear perturbation theory 0-48858  
 superionic conductors, ionic plasma oscils. 0-29212  
 transversely magnetised semiconductor plasma, instability of EM waves 0-2411  
 weakly-ionised, three-component, ionis. equilib. instability 0-10877  
 Ag, microcrystals on C foil, size distrib. from electron micrograph obs., UV absorpt. spectra obs. 0-55121  
 Al caesiated thin film, surface plasma wave excitation by polarised light, photoemission obs. 0-50518  
 Bi, Alfvén wave dispersion, non-local, freq. and relax. time depend. effects 0-29429  
 Bi, Alfvén-like waves, new branch obs. at 300 GHz 0-49794  
 Bi, Bernstein waves, electrostatic wave dispersion relation in mag. field 0-34471  
 Bi, magnetoplasma effects at 300 GHz in Voigt configuration 0-39619  
 Bi, plasma echo for elliptic Fermi surface, echo coordinates (Russian) 0-44633  
 Bi-Sb, semimetallic, magnetoplasma effects at 300 GHz in Voigt configuration 0-39619  
 Bi<sub>2</sub>Se<sub>3</sub>:Hg point defects in crystal lattice, Hall coefficient and IR spectra determ. 0-55129  
 CdS, stimulated and spontaneous emission from degenerate electron-hole plasma at 300K 0-29762  
 CdS, time-resolved spectra of spontaneous luminesc. from high density electron-hole plasma 0-40156  
 CdSe, luminesc. of high density electron-hole plasma at elevated temps. 0-20696  
 CdSe, photocond. film, plasma reson., IR refl. obs. 0-11037  
 Fe<sub>2</sub>O<sub>3</sub>, haematite, anal. of refl. spectrum by Kramers-Kronig relations 0-16058  
 GaAs, electron-hole plasma, Coulomb effects on gain and absorption spectra 0-50371  
 GaAs, spontaneous luminesc. due to high density electron-hole plasma under nano- and picosecond pulse excitation 0-40157  
 GaAs, stimulated and spontaneous emission from degenerate electron-hole plasma at 300K 0-29762  
 GaAs:Be, ion-implanted, IR refl. and transmission meas. 0-34908  
 GaP, stabilisation of electron-hole liquid by camel's back 0-6740  
 GaSe, stimulated emission due to electron-hole plasma recomb. 0-50374  
 Ge, drift velocity of plasma cloud, at high elec. field 0-6887  
 Ge, electron-hole drop and exciton atmosphere 0-6748  
 Ge, electron-hole drop recombination radiation due to heat pulse action (Russian) 0-16087  
 Ge, electron-hole droplets, luminesc. and absorpt. lineshapes, RPA theory 0-49613  
 Ge, electron-hole drops, IR magnetoplasma absorptions 0-6728  
 n-Ge, HF plasma oscils. in external mag. field 0-54731



**solid-state plasma continued**

- Ge, stressed, metal-insulator transition, luminesc. 0-20695  
 n-InSb electron heating and energy relaxation time in quantising mag. field 0-10996  
 InSb, intrinsic, photoinjected electron hole pairs, Auger lifetime, photoconductive decay obs. 0-39629  
 n-InSb, SBS of laser radiation in presence of mag. field, ion acoustic wave nonlinearity 0-45091  
 La compounds, plasma light reflection by free charge carriers 0-11403  
 Nb<sub>2</sub>Ge, electron-lifetime effects on props. 0-10951  
 Nb<sub>2</sub>Sn, electron-lifetime effects on props. 0-10951  
 PbTe-SnTe compound semiconductors, lattice instability by mm-wave magnetoplasma refl. 0-54336  
 Pr compounds, plasma light reflection by free charge carriers 0-11403  
 Si, exciton-plasma transitions, dense electron-hole system portrait composition (*Russian*) 0-49622  
 n-Si, HF plasma oscils. in external mag. field 0-54731  
 Si, p-n junction, ellipsometric method of temp. meas. rel. to secondary breakdown (*Russian*) 0-11074  
 Si, pulsed laser annealing, nonthermal, plasma annealing 0-25498  
 Ti-V-Cr, electron-lifetime effects on props. 0-10951  
 TiS<sub>2</sub>, evidence for semicond. props., Hall coeff., refl., cond., thermoelec. power 0-20220  
 ZnO epitaxial film on Al<sub>2</sub>O<sub>3</sub> substrate, recombination radiation in intense single photon excitation 0-7410  
 ZnTe, resonance Raman scatt. at high excitation levels (*Russian*) 0-55109

**solid-state rectifiers**

- see also thyristors  
 No entries

**solid structure**

- see also crystal structure; long-range order; noncrystalline state structure; short-range order  
 No entries

**solid theory**

- computer modelling of matter, conf., Anaheim, USA (March 1978) 0-51954  
 SCF theory, orbital and pot. functions calc., eq. of state 0-44463

**solid-vapour transformations**

- see also sublimation  
 ions, mol. clustering, gaseous-condensed state, nucleation and solvation 0-28129  
 propane, vapour-liquid and vapour-solid equilb. data, mass spectroscopic tracer pulse chromatography 0-37115  
 tetrachloroisophthalonitrile, vapour pres. by effusion method, solid phase eqn. of state 0-49350  
 Ar, phase transition, anharmonic cryst.-gas transition 0-6510  
 CO<sub>2</sub>, vapour-liquid and vapour-solid equilb. data, mass spectroscopic tracer pulse chromatography 0-37115  
 Pb, evaporation under action of laser beam, recoil press. behaviour 0-25501

**solidification**

- see also segregation  
 amorphous solid, supercooled liquid-glass transition region, short-range order, simulation 0-44127  
 binary alloys, solidification calc. using compensation system (*Russian*) 0-16292  
 binary melt, analytic description with melt diffusion consideration 0-24390  
 binary melt, crystallising, thermoconcentrational convection in liq., core 0-6043  
 binary melt-crystal phase transformation kinetics, stat. modelling of cryst. growth mechanism 0-24389  
 bubble departure radii at solidification interfaces 0-44295  
 cellular phase separation rate, extremum condition 0-2137  
 chemically hardening material cast in elastic cylindrical mold, transient thermal stresses 0-7589  
 dendritic growth, diffusion in semi-solid region 0-15281  
 directional solidification, processor-operated segregation of minority atoms 0-29941  
 eutectic, anomalous, acicular, nonequilib. crystn. anal. (*Russian*) 0-25678  
 eutectic alloys, unidirectionally solidified, solidification and morphology relationship 0-25684  
 glass, solidification kinetic eqn., derivation from heat transfer and viscosity eqns. 0-25679  
 ingot forming from melt, liq. containment by EM field 0-35120  
 inorganic hydrate, heat transfer processes (*Japanese*) 0-6372  
 inward cylindrical solidification, uniformly valid soln. 0-48564  
 liquid solidification about cold cylindrical pipe 0-19383  
 liquid-glass transition, free volume approach, thermodynamic behaviour 0-1940  
 metal, welded joints, pore formation mechanism evaluation, rel. to solidification 0-3017  
 metallic one component systems, normal cryst. growth fluctuations theory 0-15025  
 metals and alloys, crystn. process, X-ray fluoroscopic obs. 0-50620  
 multi-dimensional solidification, dominated by thermal cond., similarity calc. method 0-38243  
 Nimonic, IN100,  $\gamma'$  precipitates, casting conditions effect on morphology 0-7548  
 paraffin plate heat storage element, fusion, periodic solidification, heat transfer kinetics (*French*) 0-40913  
 particle rejection by solidifying melts, appl. of net repulsive van der Waals forces 0-34274  
 peritectic structure formation criteria (*Ukrainian*) 0-11636  
 polymeric solidification of low level radioactive waste, Dow process 0-37502  
 radioactive waste portable vol. reduction and solidification system 0-37515  
 radioactive waste solidification system, Dow, state-of-the-art 0-5259  
 radwaste, current concerns, treatment system design changes 0-5258  
 real liquids, quenched to glassy state, struct., one dims. Ising model appl. 0-54134  
 spherical particle, growing from a binary alloy melt, morphological stability 0-29943  
 splat cooling process, using piston and anvil technique, mathematical model 0-11679  
 steel, austenitic stainless, ferritic, single phase ferritic solidification in welds, exam. 0-7546

**solidification continued**

- steel, boride coatings, form. mechanism and struct. during crystn. of castings 0-35412  
 steel, high-speed, solidification cycle, thermal anal. 0-29945  
 steel, molten, heat loss during solidification hydrodynamic eqns., hardening front kinetics (*Russian*) 0-55385  
 steel, rimming, continuous casting and solidification (*French*) 0-25685  
 steel, rimming, teeming and solidification (*French*) 0-16296  
 steel, V, carbide eutectic presence, solidification and struct. 0-50624  
 steel forgings, expt.-calc. model of quenching, temp. meas. across cross section 0-16345  
 steel ingot, state of viscoelasticoplastic stress deformation, in process of solidification (*Russian*) 0-45295  
 supercooled, struct. refinement mech. (*Russian*) 0-20975  
 surface tension driven convection, solidification effects 0-43703  
 thermal gravitational convection, impurity distrib. and transfer processes 0-19367  
 thermal storage, high temp., latent heat method using heat exchanger (*French*) 0-40912  
 Al ingot solidification by HV pulses, impurity distrib. and conc. region formation (*Russian*) 0-20919  
 Al powder, liq.-solid phase transforms. (*French*) 0-45294  
 Al-Al<sub>3</sub>Ni directionally solidified eutectic alloy, struct. and mech. props. (*Korean*) 0-29944  
 Al-based eutectic alloys, unidirectionally solidified, solidification and morphology relationship 0-25684  
 Al-Cd hypomonotectic alloy, rapid solidification and decomposition 0-50638  
 Al-Cu alloy, cast, chilled zone composition and thickness obs. (*Japanese*) 0-7541  
 Al-Cu eutectic alloy, cooling rate in rapid solidification, estimation from cell spacing 0-50623  
 Al-Cu hypoeutectic, solidification cycle, thermal anal. 0-29945  
 Al-Cu-Zr, superplastic alloy Supral, solidification and recrystallisation 0-7550  
 Al-CuAl<sub>2</sub>, directionally solidified eutectic, structural changes during strength tests (*Russian*) 0-7543  
 Al-Mg alloy, cast, chilled zone composition and thickness obs. (*Japanese*) 0-7541  
 Al-Mg alloy, crystallisation front form. props., casting in EM field (*Russian*) 0-55384  
 Al-Pd eutectic, microstruct. morphology 0-3018  
 Al-Si eutectic, pressure effect on metal-die heat transfer coeffs. during solidification 0-7544  
 Al-Si-P (19, 0.02 wt.%), primary Si crystals in Al melt, Ostwald ripening and solidification growth 0-35179  
 Al-Zn-Mg powder, selected-area electron diffr. ring patterns 0-50642  
 Al<sub>2</sub>O<sub>3</sub>, Mo-refined single crystals, fabrication 0-16250  
 Bi-MnBi, directionally solidified composite, processing parameter role on mag. props. 0-35352  
 CBr<sub>4</sub>, bubble departure radii at solidification interfaces 0-44295  
 CBr<sub>4</sub>, low gravity solidification, bubble behaviour 0-15219  
 Cu-Ni-Al, review 0-7564  
 Cu-Zn-Al, memory alloy wire and ribbon reversible martensitic transformation, ageing effect, review 0-7564  
 Fe, cast, fused metal solidification enhancement using Bi and Te (*Italian*) 0-7540  
 Fe, pure, splat-quenched, martensite morphology, SEM study 0-7547  
 Fe-C eutectic, solidification cycle, thermal anal. 0-29945  
 Fe-C hypoperitectic, solidification cycle, thermal anal. 0-29945  
 Fe-Mn-O melts, formation of oxide inclusions, cryst. pulling, Bridgman tests (*German*) 0-35074  
 Fe-Ni (30 wt.%), Ni segregation singularities during dendrito-cellular solidification (*Russian*) 0-7542  
 Li<sub>2</sub>O.2SiO<sub>2</sub>, directionally solidified, thermal and mech. props. (*Japanese*) 0-16295  
 100(Li<sub>2</sub>O.2SiO<sub>2</sub>).3B<sub>2</sub>O<sub>3</sub>(3Na<sub>2</sub>O)(3MgO)(3Al<sub>2</sub>O<sub>3</sub>)(3SiO<sub>2</sub>)(3P<sub>2</sub>O<sub>5</sub>), directionally solidified, thermal and mech. props. (*Japanese*) 0-16295  
 Mn-Bi alloy, melting and solidification under microgravity, mag. props. (*German*) 0-45296  
 NH<sub>4</sub>Cl transparent soln., basaltic equiaxed solidification, visualisation of convection (*French*) 0-44297  
 NaNbO<sub>3</sub>-BaTiO<sub>3</sub>, unidirectionally solidified transparent ceramics 0-25677  
 Na<sub>2</sub>O-B<sub>2</sub>O<sub>3</sub>-SiO<sub>2</sub>-MoO<sub>3</sub> glass containing high level radioactive waste, phase separation 0-25683  
 Na<sub>2</sub>O-SiO<sub>2</sub>-Ga<sub>2</sub>O<sub>3</sub>-Al<sub>2</sub>O<sub>3</sub> glasses in mixed AgNO<sub>3</sub>-NaNO<sub>3</sub> melts, ion exchange 0-21282  
 Na<sub>2</sub>S<sub>2</sub>O<sub>5</sub>.5H<sub>2</sub>O, heat transfer processes (*Japanese*) 0-6372  
 Nb<sub>2</sub>Sn superconducting wire, fabrication from Cu-Nb-Sn alloy using controlled high temp. gradient 0-25056  
 Ni base superalloy, directionally solidified, struct. and props. (*Chinese*) 0-20918  
 Ni, supercooled, struct. refinement mech. (*Russian*) 0-20975  
 Ni-Al-Ti-(W) (Cr) (Co) (Mo) (Ta) (Nb), heat resist., solidification range 0-35177  
 Ni-based eutectic alloys, unidirectionally solidified, solidification and morphology relationship 0-25684  
 Ni-Nb-Al (25, 2.5 wt.%), directionally solidified  $\gamma/\gamma'$ - $\delta$  eutectic, growth conditions on struct. 0-11639  
 Pb, grain refinement, and structural stability by S, Se and Te additions (*German*) 0-55387  
 Pb, variations of energy of the {111} torsion joint as a function of the angle of torsion in metallic seeds [dendritic structure] (*French*) 0-25682  
 Pb-Cu, hypoeutectic, grain refinement, and structural stability by S, Se and Te additions (*German*) 0-55387  
 Sb-crystals, in binary or ternary alloys, shapes on solidification (*German*) 0-3020  
 Si, dislocation growth during laser melting and solidification 0-2022  
 Si, laser annealing, nonequilib. incorporation of impurities during rapid solidification 0-55286  
 Sn droplets, on Bi, Zn and Al, heterogeneous nucleation 0-44294  
 Sn-Sb-Ag, splat cooled foils, TEM study 0-40344  
 TiAl<sub>3</sub> crystals dissolution in pure Al liq., grain refinement of  $\alpha$ -Al solid-solution by Ti addition 0-35178  
 V-Ni-Mo, structure in alloy crystallisation region, peritectic equilibria (*Russian*) 0-50622  
 Zn-Al, unidirectional eutectic, FCC phase, preferred orientation 0-29973



**solidification continued**

Zn-Sn-Hg, diagram of state, melting temp., peritectic and eutectic phases (Russian) 0-55350  
 ZrO<sub>2</sub>-Nd<sub>2</sub>O<sub>3</sub>(Sm<sub>2</sub>O<sub>3</sub>)(Dy<sub>2</sub>O<sub>3</sub>) eutectic, unidirectional solidification, microstruct. and crystallographic characterization 0-35176

**solids**

*Generalities only; for specific aspects see appropriate headings see also crystals; quantum solids; solid hydrogen; solid structure; solid theory*  
 No entries

**solitons see transducers****solitons**

(1+1) dimensional model field, fermion-boson correspondence, Klein transformation 0-42379  
 $\phi^4$  behaviour in presence of an impurity potential, collective coordinate method 0-31528  
 adiabatic perturbations of solitons and shock waves 0-46830  
 adsorbed layers, two dimensional incommensurate crystal theory, thermodynamics (Russian) 0-49524  
 Alfvén waves, circular polarisation, propagation in mag. field, spiky soliton 0-28662  
 Alfvén waves, circularly polarised, spiky soliton soln. to nonlinear evolution eqn. 0-38590  
 Alfvén waves, exact, nonlinear, existence of solitons 0-24159  
 amplification in modified Korteweg-de Vries eqn. 0-27145  
 anharmonic lattices, quasisoliton solns., influence of pair pot. shape 0-22297  
 asymptotic behaviour for propag. through two different mediums, K-dV eqn. 0-43924  
 baroclinic fluid, rapidly rotating, sine-Gordon eqn. model 0-46820  
 Belousov-Zhabotruskii reaction, existence of solitary travelling wave solns. 0-35525  
 Benjamin-Ono eqn., conservation laws 0-31524  
 Benjamin-Ono equation, Backlund transform. and conservation laws 0-4540  
 Benjamin-Ono equation, internal wave solitons, linear stability 0-53802  
 Benjamin-Ono equation, meromorphic solutions 0-31980  
 bilinear soliton equations, method of constructing generalised soliton solns. 0-4541  
 bilinearisation method of analysing soliton eqns. 0-46813  
 Boson theory, quantum soliton and classical soliton 0-12986  
 boson-soliton scatt., sine-Gordon model 0-9109  
 Boussinesq type eqn., reduction to modified Hirota eqn. 0-8804  
 chaotic states of anharmonic systems in periodic fields 0-22288  
 charged scalar solitons, electrodynamics 0-42078  
 cold nuclear matter, stationary finite amplitude motions, quantum shock waves and solitons 0-42573  
 collapse, new form of nonlinear excitations 0-4876  
 computer calculations 0-46832  
 condensed matter physics, theory 0-50122  
 conference, group theoretical methods in physics, Austin, Texas, USA (Sep. 1978) 0-4474  
 conference, nonlinear problems in theoretical physics, Jaca, Gain 1978 0-4478  
 coupled intensity deviations from stationary nonlinear state, space and time soln. 0-48882  
 coupled solitary waves in neurophysics 0-51067  
 deep water gravity waves, two-dimens. nonlinear wave eqn., exact envelope soliton solns. 0-43725  
 diatomic lattice system, soliton solns. in continuum limit 0-4668  
 dissipative Toda lattice, soliton propag. using nonlinear transmission line 0-27228  
 double quadratic chain, statistical mech., nonreflectionless solitary wave 0-22518  
 dynamic stability of solitons and general nonlinear wave phenomena (German) 0-4544  
 education, soliton solns. to nonlinear wave eqns. 0-17737  
 Einstein gravitational eqns. and nonlinear scalar field, time-depend. solns. with localised energy 0-46888  
 electron holes, theory, anal. soln. 0-48879  
 equations, Hirota and inverse spectral methods 0-71  
 evolution, perturbation effects 0-46824  
 fast Langmuir solitons existence in non-equilibrium plasma 0-38604  
 Fermi gas, one dimensional with backward scatt., gap renormalisation 0-24818  
 ferromagnet, uniaxial, magneto-dipole interaction influence on one dimensional magnetisation soliton (Russian) 0-54880  
 ferromagnetic chain, characts. of soliton-like mag. excitations 0-39762  
 ferromagnetic domain wall, soliton theory and dynamics 0-29569  
 ferromagnets, magnetic vortex as topological soliton in Landau-Lifshitz eqns. (Russian) 0-7097  
 finite amplitude solitary Alfvén waves 0-53973  
 fluids of finite depth, N-soliton soln. of higher order wave eqn. 0-48724  
 formation, mth order parametric interaction, using Klein-Gordon eqns. 0-12917  
 free energies calcs., WKB approx. failure 0-42073  
 gauge phase factor operators, extended Higgs models and 't Hooft algebra 0-42324  
 gaussons, logarithmic nonlinear Schrödinger eqn. solns. 0-46865  
 general relativity, coupled scalar-vector-tensor eqns., axially symmetric soliton solns. 0-31635  
 geometrical field theories 0-27390  
 glasses, nuclear quadrupole spin-lattice relax., soliton-nucl. quadrupole moment interaction, temp. depend. 0-50220  
 gravitating disc, rotating, nonlinear stability theory 0-17488  
 gravity waves, soliton fission in channel of varying width 0-46816  
 hadrons, extended, second-quantisation of strongly interacting fields, meson state regarded as non-topological soliton 0-13270  
 harmonically coupled particle chain in double-minimum potential well exact soln. for soliton propag. in discrete case 0-34166  
 higher order Benjamin-Ono equation, N-soliton and N-periodic wave solns. 0-12915  
 Hubbard chain, modified, solitary solns. derived step-by-step 0-10849  
 hydraulic surge phenomena (Norwegian) 0-27141  
 initial-value problem for zero-area pulses, anal. props. 0-23756  
 instability in one-dimensional nonlinear systems (Russian) 0-52039  
 insulator, modulation oscils. of travelling EM wave 0-24962  
 internal waves with finite fluid depth, inverse scatt. problem, Backlund transformation 0-31517  
 inverse scattering and solitons, geometric considerations 0-4550

**solitons continued**

3X3 inverse scattering transform, soliton perturb. scheme 0-27151  
 ion acoustic soliton propag. in two-electron temp. plasma 0-33767  
 ion acoustic solitons in plasma, props., related theories 0-48877  
 ion acoustic waves, soliton-like, slow and fast, obs. 0-28654  
 ion beam-plasma system with nonisothermal electrons, ion-acoustic solitary waves 0-33784  
 ion-acoustic solitons, temporal development, initial value problem; 0-33771  
 ion-sound soliton-resonant plasma particle interactions (Russian) 0-14880  
 Ising model with competing interactions, solitons and phasons 0-34653  
 Ising-Heisenberg linear ferromagnet, excitation spectrum and thermodynamic props. 0-50118  
 Kadomtsev-Petviashvili eqn., appl of variation of action method of one field solitons 0-331  
 KdV eqn., particular N-soliton soln. 0-31971  
 Korteweg de Vries eqn., soliton soln., Hugoniot conditions for gas dynamics 0-42069  
 Korteweg de Vries equation, Pade approximants, soliton solns. 0-42071  
 Korteweg de Vries modified eqn., solitary wave solns. 0-46818  
 Korteweg-de Vries eqn., quasi-solitary wave soln. 0-70  
 Korteweg-de Vries eqn., slowly varying solitary wave solns. 0-72  
 Korteweg-de Vries eqn., weak dissipation effect on two soliton soln. 0-27143  
 Korteweg-de Vries eqns., perturbed solns. and soliton production 0-42074  
 Korteweg-de Vries equation, modified, N-soliton soln., matrix trace method 0-36871  
 Korteweg-de Vries equation, soliton soln. using matrix trace 0-36870  
 Korteweg-de Vries equation, solns. for slowly decreasing boundary conditions 0-36872  
 Korteweg-de Vries equations, N-soliton soln., functional integral representation 0-4542  
 Langmuir oblique solitons, self-contraction in free path regime (Russian) 0-43921  
 Langmuir soliton EM wave scatt., theory (Russian) 0-38564  
 Langmuir soliton solns. with high nonlinearities, energy principle 0-24156  
 Langmuir solitons, non-neutral soln. 0-33763  
 Langmuir solitons, transverse instability 0-6250  
 Langmuir standing waves instability, one dimens., soliton and collapse, numerical expt. 0-38619  
 laser physics appls. 0-48333  
 lattice solitons, scatt. from mass impurity 0-46992  
 lattice thermal conductivity theory 0-46991  
 Liapunov stability of generalized Langmuir solitons 0-38631  
 light beam self-action in nonlinear media, soliton solns. 0-14404  
 lower hybrid cones, stability anal. 0-48880  
 lower hybrid waves, modulation instability growth rates 0-48881  
 magnetic, in one-dimensional mag. systems, obs. (Japanese) 0-2555  
 magnetic flux annihilation in a large Josephson junction 0-11139  
 magnetised plasma loaded waveguide, interaction between solitary structures 0-38661  
 massive Thirring model, multisoliton solns. in Pöhlmeier-Lund-Regge system 0-47195  
 massive Thirring model, two-dimens., inverse scatt. method 0-4840  
 MHD solitons in solar wind, nonlinear dispersion eqn. qualitative anal. 0-4217  
 modified Benjamin-Ono eqn., N-periodic wave and N-soliton solns. 0-28518  
 modified Korteweg-de Vries eqn., N-soliton solns. 0-36876  
 modified Korteweg-de Vries solitary wave in a slowly varying medium 0-36873  
 molecular systems, biophys. effects of solitons and excitons 0-51044  
 motion in nonuniform, sinusoidally varying media 0-42072  
 multidimensional stable relativistic solitons (Russian) 0-13224  
 narrow magnetic domain wall material, theory of intrinsic coercivity 0-2597  
 neutron scattering observation of solitons near critical point 0-34650  
 non-Abelian gauge group theory, relationship with solitons 0-4549  
 non-Abelian internal symmetry in 3+1 dimensional space-time, quantisation, collective coord. and Lorentz covariant methods 0-47199  
 non-linear one dimensional, solitons and kink Schrödinger eqns., general method for soln. 0-46871  
 nonlinear 1D system,  $\phi^4$  chain dynamical props. 0-4655  
 nonlinear complex scalar field with nontrivial asymptotic behaviour of soliton solns. 0-4867  
 nonlinear differential evolution eqns., 3+1 dimens. 0-46828  
 nonlinear elastic dispersive media, interaction of solitary waves (Russian) 0-42076  
 nonlinear evolution equations, inverse scattering method 0-12919  
 nonlinear hydrodynamical eqn. of Kaup, periodic and N-soliton solns. (French) 0-31521  
 nonlinear kinetic equation, structural stability, soliton collisions 0-10382  
 nonlinear normal mode theory 0-48875  
 nonlinear Schrödinger eqn., appl of variation of action method of one field solitons 0-331  
 nonlinear Schrödinger eqn., slowly varying solitary wave solns. 0-73  
 nonlinear Schrödinger eqn., soliton solns. 0-27173  
 nonlinear Schrödinger equation, adiabatic invariants, deep water and spiral density waves 0-48874  
 nonlinear transmission line, solitary waves 0-4543  
 nonlinear wave equations, soliton applications in physics 0-8813  
 non-topological, hadron appl. 0-47191  
 nuclear matter, elongated soliton type wave solutions, finite amplitude wave propagation (Russian) 0-13397  
 one dimensional systems with resonance interaction, collective particle like excitations, Schrödinger eqn. 0-46868  
 one-dimensional  $\phi^4$  and double quadratic systems, kinks, quantum statistical mechanics 0-47197  
 one-dimensional complex scalar fields with phase anisotropy, statistical mech. 0-22517  
 one-dimensional molecular chain, collective model for conformons 0-15456  
 one-dimensional molecular lattice, soliton motion, thermal vibrations (Russian) 0-54321  
 one-dimensional quiescent lattices, shock profiles, end condition effects 0-34138  
 one-dimensional sine-Gordon system, kinks 0-46969  
 one-dimensional systems, with reson. interaction, soliton-like solns. 0-46831



## solitons continued

- orthorhombic ferrimagnets, domain wall motion at near sonic velocity, magnetoelastic interactions 0-34683
- $P(\phi)$  models, soliton solns. 0-42333
- Peierls dielectric, one dimensional, selftrapped excitations in Peierls-Frohlich state (*Russian*) 0-54678
- periodic solutions to classical field equations 0-46822
- perturbations, variational calcs. 0-46825
- planar ferromagnetic chain, soliton dynamic struct. factors 0-7125
- planar Langmuir solitons, 3-dimens., stability 0-46827
- plasma, ion-acoustic solitary wave, third-order corrections, reductive perturbation method 0-43898
- plasma, ion-acoustic solitary waves (*Czech*) 0-1764
- plasma, laser-irradiated, Langmuir soliton generation at crit. density 0-6267
- plasma, photon soliton and fine structure due to nonlinear Compton scattering 0-10363
- plasmas, cylindrical ion-acoustic soliton propagation 0-28632
- polyacetylene, pristine and acceptor doped isomers, EPR, DC cond., evidence against solitons 0-15782
- polyethylene, crystal, dielectric  $\alpha$ -relax., soliton as crystal defect 0-45004
- Prasad-Sommerfield soliton, excited states, SU(3) generalisation 0-4877
- quantum mechanical mass in supersymmetric theories 0-22536
- quasi one dimensional charge transfer salts, soliton model for dielectric permeability 0-40036
- radiophysics theory 0-48124
- resonant interaction of long and short waves, envelope pulse solitons and breather state 0-1616
- review of soliton theory 0-47204
- ring of torsion coupled overdamped pendulums, nucleation theory of overdamped soliton motion 0-12899
- Rossby waves in two-layer system, theory 0-17293
- Schrodinger equation with variable coefficients, differential-difference analogue, single-soliton solution behaviour 0-8819
- semiclassical soliton solns. in quantised field theories 0-4874
- sigma model, nonlinear, soliton stability in  $S^2$  0-37165
- sine-Gordon breather soliton dynamics, rel. to special relativity 0-46801
- sine-Gordon eqns., 2- and 3-dimens., ring-shaped quasisoliton solns. 0-46829
- sine-Gordon equation, approx. rotationally symmetric solns. 0-8807
- sine-Gordon equation, in one and more dimensions, break-up of quasi-soliton solns. 0-8806
- sine-Gordon equation, two soliton solutions, breather solution 0-12945
- sine-Gordon model, supersymmetric solitons and monopoles 0-31991
- sine-Gordon model for large coupling consts., soliton scatt. matrix (*Russian*) 0-13221
- sine-Gordon perturbed equation, soliton mass formulae 0-22200
- sine-Gordon system, bion dissoc. 0-13201
- single soliton cosmological waves, Friedmann cosmological model background (*Russian*) 0-17708
- Skyrme gauge model, topological solitons 0-9086
- solitary structures in magnetised plasma loaded waveguide 0-48878
- solitary wave propagation in 3-dimensional lattice 0-8929
- solitary waves in Born-Infeld electrodynamics 0-4554
- soliton lattice melting, functional integral method 0-17883
- soliton-antisoliton pair interaction in double sine-Gordon eqn., numerical simulation 0-46821
- stability, gauge theories, nonlinear Schrodinger equation 0-4881
- stability of three-dimensional nonrelativistic solitons (*Russian*) 0-4583
- static form factor, quantum correction in 2-D field theory with classical lump, asymptotic behaviour 0-52395
- stationary multisolitons, existence 0-13218
- stratified fluid in channel, wake collapse in the thermocline and internal solitary waves 0-53787
- stratified fluid of finite depth, exact multi-soliton soln. for nonlinear waves 0-22199
- stratified fluid wave propag., modified finite depth fluid eqn., exact N-soliton soln. 0-28517
- structural phase transition, intrinsic and extrinsic central peak properties, review 0-34168
- structural stability in physics (conference, Tübingen, Germany, May and Dec. 1978) 0-8739
- superposition of solitons from same nonlinear differential eqns. 0-67
- teaching, classical nonlinear field eqns. exact solns., review 0-17756
- three-level molecular system, cooperative evolution, transient effects of dephasing and relax. 0-28184
- TMMC, classical Heisenberg antiferromagnet, one-dimens., dynamic props., review 0-15737
- TMMC, one-dimensional antiferromag., solitons, neutron inelastic-scatt. meas. 0-44810
- trapped particles and waves in plasma solitons, theory and appls. 0-48876
- two-dimensional interface, sine-Gordon chain model 0-29272
- two-dimensional lattice, solitons and nonlinear resonances (*Russian*) 0-52041
- type II superconductors, resistive domain existence, current generation (*Russian*) 0-44776
- U(1) solitons, many-dimens., interactions, resons. and bound states 0-46823
- upper hybrid solitons, in warm magnetised plasma, kinetic anal. 0-38595
- Van der Pol oscillators, diffusion-coupled active medium, nonlinear waves 0-4546
- velocity and linear dispersion relation, higher order corrections 0-46826
- waveguides with prescribed propag. consts., design 0-48419
- CsNiF<sub>3</sub>, easy-plane ferromagnet, one-dimens., dynamic props., review 0-15737
- CsNiF<sub>3</sub>, one-dimens. ferromag., collective excitations in mag. field 0-44822
- Cu complex, dichloro-bis-pyridine copper II, one-dimens. antiferromagnet, dynamic props., review 0-15737
- <sup>3</sup>He, superfluid A-phase, composite solitons in presence of superflow 0-2233
- <sup>3</sup>He, superfluid A-phase, composite soliton in narrow circ. cylinder, satellite freq., thermal fluctuations 0-34266
- <sup>3</sup>He, superfluid A-phase, soliton lattice for NMR behaviour 0-2234
- <sup>3</sup>He, superfluid B phase, soliton-like spin waves 0-44385
- <sup>3</sup>He, superfluid B-phase, n solitons in crossed mag. field and superflow 0-44386
- TTF-TCNQ, pure and irradi., nonlinear transport, ESR study, 1.2-4.2K 0-20167

## sols

- see also colloids; sedimentation
- amphoter latex coagulation, reversibility and specific ion effects 0-45567
- diepoxide-diamine network polymers, chem. props. and average mol. wt. 0-37915
- diepoxide-diamine network polymers, reaction mechanism investigation using gel permeation chromatography 0-40789
- primary and secondary coagulation and heterocoagulation, role of surface chemistry 0-45551
- structure determ. by neutron diffr. and small angle scatt. 0-40748
- AgI hydrosols, appl. of radiometric method for particulate processes characterisation 0-45579
- (Th,U)O<sub>2</sub> microspheres, fabrication 0-801

## solubility

- see also phase equilibrium; solid solubility; solutions
- alkanes, in liquid O<sub>2</sub>, estimation by Preston-Prausnitz method 0-39285
- alkenes, in liquid O<sub>2</sub>, estimation by Preston-Prausnitz method 0-39285
- aromatic hydrocarbons, in liquid O<sub>2</sub>, estimation by Preston-Prausnitz method 0-39285
- As-S-Se glasses, solubility, photostimulated changes 0-24602
- benzene-hexa-n-alkylanoates, disc-like molecules, miscibility studies of mesophases 0-19696
- butene-1, in liquid N<sub>2</sub> 0-39286
- crystal habit, modifications control in growth 0-49150
- dichloromethane, solidified, solubility in liq. N<sub>2</sub> at 77.4K 0-10673
- dielectric, dipolar point defects, studied by ITC 0-6405
- electrolytes in non-ion-exchange polymers (*Russian*) 0-54391
- ethylene, in liquid N<sub>2</sub> 0-39286
- Fe-Si melts, high Si, O solubility (*Russian*) 0-15252
- gases in rabbit brain and blood, solubility and partition coeffs. 0-46116
- glass fibre, surface struct. effect in solubility in water (*Japanese*) 0-34198
- halobenzenes, aqueous molar solubilities and partitioning, 25°C obs., rel. to melting pts. 0-40803
- inert gas solubility in liquid solvents, temp. depend. from scaled particle theory 0-24604
- inert gases, solubility in homogenates of canine lung tissue 0-46117
- inorganic gases, in liq. O<sub>2</sub>, estimation by Preston-Prausnitz method 0-39285
- liquid-liquid, critical phenomena in binary mixtures 0-54376
- lung, intrapulmonary haematocrit maldistrib., effect on O<sub>2</sub>, CO<sub>2</sub>, inert gas exchange 0-8033
- metallic glass, continuous-biased sputter-deposited Kr entrapment 0-24603
- metals, FCC, under H<sub>2</sub> press., crit. phenomena and isomorphic transitions 0-49367
- methanol, in liq. O<sub>2</sub>, estimation by Preston-Prausnitz method 0-39285
- $\alpha$  methyl styrene-acrylonitrile, molecular mass determ., solubility studies (*German*) 0-23590
- micelles, reversed, solubilisation and catalysis, review 0-45545
- multi-ion system, strong electrolytes, phase diagrams and solubilities calcs. 0-25665
- naphthene hydrocarbons, in liq. O<sub>2</sub>, estimation by Preston-Prausnitz method 0-39285
- organic pollutants in water, influence of detergent traces on hydrosolubility and maintenance in suspension (*French*) 0-7961
- pleochroic dyes, dissolved in nematic liq. crystals, guest-host interactions, appl. to electrooptic displays 0-44113
- polyether sulphone, evidence for crystallinity 0-28928
- polyethersulphone dissolution in chloroform 0-21353
- polymer soln., dilute, equilibrium theory (*German*) 0-33872
- polyvinyltrimethylsilane, diffusion, sorption, solubility, permeation of hydrocarbons, Xe (*Russian*) 0-6564
- polyvinyltrimethylsilane, sorption, diffusion, solubility of hydrocarbons, Xe rel. to temp. (*Russian*) 0-6565
- propylene, in liquid N<sub>2</sub> 0-39286
- PTFE, Ne, Ar, Xe and He diffusion and solubility 0-6561
- serpentine, solubility of inert gases, meteoritic abundance 0-12712
- Sitalls, soln. rate in alkali soln. 0-16531
- sodium lauryl sulphate micelles, chlorophyll-a, soln., dilution expts., solubilisation anal. 0-35587
- steel, austenitic stainless, type 316, irradiated with 46.5 MeV Ni<sup>6+</sup> ions, soluble C effect on void swelling and low dose dislocation structs. 0-49280
- steel, carbide form. depend. on Mn, Cr, V additions, cementite stabilisation, microstruct. (*Russian*) 0-55399
- steel, solubility of W and Mo in Ti(C,N)<sub>x</sub> 0-16276
- Zircaloy, H absorption, Sn(Fe)(Cr)(Ni) effect 0-49527
- AgCl, Br<sub>1-x</sub>, binary melt, Ag solubility, temp. and conc. depend. 0-10677
- Al alloys, liquid, kinematic viscosity temp. depend., porosity, H solubility, supercooling (*Russian*) 0-54425
- Al kinematic viscosity temp. depend. porosity, H solubility, supercooling (*Russian*) 0-54425
- Al, liquid, kinematic viscosity temp. depend., porosity, H solubility, supercooling (*Russian*) 0-54425
- Al<sub>2</sub>O<sub>3</sub>, permeability and solubility of H<sub>2</sub>, 1200-1450°C 0-39351
- Al<sub>2</sub>O<sub>3</sub>, single crystals, soln. in M<sub>2</sub>O-V<sub>2</sub>O<sub>5</sub> (M=Li, Na, K) and NaVO<sub>3</sub>-KVO<sub>3</sub> melts 0-20910
- Am-La, solubility, heat of mixing and vaporisation of Am, 1200 to 1600K 0-15232
- As-S(Se) glasses, solubility, photostimulated changes 0-24602
- AsSe<sub>3</sub>Bi<sub>2</sub>O<sub>3</sub> glasses, soln. rate in alkali solns. 0-16531
- B-C system, electron probe microanalysis and destructive chem. methods of study (*French*) 0-11982
- B<sub>2</sub>O<sub>3</sub>-BaO, liquid immiscibility region, equilibration and quenching expts. 0-45288
- C, pyrolytic, tritium diffusion coeffs. and deuterium solubilities 0-37443
- CO, solution in ocean surface waters, role of homogeneous buffer factor 0-21783
- CdF<sub>2</sub>-Eu, role of solution and precipitation phenomena on ITC spectra 0-7265
- Cu liquid/liquid CuS, miscibility gap (*German*) 0-49370
- Cu-Cd(2.7 wt.%), cellular precipitation kinetics and dissolution (*German*) 0-11651
- CuCl<sub>2</sub>Br<sub>1-x</sub>, binary melt, Cu solubility, temp. and conc. depend. 0-10677
- Dy<sub>2</sub>O<sub>3</sub>, soln. in K<sub>2</sub>O.2(3)MoO<sub>3</sub>, rel. supersaturation and supercooling 0-40245
- ErFe<sub>3</sub>(BO<sub>3</sub>)<sub>4</sub>, solubility in Bi<sub>2</sub>O<sub>3</sub>-B<sub>2</sub>O<sub>3</sub> melt and crystallisation 0-19736



**solubility continued**

- Fe alloys, component interaction parameters, enthalpy and mixing energy (*Russian*) 0-54382  
 Fe and alloys, liq., C solubility, donor-acceptor mechanism 0-49365  
 Fe-Cr-Ni melts, S solubility and solid soln. precipitation (*Russian*) 0-15251  
 Fe-Ga-C melts, thermodynamics and C solubility (*Russian*) 0-39292  
 Fe-Ni-Al, liq. alloys, N solubility and AlN precipitation 0-11648  
 Fe-Ni-Cr melts, O solubility (*Russian*) 0-15250  
 GaAs epitaxial layers, from mixed Ga solns., C solubility 0-15392  
 Ga<sub>1-x</sub>In<sub>x</sub>AsSb<sub>1-x</sub>, LPE on GaSb, miscibility gap in liq. phase and lattice mismatch 0-15404  
 GdFe(BO<sub>3</sub>)<sub>4</sub>, solubility in Bi<sub>2</sub>O<sub>3</sub>-B<sub>2</sub>O<sub>3</sub> melt and crystallisation 0-19736  
 Ge-S(As)-Se glasses, solubility, photostimulated changes 0-24602  
 GeO<sub>2</sub>-K<sub>2</sub>O, glass composition effect on solubility in H<sub>2</sub>O 0-39303  
 GeO<sub>2</sub>-Na<sub>2</sub>O, glass composition effect on solubility in H<sub>2</sub>O 0-39303  
 H diffusion, and solubility in solid metals 0-49422  
 InAs<sub>2</sub>Zn<sub>3</sub>(Se), solubility and donor-acceptor interaction 0-54263  
 KCl:Pb, lead aggregation effect on yield stress, incoherent precipitates, solubility determ. method 0-50645  
 La-Ni-(Ce)-(-Co), H absorption for storage appls. 0-45790  
 LaCo<sub>5</sub>, N<sub>2</sub> absorpt. at low temps. 0-24599  
 Li<sub>2</sub>C<sub>2</sub> solubility in Li, for fusion reactor appls. 0-13840  
 Li<sub>2</sub>S, solubility in LiCl-KCl and LiCl-LiF molten eutectic mixtures 0-54387  
 Mn-Cu, alloying behaviour and high damping capacity 0-35160  
 Na-K-H system, H influence on component interactions (*Russian*) 0-54383  
 Nb<sub>2</sub>C<sub>3</sub>O<sub>7</sub>, H solubility 0-34191  
 NbO and NbO<sub>2</sub>, H solubility 0-34191  
 NdFe<sub>2</sub>(BO<sub>3</sub>)<sub>4</sub>, solubility in Bi<sub>2</sub>O<sub>3</sub>-B<sub>2</sub>O<sub>3</sub> melt and crystallisation 0-19736  
 Ni-Al, liquid, diffusion coeff. differences, rotating-disc determ. 0-39330  
 Ni-Zn-Mn-Fe spinel, solubility curve in melt of BaO-B<sub>2</sub>O<sub>3</sub>-Bi<sub>2</sub>O<sub>3</sub> 0-2945  
 Ni<sub>3</sub>P<sub>2</sub>O<sub>7</sub>-K<sub>4</sub>P<sub>2</sub>O<sub>7</sub>-H<sub>2</sub>O solubility at 25 degrees C, double phosphates formation 0-54381  
 P-Se glasses, solubility, photostimulated changes 0-24602  
 PbS, solubility products in LiCl-KCl and LiCl-LiF molten eutectic mixtures 0-54387  
 Pd-Ag, Fermi energy influence on soln. behaviour of H, B and C (*German*) 0-44323  
 Pd-Ag(V), H mobility and solubility, appearance pot. spectra obs. 0-55231  
 Si, Czochralski growth, equilb. of dissolved C and O with CO in ambient atm. 0-1949  
 β'-Si-Al-O-N, Mg-containing phases, crystn. 0-39297  
 SiC, permeability and solubility of H<sub>2</sub>, 1200-1450°C 0-39351  
 Ta-O, steady state O<sub>2</sub> solubility (*German*) 0-44322  
 TaC, solubility of H, X-ray diffr. exam. 0-44318  
 Ta<sub>2</sub>C<sub>3</sub>, solubility of H, X-ray diffr. exam. 0-44318  
 Ta<sub>2</sub>C<sub>3</sub>O<sub>7</sub>, solubility of H, X-ray diffr. exam. 0-44318  
 Ti alloy in Al alloy melt, reaction zone formation, component interaction (*Russian*) 0-54377  
 Ti alloys, fusion reactor, first wall and blanket structure, impact of H<sub>2</sub>, phase stability and solubility 0-32435  
 α-Ti, solubility of H, neutron diffr. study 0-15254  
 TiCo-H system, thermodynamic rels. and struct. transformations 0-49385  
 TiNi-H system, thermodynamic rels. and struct. transformations 0-49385  
 TiO<sub>2</sub>, solubility in KF aq. solns. 0-34197  
 U, liq., O<sub>2</sub> solubility and comp. of lower phase boundary of UO<sub>2</sub> at 1950K 0-49366  
 U solubility in the Oklo reactor 0-21756  
<sup>133</sup>Xe solubility coefficients in water, saline, dog blood and organs 0-56331  
 YFe<sub>2</sub>(BO<sub>3</sub>)<sub>4</sub>, solubility in Bi<sub>2</sub>O<sub>3</sub>-B<sub>2</sub>O<sub>3</sub> melt and crystallisation 0-19736  
 β-Zr, diffusion and solubility of H, above 1000°C and below 1×10<sup>-4</sup> mm Hg (*Russian*) 0-24671

**solute clustering** *see segregation***solution annealing**

- steel, martensitic, age hardening with Cu, Nb additions, exam. of hardness 0-7681  
 steel, Nb, controlled-rolled into ferrite temp. range, soln. temp. and rolling effects 0-11678  
 steel, stainless, type 304, corrosion fatigue and stress corrosion cracking, in boiling NaOH 0-7719  
 steel, stainless, XM19, stress corrosion resistance 0-16558  
 superconducting composites, Kirkendall void elimination by solution anneals 0-7520  
 Al alloys 2024, thixoforging into net-shapes 0-16339  
 Au-Fe-Ni layer coating, Fe and Ni conc. meas. by X-ray diffr. (*German, English*) 0-34330  
 (In+InP) melt, critical undercooling determ. and P content change after annealing (*Slovak*) 0-55430  
 Ni base superalloy, directionally solidified, struct. and props. (*Chinese*) 0-20918

**solution energy** *see heat of solution***solutions**

- see also critical mixtures; Debye-Huckel theory; heat of solution; liquids; polymer solutions; solid solutions; solvation*  
 acetone in mixed protic-aprotic solns., C=O stretching, IR spectra 0-45056  
 alcohols, dil. aqueous solns., isentropic compressibility behaviour from sound vel. meas., dissolution mechanism 0-30269  
 alkali chlorides, aq. soln., ion-solvent and solvent-solvent interactions, X-ray obs. 0-44107  
 alkali iodides in acetone, press. effects on Walden products, ion-solvent interactions 0-3398  
 alkaline frozen solutions, polycryst. and glassy, photocond. and radiometric obs. 0-45531  
 aqueous, hydrophobic apolar spheres interaction, Monte Carlo simulation 0-6335  
 aqueous, hydrophobic hydration around apolar species pair, Monte Carlo simulation 0-6336  
 aqueous, ionic crystals, precipitation, induction period 0-50882  
 aqueous multicomponent multiphase equilibria, free energy minimisation method, comput. algorithm 0-40724  
 aqueous solutions, influence of cooperative effects on props. 0-28906  
 associated, characteristic sums method in stat. theory 0-10480  
 bead solutions, quasielastic light scatt. in small wave vector limit 0-45088  
 n-butane in liq. solvents, conformational structure 0-28115

**solutions continued**

- chain molecules in soln., thermodynamic props. related to chem. pot. 0-3394  
 conductive samples, superconducting NMR spectrometer, efficient decoupler coil design to reduce heating 0-31828  
 coronene trimer radical cation, spin densities in CH<sub>3</sub>Cl<sub>2</sub>-CH<sub>3</sub>NO<sub>2</sub> solvent mixture, -100°C 0-5565  
 cryogenic solutions, spectrosc. and photochem. 0-16713  
 dilute, spheroid-cylindrical mol., dynamics 0-44090  
 DNA conformation, influence of intermol. interactions 0-16900  
 DNA-type macromolecule, melting, low mol. wt. impurity effect 0-12050  
 EBBA, binary systems with non-nematic solutes, phase transition behaviour and <sup>1</sup>H NMR anal. 0-34174  
 electrolyte, aq. soln., field-induced ion evap. from liq. surface at atm. press. 0-29859  
 electrolyte, precipitation processes, study by particle site anal. 0-50883  
 electrolyte solutions, thermodynamics, transport props., semi-phenomenological approach including short range forces 0-3353  
 electrolytes, mixed, solns., electrical transport 0-3354  
 electrolytic, thermodynamics and correlation functions 0-24132  
 ESR, bibliography of 1975-76 literature 0-51979  
 formaldehyde, solid soln. in Xe, precipitation, IR spectra obs. 0-45059  
 hard sphere solvent, dense, solute test hard sphere kinetic energy relax. 0-33864  
 histones, H2a and H4, aggregation ionic strength effect (*Russian*) 0-55697  
 hydration, hydrophobic, of nonpolar mol. in dilute aq. soln., Monte Carlo simulation 0-3314  
 inert gases, liquid phase mixtures, dipole autocorrelation function, IR absorpt. spectra obs. 0-28903  
 ion-water interactions, survey of diffr. studies 0-24347  
 ionic liquids, struct. determ., summer school lecture series 0-6349  
 ionic solvation, spectroscopic data comparison for methanolic and aqueous solns. 0-26099  
 macromolecular, gel conc. and diffusivity at gelling determ. by ultrafiltration 0-21325  
 metal-ammonia soln., ionis. equilb. instability of weakly-ionised 3-component plasma 0-10877  
 3-methoxybenzanthrone in ethanol, photoprotolytic reactions, spectra, rate consts. and lasing thresholds 0-43327  
 micellar dye soln., energy transfer 0-45581  
 molecular dynamics simulation of chemical reactions in solution 0-40673  
 naphthalene in nonpolar solvent, vibr. and reorientational relax., correl. function 0-45065  
 nitrobenzene-hexane, soln., dielec. permitt. in two phase region 0-2682  
 NMR, <sup>89</sup>Y spin-spin relax. times, no pH depend. 0-2657  
 nonelectrolyte aqueous solutions, temp. of max. density rel. to partial compressibility, struct. strengthening 0-30270  
 pentofuranosyl nucleosides, isomeric, <sup>1</sup>H NMR coupling consts., SCF FPT INDO approx. calc. 0-14156  
 piperidine solution of Pbl<sub>2</sub>, crystn. of intercalation cryst. 0-16170  
 plasmid DNA and DNA-histone chromatin-like complexes, conform. and soln. props. by laser light scatt. 0-55987  
 polar solvent reorganisation energy in inner sphere complex charge redistribution 0-40730  
 polyelectrolyte solutions, counterion nucl. mag. relax., quadrupolar mechanism 0-2659  
 protein solutions, quasielastic light scatt. in small wave vector limit 0-45088  
 proteins, globular, crystalline, intermol. interactions, denaturation, DSC and X-ray diffr. obs. 0-16897  
 solute transport in porous media, statistical theory 0-28899  
 solute-solute-solvent interaction, dielec. behaviour problems, review 0-25298  
 solute-solute-solvent interactions, introduction to symposium in Vienna, Austria (1978) 0-26098  
 solvation effects and Gurney cosphere overlaps, conductimetric approach 0-21354  
 spectrochemical analysis of biological solns. using wall stabilised arc source 0-41343  
 symmetrical electrolytes, conductance and model for ions in soln. 0-29197  
 trifluoroacetic acid-water, molecular dynamics simulation of chemical reactions in solution 0-40673  
 volatile trace organics, aqueous environmental samples, head space anal. 0-40763  
 AlCl<sub>3</sub>, aq. solns., order phenomena, X-ray diffr. obs. 0-1915  
 Ar, aqueous soln., dil., energy and struct., pair pot. energy function, Monte Carlo calc. 0-54107  
 CaCl<sub>2</sub>, aqueous soln., ion hydration 0-35518  
 CuCl<sub>2</sub>, aqueous soln., nonlinear conversion of acoustic pulses with thermo-optic excitation 0-14510  
 Dy<sub>2</sub>O<sub>3</sub>, soln. in K<sub>2</sub>O.2(3)MoO<sub>3</sub>, rel. supersaturation and supercooling 0-40245  
 Fe(CO)<sub>5</sub>, solns. with dissolved NO, photolysis, Fe(NO)<sub>3</sub>CO form. 0-53024  
 HCl aqueous solutions, diffusion coeffs. at 298K, conductimetric obs. 0-24628  
 Hf complex, Hf-EDTA 0-34837  
 HFOCl<sub>2</sub>, aqueous solns., rotational diffusion, TDPAC study 0-34837  
 MgCl<sub>2</sub> solution, initiation of SCC and pits in austenitic Cr-Ni steel at 40-90°C 0-50748  
 MoO<sub>4</sub><sup>2-</sup>, n(Sn<sup>2+</sup>), (n=0-4), <sup>17</sup>O(<sup>33</sup>S)(<sup>95</sup>Mo)(<sup>97</sup>Mo) NMR investig. 0-53022  
 NH<sub>4</sub>Cl, aq. soln., dynamical props., mol. dynamics simulation 0-1918  
 NO<sub>3</sub><sup>-</sup>, aq. soln., vibr. width and dephasing, conc. depend. 0-43029  
 NaCl aqueous soln., mol. dynamics simulation, central force model 0-49077  
 Na<sub>3</sub>PO<sub>4</sub> solution, in tap water as corrosion inhibitor of Fe 0-45424  
 Na<sub>2</sub>SO<sub>4</sub> in aqueous soln., diffusion coeffs. and Onsager-Fuoss theory disagreement 0-40729  
 NiCl<sub>2</sub>, aq. soln., Ni<sup>2+</sup> coordination from extended X-ray absorption fine struct. 0-1913  
 Zn-Ti, environmental factors affecting pitting corrosion potential in NaOH solns. 0-45423

**solvated electrons**

- acridine, aqueous soln., laser induced two-photon ionisation investig. 0-32780  
 ethanol glass, trapped and solvated electrons produced in presence of applied electric field 0-7379



**solvated electrons continued**

interaction, Coulombic component intense long-wave field effects 0-43141  
methanol glass solvated electrons, EPR,  $^1\text{H}$  spin flip satellites, geometrical model 0-7146  
optical spectra and model potentials 0-30318  
polar fluids, electronic energy levels for photoinjection 0-30319  
Raman spectrum modification, polarisation CARS obs. 0-5549  
statistical model, distrib. function of hydrated electron energy 0-30271  
trapped electrons in glassy hydrocarbons, gamma ray irradi., relax., spectral obs. 0-23416  
 $\text{H}_2\text{O}(\text{D}_2\text{O})$ , solvated electrons, optical absorpt. spectra, temp., isotope effects 0-55124

**solvated protons see hydroxonium ion**

**solvation**

*see also hydroxonium ion; solvated electrons*  
acetic acid-pyridine, H-bonding, proton transfer, isolated system, solvent effect, MO calc. 0-55629  
biomacromolecules, nonpolar groups, correl. function anal. 0-30644  
colloids, solvation force between particles, Monte Carlo calc. 0-21328  
dense Lennard-Jones fluids, solvent struct. and solvation forces between rigid particles 0-30287  
p-dioxane, aq. soln., excess molar heat capacities, 298.15K, US vel. obs. 0-6523  
fluorescein dye laser, solvation effects on tunability 0-53285  
Gurney cusp overlaps and solvation effects, conductimetric approach 0-21354  
hard particle fluids, short range solvation forces 0-38885  
ion dynamics, kinetic dielectric decrement, microscopic theory 0-7801  
ion dynamics, mol. theory, fluid struct. and ionic mobility 0-7800  
ion-molecule equilibria in solvolysis, secondary  $\beta$   $^2\text{H}$  isotope effects, hyperconjugation 0-50874  
ionic solutions, in liq. HCl, coord. sphere radius, vibr. spectrosc. investig. 0-50843  
ionic solvation, spectroscopic data comparison for methanolic and aqueous solns. 0-26099  
ionic solvation energy, statistical calc., gas approx. 0-40731  
ions, mol. clustering, gaseous-condensed state, nucleation and solvation 0-28129  
kaolinite, hydration, lattice deform., vol. expansion due to adsorbed  $\text{H}_2\text{O}$  0-45555  
micelles, surfactant,  $\text{H}_2\text{O}$  penetration, hydration 0-45572  
poly-N-vinylcarbazole, soln., picosecond time-resolved fluoresc. by pulse radiolysis 0-28122  
pyrene-3-sodium sulphate solubilised in didodecylmethylammonium bromide-benzene inverted micelles 0-3417  
skin components, rheological props. under compressive load 0-35945  
solute-solute-solvent interactions, introduction to symposium in Vienna, Austria (1978) 0-26098  
tetrabutylammonium iodide, in aq. proline soln., elec. conductance investigation 0-10692  
tetramethylammonium iodide, in aq. proline soln., elec. conductance investigation 0-10692  
 $\text{Ag}$ , and  $\text{Ag}^+$ , solvation in deuterated-ice matrices, electron spin echo obs. 0-15780  
 $\text{Br}(\text{H}_2\text{O})_n$ , hydration energies, orientation, ab initio-LCAO SCF MO calcs. 0-27944  
 $\text{CaCl}_2$ , aqueous soln., ion hydration 0-35518  
 $\beta\text{-Ca}_2\text{SiO}_4\text{-CaO-SiO}_2$  paste, hydration, compression strength and composition 0-50584  
 $\text{Ca}_2\text{SiO}_3\text{-Cr}_2\text{O}_3(\text{Al}_2\text{O}_3)(\text{Fe}_2\text{O}_3)$  solid solns., elec. cond., 800-1000°C, hydration 0-54683  
 $\text{Co}(\text{NH}_3)_6$ ,  $\text{Br}^{2+}$ , aqution, polyelectrolyte catalysis, high pressure effect 0-55656  
 $\text{Co}(\text{NH}_3)_6$ ,  $\text{Br}^{2+} + \text{OH}^-$ , polyelectrolyte catalysis, high pressure effect 0-55657  
Ge dissolution by oxidation and solvation, hole injection effect 0-26051  
 $\text{H}_2\text{O.H}_2\text{O}$  and  $\text{H}_2\text{O.Ne}$ , excited, first order interaction energy, ab initio calc. 0-32598  
 $\text{Li}^+$ , hydrated, polarisation model, review 0-54115  
 $^7\text{LiCl}$ , heavy water soln., anionic hydration, 1 bar and 1 kbar, neutron diff. obs. 0-30212  
 $\text{NiCl}_2$ , heavy water soln., anionic hydration, 1 bar and 1 kbar, neutron diff. obs. 0-30212  
 $\text{Zn}^{2+}\text{-H}_2\text{O}$  clusters, solvation, Monte Carlo simulation 0-44102  
 $\text{Zn}^{2+}\text{-CO}_2\text{-H}_2\text{O}$  clusters, solvation, Monte Carlo simulation 0-44102

**solvent effects**

alkali iodides in acetone, press. effects on Walden products, ion-solvent interactions 0-3398  
anilines, substituted, in nonpolar solvent, dielec. relax. obs. 0-55022  
4-(9-anthryl)-N,N-dimethylaniline, fluoresc., dipole moments and polarisabilities 0-1019  
benzene in dilute cyclohexane solution, fluoresc. quenching on pulsed proton irradi., temp. depend. 0-21307  
biomolecule conformational anal., solvent effects 0-3583  
butene-1, solubility in liq.  $\text{N}_2$  0-39286  
chemical reactions, semiempirical model 0-25986  
cholesteric esters, effect of nature of organic solvent on gamma radiolysis 0-7835  
dicarbaicosododecaboranes, icosahedral, electron transfer phenomena in isolated borane units 0-18871  
dicarbonitrile-anthracene solutions, absorpt. and emission spectra 0-43083  
esterification kinetic study by monitoring pitch changes in cholesteric liq. cryst. solvent 0-7786  
ethylene, solubility in liq.  $\text{N}_2$  0-39286  
glassy polymer, solvent osmotic stresses, prediction of Case II transport kinetics 0-26049  
ketocyanines alcohol solns., spectral-luminesc. props. 0-2835  
lanthanide(III) complexes, f-f transition intensities, general theory of solvent effect 0-18811  
luminescent system, orientation factor in conc. effects due to nonradiative energy transfer 0-25425  
MBBA, nematic-isotropic transition, intermolecular forces, IR  $\text{N}_2\text{O}$  mol. probe obs. 0-29155  
2-methylPOPOP, soln., anisotropic fluoresc. of prolate mol. (German) 0-1018  
molecular electronic spectra, effect of polarisation structure of solvent 0-43062  
nonradiative transitions, solvent effects, dynamic coupling model, quantum mechanical theory 0-29787

**solvent effects continued**

nucleic bases, interactions and self-organisation, ionisation and solvent salt comp. effects 0-55985  
nucleotides, interactions and self-organisation, ionisation and solvent salt comp. effects 0-55985  
phthalimide acetyl derivatives in polar solvents, luminesc. kinetics and phosphoresc. quenching 0-18885  
phthalimide derivatives, hidden vibr. band determ. method, fluorescence and excitation spectra meas. 0-40158  
pigment associations, conc. effects, luminesc., absorpt. spectra and dichroism obs. 0-1007  
pivalophenone, organic soln., triplet reactivity solvent depend., flash photolysis study 0-11902  
PMR, tunable notch filter for solvent elimination 0-22405  
polyacrylamide, gels and single chains, phase transitions and crit. behaviour 0-40759  
polymer, dil. soln., light scattering charact. of thermodynamic props., solvent and mol. wt. effect 0-16717  
polynucleotides, interactions and self-organisation, ionisation and solvent salt comp. effects 0-55985  
polyurethanes, vapour press. of solvent above swollen crosslinked networks rel. to rubber elasticity theory 0-45536  
poly[(R)-oxypropylene], opt. rot. dispersion and vac. UV circular dichroism 0-40084  
POPOP, soln., anisotropic fluoresc. of prolate mol. (German) 0-1018  
propylene, solubility in liq.  $\text{N}_2$  0-39286  
rhodamine 6G, aqueous soln., absorpt. spectra, ground and triplet state photoprotonation pH depend. 0-42961  
rhodamine 6G, fluoresc. polarisation, solvent effects 0-32755  
rhodamine 6G, orientated relax. times, streak camera meas. 0-14168  
rhodamine B and 6G, fluoresc. decay time meas. in different solns. 0-9637  
rhodamine dyes in soln., bleaching, electronic and vibr. absorpt. spectra, fluoresc. 0-42960  
solute-solute-solvent interaction, dielec. behaviour problems, review 0-25298  
solute-solute-solvent interactions, introduction to symposium in Vienna, Austria (1978) 0-26098  
transition metal complexes, reaction mechanisms and solvent effects 0-26012  
triatomic mol. in solvent, rot. induced vibr. energy relax., Coriolis effect 0-47921  
xanthene dyes, hidden vibr. band determ. method, fluorescence and excitation spectra meas. 0-40158  
xanthene dyes, internal heavy atom effect on radiative and non-radiative rate consts. 0-32765  
BN, cubic, high pressure synthesis, solvent effects 0-40310  
 $\text{CO}_2$ , in various solvents, IR absorpt. spectrum, Fermi-reson. doublet and intermolecular interactions 0-18856  
 $\text{Dy}^{3+}$ , in soln., non-radiative transitions as Forster's energy transfer to solvent vibrations 0-1014  
 $\text{Eu}^{3+}$ , in soln., non-radiative transitions as Forster's energy transfer to solvent vibrations 0-1014  
 $\text{FeBr}_4^-$ , in various solvents,  $^4\text{A}_1$   $^4\text{E}$  d-d band reson. Raman spectra, solvent depend. 0-55085  
 $\text{FeCl}_4^-$  in organic solvents, dilute, ESR linewidths (German) 0-11258  
I radical recombination in dense liquids, stochastic trajectory simulation 0-45487  
 $\text{Mn}^{2+}$ , in soln., non-radiative transitions as Forster's energy transfer to solvent vibrations 0-1014  
 $\text{O}_2$  in chloroform and carbon tetrachloride solns., sensitized luminesc. 0-32762  
OCS in Ar soln., IR spectra, solvent shifts, vibr. band assignment and anharmonic force consts. 0-9607  
OCS in n-alkane, rot. relax., solvent hydrodynamic props., Raman and IR spectra 0-45055  
 $\text{Yb}^{3+}$ , in soln., non-radiative transitions as Forster's energy transfer to solvent vibrations 0-1014

**sonar**

*see also bioacoustics; navigation; underwater sound*  
32 kW Doppler sonar for ocean internal wave meas. 0-46296  
bat, simulation in anechoic chamber, coherent processor performance estimation appl. (French) 0-56072  
beamforming by CCD scan conversion for SAW chirp-Z transform 0-43552  
C-CD appls. in sonar systems 0-53535  
C-CD beamforming and signal processing systems 0-33325  
Doppler sonar, range-gated, obs. of strongly nonlinear internal motion in open sea 0-51422  
Doppler sonar controller 0-43575  
Doppler sonar ocean current profiles 0-46311  
fish target strength functions, model for averaging 0-43512  
HF transducers, lumped bandpass filter equiv. ccts., quarter-wave matching characts. 0-1397  
high-resolution, using parametric transducer 0-14539  
horizontal array shape measurement, active/passive acoustic techniques 0-23824  
incoherent and coherent processing against echo fading in shallow water 0-19142  
linear sonar array processor finite impulse response digital filter design 0-43549  
multichannel wide-range oceanographic sonar 0-46295  
ocean surface waves remote sensing, theory 0-12564  
parametric sonar performance calculator 0-33392  
passive coherence processing sonars, near-field performance 0-33346  
passive range estimation from array of sensors 0-53583  
ranging systems, pulse compression techniques 0-33350  
sea-floor mapping in real time, sonar-microprocessor equipment 0-26646  
sector scanning sonar, use in fish heart rate telemetry 0-8225  
side scan sonar data, adaptive sample set construction 0-43554  
side scan sonar system capability improvements 0-43574  
signal processing in ultrasonics, conf., London, England, Jan. 1980 0-33351  
sodar, appl. for acoustic detection in lower atmosphere (French) 0-8435  
sodar application in aviation 0-31132  
telemetering methods for deep sea nodules deposits (German) 0-26623  
time delay design using CCD 0-43570  
US pulse-echo systems, improved sensitivity using pseudo-random binary-code phase-modulated signals 0-38182



- sonar** continued  
wideband acoustic characterisation method for fish schools and long-range propag. channels 0-43551  
Ni-Fe polycrystalline film cross-tie memory for shipborne radar/sonar 0-42204
- sonic boom** *see shock waves*
- sonic propagation** *see acoustic wave propagation*
- sonoluminescence**  
EHD visible sonoluminescence, due to collapse of cavity in liquid 0-45158  
US cavitation, production of pressure and light impulses (French) 0-33297
- Soret effect** *see thermal diffusion in liquids*
- sorption**  
*see also adsorption; chemisorption; desorption; surface diffusion*  
absorbed layer, commensurate-incommensurate transition 0-49494  
biporous sorbent, internal diffusion 0-44414  
cleaning techniques review, for atomically clean surfaces preparation 0-11804  
fission reactor primary circuits, nonlinear surface absorption activity (Russian) 0-9340  
fluid in contact with wall, nonuniform Percus-Yevick and hypernetted chain eqns. 0-15370  
gas-surface energy accommodation, hard-cube model anal. 0-50888  
glass, viscoplastic, gas-vapour interlayer problem 0-49490  
intermetallic compounds, containing d-transition metal, hydrogenated, magnetism 0-34609  
Invar, magnetic structure, absorbed H<sub>2</sub> effect 0-20534  
jet, liquid, turbulent, gas absorpt. (Japanese) 0-38473  
mass transfer mechanism, formation of new crystalline phases 0-6625  
metal, with stored H, electronic struct., many electron theory 0-49667  
metal surface, sticking coeff. and transmission problem, quadratic phonon coupling effects 0-39424  
poly-n-hexyl L-glutamate, sorption and permeation mechanism 0-26048  
polyacrylonitrile glassy polymer, energetics of gas sorption 0-29270  
polycarbonate, glassy polymer, energetics of gas sorption 0-29270  
polyesters, linear, H<sub>2</sub>O absorption and electric loss factor (German) 0-34849  
polyethylene, in toluene, pressure crystallised, swelling behaviour, rel. to densities 0-2167  
polyethylene terephthalate, glassy, energetics of CO<sub>2</sub> sorption 0-29270  
polymer, glassy, gas sorption and transport, review 0-15360  
polysiloxane dizwitterionomers, of H<sub>2</sub>O, effect on dielec., mech. relax. 0-50261  
polysiloxane dizwitterionomers, of H<sub>2</sub>O, mechanism 0-49506  
polystyrene, of organic vapours, glassy-state relaxation induction and meas. 0-44415  
polyurethanes, rigid foamed, cellular struct. effect on water absorpt. 0-39416  
polyvinyltrimethylsilane, of hydrocarbons, Xe, permeation selectivity (Russian) 0-6564  
polyvinyltrimethylsilane, of Xe, hydrocarbons, sorpt., diffusion rel. to temp. (Russian) 0-6565  
porous medium with stagnation zones 0-6139  
PVC, of organic vapours, glassy-state relaxation induction and meas. 0-44415  
pyrazine absorbed on electrode, surface enhanced Raman spectra, symmetry and polarisability changes 0-50310  
radioactive waste storage, interaction of actinides and humic acid 0-13715  
radioactive waste, geological disposal, chemical factors controlling environmental actinide sorption 0-13713  
radioactive waste, shallow land disposal, radionuclide sorption 0-16851  
radioactive waste storage, Am sorption on major rock-forming minerals 0-13716  
radioactive waste storage, mineral-contributed anion effects on the retention of trivalent actinides in the environment 0-13717  
shale investigation as radioactive waste repository, vermiculite role 0-32354  
steel, stainless, dissolution kinetics of Ti (Russian) 0-34193  
Zircaloy, H absorption, Sn(Fe)(Cr)(Ni) effect 0-49527  
Ar<sup>+</sup>, in rarefied plasma stream, energy accommodation coeffs. meas. by thermoanemometric sounding 0-16722  
C allotropes, diamond, graphite, gas-solid interface, electronic struct. HFR calc. 0-54745  
CeMg<sub>1/2</sub>V(Cr)(Mn)(Fe)(Co), of H<sub>2</sub>, and appl. in H<sub>2</sub> storage 0-51009  
CeRu<sub>2</sub>, H absorption induced Ce valence change, mag. and supercond. props. 0-50042  
Dy, and DyMn<sub>2</sub>(Fe<sub>2</sub>)(Co<sub>2</sub>)(Ni<sub>2</sub>), H<sub>2</sub> absorpt., Mossbauer study 0-44987  
Fe-Ti alloys, of H<sub>2</sub>, appl. to industrial hydride reservoirs for H storage 0-45792  
Fe-V(Cr)(Mn)(Ni), unlimited component solubility, intercrystallite internal adsorption (Russian) 0-39294  
FeTiD<sub>3</sub> (0 ≤ x ≤ 1.9), structural phase transitions, absorpt. and desorpt. isotherms 0-19948  
Gd-Al-Co, H sorption props. for H storage, influence of Al 0-45794  
H<sub>2</sub> absorption and desorption kinetics in LaNi<sub>5</sub>-type ternary alloys 0-55932  
H<sub>2</sub> sorption/desorption by ternary LaNi<sub>5</sub> type alloys, reaction kinetics 0-45813  
I<sub>2</sub> adsorption on steel in HTGR He environment 0-44233  
La<sub>0.003</sub>Ba<sub>0.66</sub>Sr<sub>0.34</sub>TiO<sub>3</sub>, water absorpt., mech. strength, stability, TCR (Russian) 0-16511  
LaCo<sub>5</sub>, N<sub>2</sub> absorpt. at low temps. 0-24599  
LaNi<sub>5</sub>, of H, rel. partial absorption (desorption) enthalpies 0-50881  
LaNi<sub>5</sub>, of H<sub>2</sub>, for storage appls., effect of Ni, Ce, Co alloying additions 0-45790  
LaNi<sub>5</sub>H<sub>2-3.0</sub>, H diffusion coeff., neutron scatt. obs. 0-24643  
LaRu<sub>2</sub>, H absorption induced Ce valence change, mag. and supercond. props. 0-50042  
Mg-Mg<sub>12</sub>Y<sub>13</sub>, of H, high temp. hydrides for H storage 0-45793  
Mg-Mg<sub>2</sub>Ni, of H, high temp. hydrides for H storage 0-45793  
MgCu<sub>2</sub>, of H<sub>2</sub>, appl. to industrial hydride reservoirs for H storage 0-45792  
N<sub>2</sub><sup>+</sup>, in rarefied plasma stream, energy accommodation coeffs. meas. by thermoanemometric sounding 0-16722  
Nb, of H, rate, metallic film effect 0-49525  
Nb-Zr-C (0.1, 0.01 wt.%) plastic deform. influence on electronic state of Nb atoms 0-40463
- sorption** continued  
Ni-Mn, hydrogenation kinetics, magnetisation, interstitial H influence 0-35528  
Ni<sub>62</sub>Ti<sub>29</sub>Zr<sub>9</sub>, amorphous, H-sorption, X-ray and DSC obs. 0-49526  
Ni<sub>64</sub>Zr<sub>36</sub>, amorphous and cryst., H-sorption, X-ray and DSC obs. 0-49526  
Pt, electrosorption of H<sub>2</sub>, oxidation, effect of soluble prods. (German) 0-55717  
Si amorphous film, vacuum deposited, microscopic voids, gas absorpt., crystn. study 0-49534  
Ta, of H, rate, metallic film effect 0-49525  
Ta wire, H-absorption kinetics between 500 and 700K 0-49528  
Ti, of H<sub>2</sub> and N<sub>2</sub>, gas-discharge device appl. 0-10796  
Ti-Co(Ni) alloys, of H<sub>2</sub>, thermodynamic parameters calc. 0-2268  
Ti-Co(Ni) alloys, press.-composition-temp. relationships, enthalpy, entropy 0-2267  
YNi<sub>3</sub>, loss of ferromagnetism after H<sub>2</sub> absorpt., Pauli paramag. props. 0-34588  
Zr-Al-Cr H sorption props. for H storage, influence of Al 0-45794  
Zr-Al-V, H sorption props. for H storage, influence of Al 0-45794  
Zr-Al-(Fe,Co), H sorption props. for H storage, influence of Al 0-45794  
ZrS<sub>2</sub>Cs<sub>0.37</sub>, lamellar cpd., gas absorpt. 0-44418
- sorting programs** *see utility programs*
- SOS integrated circuits** *see field effect integrated circuits*
- sound** *see acoustic waves; acoustics*
- sound amplification** *see acoustic wave amplification*
- sound broadcasting** *see radio broadcasting*
- sound field** *see acoustic field*
- sound generators** *see acoustic generators*
- sound intensity** *see acoustic intensity*
- sound measurement** *see acoustic variables measurement*
- sound propagation** *see acoustic wave propagation*
- sound ranging** *see sonar*
- sound reproduction**  
*see also audio acoustics; audio recording; pick-ups*  
acoustic feedback's influence on speech intelligibility 0-23859  
automatic control in cinema (Russian) 0-38212  
cinofilm, Dolby stereo procedure for optical sound prints (German) 0-18030  
dual language, Super 8, airborne cinematography appl. 0-4785  
high fidelity sound, perception of sound and music 0-42014  
listener's perception thresholds, mono, stereo, pseudo-quadrophonic, quadrophonic systems study (Polish) 0-5906  
photographic sound track, cine film KINTEK 7 channel system 0-28403  
photographic sound track quality increase (Russian) 0-22464  
studio equipment for film, TV studios, circuit diagrams (German) 0-18031  
triphonic system using coincident microphones 0-28405
- sound waves** *see acoustic waves*
- space charge**  
*see also limited space charge accumulation; space-charge-limited conduction; space-charge limited devices*  
AC corona meas. using field-filter probes 0-47082  
acetone, rel. to transient pressure-drop fluctuations in electroviscous effect 0-15286  
avalanche growth in space charge stabilised nonuniform fields, formative time-lag calc., physical model 0-49038  
cathode spot of a vacuum arc, space-charge layer at electrode surface 0-24290  
chloroform HV polarisation and space charge obs. (Russian) 0-25277  
cholesterol, dielectric props. under UV excitation 0-6912  
cholic acid, dielectric props. under UV excitation 0-6912  
collective ion acceleration using space charge waves on electron beams 0-13995  
corona, multifluid behaviour between elec.-stressed spherical cathode and spherical anode 0-10443  
DC corona discharges in coaxial cylinder electrode, time variation of ionic mobility 0-33837  
dielectric, electron beams as virtual electrodes, review 0-6861  
dielectric electret effect, homo and heterocharge charge distribution 0-11317  
dielectric film, space charge quantity meas. by Maxwell stress method 0-22389  
dielectric liquid, charge generation and transport from contacting surface, Mach-Zehnder and Schlieren obs. 0-20589  
dielectric solid, resorption current calc., boundary conditions using method of joint characts. 0-40055  
dielectric solid, resorption current due to space charges 0-40053  
dielectric solid, resorption current for steplike charge distrib. 0-40054  
dielectric solid, space charge density distrib. and I-V characts. from current injection coeff. 0-39589  
dielectric solid, space charge distrib., indeterminability limits 0-40056  
dielectric solid, space charge problems by analogue modelling on field analyser 0-40058  
dielectric solid, space-charge behaviour, effect of relax. processes 0-40057  
dielectric solid, space-charge distrib., investigative method 0-40059  
dielectric solids, space charge phenomena, decay function and resorption current 0-40052  
dielectric space charge distrib., carrier mobility and interface injection mechanism identification 0-15974  
dielectrics, potential distrib. determ., non-destructive method (French) 0-40060  
dielectrics, space charge studies of elec. phenomena 0-24939  
discharge current induced by charged particle motion in space charge filled gap 0-24283  
electrets and dielectrics, conf., Sao Carlos, Brazil, Sept. (1975) 0-7251  
electron beam, relativistic, high-current, in microwave linear accelerator, transient behaviour 0-32541  
epoxy-resin, Nomex-filled, space charge polarisation, thermal depolarisation current study 0-7282  
gyrotrons, space charge phenomena 0-28868  
haemoglobin, dielectric props. under UV excitation 0-6912  
hollow beam in magnetically insulated beam, characts. 0-5398  
II-IV p-n amorphous heterojunction, phenomenological model 0-54769  
insulators, nondestructive acoustic elec. field probe 0-47076  
interfacial polarisation effect on dielectric props., sandwich capacitor model 0-15614  
ion beam transport, shape of beam envelope, beam space charge and emittance effects 0-32901



## space charge continued

liquid dielectric, intensity of elec. field and space charge 0-11339  
 magnetron sputtering, appl. to sputtered thin compound films, review (Japanese) 0-25561  
 many-valley semiconductors, space charge, contrib. of different charge carriers (French) 0-34458  
 metal-amorphous Si barrier, electronic props. 0-11089  
 metal-insulator-semiconductor structure, DC cond. and Shubnikov-de Haas effect 0-11012  
 methylene chloride HV polarisation and space charge obs. (Russian) 0-25277  
 molecular charge distrib., quantum topology, bonding theory and molecular structure 0-5463  
 molecular crystal, band structure, excitonic processes, trap distrib. 0-6720  
 naphthalene, single crystal, anomaly in permittivity due to thermoelectric space charge 0-7258  
 oxide film, thermal and anodic, space charge effects on steady-state transport 0-11124  
 p-n hot carrier functions, effect of space charge layer defects on characts. 0-25001  
 p-n junction boundary conditions 0-20295  
 p-n junctions, linearly graded, characterisation 0-6962  
 p-n junctions, variable gap, recombination currents in space charge layer 0-20303  
 piezoelectric semiconductors, surface phonon acoustoelectric interaction, elastic anisotropy effects 0-6610  
 plasma, magnetised, double-layer characts. meas. 0-43874  
 plasma double-layer, steady-state, fluid theory 0-43873  
 plasma sheath edge theory is weakly ionised collision dominated plasma 0-43935  
 PMMA, electret, dielectric meas. at ultralow freq. by reheating 0-4741  
 PMMA, nondestructive acoustic elec. field probe meas. 0-47076  
 poly(N-vinylcarbazole) layers, supermol. struct. effect on elec. props. 0-44606  
 polyethylene, electrical capacitance under high DC elec. field 0-54705  
 polyethylene, space charge injected from electrode at low temps., luminesc. obs. 0-25464  
 polyethylene cables carrying DC current, TSC and space charge effects (French) 0-40042  
 polyethylene film, high density, corona charged, thermally stimulated surface pot. 0-11327  
 polyethylene surface field strength under DC stress 0-15967  
 polyethylene terephthalate, TSC due to mobile ions and ionic conduction (Japanese) 0-54432  
 polyethylene terephthalate, TSC meas., space charge and injected surface charge effects 0-11320  
 polyethylene terephthalate electrets, formed by electron injection, TSC meas., space charge drift 0-11321  
 polyethylene terephthalate film, space charge quantity meas. by Maxwell stress method 0-22389  
 polyethylenenaphthalate, elec. cond., appl. of model 0-24940  
 polymer, in MIS struct., charge movement study using capacitance-voltage characts. (French) 0-39575  
 polymer electret, charge dissipation, transport mechanisms 0-7268  
 polymethyl methacrylate, direct obs. of zero field surface 0-16133  
 polymonochloro-p-xylylene,  $\gamma$ -ray-induced cond., hole injection effects 0-34452  
 polypropylene film, corona-charged, TSC and space charges 0-40041  
 polystyrene,  $\gamma$ -ray-induced cond., hole injection effects 0-34452  
 polystyrene films on metal substrates, electrode effect on carrier injection, TSC, I-V characts. 0-34463  
 pyrene, band structure, excitonic processes, trap distrib. 0-6720  
 quartz, surface space-charge layer form. on  $\gamma$ -irrad. 0-10575  
 p-terphenyl, polycryst. thin layer-metal sandwich, elec. cond. 0-34526  
 relativistic electron beams, slow space-charge wave propag. 0-1115  
 RF discharge, electrode sheath 0-44052  
 schlieren method for the determination of electric field distributions in dielectrics 0-31720  
 semi-insulating material, elec. stressed, storage of charge caused by cond. gradient 0-25306  
 semiconductor, charged impurity diffusion 0-6563  
 semiconductor, energy spectrum of discrete centre in high inhomogeneous electric field of space charge region 0-10873  
 semiconductor, inhomogeneous elec. fields in oscillatory photocond. 0-2421  
 semiconductor, photocond., influence of surface space-charge layer 0-15563  
 semiconductor coatings, space charge effects on triboelec. charge exchange 0-54763  
 semiconductor surface, resonance inelastic light scattering by carriers 0-20655  
 silastic tubular electret, mag. polarised, thermal currents 0-40037  
 solid dielectrics, conference, Karpacz, Poland (Sept. 1977) 0-36766  
 solid dielectrics, electric breakdown mechanism, discharge development, electron impact ionisation 0-15961  
 space charge limited current with diffusion theory, for exponential trap distribution 0-10992  
 spatio-temporal distrib. determ. in breakdown 0-38771  
 spherical particle, max. charge imparted by pulse-charging 0-6945  
 synchrotron, effects of induced voltage and forces of space charge on motion (Bulgarian) 0-47792  
 temporal space-charge field change meas. at high voltage electrodes in negative corona 0-38770  
 testosterone, dielectric props. under UV excitation 0-6912  
 transformer oil, nondestructive acoustic elec. field probe meas. 0-47076  
 waves propagation along moving magnetoplasma slab 0-38700  
 Ar discharge, optogalvanic and excited state photoionisation signals, space charge effects 0-14947  
 $As_{35}Te_{29}Ge_{16}S_{21}$ , chalcogenide semiconductor study of electric properties (French) 0-29414  
 $Cu_{2-x}S$ /CdS heterostructures, heat treated, capacitance voltage meas. anal. 0-20292  
 p-Ga<sub>1-x</sub>Al<sub>x</sub>As crystals, spectral characts. of photosensitivity, mechanism 0-44735  
 GaAs-Ga<sub>0.1</sub>Al<sub>0.3</sub>As n-n heterojunction, LPE, rectification 0-49888  
 Ge (111) surface, n-channel inversion layer, subband energies 0-11063  
 Ge, surface, high freq. cond. and cyclotron reson. 0-11273  
 He, liquid, electrical strength, breakdown voltage depend. on electrode configuration 0-7293

## space charge continued

InP, surface space charge layers and Schottky barrier form., Raman scatt. study 0-50319  
 InSb surface, IR spectroscopy of subband levels 0-20277  
 $K_2O-SiO_2$ , glass, influence of electric charge phenomena on AES (French) 0-50478  
 LiF, space charge distribution meas. in solid dielectrics 0-50271  
 $\alpha$ -LiIO<sub>3</sub>, single crystals, light diff. under DC field 0-11367  
 NaCl, surface charge meas. in ultra high vac. 0-20287  
 n-PbTe, accumulation layer, quantised surface states 0-20279  
 p-PbTe, MIS struct. inversion layer sub-bands, IR magnetoreflectance obs. 0-44731  
 Pb(Zr,Ti)O<sub>3</sub> ceramics, space charge field meas. by ferroelec. domain switching current, piezoelec. reson. freq. ageing characts. 0-7296  
 Se-binding agent electrophotographic film characteristics and sensitivity (German) 0-4789  
 Si, accumulation layer, intersubband-cyclotron combined resonance, theory 0-20278  
 Si, plastically deformed, spin-depend. charge transport 0-6895  
 a-Si:H Schottky barrier diodes, capacitance studies 0-49908  
 Si:Na<sup>+</sup>, inversion layer, far IR optical spectroscopy 0-20680  
 Si<sub>1-x</sub>H<sub>x</sub>, amorphous, gap states, DLTS 0-49656  
 Si<sub>3</sub>N<sub>4</sub>, low press CVD film, steady-state electron and hole space charge distrib. 0-29493  
 ZnTe, photoinduced dielec. loss and capacitance changes, rel. to space charge polarisation 0-2417

**space-charge-limited conduction**  
 see also limited space charge accumulation  
 2,4-hexadiene-1, 6-diol, bis(p-toluene sulphonate), dark-current meas. 0-15520  
 cellulose acetate, I<sub>2</sub> doping effect on elec. props. 0-49757  
 current charge distribution discharge, with shorted and open electrodes 0-6863  
 deep fast trapping dielectric, SCL current injection 0-6862  
 dielectric, electron beams as virtual electrodes, review 0-6861  
 dielectric, solid, energetic struct. of traps, from SCL currents 0-24941  
 dielectric diode, Joule instability under space-charge-limited current conditions 0-15618  
 dielectrics, current injection method appl. (Portuguese) 0-20179  
 dielectrics and dielectrics, conf., Sao Carlos, Brazil, Sept. (1975) 0-7251  
 electrode and volume controlled photocurrents 0-6908  
 electron beams, annular, space-charge limiting current, upper bound 0-43245  
 insulator, current carrier trapping, SCL current-voltage characts. 0-39588  
 naphthalene, space charge transport 0-20209  
 ohmic contact, exponential trap distribution limited current with diffusion theory 0-10992  
 [p-lquinaphenyl film between metal electrodes, memory switching 0-2484  
 photoconductivity-controlled imaging systems, limitations on sensitivity 0-6907  
 polyethylene, non-isothermal currents and space charge build-up 0-39590  
 polyvinylacetate film, in MIM struct., DC cond. phenomena 0-25020  
 semiconductors, high-resistivity, carrier transport (Japanese) 0-6850  
 Al-Sb<sub>2</sub>O<sub>3</sub>-In films, negative resistance characts. 0-11103  
 B film, elec. field effect on struct. 0-20050  
 Bi<sub>2</sub>O<sub>3</sub> film, thermally grown, I-V characts., current controlled neg. resist. 0-15637  
 CdSe evaporated films, elec. props. 0-2498  
 n-GaS, TSC, electron traps 0-11002  
 (Sb<sub>2</sub>S<sub>3</sub>)<sub>0.95</sub>(Na<sub>2</sub>S)<sub>0.05</sub>, condensate, local states and switching effect 0-20336  
 Si, high resistivity, specific resistance depend. determ. using impedance freq. depend. (Czech) 0-15536  
 Si MOS struct., space-charge generation props. of Au 0-2475  
 Si:As, p-n junction form. by laser annealing, space charge region, effects on reverse current 0-54772  
 Si:H, amorphous, plasma deposited, cond. adsorbate and insulating layer effects 0-49749  
 SiO<sub>2</sub> film electron beam induced conductivity theory and expts. 0-15640  
 SnCl<sub>2</sub>·2H<sub>2</sub>O, protonic cond. in layered single cryst. 0-19983  
 TiO<sub>2</sub>, rutile ceramics, space charge effects 0-24945  
 ZnIn<sub>2</sub>S<sub>4</sub> switching investigation, negative resistance state instability, resistivity transitions 0-6920

**space-charge limited devices**  
 see also limited space charge accumulation  
 electron beam propagation in dielectric guide due to space charge neutralisation 0-18716

**space-charge limited solid state diodes** see space-charge limited devices  
**space-charge limited solid state triodes** see space-charge limited devices

**space communication links**  
 see also satellite links; space vehicles; telemetering  
 CETI from Earth satellite orbit 0-4275  
 European Space Agency activities (German) 0-8516  
 interstellar communication, theory 0-4271  
 optical tracking system for space laser communication 0-33068  
 Voyager, telecommunications system and broadcast from Jupiter 0-26715  
 Voyager Project, spacecraft communication system 0-26718

**space groups**  
 see also crystal atomic structure  
 $\alpha$ -quartz, constitutive eqns. by group theoretic methods 0-1954  
 A-15 space group struct., phase transitions, renormalisation group theory comparison with Landau theory 0-6489  
 Clebsch-Gordan coeff., crystallographic space groups 0-1955  
 cubic space groups, classification by geometrical units 0-15028  
 dibromomaleic acid thioanhydride, mol. and cryst. structs., X-ray obs. (German) 0-44199  
 1,2-diiodobenzene, vibr. spectra, packing calcs. and crystal structure investigation 0-28938  
 diiodomaleic acid thioanhydride, mol. and cryst. structs., X-ray obs. (German) 0-44199  
 direct methods, survey as number and kind of solved acentric equal atom structs. 0-38865  
 double space groups O<sub>h</sub><sup>6</sup> (Fm3c) and O<sub>h</sub><sup>8</sup> (Fd3c), selection rules 0-10518  
 elastic dielectrics, group theoretic methods 0-1954  
 Flodmark-Blokker method for irreducible representations of crystallographic space groups 0-6376  
 incommensurate crystal phases, lattice dynamics, harmonic approx. 0-29147



**space groups continued**

- internal dimensions in crystal space group symmetry 0-38983  
 irreducible linear representation, image struct. 0-6377  
 isomorphic subgroups, of  $P1$  and  $p1$  (French) 0-49155  
 monocrotaline sulphite hydrochloride, struct., space groups from X-ray crystallography (Chinese) 0-49210  
 4-nitrophenyl 4-n-octyloxybenzoate, space group unit-cell and crystallographic props. 0-6399  
 order-disorder groupoid family, parameters, stacking 0-38982  
 $Pm3n$  space group struct., phase transitions, renormalisation group theory comparison with Landau theory 0-6489  
 second order phase transitions, superspace group description (Chinese) 0-8942  
 superspace groups, mathematical struct. and props. 0-17884  
 unitary representations, Takagi construction 0-28940  
 vector system interpretation by symmetrisation, Patterson function, Harker peaks 0-33914  
 $AgNbO_3$ , single crystals, flux growth, space group determ. 0-55282  
 $AgTaO_3$ , single crystals, flux growth, space group determ. 0-55282  
 $Cd_3P_2$ , band struct., rel. to symmetry props. of  $D_{4h}^{15}$  space group 0-34357  
 Ce-Co-Al (0-33.3 at.% Ce), isothermal section, X-ray study (Ukrainian) 0-39002  
 $Cu_3As_2S_4$ , space group, determ. by convergent-beam electron diffraction 0-49154  
 $Cu_2FeGeS_4$ , crystallographic and magnetic structure (French) 0-28998  
 GaS, space group, determ. by convergent-beam electron diffraction 0-49154  
 $Hg_{1-x}AsF_6$ , space group symmetry and phase ordering 0-6396  
 $KDy(WO_4)_2$ , phase transition mechanism, absorpt. spectra, symmetry props. (Russian) 0-55130  
 $K[B(SO_4Cl)_4]$ , space group 0-33913  
 $LiAlO_3$ , ordered single crystal, struct. determ. (French) 0-15074  
 $LiCsSO_4$ , space group from optical second harmonic generation, pyroelectric meas. 0-34860  
 $MgAl_2O_4$ , spinel, space group 0-28937  
 SiC polytype 6H, space group 0-1956

**space heating**

- air-based solar heating systems with phase-change energy storage, performance anal. using computer simulation 0-35762  
 building solar-climate control systems, control options evaluation by simulation 0-40844  
 buildings, passive solar heating, transwall thermal performance 0-40840  
 climatic solar heating performance, calc. of solar fraction for building heat 0-16786  
 energy utilisation improvements using new types of construction (German) 0-40903  
 experimental installation, using solar absorbers, heat pumps, heat exchangers and measurement and control gear (German) 0-35741  
 geothermal, system design and economic anal. 0-30379  
 heat pump water-to-water, school with gymnasium, heating appl. (German) 0-16831  
 heat pumps, domestic applications (French) 0-30518  
 heat recovery/heat pump combination for sports centre heating system, operating experience (German) 0-16830  
 heat-loss index incorporating solar, temperature wind and cloud cover effects 0-53605  
 heating systems, performance mathematical simulation for optimal dimensioning (German) 0-26110  
 indoor sports centre heating, heat pump appl. (German) 0-16829  
 metal hydride solar heat pump and power system, design and costs for space heating appls. 0-30521  
 passive solar heating systems, Trombe wall control strategies 0-45737  
 passive solar heating systems design, microeconomic anal. methodology 0-35744  
 passive solar space heating, sensitivity anal. of direct gain systems 0-35647  
 photovoltaic and thermal collector system design and testing 0-45675  
 solar, correspondence between solar load ratio method for passive wall systems and f-Chart performance estimates 0-16787  
 solar, heat-pump assisted systems, perform anal. 0-35649  
 solar, office complex design, with up to 70% energy savings 0-40831  
 solar air heaters, aerodynamic drag investigation 0-40899  
 solar air heating/cooling systems for buildings, review 0-45754  
 solar augmented and assisted systems 0-7918  
 solar collector-heat storage systems for heating and ventilation of buildings 0-45758  
 solar domestic space heating in Ireland, computer simulation model of thermal performance 0-45732  
 solar energy transition and materials problems 0-26115  
 solar heat pump house, Dunham-Bush development 0-40830  
 solar heating and cooling of buildings, Shenandoah Solar Recreational Center 0-45757  
 solar heating and cooling systems design, operation, feasibility, review 0-45755  
 solar heating system, heat accumulator utilisation, calc. procedure 0-40825  
 solar heating system economic evaluation and optimisation 0-35644  
 solar heating system optimal controllers 0-45739  
 solar heating system perform. estimation using sinusoidal inputs 0-35648  
 solar heating systems, economic anal. of passive and active residential designs 0-35746  
 solar heating systems, instrumentation principles for performance meas. 0-35743  
 solar heating systems for use in Britain, collector design aspects 0-35637  
 solar heating systems performance over range of storage capacities, prediction 0-45642  
 solar hot water systems, marginal cost of electricity used for backup 0-35747  
 solar investment decision criteria, appl. to space and water heating systems 0-35643  
 solar power, appl. of flat plate collectors and thermal stores (German) 0-26152  
 solar space heating systems, load optimisation algorithms 0-45643  
 solar water and space heating, economic feasibility 0-7920  
 solar-electric heat pump for houses, design and tests (German) 0-7951  
 sports centre all-electric, heating requirements, heat pump appl. (German) 0-16827  
 sports facilities and indoor swimming pools, two heat pump appls. (German) 0-16832

**space heating continued**

- storage of thermal energy, annual cycle, ice storage and three-coil heat pump 0-55917  
 technical meteorology, technical and commercial appls. (German) 0-46231

**space research**

- see also artificial satellites; astronomy and astrophysics; space vehicles  
 asteroid missions: goals for elemental abundance analysis 0-36474  
 asteroid multiple flyby mission in main belt, feasibility study 0-36473  
 biology and medicine in space 0-41265  
 blood volume regulation, effects of space flight, review 0-3826  
 comets mission, US space agency plans for 1980 research 0-46492  
 computerised planning in ESA 0-4223  
 cosmic ray nuclei,  $Z=30-40$ , fractional cell loss, Earth orbit expt. 0-3828  
 economics, forward-looking financial planning in ESA 0-4221  
 economics, investment planning in ESA 0-4222  
 equipment for spacelab, costs, safety 0-41267  
 European Space Agency activities (German) 0-8516  
 European space technology developments, Swiss role (German) 0-4234  
 Hipparcos astrometric satellite project and space telescope astrometric program, review (French) 0-46365  
 international astronomical Federation, 29th Congress (Dubrovnik, Yugoslavia, 1-8 October 1978) 0-46723  
 International Magnetosphere Research programme, review (Russian) 0-17467  
 Jovian system, Voyager 1 encounter 0-26716  
 Jupiter, magnetosphere, low-energy charged particle environment, Voyager 1 first look 0-26797  
 Jupiter, Voyager 1 photographic obs. of atmosphere ring and major satellites 0-26788  
 Jupiter, Voyager 1 planetary radio astronomy obs. 0-26796  
 Jupiter, Voyager telecommunications system 0-26715  
 Jupiter atmosphere and ionosphere, Voyager 1 preliminary radio profiles 0-26791  
 Jupiter magnetic field studies by Voyager 1, preliminary results 0-26793  
 Jupiter magnetosphere, Voyager 1 obs. of energetic ions and electrons 0-26798  
 Jupiter magnetosphere plasma observations, Voyager 1 initial results 0-26794  
 near-Jupiter plasma, Voyager 1 plasma wave obs. 0-26795  
 Mare Crisium, view from Luna 24, conference, Houston, Texas (1977, December 1 to 3) 0-17710  
 miniaturised turbo-molecular pump, for space appl. (French) 0-42234  
 multiple-launch space research program, choice of vehicles 0-8512  
 planets gravitational spectra, determ. from planetary orbiters tracking 0-41744  
 Pluto encounter in mission beyond planets 0-17466  
 radiobiological studies in space and at ground-based accelerators 0-41266  
 recording satellites and instrumentation, 1976-8 launchings (German) 0-36471  
 satellite Fourier spectroscopy, mechanical disturbance effects on optical elements (German) 0-36478  
 satellite Fourier spectroscopy methods and problems (German) 0-36477  
 solar thermal aerostat research station (STARS) 0-17471  
 Space Shuttle project, space-oriented experimental programme 0-17465  
 Spacelab and services to users 0-31194  
 superconducting magnets, appl. 0-37058  
 superconductivity, space applications 0-41694  
 Voyager 1, IR obs. of Jupiter and satellites 0-26790  
 Zarnitsa.2 electron injection expt., circumrocket glow spectral obs. (Russian) 0-12596
- space science** see space research
- space-time configurations**  
 see also general relativity  
 $\sigma$ -model, nonlinear, superconformal invariance in 4-dimens. space-time 0-37154  
 b-boundaries of special space-time models 0-31602  
 b-boundary definition, modifications 0-31606  
 BI-SPR- $F_n$  space, theorems 0-8866  
 Bianchi cosmologies, classification in conformal flat space times 0-56985  
 Bianchi V LRS dust space-times, intermediate singularities, whimpers, instability 0-36750  
 Birkhoff's theorem generalisation 0-27187  
 black-hole space-times, mass positivity 0-8880  
 boundary definitions for space time configurations 0-31605  
 bundle boundary for the Schwarzschild and Friedmann solutions 0-31603  
 bundle completion for parallelisable space-times 0-31604  
 causal structure and four-momenta conservation law (Rumanian) 0-46887  
 charged black hole, QED effects, Cauchy horizon (Russian) 0-51803  
 coherent beam interference, phase shift in gauge and grav. fields 0-4627  
 collapsing shell, Schwarzschild-de Sitter space-time, thermodynamics and radiation 0-17607  
 complex potential eqns., all solns. to nonlinear system 0-46795  
 complex potential equations, special relativity, and complexified Minkowski space-time 0-52018  
 conformal relativity, bare mass theory 0-27417  
 conformally flat spherically symmetric space-time 0-8867  
 cosmological generic singularity studies by Belinskii, Khalatnikov and Lifschitz 0-31399  
 cosmological model without big-bang, spherical space metric (German) 0-51927  
 curved space-time, high-freq. EM waves propag. through magnetised plasma 0-48894  
 curved space-time quantum stochastic processes, covariant Kolmogorov-Klein-Fock eqn. 0-18083  
 discrete space structure dynamics 0-52392  
 divergence free tensor densities in 3-space 0-103  
 Einstein 4-D manifolds, characteristic classes 0-46886  
 Einstein eqn. spherically symm. solution in presence of conformally invariant scalar field 0-17846  
 Einstein-de Sitter model, singularity problem, book contrib. 0-46891  
 Einstein-de Sitter model and metric, book contrib. 0-22248  
 Einstein-Maxwell null fields in Newman-Penrose formalism 0-17853  
 Einstein-Yang-Mills system in six dimensions, static solution 0-8883  
 Einsteins eqns., algebraically special space-times with nontwisting rays 0-42114  
 EM fields in Godel universe 0-42125  
 energy conditions and space-time singularities 0-31608



# space-time configurations continued

energy-momentum tensors in locally isotropic space-times 0-31631  
Fermi normal coords., expansions of the affinity, metric and geodesic eqns. 0-104  
Feynman propagator in curved spacetime, momentum space representation 0-32004  
field equations for spatially homogeneous space-times 0-52083  
flat space time, conservation laws based on traceless energy momentum tensors 0-52085  
gauge field theory, space-time symmetry, Higgs model 0-52385  
generalised axisymmetric spacetimes, Einstein vacuum eqn. solns. 0-22243  
generalised Peres space-time, geometric and mathematical props. 0-22246  
geodesics in black hole space-times 0-4602  
geometric style of explanation 0-18  
gravitational field, quantisation, Hilbert space of quantised system 0-52113  
gravitational field, spherical symmetric, spin ang. momentum tensor calc. 0-42107  
gravitational field at spatial infinity asymptotically Minkowskian space-times 0-46885  
gravitational field theory, ten-dimensional manifold of local inertial reference frames 0-46903  
gravitational interaction of spin-1/2 particles, Lorentz invariant theory 0-22257  
growth of curvature near a space-time singularity 0-31612  
hadron microstructure, de Sitter microuniverse, relativistic Hooke group and nonrelativistic quark model 0-27480  
historical development (*Hungarian*) 0-46784  
inhomogeneous cosmologies, anal. of conformally flat slices 0-17704  
inhomogeneous cosmologies, conformally flat slices and invariant classification 0-17703  
inhomogeneous cosmologies, intrinsic symmetries 0-17702  
intrinsic symmetries in general relativity 0-12955  
Kerr black hole, orbits of spinning particles 0-31326  
Kruskal extension from vacuum field eqns. in Schwarzschild metric 0-42112  
Lewis metric and flat space-time 0-46877  
Lifshitz-Khalatnikov time functions in gravitational collapse 0-31615  
Lorentz-covariant model of the system of two gravitating particles 0-8865  
Mach's principle and general principle of relativity, elementary physical approach and observational basis 0-52080  
magnetofluid space-times, imperfect, spacelike, family of contracted Ricci collineations symmetry mappings 0-51650  
Marinov coupled mirrors expt., a critique, preferred cosmological reference frame 0-27120  
massive spinning particle in Minkowski space equivalence to massless particle in de Sitter space 0-119  
neutrino-generated static space-times 0-52107  
non-expanding shear free normal null congruence soln. of Einstein eqns. 0-42111  
non-flat space time, Ferraro's theorem validity 0-4247  
non-inertial framed space-time configurations, gauge theory appl. 0-22262  
nonlinear Heisenberg-Klein-Gordon equation, localised solns. in flat Schwarzschild space-time 0-4620  
nonlinear Lagrangians and Einstein spaces 0-36915  
nonuniqueness of solutions to Einstein's equations, symmetries in  $T_{ij}$  0-12953  
null strings, geometry in complex space-times 0-22241  
odd-parity perturbations, junction conditions on spherically symmetric space-times 0-42127  
Peres space-time, generalised, algebraic props. and solns. 0-106  
Petrov homogeneous vacuum space time source 0-31632  
physical operations, diagram operations 0-46846  
plane symmetric space-time of class-I and electromagnetism 0-22252  
point mass alternative space-time 0-31638  
projective geometry, Lagrangian subspaces, and twistor theory 0-52112  
pulsars, EM vars. in curved space-times 0-56866  
quantisation, projective geometry for polarisations 0-52053  
quantum field theory, Euclidean approach in curved spacetime, functional anal. 0-27181  
quantum fluctuations near the classical space-time singularity 0-8893  
quantum gravity theory at very short distances, nonlinear sigma model 0-12979  
quantum mechanics and relativity, interrelations between truth space and time space, holistic analysis of theory of measurement 0-27177  
quantum theory, origins of 0-27176  
quantum theory and structures of time and space conference, Starnberg, W.Germany (July 1978) 0-27044  
relativistic kinetic theory, thermodynamics, symmetry props. role 0-27117  
relativistic quantum mechanics, semigroup 0-27180  
Riemann-Cartan space-time with cosmological principle, torsion tensor 0-31633  
Riemannian curvature and classification of Riemann and Ricci tensors in space-time 0-36914  
Riemannian space-time cut locus 0-36910  
Robertson-Walker universes, field interaction effects on particle creation 0-42130  
Robinson-Trautman space-times, cosmic time functions 0-42113  
scalar field vacuum fluctuations in curved space-time localised region 0-42116  
Schwarzschild space-time, distant stars, distrib. seen by freely falling observer (*Polish*) 0-26897  
sigma model, nonlinear, soliton stability in  $S^2$  0-37165  
singletons and massless, integral-spin fields on de Sitter space 0-110  
singular space times, classification scheme 0-31609  
singularities, native and classes 0-31610  
singularities and causality violation 0-31607  
singularities and invariants 0-31611  
singularities in spatially homogeneous cosmologies 0-36747  
singularities in stationary, cylindrically symmetric dust solutions 0-31613  
special relativity, discrete space-time and fundamental length 0-27122  
special relativity test theory, dynamical aspects 0-17798  
spherical spacetimes for gravit. collapse to neutron stars and black holes, computer generation 0-46385  
spinor structure of space-time 0-52081  
spinors, geometrical interpretation 0-46880  
spinors, visual geometry and algebraic props. 0-31625  
stationary charged C-metric 0-17849

# space-time configurations continued

superconformal invariant two- and three-point functions, and invariant equations in 2-D space-time (*Bulgarian*) 0-47206  
supergravity, Bianchi identities and supercovariant derivative 0-17852  
surface deformations, their square root and the signature of spacetime 0-8874  
systems with Killing's property (*French*) 0-31601  
thermodynamics in multiply connected spaces 0-4606  
Thirring model of massless scalar field, conformal transformations 0-52428  
time asymmetries and classical and quantum physics 0-22216  
total mass positivity of a general spacetime 0-12965  
twistor theory of space-time 0-17843  
whimper space-time solns. to Einstein eqn. 0-31614  
Yang-Mills fields, finite, Feynman diagram theory, analogy with space-time approach 0-52400

## space vehicle power plants

dynamic isotope power system,  $\text{PuO}_2$  fuelled, organic Rankine cycle turbine power system for space appls. 0-18692  
fast spectrum reactor space power system with thermoelec. conversion, baseline design 0-37441  
fuel cell appls. in space power systems 0-30465  
heat-pipe nuclear power plants for reliable space power 0-18377  
NASA space power technology program 0-30494  
Nimbus-Landsat spacecraft power subsystems, flight performance 0-30459  
nuclear electric spacecraft propulsion, fast spectrum reactor core design 0-37440  
nuclear integrated multimission spacecraft, definition and evaluation 0-18715  
nuclear pulse propulsion, historical review of advanced consent 0-36475  
nuclear reactor plant elements for space electric power systems 0-32339  
nuclear space power, missions and planning, elect. and propulsion power requirements 0-30428  
orbital power systems, waste heat rejection development requirements for thermal control 0-30416  
photovoltaic solar arrays, appl. of thin film Kapton mirror concentrators 0-30501  
photovoltaic space power systems, 25 kW power module evolution 0-30495  
power system perform. anal. using computer modelling for geosynchronous spacecraft 0-30497  
radioisotope thermoelec. generators, design optimisation for Solar-Polar Mission 0-40880  
radioisotope thermoelectric generator cooling in the Shuttle bay 0-40881  
radioisotope thermoelectric generators, power degradation predictions using DEGRA code 0-40879  
radioisotope thermoelectric generators, SNAP 19 performance update for Pioneer and Viking missions 0-40883  
satellites photovoltaic generators, low-orbit, D2B and Signe 3, performances comparison 0-3524  
Shuttle Orbiter, solar cell array power extension package 0-30496  
solar electric propulsion, 25 kW solar array development testing 0-30500  
spacecraft, power system perform. anal. using computer modelling 0-30497  
Stirling isotope power system for space appls., development and test results 0-18693  
thermionic convertor array, efficiency optimisation using heat transfer computer modelling 0-40886  
thermionic generators for solar energy conversion 0-35714  
thermionic reactors with const. emitter heating, reflector drums as control mechanism 0-42784  
thermionic spacecraft reactors with  $^{233}\text{U}$  as fuel, reflector drums as control mechanism 0-47686  
thermoelectric generators, Voyager and LES 8/9 flight performance 0-40882  
GaAlAs solar cells, appl. for navigational satellite power systems 0-35694  
Ni-Cd, sealed aerospace cells,  $\text{H}_2$  recombination during over discharge 0-30461  
Ni-Cd battery system design for tracking and data relay satellite system 0-30460  
Ni-H<sub>2</sub>, 50 Ahr battery for low earth orbit satellite appls. 0-30463  
Ni-H<sub>2</sub>, secondary cells, characterisation and simulated low earth orbit cycling 0-30462  
Si solar cells, low mass space blanket using 50  $\mu\text{m}$  cells 0-30498  
Si solar cells, technology development of 50  $\mu\text{m}$  cells 0-30499

## space vehicles

see also artificial satellites; rockets; space vehicle power plants  
Apollo 16, magnetometer meas. rel. to elec. cond. anomaly beneath Mare Serenitatis 0-56730  
Atmospheric Cloud Physics Laboratory on Shuttle/Spacelab, droplets optical motion control appl. 0-12634  
Deep Space Net, appl. of spacecraft tracking technology to experimental gravitation 0-8895  
Halley probe, cometary micrometeoroid hazard workshop proceedings (Noordwijk, Netherlands, 18.10 April 1979) 0-36782  
Hermes, flight results on structural dynamics 0-12639  
infinite vertical limiting surface with suction, Stokes free convection effects, spacecraft reentry appl. 0-19364  
launching directions, influence on pencil of orbits 0-26723  
louvres in thermal radiating panel, temp. distrib. 0-10124  
Luna 24 and Mare Crisium, conference, Houston, Texas (1977, December 1 to 3) 0-17710  
Luna-24 site, Fahrenheit crater ejecta emplacement 0-8564  
Lunokhod 2, magnetometer meas. rel. to elec. cond. anomaly beneath Mare Serenitatis 0-56730  
motion in gravitational and mag. dipole fields (*Russian*) 0-36487  
multiple-launch space research program, choice of vehicles 0-8512  
Pioneer 10 and 11, Jupiter cloud configurations obs. interpretation in time-depend. framework 0-26787  
Pioneer 11 investig. of Saturn 0-46476  
Pioneer Venus orbiter, IR radiometer 0-36469  
Pioneer Venus orbiter, magnetometer obs. of Venus bow shock 0-36535  
Pioneer Venus results, surface and atmosphere 0-17523  
planetary probe heat shield ablation, C excited electronic states contrib. to transport props. 0-23326  
planetary spacecraft, Jovian environment simulation, materials hardening and mass shielding 0-36472  
ram effect for conducting cylinder in drifting plasma 0-54029



**space vehicles continued**

- reentry, mass loss and shape change with radiative heating 0-31198
- rotating, eigenvalue problems solution, with real symmetric matrix of same dimension 0-12895
- RPV, high-altitude, for environmental appls. 0-17470
- Salyut, international spaceport, review 0-31196
- Salyut space stations, review 0-31195
- Shuttle/Spacelab platform in near Earth ionospheric plasma, aerodynamics 0-8517
- Skylab, low energy cosmic rays meas. 0-56689
- solar radiation pressure for maximization of orbital momentum and energy 0-12640
- solar thermal aerostat research station (STARS) 0-17471
- Space Shuttle, progress report 0-12644
- Space Shuttle project, basic elements and space-oriented experimental programme 0-17465
- Spacelab and services to users 0-31194
- telescope-observatory 2.4 m, instrumentation and appl. (*French*) 0-17493
- thermal control systems, spray evaporator for transport fluid cooling 0-29160
- unpowered spaceprobe ejected from circularly orbiting space station, trajectories calc. 0-36484
- Viking, estimation of payload loads using rigid-body interface accelerations 0-10135
- Viking, Mars geological evolution data (*French*) 0-8578
- Viking 1 Orbiter encounter with Phobos, trajectory analysis 0-12641
- Viking spacecraft, Doppler and range data rel. to geocentric gravit. const. evaluation 0-3891
- Voyager, telecommunications system and broadcast from Jupiter 0-26715
- Voyager 1, currently active volcanism discovery on Io 0-26789
- Voyager 1, encounter with Jovian system 0-26716
- Voyager 1, photographic obs. of Jupiter atmosphere ring and major satellites 0-26788
- Voyager 1 encounter with Jupiter, ground-based IR imaging at 5 microns wavelength 0-26799
- Voyager 1 Jupiter cloud configurations obs. interpretation in time-depend. framework 0-26787
- Voyager 2, Jupiter's mag. tail, traversal during 1981 Saturn encounter 0-12706
- Voyager 2, obs. of solar coronal occultation, 1979 August 0-51639
- Voyager 1 and Jupiter encounter 0-12642
- Voyager Project, spacecraft communication system 0-26718

**spacecraft** *see space vehicles*

**spallation (nuclear)** *see nuclear spallation*

**spark chambers**

*see also position sensitive particle detectors*

- Cherenkov light photograms, automatic scanning by TV digitiser 0-52822
- formation time of sparks for different initial charges 0-9460
- optical chamber digitisation using CCD 0-27902
- proton spectrometer/polarimeter for photoreactions below 1 GeV 0-18751
- Fe calorimeter, hadronic cascade curves between 20 and 8000 GeV 0-36464
- He-O<sub>2</sub> chambers, ionisation discrimination 0-37700
- Ne-He high press. flash tubes, digitisation pulse characteristics 0-9455

**spark counters**

- corona counter, determ. of U content in solid waste mats. by  $\alpha$ -detection (*Russian*) 0-27904

**spark erosion machining** *see spark machining*

**spark-gap voltmeters** *see voltmeters*

**spark gaps**

- electrode shape effect on SF<sub>6</sub> dielectric strength, overvoltage protection (*Czech*) 0-10444
- laser triggered solid dielectric switches with low jitter and inductance 0-54066
- laser triggered switching of solid insulated spark gap 0-54065
- laser-triggered breakdown in gases, basic processes responsible studies 0-38794
- long, effects of neutral gas density reduction on negative pulseless glow-spark transition 0-33850
- long spark-gaps, breakdown voltage (*French*) 0-33828
- low-inductance spark gap switch for Blumlein-driven N<sub>2</sub> laser 0-33010
- resistance measurement during breakdown, time-resolved resist. meas. 0-19639
- switch for high voltages and currents, thyatron-spark gap hybrid 0-54067

**spark machining**

- electrical discharge machining, workpiece craters, electron microscopic study 0-30157
- Fe, Armcro, electron microscope object prep. method 0-50789
- refractories, erosion resistance during action of highly concentrated energy fluxes 0-55562
- steel, appl. of W, B<sub>2</sub>- and Mo, B<sub>2</sub>-based alloys as electrodes 0-21174
- Mo, dislocation structure inhomogeneity in electromachining crater zone (*Russian*) 0-16326

**sparks**

*see also electric breakdown; lightning*

- air, DC point-to-plane elec. discharge, temp. patterns, Michelson interferometry 0-54061
- air, discharge, high-current, nanosecond, explosive cathode processes and contraction 0-10449
- air, negative pulseless corona to spark breakdown transition condition 0-54062
- air-H<sub>2</sub> (methane) mixtures, ignition energy by capacitive discharge (*French*) 0-10446
- effects of neutral gas density reduction on negative pulseless glow-spark transition 0-33850
- excimer laser preionisation techniques, spark and corona preionisers 0-33016
- extended high-current discharge, initiation by long laser spark (*Russian*) 0-10404
- gas mixtures, ignition energy by capacitive discharge and through discharge of person charged with static elec. (*French*) 0-10446
- hydrocarbon liquids, electrostatically charged, incendivity of sparks from surface 0-6303
- ionised atoms, prod. by low inductance vacuum spark, spectroscopy (*Japanese*) 0-52911
- laser-produced, light pulse narrowing and power density increase 0-28862

**sparks continued**

- plasma, laser prod., holographic study at 10.6  $\mu$ m 0-38685
- shock wave degeneration to sound waves in highly-conducting spark channel 0-38428
- shock wave degeneration to sound waves in highly-conducting spark channel 0-38429
- simulated combustion gases, mode and sparking characts. of back discharges, NO conc. effects 0-6301
- sliding discharge, guided, explosive emission phenomena 0-19649
- spectral emission source, effect of strong transverse blowing 0-3441
- Stark broadening of spectral lines, electron density, determ. in stages of spark discharge (*Russian*) 0-28859
- striated elementary sparks produced by a CO<sub>2</sub> TEA laser 0-24288
- subsonic filament fluid and small spark formation 0-38792
- underwater spark discharge, vapour cavity development, bounding surface effects 0-49022
- underwater spark discharge, vapour-gas cavities generation and space-time evolution characts. 0-19650
- He, cathode spot conversion kinetics 0-44067
- N<sub>2</sub>, dense gas near metallic target, laser spark (*Russian*) 0-38682
- N<sub>2</sub>, electric breakdown, vol. discharge with external photoionisation, plasma focus spark channel (*Russian*) 0-38738
- N<sub>2</sub>, positive corona into spark, prebreakdown phase, spectroscopic anal. 0-38790

**spatial filters**

- alignment system for Helios CO<sub>2</sub> fusion laser 0-33070
- apodisation filters in optical systems with residual aberrations, image optimisation 0-53223
- apodized optical systems, frequency response and point image irradiance distrib. 0-9819
- biological specimen recognition with partially matched spatial filter 0-46113
- coherent optical matched spatial filter correlator, for microfilm data base word recognition 0-43279
- coherent optical processor for vehicle tracking and identification using laser diode light sources 0-37957
- coherent optical system, impulse response for image multiplication by spatial sampling filtration 0-33126
- coherent optics system, amplitude and phase spectra analysis (*Russian*) 0-28164
- colour coding of spatial freq. using incoherent optical processing 0-37956
- elastomer storage device evaluation for optical signal processing 0-48444
- Fraunhofer diffraction pattern of circular apertures with triangular apodisation filters, encircled energy 0-14277
- halftone images, histograms meas. 0-23631
- holographic, CAD, optimisation method (*Russian*) 0-28171
- holographic pattern recognition for 'simple' objects 0-53230
- image filtering using prism and incoherent light (*French*) 0-14450
- incoherent diffraction correlator with a holographic filter 0-37955
- incoherent image optical matched filtering 0-14286
- laser amplifier with spatial filters, graphoanalytic determ. of energy parameters 0-48322
- laser amplifier with spatial filters, optimal length and operating conditions 0-48323
- laser fusion experiments, Nd:glass laser with high flux spatial filters 0-33035
- least-mean-square spatial filter for IR sensors 0-38092
- liquid crystal polarization rotator for intermodulation spatial-bandwidth reduction holography 0-53439
- matched filter correlator memory techniques and capacity 0-43280
- matched filters for optical signal and pattern recognition 0-48392
- matched holographic filters with Pockels readout optical modulators 0-53456
- matched spatial filter optimisation for diatom recognition 0-48180
- multislit spatial filtered pseudocolour holographic imaging 0-53236
- multispectral size-averaged incoherent spatial filtering 0-33146
- nonlinear medium, loss formation with spatial filtering 0-53357
- optical, pattern recognition by means of holography (*Japanese*) 0-5699
- optical diffraction analysis, in microscopy 0-32926
- optical pseudo-colour processing of height and flow velocity (*Japanese*) 0-9826
- optical spatial domain filter theory, gas molecule images by electron holography 0-10016
- optical spatial filtering, of visualised results of flaw detection monitoring, rational regions of appl. 0-7751
- phase-inverting grating construction, use in deblurring filters 0-48398
- pinhole plasma shutter for optical isolation in high-power glass lasers 0-23733
- plasma, high density, directed, source design, characts., numerical model 0-38538
- pulse shaping and compression using electrooptic deflector with Fourier optical elements 0-53421
- scene principal vector analysis by multiple spatial filtering 0-48179
- schlieren techniques represented by phase contrast function 0-9813
- shift invariant linear matched filter for optical correlator 0-37962
- transverse analogue tomography, cross-sectional imaging of X-rays 0-56201
- turbulent atmosphere spatial filtering function for collimated laser beam amplitude fluctuations 0-9810
- vernier sine-cosine angle converters, output signal eqn. 0-10031
- visual perception appl. 0-30731
- LiNbO<sub>3</sub> volume holographic grating as spatial-freq. selector for tunable dye laser 0-53240
- Nd:glass laser amplifiers, self-focusing and suppression by spatial filtering 0-14406
- Nd<sup>3+</sup>:phosphate glass laser, brightness enhancement by spatial filtering in amplifying channel 0-48321

**spatial variables measurement**

- see also angular measurement; area measurement; curvature measurement; diameter measurement; displacement measurement; distance measurement; height measurement; length measurement; level measurement; particle size measurement; position measurement; surface topography measurement; thermal expansion measurement; thickness measurement; volume measurement*
- anatomical surface shape meas. method 0-3882
- coherent light use (*French*) 0-23641
- endoscopic contour technique for meas. dimensions of object detail (*German*) 0-31839
- fibre sizing using light scatt., error contour charts 0-4689
- laser fusion targets, X-ray meas. using least squares fitting 0-32425



**spatial variables measurement continued**

- micromovement measurement, hologram repositioning by an interferometric technique 0-23640
- powders, surface area, meas. by Monosorb surface-area analyser using Brunauer-Emmett-Teller eqn., reproducibility 0-36979
- precision measurement, image analysis of precision components (*German*) 0-42193
- surface defects in metals estimation, Rayleigh wave scattering technique (*French*) 0-55612

**speakers see loudspeakers****special purpose computers**

- pulmonary measurement system, HP model 47804A 0-36163

**special relativity**

- see also *Lorentz transformation*
- $\psi$  collapse and locality 0-372
- additivity, rapidity, relativity, teaching 0-41984
- artificial satellite tracking, relativistic Doppler shift meas. 0-46951
- ballistic theory of light based on EM force laws and Newtonian mechanics 0-50
- clock signal, light signal synchronisation, one-way light velocity meas. 0-42055
- clock synchronisation, distant simultaneity 0-27125
- common time in a four-dimensional symmetry framework 0-52016
- complex potential equations, special relativity, and complexified Minkowski space-time 0-52018
- conformal relativity, bare mass theory 0-27417
- crystal, spherical integral reps. for cond. of abruptly activated current 0-42080
- crystal optics, relativistic phenomena 0-46839
- discrete space-time and fundamental length 0-27122
- dynamics of continuum in generic motion, action of volume and surface, forces, second cardinal equation of dynamics 0-31501
- Einstein theory in relation to Newton and Maxwell (*Norwegian*) 0-27119
- Einstein-Podolsky-Rosen paradox, causal superluminal interpretation 0-45
- electron beam, relativistic, fields excited near plane magnetoeddielectric slab 0-18986
- EM permeability of vac. and light-cone structure 0-36879
- EM radiation from accelerated charge 0-31497
- EM tachyon, prep. of three-dimens. superluminal light spot in vacuum 0-42058
- EM theory based on additive light velocity and gaseous ether theories 0-51
- ether drift, historical review 0-49
- ether drift expts., using coupled mirrors interferometer 0-22193
- ether-relativity polemic, nominalism and realism 0-42110
- extended relativity, T-violation and new particle 0-37182
- fibre bundles and relativity principles 0-8783
- first-order effects, test by measuring electric field inside rotating electric screen 0-46796
- foundational problems, philosophical aspects 0-12906
- g-2 experiments as special relativity tests 0-52019
- general Sagnac effect, ring laser and interferometer study of accelerated systems 0-4520
- geometry conventionality and the ontology of special relativity 0-4521
- gravitation, gauge theory, special relativistic limit 0-22256
- gravitational compression of a body within the approximation of the special theory of relativity 0-4611
- Klein-Gordon eqn. with step nonlinearity, jetlike solutions 0-17813
- laser experiment verifying Special Theory of Relativity 0-27118
- light induced mechanical effects connected with Fresnel coeffs. of drag 0-32908
- light propagation, a ballistic theory 0-4524
- Lorentz groups, homogeneous and inhomogeneous, teaching method to illustrate difference 0-17766
- Lorentz transformations, derivation by Ives, review 0-4523
- magnetospheric ether-drag theory and the reference frames of relativistic physics 0-12905
- Marinov coupled mirrors expt., a critique, preferred cosmological reference frame 0-27120
- Michelson-Morley experiment, history of physics, role in education 0-8759
- Michelson-Morley experiment, modern version (*French*) 0-12904
- neo-Lorentzian relativity of G. Builder, review 0-46
- neutron interferometer, rotating, phase shift due to Doppler effect 0-18006
- ondulatory radiation sources, theory and appl. 0-37947
- paradoxes, cardinal equations of dynamics 0-12903
- particle decay in six-dimensional relativity 0-27121
- photon-tachyon interactions and the isotropic photon flux 0-446
- physical nonexistence of signals going backwards in time 0-42094
- quasi-Newtonian interpretation of special relativistic dynamics 0-4519
- radiation from a uniformly accelerated charge 0-31495
- reflection and elastic scatt., Compton scatt. and special relativity 0-46756
- relative simultaneity 0-27126
- relativistic particles in EM field, conservation of angular momentum 0-48129
- relativity principle verification by new Michelson-Morley expt. in Space Lab 0-27124
- sine-Gordon breather soliton dynamics, rel. to special relativity 0-46801
- space isotropy test, special relativity, laser version of Michelson-Morley expt. 0-52021
- space-time test theory, dynamical aspects 0-17798
- superluminal communication through wave function collapse in quantum theory 0-27166
- tachyons, charged extended EM radiation, collision with neutral particles 0-4522
- tachyons, emission and absorpt. in six dimensional relativity 0-31502
- teaching, developments and changes 0-8758
- teaching, event method 0-31450
- test, macroscopic and local, Stokes-Planck theory discriminated from special relativity, length contraction measurement 0-46797
- thermodynamic implications 0-47003
- time and frequency, conf., Helsinki, Finland (Aug. 1978) 0-46728
- time as three dimensional vector, arguments against the hypothesis 0-12901
- time scales and signal transmission, relativistic effects 0-46802
- two body correlations through tachyon exchange 0-42367
- ultrabaric matter, must it be superluminal 0-17796
- ultrarelativistic electron bunch in free space, lateral spreading 0-53196

**special relativity continued**

- velocity composition laws derivation 0-42056
- world line conditions for spinning particles, spin orbit forces 0-36844
- specific gravity see density**
- specific gravity measurement see density measurement**
- specific heat**
  - see also *Debye temperature*; *Gruneisen coefficient*; *specific heat of gases*; *specific heat of liquids*; *specific heat of solids*
  - absolute zero, vanishing of specific heat without invoking 3rd law, objections 0-8940
  - adsorbed gas layers on solid adsorbent, thermodynamics (*Rumanian*) 0-10786
  - Anderson model, asymmetric, perturbation theory, impurity sp. ht. 0-6766
  - Anderson-localised states, intrastate and interstate interactions 0-20113
  - boson system, plane rotator model, Hamiltonian and mol. dynamics 0-52122
  - classical planar spin model, two-dimens., Monte Carlo study 0-25147
  - DSC curves correction for thermal lag effects, sp. ht. determ. case 0-37035
  - Einstein and the quantum theory, review 0-22237
  - finite system, order parameter and sp.-ht. for epitaxial ordering renormalisation-group calc. 0-17862
  - glass fibre reinforced epoxy, thermal cond., diffusivity and sp. ht., determ. 0-24613
  - glass transition, soft-sphere model, mol. dynamics study 0-49343
  - glass-C fibre reinforced epoxy, thermal cond., diffusivity and sp. ht., determ. 0-24613
  - Hubbard model, cluster-variation method in two-site approx. at high temp. 0-7071
  - interstellar dust grains, specific heat rel. to temp. fluctuations 0-26938
  - Ising lattice, two-dimens. finite square, sp. ht. anomaly 0-27230
  - Ising model, effective field theory 0-7116
  - Ising model, one dimensional, with infinite radius of interaction in transverse magnetic field 0-2587
  - Ising O(2), O(3) and O(4) spin systems, Hamiltonian string-coupling expansions 0-20426
  - Ising systems, finite thickness, renormalization-group transformation, real-space 0-15749
  - liquid-gas system, scaling equation of state derived from the pseudospinodal 0-44286
  - localised electronic system, sp. ht., singularity at Anderson-Mott transition 0-34381
  - measurement at low temps., calorimetric and electronic system (*French*) 0-27305
  - measurement technique, computer controlled AC calorimetry (*Japanese*) 0-27306
  - mixed valence impurity model, Fermi liq. theory, Ward identities 0-34401
  - n-component spin system, energy-energy correl. function calc. 0-31697
  - one-dimensional system, Bose-Einstein condensation at const. press. 0-22276
  - one-spin ferromagnet, high temp. series expansion for mag. susceptibility and sp. ht. 0-25148
  - Potts model, Monte Carlo simulation in three dims. 0-163
  - random exchange Heisenberg antiferromagnetic chain, exchange-coupled pair model 0-20423
  - renormalisation group eqns. and thermodynamic anomalies near tricritical point (*Russian*) 0-13027
  - standards choice and certification, for liquids and vapours in 90 to 273.15K range 0-23877
  - triangular and honeycomb lattice gases, order-disorder transitions to  $2 \times 2$  struct. 0-4674
  - X-Y model, second order Green's function theory 0-54913
  - Ar monolayer adsorbed on graphite basal planes, heat capacity 0-6636
  - Ar, solid, desorption heat capacity of adsorbed  $^3\text{He}$  0-10735
  - BeCu pressure clamp cell, for low temp. specific heat and magnetisation meas. 0-17956
  - C fibre reinforced epoxy, thermal cond., diffusivity and sp. ht., determ. 0-24613
  - $^4\text{He}$  film, adsorbed on disordered substrate, heat capacity meas. 0.08-1.3K 0-2239
  - Mo, temperature standard reference material, USA National Bureau of Standards 0-47009
  - Ne, solid, desorption heat capacity of adsorbed  $^4\text{He}$  0-10736
- specific heat at constant pressure see specific heat**
- specific heat at constant volume see specific heat**
- specific heat of gases**
  - caloric function derivation for liquids and gases 0-13017
  - $\text{H}_2$  occlusion in  $\text{MoO}_3$ , molar heat content (*French*) 0-45247
  - $\text{ScI}_3$ , vaporisation thermodynamics, sublimation and formation 0-54366
- specific heat of liquids**
  - air-water droplet, heat capacity meas. (*Russian*) 0-54395
  - anthracene, chemical thermodynamic props. 0-21312
  - binary fluids, universal const.  $R_i^+$  meas. 0-19952
  - biopolymer soln. heat capacity, conformational props. temp. depend. 0-8009
  - caloric function derivation for liquids and gases 0-13017
  - p-dioxane, aq. soln., excess molar heat capacities, 298.15K, US vel. obs. 0-6523
  - ethane, use of high press. recycle-flow calorimeter 0-42228
  - glass-forming systems, structure and thermodynamics (*German*) 0-38924
  - hydrocarbons, saturated open-chain, transport behaviour of excess electrons and props. 0-39643
  - liquid metal, bulk modulus, calc. using press. fluctuation in microcanonical ensemble 0-2106
  - metal, thermophysical properties meas. by submicrosecond-pulse-heating method 0-52220
  - metals, heat capacity near melting point, vacancy mechanism of melting 0-10641
  - metals, radial distrib. function and thermodynamic characts., interparticle interaction pot. (*Russian*) 0-49086
  - mixtures, binary, excess isentropic compressibilities and isochoric heat capacities 0-21313
  - nematic liquid cryst., tricritical behaviour near transition to isotropic fluid (*Russian*) 0-15001
  - oxyloxycyanobiphenyl, nematic-smectic-A transition, high-resolution 0-10649
  - 4-n-pentyl-phenylthiol-4'-alkoxybenzoate, homologous series, specific heat meas., nematic-smectic-A tricritical point 0-15227



## specific heat of liquids continued

- phenanthrene, chemical thermodynamic props. 0-21312  
 polymers, specific heat, conform. effects 0-24607  
 rare earth metals, heat capacity near melting pt., vacancy mechanism of melting 0-15221  
 thermotropic systems of rodlike molecules with orientation-depend. interactions 0-33883  
 water, Monte Carlo simulation 0-54113  
 p-xylene, heat capacity rel. to temp. 0-44335  
 xylideneaniline-p-benzonitri 0-44328  
 Al, liquid, bulk modulus, calc. using press. fluctuation in microcanonical ensemble 0-2106  
 B, thermoelastic props. near melting point 0-19862  
 Cd-Zn(Pb)(Sn), binary metallic melt, deviation from the Kopp law, specific heat (*Russian*) 0-39305  
 Fr, properties from melting point to 7500K, prediction (*Russian*) 0-44296  
 Ge<sub>0.5</sub>Te<sub>0.5</sub>, heat capacity in solid and liq. phases, enthalpy of form. (*French*) 0-35565  
 HCl, liq. struct. simulated by a Lennard-Jones pot. 0-1917  
<sup>3</sup>He, liq., in contact with dielec. surface, mag. susceptibility enhancement, thermodynamics 0-54460  
<sup>3</sup>He, superfluid, near transition, anomalous heat capacity, 0.8-20 mK 0-15326  
<sup>3</sup>He, superfluid, sp. ht. discontinuities, rel. to Ginzburg-Landau parameters 0-54459  
<sup>4</sup>He, two-dimensional, in <sup>4</sup>He film, sp. ht. meas. 0-39382  
<sup>4</sup>He, monolayer adsorbed on Kr-plated graphite, possible Ising transition 0-34298  
<sup>4</sup>He superfluid, acoustic vibration field density of states in piecewise const. parameter media 0-6483  
<sup>4</sup>He, superfluid, two-dimens., microscopic theory, excitation spectrum and thermodynamics props. 0-24709  
 In-Sb(Sn), binary metallic melt, deviation from the Kopp law, specific heat (*Russian*) 0-39305  
 KCl, solution, apparent molar heat capacity and volume, at 298.15K 0-29179  
 KNO<sub>3</sub>, solution, apparent molar heat capacity and volume, at 298.15K 0-29179  
 NaCl, solution, apparent molar heat capacity and volume, at 298.15K 0-29179  
 UO<sub>2</sub>, thermal and transport props., electronic contrib. 0-15432

## specific heat of solids

see also Schottky anomaly

- <sup>3</sup>He, solid, two parameter model of mag. and thermal props., spin exchange 0-49461  
 , 0-29395  
 actinide compounds, specific heat meas., review 0-6524  
 actinide metals, specific heat, Debye temp. 0-15258  
 adiabatic calorimetry, high resolution heat capacity meas. (*Japanese*) 0-52218  
 alkali halide: NH<sub>4</sub><sup>+</sup>, hindered rot. energy levels calc. 0-10514  
 alkali metals, elastic and thermal props. by pseudopotential method 0-19899  
 Anderson impurities, interacting, pair, Fermi-liq. theory 0-44803  
 anharmonic crystals, Debye-Waller factor, specific heat thermal behaviour 0-54335  
 anthracene, chemical thermodynamic props. 0-21312  
 antiferromagnet, cluster approximation, Neel temp. and specific heat calc. 0-54901  
 antiferromagnetic chain, random, quantum spin-1/2 Heisenberg soln. 0-11148  
 apparatus to meas. thermophysical props. at high temps. 0-37458  
 biphenyl, heat capacity near phase transition regions 0-44330  
 carnauba wax thermoelectret, charge behaviour 0-7276  
 classical quadrupole solids, correl. effects 0-10628  
 crystalline materials, sp. ht. rel. to binding energy temp. depend. 0-54403  
 cubic Ising ferromagnet, three spin interaction effect on mag. props. 0-54910  
 Debye heat capacity, calc. using Einstein heat capacity formula 0-24608  
 differential scanning calorimetry, meas. of accurate heat capacities 0-8987  
 disordered one-dimensional conductors, interacting electron thermodynamics (*Russian*) 0-54679  
 disordered systems, localisation using random series, Anderson transition for extended states 0-44542  
 disordered systems, phonon-like excitations, dispersion and damping 0-49331  
 electron gas, two dimens., exchange interaction contrib., calc. 0-44331  
 elements, monotonous series based on atomic bond energy, for mech. and phys. props. calc. (*Russian*) 0-19740  
 entropy, free energy, sp. ht., electron-phonon interaction corrections 0-49387  
 ethylene copolymers, partially cryst. pseudoeutectoid, swelling, thermodynamics 0-39311  
 ferroelectrics, meas. by dynamic method at high hydrostatic pressures 0-47059  
 ferromagnetic classical vector model, extension of high temp. free energy series 0-7062  
 glass, insulating, thermal, acoustic props., low temp. anomaly microscopic model 0-28921  
 glycerol, cryst. and glassy states 0-2176  
 graphite, adsorbed layers of O<sub>2</sub>, heat capacity meas. 0-49511  
 graphite, with physisorbed Xe monolayer, dynamical and thermal props. 0-34292  
 guanidinium vanadium sulphate hexahydrate, singlet ground state system, low temp. mag. props. 0-44843  
 Heisenberg antiferromagnetic chain, random, low temp. thermodynamic props. in zero mag. field 0-34657  
 Heisenberg linear chain, alternating spin quantum numbers, mag. and thermodynamic props. 0-34578  
 insulator, mag. transition sp. ht. anomaly, photoacoustic meas. 0-4773  
 intermediate valence, phase diagram and Kondo behaviour 0-29366  
 intermediate valence, three-site, six-electron, even-parity model 0-20125  
 Ising model, adiabatic susceptibility and specific heat at const. magnetisation 0-7114  
 Ising model, randomly diluted, on honeycomb lattice, thermodynamic props. 0-54902  
 Ising model, three-dimens. mag. susceptibility and sp. ht., high temp. series anal. 0-22295  
 specific heat of solids continued  
 Ising quadratic two-dimensional ferromagnet with three spin interactions 0-2542  
 Kondo lattice, electron dynamics, additional sp. ht. 0-15688  
 liquid-glass transition, free volume approach, thermodynamic behaviour 0-1940  
 lysozyme, cryst., dynamic sp. ht. capacity meas. 0-21447  
 magnetic dipoles on a lattice, theory at low temps. 0-50082  
 magnetic superconductor, thermodynamics of magnetism and supercond., mol. field theory 0-34668  
 manganese zinc formate dihydrate, two-dimens. antiferromag., anomalous crit. phenomena, neutron scatt. and PMR obs. 0-50104  
 metal-hydrogen system, electronic sp. ht. meas. 0-49378  
 metallic crystal, phonon density of states determ. from heat capacity (*Russian*) 0-29131  
 metals, heat capacity near melting point, vacancy mechanism of melting 0-10641  
 metals, low temp. and high pressure techniques 0-52246  
 methane-d<sub>4</sub>, solid, thermodynamic props. calc. using significant structures method, 6 to 87K 0-24616  
 microcline, maximum, room temp. phase transition, heat capacity meas. 0-54373  
 Migdal-like approximation, quantum spin systems 0-34649  
 mixed valence cpds., mag. susceptibility and sp. ht., periodic Anderson model, CPA alloy analogue method 0-15474  
 molecular crystals, rot. and sp. ht. anomalies 0-28932  
 oligocarbonatemetacrylates, and their cross-linked polymers, thermophysical characts., temp. depend. anal. 0-19721  
 one-dimensional disordered systems, magnetism 0-25152  
 orbital degeneracy, one dimensional two spin models (*Russian*) 0-54899  
 phase transformations, thermodynamic relations, appl. to K<sub>2</sub>ReCl<sub>6</sub> 0-29164  
 phenanthrene, chemical thermodynamic props. 0-21312  
 picrite, calculation using measurement of US vel. 0-41436  
 polyalkaneimide, mech. and thermophys. props. at liq. He temps. 0-3117  
 polymer, packing coefficient determ. from acoustical meas. data 0-38959  
 polymer blends, two-component, glass transition, calorimetric investig. (*Russian*) 0-39268  
 polymer glass, sp. ht. discontinuity at glass transition 0-19954  
 powders, meas. apparatus for 4.3-300K 0-227  
 pyrazine, cryst. phases, entropy changes and struct. implications 0-54397  
 quartz ceramics, thermal and temp. cond. in range 500-1900K 0-39370  
 rare earth alloys, RFe<sub>2</sub>, (R=Gd, Tb, Dy, Ho, Er, Tm, Lu), electronic heat capacity coeffs. 0-39787  
 rare earth garnets, prep. and props. book contrib. 0-44193  
 rare earth intermetallics, low temp. sp. ht. 0-15259  
 rare earth metals, heat capacity near melting pt., vacancy mechanism of melting 0-15221  
 rare earth pnictides, prep. and props., book contrib. 0-54212  
 rare earth rhodium boride system, ternary, supercond., phase diagrams at upper crit. fields 0-2531  
 rare earth rhodium borides, RRh<sub>2</sub>B<sub>4</sub>, NMR and sp. ht. in supercond. and mag. ordered phases 0-7037  
 rare earth trihydrides, light, low-temp. sp. ht., mag., elec., and cryst. field splitting effects 0-49379  
 rare gas crystals, lattice heat capacity, thermal vibrations, Lindeman parameter, lattice dynamic model (*Russian*) 0-29141  
 Rochelle salt, high resolution heat capacity meas. (*Japanese*) 0-52218  
 S=1, singlet ground state systems, mag. props. 0-11157  
 semiconductors, elementary excitations in disordered systems with localised electrons, polarons (*Russian*) 0-49632  
 silicate minerals, heat capacities rel. to simple lattice vibrational models 0-4005  
 single-ion anisotropy, magnetic systems, high temp. series expansion 0-34576  
 smoky quartz, thermal props. at very low temp. 0-24610  
 spin glasses, phase transition, mag. susceptibility, specific heat, Ising model calcs. (*Russian*) 0-34671  
 spin glasses, RKKY Ising, sp. ht. 1/T behaviour 0-11210  
 spin glasses, sp. ht. and susceptibility, random series method 0-44542  
 spin-glass, one-dimens., sp. ht. and mag. susceptibility calcs. 0-7120  
 spin-Peierls transition in mag. field, phonon freq., Heisenberg model calcs. 0-25151  
 stored energy, and increment in heat capacity due to plastic deform. 0-54302  
 structural phase transitions, applicability of thermodynamic theory, temp. depend. of specific heat 0-2139  
 superconducting critical temp., generalised moments of phonon spectrum (*French*) 0-39702  
 superconductor with mag. impurities, Shiba theory consequences beyond s-wave scatt., sp. ht. discontinuity 0-2516  
 TCNQ salt, acridinium (TCNQ)<sub>2</sub> low temp. heat capacity, Debye temp. 0-2180  
 TCNQ salt, HMTTF-TCNQ, sp. ht., 30 to 80K 0-24614  
 TCNQ salt, MEM(TCNQ)<sub>2</sub>, phase transitions, elec. cond., ESR, mag. susceptibility study 0-24981  
 TCNQ salt, tetramethylhexamethylenediammonium-TCNQ-iodine, elec. and mag. props., struct., specific heat 0-24898  
 TGFB, high press. influence on anomalous specific heat, tricritical point 0-25322  
 TGS  $\gamma$ -ray irrad. cryst., heat capacity anomalies near phase transition (*Russian*) 0-49375  
 TGSe, deuterated, thermal and dielectric props. at high hydrostatic press. 0-34864  
 thermal insulation on metal backing, thermophys. characts., expt. determ. technique 0-4707  
 tissue-equivalent plastic, A-150, thermal diffusivity, sp. ht., thermal cond. obs. 0-34258  
 transition metal borides, narrow band types, electronic density of states, many-electron Hubbard model calcs. 0-20064  
 TTF(MBDT) spin-Peierls transition, mag. exchange interactions, mag. props. 0-25138  
 TTF-TCNQ, Landau free energy function, CDW-libron interaction, sp. ht. near phase transitions 0-19963  
 TTF-TCNQ and derivatives, 1.8 to 40K, three dimens. state, specific heats 0-44333  
 TTFcCuBDT, spin-Peierls transition in spin 1/2 Heisenberg chains, RPA calcs. 0-25150  
 TTT<sub>2</sub>-(I<sub>3</sub>)<sub>2</sub>, physical props., elec., mag. and optical meas. 0-24908  
 two dimensional periodic lattice, electron ordering, CDW-disordered state transition, Hubbard model (*Russian*) 0-6754



## specific heat of solids continued

- Wigner crystal, lattice quantum oscills. in mag. field, specific heat, mag. moments (*Russian*) 0-49636  
 xylideneaniline-p'-benzonitril 0-44328  
 Ag, specific entropy and surface heat determ. as function of temp. (*German*) 0-6619  
 Ag, two-parameter dynamical model appl 0-10597  
 AgAu, quenched, short range order effects on specific heat 0-29181  
 Ag<sub>2</sub>Si, superionic cond., phase transition and cryst. structs., sp. ht., neutron and X-ray diffr. obs. 0-10662  
 Al alloy, 51S, modified by misch metal, for space appl. 0-55466  
 Al, phonon density of states by neutron scatt., sp. ht. and Debye temp. 0-2132  
 Al, specific entropy and surface heat determ. as function of temp. (*German*) 0-6619  
 Al, two-parameter dynamical model appl. 0-10597  
 Al<sub>2</sub>O<sub>3</sub>, heat capacity laser-flash calorimetry 0-4716  
 Al<sub>2</sub>O<sub>3</sub>-SiO<sub>2</sub>-Na<sub>2</sub>O-CaO-MgO-Fe<sub>2</sub>O<sub>3</sub>-SO<sub>3</sub> glass, thermal capacity meas. at low temps. 0-44334  
 Am, superconducting critical field, sp. ht. 0-11136  
 Ar, solid, thermodynamic props. under press., multiparametric pairwise and Lennard Jones potential calcs. 0-39316  
 As-S, amorphous, glass transition and specific heat, intermolecular bond saturation 0-15011  
 As-Se, amorphous, glass transition and specific heat, intermolecular bond saturation 0-15011  
 Au<sub>1-x</sub>Fe<sub>x</sub>, 0.14 < x < 0.28, ferromagnetism study by specific heat meas. 0-7121  
 B<sub>2</sub>O<sub>3</sub> glass, effect of thermal treatment on low temp. specific heat 0-54401  
 Ba<sub>2</sub>NiF<sub>6</sub>, specific heat capacity, critical amplitude, cross-over from 2-D Ising to Heisenberg behaviour 0-39791  
 Bi, phonon density of states by neutron scatt., sp. ht. and Debye temp. 0-2132  
 CaF<sub>2</sub>:Dy<sup>3+</sup>, cubic cryst. field effects 0-2368  
 Ca<sub>10</sub>(PO<sub>4</sub>)<sub>6</sub>(OH)<sub>2-2x</sub>O<sub>x</sub>□<sub>x</sub> polycryst. sintered bodies, prep. and thermal props. 0-25624  
 p-CdCr<sub>2</sub>Se<sub>4</sub>, resistivity anomalies at mag. transitions, sp.ht. 0-39785  
 Cd<sub>0.010</sub>Fe<sub>0.990</sub>O<sub>4</sub>, heat capacity investigation of dopant effects on mag. disordering temp. 0-25143  
 CdP<sub>4</sub>, thermodynamic functions, 55-300K 0-34203  
 Cd<sub>2</sub>Re<sub>2</sub>O<sub>7</sub>, specific heats, electronic and lattice contrib. below 20K 0-34200  
 Cd<sub>2</sub>Ru<sub>2</sub>O<sub>7</sub>, specific heats, electronic and lattice contrib. below 20K 0-34200  
 Ce binary and pseudobinary intermetallics, struct. and mag. data 0-20129  
 CeAl<sub>2</sub> and CeAl<sub>3</sub>, magnetisation and sp. ht. 0-20418  
 CeAl<sub>2</sub>, antiferromag. ordering between 4f shells, Kondo effect 0-20417  
 CeIn<sub>3</sub>, magnetisation and sp. ht. 0-20418  
 Co, Co alloys, electrical resistivity and specific heat meas., anomalies rel. to thermally excited states 0-6809  
 CoB<sub>2</sub>, growth from melt and phys. props. 0-20782  
 Cr, thermal vacancies, energy of form. and conc. 0-29014  
 CrB<sub>2</sub>, CrB, and Cr<sub>2</sub>B<sub>3</sub>, mag. and thermal props. at low temps. 0-20385  
 Cr<sub>2</sub>S<sub>3</sub>, enthalpy and specific heat, temp. depend. 0-54406  
 Cr<sub>2</sub>Si, specific heat at low temps., electron density of states, Debye temp. (*Russian*) 0-54398  
 CsCaCl<sub>3</sub> crystal, sp. ht. and thermal expansion coeffs. 0-10681  
 Cs<sub>2</sub>O-SiO<sub>2</sub> glass, low temp. heat capacity 0-49373  
 Cu, lattice specific heat, from two-parameter lattice dynamical model with dispersion 0-10678  
 Cu-Fe, dilute, low temp. heat capacity in mag. field, superparamagnetism 0-39804  
 Cu-Pt, ordered equiatomic, lattice specific heat meas., Debye temp. 0-54396  
 CuAu I, ordered equiatomic, lattice specific heat meas., Debye temp. 0-54396  
 Cu<sub>0.5</sub>Fe<sub>0.5</sub>O<sub>4</sub>, ferrite, determination of specific heat at 298-800K 0-2579  
 Cu(NO<sub>3</sub>)<sub>2</sub>·2/3H<sub>2</sub>O, singlet ground state system, mag. props. 0-44850  
 Cu<sub>2</sub>Zn<sub>1-x</sub>SiF<sub>6</sub>·6H<sub>2</sub>O, heat capacities and thermodynamic props., 14 to 300K, cooperative Jahn-Teller transition 0-21314  
 Dy, critical exponents and amplitude ratios from elec. cond. data, theoretical model 0-50126  
 Dy, resistivity anomalies at mag. transitions, sp.ht. 0-39785  
 Dy<sub>12</sub>Mo<sub>6</sub>S<sub>8</sub>, low temp. heat capacity anomaly rel. to antiferromag. transition in supercond. state 0-25044  
 ErFe<sub>2</sub>, crystal field interaction contribution to specific heat 0-39788  
 Er<sub>x</sub>La<sub>1-x</sub>Cu, and Er<sub>x</sub>Y<sub>1-x</sub>Cu, antiferromag., mag. and resist. behaviour 0-34412  
 ErPd<sub>3</sub>, specific heat at low temp. 0-20413  
 Eu<sub>1-x</sub>Gd<sub>x</sub>S, concentrated system with ferromag. and antiferromag. interactions, spin-glass props. 0-34639  
 Eu(OH)<sub>3</sub>, heat capacity from near 5 to 350K, lattice and Schottky contribs. 0-49374  
 Eu<sub>2</sub>Sr<sub>1-x</sub>S, insulating spin-glass, sp. ht. near ferromag. onset 0-34667  
 Fe, electronic heating in modulation meas. method 0-24609  
 Fe, heat capacity temp. depend. meas., internal energy and entropy, anharmonic theory calcs. (*Russian*) 0-54402  
 Fe, point defect estimation from specific heat and volume in plastically deformed pure metals (*Russian*) 0-54223  
 Fe, resistivity anomalies at mag. transitions, sp.ht. 0-39785  
 Fe<sub>40</sub>B<sub>60</sub>, metallic glass, low temp. specific heat, metalloid effects 0-34654  
 Fe<sub>42</sub>B<sub>58</sub>Si<sub>2</sub>, metallic glass, low temp. specific heat, metalloid effects 0-34654  
 Fe<sub>40</sub>Ni<sub>40</sub>B<sub>20</sub>, metallic glass, low temp. specific heat, metalloid effects 0-34654  
 Fe<sub>2</sub>Ni<sub>80-x</sub>P<sub>14</sub>B<sub>6</sub> (x=0, 20, 40, 60, 80), metallic glass, low temp. sp. ht. 0-2588  
 FeS<sub>2</sub>, pyrite, heat capacity meas. by differential scanning calorimetry 0-8987  
 Fe<sub>2</sub>V<sub>2-x</sub>O<sub>4</sub> solid solutions, specific heat near semiconductor-metal transition 0-24612  
 GaP, moments of phonon spectra from specific heats 0-15203  
 GaS, lattice dynamics parameters, X-ray diffr. study (*Russian*) 0-29146  
 GaSe, lattice dynamics parameters, X-ray diffr. study (*Russian*) 0-29146  
 Gd<sub>1.2</sub>Mo<sub>6</sub>S<sub>8</sub>, low temp. heat capacity anomaly rel. to antiferromag. transition in supercond. state 0-25044  
 Gd(OH)<sub>3</sub>, heat capacity from near 5 to 350K, lattice and Schottky contribs. 0-49374

## specific heat of solids continued

- Ge-Te binary glass, eutectic, DSC obs., thermodynamic and thermokinetic characts. 0-39309  
 Ge<sub>0.5</sub>Te<sub>0.5</sub>, heat capacity in solid and liq. phases, enthalpy of form. (*French*) 0-35565  
 H<sub>2</sub>, solid quadrupolar glass, relax. time and low temp. sp.ht., computer simulations 0-49377  
<sup>3</sup>He, solid, low temp. thermal cond., structural crystalline defects 0-2240  
<sup>4</sup>He film adsorbed on graphite, transition temp., entropies, internal energies and heats of desorption 0-2238  
 Hf, HCP, lattice dynamics, thermal and elastic props., model 0-34155  
 Hf-Ni(Co), amorphous, formation, decomposition and elec. transport props. 0-20143  
 HfS<sub>2</sub>, enthalpy and specific heat, temp. depend. 0-54406  
 HoFe<sub>2</sub>, crystal field interaction contribution to specific heat 0-39788  
 In-Mg, ordered equiatomic, lattice specific heat meas., Debye temp., superconducting transition 0-54396  
 KCl:Pb<sup>2+</sup>, low temp. sp. ht. 0-2178  
 K<sub>2</sub>CoF<sub>4</sub>, specific heat capacity, critical amplitude, cross-over from 2-D Ising to Heisenberg behaviour 0-39791  
 K<sub>2</sub>Cr<sub>2</sub>O<sub>7</sub>, polymorphic behavior, depend. on thermal and prep. history 0-34184  
 K<sub>2</sub>IrCl<sub>6</sub>, sp. ht. meas. at low temp. 0-7119  
 K<sub>2</sub>MnF<sub>4</sub>, specific heat capacity, critical amplitude, cross-over from 2-D Ising to Heisenberg behaviour 0-39791  
 K<sub>2</sub>NiF<sub>4</sub>, specific heat capacity, critical amplitude, cross-over from 2-D Ising to Heisenberg behaviour 0-39791  
 K<sub>2</sub>O-SiO<sub>2</sub> glass, low temp. heat capacity 0-49373  
 K<sub>2</sub>OCl<sub>6</sub>, sp. ht. meas. at low temp. 0-7119  
 K<sub>2</sub>PtCl<sub>6</sub>, diamag. sp. ht. meas. at low temp. 0-7119  
 K<sub>2</sub>ReCl<sub>6</sub>, sp. ht. meas. at low temp. 0-7119  
 K<sub>2</sub>ReCl<sub>6</sub>, thermodynamic relations at solid state phase transitions 0-29164  
 Kr absorption on graphite, monolayer regime phase diagram 0-49507  
 La, FCC, NMR 4.2 to 296K, mag. susceptibility and sp. ht. 0-15813  
 (LaNd)Sn<sub>3</sub>, containing Nd impurities, supercond. and normal state props. 0-49967  
 LaNi<sub>5</sub>, crystal field investigation from inelastic slow neutron scatt. expts. 0-39538  
 La(OH)<sub>3</sub>, heat capacity from near 5 to 350K, lattice and Schottky contribs. 0-49374  
 LaS<sub>3.33</sub>-LaS<sub>3.40</sub>, low temp. sp. ht. 0-15259  
 La<sub>2</sub>S<sub>3</sub>, high crit. mag. field supercond., elec. resist., sp. ht. and magnetisation 0-2532  
 La<sub>2</sub>S<sub>4</sub>-La<sub>2</sub>S<sub>3</sub>, low temp. sp. ht. 0-15259  
 La<sub>1-x</sub>Sr<sub>x</sub>CoO<sub>3</sub> meas., using laser-flash method, phase transitions obs. (*Japanese*) 0-54898  
 LiAlH<sub>4</sub>, molar heat capacity, thermodynamic props., 10 to 300K 0-44329  
 Li<sub>3</sub>AlH<sub>6</sub>, molar heat capacity, thermodynamic props., 10 to 300K 0-44329  
 LiC<sub>6</sub>, intercalation compound with graphite, sp. ht. meas., 4-300K 0-44332  
 LiCsSO<sub>4</sub>, thermal and dielec. props. 0-34860  
 LiKSO<sub>4</sub>, thermal and dielec. props. 0-34860  
 Li<sub>2</sub>O, thermal decomposition and heat capacity 301 to 566K, enthalpy 0-3322  
 LiTbF<sub>4</sub>, mag. props., crit. behaviour at marginal dimensionality 0-54906  
 LuFe<sub>2</sub>, crystal field interaction contribution to specific heat 0-39788  
 Mg(AlH<sub>4</sub>)<sub>2</sub>, prep., thermal decomposition, molar heat capacity, heat of form. 0-3325  
 MnB<sub>2</sub>, growth from melt and phys. props. 0-20782  
 MnSi, amorphous, sputtered, mag., elec., struct. and thermal props., spin glass behaviour 0-50124  
 MnTe, resistivity anomalies at mag. transitions, sp.ht. 0-39785  
 MoS<sub>2</sub>, enthalpy and specific heat, temp. depend. 0-54406  
 MoS<sub>2</sub>, entropy, enthalpy and specific heat, temp. depend. 500 to 1700K 0-15260  
 Mo<sub>6</sub>S<sub>8</sub>(Se<sub>4</sub>)(Te<sub>8</sub>) and halogen substituted cpds., sp. ht. capacity 0-49986  
 NH<sub>4</sub>Cl, thermal cond. and heat capacity of solid phases under press. 0-2225  
 (NH<sub>4</sub>)<sub>2</sub>H(SO<sub>4</sub>)<sub>2</sub>, phase transitions, sp. ht. meas. 0-2157  
 NH<sub>4</sub>HgCl<sub>3</sub>, high resolution heat capacity meas. (*Japanese*) 0-52218  
 NaBr, heat capacity, Gruneisen parameters, 2 to 20K 0-29180  
 NaF, heat capacity, Gruneisen parameters, 2 to 20K 0-29180  
 Na<sub>2</sub>O-SiO<sub>2</sub>, Na<sub>2</sub>O-CaO-SiO<sub>2</sub> glasses, thermal capacity meas. at low temps. 0-44334  
 Na<sub>2</sub>O-SiO<sub>2</sub> glass, low temp. heat capacity 0-49373  
 Na<sub>3</sub>Zr<sub>2</sub>Si<sub>2</sub>PO<sub>12</sub>, NASICON, phase transition, X-ray diffr., ionic cond. and sp. ht. meas. 0-19979  
 Nb, plastic deformation effects on superconducting specific heat transition 0-20352  
 Nb, spin fluctuations effect on T<sub>c</sub>, from sp. ht. and mag. suscept. 0-7030  
 Nb/H, heat capacity and supercond. between 1.5 and 16K 0-2521  
 NbC, true heat capacity meas. by pulse method 0-19953  
 Nb<sub>2</sub>Ge, amorphous nongranular thin superconducting film, thermodynamic and resistive transitions 0-34571  
 NbS<sub>2</sub>, enthalpy and specific heat, temp. depend. 0-54406  
 Nb<sub>3</sub>S<sub>4</sub>, anisotropic superconductor, critical field and specific heat meas. 0-44779  
 Nb<sub>3</sub>Si, high T<sub>c</sub>, supercond. props. from extrapolation of sp. ht. meas. on A-15 Nb-Si 0-25045  
 NdF<sub>3</sub>, enthalpy, entropy, heat capacity and Planck function from 5 to 350K 0-15257  
 Ni, heat capacity temp. depend. meas., internal energy and entropy, anharmonic theory calcs. (*Russian*) 0-54402  
 Ni, point defect estimation from specific heat and volume in plastically deformed pure metals (*Russian*) 0-54223  
 Ni-Al alloy, solid phase reaction kinetic parameter calcs., defect formation (*Russian*) 0-54399  
 (Ni<sub>1-x</sub>Cu<sub>x</sub>)Ti, martensitic, shape memory effect kinetics and thermodynamics 0-3021  
 (Ni<sub>1-x</sub>Fe<sub>x</sub>)<sub>1-x</sub>S, anisotropic spin glass, mag. props. 0-39793  
 Ni(NO<sub>3</sub>)<sub>2</sub>·6H<sub>2</sub>O, susceptibility and specific heat meas., spin ordering, antiferromag. spin pair coupling 0-7084  
 Ni<sub>1-x</sub>S, metal-semimetal transition, lattice dynamics and thermodynamic props. 0-29324  
 NiTi, martensitic, shape memory effect kinetics and thermodynamics 0-3021  
 P-S, amorphous, glass transition and specific heat, intermolecular bond saturation 0-15011



## specific heat of solids continued

- P-Se, amorphous, glass transition and specific heat, intermolecular bond saturation 0-15011  
 PbF<sub>2</sub>, orthorhombic and cubic, heat capacity, 3 to 22K 0-19955  
 Pb<sub>2</sub>Ge<sub>2</sub>O<sub>11</sub>, ferroelectric, anharmonic effects in low freq. symm. modes, Raman study 0-25365  
 Pb(Mn<sub>1/2</sub>Ta<sub>1/2</sub>)O<sub>3</sub>, ceramic, for thermal and dielectric isolation at low temp. 0-39365  
 Pb<sub>3</sub>O<sub>4</sub>, tetragonal to orthorhombic transition, heat capacity meas. 0-20929  
 PbZrO<sub>3</sub>, pyroelectric detector, low temp. behaviour, expt. 0-31869  
 PrNi<sub>2</sub>, crystal field investigation from inelastic slow neutron scatt. expts. 0-39538  
 Pr(OH)<sub>3</sub>, low temp. heat capacity, thermophys. props. optical spectra, anal. of Schottky contributions, review 0-24611  
 Pt<sub>3</sub>Mn<sub>2</sub>Cr<sub>1-3</sub>, electronic specific heat meas. comparison with band model calcs. 0-54400  
 PuC, high temp. heat capacity 0-49384  
 PuC<sub>x</sub> (x=0.8, 1.44, 1.67), low temp. sp. ht., mag. ordering obs. 0-49372  
 PuO<sub>2</sub>, thermal and transport props., electronic contrib. 0-15432  
 Rb, specific heat at high temp., Monte Carlo calc. 0-29182  
 RbCl, sp. ht. at low temps., Debye temp. determ. 0-2177  
 RbHSO<sub>4</sub>, acoustic and dielectric props. near phase transition 0-55053  
 Rb<sub>2</sub>NiF<sub>4</sub>, specific heat capacity, critical amplitude, cross-over from 2-D Ising to Heisenberg behaviour 0-39791  
 Sc-Gd spin glass, sp. ht., 0.3-10K 0-25145  
 Se, monoclinic to trigonal conversion, thermodynamic stability and associated investigs. 0-24592  
 Se, trigonal, low temp. sp. ht. and elastic const., piezoelec. effect influence on phonons 0-54404  
 SiO<sub>2</sub>, glass, thermal capacity meas. at low temps. 0-44334  
 SiO<sub>2</sub>, vitreous, low temp. thermal props. and intrinsic defects 0-29057  
 SiO<sub>2</sub>-glass, effect of thermal treatment on low temp. specific heat 0-54401  
 SmB<sub>6</sub>, specific heat anomalies 0-34199  
 SmB<sub>6</sub>, valence fluctuating state, sp. ht. 0-20127  
 SmRh<sub>2</sub>B<sub>4</sub>, coexistence of supercond. and antiferromag. order 0-11140  
 Sm<sub>2</sub>WO<sub>6</sub> and Sm<sub>14</sub>W<sub>4</sub>O<sub>33</sub>, high-temp. enthalpy and specific heat 0-34205  
 (Sn)<sub>x</sub>, superconducting polymer, elec. cond., heat capacity and optical props. 0-7028  
 SnCl<sub>2</sub>(H<sub>2</sub>O)<sub>x</sub>(D<sub>2</sub>O)<sub>2-x</sub>, high resolution heat capacity meas. (Japanese) 0-52218  
 Sn<sub>1-x</sub>Ga<sub>x</sub>Mo<sub>2</sub>S<sub>8</sub>, heat capacity meas., singularities at low temp. 0-49985  
 SrF<sub>2</sub>Tb<sup>3+</sup>, mag., thermal and hyperfine props. 0-29368  
 TaC, true heat capacity meas. by pulse method 0-19953  
 TaSe<sub>3</sub>, enthalpy and specific heat, temp. depend. 0-54406  
 TaSe<sub>2</sub>(2H), plasmon behaviour at charge density wave onset 0-10900  
 Tb<sub>1-x</sub>Mo<sub>x</sub>S<sub>8</sub>, low temp. heat capacity anomaly rel. to antiferromag. transition in supercond. state 0-25044  
 TbPO<sub>4</sub>, phase transitions at low temp. 0-15237  
 TbPd<sub>3</sub>, specific heat at low temp. 0-20413  
 Th metallic, heat capacity from 80 to 1000K 0-34201  
 ThC<sub>0.75</sub>, specific heat, Fermi level density of states 0-10680  
 ThC<sub>0.6</sub>N<sub>0.4</sub>, specific heat, Fermi level density of states 0-10680  
 ThO<sub>2</sub>, thermal and transport props., electronic contrib. 0-15432  
 ThP, specific heat, Fermi level density of states 0-10680  
 Ti alloys, data handbook of low temp. mech. and phys. props. 0-22153  
 Ti, high purity, data handbook of low temp. mech. and phys. props. 0-22153  
 Ti, point defect estimation from specific heat and volume in plastically deformed pure metals (Russian) 0-54223  
 Ti<sub>1-x</sub>Nb<sub>x</sub>H<sub>1.94</sub>, x=0.25, 0.50, low temp. specific heat meas. 0-2179  
 Ti<sub>2</sub>O<sub>7</sub> and (Ti<sub>1-x</sub>V<sub>x</sub>)<sub>4</sub>O<sub>7</sub>, metal-insulator transitions, EPR, elec. and mag. props. 0-2336  
 TiS<sub>2</sub>, stoichiometric, heat capacity from 100 to 700K 0-10679  
 (Ti<sub>1-x</sub>V<sub>x</sub>)<sub>2</sub>O<sub>3</sub>, spin-glass props., 0.05-300K 0-25149  
 Tl, thermal and elastic props., lattice heat capacity, elastic constants and thermal expansion, model 0-39321  
 TiH<sub>2</sub>PO<sub>4</sub>, high resolution heat capacity meas. (Japanese) 0-52218  
 U metallic, heat capacity from 80 to 1000K 0-34201  
 α-U-Mo, dil., electronic properties depend. on 2<sup>1/2</sup>-th order phase transition under high press. (Russian) 0-11128  
 UAl<sub>2</sub>, transport props., susceptibility and sp. ht. 0-11174  
 UAs, sp. ht. meas., 5-300K, mag. transition obs. 0-50101  
 β-UD<sub>3</sub>, electronic props., metallic character 0-6693  
 UO<sub>2</sub>, phase, thermodynamic props. 0-13594  
 UO<sub>2</sub>, thermal and transport props., electronic contrib. 0-15432  
 U(OH)<sub>2</sub>SO<sub>4</sub>, mag. susceptibility, heat capacity anomalies at 21K 0-11151  
 V, spin fluctuations effect on T<sub>c</sub>, from sp. ht. and mag. suscept. 0-7030  
 V/H, heat capacity and supercond. from 1.5 and 16K 0-2521  
 V<sub>1-x</sub>Fe<sub>x</sub>, low temp. sp. ht. and mag. props. 0-2548  
 V<sub>1-x</sub>Fe<sub>x</sub>H<sub>1.9</sub>, low temp. sp. ht. and mag. props. 0-2548  
 VN<sub>0.74</sub> and VN<sub>0.89</sub>, low-temp. specific heat and superconducting critical temp. meas., density of states 0-54835  
 V<sub>2</sub>O<sub>7-11</sub>, insulating Magneli phases, mag. susceptibility and sp. ht. meas. 0-34604  
 V<sub>2</sub>S<sub>3</sub>, enthalpy and specific heat, temp. depend. 0-54406  
 V<sub>2</sub>Si, normal, mixed and supercond. state, specific heat meas., thermodynamic and superconducting props. 0-49987  
 WB<sub>12</sub>, growth from melt and phys. props. 0-20782  
 Y-Gd spin glass, sp. ht., 0.3-10K 0-25145  
 YAG:Nd, heat capacity and thermal diffusivity meas. 0-19956  
 YbS<sub>1.387</sub>, magnetic and thermal props. 0-34586  
 ZnFe<sub>2</sub>O<sub>4</sub>, heat capacity investigation of dopant effects on mag. disordering temp. 0-25143  
 Zn<sub>2</sub>Fe<sub>2</sub>O<sub>4</sub>, heat capacity investigation of dopant effects on mag. disordering temp. 0-25143  
 ZnSe, moments of phonon spectra from specific heats 0-15203  
 ZnTe, moments of phonon spectra from specific heats 0-15203  
 ZrC, true heat capacity meas. by pulse method 0-19953  
 ZrO<sub>2</sub>Y<sub>2</sub>O<sub>3</sub>, low-temp. specific heat, oxygen vacancy effects 0-49376

## specific volume see density

## specimen preparation

- see also biological specimen preparation; metallography; replica techniques  
 brittle materials specimen prep. for strength determ. 0-40632  
 carbides, sintered, sample prep. for metallographic structural anal. 0-13048

## specimen preparation continued

- ceramic, brittle, specimen prep. for optical and SEM obs. (German, English) 0-35457  
 ceramic, specimen prep., time saving methods (German, English) 0-35459  
 coal, synthetic, microsection prep. and struct. (German, English) 0-35458  
 composites, thermal stresses investigation, using polymer models 0-40639  
 corrosion science, surface analytic techniques 0-31929  
 deposit-substrate systems, adhesion testing 0-50814  
 dispersion staining method for refr. index meas. of a thin crystal section 0-8433  
 electron microscope specimens, vacuum pipette for processing groups 0-18052  
 EM tensile adhesion test method 0-50804  
 Fe, Armco, electron microscope object prep. method 0-50789  
 frozen hydrated specimens, mass loss and etching by electron microscopes 0-47147  
 glass-fibre reinforced plastic, three-layer cylindrical with syntactic foam base 0-3267  
 hard and brittle materials, microsection prep. technotron and polishing systems (German, English) 0-11859  
 high pressure preparation lock for surface analysis in ultrahigh vacuum chamber (German) 0-52261  
 hydrothermal etching method 0-50790  
 involatile molecule thin films, electrospray deposition for <sup>252</sup>Cf plasma desorption obs. 0-35584  
 ion implantation in samples colder than 0.5K, low temp. nuclear orientation studies 0-34033  
 metallographic specimens, automatic machine and procedure for prep. 0-13050  
 metallography, quantitative methodology (French) 0-30205  
 molecular beam mass spectrometric sampling, high press., high temp. mols., review 0-52355  
 molecular beam mass spectrometry, in situ anal. in crystal growth ambients 0-52357  
 molecular beam mass spectrometric sampling system, ion concs. in coal-fired MHD plasmas 0-52358  
 poly(4-methylpentene-1), permanganic etchant for TEM obs. 0-21132  
 polyacrylonitrile fibres, section cutting, technique (Russian) 0-7754  
 polyethylene, permanganic etchant for TEM obs. 0-21132  
 polymer treeing resistance assessment 0-15971  
 polymeric materials, partially crystalline, comparative evaluation of various prep. techniques for morphology visualisation 0-13049  
 polypropylene, permanganic etchant for TEM obs. 0-21132  
 pyroelectric polymer film for electron microscope sample preparation, rapid cooling effects (German) 0-13185  
 randomised X-ray powder diffraction patterns, adjustable sample holder 0-6317  
 Reichert FC-2 cryomicrotome attachment, improved sectioning reproducibility 0-47149  
 SEM, cryogenic stage for sample preparation for X-ray microanalysis 0-42306  
 SEM, powder scintillators, type P-47 0-22487  
 SEM, sample preparation, for materials microanal. 0-37129  
 silicate glass, low voltage electron microscopy of heated surfaces using C replica technique 0-25974  
 spark-cutter, elec. resistivity meas. (Japanese) 0-22339  
 steel, high strength, H<sub>2</sub> embrittlement due to cathodic charging during specimen prep. for SEM (German, English) 0-11760  
 Technotron system for specimen prep. (German, English) 0-30199  
 TEM, plasma etching use for foil thinning (Slovak) 0-45405  
 US test samples of different materials with equivalent vibration charact. 0-11847  
 wear test specimen, metallographic technique 0-35496  
 X-ray diffractometry handling problems, survey 0-1898  
 Ag, surface Au decoration, appl. to electrodeposits (French) 0-44445  
 Al alloys, specimen preparation for electron microscopy 0-40636  
 Al powder thin foil, prep. for TEM study 0-42310  
 Al wire, specimen preparation for TEM by ion beam thinning (German, English) 0-11861  
 BC, specimen preparation for TEM by ion beam thinning (German, English) 0-11861  
 C, pyrolytic, specimen preparation for TEM by ion beam thinning (German, English) 0-11861  
 CdTe foils, prep. for TEM, ion sputtering technique (Czech) 0-16619  
 Eu pellets, specimen preparation for TEM by ion beam thinning (German, English) 0-11861  
 Fe-base samples, for working curves, HF induction melting and centrifugal casting 0-22340  
 FeTi, H storage alloy, prep. for TEM (German, English) 0-30197  
 GaAs foils, prep. for TEM, ion sputtering technique (Czech) 0-16619  
 Mg-Al single crystal growth, specimen for tensile testing in corrosive medium (Russian) 0-20774  
 Nb, plastically deformed single crystal, foil, damage free prep. for TEM and X-ray topography (German, English) 0-30200  
 Pd-Cu-Si, laser melting and splat quenching to form foils for TEM obs. 0-29986  
 SiC, specimen preparation for TEM by ion beam thinning (German, English) 0-11861  
 Ti-Ni, laser melting and splat quenching to form foils for TEM obs. 0-29986  
 ZrO corrosion layer, specimen preparation for TEM by ion beam thinning (German, English) 0-11861

## speckle

- astronomical IR interferometry, high spatial resolution methods, speckle and aperture synthesis (French) 0-46405  
 astrophotography, isoplanicity meas., speckle holography 0-56717  
 astrophysical applications of image restoration, conf., Bordeaux, France (Mar. 1979) 0-14935  
 colour reproduction of objects by speckle interferometry in white light 0-47094  
 contrast in speckle pattern, method of meas. (French) 0-14284  
 contrast patterns rel. to surface roughness, polarisation effects obs. 0-43258  
 diffuse object, under Gaussian beam illum., laser speckles produced by longit. motion 0-48156  
 diffusely reflecting objects, deformation meas. by lasers, appl. of holography and speckle, review (Japanese) 0-9832  
 digital filtering of speckle-photography data 0-27338



## speckle continued

- displacement meas. of curved surface, using laser speckle interferometry 0-31712  
 dynamical properties study using light scatt., principles spectra derivation and applies. 0-53218  
 holographic images, diffuse noise, statistical characts. calc. 0-28176  
 holographic projection of speckle patterns applied to remote metrology 0-14299  
 image quality of coherently illuminated objects, speckled background smoothing (*Russian*) 0-28168  
 in-plane vibration measurement, real-time interferometry with aid of liq. cryst. light valve 0-53734  
 integrated speckle pattern statistics due to mixed coherent and diffused light 0-14285  
 intensity and phase of speckle pattern, second-order conditional statistics 0-37951  
 interferometric meas. of Pluto diameter 0-41763  
 interferometric obs. of solar photospheric granulation (*French*) 0-46523  
 interferometric obs. of spectroscopic binary 17  $\xi$  Cephei A 0-56874  
 interferometry, astron. appls. (*French*) 0-46404  
 interferometry, meas. of astronomical objects, simulated multiple mirror telescopes 0-56716  
 interferometry, orbital inclination and masses determ. for triple star  $\beta$  Persei (Algol) 0-36668  
 IR speckle images of  $\alpha$  Orionis, two-dimens. obs. (*French*) 0-46553  
 IR speckle interferometry, principle, performance and appl. to NML Cygni 0-31216  
 laser refraction, speckle motion, expt. obs., vision appls. 0-45879  
 laser refraction theory, speckle movement, ocular refr. determ. 0-41001  
 measurement, control and testing, coherent light appl. (*French*) 0-23641  
 mechanical translations ( $10^{-11}$  to  $10^{-3}$  m) meas. using real-time speckle method (*German*) 0-17924  
 monochromatic pattern, amplitude and intensity spatial derivatives, statistical props. 0-53216  
 monochromatic speckle patterns, statistical props. 0-53215  
 multidither adaptive optics, speckle cancellation techniques 0-48161  
 multiple image shearing interferometric camera, displacement derivative meas. 0-33549  
 non-Gaussian statistics, correlated weak scatterers, computer simulation 0-28159  
 ophthalmology and vision research, appl. of lasers, holography 0-12210  
 optical fibre modal noise anal. and meas. 0-10003  
 optical stress analysis using moiré fringe and laser speckles 0-10217  
 planar deformation analysis, speckle correlation method (*Dutch*) 0-32930  
 rotation measurement, in-plane, speckle photography appl. 0-31714  
 rough surface, exact multiple scatt., speckle contrast 0-53217  
 rough surface small vibrs., light scatt. meas. 0-1494  
 sandwich speckle photography for stress meas. (*German*) 0-10216  
 serrated apertures, monochromatic light diff. 0-43260  
 stellar interferometry data processing method 0-17498  
 Steward Observatory speckle camera 0-4254  
 stress-strain state, of machine parts, speckling application 0-19300  
 subspeckle size changes meas. by laser-speckle photography 0-31853  
 surface displacement and strain anal. by speckle interferometry 0-14635  
 surface roughness measurements by means of polychromatic speckle patterns 0-31708  
 surface structure influence on image speckle pattern contrast 0-17985  
 white light, contrast at defocused image plane 0-23621  
 white light images, speckle patterns, average contrast meas. 0-9808  
 wideband speckle interferometry, true imaging of astronomical objects 0-53226

## spectra

see also alpha-particle spectra; astronomical spectra; atmospheric spectra; atomic spectra; beam-foil spectra; beta-ray spectra; Brillouin spectra; cosmic ray energy spectra; electron spectra; energy level crossing; gamma-ray spectra; light scattering; luminescence; mass spectra; matrix isolation spectra; microwave spectra; molecular spectra; multiphoton spectra; neutron spectra; nonradiative transitions; optical double resonance; oscillator strengths; proton spectra; quantum beat spectra; Raman spectra; spectra of inorganic liquids and solutions; spectra of organic molecules and substances; spectra of solids; spectral line breadth; spectral line shift; spectrochemical analysis; Stark effect; stimulated scattering; time of flight spectra; time resolved spectra; transition moments; tunnelling spectra; X-ray spectra  
 radial integrals calc. in Coulomb approx., use of semiclassical wavefunctions 0-43025

## spectra of diatomic inorganic molecules

see also infrared spectra of diatomic inorganic molecules; radiofrequency and microwave spectra of diatomic inorganic molecules; Raman spectra of diatomic inorganic molecules  
 alkali bromides, photofragment spectra, 266 nm, bond energies and excited state symmetries 0-53072  
 inert gas dimer ions,  $A^2\Sigma_{1/2u}^+ \rightarrow D^2\Sigma_{1/2g}^+$  system, theoretical absorption spectrum 0-32734  
 inert gas halide laser, discharge excited, gas composition and lifetime studies 0-53268  
 inert gases, electron beam excited, transient absorpt. at XeF laser wavelengths 0-32644  
 ArBr, emission spectrum and chemiluminesc. 0-45508  
 ArBr, pot. curves, population distrib. and chemiluminesc. for B(1/2) and C(3/2) electronic states 0-45509  
 ArXe, continuous VUV emission spectrum 0-43066  
 BH, PE curve, spectroscopic consts., perturbation theory appl. 0-23341  
 BaH, 3800 angstrom absorption band, concave grating spectrograph obs. 0-14154  
 BiF, spectrum, 5800-6600 Å, vibr. anal., electronic transition assignment 0-992  
 C<sub>2</sub>, absorption bands in stellar spectra, 876 nm obs. 0-12805  
 CN molecular bands in N<sub>2</sub> and air-O<sub>2</sub> arcs, CN origin, band identification 0-38803  
 CN violet system, rotational and vibrational analysis 0-52961  
 CO, CO<sup>+</sup>, emission spectra, 2100-5600 Å, electronic band systems and assignments 0-5560  
 CO, K-shell photoabsorption coeffs., 500-600 eV 0-9617  
 CO<sup>+</sup> <sup>14</sup>C and <sup>18</sup>O isotope shifts, vibr. anal. of first negative, comet-tail and Balder Johnson systems 0-28029  
 CaCl, laser excitation and fluorescence spectra, rotational anal. of  $A^2\Pi \rightarrow X^2\Sigma$  transition 0-43098  
 CaF molecule, vis. spectrum,  $B^2\Sigma \rightarrow X^2\Sigma$  system 0-18863  
 CaH,  $D^2\Sigma^+ \rightarrow X^2\Sigma^+$  band system 0-18847

## spectra of diatomic inorganic molecules continued

CaO  $B^1\Pi-X^1\Sigma$  and  $C^1\Sigma-X^1\Sigma$  transition strengths, shock tube spectroscopic absorpt. meas. 0-53053  
 Cd, as 470 nm absorber, multiconfig. SCF calcs. 0-32731  
 CdHg, excimer kinetics and transmission meas. 0-37832  
 CdHg excimer system, absorpt. meas. 0-48007  
<sup>113</sup>Cd<sub>2</sub>, two-level system, absorpt. spectrum, subradiative struct. (*Russian*) 0-28008  
 Cl<sub>2</sub>, B-X transition, predissoc., laser-induced fluoresc. obs. 0-43093  
 ClO, UV spectra of C<sup>2</sup> $\Sigma^- \rightarrow X^2\Pi$  system, rot. anal. 0-996  
 Co, vacuum UV molecular photoabsorpt. cross-section meas. 0-37096  
 Cs<sub>2</sub>, rot. consts., Doppler-free polarisation spectrosc. 0-5555  
 Cu<sub>2</sub>, in supersonic free jet expansion, laser induced excitation spectrum obs. 0-14151  
 D<sub>2</sub>, predissoc. linewidths and shapes for  $3\pi D^1\Pi_u^+$  state 0-53066  
 F<sub>2</sub>, PE curve, spectroscopic consts., perturbation theory appl. 0-23341  
 GaI, A<sup>0</sup> $\rightarrow$ X<sup>0</sup> and B<sup>1</sup>-X<sup>0</sup> transitions, isotope shifts, UV and visible spectra obs. 0-53005  
 GeCl, mol., UV spectra, band assignments and rot. consts. 0-997  
 GeS, band system vibr. anal. 0-48009  
 GeTe, matrix isolated absorpt. and emission visible spectra, electronic states 0-28026  
 H<sub>2</sub> 3s, 3d: <sup>3</sup> $\Sigma$ , <sup>3</sup> $\Pi$ , <sup>3</sup> $\Delta$  complex, fine struct., Doppler-free laser-spectroscopy 0-1087  
 H<sub>2</sub> 4-0 S(1) 6368 Å quadrupole line strength and pressure shift 0-43108  
 H<sub>2</sub>, electron impact dissoci. excitation, cross sections, mechanisms 0-37895  
 H<sub>2</sub>, electron impact excited singlet-g states, optical and time resolved spectra, radiative lifetimes, quenching rates for rovibronic levels 0-23564  
 H<sub>2</sub> plasma satellites, mol. lines mole, in afterglow 0-44053  
 H<sub>2</sub>, predissoc. linewidths and shapes for  $3\pi D^1\Pi_u^+$  state 0-53066  
 H<sub>2</sub><sup>+</sup>, restricted quantum-mechanical three-body problem 0-42083  
 HCl, electronic spectrum, vac. UV absorpt. 0-9616  
 HD 4-0 and 5-0 bands, absorption strengths 0-43059  
 HD,  $\nu=0$  to  $\nu=5$  rot.-vibr. band, photoacoustic spectrosc. obs. 0-9589  
 HD, predissoc. linewidths and shapes for  $3\pi D^1\Pi_u^+$  state 0-53066  
 HF, electronic spectrum, vac. UV absorpt. 0-9616  
 HI, Rydberg states, quantum defect theory appl. 0-32700  
 He<sub>2</sub>, metastable states, laser excitation spectra 0-5578  
 Hg<sub>2</sub>, dissociative recomb. and optical transmissions meas. in high press. discharge 0-37816  
 Hg<sub>2</sub> vapour, high-press., selective refl. meas. up to 700 bar 0-28031  
 Hg<sub>2</sub><sup>+</sup>, electronic struct. and photoabsorpt. calcs. 0-27932  
 I<sub>2</sub>, Doppler-free optoacoustic spectra 0-995  
 I<sub>2</sub> folded Doppler broadened system, interaction with two reson. laser fields 0-53007  
 I<sub>2</sub>, high-dispersion polarisation-labelled spectrum 0-990  
 I<sub>2</sub>+I<sub>2</sub>, collisional energy transfer, ground and excited states, polarisation spectra 0-32805  
 InCl, discharge excited spectrum 4100-3900 Å, vibr. anal. 0-32732  
 KrF\*, oscillatory bound-free emission spectra, semiclassical anal. method 0-7799  
 Li<sub>2</sub>(A<sup>2</sup> $\Sigma_u^+$ ), state multipoles transfer following rot. inelastic He collisions, polarised emission obs. 0-5608  
 MgH(D), spectra in 230-235 nm region 0-48012  
 MgO, red and near UV bands calc., rel. to sunspot spectra 0-12736  
 N<sub>2</sub>, diffuse plasma, population densities of triplet states, correl. with electron impact processes 0-43966  
 N<sub>2</sub>, electrical discharge excitation, vibr. level population distrib., electron beam fluoresc. obs. 0-48031  
 N<sub>2</sub>, PE curve, spectroscopic consts., perturbation theory appl. 0-23341  
 N<sub>2</sub>, positive column, flowing, visible spectrum obs. 0-49026  
 N<sub>2</sub> triplet-triplet transitions, Einstein-A coeffs., oscill. strengths, lifetimes, theory and experiment comparison 0-47876  
 N<sub>2</sub><sup>+</sup>, A- and B-states interactions, time-resolved obs. 0-18862  
 N<sub>2</sub><sup>+</sup>, UV spectral line width in rarefied free jet, for rot. temp. 0-6184  
 N<sub>2</sub>-CO, electrical discharge excitation, vibr. level population distrib., electron beam fluoresc. obs. 0-48031  
 ND c <sup>1</sup> $\Pi$ -a <sup>1</sup> $\Delta$  system, new bands, spectroscopic consts. 0-9612  
 NaH, A<sup>1</sup> $\Sigma^+$ -X<sup>1</sup> $\Sigma^+$  electronic transition, spectroscopic anal. and potential energy curves 0-48102  
 Ne+HD, j=0 to 1 rot. excitation, differential cross sections, time of flight obs. 0-48104  
 NiBr, band system in near UV, vibr. analysis 0-32733  
 O<sub>2</sub> C<sup>2</sup> $\Delta_u$ -a<sup>1</sup> $\Delta_g$  band system, vibr. anal. 0-5556  
 O<sub>2</sub>, K-shell photoabsorption coeffs., 500-600 eV 0-9617  
 O<sub>2</sub>, Schumann-Runge band system in sunspots UV spectrum 0-12735  
 O<sub>2</sub>, UV absorpt. into <sup>3</sup> $\Pi_u$  state, calc., atmos. opacity 0-12582  
 O<sub>2</sub>, vacuum UV molecular photoabsorpt. cross-section meas. 0-37096  
 O<sub>2</sub><sup>+</sup>, first negative system, high-resolution photofragment spectroscopy 0-47971  
 O<sub>2</sub><sup>+</sup>, predissociated b<sup>4</sup> $\Sigma_g^-$  state, high resolution laser spectroscopy in fast ion beam 0-9656  
 OH, band oscill. strength, rot. excitation effects 0-23460  
 OH formation in H<sub>2</sub>-NO flame, OH collisional broadening parameter, curve of growth method 0-53052  
 OH rotational temp. determ., successive approx. 0-23389  
 O<sub>2</sub>(c<sup>2</sup> $\Sigma_u^-$ ), in Ar(Kr)(Ar-Kr) matrices, multiphonon vibr. relax., time-resolved emission obs. 0-18861  
 P<sub>2</sub>, intersystem transition obs. in absorpt. spectrum 0-48008  
 PO, in Ar matrix, IR and UV absorpt. spectra 0-47985  
 PrO, 0-0 band in XVII system, hyperfine splitting, visible excitation spectra 0-28028  
 S<sub>2</sub> mol. B<sup>2</sup> $\Sigma_u^- \rightarrow X^2\Sigma_g^-$  fluorescence induced by N<sub>2</sub> laser (*Japanese*) 0-14175  
 SiH, ground state,  $\Lambda$ -type doubling 0-23431  
 SiO in Ar matrix, vac. UV spectrum, vibr. progression 0-23432  
 TeF, chemiluminesc. from oxidation in F<sub>2</sub>+H<sub>2</sub>Te(D<sub>2</sub>Te) emission spectrum obs. 0-43058  
 ThO, L<sup>1</sup> $\Pi$ -<sup>1</sup> $\Sigma^+$  and N<sup>1</sup>  $\Pi$ -X<sup>1</sup> $\Sigma^+$  systems, spectra, rot. anal. 0-23430  
 TiO band absorption effect on stellar photometry with broadband filters 0-41811  
 Xe<sub>2</sub>, e-beam excited, 193 nm absorpt. studies 0-43323  
 Xe<sub>2</sub>, electron beam excited, 193 nm absorpt. meas. rel. to 172 nm laser pulse termination 0-28200  
 ZrO bands, integrated intensity meas. and effective vibr. temp. 0-43111

## spectra of inorganic liquids and solutions

see also Raman spectra of inorganic liquids and solutions  
 anharmonic molecules in condensed media, vibronic dephasing, intra- and intermolecular processes 0-2127



**spectra of inorganic liquids and solutions continued**

- cryogenic solutions, spectrosc. and photochem. 0-16713  
 inert gases, liquid phase mixtures, dipole autocorrelation function, IR absorpt. spectra obs. 0-28903  
 intermolecular interactions in condensed medium, long-wavelength IR spectroscopy 0-34927  
 ionic solutions, in liq. HCl, coord. sphere radius, vibr. spectrosc. investig. 0-50843  
 IR continua, phonon theory 0-29729  
 molecular rotation, model for IR and Raman studies in liqs. and gases 0-11390  
 polyatomic fluid, local dynamics, spectroscopic studies, summer school lecture series 0-6343  
 rare earth complexes, formation and props., book contrib. 0-43204  
 rare earth ions in soln., absorpt. and fluoresc. spectra, book contrib. 0-45112  
 semiconductors, normal refl. data and model densities of states 0-50364  
 water sorbed on DNA, temp. anomaly, IR spectroscopic obs. 0-51046  
 water-carbon tetrachloride soln., fundamental H<sub>2</sub>O IR spectrum, liq. struct. 0-23419  
 Au<sub>19</sub>/Si<sub>19</sub>, optical refl., 0.5 to 6 eV, hall coeff. and elec. resist. 0-29755  
 COF<sub>2</sub>, soln. in liquid Ar, transition freq., halfwidths and relative intensity, IR absorpt. spectra 0-55101  
 CS<sub>2</sub>, liq., props. from allowed light scatt. spectra 0-25364  
 CaO-SiO<sub>2</sub>-NiO-MgO glass melt, interaction of NiO and MgO, elec. cond. and IR spectra obs. (Japanese) 0-24632  
 Cl<sub>2</sub>, Ar matrix, vibronic dephasing 0-6469  
 Cl<sub>2</sub>-O<sub>2</sub>-H<sub>2</sub> dilute mixtures, photolysis products, Fourier Transform IR kinetic obs. 0-26033  
 Cu complex, catena- $\mu$ -isothiocyanato-(N'-pyridylmethylene-N"-salicyloylhydrazinato-NN'O) copper (II), EPR and visible spectra 0-5566  
 HCl, liq., IR spectral intensity and Raman cross-section meas. 0-2742  
 HClO<sub>4</sub>-H<sub>2</sub>O, aq. soln., IR and Raman spectra, conc. depend. (Russian) 0-53002  
 HD-T<sub>2</sub>, liq. and solid, vibr.-rot. IR spectra 0-50313  
 H<sub>2</sub>O, D<sub>2</sub>O, visible absorpt. meas., pulsed dye laser optoacoustic spectroscopy 0-11426  
 H<sub>2</sub>O, liquid, far IR optical consts. meas. with optically pumped laser 0-40082  
 HOD, IR spectra in D<sub>2</sub>O, combination vibr. 0-9609  
 H<sub>2</sub>O(D<sub>2</sub>O), solvated electrons, optical absorpt. spectra. temp., isotope effects 0-55124  
 HT-T<sub>2</sub>, liq. and solid, vibr.-rot. IR spectra 0-50313  
 IO<sub>4</sub><sup>-</sup> ion in solns., UV spectra 0-2786  
 InX(X<sub>2</sub>(X<sub>3</sub>), InAlX<sub>4</sub>, X=Cl,Br, Raman spectra, up to 1200K 0-48003  
 OCS in Ar soln., IR spectra, solvent shifts, vibr. band assignment and anharmonic force consts. 0-9607  
 PCl<sub>3</sub>-HCl<sub>3</sub>, Raman spectra, solid and melt, species identification (German) 0-45083  
 PH<sub>3</sub>, liq. and solid, Raman spectra., vibr. correl. functions, rot. motions 0-55087  
 PbO-SiO<sub>2</sub>-NiO-MgO glass melt, interaction of NiO and MgO, elec. cond. and IR spectra obs. (Japanese) 0-24632  
 Pd complex, Pd<sup>II</sup>(CNCH<sub>3</sub>)<sub>4</sub>(PF<sub>6</sub>)<sub>2</sub>, vibr. spectra, M-M bonds. (French) 0-47997  
 Pt complex, Pt<sup>II</sup>(CNCH<sub>3</sub>)<sub>4</sub>(PF<sub>6</sub>)<sub>2</sub>, Pt<sup>I</sup>(CNCH<sub>3</sub>)<sub>3</sub>(PF<sub>6</sub>)<sub>2</sub>, and Pt<sup>II</sup>Pd<sup>I</sup>(CNCH<sub>3</sub>)<sub>6</sub>(PF<sub>6</sub>)<sub>2</sub>, vibr. spectra, M-M bonds. (French) 0-47997

**spectra of inorganic molecules**

see also spectra of diatomic inorganic molecules; spectra of polyatomic inorganic molecules  
 No entries

**spectra of inorganic solids**

- see also impurity and defect absorption spectra of inorganic solids; infrared spectra of inorganic solids; luminescence of inorganic solids; radiofrequency spectra of inorganic solids; Raman spectra of inorganic solids; visible and ultraviolet spectra of inorganic solids  
 crystals, line-shape distortion on anisotropic absorpt. meas. in unpolarised light 0-2765  
 magnetic semiconductors, excitation spectrum, temp. and band occupation depend. 0-49588  
 magnetic system, amorphous, microwave absorption spectra 0-50469  
 metal film, optical absorption due to particle-hole excitations 0-45160  
 metallic thin films, granular, optical props. rel. to multipole oscills. in hemispherical particles 0-7431  
 narrow band gap semiconductors, conference, Warsaw, Poland (Sept. 1977) 0-49703  
 random alloy, optical absorption and photoemission spectra 0-45216  
 rare earth pnictides, prep. and props., book contrib. 0-54212  
 spessartine garnet, measurement of absorpt. spectra using automated microscope-spectrophotometer 0-18010  
 vibrational spectroscopy review 0-55093  
 Ag clusters on Si substrates, opt. spectra investig. of struct. (German) 0-25492  
 $\alpha$ -AgI, superionic conductor, microwave absorption spectrum 0-11515  
 $\beta$ -Al<sub>2</sub>O<sub>3</sub>-Ag<sub>2</sub>O, superionic conductor, microwave absorption spectrum 0-11515  
 $\beta$ -Al<sub>2</sub>O<sub>3</sub>-Na<sub>2</sub>O, superionic conductor, microwave absorption spectrum 0-11515  
 CdS<sub>1-x</sub>Se<sub>x</sub> mixed crystals, free excitons, disorder effects 0-34365  
 Co<sup>2+</sup> complex, ammoniated zeolite, oxygenated product form., electronic spectrosc. obs. 0-991  
 CrF<sub>3</sub>, spectra, cryst. field least squares fitting interpretation 0-44548  
 CuTeBr, superionic conductor, microwave absorption spectrum 0-11515  
 Fe<sub>2</sub>O<sub>4</sub>, optical cond. anisotropy calcs. below Verwey transition 0-50289  
 GaAs, electron-hole plasma, Coulomb effects on gain and absorption spectra 0-50371  
 GaAs:Si(Te)(S), vapour phase epitaxial grown layers, photoluminesc. and emission spectra 0-29774  
 GaSb, vibr. spectra, lattice dynamics ang. force model 0-29127  
 Ge, electron hole droplets, intervalence band absorption 0-6742  
 (NiF<sub>6</sub>)<sup>4-</sup> complex, open-shell cluster calcs., semiempirical LCAO-MO method 0-54583  
 NiF<sub>6</sub><sup>4-</sup>, spectra, cryst. field least squares fitting interpretation 0-44548  
 SiO<sub>2</sub>, vitreous, and quartz, impurity C determ. by isotopic spectral method 0-26093  
 (TiF<sub>6</sub>)<sup>3-</sup> complex, open-shell cluster calcs., semiempirical LCAO-MO method 0-54583

**spectra of organic molecules and substances**

- see also infrared spectra of organic molecules and substances; luminescence of organic solids; radiofrequency and microwave spectra of organic molecules and substances; Raman spectra of organic molecules and substances; Shpolskii spectra  
 acetic acid amides, polarisabilities and  $\pi$ - $\pi^*$  transitions, dipole interaction calcs. 0-23411  
 acetylene smoke, optoacoustic meas. of absorpt. at 0.5145, 10.6  $\mu$ m 0-43060  
 alkyl benzenes, jet-cooled, intramol. vibr. relax., reson. fluoresc. and excitation obs. 0-14152  
 alkyl substituted diacetylene radical cations, optical emission and photoelectron spectra, fragmentation decay 0-53004  
 allyl isocyanide, state-selected, visible absorption spectra and photoisomerisation kinetics 0-11879  
 anthracene, triplet-exciton fine struct., high resolution optical meas. 0-45099  
 anthracene derivative, Langmuir-Blodgett multilayer film, semiconducting props., optical and elec. meas. 0-11122  
 anthracene single cryst., Frenkel exciton spectra at dielectric and conducting layer interfaces 0-44510  
 9,10-anthraquinones,  $\Pi$ - $\Pi^*$  electronic transitions, substituent effects calcs. 0-28006  
 4-(9-anthryl)-N,N-dimethylaniline, fluoresc., dipole moments and polarisabilities 0-1019  
 aromatic, absolute fluorescence quantum yield, calorimetric determ. 0-43092  
 azulene, induced circular dichroism of  $\pi$ - $\pi^*$  bands in presence of (+)-nopinone 0-53058  
 bacteriorhodopsin Br570, bathochromic shift of absorpt. band in external elec. field 0-35838  
 BBOT dye, vapour phase, optical props. (Japanese) 0-9879  
 benzaldehyde, electronic spectra, Cl and F substitution effects 0-23456  
 benzaldehydes, o- and m-substituted fluoro- and chloro- forms, rot. isomerism,  $\pi$ - $\pi^*$  spectra obs. 0-5631  
 benzene, adsorbed on porous vycor glass, adsorpt. spectrum 0-9615  
 benzene, and methyl derivatives,  $E_{1u}$  N-V state mag. moments, MCD obs. 0-23575  
 benzene, derivatives, calc. of second-order susceptibility, using electronic spectra data 0-29756  
 benzene, optoacoustic spectroscopy using cell with ultimate corrosion resistance 0-42269  
 benzene, thermal lensing effect, absorptivity meas. at 607 nm 0-34900  
 benzene, UV photoelectron spectra, valence electron shake up approx. methods 0-18788  
 benzene and deuterates, highly vibr. excited intramolecular V-V transfer, visible and photoacoustic spectra 0-32729  
 1,3-benzodioxole, geometry, electronic absorpt. spectra 0-971  
 2-benzoylpyridine crystals, optical spectra of lowest triplet state 0-16081  
 biphenyl single crystals,  $\gamma$ -ray induced radicals, EPR and optical absorpt. studies 0-44921  
 bromobenzene, optoacoustic spectroscopy using cell with ultimate corrosion resistance 0-42269  
 bromomethane, mol. Rydberg transitions mag. circular dichroism 0-43081  
 calcium tartrate tetrahydrate:Cr<sup>3+</sup>, optical absorpt. spectrum, cryst. field parameters 0-16067  
 calcium tartrate tetrahydrate:Cu<sup>2+</sup>, spin-orbit coupling, optical absorpt. spectra 0-45120  
 catechol borane, geometry, electronic absorpt. spectra 0-971  
 chlorobenzene, optoacoustic spectroscopy using cell with ultimate corrosion resistance 0-42269  
 cofacial diporphyrins, electron transfer reactions following picosecond excitation, CT state lifetimes, optical difference spectra 0-25995  
 coumaran, geometry, electronic absorpt. spectra 0-971  
 cryogenic solutions, spectrosc. and photochem. 0-16713  
 cryptolepine derivatives, absorpt. and fluoresc. obs. of photodecomp. processes, dye laser relevance 0-55686  
 crystals, line-shape distortion on anisotropic absorpt. meas. in unpolarised light 0-2765  
 cytochrome c-serotonin soln., UV effect on optical props. 0-30663  
 cytochrome P-450, non-equilib. states formed by low-temp-reduction, absorpt. spectra 0-35837  
 p-dibromodiphenylether surface, normal and ultra-Brewster refl. spectra 0-25400  
 1,4-dibromonaphthalene, substitutionally disordered, energy localisation, optical and ODMR spectra of triplet Frenkel excitons 0-54996  
 dicarbonitrile-anthracene solutions, absorpt. and emission spectra, solvent influence 0-43083  
 dicyanodiacetylene radical cation, photoelectron and emission spectra 0-5558  
 diphenyl butadiene, absorption recovery lifetime, use in UV mode-locked lasers 0-19075  
 diphenylethylene, UV spectra, quantum-mechanical investigation of isomerisation pathways 0-43065  
 dispersion induced circular dichroism, determ. of mag. dipole allowed transitions 0-14163  
 DOBAMBC, smectic liquid crystal, ferroelectric, colour switching in elec. field 0-29719  
 dye absorpt. spectra, observation using oscillating beam spectrometer 0-31907  
 dyes, absolute fluorescence quantum yield, calorimetric determ. 0-43092  
 elastomers, relax. transitions from relax. spectrometry and internal friction (German) 0-34136  
 electron microprobes and scanning electron microscopy, conf., Orsay, France, Dec. (1978) 0-11979  
 ethanol glass, trapped and solvated electrons produced in presence of applied electric field 0-7379  
 ethylene, UV photoelectron spectra, valence electron shake up approx. methods 0-18788  
 fluoranthene, single cryst. and in fluorene matrix, polarised absorption spectra, assignments 0-55122  
 fluorobenzene, optoacoustic spectroscopy using cell with ultimate corrosion resistance 0-42269  
 formaldehyde-<sup>13</sup>C, A<sup>1</sup>A<sub>2</sub>-X<sup>1</sup>A<sub>1</sub> system, UV absorpt. spectra, rot. anal. 0-9614  
 formic acid amides, polarisabilities and  $\pi$ - $\pi^*$  transitions, dipole interaction calcs. 0-23411  
 free radicals determ., on polymer surfaces (German) 0-7892  
 haloacetylene cations, electron impact excitation A $\rightarrow$ X band system assignment 0-32766



## spectra of organic molecules and substances continued

halomethanes, synchrotron radiation photoabsorption cross sections, Rydberg states 0-28033  
 4-n-heptyl-4'-cyanobiphenyl, linear dichroism spectra in nematic and isotropic phases 0-25336  
 2-hydroxy, 3-allyl, 4,4'-dimethoxybenzophenone, methyl methacrylate copolymer, excitation singlet, internal  $H^+$  transfer, visible spectra 0-32728  
 2-hydroxybenzophenone, excitation singlet, internal  $H^+$  transfer, visible spectra 0-32728  
 ortho-hydroxybenzophenone, soln., intramol. proton transfer and energy relax. photostability, transient absorption obs. 0-28032  
 indigo dyes, triplet state config., laser flash absorpt. spectrosc. obs. 0-5557  
 large molecule, electronic struct., photoemission and optical absorpt. spectrum, CNDO/S3 model 0-53172  
 masked antifogants, hydrolysis stability, photographic process depend. (German) 0-45530  
 methane,  $\nu_4$  band, high resolution spectrosc. 0-5529  
 methane,  $\nu_4$  band Q-branch spectrum 0-5530  
 3-methoxybenzanthrone in ethanol, photolytic reactions, spectra, rate consts. and lasing thresholds 0-43327  
 methyl chloride, vacuum UV absorpt. spectrosc., Rydberg transitions obs. 0-5561  
 methyl iodide, Rydberg states, quantum defect theory applic. 0-32700  
 methylene radical, vibronic bands obs. in pulsed supersonic jet 0-28024  
 3-methylenoxetane, electron structure, orbital-O interaction, MO calcs., UV photoelectron spectra 0-28058  
 2-methyltetrahydrofuran-methanol mixed glasses, annealed,  $\gamma$ -ray produced electrons transfer from IR to visible traps 0-11440  
 methoxy radical, electronic absorpt. spectra, visible, vibr. freqs., vibronic intensities and oscill. strengths 0-28025  
 naphthalene, fluorescence and absorpt. spectra, deviations from Condon approx. 0-28004  
 naphthalene, UV spectra and extinction coeffs. for  $S_n \rightarrow S_1$  absorption 0-18866  
 naphthalene anions, electron affinities, transition energy, comparison for gaseous liquid and solid 0-29731  
 Nile Blue, subpicosecond spectroscopy, tunable probe, spectral dynamics 0-23429  
 nucleic acids, electronic absorpt. and emission spectra 0-55989  
 nucleotide bases, electronic absorpt. and emission spectra 0-55989  
 2'-oxaindan (dihydroisobenzofuran) spiropyran, photochromic transforms, spectrokinetic study 0-30259  
 3-oxetanone, electron structure, orbital-O interaction, MO calcs., UV photoelectron spectra 0-28058  
 palladium porphyrin, in n-alkane crystal, Zeeman and crystal field effects, absorpt. vibr. anal. 0-7372  
 perylene-tetracene in liquid crystals, temp. depend. of absorption and fluorescence. (German) 0-18887  
 phenazine, substitutionally disordered, energy localisation, optical and ODMR spectra of triplet Frenkel excitons 0-54996  
 (+)-(S)-2-phenyl-3,3-dimethylbutane, optical activity, circular dichroism, polarisability model 0-43082  
 phthalan, geometry, electronic absorpt. spectra 0-971  
 pigment associations, conc. effects, luminesc., absorpt. spectra and dichroism obs. 0-1007  
 pigment molecule organisation and interaction in reaction centres of Rhodospseudomonas viridis 0-35843  
 pleochroic dyes, dissolved in nematic liq. crystals, guest-host interactions, appl. to electrooptic displays 0-44113  
 poly-2-vinylnaphthalene, soln., lowest triplet props., flash photolysis and radiolysis obs. 0-32861  
 poly- $\gamma$ -benzyl-L-glutamate helices, optical activity 0-48113  
 polyacetylene, pure and heavily doped, optical and IR studies, electronic struct. calcs. 0-7347  
 st-1,2-polybutadiene, oriented film, anisotropic C 1s XUV absorpt. spectra 0-55207  
 polydiacetylene, cryst., one-dimens. conjugated semicond., vibronic coupling, Fano interference effects 0-34939  
 polyene chromophores, band broadening in electronic-vibr. absorpt. spectra 0-28003  
 polyethylene photochemical aerosol, absorbance rel. to presence in Titan atmosphere 0-31249  
 polypeptides,  $\alpha$ -helical,  $\pi\text{-}\pi^*$  absorpt. and circular dichroism spectra 0-23398  
 polystyrene, and copolymers, optical fibre waveguides, spectral characts. 0-14461  
 polystyrene solutions, dilute, diffusion coeff., solvent effect 0-19971  
 polystyrene-PMMA-benzene, soln., polystyrene diffusion, photon correl. spectroscopy 0-34220  
 poly[(R)-oxypropylene], opt. rot. dispersion and vac. UV circular dichroism 0-40084  
 porphyrins orientation in n-alkane Shpolskii hosts, spectra 0-48035  
 praseodymium  $\beta$ -ketoesters,  $Pr^{3+}$ , visible spectrum, interaction, intensity and bonding parameters 0-993  
 $\beta$ -propiolactone, electron structure, orbital-O interaction, MO calcs., UV photoelectron spectra 0-28058  
 protein secondary structure determ. by circular dichroism spectra 0-30653  
 pseudoisocyanine bound by sulphated polysaccharides, dil. aq. soln., visible and circular dichroism spectra 0-45107  
 PTZ:PMMA, purification, growth, struct., optical and elec. props. 0-54216  
 pyrazine, dispersion induced circular dichroism, determ. of mag. dipole allowed transitions 0-14163  
 pyrene-3-sodium sulphonate solubilised in didodecyldimethylammonium bromide-benzene inverted micelles 0-3417  
 pyridine, dispersion induced circular dichroism, determ. of mag. dipole allowed transitions 0-14163  
 pyridine cation radical in trichlorofluoromethane matrix, gamma irradiation, EPR and optical obs. 0-23442  
 rare earth ions, ligand-induced pseudoquadrupole absorpt., vibronic contrs. 0-52978  
 rhodamine 640, subpicosecond spectroscopy, tunable probe, spectral dynamics 0-23429  
 rhodamine 6G, aqueous soln., absorpt. spectra, ground and triplet state photoprotonation pH depend. 0-42961  
 rhodamine dyes in soln., bleaching, electronic and vibr. absorpt. spectra, fluoresc. 0-42960  
 selenophene, flash photolysis, transient absorpt. spectra 0-14153

## spectra of organic molecules and substances continued

solids, XUV photoabsorpt. spectra, at. effects 0-2785  
 solvent effects, rel. to polarisation structure 0-43062  
 strontium formate dihydrate:  $Cr^{3+}$ , optical absorption spectrum 0-50380  
 styrene anions, electron affinities, transition energy, comparison for gaseous liquid and solid 0-29731  
 styrene-acrylonitrile copolymer solutions, dilute, diffusion coeff., solvent effect 0-19971  
 tetracene in liquid crystal, absorption, fluorescence and polarisation, temp. depend. study (German) 0-18887  
 di-(tetraethylammonium)tetrahalomanganate, mag. circular and linear dichroism obs. 0-29725  
 tetrafluoromethane, gas, DID Rayleigh and Raman depolarised scatt., lattice-gas model 0-10356  
 tetramethylsilane, IR and visible spectral intensity data and the universal intensity concept 0-28066  
 tetraphenylporphyrin, dispersion induced circular dichroism, determ. of mag. dipole allowed transitions 0-14163  
 thioformaldehyde- $d_0$ ,  $-d_2$ ,  $A_1A_2-X^1A_1$ , vis. absorpt. system, rot. anal. 0-5559  
 thioindigo dyes, triplet state config., laser flash absorpt. spectrosc. obs. 0-5557  
 toluene, electronic-vibr. spectra calcs., Franck-Condon and Herzberg-Teller approx. 0-37735  
 toluene, optoacoustic spectroscopy using cell with ultimate corrosion resistance 0-42269  
 triethylamine-perfluoro-T-butanol, photoelectron and Rydberg bands, UV spectra study 0-18865  
 trifluoriodomethane, UV absorpt. spectrum broadening by laser-induced vibr. excitation 0-53050  
 UV photoelectron spectroscopy, systematic review 0-28057  
 p-xylene, electronic-vibr. spectra calcs., Franck-Condon and Herzberg-Teller approx. 0-37735  
 Ag complexes, Ag(II) porphyrins, picosec. flash photolysis, transient absorpt. 0-52976  
 $CF_2$ , time-resolved optical absorption obs. in IR multiphoton dissoc. of  $CF_2HCl$  0-16702  
 $CH^+$ , predissociation transition obs. 0-37838  
 $Cl_2$ , Ar matrix, vibronic dephasing 0-6469  
 ClFCS, second excited singlet state photophysics, laser excitation obs. 0-32758  
 Co(II) Schiff base complexes, structure and bonding, book contrib. 0-972  
 Cu, effect of impurities 0-50925  
 $Na_3Pr(C_4H_4O_5)_3 \cdot 2NaClO_4 \cdot 6H_2O$ , single cryst., forbidden  $A_1 \rightarrow A_1$  transition, mag. field induced intensification 0-50302  
 Ni complex, bis-4-dimethylaminodithiobenzyl nickel, tetrachlorethane soln., photochem. and thermal stability 0-16708  
 Ni complexes, Ni(II) porphyrins, picosec. flash photolysis, transient absorpt. 0-52976  
 $O_2$ ,  $b^2\Sigma_g^- \rightarrow X^3\Sigma_g^-$  electronic transition, absorpt. coeffs. and transition moments 0-43061  
 OCS, motion, regular and irregular spectra, theory 0-9590  
 pyrene, UV spectra and extinction coeffs. for  $S_n \rightarrow S_1$  absorption 0-18866

## spectra of polyatomic inorganic molecules

see also infrared spectra of polyatomic inorganic molecules; radiofrequency and microwave spectra of polyatomic inorganic molecules; Raman spectra of polyatomic inorganic molecules  
 cryogenic solutions, spectrosc. and photochem. 0-16713  
 inert gas halide laser, discharge excited, gas composition and lifetime studies 0-53268  
 transition metal complexes, mol. dissymmetry, book 0-27057  
 $[Re_2Cl_8]^{2-}$ , spectral assignment, metal-metal bonds, SCF X $\alpha$  SW calcs., relativistic corrections 0-53006  
 BrCN, vacuum UV photodissociation spectroscopy, quantum yield, fluorescence, polarisation 0-32736  
 $C_2N_2$ , and  $C_2N_2^+$ , electronic struct. UV and PE spectra 0-23304  
 $CO_2$ , K-shell photoabsorption coeffs., 500-600 eV 0-9617  
 $CO_2$ , photolysis, O(S) absolute quantum yield spectral depend. meas. using XeO luminesc. 0-35561  
 $CO_2$  plasma, atm. press. opt. props., 400-1200 nm spectral range and  $10^{-2} \times 10^4$  K temp. 0-33753  
 $CO_2$ ,  $\Pi_u$  symmetry transition probabilities, dipole moment and electro-optical consts. calc. 0-43115  
 $CO_2$  spectra, Fermi reson. and classical motion 0-28000  
 $CO_2$ ,  $^3A_2\Pi_u \rightarrow X^2\Pi_g$  band emission spectrum, rovibronic anal. 0-9613  
 $CS_2$ ,  $^3A_2$  state, triplet bands, MCD spectrum, near UV absorpt. spectrum 0-48010  
 $CS_2$ ,  $^3A_2$  state, MCD and UV spectrum, theoretical anal. 0-48011  
 $CS_2^+$ , photodissociation cross section, UV and visible spectral obs. 0-28077  
 ClCN, vacuum UV photodissociation spectroscopy, quantum yield, fluorescence, polarisation 0-32736  
 $FeI_3$ , vapour phase, UV-visible absorpt. spectra, absorbance peaks 0-994  
 $GeF_4$ ,  $(GeCl_4)$ , X-ray absorpt. spectra struct. 0-37819  
 $H_2$ , Rydberg spectrum, theory 0-5528  
 H $_2$ O absorption lines at ruby laser wavelengths, saturation effect 0-4098  
 HPO, in Ar matrix, IR and UV absorpt. spectra 0-47985  
 ICN, vacuum UV photodissociation spectroscopy quantum yield, fluoresc. polarisation vacuum UV photodissociation spectroscopy, quantum yield, fluoresc. polarisation 0-32736  
 $I_2$ , Ne, He, van der Waals complexes photodissoc. 0-50864  
 $Kr_2F$ , absorpt. in near UV wing of 410 nm band, fluoresc. efficiency 0-14323  
 Mg complex, bis-pyridal-Mg-tetrabenz-porphyrin, disagreement with diffuse interstellar bands 0-56905  
 $Mo_2[(CH_3)_2P(CH_3)_2]_2$ ,  $\delta\text{-}\delta^*(A_{2u} \rightarrow A_{1g})$  transition, vibr. struct. anal. 0-53006  
 $NH_3$ , ground state mol. consts., absorption spectra 0-28030  
 $NH_3$ , inversion spectra,  $\nu_4$  state 0-47965  
 $NH_3$ , optical band strengths and curves of growth rel. to spatial distrib. on Jupiter 0-46386  
 $NH_3^+$  ( $B_1 \rightarrow A_1$ ) optically-allowed transition position estimation, from UPS data 0-53047  
 NHD radical, dipole moment determ., optical Stark spectroscopy 0-23455  
 $NO_2$ , inter and intramolecular radiationless transitions, relax., time resolved excitation and fluoresc. spectra 0-27966  
 $NO_2$ , minor atm. components, visible absorpt. spectra, temp. depend. (French) 0-36355  
 $N_2O$ , K-shell photoabsorption coeffs., 500-600 eV 0-9617



**spectra of polyatomic inorganic molecules continued**

- N<sub>2</sub>O, photolysis, O(<sup>1</sup>S) absolute quantum yield spectral depend. meas. using XeO luminesc. 0-35561  
 Ni(CO)<sub>4</sub>, ppb in air meas. by chemiluminesc. detector 0-40692  
 O<sub>3</sub>, Hartley band during formation, metastable states, vibr. excitation and relax. 0-55632  
 OCS<sup>+</sup>, photodissociation cross section, UV and visible spectral obs. 0-28077  
 OsO<sub>4</sub>, HFS and fine struct., saturation spectroscopy obs. visible spectra 0-53008  
 Ru complex, ruthenium(II) tris(2,2'-bipyridine), absorption spectrum and quantum yield of formation (French) 0-5554  
 SF<sub>6</sub>, electronic props., (e,2e) spectrosc. obs. 0-5527  
 SF<sub>6</sub>, multiple-photon absorption, experimental conditions and mol. parameters depend. 0-32790  
 SF<sub>6</sub>,  $\nu_3$  bands, rot. fine struct., HFS spectroscopic consts. determ., saturation spectroscopy obs. 0-53008  
 SO<sub>2</sub>, minor atm. components, near UV absorpt. spectra, temp. depend. (French) 0-36355  
 SO<sub>2</sub>, X-A electronic absorpt. band system, non Condon effects study 0-18837  
 SiF<sub>4</sub>, (SiCl<sub>4</sub>), (SiBr<sub>4</sub>), X-ray absorpt. spectra struct. 0-37819  
 SiF<sub>4</sub>, XUV spectra, overlapping core-valence and core-Rydberg transitions and resons. 0-32735  
 UF<sub>6</sub>, photophysical props., laser study 0-28040  
 XeF<sub>2</sub>, photodissoc. yield in solid Xe and Kr, time-resolved photolum. excitation obs. 0-3372

**spectra of solids**

- see also impurity and defect absorption spectra of solids; luminescence of solids; Shpol'skii spectra; spectra of inorganic solids; spectra of organic molecules and substances*  
 absorption coefficient under laser irradi. 0-34940  
 adsorption behaviour at solid/liq. interface, IR spectra study 0-40733  
 amorphous semiconductor, configuration-coordinate model, Urbach rule 0-34948  
 amorphous solids, optical absorption tail, shape 0-34946  
 broadening, inhomogeneous and homogeneous, of optical and ODMR transitions in solids 0-32750  
 chemisorption systems, IR spectral linewidth and sticking coeffs., non-adiabatic effects 0-39423  
 cubic crystals, Raman scatt. from tunnelling of substitutional molecules 0-40107  
 disordered solid, IR and Raman spectra, analytic models 0-7336  
 dynamic Jahn-Teller systems, calc. of absorption band shapes, use of Lanczos algorithm 0-45023  
 inner level spectroscopy with synchrotron radiation, theoretical aspects, book contrib. 0-4778  
 ion beam heated thin targets, soft X-ray and VUV spectra 0-2907  
 IR reflection spectrum, dispersion formula fitting, Kramers-Kronig anal. 0-50311  
 localised electron nonequilibrium vibration interaction secondary radiation spectrum 0-2778  
 molecular crystal, calc. of second-order susceptibility, using electronic spectra data 0-29756  
 molecular crystals, spectroscopy, bibliography (1977) 0-7317  
 molecular crystals, two particle exciton-phonon interactions, optical absorpt. line shapes theory 0-55120  
 photoacoustic spectroscopy of solids immersed in transparent liquids 0-22452  
 polariton kinematical levels resulting from excitons interaction, optical absorption line broadening 0-10892  
 self-diffraction of light by excitons 0-53389  
 semiconductor, conjugated, one-dimens., vibronic coupling, Fano interference effects 0-34939  
 semiconductor, disordered, electroabsorption, contact excitons influence 0-10882  
 semiconductor, light pulse propag. inducing transitions between bands with different effective masses 0-34871  
 semiconductors, disordered, phonon-assisted interband optical absorption 0-34947  
 small metal particles, inorganic and organic, review 0-45106  
 solid state spectroscopy using synchrotron radiation, book contrib. 0-7375  
 solid/gas interfaces, in situ Fourier transform IR spectroscopy 0-37100  
 spatially dispersive medium, exciton polaritons, absorption theory 0-54618  
 surface polaritons, nonlinear optical spectroscopy, stationary and nonstationary, theory (German) 0-6922  
 surface science conference, Cambridge, England (March 1979) 0-36773  
 tetrahedron method for evaluating spectral props. of solids 0-10855  
 thermal broadening, inhomogeneous, of crystal vibr. spectrum 0-55100  
 thin films, IR absorption spectra rel. to microporosity and absorptivity 0-9053  
 zero-gap semicond., IR absorption coeff., theoretical anal. 0-20641

**spectral analysers**

- see also spectral analysis*  
 4-channel analyser for use in Thomson scattering diagnostics of plasmas 0-31905  
 acousto-optic parallel channel wideband receiver 0-48447  
 acousto-optical spectral analyser at RATAN-600 radio telescope, first test (Russian) 0-51668  
 audio spectrum analyser HP3582A using digital signal processing 0-43567  
 coherent optics system, use of spatial filtration (Russian) 0-28164  
 EEG monitor using Walsh transform on standard microprocessor 0-26399  
 EM analyser control, automatic registration of the back-scattered ions 0-18042  
 frequency-variant signal waveform processing using 2-D optical processors 0-48178  
 geodesic lens design for integrated optics signal processing 0-33247  
 guided-wave optical systems and devices, seminar, Washington, USA (April 1979) 0-31418  
 integrated optic Bragg spectrum analyser design 0-33237  
 time- and space-integrating, acoustooptic system 0-9983  
 US Doppler signals, real-time spectrum analyser, medical appls. 0-36040  
 LiNbO<sub>3</sub>, bulk, Ti-diffused integrated optical spectrum analysers, H implantation effects, pot. uses 0-43486  
 Si photodiode array for integrated optical spectrum analyser 0-33241

**spectral analysis**

- see also spectral analysers*  
 acoustic, directive spectral analysing system using moving microphone (Japanese) 0-33348  
 acoustic attenuation coefficient slope for liver tissue, statistical estimation from refl. US signals 0-46000  
 acoustics, discernibility of amplitude changes in harmonic signals (Polish) 0-38193  
 aneurysm detection using one-bit correl. 0-17175  
 angiographic I imaging using spectral anal. 0-36122  
 atmosphere spectral energetics, determ. via numerical filtering anal. 0-26577  
 atmospheric parameters over vegetated surface in sensible heat advection conditions 0-17343  
 auditory electrophysiology, spectral analysis of cochlear and brain stem evoked potentials 0-16957  
 beam generation, quasi-homogeneous Gaussian sources, spatial coherence 0-48145  
 biomedical applications, review of anal. methods 0-21560  
 biophysics, deconvolution of exponential response functions 0-16894  
 brainstem auditory evoked potentials, human, freq. comp. 0-16956  
 coherent optical hybrid space- and time-integrating spectrum analysis 0-48177  
 coherent optics system, use of spatial filtration (Russian) 0-28164  
 decomposition of two-dimensional spectra, eval. of peak volume, position and width 0-18890  
 dolphin boundary layer pulsations, results of spectral anal. (Russian) 0-41063  
 Earth mean pole position from star pair latitude obs. anal. 0-21892  
 ECG, diagnostic, classification in terms of spectral characts. 0-56264  
 EEG 0-3619  
 EEG activity comparison in right and left cerebral hemispheres by power spectrum analysis 0-45922  
 EEG alternations, power spectral analysis 0-30924  
 first-heart-sound spectra, temporal and heart-size effects 0-41276  
 geomagnetic fluctuations, spectral stacking and smoothing rel. to Earth global elec. cond. character 0-17231  
 gravity waves, spectral decomposition 0-36319  
 ionosphere waves in D- and F-regions, spectral anal. and temporal vars. 0-8483  
 landscape multispectral data, Karhunen-Loove analysis 0-48164  
 laser Doppler vibr. meas. system using bispectral anal. 0-38357  
 lateral geniculate nucleus of cat, periodic stimulation, neural activity transient persistence 0-56021  
 matched spatial filter optimisation for diatom recognition 0-48180  
 maximum entropy method and appls. 0-37006  
 maximum entropy method confidence limits 0-22284  
 maximum entropy method of period determ., accuracy 0-56712  
 microseismic events in Badra area, Iraq, spectral anal. 0-56413  
 modified-triggered photocounting and its application to optical superheterodyne spectrum analysis 0-31865  
 molecular fluorescence, nonexponential decay, method of moments for data anal. 0-55975  
 nested variances method for power spectrum calc. 0-8965  
 nuclear reactors, process monitoring and parameter estimation, multivariate signal analysis algorithms 0-47585  
 ocean semidiurnal internal waves in Polygon-70 test area of Atlantic, spatial spectra 0-31051  
 ocean wind waves, high-freq. spectra meas. in presence of currents in shallow sea 0-31053  
 oceanic magnetic anomalies recorded during deep-water mag. surveys, statistical anal. 0-36233  
 oceanography, spectral anal. of temp., salinity and sound vel. gradients in western N. Pacific 0-51429  
 physiological signals, gastro-intestinal tract, spectral analysis 0-41269  
 radar measurement of clouds and precipitation, correl. and spectral anal. 0-12529  
 radiosome meas. and spectral anal. of LOS fading 0-56568  
 rainfall in England and Wales, long-period records spectral and filter anal. 0-4080  
 rough surface power spectrum measurement 0-36989  
 SAW and optical signal processing techniques compared 0-48173  
 shoreline periodicities, spectral anal. rel. to edge waves 0-12375  
 solar flares, principal component anal. in soft X-ray flux 0-41781  
 solid state detectors spectra, fast analysis, LIZA program 0-37706  
 spectra-colour ultrasonography, instantaneous power spectra, theoretical anal. 0-51190  
 spermatozoa mobility, photon correlation study 0-12063  
 SS 0-3904  
 Sun total microwave flux, search at Toyokawa for five minute oscillations 0-4327  
 surface texture assessment, Walsh function method 0-36995  
 time and frequency stability, characterisation and meas. 0-47025  
 US A-mode echo computer spectral anal. 0-51193  
 US tissue characterisation, clinical spectrum anal. techniques 0-45998  
 Vela supernova remnant, rot. measure correl. function and assoc. power spectrum rel. to turbulence 0-51836  
 ventilation fan acoustic noise (Russian) 0-53584  
 visually evoked nonstationary EEG, anal. using max. entropy method 0-26397  
 wave perturbations in ionospheric D-layer and F-layer 0-21873  
 whistler propagation times eqn., inversion via spectral expansion 0-8495  
 whistlers, spectral-temporal anal. by digital methods 0-4175  
 Wigner distribution function, optical production, speech signal analysis 0-48521  
 Wolf sunspot numbers, freq. anal. and forecasting 0-56797  
 Fe, conversion spectrum anal., outer-shell s-electron density, ACSEMP program 0-7208

**spectral line breadth**

- see also atomic spectral line breadth; chemical shift; Davydov splitting; Doppler effect; EPR line breadth; molecular spectral line breadth; NMR line breadth; Stark effect; Zeeman effect*  
 absorption spectra, collision-broadened lines, information anal. 0-22433  
 anisotropic motion, and reson. line shape 0-7144  
 antiresonance line shapes and radiationless decay, compatibility restrictions 0-48040  
 $\alpha$  Aquarii, spectral line profiles vars. rel. to chromospheric event 0-31299  
 L-ascorbic acid, cryst. isolated OH isoscillators, IR absorption, temp. and H-bond effects 0-7351  
 astronomical line profile measurements, accuracy 0-26751



## spectral line breadth continued

atomic motion in resonant fluctuating laser radiation 0-43310  
 Bartels' theory of radiation from an inhomogeneous layer, appl. to plasma temp. meas. 0-53948  
 Be stars, electron scatt. effects on Balmer emission lines 0-17589  
 3C 33, radio galaxy, optical emission lines widths rel. to physical conditions in compact heads 0-51892  
 $\alpha$  Camelopardalis (O9.5 Ia), variable H $\alpha$  P Cygni profile 0-41818  
 $\alpha$  Canis Majoris (Sirius), Ca II K line high resolution profile obs. 0-56830  
 CARS spectroscopy linewidth parameter from laser mode structure 0-33083  
 U Cephei, eclipsing binary, gas stream effects in UV spectrum, IUE obs. 0-26898  
 chemisorption systems, IR spectral linewidth and sticking coeffs., non-adiabatic effects 0-39423  
 chromosphere flare spectrum, line broadening as electron beam diagnostic 0-26827  
 coherent optics,  $T_2$  as collision time, dephasing time, or reciprocal linewidth for teaching 0-27075  
 crystal vibrational spectrum, inhomogeneous thermal broadening effect 0-55100  
 crystals, line-shape distortion on anisotropic absorpt. meas. in unpolarised light 0-2765  
 cyclotron absorption in mag. white dwarfs, Doppler and collisional broadening effects 0-4351  
 1,4-dibromonaphthalene, k-k scatt., exciton dephasing time-resolved phosphoresc. obs. 0-11458  
 diethylammonium cadmium tetrachloride, first order phase transition, optical phonon line broadening, spin-phonon coupling model 0-7335  
 dimethyl ether, condensed multilayers, electron bombard. effects, AES line-shape anal., XPS, and desorption meas. 0-7450  
 discharge tube, hollow cathode type, with conical bottom, spectroscopic and elec. characts. 0-31891  
 dispersion vs. absorption curve method for distinguishing peak position distrib. from linewidth distrib. 0-4775  
 dye laser, difference frequency generation, degree of conversion depend. on linewidth 0-48347  
 dynamic Jahn-Teller systems, calc. of absorption band shapes, use of Lanczos algorithm 0-45023  
 excitation energy transfer and migration, spectral line broadening 0-2841  
 exciton absorption spectra, dislocations effect on band profile 0-16070  
 F-centre optical absorption bandshape calc. for transition to state with Jahn-Teller and spin orbit couplings 0-55135  
 Fabry-Perot interferometer, instrumental convolutions, linewidth anal. determ. 0-31904  
 Fabry-Perot spectrometer instrumental function determ., Voigt function assignment (Spanish) 0-52322  
 Fourier transform ion reson. spectroscopy of ions undergoing collisions with mols. 0-35598  
 G200-39, hot hybrid white dwarf, H and He I line profiles 0-26852  
 G 0-22435  
 galaxies, H I profiles appl. to mass determ. 0-56937  
 galaxies velocity dispersions and redshifts survey, data reduction techniques 0-22074  
 glass, fluoresc. linewidth 0-34978  
 glass, fluorescence linewidth, anomalous of impurity ions, theory 0-50404  
 glass targets, laser-produced plasma X-ray spectral lines identification (Chinese) 0-54036  
 graphite intercalation compounds,  $C_6M$ , (M=K, Rb, Cs), Breit-Wigner line shape anal., Raman spectra 0-50336  
 HD 50896, WN5 star, emission-line profiles vars. 0-51791  
 IC 4329A, Seyfert galaxy, optical spectrum and line profiles 0-36706  
 impurity absorption and emission in solids, Poisson distrib. moments 0-25419  
 interstellar absorption lines towards 30 Doradus central object (HD 38268), profiles 0-51839  
 interstellar matter towards  $\zeta$  Ophiuchi, narrow-lined cloud obs. from RF mol. emission spectra 0-26958  
 ions, positive, dielectronic recomb. in plasma generalised cascade theory 0-43851  
 Jahn-Teller multimode effect for E-term with strong vibronic coupling, IR and Raman spectra band shapes 0-20139  
 laser spectroscopy, finite bandwidth laser excitation, line shapes, non-perturbative effects 0-52332  
 light echo angular spectroscopy, inhomogeneously broadened lines 0-43406  
 lower main-sequence stars, line profiles Fourier anal. rel. to rot. vel. 0-51767  
 metal, ferromagnetic resonance linewidth, interaction of spin waves with conduction electron current 0-25216  
 methanol, condensed multilayers, electron bombard. effects, AES line-shape anal., XPS, and desorption meas. 0-7450  
 Mossbauer relaxation theory 0-39954  
 naphthalene, vibr. dephasing and Raman active localised internal mode temp. depend. 0-45060  
 Neptune reflected spectrum, effects of seeing rel. to rot. period determ. 0-46479  
 NGC 650/1, planetary nebula, emission line profiles and internal kinematics 0-17639  
 nonlinear absorption method in magnetic field for spectral line width and shift meas. 0-37066  
 nonlinear crystals for frequency conversion of optical radiation, review (Russian) 0-38068  
 NQR precision thermometry, freq. meas. improvement 0-22356  
 optical free induction decay, subnanosecond, with novel laser freq. shifting 0-38075  
 YY Orionis stars line profiles, spectral line form. in axisymmetric moving envelopes 0-41813  
 photoelectron, and hole recoil and vibrational shake-up, in mols. and solids 0-55265  
 plasma, Lyman- $\alpha$ , line broadening calc. 0-43984  
 plasma, nonthermal, two-temp. electron gas, collective elec. field fluctuations estimation 0-43882  
 Pleione (28 Tauri), metallic shell lines widths correl. with ionisation potential 0-8637  
 polariton kinematical levels resulting from excitons interaction, optical absorption line broadening 0-10892  
 polystyrene, O treated, interaction with vapour-deposited Cr and Ni atoms 0-3407

## spectral line breadth continued

profile recording, high resolution, using Fabry-Perot interferometer and monochromator 0-42268  
 Q 2240.9-3702, Q 2238.9-4115, QSOs, broad-lined absorpt. systems widths 0-4456  
 quasi-stellar objects, H emission line ratios implications 0-56968  
 Raman scattering of light by polaritons, reviews 0-34928  
 random arrays of grains, spectral properties 0-12727  
 resonance Raman scattering, appl. to ultrafast dephasing and relax. obs., phonon scatt. effects 0-7337  
 resonance scattering line, Monte Carlo calcs. for line width with absorpt. or differential expansion 0-21901  
 rhodamine dye polar frozen solns., luminesc. broadening 0-2834  
 ruby, Raman  $^{12}\text{C}$  and phosphorescence transitions, line widths, time correl. study 0-20621  
 WZ Sagittae, recurrent nova, Balmer emission lines double-component struct. during 1978 outburst 0-56849  
 $\zeta$  Scorpii, extreme B1 supergiant, UV reson. lines profiles 0-4349  
 semiconductor, donor van der Waals interactions, spectral lineshapes 0-11450  
 semiconductors, high density excitons and biexcitons, recomb. radiation bands profiles, time depend. 0-45140  
 semiconductors, quantum limit cyclotron resonance linewidth 0-7171  
 semiconductors and metals, Mossbauer spectra of implanted  $^{83}\text{Kr}$ , line widths, isomer shifts 0-39899  
 Si:P(As)(Sb)(Bi), high resolution study of group V impurities absorption 0-7388  
 single-mode gas laser with slightly anisotropic resonator, output polarization stability 0-43370  
 solar photosphere, 'microturbulent' vel. and damping const. rel. to lines equivalent widths (Russian) 0-12719  
 solar resonance radiation multiply scattered by nearby interstellar medium, line profiles 0-41874  
 solar spectrum, lines integral characts. rel. to solar atmosphere vel. field estimation 0-46530  
 spark discharge, electron density determ. from Stark broadening of spectral lines (Russian) 0-28859  
 Stark effect, two photon absorption spectroscopy 0-43126  
 stellar Ca II and Mg II reson. lines profiles, effects of high-pressure transition regions in model chromospheres 0-26847  
 T Tauri stars, spectral features synthesis from photosphere and low chromosphere model 0-36623  
 Taurus Molecular Cloud 2 (TMC-2),  $\text{HC}_3\text{N}$  and  $\text{NH}_3$  lines widths 0-26957  
 three two-level atoms system, continuously incoherently-pumped, radiation rate, spectrum 0-5716  
 time-resolved laser saturation spectroscopy and coherent transients survey 0-9965  
 transition quasilinear spectra of resonant secondary emission (Russian) 0-16102  
 Uranus reflected spectrum, effects of seeing rel. to period determ. 0-46479  
 78 Virginis, magnetic Ap star, high resolution polarisation obs. inside spectral lines 0-51772  
 Voigt contour of spectral line, nomogram for parameters determ. 0-52321  
 Voigt contour parameters determ. 0-943  
 water, condensed multilayers, electron bombard. effects, AES line-shape anal., XPS, and desorption meas. 0-7450  
 wavefront reversal by stimulated Brillouin scatt., four-wave process 0-53382  
 white dwarfs, DB-type, model atmospheres rel. to line profiles and equivalent widths 0-51761  
 Ag foils, polycryst. and bicrystals, grain boundaries,  $^{119}\text{Sn}$  Mossbauer anal. 0-7229  
 $\alpha$ -AgI, superionic, continuous order-disorder transition, Raman spectroscopic evidence 0-45070  
 Al, positron annihilation, effects of quenching, annealing and neutron irradi. 0-20732  
 Al-Sn alloys, heat treatment effect on  $^{119}\text{Sn}$  Mossbauer spectrum 0-7228  
 Al $_{1-x}\text{Ga}_x$ -As pulsating DH laser, spectral broadening 0-23686  
 $^{241}\text{Am}$ ,  $\alpha$ -radiation self-damage effect on hyperfine interaction and Debye-Waller factor, Mossbauer meas. 0-7230  
 a-As $_2\text{Se}_3$ , doped film, photoluminescence intensity and lineshape study 0-50448  
 Ba $_{0.54}\text{Sr}_{0.46}\text{Nb}_2\text{O}_6$ , line broadening effect in Rayleigh scatt. of Mossbauer radiation 0-50238  
 BaTiO $_3$ , line broadening effect in Rayleigh scatt. of Mossbauer radiation 0-50238  
 BeF $_2$ :Pr $^{3+}$ , glass, optical homogeneous linewidths 0-7395  
 COF $_2$ , soln. in liquid Ar, transition freq., halfwidths and relative intensity, IR absorpt. spectra 0-55101  
 Cd, Auger MNV lineshapes, hole-hole interaction 0-45177  
 CdO, Auger MNV lineshapes, hole-hole interaction 0-45177  
 CdS, high intensity excited, exciton reflection spectra, reflection struct. 0-20692  
 CdS $_{1-x}\text{Se}_x$ , mixed crystals, free excitons, disorder effects 0-34365  
 CdSe, high intensity excited, exciton reflection spectra, reflection struct. 0-20692  
 Co $^{2+}[\text{Fe}^{III}(\text{CN})_6]^{3-}$ , time depend. linewidth of Mossbauer spectrum 0-15911  
 CsF, F-centre optical absorption bandshape calc. for transition to state with Jahn-Teller and spin orbit couplings 0-55135  
 Cu, laser-produced plasma X-ray spectral lines identification (Chinese) 0-54036  
 CuCl, phonon interaction of excitonic molecule 0-50316  
 EuAsO $_4$ :Gd, dynamical interactions, EPR meas. 0-7162  
 EuVO $_4$ :Gd, dynamical interactions, EPR meas. 0-7162  
 Fe complexes, M[Fe(C $_2\text{O}_4$ ) $_3$ ].XH $_2\text{O}$ , M=Li, Na, K, Rb, Cs, NH $_4$ , Mossbauer studies of electronic relax. phenomena 0-44973  
 $\alpha$ -Fe $_2\text{O}_3$  microcrystals, surface phonon modes, IR study 0-55089  
 FeSb alloy films, vapour-deposited, formation of metastable phase 0-44437  
 GaAs, donor van der Waals interactions, spectral lineshapes 0-11450  
 GaAs, electron-exciton collision influence on luminescence line profile due to bound excitons 0-29800  
 GaSe, electron-phonon interaction and optical props. 0-34942  
 Ge, electron-hole droplets, luminesc. and absorpt. lineshapes, RPA theory 0-49613  
 Ge, electron-hole liq. thermalisation between mag. field split valleys 0-25444



**spectral line breadth continued**

- Ge, magnetoluminescence of electron-hole liq. 0-29790  
 GeO<sub>2</sub>:Pr<sup>3+</sup>, glass, optical homogeneous linewidths 0-7395  
 HCl, liq., IR spectral intensity and Raman cross-section meas. 0-2742  
 Ha line profile in Tycho SNR, model of optical emission from fast shock wave 0-46631  
 He, <sup>3</sup>D<sub>1</sub>-<sup>2</sup>P<sub>1</sub> line, press. broadening studies by saturated absorpt. techniques 0-52939  
 n-In Ar:Te(Sn), heavily doped, cathodoluminescence, doping effect on luminesc. band position and spectral profile 0-45153  
 In, Auger electron spectra, solid state effects 0-20739  
 n-InSb, cyclotron reson. of conduction electrons, strong mag. field, hot electrons 0-2640  
 n-InSb, cyclotron reson. study of conduction electrons, strong mag. field 0-2639  
 α-In<sub>2</sub>Se<sub>3</sub>, X-ray diffr. line broadening 0-49047  
 KBr:In<sup>3+</sup>, B-band, optical absorpt. and mag. circular dichroism calcs. 0-29765  
 KF(Br)(Cl)(I), K<sup>+</sup>3p core excitons, refl. spectra study, low temp. 0-29759  
 KMnF<sub>3</sub>, exciton dynamics by time resolved emission spectroscopy 0-54615  
 KTaO<sub>3</sub>:Fe<sup>3+</sup> local phase transition, EPR line temp. broadening (*Russian*) 0-54944  
 LaF<sub>3</sub>:Pr<sup>3+</sup>, optical line narrowing by nuclear spin decoupling, photon echo meas. 0-48353  
 LaF<sub>3</sub>:Pr<sup>3+</sup>, optical transition, spin decoupling and magic angle line narrowing 0-28286  
 LaF<sub>3</sub>:Pr<sup>3+</sup>, ultrahigh resolution photon echo spectroscopy 0-28285  
 La<sub>2</sub>O<sub>3</sub>:Al<sub>2</sub>O<sub>3</sub>:SiO<sub>2</sub>:Sm<sup>3+</sup>, luminesc. selective laser excitation line narrowing 0-25434  
 N<sub>2</sub>, liq., Raman lineshape 0-11384  
 Nd glasses, GLS-1 and GLS-22, luminesc. band, forced transition cross sections, laser meas. 0-40152  
 Ni, M<sub>2,3</sub> edge, temp. depend. 0-50463  
 Pd-Fe, scatt. and transmission Mossbauer spectra near Curie temp. 0-15864  
 Pt oxidation, XPS spectra study 0-3254  
 RbFeCl<sub>3</sub>·2H<sub>2</sub>O, 2D Ising system, crit. fluctuations, Mossbauer spectra study 0-44842  
 Sb, Auger electron spectra, solid state effects 0-20739  
 Si, electron-hole drops, thermodynamical parameter determ. from luminescence data 0-2845  
 Si, surface inversion layers, intersubband optical absorpt., Auger-type transition 0-29741  
 Si; Ar ion bombarded, projectile energy depend. and line shape of Ar-L AEs 0-16139  
 Sn, Auger electron spectra, solid state effects 0-20739  
 Tb(OH)<sub>3</sub>, exciton dynamics within an inhomogeneously broadened line, luminesc. spectra 0-50407  
 Te, Auger electron spectra, solid state effects 0-20739  
 Te, intervalence band absorption, press. and defects influence 0-55149  
 YAlO<sub>3</sub>:Pr<sup>3+</sup>, ultrahigh resolution photon echo spectroscopy 0-28285  
 Y<sub>3</sub>Fe<sub>5-x</sub>Ga<sub>x</sub>O<sub>12</sub>, substituted garnet, floating zone grown, FMR line width, saturation magnetisation 0-29626  
 Yb, 4f levels, hole lifetime and chemical shift, UHV study 0-20762  
 Zn<sub>1-x</sub>Cd<sub>x</sub>S, bound-exciton lines, compositional fluctuation-induced broadening 0-2846  
 ZnS, time differentiated Mossbauer spectra from <sup>57</sup>Co impurities, relaxation processes (*Russian*) 0-34834  
 ZnS:Cl, shape of self-activated cathodoluminesc. band 0-34987

**spectral line profiles** *see spectral line breadth***spectral line shift**

- see also chemical shift; isomer shift; isotope shifts; Lamb shift; radiative shifts; red shift; Stark effect; Zeeman effect*  
 active ions in crystals, spectral thermal line shift mechanism (*Chinese*) 0-7385  
 alkali metal+inert gas, collisional shifts and broadening of Voigt contour 0-27983  
 alkali metal+inert gas, line profiles, width, shift and asymmetry, square well pot. approx. 0-52936  
 atom, RF spectroscopy, nonlinear and parametric effects, review 0-18816  
 atomic excited state collisional relax., line broadening, interat. interactions, review 0-43149  
 autotype detector, spin resonance detection 0-22397  
 2-benzoylpyridine crystals, optical spectra of lowest triplet state 0-16081  
 cholesteric liquid crystals, light reflection by crystals with tilted molecular struct. 0-29713  
 complex molecules, vibr. spectra, stochastic description, appl. to optically active Brownian oscillator 0-52974  
 crystal vibrational spectrum, inhomogeneous thermal broadening effect 0-55100  
 dense polyatomic molecular systems, vibr. correl., HF band exchange dephasing 0-37803  
 1,1-difluoroethane, rot. relax., anharmonic shifts and excited state absorpt. 0-43154  
 dilute atomic gas, weak at.-at. interaction pot. from master eqn. for coupled radiation 0-23484  
 Franck-Condon effects in resonance Raman spectra and excitation profiles, appl. to CrO<sub>4</sub><sup>2-</sup> and β-carotene 0-14129  
 gas-pressure shifts of molecular lines, Stark displacements 0-23463  
 graphite-alkali metal intercalation cpds., IR, active lattice mode obs. 0-45072  
 hyper-Raman scattering, saturation effects, resonant three photon processes 0-38069  
 inorganic molecular crystals, metal complexes electronic spectra and intermolecular interactions 0-55137  
 ions, positive, dielectronic recomb. in plasma generalised cascade theory 0-43851  
 methane, saturated absorpt. reson. shape, geometry and field intensity effects (*Russian*) 0-32778  
 naphthalene, vibr. dephasing and Raman active localised internal mode temp. depend. 0-45060  
 nonlinear absorption method in magnetic field for spectral line width and shift meas. 0-37066  
 plasma negative ions, broadening of free-bound radiation threshold, quasistatic theory 0-53941  
 plasma reson. lines regularities in Stark widths and shifts, He<sup>+</sup>-Ca<sup>+</sup> 0-43881

**spectral line shift continued**

- polyethylene, H bonding effects on skeletal optical and longitudinal acoustic modes 0-34914  
 predissociating harmonic oscillator, relative line widths and level shifts 0-23469  
 propylene/butene-1 copolymers, coisotactic shift contribs. in <sup>13</sup>C NMR spectra 0-29635  
 rare earth ion energy separation, 4f<sup>N</sup>-4f<sup>N-1</sup> nl, host depend. 0-49676  
 rhodamine dye polar frozen soles., luminesc. broadening 0-2834  
 self reversal contours, use in determ. of line broadening and shift consts. 0-52940  
 solar spectrum, lines integral characts. rel. to solar atmosphere vel. field estimation 0-46530  
 TTF-TCNQ, charge transfer determ. from spectral line shift using Raman scatt. 0-25392  
 Al I resonance line profiles, influence of boundary layer of Al-seeded shock heated plasma 0-43876  
 Ar, photoionisation, Auger processes, decay lifetime, line shift, profile, X-ray photoelectron spectra 0-37798  
 BaS-CaS:Cu phosphors, X-ray diffr. and fluoresc. spectra 0-40148  
 CO<sub>2</sub> IR Zeeman spectra utilizing copropag. wave reson., diamag. shift obs. 0-53055  
 CO<sub>2</sub> laser line, electro-optic frequency shift (*Chinese*) 0-43379  
 Cd<sub>3</sub>As<sub>2</sub> film, optical absorption edge 0-50450  
 CdS, Raman shift dispersion near exciton reson., two-phonon cascade processes 0-11405  
 Cl<sup>-</sup> (Br<sup>-</sup>) (I<sup>-</sup>), in plasma, broadening of free-bound radiation thresholds 0-53940  
 Cs, four-photon ionis., strongly interacting resons. theory 0-52955  
 Cs+Ar(Xe)(He), shift, halfwidth, satellite and absorpt line in square-well pot. 0-42993  
 Eu<sub>2</sub>O<sub>3</sub>-Sc<sub>2</sub>O<sub>3</sub>-Ta<sub>2</sub>O<sub>5</sub> system, orthotantalate section, X-ray diffr. and luminesc. obs., conc., depend. 0-54205  
 Fe XXIV, dielectronic satellite spectra, solar flares appl. 0-32646  
 Ga+inert gas atom, diffuse series head lines, hyperfine components, broadening calcs. 0-32632  
 GeS<sub>2</sub> glass, melt quenched, reversible photostructural change, optical transmission spectra obs. 0-45109  
 H, hyperfine shift and interatomic pots. in inert buffer gas 0-5491  
 H, in hot plasma, elementary excitation spectrum, exchange and polarisation effects 0-43892  
 H-like ions in laser-produced plasma, Balmer fine struct. (broadening) 0-48860  
 H+He, H Balmer-α fine-struct. line shift and broadening 0-37783  
 H<sub>2</sub>, 4-0 S(1) 6368 Å quadrupole line strength and pressure shift 0-43108  
 H<sub>2</sub>, D<sub>2</sub> and HD, intermol. collision process obs. using light scatt. expts. 0-53001  
 H<sub>2</sub><sup>16</sup>O, laser spectroscopy using an optothermal receiver 0-37810  
 H<sub>2</sub>O(D<sub>2</sub>O), solvated electrons, optical absorpt. spectra, temp., isotope effects 0-55124  
 Ha(Dα) plasma red shift meas. in Ar arc, ion dynamic depend. 0-10364  
 He, <sup>3</sup>D<sub>1</sub>-<sup>2</sup>P<sub>1</sub> line, press. broadening studies by saturated absorpt. techniques 0-52939  
 He I plasma lines, Stark broadening, quantum mechanical calcs. 0-43880  
 He, isoelectronic series, ground state specific mass shift, HF variation perturbation calc. 0-47889  
 Hg<sub>2</sub>-Pt, <sup>199</sup>Hg Mossbauer meas., isomer shift and quadrupole splitting calcs. 0-28039  
 Hg<sub>2</sub>-F<sub>2</sub>, <sup>199</sup>Hg Mossbauer meas., isomer shift and quadrupole splitting calcs. 0-28039  
 I<sub>2</sub>Ne<sub>6</sub>He<sub>6</sub> van der Waals complexes photodissoc. 0-50864  
 n-In Ar:Te(Sn), heavily doped, cathodoluminescence, doping effect on luminesc. band position and spectral profile 0-45153  
 In, Auger electron spectra, solid state effects 0-20739  
 In+inert gas atom, diffuse series head lines, hyperfine components, broadening calcs. 0-32632  
 K+He(Ar)(Ne)(Xe), K 5<sup>2</sup>P level broadening and collisional relax., quant., semiclassical and expt. comparison 0-18903  
 KMnF<sub>3</sub>, exciton dynamics by time resolved emission. spectroscopy 0-54615  
 Mo<sup>32+</sup>, dielectronic recomb. rate coeffs. in plasma 0-43853  
 Mo<sup>38+</sup>, dielectronic recomb. rate coeffs. in plasma 0-43852  
 N<sub>2</sub>, solid, α- and γ-forms, Raman spectra, vibron and lattice freq. shifts, libration 0-16020  
 Nb<sub>3</sub>Ir, A-15 struct. <sup>93</sup>Nb NQR spectra 0-20496  
 Nb<sub>3</sub>Os, A-15 struct. <sup>93</sup>Nb NQR spectra 0-20496  
 Nb<sub>3</sub>Pt, A-15 struct. <sup>93</sup>Nb NQR spectra 0-20496  
 O<sub>2</sub>(c<sup>∞</sup>), in Ar(Kr)(Ar-Kr) matrices, multiphonon vibr. relax. time-resolved emission obs. 0-18861  
 Rb Doppler-free two-photon lines, self-broadening and shift meas. 0-5506  
<sup>87</sup>Rb+inert gas, D<sub>1</sub>-line hyperfine components perturbation, interferometer obs. 0-32635  
 SF<sub>6</sub> gas, CO<sub>2</sub> TEA laser-excited, slow intermol. redistrib. of vibr. energy 0-53039  
 Sb, Auger electron spectra, solid state effects 0-20739  
 Si:H(B)(P), amorphous, UV absorpt. spectra 0-25420  
 Sn, Auger electron spectra, solid state effects 0-20739  
 Te, Auger electron spectra, solid state effects 0-20739  
 Tl+inert gas atom, diffuse series head lines, hyperfine components, broadening calcs. 0-32632  
 V, atom and ions, shell energy struct., SCF calc. by Dirac-Fock-Slater method 0-52877  
 ZnS, time differentiated Mossbauer spectra from <sup>57</sup>Co impurities, relaxation processes (*Russian*) 0-34834

**spectral linewidths** *see spectral line breadth***spectral methods of temperature measurement**

- see also pyrometers*  
 combustion, coherent Raman spectrosc. obs. 0-16691  
 combustion diagnostics, laser appls. 0-16688  
 flame diagnosis, CARS appls. 0-16689  
 flame diagnostics using multichannel pulsed Raman spectroscopy 0-30237  
 hypersonic wake, excitation temp. meas. by atomic spectral line relative intensities 0-43732  
 internal combustion engine, CARS noninvasive temp. and species meas. 0-30293  
 IR pyrometer, portable, principles (*German*) 0-42229  
 IR pyrometry, calc. method for true temp. from expt. readings 0-13081  
 IR thermometry, semiconductor material temperature measurement (*Spanish*) 0-47062



## spectral methods of temperature measurement continued

- laser fluorescence temperature measurement of Na in flames 0-11893  
 laser fluorescence temperature measurements in flames 0-11892  
 laser Raman spectroscopy, flame temp. meas. 0-13074  
 multiwavelength optical pyrometer for shock compression experiments 0-52229  
 multiwavelength radiation pyrometry where reflectance is measured to estimate emissivity 0-31757  
 plasma temperature field determ., asymmetrical (*Czech*) 0-38704  
 premixed  $H_2$ - $O_2$ - $N_2$  laminar flames, temp. profiles, Raman, absorpt. and line reversal obs. 0-42227  
 pyrometer, photon counting, 1400K to above 2200K within 0.5K and 1.0K 0-52232  
 pyrometer, scale correction by electric method (*Russian*) 0-37040  
 ribbon-filament temperature lamps, measurement of characts. 0-4720  
 small volume flames, temp., temporal meas., two line at. fluoresc. technique, Raman scatt. 0-42226  
 sooty diffusion flame, CARS obs. 0-16690  
 spectral emissivity measurement device, high-temp. materials 0-37039  
 Ar-air arc, stabilised, spectroscopic methods of temp. meas. (*Russian*) 0-38854  
 $CO_2$  conc. and temp. in flames, Raman spectroscopy 0-32720  
 $CO_2$ , fast flow laser, meas. of  $N_2$  vibr. temps. 0-32955  
 $CO_2$  gasdynamic laser, vibr. temp. meas. method 0-9854  
 Cu vapour laser, gas temp. meas. using Doppler broadening of Ne buffer gas lines 0-19020  
 $H_2$  diffusion flame, Rayleigh temp. profiles meas. 0-16692  
 $H_2O$ , low density flow temp. and density meas. by submillimetre spectroscopy 0-43816  
 $N_2$ , flame temp., CARS spectra diagnostic investigation 0-43404

## spectrochemical analysis

- see also *atomic absorption spectroscopy*; *atomic emission spectroscopy*; *X-ray fluorescence analysis*  
 absorption spectra, collision-broadened lines, information anal. 0-22433  
 acetylene smoke particles, optoacoustic meas. 0-50895  
 acrylamide-acrylic acid (acrylic acid salts) copolymers, composition determ., IR spectra (*Russian*) 0-7358  
 adenylate kinase, photokinetic microassay using the firefly luciferase reaction 0-56306  
 AES, quant. depth profile (*Japanese*) 0-16751  
 air pollutants, laser spectroscopic detection 0-17366  
 archaeometry, laser microspectral analysis (*German*) 0-55750  
 atmosphere, mol. complexes presence and role in residual absorpt., light scatt. obs. 0-56607  
 atmospheric  $NO_2$  total content meas. by absorption spectroscopy (*Japanese*) 0-12469  
 atomic Faraday effect, analytical appl. 0-9538  
 Auger spectra development for derivation of chem. information 0-3434  
 benzene, bromination on zeolite adsorption complex, Raman spectroscopic anal. 0-16670  
 benzene, plasma polymerisation in glow discharge, thin film IR and free radical EPR obs. 0-2964  
 biological solutions, using wall-stabilised arc plasma source 0-41343  
 bone elemental analysis by prompt  $\gamma$ -ray spectra due to  $^{252}Cf$  neutron irradi. 0-17065  
 cell nuclei staining parameters, evaluation regarding reproducibility of fluorescence measurements 0-21590  
 cerebral cortical microfluorimetry at isosbestic wavelengths for correction of vascular artifact 0-56322  
 Cherenkov radiation light source in pulse radiolysis 0-42267  
 chlorodifluoromethane, IR multiphoton dissoci.,  $CF_2$  form., time-resolved optical absorption obs. 0-16702  
 chromatogram scanning spectrofluorimeter-densitometer 0-31901  
 coal liquids characterisation, analytical use of dialysis 0-30334  
 coherent antiStokes Raman spectroscopy use, three-wave mixing phenomenon 0-40802  
 combustion, coherent Raman spectrosc. obs. 0-16691  
 combustion diagnostics, laser appls. 0-16688  
 condensation chamber, for flame photometric analysis, exam. of design 0-21342  
 core level ligand field splittings 0-43106  
 corrosion science, surface analytic techniques 0-31929  
 crystals, electron spectroscopy, book 0-36786  
 cuvette, heated for IR spectroscopy, exam. of design. 0-18025  
 CW intracavity dye laser spectroscopy, enhancement, pumping power depend. 0-13155  
 dibromodifluoromethane, UV laser fluoresc. and photochem.,  $CF_2$ , CF and  $Br_2$  fluoresc. obs. 0-16703  
 diesel smoke particles, optoacoustic meas. 0-50895  
 diffracted stimulated emission induced by coherent crossed laser beams for conc. meas. 0-35585  
 discharge lamp, HF, with hollow electrode, for atomic spectroscopy 0-26090  
 discharges, high-freq., unipolar and electrodeless capacitively-coupled, excited at atm. press., appls. 0-1861  
 electrogenerated chromophores, electrochemical conc. profiles, mass transfer, charge transfer, laser absorpt. spectroelectrochem. obs. 0-40765  
 electron beam particulate analysis of air samples 0-40785  
 electron energy analyser based on retarding field method for use in gas medium 0-45598  
 emission spectrographic analysis system, minicomputer based, using scanning microphotometry 0-22436  
 EPR, ns time-resolved, in pulse radiolysis, via spin echo method 0-43075  
 ESCA, insulator charging, line energy corrections 0-50898  
 ESCA, surface anal. and electronic structure (*French*) 0-7891  
 ESCA appl. to thin film production, surface analysis (*Hungarian*) 0-54537  
 fast kinetics studied by NMR, review 0-55662  
 fast reaction kinetics meas. by ESR of free radicals 0-21286  
 fission reactor materials, anal. using plasma jets 0-19624  
 flame diagnosis, CARS appls. 0-16689  
 flame diagnostics using multichannel pulsed Raman spectroscopy 0-30237  
 flame spectroscopy, free atom fractions and equilib. comp. calcs. 0-22438  
 flames, temp., specie conc. meas., CARS and laser induced saturation fluoresc. spectroscopy obs. 0-45617  
 fluorescence analysis using pulse-delay data acquisition sampling system 0-37004  
 fluorescence correlation spectroscopy, profile of focused collimated laser beam near focal minimum 0-43386

## spectrochemical analysis continued

- fluorescence spectrometry, beam splitter and cell window errors 0-31897  
 fluorescent measuring equipment, selection of standard testing substances 0-7882  
 fluorometric system, nanosec. time-resolved spectrometry with tunable dye laser and pulse-gated photon counter 0-11968  
 Fourier transform IR spectrometry, absorbance subtract, wedging errors diagnosis and correction 0-11967  
 Fourier transform IR spectroscopy, use in atm. chem. 0-55743  
 Fourier transform IR spectroscopy, use in polymer research as vibr. spectroscopy tool 0-55744  
 free radicals determ., on polymer surfaces (*German*) 0-7892  
 gas chromatography/Fourier transform IR spectroscopy, review 0-55729  
 gas sampling to mass spectrometers, fast-response, using quartz tube orifice leaks 0-35609  
 geochemical sample anal. by gamma-spectrometry, data bank system 0-31120  
 glass, medieval, simulated, durability anal. using IR reflection spectroscopy 0-40777  
 halide dioxide radical form.,  $H_2O_2$  decomposition of halide-coated surface, EPR obs. 0-7851  
 high temperature gases, characterisation, reactive flow in shock tubes, laser absorpt. spectroscopy 0-45618  
 impurity microconcentrations in liquids analysis using opto-acoustic effect 0-50916  
 Incoloy 600 and 800, surface film in hot conc. NaOH, XPS study 0-11824  
 inductively coupled plasmas, optical emission spectroscopy 0-42266  
 industrial atmospheric pollutant remote analysis by Raman lidar 0-12047  
 infrared intensity reference meas., spectrophotometric data reduction, modular computer programs appl. 0-3471  
 internal combustion engine, CARS noninvasive temp. and species meas. 0-30293  
 inverse Raman scattering spectroscopy and chem. appls. 0-37094  
 IR, quantitative, microprocessor appl. and sampling technique advancements 0-16746  
 IR analytical instrumentation using tunable diode lasers 0-16762  
 IR file searching, ASTM, algorithm using peak intensity data 0-30295  
 IR reference spectra, for GC-IR, presentation specifications 0-31908  
 IR spectral analysis, background and overlapping of absorpt. bands influence on accuracy 0-55748  
 laser fusion microsphere targets, nondestructive anal. using rot. Raman spectroscopy 0-50896  
 laser Raman molecular microprobe (MOLE) 0-21330  
 laser spectroscopy, conf., San Diego, USA (Aug. 1978) 0-13153  
 laser spectroscopy applications, conf., Anaheim, USA (Mar. 1978) 0-36781  
 laser-based methods for transient chem. events meas. 0-40801  
 laser-excited luminescence spectrometry, review 0-40800  
 lubrication, spectroscopic methods for surface anal. (*French*) 0-26095  
 metal, C content determ., isotope-spectral method (*Russian*) 0-55766  
 metal substrate, thin film form., appl. of AES and ESCA (*French*) 0-50903  
 methane-air flames, OH conc. profile 0-35534  
 microfluorimetric measurements of DNA dye complex using cryostat 0-17949  
 molecular spectroscopic laboratory strategies, queueing theory and digital simulation use 0-30299  
 multicomponent, multipoint infrared ambient air monitor, microcomputer-controlled 0-40945  
 natural rubber latex  $^{13}C$  NMR spectra 0-15816  
 NMR spectrometer, for quantitative analysis, microprocessor-controlled digital integrator 0-11971  
 NMR spectroscopy, appl. to organic compounds anal. 0-16756  
 one-atom detection, reson. laser spectrosc. obs. 0-22441  
 optoacoustic signals, polymer film thickness effect on signal magnitude 0-11969  
 optoacoustic spectroscopy, direct exam. of solid and liq. samples 0-7886  
 organic compounds, IR spectra, binary coded, feature selection for automated interpretation 0-3428  
 organic sample preparation in HF discharge 0-1855  
 paddy leaves, spectrochem. anal., mineral constituents rel. to brown spot disease resistance 0-12055  
 passivation films, on Sn plate, lacquer adhesion, ESCA exam. of constitution and effects 0-40776  
 phase fluorometry as a probe of diffusion-controlled molecular encounters in dense fluids 0-32799  
 plasma emission spectroscopy, background and developments 0-45588  
 polyisocyanides, solns., struct. and acidification 0-19915  
 polystyrene lattice cleaning, dialysis, steam stripping and ion exchange effectiveness 0-3414  
 polystyrene microspheres, dye impregnated, fluoresc. spectra struct. resonances 0-50914  
 pulsed photoacoustic Raman spectrosc., gaseous trace anal. 0-40769  
 quantitative depth profile, by AES (*Japanese*) 0-16751  
 quartz, excitation in inert gas medium, detection limits of contaminants 0-55746  
 $\gamma$ -quartz, reaction, with NaCl-KCl melt, exam. of struct., IR absorption spectra 0-55706  
 Raman laser uses in molecular spectroscopy and atmospheric constituents detection 0-55762  
 Raman spectroscopy and liq. chromatography anal. (*French*) 0-45595  
 scintillation counter appl., liquid, use of miniature  $^{14}C$  and  $^3H$  standards 0-21346  
 selective excitation of probe ion luminesc. technique development 0-40797  
 self-scanning silicon photodiode array with microcomputer control 0-35612  
 single atom detection, laser reson. fluoresc. method 0-26096  
 single atom detection, using resonance ionisation spectroscopy 0-3422  
 sodium lauryl sulphate micelles, chlorophyll-a, soln., dilution expts., solubilisation anal. 0-35587  
 sooty diffusion flame, CARS obs. 0-16690  
 spectra registration system for spectrophotometers, graphical and digital forms 0-47113  
 spectra search systems, computer-aided, efficiency eval. using information theory (*German*) 0-37003  
 spectrophotometric determination of aluminium in iron alloys (*Polish*) 0-35604  
 standard paper density scaling, line spectrum intensity determ. (*Portuguese*) 0-11965



## spectrochemical analysis continued

- steel, emission spectrometric determ. of Al (*Japanese*) 0-16750  
 styrene, plasma polymerisation in glow discharge, thin film IR and free radical EPR obs. 0-2964  
 styrene, thermal polymerization, PMR obs. 0-3342  
 surface and bulk microanalysis, electron spectroscopy apparatus (*French*) 0-47151  
 dl-tartaric acid, radiation products, ESR-ENDOR OBS. 0-55682  
 tartaric acid salts, and deuterated forms, irradiated-crystals, primary reactions, EPR obs. 0-3370  
 time-of-flight spectra, fibre optic waveguides 0-23767  
 time-resolved resonance Raman spectroscopy and vidicon Raman spectrography, vibr. spectra on nsec scale 0-37095  
 toxic gas monitor based on laser photoacoustic spectrometer (*German*) 0-12046  
 toxic organic substances, detect. in water, Raman matrix isolation spectrosc. method 0-30616  
 trace analysis in gases by laser-induced schlieren technique 0-3436  
 trace gases in atmosphere, airborne laser-induced fluorescence systems 0-36425  
 tunable-diode-laser IR spectroscopy appls. 0-40798  
 two-photon excited molecular fluorescence technique 0-40799  
 vapour cell, single pass, for GC/IR spectrometer appls. 0-16743  
 Voigt effect, reson. absorpt. description 0-30302  
 X-ray, energy-dispersive, with aid of computer 0-3433  
 XPS, analytical potential, book contrib. 0-16761  
 XPS, graphite plate sample holders 0-11972  
 Al, adsorption of  $\text{NH}_3$ , KVV Auger spectra, deconvoluted spectra 0-50508  
 Al, high purity, spectrographic determination of trace impurities (*Polish*) 0-35603  
 $\text{Al}_2\text{O}_3$ , adsorption of  $\text{NH}_3$ , KVV Auger spectra, deconvoluted spectra 0-50508  
 $\text{BF}(\text{OH})_2$ , identification, rot. and centrifugal consts., mol. struct., microwave spectra obs. 0-32705  
 CO, chemisorbed on supported Rh surface, activated surface processes, IR spectra 0-16724  
 $\text{CO}_2$  conc. and temp. in flames, Raman spectroscopy 0-32720  
 Cu corrosion inhibition, by mercaptobenzothiazole, spectro-electrochem. studies 0-30138  
 Cu-Ni, sputter-induced subsurface segregation, Auger electrons obs. 0-10757  
 $\text{EsCl}_2(\text{Br})_2(\text{I})_2$ , prep., characterisation and decay of  $\text{Es}(\text{II})$  0-16727  
 FO free radical, detection by  $\text{CO}_2$  laser mag. reson. 0-45594  
 Fe and Al alloys, Mn content determ. (*Polish*) 0-31889  
 $\text{Fe/ZrB}_3$ , metal-like cpd. form. in diffusion layer during solid phase saturation 0-19994  
 $\text{Fe}_2\text{-Al}_2\text{OOH}$ , Mossbauer study, determ. of Al content and mag. props. 0-39938  
 GaAs/III-V solid soln. heterostructure composition profile by photoemission microanalysis 0-44717  
 HO fluorescence detection, interference suppression by sampling method 0-8431  
 KBr pellet, appl. to IR spectroscopy of inorganic species 0-22455  
 $\text{K}_2\text{CO}_3\text{-SiO}_2\text{-As}_2\text{O}_3$ , laser Raman spectrosc. study of ions in quenched reaction mixtures 0-25357  
 $\text{KCl-KNO}_3(\text{KNO}_3)_2$ , anion exchange during tablet pressing, IR spectroscopy appl. 0-2764  
 $\text{KEuHP}_2\text{O}_{10}$  acid, exam. of thermal decomposition 0-55638  
 KOH, beam, formed at 300-800°C, electron elastic scatt. obs., species identification 0-14231  
 $\text{LiO}_2\text{-Al}_2\text{O}_3\text{-SiO}_2$ , anal. of composition by IR reflection spectra 0-40783  
 $\text{Mo}_2$ , matrix isolated visible absorpt. spectra, electronic, vibronic and vibr. states 0-28027  
 $\text{MoN}$ , matrix isolated visible absorpt. spectra, electronic, vibronic and vibr. states 0-28027  
 $\text{MoO}_3$ , matrix isolated visible absorpt. spectra, electronic, vibronic and vibr. states 0-28027  
 $\text{NH}_3$  fragments, multiple photon dissociation of  $\text{CH}_3\text{NH}_2$  and  $\text{NH}_3$ , laser-excited fluoresc. obs. 0-11938  
 NO, chemisorption on W (110) surface, chemical changes detected by AES 0-10787  
 NO, photofragment of  $\text{NO}_2$ , Doppler spectroscopy 0-53124  
 $\text{NO}_2$ , laser and flash lamp fluoresc. monitors, comparison 0-17367  
 NaCl-KCl melt, reaction with  $\text{LiO}_2\text{-2SiO}_2$  X-ray, IR exam. 0-55706  
 $\text{NaClO}_4$ , aq. glass, formation of trapped H-atoms and electrons on X-irradiation 0-35559  
 Nb<sub>3</sub>Ge superconducting films, quantitative Auger anal. 0-55740  
 Ni-Si-B powder, oxidation at 850°C, SEM, ESCA, and elec. cond. meas. 0-7717  
 Ni<sub>3</sub>C films, form. by carburisation, characterisation 0-34337  
 NiO electrodes, effect of  $\text{Co}(\text{OH})_2$  on self-discharge, IR spectra obs. 0-21295  
 Nz pulsed laser stroboscopic fluorimeter 0-35593  
 O, conc. in lower ionosphere, fluorescence spectra 0-36434  
 $\text{PCL}_2\text{-HCl}$ , Raman spectra, solid and melt, species identification (*German*) 0-45083  
 Pd-Si (111) interface, microscopic Pd<sub>2</sub>Si form., UPS obs. 0-24743  
 Ru (~001) stepped surface, O<sub>2</sub> chemisorption, LEED and AES obs. 0-11947  
 S adsorption in coal, content meas., using X-ray radiometric analysis 0-26077  
 $\text{SF}_6\text{-Ar}$ , condensing flow, gasdynamic and IR meas. 0-6501  
 $(\text{SN})_n^*$  radicals polymerisation to  $(\text{SN})_x$  in thin films, optical spectra 0-16656  
 Si polycryst., end point detection in plasma etching by optical emission spectroscopy 0-50733  
 Si:H, amorphous, dopant conc., glow discharge optical spectroscopy 0-49546  
 $\text{Si}_3\text{N}_4$ , end point detection in plasma etching by optical emission spectroscopy 0-50733  
 $\text{SiO}_2$ , vitreous, and quartz, impurity C determ. by isotopic spectral method 0-26093  
 Ti, oxide layer growth by dry oxidation at 25°C, ESCA obs. (*French*) 0-45434  
 $\text{UO}_2(\text{NO}_3)_2$ , aq. soln., pulsed NMR relax. time,  $^{235}\text{U}$  enrichment depend. 0-2658  
 ZrC powders produced by various methods, impurities 0-11615

## spectrography see spectroscopy

## spectrometer components and accessories

- see also mass spectrometer components and accessories  
 concave grating efficiency in VUV region, diffusion pump oil contamination effect 0-14429  
 condensation chamber, for flame photometric analysis, exam. of design 0-21342  
 cuvette, heated for IR spectroscopy, exam. of design. 0-18025  
 cylindrical He absorption cell, multiple scatt. effects near reson. 0-16049  
 cylindrical mirror analyser, design and use with synchrotron radiation, autoionisation obs. 0-18049  
 DC discharge lamp, coupling to photoelectron spectrometer using differentially pumped isolating collimator 0-13156  
 decoupler coil, for supercond. NMR spectrometers 0-31828  
 digital integrator, automatically triggered, for flame AAS with discrete nebulization 0-35610  
 direct sample insertion device for inductively coupled plasma emission spectroscopy 0-42264  
 double-disc chopper with improved gating characts. for TOF spectrometer 0-37120  
 gamma-ray guide using total external refl., Mossbauer spectroscopy 0-7200  
 gas diffusion samplers, Fick's law comparison with Ohm's law 0-43819  
 graphite grids for X-ray microanalysis of biological materials 0-8232  
 grating or prism separated elements for increased spectroscopic resolution 0-43271  
 grids of fine W wire, production, use in IR spectroscopy, polarization interferometry 0-9052  
 grille filtering method and associated spectrometers, capability study, double grille monochromator 0-48427  
 heat-pipe oven, disc-shaped, used for Li excited-state lifetime meas. 0-52941  
 heated vacuum monochromator for 40-280 nm spectroscopy 0-33176  
 heating block and high-temperature cell, for spectrophotometric research of solutions, in UV and visible range 0-31899  
 high pressure cell for matrix isolation Raman spectroscopy 0-272  
 high pressure sample container for thermal neutron inelastic scattering on fluids 0-37681  
 holographic diff. gratings, Wadsworth mountings, astigmatism compensation 0-48428  
 ICP torch design method, using hydrodynamic flow patterns 0-24256  
 ion trap sensitivity for spectroscopic applications,  $^{137}\text{Ba}^+$  ground state hyperfine splitting 0-22447  
 laser microprobe, for thickness meas. using AAS 0-27355  
 laser microprobe analyser assessment for quantitative analysis in AES 0-30313  
 laser Raman spectrometer, 180° microscope sampling and viewing attachment 0-13150  
 'magic angle' spinning apparatus in solid NMR spectroscopy 0-17983  
 magic-angle rotor, using forced air bearing for NMR of solids 0-47083  
 magnetic flux stabiliser, for NMR radiospectrometers 0-52286  
 microprocessor-based spectroscopic instrumentation 0-9047  
 microwave spectrometers, modern aspects, book contrib. 0-52328  
 modulator, EPR radiospectrometer having discrete set of modulation frequencies 0-52285  
 monochromator, glancing incidence, with corrections for astigmatism and spectral-line curvature 0-43466  
 monochromator, very rapidly scanning, for IR and MM wavelengths 0-5829  
 monochromators, construction, spectrosc. appl. (*Hungarian*) 0-43478  
 multi-sample wheel for far-infrared dichroism measurements 0-47086  
 multiple optical cell for absorbance meas. of aqueous solns. 0-22450  
 NMR spectrometer, programming device for control of frequency synthesizers 0-22400  
 NQR pulse spectrometer modulator 0-17971  
 NQR spectrometer, programming device for a spin-echo installation 0-17972  
 photodiode array for radiation detection in AES and analytical appl. (*German*) 0-11992  
 physicochemical meas., modular equipment and microprocessor control (*French*) 0-30304  
 plasma jets, spectral analysis of dissolved materials 0-19624  
 preamplifier modernisation by input FET operating regime control 0-32579  
 prismatic double monochromator 0-23796  
 quick sample change probe for magic-angle-spinning NMR in a superconducting magnet 0-31834  
 radiospectrometer resonator uniaxial crystal deformation unit 0-31822  
 refractometer, SP-129, for UV region 0-31846  
 sample heating apparatus, for laser Raman spectroscopy 0-22439  
 scanning spectrometry, submillimetre, modern aspects, book contrib. 0-52329  
 shutter model, ultrafast, for resonant gamma rays 0-31955  
 SISAM employing contracircular design 0-31894  
 spectrophotometer, cutoff system for filtering out higher spectral orders in 400 to 200  $\text{cm}^{-1}$  region 0-28334  
 spectrophotometer dip probe bubble formation prevention 0-13154  
 spectrophotometer universal cryostat attachment 0-31765  
 spectrophotometer-type filters of highest possible performance, 2.5-40  $\mu\text{m}$  0-14438  
 spin-echo Fourier transform NMR spectroscopy, multiple pulse technique 0-37063  
 stroboscopic integrator for studying NQR relax. processes 0-17969  
 thermostatic control for radiospectrometer, Diapazon temperature variator 0-47160  
 time resolved EPR spectroscopy, stopped flow EPR apparatus for biological appl. 0-36206  
 transmitting TV camera, scanning nonlinearity cancellation 0-52318  
 UPS, ultrahigh vacuum, apparatus (*Japanese*) 0-37125  
 vacuum seal, with thermomechanical drive of Ti-Ni 0-31773  
 Varian Model 63 C rod atomiser, device for positioning and dispensing samples into C rods 0-42206  
 wavelength calibration device for large dispersion spectrographs 0-41728  
 HF absorption cell, appl. to precision stellar radial vels. meas. 0-12681  
 KBr pellet, appl. to IR spectroscopy of inorganic species 0-22455  
 Nd:YAG laser multipass cell for Raman scatt. diagnostics 0-1231  
 $^{67}\text{Zn}$  spectrometer, double freq. interferometer for absolute velocity calibration of piezoelectric transducer 0-37146



**spectrometers**

- see also *interference spectrometers; magnetic resonance spectrometers; mass spectrometers; microwave spectrometers; particle spectrometers; radiofrequency spectrometers; X-ray spectrometers*
- analytical atomic spectrometry, sensitivity and detection limit, review (Japanese) 0-11990
- anti-Stokes Raman, microcomputer-controlled 0-24111
- applied IR spectroscopy, instrumentation, sampling techniques and appl., book 0-46745
- automatic system for near IR stellar spectra obs. (Russian) 0-51664
- Doppler shift, particle sizing devices for research and calibration 0-4827
- double-pass, appl. to meas. of electron cyclotron emission in plasma device JIPP T-II 0-54035
- dual beam fibre optic time-of-flight spectrometer 0-52347
- echelle spectrograph, high-resolution, for far UV and visible astronomy, design and performance 0-26744
- echelle-type grating spectrograph, advantages (Polish) 0-26745
- efficiency, S/N ratio formula 0-31881
- frequency controlled saturation spectrometer, description 0-53008
- frequency-crossing phonon spectrometer for measuring magnetothermal conductivities 0-31741
- Gamma Ray Experiment on Solar Maximum Mission 0-51657
- grazing-incidence spectral region, beam-gas and beam-foil excitation obs. 0-14250
- image dissector echelle spectrometer use in flame atomic fluoresc. and emission meas. 0-11993
- instrument function of spectral devices with multiple diffraction 0-37093
- ion mobility, multielectrode, for atm. elec. meas. 0-31145
- IR scanning, for spectrally-resolved radiance 0-13164
- laser correlation spectrometer for virology and immunology 0-56158
- laser-radiation, type SKL-2 0-13151
- light scattering, quasielastic, power spectrum analyser biological appls. (German) 0-12314
- oscillating beam spectrometer for detection of very small transmission and reflection differences 0-31907
- oscillating beam spectrometer for organic thin film transmission 0-18022
- photoelectric scanning spectrometer for vacuum UV molecular photoabsorpt. cross-section meas. 0-37096
- plasma emission, background and developments 0-45588
- radial velocity spectrometer, on McDonald Observatory 2.1 m telescope 0-51667
- rocket borne resonant absorption spectrometer and photometer for geocoronal and interplanetary He obs. 0-4155
- scanning spectrometer, programmable, appl. to weak airglow emissions meas. 0-8469
- spectroradiometer for reflectance measurement 0-56658
- Ultraviolet Spectrometer and Polarimeter on Solar Maximum Mission 0-51661
- wavelength modulation reflectivity spectrometer using transmission chopper 0-13157
- CO<sub>2</sub> laser heterodyne spectrometer for examining wave-number stability of laser diode mounted in closed-cycle He refrigerator 0-31906

**spectrophotometers**

- see also *spectrophotometry*
- amplifier improved design, for SF-4 and SF-4A spectrophotometers 0-31882
- atomic absorption, positioning device for dispensing samples into C rod atomiser 0-42206
- calibration in visible range, photometric accuracy verification (Czech) 0-13159
- circular dichroism spectrophotometer, near IR, microprocessor controlled 0-22454
- cutoff system for filtering out higher spectral orders in 400 to 200 cm<sup>-1</sup> region 0-28334
- didymium glass filters for spectrophotometer wavelength scale calibration 0-43417
- dip probe bubble formation prevention 0-13154
- Fourier emission IR microspectrophotometer for surface anal., lubrication problem appls. 0-13162
- Fourier transform IR, underlying principles 0-36812
- HP 8450A, UV/visible computerised spectrophotometer 0-31883
- IL 282 CO-Oximeter for measurements on whole blood 0-56159
- microprocessor based data acquisition and control system 0-22335
- microprocessor-based spectroscopic instrumentation 0-9047
- microscope-spectrophotometer, computer processed, for measurement of absorption spectra of rock-forming minerals 0-18010
- multielement atomic spectrum anal. under computer control 0-27357
- opticophysical and physicochemical meas. instrum. 0-13121
- photochromic materials, spectrosensitometer for spectral-kinetic characts. meas. 0-27358
- photon counting microspectrophotometer for study of single vertebrate photoreceptor cells 0-12323
- portable dual-channel instrument for rapid optical spectral reflectance measurements 0-13158
- single-beam microspectrophotometer, for visible absorbance and linear dichroism meas. 0-37097
- SPECORD UV VIS, mag. micromixer attachment for immobilised cytochrome C investigations 0-56302
- universal cryostat attachment 0-31765
- UV, visible and near IR, certification of neutral light filters 0-273

**spectrophotometry**

- see also *colorimetry; spectrophotometers*
- Al-Fe alloys, spectrophotometric determ. of Al content (Polish) 0-35604
- aqueous soln. reaction kinetics meas. microwave apparatus 0-3470
- cement raw-material mix, main component determ. by atom absorption spectrophotometry 0-45615
- computer-controlled double-beam scanning microspectrophotometry for rapid microscopic image reconstructions 0-18008
- computerised colour matching, spectrophotometry 0-17995
- DNA-Au (III) interaction, rate consts., activation energies, pH, spectrophotometric obs. 0-30228
- electrogenenerated chromophores, electrochemical conc. profiles, mass transfer, charge transfer, laser absorpt. spectroelectrochem. obs. 0-40765
- galaxies, irregulars and blue compacts, chemical comp. and evolution from spectrophotometry 0-36711
- halogen tungsten lamp as radiation source for investigation of weakly reflecting materials 0-22456
- infrared, lead germanate glass, crystallisation study 0-6499
- Jupiter, spectrophotometry in 0.6 to 1.1  $\mu$  region, Jovian atmosphere optical parameters latit. vars. 0-46468

**spectrophotometry continued**

- planetary nebulae, 8 to 13 micron spectrophotometry 0-22057
- planetary nebulae, low excitation, of small ang. size, spectral studies 0-17646
- polymers, pyrolysis-mol. wt. chromatography-vapour phase IR spectrophotometry, on-line system, reviews 0-55768
- quasars of Michigan-Tololo survey, spectrophotometry 0-22105
- scintillation counter appl., liquid, use of miniature <sup>14</sup>C and <sup>3</sup>H standards 0-21346
- spectra registration system, graphical and digital forms 0-47113
- spread function, graphical representation, stray light concept 0-33198
- structural colours of beetles, analysis using reflectance measurements from macro- and microspectrophotometers 0-18023
- TU-20 turbine oil, 4-methyl-2,6-di-tert-butylphenol determ., using IR spectrophotometry (Polish) 0-13161
- two-beam, solutions in UV and visible range, high-temperature cell and heating block design 0-31899
- ultramicrospectrophotometry techniques in intravital microcirculatory studies 0-21589
- UV/vis, use of automation in achieving improved accuracy 0-27356
- As determination in seaweed and related products, hydride generation system, at absorpt. spectrometry 0-30294
- Fe and Al alloys, Mn content determ. (Polish) 0-31889
- I+HCl, quenching of I(S<sup>2</sup>P<sub>1/2</sub>), temp. depend., time resolved at. absorpt. spectrophotometry 0-32655
- Ni(H<sub>2</sub>V)<sub>2</sub>(H<sub>2</sub>O)<sub>2</sub>, synthesis and characterisation (French) 0-45225

**spectroscopes** see *spectrometers***spectroscopic light sources**

- Cherenkov radiation light source in pulse radiolysis 0-42267
- discharge lamp, HF, with hollow electrode, for atomic spectroscopy 0-26090
- discharge lamp, hollow cathode type, discharge excitation characts. obs. 0-42260
- discharge simulation, interactive programme, adaptation to disc supported microcomputer 0-24269
- discharge tube, hollow cathode type, with conical bottom, spectroscopic and elec. characts. 0-31891
- discharges, inductively-coupled, and unipolar HF, spectrum excitation 0-1855
- dye CW frequency-locked mode-locked laser, for high resolution spectroscopy in freq. domain 0-43350
- dye laser, narrow band CW oscillator/pulsed amplifier system for precision nonlinear spectrosc. 0-53318
- dye laser, narrowband CW, high output power, piezoelec. mirror translator for stabilisation 0-33036
- dye laser, two-wavelength pulsed, spectroscopic applications 0-28246
- ICP plasma source, axially viewed, for atomic emission spectroscopy 0-22434
- inductively coupled plasmas, optical emission spectroscopy 0-42266
- inert gas halide lasers, operation and use in photochem. 0-9860
- ionised atoms, prod. by low inductance vacuum spark, spectroscopy (Japanese) 0-52911
- IR Fourier spectrometer, choice of radiation source 0-27362
- metal atom conc. determ. by reson. lines broadened by Hg press. 0-43883
- mode-locked lasers for picosecond spectroscopy 0-9046
- picosecond, laser mode-locking 0-42263
- plasma source for at. emission spectrometry 0-26068
- plasma torch, reduced size inductively coupled, operation mode and detection limit 0-43994
- Pockels cell system, with 2.25 cm<sup>2</sup> aperture, for IR pulsed radiation production 0-5806
- pulsed laser excitation source for time-resolved fluoresc. spectroscopy 0-9051
- spark, high-voltage, effect of strong transverse blowing 0-3441
- submillimetric waveguide laser for gas spectroscopy 0-33022
- synchrotron radiation spectroscopy instrumentation and appls., book contrib. 0-4782
- tesla discharge as spectroscopic source for excimer laser transition study 0-274
- UV, broadly tunable, using stimulated Raman scatt. in H<sub>2</sub> 0-9963
- Ar ICP plasma, excitation source for flame at. fluoresc. spectrometry 0-37089
- CO<sub>2</sub>, continuously tunable high press. monochromatic laser for spectroscopy 0-5762
- Cs vapour tunable IR source using stimulated electronic Raman scatt., appl. to HCN (001) relax. obs. 0-9696
- D<sub>2</sub> gas discharge lamp as UV continuum source, space appls. 0-36505
- H high power arc, standard source of continuum radiation, 53-92 nm 0-44054
- H lamp using hollow lightguides, optical and operational characts. 0-53395
- H<sub>2</sub> high power tunable IR compressed laser, for spectroscopy 0-48277
- N<sub>2</sub> high power tunable liq. Raman laser, for spectroscopy 0-48277
- NH<sub>3</sub> laser, resonantly pumped, for spectroscopy 0-48277

**spectroscopy**

- see also *beam-foil spectroscopy; computerised spectroscopy; electron spectroscopy; Fourier transform spectroscopy; interference spectroscopy; magnetic resonance spectroscopy; mass spectroscopy; matrix isolation spectroscopy; microwave spectroscopy; modulation spectroscopy; optical double resonance; photoacoustic spectroscopy; quantum beat spectroscopy; radiofrequency spectroscopy; Raman spectroscopy; spectroscopy computing; time resolved spectroscopy; tunnelling spectroscopy; two-photon spectroscopy; X-ray spectroscopy*
- absorption spectra, collision-broadened lines, information anal. 0-22433
- acoustic spectroscopy, H bonds investigation, N-butyl acetamide association in solns. 0-5891
- advances in electron physics, book 0-8742
- anticrossing spectroscopy appls. 0-23379
- applied IR spectroscopy, instrumentation, sampling techniques and appl., book 0-46745
- astronomy, spectrograph with echelle-type grating (Polish) 0-26745
- atomic hyperfine structure, long isotopic chains, on-line spectroscopy 0-37903
- atomic spectroscopy using synchrotron radiation, book contrib. 0-4779
- atoms, absorpt. spectra, flame and discharge laser irradi., opto-galvanic spectroscopy 0-42272
- Brillouin scattering frequency high-precision meas., rel. to hypersound velocity meas. 0-27349
- chemistry, laser applications, review 0-45535



**spectroscopy continued**

- collision effects on nonreson. interactions, nonlinear spectrosc. obs. 0-23496  
 conference, group theory and application to spectroscopy, Nova Scotia, Canada (Aug. 1978) 0-41947  
 correlation spectroscopy, rotational and vibrational relaxation autocorrelation functions 0-32856  
 crystal field theory, finite symmetry adaptation in spectroscopy 0-43032  
 diatomic molecules, sub-Doppler laser spectrosc. 0-52320  
 dispersion vs. absorption curve method for distinguishing peak position distrib. from linewidth distrib. 0-4775  
 Doppler free intermodulated optogalvanic spectroscopy, technique description and sensitivity 0-52333  
 Doppler-free, feats and fancies 0-43001  
 Doppler-free intracavity polarization spectroscopy using elliptically polarized light 0-5537  
 echelle spectrograms reduction, single procedure 0-56713  
 electrical engineering material structure research, spectroscopy appln. (Rumanian) 0-4774  
 electro-optics, conference, Utrecht, Netherlands (Oct. 1978) 0-31420  
 electrographic instrumentation for ultraviolet imaging and spectrography 0-46399  
 exciton spectroscopy, polariton dispersion 0-54613  
 extremum position and confidence limits, determ. of absorpt. max. in wide bands 0-22188  
 far IR, appl. of far IR lasers in semiconductor research 0-31914  
 flame spectroscopy, free atom fractions and equilib. comp. calcs. 0-22438  
 fluorescence correlation, clip-correlator (Russian) 0-42270  
 fluorescence correlation spectroscopy, profile of focused collimated laser beam near focal minimum 0-43386  
 fluorescence intensity correlation, photon counting using clip-correlator (Russian) 0-42271  
 fluorescence spectrometry, beam splitter and cell window errors 0-31897  
 generating function techniques 0-44162  
 high temperature gas and vapour characterisation, conf., Gaithersburg, USA (Sept. 1978) 0-53910  
 hot gases, tunable diode laser spectrometry, noise reduction 0-31909  
 inner level spectroscopy with synchrotron radiation, theoretical aspects, book contrib. 0-4778  
 internal-reflection spectroscopy 0-18019  
 intracavity absorption, CW dye laser, Ba at. beam line shape obs. 0-47120  
 intracavity absorption model in CW multimode dye laser 0-47119  
 intracavity absorption spectroscopy at reduced pressures, using dye laser 0-47118  
 intracavity absorption spectroscopy theory with singly resonant optical parametric oscillator 0-23742  
 intracavity laser spectroscopy, appl. of OH-stabilised  $F_2^+$ -centre laser 0-32999  
 IR, gas phase species, in high temp. flow tube 0-52235  
 IR, simultaneous computer acquisition of IR, microwave and Raman spectral data (Japanese) 0-4776  
 IR, ultra-high resolution, review (Japanese) 0-31912  
 IR, with tunable diode laser (German) 0-43361  
 IR ellipsometric spectroscopy, appl. to study of adsorbed species 0-39434  
 IR instrumentation, design study, for stratospheric research 0-17391  
 IR physics, conference, Zurich, Switzerland (Mar. 1979) 0-4783  
 IR reference spectra, for GC-IR, presentation specifications 0-31908  
 isotopic isomers, spectroscopic obs. 0-53009  
 Jahn-Teller, research projects at IROE Institute (Firenze) (Italian) 0-56668  
 laser fluoresc. spectroscopy using pulse hollow cathode lamp 0-27973  
 laser polarisation, level crossing in forward scatt. 0-43004  
 laser saturation spectroscopy with optical pumping, Na, Ba atomic-resonance absorption transitions 0-47121  
 laser saturation spectroscopy with optical pumping in Na and Ba reson. transitions 0-52334  
 laser spectroscopy, atom and mol. interactions, conf., Zaragoza, Spain (June 1979) 0-27041  
 laser spectroscopy, conf., Rottach-Egern, Germany (Jun. 1979) 0-51957  
 laser spectroscopy, conf., San Diego, USA (Aug. 1978) 0-13153  
 laser spectroscopy, finite bandwidth laser excitation, line shapes, non-perturbative effects 0-52332  
 laser spectroscopy, historical perspective 0-52331  
 laser spectroscopy in mol. beams, review 0-22446  
 laser spectroscopy using an optothermal receiver 0-37810  
 layer surfaces, reflectivity at 3.39  $\mu$ m, meas. method, relevance to pipelines 0-52340  
 line position, identification and comparison of two spectra 0-47956  
 line spectrum intensity determination by standard paper density scaling (Portuguese) 0-11965  
 linear laser spectroscopy in collimated mol. beams, single mode tunable lasers appl. to small mols. 0-52339  
 long-wavelength IR spectroscopy, obs. of intermol. interactions in condensed medium 0-34927  
 molecular, synchrotron radiation appls. 0-53166  
 molecular spectroscopy, conf. Frankfurt, Germany (Sept. 1979) 0-51948  
 molecular spectroscopy using synchrotron radiation, book contrib. 0-4780  
 molecule, absorpt. spectra, flame and discharge laser irradi., opto-galvanic spectroscopy 0-42272  
 myristyltrimethylammonium bromide, micelle size, press. dependence, photon correlation spectrosc. 0-11953  
 nonlinear optical echo spectroscopy 0-48357  
 nonlinear polarisation spectroscopy, appl. to small mols. 0-52339  
 nonlinear spectroscopy of  $OsO_4$ ,  $SF_6$  mols., using tunable high-press.  $CO_2$  waveguide laser 0-43054  
 optical, CW intracavity dye laser spectroscopy, enhancement, pumping power depend. 0-13155  
 Optical Society of America meeting, Rochester, USA (Oct. 1979) 0-12841  
 optical spectroscopy technique, multiple coherent interaction in separated fields 0-52338  
 optogalvanic, CW dye laser appl. 0-43383  
 photoelectric convertor for automated spectral measurements 0-22449  
 photoelectric spectrographic detection, direct reading attachment 0-275  
 photon correlation, appl. to polarised Rayleigh scatt. in polystyrene near glass-rubber relax. 0-40124  
 photon correlation, digital correlator with blinker facility 0-37092  
 photon correlation spectroscopy, description and applications 0-52337  
 photothermal spectroscopy, thermal diffusion model 0-9045  
 picosecond spectroscopy, anal. using polarisation method 0-13152

**spectroscopy continued**

- polarisation labelling, simplification of  $NO_2$  visible spectrum, rot. vibr. spectra obs. 0-32730  
 polarisation spectroscopy, Doppler free intracavity 0-52335  
 polarisation spectroscopy and forward scatt., in Na gas 0-52336  
 polarisation-sensitive nonlinear spectroscopy, improved geometry 0-1285  
 polarised photofluorescence excitation spectroscopy, triatomic mol. photodissociation to diatomic fragments 0-28054  
 polarization props. of spectral apparatus, influence on results of luminescence spectral measurements 0-31900  
 pulse-height anal., multichannel scaling, signal averaging, SAMCSI 0-47112  
 resonance ionization spectroscopy and one-atom detection 0-22441  
 saturation spectroscopy, developments and applcs. (Japanese) 0-4777  
 saturation spectroscopy, hyperfine component intensities 0-31886  
 saturation spectroscopy including collisional effects, for three-level atomic system 0-37099  
 solar spectrometric research, automation system for on-line signal processing (Russian) 0-12659  
 spectrum-hologram, prod. and practical possibilities 0-37098  
 stellar radial velocities, meas. via HF absorpt. cell 0-12681  
 superhigh resolution spectroscopy, coherent phenomena 0-22445  
 superradiance triggering spectroscopy 0-52324  
 supersonic jet spectroscopy, appls., teaching approach 0-41996  
 synchrotron radiation, techniques and appls., book 0-5668  
 thermo-optical spectroscopy, detection by mirage effect 0-47116  
 trapped cyclotron resonance spectroscopy of Ar ions 0-53140  
 triatomic molecules, sub-Doppler laser spectrosc. 0-52320  
 vibrational spectroscopy of single crystals, review 0-55093  
 visible and UV, liq. crystal matrix optical props. 0-45102  
 H, Balmer- $\alpha$  line, high resolution spectroscopy techniques 0-52915  
 $I_2$  saturation, multiwavelength stabilisation of an Ar-Kr ion laser 0-28282

**spectroscopy applications of computers** *see computerised spectroscopy***spectroscopy computing**

- see also computerised spectroscopy*  
 A/D conversion, improved pulse height store 0-14054  
 ABSORB, absorption of muonic X-rays in P and Se allotropic modifications 0-23577  
 AES, by computer (French) 0-7890  
 alkenes, IR absorpt. curves calc. using standard fragments computer library 0-982  
 atomic emission spectrometry, blackening transformation parameters and computers use (German) 0-30300  
 2-benzoylpyridine crystals, lowest triplet state, optically detected EPR 0-15827  
 chemical analysis, energy dispersive electron probe X-ray, quantitative, compact procedure 0-40793  
 chlorotrifluoromethane, IR rovibr. spectrum (German) 0-47998  
 DOMUS, analysis of two-dimensional mol. spectra 0-18890  
 electro-optical multichannel spectrometer for transient resonance Raman and absorption spectroscopy 0-31890  
 EPR digital data acquisition using microprocessor 0-17975  
 EPR spectra, significance plots use 0-22409  
 gamma ray spectra goodness of fit anal. with IFOM program 0-27912  
 gamma-ray, instrumental neutron activation anal., improvements to basic advance prediction program 0-14042  
 gas chromatography-mass spectrometry data system, research-oriented, principles and applcs. 0-40770  
 graphite furnace peak shape study using computer 0-21331  
 IFOM, a formula for universal assessment of goodness-of-fit of gamma ray spectra 0-27912  
 infrared intensity reference meas., spectrophotometric data reduction, modular computer programs appl. 0-3471  
 IR file searching, ASTM, algorithm using peak intensity data 0-30295  
 IR filter preparation using computer, GaAs-polyethylene mixture appl. 0-2763  
 IR reflection spectrum, dispersion formula fitting, Kramers-Kronig anal. 0-50311  
 IR spectra, binary coded, feature selection for automated interpretation 0-3428  
 LINFIT, muonic X-ray spectra analysis, P and Se allotropic modifications 0-23577  
 magnetic resonance, two-centre integrals involving one-electron dipolar coupling and Slater AOs, computational procedure 0-23291  
 mass spectra, computer-aided classif., pattern recognition techniques, decision-tree approach 0-40774  
 mass spectra, low-resolution, identification using combined forward-reverse library search system 0-30296  
 mass spectral data bases, information content of retrieval procedures calc. 0-30297  
 mass spectroscopy for organic analysis, computer data search system, based on catalogue of compressed mass spectra (Russian) 0-30292  
 $^{13}C$ -methane,  $\nu_1$  fund., quasi-CW inverse Raman spectra 0-48004  
 microwave spectrometers, modern aspects, book contrib. 0-52328  
 molecular spectroscopic laboratory strategies, queueing theory and digital simulation use 0-30299  
 Mossbauer spectroscopy, data acquisition and processing system 0-18061  
 multiconfiguration Dirak-Fock program, appl. to Ba X-ray levels and 5p excited spectra 0-47865  
 multielement atomic emission/fluoresc. spectrometer system, computer-controlled 0-45587  
 multilayer dielectric microwave reflectance and transmittance, characteristic matrix formalism 0-239  
 NMR, pulsed gradient diffusion meas. with microcomputer 0-17973  
 NMR data bank,  $^{13}C$ , DARC PLURIDATA system 0-30298  
 NMR in undergrad. instruction, general purpose microcomputers use for hypothetical spectra synthesis 0-42009  
 nuclear instrumentation, standard microprocessor based 0-36822  
 organic, neutron response functions, Monte Carlo program 0-14047  
 polyatomic molecule, vibr. struct. of electronic spectra, FORTRAN programs 0-32699  
 pulse-height anal., multichannel scaling, signal averaging, SAMCSI 0-47112  
 quartz, irradiated, fused, crystalline, absorpt. spectra, colour centres 0-7384  
 random search algorithm for 2-D data fitting 0-27915  
 solar emission lines of NeV, MgVII, SiIX, SXI, population levels as function of electron density and temp. 0-21963  
 spectra, multidimensional, identification and comparison 0-47956



**spectroscopy computing continued**

- spectra search systems, computer-aided, efficiency eval. using information theory (*German*) 0-37003
- steel, standard, energy dispersive X-ray fluoresc. spectrometry, computer directed optimisation 0-45585
- triatomic linear mol., parallel bands, band model parameters 0-43026
- X-ray fluorescence anal., matrix correction, computer program (*German*) 0-3427
- X-ray spectra analysis, energy-dispersive 0-3433
- X-ray spectrometry, data interpretation, online system using multivariate statistical anal. and pattern recognition 0-3461
- Al alloys, energy dispersive X-ray fluoresc. spectrometry, computer directed optimisation 0-45585
- CO<sub>2</sub>, band model parameters prediction, 4.3 micron, 200-3000K 0-43047
- Fe, conversion spectrum anal., outer-shell s-electron density, ACSEMP program 0-7208

**spectrum** *see spectra*

**spectrum analysers** *see spectral analysers*

**speech**

*see also hearing*

- acoustic invariance in speech production, measurements of spectral char-acts. of stop consonants 0-10089
- auditory discrimination of rise and decay times in tone and noise bursts 0-19166
- bimodal cues for speech loudness 0-10090
- deaf children training to comprehend passive voice 0-33372
- deaf speech and hearing aids, vocoders, frequency lowering and lipreading cues 0-12309
- deafness effects on generation of voice 0-33361
- digital coders, optimization by exploiting human auditory masking 0-33356
- EEG activity comparison in right and left cerebral hemispheres by power spectrum analysis 0-45922
- encoding, predictive and residual 0-33354
- encoding using freq. domain techniques 0-33355
- Glossynograph system for presenting printed text synchronously with speech for hearing-impaired persons 0-56153
- hemispheric speech organisation in left- and right-handed, test of models 0-8071
- larynx, electronic, Polish developed, design and operation 0-46098
- lingual tactile sensory system, automated instrumentation for research 0-8205
- movement-related tonal signal processing, left hemisphere superiority 0-35913
- nasalisation in normal and hypernasal speakers, effects of feedback filtering 0-35921
- phonetic defects caused by facial gaps, correction using prosthetics (*French*) 0-51298
- phrase-level timing patterns in English: effects of emphatic stress location and speaking rate 0-51128
- preadolescent children's voices, acoustic correlates of perceived sexual identity 0-10088
- production, physiology and acoustical props. of vocal system (*Japanese*) 0-26242
- robotic arm voice command system, 6 degrees of freedom 0-12313
- signal modelling and recognition, system identification approach 0-51286
- stammerer fluency aid using delayed auditory feedback, body-worn aid 0-56283
- steady-state vowel representation in temporal aspects of discharge patterns of populations of auditory nerve fibres 0-21479
- stuttering, fundamental freq., effects of delayed auditory feedback and masking 0-35922
- syllable duration effects using Melodic Intonation Therapy technique 0-35920
- syllable-final position, investigations of place and manner 0-10095
- training patterns for deaf people, computer generated 0-51290
- ventilatory phonotory conflict, investigation using glottoscope 0-51145
- waveform coding technique developments in Japan, review 0-33353
- weak speech amplification device with suppression of respiration noise 0-30929

**speech amplifiers** *see audio-frequency amplifiers*

**speech analysis**

- American English, acoustic study of medial /t,d/ as function of phonetic environment 0-10093
- articulatory characteristics of tongue and jaw point movements in connected sounds of Japanese 0-26243
- CRO synthesis of optical lip shapes from vowel sounds 0-19170
- deafness effects on generation of voice 0-33361
- dysarthria associated with cerebellar disease, acoustic characts. 0-56067
- equal-articulation segment determination 0-5880
- equalizer in spectral domain for speech processing by autocorrelation function 0-1383
- Estonian, statistical data (*Russian*) 0-45923
- laryngeal prosthesis, internally worn, design and construction 0-41318
- lip motor control using mechanoreceptor feedback 0-33367
- phonation acoustic qualities in young hearing-impaired children 0-33373
- pitch-synchronous coding, linear prediction coding, analysis frame position influence 0-14523
- Russian VCV utterances, formant frequency patterns 0-33362
- spectral analysis, review of methods 0-21560
- spectral noise levels and roughness severity ratings for vowels produced by male children 0-51129
- spectral properties of fricative consonants in children 0-33364
- stop consonant production errors in developmentally dysphasic children 0-33363
- stutterers' fluent speech, voice onset time, frication and aspiration 0-51130
- ventilatory phonetics, analogic 0-51131
- vocal tract, computer representation of geometrical configuration (*Russian*) 0-46111
- vowel formation by profoundly deaf children, Argentine Spanish appl. (*Spanish*) 0-30734

**speech compression** *see bandwidth compression*

**speech intelligibility**

*see also hearing*

- acoustic feedback's influence on speech intelligibility 0-23859
- ADPCM coded speech, segmental SNR measure as indicator of quality 0-33359
- articulation loss of consonants, computation methods (*Czech*) 0-43557

**speech intelligibility continued**

- auditorium acoustics design index, S/N ratio for speech intelligibility 0-19156
- auditory-visual perception of speech with reduced optical clarity 0-35919
- binaural critical masking bands 0-21475
- coarticulatory cue decoding rel. to age 0-51126
- deaf children's speech, effect of timing errors on intelligibility 0-19167
- deep-sea diver speech distortion, chemical and physiological stress correlation 0-45924
- Dutch vowel lengths production and perception in spoken sentences 0-38185
- English consonant dissimilarity ratings by normal and hearing-impaired subjects 0-35914
- hearing tests, word list formats 0-33370
- intensity discrimination with gated and continuous sinusoids 0-10094
- low-frequency hearing loss, filtered speech, psychophysical tuning curves and masking 0-51121
- noise induced hearing listeners, effects of high-freq. compensation 0-38186
- objective measures for speech quality testing 0-33358
- perceptual invariance and onset spectra for stop consonants in different vowel environments 0-48523
- saturation diving communications system 0-43558
- sentence comprehension, multiplicative effects for combined acoustic disturbances 0-35915
- SPAC, speech processing using the autocorrelation function, noise reduction in speech communication (*Japanese*) 0-33371
- spectral integration 0-21477
- stimulus dominance in fused dichotic syllables, category goodness hypothesis 0-33368
- stimulus-onset asynchrony effect on dichotic performance of children with auditory-processing disorders 0-41044
- temporal modulation transfer functions based upon modulation thresholds 0-21478
- tones, discrimination of relative onset time of two-component tones by infants 0-33366
- transmission channel quality determining physical method 0-33369
- visual vowel and diphthong perception from two horizontal viewing angles 0-35923
- vowel normalization procedures eval. 0-33365
- word discrimination scores, effect of marking by noise 0-41047
- He speech distortion correction by vocal tract area function conversion (*Japanese*) 0-19171

**speech recognition**

- computer-aided recognition of Polish vowels in continuous speech 0-33380
- discrimination tests using programmable hearing aid with multichannel compression, children 0-17202
- distorted speech perception, role of training 0-5881
- infant perception, constancy for spectrally dissimilar vowel categories 0-33360
- information from data banks over telephone 0-1384
- linguistically oriented computer system for recognition natural continuous speech 0-23845
- speaker identification, effects of selected vocal disguises 0-10091
- visual perception of syllables and sentences, age effects 0-16943
- Wigner distribution function, optical production, speech signal analysis 0-48521

**speech synthesis**

- autoregressive system, vowel sound synthesis, adaptive filter method (*Spanish*) 0-43556
- dyad boundaries, linear interpolation of spectral parameters 0-19168
- dynamic vowels, human auditory system perceptual mechanism, dichotic fusion expts. (*Japanese*) 0-53569
- encoding voice fundamental freq. into vibrotactile freq. 0-10092
- Estonian, statistical data (*Russian*) 0-45923
- information from data banks over telephone 0-1384
- optical lip shapes from vowel sounds, synthesis using CRO 0-19170
- portable equipment (*French*) 0-51291
- portable speech synthesizer for severely handicapped children 0-56154
- programmable filter synthesiser (*French*) 0-48524
- speaking machines, historical overview (*Japanese*) 0-23846

**speech transmission** *see voice communication*

**speed** *see velocity*

**speed indicating instruments** *see velocity measurement*

**speed measurement** *see velocity measurement*

**spelter** *see zinc*

**spherical aberration** *see aberrations*

**spheroidizing**

- ceramic powder, thermal stresses during spheroidisation process (*Russian*) 0-40386
- steel, alloy, type 11Kh18M, eutectic carbide composition change due to heating 0-16353
- steel, hypereutectoid, austenite dissociation depend. on strain at intercritical temps., pearlite transform. (*Russian*) 0-40362
- steel, ultrahigh C, superplastic struct. development by heat treatment 0-11703
- Fe, cast, influence of interfacial energy on shape of graphite 0-16360
- Fe, cast, spheroidizing effect of Mg and Ce modifiers 0-35193
- ZrO<sub>2</sub>-Y<sub>2</sub>O<sub>3</sub> powder, prep. for plasma spheroidisation, sputter drying (*Russian*) 0-55324

**spicules** *see solar prominences*

**spin**

- see also baryon spin and parity; electron spin; isotopic spin (elementary particles); lepton spin and parity; meson spin and parity; nuclear spin and parity; spin density waves; spin hamiltonians*
- hadrons, relation between spin, isospin, strangeness and charm 0-37183
- neutron, electric and magnetic dipole moments 0-4993
- Poincare covariant particle model with mass and spin mixing 0-32016
- proton, outcome of violent collisions 0-434
- translational gauge theory of gravity: post-Newtonian approximation and spin precession 0-46945
- unstable particles, dynamical spin spreading 0-9117
- world line conditions for spinning particles, spin orbit forces 0-36844
- $\gamma^*N \rightarrow \psi N$ , gluon momentum, spin, parity and coupling 0-42395
- NN $\rightarrow$ NN, large momentum transfer, spin effects 0-22577
- pp $\rightarrow$ pX, high  $p_T$ , spin-spin asymmetries, polarisation, hard scatt model with QCD 0-13339



spin arrangements *see magnetic structure*

spin decoupling (NMR) *see double nuclear magnetic resonance*

### spin density waves

- conduction-electron polarisation at nucl. sites due to indirect exchange interaction 0-34619
- electron gas, one dimensional, dynamic interaction screening, spin and charge density wave instabilities 0-24819
- exciton ferromagnet, incommensurate mag. structs., inhomogeneous magnetisation (*Russian*) 0-29566
- Fermi gas, one dimensional with backward scatt., gap renormalisation 0-24818
- Hubbard model, one-dimens., extended,  $2k_F$  and  $4k_F$  correl. functions, computer renormalisation group calcs., appl. to one-dimens. conductors 0-54625
- itinerant electron antiferromagnetic matrix, local moments, spin Hamiltonian 0-34626
- one dimensional Fermi gas model in relation to spin and field theoretical models 0-24816
- one-dimensional Fermi gas with backscattering, coupling between charge and spin degrees of freedom 0-17861
- one-dimensional Hubbard model, Friedel oscills. around a nonmagnetic impurity 0-25073
- one-dimensional systems, impurity effects on ordered phases 0-24905
- organic linear chain cpds., diffuse  $4k_F$  refls., small intramolecular Coulomb interaction 0-34376
- quasi one-dimensional spin lattice coupled system, collective modes 0-24896
- spinless fermion systems, Coulomb repulsion, bond alternation, Peierls distortion, HF approx. 0-44524
- superconductor, magnetic, Fermi surface nesting effect on mag. instability 0-54831
- Cr alloys, localised magnetic moments in band antiferromagnets, impurity interactions (*Russian*) 0-54888
- Cr, antiferromag., electron interference oscills. and spin-density-wave energy gaps at Fermi surface 0-49574
- Cr, antiferromagnetic, pressure effect on Fermi surface by de Haas-van Alphen effect (*Russian*) 0-6701
- Cr, electronic structure model, Invar effect, antiferromagnetic-non mag. transitions 0-20370
- Cr, incommensurate antiferromag., inelastic neutron scatt. meas. 0-25088
- Cr, inelastic neutron scatt. expts., spin density waves 0-44818
- Cr, magnetic excitations of incommensurate spin density wave 0-11183
- Cr, magnetic phase diagram in external mag. field, spin reorientation curve, critical point coordinates (*Russian*) 0-29548
- Cr, paramagnetic, Hartree band struct., Fermi surface, nesting wave vector 0-49583
- Cr, spin density wave Q-vector, temp. and press. depend. 0-11167
- Cr-Co (4.0 at.%) alloy, antiferromag., disappearance of resist. min. under press., and press. coeff. of  $T_N$  0-10960
- Cr-Co (up to 8 at.%), antiferromagnetic, resist. minimum, Kondo effect by pairs of Co atoms 0-39566
- Cr-Fe, dilute, localised moment cluster model, ferromagnetic exchange coupling 0-39774
- Cu, fluctuations in nuclear spins, susceptibility, internal energy 0-50115
- Fe,NbSe<sub>2</sub> (2H), mag. susceptibility meas., 1.3-300K 0-39740
- $\alpha$ -Mn, electronic structure model, Invar effect, antiferromagnetic-non mag. transitions 0-20370
- TiBe<sub>2</sub>, neutron diffr. study of mag. ordering 0-44811
- V<sub>2</sub>O<sub>5-1</sub> ( $3 \leq x \leq 9$ ), Magneli phases, mag. susceptibilities at low temp. 0-20389

### spin disorder resistivity

- amorphous Heisenberg ferromagnet, force-force correl. function method 0-24918
- disordered systems, Anderson localisation theory in two dims., real space scaling method 0-44540
- rare earth metals, electrical resistivity, high temp., scatt. mechanisms 0-39553
- rare earth metals, HCP, point defect production during electron irradi. at low temp. 0-49273
- transition metal alloys, ferromagnetic, low temp. resist. calc. 0-24919
- Au-Fe(Co)(Mn), residual resistivity conc. depend. 0-2382
- Gd, liquid, electrical resistivity calc., spin disorder contrib. 0-6803
- Mg-Yb, dil., Kondo scatt. from Yb, low temp. elec. resist. meas. 0-44578
- Mn-Zn ferrospones, carrier transfer phenomena 0-54727
- NbS<sub>2</sub>(Se<sub>2</sub>) intercalation complexes with 3d transition metals, mag. and metallic transport props. 0-44814
- Ni, ferromagnetic, Hall effect, anomalous, rel. to scatt. processes 0-44572
- Ni-Cu, ferromagnetic, Hall effect, anomalous, rel. to scatt. processes 0-44572
- TaS<sub>2</sub> intercalation complexes with 3d transition metals, mag. and metallic transport props. 0-44814

### spin dynamics

- see also spin density waves; spin disorder resistivity*
- anisotropic paramagnet with exchange-bond dilution, sixth freq. moments 0-44789
- antiferromagnet, magnetisation, crit. spin-flop angle, temp. and field depend. (*Russian*) 0-7111
- biological macromolecule, truncated driven nucl. Overhauser effect in presence of spin diffusion 0-1095
- chromium phosphinate polymer, one-dimensional antiferromagnet, spin-flop 0-50131
- Coulomb gas in strong mag. field analogy with electron gas with backward scatt. 0-24817
- cubic Ising ferromagnet, three spin interaction effect on mag. props. 0-54910
- diethylammonium manganese chloride, planar Heisenberg magnet, spin diffusion, EPR study 0-15793
- diffusion, effect of spin-photon and spin-phonon interactions 0-44849
- dimethyl ammonium copper chloride, spin dynamics near crit. pt. 0-7112
- electron spin density functional gradient expansion, local approx. calcs. 0-44792
- ferromagnet, anisotropic Landau-Lifshitz, quasiclassical spectra (*Russian*) 0-15678
- ferromagnetic phase transitions, nucl. spin dynamics in anisotropic systems 0-11205
- ferromagnetic phase transitions, nucl. spin dynamics in isotropic systems 0-11204
- ferromagnets, exchange and dipolar coupled, spin wave renormalisation, Damon-Eshbach surface spin waves 0-2564

### spin dynamics continued

- frustrated two-dimensional planar model, spin-spin correl. 0-11212
- Heisenberg antiferromagnetic chain, spin dynamics, quantum effects 0-34651
- Heisenberg chain, classical, higher moments and spectral shape 0-11147
- Heisenberg ferromagnet, spin configurations near singularities in micro-magnetism 0-54908
- Heisenberg model, classical antiferromag. chain, low temp. dynamics 0-39803
- Heisenberg paramagnet, exchange bond dilution, freq. moments of spin correl. function 0-50030
- induced moment systems, effect of spin fluctuations 0-2585
- Ising 2D regular model, frustration effects 0-39784
- Ising O(2), O(3) and O(4) spin systems, Hamiltonian string-coupling expansions 0-20426
- Ising square frustration model, numerical study of ground state correl. 0-34638
- itinerant electron system, mag. excitations, neutron scatt. studies 0-44838
- itinerant localised systems, dynamic magnetic response 0-34583
- Jeener-Broekaert three-pulse sequence, inhomogeneous lineshapes, second rank spin interactions 0-39891
- kinetic Ising chain, renormalisation group transform. for master eqn. 0-11214
- long wavelength spin susceptibility from particle-particle scattering, logarithmic temp. control 0-7124
- magnetic crystal, perfect, spin rot. of forward transmitted beam in neutron diffr. 0-50113
- magnetic excitations, polarised neutron inelastic and quasi-elastic scattering 0-50045
- many-spin system, group approach in dynamics (*Russian*) 0-4579
- many-spin system, group approach in dynamics (*Russian*) 0-44900
- many-spin system dynamics, group approach (*Russian*) 0-50221
- metastable spin-aligned crystals, decay kinetics 0-34669
- <sup>13</sup>C-methane-d<sub>4</sub>O, annealed, spin conversion and proton 2nd moment time-depends. 0-11283
- NMR relaxation processes, macroscopic evolution eqns. and virtual spins importance (*French*) 0-32739
- nonstationary nutations in heteronuclear double resonance 0-20516
- one-dimensional antiferromagnet, interchain coupling, effect on US attenuation 0-19880
- one-dimensional classical planar model in applied magnetic field 0-15729
- one-dimensional mag. systems, neutron scatt., review 0-50103
- one-dimensional organic semiconductors, resonant states, mag. excitations and impurities 0-24839
- orbital degeneracy, one dimensional two spin models (*Russian*) 0-54899
- paramagnetic system, spin waves, classical approach 0-29519
- planar ferromagnetic chain, soliton dynamic struct. factors 0-7125
- polyacetylene and polyacetylene: AsF<sub>5</sub>, one-dimens. spin diffusion, NMR  $T_1$  and dynamic nuclear polarisation meas. 0-44946
- pseudo one-dimensional kinetic Ising model, dynamic susceptibility 0-50025
- quasi-localised spin system, mag. excitations, neutron scatt. studies 0-44838
- rare earth intermediate valence systems, neutron scatt., review 0-49674
- rare earth mixed valence compounds, spin dynamics, mag. neutron scatt., Mossbauer effect, XPS studies 0-39786
- redox enzyme, Fe-, Cu-, or Mo-containing, electron transfer peculiarities 0-16896
- ruby NMR laser, <sup>27</sup>Al nucl. spin system, collective ordering phenomena, instabilities 0-11278
- semiconductor, antiferromagnetic, spin-magnetomagnon resonance 0-2566
- TANOL, free radical, spin flopping transition, temp. depend., mag. anisotropy energy 0-54890
- TCNQ salts, proton nucl. relax. meas. 0-20484
- TMMC:Cu, EPR lines, dynamic effect of low-symmetric spin distrib. 0-39854
- TMMC:Cu, EPR linewidth freq. depend., spin dynamics 0-15794
- TMMC, EPR lines in one-dimensional mag. systems, dynamic effect of low-symmetric spin distrib. 0-39853
- TTF-Cu bis-dithiolene, dimer, mol. displacements at 4.2K 0-10539
- TTFCuBDT, spin-Peierls transition in spin 1/2 Heisenberg chains, RPA calcs. 0-25150
- uniaxial Heisenberg antiferromagnet, phase diagrams 0-15730
- X-Y quasi-one-dimens. system anisotropic, spin-Peierls phase transition, tricritical point 0-25142
- Al<sub>2</sub>Mn<sub>2</sub>Si<sub>2</sub>O<sub>12</sub> amorphous spin glass, spin dynamics, neutron scatt. meas. 0-15741
- Al<sub>2</sub>O<sub>3</sub>, corundum, acoustic enhancement of NMR lines 0-29632
- Ca<sub>3</sub>Mn<sub>2</sub>Ge<sub>2</sub>O<sub>12</sub>, antiferromagnetic garnet, neutron diffr. study in mag. field 0-50060
- CeIn<sub>3-x</sub>Sn<sub>x</sub>, scaling behaviour near valence instability, mag. susceptibility and mag. transitions 0-25111
- Co, internal friction anomalies in spin reorientation temp. range (*Russian*) 0-49299
- Co, spin fluctuations above Curie temp., diffuse mag. neutron scatt. obs. 0-50102
- Co-Fe, internal friction anomalies in spin reorientation temp. range (*Russian*) 0-49299
- CoBr<sub>2</sub>, magnetic excitations, neutron scatt. investigation 0-39761
- Cr, magnetic phase diagram in external mag. field, spin reorientation curve, critical point coordinates (*Russian*) 0-29548
- CrFe, mag. correls. and onset of ferromag., neutron scatt. study 0-50105
- Cr<sub>2</sub>O<sub>3</sub>, antiferromag., muon spin rotation (*German*) 0-54877
- Cr<sub>1-x</sub>V<sub>x</sub>, nucl. spin relax., spin fluctuation effect 0-34811
- CsCoCl<sub>3</sub>, Ising like antiferromag., mag. phase transition, <sup>133</sup>Cs NMR 0-7184
- CsNiF<sub>3</sub>, one-dimensional magnet, dynamics, mol. field theory approach 0-34614
- Cu-Mn spin glass alloy, spin correl. function, combined neutron spin echo and polarisation anal. 0-50107
- CuMn, spin glass, mag. correls., neutron scatt. study 0-50105
- Cu<sub>0.95</sub>Mn<sub>0.05</sub>, spin glass, low temp. mag. excitation spectrum, inelastic neutron scatt. obs. 0-50109
- Cu(NO<sub>3</sub>)<sub>2</sub>·2<sup>1</sup>/<sub>2</sub>H<sub>2</sub>O, singlet ground state system, mag. props. 0-44850
- CuSO<sub>4</sub>·3H<sub>2</sub>O, S = 1/2 antiferromag. Heisenberg chain, spin dynamics 0-11285
- DyFeO<sub>3</sub>, non Heisenberg R-Fe exchange interaction, behaviour in mag. field (*Russian*) 0-2568
- Dy<sub>0.7</sub>La<sub>0.3</sub>FeO<sub>3</sub>, reorientational phase transitions, influence of La<sup>3+</sup> ions 0-7108



## spin dynamics continued

- ErCrO<sub>3</sub>, magnetisation, NMR freq. temps. depend. weak ferromagnetic-antiferromagnetic spin reorientation transition 0-29631  
Er(Fe<sub>1-x</sub>Co<sub>x</sub>)<sub>3</sub>, spin reorientation, easy axis of magnetisation 0-25144  
Fe, spin fluctuations above Curie temp., diffuse mag. neutron scatt. obs. 0-50102  
FeCO<sub>3</sub>, metamagnetic insulator Neel temp. anal. by model including spin fluctuations (*Russian*) 0-15715  
Fe<sub>1-x</sub>M<sub>x</sub>Cl<sub>2</sub>, disordered, Mn spin excitations by microwave absorption at high freqs. 0-34759  
α-Fe<sub>2</sub>O<sub>3</sub>, antiferromag., muon spin rotation (*German*) 0-54877  
Fe<sub>2</sub>Pd<sub>2</sub>-Si<sub>18</sub>, amorphous, magnetisation, magnetoresist., spin glass and ferromag. phases 0-34697  
Gd, optical conductivity, direct interband transitions 0-15488  
He, liq., spin fluctuation peak obs. by inelastic neutron scatt. 0-49447  
He, liquid, low-energy spin fluctuation peak, theoretical anal. of neutron obs. 0-6584  
He, superfluid, A-phase, orbital dynamics in spin fluctuation feedback approx., out-of-phase mode 0-54457  
He, superfluid, spin and orbital dynamics, book contrib. 0-2236  
He, superfluid B-phase, spin oscils. in the presence of dipole forces 0-6583  
He-A, superfluid, spin dynamics, spin-orbit configurations, spin waves (*Russian*) 0-54462  
HgTe type semiconductors, spin-flip transitions in magneto-optics and magneto-transport 0-50306  
InSb type semiconductor, spin-flip transitions in magneto-optics and magneto-transport 0-50306  
K<sub>2</sub>CuF<sub>4</sub>, two-dimensional planar ferromagnet, giant fluctuation of spins (*Japanese*) 0-54894  
K<sub>2</sub>Cu<sub>1-x</sub>Zn<sub>x</sub>F<sub>4</sub>, two-dimens. ferromag., spin correls. near percolation limit 0-44840  
Ni-Pt disordered alloy, off-diagonal, T-matrix itinerant electron ferromagnetism calcs. 0-25067  
Ni<sub>0.95</sub>S Fe, spin glass, spin flop in exchange field 0-34640  
NiO (111) platelets, antiferromag. S domains, optical obs., spin flop 0-54915  
NiO (111) platelets, magnetic anisotropy investigation by torque and mag. susceptibility meas. 0-54885  
NiWO<sub>4</sub> monoclinic antiferromagnet, orientational phase transition and intermediate state (*Russian*) 0-15725  
Pd<sub>3</sub>Mn, disordered, mag. correls., neutron scatt. study 0-50105  
Rb<sub>2</sub>CoF<sub>4</sub>,<sup>57</sup>Fe, Ising antiferromag., Mossbauer spectra, critical dynamics 0-15884  
Rb<sub>2</sub>Co<sub>1-x</sub>Mg<sub>x</sub>F<sub>4</sub>, random two-dimens. Ising antiferromag., unstable mag. long-range order, neutron scatt. obs. 0-44839  
Rb<sub>2</sub>Mn<sub>1-x</sub>Mg<sub>x</sub>F<sub>4</sub>, two-dimens. antiferromag., spin fluctuations, neutron diff. study 0-44846  
Rb<sub>2</sub>Mn<sub>1-x</sub>Mg<sub>x</sub>F<sub>4</sub>, spin dynamics near percolation threshold, EPR study 0-39859  
Sm<sup>2+</sup>, Zeeman energy transfer at surface layer 0-11247  
Sm<sub>2</sub>Tb<sub>1-x</sub>FeO<sub>3</sub>, gyrotropic props. and birefringence, in spin reorientation range 0-7324  
SrEuFeO<sub>4</sub>, Neel temp. and spin reorientation, Mossbauer study 0-39934  
SrGdFeO<sub>4</sub>, Neel temp. and spin reorientation, Mossbauer study 0-39934  
SrRFeO<sub>4</sub>, (R=La,Pr,Nd), Mossbauer spectra, spin reorientation 0-15880  
TaS<sub>2</sub>(NH<sub>3</sub>)<sub>3</sub>, NMR spectral densities and two-dimens. diffusion 0-50215  
TbI<sub>2</sub>, Faraday rotation and transition of spin config. at high mag. fields 0-39776  
TbP, mag. excitations above antiferromag. ordering temp., inelastic neutron scatt. obs. 0-50112  
Tb<sub>1-x</sub>Y<sub>x</sub>Co<sub>5+0.1x</sub>, exchange interactions and magnetocrystalline anisotropy 0-34618  
TiS<sub>2</sub>(NH<sub>3</sub>)<sub>1.0</sub>, NMR spectral densities and two-dimens. diffusion 0-50215  
TiCoF<sub>3</sub> paramagnetic, nonmagnetic atomic nuclei spin density, NMR study 0-29633  
Y(Co<sub>1-x</sub>Ni<sub>x</sub>)<sub>5</sub>, spontaneous magnetisation mag. anisotropy, spin reorientation transformation (*Russian*) 0-7082  
YCrO<sub>3</sub>, magnetisation, NMR freq. temps. depend. weak ferromagnetic-antiferromagnetic spin reorientation transition 0-29631  
YFe<sub>2</sub>, amorphous concentrated spin glass, susceptibility, Mossbauer and neutron scatt. meas. 0-39783  
Y<sub>1-x</sub>Gd<sub>x</sub>Co<sub>5</sub>, exchange interactions and magnetocrystalline anisotropy 0-34618  
YIG, Si substituted, spin reorientation, Mossbauer spectroscopy obs. 0-44989  
Y<sub>1-x</sub>Nd<sub>x</sub>Co<sub>5</sub>, exchange interactions and magnetocrystalline anisotropy 0-34618  
Y<sub>1-x</sub>Tb<sub>x</sub>Co<sub>5</sub>, spontaneous magnetisation anisotropy, spin reorientation transforms. (*Russian*) 0-7082

## spin echo (EPR)

- diffusion of radical-ion pairs, spatial distrib., electron spin echo obs. 0-29622  
EPR, ns time-resolved, in pulse radiolysis, via spin echo method 0-43075  
EPR/ENDOR, modified Ka-band spectrometer, obs. of electron spin echoes at 35 GHz 0-13113  
metal particles, conduction electron spin echo modulation, theory 0-39872  
TGS X-irradiated, paramag. relax, spin-echo study 0-7168  
Ag, and Ag<sup>+</sup>, solvation in deuterated-ice matrices, electron spin echo obs. 0-15780  
CaMoO<sub>4</sub>:Er<sup>3+</sup>, phase relax. time rel. to g-factor anisotropy, electron spin echo obs. 0-29615  
CaWO<sub>4</sub>:Yb<sup>3+</sup>, Nd<sup>3+</sup> phase relaxation electron spin echo spectra 0-29613  
CaWO<sub>4</sub>:Yb<sup>3+</sup>(Nd<sup>3+</sup>), phase relax. time rel. to g-factor anisotropy, electron spin echo obs. 0-29615  
CsZnCl<sub>2</sub>:Cu<sup>2+</sup>, electron spin echo, 35 GHz 0-13113  
Cs<sub>2</sub>ZnCl<sub>2</sub>:Cu<sup>2+</sup>, single cryst. and powdered single cryst., EPR, linear elec. field effect 0-11250

## spin echo (NMR)

- acetic acid, -d<sub>1</sub>(=d<sub>4</sub>) liquid, molecular motion, proton spin echo study (*Russian*) 0-32745  
alkali metal bromates and chlorates, alkali and <sup>17</sup>O NQR, spin echo double reson. method, electronegativity 0-54970  
coherent NQR relaxometer, two freq. processes by multichannel analyser 0-20498  
diffusion in bounded heterogeneous media, stochastic Liouville eqn., spin quantum phenomena 0-54992

## spin echo (NMR) continued

- dimethylammonium copper chloride bromide, mag. props., pulsed NMR expts. 0-11292  
fluorite lattices, <sup>19</sup>F<sup>-</sup>, self-diffusion, spin lattice relax., NMR techniques 0-34801  
Fourier transform spin-echo NMR spectroscopy, multiple pulse technique 0-37063  
hydrazide derivatives, symm., <sup>14</sup>N NQR echo envelope slow beats 0-29643  
hydrazine monohydrate, <sup>14</sup>N NQR, echo envelope modulation obs. 0-50218  
Jeener-Broekaert three-pulse sequence, inhomogeneous lineshapes, second rank spin interactions 0-39891  
liquid, Earth field range, review 0-50206  
liquid, undergoing inhomogeneous Poiseuille flow, spin echo signal shape (*Russian*) 0-50225  
liquid crystal, thermotropic mesophase, DMR chain segments assignment 0-24356  
lysozyme, tryptophan residues, H exchange for D, relax., proton NMR spectra 0-35846  
methylcyclohexane, dense liq., self-diffusion and viscosity 0-15278  
molecular crystals, chem. shielding, spin-lattice, quadrupole interactions, <sup>2</sup>D NMR spin echo spectroscopy 0-34817  
multicomponent self-diffusion measurement using spin echo expts. on standard Fourier transform NMR spectrometers 0-22401  
multiple-quantum transition orders separation, using pulsed field gradients 0-50222  
nematic liquid cryst., one-deuteron system, multiple quantum spin-echo spectroscopy 0-31832  
neutron spin-echo integral transform spectroscopy 0-4748  
NQR, at multiple and combination frequencies 0-20499  
NQR spectrometer, programming device for a spin-echo installation 0-17972  
NQR-NQR double resonance, double quadrupole spin echo resonance 0-20513  
PAA, homologous series, isotropic phase, mol. self diffusion by spin echo method 0-44109  
phase-modulated spin echoes, derivation of pure absorpt. spectra 0-22410  
polyethylene cocrystals, partially and fully deuterated, chain folding, <sup>1</sup>H NMR solid echo technique 0-20507  
polymers, semicrystalline, partially and fully deuterated, chain folding, <sup>1</sup>H NMR solid echo technique 0-20507  
quadrupole spin echo envelope EFG tensor axisymmetry in mag. field 0-20497  
quadrupole spin-system, and energy levels in interaction representation 0-20492  
rare earth rhodium borides, RRh<sub>4</sub>B<sub>4</sub>, NMR and sp. ht. in supercond. and mag. ordered phases 0-7037  
small molecules in protein solns., spin-lattice relax. times, inversion recovery spin-echo sequence 0-21446  
solid, mol. and complex ion intramolecular configs., nucl. quadrupole double reson. obs. intramolecular configs., nucl. quadrupole double reson. obs. 0-34821  
solution NMR, enhanced selection of non protonated C resonances, <sup>13</sup>C spin echo obs. 0-31835  
1,1,2-trichloroethane, phase-modulated spin echoes, derivation of pure absorpt. spectra 0-22410  
two frequency spin echo spectroscopy, review 0-20506  
two-dimensional NMR spectra, elimination of dispersion-mode contribs. 0-20508  
two-dimensional spectra, anomalous spinning sidebands 0-17976  
water, diffusion const. in presence of large background gradients, modified pulsed gradient technique 0-31831  
water, flow through circular pipe, pulsed NMR study 0-28566  
water, self-diffusion coeff., pressure and temp. depend. meas. by proton spin echo 0-39328  
water molecules in biological systems, relax. rel. to vol., pulse NMR obs. 0-40960  
AgClO<sub>4</sub>, structural phase transition, <sup>35</sup>Cl NQR meas. 0-15819  
(Co<sub>1-x</sub>M<sub>x</sub>)<sub>2</sub>B, M=Mn or Fe, paramag., spin echo NMR spectra, ferro-mag. transition, spin-lattice relax. 0-29645  
(Co<sub>1-x</sub>M<sub>x</sub>)<sub>2</sub>B, M=Mn or Fe, ferromag., internal fields meas. by NMR spin echo 0-29646  
Cs atoms, nonresonance spin echo, transverse relaxation time (*Russian*) 0-50224  
Cu-Ga, high dislocation density alloys and oxide precipitated struct., NMR, spin echo 0-39892  
Cu-Si, high dislocation density alloys and oxide precipitated struct., NMR, spin echo 0-39892  
D NMR spin echo response in solids 0-25248  
DCl, liq., self-diffusion coeffs., NMR spin-echo meas. 0-50223  
EuCu<sub>2</sub>(Pt<sub>2</sub>)(Pd<sub>2</sub>), indirect exchange, spin echo NMR meas. 0-15822  
EuPd<sub>2</sub>, elec. field gradient, spin echo NMR meas. 0-20509  
EuPt<sub>2</sub>, elec. field gradient, spin echo NMR meas. 0-20509  
Fe-Al, dil., film, NMR spin echo, rel. to struct. inhomogeneities (*Russian*) 0-29644  
Fe-Co, dil., film, NMR spin echo, rel. to struct. inhomogeneities (*Russian*) 0-29644  
(Fe<sub>100-x</sub>Co<sub>x</sub>)<sub>79</sub>P<sub>11</sub>B<sub>8</sub>, amorphous, hyperfine field distrib., <sup>59</sup>Co NMR spin-echo meas. 0-34818  
FeF<sub>3</sub>, canted antiferromag., spin echo spectra of <sup>57</sup>Fe and <sup>19</sup>F nuclei 0-2662  
FeP(Ga)(As)(Sb), dil., short-range order, neutron diffuse scatt. and spin echo NMR 0-50106  
HCl, liq., self-diffusion coeffs., NMR spin-echo meas. 0-50223  
La<sub>1-x</sub>Gd<sub>x</sub>Ag, antiferromagnet, spin echo NMR anal. 0-15821  
LaNi<sub>5</sub>H<sub>6</sub>, diffusion const. in presence of large background gradients, modified pulsed gradient technique 0-31831  
LaNi<sub>1-x</sub>Mn<sub>x</sub>O<sub>3</sub>, <sup>55</sup>Mn NMR study, magnetisation meas., ferromag. and Pauli paramag. components 0-7191  
MnFe<sub>2</sub>O<sub>4</sub>, ferrite, dynamic shift of NMR freq. of nuclei located in domain walls 0-15823  
<sup>14</sup>N pulsed NQR-FFT radiofrequency spectrometer description and operation 0-17982  
Na<sub>2</sub>WO<sub>3</sub>, Knight shift, spin-lattice and spin-spin relax., high press. NMR obs. 0-50211  
α-NbH<sub>2</sub>D<sub>2</sub>, H diffusion, NMR spin echo obs. 0-34228  
(Ni<sub>1-x</sub>Rh<sub>x</sub>)<sub>99</sub>Mn, ferromagnetic, NMR study of local environment effect 0-7192  
(Ni<sub>1-x</sub>Ru<sub>x</sub>)<sub>99</sub>Mn, ferromagnetic, NMR study of local environment effect 0-7192



## spin echo (NMR) continued

- $\text{Ni}_{1-x}\text{Si}_x$ , electronic states of Si NMR study 0-50216  
 $(\text{Ni}_{1-x}\text{X})_{99}\text{Mn}$ ,  $\text{X}=\text{Rh}, \text{Fe}, \text{Mn}$ , ferromagnetic, NMR study of local environment effect, relaxation mechanism 0-7193  
 $\text{Pb}_{1.125}\text{Mo}_0.875$ , Chevrel phase supercond., NMR study 0-49989  
 Pt cluster, conduction electron density oscills., NMR spin-echo meas., indirect exchange interaction 0-44954  
 $(\text{Y}_{1-x}\text{Gd}_x)\text{Co}_2$ , spin echo NMR of mag. states 0-7190  
 YIG, domain boundary nuclear spin echo excitation, NMR domain freq. capture effect (Russian) 0-44955

## spin glasses

see also mictomagnetism

- anomalous Hall effect including Kondo effect in molecular field approx. (Russian) 0-34424  
 binary mixture at  $T=0$ , energy and variational props. 0-39794  
 Bose glass, marginal fluctuations 0-2586  
 defect hydrodynamics in nonplanar magnetic media (Russian) 0-49445  
 dilute frustrated lattice, spin-glass ordering, triangle and FCC lattices, Monte Carlo simulation 0-15746  
 diluted Ising and Heisenberg magnets with competing interactions, phase diagrams and mag. props. 0-34672  
 dirty, paramagnetic reson. 0-11264  
 EPR frequency and mag. transverse susceptibility with remanent magnetisation (French) 0-7145  
 FCC lattice, phase transitions of fully frustrated models 0-29517  
 frustrated two-dimensional planar model, spin-spin correl. 0-11212  
 frustration model, lifetime of excited states 0-15750  
 frustration network, phase transitions 0-2596  
 frustrationless models, rel. to spin glasses 0-29561  
 Heisenberg, two-level systems, evidence for existence 0-15736  
 Heisenberg  $S=1/2$  spins 0-2581  
 Heisenberg-Ising magnets, random, critical temps., binary mixture, amorphous magnet and spin glasses 0-54911  
 induced-moment spin glass, simple mean-field theory 0-29553  
 infinite-range spin glass, internal field distrib. hole, analytical treatment 0-29554  
 Ising ferromagnet and spin glass systems, random, crit. dynamics 0-34666  
 Ising frustration pots., phase transition 0-52142  
 Ising long and short ranged bond models in cluster approx. 0-20419  
 Ising spin glass, Sherrington Kirkpatrick model, entropy calc. 0-20411  
 Ising two-dimens. random bond model, evidence against spin-glass order 0-15747  
 long-range models, Ising spins and classical m-vector spins 0-15739  
 low temperature nuclear orientation investigation 0-15825  
 magnetisation relaxation time near freezing temp., HF calc. 0-34665  
 manganese aluminosilicate glass, insulating spin glass, exchange dipole optical transition 0-40136  
 mean field theory, broken replica symmetry 0-34659  
 mean field theory, replica method 0-34658  
 metallic rare earths, conference, St. Pierre-de-Chartreuse, France (Sept. 1978) 0-12844  
 mixed magnets, competing spin glass and mag. order, phase diagrams, crit. points 0-39802  
 Monte Carlo simulation appl. 0-20421  
 nuclear magnetic relaxation calcs. (French) 0-34797  
 one-dimensional, sp. ht. and mag. susceptibility calcs. 0-7120  
 one-dimensional, with antiferromag. exchange 0-25231  
 order parameter for replica symmetry breaking 0-44835  
 order parameters, infinite no. in mean-field approx. 0-25146  
 phase diagrams and order parameters, Oguchi-Kaneyoshi method 0-15727  
 phase transition, fluctuations of local spins, mean-field theory 0-34661  
 phase transition, mag. susceptibility, specific heat, Ising model calcs. (Russian) 0-34671  
 Poisson brackets, nonlinear hydrodynamics eqns. in condensed matter physics 0-54296  
 polarisation analysis of diffuse neutron scattering from magnetic systems 0-25098  
 quantum spin glass, frustration, 2-D lattice, functional integration technique (French) 0-39789  
 quenched random impurities, dynamics, replicas and frustration approaches 0-34673  
 random spherical model, crit. dynamics 0-44844  
 rare earth alloys, bulk mag. props. in amorphous and cryst. systems 0-20415  
 rare earth metal based compounds, spin glasses 0-50132  
 relaxation times, influence of spectral distrib. on freq. depend. of freezing temp. 0-44848  
 remanence magnetisation, slow decay theory 0-11211  
 RKKY Ising, sp. ht. 1/T behaviour 0-11210  
 Sherrington-Kirkpatrick model, Thouless-Anderson-Palmer eqn. solution (French) 0-39781  
 specific heat and susceptibility, random series method 0-44542  
 spin exchange scatt. time calcs. 0-50127  
 spinels, domain wall formation inhibition, effect on bulk mag. props. 0-11220  
 steel, austenitic stainless, magnetic susceptibility and magnetisation, low temp. 0-25102  
 superconductivity, total compensation of paramag. effect 0-7021  
 susceptibility, wave-vector-depend., theory 0-11209  
 TCNQ salt,  $\text{Qn}(\text{TCNQ})_2$ , one-dimens. spin glass with antiferromag. exchange, Knight shift meas. 0-25231  
 transition metal compounds and dil. alloys, mag. ordering phenomena in high mag. fields 0-50075  
 transition metal magnetic clusters, neutron inelastic scatt., review 0-50083  
 transition temperature and magnetisation curves 0-34628  
 two-dimensional Ising frustration model, ground-state correl. 0-15732  
 two-dimensional Ising model, low temp. dynamic props. 0-20425  
 two-dimensional Ising spin glass, crit. temp. 0-11206  
 Ag-Mn, dil. alloy, transverse magnetoresist. in spin glass regime 0-34417  
 Ag-Mn, spin glass, mag. susceptibility hydrostatic press depend., RKKY interaction 0-44845  
 $\text{Al}_2\text{Mn}_2\text{Si}_2\text{O}_{12}$ , amorphous, spin dynamics, neutron scatt. meas. 0-15741  
 $\text{Al}_{0.35}\text{V}_{0.65}$ , spin glass phase, low temp. mag. susceptibility meas. 0-29565  
 Au-Cr, dil. spin glass elec. resist., press. and conc. depend. 0-24864  
 Au-Fe, dil. alloy, transverse magnetoresist. in spin glass regime 0-34417  
 Au-Fe (16.2 at.%), cluster glass, mag. small angle neutron scatt. 0-50111

## spin glasses continued

- Au-Fe (3.1-10.4 at.%) spin glass alloys, high field magnetisation curves 0-11213  
 Au-Fe spin glass, energy flux associated with remanent magnetization relaxation (French) 0-7110  
 Au-Fe(Co)(Mn), residual resistivity conc. depend. 0-2382  
 $\text{Co}_2\text{Ga}_{1-x}$ ,  $\beta$ -phase, spin glass behaviour 0-44837  
 $\text{Co}_2\text{Ga}_{1-x}$ , cluster spin glass, AC susceptibility in DC mag. fields, 77 to 500K 0-34670  
 Cr-Fe, spin-glass phase, magnetisation curve test for mag. ordering 0-11201  
 Cu-Co superparamagnetic particles, macrospin glass form. (Russian) 0-25165  
 Cu-Mn, hysteresis loops, temp. and field depend. 0-15742  
 Cu-Mn, magnetisation curves, time depend. 0-15743  
 Cu-Mn, spin glass, meas. of order parameter 0-34642  
 Cu-Mn spin glass alloy, spin correl. function, combined neutron spin echo and polarisation anal. 0-50107  
 CuMn, magnetisation processes below freezing temp. 0-15748  
 CuMn, spin glass, mag. correls., neutron scatt. study 0-50105  
 CuMn, spin glass, mag. hysteresis meas. 0-34691  
 CuMn, spin glass, remanence, new approach from zero field NMR 0-34785  
 $\text{Cu}_{0.95}\text{Mn}_{0.05}$ , inelastic neutron scatt., time-of-flight and three-axis techniques 0-50108  
 $\text{Cu}_{0.95}\text{Mn}_{0.05}$ , low temp. mag. excitation spectrum, inelastic neutron scatt. obs. 0-50109  
 $\text{Er}_x\text{Y}_{1-x}\text{Al}_2$ , mag. props. meas. and neutron diffr. data 0-7126  
 $\text{Eu}_{1-x}\text{Gd}_x\text{S}$ , concentrated system with ferromag. and antiferromag. interactions, spin-glass props. 0-34639  
 $\text{Eu}_x\text{Sr}_{1-x}\text{S}$ , chalcogenide-like system, crit. conc. for ferromagnet-spin glass transition 0-34662  
 $\text{Eu}_x\text{Sr}_{1-x}\text{S}$ , dil. insulator spin-glass versus blocking 0-34641  
 $\text{Eu}_x\text{Sr}_{1-x}\text{S}$ , dilute Heisenberg magnet, complex susceptibility of blocked spins 0-15740  
 $\text{Eu}_x\text{Sr}_{1-x}\text{S}$ , ferromagnet-spin glass transition, mag. ordering, mag. susceptibility and neutron scatt. meas. 0-50135  
 $\text{Eu}_x\text{Sr}_{1-x}\text{S}$ , insulating spin glass, mag. props. 0-2589  
 $\text{Eu}_x\text{Sr}_{1-x}\text{S}$ , insulating spin-glass, sp. ht. near ferromag. onset 0-34667  
 Fe-Al, spin glass transition, Monte Carlo study 0-39801  
 Fe-Al (0.27 to 0.50 at.%), spin glass behaviour, microscopic model, Ising lattice, exchange and superexchange 0-39800  
 $(\text{Fe}_{1-x}\text{Mn}_x)_{75}\text{P}_{16}\text{B}_9\text{Al}_1$ , amorphous, spin-glass-ferromag. multicritical point, AC susceptibility meas. 0-50117  
 $\text{Fe}_2\text{NbSe}_2$  (2H), mag. susceptibility meas., 1.3-300K 0-39740  
 $\text{Fe}_2\text{Ni}_{1-x}\text{P}_{1-x}\text{B}_6$ , amorphous, spin-glass regime, magnetoresist. meas. 0-34418  
 $\text{Fe}_2\text{Pd}_{82-x}\text{Si}_{18}$ , amorphous, magnetisation, magnetoresist., spin glass and ferromag. phases 0-34697  
 $\text{Fe}_2\text{Pd}_{82-x}\text{Si}_{18}$ , metallic glass, mag. phase diagram, weak ferromagnet-spin glass transition 0-54893  
 $\text{Fe}_{0.35}\text{V}_{0.65}$ , spin glass phase, low temp. mag. susceptibility meas. 0-29565  
 $\text{Ga}_{0.6}\text{Cr}_{2.4}$ , semiconducting thiospinelide, spin glass type mag. ordering (Russian) 0-50123  
 $\text{Gd}_{37}\text{Al}_{63}$  amorphous film, spin glass, microwave mag. resonance, freq. dependence 0-39798  
 $(\text{La}_x\text{Gd}_{1-x})\text{Al}_2$ , reversible and irreversible mag. susceptibility 0-15738  
 MnSi, amorphous, sputtered, mag., elec., struct. and thermal props., spin glass behaviour 0-50124  
 MnSi, amorphous magnetisation meas. 0-34599  
 $\text{Ni}_{0.95}\text{S}$  Fe, spin glass, spin flop in exchange field 0-34640  
 $(\text{Ni}_{1-x}\text{Fe}_x)_{1-x}\text{S}$ , anisotropic spin glass, mag. props. 0-39793  
 Pd-Fe-Mn, ferromag. and spin-glass props; comment 0-2591  
 Pd-Mn, dil. alloy, very temp. magnetisation 0-34692  
 Pd-Mn(Fe), mag. ordering phenomena, neutron scatt. obs. 0-44812  
 $(\text{Pd}_{0.996}\text{Fe}_{0.0035})\text{Mn}_{0.05}$ , ferromag. and spin-glass props. 0-2590  
 $\text{PdH}_{0.97}\text{Fe}(\text{Cr})$ , supercond. transition temp. depression, coexistent mag. behaviour 0-49976  
 $\text{PdH}_x\text{-Fe}$ , dil., Kondo system, local moment hyperfine studies, Mossbauer expt. 0-39908  
 $\text{Pd}_3\text{Mn}$ , disordered, mag. correls., neutron scatt. study 0-50105  
 Sc-Gd spin glass, sp. ht., 0.3-10K 0-25145  
 Sc-Tb, induced-moment spin glass, simple mean-field theory 0-29553  
 $(\text{Ti}_{0.9}\text{V}_{0.1})_2\text{O}_3$ , spin glass, dynamic mag. susceptibility meas. 0-39792  
 $(\text{Ti}_{1-x}\text{V}_x)_2\text{O}_3$ , spin-glass props., 0.05-300K 0-25149  
 W-Fe, optical props. and electronic states 0-20412  
 W-Fe alloys, spin glass props., DC susceptibility and remanence meas., 1.6 to 295K 0-29560  
 Y-Gd spin glass, sp. ht., 0.3-10K 0-25145  
 $\text{YFe}_2$ , amorphous concentrated spin glass, susceptibility, Mossbauer and neutron scatt. meas. 0-39783  
 $\text{Y}(\text{Fe}_x\text{Al}_{1-x})_2$ , Mossbauer spectra and mag. props. 0-39950  
 $\text{Y}_6(\text{Fe}_{1-x}\text{Mn}_x)_{23}$ , struct. and mag. props. 0-25083  
 $\text{Y}_{1-x}\text{Gd}_x\text{Rh}_2\text{B}_6$ , mag. supercond., anomalous temp. depend. of upper crit. fields 0-29510  
 $\text{Zr}(\text{Fe}_{1-x}\text{Al}_x)_2$ , transition region, spin glass or long range mag. order 0-44841  
 $\text{Zr}(\text{Fe}_{1-x}\text{Co}_x)_2$ , transition region, spin glass or long range mag. order 0-44841

## spin Hamiltonians

- alloy with two ferromagnetic components, surface excitations 0-25179  
 alloys, dilute mag., local moment formation, nonequivalent orbitals model 0-11164  
 Anderson-localised states, intrastate and interstate interactions 0-20113  
 antiferromagnets,  $n=4$  type II, phase transitions, Landau Ginzburg Wilson Hamiltonian 0-15735  
 coupled rotational bands in even-even nuclei, model 0-27529  
 dislocation scattering, new Hamiltonian for describing multivalued elastic displacement fields 0-24862  
 EPR, perturbation treatment,  $M=0$  electronic state, HFS of triplet state EPR 0-25185  
 EPR quintet transition, exact axial reson. fields calc., rel. to powder spectra 0-2622  
 ferromagnetism, itinerant, effective Hamiltonian 0-11150  
 fluorene:pyrene- $\text{d}_{10}$  cryst., magnetic resonance absorpt. of host-guest triplet paired centres 0-34750  
 Heisenberg ferromagnet, biquadratic exchange, Green's function method, Hamiltonian and Curie temp. 0-15675  
 Heisenberg  $S=1/2$  spins 0-2581



**spin Hamiltonians continued**

- Heisenberg-Mattis model, long-wavelength dynamic response 0-20409  
ions in  $^6\text{S}_{5/2}$  ground state, ESR line with 3.33 isotropic g-factor 0-15787  
Ising and Heisenberg model, threshold inequalities for ground state 0-7064  
Ising O(2), O(3) and O(4) model, Hamiltonian string-coupling expansions 0-20426  
itinerant electron antiferromagnetic matrix, local moments, spin Hamiltonian 0-34626  
Kondo Hamiltonians, s-d exchange, ground states, renormalisation group calcs. 0-50046  
least-squares fitting for Hamiltonian parameters from resonance data 0-20448  
many-spin system, group approach in dynamics (*Russian*) 0-4579  
many-spin system dynamics, group approach (*Russian*) 0-50221  
mixed ferromagnetic Heisenberg and Ising bonds, appl. of effective Hamiltonian method 0-50023  
NMR, multiple pulse, of solids, average Hamiltonian theory and phase adjustment 0-22404  
one-dimensional classical planar model in applied magnetic field 0-15729  
planar spin two-dimens. model, mag. correlation function, self-consistent calc. 0-29563  
random bond systems, effective Hamiltonian method appl. 0-50023  
rare earth trichloride hexahydrate  $\text{Gd}^{3+}$  EPR, linear point charge model predictions 0-25200  
relativistic Hamiltonian theory, covariant formulation, on light cone, fields with spin (*Russian*) 0-9087  
Rochelle salt,  $\text{VO}^{2+}$ -doped, EPR study 0-34762  
 $S=1$  generalised Ising model, stability conditions 0-20427  
sandwich complexes, mag. props., effective Hamiltonian method 0-37731  
singlet-triplet ferromagnet hydrodynamics 0-11142  
strontium acetate hemihydrate:  $\text{Mn}^{2+}$  ( $\text{Cu}^{2+}$ ), EPR, spin Hamiltonian anal. and unit cell symmetry 0-29603  
 $\beta$ -B, rhombohedral, EPR anisotropy 0-25183  
 $\text{BaO-Al}_2\text{O}_3\text{-B}_2\text{O}_3$ :Ag, X-ray irradi., atomic centre interactions, EPR spectra 0-25207  
 $\text{CaCo}_2$ , aragonite, EPR of  $\text{Mn}^{2+}$  impurities, orthorhombic spin-Hamiltonian parameters 0-2631  
 $\text{CaF}_2$ : $\text{Pr}^{3+}$ , EPR data interpretation for octahedral  $\Gamma_8$  state in cubic cryst. field 0-2634  
 $\text{CoBr}_2$ , magnetic excitations, neutron scatt. investigation 0-39761  
 $\text{Cs}_2\text{ZrCl}_6$ : $\text{Np}^{4+}$ , EPR data interpretation for octahedral  $\Gamma_8$  state in cubic cryst. field 0-2634  
Cu complex, Cu-glycine in water, EPR spectral parameters, temp. depend. 0-2623  
 $\text{DyFeO}_3$ , non Heisenberg R-Fe exchange interaction, behaviour in mag. field (*Russian*) 0-2568  
 $\text{Fe}^{3+}$ , cubic spin-Hamiltonian parameters in inorganic compounds, superposition model anal. 0-20367  
 $\text{Fe}_{1-x}\text{M}_x\text{Cl}_2$ , disordered, Mn spin excitations by microwave absorption at high freqs. 0-34759  
 $\text{FeSiF}_6\cdot 6\text{H}_2\text{O}$ , submillimetre EPR and zero field spectra, spin Hamiltonian 0-29604  
 $\text{KCN}:\text{HCN}^-$ , structural props. using ESR 0-25205  
 $\text{KH}_2\text{PO}_4$ -type crystal, LF dynamics 0-10602  
 $\text{K}_2\text{O-B}_2\text{O}_3\text{:Mn}^{2+}$  glass, fine struct. parameter distrib., EPR meas. 0-11256  
 $\text{Li}_2\text{O-B}_2\text{O}_3\text{:Mn}^{2+}$  glass, fine struct. parameter distrib., EPR meas. 0-11256  
 $\text{MgO}:\text{Cr}^{3+}$  ( $\text{Mn}^{2+}$ ) spin Hamiltonian parameters, lattice expansion and vibr. effects 0-24851  
 $\text{MgO}:\text{Pt}^{3+}$ , Jahn-Teller effect in EPR spectrum 0-7160  
 $\text{Mn}^{2+}$ , cubic spin-Hamiltonian parameters in inorganic compounds, superposition model anal. 0-20367  
 $\text{Na}_2\text{O-B}_2\text{O}_3\text{:Mn}^{2+}$  glass, fine struct. parameter distrib., EPR meas. 0-11256  
 $\text{Ni}(\text{NH}_4)_2(\text{SO}_4)_2\cdot 6\text{H}_2\text{O}$ ,  $\text{Mn}^{2+}$  doped, EPR study 0-34763  
 $\text{NiSO}_4\cdot 7\text{H}_2\text{O}$ ,  $\text{Mn}^{2+}$  doped, EPR study 0-34763  
 $\text{Pb}_3(\text{PO}_4)_2\text{:Gd}^{3+}$  ( $\text{Eu}^{2+}$ ), EPR spectra of  $\alpha$ - and  $\beta$ -phases 0-11261  
 $\text{RbCl}:\text{Eu}^{2+}$ , EPR of  $^{153}\text{Eu}^{2+}$  and  $^{151}\text{Eu}^{2+}$  0-11259  
 $\text{RbCl}:\text{Eu}^{2+}$ , tetragonal sites, spin Hamiltonian parameters, EPR and UV absorpt. spectra obs. 0-50177  
 $\text{RbIn}(\text{MoO}_4)_2\text{:Fe}^{3+}$  monocystals, EPR spectrum in the phase transition neighbourhood 0-2624  
 $\text{RbMgF}_3\text{:Mn}^{2+}$ , EPR obs. and struct. interpret. (*French*) 0-50167  
 $\text{TGS}:\text{Cu}^{2+}$ , EPR studies, spin Hamiltonian parameters 0-7153  
 $\text{YIG}:\text{Si}(\text{Ge})$ ,  $\text{Fe}^{2+}$  spectroscopic props., nontrigonal cryst. field effects 0-44553  
 $\text{ZnGa}_2\text{O}_4\text{:Fe}^{3+}$  ( $\text{Mn}^{2+}$ ), EPR, spin Hamiltonian parameters 0-25195

**spin-lattice relaxation**

- see also electron spin-lattice relaxation; nuclear spin-lattice relaxation  
acetic acid,  $-d_1(=d_4)$  liquid, molecular motion, proton spin echo study (*Russian*) 0-32745  
antiferromagnet, phonon-magnon relaxation times, external mag. field depend. 0-44898  
blood plasma  $^1\text{H}$  NMR relax. rates, cancer-induced decrease obs. 0-56075  
intracellular water, effect of paramag. impurities on proton spin-lattice relax. 0-51134  
magnetic susceptibility, AC, depend. on magnitude meas. field 0-241  
MBBA, dynamic critical behaviour in NLC above nematic-isotropic transition 0-49096  
muscle, mouse, NMR multiwindow anal. and proton local fields and magnetisation distrib. 0-21444  
muscle water, study of spin-lattice and spin-spin relax. times of  $^1\text{H}$ ,  $^2\text{H}$ , and  $^{17}\text{O}$  0-21443  
phosphatidylcholine-cholesterol vesicles interacting with lucensomycin, PMR obs. 0-40954  
pulsed NMR data acquisition system, devel., appl. to polyisobutylene 0-34807  
quantum lattice systems, linear response and relaxation functions 0-4659  
three-level system transition probabilities, molecular motion anisotropy by quadrupole relaxation 0-18867  
ultraslow motion, Slichter and Ailion spin-lattice relaxation times 0-44899  
vinyl bromide- $d_3$ ,  $^{13}\text{CBr}$  bond, coupling const., correl. with C hybridisation s-character 0-34806  
water molecules in biological systems, relax. rel. to vol., pulse NMR obs. 0-40960

**spin-lattice relaxation continued**

- $\text{K}_2\text{Pt}(\text{CN})_4\text{Br}_{0.3}\cdot 3\text{H}_2\text{O}$ , quasi one-dimens. conductor, EPR linewidth 0-54938  
 $\text{NH}_3(\text{D}_3)$ , liq., longitudinal proton and deuteron relaxation rates, press. and temp. depend. 0-44941  
 $(\text{Ni}_{1-x}\text{X}_x)_{99}\text{Mn}$ ,  $\text{X}=\text{Rh}$ ,  $\text{Fe}$ ,  $\text{Mn}$ , ferromagnetic, NMR study of local environment effect, relaxation mechanism 0-7193  
 $\text{PdGdH}$ , diagram of state elec. props., indirect exchange interaction, EPR study (*Russian*) 0-50179  
 $\text{Si}$ , Jahn-Teller  $\text{Mn}^0$  centre ESR spectrum, depend. on axial press. 0-44911  
 $\text{Si}:\text{Cr}^{3+}$  EPR spectra and spin state population inversion with unpolarised optical lighting (*Russian*) 0-44909  
 $\text{Zn}_x\text{Cn}_{0.1}\text{Fe}_{2.9}\text{O}_4$ , Cu, Zn substituted magnetite, domain wall resonance, mag. props. 0-15756
- spin-orbit interactions**  
6d metal superheavy hexafluorides, relativistic mol. calcs. 0-5484  
actinide oxides, chem. bonding, mol. cluster theory 0-10526  
alkali metal atom, outer-shell photoelectron ang. distrib. 0-37797  
atom, transition array and energy level distrib. variance, Mo VX-XIV appl. 0-37767  
atomic structure, spin-other orbit and spin-spin interactions 0-913  
aza-aromatic molecules, intersystem crossing, quantum interference effects 0-53037  
 $^3\pi^*\text{-benzaldehyde}$ , zero field splitting and sublevel decay rates, deuteration and host effect 0-37750  
broadening, inhomogeneous and homogeneous, of optical and ODMR transitions in solids 0-32750  
calcium tartrate tetrahydrate:  $\text{Cu}^{2+}$ , spin-orbit coupling, optical absorpt. spectra 0-45120  
copperporphyrin, metastable quartet state radiative decay 0-23453  
coronene, luminesc., spin-orbit coupling perturbation by metal chlorides (*German*) 0-1021  
critical molecules, neutron scatt., 'optical activity' 0-23567  
diamond, natural, free exciton luminesc. line shape 0-40165  
diamond and sphalerite type crystals, energy levels of indirect excitons 0-15457  
diamond and sphalerite type crystals, with spin-orbit interaction, indirect exciton energy levels 0-24804  
diatomic molecule, nucl. spin-rot. interaction const., electron spin current contrib. 0-23441  
dimer triplet state line shape, small excitons, appl. to phenazine, naphthalene, tetrachlorobenzene 0-48041  
double folding pot. for inelastic scatt. between nuclei 0-13425  
dynamic Jahn-Teller systems, calc. of absorption band shapes, use of Lanczos algorithm 0-45023  
EPR spectra of stable radicals, slow molecular motion study, review 0-25212  
exponential transformation, quadratically convergent SCF procedure, appl. to closed shell ground states 0-47875  
F-centre optical absorption bandshape calc. for transition to state with Jahn-Teller and spin orbit couplings 0-55135  
Fano effect in photonic nuclear reactions? 0-519  
ferrous porphyrin, intermediate ( $S=1$ ) spin state, PMR characterisation 0-48014  
haloaceneaphthenes in n-heptane, quasi-line phosphoresc. spectra, vibronic spin-orbit interaction 0-43096  
HCP metals, mag. susceptibility near  $2^{1/2}$ th order electron transition, non-linear magnetisation anal. (*Russian*) 0-44859  
heteroaromatic molecules, planar, orientation and phosphoresc. polarisation in stretched film 0-14169  
induced electronic transitions, radiative lifetimes, non-Condon effects 0-53051  
inert gas dimer ions,  $\text{A}^2\Sigma_{1/2u} \rightarrow \text{D}^2\Sigma_{1/2g}^+$  system, theoretical absorption spectrum 0-32734  
Jahn-Teller centre optical band polarisation dichroism, forbidden transitions 0-55062  
liquid metals, spin-orbit interactions effect on mag. susceptibility, effective pseudohamiltonian 0-29299  
magnon relaxation, spin-orbit interaction, itinerant electron ferromagnets 0-11179  
metal, spin scattering and spin-orbit coupling 0-29369  
methanol, mol., nucl. spin-spin coupling const., Hartree-Fock calc. 0-9618  
mixed valence state, electronic structure, spin-orbit interaction effects, mag. susceptibility 0-54657  
molecular vibronic level mixing, under electronic coupling operator 0-52968  
narrow gap semiconductors, two-dimensional electron spectrum, spin splitting 0-24861  
nonlinear polarisation resonances in a continuum, optical activity, spin-orbit interactions (*Russian*) 0-53391  
nuclear, matter,  $V^8$  models, variational calcs. for binding energy and density 0-42571  
nuclear Dirac phenomenology and the  $\Lambda$ -nucleus potential, anomalous mag. moment 0-37344  
nuclear matter, variational techniques, review 0-22748  
nucleon optical pot., spin-orbit term 0-7606  
pyrazine, vibronic and spin-orbit coupling interaction 0-14126  
radial reduced Coulomb Green's function 0-31559  
rare earth ion energy separation,  $4f^N-4f^{N-1}$  nl, host depend. 0-49676  
rare earth metals, excitation energies, 3d electrons, relativistic calcs. 0-20109  
relativistic electron wave diffraction by cylindrical capacitor 0-5671  
ruby, spin-strain coupling tensor meas. US modulated EPR obs. 0-50170  
sandwich complexes, mag. props., effective Hamiltonian method 0-37731  
Schrodinger representation, spin-orbit coupling origin 0-42914  
spin-spin integrals, one- and two-centre, analytical evaluation over Slater-type orbitals (*Russian*) 0-9491  
spin-unsaturated subshells and the nucleon-nucleus optical-model spin-orbit potential 0-18259  
di-(tetraethylammonium)tetrahalomanganate, mag. circular and linear dichroism obs. 0-29725  
thiomethoxyl anion, and deuteration, electron photodetachment, affinities, vibr. freq. and spin-orbit splitting 0-53063  
transition metal complexes, ligand field spectroscopy, selection rules, intensity enhancement of forbidden transitions 0-45049  
transition metal monosulphides of first-row, XPES and UV PES 0-20760  
transition metals, theory of ferromagnetism involving spin-orbit and crystal field interactions 0-2541



**spin-orbit interactions continued**

- transition metals and alloys, 3d, Hall effect, electron scatt. processes 0-34419  
 two-body spin-orbit interaction matrix elements, shell model (*Chinese*) 0-47356  
 $\mu$  breakup effect on spin orbit and tensor pots. 0-32286  
 $\mu^-$  depolarisation, exotic at. orbital ang. momentum alignment effect 0-18946  
 (p, p), 1 GeV, polarisation data, Glauber anal. spin-orbit parameters, matter distrib. 0-52655  
 $\text{AlNH}_3(\text{SO}_4)_2 \cdot \text{Cr}^{3+}$ , optical spectral, crystal field, spin orbit and exciton interactions 0-34958  
 Ar, ns $\rightarrow$ sp photoelectrons, spin polarisation 0-37792  
 Au-Fe, spin-orbit coupling and electron scatt. 0-2370  
 Au-Mn, spin-orbit coupling and electron scatt. 0-2370  
 Bi II ion, relativistic effects in hyperfine splitting of second spectrum 0-23344  
 Br + O<sub>2</sub>(NO), quencher paramagnetism, deactivation rate const., spin-orbit relax. study 0-21263  
 CS<sub>2</sub>, photoelectron spectrum, spin-orbit splitting, excited state form. 0-43102  
 $\text{CaCO}_3 \cdot \text{Fe}^{2+}$ , electronic spin relax., effect of second-order spin-orbit coupling 0-10935  
 $\text{CaWO}_4 \cdot \text{Er}$ , spectroscopic parameters calcs. 0-50379  
 Cd I, 4d<sup>10</sup> subshell photoelectron ang. distrib. 0-14123  
 $\text{CdCo}_2 \cdot \text{Fe}^{2+}$ , electronic spin relax., effect of second-order spin-orbit coupling 0-10935  
 $\text{CdGa}_2\text{Se}_4$ , thermoreflectance and visible absorpt. spectra, energy gap, cryst. field splitting 0-34945  
 $\text{Cd}_{1-x}\text{Mn}_x\text{Te}$ , spin-orbit coupled bands, indirect exchange interaction via electrons 0-34407  
 CeCoSi, film, Hall effect and magnetoresist. (*Russian*) 0-11109  
 C1CN, ground and first excited bending, vibr. state, props., mol. beam elec. reson. 0-37823  
 ClO, UV spectra of  $\text{C}^2\Sigma^- \rightarrow \text{X}^2\Pi$  system, rot. anal. 0-996  
 Cs, four-photon ionis., strongly interacting resons. theory 0-52955  
 CsF, F-centre optical absorption bandshape calc. for transition to state with Jahn-Teller and spin orbit couplings 0-55135  
 $\text{Cs}_2\text{SiF}_6 \cdot \text{Mn}^{4+}$ , Jahn-Teller effect in  $^4\text{T}_{2g}$  state, Zeeman meas. 0-29367  
 Cu-Co heterobinuclear complex, cryst., mag. susceptibility of Cu-Co(fsa)<sub>2</sub>, en, 3H<sub>2</sub>O 0-2556  
 Cu-transition metal, alloys, satellite NMR study, lineshifts and splitting 0-34786  
 $^{19}\text{F} + ^{28}\text{Si}$  spin orbit pot., single folding model and cluster model 0-9196  
 $\text{FeBr}_4^-$ , in various solvents,  $^4\text{A}_1$  E d-d band reson. Raman spectra, solvent depend., spin-orbit coupling 0-55085  
 Gd, optical conductivity, direct interband transitions 0-15488  
 Ge, electron-hole droplets, luminesc. and absorpt. lineshapes, RPA theory 0-49613  
 H halides, spin-orbit coupling effect on proton mag. shielding 0-23440  
 HD, spin-spin coupling const., convergence of calc. 0-9506  
 $^3\text{He-A}$ , superfluid, spin dynamics, spin-orbit configurations, spin waves (*Russian*) 0-54462  
 $\text{Hg}_{1-x}\text{Mn}_x\text{Se}$ , spin-orbit coupled bands, indirect exchange interaction via electrons 0-34407  
 $\text{Hg}_{1-x}\text{Mn}_x\text{Te}$ , spin-orbit coupled bands, indirect exchange interaction via electrons 0-34407  
 HgTe type semiconductors, spin-flip transitions in magneto-optics and magneto-transport 0-50306  
 InSb type semiconductor, spin-flip transitions in magneto-optics and magneto-transport 0-50306  
 InSe, reflectivity and low energy absorption 0-34944  
 InSe, spin orbit split off valence bands, exciton transitions, Hopfield's quasicubic model, visible absorpt. spectrum 0-50370  
 $\text{K}_2\text{Sb}$ , optical and dielectric props., energy spectra, density of states calcs. 0-20083  
 Kr, ns $\rightarrow$ sp photoelectrons, spin polarisation 0-37792  
 $\text{Li}_2\text{Br}_2$ , UPS of dimeric mol., expt. and X $\alpha$  calc. 0-9640  
 $\text{Li}_2\text{Cl}_2$ , UPS of dimeric mol., expt. and X $\alpha$  calc. 0-9640  
 $\text{Li}_2\text{F}_2$ , UPS of dimeric mol., expt. and X $\alpha$  calc. 0-9640  
 $\text{Li}_2\text{I}_2$ , UPS of dimeric mol., expt. and X $\alpha$  calc. 0-9640  
 $\text{Mg}^{9/2}$ , beam-foil excited, spin orbit-forbidden X-ray transition obs. 0-23537  
 $\text{MgO} \cdot \text{Cr}^{3+}(\text{V}^{2+})$ ,  $^4\text{A}_{2g} \rightarrow ^4\text{T}_{2g}$  spectra, new expt. results 0-11441  
 $(\text{Mo}, \text{V}_{1-x})_2\text{O}_5$ , mag. and spectroscopic investigation 0-25206  
 $^{15}\text{N}$  3/2 state spin alignment and polarisation, 1/2-spin orbit interaction from  $^{27}\text{Al}$ ,  $^{88}\text{Sr}(^{16}\text{O}, ^{15}\text{N})$  0-27622  
 Ni, ferromagnetic, Hall effect, anomalous, rel. to scatt. processes 0-44572  
 Ni, magnetic surface anisotropy of transition metals, model calc. 0-34625  
 Ni, optical const., influence of temp. and relation to bandstruct. 0-25403  
 Ni-Cu, ferromagnetic, Hall effect, anomalous, rel. to scatt. processes 0-44572  
 NiFe, magnetic surface anisotropy of transition metals, model calc. 0-34625  
 $\text{O}(\text{D}) + \text{Ar}(\text{Kr})(\text{Xe})$ , inelastic collisions, spin-orbit coupling 0-5605  
 Pr, soft mode excitation behaviour under press., long range order 0-39838  
 $\text{Pr}^{3+}$  aquo ion spectra, MCD of  $^3\text{P}_0 \rightarrow ^3\text{H}_4$  transition 0-7331  
 $(\text{SNBr}_{0.4})_x$ , supercond. props., dimensionality 0-20344  
 SnTe-MnTe, degenerate semicond., anomalous Hall effect 0-29420  
 Te inversion layers in mag. fields 0-44690  
 Te, valence band struct. under press., spin-orbit splitting, intraband absorpt. spectra 0-2330  
 TeF, chemiluminesc. from oxidation in  $\text{F}_2 + \text{H}_2\text{Te}(\text{D}_2\text{Te})$  emission spectrum obs. 0-43058  
 W films, (010), energy band calc. including spin-orbit interactions 0-20274  
 Xe, ns $\rightarrow$ sp photoelectrons, spin polarisation 0-37792  
 Xe, photoelectron studies of 5p branching ratio 0-37793  
 Yb, 4f levels, hole lifetime and chemical shift, UHV study 0-20762  
 Zn-Mn(Cr), dil. mag. anisotropy, Hartree-Fock calcs. 0-11162  
 $\text{Zn}_3\text{P}_2$  bulk and thin film, UV reflectivity spectra, photovoltaic effects, optical const. 0-25472  
 $^A\text{Zr}$ , A=90, 92 and 94, charge densities and single-particle structure 0-9224

**spin-phonon interactions**

see also spin-lattice relaxation

- alkali halides, spin lattice relax. and g-shift 0-15799  
 ammonium halides, cryst., H bonding, order-disorder phenomena 0-6379  
 diethylammonium cadmium tetrachloride, first order phase transition, optical phonon line broadening, spin-phonon coupling model 0-7335  
 diffusion, effect of spin-phonon and spin-phonon interactions 0-44849  
 ferromagnet, planar, US attenuation, spin-phonon coupling, magnons and magnetostriction contrib., calc. 0-34611  
 impurity centres exchange interaction caused by elementary excitations in solids, temp. depends. 0-25193  
 linear spin chain in uniform mag. field (*Russian*) 0-2594  
 nonmetallic crystals, ENDOR of impurity centres 0-25249  
 self-trapping transition, spin 1/2 system 0-10606  
 spin-Peierls transition in mag. field, phonon freq., Heisenberg model calcs. 0-25151  
 thiourea, phonon modes near order-disorder transforms., hard-core modes due to pseudospin-phonon coupling 0-44285  
 TTFCuBDT, spin-Peierls transition in spin 1/2 Heisenberg chains, RPA calcs. 0-25150  
 $\text{CsNiCl}_3$ , linear-chain antiferromag., low temp. thermal expansion 0-39326  
 $\text{ErVO}_4$ , phonon resistivity mag. field depend. in paramag. phase 0-2226  
 EuTe, antiferromagnet, phonon Raman scatt. from spin superstructures 0-16030  
 Si, Jahn-Teller Mn<sup>0</sup> centre ESR spectrum, depend. on axial press. 0-44911  
 $\text{VI}_2$ , antiferromag., zone-boundary phonon Raman scattering, modulation of exchange interaction 0-11386  
 $\text{VI}_2$ , antiferromagnet, phonon Raman scatt. from spin superstructures 0-16030  
 YAG: rare earth metal, US absorpt. meas., relax. model 0-24539  
 $\text{ZnSiF}_6 \cdot 6\text{H}_2\text{O}$ , spin-phonon interaction between  $\text{Ni}^{2+}$  ions, phonon bottleneck effects, splitting parameters (*Russian*) 0-15796

**spin polarised electron emission**

- alkali metal atom, spin polarisation of photoelectrons, one-quantum photoeffect 0-37790  
 alkali metal atom, two-photon ionis. with two light beams, photoelectron polaris. 0-43011  
 ferromagnet, spin polarisation of emitted photoelectrons 0-45215  
 metal surface, clean, spin polarised electron field emission 0-45221  
 photoemission, spin energy analysed, feasibility anal. 0-55271  
 Ar, photoelectron emission, polarisation depend. on incident unpolarised VUV radiation wavelength 0-52952  
 Ar, plane polarised VUV irradi., emitted photoelectron polarisation, ang. depend. 0-47952  
 CO<sub>2</sub>, spin polarised photoelectrons, synchrotron excited 0-43101  
 Cs, polarised photoelectrons produced by circ. polarised synchrotron radiation 0-18830  
 ErFe<sub>2</sub> surface, effect of H and O adsorption, spin polarised photoemission study 0-29854  
 Fe (111), spin polarised photoemission 0-45221  
 Fe, field-emitted electron spin polarisation by tunnelling through surface pot. 0-29861  
 GaAs (100) and (110), photoelectrons spin polarisation 0-11530  
 $\text{GaAs}_{0.62}\text{P}_{0.38}$ , negative electron affinity, photoemission of spin polarised electrons 0-2916  
 Kr, photoelectron emission, polarisation depend. on incident unpolarised VUV radiation wavelength 0-52952  
 N<sub>2</sub>O, spin polarised photoelectrons, synchrotron excited 0-43101  
 Ni (100), spin polarised photoemission 0-45221  
 Ni (111), electron spin polarised photoemission spectrum 0-25525  
 Ni (111), single crystal, spin polarisation of emitted photoelectrons 0-45215  
 Ni, field-emitted electron spin polarisation by tunnelling through surface pot. 0-29861  
 Ni surface (111), photoyield near threshold negative-positive spin polaris. crossover 0-2922  
 US(Se)(Te), photoelectron energy distrib. and spin polarisation, electronic and mag. props. 0-16146  
 US(Se)(Te), spin polarisation and magnetism, photoelectron study 0-40219  
 UTe, Sb<sub>1-x</sub>, photoemission, densities of states 0-16147  
 W, spin filter effect of EuS 0-45221  
 Xe, plane polarised VUV irradi., emitted photoelectron polarisation, ang. depend. 0-47952

spin polarised electron phenomena see electron spin polarisation

spin-spin nuclear coupling in molecules see molecular nuclear coupling

**spin-spin relaxation**

- adenosine 5'-diphosphate, interactions with kyosin, intermolecular spin diffusion study 0-18951  
 anisotropic fluid, diffusion, EPR spin exchange and nuclear spin relax., theory 0-34753  
 apparent spin-spin relaxation time, super-regenerative NQR spectrometric obs. 0-54963  
 bromobenzenes  $^{13}\text{C}$ Br bond, spin-spin coupling const., correl. with C hybridisation s-character 0-34806  
 chloroplast, mag. relax. of water protons and state of water photo-dissociation system 0-51133  
 coherent series, T<sub>2</sub> as collision time, dephasing time, or reciprocal linewidth, for teaching 0-27075  
 p-dihalobenzenes, apparent NQR spin-spin relax. times obs. 0-54991  
 dynamic magnetoresonance effects in solids 0-20447  
 elastomer, segmented block, morphology, pulsed proton NMR study 0-33907  
 epoxy polymers, cured spin-spin and lattice relax., proton coupling,  $^{13}\text{C}$  NMR obs. 0-34799  
 ethylene oxide,  $^{13}\text{C}$  and D variants, T<sub>2</sub>-relax., 2<sub>20</sub>-2<sub>11</sub> rot. transition by microwave pulse spectrometer 0-47976  
 ethylene oxide, gas, EPR rot. transitions, T<sub>1</sub> and T<sub>2</sub> relax. 0-9622  
 fluorite lattices,  $^{19}\text{F}$ , self-diffusion, spin lattice relax., NMR techniques 0-34801  
 formic acid,  $^{13}\text{C}$  NMR spectra and relax. under intermediate decoupling power conditions 0-20515  
 II-VI semiconductors, electron-electron spin-flip scatt. and spin relax. 0-44916  
 III-V semiconductors 0-44916  
 ionic conductors, central component NMR relax. rates 0-29640  
 Ising square lattice, phase transitions, next nearest neighbour interactions 0-50128



## spin-spin relaxation continued

- lipid bilayers, D relax. rates and mol. dynamics 0-26206  
 methanol, mol., nucl. spin-spin coupling const., Hartree-Fock calc. 0-9618  
 monovalent ions in aq. metal ion solns.,  $^{14}\text{N}$  NMR relax. 0-20481  
 multiple and combinational freq. NQR, dipole-dipole, spin-spin interactions 0-20499  
 multipulse NMR, relax. processes anal. 0-34798  
 muscle, mouse, NMR multiwindow anal. and proton local fields and magnetisation distrib. 0-21444  
 muscle water, study of spin-lattice and spin-spin relax. times of  $^1\text{H}$ ,  $^2\text{H}$ , and  $^{17}\text{O}$  0-21443  
 myosin, interaction with adenosine 5'-diphosphate, intermolecular spin diffusion study 0-18951  
 myosin, interactions with HDO, intermolecular spin diffusion study 0-18951  
 NMR line profile, paramagnetic ion nuclei in magnetically conc. solid, theory 0-25238  
 NQR-NMR double resonance line intensities, level crossing method, two freq. saturation 0-20514  
 NQR-NQR double resonance, double quadrupole spin echo resonance 0-20513  
 nucleic acid bases,  $^{14}\text{N}$  relax. and N-proton spin coupling, NH-proton spin-lattice relax. 0-26202  
 one-dimensional planar magnets, low temp. NMR 0-44943  
 organic paramagnetic systems, multiple internal motions, nucl. spin dipolar relax. obs. 0-28037  
 paramagnetic nonresonance absorpt., kinetic eqns. 0-7151  
 paramagnetic substance, single spin cross-relax., temp. depend. of transition probability 0-25184  
 perdeuterobenzophenone, in 4,4'-dibromodiphenylether, cross-relax., microwave pulse obs. 0-53031  
 photoexcited triplet state molecules, in cryst., cross-relax., variable freq. ODMR obs. 0-53031  
 polyethylene,  $^{13}\text{C}$  NMR rotating frame relaxation 0-7182  
 polyethylene, linear, melt props. correl. with chain length distrib. (*Russian*) 0-37920  
 polyethylene, linear, nuclear relaxation, mol. motion (*Russian*) 0-44949  
 polymer glassy and crystalline, relax. process characterisation,  $^{13}\text{C}$  NMR obs. 0-34802  
 pulsed NMR data acquisition system, devel., appl. to polyisobutylene 0-34807  
 rare earth systems, NMR, EPR, and Mossbauer effect, book contribs. 0-39883  
 rotating coordinate system, phenomenological approach 0-39887  
 solution,  $^{89}\text{Y}$  spin-spin relax. times, no pH depend. 0-2657  
 spin systems under multiple pulse NMR conditions, chem. shift relax. 0-34808  
 spin-1/2 systems, strongly coupled, perturbation response symmetries (*French*) 0-43069  
 spin-echo Fourier transform NMR spectroscopy, multiple pulse technique 0-37063  
 superionic conductors, mag. reson., book contrib. 0-25240  
 1,1,2-trichloroethane, phase-modulated spin echoes, derivation of pure absorpt. spectra 0-22410  
 vinyl bromide- $\text{d}_3$ ,  $^{13}\text{C}$ Br bond, coupling const., correl. with C hybridisation s-character 0-34806  
 water molecules in biological systems, relax. rel. to vol., pulse NMR obs. 0-40960  
 $^{13}\text{C}$  NMR in solids, high-resolution 0-34802  
 $\text{Cd}_{0.8}\text{Ni}_{0.2}\text{Fe}_2\text{O}_4$  ferrite, Fe spin relaxation Mossbauer study, mag. hyperfine struct. (*Russian*) 0-15932  
 Co complex, tris(ethylenediamine)cobalt(III) ion in complex anion solns.,  $^{59}\text{Co}$  NMR relax. obs. 0-25234  
 Cu, NMR at high polarisation and low field, nuclear spin exchange interaction 0-34790  
 $\text{DyAlO}_3\text{:Yb}^{3+}$ , Mossbauer relax. 0-15875  
 $\text{FeF}_3$ , canted antiferromag., spin echo spectra of  $^{57}\text{Fe}$  and  $^{19}\text{F}$  nuclei 0-2662  
 o- $\text{H}_2$  dilute impurity in rare gas solids and p- $\text{H}_2$ , NMR study 0-25228  
 o- $\text{H}_2$  molecules in solid nonmagnetic host, nucl. spin lattice relax. times calc. 0-20483  
 HDO, interactions with myosin, intermolecular spin diffusion study 0-18951  
 $\text{H}(\text{UO}_2\text{PO}_4)_4\text{H}_2\text{O}$ , solid, fast hydrogen ion diffusion, NMR relax. time meas. 0-2205  
 $^3\text{He}$ , adsorbed, on MgO, nucl. mag. relax. props. 0-49457  
 $^3\text{He}$  film, submonolayer and multilayer, adsorbed on Grafoil, pulsed NMR study 0-49456  
 $^3\text{He}$  film, theory of motional inhibition of interlayer quantum tunnelling 0-54466  
 $^3\text{He}$ , superfluid, B-phase, low temp. spin relax. 0-15323  
 $^{199}\text{Hg}$  optically oriented atom interaction with cell wall paramag. centres 0-37762  
 $\text{HoAlO}_3\text{:Yb}^{3+}$ , Mossbauer relax. 0-15875  
 InSb, electron spin relaxation 0-25187  
 InSb, electron-electron spin-flip scatt. and spin relax. 0-44916  
 $\text{K}_2\text{Pt}(\text{CN})_4\text{Br}_{0.30}\cdot 3\text{H}_2\text{O}$ , dynamic  $^{195}\text{Pt}$  NMR meas. below metal-insulator transition 0-34810  
 $\text{K}_2\text{Pt}(\text{CN})_4\text{Br}_{0.3}\cdot 3\text{H}_2\text{O}$ , quasi one-dimens. conductor, EPR linewidth 0-54938  
 $^{83}\text{Kr}$  spin dephasing 0-38524  
 $\beta\text{-LaNi}_{5-y}\text{Al}_y$  hydrides, H diffusion, NMR studies 0-15298  
 LiTi ferrite, Mossbauer study, relax. and supertransferred hyperfine fields 0-39941  
 LiZn ferrite, Mossbauer study, relax. and supertransferred hyperfine fields 0-39941  
 $\text{NH}_3$ , magnetic relaxation rates for microwave spectrum and contributions to linewidth 0-5564  
 $\text{Na}_2\text{WO}_3$ , Knight shift, spin-lattice and spin-spin relax., high press. NMR obs. 0-50211  
 $(\text{NbCl}_4\text{Br}_{6-n})^-$  complexes in acetonitrile soln.,  $^{93}\text{Nb}$  spin relax. and mag. shielding 0-44944  
 Ni-b, hyperfine interactions from 6 to 730K,  $^{12}\text{B}$  NMR 0-29372  
 $\text{PF}_3\text{Br}_2$ , spin systems under multiple pulse NMR conditions, chem. shift relax. 0-34808  
 $\text{PbSnF}_6$ , fast ionic cond. of  $\text{F}^-$  ions, NMR study (*French*) 0-39345  
 $\text{PrNi}_2$ , nucl. cooling agent, relax. and exchange, EPR and NMR study 0-25237  
 $\text{Rb}+^{131}\text{Xe}$ , spin-exchange cross section,  $^{131}\text{Xe}$  nucl. spin relax. obs. 0-37868

## spin-spin relaxation continued

- $\text{TbAlO}_3\text{:Yb}^{3+}$ , Mossbauer relax. 0-15875  
 $\beta\text{-TiFeH}_{1.03}$ , H diffusion, NMR meas. 0-10707  
 TiBr melts, Ti doped and pure, stoichiometric, nucl. spin relax. 0-25236  
 TiCl<sub>4</sub> melts, stoichiometric, nucl. spin relax. 0-25236  
 $\text{UO}_2(\text{NO}_3)_2$ , aq. soln., pulsed NMR relax. time,  $^{235}\text{U}$  enrichment depend. 0-2658  
 $\text{V}_3\text{Si}$ , NMR meas. near struct. transform. (*Russian*) 0-44942  
 $\text{V}_3\text{Si}$ , NMR of  $^{51}\text{V}$  above and below 21K struct. transition (*Russian*) 0-34796
- spin systems**  
 see also *magnetic properties of substances; magnetism*  
 absorption of energy under parallel pumping conditions 0-2592  
 abstract three-level system, group approach in dynamics (*Russian*) 0-4579  
 atom spin transition, nonadiabatic, in time-depend. mag. field 0-9576  
 Bose expansion for general spin, exact 0-31662  
 boson expansion for general spin operators, coeff. 0-42141  
 Bravais lattice, ferromagnetic ground state conditions in Ising and Heisenberg models 0-50129  
 classical planar spin model, two-dimens., Monte Carlo study 0-25147  
 conference on dynamical critical phenomena, Geneva (Apr. 1979) 0-27040  
 continuum Heisenberg spin system, stationary spherically and axially sym. spin waves 0-34615  
 copolymer model with alternating spins, kinetics 0-9768  
 correlation inequalities for n-vector spin models 0-54860  
 coupled system, ABC type, matrix elements of tensor operators calc., transition probability matrix 0-25182  
 crossover, field-induced, in mag. chain, scaling theory 0-54904  
 cubic model, Monte Carlo simulation, phase transitions 0-34646  
 diffusion, effect of spin-photon and spin-phonon interactions 0-44849  
 dissipative, oscillations and fluctuations 0-27224  
 distribution function of spin/isospin saturated system, direct and exchange sum rules 0-27212  
 electron spin density functional gradient expansion, local approx. calcs. 0-44792  
 ferroelectric ferromagnet, soft modes and ferromag. reson. 0-11275  
 ferromagnet, Ising model, nonuniform mag. field method, crit. correlation function approximations, calc. 0-20407  
 ferromagnet, Ising model, transition point calc. 0-20408  
 ferromagnetic metal, anomalous magneto-optic effects near Curie temp., s-f exchange model 0-2736  
 functional integral method appl. to classical and quantum spin models 0-15676  
 Heisenberg linear chain, alternating spin quantum numbers, mag. and thermodynamic props. 0-34578  
 Heisenberg spin 1/2 system, recursion relations, Migdal renormalisation group approach 0-20368  
 Heisenberg spin system, one-dimensional, dynamical behaviour 0-29567  
 Hubbard model, cluster-variation method in two-site approx. at high temp. 0-7071  
 Ising and Heisenberg model, threshold inequalities for ground state 0-7064  
 Ising ferromagnet with two- and four-spin interaction, improved product average decomposition method 0-20406  
 Ising model, random magnetic system, correlation function, upper and lower bounds 0-25063  
 Ising model, Yang-Lee edge singularity, real-space renormalisation group method 0-34643  
 Ising O(2), O(3) and O(4) model, Hamiltonian string-coupling expansions 0-20426  
 Ising spin 1/2 model, renormalisation group approach 0-2582  
 isotropic N-component spin systems with long and short range interaction, critical behaviour 0-54907  
 itinerant localised systems, dynamic magnetic response 0-34583  
 Jeener-Broekaert three-pulse sequence, inhomogeneous lineshapes, second rank spin interactions 0-39891  
 Kondo Hamiltonians, s-d exchange, ground states, renormalisation group calcs. 0-50046  
 lattice gauge theory and spin systems, review 0-22528  
 lattice spin systems, matching conditions for crit. props., group struct. of block transforms 0-22305  
 layered spin systems, phase transitions, partition functions and binary correlation functions 0-50133  
 linear spin chain in uniform mag. field, spin-phonon interactions (*Russian*) 0-2594  
 magnetic crystal, perfect, spin rot. of forward transmitted beam in neutron diffr. 0-50113  
 magnetic excitations, polarised neutron inelastic and quasi-elastic scattering 0-50045  
 magnetic structure elastic polarised neutron scatt. atomic mag. moments 0-29531  
 magnon kinetic eqns. in parametric ultrasonically excited ferromagnets 0-44820  
 many-spin system, group approach in dynamics (*Russian*) 0-44900  
 metastable polarised crystals, decay kinetics, exchange magnon-phonon interactions (*Russian*) 0-7060  
 metastable spin-aligned crystals, decay kinetics 0-34669  
 Migdal-like approximation, quantum spin systems 0-34649  
 multipion system, time development of nuclear Overhauser effects 0-34822  
 n-component spin system, energy-energy correl. function calc. 0-31697  
 nuclear, in spherical conductor, free induction decay and skin effect 0-2649  
 one dimensional Fermi gas model in relation to spin and field theoretical models 0-24816  
 one-dimensional, disordered, magnetism 0-25152  
 one-dimensional electron system, with attractive interaction in mag. field, paramag. transition 0-7072  
 one-dimensional magnetic system, spin anisotropy and exchange alternation 0-34644  
 optical-acoustic two-phonon relaxation 0-11244  
 orbital degeneracy, one dimensional two spin models (*Russian*) 0-54899  
 paramagnetic substance, single spin cross-relax., temp. depend. of transition probability 0-25184  
 polarisation analysis of diffuse neutron scattering from magnetic systems 0-25098  
 quantum, frustration effect in s=1/2 XY and Heisenberg models 0-15677



**spin systems continued**

- quantum anisotropic antiferromag. Heisenberg model, Gibbs state limitation 0-50027  
 quenched random impurities, dynamics, replicas and frustration approaches 0-34673  
 random Ising ferromagnet, upper bounds 0-34663  
 randomly distributed interaction centres, mol. field distrib. function (*Russian*) 0-44834  
 rare earth mixed valence compounds, spin dynamics, mag. neutron scatt., Mossbauer effect, XPS studies 0-39786  
 rare-earth, mag. supercond., appl. of boson theory to mixed state 0-7050  
 rotating coordinate system with quadrupole splitting, paramag. susceptibility 0-11178  
 S=1 generalised Ising model, stability conditions 0-20427  
 semiconductors, many-valley, magnetic electron fluctuation states spin direct interactions 0-29364  
 Sherrington-Kirkpatrick model, Thouless-Anderson-Palmer eqn. solution (*French*) 0-39781  
 single-ion anisotropy, magnetic systems, high temp. series expansion 0-34576  
 solids, averaging method application to high resolution NMR, Magnus expansion (*Russian*) 0-34793  
 spin glasses, spin exchange scatt. time calcs. 0-50127  
 spin-glass, two-dimensional Ising model, low temp. dynamic props. 0-20425  
 spin-phonon system, transition to self-trapping 0-10606  
 surface tension and phase transition in lattice systems 0-27226  
 tetrahedral four spin  $1/2$  systems, Zeeman and tunnel system reson., coupled and uncoupled relax. 0-50214  
 transient phenomena, soln. using eigen-coordinate system of magnetisation vector 0-25116  
 transition metal elements and alloys, spin distribution, neutron diffraction expts. 0-25097  
 transition metal magnetic clusters, neutron inelastic scatt., review 0-50083  
 two-dimensional spin system on square lattice, exact duality-decimation transform. 0-17890  
 unidimensional xy-chain, impurity zone fine struct. (*Russian*) 0-6787  
 X-Y quasi-one-dimens. system anisotropic, spin-Peierls phase transition, tricritical point 0-25142  
 CdCr<sub>2</sub>Se<sub>4</sub>, spin system heating by drifting current carriers, magnon-phonon system energy transfer (*Russian*) 0-29541  
 Cu-Cs diluted deuterated Tutton salts, electron non-Zeeman system, nuclear relaxation study 0-44951  
 Dy, critical exponents and amplitude ratios from elec. cond. data, theoretical model 0-50126  
 EuO, spin system heating by drifting current carriers, magnon-phonon system energy transfer (*Russian*) 0-29541  
 FeAs, Mossbauer spectra of paramag. and ferromag. states, helimagnetic spin ordering 0-7197  
 (La,Gd)Al<sub>2</sub>, reverse Kondo alloy, transport props. at finite mag. field 0-6812  
 Si:Cr<sup>3+</sup> EPR spectra and spin state population inversion with unpolarised optical lighting (*Russian*) 0-44909  
 V<sub>2</sub>O<sub>5</sub>, spin order, one-dimensional, Neel transition 0-39799
- spin tickling (NMR)** see double nuclear magnetic resonance
- spin wave resonance** see ferromagnetic resonance
- spin waves**  
 see also magnetostatic waves; magnons  
 advances in basic magnetism during past twenty-five years 0-36791  
 amorphous ferromagnets with random anisotropy axes, spin waves 0-7096  
 antiferromagnet, high frequency properties, spin wave spectra corrections magnon interactions (*Russian*) 0-54876  
 antiferromagnetic semiconductor, spin-wave amplification 0-7099  
 antiferromagnets, low anisotropy, nuclear spin waves spectra, relaxation, parametric excitation, NMR dynamic shift (*Russian*) 0-11180  
 Bloch wall bound spin waves, equations of motion 0-34612  
 bootstrap percolation conductivity on Cayley tree, rel. to spin wave stiffness 0-54743  
 continuum Heisenberg spin system, stationary spherically and axially symm. spin waves 0-34615  
 cubic ferrite garnet, diffracted light polarisation characts., spin and magnetoelastic waves 0-20614  
 damping, magnetic materials with canted mag. struct., thermodynamic and high freq. props. 0-11184  
 dilute ferromagnet, linear spin-wave theory, effective medium approach 0-20393  
 diluted antiferromagnet, linear spin-wave theory, effective medium approach 0-20393  
 dislocated ferromagnet, inhomogeneous magnetisation near dislocation effect on FMR linewidth 0-25213  
 disordered, magnet, collective modes, Heisenberg-Mattis model 0-39797  
 domain wall velocity, damping parameter meas. from low field microwave excitations 0-34676  
 exciton dielectric type system with doping, low freq. excitations (*Russian*) 0-15459  
 ferrite, magnetoacoustic reson. in strong mag. field 0-11309  
 ferrite-semicond. layer struct. with negative differential conductance, instability 0-25118  
 ferroinsulators, spin waves and uniform transverse magnetization, oscillatory eigenstates (*Russian*) 0-11181  
 ferromagnet, domain wall retardation by spin waves (*Russian*) 0-25154  
 ferromagnet, itinerant electron, surface spin waves, tight-binding Hubbard model 0-39763  
 ferromagnet, light scatt. by spin waves 0-45086  
 ferromagnet, spin waves with moving domain wall 0-39764  
 ferromagnet, uniaxial dipolar, crossover behaviour, theory 0-29559  
 ferromagnetic alloys, itinerant electron model, spin wave stiffness const. calc. 0-34613  
 ferromagnetic chain, anisotropic, kink excitations, nonlinear model 0-54881  
 ferromagnetic films, spin wave excitation by microwave antenna field 0-44816  
 ferromagnetic nonmetallic film, stand exchange mode determ. 0-2565  
 ferromagnetic plate, with anisotropic surface discontinuities, spectrum and damping of quasi-surface spin waves 0-11185  
 ferromagnetism, itinerant electron model, spin quantization direction fluctuations, short range order. 0-34582  
 ferromagnets, domain struct. effects on dynamic props., review 0-34678

**spin waves continued**

- ferromagnets, exchange and dipolar coupled, spin wave renormalisation, Damon-Eshbach surface spin waves 0-2564  
 finite sample, mag. rearrangements near surface 0-11240  
 frustrated two-dimensional planar model, spin-spin correl. 0-11212  
 Heisenberg antiferromagnet, one-dimensional, spin waves in spin-flop phase 0-44817  
 Heisenberg antiferromagnetic chain, spin dynamics, quantum effects 0-34651  
 Heisenberg continuous ferromagnetic chain, finite amplitude spin wave, stability 0-20395  
 Heisenberg ferromagnet, dil., spin wave localisation near percolation threshold 0-25120  
 Heisenberg ferromagnet, spin operator study by small angle mag. neutron scatt. 0-15700  
 Heisenberg linear chain, alternating spin quantum numbers, mag. and thermodynamic props. 0-34578  
 Heisenberg-Ising chain, bosonisation, spin wave vel. calc. 0-54905  
 Heisenberg-Mattis model, long-wavelength dynamic response 0-20409  
 induced moment systems, effect of spin fluctuations 0-2585  
 Ising ferromagnet, high-freq. props. quantum theory, susceptibility tensor calcs. (*Russian*) 0-11143  
 Jahn-Teller cooperative T-(e+t) systems, pseudo spin thermal cond. 0-34406  
 localised spin excitations 0-15708  
 magnetic dipoles on a lattice, theory at low temps. 0-50082  
 magnetic film, complex surface pinning parameter and quasi-localised surface spin wave modes 0-50150  
 metal, ferromagnetic resonance linewidth, interaction of spin waves with conduction electron current 0-25216  
 metastable polarised crystals, decay kinetics, exchange magnon-phonon interactions (*Russian*) 0-7060  
 metastable spin-aligned crystals, decay kinetics 0-34669  
 neutron studies of magnetic densities and magnetic excitations, book contrib. 0-11170  
 nonexchange surface spin waves at interface between two ferromagnets 0-29544  
 one-dimensional mag. systems, neutron scatt., review 0-50103  
 paramagnetic system, spin waves, classical approach 0-29519  
 parametric excitation by noise pumping (*Russian*) 0-34617  
 parametrically excited waves, interaction with defects exhibiting internal structure 0-7173  
 Poisson brackets, nonlinear hydrodynamics eqns. in condensed matter physics 0-54296  
 quasi one-dimensional spin lattice coupled system, collective modes 0-24896  
 rare earth metal, magnetic properties, nonlinear s-f exchange interaction effect 0-15711  
 semi-infinite Heisenberg ferromagnet, macroscopic theory of response functions and appl. to light scatt. 0-20410  
 semiconductor-ferrite layer structure, EMF created by spin-wave, effect of current 0-11072  
 semiconductors, ferromagnetic, parametric amplification of coupled spin, helical and acoustic waves (*Russian*) 0-2621  
 space disordered media phenomenological Lagrangian, exchange, relativistic interactions (*Russian*) 0-29537  
 superconducting ferromagnet, magnetic ordering, spin wave dispersion (*Russian*) 0-54818  
 superconductivity-ferromagnetism coexistence, transition temp., magnon freq., indirect exchange 0-44757  
 thin films, ferro- and antiferromagnetic, two dimens. spin-wave theory, spontaneous magnetisation parameter depend. 0-34714  
 TMMC:Cu, dynamic props. using local-moment pair correl. functions 0-15728  
 TMMC, classical Heisenberg antiferromagnet, one-dimens., dynamic props., review 0-15737  
 transition metals, 3d, ferromag., itinerant electron magnetism, magnetic excitation props., theory 0-34581  
 trimethylammonium cobalt trichloride dihydrate, Ising-like system, nucl. spin-lattice relax. of <sup>1</sup>H and <sup>55</sup>Co 0-29638  
 XY model, spin 1/2, spin wave theory 0-7068  
 Co<sub>1-x</sub>B<sub>x</sub>, polycrystalline and amorphous sputtered films, Brillouin spectra 0-2775  
 CoBr<sub>2</sub>, magnetic excitations, neutron scatt. investigation 0-39761  
 CoCO<sub>3</sub>, light scatt. expts., review 0-50081  
 (Co<sub>1-x</sub>Fe<sub>x</sub>Ni<sub>20</sub>)(Si<sub>1-x</sub>B<sub>20</sub>)<sub>20</sub>, amorphous films, spin wave spectra 0-34777  
 Cr-Re, mag. excitations in commensurate antiferromag. phase 0-50079  
 CsCoCl<sub>3</sub>, mag. excitation spectrum, spin-wave response, neutron scatt. study 0-50080  
 CsCrCl<sub>3</sub>, mag. structure and excitations, neutron diffr. and susceptibility meas. 0-44806  
 CsMnF<sub>3</sub>, NMR saturation, nuclear spin wave excitation, large freq. shifts (*Russian*) 0-50207  
 CsMnF<sub>3</sub>, spin wave spectrum obs., review 0-50081  
 CsNiF<sub>3</sub>, easy-plane ferromagnet, one-dimens., dynamic props., review 0-15737  
 CsNiF<sub>3</sub>, one-dimens. ferromag., collective excitations in mag. field 0-44822  
 CsNiF<sub>3</sub>, one-dimensional magnet, dynamics, mol. field theory approach 0-34614  
 Cu complex, dichloro-bis-pyridine copper II, one-dimens. antiferromagnet, dynamic props., review 0-15737  
 Cu<sub>2</sub>MnAl, dynamical mag. susceptibility, spin waves, calc. from band struct. 0-54871  
 dimethylammonium manganese tetrachloride, 2D Heisenberg antiferromag., spin wave anal. 0-54879  
 ErCrO<sub>3</sub>, magnetisation, NMR freq. temps. depend. weak ferromagnetic-antiferromagnetic spin reorientation transition 0-29631  
 ErFeO<sub>3</sub>, weak ferromag., high freq. props. in ordering region of spin system, antiferromag. reson. study (*Russian*) 0-2644  
 EuO, light scatt. by spin waves 0-45086  
 EuS films, ferromag., optical spectra and light scatt. from spin waves 0-16116  
 Fe, band theoretic interpretation of neutron scatt. expts., spin wave modes 0-44791  
 Fe, ferromagnetic, chemisorption of H, spin-spin interactions, UPS spectra calc. 0-6630  
 Fe, light scatt. by spin waves 0-45086  
 Fe-Cr, spin waves by neutron spectrometry 0-44819  
 Fe<sub>1-x</sub>B<sub>x</sub>, polycrystalline and amorphous sputtered films, Brillouin spectra 0-2775



## spin waves continued

- $\text{Fe}_2$ , neutron inelastic scatt. from mag. excitations 0-50078  
 $\text{Fe}_{40}\text{Ni}_{40}\text{B}_{20}$ , amorphous, high-field magnetisation curve, spin wave spectrum and microstructural inhomogeneities 0-15702  
 $\text{Fe}_{40}\text{Ni}_{38}\text{Mo}_{18}\text{B}_{4}$  ribbon, magnetic characterisation 0-34680  
 $\text{Fe}_{40}\text{Ni}_{40}\text{P}_{14}\text{B}_6$  metallic glass, ferromag. reson., spin waves, thermal ageing and long-range order effects 0-25214  
 $\text{Fe}_x\text{Ni}_{1-x}\text{P}_{14}\text{B}_6$  ( $x=0, 20, 40, 60, 80$ ), metallic glass, low temp. sp. ht. 0-2588  
 $(\text{Fe}_x\text{Ni}_{1-x})_{75}\text{P}_{16}\text{B}_6\text{Al}_3$ , magnetisation temp. depend., spin wave theory 0-44927  
 GdIG, spin wave intrinsic relaxation, magnon damping at low temps. 0-29543  
 He, superfluid B phase, spin wave breathers, double sine-Gordon equations 0-15329  
 $^3\text{He}$ , A<sub>1</sub> phase, broken relative symmetry and dynamics 0-24705  
 $^3\text{He}$ , superfluid A-phase, composite soliton in narrow circ. cylinder, satellite freq., thermal fluctuations 0-34266  
 $^3\text{He}$ , superfluid B phase, soliton-like spin waves 0-44385  
 $^3\text{He}$ -A, superfluid, spin dynamics, spin-orbit configurations, spin waves (Russian) 0-54462  
 $\text{HoCo}_5$ , ground state spin excitations, inelastic neutron scatt. study 0-50077  
 $\text{KCuF}_3$ , nearly 1-D spin- $1/2$  antiferromagnet, spin wave energy dispersion 0-2551  
 $\text{K}_2\text{CuF}_4$ , microwave excitation, optical detection of ferromagnetic reson. 0-50197  
 $\text{K}_3\text{Mn}_2\text{F}_7$ , two magnon Raman scatt., magnon dispersion, susceptibility, Green's function methods 0-50340  
 Mn, antiferromag., spin wave mode, wave function calcs. 0-20098  
 $\text{MnCO}_3$ , NMR saturation, nuclear spin wave excitation, large freq. shifts (Russian) 0-50207  
 $\text{MnCO}_3$ , spin wave spectrum obs., review 0-50081  
 $\gamma\text{-MnCu}$ , antiferromag., stressed, mag. defects meas. by neutron polarisation anal. 0-50076  
 Ni alloys, mag. props. of alloys, review 0-44823  
 Ni, band theoretic interpretation of neutron scatt. expts., spin wave modes 0-44791  
 Ni, ferromagnetic, chemisorption of H, spin-spin interactions, UPS spectra calc. 0-6630  
 Ni, Landau-Lifshitz damping, wave no. and temp. depend. 0-34779  
 Ni, magnetic susceptibility, generalised, neutron scatt. meas. 0-34606  
 Ni, rel. to deformation in const. mag. field, 4.2K (Russian) 0-29591  
 Ni-Pt disordered alloy, off-diagonal, T-matrix itinerant electron ferromagnetism calcs. 0-25067  
 $\text{Ni}_{50}\text{Co}_{40}\text{P}_{10}$  amorphous film, spin wave excitation, ferromagnetic resonance study 0-50198  
 $\text{Ni}_3\text{Mn}$ , partially ordered, spin-wave dispersion relation, inelastic neutron scatt. meas. 0-20394  
 $\text{O}_2$ , solid,  $\beta$ -phase, mag. excitations spectrum (Russian) 0-7101  
 $\text{Rb}_5\text{MnCl}_4$ , 2D Heisenberg antiferromag. spin wave analysis 0-54879  
 $\text{RbMnF}_3$ , nuclear spin waves spectra, relaxation, parametric excitation, NMR dynamic shift (Russian) 0-11180  
 $\text{YCrO}_3$ , magnetisation, NMR freq. temps. depend. weak ferromagnetic-antiferromagnetic spin reorientation transition 0-29631  
 $\text{Y}_3\text{Fe}_{5-x}\text{Ga}_x\text{O}_{12}$  garnet, spin wave parametric excitation threshold anisotropy in second region 0-29542  
 $\text{YFeO}_3$ , weak ferromagnet, domain wall motion and velocity (Russian) 0-54917  
 YIG bubble films, light scatt. from spin waves, hysteresis meas. by Voigt effect 0-15770  
 YIG ferromagnetic film, quasi surface spin wave giant oscills. (Russian) 0-15767  
 YIG, subsidiary absorpt. spin-wave instability threshold, anomalous struct. 0-34776  
 $\text{Y}_{1.62}\text{Sm}_{0.21}\text{Lu}_{0.27}\text{Cu}_{0.9}\text{Ge}_{0.5}\text{Fe}_{4.1}\text{O}_{12}$ , implanted bubble garnet, anisotropy profile, FMR study 0-7103

## spinodal decomposition

- Alnico 5, two-phase separation during ageing, Mossbauer study 0-7533  
 conference, phase transformations in metallurgy, York, England (Apr. 1979) 0-2994  
 interface, continuum mechanics (German) 0-45272  
 interphase boundary structure in solids, investig. 0-15112  
 Ising lattice, thermal relaxation, nonideal behaviour, stochastic theory 0-22312  
 mag. props. after isothermal thermomag. treatment (Russian) 0-25159  
 microstructure characterisation, review 0-50588  
 orderable system, influence of heat cond. on spinodal decomp. 0-2169  
 phase transformations in metals and alloys, thermodynamic and mechanistic classification, review 0-2995  
 poly(vinyl methyl ether)-polystyrene mixture, electric field depend. of cloud point temp., laser scatt. meas. 0-6519  
 scaling equation of state derived from the pseudospinodal, liq.-gas system 0-44286  
 Al alloys, continuous precipitation, nucleation, spinodal decomposition 0-3061  
 Al-Zn alloys, spinodally decomposing, resistivity behaviour 0-45271  
 Au-Cu (50% at.), pretransitional fluctuations (French) 0-2160  
 Cr-Co-Fe, for telephone receiver mag. use 0-45318  
 Cu alloys, continuous precipitation, nucleation, spinodal decomposition 0-3061  
 Cu-Ni-Sn (10, 6 wt.%), temp. depend. of yield stress and work hardening 0-21026  
 Cu-Ni-Sn (4-15, 4-8 wt.%), strip strengthened by spinodal decomp., stress relax. in bending 0-7616  
 Cu-Ni-Sn (9, 6 wt.%), decomposition, initial stages, TEM study 0-2992  
 Fe-Cr-Co, mechanism of coercive force 0-34674  
 Fe-Cr(55 wt.%), phase decomp. early stages and clustering (Japanese) 0-55403  
 $^3\text{He}$ -He, superfluid mixture, early stages of spinodal decomposition, calc. 0-20004  
 $\text{MgO-Al}_2\text{O}_3\text{-SiO}_2\text{-ZrO}_2\text{-TiO}_2$ , glass, phase separation (German) 0-38932  
 Ni-Al, spinodal decomposition, atom probe field ion microscopy study 0-3028  
 Ni-Ti (9.6 wt.%), mag. study on phase decomposition (Japanese) 0-15758  
 $\text{PbO-B}_2\text{O}_3\text{-Al}_2\text{O}_3$  glass, spinodal decomp. during continuous cooling, theoretical anal. 0-1935

## spinodal decomposition continued

- $\text{SiO}_2\text{-Al}_2\text{O}_3$  (36.6 wt.%) plasma prep. powder, metastable immiscibility and microstruct. during sintering 0-35143  
 $\text{Zr-Al}$  (14 wt.%), transformation sequence from Zr-Al martensite to  $\text{Zr}_3\text{Al}$  phase 0-3027  
 spinor groups see group theory  
 spirality see elementary particle theory  
 splines (mathematics)  
   see also function approximation; interpolation  
   anatomy, 3D display for radiotherapy treatment planning 0-3773  
   appearance potential spectra, deconvolution using cubical spline functions, stability, error propagation 0-25487  
   barotropic primitive equation model using splines for typhoon prediction (Chinese) 0-4063  
   bicubic spline interpolation, quantitative accuracy and efficiency test 0-17405  
   biomechanical movement data smoothing, use of spline functions 0-3699  
   cubic spline, approx. of inaccurate r.m.s. vel. data 0-17406  
   differential equations solution, linear multistage formulae (German) 0-34  
   free vibration calculation for rotating non-uniform disc using spline interpolation technique 0-43656  
   Galerkin methods, quadrature rules using B-spline basis functs. 0-30  
   seismic data migration, collocation formulation of wave equation migration 0-4126  
   skew plate structures, buckling anal. using B-spline functions 0-28446  
 sponges see porous materials  
 sponginess see porosity  
 spontaneous fission  
   FFTF fuel, neutron source strength as function of irradiation 0-22929  
   mass and charge division, asymmetry, order-disorder model 0-22866  
   mass parameters, cranking and hydrodynamic models, deformation depend. (Russian) 0-13511  
   slope constant of the exponential prompt-neutron yield formula 0-22806  
   superheavy nuclei, stability and fission barriers, crit. ang. momentum depend. 0-32262  
    $^{240}\text{Am}^m$ , spontaneously fissioning isomer optical shift in pumped  $^{85}\text{Sr}_{1/2} \rightarrow ^{10}\text{P}_{1/2}$  transition, nuclear deformation 0-27971  
    $^{28}\text{Be}$  spontaneous fission pot. energy curve, cluster shell model (Chinese) 0-22867  
    $\text{Bi}_2\text{S}_3$ , superheavy element search using neutron multiplicity counter 0-4011  
    $^{254}\text{Cf}$ , A=250, 252, 254, spontaneous fission fragment kinetic energy and neutron multiplicity meas. 0-42717  
    $^{254}\text{Cf}$  fission-neutron spectrum unfolding experiment 0-13514  
    $^{254}\text{Cf}$ , neutron emission 0-37405  
    $^{254}\text{Cf}$  spontaneous fission, meas. of fission neutron spectra 0-22873  
    $^{254}\text{Cf}$ , spontaneous fission, scission point configuration, evaluation anal. 0-37361  
    $^{252}\text{Cf}(\text{sf})$ , energy dissipation in fission, comments 0-42719  
    $^{252}\text{Cf}(\text{sf})$ , scission, energy dissipation magnitude during descent from saddle point 0-42718  
    $^{256}\text{Cf}$ , spontaneous fission, fission barriers and products 0-18355  
    $^{256}\text{Cf}$  spontaneous fission, mass and kinetic energy distrib. from  $^{254}\text{Cf}(\text{t,p})$  0-47518  
    $^{258}\text{Fm}$ , A=258, 259, spontaneous fission, fission barriers and products 0-18355  
    $^{258}\text{Fm}(\text{sf})$ , A=254, 256, 258, 260, fission mass distrib. transition, liquid drop and shell model calcs. 0-32310  
    $^{257}\text{Fm}$ , spontaneous fission fragment kinetic energy and neutron multiplicity meas. 0-42717  
    $^{258}\text{Fm}$  spontaneous fission, mass and kinetic energy distrib. from  $^{258}\text{Md}^m$  decay 0-47518  
    $^{259}\text{Fm}$  spontaneous fission,  $T_{1/2}$  and kinetic energies from  $^{257}\text{Fm}(\text{t,p})$  0-47517  
    $^{235}\text{U}$ , A=236, 238, strength function of  $\beta$ -transitions, probability of delayed fission 0-22764  
 spontaneous magnetisation  
   amorphous ferromagnetic alloys, domain struct. and mag. microstruct., review 0-15751  
   amorphous ferromagnetic alloys, micromagnetic eqns. for case of dipolar and magnetocryst. fluctuations 0-11171  
   antiferromagnetic heavily doped semiconductors, Faraday light depolarisation in mixed mag. states 0-29726  
   ferromagnet, inhomogeneous, Landau's theory of second-order phase transition 0-50092  
   ferromagnetic films, spin correl. functions, crit. indices 0-7133  
   ferromagnets, conducting, magnon spectra and magnetoacoustic reson. singularities (Russian) 0-50154  
   Ginzburg-Landau-Wilson model, n-component, derivation of nonlinear  $\sigma$ -model, in low temp. limit 0-44787  
   surface magnetisation profile, in crit. region by  $\epsilon$ -expansion, Wilson perturbation theory calc. 0-50100  
   thin films, ferro- and antiferromagnetic, two dimens. spin-wave theory, spontaneous magnetisation parameter depend. 0-34714  
    $\text{CdCr}_2\text{Se}_4$ , ferromagnetic low anisotropy semicond., spontaneous magnetisation RF determ. 0-22396  
   CuMn, spin glass, mag. hysteresis meas. 0-34691  
    $\text{Cu}(\text{NO}_3)_2 \cdot 2^{1/2}\text{H}_2\text{O}$ , singlet ground state system, mag. props. 0-44850  
    $\text{Fe}_{40}\text{Ni}_{40}\text{B}_{20}$ , amorphous, high-field magnetisation curve, spin wave spectrum and microstructural inhomogeneities 0-15702  
    $\text{Fe}_3\text{O}_4$ , inverse spinel ferrite, mag. field theory 0-25104  
   LiTbF<sub>4</sub>, mag. props., crit. behaviour at marginal dimensionality 0-54906  
   Ni-Co-H, solid soln., Curie points and spontaneous magnetisation behaviour 0-50093  
    $\text{Pt}_3\text{Mn}_x\text{Cr}_{1-x}$  alloys, mag. props. 0-2562  
    $\text{ThCo}_5$  itinerant electron metamagnetism, polarised neutron study 0-39742  
    $\text{TmSe}_{1-x}\text{Te}_x$ , mixed-valent cpd., spontaneous magnetisation 0-20392  
   W/EuS field emitters, electron emission current depend. on annealing temp., mag. props. 0-16160  
    $\text{Y}(\text{Co}_{1-x}\text{Ni}_x)_2$ , spontaneous magnetisation mag. anisotropy, spin reorientation transformation (Russian) 0-7082  
    $\text{Y}_{1-x}\text{Tb}_x\text{Co}_3$ , spontaneous magnetisation anisotropy, spin reorientation transforms. (Russian) 0-7082  
 spontaneous symmetry breaking  
    $\sigma$  model,  $\text{SU}_2 \times \text{SU}_2$ , modified Goldberger-Treiman relation, pseudoscalar form factor 0-27421  
    $\sigma$  model representation of Yang-Mills theory as a spontaneous violation (Russian) 0-13220



**spontaneous symmetry breaking continued**

$\sigma$  SU(N) model, spontaneous symmetry breaking, renormalisation 0-42340  
 $(\psi\psi)^2$  model, spontaneous symmetry breaking, renormalisation 0-42340  
 additive quark model with six flavours 0-27455  
 atomic and molecular physics, dynamical groups 0-42362  
 axial current in dimensional regularization 0-13233  
 baryons, current status, additional symmetry breaking assumptions 0-4995  
 bilocal gauge field theory 0-31986  
 broken supersymmetry mass formula, quantum corrections 0-27424  
 conformal and gauge spontaneous symm. breaking, cosmology quantum effects 0-37185  
 cosmological models, spontaneous symmetry breakdown, open and closed Friedmann model 0-51929  
 current quark masses and symmetry-breaking effects 0-4952  
 duality invariance, simple gauge theories including EM-type fields with sources 0-27440  
 dynamical groups of completely integrable eqns., nonlinear realisations 0-4885  
 dynamically broken chiral symmetry and the gauge technique for Ward identities 0-47211  
 dynamically broken-gauge theories, P and T violation in QCD 0-9093  
 E(6) grand unified theories, one loop renormalisation effects, stepwise symmetry breaking 0-32058  
 effective potential for non-Abelian gauge theories and spontaneous symmetry breaking 0-4863  
 effective potential for spontaneously broken gauge theories and gauge hierarchies 0-18080  
 exceptional groups, patterns of symmetry breaking 0-42356  
 extended relativity, T-violation and new particle 0-37182  
 extended spontaneously broken supergravity models, properties 0-46924  
 fermion mass, unified gauge model based on E6 0-32053  
 gauge fields, chiral fields on loop space, colour-electric flux rings 0-42327  
 gauge theories, quantised, large time behaviour, asymptotic anal. 0-27395  
 Goldstone theorem in classical statistical mech., correl. function non-vanishing boundary terms as phase transition origin 0-27253  
 gravitational theory of symmetry breaking of transformation intransitive groups 0-36912  
 Gross-Neveu model, renormalisation, mass generation 0-27393  
 hadron masses and current algebra quark masses 0-42436  
 hadron microstructure, de Sitter microuniverse, relativistic Hooke group and nonrelativistic quark model 0-27480  
 hadron spectroscopy, quark models and SU(5) grand unification scheme 0-4958  
 Higgs bosons, effects on experimental observables, and fermion mass scale 0-32061  
 Higgs bosons, masses, gauge hierarchies,  $SU_3$  model 0-47236  
 Higgs lattice abelian model, finite temp. behaviour 0-13260  
 high temperature symmetry breaking 0-42357  
 instantons and quark-mass generation—the how of spontaneous chiral symmetry breaking 0-4963  
 isospin violation, induced by current quark mass 0-32069  
 Lewis Riesenfeld oscillator, dynamical symmetry breaking 0-47210  
 light quarks and QCD Boson representation, dynamical symmetry breaking 0-52472  
 linear SU(4) meson  $\sigma$ -model, one-loop approx., spin zero mass spectrum and leptonic-decay 0-47278  
 low energy light particle processes in spontaneously broken gauge theories, heavy particle effects 0-22521  
 magnetic monopole long range interactions in non-Abelian gauge fields 0-22520  
 magnetic monopoles, non-Abelian, stability analysis, Yang-Mills equations 0-31987  
 many-boson model, spontaneous symmetry breakdown and restoration 0-52123  
 mass generation for fermion field in absence of chiral symmetry breaking 0-347  
 massive vector boson field theory with spontaneous symmetry breaking 0-52443  
 massless quarks in QCD, dynamical symmetry breakdown 0-52471  
 meson weak and EM decays, relativistic confined quarks, MIT bag model 0-47277  
 non-relativistic model, spontaneous supersymmetry breaking and superconductivity 0-32031  
 $OSp(1,4)$  supergroup, Wess-Zumino model classical solns. 0-36928  
 physical pion low energy electro- and photoprod., Ward identity, chiral symmetry breaking struct. 0-5003  
 QCD, quark and gluon propagators 0-52469  
 QCD theory for the strong interaction 0-4962  
 quantum corrections to the quadratic mass formula of broken supersymmetry 0-46942  
 quantum SU(2) gauge theory, vacuum stability, dynamical symmetry breaking 0-32000  
 quark and lepton masses, chiral charge space, statistical analysis 0-42428  
 quark strong interactions as weak interaction symmetry breaking mechanism 0-18117  
 quarks, flavour number determination using Higgs scalar particle 0-13288  
 relativistic QFT, spontaneous symmetry violations 0-52411  
 renormalisation group eqn., spontaneously broken symmetry and heavy scalar particle decoupling 0-47189  
 $SO_{10}$  hierarchical breaking 0-22550  
 $SO(10)$  grand unified theories, one loop renormalisation effects, stepwise symmetry breaking 0-32058  
 $SO(10)$  grand unified theory, breaking scheme and neutrino mass 0-47230  
 spontaneously broken gauge theories with heavy Higgs bosons 0-13209  
 strong coupling constants in broken SU(3) 0-27423  
 $SU_3$  theorems, baryon octets, semileptonic decays 0-32030  
 $SU_L(2) \times SU_R(2) \times U(1) \times [SU(3) \times SU(3)]_c$  gauge model, chiral colour symmetry breaking 0-47234  
 SU(2), unification of isospin and hypercharge, electroweak interactions of leptons 0-27439  
 SU(4)  $\times$  SU(4) symmetry breaking, Cabibbo angle, nonlinear hadronic Lagrangian, PCAC (Russian) 0-42360  
 SU(5), broken, meson mass formulae 0-47267  
 SU(6) grand unification model, hierarchy of symmetry breakings and neutral currents 0-52446

**spontaneous symmetry breaking continued**

SU(6) grand unified theories, one loop renormalisation effects, stepwise symmetry breaking 0-32058  
 SU(8) supergravity supersymmetry breaking 0-46908  
 SU(N)  $\times$  SU(N) chiral symmetry, spontaneous breaking, instanton role 0-47219  
 SU(n) gauge theories, directions of spontaneous symmetry breaking 0-13228  
 SU(N) unification of extra strong interactions, no-go theorem 0-32056  
 superconductivity and elementary particles theory, review 0-4911  
 superconformal symmetry breakdown as guide to supergravity constraints 0-46930  
 supergraph anal., gauge supersymmetry, S-matrix 0-27422  
 supergravity, massive vector multiplets, lagrangian construction 0-31645  
 supersymmetry, expanded, spontaneous violation, Goldstone fields (Russian) 0-47218  
 unification of fundamental forces in nature, elementary particle constituents SU(3)<sub>c</sub> gauge symmetry, review 0-27448  
 unified gauge model with a nonlinear chiral hadron Lagrangian,  $SU_3 \times SU_3$  symmetry-breaking 0-42378  
 unitarity and renormalized 't Hooft identities 0-13205  
 wave function choice, effect on predictions, DKP formalism view 0-9120  
 weak interactions and symmetry breaking 0-27428  
 weak quark and lepton chiral symmetries, dynamical breaking gauge interaction 0-47215  
 Weinberg-Salam theory, spontaneous symmetry breaking dynamics 0-32060  
 Wightman theory, all spontaneously broken symmetries for noncovariant currents 0-31975  
 X-Y model, gauge theory analogue, 4-D self-dual gauge model, phases and transitions 0-27399  
 zero-fermion modes in models with spontaneous symmetry-breaking 0-18105  
 $\Delta^+ \rightarrow p\gamma$ , ground and radially excited states, broken symmetry treatment 0-9174  
 $e^+e^- \rightarrow \mu^+\mu^- X$ , search for Higgs boson 0-27496  
 $\eta \rightarrow 3\pi^0$ , chiral SU(4)  $\times$  SU(4) breaking and tadpole term 0-22532  
 $K \rightarrow \pi e(\mu)\nu$ , form factors, SU(3)  $\sigma$ -model one loop calc., chiral symmetry breaking 0-52506  
 KN  $\sigma$ -term, uncertainties in determ., K-matrix formalism 0-27522  
 NN charge symmetry breaking, nn and pp scatt. length difference, meson mixing 0-13325  
 $\nu$ , massless, left-right symmetric gauge models,  $SU_{2L} \times SU_{2R} \times U_1$  0-27461  
 $\pi$  decay constant, EM form factor, quark EM self-energy in QCD 0-37242  
 $\pi^+ p \rightarrow \pi^+ \pi^+ n$ , 203-357 MeV, integrated cross section, chiral symmetry breaking parameter 0-32125  
 $\pi^+ p \rightarrow \pi^+ \pi^+ n$ , below 1400 MeV, PS11 contrib. threshold K-matrix, chiral symmetry breaking 0-32126  
 $\psi \rightarrow (\eta/\eta')\gamma$ ,  $SU_3$  violation, symmetry breaking and decay amplitudes 0-52499  
 $\psi \rightarrow \psi\pi^0(\eta)$ ,  $SU_2$  violation, symmetry breaking and decay amplitudes 0-52499

**spooling** see winding (process)

**sporadic-E layer**  
 $E_s$ -layer of auroral ionosphere, large-scale inhomogeneities 0-4171  
 electron density explained by wind shear acting on metallic ions 0-46338  
 high-latitude types of  $E_s$ , occurrence,  $f_oE_s$  and  $h'E_s$  0-51595  
 meteor activity metallic ions rel. to sporadic-E occurrence 0-46336  
 radiowave propagation above 30 MHz, role of sporadic-E layer and troposphere 0-41636

**sports and entertainment**  
 tennis, probability and statistics teaching illustration 0-41997

**spray coating techniques**  
 see also electrostatic coating techniques; flame spraying; plasma arc spraying; powder spraying  
 ion plating by field emission deposition 0-35110

**spray coatings**  
 see also electrostatic coatings; flame sprayed coatings; plasma arc sprayed coatings; powder sprayed coatings  
 lens, water soluble cryst., protective coating to aid polishing 0-33250  
 oxide thermal-sprayed coating on steel, acoustic emission 0-21247  
 temperature measurement of spherical or near-spherical particles in plasma stream 0-21138  
 Al-PbS selective surfaces for solar photothermal conversion, prep., emissivity, absorptivity 0-12030  
 CdS, chemically sprayed, carrier conc. and mobility, thermoelec. and photothermoelectric meas. 0-2503  
 CdS solar photovoltaic panels, deposited by spray pyrolysis, film and junction structure studies 0-45689  
 $Cr_2C_3$ -(Ni-Cr), for gas cooled reactor heat exchangers, factors affecting performance 0-40609  
 $SnO_2$ -n-Si spray-deposited solar cells 0-12007  
 ZnO, film for solar cell appl. structural, optical and elec. props. 0-2294

**sprays**  
 see also aerosols; drops; jets  
 condensation-evaporation of multidroplet system, by kinetic theory 0-7873  
 hollow cone sprays, induced air flows 0-53846

**spurious** see elementary particles

**sputter etching**  
 aromatic polyamide fibre, surface struct. 0-21147  
 blazed ion-etched holographic grating, prod. methods, optical props. (Japanese) 0-10021  
 cementitious materials, ion beam etching 0-30117  
 corrosion science, surface analytic techniques 0-31929  
 diamond, cryst. surface layers treatment and study by HF ion-plasma etching (Russian) 0-16517  
 diffraction grating form. on optical waveguide surface, ion-beam etching through photoresist mask 0-14492  
 metals, dispersion coefficient determ. (German) 0-40597  
 plasma etching, MOS processing appl. 0-40577  
 polyamide fibre, surface struct. 0-21147  
 polyester fibre, surface struct. 0-21147  
 Re-sputtering and implanting sputtered atoms during deposition 0-16137  
 reactive plasma etching, mag. field control 0-11796  
 sapphire, cryst. surface layers treatment and study by HF ion-plasma etching (Russian) 0-16517



# sputter etching continued

- SEM dynamic study 0-50734
- TEM specimen preparation, plasma etching use for foil thinning (*Slovak*) 0-45405
- Al films, plasma etching, MOS processing appl. 0-40577
- Al-Cu alloy layer, photolithographically patterned, separation from substrate using plasma etching (*Slovak*) 0-45405
- Au-TiC, multilayer struct., microhardness and elec. resist. 0-2950
- BaT<sub>2</sub>O<sub>3</sub>, surface microrelief revealed by ion irradiation 0-54485
- C, diamond-like, produced by RF glow discharge of hydrocarbon gases, props. and coating rates 0-21146
- Cr, cryst. surface layers treatment and study by HF ion-plasma etching (*Russian*) 0-16517
- GaAs, interference grating blazed by ion-beam erosion 0-1302
- Ge, cryst. surface layers treatment and study by HF ion-plasma etching (*Russian*) 0-16517
- InP surface preparation for Schottky barrier and ohmic contact formation 0-39671
- Si, cryst. surface layers treatment and study by HF ion-plasma etching (*Russian*) 0-16517
- Si, dry etching induced surface contamination, SIMS, AES, and XPS obs. 0-11810
- Si, etch rate uniformity in CF<sub>4</sub>+4% O<sub>2</sub> plasma 0-40568
- Si film, polycryst., thinning using plasma etching (*Slovak*) 0-45405
- Si, fluorocarbon ion beam etching characts. 0-35363
- Si polycryst., end point detection in plasma etching by optical emission spectroscopy 0-50733
- Si, reactive plasma etching with CF<sub>4</sub>, mag. field control 0-11796
- Si single crystal, Ar<sup>+</sup> ion sputter-machined surface, lattice disordering obs. (*Japanese*) 0-3228
- Si, substrate, sputtering and sputter etching and thermal history 0-25562
- Si textured wafer, selective absorber for solar thermal conversion 0-30544
- Si wafers, microwave plasma etching, role of ions and neutral active species 0-3217
- SiC, cryst. surface layers treatment and study by HF ion-plasma etching (*Russian*) 0-16517
- Si<sub>3</sub>N<sub>4</sub>, end point detection in plasma etching by optical emission spectroscopy 0-50733
- Si<sub>3</sub>N<sub>4</sub> films, plasma etching, MOS processing appl. 0-40577
- SiO<sub>2</sub>, dry etching induced surface contamination, SIMS, AES, and XPS obs. 0-11810
- SiO<sub>2</sub> films, plasma etching, MOS processing appl. 0-40577
- SiO<sub>2</sub>, fluorocarbon ion beam etching characts. 0-35363
- SiO<sub>2</sub>, selective etching, using reactive ion etching with CF<sub>4</sub>-H<sub>2</sub> 0-3224
- SiO<sub>2</sub> blazed holographic gratings, fabrication by reactive ion etching 0-53484
- SrTiO<sub>3</sub>, surface microrelief revealed by ion irradiation 0-54485

# sputtered coatings

- see also reactively sputtered coatings
- actinide target preparation by focused ion beam sputtering 0-23219
- coated Mo tips characterised by atom probe FIM, atomic clusters, voids 0-33863
- compound films, prep. by magnetron sputtering, and special features 0-11565
- diamond-Si heterostructure, Auger spectra electron microscopy study 0-34340
- ferromagnetic alloys, amorphous, sputter-deposited, soft mag. props., magnetostriction 0-34696
- hard coating deposition 0-40544
- isotopic target preparation by ion beam sputtering 0-23220
- magnetic anisotropy rel. to columnar microstruct., calc. 0-39822
- manganin thin film microtransducers for elastohydrodynamic lubrication studies 0-37048
- metallic films, deposited by cylindrical magnetron sputtering, internal stresses 0-24773
- metallic glass, continuous-biased sputter-deposited Kr entrapment 0-24603
- optical, production and props. (*Hungarian*) 0-53483
- semiconductors, EPMA of inert gas content 0-3443
- a-Si:H<sub>x</sub> structure, effect of H-Ar plasma contact on elec. props., and optical gap 0-34533
- steel, stainless, alloyed with C, magnetron-sputtered, microstruct., and cryst.-amorphous transition 0-19719
- steel, stainless types 321-SS and 430-SS, alumina coated, H<sub>2</sub> permeation 0-34244
- thermoregulating plasma coatings, UV irradiation influence on optical parameters (*Russian*) 0-40259
- Ag, electron beam plasma sputtered coatings on KCl substrate, islet struct. (*Russian*) 0-39460
- Ag films, hillock form, hole growth and agglomeration 0-44455
- Ag, hillock growth and agglomeration by annealing, SEM obs. 0-2309
- Ag thin films, deposited by cathodic sputtering using high-resolution electron microscopy, voids obs. 0-49557
- Al coating development, porosity, durability temp. depend., electric arc metallisation regime (*Russian*) 0-39402
- Al, electron beam plasma sputtered coating, islet struct. (*Russian*) 0-39460
- Al on Al<sub>2</sub>O<sub>3</sub> and on ZrO<sub>2</sub> particles, influence of ionic treatment on formation of Al coatings (*Russian*) 0-50552
- Al-Ag alloy mirror for use as solar reflector, co-sputtering 0-20789
- Al-Zn-Mg plasma sputtered, mech. props. rel. to heat treatment (*Russian*) 0-40387
- AlN encapsulation of GaAs:Si, photolum., annealing effects 0-20681
- As, amorphous, photoluminescence, bulk and sputtered thin films 0-25457
- Au, hardening mechanisms, grain size effect 0-35302
- C, amorphous, diamond-like 3-fold coord. 0-50323
- CdO-SnO<sub>2</sub> film, prep. by RF sputtering, elec. cond. and transparency 0-7492
- CdS monocrystalline sputtered X-ray transducer characteristics (*Russian*) 0-47162
- CdS:Cu<sub>2</sub>S sputtered solar cells, energy anal. of cell fabrication techniques 0-50966
- CdS,Se<sub>1-x</sub> photosensitive films, prep., props., and use for photodetectors 0-55298
- CdSe, photocond. film, plasma reson., IR refl. obs. 0-11037
- CdTe sputtered films, struct., photocond., and trap distrib. 0-29489
- Co, on Ni-Cr type alloys, surface pretreatment to attain pore-free aluminised coatings 0-40612

# sputtered coatings continued

- Co<sub>79</sub>Fe<sub>6.5</sub>B<sub>14.5</sub> amorphous thin films, zero magnetostriction, high magnetisation 0-34708
- (CoFeB)<sub>100-x</sub>Cr<sub>x</sub> thin films, magnetic props. and corrosion resist. 0-34709
- Cr, defects and mechanical stability, different deposition methods (*Bulgarian*) 0-44438
- Cr, growth struct., influence of substrate surface topography and ang. of adatom incidence 0-20058
- Cr-Si, deposition method, for controllable comp. with given elec. props. 0-35087
- Cr-SiO<sub>2</sub>, electrical and struct. props. 0-39694
- CrO<sub>2</sub> amorphous thin films, Mossbauer and magnetisation data 0-34712
- Cr<sub>2</sub>O<sub>3</sub>, RF sputtered coating for wear appls., on Inconel X-750 foil, prep. and props. 0-40605
- Cu-plated C fabric, plasma sputtering influence on strength and elec. cond. (*Russian*) 0-21008
- Cu-Ti-Fe (0.7, 0.9 wt.%) film, dispersion-strengthened, form. by high rate magnetron/plasmatron sputtering, and props. 0-25715
- Cu<sub>2</sub>O, sputter deposited on Cu, induced stresses 0-24774
- DyIG, non-cryst., Mossbauer and magnetisation studies 0-44979
- EuIG, non-cryst., Mossbauer and magnetisation studies 0-44979
- Fe-Co-Si-B sputtered amorphous thin film, coercivity, galvanomagnetic props., resistivity 0-29578
- Fe-Si-B amorphous films, mag. props. 0-34710
- Fe<sub>40</sub>Ni<sub>40</sub>B<sub>20</sub> glass, <sup>10</sup>B self-diffusion, meas. by SIMS 0-49406
- Fe<sub>2</sub>O<sub>3</sub> amorphous RF sputtered thin films, Mossbauer and mag. study 0-34711
- Fe<sub>2</sub>O<sub>3</sub> amorphous thin films, Mossbauer and magnetisation data 0-34712
- GaAs, amorphous sputtered films, hydrogenated, photoinduced optical absorpt. 0-50362
- GaAs, RF sputtered, ESCA, surface chemistry suitability for photovolt. appl. 0-7476
- GaAs:HF amorphous sputtered films, high field cond. props. 0-44607
- GaP, RF sputtering on glass and Au film substrates, struct. and elec. props. 0-2311
- GaSb, sputtered films, on GaAs, growth, Hall effect, impurity levels 0-20334
- GaSe sputtered film microhardness, influence of gas discharge (*Russian*) 0-49560
- Gd-Co amorphous films, RF sputtered, magnetisation ripple effects 0-11232
- Gd-Co amorphous films, struct. and mag. anisotropy 0-20438
- Gd-Co amorphous sputtered film, magnetostriction and anisotropy 0-39821
- Gd-Co sputtered amorphous films, resistivity anomalies, 42 to 300K (*Chinese*) 0-7001
- Gd-Co thin films sputtered from mosaic target, thickness and composition distrib. 0-6676
- GdCo amorphous film mag. props. from Mossbauer effect obs. (*Japanese*) 0-15933
- Gd<sub>0.25</sub>Co<sub>0.64</sub>Kr<sub>0.09</sub>, amorphous film, thermal release of Kr and H, meas. using UHV mass spectrometric technique 0-3439
- Ge, amorphous sputtered films, hydrogenated, photoinduced optical absorpt. 0-50362
- Ge condensation, nucleation, growth and transform. of amorphous and crystalline solids 0-24745
- Ge:Sb, amorphous, electronic transport props. 0-44589
- Ge<sub>0.5</sub>Te<sub>0.5</sub>, structural anal. by neutron diffr., radial distribution functions 0-15010
- H<sub>x</sub>WO<sub>3</sub> films, proton diffusion coeffs. 0-6548
- In<sub>2</sub>O<sub>3</sub> thin film on polyester substrate, struct. determ. by TEM 0-6674
- In<sub>2</sub>O<sub>3</sub>:Sn, electro-reflectance meas. 0-11496
- In<sub>2</sub>O<sub>3</sub>-SnO<sub>2</sub>, on Si, antireflection props. for photovolt. appl. 0-3513
- MnSi, amorphous, mag., elec., struct. and thermal props., spin glass behaviour 0-50124
- MoS<sub>2</sub>, RF sputtered layers with variable stoichiometry, lubrication props. 0-40557
- MoS<sub>2</sub>, RF sputtered lubricant, wear life, sputtering parameter effects 0-40558
- NaTiO<sub>3</sub>/SiO<sub>2</sub> charge storage memory films for IGFETs 0-11566
- Nb, magnetron-sputtered, intrinsic stresses and supercond. props. 0-24772
- Nb-Ge film, phase transformations due to annealing, electron diffr. study 0-54551
- NbGe<sub>2</sub>, superconducting transition temp. meas. 0-7019
- Nb<sub>2</sub>Ge superconducting film, Nb<sub>2</sub>Ge<sub>3</sub> and NbO content, X-ray diffr. obs. 0-2515
- Nb<sub>2</sub>Ge superconducting film, crit. temp. correl. with resist. relations and film struct. (*Russian*) 0-15646
- Nb<sub>2</sub>Ge superconducting films, quantitative Auger anal. 0-55740
- NbSi<sub>3</sub>, superconducting transition temp. meas. 0-7019
- Nb<sub>3</sub>Sn, high-rate sputter-deposited, effect of oxygen on microstruct. 0-20343
- Ni films, HCP and amorphous, RF sputtered, O<sub>2</sub> incorporation, ESCA obs. 0-10832
- Ni, sputter deposited on Cu, induced stresses 0-24774
- Ni/ZrO<sub>2</sub>-Y<sub>2</sub>O<sub>3</sub> multilayered ceramic/metal coatings, props. 0-40620
- Ni-Cr/ZrO<sub>2</sub>-Y<sub>2</sub>O<sub>3</sub> multilayered ceramic/metal coatings, props. 0-40620
- Ni-Fe-Rh films, mag. and corrosion props. 0-34702
- NiCr, sputtered, detection by electron probe microanal., substrate depend. 0-35607
- Ni<sub>3</sub>Si coatings, form. and stability during high temp. irradiation 0-35088
- PbS sputtered film microhardness, influence of gas discharge (*Russian*) 0-49560
- Pb<sub>1-x</sub>Sn<sub>x</sub>Te, for IR detector appl. elec. and optical props. 0-35084
- PbTe, semiconductor polycrystalline thin films, low-frequency 1/f noise meas. 0-15629
- Pd<sub>2</sub>Si, on Si substrate, thermally induced Si accumulation, AES study 0-24718
- PrO<sub>2</sub>, sputtered film, optical props. under H<sub>2</sub> reduction 0-20728
- Si, amorphous, control of dihydride bond density using RF sputtering, dark anal. and photocond. 0-34327
- Si, amorphous, hydrogenated, soft H plasma effect, IR absorpt. (*French*) 0-45054
- Si, amorphous, Schottky barrier solar cell, large-area RF sputtered, contact form, scaling and optimisation 0-45679
- Si, amorphous, sputter deposited, O<sub>2</sub> incorporation during and after fabrication 0-49541
- Si, amorphous sputtered films, hydrogenated, photoinduced optical absorpt. 0-50362



**sputtered coatings continued**

- Si, amorphous sputtered thin film, US anomalies, 0.5-300K 0-34145
- Si and Si:H amorphous films, porosity and oxidation of evap., sputtered and plasma-deposited films 0-10838
- Si:H, amorphous, Auger surface spectroscopy 0-50472
- Si:H, amorphous sputtered, excitation spectra and photoluminesc. 0-50396
- Si:H:P, amorphous, heavily hydrogenated, high gap state densities 0-49803
- Si:H amorphous film, luminesc. and non-radiative decay 0-50395
- Si:H amorphous sputtered films, optical gap, IR absorpt. meas. 0-50320
- a-Si:H sputtered films, ohmic contacts by H depletion, H diffusion 0-34511
- Si:Mn(Fe)(Ni) amorphous films, ESR and elec. cond. 0-50171
- Si:Ne(Ar)(Kr), amorphous, implanted and sputtered, epitaxial regrowth, influence of noble gas atoms 0-2289
- Si:O, amorphous, sputtered, influence of O and deposition conditions 0-54693
- Si:Sb, amorphous, electronic transport props. 0-44589
- Si-Au films, quenched condensed, elec. resist. and supercond. 0-54669
- a-Si-H sputtered solar cells, temp. depend. of Schottky barrier characts. 0-45669
- Si<sub>100-x</sub>Al<sub>x</sub>, RF sputtered, amorphous, props. 0-34754
- SiC, comp. and struct. props., effect of target materials 0-54549
- SiH<sub>4</sub>, amorphous reactively sputtered films, in Pd Schottky barrier devices, photovoltaic props. 0-49910
- Si<sub>3</sub>N<sub>4</sub> encapsulation of GaAs:Si, photolum., annealing effects 0-20681
- Si<sub>3</sub>N<sub>4</sub>, preparation, characterisation and appl. 0-40268
- SiO<sub>2</sub>, and SiO<sub>0.7</sub>, amorphous sputtered thin film, US anomalies, 0.5-300K 0-34145
- SiO<sub>2</sub> film on thermally oxidised Si substrate, interface props., sputter deposition parameters effects (*German*) 0-40257
- SiO<sub>2</sub> magnetron sputtered film, oblique deposition effect on growth rate, etching rate, and struct. (*Japanese*) 0-54555
- SiO<sub>2</sub> RF magnetron sputtered coatings for laser fusion targets 0-35089
- SiO<sub>2</sub>, RF sputtered films, anomalous etching phenomenon 0-3226
- SiO<sub>2</sub>, RF sputtered films, AC conductivity and conduction mechanisms 0-20338
- SiO<sub>2</sub> sputtered film as Zn-diffusion mask for GaInAsP-InP planar stripe lasers 0-48249
- SiO<sub>2</sub> sputtered films in thin film transistors, trapping centres 0-7014
- SiO<sub>2</sub> thin films, comparison of RI and IR spectra 0-11497
- SnO<sub>2</sub> thin films, analytical characterisation 0-20053
- SnO<sub>2</sub> films, phase composition, Mossbauer spectra 0-20051
- Sr<sub>2</sub>Nb<sub>2</sub>O<sub>7</sub>, sputtered films, amorphous, dielec. props. 0-54573
- $\beta$ -Ta film, stabilisation by Ta-Si interlayer, SIMS depth profiling 0-54568
- Ta, planar-magnetron-sputtered, phys. and elec. props. 0-6673
- TaGe<sub>2</sub>, superconducting transition temp. meas. 0-7019
- TaSi<sub>3</sub>, superconducting transition temp. meas. 0-7019
- Ti, diffusion in LiNbO<sub>3</sub> planar and channel optical waveguides 0-19096
- Ti-Si cosputtered films, silicide form., X-ray diffr. and resist. study 0-54546
- Ti-W, bias-sputtered, resist. and comp. 0-25023
- Ti-W magnetron sputtered films metallisation 0-45231
- TiO<sub>2</sub> film, photocond. and TSC meas. 0-15560
- WSi<sub>2</sub>, sputtered film on Si and SiO<sub>2</sub> substrate, thermal oxidation kinetics 0-3208
- ZnO thin piezoelectric film, SAW devices for HF range (*Japanese*) 0-53598

**sputtered layers** *see* sputtered coatings**sputtering**

- see also d.c. sputtering; diode sputtering; radiofrequency sputtering; reactive sputtering; sputter etching; triode sputtering*
- alkali halides, interstitial motion during radiation damage and sputtering processes 0-54230
- alkali halides, photon induced sputtering 0-35013
- alkali halides, sputtering, thermal effects, review 0-35033
- alkali halides, sputtering of molecules, low-energy electron bombardment 0-35026
- alloy, surface composition changes 0-2913
- alloy sputtering 0-50503
- alloy surfaces, sputtering process and sputtered ion emission models 0-35044
- alloys and compounds, recoil implantation and ion-beam-induced comp. changes 0-34021
- binary alloy, time const. for preferential sputtering 0-2912
- closed field sputtering equipment 0-50556
- compound, surface composition changes 0-2913
- conference on inelastic ion surface collisions, Hamilton, Ontario, Canada (Aug. 1978) 0-31402
- cryogenic thin film ultrahigh-vacuum evaporation/sputtering apparatus 0-20790
- depth profiles distortions 0-55249
- depth profiles obtained by ion-beam sputtering, edge-effects correction 0-55757
- depth profiling, review 0-40214
- detonation sputtering, gas flow parameters calc. (*Russian*) 0-16181
- detonation sputtering, interaction between detonation waves and gas and powder flows (*Russian*) 0-16182
- elements, sputtering process and sputtered ion emission models 0-35044
- energy efficiency of ion sputtering processes (*Russian*) 0-7457
- evaporation chamber LV electron guns with longitudinal compression (*Russian*) 0-50551
- film deposition, ion beam techniques 0-11564
- film deposition, trend of new techniques (*Japanese*) 0-11563
- film deposition method, for controllable comp. with given elec. props. 0-35087
- film island coalescence of real cryst. surface, unattenuated sputtered atom source 0-6672
- fusion reactor first wall materials, light ion sputtering studies 0-18647
- fusion reactors, blister-induced first wall erosion, alpha incident velocity and poloidal angle distrib. 0-37583
- fusion technology, surface studies 0-23149
- graphite, D<sup>+</sup> bombardment, surface damage, sputtering, SEM study 0-32459
- implant ion collection with radn. enhanced diffusion and sputtering of implant 0-2055
- inhomogeneous rod in complex heat exchange conditions, temp. calcs., film sputtering evaporators (*Russian*) 0-38230

**sputtering continued**

- insulators, fission fragment sputtering 0-40207
- ion beam sputtering, appl. to surface machining 0-30129
- ion beam sputtering, combination with AES, surface anal. 0-50474
- ion bombardment, electron microscopical anal. of surface effects and volume defects, review (*Rumanian*) 0-29093
- ion emission, sputtered, universal model 0-55248
- ion microprobe analysis using ion-induced AES 0-30305
- isotopic fractionation, sputter-induced, at solid surfaces 0-55244
- Josephson junction, sputtering system for fabrication (*Japanese*) 0-55293
- light emission from solid bombarded with atomic particles, review 0-35036
- magnetron ion sputtering, thin film layers deposition uniformity investigation (*Russian*) 0-20787
- mechanisms, review 0-40213
- metal, with adsorbed Cs effects on photon and secondary ion emission during sputtering 0-35038
- metal layer growth by sputtering, corpuscular diagnostics of hollow cathode discharge 0-16180
- metal oxide layers, obtained by cathode and HF sputtering, light scattering and refr. index reduction 0-29877
- metal vapour production by sputtering in hollow-cathode discharge 0-1868
- metal-adsorbed gas systems, sputtering effects, combined analytical techniques 0-35047
- metallurgical coatings, vapour deposition processes in vac. 0-35430
- metals, erosion accompanying simultaneous action of laser emission and ultrasound (*Russian*) 0-7442
- Monte Carlo analysis of backscattering and sputtering in vacuum systems 0-235
- nonmetal, Coulomb explosion sputtering by intermediate energy multiply charged ions 0-35049
- optical films production and props. (*Hungarian*) 0-53483
- overheating influence of sputtered particles and oxidised films on heat processes (*Russian*) 0-40385
- oxide glasses, ion-bombarded, optical line intensities 0-35037
- oxides, sputtering, thermal effects, review 0-35033
- oxides, sputtering effects, combined analytical techniques 0-35047
- oxidised surfaces, sputtering process and sputtered ion emission models 0-35044
- Permalloy films, oxidation effects on atmospheric corrosion, AES, XPS and ion sputtering anal. 0-11829
- photon yield relation to population distribution and excitation function 0-34989
- plasma solid interaction, surface erosion 0-38665
- polymer coatings deposition, choice of type of electrostatic sputter (*Russian*) 0-50553
- preferred, phenomenological model for SIMS and Auger profiling 0-55254
- pulse plasma sputtering, particle velocity and disperse composition (*Russian*) 0-40258
- sample contamination, during ion implantation 0-54274
- secondary ion and photon emission, energetic particle irradiation cascade 0-45186
- steel, stainless, low energy H<sup>+</sup> sputtering 0-40198
- steel, stainless, sputtering yield meas. using AES 0-18654
- steel target, stainless, deuteron trapping model, of gas sputtering 0-49398
- surface composition changes during Ar<sup>+</sup> ion sputtering of alloys 0-49470
- surface composition depth profiles, ion sputtering effects 0-35616
- surface ionisation, elemental anal. of sputtering products (*French*) 0-50905
- thin film deposition technique, review (*Japanese*) 0-35107
- thin films, thickness meas. anal. characterisation using proton-induced X-ray emission 0-35618
- Tokamak limiter, surface observation, infrared techniques 0-38693
- Tokamak scrape-off plasma, metal impurity recycling effect 0-10421
- turbulent stream of high temp. gas with particles, modelling (*Russian*) 0-38572
- ultra cold neutron container materials, surface conc. of H atoms by ion bombardment 0-9446
- vacuum deposited film, as first wall material, sputtering yield meas. (*Japanese*) 0-25513
- yield, absolute meas., UHV microbalance, with ion gun (*Japanese*) 0-17951
- Ag, film, sputtering mechanism, SEM 0-29839
- Ag, ion bombardment, sputtering, re-emitted kinetic energy ang. distrib. 0-2910
- Ag, polycryst., sputtering rate on Ar ion bombard. 0-55245
- Ag surfaces, temp. depend. of sputtering based on thermal spike effect 0-50491
- Ag, temp. depend. 0-2914
- Ag thin films, spike effects of heavy ion sputtering 0-35034
- Ag-Au, surface layer, effect of Ar<sup>+</sup> bombardment, AES and SIMS 0-25504
- Ag-Au-Cu, sputtering and AES 0-50503
- Ag-Pu (0.5 wt.%) deposited profiles, homogeneity, from hexagonal point source array 0-25559
- Al, ion bombardment, sputtering, re-emitted kinetic energy ang. distrib. 0-2910
- Al, polycryst., sputtering rate on Ar ion bombard. 0-55245
- Al sintered powder coatings, form. and behaviour under particle bombard. 0-35029
- Al, surface ionisation, elemental anal. of sputtering products (*French*) 0-50905
- Al-Ag alloy mirror for use as solar reflector, co-sputtering 0-20789
- Al-Cu-Si, effect of sample conditions on sputtering and intensities, emission spectrochem. anal. using glow discharge (*Japanese*) 0-21349
- Al-Si coatings, form. and behaviour under particle bombard. 0-35029
- Al<sub>2</sub>O<sub>3</sub> coatings, form. and behaviour under particle bombard. 0-35029
- Ar glow discharge, metastable and reson. states density meas. (*French*) 0-14955
- Au films, (111), sputtering in high voltage electron microscope 0-35027
- Au, low energy H<sup>+</sup> sputtering 0-40198
- Au, polycrystalline foil, sputtering yield meas. by UHV microbalance with ion gun (*Japanese*) 0-17951
- Au sputtered with Xe<sup>+</sup>, Xe<sup>2+</sup>, nonlinear effects 0-20748
- Au thin films, spike effects of heavy ion sputtering 0-35034
- Be, sputtering by H<sup>+</sup>, D<sup>+</sup>, He<sup>+</sup>, weight loss measurements 0-35028
- Be surfaces, O and H covered, secondary ion emission, coverage dependence 0-35043
- BeO, sputtering by H<sup>+</sup>, D<sup>+</sup>, He<sup>+</sup>, weight loss measurements 0-35028



## sputtering continued

- CO<sub>2</sub> laser bimetallic mirror coating vacuum sputtering technology 0-35086
- CaF<sub>2</sub>, appl. of theory of sputter-induced isotopic fractionation at solid surfaces 0-55244
- Cd, ion bombardment, sputtering, re-emitted kinetic energy ang. distrib. 0-2910
- (CdGeAs<sub>2</sub>)<sub>1-x</sub>D<sub>x</sub> amorphous films, property control in common target sputtering, elec. cond. 0-7494
- CdTe foils, prep. for TEM, ion sputtering technique (*Czech*) 0-16619
- Co film, ion beam sputtering prep., struct. and mag. props. 0-35085
- Cr, film, sputtering yields, proton-induced X-ray meas. 0-50488
- Cr, gas-phase, plasma, sputtering and beam-foil excitations 0-32820
- Cr-Si, thin films, deposition method, for controllable comp. with given elec. props. 0-35087
- Cu (110), O adsorption, low-energy ion bombardment investigation 0-34302
- Cu, film, sputtering mechanism, SEM 0-29839
- Cu, polycryst., sputtering rate on Ar ion bombard. 0-55245
- Cu, sputtered, ionisation probability, energy dependence 0-35041
- Cu, sputtering, surface topography, appl. of thermodynamics of capillarity 0-20749
- Cu, surface ionisation, elemental anal. of sputtering products (*French*) 0-50905
- Cu-Al, surface ionisation, elemental anal. of sputtering products (*French*) 0-50905
- Cu-Ni, sputter-induced subsurface segregation, Auger electrons obs. 0-10757
- Cu-Ni, sputtering yield, surface binding energies 0-50503
- Cu-Ni, surface layer, effect of Ar<sup>+</sup> bombardment, AES and SIMS 0-25504
- Fe alloys, ion-implanted, depth profile, ion sputtering study 0-54277
- Fe and Fe alloys, passive films studied using AES combined with ion sputtering technique 0-35378
- Fe, and Fe-Cr, film, sputtering yields, proton-induced X-ray meas. 0-50488
- Fe, film, ion beam sputtering prep., struct. and mag. props. 0-35085
- Fe, passive films and phosphate layers, sputtering rate evaluation in glow discharge lamp 0-45443
- Fe-Ar low press. flow discharge, axial density profiles of sputtered cathode atoms 0-49029
- Fe-Cr-Mo, sputtering effect on surface comp., AES obs. 0-6601
- Fe-Zn intermetallics, initial stages of form. (*Russian*) 0-20889
- GaAs foil, prep., for TEM obs., by ion sputtering (*Czech*) 0-16619
- GaAs, sputtering at elevated temps. 0-7456
- GaSb, sputtered films, on GaAs, growth, Hall effect, impurity levels 0-20334
- GdCo, amorphous thin film, for thermomagnetic recording (*Japanese*) 0-11562
- In<sub>2</sub>O<sub>3</sub>-SnO<sub>2</sub>/GaAs, solar cell, fabrication, characts. and interfacial chemistry 0-21401
- In<sub>2</sub>O<sub>3</sub>-SnO<sub>2</sub>/InP, solar cell, fabrication, characts. and interfacial chemistry 0-21401
- Kr immobilisation by incorporation into metallic matrix by ion implantation and sputtering 0-27794
- Mo surface, 40 keV Ar<sup>+</sup> bombarded, excited at. emission 0-11481
- Mo, TFR protective plate, sputtering and surface damage by D<sup>+</sup> irradiation 0-18645
- Mo:He, accumulation and distrib., monolayer conc. by sputtering quantitative anal. 0-49253
- NaCl, sputtering of atoms by 540 eV electrons, delay times 0-35025
- Nb, ion bombardment, sputtering, re-emitted kinetic energy ang. distrib. 0-2910
- Nb thin foils, surface segregation during sputtering at elevated temps., Auger study 0-54386
- Ni film, ion beam sputtering prep., struct. and mag. props. 0-35085
- Ni low energy H<sup>+</sup> sputtering 0-40198
- Ni, polycryst., sputtering rate on Ar ion bombard. 0-55245
- Ni, sputtered, ionisation probability, energy dependence 0-35041
- Ni wire plasma sputtering with W particles, coagulation, struct. and particle size (*Russian*) 0-40260
- Ni-Cu, sputtering rate, radiation-induced segregation and preferential sputtering effects, kinetic model 0-40199
- Ni-Mo, sputtering rate, radiation-induced segregation and preferential sputtering effects, kinetic model 0-40199
- Pb, film, sputtering mechanism, SEM 0-29839
- Pb, ion bombardment, sputtering, re-emitted kinetic energy ang. distrib. 0-2910
- Pb(Zr,Ti<sub>1-x</sub>)O<sub>3</sub> films, ion beam deposition, struct., dielec. and ferroelec. props. 0-20788
- Pt thin films, spike effects of heavy ion sputtering 0-35034
- RbBr, sputtering of atoms by 540 eV electrons, delay times 0-35025
- RbI, sputtering of atoms by 540 eV electrons, delay times 0-35025
- Si, minority carrier lifetime, effect of SiO<sub>2</sub> coating deposited by magnetron sputtering 0-11003
- Si, semi-insulating polycrystalline CVD layers, AES and XPS characterisation 0-16129
- Si, single cryst., sputtering rate on Ar ion bombard. 0-55245
- Si substrates, thermal history 0-25562
- Si:As sputter rate meas. SIMS combination with Rutherford backscatter 0-21334
- Si:B sputtering by Ar<sup>+</sup>, computer simulation of sputter broadening in impurity depth profiling 0-2908
- SiC, sputtering processes by energetic ions, combined SIMS-AES study 0-40201
- SiO<sub>2</sub> film, effect of ion implanted O<sub>2</sub> on optical props. 0-45027
- Ti, polycryst., sputtering rate on Ar ion bombard. 0-55245
- TiO<sub>2</sub>, (100) surfaces, ionisation of sputtered-atomic particles 0-20750
- U, sputtered, absorpt. spectra in hollow cathode glow discharge 0-32643
- V surface, particle release by neutrons 0-25493
- W (100), coadsorption of Zr and O<sub>2</sub> at high temp. 0-6653
- W, adsorption of N<sub>2</sub>, effect of SIMS, sputtering induced recomb. anal. 0-55243
- Zn, film, sputtering mechanism, SEM 0-29839
- Zn, gas-phase, plasma, sputtering and beam-foil 0-32820
- Zn I, relative populations in arc, sputtering and gas phase collisions 0-934
- ZnS, epitaxial growth, appl. to electronic devices, review (*Japanese*) 0-55281
- ZrO<sub>2</sub>-Y<sub>2</sub>O<sub>3</sub> powder, prep. for plasma spheroidisation, sputter drying (*Russian*) 0-55324

## SQUIDS see superconducting junction devices

## stabilisation see stability

## stabilisers see controllers

## stability

- see also flow instability; frequency stability; limit cycles; Lyapunov methods; plasma instability
- amorphous Lennard-Jones solid, edge and screw dislocation, stability, elasticity, simulation 0-15099
- analytic extrapolations towards interior points from a cut, applic. to elementary particle scatt. theory 0-12952
- arches, flat, sandwich-type, elastic equilibrium states 0-48570
- artificial satellite, spinning, symmetric, in planar periodic orbit, attitude stability 0-4220
- autonomous Hamiltonian system, gyroscopic forces, effect on stability (*Russian*) 0-17794
- barrier island breach morphology and dynamics, study in stability 0-12371
- beams, dynamic stability with shearing strains and rot. inertia 0-33498
- beams, non-linear vibrations, stability analysis method 0-53686
- biaxial plastic tension, instability calc. (*Russian*) 0-23920
- bicycle stability, teaching approach—using unsuccessful nongyroscopic theory 0-42001
- black hole accretion discs, Lightman-Eardley instabilities rel. to disc thickening 0-31324
- blanks clogged into conical matrix, stability anal. (*Russian*) 0-43636
- buckling, cylindrical shell and spherical panel, stability, critical loading density 0-53664
- buckling of elastic beams, analysis using theory of quadratic operator pencils 0-48607
- BWR stability monitoring using time series anal. of neutron noise 0-47625
- camera, aerial, stabilised mount anal. 0-9059
- cantilever under multiple loads, postbuckling and stability anal. 0-48617
- chaos, reinjection principle, folded and cut chaotic flows 0-12996
- collapsing sphere, shape instability pressure stabilisation 0-8537
- columns, Beck and Leipholz types, stability, shear deformation and rot. inertia effects 0-48610
- composite material cylindrical shells, stability during nonsteady heating and transverse flexure 0-40445
- compressed air energy storage in hard rock caverns, stability and design criteria 0-30574
- continuous elastic systems under multiple loads, postbuckling anal., stability theory 0-48616
- cryogenic system, thermally driven acoustic oscillation, stability limit 0-8992
- cubic crystal under hydrostatic loading, Born and classical stability criteria divergences 0-10595
- cylinder, stable conditions for phase change problem with internal heat generation 0-10130
- cylindrically symmetric bubbles, static and dynamic props. 0-39835
- damage induced structural instability 0-28445
- deformable bodies, three-dimens., stability study 0-14596
- deformable body three dimensional stability theory, variational principles 0-38300
- distributed systems, stability of spatially inhomogeneous states 0-30629
- dynamic instability region, computation by finite element method 0-23927
- elastic body stability under isotropic uniform compression 0-4531
- elastic compressible bodies under all-around compression, stability for rods and plates 0-43633
- elastic incompressible bodies under isotropic compression 0-14597
- elastic structs., stability, buckling and postbuckling 0-1454
- energy-balance climate models, stability theorem 0-56594
- fine reinforced cylindrical shells, stress strain state and stability 0-14598
- forced oscillations, lower bound on forcing amplitude for stability, third order non-linear system 0-52013
- free circular plate, stability under non-conservative edge loading 0-23948
- frustrated two-dimensional planar model, spin-spin correl. 0-11212
- garnet, Permalloy-coated film, bubble vel. and stability, influence of planar domains 0-39831
- glass fibre reinforced plastic shell with rubber filler, stability under axial compression 0-7643
- gyrostat, symmetric satellite, uniaxial stabilisation at libration points 0-14560
- hard superconductor flux jumps under time depend. external conditions 0-7038
- heavy gyrostat, steady motion stability for free and restrained dynamical systems 0-46791
- high current density magnet, thermal stability 0-37057
- infinite dimensions and the fold catastrophe, particle modelling 0-8788
- integro-differential coupled-core reactor models, asymptotic stability 0-13531
- interstellar magnetised gaseous discs, gravitational instability 0-4424
- ionic crystal, surface stability 0-20016
- laminar blocks with plastic deformations, instability 0-43629
- laminar shells, with viscoelastic binder, stability 0-10165
- laser instability, example from synergetics 0-9848
- liquid film, thickness and stability, on nonplanar surfaces 0-10755
- load stability problems, power method modification (*Russian*) 0-28444
- magnetic bubble, transverse mass in rotating gradient 0-39832
- magnetic monopoles, non-Abelian, stability analysis, Yang-Mills equations 0-31987
- magnetic-binary problem, stationary solns. and stability when primaries are oblate spheroids 0-41697
- MOSFET, piezoresistivity effects and use as press. transducers 0-4695
- motion on ring (*Russian*) 0-42052
- moving thin elastic strip subjected to random parametric excitation, dynamic stability 0-48618
- multilayer shells with fillers, exam. of stability under axial compression comparison to theory 0-7643
- N-body problem, restricted, libration points stability in perturbed potentials case 0-4241
- Newtonian stellar dynamics, maximizing functionals, rel. to thermodynamic and dynamical stability 0-12782
- nonconservative simple frame, nonlinear divergence buckling, critical load 0-14594
- nonconservative systems, simplified stability criterion from Lyapunov's method 0-46790
- nonisolated equilibrium with max. pot. stabilised by dissipative forces 0-14599



## stability continued

nonlinear oscillators, normal modes, uncoupling and stability 0-27115  
 optimization of practical stability problems 0-5966  
 oscillating system, light damping, influence of eigenvalues (*German*) 0-31490  
 panels with openings, stability loss and critical stresses 0-10219  
 perturbation theory, quasi-periodic motion, asymptotic expansion method 0-17877  
 perturbed Hamiltonian system, stability criterion 0-17793  
 plasma flute oscillation suppression, regulator synthesis (*Russian*) 0-24212  
 plate, prestressed elastic, homogeneous solns. for bending and stability 0-43610  
 plate with crack close to one edge, elastoplastic equilb. 0-14624  
 plates, annular, dynamic stability numerical soln. (*Polish*) 0-10173  
 plates, flat, stability of postbuckling behaviour 0-1453  
 plates, rectangular, stability anal. by complementary energy method 0-48611  
 plates, rectangular, stability and vibrations (*Chinese*) 0-43644  
 plates and shells, elastoplastic, with hydrostatic press. depend. mech. props., stability problem soln. (*Russian*) 0-53668  
 plates with cut, stability loss critical stresses for steel, Ti and Al alloys 0-11690  
 polyamide mixtures, thermodynamically incompatible, composition-prop. relationship (*Russian*) 0-7872  
 polyethylene films, fibres, radiation initiated graft polymerisation of acrylonitrile, initiation rate rel. to props. (*Russian*) 0-7531  
 postbuckling behavior of thin-walled open cross-section compression members 0-5963  
 probkotron plasma stabilisation system, automatic, against flute oscills. (*Russian*) 0-24211  
 PVC, chlorinated, fibres, radiation initiated graft polymerisation of acrylonitrile, initiation rate rel. to props. (*Russian*) 0-7531  
 quasars, radiatively driven gas clouds dynamics and stability, plane-parallel slabs theory 0-22107  
 rod, short elastic, in viscous liquid axial flow, stability and transverse oscillations 0-33521  
 rod, thermal conduction, dynamic behaviour of distributed systems (*Dutch*) 0-28407  
 rods, simple orthotropic elastic, shock waves and wave-type instability 0-48622  
 rotating cantilever, stability and instability conditions, Lyapunov function method (*Russian*) 0-36840  
 rotating stars, perturbs. and stability, eigenvalues and perturb. theory 0-46538  
 rotating stars, perturbs. and stability, eigenvectors and variational principle 0-46537  
 S=1 generalised Ising model, stability conditions 0-20427  
 second law of thermodynamics and stability in thermoelasticity theory 0-31689  
 second order linear systems with periodic coeffs., approx. method for stability anal. 0-12892  
 shallow arch under multiple loads, postbuckling and stability anal. 0-48617  
 shell, cylindrical, dynamic instability due to attached mass (*Ukrainian*) 0-38297  
 shell, cylindrical, fibre reinforced, fluid conveying, vibr. characts., flow effects 0-14600  
 shell, cylindrical, under axial shock, unsymmetrical bulging and buckling (*Russian*) 0-33492  
 shell, multilayer composite, optimisation, buckling under stability and vibr. conditions (*Russian*) 0-53667  
 shell, spherical, with reinforced holes, local stability 0-50686  
 shell, spherical transversally isotropic stability (*Ukrainian*) 0-10171  
 shell and surface rigidity, pseudobending, vibrs. and stability loss (*Russian*) 0-33470  
 shells, imperfect long cylindrical, lower critical hydrostatic press., stability 0-33491  
 shells, thin circular cylindrical, stability problem soln. method (*Chinese*) 0-5928  
 shells, thin stiffened reinforced, stability and vibrs. 0-14610  
 shells of revolution (*Russian*) 0-43638  
 shells under external press., stability 0-23898  
 slamming safety membrane, stability loss in elastoplastic and elastic regions, expt. coeffs. 0-33496  
 solitons, Poincaré stability, gauge theories, nonlinear Schrödinger equation 0-4881  
 spherical shell, buckled states, under uniform external pressure, asymptotic methods and Newton's method 0-43635  
 spherically symmetric accretion flows, stability anal., X-ray sources appl. 0-46387  
 springs, helical, under compression and twist, stability, nonlinear Kirchhoff-Clebsch equations (*German*) 0-33443  
 stars, rigidly rotating, secular instabilities in general relativity, theoretical formalism 0-4341  
 stars, rigidly rotating, secular instabilities in general relativity, numerical results 0-4342  
 stars, rotating, secular instability from thermal cond. 0-21986  
 statistical mechanics, stability, equilb., and metastability 0-31659  
 statistical mechanics, structural stability 0-8932  
 statistical-kinematic analysis and limit equilibrium of systems with unilateral constraints 0-1451  
 stochastic differential eqns., stability and boundedness rel. to generalised norm 0-12993  
 stochastic input-output stability and instability, second-order, of interconnected systems 0-52133  
 storage ring, feedback-stabilised, resonator wall instability caused by ponderomotive forces 0-5418  
 structural stability in physics (conference, Tübingen, Germany, May and Dec. 1978) 0-8739  
 system with nonconserved order parameter, influence of heat cond. on relax. of unstable states 0-10637  
 Teflon FEP, annealed electret, charge stability 0-6943  
 thermoelasticity, stability of some plane deform. states 0-43634  
 thick-walled cylinder, stability loss, three-dimens. form 0-5965  
 three-body problem, unrestricted, Lagrangian solns. stability problem (*Russian*) 0-4245  
 three-body problem, unrestricted, Laplace solns. stability (*Russian*) 0-8529  
 transient laser radiation, stochastic process near an instability point, numerical solution 0-23658

## stability continued

Trojan asteroids motion, long-period effects and 1/1 resonance stability 0-41755  
 two layered parallelepiped under large elastoplastic deformations, deformation instability 0-33499  
 unstable modes of an equilibrium, number calc. 0-36493  
 unsteady aerodynamic modelling for arbitrary motions 0-19433  
 Van Allen radiation belt 0-31177  
 viscoelastic, bars with nonlinear characteristics, stability 0-10174  
 viscoelastic structures, strength and stability, a method of solving integral eqns. used 0-10167  
 viscoelasticity, nonlinear, bifurcation and uniqueness, Hadamard stability 0-43621  
 viscoelasticity, stability problems in mathematical theory 0-27133  
 VLBI, improvement of freq. stability of local oscillators (*Japanese*) 0-17504  
 C, glass tip, field emission current stability 0-11544  
 H, stabilisation at low temp. 0-44390  
 Ni complex, bis-4-dimethylaminodithiobenzyl nickel, tetrachlorethane soln., photochem. and thermal stability 0-16708

**stability criteria**  
 see also Nyquist criterion  
 brain injury and instabilities 0-45943

**stability of numerical methods** see convergence of numerical methods

**stacking faults**  
 Ag-Cu fibre composites, highly deformed, lattice defects, X-ray interference lines anal. 0-10559  
 bis(benzonitrile)trichloromonoovanadium(V), cryst., stacking faults (*French*) 0-49238  
 $\alpha$ -brass, dislocation struct., deform. (*Polish*) 0-24454  
 $\alpha$ -brasses, cold worked, atomic diffusion kinetics to stacking faults, Laplace transformation method 0-19977  
 coherent phase form. at stress concentrators, effect of dislocation splitting, dislocation pile-ups, and phase elastic moduli (*Russian*) 0-49356  
 crystallite, cylindrical, layer disorder, X-ray diff. intensity effect 0-39113  
 crystallites, curved, cluster with layer shift, X-ray diff. intensities 0-39114  
 disordered crystals, 2H to 6H solid state transformation, deformation mechanism, X-ray diffraction study 0-33921  
 disordered crystals, 2H to 6H solid state transformation, layer displacement, X-ray diffraction study 0-33920  
 fatigue failure mechanisms, thermally activated, activation energy calcs. (*Russian*) 0-16436  
 graphite, anisotropic elec. cond. rel. to stacking disorder 0-34437  
 heteroepitaxial layers, dislocation structures, problems of formation 0-15100  
 metal, FCC, vacancy migration near twin boundaries and stacking faults 0-39075  
 metals, FCC, stacking faults energies in pair potentials calc., appl. to point defect props. 0-19798  
 order-disorder groupoid family, parameters, stacking 0-38982  
 order-disorder structures, layer stacking 0-38981  
 shear band formation models, in rolling and extrusion 0-11666  
 steel, austenitic, Ni alloy, stacking fault energy of austenite, high resolution electron microscopy (*Russian*) 0-44219  
 steel, austenitic stainless, stacking fault effect on martensitic transform. during plastic deform. (*Russian*) 0-25696  
 steel, high C, high alloy,  $M_{23}C_6$  type carbides, effect of alloying elements on defect struct. and hardness 0-16481  
 steel, stainless, martensite formation, in situ obs. 0-25692  
 steel, stainless, martensite nuclei obs., role of defects in nucleation 0-25693  
 steel, stainless type 03Kh13AG19, deformation temp. influence on dislocation struct. (*Russian*) 0-11698  
 tetrahedra, displacement field construction from angular dislocation segments, electron microscope image simulation 0-6325  
 tetrahedra, electron microscope image contrast 0-6326  
 transition metal dichalcogenide, stacking layer study, appl. of convergent beam electron diff. 0-39116  
 Ag-Sn (68.2)(11) wt.%, splat-quenched, X-ray line broadening 0-40397  
 Ag<sub>3</sub>Mg, two different types of long-period ordered alloys, characterisation by high resolu. electron microscopy 0-49181  
 Au, atomic arrangements of defects, dynamic obs. of atom movement 0-39108  
 Au, thin foil, growth of stacking fault tetrahedra 0-19815  
 BN powder, wurtzite sphalerite struct. phase transition, effect on substruct. 0-25690  
 BN wurtzite-sphalerite phase transition, stacking fault role 0-6418  
 BaTiO<sub>3</sub>, surface microrelief revealed by ion irradiation 0-54485  
 BaTiO<sub>3</sub>-Hf, crystal field distortion by stacking faults, PAC meas. 0-11306  
 BiI<sub>3</sub>, layered compound, exciton spectra, surface and stacking fault effects 0-40134  
 CaBSi<sub>2</sub>O<sub>6</sub>, B=Mg, Fe<sup>3+</sup>, Al, pyroxenes, order-disorder interpretation 0-38987  
 CdS-CdTe double layers on various GaAs surfaces, morphology and crystallography 0-34326  
 Ce, cold working, deform. induced struct. effects 0-25719  
 Co-Ni alloy, slip charact., and fatigue, FCC twinning and FCC to HCP martensite transform. effect 0-35182  
 Co-Ni(Ti)(Cu)(Mn), cryst. struct. and stacking fault influence on mag. props. (*Russian*) 0-25164  
 Cr, twin and stacking fault energies calc. 0-2038  
 $\beta$ -Cu-Al martensite, stacking order, disorder anal. by continuous Fourier transformation of diffracted intensities 0-39115  
 Cu-Al-Ni, long period martensite phases, X-ray diff. obs. 0-7571  
 Cu-Ge single cryst. containing heavily faulted regions, X-ray diff. profiles 0-24462  
 Cu-Zn-Sn (24-34, 1.0 wt.%), cold-worked microstruct., X-ray diff. obs. 0-3088  
 Fe, twin and stacking fault energies calc. 0-2038  
 Fe<sup>3+</sup>BSi<sub>2</sub>O<sub>6</sub>, B=Mg, Fe<sup>3+</sup>, Al, pyroxenes, order-disorder interpretation 0-38987  
 FeS<sub>2</sub>, pyrite, stacking fault model (*French*) 0-39117  
 GaP crystal, structure defect formation due to annealing and stress, dendrites, slip, dislocations 0-29026  
 GaSe, photocond., influence of stacking disorder 0-2422  
 InGaAsP, epitaxial layer, defect evaluation by cathodoluminescence 0-2866



**stacking faults continued**

- InP, damage induced during handling for TEM obs. 0-2024  
 $K_8Nb_8Si_4O_{26}$ , luminesc. bands, Stokes shift, rel. to crystal struct., stacking faults 0-34974  
 $K_8Nb_{14}Si_4O_{47}$ , luminesc. bands, Stokes shift, rel. to crystal struct., stacking faults 0-34974  
Mg-Al spinel, non-stoichiometric, climb dissociation of network dislocations 0-2031  
 $MgBSi_2O_6$ , B=Mg,  $Fe^{3+}$ , Al, pyroxenes, order-disorder interpretation 0-38987  
 $Mg(Cu_{0.535}Al_{0.465})_2$ , 2D lattice images of Friauf-Laves phase and defect type 0-24324  
Mo deformed single crystals, struct. state and dislocation splitting (*Russian*) 0-29029  
Mo, twin and stacking fault energies calc. 0-2038  
 $NaBSi_2O_6$ , B=Mg,  $Fe^{3+}$ , Al, pyroxenes, order-disorder interpretation 0-38987  
 $Nb_{0.87}V_{0.13}Se_2(4Hb)$ , stacking layer study, appl. of convergent beam electron diffraction 0-39116  
Ni, thin film, growth on Au (001) substrates (*French*) 0-44446  
NiCoPd, anodic dissolution, SFE effect (*German*) 0-25924  
 $Ni_{7/13}Fe_{7/13}O_4$ , precipitation of  $\alpha-Fe_2O_3$ , optical microscopy, SEM and TEM studies (*French*) 0-11650  
NiSe film, vac. deposited, phase transformation, electron microscope studies 0-2302  
 $PbI_2$ , layered compound, exciton spectra, surface and stacking fault effects 0-40134  
 $SbI_3$ , layered compound, exciton spectra, surface and stacking fault effects 0-40134  
Si Czochralski wafers, thermally oxidized, stacking fault distrib., O conc. depend. 0-2042  
Si, dislocation-free,  $O_2$  precip., IR and TEM obs. 0-29173  
n-Si, edge dislocation and stacking fault defect electrical recombination efficiency 0-15106  
Si epitaxial layers, development, structure and props. of stacking faults (*Russian*) 0-24461  
Si, oxidation with trichloroethylene additive to eliminate oxidation induced stacking faults 0-39118  
Si, oxidation-induced stacking faults, nucleation mechanism 0-15122  
Si, oxidation-induced stacking faults, influence of annealing ambient on shrinkage kinetics 0-29035  
Si, stacking fault energies, intrinsic and extrinsic, by TEM 0-10562  
Si, stacking fault growth, oxidation-induced, HCl and interstitial effects 0-49241  
Si, surface, stacking fault generation due to mech. damage, preoxidation annealing influence 0-54261  
Si, thermal oxidation in wet  $O_2$ /trichloroethylene mixtures at 1200°C 0-16522  
SiO wafer, annealed, surface- and inner-microdefects, TEM obs. 0-54236  
Si-SiO<sub>2</sub> interface, oxidation stacking faults, growth rel. to self-diffusion 0-49239  
Si-undoped poly Si interface, in oxidation process, defects generation 0-40571  
SiC crystals, 2H to 6H solid-state transformation, X-ray diffraction study 0-28943  
 $SrTiO_3$ , surface microrelief revealed by ion irradiation 0-54485  
 $TaSe_2(6R)$ , stacking layer study, appl. of convergent beam electron diffraction 0-39116  
Ti-S system, nonstoichiometric, containing stacking faults, X-ray diffraction intensity distrib. calc. 0-28872  
 $TiCo_{2+x}$  ( $x=-0.06, 0.0, 0.13$ ), stacking faults in cubic Laves phase 0-19816  
V, twin and stacking fault energies calc. 0-2038  
W, twin and stacking fault energies calc. 0-2038  
Zn, stacking faults, plastic deformation, due to laser beam irradiation (*Russian*) 0-15121  
ZnS, Zn(S,Se), large single crystals, vapour growth and defect characterization 0-25540  
ZnS:Mn, dopant conc. effect on stacking fault energy 0-2041

staff see personnel

**stainless steel**

see also austenitic stainless steel; martensitic steel

- adhesive energy, meas. techniques, appl. to stainless steel/ $Al_2O_3$  system 0-50803  
AGR fuel cladding, development of high strength, ductile stainless steel alloys 0-45367  
AGR steam generators, materials specifications 0-42772  
alloyed with C, magnetron-sputtered, microstruct., and cryst.-amorphous transition 0-19719  
alumina coated, types 321-SS and 430-SS,  $H_2$  permeation 0-34244  
amorphous metal-metalloid alloys production by ion implantation, TEM study 0-15128  
Auger electron appearance potential spectroscopy (*Japanese*) 0-50473  
austenitic, type 316, high velocity tensile test at elevated temp. 0-35194  
autoradiography of thin laminars, resolution improvement (*French*) 0-35438  
biaxial fatigue, initiation and growth of cracks 0-30064  
blistering on irradiation with  $He^+$  ions annealing, surface struct. damage, in type 0Kh16N15M3B (*Russian*) 0-39170  
blistering owing to  $He^+$  bombardment, 2 MeV 0-49279  
blistering under high  $He^+$  irradiation of type 0Kh16N15M3B 0-29095  
brazed joints, strength of Ni base filler metals (*Japanese*) 0-16636  
BWR coolant pipe, critical strength under stress corrosion cracking 0-52743  
carbide precipitates, and Cr carbides at grain boundaries of type 304, AES study 0-3055  
cavitation-erosion in fresh water, electron microscope and electrochem. study 0-55580  
clad Al, sandwich sheet material, forming limits 0-3131  
cladding, cracks under stainless steel cladding of pressure vessel, detection, causes, danger 0-52760  
coated with  $Cr_3C_2$  ( $Cr_7C_3$ ) based coatings, detonation deposited, wear resist., 20-1000°C 0-11843  
coated with Pd, interdiffusion at reactor wall temps., Rutherford backscattering, obs. 0-39361  
cold plastic deform. effect on struct. and props. 0-29113  
cold worked type 316, precipitation response to neutron irradiation 0-34073  
cold worked type 316, temp. effects on swelling in nucl. reactor 0-32347
- stainless steel continued
- consistent creep and rupture properties for creep-fatigue evaluation of nuclear components 0-35329  
constitution changes due to radiation effects 0-34048  
corrosion,  $H_2SO_4$  vapour corrosion, in general atomic S-I thermochem. water-splitting cycle 0-45449  
corrosion, intercrystalline, electrochemical testing method 0-55611  
corrosion fatigue and stress corrosion cracking, in boiling NaOH, for type 304 steel 0-7719  
corrosion in flowing Li 0-35399  
corrosion in seawater circulation plant, comparison with Ti (*German*) 0-25897  
corrosion of electrolytic coatings in 40% wt. KOH 0-30175  
corrosion rates in molten Li salts 0-35400  
corrosive environment effect on fatigue crack growth rate 0-55584  
corrosive reactions obs. by polarimetric Mossbauer spectroscopy 0-40594  
crack blunting, role in sustained load crack growth 0-21098  
crack resistance in chloride soln., electrochem. protection, polarization effect 0-55589  
creep and long term strength tests for type KH18N10T (*Russian*) 0-3123  
creep behavior of ribbed cladding in prototypic GCFR coolant environment 0-16480  
creep crack extension rates in type 304 steel, as function 0-3160  
creep crack propagation, J-integral application to type 304 and 316 0-35331  
creep ductility, intergranular particle size and spacing effect 0-40461  
creep ductility, signal phase influence 0-55478  
creep fracture maps, of type 316 0-30083  
crevice corrosion rate prediction, short duration test method 0-30179  
cyclic deformation behaviour under biaxial loading, AISI 316 type 0-16431  
deuteron trapping model, of gas sputtering 0-49398  
diffusion of  $H_2$ , induced tip deflection of steel beam 0-39360  
dissolution of Ti, kinetics, steel component absorpt. (*Russian*) 0-34193  
ductile fracture, in situ obs. of microprocess of failure (*Chinese*) 0-55492  
duplex type 304, strain rate effect on stress corrosion cracking, in boiling  $MgCl_2$  0-21180  
durability in  $H_2$  up to 500°C 0-30170  
EBR-II fuel pin cladding, obs. of in-reactor creep and swelling 0-13600  
emissivity, total hemispheric, temp. variation, for steel AISI 304 0-15271  
epoxide butt joints, effect of abraded and Ar ion bombarded surfaces on ultimate tensile strength 0-16638  
failure analysis at elevated temps. 0-55499  
fast reactor cladding tubes subjected to thermal transients, rupture behaviour 0-37465  
fast reactor structural material, integral expts. 0-13612  
fast reactor structural materials, energy-averaged neutron cross sections 0-13628  
fatigue, high temp. low cycle biaxial 0-30063  
fatigue crack growth behaviour in air and high-C liquid Na, carburization studies 0-40625  
fatigue crack growth data, three component model anal. 0-3161  
fatigue crack growth in A612 grade B steel, effect of temp. and R-ratio 0-3159  
fatigue crack growth rate in high temp., high purity oxygenated water 0-40622  
fatigue crack propagation, work coeff. of type SUS 304 0-16422  
fatigue crack propagation, J-integral application to type 316 0-35332  
fatigue failure kinetics, effect of water 0-55585  
FBR cladding stress distrib., effect of irradiation-induced swelling 0-19850  
FBR fuel pin cladding, in-reactor endurance and rupture life 0-13599  
FBR fuel pin cladding strain under transient testing 0-18425  
FBR fuel rod cladding damage correl. for rod perform. predictions 0-18424  
FBR materials, correl. between void swelling and thermodynamic stability 0-641  
ferrite to austenite decomposition 0-3073  
ferritic, 430 Zr, oxidation, forming and mech. props. 0-11680  
ferritic, drawability, mech. props., and grain boundaries in 08Kh16AMT and 08Kh18T1 0-35270  
ferritic, passivity in 1N HCl, X-ray photo-electron spectroscopic study 0-11817  
ferritic, swelling and radiation induced creep, fundamental mechanisms (*Italian*) 0-55457  
ferritic SUS 410 type, coated with organometallic complexes and Ti alkoxides, neutron irradiation effects on mechanical props. 0-34078  
fibre reinforced Al alloy, exam. of deformation, fracture and forging behaviour 0-11681  
fibre reinforced porous coating, isostatically compressed for bone ingrowth 0-35134  
fission reactor material, ( $n, \alpha$ ) cross sections importance for radiation damage prediction 0-13625  
fusion blanket structures, NAA 0-23145  
fusion reactor, stainless steel first wall, swelling and irradiation creep, FWLTB computer code 0-32446  
fusion reactor blanket materials for Argonne Experimental Power Reactor 0-32450  
fusion reactor first wall material, Li compatibility,  $H_2$  influence 0-23149  
fusion reactor first wall materials, compatibility with impure He 0-32469  
fusion reactor first-wall structural mats., stress and lifetime limitations 0-32447  
fusion reactor He embrittlement simulation, splat cooling in development of B doping 0-30072  
fusion reactor material, D trapping, temp. depend. 0-37577  
fusion reactor materials, performance and economics 0-32433  
galvanic corrosion, electrochem. characts. rel. to Al alloys 0-21162  
gas liberation in vac., effect of different methods of surface treatment (*Russian*) 0-45429  
gas liberation in vacuum, depend. on oxidation process (*Russian*) 0-25901  
GCFR ribbed cladding, post-irradiation creep rupture tests 0-18430  
GCFR ribbed claddings, tensile props. at 650°C 0-45364  
He cavitation, rel. to TiC precipitation 0-45399  
heat treatment, evaluating tendency for sensitization using Jominy bar test 0-16337  
high strength stainless, types 1Kh15N5AM3 and 1Kh16N4AB, phase transformations 0-20931  
hot ductility, B effect 0-30038



## stainless steel continued

in-reactor deformation and fracture behaviour of EBR-II driver fuel cladding 0-42769  
 intercrystalline corrosion, depletion theory (Czech) 0-35408  
 ion bombarded, He effects 0-29076  
 ion bombardment, depth distrib. of swelling, TEM exam. 0-15165  
 ion implantation produced crystalline phase transitions in 316 stainless steel 0-7558  
 ion irradiated with He, fracture behaviour, in-situ HV electron microscopy 0-29089  
 irradiation creep in deuteron and proton bombarded 316 steel 0-39209  
 laser fusion reactor first wall, void growth charact. 0-34042  
 liner for TFR 400, D, O, and limiter material spatial and depth implantation distrib. 0-18648  
 martensite formation, in situ obs. 0-25692  
 martensite nucleation, in situ electron microscope obs. 0-7572  
 martensite nuclei obs., role of defects in nucleation 0-25693  
 microstructure evolution in ion-irrad., He effects 0-29078  
 microwave detection of third-order nonlinearities 0-55594  
 Mossbauer effect at high press. 0-15858  
 multicomponent duplex stainless, high temp. precipitation of  $\alpha'$  0-20939  
 N toughened, electron beam welding, fusion reactor component fabrication 0-32472  
 neutron irradiated, microstruct. and mech. props. of type 1Kh18N9T (Russian) 0-24503  
 neutron irradiated, Ni ion bombard. effects of injected interstitials on void volume 0-34092  
 neutron irradiated, rel. between irradiation induced swelling and shear modulus 0-15157  
 neutron irradiated, type 316, microstruct. and tensile props. 0-34077  
 neutron irradiation effect on low cycle fatigue and tensile props. at 298K 0-30059  
 neutron irradiation embrittlement, pre-irradiation treatment and composition modification for type 316 0-3171  
 nickelless, low cycle fatigue 0-35326  
 nitriding in glow discharge in crossed electric and magnetic fields 0-16578  
 Norton-Bailey parameters, from creep rupture data from type 304 0-30098  
 oxidation, type 316 0-16606  
 oxidation resistance, effect of C, Zr, Ti and Nb 0-35394  
 passivated 304 film, inhibitive action of bound water against Cl corrosion 0-35372  
 permeation by  $^3\text{H}$  ( $^3\text{H}$ ) in fusion reactor, oxide film influence 0-34241  
 physicochemical and wear props., influence of ion implantation and overlay coatings 0-40603  
 pitting potential of single and duplex phase, test method and surface cond. effect 0-16550  
 plasma chamber material for power generating Tokamak, suitability tests 0-32449  
 polycrystalline, elastic consts., inelastic coherent neutron scatt. meas. 0-34122  
 PWR primary corrosion products 0-13578  
 radiation effects on nucl. reactor driver fuel 0-32346  
 radiation induced outgassing from type 304 steel 0-624  
 recovery by annealing of creep produced dislocations of type 316 0-11702  
 reinforced glass matrix, vibr. damping anal. rel. to internal friction 0-40413  
 ring notched samples, change in fatigue crack growth rate 0-50716  
 roughness factor measurement, energetic  $\text{D}^+$ ,  $\text{He}^+$ ,  $\text{Ar}^+$  irradiation of 304 stainless steel 0-39172  
 secondary electron emission, ion-induced for cluster ions  $\text{V}_n^+$ ,  $\text{Nb}_n^+$ , and  $\text{V}_n\text{Nb}_n^+$  0-35035  
 shear cracks, electron microscope study of single cryst. 0-40522  
 sheet deformation, criteria for determ. of deformation limit  $G$  (German) 0-21000  
 shell, spherical, with reinforced holes, local stability 0-50686  
 shock hardening, anomalous residual, at short pulse duration 0-20942  
 solar absorber-convertors, reflectance meas. of coloured stainless steel 0-7958  
 sputtering by low energy  $\text{H}^+$ , Rutherford backscattering technique 0-40198  
 sputtering yield meas. using AES 0-18654  
 stainless steel-C, surface, obs. at very low accel. voltage (200 V-1 kV) by SEM 0-10764  
 steel, maraging, heated to high temperatures,  $\gamma$  to  $\delta$  transformations 0-20930  
 steel, stainless, LMFBR fuel pin cladding long-term in-reactor corrosion by liquid Na 0-16593  
 steel, stainless AISI 316, biaxial cyclic deformation behaviour 0-21057  
 stress corrosion, high temp. electrochemical studies 0-30146  
 stress corrosion cracking, oxyanions inhibitive effect in type 304 0-35374  
 stress corrosion cracking, prestrain effect, stress relaxation study 0-35384  
 stress corrosion cracking and anodisation during straining in boiling NaOH soln. 0-30140  
 stress corrosion cracking avoidance by improved welding in BWR pipes 0-42838  
 stress corrosion cracking susceptibility, in water 0-45428  
 stress corrosion cracks initiation, in type 304 steel, in 25%  $\text{MgCl}_2$  solution at 80°C (Japanese) 0-10593  
 stress corrosion resistance, type XM19 0-16558  
 substrate, HfN activated reactive evaporated coatings, high rate deposition, microhardness 0-25580  
 surface, reduction of oxide layer by H atoms 0-40738  
 surface, rough, liq. spreading 0-39389  
 surface, SiC coatings, deposition by RF sputtering 0-25563  
 surface coated with C, damage by  $\text{D}^+$  and  $\text{He}^+$  ion irrad. 0-23146  
 surface coated with plasma-sprayed TiC,  $\text{TiB}_2$  Be and  $\text{VBe}_{12}$  coatings, fusion reactor appl. 0-18619  
 surface Cu barrier influence on C diffusion in type 1Kh18N9T steel (Russian) 0-54434  
 surface damage and mech. changes after H atom irrad. of AISI 321 0-39182  
 surface oxide characterisation by Raman spectroscopy 0-50308  
 surface treatment, X-ray photoelectron spectrosc. study 0-50764  
 surface W-Ni alloy barrier influence on C diffusion in type 1Kh18N9T steel (Russian) 0-54434  
 tensile properties of type 316 steel irradiated in simulated fusion reactor environment 0-34076

## stainless steel continued

thermal ageing effect on high temp. low cycle fatigue life (Japanese) 0-29988  
 thermal outgassing properties of type 316L, fusion reactor appl. 0-18649  
 tip, exposed to ISX and PLT plasmas, field desorption and field ion surface studies 0-34295  
 Tokamak blanket design concept 0-13815  
 Tokamak fusion reactor first walls, hydrogen profiles 0-37578  
 Tokamak limiter, plasma interaction, current profile evolution effects 0-10420  
 tubular 304 L, mech. behaviour under constant stress associated with cyclic strain 0-25767  
 Type 304, pitting corrosion in  $\text{Na}_2\text{SO}_4$  soln. (French) 0-40581  
 void swelling, Si point defect trapping, interstitial loop growth rate temp. depend. obs. 0-49270  
 void swelling obs. under HV electron microscope (Japanese) 0-54218  
 void swelling response after fast reactor irradiation 0-6437  
 wear against graphite filled rubber sliding material, water lubrication conditions 0-21123  
 wear and fatigue, improvement of props. by ion implantation 0-16601  
 weld metal, type 316,  $\text{M}_{23}\text{C}_6$  carbide precipitation, intermetallic phases, X-ray diffr. study 0-7586  
 weld metal, Type 316, transformation of  $\delta$ -ferrites, diffusion model 0-40347  
 welds, type 316, post weld heat treatments on struct., composition and ferrite amount 0-29992  
 wire, cold drawing 0-50650  
 wire for high-speed matrix printers, wear resistivity obs. (Japanese) 0-55540  
 X-ray diffraction patterns, residual stress meas., use of position sensitive proportional counter (Japanese) 0-11853  
 X-ray fluorescence anal., energy dispersive, of 300 and 400 series 0-3465  
 X-ray fluorescence anal., matrix corrections, minicomputer program 0-3458  
 B-Cr-Ni steel, neutron irradiation and  $\text{N}_2\text{O}_4$  corrosion effects (Russian) 0-52741  
 Cr (10 to 30 wt.%) ferritic, ductile-brittle transition temp. 0-30095  
 Cr (17 wt.%), hot-rolled texture, effect on cold-rolled and annealed textures 0-55425  
 Cr, ferritic, corrosion morphology, electrochem. pot. and Mo additions effect (French) 0-45439  
 Cr ferritic, meas. of alloy and impurity elemental distrib. using STEM 0-35601  
 Cr, type 403, backscatter Mossbauer spectroscopy 0-40001  
 Cr-Al (12, 6 wt.%) ferritic, high temp. treated, strengthening mechanisms 0-3106  
 Cr-ferritic, critical strain rate 0-16399  
 Cr-Mn, type 03Kh13AG19, deformation temp. influence on dislocation struct. (Russian) 0-11698  
 Cr-Mn-C-Si (20, 14, 0.2, 0 to 3 wt.%), high-temp. oxidation (Russian) 0-25904  
 Cr-Ni (18, 10 wt.%), long-term strength in H at high pressure 0-55485  
 Cr-Ni-Mo-N, phase diagrams 0-35161  
 $\text{Cr}_2\text{O}_3$ -stainless steel system under fusion reactor first wall condition, oxide dispersoid stability 0-40374  
 He ion bombard., in situ electron microscope examination 0-34094  
 Ni free acid mixture electrolyte, for polishing 0-25902  
 Ni-Cr-Mo-W (29, 13, 3, 2 wt.%), long-term strength in H at high pressure 0-55485  
 $\text{Ni}^+$ -implanted type-430 steel, struct., comp. and electrochem. anal. of surface alloy 0-16603

standard microphones see microphones

standard voltage generators see signal generators

## standardisation

B and W viewpoint of standardisation in licensing 0-23023  
 communication/control systems for motor impaired people 0-17198  
 electrical engineering dimensional unification (Italian) 0-27266  
 fibre optic connectors, update 0-5830  
 fossil fuel fired power plants, standardisation, feasibility, advantages, limitations 0-16775  
 laboratory, test results, international acceptance (Danish) 0-8952  
 measurement theory contribution to measuring process intensification (German) 0-36966  
 movie projector objective lenses, standardisation of optotechnical parameters and testing methods 0-28301  
 nuclear plant startup, benefits of standardisation 0-13686  
 nuclear power conf., Chicago, United States, July 1979 0-794  
 optical fibre standardisation of components, EIA P-6 committee 0-1352  
 optical instrument manufacture based on unitized components 0-9016  
 optical system for plasma temperature field determ., asymmetrical (Czech) 0-38704  
 powder diffraction data, American Crystallographic Association recommendations (Czech) 0-24306  
 quick calibration checks, devices to calibrate commonly used meas. instruments 0-47010  
 SI system, need for periodic recalibration of laboratory equipment 0-31705

## standards

see also CAMAC; constants; measurement standards; units (measurement)  
 acoustic noise, activities of ISO (Japanese) 0-19154  
 acoustics, International Standards organisation (Japanese) 0-14502  
 antennas safety, 10MHz to 1GHz, ANSI and EPA recommendations 0-30765  
 atmosphere standard, International and Soviet 0-26612  
 automated perimetry standards 0-46084  
 electrical engineering dimensional unification (Italian) 0-27266  
 EM fields, range 3-30 MHz, exposure, maximum permissible intensity and duration, physiological effects (German) 0-12179  
 environmental analysis reference materials, based on river sediment and urban particulate matter (SRM 1645 and SRM 1648) 0-21831  
 environmental noise pollution, new housing sites 0-48505  
 fluorescent X-ray intensifying screen, efficiency determ., standard method 0-37140  
 industrial compressor sound level meas. (German) 0-14520  
 International Commission on Radiological Protection, dose limits (1934-77) 0-12266  
 light source colour rendering, international standards (Russian) 0-43423  
 lighting equipment, classification and terminology, new Soviet standards (Russian) 0-31706



## standards continued

- mass-produced camera objectives, effects of cosmetic defects 0-47135  
 medical electrical equipment, safety problems 0-56228  
 microwave radiation exposure protection and need for field measurements 0-26377  
 nonionising radiation hazard definition problems 0-3823  
 nuclear power plant design and operation, new security regulations in United States, impact 0-796  
 nuclear power stations, nuclear materials, safeguarding experiences (*German*) 0-611  
 nuclear power stations safety, leakage tests, Spanish policies (*Spanish*) 0-5247  
 occupational noise standard, 29 CFR 1910.95, problems in enforcement 0-43528  
 radiographic phantoms for testing X-ray imaging performance 0-51229  
 RF and microwave exposure, USA occupational safety and health standards 0-3727  
 safety-system instruments for nuclear plants, impact of IEEE Std. (323-1974) 0-52753  
 solar collectors, for heating and cooling appl. 0-7915  
 substrate dielectric constants, standard specimens 0-13038  
 visual system quantitative tolerance specification and standard development 0-48384

standby power supply *see* emergency power supply

Stark broadening *see* Stark effect

## Stark effect

*see also* atomic spectra

- alkali metal atom, Rydberg state Stark struct. 0-37754  
 alkali metals, Rydberg states, Stark ionisation 0-52933  
 anthracene film, electroabsorption spectra obs. 0-50301  
 atmospheric thermal plasma, continuous emission, ionisation potential lowering and total excitation cross section 0-38705  
 atom, AC Stark effect, fluoresc., in modulated laser beams, two-photon stepwise excitation 0-42989  
 atom, bound-continuum decay, AC Stark splitting 0-5502  
 atom, resonant ionisation under adiabatic level inversion conditions (*Russian*) 0-32691  
 atomic resonance fluorescence, laser excitation time-dependent spectrum 0-37770  
 atomic spectra and radiative transitions, book 0-22159  
 atomic transition in stochastic field, saturation and Stark splitting 0-9546  
 atomic vapour quantum counter, Stark tuning 0-53242  
 Bloch electron Stark ladders via evolution operator 0-44554  
 t-butyl cyanide-HF, hydrogen bonded heterodimer, spectroscopic consts. from IR and microwave spectra 0-43039  
 crystal lattice electron energy spectrum depend. on external electric field (*Russian*) 0-34498  
 cyanomethane-HF, hydrogen bonded heterodimer, spectroscopic consts. from microwave spectrum 0-43038  
 degenerate semiconductors, electric field influence on exciton states, Stark effect 0-54617  
 diatomic molecule, Stark effect calcs., rigid rotator rotational levels in asymmetric potential well 0-5580  
 diatomic molecules, Stark effect variational and perturbational calcs. 0-1022  
 difluoromethylborane, microwave spectra and struct. obs. 0-43036  
 dimers, electronic transitions 0-9639  
 fluoromethane,  $\nu_2$  band Lamb dips, effects of RF elec. field modulation on Stark spectra 0-52989  
 fluoromethane, optically pumped laser, IR-FIR transferred Lamb dip spectra 0-1193  
 gas, Stark tunable, mirrorless optical bistability and optical limiting, obs. 0-38056  
 gas-pressure shifts of molecular lines 0-23463  
 highly excited atoms, review of recent expts. 0-23325  
 homogeneously broadened three level atoms, intense standing wave saturated, spatial inhomogeneity, mode competition 0-23646  
 homonuclear molecules, vibrs. excitation by IR radiation 0-28068  
 iodomethane- $d_3$ , Stark tuned level crossings and saturated absorpt., RF elec. field modulation effects 0-52989  
 IR laser Stark spectroscopy, RF elec. field modulation effects 0-52989  
 laser fields, stochastically fluctuating, saturation and Stark splitting of resonant transitions 0-53245  
 metallic surface, dispersion of surface plasmons 0-2440  
 methanol, optically pumped laser, IR-FIR transferred Lamb dip spectra 0-1193  
 methyldichlorosilane, Stark effect and microwave-microwave double reson., struct. (*German*) 0-47975  
 microwave spectrometer, with electric molecular modulation (*Russian*) 0-9003  
 molecular FIR laser design, freq. tunable by Stark effect 0-5750  
 molecular rotational coherence, reson. collisional exchange, time resolved microwave obs. 0-23525  
 neutral atom lines, Stark broadening, adiabatic theory, classical trajectories of electrons 0-18936  
 neutral atom reson. lines, Stark widths and shifts, regularities from He to Ca 0-47939  
 nonmonochromatic chaotic field, double optical reson. and reson. fluoresc., AC Stark splitting 0-9547  
 one-dimensional model system, Stark effects eigenvalues, Pade approximants calcs. 0-4561  
 perturbation and variation treatments, appl. to H(1s) reson. 0-14105  
 plasma, atomic absorption spectra, high freq. Stark effect 0-23359  
 plasma, H line Stark broadening, role of ion dynamics simulation 0-24144  
 plasma, laser produced, space depend. shift of spectral lines 0-6268  
 plasma, nonthermal, two-temp. electron gas, collective elec. field fluctuations estimation 0-43882  
 plasma, of theta pinch,  $N^{7.2+3+}$  lines Stark broadening, He(II) line diagnostics 0-24249  
 plasma, photon escape probabilities for Stark-broadened Lyman series lines 0-24143  
 plasma lines, electron impact width of multiply ionised ats., semiclassical formula 0-43972  
 plasma reson. lines regularities in Stark widths and shifts, He<sup>+</sup>-Ca<sup>+</sup> 0-43881  
 polyatomic molecule, multiphoton absorpt. resons., dynamic Stark splitting 0-9670  
 Stark effect continued  
 post-collisionally Stark mixed states, autoionisation electron energy and ang. distrib. 0-18829  
 rare earth ions in cubic field, anal. of absorption spectra  $4f^{N+1} \rightarrow 4f^N 5d-6s$  0-7382  
 ruby, optical free induction decay modulation and absorpt. line struct. due to superhyperfine interaction 0-33091  
 ruby, optical hole burning, Stark and pump-probe studies 0-48356  
 Schottky barrier, excitonic refl. of light 0-10885  
 semiconductor, interband absorpt. in strong parallel mag. and elec. fields 0-6799  
 semiconductor superlattice, phonon spectrum, effect of strong elec. field, parametric reson. 0-44273  
 spark discharge, electron density, determ. from Stark broadening of spectral lines (*Russian*) 0-28859  
 two photon absorption spectroscopy, motional Stark effect 0-43126  
 two-electron ions, ground state, quadratic Stark effect 0-37775  
 Zeeman degeneracy, effects on optical dynamic Stark splitting 0-37774  
 [ $^{15}$ N]NH $_3$ , modulated coherent Raman beats 0-23464  
 Al I resonance line profiles, influence of boundary layer of Al-seeded shock heated plasma 0-43876  
 Ar, Stark shift and splitting in visible spectra 0-32659  
 Ar-O $_2$  Van der Waals complex, struct. and props., RF and microwave obs. 0-32704  
 Ar.HBr(DBr), van der Waals complexes, rot. spectra and struct. 0-48055  
 BF(OH) $_2$ , identification, rot. and centrifugal consts., mol. struct., microwave spectra obs. 0-32705  
 Ba atomic beam, light-shift induced zero-field level crossing, optical Hanle effect 0-52947  
 $^{79}$ BrF, ( $^{81}$ BrF), hyperfine struct., elec. dipole moment, rot. transitions, microwave spectral obs. 0-32695  
 C, vac. UV spectral line broadening parameters meas. 0-23352  
 CO, hole burning in single quantum power spectrum due to Autler-Townes splitting 0-9671  
 Cd, 5s5d states, Stark effect (*French*) 0-9543  
 CdSe epitaxial layers, on GaP-CdS substrates, absorption and electroabsorption 0-40178  
 Cs I, three-photon 16p reson. ionis. and DC Stark effect 0-14124  
 Cs $_2$ ZnCl $_4$ :Cu $^{2+}$ , single cryst. and powdered single cryst., EPR, linear elec. field effect 0-11250  
 Ga, ground-state hyperfine struct., differential Stark effect 0-42990  
 GaP, Stark effect at H-like impurity centres, forbidden electron transitions (*Russian*) 0-16009  
 GaP:S, shallow donor states, Stark effect and inversion splitting, electroabsorption spectral obs. 0-50385  
 GdAlO $_3$ :Er $^{3+}$ ,  $^4S_{3/2}$  to  $^1I_{9/2}$  transition laser action, optical and luminescence spectra 0-16082  
 H I ( $3^1P^0 \rightarrow 2^1S$ ) line, Stark broadening parameters, modified adiabatic theory, electron scatt. phase shifts 0-43879  
 H, Rydberg levels, selective excitation by three-photon absorpt., AC Stark effect obs. 0-5518  
 H, Stark broadening by ion impact on moving emitter, Doppler H shift, theory 0-47940  
 H, Stark effect, dispersion relation, asymptotic formulae, ionis. rate, perturbation theory calc. 0-14106  
 H, Stark effect resons., strongly asymptotic approximants 0-52931  
 H, Stark-induced quantum beats in H $_2$  0-9757  
 H-like atoms, Stark effect and perturbation approxs. 0-52932  
 H-like ions in laser-produced plasma, Balmer fine struct. (broadening) 0-48860  
 HCN...HF, hydrogen bonded heterodimer, spectroscopic consts. from microwave spectrum 0-43037  
 HNO $_2$ , trans and cis,  $\nu_2$  fundamental vibrational bands, intracavity CO laser Stark spectroscopy 0-47992  
 Ha(Da) plasma red shift meas. in Ar arc, ion dynamic depend. 0-10364  
 He I line profiles, ion motion effect in low electron density plasma 0-43877  
 He I plasma lines, Stark broadening, quantum mechanical calcs. 0-43880  
 He, Stark effect, high-freq., mol. lines effects on meas. 0-9544  
 $^3$ He liquid, electron spectra of localised electrons above surface (*Russian*) 0-29241  
 $^4$ He II, widths of Stark components calc., beam-foil data comparison (*French*) 0-9545  
 LaCl $_2$ :U $^{3+}$ ( $5f^3$ ), polarised absorption spectra and energy levels 0-16063  
 LaCl $_3$ (Br $_3$ ):Pr $^{3+}$ , IR absorption, energy values for Stark manifolds 0-34955  
 LuAlO $_3$ :Er $^{3+}$ ,  $^4S_{3/2}$  to  $^1I_{9/2}$  transition laser action, optical and luminescence spectra 0-16082  
 N I plasma jet, spectroscopic diagnostics, Stark broadening and shift, study 0-38727  
 NH $_3$  inverse level doubling mol., space and combined parity nonconservation (*Russian*) 0-52879  
 $^{14}$ NH $_3$ ,  $^{15}$ NH $_3$  and  $^{14}$ NH $_2$ D, IR laser Stark spectroscopy 0-47978  
 NHD radical, dipole moment determ., optical Stark spectroscopy 0-23455  
 NH $_2$ D, dipole moments effects of RF elec. field modulation on IR stark spectroscopy 0-52989  
 Na gas, polarisation spectroscopy and forward scatt. 0-52336  
 Na, laser temporal coherence effects in two-photon resonant three-photon ionisation 0-32686  
 Na, Stark shifts, absolute and differential, coherent optical transient meas. 0-37773  
 Na, three-photon ionisation, laser bandwidth and intensity effects 0-52956  
 Nd(BO $_3$ ) $_3$ , single cryst., IR absorpt. spectra 0-34903  
 PH $_3$ , dipole moment in ground and excited states, submm. spectrum obs. 0-28056  
 POCl $_3$ -SnCl $_4$ (ZrCl $_4$ )(TiCl $_4$ ), splitting of Sm $^{3+}$  near IR absorpt. bands 0-2750  
 POF $_3$ , level anticrossing effects, vibr., laser Stark spectra obs. 0-32771  
 Pb I and II, transition probabilities, Stark broadening parameters 0-23367  
 Pr(BO $_3$ ) $_3$ , single cryst., IR absorpt. spectra 0-34903  
 Rb, photoionis. cross section, elec. field depend. 0-37796  
 Rb, Stark shift of  $6^2P_{1/2}$  to  $5^2S_{1/2}$  line, mag. scanning meas. 0-27977  
 Sm(BO $_3$ ) $_3$ , single cryst., IR absorpt. spectra 0-34903  
 SrF $_2$ :Tb $^{3+}$ , mag., thermal and hyperfine props. 0-29368  
 Xe, s-p transitions, Stark consts. and oscill. strengths, shock tube meas. 0-18822



## Star-Object continued

YA-O<sub>2</sub>;Er<sup>3+</sup>, pulsed laser action,  $^4S_{3/2}$  to  $^4I_{9/2}$  transition laser action, optical and luminescence spectra 0-16082  
 YAIO<sub>3</sub>;Yb<sup>3+</sup>, absorption and luminescence spectra, electron-phonon resonances, Stark splitting (*Russian*) 0-20674

## stars

see also stellar .....  
 see also dwarf stars; giant stars; magnetic stars; multiple stars; neutron stars; novae; Sun; variable stars  
 OB-type stars, O VI obs. in stellar winds 0-8630  
 2A 0526-328 optical counterpart, identification and spectrum 0-22118  
 AF-type stars in solar vicinity, photometric survey rel. to low mass interstellar clouds catalogue 0-36512  
 AGK3+19°599, occultation by 65 Cybele, 1979 October 17, obs. 0-31237  
 AGK3 +0°1022, occultation by Juno, obs. 0-26773  
 AGK3 stars, proper motion system in polar region (*Russian*) 0-12647  
 $\sigma$  Andromedae, rapid spectral line variability disproved 0-8625  
 B-type, H $\beta$  indices for model atms. 0-31292  
 B-type stars, luminosity and effective temp. determ. 0-17582  
 B-type stars, pole-on, rapidly rot., spectral inconsistencies due to gravity darkening 0-17581  
 B-type stars embedded in R-associations, free-free emission obs. 0-26851  
 Be and Bn stars, 206-287 nm UV spectra 0-51776  
 Be stars, electron scatt. effects on Balmer emission lines 0-17589  
 Be stars, emission line profiles from envelopes, elliptical gaseous ring model 0-4373  
 Be stars, emission line profiles from envelopes, theoretical profiles 0-4374  
 Be stars, emission shell diameter meas. possibility by lunar occultation method 0-56839  
 Be stars, photometric behaviour, UV excess, emission indices, galactic distrib. 0-36637  
 Beals' Type III P Cygni line profiles 0-51771  
 Becklin-Neugebauer source in Orion, 3.3 to 5.5 microns spectrum 0-12796  
 blue stragglers as long-lived stars 0-46542  
 bright northern stars with interesting Stromgren indices, spectral classifications 0-56817  
 5C3 sources, optical ident., spectroscopic results 0-46689  
 C- and M-type stars near globular cluster NGC 419 in SMC, cluster membership 0-26921  
 $\alpha$  Canis Majoris (Sirius), Ca II K line high resolution profile obs. 0-56830  
 Carina spiral feature, distrib. of stars and interstellar dust along inner side 0-51871  
 catalogue coord. system orientation errors, effect on planetary ephemerides (*Russian*) 0-51640  
 central stars of planetary nebulae, kinematics 0-51762  
 central stars of planetary nebulae, UV spectral obs. from TD-1 satellite 0-31300  
 Cepheus OB2 association stars, interstellar line spectra 0-22052  
 conference, stars and star systems, Uppsala, Sweden (1978 August 7 to 12) 0-51959  
 cool stars outer atmospheres, Mg II flux profiles and chromospheric radiative loss rates 0-36611  
 CPD-26°389, central star of NGC 1360, radial vel. obs. 0-4350  
 differentially rotating gaseous polytropes, Eulerian eqns. 0-51739  
 discrimination from galaxies on astronomical plates, Bayesian approach to optimal classification 0-21920  
 distances, max. likelihood regression model 0-51745  
 distant stars distribution, evolution seen by observer falling freely into nonrotating black hole (*Polish*) 0-26897  
 30 Doradus central object (HD 38268), interstellar and nebular lines obs. 0-51839  
 early type stars, 'normal', with anomalous mid UV spectra 0-26857  
 early type stars, mid UV spectra obs. 0-21995  
 early type stars, normal, near UV line blocking depend. on spectral type and luminosity 0-36619  
 early-type, northern intermediate galactic latit., H $\beta$  photometry, rel. to galactic struct. 0-36631  
 early-type star in W49A, mass loss phase from H $\alpha$  radio recomb. line obs. 0-26998  
 early-type stars, Copernicus UB obs. of He I lines 0-41825  
 faint early-type stars in neighbourhood of H II region RCW 38, UVB photometry 0-4352  
 emission-line stars in NGC 4755, southern open cluster, Balmer line photoelectric photometry 0-56892  
 F0 to M2-type stars, Ca II H and K lines absolute flux profiles rel. to model chromospheres 0-26842  
 faint blue stars in high galactic latits., search of PSS fields near South Galactic Pole 0-46415  
 faint proper-motion stars, spectra and photometry to very low luminosity degenerates deficiency 0-17575  
 faint stars, spectral-type standards for objective prism plates 0-46539  
 faint UVRI standard stars, photometric obs. 0-51813  
 FK4 supplementary stars, right ascensions obs., definitive results 0-17473  
 G133.982+1.14 (BS4), far IR source in W3, near IR obs. and identification as massive pre main sequence star 0-22058  
 galactic centre, star density rel. to nature of IR source IRS 16 0-46671  
 galactic distribution, rel. to integrated starlight synthetic spectrum between 3000 and 10000 Å 0-46536  
 galactic distribution, statistics rel. to gamma-ray burst sources distrib. 0-22117  
 globular cluster horizontal branch stars, effects of forced mixing on evolution 0-56818  
 gravitational radiation from collapsing relativistic star with rotation 0-56816  
 H-H 7 and 11, spectrophotometry of very low-excitation objects 0-46549  
 HD 15570, Of/WN7 spectral classification problem 0-51786  
 HD 192163, 191765, Wolf-Rayet stars, optical interstellar spectra obs. 0-17640  
 HD 192273, high latitude EUV source, low-mass binary 0-4353  
 HD 193077, probable single WN 5 star with absorption lines 0-56834  
 HD 200775/NGC 7023 complex, star intrinsic and interstellar reddening 0-51832  
 HD 37903, far IR study of nearby refl. nebula (NGC 2023) 0-51831  
 HD 38268, in 30 Doradus, unique interstellar Ca II K-line profile obs. 0-51850  
 HD 50896 (WN5), variable emission-line spectrum obs. 0-51791

## stars continued

HD 51480, shell star, spectroscopic obs., atmospheric struct. and distance 0-31305  
 Herbig-Haro object 1 exciting star, identification as T Tauri star 0-17633  
 Herbig-Haro object 24, emission/reflection nature 0-41829  
 Herbig-Haro objects, radio obs. and nearby compact H II regions 0-51756  
 Herbig-Haro objects, stellar wind dynamics 0-56822  
 Herbig-Haro objects in molecular clouds, mol. obs. and physical props. 0-36689  
 high mass stars, evolution including stellar wind effects 0-21982  
 high-velocity stars, southern, radial vels. 0-21988  
 high-velocity stars, southern, UVB colours 0-21989  
 horizontal branch stars and RR Lyrae variables in globular cluster NGC 6121 (M4), UVB photometry 0-22018  
 interstellar linear polarisation, wavelength depend. at near IR wavelengths 0-51833  
 luminous stars in symmetric nebulae, IUE low-dispersion spectra 0-46560  
 $\alpha$  Lyrae (Vega), spectral anal. from Copernicus 0-26856  
 metal-poor late-type stars, MK spectral classification 0-4340  
 metal-poor stars, O abundances from O I IR triplet 0-36610  
 Michigan 239, peculiar extragalactic or extreme halo emission-line star, obs. 0-4380  
 MWC 349, IR source optical identification with reddened high-luminosity star 0-56971  
 nearby low galactic latitude stars, linear polarization meas. 0-46641  
 nearby star data published 1969-1978, catalogue 0-36513  
 nearby stars brighter than tenth mag. 0-56825  
 northern FK4 stars, radial vel. meas. 0-26848  
 O-type stars in giant H II regions IC 1805, 1848, evidence from radio obs. 0-36695  
 O-type stars in open cluster IC 1805, C IV UV reson. line P Cygni profiles 0-31296  
 OB-type stars, effective temps., ang. diameters, distances and linear radii 0-17584  
 OB-type stars, form. in stellar system rel. to mass loss and dynamical evolution 0-51815  
 OB-type stars, radial vels. rel. to force field normal to galactic plane 0-46669  
 OB-type stars in SA 98, UVB photoelectric meas. 0-46535  
 occultations by asteroids, satellites discovery 0-4286  
 $\zeta$  Ophiuchi, spectral vars. related to rot. 0-22000  
 $\zeta$  Ophiuchi direction, RF mol. emission spectra obs. 0-26958  
 pairs of stars latit. obs. anal., mean pole position calc. 0-21892  
 parallax stars with MK spectral classifications 0-56721  
 $\theta$  Pegasi, rapid spectral line variability disproved 0-8625  
 $\gamma$  Persei cluster, stellar membership determ. by proper motion meas. 0-56890  
 planet detection by astrometry, photoelectric equipment 0-56882  
 planetary nebulae, low excitation, central stars, continuous energy distrib. and temps. 0-17646  
 planetary nebulae central stars, evolutionary tracks rel. to nebulae radio flux density distrib. 0-56913  
 pre-main-sequence stars, early evolution with D burning 0-51736  
 pre-main-sequence stars in NGC 2264, metallicity and circumstellar dust shells 0-26916  
 protostar, rotating, fragmentation, comparison of two three-dimensional computer codes 0-26850  
 protostars, disc accretion in soft potential well 0-8532  
 protostars, hydrostatic models evolution rel. to star form. process simulation (*Polish*) 0-21998  
 protostars, IR polarisation rel. to nearby interstellar polarisation 0-4347  
 QSO candidates, spectroscopic obs., identifications 0-31385  
 quark stars, neutrino cooling 0-56858  
 quark stars, possible existence, 2nd order perturbation theory 0-26889  
 red and nebulous objects in dark clouds, survey, catalogue of 150 objects 0-56904  
 S106 IR, S235 B, obscured IR point sources, spectra rel. to circumstellar compact H II regions model 0-12795  
 S-type, revised spectral classification system in red 0-46541  
 SA 133 field near galactic centre, three-colour stellar photometry (*German*) 0-36618  
 Santiago astrolabe observations from 1972 to 1976, results 0-46363  
 SAO 120836, occultation by Pallas, 1973 February 6, reliability of obs. 0-46460  
 SAO 158687, occultation by Uranus, obs. rel. to Uranian upper atmosphere struct. 0-17547  
 SAO 158687, occultation by Uranus rel. to planet upper atmosphere mean temp. and temp. vars. 0-46477  
 SAO 80950, occultation by 9 Metis, Guianan obs. 0-31236  
 SAO 92603, occultation by 13 Egeria, photoelectric obs. rel. to minor planet possible satellite 0-46460  
 shell stars, 206-287 nm UV spectra 0-51776  
 single main sequence stars (A0 V to G2 V), radii compared with radii determined using binary systems 0-51758  
 southern metal-poor stars, UVRI photometry and UV excesses 0-56828  
 southern peculiar emission-line stars, observational data rel. to mass ejection 0-41843  
 southern standard stars, monochromatic flux from 3200 Å to 8800 Å 0-51742  
 in spiral galaxies nuclei, stellar population 0-56926  
 SS 433, evidence for association with supernova remnant (W50) 0-51851  
 SS 433, radio and optical positions coincidence 0-56840  
 standard stars for Washington Photometric System 0-31213  
 Stromgren four colour indices, grid for calc. of log g and effective temp. 0-36507  
 super-metal-rich stars, boundary cooling and supermetallicity 0-56821  
 supernovae stellar remnants, spectroscopic search 0-26890  
 T Tauri stars, props. of assoc. ionized regions 0-36624  
 tidally distorted configurations, external form and potential, third-order approx. 0-41714  
 time service, data acquisition and real time processing system (*Italian*) 0-8549  
 Tokyo Astronomical Obs., Time and Latitude Bulletins (Jan-Mch. 1978) 0-17476  
 Tokyo Astronomical Obs., Time and Latitude Bulletins (July-Sept. 1978) 0-4239  
 UVB photoelectric sequences, in fields of eight low-red shift quasars (*French*) 0-51904



- stars continued**  
 UV survey of high-latitude regions, balloon-borne obs. 0-41891  
 Wolf-Rayet stars, ANS UV spectrophotometric obs. 0-22023  
 Wolf-Rayet stars in galactic-centre field, new discoveries from spectroscopic obs. 0-8674  
 Wolf-Rayet stars in LMC, new discoveries, positions, spectra and magnitudes 0-46569  
 young stars, high-freq. radio continuum obs. 0-51766
- starters** *see starting*
- starting**  
*see also actuators; ignition*  
 BWR, Brunswick Unit No.1, startup test experience 0-9353  
 BWR, startup control rod programming code system 0-13688  
 BWR, TVO 1, startup principles 0-9372  
 BWR, Wm. H. Zimmer nuclear power station, startup and testing 0-9373  
 FFTF startup, instrument calibration program 0-9337  
 fission reactor boron thermal regeneration system, operating experience 0-13683  
 fission reactor Crystal River Unit 3, startup experience 0-13684  
 HTGR, 330 MWe nuclear power station, start-up and operating experience since 1975 0-830  
 LWBR, startup and initial operating experience 0-13682  
 nuclear plant startup, benefits of standardisation 0-13686  
 nuclear power plant, startup planning 0-9371  
 nuclear power plant startup scheduling 0-13687  
 PWR, Salem Unit No.1, startup and operating experience 0-13685  
 PWR, startup, secondary-side corrosion product transport 0-9377  
 PWR transient anal. methods, qualification with plant startup meas. 0-18508
- startup** *see starting*
- state estimation**  
 human motion and force sensory mechanism model 0-8094  
 nuclear reactor, digital control using linear quadratic Gaussian regulator 0-37554
- state of the art studies** *see reviews*
- static (atmospheric)** *see atmospheric*
- static electricity** *see electrostatics*
- static electrification**  
*see also triboelectricity*  
 ACS blender and chlorine containing polymers, electrostatic property 0-54764  
 ESCA, insulator charging, line energy corrections 0-50898  
 insulating film moving over grounded metal rollers, electrostatic behaviour 0-49873  
 insulators, role of surface ions in contact electrification 0-54762  
 metal-insulator contact, electron tunnelling and its role in contact electrification 0-2453  
 polarisation charge build-up on air/dielectric separation surfaces 0-25288  
 polyethylene: octadecanol, contact charging and donor impurity conc. relationship 0-20286  
 polyethylene-metal contact charging, electron transfer mechanism, PES characts. 0-35055  
 PVC, rubbed, TSC meas. 0-55017  
 semiconductors and insulators in contact with metals, charging of bulk states 0-54781
- statics**  
*see also hydrostatics*  
 No entries
- stations, power** *see power stations*
- stations, radar** *see radar stations*
- statistical analysis**  
*see also measurement errors; probability; random processes; statistical theory of nuclear reactions and scattering*  
 acoustic attenuation coefficient slope for liver tissue, statistical estimation from refl. US signals 0-46000  
 adsorption, molecular-statistical description, ensemble of excess systems 0-10776  
 air pollutants, ambient, statistical models with reference to Los Angeles Catalyst Study (LACS) data 0-30620  
 asymptotic theory of statistical estimation, regularity versus nonregularity comparison 0-52003  
 atmospheric aerosol attenuation spectral struct. (Russian) 0-4104  
 atom stripping in gaseous targets, equilib. charge state distrib., statistical anal., appl. to Cl, I and Br data 0-5610  
 biomedical research, basic statistical data analysis techniques 0-42046  
 blood cell anal., weighted chi-squared test 0-30925  
 bottom settling of solid particles in turbulent shear flow, distribution statistical properties (Japanese) 0-19344  
 brittle rotating disk, probability theory appl. to rupture strength 0-43662  
 bubbly flow, void fraction meas. by light attenuation technique derivation of transmission rate reln. (Japanese) 0-48795  
 BWR, min. critical power ratio thermal limit 0-18398  
 clinopyroxenes from deep-sea basalts, statistical anal. of chemistry 0-41437  
 comets, long-period, perihelion points distrib. statistical tests 0-4304  
 community noise abatement, estimation of  $L_{eq}$  using Weibull distribution (Japanese) 0-55964  
 Cornish-Fisher expansions, generalised 0-52004  
 cosmic ray interplanetary scintillations at 250 GV, statistical props. 0-8496  
 crystallographic orientation, distribution function generalisation using rotation matrix 0-11665  
 curve fitting to data with low statistics 0-9471  
 dead time corrections in coincidence measurements by time-to-pulse-height converters or standard coincidence systems 0-9472  
 definitions, normal distrib. and signal detect. for astronomers 0-17500  
 delayed coincidence expts., precision of half life estimation 0-27908  
 diffracted amplitude and intensity, inhomogeneous and randomly distributed media (Spanish) 0-48151  
 diffusion from ground-level source in turbulent boundary layer, Lagrangian statistical anal. 0-12517  
 distribution function parameters determ. in real time, instrument description 0-202  
 double galaxies, data anal. and galaxian mass (M/L) determ. 0-4428  
 double galaxies, observational data on well-defined sample 0-17674  
 EBR-II driver fuel lifetime, cumulative damage anal. and Weibull statistical anal. 0-13601  
 EEG-like data, Gaussian amplitude distrib., new test 0-30915
- statistical analysis continued**  
 elliptical galaxies, three-dimensional figures anal. 0-36704  
 enzyme dynamics, statistical phys. 0-21439  
 equations of state, search procedure, based on step-wise least-squares technique 0-19900  
 European air temperature band-pass filtered series, correls. and phases 0-26579  
 experimental design and statistical analysis of data, measurement of period of simple pendulum 0-42017  
 expt. data analysis, normal distribution verification algorithm (Bulgarian) 0-27261  
 fatigue crack growth data, three component model anal. 0-3161  
 film absorptive laser damage analysis by Weibull distrib. 0-33061  
 fracture, extensions of a statistical approach 0-1487  
 galaxy catalogues, statistical anal. 0-46417  
 galaxy clustering, statistical test, covariance 0-56955  
 gamma-ray counting, Poisson and Brockwell-Moyal freq. distrib.,  $\chi$ -square test 0-5430  
 Gaussian integrals, evaluation by backwards recursion or Taylor expansion 0-31488  
 glow discharge cleaning effectiveness rel. to base material atomisation rate (Russian) 0-20797  
 hydrological processes, computer simulation using super-kurtic probability density function 0-26558  
 impurity absorption and emission in solids, Poisson distrib. moments 0-25419  
 internal friction, amplitude dependence data 0-3114  
 interstellar polarisation in irregularly fluctuating medium, statistical anal. 0-26926  
 irradiated tumours, dose/cure relationship 0-46052  
 Lisbon solar radiation climate, direct, diffuse and global intensities 0-36383  
 LWR, statistical techniques for core thermal hydraulic design 0-18399  
 machined surface time series modelling 0-36998  
 macromolecular system, critical branching, a statistical theory 0-3413  
 magnetic storms prediction by multivariate statistical anal. (Chinese) 0-12614  
 maximum entropy method confidence limits 0-22284  
 meas. fundamentals of mean values and standard deviations, of stochastic processes (German) 0-13031  
 measurement results evaluation, aberrant values elimination (Rumanian) 0-47008  
 mechanical experimental data, statistical treatment techniques 0-53644  
 metal powders, particle profiles, morphological characts. derived from Walsh coeffs. 0-50816  
 metastable state relaxation, critical point region nucleation in thermodynamic systems (Russian) 0-13026  
 Mira variables, statistical anal. of galactic concentration (German) 0-4390  
 mixed crystals, 1D and 2D, ion distrib. statistics 0-49167  
 mixing of multicomponent solids, mixing index and contact number estimation by spot sampling 0-16214  
 monochromatic speckle patterns, statistical props. 0-53215  
 Monte Capellino, ice formation, meteorological conditions statistical analysis (Italian) 0-12471  
 motor units characts. determ. from low freq. EMG power spectra 0-3626  
 neural multiunit signals, educable waveform recognition system for sorting unit discharges 0-51312  
 neuronal activity model, Ornstein-Uhlenbeck process 0-51030  
 neuronal waveforms, optimal recognition 0-56003  
 noise reduction, acoustic paths between two rooms connected by ventilation duct 0-10074  
 North Sea, wave height statistics using hindcast wave data 0-17273  
 nozzle fluid concentrations, probability density functions in free-diffusion flames, laser-light technique 0-10235  
 nuclear gauge, with digital response, statistical method for stability testing (Rumanian) 0-9459  
 nuclear power, probabilistic risk assessment techniques in Japan 0-18515  
 nuclear power station forced outages, statistical data anal. 0-13776  
 nuclear power station security, sabotage and terrorist attack, statistical anal. of threat reality and consequences 0-13727  
 nuclear reactor, core thermal performance assessment, acceptance of statistical techniques 0-18394  
 nuclear reactors, statistical aspects of uncertainty anal. 0-18395  
 ocean small-scale turbulence, horizontal struct. statistical characts. (Russian) 0-4020  
 optical image quality enhancement, adaptive methods (Russian) 0-28163  
 paper sheet, elastic props., inhomogeneity with reference to basis wt. depend. of elastic moduli (Japanese) 0-2110  
 particle population statistical inference from scattered light 0-37950  
 plasmatron channel, spatial-temporal pulsations of arc plasma pinch 0-24210  
 polynomials, smoothing, averaging method 0-31  
 power plants, operational danger levels, mathematical model determ. (German) 0-13633  
 primary auditory neurons, preferred intervals in spontaneous activity 0-45921  
 PWR, effects of probabilistic design methods on operating characteristics 0-18397  
 quasar red shift parameter  $\ln(1+z)$ , statistical anal. rel. to periodicity 0-17687  
 radiometeors characts. assessment, weak, w.r.t. seasonal variations (Russian) 0-56777  
 radionuclide migration from repository sites, stochastic anal. 0-37486  
 random freq. modulation wave propagation in dispersive medium, statistical props. 0-32889  
 random processes, statistics of, use of stochastic occupation densities and local times (French) 0-46972  
 reduced model theory, hydrodynamical approach for vel. autocorrelation functions 0-27135  
 reliability in metrology (Russian) 0-22317  
 repetitive firing mechanism excitation parameters, nerve impulse trains statistical evaluation 0-40986  
 road traffic noise, prediction of time pattern of fluctuating sound levels (Japanese) 0-55965  
 roughness profile description, separation of random and periodic components 0-36997  
 rubbers, swollen, low-freq. dynamics, optical and mech. props. 0-43626  
 sampling theorems in polar coordinates 0-28169  
 semiclassical fluid, with square-well plus hard core potential, equilib. props. 0-10479



**statistical analysis continued**

- shadow optical method for turbulent flow microstruct. investig., stat. analysis problems 0-19534  
 signal detection characteristics, evolution of influence of destabilising factors 0-9825  
 solar 146 MHz C-type bursts correl. with mag. storms (*Chinese*) 0-4321  
 solar granulation morphology and granule spatial distrib. 0-26830  
 solar insolation, daily irradi., ARIMA modelling with constant and seasonal parameters 0-55821  
 solar microwave burst spectra, source inhomogeneities 0-41805  
 solar noise storms and radio bursts during cycle 20, statistical anal. 0-56794  
 solar radiation data, statistical correl. between daily and monthly averages 0-8409  
 solar soft X-ray bursts 0-26839  
 speckle pattern intensity and phase, second-order conditional statistics 0-37951  
 spoken Estonian, statistical data (*Russian*) 0-45923  
 steel, low C, increased damping capacity, mathematical planning method (*Russian*) 0-45332  
 sunspot size and facular areas per solar cycle 0-41796  
 tectonic fracture system, statistical anal. (*Chinese*) 0-41417  
 toughness data, fitting curves 0-40511  
 turbulence, non Gaussian variation models, 1-D distributions 0-6032  
 turbulence, two-dimens., ergodic behaviour 0-28494  
 Visible and Infrared Radiometer evaluation from SeaSat-A surface temp. obs. 0-46325  
 wave field statistical moments in medium with large-scale inhomogeneities 0-37953  
 weather-solar activity relationships, possible mechanisms 0-17341  
 Weibull wind speed distrib. parameters, estimation using Weibull prob. paper and percentile estimators 0-50931  
 X-ray spectrometry, data interpretation, online system using multivariate statistical anal. and pattern recognition 0-3461  
 CO<sub>2</sub> gas flow impinging on heating surface, heat transfer radiation 0-43710  
 Pu in waste, anal. of enhanced variance and twin gate methods 0-5454  
 UO<sub>2</sub> reactor material, contact conductivity between core and cladding, statistical processing of experimental data 0-5238

**statistical distributions** *see statistical analysis; statistics***statistical mechanics**

- see also classical theories of fluid structure; lattice theory and statistics; Liouville equation; liquid theory; master equation; quantum statistical mechanics; renormalisation*  
 adsorption, gas on solid substrate, Van der Waals model 0-29271  
 alkali halides, molten, statistical mechanics 0-19683  
 anisotropic paramagnet, statistical mechanics using second order Green's function theory 0-25074  
 Brownian motion, generalised Einstein theory for nonequilibrium fluctuations 0-31672  
 Brusselator, dynamic correl. functions, Mori-Zwanzig formalism 0-25988  
 chemical reaction statistical models 0-27208  
 classical hard sphere system, statistical theory of freezing 0-33868  
 cluster operator bound states 0-8899  
 coherence and randomness in quantum theory, uncertainty relations 0-22231  
 colloidal soln. phase transitions 0-40749  
 constraints, flexible vs. rigid 0-31658  
 Coulomb systems, statistical mechanics, review 0-52119  
 covariance operators, reflection positivity using Dirichlet or Neumann boundary data 0-131  
 critical exponents in three dimensions, derivation from  $\phi^4$  field theory with Gaussian propagator 0-4686  
 crystal thermodynamics in statistical theory, density Fourier coeffs., stress tensor, internal energy 0-13025  
 crystal-liquid phase boundary, pair distrib. functions and free energy functionals 0-24734  
 dense Lennard-Jones fluids, solvent struct. and solvation forces between rigid particles 0-30287  
 deterministic mechanical systems, statistical concepts 0-22271  
 disequilibrium theory applied to two-spin Glauber model 0-31669  
 disordered multicomponent solid solutions conc. fluctuation waves, microscopic theory 0-44327  
 dissipative operators for infinite classical systems and equilibrium 0-12982  
 double quadratic chain, statistical mech., nonreflectionless solitary wave 0-22518  
 dynamical fluctuation theory basic eqn. physical anal. 0-36946  
 Einstein's nonrelativistic work (*Czech*) 0-27095  
 elastic phase transitions, crit. dynamics 0-2146  
 electrolyte solutions, thermodynamics, transport props., semi-phenomenological approach including short range forces 0-3353  
 electron scattering by Coulomb potential in Born approx., bremsstrahlung statistics 0-5665  
 ergodicity, classical, quantum mech. implications 0-8898  
 ferromagnetic Heisenberg chains with easy plane, validity of classical statistical mechanics 0-44786  
 fluid, hard dumbbell mols., reference pot., perturbation theories, spherical reference systems 0-28898  
 fluid struct., variational optimization of truncated approximations 0-44097  
 fluids, semiclassical statistical mechanics, mean field effective pair pot. 0-54087  
 Fokker-Planck equation, manifolds of equivalent path integral solns. 0-4687  
 generating functionals in nonequilibrium statistical mechanics (*German*) 0-12981  
 Gibbs (1839-1903), biography (*Czech*) 0-22180  
 Gibbs ensembles equivalence, phase transitions 0-134  
 Gibbs random fields described by generating functional method 0-31698  
 Gibbs states, classical approximations 0-132  
 Goldstone theorem in classical statistical mech., correl. function non-vanishing boundary terms as phase transition origin 0-27253  
 hard sphere fluid, locally inhomogeneous, Percus-Yevick eqn. soln. 0-10474  
 hard sphere-spherocylinder equimolecular mixture, Monte Carlo simulation of fluids 0-44088  
 heat transfer in linear harmonic chain, nonequilib. steady states, information theoretic approach 0-19214

**statistical mechanics continued**

- helical wormlike chain, dipole moment, elec. birefringence, elec. dichroism, statistical mech. calcs. 0-14262  
 heterogeneous solid media, statistical continuum theory, information theory approach, static field theory 0-22198  
 infinite harmonic crystal, dynamics and ergodicity 0-10598  
 inversion problems, information theoretical approach 0-27210  
 ionised mixture, dense, binary, dynamical props., statistical mechs. 0-43895  
 lattice gauge theory and spin systems, review 0-22528  
 LF current fluctuations in stationary states (*Japanese*) 0-15658  
 liquid metal, bulk modulus, calc. using press. fluctuation in microcanonical ensemble 0-2106  
 liquid-vapour interface, surface tension-compressibility relation 0-44397  
 locally perturbed 1-D system of elastic spheres 0-4631  
 martingales, set function processes, vector lattices, Riesz decomposition and characts. (*French*) 0-8908  
 Maxwell-Boltzmann statistical distrib. function of ideal gaseous assembly 0-17858  
 metals, zero-temperature equation of state, statistical model with density gradient correction 0-15215  
 microcanonically distributed plasma, reduced distrib. functions 0-28604  
 molecular dynamics method in statistical physics, review 0-18895  
 molecular liquids and liq. crystals, theory of irreversible processes 0-54125  
 molten salt, possibility of plasmon mode obs., struct. dynamics 0-10477  
 monolayer, anomalous thermal effects, statistical mechanics 0-15367  
 Monte Carlo methods, quantum mechanical corrections to classical equilibrium statistical-mechanical results 0-135  
 N-particles connected by exponential springs, solns. by inverse method 0-46955  
 nematic solution, hard rigid/flexible mols. mixture, unathermal, lattice model (*Russian*) 0-54129  
 Newtonian system statistical mechanics, Lie-admissible struct. 0-42136  
 non-spherical molecule ensemble, background correl. in statistical thermodynamic calcs. 0-36958  
 nonequilibrium statistical mechanics, review 0-12983  
 nonlinear evolution eqns., soliton solns. 0-12919  
 one component plasma, dynamical struct. factor, collective modes 0-28607  
 one-component plasma, internal energy, mean spherical approx., asymptotic form 0-1742  
 one-dimensional complex scalar fields with phase anisotropy, statistical mech. 0-22517  
 Onsager-Machlup Lagrangian in theory of stationary diffusion processes 0-128  
 open system, new classical Hamiltonian-Lagrange mechanics 0-36900  
 oscillator, linear, excitation by stationary random force (*Russian*) 0-27116  
 oscillators, coupled, stochasticity thresholds 0-46977  
 parametric amplifier, damping theory anal. 0-52118  
 particle motion through matter, fluctuations in cascade processes 0-5456  
 percolation concept (*Czech*) 0-127  
 Percus-Yevick eqn., existence and local uniqueness of solutions 0-36936  
 Percus-Yevick eqn., orthonormal series expansion soln. 0-49065  
 phase space and Liouville theorem of classical statistics, relativistic analog 0-27184  
 phenomenological thermodynamics to canonical ensemble 0-22269  
 physical growth laws, equations for the growth of a distribution of small physical objects 0-4630  
 plasma, one-component, virial pressure 0-38536  
 polar fluids in elec. fields, statistical mechanics 0-54085  
 polymer linear chains, excluded vol. problem 0-5650  
 potential fields, nonstationary, nonlinear distrib. function, hydrodynamic eqns. (*Russian*) 0-52033  
 probability derivation in statistical mechanics, distribution function coarsening evolution 0-36937  
 probability foundations, modal frequency interpretation 0-12885  
 projective limits 0-27209  
 pseudo-first-order phase transitions in one dimension 0-22270  
 radiation problems transport eqns., using Wigner distribution 0-168  
 relaxation process as contraction of Markovian type multidimensional one 0-31671  
 response theory for systems nonlinearly displaced from equilibrium, graphical approach 0-22285  
 semiconductor, hot electron fluctuations with displaced Maxwellian distrib. 0-29418  
 simple classical, liquids, Bogolyubov method, equilibrium system many body correlation function contracted description (*Russian*) 0-38888  
 simple fluid, one-component, liquid-vapour phase coexistence, surface tension determ. from many body pot. 0-49465  
 sine-Gordon field theory Coulomb gas equivalence, classical gas with logarithmic pot. 0-4850  
 soft rods, one-dimensional, exact partition and thermodynamic functions 0-46953  
 solitons in condensed matter physics, theory 0-50122  
 spectral entropy method for distinguishing regular and irregular motion of Hamiltonian systems 0-4629  
 stability, equilb., and metastability 0-31659  
 stationary states far from equilb., regression of fluctuations 0-42138  
 statistical equality connecting zero Fourier harmonics with average quantities 0-133  
 stellar atmosphere in statistical equilb., effects of deviations from LTE 0-31290  
 stochastic Hamiltonian classical and quantum, systems, Volta Memorial Conf. 0-8738  
 structural stability, phase transitions 0-8932  
 superionic conductors, lattice gas models, book contrib. 0-24661  
 surface tension, Fowkes' hypothesis, statistical mechanics basis 0-2249  
 surface tension and phase transition in lattice systems 0-27226  
 symmetry breaking, kinetic model 0-129  
 thermal radiation of nonlinear material, generalised Kirchhoff law, fluctuation-dissipation theorem 0-4679  
 turbulence theory, review 0-4536  
 Ursell functions and cluster estimates, representations 0-8900  
 virial theorem and scale transformations, for teaching 0-17763  
 weakly relativistic statistical mechanics, choice of measure and Liouville eqn. 0-46956  
 Al, liquid, bulk modulus, calc. using press. fluctuation in microcanonical ensemble 0-2106  
 Cr binary substitutional solutions, thermodynamics 0-54410



# statistical mechanics continued

- Fe-bearing binary, substitutional liq. and solid solns., statistical thermodynamics 0-11630
- H plasma, pair correlations down to  $r=0$  0-14883
- H<sub>2</sub>, many electron systems, chem. binding, local stresses and force densities 0-27920
- Ni-bearing substitutional binary solutions, thermodynamics 0-44336
- Zn-bearing binary substitutional solutions, thermodynamics 0-44337

# statistical methods see statistical analysis

# statistical models

- (2+1) dimensional Georgi-Glashow model, critical Higgs mass, clustering, monopoles 0-52441
- Bose-Einstein statistics, wave packet formulation of multiparticle production at high energies 0-13338
- Chao-Yang statistics, particle ratios and quarks 0-27486
- dihadron high mass continuum, phenomenological anal. of Fermilab data 0-42511
- explosive quark matter, hypothesis for Centauro event 0-22648
- hadron+hadron, high-energy, inclusive spectra of secondary pions, Feynman scaling and statistical model 0-42502
- hadron+hadron, jet production, large transverse momentum 0-42503
- hadron interactions, local thermodynamic equilibrium (Russian) 0-9155
- hadron-nucleus reactions, 20-400 GeV, multiplicity of relativistic charged particles (Russian) 0-5191
- hadronic matter, phase transition of second band, anal. in one-loop theory in renormalisable field theory 0-4930
- hadronic matter, statistical bootstrap model and critical behaviour 0-42430
- hadronic reactions, trajectory slopes in gauge-dual-topological approach, jet multiplicity 0-18142
- Hagedorn Frautschi statistical bootstrap model, modification for baryon charge and strangeness conservation (Russian) 0-27489
- Hagedorn model, topological cross sections in multiplicity asymptotics (Russian) 0-9154
- hydrodynamic theory of high energy interactions (German) 0-406
- instantons and the 1/N expansion 0-400
- jet analysis, QCD calcs. and phenomenological models 0-52523
- jet production in  $e^+e^-$  collisions to order  $\alpha^3$  and  $\alpha^4$  and including QCD corrections 0-13322
- jet quantum number identification event by event, original parton and gluon jets 0-52466
- jet-mass effects and high- $p_T$  jet production 0-52473
- lepton+hadron, deep inelastic scatt., QCD event states, 3-jet events 0-52515
- lepton+nucleon, jet structure, cascade model and jet model 0-42471
- multiperipheral production of large and small fireballs at very high energies 0-47264
- n-body decay distribution function, approx. formula 0-27488
- perturbative QCD, jets, inelastic distrib., colourless clusters, scaling, multiplicity and tree evolution 0-52459
- QCD, two jet process noncollinearity in first order perturbation theory 0-22567
- QCD Compton effects, quark and gluon jets 0-32101
- QCD jet calculus, inclusive  $p_T$  distrib. with exclusive form factors consistency 0-391
- QCD jets, Markov branching processes 0-27463
- QCD jets from coherent states 0-13266
- QCD multijet model, universal quark-jet fragmentation in soft hadronic reactions 0-13285
- quantum particles in a stochastic linear potential and the temperature of hadrons 0-32087
- quantum-chromodynamic phenomenology of gluon jets 0-4941
- quark and gluon jet longitudinal momenta, QCD anal. 0-22571
- quark and lepton masses, chiral charge space, statistical analysis 0-42428
- quark form factor and jet cross sections, high energy asymptotics 0-32112
- quark jet,  $q\bar{q}$  pair production mechanism, average transverse momenta 0-18118
- quarkonia, S- and P-wave, gluon jets, perturbative QCD anal. 0-32070
- string-junction model, hair pin line rule and baryonium decay 0-27487
- uncorrelated jet model, Bose-Einstein and Boltzmann statistics calc. for rapidity spectrum 0-4969
- urn model, modified, dims. counting rule, pp elastic scatt. appl. 0-27485
- $e^+e^-$ →hadron jet, 3 to 17 GeV, including charm threshold and upson resonances, review 0-47321
- $e^+e^-$ →hadron jets, QCD, Monte Carlo model 0-27514
- $e^+e^-$ →hadron jets, two fireball model anal., Monte Carlo method (Russian) 0-37288
- $e^+e^-$ →jets, two photon four jet anal. 0-27513
- $K^-p \rightarrow pK^0 \pi^+ \pi^-$ , 10 GeV/c, dynamical mechanism from cluster anal. (Russian) 0-42499
- NN→X, nuclear size dependence of particle prod., hydrodynamical model 0-22593
- $p\bar{p}$  annihilation, pion rescatt. effect at intermediate energies 0-5010
- $p\bar{p}$ , hadronic jets, possible intermediate bosons 0-18149
- $p\bar{p}$ , jet thrust spectrum, 3-jet structure, QCD calc. 0-47333
- $p\bar{p}$ ,  $Z^0$  high  $p_T$  bremsstrahlung, Higgs versus quark or gluon jets 0-32063
- $p\bar{p}$  interactions, cluster mass spectrum 0-37307
- $p\bar{p}$  multiple hadron prod. up to 1500 GeV, hadronic matter eqn. of state (Russian) 0-32085
- $\pi^+p \rightarrow p\pi^+\pi^+\pi^-$ , 16 GeV/c, clustering, multidimens. study using Yang variables 0-5020
- $\pi^+p \rightarrow p\pi^+\pi^+\pi^-$ , 16 GeV/c, dynamical mechanism from cluster anal. (Russian) 0-42499
- O<sub>3</sub> formation dynamics in cities 0-31112

# statistical tests see statistical analysis

# statistical theory see statistical analysis

# statistical theory of nuclear reactions and scattering

- ( $\pi,\pi$ ), inelastic scatt. in Fermi liquid, nucleon-nucleon interaction effects 0-22862
- average resonance parameter eval. and calcs., statistical model for capture process 0-18271
- bound state poles, effect on N-body scatt. amplitudes (Chinese) 0-5111
- cluster cascade model, single particle distributions and two-particle correlations 0-18300
- clustering aspects in nuclei and their microscopic description, review 0-487

# statistical theory of nuclear reactions and scattering continued

- cold nuclear matter, stationary finite amplitude motions, quantum shock waves and solitons 0-42573
- collective modes in fission and deep inelastic scatt., ang. momenta equilb. statistical treatment 0-42688
- collective tube model, multiparticle prod. off hadrons and nuclei 0-5112
- collision expts. with final state partial resolution, maximal entropy procedure and surprisal anal. 0-18279
- deep inelastic heavy ion collisions, mass and charge distrib., statistical model 0-18332
- dissipative heavy ion collisions, dynamical description in adiabatic representation, statistical theory 0-5161
- dissipative heavy ion collisions, nuclear dynamics 0-42696
- dominant partition method 0-47455
- Doppler effect calcs., resonance data set choice in unresolved resonance region, sensitivity study 0-52651
- droplet-model theory of the neutron skin 0-47416
- Ericson fluctuations in polarised (p,p) reactions (Rumanian) 0-5113
- excited nuclei, self-consistent theory of giant dipole resonance, thermodynamic RPA (Russian) 0-5106
- exciton model, preequilibrium reactions, angular distrib. 0-52652
- expanding fireball in high energy heavy ion reactions, pion radiation 0-5155
- Fermi model for high multiplicity compound nucleus decay 0-22799
- fission, isobaric widths, frozen quantal fluctuations, charge equilibration 0-37365
- fission rate analysis from point of view of Brownian motion (Chinese) 0-52657
- fission width distribution, statistical properties, effect on cross-section calcs. (Russian) 0-518
- fixed angular momentum moments and level densities, statistical spectroscopic methods 0-467
- generalised exciton model, pre-equilibrium components of the fluctuation cross section 0-18278
- giant resonances, electric monopole and dipole vibrations, TDHF equations, fluid dynamical Lagrangian 0-47447
- hadron-nucleus inelastic interactions, high energy, mean normalised multiplicity target depend. 0-47454
- Hauser-Feshbach calculation of the fission neutron spectrum 0-22801
- heavy ion collisions, composite particle formation, direct, classical thermodynamic and quantum statistical theories 0-32297
- heavy ion collisions, fluid dynamical and TDHF models, abnormal nuclear matter, density isomers 0-47502
- heavy ion energetic reactions, relativistic hydrodynamical description 0-37362
- heavy ion fusion reactions, statistical model calcs. 0-42726
- heavy ion reactions, energy depend. struct., review, book contrib. 0-27671
- heavy ion reactions, nucleon emission from localised hot zone, fireball model 0-42686
- heavy ion transfer reactions, energy disposal, information theoretic anal., surprisal approach 0-18326
- heavy ions in low energy region, expt. and theoretical range comparison 0-32257
- inelastic collisions, heavy ion-light particle angular correlations, sequential three-body reaction 0-42677
- kinetic energy distrib. of fission fragments, thermal fluctuation influence 0-22865
- leading proton spectrum at high energies in (p,X) reactions, intranuclear cascade model anal. 0-5139
- mass distribution widths in statistical theory of fission, nucleon tunnelling (Russian) 0-5121
- medium nuclei, photoproton spectra and preequilb. decay, microscopic theory 0-47464
- neutron induced fission cross sections, parameter testing (Russian) 0-52653
- nuclear fluid dynamics, extended TDHF for approach to thermal equilibrium 0-13448
- nuclear size dependence of particle prod., hydrodynamical model 0-22593
- photon backscattered ang. distrib. for oblique incidence (Rumanian) 0-47456
- pre-equilibrium decay, time dependence of soft and hard parts of particle spectrum 0-22800
- preequilibrium decay models (Rumanian) 0-47457
- prompt fission neutron spectra calc., nucl. evaporation theory 0-22870
- quantal fluctuation squeezing, Schrodinger eqn., deep inelastic reactions 0-47444
- relativistic heavy ion collisions, charge multiplicity fireball and statistical model anal. 0-537
- relativistic heavy ion collisions, charged particle emission multiplicities and ang. correlations, firestreak models 0-18328
- relativistic heavy ion collisions, viscous hydrodynamical model 0-5163
- relativistic light ion collisions, two-fireball model improvements, p and  $\pi$  spectra 0-5158
- relativistic nuclear matter, shock waves, heavy ion collision hydrodynamics 0-52602
- soft nuclear matter eqn. of state, from heavy nuclei central collision fireballs 0-13395
- spherical nuclei, giant monopole resonance transition densities, dynamical Thomas-Fermi theory 0-9278
- spontaneous fission mass parameters, cranking and hydrodynamic models, deformation depend. (Russian) 0-13511
- statistical significance of spreading widths for doorway states, comments 0-27611
- stellar interiors, thermonuclear reaction rate enhancement due to strong screening, ionic mixtures case 0-36613
- strong compression effects in high energy heavy ion reactions, nuclear fluid dynamics anal. 0-18341
- thermonuclear reaction rate data for intermediate mass nuclei 0-31427
- time delay and correlation length of cross section fluctuations 0-517
- time delay of resonance wave packets, stat. model anal. 0-22802
- two-step direct reactions through doorways, fluctuation effects 0-13445
- volume and surface vibr. relations, quantum hydrodynamics 0-9227
- Z=103, 105, 107 element prod. from heavy ion fusion, cross sections from statistical model 0-32313
- (n, $\gamma$ ), A=75 to 103,  $\gamma$ -strength functions and stat. model cross section calcs. 0-52612
- (n, $\gamma$ ), A=94-190, resonance capture, low lying level population fluctuations,  $\gamma$ -rays 0-52619
- (n, $\gamma$ ), mechanism in 3s size resonance, s-wave radiative width partition 0-37387



**statistical theory of nuclear reactions and scattering continued**

- (n, $\gamma$ ), mechanism in 3s size resonance, radiative width statistical and valence effects 0-37388  
 ( $\pi,\pi$ ), microscopic theory, review 0-47511  
<sup>107</sup>Ag(p,n), A=107,109, 2.0-6.7 MeV, cross sections, Hauser-Feshbach optical calcs. for p absorption systematics 0-47483  
<sup>107</sup>Ag(n,n), 0.25-4.5 MeV, total, elastic and inelastic cross sections, optical-statistical anal. 0-27639  
<sup>107</sup>Ag(p, $\alpha$ X), 20-45 MeV,  $\alpha$  spectra, exciton model anal. 0-18306  
<sup>21</sup>Al(<sup>3</sup>He,p) 9-14 MeV, stat. multistep compound emission, residual two-body interaction 0-47493  
<sup>243</sup>Am( $\alpha$ ,f), fragment mass distrib., and yield, statistical anal. (Russian) 0-5183  
 (Ar,  $\pi^-$ X), 800 MeV/A,  $\pi^-$  energy and ang. distrib., firebreak and hard scatt. model anal. 0-13498  
<sup>76</sup>As, level structure, transitions and J <sup>$\pi$</sup> , from <sup>76</sup>Ge(p,n $\gamma$ ) 0-47379  
 Au(<sup>16</sup>O,Kr,X), 724 MeV, deeply inelastic, <sup>4</sup>He, <sup>1</sup>H emission, fragment spin, semiempirical method 0-47366  
<sup>197</sup>Au(<sup>13</sup>C,Xe,X), damped collisions, charge distrib. second moments and giant E1 quantal fluctuations 0-27547  
 ( $\alpha,\gamma$ ), excitation function competition cusps, Mauser-Feshbach calcs. 0-13404  
<sup>209</sup>Bc(<sup>36</sup>Xe,X), statistical fluctuations in dissipative collisions, multidifferential cross sections 0-37399  
 (C,  $\pi^-$ X), 800 MeV/A,  $\pi^-$  energy and ang. distrib., firebreak and hard scatt. model anal. 0-13498  
<sup>1</sup>C(<sup>16</sup>O,X), A=12, 13 exit channel competition for some residual nucleus 0-47499  
<sup>12</sup>C(<sup>12</sup>C,p)X, 800 MeV/N, fireball and preequilibrium cross sections,  $\pi$  condensation proximity influence 0-27659  
<sup>252</sup>Cf, spontaneous fission, scission point configuration, evaluation anal. 0-37361  
 C(n,n), total cross sections below 2 MeV, R-matrix fits to data 0-13466  
<sup>58</sup>Cr(p, $\gamma$ ), 1.0-3.8 MeV,  $\gamma$ -yields, cross sections, predicted (p,n) cross section, Stat. anal. 0-5136  
<sup>64</sup>Cu levels and transitions, stat. anal. of <sup>64</sup>Ni(p,n $\gamma$ ) (Russian) 0-5104  
<sup>64</sup>Cu analogue resonance direct n decay, stat. anal. from <sup>64</sup>Ni(p,n $\gamma$ ) (Russian) 0-5104  
<sup>1</sup>Dy( $\alpha$ ,n $\gamma$ ), A=162,164, Er yrast levels, spin alignment 0-52557  
<sup>166</sup>Er(<sup>60</sup>Kr,X), statistical fluctuations in dissipative collisions, multidifferential cross sections 0-37399  
<sup>69</sup>Ga(n,n' $\gamma$ ), fast n, levels, J <sup>$\pi$</sup> , transitions and mixing ratios, statistical anal. (Russian) 0-13382  
<sup>165</sup>Ho(p, $\alpha$ X), 20-45 MeV,  $\alpha$  spectra, exciton model anal. 0-18306  
<sup>115</sup>In(p,n), 2.0-6.7 MeV, cross sections, Hauser-Feshbach optical calcs. for p absorption systematics 0-47483  
<sup>74</sup>Kr, charged particle evaporation following form. from <sup>58</sup>Ni+<sup>16</sup>O 0-47453  
<sup>24</sup>Mg high spin states from selective compound reactions, stat. anal. from <sup>10</sup>B(<sup>16</sup>O,d) 0-18180  
<sup>24</sup>Mg(p,p), 15 MeV, excitation functions, Ericson theory for fluctuations 0-22825  
<sup>27</sup>Mg energy levels, spectroscopic factors, DWBA, Hauser-Feshbach anal. from <sup>26</sup>Mg(d,p) 0-52581  
 Mo stable isotope eval., 5 keV-5 MeV neutrons, rel. to reactor structural steel 0-13620  
 Mo(n,X), 2 keV-20 MeV cross sections, coherent optical and statistical model calcs. 0-18318  
<sup>93</sup>Nb B(E $\lambda$ ) transitions, quasiparticle-phonon multiplet, nuclear field theory for superfluid nuclei 0-47427  
<sup>93</sup>Nb(p, $\alpha$ X), 20-45 MeV,  $\alpha$  spectra, exciton model anal. 0-18306  
<sup>93</sup>Nb(p,n)<sup>93</sup>Mo, direct neutron decay of analogue resonances of <sup>94</sup>Mo 0-22824  
 (Ne,  $\pi^-$ X), 800 MeV/A,  $\pi^-$  energy and ang. distrib., firebreak and hard scatt. model anal. 0-13498  
<sup>20</sup>Ne(d,d), pol. d, 10-12 MeV, cross section, coupled channel and fluctuations anal. 0-27617  
<sup>21</sup>Ne states cross section, coupled channel and fluctuations anal. from <sup>20</sup>Ne(d,p) 0-27617  
<sup>4</sup>Ni(n,n), A=58,60,62,64, 5 MeV, differential cross sections, optical, statistical and coupled channel calcs. (Russian) 0-37377  
<sup>60</sup>Ni+n, total and differential cross-sections, optical-statistical and coupled-channel models 0-13472  
<sup>23</sup>Np( $\alpha$ ,f), fragment mass distrib., and yield, statistical anal. (Russian) 0-5183  
<sup>16</sup>O levels and ang. distrib., <sup>3</sup>He spectroscopic strengths, Hauser-Feshbach/DWBA anal. of <sup>13</sup>C(<sup>6</sup>Li,t) 0-47390  
<sup>208</sup>Pb(<sup>40</sup>Ar,X), deeply inelastic collisions, form factors, microscopic calcs. 0-18339  
<sup>239</sup>Pu(n,X), nuclear reaction statistical model parameters (Russian) 0-18280  
<sup>243</sup>Pu( $\alpha$ ,f), fragment mass distrib., and yield, statistical anal. (Russian) 0-5183  
 Pu(n,f), 0-18 MeV, prompt neutron spectrum, evaporation model (Chinese) 0-42721  
<sup>28</sup>Si(<sup>12</sup>C,<sup>12</sup>C), 27.8-31.5 MeV, elastic and inelastic excitation functions, fine struct., statistical anal. 0-18269  
<sup>28</sup>Si(<sup>16</sup>O,<sup>16</sup>O), 30-32.7 MeV, elastic and inelastic excitation functions, fine struct., statistical anal. 0-18269  
<sup>28</sup>Si(p,p), pol. p, 12-18 MeV, cross section, anal. power and states, <sup>29</sup>P resonance coherence widths 0-32258  
<sup>147</sup>Sm(n,  $\alpha$ )<sup>144</sup>Nd, 12 to 18 MeV, energy and angular distribution of  $\alpha$ -particles, statistical, pre-equilibrium and knock-on models 0-13477  
<sup>152</sup>Sm(n,n), 2.4-7.2 MeV, inelastic and elastic optical model and deformation parameter depend. (Russian) 0-13481  
<sup>118</sup>Sn(p, $\alpha$ X), 20-45 MeV,  $\alpha$  spectra, exciton model anal. 0-18306  
<sup>120</sup>Sn(<sup>40</sup>Ar,X), deeply inelastic collisions, form factors, microscopic calcs. 0-18339  
<sup>4</sup>Tc, A=93-96, excitation functions and isomer ratios from <sup>93</sup>Nb( $\alpha$ ,xn) (x=1 to 4) 0-492  
<sup>46</sup>Ti(d,d), 7,10 MeV, ang. distrib., DWBA and Hauser Feshbach anal. 0-47377  
<sup>47</sup>Ti levels, DWBA and Hauser Feshbach anal., compound nucleus cross sections from <sup>46</sup>Ti(d,p) 0-47377  
<sup>4</sup>Ti, A=199, 200 cross section and excitation function statistical anal. from <sup>197</sup>Au( $\alpha$ ,xn) (Rumanian) 0-22846  
<sup>169</sup>Tm(p, $\alpha$ X), 20-45 MeV,  $\alpha$  spectra, exciton model anal. 0-18306  
 U+<sup>20</sup>Ne, quark matter, signature in nuclear fireball model 0-37395  
<sup>238</sup>U( $\alpha$ ,f), fragment mass distrib., and yield, statistical anal. (Russian) 0-5183

**statistical theory of nuclear reactions and scattering continued**

- U(n,f), 0-18 MeV, prompt neutron spectrum, evaporation model (Chinese) 0-42721  
 Y isotopes, Hauser Feshbach calcs., of neutron cross sections 0-22839  
 Zr isotopes, Hauser Feshbach calcs., of neutron cross sections 0-22839  
<sup>1</sup>Zr(p,p'), A=94,96, 11.2-13.4 MeV, anal. power and excitation function  
<sup>T</sup> fluctuations 0-42626  
**statistical thermodynamics** see *statistical mechanics*  
**statistics**  
 see also *error statistics; game theory; Monte Carlo methods; probability; queueing theory; time series*  
 cloud seeding experimental results analysis 0-8389  
 cloud seeding experiments, statistics appl. 0-8438  
 definitions, normal distrib. and signal detect. for astronomers 0-17500  
 eclipsing binary stars, period statistics rel. to form. and evolution 0-36662  
 extremum position and confidence limits, determ. of absorpt. max. in wide bands 0-22188  
 galaxies, faint, number magnitude counts 0-26976  
 K-distributed noise, statistics 0-27220  
 linear least squares parameters, stat. significance, student guide 0-17770  
 Mediterranean earthquake catastrophes, statistics 0-3955  
 multiple quadratic regressions, programmable desk calculators in the laboratory 0-42048  
 neutron counting statistics in subcritical cyclo stationary multiplying system 0-32323  
 nuclear medicine, understanding and using statistics 0-12233  
 radiation therapy, dose/cure relationships study 0-56218  
 radio sources, faint, statistical study of mean ang. size and sky density at 181.5 MHz 0-51893  
 strip rolling, kinestostatics (Russian) 0-38348  
 superposition of epochs, statistical method, anal. and appl. 0-4267  
 tennis, probability and statistics teaching illustration 0-41997  
 visual analyser space-frequency filter harmonisation with statistics of images 0-30726  
 visual response, expected waiting time 0-51091  
 weather experimentation, statistical issues 0-8439  
**stators**  
 bar insulation in stator winding of large turbogenerator, inspection using microwave defectoscope 0-35474  
**steady-state theory** see *cosmology*  
**steam**  
 critical behaviour of thermodynamic potential 0-42175  
 equation of state, between 350 and 1000°C (0 to 10 GPa) and between 100 to 350°C (200 MPa to melting curve) 0-15214  
 generator, accumulation type, using NaOH as thermal storage material (French) 0-40914  
 low and moderate density, compressibility factor and viscosity coeff. eqn. 0-33722  
 shock wave induced condensation 0-34177  
 supercooled, thermodynamic props., virial eqn. of state 0-14872  
 supercritical, compressed, proton spin-lattice, relax. time meas. 0-22403  
 superheated, AFCRL atm. absorpt. line parameters in 2900-3000 cm<sup>-1</sup> atm. window 0-36396  
 thermal conductivity equation, 0 to 800°C, triple pt. press. to 1000 bars, crit. region 0-39364  
 treatment of SiO<sub>2</sub> gel, struct. changes 0-35579  
 Zircaloy-2 claddings, oxidation reaction kinetics in steam environment in temp. range 1273-1673K 0-35401  
 H production from H<sub>2</sub>O by two-stage plasmochemical cycle 0-45772  
 H, thermochemical production by steam reforming of methane, kinetic anal. 0-35788  
 H, thermochemical production by coal gasification using steam 0-35789  
 SiO<sub>2</sub>, vaporisation in steam atmosphere 0-44306  
 ZrO<sub>2</sub>, cell electrolysis of H<sub>2</sub>O at 800° to 1000°C (French) 0-26024  
**steam boilers** see *boilers*  
**steam generators** see *boilers*  
**steam plants**  
 see also *boilers; condensers (steam plant)*  
 1300 MW cross compound turbine unit IP rotor coupling, fatigue crack due to combined corrosion and low alternating stresses, report 0-16611  
 1300 MW nuclear reactor steam isolating valve blowdown tests (German) 0-22967  
 heat pump for steam generation from industrial waste heat 0-35732  
 heat pump system for process steam generation 0-35729  
 HTGR 900-MW(e) steam cycle plant design 0-592  
 MHD combined, single-load, performance and efficiency obs. (Italian) 0-26148  
 solar steam generation system for industrial appls. 0-55825  
**steam power stations**  
 coal gasification/combined cycle power generation test facility, preview 0-16773  
 coal-fired, financial impact of air pollution control costs 0-3497  
 fossil fuel fired power plants, standardisation, feasibility, advantages, limitations 0-16775  
 KILnGAS coal conversion system for low BTU gas production, electricity generation appls. 0-16776  
 MHD/steam power generation systems, commercial viability 0-35701  
 supplementary steam generation using H<sub>2</sub>/O<sub>2</sub> combustors, a viable H power generation concept 0-30330  
 H<sub>3</sub>PO<sub>4</sub> fuel cell power plant with high temp. steam reforming and autothermal reforming 0-30466  
**steam turbines**  
 see also *turbogenerators*  
 1300 MW cross compound turbine unit IP rotor coupling, fatigue crack due to combined corrosion and low alternating stresses, report 0-16611  
 heat transfer in tubular condenser apparatus (Russian) 0-1411  
 nozzle cascades, local heat transfer, approach flow turbulence effects 0-38381  
 solar thermal power plant turbine sizing, performance and economic anal. 0-30403  
 vibration and noise review, central power station large turbomachinery 0-23835  
**steel**  
 see also *alloy steel; austenitic steel; carbon steel; stainless steel*  
 ablation and fuel-steel mixing phenomena following LMFBR accident 0-47649  
 AE use for mech. tests 0-35467  
 aluminising by circulation method, thermodynamics 0-30163



## steel continued

anisotropic sheet, strain hardening, stress state depend. 0-55421  
 austenite-martensitic, struct. changes during plastic deform., mutual influence of phases (*Russian*) 0-30015  
 austenization heat treatment effect on microstruct. and mech. prpss. 0-29993  
 bainite,  $^{57}\text{Fe}$  Mossbauer spectra 0-15051  
 ball-bearing, ESR, martensitic, size effect during rotating beam fatigue tests 0-7674  
 bearing materials, rolling, effects of high temperature operation 0-21124  
 belt grinding, struct. transformations in type 12Kh2N4A 0-30169  
 boride coatings, form. mechanism and struct. during crystn. of castings 0-35412  
 boride coatings, under elec. heating conditions, hydroabrasion wear resist. 0-55543  
 boride coatings on steel effect of Cu impurities in reaction mixture on brittleness, acoustic emission meas. 0-16581  
 boriding with  $\text{B}_4\text{C}$  based paste 0-16583  
 brittle and tough fracture depend. on C content, heat treatment (*Russian*) 0-40500  
 brittle fracture resistance, welding and heat treatment effects 0-50723  
 brittleness dependence, high temp. deform. in 3Kh2V8F steel at high stress. temp. (*Russian*) 0-50698  
 C content effect on annealing texture, plastic anisotropy and mechanical props. 0-29976  
 carbide and nitride phases dissolution (*Russian*) 0-20888  
 carbide particles, fine microstructural details, characterisation, using EM400 electron microscope 0-24328  
 carbide structure quantitative analysis using Epiquant analyser quantitative analysis using Epiquant analyser (*German*) 0-3284  
 carbonitrided, case struct. investigation by warm electrolytic etching 0-35414  
 carburisation, calc. of mass transfer in diffusional saturation 0-24676  
 carburisation by polymer paste, exam. of saturation 0-16582  
 carburizing, composition effect 0-35432  
 case hardened cylinders, heat treated, residual stress fields 0-3102  
 cast, equipment for thermal shock resistance determ. 0-55614  
 cast, high tensile strength, heat treatment 0-16358  
 cast iron-steel mixture, interaction of Zr, formation reaction thermodynamics (*Russian*) 0-55645  
 cast structural, 20KhGSL, 30KhNML and 40KhL types, heat treatment and mech. working influence on mech. props. (*Russian*) 0-40392  
 casting, meas. and significance of residual stresses 0-21253  
 cleavage fracture model at low temperatures (*German*) 0-35293  
 coating,  $\text{TiC}$ , refractory layers by CVD 0-39471  
 cold-rolled sheet, St10 kp, St10 sp, mag. inspection by ferroprobe coercimeters 0-21234  
 components, dimensional stabilisation, thermoplastic treatment (*Russian*) 0-20960  
 concrete, prestressed, low-temp. tensile strength and linear expansion coeff. of reinforcing steel 0-30051  
 constructional, nitriding process in glow discharge (*Russian*) 0-55560  
 continuously cast, tensile strength and ductility above  $800^\circ\text{C}$  0-55476  
 corrosion and organic coatings, possible Mossbauer studies 0-39988  
 corrosion by seawater, cathode protection using Si solar cells 0-40859  
 corrosion cracking of 20GS2 and 20KhGS2 high-strength reinforcing bar steels 0-55578  
 corrosion of radioactive waste form containers 0-18493  
 corrosion potential/time, and potentiostatic polarisation curves as a method of predicting corrosion 0-45419  
 corrosion stability to double iodate-iodide salt melt in H prod. (*Russian*) 0-55593  
 crack electrochemistry model in active state 0-21192  
 crack growth velocity in gaseous  $\text{H}_2$  embrittlement, rel. to chemisorption 0-11831  
 crack initiation detection by AC potential method (*Chinese*) 0-21196  
 cracks, steady diffusion-migration eqns., representing mass conc. of dissolved species 0-30108  
 critical strain rate in type 20 steel 0-16399  
 cyclic crack opening displacement behaviour during high-amplitude block loading 0-45375  
 cylinder, quenched without transform., residual stresses (*German*) 0-25725  
 defects, microdefect behaviour in steel 12X18H10T (*Russian*) 0-19793  
 deform. resist., softening effects, analytical depend. calcs. (*Russian*) 0-49293  
 deformation, under conditions of superplasticity of type 0Kh12G14N4Yu2, struct. 0-21031  
 deformation and stresses during elongation, application of Ludwig eqn. (*German*) 0-40475  
 deformation process, stage-by-stage nature investigation using acoustic emission (*Russian*) 0-40434  
 deoxidation by Ca-Si alloy, thermodynamics (*Russian*) 0-16268  
 deoxidised, AlN and V carbonitrides precip. effect on mech. props. (*French*) 0-45311  
 dies, durability improvement using isothermal hardening in salt bath 0-35198  
 dual phase, C1020, mech. behaviours and structs. (*Korean*) 0-25779  
 dual phase, improved etching technique for percent martensitic determ. 0-16624  
 ductile fracture in presence of elongated sulphides (*French*) 0-45394  
 ductile structural, crack resistance and cohesive strength 0-50722  
 dynamic fracture initiation in types 4340 and 1018 0-35333  
 elastic moduli, temp. depend.,  $-196$  to  $1000^\circ\text{C}$  0-6451  
 elastic moduli, temp. depend. (*Japanese*) 0-25750  
 electric field effect on strength, hardness 0-50714  
 electric generator type, anisotropic mag. props. obs. using NDT 0-21212  
 electrical steel sheet, magnetostriiction meas. using Hall effect transducer (*German*) 0-13111  
 electrical steel sheets, specific core loss meas. using analogue wattmeter (*German*) 0-13099  
 electrode material, influence on electric breakdown in dielectric liquids (*Russian*) 0-50265  
 electroplastic drawing, type of Kh13N13M2, magnetically hard wire (*Russian*) 0-20967  
 electroplated with Cr, laser treatment 0-21191  
 electrospark machining, appl. of  $\text{W}_2\text{B}_5$  and  $\text{Mo}_2\text{B}_5$ -based alloys as electrodes 0-21174  
 electrotechnical steel, quality significance on energy and materials savings in magnetic circuits (*Czech*) 0-20947  
 elemental distribution measurement, using STEM 0-35601

## steel continued

emission spectrometric, determ. of Al (*Japanese*) 0-16750  
 energy dispersive X-ray fluoresc. spectrometry, computer directed optimisation 0-45585  
 eutectic, fatigue life improvement by thermomech. processing 0-25732  
 faceted Mn sulphides in 45, 17G2AF, 55S2 and 60S2, formation on crystn. dendrites (*Russian*) 0-50621  
 fast reactor structural materials, meas. and calcs. of integral capture cross-sections 0-13613  
 fatigue crack growth rate, intensity of random fluctuation in type CSN 12060 (*Czech*) 0-30079  
 fatigue crack propag. data, Weibull anal. 0-16416  
 fatigue in surface active media, adsorption facilitation mech. 0-55586  
 fatigue strength testing of steel shafts up to 280 mm diameter 0-3184  
 ferritic, base material for powder flame spraying process, intercrystn. corrosion (*Czech*) 0-30158  
 ferritic, C and N migration at low temps., monograph 0-22149  
 ferritic, criteria for Charpy impact testing 0-7752  
 ferritic, impurity defect interaction influence on radiation hardening and embrittlement 0-35199  
 ferritic, with interstitial N, continuous precipitation and clustering 0-7585  
 ferritic-pearlitic, X-ray elasticity constants (*German*) 0-30004  
 fibre reinforced  $\text{Al}_2\text{O}_3$ -Al, production and mech. props. 0-11619  
 fibre reinforced Al, fibre orientation effect on strength (*Korean*) 0-30027  
 fibre reinforced Al alloy, corrosion resistance, electrochemical characts. 0-11806  
 fibre reinforced Al alloy, stressed state nondestructive testing method (*Russian*) 0-40631  
 fibre reinforced concrete, tensile strength and ultimate strain (*Polish*) 0-21027  
 fibre reinforced Mg, fibre-matrix interfacial reactions 0-20043  
 fibres, polycrystalline, Mossbauer spectroscopy 0-44959  
 forgings, expt.-calc. model of quenching 0-16345  
 formability sheet, rapid test for props. assessment 0-40650  
 fracture mode, tearing topography surface fracture 0-7670  
 fracture toughness and impact strength, correl. breakdown 0-55523  
 free-cutting type, inclusion investigs. using EPIQUANT automatic structure analyser 0-55609  
 friction, lubrication and wear studies, Mossbauer spectroscopy appl. 0-40547  
 friction of rubber containing  $\text{CuSO}_4$  paired with steel, selective transfer mechanism 0-55544  
 friction pair with polymer, temp. calc. under severe friction 0-40550  
 galvanic corrosion, electrochem. characts. rel. to Al alloys 0-21162  
 galvanised, interface struct., scanning Auger microprobe study 0-34322  
 galvanised, with paint coating, adhesion failure, XPS study 0-40671  
 galvanised coatings, thickness meas. using X-ray fluorescence radiation, apparatus design 0-21202  
 galvanised, thermal oxidation affect on adhesion of polyethylene coating (*German*) 0-35419  
 gas boronized, sliding wear charact. 0-16499  
 glass fibre reinforced plastics, laminated ring with extra steel pin radial reinforcement, mech. props. 0-11714  
 grain boundary failure model for intergranular fracture modes 0-25825  
 grain boundary segregation of C, atom probe FIM study 0-37134  
 grain boundary strengthening mechanism 0-35207  
 granular model material, equipment for shear deform. investigation (*German*) 0-35449  
 H effect on weldability 0-50720  
 hardened, X-ray elasticity constants (*German*) 0-30004  
 heat treated high strength, X-ray diffr. anal. of residual stress 0-3200  
 heat treatment, high-temp. isothermic, and mech. working influence on struct. and mech. props. of 60S2 (*Russian*) 0-20969  
 high purity, low S content, for tough semi-finished products in nuclear power plant (*German*) 0-45393  
 high strength,  $\text{H}_2$  embrittlement due to cathodic charging during specimen prep. for SEM (*German, English*) 0-11760  
 high-speed, solidification cycle, thermal anal. 0-29945  
 high-temperature materials, technological requirements, R and D, report 0-45222  
 hollow cylinders, thick walled, effect of thermomech. treatment 0-11674  
 hot deformed austenite, transition from discontinuous to continuous formation of pearlite (*German*) 0-35214  
 hot forming property and struct. (*German*) 0-25730  
 hot plastic strain, stress-strain-time dependences (*Russian*) 0-40430  
 hot rolled strip and plate shape meas. device 0-35498  
 hydrogen embrittlement, method of fixing reversible to irreversible transition 0-25840  
 hydrogen embrittlement (*French*) 0-16460  
 hydrogen embrittlement (*French*) 0-16462  
 hydrogen traps, classification 0-19792  
 inclusion cleanliness, US meas. 0-25978  
 inclusion effect on cold formability 0-29975  
 inclusions and plasticity, crystn. conditions influence (*Russian*) 0-20923  
 induced anisotropy influence on mag. props., thermomagnetic working (*Russian*) 0-55549  
 industrial tests for determining lamellar testing susceptibility (*French*) 0-21250  
 ingot, state of viscoelasticoplastic stress deformation, in process of solidification (*Russian*) 0-45295  
 ionic nitriding, procedure and equipment, nitrided layer hardness obs. 0-45414  
 lamellar pearlite, containing proeutectoid ferrite, prestrain effect on brittle fracture (*Japanese*) 0-45388  
 linepipe, S content influence on  $\text{H}_2$  induced fracture 0-30088  
 liquid, Stokes coagulation model, particle motion according to Boltzmann eqn. (*German*) 0-40357  
 low strength, fracture toughness value determination by compact testing 0-45451  
 low strength, impact tests with oscillography, exam. of fracture toughness using new method 0-21215  
 low-temperature materials, mechanical, electrical and magnetic props. (*German*) 0-3081  
 magnetic inspection, of hardness and struct. of type KhVG annealed 0-7750  
 medium C, isothermally quenched, high-temp. deform. effects on struct. and props. (*Russian*) 0-25760  
 microhole working by laser irradi., accuracy increase (*Russian*) 0-55434  
 microstructure determ., transmission type electron microscope appl. (*German*) 0-15089



## steel continued

migration of C during shock compression of steel clad glassy C 0-24679  
 mild, cyclic creep reversal 0-25766  
 mild, materials specifications for AGR steam generators 0-42772  
 mild, plates, fatigue crack propag. estimation method in pre-strained and mean stressed samples 0-21067  
 mild, Ta coating at atm. press. using CVD method 0-55591  
 mild, tensile deformation, behaviour under high pressure (*Japanese*) 0-16381  
 mild, with small flaws elastic-plastic anal. of fatigue limit 0-21069  
 molten, heat loss during solidification hydrodynamic eqns., hardening front kinetics (*Russian*) 0-55385  
 morphology of inclusions changes obs., due to heating, influence on ductile fracture (*Spanish*) 0-25744  
 neutron activation anal. in VVER reactor (*Czech*) 0-5234  
 nitriding in molten nitrates 0-35417  
 non-irradiated and irradiated specimens, autoclaves for fatigue crack growth tests (*German*) 0-45467  
 nonmetallic inclusion effect on hot ductility 0-29999  
 nonmetallic inclusions effect on ductility 0-30042  
 pearlitic, partitioning, atom probe microanal. 0-3079  
 pearlitic eutectoid, crack initiation and effective grain size for cleavage fracture 0-30085  
 phase conversion kinetics, exam. using ultrasonic method, apparatus design 0-21203  
 plane strain fracture mode criterion based on plastic zone size-thickness correlation 0-43670  
 plastic deform. effect on third-order elastic moduli, dislocation anharmonism (*Russian*) 0-50786  
 plastic deform. resist. during continuous hot rolling (*Russian*) 0-55462  
 plastic deformation, C distrib. (*Ukrainian*) 0-50668  
 plastic deformation, cyclic stress anal. within hysteresis loop of type 11423 (*Czech*) 0-30031  
 plastic deformation zone, caused by crack, extent determ. with microhardness, surface roughness, measurements (*French*) 0-7682  
 plastically deformed, force and speed criteria interactions during hot rolling (*Russian*) 0-55463  
 plastically deformed, magnetoelastic props. of types 45 and U8 (*Russian*) 0-44893  
 plasticity indices in anisothermal extension (*Russian*) 0-16378  
 plate, thin, in compression, initial deflection and postbuckling behaviour analysis 0-50666  
 plates with cut, stability loss critical stresses for 20, 08 kp and 65G steels 0-11690  
 porous gauze materials, struct. and hydraulic characts. 0-11729  
 prow formation processes, sliding against mild steel (*Japanese*) 0-35336  
 quasi-cleavage fracture (*Chinese*) 0-21060  
 quenched, local H distrib. and internal microstresses (*Russian*) 0-50654  
 quenched, surface layer hardness rel. to adsorption contact fatigue (*Ukrainian*) 0-40478  
 rapid, contrib. to assimilation of new labels (*Rumanian*) 0-35216  
 reactor pressure vessel failure and radiation damage (*Czech*) 0-619  
 recrystallisation kinetics, of unkilld deep drawing sheets, N-content influence (*German*) 0-40376  
 reinforcement in concrete, fatigue crack growth 0-30060  
 reinforcement of concrete slabs, subjected to biaxial moments, optimum design using analytical and graphical methods 0-50664  
 residual quenching stress determ. in cylinder, consideration of transform. (*German*) 0-35213  
 resulphurised, fractography and X-ray photoelectron spectroscopy 0-7673  
 rimming, continuous casting and solidification (*French*) 0-25685  
 rimming, teeming and solidification (*French*) 0-16296  
 rolling, controlled, correlation links between mech. props. 0-35234  
 rolling texture, neutron diffr. analysis, steels with micro-duplex structure 0-16327  
 ruled steel grating system for length meas. 0-13039  
 scoring and scuffing on lubricated sliding surfaces, Mossbauer study 0-7690  
 self-consistent junctions and spatial relative organisation in type 50N29 0-19750  
 self-lubricating Ni coating 0-21189  
 shear-band temp. meas. of type 4340 0-48655  
 shot-peened, type JAE 1144, fatigue damage, development rate by exoelectron meas. 0-25835  
 signature response, for friction and wear 0-40541  
 siliconised, alloy formation kinetics at solid cathodes, metal electrodeposition from molten salt electrolytes 0-26028  
 sleeve, type St 37, deformation behaviour contrib. in rod drawing (*German*) 0-11684  
 steel, carburising, carbide-austenite layers, form. and development 0-35413  
 steel, Ck 45, cylindrical bodies rolling over one another, plastic deformations caused by frictional forces 0-11735  
 steel, heat-resist., C replica method of investigating creep damage in TEM 0-21012  
 steel, long-term strength, H effect 0-55581  
 steel, plastic deformation and cryst. texture in equibiaxial expsn. 0-7653  
 steel, structural, grain size depend. of yield stress in homogeneous deformation range (*German*) 0-30013  
 steel-Cu M3 bimetal, eutectic alloy, crack development, failure energy capacity (*Russian*) 0-40480  
 steels, 2Kh13 and 20Kh1MIFTR, sulphide cracking resistance, strengthening method influence 0-55577  
 steels, spring, 60S2A and 50KhFA, heat treatment and mech. working effect on mech. props. (*Russian*) 0-20962  
 strength, acoustic monitoring 0-35479  
 strengthening type Kh18N9T by vibrational stirring effect 0-40405  
 stress and strain intensity, determ. after plastic deform. using microhardness meas. 0-40641  
 stress corrosion cracking, intercrystalline, in  $\text{Ca}(\text{NO}_3)_2$  soln. (*German*) 0-30130  
 stress distribution, calcs., during cooling, program system THEPLA (*German*) 0-35237  
 stress meas. and calc. around drilled hole, with hole-gage-rosettes aid (*German*) 0-25757  
 stress measurement, US method, calibration expt. results (*German*) 0-53725  
 stress relaxation, short-term, creep and strain hardening (*Russian*) 0-30005  
 stress relaxation in cyclic deformation 0-3119  
 struct. type 05KhGM 0-35313

## steel continued

structural, brittle fracture, conditions for prediction in welded structures (*French*) 0-25867  
 structural, corrosion fatigue strength, effect of medium temp. 0-55583  
 structural St 37-2, cleavage fracture, report 0-25868  
 substrate, acoustic emission of thermal-sprayed oxide coating 0-21247  
 substrate for Cv vacuum coatings, influence of precipitation conditions on porosity (*Russian*) 0-54578  
 sulphide stress corrosion cracking, threshold stress and crack initiation stress intensity comparison 0-21158  
 surface, nitrided, chem. state anal. by conversion electron Mossbauer spectrometry 0-7718  
 surface wearing ability, finished surface direction effect on wearing ability 0-11793  
 thermal props. meas. (*French*) 0-25977  
 thermoelastic problem for Griffith crack, temp. dependent props. under linear temp distrib. 0-48579  
 thread rolled, Moire fringe method for examining local deform. zones 0-21220  
 time and spatially resolved at. absorpt. anal. 0-40760  
 tool, type NC6, cementite network separation, kinetics (*Polish*) 0-25698  
 transition element depth profile meas. using (p,y) react. 0-50910  
 tubes, square section, collapse in bending 0-25792  
 tubular, type 0Kh16N15M3B, reactor irradiated, creep resist. (*Russian*) 0-25762  
 ultra-high strength, H induced delayed plasticity and cracking 0-21100  
 ultrahigh strength, historical case study 0-7609  
 ultrahigh strength, monotonic and cyclic stress strain curves 0-35268  
 US attenuation, precrack damage and crack propag. study 0-40656  
 US inspection of hot thick steel products 0-40661  
 wear resistance, determ. using MI-IM machine 0-25943  
 wear resistance during abrasive wear, comp. and struct. effects 0-35337  
 wedged crack propagation, in type AISI 1018 0-2115  
 welded steels, types D36, D50, secondary ion anal. of segregation 0-7580  
 white zone formation, in type 1Kh17N2, and props. during friction in vac. (*Russian*) 0-40542  
 wire, drawn, age hardening props. obs., mechanical and electrical props. relationship 0-50662  
 yield strength, statistical treatment of experimental data 0-53644  
 Al coated, porosity evaluation, micro X-ray spectral anal. (*Russian*) 0-35389  
 Al-steel bimetallic wire for overhead lines, manufacturing methods 0-16247  
 Cr, stress relaxation, superplasticity and thermal cycling (*Russian*) 0-21019  
 Cu clad pipe, determ. of yield, tensile strength 0-25771  
 Fe, Armco, boride coatings, under elec. heating conditions, hydroabrasion wear resist. 0-55543  
 $\text{Fe}_2\text{O}_3$ , transformation to  $\text{Fe}_3\text{O}_4$  in oxide scales on steel, conversion kinetics 0-7561  
 H assisted cracking, mechanisms, review 0-50721  
 H discharging phenomena, effect of  $\alpha$ -Cu precipitates (*Japanese*) 0-7583  
 I<sub>2</sub> adsorption on steel in HTGR He environment 0-44233  
 $\text{Mn}_3(\text{PO}_4)_2$  coating on steel, wear resistant appl. 0-16609  
 $\text{Mo}^{+}$  ion bombardment, phase composition and struct. change of surface layers (*Russian*) 0-24506  
 Na-cooled fast reactor, structural steel properties 0-22942  
 $\text{Ti}_3\text{N}_4$  plasma condensation on steel and carbide (*Russian*) 0-20796  
 Zn coated, cold rolling influence on struct. and deform. of diffusional layer (*Russian*) 0-55465  
 Zn coated strips, plastic deform. influence on struct. and quality (*Russian*) 0-40377

**steel industry**  
 EPIQUANT automatic structure analyser for inclusion investigs. in free-cutting steel 0-55609

**steel manufacture**  
 hardening, secondary, of hot worked and rapidly worked steels (*German*) 0-3083  
 high-temperature working, effects on products props. (*German*) 0-3108  
 killed ingot, freezing process liq. core movement (*Russian*) 0-20921  
 respirable airborne crystalline silica, silicosis in steelmaking environments 0-45832

**stellar atmospheres**  
 see also solar atmosphere  
 OB-type stars, O VI obs. in stellar winds 0-8630  
 accreting compact object in binary system, magnetosphere theory, X-ray sources 0-46394  
 accretion disks, theoretical review (*Polish*) 0-26739  
 $\alpha$  Aquarii, chromospheric event detect. from UV spectrum obs. 0-31299  
 56 Arietis, spectrophotometry of Ap star, continuum features vars. 0-36638  
 $\alpha$  Aurigae (Capella), X-ray line emission obs., corona models 0-26905  
 axisymmetric moving envelopes, spectral line form. numerical method and appl. to YY Orionis stars 0-41813  
 B-type stars, pole-on, rapidly rot., spectral inconsistencies due to gravity darkening 0-17581  
 baryon star magnetospheres, inclined rotator case 0-26887  
 Be stars, electron scatt. effects on Balmer emission lines 0-17589  
 black hole accretion discs, boundary-layer behaviour of flow at disc inner edge 0-46598  
 black hole accretion discs, rapid X-ray variability and dying pulse trains 0-56872  
 $\xi$  Bootis A, active dwarf star, chromospheric emission lines obs. 0-12762  
 $\alpha$  Camelopardalis (O9.5 Ia), expanding envelope rot. rel. to variable H $\alpha$  P Cygni profile 0-41818  
 $\alpha$  Camelopardalis (O9.5 Ia), stellar wind terminal vel. short time changes from UV spectrum 0-36625  
 49 Cancri, spectrophotometry of Ap star, continuum features vars. 0-36638  
 $\alpha$  Canis Majoris (Sirius), Ca II K line profile rel. to atmospheric rel. fields 0-56830  
 Y Canum Venaticorum, C star, IR spectrum rel. to photosphere and circumstellar shell 0-46544  
 RS Canum Venaticorum systems, X-ray obs. and coronal model development 0-56873  
 $\gamma$  Cassiopeiae, Be star, polarisation rapid vars. rel. to rot. circumstellar envelope inhomogeneities 0-22022  
 RZ Cassiopeiae, eclipsing binary, spectroscopic orbit and evidence for circumstellar matter 0-22040  
 $\kappa$  Cassiopeiae, effective temp. radius, mass loss and luminosity 0-51748



## stellar atmospheres continued

- 6 Cassiopeiae, spectroscopic obs. of supergiant star, equivalent widths, microturbulence and radial vel. 0-22006  
 cataclysmic binary formation through common envelope evolution 0-8651  
 cataclysmic variables, emission lines from accretion discs 0-51774  
 proxima = V645 Centauri, dMe flare star, quiescent corona, transition region, and chromosphere obs. 0-56850  
 $\alpha$  Centauri A and B, IUE spectra and transition region models 0-46543  
 Centaurus X-3, stellar wind vel. change during transition 0-12829  
 U Cephei, eclipsing binary, gas stream effects in UV spectrum, IUE obs. 0-26898  
 $\delta$  Cephei, H $\alpha$  radial vel. curve rel. to form. in stellar outer atmosphere 0-51788  
 Cepheid variables, He enrichment effects in atm., models 0-26884  
 $\alpha$  Ceti, atmosphere expansion vel. from IUE obs. 0-22027  
 chromosphere models, Ca II H and K lines absolute flux profiles in F0 to M2-type stars 0-26842  
 chromosphere models, high-press. transition regions theory 0-26847  
 chromospheres, observational indicators, empirical models 0-12755  
 chromospheres and convection theory, H-R diagram boundary line 0-56823  
 circumstellar dust grains formation, influence of Fe condensation 0-26927  
 CIT 6 (IRC+30219), IR C star, CO obs. of mass outflow 0-12761  
 classical novae, optically thin winds struct. 0-36643  
 collisionless subsonic accretion, stellar appl. 0-46380  
 cool stars outer atmospheres, Mg II flux profiles and chromospheric radiative loss rates 0-36611  
 cool stellar wind models for late type stars 0-51733  
 coronae, evidence for existence from X-ray and UV obs. 0-12756  
 coronae, IUE search 0-4233  
 coronae, two-parameter models 0-8619  
 $\sigma$  Coronae Borealis (HD 46361) spectroscopic binary, coronal X-ray emission obs. 0-56886  
 SS Cygni, dwarf nova, spectrophotometry rel. to accretion disc models in eruption and at min. light 0-36635  
 P Cygni, effective temp. radius, mass loss and luminosity 0-51748  
 P Cygni, extreme B-type supergiant, UV spectroscopy rel. to low-vel. stellar wind 0-22004  
 V1057 Cygni, FU Orionis star, IR spectroscopy rel. to expanding envelope 0-17587  
 32 Cygni, IUE obs. and effects of B-type star within late-type supergiant upper chromosphere 0-22036  
 V832 = 59 Cygni, mass-losing Be star, changes in UV spectrum 0-46561  
 P Cygni, UV spectrum rel. to expanding circumstellar shell struct. 0-26873  
 59 = V832 Cygni, variable mass flux from spectroscopic obs. 0-41840  
 V1500, Cygni (Nova 1975), radio emission from expanding shell 0-26868  
 V1668 Cygni (Nova 1978), dust form. phase time from linear polarisation obs. 0-26875  
 V 1668 Cygni (Nova 1978) ejecta shell, dust form. rel. to spectral development 0-51789  
 Cygnus OB2 number 12, spectrum rel. to mass loss and possible duplicity 0-51760  
 degenerate stars with H atmospheres, props. rel. to theoretical models 0-17576  
 HR Delphini, UV spectrum, stellar wind 0-26880  
 HR Delphini (Nova 1967), photoionisation models, binary system evolution 0-17590  
 HR Delphini (Nova 1967), physical conditions of different regions of envelope 0-4369  
 HR Delphini (Nova 1967), radio emission from expanding shell 0-26868  
 HR Delphini (Nova 1967), spectra, line identification, radial vels. 0-17594  
 dust grains, IR spectra and props 0-26943  
 early type stars, line blanketed model atmospheres rel. to mid UV spectra 0-21995  
 eclipsing variable stars with extended atmospheres, Fourier anal. of light curves 0-46604  
 expanding and rotating atmospheres, curves of growth and line profiles 0-31295  
 flare stars, model chromospheres, Balmer-line profiles 0-46558  
 free convection effects on MHD accel. flow past vertical porous limiting surface 0-23996  
 free convection in Stokes' problem for infinite vertical limiting surface, mass transfer effects 0-28501  
 G200-39, hot hybrid white dwarf, spectroscopic obs. and atmospheric props. 0-26852  
 giant stars, model envelopes, physical props. (Portuguese) 0-22014  
 globular cluster giant stars, blanketing differences meas. 0-4345  
 grain formation in cool stellar envelopes 0-56814  
 HD 153919 (3U 1700-37), spectroscopic obs. rel. to mass loss rate and corona 0-4358  
 HD 190603, effective temp. radius, mass loss and luminosity 0-51748  
 HD 193793, Wolf-Rayet star, circumstellar dust form. episode 0-31301  
 HD 193793, Wolf-Rayet star, graphite grains form. rel. to C rich dust cloud 0-26861  
 HD 51480, shell star, spectroscopic obs., atmospheric struct. and distance 0-31305  
 high mass stars, stellar wind effects on evolution 0-21982  
 hot massive stars, stellar wind mass loss, evolution study 0-17578  
 W Hydrae, circumstellar envelope mag. field rel. to OH masers suspected Zeeman splitting 0-36632  
 ionization front propag. in inhomogeneous medium 0-46379  
 IRC+10216, circumstellar dust shell model rel. to IR energy distrib. 0-56972  
 irradiated stars in active galactic nuclei, mass loss and evolution 0-56949  
 late type stars chromospheres, struct. from Ca II H and K lines photoelectric calibration 0-36617  
 late-type stars, extended atmospheres, sphericity effects in red giants, model study 0-22012  
 late-type stars, He abundance effects on spectrum appearance 0-46540  
 late-type stars, O-rich, 16 to 39 micron spectroscopy rel. to circumstellar silicate dust 0-22002  
 $\rho$  Leonis, effective temp. radius, mass loss and luminosity 0-51748  
 luminous stars in symmetric nebulae, IUE spectra rel. to stellar wind props. 0-46560  
 RU Lupi, T Tauri star, chromosphere and corona parameters and expected X-ray fluxes (Russian) 0-51770

## stellar atmospheres continued

- Lyman continuum in atmosphere in statistical equilib., effects of deviations from LTE 0-31290  
 $\alpha$  Lyrae (Vega), LTE blanketed models rel. to visible and UV continuous energy distrib. 0-26856  
 magnetospheres and radio emissions, conf. Snowmass, Colorado, USA (Aug. 1978) 0-41939  
 massive eclipsing binary stars, spectrophotometry and search for circumstellar matter 0-26900  
 massive white dwarfs, mass accretion, rel. to thermonuclear runaways 0-41822  
 metal-poor late-type stars, model atmospheres rel. to MK spectral classification 0-4340  
 minimum flux corona theory 0-26844  
 multidimensional radiative transfer in stratified atmosphere, grey radiative equilib. 0-26845  
 neutron star, interaction between accretion disc and mag. field (Russian) 0-51799  
 neutron star magnetosphere, plasma dynamics and accretion, fate of sinking filaments 0-51798  
 neutron stars, accretion disc torques rel. to pulsating X-ray sources period changes 0-31320  
 nova ejecta, dust grains sudden nucleation and growth 0-26941  
 Nova Serpentis 1978, IR photometry rel. to dust shell condensation 0-4365  
 nova shells, radio emission obs. 0-26868  
 NP 0532 magnetosphere, cyclotron instability rel. to origin of radiation (Russian) 0-8645  
 O-type stars in open cluster IC 1805, C IV line P Cygni profiles and mass loss indices 0-31296  
 $\zeta$  Ophiuchi, spectral vars. related to rot. 0-22000  
 $\alpha$  Orionis, CO circumstellar absorpt. obs. in 4.6 micron spectrum 0-26858  
 U Orionis, Mira variable, atmospheric perturbation rel. to 1612 MHz flare and light curve 0-56844  
 $\alpha$  Orionis (Betelgeuse), optically thin dust shells 0-22011  
 EQ Pegasi, active dwarf binary star, chromospheric emission lines obs. 0-12762  
 21 Persei, spectrophotometry of Ap star, continuum features vars. 0-36638  
 plasma, highly ionized, ionization equilib. validity 0-21906  
 Pleione (28 Tauri), envelope behaviour in 1976, spectroscopic obs. 0-8636  
 Pleione (28 Tauri), metallic-line shell spectrum anal., (1973-1976) 0-8637  
 polarisation of light in atmospheres and circumstellar envelopes (Russian) 0-17573  
 pre-main-sequence stars in NGC 2264, metallicity and circumstellar dust shells 0-26916  
 pulsar atmospheres, numerical solns. of trans-relativistic shock relations 0-31202  
 pulsar electron cap, electrons accel. in internal zone 0-46592  
 pulsar emission, mag. bremsstrahlung of ultrarelativistic particle beam in relativistic plasma 0-46390  
 pulsar magnetosphere, electron absorpt. rel. to spectra low-freq. dropout 0-17602  
 pulsar magnetosphere, magnetoactive plasma equilib. in gravit. field (Russian) 0-26895  
 pulsar magnetosphere, quasi-transverse propag. theory rel. to individual pulse-polarisation patterns 0-46591  
 pulsar magnetosphere models, interior and exterior struct., pair prod. 0-46594  
 pulsar magnetosphere radio emission, plasma supply and elec. forces, review 0-46595  
 pulsar magnetospheres, axisymmetric, self-consistent description 0-31318  
 pulsar magnetospheres, narrowband versus broadband emission processes rel. to luminosities 0-51797  
 pulsar magnetospheres, propag. effects in shearing field-free plasma rel. to microstruct. 0-17483  
 pulsar magnetospheres, relativistic MHD wind or plasma wave 0-31317  
 pulsar magnetospheres, stellar-wind model for plasma-EM fields 0-22031  
 radiation field in semi-infinite atmosphere containing energy sources 0-21907  
 radiation scattering, approx. soln. (Russian) 0-36621  
 radiative transfer, non-conservative problem 0-36492  
 radiative transfer, Unno-Kondo generalized Eddington approx. in extended atmospheres 0-21997  
 radiative transfer in magnetic atmospheres, analytical soln. 0-36494  
 S-type stars, molecular spectra and model atmospheres 0-51764  
 HM Sagittae, emission-line star, polarimetry rel. to circumstellar dust shell (Russian) 0-36649  
 XZ Sagittarii, Algol system, UV photometry rel. to circumstellar matter 0-22041  
 RY Sagittarii, spectra near min. light 0-36642  
 Schwarzschild black hole, gas accretion 0-56871  
 $\zeta^1$  Scorpii, B1 supergiant, UV reson. lines rel. to expanding envelope struct. 0-4349  
 $\alpha$  Scorpii, circumstellar absorption lines in UV spectrum 0-51804  
 $\zeta^1$  Scorpii, extreme B1 supergiant, IUE obs. rel. to mass loss mechanism 0-17583  
 $\zeta^1$  Scorpii, extreme B-type supergiant, UV spectroscopy rel. to low-vel. stellar wind 0-22004  
 RY Scuti, silicate grains IR emission from early-type supergiant binary system 0-41827  
 self-gravitating rotating masses, book contrib., review 0-21915  
 RT Serpentis (Nova 1909), ionised envelope props. from spectrum in 1964, 1975 and (1978) 0-46566  
 FH Serpentis (Nova 1970), radio emission from expanding shell 0-26868  
 spectral line formation in microturbulent magnetic fields 0-31201  
 Stromgren four colour indices, grid for calc. of log g and effective temp. 0-36507  
 structure, mol. effects 0-21999  
 super-metal-rich stars, boundary cooling and supermetallicity 0-56821  
 supercritical accretion discs winds struct. and appearance, numerical models 0-21984  
 supergiants of O- and B-type in Magellanic Clouds, stellar winds 0-51863  
 supernova ejecta, dust grains sudden nucleation and growth 0-26941  
 supernovae, type II, nonequilibrium processes in evolution 0-46586  
 V471 Tauri, eclipsing binary, K-type star chromospheric Mg II emission obs. 0-26912



**stellar atmospheres continued**

- RV Tauri and yellow semiregular variables, circumstellar dust prod. rel. to metallicity 0-26865  
 T Tauri stars, props. of assoc. ionized regions 0-36624  
 T Tauri stars atmospheres, sphere and low chromosphere model 0-36623  
 thermal-convective instability through porous medium 0-53769  
 4U 1626-67, X-ray pulsar, X-ray and optical obs. rel. to accretion disc optical emission 0-51914  
 wave propag. with high radiation pressure 0-26729  
 wave propagation with magnetic field, Lagrangian procedure 0-8620  
 white dwarf stars, model atmospheres rel. to two-colour diagram, masses and radii 0-46547  
 white dwarfs, DB-type, model atmospheres 0-51761  
 white dwarfs, magnetic, model atmospheres calc. of cyclotron absorpt. spectra 0-4351  
 white dwarfs, minimum-flux coronal models for H and He atmospheres 0-8626  
 white dwarfs chem. evolution, diffusion and accretion 0-36628  
 wind flow past compact object, X-ray intensities 0-22116  
 winds in massive binary stars, effects on heavy elements prod. 0-46534  
 Wolf-Rayet stars, He rich-expanding atmosphere model rel. to UV energy distrib. obs. 0-22023  
 X-ray pulsars, vacuum polarisation effect rel. to radiative transfer and X-ray spectra 0-27015  
 X-ray sources, compact, optically thick radiative transfer rel. to X-ray spectra form. 0-22115  
 X-ray sources, strongly magnetised plasma collisional relax. of ion beam 0-33785  
 yellow semiregular and RV Tauri variables, circumstellar dust prod. rel. to metallicity 0-26865  
 young stars, circumstellar dust rel. to interstellar gas and EHF continuum emission 0-51766  
 young stars, circumstellar mols. 0-22013  
 C stars, determination of  $^{12}\text{C}/^{13}\text{C}$  and N/C ratios in atm. 0-17580  
 H $\beta$  indices for model atms., B-type stars appl. 0-31292  
 HgMn stars, line blanketed model atmospheres rel. to spectrophotometry 0-26867  
 SiO maser stars,  $J=1-0$   $\nu=1$  and 2 masers obs. and spatial coincidence 0-4339

**stellar binaries** *see binary stars***stellar clusters and associations***see also globular star clusters*

- axisymmetrical stellar systems, periodic orbits of stars 0-17619  
 binary stars on main sequence, freqs. among cluster and field stars 0-26901  
 Canis Major OB1 association, probable membership of shell star (HD 51480) 0-31305  
 Canis Major R1, anomalous diffuse bands 0-51820  
 Carina spiral feature inner side, star groups and interstellar dust distrib. 0-51871  
 Cepheus OB2 association stars, interstellar line spectra 0-22052  
 Cepheus OB3 association, near main line OH maser with Zeeman pattern in assoc. mol. cloud 0-56908  
 Cepheus OB3 association molecular cloud, mol. obs. rel. to star form. 0-12798  
 Cygnus OB2, spectral type and membership of star number 12 0-51760  
 Cygnus OB2 (VI Cygni), soft X-ray emission sources discovery 0-26918  
 Cygnus OB2 association, possible membership of IR source (MWC 349) 0-56971  
 30 Doradus cluster, relation to foreground unique interstellar Ca II K-line profile 0-51850  
 dynamical evolution, analytical approximations for effect of mass loss 0-51815  
 ESO/Uppsala survey of ESO (B) Atlas of S. sky, pt. VII 0-56722  
 G133.8+1.4 (W3N), far IR source, near IR obs. and identification as OB stars cluster 0-22058  
 Hyades, late-type stars intermediate-band photometry 0-31289  
 Hyades, photometric survey for  $\delta$  Scuti variable stars 0-36677  
 Hyades, shape and luminosity distrib. 0-17622  
 Hyades, UV spectra of white dwarf eclipsing binary V471 Tauri 0-26912  
 Hyades cluster, possible members BVRI photometry 0-51821  
 IC 1805, 1848, OB-associations and giant H II regions, physical anal. from radio obs. 0-36695  
 IC 1805, open cluster, O-type stars C IV UV reson. line P Cygni profiles 0-31296  
 IC 2391, relative proper motions of stars, ident. of member stars 0-51818  
 IRC-10442 (GL5268S), possibly two star clusters, near IR and radio obs. 0-4412  
 loose clusterings in southern Milky Way, continued photometric studies 0-36679  
 in M31, studies of luminous stars in associations in Baade's Field IV 0-36622  
 M36, photographic obs., mass, radius, central density, stellar vels. of open cluster (*German*) 0-31333  
 M38, photographic obs., mass, radius, central density, stellar vels. of open cluster (*German*) 0-31333  
 Melotte 66, oldest open cluster, colour-magnitude diagram rel. to age 0-17621  
 membership probabilities, photographic meas. of relative proper motions of stars 0-51817  
 Monoceros OB2 association, evidence for supernova-induced star form. 0-31334  
 Monoceros R1 molecular clouds ring struct., CO obs. 0-12784  
 NGC 2264, open cluster, reddening, blanketing and metallicity from spectroscopic obs. 0-26916  
 NGC 2264, UBVR photometry of 70 field stars in young cluster 0-51819  
 NGC 2264 formaldehyde kinematics and distrib. near IR source 0-4418  
 NGC 2287, open cluster, spectral classification of brightest stars 0-26919  
 NGC 2420, old disc cluster, chemical comps. of stars 0-46620  
 NGC 2423, 2482, Hyades-like clusters, late-type stars intermediate-band photometry 0-31289  
 NGC 2477, photographic obs., mass, radius, central density, stellar vels. of open cluster (*German*) 0-31333  
 NGC 2669, relative proper motions of stars, ident. of member stars 0-51818  
 NGC 3532, southern open cluster, UBVR photometric study 0-46621

**stellar clusters and associations continued**

- NGC 4755, southern open cluster, Balmer line photoelectric photometry 0-56892  
 NGC 6231, young open cluster, new  $\beta$  Canis Majoris star (HDE 326333) discovery and photometry 0-17595  
 NGC 6530 in M8 (Lagoon Nebula), rel. to nebula far IR emission 0-4413  
 NGC 6611, young open cluster, UBVR magnitudes and colours, reddening, distance, luminosity 0-31332  
 NGC 663, galactic cluster, emission line stars spectroscopic obs. 0-4363  
 NGC 6823, UBVR photometry and spectra, extinction study of young open cluster 0-4407  
 NGC 6913, photoelec. photometry of brighter stars, variability obs. 0-46625  
 NGC 7789, metal abundance and He content of open cluster, mass loss 0-31335  
 OB and T associations, membership in star form. regions rel. to population categories 0-17645  
 OB associations, mag. fields influence on subgroups sequential form. 0-4408  
 open cluster, proper motions rel. to solar motion and apex determ. 0-46418  
 open clusters, blue stragglers as long-lived stars 0-46542  
 open clusters, H-R diagrams anal. rel. to Galaxy chemical abundance gradient 0-56938  
 open clusters, white dwarf members obs. rel. to progenitor stars upper mass limit 0-51738  
 Orion OB1 (Belt), photometric studies 0-46618  
 $\gamma$  Persei, cluster membership determ. by proper motion meas. 0-56890  
 Perseus OB1 assoc., new H $\alpha$ -emission stars 0-56855  
 Perseus OB2 association molecular cloud, mol. obs. rel. to star form. 0-12798  
 Pleiades, reddening-face colours, photometric zero age main sequence definition 0-26920  
 Praesepe, photometry in BVRI colours 0-26917  
 protosolar OB association supernovae, rel. to Allende isotopic anomalies and cosmochronology 0-4462  
 R associations in southern dust clouds study of stars and bright nebulosities 0-56893  
 R-associations, obs. of free-free emission from embedded B-type stars 0-26851  
 relict circumstellar matter in young clusters 0-41865  
 rotation, ang. moments mass depend. rel. to self-similarity 0-36490  
 scale-covariant dynamics of stellar systems 0-26913  
 southern open clusters, search for interstellar H I 0-46619  
 star escape from isolated clusters, numerical methods (*Polish*) 0-26922  
 UBVR photoelectric photometry of M31 clusters (*Russian*) 0-36680  
 Vulpecula OB2, case for membership of 67 day Cepheid S Vulpeculae 0-41831  
 William Herschel's early investigations of nebulae 0-12876  
 young stellar groups towards galactic anticentre, photometry and spectra rel. to outer Galaxy struct. 0-22079

**stellar composition***see also element origin; solar composition*

- Am-type stars, mol. weight gradient effect on envelope meridional circulation 0-4370  
 Ap and Am stars, numerical taxonomy 0-22015  
 U Aquarii, R Coronae Borealis star, extraordinary comp. rel. to unusual s-processing event 0-17588  
 atmospheric structure, mol. effects 0-21999  
 BDS 1269, visual binary, metal abundances and characts. of components 0-4397  
 binary stars on main sequence, freq. depend. on metallicity 0-26901  
 V553 Centauri, C rich Cepheid, C and N abundances 0-4378  
 Cepheid instability strip 0-56833  
 Cepheid variables, He enrichment effects in atm., models 0-26884  
 CIT 6 (IRC+30219), IR C star,  $^{12}\text{C}/^{13}\text{C}$  lower limit from CO obs. 0-12761  
 V1057 Cygni, FU Orionis star, IR spectroscopy with contact-type image tube 0-17587  
 degenerate stars with H atmospheres, spectra rel. to comp. and theoretical models 0-17576  
 dust grains composition, evidence from IR spectra 0-26943  
 dwarf Cepheids, metal abundances rel. to evolutionary stage 0-46562  
 evolutionary models from zero age main sequence to red giant branch 0-21987  
 F- and G-type supergiants, enhanced He abundance effects on visible spectra 0-12759  
 Fornax dwarf elliptical galaxy, abundance range from giant branch photometry 0-4431  
 G200-39, hot hybrid white dwarf, He/H ratio 0-26852  
 G and K-type giant stars, Li abundances 0-41819  
 giant stars in open cluster NGC 7789, metal abundance, He content and mass loss 0-31335  
 GK-type dwarf stars, Mg isotopic abundances 0-51757  
 globular cluster giant stars, metal abundance parameter determ. from blanketing differences 0-4345  
 globular clusters, He content from RR Lyrae stars evolution 0-51778  
 HD 94033 ultra short period cepheid, metal deficiency 0-22024  
 heavy-element excess in late spectral class stars 0-26854  
 intermediate-mass stars asymptotic giant branch evolution as function of mass and comp. 0-12749  
 IRC+10216, circumstellar graphite dust shell model 0-56972  
 IRC+10216, molecular abundances in cool C star 0-4354  
 K-type giant stars polulation at South Galactic Pole, CN anomalies and distances 0-8622  
 late-type stars, He abundance effects on spectrum appearance 0-46540  
 late-type stars, O-rich, 16 to 39 micron spectroscopy rel. to circumstellar silicate dust 0-22002  
 $\alpha$  Lyrae (Vega), spectral anal. from Copernicus 0-26856  
 RR Lyrae stars, effective temp. and colour, metallicity effects 0-56841  
 RR Lyrae stars, period-luminosity-colour relations, metallicity effects 0-56842  
 RR Lyrae variables, metallicity rel. to three-dimensional motion 0-12754  
 RR Lyrae variables in globular cluster NGC 6121 (M4), metal and He abundances 0-22018  
 magnetic stars, equatorially symmetric rotator model, inhomogeneous element distrib. 0-4371  
 Melotte 66, oldest open cluster, metallicity from colour-magnitude diagram 0-17621



**stellar composition continued**

- metal rich globular cluster NGC 5927, colour-magnitude diagram 0-36678
- metal-poor late-type stars, metal content effects on spectral classification 0-4340
- metal-poor stars, O abundances from O I IR triplet 0-36610
- neutron stars, inner crust nuclear compositions 0-31322
- NGC 1261, globular cluster, metallicity rel. to colour-magnitude diagram 0-17623
- NGC 2264, open cluster, reddening, blanketing and metallicity from spectroscopic obs. 0-26916
- NGC 2420, old disc cluster, chemical comps. of stars 0-46620
- NGC 2423, 2482, Hyades-like clusters, metal abundance from intermediate-band photometry 0-31289
- NGC 6144, globular cluster, photometric obs. rel. to metal deficiency 0-51816
- NGC 6528, globular cluster, colour-magnitude diagram rel. to metallicity 0-4406
- NGC 6717, globular cluster, colour-magnitude diagram, distance and metallicity 0-46624
- open cluster, galactic chemical abundance gradient from H-R diagrams 0-56938
- $\alpha$  Orionis, CO circumstellar absorpt. obs. in 4.6 micron spectrum 0-26858
- FU Orionis, IR spectroscopy with contact-type image tube 0-17587
- pre-main-sequence stars, D abundance and D burning rel. to early evolution 0-51736
- S-type stars, revised spectral classification system in red 0-46541
- southern metal-poor stars, UBVR photometry and UV excesses 0-56828
- spiral galaxies nuclei, stellar population and metal abundance 0-56926
- subdwarfs, He abundance and galactic halo 0-22003
- subdwarfs, UV excesses and metal abundances 0-17574
- super-metal-rich stars, boundary cooling and supermetallicity 0-56821
- supergiant stars, southern, late-type, chem. comp., solar neighbourhood metallicity distrib. 0-12758
- V471 Tauri, eclipsing binary, UV spectra rel. to white dwarf atmospheric comp. 0-26912
- RV Tauri and yellow semiregular variables, metallicity and mass from photometric investigations 0-26865
- 47 Tucanae, globular cluster, chemical comps. of stars 0-46620
- turbulent diffusion and  $^{12}\text{C}/^{13}\text{C}$  abundance ratio 0-21993
- white dwarfs, atm. chem. evolution, diffusion and accretion 0-36628
- Wolf-Rayet binaries, evolution of mass losing massive He burning stars rel. to comp. 0-36615
- Wolf-Rayet stars, He/H ratios rel. to UV energy distrib. obs. 0-22023
- yellow semiregular and RV Tauri variables, metallicity and mass from, photometric investigation 0-26865
- Ba II stars and s-process calcs. 0-56824
- C stars, determination of  $^{12}\text{C}/^{13}\text{C}$  and N/C ratios in atm. 0-17580
- C/O ratio in massive stars, core convection effects 0-17579
- C, white dwarfs, evolutionary status 0-4355
- H burning stars, comps. rel. to Hertzsprung-Russell diagram age and mass calibrations 0-51744
- He abundance anomalies, radiative forces calcs. in stellar envelopes 0-31291
- Hg-Mn stars, chemical abundances 0-56838
- Li in weak G-band stars, spalitative origin 0-51752
- Tc in late-type stars, spectral analysis 0-8623
- Ti, isotopic abundance ratios in cool stars 0-26840

**stellar dimensions**

- AGK3+19°599, ang. dia. from occultation by 65 Cybele 0-31237
- Ap stars, angular diameters, radii, and effective temps. 0-26870
- Be stars, emission shell diameter meas. possibility by lunar occultation method 0-56839
- $\alpha$  Bootis, ang. dia. and mass from predicted and observed spectral energy distrib. 0-46546
- VY Canis Majoris, OH/IR star, 1612 MHz OH maser multibaseline VLBI obs. 0-12766
- OX Cassiopeiae, eclipsing binary, photometric radii and luminosities 0-56877
- $\kappa$  Cassiopeiae, effective temp. radius, mass loss and luminosity 0-51748
- AZ Cassiopeiae, long-period eclipsing system, stellar radii ratio from photoelectric obs. 0-46608
- SU and TU Cassiopeiae, short-period Cepheids, photometry and spectra rel. to radius anomalies 0-26864
- BV Centauri, dwarf nova and spectroscopic binary, masses and absolute dimensions 0-51775
- Cepheid variables, double-mode, Wesselink radii 0-31311
- Cepheid variables, short-period, radial vels., BVRI photometry, radii 0-31309
- Z Chamaleontis, cataclysmic binary, masses radii, and mass exchange rel. to gravit. radiation 0-4386
- P Cygni, effective temp. radius, mass loss and luminosity 0-51748
- NML=V1489 Cygni, OH/IR star, 1612 MHz OH maser multibaseline VLBI obs. 0-12766
- NML Cygni, power spectrum and dia. from IR speckle interferometry 0-31216
- V 1668 Cygni (Nova 1978), photospheric radius at max. brightness 0-51789
- V1668 Cygni (Nova 1978), temps. and radii from UVB light curve 0-46565
- WW Draconis, eclipsing binary, masses, radii and luminosities from photoelectric lightcurves 0-46606
- BY Draconis, spotted flare star, primary rot. vel. and radius rel. to pre-main-sequence nature 0-36633
- dwarf novae, quasi-periodic oscills. and nonradial pulsations of accretion disks 0-46568
- flare stars in solar neighbourhood, physical parameters 0-51777
- HD 190603, effective temp. radius, mass loss and luminosity 0-51748
- u Herculis, BVR lightcurves interpreted 0-41856
- LT Herculis, eclipsing binary, photometric elements 0-31328
- IRC+10216, spatial spectra from 2.2 to 20 microns, deviations from spherical symmetry 0-41911
- $\rho$  Leonis, effective temp. radius, mass loss and luminosity 0-51748
- Mira variables and IR sources, angular dia. in near IR, 2-5  $\mu\text{m}$  speckle interferometry 0-27010
- 1 Monocerotis,  $\delta$  Scuti star, oscill. modes and radius 0-51787
- MXB 1728-34, emission region apparent radius from type I X-ray burst obs. 0-17692

**stellar dimensions continued**

- neutron stars, mass-radius relation, obs. constraints, dense matter eqn. of state 0-46597
- non-radial oscillations, linear eigenvalue problem props. study, model 0-17571
- nonradial oscills., eigenvalue multiplicity 0-51740
- nonradial oscills., modal analysis by asymptotic method 0-21996
- nonradial pulsation hypothesis with simulated line profile vars. 0-8618
- NP 0532, Crab pulsar, mass and radius from supernova remnant physical theory 0-51834
- OB-type stars, effective temps., ang. diameters, distances and linear radii 0-17584
- $\xi$  Ophiuchi, rot.-related spectral vars. rel. to stellar radius 0-22000
- optical interferometry with two telescopes (French) 0-46403
- $\alpha$  Orionis, IR speckle images, two-dimens. obs. (French) 0-46553
- oscillations of main sequence stars, observability by photometry and spectra 0-51724
- 53 Persei, nonradial pulsator, light var. rel. to line profile changes 0-4362
- photospheric expansion and macroturbulence, line broadening effects 0-56813
- radial and nonradial stellar oscills. effect on light, colour and vel. vars. 0-31310
- AQ Sagittarii, C star, ang. dia. from lunar occultation meas. 0-22008
- $\zeta^1$  Scorpii, extreme B1 supergiant, IUE obs. rel. to mass, radius and bolometric luminosity 0-17583
- single main sequence stars (A0 V to G2 V), radii compared with radii determined using binary systems 0-51758
- SS 433, emitting region dia. and electron density from IR energy distrib. 0-31312
- U Trianguli Australis, UBVR obs. of beat Cepheid, pulsation energy changes 0-4360
- AH Velorum, radius, delta luminosity and pulsation mode of  $\delta$  Cepheid 0-46572
- very close binary systems, struct. eqns. including rot. and tidal distortions for ZAMS stars 0-22037
- white dwarf stars, masses and radii from two-colour diagram 0-46547
- X-ray bursters, radius and mass, general relativistic effects 0-8712

**stellar evolution**

- anisotropic spheres, adiabatic contraction in general relativity 0-36489
- asymptotic giant branch evolution with steady mass loss 0-26846
- B-type stars, evidence for form, in R-associations 0-26851
- birthrate and nucleosynthetic yields of metals 0-51741
- blue stragglers as long-lived stars 0-46542
- SU and TU Cassiopeiae, short-period Cepheids, radius anomalies investigations rel. to evolution 0-26864
- cataclysmic binaries, evolution and origin 0-56885
- cataclysmic binary formation through common envelope evolution 0-8651
- V553 Centauri, C rich Cepheid, C and N abundances rel. to nuclear processes and evolutionary status 0-4378
- SV Centauri, early-type contact binary, evolutionary models 0-4403
- Cepheid instability strip 0-56833
- Cepheus A mol. cloud, OH maser lines obs., star form. region 0-36691
- collapse, adiabatic hydrodynamics and shock wave propag. 0-56861
- collapse generating gravitational radiation, strength estimate 0-46584
- collapse of massive star cores, supernova explosion from shock heating 0-56863
- contact binaries, solar type, ang. momentum controlled evolution 0-36670
- convective stars, forced mixing effects on evolution 0-56818
- core collapse, limits on nuclei excitation energies in hot matter 0-56703
- core collapse, neutral currents and neutrino Comptonisation in high-temp. nuclear matter 0-21905
- core collapse, neutrino prod. and inelastic scatt. by nuclei at extreme temps. 0-36488
- core collapse, Thomas-Fermi model of warm nuclei 0-51648
- core collapse, vacuum neutrino oscills, inhibition by high matter density 0-36496
- degenerate stars with H atmospheres, cooling law from space freq. 0-17576
- HR Delphini (Nova 1967), photoionisation models, binary system evolution 0-17590
- BY Draconis, prototype spotted flare star, pre-main-sequence nature 0-36633
- dwarf Cepheids evolutionary stage, anal. and conclusions 0-46562
- eclipsing binary stars, period statistics rel. to form. and evolution 0-36662
- explosion models, new solns. 0-12751
- formation, gravit. instability of interstellar magnetised gaseous discs 0-4424
- formation, supernova trigger 0-26891
- formation and early evolution in NGC 1333, colliding molecular clouds 0-12757
- formation by spiral density wave in disc of Galaxy 0-12812
- formation in Cepheus OB3 and Perseus OB2 mol. clouds, evidence from mol. obs. 0-12798
- formation in dust clouds with bright nebulosities 0-56893
- formation in inner Milky Way, evidence from CO obs. of interstellar mol. clouds 0-4425
- formation in M8 (Lagoon Nebula), evidence from far IR obs. 0-4413
- formation induced by galactic density wave 0-17649
- formation mechanisms and galactic evolution 0-12811
- formation rate in M83 and Milky Way 0-51870
- formation regions structure, population categories and mol. clouds evolution 0-17645
- formation through accretion shock, model for H II blisters 0-21994
- giant stars, ages determ. via photoelectric MgH+Mgb index 0-12753
- giant stars in open cluster NGC 7789, metal abundance, He content and mass loss 0-31335
- gravitational collapse to neutron stars and black holes, computer generation of spherical spacetimes 0-46385
- gravitational instability role in galaxy and star form. theories (Czech) 0-41718
- H-R diagram boundary for chromospheres and convection theory 0-56823
- high mass stars, evolution including stellar wind effects 0-21982
- hot massive stars, stellar wind mass loss, evolution study 0-17578
- intermediate-mass stars asymptotic giant branch evolution as function of mass and comp. 0-12749
- irradiated stars in active galactic nuclei, mass loss and evolution 0-56949



**stellar evolution continued**

- in irregular and blue compact galaxies, evolutionary models rel. to galaxies chemical comp. 0-36711
- LB 3459, subdwarf eclipsing binary, evolutionary model 0-51808
- LMC, blue to red supergiant star ratio across face, rel. to star form. 0-26984
- low-mass stars formation, evidence from  $\text{NC}_5\text{N}$  and  $\text{NH}_3$  obs. in Taurus 0-26957
- lower main-sequence stars, age-rot. vel. rotation 0-51767
- luminous stars in M31, evolution from studies in Baade's Field IV 0-36622
- main sequence stars, single, (A0 V to G2 V), evolutionary effects on radii 0-51758
- mass loss by stellar wind, effect on Galaxy chemical enrichment 0-41814
- mass loss rates, constraints from white dwarf data 0-46548
- massive He burning stars losing mass by stellar wind, evolution rel. to Wolf-Rayet binaries 0-36615
- massive stars, effects of binary evolution on heavy elements prod. 0-46534
- massive stars nucleosynthesis, effect of mass loss on chemical yields 0-36614
- massive X-ray binaries, evolution of optical components 0-41857
- Melotte 66, oldest open cluster, colour-magnitude diagram rel. to age 0-17621
- Mira variables, envelope pulsational instability rel. to planetary nebula form. 0-26928
- Monoceros OB2 association, evidence for supernova-induced star form. 0-31334
- NGC 604, giant H II region in M33, SNRs rel. to content of high mass stars 0-31340
- NGC 6052, complex galaxy, star form. burst rel. to late-type spirals collision 0-8681
- nonradial oscillations, avoided level crossing 0-31294
- O-type main sequence stars, rotational vel. evolution 0-51759
- OB associations, mag. fields influence on subgroups sequential form. 0-4408
- open clusters, H-R diagrams anal. rel. to Galaxy chemical abundance gradient 0-56938
- Orion Nebula, low-luminosity X-ray sources obs., assoc. with star form. 0-26959
- $\beta$  Persei type systems, orbital period changes and evolutionary status 0-4396
- SX Phoenicis, evolutionary stage of RRs star 0-46583
- planetary nebulae central stars, evolutionary tracks rel. to nebulae radio flux density distrib. 0-56913
- pre-main sequence, observational studies for  $\text{H}\alpha$  emission stars 0-56827
- pre-main-sequence stars, early evolution with D burning 0-51736
- presupernova models and supernovae 0-56864
- protostar, rotating, fragmentation, comparison of two three-dimensional computer codes 0-26850
- protostellar envelopes of masses 3  $M_\odot$  and 10  $M_\odot$ , struct. and hydrodynamic evolution 0-36616
- protostellar rotating gas clouds, fragmentation 0-51827
- red giant stage 0-12752
- red giants, peculiar, constraints on evolution from masses and space densities 0-22001
- Reissner-Norstrom black hole, interior final state evolution 0-8648
- rotating stars, secular instability from thermal cond. 0-21986
- solar neighbourhood initial mass function determ. from upper H-R diagram study 0-36626
- spectroscopic binaries, evolution rel. to primary mass, mass ratio and orbital semiaxis distrib. 0-46616
- SS 433, early-type binary model and evolutionary state 0-56843
- SS 433, lifetime against gravit. radiation in ultra-close binary system model 0-4384
- SS 433, mass loss rates and lifetime from W50 optical filaments 0-12804
- SS 433, nature and evolutionary state (*Russian*) 0-36647
- star formation, in galactic dust/molecular clouds 0-26925
- star formation, influence of initial vel. fields in interstellar medium 0-21985
- star formation, ring form. in rotating protostellar clouds 0-56820
- star formation, stochastic model rel. to spiral galaxies props. 0-12818
- star formation bursts in Markarian galaxies, evidence from radio continuum obs. 0-46668
- star formation from collapsing turbulent interstellar clouds, three-dimensional numerical models 0-56910
- star formation in binary galaxies, rel. to galaxies peculiar luminosity function and colours 0-41900
- star formation in galactic centre, rate 0-36713
- star formation in W3, near IR obs. of two far IR sources 0-22058
- star formation process simulation, hydrostatic models evolution (*Polish*) 0-21998
- star formation regions,  $\text{H}_2\text{O}$  maser sources evolutionary sequence from VLBI obs 0-26954
- star-forming complex in S252 (NGC 2175), mol. line obs. 0-4411
- stochastic self-propagating star formation rel. to evolution of galaxies 0-12810
- stochastic stellar evolution, fluctuations due to convection 0-31293
- successive He shell flashes, anal. rel. to stationary shell burning 0-51737
- supermassive star collapse to black hole, Einstein eqns., numerical soln. 0-41851
- supernova off-centre explosions, rel. to high vel. pulsars form. 0-46587
- supernovae influence 0-31315
- DR Tauri, pre-main-sequence star, brightening, 1970 to 1979, and historical light curve 0-31297
- turbulent diffusion and  $^{12}\text{C}/^{13}\text{C}$  abundance ratio 0-21993
- $\gamma^2$  Velorum, WC+O binary, evolutionary model for mass-losing massive He star 0-36615
- very close binary systems, struct. eqns. including rot. and tidal distortions for ZAMS stars 0-22037
- W51 Main as expanding bubble around young massive O-star 0-8701
- white dwarf formation rate in globular clusters 0-4346
- white dwarf remnants production, progenitor stars upper mass limit determ. 0-51738
- white dwarfs, ages and cooling rel. to very low luminosity degenerates deficiency 0-17575
- zero age main sequence to red giant branch, evolutionary sequences 0-21987
- ( $n, \gamma$ ) for  $A=138-181$ , stellar nucleosynthesis and s-process neutron flux 0-42663
- C burning in degenerate core, convection effects 0-41810

**stellar evolution continued**

- $\text{C}_2$  white dwarfs, evolutionary status 0-4355
  - H burning evolutionary stages, Hertzsprung-Russell diagram age and mass calibrations 0-51744
  - He core flash onset and  $^{14}\text{C}(\alpha, \gamma)^{18}\text{O}$  in low-mass stars 0-51735
  - He shell burning stages, core mass-luminosity relations 0-21983
  - He shell flashes in red supergiants, convective penetrations and observable effects 0-51755
  - Hg-Mn stars, absolute magnitude and evolutionary status 0-46564
  - $^{40}\text{Ar}(n, \gamma)$ ,  $A=186-188$ , 2.6-800 keV, capture Maxwellian cross sections, galactic nucleosynthesis 0-42664
- stellar interiors** *see stellar internal processes*
- stellar internal processes**  
*see also solar interior; stellar evolution*
- Am-type stars, envelopes circulation 0-4370
  - Ap stars, radiative forces in stellar envelopes rel. to He abundance anomalies 0-31291
  - U Aquarii, R Coronae Borealis star, extraordinary comp. rel. to unusual s-processing event 0-17588
  - Boussinesq turbulence, statistical theory, appl. to stellar convection 0-48713
  - Cassiopeia A supernova, O burning rel. to remnant abundance inhomogeneities 0-12797
  - V553 Centauri, C rich Cepheid, C and N abundances rel. to nuclear processes and evolutionary status 0-4378
  - Cepheid pulsation period variability and convective efficiency 0-26885
  - collapse of massive star cores, supernova explosion from shock heating 0-56863
  - collapsed stars, neutrino flux from quark matter 0-22028
  - connection, random fluctuations rel. to stochastic evolution and oscill. props. 0-31293
  - contact binary stars, temp. discontinuity maintenance 0-8655
  - convection, fundamental hit correctable inconsistency of local mixing-length theory 0-26841
  - convection, mixing length parameter rel. to Hertzsprung-Russell diagram age and mass calibrations 0-51744
  - convection in massive star cores, effect on C/O ratio 0-17579
  - convection in rotating magnetic star, toroidal field effect 0-41816
  - convection onset in radially pulsating star 0-41809
  - convection zones dynamics, effect of rot. on turbulent viscosity and cond. 0-36612
  - core collapse, limits on nuclei excitation energies in hot matter 0-56703
  - core collapse, neutral currents and neutrino Comptonisation in high-temp. nuclear matter 0-21905
  - core collapse, neutrino prod. and inelastic scatt. by nuclei at extreme temps. 0-36488
  - core collapse, shape instability pressure stabilisation 0-8537
  - core collapse, Thomas-Fermi model of warm nuclei 0-51648
  - core collapse, vacuum neutrino oscills, inhibition by high matter density 0-36496
  - ellipsoidal potentials of polynomial distributions of matter 0-46532
  - evolutionary models from zero age main sequence to red giant branch 0-21987
  - forced mixing in convective stars, theory and effects on evolution 0-56818
  - gravitational waves generated by collapse, wave strength estimate 0-46584
  - heavy elements production in massive stars, effects of binary evolution 0-46534
  - high mass stars, semiconvection and convection rel. to evolutionary effects of stellar wind 0-21982
  - hot dense stellar matter, adiabatic index with full nuclear interaction 0-36620
  - intermediate-mass stars asymptotic giant branch evolution as function of mass and comp. 0-12749
  - isotopic anomalies from neutron reactions during stellar explosive C burning 0-12651
  - Mira variables, nuclear shell flashes rel. to planetary nebula form. 0-26928
  - neutrino capture rate problem, role of phonon in composite neutron mode 0-41808
  - neutron star interior plasma, mag. field rel. to pulsar periods long-term changes 0-22029
  - neutron stars, heating and cooling processes rel. to thermal props. and detectability 0-31323
  - neutron stars, inner crust nuclear compositions 0-31322
  - neutron stars, thermonuclear runaways rel. to X-ray bursts 0-22032
  - nucleosynthesis, effect of mass loss by stellar wind on Galaxy chemical enrichment 0-41814
  - nucleosynthesis in massive stars, effect of mass loss on chemical yields 0-36614
  - pre-main-sequence stars, early evolution with D burning 0-51736
  - quark stars, neutrino cooling 0-56858
  - Rayleigh-Taylor convective overturn in stellar collapse 0-41815
  - reactions producing D, T, and  $^3\text{He}$  in advanced stellar evolution, cross sections 0-56815
  - red giants, peculiar, constraints on evolution from masses and space densities 0-22001
  - resonant thermonuclear reaction rate integrals, closed-form evaluation and approximation considerations 0-8535
  - s-process calcs. and Ba II stars 0-56824
  - s-process nucleosynthesis in giant stars, implications of Ti isotopic abundance ratios 0-26840
  - spallative origin of Li in weak G-band stars 0-51752
  - stellar collapse, adiabatic hydrodynamics and shock wave propag. 0-56861
  - successive He shell flashes, anal. rel. to stationary shell burning 0-51737
  - superdense magnetised astrophysical objects, interiors physical conditions 0-17603
  - supernova off-centre explosions, rel. to high vel. pulsars form. 0-46587
  - supernovae, MHD model 0-46588
  - thermonuclear flashes on accreting neutron stars 0-31321
  - thermonuclear reactions, rate enhancement due to strong screening, ionic mixtures case 0-36613
  - turbulent diffusion and  $^{12}\text{C}/^{13}\text{C}$  abundance ratio 0-21993
  - turbulent thermal convection in presence of rot. and mag. field, stellar and planetary dynamos appl. 0-6042
  - white dwarf envelopes, heavy ion diffusion 0-51754
  - ( $n, \gamma$ ) for  $A=138-181$ , stellar nucleosynthesis and s-process neutron flux 0-42663



**stellar internal processes continued**

- pp reaction, exchange current corrections  $\pi$  and  $\rho$  exchange 0-26733
- C burning in degenerate core, convection effects 0-41810
- C-O dwarf, H and He burning in degenerate envelope (*Russian*) 0-17585
- $^{14}\text{C}(\alpha,\gamma)^{18}\text{O}$  and onset of core He flash in low-mass stars 0-51735
- He shell burning, thermal pulses in accreting white dwarf 0-22009
- He shell burning stages, core mass-luminosity relations 0-21983
- He shell flashes in red supergiants, convective penetrations and observable effects 0-51755
- Li production by weak G-band stars, results from abundance meas. 0-41819
- $^{40}\text{Os}(n,\gamma)$ ,  $A=186-188$ , 2.6-800 keV, capture Maxwellian cross sections, galactic nucleosynthesis 0-42664
- $^{32}\text{S}(n,X)$ , 2.5-1100 keV, resonance struct. from total and capture cross sections 0-42620

**stellar light curves** *see stellar photometry***stellar magnetism***see also solar magnetism*

- 2A 0311-227, high-speed photometry of AM Herculis-type binary 0-41912
- accreting compact object in binary system, magnetosphere theory, X-ray sources 0-46394
- accreting magnetic degenerate dwarfs, X-ray and UV emission 0-41826
- angular momentum and magnetic moment from superheavy hadrons 0-26843
- Ap-stars, photometry and surface magnetic fields 0-56847
- baryon star magnetospheres, inclined rotator case 0-26887
- Cepheid variables, mag. fields effects on pulsational behaviour 0-31302
- convection in rotating magnetic star, toroidal field effect 0-41816
- cosmological interpretation 0-46714
- Crab Nebula, central mag. dipole rot. neutron star theory for supernova remnant 0-51834
- cyclotron self-absorption in accretion columns of magnetic degenerate stars, X-ray sources appl. 0-12760
- V1057 Cygni, OH line Zeeman splitting and stellar mag. field 0-36629
- $\gamma$  Equulei, magnetic field obs. of Ap-star 0-51782
- field generation by close binary interaction 0-26903
- HD 215441 (Babcock's star), magnetic vars., non-axisymmetric eccentric dipole model 0-51779
- HD 3980, late Ap star, photometric and mag. variability obs. 0-56845
- HD 4174, peculiar M-giant, magnetic field 0-8631
- Hercules X-1, cyclotron self-absorpt. in accretion column of mag. degenerate star 0-12760
- AM Herculis type binaries, cyclotron self-absorption in accretion columns of magnetic degenerate stars 0-12760
- W Hydrae, long-period variable, suspected Zeeman splitting in OH masers 0-36632
- hydromagnetic phenomena described by elec. currents 0-36495
- magnetic binary problem, charged particle motion stationary solns. for oblate spheroid primaries 0-41697
- magnetic stars, equatorially symmetric rotator model, inhomogeneous element distrib. 0-4371
- neutron star, interaction between accretion disc and mag. field (*Russian*) 0-51799
- neutron star interior plasma, mag. field rel. to pulsar periods long-term changes 0-22029
- neutron star magnetosphere, plasma dynamics and accretion, fate of sinking filaments 0-51798
- neutron stars, electron solids in superstrong mag. fields, bifurcation-theory approach 0-4640
- neutron stars, EM multipole fields 0-26896
- neutron stars, mag. field effects on thermal radiation 0-56869
- neutron stars, superdense quark core, spontaneous magnetisation possibilities 0-8646
- neutron stars, torques rel. to pulsating X-ray sources period changes 0-31320
- NP 0532 magnetosphere, cyclotron instability rel. to origin of radiation (*Russian*) 0-8645
- oblique rotator with irrotational axisymmetric mag. field surface distrib., effective mag. field 0-26872
- protostellar sources, IR polarisation rel. to nearby interstellar polarisation 0-4347
- pulsar electron cap, electrons accel. in internal zone 0-46592
- pulsar magnetosphere, electron absorpt. rel. to spectra low-freq. dropoff 0-17602
- pulsar magnetosphere, magnetoactive plasma equilib. in gravit. field (*Russian*) 0-26895
- pulsar magnetosphere, quasi-transverse propag. theory rel. to individual pulse-polarisation patterns 0-46591
- pulsar magnetosphere models, interior and exterior struct., pair prod. 0-46594
- pulsar magnetospheres, narrowband versus broadband emission processes rel. to luminosities 0-51797
- pulsar magnetospheres, stellar-wind model for plasma-EM fields 0-22031
- radiative transfer in magnetic atmospheres, analytical soln. 0-36494
- spectral line formation in microturbulent magnetic fields 0-31201
- SS 433, accreting mag. neutron star model (*Russian*) 0-36647
- SS 433, dipole mag. field rel. to mass accel. and collimation mechanisms 0-4368
- superdense magnetised astrophysical objects, interiors physical conditions 0-17603
- supernovae, MHD model 0-46588
- 78 Virginis, Ap star, mag. field geometry, oblique rotator model 0-51773
- 78 Virginis, magnetic Ap star, high resolution polarisation obs. inside spectral lines 0-51772
- white dwarfs, mag. fields rel. to cyclotron absorpt. spectra 0-4351
- X-ray pulsars, mag. fields rel. to vacuum signature in spectra 0-27015
- X-ray sources, steady accretion discs general struct. with mag. field 0-8714

**stellar mass**

- ADS 4299, 8048 and 9352, parallaxes and masses for visual binaries 0-4402
- AE Aquarii, cataclysmic variable, rapid light oscills. obs. rel. to masses 0-36634
- binary stars on main sequence, secondary masses freq. distrib. 0-26901
- black holes, mass rel. to time-scale of rapid X-ray variability and dying pulse trains 0-56872
- blue stragglers as long-lived stars 0-46542
- $\alpha$  Bootis, ang. dia. and mass from predicted and observed spectral energy distrib. 0-46546

**stellar mass continued**

- OX Cassiopeiae, eclipsing binary, masses and photometric elements 0-56877
- RZ Cassiopeiae, eclipsing binary, spectroscopic orbit and mass 0-22040
- cataclysmic binaries, evolution and origin rel. to period/secondary mass relation 0-56885
- BV Centauri, dwarf nova and spectroscopic binary, masses and absolute dimensions 0-51775
- 17= $\xi$  Cephei A, speckle interferometry, mass-luminosity relation 0-56874
- Cepheid variables, mag. fields rel. to pulsational and evolutionary masses discrepancy 0-31302
- Z Chamaeleontis, cataclysmic binary, masses radii, and mass exchange rel. to gravit. radiation 0-4386
- 35 Comae Berenices, masses and K-line absolute magnitudes 0-8649
- core mass-luminosity relations, for He shell burning stars 0-21983
- BY Draconis, binary spotted flare star, mass and luminosity ratios rel. to pre-main-sequence nature 0-36633
- WW Draconis, eclipsing binary, masses, radii and luminosities from photoelectric lightcurves 0-46606
- dwarf Cepheids, mass and evolutionary stage 0-46562
- evolutionary models from zero age main sequence to red giant branch 0-21987
- G and K-type giant stars, mass correl. with Li abundance 0-41819
- giant stars in open cluster NGC 7789, metal abundance, He content and mass loss 0-31335
- HD 96953, spectroscopic binary, secondary component mass from photoelectric radial vels. 0-56887
- LT Herculis, eclipsing binary, photometric elements 0-31328
- DQ Herculis (Nova 1934), spectrophotometry rel. to red dwarf companion nature and mass 0-22017
- DQ Herculis (Nova 1934), UVB photometry of visual binary 0-8661
- hot massive stars, stellar wind mass loss, evolution study 0-17578
- HR 2081, double-lined spectroscopic binary, radial vel. orbit and min. masses 0-51811
- intermediate-mass stars asymptotic giant branch evolution as function of mass and comp. 0-12749
- $\gamma$  Leonis, masses and K-line absolute magnitudes 0-8649
- RR Lyrae variables in globular cluster NGC 6121 (M4), masses from UVB photometry 0-22018
- M36, photographic obs., mass, radius, central density, stellar vels. of open cluster (*German*) 0-31333
- M38, photographic obs., mass, radius, central density, stellar vels. of open cluster (*German*) 0-31333
- massive stars, core convection, effect on C/O ratio 0-17579
- massive white dwarfs, mass accretion, rel. to thermonuclear runaways 0-41822
- neutron star mass, determ. from theory for cold spherical stars 0-56859
- neutron stars, mass-radius relation, obs. constraints, dense matter eqn. of state 0-46597
- NGC 2477, photographic obs., mass, radius, central density, stellar vels. of open cluster (*German*) 0-31333
- NP 0532, Crab pulsar, mass and radius from supernova remnant physical theory 0-51834
- AU Pegasi, binary Type II cepheid, companion mass and nature 0-26866
- $\phi$  Persei, binary Be star, He II emission obs. rel. to components masses 0-12768
- $\beta$  Persei (Algol), orbital inclination and masses determ. from speckle interferometry 0-36668
- PSR 0820+02, long-period binary pulsar, orbital period and mass function 0-56867
- red giants, peculiar, constraints on evolution from masses and space densities 0-22001
- Rst 4036, red-dwarf binary star, orbital period and total mass 0-12780
- $\zeta^1$  Scorpii, extreme B1 supergiant, IUE obs. rel. to mass, radius and bolometric luminosity 0-17583
- solar neighbourhood initial mass function determ. from upper H-R diagram study 0-36626
- spectroscopic binaries, models for distrib. with respect to primary mass, mass ratio and orbital semiaxis 0-46616
- supergiant stars, pulsation mass calcs. 0-46556
- RV Tauri and yellow semiregular variables, metallicity and mass from photometric investigations 0-26865
- white dwarf progenitors, upper mass limit determ. 0-51738
- white dwarf stars, masses and radii from two-colour diagram 0-46547
- white dwarfs, mass distrib. rel. to stellar mass loss rates and galactic evolution models 0-46548
- Wolf 922, nearby red dwarf, evidence for low-mass unseen companion 0-51809
- X-ray bursters, radius and mass, general relativistic effects 0-8712
- yellow semiregular and RV Tauri variables, metallicity and mass from, photometric investigation 0-26865
- 1228, nearby red dwarf, evidence for low-mass unseen companion 0-51809
- H burning stars, Hertzsprung-Russell diagram age and mass calibrations 0-51744

**stellar models**

- adiabatic non-radial oscillations with moderate or large  $l$ , theory 0-56819
- AE Aquarii, cataclysmic variable, rapid light oscills. rel. to white dwarf oblique rotator model 0-36634
- B-type stars, pole-on, rapidly rot., spectral inconsistencies due to gravity darkening 0-17581
- Be stars, emission line profiles from envelopes, elliptical gaseous ring model 0-4373
- Be stars, emission line profiles from envelopes, theoretical profiles 0-4374
- black holes, X-ray polarisation features for geometrically thick clouds and accretion disc model 0-46700
- $\alpha$  Bootis, comparison of predicted and observed spectral energy distrib. 0-46546
- RS Canum Venaticorum systems, X-ray obs. and coronal model development 0-56873
- cataclysmic variables, accretion discs models rel. to emission line spectra 0-51774
- SV Centauri, early-type contact binary, evolutionary models 0-4403
- $\alpha$  Centauri A and B, IUE spectra and transition region models 0-46543
- Cepheid variables, He enrichment effects in atm., models 0-26884
- Cepheids, multimode, two-zone models, resonances 0-36641
- Cepheids in Magellanic Clouds, extrinsic model of anomalies 0-4361
- Cepheids pulsating envelopes models, mag. field effects 0-31302



## stellar models continued

- chromosphere models, Ca II H and K lines absolute flux profiles in F0 to M2-type stars 0-26842  
 chromosphere models, high-press. transition regions theory 0-26847  
 chromospheres, observational indicators, empirical models 0-12755  
 contact binary stars, discontinuity model internal inconsistencies 0-46613  
 convective models, fundamental hit correctable inconsistency of local mixing-length theory 0-26841  
 cool stellar wind models for late type stars 0-51733  
 coronae, two-parameter models 0-8619  
 SS Cygni, dwarf nova, spectrophotometry rel. to accretion disc models in eruption and at min. light 0-36635  
 Cygnus X-1, inverse Compton model 0-51918  
 Cygnus X-1, model of neutron star surrounded by massive disc 0-36736  
 degenerate stars with H atmospheres, props. rel. to theoretical models 0-17576  
 HR Delphini (Nova 1967), photoionisation models, binary system evolution 0-17590  
 differentially rotating gaseous polytropes, second-order perturb. theory 0-21990  
 Earthlike planets, prevalence in Universe 0-41735  
 evolutionary models from zero age main sequence to red giant branch 0-21987  
 F- and G-type supergiants, enhanced He abundance effects on visible spectra 0-12759  
 HD 184927, He variable star; oblique rotator model rel. to spectroscopic props. 0-51790  
 HD 215441 (Babcock's star), magnetic vars., non-axisymmetric eccentric dipole model 0-51779  
 HD 44179 (Red Rectangle), precessing jets model 0-4422  
 VW Hydris, cataclysmic variable, light curve superhumps model 0-4381  
 intermediate-mass stars asymptotic giant branch evolution as function of mass and comp. 0-12749  
 IRC+10216, circumstellar dust shell model rel. to IR energy distrib. 0-56972  
 late-type stars, extended atmospheres, sphericity effects in red giants, model study 0-22012  
 LB 3459, subdwarf eclipsing binary, evolutionary model 0-51808  
 $\alpha$  Lyrae (Vega), LTE blanketed models rel. to visible and UV continuous energy distrib. 0-26856  
 RR Lyrae stars models, radial pulsations 0-26863  
 magnetic stars, equatorially symmetric rotator model, inhomogeneous element distrib. 0-4371  
 magnetic white dwarfs, gamma ray burst model (Chinese) 0-12831  
 mass-radius relations for cold spherical body, relativistic effects 0-26730  
 massive He burning stars losing mass by stellar wind, evolution rel. to Wolf-Rayet binaries 0-36615  
 metal-poor late-type stars, model atmospheres rel. to MK spectral classification 0-4340  
 Mira variables, envelope pulsational instability rel. to planetary nebula form. 0-26928  
 neutron star models, theory for cold spherical stars 0-56859  
 non-radial oscillations, linear eigenvalue problem props. study, model 0-17571  
 nonradial oscillations, avoided level crossing 0-31294  
 nonradial oscillations of generalized Roche series models 0-21992  
 oblique rotator with irrotational axisymmetric mag. field surface distrib., effective mag. field 0-26872  
 FU Orionis mechanism 0-51763  
 SX Phoenicis, evolutionary stage of RRs star 0-46583  
 presupernova models and supernovae 0-56864  
 protostars, hydrostatic models evolution rel. to star form. process simulation (Polish) 0-21998  
 pulsar magnetosphere models, interior and exterior struct., pair prod. 0-46594  
 pulsar magnetospheres, stellar-wind model for plasma-EM fields 0-22031  
 pulsars, particle acceleration by DC electric fields 0-31316  
 pulsars, Ruderman-Sutherland model, emission zone limits 0-51795  
 response functions and secular modes 0-17572  
 rotating stars, perturbs. and stability, eigenvalues and perturb. theory 0-46538  
 rotating stars, perturbs. and stability, eigenvectors and variational principle 0-46537  
 S-type stars, molecular spectra and model atmospheres 0-51764  
 WZ Sagittae, cataclysmic variable, light curve superhumps model 0-4381  
 spectroscopic binaries, models for distrib. with respect to primary mass, mass ratio and orbital semiaxis 0-46616  
 SS 433, accreting mag. neutron star model (Russian) 0-36647  
 SS 433, binary star model including mag. white dwarf 0-4385  
 SS 433, early-type binary model 0-56843  
 SS 433, Of star orbited by neutron star, model 0-22025  
 SS 433 model, precessing jets in ultra-close binary system 0-4384  
 Stromgren four colour indices, grid for calc. of log g and effective temp. 0-36507  
 supercritical accretion discs winds struct. and appearance, numerical models 0-21984  
 supernovae, MHD model 0-46588  
 T Tauri stars atmospheres, sphere and low chromosphere model 0-36623  
 tidally distorted stars, form factor method for struct. determ. 0-21991  
 4U 2129-47, X-ray light curve and binary model 0-46704  
 very close binary systems, struct. eqns. including rot. and tidal distortions for ZAMS stars 0-22037  
 $\alpha$  Virginis,  $\beta$  Cephei type pulsation characts. 0-56835  
 78 Virginis, Ap star, mag. field geometry, oblique rotator model 0-51773  
 white dwarf stars, model atmospheres rel. to two-colour diagram, masses and radii 0-46547  
 white dwarfs, DB-type, model atmospheres 0-51761  
 white dwarfs, minimum-flux coronal models for H and He atmospheres 0-8626  
 white dwarfs, rapidly rotating, oscills., numerical calc. 0-46554  
 white dwarfs, slowly rotating, nonradial oscills. 0-4348  
 white dwarfs seismological theory for 1  $M_{\odot}$  model with crystalline core 0-17577  
 Wolf-Rayet stars, He rich-expanding atmosphere model rel. to UV energy distrib. obs. 0-22023  
 X-ray bursters 0-4460  
 X-ray source, intensities from stellar wind flow past compact object 0-22116  
 H burning stars, Hertzsprung-Russell diagram age and mass calibrations 0-51744

## stellar models continued

- H $\beta$  indices for model atms., B-type stars appl. 0-31292  
 HgMn stars, line blanketed model atmospheres rel. to spectrophotometry 0-26867
- stellar motion  
*see also celestial mechanics*  
 absolute proper motion compiled catalogue, composition method (Russian) 0-51747  
 ADS 11871 ( $\beta$  648), visual binary star, orbital elements, determ. using two methods 0-51805  
 U Aquilae, Cepheid variable, detect. as long-period binary by radial vel. spectrometer 0-51667  
 astrometric detection of planets, photoelectric detection equipment 0-56882  
 IU Aurigae, eclipsing binary, two-colour photometry and third component orbit 0-36669  
 $\alpha$  Aurigae (Capella), orbital motion determ. using phase effect detect. at CERGA stellar interferometer (French) 0-36508  
 axisymmetrical stellar systems, periodic orbits of stars 0-17619  
 BD+57° 1942, faint short-period binary, influence of Schwarzschild effect on orbital and system elements (German) 0-8653  
 BD+61° 1211 (2A 1052+606), RS Canum Venaticorum binary star, spectroscopic obs. 0-36663  
 binary star light and velocity curves simultaneous solution, eccentric orbit generalisation 0-36664  
 binary star orbits solution, Fourier transform method 0-26899  
 binary stars, minimum projected distance in eccentric orbits 0-26904  
 binary stars, Newtonian attraction of two adjacent round ellipsoidal segments (Italian) 0-8531  
 $\theta$  Carinae, radial vel. of chemically-peculiar B-type star 0-8635  
 RZ Cassiopeiae, eclipsing binary, spectroscopic orbit 0-22040  
 BV Centauri, dwarf nova and spectroscopic binary, radial vel. orbits 0-51775  
 $\alpha$  and Proxima Centauri, radial vels. and bound state 0-41859  
 central stars of planetary nebulae, kinematics 0-51762  
 17= $\xi$  Cephei A, speckle interferometry, visual orbital elements 0-56874  
 Cepheid variables, double-mode, freq. anal. 0-31308  
 Cepheid variables, short-period, radial vels., BVRI photometry, radii 0-31309  
 clusters, isolated, numerical methods of star escape rate determ. (Polish) 0-26922  
 clusters containing massive central black holes, dynamical simulations with self-consistent potentials 0-26915  
 CPD-26°389, central star of NGC 1360, radial vel. obs. 0-4350  
 57 Cygni, spectroscopic binary, search for systematic radial vel. anomalies 0-17617  
 detached systems, revised photometric elements for 8 double-line binaries 0-46610  
 BY Draconis, binary spotted flare star, orbital elements and pre-main-sequence nature 0-36633  
 dwarf Cepheids, space motions rel. to evolutionary stage 0-46562  
 dwarf stars, three-dimensional motion 0-12754  
 dynamical astronomy, integrable and stochastic behaviour 0-12650  
 eclipsing binaries, photoelectric lightcurves of possible sd-d systems, revised elements 0-56879  
 elliptical galaxies, anisotropic vel. distrib. generation 0-36715  
 faint short-period spectroscopic binaries, influence of Schwarzschild effect on orbital and system elements (German) 0-8653  
 galactic clusters, membership probabilities, photographic meas. of relative proper motions of stars 0-51817  
 galactic density waves, excitation at Lindblad and corotation resons. by external potential 0-22072  
 galaxies active nuclei, irradiated stars motion rel. to emission line broadening 0-56949  
 Galaxy dynamics, appl. of generalised twice restricted three-body problem (Russian) 0-51643  
 GCl 0422-213, distant globular cluster in Eridanus, heliocentric radial vel. 0-17624  
 galaxy collisions, numerical expts. 0-51864  
 globular clusters, late core collapse in gravitating systems 0-22048  
 HD 11579, spectroscopic binary orbit from photoelectric radial vels. 0-41862  
 HD 14969, IAU radial-velocity standard star, orbit from photoelectric radial vels. 0-56884  
 HD 175742, spectroscopic binary, orbit determ. with CORAVEL photoelectric radial vel. spectrometer (French) 0-36671  
 HD 197406, Wolf-Rayet spectroscopic binary, radial vels. and orbital elements 0-51812  
 HD 2343, spectroscopic binary, orbit from photoelectric radial vels. 0-8656  
 HD 50896 (WN5), emission-line spectrum and radial vel. vars. 0-51791  
 HD 77581 (4U 0900-40), apsidal motion test of eclipsing binary 0-51908  
 HD 94033 ultra short period cepheid, radial vel. and galactic orbit 0-22024  
 HD 96953, spectroscopic binary orbit from photoelectric radial vels. 0-56887  
 high-velocity stars, southern, radial vels. 0-21988  
 HR 2081, double-lined spectroscopic binary, radial vel. orbit and min. masses 0-51811  
 HR 5161, spectroscopic binary star, radial vel. orbit 0-12781  
 HR 9049, (HD 224113), eclipsing spectroscopic binary star, period and orbital elements 0-46609  
 VW Hydris, cataclysmic variable, orbital eccentricity rel. to light curve superhumps model 0-4381  
 hydrodynamic equations, rel. to radius depend. of elliptical galaxies vel. dispersion 0-51876  
 IAU Radial Velocity Standard stars, radial vels. meas. (French) 0-51743  
 IC 2391, relative proper motions of stars, ident. of member stars 0-51818  
 inhomogeneous spherical gravitating systems dynamics, simplest hydrodynamic models 0-17620  
 kinematics, appl. to galactic spiral structure parameters derivation 0-17665  
 RR Lyrae variables, three-dimensional motion 0-12754  
 M31 nuclear bulge, rotational vels. meas. 0-41888  
 M36, photographic obs., mass, radius, central density, stellar vels. of open cluster (German) 0-31333  
 M38, photographic obs., mass, radius, central density, stellar vels. of open cluster (German) 0-31333



**stellar motion continued**

- Me, globular cluster, stellar proper motions, membership and cluster internal motions 0-8665  
 Mira variables kinematics towards galactic centre 0-46578  
 1 Monocerotis,  $\delta$  Scuti star, oscillation modes from photoelectric radial vels. and BVRI photometry 0-51787  
 neutron stars space velocities, role of EM multipole fields 0-26896  
 Newtonian stellar dynamics, maximizing functionals, rel. to thermodynamic and dynamical stability 0-12782  
 NGC 2477, photographic obs., mass, radius, central density, stellar vels. of open cluster (*German*) 0-31333  
 NGC 2669, relative proper motions of stars, ident. of member stars 0-51818  
 northern FK4 stars, radial vel. meas. 0-26848  
 OB-type stars, radial vels. rel. to force field normal to galactic plane 0-46669  
 UZ Octantis, W Ursae Majoris system, UBV light curves and orbital elements 0-22042  
 open cluster, proper motions rel. to solar motion and apex determ. 0-46418  
 orbits in rotating galactic bar, isolating integrals of motion 0-4404  
 orbits near galaxy particle resonance, theoretical study 0-26914  
 parallax stars with MK spectral classifications 0-56721  
 AU Pegasi, binary Type II cepheid, photometric and spectroscopic study 0-26866  
 $\gamma$  Persei cluster, stellar membership determ. by proper motion meas. 0-56890  
 plane galactic orbits, epicyclic approx. 0-36674  
 proper motion of circumpolar stars, precessional corrections and solar motion const. rel. to AGK3 system (*Russian*) 0-12647  
 proper motions, membership and internal motions in M5 globular cluster 0-41864  
 PSR 0820+02, long-period binary pulsar, orbital period and mass function 0-56867  
 radial and nonradial stellar oscills. effect on light, colour and vel. vars. 0-31310  
 radial velocities, meas. via HF absorpt. cell 0-12681  
 radial velocity measurement via slitless fieldspectroscopy, focal-reducer system appl. 0-36504  
 radial-velocity standard stars, list of 200 stars 0-26849  
 resonant orbits comparison, theoretical results 0-56889  
 Rst 4036, red-dwarf binary star, orbital period and total mass 0-12780  
 runaway planetary nebula ejection from M32 0-46626  
 WZ Sagittae, cataclysmic variable, orbital eccentricity rel. to light curve superhumps model 0-4381  
 scale-covariant stellar dynamics, theory 0-26913  
 self-gravitating star system dynamics, time depend. soln. 0-4405  
 semi-detached systems, revised photometric elements for 8 single-line binaries 0-46611  
 semi-detached systems, revised photometric elements for 9 binaries 0-46612  
 solar apex, correl. with long-period comets perihelion points distrib. 0-4304  
 solar motion, vel. and apex determ. from open clusters proper motions 0-46418  
 solar system, motion rel. to extragalactic redshifts interpretation 0-4427  
 spectroscopic binaries, Barr effect anal. 0-8650  
 SS 433, period and evidence for eccentric orbit from IR light curves 0-8642  
 star clusters, evolution, Fokker-Planck eqn. numerical integration 0-36675  
 stellar systems dynamical evolution, analytical approximations for effect of mass loss 0-51815  
 subdwarfs, kinematics rel. to galactic halo rot., also He abundance 0-22003  
 T Tauri stars assoc. with Taurus-Auriga dark clouds, proper motions 0-41821  
 Trapezium member stars, space motions (*Chinese*) 0-8654  
 trapped orbits in time-dependent potential 0-8664  
 tube orbits, three-dimensional, around intermediate axis in triaxial galaxy model, nonexistence 0-22046  
 two point-masses bound system, influence of weak gravit. wave 0-21903  
 CQ Ursae Majoris, line identification list and radial vel. of Ap-star 0-41841  
 visual binary stars, orbital elements 0-46607  
 Wolf 922, nearby red dwarf, evidence for low-mass unseen companion 0-51809  
 $\mu$  Draconis (ADS 10345), radial vel. var. from spectra in visible 0-17612  
 1228, nearby red dwarf, evidence for low-mass unseen companion 0-51809

**stellar multicolour photometry** *see stellar photometry*

**stellar origin** *see stellar evolution*

**stellar photometry**

*see also stellar radiation; stellar spectra*

- 2A 0311-227, high-speed photometry of AM Herculis-type binary 0-41912  
 2A 0526-328 optical candidate, high speed optical photometry 0-51917  
 2A 0526-328, optical photometry of assoc. star 0-22120  
 2 A 1052+606, X-ray and optical variability of RS CVn star 0-31331  
 A-type stars, uvby $\beta$  calibrations 0-41820  
 AE 1, He-rich variable, spectroscopy and photometry 0-41836  
 RT Andromedae, eclipsing binary, three-colour photoelectric obs. and improved ephemeris 0-22043  
 RT Andromedae, light curve anal. of short period eclipsing binary 0-46603  
 ET Andromedae (HR 8861), Ap star, light vars. and period 0-46571  
 Ap-stars, photometry and surface magnetic fields 0-56847  
 56 Arietis, spectrophotometry of Ap star, continuum features vars. 0-36638  
 IU Aurigae, eclipsing binary, two-colour photometry rel. to presence of third body 0-36669  
 B-type stars, luminosity and effective temp. determ. 0-17582  
 BDS 1269, visual binary, metal abundances and characts. of components 0-4397  
 Be stars, photometric behaviour, UV excess, emission indices, galactic distrib. 0-36637  
 Be stars, variability search, 1971-8 photometric obs. 0-36650  
 binary stars, JHKLM photometry of close systems 0-46614  
 blue star in SNR 1006, spectral features and UBV photoelectric meas. 0-41830

**stellar photometry continued**

- i Bootis, light curve and period vars. of W Ursae Majoris type star 0-4398  
 SS Bootis, UBV obs. and Fourier anal., eclipsing RS Canum Venaticorum binary 0-17613  
 broadband filter photometry, TiO band absorption effect 0-41811  
 C- and M-type stars near globular cluster NGC 419 in SMC, cluster membership 0-26921  
 53 Camelopardalis, photometric vars. 0-4367  
 SS Camelopardalis, UBV photometry and light curve soln. for eclipsing RS Canum Venaticorum binary 0-41854  
 38 Cancrri,  $\delta$  Scuti star, UBV photometric obs. of variability 0-22021  
 49 Cancrri, spectrophotometry of Ap star, continuum features vars. 0-36638  
 $\beta$  Canis Majoris stars, ANS UV photometry 0-26871  
 AM Canum Venaticorum, orbital period increase 0-12765  
 Carina spiral feature, photometry and spectra rel. to stars and interstellar dust distrib. 0-51871  
 OX Cassiopeiae, eclipsing binary, photometric elements from UBV light curves 0-56877  
 AZ Cassiopeiae, long-period eclipsing system, photoelectric obs. 0-46608  
 SU and TU Cassiopeiae, short-period Cepheids, photometry and spectra rel. to radius anomalies 0-26864  
 cataclysmic variables, visual continuum flux distrib. 0-36636  
 V553 Centauri, C rich Cepheid, VRI photometry rel. to C and N abundances 0-4378  
 V436 Centauri, dwarf nova, photometry during superoutburst (May 1978) 0-46570  
 BV Centauri, dwarf nova and spectroscopic binary, UBV photometry, spectral types and orbit 0-51775  
 U Cephei, period changes in 1972-7 interval 0-8657  
 VW Cephei, periodic vars. in light curve of W Ursae Majoris system 0-36667  
 XY Cephei, photoelec. elements of semidetached binary system 0-31327  
 VV Cephei, UBV obs. of eclipsing binary, 1976-8 eclipse 0-17611  
 VV Cephei system, distant, in Puppis, spectral classification, UBV photometry and polarimetry 0-51810  
 Cepheid variables, short-period, radial vels., BVRI photometry, radii 0-31309  
 ZZ Ceti stars search, photometric obs. of apparently quiescent stars 0-22005  
 comparison stars near OJ287 and ON325, variability, period determ. 0-26882  
 Cousins VRI system, temp. and absolute flux calibration, appls. 0-26750  
 $\beta$  Crucis,  $\beta$  Canis Majoris star, photometric obs. 0-17595  
 SS Cygni, dwarf nova, spectrophotometry rel. to accretion disc models in eruption and at min. light 0-36635  
 NML Cygni, IR speckle interferometry 0-31216  
 UZ and VW Cygni, UBV light curve solns. for Algol-like systems 0-41855  
 V1500 Cygni (Nova 1975), light curve for 1975 Aug.-1977 July period 0-4372  
 V1668 Cygni (Nova 1978), photoelec. photometry, rapid flickering 0-36640  
 V1668 Cygni (Nova 1978), UBV light curve 0-46565  
 degenerate star candidates, photoelectric and spectroscopic obs. 0-12763  
 $\delta$  Delphini stars in Michigan Spectral Catalogue, uvby $\beta$  photometry rel. to spectral types 0-4377  
 detached systems, revised photometric elements for 8 double-line binaries 0-46610  
 S Doradus (HD 35343), luminous LMC supergiant, long time baseline VBLUW photometry 0-22007  
 S Doradus (HD 35343), luminous LMC supergiant, long time baseline VBLUW photometry 0-36630  
 WW Draconis, RS Canum Venaticorum type star, two-colour photoelectric lightcurves and elements 0-46606  
 BY Draconis, spotted flare star, spectra and photometry rel. to pre-main-sequence nature 0-36633  
 dwarf nova outbursts, colour vars. 0-46576  
 dwarf novae, spectrophotometry, 1250-7500 Å region 0-46577  
 early-type stars, northern intermediate galactic latit., H $\beta$  photometry, rel. to galactic struct. 0-36631  
 faint early-type stars in neighbourhood of H II region RCW 38, UBV photometry 0-4352  
 WX Eridani light curves, period, orbital elements of eclipsing binary 0-26902  
 extinction, oscills. caused by atmospheric disturbances, obs. 0-56606  
 faint proper-motion stars, spectra and photometry to very low luminosity degenerates deficiency 0-17575  
 faint UVBRI standard stars, photometric obs. 0-51813  
 FJM 6 region, reddened stars near IR photometry 0-26929  
 galactic anticentre direction, young stars photometry and spectra rel. to outer Galaxy struct. 0-22079  
 galactic G-type supergiants, UBV photometry 0-41824  
 GCl 0422-213, distant globular cluster in Eridanus, preliminary photometry and spectroscopy 0-17624  
 giant branch of Fornax dwarf elliptical galaxy, colour-magnitude diagram 0-4431  
 giant stars in open cluster NGC 7789, metal abundance, He content and mass loss 0-31335  
 giants in globular cluster  $\omega$  Centauri, CO absorption and effective temp. 0-51749  
 globular cluster giants, intermediate-band photometry rel. to blanketing differences 0-4345  
 globular clusters, in M31, luminosity distrib. 0-36708  
 HD 01891, subdwarf, photometry and spectrum rel. to UV excess and metal abundance 0-17574  
 HD 170899, possible halo population giant star 0-26859  
 HD 193793, Wolf-Rayet star, photometric evidence for C-rich dust cloud 0-26861  
 HD 31908, freq. analysis of  $\delta$  Delphini star 0-46581  
 HD 33579, 35343, HDE 286757, 269006, most luminous LMC supergiants, long time baseline VBLUW photometry 0-22007  
 HD 33579, HD 35343 (S Doradus), HDE 268757, HDE 269006, most luminous LMC supergiants, long time baseline VBLUW photometry 0-36630  
 HD 3765, variability due to eclipsing star or planetary system, BV photometry 0-17615  
 HD 3980, late Ap star, photometric and mag. variability obs. 0-56845  
 HD 63791, probable metal-poor halo G-type giant field star 0-26859  
 HD 80383, UBV photometry of  $\beta$  Cephei type star 0-36644



## stellar photometry continued

- HD 8781, freq. anal. of low-amplitude  $\delta$  Scuti star 0-46575  
 HD 94033 ultra short period cepheid, UVB and uvby $\beta$  photometry 0-22024  
 HDE 326333, new  $\beta$  Canis Majoris star, photometric obs. 0-17595  
 u Herculis, BVR lightcurves interpreted 0-41856  
 LT Herculis, eclipsing binary, photometric elements 0-31328  
 AC Herculis, RV Tauri star, UVB obs. 0-56857  
 DQ Herculis (Nova 1934), high time resolution spectrophotometry 0-22017  
 DQ Herculis (Nova 1934), UVB photometry of visual binary 0-8661  
 V533 Herculis (Nova 1963), 63 sec. oscill., UVB photometry 0-17592  
 high-velocity stars, southern, UVB colours 0-21989  
 HR 9049, (HD 224113), eclipsing spectroscopic binary star, period determ. 0-46609  
 Hyades, late-type stars intermediate-band photometry 0-31289  
 Hyades cluster, possible members BVRI photometry 0-51821  
 Hyades cluster, shape and luminosity distrib. 0-17622  
 IR photometry of late type stars 0-41823  
 K-type giant stars at South Galactic Pole, DDO photometry rel. to CN anomalies and distances 0-8622  
 Kottamia Observatory site, seasonal atm. extinction due to aerosol 0-46253  
 late-type (K0 to M6) giant stars, IR photometry and effective temps. 0-46545  
 late-type stars, balloon-borne near IR multicolour photometry 0-4356  
 late-type stars, near IR multicolour photometry from BAT (*Japanese*) 0-31298  
 late-type stars, near IR photometry with balloon-borne telescope 0-4357  
 late-type stars photometry, photoelectric MgH+MgB index meas. 0-12753  
 LMC, stellar photoelectric UVB photometry (*German*) 0-21932  
 loose clusterings in southern Milky Way, continued photometric studies 0-36679  
 luminous stars in M31 0-36622  
 $\alpha, \tau$  Lupi,  $\beta$  Canis Majoris stars, photometric obs. 0-17595  
 $\beta$  Lyrae, narrow-band photometry in (1971) 0-46605  
 RR Lyrae star in globular cluster NGC 6717, photometric investigation 0-46624  
 RR Lyrae stars in Microscopium, VBLUW photometry and proposed intergalactic dust cloud 0-56851  
 RR Lyrae variables in globular cluster NGC 6121 (M4), UVB photometry 0-22018  
 main sequence stars, oscills., observability by photometry and spectra 0-51724  
 Melotte 66, oldest open cluster, colour-magnitude diagram rel. to age 0-17621  
 Michigan 239, peculiar extragalactic or extreme halo emission-line star, IR photometry 0-4380  
 N Monoceros region, two-micron IR objects survey 0-8555  
 19 Monocerotis,  $\beta$  Canis Majoris variable, photometric obs. 0-4379  
 1 Monocerotis,  $\delta$  Scuti star, oscillation modes from photoelectric radial vels. and BVRI photometry 0-51787  
 V616 Monocerotis (A 0620-00), UVB photometry 0-56846  
 narrow-band photometry in O6 to G2 stars 0-8621  
 near IR photometry, effects of atmospheric extinction 0-51539  
 nearby stars, spectroscopic and photometric data published (1969-1978) 0-36513  
 NGC 1261, globular cluster, colour-magnitude diagram 0-17623  
 NGC 1868 in LMC, BV photometry of metal-poor intermediate-age cluster 0-51814  
 NGC 2264, UVBRI photometry of 70 field stars in young cluster 0-51819  
 NGC 2420, old disc cluster, photometry and spectra rel. to stars chemical comp. 0-46620  
 NGC 2423, 2482, Hyades-like clusters, late-type stars intermediate-band photometry 0-31289  
 NGC 3532, southern open cluster, UVB photometric study 0-46621  
 NGC 4755, southern open cluster, Balmer line photoelectric photometry 0-56892  
 NGC 6144, globular cluster, and neighbouring region, photometric obs. 0-51816  
 NGC 6528, metal-rich globular cluster, colour-magnitude diagram from UVB photometry 0-4406  
 NGC 6611, young open cluster, UVB magnitudes and colours, reddening, distance, luminosity 0-31332  
 NGC 6717, globular cluster, colour-magnitude diagram, distance and metallicity 0-46624  
 NGC 6823, UVB photometry and spectra, extinction study of young open cluster 0-4407  
 NGC 6913 galactic cluster, photoelec. photometry of brighter stars, variability obs. 0-46625  
 Nova Serpentinis 1978, IR photometry 0-4365  
 novalike object in Vulpecula, UVB photometry (1979 August 6 to September 20) 0-8644  
 OB-type stars, spectrophotometry rel. to effective temps., ang. diameters, distances and linear radii 0-17584  
 OB-type stars in SA 98, UVB photoelectric meas. 0-46535  
 UZ Octantis, W Ursae Majoris system, UVB light curves 0-22042  
 U Ophiuchi, massive eclipsing binary star, spectrophotometry 0-26900  
 Orion OBI (Belt), photometric studies 0-46618  
 YY Orionis stars in Orion population, UVB photometry of young emission-line objects 0-46552  
 AU Pegasi, binary Type II cepheid, photometric and spectroscopic study 0-26866  
 BB Pegasi, photoelectric photometry of totally eclipsing W Ursae Majoris systems, 1978 Oct. to Nov. (*Chinese*) 0-31330  
 AQ Pegasi, UVB light curve solns. for Algol-like system 0-41855  
 AG Persei, massive eclipsing binary star, spectrophotometry 0-26900  
 53 Persei, nonradial mode identification 0-8632  
 21 Persei, spectrophotometry of Ap star, continuum features vars. 0-36638  
 b Persei, UVB photometry and spectroscopic study of ellipsoidal variable 0-36666  
 X Persei (3U 0352+30), simultaneous X-ray and ground-based optical obs. 0-17591  
 Pleiades cluster, reddening-face colours, photometric zero age main sequence definition 0-26920  
 Praesepe, photometry in BVRI colours 0-26917  
 Przybylski's star (HD 101065),  $\beta$  photometry and period determ. 0-41835

## stellar photometry continued

- R Puppis (HD 62058), G-type supergiant, UVB photometry and variability confirmation 0-41824  
 very red giant stars in Fornax galaxy, discovery and BV photometry 0-51768  
 RI photometry, response functions from observed and computed (V-R) and (V-I) colour indices 0-56715  
 SA 133 field near galactic centre, three-colour stellar photometry (*German*) 0-36618  
 HM Sagittae, emission-line star, UVB photometry and spectral obs. in (1978) (*Russian*) 0-36648  
 HM Sagittae, emission-line star, polarimetry, (1977 to 1978) (*Russian*) 0-36649  
 HM Sagittae, variable emission object, spectrophotometry 0-17599  
 XZ Sagittarii, Algol system, UVB photometric investigation 0-22041  
 AQ Sagittarii, C star, visible and IR photometry rel. to ang. dia. 0-22008  
 V356 Sagittarii, massive eclipsing binary star, spectrophotometry 0-26900  
 MV Sagittarii, R Coronae Borealis variable, brightness decline obs. and UVB photometry 0-8641  
 $\delta$  Scuti variables, photometric search of Hyades cluster 0-36677  
 semi-detached systems, revised photometric elements for 8 single-line binaries 0-46611  
 semi-detached systems, revised photometric elements for 9 binaries 0-46612  
 SN in NGC 4321, JHKL mags., 1980 Jan. obs. 0-41847  
 solar vicinity stars, photometric survey rel. to low mass interstellar clouds catalogue 0-36512  
 southern metal-poor stars, UVBRI photometry and UV excesses 0-56828  
 southern standard stars, monochromatic flux from 3200 Å to 8800 Å 0-51742  
 SS 433, IR and visible obs., IR excess and emission processes 0-4387  
 SS 433, IR light curves from BVJHK photometry, period and ephemeris 0-8642  
 Stepanyan's star, spectrophotometric and photometric obs., 228-min period 0-56883  
 Stephenson-Sanduleak 433, 1.2-2.5  $\mu$ m spectroscopy, photometry and polarimetry 0-41838  
 Stromgren four colour indices, grid for calc. of log g and effective temp. 0-36507  
 Stromgren uvby photoelectric obs. of stars in dust clouds with bright nebulosities 0-56893  
 SU Tauri, emission lines at min. and BV photoelectric photometry 0-8640  
 $\lambda$  Tauri, massive eclipsing binary star, spectrophotometry 0-26900  
 RR Tauri, rapid periodicity, photometric investigations 0-26853  
 RV Tauri and yellow semiregular variables, photometric investigations 0-26865  
 T Tauri stars in Orion population, UVB photometry of young emission-line objects 0-46552  
 U Trianguli Australis, UVBRI obs. of beat Cepheid, pulsation energy changes 0-4360  
 47 Tucanae, globular cluster, photometry and spectra rel. to stars chemical comp. 0-46620  
 4 U 2129+47 optical counterpart, spectrum and photometry rel. to 0-17693  
 UVB photoelectric photometry of M31 clusters (*Russian*) 0-36680  
 UVB photoelectric sequences, in fields of eight low-red shift quasars (*French*) 0-51904  
 UVB photoelectric standards in SA 1-115, final catalogue 0-41733  
 uvby photometry of bright northern stars with interesting Stromgren indices 0-56817  
 variable stars in globular cluster NGC 6934, photometry 0-56891  
 VBLUW photoelectric photometric catalogue on mag. tape 0-36515  
 AH Velorum, radius, delta luminosity and pulsation mode of  $\delta$  Cepheid 0-46572  
 Vulpecula OB2 stars, photometry and spectra rel. to membership of 67 day Cepheid S Vulpeculae 0-41831  
 21 Vulpeculae, new luminous long period  $\delta$  Scuti star, photometry 0-31306  
 BW Vulpeculae, V photometry, light curve, quadratic ephemeris 0-26881  
 Washington Photometric System, props. and standard stars 0-31213  
 white dwarf stars, two-colour diagram rel. to masses and radii 0-46547  
 white dwarfs, uvby photometry of 112 southern objects 0-8624  
 white dwarfs in open clusters, obs. rel. to progenitor stars upper mass limit 0-51738  
 Wolf-Rayet stars, ANS UV spectrophotometric obs. 0-22023  
 yellow semiregular and RV Tauri variables, photometric investigations 0-26865  
 C stars, JHKL photometry 0-46555  
 C stars in Cygnus, new discoveries and BV photometry 0-46551  
 H deficient and He weak stars, uvby photometry, variability 0-46579  
 H $\beta$  indices for model atms., B-type stars appl. 0-31292  
 HgMn stars, spectrophotometry 0-26867

stellar positions *see astrometry*

## stellar radiation

- see also solar radiation; stellar photometry*  
 2A 0526-328 optical candidate, rapid brightness vars. obs. 0-51917  
 A 0535+26, transient X-ray source, flare obs. by (Prognoz 6) (*Russian*) 0-51920  
 A-type stars, uvby $\beta$  calibrations 0-41820  
 accreting magnetic degenerate dwarfs, X-ray and UV emission 0-41826  
 RT Andromedae, light curve anal. of short period eclipsing binary 0-46603  
 Ap stars, radiative forces in stellar envelopes rel. to He abundance anomalies 0-31291  
 AE Aquarii, cataclysmic variable, rapid light oscills. rel. to white dwarf oblique rotator model 0-36634  
 R Aquarii, UVBRI polarimetric obs., orbital motion effect (*Russian*) 0-36646  
 atmosphere in statistical equil., effects of deviations from LTE on emergent spectrum 0-31290  
 atmospheric scatt., approx. soln. (*Russian*) 0-36621  
 B 1900+14, soft gamma-ray bursts obs. (*Russian*) 0-36742  
 B-type stars, luminosity and effective temp. determ. 0-17582  
 B-type stars embedded in R-associations, free-free emission obs. 0-26851  
 binary star light and velocity curves simultaneous solution, eccentric orbit generalisation 0-36664



## stellar radiation continued

- black holes, rotating, neutrino fluxes resulting from macroscopic parity violation 0-22034  
 black holes, theory, of rapid X-ray variability and dying pulse trains 0-56872  
 black holes, X-ray radiation polarisation features 0-46700  
 black holes in binary stellar systems, gamma emission during spherically symmetric accretion 0-17608  
 UZ Bootis, cataclysmic variable similar to WZ Sagittae, outburst characteristics. 0-17596  
 $\alpha$  Bootis, comparison of predicted and observed spectral energy distrib. 0-46546  
 SS Bootis, UVB obs. and Fourier anal., eclipsing RS Canum Venaticorum binary 0-17613  
 Z Camelopardalis, dwarf nova, photometric obs. and light curve (1973-77) 0-56853  
 VY Canis Majoris, OH/IR star, 1612 MHz OH maser multibaseline VLBI obs. 0-12766  
 $\alpha$  Canis Majoris B (Sirius B), minimum flux H coronal model rel. to X-ray emission 0-8626  
 $\beta$  Canis Majoris stars, UV flux obs., basic data obtained with TD-1A satellite 0-51783  
 Y Canum Venaticorum, C star, IR spectrum between 1.2 and 30 microns 0-46544  
 RS Canum Venaticorum, intrinsic linear polarization of eclipsing binary 0-4394  
 $\eta$  Carinae, high-resolution IR radiation maps of homunculus, spectral and spatial distrib. 0-12767  
 $\nu$  Carinae, X-ray emission obs. from star and surrounding nebula 0-26876  
 $\gamma$  Cassiopeiae, Be star, polarisation rapid vars. 0-22022  
 OX Cassiopeiae, eclipsing binary, photometric radii and luminosities 0-56877  
 $\kappa$  Cassiopeiae, effective temp. radius, mass loss and luminosity 0-51748  
 cataclysmic variables, emission lines from accretion discs 0-51774  
 proxima = V645 Centauri, dMe flare star, quiescent corona, transition region, and chromosphere obs. 0-56850  
 SV Centauri, early-type contact binary, evolutionary models, luminosities and effective temps. 0-4403  
 V78 in  $\omega$  Centauri, light curve anal. in freq. domain by automatized Fourier technique 0-22039  
 $\alpha$  Centauri A and B, UV line fluxes from IUE spectra, and transition region models 0-46543  
 EM Cephei, B-type eclipsing binary system, investigation of period and min. 0-17614  
 VW Cephei, periodic vars. in light curve of W Ursae Majoris system 0-36667  
 VW Cephei, W Ursae Majoris star, identification with faint X-ray source 0-51913  
 17 =  $\xi$  Cephei A, speckle interferometry, mass-luminosity relation 0-56874  
 Cepheid variables, double-mode, freq. anal. 0-31308  
 WX Ceti, cataclysmic variable similar to WZ Sagittae, outburst characters. 0-17596  
 $\sigma$  Ceti, SiO maser variability at 86 GHz 0-41839  
 $\sigma$  Ceti AB, IUE obs. of UV spectrum 0-22027  
 Z Chamaeleontis, cataclysmic binary, possible gravit. radiation emission 0-4386  
 chromosphere Ca II H and K line radiation, absolute flux profiles in F0 to M2-type stars 0-26842  
 chromosphere radiative loss rates in cool stars, rel. to Mg II flux profiles 0-36611  
 CIT 6 (IRC+30219), IR C star, CO obs. of mass outflow 0-12761  
 collapsed stars, neutrino flux from quark matter 0-22028  
 35 Comae Berenices, masses and K-line absolute magnitudes 0-8649  
 comparison stars near OJ287 and ON325, variability, period determ. 0-26882  
 contact binaries, theoretical atlas of light curves and rot. broadening functions 0-17610  
 $\epsilon$  Coronae Austrinae, polarimetric obs. of eclipsing binary 0-56888  
 $\sigma$  Coronae Borealis (HD 146361), spectroscopic binary, soft, X-ray obs. with (HEAO-1) 0-56886  
 cyclotron self-absorption in accretion columns of magnetic degenerate stars, X-ray sources appl. 0-12760  
 SS Cygni, dwarf nova, accretion disc radiation models in eruption and at min. light 0-36635  
 SS Cygni, dwarf nova, soft X-ray pulsation obs. 0-46563  
 P Cygni, effective temp. radius, mass loss and luminosity 0-51748  
 V1057 Cygni, OH obs. 0-36629  
 NML = V1489 Cygni, OH/IR star, 1612 MHz OH maser multibaseline VLBI obs. 0-12766  
 CH Cygni, symbiotic star, rapid and slow light vars. 0-51792  
 V1357 Cygni (Cygnus X-1), no long-term light vars. (1928-77) 0-41861  
 V1341 Cygni (Cygnus X-2), shortest optical variability (*Russian*) 0-17695  
 V1500 Cygni (Nova 1975), light curve for 1975 Aug.-1977 July period 0-4372  
 V1500 Cygni (Nova 1975), radio emission from expanding shell 0-26868  
 V1500 Cygni (Nova 1975), visible and UV spectra and light curve 0-12771  
 V1668 Cygni (Nova 1978), linear polarisation obs. 0-26875  
 V 1668 Cygni (Nova 1978), visual light curve correl. with spectral development 0-51789  
 Cygnus X-1, evidence for new variability in hard X-ray emission 0-27011  
 Cygnus X-1, extended-bandwidth X-ray obs. 0-17689  
 Cygnus X-1, neutron star plus massive disc model rel. to light curve 0-36736  
 Cygnus X-1, UV shot noise upper limit 0-4458  
 Cygnus X-1, X-2 and X-3, long-term-studies with Ariel 5 All-Sky Monitor (ASM) 0-17688  
 Cygnus X-1, X-ray flux time variability struct. (*Russian*) 0-51921  
 Cygnus X-2, rapid UV flux vars., IUE obs. 0-12833  
 Cygnus X-3, 4.8 hour modulation period change disproved 0-8713  
 Cygnus X-3, hard X-ray spectrum obs. 0-31388  
 degenerate stars with H atmospheres, props. rel. to theoretical models 0-17576  
 HR Delphini (Nova 1967), radio emission from expanding shell 0-26868  
 BY Draconis, binary spotted flare star, mass and luminosity ratios rel. to pre-main-sequence nature 0-36633

## stellar radiation continued

- WW Draconis, eclipsing binary, masses, radii and luminosities from photoelectric lightcurves 0-46606  
 CR Draconis, UV Ceti variable, flares colour behaviour 0-22020  
 dwarf nova outbursts, colour vars. 0-46576  
 dwarf novae, HEAO-A2 soft X-ray survey during optical outburst 0-46574  
 early type stars, mid UV spectra obs. 0-21995  
 early type stars, normal, near UV line blocking depend. on spectral type and luminosity 0-36619  
 eclipsing binaries, photoelectric lightcurves of possible sd-d systems, revised elements 0-56879  
 eclipsing variable stars, Fourier analysis of light curves, error anal. in freq. domain 0-31214  
 eclipsing variable stars with extended atmospheres, Fourier anal. of light curves 0-46604  
 EXP 0520-66, flaring X-ray pulsar, recurrent gamma-ray bursts obs. (*Russian*) 0-36741  
 flare stars in Orion Nebula region, new objects and repeated outbursts 0-56852  
 flare stars in solar neighbourhood, physical parameters 0-51777  
 galactic 2  $\mu$ m radiation, mean intensity in solar neighbourhood 0-36744  
 galactic photometric disc model, direct starlight intensities and interstellar dust clumping effects 0-22077  
 gravitation radiation from homologous oscill. of compressible Newtonian spheroid 0-46533  
 gravitational radiation energy loss from binary stars, free-fall sources model 0-51647  
 gravitational waves generated by collapse, wave strength estimate 0-46584  
 HD 153919 (3U 1700-37), X-ray luminosity rel. to forbidden Fe XIV and Fe X emission 0-4358  
 HD 190603, effective temp. radius, mass loss and luminosity 0-51748  
 HD 193793, Wolf-Rayet star, IR brightening rel. to circumstellar dust form. 0-31301  
 HD 200775/NGC 7023 complex, intrinsic and interstellar reddening components 0-51832  
 HD 221568, Ap star, light var. period 0-56856  
 HD 31908, freq. analysis of  $\delta$  Delphini star 0-46581  
 HD 3765, variability due to eclipsing star or planetary system, BV photometry 0-17615  
 HD 8781, freq. anal. of low-amplitude  $\delta$  Scuti star 0-46575  
 HDE 245770, possible counterpart of variable X-ray source A 0535+26, line and continuum vars. 0-17600  
 HZ Hercules (Hercules X-1), 70 day period refuted 0-56975  
 Hercules X-1, cyclotron line form. by reson. Compton cyclotron scatt. 0-8711  
 Hercules X-1, cyclotron self-absorpt. in accretion column of mag. degenerate star 0-12760  
 Hercules X-1 (HZ Herculis), periodic mass transfer rel. to X-ray light curve 0-51911  
 $\mu$  Herculis, BVR lightcurves interpreted 0-41856  
 LT Herculis, eclipsing binary, photometric elements 0-31328  
 $\mu$  Herculis, synthetic light curve soln. of OAO-2 UV light curves 0-4399  
 AM Herculis (4U 1813+50), rapid light variability obs. (*Russian*) 0-8662  
 DQ Herculis (Nova 1934), short-period oscills. modulation and pulsed emission lines asymmetry interpretation 0-22044  
 AM Herculis type binaries, cyclotron self-absorption in accretion columns of magnetic degenerate stars 0-12760  
 high luminosity stars in Galaxy and Magellanic Clouds, UVB intrinsic colours 0-26855  
 hot white dwarfs, EUV flux interstellar absorpt., local clumpiness factor determ. 0-36627  
 HR 1099, RS Canum Venaticorum binary, February 1978 radio flare obs. 0-26911  
 HR 1217, Ap star, spectrum and light vars. relationship 0-26878  
 HR 4665, spectroscopy of bright long-period RS Canum Venaticorum system 0-36665  
 EX Hydrae, 2:3 period ratio in light curve 0-46580  
 W Hydrae, long-period variable, suspected Zeeman splitting in OH masers 0-36632  
 VW Hydri, cataclysmic variable, light curve superhumps model 0-4381  
 integrated starlight synthetic spectrum between 3000 and 10000 Å, calc. method and results 0-46536  
 interferometry, long baseline, S/N ratio 0-26749  
 interstellar diffuse starlight, inverse Compton interactions with relativistic electrons rel. to gamma-ray prod. 0-17448  
 interstellar linear polarisation, wavelength depend. at near IR wavelengths 0-51833  
 interstellar polarisation in irregularly fluctuating medium, statistical anal. 0-26926  
 interstellar UV radiation field, in clouds cooled by C atoms and ions (*Russian*) 0-12801  
 inverse Compton effect of electrons on starlight 0-26702  
 IR fluxes of single main sequence stars (A0 V to G2 V), rel. to radii determ. 0-51758  
 IRC+10216, circumstellar dust shell model rel. to IR energy distrib. 0-56972  
 IRC-10442 (GL5268S), possibly two star clusters, near IR and radio obs. 0-4412  
 K1082, in globular cluster M15, suspected ultrashort period variable star 0-26883  
 12 Lacertae, nonradial oscills. of  $\beta$  Cephei type star 0-4366  
 DD=12 Lacertae, obs. study of secular var. and pulsational stability 0-41833  
 EV Lacertae, UV Ceti variable, flares colour behaviour 0-22020  
 late type stars, Ca II H and K lines and nearby continuum photoelectric calibration 0-36617  
 $\rho$  Leonis, effective temp. radius, mass loss and luminosity 0-51748  
 $\gamma$  Leonis, masses and K-line absolute magnitudes 0-8649  
 R Leonis, SiO maser variability at 86 GHz 0-41839  
 AD Leonis, UV Ceti variable, flares colour behaviour 0-22020  
 linear polarization of 313 nearby low galactic latitude 0-46641  
 luminosity systems calibration, trigonometric parallaxes appl. 0-4343  
 RU Lupi, T Tauri star, chromosphere and corona parameters and expected X-ray fluxes (*Russian*) 0-51770  
 $\alpha$  Lyrae (Vega), continuous energy distrib. rel. to LTE blanketed models predictions 0-26856  
 RR Lyrae stars, period-luminosity-colour relations, metallicity effects 0-56842



## stellar radiation continued

- RR Lyrae variables,  $\delta(0.6)$  UV excess rel. to metallicity and three-dimensional motion 0-12754  
 M17, exciting stars radiation rel. to far IR obs. and H II region/mol. cloud interaction 0-22053  
 magnetic white dwarfs, gamma ray burst model (*Chinese*) 0-12831  
 Melotte 66, oldest open cluster, giant branch clump luminosity rel. to age 0-17621  
 MWC 349, IR source optical identification with reddened high-luminosity star 0-56971  
 MXB 1728-34, type I X-ray burst obs. by (HEAO-1) 0-17692  
 MXB 1730-335, Rapid Burster, IR bursts detect. confirmation 0-27020  
 MXB 1730-335 (Rapid Burster), steady X-ray emission obs. 0-22119  
 MXB 1837+05 (Serpens X-1), detect. of optical burst coincident with X-ray burst 0-27013  
 neutrinos and cosmic rays from pulsars 0-31319  
 neutron stars, highly magnetised, thermal radiation 0-56869  
 neutron stars, thermonuclear runaways rel. to X-ray bursts 0-22032  
 neutron stars EM recoil radiation, role of EM multipole fields 0-26896  
 neutron stars surface radiation, detectability rel. to cooling and heating processes 0-31323  
 NGC 253, Sc-type galaxy, stellar content determ. from two-micron spectrophotometry 0-4442  
 NGC 6611, young open cluster, UVB magnitudes and colours, reddening, distance, luminosity 0-31332  
 nova shells, radio emission obs. 0-26868  
 Nova Vulpeculae 1979, slow nova, pre-maximum light curve 0-4364  
 novlike object in Vulpecula, UVB photometry (1979 August 6 to September 20) 0-8644  
 NP 0532, Crab pulsar, radiation, role of magnetosphere cyclotron instability (*Russian*) 0-8645  
 NP 0532, Crab pulsar, gravitational radiation obs., energy flux upper limit 0-36655  
 O-type stars in open cluster IC 1805, luminosities rel. to C IV line P Cygni profiles 0-31296  
 OB-type stars, effective temps., ang. diameters, distances and linear radii 0-17584  
 OH maser emission from late-type stars, UHF obs. 0-56826  
 opacity in dense plasma 0-26731  
 open clusters, H-R diagrams anal. rel. to Galaxy chemical abundance gradient 0-56938  
 U Orionis, Mira variable, relation between 1612 MHz flare and light curve 0-56844  
 $\lambda$  Orionis, obs. of UV radiation scattered by interstellar dust 0-56918  
 53 Persei, nonradical pulsator, light var. rel. to line profile changes 0-4362  
 $\beta$  Persei (Algol), radio outbursts and possible period change 0-26907  
 $\beta$  Persei type systems, orbital period changes and evolutionary status 0-4396  
 planetary nebulae, low excitation, central stars, continuous energy distrib. and temps. 0-17646  
 Pleiades cluster, reddening-face colours, photometric zero age main sequence definition 0-26920  
 protostellar envelopes of masses 3  $M_{\odot}$  and 10  $M_{\odot}$ , coupled radiative transfer/hydrodynamics eqns. and IR appearance 0-36616  
 protostellar sources, IR polarisation rel. to nearby interstellar polarisation 0-4347  
 PSR 0531+21, Crab pulsar, optical light curve changes in 1970-7 period 0-36654  
 PSR 0820+02, period vars. rel. to membership of long-period binary system 0-56867  
 PSR 0833-45, Vela pulsar, optical pulse profile 0-46593  
 PSR 0833-45, Vela pulsar, pulsed high energy gamma rays 0-41848  
 PSR 0950+08, pulsar, micropulses freq. struct. 0-22030  
 pulsar, mag. bremsstrahlung of ultrarelativistic particle beam in relativistic plasma 0-46390  
 pulsar magnetosphere, magnetoactive plasma equilib. in gravit. field (*Russian*) 0-26895  
 pulsar microstructure, propag. effects in shearing field-free plasma 0-17483  
 pulsar scintillations, freq. cross-correl. and finite bandwidth effects 0-4392  
 pulsar signals interstellar scintillation, analytic soln. of second-order moment eqn. 0-26726  
 pulsar spectra, nature of low-freq. dropoff 0-17602  
 pulsars, individual pulse-polarisation patterns and quasi-transverse propag. theory 0-46591  
 pulsars, interpulse emission struct. 0-36652  
 pulsars, narrowband versus broadband emission processes rel. to luminosities 0-51797  
 pulsars, radio flux density and pulse profile at 102.5 and 61 MHz 0-17601  
 pulsars, timing measurements appl. to search for gravit. waves 0-36743  
 radial and nonradial stellar oscils. effect on light, colour and vel. vars. 0-31310  
 WZ Sagittae, cataclysmic variable, light curve superhumps model 0-4381  
 $\mu$  Sagittarii, binary star, obs. of eclipse of unseen companion 0-4401  
 AQ Sagittarii, C star, ang. dia. and effective temp. 0-22008  
 MV Sagittarii, R Coronae Borealis variable, brightness decline obs. and UVB photometry 0-8641  
 $\zeta$  Scorpii, extreme B1 supergiant, IUE obs. of line spectrum and continuum energy distrib. 0-17583  
 FH Serpentis (Nova 1970), radio emission from expanding shell 0-26868  
 SN 1181 (3C 58), absolute magnitude and type classification 0-56862  
 spectroscopic binaries, single-line, nature of secondary stars from X-ray obs. 0-31329  
 SS 433, assoc. radio jet flux density vars. 0-31381  
 SS 433, IR energy distrib. obs. 0-31312  
 SS 433, light minimum epoch and period 0-26886  
 SS 433, photometry, 1979 July to October, and 6.5 day period identification 0-8643  
 SS 433, radiation press. rel. to mass accel. and collimation mechanisms 0-4368  
 SS 433, short term H $\alpha$  central intensity increases 0-4375  
 subdwarfs, luminosity-temp. diagram locus rel. to He abundance 0-22003  
 subdwarfs, UV excesses and metal abundances 0-17574  
 supercritical accretion discs struct. and appearance, numerical models 0-21984  
 supernova in ESO 153-G27, discovery and magnitudes (1979 August 19 to October 15) 0-26892  
 symbiotic stars, survey at 1612 MHz 0-12774

## stellar radiation continued

- synchrotron neutrino emission, charge collision emission, star neutrino luminosity 0-41719  
 V711 Tauri, change in nature of light curve, and flare, 1979 October to December 0-26906  
 V471 Tauri, period var. and light curves of eclipsing binary system 0-22038  
 DR Tauri, pre-main-sequence star, brightening, 1970 to 1979, and historical light curve 0-31297  
 RR Tauri, rapid periodicity, photometric investigations 0-26853  
 T Tauri stars, continuum emission synthesis from photosphere and low chromosphere model 0-36623  
 thermal X-ray emission 0-41849  
 Tycho's supernova, distance and luminosity from fast shock wave model for remnant 0-46631  
 4U 1626-67, 7.7-second X-ray pulsar, simultaneous X-ray and optical obs. 0-51914  
 4U 1626-67, light pulses from optical counterpart 0-51916  
 4U 2129+47, X-ray light curve and binary model 0-46704  
 AW Ursae Majoris, light curve anal. of contact binary 0-56875  
 SU Ursae Majoris, probable 1980 March super outburst 0-51785  
 W Ursae Majoris stars, atm. parameters of A-type systems 0-36672  
 UV chromospheric and transition-layer emission 0-56823  
 UV radiation, interstellar grains scatt. props. rel. to particle size distrib. 0-26932  
 variable stars period determination, maximum entropy method accuracy 0-56712  
 AH Velorum, radius, delta luminosity and pulsation mode of  $\delta$  Cepheid 0-46572  
 XX Virginis, field Population II Cepheid, absolute mag. 0-41832  
 78 Virginis, magnetic Ap star, high resolution polarisation obs. inside spectral lines 0-51772  
 AR Virginis, RR Lyrae variable, photographic photometry and mean light curve (*Russian*) 0-12769  
 S Vulpeculae, 67 day Cepheid, luminosity from membership in (Vulpecula OB2) 0-41831  
 white dwarfs, DB-type, model atmospheres rel. to emerging fluxes and colours 0-51761  
 Wolf-Rayet stars in LMC, new discoveries, positions, spectra and magnitudes 0-46569  
 X-ray pulsator, 38.22 second period, in vicinity of OAO 1653-40, very hard spectrum 0-27014  
 X-ray source, intensities from stellar wind flow past compact object 0-22116  
 young stars, high-freq. radio continuum obs. 0-51766  
 ZB 33, RR Lyrae type star, light curve study (*Chinese*) 0-8633  
 C stars, search for HCN and CH maser emissions 0-51856  
 SS Cygni, soft X-ray emission detect. during optical outburst 0-46574  
 U Geminorum, soft X-ray emission detect. during optical outburst 0-46574  
 H burning stars, Hertzsprung-Russell diagram age and mass calibrations 0-51744  
 He shell burning stars, core mass-luminosity relations 0-21983  
 Hg-Mn stars, absolute magnitude 0-46564  
 O-rich late-type stars, 16 to 39 micron spectroscopy 0-22002  
 SiO 86.2 GHz maser sources, polarisation props. 0-4449  
 SiO masers,  $J=1-0$   $\nu=1$  and 2 masers relative intensity and vel. 0-4339

## stellar rotation

- see also solar rotation  
 Am-type stars, rot. vels. and spectral types catalogue 0-36514  
 Am-type stars, rotationally driven envelope circulation 0-4370  
 ET Andromedae (HR 8861), Ap star, light vars. and period 0-46571  
 angular momentum and magnetic moment from superheavy hadrons 0-26843  
 AE Aquarii, cataclysmic variable, rapid light oscils. rel. to white dwarf oblique rotator model 0-36634  
 B-type stars, pole-on, rapidly rot., spectral inconsistencies due to gravity darkening 0-17581  
 binary stars, nonsynchronous rot. generalisation of light and vel. curves simultaneous soln. technique 0-36664  
 binary stars on main sequence, freq. depend. on mean rot. vel. 0-26901  
 black holes, rotating, neutrino fluxes resulting from macroscopic parity violation 0-22034  
 $\alpha$  Camelopardalis (O9.5 Ia), expanding envelope rot. rel. to variable H $\alpha$  P Cygni profile 0-41818  
 $\gamma$  Cassiopeiae, Be star, polarisation rapid vars. rel. to rot. circumstellar envelope inhomogeneities 0-22022  
 contact binaries, solar type, ang. momentum controlled evolution 0-36670  
 contact binaries, theoretical atlas of light curves and rot. broadening functions 0-17610  
 convection in rotating magnetic star, toroidal field effect 0-41816  
 convection zones dynamics, effect of rot. on turbulent viscosity and cond. 0-36612  
 Crab Nebula, central mag. dipole rot. neutron star theory for supernova remnant 0-51834  
 Cygnus X-1, rapidly rotating neutron star plus massive disc model 0-36736  
 differentially rotating gaseous polytropes, Eulerian eqns. 0-51739  
 differentially rotating gaseous polytropes, second-order perturb. theory 0-21990  
 BY Draconis, spotted flare star, primary rot. vel. and radius rel. to pre-main-sequence nature 0-36633  
 ellipsoidal potentials of polynomial distributions of matter 0-46532  
 G200-39, hot hybrid white dwarf, rot. rel. to atmospheric mixing 0-26852  
 HD 184927, He variable star; oblique rotator model rel. to spectroscopic props. 0-51790  
 HD 221568, Ap star, light var. period 0-56856  
 HD 3980, late Ap star, photometric and mag. variability obs. 0-56845  
 HD 64740, He rich star, UV spectral vars. 0-22016  
 HZ Herculis (Hercules X-1), precessing twisted accretion disks 0-56973  
 lower main-sequence stars, rot. studies 0-51767  
 magnetic stars, equatorially symmetric rotator model, inhomogeneous element distrib. 0-4371  
 I Monocerotis,  $\delta$  Scuti star, evidence for dipole mode oscils. split by stellar rot. 0-51787  
 neutron star, accretion disc/mag. field interaction rel. to spin-up and spin-down (*Russian*) 0-51799  
 neutron stars, EM multipole fields rot. rel. to vel. 0-26896



## stellar rotation continued

- neutron stars, magnetic, accretion torques rel. to pulsating X-ray sources period changes 0-31320
- Newtonian spheroid, homologous oscill., gravit. radiation 0-46533
- normal modes of rotating stars, general variational principle 0-12750
- O-type main sequence stars, rotational vel. evolution 0-51759
- oblique rotator with irrotational axisymmetric mag. field surface distrib., effective mag. field 0-26872
- † Ophiuchi, spectral vars. related to rot. 0-22000
- YY Orionis stars, rot. rel. to spectral line form. in axisymmetric moving envelopes 0-41813
- perturbations and stability of rot. stars, eigenvalues and perturb. theory 0-46538
- perturbations and stability of rot. stars, eigenvectors and variational principle 0-46537
- protostar, rotating, fragmentation, comparison of two three-dimensional computer codes 0-26850
- PSR 0329+54, binary motion to explain freq. variations 0-26894
- pulsar electron cap, electrons accel. in internal zone 0-46592
- pulsar magnetosphere models, interior and exterior struct., pair prod. 0-46594
- pulsar NP 0531, distrib. model of press., density, ang. vel., matter rot., grav. field (*Ukrainian*) 0-12775
- pulsar polar caps as foil-less diodes, nonneutral relativistic beam accel. 0-17604
- pulsars, long-term changes in periods and neutron star interior plasma 0-22029
- rigidly rotating stars, secular instabilities in general relativity, theoretical formalism 0-4341
- rigidly rotating stars, secular instabilities in general relativity, numerical results 0-4342
- secular instability in rotating stars, resulting from thermal cond. 0-21986
- self-gravitating rotating masses, book contrib., review 0-21915
- spectral line broadening effects of macroturbulence and rotation 0-56813
- SS 433, black hole rot. rel. to precessing jets model in ultra-close binary system 0-4384
- stability and perturbations, normal mode completeness 0-4344
- tidally distorted stars, form factor method for struct. determ. 0-21991
- very close binary systems, struct. eqns. including rot. and tidal distortions for ZAMS stars 0-22037
- 78 Virginis, Ap star, mag. field geometry, oblique rotator model 0-51773
- white dwarfs, rapidly rotating, oscills., numerical calc. 0-46554
- white dwarfs, slowly rotating, nonradial oscills. 0-4348

stellar size see stellar dimensions

## stellar spectra

see also solar spectra; stellar photometry

- OB-type stars, O VI obs. in stellar winds 0-8630
- 2A 0526-328 optical counterpart, identification and spectrum 0-22118
- A 0535+26, transient X-ray source, flare energy spectra obs. by (Prognoz 6) (*Russian*) 0-51920
- 2 A 1052+606, X-ray and optical variability of RS CVn star 0-31331
- AE 1, He-rich variable, spectroscopy and photometry 0-41836
- Am-type stars with known spectral types, second catalogue 0-36514
- † Andromedae, rapid spectral line variability disproved 0-8625
- Ap and Am stars, numerical taxonomy 0-22015
- α Aquarii, chromospheric event detect. from UV spectrum obs. 0-31299
- U Aquarii, R Coronae Borealis star, extraordinary comp. rel. to unusual s-processing event 0-17588
- R Aquarii, UV obs. of hot component 0-56854
- 56 Arietis, spectrophotometry of Ap star, continuum features vars. 0-36638
- atmospheric structure, mol. effects 0-21999
- α Aurigae (Capella), X-ray line emission obs., corona models 0-26905
- B-type stars, pole-on, rapidly rot., spectral inconsistencies due to gravity darkening 0-17581
- BD+61° 1211 (2A 1052+606), RS Canum Venaticorum binary star, spectroscopic obs. 0-36663
- Be stars, electron scatt. effects on Balmer emission lines 0-17589
- Be stars, emission line profiles from envelopes, elliptical gaseous ring model 0-4373
- Be stars, emission line profiles from envelopes, theoretical profiles 0-4374
- Beals' Type III P Cygni line profiles 0-51771
- Becklin-Neugebauer source in Orion, 3.3 to 5.5 microns spectrum 0-12796
- black holes in binary stellar systems, gamma emission during spherically symmetric accretion 0-17608
- blue star in SNR 1006, spectral features and UVB photoelectric meas. 0-41830
- α Bootis, search for Ti II 3080 Å multiplet emission 0-51769
- α Bootis (Arcturus), spectral line asymmetry meas. rel. to Sun 0-51753
- ξ Bootis A, active dwarf star, chromospheric emission lines obs. 0-12762
- α Camelopardalis (O9.5 Ia), stellar wind terminal vel. short time changes from UV spectrum 0-36625
- α Camelopardalis (O9.5 Ia), variable Hα P Cygni profile 0-41818
- 49 Cancri, spectrophotometry of Ap star, continuum features vars. 0-36638
- Canis Major R1, anomalous diffuse bands 0-51820
- VY Canis Majoris, OH/IR star, 1612 MHz OH maser multibaseline VLBL obs. 0-12766
- α Canis Majoris (Sirius), Ca II K line high resolution profile obs. 0-56830
- α Canis Majoris (Sirius B), spectral energy distrib. 0-8629
- α Canis Minoris, flux spectrogram, UV line blending and wavelengths, spectral resolution influence 0-56811
- Y Canum Venaticorum, C star, IR spectrum between 1.2 and 30 microns 0-46544
- Carina spiral feature, photometry and spectra rel. to stars and interstellar dust distrib. 0-51871
- η Carinae, high-resolution IR radiation maps of homunculus, spectral and spatial distrib. 0-12767
- AG Carinae, luminous star in symmetric nebulae, IUE low-dispersion spectrum 0-46560
- θ Carinae, radial vel. of chemically-peculiar B-type star 0-8635
- RZ Cassiopeiae, eclipsing binary, spectroscopic orbit 0-22040
- γ Cassiopeiae, N I interstellar absorption, UV obs. 0-51823
- SU and TU Cassiopeiae, short-period Cepheids, photometry and spectra rel. to radius anomalies 0-26864
- 6 Cassiopeiae, spectroscopic obs. of supergiant star, equivalent widths, microturbulence and radial vel. 0-22006
- cataclysmic variables, emission lines from accretion discs 0-51774
- stellar spectra continued
- V553 Centauri, C rich Cepheid, C and N abundances 0-4378
- proxima=V645 Centauri, dMe flare star, quiescent corona, transition region, and chromosphere obs. 0-56850
- BV Centauri, dwarf nova and spectroscopic binary, UVB photometry, spectral types and orbit 0-51775
- α Centauri A and B, IUE spectra and transition region models 0-46543
- central stars of planetary nebulae, UV spectral obs. from TD-1 satellite 0-31300
- U Cephei, eclipsing binary, gas stream effects in UV spectrum, IUE obs. 0-26898
- δ Cephei, Hα radial vel. behaviour 0-51788
- DI Cephei, spectrum vars. in T Tauri star 0-8628
- VV Cephei system, distant, in Puppis, spectral classification, UVB photometry and polarimetry 0-51810
- Cepheid variables, He enrichment effects in atm., models 0-26884
- classical Cepheids, nonvariable supergiants and bright giants, spectrophotometric comparison 0-56837
- τ Ceti, Ca II 866.2 nm emission event 0-26860
- κ Ceti, IUE obs. of far UV spectra of G-type dwarf 0-56831
- o Ceti AB, IUE obs. of UV spectrum 0-22027
- chromosphere lines, high-press. transition regions rel. to Ca II and Mg II reson. lines profiles 0-26847
- CIT 6 (IRC+30219), IR C star, CO obs. of mass outflow 0-12761
- classifications for bright northern stars with interesting Stromgren indices 0-56817
- composite spectra stars, new classification scheme for bright stars of Hynek's (1938) list (*French*) 0-56876
- cool stars, Ti isotopic abundance ratios 0-26840
- β Coronae Borealis, H I Paschen lines and Ca II triplet study 0-26869
- σ Coronae Borealis (HD 146361), spectroscopic binary, soft, X-ray obs. with (HEAO-1) 0-56886
- R Coronae Borealis in quiet state, spectral energy distrib. (*Russian*) 0-51781
- coude spectrograms of stars in dust clouds with bright nebulosities 0-56893
- P Cygni, extreme B-type supergiant, UV spectroscopy 0-22004
- V1057 Cygni, FU Orionis star, IR spectroscopy with contact-type image tube 0-17587
- P Cygni, high resolution UV spectrum obs. 0-26873
- V1016 Cygni, image-tube spectrograms 0-8639
- 32 Cygni, IUE obs. and effects of B-type star within late-type supergiant upper chromosphere 0-22036
- V382 Cygni, IUE spectra of massive close binary 0-8659
- V832-59 Cygni, mass-losing Be star, changes in UV spectrum 0-46561
- V1016 Cygni, new spectroscopic obs., simultaneous presence of increasing excitation and cool features 0-26874
- V1057 Cygni, OH obs. 0-36629
- NML=V1489 Cygni, OH/IR star, 1612 MHz OH maser multibaseline VLBL obs. 0-12766
- α Cygni, radial vel. and line profile vars. in supergiant 0-22010
- 57 Cygni, spectroscopic binary, search for systematic radial vel. anomalies 0-17617
- 59=V832 Cygni, variable mass flux from spectroscopic obs. 0-41840
- V1500 Cygni (Nova 1975), Hα and Hβ emission line vars. 0-4389
- V1500 Cygni (Nova 1975), visible and UV spectra and light curve 0-12771
- V 1668 Cygni (Nova 1978), spectral development 0-51789
- Cygnus OB2 number 12, spectral classification and membership of association 0-51760
- Cygnus X-3, hard X-ray spectrum obs. 0-31388
- degenerate star candidates, photoelectric and spectroscopic obs. 0-12763
- degenerate stars with H atmospheres, spectra rel. to comp. and theoretical models 0-17576
- HR Delphini, UV spectrum, stellar wind 0-26880
- HR Delphini (Nova 1967), cataclysmic binary spectrum 0-4359
- HR Delphini (Nova 1967), emission lines at nebular stage (*Russian*) 0-17597
- HR Delphini (Nova 1967), nebular stage spectra rel. to envelope regions physical conditions 0-4369
- HR Delphini (Nova 1967), spectra, line identification, radial vels. 0-17594
- δ Delphini stars in Michigan Spectral Catalogue, uvbyβ photometry rel. to spectral types 0-4377
- diffuse interstellar line at 6284 Å, obs. and relation to interstellar reddening 0-51843
- 30 Doradus central object (HD 38268), interstellar and nebular lines obs. 0-51839
- BY Draconis, spotted flare star, spectra and photometry rel. to pre-main-sequence nature 0-36633
- dwarf novae, spectra (*Russian*) 0-8638
- dwarf novae, spectrophotometry, 1250-7500 Å region 0-46577
- early type stars, 206-287 nm UV spectra of Ap, Bp, Be, Bn and shell stars 0-51776
- early type stars, 'normal', with anomalous mid UV spectra 0-26857
- early type stars, mid UV spectra obs. 0-21995
- early type stars, normal, near UV line blocking depend. on spectral type and luminosity 0-36619
- eclipsing binary stars, period distrib. rel. to components spectral types 0-36662
- emission lines near Ca II H and K, obs. of spatial intensity vars. on solar limb 0-51720
- emission-line stars in galactic cluster NGC 663, spectroscopic obs. 0-4363
- eruptive variable stars, IR spectra rel. to grains props. 0-26943
- expanding and rotating atmospheres, curves of growth and line profiles 0-31295
- F- and G-type supergiants, enhanced He abundance effects on visible spectra 0-12759
- faint blue stars in high galactic latits., search of PSS fields near South Galactic Pole 0-46415
- faint proper-motion stars, spectra and photometry to very low luminosity degenerates deficiency 0-17575
- faint short-period spectroscopic binaries, influence of Schwarzschild effect on orbital and system elements (*German*) 0-8653
- faint stars, spectral-type standards for objective prism plates 0-46539
- Feige 86, UV high-resolution spectrum 0-41834
- flare stars, model chromospheres, Balmer-line profiles 0-46558
- G200-39, hot hybrid white dwarf, spectroscopic obs. 0-26852
- G and K-type giant stars, Li abundances 0-41819
- G-type dwarf stars, far UV Si emission line analysis 0-56829



## stellar spectra continued

- galactic anticentre direction, young stars photometry and spectra rel. to outer Galaxy struct. 0-22079  
 GCl 0422-213, distant globular cluster in Eridanus, preliminary photometry and spectroscopy 0-17624  
 giants, CN strength differences in disk and halo 0-51750  
 giants in globular cluster  $\omega$  Centauri, CO absorption and effective temp. 0-51749  
 GK-type dwarf stars, Mg H lines obs. rel. to Mg isotopic abundances 0-51757  
 globular cluster giant stars, blanketing differences meas. 0-4345  
 GX304-1 (4U 1258-61), shell spectrum of optical counterpart 0-46582  
 H-H 7 and 11, spectrophotometry of very low-excitation objects 0-46549  
 HD 01891, subdwarf, photometry and spectrum rel. to UV excess and metal abundance 0-17574  
 HD 149499 B, IUE obs. of hottest white dwarf 0-41828  
 HD 153919 (3U 1700-37), further spectroscopic obs. 0-4358  
 HD 15570, Of/WN7 spectral classification problem 0-51786  
 HD 175742, spectroscopic binary, orbit and components spectral types (French) 0-36671  
 HD 184927, He variable star, spectroscopic props. 0-51790  
 HD 192163, 191765, Wolf-Rayet stars, optical interstellar spectra obs. 0-17640  
 HD 193077, probable single WN 5 star with absorption lines 0-56834  
 HD 197406, Wolf-Rayet spectroscopic binary, radial vels. and orbital elements 0-51812  
 HD 200775/NGC 7023 complex, interstellar reddening and 2200 Å feature strength 0-51832  
 HD 38268, in 30 Doradus, unique interstellar Ca II K-line profile obs. 0-51850  
 HD 4174, peculiar M-giant, magnetic field 0-8631  
 HD 50896 (WNS), variable emission-line spectrum obs. 0-51791  
 HD 51480, shell star, spectroscopic obs., atmospheric struct. and distance 0-31305  
 HD 64740, He rich star, UV spectral vars. 0-22016  
 HDE 226868 (Cygnus X-1), H $\alpha$  emission in (1977) 0-51919  
 HDE 245770, possible counterpart of variable X-ray source A 0535+26, line and continuum vars. 0-17600  
 HeH<sup>2+</sup>, photodissoc., rel. to UV flux deficiency of stellar spectra 0-9654  
 Herbig-Haro object 1 exciting star, identification as T Tauri star 0-17633  
 Herbig-Haro object 24, emission/reflection nature 0-41829  
 Hercules X-1, cyclotron line form. by reson. Compton cyclotron scatt. 0-8711  
 AC Herculis, curve-of-growth analysis of RV Tauri variable 0-22026  
 LT Herculis, eclipsing binary, photometric elements and spectral types 0-31328  
 DQ Herculis (Nova 1934), high time resolution spectrophotometry 0-22017  
 DQ Herculis (Nova 1934), short-period oscils. modulation and pulsed emission lines asymmetry interpretation 0-22044  
 high dispersion studies using anamorphic camera 0-41727  
 high-velocity stars, southern, radial vels. 0-21988  
 HR7922, B-type spectroscopic binary, orbital soln. 0-26910  
 HR8891, B-type spectroscopic binary, orbital soln. 0-26910  
 HR 1105, He I 10830 Å line obs. of cold giant (Russian) 0-17586  
 HR 1217, Ap star, spectrum and light vars. relationship 0-26878  
 HR 432, 515 and 8006,  $\delta$  Scuti stars, spectrographic obs. 0-36639  
 HR 4665, spectroscopy of bright long-period RS Canum Venaticorum system 0-36665  
 HR 8752 (V509 Cassiopeiae), emission-line spectrum rapid changes 0-36645  
 HR 9070, Be star, spectral vars. obs. 0-12773  
 W Hydrae, long-period variable, suspected Zeeman splitting in OH masers 0-36632  
 IAU Radial Velocity Standard stars, radial vels. meas. (French) 0-51743  
 interstellar absorption lines of Na I, K I, Ca II, in stellar spectra rel. to galactic gas distrib. 0-26963  
 interstellar lines towards Cepheus OB2 association, anal. 0-22052  
 IR stars, unidentified spectral features 0-26936  
 IRC+10216, circumstellar dust shell model rel. to IR energy distrib. 0-56972  
 K-type giant stars at South Galactic Pole, spectral types from DDO photometry 0-8622  
 late type stars, Ca II H and K lines and nearby continuum photoelectric calibration 0-36617  
 late-type stars, He abundance effects on spectrum appearance 0-46540  
 late-type stars, search for Ti II 3080 Å multiplet emission 0-51769  
 R Leonis, IR atomic line spectrum of Mira variable 0-46557  
 AD Leonis, X-ray emission from flares, HEAO 1 obs. 0-41837  
 line broadening effects of macroturbulence and rotation 0-56813  
 line formation in axisymmetric moving envelopes, numerical method and appl. to YY Orionis stars 0-41813  
 line formation in microturbulent magnetic fields 0-31201  
 line profile calc. for close systems with mass transfer 0-41860  
 line profile measurements, accuracy 0-26751  
 lower main-sequence stars, spectral lines Fourier anal. rel. to rot. vels. 0-51767  
 LS I +61°303, radio variable Be star, UV spectrum, stellar models 0-26879  
 luminous stars in M31 0-36622  
 luminous stars in symmetric nebulae, IUE low-dispersion spectra 0-46560  
 $\beta$  Lyrae, narrow-band photometric index of emission line strength 0-46605  
 $\alpha$  Lyrae (Vega), Copernicus UV obs. of C II and Si II lines 0-8627  
 $\alpha$  Lyrae (Vega), spectral anal. from Copernicus 0-26856  
 M22, comparison with  $\omega$  Centauri, spectroscopic evidence 0-46617  
 main sequence stars, oscils., observability by photometry and spectra 0-51724  
 metal-poor dwarfs, Fe/H abundances from red spectra of nine objects 0-51751  
 metal-poor late-type stars, MK spectral classification 0-4340  
 metal-poor stars, O abundances from O I IR triplet 0-36610  
 Michigan 239, peculiar extragalactic or extreme halo emission-line star, obs. 0-4380  
 AT Microscopii, X-ray emission from flares, HEAO 1 obs. 0-41837  
 N Monoceros region, two-micron IR objects survey 0-8555  
 MXB 1728-34, type I X-ray burst spectral evolution, HEAO-1 obs. 0-17692

## stellar spectra continued

- nearby stars, spectroscopic and photometric data published (1969-1978) 0-36513  
 neutron stars, highly magnetised, thermal radiation spectrum 0-56869  
 NGC 2264, open cluster, reddening, blanketing and metallicity from spectroscopic obs. 0-26916  
 NGC 2287, open cluster, spectral classification of brightest stars 0-26919  
 NGC 2420, old disc cluster, photometry and spectra rel. to stars chemical comp. 0-46620  
 NGC 6823, UV photometry and spectra, extinction study of young open cluster 0-4407  
 nonradial pulsation hypothesis with simulated line profile vars. 0-8618  
 nova in Sagittarius, discovery of probable declining nova (1978 March) 0-4376  
 O-type stars in open cluster IC 1805, C IV UV reson. line P Cygni profiles 0-31296  
 $\zeta$  Ophiuchi, spectral vars. related to rot. 0-22000  
 $\alpha$  Orionis, CO circumstellar absorpt. obs. in 4.6 micron spectrum 0-26858  
 $\kappa$  Orionis, interstellar B II 1362 Å detect. 0-51841  
 FU Orionis, IR spectroscopy with contact-type image tube 0-17587  
 $\beta$  Orionis, mass loss and shell, IUE and balloon UV obs. 0-51765  
 U Orionis, Mira variable, relation between 1612 MHz flare and light curve 0-56844  
 $\pi^5$  Orionis, Orion OB1 association star, interstellar lines obs. by Copernicus 0-22050  
 oscillator strengths of astrophysical interest 0-12656  
 parallax stars with MK spectral classifications 0-56721  
 EQ Pegasi, active dwarf binary star, chromospheric emission lines obs. 0-12762  
 AU Pegasi, binary Type II cepheid, photometric and spectroscopic study 0-26866  
 $\theta$  Pegasi, rapid spectral line variability disproved 0-8625  
 $\phi$  Persei, binary Be star, He II emission obs. rel. to components masses 0-12768  
 53 Persei, nonradical pulsator, light var. rel. to line profile changes 0-4362  
 21 Persei, spectrophotometry of Ap star, continuum features vars. 0-36638  
 b Persei, UVB photometry and spectroscopic study of ellipsoidal variable 0-36666  
 X Persei (3U 0352+30), simultaneous X-ray and ground-based optical obs. 0-17591  
 Pleione (28 Tauri), envelope behaviour in 1976, spectroscopic obs. 0-8636  
 Pleione (28 Tauri), metallic-line shell spectrum anal., (1973-1976) 0-8637  
 PSR 0950+08, pulsar, micropulses freq. struct. 0-22030  
 pulsar spectra, nature of low-freq. dropoff 0-17602  
 pulsars, narrowband versus broadband emission processes rel. to luminosities and spectra 0-51797  
 pulsars, radio flux density and spectral index from obs. at 102.5 and 61 MHz 0-17601  
 red and nebulous objects in dark clouds, survey, catalogue of 150 objects 0-56904  
 S106 IR, S235 B, obscured IR point sources, ZAMS spectral types from Br fluxes 0-12795  
 S-type stars, molecular spectra and model atmospheres 0-51764  
 S-type stars, revised spectral classification system in red 0-46541  
 HM Sagittae, emission-line star, UVB photometry and spectral obs. in (1978) (Russian) 0-36648  
 HM Sagittae, new spectroscopic obs., simultaneous presence of increasing excitation and cool features 0-26874  
 WZ Sagittae, recurrent nova, spectroscopic obs. during 1978 outburst 0-26862  
 WZ Sagittae, recurrent nova, spectroscopic study during 1978 outburst 0-56849  
 HM Sagittae, variable emission object, spectrophotometry 0-17599  
 $\mu$  Sagittarii, eclipsing binary star, unseen companion spectral type 0-4401  
 RY Sagittarii, spectra near min. light 0-36642  
 SAO 015338, possible RS Canum Venaticorum star and counterpart of 2A 1052+606, spectrum 0-22118  
 $\alpha$  Scorpii, circumstellar absorption lines in UV spectrum 0-51804  
 $\zeta^1$  Scorpii, extreme B1 supergiant, IUE obs. of line spectrum and continuum energy distrib. 0-17583  
 $\zeta^2$  Scorpii, extreme B1 supergiant, UV reson. lines obs. 0-4349  
 $\zeta^3$  Scorpii, extreme B-type supergiant, UV spectroscopy 0-22004  
 Scorpius X-1, high energy X-ray obs. with Ariel V 0-17694  
 RT Serpentis (Nova 1909), spectrum in 1964, 1975 and (1978) 0-46566  
 SIMS, C and SC stars, new discoveries on southern, red-sensitive objective-prism plates 0-36511  
 slitless field spectroscopy, focal-reducer system appl. 0-36504  
 SN 1972e in NGC 5253, spectrum 0-41844  
 SN in NGC 4321 (M100), interstellar Na I and Ca II absorption 0-51847  
 southern peculiar emission-line stars, observational data rel. to mass ejection 0-41843  
 speckle interferometry data processing method 0-17498  
 SS 433, 6.55 day periodicity in emission line wavelengths 0-51784  
 SS 433, enormous periodic Doppler shifts obs. 0-17593  
 SS 433, IR spectral obs., reddening and emission 0-4388  
 SS 433, precessing jets in ultra-close binary system rel. to spectrum 0-4384  
 SS 433, short term H $\alpha$  central intensity increases 0-4375  
 SS 433, spectroscopic obs. and probable binary nature 0-51780  
 Stepanyan's star, spectrophotometric and photometric obs., 228-min period 0-56883  
 Stepanyan's star found to be eclipsing binary, possibly cataclysmic 0-51806  
 Stephenson-Sanduleak 433, 1.2-2.5  $\mu$ m spectroscopy, photometry and polarimetry 0-41838  
 supergiants, C IV resonance lines in B- and early A-type objects 0-46550  
 supergiants of O- and B-type in Magellanic Clouds, stellar winds 0-51863  
 supernovae, spectrum before max. luminosity in Type I objects 0-41845  
 supernovae stellar remnants, spectroscopic search 0-26890  
 symbiotic stars, obs. of unidentified bands at 6830 and 7088 Å 0-46573  
 SU Tauri, emission lines at min. and BV photoelectric photometry 0-8640



## stellar spectra continued

- DR Tauri, pre-main-sequence star, brightening, 1970 to 1979, and spectrum 0-31297  
 $\alpha$  Tauri, search for Ti II 3080 Å multiplet emission 0-51769  
 V471 Tauri, white dwarf eclipsing binary, IUE UV spectra 0-26912  
 T Tauri stars, spectral features synthesis from photosphere and low chromosphere model 0-36623  
 47 Tucanae, globular cluster, photometry and spectra rel. to stars chemical comp. 0-46620  
 4 U 0115+63, absorption line in pulsed hard X-ray spectrum, HEAO 1 obs. 0-27017  
 4U 1702-36, Scorpius X-1 like source, high energy X-ray obs. with Ariel V 0-17694  
 4 U 2129+47 optical counterpart, spectrum and photometry rel. to 0-17693  
 CQ Ursae Majoris, line identification list and radial vel. of Ap-star 0-41841  
 $\gamma$  Ursae Minoris, high dispersion spectroscopy 0-41853  
 UV chromospheric and transition-layer emission 0-56823  
 AH Velorum, radius, delta luminosity and pulsation mode of  $\delta$  Cepheid 0-46572  
 78 Virginis, Ap star, lines circular polarisation profiles rel. to mag. field geometry 0-51773  
 78 Virginis, magnetic Ap star, high resolution polarisation obs. inside spectral lines 0-51772  
 Vulpecula OB2 stars, photometry and spectra rel. to membership of 67 day Cepheid S Vulpeculae 0-41831  
 NQ Vulpeculae (Nova 1976), UV and visual spectra analysis (Chinese) 0-12770  
 VV Puppis, 3470 Å emission as cyclotron line 0-36673  
 white dwarfs, DB-type, model atmospheres rel. to line profiles and equivalent widths 0-51761  
 white dwarfs, magnetic, cyclotron absorpt. spectra theory 0-4351  
 Wolf-Rayet stars in galactic-centre field, new discoveries from spectroscopic obs. 0-8674  
 Wolf-Rayet stars in LMC, new discoveries, positions, spectra and magnitudes 0-46569  
 X-ray pulsars spectra, possible vacuum signature 0-27015  
 X-ray pulsator, 38.22 second period, in vicinity of OAO 1653-40, very hard spectrum 0-27014  
 X-ray sources, compact, spectra form. 0-22115  
 $\mu$  Draconis (ADS 10345), radial vel. var. from spectra in visible 0-17612  
 C stars, search for HCN and CH maser emissions 0-51856  
 C stars, spectroscopic problems 0-56832  
 C stars in Cygnus, new spectroscopic discoveries 0-46551  
 C<sub>2</sub> (4670 Å band) stars, evolutionary status 0-4355  
 C<sub>2</sub> absorption bands in stellar spectra, 876 nm obs. 0-12805  
 Ca II H and K lines in F0 to M2-type stars, high resolution absolute flux profiles 0-26842  
 Dy III lines in spectra of Ap and Bp stars 0-12764  
 H I Balmer  $\alpha$  and  $\beta$  lines in O6 to G2 stars, equivalent widths and narrow-band photometry 0-8621  
 H $\alpha$ -emission stars in Perseus OB1 assoc. region 0-56855  
 He I lines in early-type stars, Copernicus UV obs. 0-41825  
 HgMn stars, spectrophotometry 0-26867  
 Mg II flux profiles in cool stars, obs. rel. to chromospheric radiative loss rates 0-36611  
 O I 7774 Å line in O6 to G2 stars, equivalent widths and narrow-band photometry 0-8621  
 O-rich late-type stars, 16 to 39 micron spectroscopy 0-22002  
 SiO 86.2 GHz maser sources, polarisation props. 0-4449  
 SiO masers, J=1-0  $\nu$ =1 and 2 masers relative intensity and vel. 0-4339  
 Tc in late-type stars, spectral analysis 0-8623  
 TiO band absorption effect on stellar photometry with broadband filters 0-41811

stellar spectrophotometry *see stellar photometry*

## stellar structure

*see also solar interior*

- adiabatic non-radial oscillations with moderate or large l, theory 0-56819  
 anisotropic spheres, adiabatic contraction in general relativity 0-36489  
 atmosphere in statistical equil., effects of deviations from LTE on struct. 0-31290  
 black hole accretion discs, Lightman-Eardley instabilities rel. to disc thickening 0-31324  
 38 Cancri,  $\delta$  Scuti star, UVB photometry and possible non-radial pulsation 0-22021  
 U Cephei, eclipsing binary, G-type star g-mode oscills. rel. to gas stream effects 0-26898  
 $\beta$  Cephei stars, nonradial oscills., linear nonadiabatic analysis 0-56836  
 Cepheids, multimode, two-zone models, resonances 0-36641  
 cepheids, northern hemisphere, double mode excitation search using existing obs. 0-8634  
 Cepheids pulsating envelopes models, mag. field effects 0-31302  
 collapsed stars, limits on nuclei excitation energies in hot matter 0-56703  
 collapsed stars, neutrino flux from quark matter 0-22028  
 collapsing core, shape instability pressure stabilisation 0-8537  
 contact binary stars, temp. discontinuity maintenance 0-8655  
 convection in massive star cores, effect on C/O ratio 0-17579  
 convection onset in radially pulsating star 0-41809  
 convection zones dynamics, effect of rot. on turbulent viscosity and cond. 0-36612  
 convective elements, fluctuations rel. to stochastic evolution and oscill. props. 0-31293  
 convective models, fundamental hit correctable inconsistency of local mixing-length theory 0-26841  
 core mass-luminosity relations, for He shell burning stars 0-21983  
 differentially rotating gaseous polytropes, second-order perturb. theory 0-21990  
 double shell source star, successive He shell flashes anal. rel. to stationary shell burning 0-51737  
 dwarf novae, quasi-periodic oscills. and nonradial pulsations of accretion disks 0-46568  
 ellipsoidal potentials of polynomial distributions of matter 0-46532  
 HZ Herculis (Hercules X-1), precessing twisted accretion disks 0-56973  
 DQ Herculis (Nova 1934), short-period oscills. modulation and pulsed emission lines asymmetry interpretation 0-22044  
 IRC+10216, spatial spectra from 2.2 to 20 microns, deviations from spherical symmetry 0-41911  
 RR Lyrae stars models, radial pulsations 0-26863

## stellar structure continued

- massive cold spherical stars, rest-mass density and redshift 0-56859  
 Mira variables, envelope pulsational instability rel. to planetary nebula form. 0-26928  
 1 Monocerotis,  $\delta$  Scuti star, oscillation modes from photoelectric radial vels. and BVRI photometry 0-51787  
 neutron star interior plasma, mag. field rel. to pulsar periods long-term changes 0-22029  
 neutron stars, disk accretion, transition zone radial and vertical structure 0-4393  
 neutron stars outer crust, theory of electron solids in superstrong mag. fields 0-4640  
 neutron stars thermal properties and detectability, cooling and heating processes 0-31323  
 Newtonian spheroid, homologous oscill., gravit. radiation 0-46533  
 nonradial oscills., eigenvalue multiplicity 0-51740  
 nonradial oscills., modal analysis by asymptotic method 0-21996  
 protostars, hydrostatic models evolution rel. to star form. process simulation (Polish) 0-21998  
 protostellar envelopes of masses 3 M $\odot$  and 10 M $\odot$ , struct. and hydrodynamic evolution 0-36616  
 pulsars, interpulse emission struct. 0-36652  
 response functions and secular modes 0-17572  
 rigidly rotating stars, secular instabilities in general relativity, theoretical formalism 0-4341  
 rigidly rotating stars, secular instabilities in general relativity, numerical results 0-4342  
 Roche lobe formation in highly eccentric X-ray binary systems 0-41858  
 rotating stars, secular instability from thermal cond. 0-21986  
 self-gravitating rotating masses, book contrib., review 0-21915  
 spotted stars, spot sizes 0-41812  
 superdense magnetised astrophysical objects, interiors physical conditions 0-17603  
 tidally distorted configurations, external form and potential, third-order approx. 0-41714  
 tidally distorted stars, form factor method for struct. determ. 0-21991  
 Universe, high density matter, many body treatment, pulsars 0-26738  
 unstable modes of an equilibrium, number calc. 0-36493  
 very close binary systems, struct. eqns. including rot. and tidal distortions for ZAMS stars 0-22037  
 $\alpha$  Virginis,  $\beta$  Cephei type pulsation characts. 0-56835  
 white dwarfs seismological theory for 1 M $\odot$  model with crystalline core 0-17577  
 X-ray sources, steady accretion discs general struct. with mag. field 0-8714

stellar variables *see variable stars*

## stellarators

- AC Tokamak, design criterion 0-38726  
 Asperator NP-3, toroidal device with nonplanar mag. axis, current equilb. 0-48932  
 CLEO, helical winding, design, construction and installation 0-43958  
 CLEO stellarator, heating, confinement and fluctuations 0-24225  
 Cleo stellarator, neutral beam injection heating 0-28714  
 coil systems, modular, for stellarator fields 0-6274  
 current-free stellarators, RF and neutral beam heating 0-28853  
 cyclotron self-absorption in two-temp. plasma, temp. and density meas. 0-48987  
 divertor fluxes in stellarators and torsatrons, azimuthal distrib. 0-6216  
 ferromak, ferromag. wall shaping for linked min-B config. 0-24233  
 Ferromak, helical mag. configuration produced by ferromagnetic materials 0-48936  
 high beta MHD theory, stellarator equilibrium and stability, mirror traps and reverse field machines 0-28778  
 high beta stellarator, l=2,3 helical fields, stabilisation effects 0-28779  
 high beta stellarator stability theory 0-28797  
 L-2 stellarator, current equilibrium and effective ion charge 0-24228  
 L-2 stellarator, solid H<sub>2</sub> pellet injection parameters and effects 0-28775  
 low frequency parametric processes in magnetically confined plasmas 0-28827  
 neutral injection heating of CLEO stellarator-theory and experiment 0-28755  
 pressure effects, plasma equilb. evolution (Russian) 0-10418  
 toroidal field production by modular systems 0-10441  
 torsatrons, neutral beam injection calcs. 0-48949  
 Uranan-2 helical winding, metal-GRP struct. form. 0-6289  
 W VII-A stellarator, m=2 mode at q=2 0-24227  
 W VII-A stellarator, Ohmic heating, energy and particle confinement 0-24226

STEM *see scanning-transmission electron microscopy*

step motors *see stepping motors*

step-recovery diodes *see charge storage diodes*

Stepanov method *see crystal growth from melt*

stepped motors *see stepping motors*

## stepping motors

- differential ball screw actuator driven deformable mirror design and performance 0-33137  
 microcomputer mechanical proportional control for solar energy appls. 0-50987

stereo amplifiers *see audio-frequency amplifiers*

stereoisomerism *see isomerism*

stereoscopy *see vision*

stiffness constants *see elastic constants*

## stimulated Brillouin scattering

- backward stimulated scattering, comments 0-9953  
 backward stimulated scattering, reply to comments 0-9954  
 benzaldehyde, wavefront reprod. obs. by stimulated Brillouin, Raman scatt. 0-53369  
 coupled Stokes-antiStokes processes 0-9943  
 EM wave, stimulated Brillouin scatt., transverse static mag. field effect 0-50355  
 fibre Raman and Brillouin laser gains, polarisation effects 0-9887  
 internal Raman resonator, stimulated Mandelstam Brillouin scatt. component self-synchronisation (Russian) 0-48345  
 laser beam intensity ratio increase by possible use of stimulated Brillouin and Raman scatt. 0-5796  
 laser resonator, stimulated Mandelstam-Brillouin scatt. component synchronisation (Russian) 0-48346  
 laser system with phase conjugation, stimulated Mandelstam-Brillouin scatt. 0-5786



**stimulated Brillouin scattering continued**

- molecular crystal, Mandelstam-Brillouin scatt., dipole-plasma oscill. 0-1278  
 N two-level atoms, quantum theory of nonlinear optical phenomena 0-5790  
 nonlinear selection of optical radiation on refl. from stimulated Mandelstam-Brillouin scatt. mirror (*Russian*) 0-28280  
 optical fibre, high power narrow band laser radiation transmission, nonlinear optical processes 0-53443  
 phase conjugated wavefronts by stimulated Brillouin and Raman scatt. 0-5791  
 plasma, Brillouin backscatt. depend. on density scale lengths near crit. density 0-43888  
 plasma,  $H_2$ , underdense,  $CO_2$ -laser radiation filamentation 0-14941  
 plasma, laser prod., z-depend. absorpt. and stimulated backscatter processes 0-43944  
 plasma, parametric instability saturation by electrostatic daughter wave nonlinear decay 0-53945  
 plasma, weakly inhomogeneous laser-produced, stimulated Brillouin back-scatt. losses 0-19561  
 plasma critical surface, enhanced stimulated Brillouin scatt. due to light refl. 0-1750  
 pump wave wavefront reversal in Brillouin mirror, influence of certain radiation parameters 0-9961  
 Raman laser, CW fibre, bandwidth reduction using prisms, gratings and etalons 0-53366  
 semiconductor plasma, magnetised, stimulated Brillouin scatt. 0-33085  
 wavefront inversion in Stokes wave Raman conversion in oppositely directed pump beams 0-5797  
 wavefront reversal and short pulse generation using steady-state stimulated Brillouin scatt. 0-53381  
 wavefront reversal by stimulated Brillouin scatt., four-wave process 0-53382  
 $CO_2$  laser-plasma interaction, stimulated Brillouin backscatter saturation 0-24175  
 $CS_2$ , wavefront reprod. obs. by stimulated Brillouin, Raman scatt. 0-53369  
 n-InSb, SBS of laser radiation in presence of mag. field, ion acoustic wave nonlinearity 0-45091

**stimulated dielectric relaxation currents** *see thermally stimulated currents***stimulated emission**

- see also laser theory; lasers; population inversion*  
 alkali halides, coloured, light amplification at activator centres 0-2795  
 bremsstrahlung, resonator consideration (*Japanese*) 0-5721  
 carbon tetrafluoride laser, emission spectrum in 16 micron range,  $CO_2$  laser stimulation 0-9870  
 cooperative emission of excited mol. monolayer into surface plasmons of metallic substrate 0-20666  
 diffracted stimulated emission induced by coherent crossed laser beams for conc. meas. 0-35585  
 diphenyl:pyrene, self induced transparency under nonreson. excitation, luminesc. and stimulated emission 0-11436  
 diphenyl:pyrene, stimulated emission at 0-0 transition, 4.2K 0-11437  
 diphenyl with pyrene cryst., self induced transparency self stimulated excitation (*Russian*) 0-14403  
 N two-level atoms, interaction with radiation field in restricted rotating wave approx. 0-5713  
 N-two level atoms, interaction with radiation field in restricted rotating wave approx., numerical anal. 0-5714  
 naphthalene:pentacene, zero-phonon transition bottlenecks, photon echo detect. 0-33092  
 optically pumped lasers utilizing self-terminating transitions, CW stimulated emission possibility 0-14329  
 organic compounds, complex, nuclear relaxation influence on stimulated emission 0-48019  
 pendulum effect influence on optical modulation of diff. electron beam in cryst. (*Russian*) 0-55219  
 plasma turbulence stimulation, phase space granulation due to mode-mode coupling 0-38651  
 rare earth doped  $Bi_4Ge_3O_{12}$ , cryst. growth, spectral and laser props. 0-51115  
 ring laser with spontaneous emission in generation channel, semiclassical eqns. of motion 0-1240  
 ruby, phonons, at  $29\text{ cm}^{-1}$ , stimulated emission 0-45114  
 semiconductor, radiative and nonradiative recomb., spontaneous and stimulated emission (*Polish*) 0-53293  
 semiconductors, exciton condensation and electron hole liquids, state-of-the-art 0-49625  
 $AlGa_{1-x}AsGaAs$ , p-n heterojunction laser, low temp. operation 0-1204  
 $AlGa_{1-x}AsGaAs$ , p-n heterostruct. laser, tunnel injection and phonon-assisted recomb. 0-5733  
 $AlGa_{1-x}AsGaAs$  heterostructures, MO-CVD, phonon assisted recomb. and stimulated emission 0-1205  
 $As_{50}Te_{50}$ , amorphous films, metal and semicond. contacts, threshold switching, IR emission 0-49831  
 Cd II, A factors of  $^{111}Cd$  and  $^{113}Cd$  isotopes by hyperfine level crossing, stimulated emission 0-9564  
 CdS active surface, exciton stimulated emission and superradiance refl. spectra, props. 0-25411  
 CdS, doped laser mechanism and output study 0-43340  
 CdS, excitonic mol. transitions, optical gain and induced absorpt. spectra 0-11438  
 CdS, pure and Cl doped, stimulated emission due to indirect band-band transitions 0-7376  
 CdS, size effect of dense electron hole systems 0-7413  
 CdS, stimulated and spontaneous emission from degenerate electron-hole plasma at 300K 0-29762  
 CdS, two-photon-excitation, tunable laser emission, luminesc. processes 0-55127  
 $CdS_{1-x}Se_x$ , strongly excited by electron beam, determ. of nonequilibrium carrier lifetime 0-39603  
 CdSe, excitonic mol. transitions, optical gain and induced absorpt. spectra 0-11438  
 $Er^{3+}:Lu_2AlO_{12}$ , 3- $\mu m$  crystal laser functional scheme, stimulated emission 0-43339  
 $Eu^{2+}$  metastable states in discharge plasma, anomalously high speed deexcitation, modulation of induced radiation obs. 0-44014  
 GaAs injection laser, active region effect on single-freq. stimulated emission conditions 0-9884

**stimulated emission continued**

- GaAs, stimulated and spontaneous emission from degenerate electron-hole plasma at 300K 0-29762  
 GaSe, optical excitation, excitonic spectra, stimulated luminesc. 0-40132  
 GaSe, stimulated emission due to electron-hole plasma recomb. 0-50374  
 $GdAlO_3:Er^{3+}$ ,  $^4S_{3/2}$  to  $^4I_{9/2}$  transition laser action, optical and luminescence spectra 0-16082  
 Ge, far IR radiation amplification on hot hole population inversion (*Russian*) 0-16060  
 H II region, H137 $\beta$ /109 $\alpha$  intensity ratio interpretation 0-31344  
 $He_2$  dimer, electron-beam pumped, anal. of feasibility of stimulated vacuum UV radiation 0-9857  
 $Ho^{3+}:LiYF_4$ , 1.392, 1.673 and 3.914  $\mu m$  stimulated emission, laser cascades 0-9886  
 $I_2$  molecule pumped by Cu vapour laser, pulsed stimulated emission due to electronic transitions 0-14330  
 InAs, epitaxial, laser action mechanisms with electron beam excitation 0-28240  
 $KCl:Eu^{2+}$ ,  $\gamma$ -irrad., photostimulated low temp. recomb. luminesc. 0-11435  
 $KEr(WO_4)_2$ , crystallisation cond., stimulated emission in 2.8  $\mu m$  band 0-53301  
 $KNdP_4O_{12}$ , determ. of fluoresc. quantum efficiency and laser emission cross sections 0-48264  
 $KNdP_4O_{12}$ , laser emission cross sections, fluorescence spectra, radiative lifetimes, quantum efficiency 0-23694  
 $KY(WO_4)_2:Er^{3+}$ , stimulated emission at 300K 0-34951  
 $KY(WO_4)_2:Ho^{3+}$ , 3  $\mu m$  stimulated emission at 300K 0-20667  
 $LiNdP_4O_{12}$ , laser emission cross sections, fluorescence spectra, radiative lifetimes, quantum efficiency 0-23694  
 $LuAlO_3:Er^{3+}$ ,  $^4S_{3/2}$  to  $^4I_{9/2}$  transition laser action, optical and luminescence spectra 0-16082  
 $Lu_2Al_2O_5:Ho^{3+}(Er^{3+})$ , sensitized stimulated emission at 3 microns 0-53302  
 $NH_3$ , J=K=1 line mol. beam maser emission, ring-type focusing 0-28119  
 $NaNdP_4O_{12}$ , laser emission cross sections, fluorescence spectra, radiative lifetimes, quantum efficiency 0-23694  
 Nd crystals, determ. of fluoresc. quantum efficiency and laser emission cross sections 0-48264  
 $Nd^{3+}:Ca_2Ga_2Ge_2O_{12}$ , stimulated emission at 300K 0-38019  
 $Ni^{2+}:MgO$  laser system, optical parameters 0-48260  
 O I 6300 Å in type A aurora rays, emission intensification 0-4163  
 Te, opt. props. under high press., band struct. transform. 0-55112  
 $YAlO_3:Er^{3+}$ , pulsed laser action,  $^4S_{3/2}$  to  $^4I_{9/2}$  transition laser action, optical and luminescence spectra 0-16082  
 ZnO, excitonic mol. transitions, optical gain and induced absorpt. spectra 0-11438  
 ZnO, two-photon-excitation, tunable laser emission, luminesc. processes 0-55127
- stimulated Raman scattering**  
*see also coherent antiStokes Raman scattering*  
 absorbing media, ultrashort laser pulse excited, fluctuation-dissipation theory (*Russian*) 0-23753  
 anti-Stokes radiation spatial distrib., expt. and four-photon model 0-28270  
 backward Raman amplifier, technique for parasitic superfluoresc. suppression 0-38073  
 backward stimulated scattering, comments 0-9953  
 backward stimulated scattering, reply to comments 0-9954  
 beat wave imaging props., in stimulated Raman scatt. medium, holographic appl. 0-5709  
 benzaldehyde, wavefront reprod. obs. by stimulated Brillouin, Raman scatt. 0-53369  
 benzene, anti-Stokes components, class II radiation cones 0-28276  
 benzene, high-order stimulated Raman scatt. obs. (*Chinese*) 0-45053  
 benzene, ultrahigh sensitivity stimulated Raman gain spectroscopy 0-48337  
 coherent Raman spectroscopy techniques, review 0-22440  
 colliding particle system, two-photon transition, stimulated Raman scatt. 0-9663  
 coupled waves, dispersion functions, rel. to dielec. dispersion (*German*) 0-1281  
 dispersive medium, incoherent, coherent stimulated Raman scatt. with multimode pump (*Russian*) 0-38063  
 Doppler broadening at electronic resonance 0-38065  
 fluorescent organic molecules, excited state intramol. vibr. 0-32717  
 frequency shifts, nonreson. contribs. to nonlinear susceptibility 0-53373  
 IR and far IR source, powerful and tunable 0-5787  
 Kerr effect, Raman induced, with monochromatic waves 0-48359  
 laser beam intensity ratio increase by possible use of stimulated Brillouin and Raman scatt. 0-5796  
 MBBA, nematic liq. cryst., nonlinear optical suscept. using light combination scatt. (*Russian*) 0-38064  
 methane, scaled Raman pulse compression experiments at 248 nm, KrF pump laser 0-38071  
 methyl thionine chloride, intramol. vibr. spectra 0-977  
 molecules, stimulated Raman and two-photon absorpt. 0-52999  
 multiple-pass Raman gain cell 0-48334  
 multiplicative stochastic processes in statistical physics appl. 0-22289  
 N two-level atoms, quantum theory of nonlinear optical phenomena 0-5790  
 optical fibre guide, stimulated Raman scatt. dynamics by Stokes component detect. 0-14394  
 phase conjugated wavefronts by stimulated Brillouin and Raman scatt. 0-5791  
 phosphate glass laser, statistical props. and stabilisation 0-48266  
 picosecond laser techniques for obs. of vibr. modes in liqs. 0-5800  
 picosecond Raman techniques, vibr. dynamics in liqs. 0-52325  
 plasma, parametric instability saturation by electrostatic daughter wave nonlinear decay 0-53945  
 polyatomic molecule, ultrafast vibr. using laser light pulses 0-9699  
 pump beam, spatially inhomogeneous, enhanced gain of stimulated Raman scatt. 0-28279  
 resonant scatt. in noise pump field 0-9944  
 saturation effects in hyper-Raman scatt., resonant three photon processes 0-38069  
 scaled Raman pulse compression experiments at 248 nm, KrF pump laser 0-38071  
 sensitivity enhancement by quasi CW laser scheme 0-53003



**stimulated Raman scattering continued**

- solitons, laser physics appls. 0-48333  
 spatial structure of first Stokes component 0-14398  
 stationary mode, scatt. inside laser cavity (*Russian*) 0-38067  
 Stokes pump wave capture in stimulated Raman scatt. amplifier 0-23749  
 superradiance in Raman light scatt., pump depletion effect 0-9957  
 surface vibrational spectroscopy using stimulated Raman scatt. 0-38062  
 synchronously pumped stimulated Raman oscillator, for liq. group refr. index meas. 0-55059  
 thresholds for ultra-short excitation 0-33078  
 trifluoriodomethane, molecular vibration energy stochasticization in intense IR laser field by Raman spectroscopy (*Russian*) 0-14149  
 ultrahigh sensitivity stimulated Raman gain spectroscopy 0-48337  
 wavefront reconstruction and self-focusing of light 0-23752  
 wavefront registration and volume object image reconstruction (*German*) 0-53367  
 CO<sub>2</sub>, pure rotational stimulated Raman photoacoustic spectroscopy 0-32724  
 CS<sub>2</sub>, wavefront reprod. obs. by stimulated Brillouin, Raman scatt. 0-53369  
 CdS, resonance hyper-Raman light scatt. on optical photons (*Russian*) 0-14396  
 Cs vapour, IR picosecond pulse generation 0-53371  
 Cs vapour, tunable IR generation using 6s-5d Raman transition 0-53365  
 Cs vapour tunable IR source using stimulated electronic Raman scatt., appl. to HCN (001) relax. obs. 0-9696  
 H<sub>2</sub>, freq. shifting of tunable dye laser radiation 0-9963  
 H<sub>2</sub> gas, efficient higher-Stokes-order Raman conversion 0-33082  
 H<sub>2</sub> gas in multiple-pass Raman gain cell 0-48334  
 H<sub>2</sub>, tunable efficient VUV generation using ArF pumped stimulated Raman scatt. 0-38072  
<sup>3</sup>He-<sup>4</sup>He, superfluid solns., nonlinear sound interaction 0-34267  
 LiIO<sub>3</sub>, simultaneous stimulated Raman scatt. and optical freq. mixing using three-mirror config. 0-48342  
 LiNbO<sub>3</sub>, optical const. determ. by background stimulated Raman scatt. 0-48336  
 N<sub>2</sub>, liq., Raman lineshape 0-11384  
 N<sub>2</sub>, vibration stimulated Raman scatt., four photon parametric effects 0-33087  
 N<sub>2</sub>O, pure rotational stimulated Raman photoacoustic spectroscopy 0-32724  
 O<sub>2</sub>, liq., stimulated Raman scatt., vibr.-translational relax. rate, schlieren technique meas. 0-9955  
 Pb vapour, XeCl laser pulse backward Raman compression 0-19068  
 SF<sub>6</sub>, molecular vibration energy stochasticization in intense IR laser field by Raman spectroscopy (*Russian*) 0-14149

**stimulated scattering**

- see also *stimulated Brillouin scattering; stimulated Raman scattering*  
 absorbing liquid, coherent light transient self-diff., simulated thermal scatt. laser expt. 0-48361  
 laser beam, spatially inhomogeneous, induced scatt. 0-28274  
 nonmonochromatic spatially inhomogeneous radiation, wavefront reconstruction and reversal 0-9952  
 phase conjugation, reprod. of light field weak components at stimulated scatt. 0-5792  
 phase locking in transient stimulated scattering 0-53378  
 Rayleigh scattering, principle techniques and expts., review 0-34938  
 Stokes radiation spatial charact., saturation conditions 0-53379  
 weak beam wavefront inversion in stimulated light scatt. 0-5798  
 Ge, picosecond optical response, effects of parametric scatt., energy-gap narrowing and state filling 0-11424

**STO calculations**

- AB system, molecular calcs., electric dipole moments and electronic valence population, CNDO study 0-37742  
 addition theorems of spatial functions, multicentre integrals of arbitrary atomic functions, symmetry and analytical struct. (*German*) 0-37729  
 AH system, molecular calcs., electric dipole moments and electronic valence population, CNDO study 0-37742  
 analytic radial orbitals, optimisation on variational parameters 0-42941  
 18-annulene, geometrical parameters, STO-3G ab initio calc. 0-52867  
 chemical shift, two-centre integrals calculation method including ang. momentum (*French*) 0-32601  
 Compton profiles using Gaussian expansion of at. orbitals, appl. to He, Ne, Ar, Kr, Na, and Al 0-945  
 configuration interaction calc., atoms and atomic complexes confined in spherical boxes, Hartree-Fock-Slater potential 0-47898  
 correlation energy for closed and open shells, approx. calcs. 0-42942  
 dihydroxycarbene, singlet and triplet state rot. pot. surfaces 0-32627  
 electric field variant orbitals, STO field gradient depend., atomic quadrupole polarisability 0-23295  
 electrostatic isopotential maps for large biomolecules, STO transferable bond calc. 0-3571  
 film, HF formalism for calc. of total energies and charge densities 0-49850  
 internal conversion calc., Hartree-Fock-Slater and Hartree-Fock models 0-18238  
 lactam-lactim tautomeric equilibria, quantum chem. calcs. 0-50833  
 LCAO Slater-type orbital band structure calcs., computable expressions, derivation 0-24776  
 magnetic resonance, two-centre integrals involving one-electron dipolar coupling and Slater AOs, computational procedure 0-23291  
 methanol dimer, intermol. function from ab initio calcs. 0-32629  
 3-methyleneoxetane, electron structure, orbital-O interaction, MO calcs., UV photoelectron spectra 0-28058  
 one centre pot. energy functions and two electron integrals for STO's 0-14070  
 3-oxetanone, electron structure, orbital-O interaction, MO calcs., UV photoelectron spectra 0-28058  
 polyacetylene, band struct. valence Hamiltonian minimal STO-3G basis calc., nonempirical model pot. 0-54596  
 polyethylene, band struct. valence Hamiltonian minimal STO-3G basis calc., nonempirical model pot. 0-54596  
 $\beta$ -propiolactone, electron structure, orbital-O interaction, MO calcs., UV photoelectron spectra 0-28058  
 radical, small, isotropic hyperfine coupling const., MINDO/3 calcs. 0-52894  
 spin-spin integrals, one- and two-centre, analytical evaluation over Slater-type orbitals (*Russian*) 0-9491  
 subtilisin charge-relay system, electrostatic pot. map, STO transferable bond calc. 0-3571

**STO calculations continued**

- thiocarbonates, mol. struct., S-substitution effect (*French*) 0-23335  
 thionitrates, mol. struct., S-substitution effect (*French*) 0-23335  
 transition metal complex, LCAO-HFS-STO calc., basis set effects 0-52882  
 two centre and three centre integrals for attraction of Slater type orbitals to nucleus, coord. systems 0-14068  
 two centre integrals for attraction of STO to nucleus 0-14069  
 vinyl isocyanate, and vinylcyano ether, geometry and conform., ab initio minimal STO-3G MO calcs. 0-23337  
 vinylcyano ether, and vinyl isocyanate, geometry and conform., ab initio minimal STO-3G MO calcs. 0-23337  
 water, liq., structure and props., minimal basis set description 0-6347  
 Al<sub>2</sub>, repulsive region ground state pot. curves, SCF with STO basis set calc. 0-14188  
 Al<sub>2</sub><sup>3+</sup>, repulsive region ground state pot. curves, SCF with STO basis set calc. 0-14188  
 CaO, electronic structure 0-2332  
 Cr(CO)<sub>6</sub>, LCAO-HFS-STO calc., basis set effects 0-52882  
 H<sub>2</sub>O dimer, intermolecular pot. functions from ab initio calcs. 0-5473  
 H<sub>2</sub>SO hypothetical molecule, nonempirical STO calc. of chem. bonds 0-23307  
 He-like ions, ground-state electron impact excitation strengths, close-coupling calcs. 0-23561  
 Li, B<sub>4</sub>, molecular and electronic struct. 0-20107  
 NH<sub>3</sub>, IR absorption band integrated intensities, ab initio and LMO studies 0-23458

**stochastic processes**

- see also *random processes*  
 additive and cancellable interacting particle systems, book 0-41960  
 atom+diamon trajectories, collinear, pattern recognition appl. to H<sub>2</sub>+F(I), He+H<sub>2</sub><sup>+</sup> 0-45481  
 atomic motion in resonant fluctuating laser radiation 0-43310  
 atomic transition in stochastic field, saturation and Stark splitting 0-9546  
 bifurcations inducing attractor in Oboukhov's turbulence system 0-1536  
 binomial redistribution process, Ehrenfest urn problem 0-52144  
 bistable reaction system, stochastic dynamics investig. of discrete trimolecular chemical model 0-16645  
 Brownian motion, fast variables elimination using time-convolutionless projection operator formalism 0-8913  
 Brusselator, dynamic correl. functions, Mori-Zwanzig formalism 0-25988  
 Burgers equation, relationship to differential stochastic eqn. 0-36869  
 charged particles in single wave fields, adiabatic and stochastic motion 0-9795  
 chemical system far from equilibrium, stochastic simulation 0-3339  
 collisional drift waves, nonlinear evolution, bifurcations to chaotic state 0-14666  
 column, stochastically imperfect finite, on nonlinear elastic foundation, buckling 0-48619  
 compartmental analysis, stochastic contributions 0-27215  
 complex nonlinear oscillation regimes 0-8919  
 condensation, homogeneous, cluster size distrib., stochastic model 0-22311  
 construction by Dirichlet forms 0-8921  
 critical points, relaxation phenomena, stochastic and deterministic theory 0-182  
 crystallographic structures, non-linear physics anal. 0-10631  
 curved space-time quantum stochastic processes, covariant Kolmogorov-Klein-Fock eqn. 0-18083  
 deterministic motion of macrovariables inequality 0-42147  
 dielectric charge carrier drift simulation using stochastic graphs 0-15539  
 diffusion processes with two-point boundary conditions, probability distrib. 0-42144  
 dissipative structures, origins and perspectives (*French*) 0-151  
 dissipative systems, dynamical description 0-17867  
 dynamic system, classical quantisation conditions with stochastic behaviour anal. 0-8922  
 dynamical astronomy, integrable and stochastic behaviour 0-12650  
 dynamical systems, kinetic eqn. derivation based on cumulant function props. 0-12995  
 education, stochastic model, radioactive decay, difference-differential eqns. 0-51992  
 EEG analysis by all-pole model 0-41287  
 eigenvalue problem, stochastic, limit distribution (*German*) 0-52134  
 elastic phase transitions, crit. dynamics 0-2146  
 electromagnetic wave propagation, local energy density distribution using Wigner distribution functions 0-9781  
 EM wave propagation in stochastically stratified medium, transmission coeff. 0-32887  
 extrema, asymptotic analytic theory for Fokker-Planck processes 0-12992  
 fatigue crack propag., stochastic model 0-53701  
 fermion system, tight-binding spinless, many particle quantum diffusion in stochastic medium 0-42143  
 fission, spontaneous, mass and charge division, asymmetry, order-disorder model 0-28866  
 Fokker-Planck dynamics, stochastic quantisation and detailed balance 0-4645  
 fracture models, appl. to composites and polymers 0-10198  
 friction, stochastic quantisation, nonlinear Schrödinger equation 0-27164  
 Gaussian quantum stochastic processes on the CCR algebra 0-12985  
 geophysical potential fields on sphere, stochastic props. study 0-56338  
 gradient problems, error of estimation of direction 0-22282  
 Hamilton function, conditionally periodic movement presentation 0-8915  
 Hamiltonian, classical with two degrees of freedom near an equilibrium point 0-8916  
 Hamiltonian, Henon-Heiles, survey and applications to related examples 0-8917  
 Hamiltonian classical and quantum systems, Volta Memorial Conf. 0-8738  
 Hamiltonian system, ergodic components in the stochastic region 0-8918  
 harmonic oscillations of single degree of freedom systems 0-33516  
 Holder continuity of sample paths in Euclidean field theory 0-9085  
 infinite harmonic crystal, dynamics and ergodicity 0-10598  
 infinite nonlinear lattice, localised mode due to a light impurity 0-10624  
 instability theory applies. to nonlinear plasma systems, review (*Czech*) 0-38580  
 ion heating by a perpendicularly propagating electrostatic wave 0-10410  
 Ising lattice, thermal relaxation, nonideal behaviour, stochastic theory 0-22312



**stochastic processes continued**

- Ising model, magnetisation probabilities and metastability 0-29516  
 isotropic turbulence, conditional flow struct., anal. 0-19335  
 Kolmogorov direct equation, solution, Galerkin measures (Russian) 0-46981  
 Lagrangian for non dimensional non constant diffusion processes 0-31688  
 laser fields, stochastically fluctuating, saturation and Stark splitting of resonant transitions 0-53245  
 laser instability, example from synergetics 0-9848  
 linear response theory, master eqn. approach 0-31663  
 linear transport relaxation equations, matrices, variational principle 0-17785  
 loose medium, discontinuity of displacements, interpretation 0-12990  
 Lotka-Volterra eqns. with stochastic approx., numerical soln. 0-8912  
 Lyapunov characteristic numbers and Kolmogorov entropy of a four-dimensional mapping 0-46978  
 magnetic flux annihilation in a large Josephson junction 0-11139  
 martingales, set function processes, vector lattices, Riesz decomposition and characs. (French) 0-8908  
 Maxwell field, stochastic mechanics in Euclidean formulation 0-42081  
 meas. fundamentals of mean values and standard deviations (German) 0-13031  
 metal-composite shell, three-layer, stochastic formulation of optimisation using heuristic methods 0-38268  
 metallic one component systems, normal cryst. growth fluctuations theory 0-15025  
 methanol- $d_3(d_1)$  in freon 11, self-associated, OH frequency temp. depend. 0-37809  
 methods and techniques for quantum mechanics, book 0-4584  
 micellar phase dissoc.-recombination kinetics, stochastic model 0-55628  
 micelle dissociation-recombination kinetics, stochastic model 0-30291  
 molecular dynamics, semiclassical study of bound states 0-9693  
 molecular pair, fluoresc. depolarisation, using stochastic Liouville eqn. with radiative terms 0-16074  
 molecules, Fokker-Planck eqns., stochastic modeling 0-43128  
 moving thin elastic strip subjected to random parametric excitation, dynamic stability 0-48618  
 multiphoton resonance interaction with matter 0-33073  
 multiplicative stochastic processes in statistical physics, appls. 0-22289  
 neuronal activity model, Ornstein-Uhlenbeck process 0-51030  
 neutron stochastic transport, functional theory 0-37413  
 non-Markovian Langevin equations, new approach 0-27222  
 nonequilibrium transitions induced by external noise 0-152  
 nonlinear birth and death models, controlled truncation global bounds 0-52130  
 nonlinear filtering equations for two parameter doubly stochastic Poisson processes (French) 0-17870  
 nonlinear oscillators, limit cycle, chaotic response 0-148  
 nonlinear systems, vibrations under space-time stochastic loads 0-33524  
 nonlocal stochastic equation of motion with damping in electrodynamics 0-17872  
 nonstationary stochastic process, computer programme for statistical characs. 0-22283  
 Onsager-Machlup Lagrangian in theory of stationary diffusion processes 0-128  
 optical frequency up-conversion with stochastic pumping, exactly soluble model 0-23744  
 oscillators, coupled, stochasticity thresholds 0-46977  
 oscillators, nonlinear stochastic, triangular wave, optimally controlled, Weiner process and Poisson process, numerical studies 0-52128  
 oviductal egg transport, stochastic model 0-51059  
 parametric frequency up-conversion with stochastic pumping, canonical model 0-53368  
 parametric resonance, wave intensity fluctuations in one-dimensional randomly inhomogeneous medium 0-18970  
 particle accel. by MHD turbulence 0-31203  
 particle beam, stochastic cooling, review 0-37675  
 particle motion in two waves, numerical study 0-8914  
 particle transport, stochastic theory, appl. to radiation damage cascades 0-54291  
 pendulum, double with varying length, probabilistic characteristics of solns. (Polish) 0-8781  
 periodic potential, stochastic diffusion 0-12994  
 perturbation theory, quasi-periodic motion, asymptotic expansion method 0-17877  
 plane orbit estimation using discrete timing of range measurements, Hermite polynomials appl. 0-21890  
 plasma, renormalised Vlasov turbulence 0-19579  
 plasma, SS 0-14927  
 plasmas, stochastic ion heating by lower hybrid wave 0-28707  
 polystyrene, glassy state, relax., free vol. fluctuations effect 0-19722  
 probability density, time dependent, for nonlinear non-Markovian stochastic process, coloured noise effect 0-22281  
 proton (antiproton) beam in storage ring, stochastic cooling anal. 0-5420  
 quantisation, semiclassical, periodic orbit role for the quantal bound state 0-8831  
 quantum intramolecular dynamics: criteria for stochastic and nonstochastic flow 0-53082  
 quantum mechanics, stochastic formulation, quantum operator algebra origin 0-88  
 quantum pendulum under periodic perturbation, stochastic behaviour 0-8834  
 quantum theory, physical foundations, stochastic formulation, proposed expt. test 0-52049  
 radionuclide migration from repository sites, stochastic anal. 0-37486  
 random processes, statistics of, use of stochastic occupation densities and local times (French) 0-46972  
 randomly inhomogeneous medium with reflecting boundary, wave intensity fluctuations 0-42075  
 Rayleigh-Benard system, turbulence near onset of convection 0-48686  
 relativistic Brownian motion, space-time approach to quantum mechanics 0-31567  
 RF plasma heating, stochasticity role 0-28752  
 Rutherford  $180^\circ$  backscatt. anomaly in solid, Monte Carlo simulation 0-45189  
 Schrodinger eqn., model of stochastic origins 0-81  
 Schrodinger equation, stochastic solution, asymptotic behaviour (French) 0-46844  
 Schrodinger equation nonseparable potentials, vibr. energy level semiclassical calc. 0-8832  
 self-consistent analysis for two-dimensional hydrodynamics 0-4533

**stochastic processes continued**

- semiclassical laser theory in the stochastic and thermodynamic frameworks 0-1178  
 separated hypotheses for stochastic processes, tests (French) 0-17871  
 slightly dissipative systems, stochastic behaviour 0-22290  
 solar cooling performance predictions via stochastic weather algorithms 0-35642  
 solar flare protons, stochastic accel. 0-21953  
 solar water heating models comparison 0-30387  
 stability, input-output, of continuous time and discrete time interconnected stochastic systems 0-52133  
 star formation, stochastic model rel. to spiral galaxies props. 0-12818  
 stars, stochastic marginal forced mixing rel. to evolution 0-56818  
 stellar evolution, fluctuations due to convection 0-31293  
 stochastic differential eqns., Green's function soln. by hierarchy method, closure approx. error 0-149  
 stochastic differential eqns., stability and boundedness rel. to generalised norm 0-12993  
 Stokes' formula, stochastic integrals and path independence (French) 0-27216  
 superionic conductors, continuous stochastic models, book contrib. 0-24663  
 system influenced by time dependent electric field, fourth order variation perturbation theory 0-22230  
 tensors, geodesic connection to stochastic parallel displacement 0-8920  
 terrestrial catastrophism, theory incorporating galactic modulation 0-31043  
 thermal conduction of solids, temperature stochastic field in cylinder computing, digital simulation algorithm (Polish) 0-17879  
 thermal mechanics: a quantum mechanical analogue of nonequilibrium statistical thermodynamics 0-52125  
 time ordered operator cumulants, statistical independence and noncommutativity 0-31670  
 transient laser radiation, stochastic process near an instability point, numerical solution 0-23658  
 triatomic molecules, motion, regular and irregular spectra, theory 0-9590  
 two component Boltzmann gas, fluctuating kinetic eqn. 0-171  
 two-level atoms, saturation in chaotic field 0-37982  
 unsteady state age distrib. of particles in flow systems 0-12991  
 Van der Pol oscillator, renormalised perturbation theory 0-27225  
 viscoelasticity, stress/strain relationships, fluctuations 0-17802  
 wave field statistical moments in medium with large-scale inhomogeneities 0-37953  
 Wigner representation, semi-classical ergodicity of quantum eigenstates 0-8833  
 $SF_6$ , breakdown voltages dispersion, anal. 0-38772
- stochastic systems**  
*see also random processes*  
 catastrophe and stochasticity in semiclassical quantum mechanics 0-8861  
 dissipative systems, canonical quantisation, von Neumann equation 0-52132  
 gravitational waves stochastic background, energy density upper limit from pulsar timing meas. 0-36743  
 multivariate joint probability function of state variables with quantized levels for environmental system with discrete data 0-36836  
 nonordinary Poisson flows, moment dynamics 0-22280  
 river basin water resource, Pareto region, stochastic multicriterial problem in control 0-4055  
 stability, input-output, of continuous time and discrete time interconnected stochastic systems 0-52133  
 turbulence and stochastic self oscillations, review 0-4537
- Stockbarger method** *see crystal growth from melt*
- Stokes flow** *see flow*
- Stokes law (fluid mechanics)** *see flow*
- Stokes law (optical)** *see luminescence*
- Stokes lines** *see spectra*
- Stokes optical law** *see luminescence*
- stopping of particles** *see energy loss of particles*
- storage, digital** *see digital storage*
- storage devices**  
*see also energy storage devices; magnetic storage devices; optical storage devices; semiconductor storage devices*  
 Harris data memory, operation and educational uses 0-17779  
 p<sup>+</sup>n SAW memory correlators, modified theory 0-43563
- storage rings**  
 Adone  $e^+e^-$  ring, beam-beam effects 0-37649  
 ALFA, electron pulse stretcher to increase Frascati Linac duty factor, feasibility study 0-23237  
 beam-beam interaction, radical diffusion simulation 0-37653  
 beam-beam interactions, perturbation method solns. 0-37667  
 CERN, comparison of characteristics of X-ray and  $\gamma$ -ray sources 0-14030  
 CERN ISR, facility and hadron physics program review 0-873  
 colliding beam facilities, overview 0-37642  
 conference, storage ring beam-beam interactions and nonlinear dynamics, Upton, NY, USA (March 1979) 0-36758  
 DESY  $e^+e^-$  experiments, QED checks,  $\tau$  and T studies 0-18111  
 DORIS, luminosity limitations 0-37648  
 electron and positron depolarisation suppression in storage rings and cyclic accelerators 0-42882  
 electron polarisation by circularly polarised EM waves 0-14020  
 filamentation instability of electron and positron colliding beams in storage rings 0-872  
 free electron laser amplifier, storage ring appl. 0-871  
 hadronic and nuclear EM probe system using electron accelerator and storage ring 0-23200  
 interacting beam models, summary 0-37644  
 interaction effects of EM fields on particle beams 0-37643  
 ion storage in electron ring, ion-ion interaction effects 0-52796  
 ISABELLE, beam-beam interaction, transfer map approach 0-37651  
 ISABELLE, bunched beams, instability threshold 0-37652  
 ISABELLE, linear and nonlinear beam-beam effects 0-37656  
 ISABELLE, nonlinear beam-beam interaction, computer model 0-37654  
 ISR, beam-beam investigations, review 0-37645  
 laser, isochronous storage ring type 0-48204  
 NUMATRON project test accumulation ring, vacuum system (Japanese) 0-18724  
 Orsay,  $e^+e^-$  interactions, beam-beam effect observations, review 0-37650  
 PEP, comparison of characteristics of X-ray and  $\gamma$ -ray sources 0-14030



## storage rings continued

- PEP, high-speed data acquisition and analysis system 0-23194  
 PETRA, comparison of characteristics of X-ray and  $\gamma$ -ray sources 0-14030  
 PETRA, luminosity limitations 0-37648  
 photon, electron and positron prod. from primary proton beams, Monte Carlo calcs. 0-32555  
 polarised positron, electron production by colliding photon beams 0-5426  
 proton (antiproton) beam in storage ring, stochastic cooling anal. 0-5420  
 proton (antiproton) storage ring, incoherent motion damping by dissipative elements 0-5419  
 proton accelerator ISABELLE, review 0-32545  
 resonator wall instability caused by ponderomotive forces, feedback-stabilised system 0-5418  
 review of ISR projects situation (1979) (*Czech*) 0-870  
 Sendai 1.5 GeV linac electron accelerator with pulse-beam stretcher ring 0-23188  
 SPEAR, backscatt. laser polarimeter for transverse beam polarisation meas. 0-14019  
 SPEAR, beam-beam functional dependencies of machine parameters 0-37647  
 SPEAR beam-beam effects expts. 0-37646  
 SPEAR I, beam-beam limit simulation 0-37655  
 SRS, shielding design 0-37659  
 stable and unstable beam motions, mathematical statements 0-37663  
 time resolved spectroscopy with synchrotron radiation 0-31902  
 undulator radiation, hard, in dispersive medium, in dipole approx. 0-23608  
 X-ray/ $\gamma$ -ray region source characteristics 0-14030

## storage tubes

see also image storage tubes

- tera-bit electron beam memory realization 0-53198

## stores (computer) see digital storage

## storms

see also magnetic storms; thunderstorms

- Baltic beach scouring and detritus accumulation in short-term disturbance (*Russian*) 0-36288  
 Bay of Bengal, forecasting tropical storm movements 0-41531  
 Bay of Bengal, storms rel. to wave characts. off Paradip Port 0-41450  
 blizzard, 1978 February 18 to 19, in SW.England and S.Wales 0-12507  
 S.California, 1978 February 10, forecasting, satellite imagery rel. to model initial conditions 0-31084  
 convective storm environment, large aerosol particles meas. 0-41512  
 cyclogenesis, asymmetric jets instability theory 0-56537  
 cyclone centre location using kinematical determinant 0-56535  
 cyclones, unstable baroclinic waves downstream and upstream development 0-56540  
 detection, National Weather Service's training programme 0-8382  
 diagnostic analysis in weather forecasting, appl. to storms (*Chinese*) 0-12467  
 E.England coast, storm surge (1978 January 11 to 12) 0-12419  
 extratropical cyclone, enhancement after separation from polar front (*French*) 0-56517  
 flash floods, synoptic and mesoscale mechanisms for heavy rainfalls 0-8385  
 NW.Georgia, prevailing storm tracks rel. to monthly rainfall spatial correls. 0-51479  
 Great Britain, northerly gales of (1978 January 11 to 12) 0-12508  
 W.Gulf of Maine, storms rel. to gulf winter circulation 0-51430  
 hail showers in Rumania (*French*) 0-4061  
 hurricane, estimation of eddy viscosity and  $H_2O$  vap. flux 0-51503  
 hurricane cloud system, model of cloud-group activity 0-26601  
 hurricane sea surface wind speed, L-band radar backscatt. obs. 0-56561  
 hurricane surge potentials over SE.Louisiana, forecast model 0-46216  
 hurricanes, spiral bands excitation by interaction between symmetric mean vortex and shearing steering current 0-56538  
 India, November 1977 Andhra Pradesh cyclone and associated storm surge 0-51499  
 Indian sea areas, 1976 cyclonic storms and depressions 0-56533  
 Kouchibouguac Bay, New Brunswick, storms rel. to barrier island breach morphology and dynamics 0-12371  
 North Sea, wave height statistics using hindcast wave data 0-17273  
 precipitation in small mountain watershed, storm type effect, theoretical study 0-8355  
 precipitation scavenging of urban pollutants, inorganic nonmetallic species 0-12039  
 radar estimation of precipitation, using dual-wavelength radar 0-46220  
 radar remote sensing, optimal positions of multiple-Doppler system 0-31140  
 rainfall, maximum possible in Great Britain—time limited, determ. methods 0-4091  
 rainfall, spatial distrib. in small catchment, influence on storm runoff 0-8357  
 runoff, flow component separation, solute conc. and contact time study 0-8358  
 sea foam microwave emission, remote monitoring of storm intensity 0-41528  
 sea surge produced by storm, theory for stratified sea 0-51437  
 shallow sea thermal structure, during heating and storms (*Russian*) 0-56480  
 snowfall systems induced by Lake Ontario, objective forecast method 0-51484  
 squall line, formation from boundary layer forcing and temp. gradient, model 0-8396  
 surge prediction using vertical pendulums 0-36764  
 tornadic storms on 1976 January 13, assoc. gravity waves 0-41515  
 tornadic flowfield struct., laboratory expts. 0-56566  
 tornado life cycle, photographic sequence 0-41537  
 tornado vortex, barotropic instability theory 0-51458  
 tornado watches compared to observed tornadoes, rel. to weather modification 0-12505  
 tropical cloud cluster, struct. and evolution 0-12488  
 tropical cyclone, three-dimens. dynamic models and track prediction 0-56508  
 typhoon movement affected by equatorial anticyclone, Pacific and S.China Sea (*Chinese*) 0-46236  
 typhoon Ora, form. in intertropical convergence zone under influence of midlevel jets 0-12527  
 typhoon prediction by barotropic primitive equation model using splines (*Chinese*) 0-4063

## storms continued

- typhoon Tess wake vertical struct. in upper layer of Pacific Ocean 0-26538  
 urban storm water management, flood vol. distrib. 0-8361  
 USA, National Severe Storms Forecast Centre, 1970-9, predictive success 0-46214  
 waterspout in association with large cumulus congestus 0-41473  
 wind turbulence, characts. near top of spruce forest 0-17349  
 windstorm downslope from mountain 0-56551

## strain ageing

- steel, austenitic, Cr-Ni-Mn-V, X-ray anal. of carbide phases formed during ageing (*Russian*) 0-20936  
 steel, C, strain ageing and fatigue limit 0-40378  
 steel, low C and alloy, serrated flow and thermomechanical treatment (*Korean*) 0-30026  
 steel, V containing dual-phase, yielding and strain ageing, early stages 0-25794  
 steels, spring, 60S2A and 50KhFA, heat treatment and mech. working effect on mech. props. (*Russian*) 0-20962  
 Zircaloy-4,  $\beta$ -transformed, flow stress and dynamic strain ageing 0-3101  
 Al alloy 7075, serrated flow and thermomechanical treatment (*Korean*) 0-30026  
 Al-alloys, precipitation hardening, effect on dynamic strain ageing and jerky flow 0-20945  
 Cu-Cr (0.55 wt.%), crystallography of precipitates, strain field study 0-25699  
 Fe, cast, ductile, strain rate and temp., influence on strength, elongation and deformation (*Japanese*) 0-45356  
 Fe-Cu alloy, effect of  $\epsilon$ -Cu phase on strain ageing (*Japanese*) 0-7582  
 Ni-alloys, precipitation hardening, effect on dynamic strain ageing and jerky flow 0-20945  
 Ta-O, relaxation anal. after ageing under stress (*French*) 0-16365  
 Ti, dynamic annealing, effect on dynamic strain ageing phenomena 0-7594  
 $TiO_2$  rutile single crystals, stoichiometric, dynamic strain ageing 0-50661

## strain control

- epoxy resin, heat generated by fatigue (*Spanish*) 0-11736

## strain gauges

- see also strain measurement  
 application on compact bone 0-3883  
 atomic resistance transducers (wire), effect of loops 0-22346  
 calibration machine construction and parameters (*German*) 0-36970  
 compensation for temp. effects, cable capacitance and hysteresis in strain gauge meas. (*German*) 0-31734  
 creep meas., high temp., use of capacitance type strain gauges 0-21256  
 cylindrical tensoresistive pressure transducer 0-8978  
 design formulae 0-22354  
 dynamic signals treatment (*French*) 0-22352  
 error estimation for strain-gauge measurements in heat-resistance tests 0-4703  
 fluidic strain gauge load cell 0-37024  
 foil, use on materials with heat constraints during heat treatment 0-25938  
 high-temperature without base, manufacture 0-37018  
 holographic optical strain gauge 0-52182  
 mechanical strain indicators and recorders 0-13054  
 noncontact strain meter, exam. of design 0-7740  
 optoelectronic meas. methods appl. with twin diodes (*German*) 0-13064  
 orthopaedic load meas. using strain gauges 0-56262  
 piezoresistive strain gauges, biaxial gauge factors 0-52185  
 plastic model meas. use of strain gauges, instrumentation, accuracy 0-21255  
 plethysmograph, calibration-free Hg strain-gauge device 0-17161  
 polymer material bending strain, strain gauge to meas. reliably 0-25948  
 pressure pick-up with Si column strain-gauge convertor 0-31732  
 pressure transducer performance, effect of zero offset changes 0-56255  
 resistance wire, strain meas. in optical fibres and cables 0-23804  
 Sappir semicond. transducers, development and appls. 0-13059  
 semiconductor pressure transducers, temp. compensation, strain gauge appls. (*Polish*) 0-31726  
 tensoresistors, measuring force 0-17930  
 transducers in testing machine and as force standards 0-42215

## strain hardening see work hardening

## strain measurement

- see also strain gauges  
 accelerometer base strain sensitivity test device 0-52173  
 elasto-plastic strain eval. by strain gauge 0-28473  
 elastoplastic strain meas., elastic and residual components, single plate hologram interferometry 0-32932  
 floor reaction, medical appl. (*Japanese*) 0-12291  
 fluidic strain gauge load cell 0-37024  
 gravitational radiation detection method, elasto-optical antenna, photoelastic effect 0-46947  
 moire fringe method, strain anal. by multipurpose optical moire processor 0-9028  
 moire fringe methods 0-28476  
 moire gratings strain meas., long time high temperature appl. 0-38361  
 moire interferometry strain meas. in elastic thin membranes, appl. to human skin 0-30828  
 Moire method using diffraction beams, compensation of errors 0-13068  
 opposed-anvil high-pressure devices, material strength effect 0-47068  
 optical fibres and cables using resist. wire 0-23804  
 polymeric, liq., spike-strain test relevance for network connectivity destruction by deformation 0-6001  
 rheological property meas. apparatus (*French*) 0-14644  
 shear-band temp. meas., appl. to 4340 steel and 2014-T6 Al 0-48655  
 shell reinforced around hole, deformability meas. 0-16371  
 speckling application, for stress-strain state of parts 0-19300  
 steel, austenitic stainless, microdeform. meas. using method of grids 0-55615  
 surface displacement and strain anal. by speckle interferometry 0-14635  
 tensoresistors, measuring force 0-17930  
 whisker crystals uniaxial deformation, at He temperatures in magnetic field, mechanical displacement transformers design 0-50788

## strange particles

- see also hyperons; kaons  
 axial vector meson non-diffractive prod. in Kp and  $\pi$ p interactions 0-32122  
 condensation in dense nucleonic matter (*Russian*) 0-5086  
 hadrons, relation between spin, isospin, strangeness and charm 0-37183



**strange particles continued**

- Hagedorn Frautschi statistical bootstrap model, modification for baryon charge and strangeness conservation (*Russian*) 0-27489  
 long lived hyperstrange multiquark droplets in MIT bag model 0-9137  
 $K^0$ - $\bar{K}^0$  system, flavour-changing neutral currents 0-22553  
 $K^0$ - $p\bar{p}$ ( $\Delta p$ ), 50 GeV/c, strange bosons decaying into baryon-antibaryon pairs 0-37306  
 $p\bar{p}$ - $\Delta^0 X$ , small-angle production from nuclear and nucleon targets, collective tube model and triple-Regge picture 0-52538

**strangeness see strange particles****stratified flow**

- acoustic field in stratified media of variable viscosity, Green's functions 0-4545  
 Benjamin-Ono equation, Backlund transform. and conservation laws 0-4540  
 Benjamin-Ono equation, internal wave solitons, linear stability 0-53802  
 Benjamin-Ono equations, two-parameter Miura transform. 0-14720  
 boundary layers, stratified, stability calc., numerical integration (*German*) 0-53834  
 Boussinesq fluid, in rotating spherical annuli, small Reynolds number convection 0-6047  
 buoyancy effects in entraining turbulent boundary layers: a second-order closure study 0-21815  
 buoyant surface jet, 2-D flow props. (*Japanese*) 0-48762  
 cold gas, noninteracting particles, nonlinear periodic motion (*Russian*) 0-14868  
 concentration interface in turbulent mixing layer, visual growth 0-38392  
 Coriolis force blocking attenuation, wakes, baroclinic vorticity and boundary layers 0-6129  
 Czochralski bulk flow in the growth of garnet crystals 0-38979  
 density stratification as catalyst for instability 0-48676  
 disc rotating in fluid with surfactant surface layer 0-10284  
 dynamo action associated with random waves in a rotating stratified fluid 0-33687  
 entrainment process, laboratory expts. reinterpretation for stratified fluid 0-51405  
 FFTF upper-plenum mixing and stratification, comparative studies 0-583  
 finite depth stratified flow over topography on a beta-plane 0-6128  
 fluids of finite depth, exact one- and two-periodic wave solns. 0-53797  
 fluids of finite depth, N-soliton soln. of higher order wave eqn. 0-48724  
 gas and non-Newtonian liquid, stratified flow in horizontal pipes 0-48787  
 gas/liquid flow, heat transfer, local Nusselt number prediction 0-38393  
 generalised Benard problem for stratified fluid, rotation effects 0-24031  
 hydrostatic mountain waves, terrain shape effects for stratified fluid 0-21804  
 internal wave motion in a periodic stratification 0-1672  
 internal waves in stratified fluid, tank wall effect 0-53799  
 internal waves with finite fluid depth, inverse scatt. problem, Backlund transformation 0-31517  
 jet entrainment at density interface in thermally stratified vessel 0-6119  
 Jupiter atmosphere zonal flow, baroclinic instabilities 0-31245  
 lakes, stagnant, thermal stratification 0-36340  
 linear wave theory, internal wave operator solution 0-43759  
 linearly stratified fluid, gravitational collapse of mixed region 0-33653  
 MHD stratified flow between oscillating disks, boundary layers 0-28570  
 mixed fluid, nonlinear internal wave formation from gravitational collapse 0-33619  
 multilayered stratified flow investigation using water tunnel (*Russian*) 0-1703  
 natural convection from spheres and cylinders immersed in a thermally stratified fluid 0-6059  
 natural convective transfer at low temp., thermal stratification effect 0-6039  
 obstacle in weakly stratified flow, upstream influence, theory 0-56527  
 ocean, wind-driven flow in zonal channel with stratification and bottom topography 0-51402  
 ocean small-scale stratification, study via towed instruments carrier 0-36423  
 parallel flow normal modes in inviscid stratified fluid with propagation at infinity 0-24071  
 planetary atmosphere, convective instability of fluid layers 0-56754  
 plates, flat, rotating stratified flow, boundary layers 0-53793  
 point force in a stratified fluid in a cylinder under a magnetic field 0-14776  
 propagative thermal excitations, Rayleigh scatt. meas. (*French*) 0-33590  
 rotating fluid, vortex created by mass transfer between layers 0-12401  
 stable salinity gradient heated from below, convection and layers 0-24016  
 stably and neutrally stratified flow over three dimens. hill 0-48770  
 Stewartson vertical layers 0-48772  
 thermally stratified enclosures with localised heating from below, natural convection 0-24017  
 thermoconvective waves in stratified compressible fluid, stability criterion contradiction 0-19414  
 three-dimensional barrier in flow-field 0-48769  
 two layer system with baroclinic mean shear flow, solitary Rossby waves theory 0-19793  
 two-layer shallow water flow, internal and surface waves, numerical anal. 0-19472  
 two-layered, at outlet of open channel, dynamical singularities analysis (*Japanese*) 0-10285  
 two-layered flow, internal waves at interface, statistical props. (*Japanese*) 0-1673  
 unstable displacement problem for porous media with different permeability layers, developed stage anal. 0-14813  
 valley ventilation by cross winds 0-48771  
 vertical coplanar Y-junctions, two-phase steam-water flow 0-38478  
 viscous two-layer flow, stability to small perturbations, neutral stability curve 0-33652  
 wake collapse in the thermocline and internal solitary waves in stratified fluid in channel 0-53787  
 wakes in stratified flow, book contrib., review 0-19473  
 wave propagation, modified finite depth fluid eqn., exact N-soliton soln. 0-28517

**stratosphere**

see also ozonosphere

-Z 0-4074

- acetylene, tropospheric and lower stratospheric vertical profiles 0-4073  
 aerosol global distribution, 162-238 millibar altitude 0-56591  
 aerosol, determ. of characteristic parameters (*French*) 0-8387

**stratosphere continued**

- aerosol, laser radar meas. (*Japanese*) 0-21810  
 aerosol, sulphate, contrib. of OCS emissions rel. to climate 0-41524  
 aerosol detection, ground based techniques, laser usage 0-17390  
 aerosol formation and evolution model,  $SO_4^{2-}$  particles 0-17327  
 aerosol layer, Earth zonal radiation balance perturbation 0-56602  
 aerosol microstructure, lower stratosphere, sounding with multifreq. lidar. 0-56645  
 aerosol particle size distrib. meas. 0-51578  
 aerosol particles, collection and analysis techniques 0-17306  
 aerosol particles, optical props., instrumentation and techniques for meas. 0-17389  
 air collection and analysis techniques, troposphere and stratosphere 0-26566  
 barotropic 3-dimens. instability in upper stratosphere 0-41498  
 composition investigation using gas expansion and mass spectrometer beam system 0-31934  
 composition of middle atm., in situ meas. 0-17339  
 composition perturbations and temp. feedback, climatic effects 0-41525  
 cosmic ray and pressure oscills., balloon obs. (*Japanese*) 0-31182  
 cosmic rays, eleven-year cycle 0-4212  
 data compatibility used in meteorological analysis, empirical study 0-17308  
 dust loading index, 1923-54, pyrheliometric and circumsolar sky radiation obs. 0-46240  
 dynamics of middle atmosphere, review 0-17338  
 electrical conductivity, solar modulation rel. to atmospheric electricity supply current 0-17329  
 electrical parameters and aerosols, meas. (*Japanese*) 0-31087  
 equatorial wave mean-flow interaction, role of latitudinal shear 0-51461  
 ethane, tropospheric and lower stratospheric vertical profiles 0-4073  
 W.Europe, atmos. temp. 20-110 km altitude, 1975/6 winter anomaly 0-36356  
 fallout residence time, 1965-1971 obs. made in India 0-41526  
 fission products, removal rate seasonal vars. 0-55957  
 gamma-ray lines observed in balloon flights at high rigidity, extraterrestrial line flux upper limit 0-21882  
 halocarbons, hydrocarbons and  $SF_6$ , global distrib., sources and sinks, rel. to  $O_3$  depletion 0-4088  
 HAPP wind study, high-altitude platform operation feasibility 0-17369  
 internal inertia-gravity waves in tropics 0-41497  
 ion mobility and concentration, and conductivity, 10-70 km altitude 0-36358  
 IR spectroscopy instrumentation, design study 0-17391  
 jet stream, different, theory 0-46242  
 Kelvin waves, struct. and behaviour from Nimbus 5 IR meas. 0-8394  
 mass spectrometry for in situ meas. 0-17388  
 methyl chloride conc. profile up to 32 km. altitude 0-36368  
 Michelson interferometer, use as selective filter for stratospheric trace gas concs. meas. 0-17408  
 minor constituents, concs., chemiluminescence in situ instrums. and techniques 0-16886  
 minor constituents detection using tunable spin flip Raman laser, review 0-55762  
 nightglow intensity fluctuations during stratospheric warmings 0-4162  
 planetary waves at 20-80 km altitude rel. to ionospheric absorpt. winter anomaly 0-36359  
 radar observation of fine struct., pulsed VHF radar method 0-51566  
 radicals, atomic and diatomic, meas. 0-17307  
 remote sensing by two satellites, radio illumination method 0-51550  
 satellite observations, instrum. description 0-26713  
 satellite observations of middle atmosphere processes 0-21803  
 solar MUV photometer, rocket borne, stratospheric ozone concentration measurement 0-52292  
 structure in presence of noctilucent clouds 0-8412  
 temperature fluctuations, latitudinal-wavenumber power spectra 0-41499  
 trace gas sampling, chemical absorption filter techniques 0-17305  
 trichlorofluoromethane, 8-12  $\mu m$  band model calcs. 0-43112  
 trichlorofluoromethane, 8-12  $\mu m$  bands intensities, temp. depend. 0-43048  
 tropical stratopause, 2-day oscill. of meridional wind 0-56557  
 tropopause, detect. by partial specular refl. with VHF radar 0-8411  
 turbulence from IR astronomy data 0-12475  
 volcanic plume contributing sulphur and halogen to atmos. 0-51474  
 warming, Eulerian and Lagrangian mean meridional circulations 0-21799  
 water vapour 0.94  $\mu m$  absorption cross-section obs. (*Japanese*) 0-17427  
 wave motion, balloon obs. using data storage system on balloon 0-46263  
 wind and thermal structure, W.Europe 1975/6 winter anomaly obs. 0-36438  
 wind monitoring using Concorde-generated infrasound 0-51492  
 winds and turbulence continuous meas. using VHF Doppler radar, preliminary results 0-8444  
 winter warmings in N.Hemisphere 0-26591  
 $^{7}Be$ , stratospheric tracer, distrib. within high-press. systems in E.United States 0-4072  
 $Br+H_2O_2$ , rate constant upper limit, stratospheric chemistry implication 0-30216  
 $CO$ , content observed on circumpolar airliner flight 0-51475  
 $CIO$ , aircraft search for 3 mm emission 0-41510  
 $ClONO_2$ , stratospheric distrib. at sunset, balloon borne IR spectra obs. 0-41487  
 $HNO_3$ , IR spectra rel. to abundance 0-12464  
 $HO_2$  radical, atmospheric reactions studied by laser mag. reson. spectroscopy 0-12511  
 $H_2SO_4$  gas phase meas. 0-36366  
 $NO$ , photodissoc. in mesosphere and stratosphere, theory 0-41580  
 $NO$ , photodissoc. rate, calc. 0-51498  
 $NO$  predissociation, photochemistry 0-21802  
 $NO+BrO$ , controlling  $[BrO]/[Br]$  and  $[BrO]/[HBr]$  ratios in stratosphere 0-50866  
 $NO+BrO$ , temp. depend. kinetic study, stratospheric Br photochemistry implication 0-50866  
 $NO_2$  content during stratospheric warming, 1979 obs. 0-51476  
 $NO_2$  determination, observational method and behaviour at mid-latit. 0-17414  
 $NO_2$ , global behaviour 0-17334  
 $NO_2$ , minor atm. components, visible absorpt. spectra, temp. depend. (*French*) 0-36355  
 $NO_2$  transport, production in thunderstorms 0-8376  
 $NO_2$  vertical profile, balloon obs. (*Japanese*) 0-31086



**stratosphere continued**

- NO<sub>3</sub> in nighttime stratosphere, composition change following sunset 0-31097
- N<sub>2</sub>O, global atmos. composition and residence time 0-51519
- N<sub>2</sub>O, instantaneous global photochemical reaction rates 0-17335
- O<sub>3</sub>, photodissoc. and spectral absorpt. in stratosphere and mesosphere 0-51497
- O<sub>3</sub>, composition observed on circumpolar flight 0-51475
- O<sub>3</sub> content, CO<sub>2</sub> cooling affecting chem. production and loss rates 0-36369
- O<sub>3</sub> content affected by N<sub>2</sub>O from fertilisers, latitudinal effects 0-36370
- O<sub>3</sub> content in tropics, during March-April 1976 stratospheric warming 0-12494
- O<sub>3</sub> depletion by halomethanes 0-16866
- OCS, stratosphere content, solar spectra meas. by 12 km altitude aircraft 0-41486
- O(<sup>3</sup>P) translationally hot, energy distrib. function 0-21811
- O(2<sup>1</sup>D<sub>2</sub>)+N<sub>2</sub>(O<sub>2</sub>)(CO<sub>2</sub>)(H<sub>2</sub>O)(methane), collisional deactivation meas., 295K, rel. to atmospheric processes 0-16663
- SO<sub>2</sub>, minor atm. components, near UV absorpt. spectra, temp. depend. (French) 0-36355
- SO<sub>4</sub><sup>2-</sup> aerosol layer, form. and evolution model 0-21801

**strays (atmospherics) see atmospherics**

**streak photography**

- Agat, streak image camera with picosecond time resolution used in plasma investig. 0-38717
- arc, high current, rotating, hot wake investigation by streak photography and schlieren systems 0-1862
- camera synchronisation using picosecond laser pulse activated Si switch, jitter reduction 0-53440
- picosecond light pulse, meas. techniques (Japanese) 0-52291
- space charge field, spatio-temporal distrib. determ. in breakdown 0-38771
- time resolved spectroscopy, high-sensitivity streak camera, design (Japanese) 0-52327
- (Y, Gd, Yb, Bi)<sub>3</sub>(Fe, Al)<sub>2</sub>O<sub>12</sub> epitaxial film, domain wall motion and oscill. 0-2616
- (YGdYbBi)<sub>3</sub>(FeAl)<sub>2</sub>O<sub>12</sub> epitaxial film, diffuse domain wall, bubble domain expansion 0-25170

**streamer chambers**

- 2 m chamber in mag. field for  $\alpha$ -particle spectrometer installation, SKM-200 0-23241
- laser registration method for nuclear reactor detection (Russian) 0-18765
- track integral brightness, measurement using installation incorporating multiplier 0-27882
- Ne-He high press. flash tubes, digitisation pulse characteristics 0-9455

**streamers see discharges (electric)**

**streaming, acoustic see acoustic streaming**

**street lighting**

- urban, large orbiting mirrors for night illumination 0-45632

**strength (mechanical) see mechanical strength**

**stress see internal stresses; stress effects; stress/strain relations; yield stress**

**stress analysis**

- see also bending; crack-edge stress field analysis; photoelasticity; photo-plasticity; strain gauges; thermal stresses; torsion; yield strength; yield stress

- Alpine fault, New Zealand, frictional metamorphism, Ar depletion and tectonic stress 0-41440
- anisotropic plate with curvilinear holes, plane elasticity problem, soln. approach (Russian) 0-33457
- anisotropic plate with curvilinear holes, plane elasticity problem, comment (Russian) 0-38260
- anisotropic plate with curvilinear holes, plane elasticity problem, basis of soln. (Russian) 0-38261
- aortic valve mechanics, anal. in diastole 0-35928
- axisymmetric cylinder, experimental numerical hybrid method 0-48657
- axisymmetric thermoelasticity problem for two-temperature hollow cylinder 0-5941
- bar, elastic, prismatic, with rigid ends, lower and upper bounds for torsional rigidity 0-48568
- bar, round, subject to combined static and repeated bending and torsion, fatigue strength criterion 0-40496
- bar, thin-walled, effective torsional rigidity optimisation (Russian) 0-19245
- beam, Timoshenko, non-stationary loaded, use of Laplace transformation and classical method 0-14564
- beams, pure elastic-plastic bending diagram, general relationships 0-14588
- body with array of fine elastic inclusions, elongation and stress concentration 0-33466
- bonded sector plates, stress anal., soln. of elastostatic boundary value problems 0-1425
- caustics equations for crack and dynamic plane elasticity problems 0-43669
- chemically hardening material cast in elastic cylindrical mold, transient thermal stresses 0-7589
- circular bar of rate sensitive material, elastic-plastic tension-torsion 0-48602
- circular plates, thermoviscoelastic anal. of a thermorheologically simple material 0-10161
- coated fibre and cable unit structure optimisation 0-53466
- composite, laminate, crack normal to interface, impact response 0-14628
- composite inhomogeneous anisotropic body, stress singularity near rib (Russian) 0-19243
- composite wedge, stress state anal. near vertex (Russian) 0-19242
- composites, strength criteria, stress anal. (Russian) 0-1482
- composites, stretching, zone of disturbed stress state calc. 0-39206
- composites transient hygrothermal stresses, coupled diffusion of heat and moisture 0-33451
- compound arbitrary anisotropic body, stress singularity, composites appl. (Russian) 0-33455
- concentration around plane slit-shaped cavities (Russian) 0-28417
- concrete, reactor shielding thermal stress cracking anal. (German) 0-5232
- conference, computational methods in nonlinear problems in mechanics and engineering, Austin, Texas, USA (March 1979) 0-51945
- conference, reliability and stress anal., San Francisco, CA, USA, 1975 0-8740
- corrugated tubes, semi-circular, slender ring shell theory (Chinese) 0-19234

**stress analysis continued**

- Cosserat composite elastic cylinders, thermal stresses 0-5937
- creep analysis of rotating orthotropic disks 0-33476
- cup wall ironing, stress calc. 0-29989
- curved plates, subject to arbitrary temp. distrib., stresses and displacements 0-5938
- curvilinear aeolotropic solids, 3-D thermoelasticity 0-56
- cylinder, circular embedded in resisting medium, twisting, stress anal. 0-53637
- cylinder, clamped heterogeneous, stresses and displacement anal. 0-14571
- cylinder, hollow, nonlinear viscoelastic material, dynamic pressure loading 0-38289
- cylinder, hollow infinite, with temp. depend. thermal cond., thermal stress anal. 0-14575
- cylinder, transversely isotropic with circumferential edge crack, singular stresses 0-19284
- cylinder under uniform pressure, transition functions 0-10158
- cylindrical shell, stress concentration near inclined holes 0-33460
- cylindrical shell and belt, interaction contact stresses, elastic layer model 0-33543
- cylindrical shells, calc. of stresses (German) 0-33454
- cylindrical shells under internal pressure, approx. anal. 0-5943
- defect geometry, stress intensity factors, photoelastic meas. correlation (German) 0-53727
- dental implants, stress anal.; effect of elastic parameters and geometry 0-30930
- dental implants, stress anal., effect of root-length and pseudo periodontal ligament incorporation 0-30931
- dielectric bodies stress determ. using EM waves 0-38370
- dielectric parts, stress patterns and deformation characts., computer anal. 0-17787
- dielectrics, elastic, stress tensor, polarisation vector, electric tensor 0-55018
- direct and variational principles rel. to approx. techniques 0-28420
- Earth crust, aseismic geodynamics in Urals rel. to geomag. secular var. anomalies 0-26447
- elastic, with aid of computer, axisymmetric pressure vessels with structural discontinuities (Japanese) 0-38265
- elastic circular cylinder with prolate spheroidal cavity under tension, stress distrib. 0-19236
- elastic fracture mechanics, boundary integral eqn. anal. 0-14622
- elastic half space, ring shaped punch contact stress determ. 0-38356
- elastic half space containing embedded rigid block 0-23890
- elastic half-space containing axially loaded rigid cylindrical rod 0-1423
- elastic transient waves in medium with axisymmetric cavities, stress anal. (Ukrainian) 0-33503
- elastic-plastic materials, K<sub>IC</sub>-value determination, fracture mechanics method 0-45376
- elasticity, fundamental theory, and applications, book 0-22158
- elasticity equations for cubic cavities in elastic space (Russian) 0-1430
- elastoplastic strip or half-plane under moving load, residual stresses and plastic zones 0-53645
- experimental, conf., Bradford, England (Sept. 1978) 0-17718
- fatigue fracture analysis of rotating disks under torque 0-43668
- fibre reinforced cylindrical shells, stress strain state and stability 0-14598
- first wall model, mechanical anal. using state variable approach 0-32452
- fission reactor, FEM anal. of pellet-clad bonding 0-42765
- fusion reactor first-wall structural mats., stress and lifetime limitations 0-32447
- fusion reactor toroidal field coils, stress anal. by finite element method 0-13926
- glass fibre reinforced plastic, dynamic stress conc. around defects, discrete model 0-30024
- glass segment, resting on elastic ring, structural strength 0-14630
- graphite materials, isotropic, resist. to deformation and fracture under complex stress conditions 0-16479
- harmonic extensions of body under variable traction and no body force 0-8792
- hip prostheses femoral component biomechanics, bone cement stress 0-56285
- hoop stresses at tee intersections of cylindrical shells, approx. prediction 0-5942
- infinite elastic strip, circular inclusion undergoing dimensional changes, stress components 0-48590
- inhomogeneous materials, elastic deform. under multiaxial stress, analytical relations 0-44247
- inhomogeneous strips, elastic equilibrium, stress (Russian) 0-19244
- isotropic plate, stresses under concentrated forces 0-48572
- isotropic semiinfinite plate heated by moving point source of heat, temperature stresses 0-43628
- isotropic thin shells with circular hole, stress state, numerical investigation 0-48586
- JET vacuum vessel, mechanical reliability in disruptive instability 0-18643
- joints, double adhesive bonded, loaded in shear tension (French) 0-23968
- Lamb's problem, line load suddenly applied on micropolar elastic half-space 0-12907
- laminated anisotropic plates, transverse shear deformation effect 0-19237
- laminated cylindrical shell, coupling effect under internal press. (Japanese) 0-55449
- layered beams, interlaminar thermoelastic stresses 0-1432
- layered system, thermal stresses and displacements 0-23891
- Love waves, propagation in elastic isotropic incompressible medium 0-23929
- machine parts, safety factor determ. during cyclic loading taking account of initial stresses 0-43675
- martensite, microstresses associated with tempering 0-3111
- Maxwells stress function representation, completeness 0-36851
- metal, BCC, polycrystalline aggregate, prediction of plastic props., deformation by {111} pencil glide 0-11731
- metal fatigue analysis, inversion of strain-life and strain-stress anal. 0-19289
- micropolar semispace, effect of heated boundary on normal stress distrib. 0-1433
- Mindlin plate, transient and pseudotransient anal. 0-36850
- moire fringe and laser speckles, optical stress anal. 0-10217
- moire stress analysis interferometer with microprocessor 0-31858
- myocardium of human left ventricle, stiffness distrib. rel. to shape change in diastole 0-41095
- necked cylindrical bar, elastic-plastic, residual stresses after unloading 0-38284



## stress analysis continued

necking, dynamic analysis based on stress wave propagation 0-1440  
 necking, loading history depend. 0-5957  
 nonlinear photomechanics, birefringence in polymers, stress anal. appl. 0-33545  
 nuclear reactor pressure vessels, stress analysis program, STANSAS (Japanese) 0-22969  
 optimization of geometric discontinuities in stress fields [and reply] 0-14569  
 orthotropic cylindrical shell acted upon by local load 0-43617  
 orthotropic cylindrical shells, periodic problems, computer anal. (Russian) 0-23889  
 orthotropic rotating discs, flexure, stresses and deflection 0-5927  
 panels with openings, stability loss and critical stresses 0-10219  
 patella stress analysis, rel. to patellar articular cartilage lesions 0-35942  
 perforated plate, global stress strain behaviour 0-10169  
 perforated plates, finite element elasto-plastic anal. 0-10168  
 photoelastic load meas. and testing (German) 0-19297  
 pipe, layered, support layer thickness effect on stress-strain state (Russian) 0-43614  
 plane elasticity, mixed finite element method, convergence and performance 0-38258  
 plate, annular, bending anal., closed form solns. 0-38263  
 plate, infinite, with circular disc, tensile and compressive stress problems 0-38255  
 plate, rectangular with stiffening ribs, stress-strain state, elasticity eqns. (Russian) 0-1427  
 plate, semi-infinite, joint with strip plate, analytical solution 0-10139  
 plate of variable thickness, defined applied theories construction, asymptotic method (Russian) 0-53634  
 plate with bend interaction, numerical calc. method for stress and deflection (Japanese) 0-23919  
 plate with hole, contour reinforcement, plane stress state anal. (Russian) 0-33447  
 plate with two circular holes having tangential stresses, stress anal., electrostatics 0-48571  
 plates, isoparametric finite elements, variational formulation of plate equilibrium problem (French) 0-43608  
 plates, open and loaded holes, exam. of part elliptical cracks 0-10195  
 plates, rectangular orthotropic, stress anal. and generalised orthogonality relations 0-38252  
 plates, thin, converged stress solns. by extended field method 0-38306  
 plates, thin, harmonic buckling due to constrained thermal expansion 0-48620  
 plates and shells, viscoelastic, flexible, thermomech. behaviour during cyclic loading 0-33478  
 plates with cut, stability loss critical stresses for steel, Ti and Al alloys 0-11690  
 polybutadienes, use of high modulus inclusion gauge, in stress analysis 0-21254  
 polymer composite anisotropic plates, stress conc. around holes with shear strain taken into account 0-43618  
 polymer granules, compression, stress state 0-10218  
 polymer solns., dilute, Hartree self-consistent field analysis 0-5648  
 pressure vessel, structural representation in stress anal. 0-27703  
 pressure vessels, creep bounds and brittle damage estimates 0-23908  
 quarter plate support, planar flexibility depend. on fillet radius 0-5944  
 reactor fuel pins, internal and external press. effects (Czech) 0-5233  
 reactor fuel rods, cladmed, thermo-irradiation induced creep, stress analysis 0-35275  
 reactor vessel, determ. of stress intensity factor 0-37455  
 refractory, thermal stresses produced by temp. gradient, finite element anal. (Japanese) 0-33538  
 relaxation calculations in strips, errors due to approxs. 0-23909  
 rigid punch problem on non-homogeneous elastic half-space 0-53720  
 rod, conical, nonlinear viscoelastic materials, soln. using generalised correspondence principle 0-38288  
 rod-shaped elements, under simultaneous static loads and elevated temps., linear limited stress relax. 0-14590  
 rolling, determ. of stress distrib. in rolled material 0-48651  
 rotating deformable elastic disc, vibr. stress anal. (Russian) 0-19265  
 rough curved surfaces, elastic contact stresses calc. 0-10213  
 round tubes in flexure, critical buckling strains 0-23921  
 San Andreas fault, local mag. field vars. and stress changes near slip discontinuity 0-26448  
 sea ice, relationship between mean stresses and internal forces local values in drifting cover 0-31056  
 semi-infinite medium with anisotropic elasticity, 1st and 2nd periodic fundamental problems (Chinese) 0-5931  
 shaft with regular round polygon, stress state 0-35284  
 shell, conical, stress distrib. near hole, orthotropic effect 0-43630  
 shell, cylindrical, in vicinity of supporting elements, stress state 0-48585  
 shell, reinforced plastic, optimisation with allowance for geometrically non-linear factors 0-38270  
 shell, spherical, glass, with metal insert, design strength parameters 0-14576  
 shell, spherical, with elliptical hole, stress state 0-33449  
 shell subjected to centrifugal force, stress anal. (German) 0-23900  
 shells, cylindrical, thermoelastic problem 0-38273  
 shells, transversely isotropic, elastically deformed, optimal reinforcement of openings 0-38269  
 shells of revolution, state of stress by min. energy and orthogonal proj. method 0-28415  
 shells of revolution, variable thickness, stress state determ. 0-38275  
 short fatigue cracks, exam. of propagation 0-10196  
 simple plate bending theory, approx. stress intensity factors 0-43612  
 slip zones along interface, caused by plane horizontally polarised SH stress pulse 0-53648  
 snow, shear stress rel. to strain softening precipitated shear fracture and dry slab avalanche release 0-8338  
 space truss analysis in post-buckling range in dual load method 0-38298  
 spherical shell, shallow radially ribbed, stress state, struct. parameters influence 0-14581  
 statistical treatment of experimental data 0-53644  
 steel, austenitic stainless, X-ray stress anal. by new position sensitive proportional counter with uniform angular resolution (Japanese) 0-30190  
 steel, parts, stress calcs. during cooling, program system THEPLA (German) 0-35237  
 steel case hardened cylinders, heat treated, residual stress fields 0-3102  
 stranded wire helical spring, general axial response 0-33453  
 stratified material, compressed, stress determ. (Rumanian) 0-28434

## stress analysis continued

strip weakened by identical circular transverse openings, stress state 0-43606  
 tape twist induced stress estimation and reduction by pretwisting 0-53471  
 thermal emission for stress pattern analysis 0-33552  
 thermodiffusion in elastic cylinder, quasistatic problem (Polish) 0-10150  
 thermoelastoplastic solution for a circular solid cylinder subjected to heating and cooling 0-5952  
 thermoplastic beams, constant stress, design 0-38248  
 transversely isotropic medium with closed conical cavity, stressed state (Russian) 0-43616  
 trigonal monocrystals, classes 3 and  $\bar{3}$ , elastic potential and yield condition (Russian) 0-29108  
 tube, porous, nonlinear viscoelastic materials, soln. using generalised correspondence principle 0-38288  
 twisted circular cylinder with radiating internal cracks stress intensity factor (Chinese) 0-5984  
 two-phase nodules, heat treatment, stressed state, connection with nodule size, cooling rate and phase ratio (Russian) 0-16334  
 underwater acoustical compliance tube for sound projectors, stress and deformation analysis 0-33310  
 unhomogeneous bars, normal mode response, stress anal. by boundary operator method 0-19239  
 vacuum vessel for ASDEX fusion reactor, finite element stress anal. 0-18655  
 viscoelastic bodies, deformation taking into account influence of accumulated defects 0-19252  
 viscoelastic half-space, stress field in randomly varying temp. field (Ukrainian) 0-33467  
 weakly absorbing solid medium, opacity fluctuations, heating by intense radiation and thermoelastic stresses problem 0-38048  
 wedge, composite, plane elasticity stress singularities 0-38262  
 wedge, infinite, stress distrib. 0-23885  
 wedge, plane, nonlinear viscoelastic materials, soln. using generalised correspondence principle 0-38288  
 Zircaloy cladding, stresses due to pellet cladding interaction 0-42762  
 C fibre-reinforced plastic joints, fatigue life, stress distrib. analysis 0-55497  
 Ga<sub>1-x</sub>In<sub>x</sub>As-GaAs epitaxial interface with small misfits, TEM image contrast 0-2275  
 Ti-6Al-4V, stress distrib. for steady axisymmetric extrusion 0-3103  
 Ti-Al-V (6, 4 wt.%), temp. distrib. for steady axisymmetric extrusion 0-11670  
 Ti-Al-V (6, 4 wt.%), temp. distrib. for steady axisymmetric extrusion numerical results 0-11671

stress birefringence see mechanical birefringence

## stress corrosion cracking

1300 MW cross compound turbine unit IP rotor coupling, fatigue crack due to combined corrosion and low alternating stresses, report 0-16611  
 adhesive bonds, stress corrosion testing 0-16514  
 alloys, passivatable, role of oxide films in stress corrosion cracking initiation 0-50762  
 alloys testing, for coal gasifiers appl. 0-7726  
 biotite stress corrosion cracking, seen in granodiorite 0-36299  
 $\alpha$ -brass, mechanically assisted dezincification during stress corrosion in ammoniacal solns. 0-3243  
 $\alpha$ -brass, stress corrosion cracking in 15N ammonia solns., fractographic aspects 0-16547  
 $\alpha$ -brass, stress corrosion cracking in Mattsson's soln., benzotriazole inhibitive effect 0-16554  
 Br.AZnMts 7-2.5-1.5-9 bronze, Mg-Al, type, fatigue and stress corrosion cracking, welding effects 0-3233  
 concrete, cracking in seawater due to embedded metal corrosion 0-30116  
 fatigue failure, flat specimens and struct. elements in liq. corrosive media, test method 0-40646  
 feldspar stress corrosion cracking, seen in granodiorite 0-36299  
 fission reactor fuel performance anal. by finite element method 0-42750  
 fission reactor fuel rod deformation code FEMAXI-II and its application 0-37446  
 fission reactor pellet-clad interaction modelling 0-37445  
 fission reactor half-shell fuel model, FRP 0-42748  
 Hastelloy C-276 and G, accelerated H<sub>2</sub> charging in aq. H<sub>2</sub>SO<sub>4</sub> at 0.2% yield stress 0-30144  
 Incoloy 800, stress corrosion cracking and anodisation during straining in boiling NaOH soln. 0-30140  
 Incoloy 800 in 50% NaOH, stress corrosion cracking, slow strain rate method (Japanese) 0-55575  
 Inconel 600, corrosion fatigue crack propag. at 85°C in 50% NaOH, potential effect (Japanese) 0-11834  
 Inconel 600, oxide layer, mechanical impedance meas. method 0-45444  
 Inconel 600, stress corrosion cracking and anodisation during straining in boiling NaOH soln. 0-30140  
 Inconel 600 and 718 in liquid Na environment, fatigue crack propag. 0-40624  
 Inconel 600 in 50% NaOH, stress corrosion cracking, slow strain rate method (Japanese) 0-55575  
 Inconel 625, accelerated H<sub>2</sub> charging in aq. H<sub>2</sub>SO<sub>4</sub> at 0.2% yield stress 0-30144  
 LWR fuel rod failure associated with power changes 0-16525  
 metals, H effect on mech. props., review 0-50718  
 nuclear reactor vessel, corrosion fatigue crack growth rate data, appl. to integrity anal. 0-32353  
 pellet cladding interaction failures, stress corrosion of fission reactor cladding tubes 0-16526  
 plane strain fracture mode criterion based on plastic zone size-thickness correlation 0-43670  
 PMMA, unstable crack propagation in liq. environment, fractographic study 0-30155  
 polyethylene, environmental stress cracking, liq. efficiency criteria 0-21134  
 polyethylene insulation of HV cables, water-treeing, environmental stress cracking phenomenon of elec. origin 0-40575  
 polystyrene, stress cracking, pressure-induced, mechanism 0-35361  
 proportional counter appl., position sensitive (Japanese) 0-11853  
 resistance in materials under long term static loading, evaluation methods 0-45461  
 specimen configuration effects, tensile and precracked data 0-16413  
 steel, 30CrMnSiNi2A, fracture toughness parameter K<sub>ISCC</sub> 0-21099



# stress corrosion cracking continued

steel, alloy 40Kh, sulphide cracking resistance, strengthening method influence 0-55577

steel, alloy D6AC, fatigue, under const. and variable amplitude loading, air environment effect 0-35386

steel, austenitic and austenitic-ferritic Mn-Cr, stress corrosion cracking resistance (*Czech*) 0-45437

steel, austenitic Cr-Ni, SCC and pits in  $MgCl_2$  solns. at 40-90°C 0-50748

steel, austenitic stainless, AISI 304, stress corrosion cracking and electrochem. behaviour in  $(NH_4)_2SO_4$ -Cl solns. 0-55566

steel, austenitic stainless, analysis of fracture surface in stress corrosion cracking (*Japanese*) 0-16573

steel, austenitic stainless, hydride phases rel. to SCC 0-35385

steel, austenitic stainless, stress corrosion cracking, mixed mode, fractographic evidence in surgical implant 0-30156

steel, austenitic stainless, stress corrosion cracking by polythionic acid (*Korean*) 0-21179

steel, austenitic stainless 12Kh18N10T and 15Kh17N2, corrosion cracking in chloride and alkaline solutions 0-55576

steel, austenitic stainless type-316, fracture mechanics study of stress corrosion cracking 0-16580

steel, C, corrosion cracking by sulphide, effect on props. 0-55587

steel, C, fatigue crack growth rate in high temp., high purity oxygenated water 0-40622

steel, C-Mn, accelerated  $H_2$  charging in aq.  $H_2SO_4$  at 0.2% yield stress 0-30144

steel, Cr-Mo (2.25, 1 wt.%), exposed to  $H_2$ - $H_2O$ - $H_2S$  environment, fatigue crack growth 0-40623

steel, Cr-Mo (2.25, 1 wt.%), SCC and temper brittleness, P grain boundary segregation effect 0-55571

steel, crack electrochemistry model in active state 0-21192

steel, crack growth velocity in gaseous  $H_2$  embrittlement, rel. to chemisorption 0-11831

steel, high strength, type 90 Mn V8, stress corrosion crack velocities in NaCl soln. 0-21161

steel, hollow cylinder, thick walled, effect of thermomech. treatment 0-11674

steel, low alloy, fatigue crack growth rate in high temp., high purity oxygenated water 0-40622

steel, low C, and alloy, corrosion fatigue strength determ. (*Japanese*) 0-25910

steel, low C, fatigue endurance limit, metallurgical technology and mech. treatment effect 0-55536

steel, low C, fatigue strength, influence of mech. stress level in preliminary corrosion 0-55579

steel, low C alloy, SNCM2, waveform effect on corrosion fatigue crack growth in NaCl soln. 0-21163

steel, maraging, 18 Ni, welded joints ageing props. obs. (*Japanese*) 0-40401

steel, martensitic, low C without Ni, for deep-well sucker rods, corrosion fatigue 0-55588

steel, martensitic, stainless, CrMoV, stress effect on pitting susceptibility 0-16542

steel, martensitic 07Kh16N4B, corrosion cracking in chloride and alkaline solutions 0-55576

steel, martensitic low C, development and props. (*Russian*) 0-20933

steel, mild, corrosion in lime water, stress effect 0-11815

steel, mild, mild, transgranular stress corrosion cracking in  $H_2SO_4$ -KCl soln., XPS obs. 0-16556

steel, Mo-Nb (2.5, 0.035 wt.%) Mo content effect on sulphide stress cracking resistance 0-21157

steel, Nb-Mo, Mo effect on sulphide stress cracking resistance 0-16552

steel, Ni-Cr, SCC, grain boundary impurity effect 0-30150

steel, Ni-Cr-Mo (11, 5, 3 wt.%), maraging, corrosion cracking in chloride and alkaline solutions 0-55576

steel, non-irradiated and irradiated specimens, autoclaves for fatigue crack growth tests (*German*) 0-45467

steel, reinforcing bar, high-strength 20GS2 and 20KhGS2 0-55578

steel, stainless, 304 type, cracks initiation in 25%  $MgCl_2$  solution at 80°C (*Japanese*) 0-10593

steel, stainless, corrosive environment effect on fatigue crack growth rate 0-55584

steel, stainless, crack resistance in chloride soln., electrochem. protection, polarization effect 0-55589

steel, stainless, duplex type 304, strain rate effect on stress corrosion cracking, in boiling  $MgCl_2$  0-21180

steel, stainless, fatigue crack growth behaviour in air and high-C liquid Na, carburization studies 0-40625

steel, stainless, fatigue crack growth rate in high temp., high purity oxygenated water 0-40622

steel, stainless, fatigue failure kinetics, effect of water 0-55585

steel, stainless, sensitised type 304, cyclic loading effect of SCC susceptibility in water 0-45428

steel, stainless, stress corrosion cracking, prestrain effect, stress relaxation study 0-35384

steel, stainless, stress corrosion cracking and anodisation during straining in boiling NaOH soln. 0-30140

steel, stainless, stress corrosion cracking avoidance by improved welding in BWR pipes 0-42838

steel, stainless, type 304, BWR coolant pipe, critical strength under stress corrosion cracking 0-52743

steel, stainless, type 304, corrosion fatigue and stress corrosion cracking, in boiling NaOH 0-7719

steel, stainless, type 304, oxyanions inhibitive effect on stress corrosion cracking 0-35374

steel, stainless, XM19, stress corrosion resistance 0-16558

steel, stainless 304, stress corrosion, high temp. electrochemical studies 0-30146

steel, steady diffusion-migration eqns., representing mass conc. of dissolved species in cracks 0-30108

steel, struct., corrosion fatigue strength, effect of medium temp. 0-55583

steel, sulphide stress corrosion cracking, threshold stress and crack initiation stress intensity comparison 0-21158

steel intercrystalline stress corrosion cracking in a  $Ca(NO_3)_2$  soln. (*German*) 0-30130

steels, stainless, accelerated test for susceptibility to  $Cl_2$  stress corrosion cracking 0-21199

steels 2Kh13 and 20Kh1M1FTR, sulphide cracking resistance, strengthening method influence 0-55577

Zircaloy clad  $UO_2$  fuel elements, irradi. effects 0-666

# stress corrosion cracking continued

Zircaloy cladding, stress corrosion cracking due to I and Cs redistrib. in LWR fuel rods 0-32343

Zircaloy cladding, stresses due to pellet cladding interaction 0-42762

Zircaloy tubing,  $I_2$  stress corrosion cracking, pellet cladding interaction mechanism (*German*) 0-16565

Zircaloy-2, deformation and fracture behaviour, uniaxial tension test in  $I_2$  environment 0-13580

Zircaloy-2, embrittlement in  $I_2$ , environmental purity effect 0-30149

Zircaloy-2,  $I_2$  stress corrosion cracking,  $Cs_2O$  and Cs influence, in- and out-of-pile 0-3252

Zircaloy-2, iodine environment, plane strain tension test 0-22944

Zircaloy-4 cladding rubes, burst strain and stress corrosion cracking, I influence 0-3248

Al alloy, 7175 T 651, crack tip opening under cyclic loading, effect of environmental and R-ratio 0-45377

Al alloy, fracture mechanisms review 0-35296

Al alloy, surface layer influence on corrosion fatigue strength (*Japanese*) 0-16574

Al-Cu-Mg, aged, stress corrosion cracking in NaCl soln. 0-7709

Al-Cu-Mg-Fe-Ni, Hyduminium RR58, crack propag. rates in air and salt soln. 0-21063

Al-Cu-Mn-Mg-Fe-Si, corrosive environment effect on fatigue crack growth rate 0-55584

Al-Mg (7wt.%), corrosion fatigue crack propag. 0-30145

Al-Mg-Zn, granulated, degassing atm. effect on mech. props. of semifinished products 0-7720

Al-Mg-Zn alloy 7179-T651, reduced ductility under tensile after exposure to water 0-11835

Al-Si-Cu, LM30, crack propag. rates in air and salt soln. 0-21063

Al-water vapour reaction, stress corrosion susceptibility STEM study, Mg addition effect 0-3247

Al-Zn-Mg, stress conversion cracking based on micromech. surface reactions 0-7716

Al-Zn-Mg, welded section stress in rolled plate edges, mechanical surface treatment and environment effects 0-21193

Al-Zn-Mg alloys 0-35395

Al-Zn-Mg-Cu, age hardened, effect of strain rate, temp. and environment on ductility 0-45368

Al-Zn-Mg-Cu, type 7075, microstruct. role in hydrogen assisted fracture 0-30091

Al-Zn-Mg-Cu (6.76, 2.37, 1.80 wt.%), cyclic SCC in salt water (*Japanese*) 0-45435

Al-Zn-Mg-Cu age-hardened alloys, fatigue crack propagation rel. to grain size in vac. and NaCl soln. 0-16538

$Al_2O_3$ , dense, exposed to steam, influence of Ca migration on strength reduction 0-11797

Cu-Mn(Ti)(Sn)(Si), dil., oxide film form. in ammoniacal Cu(II) solns., AES obs. 0-45415

Fe-Cr-Ni austenitic alloys, environment sensitive cracking, metallurgical variables effect 0-35391

Ni-Cr-Co-Mo alloy MP35N, accelerated  $H_2$  charging in aq.  $H_2SO_4$  at 0.2% yield stress 0-30144

Ni-Cr-Mo-Mn alloy 02KhN40MB, corrosion-resist, heat-resist., phys. and mech. props. 0-35411

(NiCo)-Cr-Al-Y/ $ZrO_2$ - $Y_2O_3$  plasma sprayed ceramic coating for turbine engine components 0-40616

$Si_3N_4$ - $CoO_2$ , surface stress development during oxidation 0-50736

Ti alloy type TA6V, hot salt stress corrosion cracking (*French*) 0-21185

Ti, corrosion resist. in marine environments (*French*) 0-50767

Ti-Al age-hardened alloys, fatigue crack propagation rel. to grain size in vac. and NaCl soln. 0-16538

Ti-Al-Mo-V, crack resistance in chloride soln., electrochem. protection, polarization effect 0-55589

Ti-Al-Sn(V), corrosion resist. in marine environments (*French*) 0-50767

Ti-Al-V-Sn (6.6, 2 wt.%), depend. of  $K_{ISCC}$  on loading rate and crack orientation 0-45427

Ti-Cu, corrosion resist. in marine environments (*French*) 0-50767

Ti-V-Cr-Al (13, 11, 3 wt.%), stress corrosion cracking in methanolic solutions 0-50752

W arc welds, fatigue crack growth behaviour in air and high-C liquid Na, carburization studies 0-40625

Zircaloy,  $I_2$  stress corrosion cracking, temp. and stress depend., threshold press. determ. 0-16595

Zr, embrittlement in  $I_2$ , environmental purity effect 0-30149

## stress effects

see also cavitation; deformation; elastic waves; heat treatment; high-pressure phenomena and effects; magnetomechanical effects; materials testing; mechanical properties of substances; mechanical testing; piezoelectric effects; piezoelectricity; piezoresistance; shock wave effects; stress analysis; stress measurement; stress/strain relations; tribology

bone, human, acoustic emission in restressing 0-3704

bone, radius remodelling, sheep, rel. to functional stress and strain 0-35939

elastic cylinder under stress, biharmonic problem solution 0-4532

thick membrane strip, effect of shearing prestress, static case 0-10137

Cu-Zn-Al, single cryst., stress induced martensitic transformation 0-45308

$Pb_{0.97}La_{0.02}(Zr_{0.92}Ti_{0.08})O_3$ , ferroelec. ceramic, stress effects 0-2119

$Pb_{0.99}Nb_{0.02}(Zr_{0.95}Ti_{0.05})O_3$ , ferroelec. ceramic, stress effects 0-2119

$V_3Ga$  superconducting tape, stress effect on critical current (*Japanese*) 0-50020

## stress field analysis at cracks see crack-edge stress field analysis

## stress measurement

aqueous polymer solns., shear stress and normal stress meas. using cone-and-plate rheogoniometer 0-1496

blind hole drilling technique for residual stress measurement: application in NDT 0-40660

circular ring, inner boundary shapes, optimised, diametral compression 0-38369

crack growth, 3-D geometric effects, implications for composite material structures 0-10204

dielectric bodies stress determ. using EM waves 0-38370

diffusely reflecting objects, deformation meas. by lasers, appl. of holography and speckle, review (*Japanese*) 0-9832

drill hole method, comprehensive extension to the photo-stress process of investigating surface layers (*German*) 0-33551

epoxy resin (Araldite B), photothermoelasticity meas. by heating method 0-6000



**stress measurement continued**

- fission reactor irradiated cladding, in-cell facility for mechanical testing 0-21244
- glass, chem. tempered, surface stress meas. using opt. waveguide effect (*Japanese*) 0-45473
- glass, chemically strengthened, stress profile determ. using scatt. light 0-30186
- glass, float, optical waveguide effect 0-43681
- glass, thermally tempered sheet and plate, surface stress meas. using optical waveguide effect 0-25967
- heteroepitaxial system, dislocation struct. at stress meas., theory 0-2017
- integrated retardation technique, rotationally symmetrical bodies, thermal stresses 0-38362
- intensity factors at arched crack tip, caustics method 0-19298
- internal stress measurement using optical microscope stage polarisation adapter 0-31863
- internal stresses, cracking temps., automatic installation 0-55605
- jacketed optical fibre residual stress diagnosis, pulse delay technique 0-53469
- metal, residual stresses determ. using internal boring technique 0-3263
- mode I stress intensity factors, method of caustics 0-38364
- non-Newtonian fluids, capillary and slit methods of normal stress measurements 0-43807
- opposed-anvil high-press. devices, material strength effect 0-47068
- photoelastic dynamic studies of fracture 0-38358
- photoelastic fringe pattern analyzer, computer aided 0-38359
- photoelastic fringes, automatic stress analysis method 0-14639
- photoelastic isodynes method, integrated plane stress field components 0-14638
- photoelastic load meas. and testing (*German*) 0-19297
- photoelastic measurement for crystals, appl. to Si 0-48656
- photoelastic method of thermal stress determ. circumferentially grooved cylinder 0-38363
- plastics, anisotropic reinforced, stress distrib., using mm region of EM waves 0-25968
- polarisation device application, by compensation method 0-40643
- polariscopes interactive control system to evaluate stresses 0-19299
- polycrystals, single phase, stress strain relations by X-ray diffraction (*Russian*) 0-5999
- polymers, stress-enhanced chemiluminesc. 0-40628
- reactor vessel, determ. of stress intensity factor 0-37455
- relaxation, by cone-plate instrument 0-28477
- residual, use of position sensitive proportional counter (*Japanese*) 0-11853
- residual stress, X-ray evaluation, treatments for nonlinear distrib., review 0-25966
- residual stresses, review 0-44245
- rheological property meas. apparatus (*French*) 0-14644
- sandwich speckle photography (*German*) 0-10216
- scattered-light photoelasticity, for meas. of stress distrib. in cubic single crystals (*Russian*) 0-7326
- seals, glass-metal and glass-ceramic, annealing effect on internal stresses 0-40389
- self-contained stress determination by means of hardness measurements (*German*) 0-21200
- shear stress of solids, at 120 to 300K and up to 100 kbar 0-50787
- shell reinforced around hole, deformability factor 0-16371
- shock-wave environments, use of low-impedance Mn stress gauges in 1.0 to 40.0 GPa range 0-38367
- speckling application, for stress-strain state of parts 0-19300
- steel, austenitic, X-ray elasticity constants (*German*) 0-30004
- steel, austenitic stainless, X-ray stress anal. by new position sensitive proportional counter with uniform angular resolution (*Japanese*) 0-30190
- steel, ferritic-pearlitic, X-ray elasticity constants (*German*) 0-30004
- steel, flat bars, stress meas. and calc. around drilled hole, with hole-gage-rosettes aid (*German*) 0-25757
- steel, hardened, X-ray elasticity constants (*German*) 0-30004
- steel, heat treated high strength, X-ray diffr. anal. of residual stress 0-3200
- steel, plain C, type 304 and type 316 stainless, fatigue damage indicators, non-destructive 0-25932
- steel casting, meas. and significance of residual stresses 0-21253
- stress analysis, experimental, conf., Bradford, England (Sept. 1978) 0-17718
- subsurface stress meas. 0-21252
- textures materials, residual stress evaluation by X-rays (*German*) 0-40670
- US method, calibration expt. results (*German*) 0-53725
- X-ray portable stress analyser using position-sensitive scintillation detector 0-13190
- X-ray stress anal. using position-sensitive proportional counter 0-1498
- X-ray stress measurement, error caused by side declining angle of counter scanning plane (*Chinese*) 0-52373
- X-ray stress measurement method, appl. to practical materials (*Japanese*) 0-52379
- X-ray technique, comparison with three different detectors 0-1499
- X-ray tensometric measurement, reliability (*Czech*) 0-27382
- Zircaloy-4, microstrain and particle size meas. by Warren-Averbach method 0-55420
- Ag film, electroplated, using holographic interferometry 0-20806
- Fe, slip-initiation phenomenon by fatigue, appl. to stress meas. 0-45342
- Ge-GaAs heteroepitaxial system, dislocation struct. in stress measurements 0-29030
- KCl, stress distrib., meas. by scattered light photoelasticity (*Russian*) 0-7326
- Ni, electrodeposited in sulphamate bath, cyclic stress, meas. appl. at 125-200°C 0-19295

**stress-optical effects** see *piezo-optical effects*

**stress relaxation**

- see also *anelastic relaxation; creep; viscoelasticity*
- activation volume stress depend. 0-54304
- butyl rubber, resin cured, filled, relaxation study (*German*) 0-35243
- cable insulation for nuclear power station, deterioration testing (*Japanese*) 0-27743
- ceramic nuclear fuels, mech. props. at compressive deformation 0-651
- concrete, prestressed, low-temp. tensile strength and linear expansion coeff. of reinforcing steel 0-30051
- crystal growth from melt, stress form., dislocation density estimation (*German*) 0-15022

**stress relaxation continued**

- elastic-plastic torsion, variational inequality concept, finite element anal. 0-23907
- elastomeric network, finite linear viscoelastic theory, time-depend. deform. behaviour 0-38292
- elastomers, relax. transitions from relax. spectrometry and internal friction (*German*) 0-34136
- epichlorohydrin/bisphenol A epoxy polymer concrete, viscoelastic props. 0-45340
- epoxy resin, Cl-containing, relation between static and dynamic deform. characts. 0-3137
- epoxy resin systems, synthesis review, phys. and mech. props. at low temps. 0-25650
- filamentary crystals, complex stressed state, method of investigating mech. props. 0-3264
- film/substrate, two-layer structs., relaxation of internal stresses 0-34341
- Maxwell fluid, Rayleigh-Taylor instability 0-33631
- measurement by cone-plate instrument 0-28477
- metal, FCC, polycrystn., fatigued, behaviour model during plastic deformation (*German*) 0-21023
- plastic flow, order-disorder transform. effect on creep, traction and relaxation (*French*) 0-35180
- PMMA, piezobirefringence, optical and mech. relaxations, temp. depend. 0-34885
- PMMA, viscoelastic props. in plastic zone, cooling rate effect 0-40418
- polycarbonate, viscoelastic props. in plastic zone, cooling rate effect 0-40418
- polyethylene, effect of ketones, temp. depend., environmental stress relax. study 0-45336
- polyisobutylene, in simple extension, nonlinear stress relax., recovery after partial relax. 0-5949
- polymer relaxation props., automatic assembly for exam. over wide range of temp., and medium moisture contents 0-7739
- polymer viscoelasticity and strength characterisation, advanced light scatt. techniques 0-11857
- polymers, entangled, ternary blends of monodisperse homopolymers, viscoelastic props. 0-19301
- polymers, partially crystalline, nonlinear mech. relax. (*Russian*) 0-40467
- polymers, relaxation props., photometric transducer method of meas. 0-3268
- polyisloxane dizwitterionomers, mech., dielec. relax., effect of H<sub>2</sub>O sorpt., thermal history 0-50261
- polystyrene melt, carbon-black filled, rheological study 0-48665
- polyurethane, filled, relation between static and dynamic deform. characts. 0-3137
- powder, compacted, stress relaxation pattern, moisture effect 0-20994
- PVC, stress relaxation in macrodeformation range 0-16370
- PVC, unplastitized, evaluation method for chemical resistance (*Japanese*) 0-25893
- rod-shaped elements, under simultaneous static loads and elevated temps., linear limited stress relax. 0-14590
- roving glass cloth fibre reinforced plastic, fracture mech., time depend. (*Japanese*) 0-55508
- rubbers, swollen, low-freq. dynamics, optical and mech. props. 0-43626
- steel, austenitic, cold worked 10Kh11N23T3MR, structural transformations, aging effect, electron microscope obs. 0-40402
- steel, Cr, stress relaxation, superplasticity and thermal cycling (*Russian*) 0-21019
- steel, Cr-Mo-V, high temp. main steam pipe, residual stresses in butt welds 0-21059
- steel, stainless, stress corrosion cracking, prestrain effect, stress relaxation study 0-35384
- steel, stainless ferritic, drawability, mech. props., and grain boundaries in 08Kh16AMT and 08Kh18T1 0-35270
- steel, stress relaxation, short-term, creep and strain hardening (*Russian*) 0-30005
- steel, stress relaxation in cyclic deformation 0-3119
- stress dip technique for effective stress determination in cyclic straining 0-2113
- strips, errors occurring due to approx. formula, for radius of curvature 0-23909
- styrene-butadiene rubber, vulcanised CaCO<sub>3</sub> filled, stress/strain relations (*Japanese*) 0-40443
- tetrafluoroethylene-vinylidene fluoride mixture, in epoxide-diphenylene propane resin, exam. of temp. depend. of stress relaxation, viscoelasticity 0-11688
- viscoelastic bodies, deformation taking into account influence of accumulated defects 0-19252
- viscoelasticity, nonlinear, stress relaxation, Volterra integral equation, numerical analysis 0-53646
- Ag film, sputtered, hillock growth and agglomeration by annealing, SEM obs. 0-2309
- Ag films, hillock form. hole growth and agglomeration 0-44455
- Al-alloy, type 6351 and 6061, stress relaxation in cyclic deformation 0-3119
- Al-Cu-Mg, acoustic emission during tensile testing 0-7632
- Al-Mg, acoustic emission during tensile testing 0-7632
- Be-Cu alloy stress relaxation in bending, 63° to 343°C 0-50693
- Co, deformed, microstruct. singularities in pre-transform. temp. range (*Russian*) 0-45347
- Cu alloys, strain hardened, struct. factor effect on stress relaxation (*Russian*) 0-25748
- Cu, polycrystn., stress relaxation in cyclic deformation 0-3119
- Cu-BeCo (1.85, 0.29 wt.%), type CA172 (TH04), strengthened by spinodal decomp., stress relax. in bending 0-7616
- Cu-Ni-Sn (4-15, 4-8 wt.%), strip strengthened by spinodal decomp., stress relax. in bending 0-7616
- Cu-Zn (30 wt.%), slip band growth, thermally activated 0-40457
- Fe-B-Si amorphous ribbon, strain induced anisotropy, and toroid diam. effect on mag. props. 0-34623
- Fe-Co-V, ordered and disordered, dynamic ageing (*French*) 0-16355
- Fe-Ni austenitic, effect of Al and Ti on relaxation resist. 0-20993
- Fe<sub>100-x</sub>, amorphous, stress relax. after annealing 0-55447
- KCl, annealed in KBr vapour, crack and pore formation, diffusionaly induced stress relaxation (*Russian*) 0-40388
- KCl with Al<sub>2</sub>O<sub>3</sub> disperse spheres, dislocation mechanism for stress relaxation in cooling crystal (*Russian*) 0-54347
- MgO single cryst., internal stresses and dislocation mobility, stress relaxation method 0-6413
- Mo, mechanical props. and dislocation struct., mag. field effect 0-54935
- Nb, mechanical props. and dislocation struct., mag. field effect 0-54935



# stress relaxation continued

- Ni-Co (25 wt.%), single crystals, mag. annealing effect on magnetostriction and magnetisation (*Japanese*) 0-34744
- Ni<sub>3</sub>Fe, ordered, monocrystals, thermally activated deform. processes 0-50684
- Pb, work hardening, and recovery rates during steady state deformation, temp. and stress effect 0-45319
- PdSi, amorphous, structural relaxation enhancement following stress reduction 0-3118
- Si, near (111) surface, dislocation movement at annealed scratches, X-ray topography obs. 0-2029
- Ta-O, relaxation anal. after ageing under stress (*French*) 0-16365
- Ti-Al-Mo, type Ti-6242S, irradi. induced creep 0-39163
- Ti-Al-Sn, type Ti-5621S, irradi. induced creep 0-39163
- Ti-Al-V, irradi. induced creep 0-39163
- Ti-Al-V(Sn) alloys, plastic deformation and fracture characts. at low temps. (*Russian*) 0-7624
- Ti-V-Cr, type Ti-15-333, irradi. induced creep 0-39163
- TiO<sub>2</sub>, rutile single crystals, stoichiometric, dynamic strain ageing 0-50661
- W, plasma spray coatings, relaxation phenomena 0-19876

# stress wave emission testing see ultrasonic materials testing

# stress/strain curves see stress/strain relations

# stress/strain diagrams see stress/strain relations

# stress/strain relations

- see also elastic constants; elastic limit; serrated yielding; yield point; yield stress
- acrylic, denture base, tensile testing 0-16621
- adhesive tubular lap joint, nonlinear stress-strain anal. 0-16637
- alloy, space lattice types A<sub>1</sub>, A<sub>2</sub> and A<sub>3</sub>, strain hardening function (*German*) 0-20955
- alloys, hot plastic strain, stress-strain-time dependences (*Russian*) 0-40430
- anisotropic elastic deformation, effective stress law, appl. to saturated porous rocks 0-51385
- anisotropic metal blanks, plastically deformable, stress/strain relations (*Russian*) 0-1438
- arterial grafts, synthetic, mech. props. 0-17192
- beam, thin wall, bending stiffness 0-28425
- beam element in space, geometrical stiffness, virtual work approach 0-14567
- beams, thin walls, stress-strain state determ., method of segments 0-28424
- blood vessel dynamic strain tolerance at different post mortem conditions 0-16988
- blood vessels, exam. of mech. props 0-12175
- bodies in plane strain, stress-strain state calcs. 0-14574
- $\gamma$ -brass, brittle to ductile transition under high hydrostatic pressure and high temp. (*Japanese*) 0-35305
- $\alpha$ - $\beta$ -brass, two phase bccryst., deform. and fracture at 150K 0-16388
- brittle rod, optimum specimen shape for compression tests, gluing technique effects 0-50797
- brittle rod, optimum specimen shape for compression tests, struct. and technological parameters 0-50798
- carbonate rock, interrelation of flow or fracture and phase transition during deform. 0-51389
- ceramic nuclear fuels, mech. props. at compressive deformation 0-651
- circular plate, anisotropic and homogeneous, with circular hole at centre, creep behaviour 0-48597
- composite cylindrical shell, stiffened and stable, rational design using elasticity 0-5954
- composite material, in-plane shear charact. 0-35251
- composite spherical pressure vessels with hardening metal liners 0-7655
- compressible rubberlike materials, determination of elastic potential function 0-10159
- concrete, deformation under complex loading, mathematic description 0-25783
- concrete, reinforced slabs, nonlinear statical props. anal. 0-25809
- concrete, uniaxial compression, finite element failure anal. (*Japanese*) 0-35265
- conference, reliability and stress anal., San Francisco, CA, USA, 1975 0-8740
- crack tip plastic zone, thermal props. calcs. 0-7659
- curved structural members, large displacement theory, applic. to lateral-torsional buckling anal. of circular arches 0-23924
- cylinder, hollow, nonlinear viscoelastic material, dynamic pressure loading 0-38289
- cylinder, thick-walled, creep transition under internal pressure 0-53659
- cylindrical notched specimen, four-point bending, crack resist. tests 0-53735
- deposits, spontaneous mactrostress calc., from substrate deform. 0-15412
- dislocation gliding, by-passing of hardened particles, coplanar Orowan loops form., stress-strain curves 0-49226
- dislocation theory, nonlinear elastic problems, book contrib. 0-39093
- dislocations, elastic theory, book 0-36784
- Earth interior, stress/strain relation for anelasticity 0-26471
- elastic, linear and nonlinear solids, stress and strain fields at crack tip (*French*) 0-14615
- elastic body, system of curved cracks under different boundary conditions on their lips 0-53713
- elastic members, thin-walled, displacement theories for straight and circ. curved members (*Japanese*) 0-43615
- elastic springback in beams and plates, bending 0-38256
- elastic-plastic body, weakened by double periodic slit system, antiplane strain 0-53657
- elastically loaded polycrystal, stress state by contact problem theory 0-14573
- elastomeric network, finite linear viscoelastic theory, time-depend. deform. behaviour 0-38292
- elastoplastic bodies with cracks in complex states of stress, limiting equilib. 0-53715
- elastoplastic structures, stresses and strains during loading, mathematical programming, pivoting procedure 0-53641
- epoxy resin, deform. rate depend. of mech. props. at cryogenic temps. 0-55456
- epoxy resins, fracture props. study at cryogenic temps. 0-25869
- epoxy resins, mech. and elec. low temp. props. 0-25814
- fatigue, cumulative damage, under random loads algorithm of hysteresis loop counting 0-21064
- fatigue life predictions using computer modelling, cyclic stress/strain curves 0-19290

# stress/strain relations continued

- fibre reinforced composite, fibre pull-out at high loading rate (*Japanese*) 0-45357
- fibre reinforced composites, viscoelastic thermal shrinkage stresses 0-38287
- fibre reinforced composites, weakened by periodic system of cracks, longitudinal shear 0-35323
- fibre reinforced laminate, elastic law for materials with different tensile and compressional moduli 0-11713
- fibre reinforced plastics, optimum reinforcement laydown 0-38267
- filled rubber, stress/strain behaviour at moderate strains 0-38293
- flat cylindrical shell, with infinite series of cracks, stress state 0-53716
- fusion reactor limiters; thermal and stress environment effects 0-32461
- geological media, hysteresis behavioural effects 0-21712
- glass, rupture behaviour, long-term strength, thermofluctuation theory (*Russian*) 0-40536
- glass fibre reinforced plastic, laminate, fatigue strength under normal and interlaminar shear stresses 0-11758
- glass fibre reinforced polyamide, GFPA 66, rel. strain meas. during creep in liq. environments 0-30046
- glass shells with metallic inserts, structural strength 0-35283
- granular materials shear deformation microscopic and macroscopic exam. (*Japanese*) 0-11691
- granular mats., stress-strain relations, intergrain slip 0-16374
- graphite/epoxy composite laminates, splitting process charact. 0-25843
- graphitic materials deformation, crack and fracture behaviour, SEM exam 0-11706
- homogeneous simple strain in elastic-plastic media, necessary and sufficient conditions 0-28427
- hydraulic bulge test, use in biaxial tensile testing 0-1493
- hydrogels, two-component, elasticity theory and compress. meas. 0-44246
- infinite plane with crack in nonuniform steady field, stress intensity coeffs. 0-38343
- Kapton (polyimide), insulators for superconducting magnets, effect of low temp. irradiation 0-25817
- kinematic hardening models, use in multi-axial cyclic plasticity 0-25717
- laminates, plane strain state with transverse crack 0-38338
- large strain inelastic anal., dynamic problems 0-38278
- large strain inelastic analysis, quasi-static problems, finite element anal. 0-14568
- metal, space lattice types A<sub>1</sub>, A<sub>2</sub> and A<sub>3</sub>, strain hardening function (*German*) 0-20955
- metal ductile fracture, void growth stress/strain relations (*French*) 0-19280
- metal fatigue analysis, inversion of strain-life, and strain-stress relationships 0-16428
- metal fatigue analysis, inversion of strain-life and strain-stress anal. 0-19289
- metals, determ. of yield strength 0-25937
- metals, dynamic compression testing, mech. behaviour 0-40464
- metals, hot plastic deform., stress/strain/time relations (*Russian*) 0-20968
- Mylar (polyester), insulators for superconducting magnets, effect of low temp. irradiation 0-25817
- necking, dynamic analysis based on stress wave propagation 0-1440
- necking, loading history depend. 0-5957
- Nomex (nylon paper), insulators for superconducting magnets, effect of low temp. irradiation 0-25817
- nonlinear aftereffect medium, longitudinal one-dimens. wave propagation 0-5974
- notch-tip geometry, influence on stress and strain distrib. 0-33535
- orthotropic cylindrical shells, periodic problems, computer anal. (*Russian*) 0-23889
- orthotropic dilatant bodies, plasticity theory, plane problems (*Russian*) 0-23910
- paper sheet, elastic props., inhomogeneity with reference to basis wt. depend. of elastic moduli (*Japanese*) 0-2110
- perforated plate, global stress strain behaviour 0-10169
- photopolymer, biaxial stress-strain test 0-40417
- plane triangular element, stress-strain finite dynamic element, FORTRAN IV program 0-53
- plastic solids, stress and strain fields at crack tip (*French*) 0-14615
- plastic stress-strain relation anal. using anisotropic hardening plastic pot. 0-19250
- plastic/elastic transition, strains and stresses (*German*) 0-28431
- plasticised cellulose acetate sheet, post-yield fracture 0-25859
- plate, elastic circular cylindrical, with arbitrary transference, stress-strain state (*Russian*) 0-23895
- plate, rectangular with stiffening ribs, stress-strain state, elasticity eqns. (*Russian*) 0-1427
- plotting device for stress-strain diagrams in tensile testing 0-3269
- polyamide, PA 66, rel. strain meas. during creep in liq. environments 0-30046
- polyamide-polyoxirane copolymers, mechanical properties evaluated 0-11700
- polycarbonate, effect of mol. weight on craze shape and fracture toughness 0-25858
- polycarbonate, insulators for superconducting magnets, effect of low temp. irradiation 0-25817
- polycrystals, single phase, stress strain relations by X-ray diffraction (*Russian*) 0-5999
- polyester-polyurethane semi-interpenetrating networks, mech. props., morphology 0-45362
- polyethylene, doubly oriented, low density, deformation and structure, exam. 0-11705
- polyethylene, high-density, damage accumulation kinetics under creep during prolonged loading 0-40447
- polyethylene, mech. and elec. low temp. props. 0-25814
- polyethylene, ultra-high-strength filaments, soln. spun/drawn, mech. and thermal props. 0-40440
- polyethylene, ultra-oriented high density, shrinkage as meas. of deformation efficiency 0-40398
- polymer film elasto-plastic deformation calc., in re-drawing stretched film, finite element analysis calc. (*Japanese*) 0-7621
- polymer network, crosslinks and trapped entanglements, two-network model 0-38962
- polymers, anal. of mechanics of solid phase extrusion 0-39204
- polypropylene, insulators for superconducting magnets, effect of low temp. irradiation 0-25817
- polypropylene films, hard elastic, gas permeability, extension effects 0-40412



## stress/strain relations continued

- polyisiloxane diwittierionomers, mech. props., microstruct. 0-49131  
 polystyrene, swollen network in benzene, pendent chains, influence on thermodynamic and viscoelastic props. 0-28481  
 polyvinyl-pyrrolidone/polyethylene glycol oligomers, elasticity theory, and compression meas. 0-44246  
 porous bodies, stresses induced by drying, elastoviscoplastic model, finite element anal. 0-23904  
 porous deep drawn conical shells, permeability 0-11728  
 pressure vessels, creep bounds and brittle damage estimates 0-23908  
 prismatic beams with circular cracks under tensile loading 0-53714  
 rate and temp. depend., analytic formulation 0-40466  
 rod in penetrating liquid, exam. of lengthwise bending 0-5955  
 roving glass cloth fibre reinforced plastic, fracture mech., time depend. (Japanese) 0-55508  
 rubber, strain-energy density function 0-25773  
 rubber balloon bursting under biaxial strain, tear behaviour 0-19287  
 rubber under biaxial strain, non Gaussian theory, mechanical props. 0-16366  
 rubber under biaxial strain, nonGaussian theory, optical props. 0-16367  
 rubbers, swollen, low-freq. dynamics, optical and mech. props. 0-43626  
 SEM attachment to record stress-strain diagram 0-25961  
 shape memory effect, criteria for efficiency assessment (Russian) 0-21015  
 shell, cylindrical, optimisation of strong loading modes, stress/strain state 0-10136  
 shells, thin shallow axisymmetric, strain displacement equations, incremental anal. 0-53628  
 shells, two-layer cylindrical, stress-strain state, elasticity theory eqns. 0-33462  
 shells of revolution with inhomogeneous boundary conditions, deformation 0-33480  
 skin rheological behaviour, expt. results and struct. model 0-16968  
 spherical shell, shallow radially ribbed, stress state, struct. parameters influence 0-14581  
 split Hopkinson pressure bar use in obtaining dynamic stress/strain data at const. strain rates (Japanese) 0-16630  
 steel, anisotropic sheet, strain hardening, stress state depend. 0-55421  
 steel, austenitic, variation coeffs. of permissible stresses, at low temps. 0-16402  
 steel, austenitic stainless, fatigue and cyclic stress-strain characts. austenite-martensite transform. effect 0-21109  
 steel, C, deformation strength and strain rate depend. under plain strain state (Japanese) 0-30028  
 steel, C, failure mechanisms in impact fatigue 0-40493  
 steel, Cr, stress relaxation, superplasticity and thermal cycling (Russian) 0-21019  
 steel, Cr-Mo (2.25, 1 wt.%), strain hardening shakedown load during bending 0-20958  
 steel, Cr-Mo-V, biaxial cyclic deformation behaviour 0-21057  
 steel, Cr-Mo-V, cyclic deformation under out-of-phase loads 0-40428  
 steel, Cr-Mo-V and stainless, biaxial cyclic deformation behaviour 0-16431  
 steel, Cr-Ni-Mo, dynamic and static softening behaviour at hot forming temp. (German) 0-25728  
 steel, deformation and stresses during elongation, application of Ludwig eqn. (German) 0-40475  
 steel, high Si dual-phase, mech. props and microstruct. anal. 0-40444  
 steel, high-strength structural, stress-strain curves, shape effects (German) 0-45343  
 steel, low alloy, elastoplastic strain evaluation in crack weakened cross sections by fracture mechanics 0-45380  
 steel, low C, cyclic plasticity and low cycle fatigue life 0-21058  
 steel, low C, cyclic plasticity and low cycle fatigue life in variable amplitude loading 0-16433  
 steel, low C, instability obs. by large strain compression 0-35253  
 steel, low C, low cycle fatigue props. with variable strain ranges (Czech) 0-45390  
 steel, maraging type with 18% Ni, ageing treatment effect on fatigue crack propag. 0-16411  
 steel, parts, stress calcs. during cooling, program system THEPLA (German) 0-35237  
 steel, plain C, cyclic induced creep at room temp. 0-25765  
 steel, quasi-cleavage fracture (Chinese) 0-21060  
 steel, stainless AISI 316, biaxial cyclic deformation behaviour 0-21057  
 steel, stainless type 304 L, mech. behaviour under constant stress associated with cyclic strain 0-25767  
 steel, stress and strain intensity, determ. after plastic deform. using microhardness meas. 0-40641  
 steel, ultrahigh strength, monotonic and cyclic stress strain curves 0-35268  
 steel fatigue in surface active media, adsorption facilitation mech. 0-55586  
 steels, hot plastic strain, stress-strain-time dependences (Russian) 0-40430  
 steels, structural St 37-2, cleavage fracture, report 0-25868  
 steels, ultrahigh C, superplastic, mech. behaviour at elevated temps 0-21028  
 strain trajectories of constant curvature for plastic deformation 0-48591  
 stress analysis, experimental, conf., Bradford, England (Sept. 1978) 0-17718  
 styrene-butadiene rubber, vulcanised CaCO<sub>3</sub> filled, stress/strain relations (Japanese) 0-40443  
 superplastic materials, flow and failure, review 0-50690  
 superplasticity, deformation mechanisms, review 0-50691  
 tensile bond strength, effect of aspect ratio, for butt joint of internal fracture 0-50823  
 tension test, computer simulation, effect of testing conditions 0-7729  
 tension tests, analysis of misalignment 0-11864  
 thermoplastic elastomers, crosslinked by secondary valence interactions, elasticity and processing, crosslinking behaviour 0-40320  
 thin shells, heterogeneous stress/strain state, stability eqns. for small deformations (Russian) 0-1426  
 torsional strain curves plotting 0-40638  
 TV screen displaying instrument, exam. of design 0-21222  
 unbounded body, weakened by circular cracks, elastic equilb. 0-53717  
 unidirectionally reinforced composites, large deflection, plastic constitutive relations 0-43624  
 upsetting tests developments for better stress/strain curve results (German) 0-38368  
 viscoelastic linear solids, stress/strain tensor eqns. (French) 0-53656

## stress/strain relations continued

- viscoelastic material, stress-strain behaviour, mathematical simulation (German) 0-1442  
 viscoelastic rod, shock rel. to hard obstacle (Russian) 0-23911  
 viscoelasticity, nonlinear, stress relaxation, Volterra integral equation, numerical analysis 0-53646  
 viscoelasticity, stress/strain relationships, fluctuations 0-17802  
 viscoelasticity linear theory, variational and minimum principle applications (Japanese) 0-48599  
 viscous solids, stress and strain fields at crack tip (French) 0-14615  
 Westerly granite, stress-strain hysteresis loops shapes 0-26499  
 Zircaloy-2, deformation and fracture behaviour, uniaxial tension test in I<sub>2</sub> environment 0-13580  
 Zircaloy-2, neutron irradiated, inhomogeneous deformation behaviour 0-50679  
 Al alloy, reverse loading stress/strain curve, w.r.t. prestrain (Japanese) 0-7622  
 Al alloy, spherical shell, three layer, stress/strain relations (Russian) 0-3122  
 Al alloy 6061-T6, yielding of tubing under dynamic biaxial loading 0-16377  
 Al alloys, stress-strain state after treatment by pressure, moire strip method appl. (Russian) 0-40648  
 Al, circular tube, forming limit of free bulge-forming (Japanese) 0-55477  
 Al, crit. resolved shear stress, orientation depend. 0-21001  
 Al, deformed, thermal recovery, microstruct. and stress-strain relations 0-16325  
 Al, pure, polycryst., steady-state flow, stress and temp. depend. 0-45341  
 Al, pure, texture influence on stress/strain curves, prestrain, solid soln. and particle hardening effect on inhomogeneous deform. (German) 0-30014  
 Al-alloy, type PA6, under complex cyclic loading, behaviour of stress strain diagrams 0-16372  
 Al-Cu full coherent precipitation hardened alloy, high temp. cyclic deform. 0-25711  
 Al-Cu-Mg, acoustic emission during tensile testing 0-7632  
 Al-Mg, acoustic emission during tensile testing 0-7632  
 Al-Zn (20 (30) (35) (40) (60) at.%), effect of UTS on cyclic creep strength (Korean) 0-25778  
 Al<sub>2</sub>O<sub>3</sub>-SiO<sub>2</sub>-Fe<sub>2</sub>O<sub>3</sub>-CaO-MgO-TiO<sub>2</sub>, refractory, corrosion and mech. behaviour correlations 0-40563  
 Au<sub>52.5</sub>Ag<sub>47.5</sub>, pseudoelastic behaviour associated with thermoelastic martensitic transform. 0-16304  
 C fibre reinforced C, processing, room temp. mech. props., and low temp. expansion 0-25820  
 C-C composite, structure model, Rosen model with fractional matrix 0-11719  
 (Co,Ni)-Cr<sub>23</sub>C<sub>6</sub> eutectic, microstruct. effect on fracture energy 0-7662  
 Cr-Mo-Nb, elastic-plastic mathematical model response on quasistatic loading (Czech) 0-29111  
 Cr-Ni, elastic-plastic mathematical model response on quasistatic loading (Czech) 0-29111  
 CsI, exam. of kinking process, using cholesteric liquid crystals 0-7629  
 Cu, friction stress in high temp. creep 0-11723  
 Cu, microplastic deform. and amplitude depend. of internal friction (Russian) 0-45349  
 Cu, pure, dynamic stress strain relations in combined tension and torsion, testing device 0-21197  
 Cu wires, electrolytic, Young's modulus, working temp. effects 0-50667  
 Cu-Al, two-phase Cu-rich alloy, influence of microstruct. on stress-strain behaviour 0-7631  
 Fe, cast, ductile, strain rate and temp., influence on strength, elongation and deformation (Japanese) 0-45356  
 Fe, high purity single crystals, thermally activated slip deformation between 4.2 and 300K 0-25801  
 Fe single crystals, size effect on slip deformation ability at very low temps. 0-21049  
 Fe-Co-V, ordered and disordered, dynamic ageing (French) 0-16355  
 Fe-Cr-Al-Ti-Y<sub>2</sub>O<sub>3</sub> (20, 4.5, 0.5, 0.5) type MA956, strain rate effect on fracture behaviour at 1366K 0-16458  
 Fe-Mn (15(24)(30)wt.%), high hydrostatic pressure influence on stress-strain curve 0-25805  
 Fe-Si, microplastic deform. and amplitude depend. of internal friction (Russian) 0-45349  
 Fe<sub>3</sub>O<sub>4</sub>, Fe<sub>2</sub>O<sub>3</sub>, magnetite and haematite nodules with fayalite and Ca ferrite additives, stressed state parameters (Russian) 0-45352  
 Hf, oxidation, microstructural study (French) 0-45436  
 KCl, stress distrib., meas. by scattered light photoelasticity (Russian) 0-7326  
 LiF single crystals, glide band sources, work hardening 0-34126  
 MgO, compressive stress-strain behaviour at high temps. 0-25774  
 MgO, hot-pressed, elasticity props. of polycrystals and single crystals 0-54301  
 MgO(Al<sub>2</sub>O<sub>3</sub>)<sub>n</sub> spinel, plastic deformation at 400°C 0-40453  
 Nb, local heating during abrupt strain, catastrophic slip band formation 0-7652  
 Ni base superalloy, fatigue crack opening load variation with meas. location 0-16425  
 Ni, single crystals, strengthening, tested under compression at 293 and 77K (German) 0-50689  
 Ni-Ti alloys, shape memory effect materials, criteria for efficiency assessment (Russian) 0-21015  
 Pb, work hardening, and recovery rates during steady state deformation, temp. and stress effect 0-45319  
 Pb-Sn, eutectic, superplastic behaviour, grain size effect 0-7635  
 PbI<sub>2</sub> layered cryst. under uniaxial compression, low temp. thermal cond. (Russian) 0-44374  
 Si, mechanical strength, origin of difference in Czochralski grown and float-zone-grown cryst. 0-44212  
 Si<sub>3</sub>N<sub>4</sub>-Mg<sub>2</sub>SiO<sub>4</sub>-Si<sub>3</sub>N<sub>2</sub>O<sub>7</sub>, compressive creep, composition effect 0-50674  
 SiO<sub>2</sub> glass, strengthened by ion exchange and quenching brittle destruction theory 0-45398  
 Sn-Pb eutectic, strain rate sensitivity of flow stresses, grain boundary sliding during superplastic, non-superplastic deform. 0-7645  
 Ti, metal and alloys, compression at high strain rate, deformation anal. 0-25769  
 Ti-Al-Mo-Sn alloy, elastically and plastically deformed, positron annihilation meas. of deformation 0-21038  
 Ti-Al-V, alloy 685, fatigue life, creep and dynamic strain ageing effect, 25 to 400°C (French) 0-45384



**stress/strain relations continued**

- $\alpha$ - $\beta$  Ti-Mn (8 wt.%), calcs. of stress-strain curve, stress and strain distrib., discussion 0-7637  
 $\alpha$ - $\beta$  Ti-Mn (8 wt.%), stress-strain curve and stress and strain distrib. calcs., reply to discussion 0-7638  
 WC-Co hard alloy composite, calc. of weakest link in struct. 0-11730  
 Zn single crystals, temp. and strain rate effects on strength, slip and twinning 0-16373

**stresses, internal** *see internal stresses*

**stretch receptors** *see mechanoreception*

**striations** *see discharges (electric)*

**striking** *see impact (mechanical)*

**strip line components**

- Mach-Zehnder waveguide modulators in Ti-diffused LiNbO<sub>3</sub> 0-33203  
 microstrip antennas for biomedical applications of microwaves 0-3762

**strip lines**

- antennas, asymptotic expansions for Sommerfeld integrals 0-14272  
 EM strip transmission line energy coupler, for medical diagnostic appls. 0-17045  
 enclosed dielectric microstrip, Schelkunoff analysis (*Spanish*) 0-45005  
 self-filtering S-type strip waveguides 0-33219

**stripping reactions**

- few body systems, anal. coupling constant continuation for resonance and stripping reactions (*Russian*) 0-13435  
 (d,p) reacts. at intermediate energies, triangle graph model 0-27616  
 (dx) breakup on nucleus, adiabatic treatment stripping and forbidden transition cross section 0-9299  
<sup>52</sup>Cr(d,p)<sup>53</sup>Cr, Coulomb stripping, 2.12-2.48 MeV, DWBA anal., spectroscopic strengths 0-516  
<sup>20</sup>F cross sections and anal. power, compound nucleus contrib. Ericson fluctuations from <sup>18</sup>O(d,p), pol. d. 0-22803  
<sup>24</sup>Mg(p,p'), 40 MeV, two step pickup-stripping process, negative parity states 0-32256  
<sup>26</sup>Mg(d,p), 3.1, 3.5 MeV <sup>27</sup>Mg energy levels, spectroscopic factors, DWBA, Hauser-Feshbach anal. 0-52581  
<sup>20</sup>Ne(d,p), 10-12 MeV, pol. d., <sup>21</sup>Ne states cross section, anal. power, coupled channel and fluctuations anal. 0-27617  
<sup>16</sup>O(d,p), 12 MeV, stripping reaction differential cross section, d distortion effect (*Japanese*) 0-22796  
<sup>17</sup>O, cross sections to ground, 0.87 and 5.09 MeV states, neutron strength from <sup>16</sup>O(d,p) 0-5066  
<sup>28</sup>Si(<sup>15</sup>N,<sup>14</sup>N), 44 MeV, modified optical pot. from backward elastic scatt. 0-32255  
<sup>28</sup>Si(d,p), 8.05 MeV, stripping reaction differential cross section, d distortion effect (*Japanese*) 0-22796

**stroboscopes**

*see also velocity measurement*

- US delay line trimming using stroboscopic method of signal-to-time conversion 0-19191  
 Nz pulsed laser stroboscopic fluorimeter 0-35593

**strong-coupling superconductors**

- critical temperature formula discussion (*Chinese*) 0-7017  
 pressure coefficients of critical field, Ginzburg-Landau parameter, penetration depth 0-54833  
 superconducting short bridges, critical current depend. on high. freq. field 0-44774  
 thin film, critical mag. field (*Chinese*) 0-54849  
 transition temperature eqn. 0-25032  
 CuCl, high-temp. supercond., BCS strong-coupling limit for transition temp. 0-2511  
 La<sub>2</sub>S<sub>4</sub>, high crit. mag. field supercond., elec. resist., sp. ht. and magnetisation 0-2532  
 Nb<sub>0.75</sub>Zr<sub>0.25</sub>, effect of force constant, disorder on Eliashberg function 0-29504  
 YRh<sub>4</sub>, supercond., anomalous cond.-electron polaris. 0-25047

**strong interactions, elementary particle** *see elementary particle strong interactions*

**strontium**

*see also nuclei with .....*

- atom, efficient ionis. by reson. laser pumping 0-32685  
 atom, K $\beta$ /K $\alpha$  rel. intensity obs. 0-32665  
 atom, L-shell soft X-ray emission spectra, oscillator strengths 0-32651  
 atom, multichannel quantum defect theory anal. to predict Ra states 0-52918  
 basalt isotopic and element composition, Reykjanes Peninsula, Iceland 0-21725  
 behaviour in subsurface CaCl<sub>2</sub> brines, model, Dead Sea rift valley 0-17295  
 coral aragonite Sr/Ca ratio, ocean temp. determ. 0-12568  
 diffusion in bitumen block coating, radioactive waste treatment (*Russian*) 0-52771  
 laser action mechanism due to 3066.2, 3011.1 nm 4d<sup>3</sup>D<sub>1,2</sub>-5pP<sub>2</sub> transitions 0-9869  
 laser spectroscopic anal. of Rydberg series, multichannel quantum defect theory 0-18815  
 lattice dynamics, phenomenological model 0-44265  
 metallic compressibilities, general pseudopotential approach 0-54631  
 submonolayers adsorbed on Mo crystal, LEED and contact pot. study 0-2271  
 volcanic rock isotopic composition, Grenada, Lesser Antilles 0-21724  
 He-Sr pulsed laser, pumping rate and electron density meas. 0-9868  
 KBr:Sr, thermally stimulated luminesc., accompanying recomb. of V<sub>F</sub> and F centres 0-55201  
 KCl:Ba(Sr), Z-centre, luminesc. and absorpt. spectra obs. 0-49221  
 KCl:Sr, microcrystalline powders, role of Z-centres in stabilizing coloration 0-54227  
 KCl:Sr, thermally pre-treated, glow curves 0-25470  
 KCl:Sr, thermally stimulated luminesc. accompanying recomb. of V<sub>F</sub> and F centres 0-55201  
 KCl:Sr, triplet state of F<sub>2</sub>-centres, ESR spectra 0-29616  
 KCl(Br):Sr<sup>2+</sup>, BeF<sub>4</sub><sup>2-</sup>, IR absorpt. spectra, impurity cation rel. to degenerate vibr. splitting (*Russian*) 0-2807  
 LaCoO<sub>3</sub>:Sr, anomalous <sup>57</sup>Fe<sup>m</sup> charge states, Mossbauer study 0-40017  
 NaCl:Sr, dimer and trimer aggregate formation by NMR, ionic cond. and dielectric losses 0-15094  
 Sr+Ca, laser induced collisional and radiative energy transfer 0-53108  
 Sr+F<sub>2</sub>, crossed beam chemilum., kinetics and mechanisms 0-21264  
 Sr+He, Sr, <sup>1</sup>P, level lifetime, Hanle measurement 0-23365

**strontium continued**

- Sr+He(2<sup>3</sup>S<sub>1</sub>), coherent <sup>2</sup>P<sub>3/2</sub> levels excitation by Penning ionis., Hanle effect 0-5520  
 Sr+He(2s<sup>2</sup>S<sub>1</sub>), alignment of ions in Penning collisions, polarised emission obs. 0-23533  
 Sr+N<sub>2</sub>, A<sup>2</sup> $\Sigma_u^+$  state, vibr. excitation 0-1054  
 SrII, near IR laser transitions in hollow cathode discharge 0-1194  
 Sr<sup>+</sup>(<sup>2</sup>P<sub>3/2</sub>), Penning ion, polarised emission, Hanle effect obs., radiative decay rate meas. 0-5520  
<sup>82</sup>Sr, radioactive, adsorption on alumina column for <sup>82</sup>Rb generator prod. 0-12257  
<sup>82</sup>Sr-<sup>82</sup>Rb generator improvement using inorganic exchangers 0-17135  
<sup>85</sup>Sr, blood flow and tracer uptake in normal and abnormal canine bone 0-17072  
<sup>87</sup>Sr/<sup>86</sup>Sr, geochemistry in hydrous mantle nodules and host alkali basalts 0-56420  
<sup>87</sup>Sr/<sup>86</sup>Sr ratios in granites from British Late Caledonian 0-36276  
<sup>88</sup>Sr/<sup>86</sup>Sr, thermal ionis. mass spectrometer obs., controllable isotope fractionation (*German*) 0-42299  
<sup>89</sup>Sr therapy of bone metastases of prostatic gland carcinoma 0-36076  
<sup>90</sup>Sr, effect on fetal mouse ovary rel. to time administered during pregnancy 0-51163  
<sup>90</sup>Sr, fast neutron influence on fission product transport in UO<sub>2</sub> pyrocarbon-coated HTR fuel particles 0-42777

**strontium alloys**

*see also strontium compounds*

- Al-Sr-Nd phase diagram (*Russian*) 0-20893  
 Mg-Sr, liq. alloys, thermodynamic activities determ. 0-50604

**strontium compounds**

*see also strontium alloys*

- formate dihydrate:Cr<sup>3+</sup>, optical absorpt. spectrum 0-50380  
 oxides, Sr<sub>2</sub>MO<sub>4</sub>, M=Mn, Cr, Ti, Ru, Hf, Mo, K<sub>2</sub>NiF<sub>4</sub> structure, study by method of invariants (*French*) 0-33959  
 rare earth orthocobaltites, R<sub>1-x</sub>Sr<sub>x</sub>CoO<sub>3</sub>, ferromag. reson., Lande g-factor 0-25215  
 strontium calcium tartrate tetrahydrate, gel grown mixed single crystals, defect characterisation 0-2027  
 BaO-SrO-Al<sub>2</sub>O<sub>3</sub>-TiO<sub>2</sub>-SiO<sub>2</sub> glass ceramics, cryst. phases form., BaO/SrO ratio influence 0-19705  
 Ba(PO<sub>3</sub>)<sub>2</sub>-SrF<sub>2</sub>, IR absorption spectra exam. of hydrolytic stability 0-39291  
 Ba<sub>0.39</sub>Sr<sub>0.61</sub>Nb<sub>2</sub>O<sub>6</sub>, electro-optical props. 0-2728  
 Ba<sub>0.54</sub>Sr<sub>0.46</sub>Nb<sub>2</sub>O<sub>6</sub>, line broadening effect in Rayleigh scatt. of Mossbauer radiation 0-50238  
 (Ba<sub>1-x</sub>Sr<sub>x</sub>)<sub>1-y</sub>(Nb<sub>2</sub>O<sub>6</sub>)<sub>y</sub>:CeO<sub>3</sub> crystals, photoelectric and photorefractive props., hologram recording 0-53239  
 Ba<sub>2</sub>Sr<sub>1-x</sub>Nb<sub>2</sub>O<sub>6</sub> (x=0.27 to 0.54) exam. of freq. dependence of permittivity diffuse ferroelectric phase transition kinetics 0-2703  
 Ba<sub>2</sub>Sr<sub>1-x</sub>Nb<sub>2</sub>O<sub>6</sub> crystals, optical defects and edge dislocation distributions 0-19806  
 Ba<sub>2</sub>Sr<sub>1-x</sub>Nb<sub>2</sub>O<sub>6</sub>, ferroelectric with diffused phase transition, photoelectret states 0-20583  
 Ba<sub>1-x</sub>Sr<sub>x</sub>Pb<sub>0.75</sub>Bi<sub>0.25</sub>O<sub>3</sub>, superconductivity, rel. to lattice const. 0-49966  
 (Ba<sub>1-x</sub>Sr<sub>x</sub>)<sub>2</sub>SO<sub>4</sub>:Eu mixed crystal series, X-ray diff. study of miscibility 0-2168  
 Bi<sub>1-x</sub>Sr<sub>x</sub>O<sub>1.5-x/2</sub> vacancy-type solid soln., anionic cond. (*French*) 0-49407  
 CaAl<sub>2</sub>O<sub>4</sub>-SrAl<sub>2</sub>O<sub>4</sub>-BaAl<sub>2</sub>O<sub>4</sub>, binary and ternary systems, solid solubility (*Japanese*) 0-35174  
 Ca<sub>1-x</sub>Sr<sub>x</sub>FeO<sub>3</sub>, Mossbauer spectra, charge disproportionation 0-15891  
 Ca<sub>1-x</sub>Sr<sub>x</sub>FeO<sub>3</sub>, Mossbauer spectra, charge disproportionation 0-20542  
 Eu<sub>1-x</sub>Sr<sub>x</sub>S, exciton refl. spectra 0-2782  
 Eu<sub>1-x</sub>Sr<sub>x</sub>S, chalcogenide-like system, crit. conc. for ferromagnet-spin glass transition 0-34662  
 Eu<sub>1-x</sub>Sr<sub>x</sub>S, dil. insulator spin-glass versus blocking 0-34641  
 Eu<sub>1-x</sub>Sr<sub>x</sub>S, dilute Heisenberg magnet, complex susceptibility of blocked spins 0-15740  
 Eu<sub>1-x</sub>Sr<sub>x</sub>S, ferromagnet-spin glass transition, mag. ordering, mag. susceptibility and neutron scatt. meas. 0-50135  
 Eu<sub>1-x</sub>Sr<sub>x</sub>S, insulating spin-glass, sp. ht. near ferromag. onset 0-34667  
 Eu<sub>1-x</sub>Y<sub>x</sub>S (X=Sr,Gd), spin-disorder-induced Raman scatt. from phonons, expt. investigation 0-20635  
 Eu<sub>1-x</sub>X<sub>2</sub>S (X=Sr,Gd), spin-disorder-induced Raman scatt. from phonons, theory 0-20636  
 La<sub>0.03</sub>Ba<sub>0.66</sub>Sr<sub>0.34</sub>TiO<sub>3</sub> ceramic, positive TCR near Curie temp. rel. to charge dispersion (*Russian*) 0-16511  
 La<sub>1-x</sub>Sr<sub>x</sub>CoO<sub>3</sub>, specific heat meas., using laser-flash method, phase transitions obs. (*Japanese*) 0-54898  
 La<sub>1-x</sub>Sr<sub>x</sub>CoO<sub>3-y</sub>, Seebeck coeff. meas., small polaron hole conduction model 0-20233  
 La<sub>1-x</sub>Sr<sub>x</sub>CrO<sub>3</sub> (0≤x≤0.4), localised level hopping transport 0-10974  
 La<sub>1-x</sub>Sr<sub>x</sub>CrO<sub>3</sub>, electronic struct. study by XPS 0-25518  
 M<sub>1-x</sub>Sr<sub>x</sub>Si<sub>2</sub> (M=Ca, Eu, Ba), solid solution with type SrSi<sub>2</sub> struct., lattice parameters at high press. 0-54203  
 Pb<sub>0.94</sub>Sr<sub>0.06</sub>(Ti<sub>0.47</sub>Zr<sub>0.53</sub>)O<sub>3</sub>-NiO, modified, dielec. and piezoelec. props. 0-11342  
 Pt-SrTiO<sub>3</sub> (100) interface, struct. and electronic props., AES, LEED, EELS, and UPS study 0-24986  
 Pt-SrTiO<sub>3</sub> (100) interface, Auger and photoemission studies, relax. and chem. shift effects 0-54749  
 SiO<sub>2</sub>-CaO-ZnO-B<sub>2</sub>O<sub>3</sub>-Na<sub>2</sub>O-S, SrO effect on crystallisation 0-54135  
 Sr-SiO<sub>2</sub> glasses, morphology effects on props. 0-49118  
 Sr<sub>5</sub> (PO<sub>4</sub>)<sub>3</sub>OH, prep. from sulphate, X-ray diff. and IR spectrosc. 0-29893  
 SrBi<sub>2</sub>H<sub>12</sub>·10H<sub>2</sub>O, struct. dehydration, intermediate phases and thermooxidative degradation 0-33951  
 Sr<sub>0.61</sub>Ba<sub>0.39</sub>Nb<sub>2</sub>D<sub>6</sub>, photoinduced birefr. 0-7325  
 Sr<sub>0.61</sub>Ba<sub>0.39</sub>Nb<sub>2</sub>O<sub>6</sub>, electromechanical props., permittivity, elastic compliance, piezoelectric moduli 0-29691  
 Sr<sub>1-x</sub>Ba<sub>x</sub>ZrO<sub>3</sub>, struct., X-ray powder diff. study 0-1989  
 SrCl<sub>2</sub>, anion diffusion mechanism 0-2201  
 SrCl<sub>2</sub> film, non-cryst., very-low-freq. inelastic light scatt. 0-25367  
 SrCl<sub>2</sub>, molten, struct., electrolyte 'general primitive model' prediction test 0-28902  
 SrCl<sub>2</sub>, non-crystalline film, disorder-induced Raman scatt. 0-11387  
 SrCl<sub>2</sub>:Gd<sup>3+</sup>, small dielec. particles, cryst. field size effects 0-44913  
 SrClF, cryst., elastic consts. 0-19863  
 SrClF, long wavelength dynamics, shell model calc. 0-29134  
 Sr(ClO<sub>4</sub>)<sub>2</sub>, mol. torsional oscills., cooperative study by NQR 0-25244  
 SrCl<sub>2</sub>·2(H<sub>2</sub>D)<sub>2</sub>O, IR and Raman spectra, force fields 0-2753  
 SrCl<sub>2</sub>·2H<sub>2</sub>O, IR and Raman spectra, force fields 0-2753



## strontium compounds continued

- SrCoO<sub>3</sub>:Fe<sup>3+</sup>, ferromag., sign of Fe<sup>4+</sup> hyperfine field, spin struct., Mossbauer study 0-39933
- Sr<sub>1-x</sub>Eu<sub>x</sub>B<sub>6</sub>, EPR linewidth conc. depend., La<sub>x</sub>Eu<sub>1-x</sub>B<sub>6</sub> comparison, exchange interaction in EuB<sub>6</sub> 0-20457
- Sr<sub>1-x</sub>Eu<sub>x</sub>B<sub>2</sub>O<sub>4</sub>, luminesc. props. 0-34972
- Sr<sub>1-x</sub>Eu<sub>x</sub>B<sub>2</sub>O<sub>7</sub>, luminesc. props. 0-34972
- Sr<sub>1-x</sub>Eu<sub>x</sub>B<sub>6</sub>O<sub>10</sub>, luminesc. props. 0-34972
- SrEuFeO<sub>4</sub>, Neel temp. and spin reorientation, Mossbauer study 0-39934
- Sr<sub>2</sub>EuFeO<sub>5</sub>-SrO-PbO, quasi-ternary system comp. diagram, rel. to Sr<sub>2</sub>RFeO<sub>5</sub>, Sr<sub>2</sub>RAIO<sub>5</sub>, cryst. growth 0-20776
- SrF<sub>2</sub>, excited state spectroscopic consts., dissoc., chemilum. obs. 0-21264
- SrF<sub>2</sub>, antireflection coated, 3.8 μm CW laser damage threshold obs. 0-33053
- SrF<sub>2</sub>, dielec. const., 5.5 to 400K 0-50249
- SrF<sub>2</sub> fusion-cast prism refractive index obs., 0.2138 to 11.475 μm 0-34882
- SrF<sub>2</sub> piezo-optical coeffs. meas. at 0.6328, 1.15 and 3.39 μm 0-34888
- SrF<sub>2</sub>, thermoluminesc. and F-centre annealing, after neutron irradiation 0-7422
- SrF<sub>2</sub>, third-order elastic consts. from Lundqvist pot., many-body effects 0-39201
- SrF<sub>2</sub>, vibr. anal., kinetic consts. method 0-18838
- SrF<sub>2</sub>:Er, activation vol. for interstitial motion, dielec. const. meas. 0-49412
- SrF<sub>2</sub>:Gd<sup>3+</sup>, Na<sup>+</sup>(Kr<sup>+</sup>)(Rb<sup>+</sup>)(Ag<sup>+</sup>), EPR of orthorhombic Gd<sup>3+</sup>-univalent metal ion complexes 0-11262
- SrF<sub>2</sub>:Pr<sup>3+</sup>, wavelength and temp.-modulated UV absorpt. 0-2799
- SrF<sub>2</sub>:Tb<sup>3+</sup>, mag., thermal and hyperfine props. 0-29368
- SrF<sub>2</sub>-H<sub>2</sub>, synthesis and struct. determ. using neutron diffr. (French) 0-24425
- SrFe<sub>2-x</sub>Cr<sub>x</sub>O<sub>9</sub>, effects of substitution of Fe by Cr, Mossbauer spectra 0-2674
- Sr<sub>2</sub>FeUO<sub>8</sub>, <sup>57</sup>Fe Mossbauer study 0-39976
- SrFe<sub>2</sub>O<sub>9</sub> and Sr<sub>4</sub>Fe<sub>2</sub>O<sub>13</sub>, Mossbauer spectra 0-15882
- SrFe<sub>2</sub>O<sub>9</sub>, hysteresis loops, formation processes 0-39813
- SrFe<sub>2</sub>O<sub>9</sub>, powder, chemical plating with Co, Co-P, Ni-P and Cu 0-25593
- Sr<sub>2</sub>Fe<sub>2</sub>Ru<sub>1-x</sub>O<sub>4</sub> solid soln., Mossbauer spectrosc. study 0-50235
- Sr<sub>2</sub>FeS<sub>2</sub> cathodes for nonaqueous Li batteries 0-3506
- SrGa<sub>2</sub>O<sub>9</sub>, single crystal growth, lattice const. meas. (German) 0-44159
- SrGdFeO<sub>4</sub>, Neel temp. and spin reorientation, Mossbauer study 0-39934
- SrI<sub>2</sub> mol. struct. parameters and geom. config., gaseous electron diffr. obs. 0-37883
- Sr<sub>2</sub>KNb<sub>2</sub>O<sub>7</sub>, Raman scatt. experiments in tetragonal tungsten bronze compounds 0-40113
- SrLaFeO<sub>4</sub>, mag. and cryst. struct. determ. (French) 0-54866
- Sr<sub>1-x</sub>La<sub>x</sub>FeO<sub>3</sub>, Mossbauer spectra, charge disproportionation 0-20542
- Sr<sub>2</sub>MTa<sub>2</sub>O<sub>15</sub> (M=K, Rb, Tl, Cs), relative stability of struct. types, and piezoelec. props. (French) 0-49206
- Sr<sub>2</sub>NaNb<sub>2</sub>O<sub>7</sub>, Raman scatt. experiments in tetragonal tungsten bronze compounds 0-40113
- Sr<sub>2</sub>Nb<sub>2</sub>O<sub>7</sub>, crystal struct. and phase transitions, rel. to isomorphous crystals (Japanese) 0-49208
- Sr<sub>2</sub>Nb<sub>2</sub>O<sub>7</sub>, ferroelects., nonlinear optical props. 0-33086
- Sr<sub>2</sub>Nb<sub>2</sub>O<sub>7</sub>, normal-incommensurate phase transition, electron microscopy and diffraction study 0-39277
- Sr<sub>2</sub>Nb<sub>2</sub>O<sub>7</sub>, optical mode softening in incommensurate phase 0-7352
- Sr<sub>2</sub>Nb<sub>2</sub>O<sub>7</sub>, sputtered films, amorphous, dielec. props. 0-54573
- SrO, effect on props. of PbO containing cryst. glass 0-24637
- SrO, effect on viscosity of PbO containing crystal glasses 0-19973
- SrO, electronic struct. of V<sup>-</sup> and related centres 0-2355
- SrO, logarithmic derivative reflectance spectra 0-11429
- SrO, luminesc. band edge, 4-6.5 eV, optical absorpt., photoluminesc., cathodoluminescence, photocond. obs. 0-50411
- SrO, neutron- or proton-irrad., F<sup>+</sup> centre fluoresc. yield and lifetime, 5 to 140K 0-55181
- SrO, neutron-irradiated single cryst., F<sup>+</sup> centres, ENDOR obs. 0-15824
- SrO:Ni, optical absorption spectra in visible and near IR region 0-45119
- SrO:Ni<sup>2+</sup>, noncentral Jahn-Teller ion, energy minimum localisation, ESR study 0-25198
- SrO:Ni<sup>2+</sup>(Cu<sup>2+</sup>) noncentral Jahn-Teller ion, coupled polar-tetragonal strains 0-44555
- SrO:Pb<sup>2+</sup>(Bi<sup>3+</sup>), impurity centres vibronic spectra, lattice dynamics and electron-phonon interactions 0-7396
- SrO-Al<sub>2</sub>O<sub>3</sub>-P<sub>2</sub>O<sub>5</sub>, irradiated electret glasses, relax. of external field intensity on heating 0-25282
- SrO-Al<sub>2</sub>O<sub>3</sub>-TiO<sub>2</sub>-SiO<sub>2</sub>, glass formation, structure of cations (Russian) 0-38933
- SrO-Fe<sub>2</sub>O<sub>3</sub> system, non-existence of single phase SrFe<sub>2</sub>O<sub>4</sub>, Mossbauer expts. 0-29178
- SrO-SiO<sub>2</sub> glass, effect of high-dose X-rays and reactor radiation 0-19838
- SrO+ZrC, high temp. reactions 0-3320
- 4 SrO.B<sub>2</sub>O<sub>3</sub>.SiO<sub>2</sub>, crystal struct., X-ray powder diffr. patterns (Japanese) 0-54209
- SrO.nFe<sub>2</sub>O<sub>3</sub> isotropic ferrite magnets, manuf. process and mag. props. (Japanese) 0-29915
- Sr(PO<sub>3</sub>)<sub>2</sub>, vitreous, microhardness 0-25864
- Sr<sub>2</sub>Pb<sub>1-x</sub>(Zr<sub>0.545</sub>Ti<sub>0.455</sub>)O<sub>3</sub>, piezoelec. resonator, preparation and props. (Rumanian) 0-28402
- Sr<sub>2</sub>RAIO<sub>5</sub> (R=La, Pr, Nd, Sm, Eu, Ga, Tb), monocystals growth by flux method 0-20776
- SrRFeO<sub>4</sub> (R=La, Pr, Nd), Mossbauer spectra, spin reorientation 0-15880
- Sr<sub>2</sub>RFeO<sub>5</sub> (R=Nd, Sm, Eu, Gd), monocystal growth by flux method 0-20776
- SrSO<sub>4</sub>, surface crystn., on BaSO<sub>4</sub>, isotope exchange and electron microscopy study 0-34332
- SrSi<sub>2</sub>, phase diagram, 10 to 40 kbar, 600 to 1200°C, polymorphic transform. 0-29165
- SrSi<sub>2</sub>, superconducting temperature depression due to mag. field 0-54820
- Sr<sub>2</sub>SiAl<sub>10</sub>O<sub>20</sub>, Ce<sup>3+</sup> activated, X-ray diffr. and luminesc. props. 0-49199
- Sr<sub>2</sub>Ta<sub>2</sub>O<sub>7</sub>, crystal struct. and phase transitions, rel. to isomorphous crystals (Japanese) 0-49208
- Sr<sub>2</sub>Ta<sub>2</sub>O<sub>7</sub>, structural phase transition to superlattice, electron microscopy and diffraction study 0-39277
- SrTiO<sub>3</sub> (100) surface, struct. and electronic props., AES, LEED, EELS, and UPS study 0-24986
- SrTiO<sub>3</sub> (100) surface electronic structure, DV-Xα cluster method 0-39646
- SrTiO<sub>3</sub>, EPR of Fe<sup>3+</sup>-V<sub>O</sub> centre, above T<sub>c</sub> 0-39870
- SrTiO<sub>3</sub>, electro-optic crystals, mechanical grinding and polishing 0-48471

## strontium compounds continued

- SrTiO<sub>3</sub>, energy band struct., two-photon absorption spectra study 0-15453
- SrTiO<sub>3</sub>, form. entropy and tolerance factor 0-34204
- SrTiO<sub>3</sub>, hyper Raman scatt. on polaritons, polariton branches (Russian) 0-50334
- SrTiO<sub>3</sub>, hyper-Raman scatt. spectra due to lattice vibr. 0-29732
- SrTiO<sub>3</sub>, semicond. electrode, electrochem., photoelectrochem. props. 0-3352
- SrTiO<sub>3</sub>, structural phase transition, intrinsic and extrinsic central peak properties 0-34168
- SrTiO<sub>3</sub>, surface microrelief revealed by ion irradiation 0-54485
- SrTiO<sub>3</sub>, tetragonal, effect of impurities on Raman spectrum 0-2770
- SrTiO<sub>3</sub>:Cr<sup>3+</sup>, nonlinear Jahn-Teller coupling, local dynamics, near struct. transition 0-2625
- SrTiO<sub>3</sub>:V, Jahn-Teller impurity, V<sup>4+</sup> EPR 0-29608
- SrTiO<sub>3-x</sub>, in contacts, differential capacitance, elec. field depend. permittivity effect 0-54779
- Sr<sub>0.15</sub>VO<sub>2</sub>, electrical cond., thermo-EMF, and lattice consts. 0-54685
- Sr<sub>3</sub>(VO<sub>4</sub>)<sub>2</sub>, determination of enthalpies of formation, from heats of solution 0-2182
- SrW<sub>2</sub>O<sub>4</sub>, kinetics of crystal growth from solns. in Na<sub>2</sub>W<sub>2</sub>O<sub>4</sub> melts, by continuous cooling 0-11550
- Sr<sub>2</sub>YRuO<sub>6</sub>, <sup>99</sup>Ru Mossbauer spectra and other techniques 0-29659
- Sr<sub>2</sub>Zn<sub>2</sub>(Y=Ba<sub>2-x</sub>Fe<sub>12</sub>O<sub>22</sub>), x=0, 1, 1.6, mag. moments reorientation 0-44851
- SrZrO<sub>3</sub>, form. entropy and tolerance factor 0-34204
- Sr<sub>2</sub>ZrO<sub>3</sub>, resist. to corrosion by Al<sub>2</sub>O<sub>3</sub>, CaO, MgO, SiO<sub>2</sub>, K<sub>2</sub>CO<sub>3</sub> and coal ash 0-16516
- Y<sub>6</sub>WO<sub>12</sub>:SrO, polycryst., elec. cond., 800-7400°C 0-15517
- ZnS-SrF<sub>2</sub>, multilayer dielec. coatings, radiation breakdown and microinhomogeneities 0-7294

structural transformations see solid-state phase transformations

structure (chemical) see chemical structure

structure factors (crystals) see crystal atomic structure

## structure functions

- asymptotically free parton model, struct. function transverse momentum behaviour, SU(3) gauge model 0-27469
- deep inelastic struct. functions 0-42461
- deep inelastic structure function moments, QCD expt. test 0-22610
- deep inelastic structure functions and the quark parton model 0-4992
- diquark contribs. to scaling violation and deep inelastic  $\sigma_L/\sigma_T$ , structure functions, QCD 0-22573
- high p<sub>T</sub> jet pairs, parton-parton scattering and  $\pi$  quark struct. functions 0-47248
- Jost-Lehmann-Dyson representation, scale invariance breaking and spectral function 0-13316
- MIT bag model, G<sub>2</sub> struct. function 0-4947
- moments prediction by general assumptions 0-42460
- neutron EM structure functions from electron scatt. data 0-13306
- perturbative QCD in a covariant gauge, moments of struct. functions 0-32073
- photon, function parametrisation 0-37267
- pion, from nucleon low energy relation 0-52507
- pion EM props., dressed quark model (Russian) 0-52508
- point like spin-3/2 quarks, contrib. to deep inelastic struct. functions 0-47250
- proton EM structure functions from electron scatt. data 0-13306
- QCD calc. of structure function moments, renormalisation prescription depend. 0-4948
- QCD structure function relation between deep inelastic  $\nu$  reactions and polarised electroprod. 0-37221
- quark masses and structure functions 0-22585
- quark parton model with large parton k<sub>T</sub> 0-42412
- renormalisation group sum rules for deep inelastic structure functions 0-22611
- d, polarisation meas. in ed scatt. and d percentage D state 0-420
- e<sup>+</sup>e<sup>-</sup> →  $\gamma$ +hadrons, high energy, lepton radiation and  $\gamma$  struct. functions, quark parton model 0-32113
- e<sup>+</sup>e<sup>-</sup> → hadrons+X, structure functions in next to leading logarithm approx.,  $\phi^3$  field theory 0-37268
- e<sup>+</sup>e<sup>-</sup> h → e<sup>+</sup>X, h=hadron, structure functions in next to leading logarithm approx.,  $\phi^3$  field theory 0-37268
- eN deep inelastic polarised scatt., QCD corrections 0-52517
- eN → eX, form factors and structure functions, review, book contrib. 0-47294
- ep deep inelastic scatt., scaling violations and QCD parametrisations, struct. functions (Russian) 0-37277
- ep inclusive scatt., QCD predictions 0-13314
- $\gamma$ , struct. function determ. in  $\gamma p \rightarrow \mu^+ \mu^- X$  expts. 0-42473
- $\gamma\gamma$  collision, deep inelastic, helicity method 0-22606
- LN scattering, structure and fragmentation function moments, meas. and QCD predictions 0-37274
- $\mu$ N, deep inelastic struct. function, Nachtmann moments in QCD 0-27510
- $\mu$ N, inclusive scatt. 96, 147, 219 GeV, nucleon struct. function determ. 0-42472
- $\mu$ p inclusive scatt., QCD predictions 0-13314
- n, polarisation meas. in ed scatt. and d percentage D state 0-420
- $\bar{\nu} p \rightarrow \mu^+ + X$ , 4.5 GeV<sup>2</sup>, p struct. functions x depend., quark distrib. 0-32097
- p, polarisation meas. in ed scatt. and d percentage D state 0-420
- pN, pN, 200 GeV/c, dimuon prod. cross section, Drell-Yan predictions, struct. functions 0-37300
- pp(p) → W<sup>±</sup>(Z<sup>0</sup>)X, QCD perturbation theory struct. function predictions 0-42505
- $\pi$ , comparison between results from ep → epX and Kutl-Weisskopf model (Russian) 0-13291
- $\pi$  longitudinal struct. function, exclusive and almost exclusive process asymptotic behaviour, renormalisation group 0-42464
- $\pi$  structure function and scaling phenomena in Drell-Yan lepton pair prod. processes 0-405
- $\pi^+N$ , 200 GeV/c, dimuon prod. cross section, Drell-Yan predictions, struct. functions 0-37300
- K, comparison between results from ep → epX and Kutl-Weisskopf model (Russian) 0-13291



structure of alloys, crystal *see crystal atomic structure of alloys*  
structure of elements, crystal *see crystal atomic structure of elements*  
student experiments *see demonstrations*  
student laboratory apparatus  
air track, linear, design and construction 0-17750  
boxcar integrator/US recording unit using sample-and-hold circ. 0-27083  
diffraction grating, electronic analog 0-46753  
electron gun for electron motion obs. in elec. and mag. fields expt. 0-27076  
infrared telescope, 6032 image conversion tube 0-42020  
instrument simulator, design and use 0-4490  
laser power meter, calibration, Si solar cell 0-46780  
light-activated switch, photo-gate, pulse method of switching, circuit 0-42021  
Millikan experiment, analogy using quanta of mass, milli-can experiment 0-46778  
NMR detector, transistorised marginal oscillator 0-27078  
NMR in undergrad. instruction, general purpose microcomputers use for hypothetical spectra synthesis 0-42009  
sound-level meter, innovative high school teaching project 0-4495  
Tel-X-Ometer apparatus for educational demonstrations 0-8763  
trajectory model device 0-46759  
studios  
*see also television studios*  
film production technique and technology at Russian Mosfilm studio (*Russian*) 0-22462  
SU<sub>2</sub> theory  
axially symmetric multi-instanton solutions generated by conformal mappings in SU(2) Yang-Mills field 0-42337  
b-quark, horizontal gauge symmetry, Cabibbo universality and fermion masses 0-22583  
classical gauge field with sources 0-52416  
colour Yang-Mills theory, quark source charge screening, confinement 0-22565  
constant SU(2) non-Abelian gauge pot., vacuum polarisation by fermions, integral representation 0-22543  
dimensional regulation, SU<sub>2</sub> gauge theory, instantons 0-18066  
EM interactions, gauge formulation, SU<sub>2</sub>(2) internal symmetry and P- and CP-violation (*Russian*) 0-42368  
gauge field configurations in curved spacetimes 0-18077  
gauge hierarchy in presence of discrete symmetry, U(1)<sub>L</sub> × U(1)<sub>R</sub> and SU(2)<sub>L</sub> × SU(2)<sub>R</sub> × U(1) 0-9094  
gauge invariant S-matrix elements with Yang-Mills SU(2) instantons and antiinstanton 0-22511  
gauge transformation, continuous, SU<sub>2</sub> as an example which cannot be continuously lifted to Lie algebra 0-52396  
general Taub-NUT-De Sitter metric, self-dual Yang-Mills soln. of gravity 0-46946  
harmonic analysis as basis for quantisation 0-9116  
Higgs induced neutral currents, natural flavour conservation and quark mixing angles 0-42392  
instantaneous Coulomb interaction in SU(2) Yang-Mills QCD 0-22574  
instantons, dynamical role in quarkless chromodynamics, bag model test 0-47246  
Kaluza-Klein bundle, unified theory 0-37153  
lattice gauge theories, U(N) and SU(N), non-planar diagrams in large N limit 0-47187  
lattice gauge theory with fermions, renormalised phases, vacuum polarization 0-13198  
Lienard-Wiechert type of solution in SU(2) 0-4879  
many-spin system dynamics, group approach (*Russian*) 0-50221  
neutral currents, flavour-changing, Weinberg-Salam model 0-22553  
non-self-dual static gauge fields 0-52421  
nonlocal conserved currents for two-dimensional chiral theories 0-52413  
nucleonic form factor, pion exchange, model 0-22608  
O(4) Yang-Mills, Higgs system, topologically stable solns. 0-52382  
Pauli's exclusion principle for strong interactions in hadrons, nuclei, and astrophysics 0-37206  
plethysms of finite and continuous groups, generating functions 0-31548  
QCD vacuum, quantum liq. model, gauge and rotational invariances of colour fields 0-13283  
quantum SU(2) gauge theory, vacuum stability, dynamical symmetry breaking 0-32000  
quark-lepton correspondence, multigeneration SU(2)<sub>L</sub> × U(2)-based model 0-22584  
random walk and SU(2) Clebsch-Gordan coefficients 0-17822  
reggeisation in theories with broken global symmetries, nondegeneracy of vector meson masses, non-trivial mixing 0-13236  
Skyrme gauge model, topological solitons 0-9086  
soliton, non-topological, non-Abelian internal symmetry in 3+1 dimensional space-time, quantisation, collective coord. and Lorentz covariant methods 0-47199  
spectroscopy and crystal physics, generating function techniques 0-44162  
stability of solitons, Poincare stability, gauge theories, nonlinear Schrödinger equation 0-4881  
SU(2)<sub>L</sub> × (T<sub>3</sub>)<sub>R</sub> × U<sub>V</sub>(1) gauge unified model, neutral current interactions, ed and  $\nu$  scatt. 0-18107  
SU(2)<sub>L</sub> × SU(2)<sub>R</sub> × U(1) gauge with permutation symmetry, quark mass and Cabibbo angles 0-47232  
SU(2)<sub>L</sub> × U(1), natural flavour conservation of Higgs couplings and Cabibbo mixing conflict 0-37200  
SU(2)<sub>L</sub> ⊗ SU(2)<sub>R</sub> ⊗ U(1) calculability, fermion mass matrix and CP invariance violation 0-13252  
SU(2)<sub>L</sub> ⊗ U(1) theory, CP violation and Cabibbo angle 0-52447  
SU(2) × U(1) unified theory, symmetry and renormalisation 0-22551  
SU(2) × U(1) × G expanded gauge models of neutral currents, propagator momentum transfer 0-47237  
SU(2) × U(1) × U(1) model, Cabibbo angle and Higgs coupling strangeness conservation 0-47233  
SU(2) × U(1) gauge theories, successes and current issues 0-18064  
SU(2) × U(1) scheme, CP violation parametrization, quark n-doublet weak interaction (*Russian*) 0-13231  
SU(2) ⊗ U(1) gauge models of weak and electromagnetic interactions and the  $\mu e$  universality (*Russian*) 0-13257  
U(1) × SU(2) unified gauge field theories, field function O(4) invariance 0-37201  
unification of isospin and hypercharge, electroweak interactions of leptons 0-27439  
unified model for atomic parity violation and neutral currents in gauge theories 0-4912

SU<sub>2</sub> theory continued  
unifying mass scales without intermediate schiral colour symmetry, SU(2) × SU(1) × SU(3), [SU(2n)]<sup>4</sup> unified model 0-22555  
Weinberg-Salam model, Yang-Mills theory, Higgs particle 0-4905  
Yang-Mills equations, classical solns. 0-4875  
Yang-Mills field eqn. configurations in curved spacetimes 0-18076  
Yang-Mills lattice gauge theories, comparison with gauge groups SU(2) and Z<sub>2</sub> 0-31966  
zero energy fermions in U(1) pointwise monopole field (*Chinese*) 0-42345  
NN-NN, large momentum transfer, spin effects 0-22577  
 $\psi \rightarrow \psi \pi^0(\eta)$ , SU<sub>2</sub> violation, symmetry breaking and decay amplitudes 0-52499  
T, quixotic interpretation as QQ bound state 0-13280  
SU<sub>3</sub> theory  
asymptotically free parton model, struct. function transverse momentum behaviour, SU(3) gauge model 0-27469  
b-mesons, mass splitting, SU<sub>3</sub> nonet of SU<sub>6</sub> 0-47288  
band structures, generalised HFB approach in SU(3) framework 0-22663  
baryon octets, semileptonic decays 0-32030  
charmed baryon decays, EM and weak, U- and V-spin generalisations 0-47284  
chiral SU(3) × SU(3),  $\rho$ -meson as dormant Goldstone boson 0-368  
Clebsch-Gordan coefficients, of SU<sub>3</sub> group 0-36906  
constituent quarks in SU(3) and SU(6), current algebra, hadron decays, review, quark contrib. 0-47259  
Coulomb gauge vacua of SU(3) gauge theory 0-47188  
coupling S\* and  $e$  to  $\pi\pi$  and KK, SU<sub>3</sub> couplings 0-22580  
decomposition theorem, appl. to CP violation through quark mass diagonalisation 0-47216  
double folding pot. for inelastic scatt. between nuclei 0-13425  
E<sub>7</sub> grand unification using SU(3) × U(1)<sup>3</sup> gauge group, neutral currents 0-27444  
effective potential for non-Abelian gauge theories and spontaneous symmetry breaking 0-4863  
first order SU(3) theorem for weak and EM form factors, possible expt. verification 0-415  
gauge model of weak and EM interactions, Weinberg angle, Han-Nambu quarks 0-52452  
gauge theory, current synchrospherical symmetrical monopole in multi-synchrospherical symmetrical case (*Chinese*) 0-22527  
group symmetries in nuclear struct., book 0-41963  
hadron masses and current algebra quark masses 0-42436  
hadron multiplets, realisations in SU(3) from stable particles 0-9159  
hadrons with charm, beauty and taste, SU<sub>3</sub> subalgebras of SU<sub>6</sub> 0-9152  
Han-Nambu and SUB quark models, modified, appl. to Weinberg-Salam unified gauge model 0-22562  
hypercharge-exchange reactions, K<sup>-</sup>p, and  $\pi^+$  p, SU<sub>3</sub> prediction 0-13335  
hyperon semileptonic decay, SU(3) spectrum generation, Cabibbo angle 0-9119  
irreducible representations, commutation relations (*Chinese*) 0-52434  
lepton interaction gauge model in SU<sub>3</sub> with 30° Weinberg angle 0-4903  
Lewis Riesenfeld oscillator, dynamical symmetry breaking 0-47210  
many-spin system, group approach in dynamics (*Russian*) 0-4579  
massless non-abelian gluon confinement and rising total cross sections 0-13264  
MIT bag model, coloured quark and gluon constituents of mesons 0-4929  
noncanonical bases, of group SU<sub>3</sub> × SO<sub>3</sub> and their interconnections 0-42359  
nonlocal quark model in SU(3) × SU<sup>3</sup>(3) × U(1), meson decay and mass correction (*German*) 0-27456  
nuclear cluster problems, SU(3) symmetry and integral kernels 0-9251  
nuclear physics and elementary particle physics, dynamical groups 0-42362  
nuclear states, maximal restriction of basis 0-42552  
octonions in quantum mechanics 0-27479  
one-boson-exchange-potential model of baryon-baryon scatt. 0-13295  
Prasad-Sommerfield soliton, excited states, SU(3) generalisation 0-4877  
QCD, six-quark model,  $\Delta S = 1$  weak nonleptonic decays 0-22582  
QCD theory for the strong interaction 0-4962  
quark mass ratio, chiral perturbation in new key 0-37208  
quark masses and structure functions 0-22585  
quark-meson  $\sigma$ -model, quark masses 0-47178  
quark-parton model, EM mass shifts of pseudoscalar mesons 0-42459  
quarks with more than three colors in a class of asymptotically free gauge theories 0-394  
quaternionic Hilbert space and colour confinement, admissible symmetry groups 0-27458  
quaternionic Hilbert space and colour confinement 0-27457  
spectrum-generating SU(3) and local current algebra 0-9128  
spectrum-generating SU(3) and SU(4), idea and appl. 0-9118  
strong coupling constants in broken SU(3) 0-27423  
strong gravity contrib. to nucleonic axial-vector form factor in SU(3) 0-4902  
SU<sub>L</sub>(2) × SU<sub>R</sub>(2) × U(1) × [SU(3) × SU(3)]<sub>c</sub> gauge model, chiral colour symmetry breaking 0-47234  
SU<sub>L</sub>(3) ⊗ U(1) gauge model, exact Cabibbo universality,  $\tau^-$  and  $X^-$  0-4852  
SU(4) ⊗ SU(3)' model, T particles and SU(3)' colour space (*Chinese*) 0-42409  
sum rules for matrices of generators in SO(3) basis 0-13226  
unification of fundamental forces in nature, elementary particle constituents SU(3)<sub>c</sub> gauge symmetry, review 0-27448  
unified gauge model with a nonlinear chiral hadron Lagrangian 0-42378  
unifying mass scales without intermediate schiral colour symmetry, SU(2) × SU(1) × SU(3), [SU(2n)]<sup>4</sup> unified model 0-22555  
unitary space of particle internal states 0-18119  
 $\eta$ , vacuum symmetry, decay consts., mixing consts. in SU(3) × SU(1) QCD 0-27483  
 $\eta \rightarrow \gamma\gamma$ , radiative widths,  $\delta$  and S\* background, SU(3) and VDM anal. 0-419  
 $\eta(958) \rightarrow \gamma\gamma$ , evaluation of decay rate 0-9172  
 $\eta' \rightarrow \rho\gamma$ , radiative widths,  $\delta$  and S\* background, SU(3) and VDM anal. 0-419  
 $\gamma(10.0)$ , two-body hadronic and radiative decays, pseudo-dimension rule,  $\pi\pi$  and KK suppression, SV<sub>3</sub> singlet 0-52495  
K $\rightarrow \pi e(\mu)\nu$ , form factors, SU(3)  $\sigma$ -model one loop calc., chiral symmetry breaking 0-52506



- SU<sub>3</sub> theory continued**  
 pp-pX, diquark fragments, large transverse momentum baryon production 0-47330  
 $\pi$ p, quark-diquark elastic scatt., diquark fragments, large transverse momentum baryon production 0-47330  
 $\psi \rightarrow \eta(\eta')\gamma$ , SU<sub>3</sub> violation, symmetry breaking and decay amplitudes 0-52499  
 t-quark, mass in SU(3) horizontal symmetry 0-37230
- SU<sub>4</sub> theory**  
 $1/2^+$ , baryons, vector mesonic decay, charm changing mode, SU(4) and SU(8) 0-47283  
 A=60-260 nuclei, violated Wigner SU(4) symmetry reconstruction from mass data (*Russian*) 0-37336  
 baryons, ordinary and charmed, magnetic moments in broken SU(4) 0-18136  
 gauge theory, current synchrospherical symmetrical monopole in multi-synchrospherical symmetrical case (*Chinese*) 0-22527  
 linear SU(4) meson  $\sigma$ -model, one-loop approx., spin zero mass spectrum and leptonic-decay 0-47278  
 mass formula in SU(4), flavour symmetry breaking 0-37250  
 meson isosinglets, mixing angles, non-relativistic quark model, Schwinger-type mass relations for SU<sub>4</sub> and SU<sub>5</sub> 0-18125  
 nonleptonic weak interaction, SU(4) symmetry struct., parity violating Hamiltonian 0-52456  
 quark masses and structure functions 0-22585  
 quarks, mass of u and d quarks from weak and EM interaction model 0-13254  
 reducible representations, projector definitions, calc. method 0-9126  
 spectrum-generating SU(3) and SU(4), idea and appl. 0-9118  
 SU<sub>3</sub> subsectors, U- and V-spin generalisations 0-47284  
 SU(4)<sub>F</sub>×SU(4)<sub>C</sub> synthesis of strong, weak, and electromagnetic interactions 0-13255  
 SU(4)<sub>W</sub> symmetry, dibaryon coupling constants for  $\gamma$ ,  $\pi$  and baryon interactions (*Russian*) 0-13329  
 SU(4)×SU(1,1) for O(4) supergravity 0-12975  
 SU(4)×SU(4) symmetry breaking, Cabibbo angle, nonlinear hadronic Lagrangian, PCAC (*Russian*) 0-42360  
 SU(4)⊗SU(3)' model, T particles and SU(3)' colour space (*Chinese*) 0-42409  
 unified gauge model with a nonlinear chiral hadron Lagrangian 0-42378  
 unified theory of weak interactions of leptons and quarks, gauge model 0-22556  
 D meson decay, SU<sub>4</sub> 20-plet dominance model, inclusive branching ratios 0-13299  
 $\eta \rightarrow 3\pi^0$ , chiral SU(4)×SU(4) breaking and tadpole term 0-22532  
 F $\pi^0$  decay, SU<sub>4</sub> 20-plet dominance model, inclusive branching ratios 0-13299
- SU<sub>n</sub> theory**  
 see also elementary particle symmetry; SU<sub>2</sub> theory; SU<sub>3</sub> theory; SU<sub>4</sub> theory  
 $1/2^+$ , baryons, vector mesonic decay, charm changing mode, SU(4) and SU(8) 0-47283  
 $\sigma$  models, nonlinear, soft mass renormalisation of 1/N expansion 0-47164  
 $\sigma$  SU(N) model, spontaneous symmetry breaking, renormalisation 0-42340  
 ( $\bar{\psi}\psi$ )<sup>2</sup> model, spontaneous symmetry breaking, renormalisation 0-42340  
 additive quark model with six flavours 0-27455  
 asymptotic freedom in the infinite-momentum frame, SU(N) Yang-Mills theory renormalisation 0-22519  
 b-mesons, mass splitting, SU<sub>3</sub> nonet of SU<sub>6</sub> 0-47288  
 bilocal gauge field theory 0-31986  
 chiral SU(N) Thirring model, S-matrix bound state poles fixing 0-360  
 classical SU(2) Yang-Mills field, ignorable variables extraction from Hamiltonian 0-328  
 classical SU(2) Yang-Mills field eqns., periodic solns. in Minkowski space-time 0-4854  
 constituent quarks in SU(3) and SU(6), current algebra., hadron decays, review, book contrib. 0-47259  
 decomposition theorem, appl. to CP violation through quark mass diagonalisation 0-47216  
 density matrix for arbitrary spin, equations of motion for new SU(n) parameters 0-52592  
 dual topological unitarisation, higher rank cylinder kernel 0-27492  
 dynamical Higgs mechanism, weak  $\Delta I=1/2$  rule, sum rules, heavy quarks and leptons 0-27442  
 effective potential for non-Abelian gauge theories and spontaneous symmetry breaking 0-4863  
 elliptic meron-antimeron soln. of Minkowski SU(2) gauge theory 0-337  
 fermion mass, unified gauge model based on E<sub>6</sub> 0-32053  
 gauge theory, current synchrospherical symmetrical monopole in multi-synchrospherical symmetrical case (*Chinese*) 0-22527  
 Gelfand pattern, charmed hadrons and magnetic moment 0-398  
 generalized coherent states and generating invariants 0-18089  
 Gln basis labelling, Racah algebra identification with S<sub>N</sub> 0-8835  
 hadron spectroscopy, quark models and SU(5) grand unification scheme 0-4958  
 Heisenberg spin chain derivation from nonlinear Schrodinger eqn. 0-37184  
 Higgs bosons, masses, gauge hierarchies, SU<sub>3</sub> model 0-47236  
 high energy meson elastic scatt. amplitude, leading term approx. in SU(2) Yang-Mills theory 0-5017  
 instantaneous Coulomb interaction in SU(2) Yang-Mills QCD 0-396  
 instanton distribution, external field effects in SU(2) gauge field 0-4849  
 instantons and quark-mass generation—the how of spontaneous chiral symmetry breaking 0-4963  
 interacting boron model of collective state, O(6) limit 0-32214  
 irreducible representations of compact groups, tensor product decomp. and holomorphic induction 0-47205  
 Lewis-Riesenfeld time-depend. harmonic osc., dynamical symmetries 0-4588  
 light quarks and QCD Boson representation, dynamical symmetry breaking 0-52472  
 many-spin system, group approach in dynamics (*Russian*) 0-4579  
 massless quarks in QCD, dynamical symmetry breakdown 0-52471  
 meson isosinglets, mixing angles, non-relativistic quark model, Schwinger-type mass relations for SU<sub>4</sub> and SU<sub>5</sub> 0-18125  
 meson isosinglets, mixing angles, non-relativistic quark model, SU<sub>5</sub> and SU<sub>6</sub> 0-22591  
 nuclear force, parity violating, unified treatment 0-47400  
 O(2) symmetric connections in an SU(2) Yang-Mills theory 0-4839
- SU<sub>n</sub> theory continued**  
 Pauli-Lenz vector, extension of SO(3) to SO(4) 0-31550  
 Prasad-Sommerfield dyon (monopole) soln. of SU(2) Yang-Mills field with Higgs multiplet 0-339  
 precocious chiral grand unification based on SU(8)<sub>L</sub>×SU(8)<sub>R</sub> semi-simple gauge group (*Russian*) 0-42382  
 proton half life, Dirac approach to large number coincidences 0-27501  
 pseudo-oscillators, group theory 0-22226  
 QCD, 2-dimens., Bose form, SU(N) confining phase 0-52463  
 quark confinement, Dirac equation with relativistic linear potential, baryon properties, SU<sub>n</sub> representations 0-47261  
 quark field quantum fluctuation computation in arbitrary Yang-Mills instanton background 0-13268  
 Racah algebra of Gln, generalised back coupling rules 0-47208  
 self dual SU(N) Yang-Mills fields, nonlocal continuity eqns. 0-9096  
 SO<sub>10</sub> hierarchical breaking and neutrino masses 0-22550  
 SO(8) supergravity derivation 0-12975  
 static Euclidean SU(2) solns., global struct. 0-4862  
 (SU<sub>2</sub>×U<sub>1</sub>)×S<sub>n</sub> flavour dynamics, flavour number bound, n quark and n lepton generations unification 0-4907  
 SU<sub>5</sub> theory, superheavy particles, decoupling at low momenta 0-52431  
 SU<sub>6</sub>, SU<sub>3</sub>, subalgebras and mass sum rules for hadrons with charm, beauty and taste 0-9152  
 SU(2)<sub>L</sub>×SU(2)<sub>R</sub>×U(1) six quark gauge models, flavour violation 0-4951  
 SU(2), generalised 6-j symbols 0-31557  
 SU(2) magnetic monopole solns., parameter counting in Prasad Sommerfield limit 0-352  
 SU(2) theory with four fermion interaction and asymptotic freedom, exact soln. 0-4858  
 SU(5), broken, meson mass formulae 0-47267  
 SU(5), Clebsch-Gordan series, quark model appl. 0-47256  
 SU(5) combined quark-lepton decuplets, particle families (*Russian*) 0-47217  
 SU(5) grand unification, fermion mass and Higgs representations 0-27446  
 SU(5) grand unification, nucleon lifetime, bag model calc. 0-52450  
 SU(5) grand unification, strong CP violation, quark-lepton mass ratio 0-32057  
 SU(5) grand unification embedding in SU(N), SU(9) theory, flavour unification 0-32059  
 SU(5) grand unified theories, proton decay, flavour mixing effects 0-377  
 SU(5) grand unified theory, flavour number limit from fermion mass higher order corrections 0-4904  
 SU(5) grand unified theory, p decay modes 0-13301  
 SU(6)×O(3)<sub>L</sub> multiplets, semilocal duality, quark-orbital Regge trajectories 0-27490  
 SU(6) grand unification model, hierarchy of symmetry breakings and neutral currents 0-52446  
 SU(6) grand unified theories, one loop renormalisation effects, stepwise symmetry breaking 0-32058  
 SU(7) grand unified theory with heavy colour 0-42380  
 SU(8) supergravity on mass shell in superspace 0-46907  
 SU(8) supergravity supersymmetry breaking 0-46908  
 SU(8) unification and supergravity 0-46928  
 SU(9) grand unification of flavor with three generations 0-13251  
 SU(N)×SU(N) chiral symmetry, spontaneous breaking, instanton role 0-47219  
 SU(N) chiral Gross-Neveu spectrum derivation 0-47176  
 SU(N) colour groups, N>3, quark content 0-4938  
 SU(n) gauge theories, directions of spontaneous symmetry breaking 0-13228  
 SU(N) grand unification with several quark-lepton generations 0-27443  
 SU(N) unification of extra strong interactions, no-go theorem 0-32056  
 SU(s) grand unification, neutrino mass and oscillations, B-L nonconservation 0-52449  
 two dimensional field theories with infinite number of conservation laws and Backlund transformations 0-9095  
 unified theories, mass scales, alternatives to SU(5) 0-27441  
 Universe baryon number asymmetry mechanism, unified calibration theory calcs. (*Russian*) 0-36756  
 very early Universe, phase transitions and mag. monopole prod., grand unification 0-51934  
 weak and EM interaction unification with strong interactions following  $\tau$  and T, book contrib. 0-47235  
 Yang-Mills fields, stability and gap phenomena 0-18073  
 $e^+e^- \rightarrow \mu^+(\tau^+)\mu^-(\tau^-)$ , neutral current couplings, lepton polarisation, p violation in SU(2)×U(1) model 0-4975  
 ep deep inelastic scatt., pol. p and e, straton model, sum rule (*Chinese*) 0-42475  
 K=2 $\pi$ , decay amplitudes in SU(2)×U(1)×U(1) model with new neutral current 0-4986  
 KN, below 1 GeV/c, Y\* states, SU(6)⊗O(3) quark model classification 0-27523  
 $\theta$  vector particles, calibration interaction macroscopic confinement radius (*Russian*) 0-47257
- subboundary structure**  
 fatigue crack propagation, new measurement and observation techniques 0-45463  
 Invar N36 melt, cast metal struct. depend. on heat treatment, subgrain struct. (*Russian*) 0-40343  
 steel, high C, high alloy, M<sub>23</sub>C<sub>6</sub> type carbides, effect of alloying elements on defect struct. and hardness 0-16481  
 Al, deformed, thermal recovery, microstruct. and stress-strain relations 0-16325  
 Au-Er, dil., cold-worked, EPR expts. 0-39864  
 Na<sub>x</sub>WO<sub>3</sub> bronzes (0.4<x<1), domain, surface and substrate structs. 0-34281  
 ZnTe, elec., SEM and TEM studies of impurity segregation during long annealing 0-30001  
 $\alpha$ -Zr monocrystal perfection using Berg method and diffractometer with omega device (*French*) 0-2035
- subgrain structure** see subboundary structure
- sublimation**  
 see also heat of sublimation  
 ceramic powders, equipment for sublimation drying, exam. 0-25733  
 cometary nucleus, effect on orbital evolution of Periodic Comet Encke 0-46483  
<sup>18</sup>F-5-fluorouracil, synthesis and purification by fractional sublimation 0-17134



**sublimation continued**

- magnetic solids, surface rate processes and vapour press. 0-34182  
 snow, rel. to grain growth 0-26553  
 solid solutions, freeze drying in semiconducting powder prep., solvent choice 0-11583  
 ternary gas mixture, natural convection, naphthalene sublimation appl. 0-6511  
 $\text{Al}_2\text{O}_3$ , sublimation growth, cryst. struct. determ. 0-19751  
 $\text{Al}_2\text{N}_3\text{O}_3$ , sublimation growth, cryst. struct. determ. 0-19751  
 $\text{CdS}$ ,  $\text{CdSe}$ , growth rate, sublimation rate and etching behaviour along polar axis 0-24387  
 $\text{Co}$ , sublimation rate near Curie temp. 0-49351  
 $\text{CsAlSiO}_3$ , and  $\text{CsAlSi}_2\text{O}_7$ , cryst. evap., mass spectral investig. 0-49353  
 $\text{Cu-Ni}$  (50 wt.%) alloys, estimation of sublimation energy of Cu atoms, evaporation rate and surface composition, AES meas. (Japanese) 0-49352  
 $\text{GeO}$  formation from  $\text{Ge-GeO}_2$  mixtures, gasification kinetics (Russian) 0-21273  
 $\text{O}_2^+$   $\text{AsF}_6^-$ , thermal decomposition, Raman spectra study, free radical mechanism 0-55652  
 $\text{SiCl}_4$ , vaporisation thermodynamics, sublimation and formation 0-54366  
 $\text{SiC}$ , epitaxial growth by sublimation sandwich method, effect of impurities 0-25568  
 $\text{SiC}$  epitaxial layer growth from sublimation in vac., kinetics 0-20791  
 $\text{SmF}_3$ , vaporisation, Knudsen effusion method 0-6508  
 $\text{WO}_3$  amorphous film, sublimed under different conditions, elec. transport props. 0-7015  
 $\text{ZnCd}_{1-x}\text{S}$ , film, single-thermal-source form. 0-2492  
 $\text{ZnO}$ ,  $\text{ZnS}$ , growth rate, sublimation rate and etching behaviour along polar axis 0-24387  
 $\text{ZnP}_2$ , sublimation 0-34181

**submarine cables**

- fibre optic, small, recent experiences 0-14488  
 low dielectric loss meas. apparatus for 0.1 to 200 MHz 0-15958  
 PFM fibre-optic video transmission to and from undersea vehicles 0-46310  
 telecommunication, dielec. loss measurements of polyethylene at high pressure and freq. 0-27316

**submillimetre waves** see microwaves**suboptimal control** see optimal control**subroutines**

- binary mixture, internal consistency of activity coefficients program in BASIC 0-54364  
 computer modelling of matter, conf., Anaheim, USA (March 1978) 0-51954  
 equations of state, search procedure, based on step-wise least-squares technique 0-19900  
 molecular fluid, computer simulation of liquid-vapour surface 0-54478  
 MORPHOQUANT automatic microscope image analyser, universal program system 0-56160  
 quantum liquids and crystals, computer modelling 0-54472  
 radiographs processing, computer appl. 0-3259  
 X-ray powder diffractometer, APD3600, file searching techniques 0-24319

**subsets (mathematics)** see set theory**substrates**

- see also semiconductor device manufacture  
 adsorbed layers, two dimensional incommensurate crystal theory, thermodynamics (Russian) 0-49524  
 bending during thin film evaporation due to temp. difference between substrate faces 0-54571  
 crystalline-amorphous film system, relaxation process dislocation misfit theory (Russian) 0-39461  
 deformation, deposits spontaneous macrostress calc. 0-15412  
 deposit-substrate systems, adhesion testing 0-50814  
 dielectric constants, standard specimens 0-13038  
 dielectric multilayers, optical and geometrical thickness monitoring using monochromatic maximeter, substrate effects (French) 0-38140  
 electrodeposit, on metallic substrate, peel test for determ. adhesion 0-50815  
 electron-probe microanalysis of thin coatings, charact. fluoresc. correction 0-7881  
 epitaxial layers, on monocryst. supports, degree of disorientation, determ. by interferometry (Russian) 0-24748  
 film-substrate bond strength, meas. by laser spallation 0-50821  
 glass,  $\text{Cr(Ti)}$  films electron-beam deposition techniques improvement 0-7496  
 glass, for  $\text{Mn}_2\text{O}_4$  film form. from  $\text{Mn}^{2+}$  ions in water (Japanese) 0-45411  
 graphite, Si dip-coated, photovoltaic effects 0-29442  
 holographic image and plate substrate quality relationship 0-48193  
 instantaneous bending during thin film deposition, intrinsic stresses, cantilevered plate method anal. 0-54570  
 leucosapphire, crystal growth by Kypoulous method, temp. effect on structural and optical quality 0-20784  
 metals for polystyrene films, electrode effect on carrier injection, TSC, I-V characts. 0-34463  
 misorientation for  $\text{GaAs:Si}$  LPE layers, surface morphology, initial supercooling effects 0-34329  
 noble metal contact, substrate material diffusion and corrosion film formation, model 0-2312  
 non-metallic, temp. and pressure sensitive, micro-contacting problems with metallic layers (German) 0-55624  
 piezoelectric film, third-order piezoelec. and dielec. const. meas. using surface acoustic waves (Japanese) 0-55042  
 polyethylene/metal substrate, adhesion, role of surface topography 0-35500  
 polymeric systems, supported on inert substrates, dynamic thermomech. study 0-55623  
 quartz,  $\text{Cr(Ti)}$  films, electron-beam deposition techniques improvement 0-7496  
 rough boundary substrate-thin film system, ellipsometric obs. using equiv. film theory 0-2310  
 semiconductor substrate, measurement of contact angle between water droplets and surface (German) 0-34276  
 semiconductor substrate, work function rel. to AES (French) 0-50479  
 sputtered particles-substrate, temp. overaging (Russian) 0-40385  
 stainless steel, HFN activated reactive evaporated coatings, high rate deposition, microhardness 0-25580

**substrates continued**

- steel for Cu vacuum coatings, influence of precipitation conditions on porosity (Russian) 0-54578  
 water supercooled droplets, on ice substrate after low speed collision, freezing behaviour, cryst. struct. 0-29152  
 Al sputtered coating development, porosity, durability temp. depend., electric arc metallisation regime (Russian) 0-39402  
 Al-Zn-Mg plasma sputtered, mech. props. rel. to heat treatment (Russian) 0-40387  
 $\text{Al}_2\text{O}_3$ ,  $\text{Cr}$  (Ti) films electron-beam deposition techniques improvement 0-7496  
 $\text{Al}_2\text{O}_3$  for  $\text{W-Al}_2\text{O}_3$  composite films, oxide evaporation deposited, struct., props. 0-25581  
 $\text{Al}_2\text{O}_3$  substrates, grain growth during sintering 0-40302  
 Au coated Si for amorphous Si, whisker growth characts. by  $\text{SiH}_4$  thermal decomposition 0-34342  
 Au, substrate for VPE Pt, crit. thickness of pseudomorphic film growth, substrate size depend. (Russian) 0-29286  
 $\text{BaSO}_4$ ,  $\text{SrSO}_4$  surface crystn. 0-34332  
 $\text{Bi}_2\text{GeO}_{20}$ , for interdigital transducer (Czech) 0-19201  
 Cu, electrodeposit on (111) Cu substrate in presence of halo-compd. of acetic acid 0-15413  
 Cu plated substrates for Antares  $\text{CO}_2$  laser mirrors 0-14349  
 Cu substrate, ion induced intermixing of Au or Ag surface film 0-15420  
 Cu, surface topography influence on growth struct. of sputtered Cr 0-20058  
 Cu-benzotriazole (benzimidazole) thin films, ellipsometric study 0-35114  
 GaAs, for sputtered GaSb film, growth, Hall effect, impurity levels 0-20334  
 GaAs, out-diffusion of Cr 0-10708  
 GaAs, selective in situ vapour etching and growth 0-2958  
 GaAs substrate, Al MBE growth 0-24757  
 GaAs substrate, plasma polymerised polysiloxane film growth, dry etching process 0-25575  
 GaAs temp. influence on Hall mobilities of GaAs and GaAs:Cr epitaxial layers 0-20335  
 GaAs/ $\text{SiO}_2$  substrate/film system, interface formation during CVD, modelling 0-24764  
 Ge (111)-amorphous  $\text{SiO}_2$  or  $\text{Si}_3\text{N}_4$  film, dislocation interactions, substrate bending and edge effects 0-39472  
 Ge substrate for GaAs solar cells, thin film shallow homojunction struct., quantum efficiencies 0-35677  
 H, solid for liquid  $^4\text{He}$  film, film transfer velocity, Van der Waals interaction (Russian) 0-54465  
 InAs, heteroepitaxial layers,  $\text{AsCl}_3$  mole, fraction and substrate orientation effects on elec. parameters 0-39690  
 InP substrates, chem. etching by  $\text{H}_2\text{O}_2\text{-H}_2\text{SO}_4\text{-H}_2\text{O}$  soln. 0-35360  
 InP/ $\text{SiO}_2$  substrate/film system, interface formation during CVD, modelling 0-24764  
 n-InSb, surface quality improvement by low temp. CVD of  $\text{SiO}_2$ , and characterisation 0-49932  
 KBr, electron irradi., epitaxial growth and surface coverage of Te films 0-10825  
 KI, doped substrate for vac. deposition of Ag oriented films 0-2303  
 $\text{LiNbO}_3$  substrate for InSb films, prep. and props. 0-35093  
 $\text{LiNdP}_4\text{O}_{12}$  growth of  $\text{LiBiNd}_{1-x}\text{P}_4\text{O}_{12}$  waveguide laser layer 0-23709  
 Mo alloy, interaction with  $\text{Mo}_3\text{Si}_3$  based coating (Russian) 0-21167  
 Mo, for  $\text{W-Al}_2\text{O}_3$  composite films, oxide evaporation deposited, struct., props. 0-25581  
 NaCl (001) substrate, preferential epitaxy of evaporated films induced by electron bombard. or elec. field 0-10824  
 NaCl, (111) surfaces, electron bombard. effects and subsequent Ag epitaxial growth, RHEED and AES 0-15419  
 NaCl, doped substrate for vac. deposition of Ag oriented films 0-2303  
 Ni-Cr-Mo-Ti (19,11,3 wt.%) for TiC reactively sputtered coatings, adherence, XPES and wear study 0-25565  
 Se, amorphous, vac. deposition on polymer substrates, use of temp. gradient vac. coating device 0-35099  
 Si (111) substrate, MBE deposition kinetics of Bi film 0-10817  
 Si, conditions and growth mechanism for autoepitaxial thin layers at low temp. from  $\text{SiCl}_4\text{-H}_2$  system 0-20795  
 Si, effect of surface conditions on plasma sprayed metal coatings 0-21145  
 Si, epitaxial film growth and p-n junction formation by Si beam epitaxy in high vacuum 0-16187  
 Si, for Pb, Sb, and Bi silicate films, form. kinetics and props. 0-35358  
 Si, local mechanical defects, annealing and effect on autoepitaxial growth (Russian) 0-7701  
 Si, nucleation controlled interaction with metal film, silicide form. 0-10711  
 Si, process-induced in-plane distortion, correl. with wafer bowing 0-54579  
 Si, solid state reaction with Ti film, backscatt. anal. 0-34257  
 Si, sputtering and sputter etching and thermal history 0-25562  
 Si substrate, ion induced intermixing of Pd or Pt film 0-15420  
 Si, thermally oxidised, interface props., sputter deposition parameters effects (German) 0-40257  
 Si:Sb, ion implanted doping, isotopic composition shifts on neutron activation determination 0-24487  
 SiC CVD substrate, Cu mirror vapour deposition, pulsed laser damage characts. 0-48314  
 $\text{SiO}_2$ , for interdigital transducer (Czech) 0-19201  
 $\text{SiO}_2$ , interfacial chemistry with deposited Ba, AES obs. 0-44434  
 $\text{SiO}_2$ , solid state reaction with Ti film, backscatt. anal. 0-34257  
 Ti for  $\text{W-Al}_2\text{O}_3$  composite films, oxide evaporation deposited, struct., props. 0-25581  
 Ti-Al-V (6.4 wt.%) alloy foil, substrate temp. effect on struct. 0-7497  
 Ti-Al-V (6.4 wt.%) for TiC reactively sputtered coatings, adherence, XPES and wear study 0-25565  
 W, for Cu cementation, field ion microscopy of cementation vs. substrate dissolution, pH effect 0-16206  
 W substrate-oxide film system with rough boundaries, ellipsometric obs. using equiv. film theory 0-2310  
 YIG, magnetoelastic surface waves, magnetostatic reson. anal. 0-20441  
 Zn surface, Ni solar selective black coatings, electrochem. deposition 0-29885  
 ZnO, for Ni films, band bending, UPS study 0-7472

**sudden commencement** see magnetic storms**Suhl effect**

No entries



## sulphur

- see also nuclei with .....
- adsorbed ( $\sqrt{3} \times \sqrt{3}$ )R30° overlayer struct. on Ir (111) 0-15365
- adsorbed layer, ( $\sqrt{2} \times \sqrt{2}$ )R45°, and Pd(100), adsorbate induced surface reson. obs. in photoemission 0-7470
- adsorbed on Ni, photoelectron diffr. data 0-29851
- adsorbed on Ni (110) and Rh (110), surface struct. anal. using hybridisation model 0-44423
- adsorbed on Rh (110), LEED crystallographic determ. of surface struct. 0-44422
- adsorption and desorption kinetics of CO from clean and S covered Ru 0-6643
- adsorption and desorption kinetics of H<sub>2</sub> from clean and S covered Ru 0-6644
- adsorption on metals, thermodynamics of two-dimen. and three-dimen. sulphides 0-20036
- adsorption on Ni (111), angle-resolved photoemission 0-40230
- atom, chemisorption on Cu, cluster theory 0-29264
- atom, chemisorption on Ni, cluster theory 0-29264
- atom, one-electron binding and Auger energies 0-52872
- atom, photoionisation cross sections and ang. distrib., outer p subshell 0-9572
- charge-transits, flash excited, electrode-edge effects, meas. 0-2396
- chemical reaction involving S, sulphide, sulphate, sulphite, application to Venus and Io 0-50837
- defects predeposited in Si p<sup>+</sup>-n junction diodes by low fluence ion implantation, unequal densities 0-20293
- determination, combustion-gas chromatographic method, data processing 0-40762
- electrode, miniature, recharging characts. in two liquid phase region 0-26127
- geochemistry, influence man-made sources on S cycle of NE United States 0-26178
- high-S coal, continuous sorbent regeneration in pressurized fluid bed combustion 0-30351
- human hair surface, determination of content using minimum depth electron probe X-ray microanalysis 0-22500
- interstellar S, depletion on oxide grains 0-17635
- ions in Jupiter's S nebula, temp. anisotropy 0-17539
- isotope separation, multiphoton molecular dissociation using high-power CO<sub>2</sub> laser radiation 0-9657
- laser, atomic, pulsed microwave discharges of SF<sub>6</sub> and CS<sub>2</sub> source gases 0-48233
- lattice statics of  $\alpha$ -type under hydrostatic press. 0-49175
- liquid, eqn. of state determ., crit. props. and mol. comp. 0-49336
- measurement, model XA-300 meter for laboratory use 0-26085
- oceanic crust layer 2 S distrib., effect of low temp. seawater-basalt interaction 0-41432
- Orion Nebula, Ne, S and O abundances from fine-struct. lines obs. 0-4410
- production and props. in liq. Ar and N<sub>2</sub> by OCS photodissociation 0-43064
- rain and snow acidity, release by burning of fossil fuels 0-26590
- segregation in Ni, effect on intergranular corrosion in dil. H<sub>2</sub>SO<sub>4</sub> 0-30152
- segregation on Fe(111) surface, LEED, AES and work-function change 0-15350
- shock wave method observation of transition to highly conducting state 0-4738
- steel, C, friction faces, S, O content, secondary ion-ion emission obs. 0-55545
- troposphere, global S cycle linear eight-box model 0-56506
- Venus atmosphere, role of gaseous S<sub>2</sub>, S<sub>3</sub>, S<sub>4</sub> and H<sub>2</sub>S<sub>n</sub> 0-17518
- XPS, in BaS and BaSO<sub>4</sub> 0-43104
- zeolite-S layers, high-temp. activated dipole moments in S clusters (*Russian*) 0-20575
- zone-centre lattice vibrs. of  $\alpha$ -type, hydrostatic press. effects 0-49314
- As-S film, amorphous, chemical modification of props. 0-49250
- CoO<sub>2</sub>S, acceptor properties of S, free electron concentrations 0-34395
- CoO<sub>2</sub>S, in O<sub>2</sub>+CO<sub>2</sub>+SO<sub>2</sub> atmosphere, elec. cond. study 0-39583
- Co<sub>2</sub>O<sub>4</sub>S, defect struct. and elec. props., electron, hole conc. 0-44601
- Cr<sub>2</sub>O<sub>4</sub>S, elec. cond. and thermo-EMF 0-20231
- Fe, (100) surface, S segregation and 2D compounds precipitation (*Japanese*) 0-35188
- Fe, embrittlement, fracture mode transition as function of grain boundary sulphur 0-55520
- Fe-Ni-Sb-S, S/Sb surface site competition in segregation 0-40366
- GaAs-S, ion-implanted, capless anneal, effect of As partial press. 0-29038
- GaAs-S epitaxial, VPE growth, photoluminesc. and emission spectra 0-29774
- GaAs<sub>1-x</sub>P<sub>x</sub>S, deep level, photoconductivity, carrier nonradiative recombination 0-20112
- GaP-S, nucl. relax. rel. to donor density 0-11284
- GaP-S, shallow donor states, Stark effect and inversion splitting, electroabsorption spectral obs. 0-50385
- GaP-S,C(Cd)(Zn), donor-acceptor pair luminesc., excitation spectroscopy 0-25440
- GaSb-S, cond. and Hall coeff. relax., impurity config. model 0-6786
- H production, thermochem. H<sub>2</sub>O decomposition using S-I cycle, process eng. and bench-scale studies 0-35770
- InAs:Te(Se)(S), intrinsic pt. struct. defects 0-33998
- InAs:ZnS, solubility and donor-acceptor interaction 0-54263
- InP:Te(S), heavily doped, dislocation imaging using transmission cathodoluminesc. 0-29023
- InSb-S, reson. states and reson. scatt. 0-49738
- KI:S<sup>2-</sup>, vacancy dipoles, photo-induced polarisation and depolarisation 0-2690
- MgO-S, cathodoluminesc. spectrum (*Russian*) 0-55197
- Mn<sub>2</sub>O<sub>4</sub>S, defect struct. and elec. props., electron, hole conc. 0-44601
- Mn<sub>2</sub>O<sub>4</sub>S, elec. cond. and thermo-EMF 0-20231
- Na/S batteries, load levelling and traction 0-21391
- NaCl:S<sup>2-</sup>, enthalpy of anion vacancy migration 0-15309
- S adsorption in coal, content meas., using X-ray radiometric analysis 0-26077
- S II plasma in Jupiter magnetosphere, radial discontinuities obs. 0-4291
- S III, CI calcs. of oscillator strengths, L-S framework 0-14089
- S III, S IV in Io plasma torus, Voyager 1 EUV emission lines obs. 0-26792
- S IV, P, D-, S-states, oscillator strengths, transition strengths, CI calcs. 0-922

## sulphur continued

- S IX, excited level populations, line intensity ratios, solar corona appl. 0-32637
- S X, ground configs., forbidden line intensities calcs. 0-23362
- S XIII, beam-foil obs. of oscillator strengths for E1 transitions 0-14112
- S XV, 1s<sub>2</sub>s<sup>2</sup> 3s-1s2p <sup>3</sup>P transitions, Lamb shift, VUV beam foil spectra obs. 0-52919
- S<sup>+</sup>, mobility in He, flow-drift tube meas. 0-43831
- S<sup>+</sup>, reson. line regularities in plasma Stark widths and shifts 0-43881
- S<sup>2-</sup>, positronium formation, Doppler broadened positron annihilation line shapes 0-45164
- S/N gradient in M33 galaxy, supernova remnant evidence 0-56929
- S-I cycle for thermochem. prep. of H<sub>2</sub> by H<sub>2</sub>O dissociation 0-16823
- S<sup>+</sup>+SF<sub>6</sub>→SF<sub>5</sub>+F+S, electron affinity of SF<sub>5</sub> radical 0-45495
- S<sup>+</sup>+NO→NO<sup>+</sup>+S+1.1 eV, rate consts. kinetic energy depend., drift tube meas. 0-7778
- S<sup>+</sup>+O<sub>2</sub>→SO<sup>+</sup>+O+0.26 eV, rate consts. kinetic energy depend., drift tube meas. 0-7778
- S<sup>15+</sup>+Ar, K-shell vacancy sharing, interference effects 0-5606
- S<sup>n+</sup>+inert gas atom (n=5 to 9), small impact parameter collisions, charge exchanging processes 0-14227
- S<sub>2</sub>,  $\Delta_g$  and  $\Sigma_g^+$  states, near IR emissions 0-18852
- S<sub>2</sub> mol. B<sup>3</sup> $\Sigma_u^-$ →X<sup>3</sup> $\Sigma_g^-$  fluorescence induced by N<sub>2</sub> laser (*Japanese*) 0-14175
- S<sub>2</sub>, optically pumped CW dimer lasers 0-14322
- S<sub>8</sub><sup>2+</sup>, electronic struct. and localised MOs, bonding nature and geom. struct. 0-18798
- S<sub>8</sub>+4H<sub>2</sub>O→3H<sub>2</sub>S+H<sub>2</sub>SO<sub>4</sub>, chem. equil. of aq. system, application to Venus and Io 0-50837
- S(D, <sup>3</sup>P) isoelectronic series, Sternheimer valence shielding and anti-shielding factors 0-18807
- SXI, solar emission lines, density dependence 0-21963
- <sup>34</sup>S/<sup>32</sup>S ratio in magmatic gases of Afar ridge volcanism 0-21732
- Si:S,  $\gamma$ -irrad. influence on elec. props. 0-6845
- TiO<sub>2</sub>:S, acceptor properties of S, free electron concentrations 0-34395
- TiO<sub>2</sub>:S, in O<sub>2</sub>+CO<sub>2</sub>+SO<sub>2</sub> atmosphere, elec. cond. study 0-39583
- sulphur compounds**
- air pollutants, conc. meas. with flame photometric apparatus 0-16883
- atmosphere, information exchange concerning S compounds pollution in European Community 0-7979
- one-electron binding and Auger energies 0-52872
- polynaphthoquinone-SO<sub>2</sub>-I<sub>2</sub> system for H<sub>2</sub>O decomposition for H<sub>2</sub> production 0-16825
- sulphate aerosols, atmospheric, diurnal var. at rural sites in E. United States 0-30621
- sulphate concentration, Southwestern Desert of US, X-ray emission anal. 0-8378
- sulphate particle formation by heteromol. nucleation and condensation in cavities 0-26183
- thiocyanate complexes at Ag electrode surface, Raman spectroscopic study 0-37813
- Al<sub>2</sub>O<sub>3</sub> production, removal of S compounds in Na<sub>2</sub>O-CaO sintering (*Chinese*) 0-55323
- As-S, amorphous, glass transition and specific heat, intermolecular bond saturation 0-15011
- As-S glasses, acousto-induced structural changes, optical props. 0-49122
- As-S glasses, resonance Raman scatt. 0-50325
- As<sub>2</sub>S<sub>3</sub>-Ag light sensitive material, development of non-interchangeability under continuous laser radiation (*Russian*) 0-50870
- As<sub>2</sub>S<sub>1-x</sub>, chalcogenide, covalent non crystalline topology, short range order 0-15009
- As<sub>2</sub>S<sub>100-x</sub>, amorphous film, photoinduced changes in optical props. 0-50445
- Ba+SO<sub>2</sub>→BaO+SO reaction, laser-induced fluoresc. obs., vibronic distrib. of BaO, collisional energy depend. 0-11917
- CdS<sub>1-x</sub>Se<sub>x</sub> film, resonance between Se atom dipole vibr. and interference modes, IR spectra obs. (*Russian*) 0-2888
- Cu-Ni sulphidised alloys, Ru and Os behaviour during carbonylation (*Russian*) 0-40584
- Ge-S, amorphous, photocond., photo-induced ESR, optical edge shift 0-49809
- Ge-S amorphous film, defect states, ESR 0-49670
- Ge-S-Ga(In) system glasses, photoinduced changes 0-24365
- Ge-S-Sb glasses, microgravity effect on recrystn., optical and elec. props. 0-49127
- Ge<sub>30</sub>S<sub>70</sub> glass film, Ag photodoping sensitivity 0-39121
- Ge<sub>2</sub>S<sub>1-x</sub>, chalcogenide, covalent non crystalline topology, short range order 0-15009
- H production, thermochem. H<sub>2</sub>O decomposition using S compounds, feasibility anal. 0-35768
- H, thermochemical prod. using S-Br cycle, development of lab-scale plant 0-35774
- H<sub>2</sub>S, S K-LL Auger energies and chemical shifts 0-28069
- H<sub>2</sub>SO hypothetical molecule, nonempirical STO calc. of chem. bonds 0-23307
- H<sub>2</sub>SO<sub>4</sub>, Fe passivation, model for anodic dissolution 0-35545
- H<sub>2</sub>SO<sub>4</sub> gas phase meas. in stratosphere 0-36366
- Li/SO<sub>2</sub> cells, safety studies, DTA of constituents 0-16795
- Li/SOCl<sub>2</sub> hermetic primary cells, effect of type of C on performance 0-35661
- Li/SOCl<sub>2</sub> primary cell, cyclic voltammetric and coulometric obs. of SOCl<sub>2</sub> reduction 0-30440
- Li-SOCl<sub>2</sub> battery for implantable cardiac pacemakers 0-30939
- Li-SOCl<sub>2</sub> hermetic D cells, effect of Li<sub>2</sub>B<sub>10</sub>Cl<sub>10</sub> and Li<sub>2</sub>B<sub>12</sub>Cl<sub>12</sub> on performance 0-12000
- Mn, corrosion, at high temp. in pure SO<sub>4</sub> 0-50774
- P-S, amorphous, glass transition and specific heat, intermolecular bond saturation 0-15011
- S-Se(Te)(Ti), liq. semicond., bonding energies and entropies, mag. susceptibility meas. 0-49082
- SB<sub>2</sub> photoelectron spectra, visual assessment stripping program anal. 0-28062
- SCN<sup>-</sup>, positronium formation, Doppler broadened annihilation line shapes 0-45164
- (SCN)<sub>2</sub>, prep., UV photoelectron spectrum and structure 0-28059
- SCI(Br), unstable radicals, matrix-isolated, IR spectra force const. (*German*) 0-43053
- SF<sub>6</sub><sup>+</sup> ion-molecules, IR multiple-photon dissoc., lifetime meas. 0-28072
- SF<sub>6</sub>, absorpt. of intense laser radiation, vibr. excitation 0-9667



**sulphur compounds continued**

- $\text{SF}_6$  addition to  $\text{N}_2$  laser discharge, negative ion prod., altered discharge parameters 0-38818  
 $\text{SF}_6$ , atmospheric global distrib., sources and sinks, rel. to  $\text{O}_3$  depletion 0-4088  
 $\text{SF}_6$  axially blown arc, current-zero behaviour, theoretical model 0-38789  
 $\text{SF}_6$  breakdown voltages dispersion, anal. 0-38772  
 $\text{SF}_6$  clusters, collision induced polarisability, mol. frame distortion 0-32798  
 $\text{SF}_6$  collisions, laser spectroscopy investig. 0-9697  
 $\text{SF}_6$  compressed, influence of electrode macroscopic curvature upon surface roughness effects 0-40693  
 $\text{SF}_6$  compressed, low probability first breakdown voltage determ. 0-38787  
 $\text{SF}_6$  compressed in positive rod-to-plane gaps, static breakdown anal. 0-38796  
 $\text{SF}_6$  cooled gas, multiphoton dissociation with  $\text{CO}_2$  laser, enrichment with  $^{33}\text{S}$  0-14245  
 $\text{SF}_6$  dielec. strength, electrode shape effect, overvoltage protection (*Czech*) 0-10444  
 $\text{SF}_6$  dielectric strength, conductor surface irregularities influence 0-14946  
 $\text{SF}_6$  dissociation, infrared multiphoton processes, apparent step cross-sections, pulse spatial structure, irradiation techniques 0-32792  
 $\text{SF}_6$  electron elastic scatt. resons. 0-53133  
 $\text{SF}_6$  electron swarm development, Boltzmann eqn. anal. 0-6205  
 $\text{SF}_6$  electronic props., (e,2e) spectrosc. obs. 0-5527  
 $\text{SF}_6$  energy-dependent absorption cross sections, use in multiphoton absorption modelling 0-32789  
 $\text{SF}_6$  excitation by strong IR laser field, spectral characts. 0-32713  
 $\text{SF}_6$  gas,  $\text{CO}_2$  TEA laser-excited, slow intermol. redistrib. of vibr. energy 0-53039  
 $\text{SF}_6$  gas, compressed, initial corona voltage increase due to electrode surface roughness (*Croatian*) 0-54074  
 $\text{SF}_6$  gas, dispersion relation of spontaneous oscill., unstable regions 0-1875  
 $\text{SF}_6$  gas, thermodynamical and spectral props., effect of angle-dependent part of dispersion forces 0-43138  
 $\text{SF}_6$  gas blast breaker, current zero meas. 0-38795  
 $\text{SF}_6$  high-resolution IR Ar matrix-isolation spectra, 10K 0-32708  
 $\text{SF}_6$  highly excited, time-resolved IR absorpt. obs. 0-9666  
 $\text{SF}_6$  IR double reson. with tunable diode laser 0-14160  
 $\text{SF}_6$  impulse breakdown, polarity effect, thin dielectric coating influence 0-38773  
 $\text{SF}_6$  intramode anharmonicity const., vibr. linear absorpt. spectrum 0-18893  
 $\text{SF}_6$  isotope separation, TEA  $\text{CO}_2$  laser irradiation (*Japanese*) 0-11885  
 $\text{SF}_6$  laser spectroscopy using an optothermal receiver 0-37810  
 $\text{SF}_6$  laser-irrad., high-resolution double-reson. spectroscopy, collisionless multiphoton dissoc. 0-9623  
 $\text{SF}_6$  model system, coherent pulse propag. effects 0-9968  
 $\text{SF}_6$  molecular vibration energy stochastization in intense IR laser field by Raman spectroscopy (*Russian*) 0-14149  
 $\text{SF}_6$  molecule, resonant energy absorpt. struct. in IR laser field (*Russian*) 0-5592  
 $\text{SF}_6$  molecule absorption of IR laser radiation (*Russian*) 0-986  
 $\text{SF}_6$  multiphoton absorpt., pulsed  $\text{CO}_2$  laser radiation absorpt., press., freq., fluence depend. 0-28080  
 $\text{SF}_6$  multiphoton absorpt. meas. by third harmonic generation 0-1036  
 $\text{SF}_6$  multiphoton absorpt., energy transfer, dissoc. probability, laser field interaction, classical trajectory approx. 0-37730  
 $\text{SF}_6$  multiphoton dissoc., unified dynamical model 0-5587  
 $\text{SF}_6$  multiphoton dissoc., collision effects 0-23467  
 $\text{SF}_6$  multiphoton dissoc., classical model 0-53076  
 $\text{SF}_6$  multiphoton excited, IR fluoresc. spectrum meas. 0-37828  
 $\text{SF}_6$  multiple photon excitation, collisionless 0-53079  
 $\text{SF}_6$  multiple-photon absorption, experimental conditions and mol. parameters depend. 0-32790  
 $\text{SF}_6$  multiple-photon excited, double reson. spectroscopy 0-53030  
 $\text{SF}_6$  multiple-photon IR laser pumping, collisional effects 0-9668  
 $\text{SF}_6$  narrow reson., elastic scatt., spectroscopic studies 0-53094  
 $\text{SF}_6$  nonradiative collisionless dephasing rate, two-photon coherent transient meas. 0-14176  
 $\text{SF}_6$   $\nu_2$  bands, rot. fine struct., HFS spectroscopic consts. determ., saturation spectroscopy obs. 0-53008  
 $\text{SF}_6$  photoionisation spectra in XUV region 0-37837  
 $\text{SF}_6$  photon-enhanced dissociative electron attachment 0-9749  
 $\text{SF}_6$  photon-enhanced dissociative electron attachment, isotope selectivity 0-18939  
 $\text{SF}_6$  plasma column, in Maecker type arc, diagnostics and model (*French*) 0-19652  
 $\text{SF}_6$  polarization-rotation and thermal-motion studies via resonant degenerate four-wave mixing 0-5779  
 $\text{SF}_6$  positive-point corona phenomena, breakdown voltage/press. characts. 0-38859  
 $\text{SF}_6$  pure and mixtures, dielec. props., ionisation and attachment coeffs. 0-33726  
 $\text{SF}_6$  refractive index meas., intermolecular interaction effects 0-33728  
 $\text{SF}_6$  resonant single-photon dissoc. route using prelim. electron excitation 0-9662  
 $\text{SF}_6$  S isotope separation, multiphoton molecular dissociation using high-power  $\text{CO}_2$  laser radiation 0-9657  
 $\text{SF}_6$  spectroscopy using tunable high-press.  $\text{CO}_2$  waveguide laser 0-43054  
 $\text{SF}_6$  supersonic jet, condensation and gasdynamic cooling 0-6089  
 $\text{SF}_6$  supersonic jet expanding into vac., interaction with  $\text{CO}_2$  laser beam 0-5584  
 $\text{SF}_6$  time-resolved IR absorpt. meas. using injection-locked single mode TEA  $\text{CO}_2$  laser 0-9665  
 $\text{SF}_6$  very high current gas blast arcs, local voltage and cross-sectional areas correlation 0-38779  
 $\text{SF}_6$  vibr. spectra, rot. consts., IR spectra, Raman spectra obs. 0-32719  
 $\text{SF}_6$  viscosity meas. at low temps. 0-6193  
 $^{33}\text{SF}_6$  dissociation, infrared multiphoton processes, reaction rate, scale factors, pulse structure 0-32791  
 $\text{SF}_6$ -Ar, condensing flow, gasdynamic and IR meas. 0-6501  
 $\text{SF}_6$ -ethane mixtures, viscosity, diffusion coeffs. 0-1722  
 $\text{SF}_6$ - $\text{H}_2$  mixtures, laser irradiated, IR energy deposition and HF fluoresc. 0-23454  
 $\text{SF}_6$ -He hollow-cathode laser using F transitions 0-48289  
 $\text{SF}_6$ - $\text{N}_2$  mixtures, effective ionisation coeff. and static breakdown voltage meas. 0-19549  
 $\text{SF}_6$ +CsF, rot. inelastic collisions, mol. beam meas. 0-1049

**sulphur compounds continued**

- $\text{SF}_6$ +K, ion-pair form. reaction, energy loss spectra 0-55630  
 $\text{SF}_6$ +Ne, metastable state de-excitation, rate consts., radiolysis obs. 0-40709  
 $\text{SF}_6$ +X $\rightarrow$  $\text{SF}_5^-$ +F+X (X=O, S, F, Br, I), electron affinity of  $\text{SF}_5$  radical 0-45495  
 $\text{S}_2\text{F}_{10}$  absorpt. of intense laser radiation, vibr. excitation 0-9667  
 $\text{S}_2\text{F}_{10}$  multiple-photon IR laser pumping, collisional effects 0-9668  
 $\text{SF}_5\text{Cl}$  pure rot. spectra, 300 GHz, isotope effects 0-5533  
 $(\text{SN})_x$  brominated, struct. and elec. props. 0-24914  
 $(\text{SN})_x$  deform. and defects, lattice strain, fibrillation 0-3139  
 $(\text{SN})_x$  halogenated derivatives, cond. and magnetoresist., 4.2-300K 0-24915  
 $(\text{SN})_x$  Meissner effect, mag. susceptibility meas. 0-20351  
 $(\text{SN})_x$  single crystals, tunnelling spectroscopy investigation (*Japanese*) 0-49954  
 $(\text{SN})_x$  supercond., fluctuation cond., crit. mag. fields 0-39712  
 $(\text{SN})_x$  thermopower from 0.15 to 4.2K 0-34427  
 $(\text{SN})_x$  with H impurities, CPA calculations 0-44468  
 $(\text{SN})_x$ -Br, X-ray absorpt. meas. of mol. struct., orientation and charge transfer 0-25486  
 $\text{S}_2\text{N}_4$  effects of pressure and temp. on phonons, Raman scattering study 0-7360  
 $(\text{SNBr}_{0.4})_x$  supercond. props., dimensionality 0-20344  
 $(\text{SN})_x$  radicals polymerisation to  $(\text{SN})_x$  in thin films, optical spectra 0-16656  
 $\text{S}_2\text{N}_4\text{AsF}_6$  molecular adduct cyclotetra(azathiene), X-ray cryst. struct. determ. 0-54180  
 $\text{SO}$   $1_0-0_1$  transition in dark and molecular clouds, 30 GHz obs. 0-46639  
 $\text{SO}$  36 GHz emission line detect. in Orion nebula, rel. to mag. fields 0-46642  
 $\text{SO}$  ( $^1\Delta_g$ ,  $^1\Sigma_g^+$ ) chemiluminescence sensitised by metastable  $\text{O}_2(^1\Delta_g)$ , energy pooling 0-26016  
 $\text{SO}$  and isotopic forms,  $\text{X}^3\Sigma^-$  state,  $\text{CO}_2$  laser mag. reson. spectroscopy 0-9602  
 $\text{SO}$  interstellar abundances rel. to interstellar shocks mol. diagnostics 0-56899  
 $\text{SO}$  low lying bound mol. electronic states, SCFCI calc. 0-23314  
 $\text{SO}_2$   $2^1A'$  state, electron correl. variational description, loop driven graphical unitary group approach 0-47903  
 $\text{SO}_2$  air pollution model prediction for industrial-residential area (*Chinese*) 0-3546  
 $\text{SO}_2$  and sulphates in rain, urban and rural Norfolk, England 0-55955  
 $\text{SO}_2$  atmospheric, long-term monitoring method using permeation sampling, development 0-26189  
 $\text{SO}_2$  atmospheric, sources in  $\text{CS}_2$  and  $\text{COS}$  oxidation 0-4085  
 $\text{SO}_2$  atmospheric transmittance over IR spectral bands, model 0-51535  
 $\text{SO}_2$  catalytic surface activity,  $\text{LaNi}_5$  surface segregation (*German*) 0-51008  
 $\text{SO}_2$  city concs., box model and acoustic sounder anal. 0-7982  
 $\text{SO}_2$  complete quartic force field calc., algorithm 0-37736  
 $\text{SO}_2$  concentrations, maximum, and averaging time, in industrialised area of Bilbao (Spain) 0-51020  
 $\text{SO}_2$  dispersion and wet deposition from power plant plume 0-16861  
 $\text{SO}_2$  downwind conc. from Four Corners Generating Station 0-47620  
 $\text{SO}_2$  electron attachment processes investig. and mobility of negative ions 0-38518  
 $\text{SO}_2$  gas complex analysis method, resonance absorption with pulsed laser light (*Japanese*) 0-36421  
 $\text{SO}_2$  in atmospheric samples, meas. using luminescence (*Dutch*) 0-3565  
 $\text{SO}_2$  inertia defects and dipole moments by kinetic consts. method 0-928  
 $\text{SO}_2$  laser-induced phosphoresc.-excitation spectra of vibr. bands of ( $^3B_1$ )-(X, $^1A_1$ ) transition 0-18879  
 $\text{SO}_2$  lattice dynamics, rigid mol. model 0-44266  
 $\text{SO}_2$  liq., vibr. relax., US absorpt. and vel. meas. 0-34147  
 $\text{SO}_2$  liquid, short range orientation effects, vibr. Raman spectra 0-2759  
 $\text{SO}_2$  measurements for stability classification schemes, stack plume dispersion, Maryland 0-16862  
 $\text{SO}_2$  minor atm. components, near UV absorpt. spectra, temp. depend. (*French*) 0-36355  
 $\text{SO}_2$  nonradiative transitions and intersystem crossing rates in gas phase, theory 0-23451  
 $\text{SO}_2$  on gas covered Pt surface, thermal conductivity and thermal accommodation coeff. 0-10346  
 $\text{SO}_2$  on Io, evidence from UV obs. 0-36561  
 $\text{SO}_2$  plume in atmosphere, remote sensing mask correl. spectrosc. method 0-55966  
 $\text{SO}_2$  pollution electricity generation, policy options for control 0-51022  
 $\text{SO}_2$ , S K-LI Auger energies and chemical shifts 0-28069  
 $\text{SO}_2$ ,  $T_2$ -relax., rot. transitions, time resolved spectra, microwave pulsed spectrometer study 0-18846  
 $\text{SO}_2$  teledetection of gaseous atmos. pollutants, data acquisition and anal., pollution mapping (*French*) 0-7989  
 $\text{SO}_2$  Venice area air pollution, real time prediction of conc. 0-55953  
 $\text{SO}_2$ , X $\rightarrow$ A electronic absorpt. band system, non Condon effects study 0-18837  
 $\text{SO}_2/\text{H}_2\text{O}/\text{X}_2$  reactions ( $\text{X}_2=\text{Br}_2$ ,  $\text{I}_2$ ), appl. to thermochem. H prod. 0-35773  
 $\text{SO}_2$ - $\text{I}_2$  water splitting cycle, thermochem. H prod. 0-30600  
 $\text{SO}_2$ +Al, high temp. fast flow reactor obs. of kinetics 0-30226  
 $\text{SO}_2$ + $\text{CO}_2$ ,  $\text{CO}_2^+$ , reaction rate coeff. and product distrib. 0-3305  
 $\text{SO}_2$ +fluoromethane, collisionally induced relax. processes and vibr. energy transfer 0-53107  
 $3\text{SO}_2+\text{H}_2\text{O}\rightarrow 2\text{H}_2\text{SO}_4+\text{S}_n$ , chem. equilib. of aq. system, application to Venus and Io 0-50837  
 $\text{SO}_2$ + $\text{NO}^+$ , reaction rate consts. meas. 0-7782  
 $\text{SO}_2$ + $\text{SO}_2(\text{Ar})(\text{He})$ , vibr. relax., shock tube study 0-48062  
 $\text{SO}_4^{2-}$  aerosol layer, form. and evolution model for stratosphere and troposphere 0-21801  
 $\text{SO}_4^{2-}$  aerosol layer in stratosphere, formation and evolution model 0-17327  
 $\text{SO}_4^{2-}$ , level in reacting atmospheric aerosol, calcs. 0-26056  
 $\text{SOCl}_2$ , microwave discharge, chemiluminescence of  $\text{SO}(^1\Delta_g)$ ,  $^1\Sigma_g^+$  0-26016  
 $\text{SO}_2$  laser fluoresc. spectrum 0-28047  
 $\text{S}^{16}\text{O}_2(\text{S}^{18}\text{O}_2)$ ,  $\text{B}_2(\text{A}')$  state, force field for large amplitude motions 0-43023  
 $\text{SO}$  in Orion Molecular Cloud, line profile rel. to rotational explanation of high-vel. mol. emission 0-36688



**suphur compounds continued**

- $\text{SiO}_2\text{-Na}_2\text{O-CaO-MgO-Fe}_2\text{O}_3\text{-Al}_2\text{O}_3\text{-SO}_3\text{-Sn}$  thermally polished, exam. of strength of surfaces 0-25887  
 (Sn)<sub>x</sub>, superconducting polymer, elec. cond., heat capacity and optical props. 0-7028

**sum rules**

- additive quark model with six flavours 0-27455  
 b-mesons, mass splitting,  $\text{SU}_3$  nonet of  $\text{SU}_6$  0-47288  
 baryon magnetic moments, implications for quark model 0-13290  
 beautyonium bound states,  $T$ ,  $T'$ ,  $T''$ , dispersion sum rules (*Russian*) 0-13235  
 charmed hadron masses, from effective quark masses, sum rules 0-4965  
 Compton profiles, directional, sum rule based on kinetic energy integral 0-2889  
 conserved axial second class current, sum rule, commutation relations and axial formfactor 0-18090  
 current algebra and electromagnetic hadron interactions, review, book contrib. 0-47240  
 dipole sum rule schematical eval., collective isovector quadrupole strength 0-47428  
 dynamical Higgs mechanism, weak  $\Delta I=1/2$  rule, sum rules, heavy quarks and leptons 0-27442  
 electro- and photonuclear EM sum rules 0-22810  
 electroproduction, polarised, flavour singlet coefficient functions, QCD corrections, sum rules 0-47301  
 electroproduction above pion threshold, EM interactions and mag. sum rules 0-42639  
 energy weighted electronuclear sum rules, centre-of-mass corrections 0-5091  
 even nuclei,  $2^+$  excited states quadrupole moments, energy weighted sum rule appl. 0-9229  
 Gelfand pattern, charmed hadrons and magnetic moment 0-398  
 gluonium, scalar,  $J/\psi$  radiative decay as gluon source, QCD sum rules 0-47296  
 hadron spectrum, planar amplitudes without Regge cuts 0-27464  
 hadrons, multipole polarisabilities from Compton scatt. amplitudes 0-13311  
 hadrons with charm, beauty and taste,  $\text{SU}_3$  subalgebras of  $\text{SU}_6$  0-9152  
 Heisenberg ferromagnet system, temp. Green's function sum rules (*Chinese*) 0-31678  
 hyperon radiative weak decays sum rules, branching fractions and asymmetry parameters 0-410  
 $I=1$  bosonic reggeon-particle scatt., dispersion sum rules (*Russian*) 0-32089  
 $I=1$  reggeon-baryon scatt., superconvergent dispersion sum rules and vertices struct. (*Russian*) 0-27494  
 ionisation potentials, sum rule, Manne Åberg theorem connection, many body Green's function formalism 0-27930  
 Ising model with transverse field, method of two-time Green's functions 0-2543  
 jet cross sections and quark current-photon pointlike coupling, sum rules 0-32104  
 large-amplitude collective nuclear motion in fission and heavy ion reactions 0-22675  
 mesonic effects in photonuclear sum rules, book contrib. 0-476  
 multipole moments, form factors, energy weighted sum rules, centre-of-mass bounds 0-27590  
 nuclear EM sum rules for  $(\gamma,\gamma)$ ,  $(e,e)$ , transitions and giant resonances 0-5090  
 null plane current anticommutators, sum rules and appls. 0-52436  
 photonuclear sum rule, spin current contribs., strong violations 0-18291  
 photonuclear sum rules from continuum calcs., dependence on residual interactions 0-22807  
 pion-charmed baryon scatt. and coupling strengths, superconvergence sum rules 0-52532  
 quark recombination model, meson and baryon prod. sum rules 0-4922  
 quarkonia, spectra, decays, levels, jets, sum rules 0-18112  
 quarkonium, quantum mechanical applications, masses and leptonic widths of  $\psi$  and  $T$  0-27484  
 quarkonium radiative transition amplitudes, QCD dispersion sum rules 0-52511  
 Racah algebra of  $\text{Gln}$ , generalised back coupling rules 0-47208  
 Reggeon vertices and finite mass sum rule, bootstrap eqn., dual resonance model 0-13292  
 S- and P-wave hyperon decay amplitudes,  $\Delta I=1/2$  rule deviations, weak current-current interactions 0-9166  
 spin/isospin saturated system, two-body distribution function, direct and exchange sum rules 0-27212  
 structure functions, deep inelastic renormalisation group sum rules 0-22611  
 $\text{SU}(3)$  in  $\text{SO}(3)$  basis, sum rules for matrices of generators 0-13226  
 $T^*$  (10040) as an  $I=1$  vector meson resonance 0-47241  
 two-particle scattering systems, general, sum rules 0-8862  
 vector mesons, leptonic decays, six-quark sequential model 0-52490  
 $A_1$ , spectral function sum rules and  $A_1$ -W coupling const. 0-27429  
 $\chi_{J=1}$ , charmonium states radiative and hadronic widths, gluon spin 0-4998  
 $(e,e'p)$  quasi-free scatt., spectral function, sum rule discrepancy, shell model deviation 0-42641  
 ed scatt., energy weighted sum rules, almost realistic NN pot. anal. (*Russian*) 0-13465  
 $e^+e^-$ , jet cross sections and quark current-photon pointlike coupling, sum rules 0-32104  
 $e^+e^-$  calorimetric experiments,  $\gamma\gamma$  processes, tests of QCD 0-22628  
 eN deep inelastic polarised scatt., QCD corrections 0-52517  
 ep deep inelastic scatt., pol. p and e, straton model, sum rule (*Chinese*) 0-42475  
 $ep \rightarrow \pi^0 X$ , duality and finite energy sum rules 0-42477  
 $\eta$ , QCD sum rules for mass, possible pseudoscalar gluonium, instanton effects 0-388  
 $\gamma\gamma$ , jet cross sections and quark current-photon pointlike coupling, sum rules 0-32104  
 $\gamma p \rightarrow \pi^0 X$ , duality and finite energy sum rules 0-42477  
 $J/\psi \rightarrow \eta(\eta') \gamma$  decay rate, QCD sum rules 0-52497  
 $p\bar{p} \rightarrow \gamma\gamma$  annihilation, influence on sum rule proton polarisability 0-18143  
 $\rho^0$  radiative decay amplitude, low-energy expansion, currents, sum rules 0-52509  
 $^9\text{Be}(\gamma,\pi)$ , photoabsorption and sum rules, structure, RMS radius, polarisability and exchange parameters 0-22686  
 $^2\text{H}(e,e)$ , EM interactions and mag. sum rules 0-42639

**sum rules continued**

- $^2\text{H}(e,e)$ , energy weighted sum rules, almost realistic NN pot. anal. (*Russian*) 0-13465  
 $^4\text{He}$ , superfluid, singular f-sum rule, applicability to inelastic neutron scatt. 0-6577  
 $^7\text{Li}(\gamma,\pi)$ ,  $A=6$ ,  $7$  0-22686  
 $^{18}\text{O}$  1.98 MeV  $2^+$  state static quadrupole moment, from nuclear sum rules 0-13374
- Sun**  
 see also solar .....  
 see also cosmic ray solar modulation  
 brightness distrib. at 8.6 mm, interferometer obs. 0-56800  
 companion star influencing comet orbits 0-31260  
 Einstein effect (gravitational deflection of light), obs. at solar eclipse (1981 July 31) (*Russian*) 0-51651  
 equator orientation errors not cause of sunspot drift oscillation 0-41786  
 mass loss rel. to meteoroid swarm evolution 0-8592  
 models, H-R diagram fits rel. to He content and convective mixing length 0-26835  
 oscillation frequencies, line broadening due to convective fluctuations 0-31293  
 radial velocity, meas. using HF absorpt. cell 0-12681  
 radio obs. of quiet Sun using student-designed radiotelescope, multidisciplinary exercise 0-17759  
 radio radius at centimetre wavelengths, and brightness distrib. across disc 0-21968  
 radio signal retardation by solar gravity, Viking expt. results 0-36933  
 ring of rocky material, hypothesis 0-21961  
 Saturn's rings, thickness caused by satellite and solar perturb. and planetary precession 0-36569  
 semidiameter meas., light deflection effects (*German*) 0-46531  
 solar constant, Smithsonian Astrophysical Observatory program, (1902 to 1962) 0-36606  
 solar motion, vel. and apex determ. from open clusters proper motions 0-46418  
 spectrometric research, automation system for on-line signal processing (*Russian*) 0-12659  
 structure from global studies of 5-min. oscills. 0-26838  
 three-body problem, restricted, families of three-dimens, double-symm. periodic orbits, Sun-Jupiter case 0-26722
- sunlight**  
 see also atmospheric optics; sky brightness  
 absorption in Venus atmosphere 0-46434  
 atmosphere, sunlight scattering, Rayleigh and Mie theory 0-56605  
 atmosphere transmission, 1923 to 1957, from Smithsonian Astrophysical Observatory pyrheliometric meas. 0-17374  
 climate sensitivity to incident radiation vars. 0-56595  
 clouds, solar radiation refl., transmission and absorpt. props. parameterisation 0-56601  
 daily irradiation, ARIMA modelling with constant and seasonal parameters 0-55821  
 direct solar irradiance, indirect meas. 0-45644  
 Earth zonal radiation balance, perturbation by stratospheric aerosol layer 0-56602  
 global solar radiation at Lyon and at Macon, France, for (1978) (*French*) 0-55812  
 insulation modelling, review of solar radiation resource assessments 0-35640  
 intensity, data rehabilitation, SOLMET-2 procedures criticised 0-4071  
 Io Na cloud, solar radiation press. as cause of east-west asymmetries 0-36560  
 Jupiter reflected sunlight, absorpt. bands rel. to atmospheric comp. and cloud struct. deduced from absorpt. bands in refl. sunlight 0-56758  
 monthly mean solar radiation calc. using daily time intervals 0-17353  
 radiation loading on fixed, tracking surfaces, solar energy availability investig. 0-40838  
 radiative transfer under cumulus cloud conditions, Monte Carlo method (*Russian*) 0-21793  
 radiative transfer under fractional cloud cover, two-stream approx. 0-51534  
 reflected sunlight from Venus, polarisation, planetary atm. struct. and comp. determ. 0-36533  
 reflection by clouds, fast azimuthally dependent model 0-51532  
 reflection from Earth, brightness field, atm. transmission function calc. (*Russian*) 0-4105  
 solar constant, Smithsonian Astrophysical Observatory program, (1902 to 1962) 0-36606  
 solar radiation, monthly mean calcs. on vertical and inclined surfaces 0-45746  
 solar radiation characts. and intensity calc. 0-45649  
 solar radiation data, statistical correl. between daily and monthly averages 0-8409  
 solar radiation levels on tilted surfaces, computer model validation 0-35641  
 spectral attenuation at Mauna Loa by aerosols 0-41494  
 total solar radiation at Earth's surface using satellite measurements 0-4147  
 UV meas. and physics 0-41784  
 water suspensions, radiative property measurements 0-9811
- sunshine** see sunlight
- sunspots**  
 see also solar activity  
 annual mean numbers, max. entropy spectral anal., confidence limits 0-22284  
 axisymmetric convection in prescence of mag. field, solar granulation and sunspots appl. 0-12724  
 chromosphere, radial vel. and brightness oscills. regimes (*Russian*) 0-51727  
 convective propulsion of magnetic flux tubes 0-4313  
 coronal magnetic field, struct. rel. to local sources of solar radio emission S-component 0-46528  
 Cycle 21 prediction, comparison with previous cycles (*Chinese*) 0-8608  
 cycle morphology, theory (*Chinese*) 0-12722  
 drift oscillation not explained by solar equator orientation errors 0-41786  
 effects on satellite performance 0-56812  
 faculae and sunspots, mag. field effects on solar luminosity 0-46515  
 flare-sunspot associations rel. to Ha-flare visual features 0-41803  
 granule diameters near penumbra 0-8607  
 group rotation rates 0-41797  
 heat flow in convective downdraught 0-4314



## sunspots continued

- IR opacity due to molecular vibration rotation bands 0-41798  
largest area per solar cycle, statistics 0-41796  
line shifts and asymmetries in sunspot penumbrae 0-51715  
linearly polarised light intensity distribns., influence of magneto-optical effects 0-21965  
magnetic field for August 1972 flare-active region 0-46521  
magnetic fields higher rot. rate at photosphere, Doppler meas. 0-46516  
magnetic flux tube physics, connective overstability in mag. field in down-draft 0-21960  
magnetic flux tubes physics, umbral dots and longitudinal overstability 0-26825  
mass flow in complex sunspot 0-51732  
Maunder Minimum, catalogues of auroral obs. 0-51722  
Maunder Minimum, rel. to Andrew Marvell's poetry 0-12877  
moats, lifetimes from magnetograph obs. 0-21966  
morphological features of large solar active region, 1978 April to May (Chinese) 0-8613  
pores in sunspot groups, proper motion meas. 0-12733  
radiative transfer, through model sunspot 0-21964  
SHF emission at 6 cm wavelength, model 0-51712  
solar cycle 21, sunspot number prediction from polar coronal holes and geomag. activity 0-21979  
turning points and aurorae since (AD 1510) 0-21980  
twisted magnetic fields 0-41799  
umbral area/penumbral area ratio, vars. correl. with Earth climate 0-31272  
umbral brightening assoc. with two-ribbon flare 0-41804  
umbral dots, improved obs. 0-26831  
umbral flashes and overstable magnetoacoustic modes 0-12734  
Wilson effect (Chinese) 0-12721  
Wolf sunspot numbers, freq. anal. and forecasting 0-56797  
X-ray bright points correl. with sunspot intensity, cycle var. 0-41783  
Zurich annual sunspot number link with temp. and precipitation for USA 0-17328  
He I 10830 Å triplet in umbral spectrum (Russian) 0-36604  
MgO red and near UV bands calc. rel. to umbral spectrum 0-12736  
O<sub>2</sub> Schumann-Runge band system in umbral UV spectrum 0-12735

## superaerodynamics see rarefied fluid dynamics

## superalloys

- IN-100, fatigue crack growth retardation at elevated temp. 0-3158  
Inconel 718, environment effect on high temp. fatigue crack growth 0-30090  
Nimonic, IN100,  $\gamma'$  precipitates, casting conditions effect on morphology 0-7548  
Nimonic 80 A, TEM obs. of cellular transformation products 0-3045  
Nimonic 80A, struct., fracture characts. 0-3071  
Rene 95, as hot isostatically pressed (HIP) and HIP+forged, low cycle fatigue 0-25854  
steel, ultrahigh C, superplastic struct. development by heat treatment 0-11703  
Udimet 520, Nicalloy-coated, microstruct. degradation, influence of corrosion protective coating 0-40611  
Al-Cu-Zr, superplastic alloy Supral, solidification and recrystallisation 0-7550  
Co base, cast, high temperature fatigue behaviour 0-40485  
Co-based, low temp. hot corrosion, Na<sub>2</sub>SO<sub>4</sub>-induced, mechanism, burner rig tests 0-40610  
Co-Ni-Cr-Al-Ta, S-57 alloy hot corrosion, cyclic oxidation, depth of attack determinations 0-11837  
Co-Ni-Cr-W-Fe, HA-188 alloy, hot corrosion, cyclic oxidation, depth of attack determinations 0-11837  
Fe alloys, Al-based coatings for high temp. appl., process development and props. 0-40614  
Fe-Ni-Cr-Mo superalloy, mech. props.,  $\eta$ -phase form. effect (Chinese) 0-20925  
Fe-Ni-Cr-ZZ 0-5242  
Ni alloy, IN-100, aluminised, microstruct. degradation, influence of corrosion protective coating 0-40611  
Ni alloys, Si-based coatings for high temp. appl., process development and props. 0-40614  
Ni base superalloy, directionally solidified, struct. and props. (Chinese) 0-20918  
Ni base superalloy, fatigue crack opening load variation with meas. location 0-16425  
Ni base superalloy,  $\gamma'$ -precipitation influence on recrystallisation 0-29955  
Ni based superalloys, sigma phase prediction techniques 0-7567  
Ni-base superalloy, conventional and powder metallurgical,  $\sigma$ -phase precipitation 0-11646  
Ni-base superalloy, effects of grain boundary carbides on creep and back stress 0-3130  
Ni-base superalloy, microscopic inhomogeneity of plastic strain influence on fatigue cracks (German) 0-40470  
Ni-base type IN 718, acoustic emission interpretation of ductile fracture processes 0-35300  
Ni-based, low temp. hot corrosion, Na<sub>2</sub>SO<sub>4</sub>-induced, mechanism, burner rig tests 0-40610  
Ni-based superalloys, TEM obs. of cellular transformation products 0-3045  
Ni-Co-Cr superalloy, powder produced, necklace struct. development 0-40395  
Ni-Co-Cr-Al-Ti-Mo superalloy IN738, caking porosity removal using hydrostatic press. sintering 0-55322  
Ni-Cr-Al-ThO<sub>2</sub>, hot corrosion, cyclic oxidation depth of attack determinations 0-11837  
Ni-Cr-Al-Y<sub>2</sub>O<sub>3</sub> superalloy, recrystn. and texture development 0-16328  
Ni-Cr-Co-Mo-Al, IN-67 alloy, hot corrosion, cyclic oxidation, depth of attack determinations 0-11837  
Ni-Cr-Co-Ti, superalloy sintering thermochemical surface treatment 0-25617  
Ni-Cr-W-Mo-Al-Ti (15,6,3,2,2, wt.%), wrought, Si effect on transition brittleness (Chinese) 0-55491  
Ni-Cr-ZZ 0-5242  
Ni-Fe-Cr base superalloy, addition effect on mech. props. (Chinese) 0-20998  
NiTaC eutectics, high cycle fatigue at room temp. 0-16459  
SiC-Ni based superalloy reaction, at elevated temps. 0-3287  
SiO<sub>2</sub>-base cores, for superalloys, high temp. characterisation 0-10640  
Zn-Al (22 wt.%) superplastic alloy, cavitation and neck form. 0-30022

## superconducting cables

- magnetisation anisotropy meas. in hysteresis loss using Hall sensors 0-17966  
polycarbonate, plastic insulation for cryogenic power cable, exam. of dielectric, tensile props. 0-25823  
polyester (Mylar), plastic insulation for cryogenic power cable, exam. of dielectric, tensile props. 0-25823  
polyethylene, plastic insulation for cryogenic power cable, exam. of dielectric, tensile props. 0-25823  
polyethylenes, dielec. losses, for use in AC superconducting power transmission lines 0-25302  
polypropylene, plastic insulation for cryogenic power cable, exam. of dielectric, tensile props. 0-25823  
polypropylene-polyurethane laminates, meas. of dielectric losses at cryogenic temps. 0-25301  
polysulphone, plastic insulation for cryogenic power cable, exam. of dielectric, tensile props. 0-25823  
Nb<sub>3</sub>Sn monofilamentary wires, supercond. crit. current density, bending effects 0-50018  
Nb<sub>3</sub>Sn, multifilament, production and props. (German) 0-3081

## superconducting critical field

- anisotropic lower critical field, orientation depend. 0-20361  
antiferromagnetic superconductors, new pairing state, pair destruction, theory 0-54847  
dislocation systems, superconducting states, impurity effects (Russian) 0-11131  
filamentary superconductor, upper and lower crit. fields 0-25053  
hard superconductor flux jumps under time depend. external conditions 0-7038  
Josephson self-resonant modes analysis, using mechanical analogue model (Chinese) 0-34563  
layered superconductors, effect of random distortions on crit. field 0-54851  
paramagnetic limit, Fermi surface dielectric gap (Russian) 0-2533  
polysulphur nitride, temp. depend. and anisotropy of H<sub>c2</sub> 0-25054  
rare earth rhodium boride system, ternary, supercond., phase diagrams at upper crit. fields 0-2531  
rare earth ternary compounds, supercond. and antiferromag. coexistence 0-25030  
rare-earth, mag. supercond., appl. of boson theory to mixed state 0-7050  
strong coupling superconductor thin film, critical mag. field (Chinese) 0-54849  
type I superconducting film, cylindrical domain struct. in mag. field 0-15666  
type II superconductor, fluctuations in crit. region near upper crit. field 0-25048  
type-II superconductor, magnetisation, rel. to anisotropy of upper crit. field 0-54832  
Al-formvar superconductive junction, Ginzburg's generalised jellium model 0-15663  
Am, superconducting critical field, sp. ht. 0-11136  
C<sub>6</sub>K, intercalation cpd. with graphite, supercond. props. 0-44755  
Cs<sub>2</sub>WO<sub>6</sub>, normal phase and supercond. props 0-25035  
Cu-Nb<sub>3</sub>Sn superconducting composite, crit. props., AC hysteretic losses 0-50014  
Cu<sub>2</sub>Mo<sub>6</sub>S<sub>8</sub>, supercond., two-phase, upper crit. field meas. 0-29509  
(Er<sub>0.6</sub>Hf<sub>0.4</sub>)Rh<sub>2</sub>B<sub>4</sub>, reentrant supercond., magnetisation meas. near lower crit. temp. 0-25043  
Ga film, crit. transverse mag. fields and transition temp. (Russian) 0-7048  
Hf-V foil, rapidly quenched and heat treated, supercond. props. 0-54852  
I, metallic Al-type modification, normal conductivity and superconductivity 0-20348  
In, divided superconducting thin film, superheating and supercooling field resistive meas. (French) 0-44751  
In<sub>3</sub>Sn, anisotropy of upper crit. field 0-20360  
La<sub>2</sub>S<sub>4</sub>, high crit. mag. field supercond., elec. resist., sp. ht. and magnetisation 0-2532  
Mo-Re,  $\sigma$  phase alloy, critical mag. field, elec. resistance 0-54850  
Nb, critical field, muon spin relaxation (German) 0-50015  
NbB<sub>2</sub>, superconductivity below 1K 0-20342  
Nb<sub>72</sub>Ga<sub>72-x</sub>Mn<sub>x</sub>, supercond. props., influence of Mn mag. impurities 0-54825  
Nb<sub>80</sub>Ga<sub>20-x</sub>Mn<sub>x</sub>, supercond. props., influence of Mn mag. impurities 0-54825  
Nb<sub>1-x</sub>Ge<sub>x</sub>, supercond., mag. field props. 0-54822  
Nb<sub>2</sub>S<sub>4</sub>, anisotropic superconductor, critical field and specific heat meas. 0-44779  
Nb<sub>3</sub>Sn, current carrying capacity increase by Hf addition 0-7056  
Nb<sub>1-x</sub>Ta<sub>x</sub>Sn<sub>2</sub>, supercond. transition temp. and upper crit. field 0-39723  
(Nb<sub>0.99</sub>Ti<sub>0.01</sub>)<sub>1-x</sub>Ge<sub>x</sub>, supercond., mag. field props. 0-54822  
(Nb<sub>0.99</sub>Zr<sub>0.01</sub>)<sub>1-x</sub>Ge<sub>x</sub>, supercond., mag. field props. 0-54822  
Pa, superconducting transition temp. and upper critical mag. field 0-44756  
Pb-In, superconductive to normal transition due to external mag. fields, dynamic behaviour 0-39722  
Pb-Sb, dynamic destruction of supercond. 0-2529  
Rb<sub>2</sub>WO<sub>6</sub>, anisotropy in H<sub>c2</sub> 0-6879  
(SN)<sub>2</sub>, supercond., fluctuation cond., crit. mag. fields 0-39712  
(SNB<sub>0.4</sub>)<sub>x</sub>, supercond. props., dimensionality 0-20344  
SmRh<sub>2</sub>B<sub>4</sub>, coexistence of supercond. and antiferromag. order 0-11140  
Ta, critical field, muon spin relaxation (German) 0-50015  
Ta-N, superconductive to normal transition anisotropy 0-25031  
Tc-Fe dilute alloys, supercond. and mag. props. 0-29494  
Ti<sub>2</sub>Mo<sub>6</sub>Se<sub>6</sub>, one dimensional supercond. crystal struct., resist. and upper crit. field 0-50016  
Y<sub>1-x</sub>Gd<sub>x</sub>Rh<sub>2</sub>B<sub>4</sub>, mag. supercond., anomalous temp. depend. of upper crit. fields 0-29510  
Y<sub>2</sub>O<sub>3</sub>, synthesis at high-pressure and temp., supercond. 0-2513  
Zr-V foil, rapidly quenched and heat treated, supercond. props. 0-54852  
(Zr<sub>1-x</sub>Er<sub>x</sub>)Rh, amorphous, influence of mag. ordering on supercond. props. 0-29511

## superconducting critical temperature see superconducting transition temperature

## superconducting devices

- see also cryotrons  
coil simulation, AC loss meas. 0-37050  
field-emission cathode peak current, size effect 0-29863  
gyroscope, to test Einstein's general theory of relativity 0-8897



**superconducting devices continued**

NMR spectrometer, efficient decoupler coil design to reduce heating in conductive samples 0-31828  
 powered superconductor MM range receiver for radio astronomy 0-21919  
 QED circuits at ultralow temp. 0-13247  
 reference temperature, 0.015 to 0.21K, based on superconducting phase transitions 0-17948  
 superheated superconducting detectors, magnetic field dependence 0-27893  
 thermometer, sensitivity, temp. and field depend. 0-4708

**superconducting energy gap**

A-15 compound, defect influence on  $T_c$  0-20345  
 Cooper coupling, increase due to strong longitudinal sound 0-49990  
 kinetic eqns., nature and decay rate of new mode 0-49978  
 kinetic eqns. for electron excitations and phonons 0-7032  
 magnetic properties of superconductors, effect of insulating pairing of electrons 0-15651  
 metallic thin film, superconducting state realisation 0-49977  
 paramagnetic limit, Fermi surface dielectric gap (*Russian*) 0-2533  
 stability of superconducting states out of thermal equilib. 0-2526  
 Al, energy gap enhancement by tunnelling extraction 0-34564  
 Al-formvar superconductive junction, Ginzburg's generalised jellium model 0-15663  
 Fe-In, superconducting Kondo alloys and alloys with strong electron-magnetic impurity interaction, EM absorpt. of light 0-39711  
 Ga-Ag tunnel junction, evidence for existence of anisotropy of supercond. energy gap 0-20357  
 In-Mn, dilute alloy, local excited states, electron tunnelling observation 0-34565  
 Nb<sub>3</sub>Ge, superconducting thin films, energy gaps from tunnelling meas. 0-25050  
 Nb<sub>3</sub>S<sub>n</sub>, anisotropic superconductor, critical field and specific heat meas. 0-44779  
 Nb<sub>3</sub>Sn, supercond., thin film, US attenuation of SAWs 0-49988  
 Nb<sub>3</sub>Sn, superconducting thin films, energy gaps from tunnelling meas. 0-25050  
 Pb-Cd thin films, electron tunnelling study of supercond. proximity effect 0-2525  
 PbMo<sub>0.5</sub>S<sub>0.5</sub>Gd<sup>3+</sup>, powder EPR spectra, cryst. field, supercond. energy gap 0-34769  
 Pb<sub>1.25</sub>Mo<sub>0.75</sub>Se<sub>7.5</sub>, Chevrel phase supercond., NMR study 0-49989  
 Sn film, energy gap suppression and instability under strong quasiparticle injection 0-7042  
 SnMo<sub>0.5</sub>S<sub>0.5</sub>Gd<sup>3+</sup>, powder EPR spectra, cryst. field, supercond. energy gap 0-34769  
 V/Al-Al<sub>2</sub>O<sub>3</sub>-Pb tunnel junction, superconducting transition, critical currents, Josephson effect (*Russian*) 0-29507  
 V<sub>3</sub>Si, single crystals, supercond. tunnel characts. 0-7044  
 V<sub>3</sub>Si, superconducting thin films, energy gaps from tunnelling meas. 0-25050

**superconducting junction devices**

bidimensional junction lattices, proximity effects (*French*) 0-49998  
 cavity-coupled Josephson device, parametric dependences, I-V characts. 0-20356  
 compact preset SQUID for total field measurement 0-22392  
 DC SQUID, ultra-low-noise tunnel junction, design, fabrication and noise props. 0-29506  
 dirty superconductor-normal metal interface, boundary conditions, potential barriers effects 0-34554  
 edge-grown low-capacitance supercond. tunnel junctions props. 0-54837  
 film structure with degenerate semiconductor bridge, Josephson effect 0-20359  
 impurities in normal metal layer of supercond.-normal metal-supercond. junction, pair penetration depth determ. 0-29508  
 interferometers, threshold curve anal. 0-49999  
 Josephson interferometer flux detrapping by ground plane thickness modulation 0-2523  
 Josephson interferometer resonance amplitude theory, SFQ memory cells 0-27317  
 Josephson junction, finite length, steady oscillatory states 0-44773  
 Josephson junction, mag. flux annihilation 0-11139  
 Josephson junction, oxide formation process, ellipsometric meas. (*Japanese*) 0-11561  
 Josephson junction, sputtering system for fabrication (*Japanese*) 0-55293  
 Josephson junction parametric inductance fluctuations, upconverter 0-25052  
 Josephson junctions, half-harmonic parametric oscils. 0-50001  
 Josephson junctions, long, current thresholds, resonant fluxon propagation, loss, bias, and open-circuit boundary conditions 0-50003  
 Josephson junctions in self-pumping mode of operation, anomalies of freq. conversion 0-54839  
 Josephson junctions mounted in a waveguide, wide-band detect. characts. 0-4767  
 Josephson microbridge, I-V characts. microwave irradiation depend. 0-25051  
 Josephson nondestructive readout RAM cells, design criteria 0-50000  
 Josephson tunnel junction parameters, microwave freq., temp. depend. 0-34561  
 Josephson video-detector, optimisation for mm wavelengths 0-4768  
 microbridge Josephson junction, current-phase relation, size dependence 0-44767  
 microbridges, non-equilib. effects, superconductivity stimulation by RF radiation and DC current (*Russian*) 0-39714  
 point contacts, DC Josephson effect investig. (*German*) 0-39713  
 point-contact Josephson junctions, capsule type, MM-wave video detection 0-13141  
 quasiparticle nonlinear relax. to nonequilibrium state (*Russian*) 0-7040  
 RF-biased SQUID, with half-wavelength transmission line 0-22342  
 S-C-S(N) pure short microjunctions, nonstationary Josephson effect theory (*Russian*) 0-50010  
 short bridges, critical current depend. on high. freq. field 0-44774  
 space applications of LF supercond. sensors inc. SQUID devices 0-56691  
 spectroscopy of high-frequency phonons, transport phenomena, review 0-49325  
 SQUID, DC, voltmeter and magnetometer circuits optimisation 0-13056  
 SQUID, gravitational wave detector, resonant transducer matching between cryogenic antenna and low-noise amplifier 0-46949  
 SQUID, medical application (*Japanese*) 0-12290  
 SQUID, use in NMR spectrometer 0-37064  
 SQUID adjustment using cryostat (*Polish*) 0-31768

**superconducting junction devices continued**

SQUID appls. portable refrigerator 0-27313  
 SQUID in mag. field, stationary and transport currents (*Russian*) 0-50009  
 SQUID using Nb thin film microbridge (*Japanese*) 0-31816  
 superconducting-normal metal-superconducting junction, crit. currents, mag. field depend. 0-50008  
 superconductor-metal-insulator-metal-superconductor system, Josephson current, weak supercond. (*Russian*) 0-54842  
 superconductor-normal metal interface, boundary conditions and critical currents (*Russian*) 0-15665  
 tunnel junction, supercond.-insulator-supercond., optically irradiated, quasiparticle energy distrib. function 0-2527  
 tunnel junction fabrication, two-level e-beam resist process with 1000 Å resolution 0-49996  
 tunnel junction mixers, quantum limited detection 0-18015  
 UHF SQUID magnetometer using coded (4.2K) GaAs FET preamplifier, biased at 430 MHz 0-52282  
 UHF SQUID magnetometer using varactor-tuned 4.2K GaAs FET amplifier 0-31814  
 voltage locking and other interactions in coupled superconducting weak links 0-39719  
 weak link, short, with distinct chem. potentials at boundary 0-2528  
 Ag-Sn proximity-effect bridges,  $T^*$  anomaly under phonon injection 0-34566  
 Ag-Sn proximity-effect bridges, phonon-injection-induced first-order transition obs. 0-39718  
 Al-C-Al sandwich, microwave irradiated, superconductivity at room temp. (*Russian*) 0-11138  
 In superconducting microbridge, voltage locking and other interactions 0-39720  
 In, superconducting-normal interface, boundary resist. 0-50006  
 Nb, nanobridges Josephson effect, quasiparticle diffusion time, inelastic scatt. time 0-34556  
 Nb, superconducting bridges by electron beam lithography and ion implantation Josephson effect 0-20355  
 Nb superconducting point contact, high freq. props. in far IR 0-54840  
 Nb-Nb<sub>3</sub>O<sub>4</sub>-Pb, two-dimens. Josephson junction, supercurrent vs. mag. field characts. 0-34562  
 Nb-NbO<sub>x</sub>-Pb Josephson tunnel junctions, fabrication using FR glow discharge oxidation 0-34559  
 Pb microbridges, two-dimens. imaging of resist. voltage changes caused by electron irradi. 0-15659  
 Pb/Bi-I-Al tunnel injected nonequilibrium supercond. struct., diffusive quasiparticle instability, multiple gap states 0-50005  
 Pb-Sn Josephson junctions, small area high current density normal resistance, RC times 0-34555  
 Pb<sub>0.99</sub>Bi<sub>0.01</sub>-Cd, superconductor-normal-metal boundary resist., mag. field depend. 0-44772  
 Pb<sub>0.99</sub>Bi<sub>0.01</sub>, superconducting-normal interface, boundary resist. 0-50006  
 Sn, and Sn<sub>0.99</sub>In<sub>0.01</sub>, superconducting-normal interface, boundary resist. 0-50006  
 Sn double tunnel junction, film energy gap suppression and instability under strong quasiparticle injection 0-7042  
 Sn film, vac. deposition rate effect on supercond. Josephson tunnel junctions 0-2954  
 Sn superconducting thin-film bridge, IV curves oscill. instability and quasi-particle recomb. (*Russian*) 0-44769  
 V/Al-Al<sub>2</sub>O<sub>3</sub>-Pb tunnel junction, superconducting transition, critical currents, Josephson effect (*Russian*) 0-29507

**superconducting lenses** *see magnetic lenses***superconducting machines**

optimisation, of the refrigerators and liquefiers 0-8994

**superconducting magnets**

*see also superconducting machines*

conductor materials, review (*Japanese*) 0-25042  
 DEALS, demountable superconducting magnet system, for fusion reactors 0-52777  
 dipole, cooled by forced circulation of two-phase He 0-9009  
 emergency cold valve, operating in He II 0-22367  
 energy storage appl., 1970-9 development at Wisconsin University, Madison (USA) 0-26176  
 epoxy impregnated superconducting composites, mech. props., strain effect at 4K 0-25822  
 epoxy resin, for supercond. magnet, deform. rate depend. of mech. props. at cryogenic temps. 0-55456  
 epoxy resin based composites, superconducting magnet insulators, gamma-ray radiation effects 0-24495  
 fusion reactor, field-reversed mirror 0-42857  
 fusion reactor, mirror machine, supercond. mags. 0-42862  
 fusion reactor, reversed-field-pinch, superconducting windings 0-27804  
 fusion reactor large system, structure, insulators, conductors 0-32471  
 fusion reactors, differences between mirror and toroidal fusion systems, superconducting magnets 0-32429  
 gas-cooled current leads 0-37056  
 glass fibre reinforced epoxy, struts for superconductive storage magnets, mech. props. 0-25824  
 glass fibre reinforced polyester, struts for superconductive storage magnets, mech. props. 0-25824  
 glass-epoxy laminate, superconducting magnet insulators, gamma-ray radiation effects 0-24495  
 high current density magnet, thermal stability 0-37057  
 high energy accelerators, superconducting dipole magnets with high field uniformity, development and investigation (*Russian*) 0-5416  
 hybrid magnets for high mag. field generation, polyhelix coils, optimisation calcs. 0-240  
 Kapton (polyimide), insulators for superconducting magnets, effect of low temp. irradiation 0-25817  
 magnetic field inhomogeneity measurement method, Hall probe appln. (*Czech*) 0-13107  
 mirror fusion test facility 0-43962  
 Mylar (polyester), insulators for superconducting magnets, effect of low temp. irradiation 0-25817  
 Nomex (nylon paper), insulators for superconducting magnets, effect of low temp. irradiation 0-25817  
 polycarbonate, insulators for superconducting magnets, effect of low temp. irradiation 0-25817  
 polymer films, superconducting magnet insulators, gamma-ray radiation effects 0-24495



**superconducting magnets continued**

- polypropylene, insulators for superconducting magnets, effect of low temp. irradiation 0-25817  
 portable self-contained refrigerants transfer system, for use with supercond. magnet dewars 0-8993  
 precooling using Cryomech GB02 cryocooler and gas-filled thermal switches 0-52245  
 protection device, with superconducting switch 0-9007  
 solenoid, biaxial sample rot. use (*Czech*) 0-37010  
 solenoid, optimisation of aperture solenoid with rectangular windings 0-4747  
 solid state physics, high mag. fields, generation and application 0-27321  
 space applications 0-37058  
 space applications 0-41694  
 spacers, epoxy resin, powder filled, exam. of mech. props., thermal contraction 0-25821  
 stability, critical current margin design criterion 0-31807  
 systems 0-9008  
 Tokamak toroidal field coils, reduction of bending moments 0-47697  
 transformer-rectifier flux pump using inductive current transfer and thermally controlled Nb<sub>3</sub>Sn cryotrons 0-4727  
 Nb-Ti superconducting magnet system, for short sample test on Tokamak superconductor 0-9010  
 Si(Li) electron spectrometer with superconducting transporting magnets 0-27376  
 V<sub>3</sub>Ga superconducting tape, stress effect on critical current (*Japanese*) 0-50020

**superconducting materials**

- see also composite superconductors; dirty superconductors; strong-coupling superconductors; superconducting semiconductors; superconducting thin films; type I superconductors; type II superconductors  
 AC conductor, cooled by cryogenic liq., heat transfer models 0-5926  
 anisotropic superconductor, functional derivative of critical temp. with electron phonon spectral density 0-49971  
 borides, conference, Varna, Bulgaria (Oct. 1978) 0-12842  
 epoxy impregnated superconducting composites, mech. props., strain effect at 4K 0-25822  
 magnet conductors, review (*Japanese*) 0-25042  
 polysulphur nitride, temp. depend. and anisotropy of H<sub>c2</sub> 0-25054  
 small metal particles ground state energy and orbital mag. susceptibility 0-49983  
 soldering superconducting wire to cryogenic leads, simple repeatable method 0-4728  
 ternary compounds, supercond., p-state pairing and magnetism 0-54819  
 (TMTSF)<sub>2</sub>PF<sub>6</sub>, one dimens. conductor, superconds., resist. meas. and mag. field effects (*French*) 0-44753  
 TTF-TCNQ, effect of benzene ring substitution on supercond. and metallic props. 0-20193  
 CuCl, disordered, diamag. transition 0-34636  
 CuCl, interface superconductivity? 0-39696  
 (SN)<sub>x</sub>, thermopower from 0.15 to 4.2K 0-34427

**superconducting quantum interference devices see superconducting junction devices****superconducting semiconductor materials see superconducting semiconductors****superconducting semiconductors**

- high-temperature electron-hole supercond. 0-2512  
 CuCl, amorphous/cryst. interface, supercond. mechanism 0-44783  
 CuCl, high-temp. supercond., BCS strong-coupling limit for transition temp. 0-2511  
 Ge, amorphous, possible ABB-type excitonic superconductor (*Chinese*) 0-7029  
 Ge, amorphous/cryst. interface, supercond. mechanism 0-44783  
 Si, amorphous, possible ABB-type excitonic superconductor (*Chinese*) 0-7029  
 Si, amorphous/cryst. interface, supercond. mechanism 0-44783

**superconducting thin films**

- acoustic matching to substrates 0-15652  
 contacts, critical currents, density, penetration depth 0-25059  
 ferromagnetic, long reentrant, self-heating-induced phenomena 0-50013  
 hotspot minimum current in long, thin-films superconductors 0-15656  
 melting of two-dimensional vortex lattices 0-2539  
 metal film, effect of chemisorption on supercond. 0-39703  
 metallic, superconducting state realisation 0-49977  
 photoexcited, phonon spectrum 0-11132  
 quasiparticle charge imbalance induced by supercurrent with thermal gradient 0-34546  
 quasiparticle energy distrib. function in optically irradi. films 0-2527  
 rare earth lead molybdenum sulphides, R<sub>x</sub>Pb<sub>1-x</sub>Mo<sub>6-y</sub>S<sub>8</sub>, R=La, Nd, Pr, Gd, sputtered, supercond. props. 0-50019  
 resistive transition 0-7049  
 strong coupling superconductor thin film, critical mag. field (*Chinese*) 0-54849  
 superconducting fluctuation influence on magnetoresistance (*Russian*) 0-54815  
 surface impedance, effects of quasiparticle redistrib. 0-44764  
 tilted vortices, mixed state features in surface layers (*Russian*) 0-29512  
 type I superconducting film, cylindrical domain struct. in mag. field 0-15666  
 type I-superconductors, cylindric superconducting domain lattices in mag. field, lattice stability determ. (*Russian*) 0-44775  
 Al, cylindrical, granular, crit. currents and electron mean free paths 0-7057  
 Al, dielectric coating effect on superconductivity 0-7026  
 Al film, metastable current states, mean free path variation (*Russian*) 0-2538  
 Al films, Al<sup>2+</sup> irradi., increase of resist. and supercond. transition temp. 0-7027  
 Al, superconducting thin film, evidence for Kosterlitz-Thouless transition 0-39721  
 ErRh<sub>2</sub>B<sub>4</sub>, film, sputter deposition and low temp. props. 0-2948  
 Ga film, crit. transverse mag. fields and transition temp. (*Russian*) 0-7048  
 Hg-Xe film, random mixtures, superconducting transition temp. and metal-nonmetal transition 0-29498  
 In, divided superconducting thin film, superheating and supercooling field resistive meas. (*French*) 0-44751  
 In film, metastable current states, mean free path variation (*Russian*) 0-2538  
 LaMo<sub>6</sub>S<sub>8</sub> thin films, crit. currents and pinning forces 0-34575  
 Nb film, critical currents due to microwave field 0-25058

**superconducting thin films continued**

- Nb heteroepitaxial layers on sapphire, residual mechanical stress and strain influence on superconductivity 0-15644  
 Nb, magnetron-sputtered, intrinsic stresses and supercond. props. 0-24772  
 Nb, nanobridges Josephson effect, quasiparticle diffusion time, inelastic scatt. time 0-34556  
 Nb superconducting amorphous film, conductivity and transition temp., ion bombardment effects (*Russian*) 0-49969  
 Nb, superconducting bridges by electron beam lithography and ion implantation Josephson effect 0-20355  
 Nb superconducting films, crit. depairing currents, temp. and mag. field depend. 0-7058  
 Nb, vacuum deposited, deposition parameter effects on crit. temp. 0-2514  
 Nb-Al proximity sandwiches, supercond. transition temp. and tunnelling meas. 0-7045  
 Nb-Ge, Al<sub>15</sub> struct. superconductor, high field transport props. TEM study 0-34574  
 Nb-Ge-Si, Al<sub>15</sub> struct. superconductor, high field transport props. TEM study 0-34574  
 Nb-Ge-Si, CVD, struct., comp., stability and homogeneity 0-15421  
 Nb-NbO<sub>x</sub>-Pb tunnel junctions at 4.2K, conductance of oxide barrier 0-7046  
 NbGe<sub>2</sub>, sputtered, supercond. transition temp. meas. 0-7019  
 Nb<sub>3</sub>Ge, amorphous nongranular thin superconducting film, thermodynamic and resistive transitions 0-34571  
 Nb<sub>3</sub>Ge, energy gap from tunnelling meas. 0-25050  
 Nb<sub>3</sub>Ge, Nb<sub>3</sub>Ge<sub>2</sub> and NbO content, X-ray diffr. obs. 0-2515  
 Nb<sub>3</sub>Ge supercond. film, of high transition temp., US attenuation 0-49991  
 Nb<sub>3</sub>Ge supercond. thin films, He- and Ar-irradiated, X-ray diffr. studies 0-29503  
 Nb<sub>3</sub>Ge superconducting film, crit. temp. correl. with resist. relations and film struct. (*Russian*) 0-15646  
 Nb<sub>3</sub>Ge superconducting films, high critical temp., optimum sputtering conditions 0-15647  
 Nb<sub>3</sub>Ge superconducting films, quantitative Auger anal. 0-55740  
 Nb<sub>3</sub>N granular films, crit. current behaviour 0-15672  
 NbSi<sub>2</sub>, sputtered, supercond. transition temp. meas. 0-7019  
 Nb<sub>3</sub>Si, supercond., Al<sub>15</sub> film, electron beam evaporation 0-29284  
 Nb<sub>3</sub>Sn, atomic displacements induced by radiation damage, X-ray study 0-2085  
 Nb<sub>3</sub>Sn, energy gap from tunnelling meas. 0-25050  
 Nb<sub>3</sub>Sn films, deposition by quasi-closed vol. method, supercond. crit. temp. 0-15645  
 Nb<sub>3</sub>Sn, high-rate sputter-deposited, effect of oxygen on microstruct. 0-20343  
 Nb<sub>3</sub>Sn, O<sup>4+</sup> bombarded, Mossbauer studies 0-2672  
 Nb<sub>3</sub>Sn, supercond., thin film, US attenuation of SAWs 0-49988  
 Nb<sub>3</sub>Sn<sub>4</sub> film, critical currents due to microwave field 0-25058  
 Pb, granular film, superconducting, Josephson-coupled, role of clusters in localisation 0-39716  
 Pb superconducting amorphous film, conductivity and transition temp., ion bombardment effects (*Russian*) 0-49969  
 Pb thin strips, supercond., optical wave illum., critical current behaviour 0-50012  
 Pb/Bi-I-Al tunnel injected nonequilibrium supercond. struct., diffusive quasiparticle instability, multiple gap states 0-50005  
 Pb-Cu contacts, proximity effect (*Russian*) 0-34558  
 Pd, confined geometry, p-wave supercond. or itinerant ferromag. 0-11129  
 PdH<sub>x</sub>(D<sub>x</sub>) films, electron-phonon coupling, elec. cond. obs. 0-50011  
 Re, plasma deposited, from Re<sub>2</sub>(CO)<sub>10</sub> vapour decomp. 0-20799  
 Sb-Te, Al<sub>15</sub>-type, superconductivity 0-29496  
 Si-Au films, quenched condensed, elec. resist. and supercond. 0-54669  
 Sn, energy gap suppression and instability under strong quasiparticle injection 0-7042  
 Sn film, effect of rate of deposition on supercond. props. and struct. 0-2954  
 Sn film, metastable current states, mean free path variation (*Russian*) 0-2538  
 Sn microstrip, optically illuminated, resistive transition and supercond. props. 0-54821  
 Sn, paraconductivity 0-54845  
 Sn, phonon-injection-induced destruction of supercond. 0-6956  
 Sn, superconducting current carrying film, resistive region boundary movement, ambient media depend. 0-44763  
 Sn superconducting thin-film bridge, IV curves oscill. instability and quasi-particle recomb. (*Russian*) 0-44769  
 Sn-Sb, Al<sub>15</sub>-type, superconductivity 0-29496  
 TaGe<sub>2</sub>, sputtered, supercond. transition temp. meas. 0-7019  
 TaSi<sub>2</sub>, sputtered, supercond. transition temp. meas. 0-7019  
 Tc film, supercond. transition, complex susceptibility 0-29495  
 Te-Au, ion irradi. induced supercond. 0-34544  
 Te-I, Al<sub>15</sub>-type, superconductivity 0-29496  
 U<sub>x</sub>Pb<sub>1-x</sub>Mo<sub>6-y</sub>S<sub>8</sub>, sputtered supercond. props. 0-50019  
 V film, resist. supercond. transition 0-25033  
 V<sub>3</sub>Si, energy gap from tunnelling meas. 0-25050  
 V<sub>3</sub>Si, ion irradiated, influence on struct., resist., and supercond. transition temp. 0-54823  
 Y<sub>x</sub>Pb<sub>1-x</sub>Mo<sub>6-y</sub>S<sub>8</sub>, sputtered supercond. props. 0-50019

**superconducting transition temperature**

- A-15 compound, defect influence on T<sub>c</sub> 0-20345  
 A-15 compounds, disordered, T<sub>c</sub> depression, appl. to Nb<sub>3</sub>Ge 0-7020  
 A-15 diffusion layers, influence of additions of growth and supercond. props. (*German*) 0-11130  
 A-15 type compounds, relation between martensitic and supercond. phase transition 0-29497  
 anisotropic superconductor, functional derivative of critical temp. with electron phonon spectral density 0-49971  
 critical dynamics far from equilibrium 0-27258  
 critical temperature depend. on radiation defects, electron density of states calcs. 0-44758  
 critical temperature mag. field depend., strong diamagnetism (*Russian*) 0-7022  
 cybernetic prediction of supercond. cpds. 0-39697  
 dipstick cryostat, with temp. controller for high thermal stability 0-37044  
 dirty layer superconductors, fluctuation sound attenuation, depend. on critical temp. (*Russian*) 0-34553



**superconducting transition temperature continued**

- dislocation systems, superconducting states, impurity effects (*Russian*) 0-11131
- graphite, phonon thermal conductivity, rel. to elec. cond., possible supercond. 0-49434
- high-Tc superconductors role of quasilocated excitations 0-2508
- high-temperature electron-hole supercond. 0-2512
- Josephson tunnel junction parameters, microwave freq., temp. depend. 0-34561
- magnetic properties of superconductors, effect of insulating pairing of electrons 0-15651
- melting of two-dimensional vortex lattices 0-2539
- metal film, effect of chemisorption on supercond. 0-39703
- metal-semiconductor interface, disordered, supercond. 0-20347
- metallic thin film, superconducting state realisation 0-49977
- metals, triplet supercond. transition in strong mag. field 0-25040
- one-dimensional systems, impurity effects on ordered phases 0-24905
- paramagnetic limit, Fermi surface dielectric gap (*Russian*) 0-2533
- periodic lattice, theory of coexistence of supercond. and magnetism, supercond. transition temp. 0-34543
- perturbative corrections, direct and indirect ladder diagrams 0-49979
- phonon spectrum, generalised moments, in Allen-Dynes formula for crit. temp. (*French*) 0-39702
- polysulphur nitride, low temp. thermal cond. 0-24689
- polysulphur nitride, temp. depend. and anisotropy of  $H_{c2}$  0-25054
- pseudopotential, Bragg planes, effect on superconducting pairing and crit. temp. 0-15648
- rare earth cpds.,  $RRh_4B_4$  and  $RMo_6X_8$  ( $X=S, Se$ ), mag. order and supercond., neutron scatt. studies 0-44807
- rare earth iridium borides,  $RIr_4B_4$ , supercond., magnetism and metastability 0-29501
- rare earth iron silicides,  $R_2Fe_3Si_5$ , superconductivity 0-49968
- rare earth lead molybdenum sulphides,  $R_2Pb_{1-x}Mo_{6+y}S_8$ ,  $R=La, Nd, Pr, Gd$ , sputtered, supercond. props. 0-50019
- rare earth molybdenum chalcogenides, Chevrel phase correlation between struct. and supercond. transition temp. 0-7023
- rare earth rhodium borides,  $RRh_4B_4$ , NMR and sp. ht. in supercond. and mag. ordered phases 0-7037
- second order phase transitions, superspace group description (*Chinese*) 0-8942
- semimetal, mixed superconducting-excitonic insulator phase, diamagnetism, virtual intraband transitions 0-2520
- series formula of supercond. critical temp. applications (*Chinese*) 0-54816
- strong coupling supercond., transition temp. eqn. 0-25032
- strong coupling superconductors, critical temperature formula discussion (*Chinese*) 0-7017
- strong-coupling superconductors, press. coeffs. of critical field, Ginzburg-Landau parameter, penetration depth 0-54833
- superconductivity-ferromagnetism coexistence, transition temp., magnon freq., indirect exchange 0-44757
- ternary compounds, supercond., p-state pairing and magnetism 0-54819
- tilted vortices, mixed state features in surface layers (*Russian*) 0-29512
- (TMTSF) $_2PF_6$ , one dimens. conductor, superconds., resist. meas. and mag. field effects (*French*) 0-44753
- (TMTSF) $_2PF_6$ , organic one-dimensional superconductor, transition temp. 0-44754
- transition metal-metalloid glasses, struct., elec., supercond., and mech. props. 0-6365
- transition metals, amorphous, superconducting transition temp. (*Chinese*) 0-54817
- transition metals, supercond. transition temp., ab initio calc. 0-25036
- tungsten bronzes, hexagonal, supercond. and special phonons, neutron scatt. obs. 0-15643
- type II materials, radiation-induced changes in crit. props., radiation defects (*Russian*) 0-25027
- Ag-In (Sn) multilayers, vapour quenched, supercond. transition temp. 0-20346
- Al, energy gap enhancement by tunnelling extraction 0-34564
- Al films,  $Al^{2+}$  irradi., increase of resist. and supercond. transition temp. 0-7027
- Al strips, microwave-enhanced supercond. meas. 0-2509
- Al, superconducting transition, effect on jump-like deform. (*Russian*) 0-34538
- Al thin films, dielectric coating effect on superconductivity 0-7026
- $BaGe_2$ , superconducting temperature depression due to mag. field 0-54820
- $Ba_{1-x}Sr_xPb_{0.75}Bi_{0.25}O_3$ , superconductivity, rel. to lattice const. 0-49966
- Bi, band structure model 0-25034
- $C_8K$ , intercalation cpd. with graphite, supercond. props. 0-44755
- Cd, electronic properties depend. on  $2/2'$ -th order phase transition under high press. (*Russian*) 0-11128
- $CeCu_2Si_2$ , strong Pauli paramagnetism, superconductivity obs. 0-29499
- $Ce_{0.7}Ho_{0.3}Ru_2Co$ , spontaneous mag. order below superconducting transition temp., Mossbauer study 0-39701
- $CeRu_2$ , H absorption induced Ce valence change, mag. and supercond. props. 0-50042
- $Cs_2WO_3$ , normal phase and supercond. props. 0-25035
- Cu-Ga porous solid formed by shock compression 0-29905
- Cu-Nb-Sn system, phase equilibria and supercond. props. (*Russian*) 0-50589
- Cu-V-Si, two-step supercond. transition 0-34539
- CuCl, high-temp. supercond., BCS strong-coupling limit for transition temp. 0-2511
- ( $Er_{1-x}Ho_x$ ) $Rh_4B_4$ , superconductive and mag. interactions, hydrostatic press. effect 0-49973
- $ErRh_4B_4$ , film, sputter deposition and low temp. props. 0-2948
- $Er_2Y_{1-x}Rh_4B_4$ , supercond. phase transitions, recentering temp. to normal ferromag. state 0-7024
- e-Fe, low temp. supercond., transition temp. estimated 0-34540
- $FeMo_6S_8$ , mixed Chevrel phases, crystallography 0-39038
- $FeZnMo_6S_8$ , mixed Chevrel phases, crystallography 0-39038
- Ga film, crit. transverse mag. fields and transition temp. (*Russian*) 0-7048
- HfV $_2$ , C-15 struct., phase transitions, elec. cond., crystal lattice parameters (*Russian*) 0-54826
- Hg-Xe film, random mixtures, superconducting transition temp. and metal-nonmetal transition 0-29498
- I, metallic A1-type modification, normal conductivity and superconductivity 0-20348
- In, Lifshits transition, electron-phonon interaction 0-29502

**superconducting transition temperature continued**

- In-Mg, ordered equiatomic, lattice specific heat meas., Debye temp., superconducting transition 0-54396
- In-Sn alloy, Lifshits transition, electron-phonon interaction 0-29502
- La particles, supercond. props. (*Russian*) 0-7018
- ( $LaNd$ ) $Sn_3$ , containing Nd impurities, supercond. and normal state props. 0-49967
- $LaRu_2$ , H absorption induced Ce valence change, mag. and supercond. props. 0-50042
- $LiTi_2O_4$ , single-phase, prep., crystal struct. and superconducting transition characts. 0-50583
- Mo-Re,  $\sigma$  phase alloy, critical mag. field, elec. resistance 0-54850
- ( $Mo_{0.6}Ru_{0.4}$ ) $B_{18}$ , supercond. metallic glass, neutron irradi. effects 0-29060
- Nb film, magnetron-sputtered, intrinsic stresses and supercond. props. 0-24772
- Nb film, vac. deposited, deposition parameter effects on crit. temp. 0-2514
- Nb heteroepitaxial layers on sapphire, residual mechanical stress and strain influence on superconductivity 0-15644
- Nb, optical props. and electron-phonon interactions 0-2510
- Nb, plastic deformation effects on superconducting specific heat transition 0-20352
- Nb, spin fluctuations effect on  $T_c$ , from sp. ht. and mag. suscept. 0-7030
- Nb superconducting amorphous film, conductivity and transition temp., ion bombardment effects (*Russian*) 0-49969
- Nb, superconducting bridges by electron beam lithography and ion implantation Josephson effect 0-20355
- Nb/Cu-Sn-Mg, superconductor, effect of Mg addition to Cu-Sn matrix 0-25028
- Nb-Al proximity sandwiches, supercond. transition temp. and tunnelling meas. 0-7045
- Nb-Ga-Fe ternary system, phase equilib. at 1000°C, supercond. transition temp. 0-35158
- Nb-Ge, A15 struct. superconductor, high field transport props. TEM study 0-34574
- Nb-Ge, supercond. A-15 phase, supercond. transition temp. after ion implantation 0-49972
- Nb-Ge-Cu, phase equilib. and supercond. props. (*Russian*) 0-40332
- Nb-Ge-Ni, phase composition and superconducting props., influence of Ni (*Russian*) 0-20898
- Nb-Ge-Si, A15 struct. superconductor, high field transport props. TEM study 0-34574
- Nb-Mo system, electron-phonon coupling const. and supercond. transition temp., average T-matrix approx. 0-39707
- Nb-Pt-O system, phase equilibria, diagram, unit cell parameters, supercond. 0-55352
- Nb $_3$ Al core wires and pressed powder compacts, supercond. transition 0-34541
- Nb $_3$ As, structural and supercond. props. press. effects 0-39700
- NbB $_2$ , superconductivity below 1K 0-20342
- NbC, electronic struct. of vacancies, effect on supercond. transition temp. 0-29347
- NbC(N), critical temp. enhancement, surface effect on phonon spectrum and electronic state density (*Chinese*) 0-2507
- $Nb_{78}Ga_{22-x}Mn_x$ , supercond. props., influence of Mn mag. impurities 0-54825
- $Nb_{80}Ga_{20-x}Mn_x$ , supercond. props., influence of Mn mag. impurities 0-54825
- NbGe $_2$ , superconducting transition temp. meas. of sputtered films and bulk 0-7019
- Nb $_1-x$ Ge $_x$ , supercond., mag. field props. 0-54822
- Nb $_3$ Ge, amorphous nongranular thin superconducting film, thermodynamic and resistive transitions 0-34571
- Nb $_3$ Ge, and Nb $_{0.82}$ , structural and supercond. props. press. effects 0-39700
- Nb $_3$ Ge supercond. film, of high transition temp., US attenuation 0-49991
- Nb $_3$ Ge supercond. thin films, He- and Ar-irradiated, X-ray diffr. studies 0-29503
- Nb $_3$ Ge, superconducting A-15 type compounds, transition temp., radii ratio and structure (*Chinese*) 0-44752
- Nb $_3$ Ge superconducting film, Nb $_3$ Ge $_2$  and NbO content, X-ray diffr. obs. 0-2515
- Nb $_3$ Ge superconducting film, crit. temp. correl. with resist. relations and film struct. (*Russian*) 0-15646
- Nb $_3$ Ge superconducting films, high critical temp., optimum sputtering conditions 0-15647
- Nb $_3$ Ge(Sn), optical props. and electron-phonon interactions 0-2510
- NbSe $_3$ , Fermi surface, press. effects, supercond. transition at 3.5K 0-20068
- NbSe $_3$ Zr, dopant effect on supercond. transition temp. rel. to CDW 0-39699
- NbSi $_2$ , superconducting transition temp. meas. of sputtered films and bulk 0-7019
- Nb $_3$ Si, high T $_c$ , supercond. props. from extrapolation of sp. ht. meas. on A-15 Nb-Si 0-25045
- Nb $_3$ Si, metastable A-15 struct. synthesis by ion implantation, supercond. transition temp. 0-55319
- Nb $_3$ Si, structural and supercond. props. press. effects 0-39700
- Nb $_3$ Si, superconducting A-15 type compounds, transition temp., radii ratio and structure (*Chinese*) 0-44752
- Nb $_3$ Sn, A-15 struct. Nb based superconductors, irradi. type influence on radiation defects 0-15093
- Nb $_3$ Sn, alloying agent influence on struct. and supercond. props. (*Russian*) 0-39698
- Nb $_3$ Sn, Cu admixture in Sn bath effect on critical current and stability temp. 0-7059
- Nb $_3$ Sn films, deposition by quasi-closed vol. method, supercond. crit. temp. 0-15645
- Nb $_3$ Sn, high-rate sputter-deposited, effect of oxygen on microstruct. 0-20343
- Nb $_3$ Sn, O $^{4+}$  bombarded, Mossbauer studies, supercond. transition determ. 0-2672
- Nb $_3$ Sn, supercond., thin film, US attenuation of SAWs 0-49988
- Nb $_{1-x}Ta_xSn_2$ , supercond. transition temp. and upper crit. field 0-39723
- ( $Nb_{0.99}Ti_{0.01}$ ) $_{1-x}Ge_x$ , supercond., mag. field props. 0-54822
- ( $Nb_{0.99}Zr_{0.01}$ ) $_{1-x}Ge_x$ , supercond., mag. field props. 0-54822
- Pa, superconducting transition temp. and upper critical mag. field 0-44756



**superconducting transition temperature continued**

- Pb superconducting amorphous film, conductivity and transition temp., ion bombardment effects (*Russian*) 0-49969  
 Pb-Cd thin films, electron tunnelling study of supercond. proximity effect 0-2525  
 Pb-Sn system, soft solder, elec. and thermal cond. at low temps., superconducting transition temp. 0-20150  
 PbMo<sub>6</sub>S<sub>8</sub>(Se<sub>8</sub>)(Te<sub>8</sub>), Chevrel phase correlation between struct. and supercond. transition temp. 0-7023  
 Pd-H(D), superconductivity and electron-phonon interaction 0-49975  
 PdH, supercond., book contrib. 0-25037  
 PdH<sub>0.97</sub>Fe(Cr), supercond. transition temp. depression, coexistent mag. behaviour 0-49976  
 PdH<sub>2</sub>(D<sub>x</sub>) films, electron-phonon coupling, elec. cond. obs. 0-50011  
 Rb<sub>2</sub>WO<sub>3</sub>, anisotropy in H<sub>2</sub> 0-6879  
 (SN)<sub>x</sub>, brominated, struct. and elec. props. 0-24914  
 (SN)<sub>x</sub>, thermopower from 0.15 to 4.2K 0-34427  
 (SNBr<sub>0.4</sub>)<sub>x</sub>, supercond. props., dimensionality 0-20344  
 Sb-Te, Al-type, superconductivity 0-29496  
 Si-Au films, quenched condensed, elec. resist. and supercond. 0-54669  
 Sn-Bi, crystal struct. and superconductivity after appl. of high press. and quenching 0-10531  
 Sn-Sb, Al-type, superconductivity 0-29496  
 (Sn)<sub>x</sub>, superconducting polymer, elec. cond., heat capacity and optical props. 0-7028  
 SnMo<sub>6</sub>S<sub>8</sub>, mixed Chevrel phases, crystallography 0-39038  
 SnMo<sub>6</sub>S<sub>8</sub>(Se<sub>8</sub>)(Te<sub>8</sub>), Chevrel phase correlation between struct. and supercond. transition temp. 0-7023  
 SrSi<sub>2</sub>, superconducting temperature depression due to mag. field 0-54820  
 Ta-N, superconductive to normal transition anisotropy 0-25031  
 TaGe<sub>2</sub>, superconducting transition temp. meas. of sputtered films and bulk 0-7019  
 TaS<sub>2</sub>, alkali metal and alkali metal hydroxide intercalates, lattice parameters, supercond. transition temps. 0-25029  
 TaSi<sub>2</sub>, superconducting transition temp. meas. of sputtered films and bulk 0-7019  
 Tc film, supercond. transition, complex susceptibility 0-29495  
 Tc-Fe dilute alloys, supercond. and mag. props. 0-29494  
 Te-Au film, supercond. by ion irradi. 0-34544  
 Te-I, Al-type, superconductivity 0-29496  
 Th-H system, supercond., book contrib. 0-25037  
 ThH<sub>15</sub>, superconductivity and electron-phonon interaction 0-49975  
 Ti<sub>1-x</sub>Co<sub>x</sub>, electronic struct. and anomalies of elec. and mag. props. 0-6710  
 Ti<sub>1-x</sub>Ni<sub>x</sub>, electronic struct. and anomalies of elec. and mag. props. 0-6710  
 α-U-Mo, dil., electronic properties depend. on 2<sup>1</sup>/<sub>2</sub>-th order phase transition under high press. (*Russian*) 0-11128  
 U<sub>1-x</sub>Pb<sub>x</sub>Mo<sub>6</sub>+<sub>8</sub>S<sub>8</sub>, sputtered supercond. props. 0-50019  
 V film, resist. supercond. transition 0-25033  
 V, spin fluctuations effect on T<sub>c</sub>, from sp. ht. and mag. suscept. 0-7030  
 V/Al-Al<sub>2</sub>O<sub>3</sub>-Pb tunnel junction, superconducting transition, critical currents, Josephson effect (*Russian*) 0-29507  
 V<sub>1-x</sub>Cr<sub>x</sub>Si<sub>2</sub>, x=0 to 3, struct., supercond. and mag. props. 0-1962  
 V<sub>2</sub>Ge, A-15 cpds., nucl. mag. relax. in normal and supercond. state 0-49993  
 V<sub>2</sub>Ge, anisotropic thermal vibrations, lattice const. X-ray study 0-34164  
 V<sub>2</sub>Ge, superconducting A-15 type compounds, transition temp., radii ratio and structure (*Chinese*) 0-44752  
 VN, electronic struct. of vacancies, effect on supercond. transition temp. 0-29347  
 VN<sub>0.74</sub> and VN<sub>0.89</sub>, low-temp. specific heat and superconducting critical temp. meas., density of states 0-54835  
 V<sub>1-x</sub>Pt<sub>x</sub>(Ga<sub>1-x</sub>Si<sub>x</sub>), A-15 cpds., nucl. mag. relax. in normal and supercond. state 0-49993  
 V<sub>2</sub>Si, ion irradiated, influence on struct., resist., and supercond. transition temp. 0-54823  
 V<sub>2</sub>Si, optical props. and electron-phonon interactions 0-2510  
 V<sub>2</sub>Si, plastic deform. effect on supercond. props. 0-29500  
 V<sub>2</sub>Si, US anomaly when cooled below martensitic and supercond. transition temps. 0-20354  
 V<sub>2</sub>(Si<sub>1-x</sub>C<sub>x</sub>)<sub>2</sub>, bulk, effect of C on supercond. transition temps. and microstructure 0-54824  
 (V<sub>1-x</sub>Ti<sub>x</sub>)Ge, pseudobinary A15 compound, supercond. transition temp. 0-49970  
 (Y,La)B<sub>6</sub>, superconducting transition temps., impurity effects 0-20341  
 Y<sub>1-x</sub>Lu<sub>x</sub>Ir<sub>4</sub>B<sub>4</sub>, supercond., magnetism and metastability 0-29501  
 Y<sub>2</sub>O<sub>3</sub>, synthesis at high-pressure and temp., supercond. 0-2513  
 Y<sub>1-x</sub>Pb<sub>x</sub>Mo<sub>6</sub>+<sub>8</sub>S<sub>8</sub>, sputtered supercond. props. 0-50019  
 YRh<sub>4</sub>B<sub>4</sub>, supercond., anomalous cond.-electron polaris. 0-25047  
 ZnMo<sub>6</sub>S<sub>8</sub>, mixed Chevrel phases, crystallography 0-39038  
 Zr<sub>x</sub>Be<sub>1-x</sub>, noncrystalline alloy, phonon-electron scatt., superconducting temp. 0-54330  
 Zr<sub>2</sub>Hf<sub>1-x</sub>V<sub>2</sub>, polycrystalline superconductor, resist. and mag. susceptibility, transition temp., temp. depend. 0-25113  
 ZrV<sub>2</sub>, C-15 struct., phase transitions, elec. cond., crystal lattice parameters (*Russian*) 0-54826

**superconductive tunnelling**

- see also Josephson effect; proximity effect; superconducting junction devices; tunnelling spectra; tunnelling spectroscopy  
 A15 type compound, props. and one-dimensionality 0-2530  
 branch-imbalance relaxation times 0-20358  
 dirty type I superconductors, Al-Formvar-Sn junctions, mode propagation, well below Al transition temp. 0-15662  
 dynamical problems, approx. Hamiltonian, variational method (*Chinese*) 0-44768  
 junction, two-band model 0-2524  
 metal-semiconductor interface, disordered, supercond. 0-20347  
 quasiparticle charge imbalance induced by supercurrent with thermal gradient 0-34546  
 ring with low capacitance Josephson point contact junction, flux transition mechanisms 0-44770  
 stability of superconducting states out of thermal equil. 0-2526  
 superconducting-normal interface, boundary resist. 0-50006  
 Al, superconducting, quasiparticle charge distrib. due to tunnel injection 0-44771  
 Al-formvar superconductive junction, Ginzburg's generalised jellium model 0-15663  
 Ga-Ag tunnel junction, evidence for existence of anisotropy of supercond. energy gap 0-20357

**superconductive tunnelling continued**

- In-Mn, dilute alloy, local excited states, electron tunnelling observation 0-34565  
 Nb-NbO<sub>2</sub>-Pb tunnel junctions at 4.2K, conductance of oxide barrier 0-7046  
 Nb<sub>2</sub>Ge, superconducting thin films, energy gaps from tunnelling meas. 0-25050  
 Nb<sub>2</sub>Sn, superconducting thin films, energy gaps from tunnelling meas. 0-25050  
 Nb<sub>2</sub>Zr<sub>80</sub>, supercond., US attenuation 0-44766  
 Pb/Bi-I-Al tunnel injected nonequilibrium supercond. struct., diffusive quasiparticle instability, multiple gap states 0-50005  
 Pb-Cd thin films, electron tunnelling study of supercond. proximity effect 0-2525  
 Pb-Fe multilayers, zero pair pot. verification by supercond. tunnelling 0-54841  
 Pb-Si:Sb Schottky tunnel junction, variable range hopping assisted tunnelling 0-39670  
 PdH<sub>2</sub>(D<sub>x</sub>) films, electron-phonon coupling, elec. cond. obs. 0-50011  
 PdZr, amorphous, supercond., US props. 0-44765  
 Sn, superconducting film, energy gap suppression and instability under strong quasiparticle injection 0-7042  
 V<sub>2</sub>Si, single crystals, supercond. tunnel characts. 0-7044  
 V<sub>2</sub>Si, superconducting thin films, energy gaps from tunnelling meas. 0-25050
- superconductivity**  
 see also BCS theory; coherence length; composite superconductors; Cooper pairs; critical currents; dirty superconductors; fluctuations in superconductors; Ginzburg-Landau theory; Meissner effect; penetration depth (superconductivity); strong-coupling superconductors; superconducting critical field; superconducting devices; superconducting energy gap; superconducting materials; superconducting transition temperature; superconductive tunnelling; type I superconductors; type II superconductors  
 A-15 type compounds, props. and one-dimensionality, book 0-3  
 absorbed film, disordering due to supercond. transition in metal substrate 0-50022  
 AC superconductor, uniform, behaviour of normal zones 0-11127  
 amorphous superconductivity (*Chinese*) 0-44759  
 biological materials, remanent magnetization as evidence for room temp. superconduction 0-35926  
 branch-imbalance relaxation times 0-20358  
 current variation with gravitational field variation, general relativistic phenomenological theory 0-54827  
 dislocation systems, superconducting states, impurity effects (*Russian*) 0-11131  
 electrically conducting body, forces in mag. field using hydrodynamic analogy 0-34551  
 electron-phonon system, parallel spin electron-electron interaction 0-10622  
 Fermi liquids at surfaces quasiclassical boundary conditions 0-4641  
 ferromagnet, magnetic ordering, spin wave dispersion (*Russian*) 0-54818  
 ferromagnetic superconductor, mag. domain struct., sample thickness effects 0-39704  
 ferromagnetic superconductor, uniaxial, domain struct. parameters 0-39705  
 ferromagnetic superconductors, phase transitions, renormalisation group treatment 0-29505  
 filamentary superconductor, upper and lower crit. fields 0-25053  
 hard superconductor flux jumps under time depend. external conditions 0-7038  
 HF cut offs of Coulomb interaction, real freq. Coulomb pseudopotential derivation 0-49980  
 kinetic eqns., nature and decay rate of new mode 0-49978  
 layered compound, supercond. and charge-density waves 0-34542  
 magnetic fields, calculation method from boundary conditions (*Ukrainian*) 0-34545  
 magnetic instability of superconducting wire in the changing magnetic field 0-34569  
 magnetic superconductor, Fermi surface nesting effect on mag. instability 0-54831  
 magnetic superconductor, spin-spiral ordering 0-2517  
 magnetic superconductor, thermodynamics of magnetism and supercond., mol. field theory 0-34668  
 metal-H systems at high H press., physicochemical props., book contrib. 0-24535  
 non-equilibrium superconductivity 0-44762  
 nonequilibrium distribution, electron-electron collisions effect (*Russian*) 0-7033  
 nonequilibrium phenomena in superconductors, review 0-49982  
 nonequilibrium superconductors, T\* model of quasiparticle and phonon distrib. 0-25039  
 nonequilibrium superconductors, microscopic and Boltzmann eqn. approach 0-15649  
 nonequilibrium superconductors hypersound enhancement (*Russian*) 0-34552  
 phase slip centre, charge imbalance waves and nonequilib. dynamics 0-54830  
 phenomenological generalised theory, superdiamagnet theory (*Russian*) 0-7031  
 plastic deformation of superconductors, Cooper pair scatt. model 0-39709  
 polyvalent metals, Brillouin zone boundary influence on Coulomb interactions 0-24827  
 practical applications of superconductivity 0-49965  
 quantum defects, electron defect interactions (*Russian*) 0-15650  
 rare-earth, mag. supercond., appl. of boson theory to mixed state 0-7050  
 response functions of superconductors and <sup>3</sup>He(B), autocorrelation functions of density and transversal current, acoustic and quasihomogeneous 0-49449  
 response functions of superconductors and <sup>3</sup>He(B), density and current correlation functions 0-49448  
 small superconductor, phase transitions in mag. field, book 0-3  
 small superconductor in magnetic field, first and second order phase transitions 0-2519  
 space applications 0-41694  
 sphere rot. in mag. field, induced EM field (*German*) 0-54828  
 spin glasses, superconductivity, total compensation of paramag. effect 0-7021  
 superconductivity, general relativistic phenomenological theory 0-2518  
 superconductivity and elementary particles theory, review 0-4911



**superconductivity continued**

- superstructures, condensate band spectrum and current carrying states anal. (*Russian*) 0-39706
- symposium contrib., Florida, USA (March 1979) 0-51946
- terminology for practical superconductors 0-7034
- thermal conductivity at Lifshitz electronic transition point (*Russian*) 0-11135
- thermoelectric and acoustoelectric effects, influence of mutual drag of excitations and phonons 0-44761
- thermoelectric effects in superconductors, general and theoretical anal., review 0-11133
- two-band system, coexistence of dielec. and supercond. ordering 0-10853
- weak superconductor with current in external mag. field, free energy 0-25046
- Nb/H, heat capacity and supercond. between 1.5 and 16K 0-2521
- Pb-Sb, dynamic destruction of supercond. 0-2529
- $\text{PdAg}_{1-x}$ , possibility of superconductivity 0-10862
- V/H, heat capacity and supercond. between 1.5 and 16K 0-2521
- $\text{Y}_2\text{O}_3$ , synthesis at high-pressure and temp., supercond. 0-2513
- $\text{ZrZn}_2$ , phonon contrib. to Stoner enhancement factor, ferromag. and possible superconductivity 0-25070

**superconductors see superconducting materials; superconductivity****supercooling**

- benzyl benzoate, supercooled, depolarised lines in quasielastic light scatt. 0-45095
- crystallisation of supercooled liquid in sound field, steady-state dynamics 0-15223
- eutectic colony growth, supercooling dynamics, stability in presence of external perturbations (*Russian*) 0-16291
- gases, high velocity flows, nonequilibrium homogeneous condensation, determ. of maximal supercooling 0-6086
- glass transition, soft-sphere model, mol. dynamics study 0-49343
- inorganic hydrate, solidification, heat transfer processes (*Japanese*) 0-6372
- Lennard-Jones liquid, mol. dynamics studies of glass form. 0-38896
- metals, supercooling on homogeneous crystn. (*Russian*) 0-19914
- steam, thermodynamic props., virial eqn. of state 0-14872
- steel, pearlitic and bainitic transformations in austenite, processes during incubation period 0-40348
- supercooled, struct. refinement mech. (*Russian*) 0-20975
- water, appl. of polychromatic correlated site percolation 0-22296
- Al alloys, liquid, kinematic viscosity temp. depend., porosity, H solubility, supercooling (*Russian*) 0-54425
- Al kinematic viscosity temp. depend. porosity, H solubility, supercooling (*Russian*) 0-54425
- Al, liquid, kinematic viscosity temp. depend., porosity, H solubility, supercooling (*Russian*) 0-54425
- $\text{Ca}(\text{NO}_3)_2 \cdot \text{H}_2\text{O}$  system, induction period supercooling depend. meas. 0-19918
- Co-C alloys, graphite nucleation on surface (*Russian*) 0-40360
- $\text{D}_2\text{O}$ , appl. of polychromatic correlated site percolation 0-22296
- $\text{Dy}_2\text{O}_3$ , soln. in  $\text{K}_2\text{O} \cdot 2(3)\text{MoO}_3$ , rel. supersaturation and supercooling 0-40245
- Fe-Mg, cast ferrite-based, graphite nucleation on surface (*Russian*) 0-40360
- Hg, liquid structure, X-ray diff. obs., 173-473K 0-14997
- $\text{Na}_2\text{S}_2\text{O}_8 \cdot \text{SH}_2\text{O}$ , solidification, heat transfer processes (*Japanese*) 0-6372
- $\text{NdAl}[\text{BO}_3]_4$ , single phase crystallisation region from solvent melt 0-38977
- Ni alloy powder, crystallised by supercooling methods, struct. props. (*Russian*) 0-54483
- Ni, supercooled, struct. refinement mech. (*Russian*) 0-20975
- Ni-C alloys, graphite nucleation on surface (*Russian*) 0-40360
- Pb, supercooled liquid thin films, liq. struct. factor determ. by STEM 0-10487
- steel, high C, graphite nucleation on surface (*Russian*) 0-40360
- ZnAl (18.75 wt.%), supercooling phase  $\beta$  break up kinetics (*Polish*) 0-25654

**superexchange interactions**

- 1,4-dibromonaphthalene, highly disordered quasi-one-dimens., excitation transport 0-34961
- insulating solids, long-range ferromag., antiferromag. superexchange, limit function 0-54883
- tri-p-tolylamine and its paramag. radical cation, disordered mol. solid, direct obs. of superexchange 0-39848
- xanthine oxidase (dehydrogenase), EPR, mag. spin-spin dipolar interaction 0-53026
- $\text{Cs}_2\text{CuCl}_4 \cdot 2\text{H}_2\text{O}$ , ferromag., hyperfine and exchange interactions, NMR study 0-50208
- Fe-Al, spin glass transition, Monte Carlo study 0-39801
- Fe-Al (0.27 to 0.50 at.%), spin glass behaviour, microscopic model, Ising lattice, exchange and superexchange 0-39800
- $\text{Fe}_{1-x}\text{Cr}_x\text{Se}_2$ , crystallographic and image props. 0-39049
- $\text{K}_2\text{CuCl}_4 \cdot 2\text{H}_2\text{O}$ , ferromag., hyperfine and exchange interactions, NMR study 0-50208
- $\text{KMnF}_6$ , exchange interaction of excited  $\text{Mn}^{2+} ({}^4\text{A}_1)$  ions, Anderson model 0-25124
- $(\text{NH}_4)_2\text{CuBr}_4 \cdot 2\text{H}_2\text{O}$ , ferromag., hyperfine and exchange interactions, NMR study 0-50208
- $(\text{NH}_4)_2\text{CuCl}_4 \cdot 2\text{H}_2\text{O}$ , ferromag., hyperfine and exchange interactions, NMR study 0-50208
- $\text{Rb}_2\text{CuBr}_4 \cdot 2\text{H}_2\text{O}$ , ferromag., hyperfine and exchange interactions, NMR study 0-50208
- $\text{Rb}_2\text{CuCl}_4 \cdot 2\text{H}_2\text{O}$ , ferromag., hyperfine and exchange interactions, NMR study 0-50208

**superfluid helium-3**

- 5-d spin theory 0-49450
- A<sub>1</sub> phase, broken relative symmetry and dynamics 0-24705
- A phase, theory of orbital dynamics, hydrodynamic eqns. 0-54461
- A- and B- phases, book 0-2227
- A-phase, composite solitons in presence of superflow 0-2233
- A-phase, Cooper pairs vs. Bose condensed mols., ground-state current 0-49451
- A-phase, have persistent currents been obs.? 0-10731
- A-phase, instability of persistent currents and heat flow 0-15327
- A-phase, new phase-transfer decay mechanism for persistent currents 0-6586
- A-phase, orbital dynamics 0-2232
- A-phase, orbital dynamics in spin fluctuation feedback approx., out-of-phase mode 0-54457

**superfluid helium-3 continued**

- A-phase, phase diagram for helical texture 0-24704
- A-phase, rotating, vortex lattice detectability 0-29240
- A-phase, soliton lattice for NMR behaviour 0-2234
- A-phase, textures in narrow cylinders 0-24703
- A-phase, transverse magnetisation relaxation and superfluid spin flows (*Russian*) 0-34265
- A-phase, viscosity tensor, generalised paramagnon model 0-39379
- A-phase slab, mag.-field-induced cellular superflow, periodic texture 0-24706
- A-phase texture elec. orientation 0-6585
- B phase, soliton-like spin waves 0-44385
- B-phase, crit. current obs. 0-15328
- B-phase, gap parameters and collective modes in strong mag. field 0-15325
- B-phase, low temp. spin relax. 0-15323
- B-phase, n solitons in crossed mag. field and superflow 0-44386
- B-phase, spin wave breathers, double sine-Gordon equations 0-15329
- B-phase spin oscils. in presence of dipole forces 0-6583
- Bose spectra stability, phonon branches, dispersion coeff. (*Russian*) 0-49452
- dynamic orbital effects, US propag. and viscosity, book contrib. 0-2235
- Fermi liquids at surfaces quasiclassical boundary conditions 0-4641
- fifth sound propag. 0-6580
- heat capacity anomalous near transition, 0.8-20 mK 0-15326
- heat transfer with solids below 100 mK 0-24701
- hydrodynamics and inhomogeneous states, review 0-49453
- oscillatory flow, temp. depend. of crit. vel. 0-10732
- planar textures, Ginzburg-Landau eqn. solns. 0-10729
- Poisson brackets, nonlinear hydrodynamics eqns. in condensed matter physics 0-54296
- response functions of superconductors and  ${}^3\text{He}(\text{B})$ , autocorrelation functions of density and transversal current, acoustic and quasihomogeneous 0-49449
- response functions of superconductors and  ${}^3\text{He}(\text{B})$ , density and current correlation functions 0-49448
- soliton-antisoliton pair interaction in double sine-Gordon eqn., numerical simulation 0-46821
- sound propagation and kinetic coeff., book contrib. 0-2237
- specific heat discontinuities, rel. to Ginzburg-Landau parameters 0-54459
- spin and orbital dynamics, book contrib. 0-2236
- spin dynamics theory, spin-orbit interactions, spin waves (*Russian*) 0-54462
- spin fluctuation peak, low-energy, theoretical anal. of neutron obs. 0-6584
- superfluid A-phase, composite soliton in narrow circ. cylinder, satellite freq., thermal fluctuations 0-34266
- surface energy and textural boundary conditions between A and B phases 0-54458
- ${}^3\text{He}$ , solid, possible explanation for recently obs. phase transition in high mag. fields 0-20006
- ${}^3\text{He}$ -HeII solutions, van der Waals molecular dimers ( ${}^3\text{He}$ )<sub>2</sub>, bound states (*Russian*) 0-49454
- ${}^4\text{He}$ - ${}^3\text{He}$ , dilute soln., low temp.,  ${}^4\text{He}$  effective interaction 0-10734

**superfluid helium-4**

- $\lambda$  point, US absorption, dynamic scaling 0-44380
- acoustic vibration field density of states in piecewise const. parameter media 0-6483
- cable-in-conduit conductor, heating-induced flows 0-38229
- charged surface stability breakdown, He ion geyser ejection (*Russian*) 0-15320
- condensate fractions and pair correlations 0-39375
- continuum theory, classical theory of irreversible processes 0-29236
- cooled colour centre laser cavity 0-48282
- critical superflow through Grafoil, two-dimens. random bond model 0-15319
- critical thermal cond. near  $\lambda$ -point, light scatt. spectrum 0-24697
- dynamic scaling near  $\lambda$  point 0-15321
- dynamic scaling near  $T_\lambda$  0-34264
- electron escape from image-potential-induced surface states 0-49440
- excitation energy spectrum, roton contrib. 0-24699
- fifth sound, vel. meas. 0-39377
- film, adsorbed on  $\text{Al}_2\text{O}_3$  powder, surface tension sound 0-24691
- film, Brownian motion, boundary layers and quantised vortex prod. 0-6579
- film, jump in superfluid density 0-44387
- film, modified eqn. of state, mech. reson. meas. 0-24692
- film, rotating, melting of two-dimensional vortex lattices 0-2539
- film, superfluid healing length and density, ring diagram approx. 0-54452
- film adsorbed on Grafoil, onset and third sound vel. meas. 0-44388
- film boiling anal. 0-10716
- film in zero gravity 0-54464
- film thinning during crit. and subcrit. flow 0-20002
- first sound, order parameter fluctuation critical attenuation near critical temp. 0-2229
- flow through porous Vycor glass under small press. gradient 0-49442
- fourth sound propag. and flow props. in very long capillaries 0-44384
- fourth-sound-like propagation in grafoil-filled resonators 0-34263
- free surface, book contrib. 0-2231
- free surface, crit. behaviour near  $\lambda$  point 0-2228
- gauge wheel of superfluid  ${}^4\text{He}$ , two fluid model 0-44379
- heat transport in restricted geometries, 0.8-2K 0-29237
- hydrodynamics, Zilsel's variational principle derived from Lin's principle 0-24695
- hydrodynamics quantisation for superfluid helium (*German*) 0-39371
- interface conditions between liq. and vapour 0-10723
- isotopically pure, vortex nucleation 0-44378
- Kapitza conductance of Ag, proof of surface superfluidity in enhanced power anomaly 0-15359
- light scattering, near  $T_\lambda$  0-29238
- neutron scattering, book contrib. 0-2230
- normal fluid heat-exchange drag 0-49441
- one phonon excitation spectrum and interaction pot. 0-54455
- phonon dispersion in He II 0-10722
- Poisson brackets, nonlinear hydrodynamics eqns. in condensed matter physics 0-54296
- pressure release superleak sound modes 0-54453
- pressure-volume and acoustic virial coeffs., temp. depend., quantum range 0-47056



**superfluid helium-4** continued

- pressurised, cooling of composite superconductor, triple-phase phenomena 0-20364
- pressurised, vortex nucleation by neg. ions, thermal roton influence 0-10721
- rotating, Tkachenko waves 0-39376
- rotating cylinder, vortex patterns and energies 0-6578
- rotating system, equilibrium Onsager-Feynman vortex lattice (*Russian*) 0-29234
- rotating with vortices, defect hydrodynamics (*Russian*) 0-49445
- second sound damping, crit. dynamics below  $T_\lambda$  0-10727
- second sound damping near superfluid transition, rel. to renormalisation gp. predictions 0-10725
- single atom neutron scatt. and two roton connected state branches (*Russian*) 0-44381
- singular f-sum rule, applicability to inelastic neutron scatt. 0-6577
- sound transformation at free surface 0-54451
- spatial order, temp. depend. 0-39374
- stationary flow, combined meas. 0-49446
- superflow into a solid superleak 0-39372
- surface, ripplons, adsorbed  $^3\text{He}$  and heat conduction meas. 0-49459
- theory of superfluidity 0-39378
- third sound measurement as capillary condensation probe in porous material 0-20005
- transient heat transport 0-10715
- turbulence, electron photography (*French*) 0-54456
- turbulence, vel. and temp. depend. from thermal resist. meas. 0-20003
- turbulence during rotation, critical lengths 0-49443
- two dimensional system, phase transitions review 0-52149
- two-dimensional, microscopic theory, excitation spectrum and thermodynamics props. 0-24709
- velocity fluctuation spectrum 0-34262
- Venturi level differences 0-24698
- viscosity and thermal conductivity (*Russian*) 0-10720
- viscosity properties depend. on oscill. freq. 0-6576
- vortices pinning in nucleopores, effect on second sound resonators 0-49439
- $^3\text{He}$ - $^4\text{He}$ , superfluid soln., dil., low temp. props., book contrib. 0-15330
- $^3\text{He}$ -HeII solutions, van der Waals molecular dimers ( $^3\text{He}$ )<sub>2</sub>, bound states (*Russian*) 0-49454
- $^4\text{He}$  film, adsorbed, few atomic layers, excitations, two-dimensional roton. 0-39381
- $^4\text{He}$ - $^3\text{He}$ , dil. soln.,  $^3\text{He}$  quasiparticle excitation spectrum and second sound vel. meas. 0-24708
- $^4\text{He}$ - $^3\text{He}$ , dilute soln., low temp.,  $^4\text{He}$  effective interaction 0-10734

**superfluidity**

see also *quantum fluids*; *superfluid helium-3*; *superfluid helium-4*; *vortices*

- boson system, superfluid flow rel. to local gauge invariance 0-54450
- degenerate fermi gas, hydrodynamic eqns. allowing for finite coherence length (*Russian*) 0-12989
- Dirac's monopole analogy 0-6575
- flow birefringence, depend. on normal-superfluid component relative motion (*Russian*) 0-45032
- Gross Pitaevskii eqn., generalised solns. 0-49437
- hadronic matter, Pomeron and critical temp. 0-22566
- hydrodynamics quantisation for superfluid helium (*German*) 0-39371
- isotopic invariance and pairing energies 0-22687
- model Hamiltonian for one- and two-dimensional superfluids 0-44377
- neutron  $^3\text{P}_2$  superfluidity under  $\pi^0$  condensation in neutron star matter 0-47417
- rotational speedups accompanying angular deceleration 0-10738
- He, fifth sound propag. 0-6580
- He, film, superfluid props. 0-34270
- $^3\text{He}$ , Bose spectra stability, phonon branches, dispersion coeff. (*Russian*) 0-49452
- $^3\text{He}$ - $^4\text{He}$  mixture, transport props. near superfluid transition and tricritical point 0-29242
- $^3\text{He}$ - $^4\text{He}$  superfluid mixture, early stages of spinodal decomposition, calc. 0-20004

**supergiant stars**

- A, F, G-type supergiants kinematics, appl. to galactic spiral structure parameters derivation 0-17665
- $\alpha$  Aquarii, chromospheric event detect. from UV spectrum obs. 0-31299
- $\alpha$  Camelopardalis (O9.5 Ia), stellar wind terminal vel. short time changes from UV spectrum 0-36625
- $\alpha$  Camelopardalis (O9.5 Ia), variable H $\alpha$  P Cygni profile 0-41818
- VY Canis Majoris, OH/IR star, 1612 MHz OH maser multibaseline VLBI obs. 0-12766
- $\kappa$  Cassiopeiae, effective temp. radius, mass loss and luminosity 0-51748
- 6 Cassiopeiae, spectroscopic obs., equivalent widths, microturbulence and radial vel. 0-22006
- $\delta$  Cephei, H $\alpha$  radial vel. behaviour 0-51788
- VV Cephei, UVB obs. 0-17611
- VV Cephei system, distant, in Puppis, spectral classification, UVB photometry and polarimetry 0-51810
- P Cygni, effective temp. radius, mass loss and luminosity 0-51748
- P Cygni, extreme B-type supergiant, UV spectroscopy 0-22004
- P Cygni, high resolution UV spectrum obs. 0-26873
- NML Cygni, IR speckle interferometry 0-31216
- $\alpha$  Cygni, radial vel. and line profile vars. in supergiant 0-22010
- Cygnus OB2 number 12, spectral classification and membership of association 0-51760
- S Doradus (HD 35343), luminous LMC supergiant, long time baseline VBLUW photometry 0-36630
- extended atmospheres, sphericity effects in red giants, model study 0-22012
- F- and G-type, enhanced He abundance effects on visible spectra 0-12759
- galactic G-type supergiants, UVB photometry 0-41824
- HD 190603, effective temp. radius, mass loss and luminosity 0-51748
- HD 33579, 35343, HDE 286757, 269006, most luminous LMC supergiants, long time baseline VBLUW photometry 0-22007
- HD 33579, HD 35343 (S Doradus), HDE 286757, HDE 269006, most luminous LMC supergiants, long time baseline VBLUW photometry 0-36630
- HDE 226868 (Cygnus X-1), H $\alpha$  emission in (1977) 0-51919
- AC Herculis, curve-of-growth analysis of RV Tauri variable 0-22026
- AC Herculis, RV Tauri star, UVB obs. 0-56857

**supergiant stars** continued

- high luminosity stars in Galaxy and Magellanic Clouds, UVB intrinsic colours 0-26855
- HR 8752 (V509 Cassiopeiae), emission-line spectrum rapid changes 0-36645
- late-type southern stars, chem. comp., solar neighbourhood metallicity distrib. 0-12758
- late-type stars, near IR multicolour photometry from BAT (*Japanese*) 0-31298
- late-type supergiants, near IR photometry with balloon-borne telescope 0-4357
- $\rho$  Leonis, effective temp. radius, mass loss and luminosity 0-51748
- LMC, blue to red supergiant star ratio across face, rel. to star form. 0-26984
- in LMC, photoelectric UVB photometry (*German*) 0-21932
- LS I +61°303, radio variable Be star, UV spectrum, stellar models 0-26879
- in M31, photometric and spectroscopic studies in Baade's Field IV 0-36622
- nonvariable supergiants, classical Cepheids and bright giants, spectrophotometric comparison 0-56837
- OB supergiants, minimum flux corona theory 0-26844
- OB-type supergiants, effective temps., ang. diameters, distances and linear radii 0-17584
- OH maser emission from late-type stars, UHF obs. 0-56826
- $\alpha$  Orionis, CO circumstellar absorpt. obs. in 4.6 micron spectrum 0-26858
- $\kappa$  Orionis, interstellar B II 1362 Å detect. 0-51841
- $\alpha$  Orionis, IR speckle images, two-dimens. obs. (*French*) 0-46553
- $\beta$  Orionis, mass loss and shell, IUE and balloon UV obs. 0-51765
- $\epsilon$  Orionis, Orion OBI association star, interstellar lines obs. by Copernicus 0-22050
- $\alpha$  Orionis (Betelgeuse), optically thin dust shells 0-22011
- pulsation mass calcs. 0-46556
- R Puppis (HD 62058), G-type supergiant, UVB photometry and variability confirmation 0-41824
- $\mu$  Sagittarii, binary star, obs. of eclipse of unseen companion 0-4401
- RY Sagittarii, spectra near min. light 0-36642
- $\alpha$  Scorpii, balloon-borne near IR multicolour photometry 0-4356
- $\alpha$  Scorpii, circumstellar absorption lines in UV spectrum 0-51804
- $\zeta^1$  Scorpii, extreme B1 supergiant, IUE obs. of line spectrum and continuum energy distrib. 0-17583
- $\zeta^2$  Scorpii, extreme B1 supergiant, UV reson. lines obs. 0-4349
- $\zeta^3$  Scorpii, extreme B-type supergiant, UV spectroscopy 0-22004
- RY Scuti, silicate grains IR emission from early-type supergiant binary system 0-41827
- solar neighbourhood initial mass function determ. from upper H-R diagram study 0-36626
- RV Tauri and yellow semiregular variables, photometric investigations 0-26865
- S Vulpeculae, 67 day Cepheid, case for membership in (Vulpecula OB2) 0-41831
- winds from O and B supergiants in Magellanic Clouds 0-51863
- yellow semiregular and RV Tauri variables, photometric investigations 0-26865
- C IV resonance lines in B- and early A-type objects 0-46550
- He shell flashes in red supergiants, convective penetrations and observable effects 0-51755
- O-rich late-type stars, 16 to 39 micron spectroscopy 0-22002
- SiO 86.2 GHz maser sources, polarisation props. 0-4449

**supergravity**

- (3/2,1) superfield of O(2) supergravity 0-52105
- $\alpha$  model, supersymmetric nonlocal conservation laws 0-46938
- algebraic approach to supergravity in superspace 0-46915
- antigravity as extension of supergravity 0-46911
- antigravity from supergravity with N=2-8 fermionic generators 0-27198
- antisymmetric tensor gauge fields, local supersymmetry without gravity 0-46910
- asymptotically flat instantons 0-46932
- auxiliary fields and tensor calculus for N=2 extended supergravity 0-46920
- axial currents, supercurrents and anomalies in supersymmetric QED 0-46933
- background field gauge in supergravity 0-46912
- Bargmann-Wigner and Weyl spin-3/2 fields, spinors, chiral operator 0-31981
- Bianchi identities and supercovariant derivative 0-17852
- Bose analogs to supergravity, construction problems 0-46926
- classical field theories, non-signification of super gravitation 0-27193
- complex and quaternionic supergeometry 0-46941
- complex spinors and unified theories 0-46943
- conference, supergravity, Stony Brook, USA (Sept. 1979) 0-46738
- conformal supergravity, constraints and invariance 0-46917
- constraints for supergravity 0-46918
- covariance group structure, graded conformal, affine groups 0-22264
- covariant canonical formulation, subsidiary conditions and physical S-matrix unitarity 0-12974
- differential forms on supermanifolds (*Russian*) 0-4889
- dimensional regularization and supersymmetry at the two-loop level 0-17854
- Einstein's theories extended, book 0-22164
- Einstein supergravity, symmetry, spin connection simplifications 0-22258
- Einstein supergravity supergroup, simplest example (*Russian*) 0-36929
- extended geometric supergravity on group manifolds with spontaneous fibration 0-31649
- extended spontaneously broken supergravity models, properties 0-46924
- extended supergravity, auxiliary fields 0-46919
- extended supergravity, dimensional reduction simplifications 0-52110
- extended supersymmetry invariants by dimensional reduction 0-47213
- fiber bundle model of the gravitational field 0-46923
- G-index theorem for natural operators on ALE gravitational instanton spaces 0-46940
- gauge group and geometry of supergravity 0-8888
- gauge invariance and spinor calculus, de Sitter, gravitation theory 0-12978
- geometrical formulation on supergroup manifold 0-46916
- geometrization in superspace and local supersymmetry 0-8890
- globally supersymmetric multiplets without local extensions 0-17856
- higher spin gauge fields, beyond 3/2, systematics 0-46937
- hypergravity, consistency requirements 0-46936



**supergravity continued**

- massive spinning particle in Minkowski space equivalence to massless particle in de Sitter space 0-119
- massive vector multiplet coupled to supergravity 0-17855
- massive vector multiplets, lagrangian construction 0-31645
- massive vectormultiplets in supergravity 0-46927
- N=8, on-shell theory in superspace 0-27199
- no-hair conjecture example, Schwarzschild background, static helicity 3/2 perturbation 0-31647
- open problems with spins  $>2$  0-46934
- OSp(1,4) renormalisable theory with higher derivatives 0-36930
- OSp(1,4) supergroup, Wess-Zumino model classical solns. 0-36928
- post-Einstein unified theory, book contrib. 0-22260
- quantum corrections to the quadratic mass formula of broken supersymmetry 0-46942
- Rarita Schwinger eqn. solns. in Kerr Newman space 0-116
- self-duality and helicity in supergravity 0-46929
- self-duality in superspace, functional anal. 0-46902
- six dimensional, superspace torsion and curvature constraints 0-52104
- SO(8) extended supergravity 0-4914
- SO(8) supergravity derivation 0-12975
- space-time properties of supergravity 0-8887
- spin 2 matter-gravity coupling problems 0-46939
- spin 5/2 theories, supergravity extensions beyond SO(8) 0-46935
- status as unified gauge theory 0-46925
- SU(8) supergravity on mass shell in superspace 0-46907
- SU(8) supergravity supersymmetry breaking 0-46908
- SU(8) unification and supergravity 0-46928
- superalgebra stability in supergravity models (Russian) 0-52109
- superconformal gravity advantages over normal supergravity 0-8889
- superconformal symmetry breakdown as guide to supergravity constraints 0-46930
- superconnections in extended supergravity 0-36927
- superfield covariant derivatives for O(1) and O(2) supersymmetry 0-46914
- superfield Feynman graphs, loop calculations 0-46906
- superfield supergravity with symmetry 0-8891
- supergraph formalism UV finiteness in gauge supersymmetry 0-46913
- superspace action for simple supergravity 0-27197
- superspace formulation for supergravity, book contrib. 0-22261
- superspace formulations 0-46931
- superspace geometry of supergravity 0-46909
- superspace tensor calculus formulations, relations to supergravity 0-46922
- supersymmetry, physico-geometrical comments, unified field theories and supergravity, gauge transformations 0-364
- supersymmetry constraints, algebraic understanding 0-46921
- surface deformations, their square root and the signature of spacetime 0-8874
- tachyon solns. in classical relativity 0-36917
- unification of laws of physics (Polish) 0-36926
- weak field approximation (Russian) 0-27201
- Wess-Zumino constraints, superconformal transformations and six-dimensional spacetime 0-27196

**superheating** *see* **heat transfer****superheavy nuclei**

- see also* **nuclei with mass number 220 or higher**
- bound states of superheavy nuclei from weak unsaturated two nucleon forces (Russian) 0-462
- collective motion, stability and prod. in heavy ion collisions 0-18169
- meteorites of iron type, superheavy element fission tracks 0-26821
- monazites examination in search for superheavy elements 0-36297
- nonexistence in UNILAC expts. (German) 0-42731
- production and natural searches, review 0-37411
- search in Allende meteorite and cordierite giant halos 0-21752
- stability and fission barriers, crit. ang. momentum depend. 0-32262
- Z=118, 172, 226, symm. and stability of 2(2l+1) electron configurations of elements 0-1100
- Bi<sub>2</sub>S<sub>3</sub>, superheavy element search using neutron multiplicity counter 0-4011
- <sup>252</sup>Cf source in tissue-equivalent phantom, neutron absorbed dose obs. 0-12278

**superionic conducting materials**

- see also* **ionic conduction in solids; mixed conductivity**
- $\beta$ -Al<sub>2</sub>O<sub>3</sub>-Ag<sub>2</sub>O, antiferroelectric transformation, Potts' model universality class 0-50277
- alkaline earth fluoride based solid electrolytes, in galvanic cells 0-3501
- applications, accumulator with high energy density (French) 0-26131
- book 0-22156
- continuous stochastic models, book contrib. 0-24663
- current-pot. curves discontinuities in solid electrolyte systems 0-24660
- dielectric response 0-10899
- electrode preparation techniques, in solid electrolytes (Japanese) 0-24658
- EXAFS studies of struct. and cond. process, book contrib. 0-25485
- frequency dependent cond., correl. effect, Scher-Lax model 0-34238
- hard sphere fluid model 0-44363
- high temperature meas., solid electrolytic cell, meas. at 700K and higher 0-31760
- independent particle model 0-6551
- interacting Brownian particles and correlations 0-29202
- introduction to fast ion conductors 0-6549
- ionic plasma oscils. 0-29212
- lattice gas models, book contrib. 0-24661
- light scatt. and IR absorpt. book contrib. 0-25382
- linear chain, two-sublattice, hopping particle occupancy correlation function normal modes 0-49402
- magnetic resonance, book contrib. 0-25240
- mixed conductivity, superionic-electronic, electrodes, partial cond. meas. technique 0-44360
- oxides, review 0-49414
- paramagnetic impurity contribution is NMR relaxation in one-dimension 0-20477
- phase transitions, book contrib. 0-24662
- polyamine iodide/AgI solid electrolytes, conc. depend. of elec. cond. 0-24647
- quasi-lattice gas model 0-44364
- sine-Gordon model, overdamped, Brownian diffusion 0-27223
- soft-core model for ionic crystals, normal ionic salts and superionic conductors 0-49411

**superionic conducting materials continued**

- solid electrolyte dielectric permeability, phase transition to superionic state (Russian) 0-49403
- solid electrolyte with structural disorder, current flow mechanism 0-19982
- structure and dynamical props., X-ray and neutron scatt. studies, book contrib. 0-24433
- summer school, Aleria, Corsica, France (Sept. 1977) 0-6339
- theory of superionic conduction, including struct. principles 0-6550
- transition temperature to high cond. state as function of press. 0-44365
- [ $\beta''$ ]-Al<sub>2</sub>O<sub>3</sub>-H<sup>+</sup>(H<sub>2</sub>O)<sub>n</sub>, IR study 0-16037
- Ag-Ge-S glasses, X-ray determ. of struct. (Japanese) 0-10501
- AgI, conductivity, hopping system, master equation 0-39348
- AgI, density of valence states, photoelectron spectra meas. 0-25523
- $\alpha$ -AgI, ionic cond. in 8-40 GHz range 0-44358
- $\alpha$ -AgI, neutron scatt. expts., Ag<sup>+</sup> ion motion 0-6552
- AgI, phase transition, statics and local dynamics, mean field and Mori theory 0-39347
- $\alpha$ -AgI, single particle and collective aspects of Ag<sup>+</sup> ion motion 0-6553
- AgI solid electrolyte  $\alpha$ -phase stabilisation 0-29209
- $\alpha$ -AgI, state of order, config. model 0-6390
- $\alpha$ -AgI, struct. and dynamics, two-dimens. mol. dynamics model 0-49413
- $\alpha$ -AgI, structure, X-ray scatt. anal. 0-28983
- $\alpha$ -AgI, superionic, continuous order-disorder transition, Raman spectroscopic evidence 0-45070
- $\alpha$ -AgI, superionic conductor, microwave absorption spectrum 0-11515
- $\alpha$ -AgI, superionic conductor, soft-core model, Monte Carlo study 0-54430
- $\alpha$ -AgI, superionic phase, struct., X-ray scatt. anal. 0-28983
- AgI-based solid electrolyte cell discharge mechanism 0-35663
- AgI-type solid electrolytes, introductory survey 0-6549
- (AgI)<sub>1</sub>(Ag<sub>2</sub>O.B<sub>2</sub>O<sub>3</sub>)<sub>1-x</sub> glass, ionic cond. and disorder modes 0-39344
- Ag<sub>2</sub>I<sub>2</sub>PO<sub>4</sub> film formation from electrolysis of HI-H<sub>3</sub>PO<sub>4</sub> soln., electrocodepositional method 0-55315
- Ag<sub>2</sub>I<sub>2</sub>PO<sub>4</sub>, solid electrolyte, ionic cond. meas., 4-79°C 0-54433
- Ag<sub>2</sub>Rb(PO<sub>3</sub>)<sub>2</sub>, struct., density and elec. cond. 0-33952
- $\beta$ -Ag<sub>2</sub>S, fast-ion conductor, Ag ion density, neutron diffr. study 0-34234
- Ag<sub>2</sub>S, liquid, ionic and electronic cond., thermoelec. power 0-39329
- Ag<sub>2</sub>S-As<sub>2</sub>S<sub>3</sub>-AgI glasses, temp. and comp. depend. of ionic cond. (French) 0-34229
- Ag<sub>2</sub>SI, superionic cond., phase transition and cryst. structs., sp. ht., neutron and X-ray diffr. obs. 0-10662
- Ag<sub>2</sub>Se, liquid, ionic and electronic cond., thermoelec. power 0-39329
- Ag(T<sub>1</sub>)/AgI(Ag(T<sub>2</sub>)) cell, thermo-EMF of highly conducting solid electrolytes 0-24659
- Ag<sub>2</sub>Te, liquid, ionic and electronic cond., thermoelec. power 0-39329
- $\beta$ -Al<sub>2</sub>O<sub>3</sub>-Na<sub>2</sub>O, between metal electrodes, cell complex admittance diagrams, grain boundary effect (French) 0-45653
- $\beta$ -Al<sub>2</sub>O<sub>3</sub>, field assisted bonding to metals 0-45474
- $\beta$ -Al<sub>2</sub>O<sub>3</sub>, ionic superconductors (French) 0-39346
- $\beta''$ -Al<sub>2</sub>O<sub>3</sub>, Li<sub>2</sub>O-stabilised, deterioration under electrolytic conditions 0-40592
- $\beta$ -Al<sub>2</sub>O<sub>3</sub>, stoichiometric, Raman and IR spectra, Frenkel defects, order-disorder transition and cation cond. 0-55086
- $\beta$ -Al<sub>2</sub>O<sub>3</sub>-Ag<sub>2</sub>O, superionic conductor, microwave absorption spectrum 0-11515
- $\beta$ -Al<sub>2</sub>O<sub>3</sub>-H<sub>2</sub>O<sup>+</sup>, ESR of paramag. defects in cond. planes 0-29617
- $\beta$ -Al<sub>2</sub>O<sub>3</sub>-K<sub>2</sub>O, ESR of paramag. defects in cond. planes 0-29617
- $\beta$ -Al<sub>2</sub>O<sub>3</sub>-Na<sub>2</sub>O-CaO, microstruct. and ionic resistivity 0-44357
- Al<sub>2</sub>O<sub>3</sub>-Na<sub>2</sub>O,  $\beta$  and  $\beta''$  phases, formation by solid state reaction between NaAlO<sub>2</sub> and  $\gamma$ -Al<sub>2</sub>O<sub>3</sub> 0-29912
- Al<sub>2</sub>O<sub>3</sub>-Na<sub>2</sub>O,  $\beta'$  and  $\beta''$  phases, engineering props. data compilation, rel. to energy storage 0-49415
- $\beta$ -Al<sub>2</sub>O<sub>3</sub>-Na<sub>2</sub>O, ESR of paramag. defects in cond. planes 0-29617
- $\beta$ -Al<sub>2</sub>O<sub>3</sub>-Na<sub>2</sub>O, layered material, contact free conductivity 0-2195
- $\beta''$ -Al<sub>2</sub>O<sub>3</sub>-Na<sub>2</sub>O, Li<sub>2</sub>O stabilised, electrolyte polarisation anal. by complex admittance method 0-2689
- $\beta$ -Al<sub>2</sub>O<sub>3</sub>-Na<sub>2</sub>O, non-stoichiometric, amorphous, US attenuation and velocity 0-39228
- $\beta$ -Al<sub>2</sub>O<sub>3</sub>-Na<sub>2</sub>O, preferable orientation for Na<sup>+</sup> cond. 0-35144
- $\beta''$ -Al<sub>2</sub>O<sub>3</sub>-Na<sub>2</sub>O, rapid ion conductor, Na penetration 0-24653
- $\beta$ -Al<sub>2</sub>O<sub>3</sub>-Na<sub>2</sub>O, superionic conductor, microwave absorption spectrum 0-11515
- $\beta$ -Al<sub>2</sub>O<sub>3</sub>-Na<sub>2</sub>O <sup>23</sup>Na asymmetry parameter, temp. variations 0-6540
- $\beta''$ -Al<sub>2</sub>O<sub>3</sub>-Na<sub>2</sub>O-Li<sub>2</sub>O (8.85, 0.75 wt.%) pressing powders, prep. by spray drying 0-40294
- B<sub>2</sub>O<sub>3</sub>-Li<sub>2</sub>O-LiCl glasses, solid electrolyte, NMR meas. 0-29208
- BaF<sub>2</sub> solid electrolyte, n-type electronic cond., 700-900°C 0-29448
- CaF<sub>2</sub> solid electrolyte, meas. of O chem. pot. 0-3359
- CaS-Y<sub>2</sub>S<sub>3</sub> (1 wt.%), solid electrolyte, elec. cond. under low partial pressures of S (Japanese) 0-49409
- CeO<sub>2</sub>, ionic conduction, doping effects and defect interactions 0-19978
- Cu free electrolytic films, tensile creep for various film thicknesses calcs. (Russian) 0-11697
- CuI solid electrolyte  $\alpha$ -phase stabilisation 0-29209
- CuI, superionic cond., EXAFS study 0-50462
- CuTeBr, superionic conductor, microwave absorption spectrum 0-11515
- DAI<sub>1</sub>O<sub>7</sub>, anhydrous, cryst. struct. from powder neutron diffr. 0-1983
- K-Hollandite, one-dimens. ionic conductor, modulation and incommensurability 0-19980
- KAgI<sub>5</sub>, superionic film, elec. ionic cond. and electron spectra 0-6543
- Li<sub>2+x</sub>B<sub>2</sub>O<sub>3</sub>Li<sub>2+2x/2</sub>Cl, solid electrolyte, NMR meas. 0-29208
- LiF-Al(PO<sub>3</sub>)<sub>3</sub> glass, phase decomp., X-ray diffr. and IR spectra study 0-30003
- Li<sub>2</sub>In<sub>2</sub>O<sub>6</sub>, pseudo-two-dimens. electrolytic solid, Li ion mobility, NMR study (French) 0-34235
- Li<sub>3</sub>N, photoluminesc. props. 0-50414
- Li<sub>3</sub>NbO<sub>6</sub>, pseudo-two-dimens. electrolytic solid, Li ion mobility, NMR study (French) 0-34235
- Li<sub>2</sub>O-Li<sub>2</sub>SO<sub>4</sub>-B<sub>2</sub>O<sub>3</sub>, vitreous electrolytes, ionic cond. and Raman spectra (French) 0-24656
- Li<sub>2</sub>O-LiCl-B<sub>2</sub>O<sub>3</sub> system, fast Li<sup>+</sup> ion vitreous superconductors, EPR study (French) 0-11269
- Li<sub>3</sub>SnO<sub>6</sub>, pseudo-two-dimens. electrolytic solid, Li ion mobility, NMR study (French) 0-34235
- Li<sub>2</sub>Ti<sub>2</sub>O<sub>7</sub>, channel-structured superionic conductor, anisotropic conductivity 0-6546
- NH<sub>4</sub>AgI<sub>5</sub>, superionic solid film, prep. and elec. cond. 0-54431
- 6NaCl.CdCl<sub>2</sub>, 60 wt.% powders, Suzuki phases prep. and stability 0-35123



# superionic conducting materials continued

- Na<sub>3</sub>RSi<sub>3</sub>O<sub>12</sub> (R=Sm to Lu, Y, Sc), solid electrolytes, struct. characts. 0-1997
- Na<sub>3</sub>Zr<sub>2</sub>Si<sub>2</sub>PO<sub>12</sub>, NASICON, phase transition, X-ray diffr., ionic cond. and sp. ht. meas. 0-19979
- Pb<sub>1-x</sub>Al<sub>1-x</sub>F<sub>2+x</sub>, ionic cond. of quenched and annealed specimens, interstitial cond. mechanism 0-2199
- PbSnF<sub>4</sub>, fast ionic cond. of F<sup>-</sup> ions, NMR study (*French*) 0-39345
- RbAg<sub>4</sub>I<sub>5</sub>, phase transition, statics and local dynamics, mean field and Mori theory 0-39347
- RbAg<sub>4</sub>I<sub>5</sub> solid electrolyte, interface with metal, photocurrent obs. on illumination 0-34513
- Rb<sub>3</sub>Cu<sub>4</sub>I<sub>3</sub>Cl<sub>13</sub> in CuCl-CuI-RbCl system, high Cu ion cond. solid electrolyte, elec. props. and powder X-ray diffr. anal. 0-15295
- ThO<sub>2</sub>, ionic conduction, doping effects and defect interactions 0-19978
- ZrO<sub>2</sub>, cell electrolysis of H<sub>2</sub>O at 800° to 1000°C (*French*) 0-26024
- ZrO<sub>2</sub>:Cu, point defects, electrochem. characterisation 0-35599
- ZrO<sub>2</sub>-Y<sub>2</sub>O<sub>3</sub> superionic cond. cell, complex impedance 0-10702

# superlattices

- Bravais-lattice operator in one band of solid 0-10519
- FCC lattices, ordered superstruct., phase diagrams, cluster variation calc. 0-39256
- graphite intercalation compound C<sub>24</sub>K, order-disorder transition, X-ray study 0-33922
- graphite intercalation compounds, low energy optical transitions, refl. spectra and X-ray diffr. 0-25371
- graphite-AsF<sub>3</sub> intercalation compounds, de Haas-van Alphen effect, charge transfer rate 0-54595
- heterojunction superlattices, Green's function of electron in periodic field 0-49857
- hypersound amplification by a quantizing electric field 0-6915
- III-V compounds and alloys, MBE process and problem areas, review 0-10815
- narrow band gap semiconductor, high elec. field conduction in space and time superlattices 0-49756
- 4-n-octyloxybenzoyloxy-4'-cyanostilbene, re-entrant polymorphism, nematic-smectic A-nematic-smectic A, X-ray study 0-34172
- plasma oscillations under strong high freq. elec. field 0-10904
- semiconductor, electroplasma parametric resonance 0-34475
- semiconductor, optical props. with electron temp. superlattice (*Russian*) 0-34879
- semiconductor, plasma oscills. in strong elec. field 0-44637
- semiconductor, temperature superlattice with hot electrons 0-20202
- semiconductor multilayer heterojunction struct., impurity and phonon scatt. 0-2456
- semiconductor superlattice, phonon spectrum, effect of strong elec. field, parametric reson. 0-44273
- semiconductor superlattice microwave/infrared detectors 0-13138
- semiconductor superlattices, optical and transport props., review (*Slovak*) 0-20288
- semiconductor with superlattice, Hall effect 0-39612
- semiconductor with superlattice, impurity photocond., electron spectrum reconstruction 0-24966
- semiconductor with superlattice, optical phonon excitation by light absorpt., impurity photoionisation 0-44275
- semiconductors, narrow band gap, superlattices, acoustic wave absorpt. and amplification 0-29445
- superconducting superstructures, condensate band spectrum and current carrying states anal. (*Russian*) 0-39706
- tetramethylammonium tetrachlorozincate, low temp. phases, superstruct., X-ray study 0-39065
- TTF-SCN, quasi one-dimens. conductor, CDW phase transform., X-ray scatt. study 0-24594
- two dimensional superlattice of misfit dislocations, possibility of X-ray and electron diffr. struct. determ. 0-54560
- Ba<sub>2</sub>XRuO<sub>6</sub> (X=La,Eu), <sup>99</sup>Ru Mossbauer spectra and other techniques 0-29659
- Ca<sub>2</sub>XRuO<sub>6</sub> (X=Y,La,Eu), <sup>99</sup>Ru Mossbauer spectra and other techniques 0-29659
- CdTe-HgTe ideal superlattice, electronic props. calc. 0-49885
- CdTe-PbTe(InSb) superlattices, laser deposition of multilayer heteroepitaxial struts. 0-44450
- Co<sub>2</sub>ZrS<sub>2</sub>, (0<x≤0.50), intercalation compounds, ordered phases obs. 0-33962
- Co<sub>0.83</sub>[Pt(C<sub>2</sub>O<sub>4</sub>)<sub>2</sub>].6H<sub>2</sub>O, quasi-one-dimens. conductor, Peierls distortion and superlattice, X-ray study 0-29397
- Cs(B<sub>3</sub>W<sub>3-x</sub>)O<sub>9</sub> (B=Na, Ca, Co, Ni, Cd, Ga, Bi, Nb, Ta) cryst. struct., temp. dielec. anomalies 0-1998
- Cu, He gas-bubble superlattice form. 0-2086
- Cu-Pd, mag. susceptibility and electronic struct. of ordering (*Russian*) 0-11161
- CuAu, mag. susceptibility and electronic struct. of ordering (*Russian*) 0-11161
- Cu<sub>3</sub>Au, mag. susceptibility and electronic struct. of ordering (*Russian*) 0-11161
- Cu<sub>2</sub>Au-Cu<sub>3</sub>Pd(Pt), quasibinary system, order-disorder transform., superlattice form. 0-2159
- Cu<sub>2</sub>MS<sub>2</sub>, (0<x≤0.50) (M=Zr, Hf), intercalation compounds, ordered phases obs. 0-33962
- Fe-Ni, ordered phase, Llo superstruct., Mossbauer spectrum, Debye-Scherrer pattern from LL-chondrite 0-50241
- Fe<sub>2</sub>ZrS<sub>2</sub>, (0<x≤0.50), intercalation compounds, ordered phases obs. 0-33962
- GaAs-Al<sub>1-x</sub>Ga<sub>1-x</sub>As, heterojunction and superlattice, magnetophonon reson., polaron mass 0-44715
- GaAs-Al<sub>1-x</sub>Ga<sub>1-x</sub>As superlattice, electronic props. 0-11080
- GaAs-AlGaAs heterojunction superlattices, electron mobilities 0-29473
- GaAs-AlGaAs heterojunction superlattices, obs. of intersubband excitations in multilayer two dimensional electron gas 0-29753
- GaAs-AlGaAs superlattice, selective transmission of HF phonons 0-34154
- n-GaAs-Ga<sub>1-x</sub>Al<sub>x</sub>As, superlattice, subband struct. and optical spectra, self-consistent calc. 0-15443
- GaAs-Ga<sub>1-x</sub>Al<sub>x</sub>As heterostructures, quantum size effect in superlattices, electronic props. 0-29471
- GaAs-Ga<sub>1-x</sub>Al<sub>x</sub>As superlattice, Raman scatt., polar phonon anisotropy 0-45052
- GaAs-GaAlAs, subband related anisotropy in negative magnetoresistivity 0-11082

# superlattices continued

- GaP,As<sub>1-x</sub>-GaAs one dimens. superlattice, possibility of X-ray and electron diffr. struct. determ. 0-54560
- <sup>4</sup>He, on graphite, ground-state energy, variational calc. 0-24710
- InAs/GaSb (001) superlattices, electronic struct., two dimensional effects 0-11064
- InAs-GaSb, semiconductor-semimetal transition obs. 0-44710
- InAs-GaSb (001) superlattices, two-dimens. effects and effective masses 0-49883
- InAs-GaSb (100) superlattice, electronic struct., self-consistent pseudopot. method 0-49884
- InAs-GaSb superlattice, electronic struct., self-consistent pseudopot. calc. 0-29470
- InAs-GaSb superlattices, crystallography, Rutherford backscatt. and channelling obs. 0-49533
- InAs-GaSb superlattices, semicond.-semimetal transition obs. 0-49882
- InSb-CdTe(PbTe) superlattices, laser deposition of multilayer heteroepitaxial struts. 0-44450
- K(B<sub>3</sub>W<sub>3-x</sub>)O<sub>9</sub> (B=Na, Ca, Co, Ni, Cd, Ga, Bi, Nb, Ta) cryst. struct., temp. dielec. anomalies 0-1998
- β-LiAlSiO<sub>4</sub>, eucryptite, one-dimensional ionic conductor, neutron scatt. study 0-49361
- Nb-Zr, acoustic phonon anomalies and superstructure, neutron inelastic scatt. meas. 0-19892
- NbSe<sub>2</sub>, quasi one-dimens. conductor, CDW phase transform., X-ray scatt. study 0-24594
- Ni, He gas-bubble superlattice form. 0-2086
- Ni<sub>2</sub>ZrS<sub>2</sub>, (0<x≤0.50), intercalation compounds, ordered phases obs. 0-33962
- PbTe-CdTe(InSb) superlattices, laser deposition of multilayer heteroepitaxial struts. 0-44450
- Pt (111) and (100) superlattices formed by dissociative adsorption of HI, LEED, AES, and thermal desorption studies 0-55715
- Rb(B<sub>3</sub>W<sub>3-x</sub>)O<sub>9</sub> (B=Na, Ca, Co, Ni, Cd, Ga, Bi, Nb, Ta) cryst. struct., temp. dielec. anomalies 0-1998
- RbCaF<sub>3</sub>, structural phase transition, superlattice points, neutron diffr. obs. 0-19944
- Si, periodic stepped structure, on vicinal planes, LEED obs. 0-24725
- SiC (1 OH), phonon spectrum, dispersion curves energy discontinuity and vibr. modes, IR spectra obs. 0-44274
- Sr<sub>2</sub>Ta<sub>2</sub>O<sub>7</sub>, structural phase transition to superlattice, electron microscopy and diffraction study 0-39277
- Sr<sub>2</sub>YRuO<sub>6</sub>, <sup>99</sup>Ru Mossbauer spectra and other techniques 0-29659
- Ta<sub>2</sub>H<sub>2</sub>, ordered, distortion-induced superstruct. modulation, from X-ray scatt. 0-49186
- TaSe<sub>2</sub> (2H), optical absorpt., band struct., plasmons, and CDW 0-45104
- Ti<sub>1-x</sub>Hf<sub>x</sub>Se<sub>2</sub> mixed cryst., elec. resist. and phase transition temp. 0-24928
- TiSe<sub>2</sub> (1T), electronic and vibronic struct. 0-44500
- Ti<sub>1-x</sub>V<sub>x</sub>Se<sub>2</sub> (0≤x≤0.1), elec. resist. and Hall effect 0-2386
- V<sub>2</sub>D<sub>2</sub>, ordered, distortion-induced superstruct. modulation, from X-ray scatt. 0-49186

# supernova remnants

- blast waves, propag. rel. to interstellar medium mechanical heating 0-36682
- blast waves, propagation rel. to hot interstellar medium filling factor 0-17634
- 3C 391, obs. at 1.4 and 10.7 GHz 0-4417
- 3C 58, soft X-ray flux upper limits 0-56915
- 3C 58 (SN 1181), plerionic supernova remnant, supernova absolute magnitude and type classification 0-56862
- Cassiopeia A, weak X-ray source, ANS meas. 0-46701
- Cassiopeia A, <sup>14</sup>N radioemission at 26 MHz 0-41886
- Cassiopeia A, anal. of motion of details in thin shell model (*Russian*) 0-56920
- Cassiopeia A, high-resolution X-ray obs., struct., expansion phase, mass 0-26960
- Cassiopeia A, intensity and polarisation at 9 mm wavelength 0-36732
- Cassiopeia A, numerical model 0-12790
- Cassiopeia A, secular decrease in radio emission flux density at 437 and 510 MHz (*Russian*) 0-8702
- Cassiopeia A, X-ray spectrum, line emission obs. 0-26961
- Cassiopeia A supernova remnant, abundance inhomogeneities 0-12797
- cosmic rays, trapping by hydromag. waves in high β plasmas 0-17482
- Crab, near IR photometry and spectral index 0-8675
- Crab Nebula, emission line spectrum 0-22068
- Crab Nebula, lunar occultation obs. at 114 and 26.3 MHz, small-scale struct. 0-46627
- Crab Nebula, physical theory rel. to optical and X-ray surface brightness 0-51834
- Crab Nebula, radiation origin through pulsar magnetosphere cyclotron instability (*Russian*) 0-8645
- Crab Nebula, radio emission from compact source, HF meas. with URAN-1 interferometer 0-31343
- Crab Nebula, X-ray line emission, balloon-borne obs. 0-41884
- Crab Nebula plasma model and NP 0532 X-ray and gamma-ray radiation 0-41885
- CTB 80, as possible remnant, optical emission and historical evidence 0-51853
- CTB 80, peculiar supernova remnant, central radio source optical and H I obs. 0-56896
- Cygnus Loop, high-rel. gas Hα emission origin 0-41873
- Cygnus Loop, imaging X-ray obs., temp. struct. 0-41876
- Cygnus Loop, radial distrib. of Fe X and XIV forbidden line emission 0-51828
- electron-ion equilib. and ionization nonequilib., X-ray evidence 0-41879
- energetic particle trapping by Alfvén wave instabilities 0-31205
- G126.2+1.6 near 4U 0115+63 X-ray transient 0-8668
- G292.0+1.8, abundance anomalies, radial vels., possible Crab-like SNR 0-46628
- G292.0+1.8, young supernova remnant, high vel. material obs. 0-22064
- G339.2-0.4, radio recombination line obs. refutes SNR nature 0-46650
- G339.2-0.4, supernova remnant or planetary nebula, radio and optical obs. 0-22104
- G78.2+2.1 in Cygnus X region, H I 21 cm line emission maps 0-56917
- galactic coronae, production by supernovae rel. to intracluster medium origin and quasar absorpt. lines 0-31355
- galactic supernova remnants, new optical obs. 0-17636
- galactic supernova remnants, search for stellar remnants 0-26890
- Gum Nebula, temp. and density vars. (*French*) 0-26951



**supernova remnants continued**

- H 1538-32, new extended soft X-ray source detect., possible old supernova remnant 0-51912  
 HB 3, soft X-ray obs. 0-56915  
 HB 9, soft X-ray emission obs. 0-36697  
 high-velocity H I clouds, map and local supernovae shell model 0-26923  
 IC 443, H<sub>2</sub> detection at 2.1  $\mu$ m 0-17630  
 IC 443, high-rel. gas H $\alpha$  emission origin 0-41873  
 IC 443, shocked CO discovery 0-8669  
 interacting supernova remnants, struct. and evolution 0-4423  
 interacting supernova remnants, tunnels in sky 0-4409  
 Kepler's SNR, distance from interstellar absorption determ. 0-46651  
 LMC, SNRs identification from Einstein Obs. X-ray meas. 0-26980  
 LMC N 49, X-ray source 0525.9-66.1, gamma-ray burst obs. (*Russian*) 0-36739  
 Loop I, X-ray features, SNR model 0-22066  
 in M33, emission regions catalogue 0-46416  
 in M33, N/S abundance gradient, SNR evidence 0-56929  
 in M33, supernova remnants catalogue 0-41734  
 Milky Way near l=333°, 8.87 GHz obs. 0-22102  
 Monoceros ring, rel. to supernova-induced star form. in Monoceros OB2 assoc. 0-31334  
 N49 SNR in LMC, X-ray obs. of gamma-burst field 0-27019  
 in NGC 4449, extraordinary extragalactic supernova remnant spectrophotometry 0-56895  
 NGC 604, giant H II region in M33, SNRs rel. to content of high mass stars 0-31340  
 Orion OB1 association, direction, supernova remnants rel. to Copernicus obs. of interstellar matter 0-22050  
 primaeval galaxies, model emission spectra 0-46655  
 Puppis A, X-ray and Fe XIV 5303 Å emission 0-26962  
 southern supernova remnants, high resolution radio obs. 0-51849  
 Taurus A, intensity and polarisation at 9 mm wavelength 0-36732  
 Tycho's SNR, HEAO 1 obs. and structure study 0-51842  
 Tycho's supernova remnant, radio flux density meas. separated by 15-year interval 0-26955  
 Tycho SNR, weak X-ray source, ANS meas. 0-46701  
 Tycho SNR spectrum, model of optical emission from fast shock wave 0-46631  
 Tycho supernova remnant, radio struct. 0-56919  
 Tycho supernova remnant, Type I SNR, elemental abundances from X-ray spectrum 0-46635  
 Tycho supernova remnant, X-ray line emission obs. 0-46636  
 Vela supernova remnant, rot. measure and turbulent struct. 0-51836  
 Vela supernova remnant, X-ray maps 0-51838  
 Vela X supernova remnant, radio polarisation maps 0-56909  
 W28, RATAN-600 2-13 cm wavelength obs. of W28 A<sub>2</sub> H II region (*Russian*) 0-17642  
 W50, extended struct. correl. with SS 443 radio jet 0-31381  
 W50, optical filaments spectra rel. to SS 433 mass loss rates and lifetime 0-12804  
 W50, spectrum of optical nebulosity 0-51851  
 W50 (SS 433), optical remnant discovery 0-56916  
 X-ray obs. and quark stars in young SNRs, neutrino cooling 0-56858

**supernovae**

- see also supernova remnants*  
 in anonymous galaxies, three new discoveries 0-46589  
 Cassiopeia A supernova, O burning rel. to remnant abundance inhomogeneities 0-12797  
 collapse of massive star cores, supernova explosion from shock heating 0-56863  
 core collapse, neutral currents and neutrino Comptonisation in high-temp. nuclear matter 0-21905  
 core collapse, neutrino prod. and inelastic scatt. by nuclei at extreme temps. 0-36488  
 core collapse, shape instability pressure stabilisation 0-8537  
 core collapse, Thomas-Fermi model of warm nuclei 0-51648  
 Earth showered by lunar  $\gamma$ -ray ablation debris 0-56731  
 ejecta, dust grains sudden nucleation and growth 0-26941  
 in ESO 153-G27, discovery and magnitudes (1979 August 19 to October 15) 0-26892  
 explosion models, new solns. 0-12751  
 explosions, effect on stellar evolution 0-31315  
 explosions, off-center, rel. to high vel. pulsars form. 0-46587  
 extragalactic, X-ray bursts search using HEAO-1 satellite 0-46585  
 in galaxies, rel. to galactic coroneae and intracluster medium origin 0-31355  
 gas ejection from dwarf spheroidal galaxies driven by supernovae 0-22088  
 hydrodynamical acceleration of particles in supernovae and extragalactic radio sources 0-31313  
 interstellar medium, mechanical heating rate by supernova blast waves 0-36682  
 in M33, freq. from supernova remnants catalogue 0-41734  
 maximum of outburst as opportunity for mutual CETI search strategy 0-56723  
 MHD model, numerical anal. 0-46588  
 Monoceros OB2 association, evidence for supernova-induced star form. 0-31334  
 in NGC 1199, mag. 17 object, 1979 Sept. obs. 0-41846  
 in NGC 3733, discovery of mag. 15 object (1980 March 17) 0-51793  
 in NGC 4321, JHKL mags., 1980 Jan obs. 0-41847  
 in NGC 4321 (M100), interstellar Na I and Ca II absorption in spectrum 0-51847  
 in NGC 5854, discovery of mag. 15 Type I object (1980 March 20) 0-51793  
 nucleosynthetic yields of metals and stellar birthrate 0-51741  
 in planetary systems 0-56860  
 presupernova models and supernovae 0-56864  
 protosolar OB association supernovae, rel. to Allende isotopic anomalies and cosmochronology 0-4462  
 Rayleigh-Taylor convective overturn in stellar collapse, supernova explosion mechanism 0-41815  
 remnants evolution, hydrodynamic code for interacting remnants 0-4423  
 shell shock waves, cosmic ray acceleration, energy loss effects (*Russian*) 0-17449  
 shock wave acceleration of energetic charged particles 0-31189  
 shock waves in interstellar medium, cosmic ray acceleration 0-31179  
 SN 1181 (3C 58), absolute magnitude and type classification 0-56862  
 SN 1972e in NGC 5253, spectrum 0-41844

**supernovae continued**

- solar system origin, relation to supernova explosions 0-17509  
 spectrum before max. luminosity in Type I objects 0-41845  
 star formation trigger 0-26891  
 stellar, A>20 nuclei in advanced stellar evolution and supernovae 0-41817  
 stellar collapse, adiabatic hydrodynamics and shock wave propag. 0-56861  
 stellar remnants, spectroscopic search 0-26890  
 trigger for solar system formation, Allende meteorite evidence 0-12683  
 Tycho's supernova, distance and luminosity from fast shock wave model for remnant 0-46631  
 Tycho supernova, Type I supernova, nucleosynthesis rel. to remnant elemental abundances 0-46635  
 type II, nonequilibrium processes in evolution 0-46586  
 Virgo cluster supernovae, gravit. waves detectability by reson. antennas 0-8545  
 X-rays and gamma-rays recorded in Antarctic ice core 0-31314  
 C ignition in stellar C-O core, reaction rate enhancement due to strong screening 0-36613

**superparamagnetism**

- see also magnetic properties of fine particles*  
 crystals with dislocations, phase transitions of the second kind, dislocation superparamagnetism (*Russian*) 0-1957  
 Fe particles in glass-like C matrix, identification and props. 0-11229  
 frustrationless models, rel. to spin glasses 0-29561  
 particles, Mossbauer spectra, magnetisation vector precession 0-15872  
 particles, mutual attraction 0-29581  
 spinels, domain wall formation inhibition, effect on bulk mag. props. 0-11220  
 Co<sub>3</sub>Ga<sub>46</sub>, superparamag. response to low DC fields 0-44860  
 Co<sub>2</sub>Ga<sub>1.95</sub>Fe<sub>0.05</sub>, mag. behaviour, Mossbauer effect and DC magnetisation meas. 0-50244  
 Cu-Co, superparamagnetic, mag. aftereffects, dynamic neutron depolarisation study 0-50147  
 Cu-Co superparamagnetic particles, macrospin glass form. (*Russian*) 0-25165  
 Cu-Fe, dilute, low temp. heat capacity in mag. field, superparamagnetism 0-39804  
 Eu, Sr<sub>1-x</sub>S, insulating spin glass, mag. props. 0-2589  
 Fe clusters, supported, Mossbauer spectra 0-7220  
 Fe colloidal dispersion, mag. props., struct. and oxidation 0-34699  
 Fe film, on Cu and Ag substrates, mag. props., Mossbauer spectra meas. 0-11233  
 Fe-Al<sub>2</sub>O<sub>3</sub> granular film, interface props., Mossbauer spectroscopy 0-34336  
 Fe-SiO<sub>2</sub> granular film, interface props., Mossbauer spectroscopy 0-34336  
 Fe-SiO<sub>2</sub>(Al<sub>2</sub>O<sub>3</sub>)(ZrO<sub>2</sub>) granular films, superparamag., Mossbauer effect 0-7131  
 Fe-ZrO<sub>2</sub> granular film, interface props., Mossbauer spectroscopy 0-34336  
 Fe<sub>1-x</sub>Al<sub>x</sub>OOH, Mossbauer study, determ. of Al content and mag. props. 0-39938  
 Fe<sub>2(1-y)/3</sub>Mg<sub>(1+y)/3</sub>Ti<sub>2</sub>O<sub>4</sub>, Mossbauer spectra anal., model 0-20560  
 (Fe<sub>0.04</sub>Ni<sub>0.96</sub>)<sub>80</sub>P<sub>10</sub>B<sub>10</sub>, amorphous magnetisation, field and temp. depend. 0-39755  
 (Fe<sub>x</sub>Ni<sub>100-x</sub>)<sub>80</sub>P<sub>10</sub>B<sub>10</sub>, amorphous, elec. resist., 2 to 300K, composition depend. 0-44562  
 FeS<sub>2</sub>, oxidation, Mossbauer spectroscopic and magnetokinetic studies, 400-500°C 0-44880  
 Hg, liquid, ferromag., containing Fe particles, time depend. magnetisation 0-44877  
 MnBi, mictomag. alloys, elastic props. (*Russian*) 0-7141  
 Ni dispersions, semi-amorphous, on Al<sub>2</sub>O<sub>3</sub>-graphite, mag. characterisation 0-44876  
 NiFe<sub>2</sub>O<sub>4</sub>, precipitation from silicate glass, Mossbauer study 0-54998  
 RbFeCl<sub>2</sub>·2H<sub>2</sub>O, 2D Ising system, crit. fluctuations, Mossbauer spectra study 0-44842  
 V<sub>1-x</sub>Fe<sub>x</sub>, low temp. sp. ht. and mag. props. 0-2548  
 V<sub>1-x</sub>Fe<sub>x</sub>H<sub>n</sub>, low temp. sp. ht. and mag. props. 0-2548

**superplasticity**

- alloy, flow and failure, review 0-50690  
 brass  $\alpha/\beta$ , two-phase superplastic alloy, hydrodynamical behaviour, constitutive law 0-40452  
 deformation mechanisms, review 0-50691  
 finely crystalline materials rel. to displacement along grain boundary (*Russian*) 0-15184  
 heat-resistant alloys, installation for mech. tests under superplasticity conditions 0-55603  
 metals, mechanical props., testing and modelling 0-25811  
 refractory multiphase systems, infusible, some novel effects, rel. to practical appls. 0-55460  
 steel, 0Kh12G14N4Yu2, struct. after deformation under conditions of superplasticity 0-21031  
 steel, Cr, stress relaxation, superplasticity and thermal cycling (*Russian*) 0-21019  
 steel, stainless, ferrite to austenite decomposition 0-3073  
 steels, ultrahigh C, superplastic, mech. behaviour at elevated temps 0-21028  
 structural, theory 0-16386  
 Al-Cu, single and two phase, superplastic behaviour 0-11709  
 Al-Cu-Zr, superplastic alloy Supral, solidification and recrystallisation 0-7550  
 Al-Cu-Zr (6, 0.4 wt.%), superplastic flow activation energy 0-11701  
 Al-Cu-Zr (6, 0.4 wt.%), superplastic deformation characts. 0-16387  
 Al-Ge (0 to 8 wt.%), superplastic props. (*Russian*) 0-45345  
 Al-Si eutectic alloys, superplasticity 0-11710  
 Al-Zn alloys, recrystallisation and superplasticity, HVEM straining 0-39207  
 C steel, superplasticity due to successive deformations (*Russian*) 0-55464  
 Cu alloy, superplastic, microscopic examination of internal void formation 0-16383  
 Fe laminates, superplastic bonding 0-25981  
 Pb-In (40 wt.%), solid soln., single phase, superplastic behaviour 0-21048  
 Pb-Sn, eutectic, superplastic behaviour, grain size effect 0-7635  
 Pb-Sn eutectic, strain rate sensitivity index, expt. comparison of different methods 0-3144  
 Sn-Bi, eutectic, superplastic anisotropy (*German*) 0-25808  
 Sn-Pb eutectic, strain rate sensitivity of flow stresses, grain boundary sliding during superplastic, non-superplastic deform. 0-7645  
 Ti alloy OT4, high plasticity effect 0-35272



**superplasticity continued**

- Ti-Al-V (6.4 wt %), superplasticity, effect of temp. 0-7639  
 Zn-Al (22 at %) eutectic, superplastic, microscopic examination of internal void formation 0-16383  
 Zn-Al superplastic eutectoid alloy, low strain rate behaviour 0-40458  
 Zn-Al-Cu (18, 4 wt %), plastic deform. at room temp., superplastic props., tensile strength (*Czech*) 0-45360  
 Zr-Nb (2.5 wt %), superplastic and strain rate depend. plastic flow, 873 to 1373K 0-30052

**superradiance**

see also *acoustic superradiance*

- alkali metal, Rydberg states and microwaves, spectroscopy, masers and superradiance study 0-53248  
 amplified spontaneous emission in spherical and disk-shaped laser media 0-1177  
 atomic oscillatory superfluorescence, statistical props. 0-47938  
 bidirectional laser amplifiers, amplified spontaneous emission intensity fluctuations 0-37988  
 dye solution amplifying dynamic holograms, wavefront reversal 0-48331  
 N two-level atoms, interaction with radiation field in restricted rotating wave approx. 0-5713  
 N-two level atoms, interaction with radiation field in restricted rotating wave approx., numerical anal. 0-5714  
 parasitic superfluorescence suppression in backward Raman amplifiers 0-38073  
 phase transition problem, applicability of Wang-Hion method 0-31695  
 plasma, nonideal, in electric field 0-38568  
 POPOP dye vapour lasers, optical and electron beam pumping, review 0-48237  
 POPOP vapour, picosecond generation of radiation 0-48238  
 pump depletion effect, superradiance in Raman light scatt. 0-9957  
 ruby laser, generation, amplification of high power picosecond, pulses depend. on superluminescence 0-53305  
 ruby NMR laser, dynamic props. from point of view of synergetics 0-43341  
 Schwinger source theory 0-48195  
 slightly detuned sources, quantum theory 0-14307  
 spatially extended medium, oscillating superfluoresc., leading pulse shape and delay 0-23648  
 spectroscopy, superradiance triggering 0-52324  
 superfluorescence, phase-wave fluctuations 0-23652  
 superfluorescence, tipping angle and quantum fluctuations, pumping process effects 0-5718  
 three-level molecular system, cooperative evolution, transient effects of dephasing and relax. 0-28184  
 transverse effects in superfluorescence 0-37979  
 two-level atomic system, superfluoresc. fluctuations 0-23651  
 CdS active surface, exciton stimulated emission and superradiance refl. spectra, props. 0-25411  
 Cs atom, F-levels lifetime meas. using partially superradiant population 0-9575  
 Cs, superradiance triggering spectroscopy 0-52324  
 Eu, visible superfluorescence cooperative reson. Stokes radiation 0-5500  
 La<sub>2</sub>Mg<sub>3</sub>(NO<sub>3</sub>)<sub>12</sub>·24H<sub>2</sub>O:Nd<sup>3+</sup>, proton raser, self-radiating nuclear spin system (*German*) 0-53298  
 NH<sub>3</sub>, efficient energy extraction by superradiant emission 0-53271  
 Xe-He source, intensity fluctuations of amplified spontaneous emission at 3.51  $\mu$ m 0-32957

**supersaturation control** see *chemical variables control*

**supersaturation measurement** see *chemical variables measurement*

**supersonic flow**

see also *shock waves*

- aerodynamic shape optimisation for bodies in supersonic flow 0-38438  
 air scoops at supersonic and hypersonic vels., throttling, separation and central body cooling 0-14739  
 amplification coefficient, effect of mixing conditions in a laval nozzle 0-6085  
 analogue modelling, supersonic flow around a wing 0-28530  
 asymptotic, supersonic, 2-dimens. turbulent wakes, fully developed mean flow criteria 0-14706  
 attached supersonic turbulent boundary-layer/flap interaction pressures, correlation technique 0-48683  
 blunt axisymmetric bodies, supersonic flow modelling, drag and entropy layer 0-48740  
 blunt body, boundary and wake, supersonic viscous gas flow, numerical soln. 0-38441  
 blunt body, unsteady supersonic flow, grid characteristic method 0-38442  
 blunt body flow of viscous perfect gas and nonequib. gas mixture 0-28578  
 blunt body in supersonic flow, Navier-Stokes eqns. numerical computation 0-10263  
 blunt cone hypersonic and supersonic flow, near wake Reynolds number effects, interferometric obs. 0-43733  
 boundary layer, Reynolds number effects on turbulence field 0-19434  
 boundary layer visualisation in shock tube, book contrib. 0-1715  
 cascade deviation, prediction and measurement 0-24049  
 cascades, supersonic and transonic compressor, unstarted choked regime calc. (*Chinese*) 0-43730  
 chemical laser flowfield, laser induced I<sub>2</sub> fluorescence meas. 0-38008  
 circuit breaking arcs, current zero arc model based on forced convection 0-33831  
 combined bodies, supersonic inviscid flow, shock interactions (*Chinese*) 0-6084  
 compressible and incompressible flows, recent theoretical and expt. developments, book 0-1620  
 cones, axisymmetric impingement of supersonic air jets, shock pattern 0-48741  
 cones at incidence, supersonic viscous flow 0-38439  
 continuum source particle beam properties, comput. modelling 0-26062  
 control jets, gasdynamic features, 3-D subsonic and supersonic flows 0-6112  
 cylindrical channel, sudden expansion of supersonic jet 0-48800  
 delta wings in supersonic flow, crossflow shocks 0-48749  
 density distribution for free supersonic jet emerging against pressure difference (*German*) 0-1666  
 electrodynamic supersonic flow over wedge in presence of charged massive particles 0-33685  
 expansion corner effect on shock-wave and boundary layer interactions 0-14737  
 finite element formulation for subsonic and transonic flow 0-28526  
 finite length plate in supersonic low density flow, surface pressures and corrections 0-14741  
 flat plate trailing edge in rarefied supersonic airflow, boundary layer 0-24046  
 floating heat layer interaction with solid wall, computation, book contrib. 0-1642  
 freon gas flow around blunt object, bow shock instability 0-10266  
 gas flows, selfgravitating, thermodynamic processes and radiation, numerical method, shock fronts 0-14848  
 gas particle flows over wedge (*German*) 0-43731  
 gases, high velocity flows, nonequib. homogeneous condensation, determ. of maximal supercooling 0-6086  
 heavy-particle impurity suspension effect on viscous shock layer gas flow 0-28554  
 high Reynolds number supersonic flow, compression corner flowfields, turbulent boundary layer separation 0-14735  
 ideal gas flow, choked and supercritical, through orifices and convergent conical nozzles, numerical soln. 0-38474  
 inlet, flowfield computation using bicharacteristics method with shock wave fitting 0-38443  
 inviscid conical corner flowfields, complex shock interactions 0-48739  
 inviscid hyperbolic flow, computational algorithms tests 0-27140  
 ionised gas, nonequilibrium, supersonic, corner expansion flow, physical aspects 0-1639  
 jet, nonsteady interaction with barrier, math. model of oscillatory cycle 0-19462  
 jet, supersonic, cold, coaxial, acoustic, flow characts. 0-1656  
 jet, supersonic gas, penetration into the ground (*Russian*) 0-28544  
 jet, underexpanded, discharging into opposing supersonic stream, wave structure anal. 0-19461  
 jet injection, separation zone, boundary layer thickness and transverse curvature effects 0-48745  
 jets, acoustic radiation using double-pulse holographic interferometry 0-14678  
 jets, two-phase supersonic flow around a sphere 0-6114  
 laminar boundary layer reattachment, num. soln. 0-53809  
 laminar boundary layers, strong slot injection, flow separation 0-48738  
 laminar separation of supersonic stream, Reynolds no. effect 0-19432  
 laminar viscous, numerical anal., separation 0-24062  
 Laval nozzle, supercritical steam supersonic discharge 0-48765  
 linearised, improved higher-order panel method 0-6082  
 liquid containing gas bubbles, struct. of supersonic waves and cavitation development 0-33643  
 low Reynolds number supersonic air jets, noise generation by instabilities 0-23831  
 Mach waves, kinematics inside and outside supersonic jets, book contrib. 0-1640  
 microwave discharge, supersonic flow in waveguide, electron densities, possible laser 0-38842  
 multiphase mixture, two-dimens. nozzle and jet supersonic flows 0-48780  
 near-sonic region, steady inviscid flow field calc. (*German*) 0-1643  
 near-wake phenomena, with and without external compression, axial and radial air injection effects 0-10273  
 nozzle flowfields, fully viscous and Navier-Stokes solns., comparison, book contrib. 0-1641  
 nozzle flows with boundary layer, CO<sub>2</sub>-N<sub>2</sub>-He, gain coefficients 0-14312  
 nozzles, supersonic axisymmetric, film cooling efficiency 0-48710  
 plane flow, past a curved wedge, quasi-linear hyperbolic systems (*French*) 0-10261  
 plasma jet, supersonic damaging of metals, mech. momentum hole 0-2065  
 plasma stream, dense, shock braking processes, radiation-gasdynamic obs. 0-19635  
 plate with vertical cylindrical projection, aerodynamic coeffs., approx. method 0-48746  
 Prandtl supersonic jet problem, linear aerodynamic theory formulae, validity, book contrib. 0-6090  
 quasihomogeneous flow, turbulence in presence of density and vel. fluctuations 0-1638  
 resonance tube, oscillation excitation from supersonic jet (*Japanese*) 0-24116  
 rotating propulsive nozzle flowfields for nonequilibrium chemically reacting supersonic flow 0-48764  
 shell, cylindrical in supersonic flow, vibration, finite element anal. 0-5973  
 shock wave analysis flow through body wall 0-38447  
 sonic boom propag. in thermosphere 0-33305  
 sphere, flow pattern visualisation by broad light source holographic interferometry 0-19008  
 spherically blunted cone with massive surface blowing, laminar and turbulent flows, shocks 0-38445  
 spiked bodies in supersonic flow, nonstationary separation 0-38460  
 supersonic to subsonic transition with local supersonic regions, book contrib. 0-1627  
 three dimensional separated turbulent flows at supersonic speeds 0-19435  
 triple deck problem for supersonic and subsonic flow, numerical technique for separation 0-14757  
 turbulent shear stresses in compressible boundary layers 0-14736  
 turbulent skin friction at subsonic and supersonic speeds, wake component influence 0-19340  
 two-dimensional transverse sonic jet interaction with supersonic stream, application factor 0-24047  
 underexpanded gas jet issuance into supersonic flow 0-38468  
 unsteady aerodynamic modelling for arbitrary motions 0-19433  
 unsteady lifting surface theory in subsonic and supersonic flow, integral transform method 0-19437  
 unsteady-state flow around bodies of variable form 0-6087  
 viscous compressible flow at high Reynolds number, global approach and coupling approach 0-48742  
 viscous gas flow, subsonic and supersonic, simplified Navier-Stokes eqns. 0-31520  
 viscous supersonic flow over external axial corners, shock and bubble generation computation 0-14734  
 water flow with air contents, partially- and super-cavitating hydrofoils in cascade, analysis method (*Japanese*) 0-14763  
 wind tunnel test program for determining effect of spin on boundary-layer transition at Mach numbers 5 and 8 on 9-deg. cone configurations 0-14864  
 wing, supersonic gas flow, numerical method and routine 0-38440  
 Ar arcs in supersonic flow, numerical analysis 0-38776



**supersonic flow continued**

- H<sub>2</sub>O low density flow temp. and density meas. by submillimetre spectroscopy 0-43816
- N<sub>2</sub> plasma, spatial distrib. in transverse-discharge supersonic stream, continuum theory and probe meas. 0-48866
- Na vapour jet target, gating and pumping action 0-10281
- SF<sub>6</sub>, supersonic jet, condensation and gasdynamic cooling 0-6089
- SF<sub>6</sub>, supersonic jet expanding into vac., interaction with CO<sub>2</sub> laser beam 0-5584
- XeF, supersonic expansion jet, B-X system rot. and vibr. anal., isotope intervals, fluoresc. spectra 0-14174

**supersonics** *see* **supersonic flow****supersymmetry***see also* **supergravity**

- $\sigma$  model, nonlocal charges from zero curvature 0-31995
- $\sigma$  model, supersymmetric nonlocal conservation laws 0-46938
- $\sigma$ -model, nonlinear, superconformal invariance in 4-dimens. space-time 0-37154
- $\sigma$ -models, nonlinear, with  $N=Z$  extended supersymmetry in 4-dimens. 0-47174
- A(0,1) Lie superalgebra, Fock-type representation 0-37181
- algebraic approach to supergravity in superspace 0-46915
- algebras, unusual, appls. in particle physics 0-27419
- antisymmetric tensor gauge fields, local supersymmetry without gravity 0-46910
- auxiliary fields and tensor calculus for  $N=2$  extended supergravity 0-46920
- axial currents, supercurrents and anomalies in supersymmetric QED 0-46933
- Bose analogs to supergravity, construction problems 0-46926
- broken supersymmetry mass formula, quantum corrections 0-27424
- Casimir invariants and characteristic identities for generators of graded Lie algebras 0-13227
- classical field theories, non-signification of super gravitation 0-27193
- complex and quaternionic supergeometry 0-46941
- complex spinors and unified theories 0-46943
- conference, supergravity, Stony Brook, USA (Sept. 1979) 0-46738
- constraints for supergravity 0-46918
- covariance group structure, graded conformal, affine groups 0-22264
- differential forms on supermanifolds (*Russian*) 0-4889
- dimensional regularization and supersymmetry at the two-loop level 0-17854
- Dirac particle propagator, supersymmetric methods 0-342
- expanded, spontaneous violation, Goldstone fields (*Russian*) 0-47218
- extended supergravity, dimensional reduction simplifications 0-52110
- extended supersymmetry invariants by dimensional reduction 0-47213
- exterior calculus and two-dimensional supersymmetric models, super sine-Gordon model 0-47214
- gauge supersymmetry, supergraph anal. 0-27422
- globally supersymmetric multiplets without local extensions 0-17856
- higher spin gauge fields, beyond 3/2, systematics 0-46937
- hypergravity, consistency requirements 0-46936
- massive spinning particle in Minkowski space equivalence to massless particle in de Sitter space 0-119
- massive vectormultiplets in supergravity 0-46927
- non-perturbative quantum field theory, lattice renormalisation construction 0-9098
- non-relativistic model, spontaneous supersymmetry breaking and superconductivity 0-32031
- nonlinear  $\sigma$  model, nonlocal charges and currents 0-27410
- nonlinear model supersymmetric extension, Kahler manifolds, Grassmann manifolds and  $CP^{n-1}$  models 0-9113
- nonlinear superfields and quark confinement (*Chinese*) 0-42346
- nonlocal currents for supersymmetric nonlinear models 0-52414
- nonrelativistic supersymmetry, relevance to many-body problems 0-22537
- OSp(1,4) supergroup, Wess-Zumino model classical solns. 0-36928
- perturbation theory supergraphs 0-13229
- physico-geometrical comments, unified field theories and supergravity, gauge transformations 0-364
- QED, absence of radiative corrections to axial current anomaly 0-13242
- quantum corrections to the quadratic mass formula of broken supersymmetry 0-46942
- quantum parafield theory and supergroup transformations 0-9124
- relativistic string quantized in four-dimensional space, supersymmetrical Lagrangian in QCD principles (*Russian*) 0-13276
- scalar supersymmetric theories, characterisation by Bose field transformation 0-32033
- self-duality and helicity in supergravity 0-46929
- sine-Gordon eqn., inverse scatt. in higher dimensions 0-47165
- sine-Gordon eqn., prolongation struct. and inverse scatt. formalism 0-47173
- Sine-Gordon model, infinite set of local quantum conservation laws 0-47207
- sine-Gordon model, supersymmetric solitons and monopoles 0-31991
- sine-Gordon supersymmetric model, higher local quantum conserved currents 0-52435
- SO(8) extended supergravity 0-4914
- SO(8) supergravity derivation 0-12975
- soliton quantum mechanical mass in supersymmetric theories 0-22536
- spin 5/2 theories, supergravity extensions beyond SO(8) 0-46935
- SU(8) supergravity supersymmetry breaking 0-46908
- superconformal symmetry breakdown as guide to supergravity constraints 0-46930
- superfield covariant derivatives for O(1) and O(2) supersymmetry 0-46914
- superfield Feynman graphs, loop calculations 0-46906
- superfield supergravity with symmetry 0-8891
- supergraph formalism UV finiteness in gauge supersymmetry 0-46913
- supergravity, geometrization in superspace and local supersymmetry 0-8890
- supergravity constraints, algebraic understanding 0-46921
- supermanifolds, Lie superalgebras and superspace 0-9125
- superspace formulation for supergravity, book contrib. 0-22261
- superspace geometry of supergravity 0-46909
- superspace tensor calculus formulations, relations to supergravity 0-46922
- supersymmetric point particles and monopoles with no strings 0-52432
- unification of fundamental forces in nature, elementary particle constituents SU(3)<sub>c</sub> gauge symmetry, review 0-27448

**supersymmetry continued**

- universal supersymmetry and its need for grand unification theories 0-13230
- Wess-Zumino model, massive, dimensional regularisation, supersymmetry 0-27398
- $e^+e^-$  annihilation, spin-0 electron or muon pair prod., cross section supersymmetry predictions 0-32092
- supply systems (electric)** *see* **power systems**
- suppression wavemeters** *see* **wavemeters**
- suppressors (surge)** *see* **surge protection**
- surface acoustic wave devices**  
*see also* **acoustic microwave devices**; **acoustic parametric amplifiers**; **acoustic parametric devices**; **acoustic parametric oscillators**
- acoustic focusing device with IDT on thin piezoelectric plate 0-1398
- acousto-optic tunable TE-TM mode convertor on diffused waveguide 0-53477
- acousto-optical devices critical assessment and development trends (*Czech*) 0-23777
- acousto-optical devices for real- and near-real-time signal processing 0-10024
- acoustooptic Bragg deflector, wide-band guided wave, using tilted-finger chirp transducer 0-14440
- bandpass filters, approx. parameter anal. (*Russian*) 0-23858
- bandpass filters with quarter wave reflections, design 0-19183
- Bleustein-Gulyaev waveguides with gratings, anal. Bleustein-Gulyaev waveguides with gratings, anal. 0-1391
- conversion to bulk plate modes in shallow gratings 0-1385
- convolvers, enhancement of convolution voltage due to transverse drift of carriers 0-1381
- delay line filters, wideband, low insertion loss, VHF band 0-28398
- delay line signal processors using acousto-optic interactions, real time system 0-28384
- delay lines, appls. of amorphous magnetic-layers 0-28389
- delay lines, combined triple-transit and bulkwave suppression 0-53565
- dispersive delay lines, new cut of quartz for temperature stability 0-19185
- edge-bonded surface-acoustic-wave transducer array 0-1395
- elastic surface waves propag., characts. for SAW filters, book contrib. 0-1378
- electrode-withdrawal weighted filters, method for reducing sidelobes 0-5875
- filter, band-pass, design and expt. results (*Czech*) 0-19201
- filter design and implementation, book contrib. 0-1394
- filter design for TV, CATV and radar appls. 0-53579
- filters, design, construction, appl., book 0-1393
- filters, low insertion loss, using multiphased unidirectional transducers 0-28397
- filters, narrow band transversal types and interdigital transducers, review 0-28395
- filters, synthesis, limitations of phys. model in terms of number of fingers and material const. 0-28399
- finite SAW transducer, surface charge density and elec. field distrib., moment method 0-23857
- frequency to voltage convertor using SAW linear FM chirp filter 0-19182
- grating-resonator filter, behaviour of unidirectional transducers 0-5877
- IDT, electrode charge distrib. as element factor, anal. 0-1396
- integrated optic Bragg spectrum analyser design 0-33237
- interdigital transducer, book contrib. 0-1400
- Lamb wave transducer with three operation modes, communication system appls. 0-43583
- memory correlator using nonlinear interactions (*French*) 0-33294
- memory correlators, p<sup>n</sup>n SAW, modified theory 0-43563
- metal-ZnO-SiO<sub>2</sub>-Si structures, charge injection 0-49919
- metallic gratings, equivalent circuit of step discontinuity, rel. to SAW devices 0-33389
- metallisation, use of Cu-doped Al 0-23856
- multichannel signal processing using acoustooptic techniques 0-19160
- narrowband matched SAW filters realisation (*Russian*) 0-23850
- optical processing systems, seminar, Huntsville, USA (May 1979) 0-46732
- physical props. and communication signals processing applications and devices 0-38162
- piezoelectric film, third-order piezoelec. and dielec. const. meas. using surface acoustic waves (*Japanese*) 0-55042
- piezoelectric semiconductor SAW convolver, effect of transverse drift of carriers on operation, theory and expt. 0-14529
- quartz, delay line second harmonic generation in SAW (*French*) 0-34285
- resonator, distributed-feedback, design, computer model and construction (*Flemish*) 0-5899
- resonator filters, improved temp. stability using multiple coupling paths 0-19175
- resonator filters with enhanced out-of-band rejection 0-19179
- resonators using withdrawal weighted reflectors 0-19180
- SAW/CCD programmable matched filter 0-5896
- side-entry surface acousto-optic interaction signal processor 0-48174
- signal processing, comparison of optical and SAW techniques 0-48173
- signal processing appls., review 0-38204
- signal processing research programme of United States Air Force 0-48171
- slanted device technology for radar system appl. 0-19181
- sonar beamforming by CCD scan conversion for SAW chirp-Z transform 0-43552
- status report of SAW and magnetostatic wave devices, transversal filters appl. 0-28394
- thin film interdigital transducers for SAW devices at GHz freqs. form. by electron beam lithography 0-4702
- transducer, mixed matrix representation of interdigital transducers 0-19184
- transducer with capacitive electrode weighting, band-pass filters 0-48544
- transversal filters, interdigital transducer models for accurate design implementation 0-28396
- transversal filters, synthesis using interdigital transducer models 0-5897
- tunable resonator oscillator, appls. of amorphous magnetic-layers 0-28389
- TV IF filter, temp. stable ZnO/Pyrex glass substrate 0-43566
- two-phase PSK modulator employing SAW delay line, fundamental performance 0-33398
- As<sub>2</sub>S<sub>3</sub>, film waveguide, acoustooptic deflection and modulation of light by stationary phase grating struct. 0-5841



surface acoustic wave devices continued

- CdS SAW convolver, effect of transverse drift of carriers on operation 0-14529
- InAs/LiNbO<sub>3</sub> structure, SAW generated transverse acoustoelectric voltage, image scanning and signal processing appl. 0-49826
- Y-Z LiNbO<sub>3</sub>, radiation patterns of bulk acoustic modes from finite interdigital transducer 0-43491
- LiNbO<sub>3</sub> SAW plate convolvers at 1 GHz 0-1382
- LiNbO<sub>3</sub>-CdSe structure, electroacoustic effects and signal convolution 0-10098
- ZnO thin-film, for HF range (*Japanese*) 0-53598

surface acoustic waves

- see also *acoustic waves*; *Rayleigh waves*; *surface acoustic wave devices*; *surface phenomena*
- anisotropic graded index waveguide, acoustooptic interaction efficiency freq. depend. 0-23776
- Brillouin scattering from surface waves, appl. of surface Green's function mapping method 0-40125
- bulk particle motion fields induced in optically transparent plate, differential optical measurements 0-53576
- colinear interaction between acoustic and optical waves in planar waveguide, radiation into substrate 0-53452
- diffraction in quartz 0-38160
- end-fire piezoelectric transducers, wideband excitation of surface elastic waves in microwave range 0-10105
- Franz-type wave, rel. and attenuation, generation on outside of solid cylinders in water (*French*) 0-28370
- GHz quartz transversal filters, fabrication limits and characteristics 0-43562
- nonlinear acoustics 8th symposium, conf., Paris, France, July 1978 0-33277
- nonlinear acoustoelectro-luminescence excited by SAW 0-45143
- nuclear reactor pressure vessels, US pulses propag. by means of acoustic emission (*German*) 0-3274
- phosphor, EL-590 M type, electroluminesc. excitation by SAW, nonlinear effects 0-16104
- photochromic film waveguide, acousto-optical props., integrated optics appl. 0-33207
- physical props. and communication signals processing applications and devices 0-38162
- piezoelectric crystals, surface modes, acoustic wave propagation 0-20026
- piezoelectric crystals, surface wave solns. nonexistence example 0-6611
- piezoelectric film, third-order piezoelec. and dielec. consts. meas. using surface acoustic waves (*Japanese*) 0-55042
- piezoelectric semiconductor plates, natural oscils. modulated by charged particle beam, energy losses (*Russian*) 0-2259
- piezoelectric semiconductors, surface phonon acoustoelectric interaction, elastic anisotropy effects 0-6610
- plasma ion-acoustic waves excitation by piezoelectric surface acoustic wave 0-10381
- plasmon-acoustic wave interactions due to deformation potential (*Russian*) 0-15356
- powders, SAW interactions, for various directions of propagation 0-49486
- quartz, SAW cut with orthogonal temp. compensated propag. directions 0-10770
- quartz wedge, reflection, transmission and conversion of normally incident SAW 0-2257
- reflection from finite system of periodic perturbations 0-10059
- reflection from thin-strip overlays, first-order coeff. 0-1376
- rough surface sound reflection, surface wave effects (*Russian*) 0-1377
- scattering, surface wave formation and resonance relation (*French*) 0-8809
- scattering from elliptical cracks for failure prediction 0-55608
- second harmonic generation in finite amplitude SAW, anisotropic media (*French*) 0-34285
- semiconductor surface characterisation using SAW 0-11069
- shear waves in periodic structures, electronic damping and amplification
- shear waves in periodic structures, electronic damping and amplification 0-19124
- Stoneley wave study of adhesively bonded interface 0-49530
- strength of nonlinear interaction between collinear surface acoustic waves 0-33295
- surface skimming bulk waves, excitation and detection on rotated Y-cut quartz 0-43492
- surface-skimming bulk wave excitation, analysis using Green's function formulation 0-53519
- thermopiezoelectric material, monoclinic symmetry, surface wave propag. 0-44403
- transition metal dichalcogenides, layered, surface Brillouin scatt. obs., surface ripple and elasto-optic mechanisms 0-16048
- US, nonlinear interaction in 2-6 MHz range (*French*) 0-33296
- US wave diffraction, expt. and anal. 0-5898
- velocity measurement, high accuracy method 0-38189
- Al alloys, fatigue, microcrack development, acoustic SHG study 0-35440
- Al, surface wave scatt. from elliptical cracks for failure prediction 0-55608
- AIN, epitaxial film growth by MBE, physical and optical props. 0-2293
- Au film on (100) Si, measurement of SAW dispersion using acoustic microscopy 0-53575
- Au film on Si, SAW dispersion and film thickness meas. 0-10769
- Bi<sub>12</sub>GeO<sub>20</sub>, finite amplitude SAW distorted rippling profiles, optical probing obs. 0-34287
- CdS crystal, SAW amplification, bulk and acoustic noise 0-39637
- CdS, semicond., coexistence of surface and bulk acoustic waves in acoustoelec. domains 0-44404
- GaAs, surface characterisation using SAW 0-11069
- GaP, powder, electroluminesc. excitation by SAW, nonlinear effects 0-16104
- GaP, surface characterisation using SAW 0-11069
- InAs/LiNbO<sub>3</sub> structure, SAW generated transverse acoustoelectric voltage, image scanning and signal processing appl. 0-49826
- LiNbO<sub>3</sub>, and LiTaO<sub>3</sub>, finite amplitude SAW distorted rippling profiles, optical probing obs. 0-34287
- LiNbO<sub>3</sub> interfaces, SAW reflection, light scatt. meas. 0-34286
- LiNbO<sub>3</sub>, SAW convergence props. 0-24726
- LiNbO<sub>3</sub>, SAW propagation and scatt., finite difference anal. 0-20595
- LiNbO<sub>3</sub>, SAW reflection from conducting strips 0-5853
- LiNbO<sub>3</sub>:Na<sup>+</sup>(Co<sup>2+</sup>,Zr<sup>4+</sup>) films, LPE growth from Li<sub>2</sub>O-V<sub>2</sub>O<sub>5</sub> flux, X-ray and acoustic characterisation 0-15383

surface acoustic waves continued

- Nb<sub>3</sub>Sn, supercond., thin film, US attenuation of SAWs 0-49988
- Ni crystals in strong mag. field, EM excitation and vel. dispersion of sound (*Russian*) 0-39837
- PbTiO<sub>3</sub> ceramics, temp.-compensated, for SAW appl. 0-15355
- Si, surface characterisation using SAW 0-11069
- Si:H, amorphous, Brillouin scattering from acoustic bulk and surface waves 0-11425
- SiC, power, electroluminesc. excitation by SAW, nonlinear effects 0-16104
- Si<sub>3</sub>N<sub>4</sub>, hot pressed, surface wave scatt. from elliptical cracks for failure prediction 0-55608
- SiO<sub>2</sub>, and SiO<sub>0.7</sub>, amorphous sputtered thin film, US anomalies, 0.5-300K 0-34145
- SiO<sub>2</sub>, finite amplitude SAW distorted rippling profiles, optical probing obs. 0-34287
- Tl<sub>3</sub>VS<sub>4</sub>, growth of inclusion free crystals, for surface wave and bulk wave acoustic devices 0-25549
- YIG, dilute, magnetoacoustic surface wave excitation by RF field on Bloch walls 0-25178
- YIG substrates, magnetoelastic surface waves, magnetostatic reson. anal. 0-20441

surface activity see *surface energy*

surface-atomic beam collisions see *atom-surface impact*

surface chemistry

- see also *chemisorption*; *corrosion*; *oxidation*
- ablating layer, rate of physical and chemical transformation (*Ukrainian*) 0-50887
- alien layer build-up on contact materials (*German*) 0-7852
- alkali silicate glasses in aqueous solutions, leaching kinetics rel. to surface pot. 0-11803
- boriding, with a thermally unstable gas (B<sub>2</sub>H<sub>6</sub>) 0-30159
- catalysis and surface science, review 0-40740
- catalyst, granular bed, static, flow transfer processes 0-45554
- catalyst surface mag. field effect on mol. dissociation rate 0-16721
- chemisorption kinetics, power adsorption isotherm, entropy correction 0-40734
- conference on surface science, Cambridge, England (March 1979) 0-36773
- crystal growth and deposition, gaseous phase, chem. transport reaction 0-44161
- cyclobutene, strong collision and thermal decomp. on surface, variable encounter method calcs. 0-50885
- gas mixture, multicomponent, transport equations near catalytic surfaces 0-43821
- gas-solid interface, electronic struct. HFR calc. 0-54745
- haematite particles, crud deposition on heat transfer surface, surface chemistry 0-35376
- halide dioxide radical form., H<sub>2</sub>O<sub>2</sub> decomposition of halide-coated surface, EPR obs. 0-7851
- heterogeneous catalysis reaction mechs., electron pair behaviour and surface orbitals 0-55705
- high temperature metallic species, absorpt. and fluoresc., high temp. fast flow reactor technique 0-42231
- hydrocarbons, formation on metal surfaces in fusion reactors 0-21322
- hydrocarbons, reactions, rate consts., temp. depend., photolysis, high temp. fast flow reactor technique 0-42231
- interface, stability problem, diffusion, reaction and convection 0-33567
- interfacial organic chem. processes 0-26050
- interstellar dust, surface chemistry in mixed oxide grains model 0-26934
- metal, H<sub>2</sub>-diffusion-rate-limited hydriding and dehydriding kinetics 0-35764
- metal-gas reactions, surface chemiluminesc. study 0-55708
- metals and alloys, sulphidation mechanism, review (*Polish*) 0-45413
- molecule-metal interaction and surface reactions, theoretical description 0-39652
- multivalent binding to substrate, linear differential equations in chemical equilibrium calculations 0-30279
- propionic acid, adsorbed in thin film tunnel junctions, hydrogenation and deuteration, IETS obs. 0-45547
- protein-substrate binding, linear differential equations in chemical equilibrium calculations 0-30279
- γ-quartz, reaction, with NaCl-KCl melt, exam. of struct., IR absorption spectra 0-55706
- rheological props., terminology and symbols 0-26065
- SiC-ZZ 0-42744
- silicidic formation in thin layers of W or Mo (*German*) 0-7859
- SIMS, appl. to surface reactions (*French*) 0-45603
- solar energy utilisation, photoelectrochemical systems (*German*) 0-45713
- solid-gas reactions, existence of instabilities 0-7861
- sol, primary and secondary coagulation and heterocoagulation, role of surface chemistry 0-45551
- steel, stainless, reduction of oxide layer by H atoms 0-40738
- surfactant inhibition of electrochem. reaction rate, random error effect on characteristic parameters 0-40705
- temperature programmed desorption with reaction 0-6621
- triboelectric charging technique for surface contamination analysis 0-11966
- two-dimensional colloidal state concept and role in activity of solids 0-55704
- Zircaloy-4, heat treatment in SiO<sub>2</sub> capsules, vapour transport of Zr and Si 0-55437
- Ag (110), adsorption, O<sub>2</sub>-induced, and reaction of H<sub>2</sub>, water, CO, and CO<sub>2</sub> 0-55714
- Ag, adsorption and surface reaction of formic acid 0-40741
- Al-C-siliceous sand mixture in N<sub>2</sub> atmos., weight loss during heating, compaction (*Japanese*) 0-35151
- Al-SiO<sub>2</sub>, surface reactions and interdiffusion, photoemission study 0-49532
- Al<sub>2</sub>Ge<sub>2</sub>O<sub>7</sub> reduction by C, gaseous and metallic Ge yields (*Russian*) 0-40737
- Al-AlOOH, disappore, superstructure form. on dehydration, electron microscopy obs. 0-3327
- Au/Ti thin films, effect of Cl<sub>2</sub> on elec. resistance, Ti atom migration and preferred orientation 0-34530
- B<sub>2</sub>C-Ti(V)(Cr), contact reaction with liq. Ni 0-55707
- BaF<sub>2</sub>, formation and growth of oxidation centres result of O<sub>2</sub><sup>2-</sup> diffusion 0-7706
- CO, hydrogenation on Fe foil, AES and XPS study 0-7858



## surface chemistry continued

- CaO+CO<sub>2</sub>→CaCO<sub>3</sub>, reaction kinetics, effect of temp. and CO<sub>2</sub> press. 0-45552  
 Ca<sub>2</sub>O·Bi, positive ion nonequilibrium emission in heterogeneous chemical reaction, mass spectra 0-55277  
 Co<sub>3</sub>O<sub>4</sub>-H<sub>2</sub>, interaction with surface, quantum chemical study 0-45549  
 Cr, CVD on Ni, reaction mechanism, growth rate and struct. obs. 0-39476  
 Cr<sub>2</sub>O<sub>3</sub> dissociation in presence of C in Ar, CO and vac. atm., Cr<sub>3</sub>C<sub>2</sub> form. (Russian) 0-35570  
 Cr<sub>2</sub>O<sub>3</sub>-H<sub>2</sub>, interaction with surface, quantum chemical study 0-45549  
 Cu (100), chemisorption and decomp. of formic acid, EELS study 0-16729  
 Cu (100) reaction with ethanol and methanol, EELS study 0-16728  
 Cu (100) surface, interaction with O<sub>2</sub>, AES, EELS, LEED and work function studies 0-24731  
 Cu (111), hydroxylation and dehydroxylation, XPS obs. 0-7850  
 Cu, adsorption and surface reaction of formic acid 0-40741  
 Cu surface, interacting mechanisms with organic sulphides rel. to friction and lubrication behaviour 0-45546  
 Cu<sub>2</sub> surface film of 2-mercaptobenzothiazole and 2-mercaptobenzimidazole, XPS and X-ray induced Auger spectra obs. 0-40600  
 Cu-Fe (0.2 at.%), surface oxidation, Mossbauer obs. 0-55564  
 Cu(110), adsorption of O<sub>2</sub> and its reaction with CO 0-15373  
 D exchange reaction between H<sub>2</sub> and water a hydrophobic catalyst supporting Pt 0-30208  
 EsCl<sub>3</sub>(Br<sub>2</sub>)(I<sub>2</sub>), prep., characterisation and decay of Es(II) 0-16727  
 F+SiO<sub>2</sub>, heterogeneous reaction, discharge-flow tube meas. 0-21274  
 Fe, adsorption and surface reaction of formic acid 0-40741  
 Fe, carburization, methane gas→C(dissolved)+2H<sub>2</sub> (gas), kinetics 0-55712  
 Fe, pure circular disc electrodes in (Na, H)ClO<sub>4</sub> solns., complex formation meas. 0-55569  
 Fe surface, interacting mechanisms with organic sulphides rel. to friction and lubrication behaviour 0-45546  
 Fe surface, nitride layer formation, activated surface, passivation 0-16577  
 Fe-Ni, carburization, methane gas→C(dissolved)+2H<sub>2</sub> (gas), kinetics 0-55712  
 FeO surface, water-gas shift reaction kinetics 0-11949  
 Fe<sub>2</sub>O<sub>3</sub>-H<sub>2</sub>, interaction with surface, quantum chemical study 0-45549  
 Fe<sub>2</sub>O<sub>3</sub>-FeAl<sub>2</sub>O<sub>4</sub>-FeTiO<sub>3</sub> titaniferous magnetite, chlorination, 1273 to 2273K 0-55752  
 α-FeOOH, goethite, surface OH groups, D<sub>2</sub>O isotopic exchange, IR investig. 0-2254  
 α-FeOOH, goethite, superstructure form. on dehydration, electron microscopy obs. 0-3327  
 FeS<sub>2</sub>, oxidation, Mossbauer spectroscopic and magnetokinetic studies, 400-500°C 0-44880  
 FeTi, surface segregation, catalytic effect on hydrogenation 0-45814  
 GaAs film, RF sputtered, ESCA, surface chemistry suitability for photovolt. appl. 0-7476  
 GaAs-Al(Ga)(Ge), surface reactions and interdiffusion, photoemission study 0-49532  
 Ge+Br<sub>2</sub>, rate-limiting step, ellipsometric and photochem. meas. 0-16730  
 H<sub>2</sub>+O<sub>2</sub>, on Pd (111), mol. beam relax. and isotopic exchange meas. 0-35575  
 H<sub>2</sub>+O<sub>2</sub>, on polycryst. Ni surface, SIMS and thermal desorption meas. 0-40742  
 HI-H<sub>2</sub>-I<sub>2</sub>, H<sub>2</sub> separation in thermogravimetric column 0-45561  
 Hf, decomp. of hydrocarbons, O or N surface segregation effects 0-55654  
 Ir (110), adsorption of CO and reaction with O<sub>2</sub>, transient study 0-30284  
 K<sub>2</sub>O glasses, partially leached, dehydrated surface reaction with water 0-3406  
 LaNi<sub>5</sub>, H storage using metal hydrides, self restoring of active surface 0-45815  
 LiO<sub>2</sub>, reactions with Mo in fusion blanket feasibility tests 0-26055  
 Li<sub>2</sub>Pb<sub>2</sub>, fusion reactor breeding material, reaction with H<sub>2</sub>O 0-13830  
 Mg nitridation in HF discharge, temp. effect 0-3399  
 Mg/Mg<sub>2</sub>Cu eutectic, hydriding and dehydriding kinetics obs. by press. sweep method 0-35765  
 MgO, dissolution mechanism in acids 0-39296  
 MnO-H<sub>2</sub>, interaction with surface, quantum chemical study 0-45549  
 Mn<sub>2</sub>O<sub>4</sub> film, form. on glass surface from Mn<sup>2+</sup> ions in water (Japanese) 0-45411  
 MoF<sub>6</sub> reduction by H, chemical kinetics eqn., adsorbed component interactions (Russian) 0-35569  
 N<sub>2</sub> fixation using fusion energy heat source 0-32510  
 NaCl-KCl melt, reaction with LiO<sub>2</sub>·2SiO<sub>2</sub> X-ray, IR exam. 0-55706  
 Na<sub>2</sub>O glasses, partially leached, dehydrated surface reaction with water 0-3406  
 Na<sub>2</sub>O-Al<sub>2</sub>O<sub>3</sub>-SiO<sub>2</sub> glass, leaching in HCl solns., Na conc. distrib. in surface layers 0-21141  
 Ni (111), dehydrogenated adsorption of ethylene, thermal desorption and AES study 0-29274  
 Ni-Cr alloy, phosphidation in P vapour, 700°C, phosphide layer struct. and kinetics 0-25906  
 Ni-Si-B powder, oxidation at 850°C, SEM, ESCA, and elec. cond. meas. 0-7717  
 Ni<sub>1-x</sub>Cu<sub>x</sub>+CO, Ni(CO)<sub>4</sub> form. activation energy, mag. phase depend. 0-3409  
 NiO-H<sub>2</sub>, interaction with surface, quantum chemical study 0-45549  
 O<sub>2</sub> adsorbed on Cu (110) surface reaction with CO, ellipsometry, AES, LEED study 0-6635  
 Pb<sub>1-x</sub>Sn<sub>x</sub>Te anodic oxide film form. conditions, IR absorpt. spectra 0-11494  
 Pd (111), scattering, adsorption, and absorpt. of H<sub>2</sub> and D<sub>2</sub>, mol. beam study 0-29277  
 Pt, adsorption of water, H<sub>2</sub> and reaction between H<sub>2</sub> and adsorbed O 0-49514  
 Pt oxidation, XPS spectra study 0-3254  
 Pt(IV), reduction to Pt(II), X-ray irradiat., Ar ion bombardment, XPS obs. 0-35573  
 Si, dry etching induced surface contamination, SIMS, AES, and XPS obs. 0-11810  
 Si, thermal oxidation in O<sub>2</sub>-trichloroethylene mixture, 900, 1000 and 1100°C 0-3221

## surface chemistry continued

- Si+NH<sub>3</sub>, surface nitride form., XPS excited by Zr M<sub>5</sub> radiation 0-40236  
 SiC-fission product reaction kinetics in HTGR TRISO UC<sub>2</sub> and UC<sub>3</sub>O<sub>2</sub> fuel in thermal gradient 0-47570  
 SiO<sub>2</sub>, dry etching induced surface contamination, SIMS, AES, and XPS obs. 0-11810  
 SiO<sub>2</sub>, on Si, reduction by heating in Ga mol. beam at 800°C 0-50730  
 SiO<sub>2</sub>, vaporisation in steam atmosphere 0-44306  
 SmCo<sub>5</sub> hydriding kinetics, inverse over pressure effect 0-55944  
 SmCo<sub>5</sub> thin film, hydride form., kinetics, mag. monitoring 0-35571  
 Ta, decomp. of hydrocarbons, O or N surface segregation effects 0-55654  
 Ti film, ion stimulated N<sub>2</sub> sorption, TiN<sub>x</sub> form., sorption ratio, capture coeff. anal. 0-39411  
 Ti, nitriding, ESCA study (Japanese) 0-11833  
 TiO<sub>2</sub>, photodesorption of H<sub>2</sub>O, pulsed-laser-dynamic-mass-spectrometer study 0-35568  
 U powder, hydriding kinetics, 13.3 and 26.6 kPa, 50-250°C 0-16725  
 UO<sub>2</sub>-UC<sub>2</sub>-C microspheres, carbothermic prep., rate-controlling preps. 0-45257  
 V<sub>2</sub>O<sub>5</sub>-H<sub>2</sub>, interaction with surface, quantum chemical study 0-45549  
 W, carburization, catalytic Co effect 0-3255  
 W, catalytic decomp. of NH<sub>3</sub> single pulses, mol. beam relax. spectrometry 0-21321  
 W surface wetting by liquid Cu depend. on preliminary surface treatment (Russian) 0-35388  
 W(110) vicinals, adsorption of N<sub>2</sub>, step sites as dissociation centres 0-6642  
 Zn, phosphidation in P vapour, kinetics and associated diffusion coeffs. 0-3405  
 ZnO, photodesorption of CO<sub>2</sub>, pulsed-laser-dynamic-mass-spectrometer study 0-35568  
 ZnS 0-35096  
 ZrN-Al<sub>2</sub>O<sub>3</sub>, sintering reaction thermodynamics 0-2989  
 ZrN-Mo, cermet, sintering reaction thermodynamics 0-2989

## surface composition see surface structure

## surface conductivity

- see also surface scattering  
 dielectric, irradiat. by electron beams, effect of bulk and surface cond. on pot. 0-2446  
 electron gas, semi-infinite, nonlocal cond. tensor calc., effective optical surface region 0-20283  
 electron gas, two dimensional, elec. cond., mean free path (Russian) 0-44702  
 flat capillary, ion transport numbers, surface conductance 0-11071  
 metal film, surface impedance oscillation effects due to one sided RF excitation (Russian) 0-11106  
 metal surface problems in microwave region, theory and meas. (Chinese) 0-44704  
 metal-insulator-semiconductor structure, DC cond. and Shubnikov-de Haas effect 0-11012  
 metals, cyclotron resonance in weak mag. fields surface impedance, current density asymptotic (Russian) 0-2641  
 metals, surface impedance, extreme anomalous limit, diffuse refl. from boundary 0-29460  
 polymers, oriented, conduction anisotropy meas. (Japanese) 0-54707  
 porcelain, charge carrier prod. by degradation in SF<sub>6</sub> 0-7707  
 semiconductor, surface helicon waves in Faraday geometry, existence 0-44703  
 semiconductors, antiferromagnetic resonance rel. to surface impedance, magnetoelastic contrib. 0-50200  
 semiconductors, surface magnetoplasma wave spectrum in HF mag. field 0-24995  
 vacuum deposited resistive foils, manufacture and props. of multicomponent alloys (Polish) 0-35131  
 Al thin films, HF induction plasma treatment, effect on phys. props. (Russian) 0-24961  
 Cu surface, fine interaction of conduction electrons 0-34500  
 GaAs, surface, distrib. of surface states 0-44692  
 GaAs, surface recombination rate reduction by Ru chemisorption 0-49866  
 Ge, cleaved in liquid He, surface elec. cond. (Russian) 0-15588  
 n-Ge surface, chemical channel of recombination 0-39656  
 Ge surface Hall effect and cond., electron, hole conc. and mobility (Russian) 0-44619  
 Ge surface microwave cond. observations (Russian) 0-2447  
 He, liquid, surface electron high freq. cond., electron system heating, I-V chars. (Russian) 0-29244  
 InSb (110), ion bombard. effect on surface struct. and electronic props. 0-6923  
 InSb (110) surface, struct. and electronic props., RHEED and field effect meas. 0-11068  
 InSb, MISS struct., surface electron and hole mobility and conc. (Russian) 0-44701  
 KCl crystal, use of photoelectrons to investigate surface charges 0-2444  
 MgO single cryst., γ-irrad. in presence of O<sub>2</sub>, H<sub>2</sub> and H<sub>2</sub>O adsorbates, thermostimulated surface cond. 0-34499  
 Mo, surface thermoelectrotransport of atoms 0-2448  
 NiO:C, surface charge, O(1s), C(1s) and Ni(2p) XPS 0-45196  
 Si, two-dimensional inversion layer on surface, minigap and conductivities 0-20267  
 SiO<sub>2</sub>-Li<sub>2</sub>O-Al<sub>2</sub>O<sub>3</sub>-K<sub>2</sub>O:Ag<sub>2</sub>O-(CeO<sub>4</sub>)<sub>x</sub>-(Sb<sub>2</sub>O<sub>3</sub>)<sub>y</sub>, surface resist. meas. 0-44700  
 W, chemisorbed H, surface cond. and intrinsic surface states, surface refl. spectra 0-15378  
 W, surface thermoelectrotransport of atoms 0-2448  
 ZnO crystals, adsorbed dye laser, charge transfer, field effect and spectrally sensitised photocond. meas. 0-49815  
 ZnO film, prep. by reactive ionized cluster beam deposition, and characterisation 0-10829

## surface contours

- see also surface structure; surface topography measurement  
 B<sub>2</sub>O<sub>3</sub>-SiO<sub>2</sub> glass, surface flattening kinetics by sinusoidal profile decay method (Japanese) 0-34284  
 computer-controlled machine tool for diamond-turned surface accuracy improvement 0-1367  
 discrete actuator deformable mirror 0-33133  
 glass, polished, 1.064 μm laser damage threshold rel. to pulse duration and surface roughness 0-33055  
 Inconel 625, plasma nitriding, surface topography obs. by SEM 0-45442



**surface contours continued**

- metals, abrasive finishing with refractory carbide micropowders 0-11842
- mica, metamorphic white, surface microtopography 0-54493
- NC diamond turning system evolution 0-1369
- ophthalmic lens surface working machinery 0-28363
- optical surface microtopography, generated by diamond turning machine 0-33263
- plotting, moire technique 0-42002
- Al-Cu-Si, effect of sample conditions on sputtering and intensities, emission spectrochem. anal. using glow discharge (*Japanese*) 0-21349
- Fe-Cu-Ni-Cr<sub>2</sub>C<sub>2</sub>-C based sintered friction material, wear, surface geometry and struct. effects 0-25875
- Pb surface erosion by supersonic plasma stream, mech. momentum role 0-2065
- PbO-SiO<sub>2</sub>, surface flattening kinetics by sinusoidal profile decay method (*Japanese*) 0-34284

**surface diffusion**

- see also sorption
- adsorbed atoms, diffusion and density fluctuations on solid surfaces 0-39452
- alkali silicate glasses in aqueous solutions, leaching kinetics rel. to surface pot. 0-11803
- CIDN(E)P, in two-dimensional fluid, and Heisenberg spin exchange 0-14157
- crystal surface, (1n0), stepped relief machine model 0-34283
- disordered surfaces, atomic migration, theory 0-54516
- epitaxial island mobility, one-dimens. model sinusoidal pot. 0-44457
- flavanthrene molecules, stationary stochastic adparticle flip-flop as a precursor to surface diffusion 0-15371
- gas diffusion through surfactant films, interfacial resistance 0-39385
- glass, conc. distrib. in surface layer after contact with AgNO<sub>3</sub> melt, AgNO<sub>3</sub>/NaNO<sub>3</sub> mixture 0-44372
- grain boundary grooving under action of surface diffusion and evaporation or corrosion 0-39397
- hydrodynamic interfacial instability, mechanical, chem. and elec. constraints, review 0-34278
- interface, stability problem, diffusion, reaction and convection 0-33567
- ion, near metal surface, friction parameter and Brownian motion 0-15584
- ionic crystal, gas-solid interaction potential, adsorption sites and surface migration 0-24738
- ionic crystal, phys. adsorption of nonpolar gases, localised and mobile phases, hopping adsorbates 0-24739
- island films, diffusive mass transfer, review 0-20054
- islands, rotation and translation on substrate 0-10811
- metal, with low and adsorption activity, diffusion coeff. of H, steady-state flow method 0-10795
- metal surface, electron density depend. on modulation, adsorption, diffusion 0-54526
- metal surfaces self-diffusion of single atoms and diffusion of adatoms, activation energies calc. 0-24732
- metallic thin film, vacuum deposition, early stage obs. using microbalance technique and electron microscopy (*Japanese*) 0-54554
- methane, adsorbed on graphite, NMR pulsed field gradient method, diffusion coeff. meas. 0-15362
- molecular sieves, 5A, modelling, appl. to Ar diffusion coeff. determ. (*French*) 0-54508
- neopentane, adsorbed on graphite (TiO<sub>2</sub>), NMR pulsed field gradient method, diffusion coeff. meas. 0-15362
- oxides at high temperatures obs., crystalline and non-crystalline, use of sinusoidal profile decay method (*Japanese*) 0-54479
- pore velocity, due to surface diffusion under temp. gradient, finite thermal conductivity correction 0-15428
- sintering, diffusion controlled sphere-sphere, simulation 0-20814
- steel, ionic nitriding, procedure and equipment, nitrided layer hardness obs. 0-45414
- thin film growth due to crystallite surface migration, review 0-10810
- transition metals, adatom surface diffusion characts., pair potential calcs. 0-39446
- Ag films, hillock form. hole growth and agglomeration 0-44455
- Ag surface, diffusion of labelled adsorbed Cl<sup>-</sup>, I<sup>-</sup> ions 0-39413
- Ag, surface self-diffusion coeff., O<sub>2</sub> potential effect 0-15354
- Ag, vacuum deposition, on evaporated AgBr layers, growth mechanism 0-35095
- Ag-Au, surface layer, effect of Ar<sup>+</sup> bombardment, AES and SIMS 0-25504
- Co-C alloys, graphite nucleation on surface (*Russian*) 0-40360
- Cu-Ni, clean surface, surface segregation and growth process of altered layer (*Japanese*) 0-24720
- Cu-Ni, surface layer, effect of Ar<sup>+</sup> bombardment, AES and SIMS 0-25504
- α-Fe, O<sub>2</sub> potential effect on surface self-diffusion coeff. 0-15353
- Fe-Mg, cast, ferrite-based, graphite nucleation on surface (*Russian*) 0-40360
- GaAs, rel. to VPE in CVD systems, anisotropic phenomena 0-54563
- Gd<sub>3</sub>Ga<sub>5</sub>O<sub>12</sub>, interface processes with (YSm)<sub>3</sub>(FeGa)<sub>5</sub>O<sub>12</sub> film, LPE, horizontal dipping obs. 0-49552
- Mo (011) face, surface diffusion and interaction between adsorbed Ba atoms (*Russian*) 0-6658
- Mo, surface thermoelectrotransport of atoms 0-2448
- NH<sub>3</sub>, adsorbed on graphite, NMR pulsed field gradient method, diffusion coeff. meas. 0-15362
- NaCl, of CO<sub>2</sub>, gas-solid interaction potential, adsorption sites and surface migration 0-24738
- NaCl, of methane, adsorpt. pot., localised and mobile phases, hopping adsorbates 0-24739
- Na<sub>2</sub>O.2SiO<sub>2</sub> glass, diffusion of Ag into surface layer from AgNO<sub>3</sub> melt 0-44371
- Nb, H absorption rate, metallic film effect 0-49525
- Ni, surface self-diffusion in presence of adsorbed halogens (*French*) 0-24723
- Ni-C alloys, graphite nucleation on surface (*Russian*) 0-40360
- NiO, grain boundary thermal grooving, mass transport, self-diffusion coeffs. 0-44217
- PbTe (111) epitaxial films, localised electron irradi. effects on elec. props. and O<sub>2</sub> sorption 0-49472
- Pt-Rh alloys, surface comp. determ. by ion scatt. spectroscopy 0-6602
- Rn, diffusion coefficient and exhalation rate from building materials, meas. technique 0-4694
- Si, epitaxial layer, growth mechanism from ion-molecular beams 0-2299

**surface diffusion continued**

- Si:B, inhomogeneous surface layer, diffusion and implanted, X-ray rocking curves 0-6603
- SiO<sub>2</sub> film on Si substrate, Na transport caused by ion and atom impact 0-6682
- steel, high C, graphite nucleation on surface (*Russian*) 0-40360
- Ta, H absorption rate, metallic film effect 0-49525
- Ti fibres, high-temp. nitriding kinetics (*Russian*) 0-21166
- UO<sub>2</sub>-zircaloy-4, reaction kinetics at high temps., O<sub>2</sub> diffusion 0-16667
- V, oxidised in air during laser irradiation, switching effect (*Russian*) 0-24977
- W (100), coadsorption of Zr and O<sub>2</sub> at high temp. 0-6653
- W (111), (211), and (311), adsorption of W single atoms, surface site geometry determ. by FIM 0-39447
- W adatoms, on Ir(110), surface diffusion by atomic exchange mech. 0-49508
- W, surface thermoelectrotransport of atoms 0-2448
- (YSm)<sub>3</sub>(FeGa)<sub>5</sub>O<sub>12</sub> film, LPE on Gd<sub>3</sub>Ga<sub>5</sub>O<sub>12</sub>, interface processes, horizontal dipping obs. 0-49552
- Zr fibres, high-temp. nitriding kinetics (*Russian*) 0-21166

**surface discharges**

- see also corona
- air/glass interface, ns. grazing discharge, X-ray emission 0-33846
- creep discharge, probability of discharge phenomena, theory and obs. 0-38838
- creep discharge plasma channel props., dielectric surface effects 0-15973
- creep discharge self-sustaining at dielectric surface, Paschen's law 0-38837
- creep discharge surface injected carrier half-life meas. 0-15972
- dielectric in vacuum, surface breakdown, dielectric strength calc., quantitative model 0-34855
- dielectric surface grazing discharge, elec. field config. 0-44069
- electrostatically rechargeable liquids, max. discharge energy estimate (*German*) 0-38737
- gliding linear discharge over dielectric surface, obs. 0-38826
- high-pressure atomic and molecular impurities, preionisation by UV irradi. of surface discharge 0-38847
- hydrocarbon liquids, electrostatically charged, incendivity of sparks from surface 0-6303
- insulator surface flashover in vacuum, electro-optical meas. 0-38823
- Kapton H, discharge area scaling and surface/subsurface damage due to electron beam irradi. 0-34853
- metal cathode, electrically stressed surface elec. phenomena, electrolum. and breakdown with medium gap spacings 0-20710
- Mylar, discharge area scaling and surface/subsurface damage due to electron beam irradi. 0-34853
- PMMA, immersion in high press. gaseous media, breakdown characts. for direct voltages with ripple 0-45009
- polyethylene surface field strength under DC stress 0-15967
- Rochelle salt ferroelectric surface creep discharge plasma channel and domain interactions 0-15996
- sliding discharge, guided, explosive emission phenomena 0-19649
- smouldering discharge at O<sub>3</sub> liq. surface in N<sub>2</sub>, thin solid pellicle formation of N<sub>2</sub>O<sub>5</sub> 0-38827
- Teflon FEP, discharge area scaling and surface/subsurface damage due to electron beam irradi. 0-34853
- Townsend discharge spark voltages, cathode surface state effects (*Korean*) 0-19643
- CO<sub>2</sub> TEA laser, laser output depend. on initial photoelectron density 0-43320
- N<sub>2</sub>, liq., dielectric breakdown, using discharge figures 0-11338
- SnO<sub>2</sub> coated glass, surface elec. breakdown 0-25303
- ZnS, single crystals, excited by laser beam and elec. field, streamer luminesc. and photolum. obs. 0-34986

**surface electron states**

- see also interface electron states; surface scattering
- adatom, electronic states, correlation effects, self-consistent T-matrix calc. 0-44691
- adatom on transition metal surface, vibr. model using pair interactions 0-15357
- adatom pair interaction asymptotics, degenerate electron gas permittivity 0-29281
- adsorbate on single crystal, anal. of electronic state by angle-resolved photoelectron spectroscopy 0-11541
- adsorbates, photoexcitation theory rel. to angle-resolved UPS and surface EXAFS 0-39426
- adsorbates deep level spectroscopy, many body effects 0-39441
- adsorbed atom on solid surface, photoemission from valence band, surface plasmon emission, model Hamiltonian calcs. 0-50525
- adsorbed atoms and molecules XPS, many-body effects 0-55266
- adsorbed layer, nonuniform charge distribution, phase transitions, Hartree-Fock calcs. 0-54525
- adsorbed molecules, surface plasmon enhanced light absorption 0-40176
- alloy surfaces, sputtering process and sputtered ion emission models 0-35044
- angle-resolved photoemission, review 0-45214
- atomic and electronic struct. 0-54746
- atomic cluster on metallic surface, density functional calculations 0-44699
- bimetallic junctions, interface plasmon modes, theoretical anal. 0-54767
- p-CdTe, surface photovoltage spectroscopy in IR and visible range 0-39632
- charged particle interaction with surface modes 0-20275
- charged particles surface excitation system, ground-state energy 0-15462
- chemisorption, electronic and ionic motion, exact unidimensional model 0-15369
- chemisorption systems, IR spectral linewidth and sticking coeffs., non-adiabatic effects 0-39423
- cluster Bethe-lattice method appl. 0-49852
- complex tight binding systems, surface density of states determ. 0-20272
- cooperative emission of excited mol. monolayer into surface plasmons of metallic substrate 0-20666
- crystal lattice electron energy spectrum depend. on external electric field (*Russian*) 0-34498
- deep levels, effect of vibration of adsorbed molecules on electron capture 0-29458
- degenerate semiconductor, with surface depletion layer, surface polaritons, hydrodynamical model 0-6752
- diamond-type crystals, LCAO band structure, overlap and distant neighbour effects 0-49585



## surface electron states continued

- dielectric films, transition layer vibrs., resonance region auxiliary surface polaritons (*Russian*) 0-2347
- dielectric surfaces, phenomenological model for optical props. 0-20605
- electron spectroscopic analysis of surfaces (*French*) 0-16153
- electron spectroscopy and surface chemical bonding, book contrib. 0-24992
- elements, sputtering process and sputtered ion emission models 0-35044
- energy conversion radiation enhancement using surface polaritons 0-7941
- energy spectrum in periodic magnetic field, band struct., surface states anal. (*Russian*) 0-39645
- ESCA, surface anal. and electronic structure (*French*) 0-7891
- ferroelectric semiconductor, spontaneous polarisation field screening by free charge carriers (*Russian*) 0-50274
- film, HF formalism for calc. of total energies and charge densities 0-49850
- films, thin, quantised, electronic energy spectrum (*Russian*) 0-44688
- gas-solid interface, electronic struct. HFR calc. 0-54745
- graphite, chemisorption of CO, CNDO calc. using cluster model 0-54522
- graphite (0001) surface, He atom scatt., bound state reson., interaction pot., band struct. effects 0-29840
- Green's function for surface physics, partial differential eigenvalue eqn. 0-6929
- halides, electron spectroscopy of crystals, book 0-36786
- heterogeneous catalysis reaction mechs., electron pair behaviour and surface orbitals 0-55705
- III-V semiconductor, cubic, high symmetry surface, dispersion law calc. for Tamm states 0-15587
- III-V semiconductor, theory for surface (110), relax. effects 0-6938
- III-V semiconductor surfaces and interfaces, Green's function technique, tight binding approx. 0-49855
- inhomogeneous electron systems, exchange and correlation effects calc. 0-20104
- ion, near metal surface, friction parameter and Brownian motion 0-15584
- ionically bonded surfaces, stability in ionising environments, core hole Auger decay mechanism 0-29457
- itinerant-electron ferromagnetic film on nonmagnetic metallic substrate, mag. props. 0-20371
- jellium metal, surfaces props., statistical calc. 0-24987
- laminated systems, two dimensional and surface plasmon mixing (*Russian*) 0-15466
- liquid, surface CARS 0-1280
- metal, density functional theory, review 0-44698
- metal, electron gas, local density functional for kinetic energy near defect, metal surface 0-20105
- metal, energetics of chemisorption, book contrib. 0-24740
- metal, FCC, (100) surface, chemisorption-induced interaction between electronic levels of two-level adsorbate 0-39644
- metal, physisorbed inert atoms, polarisation due to short range interaction with substrate 0-39428
- metal, plasmon mechanism for energy loss, dissoc. and orientation of fast ions excited by grazing collisions 0-11523
- metal, sticking probability, correl. with adsorbate-induced electron struct. 0-39425
- metal, surface energies and work function, simple analytic model 0-49862
- metal, surface excitations in contiguous plasma 0-38667
- metal circular cylinders, inhomogeneous, non-radiative surface plasmon-polariton modes 0-29455
- metal film, surface impedance oscillation effects due to one sided RF excitation (*Russian*) 0-11106
- metal films, one-dimens., electronic states 0-54758
- metal surface, electron-phonon coupling in image-potential bound states 0-54752
- metal surface, electron-plasmon interaction 0-39649
- metal surface, fast ion scatt. by plasmons, theory 0-45190
- metal surface, integro-differential eqn. for electron density and formula for surface tension of jellium 0-44689
- metal surface, positron-electron correlations, RPA calc. 0-40181
- metal surface bonding, book contrib. 0-24990
- metal surface electronic barrier, elec. field effect in presence of adsorbate, Thomas-Fermi model 0-49864
- metal surface energy, gradient corrections in interpolation formulae, surface plasmons 0-2441
- metal surfaces, exchange and correlation energy, wave vector anal. 0-20273
- metal-adsorbate system, appl. of cluster model theory, book contrib. 0-24991
- metal-insulator-semiconductor structure, DC cond. and Shubnikov-de Haas effect 0-11012
- metallic interfaces, conf., Ghent, Belgium (Sept. 1978) 0-41946
- metallic surface, dispersion of surface plasmons 0-2440
- metallic surface, electrodynamics, microscopic effects (*Russian*) 0-6936
- metallic surface state, influence of refr. of p-polarised light on photoemission 0-20772
- metals, adhesion theory for two surfaces 0-20270
- metals, liq., charge density fluctuations in surface layer (*Russian*) 0-15580
- Mg, K X-ray emission spectra, double plasmon high energy satellite 0-11510
- MIS structure, calc. of surface states in band gap by Green's function method 0-15611
- MIS structure, capacitance-voltage characs., built-in charge fluctuation effects, negative surface state density 0-6992
- MIS structure, determ. of deep level parameters in surface layer of semiconductor 0-15612
- MIS structure, high- and low-freq. steady state capacitance 0-54796
- MIS structure, semicond. surface states, capacitance, admittance, freq. depend. 0-49940
- molecular crystal, surface exciton levels, radiation corrections 0-34962
- molecular crystals, semi-infinite, with surface point defect, exciton states 0-20271
- molecule-metal interaction and surface reactions, theoretical description 0-39652
- MOS surface states, DLTS spectra synthesis and anal. 0-11090
- MOS transistor, Au-doped, Au surface-state energy levels 0-11092
- Mossbauer spectroscopy and surface phenomena study 0-39916
- MOST channels, quasi-Fermi level gradient distrib., Hall voltage 0-29481
- MOST structures with process-induced defects, elec. props. 0-54788

## surface electron states continued

- multi-scattering method for cryst. surface band struct. calc. 0-2439
- n-type semiconductor anode, illum., charge transfer modes, digital simulation 0-2464
- narrow band gap semiconductors, conference, Warsaw, Poland (Sept. 1977) 0-49703
- neutral particles interaction pot. with surfaces (*Russian*) 0-6937
- one-dimensional crystals, matching conditions, Bloch functions, logarithmic derivatives 0-15475
- oxidised surfaces, sputtering process and sputtered ion emission models 0-35044
- photoelectron spectroscopy of clean and adsorbate covered surfaces (*French*) 0-50519
- piezoelectric semiconductors, surface phonon acoustoelectric interaction, elastic anisotropy effects 0-6610
- plasmon-acoustic wave interactions due to deformation potential (*Russian*) 0-15356
- plasmons, counterpropagating, for coherent SHG 0-33081
- polar semiconductor surface, energy levels and geometry, theory 0-49481
- polariton frequency shift, cryst. surface and dielec. function depend. 0-44522
- polariton use in optical storage 0-48414
- polaritons, hybrid bulk-surface type 0-49626
- polaritons, hybrid bulk-surface type 0-49627
- polaritons, linear photon and two photon absorpt. 0-49863
- polaritons, nonlinear optical spectroscopy, stationary and nonstationary, theory (*German*) 0-6922
- polars and excitons, surface self-trapped states (*Japanese*) 0-2445
- polyethylene, surface charge release, crossover phenomenon, thermally stimulated discharge current study 0-50255
- polymers powders, corona-charging props. 0-6946
- positron surface states, emission of positrons, positronium 0-54655
- pseudopotential surface and interface calculations 0-49853
- pseudopotentials, reliability criteria 0-49563
- quantum chemical calc. methods 0-49849
- quasi-two-dimensional system in perpendicular elec. field, hydrogenic model 0-29454
- random alloy, optical absorption and photoemission spectra 0-45216
- rare earth element submonolayer films, electronic phase transitions, heat of absorption 0-24736
- rhodamine B surface state hole traps, surface photovoltage meas. 0-39654
- Schottky barrier, mag. surface levels in presence of depletion-type band bending 0-20285
- semiconductor, covalent, non-orthogonal tight-binding approach 0-2442
- semiconductor, generalised tridiagonal Hamiltonian resolvent matrix, exact soln. 0-29307
- semiconductor, interface form., initial steps, surface states and thermodynamics 0-49503
- semiconductor, meas. of surface and interface states (*Japanese*) 0-20269
- semiconductor, photocond., influence of surface space-charge layer 0-15563
- semiconductor, photoemission meas. of surface and bulk states 0-25527
- semiconductor, surface electronic props., optical spectroscopic techniques, review 0-11070
- semiconductor, surface reconstruction, dynamical theory 0-10773
- semiconductor, unipolar, n-type, field-effect mobility, energy spectrum of surface states 0-39657
- semiconductor interface and overlayer electronic struct., review 0-49841
- semiconductor surface, macroscopic recomb. centres 0-6933
- semiconductor surface, resonance inelastic light scattering by carriers 0-20655
- semiconductor surface characterisation using SAW 0-11069
- semiconductor surface spectroscopy, exciton effects, theory 0-49856
- semiconductor surfaces and interfaces, electronic struct. calc., scattering theoretic approach 0-6940
- semiconductors, empirical tight-binding method, critique 0-49854
- semiconductors, photoelectron spectra, book contrib. 0-16155
- semiconductors, surface potentials using electron energy anal., SEM study 0-15582
- n-Si-electrolyte junction, Schottky barrier height and reverse current 0-6979
- solid surface studies, recent progress (*Japanese*) 0-15347
- solid surfaces props. characterisation, structural, chemical and electronic, use of LEED methods (*Italian*) 0-49467
- specific heat of two dimens. electron gas, exchange interaction contrib., calc. 0-44331
- spherical particle, max. charge imparted by pulse-charging 0-6945
- spherical particle with extremely high resistivity, corona charging 0-6944
- SrTiO<sub>3</sub> (100) surface electronic structure, DV-X $\alpha$  cluster method 0-39646
- surface chemical bond, book 0-22147
- surface roughness effect on image potential electron energy loss, plasmon electron scatt. 0-54748
- Teflon FEP, annealed electret, charge stability 0-6943
- tetracene surface states, electric field effects, exciton-charge carrier interactions (*Russian*) 0-24989
- theory of solid surfaces, book 0-36787
- thin surface layer, interactions between nondegenerate electrons, effect on cyclotron resonance, mag. cond. (*Russian*) 0-15802
- three-dimensional crystal, Hartree-Fock theory of surface states 0-44468
- tight binding method, first principles 0-49564
- tight-binding Green's functions for surfaces, thin films, and solid interfaces using random-walk theory 0-54753
- transition metal, adsorption of CO, electronic struct., localised orbital pseudopot. method 0-39653
- transition metal, chemisorption of ordered atomic layers, HF Green's function formalism and phase shift technique 0-24733
- transition metals, chemisorption on, theoretical model, formalism 0-6651
- transition metals, surface states, qualitative theory, Shockley model 0-6924
- two atom surface coupling, double reson. at plasmon freq., collective effects 0-34934
- two dimensional electron spectrum spin splitting, specified by surface potential (*Russian*) 0-15583
- uniaxial crystal foil, electron energy loss probability at oblique incidence 0-25506
- UPS, angle-resolved, initial state symmetries from polarisation effects 0-40227
- Wigner crystal on liq. He surface, cond. (*Russian*) 0-6594



## surface electron states continued

- Ag, electroreflectance spectroscopy, longitudinal surface plasmons 0-40137  
 Ag, single cryst. electrodes, electroreflectance obs. in aqueous solns. 0-25342  
 Ag surfaces, Cs and Cs-O covered, surface plasma waves, ATR study 0-39451  
 Ag-Cu, surface segregation, electronic theory, density of states, cluster-Bethe-lattice approx. 0-49369  
 Al (100), photoemission, ang. terms in optical pot. 0-55269  
 Al (111), ordered O overlayer, angle-resolved photoemission, band struct. 0-40229  
 Al, surface broadening of 2p core level photoemission spectra 0-25524  
 Al-Al<sub>2</sub>O<sub>3</sub>-SnTe, junction, tunnelling, Fermi level depend. on carrier conc., influence of surface states 0-25016  
 Al-Si<sub>3</sub>N<sub>4</sub>-Si struct., surface energy bands under step function illumination 0-49840  
 Al<sub>2</sub>O<sub>3</sub> monolayer, core excitons and inner well resonances in surface soft X-ray absorpt. spectra 0-40187  
 As<sub>2</sub>Se<sub>3</sub> amorphous thin films, illumination-induced change in contact pot. 0-20251  
 Au (100), normal and reconstructed, electronic struct. changes, ang. resolved photoemission obs. 0-25520  
 Au, photoelectron spectra, bulk and surface, rel. to band struct. 0-20770  
 Au, single cryst. electrodes, electroreflectance obs. in aqueous solns. 0-25342  
 Au surface electronic structure, XPS study 0-55259  
 Au-Ag(Cu), surface segregation, electronic theory, density of states, cluster-Bethe-lattice approx. 0-49369  
 Au-oxide-n-GaAs structs., reverse-bias depend. photocurrent, photoionisation of surface states 0-20323  
 Au(111) and polycrystalline surfaces, O<sub>2</sub> adsorption, LEED, AES and energy loss spectra 0-34310  
 Bi film, quantum size effect and band struct. Bi-dielec.-metal system obs. 0-54811  
 Bi, skipping electrons cyclotron resonance, electron-electron interaction parameter determ. 0-34351  
 BiI<sub>3</sub>, layered compound, exciton spectra, surface and stacking fault effects 0-40134  
 Bi<sub>1-x</sub>Sb<sub>x</sub> alloy films, quantum resistance oscils. at low temps., surface band distortion (*Russian*) 0-11110  
 Bi<sub>2</sub>Te<sub>3-x</sub>Se<sub>x</sub> films, surface band struct. and scatt. mechanism 0-34535  
 C allotropes, diamond, graphite, gas-solid interface, electronic struct. HFR calc. 0-54745  
 CaO, chemisorption of O<sub>2</sub>, adsorboluminescence from surface F-centres 0-20723  
 CdS, polycrystalline evaporated layers, donor and trap densities 0-20213  
 CdS, surface electronic struct., slow electron reflection, total current spectroscopy (*Russian*) 0-54759  
 CdTe, clean and oxidised surfaces, surface states, low-energy EELS study 0-11522  
 Co (0001) surface state, photoemission and synchrotron radiation obs., symmetry determ. 0-20771  
 Cr, (100) surface, clean ( $\sqrt{2} \times \sqrt{2}$ )R45° struct. 0-2255  
 Cr, antiferromagnetic, surface Raman scatt., calc. 0-45069  
 Cr, surface atom electron binding energy depend. on composition, Auger spectra, APS spectra 0-39655  
 Cu (001), electronic surface barrier resons., LEED study 0-39651  
 Cu, (100) and (111), surface states, d-band, angle-resolved photoemission spectra obs. 0-20768  
 Cu (100) monolayer, self consistent electronic struct. 0-6926  
 Cu (100) surface, angle-resolved PES study 0-55273  
 Cu (110), adsorption of pyridine, angle-resolved photoemission, selection rules 0-40231  
 Cu (111), Cs adsorption system, electronic surface band energy 0-2443  
 Cu (111) surface band energy shift upon adsorption of Cs and O, angle-resolved UPS study 0-40228  
 Cu (111)/Cs, adsorption-induced changes of photoemission spectra and surface electronic struct. 0-55260  
 Cu, chemisorption of H, density of states and chemisorption energy calc. 0-34315  
 Cu, d-band narrowing, obs. using angle-resolved XPS 0-11062  
 Cu, single cryst. electrodes, electroreflectance obs. in aqueous solns. 0-25342  
 Cu, surfaces and twin faults, electronic states calc. by surface Green's functions 0-39647  
 Cu-Ni, optical absorption and photoemission spectra 0-45216  
 Cu(111) frequency depend. photoelectric surface state cross section periodic oscils., PES study 0-50522  
 Cu(111) surface, UPS at const. wavevector component 0-16151  
 Fe, ferromagnetic, chemisorption of H, spin-spin interactions, UPS spectra calc. 0-6630  
 Fe, field-emitted electron spin polarisation by tunnelling through surface pot. 0-29861  
 Fe, surface atom electron binding energy depend. on composition, Auger spectra, APS spectra 0-39655  
 Fe-Cr, surface atom electron binding energy depend. on composition, Auger spectra, APS spectra 0-39655  
 Fe<sub>1-x</sub>O<sub>x</sub> surface struct., XPS study 0-20759  
 n-Fe<sub>2</sub>O<sub>3</sub> electrodes, characterisation and behaviour in acetonitrile solns. 0-25004  
 GaAs (100), angle-resolved photoemission spectra 0-50516  
 GaAs, (100) surfaces, reconstructed, ang. resolved photoemission from surface states, adsorption and annealing effects 0-16143  
 GaAs (110), adsorption of In, N, P, and As, UPS and EELS study, tight-binding calcs. 0-49496  
 GaAs (110), adsorption of O<sub>2</sub>, H<sub>2</sub>, H<sub>2</sub>O and H<sub>2</sub>S, surface photovolt. spectroscopy 0-49499  
 GaAs (110), chemisorption of Cl, photoemission spectra and tight-binding calcs. 0-6629  
 GaAs (110), chemisorption of Al, electronic struct., tight binding calc. 0-49842  
 GaAs (110), chemisorption site geometry and interface electronic struct. of Al and Ga, photoelectron spectra 0-49843  
 GaAs (110), clean, cleaved, surface states, work function meas. 0-49847  
 GaAs (110), optical technique, detection of external reflectivity change on oxidation 0-6939  
 GaAs (110), reconstruction and oxidation initial stages, ab initio calc. 0-49473  
 GaAs (110), self-consistent pseudopotential calcs., electronic struct. and atomic co-ords. 0-49848

## surface electron states continued

- GaAs (110), steps 0-49846  
 GaAs (110) surface, electronic struct., pseudopot. calc., surface relax. model 0-29456  
 GaAs (110)-Al(Ga)(In), Schottky barrier form., defect mechanism 0-49902  
 GaAs, MBE (001) layers, work function meas. 0-49870  
 GaAs Schottky-contact, influence of surface states and hole traps (*Bulgarian*) 0-25006  
 GaAs, semi-insulating, surface layer thermal conversion mechanism, Hall effect meas. 0-49772  
 GaAs, surface, distrib. of surface states 0-44692  
 GaAs, surface, electron struct. and Fermi level pinning by O<sub>2</sub> and metals 0-11066  
 GaAs, surface, vacancies, bound state energy level calcs., tight binding approx. 0-44694  
 GaAs, surface characterisation using SAW 0-11069  
 GaAs, surface electron states, (110), photoemission 0-25529  
 GaAs, surface states, band struct. by discontinuous potential method 0-20276  
 GaAs surface states obs. by XPS 0-50515  
 GaAs, surface states XPS 0-25528  
 GaAs surfaces, electronic struct., tight-binding calc. 0-54755  
 p-GaAs: Cd, (110) cleaved surface, defect-induced surface states 0-6925  
 GaAs-AlGaAs heterojunction superlattices, obs. of intersubband excitations in multilayer two dimensional electron gas 0-29753  
 n-GaAs-oxide, plasma-grown, surface states, modified DLTS meas. 0-11094  
 GaP (110), electronic surface states, initial steps of O<sub>2</sub> chemisorption 0-49844  
 GaP, cleaved (110) surface, electron surface props. 0-11067  
 p-GaP electrodes with metal adatoms, surface states form. due to impregnated H 0-54778  
 GaP, surface characterisation using SAW 0-11069  
 GaP, surface polariton linear photon and two photon absorpt. 0-49863  
 GaP, surface polaritons, light scattering studies, effect of surface roughness 0-6753  
 GaSb (110), chemisorption of Cl, photoemission spectra and tight-binding calcs. 0-6629  
 GaSb (110), oxidation, initial stages, photoemission study 0-16529  
 GaSb, surface, electron struct. and Fermi level pinning by O<sub>2</sub> and metals 0-11066  
 Ge (111) surface, clean and CO-covered, UPS and ion-neutralisation spectroscopy 0-10785  
 Ge (111) surface, n-channel inversion layer, subband energies 0-11063  
 Ge, LCAO band structure, overlap and distant neighbour effects 0-49585  
 Ge surface, adatom indirect interaction 0-44696  
 n-Ge surface, chemical channel of recombination 0-39656  
 Ge, surface, high freq. cond. and cyclotron reson. 0-11273  
 Ge, surface states, recombination centre formation (*Russian*) 0-29459  
 Ge surfaces, electronic struct., tight-binding calc. 0-54755  
 Ge(100) surface electronic state localisation, layer density of states calcs. 0-6931  
 Ge(111)2×1, oxide layer, surface states detect optical reflectivity obs. 0-50368  
 He, liq., electrons localised at surface, cyclotron freq. shift (*Russian*) 0-6582  
 He, liq., surface electron system, liq. to cryst. phase transition (*Russian*) 0-6593  
 He, liquid, charged surface, current instability theory (*Russian*) 0-29243  
 He, liquid, short-wave surface excitation study using electron gas non-linear I-V characts. (*Russian*) 0-10717  
 He, liquid, surface electron high freq. cond., electron system heating, I-V characts. (*Russian*) 0-29244  
<sup>3</sup>He, liq., electron escape from image-potential-induced surface states 0-49440  
<sup>3</sup>He, liq., localised electron states, cyclotron reson. above surface (*Russian*) 0-6587  
<sup>4</sup>He, liq., electron escape from image-potential-induced surface states 0-49440  
<sup>4</sup>He, liq., localised electron states, cyclotron reson. above surface (*Russian*) 0-6587  
<sup>4</sup>He, liquid, surface electron interaction with EM radiation (*Russian*) 0-54449  
 Hg<sub>1-x</sub>Cd<sub>x</sub>Te, n-surface inversion layers study 0-25017  
 InP (110), oxidation, initial stages, photoemission study 0-16529  
 InP, cleaved surface, angle resolved photoelectron spectroscopy 0-55258  
 InP, surface, electron struct. and Fermi level pinning by O<sub>2</sub> and metals 0-11066  
 InP, surface space charge layers and Schottky barrier form., Raman scatt. study 0-50319  
 InSb (110), chemisorption of Cl, photoemission spectra and tight-binding calcs. 0-6629  
 InSb (110), clean, O<sub>2</sub> adsorption, AES, LEED, RHEED and field effect meas. 0-49501  
 InSb (110), ion bombard. effect on surface struct. and electronic props. 0-6923  
 InSb (110) surface, struct. and electronic props., RHEED and field effect meas. 0-11068  
 InSb surface, IR spectroscopy of subband levels 0-20277  
 InSb, surface, reson. excitation of electron subbands 0-49865  
 InSb surface magnetoplasma wave struct. 0-6934  
 Ir, clean and adsorbate covered surfaces, field emission energy distrib. spectra 0-25535  
 K, surface electron states and optical props. in IR spectral range (*French*) 0-54757  
 KCl crystal, use of photoelectrons to investigate surface charges 0-2444  
 LaB<sub>6</sub> (100) surface, O<sub>2</sub> adsorption, UPS and LEED study 0-49519  
 MgO, chemisorption of O<sub>2</sub>, adsorboluminescence from surface F-centres 0-20723  
 Mo, (001) surface, electronic origin of reconstruction 0-11065  
 Mo (001) surface with saturated H adsorption, band structure self-consistent calc. 0-15585  
 Mo (100), adsorption of CO<sub>2</sub> and trimethylamine, adsorbed O effect, LEED and AES obs. 0-39443  
 Mo (100) clean surface electron struct., positron annihilation study 0-24988  
 Mo, adsorption of CO, O<sub>2</sub>, metastable He de-excitation spectroscopy and UPS study 0-34314



## surface electron states continued

- MoS<sub>2</sub>, surface electronic struct., slow electron reflection, total current spectroscopy (*Russian*) 0-54759  
 Mo(001), H chemisorbed, self-consistent electron struct. 0-44693  
 Na, adsorbed on Ni, substrate, hybridisation between s and p reson., jellium model 0-6932  
 Na film, slow electron bombarded, light radiation 0-40168  
 Na surfaces, (100) and (111), electron energy states (*French*) 0-34496  
 NaCl, quantum-chem. calcs. of electronic and hole centres and surface 0-20118  
 Ni (001), adsorbed c(2×2) Na overlayer, core level excitation effects, synchrotron radiation UPS study 0-40234  
 Ni (111), adsorption of chalcogens, angle-resolved photoemission 0-40230  
 Ni (111), isothermal desorption of CO, UPS study, time-resolved approach 0-39440  
 Ni, adsorbed CO, core level spectrum, satellite struct., ab initio HF-LCAO calc. 0-40233  
 Ni, chemisorption of H, embedded cluster model 0-39427  
 Ni, d-band narrowing, obs. using angle-resolved XPS 0-11062  
 Ni, ferromagnetic, chemisorption of H, spin-spin interactions, UPS spectra calc. 0-6630  
 Ni, field-emitted electron spin polarisation by tunnelling through surface pot. 0-29861  
 Ni, magnetic surface anisotropy of transition metals, model calc. 0-34625  
 NiFe, magnetic surface anisotropy of transition metals, model calc. 0-34625  
 NiNO, ground and core hole states, config. depend. HF LCAO SCF calc., relax. and binding energy 0-29453  
 Ni(100) magnetic surface states, photoelectron spectra, surface Brillouin zones 0-6928  
 PbI<sub>2</sub>, layered compound, exciton spectra, surface and stacking fault effects 0-40134  
 PbS (100) surface, electronic struct., O<sub>2</sub> adsorption effects, UPS study 0-54756  
 Pb<sub>1-x</sub>Sn<sub>x</sub>Te: Cd, photoelec. props., surface recomb. effect 0-44659  
 n-PbTe, accumulation layer, quantised surface states 0-20279  
 Pd (111) surface, adsorbed O<sub>2</sub>, UPS and thermal desorpt. characts. 0-54754  
 Pd, chemisorption of H, embedded cluster model 0-39427  
 Pd overlayers, on Nb, form. of Pd (111) surface states and reson. d-levels, photoemission obs. 0-50523  
 Pd-Si (111) interface, microscopic Pd<sub>2</sub>Si form., UPS obs. 0-24743  
 Pt, chemisorption of H, embedded cluster model 0-39427  
 Pt cluster, conduction electron density oscils., NMR spin-echo meas., indirect exchange interaction 0-44954  
 Pt(111) surface, identification of adsorbed OH species 0-49509  
 Re (0001), chemisorption of CO, role of d-orbitals, angular resolved UPS and thermal desorption meas. 0-40232  
 SbI<sub>3</sub>, layered compound, exciton spectra, surface and stacking fault effects 0-40134  
 Si (100), atomic and electronic structs., energy minimisation calc. 0-49480  
 Si (100), intrinsic surface states, photoemission study 0-50514  
 Si (111), chemisorbed O<sub>2</sub> electronic struct. tight-binding calc., XPS and UPS meas. 0-49845  
 Si (111), chemisorption of H, localised model, ab initio HF-LCAO calc. 0-6930  
 Si (111) 7×7 surface electronic struct., angle-resolved UPS study 0-50513  
 Si (111) (7×7) surface structs., LEED anal. and energy minimisation calcs. 0-49478  
 Si (111) surface, clean and O<sub>2</sub>-chemisorbed, electron states by AES 0-54747  
 Si, (111) surface, low press. baked, dominant interactions and average distances between paramag. centres 0-15783  
 Si (111) surface, with Al overlayers, electronic states 0-11061  
 Si (111)7×7 surface electronic struct., angle-resolved UPS study 0-40226  
 Si amorphous film, optical props., electronic states 0-25475  
 Si, clean and gas (O<sub>2</sub> and H<sub>2</sub>O) covered surface, appl. of UPS ultrahigh vacuum apparatus (*Japanese*) 0-37125  
 Si, inversion layer, polaron model for localisation 0-20280  
 Si, inversion layer, voltage tunable far IR emission 0-25018  
 n-Si, inverted MOSFET surface, evidence for Lande factor g=2, finite valley splitting 0-6989  
 Si surface, (111)7×7, electronic struct. calc. 0-24993  
 Si surface, adatom indirect interaction 0-44696  
 Si surface, electron states, surface photovoltage spectroscopy study, doping effects 0-49860  
 Si, surface characterisation using SAW 0-11069  
 Si surfaces, electronic struct., tight-binding calc. 0-54755  
 Si, under stress, density functional calc. of subband struct. 0-20321  
 Si:H, amorphous, surface activated, photoemission spectra, minority carrier diffusion length 0-40235  
 Si:Zn (Mn) (In), surface characterised by negative electrochemical pot., electronic props. 0-44695  
 n-Si-SiO<sub>2</sub> interface, hot carrier surface thermo EMF depend. on surface band bending 0-44734  
 SiO<sub>2</sub>, electron irradi. effects, EELS study 0-24985  
 SiO<sub>2</sub> monolayer, core excitons and inner well resonances in surface soft X-ray absorpt. spectra 0-40187  
 SiO<sub>2</sub>, surfaces, electronic struct. calc., scattering theoretic approach 0-6940  
 Si(111), surface density of states from soft X-ray absorpt. spectra 0-40187  
 Si(111)2×1, oxide layer, surface states detec., optical reflectivity obs. 0-50368  
 Sm surface electronic structure, XPS study 0-55259  
 Sm, XPS, electronic struct. determ. for surface 0-20765  
 SrTiO<sub>3</sub> (100) surface, struct. and electronic props., AES, LEED, EELS, and UPS study 0-24986  
 SrTiO<sub>3</sub>, semicond. electrode, electrochem., photoelectrochem. props. 0-3352  
 Te inversion layers in mag. fields 0-44690  
 Ti (0001), valence band struct. and chemisorption, XPS and UPS study 0-35062  
 Ti (0001), with adsorbed N (1×1) layer, underlayer geometry, electronic struct. calcs. and UPS meas. 0-54751  
 Ti (0001) film, electronic struct., Fermi level, surface states, GO calcs. 0-6927

## surface electron states continued

- Ti (0001) film, with adsorbed H (1×1) monolayer, electronic struct., surface geometry 0-54750  
 TiO<sub>2</sub> (rutile), (001) and (110) faces, UPS and LEED obs. 0-45206  
 TiO<sub>2</sub> (rutile), (001) and (110) surfaces, surface and bulk density of states calcs. 0-49858  
 TiO<sub>2</sub>, clusters, surface electron struct. and defect states, DV-X $\alpha$  calc. 0-20268  
 TiO<sub>2</sub> electrodes, in aq. electrolytes, surface states, photocurrent obs. 0-49895  
 TiO<sub>2</sub>, rel. to elec. props. of Ti-TiO<sub>2</sub>-Au diode 0-15617  
 n-TiO<sub>2</sub>-electrolyte interface, charge-transfer-controlled photocurrent 0-50992  
 W (001), chemisorption of H, HF Green's function formalism and phase shift technique 0-24733  
 W (001), surface phase transition, electronic contribs., surface susceptibility, ab initio self-consistent thin-film energy band calc. 0-29255  
 W, (001) surface, electronic origin of reconstruction 0-11065  
 W (110) surface, adsorption of H, band struct. and adsorbate geometry, surface-reflectance-spectroscopy 0-44416  
 W, chemisorbed H, surface cond. and intrinsic surface states, surface refl. spectra 0-15378  
 W films, (010), energy band calc. including spin-orbit interactions 0-20274  
 W, surface state transferability, UPS meas. for (011) states 0-39650  
 YbAu, surface electronic structure, XPS study 0-55259  
 Zn<sub>0.9</sub>Cd<sub>0.1</sub>S:Cu crystalline phosphors, spectra of IR electrophotographic sensitivity (*Russian*) 0-50423  
 ZnO substrate, for Ni films, band bending, UPS study 0-7472  
 ZnSe(Te), clean and oxidised surfaces, surface states, low-energy EELS study 0-11522  
 ZnTe, luminescence spectra struct. surface and volume polaritons (*Russian*) 0-16089

## surface energy

- see also surface electron states; surface energy measurement  
 adsorption system surface properties variational calcs., binding energy, Lang model 0-29279  
 aliphatic acids, thermodynamics of adsorption at air/aqueous soln. interface 0-10752  
 aliphatic alcohol, thermodynamics of adsorption at air/aqueous soln. interface 0-10752  
 artificial blood substitutes, surface energetics anal. 0-41321  
 brittle materials, effective surface energy of rupture determ. 0-21074  
 charged particles surface excitation system, ground-state energy 0-15462  
 coherent interphase boundary energy anisotropy between cubic-type crystals 0-54252  
 crack resistance, characteristics correlation of material  $\alpha_p$  and  $\gamma$  0-21075  
 crystal surface-electron-hole drop interactions, interaction energy 0-29335  
 4,4-dihexyloxybenzene, nematic liq. cryst., alignment on surfactant treated obliquely evaporated surfaces 0-49092  
 dipolar crystal, surface local field effect, dipole moment, self consistent electric field calcs. 0-49178  
 fatty alcohol solid monolayers in H<sub>2</sub>O, interface struct., model 0-54505  
 FCC crystal, surface energy and chem. pot., microscopic capillarity approx. 0-5654  
 gas-liquid interface of rising bubbles, adsorption rate determ. (*Japanese*) 0-6595  
 gas-liquid surface of mol. fluids, mol. dynamics computer simulations 0-39387  
 graphite fibres, HM, surface comp. and energetics 0-54480  
 4-heptyl-4'-cyanobiphenyl, nematic liq. cryst., alignment on surfactant treated obliquely evaporated surfaces 0-49092  
 interfaces of two bulk phases, non-equilibrium thermodynamics including EM effects 0-13021  
 ionic crystal, surface stability 0-20016  
 ionic crystals, statistical theory calcs. of surface energy and surface tension 0-17894  
 jellium metal, surfaces props., statistical calc. 0-24987  
 liquid crystal, isotropic phase, surface induced ordering, birefringence obs. 0-14998  
 liquid crystals, surface alignment using polynuclear metal complexes 0-1924  
 macroscopic metal catalysts, morphology and etching processes, review 0-7856  
 magnetisation theory, of slab of finite thickness, role of positive surface energy 0-15724  
 metal, gradient corrections in interpolation formulae, surface plasmons 0-2441  
 metal, surface energies and work function, simple analytic model 0-49862  
 metal surface, influence of submonolayer films on props., calc. (*Russian*) 0-2273  
 metal surface free energy for BCC, FCC and HCP structs. etch pit depend. 0-29258  
 metals, adhesion theory for two surfaces 0-20270  
 microindentation method, for surface energy evaluation 0-16473  
 naphthalene single crystals, surface active substances effect on plastic flow 0-44248  
 nuclear ceramics, grain boundary energy to surface energy ratio, as determ. from pore geometry 0-34291  
 nucleation processes, and surface energy values for substance of different crystn. struct. 0-49144  
 pentylcyanobiphenyl, isotropic phase, surface induced ordering, birefringence obs. 0-14998  
 pentylcyanobiphenyl, liquid crystal, isotropic phase, surface induced ordering, birefringence obs. 0-14998  
 phyllosilicates, dioctahedral and trioctahedral, calc. of electrostatic energy relations 0-19743  
 polar liquids, electrostatic contrib. 0-20014  
 trans-1,4-polyisoprene, kinetics of thin film growth from melt 0-10505  
 polymer-water interfaces, contact angle 0-20010  
 powder science, laboratory techniques for handling powders 0-45475  
 pure liquids, predictions of total surface energy 0-29250  
 rare earth hexaborides, obtained by melting, micromech. props., rel. to bonding 0-21082  
 rods, with anisotropic surface free energy, stability 0-20013  
 solid, universal model 0-39409  
 solid surfaces props. characterisation, structural, chemical and electronic, use of LEED methods (*Italian*) 0-49467



## surface energy continued

- steel, stainless, creep ductility, intergranular particle size and spacing effect 0-40461  
water, electrostatic contrib. 0-20014  
Ag epitaxial films, grain boundary struct. evolution during recrystn., interface energy effect (*Russian*) 0-15387  
AgBr melts, surface energy and surface tension coeffs., effect on photographic emulsion microcryst. growth rate (*Russian*) 0-47132  
AgCl melts, surface energy and surface tension coeffs., effect on photographic emulsion microcryst. growth rate (*Russian*) 0-47132  
Al, adhesion props. 0-10774  
Al epitaxial films, grain boundary struct. evolution during recrystn., interface energy effect (*Russian*) 0-15387  
Al powder, liq.-solid phase transforms. (*French*) 0-45294  
Au epitaxial films, grain boundary struct. evolution during recrystn., interface energy effect (*Russian*) 0-15387  
Co<sub>2</sub>Ge<sub>3</sub>, solid and liquid, physicochemical props. and structure 0-39548  
Fe, cast, influence of interfacial energy on shape of graphite 0-16360  
Fe-Si-B, surface tension, density, and oxidation kinetics 0-20028  
H<sub>2</sub>O, surface tension and energy, Fowler model 0-10754  
<sup>3</sup>He, superfluid, surface energy and textural boundary conditions between A and B phases 0-54458  
LaNi<sub>3</sub>, surface segregation, influence of O<sub>2</sub>, H<sub>2</sub>, H<sub>2</sub>O, SO<sub>2</sub> (*German*) 0-51008  
Ni<sub>3</sub>Ge<sub>3</sub>, solid and liquid, physicochemical props. and structure 0-39548  
Si (100), atomic and electronic structs., energy minimisation calc. 0-49480  
Si (111) (7×7) surface structs., LEED anal. and energy minimisation calcs. 0-49478  
Si (111) surface reconstruction, milk-stool model, quantum chem. ab initio calc. 0-49477  
Si, reconstructed surface physics, review 0-10766  
Si, structurally related bulk and surface props., self-consistent pseudopot. method 0-54632  
UO<sub>2</sub>, surface props. of low index faces, calc. 0-6604

## surface energy measurement

- adhesive energy measurement techniques 0-50803

## surface hardening

- brass, surface hardening by electrohydraulic forming (*Japanese*) 0-16571  
case carburising, in commercial elec. furnaces 0-27310  
Inconel 625, nitriding in N<sub>2</sub>-H<sub>2</sub> glow discharge 0-16590  
metal, cavitation erosion resist., increase by case hardening, possible mechanism 0-11845  
steel, austenitic stainless, nitrided, type 03kh17N8G5MFAB, alloying characts. and phase comp. 0-30166  
steel, austenitic stainless, surface hardening by electrohydraulic forming (*Japanese*) 0-16571  
steel, C, induction hardened, surface durability, optimum case depth 0-30137  
steel, C, spinning machine ring, increasing wear resist. by boring 0-21115  
steel, C and alloy, nitriding, effect on struct. and internal stresses 0-30162  
steel, carbonitrided, case struct. investigation by warm electrolytic etching 0-35414  
steel, composition effect on carburizing 0-35432  
steel, Cr plated, laser treatment 0-21191  
steel, die types 4Kh5MFS and 5Kh2MNF, nitriding in vibrofluidised bed 0-35410  
steel, ionic nitriding, procedure and equipment, nitrided layer hardness obs. 0-45414  
steel, Ni (21 wt.%), ageing, nitrided case struct. investigation 0-35416  
steel, stainless, nitriding in glow discharge in crossed electric and magnetic fields 0-16578  
steel, stainless martensitic, nitriding in metastable condition 0-30167  
steel, tool, type KhBG, carburising and quenching, effect on fracture toughness 0-29997  
steel, type 12Kh2N4A, belt grinding, struct. transformations 0-30169  
steels, N-implanted, surface hardness and abrasive wear resist. 0-50746  
Be, surface hardening by B ion implantation 0-16604  
Fe, cast, nitrided, wear resistance (*Korean*) 0-21178  
SiO<sub>2</sub>-Na<sub>2</sub>O-CaO-MgO-Al<sub>2</sub>O<sub>3</sub>, toughening by electrochemical treatment in Sn melt 0-11800  
steel, Ni-Cr, rolling contact fatigue failure 0-16608  
Ti-Al-V (6, 4 wt.%), friction characts. improvement by O<sub>2</sub> dissolution and controlled surface hardening (*French*) 0-45401  
W, carburization, catalytic Co effect 0-3255

## surface-ion beam collisions see ion-surface impact

## surface ionisation

- dynamic characts. of neutral particle desorption by surface ionisation voltage method 0-44426  
ion trap sensitivity for spectroscopic applications, <sup>137</sup>Ba<sup>+</sup> ground state hyperfine splitting 0-22447  
ionisation density, spatial distrib. calc. in a material due to electron beam irradiation 0-55234  
isobar nuclei, separation of alkali and alkaline earth elements using surface ion source 0-37688  
radiation damage, defects and surfaces in bulk metallic, covalent and ionic systems, review 0-34049  
sputtering products, elemental anal. (*French*) 0-50905  
Al, elemental anal. of sputtering products (*French*) 0-50905  
Cu, elemental anal. of sputtering products (*French*) 0-50905  
Cu-Al, elemental anal. of sputtering products (*French*) 0-50905  
H<sub>2</sub><sup>+</sup>, negative surface ionisation on ThO<sub>2</sub>, plasma diagnostics appl. 0-6280  
In, surface ionisation meas. after ion sputtering (*French*) 0-27374  
W, desorption of Cs, dynamic characts. of neutral particle desorption by surface ionisation voltage method 0-44426

## surface-molecular beam collisions see molecule-surface impact

## surface phenomena

- see also surface.....  
see also atom-surface impact; capillarity; crazing; crystal surface and interface vibrations; emissivity; field evaporation; interface phenomena; ion-surface impact; magnetic surface phenomena; molecule-surface impact; sorption; surface acoustic waves  
ablation of melting solid surfaces, in impingement region of H<sub>2</sub>O jet 0-14766  
atomically clean surface environment, confirmation using field electron emission 0-52250

## surface phenomena continued

- binary metal alloys, surface segregation correlation with bulk diffusion 0-54388  
composite materials, surface, flame propagation velocity rel. to thermal props. (*Russian*) 0-7797  
conference, Cambridge, England (March 1979) 0-36773  
conference, Gothenburg, Sweden, June 1979 0-51950  
conference, trends in physics, York, England (Sep. 1978) 0-31416  
elastic wave propagation, free surface of cryst., spatial dispersion 0-54310  
electrolyte soln. surface interaction, grand canonical ensemble method appl. 0-54092  
ellipsometry work at Gakushuin University from 1955, review 0-9019  
ferroelectric films, surface effects on phase transitions, local spontaneous polarisation 0-2708  
Fourier emission IR microspectrophotometer for surface anal., lubrication problem apps. 0-13162  
glass, thermally tempered sheet and plate, surface stress meas. using optical waveguide effect 0-25967  
glass liquid-liquid immiscible regions, surface effects on energetics 0-33903  
layer surfaces, reflectivity at 3.39  $\mu$ m, meas. method, relevance to pipelines 0-52340  
liquid surface deform. due to laser radiation thermal action, lens effect 0-33048  
liquid-liquid system interfacial instability and longitudinal waves 0-33566  
liquid-solid interaction forces, meas. by detachment of liq. from solid substrate 0-10740  
meas. of lubricated sliding surfaces (*German*) 0-14643  
molecular processes on surfaces 0-34339  
Mossbauer effect appl., conference, Kyoto, Japan (Aug.-Sept. 78) 0-7199  
photoelectron spectrometer for surface studies, gas press. up to 1 Torr 0-4822  
polyethylene, effect of ketones, temp. depend., environmental stress relax. study 0-45336  
polymer surface, flame propagation velocity rel. to thermal props. (*Russian*) 0-7797  
powders and porous materials, specific surface, determ. using Hg porosimetry 0-29896  
semiconductor, struct. and props., review (*Japanese*) 0-49483  
semiconductors, conference, Pacific Grove, USA (Jan.-Feb. 1979) 0-46725  
semiconductors, interface and surface physics, review 0-49872  
skinned sintering kinetics, cryst. surface calcs. (*Russian*) 0-40276  
solid films and surfaces, conference, Tokyo, Japan (Jul. 78) 0-10739  
steel, austenitic, thermonuclear reactor walls, ferromagnetic layer form. magneto-optical testing method 0-35465  
steel, stainless, gas liberation, 20°C, surface oxide effects (*Russian*) 0-3286  
steel, stainless, surface roughness influence on equilib. of liq. spreading 0-39389  
survey of recent research 0-39384  
suspended particles in estuarine and coastal waters, surface films form. rel. to elec. charge 0-36331  
thermoplastic recording material, latent image and surface deformation (*German*) 0-42284  
Al, surface roughness influence on equilib. of liq. spreading 0-39389  
He, liquid, charged surface vibrations in metal approx. (*Russian*) 0-10718  
<sup>4</sup>He superfluid, charged surface stability breakdown, He ion geyser ejection (*Russian*) 0-15320  
Si<sub>3</sub>N<sub>4</sub>-CeO<sub>2</sub>, surface stress development during oxidation 0-50736  
VH<sub>0.55</sub>, ultra-high vacuum cleavage, H<sub>2</sub> desorption 0-54514  
Zn, strengthening by electroplastic strain, surfactant effect (*Russian*) 0-20953

## surface phonons see crystal surface and interface vibrations

## surface potential

- adatom on transition metal surface, vibr. model using pair interactions 0-15357  
alkali silicate glasses in aqueous solutions, leaching kinetics rel. to surface pot. 0-11803  
alkaline earth phosphate (MO-Al<sub>2</sub>O<sub>3</sub>-P<sub>2</sub>O<sub>5</sub>) irradiated electret glasses, relax. of external field intensity on heating 0-25282  
biomembranes, potential, rel. to surface pot., ionic permeab. 0-35853  
corona charged polyethylene thermally stimulated current and surface potential decay obs. 0-15945  
dielectric, electron penetration, 20-50 keV, sandwich method meas. 0-6436  
dielectric, irradi. by electron beams, effect of bulk and surface cond. on pot. 0-2446  
flat capillary, ion transport numbers, surface conductance 0-11071  
graphite (0001) surface, He atom scatt., bound state reson., interaction pot., band struct. effects 0-29840  
hydrocarbon liquids, electrostatically charged, incendivity of sparks from surface 0-6303  
hydrodynamic interfacial instability, mechanical, chem. and elec. constraints, review 0-34278  
ice, surface pot. obs., rel. to thunderstorm charge separation 0-51495  
ion beam, scatt. by solid surface, skipping motion due to surface pot. 0-45191  
ionic crystals, mirror chips, in contact with liq. phase, ellipsometric investigation 0-11516  
jellium surface, interaction of H<sub>2</sub> 0-29259  
LiF, mirror chips, wetting contact angle 0-10746  
metal and semiconductor surfaces, electrostatic interaction of charges 0-24996  
metallic surface, anisotropic contrib. to optical pot., in electron spectroscopy, theory 0-44086  
metals, liq., charge density fluctuations in surface layer (*Russian*) 0-15580  
microporous solid, electrical double layer on surface 0-11955  
MIS structure, MM wave modification by surface carrier scatt., surface pot. depend. 0-44736  
monolayers, elastic and viscoelastic, dynamic surface potentials 0-3603  
MOS devices, inversion layer, pot. and carrier distrib., quantum mechanical determ. 0-29483  
MOS structures with superthin gate dielectric, hole mobility in inversion layers 0-29482  
organic adsorbed layers, Si-SiO<sub>2</sub> interface as electrode for electrical and ellipsometric meas. 0-15366



**surface potential continued**

- photoconductor-air gap-semiconductor system, calc. of surface charges under voltage in darkness 0-6905  
 PLZT electrooptic ceramic, electron beam surface charging, rel. to optical modulation 0-6952  
 poly(alkyl methacrylate)s, corona charged, decay of surface charge and TSC (*Japanese*) 0-54712  
 polyethylene, surface charge release, crossover phenomenon, thermally stimulated discharge current study 0-50255  
 polyethylene film, effect of corona generated excited molecules on surface pot. decay 0-6941  
 polyethylene film, high density, corona charged, thermally stimulated surface pot. 0-11327  
 polyethylene terephthalate, TSC due to mobile ions and ionic conduction (*Japanese*) 0-54432  
 polyethylene terephthalate film, corona charged, surface voltage decay mechanism, TSC meas. 0-11326  
 polymer electret, absorpt. and relax. of charge 0-6942  
 polymer electret, charge dissipation, transport mechanisms 0-7268  
 polyvinylidene fluoride film, uniaxially stretched and corona poled, piezoelec. meas. 0-25311  
 rare earth-transition metal amorphous thin films, mag. potential distribution and wall velocity meas. 0-34725  
 Schottky barrier, excitonic refl. of light 0-10885  
 semiconductor, surface potentials using electron energy anal., SEM study 0-15582  
 solid surface in localised physi-sorption, gas desorption times, local or nonlocal surface pot. calcs. 0-54499  
 sols, primary and secondary coagulation and heterocoagulation, role of surface chemistry 0-45551  
 stratified spheroidal volume conductors excited by electric dipole source 0-32867  
 two dimensional electron spectrum spin splitting, specified by surface potential (*Russian*) 0-15583  
 water interface, mol. orientation and surface pot. at 4°C 0-15339  
 Al alloys, contamination, automated nondestructive inspection 0-16629  
 Al plasma anodisation forming voltage limitation mechanism (*Japanese*) 0-16579  
 As<sub>2</sub>Se<sub>3</sub>, amorphous, dark discharge, relaxation current meas. (*German*) 0-49760  
 As<sub>2</sub>Se<sub>3</sub> layers for electrophotographic use (*German*) 0-42283  
 BaSO<sub>4</sub>, TSEE and surface charging, simultaneous meas. 0-29864  
 Bi, spheres, mean inner pot., elec. biprism and interf. electron microscopy 0-49063  
 CaF<sub>2</sub>, mirror chips, wetting contact angle 0-10746  
 CdS powder layers, surface pot. dark decay, moisture sorption and heat treatment effects 0-18038  
 Cu (111), chemisorption of CO, IR spectra, LEED, and surface pot. meas. 0-39438  
 Fe, field-emitted electron spin polarisation by tunnelling through surface pot. 0-29861  
 n-InSb, photoconductive lifetime, surface pot. effects 0-11029  
 Ni (110), chemisorption of N<sub>2</sub>, mol. and dissociative mechanisms 0-39431  
 Ni, field-emitted electron spin polarisation by tunnelling through surface pot. 0-29861  
 n-PbTe, accumulation layer, quantised surface states 0-20279  
 Se photoreceptors, phthalocyanine sensitized, elec. cond., charge decay characts. 0-15630  
 Si solar cells, effect on surface recombination 0-12017  
 Si:Zn (Mn) (In), surface characterised by negative electrochemical pot., electronic props. 0-44695  
 Si-SiO<sub>2</sub> interface, thermally grown, inhomogeneities of surface potential 0-34524  
 SiO<sub>2</sub>, surface pot. during ion implantation 0-19826  
 ZnCdS:(Cu+Ag) binder layer for electrophotography 0-4797

**surface scattering**

- used for carrier scattering by surfaces  
 see also surface conductivity  
 disorder metal systems, conduction electron surface scatt. (*Russian*) 0-24917  
 ferromagnetic metal slab, transmission of 24 GHz radiation, effect of diffuse surface scatt. of carriers, calc. 0-34780  
 metal, US generation by EM radiation, surface scatt. effects 0-24973  
 metal surface, disordered, multiple scatt. of cond. electrons 0-10959  
 metallic film, conduction electron surface scatt. process, magnetoacoustic oscillations (*Russian*) 0-15575  
 metallic thin films, free-electron, optical props., theory including electron surface scatt. 0-29817  
 metallic thin films, unlike surface properties, transport coeffs., diffuse surface scatt. 0-20331  
 metals, surface impedance, extreme anomalous limit, diffuse refl. from boundary 0-29460  
 MIS structure, MM wave modification by surface carrier scatt., surface pot. depend. 0-44736  
 Ag, transverse electron focusing and specular refl. from cryst. faces 0-6823  
 Au, films, optical props. meas. rel. to electron surface scatt. theory 0-29818  
 Bi, thin film, 1/f noise, boundary scatt. effect 0-49836  
 Bi<sub>2</sub>Te<sub>3</sub>-Se, films, surface band struct. and scatt. mechanism 0-34535  
 W, RF size effect, surface electron scatt. influence (*Russian*) 0-2414

**surface structure**

- see also interface structure; surface texture  
 absorbed film, disordering due to supercond. transition in metal substrate 0-50022  
 AES, by computer (*French*) 0-7890  
 AES and ESCA combined with SEM (*French*) 0-47154  
 alkali chlorides, thin film, crystal-vacuum (100) surfaces, mol. dynamics computer simulation 0-34288  
 alkali halides, thin films, crystal-vacuum (110) interfaces, mol. dynamics computer simulation 0-34289  
 alkaline silicate glass, surface layers, plasticity and microcrack formation, electron microscopy (*German*) 0-40469  
 alloy, surface composition changes on ion bombardment 0-2913  
 alloy sputtering 0-50503  
 alloy surface, free energy of segregation 0-29256  
 analysis by photon-induced field ionisation mass spectroscopy 0-40780  
 anodic oxide superficial layer, X-ray emission spectroscopy and ion back-scattering (*French*) 0-49482

**surface structure continued**

- atomic and electronic struct. 0-54746  
 Auger electron appearance potential spectroscopy, core level spectroscopy (*Japanese*) 0-50473  
 Auger spectrometry, analytic approach 0-50474  
 bonding and crystallography of surfaces, book contrib. 0-24724  
 borided surface layers, Mossbauer and metallographic anal. 0-50769  
 cast Fe, grey and ductile, subsurface defects, SEM and EDAX study 0-44400  
 catalysis and surface science, review 0-40740  
 characterisation, physical methods, review (*French*) 0-7889  
 coeff. and surface conc. 0-39122  
 composition depth profiles, ion sputtering effects 0-35616  
 compound, surface composition changes on ion bombardment 0-2913  
 conducting and semiconducting materials, surface study using Johansson three-electrode objective (*French*) 0-47152  
 conference, Gothenburg, Sweden, June 1979 0-51950  
 crystal surface, (1n0), stepped relief machine model 0-34283  
 cubic crystals, microfacet rotation for high Miller-index surfaces with terrace, step, and kink struts. 0-54495  
 diamond, cryst. surface layers treatment and study by HF ion-plasma etching (*Russian*) 0-16517  
 diamond, identification by electron refl. (*German*) 0-54080  
 diatomic surfaces, LEED/MEED intensity calcs. 0-44083  
 dielectric solid, absorpt. of laser radiation by defects in surface layer (*Russian*) 0-25497  
 elastic crystal, relationship between dislocations and surfaces 0-24446  
 electron spectroscopy, for bulk and surface microscopy and microanal. 0-52367  
 ESCA, surface anal. and electronic structure (*French*) 0-7891  
 extended appearance pot. fine struct. surface anal. 0-11512  
 film surface analysis techniques survey, for development and production (*Hungarian*) 0-54537  
 Gaussian TEM<sub>00</sub> mode laser beam scatt. from surface defect, normaliza-tion 0-48313  
 glass, chem. tempered, surface stress meas. using opt. waveguide effect (*Japanese*) 0-45473  
 glass, structure and processes (*German*) 0-38928  
 glass fibre, surface struct. effect in solubility in water (*Japanese*) 0-34198  
 glass tip, surface and crystallographic struct. using field-ion and electron microscopy 0-10767  
 grain boundary grooving under action of surface diffusion and evaporation or corrosion 0-39397  
 graphite, Auger electron appearance potential spectroscopy (*Japanese*) 0-50473  
 graphite fibres, HM, surface comp. and energetics 0-54480  
 hexamethylcyclotrisilazane film, plasma-polymerised, TEM study 0-44456  
 ice surface layer, viscosity, from thermal contraction meas., 0 to -50°C 0-49469  
 influence on image speckle pattern contrast 0-17985  
 interior planes acoustic microscopy 0-5886  
 ion beam analysis (*Japanese*) 0-20021  
 ion bombardment, electron microscopical anal. of surface effects and volume defects, review (*Rumanian*) 0-29093  
 ion induced Auger spectroscopy for surface anal. 0-55756  
 ion scattering, atomic chain model, surface semi-channelling (*Japanese*) 0-50501  
 ion-surface impact, surface atomic struct., effect on recoil atom energy distrib. 0-35050  
 ionic compounds, monovalent, solid soln., surface comp. calc. using monolayer model 0-6607  
 ionic crystal, surface stability 0-20016  
 ionic crystals, layer spacing relax. at surfaces 0-6609  
 ionically bonded surfaces, stability in ionising environments, core hole Auger decay mechanism 0-29457  
 LEED, defects in surface structure 0-44402  
 LEED, dynamic installation 0-44399  
 LEED, single-reflection layer scatt. theory 0-49059  
 LEED analysis method, comparison of rel. intensities of diffraction beams 0-54082  
 LEED reliability determ. 0-49474  
 low energy ion scattering spectroscopy, UHV apparatus (*Japanese*) 0-20746  
 macroscopic metal catalysts, morphology and etching processes, review 0-7856  
 melt fragmentation, initiation in fuel-coolant interactions, mixing of drops of hot liquid fuel with volatile coolant 0-13537  
 metal, radiation blistering developments, review 0-44239  
 metal and oxide surfaces, and interfaces, slow exchange processes study using SIMS 0-55653  
 metal films, on alkali halide substrates, nucleation and growth, surface study techniques, review 0-10809  
 metal surface, order-disorder phase transforms., CDW and mass density waves 0-39281  
 metal with terraced surface, work function calc. 0-6950  
 metallic surface, electrodynamics, microscopic effects (*Russian*) 0-6936  
 metals, abrasive finishing with refractory carbide micropowders 0-11842  
 metals, slow positron studies 0-55223  
 mica, metamorphic white, surface microtopography 0-54493  
 microanalysis, electron spectroscopy apparatus (*French*) 0-47151  
 nuclear fuel and materials, nondestructive surface exam. 0-21246  
 nylon 66 films, superstructural ordering 0-15344  
 photoelectron spectroscopy of clean and adsorbate covered surfaces (*French*) 0-50519  
 planar structures, hexagonal and cubic models, surface forces 0-20022  
 PMMA, crack growth rate effect, fracture surface structure 0-16466  
 PMMA, solvent cast, surface characts., chromatographic study 0-20020  
 PMMA, uniaxial tension, fractographic anal. of crack growth kinetics 0-40519  
 point defects, elastic interactions in semi-infinite medium 0-39146  
 polar semiconductor surface, energy levels and geometry, theory 0-49481  
 poly-γ-benzyl-L-glutamate, monolayers, struct. studies, IR, ATR, and TEM obs. 0-44396  
 polymethyl methacrylate, direct obs. of zero field surface 0-16133  
 probing and imaging techniques 0-54487  
 quartz, microtopographical obs. of 2nd order prism faces, hydrother-mally-grown crystals 0-54481  
 quartz, synthetic, Z-surfaces, SEM examination (*French*) 0-24719



## surface structure continued

- quartz, twinned crystals, after Japan Law, investigation of regrowth 0-54162  
 reconstruction, physical realisation of two-dimensional Ising and X-Y models 0-15351  
 resistive layer microstructure on superconducting Al surface (*Russian*) 0-34567  
 resistivity relaxation measuring system, for surface reaction meas. 0-55718  
 Rutherford backscattering spectrometry, signal overlap subtraction, surface struct. studies 0-50486  
 sapphire, cryst. surface layers treatment and study by HF ion-plasma etching (*Russian*) 0-16517  
 semi-infinite isotropic elastic medium, reson. scatt. of Rayleigh waves by mass defect 0-20025  
 semiconductor, struct. and props., review (*Japanese*) 0-49483  
 silicates, core-level XPS peak intensity ratio ang. variations rel. to surface anal. and chemisorption 0-40225  
 SIMS, appl. to surface anal., review 0-40204  
 SIMS, solid surface investig. applications (*Rumanian*) 0-49510  
 solid state physics, conf. Munster, Germany (March 1979) 0-41941  
 solid surface studies, recent progress (*Japanese*) 0-15347  
 solid surfaces props. characterisation, structural, chemical and electronic, use of LEED methods (*Italian*) 0-49467  
 spectroscopy, total current, study of surface regions and bulk physics 0-31952  
 sputter induced surface composition changes, in alloys 0-49470  
 stainless steel: C, surface, obs. at very low accel. voltage (200 V-1 kV) by SEM 0-10764  
 stainless steel, coated with C, surface damage by D<sup>+</sup> and He<sup>+</sup> ions irradi. 0-23146  
 steel, austenite, blistering after 40 keV He ion bombard. 0-39175  
 steel, austenitic stainless type AISI 304, surface comp. after different surface treatments 0-3253  
 steel, austenitic stainless type AISI 316, L sheet and LN plate surface comp. after different surface treatments 0-3253  
 steel, C, machined, microdefects on surface 0-16607  
 steel, C, pore formation in surface layers, during As diffusion redistrib. 0-49421  
 steel, C and Cr, surface damage during friction, struct. effect 0-35339  
 steel, Cr, exam. of surface layer after electrochemical treatment, effect on mech. props. (*Russian*) 0-7727  
 steel, mild, AISI 1009 and 1018, corrosion incipient processes in hypersaline geothermal brine at 90°C 0-50753  
 steel, Mo<sup>+</sup> ion bombardment, phase composition and struct. change of surface layers (*Russian*) 0-24506  
 steel, nitrided, chem. state anal. by conversion electron Mossbauer spectrometry 0-7718  
 steel, stainless, OKh16N15M3B (*Russian*) 0-39170  
 steel, stainless, surface treatment, X-ray photoelectron spectrosc. study 0-50764  
 steel, stainless, type 430, Ni<sup>+</sup>-implanted, struct., comp. and electrochem. anal. of surface alloy 0-16603  
 steel, stainless 304, Auger electron appearance potential spectroscopy (*Japanese*) 0-50473  
 steel, type 1Kh17N2, white zone formation and props. during friction in vac. (*Russian*) 0-40542  
 steel, W-Mo, types R6M5 and R6M5K5, decarburising layer evaluation 0-21164  
 steel, Zn coated, cold rolling influence on struct. and deform. of diffusional layer (*Russian*) 0-55465  
 subsurface structure detection by scanning photoacoustic microscopy 0-6323  
 surface (100), atomic struct., angle-resolved XPS, LEED and ISS investigation 0-10765  
 surface chemical bond, book 0-22147  
 surface dislocation model, Z-phase interface boundary problem 0-39085  
 surface layer, segregation of ferromag. Ni, magneto-optic investigation 0-2256  
 surface-dynamics of growing crystals 0-44160  
 thin film, and surface anal., modern methods 0-54486  
 thin film surface anal. and depth profiling by spark-source mass spectrography, discharge model 0-40781  
 thin films, segregation effects at surfaces and interfaces 0-39475  
 threshold-potential spectrometer appl., based on Auger electron spectrometer 0-52365  
 total current spectroscopy, review 0-45185  
 USB<sub>2</sub>, single crystal growth, structural perfection 0-15024  
 vicinal surface, system of regularly spaced steps, LEED (*French*) 0-49060  
 wedge disclinations near surface of semi-infinite cryst. (*Russian*) 0-49224  
 Zircaloy-2, neutron irradiated, inhomogeneous deformation behaviour 0-50679  
 Ag, film, sputtering mechanism, SEM 0-29839  
 Ag, surface roughness induced electronic Raman scatt. 0-50347  
 Ag-Au, surface layer, effect of Ar<sup>+</sup> bombardment, AES and SIMS 0-25504  
 Ag-Pd, surface comp. changes under ion bombardment, AES study 0-55250  
 Al, and Al-Cu(Pb) dil. alloys, pulsed ruby laser irradi., noncryst. phase form 0-35012  
 Al lithographic sheet, AC etching 0-35547  
 Al sputtered coating development, porosity, durability temp. depend., electric arc metallisation regime (*Russian*) 0-39402  
 Al surface, (111), interlayer spacing, LEED data anal. 0-54484  
 Al-Sb, laser induced surface alloy formation and Sb diffusion 0-54439  
 Al<sub>2</sub>O<sub>3</sub>, adsorbed ethanol, acetic acid and acetaldehyde, inelastic electron tunnelling spectra, surface vibr. struct. determ. 0-35572  
 Au (110), (1×2) and (1×3) superstructures, LEED study 0-20024  
 Au (111), anomalous surface superstruct., UHV electron microscope obs. 0-10760  
 Au film, surface step structure imaging by dark field electron microscopy 0-15346  
 Au film (001) surface, computer modelling of high resolution TEM images 0-6330  
 Au films, (111), sputtering in high voltage electron microscope 0-35027  
 Au-Pd, surface comp. changes under ion bombardment, AES study 0-55250  
 B fibres, surface morphologies rel. to mech. props. 0-11749  
 BaB<sub>6</sub> powder, surface struct. effects on thermionic emission characts. and vapour pressure (*Japanese*) 0-50506

## surface structure continued

- BaTi<sub>2</sub>O<sub>7</sub>, surface microrelief revealed by ion irradiation 0-54485  
 Be-Cu dynode, depth profiling anal. of surface layer 0-2253  
 Bi, single crystal from Bridgman's method, triangular facet formation 0-28933  
 C, (001)-(2×1) surface, reconstruction-induced mean-square displacements 0-15343  
 CaC<sub>2</sub>O<sub>4</sub>·2xH<sub>2</sub>O (0<x<5 zeolite water fraction), weddellite, growth morphology, PBC analysis 0-24388  
 CaO (100), surface struct., LEED study 0-39396  
 CaO, (100) surface struct. using LEED meas. and rumpled ionic models 0-20019  
 CaO, produced from CaCO<sub>3</sub> powder decomp. in vac. and in CO<sub>2</sub> 0-45255  
 Cd<sub>2</sub>Hg<sub>1-x</sub>Te, correlation between structural and chemical inhomogeneity (*Russian*) 0-49484  
 CdS, clean surface, AES and LEED exam. 0-10762  
 CdS, film, surface struct. and elec. props. 0-34531  
 CdS, single cryst., polar (0001) and (000 $\bar{1}$ ) surfaces, comparison of AES signals 0-16130  
 CdTe epitaxial films, surface morphology, layer and spiral growth 0-10823  
 CeTe, surface characterisation by high resolution Rutherford backscatt. 0-25511  
 Co, corrosion in Ar-SO<sub>2</sub> atmospheres, scale struct. obs. (*Japanese*) 0-55568  
 Co-C, dil., C segregation to single cryst. surfaces 0-39301  
 CoO (100), LEED anal. 0-15352  
 CoO (100), surface struct., LEED study 0-39396  
 CoO (111), surface relax., ionic model 0-6608  
 Cr, (100) surface, clean ( $\sqrt{2}\times\sqrt{2}$ )R45° struct. 0-2255  
 Cr, cryst. surface layers treatment and study by HF ion-plasma etching (*Russian*) 0-16517  
 Cr-Ni, blistering after 40 keV He ion bombard. 0-39175  
 Cr<sub>2</sub>O<sub>3</sub>/γ-Fe<sub>2</sub>O<sub>3</sub>/Pt electrode, two layer oxide surface film anal. by modulation spectroscopy (*Japanese*) 0-11491  
 Cr<sub>2</sub>O<sub>3</sub> anode, wear-resistant, use in applied electrochem. 0-40701  
 Cu (001), adsorbed O c(2×2), surface geometry determ. by deep-core-level XPS 0-40224  
 Cu (100), chemisorption and decomp. of formic acid, EELS study 0-16729  
 Cu, (100) single crystal surface oxidation 0-11846  
 Cu (111)/Cs, adsorption-induced changes of photoemission spectra and surface electronic struct. 0-55260  
 Cu (410) surface, edge atom depression, ion scatt. spectroscopy study 0-54492  
 Cu, film, sputtering mechanism, SEM 0-29839  
 Cu, ion irradi., topographical features relative stability 0-2092  
 Cu, sputtering, surface topography, appl. of thermodynamics of capillarity 0-20749  
 Cu, surface contaminant anal. by ion-electron spectroscopy 0-54490  
 Cu:Au:C, surface, obs. at very low accel. voltage (200 V-1 kV) by SEM 0-10764  
 Cu-Au(Pd), surface structures, LEED obs. 0-10761  
 Cu-Mn-S, Mn surface segregation and Mn/S cosegregation 0-40367  
 Cu-Ni, clean surface, surface segregation and growth process of altered layer (*Japanese*) 0-24720  
 Cu-Ni, sputter-induced subsurface segregation, Auger electrons obs. 0-10757  
 Cu-Ni, surface layer, effect of Ar<sup>+</sup> bombardment, AES and SIMS 0-25504  
 Cu-Ni (50 wt.%) alloys, estimation of sublimation energy of Cu atoms, evaporation rate and surface composition, AES meas. (*Japanese*) 0-49352  
 Cu-Ni:polyethylene, surface, obs. at very low accel. voltage (200 V-1 kV) by SEM 0-10764  
 Cu-Pd, surface comp. changes under ion bombardment, AES study 0-55250  
 Cu-Sn-P (5, 1-5 wt.%), effect of P on friction and wear characts. 0-16494  
 EuO (100), surface struct., LEED study 0-39396  
 Fe (100), adsorption of Br<sub>2</sub>, AES, LEED, work function, and thermal desorption study 0-15375  
 Fe (100), adsorption of carbon tetrachloride, AES, LEED, work function, and thermal desorption study 0-15376  
 Fe (100), adsorption of I<sub>2</sub>, AES, LEED, thermal desorption, and work function study 0-15374  
 Fe, (100) surface, S segregation and 2D compounds precipitation (*Japanese*) 0-35188  
 Fe, cast, structural changes, due to pulsed action of high temps. and pressures (*Russian*) 0-7554  
 Fe surface, adsorbed O<sub>2</sub> effect on chem. reaction kinetics 0-55572  
 Fe, surface, contamination in vac. depth selective conversion electron Mossbauer spectroscopy 0-2671  
 Fe-Co, surface comp. and surface segregation 0-34280  
 Fe-Cr, Auger electron and appearance pot. spectroscopic study of surfaces 0-11520  
 Fe-Cr, surface covered with anodic oxide film, in-depth composition profiles 0-10763  
 Fe-Cr-Al(-Y), isothermal oxidation behaviour at 1200°C, SEM 0-50755  
 Fe-Cr-Al(-Y), thermal cycling influence on oxidation behaviour at 1200°C, SEM 0-50756  
 Fe-Cr-Mo, sputtering effect on surface comp., AES obs. 0-6601  
 Fe-Mn, high-temp. sulphidation, scale struct., corrosion kinetics 0-50777  
 Fe-Ni-Mn (20, 5 wt.%), surface martensite, crystallography and morphology 0-40354  
 Fe-Ni-Sb-S, S/Sb surface site competition in segregation 0-40366  
 Fe-Si-B, surface tension, density, and oxidation kinetics 0-20028  
 Fe<sub>1-x</sub>O, surface struct., XPS study 0-20759  
 α-FeOOH, goethite, surface OH groups, D<sub>2</sub>O isotopic exchange, IR investig. 0-2254  
 GaAs (100) surface struct. determ. by LEED, UPS, and EPR 0-49475  
 GaAs, (100) surfaces, reconstructed, ang. resolved photoemission from surface states, adsorption and annealing effects 0-16143  
 GaAs (110), atomic struct. of clean and As covered surfaces, LEED study 0-49476  
 GaAs (110), reconstruction and oxidation initial stages, ab initio calc. 0-49473  
 GaAs (110), self-consistent pseudopotential calcs., electronic struct. and atomic co-ords. 0-49848



## surface structure continued

- GaAs (110), surface struct., LEED and AES study, comparison of MBE and ion bombard. surface prep. 0-54496  
 GaAs (110) surface, O<sub>2</sub> interaction, order-disorder effects, LEED, UPS anal. 0-6634  
 GaAs, diffusion of Sn effect of ambient As vapour press. on surface stability 0-2208  
 GaAs, ion-implanted, laser pulse annealing of amorphous surface layer, TEM 0-55436  
 GaAs layers, from gas phase, impurity influence on growth micromechanism 0-45237  
 GaAs, MBE (001) layers, work function meas. 0-49870  
 GaAs, surface characterisation by high resolution Rutherford backscatt. 0-25511  
 GaAs surface morphology during etching with H<sub>2</sub>O vapour 0-39094  
 GaAs:Cu, back surface gettering 0-10758  
 GaAs:Cr, gettering by back surface mech. damage 0-10759  
 GaAs:Se, TEM structural study, surface and interior damage 0-34025  
 GaAs:Si LPE layers, surface morphology, substrate misorientation, initial supercooling effects 0-34329  
 GaP (100), prep. of negative electron affinity surface by Cs adsorption 0-10768  
 Gd, AES, by computer (*French*) 0-7890  
 Ge, (001)-(2×1) surface, reconstruction-induced mean-square displacements 0-15343  
 Ge (111) surface, clean and CO-covered, UPS and ion-neutralisation spectroscopy 0-10785  
 Ge, cryst. surface layers treatment and study by HF ion-plasma etching (*Russian*) 0-16517  
 In film, RF plasma oxidised, surface analysis using ESCA 0-50742  
 InGaAsP, LPE grown, impurity effect on surface morphology 0-29291  
 InGaSb, LPE growth characteristics, substrate surface contamination dependence 0-39470  
 InP, LPE grown, impurity effect on surface morphology 0-29291  
 InSb (110), clean, O<sub>2</sub> adsorption, AES, LEED, RHEED and field effect meas. 0-49501  
 InSb (110), ion bombard. effect on surface struct. and electronic props. 0-6923  
 InSb (110) surface, struct. and electronic props., RHEED and field effect meas. 0-11068  
 InSb (110) surface struct. determ. by LEED, UPS, and EPR 0-49475  
 InSb, (111) surface, anal. by low energy ion scattering spectroscopy, LEED and AES (*Japanese*) 0-20746  
 InSb, ion implanted, efficient void form., TEM obs. 0-44237  
 InSb, LPE growth characteristics, substrate surface contamination dependence 0-39470  
 In<sub>2-x</sub>Sn<sub>x</sub>O<sub>3-y</sub>-ZnS:Mn thin film structure, surface morphology and electro-optical props. (*Russian*) 0-49554  
 Ir (100), adsorption of Xe, local surface struct., UPS study 0-39429  
 Ir (110), O adsorbed, surface struct. anal. using hybridisation model 0-44423  
 Ir (110) 1×2 reconstructed surface, struct. study by LEED, reliability factor anal. 0-39399  
 Ir (111), ( $\sqrt{3}\times\sqrt{3}$ )30° S overlayer struct., LEED obs. 0-15365  
 Ir (111) surface, structural anal. of (2×2) O overlayer, LEED study 0-2264  
 Ir, surfaces (111), (100)-(5×1) and metastable (100)-(1×1) struct. depend. 4f-core-level binding energies for surface atoms 0-44406  
 Ir, with adsorbed Xe, 5p photoemission, local surface struct. influence 0-2920  
 KCl crystal, surface elementary steps interaction with Au particles 0-39400  
 LaB<sub>6</sub>, surface (100), atomic struct., angle-resolved XPS, LEED and ISS investigation 0-10765  
 LaNi<sub>3</sub>, surface segregation, influence of O<sub>2</sub>, H<sub>2</sub>, H<sub>2</sub>O, SO<sub>2</sub> (*German*) 0-51008  
 Li electrode, in lithium perchlorate-propylene carbonate solution, surface anal. (*French*) 0-50859  
 LiF, single crystal, neutron and gamma irradiation, SEM and Bragg profile anal. 0-15158  
 Li<sub>3</sub>N:H, ionic cond., nuclear reaction anal. 0-34454  
 Lu, crystal surface study from refl. electron energy loss spectra obs. 0-20742  
 Mg-Mg<sub>2</sub>Ni eutectic alloy and Mg<sub>2</sub>Ni, catalytic effect in hydrogenation, surface analysis 0-30283  
 MgO (100), chain method of LEED/MEED intensity anal. 0-20018  
 MgO (100), surface struct., LEED study 0-39396  
 Mg<sub>2</sub>SiO<sub>4</sub> crystals, morphology and dislocation etch pits, (010) surface 0-24457  
 Mn-substituted garnet film, growth characts. and mag. props. 0-39826  
 Mn-Zn ferrite single crystals, mech. polishing effect on mag. props. (*Japanese*) 0-16569  
 MnO (100), surface struct., LEED study 0-39396  
 Mo, (001) surface, electronic origin of reconstruction 0-11065  
 Mo (001) surface struct., LEED anal. 0-34282  
 Mo (112) surface adsorption of Li film, LEED and contact pot. method 0-10794  
 Mo, surface impurities, depend. on prep. method, ion scatt. spectroscopy 0-40200  
 Mo Tokamak limiter, surface observation, infrared techniques 0-38693  
 Mo-Fe metal/ceramic alloy, brittle fracture investigation, segregation, morphology, struct. (*Russian*) 0-55503  
 Mo-Mn metal/ceramic alloy, brittle fracture investigation, segregation, morphology, struct. (*Russian*) 0-55503  
 Mo-Re-C (0.3, 0.2 at.%) time-of-flight atom-probe expts. 0-55741  
 Mo-TiC(ZrC)(HfC), thermionic emission, surface structural characts. after prolonged use, work function variation 0-20758  
 MoS<sub>2</sub>, clean surface, AES and LEED exam. 0-10762  
 N<sub>2</sub> overlayer on graphite, orientational ordering, neutron scatt. meas. 0-10783  
 NH<sub>4</sub>HSO<sub>4</sub>, ferroelectric powder dielectric behaviour particle size depend. 0-55046  
 NaCl crystal surface struct., effect of ionic bombardment (*German*) 0-24507  
 NaCl, evaporating cryst. surfaces, successive monatomic step trains with different density 0-29254  
 NaCl surface conditions of step decoration 0-15349  
 NaCl type structure, chain method of LEED/MEED intensity anal. 0-20018  
 NaO-CaO-SiO<sub>2</sub> glasses, fluorinating agents effect on comp. and surface struct. 0-35364

## surface structure continued

- Na<sub>2</sub>O-Al<sub>2</sub>O<sub>3</sub>-SiO<sub>2</sub> glass, leaching in HCl solns., Na conc. distrib. in surface layers 0-21141  
 Na<sub>2</sub>O-Al<sub>2</sub>O<sub>3</sub>-SiO<sub>2</sub> glass, interaction with aq. salt solns., alkali ions distrib. in surface layers 0-21142  
 Na<sub>2</sub>O-NaF-CaO<sub>2</sub>ZnO<sub>1-x</sub>-Al<sub>2</sub>O<sub>3</sub>-SiO<sub>2</sub>, opal glasses, strength, surface composition 0-30066  
 Na<sub>2</sub>O-ZrO<sub>2</sub>-SiO<sub>2</sub> glass, treated with 2 N solns. of NaCO<sub>3</sub> and NaOH, surface layer comp. 0-35366  
 Na<sub>x</sub>WO<sub>3</sub> bronzes (0.4<x<1), domain, surface and substrate structs. 0-34281  
 Na<sub>x</sub>WO<sub>3</sub>, x=0.6 and 0.8, surface characts. 0-39392  
 Nb (110) and (750), interaction with O<sub>2</sub>, LEED, AES, SIMS, and EELS obs. 0-44408  
 Nb, surface damage caused by He<sup>+</sup> ion bombard. 0-39177  
 Nb, surface topography formation due to elec. transfer processes (*Russian*) 0-54482  
 Nb-Mo(Ti)(Zr), nitriding, diffusive saturation, lattice spacing and activation coeffs. (*Russian*) 0-21168  
 Nb-Zr (1.5 wt.%) alloy, field ion microscopy investigation, surface struct. 0-45220  
 Ni (001), adsorbed CO c(2×2), surface geometry determ. by deep-core-level XPS 0-40224  
 Ni (001), surface barrier struct., LEED anal. 0-20023  
 Ni (001) surface, adsorbed N<sub>2</sub>, p(2×2) struct., LEED and AES study 0-54515  
 Ni (001)/CO(O) system, adsorbate geometries determ. from final state scattering in X-ray photoemission 0-54488  
 Ni (100), adsorption of C, substrate reconstruction, LEED constant momentum transfer averaging study 0-39445  
 Ni (100), clean surface and with chemisorbed O, rapid LEED intensity meas. 0-44420  
 Ni (100)-c(2×2)CO, LEED meas. 0-6647  
 Ni (110), adsorption of H, substrate reconstruction, LEED constant momentum transfer averaging study 0-39445  
 Ni (110), S and O adsorbed, surface struct. anal. using hybridisation model 0-44423  
 Ni (111) surface, C interaction, monolayer form. and struct. stability 0-10756  
 Ni (100), adsorption of O, low energy ion scatt. study 0-39420  
 Ni, adsorbed S and Se, photoelectron diff. data 0-29851  
 Ni alloy powder, crystallised by supercooling methods, struct. props. (*Russian*) 0-54483  
 Ni single crystal, surface hyperchannelling, scatt. of low energy Ar ions, computer simulation 0-34110  
 Ni surface, oxidation, structural changes, low energy ion scatt. study 0-35423  
 Ni, surface self-diffusion in presence of adsorbed halogens (*French*) 0-24723  
 Ni-Cu, sputtering rate, radiation-induced segregation and preferential sputtering effects, kinetic model 0-40199  
 Ni-Cu alloy, surface comp. and catalysis 0-54489  
 Ni-Fe-Pd thin films, mag., surface and corrosion props. 0-34707  
 Ni-Mo, sputtering rate, radiation-induced segregation and preferential sputtering effects, kinetic model 0-40199  
 Ni-Pd surfaces, electrochem. passive film form. and comp. determ. by SEM, SIMS, XPS 0-39401  
 Ni-Ti (1.6, 7.64 wt.%), monophase high temp. scaling, metallography study 0-21159  
 NiO (100), surface struct., LEED study 0-39396  
 Pb, film, sputtering mechanism, SEM 0-29839  
 PbCO<sub>3</sub>, cryst. growth, Liesegang ring form., pH effect 0-49140  
 PbInAu film, RF plasma oxidised, surface analysis using ESCA 0-50742  
 PbMoO<sub>4</sub>, hollock growth origin in gel growth 0-49139  
 PbS, clean surface, AES and LEED exam. 0-10762  
 Pb<sub>1-x</sub>Sn<sub>x</sub>Te layers, LPE growth on metal-etched substrates 0-55313  
 PbTe (111) epitaxial films, localised electron irradi. effects on elec. props. and O<sub>2</sub> sorption 0-49472  
 Pd (100), adsorption struct. of CO, LEED and high-resolution EELS study 0-20037  
 Pd crystallite morphology, surface struct., electron microscopy obs. 0-29257  
 Pd-C, dil., C segregation to single cryst. surfaces 0-39301  
 Pd-Pt, with adsorbed Xe, 5p photoemission, local surface struct. influence 0-2920  
 Pd<sub>2</sub>Si, on Si substrate, thermally induced Si accumulation, AES study 0-24718  
 Pt (110) reconstructed surface, LEED-AES study, O<sub>2</sub> treatment effect 0-39398  
 Pt (111) and (100) superlattices formed by dissociative adsorption of HI, LEED, AES, and thermal desorption studies 0-55715  
 Pt (997), terrace bending obs. from He beam scatt. 0-40202  
 Pt, adsorption of CO, O<sub>2</sub>, NH<sub>3</sub>, surface composition, AES and temp. programmed desorption meas. 0-34313  
 Pt crystallite morphology, surface struct., electron microscopy obs. 0-29257  
 Pt-C, dil., C segregation to single cryst. surfaces 0-39301  
 Pt-Cu, surface composition, XPS (*Portuguese*) 0-24722  
 Pt-Rh alloys, surface comp. determ. by ion scatt. spectroscopy 0-6602  
 Pt(111), LEED, quantitative anal. 0-44085  
 Re, O<sub>2</sub> adsorption, effect of struct. defects, steps and kinks 0-29269  
 Rh (110), S adsorbed, surface struct. anal. using hybridisation model 0-44423  
 Rh (110), S-adsorbed, LEED crystallographic determ. of struct. 0-44422  
 Rh supported surface, CO chemisorption, activated surface processes, IR spectra 0-16724  
 Ru (~001) stepped surface, O<sub>2</sub> chemisorption, LEED and AES obs. 0-11947  
 Ru, with adsorbed Xe, 5p photoemission, local surface struct. influence 0-2920  
 RuO<sub>2</sub>-TiO<sub>2</sub>, anode, wear-resistant, use in applied electrochem. 0-40701  
 Se, crystal surface, N and O adsorption, refl. electron energy loss spectra obs. 0-20742  
 Se-Ge, amorphous thin film, photocontraction rel. to surface struct. 0-49551  
 Si, (001)-(2×1) surface, reconstruction-induced mean-square displacements 0-15343  
 Si (100), atomic and electronic structs., energy minimisation calcr. 0-49480  
 Si (100), intrinsic surface states, photoemission study 0-50514  
 Si (110) surface peak anal. by 100-350 keV protons 0-55247



## surface structure continued

- Si (111) 7×7, structure model from anal. of RHEED patterns 0-49471  
 Si (111) (7×7) surface structs., LEED anal. and energy minimisation calcs. 0-49478  
 Si (111) surface, O<sub>2</sub> adsorption, atomic steps and residual gas effects 0-54517  
 Si (111) surface reconstruction, milk-stool model, quantum chem. ab initio calc. 0-49477  
 Si (111) surfaces, geometric struct., LEED obs. 0-49479  
 Si, clean and gas (O<sub>2</sub> and H<sub>2</sub>O) covered, appl. of UPS ultrahigh vacuum apparatus (*Japanese*) 0-37125  
 Si, cryst. surface layers treatment and study by HF ion-plasma etching (*Russian*) 0-16517  
 Si, decontamination of Au impurities by etching 0-55559  
 Si, ion bombard. effect on surface struct., RHEED and Au decoration 0-2096  
 Si, ion-implanted, period surface struct. in laser annealing, new expt. evidence 0-29836  
 Si, local mechanical defects, annealing and effect on autoepitaxial growth (*Russian*) 0-7701  
 Si, MBE growth and surface struct. 0-10816  
 Si, periodic stepped structure, on vicinal planes, LEED obs. 0-24725  
 Si, reconstructed surface physics, review 0-10766  
 Si sputter-machined surface, Ar<sup>+</sup> ion, lattice disordering obs. (*Japanese*) 0-3228  
 Si, structurally related bulk and surface props., self-consistent pseudopot. method 0-54632  
 Si surface, (111)7×7, electronic struct. calc. 0-24993  
 Si, surface, etched and heat-treated, optically stimulated ESR investigation 0-11245  
 Si, surface, stacking fault generation due to mech. damage, preoxidation annealing influence 0-54261  
 Si surface layers, impurities, elec. and photoelec. props. 0-2298  
 Si, surface structures after pulsed laser annealing, LEED obs. 0-54494  
 Si surfaces, amorphous, hydrogenated, and monocryst., AES and LEED, comparative study (*French*) 0-44398  
 Si:B, inhomogeneous surface layer, diffusion and implanted, X-ray rocking curves 0-6603  
 SiC, cryst. surface layers treatment and study by HF ion-plasma etching (*Russian*) 0-16517  
 SiC, surface defect annealing, following Ar ion and electron irradi. 0-7603  
 SiO<sub>2</sub> glasses surface textures and defects, exam. using liq. crystals. 0-6364  
 SiO<sub>2</sub>:Na<sup>+</sup>, heat treated, heat of immersion in H<sub>2</sub>O, organic compds. 0-3396  
 SmS (001) surface, mixed valency and phase transitions 0-39658  
 Sn plate surface, ion-bombardment conditions effect on chem. profile 0-54287  
 SnO<sub>2</sub>-ZnS:Mn thin film structure, surface morphology and electro-optical props. (*Russian*) 0-49554  
 SrTiO<sub>3</sub> (100) surface, struct. and electronic props., AES, LEED, EELS, and UPS study 0-24986  
 SrTiO<sub>3</sub>, surface microrelief revealed by ion irradiation 0-54485  
 Ta<sub>2</sub>O<sub>5</sub>, hydrated, heat treatment effect on physicochem. props. 0-20966  
 (Ti,V)C, activated reactive evaporation deposited films, annealing study, microstructure 0-24762  
 Ti (0001), with adsorbed N (1×1) layer, underlayer geometry, electronic struct. calcs. and UPS meas. 0-54751  
 Ti (0001) film, with adsorbed H (1×1) monolayer, electronic struct., surface geometry 0-54750  
 Ti alloys, grinding, effect on surface struct. 0-25878  
 Ti, Auger electron appearance potential spectroscopy (*Japanese*) 0-50473  
 Ti-Al-Cr-Mo alloy VT3-1, reactions with some refractory compounds 0-16585  
 TiC, activated reactive evaporation deposited films, annealing study, microstructure 0-24762  
 TiC-Ni-Mo sintered hard alloy TN-20, fracture surfaces 0-7684  
 TiO<sub>2</sub> (rutile), (001) and (110) faces, UPS and LEED obs. 0-45206  
 TiO<sub>2</sub>:H photoanodes, diffusion and surface chemistry 0-35546  
 TiO<sub>2</sub>-RuO<sub>4</sub> anode, wear resistant, use in applied electrochem. 0-40701  
 TiS<sub>2</sub>, LEED, single-reflection layer scatt. theory 0-49059  
 UO<sub>2</sub>, (110), (100), and (111) surfaces, struct. study using He<sup>+</sup> ion scatt. spectroscopy 0-40206  
 UO<sub>2</sub> pellet surfaces, β-UO<sub>2.33</sub> formation in air at 229 to 275°C, X-ray diffr. study 0-35362  
 UO<sub>2</sub>, surface props. of low index faces, calc. 0-6604  
 (V,Ti)C+Ni cermet, binder grain size 0-44401  
 V<sub>2</sub>O<sub>5</sub>, (001) surface modification, during catalytic oxidation of propene (*French*) 0-45557  
 W (001), surface phase transition, electronic contrbs., surface susceptibility, ab initio self-consistent thin-film energy band calc. 0-29255  
 W (001) (1×1) surface contraction using LEED intensity anal 0-6606  
 W (001) clean surface displacive phase, long-range inhibition by N 0-2266  
 W, (001) surface, electronic origin of reconstruction 0-11065  
 W (001) surface structure by MeV ion backscattering, channelling 0-6605  
 W (100), LEED intensities, temp. depend., surface struct. phases and surface Debye temp. 0-39395  
 W (100), reconstruction in presence of O half monolayer, struct. props. 0-44421  
 W (100) stepped surface, adsorbed O, electron stimulated desorption ion ang. distrib. 0-20035  
 W (110), WO<sub>3</sub> and O<sub>2</sub> adsorption by LEED and AES 0-34317  
 W (111), (211), and (311), adsorption of W single atoms, surface site geometry determ. by FIM 0-39447  
 W surface layer struct. during milling, plastic deform., failure (*Russian*) 0-40586  
 W-Al<sub>2</sub>O<sub>3</sub> cermet films, oxide evaporation deposited on Mo, Ti, Al<sub>2</sub>O<sub>3</sub> substrates, struct., props. 0-25581  
 W-TiC(ZrC)(HfC), thermionic emission, surface structural characts. after prolonged use, work function variation 0-20758  
 W(110) vicinals, adsorption of N<sub>2</sub>, step sites as dissoci. centres 0-6642  
 W{001} surface, clean, reconstructed, field-ion microsc. obs., 15-400K 0-15348  
 Zircaloy-4, heat treated in SiO<sub>2</sub> capsules, Zr and Si vapour transport surface struct. anal. of deposits 0-55437  
 Zn, film, sputtering mechanism, SEM 0-29839  
 ZnO, film for solar cell appl. structural, optical and elec. props. 0-2294  
 ZnS, clean surface, AES and LEED exam. 0-10762  
 ZnTe (110) surface struct. determ. by LEED, UPS, and EPR 0-49475

## surface structure continued

- Zr, (0001) surface struct., HCP phase, LEED study 0-20017  
 Zr-Ni, surface layer, segregation of ferromag. Ni, magneto-optic investigation 0-2256  
 Zr-Ni-H, surface segregation of Ni, influence on catalytic activity 0-30275  
 ZrNi, surface segregation of Ni, influence on catalytic activity 0-30275

## surface tension

- acrylic coating, surface tension effects 0-53487  
 aliphatic acids, thermodynamics of adsorption at air/aqueous soln. interface 0-10752  
 aliphatic alcohol, thermodynamics of adsorption at air/aqueous soln. interface 0-10752  
 artificial blood substitutes, surface energetics anal. 0-41321  
 binary liquid mixture, horizontal layer, surface tension driven instability in presence of Soret effect 0-10227  
 binary metallic system, rel. to conc. profiles across solid-liq. interface 0-55382  
 black lipid membranes and bilayer vesicles in solution, thermodynamic stable states anal. 0-45856  
 capillary phenomena in cylindrical pores, appl. to pore size anal. 0-15340  
 charged fluids, theory of density profiles and surface tension 0-44689  
 convection driven by non-uniform surface tension 0-10116  
 crystal growth, diffusive, numerical soln. accounting for growth rate and surface tension anisotropy 0-33912  
 dielectric liquids, HF electric field influence on surface tension (*Russian*) 0-49463  
 diphilic polyelectrolytes, aqueous solns., Wilhelm method 0-10745  
 drops, interfacial tension inferred from quadrupole resonance props. 0-33275  
 flow, separating, fluid-surface interface, static contact line, slip at wall and shape of free surface 0-53737  
 fluid interfaces, isothermal and deformable, mass transfer and surface tension, review 0-33564  
 Fowkes' hypothesis, statistical mechanics basis 0-2249  
 free energy theory, using Lennard-Jones 6-12 pot. 0-10751  
 gas bubble, growth or dissolution, general soln., analyticity 0-10747  
 gas-liquid surface of mol. fluids, mol. dynamics computer simulations 0-39387  
 Gibbs states, non-translation invariant with coexisting phases, analyticity 0-8923  
 gravity waves, non-uniform free surface, superficial viscosity and tension (*French*) 0-48728  
 group structure for general lattice systems and surface tension 0-4675  
 hydrodynamic stability of liquid films and jets, effect of soluble surface-active substances 0-6027  
 immiscible liquids, binary system, wetting hypothesis, validity, Antonow's rule appl. (*French*) 0-49462  
 interface, stability problem, diffusion, reaction and convection 0-33567  
 ionic crystals, statistical theory calcs. of surface energy and surface tension 0-17894  
 Kelvin equation, effect of surface tension on vapour pressure, derivation 0-2248  
 lattice systems, surface tension and phase transition 0-27226  
 light modulator, using oil film deform. by surface tension var. 0-5831  
 liquid, in vessel, vibr. amplitude determ., structural damping and surface tension applied to stress anal. 0-19417  
 liquid metals, radial distrib. function and thermodynamic characts., interparticle interaction pot. (*Russian*) 0-49086  
 liquid metals, surface properties, hard-sphere and square-well models 0-19684  
 liquid penetrant testing, continuum fluid mechanics aspects 0-43818  
 liquid spreading on solid surfaces, static and dynamic contact lines, book contrib., review 0-20015  
 liquid-vapour interface, struct. at 110K, Monte Carlo method, for Ar-like fluid 0-54477  
 liquid-vapour interface, surface tension-compressibility relation 0-44397  
 lubrication, hydrodynamic, free boundary problem including surface tension 0-19542  
 measurement of low interfacial tensions from light scatt. intensity by liq. interfaces (*French*) 0-20007  
 metallic particle, surface tension depend. on size, vaporisation time (*Russian*) 0-34290  
 metals, liq., temp. depend. (*Russian*) 0-15336  
 molecular fluid, computer simulation of liquid-vapour surface 0-54478  
 molten salt mixtures, surface tensions 0-29246  
 monolayer, interfacial, thermodynamic treatment, excess quantities, adsorbed and spread layers 0-40732  
 monolayers at fluid-fluid interfaces, hydrodynamic stability, ion interactions 0-6598  
 monolayers at fluid-fluid interfaces, hydrodynamic stability, dipole interactions 0-6599  
 oil-water interface, electroadsorption and electrocapillarity 0-44393  
 optical fibre ends when fusion spliced (*Japanese*) 0-28317  
 oscillating jet method, surface elasticity effect 0-10743  
 oxides, liq., calc. (*Russian*) 0-15335  
 pentanol activity in bulk phases, distribution and surface activity (*French*) 0-24712  
 phospholipid vesicles, hydrostatic press. 0-56000  
 planar structures, hexagonal and cubic models, surface forces 0-20022  
 plane pendant drops, instability 0-29247  
 polyethylene-co-vinyl alcohol-g-ethylene oxide aq. soln., surface tension (*Japanese*) 0-24716  
 polymer, adhesion phenomena and influence of various factors, work of adhesion (*Polish*) 0-3292  
 polymeric composite, interphase, physico-chemical problems 0-16262  
 polymers, amorphous high, surface tension temp. depend., appl. of significant liquid struct. theory 0-44394  
 pulsed laser-induced shattering of water drops 0-50471  
 Rayleigh waves, surface tension dispersion effects 0-14513  
 silicone oil drop spreading on horizontal surfaces 0-2250  
 simple fluid, one-component, liquid-vapour phase coexistence, surface tension determ. from many body pot. 0-49465  
 small particles, cause of reduction in lattice spacing (*Russian*) 0-38967  
 solid, eqn. of state anal. 0-6618  
 solitons in condensed matter physics, theory 0-50122  
 specific acoustic impedance in organic liquids, interdependence on surface tension (*Polish*) 0-39223  
 steep water waves, surface tension effects 0-38424  
 submerged moving bodies, free surface and surface tension effects 0-1522



## surface tension continued

- surface tension driven convection, solidification effects 0-43703  
viscoelastic non-Newtonian liquids, resist. to tensile stress 0-1505  
wetproofed electrode, pore filling degree with electrolyte and liq. reactant 0-40702  
wetting tension depend. on meniscus curvature, adjacent liquid film disjoining press. isotherm 0-2247  
AgBr melts, surface energy and surface tension coeffs., effect on photographic emulsion microcryst. growth rate (*Russian*) 0-47132  
AgCl melts, surface energy and surface tension coeffs., effect on photographic emulsion microcryst. growth rate (*Russian*) 0-47132  
AgCl-NaCl molten solns., activities and surface tension 0-10748  
Al-halide systems, liquid-liquid interfacial tension meas. 0-10750  
Al-Pb(Sn), liquid, surface tension, size effect (*French*) 0-15341  
Ca(NO<sub>3</sub>)-H<sub>2</sub>O system, induction period supercooling depend. meas. 0-19918  
CdTi<sub>2</sub>Se<sub>3</sub>:Au(Ag)(Cu), doping effect on surface tension of melt and crust. microhardness 0-49464  
Cl<sub>2</sub>, liquid-vapour surface, computer simulation 0-54478  
Cr-Ge liquid and amorphous alloys, struct. props., cond., viscosity, surface tension (*Russian*) 0-54119  
Cu-Pb, liquid, surface tension, size effect (*French*) 0-15341  
Fe-As melts, influence of Sn, Si, Mn and Cr additions on surface tension and density (*Russian*) 0-15337  
Fe-C (graphite), adhesion and wettability of graphite (*Russian*) 0-20008  
Ge, electron-hole droplet condensation model, phase diagram and surface tension 0-6734  
H<sub>2</sub>O, surface tension and energy, Fowler model 0-10754  
He, liq. and vapour phases, thermodynamic and thermophysical props. calc. using HEPROP computer program 0-6529  
He, liquid, free surface, book contrib. 0-2231  
<sup>3</sup>He-<sup>4</sup>He mixtures, free surface, book contrib. 0-2231  
<sup>4</sup>He, liq., free surface, crit. behaviour near  $\lambda$  point 0-2228  
<sup>4</sup>He superfluid film, adsorbed on Al<sub>2</sub>O<sub>3</sub> powder, surface tension sound 0-24691  
Hg, in Rankine-type capillary viscometer (*Japanese*) 0-14859  
KCl, molten, vapour-liq. interface, mol. dynamics model 0-54362  
La<sub>2</sub>O<sub>3</sub>-Na<sub>2</sub>Si<sub>2</sub>O<sub>5</sub> molten glasses, surface tension and density, 900-1500°C 0-15334  
Mo, doped, surface tension driven flow in electron beam floating zone expts. 0-19731  
N<sub>2</sub>, liquid-vapour surface, computer simulation 0-54478  
Ni epitaxial electrodeposition, surface-stress phenomena at start 0-35542  
Pd-C (graphite), adhesion and wettability of graphite (*Russian*) 0-20008  
Pt-C (graphite), adhesion and wettability of graphite (*Russian*) 0-20008  
Pt-Pd (Co)(Su)(Al)(Si) melts, surface tension and density (*Russian*) 0-39388  
Rh-C (graphite), adhesion and wettability of graphite (*Russian*) 0-20008  
Si, electron-hole droplet condensation model, phase diagram and surface tension 0-6734  
Si-B system, liq., surface tension, density, and oxidation kinetics, 1410-1700°C 0-20011  
UO<sub>2</sub>, surface props. of low index faces, calc. 0-6604  
Zn, liq., temp. depend. (*Russian*) 0-15336  
Zn-Pb(Bi), liquid, surface tension, size effect (*French*) 0-15341

## surface tension measurement

- absolute method, max. force exerted by meniscus formed by cone on free liq. surface 0-39390  
dynamic surface tension of solns., bubbles, maximal pressure, dead time of formation 0-10744  
floating foil method 0-325  
liquid dynamic surface tension meas. instrument 0-42313  
liquid interfacial tension meas. from scatt. light intensity 0-20012  
liquid-liquid interfacial tension meas., appl. to molten Al-halide systems 0-10750  
oxide melts, specific weight, electrical conductivity, viscosity and surface tension meas. methods survey (*Slovak*) 0-47079  
wall effect in surface tension determ. using Wilhelmy plate 0-2246  
water on semiconductor substrate surfaces, measurement of contact angle (*German*) 0-34276

## surface texture

- autocorrelation, surface texture assessment 0-47013  
binary liquid mixtures adsorption onto solid surface, effect of surface heterogeneity 0-44411  
cartilage, articular, meas. of surface microgeometry 0-3880  
ellipsometry for surface roughness meas. 0-52294  
glass, ground, surface height and correlation length from reflection scatt. of laser light (*French*) 0-54491  
gloss appearance by means of moiré patterns (*German*) 0-52300  
luster quality, meas. method, texture and microreflection characteristics (*Japanese*) 0-35466  
magnox fuel cladding, surface struct. data acquisition and processing system 0-898  
measurement, evaluation of fibre optic proximity transducer 0-36985  
measurement by differential light scattering 0-36991  
measurement developments, future implications 0-36984  
metal surface micro-inhomogeneity effect on optical breakdown of gas 0-48922  
meteorites regmaglyptic relief index, meas. 0-56782  
nuclear tracks, etched, statistical distrib. of quadratic holes on planar surface, computer simulation 0-37705  
orientation distribution function, calc. of odd part 0-20954  
polyethylene film, oriented, soln. growth 0-45244  
polypropylene fibre, with helical internal texture, SEM obs. of surface morphology 0-39394  
quartz, amorphous layer on mech. treated single crystals. electron microscope and RHEED obs. 0-24721  
rough curved surfaces, theoretic considerations on surface roughness meas. (*Czech*) 0-193  
sinters, texture anal., appl. to Ca ferrites in sinters of rich Fe ores 0-18009  
snad grain surface texture rel. to wind vel. conditions 0-41443  
speckle, white light, contrast at defocused image plane 0-23621  
stylus instrument developments 0-36983  
Walsh function assessment method 0-36995  
wetting, effects of solid surface roughness, expt. study 0-34275  
Ag electrone, enhanced Raman effect from adsorbed cyanide 0-50348  
Cd films, nucleation and growth, props. 0-29878  
Cr<sub>2</sub>O<sub>3</sub>-Cr black, selective coating, optical and topographical props. 0-26165

## surface texture continued

- Cu substrate, surface topography influence on growth struct. of sputtered Cr 0-20058  
 $\delta$ -FeO(OH) crystallites, TEM imaging investigation 0-39096  
GaP, surface polaritons, light scattering studies, effect of surface roughness 0-6753  
<sup>3</sup>He-A, superfluid, instability of persistent currents and heat flow 0-15327  
KCl, etching, double poison role 0-54240  
KCl surface texture and optical props. after forging between polished dies 0-33102  
Mo<sub>2</sub> single crystals, surface orientation effect as high temp. creep and fracture type 0-16403  
SF<sub>6</sub>, compressed, influence of electrode macroscopic curvature upon surface roughness effects 0-40693  
SF<sub>6</sub>/N<sub>2</sub> pressurized mixtures, electric breakdown, surface roughness effects 0-14877  
Si films, CVD, amorphous and polycryst., microscopic surface roughness, effective-medium models, ellipsometric expts. 0-24756  
Si wafer, chemically etched, surface roughness by gas adsorption techniques 0-15398  
SiO<sub>2</sub> film, on Si wafer, surface roughness by gas adsorption techniques 0-15398  
Te textured thin films, prep., high solar absorptivity by multiples refl. 0-11568

## surface topography measurement

- adhesive bondline interrogation using Stoneley wave methods 0-49530  
aspheric surface contour meas. machine and computer system 0-14494  
automatic pattern processor for simple and complex interference patterns 0-13129  
cartilage, articular, meas. of surface microgeometry 0-3880  
corneal topography using moiré contour fringes 0-26316  
developments, future implications 0-36984  
differential light scattering method 0-36991  
diffuse reflectance rel. to partial coherence and IR laser photogoniometric meas. 0-14283  
elastohydrodynamic film thickness, meas. of artificially produced dents and grooves 0-36975  
ellipsometry for surface roughness meas. 0-52294  
endoscopic contour technique for meas. dimensions of object detail (*German*) 0-31839  
fibre optic proximity transducer evaluation 0-36985  
height difference detection by digitised moiré pattern processing 0-52156  
image moiré method for determination of partial slopes in fixed plates 0-14645  
image processing of additive-obtained moiré patterns (*German*) 0-47017  
ion etching, SEM dynamic study 0-50734  
laser scanning analyser, roughness meas. 0-36992  
machined surface time series modelling 0-36998  
metal surfaces, laser technique (*German*) 0-52155  
microcomputer application to surface roughness meas. 0-47014  
mirror optical scatter meas. specification proposal 0-48390  
moiré topography, historical review 0-9024  
moiré topography, real-time and time-resolved, in microseconds region 0-52154  
noncontact optical gauging by remote image tracking in production environment 0-8961  
nonplanarity of surface plates, errors in measurement by optical planarity meter 0-17919  
optical profilometer, fast versatile, for surface roughness of workpieces meas. 0-37069  
optical surface quality standards based on total integrated scatt. 0-48391  
orientation determ. from multiple images, photometric method 0-52163  
planarity determ., by interference pattern assessment, using laser source 0-31711  
polychromatic speckle patterns, use for surface roughness meas. 0-31708  
power spectrum measurement by optical Fourier transformation 0-36989  
profile computerised meas., digital voltmeter output recording on punched tape 0-22327  
profile digitization for stylus instruments 0-36993  
profilometers 252 and 283, with direct indication 0-22329  
replica materials, film type, surface reproduction characteristics 0-36988  
replica materials and techniques, comparative study 0-36987  
rough curved surfaces, theoretic considerations on surface roughness meas. (*Czech*) 0-193  
roughness and surface slope measurement, comparison of Talysurf and optical methods 0-36990  
roughness filtering using digital filters 0-36994  
roughness meas. by reflected-light microscope (*German*) 0-31861  
roughness profile description, separation of random and periodic components 0-36997  
Rutherford proton backscatt. 0-47015  
Soviet instruments and meas. systems exhibition 0-52161  
standards development in Soviet Union, All-Union test scheme 0-22328  
steel, hot rolled strip and plate shape meas. device 0-35498  
steel, stainless, surface, roughness factor measurement, energetic D<sup>+</sup>, He<sup>+</sup>, Ar<sup>+</sup> irradiation 0-39172  
structure influence on image speckle pattern contrast 0-17985  
stylus instrument developments 0-36983  
texture, autocorrelation function appls. 0-47013  
thin wire defect parameters meas. using capacitance method 0-35489  
tunable moiré grating for optical mapping 0-5832  
US backscatter at normal incidence for randomly rough surface characteristics meas. (*French*) 0-52165  
US pulse echo techniques for flaw detection in metal components (*French*) 0-55613  
X-ray diffraction topography (*Chinese*) 0-1883  
Al alloys, contamination, automated nondestructive inspection 0-16629  
Be substrate for lightweight mirror, surface quality and thermal props. 0-23762  
C surface, pyrolytic, roughness factor measurement, energetic D<sup>+</sup>, He<sup>+</sup>, Ar<sup>+</sup> irradiation 0-39172  
Co, effect on surface roughness on backscattering spectra 0-47016  
Mo laser mirror, optical and metallurgical characterisation 0-33129  
Si, surface roughness evaluation by UV refl. 0-39393  
SiC coatings for first-wall candidate materials by RF sputtering 0-25563  
SiC surface, roughness factor measurement, energetic D<sup>+</sup>, He<sup>+</sup>, Ar<sup>+</sup> irradiation 0-39172  
SiO<sub>2</sub> film on Si, electron beam damage, obs. using scanning AES 0-2070



## surface treatment

see also etching; surface hardening

alloys, improvement of props. by ion implantation 0-16601  
 austenitic stainless steel thermal treatment for spectrally selective surface fabrication 0-35752  
 boriding, with a thermally unstable gas ( $B_2H_6$ ) 0-30159  
 cleaning (*Japanese*) 0-16527  
 cleaning techniques review, for atomically clean surfaces preparation 0-11804  
 crystal units, vacuum system for cleaning and cold welding (*Polish*) 0-31776  
 electrolytic coating, ionic evaporation, paints, organic coatings (*French*) 0-30127  
 ferrite reduction using plasma methods (*Russian*) 0-7700  
 fibre reinforced plastic laminates, US evaluation of hygrothermal effects 0-7730  
 fretting corrosion control using coatings and surface treatments 0-35368  
 glass, surface props. and contact angle after treatment with glow discharge and heating 0-21139  
 glass surface, difluorodichloromethane thermochem. treatment, mech. props. 0-40565  
 glasses, alkali-silicate, chem. stability, cations coordination, leaching vacancy mechanism 0-35526  
 glasses, alkali-silicate, chem. stability depend. on cation  $O_2$  structs. 0-35527  
 glasses, partially leached rods, contact-damage resist. 0-50707  
 glazing machine, which improves quality of glazing, exam. of design 0-11801  
 glow discharge cleaning effectiveness rel. to base material atomisation rate (*Russian*) 0-20797  
 graphite fibres, HM, surface comp. and energetics 0-54480  
 Inconel 625, plasma nitriding, hardness meas., Rutherford backscatt. surface anal. 0-45442  
 industrial, review (*French*) 0-16528  
 ion beam sputtering, appl. to surface machining 0-30129  
 ion implantation, surface treatment process in production engineering 0-34028  
 ionic deposition and electron bombardment industrial equipment, pollution control (*French*) 0-7699  
 laser material processing, workpiece focal point window tolerances 0-5776  
 metal, heating by laser emission; spatial nonlinear problems (*Russian*) 0-7440  
 metal cleaning, by electron cyclotron resonance plasma (*Japanese*) 0-16572  
 metal oxide reduction using plasma methods (*Russian*) 0-7700  
 metal surface, metastable alloy formation by ion implantation 0-15130  
 metal surface cleanliness control by photoemission recording (*Russian*) 0-49839  
 metals, abrasive finishing with refractory carbide micropowders, surface struct. 0-11842  
 metals and alloys, chemicothermal treatment, process kinetics 0-35415  
 microalloy layer formation by ion implantation 0-16600  
 oxidising metal heating by periodically pulsed  $CO_2$  laser 0-7445  
 palliative treatments for fretting fatigue, review 0-21126  
 polymer film, plasma etching and cleaning 0-1855  
 polymer film coating, electropolymerisation in aq. medium book contrib. 0-50778  
 polystyrene lattice cleaning, dialysis, steam stripping and ion exchange effectiveness 0-3414  
 quartz, grinding and surface treatment by ball mill in cetyl alcohol (*Japanese*) 0-25890  
 refractory metals, nitriding reactions and processing conditions, thermodynamic approach (*Russian*) 0-21169  
 semiconductor processing, residual film monitoring by ellipsometry 0-13124  
 steel, alloy, carburisation, internal oxidation of excess carbides (*Russian*) 0-25903  
 steel, alloy, structure and properties after nitriding in molten salts, steel 08kp with Al diffusion coating 0-35418  
 steel, alloy, types CT40, CT40X, CT45, texture form. 0-25721  
 steel, alloy cast, optimal alloying, carburising effect 0-50771  
 steel, austenitic stainless carburisation, X-ray microanalysis (*French*) 0-11981  
 steel, austenitic stainless type AISI 304, surface comp. after different surface treatments 0-3253  
 steel, austenitic stainless type AISI 316, L sheet and LN plate surface comp. after different surface treatments 0-3253  
 steel, boride coatings, form. mechanism and struct. during crystn. of castings 0-35412  
 steel, boride coatings from induction heating microstruct. and props. 0-30165  
 steel, boriding with  $B_2C$  based paste 0-16583  
 steel, C, 45, surface wearing ability, surface finishing method and running-in effects 0-11794  
 steel, C, Cr-Mo and Cr-Mo-Al,  $N_2$ - $H_2$ -( $C_2H_6$ ) gas mixture and its effect on nitrided layer (*Japanese*) 0-35403  
 steel, carburisation by polymer paste, exam. of saturation 0-16582  
 steel, carburised, transform. of residual austenite, mag. field effects (*Russian*) 0-29952  
 steel, carburising, carbide-austenite layers, form. and development 0-35413  
 steel, constructional, nitriding process in glow discharge (*Russian*) 0-55560  
 steel, Cr-Ni-Mn, type 4340, decarburisation by gaseous atomic hydrogen 0-30160  
 steel, glass-enamel coating prod. by induction fusion method, heating rate effect 0-11825  
 steel, high-strength maraging, N18K9M5T, nitriding effect on fracture resist. 0-21092  
 steel, low C, current density and voltage effect on cpd. layer growth by ion-softnitriding (*Japanese*) 0-35402  
 steel, low C, surface shot blasting, prep. for plasma deposition 0-16586  
 steel, mild, adsorbed H distrib. rel. to electrochemical treatment in pure alkali 0-16589  
 steel, nitrided, chem. state anal. by conversion electron Mossbauer spectrometry 0-7718  
 steel, nitriding in molten nitrates 0-35417  
 steel, stainless, gas liberation in vac., effect of different methods of surface treatment (*Russian*) 0-45429

## surface treatment continued

steel, stainless, surface treatment, X-ray photoelectron spectrosc. study 0-50764  
 steel, stainless, type 304, physicochemical and wear props., influence of ion implantation and overlay coatings 0-40603  
 steel, surface wearing ability, finished surface direction effect on wearing ability 0-11793  
 steel fatigue in surface active media, adsorption facilitation mech. 0-55586  
 surface structure, distribution of defects, LEED 0-44402  
 Al alloys, surface shot blasting, prep. for plasma deposition 0-16586  
 Al, physicochemical and wear props., influence of ion implantation and overlay coatings 0-40603  
 Al pretreatment and anodisation, before Cu plating (*German*) 0-45243  
 Au-CdS, Schottky junction, surface defects, photovoltaic, piezoelectric and V-I characteristics (*French*) 0-49898  
 $BaFe_{12}O_{19}$  powder, chemical plating with Co, Co-P, Ni-P and Cu 0-25593  
 C fibres and C fibre reinforced epoxy phenol, oxidation, effect on props. 0-40574  
 CdS, Au deposition, Schottky diodes and MIS devices, surface treatment effects, SEM obs. 0-54794  
 Cu surface shot blasting, prep. for plasma deposition 0-16586  
 Cu-Ni sulphidised alloys, Ru and Os behaviour during carbonylation (*Russian*) 0-40584  
 Fe and Fe-C, (0.8 wt. %), sintered, hot forging and chemicothermal treatment, effect on wear resistance 0-25606  
 Fe, Armc, borided surface layers, Mossbauer and metallographic anal. 0-50769  
 Fe, Armc, siliciding with Si- $SiO_2$  mixture, exam. of corrosion resistance 0-16584  
 Fe, carburization, methane gas—C(dissolved)+ $2H_2$  (gas), kinetics 0-55712  
 Fe, refining by electric fields in vacuum, surface active impurity elimination (*Russian*) 0-55563  
 Fe surface, nitride layer formation, activated surface, passivation 0-16577  
 Fe-Ni, carburization, methane gas—C(dissolved)+ $2H_2$  (gas), kinetics 0-55712  
 InAs anodic oxide films prep. and props. 0-55553  
 InP surface preparation for Schottky barrier and ohmic contact formation 0-39671  
 Mg nitridation in HF discharge, temp. effect 0-3399  
 $MgO-Al_2O_3-SiO_2$  based cordierite glass-ceramic, strength and thermal shock, surface treatment effect 0-25884  
 $MgSiO_3$ , kinetics of dislocation etching 0-6409  
 Mo, nitriding kinetics 0-35415  
 Mo, rolled sheet, boriding, Cu effect 0-21165  
 Mo-N, nonporous metal production accompanying arc plasma nitriding (*Russian*) 0-7712  
 $Na_2O-Al_2O_3-SiO_2$  glass, leaching in HCl solns., Na conc. distrib. in surface layers 0-21141  
 $Na_2O-Al_2O_3-SiO_2$  glass, interaction with aq. salt solns., alkali ions distrib. in surface layers 0-21142  
 Nb, nitriding kinetics 0-35415  
 Nb-Mo(Ti)(Zr), nitriding, diffusive saturation, lattice spacing and activation coeffs. (*Russian*) 0-21168  
 Ni, kinetics,  $Ni_3Al_2$  layers growth by cementation (*French*) 0-35127  
 Ni-Cr alloy, phosphidation in P vapour, 700°C, phosphide layer struct. and kinetics 0-25906  
 Ni-Cr type alloys, Co surface pretreatment to attain pore-free aluminised coatings 0-40612  
 Ni-Cr-Co-Ti, superalloy sintering thermochemical surface treatment 0-25617  
 Ni-In, protective coating on Kovar, vacuum seal for borosilicate glass appl. (*Italian*) 0-40621  
 NiAl, kinetics,  $Ni_3Al_2$  layers growth by cementation (*French*) 0-35127  
 $Pb_{1-x}Sn_xTe$ , photoelec. props., surface recomb. effect 0-44659  
 $Pb(Zr,Ti)O_3$  polycrystalline ceramic, fracture and strength, surface treatment effects 0-11704  
 Si, nitridation, fluoride accelerated 0-7705  
 Si, nitridation to form  $\alpha$ - or  $\beta$ - $Si_3N_4$  0-50609  
 Si, surface cleaning by pulsed laser irradi. 0-45173  
 p-Si, surface elec. behaviour after chem. treatment 0-20185  
 Si wafer, thermal characts. of  $H_2SO_4-H_2O_2$  cleaning soln. 0-3225  
 $Si_3N_4$  films, prep. by thermal nitridation of Si in  $NH_3$ , comp. and oxidation resist. 0-3215  
 $SiO_2$ , on Si, reduction by heating in Ga mol. beam at 800°C 0-50730  
 Sn fine powders, electrodeposition, effect of cathodic current density on structure 0-16238  
 $SrFe_{12}O_{19}$  powder, chemical plating with Co, Co-P, Ni-P and Cu 0-25593  
 Ti fibres, high-temp. nitriding kinetics (*Russian*) 0-21166  
 Ti, nitriding, ESCA study (*Japanese*) 0-11833  
 Ti, permeation of H plasma reduced by layer of interstitially built  $\epsilon$ - $Ti_2N$  0-16566  
 Ti, physicochemical and wear props., influence of ion implantation and overlay coatings 0-40603  
 Ti powder, exam. of mechanicochemical comminution, in the presence of epoxy resin or polysulphide rubber 0-16236  
 Ti-Al-V (6.4 wt. %), phase transformation after hydrogenation 0-7560  
 W, rolled sheet, boriding, Cu effect 0-21165  
 W surface layer struct. during milling, plastic deform., failure (*Russian*) 0-40586  
 WC powder, chemical plating with Co and Co-P 0-25593  
 YAG brittleness anisotropy, microcrack formation due to surface treatment 0-40526  
 Zr fibres, high-temp. nitriding kinetics (*Russian*) 0-21166

## surface vibrations see crystal surface and interface vibrations

## surface waves (fluid)

see also liquid waves; oceanography

airflow above waves, numerical simulation (*Russian*) 0-4076  
 capillary-gravity waves, exact eqn. numerical soln., closed bubbles 0-14715  
 energy flux for trains of inhomogeneous plane waves 0-46817  
 floating finite-width plate in a periodic pressure system 0-6070  
 free surface flows under gravity, exact selfsimilar solns. 0-48725  
 gravity wave diffraction by arbitrary obstacles (*Ukrainian*) 0-48722  
 gravity waves, non-uniform free surface, superficial viscosity and tension (*French*) 0-48728



- surface waves (fluid)** continued  
hydraulic surge phenomena (*Norwegian*) 0-27141  
hydrodynamic effects of a travelling wave (*Russian*) 0-38423  
infinite depth fluid, steady free surface gravity-capillary waves, integro-differential formulation 0-6072  
interaction between short surface waves and long internal waves 0-48723  
linear waves, asymptotic behaviour and wave patterns construction (*Czech*) 0-69  
liquid wave-fronts in free-flow transients, position fixing method based on Ti memory property (*Italian*) 0-43723  
liquid-liquid system interfacial instability and longitudinal waves 0-33566  
meas. using resistance wave gauge, accuracy and calibration 0-24110  
non-Newtonian incompressible liquid film, surface waves 0-43748  
nonisothermal liquid film, nonlinear dispersive surface waves 0-33617  
nonlinear stern wave production in pot. flow past flat bottomed body 0-38425  
nonlinear waves in closed basin, random behaviour 0-26557  
oil thickness variation on wavy water 0-6134  
propagation theories for water waves, variational principles 0-24043  
ripple growth to swell, ang. momentum conservation explanation 0-56478  
rotating circular cylinder, radially progressive surface waves 0-14722  
small amplitude water waves, uniqueness in region of varying depth 0-1613  
solar photosphere, props. of surface (capillary) waves (*Russian*) 0-12726  
spin and angular momentum in gravity waves 0-53798  
stationary temperature boundary layers generation by surface waves (*Russian*) 0-1611  
thinning liquid film, surface wave development 0-19416  
transient waves generated by a moving oscillatory pressure on a sloping beach 0-56476  
two-layer shallow water flow, internal and surface waves, numerical anal. 0-19472  
water wave, steady, numerical soln. using Riemann Hilbert method 0-33618  
water wave propag. over circular shoal, parabolic eqn. method 0-14717  
water wave reflexion by permeable barrier 0-14716  
wind-wave tank, microscopic and macroscopic surface structs. growth and decay rates 0-48726
- surge absorbers** *see* **surge protection**
- surge protection**  
*see also* **divertors; surges**  
neutral beam injector, high voltage series protection by cross field interrupter 0-13884
- surge suppressors** *see* **surge protection**
- surgery**  
acrylic surgical bone cement fracture behaviour 0-56277  
anaesthesia stage indicator, signal divider 0-3858  
aortocoronary saphenous bypass surgery, evaluation by <sup>201</sup>Tl myocardial perfusion scintigrams 0-12235  
crest factor definition for surgical equipment 0-56273  
cryogenic techniques, clinical appl. 0-12295  
cryoprobe, for medical surgery 0-56274  
cryosurgery, self-contained apparatus 0-56271  
cryosurgical probe, heat transfer coeff. within cavity formed by tip 0-36188  
EEG automatic pattern recognition, patients under general anaesthesia during operations 0-17154  
electrosurgery, tissue coagulation, effects of HF current parameters 0-3746  
endometrial cryosurgery of perfused human uterus, investigation of temp. field produced 0-55995  
eye operations, photographic documentation using model 310 surgical microscope 0-56161  
laser applications in clinical medicine (*Japanese*) 0-12211  
laser applications in medical research, biophysical aspects 0-51201  
laser medicine development trends 0-51198  
laser possibilities, limits and prospects (*Italian*) 0-56156  
laser scalpel and micromanipulator for neurosurgery, CO<sub>2</sub> laser system (*German*) 0-3753  
neurosurgery, laser appls., review 0-26317  
plastic surgery, biomechanical aspects 0-56103  
rehabilitation engineering (*Japanese*) 0-12304  
skin, human, reconstructive surgery, in-plane compressive strain limits prediction 0-41069  
US, refinements in methods and apparatus 0-21508  
US equipment, selection of material for concentrator-instrument section 0-21242  
wrist kinematic and kinetic analysis rel. to surgical reconstructive procedures 0-16999
- surges**  
*see also* **transients**  
explosion of double wire, optical flashes, photographic appl. 0-1865  
spark gaps, electrode shape effect on SF<sub>6</sub> dielectric strength, overvoltage protection (*Czech*) 0-10444
- surgical operations** *see* **surgery**
- surveying**  
contemporary crustal movements in Canada 0-8273  
Gauss-Helmert model, singular covariances, least-squares adjustments (*German*) 0-56340  
geological joints, mapping via photogrammetry and EDP appl. 0-56470  
German Bight, trilateration distance meas. (*German*) 0-8248  
inertial meas. systems, basic eqns. and error models (*German*) 0-56655  
inertial rotation sensors for surveying and geophysical meas. 0-12571  
inertial systems, geodetic appls. (*German*) 0-56656  
Mini Range III positioning system, meas. range improvements, technical details and characts. (*Italian*) 0-56611  
offshore surveys, accurate positioning at distances to 400 km 0-12328  
relevelling data, secular gravity var. effects, orthometric corrections (*German*) 0-56341  
theodolite, THEO 080 A, with attachable circular compass 0-56634  
theodolite, type 2T, highly unified instrum. 0-13120  
United States, western region, strain accumulation rates, 1970-78 period 0-21607
- susceptance, electric** *see* **electric admittance**
- susceptance, electric, measurement** *see* **electric admittance measurement**
- susceptibility, dielectric** *see* **optical susceptibility**
- susceptibility, magnetic** *see* **magnetic susceptibility**
- susceptibility, optical** *see* **optical susceptibility**
- suspensions**  
adsorbed polymer layer, on particles in suspension, thickness meas. by mag. birefringence 0-42191  
anisotropic micropolar fluid theory 0-31515  
aqueous suspensions, three flux method for predicting radiative transfer 0-6052  
Brownian movement of suspended particle with nonlinear friction 0-146  
ceramic, rheological properties, effect of grainy filler ceramic suspensions 0-43685  
ceramic suspensions, sputter drying (*Russian*) 0-55324  
charged particles in ionic solutions, elec. cond. 0-7866  
clay aqueous suspension turbulent flow, average velocity profile and functional loss in pipe 0-48778  
cluster settling, appl. of distrib. of kth nearest neighbours 0-40758  
colloidal, radiometric method for particulate processes characterisation, theory 0-45578  
colloidal, radiometric method for particulate processes characterisation, expt. 0-45579  
concentrates, physical stability criteria, review 0-45562  
continuous models of suspensions, nonequilib. thermodynamic approach 0-28479  
creeping flow, hindered settling, particle shape effect 0-14797  
deposition in channel entrance, combined influence of diffusion, electricity and gravity 0-1674  
deposition in entrance of diffuser, electrostatic and gravitational effects, laminar flow, numerical investigation 0-14785  
diamond, aq. suspension, particle size distrib. function electrooptical diffusion method for determ. 0-8956  
dielectric separation of solid particles 0-16213  
dielectric theory, interfacial polarisation, anal. of biological cell suspensions 0-45563  
diffuser entrance region, suspension laminar flow and particle deposition 0-53845  
dilute, of spherical particles in non-Newtonian liq., rheological behaviour 0-24058  
divinyl benzene suspension, dielectrophoresis 0-3362  
electrorheological suspension flow, vibr. effect (*Russian*) 0-53877  
elliptical particle suspensions covered with shell, dielec. behaviour, rel. to biological cells 0-51057  
ferromagnetic suspension, magnetorheological characts. meas., errors 0-33550  
ferrosuspensions, internal rotations and the other transport phenomena 0-28573  
fibre suspension, dil., mechanistic aspects of drag reduction in turbulent pipe flow 0-6102  
filtration in porous membranes, pore and particle size distrib. correl. (*Japanese*) 0-3418  
flocculent, sedimentation, review 0-35577  
flow, two-phase, in entrance region of circular pipe, effect of conc. of suspended particles 0-19481  
flow of gas with dispersed solid particle impurity in viscous shock layer 0-28554  
flow rate meas. ultrasound propagation and scatt. approach 0-43806  
fluid dynamical aspects of operating conditions of suspension stirrers (*German*) 0-26058  
gas suspension, closed dynamic eqn. system using kinetic theory 0-6190  
gas suspension flow in long horizontal pipe, heat exchange investig. 0-19388  
geophite, suspension, electrooptical diffusion method for determ. particle distrib. function 0-8956  
giant lecithin vesicles, alignment and opening by elec. field 0-3708  
NE Gulf of Alaska, processes affecting suspended matter distrib. and transport 0-12398  
heavily filled, viscosity relations 0-48776  
inclined pipe, suspension in turbulent flow, Markovian model, eddies 0-48790  
laminar flow with diffusive gravit. deposition at entrance of converging and diverging channels 0-14825  
latex sphere aggregates, dynamic shape factors determ. by sedimentation vel. meas. in capacitor 0-26063  
magnetisable suspensions, hydrodynamic in travelling mag. field 0-48807  
magneto-rheological suspensions, mag. field effects on elec. cond. 0-11960  
microfluids, theory of chemically reacting mixtures 0-14777  
movement in porous solid interior (*French*) 0-43770  
nonstationary flow, rheological behaviour 0-6130  
nonuniform suspended load, non-equilibrium transportation (*Chinese*) 0-8339  
ocean acid waste dump, particulate Fe mapping 0-56497  
organic pollutants in water, influence of detergent traces on hydrosolubility and maintenance in suspension (*French*) 0-7961  
particle distribution in Poiseuille flow of suspension in micropolar fluid model 0-10314  
particle size and number concentration, meas. method 0-9082  
poly (N,N-dipropylacrylamide), 'feathered' polymer resin, prep. from suspension 0-35533  
polystyrene sphere crystals, in aqueous suspensions, solid-like phase transition 0-50893  
polystyrene suspension, laminar flow, augmentation of heat and mass transfer, correl. of data 0-53840  
pulverised fuel gas flow distrib. in manifolds of uniformly variable section (*Russian*) 0-33666  
radiational flame propagation over gas suspension of solid combustible particles 0-53880  
rigid ellipsoidal particles in external field, dil. suspension, rheological eqns. (*Ukrainian*) 0-48661  
sea suspended material and chlorophyll conc., estimation from outgoing radiation spectrum meas. from helicopter 0-36333  
seawater, surface charge of suspended particles in estuarine and coastal waters 0-36331  
seawater from Pacific, size distrib. of suspended particles in surface water 0-4047  
sedimentation of monodisperse suspension of solid particles in viscous fluid, Markov model 0-28551  
slurries, solids content determ. by X-ray scatt. 0-3467  
solid dielectric particle dilute suspension in flat duct, electric field effect 0-53868



**suspensions continued**

- solid-liquid mixtures, rheological charact., shear stress/strain rate relationships 0-10287
- stability, net repulsive van der Waals forces between different particles, macromolecular, or biological cells in liqs., appls. 0-34274
- thermomagnetophoresis of particles in magnetic suspensions 0-35581
- thick clay suspensions, electroenforced sedimentation in consolidation region 0-26057
- turbulent energy balance in pressure pipe flow for suspension bearing flow 0-48777
- turbulent suspension flow, gravitational theory, discrete model 0-48779
- two-phase flow of particles during crystallisation in gaseous stream, modelling by aerothermochemistry of suspension eqns. (*French*) 0-53844
- water suspensions, radiative property measurements 0-9811
- water suspensions of latex spheres, laser heterodyne apparatus for small angle scatt. meas. 0-1261
- yeast cells in suspension, vacuole detect. by transmittance radiometry 0-26418
- C black conc. suspensions in low mol. wt. vehicles, rheology anal. 0-19312
- Fe<sub>2</sub>O<sub>3</sub>, flocculated suspension in ethylene glycol, intrinsic viscosity rel. to shear rate 0-1502
- Fe(OH)<sub>3</sub>-Fe(OH)<sub>2</sub> suspension system, potential-pH diagram 0-55728
- KCl, colloidal suspension, radiowave dielec. dispersion 0-11311
- LiCl, colloidal suspension, radiowave dielec. dispersion 0-11311

**swelling**

- AGR fuel cladding, development of high strength, ductile stainless steel alloys 0-45367
- biophenol-A-polycarbonate, liquid induced crystallisation 0-30125
- ceramics, technique for studying internal and external gas pressure within pores 0-11606
- correl. between void swelling and thermodynamic stability 0-641
- ethylene copolymers, partially cryst. pseudoeutectoid, swelling, thermodynamics 0-39311
- extrudate swell, inelastic theory 0-43684
- fission reactor core system, bowed, NUBOW-3D program for static anal. including irradi. creep and swelling 0-5215
- fusion materials, heavy ion irradiation, swelling theory 0-34090
- fusion reactor first wall material, mobile He inclusion in void swelling rate theory model 0-34069
- fusion reactor materials, ion bombarded, swelling induced stresses, crystalline orientation effects 0-34093
- fusion reactor metals, irradiated, defect cluster nucleation, He injection effect 0-34091
- gels, swelling kinetics device 0-21210
- glass fibre reinforced epoxy composite, unidirectional, hygroelasticity, angular depend. 0-50663
- glassy polymer, solvent osmotic stresses, prediction of Case II transport kinetics 0-26049
- irradiation effects, void nucleation, swelling, creep, rate eqns. 0-49274
- metal, radiation blistering developments, review 0-44239
- metals, irradiation induced swelling, bias factor 0-2062
- metals, radiation-induced creep and swelling, radiation dose depend. (*Russian*) 0-29050
- $\alpha,\omega$ -methoxy-poly(ethylene oxide) effect of swelling on longitudinal acoustic mode 0-29739
- multicomponent inhomogeneous system, diffusion with moving boundaries and swelling at const. volume 0-44353
- nuclear oxide fuel element in fast overpower transient, effect of solid fission products and dislocations 0-623
- PET, effect of liquid aliphatic compounds on mech. props. 0-55488
- point defect production in irradiation, swelling, cascade diffusion theory 0-34044
- polyethylene, in toluene, pressure crystallised, swelling behaviour, rel. to densities 0-2167
- polymer, glassy, sheets and spheres, gel diffusion with discontinuous swelling 0-44354
- polymer, non-ion-exchange type, electrolyte solubility (*Russian*) 0-54391
- polymer networks, deformation free energy, vol. depend. 0-40454
- polysiloxane dizwitterionomers, sorption of H<sub>2</sub>O, mechanism 0-49506
- polystyrene, swollen network in benzene, pendent chains, influence on thermodynamic and viscoelastic props. 0-28481
- polyurethanes, vapour press. of solvent above swollen crosslinked networks rel. to rubber elasticity theory 0-45536
- polyvinyl alcohol, atactic, thermoelasticity of networks swollen in water, polymer-diluent interactions 0-29102
- pulsed radiation effect on void growth and swelling 0-34043
- PVA, swollen crystallinity determ. by laser Raman spectroscopy 0-38953
- refractory fusion reactor materials, neutron irradi., microstruct., voids, nucleation TEM study 0-29065
- rubbers, swollen, low-freq. dynamics, optical and mech. props. 0-43626
- SAP 895 (Al-Al<sub>2</sub>O<sub>3</sub>) alloy containing <sup>4</sup>He and <sup>3</sup>H, tensile props. 0-34129
- stainless steel in FBRs, correl. between void swelling and thermodynamic stability 0-641
- steel, austenitic, annealed, Ni ion bombardment, swelling temp. depend. effect of He implantation 0-29080
- steel, austenitic, gas implantation effects, fusion reactor first wall damage simulation 0-29079
- steel, austenitic stainless, type 316, irradiated with 46.5 MeV Ni<sup>6+</sup> ions, soluble C effect on void swelling and low dose dislocation structs. 0-49280
- steel, austenitic type 316, continuous gas generation effects in neutron and simulation environments 0-34068
- steel, ferritic, void swelling during irradiation, suppression mechanisms 0-6441
- steel, ferritic alloy and martensitic stainless, void swelling response after fast reactor irradiation 0-6437
- steel, stainless,  $\alpha$ -irradiated, He cavitation, rel. to TiC precipitation 0-45399
- steel, stainless, depth distrib. of swelling, TEM exam. 0-15165
- steel, stainless, dilation and bowing in EBR II ducts and cladding 0-625
- steel, stainless, EBR-II fuel pin cladding, obs. of in-reactor creep and swelling 0-13600
- steel, stainless, FBR cladding stress distrib., effect of irradiation-induced swelling 0-19850
- steel, stainless, He effects on microstruct. in ion-irrad. 0-29078
- steel, stainless AISI 316, neutron irradiated, rel. between irradiation induced swelling and shear modulus 0-15157
- steel, stainless type 304, ion bombarded, He effects 0-29076
- steel, stainless type 316, temp. effects on swelling 0-32347

**swelling continued**

- steel, type FV548, 1 MeV electron irradiated, influence of pre-injected He on void nucleation and growth 0-34054
- transient fuel fission gas behaviour, NEFIG model calcs., bubbles and swelling 0-618
- void swelling rate, vacancy dislocation loop effect 0-2084
- Al, surface exfoliation and blistering induced by He ion bombard. in energy range 10-80 keV 0-39173
- $\alpha$ -Fe, irradiation induced void swelling, Cr additions effect 0-55408
- $\alpha$ -Fe, void swelling during irradiation, suppression mechanisms 0-6441
- $\alpha$ -Fe, void swelling response after fast reactor irradiation 0-6437
- Fe-Cr, irradiation induced void swelling, Cr additions effect 0-55408
- Fe-Cr-Ni, austenitic, self-diffusion and swelling under irradiation 0-39343
- Fe-Cr-Ni, neutron irradiated, rel. between irradiation induced swelling and shear modulus 0-15157
- Fe-Ni-Cr, pulsed HVEM irradi., effect on microstruct. evolution 0-34053
- Fe-Ni-Cr (20, 15 wt.%), single and dual ion irradi., microstruct. studies 0-29077
- Mo, microstruct., swelling induced by ion bombard., He injection effects 0-29083
- Mo, neutron irradiated, void swelling and shrinkage, TEM study 0-34079
- Mo-Ti-Zr (0.5, 0.1 wt.%), neutron irradiated, void swelling and shrinkage, TEM study 0-34079
- Mo-Zr, heavy ion irradiated, void swelling, phase instability 0-29084
- Mo-Zr-B, porosity and mech. props. after neutron bombard., 780-1080°C (*Russian*) 0-24502
- NaCl, single cryst. expt. on distension of gas-filled cavity 0-49286
- Ni, cavity evolution in 500 keV <sup>4</sup>He<sup>+</sup> irradi. 0-29082
- Ni, void swelling rates in self-ion irradi. sample 0-29081
- Ni-Al, neutron irradiated, rel. between irradiation induced swelling and shear modulus 0-15157
- Ti-Al-V, (6.4 wt.%), single and dual ion irradi., microstruct. studies 0-29077
- U core fuel elements, of A-1 reactor, volume growth (*Czech*) 0-27745
- UO<sub>2</sub>, microstruct. depend. model for fission product gas release and swelling 0-42757
- UO<sub>2</sub>:Cr<sub>2</sub>O<sub>3</sub>, fission gas release and swelling 0-47567
- V-Ni, ion bombard., void form. 0-34097
- V-Ni, ion bombard., void form. 0-34097

**swept-frequency oscillators**

- wideband freq.-swept marginal oscillator detector for ion cyclotron reson. spectrometer 0-9069

**swept-frequency reflectometry**

- liquid and solid complex permittivity meas., rectangular waveguide method 0-15941

**switchboxes** *see switchgear***switches**

- see also relays; semiconductor switches*
- electro-optic multimode waveguide modulator or switch 0-23783
- electro-optical channel waveguide switch for computer communication bus 0-9987
- fibre-optic switch with electrostatic deflection cantilever 0-53427
- integrated waveguide-hologram memory design approach 0-32940
- IR to visible AC Kerr efficient switches using liquid O<sub>2</sub> and liquid CS<sub>2</sub> 0-19078
- laser triggered solid dielectric switches with low jitter and inductance 0-54066
- laser triggered switching of solid insulated spark gap 0-54065
- light-activated switch, photo-gate, pulse method of switching, circuit 0-42021
- Mach-Zehnder interferometric switch for integrated optical multivibrators 0-53479
- optical fibre switch, four-way, mechanically operated 0-53464
- thermal, gas-filled, for use in precooled system for superconducting magnet 0-52245
- thyatron-spark gap hybrid for high voltages and currents 0-54067

**switchgear**

- see also circuit breakers; switches*
- quasistatic magnetic field generation using prototype switching system 0-42244

**switching**

- see also electrical conductivity transitions; ferroelectric switching; magnetic switching; switches*
- bipolar image converter, photocathode switching 0-19105
- laser emission spectrum switching by external optical signal 0-9892
- laser logic elements, transients during switching (*Russian*) 0-23697
- metal-insulator-Si(n)-Si(p<sup>+</sup>) device, switching voltage criteria 0-15610
- nematic liquid crystal adjustable access couplers for fibre-optic switching 0-33217
- optical communication, conference, Amsterdam, Netherlands (Sep. 1979) 0-46733
- photothermoplastic recording with rapid switching 0-32941
- stepped switched optical directional couplers with unequal section lengths 0-33235
- Te-Au thin film interface, evolution, switching effects (*French*) 0-6660

**switching circuits**

- see also choppers (circuits); trigger circuits*
- light-activated switch, photo-gate, pulse method of switching, circuit 0-42021
- linear transmission gate for nuclear electronics 0-23267
- respiratory flowmeter switching device incorporating delay for synchronisation with mass spectrometer 0-17160

**switching transitions** *see electrical conductivity transitions***symbol manipulation**

- problem soln. by symbolic computer processing of formulae 0-17803

**symbols** *see nomenclature and symbols***synchrocyclotrons**

- No entries

**synchronisation**

- cinematography, EBU/IRT time codes with modified setting instrument (*German*) 0-18029
- dropping Hg electrode, synchronisation in natural drop expts., high speed device 0-37049
- global coordinate time scale, practical implications of relativity 0-47030
- high-speed motion picture photography and oscillography 0-8969
- injection diode modulated laser pulse generator and digital control cct. (*Russian*) 0-14372
- intercontinental clock synchronisation, ramp method 0-47034



**synchronisation continued**

- international time synchronisation, precision tracking package TEMPUS, NAVSTAR satellite network appl. 0-22332
- lasers, injection, for optical pulses meas. 0-23711
- luminous flux meas., automatic null method (*French*) 0-27331
- masers, MCR monotron synchronisation by external harmonic signal applied to resonator 0-43312
- optical discharge image, as registered with streak camera, with electrical parameters 0-31919
- pulse synchronisation technique, dispersion meas. in single-mode optical fibres 0-48410
- respiratory flowmeter switching device incorporating delay for synchronisation with mass spectrometer 0-17160
- satellite time transfer technology, review 0-47029
- stochastic self-oscillations and turbulence, review 0-4537
- Symphonic geostationary satellite, time transfer link for atomic clock synchronisation 0-47038
- time, by VLBI technique (*Japanese*) 0-26755
- time and frequency, conf., Helsinki, Finland (Aug. 1978) 0-46728
- time comparison (*German*) 0-37000
- time synchronisation using ATA standard time broadcast 0-47024
- tissue mutual impedivity spectrometry 0-17046

**synchronism** *see* **synchronisation****synchronous generators**

- JET, large flywheel-generator-diode convertor, modelling and simulation 0-13894

**synchronous machines***see also* **synchronous generators**

- slot-less, armature and excitation field, analytical calc. method using polar coordinates (*German*) 0-32870
- slot-less, winding reactances and inductances determ. under stationary conditions (*German*) 0-32871

**synchroscopes** *see* **cathode-ray oscilloscopes****synchrotron radiation**

- accelerator source, book contrib. 0-5421
- Adone  $e^+e^-$  ring, beam-beam effects 0-37649
- applications, comparison of characteristics of X-ray and  $\gamma$ -ray sources 0-14030
- atomic photoionisation studies in extreme UV and X-ray regions 0-43017
- atomic spectroscopy using synchrotron radiation, book contrib. 0-4779
- biological structural determinations using synchrotron X-rays 0-46112
- 3C 111, 3C 236, radio galaxies, 150 GHz obs. 0-41908
- 3C 273 microwave emission, self-Compton process rel. to X-rays and  $\gamma$ -radiation 0-22106
- channelling, spontaneous radiation, coherent bremsstrahlung and synchrotron radiation 0-6446
- conference, storage ring beam-beam interactions and nonlinear dynamics, Upton, NY, USA (March 1979) 0-36758
- conference, trends in physics, York, England (Sep. 1978) 0-31416
- crystal monochromatized beams, investigation using X-ray monochromators with order sorting and polarizing props. 0-31963
- crystallite dimensions determ. using synchrotron radiation X-ray diffr. photographs 0-24313
- Cygnus A, radio galaxy, 150 GHz obs. 0-41908
- cylindrical mirror analyser, design and use with synchrotron radiation, autoionisation obs. 0-18049
- diamond, synchrotron electron beam damage, study by optical, cathodoluminesc. and X-ray topography 0-39155
- DORIS, luminosity limitations 0-37648
- electron ring optical diagnostics using synchrotron radiation and light scattering meas. 0-5405
- electron synchrotron-Cherenkov detectors 0-884
- ethene, optical synchrotron-Cherenkov radiation threshold effects 0-28154
- extragalactic IR sources, synchrotron radiation model 0-31387
- galactic non-thermal radio radiation from polar regions, spectra 0-22082
- galactic synchrotron radio emission, rel. to Galaxy cosmic rays and mag. field distrib. 0-4207
- gas-phase time-of-flight photoelectron spectrometer using synchrotron radiation 0-4818
- generation, properties and appls. (*Czech*) 0-37945
- generation and applications 0-32896
- halomethanes, synchrotron radiation photoabsorption cross sections, Rydberg states 0-28033
- heavy-ion accelerator, dimensions of electron ring meas. by synchrotron radiation 0-42877
- inner level spectroscopy with synchrotron radiation, theoretical aspects, book contrib. 0-4778
- interacting beam models, summary 0-37644
- ISABELLE, beam-beam interaction, transfer map approach 0-37651
- ISR, beam-beam investigations, review 0-37645
- M87 jet, synchrotron optical and radio emission origin (*Russian*) 0-8694
- molecular photoexcited excited states, dynamics, advances using synchrotron radiation 0-37836
- molecular spectroscopy appls. 0-53166
- molecular spectroscopy using synchrotron radiation, book contrib. 0-4780
- NP 0532, Crab pulsar, radiation, role of magnetosphere cyclotron instability (*Russian*) 0-8645
- OJ 287, BL Lacertae object, purely synchrotron interpretation for synchrotron optical-radio outbursts 0-8679
- optical synchrotron-Cherenkov radiation threshold effects 0-28154
- Orsay,  $e^+e^-$  interactions, beam-beam effect observations, review 0-37650
- PETRA, luminosity limitations 0-37648
- photoelectron spectroscopy, synchrotron radiation appls., book contrib. 0-14035
- PKS 0548-322, BL Lacertae object, synchrotron self-Compton model for X-ray spectrum 0-17654
- plasmas, laser produced, as X-ray source for synchrotron radiation research 0-320
- polyisobutylene fibres, stretched, crystn. kinetic study using synchrotron radiation 0-33909
- properties and introduction to synchrotron radiation, book contrib. 0-5669
- quantum corrections 0-37193
- quasars and active galactic nuclei, magnetic flare model, magnetised accretion disc around massive black hole 0-22113
- quasi-thermal electrons gyrosynchrotron emission, appl. to solar flares 0-36602
- radio sources, relativistic corrections in expanding synchrotron sources theory 0-12821

**synchrotron radiation continued**

- radiosources, extended, particle accel. and radiative losses effects on source dynamics 0-46687
- relativistic charged particle, effect of multiple scattering on synchrotron radiation (*Russian*) 0-13245
- resonant filtering, pure nucl. refls. and X-ray interferometry, impedance matched grazing incidence films 0-37141
- solar moving type IV bursts, gyro-synchrotron modulation obs. 0-26833
- solid state spectroscopy using synchrotron radiation, book contrib. 0-7375
- source for electronic states and struct. anal. (*Chinese*) 0-44075
- SPEAR, beam-beam functional dependencies of machine parameters 0-37647
- spectroscopy instrumentation and appls., book contrib. 0-4782
- spin-flip and normal synchrotron radiation from rot. charge in mag. plasma 0-28153
- storage rings, beam-beam interaction, radical diffusion simulation 0-37653
- storage rings, interaction effects of EM fields on particle beams 0-37643
- techniques and appls., book 0-5668
- time resolved spectroscopy at storage rings 0-31902
- undulators and 'free-electron lasers', review 0-9794
- wiggler, helical wiggler and free electron laser (*Japanese*) 0-37658
- X-ray camera, double focusing, use with synchrotron radiation 0-313
- X-ray crystallography white radiation methods using synchrotron sources 0-44076
- $e^+e^-$  storage rings, beam-beam effects expts. at SPEAR 0-37646
- Al clean films,  $O_2$  interaction study using synchrotron-radiation-induced-photoemission 0-55709
- $CO_2$ , spin polarised photoelectrons, synchrotron excited 0-43101
- Cs, polarised photoelectrons produced by circ. polarised synchrotron radiation 0-18830
- $^{57}Fe$  Mossbauer level excitation using synchrotron radiation 0-7204
- Ge, hot microdeformation and simultaneous X-ray topography apparatus (*French*) 0-38871
- $K_2$  excitation, prod. and decay of  $O_u^+$  and  $1_u$  states 0-43109
- Mg clean films,  $O_2$  interaction study using synchrotron-radiation-induced-photoemission 0-55709
- $N_2O$ , spin polarised photoelectrons, synchrotron excited 0-43101
- $SF_6$ , photoionisation spectra in XUV region 0-37837

**synchrotrons***see also* **cosmotrons**

- AGS, efficient slow extraction, nonlinear growth of betatron oscillations, magnetic septum 0-47793
- AGS slow extracted beam, size meas. 0-37672
- CERN experiments in 1979 0-408
- CERN Super Proton Synchrotron, beam observation via optical transmission system 0-38119
- colliding beam facilities, overview 0-37642
- electron relativistic beam in synchrotron, ang. spread of vel. using undulator radiation electron 0-14021
- INS electron 1.3 GeV synchrotron, polarised electron acceleration 0-37660
- photodisintegration and  $\pi$  photoprod. coincidence expts. at Bonn 500 MeV synchrotron 0-22815
- proton synchrotron, oscillations, effects of induced voltage and forces of space charge on motion (*Bulgarian*) 0-47792
- Saturn 2, 100 MeV-3 GeV proton accelerator (*French*) 0-32547
- Serpukhov proton synchrotron shield, mixed radiation dose equivalent outside 0-32530
- spin flip by adiabatic passage of depolarisation resonances 0-5415
- SPS, real-time control system, operating system principles 0-875
- synchrophasotron, system for coupling freq. of accelerating voltage with mag. field 0-23193
- wiggler, helical wiggler and free electron laser (*Japanese*) 0-37658

**synoptic climatology** *see* **climatology****synthetic rubber** *see* **rubber****system documentation** *see* **program and system documentation****systems analysis***see also* **program and system documentation**

- fission-fusion systems, laser-driven, nuclear and thermohydrodynamic calcs. 0-47696
- search for extraterrestrial intelligence 0-4274
- storage reservoir analysis, mass-curve techniques, systems and perspective 0-8457

**systems design** *see* **systems analysis****systems engineering***see also* **systems analysis**

- optical storage medium specification and performance trends, review 0-43415
- optical system tolerancing plan activities and documents 0-48382
- pacemaker automated test system developments 0-30944

**systems programming** *see* **systems analysis****Szilard-Chalmers reactions** *see* **radiochemistry****T invariance**

- atom + diatom, rot. inelastic scatt., mag. transitions, time reversal symm. 0-48066
- broken symmetries at high temperature 0-42357
- dynamically broken-gauge theories, P and T violation in QCD 0-9093
- extended relativity, T-violation and new particle 0-37182
- magnetic monopoles, PT-invariant theory of massive dually charged particles, Dirac-like eqn. 0-52429
- P and T violating electromagnetic interaction of the quark in the instanton field 0-52430
- PT asymmetry and four-fold EM degeneracy lifting, appl. to ring laser mode splitting 0-23606
- relativistic QFT, spontaneous symmetry violations 0-52411
- rotationally inelastic scattering, mag. transitions, time reversal symm. 0-53105
- time asymmetries and classical and quantum physics 0-22216
- $\pi$ , photoproduction in  $E < 450$  MeV region, dispersion relations, CT invariance, review, book contrib. 0-47311
- TIF, P- and T-violating interactions in hyperfine struct., mol. beam reson. expt. 0-53019

**Ta** *see* **tantalum****table lookup***see also* **data handling**

- holographic numerical optical processor configurations 0-48194



table-top computers *see* minicomputers

tables (data) *see* collections of physical data

tables (decision) *see* decision tables

## tachometers

*see also* angular velocity measurement

cardiotach, heart-rate monitoring cct., construction 0-30920

digital, for heart rate measurement 0-17162

Doppler effect based, microwaves non-conventional appl. survey (Italian) 0-13093

## tachyons

bradyon interactions, superluminal and subluminal EM fields 0-12902

charged extended tachyon EM radiation, collision with neutral particles 0-4522

emission and absorpt. in six dimensional relativity 0-31502

general relativistic eqn. solns. 0-36917

magnetoelectric dipole gas as explanation of biocosmic phenomena, summary of phenomena 0-8241

magnetoelectric dipole gas as explanation of biocosmic phenomena, theoretical concepts 0-8242

magnetoelectric dipole gas as explanation of biocosmic phenomena, theory development 0-8243

magnetoelectric monopoles, polymerised, delocalised clouds as possible cause of auras 0-41362

observations in nucl. emulsions possibly overlooked 0-12963

photon-tachyon interactions and the isotropic photon flux 0-446

quantum field theory description 0-18069

superluminal Lorentz transformations, imaginary quantities problem in extended relativity 0-52020

toxic air ion effects due to tachyon magnetoelectric dipoles and beta rays 0-35999

two body correlations through tachyon exchange 0-42367

tackiness *see* adhesion

TADMR *see* microwave-optical double resonance

tandem accelerators *see* particle accelerators

## tantalum

*see also* nuclei with .....

absorption rate of H, metallic film effect 0-49525

adsorption, of LaB<sub>6</sub>, work function 0-20039

atom, nuclear K-X-ray satellites, Z=50-83, by  $\alpha$ -bombard., 17.5-22.5 MeV 0-42984

autocathode, influence of electric field and heating on work 0-7478

BCC, band struct., generalised APW method using variational expression 0-6695

BCC crystal, elastic constants, thermal expansion and bulk modulus 0-6452

chemical vapour deposited, kinetics and microstruct., pressure and temp. depend. 0-11569

coating of mild steel at atm. press. using CVD method 0-55591

desorption kinetics of halogens, pulsed ion beam method 0-34300

desorption of O<sub>2</sub> in vacuum, thermodynamic props. calcs. (Russian) 0-54501

diffusion of H and D in Ta, low temp., from quenching and annealing study 0-6555

edge dislocations, study by transmission channelling of MeV ions, expt. setup 0-29098

elastic properties, at high temp. 0-30007

electrotransport of H(D) at high H concs. 0-34246

epitaxial layers, influence of formation conditions on struct. (Russian) 0-20045

film, electron beam evaporator for in situ deposition studies in UHV electron microscope 0-40264

film, planar-magnetron-sputtered, phys. and elec. props. 0-6673

foil, electron energy loss spectra 0-7452

interatomic pair potential, phonon spectra 0-33927

L-subshell ionisation cross section, branching ratios, fluoresc. yield, Coster-Kronig factors 0-43166

microvoid form., gaseous impurity atom effects, positron annihilation study 0-49275

Mossbauer states at 6.2 keV, freq. modulation 0-7212

muon trapping, Knight shift, rel. to H interstitials 0-50247

NMR- $\gamma$  double resonance, Mossbauer absorpt. spectra (Russian) 0-34824

NMR-Mossbauer double reson. 0-40019

photo field emission spectroscopy of band structure by He-Ne laser irradi. 0-55276

photoneutron yields released by incident electrons, improved calc. 0-27630

positron annihilation and vacancy formation 0-16119

positron trapping and annihilation at vacancies 0-29823

powder, cathodic electrodeposit, effect of electrolyte composition and process parameters, on particle size distribution 0-16233

rolled single crystal, recovery and recrystallization 0-3093

secondary ion emission, normalised energy spectra from Hg<sup>+</sup> impact 0-45193

sputtered film, stabilisation of  $\beta$ -modification by Ta-Si interlayer, SIMS depth profiling 0-54568

static and dynamic props. of O and H impurities, Mossbauer meas. 0-7246

superconducting, muon spin relaxation (German) 0-50015

superconducting transition temperature, ab initio calc. 0-25036

surface, decomp. of hydrocarbons, O or N surface segregation effects 0-55654

target impurity effect on laser produced expansion, ion spectrography 0-43945

vacuum technology appl., melt processing and appl. (Hungarian) 0-55318

valve metal thin films, deposited on dielectric supports, exam. of anodisation kinetics (Russian) 0-7702

wire, H-absorption kinetics between 500 and 700K 0-49528

HfC-Ta, perturbed ang. correlation spectra, elec. quadrupole interaction 0-15916

HfCo<sub>2</sub>-Ta, perturbed ang. correlation spectra, elec. quadrupole interaction 0-15916

HfFe<sub>2</sub>-Ta, perturbed ang. correlation spectra, elec. quadrupole interaction 0-15916

liquid, polyvalent, electrical resistivity by harmonic model potential 0-54668

Ta XLVI X-ray spectra from laser produced plasmas 0-42981

Ta-N, superconductive to normal transition anisotropy 0-25031

Ta-O, relaxation anal. after ageing under stress (French) 0-16365

## tantalum continued

Ta-O, steady state O<sub>2</sub> solubility (German) 0-44322

<sup>178</sup>Ta radiopharmaceuticals for lung and liver imaging, rat expts. 0-51254

<sup>178</sup>Ta, scintigraphic imaging with the Anger scintillation camera 0-12231

<sup>181</sup>Ta in Te, quadrupole interaction, TDPAC meas. 0-20521

## tantalum alloys

*see also* tantalum compounds

CC TaC based hard metal, non-stoichiometric sintering, mech. props. 0-25616

Fe-Ni-Ta (-Co), alloys, Co effect on martensite ageing at 300-600°C (Russian) 0-20972

Nb-W-Zr-Ta, long-term strength props., vac. level effect 0-55484

Nb<sub>3</sub>Ta<sub>4</sub>, pure and hydrogenated crystals, effect of pressure on elastic consts. 0-7614

Ni-Al-Ta, heat resist., solidification range 0-35177

Ni-Fe-Cr-Nb-Ta-Mo alloy, fatigue crack growth, stress ratio and hold-time effects 0-40531

Ni-Ta-Al system, phase equilibria and diagram, electron probe, X-ray diffr. anal. 0-29927

NiTaC eutectics, high cycle fatigue at room temp. 0-16459

Ta-Cr (15 wt.%), solid soln., discontinuous precipitation (German) 0-45314

Ta-H, BCC, quasimolecular Jahn-Teller reson. states 0-44550

Ta-H, electron work function, 300 to 600 degrees C, contact potential difference meas. 0-29462

Ta-Si-Cu, struct. and supercond., Cu influence 0-50592

TaGe<sub>2</sub>, superconducting transition temp. meas. of sputtered films and bulk 0-7019

TaSi<sub>2</sub>, superconducting transition temp. meas. of sputtered films and bulk 0-7019

Ti-Al-Nb-Ta-Mo (6, 2, 1, 0.8 wt.%), elevated temp. flow strength, creep resist., diffusion welding characts. 0-30033

V-Ta (5 wt.%), strain hardening, screw dislocations and microtwinning (Russian) 0-29971

WC-Co-TaC-TiC-NbC cemented carbide, microstructure, high temp. deformation, uniaxial plastic compression 0-40451

## tantalum compounds

*see also* tantalum alloys

CVD on quartz substrate from gas mixture of TaCl<sub>5</sub>-BCl<sub>3</sub>-H<sub>2</sub>-Ar 0-29880

refractory carbides, borides and nitrides, wetting by and interactions with liq. metals 0-54473

Sitalls, soln. rate in alkali soln. 0-16531

Ta<sub>2</sub>S<sub>5</sub>, amine intercalation, water effects, X-ray diffr. meas. 0-44178

BaO-Al<sub>2</sub>O<sub>3</sub>-SiO<sub>2</sub>-Ta<sub>2</sub>O<sub>5</sub>-Mo glass ceramic metal composites, cermet prep. 0-11618

Cr-Ti/MgO-TaC dispersion-strengthened, high temp. wear and oxidation resist. 0-25877

Cr-Ti/TaC dispersion-strengthened, high temp. wear and oxidation resist. 0-25877

Eu<sub>2</sub>O<sub>3</sub>-Se<sub>2</sub>O<sub>3</sub>-Ta<sub>2</sub>O<sub>5</sub> system, orthotantalate section, X-ray diffr. and luminesc. obs., conc. depend. 0-54205

IT-Fe-Ta<sub>1-x</sub>S<sub>2</sub>, Anderson localisation, elec. resist. and magnetoresist. meas. 0-44596

Nb-Ta-N sputtered films and their anodic oxides, elec. props. of resist. and dielec. films 0-11126

Nb<sub>1-x</sub>Ta<sub>x</sub>Se<sub>3</sub>, thermoelectric power meas., 10-300K 0-20177

Nb<sub>1-x</sub>Ta<sub>x</sub>Sn<sub>2</sub>, supercond. transition temp. and upper crit. field 0-39723

(Ta,Ti)B<sub>2</sub> on graphite, CVD coatings, hardness meas., SEM study 0-24760

Ta-H, electron work function, 300 to 600 degrees C, contact potential difference meas. 0-29462

Ta-O supersaturated solid solution, precipitation processes, hardness change meas. 0-25712

TaC, reactions with Ti-Al-Cr-Mo alloy VT3-1 0-16585

TaC, true heat capacity meas. by pulse method 0-19953

Ta<sub>2</sub>C<sub>1</sub>, solubility of H, X-ray diffr. exam. 0-44318

Ta<sub>2</sub>C<sub>2</sub>, solubility of H, X-ray diffr. exam. 0-44318

Ta<sub>2</sub>C<sub>3</sub>, solubility of H, X-ray diffr. exam. 0-44318

TaD, structs. phase diagrams, morphologies, prep. methods, book contrib. 0-25675

Ta<sub>2</sub>D, neutron diffr. meas. of disorder-order phase transitions 0-29947

TaH, structs. phase diagrams, morphologies, prep. methods, book contrib. 0-25675

TaH<sub>3</sub>, H diffusion and electronic struct., pulsed NMR obs. 0-54967

Ta<sub>2</sub>H, ordered, distortion-induced superstruct. modulation, from X-ray scatt. 0-49186

(TaI<sub>3</sub>)<sub>2</sub>, X-ray cryst. struct. determ. (German) 0-19754

TaN, electronic struct., relativistic energy band struct. calc. 0-34354

TaN, thin film, characteristics of Pirani type vacuum gauge (Japanese) 0-13086

TaN, thin film, in Pirani type vacuum gauge (Japanese) 0-52257

Ta<sub>2</sub>N film, high temp. nitriding kinetics depend. on press. (Russian) 0-50838

TaO, displacement function calc. 0-34047

Ta<sub>2</sub>O<sub>5</sub>, anodic film, thermally stimulated exo-electron emission 0-11546

Ta<sub>2</sub>O<sub>5</sub>, anodic oxide film, model for ionic cond. 0-2197

Ta<sub>2</sub>O<sub>5</sub>, chemical effect, influence on stopping power 0-47830

Ta<sub>2</sub>O<sub>5</sub>, elec. breakdown during anodic growth 0-55033

Ta<sub>2</sub>O<sub>5</sub>, film, atomic composition depth distrib. by energetic ion anal. 0-35617

Ta<sub>2</sub>O<sub>5</sub> films, Poole-Frenkel effect and cond., effect of heat treatment in oxygen and in vacuum 0-39693

Ta<sub>2</sub>O<sub>5</sub>, hydrated, heat treatment effect on physicochem. props. 0-20966

Ta<sub>2</sub>O<sub>5</sub>, optical waveguides, colinear interaction between acoustic and optical waves in planar waveguide, radiation into substrate 0-53452

Ta<sub>2</sub>O<sub>5</sub>, reactive DC sputtering deposited films with magnetron-plasmatron, mechanical elec., optical props. 0-25566

Ta<sub>2</sub>O<sub>5</sub>-GaAs interface, fabricated by interactive oxidation, props. 0-49935

Ta<sub>2</sub>S<sub>2</sub> (1T), nonlinear cond. in two-dimens. CDW system 0-10997

Ta<sub>2</sub>S<sub>2</sub> (1T) and (2H), bonding and charge density wave phase transitions 0-44282

Ta<sub>2</sub>S<sub>2</sub>, alkali metal and alkali metal hydroxide intercalates, lattice parameters, supercond. transition temps. 0-25029

1T-TaS<sub>2</sub>, and 1T-TaS<sub>2-x</sub>Se<sub>x</sub>, Anderson localisation, elec. resist. and magnetoresist. meas. 0-44596

Ta<sub>2</sub>S<sub>2</sub>, enthalpy and specific heat, temp. depend. 0-54406



**tantalum compounds continued**

- Ta<sub>2</sub>S<sub>5</sub> intercalation complexes with 3d transition metals, mag. and metallic transport props. 0-44814  
 TaS<sub>2</sub>, intercalation cpd. with pyridine, nucl. spin-lattice relax. meas. 0-54962  
 TaS<sub>2</sub>, nucl. spin-lattice relax. meas. 0-54962  
 1T-TaS<sub>2</sub>, pure and cation-doped, charge carrier localisation 0-44597  
 TaS<sub>3</sub>, Raman spectra, CDW induced metal-semicond. transition 0-11404  
 TaS<sub>3</sub>, transport props. 0-20175  
 TaS<sub>2</sub>(NH<sub>3</sub>)<sub>2</sub>, NMR spectral densities and two-dimens. diffusion 0-50215  
 1T-TaS<sub>2</sub>, Se<sub>1-x</sub>, electronic cond. process, resist. meas., 1.3-240K 0-44595  
 1TTa<sub>2</sub>(Se<sub>2</sub>)<sub>3</sub>, Hall effect meas., 1.4-360K 0-44616  
 TaS<sub>2</sub>(Se<sub>2</sub>)<sub>3</sub>, phase transitions and elec. props. 0-20178  
 TaS<sub>2</sub>(1T) pure and doped, Mott and Anderson localisation, commensurate phase transition 0-39641  
 TaS<sub>2</sub>(1T), surface CDW, obs. by atomic beam diffr. 0-39195  
 TaS<sub>2</sub>(1T), inequivalent lattice sites in charge density distorted phases 0-15835  
 TaS<sub>2</sub>(2H), Li intercalation, electrochemical studies 0-39048  
 TaSe<sub>2</sub>, 1T and 2H superstruct., cryst. struct. using X-ray diffr. 0-39044  
 TaSe<sub>2</sub>, 4Hb polytype, CWD induced atomic shifts 0-39045  
 TaSe<sub>2</sub>(2H), optical absorpt., band struct., plasmons, and CDW 0-45104  
 TaSe<sub>2</sub>(4Hb), atomic displacements in CDW induced superstructure 0-10536  
 TaSe<sub>3</sub>, phonon study of chemical bonding 0-20645  
 TaSe<sub>3</sub>, transport props. 0-20175  
 TaSe<sub>2</sub>(2H), plasmon behaviour at charge density wave onset 0-10900  
 TaSe<sub>2</sub>(6R), stacking layer study, appl. of convergent beam electron diffr. 0-39116  
 TaSi<sub>2</sub>, self-propag. high-temp. synthesis 0-2988  
 TaSi<sub>2</sub>-CrSi<sub>2</sub>, phase equil., struct. and props. 0-50608  
 Ta<sub>1-x</sub>Ti<sub>x</sub>S<sub>2</sub>, Li intercalation, electrochemical studies 0-39048  
 TiO<sub>2</sub>:Ta<sub>2</sub>O<sub>5</sub>(Nb<sub>2</sub>O<sub>5</sub>), rutile, defect struct. and elec. cond. at 1273K 0-44604  
 Ti<sub>1-x</sub>Ta<sub>1+x</sub>W<sub>1-x</sub>O<sub>6</sub>nH<sub>2</sub>O, pyrochlore type, stoichiometry and ionic cond. 0-24648

**tantalum electrolytic capacitors** *see electrolytic capacitors***tape recorders**

- see also magnetic heads; magnetic recording*  
 biomedical recording system, TDM multiplexing system for multichannel signal averaging of visually evoked responses 0-36165  
 magnetic head alloy Fe-Al-Pr, resist. depend. on rolling process, thermal treatment (*Polish*) 0-39555  
 meteorology radar signal recording on video machine, coherent Doppler radar 0-46275  
 physiological signals, analogue tape recorder, low cost using hi-fi cassette player 0-41282  
 seismometer stationed on ocean bed, self-contained unit with mag. recorder (*Russian*) 0-36410  
 shipboard meteorological data system 0-46299  
 slide sync tape recorder, sensory modality matching tests 0-41334  
 thermoplastic photoconductor tape performance for optical recording 0-43305

**taste** *see chemioception***Taylor instability** *see flow instability***t.d.m.** *see time division multiplexing***teaching**

- see also demonstrations; education; student laboratory apparatus; training*  
 accelerated reference frames, theory 0-41991  
 acceleration and velocity teaching, racetrack game 0-31458  
 acoustic absorption, classroom experiment 0-42016  
 additivity, rapidity, relativity, teaching 0-41984  
 American Association of Physics Teachers, 1979 winter meeting 0-42042  
 angular velocity vector, attached to moving reference frame, time variation 0-41986  
 asymptotic freedom 0-17761  
 automobile whip antenna, first overtone vibrational mode obs. 0-17747  
 bicycle stability, teaching approach using unsuccessful nongyroscopic theory 0-42001  
 bond free energies, table for chem. student use 0-22171  
 bound diatomic molecules, covalent bonding concept in undergrad. chem. courses 0-22177  
 Brecht's Galileo, changing perceptions of Galileo Galilei as scientific exemplar 0-51996  
 Brownian motion, two-dimens., simulation on micro-computer (*Japanese*) 0-31461  
 CAI, audible, use of audio or video recordings 0-42008  
 capacitor complete discharge time, thermal noise 0-17727  
 chemical reaction, complex, kinetics, Markov chain appl. 0-27085  
 chemical reaction rate eqn. integration, interactive computer program system 0-31469  
 circuit theory, DC, teaching approach using rectangle dissection 0-46757  
 classical field theory, classical deflection in a central field 0-41993  
 classical mechanics, freely moving balls on rotating discs, stable circular orbits 0-27074  
 closed universe, S<sup>3</sup> topology, rel. to Dante's Divine Comedy 0-41980  
 coherent optics, T<sub>2</sub> as collision time, dephasing time, or reciprocal line-width 0-27075  
 collisions, linear, elastic, dynamic solns. 0-17769  
 computer-assisted-learning agency, staffing needs and position in vertical organisational struct. of educational institution 0-42007  
 contour plotting, moire technique 0-42002  
 correspondence principle, rel. to potential step scattering, theory 0-46761  
 Coulomb problem, symmetry and invariance, canonical transformations 0-41989  
 data manipulation and handling problems of analogue signals, digital filtering use 0-4489  
 David Ausubel learning theory as reference system for content organisation in physics 0-22172  
 detonation, theory, one-dimensional compressible flow 0-41985  
 diamagnetic susceptibility calculation using Pascal's consts., BASIC program 0-37717  
 diffraction pattern classroom anal., image-space method 0-51983  
 Dirac delta function, appl. elec. current and mag. multipole distrib. 0-17740  
 Dirac equation for the H atom 0-46760  
 dispersion eqn., long wavelength approx., appl. EM wave in plasma 0-17735  
 Earth gravity values at poles, rel. to equator, density effects 0-46758

**teaching continued**

- eigenfunctions and eigenenergies, N-space dimensions calcs., for H and relativistic  $\pi$ -mesic atom 0-41988  
 Einstein and  $\Delta E$  0-51986  
 electric resistance, temp. depend., qualitative anal. by audible demonstration 0-46775  
 electromagnetic radiation fields: a simple approach via field lines 0-51991  
 electromagnetism, Maxwell's theory, Faraday induction term and Galilei invariance 0-41995  
 electronics design course curriculum study, overview 0-27063  
 electronics technology development, teaching 0-31470  
 electrostatic fields, points of equilb. 0-31453  
 elliptical orbits and inverse square law of gravity 0-46755  
 EM field, static, angular momentum 0-46771  
 EM vector pot., physical interpretation 0-46772  
 engineering design, creativity testing 0-27062  
 engineering design curricula, computer appls. 0-27065  
 engineering education, modern methods and instructional media roles 0-27064  
 entropy and rubbery elasticity, teacher resource paper 0-17777  
 European computer network, engineering design computer packages, teaching 0-31465  
 Fibonacci numbers, recurrence relation soln., combinatorics function anal. 0-51988  
 finite rotations and angular velocity 0-46766  
 Galileo's two bodies falling through air, numerical anal. 0-17755  
 generalized bound-state perturbation theory 0-17748  
 geometrical analogy for the formal definition of entropy 0-51990  
 glider on inclined linear air track, viscous damping and restitution coeffs. 0-46768  
 group theory in chemistry, pedagogical approach to direct product represent. 0-17771  
 Hall effect discovery 0-27099  
 Hamilton-Jacobi equation solns. in Coulomb pot. and quasiclassical approx. 0-46765  
 harmonic oscillator, damped, canonical approach, for teaching 0-17757  
 harmonic waves, introduced through Fourier synthesis 0-27080  
 heat diffusion in solid sphere, Fourier theory 0-31456  
 heat engine using clear night sky as heat sink 0-27082  
 Heisenberg microscope, crit. ang. aperture 0-41981  
 increasing weight of falling bodies, Aristotle's conclusion 0-46770  
 interference colours produced by white light refl., teaching paper from films 0-8754  
 internal forces cancellation 0-27079  
 J<sup>2</sup> eigenvalues 0-17742  
 laser driven fusion 0-42012  
 lattice vibrations, in 1-dimens. defect system 0-31454  
 linear least squares parameters, stat. significance, student guide 0-17770  
 linear systems, response to square wave force, transients, teaching appl. 0-31467  
 logical abilities and success in physics courses, correl. 0-17731  
 Lorentz groups, homogeneous and inhomogeneous, teaching method to illustrate difference 0-17766  
 Lorentz transformation without rot., matrix representation, for undergrads. 0-17760  
 magnetism w.r.t chemistry, guide to units 0-12871  
 mechanical laws, optoelectronic apparatus for classroom demonstrations 0-46773  
 mechanical resonance, J<sub>0</sub>(x) obs. on reson. rot. vertical chain 0-42006  
 microelectronics revolution, appl. in telecommunications, medicine, education 0-31446  
 Millikan experiment, analogy using quanta of mass, milli-can experiment 0-46778  
 mirrors, semireflecting lossless, transmitted and reflected optical fields phase shift 0-46769  
 molecular beam effusive flow, vector flux density distrib. calc. for any aperture 0-22165  
 molecule, diatomic, hyperfine struct. transitions, quantum theory 0-17762  
 momentum operators for curvilinear coordinate systems 0-17743  
 musical acoustics, room reverberation time meas. 0-42000  
 Newtonian motion analysis on micro-computer (*Japanese*) 0-31462  
 newtons laws of motion: some interpretations of the formalism 0-51984  
 nuclear angiocardigram anal. program for radiology trainees 0-8143  
 nuclear chain reaction demonstration model 0-46774  
 nuclear reactor analysis 0-36806  
 nuclear reactor thermal hydraulics, computer graphics 0-36824  
 nuclear structure, one-dimensional many-boson systems 0-27071  
 numerical electronic technique, in physics education 0-46777  
 one-dimensional particle-in-the-box problem, perturbation theory illustration using champagne bottle situation 0-36816  
 ophthalmological instruments and eye models in teaching, training and education 0-51993  
 organic chemistry courses, unified approach to teaching of struct. and bonding 0-17732  
 Pauli principle in Euclidean geometry 0-17768  
 pendulum, simple, large-amplitude, Fourier anal. 0-17767  
 perspective distortion in photography, eye as simple lens 0-17734  
 phase change derivation, phys. chem. textbook assumption removal 0-17772  
 photoacoustic effect and wave physics 0-42003  
 physicists' thinking skills, in laboratory 0-31443  
 physics, sequential examination processes appl. (*German*) 0-4487  
 physics teaching and Piaget, understanding students 0-31473  
 Piagetian approach to physics teaching 0-41978  
 plane wave solns., rel. to const.-identity 3-dimens. wave 0-17749  
 point groups, continuous, characters and representations 0-36809  
 point groups, continuous, reduction of representations 0-36808  
 Poynting vector introduction at elem. stage of physics courses 0-12865  
 practical work, relevance to comprehension of physics 0-27068  
 Prestel viewdata system, introduction 0-42013  
 probability and statistics, rel. to tennis 0-41997  
 problem-solving in physics, teaching and understanding 0-8752  
 QED charge-electric dipole interaction in 1 dimens. 0-42005  
 quantum statistical mechanics, Dirichlet's integral formula and phase vol. 0-17744  
 quantum transition concept in undergrad. courses, explanation of photon creation and absorpt. 0-36807  
 radiotelescope design, multidisciplinary exercise, Jupiter bursts and quiet Sun obs. 0-17759



**teaching continued**

- rare earth garnet thin films, macroscopic magn. props., magneto-optical expts. 0-46764
- reading through pinholes 0-17765
- reflection and elastic scatt., Compton scatt. and special relativity 0-46756
- relativistic massive particles, gravitational deflection, general relativistic anal. 0-46767
- relativistic quantum mechanics, free localised Dirac particle, Zitterbewegung 0-17739
- scalar diffraction theory, near-field, Fourier transform appls. 0-31455
- Schrodinger eqn. for free particle, wave packet spreading in coord. representation 0-17736
- Schrodinger wave functions at pot. discontinuities, continuity conditions 0-27077
- science and the humanities, The Two Cultures gap, teaching 0-41979
- screened Coulomb potentials, energies calcs. 0-31452
- SI units, conventions and practices, physics teacher's viewpoint 0-36968
- SI units, group props., dimensionality 0-17746
- SI units, group props. 0-17745
- SI units, rationalisation and need for approximation to SI 0-36969
- solid-state diffusion in elec. field, Monte Carlo demonstration 0-27072
- solitary wave solns. of classical nonlinear field eqns. 0-17756
- soliton solns. to nonlinear wave eqns. 0-17737
- special relativity, developments and changes 0-8758
- special relativity, event method 0-31450
- special relativity and Michelson-Morley experiment, history of physics, role in education 0-8759
- spectroscopy with supersonic jets 0-41996
- spontaneous reasoning in elementary dynamics 0-4482
- springs, static and dynamic effects, influence of mass 0-41990
- sprung pendulum, anal. of nonlinear coupling 0-51987
- square-well potential, integral eqns. and scatt. solns. 0-31451
- stochastic model, radioactive decay, difference-differential eqns. 0-51992
- student experiment, evolution of theoretical models (*Polish*) 0-36819
- superposition of acoustic or EM waves, false paradox 0-41999
- thermodynamic equilibrium 0-46751
- thermodynamics, classroom example, free energy change during liq. vaporisation 0-42010
- thermodynamics, pressure-volume work exercises illustrating the first and second laws 0-22173
- thermodynamics violation of second law, linear decompressive expansion followed by adiabatic compression, cyclic 0-42019
- Titius-Bode law, Piagetian learning cycle for astronomy study unit 0-51985
- two-electron atom, 1snl excited levels, ionisation energy calc., perturbation, Schrodinger eqn. methods 0-17728
- uncertainty relation between angular momentum and angle variable 0-27073
- university engineering course, first semester subjects and projects (*French*) 0-27066
- University of London Institute of Education, Science Department, teacher training, curriculum devel. 0-27061
- virial theorem and scale transformations 0-17763
- wave mechanics, origin, pedagogical approach (*Portuguese*) 0-22166
- H atom, variations, quantum theory calcs., generator coord. calcs. 0-41987
- H, Schrodinger eqn. in two-dimens. 0-31457
- H<sub>2</sub>, electron correl. as rot. polarisation, Heitler-London-Rosen calc. 0-4492
- <sup>3</sup>He and <sup>4</sup>He superimposed spectra, isotope shift, mass and vol. effect, Fe arc spectrum calibration 0-46763
- U isotope separation appl. to nucl. fuel cycle, teaching module 0-36805

**teaching approaches to particular topics** *see teaching*

**teaching demonstrations** *see demonstrations*

**teaching machines** *see computer-aided instruction*

**technetium**

*see also nuclei with .....*

- bleomycin-<sup>99m</sup>Tc thyroid scans, evaluation of cold areas 0-56183
- film, supercond. transition, complex susceptibility 0-29495
- paramagnetic form factor, polarised neutron diff. study 0-39745
- pertechnetate [<sup>99m</sup>Tc], evaluation of renal grafts 0-46017
- red blood cells, in vivo labelling with <sup>99m</sup>Tc with stannous pyridoxylideneamines 0-46049
- red blood cells labelled with <sup>99m</sup>Tc, evaluation of gastrointestinal bleeding 0-51219
- stannous pyrophosphate labelled with <sup>99m</sup>Tc, mouse myocardial uptake obs. 0-46019
- stellar spectral analysis and Tc in late-type stars 0-8623
- <sup>99m</sup>Tc, muco-ciliary transport monitoring method, bronchiectatic patient appl. 0-30840
- <sup>99m</sup>Tc migration potential in radioactive waste 0-3537
- <sup>99m</sup>Tc generator of higher activity 0-17136
- <sup>99m</sup>Tc, blood flow and tracer uptake in normal and abnormal canine bone 0-17072
- <sup>99m</sup>Tc, bone marrow scanning in pediatric oncology 0-17067
- <sup>99m</sup>Tc bone scintigraphy, use in uremic pulmonary calcification detect. 0-3788
- <sup>99m</sup>Tc brain scintigraphy, early and delayed image evaluation 0-3790
- <sup>99m</sup>Tc, cardiomyopathy scintigraphic diagnosis, method sensitivity 0-17061
- <sup>99m</sup>Tc DTPA, radiolabelled liposomes as metabolic and scanning tracers in mice 0-17073
- <sup>99m</sup>Tc, gamma camera array of <sup>99</sup>Mo impurities 0-36100
- <sup>99m</sup>Tc, hepatobiliary study of liver-transplant patients 0-3793
- <sup>99m</sup>Tc labelled 2,3-dimercaptopropansulphonate, prep. and distrib. in the rat 0-51244
- <sup>99m</sup>Tc labelled bovine thrombin and streptokinase-activated human plasmin, in vitro assessment 0-41238
- <sup>99m</sup>Tc labelled fibrinogen, usefulness of phlebography for pulmonary embolism patients 0-36093
- <sup>99m</sup>Tc labelled human serum albumin kits, evaluation for cardiac blood pool imaging 0-17130
- <sup>99m</sup>Tc labelled radiopharmaceuticals, comparison of 2 types for lymphoscintigraphy 0-41185
- <sup>99m</sup>Tc labelled red blood cells, ultrafiltration labelling technique 0-51243
- <sup>99m</sup>Tc labelling of red blood cells 0-41236
- <sup>99m</sup>Tc myocardial scintigraphy, use of blood-pool imaging 0-12228
- <sup>99m</sup>Tc radiopharmaceuticals, As for P substitution, bone-seeking agent analogues 0-51250

**technetium continued**

- <sup>99m</sup>Tc, rel. to <sup>123</sup>I in thyroid imaging 0-36077
- <sup>99m</sup>Tc-Ti-DTPA, prep., control and biological distrib. 0-51246
- <sup>99m</sup>Tc-labelled radiopharmaceuticals, brain uptake by passive membrane transport 0-51053

**technetium alloys**

*see also technetium compounds*

- Tc-Fe alloy, Mossbauer spectra, hyperfine field 0-20526
- Tc-Fe dilute alloys, supercond. and mag. props. 0-29494

**technetium compounds**

*see also technetium alloys*

- TcB<sub>3</sub>, electron struct., Fermi energy and surface, bonding 0-20076
- <sup>99m</sup>Tc-EDTA complex production method and renal retention obs. 0-12254
- <sup>99m</sup>Tc-radiopharmaceuticals, ligand determ., electrophoretic method 0-40699
- <sup>99m</sup>TcS colloid lymphoscintigraphy 0-36114

**technical information centres** *see information services*

**technical presentation**

No entries

**technicians** *see personnel*

**technological forecasting**

*see also research and development management*

- adaptive optics technology status and prospects 0-33132
- AGR development and exploitation prospects 0-23109
- cancer treatment by microwave hyperthermia (*French*) 0-3764
- cinematographic equipment development, 35 mm cameras appl. (*Russian*) 0-284
- coal utilisation review and forecast (1950-2000) (*French, English*) 0-21363
- energy projections for USSR and Eastern Europe 0-26100
- fibre optic communication systems, development during next decade 0-1329
- French natural gas industry developments and prospects (*French, English*) 0-21364
- integrated optics long-term role in optical and electronic systems 0-33232
- optical fibre communications history and prospects 0-9994
- optical hybrid image processing trends and prospects 0-32927
- solar cells combined with heat pumps, domestic space heating appl. (*Swedish*) 0-7919

**tectonics**

- Afar, accreting plate boundary, seismic and volcanic evidence 0-21700
- Afar region rifting, geodetic evidence and elastic-brittle model 0-21697
- African plate, deformed by post-Jurassic drift 0-17245
- E.African rift system, tectonic history, theory and laboratory expts. 0-21669
- Agulhas Basin of S.Atlantic, seafloor spreading history, geomag. study 0-21696
- Alaska, 1964 earthquake faulting mechanism regional var. from static displacement data anal. 0-30998
- central Alaska plate tectonics, implications of Bouguer anomaly map 0-51380
- Alberta, Canada, crustal stress evidenced by bore hole asymm. 0-21671
- Aleutian subduction zone seismicity, volcano-trench separation, rel. to great thrust-type earthquakes 0-21655
- Alpine fault, New Zealand, frictional metamorphism, Ar depletion and tectonic stress 0-41440
- Alps, tectonic progradation rel. to plate tectonic evolution 0-56452
- N.America, palaeopoles and palaeolatitudes, displaced terrains 0-12367
- Middle America Trench, S.Mexico, progressive accretion 0-26487
- N.American intra-plate crustal deformation, implications of VLBI meas. 0-51379
- Central American isthmus, emergence rel. to Gulf Stream Late Cenozoic vel. fluctuations 0-12432
- Andaman Sea crust, seismotectonics and tectonic history 0-8283
- Andean andesites, petrogenetic composition variations 0-8313
- Antarctic Peninsula, subduction rel. to transverse geochemical vars. and calc-alkaline magmas genesis 0-56466
- Appalachian foreland fold and thrust belt, New York State, deform. nature 0-3973
- Appalachian Orogen in Canada 0-8304
- arc-arc junction, continental plate stress state, model 0-46163
- Archaeon Superior Province, tectonic model, thermal conditions 0-31018
- Asal-Ghoubet rift zone, Afar, 1978-9 geodetic survey after seismo-volcanic activity 0-46164
- central Asia, active faulting and Cenozoic tectonics of Tien Shan, Mongolia and Baykal 0-8278
- Asia, central and south-central, large-scale Cenozoic tectonics as prods. of continental collision 0-17246
- S.E. Asia, crustal tectonic stress field details (*Chinese*) 0-56414
- Middle Asia seismotectonic regions, geomag. investigations rel. to crustal blocks compression and tension 0-26464
- asthenosphere thermal instability beneath moving plate 0-31007
- N.Atlantic crustal structure, deep drilling results 0-26478
- N.Atlantic Mesozoic crust reconstruction 0-51365
- Atlantic mid-oceanic ridge, axial temp. profile and crustal struct. 0-26476
- Atlantic Ocean, history of growth and topography of ocean bottom 0-3993
- NE Atlantic Ocean, spreading history rel. to continental margin bathymetry, around British Isles 0-12372
- Atlantic Ocean opening, palaeomag. study 0-51320
- S.Atlantic oceanic crust in Mesozoic and subsequent evolution, mag. and gravity data 0-21699
- N.Atlantic opening from palaeomagnetism of Notre Dame Bay lamprophyre dikes 0-26440
- Mid Atlantic Ridge crest, geological and geophys. investigations 0-8284
- Atlantic rifting initiation, paleomag. evidence 0-51350
- Atlantic S.E. of Azores, crustal struct. rel. to mag. anomalies and bathymetry 0-51384
- Atlantic seafloor spreading, Kane fracture zone 0-21668
- N.Australia Precambrian shields and platforms, struct. and tectonic style 0-3982
- Avalon zone, Atlantic Canada, extent determ. from mag., seismic and gravity data 0-12384
- Azores, K-Ar age of oldest volcanics, volcanic history 0-46158
- central Baffin Bay, sea-floor spreading 0-51373
- Baikal rift, deep struct. and formation mechanism from geophysical exploration (*Russian*) 0-12364



## tectonics continued

- Baltic Shield, Proterozoic tectonics from palaeomag. study of Swedish rapakivi suite 0-56346  
 Bellingshausen Sea earthquake, Feb. 1977, ocean ridge generated compression mechanism 0-46142  
 Benue Trough, Nigeria, gravity field rel. to tectonic evolution 0-21701  
 Bergell region, uplift history of Alps, apatite fission track age 0-21727  
 Bering Sea and NW.Pacific Ocean,  $S_n$  waves propag. rel. to trapped old lithospheric unit 0-51346  
 block tectonics analysis in Mongolia, appl. of two-dimensional autocorrelation anal. 0-56469  
 Cabo-Ortega mafic/ultramafic massif, emplaced nappe, gravity data 0-21689  
 S. California, crustal deformation model 0-51377  
 S. California downwarping, tectonomagnetism anomaly and seismicity 0-21626  
 E. Canada tectonically active region, magnetotelluric fields time depend. 0-26451  
 Canadian continental margins, evolution and geophys. features 0-8274  
 Canadian Cordillera, geodynamic evolution 0-8276  
 Canary Island palaeomagnetism, and continental margin evolution 0-56363  
 N. Caribbean, crustal plate subduction history 0-41429  
 Caribbean Basin, transitional intercontinental sutural geostructure model 0-31015  
 Caroline Plate, petrochem. of troughs and crustal accretion 0-12385  
 S. China Sea, 1965 October 7, intraplate thrust earthquake 0-26461  
 E. Churchill Province, Andean-type tectonism 0-36222  
 Colorado, tectonomag. study using field difference method 0-21850  
 conference on passive margins, Jun. 1978, Nova Scotia, Canada 0-36774  
 contemporary crustal movements in Canada 0-8273  
 continental coalescence of Guyana Shield and W. African Craton 0-26613  
 continental crust shortening, by reactivated basement reverse faulting 0-36284  
 continental evolution, basement and sedimentary recycling 0-56430  
 continental lithospheric boundary layer, liability to sink into less dense asthenosphere 0-56447  
 continental plates pre-Tertiary velocities from palaeomag. data 0-21848  
 convection rates of viscous fluid, upper mantle and continental drift appl. (Russian) 0-1581  
 Coral Sea basin tectonic evolution from marine mag. anomaly data 0-21698  
 Corsica-Sardinia microplate evolution from magnetisations of Tertiary volcanics 0-56343  
 Costa Rican orogen, tectonics of outer arcs 0-8311  
 crustal deformation, line length changes resolution by EM distance meas. ratio method 0-4143  
 crustal deformation by dilatancy model, earthquake precursors 0-51347  
 crustal movement data from strain meas. in Honshu, Japan 0-8277  
 Cuvier Basin, off W. Australia, crust form. by rifting, seismic study 0-12368  
 Dalradian slide, NW Ireland, strain history from deformed pebbles 0-4013  
 Damara-Ribeira orogen, continental collision interpretation 0-21703  
 diapir formation, finite element model of density instability 0-51366  
 double seismic zone in downgoing slabs and mesosphere viscosity 0-26472  
 Early Cretaceous remanent spreading centre in central Pacific Basin 0-21706  
 earthquake aftershock sequence, frictional fault model 0-30992  
 earthquake cycle in underthrust zones, model 0-26457  
 earthquake fault mapping in Japan (Japanese) 0-51348  
 earthquake faults, premonitory slip rel. to foreshocks characts. and earthquake prediction 0-3944  
 earthquake mechanisms, Izu Peninsula, Japan 0-12345  
 earthquakes at plate boundaries, magnitude-freq. relation 0-56390  
 SW. Ethiopia, dating of volcanic and rifting history 0-51369  
 evolution of surface features of Earth, endogenic and exogenic forces 0-3972  
 Falkland-Agulhas Fracture Zone, ridge-crest offset history 0-26490  
 fault blocks and plate tectonics, theory 0-46166  
 fault slip stabilisation by coupled deformation-pore fluid diffusion 0-56378  
 fault stress directions, for given fault population, theory 0-8455  
 fault termination deformation, a clay expt. 0-21734  
 faulting of geological structures, cryst. defect theory approach 0-21731  
 folding of sedimentary rocks, Malaguide Complex, Spain 0-8312  
 fracture system, statistical anal. (Chinese) 0-41417  
 Galapagos Rift at 86°W, regional morphological and struct. anal. 0-26491  
 Galapagos Rift at 86°W, rift valley sheet flows, collapse pits and lava lakes 0-21708  
 Galapagos Rift at 86°W, sealed topography and magmatic episodes 0-21681  
 Galapagos Rift at 86°W, volcanism struct. and evolution of rift valley 0-21707  
 Garm region, crustal fracturing rel. to weak earthquakes space-time sequence 0-21653  
 geodynamic monitoring and earthquake research, radiointerferometry appl. 0-31151  
 geological folding process, laboratory expt. and theory 0-21733  
 German Democratic Republic, geomag. secular var. anomalies rel. to vertical and horizontal crustal movements 0-26449  
 global geodynamics, Canadian contribs., 1971-79 period. 0-8262  
 Gondwanaland, breakup rel. to evolution of Indian Ocean 0-41428  
 SE. Gondwanaland, plate tectonics Campbell plateau and Lord Howe Rise 0-17244  
 Gondwanaland fit, plate tectonics of India and SE Asia 0-8282  
 grabens of Canyonlands National Park, Utah, geometry, mechanics, kinematics 0-21728  
 E. Greenland, continental rifting rel. to struct. of coastal dyke swarm and assoc. plutonic intrusions 0-56467  
 Gulf of Aden and Afar, mag. anomaly map and plate tectonics 0-56364  
 Gulf of Mexico-Caribbean area, Permian-Triassic continental reconstruction 0-56431  
 W. Gulf of Oman, tectonics 0-8279  
 Hawaii earthquake, Nov. 1975, low dip angle faulting mechanism 0-56406  
 Hawaiian Island chain, volcanism linear migration from Kauai shield-building volcanism age 0-36281

## tectonics continued

- Hawaiian Islands, isostasy and lithosphere flexure 0-26485  
 heat flow from tectonic units, Romania (Rumanian) 0-8268  
 Hellenic arc and trench system, key to E. Mediterranean area neotectonic evolution 0-56451  
 Hellenic trench system, subduction to transform motion, Seabeam survey 0-8285  
 Hokkaido and Tohoku, Japan, intraplate seismicity and large quakes 0-51337  
 Honshu, Japan, deep seismic zone and plate tectonics 0-8269  
 Horse Canyon earthquake, California, stress-release process 0-56387  
 E. Iceland, lava  $^{40}\text{Ar}/^{39}\text{Ar}$  age for ocean ridge spreading rate 0-36273  
 India-Asia collision from Indian apparent polar wandering path 0-26452  
 Indian Ocean, model of evolution rel. to breakup of Gondwanaland 0-41428  
 Innuitian Province, Arctic Canada, tectonic history 0-8275  
 intraplate seismicity on bathymetric features, 1968 Emperor Trough earthquake 0-30997  
 isostasy and long term flexural rigidity of crust 0-46161  
 isostasy at midocean ridge crests 0-31022  
 Izu Block, Japan, accommodation of colliding plates 0-41424  
 Izu Peninsula, Japan, geoelectric survey near anomalous upheaval zone (Japanese) 0-46122  
 Izu-Oshima-kinkai earthquake, Jan. 1978, fault mechanism 0-41390  
 Izu-Oshima-kinkai earthquake, Japan, Jan. 1978, associated surface faulting 0-41408  
 Japan, continental drift and Permian greenstone palaeomag. 0-21629  
 SW. Japan, earthquake activity rel. to plate tectonics 0-21663  
 Juan de Fuca Ridge crest, E. Pacific, tectonic topography compensation 0-56448  
 Kamchatka, volcanic zone, tilt meas. 0-3984  
 S. Kanto and Tokai districts, Japan, crustal plate dynamics (Japanese) 0-51382  
 Laramide folding and faulting in SE. Arizona, basement cored uplift model 0-8272  
 Laramide Wind River uplift, Wyoming, USA, gravity and seismic refl. data 0-21679  
 Lewisian foreland, NW. Scotland, central zone palaeomag. rel. to tectonics 0-26443  
 Los Angeles basin (California) SW block, thermal subsidence and petroleum generation 0-3967  
 magma series erupted in different marine tectonic settings, trace element anal. 0-21667  
 magnetic variation due to stress change, theory of electrokinetic-mag. anomalies 0-21627  
 upper mantle, tectonics rel. to magmas and volatile components 0-41418  
 mantle convection, depth extent from seismic energy release of deep and intermediate earthquakes 0-41404  
 mantle convection, numerical anal. 0-51371  
 mantle plume, fluid-dynamic model of ascending flow 0-12370  
 Markansu Valley earthquake, Tadzhikistan, USSR, 1974 August 11, seismotectonics 0-21659  
 meteorite craters, geophysical and geomechanical aspects 0-17265  
 trans-Mexican volcanic belt, seismic refl. and geomag., leg 17 of project CICAR (Spanish) 0-36280  
 mid-oceanic ridge axes, topography and tectonics from fluid dynamic models 0-41433  
 migmatite rise, numerical expts. based on continuum dynamics 0-51381  
 migmatite tectonics, Hidaka metamorphic belt, Japan 0-8310  
 minimum-dissipation theorem, usage in temp. depend. viscosity problems 0-12369  
 mylonites flow strength, role of grain size reduction and grain boundary sliding 0-21721  
 Nazca group volcanic rocks, Peru, volcanic history 0-12357  
 New Hebrides Island Arc, anomalous propag. through shearing contact zone 0-3948  
 E. North America, tectonic implications of earthquakes surface wave focal mechanisms 0-3942  
 North America Early Carboniferous palaeomag. field rel. to N. Appalachians tectonics 0-8249  
 North Sea, Buchan and Witchground Grabens, seismology study 0-51364  
 N. Norway, continental margin crustal struct. and tectonic history 0-51360  
 Norwegian Caledonides Trondheim Nappe melange and tectonic model 0-3985  
 Norwegian-Greenland sea, thermal evolution in sea floor spreading model 0-56427  
 oceanic aseismic ridges, isostasy anal. and tectonics implications 0-3971  
 oceanic basins, volcanic evolution of marginal and interarc basins 0-8271  
 oceanic lithosphere flexure and uplifted atolls, comment 0-26486  
 oceanic trench outer rise width, model of crust thickness as function of age 0-56426  
 Oklo natural fission reactors geological environment, tectonic anal., petrography, geochemistry (French) 0-21742  
 Oklo natural reactors, fluid phases contemporaneous with sandstone diagenesis, and tectonic movements (French) 0-21746  
 Oklo natural reactors, mining, geology and tectonics (French) 0-21743  
 NW. Ontario, granitoid complexes and Archaean tectonics 0-31019  
 Ontong Java and Manihiki Pacific oceanic plateaus, seismic struct. 0-21680  
 overthrusting, model of const. thickness overthrust on visco-plastic sole 0-51378  
 SW. Pacific basin, reverberant subbottom layers distrib. rel. to plate northward drift 0-8290  
 Pacific lithospheric plate, elastic thickness from geoid heights along Hawaiian-Emperor seamount chain 0-3899  
 NW. Pacific Ocean and Bering Sea,  $S_n$  waves propag. rel. to trapped old lithospheric unit 0-51346  
 Pacific Ocean basin, volcanic history since Jurassic, crustal loading study 0-46165  
 Pacific plate subduction beneath Japan Islands, 3-D seismic struct. 0-51376  
 E. Pacific Rise, sea-floor spreading rel. to young cratered volcanoes pair history 0-12374  
 E. Pacific Rise, struct. of crust, volcanism periodicity and magma flow 0-17243  
 Pacific-N. American plate interaction and Californian Neogene volcanism 0-21702  
 palaeomagnetism and plate tectonics, book 0-36789  
 Palaeozoic base maps, palaeogeography and plate tectonics 0-41441  
 Papua New Guinea, Late Cainozoic geotectonics and volcanism 0-51372



**tectonics continued**

- Papua New Guinea-Solomon Islands region, 1964-1973 earthquakes, seismotectonics 0-8270
- Parece Vela Basin, E. Philippine Sea, evolution and chronology 0-41431
- passive continental margin, thermal evolution in sea floor spreading model 0-56427
- Philippine Sea Plate, activity of northern boundary (*Japanese*) 0-51382
- Pine Mountain block thrust sheet, USA, energetics of driving force 0-21730
- plate bending at trenches, mechanical models constraints from earthquakes 0-41426
- plate motion and mantle return flow response 0-46152
- plate tectonic controls on diagenesis 0-12387
- plate tectonics, driving force models for plate stress, review 0-56450
- plate tectonics, theoretical problems, conf., Aug. 1978, Caracas, Venezuela 0-51400
- plates relative motions, rel. to marginal basins form. 0-41427
- Precambrian basement, W. Canada, U and Th conc., petrologic and tectonic controls 0-17257
- Precambrian polar wandering rel. to plate tectonics 0-31024
- Proterozoic rocks of Sweden indicating ancient subduction zone 0-46162
- Ridge Basin, S. California, earthquake focal mechanisms and hypocentres, tectonics 0-21695
- rift valley formation over oceanic ridge, upwelling flow model of topographic profile (*Chinese*) 0-8280
- rifted continental margins, thermal history and subsidence, Nova Scotian and Labrador Shelves 0-12353
- rock mechanics constraints on lithosphere stress and temp., consuming plate 0-31021
- rocks crenulation cleavage, mechanical significance investigations 0-21737
- Russian platform, tectonic fluctuations determ. from geological records coding (*Russian*) 0-17383
- San Andreas and Calaveras fault region, crustal deformation, 1971-8 obs. 0-56428
- San Andreas fault, local mag. field vars. and stress changes near slip discontinuity 0-26448
- San Andreas fault (central California), mag. field local vars., creep rate changes and local earthquakes 0-26450
- San Andreas fault strain accumulation 1964-1977 near 1976-7 earthquake swarm 0-36272
- San Andreas fault system, stress field and aftershocks, theory 0-36249
- Sanriku, 1933 March 2, dislocation model rel. to tsunami waves and plate tectonics 0-31000
- Sanriku-Oki region, Japan, 1965-1970 shallow earthquake source characts. 0-12346
- Scandinavian Caledonides, gabbro complex palaeomag., plate rot. or polar shift theories 0-21615
- seismic faulting mechanism, role of inhomogeneities 0-51342
- seismic gap quiescence duration determ. method 0-26627
- serpentinites, Glenrock, New South Wales, foliation development 0-21738
- Shuswap Complex, S. Okanagan, British Columbia, recumbent folding, mechanism and geometry 0-4008
- E. Siberia, tectonic activity rel. to amethysts form. (*Russian*) 0-12393
- Sierra Nevada, California, regional deform. on conjugate microfault sets 0-21729
- Sila nappes (Calabria), palaeomag. evidence for non-Apenninic origin 0-56369
- single-layer folds, shape at small but finite amplitude 0-56473
- slaty cleavage, development Fleurieu Peninsula 0-21735
- Solomon Islands, earthquake doublet mechanism in subduction zone 0-56410
- South China Sea basin, tectonics from profiler-sonobuoy meas. 0-8291
- South Sandwich arc, moderate and large earthquakes, tectonic var. along subduction zone 0-26458
- strike-slip faulting, in crust of horizontally variable rigidity, model 0-56377
- subducting slab creating deep-focus quakes, theory 0-51375
- subduction beneath W. South America, evidence from converted phases 0-26484
- subduction rel. to geoid and lower mantle convection 0-31023
- subduction zone, thermal struct. evolution 0-56440
- subduction zone topography, dynamics of subducting plate 0-51374
- subduction zones, young lithosphere thrusting rel. to struct. in ophiolitic peridotites 0-56446
- submarine lithosphere, geophys., geochem. and petrological model 0-3994
- Superior Geotraverse symposium (Toronto, 1978 October 23-26) 0-27029
- central Sverdrup Basin, crustal struct. and active intraplate tectonic feature 0-12355
- Tajikistan, tectonomagnetic studies 0-26446
- Tarbela reservoir, Pakistan Himalayas, seismicity during initial filling 0-56388
- tectonomagnetic anomaly due to lake ground loading, piezomagnetic effect 0-8346
- Tethys early development, Iranian segment, Ar isotope age of ophiolites 0-46156
- thermal evolution of continental crust during magmatic accretion and metamorphism 0-46150
- thermal evolution of ocean ridge, affected by spreading rate 0-56424
- Tibet earthquake, 14 July 1973, source mechanism and seismic wave attenuation 0-36252
- Tibetan Plateau underthrust by India, palaeomagnetic constraints 0-56449
- Tohoku district, Japan, crustal movements during 1900-1975 and tectonic implications 0-56453
- Torlesse Terrane, New Zealand, exceptionally large steeply plunging folds origin 0-12388
- Turkey's rotation, palaeomagnetism of dykes and tuffs 0-31020
- Turkish-Iranian Plateau, post-collisional tectonics, comparison with Tibet 0-3986
- two-dimensional strike-slip fault, static deform. of laterally inhomogeneous half-space 0-31012
- Tyrrhenian Sea rifting, Rayleigh wave dispersion evidence 0-56445
- W. United States, collided Palaeozoic microplate (Sonoma) 0-41415
- United States, western region, strain accumulation rates, 1970-78 period 0-21607
- Upper Proterozoic apparent polar wander, analogous loops from Laurentia, Fennoscandia and Africa 0-56360
- Urals, geomag. secular var. anomalies rel. to aseismic geodynamics 0-26447

**tectonics continued**

- vertical crustal movements Carpathian area of Rumania (*Rumanian*) 0-8281
- Walvis Ridge, S. Atlantic, gravity anomalies and origin 0-21682
- Western Australian Shield, struct. and tectonic style 0-3983
- N. Wolverine Complex, British Columbia, geochronology and tectonics 0-3961
- Yellowstone Park hot spot, volcanic and tectonic evolution 0-56472

**tektites see meteorites****telecommunication**

- see also biocommunications; communication networks; optical communication; radiocommunication; telemetering; telephony*
- long distance communications, fibre optic developments (*Norwegian*) 0-1318
- microelectronics revolution, appl. in telecommunications, medicine, education 0-31446
- photovoltaic power systems, equipment performance and manufacturing techniques improvements and system design problems for telecommunication applications 0-55843
- remote site development, solar cell power supplies 0-26133
- technical meteorology, technical and commercial appls. (*German*) 0-46231

**telecommunication cables**

- see also coaxial cables; submarine cables; telephone lines; underground cables*
- fibre optic undersea cables, small, recent experiences 0-14488
- fibre-optic, construction and props. of 140 Mb/s trial system 0-23794
- fibre-optic, measurement of baseband transfer function 0-1355
- fibre-optic, monomode, fabrication, characterization and cabling for transmission in 1.2-1.6  $\mu$ m range 0-10042
- fibre-optic, single-mode evaluation of characts. (*Japanese*) 0-28316
- fibre-optic, status of development 0-43485
- optical coated fibre and cable unit structure optimisation 0-53466
- optical fibre, metal-free, wide temperature range communications appl. 0-23795
- optical fibre cable attenuation and input and output efficiency 0-14469
- optical fibre cable transmission and strength improvement technology 0-28347
- optical fibre unit, high density low-loss, cabling 0-53468
- optical single-mode fibre cabling for low-loss communication 0-53467
- plastics, for transmission media, thermomech. reliability 0-40666
- submarine, dielec. loss measurements of polyethylene at high pressure and freq. 0-27316
- Pb sheathed, corrosion in plastic multiway ducts 0-7721

**telecommunication equipment**

- see also multiplexing equipment; radio equipment; repeaters; television equipment*
- SAW filters, design, construction, appl., book 0-1393

**telecommunication systems**

- see also data communication systems; digital communication systems; telephone systems*
- fibre-optic system components, status of development 0-43485
- fibre-optic transmission systems, development progress 0-43482

**telecommunication theory see information theory****telecontrol**

- see also alarm systems; telemetering*
- nuclear fuel pellets, automated inspection 0-13766
- nuclear power plant, instrumentation and control, remote multiplexing appl. 0-52752
- pellet fuels,  $\gamma$ -active, remotely operated plant for fabrication 0-32340
- UV spectrometers, on OSO-8, computer-controlled, mission operations 0-41723

**telecontrol equipment**

- fission reactor core, neutron detector telecontrol device with direct loading (*Russian*) 0-52770
- leaktight remote handling equipment for operations in an irradiating and contaminating environment 0-13951
- US remote control circuit using US transducer 0-10097

**teletext**

- see also telerecording*
- telex, description of Thomson-CSF flying-spot twin format telexine (*French*) 0-37110

**telemetering**

- ELF/VLF goniometer receiver, remote, unmanned, in Antarctica, UHF telemetry link 0-21854
- environmental data from satellite system 0-56592
- ion accelerator systems for ion implantation research 0-32540
- nuclear power plant, instrumentation and control, remote multiplexing appl. 0-52752
- pCM telemetry for physiological data 0-36059
- sector scanning sonar, use in fish heart rate telemetry 0-8225
- wildlife biotelemetry, reviews 0-30966
- Mn nodules deposits, deep sea telemetry (*German*) 0-26623

**telemetering equipment**

- digital frequency-to-temp. convertor for use in radio telemetry systems 0-8119
- EM, perched water table detection appl. 0-26655
- fever alarm device using telemetry 0-21556
- medical research on animals, chronically implantable instrumentation 0-30834
- Mn nodules deposits, deep sea telemetry (*German*) 0-26623

**telemetering systems**

- data buoy wideband wave directional spectra, real-time telemetry 0-46305
- electrophysiological research animal model, chronically instrumented 0-26323
- high data rate acoustic telemetry system design 0-43573
- IR system for surgical patient monitoring 0-30836
- medical system, portable, multi-sensor, for rural health network 0-30835
- ocean sediment free-fall penetrometer with Doppler telemetry 0-46320
- pCM telemetry for physiological data 0-36059
- Spar Buoy Oceanographic Telemetry System 0-46307
- Spar Buoy Oceanographic Telemetry System software engineering 0-46308



- telemeters *see* telemetering
- telemetry *see* telemetering
- telephone calling equipment *see* telephone station equipment
- telephone exchanges  
noise abatement measures in PTT premises (*French*) 0-10079
- telephone lines  
PCM 480 system for Deutsche Bundespost using fibre-optic link 0-38120
- telephone receivers  
ring armature type, use of low Co ternary Cr-Co-Fe alloy 0-45318
- telephone sets  
aids for handicapped people 0-36196  
optical fibre voice transmission using unmodulated transmission of AF, telephone terminal sets (*German*) 0-28314
- telephone station equipment  
disabled persons employment using traffic operator position system 0-36197
- telephone systems  
*see also* telephone exchanges  
saturation diving communications system 0-43558
- telephones *see* telephone sets
- telephony  
optical fibre systems, worldwide development 0-43468  
thickness meas. of Au and Ni layers on Cu substrates simultaneously 0-13041
- telerecording  
*see also* telefilming  
telecine, description of Thomson-CSF flying-spot twin format telecine (*French*) 0-37110
- telescopes  
*see also* astronomical telescopes  
alignment techniques by optical means 0-1341  
aspheric reflecting systems, geometrical design 0-38083  
cryogenic, construction, appl. of C fibre reinforced epoxy 0-22414  
high-performance telescope aspheric mirror test error budget 0-48386  
infrared telescope, 6032 image conversion tube 0-42020  
photomicrography appl., low-power, critical focusing 0-13165  
resonator, unstable telescopic, precision of some methods of adjustment (*Russian*) 0-38040  
time of flight telescope for high energy gamma-ray astronomy 0-31210
- teletypes *see* interactive terminals
- television applications  
astrophysical observations, image isocron appl. (*Russian*) 0-12671  
bistable TV-optical feedback system using optical flip-flops 0-53354  
bubble chamber, projection graphic display for computer aided image anal. 0-27895  
Cherenkov light photograms, automatic scanning by TV digitiser 0-52822  
cinematography, development and introduction of TV facilities (*Russian*) 0-22465  
communication aid for disabled, Telecad 0-17197  
computer augmented video education, project status report 0-22174  
computerised tomographic image display by TV and photography 0-8129  
distance meas. of polyhedral objects from loci of vertices 0-42195  
eye tracking raster graphics device, picture processing computer appls. 0-41330  
fluoroscopic image recording using multiformat camera 0-51234  
Fresnel holograms transmission 0-19009  
grain size determination and structural classification by visual comparative method using TV equipment (*German, English*) 0-35461  
instantaneous spectra meas., TV camera and microcomputer appl. (*Japanese*) 0-31888  
interference microscope with electronic image formation (*Slovak*) 0-31862  
Josephson video-detector, optimisation for mm wavelengths 0-4768  
laser scanning camera nuclear reactor surveys appl. 0-52748  
LEED intensity measurement using modified CCTV system 0-31946  
marine life forms obs., using CCD colour TV camera 0-51301  
microprocessor-based teleradiology system 0-26343  
microscopy and cinephotomicrography with Zeiss Axiomat 0-27343  
movement measurement, vidicon television camera appl. 0-41333  
particle tracks, time digitiser in CAMAC format 0-14062  
Perseid meteor shower, television obs. 0-4309  
planimeter for meas. and displaying slide mounted samples 0-195  
PWR steam generators, remote controlled TV for detection of leaking tubes (*French*) 0-791  
stellar objects monitoring using minicomputer-controlled photon counter (*Russian*) 0-31212  
STEM image accumulation, storage and display system 0-37132  
stress/strain display on TV screen 0-21222  
temperature meas. in polyorganosiloxane fluid friction zone (*Russian*) 0-7688  
vapour pressure measurement, torsion-effusion method, automatic data acquisition 0-52188  
wind speed remote meas. using video equipments (*French*) 0-7990  
X-ray colour TV system with soft X-ray preferred display 0-56186  
X-ray TV chain MTF and image quality determ. factors 0-36126
- television camera tubes  
*see also* image storage tubes  
IR imaging, imaging systems design, operation and performance, applications 0-47111  
isocron plus image intensifier, appl. in astrophysical obs. (*Russian*) 0-12671  
vidicon Raman spectrography detection system 0-37095  
vidicon-camera parallel-detection system for angle-resolved electron spectroscopy 0-4817  
Si:H film, amorphous, photocond. imaging 0-1300
- television cameras  
*see also* colour television cameras  
balloon-borne slow-scan TV camera performance test (*Japanese*) 0-12635  
laser, with scanning head and photosensitive detector, nuclear reactor surveys appl. 0-52748  
lens performance meas. system, routine checking appl. 0-277  
objective lenses testing by projection 0-9060  
planetary observation appls. 0-31197  
scanning nonlinearity cancellation, transmitting TV camera 0-52318
- television equipment  
holographic TV, appl. of CRT with electro-optic crystal (*Russian*) 0-37974
- television equipment continued  
SAW filter design for TV, CATV and radar appls. 0-53579  
telecine FDL 60, CCD line scanning, digital frame store 0-278
- television picture tubes  
*see also* cathode-ray tubes; fluorescent screens  
cathodoluminescence of BeO with/without admixtures (*Polish*) 0-2869
- television signals *see* video signals
- television studios  
acoustically optimal room proportions with regard to normal frequency spacing (*German*) 0-14522  
rapid processing technique for colour reversal cinefilm (*Russian*) 0-3385  
receiver for parallel operation of radiomicrophones (*German*) 0-4787  
sound processing circuit diagrams (*German*) 0-18031
- tellurium  
*see also* nuclei with .....  
adsorbed on Ni (001), photoelectron diff. obs. 0-40223  
adsorption on Ni (111), angle-resolved photoemission 0-40230  
amorphous, Rayleigh scatt. of Mossbauer radn., lattice dynamics 0-15845  
amorphous film, vac. deposited, phonon-assisted hopping cond. 0-2392  
atom, photoionisation cross sections and ang. distrib., outer p subshell 0-9572  
atom, XPS and XES, dynamical effects 0-52924  
Auger electron spectra, solid state effects 0-20739  
chemical bonding in group V and VI elements and compounds with tetradymite structure 0-15036  
coating of PbTe surfaces, struct. and junction characts. 0-50743  
Compton profile, charge and momentum density 0-55220  
dislocations influence on galvanomag. props. 0-54722  
electron irradi., mobility increase due to defect prod. 0-24501  
facet coating, for side lobe suppression in far field of AlGaAs DH stripe laser 0-5744  
film, gas-evaporated, selective absorpt. characts. and emissivity 0-50998  
film, interference enhanced Raman scatt. 0-42273  
film, on electron irradi. KBr, epitaxial growth and surface coverage 0-10825  
film condensed on mica, struct. and electrophysical props. 0-39688  
films, evaporated deposition, absorptivity and emissivity 0-25473  
high pressure metallic phase, cryst. struct. 0-49161  
hole mobility anisotropy in edge dislocated cryst. 0-24936  
impurity state and impurity cond., press. effect, pure and Sb doped crystals. 0-54723  
intervalence band absorption, press. and defects influence 0-55149  
inversion layers in mag. fields 0-44690  
isomer shift values of implanted  $^{133}\text{Xe}/^{133}\text{Cs}$ , Mossbauer spectra 0-7240  
liquid, structure metallic constituent calcs. hard sphere model (*Russian*) 0-24349  
optical activity, de Haas-van Alphen oscillations and cond. band parameters 0-54605  
optical bleaching near fundamental absorpt. edge at 80K 0-28287  
optical properties under high press., band struc. transform. 0-55112  
optically active crystals, circular photogalvanic effect 0-54739  
overlay,  $c(2\times 2)$  on Ni surface, 4d levels, angle resolved photoemission cross section, atomic and solid-state effects 0-29853  
p-type, impact ionization rate of holes at 77K 0-10993  
phonon dispersion curves, scaling formalism 0-54326  
photo-excited carriers, far IR magneto-spectroscopy 0-50343  
photoconductivity under pulse excitation conditions 0-2425  
photoelasticity and acousto-optic diff. in piezoelec. semiconds. 0-29715  
photovoltaic effect in thin films, 10.6  $\mu$ , prep. methods 0-20252  
physics, conf., Konigstein, Germany (May 1979) 0-51958  
piezoelectrical free-carrier scatt. by screw dislocations, Hall effect and cond. meas. 0-24926  
thin films, textured, prep., high solar absorptivity by multiple refl. 0-11568  
trigonal,  $^{129}\text{I}$  Mossbauer obs. at high press. 0-55005  
trigonal, dielec. matrix calcs. 0-54630  
trigonal, self-consistent ground state,  $X_\alpha$  calcs. 0-54604  
trigonal, state-of-the-art review of model calcs. 0-54327  
trigonal, surface lattice dynamics, mean square displacement spectra in long wavelength limit 0-54498  
uniaxially stressed, submm. cyclotron reson., deform. pots. and k.p coeffs. 0-54606  
valence band struct. under press., spin-orbit splitting, intraband absorpt. spectra 0-2330  
Ag-Te thin film couple, room temp. interactions 0-2220  
 $\text{Al}_2\text{Ga}_{1-x}\text{As}_x$ :Te, persistent photocond., due to donor-related centres 0-15558  
 $\text{Al}_2\text{O}_3$ -Si-Te- $\text{Al}_2\text{O}_3$  layered apertured facet reflector, for lateral mode stabilisation of diode lasers 0-23708  
As:Te film, amorphous, chemical modification of props. 0-49250  
a-As $_2$ Se $_3$ :Te, doped film, photoluminescence intensity and lineshape study 0-50448  
CdS-Te, heterostructure, effect of low cond. CdTe interlayer on charact. 0-44721  
FeP:Te, nucl. relax. rel. to donor density 0-11284  
 $\text{Ga}_{1-x}\text{Al}_x\text{As}$ :Te, plasmon-LO-phonon coupling, IR refl. obs. 0-50335  
n-GaAs:Te, radiative transitions induced by modest annealing, photoluminesc. spectra 0-55158  
GaAs:Te, recombination barrier, dark cond., photocond., and Hall mobility meas. 0-15559  
GaAs:Te, superdilation and defects, lattice parameter meas. and carrier mobility 0-10569  
GaAs:Te diffused LED, electron irradi. effect on characts. 0-39667  
GaAs:Te substrate, VPE growth, photoluminesc. and emission spectra 0-29774  
GaP:Ae,C(Mg), donor-acceptor pair luminesc., excitation spectroscopy 0-25440  
GaP:Te, VPE grown layers, precision lattice parameter determination 0-24429  
GaSb:Te, indirect gap photolum. 0-29797  
Ge:Te $^{+}$ , ion implanted, alignment of irradi. induced defects, TEM obs. 0-15168  
InAs:Cd,Te interaction between impurities, effect on elec. props., Hall effect. 0-19832  
n-InAs:Te, heavily doped, cathodoluminescence, doping effect on luminesc. band position and spectral profile 0-45153  
InAs:Te(Se)(S), intrinsic pt. struct. defects 0-33998  
InP:Te, quadrupole struct. of NMR line 0-20505



**tellurium continued**

- InP:Te(S), heavily doped, dislocation imaging using transmission cathodoluminesc. 0-29023  
 InSb:Te, reson. states and reson. scatt. 0-49738  
 Li ions stopping power and straggling 0-42908  
 Sb:Te vapour saturation, diffusion zone struct. crystallisation orientation (Russian) 0-54438  
 Si:Te, implanted impurity location, Mossbauer and channelling expts. 0-39128  
 Si:Te implanted, laser annealing, Mossbauer obs. 0-39127  
 $\alpha$ -Sn:Te, implanted, impurity-defect structs., Mossbauer expts. 0-39129  
 Te VII, 4d<sup>5</sup>d config., UV spectrosc. obs. 0-18817  
 Te:Sb, impurity states and impurity conduction, hydrostatic pressure 0-39521  
 Te-Au thin film interface, evolution, switching effects (French) 0-6660  
 Te+Cd,  $\pi^-$  capture, radioactivity meas. 0-47831  
 Te<sub>2</sub>, optically pumped CW dimer lasers 0-14322  
 ZnS:Te phosphors, luminesc. excitation spectra and exciton struct. 0-55165

**tellurium alloys**

see also tellurium compounds

- Ag-Te, liq., struct. and elec. props. 0-49083  
 Au-Te, elec. field gradients and charge transfer, Mossbauer spectra 0-25268  
 AuTe<sub>2</sub>, core-level binding energy shifts and charge transfer 0-25268  
 Bi-Te, dilute, oxidation kinetics 0-25914  
 Cu-Te, liq., struct. and elec. props. 0-49083  
 Fe, cast, fused metal solidification enhancement using Bi and Te (Italian) 0-7540  
 FeNiTe alloys, disordered, polycrystalline, elec. resist., temp. depend. 0-49692  
 Ga-Te, solid and liq., thermodynamic props. 0-35567  
 Hg-Cd-Te, partial vapour pressure, determ. for volatile component by static method 0-37150  
 Ni-Te, liq., struct. and elec. props. 0-49083  
 Sb-Te, Al-type, superconductivity 0-29496  
 SeTe liquid alloy, effect of branched chain polymers on bond equilib. 0-24348  
 Te-Au film, supercond. by ion irradiation 0-34544  
 Te-In alloys, direct reaction calorimetric study, 737 to 1340K (French) 0-49382

**tellurium compounds**

see also tellurium alloys

- chemical bonding in group V and VI elements and compounds with tetradymite structure 0-15036  
 halides, Wasastjerna pot. function, force consts., internuclear separations and binding energies 0-14187  
 As-Se-Te, amorphous, electron and hole drift mobilities 0-34442  
 As-Te-Ga, glass, elec. cond., 190-300K (Russian) 0-54702  
 As-Te-Ga system, glass-forming region and props. 0-25674  
 As<sub>2</sub>Ge<sub>10</sub>Te<sub>65</sub>, chalcogenide glasses, dielectric relaxation 0-55027  
 As<sub>2</sub>(Se,Te)<sub>3</sub> glasses, X-ray absorption and photoelectron spectroscopy study 0-7463  
 As<sub>2</sub>Se<sub>20</sub>, amorphous films, metal and semicond. contacts, threshold switching, IR emission 0-49831  
 As<sub>2</sub>Te<sub>28</sub>Ge<sub>16</sub>S<sub>21</sub>, chalcogenide semiconductor study of electric properties (French) 0-29414  
 Bi<sub>2</sub>Te<sub>2</sub>Se<sub>0.3</sub>, magnetoresistance and Hall EMF meas., using AM method 0-52278  
 n-Bi<sub>2</sub>Te<sub>2.88</sub>Se<sub>0.12</sub>, extrusion deformed, powder dispersion degree influence on thermal and elec. props. (Russian) 0-39366  
 Bi<sub>2</sub>Te<sub>3-x</sub>Se<sub>x</sub> films, surface band struct. and scatt. mechanism 0-34535  
 Ga<sub>2</sub>As<sub>9</sub>Te<sub>49</sub> glassy film, nonlinear current voltage characts., Poole-Frenkel effect 0-7007  
 Ge<sub>15</sub>As<sub>4</sub>Te<sub>81</sub> glassy film, nonlinear current voltage characts., Poole-Frenkel effect 0-7007  
 (Ge<sub>0.32</sub>Se<sub>0.32</sub>Te<sub>0.32</sub>As<sub>0.4</sub>)<sub>100-x</sub>Ni<sub>x</sub>, ESR, rel. to elec. cond. 0-7155  
 Ge<sub>0.5</sub>Te<sub>0.5</sub>, heat capacity in solid and liq. phases, enthalpy of form. (French) 0-35565  
 Mn<sub>2</sub>TeO<sub>6</sub>, magnetic structure, stability of mag. modes, neutron diffraction study (French) 0-39744  
 P-Se-Te system glasses, mag. susceptibility and opt. props. 0-25079  
 S-Te, liquid semicond., bonding energies and entropies, mag. susceptibility meas. 0-49082  
 Se-Te crystallised glasses, struct. transforms. and IR spectra 0-19712  
 Se<sub>1-x</sub>Te<sub>x</sub> systems, amorphous and liq. states, short range order, neutron scatt. study 0-49124  
 Se<sub>2</sub>Te<sub>1-x</sub> liq., thermoelec. transport at mobility edge 0-49787  
 Te (IV) compounds, Mossbauer spectra, direct population of solid-state bands 0-15905  
 Te complex, bis(pyridium) hexachlorotellurate(IV), cryst. struct. (French) 0-28965  
 Te complexes of thiourea, Mossbauer spectra 0-15914  
 Te-I, Al-type, superconductivity 0-29496  
 Te-Se mixtures, liquid, electrical conductivity and thermoelectric power, high temps. and pressures 0-39639  
 Te<sub>40</sub>As<sub>35</sub>Ge<sub>18</sub>, amorphous, threshold switching, expt. 0-49830  
 TeCl<sub>4</sub>, chem. transport with equilib. NbO<sub>2.417</sub> to NbO<sub>2.5</sub> 0-2934  
 TeD<sub>2</sub>+F<sub>2</sub> TeF radical form., chemiluminescence obs. 0-43058  
 TeF, chemiluminesc. from oxidation in F<sub>2</sub>+H<sub>2</sub>Te(D<sub>2</sub>Te) emission spectrum obs. 0-43058  
 Te<sub>81</sub>Ge<sub>15</sub>As<sub>4</sub>, Hall effect in electrically switched memory state 0-2403  
 TeH<sub>2</sub>+F<sub>2</sub>, TeF radical form., chemiluminescence obs. 0-43058  
 TeO<sub>2</sub> acousto-optic laser deflector scanning 0-14486  
 TeO<sub>2</sub>, band struct., tight-binding calc. 0-24796  
 TeO<sub>2</sub>, elastic wave parametric instability kinetics in dielectrics (Russian) 0-45035  
 TeO<sub>2</sub>, electronic struct. and densities of states, tight-binding calcs. 0-15447  
 TeO<sub>2</sub>, ligat diff. by slow acoustic waves 0-29717  
 TeO<sub>2</sub>, paratellurite, optical absorpt. and refl. spectra, 80-500K, optical consts. determ. 0-50359  
 TeO<sub>2</sub> paratellurite crystals, parametric excitation of sound, calc. 0-24537  
 TeO<sub>2</sub>, structure simulation of some tellurite and chalcogenide glasses quasi-crystalline structural diffusion method (Russian) 0-54147  
 TeO<sub>2</sub> thin film, Al-TeO<sub>2</sub>-Al, field-assisted cond. mechanism 0-11105  
 TeO<sub>2</sub>-BaO, cryst. chem. study, X-ray diff. powder data (French) 0-15080  
 TeO<sub>2</sub>-CaO, cryst. chem. study, X-ray diff. powder data (French) 0-15080

**tellurium compounds continued**

- TeO<sub>2</sub>-CdO, cryst. chem. study, X-ray diff. powder data (French) 0-15080  
 TeO<sub>2</sub>-Li<sub>2</sub>O glassy system, struct. recomb. model 0-19707  
 TeO<sub>2</sub>-NaCl(-NaBr), condition diagram, thermographic obs. (Russian) 0-55377  
 TeO<sub>2</sub>-V<sub>2</sub>O<sub>5</sub> glass threshold devices, reversible monopolar switching 0-2434  
 TeO<sub>2</sub>-ZnO, cryst. chem. study, X-ray diff. powder data (French) 0-15080  
 Te(OH)<sub>6</sub>-Na<sub>2</sub>HAsO<sub>4</sub>·H<sub>2</sub>O, Te(OH)<sub>4</sub>-4.6Rb<sub>2</sub>HAsO<sub>4</sub>·Rb<sub>2</sub>H<sub>2</sub>AsO<sub>4</sub> and Te(OH)<sub>6</sub>·2(NH<sub>4</sub>)<sub>2</sub>HAsO<sub>4</sub>, synthesis and cryst. data (French) 0-33948  
 Te(OH)<sub>6</sub> diurea complex, cryst. struct. determ. 0-28971  
 TeSe, valence fluctuation system, ground state and elementary excitations, Anderson lattice model Hamiltonian, dense Kondo problem 0-54656  
 Te<sub>2</sub>Si<sub>2</sub>, (x=78.87, y=22.13), amorphous, struct., X-ray diff. study 0-6362

TEM see transmission electron microscopy

temper brittleness see brittleness

**temperature**

see also atmospheric temperature; boiling point; critical points; Debye temperature; ferroelectric Curie temperature; magnetic transition temperature; melting point; superconducting transition temperature; temperature scales

- astronomical observatories, telescope and dome temps. rel. to dome seeing 0-12657  
 galaxies active nuclei, temp. and electron density in narrow line region 0-31364  
 integral, approximative eqns., accuracy analysis 0-36834  
 intergalactic hot gas in clusters of galaxy, temp. and entropy 0-17660  
 interstellar dust grains, temp. fluctuations 0-26938  
 interstellar grains, temperatures in diffuse clouds rel. to interstellar Ar depletion 0-51848  
 late-type (K0 to M6) giant stars, effective temps. 0-46545  
 planetary nebulae, electron density and temp. from absolute flux densities for emission lines in 6000-11000 Å range 0-51857  
 quasars, temp. and electron density in narrow line region 0-31364  
 school physics, elementary presentation by theory of heat, thermodynamics, and thermometry (Danish) 0-4483

temperature compensation see compensation

**temperature control**

see also thermostats

- Atmospheric Cloud Physics Laboratory 0-4090  
 cryostat with optical high-pressure chamber 0-31767  
 diamond turning, Honeywell Corporation facilities 0-5852  
 dipstick cryostat, with temp. controller for high thermal stability 0-37044  
 extracorporeal circulation apparatus using thermoelec. heat regulating systems 0-3870  
 extracorporeal circulation system, energy parameters of temp. stabilisation system 0-3867  
 furnace thyristor temp. regulation circuits, for creep testing devices 0-25956  
 furnaces, elec. resist. 0-27307  
 gas chromatograph system development (Japanese) 0-50922  
 high temp. furnace control methods in creep testing 0-30187  
 induction salt baths, automatic temp. control 0-27300  
 industrial, thermocoupler and resistance thermometer 0-42221  
 LMFB, Na loop temp. control using 100 kW elect. heater (Czech) 0-5203  
 plate heating, optimal fast response control under temp. field gradient constraints 0-38232  
 radiospectrometer, automatic thermostatic control, using Diapazon variator 0-47160  
 rotary tube photographic processor design 0-4795  
 solar central receiver plant, dynamic simulation of thermal-hydraulic characts. of Na-cooled plant 0-30400  
 thermophysical testing device, rate of change of temp. in time (Russian) 0-208  
 InGaAsP InP DH lasers, optical power and wavelength stabilisation 0-38036  
 Si substrates during sputtering and sputter etching, thermal history of substrates 0-25562

**temperature distribution**

- altitudinal temp. gradients for N.Pennines in Britain 0-4094  
 E. central Atlantic, horizontal temp. in upper ocean layer (Russian) 0-17283  
 NE tropical Atlantic, thermohaline structure (Russian) 0-17281  
 Atlantic mid-oceanic ridge, axial temp. profile and crustal struct. 0-26476  
 Atlantic Ocean, temp. fluctuations rel. to semidiurnal internal waves in Polygon-70 test area 0-31051  
 atmosphere, Mason method for lidar temp. profiling, computer simulation 0-21827  
 atmosphere and ocean surface, canonical correl. method study 0-26593  
 atmosphere temperature profile retrieval, generalized inverse theory appl. and spectral expansion method 0-17412  
 BWR four-rod bundle burnout and heat removal intensification with water and freon-12 flows 0-18413  
 chemically hardening material cast in elastic cylindrical mold, transient thermal stresses 0-7589  
 chromosphere spicules, temp. struct. rel. to contrib. to solar EUV line emission 0-4325  
 clinical microwave focusing thermography 0-3771  
 coastal surface water temp., spatial var. during upwelling 0-36322  
 compressible laminar wall jet 0-28542  
 condensed medium, semitransparent, plane layer radiative-conductive heat transfer 0-43590  
 contact binary stars, temp. discontinuity maintenance 0-8655  
 convection, natural, transient and steady-state numerical solns. 0-10119  
 converse problems, initial temp. distrib. determ. by optimal dynamic filtering 0-19208  
 Cygnus Loop, supernova remnant, imaging X-ray obs., temp. struct. 0-41876  
 cylinder, circ., impulsively started from rest, heat transfer, numerical anal. 0-10248  
 cylinder, hollow, unsteady axially nonsymmetric temp. distrib. (Polish) 0-10152  
 HR Delphini (Nova 1967), electron temps. in different regions of envelope 0-4369  
 dielectric mirror, temp. field during laser radiation absorpt. 0-19063



**temperature distribution continued**

- diffusion furnace temp. profile meas. systematic errors, theoretical model (German) 0-8989  
 fibre reinforced materials, therm. stresses in unit cell 0-10160  
 flat layer of selective medium with semitransparent boundaries, radiative-conductive heat transfer 0-19227  
 flow, in channel, turbulent vel., press., and temp. fields, direct numerical simulation 0-19361  
 W. Gulf of Maine, current, temp. and press. obs. rel. to winter circulation 0-51430  
 heat pipe, evaporator section, evap. and vap. flow between parallel planes 0-10115  
 heat sources method, appl. in temp. field anal. (Russian) 0-28410  
 icy satellites, mass-radius relationships, density and temp. profiles 0-31222  
 inhomogeneous rod in complex heat exchange conditions, temp. calcs., film sputtering evaporators (Russian) 0-38230  
 interstellar shocks, post-shock gas temp., density and vel. profiles, analytical results 0-56911  
 inverse nonlinear heat cond. problem, thermal gas dynamic testing 0-23862  
 Io, surface temp. distrib. rel. to UV obs. of SO<sub>2</sub> 0-36561  
 ionosphere, day-night terminator 0-4186  
 Jupiter atmosphere, high resolution obs. between 30 and 50  $\mu$ m rel. to temp. profiles 0-46462  
 Jupiter atmosphere and ionosphere, temp. struct. from Voyager 1 preliminary radio profiles 0-26791  
 lakes, stagnant, thermal stratification 0-36340  
 laminar circular jets, friction heat effect on temp. distrib., anal., forced convection 0-10279  
 liquid crystal improved technique for thermal field measurements 0-216  
 liquids, throttling, temp. field near boundary 0-43757  
 local heat flux distributions, highly inhomogeneous, auxiliary-wall meas. method 0-5917  
 louvers in thermal radiating panel 0-10124  
 LPE system, temp. gradient meas. using W-graphite thermocouple 0-25584  
 marine thermocline evolution, study using Mellor-Durbin theory 0-4041  
 melt, temp. field calc. by numerical implicit method 0-44342  
 melt adjoining solid phase, inhomogeneous temp. field influence on capillary phenomena (Russian) 0-20029  
 microwave irradiated breast tumour thermal pattern calc. (French) 0-3759  
 microwave-irradiated cylinders simulating living tissues 0-3760  
 ocean, seasonal thermocline, temp. field fine structure (Russian) 0-17278  
 ocean, thermocline affecting vertical distrib. of oscils. (Russian) 0-21777  
 ocean, vertical temp. gradients meas. via moored instrument 0-12561  
 ocean, water temp. rel. to irradiance in Norwegian and Barents Sea 0-31055  
 ocean surface, satellite data processing (Russian) 0-17417  
 ocean thermocline, temp. fluctuations and internal waves rel. to wind field variability 0-31052  
 ocean thermocline and mixed layer, model of seasonal evolution 0-26546  
 Orion Molecular Cloud, NH<sub>3</sub> emission obs. and rot. temps. distrib. 0-36687  
 N. Pacific mesoscale phenomena, oceanographic model and acoustic survey comparison 0-46195  
 tropical Pacific Ocean, climatological usefulness of satellite-determined sea-surface temps. 0-31044  
 N. Pacific Ocean, west, depth, var. of temp., salinity and sound vel. meridional gradients 0-51429  
 particles in nonisothermal plasma jet, trajectory and temp. calcs. (Russian) 0-7514  
 plane steady temp. field, effect of bi-periodic system of plane inclusions 0-19224  
 plate, approx. soln. method for heat cond. problems 0-33415  
 plate, thin semiinfinite, mobile normally-distributed heat source on lateral surface (Russian) 0-23870  
 pore velocity, due to surface diffusion under temp. gradient, finite thermal conductivity correction 0-15428  
 rectangular jet distrib. in cross flow, expt. 0-19465  
 regenerative heater, high-temp., refined math. model 0-22365  
 RF plasma torch, one dimensional analysis using finite element method 0-24264  
 Ross Ice Shelf temperature in bore holes, ice thickening history 0-31072  
 sea surface, tropical anomaly effect in ocean-atmosphere coupled model 0-12418  
 seawater, Mangalore coast, India, 1976-7 nearshore water conditions 0-8315  
 semi-infinite medium, transient thermal loadings, stress intensity factors 0-10193  
 semiconductors, laser annealing after ion implantation, temp. distrib. 0-54265  
 shell enclosures, temp. distrib. calcs. under thermal radiation, numerical calcs. 0-38241  
 Shinnecock Inlet, radiometric sea surface temp. distrib. 0-41454  
 shock wave, strong, piston struct. and gas distrib. 0-10265  
 solar X-ray flares, temp. and thermal energy content profiles 0-17561  
 steel, alloy, nonsteady temp. fields during cooling, calc. 0-16346  
 stress pattern analysis by thermal emission 0-33552  
 subduction zone, thermal structs. evolution 0-56440  
 thermal diffusion cloud chambers, wall linear temp. gradient rel. to super-saturation distrib. 0-56631  
 thermotechnical equipment, radiant heat exchange modelling in rectangular chamber with attenuating medium 0-33433  
 thermoviscous fluid, steady flow through straight tubes 0-33636  
 tissue, soft, temp. distrib. monitoring by temp. depend. of US vel. 0-45994  
 troposphere, temp. profiles from ground-based angular microwave meas. 0-51551  
 turbulent boundary layer, nominally steady, two-dimens., vel. and temp. profile prediction method 0-1624  
 Uranus upper atmosphere, mean temp. and temp. vars. 0-46477  
 Venus, atmosphere thermal contrast from Pioneer probe data 0-46229  
 weldable butt joints, calc. of temp. field for nonideal thermal contact (Russian) 0-10121  
 World Ocean, waters heat and salt content 0-31054  
 X-ray sources, compact, temp. and ionisation struct. rel. to X-ray spectra form. 0-22115  
 Al plates with air gap, temp. field for microplasma welding of edge joints (Russian) 0-7755

**temperature distribution continued**

- Al-SiC fibre reinforced materials, therm. stresses in unit cell 0-10160  
 CO<sub>2</sub> gas flow impinging on heating surface, heat transfer radiation 0-43710  
 H plasma plane and cylindrical layer emission field calc. (Russian) 0-33755  
 Hf electron field emitter, temp. drop meas., allotropic transform. temp. 0-2931  
 Hg, turbulent flow on stabilising thermal section, temp. fields and heat transfer 0-19366  
 Si, p-n junction, ellipsometric method of temp. meas. rel. to secondary breakdown (Russian) 0-11074  
 Si temperature field determ. under laser irradiation (German) 0-25496  
 Ti-Al-V (6, 4 wt.%), temp. distrib. for steady axisymmetric extrusion 0-11670  
 Ti-Al-V (6, 4 wt.%), temp. distrib. for steady axisymmetric extrusion numerical results 0-11671

**temperature measurement**

- see also pyrometers; spectral methods of temperature measurement; temperature scales; thermocouples; thermometers  
 accuracy, additive and multiplicative meas. errors influence (German) 0-8985  
 acoustic noise in electric arcs, arc temp. meas. appl. (French) 0-28865  
 acoustic temp. indicator, consisting of temp. sensitive resistor and operational amplifiers (Spanish) 0-13061  
 cancerous mouse hyperthermia meas., microwave, IR and thermocouple methods (French) 0-3768  
 correlation at high press., belt apparatus temp. meas. (Chinese) 0-52200  
 cryotron temperature-to-time interval convertor (Russian) 0-222  
 deep tissue temp. monitoring by ultraminiature thermistors 0-3761  
 diffusion furnace temp. profile meas. systematic errors, theoretical model (German) 0-8989  
 diffusion furnaces, temp. profile meas., systematic errors (German) 0-37030  
 digital recorders, advantages over analogue instruments 0-210  
 digital thermometer, for 4 to 300K range 0-4709  
 diode sensor based on const. leakage current with negative temp. coeff. 10 V analogue output (German) 0-47052  
 Drifting Oceanographic Profile Buoy with minimum vertical motion 0-46306  
 EBR-II, comparison of XX08 steady-state temp. meas. with anal. predictions 0-579  
 electronic instruments developments (German) 0-8986  
 expendable bathythermograph digital recording and display system 0-46318  
 fever alarm device using telemetry 0-21556  
 frequency response of cold-wire thermometers used for atmospheric turbulence meas. in marine environment 0-56650  
 furnaces, temp. distrib. measurement using thermocouples and wire bridge cct. 0-31758  
 gas thermometry, constant volume valve design 0-4711  
 gases, dilute, temp. and thermophysical prep. meas., using acoustic resonators 0-53573  
 geothermal well logging, temp. meas. utilising melting props. of materials 0-56659  
 glass track detectors, thermometry appl. 0-37031  
 heat filters for bolometers cooled to very low temperatures 0-52315  
 high temperature, solid electrolytic cell, meas. at 700K and higher 0-31760  
 high temperature, using Mossbauer, noise and US thermometers 0-52202  
 high-pressure liquid MP determ. centrifuge cell 0-31783  
 high-pressure temperature meas. in liquid He region 0-31748  
 induction salt baths, automatic temp. control 0-27300  
 industrial, thermocouple and resistance thermometer 0-42221  
 instrument for temperature measurement using temperature-sensitive magnetic fluid 0-31745  
 internal combustion engine, measurement of pulsating temp. and vel. using US flowmeter 0-1704  
 internal contraction engine, highly loaded, exhaust gases temp. and velocity meas. using two thermometer method (German) 0-31754  
 ion implantation, target heating, temp. measurement 0-34032  
 IR detectors, temperature distribution in weld of thermoplastic foil (Polish) 0-22362  
 laser nozzle, chemical, temperature profiles meas. by thermal imaging system 0-14376  
 laser pulse heating, high speed pyrometry and spectroscopy, review of techniques 0-52225  
 liquefied natural gas, level, density and temperature measurement, prediction of roll-over 0-27269  
 liquid crystal improved technique for thermal field measurements 0-216  
 LMFBR coolant temp. meas. using high integrity coaxial thermocouples 0-32410  
 low temperature rise heating of a field emission tip 0-52371  
 low-temperature measurements between 0.5 and 30K 0-42225  
 low-temperature meter, digital, 4 to 300K, with Ge pickups 0-31747  
 measuring cycle improvement, correction of measurement path (Polish) 0-22318  
 medical appls., radiation balance microwave thermograph 0-26315  
 medical temperature measurement, electrical measurement techniques (Hungarian) 0-30910  
 melting point standards, secondary, for temp. range 2000-3000°C, chemical aspects of choice 0-52226  
 metal forming, instrument for temp. determ. in deformed space 0-17938  
 metals, working, method of applying fusion thermal indicators to surfaces, including heated surfaces 0-17937  
 microprocessor-controlled system for precise meas. of temp. changes 0-22361  
 microwave thermography, principle and biomedical appls. (French) 0-30957  
 molecular torsional oscils., NQR freq. temp. depend. electric field gradient asymmetry 0-18868  
 NQR methods (Russian) 0-223  
 NQR precision thermometry, freq. meas. improvement 0-22356  
 NQR spectrometers, optimisation (Russian) 0-22412  
 ocean surface layer remote sounding (Russian) 0-4138  
 ocean surface meteorological buoy and aircraft VHF link 0-46298  
 ocean temperature, by coral skeletal aragonite Sr/Ca ratio 0-12568  
 optoelectronic meas. methods appl., with twin diodes (German) 0-13064  
 p-n series-connected junctions method (Polish) 0-13075



**temperature measurement continued**

- particles in flight, temp. meas. by monochromatic photographic pyrometry (*French*) 0-27312
- perfusion blood temp. monitoring, zero-heat-flow transducer 0-8201
- platinum resistance thermometers, state of the art review (*Spanish*) 0-52212
- polyorganosiloxane fluids, temp. determ. in friction zone accompanying breakdown, using TV (*Russian*) 0-7688
- powders, in detonation deposition of coatings 0-11559
- power, nonconducting, in detonation deposition 0-226
- power plant cooling water, thermal IR scanner meas. technique 0-40947
- pressure-volume and acoustic virial coeffs. for  $^4\text{He}$ , temp. depend., quantum range 0-47056
- pyrometer photoelectric, using radiation invariant method, true temp. meas. of metals 0-52223
- radiation thermometry, applied precision, current status 0-52224
- radiometer, low-temperature, with conical light pipe, IC manufacture appl. 0-47105
- reference standard for use below 0.5K, SRM 768 0-27303
- resistance thermometry, review 0-52206
- review, techniques and instruments (*German*) 0-22358
- sea temperature gradient meas., anal. of two methods 0-31149
- semiconductor temperature testing probes, accuracy and thermal characts. 0-52201
- semiconductor thermometry at low and very low temperatures 0-4713
- semiconductors temperature dependences meas., of electric conductivity, Hall coeff. and magnetoresistance 0-31792
- sensors, determination of dynamic behaviour (*German*) 0-17940
- shear-band temp. meas., appl. to 4340 steel and 2014-T6 Al 0-48655
- shipboard meteorological data system 0-46299
- skin temperature measurements using a disc sensor, effect of press. 0-56259
- sliding surfaces with lubrication, stationary and non-stationary meas. (*German*) 0-23975
- Spar Buoy Oceanographic Telemetry System 0-46307
- state of art and research appl. 0-31743
- steel forgings, expt.-calc. model of quenching, temp. meas. across cross section 0-16345
- subcutaneous, on living samples, microwaves non-conventional appl. survey (*Italian*) 0-13093
- superconducting transition temperature, dipstick cryostat 0-37044
- superthermal electrons in laser-produced plasmas 0-1822
- surface temp. meas., temp. contact methods using thermistor and thermoindicators (*Russian*) 0-27295
- surface temperature meas. through radiance temp. and emissivity, algorithm for calc. 0-52209
- surfaces, sliding, lubricated (*German*) 0-14643
- temperature probe design, exptl. calibration results and numerical model predictions 0-56258
- thermocouple thermometry, accurate, review 0-52207
- thermocouples, temperature of oil in sliding friction bearings 0-31753
- thermodynamic temperature, meas. techniques and concept. 0-52204
- thermophysical properties, conf., Dubrovnik, Yugoslavia (June 1978) 0-51944
- thermophysical properties, temp. measurement methods at high temp. 0-52208
- thermophysical testing device, rate of change of temp. in time (*Russian*) 0-208
- thermosensitive film coating, dispersed liq. cryst. microdroplets in gelatin matrix, exam. of preps. 0-42220
- tissue, soft, temp. distrib. monitoring by temp. depend. of US vel. 0-45994
- transparent materials, laser irradiated, in-depth and surface temp. meas. by Moire-Schlieren technique 0-53392
- velocimeter for fluctuating temp. and vel. meas. in combustion field 0-14856
- water quality monitoring, modular system (*German*) 0-26186
- well temperature measurement, bottom-hole temperature stabilisation model 0-51356
- wire sensors, frequency response meas. by internal and acoustic heating 0-31123
- $\text{BaTiO}_3$ , semiconducting ceramic, AC thermopower measurement 0-44624
- Ga triple point temp. determ. 0-42223
- GaAs diode temperature sensors, characts. obs. at 4.2 to 393K 0-47054
- $^4\text{He}$ , liquid, thermodynamic temp. meas. by noise thermometry at various vapour pressures 0-27298
- Hg-in-glass thermostat 0-22359
- $\text{N}_2$   $\alpha$ - $\beta$  transition, applicability as thermometric fixed point 0-13076
- $\text{O}_2$ , triple point, determination at low temp. (*Japanese*) 0-31749
- Pt resistance elements 0-27296
- Pt resistance temperature probes, constructional types and state of technique (*German*) 0-52213
- Pt resistance thermometers, linearisation technique (*German*) 0-42224
- Si diodes as low temperature sensors (*German*) 0-31744
- Si, p-n junction, ellipsometric method of temp. meas. rel. to secondary breakdown (*Russian*) 0-11074
- Si p-n junction local temp. meas. using pulsed SEM, induced-current mode 0-54775
- Si substrates during sputtering and sputter etching, thermal history of substrates 0-25562
- Xe discharge lamps, large, electrode temp. meas. by photographic method (*Russian*) 0-47057

**temperature scales**

- 0.5K to 30K, 1976 provisional scale 0-13034
- 0.5K to 30K, 1976 provisional scale derivation and development 0-13033
- Celsius, Kelvin, Fahrenheit and Rankine, definitions and comparisons (*German*) 0-36972
- cryogenic, 0.015 to 0.21K, based on superconducting phase transitions 0-17948
- gas thermometry, constant-volume, 2.6K to 27.1K (NPL-75) 0-13035
- high-temperature meas. and calibration, above 1000°C, based on Au melting point (*Rumanian*) 0-47061
- International Practical Temperature Scale of 1968, future development 0-52205
- IPTS, suitability of W strip lamps as secondary standard sources below 1064 degrees C 0-27297
- NQR methods of establishment (*Russian*) 0-223
- primary thermometry, 2.5-27K, isotherm smoothing,  $^4\text{He}$  0-47056
- thermodynamic temperature, meas. techniques and concept. 0-52204

**temperature scales continued**

- thermophysical properties, conf., Dubrovnik, Yugoslavia (June 1978) 0-51944
- Ga triple point temp. determ. 0-42223
- $\text{H}_2$  triple, boiling and 17K equilib. points realization, cryostat and method 0-27314
- Pd melting point, effect of surrounding  $\text{O}_2$  0-27299
- tempering**
- butadiene nitrile, soot filled, thermal treatment influence on mech. props. (*German*) 0-30000
- glass, chem. tempered, surface stress meas. using opt. waveguide effect (*Japanese*) 0-45473
- glass, thermally tempered sheet and plate, surface stress meas. using optical waveguide effect 0-25967
- isoprene rubber elastomers, thermal treatment influence on mech. props. (*German*) 0-30000
- martensite, microstresses associated with tempering 0-3111
- steel, OKh12G14N4Yu2, struct. after deformation under conditions of superplasticity 0-21031
- steel, alloy, austenitic, grain size, tempering effect on brittle fracture susceptibility 0-55534
- steel, alloy, W-Mo-Cr-V, blanks welded to steel 45, optimal high temp. tempering 0-16351
- steel, alloy low, Ni-Cr, tempered martensite embrittlement 0-7669
- steel, alloy type 25KhN3MFA, tempering of bainitic structure 0-20983
- steel, austenitic, tempering cavity condensation (*French*) 0-55442
- steel, C, austempered, exam. of running in and wear 0-16485
- steel, C, martensitic, tempering induced decomposition and segregation, atom probe study 0-3112
- steel, C type 45, martensitic needle size, effect on mech. props. after induction hardening 0-11672
- steel, Co-Cr-Ni-Mo-Mn (39.65, 20.25, 15.33, 7.08, 1.9 wt.%) carbide formation during tempering after plastic deformation 0-16330
- steel, Cr, corrosion resist., tempering after air-hardening in rolling heat (*German*) 0-45324
- steel, Cr-Mo (2.25, 1 wt.%), strain hardening shakedown load during bending 0-20958
- steel, Cr-Mo-V, excessive temp. effect on creep behaviour, structure and hardness (*German*) 0-30054
- steel, Cr-Mo-V, heat treated, mech. props. (*German*) 0-25724
- steel, Cr-Ni, effect of tempering under load on mech. props. 0-16354
- steel, Cr-W-V-Mo (3.9 to 4.5, 1.5 to 2, 0.9 to 1.2, 3.9 to 4.4 wt.%), heat resistant, type 8Kh4M4V2F1-Sh, mech. props. 0-16464
- steel, heat treated high strength, X-ray diffr. anal. of residual stress 0-3200
- steel, high purity, low S content, for tough semi-finished products in nuclear power plant (*German*) 0-45393
- steel, high speed, type R6MSK5, secondary and red hardness of marquenching 0-16350
- steel, high-alloy die, electrothermal treatment 0-29996
- steel, HSLA, V effect on mech. props. (*Korean*) 0-29987
- steel, low alloy, brittle fracture, quenched and tempered 0-11677
- steel, low alloy structural, type 30KhGSA, effect of thermomech. treatment on strength, fracture toughness and fatigue props. 0-11676
- steel, low alloy type 14Kh2GMR, high strength, welded joint, impact toughness, welding thermal cycle and tempering effects 0-3157
- steel, low C, effect of heat treatment on resistance to fatigue crack propagation. 0-11675
- steel, martensitic, age hardening with Cu, Nb additions, exam. of hardness 0-7681
- steel, martensitic, fatigue crack propag., effect of intercrystalline fracture associated with temper brittleness (*French*) 0-16463
- steel, medium C 0-11752
- steel, Mn-Cr-V, tool, quenched and tempered, fracture toughness (*German*) 0-25726
- steel, Mn-Mo-Ni-Cr, bainitic, microstruct. and mech. props. (*French*) 0-16362
- steel, Mo-Cr (3 wt.%), CrC formation in isochronal tempering, electron microscope study 0-7584
- steel, Ni(9 wt.%), isothermal bainitic transform., thermomechanical effects on mech. props. (*German*) 0-40383
- steel, Ni (3.5 wt.%), heavy rotor forgings, temper embrittlement, metallurgical investigations (*German*) 0-16471
- steel, Ni and W, recrystallisation mech. during laser treatment 0-50658
- steel, Ni-Cr, cast, tempering embrittlement due to impurities, Auger spectroscopy exam. 0-11683
- steel, Ni-Cr, P doped, tempered martensite embrittlement 0-30089
- steel, Ni-Cr low alloy, effect of Mo on tempered martensite embrittlement 0-3187
- steel, Ni-Cr-Mo, quenched and tempered, notched bar tensile tests (*German*) 0-35247
- steel, pressure tank, heat-treatment effects and mech. props. (*German*) 0-40409
- steel, reinforcing bar, high-strength 20GS2 and 20KhGS2, corrosion cracking 0-55578
- steel, Si-Cr-Mo-W-V (2.4, 1.3, 2 wt.%), heat treatment and props. 0-16349
- steel, stainless ferritic, drawability, mech. props., and grain boundaries in 08Kh16AMT and 08Kh18T1 0-35270
- steel, structural, addition of solid  $\text{SiO}_2$ , effect on ductile fracture 0-16465
- steel, temper embrittled, grain boundary failure model for intergranular fracture modes 0-25825
- steel, tempering effect on struct. and mech. props. of types 70, U8, and U12 (*Russian*) 0-50655
- steel, tool, W-Mo, heat treatment effect on props. 0-50656
- steel, TRIP, warm extrusion, process control and tensile props. 0-16338
- steel, type 28Kh3SNMVFA, strain hardened martensite, resist. to tempering, exam. 0-16348
- steel, type 52100, heat treatment effect on microstruct. and mech. props. 0-29993
- steel, ultra high strength, historical 0-7609
- steel, ultrahigh strength, monotonic and cyclic stress strain curves 0-35268
- steel, W-Cr (3 wt.%), CrC formation in isochronal tempering, electron microscope study 0-7584
- steel, W-Mo, tool, hydrostatic extrusion and tempering, wear resistance effect 0-50728
- steel 30KhGSNA, low alloy, quenched, grain refinement influence on impact strength (*Russian*) 0-20974
- steel tubes, square section, collapse in bending 0-25792



**tempering continued**

- steels, C, quenched and tempered, struct.-prop. relationships 0-7599  
 steels, high-purity and commercially based, containing 10 wt.%W or 5 wt.%Mo, tempering behaviour 0-7600  
 steels, secondary hardened, microstruct. rel. to mech. props. 0-25851  
 surface stress meas. by optical waveguide effect 0-43681  
 Al-Mg-Zn alloys, liq./solid phase equilibria determ. (German) 0-50601  
 Cu-Al (21 at.%) transition state (French) 0-55392  
 Fe-C (1.2 wt.%), Mossbauer study of early stages of tempering 0-16342  
 Fe-Cu alloys, transform. substruct., lath microstructure after quenching 0-16298  
 Fe-Mn (2 to 8 wt.%) alloys, phase transformations, tempering influence (Russian) 0-25735  
 Fe-Ni austenitic, effect of Al and Ti on relaxation resist. 0-20993  
 Fe-Ni-Cr, Elinvar, struct. and mag. props., singularities during tempering (Russian) 0-50627  
 Fe-Ni-P, segregation kinetics, theory, and temper brittleness 0-11649  
 Sm( $\text{Co}_{0.83}\text{Cu}_{0.16}$ )<sub>6.9</sub>, microstruct. and domain struct., mag. reversal (Russian) 0-20429

**tenacity** *see* **tensile strength****tensile strength**

- see also fracture; yield strength*  
 acrylic, denture base, tensile testing 0-16621  
 Al-alloys, influence of strain path on mech. props., orthogonal tensile paths 0-30035  
 alloys for fission reactor components, mech. props. at high temp., failure prediction 0-5241  
 aramid/epoxy composite, tensile test 0-11778  
 bone, mechanical properties rel. to density and mineral phase orientation and particle size 0-16989  
 bone/porous polyethylene interface, tensile strength 0-30737  
 $\alpha$ -brass, Portevin-LeChatelier effect (Japanese) 0-11724  
 $\alpha$ - $\beta$  brass, two phase bicrystal, deform. and fracture at 450K 0-16409  
 $\alpha$ - $\beta$ -brass, two phase bicryst., deform. and fracture at 150K 0-16388  
 butt joint, tensile bond strength, effect of aspect ratio 0-50823  
 carotid arteries, human, strength props., changes with age 0-16993  
 cellulose acetate films, light scatt., tensile creep, desalination 0-16050  
 cellulose film, moisture effect on phys. and mech. props. 0-40450  
 ceramic, tensile strengths, uniaxial and equibiaxial in bending statistical comparison 0-25775  
 circular ring, inner boundary shapes, optimised, diametral compression 0-38369  
 concrete, prestressed, low-temp. tensile strength and linear expansion coeff. of reinforcing steel 0-30051  
 diffusion welded joints, creep deformation effect on characts. 0-25806  
 elastic springback in beams and plates, bending 0-38256  
 EM tensile adhesion test method 0-50804  
 epoxy impregnated superconducting composites, mech. props., strain effect at 4K 0-25822  
 epoxy laminate, glass-fibre reinforced, with circular holes, tensile fracture 0-25789  
 epoxy resin, powder filled, exam. of mech. props., thermal contraction 0-25821  
 epoxy resin EHD-10, temp.-time rel. of strength 0-25798  
 epoxy resin systems, synthesis review, phys. and mech. props. at low temps. 0-25650  
 epoxy resins, correlation between valence energies and low temp. flexibility 0-25815  
 ferrite-pearlitic grey Fe, tensile testing of mechanical props., from room temp. to liquidus (Japanese) 0-7728  
 ferritic grey Fe, tensile testing of mechanical props., from room temps. to liquidus (Japanese) 0-7728  
 fibre composites impetus of composite mechanics on test methods 0-11868  
 fibre reinforced composites, transverse strength rel. to fracture mech., stress interactions 0-16421  
 fibre reinforced composites, unidirectional, tensile testing 0-40664  
 fibre reinforced nonlinearly elastic matrix, unidirectionally reinforced, deform., strength, and failure 0-3134  
 fibrous composite materials, brittle interlayers influence on tensile strength (Russian) 0-21006  
 fission reactor irradiated cladding, in-cell facility for mechanical testing 0-21244  
 fluorocarbon foil, Ftoroplast, homogeneity study (Polish) 0-35278  
 glass fibre, tensile strength meas. using chain-loading fibre tensometer (Japanese) 0-55610  
 glass fibre for optical communications, statistics of tensile strength (German) 0-38121  
 glass fibre reinforced epoxy, wound, strength in twisting, stretching and transverse bending 0-11622  
 glass fibre reinforced plastics, cyclic strength in complex stressed state 0-3181  
 glass fibre reinforced plastics, laminated ring with extra steel pin radial reinforcement, mech. props. 0-11714  
 glass fibre reinforced polyester, compressive fatigue tests at cryogenic temps. 0-25870  
 glass/epoxy composite, tensile test 0-11778  
 graphite, ATJS, oxidation effects up to 2500K 0-3209  
 graphite, diametral compressive testing method 0-35495  
 graphite fibre/epoxy laminates, free edge induced failure 0-11775  
 PAN graphite-Al composites, fracture characteristics and props. 0-11779  
 hard metal, bend test-piece geometry appl. to tensile strength meas. 0-30184  
 Hastelloy C-4, loaded at high temp., useful life 0-40523  
 hydraulic bulge test, use in biaxial tensile testing 0-1493  
 hydrogel of high water content as a material for the soft contact lens (Japanese) 0-12300  
 iliac arteries, human, strength props., changes with age 0-16993  
 izod polystyrene, influence of dimensions in mech. props. (German) 0-21039  
 Kapron fibres, elongation and tensile strength rel. to UV irradiation 0-25796  
 marble, diametral compressive testing method 0-35495  
 metacarpi, equine, fracture toughness 0-3694  
 metal mechanical property effects on frictional behaviour 0-55548  
 metals, deformation resistance, rel. between uniaxial stress state and breaking stresses in shear 0-3147  
 metals, in-situ deform., 200 kV STEM study 0-47155  
 Ni alloy KhN45Yu, tensile strengths, dispersity of struct. effect 0-55486
- tensile strength continued**  
 Nylons, morphology and crack propag. in inorganic salts 0-30118  
 optical fibre, mech. deform. meas. by light scatt. method 0-14452  
 optical fibre strength distribution description using upper and lower limits 0-53470  
 optical fibres, preparation conditions influence 0-33205  
 PAN fibres, neutron irradiated, struct. and props. (Russian) 0-25763  
 pentaplast, plasticised, thermal treatment effect on props. 0-40324  
 Permandur 49, ordered and disordered, clean mild wear 0-16508  
 PET, effect of liquid aliphatic compounds on mech. props. 0-55488  
 photoelastic load meas. and testing (German) 0-19297  
 plant fibres, fracture mechanism 0-35931  
 plastics, tensile and flexural testing device, incorporating an impactor (German) 0-3276  
 plastometer, electronically controlled, for tensile and compression tests (German) 0-3273  
 polyamide-polyoxirane copolymers, mechanical properties evaluated 0-11700  
 polyester-polyurethane semi-interpenetrating networks, mech. props., morphology 0-45362  
 polyethylene: (Dy<sub>2</sub>O<sub>3</sub>), mech. props. and transfer to steel surfaces 0-16496  
 polyethylene, correlation between valence energies and low temp. flexibility 0-25815  
 polyethylene, deformation, Hartree-Fock SCF calcs. 0-18949  
 polyethylene, filled, mech. props., cyclic heating effect 0-55526  
 polyethylene, high density, influence of dimensions in mech. props. (German) 0-21039  
 polyethylene, ultra-high-strength filaments, soln. spun/drawn, mech. and thermal props. 0-40440  
 polyethylene fibres, high density, ultra oriented, physical, mech. props. 0-25649  
 polyethylene filaments, ultrahigh-strength, from soln. spinning and hot drawing 0-45268  
 polyimide fibre reinforced polyamide-12 0-11754  
 polyisocyanurate foams, strength, cellular struct. effect 0-40518  
 polymer, filled, tensile strength calc., rel. to fracture (German) 0-25795  
 polymer, semicryst., and filled, elastic modulus, strength, rel. to crystallite shape 0-45335  
 polypropylene powder, cold compaction, product strength, heat treatment effects 0-11621  
 polystyrene, cryogenic foam insulators, low temp. props. 0-25818  
 polystyrene, props. changes upon photooxidation 0-30123  
 polytrifluoroethylene, dielectric relax. processes above and below glass trans. (Japanese) 0-55028  
 polyurethane, cryogenic foam insulators, low temp. props. 0-25818  
 polyurethane foams, strength, cellular struct. effect 0-40518  
 polyvinylidene chloride co-polymer powder, cold compaction, product strength, heat treatment effects 0-11621  
 porcelain, elec., comparative assessment of methods of determ. strength 0-40429  
 porous materials, pore geometry effects on tensile strength 0-30048  
 porous sintered materials, mech. testing device for hydrostatic pressure conditions 0-40645  
 powder, tensile and compressive strength meas. (Japanese) 0-25780  
 prealloyed powder blending, composite materials fatigue and tensile props. (French) 0-20850  
 PVC powder, cold compaction, product strength, heat treatment effects 0-11621  
 rock, mech. props. rel. to cooling (Japanese) 0-31036  
 SAP 895 (Al-Al<sub>2</sub>O<sub>3</sub>) alloy containing <sup>4</sup>He and <sup>3</sup>H, tensile props. 0-34129  
 sheet moulding compound, laminate, charge pattern influence on tensile strength (Japanese) 0-55513  
 shell buckling rigidity characts. (German) 0-48608  
 silk, natural, elongation and tensile strength rel. to UV irradiation 0-25796  
 silk, spider, tensile, fracture strength, elongation and ageing effects 0-41072  
 steel, 0.2 to 0.8% C, ferrite-pearlite transformation, tensile strength, cooling rate effect 0-7549  
 steel, 15NiCrMo 106, struct. changes, through simulated multiple layer welding, micro-tensile and shearing tests (German) 0-35215  
 steel, alloy, low, dual phase, high strength, exam. of energy absorption by structural collapse 0-7640  
 steel, austenitic stainless, type 316, hydrogen embrittlement, tensile testing 0-7671  
 steel, austenitic stainless, types 304, 316, tensile props., effect of exposure to Li and LiH 0-35219  
 steel, austenitic stainless Kh18N10T, strength properties, dispersity of struct. effect 0-55486  
 steel, brass clad plate/roll bonded Ni clad, fatigue crack growth behaviour 0-40484  
 steel, C1020, dual phase, mech. behaviours and structs. (Korean) 0-25779  
 steel, C, thermomechanically treated, in situ composite material description 0-7649  
 steel, cast, 80 kg/mm<sup>2</sup>, heat treatment 0-16358  
 steel, cast structural, heat treatment and mech. working influence on mech. props. (Russian) 0-40392  
 steel, continuously cast, tensile strength and ductility above 800°C 0-55476  
 steel, Cr, corrosion resist., tempering after air-hardening in rolling heat (German) 0-45324  
 steel, Cr-Mo, toughness of heat treated steels of equal tensile strength (German) 0-25727  
 steel, Cr-Mo-Ni-Nb, Nb effect on mech. props. (German) 0-30012  
 steel, Cr-Ni-Ti-B, grain size effect on mech. and struct. props. (French) 0-45361  
 steel, Cu-Zn, brass clad, fatigue crack growth behaviour 0-40484  
 steel, duplex ferrite-martensite, microstructure resistance optimisation 0-40482  
 steel, eutectoid, anisothermal strain with phase transform., effect on tensile strength (Russian) 0-40431  
 steel, ferritic/austenitic high Cr, development, mech. props. and corrosion resist. 0-45422  
 steel, for pressure tanks, yield point influence on brittle fracture, tensile strength (German) 0-40539  
 steel, high speed type M-50 and 18-4-1, fracture and fatigue 0-16457  
 steel, HSLA, V effect on mech. props. (Korean) 0-29987  
 steel, low-alloy, props. with nitride and Cu hardening at low temps. (Russian) 0-40372



**tensile strength continued**

- steel, low-C, fully pearlitic, struct. and mech. characts. rel. to cooling conditions (*French*) 0-40425
- steel, martensitic low C, development and props. (*Russian*) 0-20933
- steel, martensitic stainless, type 05Kh13N4m, strength and embrittlement, early stages of martensite decomp. effect 0-35227
- steel, medium C, Nb addition, effect on transformation and strength 0-7607
- steel, mild, AC effect on fatigue and static props. 0-45372
- steel, mild, subject to three point bending and tensile load, acoustic emission 0-3154
- steel, Mn, acicular ferrite high-strength low-alloy, low temp. mech. props., pipe-line appl. 0-55472
- steel, Mn-Cr-Mo, Mn-V-Mo, high-strength heat-treatable sintered 0-50575
- steel, Ni-Cr-Mo, quenched and tempered, notched bar tensile tests (*German*) 0-35247
- steel, nonmetallic inclusion, effect on hot ductility 0-29999
- steel, nonmetallic inclusions effect on ductility 0-30042
- steel, sheet, rapid test for props. assessment 0-40650
- steel, stainless, austenitic, type 316, high velocity tensile test at elevated temp. 0-35194
- steel, stainless, epoxide butt joints, effect of abraded and Ar ion bombarded surfaces on ultimate tensile strength 0-16638
- steel, stainless, neutron irradiation effect on low cycle fatigue and tensile props. at 298K 0-30059
- steel, stainless, tensile props. of GCFR ribbed claddings at 650°C 0-45364
- steel, stainless type 304 L, mech. behaviour under constant stress associated with cyclic strain 0-25767
- steel, tempered, high strength, internal stresses and mech. props. 0-3200
- steel, TRIP, warm extrusion, process control and tensile props. 0-16338
- steel, type 28Kh3SNMVFA, strain hardened martensite, resist. to tempering, exam. 0-16348
- steel, type 52100, heat treatment effect on microstruct. and mech. props. 0-29993
- steel alloy, type 30 KhGSA, expt. functions of resist. in tension and torsion 0-16397
- steel fibre reinforced Al, fibre orientation effect on strength (*Korean*) 0-30027
- steel fibre reinforced concrete, tensile strength and ultimate strain (*Polish*) 0-21027
- steel intercrystalline stress corrosion cracking in a  $\text{Ca}(\text{NO}_3)_2$  soln. (*German*) 0-30130
- steel tubes, square section, collapse in bending 0-25792
- steel wire, drawn, age hardening props. obs., mechanical and electrical props. relationship 0-50662
- steel/Cu bimetallic pipe, determ. of yield, tensile strength 0-25771
- superplastic materials, flow and failure, review 0-50690
- toluene sulphonate diacetylene polymer, vibr. modes, strain depend. using Raman spectra 0-20626
- viscoelastic non-Newtonian liquids, resist. to tensile stress 0-1505
- water, free surface, metastable effects associated with press. pulse refl. 0-6463
- yarns, multi-filament, twisted, modified Platt's equation (*Japanese*) 0-5985
- Zircaloy-2, effect of simulated fission products on elongation fractography and metallography 0-649
- Zircaloy-2, effects of simulated fission products on mechanical props. 0-52740
- Al alloy, 51S, modified by misch metal, for space appl. 0-55466
- Al alloy 6061-T6, yielding of tubing under dynamic biaxial loading 0-16377
- Al, Bauschinger effect, temp. influence, combined tension-torsion testing machine 0-45453
- Al, deformed in tension, elec. cond. changes at 78 and 283K, grain boundary effect (*Japanese*) 0-30029
- Al, electroplastic effect 0-7647
- Al foil, alloying additions (Si, Mg, Y, Se, Sc) effect, on tensile strength, weldability 0-55475
- Al single crystals, liq. metal embrittlement by Ga, tensile tests 0-7675
- Al-Al<sub>3</sub>Ni directionally solidified eutectic alloy, struct. and mech. props. (*Korean*) 0-29944
- Al-alloys, biaxial prestrain influence on tensile props. 0-30036
- Al-C, dispersion hardened, effect of processing parameters on mech. props. 0-20826
- Al-Cu, single and two phase, superplastic behaviour 0-11709
- Al-CuAl<sub>3</sub>, directionally solidified eutectic, structural changes during strength tests (*Russian*) 0-7543
- Al-Fe<sub>78</sub>Mo<sub>20</sub>B<sub>20</sub> wire composite, mech. props. 0-40441
- Al-Ni-Co(Si), directionally solidified eutectic, morphological and mech. props. (*Russian*) 0-30057
- Al-rare earth alloys, granules, rolling to form foil, exam. 0-20825
- Al-Zn-Mg plasma sputtered, mech. props. rel. to heat treatment (*Russian*) 0-40387
- Al-Zn-Mg-Cu, age hardened, effect of strain rate, temp. and environment on ductility 0-45368
- B fibre reinforced Al, impact behaviour under fatigue 0-7661
- B fibre reinforced Al, tensile strength and brittle fracture 0-11707
- B fibre reinforced Al composite, strength of fibre-matrix interface and tensile strength (*Russian*) 0-21005
- B fibre reinforced Al-Mg, heat treatment effect on struct., tensile strength 0-55487
- B fibres, surface morphologies rel. to mech. props. 0-11749
- B thin wires, fatigue limit and tensile strength 0-25834
- Be-bronze BrB2, struct. and phase transform. during mechano-thermal treatment (*Russian*) 0-11667
- C fibre reinforced epoxy, wound, strength in twisting, stretching and transverse bending 0-11622
- C fibres, durability, elastic props. and struct., heat treatment temp. effect, US meas. methods 0-40446
- C fibres and C fibre reinforced epoxy phenol, oxidation, effect on props. 0-40574
- C, vitreous, oxidation effects up to 2500K 0-3209
- C-fibre reinforced epoxy resin, laminated structs. mech. props. 0-50672
- CU-Zr-(Cr), powder metallurgical alloys, thermomech. treatment effect on props. 0-50660
- Cu, crystalline FCC, theoretical tensile strength, three separate first-principles calcs. 0-50683
- Cu, diffusion welding, tensile fracture strength (*Japanese*) 0-7663
- Cu, on thermally oxidised Si, EM tensile adhesion test method 0-50804

**tensile strength continued**

- Cu-Al-Fe, mech. props. rel. to heat treatment 0-50682
- Cu-BeCo (1.85, 0.29 wt.%), type CA172 (TH04), strengthened by spinodal decomp., stress relax. in bending 0-7616
- Cu-Fe<sub>78</sub>Mo<sub>20</sub>B<sub>20</sub> wire composite, mech. props. 0-40441
- Cu-Nb-Sn, multifilamentary supercond. composite wires, fabrication on laboratory scale and mech. props. 0-29897
- Cu-Ni-Sn (4-15, 4-8 wt.%), strip strengthened by spinodal decomp., stress relax. in bending 0-7616
- Cu-Ni-Sn spinodal substitute for Be-Cu alloy 0-35217
- Cu<sub>46</sub>Zr<sub>54</sub>, devitrification effect on mech. props. 0-30082
- Cu<sub>56</sub>Zr<sub>44</sub> metallic glass, devitrification and its effect on mech. props. 0-33893
- (Fe,Ni,Co)<sub>3</sub>V, long-range ordered alloy for fusion reactor appl. 0-32481
- Fe atomised powder, sintering effect on recrystn., mech. props. 0-40292
- Fe, cast, grey, tensile strength, surface area to volume ratio effect (*Japanese*) 0-45389
- Fe, cast, thermal treatment influence on mechanical props. (*German*) 0-29980
- Fe, grey cast, tensile testing of mechanical props., from room temp. to liquidus (*Japanese*) 0-7728
- Fe, sintered, strength and elongation, rel. to density 0-30047
- Fe, sintered and pressed, props., effect of atomised Fe powder particle size distrib. 0-11601
- Fe/zinc stearate, compacts, admixing, effect on mech. props. 0-45402
- Fe-C-Mn (0.5, 0.6 wt.%), powder forged, mech. props. 0-21096
- Fe-C(0.001 to 0.44 wt.%), C effect on low temp. brittleness (*Japanese*) 0-50711
- Fe-Cr-Al-Ti-Y<sub>2</sub>O<sub>3</sub> (20, 4.5, 0.5, 0.5) type MA956, strain rate effect on fracture behaviour at 1366K 0-16458
- Fe-Cu, precipitation hardening of  $\alpha$ -Fe containing weak and strong particles 0-20946
- Fe-Ni-C (31, 0.1 wt.%), pre-deformation and temp. effect on transformation-deformation behaviour 0-3127
- Fe-Ti, precipitation hardening of  $\alpha$ -Fe containing weak and strong particles 0-20946
- Mg-Al single crystal growth, specimen for tensile testing in corrosive medium (*Russian*) 0-20774
- Mg-Ce, workability, aging characts. and tensile strength 0-55416
- Mg-La, workability, aging characts. and tensile strength 0-55416
- Mg-Sm, phase diagram and mech. props. (*Russian*) 0-20892
- Mo, neutron irradiated, radiation softening and hardening 0-34083
- Mo-Ti-Zr (0.5, 0.7 wt.%) alloy TZM, props. and appl. (*German*) 0-21040
- NaCl whiskers, plastification in elec. field (*Russian*) 0-21010
- Ni powders, stereological appl. in study of compacting process, elec. and mech. props. (*French*) 0-40286
- Ni-Cr-Mn-Fe-Nb (20,3,3,2.5 wt.%), short-range order effects on tensile behaviour 0-25793
- Ni-Cr-W (20, 10 to 40 wt.%), phase composition, struct. and props. 0-21034
- Ni-Cr-W-Mo-Al-Ti (15,6,3,2,2, wt.%), wrought, Si effect on transition brittleness (*Chinese*) 0-55491
- Ni-Fe-Cr base superalloy, addition effect on mech. props. (*Chinese*) 0-20998
- Ni<sub>3</sub>Al-B, L1<sub>2</sub> type intermetallic cpd. room temp. ductility improvement by B addition (*Japanese*) 0-35263
- Pt-Rh-W (30, 8 wt.%), intergranular embrittlement by Se vapour 0-3185
- SiC continuous fibres, mech. props. depend. on testing conditions (*Russian*) 0-35297
- SiC fibre reinforced Al-Mg, heat treatment effect on struct., tensile strength 0-55487
- SiC, tensile strength distrib. 0-40471
- Si<sub>3</sub>N<sub>4</sub>, tensile strength distrib. 0-40471
- Si<sub>3</sub>N<sub>4</sub>-MgO (2-5 wt.%) hot pressed, tensile creep testing 0-40423
- Si<sub>3</sub>N<sub>4</sub>-SiC-Y<sub>2</sub>O<sub>3</sub> (La<sub>2</sub>O<sub>3</sub>)(Ce<sub>2</sub>O<sub>3</sub>)(Eu<sub>2</sub>O<sub>3</sub>)(Gd<sub>2</sub>O<sub>3</sub>), reactively sintered, microstruct. and strength 0-25631
- SiO<sub>2</sub>B<sub>2</sub>O<sub>3</sub>-K<sub>2</sub>O-Al<sub>2</sub>O<sub>3</sub>-As<sub>2</sub>O<sub>3</sub> glass fibres containing metallic granules, tensile strength, Young's modulus, DC conductivity 0-30023
- Sn plate, rapid test for props. assessment 0-40650
- steel, C, castability, in metal mould, mechanical props. (*Japanese*) 0-25681
- Ti alloys, data handbook of low temp. mech. and phys. props. 0-22153
- $\alpha$ - $\beta$ Ti alloys, high strength, heat-treated weldments, intergranular fracture 0-21097
- Ti, high purity, data handbook of low temp. mech. and phys. props. 0-22153
- Ti, IMI-125, strain rate effect on mech. behaviour 0-3153
- Ti, type 70A, containing 0-6000 ppm <sup>3</sup>He, sensitivity of tensile props. 0-39197
- Ti-Al (4 wt.%), sintered, long-time strength 0-40529
- Ti-Al-Mo alloy VT-14, spherical pressure vessel, correlation between fracture stresses and mech. laboratory characts. 0-25838
- Ti-Al-V, containing 0-6000 ppm <sup>3</sup>He, sensitivity of tensile props. 0-39197
- Ti-Al-V (6.4 wt.%),  $\alpha/\beta$  interface phase influence on tensile props. 0-30034
- Ti-Al-V (6.4 wt.%), strongly textured, influence of crystallographic orientation on tensile behaviour 0-7633
- Ti-Al-V (6.4 wt.%), to H effect on fracture props. and microstruct. 0-40512
- Ti-Pd (0.15 wt.%), IMI-260, strain rate effect on mech. behaviour 0-3153
- $\alpha$ -Ti-Zr-W, effect of W impurity on mech. props. 0-16392
- W, sintered, brittle fracture, statistical anal. 0-11744
- W wire from rolled rods, mech. props. and struct. 0-25743
- W, with different microstructs., temp. depend. of yield strength 0-16404
- W-Ni-Fe (5(2), 5(2) wt.%) pore formation, effect on mech. props. 0-45396
- W-Re, thin wires, fatigue limit and tensile strength 0-25834
- YH<sub>1.92</sub>, tensile strength and creep 0-55459
- Zn-Al (10,22,50wt.%), low temp. mech. props. plastic deformation, glissile dislocation nucleation (*Russian*) 0-11695
- Zn-Al-Cu (18, 4 wt.%), plastic deform. at room temp., superplastic props., tensile strength (*Czech*) 0-45360
- Zr-Al (8.0 wt.%), tensile props. and fracture toughness after fast neutron irradiation 0-3198
- Zr-H, tensile strength and creep 0-55459
- Zr<sub>3</sub>Al, neutron irradi. effect on tensile props. 0-3156
- Zr<sub>3</sub>Al, tensile props., surface preparation depend. 0-3155



tensimeters *see* vapour pressure measurement

## tensors

- almost contact manifold, generalised S-curvature like tensor field 0-36909
- anisotropic media, piezomagnetolectric effects 0-25174
- bi-recurrent Finsler space, basic props. 0-12958
- Clifford algebra and Dirac matrices in a tensor formulation (*Russian*) 0-12966
- complex electron configurations, quasispin method, mixing configurations 0-42953
- differential geometry of deformed crystals 0-19867
- divergence free tensor densities in 3-space 0-103
- EM field energy-momentum tensor in phenomenological electrodynamics (*Czech*) 0-27146
- energy momentum tensor, nominal source of the Kruskal metric 0-12956
- energy-momentum tensor vac. expectation values, depend. on manifold geom. and topology 0-355
- Feynman diagrams, dimensionally regularised, symbolic evaluation, quantum gravity application 0-13259
- fractional-parentage coefficients, reduced in quasi-spin space, submatrix elements of tensor operators 0-4578
- geodesic corrections to stochastic parallel displacement of tensors 0-8920
- left Cauchy-Green tensor history, viscoelastic fluid theories 0-4534
- ligand fields calcs., strong and intermediate field theories, tensor algebra 0-42922
- liquid-solid phase transition, dynamic Ginzburg-Landau theory 0-44292
- many-electron atom, tensorial props. of operators in quasi-spin space 0-42925
- molecular energy level clustering, qualitative theory of irreducible tensor operators spectra 0-28001
- molecular rotationally inelastic collisions, tensorial factorisation 0-28096
- non-linear model, constitutive equation testing with free. vol. relax. spectrum 0-6011
- plasticity problem soln. by symbolic computer processing of formulae 0-17803
- quartz resonator, large mag. field effect on rate of time 0-27195
- s-recurrent Finsler space, tensor field props. 0-12959
- spin system, ABC type, matrix elements of tensor operators calc., transition probability matrix 0-25182
- stress energy tensor symmetries, Einstein's equations, nonuniqueness of solutions 0-12953
- SU(5), Clebsch-Gordan series, quark model appl. 0-47256
- Warm nonuniform plasma, stress tensor for high freq. wave propag. 0-33764
- Weyl tensor in gravitational field, vector fields and ideal reference frames 0-36918

## terbium

- see also nuclei with .....*
- critical magnetic studies 0-15745
- doped La-Al(Ag)(Sn)(Pb) superconductors, cryst. field transitions line-widths 0-24854
- elastic constants, magnetoelastic contrib. 0-15777
- ferromagnet, field depend. of elastic const.  $c_{66}$  0-15181
- ferromagnetic, mag. dipole and elec. quadrupole hyperfine fields, NMR obs. 0-34791
- film, thermorefectance dispersion curves at 315K and 97K 0-7332
- lattice dynamics, phonon freqs., calc. 0-15206
- liquid, mag. susceptibility, elec. resistivity 0-20377
- magnetic phase diagram, US meas. of elastic const. 0-15721
- magnetocaloric effect in high magnetic fields 0-25140
- magnon lifetimes at 4.2K 0-15710
- microcontact magnon spectra, electron-magnon interaction (*Russian*) 0-54768
- point defect production during electron irradi. at low temp. 0-49273
- CaF<sub>2</sub>:Tb, spectra of radn.-induced defect form. 0-2801
- CaO:Tb, phosphor, isothermal decay 0-55156
- CaS:Tb, Eu phosphors, fluoresc. spectra under X-ray excitation 0-16083
- Gd<sub>2</sub>O<sub>3</sub>:B<sup>3+</sup>, Tb<sup>3+</sup>, energy transfer from sensitiser to activator, intermediate role of Gd<sup>3+</sup> 0-50389
- Mg<sub>2</sub>SiO<sub>4</sub>:Tb, TLD phosphor response, heating rate effect 0-26359
- Na<sub>2</sub>O-B<sub>2</sub>O<sub>3</sub>-SiO<sub>2</sub>:Yb(Tb), luminesc. cooperative processes, glass struct. and comp. effect 0-16101
- SrF<sub>2</sub>:Tb<sup>3+</sup>, mag., thermal and hyperfine props. 0-29368
- Tb<sup>3+</sup> soln., luminesc. quantum yield spectral depend. 0-2838
- Tb<sup>3+</sup>:Yb<sup>3+</sup> in liq. media, luminesc. cooperative sensitisation 0-2827
- <sup>160</sup>Tb, hyperfine interaction parameters in Gd matrix 0-18240
- Tm IV 4f<sup>12</sup> configuration, spectra calcs. by configuration superposition (*Russian*) 0-14080
- YAG:Tb<sup>3+</sup>, cathodolum. efficiency rel. to activator conc. 0-11479
- Y<sub>2</sub>O<sub>3</sub>:Tb<sup>3+</sup>, temp. and viscosity depend. of colour coords. 0-40149
- Zn<sub>2</sub>O(BO<sub>2</sub>)<sub>2</sub>:Tb, phosphoresc. study (*Spanish*) 0-16105
- ZnS:Tb<sup>3+</sup>, NdF<sub>3</sub> film, vac. deposited, electrolum. energy transfer 0-2861

## terbium alloys

- Dy-Er, Kaufman approach to calc. of intra-rare earth phase diagrams 0-25657
- La<sub>1-x</sub>Tb<sub>x</sub>Ag(Sn<sub>3</sub>)(Al<sub>2</sub>), paramag. anisotropy of Tb<sup>3+</sup> in cubic cryst. field 0-15687
- Mg-Tb, (up to 45 wt.%), phase diagram, and mech. props. 0-16277
- Mn-Tb, dil., hyperfine interactions, nuclear orientation 0-15929
- Sc-Tb, induced-moment spin glass, simple mean-field theory 0-29553
- Tb-Al<sub>3</sub>, cubic Laves phase compounds, exchange striction determ. 0-44895
- Tb-Er, Kaufman approach to calc. of intra-rare earth phase diagrams 0-25657
- Tb-Gd, elec. resistivity and thermopower critical behaviour 0-15499
- Tb-Ho, Kaufman approach to calc. of intra-rare earth phase diagrams 0-25657
- Tb-Sc(Y)(La)(Lu)(Yb)(Mg)(Th), mag. ordering temps., susceptibility meas. 0-25136
- Tb-Sm (*Russian*) 0-34608
- Tb-Y(Gd), mag. anisotropy, contrib. from single-ion cryst. anisotropy and anisotropic exchange (*Russian*) 0-29546
- Tb<sub>2</sub>Ag<sub>48</sub>, amorphous, mag. aftereffect 0-20435
- TbAl<sub>2</sub>, ferromagnetic, extraordinary Hall effect 0-39560
- TbAl<sub>3</sub>, polytypism occurrence 0-44164
- TbAl<sub>3</sub>Ga<sub>2-x</sub>, mag. props. and phase transitions 0-25133
- TbBe<sub>13</sub>, magnetic structure at low temps., antiferromagnetic, neutron diffraction study (*French*) 0-39743
- TbCo<sub>2</sub>, elec. resistivity, thermopower, X-ray struct. meas. 0-24874
- TbCo<sub>2</sub>, rhombohedral distortion at low temp. 0-34743

## terbium alloys continued

- TbCo<sub>3</sub>, X-ray absorpt. edge shifts 0-25483
- TbCo<sub>3</sub>-H<sub>2</sub>, phase equilibria, from dissociation isotherms 0-50591
- (Tb<sub>0.27</sub>Dy<sub>0.73</sub>)Fe<sub>2</sub>, magnetisation, ferromag. domains 0-25162
- Tb<sub>0.3</sub>Dy<sub>0.7</sub>Fe<sub>2</sub>, sound velocity mag. field and temp. depend. elastic moduli calcs. 0-39839
- TbFe<sub>2</sub>, amorphous, Mossbauer spectra (*French*) 0-25261
- TbFe<sub>2</sub>, electronic heat capacity coeffs. 0-39787
- TbFe<sub>2</sub>, magnetisation, ferromag. domains 0-25162
- TbFe<sub>2</sub>, magnetoelastic props., magnetostriction hysteresis (*Russian*) 0-29590
- TbNi<sub>5</sub>, ferromag., magnetisation and paramag. susceptibility 0-25082
- TbPd<sub>3</sub>, specific heat at low temp. 0-20413
- TbSi<sub>2</sub>,  $\gamma$ - $\gamma$  ang. correl. obs. of polymorphic transition, 200-900°C 0-29653
- Tb<sub>2</sub>Y<sub>1-x</sub>Co<sub>5+0.1x</sub>, exchange interactions and magnetocrystalline anisotropy 0-34618
- Tb<sub>2</sub>Y<sub>1-x</sub>Sb<sub>x</sub>, elec. resist., cryst. field and exchange interaction contribs. 0-39556
- TbZn, ferromag., elec. resist., just below crit. temp., effect of mag.-domains 0-39557
- TbZn, ferromag. transition, transport coeffs. critical behaviour 0-15498
- Y<sub>1-x</sub>Tb<sub>x</sub>Co<sub>5</sub>, spontaneous magnetisation anisotropy, spin reorientation transforms. (*Russian*) 0-7082

## terbium compounds

- see also terbium alloys*
- metaphosphate glasses, n(M<sub>2</sub>O.P<sub>2</sub>O<sub>5</sub>).(1-x)Y<sub>2</sub>O<sub>3</sub>.xTb<sub>2</sub>O<sub>3</sub>.3P<sub>2</sub>O<sub>5</sub>, M=Li, Na, K, excitation and emission spectra 0-40150
- mixed valence compounds, charge dominated fluctuation props. comparison, mag. moments and ordering 0-54659
- (Er,Tb,Gd<sub>3</sub>)Fe<sub>2</sub>O<sub>12</sub> plate, pseudouniaxial, domain struct., magneto-optical obs. 0-11221
- (Gd<sub>1-x</sub>Tb<sub>x</sub>)<sub>2</sub>O<sub>2</sub>S phosphor, concentration quenching of Tb<sup>3+</sup> luminesc. 0-29785
- La<sub>1-x</sub>Tb<sub>x</sub>OBr phosphor, concentration quenching of Tb<sup>3+</sup> luminesc. 0-29785
- LiTb<sub>0.5</sub>Y<sub>0.5</sub>F<sub>4</sub>, mag. susceptibility, dilution effect on critical behaviour of dipolar uniaxial ferromagnet 0-34635
- Sm,Tb<sub>1-x</sub>FeO<sub>3</sub>, gyrotropic props. and birefringence, in spin reorientation range 0-7324
- Sm<sub>0.8</sub>Tb<sub>0.2</sub>S, resistivity and thermopower 0-20260
- Tb complex, in Cs<sub>2</sub>NaTbCl<sub>6</sub>, f-f transitions, mag. dipole intensities, vibronic coupling model 0-25404
- Tb complex of L-histidine, influence of metal-to-ligand ratio on energy transfer to Eu complex of L-histidine 0-32763
- Tb complexes, intermol. energy transfer to Eu complexes in aq. soln. 0-25426
- Tb complexes, intermol. energy transfer to Eu complexes in aq. soln. 0-25427
- TbAlO<sub>3</sub>:Yb<sup>3+</sup>, Mossbauer relax. 0-15875
- TbAsO<sub>4</sub>, ferromag., static and AC susceptibility meas. 0-29533
- Tb<sub>2</sub>, mag. struct., ferromag. ordering, neutron diff. study 0-15692
- TbB<sub>4</sub>, mag. and elec. props., metallic character 0-20386
- TbCl<sub>3</sub>.6H<sub>2</sub>O-PrCl<sub>3</sub>.6H<sub>2</sub>O(ErCl<sub>3</sub>.6H<sub>2</sub>O) in DMSO soln., Tb<sup>3+</sup>→Pr<sup>3+</sup>(Er<sup>3+</sup>) energy transfer mechanism 0-5498
- TbCrO<sub>4</sub>, valence states of Cr, XPS obs. 0-40216
- TbD<sub>3</sub>, non-stoichiometric, complex antiferromag. struct., neutron diff. study 0-50061
- Tb<sub>0.9</sub>Er<sub>0.1</sub>Gd<sub>0.1</sub>Al<sub>0.2</sub>Fe<sub>0.8</sub>O<sub>12</sub>, garnet plate, domain struct. 0-2602
- TbF<sub>3</sub>, crystal structure by powder neutron diff. study 0-15077
- Tb<sup>3+</sup>Fe<sub>1-x</sub>Cr<sub>x</sub>O<sub>3</sub> mag. props. from Mossbauer effect obs. (*Japanese*) 0-15933
- TbGa<sub>3</sub>(BO<sub>3</sub>)<sub>4</sub>, luminesc. spectra, local symmetry of rare earth ion determ. 0-16095
- TbIG, Faraday rotation and transition of spin config. at high mag. fields 0-39776
- Tb<sub>2</sub>(MoO<sub>4</sub>)<sub>2</sub>, ferroelectric-ferroelastic crystal, room temp. crystal struct., X-ray scatt. 0-28978
- Tb<sub>2</sub>MoO<sub>5</sub>, cryst. struct., IR spectra, elec. and mag. props. 0-33954
- Tb<sub>1.2</sub>Mo<sub>0.8</sub>S<sub>8</sub>, low temp. heat capacity anomaly rel. to antiferromag. transition in supercond. state 0-25044
- TbNbO<sub>4</sub>-CaWO<sub>4</sub>, phase transitions of fergusonite-scheelite (*French*) 0-19942
- Tb(OH)<sub>3</sub>, exciton dynamics within an inhomogeneously broadened line, luminesc. spectra 0-50407
- Tb(OH)<sub>3</sub>, powder and single crystal, mag. props. 0-2558
- TbP, mag. excitations above antiferromag. ordering temp., inelastic neutron scatt. obs. 0-50112
- TbP, magnetic  $\Gamma_1$ - $\Gamma_4$  exciton, inelastic neutron scatt. study 0-11159
- TbP, singlet-groundstate magnetism, static mag. props. 0-7109
- TbPO<sub>4</sub>, IR and Raman spectra 0-34904
- TbPO<sub>4</sub>, linear optical birefr. meas. near bicritical point 0-15719
- TbPO<sub>4</sub>, phase transitions at low temp. 0-15237
- TbP<sub>2</sub>O<sub>14</sub>, IR absorpt. and luminesc. spectra 0-55079
- TbRh<sub>2</sub>B<sub>4</sub>, NMR and sp. hf. in supercond. and mag. ordered phases 0-7037
- Tb<sub>2</sub>(SeO<sub>4</sub>)<sub>3</sub>.8H<sub>2</sub>O, thermal decomp. and IR spectra 0-3319
- Tb<sub>2</sub>Si<sub>2</sub>O<sub>7</sub>N<sub>2</sub>, prop. and X-ray diff. powder data 0-33944
- ZnS:TbF<sub>3</sub> film between semicond. Y<sub>2</sub>O<sub>3</sub> layers, bright green electrolum. 0-2859

terminals, interactive *see* interactive terminals

## ternary semiconductor

for pseudobinary semiconductors, *see* II-VI semiconductors, III-V semiconductors, III-VI semiconductors, IV-VI semiconductors and semiconductor materials

*see also chalcogenide glasses*

- A<sup>11</sup>B<sup>11</sup>C<sup>11</sup> semiconductor, crystal structure effects in electronic states 0-20085
- CoCr<sub>2</sub>S<sub>4</sub> films, galvanomagnetic and thermoelec. props. 0-54717
- p-CuInTe<sub>2</sub>, single cryst., IR study of lattice and free carrier effects 0-45074
- heteroepitaxial layer, measurement of lattice parameters, RHEED technique 0-15406
- II-III<sub>2</sub>-VI<sub>4</sub> compounds, electronic states, sensitivity to cryst. struct. 0-45209
- tC FeCr<sub>2</sub>S<sub>4-x</sub>Se<sub>x</sub> chalcospinel, ESR spectrum and paramag. susceptibility 0-15789
- Ag<sub>3</sub>AsS<sub>3</sub>, SHG, absorpt. coeffs. and temp. variation of refr. index difference 0-14390
- AgFeTe<sub>2</sub>, Mossbauer parameters in phase-transition region 0-11308



## ternary semiconductors continued

- AgGaS<sub>2</sub>, iso-index coupled-wave electrooptic filter 0-1324  
 AgGaSe<sub>2</sub>, SHG, absorpt. coeffs. and temp. variation of refr. index difference 0-14390  
 $\beta$ -AgSbS<sub>2</sub>, phase transitions, electrophysical props. 0-44316  
 Ag<sub>3</sub>SnSe<sub>6</sub>, cryst., Hall effect investigation of polymorphic transform. 0-39605  
 CdCr<sub>2</sub>Se<sub>4</sub>, ferromag. semicond., photoinduced mag. anisotropy 0-50086  
 CdCr<sub>2</sub>Se<sub>4</sub>, refr. index variation in strong alternating mag. field 0-23741  
 p-CdCr<sub>2</sub>Se<sub>4</sub>, resistivity anomalies at mag. transitions, sp. ht. 0-39785  
 CdCr<sub>2</sub>Se<sub>4</sub>, single cryst. growth by chem. transport reactions 0-16163  
 p-CdCr<sub>2</sub>Se<sub>4</sub>:Ag, electrical props., 100-300K 0-54692  
 CdCr<sub>2</sub>Se<sub>4</sub>:Ag, magneto-electrical props. temp. behaviour depend. on dopant conc. (*Russian*) 0-11006  
 n-CdCr<sub>2</sub>Se<sub>4</sub>:In, electrical props., 93-168K 0-49713  
 CdCr<sub>2</sub>Se<sub>4</sub>:In (Ga)(Ag), and undoped, elec. prop., vac. heat treatment effect 0-15518  
 CdGaS<sub>2</sub>, single crystals, peculiarities of photocond. in strong elec. field 0-54736  
 CdGa<sub>2</sub>Se<sub>4</sub>, IR refl. spectra, optical phonon dispersion 0-29746  
 CdGa<sub>2</sub>Se<sub>4</sub>, struct. of valence band, photocond. and reflection spectra meas. 0-6719  
 CdGa<sub>2</sub>Se<sub>4</sub>, thermoreflectance and visible absorpt. spectra, energy gap, cryst. field splitting 0-34945  
 CdGeAs<sub>2</sub>, SHG, absorpt. coeffs. and temp. variation of refr. index difference 0-14390  
 CdGeP<sub>2</sub>, crystals, prep. by chem. vapour transport 0-55280  
 n-CdGeP<sub>2</sub>-p-CdGeAs<sub>2</sub> heterojunction photocells, polarisation-sensitive 0-11075  
 CdIn<sub>2</sub>S<sub>4</sub>, electronic states, sensitivity to cryst. struct., UPS study 0-45209  
 CdIn<sub>2</sub>S<sub>4</sub> film, vac. deposited, growth, struct., optical and photoelectronic props. 0-10831  
 CdIn<sub>2</sub>S<sub>4</sub>, photoconducting semiconductors, fundamental absorption edge 0-40130  
 n-CdIn<sub>2</sub>S<sub>4</sub>/p-CuInSe<sub>2</sub> heterostructure, form. and photovolt. meas. 0-10831  
 Cd<sub>1-x</sub>M<sub>x</sub>S (M=Sr, Ca, Mg, Pb, Sn), solid soln., prep. and semicond. props. 0-2383  
 Cd<sub>3</sub>P<sub>2</sub>Cl<sub>3</sub>(Br<sub>3</sub>)(I<sub>3</sub>), elec. and photoelec. props. 0-34480  
 CdSiP<sub>2</sub>, birefringence, effects on hydrostatic pressure and temp. 0-45033  
 CdSiP<sub>2</sub>, pseudodirect chalcopyrite semicond., electronic band struct. 0-20079  
 CdSiP<sub>2</sub>, reflectance spectra at 300K 0-25407  
 CdSiP<sub>2</sub>:Na(Bi), single crystal, photocond. under laser excitation 0-44661  
 CdSnO<sub>3</sub>, single crystals, elec. props. 0-6978  
 Cd<sub>2</sub>SnO<sub>4</sub>, single crystals, elec. props. 0-6978  
 CdSnP<sub>2</sub>, crystal growth, DTA obs. of Cd-Sn-CdSnP<sub>2</sub> phase diagram 0-24394  
 CdTi<sub>2</sub>Te<sub>4</sub>, Hall and thermo-EMF coeffs., in solid, liquid states 0-54704  
 Co-Ge-Te system, phase equilib. 0-20908  
 CsPbBr<sub>3</sub>, electronic and optical props. 0-25414  
 CsPbCl<sub>3</sub>, electronic and optical props. 0-25414  
 CsPbCl<sub>3</sub>Br<sub>3-x</sub>, optical meas., LCAO band scheme 0-25437  
 Cu<sub>1-x</sub>Ag<sub>x</sub>In<sub>2-x</sub>Se<sub>2x</sub>, for solar photovoltaic cells 0-10982  
 Cu<sub>1-x</sub>Ag<sub>x</sub>In<sub>2-x</sub>Se<sub>2x</sub> pentenary alloy system, appl. to photovoltaic solar-energy conversion 0-35680  
 Cu<sub>3</sub>AsS<sub>4</sub> and Cu<sub>3</sub>SbS<sub>4</sub>, thermal cond. in solid and liq. phases, 300 to 1100K, thermoelec. Q-factor 0-19997  
 CuCrS<sub>2</sub>, single cryst., spectral study and phys. props. (*French*) 0-29002  
 (CuCr<sub>2</sub>S<sub>4</sub>)<sub>1-x</sub>(Cu<sub>0.5</sub>In<sub>0.5</sub>Cr<sub>2</sub>S<sub>4</sub>)<sub>1-x</sub> solid solution, piezoelectric effect, X-ray struct. anal. (*Russian*) 0-15978  
 CuCr<sub>2</sub>Se<sub>4</sub>(S<sub>4</sub>)(Te<sub>4</sub>), binary and ternary solid solns., mag. and elec. props. 0-2407  
 CuGaS<sub>2</sub>, crystal growth by solid phase crystallisation 0-25556  
 CuGaSe<sub>2</sub> crystals, electron probe microanal., correction procedure 0-2171  
 CuGaSe<sub>2</sub> single crystals, Hall effect and resist., acceptor states 0-10975  
 CuGaSe<sub>2</sub> single crystals, elect. and optical props. for solar cell appl. 0-10981  
 CuGaTe<sub>2</sub>, elec. and optical props. 0-6829  
 CuGaTe<sub>2</sub> films deposited on GaAs substrates by flash evaporation, struct. and elec. cond. 0-24755  
 Cu<sub>0.5</sub>In<sub>0.5</sub>Cr<sub>2</sub>S<sub>4</sub>, piezoelectric effect, X-ray struct. anal. (*Russian*) 0-15978  
 CuInS<sub>2</sub>, epitaxial thin film on GaAs, exam. of growth, electrical props. 0-24754  
 CuInSe<sub>2</sub>, acceptor levels, elec. props. study 0-39578  
 CuInSe<sub>2</sub> crystals, electron probe microanal., correction procedure 0-2171  
 CuInSe<sub>2</sub> film, evaporation source temp. effect, on comp. 0-39478  
 Cu<sub>0.5</sub>In<sub>0.5</sub>Se<sub>4</sub>, transition state and domain struct. by electron microscopy and diff. studies 0-15095  
 Ga<sub>0.67</sub>Cr<sub>0.33</sub>S<sub>4</sub>, semiconducting thiospinelide, spin glass type mag. ordering (*Russian*) 0-50123  
 (Ga<sub>1-x</sub>In<sub>x</sub>)<sub>2</sub>Se<sub>3</sub>, 1  $\leq$  x  $\leq$  0, phases, lattice parameters and thermal expansion between room temp. and melting point 0-39031  
 GeBi<sub>2</sub>Te<sub>4</sub>, Hall const., thermoelec. power, and elec. cond. 0-29407  
 Ge<sub>1.5</sub>Te<sub>0.5</sub>X<sub>4</sub> amorphous semicond. switches, fabrication technology (*German*) 0-7493  
 HgGa<sub>2</sub>S<sub>4</sub>, melt growth, optical props. and SHG, HgS-HgGa<sub>2</sub>S<sub>4</sub> phase diagram 0-50548  
 HgGa<sub>2</sub>S<sub>4</sub>, energy band struct. calc., empirical pseudopot. method 0-24793  
 HgGa<sub>2</sub>Se<sub>4</sub>, energy band struct. calc., empirical pseudopot. method 0-24793  
 In<sub>1-x</sub>Ga<sub>x</sub>P, epitaxial growth on GaAs substrate, formation of intermediate layers 0-2304  
 Nd<sub>2</sub>In<sub>2</sub>S<sub>3</sub>, chalcogenide cryst. struct., diff. and Patterson function anal. 0-39056  
 Pb<sub>1-x</sub>Sn<sub>x</sub>Te anodic oxide film form. conditions, IR absorpt. spectra 0-11494  
 SrTiO<sub>3</sub> semicond. electrode, electrochem., photoelectrochem. props. 0-3352  
 Ti<sub>3</sub>AsSe<sub>3</sub>, SHG, absorpt. coeffs. and temp. variation of refr. index difference 0-14390  
 TiGaS<sub>2</sub>-TiGaSe<sub>2</sub>, phase and composition-property diagrams 0-55366  
 TiGaS<sub>2</sub>(Se<sub>2</sub>), phase transforms. under hydrostatic press., Raman scatt. study 0-25366  
 TiGaS<sub>2</sub>Se<sub>2(1-x)</sub>, layer solid soln., long wave lattice vibrs., IR reflection spectra 0-11388  
 TiGaTe<sub>2</sub>, IR refl. and Raman scatt. spectra, lattice vibrs. 0-40108  
 TiInS<sub>2</sub>-TiInSe<sub>2</sub>, phase and composition-property diagrams 0-55366

## ternary semiconductors continued

- TiInS<sub>2</sub>Se<sub>2(1-x)</sub> layer solid soln., long wave lattice vibrs., IR reflection spectra 0-11388  
 TiInTe<sub>2</sub>(Se<sub>2</sub>), IR refl. and Raman scatt. spectra, lattice vibrs. 0-40108  
 ZnGeP<sub>2</sub>, birefringence, effects on hydrostatic pressure and temp. 0-45033  
 ZnIn<sub>2</sub>S<sub>4</sub>, cond. and valence band states, photoemission study 0-35054  
 ZnIn<sub>2</sub>S<sub>4</sub>, electronic props. of polytypic forms, pseudopot. calc. 0-38997  
 ZnIn<sub>2</sub>S<sub>4</sub>, III(a) polytype, absorpt. spectrum tail changes due to microstresses 0-2788  
 ZnIn<sub>2</sub>S<sub>4</sub> single cryst., intense radiation effect on optical transmission, absorpt. saturation 0-53385  
 ZnIn<sub>2</sub>S<sub>4</sub> switching investigation, negative resistance state instability, resistivity transitions 0-6920  
 ZnSiAs<sub>2</sub>, birefringence, effects on hydrostatic pressure and temp. 0-45033  
 ZnSiP<sub>2</sub>, birefringence, effects on hydrostatic pressure and temp. 0-45033  
 ZnSiP<sub>2</sub> crystal growth, DTA obs. of Sn-Zn-ZnSiP<sub>2</sub> phase diagram 0-24394  
 ZnSiP<sub>2</sub>, pseudodirect chalcopyrite semicond., electronic band struct. 0-20079  
 ZnSiP<sub>2</sub>, reflectance spectra at 300K 0-25407  
 ZnSiP<sub>2</sub>-In Schottky diode, photovoltaic spectra 0-2423

## terrestrial age see geochronology

## terrestrial atmosphere

- see also air; clouds; stratosphere; troposphere; upper atmosphere  
 acetonitrile, possible source of amino acids on primitive Earth 0-4112  
 albedo change due to aerosol 0-56604  
 circulation, by two-level quasi-geostrophic model 0-56546  
 global energy balance, environmental fluctuation effects 0-4084  
 IR radiation absorpt. induced by press., mol. collision between CO<sub>2</sub>, N<sub>2</sub>, O<sub>2</sub> (*Russian*) 0-56600  
 magnetosphere corotation lag, inertial limit, theory 0-41660  
 origin, implications of <sup>36</sup>Ar excess on Venus 0-12700  
 origin, theory based on protoplanetary cloud history 0-12549  
 palaeoatmosphere O<sub>2</sub> content, since Lower Carboniferous, fossil charcoal evidence 0-51542  
 physics, book 0-51976  
 remote sensing, conf. (Innsbruck, 1978 May 29-June 10) 0-31415  
 standard atmosphere, International and Soviet 0-26612  
 Tunguska catastrophe, computational modelling 0-41779  
 VHF radar studies (*German*) 0-46294  
 CO<sub>2</sub> cycling in environment, non-proportionality between flux and reservoir content 0-46261  
<sup>15</sup>N/<sup>14</sup>N ratio rel. to solar nebula differentiation 0-36519

## terrestrial composition see Earth composition

## terrestrial electricity

- Middle Asia seismoactive regions, geomag. investigations rel. to rock cond. 0-26464  
 asthenosphere under NE.Pacific, magnetotelluric sounding obs. 0-46123  
 Azov Sea, magnetotelluric soundings and dipole mag. profiling 0-3926  
 Baikal region, USSR, geoelectrical model 0-56365  
 Baikal rift zone, elec. anomalies rel. to continental rift form. (*Russian*) 0-12364  
 bay phenomena, theory of equivalent current systems including ground induction 0-41610  
 British Isles region, EM induction by analogue model 0-56368  
 Carpathians deep crustal struct., elec. cond. anomaly, numerical electromagnetic modelling 0-31008  
 coal fields of India, seam thickness by elec. and  $\gamma$ -logging 0-51394  
 coastal effect on geoelectrical soundings 0-46128  
 conducting sphere in mag. dipole field, general soln. 0-3921  
 conductivity in mantle, from heat transport processes 0-3929  
 conductivity profile, meas. via geomag. D<sub>SI</sub> vars. anal. comparison 0-17419  
 core-mantle system, conductivity profile 0-36238  
 Earth core electric current and zonal mag. fields, theory 0-36240  
 EM sounding, multicoil II airborne system 0-51554  
 EM sounding, numerical modelling of new multi-freq. system 0-56623  
 EM sounding of kimberlite pipes, prospecting techniques and EM signature 0-51393  
 Etna volcano, shallow geological struct. by elec. sounding 0-41419  
 galvanic prospecting effects, calc. via method of sub-areas 0-56348  
 geoelectric potentials and their derivatives, appl. to deep crustal sounding (*German*) 0-56626  
 global electrical conductivity, qualitative character 0-17231  
 HF EM induction profiling, of boreholes in underground mines (*Polish*) 0-51547  
 horizontally stratified media sounding, geophysical problems unification 0-56622  
 induced polarisation soundings interpretation, freq.-effect transform function definition and appl. 0-56624  
 Iturup Island, magnetotelluric soundings, geoelectric horizon and sedimentary layer 0-3925  
 Izu peninsula, Japan, elec. resistivity along Inatori-Omineyama fault (*Japanese*) 0-46121  
 Izu Peninsula, Japan, geoelectric survey near anomalous upheaval zone (*Japanese*) 0-46122  
 Izu Peninsula, Japan, geomag. variations rel. to earthquakes (*Japanese*) 0-41396  
 Izu-Hanto-Oki earthquake, May 1974, precursory resist. changes 0-51336  
 Izu-Oshima-kinkai earthquake, Jan. 1978, associated 73 Hz elec. resist. changes (*Japanese*) 0-46133  
 Izu-Oshima-kinkai earthquake, Jan. 1978, precursory elec. fields obs. (*Japanese*) 0-46131  
 Izu-Oshima-kinkai earthquake, Jan. 1978, precursory mag. variations and electricity (*Japanese*) 0-41397  
 Jharia Coalfield, India, coal seam mapping by elec. resist. methods 0-4133  
 lower mantle conductivity, comments and reply 0-30988  
 magneto-telluric surface impedance, calcs. by layered Earth model 0-56349  
 magnetometric resistivity anomalies, two-dimensional struct., mag. field determ. method 0-12334  
 magnetotelluric and geothermal surveys in NW Germany, comparisons 0-12336  
 magnetotelluric field variations due to atmospheric discharges and ionosphere elec. currents (*Danish*) 0-8250  
 magnetotelluric fields in E.Canada tectonically active region, time depend. 0-26451



**terrestrial electricity continued**

- magnetotelluric prospecting methods, exact surface impedance for spherically concentric Earth model 0-46129  
 magnetotelluric sounding, affected by resistivity freq.-dispersion 0-41368  
 magnetotelluric sounding, audio-frequency, case history at Cavendish geophysical test range 0-51324  
 magnetotellurics, crustal resistivity and conductivity variations, thin sheet anal. 0-51329  
 mantle conductivity anomaly interacting with ionosphere current to form geomag. variation 0-30985  
 Nakaizu, Izu Peninsula, repeated resistivity meas. (*Japanese*) 0-41370  
 ocean electric current, induced in insulated oceans 0-51407  
 oceanic dynamo, contrib. to  $O_1$  tidal component of geomag. lunar daily var. at Alibag 0-56355  
 Oshima Volcano, Japan, elec. resist. changes and 1978 Jan. 14 earthquake (*Japanese*) 0-46132  
 prospecting in marine areas, dipole and unipole resistivity methods 0-56641  
 remote reference magnetotellurics, random error derivations relating to impedance 0-12335  
 resistivity, airborne survey using VLF plane waves, resolution studies 0-12333  
 resistivity curves of horizontally multilayered models, calc. methods 0-46283  
 resistivity methods for subterranean cavity research, theoretical and exptl. investigation 0-56625  
 resistivity modelling for arbitrarily shaped three-dimens. structs. 0-3920  
 resistivity prospecting, use of signal contrib. sections 0-21836  
 resistivity sounding master curves, rapid computation 0-51560  
 Rhinegraben mag. anomaly, responsible elec. currents 0-46124  
 rocks, complex resistivity meas. by freq. domain method (*German*) 0-4001  
 rocks with fibrous dissemination, models 0-4002  
 Rybachy peninsula, USSR, geoelectric freq. soundings (*Russian*) 0-36230  
 self-potential anomalies near vertical contacts 0-3919  
 self-potential method in geothermal exploration 0-4125  
 W Sicily, Palermo-Sciaccia vertical electric sounding profile 0-56344  
 stationary well quadrupole logging in layers of restricted thickness (*Polish*) 0-12556  
 surface of Earth with variable conductance, 3D-model of EM induction 0-30983  
 transient EM fields about a grounded elec. dipole 0-56350  
 transient EM response of anisotropic rock to vertical electric dipole (*Polish*) 0-41367  
 Urals, aseismic geodynamics rel. to rock cond. changes and geomag. secular var. anomalies 0-26447  
 Vancouver Island region, analogue model study of EM induction 0-56356  
 Vancouver Island region, electromagnetic induction model 0-56367  
 Yerington mine, Nevada, in situ induced polarisation and mag. susceptibility meas. 0-51323  
 Yoshioka-Shikano Fault, seismically active fault along Japan Sea coast, geomag. induction study 0-26475

**terrestrial heat**

- see also volcanology*  
 Alpine fault, New Zealand, frictional metamorphism, Ar depletion and tectonic stress 0-41440  
 Archaean sialic crust, southern West Greenland, chemical and thermal evolution 0-31016  
 E.Arizona, USA, heat flow rel. to subsurface struct. 0-21686  
 artificially fractured rock, heat transfer agents flow patterns 0-17239  
 asthenosphere thermal instability beneath moving plate 0-31007  
 Atlantic mid-oceanic ridge, axial temp. profile and crustal struct. 0-26476  
 Atlantic Ocean, history of growth and topography of ocean bottom 0-3993  
 Mid Atlantic Ridge crest, geological and geophys. investigations 0-8284  
 Australia, regional heat flow maps 0-51351  
 Baikal rift zone, heat flux anomalies rel. to continental rift form. (*Russian*) 0-12364  
 basalt sheets, thermal effect on adjacent rock, heat flow model 0-46181  
 borehole meas., high temperature electronics for geothermal energy 0-11997  
 Bournac, Haute-Loire, heat flow determ., geotherm proposal 0-8259  
 E. Canada, thermal struct. of upper crust 0-31013  
 Canadian Shield, Superior Province lakes, heat flow meas. 0-31003  
 Ceylon-Cocos Zone, thermal regime and nascent island arc 0-56418  
 N.China, heat flow obs. (*Chinese*) 0-56416  
 Coast Plutonic Complex, British Columbia, geochronology and thermal history 0-12351  
 continental crust during magmatic accretion and metamorphism, thermal model 0-46150  
 continental crust heat production model 0-21690  
 core cooling by subsolidus mantle convection 0-36278  
 core thermal evolution 0-21674  
 crustal rocks, critical thermal gradients for seismic low-vel. zones 0-41435  
 deep-sea hydrothermal site on strike-slip fault, discovery 0-21710  
 desaturating geothermal reservoir, numerical modelling 0-12363  
 dynamothermal aureole of the Bay of Islands ophiolite suite 0-51355  
 Earth core, outward heat flow rel. to geomag. field origin 0-8251  
 Earth-atmosphere radiative heating effects on climate, NOAA radiometer meas. 0-8425  
 Galapagos hydrothermal mounds, sediment U content anomaly 0-56434  
 Galapagos Rift, submarine thermal springs 0-8295  
 Galapagos Rift hydrothermal mounds, obs. with DSRV Alvin and detailed heat flow studies 0-51383  
 garnet and clinopyroxene solid solns., geothermometry based on Fe-Mg distrib. 0-46151  
 geothermal and magnetotelluric surveys in NW Germany, comparisons 0-12336  
 geothermal gradient at 1000 km depth 0-8260  
 geothermal power plants flash cycle optimisation, analytical expression in terms of temp. only 0-40894  
 geothermal region, thermal-convective instability through porous medium 0-53769  
 geothermal reservoir exploitation, finite difference modelling 0-55798  
 geothermal reservoir simulation, math. models 0-12446  
 geothermal reservoir simulation, numerical soln. techniques 0-12447  
 geothermal steam pipeline network, numerical simulation 0-40822

**terrestrial heat continued**

- geothermally active fault zone, water convection 0-19375  
 German Democratic Republic, geomag. secular var. anomalies rel. to heat flow positive anomalies 0-26449  
 geyser vent, pre-boiling convection, mathematical model 0-31067  
 Geysers geothermal field, California, explosions and microearthquakes study 0-3964  
 global geodynamics, Canadian contribs., 1971-79 period. 0-8262  
 Grass Valley, Nevada, USA, microseisms in geothermal exploration 0-21647  
 Grassy granodiorite, Tasmania, thermal history meas. using garnet fluid inclusion data 0-4012  
 groundwater chemical geothermometer, Na-K-Ca temp. with Mg correction 0-51357  
 Guaymas Basin, Gulf of California, basaltic sill intrusion into sediments, hydrothermal activity 0-46154  
 Guaymas Basin, Gulf of California, heat flow at spreading centres 0-41411  
 central Gulf of California, heat flow meas. 0-3968  
 heat flow measurement, vertical groundwater movement correction 0-3969  
 Jordan-Dead Sea Rift Valley warm springs, correl. between  $SiO_2$  conc. and orifice temp. 0-41464  
 Lehmann discontinuity, mantle props. beneath continents 0-56425  
 Los Angeles basin (California) SW block, thermal subsidence and petroleum generation 0-3967  
 lower mantle, convection, composition and thermal state 0-21678  
 lower mantle, thermodynamically based eqn. of state 0-26473  
 lower mantle Gruneisen parameter, evidence for approximation  $\gamma p = \text{const.}$  0-3970  
 mantle plume, fluid-dynamic model of ascending flow 0-12370  
 marginal seas, heat flow correl. with underlying mantle density inhomogeneities 0-21676  
 multi-layered geothermal reservoir, natural convection 0-8347  
 Nevada, gravity surveys in Grass and Buena Vista Valleys rel. to geothermal resources 0-41365  
 North Sea, Buchan and Witchground Grabens, seismology study 0-51364  
 Norwegian-Greenland sea, thermal evolution in sea floor spreading model 0-56427  
 ocean crust heat flow from U abundance 0-8287  
 ocean floor hot spring created by drill hole 0-55951  
 ocean ridge thermal evolution, affected by spreading rate 0-56424  
 ocean spreading ridge crests, hydrothermal activity rel. to ocean major and minor elements balance 0-41459  
 oceanic ridge crests, hydrothermal activity rel. to metal-rich deposits form. 0-41430  
 passive continental margin, thermal evolution in sea floor spreading model 0-56427  
 plutons undergoing hydrothermal cooling and thermal cracking, heat transfer 0-12362  
 Proterozoic era, crustal temp. gradients rel. to tectonics and apparent polar wander loops 0-56360  
 Quottoon pluton, British Columbia, thermal effects of igneous intrusion and uplift 0-12352  
 Raft River geothermal area, Idaho, seismic refr. study 0-3963  
 Raft River geothermal reservoir, Idaho, USA, borehole geophys. study 0-21672  
 rifted continental margins, thermal history and subsidence, Nova Scotian and Labrador Shelves 0-12353  
 Roosevelt hot springs, Utah, seismic noise study 0-56399  
 Salton Sea geothermal area, California, temp. gradients, onshore and offshore meas. 0-3962  
 self-potential anomalies near vertical contacts 0-3919  
 self-potential method in geothermal exploration 0-4125  
 E.Siberia, amethysts form. temps. and history (*Russian*) 0-12393  
 standard geothermal provinces, heat flow-generation relation (*Polish*) 0-36271  
 subduction zone, thermal structs. evolution 0-56440  
 tectonic unit heat flow, Romania (*Rumanian*) 0-8268  
 temp. gradient distrib. and geological struct. Izmir-Seferihisar geothermal area, Turkey, relation between temp. gradient distrib. and geological struct. 0-56441  
 thermal effects on surface waves in stressed conducting media, theoretical study 0-8253  
 thermal history model of Earth with parameterized convection 0-26470  
 topographic corrections to geothermal obs., analytical method 0-46282  
 UK mainland, heat flow field 0-26477  
 western Virginia, heat flow rel. to origin of thermal springs in folded Appalachians 0-41414  
 water convection, simple theoretical and expt. study, geophysical appl. and analogies 0-24018  
 wells, bottom-hole temperature stabilisation model 0-51356  
 N.Wolverine Complex, British Columbia, geochronology rel. to thermal history and tectonics 0-3961  
 Yellowstone National Park as continental hot spot 0-3981

**terrestrial magnetic field** *see geomagnetism***terrestrial magnetism** *see geomagnetism***test equipment**

- see also automatic test equipment*  
 acoustic microscopy, nondestructive testing appl. 0-16612  
 cardiac activity signal simulator 0-56230  
 conductometric instruments metrological monitoring, for environmental contaminants control 0-55973  
 cylinder, rectilinearity meas. using equal chromatic order fringes 0-27286  
 cylindrical part edge quality determ., acoustic method and equipment 0-35491  
 digital cardiac defibrillator tester 0-41286  
 disperse materials, fine layers, autohesive strength, meas. installation 0-40644  
 eddy current probe, high saturation with internal reference, design and specifications 0-40658  
 fatigue test machine, low-cycle, far sheet material bending to  $-196^\circ\text{C}$  0-55616  
 ferromagnetic probe coercimeter for inspecting the quality of parts with variable geometric dimensions 0-35488  
 interleaved glass layer prism for semiconductor mask testing 0-43425  
 microhardness measurement, bicylindrical indenter, 0-40642  
 negatoscope, 0D-10N, for scanning radiograph 0-35494  
 nuclear power stations, fission reactors testing using ultrasonic test apparatus (*German*) 0-13730



**test equipment continued**

- pacemaker patient simulator 0-41322
- passive solar building thermal performance modelling by passive solar test boxes, expt. 0-3494
- passive solar building thermal performance modelling by passive solar test boxes, theory 0-7921
- random vibration simulator, practical realisation 0-53732
- spectral response, pulsed measurement, test set-up and apparatus, shortcomings and planned improvements 0-45695
- split Hopkinson pressure bar use in obtaining dynamic stress/strain data at const. strain rates (*Japanese*) 0-16630
- steel granular model material, equipment for shear deform. investigation (*German*) 0-35449
- table top pulsed solar simulator, design and construction, for testing solar cell arrays powering artificial satellites 0-45696
- Pt-alloy thermocouples, reference-standard testing apparatus 0-13077

**test facilities**

- see also *aerospace test facilities; anechoic chambers*
- Battery Energy Storage Test facility, test programs and data processing 0-30449
- coal gasification/combined cycle power generation test facility, preview 0-16773
- FBRs, testing full-scale components for sodium reactors 0-828
- flat-plate solar collector test facility to determine thermal performance characts. 0-45730
- fusion energy, Engineering Test Facility work on magnetic confinement 0-52787
- low dielectric loss meas. apparatus for 0.1 to 200 MHz 0-15958
- marine environment test facility for electro-optical systems 0-45847
- moving material fault test rig (*German*) 0-11855
- nuclear power stations, fission reactors testing using ultrasonic test apparatus (*German*) 0-13730
- nuclear safety testing, LOFT (loss-of-fluid) project at INEL 0-32386
- OTEC, design of seacoast test facility, Hawaii 0-55888
- reactor testing, fast flux, research-type, neutron radiography facility 0-18371
- solar cells, testing using plane mirror heliostat 0-45668
- solar simulator design for testing solar collectors 0-50996
- solar standards and testing activities in developed and developing countries 0-55819
- Na ML-3 circuit for testing mech. props. of structural materials of LMF-BRs (*Spanish*) 0-55595

**testers see test equipment****testing**

- see also *automatic testing; electron device testing; electronic equipment testing; environmental testing; impulse testing; inspection; integrated circuit testing; logic testing; machine testing; materials testing; mechanical testing; nondestructive testing; optical testing; production testing; program testing*
- 1300 MW nuclear reactor steam isolating valve blowdown tests (*German*) 0-22967
- angular meas., testing instrument for errors 0-42186
- computed tomography scanner, fourth-generation, performance evaluation 0-46035
- computer tomography head scanner, translate-rotate type with Xe detectors, performance characts. 0-46036
- conductometric instruments metrological monitoring, for environmental contaminants control 0-55973
- dielectric constant meas., test scheme design 0-13101
- FBR blanket, integral neutron reaction rate meas., in FBBF facility 0-22887
- laboratory, test results, international acceptance (*Danish*) 0-8952
- land-use map accuracy testing, sampling designs 0-17226
- light sources, photometric laboratory equipment requirements and standards (*Slovak*) 0-17990
- magnets, permanent, meas. errors determ. 0-52280
- nuclear power stations, seismic design and testing of equipment and components, Japan 0-52763
- nuclear power stations, fission reactors testing using ultrasonic test apparatus (*German*) 0-13730
- nuclear power stations safety, leakage tests, Spanish policies (*Spanish*) 0-5247
- power transformers, fault diagnosis, dissolved gas analysis of insulating oils 0-26097
- radiographic phantoms for testing X-ray imaging performance 0-51229
- radioisotope thermoelectric generator shock and vibration test program for MB-M75(A) 0-35711
- solar water heater, low-cost unit development (*Afrikaans*) 0-7925
- solar-electric heat pump for houses, design and tests (*German*) 0-7951
- spectral response, pulsed measurement, test set-up and apparatus, shortcomings and planned improvements 0-45695
- terrestrial solar modules, sandwich type glass encapsulation, climatic parameters effect, economic anal. 0-45673
- unfolding codes for benchmark gamma spectrometry 0-47807
- Ni-Cd 6.0 Ah cells, accelerated testing of cell failure for life prediction 0-35670

**testing apparatus see test equipment****testing equipment see test equipment****testing machines see test equipment****tetramethylammonium manganese chlorides see organic compounds****tetraneutrons see neutrons****tetrodes**

- reflex tetrode, ion beam extraction anal. 0-48903
- reflex tetrode ion-beam source, extracted ion beam anal. 0-23236

**textile fibres see fibres****textile industry**

- agitating type polymerizer, synthetic resins and fibres manufacturing process 0-3341
- electrical resistance of textiles, meas. device using operational amplifiers 0-42240

**texture**

- see also *recrystallisation texture; surface texture*
- BCC metals, plastic deform., computer simulation 0-40456
- brass, 70:30, rolled, nucleation and annealing texture development 0-45320
- $\alpha$ - $\beta$  brass, cold-rolled, energy dispersive X-ray diffr. studies 0-40379
- $\alpha$ -brass, texture, recrystallised orientation distrib. function comparison with 40°(111) rolling texture 0-25723

**texture continued**

- cholesteric planar texture, planar-finger print texture transform. around Cano disclinations 0-14999
- copper phthalocyanin, thin film, thermal behaviour (*Japanese*) 0-24753
- cross-rolling and compression textures, numerical prediction 0-40382
- crystals, textural defects 0-49158
- cubic polycrystal, anal. of orientation distribution plots obtained by vector method 0-29977
- deformation textures, eulerian simulation 0-3096
- fibre, quantitative determ. of volume fraction, analytical method by pole figures 0-11863
- goniometer for analysis of rocks 0-26630
- inverse pole figures, calc. method on digital computer 0-20950
- metals, FCC nonhomogeneous sheet, orientational distrib. function calc. of mean texture 0-11659
- Mossbauer absorbers, deformation induced texture 0-7214
- Mossbauer effect, texture problem and Goldanskii-Karagin effect, intensity matrix method 0-7215
- non-random orientation distribution functions with random pole figures 0-6320
- PNAOBA, type C smectic liq. crystals, electrohydrodynamic instability 0-1927
- polycrystalline material, texture and anisotropy (*German*) 0-3097
- polyethylene, doubly oriented, low density, deformation and structure, exam. 0-11705
- polypropylene, injection moulded, texture (*Japanese*) 0-25722
- polystyrene filament, melt spun, struct. and mech. props., effect of drawing, twisting, annealing, untwisting 0-45331
- powders, spray drying to minimize preferred orientation 0-3098
- refractories, fatigue, effect of texture/crack relationship (*German*) 0-25829
- refractories, fatigue behavior, effect of texture and crack kinetics, AE anal. (*German*) 0-21061
- shear band formation models, in rolling and extrusion 0-11666
- sheet metals, X-ray diffr. anal. 0-6316
- steel, alloy, types CT40, CT40X, CT45, texture form. 0-25721
- steel, austenitic stainless, ferritic, single phase ferritic solidification in welds, exam. 0-7546
- steel, bainitic, invariant plane strain theory, determ. of habit planes and orientation relationships 0-55388
- steel, C content effect on annealing texture, plastic anisotropy and mechanical props. 0-29976
- steel, Cr (17 wt.%), stainless, hot-rolled texture, effect on cold-rolled and annealed textures 0-55425
- steel, eutectoid thermomechanically treated, textural studies 0-29978
- steel, low C, Mn effect on recrystallisation and texture (*French*) 0-3110
- steel, mild, orientation distribution function, representation of texture and slip directions 0-11665
- steel, plastic deformation and cryst. texture in equibiaxial exspn. 0-7653
- steel low C, rolled, analytical vectorial method for crystallographic texture (*French*) 0-20956
- steel with micro-duplex structure, neutron diffraction analysis of rolling texture 0-16327
- steels, hot forming property and struct. (*German*) 0-25730
- Teflon foils, cryst. struct. and texture changes due to polarisation process (*Polish*) 0-35209
- tetragonal powder, preferred orientation, X-ray intensity corrections 0-1880
- textures materials, residual stress evaluation by X-rays (*German*) 0-40670
- X-ray quantitative phase anal. (*Chinese*) 0-21195
- X-ray topography (*German*) 0-1894
- Zircaloy-4 tubes, texture influence on anal. of thermoelastic/plastic anisotropy and initial yielding 0-35260
- Ag, (211)[111] single crystals, shear band effects on rolling deformation 0-50651
- Al, cyclic torsional deformation, final texture 0-7595
- Al, pure, hydroextrudates, incomplete axial orientation (*Russian*) 0-20949
- Al, pure, texture influence on stress/strain curves, prestrain, solid soln. and particle hardening effect on inhomogeneous deform. (*German*) 0-30014
- Al, rolled, analytical vectorial method for crystallographic texture (*French*) 0-20956
- Al-Zn (40 wt.%), plastic deform. effect on discontinuous precipitation 0-3053
- Al<sub>2</sub>O<sub>3</sub>, hot pressing, microstruct., texture 0-40299
- B films, prep. by H reduction of BCl<sub>3</sub>, struct. and hardness 0-54543
- Be<sub>2</sub>Ti<sub>2</sub>O<sub>12</sub> grain oriented ferroelectric ceramic, prep. by molten salt synthesis-tape casting method 0-40296
- Bi foil, sputat quenched, preferred orientation 0-40381
- Bi<sub>2</sub>WO<sub>6</sub> grain oriented ferroelectric ceramic, prep. by molten salt synthesis-tape casting method 0-40296
- Cd, cold rolling texture development 0-25720
- Cd foil, sputat quenched, preferred orientation 0-40381
- Co evaporated film, X-ray diffr. study 0-6663
- Co film, evaporated, columnar struct. depend. on degree of texture 0-54567
- Co film, evaporated, texture and columnar struct. 0-54566
- Co, magnetic anisotropy induced by mag. annealing and cold rolling, expt. 0-7695
- Co, magnetic anisotropy induced by mag. annealing and cold rolling, calc. 0-7696
- Co-Ni, magnetic anisotropy induced by mag. annealing and cold rolling, expt. 0-7695
- Co-Ni, magnetic anisotropy induced by mag. annealing and cold rolling, calc. 0-7696
- Cr, sputtered, growth struct. influence of substrate surface topography and ang. of adatom incidence 0-20058
- Cu cyclic torsional deformation, final texture 0-7595
- Cu film, effect of thermal strain on orientation 0-49294
- Cu-Ag (8 wt.%), plastic deform. effect on discontinuous precipitation 0-3053
- Cu-In eutectoid, directional eutectoid decomposition growth, crystallography 0-29874
- Fe-Al, hot- and cold-rolled, texture form., pole figures method (*Russian*) 0-45317
- Fe-Co-Ni-Al (35, 14.5, 7.2 wt.%), high-coercivity, substructure and texture change during bending and upsetting 0-21037
- Fe-Ni-Co, texture form. after cold working and annealing (*German*) 0-3089



## texture continued

- Fe-Zn, crystallographic relations by X-ray diff. 0-24408  
<sup>3</sup>He, A-phase slab, mag.-field-induced cellular superflow, periodic texture 0-24706  
<sup>3</sup>He, superfluid, planar textures, Ginzburg-Landau eqn. solns. 0-10729  
Mg cold rolling texture development 0-25720  
Mg, HCP, computer simulation of rolling texture formation 0-3095  
Mg-Al-Zn (9wt.%Al), sand cast, preferred orientation and mechanical props. (Japanese) 0-20979  
Mo, orientation distrib. function depend. on deform. during cold rolling (Russian) 0-50647  
MoSe<sub>2</sub> coating, on Mo, support annealing influence on orientation, texture and hardness (Russian) 0-20961  
MoSi<sub>2</sub>, ceramic additives effect on sintering, recrystallisation 0-40306  
NaCl, halite, dynamic recrystn. during compression creep, geophys. appl. 0-25772  
Ni, yield point, effect of alloying elements (Russian) 0-50670  
NiF<sub>2</sub>, powder, preferred orientation, X-ray intensity corrections 0-1880  
NiO, lattice parameters, microstrains, non-stoichiometry, comparison between mosaic microcrystals and quasi-perfect single microcrystals. 0-24414  
PbBi<sub>2</sub>Nb<sub>2</sub>O<sub>6</sub>, bend strength, grain orientation effects 0-40375  
SiO<sub>2</sub>, glasses surface textures and defects, exam. using liq. crystals. 0-6364  
Sn-Bi, eutectic, superplastic anisotropy (German) 0-25808  
Ta, rolled single crystal, recovery and recrystallization 0-3093  
Ti-Al-V (6.4 wt.%), strongly textured, influence of crystallographic orientation on tensile behaviour 0-7633  
Ti-Al-V(Sn) alloys, plastic deformation and fracture characts. at low temps. (Russian) 0-7624  
Ti-Al(Mo), swaged and recrystallized, grain growth 0-3092  
Ti-Al(-V)(Mo), impact strength anisotropy, influence of texture (Russian) 0-20952  
α-U, orthorhombic, computer simulation of rolling texture formation 0-3095  
Zn, cold rolling texture development 0-25720  
Zn foil, splat quenched, preferred orientation 0-40381  
Zn, HCP, computer simulation of rolling texture formation 0-3095  
Zn-Al, unidirectional eutectic, FCC phase, preferred orientation 0-29973  
ZnF<sub>2</sub>, powder, preferred orientation, X-ray intensity corrections 0-1880  
Zr, HCP, computer simulation of rolling texture formation 0-3095

## texture, surface see surface texture

## thallium

- see also nuclei with .....  
alkali halide: Tl<sup>+</sup>-like ions, triplet state lifetime, hyperfine interaction 0-2844  
atom, 6<sup>2</sup>P<sub>3/2</sub>-6<sup>2</sup>P<sub>1/2</sub> transition, population inversion 0-950  
atom, hyperfine struct. optical pumping, O-O transition perturbation 0-949  
atom, in gas discharge, optical self pumping, hyperfine struct., microwave-optical spectroscopy 0-32680  
atom, optical excitation, Landau-Zener nonlinearity, fluoresc. obs. (Russian) 0-52948  
atom, parity non-conserving E1 matrix elements, many body calcs. 0-47924  
atom, reson. lines, perturbing gas and self-broadening, temp. effects 0-42979  
atom, Tl 5d XPS comparison with TlI 0-43099  
atom λ<sub>max</sub>=251.3 nm absorption band, rel. to Tl atom conc., temp. and disturbing gases 0-42980  
atomic beam tubes, freq. pulling effect with mag. double reson. 0-37802  
atoms, axial distrib. in unipolar arc discharge, influence of Li conc. 0-19656  
electrical resistivity, 300-1050K 0-24868  
HCP, lattice dynamics, local pseudopotential approach, dielectric functions 0-34151  
liquid and solid, UPS, optical densities of states 0-2924  
nonlinear helicon resonance due to open-orbit conduction 0-2324  
normal atom conc. determ. by resonance line broadening with Hg press. 0-43883  
photoemission, transition from ordered solid to disordered liquid 0-45217  
thermal and elastic props., lattice heat capacity, elastic constants and thermal expansion, model 0-39321  
vapour, coherent anti-Stokes scatt. four-photon parametric oscill. 0-9959  
vapour, ruby laser third harmonic generation, focusing degree influence 0-48348  
As<sub>2</sub>Se<sub>3</sub>:X (X=Cu, Ag, Tl, I, Ge), effect of doping, NMR meas. 0-11282  
Bi:Ti, microhardness anisotropy 0-21079  
CsI:Ti, crystallophosphor, luminesc. characts., temp. and conc. depend. 0-55175  
CsI:Ti, gamma-scintillation growth front, external elec. field effect 0-34984  
Cs<sub>2</sub>O-B<sub>2</sub>O<sub>3</sub>:Tl<sup>+</sup> glass, optical basicity, variation with probe ion and comp. 0-2800  
Hg-Tl-I discharges, 50 Hz, Tl atoms axial segregation 0-38781  
KBr:Ti excitation in fund. absorpt. region, luminesc. and thermolum. 0-50433  
KBr:Ti<sup>+</sup>, quadratic Jahn-Teller effect, totally symm. vibr. mode effect, ang. overlap model 0-49680  
KBr:Ti<sup>2+</sup>, relation between bonding and g-shift 0-39492  
KCl:Ti, energy level scheme, mol. orbital model 0-10912  
KCl:Ti, excitation in fund. absorpt. region, luminesc. and thermolum. 0-50433  
KCl:Ti, hole capture kinetics, influence of autolocalised and zone holes (Russian) 0-54714  
KCl:Ti<sup>+</sup>, quadratic Jahn-Teller effect, totally symm. vibr. mode effect, ang. overlap model 0-49680  
KCl:Ti<sup>+</sup> cryst., A band, mag. field effect 0-34897  
KCl:Ti<sup>2+</sup>, optical absorpt. spectra interpretation mol. orbital scheme 0-20671  
KCl:Ti<sup>2+</sup>, relation between bonding and g-shift 0-39492  
KCl(Br)(I):Ti, Jahn-Teller system, negative mag. circular polarisation in emission spectrum 0-20694  
KI:Ti<sup>+</sup>, A<sub>1</sub> emission, mag. circular polarisation, WKB approx. for non-radiative transition rate 0-55180  
KI:Ti, A<sub>1</sub> emission, linear polarisation, appl. of semi-classical WKB formalism 0-45134  
KI:Ti, electron-hole and V<sub>K</sub>-Ti recomb., TSC and thermolum. study (French) 0-34461  
KI:Ti<sup>+</sup>, pre-resonant enhancement of Raman scatt. 0-7354  
KI:Ti, excitation in fund. absorpt. region, luminesc. and thermolum. 0-50433

## thallium continued

- LiI:Ti, absorpt. spectrum obs. 0-50378  
Li<sub>2</sub>O-B<sub>2</sub>O<sub>3</sub>:Tl<sup>+</sup> glass, optical basicity, variation with probe ion and comp. 0-2800  
NaCl:Ti<sup>+</sup>, γ-irrad., aquoluminesc. obs. 0-2856  
NaI:Ti, scintillation excitation mechanism 0-2857  
PbS:Ti, Hall and Seebeck coeffs., Hall mobility, impurity states 0-15545  
PbTe:Ti, influence of Tl impurity states 0-20121  
PbTe:Ti, thermoelectric power, elec. cond., Hall coeff. and optical absorpt. coeff. 0-39584  
RbCl:Ti, origin of 3.55 eV emission band 0-7401  
Si:Ti, binding energy, excited state spectra, photolum., semi-empirical short range pot. 0-44534  
Si:Ti, ion implantation, indirect doping method 0-10568  
Tl, elec. field gradient at <sup>111</sup>Cd, effects of high press., TDPAC meas. 0-25266  
Tl<sup>+</sup> in hollow-cathode Ne-TlCl discharge, 594.9, 695.1 nm CW laser oscill. 0-23674  
Tl-Xe, electric discharge excitation of Tl in high-press. Xe 0-49025  
Tl+Ba, laser induced collisional and radiative energy transfer 0-53108  
Tl+H<sub>2</sub>, Tl atomic fluorescence, pressure and Doppler broadening 0-5504  
Tl+Hg, excitation energy transfer, excitation rate consts. 0-37772  
Tl+inert gas atom, diffuse series head lines, hyperfine components, broadening calcs. 0-32632  
<sup>199</sup>Tl, production by <sup>197</sup>Au(α, n) reaction, medical apps. 0-51245  
<sup>201</sup>Tl abnormal myocardial rest image, significance in coronary artery disease 0-17060  
<sup>201</sup>Tl myocardial images in coronary artery disease extent prediction 0-26336  
<sup>201</sup>Tl myocardial imaging, redistrib. rel. to rest images 0-12225  
<sup>201</sup>Tl, myocardial perfusion evaluation by coded aperture tomographic technique 0-21537  
<sup>201</sup>Tl, myocardial perfusion imaging, algorithm for background activity calc. 0-56195  
<sup>201</sup>Tl myocardial perfusion scintigrams in the evaluation of aortocoronary saphenous bypass surgery 0-12235  
<sup>201</sup>Tl scintigraphy of the myocardium, effect of gate width 0-41172  
<sup>201</sup>Tl, use in thyroid 'cold' areas scintigraphic evaluation 0-36078

## thallium alloys

- see also thallium compounds  
Bi-Tl, dilute, oxidation kinetics 0-25914  
Li-Tl, liquid alloys, calorimetry study (German) 0-25664  
Mg-In-Tl, phase diagrams and electrochem. props. (Russian) 0-40330  
Mg-Li-Tl, phase diagram, isothermal cross section (Russian) 0-20900  
Pb-Tl, vacancies, positron capture, function of Tl concentration (German) 0-49213  
Pb-Tl alloys, positron trapping in vacancies, varying concentration effects (German) 0-25477  
Pb-Tl-Cd(Sn) melt, short-range order struct. 0-49088  
Pb-Tl-O-Pb, Josephson tunnel junction parameters, microwave freq., temp. depend. 0-34561  
Pr<sub>3</sub>Tl, critical fluctuations temp. depend. 0-25160  
Pr<sub>3</sub>Tl, transition temp. and magnetisation 0-25161  
Tl-Bi system, phase transitions near Tl<sub>3</sub>Bi, elec. props. meas. 0-35181  
TlBi<sub>2</sub>, cryst. struct. and density (German) 0-24407  
Tl<sub>2</sub>Se<sub>1-x</sub>, liquid semiconductor, diamagnetism and paramagnetism, dangling bond paramag. centres, mag. susceptibility obs. 0-44797

## thallium compounds

- see also thallium alloys  
halides, anal. of cryst. binding and Anderson-Grüneisen parameters 0-15040  
(Ag, Tl, Ca)NO<sub>3</sub>, aqueous solutions, vapour press. meas. 0-6504  
B<sub>2</sub>S<sub>3</sub>-Tl<sub>2</sub>S system, phase diagram and verification 0-35165  
B<sub>2</sub>Se<sub>3</sub>-Tl<sub>2</sub>Se<sub>3</sub> system, phase diagram 0-35165  
CdO-GeO<sub>2</sub>:Tl-O photochromic glass for optical information retention media 0-33108  
CdTl<sub>2</sub>Se<sub>4</sub>:Au(Ag)(Cu), doping effect on surface tension of melt and cryst. microhardness 0-49464  
CsCl-TlCl solid soln., point defect parameters 0-54224  
Cu<sub>2</sub>S-Tl<sub>2</sub>S system, phase diagram 0-20906  
GdTmGa garnet bubble film, ion implanted, pot. wells under charged wells 0-34717  
HgTl optically excited excimers, upper state kinetics 0-37831  
KCl:TiCl<sub>2</sub>, lattice defects, X-ray line profile obs. 0-24455  
KTI[Fe(CN)<sub>6</sub>], isomer shift of Mossbauer spectra 0-29662  
(NH<sub>4</sub>)<sub>2</sub>Tl<sub>1-x</sub>Al(SO<sub>4</sub>)<sub>2</sub>·12H<sub>2</sub>O·Cr<sup>3+</sup>, zero field splitting, g-values, EPR spectra obs. 0-50169  
NaNO<sub>2</sub>-TiNO<sub>3</sub>-Ca(NO<sub>3</sub>)<sub>2</sub>·4.09H<sub>2</sub>O melt, mixed alkali effect 0-34219  
Ne-TlCl hollow-cathode discharge, CW laser oscill. on 594.9, 695.1 nm Tl<sup>+</sup> transitions 0-23674  
P-Se-Tl glasses, NMR of <sup>31</sup>P and <sup>205</sup>Tl 0-15812  
PbF<sub>2</sub>-TlI graded coatings on KCl laser windows, photoacoustic spectroscopy 0-33052  
S-Tl, liquid semicond., bonding energies and entropies, mag. susceptibility meas. 0-49082  
Tl-Ge-S system, glass forming 0-19716  
Tl-Pb-S system, phase diagram quasibinary Tl<sub>2</sub>S-PbS section obs. 0-55372  
Tl-Se liquid binary mixtures, phase separation under press. 0-34183  
TlAlF<sub>4</sub>, hydrothermal growth method in presence of hydrofluorhydric acid (French) 0-25543  
TlAs, possibility of existence with sphalerite struct. 0-33950  
Tl<sub>3</sub>AsS<sub>4</sub>, optical phonons, Raman and refl. spectra 0-11400  
Tl<sub>3</sub>AsSe<sub>3</sub>, SHG, absorpt. coeffs. and temp. variation of refr. index difference 0-14390  
Tl<sub>2</sub>BRCl<sub>6</sub>, B=Li, Ag, Na, systematic structs., X-ray Guinier-Simon method (German) 0-44186  
TlBi, possibility of existence with sphalerite struct. 0-33950  
TlBr, electron-hole liquid, RPA calcs. 0-6743  
TlBr melts, Tl doped and pure, stoichiometric, nucl. spin relax. 0-25236  
TlBr, reson. Raman scatt., forbidden one phonon and intervalley scatt. at direct exciton 0-45073  
TlBr, second order Raman scatt., reson. behaviour rel. to phonon bands 0-40101  
TlBr, Wannier exciton-ionised donor complexes, binding energy calc. 0-49609  
TlBr-TlI, KRS-5, periodic strain anisotropy, optical and X-ray diff. study 0-54167  
TlBr-TlI, KRS-5 crystal, refr. index temp. increments meas. 0-33098



## thallium compounds continued

- TlBr-TlI, TlBr-TlCl, KRS-5 and KRS-6 crystals, optical losses, laser calorimetric meas. 0-9973  
 TlCdF<sub>3</sub>, third and fourth order elastic consts., press. depend. near phase transition (*French*) 0-34116  
 TlCdF<sub>3</sub>, weakly discontinuous phase transition, linear birefringence obs. 0-11362  
 Tl<sub>2</sub>Cd<sub>2</sub>(SO<sub>4</sub>)<sub>3</sub>, langbeinites, symmetry limitations on choice of hypothetical protophase 0-33916  
 Tl<sub>2</sub>Cd<sub>2</sub>(SO<sub>4</sub>)<sub>3</sub>, ferroelec. langbeinites, Raman scattering 0-34926  
 TlCl, band structure and optical spectra, local field and exchange effects 0-24798  
 TlCl, Debye-Waller parameter by powder elastic neutron diff. 0-29140  
 TlCl, electron-hole liquid, RPA calcs. 0-6743  
 TlCl, melts, stoichiometric, nucl. spin relax. 0-25236  
 TlCl, role of electron-hole interaction in optical spectra, review 0-45113  
 TlCl, second order Raman scatt., reson. behaviour rel. to phonon bands 0-40101  
 TlCl, self-consistent electronic struct. and ground state props. 0-15451  
 TlCl, Urbach rule at excitonic absorpt. edge, theoretical model tests 0-50299  
 TlCl, vap. press. and thermodynamics 0-6503  
 TlCl, Wannier exciton-ionised donor complexes, binding energy calc. 0-49609  
 TlCl-CsCl solid soln., determ. and computation of phase diagram 0-55379  
 TlCl-TlBr, KRS-6 crystal, refr. index temp. increments meas. 0-33098  
 TlCl-TlBr, KRS-6/GeSe, IR multilayer partial mirrors effective from 1.3 to 16  $\mu$ m 0-9978  
 TlCl<sub>3</sub>, vap. press. and thermodynamics 0-6503  
 TlCoF<sub>3</sub>, paramagnetic, nonmagnetic atomic nuclei spin density, NMR study 0-29633  
 $\alpha$ -Tl<sub>4</sub>CrI<sub>6</sub>, prep. and cryst. struct. determ. 0-28957  
 Tl<sub>2</sub>Cr<sub>2</sub>O<sub>7</sub>, Tl<sub>2</sub>Mn<sub>2</sub>O<sub>7</sub>, pyrochlore type, synthesis and physical props. 0-33963  
 TlD<sub>2</sub>PO<sub>4</sub>, dielectric props. under hydrostatic press. up to 7 kbar 0-29696  
 TlF, electric dipole hyperfine struct. calc. 0-53162  
 TlF, P- and T-violating interactions in hyperfine struct., mol. beam reson. expt. 0-53019  
 TlGaSe<sub>2</sub>-TlGaSe<sub>3</sub>, phase and composition-property diagrams 0-55366  
 TlGaSe<sub>2</sub>(Se<sub>2</sub>), phase transforms. under hydrostatic press., Raman scatt. study 0-25366  
 TlGaSe<sub>2</sub>Se<sub>2(1-x)</sub>, layer solid soln., long wave lattice vibrs., IR reflection spectra 0-11388  
 TlGaSe<sub>2</sub>Se<sub>2(1-x)</sub>, solid soln., fundamental optical absorpt. edge 0-25408  
 TlGaTe<sub>2</sub>, IR refl. and Raman scatt. spectra, lattice vibrs. 0-40108  
 TlGaTe<sub>2</sub>, multilayer cryst., lattice vibr. symm., IR absorpt. and Raman scatt. selection rules 0-39231  
 TlH<sub>2</sub>PO<sub>4</sub>, dielectric props. under hydrostatic press. up to 7 kbar 0-29696  
 TlH<sub>2</sub>PO<sub>4</sub>, high resolution heat capacity meas. (*Japanese*) 0-52218  
 Tl<sub>2</sub>HPO<sub>4</sub>, X-ray cryst. struct. determ. and refinement (*French*) 0-19756  
 TlI coatings on KCl laser windows, photoacoustic spectroscopy 0-33052  
 TlI, impurity in AC metal halide discharge, atomic plasma characts., a priori method 0-44034  
 TlI photodissociation, Tl atomic fluorescence, pressure and Doppler broadening 0-5504  
 TlI, Tl 5d XPS comparison with Tl 0-43099  
 TlI, XPS and UPS study of phase transforms. 0-45210  
 TlI/KCl/TlI low absorpt. antireflection coatings for KCl surfaces 0-38078  
 TlI-PbF<sub>2</sub> graded-index film coating technique and results 0-33265  
 TlInSe<sub>2</sub>, electrical cond. of single crystals with symm. and asymm. Ag-In contacts 0-6835  
 TlInSe<sub>2</sub>-TlInSe<sub>3</sub>, phase and composition-property diagrams 0-55366  
 TlInSe<sub>2</sub>Se<sub>2(1-x)</sub>, layer solid soln., long wave lattice vibrs., IR reflection spectra 0-11388  
 TlInSe<sub>2</sub>, electrical cond. of single crystals with symm. and asymm. Ag-In contacts 0-6835  
 TlInSe<sub>2</sub>, IR refl. and Raman scatt. spectra, lattice vibrs. 0-40108  
 TlInSe<sub>2</sub>(Te<sub>2</sub>), multilayer cryst., lattice vibr. symm., IR absorpt. and Raman scatt. selection rules 0-39231  
 TlInTe<sub>2</sub>, IR refl. and Raman scatt. spectra, lattice vibrs. 0-40108  
 Tl<sub>2</sub>Mo<sub>6</sub>Se<sub>6</sub>, one dimensional supercond. crystal struct., resist. and upper crit. field 0-50016  
 Tl<sub>0.33</sub>(NH<sub>4</sub>)<sub>0.67</sub>H<sub>2</sub>PO<sub>4</sub>, X-ray crystallographic investig. (*French*) 0-49192  
 TIP, possibility of existence with sphalerite struct. 0-33950  
 (Tl<sub>0.75</sub>Pb<sub>0.25</sub>)Cl<sub>5</sub>, cation disordered phase, X-ray diff. determ. of cryst. struct. 0-1985  
 Tl<sub>2</sub>S-SnS, phase equilibria exam. 0-55369  
 TlSb, possibility of existence with sphalerite struct. 0-33950  
 TlSe, Raman spectra, phonon modes 0-40109  
 TlSe, amorphous phase struct., rapid electron density distrib. curves 0-33896  
 Tl<sub>2</sub>Se, fused, diffusion of <sup>204</sup>Tl, <sup>110</sup>Ag, <sup>112</sup>Sn impurities 0-54415  
 Tl<sub>2</sub>SeAs<sub>2</sub>Te<sub>3</sub>, secondary electron emission, fluctuation state effect 0-40193  
 Tl<sub>2</sub>SeAs<sub>2</sub>Te<sub>3</sub>, vitreous, thermal switching process in high electric fields 0-2432  
 Tl<sub>2</sub>Ta<sub>2</sub>O<sub>6</sub>, localisation of TlI, electrostatic energy, calc. (*French*) 0-33926  
 Tl<sub>1-x</sub>Ta<sub>1+x</sub>W<sub>1-x</sub>O<sub>6</sub>nH<sub>2</sub>O, pyrochlore type, stoichiometry and ionic cond. 0-24648  
 Tl<sub>2</sub>Te<sub>3</sub>, exam. of electrical props., in solid, liquid state 0-54686  
 TlTiMO<sub>3</sub> (M=Ta, Nb), ion exchange props., synthesis and crystallographic props. (*French*) 0-28997  
 TlUF<sub>3</sub>, X-ray cryst. struct. anal. (*French*) 0-54184  
 Tl<sub>1.74</sub>V<sub>0.16</sub>, hollandite-type struct., synthesis and cryst. struct. 0-29003  
 Tl<sub>3</sub>VS<sub>4</sub>, growth of inclusion free crystals, for surface wave and bulk wave acoustic devices 0-25549  
 Tl<sub>0.33</sub>WO<sub>3</sub>, supercond. and special phonons, neutron scatt. obs. 0-15643  
 Tl<sub>2</sub>W<sub>4</sub>O<sub>13</sub>, tunnel struct., related to hexagonal tungsten bronze 0-28988

## thawing see melting

## The Galaxy

- 2  $\mu$ m radiation, mean intensity in solar neighbourhood 0-36744  
 5 GHz galactic plane radio sources, catalogue 0-4269  
 $\gamma$ -ray sources, number intensity relation rel. to galactic disc emission 0-46702  
 abundance gradients, reassessment from spectrophotometry of Perseus arm H II regions 0-22055  
 age, determ. from <sup>187</sup>Re-<sup>187</sup>Os systematics in meteorites 0-41778

## The Galaxy continued

- Be stars, photometric behaviour, UV excess, emission indices, galactic distrib. 0-36637  
 Carina spiral feature, distrib. of stars and interstellar dust along inner side 0-51871  
 central parsec, black hole 0-22089  
 central region, gas, dust, high energy particles and star form. dust, high energy particles and star form. 0-36713  
 centre, annihilation radiation due to positron prod. by evaporating black holes 0-46599  
 centre, as possible source of ultrahigh-energy cosmic rays 0-46351  
 centre field, planetary nebulae and Wolf-Rayet stars identifications 0-8674  
 centre region, OH absorpt. struct. determ. using regularisation method 0-17505  
 centre region, radio search for planetary nebulae, implications of flux density distrib. 0-56913  
 centre region, search for H<sub>2</sub> 2.1  $\mu$  emission 0-22059  
 centre region, star density rel. to nature of IR source IRS 16 0-46671  
 chemical abundance gradient, determ. from open clusters H-R diagrams anal. 0-56938  
 chemical evolution, effect of mass loss on chemical yields from massive stars 0-36614  
 chemical evolution, effect of stars mass loss by stellar wind 0-41814  
 chemical evolution, Mg isotopic abundances in five G and K dwarf stars 0-51757  
 chemistry, workshop proc. (Frascati, Italy, 29 May-2 June 1978) (*Italian*) 0-12845  
 cosmic ray age distrib. in galactic convective halo 0-51625  
 cosmic rays and magnetic field, distrib. from synchrotron radio and gamma-ray obs. 0-4207  
 dense radio H II regions distrib. in inner Galaxy, kinematic models 0-12813  
 disc  $\alpha\omega$  dynamo theory for mag. field generation 0-46663  
 disk and halo giant, CN strength differences 0-51750  
 dust/molecular clouds in Galaxy, props. 0-26925  
 dynamics, appl. of generalised twice restricted three-body problem (*Russian*) 0-51643  
 early-type stars, northern intermediate galactic latit., H $\beta$  photometry, rel. to galactic struct. 0-36631  
 evolution and spiral structure of a spiral galaxy 0-17667  
 evolution from light-element abundances, models, cosmological constraints 0-31401  
 evolution rel. to star formation mechanisms 0-12811  
 evolutionary models, constraints from white dwarf data 0-46548  
 exponential disk, scale length 0-41901  
 faint blue stars in high galactic latits., search of PSS fields near South Galactic Pole 0-46415  
 for IR emission, balloon obs. (*Japanese*) 0-36714  
 force field normal to galactic plane, determ. from z-oscill. theory 0-46669  
 galactic  $\gamma$ -ray lines, balloon investigation using Ge(Li) spectrometer 0-8677  
 galactic  $\gamma$ -rays from low energy cosmic ray interactions with interstellar medium 0-8678  
 galactic disc structure, theory of disc accretion in soft potential well 0-8532  
 gamma-ray burst sources, galactic distrib. models 0-22117  
 gamma-rays from disk and inverse Compton effect of electrons on starlight 0-26702  
 H I subsystem, rot. curve (*Russian*) 0-36724  
 halo, rot. from subdwarf kinematics 0-22003  
 high latitude nebulosity, as source of enigmatic dark lines crossing (M81) 0-56947  
 high luminosity stars in Galaxy and Magellanic Clouds, UBV intrinsic colours 0-26855  
 high-latitude regions, balloon-borne UV survey 0-41891  
 hot white dwarfs, EUV flux interstellar absorpt., local clumpiness factor determ. 0-36627  
 interstellar absorption lines of Na I, K I, Ca II, in stellar spectra rel. to galactic gas distrib. 0-26963  
 interstellar absorption lines towards 30 Doradus central object (HD 38268), profiles 0-51839  
 interstellar Ca II K-line profile in 30 Doradus direction, obs. 0-51850  
 interstellar CO, distrib. around (l=30°, b=0°) 0-41868  
 interstellar density fluctuations effect on pulsar scintillations 0-46649  
 interstellar gaseous medium, small oscill. freqs. in cylindrically symmetrical gravit. field (*Russian*) 0-41883  
 light extinction, A<sub>B</sub> coeff. amplitude 0-17664  
 Mira variables, statistical anal. of galactic concentration (*German*) 0-4390  
 Mira variables around globular clusters, freq. distrib., cluster membership 0-36676  
 Mira variables kinematics towards galactic centre 0-46578  
 N Monoceros region, late-type giants space density from two-micron objects survey 0-8555  
 non-thermal radio radiation from galactic polar regions, spectra 0-22082  
 North Polar Spur, radio continuum obs. at 1420 MHz 0-22100  
 photometric disc model, direct starlight intensities and interstellar dust clumping effects 0-22077  
 planetary nebulae, kinematics 0-26948  
 planetary nebulae kinematics, radial vel. meas. 0-46633  
 positron production by pulsars, galactic 511 keV gamma-ray line from positron annihilation 0-46590  
 pregalactic halo objects, gravitational lens effect 0-17484  
 radio sources near l=333°, 8.87 GHz obs. 0-22102  
 reflection nebulosities, high latitude, as false companions of galaxy (NGC 772) (*Russian*) 0-36723  
 rotation and structure beyond solar circle, photometry and spectra of young stars towards galactic anticentre 0-22079  
 SA 133 field near galactic centre, three-colour stellar photometry (*German*) 0-36618  
 solar neighbourhood initial mass function determ. from upper H-R diagram study 0-36626  
 South Galactic Pole, K-type giant stars population CN anomalies and distances 0-8622  
 southern Milky Way, loose stellar clusterings continued photometric studies 0-36679  
 spiral arms and terrestrial catastrophism, theoretical mechanism 0-31043  
 spiral structure parameters, derivation from stellar kinematics 0-17665  
 star formation by spiral density wave in disc of Galaxy 0-12812



**The Galaxy continued**

- star formation rate, rotational dynamics and interstellar gas density 0-51870  
 starlight, integrated, synthetic spectrum between 3000 and 10000 Å, calc. method and results 0-46536  
 stellar disc, central density min. 0-17663  
 stellar dynamics, reson. orbits comparison 0-56889  
 stellar nucleosynthesis, cosmochronology after Allende 0-4462  
 supergiant stars, southern, late-type, chem. comp., solar neighbourhood metallicity distrib. 0-12758  
 supernova remnants, new optical obs. 0-17636  
 supernova remnants interacting, rel. to galactic tunnel system 0-4409  
 three-dimensional motion of dwarf stars and RR Lyrae variables rel. to primordial galaxy contraction 0-12754  
 UVB photoelectric standards in SA 1-115, final catalogue 0-41733  
 X-ray background radiation isotropy, 2-18 keV energy range 0-46709  
 X-ray sources at galactic bulge, black hole and orbital disk model 0-17691  
 CO, radio emission rel. to cold mol. clouds in inner Milky Way 0-4425  
 D/H ratio in galactic centre direction, 327 MHz obs. upper limit 0-26949  
 H I, column density as function of position in southern sky 0-4420  
 H I 21 cm line, radial vel. contour maps 0-17626  
 H I absorption, obs. of struct. on small ang. scales 0-22051  
 H I at high galactic latitudes, time variable 21 cm line profiles correction 0-51844  
 H I distrib. and diffuse gamma rays 0-41917  
 H I gas, pervasiveness of intercloud medium 0-51825  
 H I regions, N.galactic hemisphere 0-17643  
 H I regions, new feature discovery in Vulpecula-Delphinus (*Russian*) 0-46654  
 H II regions, gas dynamics, galactic extended low density region components 0-36694  
 H $\alpha$  background emission, high spatial and spectral resolution pictures 0-56897  
 high-velocity clouds, dynamic coronal gas flows 0-56928  
 O/H abundance ratio determ. in Galaxy from H II regions radio obs. 0-36692

**theoretical mechanics** *see mechanics***thermal analysis**

- p-alkoxy-phenyl-p-acryloyloxy benzoate polymers, mesomorphic struct. 0-38905  
 alkylammonium zinc tetrachloride cpds., high temp. phase transitions 0-54372  
 applications, review 0-26083  
 aqueous soln. reaction kinetics meas. microwave apparatus 0-3470  
 BBAA, polymorphism, radiothermoluminescence and differential scanning calorimetric study 0-24570  
 bromoform, solid, phase transform., dielec. dispersion and differential scanning calorimetric obs. 0-24582  
 ceramic technology, DTA appl. 0-20913  
 p-chlorobenzylidene-p-n-pentylaniline, metastable phases formed by rapid cooling of mesophase, IR and Raman spectra and DSC obs. 0-34919  
 Cl (Co<sub>100-x</sub>Fe<sub>x</sub>)<sub>83</sub>B<sub>17</sub>, 1≤x≤30, annealing embrittlement and crystn. 0-45329  
 combined photovoltaic/thermal flat plate collectors, extended Hottel-Whillier model 0-3520  
 condensed systems, phase equilibria, 400-1100°C, DTA method 0-218  
 DL-cysteine, phase transition obs. at 10°C (*French*) 0-49355  
 DNA, sorption and desorption of water, thermal-stimulated press. and thermogravimetric anal. 0-8008  
 DNA hydrate, stability studied by thermogravimetry 0-30650  
 DSC curves correction for thermal lag effects, sp. ht. determ. case 0-37035  
 DTA, thermal curve interpretation 0-45599  
 DTA apparatus, modelling, elec. analogue approach 0-3270  
 EBBA, metastable phases formed by rapid cooling of mesophase, IR and Raman spectra and DSC obs. 0-34919  
 EBBA, polymorphism, radiothermoluminescence and differential scanning calorimetric study 0-24570  
 ethyleneterephthalate-ethylene glycol copolyester/15% polyglycol, semicryst. melting and glass transitions 0-49346  
 FBR Sphere-Pac carbide fuels, SPECKLE-1, computer modelling of thermal aspects of fuel response 0-18427  
 ferrocene, cryst., stable low-temp. phase 0-34185  
 fission reactor materials, gamma heating-effects, meas. using calorimetric and dosimetric techniques 0-658  
 2-fluoronaphthalene-2-naphthol system, phase relations, X-ray diffr. and DTA study 0-45287  
 gas analyser, two-bridge, based on voltage ratios meas. 0-50907  
 glass-crystal transition energetics, Pilyan's method appl. 0-38916  
 heterogeneous system, melting, enthalpy and phase relations (*Czech*) 0-45543  
 hexamethylolmelamine, doped, and condensation resin, room temp. phosphoresc., thermal transforms. 0-45132  
 Inconel 600, PWR primary corrosion products 0-13578  
 irradiated nuclear fuel transport flasks 0-5281  
 liquid crystals, solid state polymorphism, differential scanning calorimetry and IR and Raman spectra obs. 0-55094  
 lysozyme, sorption and desorption of water, thermal-stimulated press. and thermogravimetric anal. 0-8008  
 MBBA, metastable phases formed by rapid cooling of mesophase, IR and Raman spectra and DSC obs. 0-34919  
 microcomputer-controlled analyser, Du Pont 1090 system 0-16613  
 nematic liquid crystal, Merck 389, polymorphism, radiothermoluminescence and differential scanning calorimetric study 0-24570  
 nylon 6, oriented glassy, mol. wt. influence on cryst. rate 0-44156  
 photothermal radiometry, contact-free condensed matter anal., K<sub>2</sub>SO<sub>4</sub> powder appl. 0-26088  
 phthalocyanides, thermal stability, DTA (*German*) 0-11945  
 pitch, coal-derived low-volatile residues, glass transition, rheological props., DSC anal. 0-39331  
 poly(vinylidene fluoride) films, poled, piezoelec. activity and field-induced cryst. struct. transitions 0-20592  
 poly(vinylidene fluoride) orientation, solid state deformation by coextrusion 0-40394  
 poly-ε-caprolactum, semicryst. melting and glass transitions 0-49346  
 polyester-organic solvent mixtures, phase diagrams, eutectic props., devitrification, crystn. (*French*) 0-3015  
 polyesters, thermotropic, quiescent crystn. 0-38937

**thermal analysis continued**

- polyethylene, crystn. under high pressure 0-38946  
 polyethylene, drawn, ultrahigh modulus, linear, melting behaviour 0-19916  
 polyethylene, fibrillar, high mol. wt., oriented crystallisation, heat treatment effect (*Japanese*) 0-25738  
 polyethylene, high- and low-density, crystallinity degree, comparative obs. (*Polish*) 0-1943  
 polyethylene, linear, glass transition temp. 0-15225  
 polyethylene, nascent, electron microscope study 0-38940  
 polyethylene, oriented, shear strain, effect on struct., props. (*Russian*) 0-7656  
 polyethylene crystal, longitudinal growth in flowing soln., melting of continuous fibrillar crystal 0-19917  
 polyethylene electrets, charge trapping mechanism, TSC, DTA and optical meas. 0-11322  
 polyethylene fibres, high density, ultra oriented, physical, mech. props. 0-25649  
 polyethylene fibril, high mol. wt., high melting point crystal (*Japanese*) 0-38954  
 polymer glasses, aged, enthalpic state determ. by scanning calorimetry 0-6528  
 polymers, crystallinity determ. by thermal method (*Russian*) 0-38966  
 polypropylene, Halen and Daplen, semicryst. melting and glass transitions 0-49346  
 polystyrene, isotactic and static cold-crystallised blends, thermal transitions 0-24381  
 polystyrene, plasticizer effect on electric strength 0-29688  
 PTFE, annealing effect on melting and crystallisation (*Japanese*) 0-20980  
 PTFE+metal, fluoride prod., DSC and XPS anal., rel. to polymer wear 0-11889  
 PVC, plasticised, foam growth, thermomech. anal. 0-3416  
 pyrazine, cryst. phases, entropy changes and struct. implications 0-54397  
 rare earth cpds., R<sub>3</sub>Fe<sub>2</sub>O<sub>x</sub>-H, TGA-DTA meas., H absorption characts. 0-24600  
 Schiff's base compounds, double axis, Siamese Twin type liq. crystals, thermal and X-ray obs. 0-39312  
 silk fibroin films, conformational changes induced by water immersion 0-10498  
 solar furnace, focal spot thermal analysis 0-21383  
 steel, high-speed, solidification cycle, thermal anal. 0-29945  
 steel, stainless, PWR primary corrosion products 0-13578  
 temperature integral, approximative eqns., accuracy analysis 0-36834  
 terephthalate copolyester, heat treatment effect on melting point (*Japanese*) 0-40400  
 thermobalance, high sensitivity for macro samples, construction, performance (*Japanese*) 0-47023  
 thermogravimetric system for investigating gas-metal reactions at elevated temps. 0-229  
 thermoset and coating technology, torsional braid and thermal anal. 0-55622  
 vinyl alcohol-vinyl acetate copolymers, mol. architecture and physicochem. props. 0-44103  
 Zircaloy, PWR primary corrosion products 0-13578  
 Ag-CdO cermets, coprecipitated carbonates and hydroxides, physicochem. props. 0-25706  
 AgI solid electrolyte α-phase stabilisation 0-29209  
 AgZr<sub>2</sub>(PO<sub>4</sub>)<sub>3</sub> system, phase charact. at different temps. 0-29936  
 Al sheet, recrystallization, DSC eval. 0-3105  
 Al-Cu hypoeutectic, solidification cycle, thermal anal. 0-29945  
 Al-Cu(Zn, Ag, Mg<sub>2</sub>Si), intermediate precipitates, stability, X-ray, elec. resist. and hardness study 0-3063  
 Al-Mg-Si, DTA exam. after small and medium deform. 0-21002  
 Al-Zn (10 wt.%), ageing behaviour, calorimetric study 0-45328  
 Al-Zn (15 wt.%), calorimetric ageing study 0-45330  
 Al-Zn-Mg (4.5, 2 to 3 at.%) solid state reactions by interrupted continuous heating 0-25737  
 Al-Zn-Mg (4.5 at.%, 2 to 3 at.%), decomp. behaviour during continuous heating 0-29922  
 α-AlH<sub>3</sub>, prep., thermal decomposition, transform., struct. (*French*) 0-3326  
 AlPO<sub>4</sub>, high temp. behaviour up to liq. state, phase relations, X-ray diffr. and therm. anal. study (*French*) 0-10660  
 As, condensed layers, low temp. allotropic phase transition (*Russian*) 0-54553  
 B<sub>2</sub>S<sub>3</sub>-Ti<sub>2</sub>S<sub>3</sub> system, phase diagram and verification 0-35165  
 B<sub>2</sub>Se<sub>3</sub>-Ti<sub>2</sub>Se<sub>3</sub> system, phase diagram 0-35165  
 BaO-Fe<sub>2</sub>O<sub>3</sub>-B<sub>2</sub>O<sub>3</sub> glass, sput coated, low temp. micromagnetism 0-34660  
 BaO-MoO<sub>3</sub>, solid phase reaction, thermal analysis 0-55639  
 BaO-SiO<sub>2</sub> glass ceramic, growth and nucleation kinetics 0-7528  
 BaO-WO<sub>3</sub>, solid phase reaction, thermal anal. 0-55639  
 Bi<sub>2</sub>CoO<sub>3</sub>, in Bi<sub>2</sub>O<sub>3</sub>-CoO system, X-ray diffr., thermal anal. and metallography obs. 0-24598  
 BiH(PO<sub>3</sub>)<sub>2</sub>, condensed, thermal behaviour and IR spectra 0-19912  
 Bi<sub>2</sub>O<sub>3</sub>-AlPO<sub>4</sub>, phase equilib. 0-35168  
 Bi<sub>2</sub>O<sub>3</sub>-CoO system, X-ray diffr., thermal anal. and metallography obs. 0-24598  
 BiP<sub>2</sub>O<sub>4</sub>, condensed, thermal behaviour and IR spectra 0-19912  
 Bi<sub>2</sub>SnO<sub>7</sub>, polymorphic phase transition, X-ray, DSC, SHG, dielec. and optical obs. 0-44163  
 CaAl<sub>2</sub>O<sub>4</sub> compounds and cements, quantitative thermogravimetry after hydrothermal treatment 0-16737  
 CaCl<sub>2</sub>-Ca phase diagram, DTA study (*French*) 0-25672  
 Ca<sub>2</sub>(PO<sub>3</sub>)<sub>2</sub>OH, prep. from sulphate, X-ray diffr. and IR spectrosc. 0-29893  
 CaWO<sub>4</sub>, crystn. from solns. in NaWO<sub>4</sub> melts, kinetics obs. by DTA 0-40246  
 CdGeAs<sub>2</sub>, amorphous, thermal gradient expts., recrystn. 0-55438  
 CdSnP<sub>2</sub> crystal growth, DTA obs. of Cd-Sn-CdSnP<sub>2</sub> phase diagram 0-24394  
 CdTe-Au system, phase diagram rel. to doping 0-16282  
 CdTe-ZnS ternary mutual system, phase diagram 0-20904  
 Ce-Ga system, phase equilib. and cryst. struct. of phases 0-35159  
 Ce-Pr powder, DHCP→FCC transition, X-ray, DTA and resistivity studies 0-50629  
 CoTe<sub>2</sub>-GeTe<sub>2</sub>, phase diagram, from thermal, X-ray, microstructural analyses 0-55367  
 CrS-FeS, sulphorspinel, struct. and elec. props. 0-49834  
 CrSe<sub>2</sub>, layered, phys. and elec. props. 0-44594  
 Cs-Sn alloy, peritectic reactions, phase diagram (*Russian*) 0-40784



## thermal analysis continued

- CsCl-CuCl, phase transform. heats, DTA obs. (*Russian*) 0-55698  
 $\text{Cs}_2\text{Ni}_3(\text{P}_2\text{O}_7)_2 \cdot n\text{H}_2\text{O}$ , thermal dehydration 0-35513  
 Cu-Al-Ni, mixed powder compacts, Ni content influence in sintering behaviour (*Japanese*) 0-35130  
 Cu-Al-Ni (13.8, 7.9 wt.%), cooling rates effect on internal friction (*Japanese*) 0-39217  
 Cu-Ni-Sn, liq. alloy, mixing enthalpies determ. using a SETARAM high temp. calorimeter (*German*) 0-44324  
 CuI solid electrolyte  $\alpha$ -phase stabilisation 0-29209  
 $(\text{CuInTe})_{1-x}(\text{ZnTe})_x$ , phase diagram and cryst. growth of  $\text{CuZn}_2\text{InTe}$  from  $\text{ZnCl}_2$  flux 0-16287  
 $\text{Cu}_2\text{O}$ -CuO-MoO<sub>3</sub>, subsolidus phase diagram, mag. props. 0-50615  
 $\text{Cu}_2\text{S}$ -Ti<sub>2</sub>S system, phase diagram 0-20906  
 DyB<sub>6</sub>, form. mechanism, reduction of Dy<sub>2</sub>O<sub>3</sub> by B, DTA appl. 0-55643  
 Dy<sub>2</sub>B<sub>3</sub>, prep. and props., DTA study 0-20859  
 Fe, cast, spheroidizing effect of Mg and Ce modifiers 0-35193  
 Fe-C eutectic, solidification cycle, thermal anal. 0-29945  
 Fe-C hypereutectic, solidification cycle, thermal anal. 0-29945  
 Fe-Cr-Al (0.3 wt.%), oxidation behaviour at high temps. (*Japanese*) 0-35404  
 Fe-Cr-Ni austenitic alloy, cold deformed,  $\alpha$ - $\gamma$  transition, calorimetric study (*Russian*) 0-55390  
 Fe-Ni-Al-Co-Ti base alloys, highly coercive, phase comp., Mossbauer meas. 0-39996  
 Fe-Zn, phase diagram, DTA, EDAX, X-ray diffr. study 0-50602  
 $\text{Fe}_{48}\text{B}_{16-x}\text{C}_x$ , amorphous alloys, short range order, Mossbauer and DSC study 0-39960  
 $(\text{Fe}_{100-x}\text{Ni}_x)_{100-y}\text{B}_y$ , metallic glass, embrittlement and crystn. 0-7685  
 FeO, wustite, invariant points between stable and metastable phases, T-P-X diagram (*French*) 0-29938  
 $\text{Fe}_2\text{O}_3$  based  $\gamma$  defective spinels, elec. cond. behaviour during transform. to  $\alpha$  rhombohedral phases (*French*) 0-49354  
 $\alpha$ - $\text{Fe}_2\text{O}_3$ -Li<sub>2</sub>O, structural and thermal phase behaviour from mag., spectral and thermal studies 0-2673  
 $\text{Fe}_3\text{O}_4$ , magnetite, Verwey transition temp., isotope effect, elec. resist. and DTA meas. 0-24976  
 $\text{GdCl}_3 \cdot 6\text{H}_2\text{O}$ , X-ray emission luminesc. (*Japanese*) 0-55763  
 $\text{Gd}_2\text{Ga}_2\text{O}_{12}$ , garnet-perovskite transform 0-15239  
 Ge-GeO<sub>2</sub> mixtures, gasification kinetics and GeO form. mechanism (*Russian*) 0-21273  
 Ge-Te binary glass, eutectic, DSC obs., thermodynamic and thermokinetic characts. 0-39309  
 GeSe<sub>2</sub>, single crystals, 3 polymorphic forms, DTA, photolum., IR and Raman spectroscopy 0-33923  
 Hf-Ni(Co), amorphous, formation, decomposition and elec. transport props. 0-20143  
 In-Pb-Sn system, thermal anal. 0-35162  
 $\text{K}_2\text{Ca}(\text{SO}_4)_2 \cdot \text{H}_2\text{O}$ , syngenite, thermal dehydration under nonisothermal conditions 0-3324  
 $\text{K}_2\text{Cr}_2\text{O}_7$ , polymorphic behavior, depend. on thermal and prep. history 0-34184  
 $\text{KEuHP}_3\text{O}_{10}$  acid, exam. of thermal decomposition 0-55638  
 $\text{KMg}_2(\text{AlSi}_3\text{O}_{10})\text{F}_2 \cdot \text{KMg}_2\text{Si}_4\text{O}_{10}\text{F}_2$ , solid soln., melting and crystn., quenching and DTA study 0-39263  
 $\text{K}_2\text{Ni}_3(\text{P}_2\text{O}_7)_2 \cdot n\text{H}_2\text{O}$ , thermal dehydration 0-35513  
 $\text{KO}_2$ , non-isothermal decomp. kinetics 0-16649  
 $\text{KO}_2$ , thermal decomp. macrokinetics, differential thermal anal. 0-16650  
 $\text{K}_2\text{O}$ , thermodynamic props. 0-29184  
 $\text{K}_{1-x}\text{Ta}_{1-x}\text{W}_{1-x}\text{O}_6 \cdot n\text{H}_2\text{O}$ , composition, struct. and ionic conductivity 0-49410  
 $\text{La}_2(\text{SO}_4)_3 \cdot 9\text{H}_2\text{O}(\text{D}_2\text{O})$ , dynamic disorder of water mols., isotope effect obs. 0-55015  
 $(\text{Li},\text{Na},\text{K})(\text{Nb},\text{Ta})\text{O}_3$ , pseudo-binary and ternary systems quenched metastable glassy and cryst. phases 0-29935  
 Li soaps,  $n\text{C}_{13}$ - $n\text{C}_{20}$ , phase transition temps. and enthalpies, DSC obs. 0-45544  
 Li<sub>2</sub>SO<sub>4</sub> cells, safety studies, DTA of constituents 0-16795  
 $\text{LiBO}_2$ -In<sub>2</sub>O<sub>3</sub>, phase composition, mag. props, elec. cond. 0-55365  
 $\text{LiF-AlF}_3$ -Na<sub>3</sub>AlF<sub>6</sub>-Al<sub>2</sub>O<sub>3</sub> system, phase equilibrium, X-ray diffr., DTA, quenching, optical microscopy study 0-50610  
 $\text{Li}_2\text{K}(\text{IO}_3)_3$  in  $\text{LiIO}_3$ -KIO<sub>3</sub> system, lattice parameter, equilb. and metastable phase diagram (*Chinese*) 0-7538  
 $\text{Li}_2\text{O-Al}_2\text{O}_3(\text{Ga}_2\text{O}_3)(\text{Bi}_2\text{O}_3)$ , quenched glasses, crystn. and ionic cond. 0-33899  
 $\text{Li}_2\text{O-SiO}_2$ -(TiO<sub>2</sub>) glass, crystn., kinetic study using differential scanning calorimetry 0-44138  
 Mg-In liquid solns., EMF and calorimetric meas. 0-55359  
 Mg-Y-Cd, phase equilibria and mech. props. (*Russian*) 0-20894  
 $\text{Mg}(\text{AlH}_4)_2$ , prep., thermal decomposition, molar heat capacity, heat of form. 0-3325  
 $\text{Mg}(\text{NO}_3)_2 \cdot 6\text{H}_2\text{O}$ , crystal structure changes due to substitution of  $\text{Mg}^{2+}$  by  $\text{Co}^{2+}$  or  $\text{Ni}^{2+}$  (*German*) 0-24428  
 $(\text{NH}_4)_2\text{Ni}_3(\text{P}_2\text{O}_7)_2 \cdot n\text{H}_2\text{O}$ , thermal dehydration 0-35513  
 $\text{NaCl-NaBr-TeO}_2$ , condition diagram, thermographic obs. (*Russian*) 0-55377  
 $\text{NaF-YF}_3$  system, fusibility diagram, quasibinary section of  $\text{NaF-YF}_3$ -YOF system characts. 0-55371  
 $\text{Na}_2\text{Ni}_3(\text{P}_2\text{O}_7)_2 \cdot n\text{H}_2\text{O}$ , thermal dehydration 0-35513  
 $\text{Na}_2\text{O}$ , non-isothermal decomp. kinetics 0-16649  
 $\text{NaO}_2$ , thermal decomp. macrokinetics, differential thermal anal. 0-16650  
 Nb-Si diagram of state, melting temp., polymorphic transform. temp. (*Russian*) 0-50594  
 $\text{NbOAsO}_4$  and  $\text{NbOAsO}_4 \cdot 4\text{H}_2\text{O}$ , crystal growth, composition, struct. and crystallographic characts. 0-54198  
 $\text{NdTiO}_3$ , physicochem. props. 0-25625  
 Ni-B amorphous films, electronic transport and crystn. activation energies (*French*) 0-6807  
 Ni-P, amorphous electrodeposited alloys, phase-separation (*Japanese*) 0-54140  
 $\text{Ni}(\text{H}_2\text{V})_2(\text{H}_2\text{O})_2$ , synthesis and characterisation (*French*) 0-45225  
 $\text{Ni}_{16}\text{Ti}_{20}\text{Zr}_9$ , amorphous, H-sorption, X-ray and DSC obs. 0-49526  
 $\text{Ni}_{16}\text{Zr}_{36}$ , amorphous and cryst., H-sorption, X-ray and DSC obs. 0-49526  
 PLZT ceramics, ferroelectric and struct. transitions, crystallographic, thermal, and dielec. anal. 0-29693  
 $\text{PbF}_2$ , polymorphic transition temps. under hydrostatic press., DTA study 0-2156  
 $\text{PbF}_2$ -AlF<sub>3</sub> glass, optical props., crystn. and thermal expansion 0-48367  
 $\text{PbS}$ , oxidation,  $\text{PbSO}_4$  distrib. in products (*Polish*) 0-25883  
 $\text{Pb}_2\text{TaMnO}_6$ , reaction of form. from oxides, ferroder. props. 0-55326

## thermal analysis continued

- PbTe-PbSe system, thermodynamic props. 0-11635  
 $\text{PbZrO}_3$ , phase transitions, X-ray, dielec., and thermal anal. 0-45020  
 $1-x\text{PbZrO}_3-x\text{PbScO}_3\text{NbO}_3$ ,  $0 \leq x \leq 1$ , phase transitions, X-ray, dielec., and thermal anal. 0-45020  
 Pd-Ag-Si alloys, amorphous, crystn. kinetics, DSC meas. 0-1933  
 Pd-Au-Si, amorphous films, RF sputter deposition, composition and thermal behaviour 0-55292  
 Pd-Si amorphous films, RF and DC sputter deposition, composition and thermal behaviour 0-55292  
 PdAl-Fe(Ni), phase diagrams, eutectic points and solubility (*Russian*) 0-40333  
 Pr-Ga (0 to 50 at.%), phase diagram and cryst. structs. of intermetallic cryst. 0-3002  
 $\text{Pr}(\text{OH})_3$ , thermal decomposition, exam. 0-55640  
 $\text{PuO}_{2.82(1.49)}$ , high temp. enthalpies 0-49384  
 $\text{RbCl-CuCl}$ , phase transform. heats, DTA obs. (*Russian*) 0-55698  
 $\text{Rb}_2\text{Ni}_3(\text{P}_2\text{O}_7)_2 \cdot n\text{H}_2\text{O}$ , thermal dehydration 0-35513  
 Sb, liquid-quenched, stabilisation and transformation kinetics of metastable phases 0-3022  
 $\text{Sb}_2\text{O}_3$ -Na<sub>2</sub>O-B<sub>2</sub>O<sub>3</sub>-SiO<sub>2</sub> glass, elec. cond. meas., -160 to 200°C 0-20190  
 $\text{Sb}_2\text{O}_3\text{Cl}_2$ , single crystals, prep. and props. 0-35067  
 Sc-H, p-T phase diagram and influence of H pressure, on decomposition temp., DTA exam. 0-29929  
 Se, monoclinic to trigonal conversion, thermodynamic stability and associated investigs. 0-24592  
 $(\text{Se})_x$ , crystn. and melting 0-40241  
 SiC fibres obtained from polycarbosilane fibre 0-50582  
 $\text{Si}_3\text{N}_4$ -Al<sub>2</sub>O<sub>3</sub>, solid soln., prep., effect of  $\text{Si}_3\text{N}_4$  powder reactivity 0-45256  
 $\text{SiO}_2$ -Li<sub>2</sub>O-K<sub>2</sub>O-ZnO glass ceramic, prep., phase transformations and physical props. 0-45299  
 $\text{SiO}_2$ -Na<sub>2</sub>O-CaO-MgO-Al<sub>2</sub>O<sub>3</sub> charge, silicate formation during heating 0-55342  
 $\text{Sm}_2\text{Ga}_2\text{O}_{12}$ , garnet-perovskite transform 0-15239  
 Sn droplets, on Bi, Zn and Al, heterogeneous nucleation 0-44294  
 Sn-F system, partial phase diagram construct. in Sn-SnF<sub>2</sub> region (*French*) 0-50605  
 Sn<sub>1</sub>-SnF<sub>3</sub> system, phase diagram construct. (*French*) 0-50605  
 Te-In alloys, direct reaction calorimetric study, 737 to 1340K (*French*) 0-49382  
 Ti-Zr-W(Al) alloys, phase struct. and props. (*Russian*) 0-16270  
 TiO<sub>2</sub>, obtained ions  $\text{Ti}_2\text{OCl}(\text{HCOO})_3(\text{OH})_2$ , by thermohydrolysis, exam. of crystallisation 0-2173  
 TiGaSe<sub>2</sub>-TiGaSe<sub>2</sub>, phase and composition-property diagrams 0-55366  
 TiInS<sub>2</sub>-TiInSe<sub>2</sub>, phase and composition-property diagrams 0-55366  
 Ti<sub>2</sub>S-SnS, phase equilibria exam. 0-55369  
 $\text{Ti}_{1-x}\text{Ta}_{1+x}\text{W}_{1-x}\text{O}_6 \cdot n\text{H}_2\text{O}$ , pyrochlore type, stoichiometry and ionic cond. 0-24648  
 U-UNi<sub>2</sub>-UCO<sub>2</sub>, system, phase equilibria, lattice constants (*German*) 0-50598  
 UO<sub>2</sub> ceramic fuel fabrication, simulation of thermal processes by emanation thermal anal. 0-811  
 UO<sub>2</sub>, sintered, production by gel calcination and drying, thermal anal. (*Czech*) 0-45260  
 V-H(D), metallographic and thermal differential anal., potential for H energy storage appls. 0-45281  
 V-Ni-Mo, structure, in alloy crystallisation region, peritectic equilibria (*Russian*) 0-50622  
 $\text{V}_2\text{O}_5$ , high-temp. phase transition, resistivity, valence photoelectron spectra 0-49357  
 WC-Co powder, prep. by direct carburisation of WO<sub>3</sub> in presence of Co<sub>2</sub>O<sub>4</sub> 0-50573  
 YAG, production of densely sintered ceramic, exam. of recrystallisation during sintering 0-11609  
 $\text{Y}_2\text{Ti}_2\text{O}_7$ , precipitation from oxalates, carbonates, exam. 0-55641  
 $\text{ZnFe}_2\text{O}_4$ -Fe<sub>2</sub>O<sub>3</sub> solid solns., form. of  $\alpha$ -Fe<sub>2</sub>O<sub>3</sub> during oxidation 0-25889  
 $\text{ZnSiP}_2$  crystal growth, DTA obs. of Sn-Zn-ZnSiP<sub>2</sub> phase diagram 0-24394  
 ZrO<sub>2</sub> gels, calcination 0-11964  
 ZrO<sub>2</sub>, stabilised, fabrication by hot petroleum drying method, X-ray diffr. and thermal anal. study 0-40297

## thermal capacity see specific heat

## thermal conductivity

- see also Kapitza resistance; Lorenz number; thermal conductivity of gases; thermal conductivity of liquids; thermal conductivity of solids; thermal diffusivity; thermal insulating materials  
 bar, cylindrical, thermal cond. calc. using numerical soln. of Boltzmann eqn. 0-44373  
 conference, Chicago, USA (Nov. 79) 0-31425  
 cylinders, perfectly conducting arrays, transport prop. investig. 0-13011  
 fluid flow in packed beds, effective heat transfer parameters, theoretical predictions 0-14802  
 heat filters for bolometers cooled to very low temperatures 0-52315  
 inhomogeneous thermal system, thermal cond. and boundary resistance at low temp., heat flow model calc. 0-10120  
 metal, effects of large scale voids on thermal magnetoresist. 0-10946  
 nonideal thermal contact, heat exchange between thin walled bodies (*Russian*) 0-14553  
 nonlinear inverse thermal cond., iterative soln. 0-23865  
 plate heating by localised volume heat source with power-time depend. (*Russian*) 0-53608  
 stars, rotating, secular instability from thermal cond. 0-21986  
 system with nonconserved order parameter, influence of heat cond. on relax. of unstable states 0-10637  
 systems analysis method, to solve thermal cond. problems (*Russian*) 0-24685  
 temperature fields in space-connected regions with alternating contact thermal resistance (*Russian*) 0-53607  
 thermionic convertors, effect of electron thermal conductivity, theory 0-40892  
 Al thin films, HF induction plasma treatment, effect on phys. props. (*Russian*) 0-24961  
<sup>3</sup>He, boundary resistance of low temp., heat flow model calc. 0-10120  
<sup>4</sup>He, boundary resistance at low temp., heat flow model calc. 0-10120  
 SiC, 6H polytype, elec. and thermal cond., carrier concentrations 0-2223

## thermal conductivity measurement

- apparatus to meas. thermophysical props. at high temps. 0-37458



**thermal conductivity measurement continued**

- Benard-Rayleigh problem, experimental system for measurement of equivalent thermal conductivity 0-33711  
 cryostat system, thermal transport in solids 0-52243  
 detector, with a narrow packed column 0-22355  
 foam insulation material, unsteady probe method (*German*) 0-31740  
 gases, thermal cond. by coaxial-cylinder method, Knudsen effect 0-42219  
 heat flux measurement based on thermoelectric props. of thin electroplated foil 0-37026  
 hot wire method for gaseous CO<sub>2</sub> and Kr at elevated temps. 0-6199  
 hot wire method for gaseous CO<sub>2</sub> and Kr at elevated temps. 0-6200  
 hot wire techniques for refractories 0-37038  
 hot-wire method for refractories, 20 to 900°C 0-31759  
 magnetothermal conductivity using frequency-crossing phonon spectrometer 0-31741  
 organic liquids, radiant heat exchange effect 0-19996  
 poor heat conductors, meas. under monotonic conditions 0-4706  
 rock sample, steady state plate method (*Chinese*) 0-56615  
 semiconductors, thermophysical props. determ. from Ettingshausen effect meas. method 0-44376  
 solidified gas constant-volume thermal conductivity meas. cell 0-31739  
 thermal insulation on metal backing, thermophys. characts., expt. determ. technique 0-4707  
 transient hot-strip method for simultaneously measuring thermal conductivity and thermal diffusivity of solids and fluids 0-1417  
 transient hot-wire technique, improvements, wire tension effect and elimination of stray electric pulses 0-48839  
 transient hot-wire technique 0-48838

**thermal conductivity of gases**

- aerosol particles, charged, effect on thermal and elec. conds. of ionised gas 0-28593  
 binary mixtures of monatomic gases, Chapman-Enskog theory 0-24118  
 inert gases, transient hot-wire technique 0-48838  
 linear mol. gas thermal cond. Senftleben-Beenakker effect, effective collision cross section 0-24117  
 polar gases in mag. field 0-1728  
 polyatomic gas, in external field, simplified expressions 0-6197  
 sonic nozzle expansions, rot. relax. theory 0-43827  
 steam, thermal cond. equation, 0 to 800°C, triple pt. press. to 1000 bars, crit. region 0-39364  
 symmetric top molecules, viscosity and thermal cond. under simultaneous elec. and mag. field 0-6188  
 transient hot-wire technique, improvements, wire tension effect and elimination of stray electric pulses 0-48839  
 water, vapour, radiation absorption capacity 0-14873  
 Ar, Lennard-Jones (12-6) pot. parameters calcs. 0-28591  
 Ar, thermal cond., 90-273K 0-48836  
 Ar<sub>2</sub>, interatomic potential single parameter 0-48059  
 CO<sub>2</sub>, thermal conductivity meas. at elevated temps. by hot wire method 0-6199  
 CO<sub>2</sub>, thermal conductivity meas. at elevated temps. by hot wire method 0-6200  
 CO<sub>2</sub>+O<sub>2</sub>(NO), Senftleben-Beenakker effect, saturation field, Kohler-Raum theory and obs. 0-28596  
 D<sub>2</sub>O, vapour, mol. association entropy and enthalpy, thermal cond. meas. 0-7777  
 H<sub>2</sub>O, vapour, mol. association entropy and enthalpy, thermal cond. meas. 0-7777  
 He-Ar, gas mixtures, thermal cond. meas. in the range 0.5-15 MPa 0-14874  
 Hg vapour, viscosity and thermal cond. meas., data anal., 694-1054K 0-19545  
 K vapour, 800-1050K 0-19546  
 Kr, Lennard-Jones (12-6) pot. parameters calcs. 0-28591  
 Kr, thermal conductivity meas. at elevated temps. by hot wire method 0-6199  
 Kr, thermal conductivity meas. at elevated temps. by hot wire method 0-6200  
 N<sub>2</sub>, rotational collision number from thermal cond., 700-2500K 0-23526  
 Ne, Lennard-Jones (12-6) pot. parameters calcs. 0-28591  
 Ne, thermal cond., 90-273K 0-48836  
 Ne-Ar, gas mixtures, thermal cond. meas. in the range 0.5-15 MPa 0-14874  
 Ne-Ar, thermal cond., 90-273K 0-48836  
 Ne-Ar-Kr, gas mixtures, thermal cond. meas. in the range 0.5-15 MPa 0-14874  
 Rb, vapour, thermal cond. meas. 0-14870  
 SF<sub>6</sub>, equivalent thermal conductivity determ. (*Czech*) 0-53911  
 SO<sub>2</sub> on gas covered Pt surface, thermal conductivity and thermal accommodation coeff. 0-10346  
 Xe, Lennard-Jones (12-6) pot. parameters calcs. 0-28591

**thermal conductivity of liquids**

- coolants and index matching media for Nd:glass laser systems 0-33015  
 organic liquids, thermal conductivity meas., radiant heat exchange effect 0-19996  
 superheated organic liquids, thermal cond. meas. 0-15316  
 water, thermal cond. equation, 0 to 800°C, triple pt. press. to 1000 bars, crit. region 0-39364  
 Widom-Rowlinson hard-sphere mixture model, transport props. 0-14981  
 As<sub>2</sub>(Se<sub>1-x</sub>Te<sub>x</sub>)<sub>3</sub> semiconducting glasses, solid and liquid, thermal cond. 0-6574  
 Cu<sub>3</sub>AsS<sub>4</sub> and Cu<sub>3</sub>SbS<sub>4</sub>, thermal cond. in solid and liq. phases, 300 to 1100K, thermoelec. Q-factor 0-19997  
 Fr, properties from melting point to 7500K, prediction (*Russian*) 0-44296  
<sup>3</sup>He-<sup>4</sup>He mixture, transport props. near superfluid transition and tricritical point 0-29242  
<sup>4</sup>He, liq., critical thermal cond. near  $\lambda$ -point, light scatt. spectrum 0-24697  
<sup>4</sup>He, liq., dynamic scaling near T <sub>$\lambda$</sub>  0-34264  
<sup>4</sup>He, superfluid, heat transport in restricted geometries, 0.8-2K 0-29237  
<sup>4</sup>He, superfluid, surface, ripplons, adsorbed <sup>3</sup>He and heat conduction meas. 0-49459  
<sup>4</sup>He, superfluid, transient heat transport 0-10715  
<sup>4</sup>He, superfluid, viscosity and thermal conductivity (*Russian*) 0-10720  
 In, thermal cond. in solid and liq. phases, Wiedemann-Franz law 0-39554  
 UO<sub>2</sub>, thermal and transport props., electronic contrib. 0-15432

**thermal conductivity of solids**

see also *thermal magnetoresistance*

- AC superconductor, uniform, behaviour of normal zones 0-11127  
 alkali metals, ideal thermal resist. and Lorenz number due to conduction electron-phonon scatt. 0-29377  
 alloys, binary, thermal cond. conc. depend., irreversible processes, thermodynamic calcs. (*Russian*) 0-39550  
 amorphous solid, phonon scatt. by density fluctuations and thermal cond. 0-10626  
 balsa wood, cryogenic insulation, exam. of strength specifications, props. 0-25819  
 Boltzmann eqn., phonon and electron transport in bounded systems 0-39545  
 brass, electronic and lattice components, separation methods 0-29380  
 brass alloys, thermal and elec. cond., 4 to 300K, Zn conc. depend. 0-29379  
 Callaway eqn., phonon scatt. in highly disordered systems 0-20000  
 coal, thermal diffusivity and cond. meas. for in situ coal gasification appls. 0-30360  
 composite materials, effective thermal conductivity 0-54447  
 composite materials, surface, flame propagation velocity rel. to thermal props. (*Russian*) 0-7797  
 cylinder, hollow infinite, with temp. depend. thermal cond., thermal stress anal. 0-14575  
 diamond, thermal cond. at low temp., correl. with IR absorpt. features 0-49435  
 dielectric, thermal cond. at low conc. of phonon scatt. centre, freq. crossing signals 0-2224  
 dielectric material, phonon thermal conductivity, Umklapp process, comparison with LiF data 0-39367  
 dilute magnetic alloy, reverse Kondo effect, magneto-transport theory 0-15509  
 dispersed materials, effective thermal conductivity (*German*) 0-33440  
 ferritic scales on steam generating tubes, thermophysical props., thermal conductivity 0-2221  
 fibreglass composite, with complex spatial struct. 0-6571  
 glass fibre reinforced epoxy, thermal cond., diffusivity and sp. ht., determ. 0-24613  
 glass-C fibre reinforced epoxy, thermal cond., diffusivity and sp. ht., determ. 0-24613  
 glass-forming polymer, paramag. spin-lattice interactions 0-7149  
 glasses, thermal cond. rel. to diffusion process due to phonon-defect interaction 0-34259  
 graphite, phonon thermal conductivity, rel. to elec. cond., possible supercond. 0-49434  
 heterogeneous matrix system, generalised conductivity and loss, tangent 0-7289  
 ice, Ih, thermal resist. near melting point meas. 0-44375  
 insulator, lattice thermal resist. due to core dislocations 0-29231  
 intermediate state superconductor, kinetic props. of corrugated and thread struct., sound attenuation (*Russian*) 0-54843  
 Jahn-Teller cooperative T-(e+t) systems, heat current operator 0-34405  
 Jahn-Teller cooperative T-(e+t) systems, pseudo spin thermal cond. 0-34406  
 lattice thermal conductivity, general transport theory, phonon Boltzmann eqn. 0-54446  
 metal, deformed in pressing process, temp. field modelling (*Russian*) 0-53602  
 metal, heating by laser emission, spatial nonlinear problems (*Russian*) 0-7440  
 metal, laser heating kinetics, influence of oxide film interf. effects 0-11841  
 metal-H systems at high H press., physicochemical props., book contrib. 0-24535  
 metallic crystal, thermomechanical deform., analytical description 0-49391  
 metallic thin films, unlike surface properties, transport coeffs., diffuse surface scatt. 0-20331  
 metals, fracture during laser working, depend. on physico-chem. props., heat cond. (*Russian*) 0-55432  
 metals, thermal conductivity models, during hot descaling (*Russian*) 0-24869  
 mixed-carbide, sphere-Pac fuel, thermal conductivity during initial stage restructuring 0-810  
 molten salt, heat storage, review (*Japanese*) 0-6573  
 non-steady state thermal conductivity in multilayer sheets (*Russian*) 0-43596  
 oligocarbonatomethacrylates, and their cross-linked polymers, thermophysical characts., temp. depend. anal. 0-19721  
 phonon conductivity correction due to three phonon normal processes in presence of dislocations 0-15318  
 phonon diffusion with freq. down-conversion 0-19886  
 polyamide, Al<sub>2</sub>O<sub>3</sub> filled, low temp. thermal and mech. props. 0-25816  
 polymer surface, flame propagation velocity rel. to thermal props. (*Russian*) 0-7797  
 polysulphur nitride, low temp. thermal cond. 0-24689  
 pore velocity, due to surface diffusion under temp. gradient, finite thermal conductivity correction 0-15428  
 quartz ceramics, thermal and temp. cond. in range 500-1900K 0-39370  
 rare earth garnets, prep. and props. book contrib. 0-44193  
 rare earth oxides, binary, struct. and props., book contrib. 0-45292  
 refractories, hot wire meas. technique 0-37038  
 refractories, hot-wire meas. method, 20-900°C 0-31759  
 refractories, microcracks contrib. 0-19999  
 refractory materials, contrib. of segregation and diffusion to heat cond. 0-20001  
 semiconductor, thermal cond. calc. using numerical soln. of Boltzmann eqn. 0-44373  
 semiconductors thermophysical props. determ. from Ettingshausen effect meas. method 0-44376  
 semiinfinite bar, boundary value inverse heat conduction problem, hyperbolic eqn. soln. 0-19210  
 sintered porous materials, effective thermal conductivities 0-19998  
 smoky quartz, thermal props. at very low temp. 0-24610  
 solidified gas constant-volume thermal conductivity meas. cell 0-31739  
 soot, granulated, thermal and elec. cond. 0-24687  
 spectroscopy of high-frequency phonons, transport phenomena, review 0-49325  
 steel forgings, expt.-calc. model of quenching, temp. meas. across cross section 0-16345



**thermal conductivity of solids continued**

- stochastic temperature field in cylinder, digital simulation algorithm (Polish) 0-17879
- superconductor, dirty, mixed state, thermal cond. anisotropy 0-7036
- superconductors, long, thin-film, min. hotspot current 0-15656
- superconductors at Lifshitz electronic transition point (Russian) 0-11135
- thermal insulation on metal backing, thermophys. characts., expt. determ. technique 0-4707
- tissue-equivalent plastic, A-150, thermal diffusivity, sp. ht., thermal cond. obs. 0-34258
- transition metal compound refractories, electron and phonon behaviour 0-54624
- transparent dielectric with metallic inclusions, light pulse shape effect on optical breakdown threshold 0-20588
- YIG, thermal cond. at low temps. 0-2222
- Al, electron-phonon enhancement of electron-electron scatt., elec. and thermal cond. 0-49326
- Al, lattice thermal cond. at low temps., Ashcroft pseudopotential method 0-19897
- Al plates with air gap, temp. field for microplasma welding of edge joints (Russian) 0-7755
- Al, thermal conductivity minimum, effect of lattice component 0-15500
- Al-Mg-Si, DTA exam. after small and medium deform. 0-21002
- As, electrical resist., thermal cond. and thermopower, low temp. transport props. 0-49708
- As<sub>2</sub>(Se<sub>1-x</sub>Te<sub>x</sub>)<sub>3</sub> semiconducting glasses, solid and liquid, thermal cond. 0-6574
- B<sub>3</sub>C, mech. and thermal props. 0-21083
- B<sub>2</sub>O<sub>3</sub>-Na<sub>2</sub>O-SiO<sub>2</sub>-Al<sub>2</sub>O<sub>3</sub>, effect of alumina dispersions on the thermal cond./diffusivity/stress resist. 0-39368
- B<sub>2</sub>O, mech. and thermal props. 0-21083
- Bi, electrical resist., thermal cond. and thermopower, low temp. transport props. 0-49708
- Bi-Sn, thermoelec. props. from 2 to 300K 0-24872
- Bi<sub>2</sub>O<sub>3</sub>, thermoelec. props., 500-1500K 0-29423
- Bi<sub>2</sub>Te<sub>3</sub>-SbTe<sub>3</sub>, ordered structure formation, heat treatment effect on thermal cond. 0-54448
- n-Bi<sub>2</sub>Te<sub>2.88</sub>Se<sub>0.12</sub>, extrusion deformed, powder dispersion degree influence on thermal and elec. props. (Russian) 0-39366
- C fibre reinforced epoxy, thermal cond., diffusivity and sp. ht., determ. 0-24613
- Ca<sub>10</sub>(PO<sub>4</sub>)<sub>6</sub>(OH)<sub>2</sub>-2xO<sub>x</sub>□<sub>x</sub> polycryst. sintered bodies, prep. and thermal props. 0-25624
- CaSO<sub>4</sub>, cryst. growth kinetics at heated metal surfaces, thermal cond. morphology and crystn. 0-29867
- CeCu<sub>2</sub>Si<sub>2</sub>, transport anomalies 0-20148
- Co, thermal diffusivity meas., 300 to 1000K, Lorenz number determ. 0-29384
- Cr<sub>2</sub>S<sub>3</sub>-Se<sub>3</sub>, elec. resist., thermal cond. and Seebeck coeff. meas. 0-24958
- Cu, sintered, in contact with <sup>3</sup>He, thermal conductance, rel. to elec. resist., heat flow model calc. 0-10728
- Cu/Sn (Pb)/W interface, thermal conductance at low temps. 0-49436
- Cu<sub>2</sub>AsS<sub>4</sub> and Cu<sub>2</sub>SbS<sub>4</sub>, thermal cond. in solid and liq. phases, 300 to 1100K, thermoelec. Q-factor 0-19997
- ErVO<sub>4</sub>, phonon resistivity mag. field depend. in paramag. phase 0-2226
- GaAs, design and fabrication of cryostatic system 0-52243
- GaAs, thermal cond. calc. using numerical soln. of Boltzmann eqn. 0-44373
- Ge, laser interaction, multiple refls. contrib. to thermal runaway, heat cond. eqn. 0-33044
- Ge, phonon cond. correction term and electron-photon scatt. relax. rate, appl. to doped and undoped samples 0-39369
- Ge, thermal cond. calc. using numerical soln. of Boltzmann eqn. 0-44373
- Ge:Ga:Sb, compensated, low temp. props. rel. to appl. in bolometry 0-31867
- <sup>3</sup>He, solid, low temp. thermal cond., structural crystalline defects 0-2240
- <sup>4</sup>He, solid, boundary limited thermal cond., Poiseuille phonon flow 0-2241
- Hf, thermal diffusivity meas., 300 to 1000K, Lorenz number determ. 0-29384
- In, thermal cond. in solid and liq. phases, Wiedemann-Franz law 0-39554
- K, high field Righi-Leduc effect and lattice thermal cond. 0-10948
- K, high field Righi-Leduc effect and lattice thermal cond., reply to comment 0-10949
- (La,Gd)Al<sub>2</sub>, reverse Kondo alloy, transport props. at finite mag. field 0-6812
- LaF<sub>3</sub>, pre and Nd<sup>3+</sup>-doped, thermal cond., 300-1450K 0-24686
- MgO-MgAl<sub>2</sub>O<sub>4</sub>(FeCr<sub>2</sub>O<sub>4</sub>), thermoplastic and thermophys. props. for steel vacuuming installations 0-35281
- Mo<sub>2</sub>B<sub>3</sub> and MoB<sub>4</sub>, thermal, elec., and mag. props. 0-20187
- NH<sub>4</sub>Cl, thermal cond. and heat capacity of solid phases under press. 0-2225
- Na<sub>2</sub>S<sub>2</sub>O<sub>3</sub>·5H<sub>2</sub>O, solidification, heat transfer processes (Japanese) 0-6372
- Nb-Mo-Al-(Cr) eutectic directionally crystallised alloy, heat resistance, alloy struct. (Russian) 0-40481
- Nb<sub>3</sub>Sn superconducting wire, fabrication from Cu-Nb-Sn alloy using controlled high temp. gradient 0-25056
- Ni-Cr-Co, Mo, Ti, Y and R alloying additions influence on oxidation (Russian) 0-40587
- Ni-Cr-Mo-Mn alloy 02KhN40MB, corrosion-resist., heat-resist., phys. and mech. props. 0-35411
- Os, electrical resistivity and thermal diffusivity meas. 0-15495
- Pb, thermal cond. measurements below 1K (German) 0-49984
- Pb, thermal conductivity, in normal and supercond. states, 0.6-7.5K (Russian) 0-6815
- Pb-Sn system, soft solder, elec. and thermal cond. at low temps., superconducting transition temp. 0-20150
- PbI<sub>2</sub> layered cryst. under uniaxial compression, low temp. thermal cond. (Russian) 0-44374
- Pb(Mn<sub>1/2</sub>Ta<sub>1/2</sub>)O<sub>3</sub>, ceramic, for thermal and dielectric isolation at low temp. 0-39365
- Pd-H, low temp. transport props., heterogeneous-mixture model 0-24871
- Sb, electrical resist., thermal cond. and thermopower, low temp. transport props. 0-49708
- p-Sb<sub>1.48</sub>Bi<sub>0.52</sub>Te<sub>3</sub>, extrusion deformed, powder dispersion degree influence on thermal and elec. props. (Russian) 0-39366
- Sb<sub>2</sub>O<sub>3</sub>, thermoelec. props., 500-1500K 0-29423
- Sb<sub>2</sub>Te<sub>3</sub>-SbSe<sub>3</sub>, ordered structure formation, heat treatment effect on thermal cond. 0-54448
- Si temperature field determ. under laser irradiation (German) 0-25496

**thermal conductivity of solids continued**

- Si, thermal cond. calc. using numerical soln. of Boltzmann eqn. 0-44373
- Si:Sn, thermal conductivity, Hall mobility depend. on Sn conc., phonon-defect scatt. 0-29232
- SiB<sub>3</sub>, mech. and thermal props. 0-21083
- SiC, chem. stability, mech. and thermal props. rel. to appls. 0-21103
- SiO<sub>2</sub>, vitreous, low temp. thermal props. and intrinsic defects 0-29057
- SmRh<sub>2</sub>B<sub>4</sub>, mag. ordered, persistence of supercond. 0-54834
- TbZn, ferromag. transition, transport coeffs. critical behaviour 0-15498
- Ti alloys, data handbook of low temp. mech. and phys. props. 0-22153
- Ti, high purity, data handbook of low temp. mech. and phys. props. 0-22153
- TiC-TiN system, electro- and thermo-phys. props. 0-34210
- TiC-N<sub>2</sub>, thermal cond., elec. cond., and thermal expansion 0-10714
- TiC-O<sub>2</sub>, thermal cond., elec. cond., and thermal expansion 0-10714
- UAl<sub>2</sub>, transport props., susceptibility and sp. ht. 0-11174
- UO<sub>2</sub>, thermal and transport props., electronic contrib. 0-15432
- VN-CrN solid solutions, thermal cond., Lorentz number 0-15317
- V<sub>2</sub>O<sub>5</sub>, thermoelec. props., 500-1500K 0-29423
- W<sub>2</sub>B<sub>3</sub> and WB<sub>4</sub>, thermal, elec., and mag. props. 0-20187
- Zr<sub>x</sub>Be<sub>1-x</sub> noncrystalline alloy, phonon-electron scatt., superconducting temp. 0-54330

**thermal convection** see convection

**thermal decomposition** see pyrolysis

**thermal diffusion**

see also thermal diffusion in gases; thermal diffusion in liquids

- Brownian motion in periodic potential, in presence of temp. and elec. potential gradients 0-4650
- cloud chamber, continuous flow parallel plate type, analysis w.r.t. atm. water droplet growth 0-36416
- nuclear fuel, transport phenomena under severe temp. gradient 0-615
- parasitic convection effects in thermal diffusion column in sampling mode 0-19386
- thermomagnetophoresis of particles in magnetic suspensions 0-35581
- As<sub>2</sub>S<sub>3</sub>(Se<sub>3</sub>):Ag glassy films, doped by photodiffusion and thermodiffusion, photocond. 0-29441
- Si, monocryst. plates, purification by thermal diffusion, impurity migration anal. 0-25553
- Si:Au, p<sup>+</sup>-n junction, quantitative study of Au atoms by TSC method 0-2458
- SiO<sub>2</sub>-FeO<sub>2</sub>, particulate mass transfer mechanism in modified CVD, thermophoresis 0-2955

**thermal diffusion in gases**

- binary gas systems, thermal diffusion factors meas. 0-10344
- binary mixtures of monatomic gases, Chapman-Enskog theory, thermal cond. calc. 0-24118
- chemically frozen multicomponent boundary layer, thermal diffusion effects behind strong shock 0-53772
- combustion front thermal propagation and thermodiffusional instability 0-7796
- fluoromethane, molecular pumping, thermal lens phenomena 0-9708
- molecular pumping, thermal lens phenomena, time-resolved geom. optics approach 0-9708
- optically active systems, transverse diffusion in electric field 0-6187
- polyatomic-noble gas mixtures, mag. field effects 0-10345
- thermal diffusophoresis of droplets of a liquid solution in a binary gas mixture 0-43766
- Ar-N<sub>2</sub>(CO<sub>2</sub>), thermal diffusion factors meas. 0-10344
- Ar-Ne mixtures, thermal diffusion 0-1726
- Ar<sub>2</sub>, interatomic potential single parameter 0-48059
- H, spin-polarised, density, magnetisation, compression and thermal leakage 0-44391
- H<sub>2</sub> separation from HI-H<sub>2</sub>-I<sub>2</sub> mixture in thermogravitational column 0-45561
- He-Ar(Ne)(N<sub>2</sub>)(CO<sub>2</sub>) mixtures, thermal diffusion 0-1726
- He-H<sub>2</sub>(N<sub>2</sub>O)(NH<sub>3</sub>), thermal diffusion factors meas. 0-10344
- Kr-N<sub>2</sub>O, thermal diffusion factors meas. 0-10344
- N<sub>2</sub>-Ar equimolar mixture, transverse Dufour effect 0-6194
- <sup>222</sup>Rn-CO<sub>2</sub>, thermal diffusion, expt. method for study 0-5922

**thermal diffusion in liquids**

- binary liquid mixture, horizontal layer, surface tension driven instability in presence of Soret effect 0-10227
- coolants and index matching media for Nd:glass laser systems 0-33015
- electrically conducting fluid, laminar flow mass transfer at high Peclet numbers 0-43784
- isobutyril acid-water, mixture, heat of transport, crit. exponent 0-15277
- lakes, stagnant, thermal stratification 0-36340
- laminar boundary layer mass transfer with thermal diffusion 0-19323
- Soret driven instability, secondary effects 0-6062
- tetrachloromethane-cyclohexane liq. mixtures, heat of transport, Dufour effect 0-44344
- volatile highly thermally conductive spherical drop, theory of diffusophoresis 0-14784
- <sup>3</sup>He-<sup>4</sup>He, anomalous cooling power of dilution refrigerators 0-37045
- <sup>3</sup>He-<sup>4</sup>He mixture, transport props. near superfluid transition and tricritical point 0-29242
- <sup>4</sup>He, superfluid, heat transport in restricted geometries, 0.8-2K 0-29237

**thermal diffusivity**

- apparatus to meas. thermophysical props. at high temps. 0-37458
- automatic meas. by pulse method using analogue computer (Japanese) 0-27294
- automatic measuring method (French) 0-14559
- coal, thermal diffusivity and cond. meas. for in situ coal gasification appls. 0-30360
- conference, Chicago, USA (Nov. 79) 0-31425
- glass, meas. by constant-rate heating method (Japanese) 0-6570
- glass fibre reinforced epoxy, thermal cond., diffusivity and sp. ht., determ. 0-24613
- glass-C fibre reinforced epoxy, thermal cond., diffusivity and sp. ht., determ. 0-24613
- glycerine, meas. by constant-rate heating method (Japanese) 0-6570
- granular materials, thermal diffusivity measurement, constant rate heating method (Japanese) 0-6572
- graphite, thermal diffusivity, high temp., meas. by radial flash method 0-52227
- measurement, transient hot-strip method for simultaneously measuring thermal conductivity and thermal diffusivity of solids and fluids 0-1417
- metallic powder, constant rate heating method (Japanese) 0-6572
- microfluids, linear theory of chemically reacting mixtures 0-14777
- polymers, thermal diffusivity, Fourier theory 0-31456



**thermal diffusivity continued**

- radial flash method for high temp. thermal diffusivity meas. 0-52227  
 sand, constant rate heating method (*Japanese*) 0-6572  
 semiconductors thermophysical props. determ. from Ettingshausen effect meas. method 0-44376  
 silicate glass, thermal diffusivity in range 0-600°C, influence of TiO<sub>2</sub> 0-29233  
 silicon oil, meas. by constant-rate heating method (*Japanese*) 0-6570  
 solid, iterative estimation method 0-43603  
 solids, meas. using modulated heating beam technique 0-52221  
 tissue-equivalent plastic, A-150, thermal diffusivity, sp. ht., thermal cond. obs. 0-34258  
 transparent materials, laser irradiated, in-depth and surface temp. meas. by Moire-Schlieren technique 0-53392  
 tubular furnace for thermal diffusivity meas., design 0-30182  
 viscous liquid, constant-rate heating method (*Japanese*) 0-6570  
 Al<sub>2</sub>O<sub>3</sub> dispersion hardened by Ba mica, thermal diffusivity 0-25713  
 B<sub>2</sub>O<sub>3</sub>-Na<sub>2</sub>O-SiO<sub>2</sub>-Al<sub>2</sub>O<sub>3</sub>, effect of alumina dispersions on the thermal cond./diffusivity/stress resist. 0-39368  
 C fibre reinforced epoxy, thermal cond., diffusivity and sp. ht., determ. 0-24613  
 Ca<sub>10</sub>(PO<sub>3</sub>)<sub>6</sub>(OH)<sub>2-2x</sub>O<sub>x</sub>□<sub>x</sub> polycryst. sintered bodies, prep. and thermal props. 0-25624  
 Co, thermal diffusivity meas., 300 to 1000K, Lorenz number determ. 0-29384  
 Fe, thermal diffusivity by pulse method 0-15497  
 Hf, thermal diffusivity meas., 300 to 1000K, Lorenz number determ. 0-29384  
 MgO-MgAl<sub>2</sub>O<sub>4</sub>(FeCr<sub>2</sub>O<sub>4</sub>), thermoplastic and thermophys. props. for steel vacuuming installations 0-35281  
 Os, electrical resistivity and thermal diffusivity meas. 0-15495  
 Pb(Mn<sub>1/2</sub>Ta<sub>1/2</sub>)<sub>2</sub>O<sub>3</sub>, ceramic, for thermal and dielectric isolation at low temp. 0-39365  
 Pd-Ag electrical resistivity, thermo-EMF and thermal diffusivity at high temps. (*Russian*) 0-6808  
 SiC, constant rate heating method (*Japanese*) 0-6572  
 Sn, thermal diffusivity by pulse method 0-15497  
 WC-Co, composition and oxidation resistance of coatings deposited by thermal diffusion, using TiB<sub>2</sub> (*Bulgarian*) 0-45430  
 YAG:Nd, heat capacity and thermal diffusivity meas. 0-19956

**thermal effects in magnetism** *see magnetocaloric effects***thermal expansion***see also Gruneisen coefficient*

- AGR fuel cladding, development of high strength, ductile stainless steel alloys 0-45367  
 alkaline earth silicate glasses, morphology effects on props. 0-49118  
 anharmonic crystals, Debye-Waller factor, specific heat thermal behaviour 0-54335  
 anthracene crystals, dilatometric studies 0-34212  
 BCC crystal, elastic constants, thermal expansion and bulk modulus 0-6452  
 carbazole, birefr. meas., 20 to 190°C, crystal-to-crystal phase transform. 0-45031  
 carbon fibre reinforced composites, filament-wound, thermal residual stresses 0-49290  
 coefficient of thermal expansion of simple bodies, correl. with electromech., thermal and erosion characts. (*Russian*) 0-49388  
 concrete, prestressed, low-temp. tensile strength and linear expansion coeff. of reinforcing steel 0-30051  
 conference, Chicago, USA (Nov. 79) 0-31425  
 cylindrical and plane parallel layered materials, thermographic determination of heat transfer coeff. 0-19221  
 diamond, semiconducting, band gap temp. depend, dilation and vibr. contrs. determ. 0-10868  
 p-dichlorobenzene, expansivity, determ. by calorimetric compression from 0 to 400 MPa 0-44339  
 epoxy resin, meas. of glass transition temp., linear viscoelasticity 0-29157  
 epoxy resin, powder filled, exam. of mech. props., thermal contraction 0-25821  
 epoxy resin systems, synthesis review, phys. and mech. props. at low temps. 0-25650  
 FCC metals, props. of vacancies and divacancies 0-10545  
 ferromagnet, metallic, correl. of temp. anomalies of hyperfine field and thermal expansion of lattice 0-20400  
 fibreglass/epoxy composites, laminates, rings, tubes, thermal contraction at low temps., report 0-19968  
 2-fluoronaphthalene, disordered form, thermal expansion, neutron and X-ray diff. study 0-24621  
 glass transition temperature, determ. from expansion and elec. cond. temp. depend. 0-19967  
 ice surface layer, viscosity, from thermal contraction meas., 0 to -50°C 0-49469  
 inorganic crystals, glasses, thermal expansion coeff. rel. to phys. props. 0-49389  
 Invar, thermal expansion coeff. relationship to magnetisation 0-15269  
 Kevlar/epoxy composites, elastic props. rel. to thermal expansion 0-24622  
 liquid, Rao's acoustical constant, temp. depend., from C<sub>1</sub>-parameter 0-6462  
 liquid metal, thermophysical properties meas. by submicrosecond-pulse-heating method 0-52220  
 liquid surface deform. due to laser radiation thermal action, lens effect 0-33048  
 metals, atomic interaction force characts., association with struct., mech. props. 0-49172  
 metals, rel. to temp. depend. of elec. resist. 0-51967  
 methane-d<sub>4</sub>, solid, thermodynamic props. calc. using significant structures method, 6 to 87K 0-24616  
 methanol-d<sub>3</sub>(d<sub>1</sub>) in freon 11, self-associated, OH frequency temp. depend. 0-37809  
 microcline, maximum room temp. phase transition, unit cell parameters, thermal expansion 0-54208  
 minerals relevant to Earth interior geophysics, Hildebrand equation of state 0-56464  
 plate temp. dependent props. under linear temp. distrib., thermoelastic problem for crack 0-48579  
 polyalkaneimide, mech. and thermophys. props. at liq. He temps. 0-3117  
 polyamide, Al<sub>2</sub>O<sub>3</sub> filled, low temp. thermal and mech. props. 0-25816  
 polyamides, 1,3-cyclohexanebis(methylamine) based, thermal props. and glass transition temp. 0-39264
- thermal expansion continued**  
 polycrystals with axial texture, heterogeneity of props. (*Russian*) 0-29192  
 polyethylene fibres, high density, ultra oriented, physical, mech. props. 0-25649  
 polymer, oriented crystalline, anisotropic thermal expansion 0-39324  
 polyvinylidene fluoride, thermodynamical model, applications (*French*) 0-39315  
 PZT, polycryst., thermal expansions, elasticity and internal friction 0-35238  
 quartz, glassy, thermal expansion coeffs., represented by Gaussian spline polynomials 0-44341  
 rare earth borides, higher types, phys. props. and electronic struct., group orbitals-LCAO calcs. 0-20077  
 rare earth compounds, binary, regression eqns., for calc. props. from electron struct. 0-39498  
 rare earth compounds, hexagonal, cryst. field effect in thermal expansion 0-49390  
 rare earth oxides, binary, struct. and props., book contrib. 0-45292  
 rare earth-Al Laves phase intermetallics, RAl<sub>2</sub>, R=Gd, Ho, Dy, Tb, cubic Laves phase compounds, exchange striction determ. 0-44895  
 refractory material, with phosphate binder base, filler content and temp. influence on strain and thermal expansion (*Russian*) 0-19964  
 rock, thermal expansion expts. at high-pressure. 0-21719  
 rocks, compressional and shear wave velocities under high press., effect of high-low quartz transition 0-12380  
 solid, difference and average temp. linear expt. coeffs. 0-24620  
 solid state phase transformations, thermodynamic relations, appl. to K<sub>2</sub>ReCl<sub>6</sub> 0-29164  
 steel, Mo and Cr-Mo, X-ray elasticity constants at high specimen temp. (*German*) 0-35239  
 stycast 1266 epoxy, thermal contraction, 4-300K 0-4724  
 substitutional impurities in solids, entropy and volume of solution 0-15253  
 thermoelastic expansion flexible acoustic probe 0-16618  
 transition metal borides, higher types, phys. props. and electronic struct., group orbitals-LCAO calcs. 0-20077  
 Vespel SP-22 resin, thermal contraction, 4-300K 0-4724  
 Al alloy, 51S, modified by misch metal, for space appl. 0-55466  
 Al<sub>2</sub>O<sub>3</sub> ceramic, thermal expansion coeffs., represented by Gaussian spline polynomials 0-44341  
 Al<sub>2</sub>O<sub>3</sub>-Cr<sub>2</sub>O<sub>3</sub>, solid soln., thermal expansion anisotropy, lattice const. 0-54411  
 Al<sub>2</sub>SiO<sub>5</sub> polymorphs (sillimanite-andalusite-kyanite), thermal expansion and high-temp. cryst. chemistry 0-39319  
 Ar, solid, self consistent field calcs. of isotherms and thermodynamic props. (*Russian*) 0-10633  
 B<sub>4</sub>C, mech. and thermal props. 0-21083  
 BN films, elastic stiffness and thermal expansion 0-49559  
 B<sub>2</sub>O, mech. and thermal props. 0-21083  
 BaGeO<sub>3</sub>-(0.25MgF<sub>2</sub>, 0.75YF<sub>3</sub>)-Ga<sub>2</sub>O<sub>3</sub> glass, synthesis and props. 0-25648  
 BaO-Al<sub>2</sub>O<sub>3</sub>-SiO<sub>2</sub>-Ta<sub>2</sub>O<sub>5</sub>-Mo glass ceramic metal composites, cermet prep. 0-11618  
 BaO-Al<sub>2</sub>O<sub>3</sub>(PbO)-GeO<sub>2</sub>-MF<sub>2</sub> (M=0.45CaF<sub>2</sub>+0.55MgF<sub>2</sub>), and MgF<sub>2</sub> and CaF<sub>2</sub> effect on physicochem. props. 0-34876  
 C fibre reinforced Al, mech. props. 0-11708  
 C fibre reinforced C, processing, room temp. mech. props., and low temp. expansion 0-25820  
 CaSO<sub>4</sub>, thermal exptn., 22-1000°C 0-6530  
 Ca<sub>2</sub>V<sub>2</sub>O<sub>7</sub>, Ca(VO<sub>3</sub>)<sub>2</sub>, and Ca<sub>3</sub>(VO<sub>4</sub>)<sub>2</sub>, thermal expansion, lattice constants temp. depend. 0-34211  
 Cd, temp. depend. Knight shift 0-2655  
 Cd<sub>6</sub>Hg<sub>35</sub> and Cd<sub>55</sub>Hg<sub>45</sub>, X-ray study of cryst. struct. and thermal expansion 0-24405  
 Ce binary and pseudobinary intermetallics, struct. and mag. data 0-20129  
 Ce, polymorphic γ↔α transform. and volume anomalies under press. 0-34189  
 CeAl<sub>2</sub>, Anderson lattice system, ground state props. 0-20443  
 CeIn<sub>3</sub>-Sn<sub>3</sub>, electrical resist. and thermal expansion meas., 1.5-300K 0-34400  
 CoS<sub>2</sub>, ferromagnet, elec. resist. and thermal expansion anomalies 0-15542  
 CrS<sub>2</sub>(Se<sub>2</sub>), physical props. 0-44179  
 CsCaCl<sub>3</sub> crystal, sp. ht. and thermal expansion coeffs. 0-10681  
 CsH<sub>2</sub>PO<sub>4</sub>, Raman scatt. and high temp. props. 0-16024  
 CsMnF<sub>3</sub>, mag. phase boundaries, XY to Ising crossover, virtual bicritical point 0-50095  
 CsNiCl<sub>3</sub>, linear-chain antiferromag., low temp. thermal expansion 0-39326  
 CsPbCl<sub>3</sub>, lattice thermal expansion, X-ray powder technique 0-19965  
 Cu(NH<sub>3</sub>)<sub>4</sub>(ClO<sub>4</sub>)<sub>2</sub>, (n=4 or 5), EPR parameters and dilatometry 0-39850  
 Fe, thermal props. at high-pressure. (150 GPa), from shock-wave expts., Earth core struct. 0-21683  
 Fe-Cr-B, amorphous, Elinvar and Invar charact. (*Japanese*) 0-11832  
 Fe-Ni, thermal expansion, ferromagnetic-paramagnetic transition (*Russian*) 0-54412  
 Fe<sub>3</sub>Al, ordered, magnetostriction and thermal expansion 0-39842  
 Fe<sub>78</sub>Mo<sub>20</sub> glass, thermal expansion, glass transform. and crystn. temps. 0-2183  
 Fe<sub>12</sub>Ni<sub>36</sub>Cr<sub>14</sub>P<sub>12</sub>B<sub>6</sub> glass, thermal expansion, glass transform. and crystn. temps. 0-2183  
 Fe<sub>40</sub>Ni<sub>40</sub>P<sub>14</sub>B<sub>6</sub> glass, thermal expansion, glass transform. and crystn. temps. 0-2183  
 GaAs homojunction LED, mechanical stress induced degradation 0-2860  
 GaAs, lattice vibration, thermal expansion and pressure effect 0-39233  
 GaBO<sub>3</sub>, coefficients of thermal expansions 0-39322  
 Ga<sub>0.47</sub>In<sub>0.53</sub>As, LPE growth and characterisation 0-10845  
 (Ga<sub>1-x</sub>In<sub>x</sub>)<sub>2</sub>Se<sub>3</sub>, 1≤x≤0, phases, lattice parameters and thermal expansion between room temp. and melting point 0-39031  
 GaS, lattice dynamics parameters, X-ray diff. study (*Russian*) 0-29146  
 GaSb, lattice vibration, thermal expansion and pressure effect 0-39233  
 GaSe, lattice dynamics parameters, X-ray diff. study (*Russian*) 0-29146  
 Hf, HCP, lattice dynamics, thermal and elastic props., model 0-34155  
 HfO<sub>2</sub>, zero and low coeff. of thermal expansion 0-39325  
 HfO<sub>2</sub>-TiO<sub>2</sub> system, zero and low coeff. of thermal expansion 0-39325  
 Hg, electrical and thermodynamic props. in metal-semicond. transition range 0-20144  
 InSb, lattice vibration, thermal expansion and pressure effect 0-39233  
 KCoF<sub>3</sub>, lattice parameter temp. depend., phase transitions and thermal expansion coeff. 0-1988



**thermal expansion continued**

- KDP monocrystal, expansion and contraction coeffs., tricritical point, Landau theory explanation (*Russian*) 0-44340  
 KMnF<sub>3</sub>, lattice parameter temp. depend., phase transitions and thermal expansion coeff. 0-1988  
 KMn<sub>0.9</sub>M<sub>0.1</sub>F<sub>3</sub>, (M=Co,Ni), lattice parameter temp. depend., phase transitions and thermal expansion coeff. 0-1988  
 KNiF<sub>3</sub>, lattice parameter temp. depend., phase transitions and thermal expansion coeff. 0-1988  
 K<sub>2</sub>ReCl<sub>6</sub>, thermodynamic relations at solid state phase transitions 0-29164  
 La<sub>1-x</sub>Ce<sub>x</sub>Sn<sub>3</sub>, electrical resist. and thermal expansion meas., 1.5-300K 0-34400  
 LiKSO<sub>4</sub>, uniaxial crystal, pyroelectric, thermal expansion, phase transition 0-19966  
 LiNH<sub>2</sub>SO<sub>4</sub>, ferroelectric phase transition, lattice parameters and thermal expansion coeffs. 0-40074  
 LiNO<sub>3</sub>·3H<sub>2</sub>O(D<sub>2</sub>O), crystals and melts, density, mol. vol., thermal coeff. of expansion, rel. to struct. 0-15270  
 Li<sub>2</sub>O·2SiO<sub>2</sub>, directionally solidified, thermal and mech. props. (*Japanese*) 0-16295  
 100(Li<sub>2</sub>O·2SiO<sub>2</sub>)·3B<sub>2</sub>O<sub>3</sub>(3Na<sub>2</sub>O)(3MgO)(3Al<sub>2</sub>O<sub>3</sub>)(3SiO<sub>2</sub>)(3P<sub>2</sub>O<sub>5</sub>), directionally solidified, thermal and mech. props. (*Japanese*) 0-16295  
 MgO:Cr<sup>2+</sup> (Mn<sup>2+</sup>), spin Hamiltonian parameters, lattice expansion and vibr. effects 0-24851  
 MgO-Al<sub>2</sub>O<sub>3</sub>-SiO<sub>2</sub>, glass ceramic, structure and props. (*German*) 0-38927  
 Mo-Ti-Zr (0.5, 0.7 wt.%) alloy TZM, props. and appl. (*German*) 0-21040  
 MoS<sub>2</sub>(2H), lattice dynamics, Coulomb and quasi-harmonic effects 0-39245  
 (NH<sub>4</sub>)<sub>2</sub>H(SO<sub>4</sub>)<sub>2</sub>, successive phase transitions, dilatometric and X-ray expts. 0-11348  
 α-NH<sub>2</sub>HgCl<sub>3</sub>, thermal expansion, lattice constants between 302 and 364K 0-15268  
 NaCl, thermal expansion meas. after X-ray irradi., F-centre bleaching 0-44338  
 NaCl, X-ray irradi., vacancy conc., thermal expansion meas. 0-6431  
 Na<sub>2</sub>O-CaO-SiO<sub>2</sub> glass, effect of phase on liquids and gas diffusion (*German*) 0-38931  
 Na<sub>1-x</sub>Si<sub>x</sub>Zr<sub>2</sub>P<sub>3-x</sub>O<sub>12</sub>; monoclinic to rhombohedral phase transformation 0-29950  
 NaYb(WO<sub>4</sub>)<sub>2</sub>, thermal expansion, X-ray determ. 0-39323  
 NbH<sub>3</sub>, harmonic and anharmonic elastic props. 0-10589  
 NbO<sub>2</sub>, semicond., thermal expansivity 0-34213  
 Ni/ZrO<sub>2</sub>-Y<sub>2</sub>O<sub>3</sub>, sputtered multilayered ceramic/metal coatings, props. 0-40620  
 Ni-Cr/ZrO<sub>2</sub>-Y<sub>2</sub>O<sub>3</sub> sputtered multilayered ceramic/metal coatings, props. 0-40620  
 Ni-Cr-Mo-Mn alloy 02KhN40MB, corrosion-resist., heat-resist., phys. and mech. props. 0-35411  
 Ni-Ti, Nitinol memory material heat engine, comment on efficiency 0-3529  
 Ni-Ti, Nitinol memory material heat engine, reply to comments on efficiency 0-3530  
 Ni<sub>3</sub>B<sub>2</sub>O<sub>7</sub>, unit cell parameters and struct. transitions, 20 to 293K, X-ray diff. study 0-24431  
 Pa, lattice parameter variation at low temp., thermal expts. 0-15046  
 PbF<sub>2</sub>-AlF<sub>3</sub> glass, optical props., crystn. and thermal expansion 0-48367  
 Pb(Mn<sub>1/2</sub>Ta<sub>1/2</sub>)O<sub>3</sub>, ceramic, for thermal and dielectric isolation at low temp. 0-39365  
 PbO-B<sub>2</sub>O<sub>3</sub>-ZnO solder glass, with admixtures, crystallisation and thermal expansion 0-24364  
 PbTiO<sub>3</sub>, anomalies in elec., photoelectric and mechanical props. 0-55051  
 Pd-H(D), thermal expansion and lattice anharmonicity 9 to 270K 0-39241  
 Pr, DHCP, cryst. field effect in thermal expansion 0-49390  
 PrNi<sub>3</sub>, hexagonal, cryst. field effect in thermal expansion 0-49390  
 Pu(C, N), PuC and PuN, lattice parameter variation at low temp., thermal expts. 0-15046  
 Si-Al(Ti)C, sintered, exam. of props. 0-25644  
 SiB<sub>4</sub>, mech. and thermal props. 0-21083  
 SiC-fibre reinforced glass, fabrication, thermal expansion, flexural and fracture toughness 0-40319  
 SiO<sub>2</sub>-base cores, for superalloys, high temp. characterisation 0-10640  
 SiO<sub>2</sub>-Li<sub>2</sub>O-K<sub>2</sub>O-ZnO glass ceramic, prep., phase transformations and physical props. 0-45299  
 SmCo<sub>5</sub>, sintered, anisotropic thermal expansion and fracture of radially oriented toroids (*Chinese*) 0-10686  
 TbPO<sub>4</sub>, phase transitions at low temp. 0-15237  
 Th, lattice parameter variation at low temp., thermal expts. 0-15046  
 Ti alloys, data handbook of low temp. mech. and phys. props. 0-22153  
 Ti, high purity, data handbook of low temp. mech. and phys. props. 0-22153  
 TiC-TiN system, electro- and thermo-phys. props. 0-34210  
 TiC-N<sub>y</sub>, thermal cond., elec. cond., and thermal expansion 0-10714  
 TiC-O<sub>2</sub>, thermal cond., elec. cond., and thermal expansion 0-10714  
 TiS<sub>2</sub>(Se<sub>2</sub>), physical props. 0-44179  
 Tl, thermal and elastic props., lattice heat capacity, elastic constants and thermal expansion, model 0-39321  
 U, vacancy formation and phase transformation by positron annihilation 0-49215  
 α-U-Mo, dil., electronic properties depend. on 2<sup>1/2</sup>-th order phase transition under high press. (*Russian*) 0-11128  
 UC 0-15046  
 UP, vol. changes at mag. transitions 0-7107  
 VS<sub>2</sub>(Se<sub>2</sub>), physical props. 0-44179  
 V<sub>2</sub>Si, thermal expansion, 20-300°C, using differential push-rod dilatometer 0-39320  
 Xe, monolayer adsorption on Ag (111), statistical mech. 0-34306  
 Y-Si-Al-O-N glass, prep. and props. 0-25647  
 Y(Co<sub>1-x</sub>Cu<sub>x</sub>)<sub>2</sub>, neutron diff., thermal expts. (*French*) 0-19749  
 ZnB<sub>2</sub>O<sub>4</sub>-MF<sub>2</sub> (M=Mg, Ca, Sr, Ba) glass system, physicochem. props. 0-34877  
 ZnSe, lattice vibration, thermal expansion and pressure effect 0-39233  
 ZnTe, lattice vibration, thermal expansion and pressure effect 0-39233  
 Zr(Fe<sub>1-x</sub>Co<sub>x</sub>)<sub>2</sub>, magnetovolume effects, thermal expansion and forced vol. magnetostriction meas. 0-29595

**thermal expansion measurement**

- fibres, determ. using optical dilatometer 0-45454  
 films, determ. using optical dilatometer 0-45454

**thermal expansion measurement continued**

- flow microcalorimeter for direct continuous meas. of coefficients for liquids and solids 0-52164  
 gamma attenuation technique for thermal expansion meas. of solids. at high temperatures 0-31960  
 linear expansion test rig 0-22324  
 low-temperature coeff. differences in 4 to 80K range, measurement using differential dilatometer 0-17922  
 polymers, determ. using optical dilatometer 0-45454  
 thermostat metals, influence of specimen curvature on sensitivity (*German*) 0-27291  
 NaCl, measurement using X-ray powder diffractometer with polythermal attachment 0-311  
 Si cell for precise measurement of thermal expansion at low temps., results for Cu, NaF 0-37027

**thermal fatigue see thermal stress cracking****thermal insulating materials**

- see also thermal conductivity  
 evacuated multilayer insulation, method for evaluation of normal heat flux 0-53610  
 foam thermal conductivity meas., unsteady probe method (*German*) 0-31740  
 phase change material wall thermal storage, design criteria 0-35759  
 phase change material wall thermal storage, modelling 0-35758  
 Pb(Mn<sub>1/2</sub>Ta<sub>1/2</sub>)O<sub>3</sub>, ceramic, for thermal and dielectric isolation at low temp. 0-39365

**thermal insulation**

- conference, nonmetallic materials and composites at low temps., Munich, Germany, July 1978 0-22139  
 gas flow in thermal insulation media, transient behaviour at rapid depressurisation 0-27701  
 hot water storage tank, heat loss rel. to thermal insulation (*Japanese*) 0-5918  
 on metal backing, thermophys. characts., expt. determ. technique 0-4707  
 periodic heat flux through a three layered slab exposed to solar radiation 0-43598  
 reactors, gas cooled, internal insulation 0-47537  
 solar heating system components, optimal insulation, numerical sensitivity anal. 0-35745  
 space heating, energy utilisation improvements using new types of construction (*German*) 0-40903

**thermal magnetoresistance**

- metal, effects of large scale voids on thermal magnetoresist. 0-10946  
 n-Ge, magnetothermal cond., 4.2K 0-24688  
 K, thermomagnetic and thermoelectric properties, phonon scatt. processes 0-29390

**thermal noise**

- education, capacitor complete discharge time, thermal noise 0-17727  
 linear quantum channel with thermal noise, quasiprobability distrib. 0-12984  
 metal, temp. fluctuations as 1/f noise origin, theory 0-11059  
 optical fibre system, timing error tolerant waveforms 0-14293  
 polymer solutions, aq., capillary flow, thermal noise, low freq. oscills. 0-48754  
 Ge:Ga,Sb, compensated, low temp. props. rel. to appl. in bolometry 0-31867

**thermal properties of substances**

- see also magnetocaloric effects; Scott effect; specific heat; thermal conductivity; thermal diffusivity; thermal expansion; thermal variables measurement  
 fibre reinforced thermoelectric materials, nonlinear thermodynamic continuum theory 0-14579  
 gas thermometry, constant volume valve design 0-4711  
 gradient index material models and exptl. verification 0-16002  
 MgO-ZrO<sub>2</sub> ceramic reinforced with filamentary crystals, mech. and thermal props. 0-45262  
 polyamides, 1,3-cyclohexanebis(methylamine) based, thermal props. and glass transition temp. 0-39264  
 steel, thermal props. meas. (*French*) 0-25977  
 Be substrate for lightweight mirror, surface quality and thermal props. 0-23762

**thermal quenching see quenching (thermal)****thermal radiation see heat radiation****thermal resistance**

- bodies in contact, heat transmission, optimal control thermoelectric stress constraint 0-19223  
 heat pipes with metal fibre wicks, thermal resist. 0-43601  
 plate-semi-infinite space, heat exchange process control, thermoelectric stresses (*Russian*) 0-53606  
 temperature fields in space-connected regions with alternating contact thermal resistance (*Russian*) 0-53607  
 GaAlAs DH laser, In solder deterioration, Au diffusion in In 0-33019

**thermal resistivity see thermal conductivity****thermal shock**

- glass bodies, heat resistance, determ. 0-24690  
 metals, working, method of applying fusion thermal indicators to surfaces, including heated surfaces 0-17937  
 refractories, fatigue behavior, effect of texture and crack kinetics, AE anal. (*German*) 0-21061  
 refractory, fracture under thermal shock, AE study 0-25865  
 refractory oxide, thermal shock resist. mechanisms 0-25860  
 steel, cast, equipment for thermal shock resistance determ. 0-55614  
 Al<sub>2</sub>O<sub>3</sub>, crack detection caused by thermal shock, AE technique (*Japanese*) 0-21248  
 Be, plasma-sprayed coatings on Cu and stainless steel, fusion reactor appl. 0-18619  
 MgO and MgO-dolomite, crack detection caused by thermal shock, AE technique (*Japanese*) 0-21248  
 MgO-Al<sub>2</sub>O<sub>3</sub>-SiO<sub>2</sub> based cordierite glass-ceramic, strength and thermal shock, surface treatment effect 0-25884  
 TiB<sub>2</sub>, plasma-sprayed coatings on Cu and stainless steel, fusion reactor appl. 0-18619  
 TiC, plasma-sprayed coatings on Cu and stainless steel, fusion reactor appl. 0-18619  
 TiO<sub>2</sub>, based construction ceramics, fibre-like cryst. reinforced, mech. props. 0-55341  
 VBe<sub>2</sub>, plasma-sprayed coatings on Cu and stainless steel, fusion reactor appl. 0-18619



**thermal shock failure** *see thermal stress cracking*

**thermal spikes** *see crystal defects; radiation effects*

### thermal stress cracking

alloys, heat-resist., evaluation method 0-3260  
central receiver solar power stations, solar receiver tube thermal stresses, fatigue aspects 0-40908  
ceramics, microcracked brittle, thermal stress resistance anal. 0-40472  
composite fusion reactor liners, thermal fatigue tests 0-32460  
concrete, reactor shielding thermal stress cracking anal. (*German*) 0-5232  
cylinder, weakened by penny-shaped cracks, thermoelastic stresses 0-10191  
disc, thermal cycling endurance, finite element method calc. 0-48646  
fatigue of high-melting material sheets, testing device 0-25955  
Fe, cast, high Cr, hardfacing of roll, wear resistance and thermal durability 0-7686  
fusion reactor limiters; thermal and stress environment effects 0-32461  
graphite, fusion reactor liners, thermal fatigue tests 0-32460  
irradiation reactor advanced fuels, effect of crack formation on fuel behaviour 0-650  
metals and alloys, testing, installation for  $-180$  to  $1100^{\circ}\text{C}$  0-3266  
optical fibre, elliptically clad borosilicate single-mode, strain birefringence 0-33148  
oxide films on  $\text{MoSi}_2$ , cracking under heat cycling, acoustic emission determ. (*Russian*) 0-30067  
porosity effect, on thermal stress resist. during steady-state heat flow 0-1488  
reinforced concrete containment model behaviour under thermal gradients and internal pressure 0-42837  
semi-infinite medium, transient thermal loadings, stress intensity factors 0-10193  
space-quality solder joints, resistance to thermal fatigue 0-25831  
steel, austenitic, high-temp. crack resist., B and Mo influence (*Russian*) 0-16435  
steel, Cr, stress relaxation, superplasticity and thermal cycling (*Russian*) 0-21019  
steel, die, thermal fatigue resistance, high temp. thermomech. treatment effect 0-50715  
steel, low alloy, welded joints, cracking during heat treatment 0-7724  
steel, low alloy type 14Kh2GMR, high strength, welded joint, impact toughness, welding thermal cycle and tempering effects 0-3157  
welded joints in dissimilar Al alloys, fishbone test piece axis of symmetry, residual stresses, cracking coefficient effects 0-7725  
 $\text{Al}_2\text{O}_3$ , crack detection caused by thermal shock, AE technique (*Japanese*) 0-21248  
 $\text{Al}_2\text{O}_3$ -Mo (20 wt.%) cermet,  $\text{ZrO}_2$  crystal addition effect on thermal fatigue resistance 0-40528  
 $\text{Al}_2\text{O}_3$ - $\text{Si}_3\text{N}_4$  preparation, compressive strength 0-25634  
GaAs, during deformation, acoustic emission rel. to cracks, dislocations 0-35441  
MgO and MgO-dolomite, crack detection caused by thermal shock, AE technique (*Japanese*) 0-21248  
Mo, candidate refractory for Tokamak, thermal fatigue failure testing 0-32454  
Ni base superalloy, directionally solidified, struct. and props. (*Chinese*) 0-20918  
Ni/ $\text{ZrO}_2$ - $\text{Y}_2\text{O}_3$ , sputtered multilayered ceramic/metal coatings, props. 0-40620  
Ni-Cr/ $\text{ZrO}_2$ - $\text{Y}_2\text{O}_3$ , sputtered multilayered ceramic/metal coatings, props. 0-40620  
Si-B based CVD coating for gas turbine blading, props. 0-40615  
 $\text{Si}_3\text{N}_4$ - $\text{Y}_2\text{O}_3$  ceramic, thermal degradation, C impurity effect 0-50708  
Sn melt in contact with Fe, Fe distrib. on thermal cycling (*Russian*) 0-16562  
W, candidate refractory for Tokamak, thermal fatigue failure testing 0-32454  
W- $\text{ThO}_2$ , candidate refractory for Tokamak, thermal fatigue failure testing 0-32454

**thermal stresses**  
*see also thermal stress cracking; thermoelasticity*  
brittle materials, grain size dependence of microcrack initiation 0-40505  
carbon fibre reinforced composites, filament-wound, thermal residual stresses 0-49290  
centre cracked plate under quadratic thermal gradient, stress intensity factors analysis 0-43665  
ceramic powder, thermal stresses during spheroidisation process (*Russian*) 0-40386  
circular cylinder with circumferential edge crack under uniform heat flow, thermal stresses 0-48641  
composites, thermal stresses investigation, using polymer models 0-40639  
concrete, bituminous, thermal stresses and brittle point, automatic installation for meas. 0-55605  
continuous elastic solids, foundations for coupled thermoelasticity 0-46807  
cylinder, hollow infinite, with temp. depend. thermal cond., thermal stress anal. 0-14575  
cylinder, weakened by penny-shaped cracks, thermoelastic stresses 0-10191  
cylinders, symmetric thermoelastic stress, Lanczos-Chebyshev method 0-33458  
cylindrical shells, calc. of stresses (*German*) 0-33454  
cylindrical shells, transient response to localised heat sources, thermal displacement and stresses 0-13538  
fibre reinforced composites, viscoelastic thermal shrinkage stresses 0-38287  
fibre reinforced materials, therm. stresses in unit cell 0-10160  
finite short circular cylinder with arbitrary heat supply, unsteady thermal stress length effects 0-13541  
fusion reactor limiters; thermal and stress environment effects 0-32461  
glass bodies, heat resistance, determ. 0-24690  
integrated retardation technique, rotationally symmetrical bodies 0-38362  
layered system, thermal stresses and displacements 0-23891  
martensite, microstresses associated with tempering 0-3111  
metal, two-way polishing, thermal stresses and surface quality (*Russian*) 0-30151  
micropolar layer, pertinent formulas for displacement vector components, force stress component distrib. 0-48581  
optical waveguide blanks, thermal and elastic stresses in a cylinder 0-14447  
optical waveguides, inhomogeneous glass sintering, self stresses producing bulk flow 0-14448

### thermal stresses continued

plate, annular elliptic heated, const. thickness, buckling and stability criterion 0-28443  
plate temp. dependent props. under linear temp. distrib., thermoelastic problem for crack 0-48579  
plate with crack or ribbon like inclusion subjected to uniform heat flow, thermoelasticity 0-48578  
plate-semi-infinite space, heat exchange process control, thermoelastic stresses (*Russian*) 0-53606  
polymers, wear in thermally stressed state 0-3202  
porosity effect, on thermal stress resist. during steady-state heat flow 0-1488  
PVC, stress relaxation in macrodeformation range 0-16370  
quartz resonators, thickness-mode, thermal stress effects on reson. freq., theory 0-50272  
refractory, thermal stresses produced by temp. gradient, finite element anal. (*Japanese*) 0-33538  
rock salt, thermomech. impact due to storage of radioactive waste 0-5278  
shell enclosures, temp. distrib. calcs. under thermal radiation, numerical calcs. 0-38241  
shells of revolution, variable thickness, stress state determ. 0-38275  
substrate bending during thin film evaporation due to temp. difference between substrate faces 0-54571  
substrates, instantaneous bending during thin film deposition, intrinsic stresses, cantilevered plate method anal. 0-54570  
two-phase nodules, heat treatment, stressed state, connection with nodule size, cooling rate and phase ratio (*Russian*) 0-16334  
unsteady thermal stress problems, numerical treatment based on Euler-Maclaurin summation formula 0-48580  
weakly absorbing solid medium, opacity fluctuations, heating by intense radiation and thermoelastic stresses problem 0-38048  
Ag films, hillock form. hole growth and agglomeration 0-44455  
Al alloy cylindrical shells, buckling under combined axial preload, nonuniform heating and torque 0-53662  
Al-SiC fibre reinforced materials, therm. stresses in unit cell 0-10160  
 $\text{Al}_2\text{O}_3$ , thermally stressed insulator surfaces, behaviour under vacuum 0-18652  
 $\text{B}_2\text{O}_3$ -Na<sub>2</sub>O-SiO<sub>2</sub>- $\text{Al}_2\text{O}_3$ , effect of alumina dispersions on the thermal cond./diffusivity/stress resist. 0-39368  
 $\text{Ba}_2\text{Sr}_{1-x}\text{Nb}_2\text{O}_6$  crystals, optical defects and edge dislocation distributions 0-19806  
Cu, thermal stress role in dislocation form. during growth from melt 0-6374  
Fe/Cu composite, prop. of fatigue crack crossing interface under residual thermal stress effect 0-45371  
GaAs homojunction LED, mechanical stress induced degradation 0-2860  
Nb heteroepitaxial layers on sapphire, residual mechanical stress and strain influence on superconductivity 0-15644  
Nd:YAG laser, thermal lens effect on emission stability 0-19064  
p-Si-In<sub>2-3</sub>-Sn<sub>x</sub>O<sub>3-y</sub> solar cells, thermal degradation mechanisms 0-55841

**thermal transformations** *see phase transformations*

**thermal variables control**  
*see also temperature control*  
production processes, nonstationary Doppler effect, freq.-phase methods of investig., control 0-45464

**thermal variables measurement**  
*see also bolometers; calorimeters; calorimetry; temperature measurement; thermal conductivity measurement; thermocouples; thermometers*  
conference, Chicago, USA (Nov. 79) 0-31425  
diffusivity, automatic measuring method (*French*) 0-14559  
diffusivity, transient hot-strip method for simultaneously measuring thermal conductivity and thermal diffusivity of solids and fluids 0-1417  
diffusivity automatic meas. by pulse method using analogue computer (*Japanese*) 0-27294  
emissivity of solar absorber coatings, optical technique for meas. (*Spanish*) 0-16835  
emissivity of solids and coatings at low temps., calorimetric technique 0-17941  
gases, dilute, temp. and thermophysical prep. meas., using acoustic resonators 0-53573  
gases, thermal activity coeff. meas., periodic-heating method, appls. 0-42218  
granular materials, thermal diffusivity measurement, constant rate heating method (*Japanese*) 0-6572  
heat capacity, true, of high-melting cpds., pulse method and meas. unit 0-19953  
heat capacity of ferroelectrics, by dynamic method at high hydrostatic pressures 0-47059  
heat pipe appls. in thermophysical props. meas. 0-23878  
high rate local heat flux meas. probe 0-47050  
hot gases, convective heat transfer coeffs. to solid surface, moving thermocouple meas. 0-42230  
metal-hydrogen system, electronic sp. ht. meas. 0-49378  
metals, specific heat meas. method of low temperatures and high pressures 0-52246  
pipes, local heat transfer using heat flux sensors 0-48709  
prediction of thermophysical properties of fluid mixtures, generic procedure 0-48563  
production processes, nonstationary Doppler effect, freq.-phase methods of investig., control 0-45464  
solid, thermal diffusivity, iterative estimation method 0-43603  
specific heat of  $\text{La}_{1-x}\text{Sr}_x\text{CoO}_3$ , using laser-flash method, at 80 to 950K, phase transitions obs. (*Japanese*) 0-54898  
thermal diffusivity in solids, meas. using modulated heating beam technique 0-52221  
thermal flux, high, using calorimeter probes 0-13080  
thermoelectric thermal flux meters, response time reduction 0-4719  
thermophysical properties, conf., Dubrovnik, Yugoslavia (June 1978) 0-51944  
thermophysical properties, standardisation of meas. methods 0-52197  
thermophysical properties dynamic meas. techniques 0-52219  
thermophysical properties of liq. metals, submicrosecond-pulse-heating method 0-52220  
tubular furnace for thermal diffusivity meas., design 0-30182  
viscous liquid, thermal diffusivity meas., constant-rate heating method (*Japanese*) 0-6570  
wet-bulb temp. and moist air heat content meas. 0-52211  
Fe, sp. ht., electronic heating in modulation meas. method 0-24609  
<sup>222</sup>Rn-CO<sub>2</sub>, thermal diffusion, expt. method for study 0-5922



**thermally stimulated capacitor discharge** *see thermally stimulated currents*

### thermally stimulated currents

amorphous materials, TSC calcs. 0-7284  
anthracene, charge storage and trapping levels, TSC studies 0-6875  
anthracene, laser excited single crystal, numerical anal. for TSC results (Japanese) 0-34464  
anthracene, single crystals, TSC excited by Q-switched ruby laser 0-29417  
anthracene, TSC and carrier retrapping 0-39599  
carnauba wax and rosin thermal electret, elec. charge studied by TSC 0-7286  
cellulose, thermally stimulated discharge studies 0-11329  
cellulose electrets, TSC and dielec. losses and relax. 0-25284  
charge storage, charge transport and electrostatics conference, Kyoto, Japan (Oct. 78) 0-7252  
cobalt naphthalate electret, thermally stimulated discharge, 55-75°C 0-25279  
corona charged polyethylene thermally stimulated current and surface potential decay obs. 0-15945  
p-cyanophenyl-p'-caproyloxybenzoate, charge carrier behaviour, thermal depolarisation current study 0-7283  
dielectric, dipolar point defects, studied by ITC 0-6405  
dielectrics, thermally stimulated depolarisation as method of studying charge trapping 0-11325  
diffusion traps for divalent ions, dielectric loss and ionic thermocurrent techniques 0-6566  
dipolar relaxation study using thermally stimulated polarisation currents 0-7278  
electrets and dielectrics, conf., Sao Carlos, Brazil, Sept. (1975) 0-7251  
epoxy-resin, Nomex-filled, space charge polarisation, thermal depolarisation current study 0-7282  
p-hexyloxyphenyl-p-pentoxibenzoate, nematic liq. cryst., elec. discharge meas. of persistent internal polarisation 0-10488  
hydrocarbon, long chain single cryst., carrier transport meas. 0-6874  
ionic electret behaviour, ionic thermoconductivity technique 0-7274  
MOS capacitor, TSC meas., suppression of meas. interferences from interface states and mobile ions 0-29479  
non-polar dielectrics, TSC and carrier retrapping 0-39599  
p-octyloxyphenyl-p-pentoxibenzoate, nematic liq. cryst., elec. discharge meas. of persistent internal polarisation 0-10488  
organic semiconductor films, relax. currents, polarisation and depolarisation currents obs. 0-49764  
paper cellulose sandwiched between metal electrodes, thermo-induced elec. current 0-25021  
Perspex magneto-electret, equiv. elec. field calc. from thermally stimulated discharge current 0-7259  
Perspex pyramid electret, thermally stimulated discharge currents 0-2688  
PET, ionic cond. current rel. to neutralisation at polymer-metal interface at elevated temps. 0-24664  
PMMA, electret, dielectric meas. at ultralow freq. by reheating 0-4741  
poly(alkyl methacrylate)s, corona charged, decay of surface charge and TSC (Japanese) 0-54712  
poly(alkyl-methacrylates), surface charge decay and TSC 0-11328  
poly(vinyl halides), surface charge decay and TSC 0-11328  
polycarbonate, TSC anal. by activation energy spectra 0-20579  
polycarbonate thin films, solution-grown, dielectric relaxations 0-55029  
polychlorotrifluoroethylene, electret, thermodepolarisation curves 0-7266  
polyethylene, high and low density, depolarisation thermocurrent study, relax. modes 0-7263  
polyethylene, high density, carrier trapping, X-ray induced TSC 0-11005  
polyethylene, surface charge release, crossover phenomenon, thermally stimulated discharge current study 0-50255  
polyethylene, TSC study of deuteration 0-20581  
polyethylene cables carrying DC current, TSC and space charge effects (French) 0-40042  
polyethylene electrets, charge trapping mechanism, TSC, DTA and optical meas. 0-11322  
polyethylene film, high density, corona charged, thermally stimulated surface pot. 0-11327  
polyethylene film electrets, polarisation obs. and influence of wax impurities, TSC obs. and analysis (French) 0-44999  
polyethylene films, elongated,  $\gamma$ -irrad., TSC meas. 0-11324  
polyethylene terephthalate, TSC due to mobile ions and ionic conduction (Japanese) 0-54432  
polyethylene terephthalate, TSC meas., space charge and injected surface charge effects 0-11320  
polyethylene terephthalate electrets, formed by electron injection, TSC meas., space charge drift 0-11321  
polyethylene terephthalate film, corona charged, surface voltage decay mechanism, TSC meas. 0-11326  
polyethylene terephthalate film, elec. cond. and space charge accumulation 0-10998  
polymer, carrier trap study by X-ray induced TSC and thermoluminescence (Japanese) 0-54713  
polymer films, carrier transport meas. 0-6874  
polymers, electrical phenomena, nature and appl., book contrib. 0-50254  
polymers powders, corona-charging props. 0-6946  
polypropylene, electron bombarded electret, trapped charges ESR study 0-7170  
polypropylene, TSC meas. of relax. modes, apparent double glass transition 0-11323  
polypropylene electrets corona charged at high temp., TSC study 0-7261  
polypropylene film, corona-charged, TSC and space charges 0-40041  
polystyrene, thin film, TSC and dielectric props. (Japanese) 0-15632  
polystyrene films on metal substrates, electrode effect on carrier injection, TSC, I-V characts. 0-34463  
polystyrene foils, breakdown-charged, surface charge densities and depths, TSC spectra 0-7260  
polystyrene-chloranil molecular complex, glass-rubber and liquid-liquid transitions 0-45002  
polyvinyl alcohol, bulk polarisation, thermally stimulated discharge current meas. 0-40039  
polyvinyl butyral film, charge storage mechanism, TSC expts. 0-25280  
polyvinylidene fluoride, dielectric relax. mechanism 0-55023  
polyvinylidene fluoride, piezoelectric effect formation due to injection process, TSC (French) 0-34856  
polyvinylidene fluoride, TSC and thermoluminescence, reln. to molecular motion (Japanese) 0-55200  
PTFE electrets corona charged at high temp., TSC study 0-7261  
PVC, rubbed, TSC meas. 0-55017

### thermally stimulated currents continued

semi-insulating material, elec. stressed, storage of charge caused by cond. gradient 0-25306  
semiconductor, deep impurities, exptl. techniques (Japanese) 0-15476  
semiconductors, local centre parameter determ. from thermally stimulated excitation curve derivative singularities 0-11004  
silastic tubular electret, mag. polarised, thermal currents 0-40037  
sisal wax thermoelectrets, thermally stimulated discharge and internal polarisation 0-55016  
styrene-acrylonitrile copolymer film, multiple relax. obs. using TSC 0-45000  
Teflon film, TSC studies of carrier trapping and mobility 0-7016  
tetracene, amorphous film, TSC meas., carrier traps 0-2496  
TGS, pyroelec. single cryst., elec. field meas., thermally stimulated charges 0-45012  
vinyl chloride-vinyl acetate copolymer film, dielec. relax. and thermally stimulated depolarisation current meas. 0-11336  
vinyl chloride-vinyl acetate copolymer film between metal electrodes, depolarisation current studies 0-2691  
 $\alpha$ -Al<sub>2</sub>O<sub>3</sub>, crystal defects from X-ray irradiation, F-centres, X-ray luminesc. obs. 0-55176  
 $\alpha$ -Al<sub>2</sub>O<sub>3</sub>:Er(Cr), crystal defects from X-ray irradiation, F-centres, X-ray luminesc. obs. 0-55176  
As<sub>2</sub>Se<sub>3</sub> amorphous film, photocond., TSC, light-induced changes 0-49810  
CaWO<sub>4</sub>:Gd, thermally stimulated depolarisation current, 100 to 300K 0-7280  
CdF<sub>2</sub>:Eu, role of solution and precipitation phenomena on ITC spectra 0-7265  
CdS:CuCl<sub>2</sub>(CdCl<sub>2</sub>) sintered layer, distrib. of energy levels of local centres 0-15568  
CdTe sputtered films, struct., photocond., and trap distrib. 0-29489  
GaAs, surface, distrib. of surface states 0-44692  
GaAs, thermally stimulated relax. under internal field conditions 0-7279  
GaP, proton implanted, thermally stimulated current meas. 0-24943  
n-GaS, TSC, electron traps 0-11002  
Ge-Si alloy p-n junction, Sb-diffused, TSC 0-20289  
GeS, Si doped and undoped, elec. cond. and thermally stimulated currents 0-20194  
In<sub>2</sub>S<sub>7</sub>, TSC at various cooling rates (Russian) 0-11000  
KBr, proton irradi., divacancies, positron capture, ionic cond. and TSC study 0-54289  
KBr:Cl<sup>-</sup>, diffusion traps for divalent ions, dielectric loss and ionic thermocurrent techniques 0-6566  
KCl:Pb, light induced ionic polarisation 0-7264  
KCl-KF:Pb<sup>2+</sup>, point defects, ionic thermal currents and optical meas. 0-6403  
KI:S<sup>2-</sup>, vacancy dipoles, photo-induced polarisation and depolarisation 0-2690  
KI:Ti, electron-hole and V<sub>K</sub>-Ti recomb., TSC and thermolum. study (French) 0-34461  
La<sub>2</sub>(SO<sub>4</sub>)<sub>3</sub>·9H<sub>2</sub>O(D<sub>2</sub>O), dynamic disorder of water mols., isotope effect obs. 0-55015  
LiF:Be(Mg), Maxwell-Wagner relax. induced by impurity clouds around dislocations, ionic thermocurrent meas. 0-7281  
MgO single cryst.,  $\gamma$ -irrad. in presence of O<sub>2</sub>, H<sub>2</sub> and H<sub>2</sub>O adsorbates, thermostimulated surface cond. 0-34499  
MgO, single crystal, thermal and optical stimulation processes of V-centres (Japanese) 0-11485  
NaCl, irradiated, at 80K, thermolum. processes 0-34990  
NaCl-NaF:Pb<sup>2+</sup>(Eu<sup>2+</sup>)(Zn<sup>2+</sup>)(Mn<sup>2+</sup>)(Sn<sup>2+</sup>), point defect ionic thermal current and optical meas. 0-6403  
NaF:Ca, migration enthalpy and entropy, TSC obs. 0-54716  
3PbO.2GeO<sub>2</sub>, TSC in thermoelectret state during ceramic synthesis, pyroelec. currents and energy struct. of capture centres 0-55014  
Pb(Zr,Ti)O<sub>3</sub> ceramics, space charge field meas. by ferroelec. domain switching current, piezoelec. reson. freq. ageing characts. 0-7296  
RbBr:Cu<sup>+</sup>, off-centre ion position, ionic thermocurrent study 0-7271  
RbCl:Cu<sup>+</sup>, off-centre ion position, ionic thermocurrent study 0-7271  
Si, amorphous, Schottky barrier solar cells, deep hole traps, spectral response and TSC meas. 0-50962  
Si:Au, p<sup>+</sup>-n junction, quantitative study of Au atoms by TSC method 0-2458  
TiO<sub>2</sub> sputtered film, photocond. and TSC meas. 0-15560  
 $\alpha$ -ZnP<sub>2</sub>, local centre parameters, photoelectron transition scheme, recomb. process anal. 0-44654  
ZnS:Ag, TSC and induced impurity photoconductivity, existence of two electron trapping centres 0-44655

**thermally stimulated depolarisation** *see thermally stimulated currents*  
**thermally stimulated discharge** *see thermally stimulated currents*  
**thermally stimulated ionic currents** *see thermally stimulated currents*  
**thermally stimulated polarisation** *see thermally stimulated currents*  
**thermally stimulated relaxation currents** *see thermally stimulated currents*

**thermionic cathodes**  
high-current multirad cathode, influence of absorption effects on characts. 0-20756  
ionisation gauges, heated cathodes, emission characteristics, selection (German) 0-236  
Knudsen converter low energy electron reflection from thermionic cathode, mag. field depend. 0-19627  
plasmatron, emission cooling (Russian) 0-54052  
LaB<sub>6</sub> cathode gun from transmission electron microscope appls. 0-18048  
Mo-TiC(ZrC)(HfC), thermionic emission, surface structural characts. after prolonged use, work function variation 0-20758  
W-ThO<sub>2</sub>-B, thermocathodes diffusion mobility, based on deboronation kinetics 0-39349  
W-Ti, Ti addition effect on heat resistance and radiative props. (Russian) 0-25515  
W-TiC(ZrC)(HfC), thermionic emission, surface structural characts. after prolonged use, work function variation 0-20758  
W-Zr, Zr addition effect on heat resistance and radiative props. (Russian) 0-25515  
W-Zr-C, Zr and C addition effect on heat resistance and radiative props. (Russian) 0-25515

**thermionic conversion**  
cermet electrode development for flame heated thermionic converters 0-40891  
cylindrical, low cost convertor for measuring lead efficiency 0-40889  
electron beam, fast, relax. cross sections energy depend. 0-43939  
electron thermal conductivity, effect on convertor performance, theory 0-40892



**thermionic conversion continued**

- flame-fired thermionic diode development 0-40890
- heat flux and electron reflectivity expts. for improved convertor efficiency 0-45719
- heat pipes, spacecraft radiator elements, NEP thermionic system design 0-40887
- hybrid mode thermionic convertor, developments 0-40888
- ignited mode of convertor, electron energy distrib. meas. of Cs plasma (Japanese) 0-3528
- ignited mode of convertor, internal phenomena and output characteristic (Japanese) 0-3527
- Knudsen converter low energy electron reflection from thermionic cathode, mag. field depend. 0-19627
- R and D at US DOE 0-35715
- sheath operating mechanism effects 0-30507
- space vehicle thermionic convertor array, efficiency optimisation using heat transfer computer modelling 0-40886
- space vehicle thermionic generators for solar energy conversion 0-35714
- thermionic spacecraft reactors with  $^{235}\text{U}$  as fuel, reflector drums as control mechanism 0-47686
- Zepo-the world's largest thermionic converter, design and testing 0-40885
- Cs convertor, pulsed, plasma parameters, operating characts. 0-6293
- Cs-Se thermionic converter, output power, vap. source depend. 0-44000

**thermionic electron emission**

- see also Schottky effect; thermionic cathodes
- high-current multirod cathode, influence of absorption effects on characts. 0-20756
- laser spark in dense  $\text{N}_2$  near metallic target (Russian) 0-38682
- laser- or black-body radiation, strong electron coupling, limitation of Fermi-Dirac statistics 0-29843
- metal, anisotropy 0-20757
- point-contact junction, influence of mech. modulation elec. transport 0-2481
- work function, local, surface with adsorbed atom islands 0-7462
- Au-Al $_2\text{O}_3$ -Al system, influence of mech. modulation on elec. transport 0-2481
- BaB $_6$  powder, surface struct. effects on thermionic emission characts. and vapour pressure (Japanese) 0-50506
- BaB $_6$  powder prep., thermionic emission charact. (Japanese) 0-11610
- $\text{CO}_2$  laser-heated electron emission from C-coated metal surface, appl. to emissive probe meas. 0-6270
- GaAs, deep centres, collective thermal emission of electrons 0-10918
- GaAs-Al $_2\text{O}_3$ -Ga $_2\text{O}_3$ -As, negative differential resist., real-space electron transfer 0-6958
- (La, Y, Sc)B $_6$  solid solns. electron work function, thermal emission technique 0-20755
- Re, thermionic work function of low index planes 0-55255
- Ta autocathode, influence of electric field and heating on work 0-7478

**thermionic emission**

- see also thermionic electron emission; thermionic ion emission
- refractory metals, work function, ionising radiation effects meas. method 0-6951
- LaB $_6$ , synthesis and props. (Japanese) 0-40255
- Mo-TiC(ZrC)(HfC), thermionic emission, surface structural characts. after prolonged use, work function variation 0-20758
- W cathode, hollow, cylindrical, heavy-current temp. condition 0-38763
- W-TiC(ZrC)(HfC), thermionic emission, surface structural characts. after prolonged use, work function variation 0-20758

**thermionic generators** see thermionic conversion**thermionic ion emission**

No entries

**thermionic power generation** see thermionic conversion**thermionic tubes**

- see also cathode-ray tubes; electron-wave tubes; gas-discharge tubes; rectifier tubes; vacuum tubes
- flame-fired thermionic diode development 0-40890

**thermionic valves** see thermionic tubes**thermistors**

- acoustic temp. indicator, consisting of temp. sensitive resistor and operational amplifiers (Spanish) 0-13061
- deep tissue temp. monitoring by ultraminiature thermistors 0-3761
- dynamic behaviour determination (German) 0-17940
- level sensing in elec. conducting liquids using PTC thermistors 0-42209
- PTC thermistor P310-C11, level sensor for liq.  $\text{N}_2$  0-52247
- semiconductor thermometry at low and very low temperatures 0-4713
- solar power measurement, microcomputer-controlled photodiode light meter and thermistors 0-50946
- surface temp. meas., temp. contact methods using thermistor and thermoinductors (Russian) 0-27295
- temp. measurement, review, techniques and instruments (German) 0-22358
- SiC thin film, RF-sputtered, highly reliable temp. sensor 0-224

**thermo-optical effects**

- see also thermorefectance
- aqueous soln. reaction kinetics meas. microwave apparatus 0-3470
- N-5-chlorosalicylideneaniline, photochromism and thermochromism, NQR spectra, temp. and UV irradiation depend. 0-54968
- crystal vibrational spectrum, inhomogeneous thermal broadening effect 0-55100
- elasto-optical constants and refractive index, thermo-optical method for meas. 0-7327
- glass, photochromatic, induced colour by optical/thermal treatment 0-34954
- glass, photochromic, thermo-optic transitions 0-50307
- IR absorption measurement, interference calorimetric method, effect of crystal thermo-optic props. 0-47096
- liquid crystal improved technique for thermal field measurements 0-216
- mirage effect spectroscopy 0-47116
- nonlinear optical crystals, SHG, absorpt. coeffs. and temp. variation of refr. index difference 0-14390
- optically thick sample, thermal lensing effect, revised model 0-34900
- phosphate laser glasses, review 0-9888
- salicylidene-2-chloroaniline, photochromism and thermochromism, NQR spectra, temp. and UV irradiation depend. 0-54968
- single-mode fibre lightguide, phase of coherent signal, temp. and stress effects 0-33208
- sound generation, nonsteady acoustic fields 0-15193
- thermal nonlinearity effects of thermooptical sound generation 0-38146

**thermo-optical effects continued**

- thermosensitive film coating, dispersed liq. cryst. microdroplets in gelatin matrix, exam. of preps. 0-42220
- As-S chalcogenide glass holographic recording efficiency, photocond. and annealing effects (Russian) 0-15556
- As $_2\text{Se}_3$  chalcogenide semicond. film, thermooptical transitions with photostructural transformations (Russian) 0-16016
- BaF $_2$  crystal, refr. index temp. increments meas. 0-33098
- $\text{CO}_2$ -N $_2$ , kinetic cooling effect by  $\text{CO}_2$  laser radiation, temp. dependence 0-10347
- Co enamel, vitreous, objective colour evaluation, rel. to firing parameters (Czech) 0-42252
- Cs $_2\text{Cr}_2\text{Cl}_6$ , thermo-optical spectroscopy, detection by mirage effect 0-47116
- CuCl $_2$ , aqueous soln., nonlinear conversion of acoustic pulses with thermooptic excitation 0-14510
- GaSe, refr. index meas., temp. variation 300 to 75K 0-25328
- MnF $_2$ , magnetic, thermal, elastic refraction of light, mag. order influence on refractive index (Russian) 0-34880
- Nd $_2(\text{MoO}_4)_3$ , thermo-optical spectroscopy, detection by mirage effect 0-47116
- TiBr-TiI, TiCl-TiBr, KRS-5 and KRS-6 crystals, refr. index temp. increments meas. 0-33098
- $\text{VO}_2$ , film, visualisation of microwave and IR radiation 0-5839
- $\text{V}_2\text{O}_5$ , FTIR spectroscopy, thermochromic materials, colour and visual contrast 0-33100
- $\text{Y}_2\text{O}_3\text{:Tb}^{3+}(\text{Eu}^{3+})$  temp. and viscosity depend. of colour coords. 0-40149
- ZnSe crystal, refr. index temp. increments meas. 0-33098

**thermochemistry**

## see also chemical reactions

- aliphatic perfluorocarbons, electron attachment, fragmentation 0-12 eV 0-5618
- heat pump/refrigerator thermodynamic analysis 0-35716
- high temperature species, JANAF thermochemical tables, thermodynamic properties evaluation and compilation 0-41959
- high temperature system characterisation, models, phys. and chem. reference data sources 0-41958
- ion+molecule, entropy change, enthalpy of form., equilib. const., thermochemistry 0-30233
- ion-molecule, flames and diagnostic techniques 0-55664
- metals, FCC, under  $\text{H}_2$  press., crit. phenomena and isomorphic transitions 0-49367
- PMMA, thermochem. instability at Pt sphere inclusions caused by CW laser beam 0-29689
- polyatomic molecule dissociation, thermochemical study of thermal negative ion production (Japanese) 0-50495
- production by Westinghouse electrochem./thermochem. S-cycle process 0-45808
- refractory compounds heat of formation determ. using self-propagating high-temp. synthesis 0-3392
- solar energy storage by  $\text{H}_2$  prod. using Mg(Al)(Fe)(Co)(Ni)(Cu)(Zn) sulphates (French) 0-55935
- turbulent diffusion, flames, high Reynolds number, rocket exhaust appl., chem. processes theory 0-45504
- $\text{Bi}_2(\text{SO}_4)_3$  thermochem. cycle, process engng. design for H prod. 0-30599
- $\text{CaCl}_2$ -methanol thermochem. cycle for solar thermal energy storage 0-30587
- $\text{Ca}_2\text{SiO}_5$ , thermochem. effects on formation 0-16666
- H, electro-/thermochemical prod. from  $\text{H}_2\text{O}$  by Westinghouse sulphur cycle 0-55940
- H, electrochemical/thermochem. prod. using S cycle, laboratory prod. model and electrolyser development 0-30602
- H production, thermochemical or hybrid cycles of hydrogen production techno-economical comparison with water electrolysis 0-45796
- H production using Ce-Cl cycle 0-35783
- H production using hybrid electrochem./thermochem. cycles, search for electrochem. reactions 0-45807
- H, thermochem. prod. by  $\text{H}_2\text{O}$  decomposition using Mg-I cycle 0-35786
- H, thermochem. prod. using the Mark-13 process, status report 0-30606
- H thermochemical prod., engineering impact on the validity of the Mark-16 thermochem. cycle 0-45806
- H, thermochemical prod. by  $\text{H}_2\text{O}$  decomposition, impact of thermal burdens and kinetics 0-35787
- H, thermochemical prod. from  $\text{H}_2\text{O}$ , noncorrosive two-reaction low temp. cycles based on mordenite-hosted redox reactions 0-55939
- H thermochemical prod. using  $\text{Bi}_2(\text{SO}_4)_3$  cycle, process engng. design 0-30599
- H, thermochemical prod. using  $\text{SO}_2$ -I $_2$  water splitting cycle 0-30600
- H, thermochemical prod. using Br-Ca-Fe  $\text{H}_2\text{O}$ -decomposition cycles 0-35784
- H, thermochemical production using Hg-I ANL-4 cycle 0-35785
- H, thermochemical production by coal gasification using steam 0-35789
- H thermochemical production using air blown coal gasification, economics 0-35790
- H, thermoelectrochemical prod. using NaCl 0-55946
- $\text{H}_2$  and power production using thermoelectrochem. cycles 0-16820
- $\text{H}_2$  production, engineering impact on the validity of the mark-16 thermochemical cycle 0-55931
- $\text{H}_2$  production by polynaphthoquinone- $\text{SO}_2$ -I $_2$  system for  $\text{H}_2\text{O}$  decomposition 0-16825
- $\text{H}_2$ , thermochemical prep. by  $\text{H}_2\text{O}$  dissoc. using S-I cycle 0-16823
- $\text{H}_2$  thermochemical prod. by  $\text{H}_2\text{O}$  dissoc. using Sb-I-Ca process 0-16824
- $\text{H}_2$ , thermochemical production, based on reactions of  $\text{CeTiO}_2$  for water-splitting 0-55929
- $\text{H}_2$  thermochemical production using open-loop cycles 0-55930
- $\text{H}_2\text{O}$ , decomp., H prod. by thermochemical and thermoelectrochemical cycles 0-26029
- W-Br regenerative cycle of linear quartz lamps, metallic impurity effects, thermochemical interpretation 0-3312
- ZnSe thermochem. cycle for H prod., chemical and process design studies 0-35782

**thermoclines** see temperature distribution**thermocouples**

## see also thermopiles

- anemometer, hot-wire, for boundary layer meas. with free convection in liquids (German) 0-10329
- cancerous mouse hyperthermia meas., microwave, IR and thermocouple methods (French) 0-3768



**thermocouples continued**

- ceramic, isolated, fault detection using computer-controlled capacitor discharging method (*German*) 0-13079
- chromel and alumel, decalibration, quantitative SIMS anal. 0-4705
- coaxial, high integrity thermocouple for LMFBR coolant temp. meas. 0-32410
- comparator for testing gemstones 0-13070
- conductor heating, similarity theory and dimensional anal. computational methods (*Rumanian*) 0-47053
- dynamic errors, 3-channel corrector 0-17939
- electronic thermometer, microprocessor based linearisation of thermocouple temp. charact. 0-221
- high-pressure temperature meas. in liquid He region 0-31748
- hot gases, convective heat transfer coeffs. to solid surface, moving thermocouple meas. 0-42230
- industrial appl., advantages 0-42221
- measurement of temperature of oil in sliding friction bearing 0-31753
- nonmetallic, differential-temp. probe for use in microwave fields 0-56320
- temp. measurement, review, techniques and instruments (*German*) 0-22358
- temperature meas. devices developments (*German*) 0-8986
- thermocouple probe, apparatus for testing under working conditions 0-22360
- thermometry, accurate, review 0-52207
- thin film fission thermocouples for energy deposition meas. in FBR safety expts. 0-47658
- thin-film fission thermocouple detectors for reactors safety expts. 0-22987
- Pt-alloy thermocouples, reference-standard testing apparatus 0-13077
- W-graphite thin film thermocouple, temp. gradient meas. in LPE system 0-25584

**thermodiffusion** see *thermal diffusion*

**thermodynamic changes of state** see *phase transformations*

**thermodynamic cooling** see *cooling*

**thermodynamic equations of state** see *equations of state*

**thermodynamic potential** see *free energy*

**thermodynamic properties**

see also *critical points; enthalpy; entropy; free energy; Gruneisen coefficient; latent heat; specific heat*

- <sup>3</sup>He, solid, two parameter model of mag. and thermal props., spin exchange 0-49461
- alcohol-unassociated active component liquid mixtures, associated soln. theory, thermodynamic parameters 0-7836
- alkali halides, cryst., pot. parameters, Hellman function calcs. 0-2181
- alkali halides, molten, crit. consts. calc., dense gas formulation 0-44100
- alkali metal actinide complex halides, thermochem. and struct. props. 0-7847
- alkali metal liq. binary systems, thermodynamic props. at high temps. 0-15262
- n-alkanes, liq. mixtures, thermodynamics 0-55700
- alloys, binary, thermal cond. conc. depend., irreversible processes, thermodynamic calcs. (*Russian*) 0-39550
- alloys, DO<sub>2</sub> and Li<sub>2</sub> superstructures, atomic ordering, multicluster approx., order-disorder transition 0-38990
- alloys, structure at high temp., microscopic theory (*Japanese*) 0-29191
- amorphous soft-core systems, low temp., mol. dynamic studies 0-6359
- benzaldehydes, para-halogenated, IR and Raman spectra, vibr. assignments, thermodynamic functions 0-14139
- benzene-chlorobenzene, benzene-toluene, perfect binary liquid mixtures on silica gel, adsorption thermodynamics 0-44428
- benzene-tetrahydrofuran, soln., excess thermodynamic props. and interactions, US vel. and density meas. 0-39288
- benzene-toluene, perfect binary liquid mixtures on silica gel, adsorption thermodynamics 0-44428
- binary lattice gas, crit. phenomena, series anal. 0-4671
- boson magnetised ideal gas, effect of confinement, anal. 0-12987
- brasses, thermodynamic anal. (*German*) 0-25663
- butanol-methylethyl ketone, soln., excess thermodynamic props. and interactions, US vel. and density meas. 0-39288
- cast iron-steel mixture, interaction of Zr, formation reaction thermodynamics (*Russian*) 0-55645
- chain molecules in soln., thermodynamic props. related to chem. pot. 0-3394
- chemoeptaxial nucleation during reaction diffusion, thermodynamic anal. (*Russian*) 0-15394
- chlorobenzene-bromobenzene, perfect binary liquid mixtures on silica gel, adsorption thermodynamics 0-44428
- classical and quantum spin models, functional integral method appl. 0-15676
- corresponding states theory, thermodynamic props. 0-54338
- cyclopropyl bromide, IR absorption, Raman scatt., assignments, thermodynamic functions 0-984
- cylinder, perforated, radiated energy anal. 0-19228
- Debye lattice, thermal props., WINIMAX approx. appl. 0-49333
- diamond, 'melting' to solid metallic C phase above graphite triple point 0-15236
- dichloroanilines, vibr. assignments, Raman spectra obs., thermodynamic functions 0-52992
- 2,3-dimethylbuta-1,3-diene, IR, Raman spectra, torsional pot. function, thermodynamic function 0-43046
- dipolar fluids, equilib. statistical mechanics, struct., dielec. and thermodynamic props. 0-6345
- dipolar liquids, hypernetted-chain eqn., perturbation theory soln. 0-49072
- electrolyte soln. grand canonical ensemble Monte Carlo method 0-54092
- electrolyte solutions, thermodynamics, transport props., semi-phenomenological approach including short range forces 0-3353
- ethylene copolymers, partially cryst. pseudoeutectoid, swelling, thermodynamics 0-39311
- extractive metallurgical processes, thermodynamic evaluations 0-11591
- ferrite systems, thermodynamic stability, dissociation and phase relations (*Japanese*) 0-55378
- ferroelectric thin film, in neighbourhood of phase transition of second kind 0-45021
- fibre reinforced thermoelastic materials, nonlinear thermodynamic continuum theory 0-14579
- fluid, binary mixture, in centrifugal field, crit. dynamics 0-44310
- fluids, thermoelastic, stability of motion anal. 0-10221
- fluoroanilines, isomers, thermodynamic functions and fundamental vibr. freqs. 0-9581

**thermodynamic properties continued**

- gases, thermal activity coeff. meas., periodic-heating method, appls. 0-42218
- granular materials, localised internal heating, thermodynamic theory 0-19230
- graphite, adsorption of methane in first monolayer domain, thermodynamic props. (*French*) 0-29275
- hard rod system, improved lattice model, nematic and isotropic phases 0-33882
- hard spherocylinders and spheres mixtures, Monte Carlo study 0-49073
- hard-core lattice gas with tricrit. point, phase transition behaviour 0-8926
- high temperature species, JANAF thermochemical tables, thermodynamic properties evaluation and compilation 0-41959
- highly degenerate multicomponent plasma thermodynamic props. 0-33739
- histones, H2a and H4, aggregation ionic strength effect (*Russian*) 0-55697
- Hubbard two-site model with orbital degeneracy, thermodynamic props. 0-2545
- hydrogen, and isotopic forms, cryogenic data relevant to mag. fusion energy 0-8746
- inert gas small clusters, three body interaction effects on thermodynamic props., comparison bulk props. 0-28128
- ionic crystal, thermodynamic props. calc., pot. energy function approach 0-54407
- ionic molecules, vapours, thermodynamic properties, classical partition function, dimens. anal. 0-43829
- Ising lattice, thermal relaxation, nonideal behaviour, stochastic theory 0-22312
- Ising-Heisenberg linear ferromagnet, excitation spectrum and thermodynamic props. 0-50118
- laser, photon distrib. with 1st-order phase-transition analogy 0-23659
- liquid crystals, solid state polymorphism, differential scanning calorimetry and IR and Raman spectra obs. 0-55094
- liquid metal, electronic theory of thermodynamics and struct., summer school lecture series 0-6353
- liquid metals, radial distrib. function and thermodynamic characts., interparticle interaction pot. (*Russian*) 0-49086
- liquid mixtures, intermol. forces effect on phase diagram and excess props., perturbation theory 0-39287
- long chain paraffins, thermodynamic functions, Monte Carlo method appl. (*German*) 0-19962
- LWR, HCDA, behaviour of concrete in contact with molten corium 0-13584
- magnet, ordering temps. determ. by Bethe-Peierls-Weiss (BPW) method 0-49912
- MBBA-n-heptane system, thermodynamic functions in lattice model (*Russian*) 0-33887
- metal oxides, diffusion activation process, interatomic bonding energy (*Russian*) 0-54428
- metal-H systems at high H press., physicochemical props., book contrib. 0-24535
- metals, enthalpy and average mass temp. on plasma-arc melting (*Russian*) 0-54405
- metals, FCC, under H<sub>2</sub> press., crit. phenomena and isomorphic transitions 0-49367
- metals, structure at high temp., microscopic theory (*Japanese*) 0-29191
- methane, compressibility isotherms, thermodynamic props., 0 to 150°C 0-6196
- methylethyl ketone-butanol, soln., excess thermodynamic props. and interactions, US vel. and density meas. 0-39288
- microfluids, linear theory of chemically reacting mixtures 0-14777
- mixture, fluid, molecular basis of activity coeff., isobaric-isothermal ensemble approach 0-55690
- molecular dynamics method in statistical physics, review 0-18895
- molecular liquids, generalised mean field theory, thermodynamic props. 0-6332
- monolayer, interfacial, thermodynamic treatment, excess quantities, adsorbed and spread layers 0-40732
- nematic solution, hard rigid/flexible mols. mixture, unathermal, lattice model (*Russian*) 0-54129
- non-spherical molecule ensemble, background correl. in statistical thermodynamic calcs. 0-36958
- nonelectrolyte aqueous solutions, temp. of max. density rel. to partial compressibility, struct. strengthening 0-30270
- nonideal gas in gravitational field, partition function, eqn. of state 0-6198
- nonpolar binary mixture, partial molar vol. prediction from Lee-Kesler eqn. of state 0-10632
- organic binary liquid mixtures, excess free vol. calcs. 0-34202
- organic binary mixtures, with weak charge transfer interactions, thermodynamic props. 0-54360
- plasma, nonideal, elem. excitations and macroscopic props., review 0-43842
- PMMA, solvent cast, surface characts., chromatographic study 0-20020
- PMMA solution, diffusion coeffs. and thermodynamic props., conc. depend. 0-15274
- polar liquids in elec. fields, statistical mechanics 0-54085
- polyelectrolyte solution, thermodynamic props. determ. from Donnon equil. obs. 0-7846
- polyethylene-polyoxymethylene mixtures connection of melt thermodynamic props. with solid state struct. (*Russian*) 0-54152
- polymer, dil. soln., light scattering charact. of thermodynamic props., solvent and mol. wt. effect 0-16717
- polyvinylidene fluoride, thermodynamical model, applications (*French*) 0-39315
- PVC solution, diffusion coeffs. and thermodynamic props., conc. depend. 0-15274
- rare earth halides, prep. and props., book contrib. 0-54211
- rare earth hydrides, props., book contrib. 0-45291
- rare earth oxides, binary, struct. and props., book contrib. 0-45292
- relativistic fluid, infinite thermal conductivity, Cauchy problem solutions, existence and uniqueness (*Italian*) 0-48821
- semiclassical laser theory in the stochastic and thermodynamic frameworks 0-1178
- semiconducting liquid alloys, anomalous thermodynamic props., theory 0-49287
- semiconductor, interface form., initial steps, surface states and thermodynamics 0-49503
- semiconductors, chemical thermodynamics, review 0-55692



## thermodynamic properties continued

- silicate glass, thermodynamic theory of structural relaxation (*German*) 0-38929
- silylacetylene, centrifugal distortion consts., thermodynamic functions 0-47959
- simple fluids, semiempirical calcs. using perturbation theory 0-28892
- small extended Hubbard rings, thermodynamic props. 0-2546
- soft rods, one-dimensional, exact partition and thermodynamic functions 0-46953
- solar energy storage by  $H_2$  prod. using  $Mg(Al)(Fe)(Co)(Ni)(Cu)(Zn)$  sulphates (*French*) 0-55935
- solid electrolyte, transition temperature to high cond. state as function of press. 0-44365
- solvation effects and Gurney cosphere overlaps, conductimetric approach 0-21354
- spin wave damping, magnetic materials with canted mag. struct., thermodynamic and high freq. props. 0-11184
- spin- $1/2$  XY model, thermodynamic quantities, high-temp. series expansions anal. 0-7067
- spin-phonon system, transition to self-trapping 0-10606
- star, cold, massive rest-mass density and redshift 0-56859
- steel, deoxidation by Ca-Si alloy, thermodynamics (*Russian*) 0-16268
- structural relaxation, order parameter model (*German*) 0-44146
- superconducting slab, type I, first stage magnetisation and metastable migration field 0-15655
- supercooled steam, thermodynamic props., virial eqn. of state 0-14872
- TCNQ salt, quinolinium, electron spin location, elec., mag., and thermal props. 0-25189
- ternary alloy of quasi-binary cross sections, thermodynamic functions calc. 0-16265
- tetrafluoromethane adsorbed on graphite, adsorption isotherms, crit. temps. (*French*) 0-34312
- tetrahydrofuran-benzene, soln., excess thermodynamic props. and interactions, US vel. and density meas. 0-39288
- thiaalkanes pure crystals, thermal press. coeffs. and expansivity at 298.15K 0-49381
- toluene-bromobenzene, perfect binary liquid mixtures on silica gel, adsorption thermodynamics 0-44428
- toluene-chlorobenzene, benzene-toluene, perfect binary liquid mixtures on silica gel, adsorption thermodynamics 0-44428
- transition metals, liq., calc. (*Russian*) 0-15264
- Van der Waals gas, thermodynamic props. review 0-31694
- van der Waals molecules, pot. functions, level spacings and thermodynamic props. 0-14185
- water, appl. of polychromatic correlated site percolation 0-22296
- water, liq., Monte Carlo-Metropolis computer simulation, convergence characts. 0-10485
- water, thermodynamic props., computer programme calcs. (*French*) 0-54409
- ( $X=H,D$ ;  $n=1,2,3$ ), thermodynamic function in ideal gas state 0-14871
- Ag-AgCl reference electrode, construction and thermodynamic props., high temp. aq. environment appl. 0-21288
- AgCl-NaCl molten solns., activities and surface tension 0-10748
- Al-Zn, liq. solutions, thermodynamic properties (*Polish*) 0-49380
- $Al_2TiO_5$ , activation energies for decomposition and nucleation (*Japanese*) 0-35156
- Ar, solid, thermodynamic props. under press., multiparametric pairwise and Lennard Jones potential calcs. 0-39316
- Ar, thermodynamic behaviour, improved analytical representation 0-54339
- Ar-Xe plasma, shock wave dynamic compression (*Russian*) 0-53931
- B fibre reinforced Al-Cr(Mg)(Mn)(Si), calc. of thermodynamic interaction potential between B fibre and matrix 0-11627
- $BBr_2 \cdot PCl_3 \cdot H_2$ , gas phase equilib. comp. 0-35166
- BN, adsorption of methane in first monolayer domain, thermodynamic props. (*French*) 0-29275
- $CX_n$  radical, ( $X=H,D$ ;  $n=1,2,3$ ), thermodynamic function in ideal gas state 0-14871
- Ca-Mg, liq. alloys, thermodynamic activities determ. using modified Ruff method (*German*) 0-11631
- $CaO-SiO_2$  glass, two phase region, expt. and thermodynamic data 0-16288
- $CaSO_4 \cdot 2H_2O$ , thermodynamic expression for crystal growth and dissolution affinity 0-24385
- Cd-In-Sb, liq. alloys, thermodynamic activity of Cd between 833 and 953K (*German*) 0-45278
- Cd-Sn-(Pb) liquid (0.03 to 0.10 at.% Cd), Cd activity coeffs., interaction parameters, EMF depend. on temp. 0-49383
- $Cl_2$ , mol. liquid, mean squared torque and mean squared force, interaction energy spherical harmonic expansion 0-54093
- B-CoTe phase, thermodynamic study by Galvanic cell meas. 0-29190
- Cr-rare earth alloys, liquid phase, topology in diagrams of state (*Russian*) 0-54121
- Cs, nonideal plasma press. ionisation, short range forces, thermodynamic props. 0-33733
- Cu-O-Zn dilute liquid alloy, Zn-O interaction parameter 0-55694
- Cu-Pb-O, liquid, dil. alloy,  $O_2$  activity, 1100 to 1200°C 0-25662
- $D_2O$ , appl. of polychromatic correlated site percolation 0-22296
- Fe, heat capacity temp. depend. meas., internal energy and entropy, anharmonic theory calcs. (*Russian*) 0-54402
- Fe-As-Su-Si (Cr)(Mn) melts, As and Sn distrib., Si, Cr, and Mn influence (*Russian*) 0-16274
- Fe-bearing binary, substitutional liq. and solid solns., statistical thermodynamics 0-11630
- Fe-C system, mixing variables, activities and entropies calc., short range order model (*German*) 0-25655
- Fe-C-Cr, pearlite reaction kinetics 0-3006
- Fe-C-Cr, thermodynamics and phase equilibria near eutectoid temp. 0-3005
- Fe-Ga-C melts, thermodynamics and C solubility (*Russian*) 0-39292
- Fe-Ni, liq. alloy, electrochem. meas. of O, thermodynamic props. at 1873K 0-30244
- Fe-Ni, thermodynamic props., anomalous 0-39313
- Fe-Ni Invar alloy, mag. phase mixing effect on thermodynamic props. 0-54891
- $Fe_3O_4-Co_3O_4$  spinels, phase diagram anal., thermodynamic props. 0-3009
- $Fe_3O_4-NiFe_2O_4$ , solid soln., activities determ. from EMF of galvanic cell 0-16290
- $H_2O$ , n-state configurational excitation model, diagnostic thermodynamic props. 0-10481

## thermodynamic properties continued

- $H_2O-HNO_3-NO_3^-$  clusters, gas phase, thermodynamic quantities, mass spectra obs. 0-50875
- He, liq. and vapour phases, thermodynamic and thermophys. props., HEPROP computer program 0-6529
- $^3He-^4He$ , dil. soln., grand partition function, ground state energy determ.,  $^3He$  conc. depend. 0-49455
- $^3He-^4He$ , superfluid, osmotic and mag. props., review (*French*) 0-10733
- $^4He$ , superfluid, continuum theory based on classical theory of irreversible processes 0-29236
- In-As system, exam. of thermodynamic consistence of models, and QCE approx. for activity coeffs. (*German*) 0-24615
- InAs-InP, phase equilib. and dissoc. 0-35170
- La-Co-O system, stability of ternary phases, nonstoichiometry 0-24434
- $LaNi_5-Al$ , alloys and related hydrides, thermodynamic and struct. props. for  $H_2$  storage appl. 0-16847
- La, Ni,  $H_2$ , thermokinetics of H evolution 0-30593
- $LiReO_4$ , thermodynamic activity in  $LiReO_4-CsReO_4$  system, mass spectra meas. 0-2174
- $Mg,U_{1-x}O_{2+x}$ , thermodynamic props., EMF meas. 0-29187
- Mn-Si(C), melt, activation determ. by vapour press. meas. 0-16279
- $Mn_3O_4-Co_3O_4$  spinels, phase diagram anal., thermodynamic props. 0-3009
- $Mo_2C$ , free energy of form. and thermodynamic props. of C in solid Mo 0-15266
- $N_2$ , liq., thermodynamic props., perturbation theory with hard dumbbell reference system 0-14991
- $N_2$ , mol. liquid, mean squared torque and mean squared force, interaction energy spherical harmonic expansion 0-54093
- $N_2O_4=2NO_2=2NO+O_2$ , working fluid for power-producing thermodynamic cycles 0-13536
- Na-Se system, liq., thermodynamic props. 0-21319
- NaCl-KCl, aq. solns., isopiestic studies, 383 to 474K 0-21320
- $Na_2O-B_2O_3$  glass-forming melts, thermodynamic functions 0-25673
- $Na_2O-MoO_3$ , melt, EMF meas., rel. partial molar thermodynamic props. 0-6526
- $Na_2O-SiO_2-Ga_2O_3-Al_2O_3$  glasses in mixed  $AgNO_3-NaNO_3$  melts, ion exchange 0-21282
- $Na_2SO_4$  in aqueous soln., diffusion coeffs. and Onsager-Fuoss theory disagreement 0-40729
- Nb-K melts, thermodynamic characts., elec. resistivity, single parameter rigid sphere calcs. (*Russian*) 0-34410
- $Nb_3Ge$ , amorphous nongranular thin superconducting film, thermodynamic and resistive transitions 0-34571
- Ne- $H_2$  mixture, liquid vapour phase equilib., sound vel., compressibility, thermodynamic perturbation theory obs. (*Russian*) 0-39306
- Ni, heat capacity temp. depend. meas., internal energy and entropy, anharmonic theory calcs. (*Russian*) 0-54402
- Ni-S melt, three-suffix Margules equations with zero ternary interactions 0-19957
- Ni-Si liquid alloys, thermodynamic props., enthalpy of mixing (*Russian*) 0-34207
- Ni-W-C(Nb) system,  $\gamma$  to ( $\gamma+W$ ) phase boundary calcs. using Wigner method (*Russian*) 0-54346
- NiO-CuO, equilibrium relations 0-55375
- Pb liquid,  $O_2$  activity from electrochem. meas. 0-55695
- Pb melts, As and Sn distrib., Si, Cr, and Mn influence (*Russian*) 0-16274
- Pb-Sb, liq. alloy, Pb thermodynamic props. (*Czech*) 0-29925
- $PbHPO_4$ -type crystals, ferroelec. transition, statistical model 0-25321
- PbTe-PbSe system, thermodynamic props. 0-11635
- Pb(Zr,Ti) $O_3$ , absolute and relative vapour pressures, thermodynamic formation data 0-29939
- Pd-Au- $H_2(D_2)$ , thermodynamic props. at 555 and 700K, vibr. freqs. and excess entropies 0-29186
- Pd-H and Pd alloy-H systems, review of props., book contrib. 0-24605
- Pr-Al liquid alloys, atomic interactions, thermodynamic props. (*Russian*) 0-39307
- Pt-Al(In)(Sn) alloys, Fermi energy influence on thermodynamic props. (*German*) 0-24619
- PuO $_2$  nuclear fuel, eqn. of state and thermodynamic props. 0-13592
- Sb, liquid,  $O_2$  activity from electrochem. meas. 0-55695
- ScI $_3$ , vapourisation thermodynamics, sublimation and formation 0-54366
- SeS $_2$  gas, thermodynamic props., quadrupole mass filter study 0-16716
- $SiX_n$  radical, ( $X=H,D$ ;  $n=1,2,3$ ), thermodynamic function in ideal gas state 0-14871
- $SnO_2$  film, deposition from vapour phase, thermodynamic anal. 0-15418
- $TeO_2-NaCl(NaBr)$ , condition diagram, thermographic obs. (*Russian*) 0-53377
- TiCo-H system, thermodynamic rels. and struct. transformations 0-49385
- TiNi-H system, thermodynamic rels. and struct. transformations 0-49385
- TiO, high temp. thermodynamics, vaporisation, and pressures over 0-10685
- TiO $_2$ -Ti-Cl $_2$  system, thermodynamic analysis, gas phase equilibrium composition 0-21317
- UO $_2$  nuclear fuel eqn. of state and thermodynamic props. 0-13592
- UO $_2$  phase, thermodynamic props. 0-13594
- UO $_2$  vapour, saturated, thermodynamic state and gas kinetic relaxation to 5000K 0-13593
- $UO_2^{2+}+UO_2NO_3^{+}$ , ground and excited state interaction, struct., thermodynamic functions, photochemistry obs. 0-32779
- V-based ternary solutions, containing H, thermodynamics 0-19961
- $VCl_4(Br_4)$ , vibronic systems, degenerate ground states, statistical sums, thermodynamic func. calcs. 0-27997
- VS through  $V_3S_4$ , nonstoichiometric, phase relations and thermodynamics 0-29188
- $V_3Si$ , normal, mixed and supercond. state, specific heat meas., thermodynamic and superconducting props. 0-49987
- $ZnF_2$ , sublimation 0-34181

## thermodynamics

- see also atmospheric thermodynamics; critical phenomena; entropy; equations of state; Joule-Thomson effect; statistical mechanics
- absolute zero, vanishing of specific heat without invoking 3rd law, objections 0-8940
- adsorbed layers, two dimensional incommensurate crystal theory, thermodynamics (*Russian*) 0-49524
- adsorption, localised, on homogeneous solid surface, Berezin-Kiselev model 0-10780
- alloy, FCC closed packed, ordering-type transitions 0-2140



## thermodynamics continued

alloys, interstitial solid solns., HCP, ordering type transitions within thermodynamics theory framework 0-49162  
 anisotropic micropolar fluid theory 0-31515  
 anisotropic spheres, adiabatic contraction in general relativity 0-36489  
 Ba-Mg, liq. alloys, thermodynamic activities determ. 0-50604  
 Belusov-Zhabotinski reaction, nonlinear effects 0-3302  
 binary alloy freezing, non-equilibrium thermodynamic processes 0-34167  
 biological longitudinal transport, electroosmotic model 0-45870  
 black hole thermodynamics, second order phase transitions 0-46897  
 black hole thermodynamics and entropy 0-4613  
 black-hole thermodynamics, general review 0-31696  
 Bose, imperfect gas, condensed state, limit Gibbs state 0-52124  
 Bose gas, weakly interacting in restricted geometries, low-temp. thermodynamics 0-34261  
 Bose-Einstein condensation of a relativistic gas in d dimensions 0-8902  
 boson gas, interacting, approx. equilib. states 0-46962  
 boson quantum thermodynamical system in one space dimension, high-order perturbation expansion 0-4636  
 carbide solid solns. decomposition temp. expression 0-55398  
 cardiac chemical power, derivation of chem. power eqn. and determ. of eqn. consts. 0-16911  
 Carnot cycle, efficiency and irreversibility (*Spanish*) 0-176  
 Carnot cycle, systematics at positive and negative Kelvin temps. 0-42178  
 cast iron-steel mixture, interaction of Zr, formation reaction thermodynamics (*Russian*) 0-55645  
 chemical, symbols and terminology 0-3296  
 chemical discontinuous systems, general inequality for irreversible processes 0-55676  
 chemical laser, mol. constraints implied by kinetic coupling schemes, maximal work 0-38010  
 chemical power, appl. of power, work and efficiency eqns. to left ventricular energetics in man 0-16912  
 chemical reaction, Eckart barrier tunnelling, Arrhenium plot curvature 0-3298  
 chemically reacting systems, sound wave attenuation, thermodynamic interpretation 0-43505  
 Clausius' inequality, formulation using nonequilibrium temp. 0-180  
 coexisting phases, interfacial profile near tricrit. points 0-19906  
 coexisting thermodynamic phase interface, Ginzburg-Landau-Wilson model, drumhead model derivation in low temp. limit 0-42180  
 collapsing shell, Schwarzschild-de Sitter space-time, thermodynamics and radiation 0-17607  
 compressible flow, steady, thermodynamic consistency, finite difference scheme 0-48732  
 continuous elastic solids, foundations for coupled thermoelasticity 0-46807  
 critical thermodynamics, phase transition in transverse field with deform. depend., phonon anomaly separation 0-39258  
 crystal growth, macroscopic equilib. and transport concepts, book 0-27054  
 crystal thermodynamics in statistical theory, density Fourier coeffs., stress tensor, internal energy 0-13025  
 crystals, velocity autocorrelation function, long-time correlation tails 0-24541  
 crystals with dislocations, phase transitions of the second kind, dislocation superparamagnetism (*Russian*) 0-1957  
 dielectric negative static permittivity possibility (*Russian*) 0-50253  
 dimensionless entropies, simplification of thermodynamic calcs. 0-13019  
 discrete systems, fundamentals of dissipation inequalities 0-27251  
 disequilibrium theory applied to two-spin Glauber model 0-31669  
 dissipation inequality fundamentals, field formulation, continuous systems case 0-36960  
 dissipative structures, non-equilibrium systems, self organisation (*Chinese*) 0-42168  
 dissipative structures, origins and perspectives (*French*) 0-151  
 dissipative structures in chemical systems, nonlinear effects 0-3302  
 distribution functions, high order, truncation procedure, compatibility problem 0-47004  
 DNA-type macromolecule, melting, low mol. wt. impurity effect 0-12050  
 dust formation in space medium thermodynamics and kinetics, workshop, Houston, Texas (1978 September 6 to 8) 0-22131  
 electric current fluctuations in extended irreversible thermodynamics 0-42177  
 electrical circuit, power conversion of energy fluctuations, rel. to 2nd law of thermodynamics 0-17911  
 electrical contact phenomena, incorporation in electrodynamics eqns. 0-29374  
 electrolyte transport, irreversible thermodynamics calcs. 0-3364  
 electrolytic solution, thermodynamics and correlation functions 0-24132  
 equilibrium, teaching 0-46751  
 ethane derivatives, diastereoselective form. and symm. props., semirigid mol. model 0-48099  
 finite system, order parameter and sp. ht. for epitaxial ordering renormalisation-group calc. 0-17862  
 Fisher's droplet model for gas above  $T_c$  and the metastable phase 0-49348  
 flow equations for membrane transport, nonelectrolyte solute plus water case 0-26205  
 fluid mixtures, thermophysical properties prediction 0-48563  
 Fokker-Planck eqn., kinetic effects due to detailed equilibrium violation, elastic scatt. (*Russian*) 0-31687  
 Fokker-Planck equation, manifolds of equivalent path integral solns. 0-4687  
 fuel cells, nonequilibrium thermodynamics, heat release mechanisms and voltage 0-45660  
 fundamental mechanics, thermodynamics and gravitation (book) 0-41964  
 G-varying cosmology, thermodynamic relations and 3K background radiation 0-56979  
 galaxy clustering and thermodynamics 0-51881  
 gas, alternant Takahashi nearest neighbour type, exactly soluble case rel. to soft rods 0-33718  
 gas kinetic boundary value problem, non-equilibrium thermodynamics 0-19544  
 general relativity conformal groups, appl. (*French*) 0-101  
 generalised Kirchhoff law 0-17912  
 geothermal power plant, energy conversion process, thermodynamic considerations 0-16779  
 geothermal power plants flash cycle optimisation, analytical expression in terms of temp. only 0-40894  
 Gibbs (1839-1903), biography (*Czech*) 0-22180

## thermodynamics continued

Gibbs random fields described by generating functional method 0-31698  
 Gibbs states, classical approximations 0-132  
 glass transition, soft-sphere model, mol. dynamics study 0-49343  
 global mean value theorems in thermodynamics 0-31690  
 grain boundary Gibbs thermodynamics anal., interaction with vacancies (*Russian*) 0-2034  
 hard-particle fluids, series representation of eqn. of state 0-6337  
 harmonic oscillators, charged, interaction with transverse EM field mode 0-5712  
 heat conduction in porous materials non-equilibrium processes (*Hungarian*) 0-178  
 heat conduction in relativistic extended thermodynamics 0-43803  
 heat engine theory, mathematical formulation including negative absolute temps. 0-27250  
 heat engine using clear night sky as heat sink for teaching 0-27082  
 heat flow in relativistic equilibrium thermodynamics 0-52017  
 heat transfer in linear harmonic chain, nonequilibrium steady states, information theoretic approach 0-19214  
 HF approximations, thermodynamic Fermi systems 0-4642  
 high temperature system characterisation, models, phys. and chem. reference data sources 0-41958  
 high-pressure systems with liq. heat carrier, thermodynamic equilibrium approach to depressurisation calc. 0-17957  
 hyperbolic balance laws in continuum physics 0-4525  
 infinite dilution activity coeffs. determ. from total press. VLE data, eqn. of state influence 0-40727  
 inhomogeneous solid solutions with conc. expansion, thermodynamics, energy defect diffusion calcs. 0-24618  
 interface phenomena singular densities and currents at dividing surface 0-17907  
 internal scalar pressure determ. in atom or molecule, density functional theory 0-47857  
 interstellar space, disequilibrium condensation environments as frontier in thermodynamics 0-26942  
 irreversible processes, time scaling 0-17906  
 irreversible processes and physical interpretation of rational thermodynamics, review 0-13020  
 isotope transport in reversibly reacting species systems, isotopically labelled solvent and friction coeffs. 0-54420  
 isotropic elastic-plastic materials, thermodynamic theory, global entropy inequality 0-1436  
 Kramers rate theory, quantisation using Wigner representation 0-52054  
 Lagrangian for non dimensional non constant diffusion processes 0-31688  
 latent heat storage materials, high temp. corrosion resistance and thermodynamic stability 0-30582  
 Lennard-Jones liquid, mol. dynamics studies of glass form. 0-38896  
 light scattering in dynamical props. study, principles spectra derivation and appls. 0-53218  
 liquid, simple, equilib. theories, review 0-38887  
 liquid mixture, near tricrit. pt., thermodynamic model and sum rules, appl. to benzene-ethanol-water-( $\text{NH}_4$ )<sub>2</sub>SO<sub>4</sub> 0-34196  
 liquid-glass transition, free volume approach, thermodynamic behaviour 0-1940  
 liquids, low-pressure, evaporation, interface thermodynamic model 0-2252  
 local equilibrium hypothesis extension 0-27249  
 locally equilibrium correlation function calc. method 0-36943  
 macromolecular thermodynamics and its possible relevance in physiology 0-53176  
 mapping relations (*Chinese*) 0-27227  
 mean field models, equilib. states 0-46961  
 membrane potentials, meas. in ionic environment, biological membrane simulation 0-3412  
 membrane potentials measurements 0-3411  
 metastable state relaxation, critical point region nucleation in thermodynamic systems (*Russian*) 0-13026  
 meteors, nonequilibrium thermodynamic model 0-4308  
 microcanonically distributed plasma, reduced distrib. functions 0-28604  
 mixtures containing polar substances, corresponding states principle use in crit. states calc. 0-39196  
 molecular relax. phenomena, quantum statistical mechanical approach, irreversible thermodynamic theory for radiationless decay 0-48028  
 molecular liquids and liq. crystals, theory of irreversible processes 0-54125  
 moving boundary problems, weak soln. 0-179  
 network thermodynamics (*Czech*) 0-177  
 neutral gravitating fermion system, equilibrium states 0-31692  
 neutron stars thermal properties and detectability, cooling and heating processes 0-31323  
 Newtonian stellar dynamics, maximizing functionals, rel. to thermodynamic and dynamical stability 0-12782  
 non-equilibrium thermodynamics, De Donder-Meixner transformations 0-8944  
 non-equilibrium thermodynamics of continuous media 0-8943  
 non-equilibrium thermodynamics of hydrodynamic instabilities 0-42184  
 non-equilibrium thermodynamics of two bulk interfaces including Em effects 0-13021  
 non-ionic reactions, temp. and press. effect on kinetic and thermodynamic parameters 0-3300  
 non-Newtonian third grade fluids, thermodynamics and stability 0-33638  
 non-stationary thermodynamics of polarisable and magnetisable dissipative fluid media 0-47002  
 nonclassical equations of state for critical and tricritical points 0-4683  
 nonequilibrium steady states, irreversible processes, Liapunov criterion 0-13023  
 nonequilibrium thermodynamics of luminescent processes in solids 0-50435  
 nonequilibrium transitions induced by external noise 0-152  
 nonisotropic systems near liquid-vapour critical point, similarity hypothesis, gravitational effects 0-17913  
 nonlinear autonomous systems, charact. functions, transformation group symmetry 0-47007  
 nonlinear fluctuation-dissipation theory 0-36963  
 normal modes in irreversible thermodynamics 0-52148  
 nuclear spin thermodynamics 0-54964  
 nucleation, theory for high and low supersaturations, review 0-49142  
 oscillating reactions, thermal props. 0-7762  
 Pade approximation method as renormalisation group method 0-17909  
 paragas thermodynamics at intermediate temps. 0-46970  
 phenomenological thermodynamics to canonical ensemble 0-22269  
 plasma, thermodynamics and correlation functions 0-24132



**thermodynamics continued**

- plasticity, constitutive equations derivation from Clausius-Duhem inequality 0-46804  
 polar fluids, continuum theory thermodynamics 0-31691  
 polydisperse systems of nonadditive hard particles, thermodynamics 0-7863  
 polymer, high-modulus, behaviour in solid state, nonlinear irreversible thermodynamics approach 0-44154  
 porous bodies, atom-atom interaction law (*Russian*) 0-19861  
 Potts model, first order phase transitions, Monte Carlo renormalisation group method 0-34645  
 pressure unit, optimum metric, for thermodynamic standard state 0-8950  
 quantum fermion thermodynamic system, high-order perturbation expansion 0-4635  
 quantum theory and time asymmetry 0-22215  
 radiative transfer, irreversible processes (*French*) 0-13002  
 radioactive material storage, thermodynamics of free-convection air-cooled storages 0-5282  
 reciprocating magnetic refrigerator for 2-4K operation 0-2577  
 refrigeration system, energy conservation estimates by second law anal. 0-45723  
 relativistic kinetic theory, thermodynamics, symmetry props. role 0-27117  
 renormalisation group eqns. and thermodynamic anomalies near tricritical point (*Russian*) 0-13027  
 Riemannian geometric model, appl. to pure fluid 0-17910  
 running crack, cohesive fracture zone, thermodynamic laws 0-43676  
 school physics, elementary presentation by theory of heat, thermodynamics, and thermometry (*Danish*) 0-4483  
 sea ice, dynamic thermodynamic model 0-51432  
 second law limitations, Maxwell's demon 0-13015  
 second law of thermodynamics, time, struct. and fluctuations (*Czech*) 0-13016  
 second law of thermodynamics and stability in thermoelasticity theory 0-31689  
 second-law analysis of solar-thermal processes 0-21378  
 second-order constitutive equations of hydrodynamics, dynamical interpret. 0-36860  
 size effect, model of dynamics, generalised thermodynamic forces 0-53627  
 soil-water system, thermodynamic state functions (*German*) 0-4056  
 solar stills, design and thermodynamic parameters, numerical anal. 0-55914  
 solar transition zone, energy balance and press. for network and active region features 0-21957  
 solid-solid reactions, analysis and reaction development, review 0-16648  
 soliton lattice melting, functional integral method 0-17883  
 special relativity, thermodynamic implication 0-47003  
 spin systems, Gibbs states, boundary condition equivalence 0-42159  
 stability conditions, complete diagonalisation 0-17908  
 statistical equality connecting zero Fourier harmonics with average quantities 0-133  
 statistical mechanics, foundations 0-22271  
 statistical mechanics, stability, equilib., and metastability 0-31659  
 stellar atmosphere in statistical equilib., effects of deviations from LTE 0-31290  
 Stirling free piston heat engines, closed-form solns. for a coupled ideal anal. 0-35721  
 stress energy finite temp. matrix elements in multiply connected spaces 0-4606  
 structural phase transitions, applicability of thermodynamic theory 0-2139  
 subsystem interacting with thermal bath. kinetic eqn., Markov approx. 0-47006  
 superconductivity, general relativistic phenomenological theory 0-2518  
 superradiance phase transition problem, applicability of Wang-Hion method 0-31695  
 teaching, classroom example, free energy change during liq. vaporisation 0-42010  
 teaching, pressure-volume work exercises illustrating the first and second laws 0-22173  
 temperature concept, meas. techniques 0-52204  
 ternary systems with two component solid phases, eutectic, peritectic curve eqns. (*Russian*) 0-54344  
 tetraphenylammonium-tetraphenylborate assumption for single ion thermodynamics in amphiprotic and dipolar-aprotic solvents 0-55675  
 thermal fluctuation of self oscillating reaction system under periodic external force 0-50828  
 thermal mechanics: a quantum mechanical analogue of nonequilibrium statistical thermodynamics, stochastic processes 0-52125  
 thermal-convective instability through porous medium 0-53769  
 thermochemical heat pump/refrigerator thermodynamic analysis 0-35716  
 thermoviscoelastic-plastic materials, constitutive reln. 0-58  
 two phase flow, constitutive laws determ. from irreversible thermodynamics 0-36861  
 two-phase dispersion, size distrib. function of bubbles/droplets in thermodynamic equil. 0-7862  
 units, SI system (*Croatian*) 0-189  
 vacuum system, rate of molecular impact on surface or orifice, possible conflict with second law of thermodynamics 0-46954  
 vapour, associated, one-component unsaturated, press., composition changes, eqns. (*Russian*) 0-55696  
 violation of second law, linear decompressive expansion followed by adiabatic compression, cyclic 0-42019  
 water equation of state, between 350 and 1000°C (0 to 10 GPa) and between 100 to 350°C (200 MPa to melting curve) 0-15214  
 water solar photodecomposition, redox reaction thermodynamics 0-35697  
 C<sub>3</sub>, linear, high temp., rot.-vibr., anharmonicity, thermodynamic function calcs. 0-43830  
 CO<sub>2</sub>, linear, high temp., rot.-vibr., anharmonicity, thermodynamic function calcs. 0-43830  
 Cr binary substitutional solutions, thermodynamics 0-54410  
 Cu-Cs diluted deuterated Tutton salts, electron non-Zeeman system, nuclear relaxation study 0-44951  
 Cu-Sn (25 wt.%), liq., struct. from thermodynamic and diff. studies 0-6350  
 Fe-C, martensitic transformation, thermodynamical study (*Chinese*) 0-55395  
 Ga<sub>1-x</sub>In<sub>x</sub>As<sub>1-y</sub>P<sub>1-y</sub>, CVD by Ga-In-P-H-Cl system, 0-54159  
 GaN, thermodynamic anal. of prep. methods 0-55328  
 H plasma, pair correlations down to  $r=0$  0-14883

**thermodynamics continued**

- H prod. by H<sub>2</sub>O pyrolysis, computer thermodynamic anal. and optimisation 0-45766  
 H<sub>2</sub> production, engineering impact on the validity of the mark-16 thermochemical cycle 0-55931  
 He, thermoacoustic oscillations in nonuniformly heated tubes 0-33441  
 Mg-Sr, liq. alloys, thermodynamic activities determ. 0-50604  
 Nb, O<sub>2</sub> desorption in a vacuum, thermodynamic props. calcs. (*Russian*) 0-54501  
 NbN preparation, by precip. from gaseous NgF<sub>3</sub>-N<sub>2</sub>-H<sub>2</sub> mixture 0-20857  
 Ni-bearing substitutional binary solutions, thermodynamics 0-44336  
 Ni(OH)<sub>2</sub> electrodes, charged, thermodynamic considerations of reversible potentials 0-55670  
 Ta, O<sub>2</sub> desorption in vacuum, thermodynamic props. calcs. (*Russian*) 0-54501  
 Ti-N-C-H-(O) system, thermodynamic anal. (*Russian*) 0-55325  
 TiC, production from tetrachloride and hydrocarbon, thermodynamic analysis (*Russian*) 0-7523  
 ZrI<sub>4</sub>, thermodynamics of vaporisation from substoichiometric solid Zr iodides 0-3393

**thermoelasticity***see also thermal stresses*

- anisotropic, at low reference temp., linear coupled theory 0-59  
 anisotropic slab, thermoelastic crack problem 0-23960  
 asymmetric elastic medium, electrically conducting, magneto-thermoelastic waves anal. 0-15772  
 axisymmetric thermoelasticity problem for two-temperature hollow cylinder 0-5941  
 beam-like lattice trusses, numerical analysis 0-14566  
 bodies in contact, heat transmission, optimal control thermoelastic stress constraint 0-19223  
 chemically hardening material cast in elastic cylindrical mold, transient thermal stresses 0-7589  
 circular cylinder with circumferential edge crack under uniform heat flow, thermal stresses 0-48641  
 circular plates, thermoviscoelastic anal. of a thermorheologically simple material 0-10161  
 continuous elastic solids, foundations for coupled thermoelasticity 0-46807  
 Cosserat composite elastic cylinders, thermal stresses 0-5937  
 coupled thermoelastic problem, formal soln. 0-4529  
 crystal growth from melt, stress form., dislocation density estimation (*German*) 0-15022  
 curved plates, subject to arbitrary temp. distrib., stresses and displacements 0-5938  
 curvilinear aeolotropic solids, 3-D thermoelasticity 0-56  
 cylinder, hollow, unsteady axially nonsymmetric temp. distrib. (*Polish*) 0-10152  
 cylinder, stresses due to plane temp. distrib. 0-5935  
 cylinder, weakened by penny-shaped cracks, thermoelastic stresses 0-10191  
 cylinders, symmetric thermoelastic stress, Lanczos-Chebyshev method 0-33458  
 cylindrical shells, calc. of stresses (*German*) 0-33454  
 decomposition theorem for thermoelasticity with finite wave speeds 0-57  
 deformable solids, singularities of dynamic processes, finite rate effect of heat propag. 0-19247  
 diatomic solids, thermoelastic, continuum theory 0-53635  
 direct anal. in 1-D 0-8797  
 elastic medium, crack propag. in dynamic thermoelasticity (*French*) 0-38327  
 electromagneto-thermoelastic plane wave propag. phase vel. and attenuation coeff. 0-48621  
 epoxy resin (Araldite B), photothermoelasticity meas. by heating method 0-6000  
 expansion flexible acoustic probe 0-16618  
 fibre reinforced materials, therm. stresses in unit cell 0-10160  
 fibre reinforced thermoelastic materials, nonlinear thermodynamic continuum theory 0-14579  
 fibreglass cross wound shell, thermoelastic consts. 0-14577  
 finite element approximations in thermo-plasticity 0-1435  
 finite short cylindrical cylinder with arbitrary heat supply, unsteady thermal stress length effects 0-13541  
 fluids, stability of motion anal. 0-10221  
 generalised thermorheologically simple porous materials, thermomechanical theory of viscoelasticity 0-33479  
 glass bodies, heat resistance, determ. 0-24690  
 glass fibre reinforced plastic cylindrical shells, temp. stresses developing during polymerisation 0-40326  
 granular materials, thermoelasticity theory 0-42066  
 harmonic wave reflection, effect of thermoelastic scatt. 0-14613  
 heat conduction, appl. of orthogonal projection methods 0-1403  
 isotropic semiinfinite plate heated by moving point source of heat, temperature stresses 0-43628  
 Kevlar/epoxy composites, elastic props. rel. to thermal expansion 0-24622  
 layered beams, interlaminar thermoelastic stresses 0-1432  
 linear, conservation laws, path independent integral generalisation 0-53626  
 linear coupled thermoelasticity with microstruct., existence and uniqueness theorems 0-60  
 linear generalized theory, stress-flux initial boundary value problem 0-61  
 machining metals, thermoelastic distortion 0-5939  
 magnetothermoelastic interactions in cylindrical conductor, mechanocaloric effect 0-7139  
 magnetothermoelastic Rayleigh waves with thermal relaxation in uniform magnetostatic field 0-2617  
 martensite crystal, dislocation representations of development kinetics 0-39086  
 micropolar layer, pertinent formulas for displacement vector components, force stress component distrib. 0-48581  
 micropolar semispace, effect of heated boundary on normal stress distrib. 0-1433  
 mixed boundary-value problems of steady-state thermoelasticity and electrostatics 0-55  
 nonlinear thermal bending of shallow sandwich shells and flat plates, numerical anal. 0-5936  
 orthotropic plate with square hole and convective heat exchange, plane static thermoelasticity (*Russian*) 0-33456



**thermoelasticity continued**

- piecewise homogeneous bodies, thermoelast. eqns., generalised conjugation prob. (*Ukrainian*) 0-53629
- planar thermoelastic contact problems, Green's function for exterior contact 0-38350
- planar thermoelastic contact problems, Green's function for interior contact 0-38351
- plane deformation states, stability 0-43634
- plane harmonic waves in pre-stressed heat cond. elastic material 0-62
- plate, annular elliptic heated, const. thickness, buckling and stability criterion 0-28443
- plate, three layer, thermoelasticity problem, soln. method (*Ukrainian*) 0-48574
- plate temp. dependent props. under linear temp. distrib., thermoelastic problem for crack 0-48579
- plate with crack or ribbon like inclusion subjected to uniform heat flow, thermoelasticity 0-48578
- plate-semi-infinite space, heat exchange process control, thermoelastic stresses (*Russian*) 0-53606
- plates, flat, stability of postbuckling behaviour 0-1453
- plates, thick, thermally loaded, 3-D anal. 0-33459
- polyurethanes, crosslinked, thermoelastic props. 0-20991
- polyvinyl alcohol, atactic, thermoelasticity of networks swollen in water, polymer-diluent interactions 0-29102
- quartz resonator, nonlinear thermoelastic couplings (*French*) 0-34118
- residual stresses in shells of revolution, cut-out element method glass-plastic composite, thermoelastic residual stresses in shells of revolution, cut-out element method 0-38271
- retrospective problem, pot.-type singular integral approx. algorithm 0-27132
- rocks, crack growth and thermoelastic behaviour 0-26502
- rods, thermomechanics, direct approach 0-10141
- second law of thermodynamics and stability in thermoelasticity theory 0-31689
- semi-infinite medium, transient thermal loadings, stress intensity factors 0-10193
- semiconductor plate, light irradiation, heating and thermoelastic stress 0-25499
- shape memory effect, criteria for efficiency assessment (*Russian*) 0-21015
- shells, cylindrical, asymptotic method 0-38273
- shells of revolution, variable thickness, stress state determ. 0-38275
- size effect, model of dynamics, generalised thermodynamic forces 0-53627
- state space approach to thermoelasticity 0-4527
- state space formulation, connection to thermoelastic pot. 0-63
- steel case hardened cylinders, heat treated, residual stress fields 0-3102
- stored energy, and increment in heat capacity due to plastic deform. 0-54302
- stress-temp. eqns. of dynamic thermoelasticity, uniqueness theorem 0-4528
- surface point source in a generalized thermoelastic half space 0-23893
- thermo-piezoelectric material, time depend. harmonically changing plane wave propag. anal. 0-15977
- thermodiffusion in elastic cylinder, quasistatic problem (*Polish*) 0-10150
- thermoelastic inclusion energy in semi-infinite solid 0-14565
- thermoelastoplastic solution for a circular solid cylinder subjected to heating and cooling 0-5952
- thermomechanical interaction effect by finite-element method 0-42067
- thermopiezoelectricity, general eqns. 0-7297
- thermorigid dielectrics, nonlinear thermodynamic theory 0-10149
- thermoviscoelastic media, dynamical problems, Volterra method generalisation 0-33481
- thermoviscoelastic transient responses, stability and accuracy of finite element solns. 0-5951
- thermoviscoelastic-plastic materials, constitutive reln. 0-58
- thermoviscoelasticity, heat liberation effect in deformable linear medium 0-33484
- thermoviscoelasticity, linear bound, minimum principle (*Ukrainian*) 0-33468
- third and fourth order elastic const. (*French*) 0-34116
- unsteady thermal stress problems, numerical treatment based on Euler-Maclaurin summation formula 0-48580
- weak nonlinear waves in homogeneously deformed heat-conducting elastic materials 0-48632
- weakly absorbing solid medium, opacity fluctuations, heating by intense radiation and thermoelastic stresses problem 0-38048
- Al-Ni, thermoelastic phase transform., acoustic emission 0-3039
- Al-SiC fibre reinforced materials, therm. stresses in unit cell 0-10160
- Au<sub>52</sub>-Ag<sub>47.5</sub>, pseudoelastic behaviour associated with thermoelastic martensitic transform. 0-16304
- B, liq., thermoelastic props. near melting point 0-19862
- Fe-Ni (31 wt.%), thermoelastic martensite obs. 0-3052
- Ni-Ti alloys, shape memory effect materials, criteria for efficiency assessment (*Russian*) 0-21015
- Ti-Ni, thermoelastic phase transform., acoustic emission 0-3039
- TiCdF<sub>3</sub>, third and fourth order elastic const., press. depend. near phase transition (*French*) 0-34116

**thermoelectrets**

- carnauba wax, thermoelectret, lattice parameter changes at elevated temps. 0-29674
- carnauba wax and rosin thermal electret, elec. charge studied by TSC 0-7286
- carnauba wax thermoelectret, charge behaviour 0-7276
- Perspex pyramid electret, thermally stimulated discharge currents 0-2688
- polypropylene, mag. polarisation, optical studies 0-55013
- sisal wax, thermally stimulated discharge and internal polarisation 0-55016
- 3PbO<sub>2</sub>GeO<sub>3</sub>, TSC in thermoelectret state during ceramic synthesis, pyroelec. currents and energy struct. of capture centres 0-55014

**thermoelectric conversion**

- see also thermoelectric devices
- cassegrain solar collector with thermoelectric module, concentration efficiency 0-35709
- efficiency, in presence of small temp. drop 0-40878
- fast spectrum reactor space power system with thermoelec. conversion, baseline design 0-37441
- generators, utilisation of amorphous semiconductors 0-35704
- heat pumps 0-35713

**thermoelectric conversion continued**

- OTEC; analysis of a heat exchanger-thermoelectric generator system 0-35710
- photovoltaic/thermoelectric refrigerator for medicine storage for developing countries 0-35712
- polyacetylene, semiconducting and metallic, thermoelec. props. 0-40884
- radioisotope thermoelec. generators, design optimisation for Solar-Polar Mission 0-40880
- radioisotope thermoelectric generator cooling in spacecraft 0-40881
- radioisotope thermoelectric generator shock and vibration test program for MB-M75(A) 0-35711
- radioisotope thermoelectric generators, power degradation predictions using DEGRA code 0-40879
- radioisotope thermoelectric generators, SNAP 19 performance update for Pioneer and Viking missions 0-40883
- single-stage thermoelectric heat pumps, design, characterisation and optimisation 0-35735
- solar, appls. to OTEC and agricultural irrigation 0-35708
- solid state heat engine, experimental demonstration of heat-to-electricity conversion within a dielectric 0-35707
- space vehicle thermoelectric generators, Voyager and LES 8/9 flight performance 0-40882
- thermoelectrochemical cycles for power and hydrogen production 0-45718
- Ag-AgCl/KCl/AgCl-Ag thermocell, and thermal liq. junction pot. for KCl solns. at high temp. 0-16819
- H<sub>2</sub> and power production using thermoelectrochem. cycles 0-16820
- LaCr<sub>2</sub> alloy development for thermoelec. appls. 0-35705
- LaCrSe<sub>3</sub> alloy development for thermoelec. appls. 0-35705
- $\beta$ -SiC, n-type, thermoelectric efficiency at high temps. 0-35706

**thermoelectric devices**

- see also thermocouples; thermoelectric conversion; thermopiles
- extracorporeal circulation apparatus using thermoelec. heat regulating systems 0-3870
- refrigerators, performance optimisation using asymptotic temp. distrib. 0-230
- thermal flux meters, response time reduction 0-4719
- thermoelectric generators, utilisation of amorphous semiconductors 0-35704

**thermoelectric effect see thermoelectricity****thermoelectric effects in metals and alloys**

- alkali metals, liquid, thermoelectric power, optimised model pot. calcs. 0-29391
- amorphous alloys, transport props., thermopower 0-34411
- amorphous metals, electron-phonon interaction effect on thermopower 0-29393
- anisotropic normal metal, thermopower calc. 0-24879
- diffusion thermopower, boundary scatt. effect 0-6817
- dilute magnetic alloy, reverse Kondo effect, magneto-transport theory 0-15509
- electroplated foil, appl. to measurement of heat flux 0-37026
- liquid alkali metals, nonlocal harmonic model potential, appl. to elec. props. 0-6802
- metal-H systems at high H press., physicochemical props., book contrib. 0-54355
- polyacetylene, semiconducting and metallic, thermoelec. props. 0-40884
- pseudopotential study of electronic props. 0-20149
- rare earth alloys, RCo<sub>2</sub>, elec. resistivity, thermopower, X-ray struct. meas. 0-24874
- rare earth metal, conduction electron interactions, anisotropic 0-15492
- Al wire, hot and cold deformation drawing strengthened, thermal EMF study (*Russian*) 0-54674
- Bi, phonon-drag low temperature thermoelectric refrigeration 0-22366
- Bi-Cd(Zn), alloy absolute thermoelectric temp. and conc. depend. (*Russian*) 0-39561
- Bi-Sn, thermoelec. props. from 2 to 300K 0-24872
- Bi-Sn, thermopower from 50 mK to 25K 0-24880
- Cd, thermopower meas. in mag. field, 1.5-4K 0-54675
- Ce, thermo-EMF up to 75 kbars 0-24882
- Ce-Co-Si, thermoelectromotive force and electrocond. (*Ukrainian*) 0-54670
- Ce-Fe-Si, thermoelectromotive force and electrocond. (*Ukrainian*) 0-54670
- Ce-Ni-Si, thermoelectromotive force and electrocond. (*Ukrainian*) 0-54670
- CeCu<sub>2</sub>Si<sub>2</sub>, transport anomalies 0-20148
- Ce<sub>1-x</sub>La<sub>x</sub>, thermoelectric power, mag. transition temps. 0-20154
- Cu, compressed powder, thermoelectric effects 0-20155
- Cu-Be-Ni-Ti-Mg bronze, alloying element influence on minimum thermo EMF, cold working (*Russian*) 0-34426
- Cu-Sn, amorphous, electron-phonon interaction effect on thermopower 0-29393
- Fe-Ni, thermodynamic props., anomalous 0-39313
- Ga, thermopower quantum oscillations 0-15505
- Gd(Al<sub>1-x</sub>Cu<sub>x</sub>)<sub>2</sub>, thermoelec. power, exchange interactions 0-24881
- Hg, electrical and thermodynamic props. in metal-semicond. transition range 0-20144
- K, liquid, thermoelectric power, optimised model pot. calcs. 0-29391
- K, thermomagnetic and thermoelectric properties, phonon scatt. processes 0-29390
- K-Rb, liq., form factors and transport coeffs., pseudopot. perturb. theory 0-44561
- (La,Gd)Al<sub>2</sub>, reverse Kondo alloy, transport props. at finite mag. field 0-6812
- La<sub>1-x</sub>Sr<sub>x</sub>CoO<sub>3-y</sub>, Seebeck coeff. meas., small polaron hole conduction model 0-20233
- Li, liq., elec. resistivity and thermoelec. power, orthogonalisation hole pseudopotential calc. 0-29376
- Na, liquid, thermoelectric power, optimised model pot. calcs. 0-29391
- Na-K(Cs), liq., form factors and transport coeffs., pseudopot. perturb. theory 0-44561
- Nd<sub>1-x</sub>La<sub>x</sub>, thermoelectric power, mag. transition temps. 0-20154
- Ni<sub>7</sub>P<sub>24</sub>, cryst. and amorphous, thermopower and resist. meas. 0-20145
- Pd films, evaporated, and thermoelec. power, annealing effects 0-39684
- Pd Ni, effect of hydrogenation on thermopower 0-39562
- Pd-Ag electrical resistivity, thermo-EMF and thermal diffusivity at high temps. (*Russian*) 0-6808
- Pd-H, low temp. transport props., heterogeneous-mixture model 0-24871
- PdCo, effect of hydrogenation on thermopower 0-39562



**thermoelectric effects in metals and alloys continued**

- (Pd,Pt)<sub>1-x</sub>Fe atomically ordered alloy, thermoelectric power, carrier energy spin shift, mag. props. 0-29394  
 Rb, liquid, expanded, eqn. of state, transport up to 1700°C, 400 bar 0-2136  
 Se-H, conc.-temp. depend. at room temp. of elec. resist. thermo-EMF, mag. susceptibility, and Hall coeff. 0-29382  
 Tb-Gd, elec. resistivity and thermopower critical behaviour 0-15499  
 TbZn, ferromag. transition, transport coeffs. critical behaviour 0-15498  
 Ti alloys, metallurgical characterisation using thermoelec. power meas. (French) 0-45462  
 Ti-Bi system, phase transitions near Ti<sub>3</sub>Bi, elec. props. meas. 0-35181  
 TmS, metallic, thermoelec. power 0-6818  
 TmSe, metallic, thermoelec. power 0-6818  
 UAl<sub>3</sub>, transport props., susceptibility and sp. ht. 0-11174  
 W, electronic transport below 1K 0-2377  
 W, thermopower meas. in mag. field, 1.5-4K 0-54675  
 W-Fe, electronic transport below 1K 0-2377  
 Y, magnetic and elec. props., 100 to 900K (Russian) 0-25077  
 Zr-Hf-ZZ (Russian) 0-39551  
 Zr-Ti, alloy, mag. susceptibility, elec. cond., Hall conc. thermoEMF conc. depend. (Russian) 0-39551

**thermoelectric effects in semiconductors and insulators**

- amorphous semiconductor thermoelec. power transport coeff. calc. by quasiclassical approx. 0-20230  
 amorphous semiconductors, appl. to thermoelec. generators 0-35704  
 CoCr<sub>2</sub>S<sub>4</sub> films, galvanomagnetic and thermoelec. props. 0-54717  
 degenerate semiconductors, longitudinal thermo-EMF in quantising mag. field, scatt. mechanism (Russian) 0-24960  
 eddy currents, thermoelec., mechs. 0-44626  
 graphite, neutron irradiation, electron transport, annealing study 0-39165  
 graphite, thermoelec. and thermomag. props., cylindrical band model 0-39616  
 heavily doped semiconductors, materials science developments, appl. to thermoelectric heat pumps 0-35713  
 high temperature meas., solid electrolytic cell, meas. at 700K and higher 0-31760  
 many-valley semiconductors, thermoelectric power, depend. of longitudinal mag. field 0-39618  
 phthalocyanine-halogen complexes, elec. props. 0-29424  
 polycyclic quinone radical polymers, elec. props. described by variable range hopping model 0-44588  
 polyacetylene, semiconducting and metallic, thermoelec. props. 0-40884  
 rare earth tungstates, elec. cond. and thermoelec. power meas., band theory 0-20191  
 semiconductor, amorphous, non-polaronic, cond. and thermopower near band edge 0-49719  
 semiconductor, inhomogeneity effects on thermoelec. and photothermoelec. power meas. 0-54728  
 semiconductor, partly disordered, with mobility threshold, transport props. and thermoelec. parameters 0-34449  
 semiconductor, thermoelectric amplification of sound 0-2427  
 semiconductor-ferrite layer structure, EMF created by spin-wave, effect of current 0-11072  
 semiconductors, thermoelectric and thermomagnetic effects, heat transfer due to quasi-particle subsystems (Russian) 0-24959  
 small-sample mag. semiconductor thermoelectric power meas. installation 0-31795  
 TCNQ, salt, DBTTF-TCNQ, elec. resistivity and thermoelec. power meas. 0-20193  
 TCNQ complexes with N-methyl derivatives of pyridine, cond. and thermoelec. power meas., band model anal. 0-10952  
 TCNQ salt, (NMP)<sub>x</sub>(phen)<sub>1-x</sub>(TCNQ), thermoelectric power temp. depend. 0-15548  
 TCNQ salt, Rb-TCNQ-II, two carrier cond. 0-44625  
 TEA(TCNQ)<sub>2</sub>, elec. cond. and thermoelec. power under hydrostatic press. 0-11024  
 zero gap semiconductors, electron scatt., thermoelec. power and Hall effect at low temp. 0-44628  
 Ag<sub>2</sub>S, liquid, ionic and electronic cond., thermoelec. power 0-39329  
 Ag<sub>2</sub>Se, liquid, ionic and electronic cond., thermoelec. power 0-39329  
 Ag(Tl)/AgI/Ag(T<sub>2</sub>) cell, thermo-EMF of highly conducting solid electrolytes 0-24659  
 Ag<sub>2</sub>Te, liquid, ionic and electronic cond., thermoelec. power 0-39329  
 α-AlB<sub>12</sub>, prep. and electrothermal props. 0-20863  
 AlH<sub>3</sub>, thermo-EMF meas. 0-39617  
 AlMgB<sub>4</sub>, prep. and electrothermal props. 0-20863  
 As, electrical resist., thermal cond. and thermopower, low temp. transport props. 0-49708  
 As<sub>2</sub>Ni(Ge)(S)(Se)(Te) film, amorphous, chemical modification of props. 0-49250  
 As<sub>2</sub>Se<sub>3</sub>-As<sub>2</sub>Te<sub>3</sub> glass thermoelec. power, and transport mechanism 0-2408  
 B, preparation and purification, physical characterisation (French) 0-16189  
 α-B, rhombohedral, elec. cond., thermoelec. power, and Hall coeff. 0-6843  
 B-Si compounds, thermoelec. material, prep. by pyrolysis of BB<sub>3</sub>-SiB<sub>4</sub> mixture 0-20862  
 Bi<sub>2</sub>C<sub>x</sub>, phonon energies and electronic props., x depend., refl. spectra and thermoelec. power meas. 0-16052  
 B<sub>2</sub>Cy, metal-insulator transition, elec. cond. and thermoelec. power, 80 to 700K 0-44673  
 Bi<sub>4</sub>Si, β rhombohedral, conduction mechanism, thermoelectric props. 0-24932  
 Bi<sub>4</sub>Si elec. props., medium range disorder model 0-15522  
 Ba<sub>1-x</sub>Sm<sub>x</sub>B<sub>6</sub>, prep., elec. cond. and thermoelec. props. 0-49697  
 BaTiO<sub>3</sub>, H<sub>2</sub>-reduced, elec. cond. mechanism, EPR, resist. and Seebeck coeff. meas. 0-10976  
 Bi, electrical resist., thermal cond. and thermopower, low temp. transport props. 0-49708  
 Bi, magneto-thermopower, weak-field, implication for scatt. mech. 0-49790  
 Bi<sub>2</sub>O<sub>3</sub>, thermoelec. props., 500-1500K 0-29423  
 Bi<sub>2-x</sub>Sb<sub>x</sub>Te<sub>3-y</sub>Se<sub>y</sub> solid solution, density-of-states effective mass, carrier mobility temp. depend. 0-24931  
 n-Bi<sub>2</sub>Se<sub>3</sub>, single cryst., new aspect of carrier scatt. 0-49707  
 Bi<sub>2</sub>Te<sub>3</sub>-Bi<sub>2</sub>Se<sub>3</sub> thermoelectric alloys, diffusion and evaporation of volatile component during prep. 0-35118  
 Bi<sub>2</sub>Te<sub>3</sub>-SbTe<sub>3</sub>, ordered structure formation, heat treatment effect on thermal cond. 0-54448

**thermoelectric effects in semiconductors and insulators continued**

- n-Bi<sub>2</sub>Te<sub>2.88</sub>Se<sub>0.12</sub>, extrusion deformed, powder dispersion degree influence on thermal and elec. props. (Russian) 0-39366  
 CaCO<sub>3</sub>, calcite, elec. cond., 300 to 1200°C at CO<sub>2</sub> pressure of 40 bars 0-20195  
 Ca<sub>0.15</sub>VO<sub>2</sub>, electrical cond., thermo-EMF, and lattice consts. 0-54685  
 CdAs<sub>2</sub>, amorphous, elec. cond. and thermopower 0-49722  
 CdAs<sub>2</sub>, thermoelec. props., anisotropy 0-34470  
 Cd<sub>3</sub>As<sub>2</sub>, band structure, pressure dependence of galvano- and thermomagnetic effects 0-6722  
 Cd<sub>3</sub>As<sub>2</sub>, electron effective mass. temp. depend., Hall effect and thermoelec. power meas. 0-39613  
 CdS, and CdS<sub>1-x</sub>Se<sub>x</sub>, thermoelec. and photothermoelec. power meas., inhomogeneity effects 0-54728  
 CdS film, chemically sprayed, carrier conc. and mobility, thermoelec. and photothermoelectric meas. 0-2503  
 CdS films, pure and Na doped, chemical bath deposited, photothermoelectric effect 0-6906  
 CdS:Li chemically deposited filter, elec. props. 0-11113  
 CdTe-Te film, prep. by combined hot-wall-flash evaporation method, and characterisation 0-55296  
 CdTi<sub>2</sub>Te<sub>4</sub>, Hall and thermo-EMF coeffs., in solid, liquid states 0-54704  
 CoB<sub>12</sub>, growth from melt and phys. props. 0-20782  
 Co<sub>1-x</sub>Fe<sub>x</sub>Si, elec. and optical props. 0-49740  
 Co<sub>2</sub>Ge<sub>2</sub>Te<sub>3</sub>, struct., resist., and thermo-EMF 0-20908  
 Co<sub>3</sub>O<sub>4</sub>:Li(Cr)(Al)(S), and pure Co<sub>3</sub>O<sub>4</sub>, elec. cond. and thermo-EMF 0-20231  
 CrSe<sub>2</sub>, layered, phys. and elec. props. 0-44594  
 CrSi, based solid solns., prep., elec. cond. and thermoelec. props. 0-49697  
 Cu<sub>3</sub>AsS<sub>4</sub> and Cu<sub>3</sub>SbS<sub>4</sub>, thermal cond. in solid and liq. phases, 300 to 1100K, thermoelec. Q-factor 0-19997  
 CuCr<sub>2</sub>Se<sub>4</sub>, crystal growth from melt, exam. of props. 0-55283  
 Cu<sub>2</sub>S, thermoelectric props. 0-54726  
 DyIG, thermoelectric power, elec. cond. charge carrier conduction mechanism 0-34441  
 Fe<sub>3</sub>O<sub>4</sub>, Coulomb gap and hopping cond., effects on thermopower and Verwey ordering 0-44583  
 Fe<sub>3</sub>O<sub>4</sub>, hopping conduction and the Coulomb gap 0-44605  
 GaSb films, amorphous and cryst., vac. evaporated, Elec. cond. thermoelec. power and optical absorpt. 0-2504  
 GaSb-GaAs-Ge system, props. and struct. 0-20232  
 n-Ge, vel. component of hot charge carriers' thermoelectromotive force 0-44630  
 Ge:Sn, amorphous, electronic transport props. 0-44589  
 Ge<sub>20</sub>Bi<sub>2</sub>Se<sub>70-x</sub>Te<sub>10</sub>, n-type semiconducting glasses, resistivity and thermoelectric power meas. 0-54695  
 GeBi<sub>2</sub>Te<sub>4</sub>, Hall const., thermoelec. power, and elec. cond. 0-29407  
 GeTe films, elec. props. and struct., influence of annealing and condensation conditions 0-15388  
 GeTe-MnTe, heat treatment effect on struct., elec. props. 0-54725  
 Hg<sub>1-x</sub>Mn<sub>x</sub>Te, Shubnikov de Haas effect and quantum oscils. of thermoelec. power 0-49781  
 HgTe film, vac. deposited, elec. props., 78-420K 0-11119  
 HgTe, magnetophonon oscils. of thermoelec. power 0-49789  
 p-InSb, mobility, diffusion and thermoelectric power of hot holes 0-35955  
 InSb:S(Se)(Te), reson. states and reson. scatt., elec. props. 0-49738  
 KNbO<sub>3</sub>, elec. and thermoelec. props., influence of O defects 0-29401  
 LaCr<sub>3</sub> alloy development for thermoelec. appls. 0-35705  
 LaCrSe<sub>3</sub> alloy development for thermoelec. appls. 0-35705  
 La<sub>1-x</sub>Sr<sub>x</sub>Co<sub>3-y</sub>, Seebeck coeff. meas., small polaron hole conduction model 0-20233  
 Mn-Zn ferrosilicates, carrier transfer phenomena 0-54727  
 MnBi<sub>2</sub>, growth from melt and phys. props. 0-20782  
 Mn<sub>3</sub>O<sub>4</sub>:Li(Cr)(Al)(S), and pure Mn<sub>3</sub>O<sub>4</sub>, elec. cond. and thermo-EMF 0-20231  
 Mo<sub>2</sub>B<sub>3</sub> and MoB<sub>4</sub>, thermal, elec., and mag. props. 0-20187  
 NaNbO<sub>3</sub>, elec. and thermoelec. props., influence of O defects 0-29401  
 NdTiO<sub>3</sub>, physicochem. props. 0-25625  
 Ni<sub>1-x</sub>Co<sub>x</sub>S<sub>2</sub>, elec. transport and semicond.-metal transition 0-10985  
 (Ni<sub>1-x</sub>Fe<sub>x</sub>)<sub>1-y</sub>S, anomalous thermal hysteresis in metal-semicond. transition 0-39640  
 p-PbS, struct. of valence band, transport processes study 0-20081  
 PbS:Ti, Hall and Seebeck coeffs., Hall mobility, impurity states 0-15545  
 PbSe<sub>0.5</sub>S<sub>0.5</sub>, valence band struct., absorpt. spectra, elec. props. 0-44505  
 Pb<sub>1-x</sub>Sn<sub>x</sub>Se, n- and p-type, with band inversion, study of transport phenomena 0-49741  
 p-Pb<sub>0.65</sub>Sn<sub>0.35</sub>Te, transport coeffs. and dispersion law 0-44629  
 Pb<sub>0.82</sub>Sn<sub>0.18</sub>Te, thermomagnetic, thermoelectric props., valence band struct. (Russian) 0-54724  
 Pb<sub>1-x</sub>Sn<sub>x</sub>Te, mag. and kinetic props. near ferroelec. transition 0-11160  
 p-Pb<sub>1-x</sub>Sn<sub>x</sub>Te, thermoelec. power, carrier conc. and temp. depend., interband scatt. 0-24957  
 Pb<sub>1-x</sub>Sn<sub>x</sub>Te: Mn, Mn mag. and elec. active states, mag. impurity behaviour 0-44627  
 p-PbTe, energy band struct. and scattering of holes 0-10874  
 PbTe:Ti, influence of Ti impurity states 0-20121  
 PbTe:Ti, thermoelectric power, elec. cond., Hall coeff. and optical absorpt. coeff. 0-39584  
 Sb, electrical resist., thermal cond. and thermopower, low temp. transport props. 0-49708  
 p-Sb<sub>1.48</sub>Bi<sub>0.52</sub>Te<sub>3</sub>, extrusion deformed, powder dispersion degree influence on thermal and elec. props. (Russian) 0-39366  
 Sb<sub>2</sub>O<sub>3</sub>, thermoelec. props., 500-1500K 0-29423  
 Sb<sub>2</sub>Te<sub>3</sub> epitaxial films, growing conditions effect on elec. cond., thermo-EMF 0-39687  
 Sb<sub>2</sub>Te<sub>3</sub>-Sb<sub>2</sub>Se<sub>3</sub>, ordered structure formation, heat treatment effect on thermal cond. 0-54448  
 Se,Te<sub>1-x</sub>, liq., thermoelec. transport at mobility edge 0-49787  
 Si, amorphous, doped, density of states determ. from transport meas. 0-49720  
 Si, amorphous, doped, non-polaronic cond. and thermopower near band edge 0-49719  
 n-Si, drag thermoelec. power, anisotropy parameter determ. 0-20235  
 Si, n-n<sup>+</sup> point junctions 0-44719  
 Si:Li(Na)(K)(F)(Cl), amorphous, implantation effects on elec. props. 0-49716  
 Si:P, impurity cond., hopping conduction and the Coulomb gap 0-44605  
 Si:Sb, amorphous, electronic transport props. 0-44589  
 Si-Ge, heavily doped, reversal of precip. 0-2409



**thermoelectric effects in semiconductors and insulators continued**

- n-Si-SiO<sub>2</sub> interface, hot carrier surface thermo EMF depend. on surface band bending 0-44734  
 Si<sub>1-x</sub>B<sub>x</sub>H, amorphous films, thermopower and cond. for mixed band and broad tail state cond. 0-49786  
 β-SiC, n-type, thermoelectric efficiency at high temps. 0-35706  
 SiTe:Ge(Sn), substitution of Si, thermoelectric props. (*Russian*) 0-11023  
 Sn<sub>1-x</sub>Mn<sub>x</sub>Te, degenerate mag. semicond., thermoelec. power meas. 0-29392  
 Sr<sub>0.15</sub>VO<sub>2</sub>, electrical cond., thermo-EMF, and lattice consts. 0-54685  
 Te film condensed on mica, struct. and electrophysical props. 0-39688  
 Th<sub>3</sub>As<sub>4</sub>-U<sub>3</sub>As<sub>4</sub> solid soln., electronic props. 0-34469  
 TiC-TiN system, electro- and thermo-phys. props. 0-34210  
 TiC-VC, mag. susceptibility, elec. cond. and thermoelec. props. 0-50033  
 TiC-ZrC, mag. susceptibility, elec. cond. and thermoelec. props. 0-50033  
 TiC-ZrC, solid soln., conc. and temp. dependence of props. 0-39736  
 TiO<sub>2</sub>-Ti<sub>2</sub>O<sub>3</sub>-P<sub>2</sub>O<sub>5</sub>, glass form., struct. and elec. props. 0-44592  
 Ti<sub>4</sub>O<sub>7</sub>, hopping conduction and the Coulomb gap 0-44605  
 TiS<sub>2</sub>, evidence for semicond. props., Hall coeff., refl., cond., thermoelec. power 0-20220  
 TiS<sub>2</sub>, transport props. and semicond. nature 0-44598  
 Ti<sub>3</sub>Te<sub>3</sub>, exam. of electrical props., in solid, liquid state 0-54686  
 V<sub>2</sub>O<sub>5</sub>, thermoelec. props., 500-1500K 0-29423  
 V<sub>2</sub>O<sub>5</sub>:Na(Li), pure and doped, elec. cond. and thermoelec. power meas. 0-10987  
 V<sub>2</sub>O<sub>5</sub>-BaO-K<sub>2</sub>O-ZnO glasses, elect. props. and struct. 0-15547  
 V<sub>2</sub>O<sub>5</sub>-MoO<sub>3</sub> solid solns., small polaron cond., elec. resist. and thermoelec. power meas. 0-34447  
 V<sub>2</sub>O<sub>5</sub>-P<sub>2</sub>O<sub>5</sub> (70-30), electrical cond. and thermoelectric meas., Au-glass-Au sandwich 0-29403  
 WB<sub>2</sub>, growth from melt and phys. props. 0-20782  
 W<sub>2</sub>B<sub>5</sub> and WB<sub>4</sub>, thermal, elec., and mag. props. 0-20187  
 WO<sub>3</sub>, amorphous film, sublimed under different conditions, elec. transport props. 0-7015  
 YH<sub>x</sub> (x=1.92 to 1.98), magnetic and elec. props., 100 to 900K (*Russian*) 0-25077  
 ZnSb, epitaxial films, growing conditions effect on elec. cond., thermo-EMF 0-39687

**thermoelectric generators** *see thermoelectric conversion***thermoelectricity**

*see also Peltier effect; Seebeck effect; thermocouples; thermoelectrets; thermoelectric effects in metals and alloys; thermoelectric effects in semiconductors and insulators; thermomagnetic effects; thermopiles; Thomson effect*

- alkaline earth halide crystals, thermal transport of charged point defects 0-15293  
 condensed systems, phase equilibria, 400-1100°C, DTA method 0-218  
 HMTSF-TNAP, one-dimens. conductor, transport props. 0-20165  
 polyacetylene film, doped, transport props. 0-24913  
 superconductor, quasiparticle charge imbalance induced by supercurrent with thermal gradient 0-34546  
 superconductors, general and theoretical anal., review 0-11133  
 superconductors, thermoelectric and acoustoelectric effects, influence of mutual drag of excitations and phonons 0-44761  
 TCNQ salt, (N-methylphenazinium)<sub>x</sub>(phenazine)<sub>1-x</sub>, 1 band filling, carrier mobility and disorder effects 0-24904  
 TCNQ salt, (NMe<sub>3</sub>H)(I)(TCNQ), one-dimens. semicond. with metal-like cond. 0-24909  
 TCNQ salt, (TSeF)<sub>x</sub>(TTF)<sub>1-x</sub>-TCNQ, struct., elec. and mag. props., review 0-20158  
 TCNQ salt, Qn(TCNQ)<sub>2</sub>, thermoelec. power and cond., large Coulomb repulsion model 0-24893  
 TCNQ salt, Qn (TCNQ)<sub>2</sub>, configurational entropy, thermoelec. power meas. 0-34432  
 TCNQ salt, TMTSF-DMTCNQ, cond. and thermopower meas. 0-20165  
 thermo-piezoelectric material, time depend. harmonically changing plane wave propag. anal. 0-15977  
 thermo-piezoelectricity, of polarised annular disc, deformation due to prescribed temp. distrib. 0-2699  
 TMTSF-DMTCNQ, metallic state, transport props. 0-24974  
 TTT<sub>2</sub>I<sub>3+δ</sub>, thermoelec. power and metal-semicond. transition 0-34431  
 TTT<sub>2</sub>I<sub>3</sub>, quasi one-dimens. organic metal, elec. cond. and thermoelec. power 0-24899  
 Al<sub>1+x</sub>O<sub>3</sub>, sintered, elec. cond. temp. and comp. depend., thermoelec. power 0-2438  
 NbSe<sub>3</sub> and Nb<sub>1-x</sub>Ta<sub>x</sub>Se<sub>3</sub>, thermoelec. power meas., 10-300K 0-20177  
 (SN)<sub>x</sub>, thermopower from 0.15 to 4.2K 0-34427  
 SmS, and Sm<sub>0.8</sub>Tb<sub>0.2</sub>S, resistivity and thermopower 0-20260  
 Te-Se mixtures, liquid, electrical conductivity and thermoelectric power, high temps. and pressures 0-39639

**thermography** *see infrared imaging***thermogravimetry** *see thermal analysis***thermoluminescence**

- adamantane, plastic cryst., thermolum. curves 0-2876  
 alkali borate binary glass, energy storage behaviour studied by thermoluminesc. 0-50432  
 BBOA, polymorphism, radiothermoluminescence and differential scanning calorimetric study 0-24570  
 chondrites, thermoluminescence 0-51706  
 dating, radiation dose-rate data 0-31964  
 EBBA, polymorphism, radiothermoluminescence and differential scanning calorimetric study 0-24570  
 exoskeletons of *Magiaca* sp., detect. of thermolum., possible use as TLDs 0-30896  
 glow curve theory, temp. depend. of pre-exponential factor, activation energy calc. 0-2878  
 halophosphate phosphors, radiation stability, recomb. processes effect (*Russian*) 0-7424  
 hydrocarbon, long chain single cryst., carrier transport meas. 0-6874  
 9-iodoanthracene, picosecond fluoresc. lifetimes, thermally activated S<sub>1</sub>→T<sub>1</sub> intersystem crossing 0-28045  
 meteorites, study of objects of known age 0-46498  
 meteorites, thermoluminesc. rel. to orbit, pre-impact history and Earth residence time 0-31262  
 meteorites, validity of irradiation history from thermoluminesc. 0-36584  
 nematic liquid crystal, Merck 389, polymorphism, radiothermoluminescence and differential scanning calorimetric study 0-24570  
 nonequilibrium thermodynamics of luminescent processes in solids 0-50435

**thermoluminescence continued**

- Oklo natural fission reactor materials, thermoluminesc. props., effect of radiation damage 0-21750  
 phosphors, thermoluminescence, UV dosimetry 0-853  
 polyethylene, low-density, α-irrad., thermolum. mechanism biphenyl anions influence 0-2880  
 polyethylene-terephthalate, field-controlled photogeneration and carrier trapping 0-25285  
 polymer, carrier trap study by X-ray induced TSC and thermoluminescence (*Japanese*) 0-54713  
 polymer films, carrier transport meas. 0-6874  
 polyoxymethylene, irradi., thermoluminesc. above room temp. 0-2871  
 polyvinylidene fluoride, TSC and thermoluminescence, reln. to molecular motion (*Japanese*) 0-55200  
 quartz, alpha particle induced radiation defects, EPR and thermoluminescence study 0-20461  
 quartz, defects growth, study by X-ray diffraction topography (*French*) 0-39095  
 quartz, natural, gamma-irradiated, stress effect on thermolum. sensitivity 0-11482  
 quartz, natural, virgin (γ-irradiated), polarisation effect on thermolum. sensitivity 0-11483  
 spatial distribution determination, using image intensifier technique 0-47115  
 triethylenediamine, plastic cryst., thermolum. curves 0-2876  
 α-Al<sub>2</sub>O<sub>3</sub>, crystal defects from X-ray irradiation, F-centres, X-ray luminesc. obs. 0-55176  
 α-Al<sub>2</sub>O<sub>3</sub>:Cr(Ti)(V), impurities effect on thermoluminesc. 0-40170  
 α-Al<sub>2</sub>O<sub>3</sub>:Er(Cr), crystal defects from X-ray irradiation, F-centres, X-ray luminesc. obs. 0-55176  
 BaF<sub>2</sub>, thermoluminesc. and F-centre annealing, after neutron irradiation 0-7422  
 BaFCl crystals, F-centres, X- and γ-irradiation, thermoluminescence and optical absorption spectra 0-45155  
 Ba<sub>3</sub>(PO<sub>4</sub>)<sub>2</sub> phosphor, ionisation of capture centres, thermolum. spectra 0-11487  
 Ba<sub>3</sub>(PO<sub>4</sub>)<sub>2</sub>, recomb. luminesc. mechanisms 0-2874  
 CaCO<sub>3</sub>, thermoluminesc. spatial distrib. using image intensifier technique 0-47115  
 CaF<sub>2</sub>, doped and gamma irradi., high temp.-peak in thermoluminescence 0-50434  
 CaF<sub>2</sub>, thermoluminesc. and F-centre annealing, after neutron irradiation 0-7422  
 CaF<sub>2</sub>:Dy, thermolum. induced by 254 nm UV photons 0-55204  
 CaF<sub>2</sub>:Eu, thermolum. in presence of lanthanide impurities 0-2870  
 CaF<sub>2</sub>:Na, single cryst., X-irrad., optical absorpt. and thermoluminesc. 0-34952  
 CaO:Dy, thermolum. induced by 254 nm UV photons 0-55204  
 CaO:Eu(Tb), phosphor, isothermal decay 0-55156  
 Ca<sub>3</sub>P<sub>2</sub>O<sub>7</sub>:Sb(Mn), luminesc., colouration 0-2828  
 β-Ca<sub>3</sub>(PO<sub>4</sub>)<sub>2</sub>:Sb(Mn), luminesc., colouration 0-2828  
 Ca<sub>10</sub>(PO<sub>4</sub>)<sub>6</sub>(OH)<sub>2</sub>, UV induced thermolumin. glow peak obs. 0-29814  
 Ca<sub>5</sub>(PO<sub>4</sub>)<sub>3</sub>OH prod. by hydrothermal synthesis, thermolum. props. 0-2877  
 CaS:Bi phosphors, UV dosimetry by thermolum. 0-55199  
 CaSO<sub>4</sub> phosphors:Ce(Eu)(Dy)(Tm), gamma-irradiated valency conversions in rare earth ions 0-55198  
 CaSO<sub>4</sub>:Ce(Eu) phosphors, fluorescence spectra, thermolum. glow curve 0-2879  
 CaSO<sub>4</sub>:Dy, γ-ray induced sensitization, competing trap model 0-2881  
 CaSO<sub>4</sub>:Dy-KBr thermolum. phosphor, thermal neutron detect. by activation 0-32581  
 CaSO<sub>4</sub>:Dy(Tm), thermolum. induced by 254 nm UV photons 0-55204  
 CaSO<sub>4</sub>:Tm/polythene mixture, thermoluminesc. response to fast neutrons 0-5340  
 CsBr:Cu<sup>+</sup>, X-ray irradi., thermoluminesc. 0-16107  
 CsCl:Cu<sup>+</sup>, X-ray irradi., thermoluminesc. 0-16107  
 KBr, excitation of thermolum. near liq. He temp. 0-40171  
 KBr, X-irrad., F-centre role in thermoluminescence 0-20720  
 KBr:TI excitation in fund. absorpt. region, luminesc. and thermolum. 0-50433  
 KBr(Cl), X-ray irradi., tunnelling recomb. luminesc. 0-2873  
 KCl (Br) crystals, thermally stimulated luminescence accompanying recombination of V<sub>F</sub> and F centres 0-55201  
 KCl, thermal annealing of F, V<sub>F</sub>, V<sub>3</sub>-centres (*Russian*) 0-54229  
 KCl:Ag(In)(Ti), excitation in fund. absorpt. region, luminesc. and thermolum. 0-50433  
 KCl:Eu<sup>2+</sup>, γ-irrad., photostimulated low temp. recomb. luminesc. 0-11435  
 KCl:Sr, thermally pre-treated, glow curves 0-25470  
 KCl-Ba, X-ray irradi. cryst., thermoluminescence spectra 0-20719  
 KCl-KBr mixed crystals, thermolum. studies 0-11486  
 KCl-Mg, thermolum. of Z-centre, optical absorpt. 0-55203  
 KCl<sub>0.5</sub>Br<sub>0.5</sub>:Ca, X-ray irradi., Z<sub>1</sub>-centres, thermoluminesc. and optical absorpt. meas. 0-16108  
 KI:TI, electron-hole and V<sub>K</sub>-TI recomb., TSC and thermolum. study (*French*) 0-34461  
 K<sub>2</sub>O-B<sub>2</sub>O<sub>3</sub> glass, γ- and UV- irradi., thermodecolorisation and thermolum. 0-20721  
 KI:TI, excitation in fund. absorpt. region, luminesc. and thermolum. 0-50433  
 LiF, non-universality of TL-LET response, effect of batch composition 0-16106  
 LiF TLD-100, thermoluminesc., kinetics and trapping parameters, dose depend. 0-2872  
 LiF, TLD-100, trapping centres, optical absorpt. spectra defect and thermolum. mechanism models 0-50436  
 LiF TLD-100 phosphor, sensitisation mechanism study, thermolum. glow peak intensity obs. 0-55202  
 LiF:Mg,Ti crystals, Z<sub>2</sub>-centres, correlation of thermoluminescence and optical absorption 0-45154  
 MgO, single crystal, thermal and optical stimulation processes of V-centres (*Japanese*) 0-11485  
 MgSiO<sub>3</sub>:Dy, thermolum. induced by 254 nm UV photons 0-55204  
 N, active condensed, thermolum. meas. (*French*) 0-11484  
 NaCl, irradiated, at 80K, thermolum. processes 0-34990  
 NaCl preirradiation effect on proton channelling, thermoluminescence study 0-19860  
 NaCl:Ag, excitation in fund. absorpt. region, luminesc. and thermolum. 0-50433



**thermoluminescence continued**

- NaCl:Ca, microhardness and thermoluminescence, hardness-quenching temp. variation 0-29813  
 NaCl:Ca,  $Z_1$  centre thermoluminescence study 0-16109  
 NaCl:(Ca), irradi. at room temp., stored energy rel. to thermolum. 0-10574  
 Na<sub>2</sub>O-3SiO<sub>2</sub> glass, high-temp. thermolum., colour centre absorpt. 0-16110  
 Na<sub>2</sub>O-SiO<sub>2</sub> glass, tunnelling recomb. luminesc. 0-2875  
 Na<sub>2</sub>SiO<sub>3</sub>-CaO glass, thermostimulated and tunnel luminesc. 0-45157  
 RbBr, suprapure, thermolum. glow and emission studies at room temp. 0-7423  
 $\alpha$ -SiC (6H) laser excited thermostimulated luminescence light sum dose depend. (Russian) 0-16111  
 $\alpha$ -SiC(6H), two stage transitions, nonlinear absorpt., thermoluminesc. method 0-7425  
 SrF<sub>2</sub>, thermoluminesc. and F-centre annealing, after neutron irradi. 0-7422  
 YPO<sub>4</sub> phosphor, ionisation of capture centres, thermolum. spectra 0-11487  
 YVO<sub>4</sub> phosphor, ionisation of capture centres, thermolum. spectra 0-11487  
 Zn<sub>2</sub>O(BO<sub>2</sub>)<sub>2</sub>Tb, phosphoresc. study (Spanish) 0-16105  
 ZnS:Ag, single crystal, ionisation mechanism of field trapping centres 0-45156  
 ZnS:Ne, implanted single crystals, photolum. and bombardment effect, thermolum. curve obs. 0-55166  
 ZnS:Pb phosphor, ionisation mechanism of field trapping centres 0-45156  
 ZnS,Se<sub>1-x</sub>, VPE, characterisation of defect centres by photoelectronic meas. 0-10914

**thermoluminescent dosimeters**

- alkali borate binary glass, energy storage behaviour studied by thermoluminesc. 0-50432  
 aluminophosphate glass, improvement of fast neutron response 0-13932  
 automated TLD processing and dose record keeping service 0-12267  
 calibration, source storage and irradiation device 0-5339  
 calibration procedures in the Studsvik standardized personnel dosimetry system, Sweden 0-9418  
 calibrator, for dosimeter element (Japanese) 0-23159  
 computerised system for automated radiological monitoring 0-27827  
 data analysis using a Texas instruments programmable calculator 0-36136  
 downward drift of IKS-A instrums. stored after irradiation 0-23157  
 environmental meas. at nucl. facilities 0-42876  
 exoskeletons of Magicicada sp., detect. of thermolum., possible use as TLDs 0-30896  
 gamma-ray dosimetry errors with thermoluminescent dose meters 0-18705  
 hardness dependence of glass dosimeters for photons with energy up to 6 MeV 0-846  
 heating rate effect on TLD phosphor response 0-26359  
 light conversion efficiency of TLD-700 for  $\alpha$  particles rel. to <sup>60</sup>Co  $\gamma$ -rays 0-13935  
 lightning, thermoluminescent dosimetry measurement of radiation 0-36361  
 mixed-field dosimetry, appl. to personnel dosimeter badges 0-23170  
 neutron irradi., response to photon component of rad. field (German) 0-23176  
 orthovoltage X-ray therapy, TLD dose intercomparison 0-12272  
 personal monitoring, judgement of uncleanness in elements by residual value method (Japanese) 0-21546  
 personnel monitoring, occupational radiation exposure in Austria (German) 0-26352  
 phosphate glass, appl. in gamma dosimetry (Slovenian) 0-32521  
 phosphors, thermoluminescence, UV dosimetry 0-853  
 phosphors, use for high-level gamma-ray dosimetry 0-13934  
 polyethersulphone, thin film TLD, skin dosimetry appl. 0-52790  
 precision dosimetry, some problems 0-13936  
 reader with photon counting and DC techniques for wide range dose meas. 0-42870  
 review, characteristics and recent trends (Korean) 0-41253  
 thin film dosimeter based on polyethersulphone and LiF 0-23156  
 thin-layer TLDs based on high-temp. self-adhesive tape 0-13933  
 total radiation monitoring using liquid crystals and thermoluminescence 0-3819  
 BeO ceramic TLD, gamma ray response 0-23153  
 BeO compared with LiF 0-26357  
 CaF<sub>2</sub>+Dy<sub>2</sub>O<sub>3</sub>+KCl, intermediate neutron detection by thermoluminescence 0-5444  
 CaS:Bi as UV dosimeter 0-34991  
 CaSO<sub>4</sub>:Dy Teflon disc based TLD cards, annealing and repeated readout 0-3812  
 CaSO<sub>4</sub>:Dy Teflon TLD discs, metal filters for compensation of photon energy depend. 0-30901  
 CaSO<sub>4</sub>:Dy thermoluminescent phosphor, effect of sensitisation on energy depend. 0-26358  
 CaSO<sub>4</sub>:Dy+Dy<sub>2</sub>O<sub>3</sub>+KCl, intermediate neutron detection by thermoluminescence 0-5444  
 CaSO<sub>4</sub>:Tm intrinsic thermoluminescence stability for UV dosimetry 0-12262  
 CaSO<sub>4</sub>:Tm/polythene mixture, thermoluminesc. response to fast neutrons 0-5340  
<sup>60</sup>Co total body irradiation, dose distrib. meas. using thermoluminescent dosimeters 0-41245  
 D-D neutron meas. on 40 kV, 60 A neutral beam test facility 0-37710  
 Li<sub>2</sub>B<sub>4</sub>O<sub>7</sub>:Mn, gamma ray response 0-23153  
 LiF, non-universality of TL-LET response, effect of batch composition 0-16106  
 LiF TLD meas. rel. to Burlin cavity theory 0-56220  
 LiF, TLD-100, trapping centres, optical absorpt. spectra defect and thermolum. mechanism models 0-50436

**thermomagnetic effects**

- Ettingshausen-Nernst detectors with one- and two-phase detector layers (German) 0-27344  
 ferromagnetic metal, dragging of domains by temp. gradient 0-34425  
 graphite, galvanomagnetic and thermomagnetic effects at low temp. 0-44618  
 graphite, thermoelec. and thermomag. props., cylindrical band model 0-39616

**thermomagnetic effects continued**

- heavily doped semiconductors, materials science developments, appl. to thermoelectric heat pumps 0-35713  
 metal, effects of large scale voids on thermal magnetoresist. 0-10946  
 motor, dynamic characts. and stable operation (Japanese) 0-16840  
 Nernst-Ettingshausen detector materials, criteria for selection 0-39615  
 semiconductor, type I zero-gap state, Nernst-Ettingshausen and Hall effects 0-44622  
 semiconductors, thermoelectric and thermomagnetic effects, heat transfer due to quasi-particle subsystems (Russian) 0-24959  
 semiconductors thermophysical props. determ. from Ettingshausen effect meas. method 0-44376  
 thermoelectromagnetic waves in conductors in a mag. field (Russian) 0-49695  
 type II superconductor, thermomag. effects and crit. state stability 0-20353  
 AS,Sb<sub>1-x</sub>, thermomagnetic EMF, temp. and mag. flux density (Russian) 0-11022  
 Bi, galvanothermomagnetic instability 0-49785  
 Bi, magnetothermal EMF, twinned layer effect 0-49784  
 Bi, radioelectric effect in far IR 0-24967  
 Bi, thermomagnetic wave dispersion, propagation (Russian) 0-49696  
 n-Bi<sub>2</sub>Se<sub>3</sub>, single cryst., new aspect of carrier scatt. 0-49707  
 CO, chemisorbed monolayer on Pt or Au, mag. phase transition, thermomagnetic study (Russian) 0-34319  
 Cd, thermopower meas. in mag. field, 1.5-4K 0-54675  
 Cd<sub>3</sub>As<sub>2</sub>, band structure, pressure dependence of galvanomagnetic effects 0-6722  
 Cd,Hg<sub>1-x</sub>Te, photothermomag. effect and photocond. in millimetre wavelength range 0-44657  
 Ga, thermopower quantum oscillations 0-15505  
 K, high field Righi-Leduc effect and lattice thermal cond. 0-10948  
 K, high field Righi-Leduc effect and lattice thermal cond., reply to comment 0-10949  
 K, thermomagnetic and thermoelectric properties, phonon scatt. processes 0-29390  
 Ni-Mn-Al-Si-Co, Almel, Ettingshausen-Nernst coeff. and transport props. from 200 to 473K 0-44573  
 Ni<sub>3</sub>(Fe,M), M=Cr,Mo,W, elec. resist., temp. depend. anomalies, Hall and Nernst-Ettingshausen effects (Russian) 0-10942  
 Pb<sub>40</sub>In<sub>60</sub>, mixed state supercond., Hall and Ettingshausen effects, vortex transport 0-44780  
 p-PbS, struct. of valence band, transport processes study 0-20081  
 PbSe<sub>0.5</sub>S<sub>0.5</sub>, valence band struct., absorpt. spectra, elec. props. 0-44505  
 Pb<sub>1-x</sub>Sn<sub>x</sub>Se, n- and p-type, with band inversion, study of transport phenomena 0-49741  
 p-Pb<sub>0.65</sub>Sn<sub>0.35</sub>Te, transport coeffs. and dispersion law 0-44629  
 Pb<sub>0.82</sub>Sn<sub>0.18</sub>Te, thermomagnetic, thermoelectric props., valence band struct. (Russian) 0-54724  
 PbTe, radioelectric effect in far IR 0-24967  
 PbTe:TI, influence of TI impurity states 0-20121  
 Ru, thermo-EMF and Nernst effect under mag. breakdown conditions (Russian) 0-24878  
 W, thermopower meas. in mag. field, 1.5-4K 0-54675
- thermomagnetic recording**  
 rare earth-transition metal amorphous thin films for thermomag. recording 0-20403  
 semiconductor optical image transducers for increased sensitivity (Russian) 0-44833  
 EuO film for thermomagnetic recording, anisotropy of resolving power 0-20404  
 GdCo, amorphous thin film, for thermomagnetic recording (Japanese) 0-11562  
 GdFe homogeneous amorphous films, compensation point switching, magneto-optical Kerr signal anal. 0-15726  
 MnBi holographic film, reduction of thermomag. recording energy threshold (Russian) 0-43302
- thermomagnetic torque** see Scott effect
- thermomagnetic treatment**  
 see also magnetic annealing; magnetocaloric effects  
 magnetic materials, sintering, structure and props., external mag. and elec. field influence 0-50570  
 steel, carburised, transform. of residual austenite, mag. field effects (Russian) 0-29952  
 steel, induced anisotropy influence on mag. props., thermomagnetic working (Russian) 0-55549  
 Ticonal, two- and one-dimens. modulated struct. after thermomag. treatment and water quenching (Russian) 0-29983  
 Fe-Ni-Al, type YuN14DK25BA, thermomag. treatment 0-16512  
 Fe-Ni-Co-Mo-Ge alloy 40NKM, excess mag. noise after various thermomag. treatments (Russian) 0-29575  
 Fe-Pt, plastic deform. effect on struct. singularities and mag. props. (Russian) 0-44892
- thermomechanical processing** see thermomechanical treatment
- thermomechanical treatment**  
 see also hot pressing; hot working  
 diamond, mechanical strength depend. on thermal working parameters, microcracks (Russian) 0-55501  
 epoxide resins, amine-hardened, heat distortion, glass transition temps., chem. cure 0-44302  
 epoxy resin, cure history effect on dynamic mech. props. 0-54356  
 eutectoid thermomechanically treated, textural studies 0-29978  
 magnetic materials, high-energy, technology developments and props. (Italian) 0-54914  
 metallic crystal, thermomechanical deform., analytical description 0-49391  
 rare earth magnetic materials, permanent magnets flux stability enhancement, gyroscope-based guidance systems performance improvement 0-50144  
 steel, austenitic Cr-Mn, M<sub>23</sub>C<sub>6</sub> carbide precipitates comp., heat and thermomech. treatment influence (Russian) 0-40361  
 steel, austenitic stainless, biphase, ferritic, ageing and thermomech. treatment effects on struct. and props. 0-35226  
 steel, austenitic stainless, blister initiation inclusion, heat treatment and thermomechanical treatment effects (French) 0-35224  
 steel, austenitic stainless, high N, plasma arc remelting, processing parameters and props. 0-16336  
 steel, C and HSLA, grain size and substruct. control by alloying and thermomech. treatment, review 0-3082



**thermomechanical treatment continued**

- steel, components, dimensional stabilisation, thermoplastic treatment (*Russian*) 0-20960  
 steel, eutectic 1080, fatigue life improvement by thermomech. processing 0-25732  
 steel, high-temp. isothermic combined heat treatment and mech. working influence on struct. and mech. props. of 60S2 (*Russian*) 0-20969  
 steel, hollow cylinder, thick walled, effect of thermomech. treatment 0-11674  
 steel, low alloy structural, type 30KhGSA, effect of thermomech. treatment on strength, fracture toughness and fatigue props. 0-11676  
 steel, low alloyed (Mo,Cr,B) structural and mech. props., report (*French*) 0-25691  
 steel, low C (0.01-0.05 wt.%), structural and mech. props., report (*French*) 0-25691  
 steel, low C and alloy, serrated flow and thermomechanical treatment (*Korean*) 0-30026  
 steel, Mn-Cr-V, tool, quenched and tempered, fracture toughness (*German*) 0-25726  
 steel, Ni, struct. change of hot-worked austenite during post-deform. holding 0-35228  
 steel, TRIP, warm extrusion, process control and tensile props. 0-16338  
 steel, wear resist., mech. props. and struct. effects 0-35338  
 thermoplastic elastomers, crosslinked by secondary valence interactions, elasticity and processing, crosslinking behaviour 0-40320  
 Al alloy 7075, serrated flow and thermomechanical treatment (*Korean*) 0-30026  
 Al wire, hot and cold deformation drawing strengthened, thermal EMF study (*Russian*) 0-54674  
 Al-Cu alloy 1201, thermomech. treatment effect on strength characts. and fracture toughness (*Russian*) 0-40391  
 B fibre reinforced Al-Zn-Mg, packet rolling, thermodeform. process parameters (*Russian*) 0-55433  
 MgO-MgAl<sub>2</sub>O<sub>4</sub>(FeCr<sub>2</sub>O<sub>4</sub>), thermoplastic and thermophys. props. for steel vacuuming installations 0-35281  
 $\alpha + \beta$  Ti alloy VT3-1, drop forgings, grain orientation and props., combined mech. working, hardening and high-temp. heat treatment influence (*Russian*) 0-20973  
 WC-Co and WC-Co-TaC-TiC-NbC cemented carbides, microstructure, high temp. deformation, uniaxial plastic compression 0-40451

**thermometers**

- see also pyrometers; resistance thermometers; temperature measurement; thermocouples; thermopiles*  
 biomedical digital thermometer, simple, inexpensive design 0-36178  
 calibration, in liq. He range, dipstick cryostat 0-37044  
 digital, electronic, with two sensors, in kit form (*French*) 0-4712  
 digital, type DTM 1, with LED display (*German*) 0-27302  
 digital, using LSI for remote sensing 0-27301  
 ferroelectric thermometer (*Polish*) 0-31750  
 grafted, for psychrometer (*Japanese*) 0-31771  
 internal contraction engine, highly loaded, exhaust gases temp. and velocity meas. using two thermometer method (*German*) 0-31754  
 ionic crystal, possible high-temp. thermometer using elec. cond. changes 0-52203  
 JFT-2 Tokamak, radiation loss meas. using thin-film thermometer 0-47698  
 magnetic, depend. of AC mag. susceptibility on magnitude of meas. field 0-241  
 medical temperature measurement, electrical (*Hungarian*) 0-30910  
 NQR thermometer, calibration in 203-398K range 0-42222  
 nuclear susceptibility thermometry using enriched <sup>119</sup>Sn 0-4710  
 sonic anemometer-thermometer, phase-locked loop CW system 0-41565  
 state of art and research appl. 0-31743  
 superconducting thermometer sensitivity, temp. and field depend. 0-4708  
 thermal noise thermometer with supercond. quantum magnetometer (*Czech*) 0-220  
 US temp. profiling system for critical heat flux meas. of nuclear reactor fuel assembly 0-37032  
 Hg-in-glass thermostat 0-22359

**thermometric conductivity** *see thermal diffusivity***thermonuclear devices** *see plasma devices***thermonuclear reactions** *see nuclear reactions and scattering***thermopiles**

- IR detectors appl. 0-47104

**thermoreflectance**

- CdGa<sub>2</sub>Se<sub>4</sub>, thermoreflectance and visible absorpt. spectra, energy gap, cryst. field splitting 0-34945  
 CdS, A<sub>1</sub>-exciton, reflectance and thermoreflectance spectra, spatial dispersion and angle of incidence effects 0-25409  
 Dy, film, thermoreflectance dispersion curves at 315K and 97K 0-7332  
 Gd, film, thermoreflectance dispersion curves at 315K and 97K 0-7332  
 Hg<sub>0.75</sub>Cd<sub>0.25</sub>Te, thermorefl. spectra, effect of excitons on E<sub>1</sub> and E<sub>1</sub> +  $\Delta_1$  structs. 0-16057  
 Nb-Mo, electronic struct., thermoreflectance meas. 0.5-5.0 eV 0-45050  
 Si-H, amorphous, refr. index, temp. depend., implications for thermoreflectance and electrorefractance 0-50290  
 TaSe<sub>2</sub> (2H), optical absorpt., band struct., plasmons, and CDW 0-45104  
 TaSe<sub>2</sub> (2H), plasmon behaviour at charge density wave onset 0-10900  
 Tb, film, thermoreflectance dispersion curves at 315K and 97K 0-7332  
 YIG, pure and Ga-substituted diffuse refl. and thermorefl. spectra near Curie point 0-40131  
 YIG, thermoreflectance spectra 0-20616  
 ZrS<sub>3</sub>, thermomodulated reflectivity and transmission 0-50357

**thermosphere**

- annual composition vars. from Aeros Nims data 0-12578  
 auroral NO densities, horizontal winds effects 0-26656  
 chemical processes 0-17431  
 circulation, seasonal and solar cycle variation 0-56661  
 circulation and comp., effects of magnetospheric elec. field and currents 0-17446  
 composition of middle atm., in situ meas. 0-17339  
 dynamics, Fabry-Perot spectrometer obs. 0-12573  
 dynamics calcs., Navier-Stokes eqns. validity 0-26659  
 dynamics of middle atmosphere, review 0-17338  
 W.Europe, atmos. temp. 20-110 km altitude, 1975/6 winter anomaly 0-36356  
 W.Europe, ion production obs., 50-120 km altitude, 1975/6 winter anomaly 0-36439  
 W.Europe, mesosphere and lower thermosphere temp. and density, 1975/6 winter anomaly 0-36357

**thermosphere continued**

- W.Europe, mesosphere and lower thermosphere trace constituents, 1975/6 winter anomaly 0-36433  
 W.Europe, neutral atmosphere composition 1975/6 winter anomaly 0-36432  
 F-region response to storm of June 1972, thermosphere-ionosphere coupling 0-41617  
 gravity wave activity effects on photochem. and comp. 0-41583  
 gravity wave propag. in diffusively separated atmosphere 0-12580  
 heating during magnetic storm, dynamic energy transport from high to low latits. 0-26657  
 ion-drag effects 0-17432  
 ionisation caused by variable solar UV flux, 1974-9 obs. 0-17430  
 neutral gas temperature, in-situ meas. by Atmosphere Explorer 0-12576  
 neutral temperature and winds, geomag. disturbances effects 0-26658  
 neutral wind, midlatitude meas. during ALADDIN programme 0-31153  
 neutral winds, tidal modes rel. to low latit. dynamo currents seasonal vars. 0-8479  
 quiet thermosphere dynamics, review 0-21866  
 resonance radiation transport with varying Doppler width, thermosphere appl. 0-26737  
 response to 1969 November 8-9 magnetic disturbances 0-12574  
 satellite observations of middle atmosphere processes 0-21803  
 sonic boom propagation 0-33305  
 temperature, turbulence and N<sub>2</sub> composition, 95-150 km altitude, 1967-75 obs. 0-51588  
 temperatures over Malvern, incoherent scatter data comparison with two global thermospheric models 0-8467  
 tides, differential operator and integro-differential eqn. (*Chinese*) 0-56660  
 wind measurement at 60-120 km, radiowave drifts technique 0-31137  
 O and O<sub>2</sub> distrib. in lower thermosphere assuming tidal effects, one dimens. nonstationary diffusion-photochemical model 0-4160  
 O content of lower thermosphere, 100-160 km, new spectral method 0-41578  
 O<sub>2</sub>, O<sub>2</sub> distribution in lower thermosphere 0-4159  
 O<sup>+</sup> energetic ions precip. during mag. storms and magnetosphere-thermosphere coupling 0-26665  
 OH emissive layer, waves, near IR photographic studies 0-51545  
 O(<sup>3</sup>P) translationally hot, energy distrib. function 0-21811

**thermostats**

- see also cryostats; temperature control; thermistors*  
 air, for reaction-solution rotating-bomb calorimeter 0-4717  
 automatic, using Diapazon temperature variator, radiospectrometer appl. 0-47160  
 sensitivity, influence of specimen curvature (*German*) 0-27291  
 Hg-in-glass thermostat 0-22359

**theta pinch** *see pinch effect***thick film circuits**

- adhesion testing, use of fracture mechanics concepts 0-50802  
 conductors, adhesion meas. 0-50808  
 optical waveguide integration with fibre-optic connectors 0-33246  
 Pt-Au, adherence meas. and evaluation 0-50813

**thick film devices**

- reed-type routing switch for multimode optical fibres 0-53463

**thick films**

- adhesion, to ceramic, destructive and nondestructive meas. 0-50809  
 adhesion measurement, conf. Philadelphia, USA (Nov. 1976) 0-46729  
 adhesion measurement 0-50817  
 diffusion experiment, introduction of weights to least squares anal. 0-49399  
 soldered thick-film conductor, adhesion meas. technique 0-50811  
 solid films and surfaces, conference, Tokyo, Japan (Jul. 78) 0-10739  
 terminations on chip components, adhesion meas. methods 0-50810  
 CdTe, prep. by sintering and elec. props. 0-29451  
 V<sub>2</sub>O<sub>5</sub>-P<sub>2</sub>O<sub>5</sub> (70-30), electrical cond. and thermoelectric meas., Au-glass-Au sandwich 0-29403

**thickness control**

- cold light production by high vacuum deposition of multilayer interference coatings (*German*) 0-53486  
 glass fibre thickness meas. and control system in production (*German*) 0-10052  
 semiconductor epitaxial layers, resistivity and thickness monitoring, use of spreading-resistance method 0-47075  
 thin film composition gradient production 0-55295

**thickness measurement**

- adsorbed polymer layer, on particles in suspension, thickness meas. by mag. birefringence 0-42191  
 annular liquid film meas. techniques 0-31439  
 antireflection coatings, thickness monitoring during deposition 0-19114  
 arterial walls, human coronary, optical density determ. 0-12173  
 contact lens radii and thickness meas. by interferometry 0-8118  
 dielectric multilayers, optical and geometrical thickness monitoring using monochromatic maximeter, substrate effects (*French*) 0-38140  
 dielectric thin film refractive index and thickness, algorithm for determ. on basis of ellipsometric meas. 0-34881  
 dielectric thin films, accurate meas. by symmetric prism wave couplers (*Chinese*) 0-2885  
 electrodeposits, multilayer, instrument based on destructive coulombmetric method (*Czech*) 0-8980  
 electron beam evaporation rate automation by ion current meas. (*Hungarian*) 0-16198  
 electron beam evaporation source with integrated rate control (*Hungarian*) 0-20798  
 electron-irradiated specimen, determ. by continuum integration 0-31713  
 fluorescent film, method for refr. index and thickness determ. 0-40175  
 fluorocarbon foil, fluoroplast, homogeneity study (*Polish*) 0-35278  
 glass fibre thickness meas. and control system in production (*German*) 0-10052  
 glass film and shell wall thickness meas., white light interferometric meas., dispersion effect 0-4757  
 glass industry, applications of gauges and optical projectors 0-21249  
 glass surface, ellipsometric study of zone of optical contact 0-4754  
 optical waveguide, thin film, with emitting diff. grating, inhomogeneity in thickness 0-48425  
 polycrystalline Si film growth, underlying oxide layer thickness effect on in-process thickness monitoring 0-6679  
 polyethylene films 4 to 100  $\mu$ m (*Japanese*) 0-52160  
 profile measurement of hot rolled strip during hot rolling (*German*) 0-25929  
 quartz crystal thickness sensor isotope target preparation 0-17923



**thickness measurement continued**

- semiconductor detectors, determination of thickness of sensitive layer with aid of  $\beta$  and  $\gamma$  sources 0-22323
- simultaneous meas. of Au and Ni layers on Cu substrates, X-ray fluorescence 0-13041
- steel, galvanised coatings, thickness meas. using X-ray fluorescence radiation, apparatus design 0-21202
- surface and surface layer measurements, ellipsometric method 0-52295
- thin film, photoacoustic microscopy appl. 0-14525
- thin film growth measurement using galvanically separated quartz monitor probe (*German*) 0-11576
- thin film permittivity and thickness determ. using differential-gap varying method (*Japanese*) 0-4739
- thin films, calibration standards for surface profile monitors 0-17918
- thin films, characterisation using proton-induced X-ray emission 0-35618
- thin films, X-ray interferometer based on small-angle scattering apparatus 0-27271
- UNIPAN 545 US gauge, with digital readout 0-47019
- various methods, critical assessment 0-47018
- Ag layers, thickness determ. by laser microprobe and flame atomic absorpt. 0-27355
- Au film on (100) Si, appl. of acoustic microscopy 0-53575
- Au film on Si, SAW dispersion and film thickness meas. 0-10769
- Au layers, thickness determ. by laser microprobe and flame atomic absorpt. 0-27355
- Cu thin layers, thickness meas. by proton-induced X-ray emission 0-4690
- Fe-Al, rate of form. and thickness of diffusion layer, 200 to 600°C 0-15315
- Ni layers, thickness determ. by laser microprobe and flame atomic absorpt. 0-27355
- Pd-H thin film system, phase diagrams using quartz crystal thickness monitor 0-7537
- Si-Al devices, thickness meter for Al contacting layers (*Russian*) 0-36980
- SiNH films, thickness and refractive index meas., comparison of techniques 0-8957
- SiO<sub>2</sub> films, thickness and refractive index meas., comparison of techniques 0-8957
- Ta, transmission channelling of MeV ions to study edge dislocations, expt. setup 0-29098
- TiC coating thickness meas. using X-ray diffr. 0-21243
- V<sub>2</sub>O<sub>5</sub> film, amorphous, thickness, density and refr. index determ. from reflectance interference spectra 0-55206

**thin film capacitors**

- CVD, high temp. instrumentation fabrication 0-40266
- Nb-Ta-N sputtered films and their anodic oxides, elec. props. of resist. and dielec. films 0-11126
- Y-Y<sub>2</sub>O<sub>3</sub>-Au, self-healing dielec. breakdown 0-11104

**thin film circuits**

- high temperature instrumentation, passive components fabrication 0-40266
- manufacture, using low-temperature radiometer, with conical light pipe 0-47105
- Cr films, on Al<sub>2</sub>O<sub>3</sub>, quartz and glass, electron-beam deposition techniques improvement 0-7496
- Ti films on Al<sub>2</sub>O<sub>3</sub>, quartz and glass substrates, electron-beam deposition techniques improvement 0-7496
- Ti-Cu thin films, oxidation kinetics in air at 100 to 300°C, meas. 0-40590

**thin film devices**

- see also *magnetic thin film devices*
- field ionisation source fabrication 0-52359
- fission thermocouple detectors for reactors safety expts. 0-22987
- image converters, solid state, with integrated fixed-pattern noise suppression 0-14458
- interdigital transducers for SAW devices at GHz freqs. form. by electron beam lithography 0-4702
- SAW, ZnO, for HF range (*Japanese*) 0-53598
- TTF polymer thin film batteries 0-45709
- Zn<sub>3</sub>P<sub>2</sub>, UV photoconductive detectors 0-4766
- Ge<sub>1-x</sub>Te<sub>x</sub>X<sub>4</sub> amorphous semicond. switches, fabrication technology (*German*) 0-7493
- HgTe thin film Hall sensor fabrication 0-2951
- VO<sub>2</sub> thin film semiconductor-metal transition applications 0-49835
- ZnS:Mn AC electrolum. device, filament behaviour 0-20712
- ZnS:Mn co-deposited electrolum. device, phys. and elec. characterisation 0-20713
- ZnS:TbF<sub>3</sub>, between semicond. Y<sub>2</sub>O<sub>3</sub> layers, bright green electrolum. 0-2859

**thin film resistors**

- CVD, high temp. instrumentation fabrication 0-40266
- Cr-SiO<sub>2</sub> sputtered, elec. and struct. props. 0-39694
- Nb-Ta-N sputtered films and their anodic oxides, elec. props. of resist. and dielec. films 0-11126
- TiN films deposited by reactive sputtering, elec. props. 0-15638

**thin film transistors**

- SiO<sub>2</sub> sputtered films in thin film transistors, trapping centres 0-7014
- SiO<sub>2</sub>-CdSe, slow states, trapping state densities and cross sections 0-15613

**thin film triodes** see *thin film transistors***thin films**

- see also *coatings; dielectric thin films; epitaxial layers; insulating thin films; magnetic thin films; metallic thin films; semiconductor thin films; semimetallic thin films; sputtered coatings; substrates; vapour deposited coatings*
- adherence, locus of failure, implications for adhesion meas. 0-50818
- adhesion measurement, conf. Philadelphia, USA (Nov. 1976) 0-46729
- adhesion measurement 0-50817
- adhesion measurement 0-50819
- adhesive failure, rel. to interfacial structure 0-50820
- alkali chlorides, thin film, crystal-vacuum (100) surfaces, mol. dynamics computer simulation 0-34288
- alkali halides, thin films, crystal-vacuum (110) interfaces, mol. dynamics computer simulation 0-34289
- amorphous film-crystalline substrate, relaxation process dislocation misfit theory (*Russian*) 0-39461
- atomic composition depth distrib. by energetic ion anal. 0-35617
- bicrystals, dislocation interaction, with grain boundaries during plastic deform., electron microscopy technique 0-54281
- characterisation and microanal. by STEM combined with other techniques 0-50901

**thin films continued**

- composition gradient production 0-55295
- detection on surface by electron probe microanal., in depend. on substrate 0-35607
- diatomic clusters, break-up in thin films, particle energy distrib., central peak nature 0-50490
- dual source evaporation, rate control 0-40263
- electron-probe microanalysis of thin coatings, charact. fluoresc. correction 0-7881
- EM tensile adhesion test method 0-50804
- ESCA, surface anal. and electronic structure (*French*) 0-7891
- film-substrate bond strength, meas. by laser spallation 0-50821
- gelatin orientating action of solid substrates, on liq. cryst. layer exam. 0-44111
- growth due to crystallite surface migration, review 0-10810
- growth measurement using galvanically separated quartz monitor probe (*German*) 0-11576
- growth parameters of isolated steps on vicinal faces, elementary rate anal. 0-10805
- hardness and adhesion meas., scratch technique 0-50805
- HF density of states 0-6689
- HF formalism for calc. of total energies and charge densities 0-49850
- interference colours produced by white light refl., teaching paper 0-8754
- interference electron microscopy and electron interferometry in thin film studies 0-6328
- intrinsic stress determ., cantilevered plate method anal. 0-54570
- ion implanted 10 nm layer production method and apparatus 0-19818
- ion plating, low-pressure, ion source design 0-35105
- laser heating of thin films on absorbent supports (*Russian*) 0-7441
- lens formation, appl. of alternating elec. field 0-12060
- magnetron ion sputtering, thin film layers deposition uniformity investigation (*Russian*) 0-20787
- mechanical testing methods, review 0-40637
- microporosity described in terms of vacancies and voids 0-24769
- microprocessing, laser microprobe mass analyser (LAMMA) appl. 0-18041
- molecular solid, 0-15 eV electron transmission spectra 0-35023
- multi-scattering method for cryst. surface band struct. calc. 0-2439
- normal-incidence Brillouin scattering by acoustic phonons 0-20648
- nucleation, growth and transform. of amorphous and crystalline solids 0-24745
- nucleation kinetics, coalesc. of mobile nuclei 0-6671
- optical constants determ. 0-2883
- optical constants measurement, Shamir-Graff method evaluation 0-11489
- organic, scanner laser marking 0-43385
- quantised, electronic energy spectrum (*Russian*) 0-44688
- rare earth hydrides and sesquioxides, prep., struct. and props., general review 0-54556
- Rutherford backscattering spectrometry, signal overlap subtraction, surface struct. study 0-50486
- segregation effects at surfaces and interfaces 0-39475
- separation from substrate using plasma etching (*Slovak*) 0-45405
- solid films and surfaces, conference, Tokyo, Japan (Jul. 78) 0-10739
- spontaneous macrostress calculation, from substrate deform. 0-15412
- substrate-thin film system with rough boundaries, ellipsometric obs. using equiv. film theory 0-2310
- surface anal. and depth profiling by spark-source mass spectrography, discharge model 0-40781
- surface analysis, modern methods 0-54486
- surface analysis techniques survey, for development and production (*Hungarian*) 0-54537
- surface and surface layer measurements, ellipsometric method 0-52295
- thermal expansion coefficient, determ. using optical dilatometer 0-45454
- thermosensitive film coating, dispersed liq. cryst. microdroplets in gelatin matrix, exam. of preps. 0-42220
- thickness meas. using X-ray interferometer based on small-angle scattering apparatus 0-27271
- thickness measurement and characterisation using proton-induced X-ray emission 0-35618
- tight-binding Green's functions for surfaces, thin films, and solid interfaces using random-walk theory 0-54753
- X-ray diffraction,  $1-\sin^2\theta/\lambda^2$  intensity eqn. verification (*German*) 0-19668
- $\beta$ -AgI thin film, exciton spectrum 0-55216
- Ag<sub>2</sub>I<sub>4</sub>PO<sub>4</sub> film formation from electrolysis of HI-H<sub>3</sub>PO<sub>4</sub> soln., electrocodepositional method 0-55315
- Au-Ag, thin film struct., Rutherford backscattering spectrometry, signal overlap subtraction 0-50486
- B and borides, conference, Varna, Bulgaria (Oct. 1978) 0-12842
- BaCl<sub>2</sub>, non-crystalline film, disorder-induced Raman scatt. 0-11387
- BaFCl, non-crystalline film, disorder-induced Raman scatt. 0-11387
- Bi<sub>2</sub>Si<sub>2</sub>O<sub>7</sub> films on Si, form. kinetics and props. 0-35358
- C, orientating action of solid substrates, on liq. cryst. layer exam. 0-44111
- Fe-Al<sub>2</sub>O<sub>3</sub> granular film, interface props., Mossbauer spectroscopy 0-34336
- Fe-SiO<sub>2</sub> granular film, interface props., Mossbauer spectroscopy 0-34336
- Fe-ZrO<sub>2</sub> granular film, interface props., Mossbauer spectroscopy 0-34336
- MgO film, graphitic C detected by surface Raman spectra 0-2297
- Ni<sub>3</sub>C films, form. by carburisation, characterisation 0-34337
- Pb-Si<sub>3</sub>N<sub>4</sub> films on Si, form. kinetics and props. 0-35358
- PdH<sub>1.18</sub>, PdH<sub>1.20</sub>, prep., cryst. struct., chem. comp. determ. by thermal decomp. 0-34334
- Sb<sub>2</sub>Si<sub>2</sub>O<sub>7</sub> films on Si, form. kinetics and props. 0-35358
- Si-Al, silumin, crystn. of eutectic phases (*Russian*) 0-29942
- SrCl<sub>2</sub>, non-crystalline film, disorder-induced Raman scatt. 0-11387
- TaN, characteristics of Pirani type vacuum gauge (*Japanese*) 0-13086
- TaN, in Pirani type vacuum gauge (*Japanese*) 0-52257
- TiO<sub>2</sub> films, refl., 2-25 eV 0-55123

**third-order optical susceptibility** see *nonlinear optical susceptibility***thixotropy**

- blood, rheological parameters for viscosity, viscoelasticity and thixotropy 0-16963
- coagulation kinetics, diffusion effects and rheological models for thixotropic fluids 0-43740
- inelastic fluid, rheological characterisation 0-38373
- AlN, thermoplastic slips, viscosity, thixotropy, dilatance determs. 0-25633
- TiN, thermoplastic slips, viscosity, thixotropy, dilatance determs. 0-25633



**Thomas-Fermi model**

- contact exciton, screening and quenching 0-29334  
 covalent semiconductors, vacancy screening, dielec. const., exchange correl. pot., Thomas-Fermi description 0-44528  
 diatomic systems, correl. diagrams, Thomas-Fermi calcs. 0-23294  
 diatomic systems, Thomas-Fermi and Thomas-Fermi-Dirac-Weizsacker eqns., solns. 0-23293  
 electron plasma, impurity screening effects in intermediate degeneracy region 0-14882  
 inhomogeneity correction for atom in strong mag. field 0-27947  
 interatomic potential for atomic pairs, Thomas Fermi model with quantum corrections 0-32797  
 local density functional theory of atomic and mol. ground electronic states 0-23286  
 many-valley semiconductor, metal-insulator transition at finite temp., calc. 0-49603  
 metal, electron gas, local density functional for kinetic energy near defect, metal surface 0-20105  
 metal, single-particle density matrix, perturbation expansion 0-54635  
 metal surface electronic barrier, elec. field effect in presence of adsorbate 0-49864  
 nucleon, EM structure 0-9170  
 positive ions, in extremely strong mag. field,  $1/Z$  expansion for total energy 0-52855  
 screening in inhomogeneous systems 0-20106  
 semiconductor, dielectric screening, Thomas-Fermi model 0-49648  
 semiconductor, electronic properties, rel. to chem. bonding and lattice dynamics 0-44169  
 superconductors, polyvalent metals, Brillouin zone boundary influence on Coulomb interactions 0-24827  
 surface properties from Thomas-Fermi calc. 0-13394  
 Al-Al, Thomas-Fermi-Dirac model, inhomogeneity corrections 0-23308  
 Ge, donor ion pot., small  $r$  behaviour of nonlinear Poisson eqns. 0-54652  
 N-N, correl. diagrams, Thomas-Fermi calcs. 0-23294  
 Ne-Ne, correl. diagrams, Thomas-Fermi calcs. 0-23294  
 Ne-Ne, Thomas-Fermi-Dirac model, inhomogeneity corrections 0-23308  
 Pb, electronic thermal Gruneisen parameters 0-39242  
 Si, donor ion pot., small  $r$  behaviour of nonlinear Poisson eqns. 0-54652  
 Si, electronic properties, rel. to chem. bonding and lattice dynamics 0-44169  
 Si, vacancy screening, dielec. const., exchange correl. pot., Thomas-Fermi description 0-44528  
 $\text{Sn}^{4+}$ , electron density function, Thomas-Fermi calc. 0-6763  
 Th, electronic thermal Gruneisen parameters 0-39242

**Thomson effect**

- semiconductor, dumb-bell shaped specimen, vol. component determ. of Seebeck effect 0-49788

**thorium**

see also nuclei with .....

- $^{232}\text{Th}$ ,  $^{238}\text{U}$  comparative breeding potential in LMFBR blankets 0-22948  
 abundance in Precambrian basement, W.Canada, petrologic and tectonic controls 0-17257  
 adsorption of  $\text{O}_2$ , XPS study 0-7473  
 density functional theory 0-15442  
 electronic states under press. 0-54600  
 electronic thermal Gruneisen parameters 0-39242  
 electrotransport purification under low press. 0-15303  
 fission reactors, integral experiments for testing Th and  $^{233}\text{U}$  data 0-27707  
 fuel cycle, U cycle comparison use in LWRs (Spanish) 0-32420  
 fusion hybrid reactor blanket, reaction rate calc., central DT neutron source, ENDF/B-IV cross sections 0-13792  
 GCFR lattice, Th reaction rate meas. 0-656  
 heat capacity, from 80 to 1000K of high purity metallic sample 0-34201  
 HTR fuel cycle program in the Federal Republic of Germany 0-644  
 lattice dynamics, unpaired forces 0-15201  
 lattice parameter variation at low temp., thermal expsn. 0-15046  
 LMFBR, effects of Th breeder material on Na-void reactivity 0-22982  
 LMFBR, heterogeneous, Th blanket zones study in ZPPR Assembly 8 0-22983  
 Oklo natural fission reactor, radioactive dating from Pb and Th meas. (French) 0-21762  
 optical reflectivity 0-16054  
 PIXE elemental anal. at  $\mu\text{g g}^{-1}$  levels in ore samples 0-55758  
 reprocessing, continuous solvent extraction feed prep. 0-13773  
 sand grains containing high  $^{238}\text{U}$  and  $^{232}\text{Th}$  concentrations, enhanced natural radiation exposure (German) 0-51018  
 tracer for atmospheric stability (Spanish) 0-51448  
 vacuum thermal reduction of Ho oxides (Russian) 0-16226  
 XPS of 5p level, screening and configuration interaction effects 0-54633  
 Th II, oscillator strengths calc. 0-27982  
 $\text{Th} + \text{H}^+(\text{D}^+)$ , L-subshell vacancy production, Coulomb deflection effects 0-9711  
 $^{230}\text{Th}$  dating of fossil corals and shells 0-12434  
 $^{232}\text{Th}$ , neutron spectra for fusion + hybrid reactor materials 0-23142  
 $^{232}\text{Th}$ , reevaluation of dose unit per unit intake 0-26356  
 $^{232}\text{Th}$ -makrofol, solid state nuclear track detector, neutron response 0-27876  
 $^{234}\text{U}$ ,  $^{230}\text{Th}$ ,  $^{226}\text{Ra}$ , superposition soln. of transport of decay chain through sorbing medium 0-37500  
 $^{234}\text{U}$ ,  $^{230}\text{Th}$ ,  $^{226}\text{Ra}$  decay chain, hydrogeological migration anal. 0-37501

**thorium compounds**

- Ni-Th $\text{O}_2$ , dispersion strengthened, high temperature cyclic deformation 0-16430  
 (Pu-Th) $\text{O}_2$ , FBR fuel pellet fabrication, control of  $\text{O}_2$ -to-metal ratio 0-13760  
 (Th,Pu) $\text{O}_2$ , nuclear fuels, economic viability of Pu recycling in LWR 0-18576  
 (Th,U) $_2$ , chemical form of solid fission product simulating high burnup 0-616  
 (Th,U) $\text{O}_2$  microspheres, fabrication 0-801  
 Th-H system, supercond., book contrib. 0-25037  
 Th,As $_2$ -U,As $_4$  solid soln., electronic props. 0-34469  
 ThBr $_4$ ·U $^{4+}$ , absorpt. spectrum, zero phonon line (French) 0-11443  
 ThC $_{0.75}$ , specific heat, Fermi level density of states 0-10680  
 ThC $_{0.6}\text{N}_{0.4}$ , specific heat, Fermi level density of states 0-10680  
 ThF $_4$ , inhomogeneous interface laser mirror coatings 0-1252  
 Th $_2\text{Fe}_3\text{H}_{14.2}$ , Mossbauer spectra, mag. props. 0-15852

**thorium compounds continued**

- ThH $_2$ ·Er $^{3+}$ , EPR of Er localised electron mag. states, Kondo effect 0-25202  
 ThH $_4$ , Dirac-Fock one-centre expsn. calc. 0-5485  
 Th $_4\text{H}_{15}$ , superconductivity and electron-phonon interaction 0-49975  
 Th $_4\text{H}_{15}$ ·Er $^{3+}$ , EPR of Er localised electron mag. states, Kondo effect 0-25202  
 ThO, L $\text{II}^+\Sigma^+$  and N $\text{I}^+\Pi\text{-X}^1\Sigma^+$  systems, spectra, rot. anal. 0-23430  
 ThO, spectroscopic data rel. to thermodynamic functions 0-34208  
 ThO $_2$  a once-through cycle for BWRs 0-18433  
 ThO $_2$  central zone is PROTEUS GCFR lattice 0-22984  
 ThO $_2$ , H $_2$  $^+$ , ion beam surface interaction, H $^-$  formation by reson. electron capture 0-40691  
 ThO $_2$ , HTR fuel particles, fission product behaviour anal. using gamma spectrometry 0-42778  
 ThO $_2$ , ionic conduction, doping effects and defect interactions 0-19978  
 ThO $_2$ , isolated rod, exptl. and calculated resonance integrals 0-22986  
 ThO $_2$  Knudsen cells heated by radiation, emissivity (Japanese) 0-13073  
 ThO $_2$  laser coating, UV damage obs. 0-33056  
 ThO $_2$ , negative surface ionisation of H $_2^+$  ions 0-6280  
 ThO $_2$  nuclear fuel production, economic and environmental anal. 0-18575  
 ThO $_2$  plasma deposition of crysts. and their characterisation 0-20800  
 ThO $_2$ , sintered, fracture props. studied by Hertzian indentation technique 0-50703  
 ThO $_2$ , spectroscopic data rel. to thermodynamic functions 0-34208  
 ThO $_2$ , thermal and transport props., electronic contrib. 0-15432  
 ThO $_2$ /Ni, adhesive energy, meas. techniques 0-50803  
 ThO $_2$ /Ni-Cr, adhesive energy, meas. techniques 0-50803  
 ThOS·Gd $^{3+}$ , EPR study, g-factor and cryst. field parameters 0-25204  
 ThP, specific heat, Fermi level density of states 0-10680  
 (U,Th) $\text{O}_2$  fuel pellet fabrication using gel microspheres 0-42844  
 (U,Th) $\text{O}_2$  fuel rods, analytical stressing in hot cell 0-18566  
 (U,Th) $\text{O}_2$ ,  $\gamma$ -active pellet fuels fabrication, conceptual design of remotely operated plant 0-32340  
 (U,Th,...)Sb, magnetisation, U valence change 0-7089  
 ( $^{233}\text{U}$ , Th) $\text{O}_2$  fuels for HTGR, remote fabrication 0-13752  
 ( $^{233}\text{U}$ , Th) $\text{O}_2$  pellet-type fuels for CANDU reactors, remote fabrication plant design 0-13751  
 W-ThO $_2$ , candidate refractory for Tokamak, thermal fatigue failure testing 0-32454  
 W-ThO $_2$ -B, thermocathodes diffusion mobility, based on deboronation kinetics 0-39349  
 Y $_{1-x}\text{Th}_x\text{Fe}_3$  system, elec. resist. meas., 77-300K 0-34413

three-phase flow see multiphase flow

three-photon spectra see multiphoton spectra

three-term control

diptick cryostat, with temp. controller for high thermal stability 0-37044

throat microphones see microphones

**thulium**

see also nuclei with .....

- atom, nuclear K-X-ray satellites, Z=50-83, by  $\alpha$ -bombard., 17.5-22.5 MeV 0-42984  
 electronic relaxation, Tm $^{3+}$  Mossbauer spectroscopy 0-39914  
 energy transfer between 5d electronic states 0-2808  
 Hall coefficient meas., 80 to 1000K 0-49694  
 Bi $_4\text{Ge}_3\text{O}_{12}$ ·Tm $^{3+}$  crystal growth, spectral and laser props. 0-45115  
 CaSO $_4$ ·Tm, gamma-irradiated valency conversions in rare-earth ions 0-55198  
 CaSO $_4$ ·Tm intrinsic thermoluminescence stability for UV dosimetry 0-12262  
 CaSO $_4$ ·Dy(Tm), thermolum. induced by 254 nm UV photons 0-55204  
 Fe: $^{169}\text{Tm}$ ( $^{175}\text{Lu}$ ), radiation-damage evolution influence on hyperfine interaction 0-6793  
 LaF $_3$ ·Tm, cryst. field anal. of triply ionised ion spectra 0-2796  
 Tm:LiYF $_4$ , XeF pumped, excimer excited storage laser 0-33003  
 YF $_3$ ·Tm, Nd, energy transfer between 5d electronic states 0-2808

**thulium alloys**

- electronic relaxation, Tm $^{3+}$  Mossbauer spectroscopy 0-39914  
 Ag-Tm, dil., high field magnetoresist. 0-15503  
 Ga-Ni-R, (R=Dy, Ho, Er, Tm, Lu), struct. determ. by X-ray powder method (Ukrainian) 0-39001  
 Pr-Tm, mag. order onset, elec. resistivity 0-20416  
 (Tm,Lu)Al $_2$ , disordered alloys, cryst. field transitions, inelastic neutron scatt. obs. 0-50055  
 TmAl $_3$ , ferromagnetic structs., elastic neutron scatt. obs. 0-50055  
 TmCd(Zn), quadrupolar phase transitions, magnetoelastic and quadrupolar coupling consts. 0-15744  
 TmFe $_2$ , electronic heat capacity coeffs. 0-39787  
 TmFe $_2$ , Mossbauer  $\gamma$  eff., combination type maxima, hyperfine interactions on nuclei 0-25263

**thulium compounds**

see also thulium alloys

- mixed valence compounds, charge dominated fluctuation props. comparison, mag. moments and ordering 0-54659  
 (BiTm) $_2$ (FeGa) $_2\text{O}_{12}$ , monocrystalline films, mag. anisotropy 0-2609  
 CaSO $_4$ ·Tm/polythene mixture, thermoluminesc. response to fast neutrons 0-5340  
 Cs $_2\text{KTmBr}_6(\text{Cl}_6)(\text{F}_6)$ , Cs $_2\text{NaTmF}_6$  and Cs $_2\text{RbTmF}_6$ , mag. behaviour 2.9 to 251.3K, cryst. field levels, ang. overlap model (German) 0-29520  
 Tm(ClO $_4$ ) $_3$ , osmotic coeffs. 0-45556  
 TmCrO $_3$ , optical-absorption spectra of Tm $^{3+}$  0-20662  
 Tm $_{1-x}\text{Eu}_x\text{Se}$ , valence changes, semicond.-metal transition 0-20086  
 TmF $_3$ , thermodynamic props., galvanic cell meas. 0-21316  
 TmFe $_2$ H $_x$ , mag. props. 0-25095  
 Tm $_2\text{Fe}_2\text{O}_{12}$ , mol. field coeffs., mag. moment/temp. relations 0-50067  
 TmH,  $^1\Sigma$  state, Dirac-Fock one-centre calcs. 0-23301  
 TmH $_2$ · $^{169}\text{Tm}$  Mossbauer studies 0-44975  
 TmH $_3$ ,  $^{169}\text{Tm}$  Mossbauer study 0-44976  
 TmNbO $_4$ -CaWO $_4$ , phase transitions of fergusonite-scheelite (French) 0-19942  
 Tm(OH) $_3$ , cryst. struct. 0-24424  
 TmPO $_4$ , IR and Raman spectra 0-34904  
 TmS, metallic, thermoelec. power 0-6818  
 TmSb, metallic, elec. resistivity, 4f-quadrupole charge distrib. 0-24873  
 TmSe, intermediate valent, Raman scatt. 0-16038  
 TmSe, Kondo lattice theory 0-20380  
 TmSe, mag. neutron scatt. 0-25096  
 TmSe, mag. props. and struct. 0-25109  
 TmSe, metallic, thermoelec. power 0-6818



**thulium compounds continued**

- TmSe, mixed valence state, ferromag. alignment 0-20133  
 TmSe, susceptibility,  $Tm^{2+}$  and  $Tm^{3+}$  characts. 0-25110  
 Tm<sub>2</sub>Se, valence instabilities, antiferromag. order 0-20128  
 Tm<sub>2</sub>(SeO<sub>4</sub>)<sub>3</sub>·8H<sub>2</sub>O, thermal decomp. and IR spectra 0-3319  
 TmSe<sub>1-x</sub>Te<sub>x</sub>, mixed-valent cpd., spontaneous magnetisation 0-20392  
 TmSe<sub>1-x</sub>Te<sub>x</sub>, phase relationships and press. induced transitions 0-19771  
 TmSe<sub>1-x</sub>Te<sub>x</sub>, valence changes, semicond.-metal transition 0-20086  
 Tm<sub>2</sub>Se<sub>1-y</sub>Te<sub>y</sub>, magnetic ordering studies (*German*) 0-54882  
 Tm<sub>2</sub>Si<sub>2</sub>O<sub>7</sub>N<sub>2</sub>, lattice consts., X-ray diffr. anal. 0-28986  
 TmVO<sub>3</sub>, Jahn-Teller distortion, RF susceptibility and NMR meas. 0-44930  
 Tm<sub>2</sub>Y<sub>1-x</sub>Se, Kondo effect, Van Vleck behaviour 0-25085  
 (Y<sub>2</sub>Sm<sub>2</sub>Lu<sub>2</sub>Tm<sub>2</sub>Ca<sub>3</sub>)(Fe<sub>2</sub>Ge<sub>2</sub>)<sub>2</sub>O<sub>12</sub>, epitaxial garnet film, temp. depend. mag. props. 0-39825  
 (YEuTm)<sub>3</sub>(FeGa)<sub>2</sub>O<sub>12</sub> film, dynamic props. of bubble domains by high speed photography 0-15771  
 (YEuTm)<sub>3</sub>(FeGa)<sub>2</sub>O<sub>12</sub> garnet film, bubble domain steady state motion on a circle 0-29589  
 YEuTmGa garnet bubble film, dynamic diffuse wall deform. 0-54927

**thunderstorms**

- see also lightning*  
 atmospheric electricity supply current, solar modulation 0-17329  
 Doppler weather radar, development of weather echo props. 0-26645  
 electric field changes, rel. to ice particles orientation and alignment rapid changes 0-17330  
 electrical conductivity, contrib. of cloud and precip. particles rel. to air relaxation time 0-17332  
 ice particle surface potential, laboratory study 0-51495  
 intensity from satellite data 0-41518  
 lightning peak current meas. and recording device results (*Japanese*) 0-46288  
 lightning study using thunder meas., thunder duration rel. to strike pt. (*Russian*) 0-56532  
 Oxford, 1682 May 31, point deluge and tornado 0-51521  
 radar and VHF emission obs. of three-dimens. motion 0-46218  
 radar observation of precipitation related depolarisation 0-51453  
 Schumann resonance noise generation, expt. data appl. to thunderstorms location and atmosphere cond. profiles 0-36360  
 tropical convection in anvil clouds, hydrometeor precipitation, melting and evaporation 0-17323  
 VLF atmospherics rel. to thunderstorms at sea, nighttime effect 0-26585  
 NO<sub>x</sub> production, transport into stratosphere 0-8376

**thyratrons**

- FX2508 for off-resonance transformer charging for 250-kV water Blumlein, Experimental Test Accelerator appl. 0-23183  
 high current discharge, in thyatron, nanosec. grid extinction time (*Russian*) 0-54057  
 switch for high voltages and currents, thyatron-spark gap hybrid 0-54067

**thyristor applications**

- furnace temp. regulation circuits, for creep testing devices 0-25956  
 sound-controlled flashlamp trigger circuit (*Spanish*) 0-13175

**thyristors**

- high-output, air cooling intensification design method (*Chinese*) 0-19229  
 lifetime profile measurements in heavily doped emitter structures using electron beams 0-15538

**ticking stars *see pulsars*****tidal power stations**

- West Bengal, siltation estimation 0-31059

**tides**

- N.Adriatic Sea, Green's function of Laplace's tidal eqn. 0-17291  
 amplitude factor, phase lag at Beijing, China (*Chinese*) 0-8246  
 aquifer storage capacity determ., well tide eqn. 0-21785  
 NW Atlantic Ocean, oceanic geoid and tides derived from Geos 3 satellite data 0-3901  
 Atlantic Ocean, spatial characts. of semidiurnal internal waves in Polygon-70 test area 0-31051  
 atmosphere, rel. to O(S) excitation mechanism 0-41588  
 atmosphere lunar O<sub>1</sub> tide, detect. in geomag. lunar daily var. at Alibag and contamination by M<sub>2</sub> component 0-56355  
 atmosphere lunar tide determination, data filtering method 0-46223  
 atmospheric tidal winds, meteor data, poleward momentum transport 0-12581  
 Bight of Abaco, Bahamas, algorithmic tidal study, expt. and harmonic anal. 0-8319  
 Bight of Abaco, Bahamas, tidal model comparison with data 0-4035  
 Caracas, gravity-tide meas. rel. to Pasadena magnitudes of earthquakes 0-51344  
 Chandler wobble affected by pole tide, theory 0-51318  
 Cochin Harbour mouth, India, hydrographic characts. and tidal prism 0-41452  
 continental shelf width affecting tidal range 0-56483  
 Earth's crust, tidal displacement, Geos-3 laser ranging obs. 0-3913  
 Earth tides, global interaction with ocean tides, model 0-51319  
 Earth tides, theoretical problems, conf., Aug. 1978, Caracas, Venezuela 0-51400  
 Earth tides anal. in Peking region before 1976 July 28 Tangshan earthquake (*Chinese*) 0-3892  
 earthquakes, tidal triggering in Swabian Jura 0-12348  
 E England coast, storm surge (1978 January 11 to 12) 0-12419  
 enhanced pole tide rel. to Chandler wobble period and damping 0-21778  
 estuarine current meter data acquisition microcomputer system 0-46265  
 gauge with fast-response characts. for shallow water 0-26639  
 Ghana shelf fortnightly wave, characts. 0-26515  
 Gironde inlet and Pertuis de Maumusson, tidal effects on estuarine waters seaward dispersion (*French*) 0-8324  
 global geodynamics, Canadian contribs., 1971-79 period. 0-8262  
 gravimetric observations, effect of the Honkasalo term in tidal corrections 0-21602  
 ice shelves tidal flexure, meas. by tiltmeter 0-31050  
 Indian Ocean, sea levels in western equatorial region rel. to tides, meteorology and ocean circulation 0-4018  
 internal wave formation, vertical diffusion driving mechanism in Oslofjord 0-26531  
 Kouchibouguac Bay, New Brunswick, tides rel. to barrier island breach morphology and dynamics 0-12371  
 Laplace tidal equation, perturbation methods, Ligurian Sea application 0-26533  
 lunar tide, semidiurnal, basic physics 0-31449

**tides continued**

- M<sub>2</sub> ocean tide parameters and Moon's meas. longit. decel. from artificial satellite orbit data 0-31048  
 old Mangalore port, tides effect on estuarine and oceanic waters hydrographic conditions 0-41451  
 Mediterranean harbour tidal harmonic constants 0-41448  
 middle atmosphere dynamics, review 0-17338  
 Msf propagation and sea temperature on Guinea Gulf northern coast 0-4033  
 ocean lunar O<sub>1</sub> tide, contrib. to geomag. lunar daily var. at Alibag 0-56355  
 ocean palaeotides and nautiloid growth, rel. to Earth-Moon system dynamics 0-41713  
 ocean tidal currents, interaction with wind-generated sea waves 0-51428  
 ocean tidal interactions in region of large bottom slope, NW Africa, JOINT-1 obs. 0-4016  
 ocean tides, vol. to lunar orbit evolution 0-8565  
 Polygon-70 in Atlantic Ocean, internal tidal structure (*Russian*) 0-51411  
 radar altimeter height and timing bias report 0-46326  
 Sea of Japan, tides rel. to seawater hydrochemical characts. and transparency distrib. 0-31057  
 solar tides effect on nightglow O I 5577 Å line, intensity var. (*Russian*) 0-12585  
 solid Earth tides, Fourier anal. applied to short data length 0-30972  
 South Pole gravity tides, long period, 1970 obs. 0-21611  
 spectral modelling by finite element method (*French*) 0-21782  
 thermosphere, differential operator and integro-differential eqn. (*Chinese*) 0-56660  
 thermosphere, midlatitude, tidal modes identification from neutral wind meas. during ALADDIN programme 0-31153  
 thermosphere neutral winds, tidal modes rel. to low latit. dynamo currents seasonal vars. 0-8479  
 tidal channel, energy dissipation due to bottom friction and eddy losses 0-31058  
 Venice, sea-lagoon exchange in modified tide regime 0-12431  
 VLBI, correction for effects of troposphere, ionosphere and Earth crustal tide (*Japanese*) 0-21926  
 O and O<sub>2</sub> distrib. in lower thermosphere assuming tidal effects, one dimens. nonstationary diffusion-photochemical model 0-4160

**tight-binding calculations**

- alloys, with off-diagonal disorder, density of states and cond., CPA calc. 0-24780  
 Anderson localisation problem, cond. numerical studies 0-49673  
 BCC and simple cubic lattice, density of states of tight-binding s-bands using modified-moments method 0-15431  
 binary alloy, ordered, electronic struct. in Bethe lattice, exact analytic treatment 0-49582  
 chemisorbed atoms on transition metal surface, interaction energy calc. 0-54507  
 complex tight binding systems, surface density of states determ. 0-20272  
 diamond, nonlinear optical susceptibility, tight binding bonding orbital model 0-5784  
 dislocation scattering, new Hamiltonian for describing multivalued elastic displacement fields 0-24862  
 (ethylene)<sub>n</sub>, mol. crystals, quantum theory, mol. tight binding method calcs. 0-49572  
 ferromagnet, itinerant electron, surface spin waves, tight-binding Hubbard model 0-39763  
 first principles method for electronic props. of surfaces, interfaces and bulk solids 0-49564  
 (formamide)<sub>n</sub>, mol. crystals, quantum theory, mol. tight binding method calcs. 0-49572  
 glass, ionicity and coordination, tight binding calcs. 0-49129  
 graphite, various modifications, electronic props. 0-49592  
 graphite intercalation compounds, band struct. model, dynamical dielec. function, reflectivity 0-34348  
 graphite intercalation cpds., mag. susceptibility, tight-binding model 0-44796  
 graphite-FeCl<sub>3</sub> intercalation cpd., electronic excitation spectrum, high resolution EELS meas. 0-45182  
 Green's functions for surfaces, thin films, and solid interfaces using random-walk theory 0-54753  
 III-V semiconductor surfaces and interfaces, Green's function technique, tight binding approx. 0-49855  
 interfaces, empirical tight-binding method, critique 0-49854  
 metal, FCC, (100) surface, chemisorption-induced interaction between electronic levels of two-level adsorbate 0-39644  
 mixed valence states, excitation mechanism in tight-binding approx., metal-insulator transition 0-10925  
 one-dimensional finite chain, boundary states and vibrs., tight-binding approx. 0-2317  
 one-dimensional molecular crystals, electronic struct., mol. orbital theory 0-54588  
 orientational metal-insulator phase transitions in quadrupolar strands with itinerant electrons 0-15455  
 overlapping potentials, tight-binding rel. to scatt. theory 0-10854  
 polar semiconductor, conduction states, pseudopot. and tight-binding calcs. 0-24785  
 polyacetylene, trans- and cis-isomer, electronic struct. calcs. 0-24788  
 protein model chain, aperiodic, electronic spectra, hopping cond. 0-5641  
 quasi-one-dimensional metals, narrow-band, exchange-correlation effects on plasmons and on CDW instability 0-44525  
 random lattice, with purely off-diagonal disorder, electron localisation 0-49672  
 rare earth compounds, valence fluctuations, electron-phonon coupling effect 0-20134  
 rare-earth metal, semi-infinite surfaces with mag. struct., density of states calc. 0-10851  
 semiconductor, covalent, non-orthogonal tight-binding approach 0-2442  
 semiconductor surfaces, empirical tight-binding method, critique 0-49854  
 semiconductors, doping of amorphous tetrahedrally bonded cpds. 0-2361  
 Slater-Koster tables for f electrons 0-44461  
 static macroscopic dielectric function, tight binding calcs., density response and local field effect 0-49644  
 superconductor, magnetic, Fermi surface nesting effect on mag. instability 0-54831  
 tetrahedron method for evaluating spectral props. of solids 0-10855  
 transition metal, dichalcogenide layer cpds., bonding and phase transitions 0-34186



**tight-binding calculations continued**

- transition metal, FCC, semi-infinite, susceptibilities near (001) surface 0-15701  
 transition metal dichalcogenides, electronic struct. and band theory 0-44497  
 transition metals, amorphous, density of electronic states, effect of struct. variation due to interatomic pot. softness 0-54597  
 transition metals, cohesive and elastic props. model (*Hungarian*) 0-34120  
 transition metals, FCC, surface relax. and force consts. 0-39404  
 TTF-TCNQ, electron-electron interaction as source of metallic resist. 0-20162  
 zinc blende type ionic semiconductors, vacancies, bound state energy level calcs., tight binding approx. 0-44694  
 Ag halides, quadrupolar deformability theory by tight binding method 0-10614  
 Ag-Cu, surface segregation, electronic theory, density of states, cluster-Bethe-lattice approx. 0-49369  
 Au-Ag(Cu), surface segregation, electronic theory, density of states, cluster-Bethe-lattice approx. 0-49369  
 C, vacancy, tight-binding calc. 0-24844  
 Cd,  $Hg_{1-x}Te$ , band struct. and optical props. 0-15450  
 CdI<sub>2</sub>, electronic struct. 0-15446  
 CdTe-HgTe ideal superlattice, electronic props. calc. 0-49885  
 Ce, Compton profile study of  $\gamma$ - $\alpha$  phase transition 0-11503  
 Cr, twin and stacking fault energies calc. 0-2038  
 Cs-Au, liquid, metal-insulator transition, mag. susceptibility, Knight shift, theory 0-44672  
 Cu, Brillouin zone integration special directions, electronic density of states calcs. application 0-49569  
 Fe, twin and stacking fault energies calc. 0-2038  
 GaAs (110), adsorption of In, N, P, and As, UPS and EELS study, tight-binding calcs. 0-49496  
 GaAs (110), chemisorption of Cl, photoemission spectra and tight-binding calcs. 0-6629  
 GaAs (110), chemisorption of Al, electronic struct., tight binding calc. 0-49842  
 GaAs, surface, vacancies, bound state energy level calcs., tight binding approx. 0-44694  
 GaAs surfaces, electronic struct., tight-binding calc. 0-54755  
 GaAs-GaAlAs (100) interfaces, carrier transport coeffs., tight binding calc. 0-49889  
 GaS(Se)(Te), electronic struct. 0-15448  
 GaSb (110), chemisorption of Cl, photoemission spectra and tight-binding calcs. 0-6629  
 Ge, amorphous, ideal network struct., electronic struct., tight-binding model 0-44485  
 Ge, nonlinear optical susceptibility, tight binding bonding orbital model 0-5784  
 Ge, phonon dispersion and microscopic screening, extreme tight-binding model 0-49324  
 Ge surfaces, electronic struct., tight-binding calc. 0-54755  
 Ge, vacancy, tight-binding calc. 0-24844  
 GeO<sub>2</sub>, band struct., tight-binding calc. 0-24796  
 GeO<sub>2</sub>, electronic struct. and densities of states 0-15447  
 Ge(100) surface electronic state localisation, layer density of states calcs. 0-6931  
 (HCN)<sub>n</sub>, mol. crystals, quantum theory, mol. tight binding method calcs. 0-49572  
 InSb (110), chemisorption of Cl, photoemission spectra and tight-binding calcs. 0-6629  
 InSe, electronic struct. 0-15448  
 InSe, energy band structure, chem. bond polarity, photoemission, semiempirical tight binding method 0-44504  
 K<sub>2</sub>Fe(CN)<sub>6</sub>, electronic struct., elec. field gradient tensor 0-15483  
 MgF<sub>2</sub>, band struct., tight-binding calc. 0-24796  
 MgF<sub>2</sub>, electronic struct. and densities of states 0-15447  
 Mo, (001) surface, electronic origin of reconstruction 0-11065  
 Mo, twin and stacking fault energies calc. 0-2038  
 Ni (111), adsorption of chalcogens, angle-resolved photoemission 0-40230  
 PbI<sub>2</sub>, electronic struct. 0-15446  
 PbO<sub>2</sub>, electronic struct. and densities of states 0-15447  
 Si (100), atomic and electronic structs., energy minimisation calcr. 0-49480  
 Si (111), chemisorbed O<sub>2</sub> electronic struct. tight-binding calc., XPS and UPS meas. 0-49845  
 Si, amorphous, ideal network struct., electronic struct., tight-binding model 0-44485  
 Si, nonlinear optical susceptibility, tight binding bonding orbital model 0-5784  
 Si surfaces, electronic struct., tight-binding calc. 0-54755  
 Si, vacancy, tight-binding calc. 0-24844  
 Si<sub>3</sub>Ge<sub>1-x</sub>O<sub>2</sub>, amorphous, electronic struct. in Bethe lattice approx. 0-44487  
 SiO<sub>2</sub>, crystalline and amorphous density of states, bulk electronic struct., tight binding calcs. 0-44502  
 SnI<sub>2</sub>, band struct., layer model 0-44501  
 SnO<sub>2</sub>, band struct., tight-binding calc. 0-24796  
 SnO<sub>2</sub>, electronic struct. and densities of states 0-15447  
 SnS<sub>2</sub>(Se<sub>2</sub>), electronic struct. 0-15446  
 TaS<sub>2</sub> (1T) and (2H), bonding and charge density wave phase transitions 0-44282  
 TeO<sub>2</sub>, band struct., tight-binding calc. 0-24796  
 TeO<sub>2</sub>, electronic struct. and densities of states 0-15447  
 TiCl<sub>3</sub>, lattice instability, d-electron-lattice interaction 0-44276  
 Ti<sub>1-x</sub>Nb<sub>x</sub>H<sub>1.94</sub>, electronic struct. MNR meas. 0-15439  
 V, twin and stacking fault energies calc. 0-2038  
 W, (001) surface, electronic origin of reconstruction 0-11065  
 W, twin and stacking fault energies calc. 0-2038

timber *see wood***time and latitude**

- see also Earth rotation; time measurement*  
 daily latitude variations anal. 0-21891  
 data acquisition and real time processing system for time service (*Italian*) 0-8549  
 Ephemeris and Universal Time, empirical difference from polynomial approx. 0-17223  
 geological time and tidal friction, evidence for Earth deceleration 0-3916  
 inertial rotation sensors for surveying and geophysical meas. 0-12571  
 latitude vars. and diurnal polar motion (*Russian*) 0-51641

**time and latitude continued**

- mean latitude, Chandler, annual and semiannual wobbles, anal. of 1957-77 data 0-30974  
 Santiago astrolabe observations from 1972 to 1976; results 0-46363  
 star pair latitude obs. anal., mean pole position calc. 0-21892  
 Tokyo Astronomical Obs., Time and Latitude Bulletins (Jan-Mch. 1978) 0-17476  
 Tokyo Astronomical Obs., Time and Latitude Bulletins (July-Sept. 1978) 0-4239  
 universal time, random function determ. 0-46120  
 Universal Time in China, short-period terms 0-12648  
 Z-term of latitude variation, nutation amplitude calcs. (*Chinese*) 0-8244  
**time delay circuits** *see delay circuits*  
**time delays** *see delays*  
**time division multiplexing**  
 biomedical recording system, TDM multiplexing system for multichannel signal averaging of visually evoked responses 0-36165  
**time-domain analysis**  
 dielectric relaxation data representation by Havriliak-Negami formalism 0-15950  
 frequency stability, characterisation and meas. 0-47025  
**time-domain reflectometry**  
 methods, appl. to dielectrics 0-52310  
 precision time-domain measurement system 0-42236  
**time interval measurement** *see time measurement*  
**time measurement**  
*see also clocks; frequency measurement; streak photography; time and latitude; time resolved spectroscopy*  
 absolute motion, detection from atomic timekeeping data 0-13045  
 accelerating atomic clock synchronisation by radiowave propag., one-way Doppler effects 0-13044  
 adjustable exposure timer, circuit diagram and operation (*Hungarian*) 0-52169  
 chronobiology in plants 0-56328  
 cinematography, EBU/IRT time codes with modified setting instrument (*German*) 0-18029  
 clock comparison by laser in the nanosecond range 0-47035  
 digital freq. counters and counter-timers, new range using MSI 0-27318  
 Ephemeris and Universal Time, empirical difference from polynomial approx. 0-17223  
 frequency and time, conf., Helsinki, Finland (Aug. 1978) 0-46728  
 frequency stability, characterisation and meas. 0-47025  
 intercontinental laser synchronisation of high precision clocks via SIRIO geostationary satellite, nanosec. accuracy (*German*) 0-37000  
 international time standard coordination (*German*) 0-52171  
 international time synchronisation, precision tracking package TEMPUS, NAVSTAR satellite network appl. 0-22332  
 interval, counter design, 1 GHz, use of custom LSI 0-8973  
 interval, counter design technology 0-8974  
 interval, counter/timers, avoiding compromises in accuracy 0-8970  
 interval, counters and timers, var. in counting cct. techniques 0-8971  
 interval, universal timer-counter, design aspects 0-8972  
 interval meter, broadband, with digital display 0-31729  
 microchannel photomultiplier, with subnanosec. characts. 0-37001  
 microprocessor-based timer interval meter (*Russian*) 0-52172  
 microwave time and frequency standards 0-47026  
 national time and frequency standards of Finland 0-47031  
 photocell pulse time resolution when optical pulse shorter than photoelectron transit time, theory (*German*) 0-9035  
 precise time dissemination via OMA-50 kHz 0-47032  
 precise time recovery from Transit satellites 0-47037  
 satellite time transfer technology, review 0-47029  
 scale generation by international organizations 0-47028  
 South African measuring standard, national and international role 0-36971  
 spark gap breakdown, time-resolved resist. meas. 0-19639  
 square root of time mark generator using TTL digital ccts. for chronocoulometry 0-35588  
 standard, establishing common scale for COMECON member countries 0-42200  
 Symphonie geostationary satellite, time transfer link for atomic clock synchronisation 0-47038  
 synchronisation using ATA standard time broadcast 0-47024  
 time to amplitude converters, precision 1 GHz time calibration 0-27903  
 TV broadcasting satellite, use for precise real-time signal dissemination 0-47033  
 universal time, random function determ. 0-46120  
 using Nova satellite time signals 0-47036  
**time of flight mass spectra**  
 aliphatic perfluorocarbons, electron attachment, fragmentation 0-12 eV 0-5618  
 amino acid valine, heavy ion induced desorption, time-of-flight mass spectrometry anal. 0-54509  
 chlorobenzene ion fragmentation, kinetic shift and phenyl ion heat at formation, photoelectron-photoion coincidence meas. 0-25998  
 ethane, H<sup>+</sup>, H<sub>2</sub><sup>+</sup>, and H<sub>3</sub><sup>+</sup> kinetic energy distrib., electron impact dissociation, time of flight mass spectra 0-32843  
 ethanol, H<sup>+</sup>, H<sub>2</sub><sup>+</sup>, and H<sub>3</sub><sup>+</sup> kinetic energy distrib., electron impact dissociation, time of flight mass spectra 0-32843  
 ethylene adsorbed on Ag, photon-induced field ionisation mass spectroscopy 0-6639  
 fluorobenzene cations, fluoresc. quantum yields and lifetimes, electronic state relax. processes 0-48027  
 methane, H<sup>+</sup>, H<sub>2</sub><sup>+</sup>, and H<sub>3</sub><sup>+</sup> kinetic energy distrib., electron impact dissociation, time of flight mass spectra 0-32843  
 methanol and deuterates, H<sup>+</sup>, H<sub>2</sub><sup>+</sup>, and H<sub>3</sub><sup>+</sup> kinetic energy distrib., electron impact dissociation, time of flight mass spectra 0-32843  
 particle identification at 2-400 keV/N 0-5435  
 CO<sub>2</sub>, C 1s<sup>-1</sup>,  $\pi^*$ -state decay, fragment ion relative abundance by electron-ion coincidence technique 0-9743  
 H<sub>2</sub>(N<sub>2</sub>)(NH<sub>3</sub>) adsorbed on W, thermal desorption and pulsed time of flight mass spectra anal. 0-30285  
 LaBr<sub>3</sub>, time of flight atom-probe FIM study 0-6652  
 N<sub>2</sub>O, N 1s<sup>-1</sup>,  $\pi^*$ -state decay, fragment ion relative abundance by electron-ion coincidence technique 0-9743  
**time of flight spectra**  
*see also atom probe field ion microscopy; time of flight mass spectra*  
 alkali halides, sputtering of molecules, low-energy electron bombardment 0-35026



**time of flight spectra continued**

- electron drift velocity in counter gas mixtures 0-28590  
 fibre optic waveguides 0-23767  
 hydrocarbon, long chain single cryst., carrier transport meas. 0-6874  
 inert gas atom +  $H^+$ , electron capture, charge-state distrib. 0-32814  
 metals, microwave transmission, time-of-flight effects in Fermi vel. determ., calc. 0-20238  
 neutron meas. of direct react. spectra, resolution improvement 0-18753  
 PANSI, polarisation anal. neutron scattering instrument, description and appls. 0-23280  
 plasma metastable at. sampling from hollow cathode arc, electron temp. probe 0-43967  
 polymer film, carrier transport meas. 0-6874  
 rubrene, orthorhombic cryst. photogenerated carriers, transit time meas. 0-49811  
 Be, phonon spectrum from inelastic coherent scatt. of cold neutrons 0-10617  
 Cl ions, multiply-charged, beam-foil obs. of allowed L-shell transitions 0-14113  
 $Cl^+ + He(Ne)(Ar)$ , highly charged low vel. recoil ion time of flight spectra, cross section energy depend. 0-14222  
 $Cu_{40}Zr_{60}$ , metallic glass, dynamical struct. factor and freq. distrib. meas. 0-54136  
 H beam, low temp., direct determ. of temp. and density 0-14875  
 $\alpha$ ,  $p$ - $H_2 + Li^+$ , rot. excitation and ang. depend. transition probabilities, time of flight spectra 0-23517  
 He, positron inelastic scatt. at intermediate energies, time of flight spectra 0-18932  
 KBr surface, residence times of Au atoms, time-of-flight meas. 0-10788  
 LiF, laser-irrad., emitted electrons and positive ions delay 0-29830  
 $Mg^{8+}$ , beam-foil excited, spin orbit-forbidden X-ray transition obs. 0-23537  
 Mo surface, metastable He atom beam contamination by fast neutral atoms, effect on secondary emission 0-55253  
 $N_2 + K$  collision, electronic excitation and energy transfer, time of flight spectra 0-43151  
 NaCl, sputtering of atoms by 540 eV electrons, delay times 0-35025  
 NaCl surface, residence times of Au atoms, time-of-flight meas. 0-10788  
 $Ne + HD$ ,  $j=0$  to 1 rot. excitation, differential cross sections, time of flight obs. 0-48104  
 Ni (001) surface,  $Ne^+$  scattering and neutralisation on first and second layers 0-35045  
 $O^+ + Ne(Ar)(Kr)$ , 0.2-1 keV, elastic and inelastic reduced differential cross-sections 0-32829  
 $O_2$  photofragment, produced by  $O_3$  photolysis at 266 nm 0-50865  
 RbBr, sputtering of atoms by 540 eV electrons, delay times 0-35025  
 RbI, sputtering of atoms by 540 eV electrons, delay times 0-35025  
 Si,  $H^+$ ,  $H_2^+$  and  $He^+$  backscattering, energy spectra and charge fractions 0-35046

**time of flight spectrometers**

- associated particle type, neutron elastic scatt. by  $^{40}Ca$  and  $^{32}S$ , 2 to 3 MeV 0-13468  
 double-disc chopper with improved gating characts. 0-37120  
 dual beam fibre optic time-of-flight spectrometer 0-52347  
 fast neutron time of flight spectroscopy, multi-angle detector system 0-52810  
 gas-phase photoelectron spectrometer using synchrotron radiation 0-4818  
 high pressure sample container for thermal neutron inelastic scattering on fluids 0-37681  
 low energy ion scattering, meas. of energy spectra of neutral particles, apparatus and expts. 0-55242  
 mass spectrometer, 3-dimens., asymmetric quadrupole lens 0-4807  
 mass spectrometer, 3-dimens., quadrupole type, theory 0-4806  
 mass spectrometer ion source, electron beam collimation, rel. to resolution and sensitivity 0-42294  
 multichannel counter for molecular beam time-of-flight experiments 0-37119  
 NE213 liquid scintillator, light output for electrons and protons 0-32564  
 neutron detectors for TOF meas. with very fast burst source (French) 0-14040  
 neutron meas., rate depend. of counting losses 0-37692  
 neutron small angle scatt. on Harwell linac 0-19675  
 particle identification at 2-400 keV/N 0-5435  
 photoelectron-photoion coincidence spectrometer for the study of translational energy release distributions 0-11974  
 reactor structural material transmission meas. using TOF spectrometer 0-18440  
 telescope for high energy gamma-ray astronomy 0-31210

**time resolved spectra**

- alkyl benzenes, jet-cooled, intramol. vibr. relax., reson. fluoresc. and excitation obs. 0-14152  
 anthracene crystals,  $\alpha$ -particle induced scintillation, mag. field effects 0-40161  
 aromatic hydrocarbon in soln., excited electronic state vibr. relax., time resolved fluoresc. 0-48024  
 atomic system, temporally limited EM radiation, time integrated spectrum (German) 0-37769  
 trans-azobenzene,  $S_2 \rightarrow S_0$  fluoresc. 0-28044  
 benzene in dilute cyclohexane solution, fluoresc. quenching on pulsed proton irradi., temp. depend. 0-21307  
 benzil, excited electronic states; conformational relax., time resolved matrix isolation spectral obs. 0-32701  
 2-benzoylpyridine crystals, lowest triplet state, optically detected EPR 0-15827  
 chlorodifluoromethane, IR multiphoton dissociation,  $CF_2$  form., time-resolved optical absorption obs. 0-16702  
 coumarin 102, excited state protonation kinetics, laser pH jump and picosecond spectroscopy 0-25992  
 1,4-dibromonaphthalene, highly disordered quasi-one-dimens., excitation transport 0-34961  
 1,4-dibromonaphthalene, k-k scatt., exciton dephasing time-resolved phosphoresc. obs. 0-11458  
 discharge, capillary pulse type, spectral chronographic-equidensitometric diagnostics 0-44055  
 elastomer, segmented block, morphology, pulsed proton NMR study 0-33907  
 ethylene, excited with parametric oscillator, vibr. relax. obs. and interpret. 0-9702  
 firefly chemiluminescence emissions, time-resolved spectra 0-35822

**time resolved spectra continued**

- formaldehyde,  $T_2$ -relax., rot. transitions, time resolved spectra, microwave pulsed spectrometer study 0-18846  
 2-hydroxy, 3-allyl, 4,4'-dimethoxybenzophenone, methyl methacrylate copolymer, excitation singlet, internal  $H^+$  transfer, visible spectra 0-32728  
 2-hydroxybenzophenone, excitation singlet, internal  $H^+$  transfer, visible spectra 0-32728  
 ortho-hydroxybenzophenone, soln., intramol. proton transfer and energy relax. photostability, transient absorption obs. 0-28032  
 inert gas plasma, weakly ionised, photon echo relax. obs. in RF discharge 0-43986  
 9-iodanthracene, picosecond fluoresc. lifetimes, thermally activated  $S_1 \rightarrow T_1$  intersystem crossing 0-28045  
 methane, energy transfer obs. using excitation of fund., overtone and combination bands 0-9704  
 molecular rotational coherence, reson. collisional exchange, time-resolved microwave obs. 0-23525  
 naphthalene, triplet state time evolution after radiationless transition, initial vibronic distrib. effects 0-23450  
 naphthyl, excited electronic states; conformational relax., time resolved matrix isolation spectral obs. 0-32701  
 Nile Blue, subpicosecond spectroscopy, tunable probe, spectral dynamics 0-23429  
 NMR multiple-quantum coherence, selective excitation, appl. to benzene 0-23439  
 NMR multiple-quantum transition orders separation, using pulsed field gradients 0-50222  
 optical absorption spectrum dynamics using sub-ps. optical pulses 0-11431  
 phase fluorimetry as a probe of diffusion-controlled molecular encounters in dense fluids 0-32799  
 photothermal radiometry, contact-free condensed matter anal.,  $K_2SO_4$  powder appl. 0-26088  
 plasma formation dynamics of underexpanded supersonic erosive laser plasma flare, high speed techniques 0-48923  
 poly-2-vinylnaphthalene, soln., lowest triplet props., flash photolysis and radiolysis obs. 0-32861  
 poly-N-vinylcarbazole, soln., picosecond time-resolved fluoresc. by pulse radiolysis 0-28122  
 propynal, energy dispersion and relax., laser IR-visible double reson. 0-48023  
 rhodamine 640, subpicosecond spectroscopy, tunable probe, spectral dynamics 0-23429  
 stilbene, cis-trans photoisomerisation rate const., direct meas. 0-30250  
 stilbene, cis- and trans-, picosecond flash photolysis, intramol. charge-reson. transition obs. 0-7810  
 trans-stilbene, time resolved fluoresc. in ps. regime 0-14164  
 s-tetrazine in n-hexane, picosecond time-resolved fluoresc., vibr. relax. 0-48025  
 thionine triplet+haloanilines, electron transfer reaction, radical yield meas. 0-3330  
 time and spatially resolved at. absorpt. anal. 0-40760  
 unimolecular reactions induced by monochromatic IR radiation, intensity and laser energy fluence influence 0-11903  
 Al alloys, time and spatially resolved at. absorpt. anal. 0-40760  
 $As_2S_3$ , amorphous, time resolved spectroscopy of valence alternation pair luminesc. 0-50400  
 $As_2Se_3$ , amorphous, time resolved meas. of photoinduced optical absorpt. and photocond. 0-49807  
 $CH_3B^{2-}$  state predissoc., calcs. and time resolved spectrosc. 0-23576  
 CN monolayer on Ag, picosecond Raman gain spectroscopy 0-25351  
 CO,  $A^1\Pi(\nu=1)$ , vibr. relax. by reversible intersystem crossing, fluoresc. obs. 0-14170  
 CO, collision-induced reorientation, direct meas. by IR double reson. 0-32800  
 CO + CO $_2$ , vibr. level depend. quenching of CO( $\nu=1-16$ ) 0-32808  
 CdS, time-resolved spectra of spontaneous luminesc. from high density electron-hole plasma 0-40156  
 CdTe, time-resolved spectra, carrier relax. time, phonon lifetime 0-11433  
 Cr, pulse hollow cathode discharge, time resolved high resolution spectroscopy 0-38759  
 $CsMnF_3$ , magnon absorption and luminesc. 0-7400  
 Cu alloys, time and spatially resolved at. absorpt. anal. 0-40760  
 GaAs, time-resolved spectra, carrier relax. time, phonon lifetime 0-11433  
 $H_2$ , electron impact excited singlet-g states, optical and time resolved spectra, radiative lifetimes, quenching rates for rovibronic levels 0-23564  
 $H_2 + Ar^+(4s)$ ,  $H_2$  continuum emission, kinetic studies in  $Ar-H_2$  mixture, e-beam pumped 0-43153  
 He and  $He^+$ ,  $3^3P$  and  $4^3F$  levels excitation with electron beams, radiation decay obs. 0-43188  
 He glow discharge, low press., excitation transfer and quenching of  $n=3$  excited states 0-38743  
 He- $N_2$ , de-excitation rate consts., energy transfer, pulse radiolysis obs. 0-30303  
 $He^+ + Ne$ , ( $3^1S$ ,  $3^3S$ ,  $3^1P$ ,  $3^3P$ ) de-excitation cross section temp. depend., time resolved spectra 0-28100  
 I, produced in UV photodissoc. of alkyl iodides, time-resolved obs. of  $I(^1P_{1/2})$  reactions 0-11940  
 I + HCl, quenching of  $I(5^3P_{1/2})$ , temp. depend., time resolved at. absorpt. spectrophotometry 0-32655  
 I + methane  $d_0(d_3)$ , ( $d_4$ ), excited atoms, quenching, isotope effects, time resolved reson. fluoresc. 0-32656  
 K, s and d state radiative lifetimes, time and wavelength resolved fluoresc. spectra 0-14104  
 $KMnF_3$ , exciton dynamics by time resolved emission spectroscopy 0-54615  
 KXe, dye laser induced emission, excimer bands and uses 0-9650  
 $N_2^+$ , A- and B-states interactions, time-resolved obs. 0-18862  
 NO $_2$ , inter and intramolecular radiationless transitions, relax., time resolved excitation and fluoresc. spectra 0-27966  
 Na, diabatic field ionisation of highly excited at. states 0-43202  
 Na, reson. two-photon ionisation via  $3p^3P_{3/2}$  state, photoelectron ang. distrib. 0-43016  
 Nb + Nb, selected MO X-ray coincidence with separated at. K X-rays 0-43148  
 Ni (111), isothermal desorption of CO, UPS study, time-resolved approach 0-39440  
 $O(2^1D_2) + N_2(O_2)(N_2O)(CO_2)(H_2O)(methane)$ , collisional deactivation meas., 295K, rel. to atmospheric processes 0-16663



**time resolved spectra continued**

- $O_2(c^2\Sigma_u^-)$ , in Ar(Kr)(Ar-Kr) matrices, multiphonon vibr. relax. time-resolved emission obs. 0-18861  
 Pb alloys, time and spatially resolved at. absorpt. anal. 0-40760  
 Rb, radiative lifetime, time resolved laser induced fluorescence 0-37781  
 SF<sub>6</sub>, highly excited, time-resolved IR absorpt. obs. 0-9666  
 SF<sub>6</sub>, time-resolved IR absorpt. meas. using injection-locked single mode TEA CO<sub>2</sub> laser 0-9665  
 SO<sub>2</sub>, T<sub>2</sub>-relax., rot. transitions, time resolved spectra, microwave pulsed spectrometer study 0-18846  
 Si, amorphous, time resolved photoluminesc. near band gap 0-25445  
 Si, amorphous, time-resolved ODMR and luminesc. 0-25254  
 Si, excitonic molecules, thermodynamics, luminesc. 0-25442  
 SiC:Al(Ga)(B) (6H) LEDs, fabrication by rotation dipping technique, electrolum. mechanisms 0-50426  
 Tb(OH)<sub>3</sub>, exciton dynamics within an inhomogeneously broadened line, luminesc. spectra 0-50407  
 XeF fragment luminescence, during XeF<sub>2</sub> photodissoc. in solid Xe and Kr 0-3372  
 Y<sub>3</sub>(Al<sub>1-x</sub>Ga<sub>x</sub>)<sub>5</sub>O<sub>12</sub>:Nd<sup>3+</sup>, time-resolved site-selection spectroscopy, energy transfer 0-2814  
 Zn, excited states, collisional quenching cross sections and exit channels, fluoresc. quenching obs. 0-18919

**time resolved spectroscopy**

- see also *streak photography*  
 benzophenone L in dibromodiphenylether, benzophenone triplet state, nanosecond resolved ODMR, freq.-agile techniques appl. 0-34825  
 Brownian motion, intensity fluctuation spectroscopy appls., review 0-52129  
 cresyl violet, rot. diffusion, picosec. saturation spectrosc. obs. 0-5634  
 DODCI+malachite green (DQOCI), electronic energy transfer obs. 0-5633  
 EPR, ns time-resolved, in pulse radiolysis, via spin echo method 0-43075  
 EPR spectroscopy, stopped flow EPR apparatus for biological appl. 0-36206  
 fluorescence spectroscopy using pulsed laser excitation source 0-9051  
 fluorometric system, nanosec. time-resolved spectrometry with tunable dye laser and pulse-gated photon counter 0-11968  
 IR time-resolved spectral photography, transient broadband absorption spectra 0-18024  
 iterative Rydberg-Klein-Dunham method calcs. and Weyl theory 0-23576  
 laser saturation spectroscopy and coherent transients survey 0-9965  
 laser-based methods for transient chem. events meas. 0-40801  
 molecular, astrophys. appls. 0-21913  
 molecular spectroscopy book 0-27052  
 NMR pulsed, automatic trigger pulse logic for pulse programmer 0-47084  
 on-line computer-based system for performing time domain spectroscopy 0-271  
 photoacoustic spectroscopy, time-domain, nonradiative lifetime meas. of condensed phases 0-55232  
 photon echoes in standing-wave fields: time separation of spatial harmonics 0-9759  
 picosecond laser techniques for obs. of vibr. modes in liqs. 0-5800  
 picosecond light pulse, meas. techniques (*Japanese*) 0-52291  
 picosecond Raman techniques, vibr. dynamics in liqs. 0-52325  
 picosecond spectroscopy, methods and appls. 0-42263  
 picosecond spectroscopy of biological systems, exptl. system and rhodopsin example 0-56312  
 picosecond time-resolved fluorescence techniques using mode-locked laser system 0-27359  
 polymethine cyanine dyes, vibronic energy relax., picosec. spectrosc. obs. 0-5526  
 pulsed laser fluorescence spectroscopy for atomic and mol. excited states obs., review, book contrib. 0-9760  
 resonance Raman spectroscopy and vidicon Raman spectrography, vibr. spectra on nsec scale 0-37095  
 resonance scattering methods in atomic spectroscopy 0-53167  
 rhodopsin, picosecond spectroscopy obs. of primary events 0-56312  
 streak camera, high-sensitivity, design (*Japanese*) 0-52327  
 streak spectroscopy, in ultrahigh mag. fields (*Japanese*) 0-18021  
 subpicosecond spectroscopy, tunable probe, spectral dynamics 0-23429  
 synchrotron radiation at storage rings 0-31902  
 tetracene-Kr(Xe), intramol. intersystem crossing in supersonic beam, external heavy atom effect 0-14167  
 time-resolved absorption spectra, with picosecond laser (*Japanese*) 0-22451  
 velocity distrib. measurements using mass filter and focusing ion detector 0-4819  
<sup>57</sup>Fe Mossbauer level excitation using synchrotron radiation 0-7204  
 Kr<sub>2</sub>, prod. and decay of O<sub>u</sub><sup>+</sup> and I<sub>u</sub> states, synchrotron excited 0-43109

**time series**

- BWR stability monitoring using time series anal. of neutron noise 0-47625  
 Earth mean pole position from star pair latitude obs. anal. 0-21892  
 geomagnetic field reversals, correl. function anal. 0-21622  
 machined surface time series modelling 0-36998  
 nuclear reactor noise analysis, time series modelling methods, comparative eval. (*Japanese*) 0-13552  
 PWR noise analysis using multivariate autoregressive time series modelling 0-23028

**time varying parameters** see *time-varying systems***time-varying systems**

- radiation of uniformly moving charge on nonstationary layer 0-32893  
 signal coherent detection using multiple obs. 0-43553

**timing** see *time measurement***timing circuits**

- adjustable exposure timer, circuit diagram and operation (*Hungarian*) 0-52169  
 avalanche transistor discriminator for low energy radiations 0-5450  
 camera shutter control, use of photosensor with IC amplifier (*German*) 0-52341  
 clock timer using thermal printer for time of day readings 0-42211  
 injection diode modulated laser pulse generator and digital control cct. (*Russian*) 0-14372

**tin**

- see also *nuclei with .....*  
 adsorption on Ni (100), effects on secondary electron spectra 0-50480  
 adsorption on P or C contaminated Ni, AES study 0-54521

**tin continued**

- anodically treated in borate buffer, passive film form., Mossbauer meas. 0-39990  
 atom, nuclear K-X-ray satellites, Z=50-83, by  $\alpha$ -bombard., 17.5-22.5 MeV 0-42984  
 atom, oscillator strengths and hyperfine splitting of  $5^3D_1^0$  and  $6^3P_2^0$  levels, line absorpt. meas. 0-18818  
 atom, XPS and XES, dynamical effects 0-52924  
 Auger electron spectra, solid state effects 0-20739  
 Auger spectra expt., fine structure anal. of clean and oxidised Sn 0-29831  
 band structure of diamond like crystals, cluster-Bethe lattice model calc. 0-6713  
 binding state of atoms segregated at boundary of Fe and Fe alloys, Mossbauer study 0-7232  
 cathode, ion generation by O low pressure reactive sputtering (*Japanese*) 0-50494  
 diffusion in Fe-C, microprobe anal. of intermediate phases (*French*) 0-50596  
 diffusion in GaAs, effect of ambient As vapour press. on surface stability 0-2208  
 diffusion in liq. Sn and Pb, <sup>113,117m,125</sup>Sn diffusion coeff. meas. (*Ukrainian*) 0-10690  
 Doppler effect meas. on solid and liquid metal 0-22933  
 droplets, on Bi, Zn and Al, heterogeneous nucleation 0-44294  
 electric field gradient, Debye model calc. 0-49682  
 electroless tinning onto Cu powder 0-25607  
 electromigration in Cu 0-6557  
 electron stopping power, continuous slowing down approx., range difference for 0.2 to 10 MeV electrons 0-39187  
 extractive metallurgy, developments, review 0-20820  
 film, effect of rate of deposition on supercond. props. and struct. 0-2954  
 film, on NaCl, preferential epitaxy induced by electron bombard. or elec. field 0-10824  
 film, reactively sputtered, discharge produce evaluation, mass spectrometer obs. 0-6668  
 fine powders, electrodeposition, effect of cathodic current density on structure 0-16238  
 gamma-ray scatt., incoherent 0-40179  
 heat pipe meas. of corrosion and vapour press. 0-23878  
 heterodiffusion in n-PbSe 0-34245  
 internal friction, time-dependent 0-7610  
 ion implanted with Sn, Sb or Te, impurity-defect structs., Mossbauer expts. 0-39129  
 ion plated soft film, initial wear rate 0-11795  
 Josephson microbridge, I-V characts. microwave irradiation depend. 0-25051  
 L-shell fluorescence yield, L<sub>3</sub> subshell yield 0-47936  
 liquid, <sup>113,117m,125</sup>Sn diffusion coeff. meas. (*Ukrainian*) 0-10690  
 liquid, electrodiffusion conc. of impurities 0-54414  
 liquid, interference functions by double hard sphere model 0-49090  
 melt, structural factors, tetrahedral concs., neutron diffr. study (*German*) 0-19688  
 melt in contact with Fe, Fe distrib. on thermal cycling (*Russian*) 0-16562  
 microstrip, optically illuminated, resistive transition and supercond. props. 0-54821  
 model pseudopotential, band struct. calcs., liquid semicond. resistivity calcs. 0-20075  
 Mossbauer effect, filtered reson. radiation, time depend. 0-7216  
 nuclear susceptibility thermometry using enriched <sup>119</sup>Sn 0-4710  
 passivation films, on Sn-plate, TEM struct. obs. 0-45416  
 plate, lacquer adhesions of passivation films, adhesion, ESCA exam. of constitution and effects 0-40776  
 plate, rapid test for props. assessment 0-40650  
 plate surface, ion-bombardment conditions effect on chem. profile 0-54287  
 polymorphic transformations ( $\beta$ - $\alpha$ ), effect of impurities, exam. 0-7557  
 powders, fine, electrodeposition from choride-fluoride electrolytes 0-11598  
 saturated vapour pressure measurement by line absorpt. method in atomic absorpt. spectroscopy of SnI 0-55747  
 $\beta$ -Sn, cryst., fatigue crack propag. mechanism 0-25861  
 $\beta$ -Sn, Fermi surface, electronic momentum densities, positron annihilation obs. 0-6696  
 sound absorption giant resonance, produced by coherent mag. breakthrough (*Russian*) 0-6700  
 sound attenuation and velocity depend. on mag. field (*Russian*) 0-29446  
 stopping power for 6.75 MeV protons 0-34107  
 superconducting current carrying film, resistive region boundary movement, ambient media depend. 0-44763  
 superconducting film, energy gap suppression and instability under strong quasiparticle injection 0-7042  
 superconducting film, metastable current states, mean free path variation (*Russian*) 0-2538  
 superconducting film, paraconductivity 0-54845  
 superconducting film, phonon-injection-induced destruction of supercond. 0-6956  
 superconducting thin-film bridge, IV curves, oscill. instability and quasiparticle recomb. (*Russian*) 0-44769  
 superconducting-normal interface, boundary resist. 0-50006  
 surface impedance change, reflected RF EM wave interaction (*Russian*) 0-49867  
 target, microwave laser irradi., plasma form., inhibited electron thermal cond., laser intensity threshold Z-depend. 0-48928  
 thermal diffusivity by pulse method 0-15497  
 vacancy formation and activation volume, macroscopic model 0-54221  
 white, Fermi surface, electronic momentum densities, positron annihilation obs. 0-6696  
 wire, elastically bent, elec. resist. in mag. field 0-44568  
 X-ray diffraction study of thermal motion of atoms in  $\beta$ -Sn 0-39243  
 XPS, electronic struct. 0-7464  
 XPS, inelastic mean free path in 700 to 1200 eV range, bulk method 0-20763  
 zero-gap semiconductor,  $\alpha$ -phase props. rel. to  $\Gamma_8$  symmetry 0-6717  
 Ag-Sn multilayers, vapour quenched, supercond. transition temp. 0-20346  
 Ag-Sn proximity-effect bridges, T\* anomaly under phonon injection 0-34566  
 Ag-Sn proximity-effect bridges, phonon-injection-induced first-order transition obs. 0-39718  
 Ag-Sn thin film couple, room temp. interactions 0-2220



## tin continued

- Al/(Al<sub>2</sub>O<sub>3</sub>)-BaSn/Sn struct., internal voltage temp. variation 0-20326  
 Al-Formvar-Sn tunnel junction, mode propag. in dirty type I supercond. 0-15662  
 Al<sub>1-x</sub>Ga<sub>x</sub>As: Sn, persistent photocond., due to donor-related centres, symmetry 0-15558  
 Au/Sn films, evaporated, microstructure and texture, TEM obs. 0-39481  
 Bi-Sn, microhardness anisotropy 0-21079  
 Cu+Fe+Sn, nuclear target preparation by evaporation and rolling 0-23224  
 EuSn:Sn<sup>2+</sup>, Mossbauer spectra, Sn<sup>2+</sup> transferred hyperfine fields 0-15887  
 EuTe:Sn<sup>2+</sup>, Mossbauer spectra, Sn<sup>2+</sup> transferred hyperfine fields 0-15887  
 Fe, pure, Sn and Cr diffusion, effect of boundary struct., autoradiography study (*Japanese*) 0-49419  
 α-Fe<sub>2</sub>O<sub>3</sub>:Sn<sup>2+</sup>, antiferromag. reson. (*Russian*) 0-7175  
 Ga<sub>1-x</sub>Al<sub>x</sub>As:Sn, layer Schottky barrier, deep level spectroscopy 0-49666  
 GaAs:Sn<sup>m</sup>, Mossbauer spectra 0-29667  
 GaAs:Cr, Sn doped LPE layers, Au film deposition and annealing, Cr redistrib. 0-15312  
 GaAs:Sn, diamagnetism quenching 0-6782  
 GaAs:Sn, dopant segregation during liq. phase electroepitaxy 0-54384  
 GaAs:Sn, implantation, annealing, impurity-defect struct., Mossbauer study 0-54269  
 GaAs:Sn, MBE layers, photoluminesc. 0-29803  
 GaAs:Sn, proton implantation and annealing behaviour (*Chinese*) 0-44224  
 n-GaAs:Sn, VPE growth, reactor design 0-2956  
 GaAs:Sn diode, LPE grown, electron irradi. effect on characts. 0-39667  
 GaP:Zn, Sn doped epitaxial layers, Hall const., hole mobility and conc. 0-15143  
 Ge:Sn, Mossbauer spectra of <sup>119</sup>Sn impurity atoms 0-15935  
 H, and He, stopping powers meas. 0-42904  
 n-InAs:Sn, heavily doped, cathodoluminescence, doping effect on luminesc. band position and spectral profile 0-45153  
 In<sub>2</sub>O<sub>3</sub>:Sn, glass like thin film, electron evaporated, conductive transport (*Chinese*) 0-49960  
 In<sub>2</sub>O<sub>3</sub>:Sn films, CVD and DC sputtered, electro-reflectance meas. 0-11496  
 In<sub>2</sub>O<sub>3</sub>:Sn films, prod. by ion plating, elec. and optical props. 0-2488  
 In<sub>2</sub>O<sub>3</sub>:Sn films, pure and doped, prod. by ion plating, elec. and optical props. 0-2488  
 In<sub>2</sub>O<sub>3</sub>:Sn-Si heterojunctions, current mechanisms and barrier height 0-11083  
 α-Sn, local field, microscopic electronic polarisation 0-25283  
 NaCl-NaF:Sn<sup>2+</sup>, point defects, ionic thermal current and optical meas. 0-6403  
 Pb, melting studies by temperature wave anal. method 0-15217  
 Pb-Sn Josephson junctions, small area high current density normal resistance, RC times 0-34555  
 Si:Sn, Mossbauer spectra of <sup>119</sup>Sn impurity atoms 0-15935  
 Si:Sn, thermal conductivity, Hall mobility depend. on Sn conc., phonon-defect scatt. 0-29232  
 α-Sn, compact prep., from β-Sn containing 0.1 at.% Ge 0-55320  
 α-Sn, dielectric polarisation calcs., microscopic local fields 0-20582  
 β-Sn, elec. field gradient at <sup>111</sup>Cd, effects of high press., TDPAC meas. 0-25266  
 Sn II, oscillator strength meas. and trends in group IV homologous ions 0-42991  
 Sn, powder particle nonequiality effect on size distrib. meas. in pulse conductometric anal. 0-20833  
 Sn<sup>4+</sup>, electron density function, Thomas-Fermi calc. 0-6763  
 Sn/Cu interface, thermal conductance at low temps. 0-49436  
 Sn-Ge, amorphous, junction, current-voltage charact. 0-44725  
 Sn-Ge-Sn system, Schottky and Poole-Frenkel cond. mechanisms 0-54799  
 Sn+N<sub>2</sub>O-SnO(a<sup>2</sup>Σ)+N<sub>2</sub>, chemiluminesc. high temp. fast flow reactor obs. 0-45493  
<sup>119</sup>Sn, isotope, fractionation during zone recrystn. 0-2946  
 Sn<sup>3+</sup>(5s5p<sup>2</sup>)P<sub>1/2</sub> level, lifetime and Lande g-factor (*French*) 0-52938  
 Y<sub>3-x</sub>Ca<sub>x</sub>(Fe<sub>2-x</sub>Sn<sub>x</sub>)Fe<sub>2</sub>O<sub>12</sub>, Mossbauer spectra, Sn hyperfine mag. field 0-15893
- tin alloys**  
 see also tin compounds  
 Br<sub>2</sub>AZnMts 7-2.5-1.5-9 bronze, Mg-Al, type, fatigue and stress corrosion cracking, welding effects 0-3233  
 bronze, Al, wear on 13% Cr steel in presence of aviation fuel 0-11781  
 corrosion resist. depend. on mech. and heat treatments 0-653  
 Dilute, Fe-X-Sn, Mossbauer meas. of Sn interaction with solute atoms 0-15856  
 mag. props. from Mossbauer effect obs. (*Japanese*) 0-15933  
 Wood's alloy, liq. enthalpy effects when solute is added 0-39314  
 Zircaloy, H absorption, Sn(Fe)(Cr)(Ni) effect 0-49527  
 Zircaloy-2, tritium diffusion 0-32341  
 Ag-Sn (6.82)(11) wt.%, splat-quenched, X-ray line broadening 0-40397  
 Ag<sub>3</sub>Sn-Hg, metallic powder-liquid system, correlation between hardness and evolution and sintering states 0-25614  
 Al-Cu-Sn, ageing process, effect of Sn atoms, <sup>119</sup>Sn Mossbauer spectra obs. 0-7598  
 Al-Ge-Sn, thermodynamic props. of mixing of binary systems, phase diagram 0-45275  
 Al-Sn, binary metallic melt, deviation from the Kopp law, specific heat (*Russian*) 0-39305  
 Al-Sn, conc. profiles across solid-liq. interfaces 0-55382  
 Al-Sn, liquid, surface tension, size effect (*French*) 0-15341  
 Al-Sn alloys, heat treatment effect on <sup>119</sup>Sn Mossbauer spectrum 0-7228  
 Al-Sn liquid alloys, diffusion of Ge, mechanism (*Russian*) 0-15276  
 AuSn, XPS, electronic struct. 0-7464  
 AuSn<sub>2</sub>, core-level binding energy shifts and charge transfer 0-25268  
 Bi-Sn, dilute, oxidation kinetics 0-25914  
 Bi-Sn, maximum diamagnetism rel. to electron density 0-54865  
 Bi-Sn, thermoelec. props. from 2 to 300K 0-24872  
 Bi-Sn, thermopower from 50 mK to 25K 0-24880  
 Bi-Sn melt structure, radial distrib. function of atoms, anal. (*Russian*) 0-14995  
 Cd-Sb-Sn ternary system, phase equilib. 0-16266  
 Cd-Sn, binary metallic melt, deviation from the Kopp law, specific heat (*Russian*) 0-39305  
 Cd-Sn-(Pb) liquid (0.03 to 0.10 at.% Cd), Cd activity coeffs., interaction parameters, EMF depend. on temp. 0-49383

## tin alloys continued

- CeIn<sub>3-x</sub>Sn<sub>x</sub>, scaling behaviour near valence instability, mag. susceptibility and mag. transitions 0-25111  
 CeIn<sub>3-x</sub>Sn<sub>x</sub>, electrical resist. and thermal expansion meas., 1.5-300K 0-34400  
 Ce<sub>1-x</sub>La<sub>x</sub>Sn<sub>3</sub> (x=0 to 1), mag. susceptibility and magnetisation, lattice parameters, X-ray and neutron diffr. meas. 0-49675  
 CeSn<sub>3</sub>, induced magnetic form factor, polarised neutron studies 0-25078  
 CeSn<sub>3</sub>, mag. susceptibility and magnetisation, lattice parameters, X-ray and neutron diffr. obs. 0-49675  
 CeSn<sub>3</sub>, polarised neutron study of induced magnetisation 0-34594  
 Ce<sub>2</sub>Sn<sub>3</sub>, low temp. modification with tetragonal struct. 0-1963  
 Cr bronze Sn, recrystn. props., hot rolling, annealing, polygonisation (*Russian*) 0-55419  
 Cs-Sn alloy, peritectic reactions, phase diagram (*Russian*) 0-40784  
 Cu-Nb<sub>3</sub>Sn superconducting composite, crit. props., AC hysteretic losses 0-50014  
 Cu-Nb-Sn, multifilamentary supercond. composite wires, fabrication on laboratory scale and mech. props. 0-29897  
 Cu-Nb-Sn system, phase equilibria and supercond. props. (*Russian*) 0-50589  
 Cu-Ni-Sn, liq. alloy, calc. and anal. of mixing enthalpies (*German*) 0-44325  
 Cu-Ni-Sn, liq. alloy, mixing enthalpies determ. using a SETARAM high temp. calorimeter (*German*) 0-44324  
 Cu-Ni-Sn (10, 6 wt.%), temp. depend of yield stress and work hardening 0-21026  
 Cu-Ni-Sn (4-15, 4-8 wt.%), strip strengthened by spinodal decomp., stress relax. in bending 0-7616  
 Cu-Ni-Sn (9, 6 wt.%), decomposition, initial stages, TEM study 0-2992  
 Cu-Ni-Sn spinodal substitute for Be-Cu alloy 0-35217  
 Cu-Sn, amorphous, electron-phonon interaction effect on thermopower 0-29393  
 Cu-Sn, dil., oxide film form. in ammoniacal Cu(II) solns., AES obs. 0-45415  
 Cu-Sn (25 wt.%), liq., struct. from thermodynamic and diffr. studies 0-6350  
 Cu-Sn warm pressed compact prep. 0-35136  
 Cu-Sn-P (5, 1-5 wt.%), effect of P on friction and wear characts. 0-16494  
 Cu-Sn-(Al), quenched and aged, struct. of phases (*Russian*) 0-49184  
 Cu-Zn-Sn (24-34, 1.0 wt.%), cold-worked microstruct., X-ray diffr. obs. 0-3088  
 e-(Cu<sub>2</sub>Sn)-Cu diffusion couples, growth of intermediate phase layers (*Japanese*) 0-49431  
 Fe-As-Sn, Sn additions to Fe-As melts, influence on surface tension and density (*Russian*) 0-15337  
 Fe-As-Su-Si (Cr)(Mn) melts, As and Sn distrib., Si, Cr, and Mn influence (*Russian*) 0-16274  
 Fe-Sn, grain boundary embrittlement by Sn segregation, Mossbauer study 0-7239  
 Fe-Sn, segregation of Sn, kinetics, theory 0-11649  
 α-Fe-Sn alloy, grain boundary hardening and segregation 0-55417  
 Fe-Sn system, Sn binding state, using segregated <sup>119m</sup>Sn, Mossbauer anal. (*Japanese*) 0-20525  
 Fe, Sn<sub>1-x</sub>, amorphous alloy, Mossbauer spectra, charge transfer and atomic vol. effects 0-39959  
 Ga-Cu-Sn solders, exam. of structural transformations due to hardening, heat treatment (*Russian*) 0-7578  
 Ga-Ge-Sn, thermodynamic props. of mixing of binary systems, phase diagram 0-45275  
 GdSn<sub>3</sub>, Neel temp., hydrostatic press. depend. 0-29549  
 Hg-Ag-Sn, dental amalgams, corrosion penetration in crevices 0-3238  
 In-Pb-Sn system, thermal anal. 0-35162  
 In-Sn, binary metallic melt, deviation from the Kopp law, specific heat (*Russian*) 0-39305  
 In-Sn, dil., intermediate state, doping effect on US attenuation 0-2522  
 In-Sn alloy, Lifshits transition, electron-phonon interaction 0-29502  
 In<sub>3</sub>Sn, anisotropy of upper crit. field 0-20360  
 La<sub>1-x</sub>Ce<sub>x</sub>Sn<sub>3</sub>, electrical resist. and thermal expansion meas., 1.5-300K 0-34400  
 (LaNd)Sn<sub>3</sub>, containing Nd impurities, supercond. and normal state props. 0-49967  
 LaSn<sub>3</sub>, inelastic neutron scatt. 0-11165  
 LaSn<sub>3</sub>, mag. susceptibility and magnetisation, lattice parameters, X-ray and neutron diffr. obs. 0-49675  
 LaSn<sub>3</sub>, Tb and Pr substituted, superconductors, cryst. field transitions line-widths 0-24854  
 La<sub>2</sub>Sn<sub>3</sub>, low temp. modification with tetragonal struct. 0-1963  
 La<sub>1-x</sub>Tb<sub>x</sub>Sn<sub>3</sub>, paramag. anisotropy of Tb<sup>3+</sup> in cubic cryst. field 0-15687  
 Nb/Cu-Sn-Mg, superconductor, effect of Mg addition to Cu-Sn matrix 0-25028  
 Nb-Sn-C, phase equilib. and supercond. 0-50593  
 Nb<sub>3</sub>Sn, A-15 struct. Nb based superconductors, irradi. type influence on radiation defects 0-15093  
 Nb<sub>3</sub>Sn, alloying agent influence on struct. and supercond. props. (*Russian*) 0-39698  
 Nb<sub>3</sub>Sn, atomic displacements induced by radiation damage, X-ray study 0-2085  
 Nb<sub>3</sub>Sn, composite supercond., powder metallurgical prep. 0-2981  
 Nb<sub>3</sub>Sn cryotron, thermally controlled, used in transformer-rectifier flux pump for superconducting magnet 0-4727  
 Nb<sub>3</sub>Sn, Cu admixture in Sn bath effect on critical current and stability temp. 0-7059  
 Nb<sub>3</sub>Sn, current carrying capacity increase by Hf addition 0-7056  
 Nb<sub>3</sub>Sn, electron-lifetime effects on props. 0-10951  
 Nb<sub>3</sub>Sn fatigue effects in unidirectional composites, computer simulated model 0-35289  
 Nb<sub>3</sub>Sn films, deposition by quasi-closed vol. method, supercond. crit. temp. 0-15645  
 Nb<sub>3</sub>Sn, flux trapping and shielding capabilities in transverse fields 0-15667  
 Nb<sub>3</sub>Sn, high-current A-15 microcomposite material 0-44781  
 Nb<sub>3</sub>Sn, high-rate sputter-deposited, effect of oxygen on microstruct. 0-20343  
 Nb<sub>3</sub>Sn monofilamentary wires, supercond. crit. current density, bending effects 0-50018  
 Nb<sub>3</sub>Sn, multifilament conductors appl., production and props. (*German*) 0-3081  
 Nb<sub>3</sub>Sn, multifilament superconductor, pulsed mag. field losses and critical current densities 0-54853



## tin alloys continued

- Nb<sub>3</sub>Sn, O<sup>4+</sup> bombarded, Mossbauer studies 0-2672  
 Nb<sub>3</sub>Sn, supercond., thin film, US attenuation of SAWs 0-49988  
 Nb<sub>3</sub>Sn, superconducting, optical props. and electron-phonon interactions 0-2510  
 Nb<sub>3</sub>Sn superconducting composite, bronze process, metallurgy 0-3004  
 Nb<sub>3</sub>Sn, superconducting thin films, energy gaps from tunnelling meas. 0-25050  
 Nb<sub>3</sub>Sn superconducting wire, fabrication from Cu-Nb-Sn alloy using controlled high temp. gradient 0-25056  
 Nb<sub>3</sub>Sn-Cu, high-current A-15 microcomposite material 0-44781  
 Nb<sub>3</sub>Sn film, critical currents due to microwave field 0-25058  
 Nb<sub>3</sub>(Sn-Al) system, X-ray spectroscopic studies of electronic struct. of A15 cpds. 0-2900  
 Nb<sub>3</sub>Su-Cu supercond. composites, fabrication, magnet appl. 0-11602  
 NdSn<sub>3</sub>, magnetoresistance 0-24877  
 NdSn<sub>3</sub>, Neel temp., hydrostatic press. depend. 0-29549  
 Ni-Ti, Nitinol memory material heat engine, comment on efficiency 0-3529  
 Ni-Ti, Nitinol memory material heat engine, reply to comments on efficiency 0-3530  
 Ni<sub>3</sub>Fe-Sn, dil., atomic order detection by <sup>119</sup>Sn spectroscopy 0-39993  
 Ni<sub>2</sub>Mn<sub>1-x</sub>M<sub>1-x</sub>Sn (M=Ti,V) mag. hyperfine fields, <sup>119</sup>Sn Mossbauer spectra study 0-55003  
 Ni<sub>2</sub>MnSn, ferromag. Heusler alloy, electronic struct., spin polarisations, theory 0-54598  
 Ni<sub>2</sub>Mn<sub>1-x</sub>Ti<sub>x</sub>Sn, Mossbauer spectra, mag. hyperfine field 0-15857  
 Pb-Sn, eutectic, superplastic behaviour, grain size effect 0-7635  
 Pb-Sn eutectic, strain rate sensitivity index, expt. comparison of different methods 0-3144  
 Pb-Sn system, soft solder, elec. and thermal cond. at low temps., superconducting transition temp. 0-20150  
 Pb-Sn-Bi-Cd low melting point alloy block for organ shielding in radiotherapy (Korean) 0-36154  
 Pb-Tl-Sn melt, short-range order struct. 0-49088  
 Pd<sub>2</sub>MnSn, ferromag. Heusler alloy, electronic struct., spin polarisations, theory 0-54598  
 Pd<sub>2</sub>Mn<sub>0.95</sub>Sn<sub>1.05</sub>, hyperfine mag. fields, Mossbauer spectra 0-15870  
 Pd<sub>2</sub>MnSn<sub>1-x</sub>Sb<sub>x</sub>, Mossbauer spectra, mag. hyperfine field 0-15868  
 PrSn<sub>3</sub>, magnetoresistance 0-24877  
 PrSn<sub>3</sub>, Neel temp., hydrostatic press. depend. 0-29549  
 Pr<sub>2</sub>Sn<sub>3</sub>, low temp. modification with tetragonal struct. 0-1963  
 Pt-Sn, Fermi energy influence on thermodynamic props. (German) 0-24619  
 Pt-Sn melts, surface tension and density (Russian) 0-39388  
 Pt-Sn/Al<sub>2</sub>O<sub>3</sub> catalyst, Mossbauer effect, reactivity 0-11298  
 Ru<sub>2</sub>FeSn, hyperfine mag. field, Mossbauer spectra 0-15865  
 Sb-Sn (0.5 to 1.0 at.%), carrier transport, magnetoresistivity, field-dependent tensor study 0-39609  
 Sn-Bi, crystal struct. and superconductivity after appl. of high press. and quenching 0-10531  
 Sn-Bi, eutectic, superplastic anisotropy (German) 0-25808  
 Sn-Bi fine alloy powder, electrodeposition, electrolyte comp. effect 0-7519  
 Sn-Co alloy plating from sulphate electrolyte 0-16597  
 Sn-Ni, electrodeposit, Mossbauer meas. 0-39990  
 Sn-Pb composition anal. of PCBs using beta-backscatter gauge 0-16631  
 Sn-Pb eutectic, strain rate sensitivity of flow stresses, grain boundary sliding during superplastic, non-superplastic deform. 0-7645  
 Sn-Pb solder on Cu plate, spreadability, effect of fluoride and iodide addition to ZnCl<sub>2</sub> flux (Japanese) 0-29251  
 Sn-Sb, A1-type, superconductivity 0-29496  
 Sn-Sb (10 wt.%), decomposition of supersaturated solid soln. 0-29960  
 Sn-Sb alloys electrodeposition 0-25586  
 Sn-Sb-Ag, splat cooled foils, TEM study 0-40344  
 Sn-Zn melts, plasticising action in deform. hardening of medium C steel 0-55415  
 Th<sub>0.99</sub>In<sub>0.01</sub>, superconducting-normal interface, boundary resist. 0-50006  
 ThSn<sub>3</sub>, inelastic neutron scatt. 0-11165  
 Ti-Al system, compact growth in liquid phase sintering 0-20835  
 Ti-Al-Mo-Cr-Fe, distrib. of Sn, Zr between phases, temp. effect. 0-55357  
 Ti-Al-Mo-Sn alloy, elastically and plastically deformed, positron annihilation meas. of deformation 0-21038  
 Ti-Al-Sn, type Ti-5621S, irradi. induced creep 0-39163  
 Ti-Al-Sn (5, 2.5 wt.%), annealing of near-basal hydrides 0-20989  
 Ti-Al-Sn (5, 2.5 wt.%), corrosion resist. in marine environments (French) 0-50767  
 Ti-Al-Sn-Zr-Mo (6, 2, 4, 6 wt.%),  $\alpha$ - $\beta$  type 6246, fusion zone fracture behaviour in weldments 0-30093  
 Ti-Al-Sn-Zr-Mo alloy, Ti-6242,  $\alpha$ + $\beta$ , creep property improvement by Pt in plating 0-16408  
 Ti-Al-Sn-Zr-Mo-Si (6, 2, 4, 2, 0.1 wt.%), effect of elevated temperature and environment on fatigue crack growth 0-40486  
 Ti-Al-V-Sn (6, 6, 2 wt.%) weldments, heat treated, transangular fracture 0-40524  
 Ti-Al-V-Sn (6, 6, 2 wt.%), fatigue crack growth, cyclic freq. and microstruct. influence 0-55515  
 Ti-Al-V-Sn (6, 6, 2 wt.%),  $\alpha$ - $\beta$  type 662, fusion zone fracture behaviour in weldments 0-30093  
 Ti-Al-V-Sn (6, 6, 2 wt.%), depend. of K<sub>ISCC</sub> on loading rate and crack orientation 0-45427  
 Ti-Al-V-Sn (6, 6, 2 wt.%) solid metal embrittlement by Cd, Ag and Au 0-16551  
 Ti-Al-V(Sn) alloys, plastic deformation and fracture characts. at low temps. (Russian) 0-7624  
 Ti-Mo-Zr-Sn (11.5, 6, 4.5 wt.%), metastable beta III phase, recrystallization and grain growth 0-3091  
 $\alpha$ -Ti-Sn, Mossbauer spectra, metastable  $\theta$ - and  $\omega$ -phases 0-20556  
 Ti-Sn, porous, effect of Al and Sn on sintering 0-20830  
 USn<sub>3</sub>, crystalline elec. field studies using neutron inelastic scatt. at NRCN 0-10931  
 USn<sub>3</sub>, inelastic neutron scatt. 0-11165  
 V-Sn-C, phase equilib. and supercond. 0-50593  
 Zircaloy-4, vapour transport of Zr and Si 0-55437  
 Zn-Sn, binary metallic melt, deviation from the Kopp law, specific heat (Russian) 0-39305  
 Zn-Sn-Hg, diagram of state, melting temp., peritectic and eutectic phases (Russian) 0-55350  
 Zr-Nb-Sn (3.0, 1.0 wt.%), oxidation kinetics in flowing CO<sub>2</sub>, 873 to 1173K 0-16596

## tin alloys continued

- Zr-Nb-Sn (3 wt.%, 1 wt.%), oxidation kinetics in flowing CO<sub>2</sub> at high temp. 0-47575  
 Zr-Sn, grain-boundary migration during fatigue at 600 to 775°C 0-16443
- tin compounds**  
 see also tin alloys  
 chalcogenides, screw dislocations in layer crystal growth from vapour (Russian) 0-1953  
 dimethyl stannous chloride di(pyridine 1-oxide), <sup>119</sup>Sn Mossbauer spectra, elec. field gradient 0-15909  
 dimethyl tin diisothiocyanate, <sup>119</sup>Sn Mossbauer spectra, elec. field gradient 0-15909  
 oxalate cryst. struct. determ. by X-ray crystallography, relations with Na<sub>2</sub>C<sub>2</sub>O<sub>4</sub>, Na<sub>2</sub>Sn(C<sub>2</sub>O<sub>4</sub>)<sub>2</sub> (French) 0-2004  
 sodium tin oxalate, cryst. struct. rel. to those of Na<sub>2</sub>C<sub>2</sub>O<sub>4</sub>, SnC<sub>2</sub>O<sub>4</sub> (French) 0-2004  
 tetrahalides of Gp.IV elements, M-X bond flexibility, by compliance scheme 0-37805  
 trimethyl tin cyanide, <sup>119</sup>Sn Mossbauer spectra, elec. field gradient 0-15909  
 tris(trimethylstannyl)phosphine, gamma irradi., free radicals, struct. and EPR spectra 0-29623  
 AgIn<sub>2</sub>Sn<sub>2</sub>, spinel phase Ag<sub>2</sub>In<sub>2</sub>Sn<sub>1-x</sub>S<sub>2</sub> obs., stoichiometry (French) 0-44326  
 CdO-SnO<sub>2</sub> film, DC reactively sputtered, transparent electrode props., optimum sputtering conditions 0-11116  
 CdO-SnO<sub>2</sub> film, prep. by RF sputtering, elec. cond. and transparency 0-7492  
 CuInS<sub>2</sub>-SnS<sub>2</sub>, spinel phase Cu<sub>2</sub>In<sub>2</sub>Sn<sub>1-x</sub>S<sub>2</sub> obs., stoichiometry (French) 0-44326  
 Cu<sub>2</sub>SnS<sub>3</sub>-CdSe, diamond-type semiconductor, Mossbauer spectrum of <sup>119</sup>Sn 0-44991  
 (Cu<sub>2</sub>SnS<sub>3</sub>)<sub>1-x</sub>(3CdS)<sub>1-x</sub>, diamond-type semiconductor, Mossbauer spectrum of <sup>119</sup>Sn 0-44991  
 (Cu<sub>2</sub>SnS<sub>3</sub>)<sub>1-x</sub>(3ZnS)<sub>1-x</sub>, diamond-type semiconductor, Mossbauer spectrum of <sup>119</sup>Sn 0-44991  
 Cu<sub>2</sub>SnSe<sub>3</sub>-CdS, diamond-type semiconductor, Mossbauer spectrum of <sup>119</sup>Sn 0-44991  
 (Cu<sub>2</sub>SnSe<sub>3</sub>)<sub>1-x</sub>(Cu<sub>2</sub>SnS<sub>3</sub>)<sub>1-x</sub>, diamond-type semiconductor, Mossbauer spectrum of <sup>119</sup>Sn 0-44991  
 Fe<sub>3</sub>-Sn<sub>2</sub>O<sub>4</sub>, mag. hyperfine fields, <sup>57</sup>Fe and <sup>119</sup>Sn Mossbauer spectra 0-39944  
 In<sub>2</sub>O<sub>3</sub>-SnO<sub>2</sub>/GaAs, solar cell, fabrication, characts. and interfacial chemistry 0-21401  
 In<sub>2</sub>O<sub>3</sub>-SnO<sub>2</sub>/InP, solar cell, fabrication, characts. and interfacial chemistry 0-21401  
 In<sub>2</sub>O<sub>3</sub>-SnO<sub>2</sub>/Si solar cells, antireflection props. of oxide film 0-3513  
 In<sub>2</sub>O<sub>3</sub>-SnO<sub>2</sub>/SiO<sub>2</sub>/Si diode solar cells, loss mechanisms, characts., band struct. 0-26135  
 (In<sub>1-x</sub>Sn<sub>x</sub>)<sub>2</sub>O<sub>3</sub>-Si solar cell efficiency and elec. props. 0-35676  
 In<sub>2</sub>-Sn<sub>2</sub>O<sub>3</sub>-y-CdTe(InP) photovoltaic heterojunctions, surface and interface studies, efficiency 0-45691  
 In<sub>2</sub>-Sn<sub>2</sub>O<sub>3</sub>-y-ZnS:Mn thin film structure, surface morphology and electro-optical props. (Russian) 0-49554  
 In<sub>2</sub>-Sn<sub>2</sub>O<sub>3</sub>-y(SnO<sub>2</sub>)-CdSe-CdS:Cd,Cl sandwich photoconductor injection obs. (Russian) 0-54773  
 KCl:SnCl<sub>2</sub>, X-ray irradi., polarised luminesc. and EPR study of Sn<sup>3+</sup> centres 0-39868  
 La<sub>0.98</sub>Sn<sub>0.02</sub>Mo<sub>6</sub>Se<sub>8</sub>, Mossbauer spectra 0-15926  
 Na<sub>2</sub>In<sub>2</sub>Sn<sub>2</sub>S<sub>2</sub>, intercalation-substitution compounds, NMR study 0-44952  
 Na<sub>2</sub>O-Al<sub>2</sub>O<sub>3</sub>-SnO<sub>2</sub>-SiO<sub>2</sub> glass, chemical stability in NaOH and Na<sub>2</sub>CO<sub>3</sub> solns. 0-16532  
 Na<sub>2</sub>O-SiO<sub>2</sub>-Ga<sub>2</sub>O<sub>3</sub>-Al<sub>2</sub>O<sub>3</sub>-B<sub>2</sub>O<sub>3</sub>-SnO<sub>2</sub> glasses, ion exchange reactions with NaNO<sub>3</sub> and KNO<sub>3</sub> melts 0-16673  
 Na<sub>2</sub>O-SnO<sub>2</sub>-ZrO<sub>2</sub>-SiO<sub>2</sub> glass, chemical stability in NaOH and Na<sub>2</sub>CO<sub>3</sub> solns. 0-16532  
 POCl<sub>3</sub>-SnCl<sub>4</sub>, splitting of Sm<sup>3+</sup> near IR absorpt. bands 0-2750  
 (Pb, Sn)Te-type semiconductors, displacive ferroelec. phase transitions, vibronic theory 0-11354  
 Pb-Sn-Te, solid solution, scattering mechanism of carriers 0-49710  
 p-Pb<sub>1-x</sub>Sn<sub>x</sub>Te, carrier mobility, acoustical phonon and impurity scatt., deform. impurity const., conc. depend. 0-39570  
 Pb<sub>1-x</sub>Sn<sub>x</sub>F<sub>2</sub>, ionic cond. of F ion (French) 0-6547  
 n-Pb<sub>0.94</sub>Sn<sub>0.06</sub>Se solid solns., Burstein-Moss effect and energy band struct. 0-40118  
 n-Pb<sub>1-x</sub>Sn<sub>x</sub>Se, absorption spectra investigation 0-2768  
 Pb<sub>1-x</sub>Sn<sub>x</sub>Se, band struct. and transport props., hydrostatic press. effects 0-15452  
 Pb<sub>1-x</sub>Sn<sub>x</sub>Se, displacive transition, temp. and press. depend., elec. meas. 0-10672  
 Pb<sub>1-x</sub>Sn<sub>x</sub>Se laser, optical feedback effects on performance, external cavity modes 0-32981  
 Pb<sub>1-x</sub>Sn<sub>x</sub>Se, material props. and use in diode lasers, review 0-5732  
 Pb<sub>1-x</sub>Sn<sub>x</sub>Se, n- and p-type, with band inversion, study of transport phenomena 0-49741  
 Pb<sub>1-x</sub>Sn<sub>x</sub>Se, small gap, band-edge parameters 0-49594  
 PbSnTe, Magneto transport anomalies at low carrier densities, Wigner crystallisation 0-20222  
 Pb<sub>0.41</sub>Sn<sub>0.59</sub>Te, Hall coeff., elec. cond. meas. 0-44615  
 p-Pb<sub>0.65</sub>Sn<sub>0.35</sub>Te, transport coeffs. and dispersion law 0-44629  
 Pb<sub>0.76</sub>Sn<sub>0.24</sub>Te single crystals, current-voltage characts. at He temps. 0-20197  
 Pb<sub>0.78</sub>Sn<sub>0.22</sub>Te:In epitaxial layers, dislocation density, Hall effect, conductivity, photoeffects 0-25024  
 Pb<sub>0.8</sub>Sn<sub>0.2</sub>Te, single cryst. and epitaxial film, far IR refl. spectra, carrier density, Hall const., and plasma freq. 0-20629  
 Pb<sub>0.8</sub>Sn<sub>0.2</sub>Te, susceptibility effective mass, carrier conc. depend. 0-20069  
 Pb<sub>0.8</sub>Sn<sub>0.2</sub>Te-Pb, Schottky barrier form., Auger depth profiling and I-V meas. 0-49903  
 Pb<sub>0.82</sub>Sn<sub>0.18</sub>Te, thermomagnetic, thermoelectric props., valence band struct. (Russian) 0-54724  
 Pb<sub>1-x</sub>Sn<sub>x</sub>Te, (x<0.35), permittivity and soft modes, carrier density and comp. effects 0-7256  
 Pb<sub>1-x</sub>Sn<sub>x</sub>Te anodic oxide film form. conditions, IR absorpt. spectra 0-11494  
 Pb<sub>1-x</sub>Sn<sub>x</sub>Te, anomalous resist. near ferroelec. phase transition 0-20196  
 Pb<sub>1-x</sub>Sn<sub>x</sub>Te, band struct. changes due to displacive phase transition, Hall coeff. meas. 0-10671



## tin compounds continued

- Pb<sub>1-x</sub>Sn<sub>x</sub>Te DH laser, minority carrier lifetimes and lasing thresholds 0-19031  
 Pb<sub>1-x</sub>Sn<sub>x</sub>Te, Faraday effect and electron gas magnetisation, Kane two band model calcs. (*Russian*) 0-34899  
 Pb<sub>1-x</sub>Sn<sub>x</sub>Te film, sputtered, for IR detector appl. elec. and optical props. 0-35084  
 Pb<sub>1-x</sub>Sn<sub>x</sub>Te films, size quantisation, optical orientation of free carriers 0-20725  
 Pb<sub>1-x</sub>Sn<sub>x</sub>Te heterojunction lasers, instantaneous vacuum evaporation grown, threshold current density 0-5759  
 Pb<sub>1-x</sub>Sn<sub>x</sub>Te, inter- and intraband magneto-optical transitions 0-25346  
 Pb<sub>1-x</sub>Sn<sub>x</sub>Te LPE grown heterostructures, dislocation etch pitch, interfaces 0-2023  
 Pb<sub>1-x</sub>Sn<sub>x</sub>Te, narrow gap, many-body interaction effects, Bloch electron scatt. lifetimes, energy renormalisation 0-49637  
 Pb<sub>1-x</sub>Sn<sub>x</sub>Te, photoelec. props. 30 to 4.2K, temp. depend. of electron density 0-20246  
 Pb<sub>1-x</sub>Sn<sub>x</sub>Te single crystals, selection using travelling solvent method (*German*) 0-2936  
 Pb<sub>1-x</sub>Sn<sub>x</sub>Te, small gap, band-edge parameters 0-49594  
 Pb<sub>1-x</sub>Sn<sub>x</sub>Te, surface photo-EMF under laser excitation conditions 0-6897  
 p-Pb<sub>1-x</sub>Sn<sub>x</sub>Te, thermoelec. power, carrier conc. and temp. depend., inter-band scatt. 0-24957  
 Pb<sub>1-x</sub>Sn<sub>x</sub>Te, VPE growth control by EM irradi. (*Russian*) 0-34338  
 Pb<sub>1-x</sub>Sn<sub>x</sub>Te: Mn, Mn mag. and elec. active states, mag. impurity behaviour 0-44627  
 Pb<sub>1-x</sub>Sn<sub>x</sub>Te: Cd, impurity photocond. spectra 0-6902  
 Pb<sub>1-x</sub>Sn<sub>x</sub>Te: Cd, photocond., photomag. effect, carrier lifetimes 0-44658  
 Pb<sub>1-x</sub>Sn<sub>x</sub>Te: Cd, photoelec. props., surface recomb. effect 0-44659  
 Pb<sub>1-x</sub>Sn<sub>x</sub>Te: In, carrier spectroscopic g-factors, magnetoresistance, temp. depend. 0-6705  
 Pb<sub>1-x</sub>Sn<sub>x</sub>Te: In, energy spectra modifications due to comp. changes and press. appl. 0-10915  
 Pb<sub>1-x</sub>Sn<sub>x</sub>Te: In, semiconductor-metal-semiconductor transitions under press. 0-34491  
 Pb<sub>1-x</sub>Sn<sub>x</sub>Te: In, with low carrier conc., transport phenomena 0-49783  
 Pb<sub>1-x</sub>Sn<sub>x</sub>Te: In epitaxial layers, growth, elec. props., and luminesc. 0-54542  
 Pb<sub>1-x</sub>Sn<sub>1-x</sub>Te, for appl. in IR detector arrays, comp. control 0-31872  
 Pb<sub>1-x</sub>Sn<sub>1-x</sub>Te, thin film, oxidation, appl. of Mossbauer method 0-45410  
 PbSnTe(Se) Schottky barrier diode and n-p diffused junction IR detectors, comparison 0-9039  
 PbTe-SnTe, solid soln., enthalpy of formation (*Russian*) 0-15267  
 PbTe-SnTe compound semiconductors, lattice instability by mm-wave magnetoplasma refl. 0-54336  
 p-Si-In<sub>1-x</sub>Sn<sub>x</sub>O<sub>3-y</sub> solar cells, thermal degradation mechanisms 0-55841  
 Sn (II) compounds, Mossbauer spectra, direct population of solid-state bands 0-15005  
 Sn (IV) in glassy aq. soln., Mossbauer spectra 0-15894  
 Sn-F system, partial phase diagram construct. in Sn-SnF<sub>2</sub> region (*French*) 0-50605  
 Sn-S system, use of boiling points to investigate vapour pressure 0-54361  
 SnBr<sub>2</sub>, <sup>81</sup>Br NQR line width obs. 0-50219  
 Sn<sub>2</sub>Br<sub>0.65</sub>Cl<sub>0.35</sub>·3H<sub>2</sub>O, X-ray cryst. struct. determ., Patterson synthesis (*French*) 0-28960  
<sup>119m</sup>SnCl<sub>2</sub> adducts with O and N containing cpds., Mossbauer emission 0-15918  
 SnCl<sub>2</sub>-TiCl<sub>4</sub> liq., beat effects, neutron diffr. studies 0-38897  
 SnCl<sub>2</sub>(H<sub>2</sub>O)<sub>x</sub>(D<sub>2</sub>O)<sub>2-x</sub>, high resolution heat capacity meas. (*Japanese*) 0-52218  
 SnCl<sub>2</sub>·2D<sub>2</sub>O, order-disorder transition, neutron diffr. study, lattice statistical model 0-24558  
 SnCl<sub>2</sub>·2H<sub>2</sub>O, protonic cond. in layered single cryst. 0-19983  
 SnCl<sub>2</sub>·2H<sub>2</sub>O, quasi two-dimensional, DC protonic cond. 0-44362  
 Sn<sub>0.75</sub>Eu<sub>0.25</sub>Mo<sub>2</sub>S<sub>8</sub>, Chevrel phase supercond., spin-depairing interaction, Mossbauer obs. 0-25258  
 α-SnF<sub>2</sub>, crystallochemistry 0-28990  
 Sn<sub>1-x</sub>Ga<sub>x</sub>Mo<sub>6</sub>S<sub>8</sub>, heat capacity meas., singularities at low temp. 0-49985  
 Sn<sub>0.9</sub>Ge<sub>0.1</sub>Te, Mossbauer spectra, soft modes 0-20550  
 Sn<sub>1-x</sub>Ge<sub>x</sub>Te, solid soln. series, Mossbauer study 0-39985  
 Sn(HPO<sub>3</sub>)<sub>2</sub>·H<sub>2</sub>O and its alkali metal salts, struct. and vibr. spectra 0-39030  
 SnI, atomic absorpt. spectroscopy, line absorpt. method use for SVP meas. of Sn 0-55747  
 SnI<sub>2</sub> band struct., layer model 0-44501  
 SnI<sub>2</sub>-SnF<sub>2</sub> system, phase diagram construct. (*French*) 0-50605  
 Sn<sub>2.8</sub>Li<sub>1.6</sub>Mg<sub>1.6</sub>O<sub>8</sub>, four layer close packing, cryst. struct. determ. (*French*) 0-28999  
 Sn<sub>2.8</sub>Li<sub>1.6</sub>Zn<sub>1.6</sub>O<sub>8</sub>, four layer hexagonal close packing, cryst. struct. determ. (*French*) 0-28999  
 Sn<sub>1-x</sub>Mn<sub>x</sub>Te, degenerate mag. semicond., thermoelec. power meas. 0-29392  
 SnMo<sub>6</sub>S<sub>8</sub>, Chevrel phase, synthesis and supercond. (*German*) 0-25038  
 SnMo<sub>6</sub>S<sub>8</sub>, Chevrel phase, RE mag. isolation and supercond. 0-44470  
 SnMo<sub>6</sub>S<sub>8</sub>, isotope effect props. (*Russian*) 0-37751  
 SnMo<sub>6</sub>S<sub>8</sub>, mixed Chevrel phases, crystallography 0-39038  
 SnMo<sub>6</sub>S<sub>8</sub>:Gd, EPR meas. (*French*) 0-54947  
 SnMo<sub>6</sub>S<sub>8</sub>:Gd<sup>3+</sup>, powder EPR spectra, cryst. field, supercond. energy gap 0-34769  
 SnMo<sub>6</sub>S<sub>8</sub>(Se<sub>8</sub>), Mossbauer spectra 0-15926  
 Sn<sub>1-x</sub>Mo<sub>x</sub>S<sub>8</sub>(Se<sub>8</sub>)(Te<sub>8</sub>), Chevrel phase correlation between struct. and supercond. transition temp. 0-7023  
 SnMo<sub>6</sub>Se<sub>8</sub>, Chevrel phase, RE mag. isolation and supercond. 0-44470  
 SnNbS(Se), struct., X-ray powder diffr. meas 0-44175  
 SnO chlorination, Mossbauer and X-ray phase anal. 0-21266  
 SnO<sub>2</sub>, <sup>119</sup>Sn-enriched, use as blackbody absorber in Mossbauer spectroscopy 0-2669  
 SnO<sub>2</sub>, adsorption anomaly of water, effects of cryst. growth of solid 0-10779  
 SnO<sub>2</sub>, band struct., tight-binding calc. 0-24796  
 SnO<sub>2</sub> coated glass, surface elec. breakdown 0-25303  
 SnO<sub>2</sub>, electro-conducting transparent film, props. rel. to production method (*Japanese*) 0-25557  
 SnO<sub>2</sub>, electronic struct. and densities of states, tight-binding calcs. 0-15447  
 SnO<sub>2</sub> film, deposition from vapour phase, thermodynamic anal. 0-15418  
 SnO<sub>2</sub> film, orientating action of solid substrates, on liq. cryst. layer exam. 0-44111  
 SnO<sub>2</sub>, finely dispersed, Lamb-Mossbauer factor 0-39930  
 SnO<sub>2</sub>, point lattice electrostatic pot. calcs. (*Russian*) 0-15044

## tin compounds continued

- SnO<sub>2</sub>, semiconductor, photoluminescence, depend. on lattice temp. and excitation intensity 0-45137  
 SnO<sub>2</sub> surface, interactions with O<sub>2</sub>, H<sub>2</sub>O and H<sub>2</sub>, desorpt., ESR and cond. meas 0-10790  
 SnO<sub>2</sub> thin film gas sensor, prep. 0-39691  
 SnO<sub>2</sub> thin films, analytical characterisation 0-20053  
 SnO<sub>2</sub> thin films, solid state gas sensor 0-40790  
 SnO<sub>2</sub>, transparent conducting film, prep. by CVD, and characterisation 0-11571  
 SnO<sub>2</sub>:As film, prep. and elec. cond. 0-2959  
 SnO<sub>2</sub>/n-Si spray-deposited solar cells 0-12007  
 SnO<sub>2</sub>-GaSe heterojunction photocell, fine struct. of photo-EMF spectra 0-6967  
 SnO<sub>2</sub>-InSe n-n heterostructures, photoelec. props., 80 to 300K 0-20297  
 SnO<sub>2</sub>-Sb<sub>2</sub>S<sub>3</sub>, Sn structures, photovoltaic effects (*Korean*) 0-44647  
 SnO<sub>2</sub>-Si, heterojunction solar cells, anomalous photocurrent 0-3515  
 SnO<sub>2</sub>-Si heterojunction solar cell, elec. props. (*Korean*) 0-45665  
 SnO<sub>2</sub>-Si heterojunctions, elec. and photovoltaic props. 0-26141  
 SnO<sub>2</sub>-Si solar cells, electron-beam deposited, struct., photovolt. props. 0-50956  
 SnO<sub>2</sub>-SiO<sub>2</sub>-n-Si heterojunction, cheap solar elements for ground-based appls. 0-40860  
 SnO<sub>2</sub>-ZnS:Mn thin film structure, surface morphology and electro-optical props. (*Russian*) 0-49554  
 SnO<sub>2</sub> films, phase composition, Mossbauer spectra 0-20051  
 Sn<sub>2</sub>P<sub>2</sub>Se<sub>6</sub>, illumination effect on soft mode and dielectric props., luminesc. study (*Russian*) 0-50420  
 Sn<sub>2</sub>P<sub>2</sub>(S<sub>1-x</sub>Se<sub>x</sub>)<sub>6</sub>, solid solutions, ferroelectric soft mode freq., dispersive transformations 0-29701  
 Sn<sub>2</sub>P<sub>2</sub>Se<sub>6</sub>, ferroelec. props. (*Russian*) 0-25313  
 Sn<sub>2</sub>P<sub>2</sub>(Se<sub>1-x</sub>S<sub>x</sub>)<sub>6</sub>, ferroelec. props. (*Russian*) 0-25313  
 (Sn<sub>1-x</sub>Pb<sub>x</sub>)<sub>2</sub>P<sub>2</sub>Se<sub>6</sub>, solid solutions, ferroelectric soft mode freq., dispersive transformations 0-29701  
 Sn<sub>1-x</sub>Pb<sub>x</sub>Se(Te) thin films, resistance to oxidation, Mossbauer study 0-39986  
 Sn<sub>1-x</sub>Pb<sub>x</sub>Te, film, production under quasi-equilibrium conditions 0-45241  
 SnS<sub>2</sub>, effect of powdering on polytypic cryst. struct. 0-1979  
 SnS<sub>2</sub>, Mossbauer spectra, vibr. amplitudes anisotropy 0-15904  
 SnS<sub>2</sub>, optical transitions from d core levels 0-45105  
 SnS<sub>2</sub>, polytypes, electronic bandgap meas. 0-34358  
 SnS<sub>2</sub>, Sn4d photoionisation, second threshold 0-40222  
 SnS(Se), electron diffr. struct. anal. 0-44449  
 SnS(Se), electronic struct., tight-binding calcs. 0-15446  
 SnS(Se)(Te), reaction with II-VI compounds, thermodynamic anal. 0-40728  
 Sn<sub>2</sub>Sb<sub>2</sub>S<sub>2</sub>, cryst. struct. (*French*) 0-1991  
 SnSe, small gap, band-edge parameters 0-49594  
 SnSe-GeSe<sub>2</sub>-As<sub>2</sub>Se<sub>3</sub> glasses, vitrification region and elec. cond. 0-15008  
 SnSe<sub>2</sub>, Mossbauer spectra, vibr. amplitudes anisotropy 0-15904  
 SnSe<sub>2</sub>, optical transitions from d core levels 0-45105  
 SnTaS(Se), struct., X-ray powder diffr. meas 0-44175  
 SnTe, <sup>119</sup>Sn diffusion coeff. meas., stoichiometric deviation, SIMS 0-34236  
 SnTe, bond gap, phase transform., optical dielec. const. meas. 0-10630  
 p-SnTe, cathodoluminescence and Fermi level hole effective mass 0-25467  
 SnTe, dispersive phase transition at 22K, Mossbauer spectra and elec. resist. meas. 0-6514  
 SnTe, enthalpy of formation (*Russian*) 0-15267  
 SnTe film, evaporated, electro-reflectance meas. 0-11496  
 SnTe film, polycrystalline, anomalous resist. at struct. phase transition 0-29488  
 SnTe, polymorphism, high press. and temp., X-ray diffr. study 0-54375  
 SnTe, self-consistent relativistic energy bands 0-10870  
 SnTe, small gap, band-edge parameters 0-49594  
 SnTe:Mn, EPR as probe of phase transitions 0-15790  
 SnTe:Mn, NMR study 4.2 to 300K (*French*) 0-54960  
 SnTe-Al<sub>2</sub>O<sub>3</sub>-Al junction, tunnelling, Fermi level depend. on carrier conc., influence of surface states 0-25016  
 SnTe-Al<sub>2</sub>O<sub>3</sub>-Al structure, tunnelling characts., model anal. 0-29480  
 SnTe-MnTe, degenerate semicond., anomalous Hall effect 0-29420  
 Sn<sub>1-x</sub>Ti<sub>1-x</sub>O<sub>2</sub>, solid soln., thermal reaction with V(V), Cr(III), Cr(VI), Mn(II), Fe(III), Co(II), Ni(II), Cu(II), Sb(III) 0-16674  
 Sn<sub>10</sub>W<sub>16</sub>O<sub>46</sub>, cryst. struct. determ. 0-33934  
 Sn<sub>10</sub>W<sub>16</sub>O<sub>46</sub>, struct. anal. and stereoactivity of Sn<sup>II</sup> lone pair 0-33935  
 TiN, synthesis using enhanced reactive evaporation 0-2953  
 Ti<sub>1-x</sub>Sn<sub>x</sub>, phase equilibria exam. 0-55369

## titanium

- see also nuclei with .....  
 annealed, high-temp., kinetics (*Russian*) 0-21166  
 anode, Pt-ir coated, corrosion and passivation behaviour in Cu electrowinning appl. 0-55573  
 anodic behaviour, steady-state, in conc. HCl 0-45515  
 anodic dissolution and passivation in acidic chloride solution 0-35541  
 anodic dissolution in SiO<sub>2</sub>-Na<sub>2</sub>O-K<sub>2</sub>O-CaO-MgO-Al<sub>2</sub>O<sub>3</sub> glass melt 0-19949  
 anodic oxidation under high voltage, porous layers (*French*) 0-54574  
 anodic oxide superficial layer, X-ray emission spectrometry and ion back-scattering (*French*) 0-49482  
 atom, rel. oscillator strengths by combined absorption/emission meas., new method 0-37784  
 Auger electron appearance potential spectroscopy (*Japanese*) 0-50473  
 CESR, prediction of obs. 0-29369  
 charged particle prod. cross sections for 14 MeV neutrons, Ti, V, Cr, Mn 0-42648  
 compression at high strain rate, deformation anal. 0-25769  
 contact with SiC single crystal, friction and fracture of SiC 0-11780  
 cool stars, Ti isotopic abundance ratios 0-26840  
 corrosion in seawater circulation plant, comparison with stainless steel (*German*) 0-25897  
 corrosion resist. in marine environments (*French*) 0-50767  
 creep behaviour, 25 to 400°C, role of impurities and/or alloying elements of commercial grade specimens (*French*) 0-45354  
 diffusion bonding, low-pressure 0-11873  
 diffusion characteristics in Ag, 1051 to 1220K 0-15308  
 diffusion of Be, temp. depend., radioactive tracer method (*Russian*) 0-10703  
 diffusion of O, atomic jumping model 0-44366



## titanium continued

- dissolution in stainless steel, kinetics, steel component absorpt. (*Russian*) 0-34193  
 dynamic annealing, effect on dynamic strain ageing phenomena 0-7594  
 electromigration of H(D) 0-34247  
 electronic structure of five and ten atom chains SCF-X $\alpha$ -SW calcs. 0-5483  
 fast reactor structural material, (n,p) cross section eval. from threshold to 20 MeV 0-13623  
 fast reactor structural material, capture cross section eval. 10<sup>-5</sup> eV to 200 keV 0-13622  
 fatigue crack closure mechanism 0-16434  
 fatigue crack closure mechanism 0-21107  
 film, interaction with O<sub>2</sub> 0-45431  
 film, interference enhanced Raman scatt. 0-40105  
 film, ion stimulated N<sub>2</sub> sorption, TiN<sub>x</sub> form., sorption ratio, capture coeff. anal. 0-39411  
 film, solid state reaction with Si or SiO<sub>2</sub> substrates, backscatt. anal. 0-34257  
 film (0001), with adsorbed H (1 $\times$ 1) monolayer, electronic struct., surface geometry 0-54750  
 film (0001) electronic struct., Fermi level, surface states, GO calcs. 0-6927  
 films, implanted inert gas desorption, reemission process 0-39453  
 fracture mechanism maps 0-3188  
 fusion reactor first wall material, thermal response 0-32456  
 fusion reactor material, D profiles after D<sub>3</sub><sup>+</sup> implantation 0-37581  
 galvanic corrosion, electrochem. characts. rel. to Al alloys 0-21162  
 glass-ceramic protective coatings, synthesis and props. 0-25900  
 grinding of type VT1, abrasive props. of ZrB<sub>12</sub> and diamond wheels 0-16489  
 heterogeneity of strain field in commercially pure alloy VTI-0 0-35286  
 hydriding, surface condition and environment influence 0-35380  
 ions, beam-foil spectra from 20 to 238 MeV energy, 5 to 60 nm, lifetime meas. problems 0-9722  
 JAERI Tokamak, Ti coating for improved plasma characts. 0-24232  
 low temperature data, handbook of mech. and phys. props. 0-22153  
 mechanical props., electrochemistry, oxidation and corrosion resist., conference, Nantes, France (Nov. 1978) 0-41932  
 Moon, regolith Ti composition, orbiting  $\gamma$ -ray expt. 0-17510  
 neutron low energy interaction cross sections, gravitational spectrometer meas. 0-24521  
 nitriding, ESCA study (*Japanese*) 0-11833  
 in oceanic phosphorites, Fe, Ti and Al behaviour during initial form. stages 0-31029  
 oxidation, reaction mechanism 0-25912  
 oxidation under hydrothermal cond. to produce brookite (*Japanese*) 0-35433  
 oxide film form. during thermal treatment, morphological and struct. study (*French*) 0-50766  
 oxide layer growth by dry oxidation at 25°C, ESCA obs. (*French*) 0-45434  
 passive oxide layer form. in H<sub>2</sub>SO<sub>4</sub>, ageing with and without photoexcitation (*French*) 0-45432  
 permeation of H plasma through Ti reduced by layer of interstitially built  $\epsilon$ -Ti<sub>3</sub>N 0-16566  
 photoemission, primary and secondary yields using low-energy monochromatic X-rays 0-35053  
 physicochemical and wear props., influence of ion implantation and overlay coatings 0-40603  
 plasma, laser-prod., space-resolved extreme UV emission 0-54015  
 plasma chamber material for power generating Tokamak, suitability tests 0-32449  
 plasma impurity, atom-electron collisions in inner discharge column (*Russian*) 0-38529  
 plastic deform. dynamics, mech. characts. and phys. props., effect of O<sub>2</sub> (*French*) 0-45353  
 point defect estimation from specific heat and volume in plastically deformed pure metals (*Russian*) 0-54223  
 porous structure, change in presence of liq. phase (*Russian*) 0-16223  
 positron annihilation study of defects 0-3281  
 powder, exam. of mechanicochemical comminution, in the presence of epoxy resin or polysulphide rubber 0-16236  
 powder, resist.-sintability (*Japanese*) 0-16228  
 pure, rapid grain growth 0-16343  
 pure plate, shear band formation in ductile fracture process (*Japanese*) 0-16445  
 reactor structural material s-wave resonance parameters from capture cross section data 0-13629  
 reactor structural material transmission meas. using TOF spectrometer 0-18440  
 recrystallised  $\alpha$ -phase of commercial purity, Fe-rich precipitates obs. (*French*) 0-50637  
 repassivation and pitting corrosion 0-30143  
 RF sputter deposition, ion bombardment and ion implanatation 0-25564  
 rolled foil preparation 0-18744  
 sapphire:Ti<sup>4+</sup>, plastically deformed, precipitation hardening, TEM study 0-7592  
 solubility of H, neutron diffr. study 0-15254  
 sorption of H<sub>2</sub> and N<sub>2</sub>, gas-discharge device appl. 0-10796  
 sputtering rate on Ar ion bombard. 0-55245  
 strain rate effect, upon mech. behaviour in type IMI-260 0-3153  
 substrate, detonation deposition of Al<sub>2</sub>O<sub>3</sub> coating, impact interaction parameters 0-40602  
 substrate for W-Al<sub>2</sub>O<sub>3</sub> composite films, oxide evaporation deposited, struct., props. 0-25581  
 superconducting transition temp., perturbative corrections, direct and indirect ladder diagrams 0-49979  
 surface, (0001), valence band struct. and chemisorption, XPS and UPS study 0-35062  
 surface (0001), with adsorbed N (1 $\times$ 1) layer, underlayer geometry, electronic struct. calcs. and UPS meas. 0-54751  
 surface oxidation reaction, surface chemiluminesc. study 0-55708  
 surfaces, clean and oxidised, refl., 2-25 eV 0-55123  
 target, microwave laser irr., plasma form., inhibited electron thermal cond., laser intensity threshold Z-depend. 0-48928  
 target impurity effect on laser produced expansion, ion spectrography 0-43945  
 thin film, electron-beam deposition on Al<sub>2</sub>O<sub>3</sub> quartz and glass 0-7496  
 Tokamak fusion reactor first walls, hydrogen profiles 0-37578  
 tritiated self supported target prep. 0-23211

## titanium continued

- US wave diffraction in penny-shaped cracks, theory and expt. 0-33267  
 vacuum technology appl., melt processing and appl. (*Hungarian*) 0-55318  
 $\alpha$ -Al<sub>2</sub>O<sub>3</sub>:Cr(Ti)(V), impurities effect on thermoluminesc. 0-40170  
 Ar-Ti hollow cathode afterglow, energy transfer mechanisms and excited metallic ion prod. 0-43857  
 Au/Ti thin films, effect of Cl<sub>2</sub> on elec. resistance, Ti atom migration and preferred orientation 0-34530  
 EuIG:Sb(Ca)(Ti), growth from PbO-B<sub>2</sub>O<sub>3</sub> based flux, prop. depend. on Pb content 0-39824  
 n-Fe<sub>2</sub>O<sub>3</sub>:Ti electrodes, characterisation and behaviour in acetonitrile solns. 0-25004  
 H impurity detection by <sup>1</sup>H(<sup>15</sup>N, $\alpha$  $\gamma$ ) reaction 0-55767  
 H<sub>2</sub> isotope release 0-37580  
 H<sub>2</sub>-D<sub>2</sub>-T<sub>2</sub> mixtures, mesic at. and mol. processes 0-23580  
 LiF:Mg,Ti crystals, Z<sub>1</sub>-centres, correlation of thermoluminescence and optical absorption 0-45154  
 LiNbO<sub>3</sub>:Ti diffused, optical directional couplers, characts. 0-33145  
 LiNbO<sub>3</sub>:Ti diffused, optical waveguide, fabrication problems (*Japanese*) 0-33256  
 LiNbO<sub>3</sub>:Ti narrow ridge optical waveguides and electro-optical, ion-bombardment-enhanced etching 0-38133  
 LiNbO<sub>3</sub>:Ti planar and channel optical waveguides, Ti diffusion coeff. meas. 0-19096  
 LiNbO<sub>3</sub>:Ti waveguide, in-plane scatt. obs. and countermeasures 0-33215  
 LiNbO<sub>3</sub>:Ti waveguide thin film electrooptic Bragg modulator, bistable optical element 0-10034  
 LiNbO<sub>3</sub>:Ti waveguide and cryst., absorpt. loss and photorefractive index changes 0-48368  
 LiNbO<sub>3</sub>:Ti waveguide directional coupler switches, optically-induced crosstalk 0-48417  
 LiTaO<sub>3</sub>:Ti, diffused waveguide prep., parameters determ. 0-14465  
 Ni-Ti multilayers for monochromators and supermirrors, neutron reflectivities 0-22880  
 Si-Ti, deep level impurity, Hall meas. 0-6768  
 Ti density, in DC sputtering discharge by atomic absorpt. spectroscopy 0-43973  
 $\alpha$ -Ti, grain size independent viscous creep 0-40460  
 Ti<sup>+</sup>, excited config. position and level struct., review 0-32621  
 Ti-Permalloy films, interdiffusion, Auger anal. and X-ray diffr. obs., degradation of mag. props. 0-34251  
 Ti-Si film thin film interaction, metallisation, X-ray diffr. and sheet resist. 0-54442  
 Ti-TiC-TiN system, phases 0-20905  
 Ti-TiO<sub>2</sub>-Au diode, spectral photoresponse and I-V characts. 0-15617  
 Ti+H<sup>+</sup>, K-shell ionisation calcs. 0-23534  
 Ti+H<sup>+</sup>, K-shell ionisation cross-section determ. 0-48077  
 Ti+He<sup>2+</sup>(C<sup>4+</sup>)(O<sup>7+</sup>)(N<sup>4+</sup>)(N<sup>5+</sup>) atom-ion collisions, ratio of single K-shell ionisation cross section to double K-shell ionisation cross section 0-53119  
 TiC-Ni-Mo sintered hard alloy TN-20, fracture surfaces 0-7684  
<sup>A</sup>Ti, A=46, 48, 50, pionic X-rays, strong interaction and isotope shifts,  $\pi$ -nuclear optical pot. 0-53169  
 ZnO-Ti transparent type MIS solar cells 0-45662

## titanium alloys

## see also titanium compounds

- $\alpha$ + $\beta$  phases, interfacial precipitation 0-3068  
 binary alloys, appl. to H storage as solid metal hydrides 0-45786  
 colony size effect, in  $\alpha$ + $\beta$  alloys, on fatigue crack growth on Widmanstätten struct. 0-30094  
 compression at high strain rate, deformation anal. 0-25769  
 creep resistance and thermal stability of Ti 685 and Ti 6242 in air and in vac. 0-30020  
 creep strain increments rel. to stresses, nonstationary loading 0-25776  
 data handbook of low temp. mech. and phys. props. 0-22153  
 disc, rotating notched, strength in quasibrittle fracture 0-55533  
 dissolving in Al alloy melt, reaction zone formation, component interaction (*Russian*) 0-54377  
 drop forgings, grain orientation and props., combined mech. workings, hardening and high-temp. heat treatment influence (*Russian*) 0-20973  
 ductility, for different phase comps. at low temps. 0-35273  
 fatigue crack propagation resistance, grain size effect, exam. 0-11765  
 ferritic alloy DT02, oxidation behaviour in CO<sub>2</sub> or Ar with H<sub>2</sub>O and H<sub>2</sub>, 823-123K 0-3249  
 fracture, intergranular, high strength, heat-treated weldments, in  $\alpha$ - $\beta$  type 6246 0-21097  
 fracture mechanics, K<sub>IC</sub> values determ. in elastic-plastic material behaviour range 0-45376  
 fracture toughness testing with eddy current sensor 0-45459  
 fusion reactor environment, first wall and blanket structure, impact of H<sub>2</sub>, phase stability and solubility 0-32435  
 fusion reactor first-wall and blanket material, mech. props. 0-34074  
 fusion reactor materials, He and simultaneous damage production simulation 0-32480  
 grinding, effect on surface struct. of VT9 0-25878  
 high plasticity effect in alloy OT4 0-35272  
 hot salt stress corrosion cracking on type TA6V (*French*) 0-21185  
 Inconel X750, positron annihilation study of ageing and creep 0-29824  
 mathematical-physical considerations rel. to metal powder prod. 0-11595  
 mechanical props., electrochemistry, oxidation and corrosion resist., conference, Nantes, France (Nov. 1978) 0-41932  
 metallurgical characterisation using thermolec. power meas. (*French*) 0-45462  
 Nimonic, IN100,  $\gamma'$  precipitates, casting conditions effect on morphology 0-7548  
 Nimonic 90, creep rate stress exponents and friction stress, comparison with Lagneborg particle by-passing model 0-55481  
 oxidation resist, 400 to 800°C 0-50768  
 plates with cut, stability loss critical stresses for VT-1-1 alloy 0-11690  
 rolled  $\alpha$ -Ti alloy, elastic stiffness and Bauschinger effect accompanying anisotropic hardening (*Russian*) 0-40435  
 steel, austenitic stainless, 08Kh18N10T, hot-worked precipitation kinetics and struct. of dispersed phases, Ti effect 0-29964  
 steel, Cr-Ni-Ti-B, grain size effect on mech. and struct. props. (*French*) 0-45361  
 steel, medium C, microalloying with V and Ti, effect on hardness and structure 0-11750  
 steel, Ni-Co-Mo-Ti, maraging, electron diffr. obs. of second phase (*Chinese*) 0-11655  
 steel, solubility of W and Mo in Ti(C,N)<sub>x</sub> 0-16276



## titanium alloys continued

- steel, stainless, oxidation effect of Ti 0-35394  
 Ti-Ni, electron emission and shape memory effect 0-50687  
 Ticonal, two- and one-dimens. modulated struct. after thermomag. treatment and water quenching (*Russian*) 0-29983  
 toughness and behaviour under dynamic loads (*French*) 0-45383  
 type 70A, containing 0-6000 ppm <sup>3</sup>He, sensitivity of tensile props. 0-39197  
 Udimet 520, Nicalloy-coated, microstruct. degradation, influence of corrosion protective coating 0-40611  
 X-ray stress analysis of strongly fluorescing specimen 0-1499  
 Al-Ti, liq., dissoln. and diffusion of alloying components, 700-1000°C (*Russian*) 0-15275  
 Al-Ti-Fe, ternary phase diagram, computer calculations 0-45274  
 Al<sub>3</sub>Ti, precipitate shape, and distribution in chill-cast Al-14 wt.% Ti alloy 0-16310  
 B<sub>2</sub>C-Ti, contact reaction with liq. Ni 0-55707  
 Co-Ti, cryst. struct. and stacking fault influence on mag. props. (*Russian*) 0-25164  
 Co-Ti (22 at.%), amorphous eutectic phase 0-55360  
 Co-Ti (9 at.%), decomp. kinetics, elec. resist., hardness, and saturation magnetisation during ageing (*Russian*) 0-50587  
 Co<sub>1-x</sub>Ti<sub>x</sub>, ferromag. props., Ti conc. effect 0-54872  
 Co<sub>2</sub>Ti, electron energy spectrum calcs. by supplementary plane wave method 0-6711  
 Cr-Ti/MgO-NbC(TaC) dispersion-strengthened, high temp. wear and oxidation resist. 0-25877  
 Cr-Ti/NbC(TaC) dispersion-strengthened, high temp. wear and oxidation resist. 0-25877  
 Cu-Be-Ni-Ti-Mg bronze, alloying element influence on minimum thermo EMF, cold working (*Russian*) 0-34426  
 Cu-Ti, dil., oxide film form. in ammoniacal Cu(II) solns., AES obs. 0-45415  
 Cu-Ti, dil. alloy, cellular precipitates, nucleation, TEM study 0-3069  
 β-Cu-Ti, dil. alloy, growth phenomena associated with precipitation, TEM study 0-3070  
 Cu-Ti, solubility of Ti, exam. using NMR of <sup>63</sup>Cu (*French*) 0-7179  
 Cu-Ti (3.5 wt.%), aged by US strain, struct. and props. (*Russian*) 0-21003  
 Cu-Ti (4 wt.%), isothermal transformation, electron and optical microscopy obs. of microstructure 0-16307  
 Cu-Ti-Fe (0.7, 0.9 wt.%) film, dispersion-strengthened, form. by high rate magnetron/plasmatron sputtering, and props. 0-25715  
 Cu<sub>60</sub>Ti<sub>40</sub>, metallic glass, neutron diffr. meas. of struct. factor 0-24367  
 Fe-Cr-Al-Ti-Y<sub>2</sub>O<sub>3</sub> (20, 4.5, 0.5, 0.5) type MA956, strain rate effect on fracture behaviour at 1366K 0-16458  
 Fe-Hl (Si) (Ti) (V), molten, gaseous O<sub>2</sub> absorption 0-11836  
 Fe-Mn-Ti alloys, austenitic, precipitation strengthened 0-25714  
 Fe-Ni-Al-Co-Ti base alloys, highly coercive, phase comp., Mossbauer meas. 0-39996  
 Fe-Ni-Al-Cu (25, 14, 4 wt.%), alloy YuND4, effect of Ti addition on structure, mag. props. 0-15714  
 Fe-Ni-Co-Ti, shape memory effect after appl. of bending moment (*Russian*) 0-45305  
 Fe-Ni-Ti-Al-Nb, struct. mechanism for inverse α-γ transform. (*Russian*) 0-40351  
 Fe-Sb-Ti, dil., interactions and precip., Mossbauer study 0-39997  
 Fe-Ti, industrial hydride reservoir, characts., technological aspects 0-45792  
 α-Fe-Ti, ion-implanted and annealed, microstruct. evolution 0-15132  
 Fe-Ti, mag. moment distrib. and environmental effects around Ti impurity 0-7092  
 Fe-Ti, precipitation hardening of α-Fe containing weak and strong particles 0-20946  
 Fe-Ti metal hydrides, numerical physical property data for H storage 0-40929  
 Fe-Ti-D, ion implanted, D trapping, 90-500K 0-15131  
 Fe-TiB<sub>2</sub>, phase composition, secondary ion-ion emission study (*Russian*) 0-20896  
 Fe-TiC-WC(VC), sintering, densification 0-25615  
 Fe<sub>0.5</sub>Co<sub>0.5</sub>TiH<sub>x</sub>, transmission Mossbauer spectra 0-44964  
 FeTi, H storage alloy, prep. for TEM (*German, English*) 0-30197  
 FeTi hydrides, struct., heat of soln., diffusion and hydriding kinetics for H storage 0-40930  
 FeTi, positronium form. after hydrogenation-dehydrogenation cycling and annealing 0-18947  
 FeTi, surface segregation, catalytic effect on hydrogenation 0-45814  
 Fe<sub>1-x</sub>Ti<sub>x</sub>, ferromag. props., Ti conc. effect 0-54872  
 FeTiB, corrosion-resistant amorphous mag. thin films 0-54923  
 α-FeTiD<sub>0.057</sub>, solid soln., interstitial D, neutron diffr. study 0-39071  
 FeTiD<sub>2</sub> (0 ≤ x ≤ 1.9), structural phase transitions, absorpt. and desorpt. isotherms 0-19948  
 FeTiH, H storage material, H diffusion, neutron diffr. obs. 0-51013  
 H assisted cracking, mechanisms, review 0-50721  
 Mn-Ti-Fe, ternary phase diagram, computer calculations 0-45274  
 Mo-Ti, irradi. between 425 and 1000°C, ductility in bending 0-39164  
 Mo-Ti-Zr, alloy TZM, polycrystalline, anal. of elastic anisotropy and microyielding 0-30050  
 Mo-Ti-Zr, D trapping in fusion reactor materials, temp. dependence 0-37577  
 Mo-Ti-Zr, fusion reactor first wall material, compatibility with impure He 0-32469  
 Mo-Ti-Zr (0.5, 0.1 wt.%), neutron irradiated, void swelling and shrinkage, TEM study 0-34079  
 Mo-Ti-Zr (0.5, 0.7 wt.%) alloy TZM, props. and appl. (*German*) 0-21040  
 Mo-TiC-Ni phase equilibria, subsolidus temp., metallographic and X-ray anal. 0-16278  
 Nb-Mo-Ti-Zr-C, work function temp. and phase depend. (*Russian*) 0-2449  
 Nb-Ti, multifilament wire, superconducting magnet system, development for physical experiments 0-9008  
 Nb-Ti, nitriding, diffusive saturation, lattice spacing and activation coeffs. (*Russian*) 0-21168  
 Nb-Ti, sheet, flux trapping, appl. to mag. shielding and levitation 0-31806  
 Nb-Ti, single core conductor, carrying DC transport current, alternating field losses 0-34550  
 Nb-Ti superconducting magnet system, for short sample test on Tokamak superconductor 0-9010

## titanium alloys continued

- Nb-Ti/Cu sheet composite, flux trapping and shielding capabilities in transverse fields 0-15667  
 Nb-Ti-Zr, superconducting wire, coil simulation meas. of losses and instabilities 0-37050  
 NbTi, superconducting multifilamentary conductors, crit. current density, bending effects (*German*) 0-39727  
 NbTi, superconductor, acoustic emission during flux jump 0-39724  
 NbTi/In granular composite, resistivity mag. field depend. 0-15654  
 (Nb<sub>0.99</sub>Ti<sub>0.01</sub>)<sub>1-x</sub>Ge<sub>x</sub>, supercond., mag. field props. 0-54822  
 Ni-Al-Ti, heat resist., solidification range 0-35177  
 Ni-Al-Ti, heat-resisting dispersion-hardening alloys, props. and struct., γ'-phase comp. influence (*Russian*) 0-20943  
 Ni-Al-Ti ferromagnetic non-homogeneous alloy, composition determination by Curie temp. meas. 0-11196  
 Ni-Ce-Fe-Ti (77, 20, 4, 2.5 wt.%), long-term strength in H at high pressure 0-55485  
 Ni-Co-Cr-Al-Ti-Mo superalloy IN738, casting porosity removal using hydrostatic press. sintering 0-55322  
 Ni-Cr-Co-Mo-Ti, oxidation depend. on alloying element, cohesion strength (*Russian*) 0-40587  
 Ni-Cr-Co-Ti, superalloy sintering thermochemical surface treatment 0-25617  
 Ni-Cr-Mo-Ti (19,11,3 wt.%) for TiC reactively sputtered coatings, adherence, XPES and wear study 0-25565  
 Ni-Cr-Ti, effect of ultrasound on crystallisation, dendritic structure, and plasticity (*Russian*) 0-11637  
 Ni-Cr-Ti, type EHL698, loading history effect on resist. to cyclic elastoplastic strain 0-16398  
 Ni-Cr-W-Mo-Al-Ti (15,6,3,2,2, wt.%), wrought, Si effect on transition brittleness (*Chinese*) 0-55491  
 Ni-Ti, mag. moment distrib. and environmental effects around Ti impurity 0-7092  
 Ni-Ti, martensitic phase transformation effect on low cycle fatigue behaviour 0-7666  
 Ni-Ti, neutron irradiated, thermally activated deform. 0-6438  
 Ni-Ti, Ni-rich, temp. depend. resist. 0-10943  
 Ni-Ti, shape memory effect, criteria for efficiency assessment (*Russian*) 0-21015  
 Ni-Ti, structural instability, deform. effects on electron energy spectrum 0-39284  
 Ni-Ti (1.6, 7.64 wt.%), monophase high temp. scaling, metallography study 0-21159  
 Ni-Ti (3 wt.%), C precipitation 0-29958  
 Ni-Ti (9.6 wt.%), mag. study on phase decomposition (*Japanese*) 0-15758  
 Ni-Ti shape memory alloy processing and medical applications (*German*) 0-17203  
 Ni-Ti shape memory alloy trigger for space satellite boom latch and release mechanism 0-7575  
 Ni<sub>3</sub>Al-Ti, powder, X-ray spectral analysis exam. 0-16239  
 (Ni<sub>1-x</sub>Cu<sub>x</sub>)Ti, martensitic, shape memory effect kinetics and thermodynamics 0-3021  
 Ni<sub>2</sub>Mn<sub>2</sub>Ti<sub>1-x</sub>Sn<sub>x</sub>, mag. hyperfine fields, <sup>119</sup>Sn Mossbauer spectra study 0-55003  
 Ni<sub>2</sub>Mn<sub>2</sub>Ti<sub>1-x</sub>Sn<sub>x</sub>, Mossbauer spectra, mag. hyperfine field 0-15857  
 NiTi, martensitic, shape memory effect kinetics and thermodynamics 0-3021  
 Ni<sub>1-x</sub>Ti<sub>x</sub>, ferromag. props., Ti conc. effect 0-54872  
 Ni<sub>3</sub>Ti, electronic struct., X<sub>α</sub> calc., photoelectron and AES spectra 0-20769  
 Ni<sub>62</sub>Ti<sub>38</sub>Zr<sub>9</sub>, amorphous, H-sorption, X-ray and DSC obs. 0-49526  
 SiC fibre reinforced Ti, effect of Al, Zr and Mo alloying additions on reaction rate of Ti with fibres 0-16249  
 TZM, fatigue and threshold behaviour under high cycle fatigue 0-40487  
 α-β-Ti alloys, stress anal. of strongly fluorescing specimen 0-1499  
 Ti-6Al-4V, stress distrib. for steady axisymmetric extrusion 0-3103  
 Ti-Al, H<sub>2</sub> diffusion at room temp. (*Japanese*) 0-19987  
 Ti-Al, structural and phase changes due to annealing (*Russian*) 0-55440  
 Ti-Al (Sn), porous, effect of Al and Sn on sintering 0-20830  
 Ti-Al (4 to 5.5 wt.%), alloy VT5 with WC-Co coating appl. by detonation, antifirthing props. 0-21188  
 Ti-Al (4 wt.%), sintered, long-time strength 0-40529  
 Ti-Al (6 wt.%), D profiles after D<sub>3</sub><sup>+</sup> implantation 0-37581  
 Ti-Al age-hardened alloys, fatigue crack propagation rel. to grain size in vac. and NaCl soln. 0-16538  
 Ti-Al film, evaporated, anodisation, anodic voltage-time dependence obs. (*Polish*) 0-55574  
 Ti-Al film, struct. and elec. props. 0-7002  
 Ti-Al-Cr-Mo alloy VT3-1, reactions with some refractory compounds 0-16585  
 Ti-Al-Cr-Mo system, VTZ-1 alloy, microstruct. influence on fatigue characts. 0-3195  
 Ti-Al-H, H effect on mech. props. and lattice constants 0-21036  
 Ti-Al-Mn, endurance with cyclic bending, effect of loading conditions 0-50724  
 Ti-Al-Mo, type Ti-6242S, irradi. induced creep 0-39163  
 Ti-Al-Mo alloy VT-14, spherical pressure vessel, correlation between fracture stresses and mech. laboratory characts. 0-25838  
 Ti-Al-Mo-Cr-Fe, distrib. of Sn, Zr between phases, temp effect. 0-55357  
 (α+β)-Ti-Al-Mo-Fe alloy VT-22, behaviour during creep testing, solid soln. dissoc. (*Russian*) 0-40346  
 Ti-Al-Mo-Sn alloy, elastically and plastically deformed, positron annihilation meas. of deformation 0-21038  
 Ti-Al-Mo-Sn-Si (2.25, 4, 11, 0.25 wt.%), type IMI 680, internal friction study of martensitic transformations 0-7573  
 Ti-Al-Mo-Sn-Si (2.25, 4, 11, 0.25 wt.%), type IMI 680, stability of martensitic phases 0-7574  
 Ti-Al-Mo-Sn-Si (4, 4, 4, 1/2 wt.%), type IMI 551, internal friction study of martensitic transformations 0-7573  
 Ti-Al-Mo-Sn-Si (4, 4, 4, 1/2 wt.%), type IMI 551, stability of martensitic phases 0-7574  
 Ti-Al-Mo-V, crack resistance in chloride soln., electrochem. protection, polarization effect 0-55589  
 Ti-Al-Mo-V based alloy BT22 quenched from 850-1200°C, X-ray study of structure (*Ukrainian*) 0-24402  
 Ti-Al-Mo-Zr SiC fibre reinforced composites, matrix selection (*Russian*) 0-35192  
 Ti-Al-Mo-Zr-Si (6.6, 3.3, 1.8, 0.3 wt.%) SiC fibrous composite, component interaction kinetics (*Russian*) 0-55364



## titanium alloys continued

- Ti-Al-Mo(Cr)(Fe), thermomechanical treatment effect on mech. props., strengthening mechanisms 0-55441
- Ti-Al-Nb-Ta-Mo (6, 2, 1, 0.8 wt.%), elevated temp. flow strength, creep resist., diffusion welding characts. 0-30033
- Ti-Al-Sn, type Ti-5621S, irradi. induced creep 0-39163
- Ti-Al-Sn (5, 2.5 wt.%), annealing of near-basal hydrides 0-20989
- Ti-Al-Sn-Zr-Mo (6, 2, 4, 6 wt.%),  $\alpha$ - $\beta$  type 6246, fusion zone fracture behaviour in weldments 0-30093
- Ti-Al-Sn-Zr-Mo alloy, Ti-6242,  $\alpha$ + $\beta$ , creep property improvement by Pt ion plating 0-16408
- Ti-Al-Sn-Zr-Mo-Si (6, 2, 4, 2, 0.1 wt.%), effect of elevated temperature and environment on fatigue crack growth 0-40486
- Ti-Al-Sn(V), corrosion resist. in marine environments (*French*) 0-50767
- Ti-Al-V, (6, 4 wt %), fracture mode, tearing topography surface fracture 0-7670
- Ti-Al-V, (6, 4 wt.%), single and dual ion irradi., microstruct. studies 0-29077
- Ti-Al-V, alloy 685, fatigue life, creep and dynamic strain ageing effect, 25 to 400°C (*French*) 0-45384
- Ti-Al-V, containing 0-6000 ppm  $^3\text{He}$ , sensitivity of tensile props. 0-39197
- Ti-Al-V, irradi. induced creep 0-39163
- Ti-Al-V, rolled, elastic stiffness and Bauschinger effect accompanying anisotropic hardening (*Russian*) 0-40435
- Ti-Al-V, VT6 alloy, butt welded joints, electron beam welding conditions effecting interstitial impurities distribution 0-39136
- Ti-Al-V (4, 7, 2 wt.%) pseudo alpha alloy, laminar struct. singularities,  $\beta$  to  $\alpha$  transformation (*Russian*) 0-7552
- Ti-Al-V (6, 4 wt.%), dynamic crit. stress intensity vs. crack vel. 0-2115
- Ti-Al-V (6, 4 wt.%), friction characts. improvement by  $\text{O}_2$  dissolution and controlled surface hardening (*French*) 0-45401
- Ti-Al-V (6, 4 wt.%), gust spectrum fatigue crack prop. 0-21105
- Ti-Al-V (6, 4 wt.%), improvement of props. by ion implantation 0-16601
- Ti-Al-V (6, 4 wt.%), repassivation and pitting corrosion 0-30143
- Ti-Al-V (6, 4 wt.%), temp. distrib. for steady axisymmetric extrusion 0-11670
- Ti-Al-V (6, 4 wt.%), temp. distrib. for steady axisymmetric extrusion numerical results 0-11671
- Ti-Al-V (6, 4 wt.%), type IMI 318, internal friction study of martensitic transformations 0-7573
- Ti-Al-V (6, 4 wt.%), type IMI 318, stability of martensitic phases 0-7574
- Ti-Al-V (6, 4 wt.%) cylinders, residual stresses introduced by quenching elastoplastic anal. (*French*) 0-45355
- Ti-Al-V (6, 4 wt.%) slow crack growth in air and fracture toughness, H content effect (*French*) 0-45385
- Ti-Al-V (6, 4 wt %), superplasticity, effect of temp. 0-7639
- Ti-Al-V (6, 4 wt.%),  $\alpha/\beta$  interface phase influence on tensile props. 0-30034
- Ti-Al-V (6, 4 wt.%), D profiles after  $\text{D}_3^+$  implantation 0-37581
- Ti-Al-V (6, 4 wt.%), D trapping in fusion reactor materials, temp. dependence 0-37577
- Ti-Al-V (6, 4 wt.%), fretting fatigue behaviour of temps. up to 600°C 0-21104
- Ti-Al-V (6, 4 wt.%), high temp. fretting fatigue, fatigue and fretting wear 0-3197
- Ti-Al-V (6, 4 wt.%), phase transformation after hydrogenation 0-7560
- Ti-Al-V (6, 4 wt.%), quenched, struct. and age hardening rel. to treatment temp. 0-11657
- Ti-Al-V (6, 4 wt.%), strongly textured, influence of crystallographic orientation on tensile behaviour 0-7633
- Ti-Al-V (6, 4 wt.%), to H effect on fracture props. and microstruct. 0-40512
- Ti-Al-V (6, 4 wt.%) alloy foil, substrate temp. effect on struct. 0-7497
- Ti-Al-V (6, 4 wt.%) for TiC reactively sputtered coatings, adherence, XPES and wear study 0-25565
- Ti-Al-V-Sn (6, 6, 2 wt.%) weldments, heat treated, transangular fracture 0-40524
- Ti-Al-V-Sn (6, 6, 2 wt.%), fatigue crack growth, cyclic freq. and microstruct. influence 0-55515
- Ti-Al-V-Sn (6, 6, 2 wt.%),  $\alpha$ - $\beta$  type 662, fusion zone fracture behaviour in weldments 0-30093
- Ti-Al-V-Sn (6, 6, 2 wt.%), depend. of  $K_{\text{ISCC}}$  on loading rate and crack orientation 0-45427
- Ti-Al-V-Sn (6, 6, 2 wt.%) solid metal embrittlement by Cd, Ag and Au 0-16551
- Ti-Al-V(Sn) alloys, plastic deformation and fracture characts. at low temps. (*Russian*) 0-7624
- Ti-Al-Zr alloy, TA6Zr5D, structural evolution during continuous cooling at different rates (*French*) 0-45300
- Ti-Al-Zr-Mo alloy 685, phase at  $\alpha/\beta$  interface (*French*) 0-25661
- Ti-Al(Fe) microprobe anal. of alloying addition distrib. 0-55358
- Ti-Al(Mo), swaged and recrystallized, grain growth 0-3092
- Ti-Al(-V)(Mo), impact strength anisotropy, influence of texture (*Russian*) 0-20952
- Ti-alloys, methods of studying effect of H on service behaviour 0-16478
- Ti-B, abrasive props. 0-16489
- Ti-Be, coupled phase diagrams and thermochemical descriptions 0-25656
- Ti-Be, metallic glass form. and props. 0-16219
- Ti-Be-Zr, coupled phase diagrams and thermochemical descriptions 0-25656
- Ti-Co, radiation disorder model of phase stability 0-16297
- Ti-Co alloys, absorpt. of  $\text{H}_2$ , press.-composition-temp. relationships, enthalpy, entropy 0-2267
- Ti-Co alloys, absorpt. of  $\text{H}_2$ , thermodynamic parameters calc. 0-2268
- Ti-Cr,  $\text{H}_2$  diffusion at room temp. (*Japanese*) 0-19987
- Ti-Cr, phase transformation, appl. of Philips STEM400 system 0-25689
- Ti-Cr-B system, self-propagating high temp. synthesis, crystallochemical and mech. props. 0-20861
- Ti-Cr-Zr, martensite formation, chemical composition effect 0-50634
- Ti-Cu (2.5 wt.%), corrosion resist. in marine environments (*French*) 0-50767
- Ti-Cu dissolution mechanisms, photoelectron spectra study (*French*) 0-45198
- Ti-Cu thin films, oxidation kinetics in air at 100 to 300°C, meas. 0-40590
- Ti-Fe, diffusion of stored H, Mossbauer study 0-34838
- Ti-Fe, dil., phase analysis by Mossbauer spectra 0-15922
- Ti-Fe, force constant change with pressure, relative Mossbauer fraction 0-34163

## titanium alloys continued

- Ti-Fe, magnetic susceptibility depend. on phase composition (*Russian*) 0-54875
- Ti-Fe corrosion resistant coating on Cu, obtained by contact eutectic fusion 0-50772
- Ti-H, diffusion in hydride phase, exam. 0-29204
- Ti-H (Ni-H)(Cu-H), catalytic props. 0-30274
- Ti-Hf, dil.,  $^{178}\text{Hf}$  Mossbauer transition, electric quadrupole interaction 0-39928
- Ti-Ir, Ti-rich, thermodynamic study at high temp. using Knudsen cell mass spectrometry 0-45539
- $\alpha$ - $\beta$  Ti-Mn (8 wt.%), calcs. of stress-strain curve, stress and strain distrib., discussion 0-7637
- $\alpha$ - $\beta$  Ti-Mn (8 wt.%), stress-strain curve and stress and strain distrib. calcs., reply to discussion 0-7638
- Ti-Mo-Fe (3, 0.13 at.%), metastable phases, Mossbauer study 0-7243
- Ti-Mo-Zr-Sn (11.5, 6, 4.5 wt.%), metastable beta III phase, recrystallization and grain growth 0-3091
- Ti-Nb-Al, decomposition during isothermal annealing 0-25653
- Ti-Nb-Zr (35, 3 wt.%), martensitic  $\tau$  phase, X-ray diffr. obs. 0-16300
- Ti-Ni, effect of alloying on crit. points and martensitic transform. hysteresis 0-20935
- Ti-Ni, electron phase transition XPS, optical spectra and mag. susceptibility meas. 0-19943
- Ti-Ni,  $\text{H}_2$  diffusion at room temp. (*Japanese*) 0-19987
- Ti-Ni, laser melting and splat quenching to form foils for TEM obs. 0-29986
- Ti-Ni, martensite transform. B2-B19', optical props. and electron struct. (*Russian*) 0-34878
- Ti-Ni, thermoelastic phase transform., acoustic emission 0-3039
- Ti-Ni, vacuum pressure seal with thermomechanical drive 0-31773
- Ti-Ni alloys, absorpt. of  $\text{H}_2$ , press.-composition-temp. relationships, enthalpy, entropy 0-2267
- Ti-Ni alloys, absorpt. of  $\text{H}_2$ , thermodynamic parameters calc. 0-2268
- Ti-Pd (0.15 wt.%), IMI-260, strain rate effect on mech. behaviour 0-3153
- Ti-Pt-Au, nonalloyed ohmic contacts to n-GaAs by pulse-electron beam annealed Se implants 0-2466
- Ti-Ru, radiation disorder model of phase stability 0-16297
- Ti-Si cosputtered films, silicide form., X-ray diffr. and resist. study 0-54546
- Ti-Si film thin film interaction, metallisation, X-ray diffr. and sheet resist. 0-54442
- Ti-V, elastic moduli, comparison with paramagnetic Cr, V-Cr, rel. to bandstructure 0-7615
- Ti-V-Cr, electron-lifetime effects on props. 0-10951
- Ti-V-Cr, type Ti-15-333, irradi. induced creep 0-39163
- Ti-V-Cr-Al (13, 11, 3 wt.%), stress corrosion cracking in methanolic solutions 0-50752
- Ti-V-Mo-Cr system,  $\beta$ -phase stability 0-55353
- $\alpha$ -Ti-V(Al)(Sn), Mossbauer spectra, metastable  $\theta$ - and  $\omega$ -phases 0-20556
- Ti-W film, bias-sputtered, resist. and comp. 0-25023
- Ti-W(-Al), mech. props. and heat treatment 0-35274
- Ti-Zr-Cr-Mn/LaNi<sub>5</sub> hydriding alloy mixtures for H energy storage 0-45788
- $\alpha$ -Ti-Zr-W, effect of W impurity on mech. props. 0-16392
- Ti-Zr-W(-Al), phase struct. and props. (*Russian*) 0-16270
- TiAl, crystals dissolution in pure Al liq., grain refinement of  $\alpha$ -Al solid-solution by Ti addition 0-35178
- TiAl<sub>2</sub>V<sub>4</sub>, H impurity detection by  $^1\text{H}(^{15}\text{N}, \alpha\gamma)$  reaction 0-55767
- TiBe<sub>2</sub>, neutron diffr. study of mag. ordering 0-44811
- TiBe<sub>2</sub>-Cu<sub>2</sub>, C-15 lower phase, itinerant ferromagnetism 0-15723
- TiC-Fe-Cr powder mixture, exam. of milling condition effects 0-16237
- TiC-Ni powder compact, wetting problems in sintering 0-11596
- TiC-TiB<sub>2</sub>, friction characts., comp. depend., 20-1000°C 0-3203
- TiC-TiB<sub>2</sub>, wear in vacuum, role of boride phase 0-21113
- TiC-TiB<sub>2</sub> alloys, composition effect on surface layer rupture at various temps. 0-25879
- TiCo-H system, thermodynamic rels. and struct. transformations 0-49385
- TiCo<sub>2-3</sub> ( $x=0.06, 0.0, 0.13$ ), stacking faults in cubic Laves phase 0-19816
- Ti<sub>1-x</sub>Co<sub>x</sub>, electronic struct. and anomalies of elec. and mag. props. 0-6710
- Ti(Fe,Co,Ni) cubic metal binary alloys for H energy storage 0-45787
- TiFeD, cryst. struct., Mossbauer and neutron diffr. obs. 0-34839
- TiMn, faceted parent martensite interface 0-6417
- Ti<sub>1-x</sub>Nb<sub>x</sub>H<sub>1.94x</sub>, electronic struct. MNR meas. 0-15439
- Ti<sub>1-x</sub>Nb<sub>x</sub>H<sub>1.94x</sub>,  $x=0.25, 0.50$ , low temp. specific heat meas. 0-2179
- TiNi-H system, thermodynamic rels. and struct. transformations 0-49385
- Ti<sub>0.60</sub>Ni<sub>0.40</sub> metallic glass, Young's modulus meas. by impulse induced resonance technique 0-40411
- Ti<sub>1-x</sub>Ni<sub>x</sub>, electronic struct. and anomalies of elec. and mag. props. 0-6710
- Ti<sub>2</sub>NiH<sub>2</sub>, H storage material, H diffusion, neutron diffr. obs. 0-51013
- Ti(Zr,Hf)-Gd-B system, phase equil. 0-11629
- (V,Ti)C+Ni cermet, binder grain size 0-44401
- V-Ti, and V-Ti-Be(Zr), 4 MeV Ni<sup>++</sup> irradi., He gas bubble form. 0-29085
- V-Ti (42 at.%), mixed state, US attenuation meas. at 4.14K 0-15657
- W-Cu-Ti exam. of mech. props. as function of temp., composition, and oxidation props. 0-16472
- W-Ti, Ti addition effect on heat resistance and radiative props. (*Russian*) 0-25515
- WC-Co-Ta-C-Ti-C-NbC cemented carbide, microstructure, high temp. deformation, uniaxial plastic compression 0-40451
- Zn-Ti, environmental factors affecting pitting corrosion potential in NaOH solns. 0-45423
- Zr-Ti, alloy, mag. susceptibility, elec. cond., Hall conc. thermoEMF conc. depend. (*Russian*) 0-39551

## titanium compounds

- see also titanium alloys
- garnets, synthetic, IR spectra, Ti struct. role 0-7346
- oxide films, anal. by AES (*French*) 0-44440
- quartz ceramic, SiO<sub>2</sub>-Cr<sub>2</sub>O<sub>3</sub>-TiO<sub>2</sub>, creep and porosity, for ceramics with different structures 0-21011
- refractory carbides, borides and nitrides, wetting by and interactions with liq. metals 0-54473
- rutile ceramic anomalous conductivity effect analysis 0-15512
- tetrahedrals of Gp.IV elements, M-X bond flexibility, by compliance scheme 0-37805



## titanium compounds continued

- TiO<sub>2</sub>, high temperature interactions with Re 0-16665  
 Zircon ceramic, exam. of development and fabrication 0-11608  
 Al-TiSi<sub>3</sub>-n-Si struct., elec. props., charge transfer mechanism across TiSi<sub>2</sub>-Si interface (*Russian*) 0-34515  
 AlN, thermoplastic slips, viscosity, thixotropy, dilatance determs. 0-25633  
 Al<sub>2</sub>O<sub>3</sub>-Ti<sub>2</sub>O<sub>3</sub>, dopant influence on struct. and mech. props. 0-24471  
 Al<sub>2</sub>O<sub>3</sub>-SiO<sub>2</sub>-Fe<sub>2</sub>O<sub>3</sub>-CaO-MgO-TiO<sub>2</sub>, refractory, corrosion and mech. behaviour correlations 0-40563  
 Al<sub>2</sub>O<sub>3</sub>-TiO<sub>2</sub>, thermal-sprayed coating on steel, acoustic emission 0-21247  
 BaO-Al<sub>2</sub>O<sub>3</sub>-TiO<sub>2</sub>-SiO<sub>2</sub>, glass formation, structure of cations (*Russian*) 0-38933  
 BaO-SrO-Al<sub>2</sub>O<sub>3</sub>-TiO<sub>2</sub>-SiO<sub>2</sub>, glass ceramics, cryst. phases form., BaO/SrO ratio influence 0-19705  
 CaO-Al<sub>2</sub>O<sub>3</sub>-TiO<sub>2</sub>-SiO<sub>2</sub>, glass formation, structure of cations (*Russian*) 0-38933  
 CoO-MgO-Cr<sub>2</sub>O<sub>3</sub>-Fe<sub>2</sub>O<sub>3</sub>-TiO<sub>2</sub>, form. and colour of spinel solid soln. (*Japanese*) 0-16059  
 Cr<sub>1-x</sub>Ti<sub>x</sub>N, cryst. and mag. struct., at low temps. (*French*) 0-29005  
 CuO-Cu<sub>2</sub>O-TiO<sub>2</sub>, phase equilibria, thermodynamics of Cu<sub>2</sub>TiO<sub>4</sub> phase 0-55374  
 (Fe, Ti) silicate glasses, optical absorption and Mossbauer spectra 0-55136  
 (Fe,Ti)O<sub>4</sub>, magnetostriction calcs. (*Dutch*) 0-2619  
 Fe-TiB<sub>2</sub>, dispersion strengthened, thick vacuum condensate, control of struct. and mech. props. 0-16324  
 Fe-TiC, dispersion strengthened, thick vacuum condensate, control of struct. and mech. props. 0-16324  
 FeTiD<sub>x</sub> (0 ≤ x ≤ 1.9), structural phase transitions, absorpt. and desorpt. isotherms 0-19948  
 Fe<sub>3-x</sub>Ti<sub>x</sub>O<sub>4</sub>, Mossbauer spectra in paramag. phase 0-39943  
 Fe<sub>(1+x)</sub>Ti<sub>(2-x)</sub>S<sub>4</sub>, non-stoichiometric cpds., vacancy-cation distrib., Mossbauer spectra 0-15900  
 HfO<sub>2</sub>-TiO<sub>2</sub> system, zero and low coeff. of thermal expansion 0-39325  
 K<sub>2</sub>O-Ti<sub>2</sub>O<sub>3</sub>-SiO<sub>2</sub> glass, Si-O bonding, SiKβ X-ray fluorescence and IR spectra 0-10500  
 LaCrO<sub>3</sub>-TiO<sub>2</sub> photoactive anode, for photoelectrolytic production of H<sub>2</sub> and electricity 0-12024  
 Li-TiS<sub>2</sub>, storage batteries (*German*) 0-12001  
 Li<sub>2</sub>O-SiO<sub>2</sub>-TiO<sub>2</sub> glass, crystn., kinetic study using differential scanning calorimetry 0-44138  
 Li<sub>2</sub>Si<sub>2</sub>O<sub>7</sub>-TiO<sub>2</sub> glasses, struct. and crystn. investigation using Raman spectra 0-38918  
 LiTi ferrite, Mossbauer study, relax. and supertransferred hyperfine fields 0-39941  
 LiTi, substituted ferrite, cation distribution, Mossbauer, X-ray, neutron diff. study 0-28975  
 Li<sub>2</sub>TiS<sub>2</sub> (0 ≤ x ≤ 3), intercalation in TiS<sub>2</sub>, possible electrochem. cathode 0-19772  
 Li<sub>2</sub>TiS<sub>2</sub>, electrochemically intercalated, ion ordering, X-ray diff. meas. 0-44177  
 Li<sub>2</sub>TiS<sub>2</sub>, struct. determ. by neutron diffraction 0-54196  
 MgO-Al<sub>2</sub>O<sub>3</sub>-SiO<sub>2</sub>: ZrO<sub>2</sub>, TiO<sub>2</sub>, glass, phase separation (*German*) 0-38932  
 MgO-Al<sub>2</sub>O<sub>3</sub>-TiO<sub>2</sub>-SiO<sub>2</sub>, glass formation, structure of cations (*Russian*) 0-38933  
 Mn<sub>0.94</sub>Ti<sub>0.06</sub>O-S system, 1380 and 1485K, phase equilib. study 0-50616  
 (N<sub>2</sub>H<sub>5</sub>)<sub>2</sub>F<sub>2</sub>[TiF<sub>6</sub>], X-ray cryst. struct. determ. 0-54182  
 Na<sub>2</sub>O-TiO<sub>2</sub>-SiO<sub>2</sub> glass, ion-bombarded, optical time intensities 0-35037  
 Na<sub>2</sub>O-TiO<sub>2</sub>-SiO<sub>2</sub> glass, Si-O bonding, SiKβ X-ray fluorescence and IR spectra 0-10500  
 Na<sub>2</sub>O-Al<sub>2</sub>O<sub>3</sub>-10TiO<sub>2</sub>, crystallized bronze, chem. comp., morphology, optical and thermal props. (*Japanese*) 0-16172  
 Na<sub>2</sub>TiS<sub>2</sub>, electrochemically intercalated, ion ordering, X-ray diff. meas. 0-44177  
 POCl<sub>3</sub>-TiCl<sub>4</sub>, splitting of Sm<sup>3+</sup> near IR absorpt. bands 0-2750  
 Pb(Zr,Ti)O<sub>3</sub> polycrystalline ceramic, fracture and strength, surface treatment effects 0-11704  
 Pt/TiO<sub>2</sub> catalyst for photoassisted decomposition at room temp. of H<sub>2</sub>O and ethylene 0-55703  
 SiO<sub>2</sub>-TiO<sub>2</sub> antireflection coating, 1.064 μm laser damage, barrier 0-33059  
 SiO<sub>2</sub>-TiO<sub>2</sub>-Na<sub>2</sub>O(-CaO), thermal diffusivity in range 0-600°C, influence of TiO<sub>2</sub> 0-29233  
 SiO<sub>2</sub>-(TiO<sub>2</sub>) glass prep., melting (*Polish*) 0-40316  
 SrO-Al<sub>2</sub>O<sub>3</sub>-TiO<sub>2</sub>-SiO<sub>2</sub>, glass formation, structure of cations (*Russian*) 0-38933  
 (Ta,Ti)B<sub>2</sub> on graphite, CVD coatings, hardness meas., SEM study 0-24760  
 Ta<sub>2</sub>Ti<sub>1-x</sub>S<sub>2</sub>, Li intercalation, electrochemical studies 0-39048  
 (Ti, Cr)B<sub>2</sub>-based alloys, densification of powder mixtures by hot-pressing, elec. and mech. props. 0-20812  
 (Ti,V)C, activated reactive evaporation deposited films, annealing study, microstructure 0-24762  
 (Ti,Zr)B<sub>2</sub> on graphite, CVD coatings, hardness meas., SEM study 0-24760  
 Ti complex, TiOCl[Co(cyclopentadienyl)]<sub>2</sub>,<sub>0.16</sub>, synthesis and struct. 0-44176  
 Ti-C-N-O-H, solid solns. of H, exam. of props. 0-29172  
 Ti-H, deposited on carriers, synthesis, structure and catalytic props. 0-29890  
 Ti-H, diffusion in hydride phase, exam. 0-29204  
 Ti-H exam. of electron structure 0-29306  
 Ti-N-C-H(-O) system, thermodynamic anal. (*Russian*) 0-55325  
 Ti-O system, intermediate oxide thermodynamics under equilibrium press. 0-55351  
 Ti-S system, nonstoichiometric, containing stacking faults, X-ray diff. intensity distrib. calc. 0-28872  
 Ti-TiC-TiN system, phases 0-20905  
 Ti-TiO<sub>2</sub>-Au diode, spectral photoresponse and I-V characts. 0-15617  
 TiB<sub>2</sub>, CVD coating, surface damage and erosion under energetic D<sup>+</sup> and <sup>4</sup>He<sup>+</sup> irradi. 0-39174  
 TiB<sub>2</sub> coated limiters, first wall protection 0-32483  
 TiB<sub>2</sub>, coating, D<sup>+</sup> and <sup>4</sup>He<sup>+</sup> irradi. effects 0-20753  
 TiB<sub>2</sub> coating, erosion rates under H<sup>+</sup> ion bombard., fusion reactor appls. 0-39179  
 TiB<sub>2</sub> coating, on WC-Co alloy cutting plates, hardness and struct. 0-21175  
 TiB<sub>2</sub> coating on graphite by CVD 0-21131

## titanium compounds continued

- TiB<sub>2</sub> coatings for Tokamaks, H trapping and re-emission, annealing effects 0-37582  
 TiB<sub>2</sub>, crystal growth by chem. vapour transport 0-16164  
 TiB<sub>2</sub>, deposition of coating on WC-Co by thermal diffusion (*Bulgarian*) 0-45430  
 TiB<sub>2</sub>, electric arc melting prep. and oxidation props. 0-20860  
 TiB<sub>2</sub>, first-wall coating for Tokamak, H retention and release 0-18620  
 TiB<sub>2</sub>, plasma-sprayed coatings on Cu and stainless steel, fusion reactor appl. 0-18619  
 TiB<sub>2</sub>, preparation method rel. to compressive strength 0-55327  
 TiB<sub>2</sub>, reactions with Ti-Al-Cr-Mo alloy VT3-1 0-16585  
 TiC (001) surface, change in work function with chemisorption of O<sub>2</sub> and H<sub>2</sub>O 0-29461  
 TiC, activated reactive evaporation deposited films, annealing study, microstructure 0-24762  
 TiC coated limiters, first wall protection 0-32483  
 TiC coating, erosion rates under H<sup>+</sup> ion bombard., fusion reactor appls. 0-39179  
 TiC coating thickness meas. using X-ray diff. 0-21243  
 TiC, deformation behaviour during rubbing in wide temp. range 0-16486  
 TiC film, CVD, on WC, diffusion processes, ion beam anal. 0-49424  
 TiC layers, on steel and cemented carbides, load-bearing capacities 0-40606  
 TiC micro powder surface finishing of metals, surface struct. 0-11842  
 TiC plasma-chemical synthesis, depend. on geometric and flow rate parameters (*Russian*) 0-40677  
 TiC, plasma-sprayed coatings on Cu and stainless steel, fusion reactor appl. 0-18619  
 TiC precipitate in austenitic stainless steel, grain boundary dislocation interaction, during creep 0-16384  
 TiC precipitation in alpha-radiated stainless steel, effect on He embrittlement 0-45399  
 TiC, production from tetrachloride and hydrocarbon, thermodynamic analysis (*Russian*) 0-7523  
 TiC, reactions with Ti-Al-Cr-Mo alloy VT3-1 0-16585  
 TiC reactively sputtered coatings on Ni-Cr-Mo-Ti (19,11,3 wt.%), adherence, XPS and wear study 0-25565  
 TiC single crystals, synthesis and impurities 0-55329  
 TiC, sintering and grain growth, metallographic anal. 0-25642  
 TiC, soft X-ray emission, excitation pot. spectra, excited level binding energy 0-35009  
 TiC sputtered coatings on Ti-Al-V (6,4 wt.%), adherence, XPS and wear study 0-25565  
 TiC-Au multilayer struct., microhardness and elec. resist. 0-2950  
 TiC-B, struct. and mech. props. 0-55461  
 TiC-TiB<sub>2</sub>, strength and antifriction props. over wider range of concs. 0-50673  
 TiC-TiN, hardness var. charact. in homogeneity field 0-3192  
 TiC-TiN, physicochem. props., comp. depend. 0-55370  
 TiC-TiN system, electro- and thermo-phys. props. 0-34210  
 TiC-VC, mag. susceptibility, elec. cond. and thermoelec. props. 0-50033  
 TiC-W(Mo), thermionic emission, surface structural characts. after prolonged use, work function variation 0-20758  
 TiC-ZrC, mag. susceptibility, elec. cond. and thermoelec. props. 0-50033  
 TiC-ZrC, solid soln., conc. and temp. dependence of props. 0-39736  
 TiC<sub>1-x</sub>, substoichiometric, electronic density of states 0-2319  
 TiC, refractory layers on steel surfaces, ESCA obs. 0-39471  
 TiC(N) overlay coating on stainless steel, Ti or Al, effect on physicochemical and wear props. 0-40603  
 TiC<sub>1-x</sub>N<sub>x</sub>, formation in high temp. N flow, ultra disperse powder, thermodynamic anal. (*Russian*) 0-55325  
 TiC<sub>x</sub>N<sub>1-x</sub>, electronic struct., theoretical approach 0-54584  
 TiC<sub>x</sub>N<sub>y</sub>, thermal cond., elec. cond., and thermal expansion 0-10714  
 TiC<sub>0.1-x</sub>, electronic struct., theoretical approach 0-54584  
 TiC<sub>0.9</sub> are TiC<sub>0.9</sub>H<sub>0.1</sub>, cubic phases, mag. susceptibility 0-15680  
 TiC<sub>0.9</sub>, thermal cond., elec. cond., and thermal expansion 0-10714  
 TiCl<sub>3</sub>, lattice instability, d-electron-lattice interaction 0-44276  
 TiCl<sub>3</sub>, phase transition, phonon dispersion curves 0-2130  
 TiCl<sub>4</sub>, electrochemical behaviour in alkali chloride baths 0-30243  
 TiCl<sub>4</sub>, t<sub>1</sub>→2e<sup>-</sup>(A<sub>1</sub>→<sup>1</sup>T<sub>2</sub>) transition, bond props. and LCAO MO calcs. 0-18889  
 TiCl<sub>4</sub>-graphite intercalation compound 0-40675  
 TiCl<sub>4</sub>-MgCl<sub>2</sub>, high activity catalyst for polyethylene, struct. and mechanism investig. 0-11951  
 TiCl<sub>4</sub>-SiCl<sub>4</sub>(SnCl<sub>4</sub>) liq., beat effects, neutron diff. studies 0-38897  
 TiCrB<sub>2</sub>-Ni(Ni-Mo) systems, interphase reactions, electron probe anal., metallography and hardness exam. 0-2990  
 TiD<sub>2</sub>, film formed during simulated Tokamak gettering cycles, desorption 0-34296  
 TiF<sub>2</sub>, TiF<sub>4</sub>, X-ray emission, core level chem. shift calcs. 0-53010  
 TiF<sub>2</sub>, vibr. anal., kinetic consts. method 0-18838  
 TiF<sub>4</sub>, equilib. config., force field, Coriolis consts., vibr. freqs. and amplitudes 0-32835  
 (TiF<sub>6</sub>)<sup>3-</sup> complex, open-shell cluster calcs, semiempirical LCAO-MO method 0-54583  
 β-TiFeH<sub>1.03</sub>, H diffusion, NMR meas. 0-10707  
 TiH, electronic structure of five and ten atom chains SCF-Xα-SW calcs. 0-5483  
 TiH<sub>2</sub>, band model of martensitic phase transition 0-29953  
 TiH<sub>2</sub>, H impurity detection by <sup>1</sup>H(<sup>15</sup>N,αγ) reaction 0-55767  
 TiH<sub>4</sub>, X-ray emission, core level chem. shift calcs. 0-53010  
 TiH<sub>4</sub>, film, anomalous H<sub>2</sub> desorption at room temp. 0-29261  
 TiH<sub>4</sub>, film, kinetics of H<sub>2</sub> interaction 0-6620  
 TiH<sub>4</sub>, H diffusion, NMR obs. 0-34813  
 TiH<sub>3</sub>F, X-ray emission, core level chem. shift calcs. 0-53010  
 Ti<sub>1-x</sub>Hf<sub>x</sub>Se<sub>2</sub> mixed cryst., elec. resist. and phase transition temp. 0-24928  
 Ti(IV)-Fe(II) oxide, U adsorption, U extraction from seawater 0-24730  
 TiN film as protective coating for vacuum deposition chamber, Auger electron spectroscopy study 0-25922  
 TiN films deposited by reactive sputtering, elec. props. 0-15638  
 TiN, from high-temp. reaction of NH<sub>3</sub> and TiCl<sub>4</sub>, physicochem. props. 0-55334  
 TiN, interatomic interactions from XPS 0-49171  
 TiN layers formation, on steel substrate, microhardness and structure obs. (*Hungarian*) 0-2965  
 TiN, RF sputter deposition, ion bombardment and ion implantation 0-25564  
 TiN, reactive ion plating with auxiliary discharge deposition conditions influence on film props. 0-20801



## titanium compounds continued

- TiN, self-propag. high-temp. synthesis under high  $N_2$  pressures 0-25630  
 TiN, soft X-ray emission, excitation pot. spectra, excited level binding energy 0-35009  
 TiN, synthesised in SHF discharge plasma, exam. of props. (*Russian*) 0-7524  
 TiN-Ti<sub>3</sub>N<sub>2</sub>, activated reactive evaporation formed deposits, microstructure, transformation depend. on depositing conditions 0-24761  
 TiN<sub>2</sub> film, reactively sputtered in Ar-N<sub>2</sub> atm., elec. and struct. props. 0-15636  
 TiN<sub>2</sub>, oxidation mechanism 0-25912  
 $\epsilon$ -Ti<sub>2</sub>N, interstitially built layer, reducing permeation of H plasma through Ti 0-16566  
 Ti<sub>3</sub>N<sub>4</sub> plasma condensation on steel and carbide (*Russian*) 0-20796  
 TiN<sub>2</sub>O<sub>1-x</sub>, electronic struct., theoretical approach 0-54584  
 TiN<sub>2</sub>O<sub>2</sub>, elec. cond., conc.-temp. depend., 25-1000°C 0-34439  
 Ti<sub>1-x</sub>Nb<sub>x</sub>H<sub>1.94</sub>,  $x=0.25, 0.50$ , low temp. specific heat meas. 0-2179  
 Ti<sub>0.5</sub>Nb<sub>0.5</sub>Se<sub>2</sub>, cryst. struct., metallic cond., mag. and phys. props. (*French*) 0-33956  
 TiO band absorption effect on stellar photometry with broadband filters 0-41811  
 TiO, electron struct. calc. 0-49587  
 TiO, energy band struct. and density of states (*Russian*) 0-44493  
 TiO, Fermi surface and de Haas-van Alphen effect (*Russian*) 0-49573  
 TiO, high temp. thermodynamics, vaporisation, and pressures over 0-10685  
 TiO, X( $\Delta$ ) state, vibrational IR spectrum using microwave powered molecular source, rotational analysis 0-9596  
 TiO<sub>2</sub>, (100) surfaces, ionisation of sputtered-atomic particles 0-20750  
 TiO<sub>2</sub> (rutile), (001) and (110) faces, UPS and LEED obs. 0-45206  
 TiO<sub>2</sub> (rutile), (001) and (110) surfaces, surface and bulk density of states calcs. 0-49858  
 TiO<sub>2</sub>, absorbing film parameters determ. by ellipsometry 0-254  
 TiO<sub>2</sub>, adsorption of neopentane, NMR pulsed field gradient method, diffusion coeff. meas. 0-15362  
 TiO<sub>2</sub>, amorphous film, vac. deposited, struct. and crystn., TEM obs. 0-2291  
 TiO<sub>2</sub>, anatase phase, lattice vibr. calcs., rigid ion model 0-2125  
 TiO<sub>2</sub> based ceramics, variation of dielectric constant and resistivity with temp. 0-2683  
 TiO<sub>2</sub> based construction ceramics, fibre-like cryst. reinforced, mech. props. 0-55341  
 TiO<sub>2</sub>, CW CO<sub>2</sub> laser deposited dielect. thin film, optical and struct. props. 0-7506  
 TiO<sub>2</sub>, chemical effect, influence on stopping power 0-47830  
 TiO<sub>2</sub>, clean and hydrated, surface sites, XPS 0-35052  
 TiO<sub>2</sub>, clusters, surface electron struct. and defect states, DV-X $\alpha$  calc. 0-20268  
 TiO<sub>2</sub>, coincidence-site lattice interfaces 0-15381  
 TiO<sub>2</sub>, elec. cond., temp. depend. resistivity meas. at 77 to 600K, unswitched samples 0-20262  
 TiO<sub>2</sub> electrode, doping density dependent attachment of rhodamine B 0-54777  
 TiO<sub>2</sub> electrodes, in aq. electrolytes, surface states, photocurrent obs. 0-49895  
 TiO<sub>2</sub> electrodes in photoelectrochem. cell, photothermal effect 0-7947  
 TiO<sub>2</sub>, energy band struct., uniaxial stress depend. 0-2334  
 TiO<sub>2</sub> film deposited on Si, SiO<sub>2</sub> growth under film during postdeposition high temp. annealing 0-15400  
 TiO<sub>2</sub>, formation by pyrolysis of tetrabutoxytitanium 0-55311  
 TiO<sub>2</sub>, H species characterisation by electron-stimulated desorption 0-34305  
 TiO<sub>2</sub> in non-aqueous liquids, effects of mol. architecture of long chain fatty acids on dispersion props. 0-40751  
 TiO<sub>2</sub>, indirect forbidden transitions, band struct. enhancement 0-44503  
 TiO<sub>2</sub>, K<sup>+</sup> implantation, extended defects and precipitates 0-49251  
 TiO<sub>2</sub> layer form. by anodic oxidation, characterisation using <sup>4</sup>He back-scatt. (*French*) 0-45433  
 TiO<sub>2</sub> layers, obtained by cathode and HF sputtering, light scatt. and refr. index reduction 0-29877  
 TiO<sub>2</sub>, obtained ions Ti<sub>2</sub>OCl (HCOO)<sub>3</sub>(OH)<sub>2</sub>, by thermohydrolysis, exam. of crystallisation 0-2173  
 n-TiO<sub>2</sub> photoanodes, corrosion suppression mechanism 0-2462  
 TiO<sub>2</sub>, photodesorption of H<sub>2</sub>O, pulsed-laser-dynamic-mass-spectrometer study 0-35568  
 TiO<sub>2</sub>, photoelectrochemical systems, solar energy utilisation (*German*) 0-45713  
 TiO<sub>2</sub>, plasmochemical synthesis, oxidised from metals, exam. of props. 0-2984  
 TiO<sub>2</sub>, reactive DC sputtering deposited films with magnetron-plasmatron, mechanical elec., optical props. 0-25566  
 TiO<sub>2</sub>, reactively sputtered optical coating for inertial confinement fusion laser components 0-23705  
 TiO<sub>2</sub>, reduction with CaH<sub>2</sub>, preparation of rolled Ti foils 0-18744  
 TiO<sub>2</sub>, rutile, defect struct. and elec. cond. at 1273K 0-44604  
 TiO<sub>2</sub>, rutile, isothermal compression under hydrostatic press. to 106 kbar 0-31035  
 TiO<sub>2</sub>, rutile ceramics, space charge effects 0-24945  
 TiO<sub>2</sub> rutile single crystals, stoichiometric, dynamic strain ageing 0-50661  
 TiO<sub>2</sub> semicond. films for water photoelectrolysis 0-26146  
 TiO<sub>2</sub>, sintering, struct., pressing, atm., and doping effects 0-20873  
 TiO<sub>2</sub>, solubility in KF aq. solns. 0-34197  
 TiO<sub>2</sub>, sputtered film, photocond. and TSC meas. 0-15560  
 TiO<sub>2</sub>, stoichiometric single crystals, anisotropy of ion transport 0-2206  
 TiO<sub>2</sub> surface crystalline, mass transport mechanisms at high temperatures (*Japanese*) 0-54479  
 TiO<sub>2</sub> transparent film photographic layers, props. (*Russian*) 0-43420  
 TiO<sub>2</sub>, two photon spectra, quantitative investigation, temp. depend. 0-50373  
 TiO<sub>2</sub>, vacuum deposited, destruction props. obs., suitability for integrated optics assessment (*Slovak*) 0-33224  
 TiO<sub>2</sub>, XPS satellite spectra, mol. orbital study 0-43100  
 n-TiO<sub>2</sub>-Be electrodes, photoassisted oxidation of water 0-30502  
 TiO<sub>2</sub>-Cu, anodic, effect of Cu on optical props., rel. to possible appl. in solar energy conversion 0-16115  
 TiO<sub>2</sub>-Fe, rutile, ESR meas. 0-54945  
 TiO<sub>2</sub>-Fe<sup>3+</sup>, low noise travelling wave maser, noise temp. 0-32945  
 TiO<sub>2</sub>-Fe<sup>3+</sup>, microwave second harmonic generation and freq. conversion 0-50166  
 TiO<sub>2</sub>-H photoanodes, diffusion and surface chemistry 0-35546  
 TiO<sub>2</sub>-S, acceptor properties of S, free electron concentrations 0-34395

## titanium compounds continued

- TiO<sub>2</sub>-S, in O<sub>2</sub>+CO<sub>2</sub>+SO<sub>2</sub> atmosphere, elec. cond. study 0-39583  
 TiO<sub>2</sub>-Ta<sub>2</sub>O<sub>5</sub>(Nb<sub>2</sub>O<sub>5</sub>), rutile, defect struct. and elec. cond. at 1273K 0-44604  
 TiO<sub>2</sub>-V(Cr)(Mn)(Fe), impurity levels, photocurrent and ESR meas. 0-29346  
 TiO<sub>2</sub>/SiO<sub>2</sub> charge storage memory films for IGFETs 0-11566  
 TiO<sub>2</sub>-aqueous electrolyte interface, pot. distrib., Mott-Schottky plots 0-11084  
 TiO<sub>2</sub>-based ceramics, impurity atoms chem. state, Mossbauer spectra 0-15902  
 n-TiO<sub>2</sub>-electrolyte interface, equivalent circuit elements from impedance meas. 0-39669  
 n-TiO<sub>2</sub>-electrolyte interface, charge-transfer-controlled photocurrent 0-50992  
 TiO<sub>2</sub>-Ge, elec. props., molecular deposition method 0-34525  
 TiO<sub>2</sub>-LaCrO<sub>3</sub>-GaP photoelectrochem. reactor for materials synthesis using solar energy 0-45712  
 TiO<sub>2</sub>-Pd Schottky barrier, work function depend. on adsorbed species 0-54782  
 TiO<sub>2</sub>-RuO<sub>2</sub> anode, wear-resistant, use in applied electrochem. 0-40701  
 TiO<sub>2</sub>-Si solar cell hybrid electrodes for photoelectrochem. H prod. 0-45775  
 TiO<sub>2</sub>-SiO<sub>2</sub> multilayered film striped optical filters, optical props. and fabrication of RF sputtering 0-10030  
 TiO<sub>2</sub>-Ti<sub>2</sub>O<sub>3</sub>-P<sub>2</sub>O<sub>5</sub>, glass form., struct. and elec. props. 0-44592  
 TiO<sub>2</sub>-Ti-Cl<sub>2</sub> system, thermodynamic analysis, gas phase equilibrium composition 0-21317  
 TiO<sub>2</sub>-ZrO<sub>2</sub>, submicron powders, vapour phase production from TiCl<sub>4</sub>-ZrCl<sub>4</sub>-O<sub>2</sub> system 0-40301  
 TiO<sub>2</sub>-x, reduced, cond. between elec. props. in equil. at 1100°C and after quenching, defects role (*French*) 0-44582  
 TiO<sub>3</sub>-Cr<sub>2</sub>O<sub>3</sub>, dielec. consts., AC and DC resist. 0-20186  
 TiO<sub>2</sub>, antireflection coatings for solar cells, optical, struct., and compositional characts. 0-55852  
 TiO<sub>x</sub> evaporated films, epitaxial growth on NaCl, electron microscopy obs. 0-10822  
 TiO<sub>x</sub> film, durable optical, ion plating onto plastics, optical and mech. props. 0-38141  
 TiO<sub>x</sub> films, refl., 2-25 eV 0-55123  
 Ti<sub>2</sub>O<sub>3</sub>, crystal and band struct. calcs. 0-49858  
 Ti<sub>2</sub>O<sub>3</sub>, metal-semicond. transition, refl. spectra study 0-10880  
 Ti<sub>4</sub>O<sub>7</sub>, hopping conduction and the Coulomb gap 0-44605  
 Ti<sub>4</sub>O<sub>7</sub>, metal-insulator transition, EPR elec. and mag. props. 0-2336  
 Ti<sub>4</sub>O<sub>7</sub> film, interference enhanced Raman scatt. 0-40105  
 TiO<sub>2</sub>-(Cr<sub>2</sub>O<sub>3</sub>), rutile, Cr<sub>2</sub>O<sub>3</sub> effects on O<sub>2</sub> tracer diffusivity, depth profile meas. by SIMS 0-24651  
 TiP, TiP<sub>2</sub>, iodide synthesis, and catalytic props. of TiP 0-55316  
 TiS, vaporisation chemistry and thermodynamics, computer-automated simultaneous Knudsen-torsion effusion 0-48837  
 TiS<sub>1.5</sub>, (4H)<sub>2</sub>-6C-type superstruct. revealed by high resolution microscopy 0-19755  
 TiS<sub>2</sub> (1T), electronic and vibronic struct. 0-44500  
 TiS<sub>2</sub>, elect. resist. at room temp., press. depend. to 80 kbar 0-49730  
 TiS<sub>2</sub>, evidence for semicond. props., Hall coeff., refl., cond., thermoelec. power 0-20220  
 TiS<sub>2</sub>, LEED, single-reflection layer scatt. theory 0-49059  
 TiS<sub>2</sub>, stoichiometric, heat capacity from 100 to 700K 0-10679  
 TiS<sub>2</sub>, transport props. and semicond. nature 0-44598  
 TiS<sub>2</sub>, valence density of states 0-44465  
 TiS<sub>3</sub> synthesis 0-35141  
 TiS<sub>2</sub>(NH<sub>3</sub>)<sub>1.0</sub>, NMR spectral densities and two-dimens. diffusion 0-50215  
 TiS<sub>2</sub>(Se<sub>2</sub>), and alkali metal intercalates, phys. props. 0-44179  
 TiSe<sub>2</sub> (1T), electronic and vibronic struct. 0-44500  
 TiSe<sub>2</sub>, lattice dynamics, charge density waves transverse phonon dispersion curves, model 0-49322  
 TiSi<sub>2</sub>, self-propag. high-temp. synthesis 0-2988  
 TiSi<sub>2</sub>-CrSi<sub>2</sub>, phase equil., struct. and props. 0-50608  
 TiSi<sub>3</sub>, self-propag. high-temp. synthesis 0-2988  
 (Ti<sub>0.9</sub>V<sub>0.1</sub>)<sub>2</sub>O<sub>3</sub>, spin glass, dynamic mag. susceptibility meas. 0-39792  
 (Ti<sub>1-x</sub>V<sub>x</sub>)<sub>2</sub>O<sub>7</sub> order-disorder and metal-insulator transition theory 0-24802  
 (Ti<sub>1-x</sub>V<sub>x</sub>)<sub>2</sub>O<sub>3</sub>, spin-glass props., 0.05-300K 0-25149  
 (Ti<sub>1-x</sub>V<sub>x</sub>)<sub>2</sub>O<sub>7</sub>, elec. cond. and phase diagram near metal-insulator transition 0-11054  
 (Ti<sub>1-x</sub>V<sub>x</sub>)<sub>2</sub>O<sub>7</sub>, metal-insulator transitions, EPR, elec. and mag. props. 0-2336  
 (Ti<sub>1-x</sub>V<sub>x</sub>)<sub>2</sub>O<sub>7</sub>, order-disorder and metal-insulator transitions 0-39504  
 Ti<sub>0.99</sub>V<sub>0.01</sub>Se<sub>2</sub>, negative magnetoresist. and nonlinear cond. 0-44617  
 Ti<sub>1-x</sub>V<sub>x</sub>Se<sub>2</sub> (0≤x≤0.1), elec. resist. and Hall effect 0-2386  
 TiO<sub>2</sub> electrodes, effect of processing variables on photoelectrochem. props. 0-6975  
 TiO<sub>2</sub> electrodes, room temp. diffusions, capacitance, spectral response and volt-ampere characts. 0-15294  
 (V<sub>1-x</sub>Ti<sub>x</sub>)Ge, pseudobinary A15 compound, supercond. transition temp. 0-49970  
 (V<sub>1-x</sub>Ti<sub>x</sub>)<sub>2</sub>O<sub>3</sub>-Fe, metallic antiferromagnetism, Mossbauer spectra 0-15881

## Tokamak devices

- AC, design criterion 0-38726  
 air-core Tokamak, optimisation of ohmic heating coil configurations 0-14914  
 Alcator, electron cyclotron emission, polarisation freq. depend. 0-33808  
 Alcator Tokamak, energy balance, MHD activity 0-28838  
 arcing observations in ISX Tokamak 0-33836  
 ballooning modes and pressure limits 0-28647  
 Berkeley multicusp ion source for use with TFTR neutral beam injector, characts. 0-54040  
 cold-banket systems, boundary layer analysis 0-28605  
 collisional divertor scrape-off layer in Tokamak, plasma transport 0-28614  
 commercial fusion reactors, small Tokamak hybrid design 0-13797  
 confinement and stability, effects of shaping and compression of plasma 0-28772  
 controlled fusion research and the Joint European Torus project 0-18593  
 CT-8, mag. field design (*Chinese*) 0-43995  
 CTR, nuclear energy strategy, Japan, possibility of FFHR 0-42868  
 Demonstration Tokamak Hybrid Reactor, design of advanced bundle divertor 0-13834



**Tokamak devices continued**

disruptions and turbulence in Tokamaks 0-28675  
 DITE, arcing, time-resolved meas. 0-10436  
 DITE Tokamak, impurity ion concentrations and diffusion, spectroscopic measurement 0-28771  
 DITE Tokamak 0-28688  
 DIVA, metal-impurity, confinement, discharges 0-28843  
 DIVA, scrape off layer, multigrid energy analyser applications 0-33818  
 divertor injection Tokamak experiment, plasma stability, energy and particle transport, and hydrogen recycling 0-28834  
 divertor Tokamaks, refuelling methods, pellet-plasma interaction 0-28841  
 Doublet III, fusion reactor, noncirc. discharge, ohmic heating 0-52785  
 driven magnetic fusion reactors, conf., Erice-Trapani, Italy (Sept. 1978) 0-41948  
 eddy currents induced in vacuum vessel, anal. 0-1832  
 electron cyclotron heating, Bernstein modes, Vlasov dispersion relation 0-33809  
 energy lifetime of plasma, T-3 scaling law 0-28635  
 first wall materials, effect on Tokamak plasmas 0-38692  
 formation of plasma in fusion devices, at. and plasma processes, diagnostic techniques 0-48915  
 French Tokamak research (*Russian*) 0-38690  
 FT Tokamak, electron energy replacement time and total energy containment time 0-28836  
 FT-1 Tokamak, lower hybrid plasma heating 0-28700  
 fusion devices, secondary ion emission, appl. to impurity control 0-37584  
 fusion possibilities and plasma confinement and interactions in mag. conf. fig. Tokamak, review (*French*) 0-54017  
 fusion reactor, design modifications to simplify remote maintenance 0-18613  
 fusion reactor, flux-conserving, high power density, performance characts. 0-23124  
 fusion reactor RIGGATRON, neutronic anal. of two-dimensional models 0-13789  
 fusion reactors, doublet research, plasma shape control, MHD stability 0-28837  
 fusion reactors, superheating-diffusion instability, thermonuclear burn 0-32500  
 fusion research, philosophy 0-42854  
 fusion test reactor, in-vessel maintenance remote manipulator system 0-18611  
 heating in toroidal plasmas 0-24239  
 high-beta Tokamaks, MHD beta limits, dependence on current density and pressure profiles, num. calc. 0-28637  
 high-beta Tokamaks, MHD eqn., stability, transport calc. 0-28848  
 impurity effects and control, neutral beam injection, computational models 0-28773  
 instabilities, thermonuclear cone microinstabilities and anomalous alpha-particle losses 0-28636  
 ISX-A Tokamak, plasma confinement and impurity flow reversal 0-28770  
 ISX-B Tokamak, intense heating, plasma position and current, feedback control modeling 0-33802  
 JAERI Tokamak, Ti coating for improved plasma characts. 0-24232  
 JET, ballooning modes, MHD theory 0-28639  
 JFT-2 Tokamak, plasma heating near lower hybrid frequency 0-28698  
 JIPP T-II, electron cyclotron emission meas. using double-pass optical spectrometer 0-54035  
 JIPP T-II torus, neutral gas injection and plasma current control, suppression of major disruption 0-28839  
 JT60 critical plasma testing device, status report 0-27801  
 magnetic diverters for experimental Tokamaks and fusion reactors 0-18621  
 magnetic islands, feedback stabilisation 0-28638  
 magnetic islands, tearing modes 0-28846  
 MHD stability limits of high- $\beta$  Tokamaks 0-28643  
 MHD-mode stability, high wave number, in high-pressure Tokamaks 0-28644  
 ORMAK, tearing mode mag. island struct. rot., diagnostics theory 0-48982  
 Petula Tokamak, lower hybrid waves, plasma heating and nonlinear effects 0-28697  
 plasma impurity diversion through ambient boundary layer flow 0-19603  
 PLT, current profile evolution effect on plasma-limiter interaction and energy confinement time 0-10420  
 PLT and ISX plasmas, field desorption and field ion surface studies of exposed stainless steel tips 0-34295  
 PLT Tokamak, energy balance 0-28733  
 PLT Tokamak, neutral beam heating 0-28701  
 PLT Tokamak, ohmically heated plasmas, radiation, impurity effects, instability and particle transport 0-28833  
 Pulsator Tokamaks, modulated runaway losses and effects of helical dipole field 0-28845  
 recycling and surface erosion processes 0-33805  
 refuelling by pellet injection, transport processes effects 0-38699  
 RF heating, supplementary, in Tokamak installations (*Czech*) 0-24258  
 shaping and internal structure in non-circular Tokamaks 0-28842  
 stability, two-fluid dissipative theory, shaped large-aspect ratio Tokamaks 0-28640  
 stability and beta limits in non-circular Tokamaks 0-28646  
 T-10, discharge dynamics, calculations of plasma energy and particle balance 0-28847  
 T-10 Tokamak, plasma X-ray emission 0-28840  
 T-11 Tokamak, neutral beam injection, plasma heating and stability 0-28702  
 T-12 Tokamak with two axisymmetric divertors, characteristics of divertor 0-28844  
 TFR 600 Tokamak, plasma confinement, low effective plasma charge 0-28769  
 TFTR, plasma generation and confinement 0-42864  
 TO-1 Tokamak, kink instability, feedback stabilisation 0-28634  
 toroidal field coils, reduction of bending moments 0-47697  
 transport losses, computer modelling and scaling 0-28612  
 TTR, Thomson scattering system based on two-detector spectrometers 0-32426  
 Tuman-2A, plasma compression particle diagnostics, density and temp. (*Russian*) 0-38677  
 Tuman-2A Tokamak, ohmic heating and compression of plasma 0-28703  
 Wega Tokamak, lower hybrid heating 0-28699

tomography, computerised *see computerised tomography*tool steel *see steel***tools***see also hand tools; machine tools*

cutting tool coating by cubic BN reactive vapour deposition 0-40545  
 elastic tools for finishing optical components with noncircular cylindrical surfaces 0-28368  
 metal cutting, separation process tool tip, fracture detection, acoustic emission method (*Japanese*) 0-1388  
 optical fibre alignment tool 0-23814  
 optical fibre cutting tool 0-1360  
 optical fibre ribbon cable cutting tool 0-19113

**topology***see also catastrophe theory; graph theory; network topology*

bifurcation diagram and non-homogeneous steady states in a system of diffusion-coupled chemical reactors 0-16647  
 Bogolyubov axiomatic approach to nonlocal field theory, CSL topologization (*Russian*) 0-47202  
 catalytic pellet, isothermal n-order decomposition reaction, steady state stability anal., topological degree and Lypunov method 0-30280  
 catastrophe theory, phase diagram classification 0-22313  
 catastrophe theory, singularities, examples, Thom 0-8785  
 catastrophe theory as a bridge between mathematics and physics 0-8786  
 chemical bonding, topological resonance energy, appl. to benzene and cyclobutadiene 0-5462  
 conjugated cpds., aromaticity determ. by topological reson. energy method 0-42915  
 conservation laws, dynamical topology for the space of states 0-27418  
 crystal vacancy modelling, topological approach 0-10543  
 fold field, evolving, structural stability 0-8802  
 measurable selection theorem, variational calculus appl. (*French*) 0-42045  
 phase transitions as catastrophes 0-8948  
 physics and topology, review (*Russian*) 0-8770  
 polymer network, Riemann's metric degeneration to graph metric demonstration, chain entanglement problems 0-38963  
 shock waves, global structure anal. 0-8800  
 Sobolev space mapping 0-12893  
 structural stability in physics (conference, Tübingen, Germany, May and Dec. 1978) 0-8739  
 Tokamak orbits, topology 0-28806  
 tops and d-functions in even spaces (*Russian*) 0-4508  
 two-dimensional electrostatic field construction for energy analysis 0-9796  
 unstable modes of an equilibrium, number calc. 0-36493

**torque***see also Scott effect*

adhesion measurement, of thin evaporated films 0-50822  
 electrostatic suspended gyroscopes, electrofield torque due to offset of envelope assembly (*Chinese*) 0-43225  
 galactic discs, torques and density waves excitation by external potential 0-22072  
 neutron stars, rotating, magnetic, accretion torques rel. to pulsating X-ray sources period changes 0-31320  
 thermomagnetic motor, dynamic characts. and stable operation (*Japanese*) 0-16840  
 wood screw, effects of crest and pilot hole in withdrawal resist. (*Japanese*) 0-3290  
 Al alloy cylindrical shells, buckling under combined axial preload, nonuniform heating and torque 0-53662

**torque measurement***see also dynamometers*

automatic torque magnetometer for vacuum-to-high-pressure  $H_2$  environments 0-4746  
 magnetic torque acting on rotating sample, measurement using air turbine 0-31811  
 polarisation torque-measuring system error anal. (*Russian*) 0-52191  
 Al alloy cylindrical shells, buckling under combined axial preload, nonuniform heating and torque 0-53662

torque meters *see torque meters***torquemeters**

strip-support self-balancing, kinematic features 0-4704

Torrey oscillations (NMR) *see double nuclear magnetic resonance***torsion***see also stress analysis*

bar, prismatic, with rigid ends, lower and upper bounds for torsional rigidity 0-48568  
 bar, thin-walled, effective torsional rigidity optimisation (*Russian*) 0-19245  
 bars, cylindrical, elastic-plastic torsion 0-33473  
 bluff structures, aerodynamic mechanism of torsional flutter 0-53689  
 composite cylindrical shell, torsional vibr. in mag. field 0-48624  
 composites, circular specimens, shear modulus determ. 0-25752  
 conic section bounded by straight line, torsion problem, St. Venant semi-inverse method 0-54  
 conical rod, dynamic torsion, exact solns. (*Russian*) 0-1461  
 cracks, circular, forced torsional oscillations at low frequencies 0-53703  
 curved structural members, large displacement theory, applic. to lateral-torsional buckling anal. of circular arches 0-23924  
 cylinder, clamped heterogeneous, stresses and displacement anal. 0-14571  
 cylinder, hollow, with external crack, axially symmetric torsion problem soln. 0-14614  
 cylinder, torsional vibr. superposed on finitely deformed state 0-19263  
 cylindrical bar, elastoplastic, with linear hardening, simultaneous torsion and tension 0-53658  
 elastic cylinder with holes, torsion problem, integral eqn. method soln. 0-36849  
 elastic prisms, minimum energy, St. Venant's solns. 0-52027  
 elastic-plastic torsion, variational inequality concept, finite element anal. 0-23907  
 epoxy resin, cure history effect on dynamic mech. props. 0-54356  
 fatigue strength criterion, of a round bar, subject to combined static and repeated bending and torsion 0-40496  
 glass fibre reinforced epoxy, wound, strength in twisting, stretching and transverse bending 0-11622  
 hot strip rolling simulation, by hot torsion technique 0-29990  
 kinematic hardening models, use in multi-axial cyclic plasticity 0-25717  
 laminated cylinder, imperfect, buckling under combined loading 0-7620  
 laminated cylindrical shell, coupling effect under internal press. (*Japanese*) 0-55449



**torsion continued**

- magnetostrictive cylinder, torsional deformation 0-53636
- metals and alloys, yield criterion, rheological interpretation (*Russian*) 0-21014
- methyl torsion modes, vibrational optical activity, inertial contrib. 0-5524
- optical fibre tape twist induced stress estimation and reduction by pre-twisting 0-53471
- optical glass K8, torsional deform. above  $T_g$  under low stresses, temp. effect 0-21052
- optical glass K8, torsional deform. above  $T_g$  under low stresses 0-25804
- plastic, integral inequality anal. 0-10155
- PMMA, unstable crack propagation in liq. environment, fractographic study 0-30155
- polymers, torsion pendulum dynamic mechanical testing 0-55620
- porous sintered materials, mech. testing device for hydrostatic pressure conditions 0-40645
- prismatic bar, finite element solution 0-38282
- rheological property meas. apparatus (*French*) 0-14644
- ring, homogeneous isotropic compressible elastic, second order torsion problem 0-14570
- shaft with regular round polygon, stress state 0-35284
- shell, conical, stress distrib. near hole, orthotropy effect 0-43630
- shell, spherical, non-shallow, torsional axisymmetric deform. subprogram 0-43607
- steel, austenite hot deformation influence on phase transformations 0-7606
- steel, C, effect of pre-straining on torsional fracture strain (*Japanese*) 0-3183
- steel, C, non-propagating microcrack, opening and closing behaviour in rotating bending and torsional fatigue (*Japanese*) 0-25846
- steel, C, torsional prework effect on fatigue strength, crack propagation (*Japanese*) 0-55514
- steel, low C, absolute dimensions effect on logarithmic decrement of torsional vibrs. 0-3150
- steel, stainless, reinforced glass matrix, vibr. damping anal. rel. to internal friction 0-40413
- steel, stainless type 304 L, mech. behaviour under constant stress associated with cyclic strain 0-25767
- steel alloy, type 30 KhGSA, expt. functions of resist. in tension and torsion 0-16397
- strain curves plotting 0-40638
- tape cores carrying current, torsional stress effects 0-34742
- transient elasto-dynamic response of circular crack in thick plate under torsion 0-5993
- tube, porous, nonlinear viscoelastic materials, soln. using generalised correspondence principle 0-38288
- two channel drive dynamics with differential wave mechanism (*Russian*) 0-28449
- unified theory of gravitation and electromag., Weyl-Dirac theory with torsion 0-52106
- viscoelastic layer, anisotropic, nonstationary torsional waves problem (*Russian*) 0-53678
- wind-induced bending torsional galloping vibration of rigid body, minimal wind velocity determ. 0-48623
- wire in torsion, installation for automated determination of yield strength 0-21221
- Al, Bauschinger effect, temp. influence, combined tension-torsion testing machine 0-45453
- Al, texture influence on stress/strain curves, prestrain, solid soln. and particle hardening effect on inhomogeneous deform. (*German*) 0-30014
- B<sub>2</sub>O<sub>3</sub>, vitreous, torsional deform. above  $T_g$  under low stresses, temp. effect 0-21052
- B<sub>2</sub>O<sub>3</sub>, vitreous, torsional deform. above  $T_g$  under low stresses 0-25804
- C fibre reinforced epoxy, wound, strength in twisting, stretching and transverse bending 0-11622
- Fe<sub>40</sub>Ni<sub>40</sub>P<sub>14</sub>B<sub>6</sub>, amorphous ribbon, influence of torsion on mag. props. 0-7138
- Na<sub>2</sub>O-SiO<sub>2</sub>-(B<sub>2</sub>O<sub>3</sub>) glass, torsional deform. above  $T_g$  under low stresses 0-25804
- V-H rods, twisting effect, anelastic deviations on thermal cycling 0-21043

**torsion loading** *see* **torsion****total energy systems**

- distributed microcomputer-based control system for a large scale solar total energy system 0-30396
- optimal development strategies for a whole energy system based on hydrogen 0-45795
- solar total energy system, Fort Hood, control system 0-30397
- solar total energy system at Georgia, USA 0-35652
- solar total energy system evaluation program 0-30402
- Stirling engine powered total energy system for recreational vehicle appls. 0-30538
- thermogravimetric reversible total energy system 0-55884

**touch** *see* **mechanoreception****town and country planning**

- Iranian solar town conceptual development 0-35645
- traffic noise, model investigation on acoustical performance of courtyard houses 0-10077
- traffic noise screening effect by buildings (*German*) 0-10076

**Townsend coefficient** *see* **Townsend discharge****Townsend discharge**

- n-heptane, Townsend primary and secondary ionisation coeffs. and spark-ignition voltages 0-1732
- n-hexane, Townsend primary and secondary ionisation coeffs. and sparking voltages 0-1732
- inert gases, Townsend avalanches, gas scintillation counter obs. 0-38805
- n-pentane, Townsend primary and secondary ionisation coeffs. and spark-ignition voltages 0-1732
- spark voltages, cathode surface state effects (*Korean*) 0-19643
- Ar discharge, optogalvanic and excited state photoionisation signals, space charge effects 0-14947
- H<sub>2</sub>, Townsend avalanches, gas scintillation counter obs. 0-38805
- He, macroscopic quantities, Boltzmann eqn. and Monte Carlo calcs. 0-38848
- Hg, electron swarm props. Boltzmann eqn. anal. 0-19648
- Ne afterglow, decay rate of metastable ats. 0-44011
- Ne-He high press. flash tubes, digitisation pulse characteristics 0-9455
- Ne-Kr Penning mixtures, Townsend ionisation coeffs. and breakdown pot. meas. 0-19641

**Townsend discharge continued**

- Ne<sub>2</sub><sup>+</sup>, formation and destruction in Townsend discharges 0-38747
- SF<sub>6</sub>, electron swarm development, Boltzmann eqn. anal. 0-6205

**tracers***see also* **radioactive tracers**

- groundwater recharge mechanism, Los Naranjos area, Mexico, using environmental isotope methods 0-12458
- nuclear microprobe anal. of stable isotope tracers spatial distrib. 0-50909
- sand tracer dispersion under progressive water waves, laboratory and field obs. 0-46170
- two-phase flow systems, tracer analysis 0-24073
- He tracers for detection of gaseous atmos. pollutant emissions (*French*) 0-7987
- Ni, oxidation transport processes using tracers in growing NiO scales 0-25913
- <sup>31</sup>Si tracer diffusivity in CaO-SiO<sub>2</sub> melt at 1600°C 0-54418

**track visualisation, particle** *see* **particle track visualisation****tracking***see also* **radar**

- coherent optical processor for vehicle tracking and identification using laser diode light sources 0-37957
- Deep Space Net, appl. of spacecraft tracking technology to experimental gravitation 0-8895
- Geos 3, calibration and evaluation of STDN S-band stations, using Doppler and laser ranging data 0-4228
- Geos 3, satellite-satellite tracking data appl. to geocentric gravit. const. (GM) determ. 0-3911
- Geos 3/ATS 6 satellite-to-satellite tracking for Geos 3 orbit determ., results 0-4225
- methane gas plumes, in atmosphere, tracking via acoustic sounder 0-55968
- planetary orbiters, tracking for planets gravit. spectra determ. 0-41744
- relativistic Doppler shift in satellite tracking 0-46951
- satellite time transfer technology, review 0-47029
- Viking Lander tracking contributions to Mars mapping 0-12702

**tracking (insulation)** *see* **surface discharges****tracking (sonar)** *see* **sonar****tracking systems***see also* **ground support systems; radar systems**

- Geos 3 tracking systems, intercomparison 0-4227
- international time synchronisation, precision tracking package TEMPUS, NAVSTAR satellite network appl. 0-22332
- optical tracking system for space laser communication 0-33068
- satellite, low-orbiting, tracking errors estimation 0-36470

**tracks, particle** *see* **particle tracks****traction**

- stress anal. in body under variable traction 0-8792
- Na/S batteries, load levelling and traction 0-21391

**tractive effort** *see* **traction****trade** *see* **commerce****trade fairs** *see* **exhibitions****trade shows** *see* **exhibitions****traffic control***see also* **air traffic control**

- noise, traffic control effect on evaluation index 0-51024

**traffic restrictions** *see* **traffic control****training***see also* **education; teaching**

- deaf children training to comprehend passive voice 0-33372
- dynamic electric and magnetic field evolutions, visualisation using computer graphics display 0-46776
- energy option for undergraduates 0-31447
- engineering education, modern methods and instructional media roles 0-27064
- industrial radiography radiation exposures, causes, safety training program 0-17141
- nuclear fuel reprocessing, analytical procedure and training material development at ICPP 0-37569
- ophthalmological instruments and eye models in teaching, training and education 0-51993
- storm spotting, National Weather Service's training programme 0-8382
- University of London Institute of Education, Science Department, teacher training, curriculum devel. 0-27061
- virtual image display using Fresnel lenses 0-1295

**trams** *see* **road vehicles****transceivers**

- logic signal transmission system for spaced cosmic ray detectors 0-52837
- US medical transceivers, gain transfer characts. 0-30814

**transducers***see also* **accelerometers; acoustic transducers; actuators; extensometers; Hall effect transducers; piezoelectric transducers; pressure transducers; strain gauges**

- angle, vernier resolvers (*French*) 0-37022
- automation in sugar industry, measuring transducers (*Polish*) 0-42212
- blood pressure measurement, noninvasive techniques 0-41298
- capacitive displacement system for UHV operation 0-31737
- capacitive displacement transducer, automatic calibration (*Russian*) 0-36981
- conductivity sensitive liquid level transducer for PWR coolant two-phase flow meas. 0-37550
- contactless electropneumatic transducer parameter determ. (*Bulgarian*) 0-47045
- displacements below 50 mm meas., types available commercially, comparative survey 0-42214
- drag disc turbine transducer calibration for mass flow rate meas. in PWR coolant two-phase flow 0-37552
- drag disc turbine transducer for PWR coolant two-phase flow meas. 0-37550
- electrochemical measurement transducers, actual distribution of errors 0-45605
- electrodiffusive flow and shear transducer electrical anal. 0-48824
- electromechanical transducers in hostile environments, review 0-37019
- ferromodulation meas., with increased temp. stability 0-52281
- fibre optic lever displacement transducer 0-5816
- fibre optic proximity transducer evaluation for surface texture meas. 0-36985
- force/tension transducer for small muscle meas. 0-41281



**transducers continued**

- frequency response measurement technique for press., vol. and flow transducers 0-41344
- gravitational wave detector, resonant transducer matching between cryogenic antenna and low-noise amplifier 0-46949
- humidity-sensing capacitance transducer, construction and characts. 0-4729
- incremental, for position measurement, analogue interpolation system (*German*) 0-17929
- induction transducer displacement/voltage proportionality improvement (*Bulgarian*) 0-52183
- inductive, technique for computing basic characts. 0-4696
- linear movement transducers, magnetic amplifier principles 0-22341
- liquid level measurement 0-31709
- magnetostrictive, transducer in presence of eddy currents, mobility analogy equivalent oct. 0-48540
- magnetostrictive transducer at air-water surface, effect of spherical scatterer on radiation reactance 0-48531
- membrane pressure gauge with displacement sensor (*Hungarian*) 0-31733
- perfusion blood temp. monitoring, zero-heat-flow transducer 0-8201
- photoelectric angular-displacement, accuracy 0-8977
- photometric, for relaxation props. determ. of polymers 0-3268
- polymer films, ultrathin, photochemical props., transducer appl. 0-37020
- resistive, force and mass measuring, normalisation (*Rumanian*) 0-4699
- surround coil transducers, optimisation for eddy current testing 0-31728
- thin film magnetic elements used in measurement transducers (*Polish*) 0-4700
- HaO samples, meas. of small difference of density by elastic vibrator method (*Japanese*) 0-27272

**transfer functions**

- see also *optical transfer function*
- 12 m discus and NOMAD buoy hull transfer function computations 0-46303
- buoy wave data analyses noise correction functions and error sources 0-46302
- compensating circuit, system function of an acoustic transmission system (*Japanese*) 0-53566
- electron microscope transfer functions in closed form with tilted illumination 0-52368
- frequency-effect transform function for Earth induced polarisation soundings, definition and appl. 0-56624
- narrowband matched SAW filters realisation (*Russian*) 0-23850
- oceanic aseismic ridges, gravity/bathymetry transfer functions rel. to isostasy 0-3971
- photoacoustic spectroscopy, time-domain, nonradiative lifetime meas. of condensed phases 0-55232
- reciprocity calibration of acoustic emission transducers 0-28401
- solar thermal systems long-term performance predictions using closed-form solutions 0-30556
- speckle interferometry application to partially-coherent sources 0-9032
- thermogenesis, harmonic analysis and inverse filter 0-27304

**transferred electron devices** see *Gunn devices***transferred electron effects** see *Gunn effect***transferred electron oscillators** see *Gunn oscillators***transfluxors** see *magnetic cores***transformations, phase** see *phase transformations***transformers**

- see also *d.c. transformers; power transformers; pulse transformers*
- electrotechnical steel, quality significance on energy and materials savings in magnetic circuits (*Czech*) 0-20947
- off-resonance transformer charging for 250-kV water Blumlein, for Experimental Test Accelerator 0-23183
- oil heat transfer efficiency from rough plate 0-48704

**transforms**

- see also *Fourier transforms; Laplace transforms; Z transforms*
- 't Hooft transformation, explicit solns. 0-345
- Adamar, image shift analysis (*Russian*) 0-1134
- ambiguity group for classical canonical transforms, role in quantum mechanics 0-8839
- Backlund, and gravitational duality 0-12971
- Backlund, local conservation laws of principal chiral fields ( $d=1$ ) 0-4888
- Backlund, symmetries of Yang eqns. 0-52393
- Backlund transform, derivation in inverse scatt. formalism 0-8810
- Benjamin-Ono equation, meromorphic solutions 0-31980
- Bonnor transform, extension 0-31643
- Borel summability, improvement on Watsons theorem,  $\phi^4$  appl. 0-52394
- classical nonconservative systems, appl. of time depend. canonical transforms 0-17792
- conference, nonlinear problems in theoretical physics, Jaca, Gain 1978 0-4478
- cracks, Griffith, at interface of two bonded dissimilar elastic wedges, stress field, inverse Mellin transforms 0-53718
- Delaunay-Zeipel transformation, use in reson. props. of celestial mechanics 0-46378
- dislocation scattering, new Hamiltonian for describing multivalued elastic displacement fields 0-24862
- edge notches, conformal transformations 0-27128
- elastic wedge, mixed boundary value problem, use of Mellin transforms 0-23884
- fast convolution by finite ring arithmetics 0-36837
- Fermat number transform for microwave holography data processing 0-43298
- general affine transform, appl. to Landsat imagery planimetric restitution using Zeiss Stereotop 0-56648
- Hadamard and M-sequence transforms are permutationally similar 0-32921
- integral, with non-standard kernels, uses, teaching appl. 0-31466
- inverse spectral transforms, nonlinear evolution equations, soliton solutions 0-12919
- Jaulent-Miodek transformation is canonical 0-36894
- Kinnersley, soln. of Einstein-Maxwell eqns. 0-4617
- Kinnersley-Chitre transformations, integral eqn. method 0-17844
- landscape multispectral data, Karhunen-Loove analysis 0-48164
- linear thermokinetics, transient conditions, resolu. using finite integral transform. method (*French*) 0-38218
- magnetogas dynamics, reciprocal type transformations 0-48804
- Melosh transformation, Eriksen like form, group theoretic interpretation 0-8859
- multiple finite spheroidal transform and its application 0-12910

**transforms continued**

- nonlinear evolution equation, exact two-periodic wave soln. 0-12914
- nonlinear optics, fast transform calcs., appl. to SHG with depletion and diffraction 0-53376
- nonlinear transformations for partial differential eqns. 0-42043
- optical processing, performance of generalised two-dimensional linear transforms 0-9824
- para-Bose states, generalised Bogoliubov transform. coeff. 0-27211
- polymer chain, self interacting, Legendre transformation 0-15018
- Schrodinger equation, discrete-time, Green functions, k-transforms 0-46859
- sequential, appls. of quantitative image analysis 0-23627
- spectral transform, nonlinear discrete evolution equations 0-4553
- spectral transform and nonlinear evolution equations 0-4551
- spectral transforms, nonlinear evolution equations 0-4552
- Walsh transform on standard microprocessor, use as EEG monitor 0-26399

**transient response**

- bistable optical device, transient response and applications 0-33214
- ionosphere, uniform, transient response to geomag. storm sudden commencement rel. to preliminary reverse impulse 0-8477
- linear systems, response to square wave force, transients, teaching appl. 0-31467
- solar cell, p-n junction, photoinjected carrier lifetime meas. by reverse voltage pulse response 0-45664

**transient stability** see *stability***transient voltages** see *transients***transients**see also *surges*

- arc plasma gun for metal cutting, transient performance, obs. 0-49017
- compensated semiconductor, theory of transient processes 0-24930
- currents and charges induced on wedges and strips 0-18974
- deep level transient spectroscopy expts., high resolution anal. of exponentially decaying transients 0-10906
- Gunn diode, anode domain disappearance dynamics, computer simulation calcs. 0-6859
- laser logic elements, transients during switching (*Russian*) 0-23697
- pulsed excitation of flexural modes in infinite plates 0-38167
- recorders for natural and induced phenomena 0-27284
- semiconductor, deep trap activation energy, effect of non-exponential transients, DLTs method 0-20115
- semiconductor diode transient process calcs., minority nonequilibrium carriers, postinjection EMF 0-6971
- skin effect transients on hollow sphere in plane field of system of conductors (*German*) 0-37927
- voltage wave propagation in mag. insulated line 0-5667
- GaAs MOS structures, props. of capacitance transient 0-25013

**transistor circuits**

## Used for general papers and papers where the use of transistors is significant

see also *field effect transistor circuits***avalanche transistor discriminator** for low energy radiations 0-5450**transistor-transistor logic**see also *logic circuits***square root of time mark generator using TTL digital ccts. for chronocoulometry** 0-35588**transistorised circuits** see *transistor circuits***transistors**see also *bipolar transistors; phototransistors; power transistors; thin film transistors; unijunction transistors***Si, microwave Stark effect spectrometer, with electric molecular modulation** (*Russian*) 0-9003**transit time devices**see also *BARITT diodes*

## No entries

**transit time noise** see *random noise***transition metal alloys**see also *alloys of individual transition metals e.g. nickel alloys*see also *copper alloys; gold alloys; silver alloys; transition metal compounds*

- 3d, Hall effect, electron scatt. processes 0-34419
- Al<sub>5</sub> compounds as Jahn-Teller systems, multiple band electron-phonon transport theory 0-24902
- amorphous, mag. props. 0-29576
- catalyst surface mag. field effect on mol. dissoci. rate 0-16721
- Curie temperature, high press. effects (*Japanese*) 0-20444
- diffusion of H transition metal-H systems 0-29219
- dilute, magnetic ordering phenomena in high mag. fields 0-50075
- disordered, bulk electronic structure 0-44467
- ferromagnetic, high-field susceptibility 0-7083
- ferromagnetic, interstitial or substitutional sp impurity doped, electronic struct. 0-34384
- ferromagnetic, mag. props., review 0-44823
- germanides, X-ray emission, absorption and photoelectron spectra (*Russian*) 0-11509
- group VIII aluminides, NMR near equiatomic composition (*Russian*) 0-20479
- heat of formation 0-7849
- hydrides and deuterides, conc.-temp. depend. of mag. susceptibility 0-29523
- intermetallic compounds, containing d-transition metal, hydrogenated, magnetism 0-34609
- metal-H system, exam. of excitation spectra and diffusion mobility of H using neutrons 0-29203
- metal-H systems, anelastic and plastic props., review 0-49298
- metal-H systems under high H pressure, phase diagrams., electrical cond., mag. props. 0-29923
- metalloid cryst. and glassy alloys, electronic struct. from magnetisation and Mossbauer meas. 0-29363
- metalloid-transition metal alloy, glass transition temp. 0-24371
- noble metal-Gd(Eu), dil., hyperfine fields of rare earth impurity, calc. 0-15486
- photoelectron energy distrib. curves, rel. to band struct., book contrib. 0-16156
- rare earth alloys, amorphous, struct. and mag. props., book contrib. 0-39818
- rare earth alloys, magnetic amorphous films for mag. bubble memories, materials review (*Polish*) 0-34715
- rare earth alloys, RM<sub>2</sub>, (M=Fe, Co, Ni), magnetism, review 0-20365



**transition metal alloys continued**

- rare earth and actinide alloys, binary system constitution diagram interrelations (*Russian*) 0-7535  
 rare earth intermetallics, H absorpt., Mossbauer studies 0-39987  
 rare earth-3d transition metal amorphous alloys, crystallisation behaviour 0-49116  
 rare earth- $M_2Al_k$  ( $M=Cr, Mn, Fe, Cu$ ) intermetallic cpd., magnetism and hyperfine interactions 0-25256  
 rare earth-transition metal (4f-3d) intermetallic cpds., mag. moment and mag. anisotropy 0-25107  
 rare earth-transition metal amorphous thin films, mag. potential distribution and wall velocity meas. 0-34725  
 rare earth-transition metal amorphous thin films for thermomag. recording 0-20403  
 rare earth-transition metal intermetallics, two sublattice system with high competing single ion anisotropies, model 0-39767  
 resistivity at low temp., disordered ferromag. alloys 0-24919  
 spin distribution in transition metal elements and alloys, neutron diffraction expts. 0-25097  
 transition metal-hydrogen systems, eqn. for multiplateau isotherm, lattice expansion role 0-39252  
 transition metal-metalloid glasses, struct., elec., supercond., and mech. props. 0-6365  
 Al-M, dil., pre-asymptotic charge oscils. 0-20099  
 B-transition metal thin films, amorphous to cryst. transformation 0-7563  
 Cu-transition metal, alloys, satellite NMR study, lineshifts and splitting 0-34786  
 H production on illuminated transition metal surfaces, tight binding model 0-45812  
 $H_2SO_4$  decomposition, corrosion tests on possible containment materials 0-45448

**transition metal compounds**

- see also compounds of individual transition metals e.g. nickel compounds*  
*see also copper compounds; gold compounds; silver compounds; transition metal alloys*  
 antifluorite, 5d transition metal crystal, struct. props. and lattice dynamics, mag. struct. 0-44268  
 borides, binding energies from X-ray photoelectron spectra 0-49170  
 borides, higher types, phys. props. and electronic struct., group orbitals-LCAO calcs. 0-20077  
 borides, narrow band types, electronic density of states, many-electron Hubbard model calcs. 0-20064  
 borides, superconductivity search below 1K 0-20342  
 borides, XPS meas. and chem. bond 0-20761  
 borohydrides, formation by reaction of transition metals with  $NaBH_4$  or  $CaBH_4$  in organic solvents 0-30223  
 carbonitrides, physicochem. props., comp. depend. 0-55370  
 chalcogenides,  $MS_2(Se_2)$ , present status of research (*Japanese*) 0-20100  
 Chevrel phase compounds, bonding and phys. props. rel. to struct., book contrib. 0-49209  
 complex, LCAO-HFS-STO calc., basis set effects 0-52882  
 complexes, discrete variational  $X\alpha$  cluster calcs. 0-15444  
 complexes, mol. dissymmetry, book 0-27057  
 complexes, reaction mechanisms and solvent effects 0-26012  
 complexes, vibronic coupling and spin relax. NMR decay rate study 0-18870  
 dichalcogenide, physical props., reviews (*Japanese*) 0-33969  
 dichalcogenide layer compounds, bonding and phase transitions 0-34186  
 dichalcogenides:  $^{57}Fe$ , Mossbauer spectra, isomer shift 0-15885  
 dichalcogenides, electronic struct. and band theory 0-44497  
 dichalcogenides, layered, surface Brillouin scatt. obs., surface ripple and elasto-optic mechanisms 0-16048  
 dichalcogenides, layered materials, struct. changes rel. to CDW, TEM, electron diffr. 0-39042  
 dichalcogenides, octahedral intercalate ordering study by electron diffr. 0-15076  
 dichalcogenides, phys. props. and CDWs, review (*Japanese*) 0-49635  
 dichalcogenides, stacking layer study, appl. of convergent beam electron diffr. 0-39116  
 diffusion of H transition metal-H systems 0-29219  
 dihalides, crystal field stabilisation energies, lattice energies 0-38994  
 dihalides, MS potential from a set of overlapping densities 0-52850  
 dihydrides, gas phase geometrical struct. calcs. 0-42951  
 electrical resistivity, saturating contrib. from electron-phonon interactions 0-2376  
 formation, Miedema's empirical theory, microscopic basis 0-45541  
 germanides, binding energies from X-ray photoelectron spectra 0-49170  
 germanides, X-ray emission, absorption and photoelectron spectra (*Russian*) 0-11509  
 halides, electron spectroscopy of crystals, book 0-36786  
 hydrides, struct. change from metal struct., due to interaction of metal with H 0-49196  
 hydrides, synthesis and physicochemical props., conf., Moscow, USSR (Jan. 1978) 0-27032  
 hydrides (binary ternary systems with metallic cond.) review of research on catalytic props. 0-30273  
 hydrides and deuterides, conc.-temp. depend. of mag. susceptibility 0-29523  
 intercalation complexes with  $TaS_2$ ,  $NbS_2$ , and  $NbSe_2$ , mag. and metallic transport props. 0-44814  
 layer dichalcogenide, diffuse intensity contours in electron diffr. patterns, struct. interpretation 0-38878  
 layered oxides, struct. classification and props. 0-39046  
 ligand field problems, group theory 0-42920  
 ligand field spectroscopy, selection rules, intensity enhancement of forbidden transitions 0-45049  
 ligand fields calcs., strong and intermediate fields, tensor algebra 0-42922  
 localisation of electrons, review 0-49650  
 magnetic clusters, neutron inelastic scatt., review 0-50083  
 magnetic ordering phenomena in high mag. fields 0-50075  
 metal-H system, exam. of excitation spectra and diffusion mobility of H using neutrons 0-29203  
 monosulphides of first-row metals, XPES and UV PES 0-20760  
 nitrosyls, appl. of HF and CI calcs. 0-9513  
 oxides, crystal field stabilisation energies, lattice energies 0-38994  
 oxides, surface oxidation, study by AES 0-45175  
 oxides+Li topochemical reactions in high energy batteries, solid state electrode materials 0-55836

**transition metal compounds continued**

- photoelectron energy distrib. curves, rel. to band struct., book contrib. 0-16156  
 pyrite structured 3d-transition metal chalcogenide mag. props. from Mossbauer effect obs. (*Japanese*) 0-15933  
 Q-switching transition-metal dithiene complex dyes for 0.9 to 1.4  $\mu$  lasers 0-1200  
 rare earth-transition metal garnets,  $R_3M_5O_{12}$ , amorphous films for mag. bubble memories, materials review (*Polish*) 0-34715  
 rare earth-transition metal hydrides, electronic and mag. props., Mossbauer study 0-34830  
 refractories, electron and phonon behaviour 0-54624  
 silicides, binding energies from X-ray photoelectron spectra 0-49170  
 silicides, self-propag. high-temp. synthesis 0-2988  
 spectra, cryst. field least squares fitting interpretation 0-44548  
 transition metal complexes, O containing, coordinate bonding, charge transfer electronic bands, complex struct. determ. 0-52977  
 transition metal complexes, octahedral substituted, ligand-fluid splittings, accidental degeneracy origin 0-10932  
 transition metal systems, ESR studies, polarised absorption, ligand field model, group theory applications 0-43077  
 transition metal-carbonyl cluster molecules, electronic struct., localised orbital pseudopot. method 0-39653  
 valence band structure, X-ray spectroscopic study 0-29319  
 X-ray emission K-lines, of transition elements, free-atom approx. applic. 0-11513  
 $Li_xMO_2$ ,  $M=Mo, W, Os, Ir, Ru$ , intercalation compounds, mag. props., decomposition effects 0-25075  
 M-R-B systems ( $R=rare\ earth$ ), phase diagrams and struct. considerations 0-16286  
 $MO_2$ , defect struct., nonstoichiometry and elec. cond., pentavalent oxide dopant effect 0-24442  
 $Sm_{1-x}M_xS$ , valence charges, band struct. 0-20131

**transition metals**

- see also the individual transition metals e.g. nickel*  
*see also copper; gold; silver*  
 3d, core electrons, Sternheimer shielding-antishielding factor 0-39534  
 3d, ESR for valency assessment, appl. to ceramics and glass industries (*German*) 0-34757  
 3d, Hall effect, electron scatt. processes 0-34419  
 3d-metals, electron impact excited soft X-ray spectra, resonances and many body effects 0-50468  
 adatom surface diffusion characts., pair potential calcs. 0-39446  
 adsorption of CO, electronic struct., localised orbital pseudopot. method 0-39653  
 alkali lime germanosilicate glasses, optical absorpt. of transition metal impurities 0-2784  
 amorphous, density of electronic states, effect of struct. variation due to interatomic pot. softness 0-54597  
 amorphous, superconducting transition temp. (*Chinese*) 0-54817  
 atom, many-config. approx. in X-ray and electronic spectra interpret. 0-32615  
 atoms, CNDO/S method extension, parametrisation procedure (*French*) 0-9511  
 Auger effect,  $K-M^2$  radiative, low energy satellites meas. 0-45174  
 Auger relaxation energy theory 0-7446  
 BCC, phonon dispersion relations, Fiełek five-const. model calc. 0-34150  
 bimetallic cluster, photoselective bimetallic aggregation, review 0-53182  
 catalyst surface mag. field effect on mol. dissoc. rate 0-16721  
 chemisorption, theoretical model, formalism 0-6651  
 chemisorption of ordered atomic layers, HF Green's function formalism and phase shift technique 0-24733  
 clusters, particle size rel. to bulk metallic props. 0-44490  
 cohesive and elastic props. model (*Hungarian*) 0-34120  
 corrosion potential/time, and potentiostatic polarisation curves as a method of predicting corrosion 0-45419  
 diffusion in Si, anomalous behaviour 0-29044  
 diffusion of H 0-29219  
 electrical properties, temp. depend. 0-15496  
 emissivity, temp. depend. 0-10688  
 FCC, surface relax. and force consts. 0-39404  
 ferromagnetic, 3d, itinerant electron magnetism, magnetic excitation props., theory 0-34581  
 ferromagnetic metal, Fano effect and hyperfine field of non-transition impurity 0-25128  
 ferromagnetic metals, dislocation drag by conduction electrons 0-24451  
 ferromagnetism, theory 0-2541  
 film, electron beam evaporator for in situ deposition studies in UHV electron microscope 0-40264  
 hydrogen embrittlement, model for metallic cohesion reduction mech. 0-7679  
 implantation of  $He^+$ , range profiles and thermal release 0-39138  
 impurities, integration with large-angle grain boundaries 0-39148  
 impurities in Ba silicate and phosphate glasses, quenching of  $Nd^{3+}$  luminesc. 0-25449  
 interatomic potentials, from phonon spectra 0-33927  
 interstitials, wave-packet motion in Eckart and quadratic pots. 0-52067  
 ion, superposition of quasidegenerate configurations, principal quantum number  $N=3$  0-14079  
 ion pairs, simply reducible symmetry group crystal fields, kinetic exchange theory 0-39541  
 ions in solids, EPR 0-51968  
 Jahn-Teller coupling constants calcs. in 3d transition metal ions in crystals 0-49679  
 lattice excitations, classical models 0-29132  
 liquid, electronic struct. and transport props. 0-29314  
 liquid, thermodynamic characts. calc. (*Russian*) 0-15264  
 magnetic surface properties, review 0-44861  
 metallic glass, short-range order, hyperfine field distrib. determ. by Mossbauer spectroscopy 0-39962  
 noble metal contact, substrate material diffusion and corrosion film formation, model 0-2312  
 noble metals, Krasko-Gurskii model potential, test of validity for Cu 0-39485  
 paramagnetic metals, polarised neutron studies of field induced magnetisation 0-25084  
 photoelectron energy distrib. curves, rel. to band struct., book contrib. 0-16156  
 photoemission spectra, core-level satellite struct. 0-29855



**transition metals continued**

- radiochemical neutron activation anal. of environmental matrices for Hg and noble metals 0-16889  
 SCF theory, orbital and pot. functions calc., eq. of state 0-44463  
 semi-infinite FCC metal, susceptibilities near (001) surface 0-15701  
 semiconductor: transition metal, Anderson model localised impurity states (*Russian*) 0-6788  
 spin distribution in transition metal elements and alloys, neutron diffraction expts. 0-25097  
 steel, depth profiles of transition elements using (p, $\gamma$ ) react. 0-50910  
 stopping power for 6.75 MeV protons 0-34107  
 surface, adatom vibr. model using pair interactions 0-15357  
 surface chemisorbed atoms, interaction energy calc. 0-54507  
 surface states, qualitative theory, Shockley model 0-6924  
 third row atoms, contracted Gaussian type orbital basis set 0-23297  
 X-ray emission K-lines, free-atom approx. applic. 0-11513  
 GaAs, VPE, hole diffusion lengths, effect of transition metal diffusional doping 0-15628  
 GaAs<sub>0.8</sub>P<sub>0.2</sub>, VPE, hole diffusion lengths, effect of transition metal diffusional doping 0-15628  
 H effect, on mech. props. review 0-50718  
 H<sub>2</sub>SO<sub>4</sub> decomposition, corrosion tests on possible containment materials 0-45448  
 M:<sup>129</sup>I, calibration of Mossbauer isomer shift 0-20520  
 Si-M system, interfacial reaction and Schottky barrier 0-39672

**transition moments**

- alkali metal atom, perturbed by rare gases, dipole moments of S-P transitions 0-27979  
 atoms, electronic transition probabilities and lifetimes, expt. determ. 0-23369  
 dyes, rot. diffusion of prolate, oblate mols. from absorpt. relax. 0-1008  
 f<sup>n</sup> systems, electron correl. effects on elec. dipole transition probabilities 0-23316  
 impurities in solids, absorption and emission spectra, bandshapes, moments 0-45122  
 inert gas dimer ions, A<sup>2</sup> $\Sigma_{1/2u}^+ \rightarrow D^2\Sigma_{1/2g}^+$  system, theoretical absorption spectrum 0-32734  
 ions, electronic transition probabilities and lifetimes, expt. determ. 0-23369  
 IR radiation, interaction with molecular system, classical/semiclassical theory challenged 0-43117  
 K level X-ray lines, relative transition probability 0-935  
 light emission by mag. and elec. dipoles, radiation patterns 0-32886  
 liquid crystal display, with dichroic dye guest, field-induced colour switching 0-1327  
 molecular collision, quasi-classical and quantum moments of distrib. of states, semiclassical comparison 0-23480  
 multiconfiguration Hartree Fock method, appl. to at. energy levels and transition probabilities calcs. 0-23318  
 polarised electronic absorption spectrum at 300 and 77K, phys. chem. lab. expt. 0-17774  
 quantum transition probabilities, two-level approx. 0-9557  
 three-level system transition probabilities, molecular motion anisotropy by quadrupole relaxation 0-18867  
 vibrational, of diatomic and polyatomic mols., elec. and mech. anharmonicity influences 0-23459  
 CO<sub>2</sub>,  $\Pi_u$  symmetry transition probabilities, dipole moment and electro-optical consts. calc. 0-43115  
 HgCl, photodissociation calcs., laser efficiency 0-48047  
 I<sup>+</sup>methane d<sub>0</sub>(<sup>-</sup>d<sub>1</sub>),(<sup>-</sup>d<sub>2</sub>), excited atoms, quenching, isotope effects, time resolved reson. fluoresc. 0-32656  
 Krl, p-s lines, transition probabilities meas. 0-23366  
 LaCl<sub>3</sub>:Pr<sup>3+</sup>, dipole transition probabilities between states, electron correl. effects 0-23364  
 O<sub>2</sub>, b<sup>2</sup> $\Sigma_g^+ \rightarrow X^3\Sigma_g^-$  electronic transition, absorpt. coeffs. and transition moments 0-43061  
 O<sub>2</sub>, UV absorpt. into <sup>3</sup> $\Pi_u$  state, calc., atmos. opacity 0-12582  
 OH, A-X system, rot. transition probabilities 0-43027  
 OH, A<sup>2</sup> $\Sigma^+ \rightarrow X^2\Pi$  system, vibrational and rotational levels, transition probability determ. 0-43034  
 SF<sub>6</sub>, IR double reson. with tunable diode laser 0-14160  
 TiCl<sub>4</sub>, t<sub>1</sub> $\rightarrow 2e(^1A_1 \rightarrow ^1T_2)$  transition, bond props. and LCAO MO calcs. 0-18889  
 XeCl, energy curves and transition moments 0-28210  
 XeF, energy curves and transition moments 0-28210

**transition probability** *see radiative lifetimes***transition probability, nuclear** *see nuclear energy level transitions***transition radiation**

- interference effects in transition radiation near Cherenkov radiation threshold 0-9454  
 metal surface plasmon light emission due to low energy electron irradi. 0-34997  
 piezoelectric semiconductor plates, natural oscils. modulated by charged particle beam, energy losses (*Russian*) 0-2259  
 uniformly moving charge on nonstationary layer 0-32893  
 Ag, surface and volume plasmon light emission due to low energy electron scatt. 0-40177

**translation (language)** *see language translation***translators (repeaters)** *see repeaters***transmission**

- see also acoustic wave transmission; light transmission; power transmission*  
 Ag-Cu-Pb coin chem. anal. by low energy  $\gamma$ -rays and neutron transmission meas. 0-35591

**transmission electron microscope examination of materials**

- see also transmission electron microscopy*  
 amorphous metal-metalloid alloys production by ion implantation 0-15128  
 book 0-17726  
 $\alpha$ -brass, 70:30, cold-worked, recrystallised grains nucleation on heating 0-29998  
 cavities observation, TEM techniques review 0-14974  
 ceramic nuclear fuels, mech. props. at compressive deformation 0-651  
 coatings, defects and their effect on props. 0-39474  
 collagen fibrils cholesteric analogue packing in *Holothuria forskali* 0-8035  
 hexamethylcyclotrisilazane film, plasma-polymerised, TEM study 0-44456

**transmission electron microscope examination of materials continued**

- II-VI semiconductors, lattice defects, X-ray diffr. and electron microscopic study 0-15088  
 image resolution and penetration in amorphous and polycrystalline materials, comparison with STEM 0-14976  
 Incoloy, alloy 800, M<sub>23</sub>C<sub>6</sub>/austenite phase boundary defect struct. resolution by weak beam microscopy 0-3046  
 Inconel X750, positron annihilation study of ageing and creep 0-29824  
 insulating films, on Si, struct. stability 0-54564  
 ion bombardment, electron microscopical anal. of surface effects and volume defects, review (*Rumanian*) 0-29093  
 Kevlar 29 and 49, aramid fibres, microvoid obs. 0-38960  
 layered materials, struct. changes rel. to CDW, TEM, electron diffr., dichalcogenides appl. 0-39042  
 macroscopic metal catalysts, morphology and etching processes, review 0-7856  
 metal crystallites, orientation and shape determ. by TEM 0-1907  
 metal films, on alkali halide substrates, nucleation and growth, surface study techniques, review 0-10809  
 metallic glasses, structure direct obs. by bright field TEM 0-10502  
 metals, metastable phases, ion implantation, review 0-49254  
 microstructures digital simulation 0-19679  
 organic crystal, appl. of TEM 0-24327  
 Permalloy RF sputtered films, struct.-sensitive mag. props. 0-34705  
 plasticised cellulose acetate sheet, post-yield fracture 0-25859  
 poly(4-methylpentene-1), permanganic etchant for TEM obs. 0-21132  
 poly- $\gamma$ -benzyl-L-glutamate, monolayers, struct. studies, IR, ATR, and TEM obs. 0-44396  
 polyacetylene, nascent morphology obs. 0-24379  
 polyester-polyurethane semi-interpenetrating networks, mech. props., morphology 0-45362  
 polyethylene, obtained from heterogeneous Ziegler-Natta catalysts, cryst. morphology and growth 0-38941  
 polyethylene crystals, plastic deformation, molecular mech., TEM obs. 0-21022  
 polyisoprene, from guayule rubber, TEM exam. of crystallisation 0-10508  
 polymers, defocus transmission electron microscopy 0-28927  
 polypropylene, permanganic etchant for TEM obs. 0-21132  
 polysiloxane dizwitterionomers, mech. props., microstruct. 0-49131  
 polystyrene, crazed, orientation and struct., electron diffr. meas. 0-30122  
 polystyrene, isotactic crystals, plastic deformation, molecular mech., TEM obs. 0-21022  
 Portland cement, HVEM and gas reaction cell for microstructural investigation 0-40649  
 pyrocarbon coatings, deposition in fluidized bed, TEM, changes by irradiation 0-34084  
 rare earth-3d transition metal amorphous alloys, crystallisation behaviour 0-49116  
 refractory fusion reactor materials, neutron irradi., microstruct., voids, nucleation TEM study 0-29065  
 refractory metal films, evaporated, optical props., rel. to struct. 0-55211  
 Rene 95, as hot isostatically pressed (HIP) and HIP+forged, low cycle fatigue 0-25854  
 SAP (Al<sub>2</sub>O<sub>3</sub>-Al) alloy, effect of high He<sup>+</sup> and H<sub>2</sub><sup>+</sup> conc. on microstruct. 0-34098  
 sapphire:Ti<sup>4+</sup>, plastically deformed, precipitation hardening, TEM study 0-7592  
 steel, 0Kh12G14N4Yu2, struct. after deformation under conditions of superplasticity 0-21031  
 steel, alloy, type AISI 4340, martensitic transformation, TEM study 0-3043  
 steel, alloy, V-W-Mo-Cr, exam. of carbide transformation 0-16299  
 steel, austenite/ferrite interface, struct. and diffr. effects, TEM exam. 0-16308  
 steel, austenitic, Cr-Ni (25, 20 wt.%) recrystallisation and sigma phase formation 0-35211  
 steel, austenitic stainless, Ni-alloyed, Cr<sub>2</sub>N precipitation, interface struct. and morphology 0-11644  
 steel, austenitic stainless, stacking fault effect on martensitic transform. during plastic deform. (*Russian*) 0-25696  
 steel, C content influence on brittle and tough fracture, heat treatment (*Russian*) 0-40500  
 steel, C martensitic, tempering induced decomposition and segregation, atom probe study 0-3112  
 steel, Cr-Mo (2.25, 1 wt.%), damage accumulation and microstruct. changes during creep 0-3129  
 steel, Cr-Ni (1.47, 1.48 wt.%), lath martensite microstruct. and props., cold rolling effect 0-55422  
 steel, Cr-Ni (2.25, 1 wt.%), role of Mo in P-induced temper embrittlement 0-35316  
 steel, CrMoV, creep-resistant, quantitative struct. parameter (*Czech*) 0-35266  
 steel, Cu-Mo, tempered, cementite precipitation along twin boundaries 0-45309  
 steel, heat-resist., C replica method of investigating creep damage in TEM 0-21012  
 steel, high C, high alloy, M<sub>23</sub>C<sub>6</sub> type carbides, effect of alloying elements on defect struct. and hardness 0-16481  
 steel, high Si dual-phase, mech. props and microstruct. anal. 0-40444  
 steel, low alloy, martensite twinning, direct anal. 0-2040  
 steel, maraging 300 grade, serrated flow in austenitic state 0-30041  
 steel, mild, AISI 1009 and 1018, corrosion incipient processes in hypersaline geothermal brine at 90°C 0-50753  
 steel, Mn-Cr-B (1.46, 1.03, 0.003 wt.%) 0-55422  
 steel, multicomponent duplex stainless, high temp. precipitation of  $\alpha'$  0-20939  
 steel, Ni-Co-Mo (17.55, 8.02, 4.92 wt.%) maraging, lath martensite microstruct. and props., cold rolling effect 0-55422  
 steel, Ni-Co-Mo-Ti, maraging, electron diffr. obs. of second phase (*Chinese*) 0-11655  
 steel, Ni-Si-Nb (1.5,0.02,0.03 wt.%), fatigue crack growth under bending (*French*) 0-21089  
 steel, pearlitic eutectoid, crack initiation and effective grain size for cleavage fracture 0-30085  
 steel, stainless, alloyed with C, magnetron-sputtered, microstruct., and cryst.-amorphous transition 0-19719  
 steel, stainless, depth distrib. of swelling, TEM exam. 0-15165  
 steel, stainless, He ion irradi., fracture behaviour, in-situ HV electron microscopy 0-29089



**transmission electron microscope examination of materials continued**

steel, stainless, stress corrosion cracking, prestrain effect, stress relaxation study 0-35384  
 steel, stainless, type 430, Ni<sup>+</sup>-implanted, struct., comp. and electrochem. anal. of surface alloy 0-16603  
 thermoplastic, partially crystalline, microscopic methods of struct. anal. (*German, English*) 0-30198  
 thin foil, quantitative microanalysis, by energy loss spectroscopy (*French*) 0-50900  
 transition metal clusters, particle size rel. to bulk metallic props. 0-44490  
 wetting, exam. of accompanying size effect (*Russian*) 0-6596  
 Zircaloy-2, neutron irradiated, inhomogeneous deformation behaviour 0-50679  
 Zircaloy-2 and -4, (c) component dislocations from TEM contrast expts. 0-6412  
 Ag, electron beam plasma sputtered coatings on KCl substrate, islet struct. (*Russian*) 0-39460  
 Ag films, hillock form. hole growth and agglomeration 0-44455  
 Ag thin films, deposited by cathodic sputtering using high-resolution electron microscopy, voids obs. 0-49557  
 Ag<sub>3</sub>Mg, two different types of long-period ordered alloys, characterisation by high resoln. electron microscopy 0-49181  
 Al, and Al-Cu(Pb) dil. alloys, pulsed ruby laser irradi., noncryst. phase form 0-35012  
 Al, anodisation in H<sub>2</sub>PO<sub>4</sub>, irregular film formation obs. 0-30153  
 Al bicrystals, [011] low-angle tilt boundaries, high resolution electron microscopy 0-34012  
 Al cell structures produced by cycling and monotonic creep 0-55452  
 Al crystals, TEM meas. of excess vol. of grain boundaries 0-15111  
 Al, deformed, thermal recovery, microstruct. and stress-strain relations 0-16325  
 Al, electron beam plasma sputtered coating, islet struct. (*Russian*) 0-39460  
 Al powder thin foil, prep. for TEM study 0-42310  
 Al, splat-cooled, grain-size distrib. function, TEM study 0-40396  
 Al, subgrain coalescence, grain boundary recrystallisation nucleation 0-3094  
 Al wire, specimen preparation for TEM by ion beam thinning (*German, English*) 0-11861  
 Al-Au (0.2 wt.%), precipitation mechanism and creep behaviour 0-3058  
 Al-Cr(Zr), simultaneous recrystallisation and precipitation (*French*) 0-16313  
 Al-Cu samples (0.5, 2.0 and 4.0 wt.%) polycryst., precipitation, positron annihilation and TEM 0-50639  
 Al-Cu-Mn-Zr, type 2219, particle, coarsening of disk shaped  $\theta'$  particles 0-45315  
 Al-Cu-Zr (6, 0.4 wt.%), superplastic deformation characts. 0-16387  
 Al-CuAl<sub>3</sub> eutectic, heat treatment and interlamellar spacing effect on tensile deformation 0-29979  
 Al-Li (2.8 wt.%), ageing in US field, precip. hardening (*Russian*) 0-29968  
 Al-Mg solid solns., decomposition studied by ultrasonic meas. of elastic props. 0-35184  
 Al-Mg/Al<sub>2</sub>O<sub>3</sub> composites, interface phase, Auger and electron diffr. study 0-25646  
 Al-Mg<sub>2</sub>Si(1.42 wt.%), aged, dislocation structs. caused by plastic deformation 0-25786  
 Al-Mn, metastable L1<sub>0</sub> phase, transformations, mag. struct., TEM study 0-3029  
 Al-Si, deformed, local lattice rotations at second phase particles 0-25709  
 Al-silicide-Si systems with CoSi<sub>2</sub>, Pt<sub>3</sub>Ni<sub>1-x</sub>Si<sub>2</sub> and MoSi<sub>2</sub> as silicide, diffusion, compound form., and microstructure 0-34253  
 Al-Zn (15 at.%), supersaturated alloy, growth and decomposition kinetics 0-29965  
 Al-Zn alloy, metastable phases formed at 200°C, room temp. stability 0-16315  
 Al-Zn alloys, recrystallisation and superplasticity, HVEM straining 0-39207  
 Al-Zn-Mg, polygonized struct. in extrusions, thermal stability and mech. props. 0-50659  
 Al-Zn-Mg, stress conversion cracking based on micromech. surface reactions 0-7716  
 Al-Zn-Mg (4.5 at.%, 2 or 3 at.%), decomposition behaviour during continuous cooling, XSAS and TEM examination 0-16264  
 Al-Zn-Mg (4.5 at.%, 2 to 3 at.%), decomp. behaviour during continuous heating 0-29922  
 Al-Zn-Mg (5.9, 2.9 wt.%), ageing effects on microstruct. 0-16306  
 Al-Zn-Mg-Cu, age hardened, effect of strain rate, temp. and environment on ductility 0-45368  
 Al<sub>2</sub>C<sub>3</sub>-3Be<sub>2</sub>C, X-ray diffr. and TEM study 0-14973  
 n-Al<sub>2</sub>Ga<sub>1-x</sub>As, Au-based ohmic contacts TEM obs. 0-34509  
 Al<sub>2</sub>O<sub>3</sub>, defect microstructure due to ion bombardment, TEM study 0-34100  
 Al<sub>2</sub>O<sub>3</sub> substrates, grain growth during sintering 0-40302  
 As<sub>2</sub>S<sub>3</sub> thin films, vacuum deposited on Ge and PbS, sealing props. and TEM 0-35097  
 Au (111), anomalous surface superstruct., UHV electron microscope obs. 0-10760  
 Au, atomic arrangements of defects, dynamic obs. of atom movement 0-39108  
 Au, electroplated, microstruct. and hardness, effect of thickness and deposition conditions 0-20057  
 Au, epitaxial film, on NaCl substrate, electrotransport inferred from void growth rate (*German*) 0-10699  
 Au film, surface step structure imaging by dark field electron microscopy 0-15346  
 Au film (001) surface, computer modelling of high resolution TEM images 0-6330  
 Au film bicrystal, grain boundary dislocations in plane matching boundaries 0-39110  
 Au fine particles, vacuum deposited, morphological features using TEM weak-beam dark-field technique 0-15410  
 Au, grain boundary struct. anal. by HVEM (*Japanese*) 0-15109  
 Au, hardening mechanisms, grain size effect 0-35302  
 Au, surface decoration, on (111) Ag surfaces, by electrodeposition (*French*) 0-44445  
 Au thin films, with nm-sized pores, prep. from Au-Ge eutectic films by etching 0-16227  
 Au/AuPd, bicrystals, in situ relax. of interphase interfaces 0-39455  
 Au/Pd, bicrystals, in situ relax. of interphase interfaces 0-39455  
 Au/Sn films, evaporated, microstructure and texture, TEM obs. 0-39481

**transmission electron microscope examination of materials continued**

B films, prep. by H reduction of BCl<sub>3</sub>, struct. and hardness 0-54543  
 B-transition metal thin films, amorphous to cryst. transformation 0-7563  
 BC, specimen preparation for TEM by ion beam thinning (*German, English*) 0-11861  
 Be-Li-V, phase diagram, metallurgical aspects for fusion blanket use 0-32467  
 Bi oxide film, struct. by electron diffr. and TEM obs. 0-6678  
 i-C, hard coating preparation by ion beam methods 0-25579  
 C, pyrolytic, specimen preparation for TEM by ion beam thinning (*German, English*) 0-11861  
 CC Al-Zn-Mg (4.5,1,2)(3) at.%, decomposition during ageing, preageing and cooling rate influence 0-20938  
 Cu-Zr-(Cr), powder metallurgical alloys, thermomech. treatment effect on props. 0-50660  
 CaCO<sub>3</sub>, calcite, form of end of free elastic twin (*Russian*) 0-6416  
 CaF<sub>2</sub>, plastic deform, work hardening regions, TEM obs. 0-3140  
 Ca<sub>3</sub>(PO<sub>4</sub>)<sub>2</sub>, soln., coagulation effects on light scatt. obs., TEM, SEM 0-45090  
 Cd films, nucleation and growth, props. 0-29878  
 CdS, deformed, dislocation struct., TEM obs. 0-54250  
 CdTe:P, annealing induced lattice defects, TEM obs. 0-2010  
 Co film, on Si substrate, laser irradi., cellular struct. and silicide form. 0-10710  
 Co-Ga  $\beta'$  quenched single crystals, annealing-out of point defects 0-55426  
 Cr film, vapour deposited on low temp. KCl substrates, struct. obs. 0-10826  
 Cr whisker cryst., growth incorporated with field electron emission 0-44458  
 Cr-C, hard coating preparation by ion beam methods 0-25579  
 Cu, Ar<sup>+</sup> ion irradiated, defects study by electron microscopy (*German*) 0-2087  
 Cu, fatigued single crystals, temp. depend. of saturation stress and dislocation substruct. 0-44211  
 Cu, friction mechanism, HV TEM expts. 0-35341  
 Cu, grain boundary anal. by TEM, CSL condition determ. 0-15117  
 Cu, ion irradi., Frank loops, electron microscope image contrast 0-6326  
 Cu-Al-Co, precipitate-free zones near grain boundaries, growth kinetics, TEM obs. 0-40368  
 Cu-Cr, age hardened, fine precipitates struct., TEM study 0-3066  
 Cu-Fe, precipitation processes during aging, TEM, resistivity, hardness study (*Japanese*) 0-35221  
 Cu-Ni alloys, artefacts in thin foil images 0-3056  
 Cu-Ni-Sn (9, 6 wt.%), decomposition, initial stages, TEM study 0-2992  
 Cu-SiO<sub>2</sub>, deformed, lattice rotations at second phase particles 0-25709  
 Cu-Ti, dil. alloy, cellular precipitates, nucleation, TEM study 0-3069  
 $\beta$ -Cu-Ti, dil. alloy, growth phenomena associated with precipitation, TEM study 0-3070  
 Cu-Ti (4 wt.%), isothermal transformation, electron and optical microscopy obs. of microstructure 0-16307  
 Cu<sub>8</sub>Pd<sub>17</sub>, Cu<sup>+</sup> (Au<sup>+</sup>) ion-bombarded, displacement cascades and disordered zones, TEM studies 0-15167  
 Eu pellets, specimen preparation for TEM by ion beam thinning (*German, English*) 0-11861  
 Fe, defect trapping of ion implanted D, depth profile, diffusion eqn. calcs. 0-2047  
 Fe film, thermally evaporated, contamination effects obs. 0-49545  
 Fe powders, prep. by BH<sub>4</sub> process, comp. and stability 0-44878  
 Fe-C (1.2 wt.%), Mossbauer study of early stages of tempering 0-16342  
 Fe-Cr-C, austenite to ferrite+precipitate reaction, TEM/STEM study 0-3075  
 Fe-Cr-C, isothermal transformations 0-16302  
 Fe-Cu alloy, effect of  $\alpha$ -Cu phase on strain ageing (*Japanese*) 0-7582  
 Fe-Cu alloys, transform. substruct., lath microstructure after quenching 0-16298  
 Fe-Cu-Ni, austenite to ferrite+precipitate reaction, TEM/STEM study 0-3075  
 Fe-Ni (23 wt.%), struct., composition changes during  $\alpha$  to  $\gamma$  transform., martensite plastic deformation influence (*Russian*) 0-11642  
 Fe-Ni-C (31, 0.28 wt.%), crossings of thin plate martensites, TEM obs. 0-25756  
 Fe-Ni-Cr (25, 15 wt.%), mobile dislocation density in steady state creep, strain transient dip test, TEM exam. 0-7650  
 Fe-Si (3.25 wt.%), dislocations in twin boundaries, electron microscopic images 0-34006  
 $\alpha$ -Fe-Ti, ion-implanted and annealed, microstruct. evolution 0-15132  
 Fe-V-C, austenite to ferrite+precipitate reaction, TEM/STEM study 0-3075  
 Fe-V-C (0.3, 0.05 wt.%), interphase precipitation obs. in assoc. with Widmanstätten ferrite lateral growth 0-40365  
 Fe<sub>2</sub>Al, Cu<sup>+</sup> (Au<sup>+</sup>) ion-bombarded 0-15167  
 Fe<sub>2</sub>O<sub>3</sub> film, thermally evaporated, contamination effects obs. 0-49545  
 $\delta$ -FeO(OH) and its solid solns. synthesis, X-ray diffr. and TEM studies 0-29891  
 $\delta$ -FeO(OH) crystallites, TEM imaging investigation 0-39096  
 FeTi, H storage alloy, prep. for TEM (*German, English*) 0-30197  
 Fe-Fe-Nb, cold-worked and aged, mag. props. and microstruct. 0-34690  
 Ga<sub>1-x</sub>Al<sub>x</sub>As DH catastrophically degraded laser, TEM obs. of defects 0-32989  
 GaAs, ion-implanted, laser pulse annealing of amorphous surface layer, TEM 0-55436  
 GaAs:Cu, back surface gettering 0-10758  
 GaAs:Cr, gettering by back surface mech. damage 0-10759  
 GaAs:Cr pulsed electron beam induced recrystallisation and damage, amorphous layer formation 0-34052  
 GaAs:Cr substrates and LPE layers, Au film deposition, Cr redistrib., TEM and SIMS 0-15312  
 GaAs:Se<sup>+</sup>, TEM structural study, surface and interior damage 0-34025  
 Ga<sub>1-x</sub>In<sub>x</sub>As-GaAs epitaxial interface with small misfits, TEM image contrast 0-2275  
 GaP crystal, structure defect formation due to annealing and stress, dendrites, slip, dislocations 0-29026  
 GaSb films, amorphous and cryst., vac. evaporated, Elec. cond. thermoelec. power and optical absorpt. 0-2504  
 Ge, amorphous film, laser pulse annealing 0-15006  
 Ge, defect form. under radiation-accelerated diffusion conditions 0-19854  
 Ge:Te<sup>+</sup> ion implanted, alignment of irradi. induced defects, TEM obs. 0-15168  
 Ge-metal films codeposited, amorphous and polycryst., struct. and elec. props. 0-24766



## transmission electron microscope examination of materials continued

- In particles, grown in ultra-high vac. on KCl substrates, struct. and orientation 0-10814  
 In<sub>2</sub>O<sub>3</sub> thin film on polyester substrate, struct. determ. by TEM 0-6674  
 InP, damage induced during handling for TEM obs. 0-2024  
 InSb, ion implanted, efficient void form., TEM obs. 0-44237  
 InSb:Se, exam. of defects in crystal 0-6423  
 LaAlO<sub>3</sub>, Pm3m to R3c or R3c phase transitions, TEM method for domain identification 0-14980  
 Li electrode, in lithium perchlorate-propylene carbonate solution, surface anal. (French) 0-50859  
 Li electrode, passivation layer, in LiClO<sub>4</sub>-propylene carbonate solution, composition (French) 0-11899  
 LiFeO<sub>2</sub>, vacuum annealed, tetragonal  $\gamma$ -phase obs. with TEM 0-11661  
 Mg-Al spinel, non-stoichiometric, climb dissociation of network dislocations 0-2031  
 MgAl<sub>2</sub>O<sub>4</sub>, microplasticity at room temp., dislocations, TEM study 0-19805  
 Mg(Cu<sub>0.535</sub>Al<sub>0.465</sub>)<sub>2</sub>, 2D lattice images of Friauf-Laves phase and defect type 0-24324  
 MgO, single cryst., order hardening by large precipitated vol. fraction of spinel particles 0-3085  
 MnZn soft ferrites, commercial grade, microstruct. rel. to mag. props. 0-34009  
 MnZn-ferroferrites, sintered, microstruct., TEM study (Dutch) 0-2036  
 Mo film, on Si substrates, laser irradi., cellular struct. and silicide form. 0-10710  
 Mo, ion irradi., dislocation loops and stacking fault tetrahedra, electron microscope image contrast 0-6326  
 Mo, neutron irradiated, void swelling and shrinkage, TEM study 0-34079  
 Mo, slip geometry, HVEM straining 0-39207  
 Mo whisker cryst., growth incorporated with field electron emission 0-44458  
 Mo-O crystals, electron microscopy study 0-28889  
 Mo-Ti-Zr (0.5, 0.1 wt.%), neutron irradiated, void swelling and shrinkage, TEM study 0-34079  
 Nb alloy SVMTs, high-temp. ageing, struct. and morphology of hardening phases (Russian) 0-40390  
 Nb, nanobridges Josephson effect, quasiparticle diffusion time, inelastic scatt. time 0-34556  
 Nb, plastic deformation effects on superconducting specific heat transition 0-20352  
 Nb, plastically deformed single crystal, foil, damage free prep. for TEM and X-ray topography (German, English) 0-30200  
 Nb-Ge, A15 struct. superconductor, high field transport props. TEM study 0-34574  
 Nb-Ge film, phase transformations due to annealing, electron diffr. study 0-54551  
 Nb-Ge-Si, A15 struct. superconductor, high field transport props. TEM study 0-34574  
 Nb-Zr (1 at.%), annealed, TEM study of ion implanted irregular He bubbles 0-15164  
 Nb<sub>3</sub>Sn, high-rate sputter-deposited, effect of oxygen on microstruct. 0-20343  
 Nd<sub>0.35</sub>Co<sub>0.65</sub> film, vac. evaporated, magnetisation ripple struct., TEM and defocused Lorentz microscopy 0-7136  
 Ni, cavity evolution in 500 keV <sup>4</sup>He<sup>+</sup> irradi. 0-29082  
 Ni electrodeposited film, appl. of stereomicroscopic method for obs. of organic molecule incorporation 0-2288  
 Ni-Al films, evaporated, grain size and microstruct. 0-15423  
 Ni-based superalloys, TEM obs. of cellular transformation products 0-3045  
 Ni-Fe films, magnetisation reversal in narrow strips, TEM study 0-34720  
 Ni-Fe-Nb (Mo), magnetic alloy, TEM and X-ray obs. (Chinese) 0-24401  
 Ni-Fe-Nb-Al(-Mo), wear resisting mag. head material, mag. props. and struct. 0-35350  
 Ni-P, amorphous electrodeposited alloys, phase-separation (Japanese) 0-54140  
 Ni-ZrO<sub>2</sub>, electron-beam-evaporated condensate, cold deform. and annealing effects on microstruct. 0-16331  
 Ni<sub>3</sub>C films, form. by carburisation, characterisation 0-34337  
 Ni<sub>2/3</sub>Fe<sub>1/3</sub>O<sub>4</sub>, precipitation of  $\alpha$ -Fe<sub>2</sub>O<sub>3</sub>, optical microscopy, SEM and TEM studies (French) 0-11650  
 NiSe film, vac. deposited, phase transformation, electron microscope studies 0-2302  
 PbTiO<sub>3</sub>, ferroelec. domain boundaries, rigid body displacement of lattice 0-40079  
 Pd film, on Si substrate, laser irradi., cellular struct. and silicide form. 0-10710  
 Pd, two-dimens. nucleus form. on Ag (111), UHV electron microscope obs. 0-10760  
 Pd/Si interface, chem. and struct. props. during silicide form., AES and TEM obs. 0-49430  
 Pd-Cu-Si, laser melting and splat quenching to form foils for TEM obs. 0-29986  
 polyethylene, permanganic etchant for TEM obs. 0-21132  
 (SN)<sub>2</sub>, deform. and defects, lattice strain, fibrillation 0-3139  
 Sb, liquid-quenched, stabilisation and transformation kinetics of metastable phases 0-3022  
 Si (100), self-ion implanted, laser annealing, channelling and TEM meas. 0-24466  
 Si amorphous film, crystn. on annealing at low temps. in contact with Al 0-24765  
 Si, Czochralski-grown crysts., thermally induced microdefects, annealing temp. and starting material effects 0-49141  
 Si, deep amorphous layer implantation, laser effects, channelling diffr. study 0-25494  
 Si, defect form. under radiation-accelerated diffusion conditions 0-19854  
 Si, dislocation-free, O<sub>2</sub> precip., IR and TEM obs. 0-29173  
 n-Si, edge dislocation and stacking fault defect electrical recombination efficiency 0-15106  
 Si films, polycryst., glow discharge deposited below 250°C, struct. and morphology 0-49535  
 Si, floating zone structural perfection changes by high temp. treatment, dendrites, dislocation interactions 0-29049  
 Si, implanted annealed layers, amorphised structure formation mechanism and crystallographic nature 0-29091  
 Si, ion implanted and laser annealed, characterisation 0-29043  
 Si MOS device, electron optical identification of precipitations 0-16309  
 Si, oxidation-induced stacking faults, nucleation mechanism 0-15122

## transmission electron microscope examination of materials continued

- Si oxides, grown in Cl-containing ambients, correl. between elec. and material props. 0-39479  
 Si, P<sup>+</sup> implantation, induced disorders. 0-6422  
 Si p-n junction, charge carrier recomb. at dislocations, combined SEM and TEM study 0-15105  
 Si, polycryst. films, transport props. and grain boundary charact. by TEM 0-50980  
 Si, porous, form. during anodic treatment in aq. HF 0-35369  
 Si, precipitation of O<sub>2</sub>, 1000°C TEM, IR absorpt. and X-ray studies 0-34194  
 Si, sintered, grain boundaries, TEM obs. 0-15118  
 Si, stacking fault energies, intrinsic and extrinsic, by TEM 0-10562  
 Si, surface, stacking fault generation due to mech. damage, preoxidation annealing influence 0-54261  
 Si, thermally induced microdefects, effect of C, TEM obs. (Japanese) 0-54244  
 Si:As, implanted through SiO<sub>2</sub> films, elec. props., defect struct. 0-54264  
 Si:As, ion-implanted, CW IR laser annealing 0-34022  
 Si:H plasma deposited film, amorphous, microstruct., TEM and SEM obs. 0-10801  
 SiO wafer, annealed, surface- and inner-microdefects, TEM obs. 0-54236  
 Si:P<sup>+</sup> ion implanted single crysts., secondary defects development during annealing 0-44228  
 Si-Al-O-N, high-temp. fracture and diffusional deform. mechanisms 0-40509  
 $\beta$ -Si-Al-O-N, Mg-containing phases, crystn. 0-39297  
 Si-Al-O-N, oxidation mechanisms 0-40570  
 Si-Al-O-N polytypes, hot-pressed, microstruct. 0-3023  
 Si-Co interface metal-semiconductor transition, rel. to first compound nucleation 0-24771  
 SiC, cubic, atomic displacement energy determ. by bracketing technique 0-49272  
 SiC, polytypic transform., interface struct. exam. by TEM 0-15033  
 SiC, specimen preparation for TEM by ion beam thinning (German, English) 0-11861  
 $\beta$ -SiC, undoped compact, microstruct. development during heating 0-25746  
 Si<sub>3</sub>N<sub>4</sub>, consolidation by hot isostatic pressing 0-11605  
 SiO<sub>2</sub>-Al<sub>2</sub>O<sub>3</sub> (36.6 wt.%) plasma prep. powder, metastable immiscibility and microstruct. during sintering 0-35143  
 SiO<sub>2</sub>-Al<sub>2</sub>O<sub>3</sub>-Fe<sub>2</sub>O<sub>3</sub>-CaO, basalt glass ceramics, crystallite form. due to heat treatment 0-38917  
 SiO<sub>2</sub>-Na<sub>2</sub>O-CaO (13, 11 wt.%) glass, phase separation, SiO<sub>2</sub> purity effect 0-44144  
 SiO<sub>2</sub>-Na<sub>2</sub>O-CaO glass, phase separation characts., melting atmosphere effect 0-44141  
 SiO<sub>2</sub>-TiO<sub>2</sub>, antireflection coating, 1.064  $\mu$ m laser damage, barrier 0-33059  
 SiO<sub>x</sub>, grown in HCl/O<sub>2</sub> ambients, phase separation and Na passivation 0-3219  
 SmS, defect struct., precipitate colonies, dislocation loops, TEM obs. 0-44214  
 Sn-plate passivation films TEM struct. obs. 0-45416  
 Sn-Sb (10 wt.%), decomposition of supersaturated solid soln. 0-29960  
 Sn-Sb-Ag, splat cooled foils, TEM study 0-40344  
 SnO<sub>2</sub> thin films, analytical characterisation 0-20053  
 steel, Cr-Ni, ferrite precip. (Japanese) 0-35187  
 Te film, on electron irradi. KBr, epitaxial growth and surface coverage 0-10825  
 (Ti,V)C, activated reactive evaporation deposited films, annealing study, microstructure 0-24762  
 Ti-Al-Sn (5, 2.5 wt.%), annealing of near-basal hydrides 0-20989  
 Ti-Al-V (4.7, 2 wt.%) pseudo alpha alloy, laminar struct. singularities,  $\beta$  to  $\alpha$  transformation (Russian) 0-7552  
 Ti-Al-V (6.4 wt.%),  $\alpha/\beta$  interface phase influence on tensile props. 0-30034  
 Ti-Al-V (6.4 wt.%), phase transformation after hydrogenation 0-7560  
 Ti-Al-V (6.4 wt.%), to H effect on fracture props. and microstruct. 0-40512  
 Ti-Ni, laser melting and splat quenching to form foils for TEM obs. 0-29986  
 Ti-V-Mo-Cr system,  $\beta$ -phase stability 0-55353  
 TiC, activated reactive evaporation deposited films, annealing study, microstructure 0-24762  
 TiN-Ti<sub>2</sub>N, activated reactive evaporation formed deposits, microstructure, transformation depend. on depositing conditions 0-24761  
 TiO<sub>2</sub>, amorphous film, vac. deposited, struct. and crystn., TEM obs. 0-2291  
 TiO<sub>2</sub>, K<sup>+</sup> implantation, extended defects and precipitates 0-49251  
 TiO<sub>2</sub> rutile single crystals, stoichiometric, dynamic strain ageing 0-50661  
 TiS<sub>2</sub>, (4H)<sub>2</sub>-6C-type superstruct. revealed by high resolution microscopy 0-19755  
 (V,Ti)C+(Ni,Mo) cermet, carbide-binder interface ledges 0-29283  
 (V,Ti)C+Ni cermet, binder grain size 0-44401  
 V, ion implanted with 2 MeV He under pulsed conditions, microstructure obs. 0-29088  
 V-Zr-C-Y alloy weld metal, hardening phase precipitates examination 0-7576  
 W, drawn wire, microstruct. effect on fracture 0-3177  
 W, vacancies, quenching and recovery invest., resist. and TEM study 0-39074  
 W whisker cryst., growth incorporated with field electron emission 0-44458  
 WC-Co and WC-Co-TaC-TiC-NbC cemented carbides, microstructure, high temp. deformation, uniaxial plastic compression 0-40451  
 W<sub>2</sub>C, oxidation, oriented struct. transform. to W, FEM and TEM obs. 0-30124  
 WO<sub>3</sub>, amorphous film, vac. deposited, struct. and crystn., TEM obs. 0-2291  
 ZnS, Zn(S,Se), large single crystals, vapour growth and defect characterisation 0-25540  
 ZnTe, elec., SEM and TEM studies of impurity segregation during long annealing 0-30001  
 ZnTe, TEM obs. of precipitates, shape of Te solidus line 0-25703  
 ZnTe:Li, diffusion investigation by SEM and TEM 0-10706  
 ZnTe:Li, impurity segregation during short annealing and quenching, SEM, TEM and elec. meas. 0-10676



**transmission electron microscope examination of materials continued**

ZrC CVD coated fuel particles, diffusion of  $^{137}\text{Cs}$ ,  $^{90}\text{Sr}$  and  $^{144}\text{Ce}$  0-13582

ZrO corrosion layer, specimen preparation for TEM by ion beam thinning (*German, English*) 0-11861

**transmission electron microscopes**

see also *transmission electron microscopy*

80 kV accelerating voltage transmission electron microscopes 0-27380

developments in instruments and techniques (*Hungarian*) 0-31949

diffraction patterns and bent contours visibility in thick composite amorphous-crystalline specimens 0-1906

high resolution, combined with nanoPROBE anal. 0-4814

LaB<sub>6</sub> cathode gun 0-18048

**transmission electron microscopy**

see also *transmission electron microscope examination of materials; transmission electron microscopes*

adhesive energy, meas. techniques for metal/ceramic system 0-50803

book 0-17726

brass, interface boundaries, TEM procedures for struct. 0-19814

computerised three-dimensional image reconstruction from projections under limited view angle 0-9078

cryomicrotome attachment, modification to Reichert FC-2 device, improved sectioning reproducibility 0-47149

defocus values, determ. using Fourier images 0-47148

electric field effects 0-4823

electrocrystallisation, recent progress in electrochem. and physical methods (*French*) 0-7510

electron energy loss analysis, developments in instruments and techniques (*Hungarian*) 0-31949

electron energy-loss spectroscopy in context of TEM, review 0-31945

energy loss spectroscopy, quant. microanal. of thin foils (*French*) 0-50900

epitaxy, growth modes, exp. techniques, book contrib. 0-49558

experience in TEM at the Univ. of California (Berkeley) 0-37130

extraction replica evaluation, Ashby-Ebeling model analysis (*Czech*) 0-49062

foils preparation, GaAs and CdTe, by ion sputtering (*Czech*) 0-16619

grain boundary anal. by TEM, CSL condition determ. 0-15117

high resolution, combined with nanoPROBE anal. 0-4814

high resolution, low-noise B supports 0-8236

HVEM straining, optimum conditions 0-39207

image resolution and penetration in amorphous and polycrystalline materials, comparison with STEM 0-14976

inelastic scattering probabilities for fast electrons in single cryst., orientation depend. 0-2905

interphase boundaries, struct. anal. 0-19813

lattice image formation, many-beam theory, TEM 0-38879

molecular solid, film, 0-15 eV electron transmission spectra 0-35023

phase transformations, direct obs., using TEM 0-2997

specimen preparation, plasma etching use for foil thinning (*Slovak*) 0-45405

stereo photo-micrographs, analysis using computerized graphical method 0-42304

stereomicroscopic method for obs. of organic molecule incorporation in electrodeposited films 0-2288

surface characterisation, physical methods, review (*French*) 0-7889

thin film, and surface anal., modern methods 0-54486

void arrays in crystals, contrast 0-14975

Au decoration technique, TEM and SEM study of localisation of decorating crystallites (*French*) 0-10470

**transmission line theory**

Maxwell's equations, numerical soln. by transmission line and lumped network models 0-27147

solitary waves in nonlinear transmission line 0-4543

superconducting phase slip centre, charge imbalance waves and nonequilibrium dynamics 0-54830

**transmission lines**

see also *cables (electric); overhead lines; power transmission lines; waveguides*

Doppler frequency shift by fast moving boundary (*Japanese*) 0-18967

optical fibre cables, 10-fibre filled, 6-fibre, connector for field installation 0-43470

RF-biased SQUID, with half-wavelength transmission line 0-22342

TEM cell for electromag. interference investigations, large, based on rectangular coaxial transmission line 0-238

**transmission networks**

see also *communication networks*

fast nuclear reactors, electrical supplies and Na pumping system 0-52723

**transmission wavemeters** see *wavemeters***transmitters**

see also *transceivers*

laser-fibre transverse coupling and front-mirror monitoring for feedback control of laser transmitters 0-33151

**transmitting** see *transmission***transonic flow**

acoustic plane wave excitation by volume sources, nonlinear 0-38154

aerodynamic wind-tunnel testing, transonic flow simulation by tracking and blowing (*German*) 0-6081

aircraft design technology, fluid dynamics computer program assessment data base 0-1637

airfoil optimisation, transonic flow finite element anal., book contrib. 0-1633

airfoils, transonic testing at high Reynolds number in shock tube 0-14852

axisymmetric transonic turbulent base pressures 0-19425

cascade shock loss location and magnitude by high speed smoke visualisation 0-24051

cascade with slender profiles, transonic flow, numerical soln. 0-38436

cascaes, supersonic and transonic compressor, unstarted choked regime calc. (*Chinese*) 0-43730

classical equivalence rule assessment for flows past nonaxisymmetric slender shapes 0-6079

compressible and incompressible flows, recent theoretical and expt. developments, book 0-1620

compressible flow of perfect gas around uniformly expanding sphere 0-28528

cone, sharply pointed, press. distrib. at attack angle 0 to 10° 0-38434

continuum source particle beam properties, comput. modelling 0-26062

cylinders and airfoils, primitive variable least-squares finite element formulation 0-33623

**transonic flow continued**

density distribution in a non-stationary bow wave in a transonic flow, book contrib. 0-1631

detached bow waves around bodies at slightly greater than sonic speed, book contrib. 0-1630

diffuser flow, shock wave oscillations 0-14729

duct with abrupt enlargement, transonic flow, self-excited oscills., model calcs. 0-28522

Euler eqns., numerical soln., Lagrangian method 0-38435

fast implicit soln. procedure 0-19430

finite element formulation for subsonic and transonic flow 0-28526

finite element method appl., shock-fitting for transonic flow with shocks 0-14730

flow field computations, heuristic obs., book contrib. 0-1626

Guderley's transonic small disturbance equation, exact solns. 0-19315

hyperbolic Laval nozzles, transonic flow in throat region (*Chinese*) 0-6122

ideal radiating gas, sonic discontinuities, shock development 0-43802

inviscid hyperbolic flow, computational algorithms tests 0-27140

jet, free, overexpanded two-dimens., eqns. formulation and soln. method 0-6109

laser velocimetry appl. for unsteady transonic flow meas. 0-10341

lifting three-dimensional wings in transonic flow 0-19428

Mach line flow, two-dimens., equivalence conditions, physical interpretation (*German*) 0-1634

non-asymptotic shock-detachment distance of slender cones in transonic flow, book contrib. 0-1632

nonequilibrium flows with transonic vel., second approx. 0-33622

nonlinear near-sonic potential flow with viscosity, solns. (*German*) 0-1646

nonsteady two-dimens. transonic flow, numerical solns., shock waves 0-53808

ogive cylinder at high angle of attack, experimental investigation of sup-orthogonal finite element method 0-28529

perturbation potential for unsteady near-sonic flows (*German*) 0-1635

post shock expansion behind normal shock on curved wall, flow separation, book contrib. (*German*) 0-1628

potential flow partial differential equatn. soln. by finite element method 0-24045

potential flows past cascades, in nozzles and channels, pseudo-unsteady method 0-14727

potential subsonic and transonic cascade flow, stability anal., finite area methods 0-48737

potential theory model for separation regions behind shock waves (*German*) 0-1636

radial turbomachine, meridian plane characts. for subsonic and transonic flow, finite element calcs. (*French*) 0-38418

relaxing gas, sonic discontinuities 0-28531

shock free flow around a convex angle 0-1625

simulation, implicit finite-difference, of steady and LF transonic flow 0-19429

sink-vortex flow in compressible medium, book contrib. (*German*) 0-1603

small disturbance theory, self-consistent formulation, book contrib. 0-1629

small-disturbance theory, leading-edge singularity, num. integration methods eval. 0-6080

steady transonic Euler eqns., Newton's method soln., nozzle appl. 0-38437

steady transonic flow past aerofoil, viscous effects, prediction model 0-14732

store configuration, critical Mach number 0-19427

sub and transonic flow over wing, flow separation, vortex struct., shock wave shape (*French*) 0-14733

supersonic to subsonic transition with local supersonic regions, book contrib. 0-1627

swept wing, finite volume method soln. 0-19431

symmetrical airfoil, transonic flow, inviscid and turbulent flow props., wake 0-48736

three-dimensional, integral eqn. derivation 0-10259

torus, axially symmetric, transonic flow 0-28527

transonic shock/boundary-layer interaction subject to large pressure fluctuations 0-38433

turbine cascades, rotating annular, test facility of DFVLR, measurement and evaluation 0-14866

unsteady transonic flow, freq. effects 0-14728

unsteady transonic shock motions in two-dimens. flow 0-14731

wing, oscillating, in transonic flow, unsteady airloads and flow linearisation 0-1426

**transparence** see *transparency***transparency**

see also *light transmission; optical constants; self-induced transparency*

trans-4-alkylcyclohexane carboxylic acids, visible and UV spectroscopy transparent matrix 0-45102

liquid irradiated, dosimetry by holographic interferometry (*Rumanian*) 0-9412

liquids for cooling and index matching of Nd:glass laser systems 0-33015

magnetic materials (*Japanese*) 0-11369

optical interference filter, effect of harmonic variation of layer thickness 0-28326

optical waveguide, conic and quasi-conic profile, calc. and construction (*Rumanian*) 0-28331

polyethylene, high density, oriented extended chain crystals, transparency (*Japanese*) 0-38955

polyethylene, lightly crosslinked, processed under mol. orient., transparent film prep. 0-38957

seawater, transparency rel. to hydrochemical characts. distrib. 0-31057

water aerosol, propagation of intense radiation at 10.6  $\mu\text{m}$  0-5692

weakly absorbing solid medium, opacity fluctuations, heating by intense radiation and thermoelastic stresses problem 0-38048

As-S-Se-Ge semiconducting glasses, IR characts. (*Czech*) 0-25332

C. vapour-deposited, transparent and hard insulating layer, struct. and props. 0-10830

CuCl, propagation process of polaritons (*Japanese*) 0-24809

Ge-S-Ga(In) system glasses, photoinduced changes 0-24365

Ge<sub>0.3</sub>As<sub>0.2</sub>Se<sub>0.5</sub>, IR optic materials, characteristics (*German*) 0-38081

GeS<sub>2</sub>, IR optic materials, characteristics (*German*) 0-38081

In<sub>0.4</sub>Ga<sub>0.6</sub>As, epitaxial solid soln. film, spectral depend. of transparency, absorpt. spectra calcs. 0-45161

In<sub>2</sub>O<sub>3</sub>, electro-conducting transparent film, props. rel. to production method (*Japanese*) 0-25557



**transparency continued**

- $\text{In}_2\text{O}_3$ , transparent conducting film, prep. by CVD, and characterisation 0-11571  
 $\text{K}(\text{Ta,Nb})\text{O}_3$ , ceramic, prep. and electro-optical props. 0-25620  
 $\text{LiF}$  mech. and optical props. rel. to forging conditions 0-33101  
 $\text{Li}_2\text{Ti}_2\text{O}_7$ , growth by Bridgman-Stockbarger technique, optical transparency 0-25548  
 $\text{MgAl}_2\text{O}_4$ , transparent ceramic, transmittance, grain size and dopant effects (Japanese) 0-19083  
 $\text{NaNbO}_3\text{-BaTiO}_3$ , unidirectionally solidified transparent ceramics 0-25677  
 $\text{PbTiO}_3$ , ferroelectric thin films, fabrication by RF sputtering, characts. 0-40261  
 $\text{SnO}_2$ , electro-conducting transparent film, props. rel. to production method (Japanese) 0-25557  
 $\text{SnO}_2$ , transparent conducting film, prep. by CVD, and characterisation 0-11571  
 $\text{Y}_2\text{O}_3$ , transparent ceramic, transmittance, grain size and dopant effects (Japanese) 0-19083

**transpiration**

see also *flow through porous media*

- high-temperature, transpiration apparatus, viscous, incongruently vapourising melts 0-52231  
 mass spectrometry, of high temp. vapours 0-52356  
 $\text{Sb}$ , vaporisation behaviour, transpiration and boiling temp. studies 0-29161

**transport** see *transportation***transport equation** see *Boltzmann equation***transport phenomena** see *transport processes***transport processes**

see also *biotransport*; *Boltzmann equation*; *cellular transport and dynamics*; *cosmic ray propagation*; *diffusion*; *electrical conductivity*; *Liouville equation*; *master equation*; *neutron transport theory*; *photon transport theory*; *plasma transport processes*; *Senfleben-Beenakker effect*; *thermal conductivity*; *thermal diffusivity*; *viscosity*

W. Atlantic Ocean, equatorial, subthermocline countercurrents mean geostrophic transport 0-51426

atmosphere, S dry deposition vels. over E United States and surrounding regions 0-56507

atmosphere large-scale eddy transports, linear parameterisation 0-17361

atmosphere  $\text{O}_3$  production transport and distribution, numerical simulations with global general circulation model 0-56544

atom-molecule anisotropic interaction pot. influence on transport cross sections, appl. to He-alkali dimer 0-9677

Baltic Sea, salt transports determ. from conservation calculations in natural coordinates 0-51433

binomial redistribution process, Ehrenfest urn problem 0-52144

bistable potential model, renormalised transport eqns. 0-36957

black hole accretion discs, boundary-layer flow rel. to energy and ang. momentum transport 0-46598

Boltzmann eqn., phonon and electron transport in bounded systems 0-39545

branching asymptotic behaviour 0-175

critical sphere problem 0-27245

cylindrical critical problem for an extremely anisotropic kernel 0-27246

dense fluid transport phenomena, generalised moment method 0-33866

dense one-component systems, low-temp., kinetic phenomena, shear viscosity (Russian) 0-10694

dilute gas mixtures, transport props., calc. prog. 0-10342

dilute gases, transport props., softness expansion for inverse power pot. 0-28589

dust grains in solar nebula, dynamics rel. to role as isotopic anomalies carriers 0-26757

eigendistributions in linear transport theory 0-13523

Einstein's contribution to twentieth century physics (Chinese) 0-17

electron transport, discrete ordinates calc. using standard  $S_n$  neutron transport codes 0-46998

electron transport and small angle collisions 0-165

electron transport by the method of condensed collisions 0-47000

electron transport in anhomogeneous anisotropically scatt. medium, medium Green's function 0-27244

electron transport in nonmonochromatic EM field 0-10937

electrons, diffusion of pencil beam, ang. distrib. model 0-23273

energy dependent transport theory, exact solns. 0-32319

energy transport by waves without spatial damping, dissipative media 0-31531

flux-corrected transport algorithm, rezoning technique 0-31516

Fokker-Planck eqn. eigenfunction expansion soln. extension, first order system 0-31668

Fokker-Planck equation, manifolds of equivalent path integral solns. 0-4687

Fokker-Planck equatn. numerical solutn. 0-18622

fusion reactors, re-entrant boundary conditions for toroidal transport and diffusion 0-18592

geochemistry, transport models rel. to mantle and crustal reservoirs mean age 0-51559

heavy ion radiation transport computer codes for thick targets 0-39180

homogenisation and approximation (French) 0-31684

hopping transport theory, master eqn. approach (German) 0-27237

hot matter, conductive opacities and free-free Gaunt factors 0-3361

interphase mass flux and mass fluxes within phases 0-48561

interstellar charged dust grains, motion in interplanetary space 0-4300

intramolecular energy transfer, quantum effects 0-42964

Jupiter, ang. momentum outward transfer rel. to atmosphere differential rot. 0-46467

K-distributed noise, statistics 0-27220

Landau-Zener problem, random nature of motion role in intersecting terms problem 0-8937

lattices, finite, with traps, random walks, Monte Carlo simulations 0-52131

light scattering in dynamical props. study, principles spectra derivation and applies. 0-53218

linear filter matrix, variational principle, functional max. value 0-27243

linear partial differential eqns. describing transport phenomena, soln. technique 0-13004

LMFBR safety, collocation method soln. of radiation-conduction problems 0-13720

LWR lattices, Monte Carlo radiation transport program for reactor bundle gamma transport and energy deposition analysis 0-22915

**transport processes continued**

marine atmosphere stratocumulus convection, turbulent fluxes in horizontally inhomogeneous solns. 0-56543

marine pollution, dynamically passive impurity propag. in sea surface layer 0-31063

Mediterranean Sea, hydrological regime during glacial periods (French) 0-4040

memory functions for transport fluxes 0-42172

molecular dynamics method in statistical physics, review 0-18895

Monte Carlo game, variance versus efficiency 0-27238

Monte Carlo importance sampling with parametric depend. 0-13013

Monte Carlo recursive methods, optimal strategies for appl. 0-13014

Monte Carlo transport calcs., second moment functionals for last event and collision estimators 0-13012

moving fluids, transport eqns. and acoustic motion 0-53523

multidimensional inverse problem in transport theory 0-174

multigroup electron transfer cross-section method 0-46999

neutrino Comptonisation in high-temp. nuclear matter, neutral current theory 0-21905

nonlinear coefficients, generalised Nernst-Einstein relations 0-52145

nonlinear evolution eqn., family of H-theorems 0-31685

nonlinear transfer processes, optimisation (Russian) 0-8934

nonlinear transport processes, hydrodynamics 0-22310

numerical solution of transfer theory problems by the direct reduction method 0-22309

ocean, advective mixed-layer model with imposed surface heating and wind stress 0-12395

ocean, barotropic transport in wind-driven zonal channel with stratification and bottom topography 0-51402

oceans in Southern Hemisphere, mean annual poleward energy transports 0-51406

one-dimensional chain of harmonically coupled Brownian particles, Smoluchowski eqn. 0-17878

one-dimensional conductor, phenomenological eqns. of motion for electrons, phonons and librions 0-10955

particle motion through matter, fluctuations in cascade processes 0-5456

particle transport theory, integro-differential eqn. soln. 0-36955

polarised radiation transport theory, charact. eqn. 0-4678

probabilistic methods for stationary problems of linear transport theory 0-167

quantum mechanical Brownian particle, tunnelling and transport problems 0-4644

radiation problems transport eqns., using Wigner distribution 0-168

radiation transport theory, tracklength biasing in Monte Carlo methods 0-5335

radionuclide geospheric transport eqn., boundary conditions 0-47611

radionuclide transport through heterogeneous media 0-32382

rarefied gas, nonisothermal flow in cylindrical capillary, calc. of vel. profile and flux 0-6098

reaction-diffusion system, global branching theorem 0-4677

resonance transfer rate of electron excitation, model of convergent terms, effect of diffusional motion of particles 0-8936

Saturn, ang. momentum outward transfer rel. to atmosphere differential rot. 0-46467

scattering expansion truncation error correction program 0-47001

slab geom., transmission and reflection coefficients in the slowing down region 0-13005

solar nebula/giant gaseous protoplanets ang. momentum transfer rel. to protoplanet evolution 0-56727

steady two-dimens. viscous boundary layer, transport physics and math. characts. 0-14673

zodiacal dust cloud, charged dust particles motion in interplanetary space 0-4299

C, excited electronic states contrib. to transport props. 0-23326

**transport properties** see *transport processes***transport theory** see *transport processes***transport theory of neutrons** see *neutron transport theory***transport through biomembranes** see *biomembrane transport***transportation**

see also *aircraft*; *marine systems*; *rail traffic*; *road traffic*

environmental noise, importance in France 0-48510

fission reactor fuel, mixed oxide, suitability of spent fuel shipping casks 0-27757

Iranian solar town conceptual development 0-35645

LNG, transport and storage hazards 0-45620

nuclear materials, SABRE II combat simulation model 0-37542

nuclear spent fuel shipping cask licensing 0-37545

nuclear waste transportation, DOE transportation technology centre 0-37537

public, fuel conservation, environmental, economic and social aspects 0-35621

radioactive contact-handled transuranic waste transportation 0-37538

radioactive low-level waste transport and disposal, logical 0-23044

reactor fuel element disposal 0-13707

spent nuclear fuel shipment, appl. of ALARA principles 0-37541

technical meteorology, technical and commercial appls. (German) 0-46231

Pu compounds 18B packagings for transportation 0-37544

Pu, transportation, effect on environment, evaluation study (French) 0-27785

**transportation networks** see *transportation***transportation services** see *transportation***transportation systems** see *transportation***transverse rupture strength** see *bending strength***trapped electron centres** see *F-centres***trapped free radicals** see *free radicals***trapped hole centres** see *V-centres***traps, electron** see *electron traps***travelling-wave-tubes**

see also *backward-wave tubes*

electron cyclotron maser as high power travelling wave amp. of MM waves 0-1176

**treatment, heat** see *heat treatment***treatment, patient** see *patient treatment*



treatment, surface *see* surface treatment

treatment, water *see* water treatment

## trees (mathematics)

*see also* network topology

QCDs, fermionic Green function and functional determinant, closed representation 0-13269

random Ising model, variational principle for distrib. function in the Bethe approx. 0-15674

supergraph anal., gauge supersymmetry, S-matrix 0-27422

triboelectric emission *see* electron emission

## triboelectricity

*see also* static electrification

acetone, electrification during laminar flow in metal pipe 0-6954

benzene, electrification during laminar flow in metal pipe 0-6954

charging technique for surface contamination analysis 0-11966

electrophotography, triboelectrical properties of toner and carrier 0-18039

ethyl alcohol, electrification during laminar flow in metal pipe 0-6954

granular bed, aerosol filtration efficiency, triboelec. effects 0-38487

n-heptane, electrification during laminar flow in metal pipe 0-6954

metal-polymer friction pairs, triboelec. effects 0-11784

nylon 6, frictional electrification between metal and polymer, depend. on temp. and friction speed, contrib. of mol. motion of polymer to electrification 0-6953

polystyrene, frictional electrification between metal and polymer, depend. on temp. and friction speed, contrib. of mol. motion of polymer to electrification 0-6953

semiconductor coatings space charge effects on triboelec. charge exchange 0-54763

silicone, electrification during laminar flow in metal pipe 0-6954

water, electrification during laminar flow in metal pipe 0-6954

LiF, crystal fracture induced surface charge, elec. signal meas., double elec. layer approx. 0-44254

## tribology

*see also* friction; lubrication; mechanical contact; wear

abrasion and erosion, superficial plastic deformations by particles (*French*) 0-40540

metrological provisions, Soviet installations and instruments development 0-23974

## triboluminescence

ammonium tartrate, triboluminescence and cryst. fracture dynamics 0-50437

benzil crystals, mol. triboluminesc. meas. 0-40172

citric acid monohydrate, triboluminescence and cryst. fracture dynamics 0-50437

erosivity and mechanoluminescence (*German*) 0-25873

ferroelectrics, triboluminescence on piezo-electrification of surfaces during fracture 0-29815

student experiment using common candies 0-17778

sugar, triboluminescence and cryst. fracture dynamics 0-50437

tartaric acid, triboluminescence and cryst. fracture dynamics 0-50437

Fe flakes, light flashes, tribo-induced discharge luminesc. rel. to astrophys. 0-25471

KI(Br), X-irradiated cryst., luminesc. during press. release 0-20722

LiF, X-irradiated cryst., luminesc. during press. release 0-20722

Li<sub>2</sub>SO<sub>4</sub>, triboluminescence and cryst. fracture dynamics 0-50437

## trigger circuits

*see also* flip flops; multivibrators

flashgun slave trigger, using Si solar cell 0-47125

HV pulser development for CS<sub>2</sub> laser cavity 0-23707

IEEE 488-1975 interface bus, high speed ADC and addressable trigger generation 0-41283

sound-controlled flashlamp trigger circuit (*Spanish*) 0-13175

X-ray tube, part of installation for rapid process frame-by-frame registration 0-47159

## triode sputtering

CdS, Se<sub>x</sub>, photosensitive films, prep., props., and use for photodetectors 0-55298

Pb<sub>1-x</sub>Sn<sub>x</sub>Te, for IR detector appl. elec. and optical props. 0-35084

## triodes

reflex triode system, generation of intense microwave radiation by relativistic electron beam 0-14887

spherical reflex triode, extraction and bunching of ion beam 0-18727

triplet point *see* critical points

triplet absorption detection of magnetic resonance *see* microwave-optical double resonance

## triplet state

<sup>3</sup>P isoelectronic series, Sternheimer valence shielding and antishielding factors 0-18807

acetaldehyde, first triplet state geometry, fragmentation into free radicals 0-47915

alkali bromides and iodides, self-trapped exciton and F-centre form. by picosecond laser pulses 0-10546

alkali halide:Ti<sup>3+</sup>-like ions, triplet state lifetime, hyperfine interaction 0-2844

alkali halides, <sup>14</sup>N impurities, molecular point defects, EPR isotropic hyperfine triplets 0-2636

alloys, dilute mag., local moment formation, nonequivalent orbitals model 0-11164

anthracene, triplet-exciton fine struct., high resolution optical meas. 0-45099

anthracene-tetracyanobenzene cryst., triplet exciton annihilation, time correlated delay fluoresc., ODMR 0-39895

anthracene-tetracyanobenzene crystals, deuteration effect on phase transition, triplet state EPR study 0-50163

aromatic hydrocarbons, singlet-triplet conversion at low temp. 0-43094

aromatic isolated mol. nonradiative conversion, internal and S-T conversion, vibr. excitation and fluoresc. quantum yield 0-43095

aza-aromatic molecules, intersystem crossing, quantum interference effects 0-53037

azulene-fluoranthene, soln., triplet energy transfer, delayed fluoresc. study of S<sub>2</sub>→S<sub>0</sub> 0-23331

bacteriorhodopsin, triplet state energy and lifetime 0-30682

bacteriorhodopsin, triplet state energy and lifetime 0-30682

benzaldehyde, electronic spectra, CI and F substitution effects 0-23456

benzaldehyde-biacetyl system, self-quenching and electronic energy transfer obs. 0-5571

1,2-benzanthracene in polystyrene films, delayed luminesc. decay kinetics 0-43088

## triplet state continued

benzil, excited electronic states; conformational relax., time resolved matrix isolation spectral obs. 0-32701

benzophenone L in dibromodiphenylether, benzophenone triplet state, nanosecond resolved ODMR, freq.-agile techniques appl. 0-34825

2-benzoylpyridine crystals, lowest triplet state, optically detected EPR 0-15827

2-benzoylpyridine crystals, optical spectra of lowest triplet state 0-16081

borazine, triplet instability, RPA calculations 0-27938

broadening, inhomogeneous and homogeneous, of optical and ODMR transitions in solids 0-32750

carbenes, triplet state g-tensors and hyperfine coupling tensors 0-52895

carbonyls, electric polarisability, in excited singlet and triplet states (*Bulgarian*) 0-52897

chlorophyll photo-oxidation, role of singlet-excited and triplet states 0-51156

CIDEP, triplet mechanism, vector model 0-48020

complex molecules, photostability and quenching effect on laser generation kinetics 0-3390

condensation in magnetic field 0-2341

diacetylene, single cryst., photopolymerisation, intermediate states, struct. changes 0-30235

dibenzofuran, cryst., phosphoresc. spectra and ODMR meas. 0-11470

dibenzofuran-fluorene, mixed cryst., phosphoresc. spectra and ODMR meas. 0-11470

1,4-dibromonaphthalene, substitutionally disordered, energy localisation, optical and ODMR spectra of triplet Frenkel excitons 0-54996

p-dichlorobenzene, in p-dibromobenzene, optical detection of CI NQR in mag. field 0-50228

dihydroxycarbene, singlet and triplet state rot. pot. surfaces 0-32627

dimer triplet state line shape, small excitons, appl. to phenazine, naphthalene, tetrachlorobenzene 0-48041

durene-naphthalene melt, exciton diffusion, percolation approach 0-2390

dye laser materials, PPP calcs., ground and excited states, triplet yields and efficiency 0-37743

dye lasers, triplet loss influence on relaxation oscils. 0-23680

education, two-electron atom, 1s1l excited levels, ionisation energy calc., perturbation, Schrodinger eqn. methods 0-17728

electrogenerated chemiluminescence, estimation of triplet energies, possibilities and restrictions 0-34992

electronic correlation, n-AO in ground state, nπ\*-excited states (*Bulgarian*) 0-32614

EPR spin Hamiltonian, perturbation treatment, M=0 electronic state, HFS of triplet state EPR 0-25185

ethylbenzocarbazole, soln., luminesc., effect of electronic excitation energy vibr. 0-55174

ethylene(-d<sub>4</sub>), Rydberg states assignments, electron energy loss spectra 0-53153

fluorene: acridene, radical pair form. from excited states, optical nucl. polarisation obs. 0-14155

fluorene:pyrene-d<sub>10</sub>, exciton-guest, triplet-triplet annihilation, impurity traps effects 0-25433

fluorene, cryst., phosphoresc. spectra and ODMR meas. 0-11470

formaldehyde, triplet instability, RPA calculations triplet instability, RPA calculations 0-27938

formaldehyde, triplet state g-tensors and hyperfine coupling tensors 0-52895

hydrocarbons, electric polarisability, in excited singlet and triplet states (*Bulgarian*) 0-52897

ortho-hydroxybenzophenone, soln., intramol. proton transfer and energy relax. photostability, transient absorption obs. 0-28032

indigo dyes, triplet state config., laser flash absorpt. spectrosc. obs. 0-5557

intermolecular triplet excitation transfer in diffusive limit 0-28046

Jahn-Teller effect, intermediate, in orbital triplet, effect on EPR 0-34756

metals, triplet supercond. transition in strong mag. field 0-25040

methylene, singlet-triplet separation, relativistic corrections 0-32618

naphthalene, triplet exciton annihilation and triplet spin relax. 0-29792

naphthalene, triplet state time evolution after radiationless transition, initial vibronic distrib. effects 0-23450

naphthyl, excited electronic states; conformational relax., time resolved matrix isolation spectral obs. 0-32701

nucleic acid components, pyrimidine and purine, electronic struct. 0-30654

open shells, RHF treatment without Lagrange multipliers 0-32589

organic charge transfer crystals, transport props., phase transitions, mol. dynamic (*German*) 0-39507

palladium-octaethylporphyrin, gas phase delayed fluoresc. and phosphoresc., triplet excimer formation 0-18884

perdeuterobenzophenone, in 4,4'-dibromodiphenylether, cross-relax., microwave pulse obs. 0-53031

phenazine, substitutionally disordered, energy localisation, optical and ODMR spectra of triplet Frenkel excitons 0-54996

photoexcited triplet state molecules, in cryst., cross-relax., variable freq. ODMR obs. 0-53031

photosynthetically relevant mols., electronic structural props. 0-16902

polar dielectrics, triplet two electron states 0-24810

poly(N-vinylcarbazole) film, fluoresc. and phosphoresc., energy transfer mechanism 0-16112

poly-2-vinylnaphthalene, soln., lowest triplet props., flash photolysis and radiolysis obs. 0-32861

poly-N-vinylbenzocarbazole, soln., luminesc., effect of electronic excitation energy vibr. 0-55174

polyarylenealkyls, colour, EPR, electron density delocalisation degree determ. (*Russian*) 0-7152

polymethine dye behaviour in lasers, efficiency and photoisomer generation 0-14335

polyvinylbenzocarbazole, weak solution, intramolecular energy transfer by singlet and triplet excitons 0-34971

polyvinylcarbazole, weak solutions, intramolecular energy transfer by singlet and triplet excitons 0-34971

POPOP laser, bleaching of vapour 0-19027

propylene, mol. disoc. on bombardment by low energy electrons 0-43845

propynal, IR photochem. in electronically excited state 0-11923

proteins, adsorbed at interfaces, fluoresc. spectroscopy study 0-12315

quinoxaline guest molecule in p-dibromobenzene, crystal nucl. spin polarisation cross relax. study 0-29647

RF saturation spectroscopy, optical nucl. polarisation detect., excited state NMR and ESR transition mechanisms 0-54995

rhodamine 101, quenching of emission in methanol and latex particle suspensions 0-3374



## triplet state continued

- rhodamine 6G, aqueous soln., absorpt. spectra, ground and triplet state photoprotonation pH depend. 0-42961  
 scandium octaethylporphyrin,  $\mu$ -oxo bridged dimer, triplet states and geometrys, ODMR obs. 0-9625  
 scandium octaethylporphyrin, triplet states and geometrys, ODMR obs. 0-9625  
 TCNQ salt, MEM(TCNQ)<sub>2</sub>, phase transition electronic struct. interpretation 0-24781  
 TCNQ salt, N-n-butyl-quinolinium (TCNQ)<sub>2</sub>, ESR spectrum fine struct. splitting 0-44904  
 TCNQ salt, N-propyl-quinolinium(TCNQ)<sub>2</sub>, defect conc. depend. phase transition 0-44577  
 p-terphenyl, triplet exciton annihilation and triplet spin relax. 0-29792  
 1,2,4,5-tetrachlorobenzene, excited triplet state dimer, intermol. exchange integral, isotope effect 0-15826  
 1,2,4,5 tetrachlorobenzene, triplet excitons, high. mag. field, spin-lattice relax. study 0-20517  
 thioindigo dyes, triplet state config., laser flash absorpt. spectrosc. obs. 0-5557  
 thionine triplet+haloanilines, electron transfer reaction, radical yield meas. 0-3330  
 TOPOT, 1,4-bis[2-(5-p-tolylloxazolyl)]benzene laser, bleaching of vapour 0-19027  
 s-triazine, triplet instability, RPA calculations 0-27938  
 trimethylenemethane, ground state triplet, HFS, EPR obs. 0-50188  
 triphenylene-(d<sub>2</sub>), lowest T<sub>1</sub>[<sup>3</sup>A<sub>2</sub>( $\pi\pi^*$ )] state vibronic coupling 0-47955  
 xanthene dyes, internal heavy atom effect on radiative and non-radiative rate consts. 0-32765  
 ( $\mu$ )<sub>15</sub> muonic atoms in gaseous H, triplet state lifetime 0-23579  
 Ag complexes, Ag(II) porphyrins, picosec. flash photolysis, transient absorpt. 0-52976  
 AgBr, new shoulder in luminesc. spectra, triplet excitons 0-20706  
 $\alpha$ -Al<sub>2</sub>O<sub>3</sub>, additively coloured single crystal, luminescence (Russian) 0-55169  
 CF<sub>2</sub>(<sup>3</sup>B<sub>1</sub>) triplet-triplet annihilation, CF<sub>2</sub>, CF<sub>2</sub>(<sup>1</sup>B<sub>1</sub>) energy distrib. 0-50861  
 CH<sub>2</sub>, photoprod. from ketene, singlet-triplet energy separation and vibronic level obs. 0-11936  
 CO, A'<sup>1</sup> $\Pi$ ( $\nu=1$ ), vibr. relax. by reversible intersystem crossing, fluoresc. obs. 0-14170  
 CO, b<sup>2</sup> $\Sigma^+$  state excitation, low-energy electron impact,  $\nu=3$  level lifetime 0-1072  
 CS<sub>2</sub>, <sup>3</sup>A<sub>2</sub> state, triplet bands, MCD spectrum, near UV absorpt. spectrum 0-48010  
 CsO, <sup>3</sup>P<sup>3+</sup> orbital triplet, intermediate Jahn-Teller effect, APR 0-34758  
 Cd(<sup>5</sup>P<sub>1/2</sub>)+methane (H<sub>2</sub>)(D<sub>2</sub>)(N<sub>2</sub>), absolute quenching cross sections 0-5604  
 Cl<sub>2</sub>CS, excitation, singlet and triplet states, two photon absorpt., singlet-singlet energy pooling, fluoresc. obs. 0-48032  
 CsI, self-trapped exciton electronic struct., semi-empirical mol. orbital method 0-49605  
 CsI:Na, self-trapped exciton emission polarisation 0-49607  
 Cu complex, Cu(II) dimers, temp. depend. PMR relax., singlet-triplet separation determ. 0-43073  
 CuBr, IS exciton triplet state, magneto-optical props. 0-25345  
 GaP:O<sup>-</sup>, two-electron O<sup>-</sup> state evidence, ODMR, IR emission, phonon replicas 0-15828  
 GaS, optical detection of triplet excitons 0-29650  
 GaSe excitonic spectra fine struct., reflection and transmission spectra (Russian) 0-55126  
 GaSe, triplet excitons ODMR 0-25252  
 H<sup>-</sup>, bound states in mag. field, binding anal., variational calcs. 0-42940  
 H<sub>2</sub> 3s, 3d: <sup>3</sup> $\Sigma$ , <sup>3</sup> $\Pi$ , <sup>3</sup> $\Delta$  complex, fine struct., Doppler-free laser spectroscopy 0-1087  
 H<sub>2</sub>, interat. pot. energy matrix elements, generalised DIM calc., ZDO approx. 0-52864  
 He, bound states in mag. field, binding anal., variational calcs. 0-42940  
 He+He<sup>+</sup>, triplet excitation cross-section, Ochkur-Rudge approx. calcs. 0-28101  
 He(2<sup>1</sup>S, 2<sup>3</sup>S), threshold to 0.10 eV, energy-integrated total cross section ratio 0-37885  
 He(2<sup>1</sup>S, 2<sup>3</sup>S)+Ne(Ar)(Kr)(Xe), Van der Waals forces, one-electron model pot. calcs. 0-14094  
 He(2<sup>1</sup>S), inelastic scatt., RPA and 1st Born approx. calcs. 0-53148  
 He(2<sup>3</sup>S), electron impact ionis. to 1s, 2s, and 2p state, autoionis. 0-1068  
 He(2<sup>3</sup>S) in alkali-He quantum magnetometer 0-17965  
 He(2<sup>3</sup>S)+Ca(Sr)(Ba), coherent <sup>3</sup>P<sub>3/2</sub> levels excitation by Penning ionis., Hanle effect 0-5520  
 He(2<sup>3</sup>S<sub>1</sub>)+Sr, alignment of ions in Penning collisions, polarised emission obs. 0-23533  
 He(3<sup>3</sup>P) electron beam-excitation 0-43188  
 KBr:PO<sub>2</sub><sup>-</sup>, phosphorescence, triplet state sublevels, mixing 0-25446  
 KCl:PO<sub>2</sub><sup>-</sup>, triplet state, level anticrossing and pseudonuclear Zeeman effect, microwave ODMR 0-39896  
 KCl:Kr, triplet state of F<sub>2</sub>-centres, ESR spectra 0-29616  
 Kr(<sup>3</sup>P<sub>2</sub>)+F<sub>2</sub>(NF<sub>3</sub>)(CF<sub>3</sub>OF), KrF\* bound-free oscill. emission spectra calcs. 0-7799  
 Li<sub>2</sub>, second virial coeffs., Konowalow MCSCF potential calcs. 0-23312  
 Li<sub>2</sub>, spectroscopy and structure, triplet excimer continuum emission 0-32769  
 Mg, hollow cathode discharge, excitation mechanisms of triplet state atoms and decay obs. 0-44015  
 N<sub>2</sub>, diffuse plasma, population densities of triplet states, correl. with electron impact processes 0-43966  
 N<sub>2</sub>, solid and matrix isolated mol., triplet state spectra (Russian) 0-5574  
 N<sub>2</sub> triplet-triplet transitions, Einstein-A coeffs., oscill. strengths, lifetimes, theory and experiment comparison 0-47876  
 NH<sub>3</sub>, first triplet state, photodissoc. and Rydbergisation investig. 0-53067  
 NH<sub>3</sub>, lowest triplet state geometry, SCF and CEPA-PNO calc. 0-914  
 NH<sub>3</sub>+2H<sub>2</sub>, triplet n3S Rydberg state, ab initio UHF CI SCF calcs. 0-53095  
 NH(A<sup>1</sup> $\Pi$ , b<sup>3</sup> $\Sigma$ ), two-photon generation in NH<sub>3</sub> UV laser photodissoc. 0-11901  
 Na<sub>2</sub>, spectroscopy and structure, triplet excimer continuum emission 0-32769  
 NaK dimer formed in supersonic beam, laser-induced emission 0-9636  
 Ne (<sup>3</sup>P<sub>2</sub>) metastable state decay in Townsend discharge afterglow 0-44011

## triplet state continued

- Ne I to Ne IV, excitation in ion-atom collisions, 100 keV region, emission spectra obs. 0-14205  
 O(<sup>3</sup>P, D)+H<sub>2</sub>(<sup>1</sup> $\Sigma_g^+$ )→H<sub>2</sub>O, potential energy surfaces, extended basis first-order CI study 0-7776  
 O(<sup>3</sup>P) translationally hot, energy distrib. function 0-21811  
 Ru complex, ruthenium(II) tris(2,2'-bipyridine), absorption spectrum and quantum yield of formation (French) 0-5554  
 SO, and isotopic forms, X<sup>3</sup> $\Sigma^-$  state, CO<sub>2</sub> laser mag. reson. spectroscopy 0-9602  
 Ti(y <sup>3</sup>D<sub>0</sub>) lifetime, in rel. oscill. strengths determ. by combined absorpt./emission meas. 0-37784  
 Xe (<sup>3</sup>P<sub>1</sub>), in afterglow 0-38742
- tritium**  
 aqueous tritiated waste management from fuel reprocessing 0-5272  
 behaviour in advanced nuclear fuel systems 0-18633  
 behaviour in pebble bed reactors, numerical calc. (German) 0-9387  
 CANDU heavy water reactors, storage and monitoring of tritium 0-5291  
 concentration meas. by portable gas radiometer 0-32570  
 counting efficiencies and sample time stabilities in a Triton X-100/toluene scintillant 0-52813  
 cryogenic data relevant to mag. fusion energy 0-8746  
 diffusion coeff. in Zr foil 0-15306  
 diffusion coefficients in pyrolytic C 0-37443  
 diffusion in Zircaloy-2 0-32341  
 environmental control of use and release at TFTR 0-13829  
 fusion fuel exchange between fusion hybrid, fission, and T producer reactors 0-13811  
 fusion reactor direct-cycle steam generating blanket design 0-37615  
 fusion reactor T breeding, comparative evaluation for Li, LiO<sub>2</sub>, Li<sub>2</sub>Pb<sub>2</sub> 0-13831  
 handling systems for fusion reactors, materials considerations 0-32463  
 HTGR, T contamination of product gas 0-13590  
 isotope separation in Ti-fluidised bed 0-18676  
 labelled biologically active compounds obtained using at. <sup>3</sup>H bundles, appls. 0-30888  
 laser fusion microsphere targets, nondestructive anal. using rot. Raman spectroscopy 0-50896  
 losses in primary and steam circuits in FINTOR-D, control system 0-18634  
 low-dose  $\beta$ -ray relative biological effectiveness 0-12190  
 E.Mediterranean Sea, T and O<sub>2</sub> profiles 0-17298  
 monitoring at nuclear power stations 0-18691  
 monitoring methodology using SiO<sub>2</sub> desiccant, appl. to research reactor facility 0-21434  
 nervous activity monitoring in Drosophila by [<sup>3</sup>H]deoxyglucose 0-56024  
 permeation in stainless steel 0-34241  
 permeation through steam generator alloys 0-34250  
 pollution in N.Pacific surface water during 1974, conc. meas. 0-26181  
 production and distrib. in Peach Bottom HTGR 0-47581  
 production in advanced stellar evolution, reaction cross sections 0-56815  
 production in fission research reactors to fuel CTR expts., feasibility 0-18632  
 production in toroidal fusion reactor, cross section sensitivity calc. using SENSITWO code 0-835  
 proportional counters, multielement, anticoincidence techniques for measuring low T activities 0-27874  
 proteins, <sup>3</sup>H-labelled, fluorography in immunoelectrophoresis 0-17220  
 PWR, T sources, releases, monitoring, management and environmental impact 0-18690  
 rabbit tritium obs. after ingestion of contaminated food and water 0-21549  
 radiation safety in nucl. fuel cycle (Russian) 0-56227  
 radioactive fallout at South Pole, 1954-1978 T content of snow 0-16867  
 radioactive target preparation and characterisation 0-18734  
 radioactive waste, leaching behaviour from hardened cement paste 0-18443  
 radioactive waste, tritiated, gas generation by autoradiolysis 0-32384  
 radioactive waste immobilisation, possible solid mats. 0-27755  
 rats, T content in organs, and DNA of rat liver cells, after doses of tritiated food, protein or water 0-56226  
 rats, T radiation dose absorbed in rat organs, after feeding with organically bound T 0-51262  
 recovery from molten Li by Y getters 0-32470  
 reflection from amorphous Be, Fe, Mo, W, Monte Carlo study 0-40197  
 release from nuclear power stations 0-23032  
 removal from solid Li compounds in fusion reactor blanket 0-32513  
 RFPR, T transport in packed bed Li<sub>2</sub>O fusion blanket 0-37612  
 self-diffusion in ZrH<sub>2</sub>, autoradiographic study, energy of soln. in H sublattice (Russian) 0-2194  
 sources and reactions of T species 0-21432  
 thermonuclear fusion plasmas, elem. processes and role of atomic, ionic and mol. data 0-14916  
 visual pigment regeneration studies, use of [<sup>15</sup>-H]all-trans-retinal tracer 0-41357  
 water cooled, water moderated reactor, coolant tritium content in first loop 0-32334  
 water pollution, T concentration in natural waters of N.Italy (Italian) 0-40933  
 D-T pellet neutron moderation on blanket neutronics of inertially-confined fusion reactors 0-836  
 D-T plasma, EM field induced resultant drift inwards from boundary 0-38577  
 H<sub>2</sub>, solid, T-impregnated, storable conc. of atomic H 0-30594  
 HT-HTO in air meas. system 0-21433  
<sup>2</sup>H<sup>3</sup>H $\mu$ →<sup>4</sup>He+n+ $\mu$ +17.6 MeV, muonic catalysis in synthesis reactions (Russian) 0-52706  
 T+D, guiding centre distrib. spatial separation, reaction rate enhancement 0-37377  
 T+HD hot atom exchange reactions, trajectory calcs. 0-26037  
 T<sub>2</sub>-HT(HD), liq. and solid, vibr.-rot. IR spectra 0-50313  
 Ti, tritiated self supported target prep. 0-23211
- tritium compounds**  
 water, tritiated, inhalation hazard from open containers 0-8240  
 HT-HTO in air meas. system 0-21433  
 HT<sub>2</sub>, storable conc. of atomic H in T-impregnated crystalline solid H<sub>2</sub> 0-30594  
 H<sub>2</sub>T, storable conc. of atomic H in T-impregnated crystalline solid H<sub>2</sub> 0-30594  
<sup>3</sup>H<sub>2</sub>O, yeast cell mutagenesis by storage in tritiated water 0-17017



**tritium compounds continued**

<sup>3</sup>HOH, effects of chronic ingestion on prenatal brain development, rat expts. 0-36004

THO, prediction of flux from air to plant leaves 0-26381

T<sub>2</sub>O, inertia defects and dipole moments by kinetic consts. method 0-928

**triton interactions** *see triton-nucleus reactions***triton-nucleus reactions**

for inelastic triton-nucleus scattering, *see* "triton-nucleus scattering"  
*see also nuclear fusion*

(t,p), even actinides, lowest 0<sup>+</sup> state excitation, collective phonon state, spectroscopic factors 0-13410

(t,p) ground state cross section systematics in 2s-1d shell 0-5148

<sup>10</sup>B(t,α)<sup>9</sup>Be\*(2s<sub>1/2</sub>), resonant spectra 0-22691

<sup>40</sup>Ca(t,p), centre of mass corrections to DWBA overlap factors 0-18319

<sup>254</sup>Cf(t,p), <sup>256</sup>Cf spontaneous fission, mass and kinetic energy distribns. 0-47518

<sup>254</sup>Es fission coincidence data from d, t, and <sup>3</sup>He induced reactions 0-42720

<sup>54</sup>Fe(t,d), 2.5-3.5 MeV, <sup>55</sup>Fe Zp<sub>3/2</sub> neutron orbit radius isotone shift from DWBA anal. 0-32172

<sup>257</sup>Fm(t,p), 16 MeV, cross section, <sup>259</sup>Fm spontaneous fission, T<sub>1/2</sub> and kinetic energies 0-47517

<sup>7</sup>Li(t,<sup>9</sup>Li), 5.43-5.95 MeV, near threshold anomaly, <sup>10</sup>Be near threshold state (Russian) 0-13484

<sup>14</sup>N(t,γ), 0.8-3.3 MeV, <sup>17</sup>O levels, resonances, J<sup>π</sup> and radiative width 0-47389

<sup>15</sup>N(t,p), 15 MeV, <sup>17</sup>N levels and ang. distribns. meas., shell model calcs. 0-9233

<sup>16</sup>O(t,γ)<sup>19</sup>F, energy levels from α-<sup>15</sup>N and t-<sup>16</sup>O coupled channel orthogonality condition model 0-37326

<sup>16</sup>O(t,p), centre of mass corrections to DWBA overlap factors 0-18319

<sup>18</sup>O(t,p), 15 MeV, <sup>20</sup>Ne, levels, J<sup>π</sup> and ang. distribns. 0-18204

<sup>189</sup>Os(t,α)<sup>188</sup>Re, 15.1 MeV, <sup>188</sup>Re energy level obs. 0-47487

Os(t,p), 17 MeV, two neutron transfer strength, O(6) limiting symmetry in IBA, Pt comparison 0-32287

<sup>208</sup>Pb(t,p), centre of mass corrections to DWBA overlap factors 0-18319

Pt(t,p), 17 MeV, two neutron transfer strength, O(6) limiting symmetry in IBA, Os comparison 0-32287

<sup>244</sup>Pu(t,p), 17 MeV, <sup>246</sup>Pu excited states, mass excess and shell gap, L=0 transition 0-9236

<sup>150</sup>Sm(t,α), pol. t, 17 MeV, <sup>149</sup>Pm single proton states, spin assignments, spectroscopic factors 0-18170

<sup>6</sup>Sn (t,α), 4.75-5.25 MeV, A=112, 116, 118, 120, 124, single proton states RMS radius 0-13350

Te(t,α), 16 MeV, <sup>125</sup>Sb, A=123,125,127,129, cross-sections, ang. distribns., spectroscopic factors, DWBA anal. 0-52572

<sup>50</sup>Ti(t,d), 2.25-3.00 MeV, <sup>51</sup>Ti Zp<sub>3/2</sub> neutron orbit radius isotone shift from DWBA anal. 0-32172

Ti(t,2n)<sup>48</sup>Ti, He, fusion cross sections and thermonuclear reaction rates 0-533

<sup>176</sup>Yb(t,α), pol. t, 17 MeV, <sup>175</sup>Tm single proton states, rot. bands, J<sup>π</sup> assignments 0-452

<sup>90</sup>Zr(t,p), centre of mass corrections to DWBA overlap factors 0-18319

**triton-nucleus scattering**

(t,t), A=40-208, 17 MeV, pol. t, cross sections and anal. powers, optical anal. 0-47462

<sup>2</sup>H(t,t)H, 0.6-3.4 MeV, differential cross-sections, <sup>5</sup>He energy levels deduced 0-47488

<sup>3</sup>H doublet scatt. length, Phillips plot, N/D input parametrisation 0-42672

**triton scattering** *see triton-nucleus scattering***tritons**

ion medium energy beam from α-particle fragmentation 0-27847

production in Br,Ag+p in 24 GeV/c reacts., role of pick-up processes 0-27632

three-particle bound states for partly nonlocal interactions with continuum bound states 0-32206

<sup>3</sup>H→n+d, s-wave asymptotic normalisation consts. in one-boson exchange model 0-37334

**trolleybuses** *see road vehicles***troposphere**

*see also atmospheric boundary layer; tropospheric electromagnetic wave propagation*

acetylene, tropospheric and lower stratospheric vertical profiles 0-4073

aerosol global distribution, 162-238 millibar altitude 0-56591

aerosol, particle size distribns. evolution via Brownian coagulation, num. simulation 0-41513

aerosol concentration above South Polar Plateau, rel. to meteorological transport of particulate material 0-51481

aerosol properties at S.Pole, 1978 obs. 0-41484

aerosols, effect on surface and surface-atmosphere radiation budgets 0-17375

air collection and analysis techniques, troposphere and stratosphere 0-26566

n-alkane pollutants, N.Atlantic gas and particle concs. 0-7969

empirical orthogonal functions of 500 mb height, truncation of series 0-56581

empirical orthogonal functions of 500 mb level, N.hemisphere 0-56580

energy balance, diurnal variation 0-56548

entraining convection at upper limit of convection 0-26568

ethane, tropospheric and lower stratospheric vertical profiles 0-4073

formaldehyde composition of air over N.Germany coast, obs. 0-26584

fronts and depressions at middle latitudes, mesoscale struct. 0-26604

geopotential height data over ocean areas, supplementary method 0-26647

gravity waves and LF oscillations, tropical lower atmos., theory 0-12496

gravity waves generated by shear flow instability 0-31098

hailstones, free-fall kinematics near ground 0-12519

high-pressure systems in E.United States, <sup>7</sup>Be distrib. 0-4072

interhemisphere transpore in troposphere, CO content study 0-31106

intrusive density flows, soliton source 0-12499

isotropic and sigma coord. hybrid numerical model 0-12485

jet stream, different, theory 0-46242

kinetic energy balance of large-scale motion over British Isles 0-56578

lee waves, models, limiting cases (Russian) 0-12480

Lee waves classical theory, asymptotic approx., upper boundary condition role 0-12472

moisture, temp., IR soundings anal. by statistical struct. and correl. functions 0-8398

mountains affecting geopotential, Coriolis force variability 0-26602

**troposphere continued**

planetary waves in middle troposphere, nonlinear interaction, theory 0-36385

planetary waves of N.Hemisphere, space time anal. 0-51468

pressure and temp. meas. by lidar differential absorpt., influence of laser emission spectral width (French) 0-41554

pressure at high altitudes, correl. with interplanetary mag. field struct. and solar wind 0-56515

radar observation of fine struct., pulsed VHF radar method 0-51566

radiative divergence in GATE, results 0-17320

radiative energy balance, affected by stratospheric O<sub>3</sub> content 0-51466

radio-acoustic sounder, metric radio wave device 0-46276

sea breezes of Alaskan Beaufort Sea Coast 0-41485

stationary waves, vorticity and heat balance calcs. 0-51460

stratified flow around three-dimens. barrier 0-48769

stratosphere warming event of January-February 1979, tropospheric-stratospheric interaction 0-4074

structure over Bay of Bengal, during Aug. 1977 active and break monsoon 0-56570

Sun-weather relation, vorticity area index to interplanetary mag. sector struct. 0-46222

synoptic windfinding using tropical constant-level balloon system 0-17395

temperature profiles from ground-based angular microwave meas. 0-51551

temperature-pressure profile meas. by microwave remote sensing (Chinese) 0-4116

tropopause, detect. by partial specular refl. with VHF radar 0-8411

troposphere and stratosphere sounding by pulsed VHF radar 0-51566

turbidity of Barcelona's air, anal. of 1971-7 obs. (Spanish) 0-36375

ultralong waves, β-effect influence on baroclinic instability (Chinese) 0-4062

UV flux calcs. and photolysis rates 0-12465

virtual temperature rel. to height of isobaric surface, theory (French) 0-21806

wave motion, balloon obs. using data storage system on balloon 0-46263

winds and turbulence continuous meas. using VHF Doppler radar, preliminary results 0-8444

winds variance spectrum over E.Europe 0-8397

winter lower atmosphere, influence of interplanetary mag. field sector struct. 0-8510

zonal and meridional large scale flow over British Isles 0-56579

CO, content observed on circumpolar airliner flight 0-51475

CO, tropospheric latitude distrib., model involving production and transport 0-41483

HO<sub>2</sub>+NO→OH+NO<sub>2</sub>, kinetics temp. depend. 0-3313

NH<sub>3</sub>+NO<sub>2</sub>, reaction rate const. meas. 0-7772

NO, troposphere content, 0-7 km altitude over clean and polluted areas 0-51478

NO<sub>2</sub>, composition of air over N.Germany coast, obs. 0-26584

N<sub>2</sub>O, global atmos. composition and residence time 0-51519

O<sub>3</sub>, composition observed on circumpolar flight 0-51475

O<sub>3</sub>, composition of air over N.Germany coast, obs. 0-26584

O<sub>3</sub>, depletion by halomethanes 0-16866

O<sub>3</sub>, differential absorption lidar meas. 0-12554

O<sub>3</sub>, photochemical prod. and influence on climate 0-36365

OH budget, reaction kinetics of OH+trichloroethanes 0-16657

OH radical concentration, determ. method using atmospheric <sup>14</sup>CO meas. (German) 0-8419

OH+NO<sub>2</sub>+M→HNO<sub>3</sub>+M, N<sub>x</sub>O<sub>y</sub>, removal from polluted atmospheres 0-50846

OH+trichloroethane→H<sub>2</sub>O+CH<sub>2</sub>CCl<sub>3</sub>, rate const. and tropospheric chem. 0-16658

S, linear eight-box model for tropospheric global cycle 0-56506

SO<sub>2</sub> in marine troposphere, sources in CS<sub>2</sub> and COS oxidation 0-4085

SO<sub>4</sub><sup>2-</sup> aerosol layer, form. and evolution model 0-21801

**tropospheric electromagnetic wave propagation**

aerosol light scattering, obs. of polarisation and intensity 0-51541

Comstar beacon cumulative slant path rain attenuation statistics, 28.56 GHz 0-26582

correlation bandwidth, empirical evaluation over troposcatter paths (French) 0-41527

ducting of HF radiowaves, numerical study 0-36378

fog, IR extinction and absorption, linear relation to water content 0-56603

hurricane sea surface wind speed, L-band radar backscatt. obs. 0-56561

IR radiative transfer, absorpt. in partial cloud cover model 0-12544

laser beam attenuation by snowfall, characts. 0-26611

numerical comparison of ray method and normal wave method 0-21858

precipitation detection by radar (German) 0-46227

radar measurement of clouds and precipitation, correl. and spectral anal. 0-12529

radar observation of cloud and precipitation particles, X- and K<sub>a</sub>-band method 0-46273

radar observation of hydrometeors 0-46219

radar reflection from cloud and clutter targets, broad-band noise techniques 0-51454

radar reflection from rain, differential refl. method 0-46221

radio and optical waves refraction in atmospheric boundary layers 0-36400

radio refractive index, calc. from temp., press. and humidity data (Czech) 0-36351

radio wave absorpt. by water vapour in atmosphere, 0.8-20 mm range 0-4086

radiosonde meas. and spectral anal. of LOS fading 0-56568

radiowave phase fluctuations in anisotropic turbulent atmosphere when emitted by moving source 0-17352

radiowave propag., angular depend. of rain scatt. at freqs. below 30 GHz 0-8416

radiowave propag., crosspolarisation and attenuation meas. at 11.6 GHz using theoretical rain model, canting angle distrib. 0-4070

radiowave propag. errors during geomag. storms 0-4077

radiowave propagation above 30 MHz, role of sporadic-E layer and troposphere 0-41636

radiowaves, propag. in ducts used for line-of-sight links (French) 0-17303

radiowaves, troposcatter developments in North Sea 0-46246

rain attenuation of radiowaves meas., microwave radio link projected design appls. (Slovenian) 0-46217

rain scattering of microwaves, drop-size and temp. effects on forward and backward scattering 0-17317



**tropospheric electromagnetic wave propagation** continued

- rain-cell modelling for earth-space links using SIRIO satellite radiowave propagation data 0-36352
- rainfall over land, microwave radiometry by Nimbus 6 ESMR 0-56635
- refraction values of radiowaves in troposphere in air temp. inversion 0-4087
- remote probing for wind and struct. const., line-of-sight method 0-36426
- remote sensing by two satellites, radio illumination method 0-51550
- satellite communications above 10 GHz, rain effects 0-8410
- SHF signal attenuation by rain, monitored by radar 0-51567
- storm precipitation observed with radar 0-46220
- thunderstorm, radar and VHF emission obs. of three-dimens. motion 0-46218
- thunderstorm observed by radar, depolarisation rel. to precipitation 0-51453
- transhorizon propag. at freqs. >1 GHz on transmission paths set up in CSSR and GDR (*German*) 0-17364
- VLBI, correction for effects of troposphere, ionosphere and Earth crustal tide (*Japanese*) 0-21926
- weather radar, Doppler, estimation of echo spectral moment 0-51563
- wind shear detection radar, for airport use 0-51565

**truth tables** see logic design**TSC** see thermally stimulated currents**TSCD** see thermally stimulated currents**TSD** see thermally stimulated currents**TTL** see transistor-transistor logic**tubes (electronic)** see electron tubes**turners** see tuning**tungsten**

## see also nuclei with .....

- adatoms, on Ir(110), surface diffusion by atomic exchange mech. 0-49508
- adsorbed Be layers on W(110) and (100), work function and loss spectra meas. 0-6638
- adsorbed O on stepped (100) surface, electron stimulated desorption ion ang. distrib. 0-20035
- adsorption of O<sub>2</sub> and CO, angle resolved electron stimulated desorption, LEED and AES 0-6645
- adsorption of Ag, substrate temp. effect on relation between work function and coverage, FEM obs. 0-2272
- adsorption of CO on (100) plane, thermal desorption and work function meas. 0-29273
- adsorption of Cs and O<sub>2</sub>, work function and thermal stability 0-44427
- adsorption of Cs on oxygenated and oxidised (110) 0-44424
- adsorption of H<sub>2</sub>(N<sub>2</sub>)(NH<sub>3</sub>), thermal desorption and pulsed time of flight mass spectra anal. 0-30285
- adsorption of N<sub>2</sub>, effect of SIMS, sputtering induced recomb. anal. 0-55243
- adsorption of N<sub>2</sub> on W(110) vicinals, step sites as dissoc. centres 0-6642
- adsorption of NO on (110) surface, chemical changes detected by AES 0-10787
- adsorption of Pb on W(100), W(110) substrates, pairwise interaction model using Morse pot. 0-6657
- adsorption of W single atoms on (111), (211), and (311), surface site geometry determ. by FIM 0-39447
- adsorption of Xe and coadsorption with O on (110) and (100), work function and thermal desorption meas. 0-39448
- adsorption of Zr on (100) surface, AES, LEED, thermal desorption, and work function meas. 0-39444
- amorphous, reflection of D and T, Monte Carlo study 0-40197
- anodic oxidation, open circuit transient anal., dielec. and elec. props. of oxide film 0-3245
- arc welds, fatigue crack growth behaviour in air and high-C liquid Na, carburization studies 0-40625
- Auger spectrum, 150 to 200 eV 0-35022
- boriding, Cu influence 0-21165
- candidate refractory for Tokamak, thermal fatigue failure testing 0-32454
- carburization, catalytic Co effect 0-3255
- catalytic decomposition of NH<sub>3</sub> single pulses, mol. beam relax. spectrometry 0-21321
- cathode, hollow, cylindrical, heavy-current temp. condition 0-38763
- cathode, motion of cathode spot of vacuum arc 0-54069
- cathodes arced in vacuum, erosion structs. 0-1872
- channelling of He atoms, calc. 0-34108
- chemisorbed H, surface cond. and intrinsic surface states, surface refl. spectra 0-15378
- chemisorbed H monolayer on (001), surface phonons, lattice dynamical model 0-39405
- chemisorbed O on (110), island form. and condensation 0-49517
- chemisorption of  $\beta$ -N<sub>2</sub> on [110] surface, underlayer mechanism 0-39432
- chemisorption of H on (001) surface, HF Green's function formalism and phase shift technique 0-24733
- chemisorption of H on (100) surface, struct. determ. by surface vibr. modes anal., EELS obs. 0-39435
- chemisorption of halogens on (100) surface, UV photoelectron spectrosc. study 0-7854
- coadsorption of Zr and O<sub>2</sub> at high temp. on (100) surface 0-6653
- codeposition of Cs and O on (110), Cs<sub>2</sub>O form. 0-44425
- combustion under CW CO<sub>2</sub> laser radiation action 0-30241
- corrosion protective coating for Al<sub>2</sub>O<sub>3</sub>-Y<sub>2</sub>O<sub>3</sub> ceramics 0-35367
- D electro-fission on relativistic channelling (*Russian*) 0-54294
- desorption dynamics of Cs, surface ionisation voltage modulation method 0-44426
- desorption kinetics of halogens, pulsed ion beam method 0-34300
- determ. by atomic absorption, using low temp. flames 0-30307
- drawn wire, microstruct. effect on fracture 0-3177
- electrode material, influence on electric breakdown in dielectric liquids (*Russian*) 0-50265
- electrolytic anodisation, production of WO<sub>3</sub> electrochromic elements 0-25921
- electron stimulated desorption of O<sup>-</sup> and O<sup>+</sup> ions from adsorbed CO 0-2270
- electronic and struct. props., nonlocal pseudopot. calc. 0-34349
- electronic transport below 1K 0-2377
- EM showers produced by electrons, positron spectral distribution (*Russian*) 0-55218
- emissivity angular dependence, meas. in IR spectral region 0-34214
- fibre, brittle to tough transition, impact strength meas. 0-40527

**tungsten** continued

- fibre reinforced Co powder alloys, reactions and recryst. 0-11603
- field cathode with (001) orientation preparation technique 0-15241
- field desorption of Ba atoms, conc. depend. 0-25533
- field emission, spin filter effect of EuS 0-45221
- field-ion emitter, determ. of precise geometry from field-ion image 0-2930
- filament, incandescent, light flux fluctuations, limiting factors in photoelectric meas. 0-13136
- film, electron beam evaporator for in situ deposition studies in UHV electron microscope 0-40264
- film, evaporated, optical props., rel. to struct. 0-55211
- film, ion plating deposition system using electron beam evaporation (*French*) 0-20802
- films, (010), energy band calc. including spin-orbit interactions 0-20274
- foil, rolling procedures 0-23225
- grids of fine W wire, production, use in IR spectroscopy, polarization interferometry 0-9052
- heat resistant particles in low temp. Ar plasma, heating, melting, vaporisation (*Russian*) 0-40384
- implantation effects of <sup>133</sup>Xe, annealing behaviour, Mossbauer study 0-40011
- interatomic pair potential, phonon spectra 0-33927
- ion induced secondary electron emission, probe for adsorbed O 0-55251
- ion irradiated, defect clusters obs. 0-2089
- ion-irradiated, recovery behaviour studied by field ion microscope 0-29074
- ions, beam-foil spectra from 20 to 238 MeV energy, 5 to 60 nm, lifetime meas. problems 0-9722
- isomer shift values of implanted <sup>133</sup>Xe/<sup>133</sup>Cs, Mossbauer spectra 0-7240
- isotopically enriched target preparation using electron gun 0-23226
- Knudsen cells heated by radiation, emissivity (*Japanese*) 0-13073
- L-subshell ionisation cross section, branching ratios, fluoresc. yield, Coster-Kronig factors 0-43166
- lattice wave dispersion, lattice const., elastic const. 0-24545
- microscopy, signal-to-noise enhancement by superposition of bright-field images obtained under different illumination tilts 0-6329
- monolayer gas adsorption, relax., electron contrib. to chemisorption, Auger shift study 0-20738
- neutron low energy interaction cross sections, gravitational spectrometer meas. 0-24521
- phonon density of states determ. from heat capacity (*Russian*) 0-29131
- photo-stimulated field emission, effect of light polarisation, pure and Ba covered W (*French*) 0-7480
- photoemission, four-photon, incident angle and polarisation depend. 0-40221
- photoneutron yields released by incident electrons, improved calc. 0-27630
- physorption of Xe on (100) surface, Lennard-Jones model, mol. dynamics study 0-34308
- plasma spray coatings, relaxation phenomena 0-19876
- plasma sprayed coating, effect of Si substrate surface conditions and impact velocity of sprayed particles 0-21145
- plasma sputtering of Ni wire, coagulation, struct. and particle size (*Russian*) 0-40260
- positron annihilation and vacancy formation 0-16119
- positron trapping and annihilation at vacancies 0-29823
- powder, subjected to vibratory milling, exam. of plastic deformation, recrystallisation, sintering 0-16234
- powder metallurgy prep. 0-29904
- powder production, H reduction of WO<sub>3</sub>, staring specific surface effect on kinetics 0-11599
- powders, defective structure and activated sintering, exam. 0-16240
- powders, influence of geometrical props. on compaction (*Russian*) 0-20818
- RF size effect, surface electron scatt. influence (*Russian*) 0-2414
- secondary emission and photoemission props., effect of one-electron density of states 0-16152
- sintered, brittle fracture, statistical anal. 0-11744
- sintering of W-spheres in liquid Ni, computer simulation of chemically driven grain growth 0-55427
- spin polarised LEED, energy and ang. distrib. (*German*) 0-49468
- steels, high-purity and commercially based, containing 10 wt.%W or 5 wt.%Mo, tempering behaviour 0-7600
- strip lamp temp.-measurement using multiwavelength radiation pyrometry 0-31757
- substrate for Cu cementation, field ion microscopy of cementation vs. substrate dissolution, pH effect 0-16206
- substrate-oxide film system with rough boundaries, ellipsometric obs. using equiv. film theory 0-2310
- superconducting transition temperature, ab initio calc. 0-25036
- surface, {001}, clean, reconstructed, field-ion microsc. obs., 15-400K 0-15348
- surface, {001}, displacive surface phases formed by H<sub>2</sub> chemisorption, LEED study 0-49520
- surface, {411} and {320}, sticking probability and coverage determ. of N<sub>2</sub> 0-54528
- surface, (001), electronic origin of reconstruction 0-11065
- surface, (001), surface phase transition, electronic contribs., surface susceptibility, ab initio self-consistent thin-film energy band calc. 0-29255
- surface, (001) clean, long-range inhibition by N of displacive phase 0-2266
- surface, (100), reconstruction in presence of O half monolayer, struct. props. 0-44421
- surface, charged-particle emission caused by laser beam scanning 0-11518
- surface, clean and H<sub>2</sub>-covered, Cl<sub>2</sub> scatt. 0-20743
- surface, Cs coated, survival probabilities of emerging H<sup>+</sup> ions 0-45187
- surface, influence of alkali films on props., calc. (*Russian*) 0-2273
- surface (100), adsorbed Na atom, binding props. calc. 0-49522
- surface (100), LEED intensities, temp. depend., surface struct. phases and surface Debye temp. 0-39395
- surface (110), H adsorption, band struct. and adsorbate geometry, surface-reflectance-spectroscopy 0-44416
- surface (110), ionisation of hyperthermal Na atoms, temp. depend. 0-50504
- surface (110), O<sub>2</sub> and WO<sub>3</sub> adsorption, LEED and AES obs. 0-34317
- surface (110), work function, Fowler-Nordheim studies 0-34501
- surface (121), Ba atom desorption in strong elec. fields 0-29280
- surface contraction of (001) (1×1) using LEED intensity anal 0-6606



**tungsten continued**

- surface layer struct. during milling, plastic deform., failure (*Russian*) 0-40586  
 surface reconstruction, physical realisation of two-dimensional Ising and X-Y model 0-15351  
 surface structure by MeV ion backscattering, channelling 0-6605  
 surface thermoelectrotransport of atoms 0-2448  
 surface wetting by liquid Cu depend. on preliminary surface treatment (*Russian*) 0-35388  
 thermal accommodation of alkali metal vap. 0-24729  
 thermal neutron irradiated, recovery processes 0-19848  
 thermopower meas. in mag. field, 1.5-4K 0-54675  
 Tokamak limiter, plasma interaction, current profile evolution effect 0-10420  
 trapping of He at Xe atoms, attachment of mobile particles to non-saturable traps 0-39418  
 twin and stacking fault energies calc. 0-2038  
 twin lamellae shape of single crystal (*Russian*) 0-19812  
 vacancies, quenching and recovery invest., resist. and TEM study 0-39074  
 whisker crystal growth incorporated with field electron emission 0-44458  
 wire, organic microneedle growth under intense elec. fields, X-ray diff. and AES 0-54580  
 wire for high-speed matrix printers (*Japanese*) 0-55540  
 wire from rolled rods, mech. props. and struct. 0-25743  
 wire grids, FIR performance and appl. 0-10012  
 work function, nonideal terraced surface, calc. 0-6950  
 yield strength, temp. depend., of W with different microstructs. 0-16404  
 zonal electronic purification, mass spectra of contaminants (*Polish*) 0-25552  
 C content determ., isotope-spectral method (*Russian*) 0-55766  
 Ge-W contacts, surface electron state spectrum surface treatment effects (*Russian*) 0-34497  
 Nb<sub>2</sub>O<sub>5</sub>·W<sup>3+</sup>, ESR obs. on B-form single crystals. 0-54946  
 Ni-W surfaces in contact, deform. and adhesion at very low loads 0-39457  
 W spheres, in liq. Ni, sintered, coalescing, crystallographic orientation, SEM study 0-45249  
 W, surface state transferability, UPS meas. for (011) states 0-39650  
 W, thermal and anodic oxidation, production of WO<sub>3</sub> layer semiconductor electrode 0-35544  
 W XLVII X-ray spectra from laser produced plasmas 0-42981  
 W-Re, polygonisation in diffusion process, glide dislocation interactions 0-38998  
 W/α-Al<sub>2</sub>O<sub>3</sub>, heteroepitaxial structs., refined formulation of relative orientation criterias 0-44448  
 W/Cu interface, thermal conductance at low temps. 0-49436  
 W/Cu powders, liq. phase sintering, particle rearrangement 0-45253  
 W/EuS field emitters, electron emission current depend. on annealing temp., mag. props. 0-16160  
 W-Al<sub>2</sub>O<sub>3</sub> cermet films, oxide evaporation deposited on Mo, Ti, Al<sub>2</sub>O<sub>3</sub> substrates, struct., props. 0-25581  
 W-Br regenerative cycle of linear quartz lamps, metallic impurity effects, thermochemical interpretation 0-3312  
 W-C point contact, compared with TGS pyroelec. detector, appl. to temporal coherence meas. of HCN laser 0-31871  
 W-ThO<sub>2</sub>, candidate refractory for Tokamak, thermal fatigue failure testing 0-32454  
 W-ThO<sub>2</sub>-B, thermocathodes diffusion mobility, based on deboronation kinetics 0-39349  
 W<sub>2</sub>, dissoc. energy, estimated from LaIr(g) thermal decomp. obs. 0-7781  
<sup>178</sup>W, productions in <sup>181</sup>Ta(p,4n), purification procedure 0-12252

**tungsten alloys***see also tungsten compounds*

- fibre reinforced Co powder alloys, reactions and recryst. 0-11603  
 ion-irradiated, recovery behaviour studied by field ion microscope 0-29074  
 steel, alloy, V-W-Mo-Cr, exam. of carbide transformation 0-16299  
 steel, alloy, W-Mo-Cr-V, blanks welded to steel 45, optimal high temp. tempering 0-16351  
 steel, Cr-Mo-V-W, crack-growth and thermal-mech. fatigue 0-21072  
 steel, Cr-W-V-Mo (3.9 to 4.5, 1.5 to 2, 0.9 to 1.2, 3.9 to 4.4 wt.%), heat resistant, type 8Kh4M4V2F1-Sh, mech. props. 0-16464  
 steel, Si-Cr-Mo-W-V (2.4,1.3,2 wt.%), heat treatment and props. 0-16349  
 steel, solubility of W and Mo in Ti(C,N), 0-16276  
 steel, stainless, Ni-Cr-Mo-W (29, 13, 3, 2 wt.%), long-term strength in H at high pressure 0-55485  
 steel, tool, W-Mo, heat treatment effect on props. 0-50656  
 steel, W and W-Mo, sintered high-speed, naphthalenelike grain form., quenching effect on fracture toughness 0-30103  
 steel, W-Cr (3 wt.%), CrC formation in isochronal tempering, electron microscope study 0-7584  
 steel, W-Mo, tool, hydrostatic extrusion and tempering, wear resistance effect 0-50728  
 Stellite, friction behavior in high temp. Na environment (*Japanese*) 0-40546  
 Al-W, struct. and props. of alloys obtained from granules 0-50717  
 Fe-Ni-Mo (16.4, 8.1 wt.%), effect of substituting Mo by W during ageing 0-29991  
 Fe-W-C(VTiC), sintering, densification 0-25615  
 Mg-Ni-W-Co-Al-Cr alloy KhN56VMKYu, Al effect on excess Mg phase 0-29926  
 Mo-W, fatigue and threshold behaviour under high cycle fatigue 0-40487  
 Mo-W-C, phase equilibria calc., line compounds 0-10638  
 Nb-W-Mo-Zr, long-term strength props., vac. level effect 0-55484  
 Nb-W-Mo-Zr-C, strength and ductility, prolonged high-temp. soaking effect 0-55483  
 Nb-W-Zr-Ta, long-term strength props., vac. level effect 0-55484  
 Ni-Al-W, heat resist., solidification range 0-35177  
 Ni-C-W-Cr(Mo), Vickers hardness and crystallisation temp. 0-16361  
 Ni-Cr-Fe-W, type EHI868, loading history effect on resist. to cyclic elastoplastic strain 0-16398  
 Ni-Cr-W (20, 10 to 40 wt.%), phase composition, struct. and props. 0-21034  
 Ni-Cr-W-Mo-Al-Ti (15.6,3.2,2, wt.%), wrought, Si effect on transition brittleness (*Chinese*) 0-55491  
 Ni-Mo-C-W, Vickers hardness and crystallisation temp. 0-16361  
 Ni-W sintered powder pressings, intermetallic phases (*Russian*) 0-55349

**tungsten alloys continued**

- Ni-W-C(Nb) system, γ to (γ+W) phase boundary calcs. using Wigner method (*Russian*) 0-54346  
 Ni<sub>3</sub>Al-W, powder, X-ray spectral analysis exam. 0-16239  
 Ni<sub>3</sub>(Fe,W), elec. resist., temp. depend. anomalies, Hall and Nernst-Ettinghausen effects (*Russian*) 0-10942  
 Pd-W/Si, contact reactions, backscattering, X-ray diff. meas. 0-20040  
 Pt-Rh-W (30, 8 wt.%), intergranular embrittlement by Se vapour 0-3185  
 Ti-W film, bias-sputtered, resist. and comp. 0-25023  
 Ti-W(-Al), mech. props. and heat treatment 0-35274  
 α-Ti-Zr-W, effect of W impurity on mech. props. 0-16392  
 Ti-Zr-W(-Al), phase struct. and props. (*Russian*) 0-16270  
 W-Cr powder alloys, sintering in presence of Cu-Ni liq. phase 0-16246  
 W-Cr solid solution, precipitation behaviour, reaction front motion, lattice parameters (*German*) 0-55401  
 W-Cu, porous material, skeletal type, produced by liquid phase sintering, exam. of mech. strength, determ. resistance 0-16245  
 W-Cu-(Ti)(Zr), exam. of mech. props. as function of temp., composition, and oxidation props. 0-16472  
 W-Fe, electronic transport below 1K 0-2377  
 W-Fe, spin glass props., DC susceptibility and remanence meas., 1.6 to 295K 0-29560  
 W-Fe spin glass, optical props. and electronic states 0-20412  
 W-Fe-Co, sintering and mechanical props. (*Japanese*) 0-21086  
 W-Hf-C, phase equilib. 0-55348  
 W-Mo, vapour deposited, long-term strength and thermocyclic creep 0-16405  
 W-Ni, liquid phase sintering 0-16232  
 W-Ni, liquid phase sintering 0-25613  
 W-Ni, MBM diode, resist. depend. of detected signals 0-2482  
 W-Ni, MOM diode, breakdown effect in visible and near-IR regions 0-6999  
 W-Ni, surface barrier influence on C diffusion in stainless steel type 1Kh18N9T (*Russian*) 0-54434  
 W-Ni compact, sintering behaviour and workability (*Japanese*) 0-20822  
 W-Ni-Fe, W-Ni-Fe-Mo (Mn), sintering and mechanical props. (*Japanese*) 0-21086  
 W-Ni-Fe (5(2), 5(2) wt.%) pore formation, effect on mech. props. 0-45396  
 W-Os system films, condensation temp., conc., and phase comp. effect on struct. and props. (*Russian*) 0-24749  
 W-Re, amorphous wire, elec. resist., 2-20K, dims. and mag. field depend., quantum localisation 0-39547  
 W-Re, ion irradiated, recovery behaviour studied by field ion microscope 0-29074  
 W-Re, thin wires, fatigue limit and tensile strength 0-25834  
 W-Re alloy, prep. by powder metallurgy technique, appl. in lighting industry 0-29904  
 W-Ru based refractory transition metal-metalloid glass, struct. 0-1938  
 W-Si-Cu, struct. and supercond., Cu influence 0-50592  
 W-Ti, Ti addition effect on heat resistance and radiative props. (*Russian*) 0-25515  
 W-TiC(ZrC)(HfC), thermionic emission, surface structural characts. after prolonged use, work function variation 0-20758  
 W-Zr, Zr addition effect on heat resistance and radiative props. (*Russian*) 0-25515  
 W-Zr-C, Zr and C addition effect on heat resistance and radiative props. (*Russian*) 0-25515  
 W<sub>2</sub>B<sub>5</sub>-based alloys, mech. props., rel. to appl. as electrodes in electrospray machining 0-21174  
 WC powder, chemical plating with Co and Co-P 0-25593  
 WC-Co, calc. of weakest link in struct. 0-11730  
 WC-Co, composition and oxidation resistance of coatings deposited by thermal diffusion, using TiB<sub>2</sub> (*Bulgarian*) 0-45430  
 WC-Co, elastic and plastic charact. 0-35280  
 WC-Co, elemental and phase comp. of diffusion-deposited boride coatings 0-15402  
 WC-Co, phase comp. and oxidation resist. of coatings deposited by thermal diffusion using TiB<sub>2</sub> 0-21173  
 WC-Co (15 wt.%), alloy VK15 coating on Ti-Al, detonation sprayed, antifraction props. 0-21188  
 WC-Co (15 wt.%) detonation spraying on to Cr-Ni steel with automatic powder feed 0-25558  
 WC-Co alloy, hard metal, resistance of cavitation erosion (*Japanese*) 0-16575  
 WC-Co and WC-Co-Ta-C-TiC-NbC cemented carbides, microstructure, high temp. deformation, uniaxial plastic compression 0-40451  
 WC-Co carbide, crack paths, SEM study (*Japanese*) 0-50710  
 WC-Co cemented carbides, transverse-rupture strength obs., w.r.t. domain size of binder phase (*Japanese*) 0-11741  
 WC-Co cemented composites, abrasion by quartz 0-16495  
 WC-Co cutting plates, hardness and struct. of TiB<sub>2</sub> coatings 0-21175  
 WC-Co from directionally carburized WO<sub>3</sub>-C-Co<sub>3</sub>O<sub>4</sub> mixtures, sinking (*Japanese*) 0-11589  
 WC-Co hard alloys, machined with polycryst. superhard materials, surface struct. using X-ray photoelectron spectroscopy 0-25919  
 WC-Co powder, prep. by direct carburisation of WO<sub>3</sub> in presence of Co<sub>3</sub>O<sub>4</sub> 0-50573  
 WC-Co powder form. from WO<sub>3</sub> and Co<sub>3</sub>O<sub>4</sub> carburization, C behaviour (*Japanese*) 0-7517  
 WC-Co substrate, load-bearing capacities of TiC layers 0-40606  
 WC-Co-C, densification kinetics, in hot pressing of VK6 hard alloy 0-11600  
 Zr-Fe-Cu-W, Mossbauer spectra parameters of Zr<sub>2</sub>Fe particles (*Russian*) 0-29654  
 Zr-C-W (75 wt.%) eutectic refractory alloys, smelting in suspended states, components distrib. (*Russian*) 0-19913

**tungsten compounds***see also tungsten alloys*

- bronzes, hexagonal, supercond. and special phonons, neutron scatt. obs. 0-15643  
 refractory carbides, borides and nitrides, wetting by and interactions with liq. metals 0-54473  
 WO<sub>3</sub> reduction with H, starting specific surface effect on kinetics 0-11599  
 BaO-WO<sub>3</sub>, solid phase reaction, thermal anal. 0-55639  
 CdO-WO<sub>3</sub>, phase diagram and prep. of CdWO<sub>4</sub> single crystals. 0-29933  
 (H<sub>2</sub>PO<sub>4</sub>)<sub>2</sub>(WO<sub>3</sub>)<sub>12</sub>·29H<sub>2</sub>O, electrochromic solid-state cells 0-2724  
 H<sub>2</sub>WO<sub>3</sub> films, proton diffusion coeffs. 0-6548



**tungsten compounds continued**

- Na<sub>2</sub>WO<sub>4</sub> bronzes ( $0.4 < x < 1$ ), domain, surface and substrate struct. 0-34281  
 V<sub>2</sub>WO<sub>6</sub>, magnetic structure, stability of mag. modes, neutron diffraction study (*French*) 0-39744  
 WB<sub>12</sub>, growth from melt and phys. props. 0-20782  
 WB<sub>2</sub> and W<sub>2</sub>B<sub>5</sub>, core of B filaments, elec. resist. 0-15523  
 W<sub>2</sub>B<sub>5</sub> and WB<sub>4</sub>, thermal, elec. and mag. props. 0-20187  
 W<sub>2</sub>B<sub>5</sub>, monocryst., grain size, abrasive and strength props. 0-11787  
 W<sub>2</sub>B<sub>5</sub>, reactions with Ti-Al-Cr-Mo alloy VT3-1 0-16585  
 WC anode, performance in fuel cells with H<sub>2</sub>SO<sub>4</sub> electrolyte 0-21293  
 WC, deformation behaviour during rubbing in wide temp. range 0-16486  
 WC micropowder surface finishing of metals, surface struct. 0-11842  
 WC powder, sintering processing conditions 0-11614  
 WC, reactions with Ti-Al-Cr-Mo alloy VT3-1 0-16585  
 WC, rolling bearing materials, effects of high temp. operation 0-21124  
 WC, single cryst. elastic constants from mech. and X-ray elastic constants of polycryst. (*German*) 0-10591  
 WC, ultrafine powder, prod. by cryochemical, freeze drying, spray drying or soln. techniques 0-55336  
 WC-Co, fracture mode determination, using Auger electron spectroscopy 0-7680  
 WC-Co particles electrophoretic deposition, on metal surfaces, wear resistant coatings preparation (*German*) 0-2969  
 W<sub>2</sub>C and WC, plastic deform. under bending, 800-2200°C (*French*) 0-55482  
 W<sub>2</sub>C, oxidation, oriented struct. transform. to W, FEM and TEM obs. 0-30124  
 WF<sub>6</sub>, mechanism of heterogeneous reduction by H<sub>2</sub> (*Russian*) 0-21265  
 WF<sub>6</sub>-graphite intercalation cpds., prep. and props. 0-40686  
 WO<sub>2</sub> and O<sub>2</sub> adsorption on W (110) LEED and AES obs. 0-34317  
 WO<sub>2</sub> film coatings for Mo tips, film characterisation by atom probe FIM atomic clusters, voids 0-33863  
 WO<sub>3</sub> addition to WC powder, sintering processing conditions 0-11614  
 WO<sub>3</sub> amorphous film, sublimed under different conditions, elec. transport props. 0-7015  
 WO<sub>3</sub>, amorphous film, vac. deposited, struct. and crystn., TEM obs. 0-2291  
 WO<sub>3</sub>, amorphous film, vac. evaporated, density meas., microcrystalline model of struct. 0-2313  
 WO<sub>3</sub>, close-spaced chem. transport rates (*Russian*) 0-11570  
 WO<sub>3</sub> electrochromic elements, prod. by electrolytic anodisation of W, and characterisation 0-25921  
 WO<sub>3</sub> electrochromics in noneaqueous acid soln. 0-2722  
 WO<sub>3</sub>, electrochromism for student lab. expt. 0-17738  
 WO<sub>3</sub> electron density map of W<sup>5+</sup> polarons, EPR and optical absorpt. obs. 0-44912  
 WO<sub>3</sub> film, evaporated, mech. of elec. cond. 0-44747  
 WO<sub>3</sub> films, ESR study after colouring by H<sub>2</sub> injection and after bleaching in air 0-39867  
 WO<sub>3</sub> films, electron struct. changes during electrocoloration, XPS obs. 0-40217  
 WO<sub>3</sub> films on Si, sapphire, glass and metal substrates, colour intensity dependence obs. (*Russian*) 0-2430  
 WO<sub>3</sub> layers, semiconductor electrodes, electrochromism and photoelectrochemistry 0-35544  
 WO<sub>3</sub>, on glass substrate, electrochromism of glass film compositions 0-29720  
 WO<sub>3</sub> powders, hopping mechanism and Poole-Frenkel effect, elec. props. determ. 0-49734  
 WO<sub>3</sub>, triclinic, condensed modes 0-15211  
 WO<sub>3</sub>, vibr. anal., mol. const., kinetic const. method 0-23393  
 WO<sub>3</sub>-LiF system, on glass substrate, electrochromism of glass film compositions 0-29720  
 WO<sub>3</sub>-MoO<sub>3</sub> system, on glass substrate, electrochromism of glass film compositions 0-29720  
 WO<sub>3</sub>-P<sub>2</sub>O<sub>5</sub> alkali glasses, electrochromic, electron-ion processes 0-25341  
 (WO<sub>3</sub>)<sub>3</sub>, identification of polymer species by vapour phase electron diffraction 0-53135  
 WO<sub>6</sub><sup>6-</sup>, electronic struct., discrete variation and scatt. wave X<sub>α</sub> methods 0-917  
 WS<sub>2</sub>, self-propag. high-temp. synthesis, wear props. 0-2975  
 WS<sub>2</sub>, amorphous struct., X-ray radial distrib. anal. and XPS 0-49115  
 WS<sub>2</sub> sputtered film on Si and SiO<sub>2</sub> substrate, thermal oxidation kinetics 0-3208  
 W(ZrO<sub>2</sub>-La<sub>2</sub>O<sub>3</sub>), structural changes during reduction and sintering 0-25636

**tuning**

see also laser tuning; receivers; resonance  
 microtrons, nondimensional tuning of coupled-cavity structs. 0-32546

**tuning forks** see vibrating bodies**tunnel diode oscillators**

No entries

**tunnel diode storage devices** see semiconductor storage devices; tunnel diodes**tunnel diodes**

see also tunnelling  
 MIS, photoionisation of states 0-11099  
 AlGaAs tunnel diode, fabrication and appl. in cascade solar cell struct. 0-35682  
 p-(GaAs)<sub>x</sub>(ZnSe)<sub>1-x</sub>-nn<sup>+</sup>.GaAs, avalanche heterojunctions, inverse branch of volt ampere characts. (*Russian*) 0-6974

**tunnel effect** see tunnelling**tunnel triodes** see thin film transistors**tunnelling**

see also superconductive tunnelling; tunnelling spectra; tunnelling spectroscopy  
 $\phi^4$  system, metastable state, decay rate calc. 0-22301  
 alkali halide: NH<sub>4</sub><sup>+</sup>, hindered rot. energy levels calc. 0-10514  
 alkali halide, electric-dipole ordering of tunnelling impurity centres 0-2215  
 ammonium compounds, rotational tunnelling, temp. dependence 0-38970  
 amorphous solids, optical absorption tail, shape 0-34946  
 atom, bound state decay in external field in semiclassical approx. 0-12941  
 chemical reaction, Eckart barrier tunnelling, Arrhenium plot curvature 0-3298  
 chemical relaxation, tunnelling, Mossbauer emission spectroscopy studies 0-40683

**tunnelling continued**

cubic crystals, Raman scatt. from tunnelling of substitutional molecules 0-40107  
 diffusion-controlled defect recombination, quasi-steady radius, tunnelling and elastic interaction (*Russian*) 0-10908  
 disordered systems, tunnel transparency, random scattering centres (*Russian*) 0-2454  
 double-well potentials, symmetric and asymmetric, periodic orbit theory 0-23488  
 eight-site order-disorder model, influence of tunnelling 0-2709  
 electron tunnelling, two band calcs., Gamow formula applications 0-54665  
 excitonic insulator, tunnel breakdown theory (*Russian*) 0-29686  
 glass, tunnelling systems, intrinsic elec. dipole moment, coherent elec. echo obs. 0-29705  
 Heisenberg spin 1 system assembly with tunneling, phase transitions, thermodynamic behavior 0-4667  
 hydrocarbons, saturated open-chain, transport behaviour of excess electrons and props. 0-39643  
 hydrogen-bonded ferroelectric, Ising model in transverse tunnelling field and proton-lattice interaction 0-7307  
 II-IV p-n amorphous heterojunction, phenomenological model 0-54769  
 Ising model, central peak with transverse field 0-7306  
 junction mixers, quantum limited detection 0-18015  
 junctions generating burst noise, existence of tunnel-effects (*Rumanian*) 0-6960  
 metal surface, dynamic image pot. for tunnelling electrons 0-49874  
 metal whisker point contact junctions, tunnelling and rectification characts. 0-6955  
 metal-insulator contact, electron tunnelling and its role in contact electrification 0-2453  
 metal-semiconductor-metal junction, tunnelling phenomena in terms of exact method and WKBJ approx. 0-20329  
 metal/PbI<sub>2</sub>/metal struct. reson. and inelastic tunnelling 0-44739  
 metals, proper EM radiation on inelastic electron tunnelling with photon emission, cond. (*Russian*) 0-54765  
 methyl compounds, rotational tunnelling, temp. dependence 0-38970  
 methyl groups in solids, reorienting and tunnelling, spin-lattice relax. 0-50217  
 methyl groups in solids, tunnelling freq. for internal rotation in pot. function 0-49134  
 methyl radical in sodium acetate, EPR spectra, anisotropic hyperfine interaction, rot. tunnelling 0-34775  
 MIM diodes, negative differential resistance, stimulated inelastic tunnelling theory 0-49951  
 MIM structure, nonequilibrium states, kinetic eqns. (*Russian*) 0-11101  
 MIM structures, zero bias anomaly due to elastic tunnelling, calc. 0-2483  
 MIM tunnel junctions, roughened, photon emission, calc. 0-44738  
 MIS tunnel diodes, photoionisation of states 0-11099  
 molecular solid, electron tunnelling, long-range electron transfer processes, orbital overlap model 0-7813  
 molecule, tetrahedral, in cryst. field, torsional ground state splitting, appl. to methane and (NH<sub>4</sub><sup>+</sup>)<sub>2</sub>SnCl<sub>6</sub><sup>2-</sup> 0-15019  
 MOS devices, inversion layer, pot. and carrier distrib., quantum mechanical determ. 0-29483  
 organic glass, electron-cation recombination; charge distrib. simulation and luminesc. kinetics 0-2855  
 paraelectric resonance of nonstationary tunnelling states (*Russian*) 0-34869  
 passive layer, on Fe electrode, semiconductor model, appl. to electrochem. reactions, review 0-26022  
 plasma, stratified, obliquely propag. extraordinary microwave Budden tunnelling 0-48895  
 point-contact junction, influence of mech. modulation elec. transport 0-2481  
 polyatomic mols., dissociation reaction path Hamiltonian 0-45486  
 polyethylene dielectric losses, at very low temperatures (*Japanese*) 0-11331  
 polymer electret, charge dissipation, transport mechanisms 0-7268  
 polyphenylacetylene films, phys. struct., AC and DC cond. 0-44750  
 polytetrahydrofuran films, electrochemically prepared between metal electrodes, DC elec. props. 0-39695  
 slow neutron scatt. by rotating systems of identical nuclei (*Russian*) 0-14968  
 small polaron tunnelling, thermally assisted, computer anal. 0-2391  
 sodium acetate trihydrate, press. depend. of methyl tunnelling motion 0-10603  
 tetrahedral four spin 1/2 systems, Zeeman and tunnel system reson., coupled and uncoupled relax. 0-50214  
 meso-tetraphenylporphine, potential parameters of H migration tunnel rates calcs. 0-5600  
 thin disordered film, electronic energy spectrum calcs. extended Halpern Green's function technique 0-20066  
 tropolone vibr. spectra and proton tunneling 0-28014  
 TTF-TCNQ, interchain tunnelling effect on nucl. spin-lattice relax. time, interchain coupling of CDW 0-20163  
 Al-Al<sub>2</sub>O<sub>3</sub>-SnTe, junction, tunnelling, Fermi level depend. on carrier conc., influence of surface states 0-25016  
 Al-Al<sub>2</sub>O<sub>3</sub>-SnTe structure, tunnelling characts., model anal. 0-29480  
 Al-Al<sub>2</sub>O<sub>3</sub>-(a-Ge)-Al, electron tunnelling into a-Ge, press. effect 0-49938  
 Al-Al<sub>2</sub>O<sub>3</sub>-Pb tunnel junction, thermal annealing effects 0-49952  
 Al-SiO<sub>2</sub> interface, internal photoemission and photon-assisted tunnelling 0-6982  
 AlGa<sub>1-x</sub>As-GaAs, p-n heterostruct. laser, tunnel injection and phonon-assisted recomb. 0-5733  
 As<sub>2</sub>S<sub>3</sub>, amorphous, temp. below 1K, props., tunnelling 0-49576  
 Au-Al<sub>2</sub>O<sub>3</sub>-Al system, influence of mech. modulation on elec. transport 0-2481  
 Ba<sub>3</sub>(PO<sub>4</sub>)<sub>2</sub>, recomb. luminesc. mechanisms 0-2874  
 Bi film, quantum size effect and band struct. Bi-dielec.-metal system obs. 0-54811  
 CdS-Te, heterostructure, effect of low cond. CdTe interlayer on charact. 0-44721  
 Cr-SiO films, sputtered, elec. and struct. props. 0-39694  
 Cr-SiO<sub>2</sub>-Si MIS solar cell, current cond. 0-7936  
 Fe, field-emitted electron spin polarisation by tunnelling through surface pot. 0-29861  
 GaAs epitaxial layers, structural defect and conc. inhomogeneities influence on barrier diode I-V characts. 0-15602



**tunnelling continued**

- GaAs, phonon assisted tunnel emission of electrons from deep levels 0-25532  
 GaAs:Cr<sup>2+</sup>, dynamic Jahn-Teller effect, relaxation time for reorientation 0-6798  
 GaSb-Pb junction, Ar ion bombard. effect on tunnelling props. 0-54783  
 Ge amorphous film, high freq. phonon scatt. 0-49328  
 n-Ge:Ni, recombination of hot electrons on Ni impurity centres 0-44612  
 H<sup>+</sup> transfer reaction tunnelling probability 0-26032  
<sup>3</sup>He film, theory of motional inhibition of interlayer quantum tunnelling 0-54466  
<sup>4</sup>He, solid, phase transition 0-15333  
 In<sub>2</sub>O<sub>3</sub>:Sn-Si heterojunctions, current mechanisms and barrier height 0-11083  
 KBr, diffusion-controlled defect recombination, quasi-steady radius, tunnelling and elastic interaction (*Russian*) 0-10908  
 KBr(Cl), X-ray irradi., tunnelling recomb. luminesc. 0-2873  
 KCl, radiative tunnel transitions in negatively charged colour centre systems 0-49655  
 KCl:CN<sup>-</sup>, paraelectric reson. study, tunnelling parameters and elec. dipole moment 0-25326  
 KD<sub>2</sub>PO<sub>4</sub>, deuteron tunnelling, barrier height and energy level calc. 0-6482  
 KH<sub>2</sub>PO<sub>4</sub>, proton tunnelling, barrier height and energy level calc. 0-6482  
 KH<sub>2</sub>PO<sub>4</sub>-type crystal, LF dynamics 0-10602  
 KI, luminesc. lines due to n=2 free exciton state of Wannier series 0-29776  
 KI:Ti, A<sub>1</sub> emission, linear polarisation, appl. of semi-classical WKB formalism 0-45134  
 KI:Ti, electron-hole and V<sub>k</sub>-Ti recomb., TSC and thermolum. study (*French*) 0-34461  
 methane, solid, librational tunnelling and proton relax. temp. 0-38969  
 MgO, electron irradiated, luminescence, radiative recombination kinetics 0-7421  
 Mn-Zn ferrosilicates, carrier transfer phenomena 0-54727  
 ND<sub>2</sub>ClO<sub>4</sub>, level-crossing relax. study of MD<sub>4</sub><sup>+</sup> ion tunnelling freq. 0-7185  
 ND<sub>2</sub>ClO<sub>4</sub>, librational tunnelling and proton relax. temp. 0-38969  
 (ND<sub>2</sub>)<sub>2</sub>PtCl<sub>6</sub>, level-crossing relax. study of MD<sub>4</sub><sup>+</sup> ion tunnelling freq. 0-7185  
 NH<sub>3</sub>, Br single cryst., low temp. PMR lineshapes of tunnelling NH<sub>4</sub><sup>+</sup> ions 0-25223  
 (NH<sub>4</sub>)<sub>2</sub>PbCl<sub>6</sub>, librational tunnelling and proton relax. temp. 0-38969  
 (NH<sub>4</sub>)<sub>2</sub>PbCl<sub>6</sub>, temp. depend. of tunnel freq. 0-1947  
 NaCl, absorpt. spectra, influence of elec. field 0-2794  
 NaCl:Ag, absorpt. spectra, influence of elec. field 0-2794  
 Na<sub>2</sub>O-SiO<sub>2</sub> glass, tunnelling recomb. luminesc. 0-2875  
 Na<sub>2</sub>SiO<sub>3</sub>-CaO glass, thermally stimulated and tunnel luminesc. 0-45157  
 Ni, field-emitted electron spin polarisation by tunnelling through surface pot. 0-29861  
 Pb<sub>1-x</sub>Ge<sub>x</sub>Te, band struct., tunnelling obs. in MIS struct. 0-54795  
 PbTe surfaces, tunnelling spectroscopy in MOS and Schottky barrier junctions 0-49945  
 Sb<sub>2</sub>Se<sub>3</sub>, polycrystalline, elec. cond. mech. 0-49705  
 Si gas-sensitive microtransducer, cond. variation with pulsed ethanol adsorption (*Russian*) 0-50915  
 Si:H, amorphous, radiative recomb. by diffusion and tunnelling, photocond. quantum efficiency 0-50394  
 a-Si:H MIS junction, electronic struct. study by tunnelling 0-44729  
 SiO amorphous film, high freq. phonon scatt. 0-49328  
 SiO<sub>2</sub>, amorphous, temp. below 1K, props., tunnelling 0-49576  
 SiO<sub>2</sub>, and SiO<sub>0.7</sub>, amorphous sputtered thin film, US anomalies, 0.5-300K 0-34145  
 SiO<sub>2</sub> sputtered films in thin film transistors, trapping centres, electron tunnelling 0-7014  
 SiO<sub>2</sub>-Si, P ion implantation, electrical transport props. 0-39130  
 SiO<sub>2</sub>B<sub>2</sub>O<sub>3</sub>-K<sub>2</sub>O-Al<sub>2</sub>O<sub>3</sub>-As<sub>2</sub>O<sub>3</sub> glass fibres containing metallic granules, tensile strength, Young's modulus, DC conductivity 0-30023  
 TiH<sub>2</sub>PO<sub>4</sub> and TiD<sub>2</sub>PO<sub>4</sub>, dielec. props. under hydrostatic press. up to 7 kbar 0-29696  
 ZnS, phosphor, voltage and temp. dependence of pre-breakdown electroluminescence 0-45147  
 ZnS, phosphor, voltage depend. of electrolum. brightness 0-45148  
 ZnSe, Gudden-Pohl effect, release of electrons from traps 0-45149

**tunnelling spectra**

- ethanol, adsorbed on Al<sub>2</sub>O<sub>3</sub>, inelastic electron tunnelling spectra, surface vibr. struct. determ. 0-35572  
 propionic acid, adsorbed in thin film tunnel junctions, hydrogenation and deuteration, IETS obs. 0-45547  
 Al-Al oxide-Pd tunnel junctions, exposed to H<sub>2</sub>, inelastic electron tunnelling spectra 0-20327  
 Fe(CN)<sub>6</sub>, adsorbed on Al<sub>2</sub>O<sub>3</sub>, tunnelling spectra, isotope shifts 0-29262  
 Ge, phonon energy variation under high press. band struct. changes, tunnel spectroscopy study (*Russian*) 0-2134  
 (SN)<sub>x</sub> single crystals, electronic structure clarification near the Fermi level (*Japanese*) 0-49954

**tunnelling spectroscopy**

- AC bridge with two-freq. modulation of supply 0-13196  
 Pb/oxide/InAs structure, effective mass determ. by tunnelling spectroscopy (*Russian*) 0-44482

**tunnels, wind** *see wind tunnels***turbidimeters** *see turbidimetry***turbidimetry**

- composition analysers, electronic self-balancing system, turbidity meter appl. 0-16754  
 digital polar nephelometer, scatt. meas. from monodisperse aerosol particles 0-9804  
 photoelectric turbidimeter (*Polish*) 0-31840

**turbidity***see also turbidimetry*

- Atlantic Ocean, anomalous bottom water south of Grand Banks due to turbidity current activity 0-4042  
 atmospheres, spherical symmetry, radiative transfer, non-conservative problem 0-36492  
 fine particles of dredger spoil, motion with current from dumping ground 0-17287  
 hot matter, conductive opacities and free-free Gaunt factors 0-3361  
 human and calf lenses, light scatt. and reversible cataracts 0-56019  
 laser backscattering from turbid water-nigrosin black dye-Teflon spheres dispersion 0-1129

**turbidity continued**

- potentiophotometric platelet aggregation meas. by turbidity change 0-36061  
 rubber, nitrite, heat ageing, light scatt. method study (*Russian*) 0-40407  
 Sargasso Sea at 3.2 km depth, organic carbon annual variation 0-41460  
 seawater, Mangalore coast, India, 1976-7 nearshore water conditions 0-8315  
 St. Lawrence Estuary turbidity maximum, sediment, salinity, suspended matter study 0-4015  
 water quality monitoring, modular system (*German*) 0-26186

**turbine generators** *see turbogenerators***turbines**

- see also compressors; gas turbines; hydraulic turbines; steam turbines; turbogenerators; wind turbines*  
 air, for measurement of magnetic torque acting on rotating sample 0-31811  
 air lubricated sample turbine for applications in solid body multipulse spectroscopy (*German*) 0-52284  
 cascade deviation, prediction and measurement 0-24049  
 cascades, rotating annular, test facility of DFVLR, measurement and evaluation 0-14866  
 flowmeters, turbine-type, made in Bulgaria, survey (*Bulgarian*) 0-6173  
 overlay coatings for turbine parts, physical vapour deposition techniques, economic evaluation 0-35429  
 ring chamber, oscillatory behaviour of confined ring vortex 0-6075  
 TU-20 turbine oil, 4-methyl-2,6-di-tert-butylphenol determ., using IR spectrophotometry (*Polish*) 0-13161

**turbogenerators** *see turbogenerators***turbogenerators**

- bar insulation in stator winding of large turbogenerator, inspection using microwave defectoscope 0-35474  
 compressed air energy storage plants, turbomachinery options 0-30578  
 cryoturbogenerator transition process simulation, cryostat damping casings electrical characteristics determination (*Russian*) 0-8996  
 wind turbine generator, control and stabilisation 0-30370  
 H production from radioactive waste heat and utilisation in gas turbines 0-30326

**turbulence**

- see also atmospheric turbulence; boundary layer turbulence; cavitation; laminar to turbulent transitions; plasma turbulence; shear turbulence; turbulent diffusion; vortices*  
 aeroacoustic measuring techniques in or outside turbulent flows 0-53534  
 aerodynamic noise from wave-turbulence interaction 0-14679  
 air flow, turbulent, in infinite medium spatial speed distrib. (*Rumanian*) 0-53826  
 air jets, interacting two-plane parallel jets, turbulence props., hot wire meas. 0-14767  
 air turbulence, effect on light flux fluctuations, limiting factors in photoelectric meas. 0-13136  
 air-water surfaces, turbulence characts., mass transfer and eddies 0-14665  
 airfoils, transonic testing at high Reynolds number in shock tube 0-14852  
 annular diffuses with conical walls, swirling flow and separation 0-43715  
 annular flow of gases with varying physical props., turbulent, heat transfer in two-sided heating 0-48702  
 annular spaces inner surface, heat transfer in turbulent flow 0-14686  
 annuli carrying turbulent flows of gases with variable physical props., heat transfer in one-sided heating 0-48701  
 annuli heated from both sides, critical heat flux density and turbulence 0-48694  
 annuli with turbulence promoters, heated, lengthwise-uniform and non-uniform heat release, boiling crisis 0-48703  
 arc, electrical characts., effects of laminar and turbulent flows 0-1870  
 arc column in free turbulent jet, electric field strength 0-49021  
 asymmetrical heated tube, turbulent airflow heat transfer characts. 0-38402  
 asymptotic, supersonic, 2-dimens. turbulent wakes, fully developed mean flow criteria 0-14706  
 axially symmetrical turbulent free jets, in wind tunnel, higher order moments measurement (*German*) 0-33648  
 axisymmetric jet, interaction with plane obstacle, Navier-Stokes eqn. solns. (*Russian*) 0-1659  
 baroclinic finite amplitude instabilities, book contrib., review 0-19328  
 bifurcations inducing attractor in Oboukhov's turbulence system 0-1536  
 bispectra, one-dimens. calcs. 0-53757  
 blood flow, contrib. of semilunar leaflets 0-3666  
 Boussinesq turbulence, statistical theory 0-48713  
 bubble and eddy heat diffusion in single phase flow 0-19477  
 buoyant surface jet, 2-D flow props. (*Japanese*) 0-48762  
 buoyant surface jets of incompressible fluid, turbulent energy balance appl. 0-38469  
 Burgers equations, in two dimens., finite element anal. 0-1532  
 bursting phenomenon in bounded turbulent shear flow, streamline vortices 0-1600  
 cavity, square, 2-D, recirculating flow of incompressible fluid, large Re, convergence of finite-difference schemes 0-33611  
 cellular flow wavelength selection, convection and turbulence 0-38380  
 channel height effect on nearcritical flow past circular cylinder 0-14818  
 chaos, reinjection principle, folded and cut chaotic flows 0-12996  
 chemically reacting flows, turbulent, steady and unsteady, computation in axi-symmetrical domains 0-1697  
 circular cylinder, turbulent crossflow in vortex zone 0-10252  
 circular cylinder with tripping wires, heat transfer, flow and wakes (*German*) 0-1589  
 coaxial jets with and without swirl 0-48759  
 collisional drift waves, nonlinear evolution, bifurcations to chaotic state 0-14666  
 combustion region of gas turbines, perturbations produced by unsteady combustion and heat addition 0-53764  
 computation, bispectral meas. 0-38382  
 conference on dynamical critical phenomena, Geneva (Apr. 1979) 0-27040  
 constricted tube, turbulent flow, haemodynamic appl. 0-53860  
 convection, turbulent, numerical models based on unsteady Navier-Stokes eqns. 0-38415  
 convection between parallel plates, result plotting method 0-24001  
 convective free and forced flow in vertical channels 0-19391  
 curved tube bank vibration in turbulent transverse water flow (*Russian*) 0-33678



## turbulence continued

- decay of grid produced turbulence, velocity correlation equations, two- and three-point 0-53741
- digital processing of unsteady periodic signals around oscillating airfoils 0-10340
- dispersion in porous media, pore distrib. and flow segregation effects 0-10302
- duct wall cavities, heated bottom surface, forced convection heat transfer 0-6048
- electrolytic cells, gas sparged, mass transport anal. 0-24004
- electrostatic precipitators, aerodynamic theory, gas turbulence, Deutsch law 0-53758
- EM or optical pulse arrival time statistics in turbulent media 0-48154
- emulsion, concentrated unstable, turbulent flow in pipes 0-28537
- equilibrium dispersed-ring water vapour flows, liq. distrib., film parameters and hydraulic resist. 0-24079
- ergodic behaviour of two-dimens. turbulence 0-28494
- ferrofluid devices, magnetostatic and centrifugal, nonmagnetic body motion 0-33700
- ferrofluid flow in circular pipe, uniform mag. field effects 0-43782
- fibre suspension, dil., mechanistic aspects of drag reduction in turbulent pipe flow 0-6102
- fission reactor 61-tube bundle with wire wrap 0-32329
- flame, mass streamline, vel. and density fluctuations correlation (*Japanese*) 0-6164
- flame, round jet type, mass exchange between recirculation zone and outer flows, stabilisation 0-14842
- flame propagation limits, mixture turbulence effects 0-16679
- flames, effects of finite reaction rate and molecular transport on premixed turbulent combustion 0-3348
- flames, premixed, structure investig. by light intensity distrib. meas. 0-16680
- flow field meas., near nozzle outlet using laser Doppler anemometer 0-28582
- flow meas., light beam coherence effect on optical method information capacity 0-1709
- flow regulating system operating with Newtonian and non-Newtonian fluids (*German*) 0-1535
- fluid flow and heat transfer around two circular cylinders of different diameters in cross flow 0-14687
- fluid stream, turbulent structure determ. using thermoprobe unit (*Bulgarian*) 0-28584
- fluidised beds, solids circulation and heat transfer to immersed tube banks 0-6141
- formation in parallel blast mixing (*Ukrainian*) 0-6033
- free convection loops, dissipation effects in laminar and turbulent flow 0-19372
- free convective heat transfer in liq. saturated porous bed at high Rayleigh number (*German*) 0-33605
- free turbulent flow of incompressible liquid, self-consistency of expt. data 0-6031
- free-stream, effect on aerodynamic characts. of circular cylinder (*Japanese*) 0-10229
- fully developed, quasi-normal Markovian approx. 0-53756
- fully turbulent free convection heat transfer, surface renewal approach 0-14697
- fully-developed, renormalisation group, review 0-28495
- galactic wake turbulence, rel. to head-tail radio sources form. 0-36703
- gas cooled rough rod bundles, thermofluid dynamic expts., evaluation with code SAGAPO 0-24002
- gas-liquid turbulent flow, friction, velocity and gas content profiles 0-14793
- geostrophic turbulence, book contrib., review 0-19336
- ground water at horizontal plane, 2-D unsteady flow (*Chinese*) 0-46205
- heat exchange between jet and obstacle, turbulence effect (*Russian*) 0-1579
- heated turbulent jet, local isotropy and large structs. 0-6116
- helical channel flow, heat transfer 0-6150
- Henon-Pomeau attractor 0-46811
- homogeneous fuel mixture, turbulent combustion theory 0-53883
- homogeneous turbulence, chemical reactions, probability approach and particle models, comparison 0-14844
- homogeneous turbulence decay from given state at higher Reynolds number 0-1534
- hot-wire anemometry using 'squared signals', comments and reply 0-28581
- hot-wire signal analysis, flow field determ. with high/low turbulence intensity 0-1719
- Howells' model for isotropic turbulence, soln. and simplification 0-48682
- hydrodynamic instabilities, transition to turbulence 0-28491
- ice layer profile on const. temp. plate in forced convection, laminar to turbulence transition regime 0-24007
- images aberrated by turbulence, undersampling errors in moments meas. 0-1137
- incompressible viscous fluid, turbulently generated sound, pressure probability struct. 0-33581
- inhomogeneous, simulation, clipping approx. 0-19331
- inhomogeneous turbulent flow scale characts., vortex struct. relationship 0-53754
- internal separated flows at large Reynolds number, Poiseuille flow development in channel 0-53755
- interplanetary plasma turbulence spectrum, determ. from radio sources scintillation spectra 0-46361
- interstellar clouds, turbulence effects on collapse, three-dimensional numerical models 0-56910
- interstellar medium turbulence rel. to scintillation, analytic soln. of second-order moment eqn. 0-26726
- inviscid, two-dimens. turbulence, equilib. energy spectra 0-38383
- isotropic turbulence, conditional flow struct., anal. 0-19335
- isotropic turbulent flowfield, smoke downstream diffusion, mass transfer characts. 0-14668
- isotropic two-dimensional, energy dissipation, correl. relationships and Taylor length scale 0-19334
- jet, air, subsonic, fully pulsed, near field vel. meas. 0-19540
- jet, axially symmetric, impingement on plate, heat transfer characts., inner peak in heat flux 0-28540
- jet, turbulent, axisymmetric, spatial correlations 0-19539
- jet, turbulent, free, three-dimens.,  $k-\epsilon$  model calc. using finite difference procedure 0-19468
- jet flow modification of uniform flow along a plane wall (*German*) 0-6120

## turbulence continued

- jet flows, correlation techniques to detect azimuthally coherent structures 0-53765
- jet structure, turbulence and coherent eddies, review 0-48760
- jets, axisymmetric and flat, heat transfer in vicinity of stagnation point, turbulence effect 0-48697
- jets, vortex-street structure 0-10280
- kinetic theory, fundamental soln. 0-27137
- large eddy simulation 0-19333
- laser beam degradation by two-dimens. turbulent jet 0-14375
- laser instability, example from synergetics 0-9848
- liquid metal jets, 3D fluid flow model induced in ladles or holding vessels 0-10278
- liquid metals, heat transfer with gas bubbled through (*Russian*) 0-38395
- liquids of different density, turbulent mixing at an accelerating interface 0-6030
- LMFBR wire-wrapped assemblies, turbulent mixing expt. and model 0-590
- log-amplitude and phase time fluctuations, turbulence spectrum parameters influence (*Czech*) 0-9774
- Lorenz model, intermittency, first limit cycle-second strange attractor transition 0-31674
- low quality flow boiling, turbulent forced convection and nucleate boiling heat transfer 0-14696
- $\alpha$  Lyrae (Vega), microturbulence parameter from Copernicus UV spectral anal. 0-26856
- magma's turbulent mixing, implications of density var. among mid-ocean ridge basalts 0-56460
- magnetic field dynamics, turbulent dynamo theory 0-32880
- main eddies of recirculating zone induced by impulsively started cylinder, origin (*French*) 0-53784
- marine thermocline, turbulent quantities computation using Mellor-Durbin theory 0-4041
- MBBA, nematic liquid crystals, wave number spectrum of dissipative structures 0-38904
- measurement by laser Doppler anemometers, book contrib., review 0-19538
- metastable chaos, transition to sustained chaotic behavior in Lorentz turbulent convection model 0-4643
- MHD flows, residual disturbances after laminarisation, entry effects 0-6160
- minicomputer-based scheme for turbulence measurements with pulsed Doppler ultrasound 0-26435
- mixing layer description from transient vortex flow results 0-1533
- modelling, subgrid, with classical closures and Burgers' eqn. 0-19332
- models, integral-relation model appl. 0-43691
- molecular gas radiation in the thermal entrance region of a duct 0-6051
- multidimensional two phase flow eqn. derivation, general constitutive principle appl., turbulent stresses 0-10297
- natural laminar and turbulent convection, from isothermal spheres, correlation eqn. (*German*) 0-33607
- Navier-Stokes equations, turbulence and infinite bifurcations, five-mode truncation 0-52031
- needle shaped particles, diffusion orientation on filtration surface in turbulent flow 0-33668
- noise generated by an eddy (*French*) 0-19363
- non isotropic homogeneous, pure rotation influence (*French*) 0-33568
- nonisothermal streams, turbulent velocity pulsations meas., procedure 0-19514
- nonisothermal turbulent jet, physicochemical processes, temp. and conc. effects 0-14849
- nonlinear internal waves, turbulence, numerical anal. 0-14721
- nonsteady turbulent MHD flows in plane channels and circular tubes 0-48810
- nozzle expansion in turbulent flow, downstream heat and mass transfer 0-1669
- nuclear reactor coolant axial flow in bare rod bundles, turbulence modelling 0-32338
- numerical simulation with three-dimens. vortex in cell method 0-19330
- observable motions, Navier-Stokes eqns. 0-10230
- ocean, vertical eddy viscosity effects on Rossby and Eady waves 0-51404
- ocean, vertical struct. characts. 0-12426
- ocean small-scale turbulence, study via towed instruments carrier 0-36423
- onset, fluctuation spectrum calc., appl. to Rayleigh Benard flow 0-23989
- open cct. wind tunnel, exptl. procedures to improve characts. (*Japanese*) 0-19528
- optical beam, diffracted rays in turbulent medium 0-48153
- optical propagation, laboratory-generated turbulence simulating atmosphere 0-9803
- orifice plate calibrations, extrapolation to high Reynolds no. 0-53833
- oscillators in convective bi-periodic regime, velocity oscils. 0-53759
- particle entrainment into fluid stream, force balance model 0-43690
- particles in turbulent fluid, statistical motion, Eulerian direct interaction 0-53841
- perturbation potential for unsteady near-sonic flows (*German*) 0-1635
- perturbation theory, quasi-periodic motion, asymptotic expansion method 0-17877
- physical and spectral space methods (*French*) 0-28493
- pipe flow, enlargement, contraction effect on flow characteristics 0-6154
- pipe-jet system in crossflow, turbulent vortex shedding modes 0-10274
- pipes, turbulence and heat exchange 0-24094
- plane symmetric sudden expansion over backward step, turbulence and separation 0-53752
- power spectra for chaotic transitions in Rossler dynamical system 0-53898
- Prandtl and Schmidt numbers from modelled transport eqns. 0-19373
- pressure fluctuations assoc. with general eddy turbulence field 0-53750
- pressure fluctuations in jets, long range effects, book contrib. 0-1663
- PWR power plant flow pressure fluctuations as vibration source, relationships (*Hungarian*) 0-47685
- radiative heat transfer between isothermal parallel plates, flow models, numerical analysis 0-14547
- random velocity fields, radiative transfer and line form., intensity moment transfer eqn. derivation 0-52967
- recirculating two-dimens. turbulent flow, numerical model calcs. 0-19358
- review of theory 0-4536
- rough surface heat transfer, turbulent flow in annular channels, result anal. 0-24003
- roughened surface, slope and intercept of dimensionless velocity profile 0-43701



**turbulence continued**

salting solid particles in turbulent flow, accel. and forces (*Russian*) 0-1675  
 scalar fields, transport eqn. for probability density function, closure 0-1585  
 sea surface layer, dynamically passive impurity propag. by currents and turbulent pulsations 0-31063  
 seawater, refractive microstructure from diffusive and turbulent mixing 0-8326  
 separated flows, upwind and central difference schemes 0-28539  
 shadow optical method for turbulent flow microstruct. investig., stat. analysis problems 0-19534  
 shaped edge cylinders in oscillatory flow, separation and vortex shedding forces 0-53825  
 single particle drag coeff. in still air 0-33620  
 skewness and flatness factors, Reynolds number dependence 0-53751  
 slightly dissipative systems, stochastic behaviour 0-22290  
 slightly heated cylinder, turbulent wake, conditional sampling study, turbulence struct. 0-6063  
 slowly moving vapour, film condensation heat transfer 0-19376  
 solar corona, turbulent heating role 0-12715  
 solar nebula, turbulent flows rel. to grains as isotopic anomalies carriers 0-26757  
 solar photosphere, complex study of 'microturbulent' vel. and damping const., introduction (*Russian*) 0-12719  
 solid and liquid particle interaction with turbulent flow field 0-43767  
 spectrally local disturbance evolution in grid generated nearly isotropic turbulence 0-48681  
 sphere motion in infinite conductive fluid, variable mag. dipole located within sphere case 0-19519  
 spherically blunted cone with massive surface blowing, laminar and turbulent flows, shocks 0-38445  
 statistical analysis, non Gaussian variation models, 1-D distributions 0-6032  
 statistical hydrodynamics for the Burgers turbulence (*Japanese*) 0-14667  
 steam jet condensation in turbulent liquid flow, heat transfer 0-33599  
 steam turbine nozzle cascades, local heat transfer, approach flow turbulence effects 0-38381  
 stellar convection zones dynamics, effect of rot. on turbulent viscosity and cond. 0-36612  
 stochastic particle accel. by MHD turbulence 0-31203  
 stochastic self-oscillations and turbulence, review 0-4537  
 Stokes flow, attached and free eddies 0-48679  
 Stokes flows, separation 0-48680  
 stratified gas/liquid flow, heat transfer, local Nusselt number prediction 0-38393  
 subsonic base pressure fluctuations on axisymmetric blunt-based body, Mach no. depend. 0-19423  
 subsonic turbulent jet, entry zone flow wave struct., eddies 0-14773  
 supersonic jet, nonsteady interaction with barrier, math. model of oscillatory cycle 0-19462  
 supersonic quasihomogeneous flow, turbulence in presence of density and vel. fluctuations 0-1638  
 suspension, dil., of spherical particles in non-Newtonian liq., rheological behaviour 0-24058  
 suspension bearing flow, turbulent energy balance in pressure pipe flow 0-48777  
 suspension flow, gravitational theory, discrete model 0-48779  
 symmetric free turbulence, similarity and weak closing relations 0-33569  
 symmetrical wake calc., two-dimens. laminar and turbulent flows 0-14707  
 Taylor-Couette flows at very high Taylor number, marginal instability 0-1599  
 temperature field fluctuations in raised temp. turbulent flow (*French*) 0-19371  
 thermal convection in presence of rot. and mag. field, stellar and planetary dynamos appl. 0-6042  
 three dimensional turbulent rectangular jets 0-14769  
 transient freezing of liquids in turbulent flow inside tubes 0-6494  
 triangular array rod bundles, fully developed turbulent flow, secondary flows 0-53753  
 turbulent combustions, problems of bias on mean meas. (*French*) 0-53879  
 two component reacting fluid, density fluctuations, light scatt. spectrum, Rayleigh lines 0-25397  
 two-dimensional space isothermal and nonisothermal turbulent flow (*German*) 0-28505  
 two-dimensional turbulent blunt body flows with impinging shock 0-38444  
 underexpanded gas jet issuance into supersonic flow 0-38468  
 unsteady Lagally theorem for multipoles and deformable bodies 0-33560  
 unsteady subsonic turbulent jets, book contrib. 0-1664  
 Vela supernova remnant, turbulent struct. from rot. meas. 0-51836  
 velocimeter for fluctuating temp. and vel. meas. in combustion field 0-14856  
 velocity sensor for three-dimensional turbulence meas. 0-46314  
 vertical buoyant jets, decay, unified correlation and prediction in turbulence model 0-6118  
 viscous compressible flows at high Reynolds number, book contrib., review 0-19424  
 viscous incompressible flow in tube, nonsteady convective heat transfer 0-19393  
 viscous incompressible liquid, vibrational displacement, wave mechanism 0-43777  
 viscous toroidal eddy generation in cylinder, Stokeslet streamlines 0-19404  
 vortex ring core, turbulence struct. 0-33615  
 vortices formation in mixing layer downstream of a separation in near wake of body (*French*) 0-48716  
 wake, of heated cylinder, turbulent temp. and thermal flux characts. using four-wire probe 0-19541  
 wake of axial flow turbomachinery rotor blades, numerical anal. 0-1596  
 wall flow direction probe for turbulent separating and reattaching flows 0-53903  
 water, flow through circular pipe, pulsed NMR study 0-28566  
 wind, crossed hot-film velocity data anal. 0-31122  
 wind energy conversion, wind driven turbines, review 0-7909  
 wrinkled flame speed and struct., turbulence effects 0-26015  
 zero-mean-shear mixed layer, turbulence meas. 0-1705  
<sup>4</sup>He, superfluid, electron photography (*French*) 0-54456  
 CO<sub>2</sub>, turbulent flow field, mol. vibr.-rot. bands, spectral absorpt. coeff., temp. depend. 0-52987

**turbulence continued**

He II superfluid, turbulence during rotation, critical lengths 0-49443  
<sup>4</sup>He, heat transfer and hydraulic drag in tubulent flow in circular tube 0-14821  
<sup>4</sup>He, superfluid turbulence, vel. and temp. depend. from thermal resist. meas. 0-20003  
 Hg, on stabilising thermal section, temp. fields and heat transfer 0-19366  
**turbulence, atmospheric** *see atmospheric turbulence*  
**turbulence in shear flow** *see shear turbulence*  
**turbulent diffusion**  
 atmosphere, turbulent viscosity rel. to turbulent thermal conductivity (*Russian*) 0-21796  
 atmospheric boundary layer, mol. resistance during diffusion, universal function determ. 0-26573  
 atmospheric boundary layer, stratified, conc. profile, admixture-underlying surface interaction effect 0-31089  
 boundary layer, drag reduction polymer molecule turbulent diffusion and degradation 0-1686  
 buoyancy effects in entraining turbulent boundary layers: a second-order closure study 0-21815  
 concentration interface in turbulent mixing layer, visual growth 0-38392  
 diffusers, optimum press. recovery 0-1539  
 diffusion flame in turbulent boundary layer on liq. propellant surface behind shock wave 0-53763  
 discrete particles dispersion in turbulent fluid field 0-33580  
 dust entrainment in shock-induced turbulent air flow, dust entrainment 0-43763  
 flame, free-jet diffusion type, ionis. meas. and combustion progress 0-30238  
 flame, turbulent diffusion, transport eqn. for probability density function, closure 0-1585  
 flames, high Reynolds number, rocket exhaust appl., chem. processes theory 0-45504  
 flames, turbulent, calc. in one-dimensional approach 0-30236  
 heat flux and temp. fluctuation prediction 0-38400  
 highly turbulent fluids, diffusion, memory and retardation effects 0-43697  
 homogeneous turbulence, diffusion of passive scalar, statistical approach 0-38391  
 hydrocarbon turbulent diffusion flame, flame-zone model anal. 0-16684  
 ion wind enhancement of evaporation into a laminar air stream 0-53773  
 jets, two-phase, turbulent, particle or droplet size effect on diffusion 0-1658  
 kinematic diffusion of scalar quantities in turbulent velocity fields 0-27235  
 mass and heat transfer between turbulent flowing fluid and solid wavy surface 0-14681  
 methane tracers, single-jet mixing in turbulent tube flow, similarity and scaling law 0-14765  
 nuclear reactors, connected flow passages, computer prediction using k-ε turbulence model 0-9331  
 nuclear reactors, connected flow passages 0-9330  
 ocean refractive index microstruct. from diffusive and turbulent ocean mixing 0-56486  
 open channel flows, junction losses, flow anal. 0-6156  
 pipe flow, drag reduction polymer molecule turbulent diffusion and degradation 0-1686  
 plumes, vertical, round, diffusion, flow props. 0-43755  
 rectangular jet distrib. in cross flow, expt. 0-19465  
 Richardson problem, soln. in one dimension (*French*) 0-23993  
 soluble flat surface stability in turbulent flow 0-14676  
 stratosphere, turbulence from IR astronomy data 0-12475  
 total dispersion of a scalar quantity in turbulent flow 0-28499  
 tubes, heat transfer laws, longitudinal turbulent diffusion influence 0-33597  
 water vapour, wet, boundary layer in compressible flow 0-10295  
**turbulent flow** *see turbulence*  
**twilight**  
*see also night sky*  
 aerosols from Perseid meteors, effect on twilight optical characts. (*French*) 0-46255  
 NO<sub>2</sub>, in stratosphere, spectroscopic determ. and behaviour at mid-latit. 0-17414  
**twin boundaries**  
 gamma-ray diffractometry, phase transitions, domain structures, twinned texture studies 0-19678  
 metal, FCC, vacancy migration near twin boundaries and stacking faults 0-39075  
 Peierls force of boundary layer, theory 0-10552  
 steel, austenitic stainless, dislocation transport and H<sub>2</sub> embrittlement 0-30087  
 steel, austenitic stainless, Ni-alloyed, Cr<sub>7</sub>N precipitation, interface struct. and morphology 0-11644  
 steel, CrNi, etchability of austenite (*German, English*) 0-11860  
 steel, Cu-Mo, tempered, cementite precipitation along twin boundaries 0-45309  
 steel, low C, ferrite grain nuclei form. during polymorphic transform. (*Russian*) 0-50626  
 steel, stainless, He ion bombard., in situ electron microscope examination 0-34094  
 Al thin foil, thin foil, electron irradi., observation of triangular loops at twin boundaries 0-34005  
 Al<sub>3</sub>Cu<sub>9</sub>, rhombohedral γ-brass, direct imaging of struct. and structural defects 0-15115  
 Al<sub>3</sub>Mn<sub>3</sub>, rhombohedral γ-brass, direct imaging of struct. and structural defects 0-15115  
 Au, atomic arrangements of defects, dynamic obs. of atom movement 0-39108  
 Au film, surface step structure imaging by dark field electron microscopy 0-15346  
 Au/AuPd, bicrystals., in situ relax. of interphase interfaces 0-39455  
 Au/Pd, bicrystals., in situ relax. of interphase interfaces 0-39455  
 Be, twin boundaries, computer simulation 0-39109  
 CaCO<sub>3</sub>, with perfect struct., temp. depend. of rate of twinning 0-10561  
 Cd, twin boundaries, computer simulation 0-39109  
 Cr, twin and stacking fault energies calc. 0-2038  
 Cu, surfaces and twin faults, electronic states calc. by surface Green's functions 0-39647  
 Fe, twin and stacking fault energies calc. 0-2038  
 Fe-Ni-Co-C, substruct. effect in mech. props. 0-30086



**twin boundaries continued**

- Fe-Si (3.25 wt.%), dislocations in twin boundaries, electron microscopic images 0-34006
- In, twin boundary movement by creep 0-24460
- Li, twin boundaries, computer simulation 0-39109
- Mg, twin boundaries, computer simulation 0-39109
- Mo, twin and stacking fault energies calc. 0-2038
- TiMn, faceted parent martensite interface 0-6417
- V, twin and stacking fault energies calc. 0-2038
- W, twin and stacking fault energies calc. 0-2038
- Zn, twin boundaries, computer simulation 0-39109

**twinning**

see also twin boundaries

- BCC metals, plastic deform., computer simulation 0-40456
- $\alpha$ -brass, 70:30, cold-worked, recrystallised grains nucleation on heating 0-29998
- brass, 70:30, rolled, nucleation and annealing texture development 0-45320
- calcite, sound emission on dislocation annihilation (Russian) 0-54246
- ceramics, polycrystn., porosity, twinning and grain-size depend. on spontaneous cracking 0-44253
- coatings, defects and their effect on props. 0-39474
- composition plane as extended defect, structure-building entity, review 0-44218
- diamond, synthetic grits, crystal morphology of cyclic twins 0-2037
- ferroelastics, incommensurate twin plane (Japanese) 0-29034
- heteroepitaxial layers, dislocation structures, problems of formation 0-15100
- metal particles produced by gas evaporation, form., growth and interaction 0-16220
- metallic polycrystals, deform. during cooling, revealed by deposited graphite layer (Polish) 0-25755
- poly-1,6-dip-toluenesulphonyloxy-2,4-hexadiyne single cryst., twinning 0-33906
- $\alpha$ -quartz, ferroelastic hysteresis 0-19869
- quartz, twinned crystals, after Japan Law, investigation of regrowth 0-54162
- SOS films, cryst. quality improvement by Si ion channelling, annealing 0-44222
- steel, alloy structural, anomalous grain growth 0-20984
- steel, austenitic stainless, stacking fault effect on martensitic transform. during plastic deform. (Russian) 0-25696
- steel, bainitic, invariant plane strain theory, determ. of habit planes and orientation relationships 0-55388
- steel, high-C, type U12, U15, U17, cementite precipitation cryst. geometry singularities during decomposition of martensite (Russian) 0-7577
- steel, low alloy, martensite twinning, direct anal. 0-2040
- Ag, (211)[111] single crysts., shear band effects on rolling deformation 0-50651
- Ag catalysts, multiply-twinned particles 0-15114
- Ag-Cd (45 at.%) martensite, shape memory mech. and related phenomena 0-30009
- $\beta$ -B, electron beam zone melting growth, crystn. and defect form. 0-15020
- $B_{12}C_3$ , sintering and subsequent high temp. annealing, struct. and props. 0-20858
- Bi, magnetothermal EMF, twinned layer effect 0-49784
- CaBSi<sub>2</sub>O<sub>6</sub>, B=Mg, Fe<sup>3+</sup>, Al, pyroxenes, order-disorder interpretation 0-38987
- CaCO<sub>3</sub>, calcite, form of end of free elastic twin (Russian) 0-6416
- CaCO<sub>3</sub>, with perfect struct., temp. depend. of rate of twinning 0-10561
- CaO, single cryst. growth from molten CaCl<sub>2</sub> in wet atmosphere, habits 0-55287
- CdI<sub>2</sub>, hexagonal-rhombohedral polytypic transformation, electron diffr. and X-ray diffr. obs. 0-49163
- CdS-CdTe double layers on various GaAs surfaces, morphology and crystallography 0-34326
- Co-Ni alloy, slip charact., and fatigue, FCC twinning and FCC to HCP martensite transform. effect 0-35182
- CsCl, twin form. by compressive stress during phase transform. 0-49358
- Cu, annealing twins density, photoemission microscopy 0-35208
- Cu-Al (3 wt.%), annealing twins density, photoemission microscopy 0-35208
- Cu-Cd, structure, electrolytic deposition on monocrystalline Cu cathodes (Polish) 0-44435
- Dy<sub>2</sub>O<sub>3</sub>, lattice conserving twin, bend contours due to upper Laue zones 0-15113
- Fe-Ni-C (31, 0.28 wt.%), crossings of thin plate martensites, TEM obs. 0-25756
- Fe<sup>2+</sup>BSi<sub>2</sub>O<sub>6</sub>, B=Mg, Fe<sup>3+</sup>, Al, pyroxenes, order-disorder interpretation 0-38987
- Fe<sub>2</sub>(MoO<sub>4</sub>)<sub>3</sub>, cryst. struct. and twinning behaviour 0-33967
- GaP crystal, structure defect formation due to annealing and stress, dendrites, slip, dislocations 0-29026
- InP, twin-free, prep. using liquid encapsulated Czochralski growth 0-50546
- InSb thin layers, directed crystn. on sapphire, struct. 0-35112
- K<sub>2</sub>SO<sub>4</sub>, thermal phase transition 0-19738
- LaTiO<sub>3</sub>, cryst. struct. and cryst. chem., cryst. showing complex twinning 0-1984
- $\beta$ Li<sub>2</sub>CoSiO<sub>4</sub>, disordered struct., twinning description 0-39017
- Mg-Ce, workability, aging characts. and tensile strength 0-55416
- Mg-La, workability, aging characts. and tensile strength 0-55416
- MgBSi<sub>2</sub>O<sub>6</sub>, B=Mg, Fe<sup>3+</sup>, Al, pyroxenes, order-disorder interpretation 0-38987
- MnCO<sub>3</sub> crystals, gel. grown, Ca<sup>2+</sup>, Ni<sup>2+</sup> impurity influence, SEM study, cause of twinning 0-20778
- (NaAl)<sub>2</sub>Si<sub>2</sub>-O<sub>6</sub>-H<sub>2</sub>O, analcite, polyhedral tilt transitions obs. at high press. 0-6515
- Na<sub>2</sub>Al<sub>2</sub>Si<sub>2</sub>O<sub>10</sub>-2H<sub>2</sub>O, natrolite, cleavage etching in acidic and neutral media 0-6407
- NaBSi<sub>2</sub>O<sub>6</sub>, B=Mg, Fe<sup>3+</sup>, Al, pyroxenes, order-disorder interpretation 0-38987
- NaNO<sub>2</sub>(NO<sub>3</sub>), linear compressibility to 27 kbar, X-ray diffr. obs. 0-34125
- Ni, (99 wt.%), annealing twins density, photoemission microscopy 0-35208
- Ni, pure, anomalous grain growth 0-20984
- RbMnCl<sub>3</sub> crystal, structural phase transition, twin struct. 0-15243
- Si, fivefold twinned crystals grown in Al-Si (16 wt.%) melt 0-2942

**twinning continued**

- Si, implanted annealed layers, amorphised structure formation mechanism and crystallographic nature 0-29091
- $\beta$ -SiC, twinned crystals, fracture characts. 0-3193
- TaSe<sub>2</sub>, 1T and 2H superstruct., cryst. struct. using X-ray diffr. 0-39044
- Ti-Al-V (6.4 wt.%), strongly textured, influence of crystallographic orientation on tensile behaviour 0-7633
- Ti-Al-V(Sn) alloys, plastic deformation and fracture characts. at low temps. (Russian) 0-7624
- Ti-Al(-V)(Mo), impact strength anisotropy, influence of texture (Russian) 0-20952
- V, strain hardening, screw dislocations and microtwinning (Russian) 0-29971
- V-Ta (5 wt.%), strain hardening, screw dislocations and microtwinning (Russian) 0-29971
- W twin lamellae shape of single crystal (Russian) 0-19812
- Zn II complex, hexamidazole-zinc(II) dichloride tetrahydrate:Cr(III), D-tensor orientation, charge-compensation vacancies 0-50172
- Zn single crystals, temp. and strain rate effects on strength, slip and twinning 0-16373

**twistors** see magnetic storage devices**two-dimensional digital filters**

- multispectral scanner imagery application 0-31152

**two-phase flow**

- accelerating bubble flow of gas-liquid mixture, phase slip 0-53838
- aerosol, large particle thermophoresis theory, comparison of two methods 0-26060
- aerosol electrostatic discharger for helicopters (French) 0-28863
- aerosol kinematic coagulation calcs. in variable-speed gas stream 0-19491
- aerosol particles, turbulent migration phenomenon 0-53836
- air-H<sub>2</sub>O injection into permeable bed for underground coal gasification, numerical model 0-30359
- air-water mixture, vertical flow, temp. influence on boundary lines between flow regimes 0-43764
- airdroplet flight in air, drift loss from spray cooling pond, numerical estimation 0-19471
- annular, crit. heat flux, swirl effect 0-10113
- annular, entrained droplets, size distrib. and entrainment rate 0-43760
- annular flow through orifices, modelling 0-28555
- aqueous fog form. in shock tube 0-19531
- balance equations, computer programs for thermal-hydraulic anal. of nucl. steam supply systems 0-9332
- blast furnace, simulated, interaction between gas and liq. flow 0-10300
- boiling, mechanism model based on rotating vortex model with spatial heating 0-14694
- bottom settling of solid particles in turbulent shear flow, distribution statistical properties (Japanese) 0-19344
- bubble, spherical gas, nonlinear response to multi-freq. acoustic excitation 0-38480
- bubble and eddy heat diffusion in turbulent flow 0-19477
- bubble cavitation in inviscid compressible liq. 0-28553
- bubble distribution, eruption diam. in fluidised bed with horizontal tube bundle 0-14781
- bubble layers in liquids, struct. of pressure pulses 0-38479
- bubbles, forced oscillation damped by acoustic radiation 0-33664
- bubbles, pulsating, motion in viscous liquid half-space near boundary with inviscid liquid 0-19494
- bubbles, pulsating, surface oscillations and jet production 0-33640
- bubbles and drops driven by modulated acoustic radiation stresses, shape oscillation and static deformation 0-33274
- bubbly, droplet and particulate flows, drag coeff. and relative vel. relations 0-24072
- bubbly flow, void fraction meas. by light attenuation technique derivation of transmission rate reln. (Japanese) 0-48795
- BWR, coolant flowrate in evaporative channel, self-oscillation parameters investigation 0-37572
- BWR, momentum coupled transient thermal-hydraulic model 0-13565
- BWR Channel, two-phase flow fluctuations and continuity 0-14786
- characterisation using neutron techniques, review (Italian) 0-19479
- compressible two-phase flow dynamics, distributed parameter model 0-24086
- compression shock stability in streams of spontaneously condensing vapour 0-28563
- constitutive laws determ. from irreversible thermodynamics 0-36861
- counter-current flow, discrete polydispersed model 0-14779
- counter-current flow, hold-up and particle size distrib. simulation 0-14780
- creeping flow mass transfer in size distrib. cloud drops, high Schmidt number 0-14783
- critical flow in long nozzles, PWR appl. 0-13550
- critical heat flux in annuli, general correlation 0-43705
- critical mass flow rate, calc. (Russian) 0-53848
- critical two-phase flow, nonequilibrium vapour production model 0-52719
- cyclohexane-aniline, crit. mixture with shear flow, light scatt. obs. 0-6521
- density wave oscillations, linear stability anal. 0-19327
- depressurised subcooled liquid, boiling boundary phase-change front transient propag. 0-43768
- detonation development in unmixed media (Russian) 0-28556
- detonation sputtering, interaction between detonation waves and gas and powder flows (Russian) 0-16182
- dispersive, coeff. of internal resistance 0-19476
- droplet deformation in extensional flow 0-19449
- droplet dynamic interaction, angle of collision effects 0-38475
- drops driven by modulated acoustic radiation pressure, quadrupole resonance, experimental props. 0-33275
- duct, horizontal, slugging onset 0-10296
- dust clouds of solid fuels, ignition and flame quenching 0-28577
- dusty fluid flow past plate, small amplitude oscillations 0-14792
- dusty gas, flow between concentric coaxial circular cylinders 0-10299
- dusty gas, hypersonic wedge flow 0-6083
- dusty gas, Stokes layer stability 0-19493
- dusty plane viscous incompressible fluid flows, kinetic, kinematic props. 0-38482
- dusty viscous flow due to torsional vibrations of a circular disc 0-28548
- emulsion, concentrated unstable, turbulent flow in pipes 0-28537
- equilibrium dispersed-ring water vapour flows, liq. distrib., film paramters and hydraulic resist. 0-24079
- ferrofluid constitution examination by rotating test tube method 0-33693



**two-phase flow continued**

ferrofluid droplet, interphase boundary hydrostatic characts. in uniform mag. field 0-33692  
 fission reactor LOCA, reflooding phenomena in single heated tool 0-27754  
 fission reactor rod bundle blowdown heat transfer instrumentation, transient two-phase flow meas. 0-685  
 flotation, noninertial, effect of particle aggregation 0-55719  
 flow regime maps for developing steady air-water two-phase flow in horizontal tubes 0-28552  
 flow visualization using two-phase flow 0-33714  
 fluid mixture, inertia coeff. and drag coeff. 0-19475  
 fluid-gas mixtures, tubular reactor layout (*German*) 0-1698  
 fluidised bed, jet penetration depth of multiple vertical grid jets 0-38486  
 forced convection in two-phase flow from jets, mass transfer near interface (*German*) 0-53782  
 forced flow laminar filmwise condensation of vapour in vertical tube 0-43762  
 forced oscillations of nonspherical bubbles 0-33663  
 free molecule heating of micron size particles at hypersonic speeds 0-19442  
 free-surface sediment conveying river bed flow, flowrate and momentum correction factors 0-36339  
 Freon-113 vapour environment, rewetting of hot surfaces, two-phase high pressure flow simulation 0-32358  
 gas, in contact with condensed phase, hydrodynamic eqn. and slip boundary condition 0-14791  
 gas and non-Newtonian liquid, stratified flow in horizontal pipes 0-48787  
 gas particulate flow on flat plate, laminar boundary layer, finite difference method 0-43688  
 gas suspension flow in long horizontal pipe, heat exchange investig. 0-19388  
 gas-liquid cocurrent downflow in fixed bed in pulsed regime, mass transfer fluctuations 0-19485  
 gas-liquid countercurrent packed column, with intermittent voids, residence time distrib. studies 0-19483  
 gas-liquid flow, hydraulic resistance 0-24077  
 gas-liquid flow in heat exchange panel (*Russian*) 0-28550  
 gas-liquid mixture, bubble mode of flow in vertical pipe 0-24081  
 gas-liquid systems, vib. stabilisation of dynamic equilib. and mixing (*Ukrainian*) 0-10291  
 gas-liquid turbulent flow, friction, velocity and gas content profiles 0-14793  
 gas-solid horizontal pipe flow, vertical concentration distrib. (*French*) 0-14824  
 gas-solid mixture hydrodynamics, use of relative velocity of gas to solids (*Croatian*) 0-14799  
 gas-solid packed column, gas and solid phase axial dispersion at trickle flow 0-14807  
 gas-solid turbulent shear channel flow, particulate motion, numerical simulation 0-53863  
 gas-water flow, heat transfer meas. (*Russian*) 0-43761  
 geothermal reservoir simulation, numerical soln. techniques 0-12447  
 gravity flow of gases, liquids and bulk solids, common eqn. represent. and exptl. test 0-38477  
 heat pipe, 2-component, heat and mass transfer 0-24021  
 heavy-particle impurity suspension effect on viscous shock layer gas flow 0-28554  
 Hele Shaw flow with horizontal temp. gradient, slow bubble motion 0-28549  
 hindered settling in a multi-species particle system 0-14782  
 hollow cone sprays, induced air flows 0-53846  
 horizontal coiled tube banks, two-phase flow boiling heat transfer and hydrodynamics 0-48708  
 horizontal pipelines, two-phase flow patterns, pipe dia. and fluid prop. effects 0-48791  
 horizontal slug or surge flow 0-48786  
 hydraulic lines, wave phenomena, coupled vibrations in bending and branching lines 0-14778  
 inhomogeneous fluidised layer in reactor, 2-point boundary value problem, asymptotic anal. 0-33654  
 instrumentation calibration for mass flow rate meas. in PWR coolant two-phase flow 0-37552  
 instrumentation for localised meas. in PWR coolant two-phase flow conditions 0-37550  
 internally finned tubes, refrigerant 22, evaporative heat transfer and pressure drop 0-5919  
 isothermal expansion of a two-phase fluid in a magnetohydrodynamic generator duct 0-1695  
 jet, laminar, in liq.-liq. system, vel. profile, numerical analysis 0-28545  
 jet, liquid, turbulent, gas absorpt. (*Japanese*) 0-38473  
 jets, two-phase, turbulent, particle or droplet size effect on diffusion 0-1658  
 jets, two-phase supersonic flow around a sphere 0-6114  
 laminar boundary layer eqns. 0-38476  
 laminar suspension flow, with diffusive gravit. deposition at entrance of converging and diverging channels 0-14825  
 liquid containing gas bubbles, struct. of supersonic waves and cavitation development 0-33643  
 liquid drop aggregate breakup in shock waves 0-24084  
 liquid film, gas entrained, combined plane parallel flow, linear and non-linear stability 0-33655  
 liquid film flowing concurrently with air in horiz. duct, flow pattern 0-43774  
 liquid metal MHD generator, wall-jet gas injection 0-28830  
 liquid-gas system between two plates, capillary curve 0-33660  
 liquids with vapour bubbles, US propag. 0-33661  
 LMFBR, flow behaviour of vol. heated boiling pools 0-13545  
 LMFBR thermal hydraulics 0-27718  
 LOCA, blowdown phase, two-phase mass flow rate meas. using true mass flowmeters 0-778  
 local density measurements, side-scatter gamma technique 0-569  
 low quality flow boiling, turbulent forced convection and nucleate boiling heat transfer 0-14696  
 LWR, analytic simulation 0-13551  
 magnetic stabilization of the state of uniform fluidization 0-19484  
 medium with low initial water saturation, end effect in two-phase flow 0-33656  
 MHD pipe flow, single and two phase 0-53869  
 mist flow over heated cylinder, particle size and temp. difference effects 0-38409

**two-phase flow continued**

multidimensional two phase flow eqn. derivation, general constitutive principle appl. 0-10297  
 Newtonian fluids, mean velocity and vol. flow rate for steady 1-D flow 0-6132  
 non-Newtonian flow through porous media, fluidised beds, solid-fluid interaction (*Portuguese*) 0-38454  
 non-Newtonian liquids, spherical gas inclusion radius change Rayleigh classical equation generalisation 0-19444  
 non-Newtonian liquids and gases, annular two-phase flow, press. drop and gas vol. fraction 0-10286  
 nonequilibrium transient flow boiling, method of characts. soln. 0-14789  
 nozzle, two phase, efficiency at high rates of heat and mass transfer 0-48767  
 nuclear power plant heat exchange problems 0-18372  
 nuclear reactor, AGR, helical monotube vapour generator, density wave instability, experimental-stochastic and theoretical anal. 0-47539  
 nuclear reactor, interfacial mass and momentum transfer in two-phase flow 0-27725  
 nuclear reactor, two-phase critical flow phenomena 0-27723  
 nuclear reactor LOCA, modelling two-phase hydrodynamic phenomena, pipe blowdown with Freon-12 0-5267  
 nuclear reactor LOCE blowdown flow meas., improved spool piece 0-27727  
 nuclear reactor transient two-phase flow, analytical modelling 0-27722  
 oil thickness variation on wavy water 0-6134  
 one dimensional, critical flowrate in channel calc. 0-10292  
 optic cavitation and laser-produced bubbles 0-38463  
 parallel channel forced convection boiling upflow system, instabilities 0-9327  
 partial differential equatn. finite difference solutn. 0-18564  
 particles in a fluid, convective diffusion and mass transfer, wakes, chemical reactions 0-38394  
 particles in turbulent fluid, statistical motion, Eulerian direct interaction 0-53841  
 pipe, circular, two phase flow in entrance region, effect of conc. of suspended particles 0-19481  
 pipes, flow of liquid and gas mixture, optical representation (*German*) 0-14800  
 polystyrene suspension, laminar flow, augmentation of heat and mass transfer, correl. of data 0-53840  
 porous media, two-phase flow with end effect allowance, numerical simulation 0-33659  
 pulsating gas bubbles in acoustic field, thresholds for surface waves 0-33665  
 pulverised fuel gas flow distrib. in manifolds of uniformly variable section (*Russian*) 0-33666  
 PWR, small scale ECC bypass data anal. 0-18505  
 PWR LOCA reflooding phase, two-phase flow and heat transfer at and near quench front 0-757  
 PWR rod bundles, radiative heat transfer calc. method 0-33602  
 RETRAN two-phase flow model, comparison with expt. 0-32330  
 rotating heat exchanger, frictionless two-phase tube flow, centrifugal accel., choked flow 0-48792  
 rotating spheres, heat transfer coeffs. for gas-solid two-phase flow 0-19369  
 saltating solid particles in turbulent flow, accel. and forces (*Russian*) 0-1675  
 saturated steam-water mixtures, void fraction relationships for upward flow 0-14790  
 separated incompressible boundary layer prediction, including viscous-inviscid interaction 0-1548  
 slowly moving vapour, film condensation heat transfer 0-19376  
 slowly rotating sphere submerged in fluid with surfactant surface layer 0-48717  
 solar nebula, grain motion through gas rel. to role as isotopic anomalies carriers 0-26757  
 solid-gas flow, fluctuation damping 0-19478  
 solid-liquid mixtures, rheological characts., shear stress/strain rate relationships 0-10287  
 solids-gas countercurrent vertical flow 0-10288  
 spherical cavity gas bubble in compressible liquid, kinematics of free vibrations (*German*) 0-24074  
 steam condensation in moving two-phase film, heat transfer, volumetric coefficient 0-48696  
 steam-water annular flow, moisture exchange, salt method 0-24078  
 steam/air mixtures, instrument for steam fraction meas. 0-52724  
 stratified gas/liquid flow, heat transfer, local Nusselt number prediction 0-38393  
 subcooled forced convection film boiling in forward stagnation region 0-43702  
 supersaturated vapour, nucleating centre nonstationary formation rate calc. 0-34178  
 suspension, dil., of spherical particles in non-Newtonian liq., rheological behaviour 0-24058  
 suspension in nonstationary flow, rheological behaviour 0-6130  
 suspension of particles during crystallisation in gaseous stream, modelling by aerothermochemistry of suspension eqns. (*French*) 0-53844  
 suspensions, creeping flow, hindered settling, particle shape effect 0-14797  
 tapered tubes, flow of closely fitting spheres and cones 0-48789  
 thermal reactor containment systems, critical flow mode for air-steam-water mixtures 0-18502  
 thermocapillary gas bubble movement, liquid screening 0-19474  
 thermomagnetoforesis of particles in magnetic suspensions 0-35581  
 thermosiphons, two-phase heat exchange in supply zone, anal. 0-19387  
 tracer analysis in two-phase flow systems 0-24073  
 transient two-phase flow system, three-dimensional numerical simulation 0-687  
 tubes, horizontal and vertical cooled, boiling crisis and critical heat flux 0-48712  
 turbulent flow field, solid and liquid particle interaction 0-43767  
 two parallel infinite plates, Couette flow of dusty gas 0-1681  
 two-fluid model calculations, stability problems 0-19489  
 upflow at atmospheric press., void fraction and pressure drop 0-48781  
 UVUTUP two-phase separated flow models 0-48793  
 vapourising liquid drops in N<sub>2</sub> gas, drag coeff. meas. 0-19486  
 vapour bubbles, analysis of oscillation 0-19487  
 vapour bubbles, oscillating, evaporation-condensation resonance frequency 0-19488  
 vapour flows with condensation 0-48794



**two-phase flow continued**

- vapour generator for K, heat transfer with drop motion in tube in supercrit. region 0-23880  
 vapour-drop flow, effect of drop conc. and dispersions 0-24082  
 vapour-gas bubbles removal in arteries of low-temp. heat pipes, anal. 0-19490  
 velocity-voidage relations for sedimentation and fluidisation 0-24076  
 vertical coplanar Y-junctions, two-phase steam-water flow 0-38478  
 virtual mass effects for interfacial transfer phenomena 0-14788  
 viscous fluid, bubbling through of air, drop entrainment 0-14787  
 volatile highly thermally conductive spherical drop, theory of diffusio-phoresis 0-14784  
 vortex breakdown flowfields, spectral characts. in water 0-19408  
 water and Freon-12, flow boiling crisis in horizontal tubes, fluid-to-fluid modelling 0-48785  
 water boiling in Laval nozzles, discharge and dynamic characteristics 0-19470  
 water flow with air contents, partially- and super-cavitating hydrofoils in cascade, analysis method (*Japanese*) 0-14763  
 water vapour, 2-D laminar boundary layer 0-19492  
 water vapour, wet, boundary layer in compressible flow 0-10295  
 water-water vapour flow through packed bed 0-38484  
 wet steam tunnel expts., low press., temp. and press. differentials 0-33667  
 wood chip refiners, cavitation effects in two-phase flow 0-35348  
 He boiling tube hydraulic resistance and burnout expt. 0-24085  
 N<sub>2</sub>-H<sub>2</sub>O mixtures, two-phase pressure drops in the low flowrate region 0-19480  
 N<sub>2</sub>O<sub>4</sub>, reactor coolant, stability in two-phase flow (*Russian*) 0-609  
 Na boiling in tubes, heat transfer and pressure drop 0-28408

**two-photon spectra**

- alkali bromides and iodides, self-trapped exciton and F-centre form. by picosecond laser pulses 0-10546  
 alkali halides, two-photon absorpt. 0-50292  
 alkyl iodides, two-photon reson. ionis. spectra 0-28071  
 aromatic hydrocarbon, centrosymmetric, two photon excited upper state fluoresc. spectra, reson. fluoresc. and vibr. mode selectivity 0-18878  
 atom, AC Stark effect, fluoresc., in modulated laser beams, two-photon stepwise excitation 0-42989  
 benzene-(d<sub>1</sub>,d<sub>2</sub>,d<sub>4</sub>), two-photon <sup>1</sup>B<sub>2u</sub>←<sup>1</sup>A<sub>1g</sub> spectrum, deuterium effect 0-32788  
 CdSe two-photon absorption, laser calorimetric obs. 0-33076  
 coherent states in degenerate four wave mixing 0-5717  
 colliding particle system, two-photon transition, stimulated Raman scatt. 0-9663  
 diatomic molecule, rot. line strengths in multiphoton transitions 0-48051  
 double beam two-photon absorption spectra, off-diagonal matrix elements 0-5517  
 homonuclear molecules, vibr. excitation by IR radiation 0-28068  
 hydrogenic atoms, metastable, Raman-like two-photon scatt., calc. 0-47953  
 II-VI semiconductor, two-photon and two-step absorption of light 0-7389  
 II-VI semiconductors, zinc blende and wurtzite struct., two photon spectra, quantitative investigation 0-50373  
 inert gas atom, two-photon excitations, interelectron correlation 0-957  
 interference in two-channel two photon ionization 0-23381  
 IV-VI semiconductors, two photon spectra, quantitative investigation 0-50373  
 organic dye molecules, two-photon absorpt. in laser fields with arbitrary statistical characts. (*Russian*) 0-37842  
 polarisation spectroscopy 0-9573  
 resonance two-photon absorption, theory 0-28268  
 semiconductor films, two-photon absorption, exciton effects (*Russian*) 0-40174  
 semiconductors, direct-gap, two-photon absorpt. 0-50292  
 semiconductors, II-VI and III-VI types, competition between two-photon absorption and two-stage absorption via deep traps 0-29764  
 semiconductors, two-photon light absorption by excitons in static elec. field 0-11364  
 simple molecules, two-photon dissoc., spectrosc. obs. 0-32787  
 Stark effect, two photon absorption spectroscopy 0-43126  
 toluene, two-photon ionisation spectrum, of <sup>1</sup>L<sub>b</sub>←S<sub>0</sub> transition 0-14180  
 As<sub>2</sub>S<sub>3</sub>, amorphous and cryst., optically induced changes, ps. spectroscopy 0-48326  
 CO, rot. line strengths in multiphoton transitions 0-48051  
 CO, two-photon spectroscopy with tunable ArF laser 0-37843  
 CdS, biexciton, low intensity nonlinear coherent mixing study 0-49619  
 CdS, biexciton levels, luminescence-assisted two-photon spectra 0-29795  
 CdS, size effect of dense electron hole systems 0-7413  
 CdS, two photon Raman scatt. at high excitation levels (*Russian*) 0-16032  
 CdS, virtually excited biexcitons polaritons dispersion, two photon Raman scatt. 0-45067  
 CdS:Cu(In), two-photon and two-step absorption of light 0-7389  
 CdTe two-photon absorption, laser calorimetric obs. 0-33076  
<sup>113</sup>Cd<sub>2</sub>, two-level system, absorpt. spectrum, subradiative struct. (*Russian*) 0-28008  
 Cl<sub>2</sub>CS, excitation, singlet and triplet states, two photon absorpt., singlet-singlet energy pooling, fluoresc. obs. 0-48032  
 Cs, two-photon ionis., profiles of 6<sup>3</sup>S<sub>1/2</sub>-7<sup>2</sup>P<sub>3/2,1/2</sub> lines 0-958  
 Cs<sub>2</sub>, two-photon dissoc., spectrosc. obs. 0-32787  
 CsPbBr<sub>3</sub>, electronic and optical props. 0-25414  
 CsPbCl<sub>3</sub>, electronic and optical props. 0-25414  
 Cu halides two photon spectra, quantitative investigation 0-50373  
 CuBr, biexciton two-photon absorpt. 0-11432  
 CuBr, P exciton fine struct. 0-20091  
 CuCl, biexciton two-photon absorpt. 0-11432  
 CuCl, excitonic molecules, secondary emission under two-photon reson. excitation 0-11468  
 CuCl, phonon interaction of excitonic molecule 0-50316  
 CuCl, two-photon absorpt. and luminesc., biexcitons 0-11434  
 Cu<sub>2</sub>O, even-parity excitons assignment, from two-photon spectrum 0-6731  
 H<sub>2</sub>, two-photon spectroscopy with tunable ArF laser 0-37843  
 He, Doppler-free two-photon optical spectroscopy 0-52960  
 Hg<sub>2</sub>, emission and form. kinetics, sequential two-photon absorpt. expt. 0-32767  
 Hg<sub>1-x</sub>Cd<sub>x</sub>Te, two-photon absorpt. spectra 0-20660  
 I<sub>2</sub>, 2- and 3-photon absorpt. obs. 0-18864  
 InSb, two-photon absorpt. spectra 0-20660

**two-photon spectra continued**

- KCl, colour centres laser spectra, induced F' band absorpt. 0-2779  
 Li, seeded flames, excitation, laser radiation absorpt., sound vel., opto-acoustic effects obs. 0-43345  
 Li, two-photon ionization spectra 0-23382  
 N<sub>2</sub>, rot. line strengths in multiphoton transitions 0-48051  
 NO, rot. line strengths in multiphoton transitions 0-48051  
 Na, Rydberg states, high resolution two-photon mm spectroscopy, metrology appl. 0-43018  
 Na seeded flames, excitation, laser radiation absorpt., sound vel., opto-acoustic effects obs. 0-43345  
 Na, two-photon absorpt. processes, polarisation selection rules 0-9574  
 Na, two-photon transition, distinction of competing processes in nonlinear resonant freq. mixing 0-33080  
 Na+inert gas, collisional redistrib., two-photon absorpt. with near-reson. intermediate state 0-23505  
 Na+Xe, nonreson. two-photon absorpt., 4s excited states and pot. energy curves, close coupled eqns. 0-48068  
 Nd<sup>3+</sup>:glass, nonlinear refractive index, two-photon resonant absorption by Nd<sup>3+</sup> (*Chinese*) 0-43387  
 Ne, atom, isotopic shift and fine struct. for 2p<sup>5</sup>4d and 2p<sup>5</sup>5s config., Doppler-free two-photon spectroscopy 0-23387  
<sup>21</sup>Ne, hyperfine interaction in 4d subconfiguration, Doppler-free two-photon spectroscopy meas. 0-18944  
 Rb, 5<sup>2</sup>S-n<sup>2</sup>S transitions, Rydberg levels, high resolution two photon spectra obs. 0-52923  
 Rb Doppler-free two-photon lines, self-broadening and shift meas. 0-5506  
 Rb, Doppler-free two-photon absorpt. spectrum 0-42975  
<sup>85,87</sup>Rb, high Rydberg levels, press. broadening and shifts 0-52902  
 RbBr (I), optical absorpt. centre formation time meas. 0-40081  
 SF<sub>6</sub>, excitation by strong IR laser field, spectral characts. 0-32713  
 SF<sub>6</sub> molecule, resonant energy absorpt. struct. in IR laser field (*Russian*) 0-5592  
 SrTiO<sub>3</sub>, energy band struct., two-photon absorption spectra study 0-15453  
 XeBr, emission and form. kinetics, sequential two-photon absorpt. expt. 0-32767  
 ZnO, biexciton levels, luminescence-assisted two-photon spectra 0-29795
- two-photon spectroscopy**  
 amorphous semiconductor, ps. spectroscopy 0-48326  
 chemical analysis, uses of two-photon excited mol. fluoresc. 0-40799  
 Doppler-free, and wave-front conjugation by four-wave mixing of monochromatic waves 0-28265  
 IR Doppler free molecular spectroscopy, two photon coherence and pumping 0-48052  
 laser, real time monitoring of atmospheric pollutants 0-7996  
 laser-radiofrequency double quantum saturation spectroscopy 0-48105  
 luminescence-assisted two-photon spectroscopy, appl. to biexciton levels in CdS and ZnO 0-29795  
 molecular, two pulse technique using ultrashort pulses 0-53165  
 molecule, using tunable spin flip Raman laser, review 0-55762  
 molecules, stimulated Raman and two-photon absorpt. 0-52999  
 nuclear laser-induced resonant absorption of γ radiation 0-18290  
 polarisation 0-9573  
 resonance scattering methods in atomic spectroscopy 0-53167  
 solids, optical absorption under laser irradi. 0-34940  
 two-photon fluorescence, contrast ratio decrease depend. on laser pulse intensity 0-1255
- TWT** see travelling-wave-tubes
- Tyndallometry** see turbidimetry
- type I superconductors**  
 see also intermediate state  
 cylindric superconducting domain lattices in magnetic field, lattice stability determ. (*Russian*) 0-44775  
 film, cylindrical, domain struct. in mag. field 0-15666  
 magnetisation, first stage, and metastable migration field in slab 0-15655  
 rare earth iridium borides, RIr<sub>2</sub>B<sub>4</sub>, supercond., magnetism and metastability 0-29501  
 Al, bulk superconducting fluctuations in elec. resist 0-49995  
 Al films, Al<sup>2+</sup> irradi., increase of resist. and supercond. transition temp. 0-7027  
 Al, fluxural oscillations in longitudinal mag. field, sound attenuation, magnetoelasticity (*Russian*) 0-54844  
 Al, resistivity well above T<sub>c</sub>, supercond. effect up to 2T<sub>c</sub> 0-6810  
 Al small particle, NMR study, Knight shift, spin-lattice relax. time, supercond. effects 0-39710  
 Al, superconducting, quasiparticle charge distrib. due to tunnel injection 0-44771  
 Al, superconducting, resistive layer microstructure (*Russian*) 0-34567  
 Al, superconducting transition, effect on jump-like deform. (*Russian*) 0-34538  
 Al thin films, dielectric coating effect on superconductivity 0-7026  
 Al, transition temp., perturbative corrections, direct and indirect ladder diagrams 0-49979  
 Am, superconducting critical field, sp. ht. 0-11136  
 C<sub>6</sub>K, intercalation cpd. with graphite, supercond. props. 0-44755  
 Cd, electronic properties depend. on 2<sup>1</sup>/<sub>2</sub>-th order phase transition under high press. (*Russian*) 0-11128  
 Cd, transition temp., perturbative corrections, direct and indirect ladder diagrams 0-49979  
 Ga film, crit. transverse mag. fields and transition temp. (*Russian*) 0-7048  
 Hg, transition temp., perturbative corrections, direct and indirect ladder diagrams 0-49979  
 In, divided superconducting thin film, superheating and supercooling field resistive meas. (*French*) 0-44751  
 In, Lifshits transition, electron-phonon interaction 0-29502  
 In, US attenuation in supercond. and normal state in transverse mag. field and zero field 0-54836  
 Pb, dislocation electron drag coeff. temp. depend., internal friction method, superconducting state 0-29031  
 Pb, fluxural oscillations in longitudinal mag. field, sound attenuation, magnetoelasticity (*Russian*) 0-54844  
 Pb, supercond. transition temp., ab initio calc. 0-25036  
 Pb superconducting amorphous film, conductivity and transition temp., ion bombardment effects (*Russian*) 0-49969  
 Pb, thermal conductivity, in normal and supercond. states, 0.6-7.5K (*Russian*) 0-6815  
 Pb thin strips, supercond., optical wave illum., critical current behaviour 0-50012



**type I superconductors continued**

- Pb, transition temp., perturbative corrections, direct and indirect ladder diagrams 0-49979  
 Pb/Cu interface, thermal conductance at low temps. in normal and supercond. states 0-49436  
 Pd, confined geometry, p-wave supercond. or itinerant ferromag. 0-11129  
 Sb, electronic band struct. changes due to plane straining effects (*Russian*) 0-54602  
 Sn film, energy gap suppression and instability under strong quasiparticle injection 0-7042  
 Sn film, phonon-injection-induced destruction of supercond. 0-6956  
 Sn, superconducting current carrying film, resistive region boundary movement, ambient media depend. 0-44763  
 Sn, superconducting film, paraconductivity 0-54845  
 Sn superconducting thin-film bridge, IV curves oscill. instability and quasi-particle recomb. (*Russian*) 0-44769  
 Ta, critical field, muon spin relaxation (*German*) 0-50015  
 Ta:N, superconductive to normal transition anisotropy 0-25031  
 Th-Dy, dil., supercond. Th, paramag. relax. of Dy moments, Mossbauer study 0-39957  
 Zn, transition temp., perturbative corrections, direct and indirect ladder diagrams 0-49979

**type II superconductors**

see also mixed state

- A15 type compound, props. and one-dimensionality 0-2530  
 A-15 compound, defect influence on  $T_c$  0-20345  
 A-15 compounds, disordered,  $T_c$  depression, appl. to  $Nb_3Ge$  0-7020  
 A-15 compounds, homogeneity range 0-2172  
 A-15 diffusion layers, influence of additions of growth and supercond. props. (*German*) 0-11130  
 A-15 phase, comment on new 3-dimens.  $k \cdot p$  model for electronic struct. 0-10865  
 A-15 phase, reply to comment on new 3-dimens.  $k \cdot p$  model for electronic struct. 0-10866  
 A-15 type compounds, relation between martensitic and supercond. phase transition 0-29497  
 amorphous metals, supercond., mag. impurity interactions 0-44777  
 antiferromagnetic superconductors, new pairing state, pair destruction, theory 0-54847  
 Chevrel phase compounds, bonding and phys. props. rel. to struct., book contrib. 0-49209  
 critical state, flux jumps and oscills. (*Russian*) 0-7052  
 cubic, flux-line lattice anisotropy, boson method calc. 0-2536  
 dilutely pinned, threshold criteria for pinning force 0-15668  
 ferromagnetic superconductor, supercond. Bloch wall 0-20349  
 fluctuations in crit. region near upper crit. field 0-25048  
 flux distribution and hysteresis loss in round supercond. wire 0-34570  
 flux-flow noise voltages, oscillations in V-I curves 0-15671  
 flux-line cutting 0-7055  
 flux-line cutting model 0-50017  
 giant-vortex state, temp. depend. 0-7051  
 Ginzburg-Landau theory, exact solns. for pure metals 0-49981  
 high- $T_c$  superconductors role of quasilocal excitation 0-2508  
 intermetallic compounds, containing d-transition metal, hydrogenated, magnetism 0-34609  
 magnetic behaviour under longitudinal mag. field, irreversible force free current 0-7053  
 magnetisation, rel. to anisotropy of upper crit. field 0-54832  
 metallic glasses props., development and appl. 0-19710  
 metastable states, boundaries 0-54848  
 molybdenum ternary sulphides, Chevrel phase, synthesis and superconductivity (*German*) 0-25038  
 oscillations, resistive state, current density 0-44782  
 paramagnetic limit, Fermi surface dielectric gap (*Russian*) 0-2533  
 $Pb_{0.7}In_{0.3}$  foil, flux-flow crit. freq. and generalised bundle size depend. on fluxoid traversal distance and length 0-7054  
 pion condensate props. in mag. field, superconductivity, mixed state (*Russian*) 0-49974  
 positive muon diffusion coeff., determ. from transverse depolarisation 0-25269  
 radiation-induced changes in crit. props., radiation defects (*Russian*) 0-25027  
 rare earth compounds,  $RMo_6X_8$ , ( $X=S, Se$ ), supercond. and long range mag. order coexistence 0-15642  
 rare earth compounds,  $RRh_4B_4$ , supercond. and long range mag. order coexistence 0-15642  
 rare earth cpds.,  $RRh_4B_4$  and  $RMo_6X_8$  ( $X=S, Se$ ), mag. order and supercond., neutron scatt. studies 0-44807  
 rare earth iron silicides,  $R_2Fe_2Si_5$ , superconductivity 0-49968  
 rare earth lead molybdenum sulphides,  $R_2Pb_{1-x}Mo_{6+y}S_8$ ,  $R=La, Nd, Pr, Gd$ , sputtered, supercond. props. 0-50019  
 rare earth molybdenum chalcogenides, Chevrel phase correlation between struct. and supercond. transition temp. 0-7023  
 rare earth molybdenum sulphides, supercond. and magnetism coexistence (*Japanese*) 0-7025  
 rare earth rhodium boride system, ternary, supercond., phase diagrams at upper crit. fields 0-2531  
 rare earth rhodium borides,  $RRh_4B_4$ , NMR and sp. ht. in supercond. and mag. ordered phases 0-7037  
 rare earth ternary compounds, supercond. and antiferromag. coexistence 0-25030  
 rare-earth compounds, supercond. pairing, mag. ordering effect 0-15641  
 resistive domain existence, current generation (*Russian*) 0-44776  
 series formula of supercond. critical temp. applications (*Chinese*) 0-54816  
 strong coupling superconductor thin film, critical mag. field (*Chinese*) 0-54849  
 thermodynamics, corrections from electron-phonon interactions 0-49387  
 thermomagnetic effects and critical state stability 0-20353  
 (TMTSF) $_2PF_6$ , organic one-dimensional superconductor, transition temp. 0-44754  
 transition metal borides, supercond. search below 1K 0-20342  
 transition metal compound refractories, electron and phonon behaviour 0-54624  
 transition metal silicides, struct. and supercond., Cu influence 0-50592  
 transition metals, amorphous, superconducting transition temp. (*Chinese*) 0-54817  
 transition metals, supercond. transition temp., ab initio calc. 0-25036  
 Al, energy gap enhancement by tunnelling extraction 0-34564  
 Al film, metastable current states, mean free path variation (*Russian*) 0-2538

**type II superconductors continued**

- Al superconducting film, cylindrical, granular, crit. currents and electron mean free paths 0-7057  
 Al, superconducting thin film, evidence for Kosterlitz-Thouless transition 0-39721  
 $BaGe_2$ , superconducting temperature depression due to mag. field 0-54820  
 $Ba_{1-x}Sr_xPb_{0.75}Bi_{0.25}O_3$ , superconductivity, rel. to lattice const. 0-49966  
 $C_8K$ , intercalation cpd. with graphite, supercond. props. 0-44755  
 $CeCu_2Si_2$ , strong Pauli paramagnetism, superconductivity obs. 0-29499  
 $Ce_{0.73}Ho_{0.27}Ru_2$ , superconductors, mag. correlations and crystal-field levels 0-34547  
 $Ce_{0.73}Ho_{0.27}Ru_2Co$ , spontaneous mag. order below superconducting transition temp., Mossbauer study 0-39701  
 $(Ce_{1-x}Ho_x)Ru_2$ , mag. props., neutron scatt. study 0-44808  
 $CeRu_2$ , H absorption induced Ce valence change, mag. and supercond. props. 0-50042  
 $Cs_{0.33}WO_3$ , supercond. and special phonons, neutron scatt. obs. 0-15643  
 $Cs_2WO_3$ , normal phase and supercond. props. 0-25035  
 Cu-Ga porous solid formed by shock compression 0-29905  
 Cu-Nb alloys for superconducting wire, casting of dendritic structure 0-2976  
 Cu-Nb $_3$ Sn superconducting composite, crit. props., AC hysteretic losses 0-50014  
 Cu-Nb-Sn, multifilamentary supercond. composite wires, fabrication on laboratory scale and mech. props. 0-29897  
 Cu-Nb-Sn system, phase equilibria and supercond. props. (*Russian*) 0-50589  
 Cu-V-Si, two-step supercond. transition 0-34539  
 CuCl, high-temp. supercond., BCS strong-coupling limit for transition temp. 0-2511  
 $Cu_{1-x}Mo_xD_8$ , triclinic struct., X-ray powder diffr. anal. 0-6388  
 $Cu_2Mo_8S_8$ , supercond., two-phase, upper crit. field meas. 0-29509  
 $Dy_{1.2}Mo_6S_8$ , low temp. heat capacity anomaly rel. to antiferromag. transition in supercond. state 0-25044  
 $(Er_{0.6}Ho_{0.4})Rh_4B_4$ , reentrant supercond., magnetisation meas. near lower crit. temp. 0-25043  
 $(Er_{1-x}Ho_x)Rh_4B_4$ , superconducting ferromag., Josephson effect, point contact junction meas. 0-7043  
 $(Er_{1-x}Ho_x)Rh_4B_4$ , superconductive and mag. interactions, hydrostatic press. effect 0-49973  
 $ErRh_4B_4$ , film, sputter deposition and low temp. props. 0-2948  
 $ErRh_4B_4$ , Mossbauer spectra 0-15926  
 $Er_2Y_{1-x}Rh_4B_4$ , supercond. phase transitions, recentering temp. to normal ferromag. state 0-7024  
 $EuMo_6S_8$ , Chevrel phase, RE mag. isolation and supercond. 0-44470  
 e-Fe, low temp. supercond., transition temp. estimated 0-34540  
 $GdMo_6S_8$ , Chevrel phase, RE mag. isolation and supercond. 0-44470  
 $Gd_{1.2}Mo_6S_8$ , low temp. heat capacity anomaly rel. to antiferromag. transition in supercond. state 0-25044  
 Hf-V foil, rapidly quenched and heat treated, supercond. props. 0-54852  
 HfV $_2$ , C-15 struct., phase transitions, elec. cond., crystal lattice parameters (*Russian*) 0-54826  
 $Hg_{3-x}AsF_6$ , linear chain compound, mag. field induced residual resist., anisotropic supercond. 0-24897  
 $Hg_{3-x}AsF_6$ , supercond., absence of surface Hg 0-20350  
 In film, metastable current states, mean free path variation (*Russian*) 0-2538  
 In-Mg, ordered equiatomic, lattice specific heat meas., Debye temp., superconducting transition 0-54396  
 In-Sn alloy, Lifshits transition, electron-phonon interaction 0-29502  
 $In_2Sn$ , anisotropy of upper crit. field 0-20360  
 $K_{0.33}WO_3$ , supercond. and special phonons, neutron scatt. obs. 0-15643  
 $(La,Gd)Al_2$ , normal and supercond. state, US attenuation, freq. depend. and mechanisms 0-49992  
 La particles, supercond. props. (*Russian*) 0-7018  
 LaAg, Tb and Pr substituted, superconductors, cryst. field transitions line-widths 0-24854  
 LaAl $_2$ , Tb and Pr substituted, superconductors, cryst. field transitions line-widths 0-24854  
 LaMo $_6S_8$  thin films, crit. currents and pinning forces 0-34575  
 $(LaNd)Sn_3$ , containing Nd impurities, supercond. and normal state props. 0-49967  
 LaPb $_3$ , Tb and Pr substituted, superconductors, cryst. field transitions line-widths 0-24854  
 La $_{1-x}Pr_xPb_3(Sn_3)$ , cryst. field excitations, inelastic neutron scatt. obs. 0-15653  
 LaRu $_2$ , H absorption induced Ce valence change, mag. and supercond. props. 0-50042  
 LaS $_{1.33}$ -LaS $_{1.40}$ , low temp. sp. ht. 0-15259  
 La $_3S_4$ , high crit. mag. field supercond., elec. resist., sp. ht. and magnetisation 0-2532  
 LaSn $_3$ , Tb and Pr substituted, superconductors, cryst. field transitions line-widths 0-24854  
 La $_{0.98}Sn_{0.02}Mo_6Se_8$ , Mossbauer spectra 0-15926  
 LiTi $_2O_4$ , single-phase, prep., crystal struct. and superconducting transition characts. 0-50583  
 Li $_{0.33}WO_3$ , supercond. and special phonons, neutron scatt. obs. 0-15643  
 Mo, transition temp., perturbative corrections, direct and indirect ladder diagrams 0-49979  
 Mo-Re,  $\sigma$  phase alloy, critical mag. field, elec. resistance 0-54850  
 $(Mo_{0.6}Ru_{0.4})_8B_{18}$ , supercond. metallic glass, neutron irradi. effects 0-29060  
 $Mo_2S_8(Se_8)(Te_8)$  and halogen substituted cpds., sp. ht. capacity 0-49986  
 $Mo_2Se_8$ , Chevrel phase, supercond. isotope effect meas. (*German*) 0-25038  
 $(NH_4)_{0.33}WO_3$ , supercond. and special phonons, neutron scatt. obs. 0-15643  
 Nb, critical field, muon spin relaxation (*German*) 0-50015  
 Nb film, critical currents due to microwave field 0-25058  
 Nb film, magnetron-sputtered, intrinsic stresses and supercond. props. 0-24772  
 Nb film, vac. deposited, deposition parameter effects on crit. temp. 0-2514  
 Nb, fluxoid lattice, eqn. props., small-angle neutron diffraction measurements 0-34573  
 Nb, fluxoid lattice, eqn. props., magnetisation measurements 0-39725  
 Nb heteroepitaxial layers on sapphire, residual mechanical stress and strain influence on superconductivity 0-15644  
 Nb, nanobridges Josephson effect, quasiparticle diffusion time, inelastic scatt. time 0-34556



## type II superconductors continued

- Nb, optical props. and electron-phonon interactions 0-2510  
 Nb, plastic deformation effects on superconducting specific heat transition 0-20352  
 Nb, spin fluctuations effect on  $T_c$  from sp. ht. and mag. suscept. 0-7030  
 Nb superconducting amorphous film, conductivity and transition temp., ion bombardment effects (*Russian*) 0-49969  
 Nb, superconducting bridges by electron beam lithography and ion implantation Josephson effect 0-20355  
 Nb superconducting films, crit. depairing currents, temp. and mag. field depend. 0-7058  
 Nb superconducting point contact, high freq. props. in far IR 0-54840  
 Nb/Cu-Sn-Mg, effect of Mg addition to Cu-Sn matrix 0-25028  
 Nb/H, heat capacity and supercond. between 1.5 and 16K 0-2521  
 Nb-Al proximity sandwiches, supercond. transition temp. and tunnelling meas. 0-7045  
 Nb-B, atomic order, stability, supercond. (*French*) 0-50021  
 Nb-Ga-Fe ternary system, phase equil. at 1000°C, supercond. transition temp. 0-35158  
 Nb-Ge, A15 struct. superconductor, high field transport props. TEM study 0-34574  
 Nb-Ge, supercond. A-15 phase, supercond. transition temp. after ion implantation 0-49972  
 Nb-Ge-Cu, phase equil. and supercond. props. (*Russian*) 0-40332  
 Nb-Ge-Ni, phase composition and superconducting props., influence of Ni (*Russian*) 0-20898  
 Nb-Ge-Si, A15 struct. superconductor, high field transport props. TEM study 0-34574  
 Nb-Ge-Si film, CVD, struct., comp., stability and homogeneity 0-15421  
 Nb-Hf (38 at.%) superconductor, peak effect, summation problem, mag. history flux pinning force 0-20362  
 Nb-Mo system, electron-phonon coupling const. and supercond. transition temp., average T-matrix approx. 0-39707  
 Nb-NbO<sub>2</sub>-Pb tunnel junctions at 4.2K, conductance of oxide barrier 0-7046  
 Nb-Pt-O system, phase equilibria, diagram, unit cell parameters, supercond. 0-35352  
 Nb-Sn(Al)(Ga)(Ge)(Si)-C, phase equil. and supercond. 0-50593  
 Nb-Ti, sheet, flux trapping, appl. to mag. shielding and levitation 0-31806  
 Nb-Ti, single core conductor, carrying DC transport current, alternating field losses 0-34550  
 Nb-Ti superconducting magnet system, for short sample test on Tokamak superconductor 0-9010  
 Nb-Ti-Zr, superconducting wire, coil simulation meas. of losses and instabilities 0-37050  
 Nb-Zr, acoustic phonon anomalies and superstructure, neutron inelastic scatt. meas. 0-19892  
 Nb<sub>2</sub>As, structural and supercond. props. press. effects 0-39700  
 NbB<sub>2</sub>, superconductivity below 1K 0-20342  
 NbC, electronic struct. of vacancies, effect on supercond. transition temp. 0-29347  
 NbC(N), critical temp. enhancement, surface effect on phonon spectrum and electronic state density (*Chinese*) 0-2507  
 Nb<sub>78</sub>Ga<sub>20-x</sub>Mn<sub>x</sub>, supercond. props., influence of Mn mag. impurities 0-54825  
 Nb<sub>80</sub>Ga<sub>20-x</sub>Mn<sub>x</sub>, supercond. props., influence of Mn mag. impurities 0-54825  
 NbGe<sub>2</sub>, superconducting transition temp. meas. of sputtered films and bulk 0-7019  
 Nb<sub>1-x</sub>Ge<sub>x</sub>, supercond., mag. field props. 0-54822  
 Nb<sub>2</sub>Ge A15 cpd., bulk modulus 0-7611  
 Nb<sub>2</sub>Ge, amorphous nongranular thin superconducting film, thermodynamic and resistive transitions 0-34571  
 Nb<sub>2</sub>Ge, and Nb<sub>0.82</sub>, structural and supercond. props. press. effects 0-39700  
 Nb<sub>2</sub>Ge, electron-lifetime effects on props. 0-10951  
 Nb<sub>2</sub>Ge, Nb<sub>2</sub>Ge<sub>3</sub> and NbO content, X-ray diffr. obs. 0-2515  
 Nb<sub>2</sub>Ge supercond. film, of high transition temp., US attenuation 0-49991  
 Nb<sub>2</sub>Ge supercond. thin films, He- and Ar-irradiated, X-ray diffr. studies 0-29503  
 Nb<sub>2</sub>Ge, superconducting A-15 type compounds, transition temp., radii ratio and structure (*Chinese*) 0-44752  
 Nb<sub>2</sub>Ge superconducting film, crit. temp. correl. with resist. relations and film struct. (*Russian*) 0-15646  
 Nb<sub>2</sub>Ge superconducting films, high critical temp., optimum sputtering conditions 0-15647  
 Nb<sub>2</sub>Ge superconducting films, quantitative Auger anal. 0-55740  
 Nb<sub>2</sub>Ge, superconducting thin films, energy gaps from tunnelling meas. 0-25050  
 Nb<sub>2</sub>Ge(Sn), optical props. and electron-phonon interactions 0-2510  
 NbN granular films, crit. current behaviour 0-15672  
 NbN preparation, by precip. from gaseous NgF<sub>3</sub>-N<sub>2</sub>-H<sub>2</sub> mixture 0-20857  
 Nb<sub>2</sub>S<sub>4</sub>, anisotropic superconductor, critical field and specific heat meas. 0-44779  
 NbSe<sub>3</sub>, Fermi surface, press. effects, supercond. transition at 3.5K 0-20068  
 NbSe<sub>3</sub>, transport props. 0-20175  
 NbSe<sub>3</sub>-Zr, dopant effect on supercond. transition temp. rel. to CDW 0-39699  
 NbSi<sub>3</sub>, superconducting transition temp. meas. of sputtered films and bulk 0-7019  
 Nb<sub>2</sub>Si, high  $T_c$ , supercond. props. from extrapolation of sp. ht. meas. on A-15 Nb-Si 0-25045  
 Nb<sub>2</sub>Si, metastable A-15 struct. synthesis by ion implantation, supercond. transition temp. 0-55319  
 Nb<sub>2</sub>Si, structural and supercond. props. press. effects 0-39700  
 Nb<sub>2</sub>Si, supercond., A15 film, electron beam evaporation 0-29284  
 Nb<sub>2</sub>Si, superconducting A-15 type compounds, transition temp., radii ratio and structure (*Chinese*) 0-44752  
 Nb<sub>2</sub>Sn, A-15 struct. Nb based superconductors, irradi. type influence on radiation defects 0-15093  
 Nb<sub>2</sub>Sn, alloying agent influence on struct. and supercond. props. (*Russian*) 0-39698  
 Nb<sub>2</sub>Sn, atomic displacements induced by radiation damage, X-ray study 0-2085  
 Nb<sub>2</sub>Sn, composite supercond., powder metallurgical prep. 0-2981  
 Nb<sub>2</sub>Sn, Cu admixture in Sn bath effect on critical current and stability temp. 0-7059  
 Nb<sub>2</sub>Sn, current carrying capacity increase by Hf addition 0-7056

## type II superconductors continued

- Nb<sub>2</sub>Sn, electron-lifetime effects on props. 0-10951  
 Nb<sub>2</sub>Sn fatigue effects in unidirectional composites, computer simulated model 0-35289  
 Nb<sub>2</sub>Sn films, deposition by quasi-closed vol. method, supercond. crit. temp. 0-15645  
 Nb<sub>2</sub>Sn, flux trapping and shielding capabilities in transverse fields 0-15667  
 Nb<sub>2</sub>Sn, high-current A-15 microcomposite material 0-44781  
 Nb<sub>2</sub>Sn, high-rate sputter-deposited, effect of oxygen on microstruct. 0-20343  
 Nb<sub>2</sub>Sn monofilamentary wires, supercond. crit. current density, bending effects 0-50018  
 Nb<sub>2</sub>Sn, multifilament conductors appl., production and props. (*German*) 0-3081  
 Nb<sub>2</sub>Sn, multifilament superconductor, pulsed mag. field losses and critical current densities 0-54853  
 Nb<sub>2</sub>Sn, O<sup>4+</sup> bombarded, Mossbauer studies 0-2672  
 Nb<sub>2</sub>Sn, supercond., thin film, US attenuation of SAWs 0-49988  
 Nb<sub>2</sub>Sn, superconducting thin films, energy gaps from tunnelling meas. 0-25050  
 Nb<sub>2</sub>Sn superconducting wire, fabrication from Cu-Nb-Sn alloy using controlled high temp. gradient 0-25056  
 Nb<sub>2</sub>Sn-Cu, high-current A-15 microcomposite material 0-44781  
 Nb<sub>2</sub>Sn film, critical currents due to microwave field 0-25058  
 Nb<sub>2</sub>(Sn-Al) system, X-ray spectroscopic studies of electronic struct. of A15 cpds. 0-2900  
 Nb<sub>2</sub>Su-Cu supercond. composites, fabrication, magnet appl. 0-11602  
 Nb<sub>1-x</sub>Ta<sub>x</sub>Sn<sub>2</sub>, supercond. transition temp. and upper crit. field 0-39723  
 NbTi, acoustic emission during flux jump 0-39724  
 NbTi, superconducting multifilamentary conductors, crit. current density, bending effects (*German*) 0-39727  
 (Nb<sub>0.99</sub>Ti<sub>0.01</sub>)<sub>1-x</sub>Ge<sub>x</sub>, supercond., mag. field props. 0-54822  
 Nb<sub>0.75</sub>Zr<sub>0.25</sub>, effect of force constant, disorder on Eliashberg function 0-29504  
 Nb<sub>0.7</sub>Zr<sub>0.3</sub>, supercond., US attenuation 0-44766  
 (Nb<sub>0.99</sub>Zr<sub>0.01</sub>)<sub>1-x</sub>Ge<sub>x</sub>, supercond., mag. field props. 0-54822  
 Pa, superconducting transition temp. and upper critical mag. field 0-44756  
 Pb/Bi-I-Al tunnel injected nonequilibrium supercond. struct., diffusive quasiparticle instability, multiple gap states 0-50005  
 Pb-In, containing Ag particles, flux pinning in superconducting matrix 0-2534  
 Pb-In, superconductive to normal transition due to external mag. fields, dynamic behaviour 0-39722  
 Pb-In (50 wt.%), supercond., pinning effect 0-15669  
 Pb-In-Ag, transport current distribution in longitudinal mag. field 0-25057  
 Pb-Sb, dynamic destruction of supercond. 0-2529  
 Pb-Sn Josephson junctions, small area high current density normal resistance, RC times 0-34555  
 PbMo<sub>6</sub>S<sub>8</sub>, temp. depend. of crit. currents 0-20363  
 PbMo<sub>6</sub>S<sub>8</sub>Gd<sup>3+</sup>, powder EPR spectra, cryst. field, supercond. energy gap 0-34769  
 PbMo<sub>6</sub>S<sub>8</sub>(Se<sub>3</sub>)(Te<sub>3</sub>), Chevrel phase correlation between struct. and supercond. transition temp. 0-7023  
 Pb<sub>1.125</sub>Mo<sub>6</sub>Se<sub>7.5</sub>, Chevrel phase supercond., NMR study 0-49989  
 Electron-phonon parameters and supercond. p-state pairing 0-25041  
 Pd-H(D), superconductivity and electron-phonon interaction 0-49975  
 PdH, supercond., book contrib. 0-25037  
 PdH<sub>0.97</sub>Fe(Cr), supercond. transition temp. depression, coexistent mag. behaviour 0-49976  
 PdH<sub>2</sub>(D), films, electron-phonon coupling, elec. cond. obs. 0-50011  
 Pd(M<sub>2</sub>Co), giant moments, Mossbauer study of <sup>57</sup>Fe 0-44969  
 PdZr, amorphous, supercond., US props. 0-44765  
 Rb<sub>0.33</sub>WO<sub>3</sub>, supercond. and special phonons, neutron scatt. obs. 0-15643  
 Rb<sub>2</sub>WO<sub>3</sub>, anisotropy in H<sub>2</sub> 0-6879  
 (SN)<sub>x</sub>, brominated, struct. and elec. props. 0-24914  
 (SN)<sub>x</sub>, Meissner effect, mag. susceptibility meas. 0-20351  
 (SN)<sub>x</sub>, supercond., fluctuation cond., crit. mag. fields 0-39712  
 (SNBr<sub>0.4</sub>)<sub>x</sub>, supercond. props., dimensionality 0-20344  
 Sb-Te, Al-type, superconductivity 0-29496  
 ScRu<sub>4</sub>B<sub>4</sub>, superconducting and crystallographic data 0-33968  
 SmRh<sub>2</sub>B<sub>4</sub>, coexistence of supercond. and antiferromag. order 0-11140  
 SmRh<sub>2</sub>B<sub>4</sub>, mag. ordered, persistence of supercond. 0-54834  
 Sn film, metastable current states, mean free path variation (*Russian*) 0-2538  
 Sn film, phonon-injection-induced destruction of supercond. 0-6956  
 Sn-Bi, crystal struct. and superconductivity after appl. of high press. and quenching 0-10531  
 Sn-Sb, Al-type, superconductivity 0-29496  
 Sn<sub>0.75</sub>Eu<sub>0.25</sub>Mo<sub>6</sub>S<sub>8</sub>, Chevrel phase supercond., spin-depairing interaction, Mossbauer obs. 0-25258  
 Sn<sub>1-x</sub>Ga<sub>x</sub>Mo<sub>6</sub>S<sub>8</sub>, heat capacity meas., singularities at low temp. 0-49985  
 SnMo<sub>6</sub>S<sub>8</sub>, Chevrel phase, RE mag. isolation and supercond. 0-44470  
 SnMo<sub>6</sub>S<sub>8</sub>Gd<sup>3+</sup>, powder EPR spectra, cryst. field, supercond. energy gap 0-34769  
 SnMo<sub>6</sub>S<sub>8</sub>(Se<sub>3</sub>), Mossbauer spectra 0-15926  
 SnMo<sub>6</sub>S<sub>8</sub>(Se<sub>3</sub>)(Te<sub>3</sub>), Chevrel phase correlation between struct. and supercond. transition temp. 0-7023  
 SnMo<sub>6</sub>Se<sub>8</sub>, Chevrel phase, RE mag. isolation and supercond. 0-44470  
 SrSi<sub>3</sub>, superconducting temperature depression due to mag. field 0-54820  
 Ta<sub>2</sub>N, superconductive to normal transition anisotropy 0-25031  
 TaGe<sub>2</sub>, superconducting transition temp. meas. of sputtered films and bulk 0-7019  
 TaS<sub>2</sub>, alkali metal and alkali metal hydroxide intercalates, lattice parameters, supercond. transition temps. 0-25029  
 TaSe<sub>3</sub>, phase transitions and elec. props. 0-20178  
 TaSe<sub>3</sub>, transport props. 0-20175  
 TaSi<sub>3</sub>, superconducting transition temp. meas. of sputtered films and bulk 0-7019  
 Tb<sub>1.2</sub>Mo<sub>6</sub>S<sub>8</sub>, low temp. heat capacity anomaly rel. to antiferromag. transition in supercond. state 0-25044  
 Tc film, supercond. transition, complex susceptibility 0-29495  
 Te-Fe dilute alloys, supercond. and mag. props. 0-29494  
 Te-Au film, supercond. by ion irradi. 0-34544  
 Te-I, Al-type, superconductivity 0-29496  
 Th-H system, supercond., book contrib. 0-25037  
 Th<sub>4</sub>H<sub>15</sub>, superconductivity and electron-phonon interaction 0-49975  
 Ti, transition temp., perturbative corrections, direct and indirect ladder diagrams 0-49979



**type II superconductors continued**

- Ti-V-Cr, electron-lifetime effects on props. 0-10951  
 Ti<sub>1-x</sub>Co<sub>x</sub>, electronic struct. and anomalies of elec. and mag. props. 0-6710  
 Ti<sub>1-x</sub>Ni<sub>x</sub>, electronic struct. and anomalies of elec. and mag. props. 0-6710  
 Ti<sub>2</sub>Mo<sub>2</sub>Se<sub>8</sub>, one dimensional supercond. crystal struct., resist. and upper crit. field 0-50016  
 Ti<sub>0.33</sub>WO<sub>3</sub>, supercond. and special phonons, neutron scatt. obs. 0-15643  
 α-U-Mo, dil., electronic properties depend. on 2<sup>1</sup>/<sub>2</sub>-th order phase transition under high press. (*Russian*) 0-11128  
 U<sub>2</sub>Pb<sub>1-x</sub>Mo<sub>6+y</sub>S<sub>8</sub>, sputtered supercond. props. 0-50019  
 V film, resist. supercond. transition 0-25033  
 V, fluxural oscillations in longitudinal mag. field, sound attenuation, magnetoelasticity (*Russian*) 0-54844  
 V, spin fluctuations effect on T<sub>c</sub>, from sp. ht. and mag. suscept. 0-7030  
 V/H, heat capacity and supercond. between 1.5 and 16K 0-2521  
 V-Sn(Al)(Ga)(Ge)(Si)-C, phase equil. and supercond. 0-50593  
 (V<sub>1-x</sub>Cr<sub>x</sub>)<sub>3</sub>Si, mag. susceptibility, 4.2 to 320K, density of states model 0-7035  
 V<sub>3-x</sub>Cr<sub>x</sub>Si, x=0 to 3, struct., supercond. and mag. props. 0-1962  
 V<sub>3</sub>Ga, high-current A-15 microcomposite material 0-44781  
 V<sub>3</sub>Ga, multifilament superconductor, pulsed mag. field losses and critical current densities 0-54853  
 V<sub>3</sub>Ga superconducting tape, stress effect on critical current (*Japanese*) 0-50020  
 V<sub>3</sub>Ga-Cu, high-current A-15 microcomposite material 0-44781  
 V<sub>3</sub>Ge, A-15 cpds., nucl. mag. relax. in normal and supercond. state 0-49993  
 V<sub>3</sub>Ge, anisotropic thermal vibrations, lattice const. X-ray study 0-34164  
 V<sub>3</sub>Ge, superconducting A-15 type compounds, transition temp., radii ratio and structure (*Chinese*) 0-44752  
 VN, electronic struct. of vacancies, effect on supercond. transition temp. 0-29347  
 VN<sub>0.74</sub> and VN<sub>0.89</sub>, low-temp. specific heat and superconducting critical temp. meas., density of states 0-54835  
 V<sub>1-x</sub>Pt<sub>x</sub>(Ga<sub>1-x</sub>Si<sub>x</sub>), A-15 cpds., nucl. mag. relax. in normal and supercond. state 0-49993  
 V<sub>3</sub>Si, d-spacing fluctuations above Martensitic phase transition 0-7570  
 V<sub>3</sub>Si, ion irradiated, influence on struct., resist., and supercond. transition temp. 0-54823  
 V<sub>3</sub>Si, normal, mixed and supercond. state, specific heat meas., thermodynamic and superconducting props. 0-49987  
 V<sub>3</sub>Si, optical props. and electron-phonon interactions 0-2510  
 V<sub>3</sub>Si, plastic deform. effect on supercond. props. 0-29500  
 V<sub>3</sub>Si, single crystals, supercond. tunnel characts. 0-7044  
 V<sub>3</sub>Si, superconducting thin films, energy gaps from tunnelling meas. 0-25050  
 V<sub>3</sub>Si, thermal expansion, 20-300°C, using differential push-rod dilatometer 0-39320  
 V<sub>3</sub>Si, US anomaly when cooled below martensitic and supercond. transition temps. 0-20354  
 V<sub>3</sub>(Si<sub>1-x</sub>C<sub>x</sub>), bulk, effect of C on supercond. transition temps. and microstructure 0-54824  
 (V<sub>1-x</sub>Ti<sub>x</sub>)Ge, pseudobinary A15 compound, supercond. transition temp. 0-49970  
 (Y,La)B<sub>6</sub>, superconducting transition temps., impurity effects 0-20341  
 Y<sub>1-x</sub>Gd<sub>x</sub>Rh<sub>2</sub>B<sub>4</sub>, mag. supercond., anomalous temp. depend. of upper crit. fields 0-29510  
 Y<sub>2</sub>Lu<sub>1-x</sub>Ir<sub>x</sub>B<sub>4</sub>, supercond., magnetism and metastability 0-29501  
 Y<sub>2</sub>Pb<sub>1-x</sub>Mo<sub>6+y</sub>S<sub>8</sub>, sputtered supercond. props. 0-50019  
 YRh<sub>2</sub>B<sub>4</sub>, supercond., anomalous cond.-electron polaris. 0-25047  
 Zr-V foil, rapidly quenched and heat treated, supercond. props. 0-54852  
 Zr<sub>2</sub>Be<sub>1-x</sub> noncrystalline alloy, phonon-electron scatt., superconducting temp. 0-54330  
 (Zr<sub>1-x</sub>Er<sub>x</sub>)<sub>3</sub>Rh, amorphous, influence of mag. ordering on supercond. props. 0-29511  
 Zr<sub>2</sub>Hf<sub>1-x</sub>V<sub>2</sub>, polycrystalline superconductor, resist. and mag. susceptibility, transition temp., temp. depend. 0-25113  
 ZrV<sub>2</sub>, C-15 struct., phase transitions, elec. cond., crystal lattice parameters (*Russian*) 0-54826

**U-centres**

- chalcogenide glasses, trap controlled transient photocond. 0-44641  
 KBr:Na, U-centres, HFS and g-factor, EPR spectra 0-39869  
 KCl:F (Br<sup>-</sup>)(I<sup>-</sup>), U-centres, local defect modes, Green's functions calcs. 0-44280  
 KCl:H, dichroic H- and U-centres by polarised bleaching of interstitial H 0-29766  
 KCl:KH, F- and U-centre redistrib. at end of proton tracks, microspectrophotometric anal. 0-10583  
 KCl(Br)(I), U<sub>2</sub> and U<sub>1</sub> centres, optical excitations 0-2803  
 LiF:OH crystals, X-irradiated, H centres formation and annealing 0-54226  
 NaBr-U-centre containing cryst., X-ray radiation induced cation vacancy generation 0-39078  
 NaCl:Li, U-centres, HFS consts., g-factor, EPR spectra 0-39869  
 NaCl(Br)(I), U<sub>2</sub> and U<sub>1</sub> centres, optical excitations 0-2803  
 RbCl:Na, U-centres, HFS consts., g-factors, EPR spectra 0-39869

**UBV photometry see stellar photometry****u.h.f. amplifiers see ultra-high-frequency amplifiers****u.h.f. tubes see ultra-high-frequency tubes****ultimate tensile strength see tensile strength****ultra-high-frequency amplifiers**

- GaAs FET amplifier, varactor-tuned, for UHF SQUID magnetometer 0-31814

**ultra-high-frequency tubes****see also microwave tubes**

No entries

**ultracentrifuges see centrifuges****ultrafiltration see filtration****ultrasonic absorption**

- adhesive bonds, transducer materials and adhesives for high temp. US generation 0-43586  
 animal tissues, freshly excised, attenuation and backscatt. obs. 0-51148  
 attenuation, of US main waves with distance 0-5859  
 austenitic steels at large strain amplitudes 0-19192  
 benzene-similar liquids, 10 to 1300 MHz 0-39229  
 blood, canine, US attenuation and speed, rel. to packed cell vol., 37°C 0-41106

**ultrasonic absorption continued**

- brain, normal and abnormal, attenuation, vel. and impedance 0-45955  
 breast cancer connective tissue content correl. with US attenuation 0-45997  
 breast malignant tumour, freq. depend. US attenuation, fast Fourier transform technique 0-45996  
 n-butanol-water-Ca (SCN)<sub>2</sub> system with hypercrit. point, US absorpt. 0-49306  
 N-n-butoxybenzylidene-n-butylaniline, US propag. near nematic-smectic A transition, mag. field effect 0-39266  
 o-chloroaniline-iso-octane, crit. system, comp. depend. of absorpt., US obs. (*German*) 0-19879  
 o-chloroaniline-n-heptane, crit. system, comp. depend. of absorpt., US obs. (*German*) 0-19879  
 dislocation internal friction in high-dislocation density crystals (*Russian*) 0-34146  
 ferromagnet, planar, US attenuation, spin-phonon coupling, magnons and magnetostriction contrib., calc. 0-34611  
 ferromagnet, pure and random uniaxial with dipolar interaction, US attenuation 0-11239  
 glass filled solids, ultrasonic absorpt., scatt., velocity and attenuation 0-44262  
 heterocyclic liquids, 10 to 1300 MHz 0-39229  
 human tissue, transmission of US beams, focusing and attenuation studies 0-45948  
 isobutyric acid-water, crit. mixture, conc. fluctuation mean relax. time, US absorpt. and vel. meas 0-29163  
 LF absorpt. in liquids at 500 kHz, determination using reverberation technique 0-38197  
 liquid, weakly assoc., US wave reson. absorpt. 0-34141  
 liquid containing gas bubbles, investigation using acoustic streaming 0-5863  
 liver tissue, attenuation coefficient slope statistical estimation from refl. US signals 0-46000  
 MBBA, pure and mixed with benzene (chlorobenzene), nematic-isotropic transition, US absorpt., visual hysteresis 0-54355  
 MBBA/EBBA binary liquid crystal mixture, US absorpt. and vel. dispersion, phase transition and alignment effects (*Korean*) 0-29121  
 measurement, pulse echo method, minicomputer program control (*Japanese*) 0-53587  
 methane, liquid, Brillouin scatt. obs., US vel. and absorpt. 0-45085  
 3-methylpentane-nitroethane crit. mixture, dynamical scaling for sound propag. 0-49305  
 micellar solutions, US absorpt. 0-45571  
 myocardium, acoustic microscopic anal. 0-45995  
 myocardium, normal and ischaemic, US attenuation 0-45954  
 nitrobenzene-n-heptane, crit. mixture, conc. fluctuation mean relax. time, US absorpt. and vel. meas 0-29163  
 nitroethane-isoctane, crit. mixture, conc. fluctuation mean relax. time, US absorpt. and vel. meas 0-29163  
 oil-polymer mixture, acoustic attenuation CW meas., tissue simulation appl. 0-35961  
 one-dimensional antiferromagnet, interchain coupling, effect on US attenuation 0-19880  
 piezoelectric semiconductor, polarisation of Maxwell-Wagner relaxation oscillators 0-44670  
 poly(4-methyl pentene-1), US props., glass transition, Gruneisen parameters 0-54316  
 polycrystalline materials, freq. and grain size dependency of US attenuation 0-50783  
 polyethylene, glass filled solids, ultrasonic absorpt., scatt., velocity and attenuation 0-44262  
 polypeptides, in aq. poly(L-glutamic acid) soln., helix-coil transition, US relax. times 0-45849  
 polyvinylidene fluoride, US transducers, dielec. and acoustic losses 0-48541  
 PVAC dispersions, US method of determining plasticiser content (*German*) 0-21257  
 quartz, US absorption, influence of plastic deform. and electrostatic field (*Russian*) 0-39226  
 rare earth alloys and intermetallic cpds., US attenuation, temp. and mag. field depend. 0-15195  
 resonance absorption of ultrasound by moving dislocation 0-54318  
 sand, fluid-saturated, viscous attenuation 0-33307  
 Schaaffs' molecular-kinetic theory of propag. in liquids, temp. and pressure changes of 'collision factor' 0-19143  
 semiconductors, narrow band gap, superlattices, acoustic wave absorpt. and amplification 0-29445  
 steel, plain C, type 304 and type 316 stainless, fatigue damage indicators, non-destructive 0-25932  
 thiophene, meas. of absorpt. coeff. in 10-60 MHz range, existence of vibrational relaxation 0-33377  
 tissue, mammalian, survey of US vel. and attenuation data 0-46744  
 tissue, mammalian, US attenuation and speed determ. as function of temp. 0-41108  
 tissue, possible mechanisms 0-45951  
 tissue, soft, attenuation 0-45952  
 tissue, soft, attenuation vs. frequency 0-45956  
 tissue, temp. and freq. dependence 0-45949  
 tissue characterization in vivo by differential attenuation measurements 0-45999  
 tissue US backscatter and attenuation distrib. mapping, digital reconstruction 0-51188  
 tissues, fixed and unfixed, US propagation, backscattering coeffs. and speech determ. 0-41109  
 tissues, mammalian, US absorpt. and attenuation determ. by thermoelectric method 0-41110  
 uniaxial ferroelectric, acoustic attenuation near transition point 0-11350  
 US relaxation of aqueous mixtures of methanol and ethanol (*French*) 0-6468  
 vinyl chloride, time-dependent spectra at 1 MHz for various polymerisation conditions 0-33299  
 vinyl-series polymer solutions, longitudinal US waves absorption 0-15192  
 Ag film, damping and vel. of longit. elastic waves at 9.4 GHz 0-10596  
 Al, dislocation and point defect interactions, US study under quasistatic stress (*French*) 0-2061  
 β-Al<sub>2</sub>O<sub>3</sub>-Na<sub>2</sub>O, non-stoichiometric, amorphous, US attenuation and velocity 0-39228  
 As, amorphous, US attenuation and sound vel. meas., 4.2 to 300K; 0-49308  
 As<sub>2</sub>S<sub>3</sub>, amorphous, shear wave attenuation 0-11027



**ultrasonic absorption continued**

- Au film, damping and vel. of longit. elastic waves at 9.4 GHz 0-10596  
 Bi, US attenuation in strong mag. fields, electron-hole correlation effects 0-11049  
 CHCl<sub>3</sub> and C<sub>2</sub>H<sub>5</sub>OH and mixtures, velocity and damping of ultrasound 0-29120  
 CO, liquid, Brillouin scatt. obs., US vel. and absorpt. 0-45085  
 CdCl<sub>2</sub>, aq. solns., sound absorpt. and relax. phenomena 0-49311  
 CdS, photoconductive, obs. of high intensity sound self-defocusing 0-24972  
 Cr film, damping and vel. of longit. elastic waves at 9.4 GHz 0-10596  
 CsNiF<sub>3</sub>, planar ferromagnet, US attenuation, spin-phonon coupling, magnons and magnetostriction contrib., calc. 0-34611  
 Cu film, damping and vel. of longit. elastic waves at 9.4 GHz 0-10596  
 Cu, HF ultrasound, viscous and relax. components of dislocation attenuation 0-15196  
 Fe<sup>2+</sup>Fe<sub>0.75</sub><sup>3+</sup>Cr<sub>0.25</sub><sup>3+</sup>O<sub>4</sub>, acoustic props. rel. to cooperative Jahn Teller effect and structural phase transform 0-24538  
 GaAs:Cr<sup>3+</sup>, dynamic Jahn-Teller effect, relaxation time for reorientation 0-6798  
 p-H<sub>2</sub>, rotational 0-2 transaction cross-sections (*Russian*) 0-32812  
 He HCP crystals, US attenuation, dislocation damping 0-24711  
 He, liq., λ point, US absorption, dynamic scaling 0-44380  
 In film, damping and vel. of longit. elastic waves at 9.4 GHz 0-10596  
 In, intermediate state, doping effect on US attenuation 0-2522  
 In, US attenuation in supercond. and normal state in transverse mag. field and zero field 0-54836  
 In-Sn, dil., intermediate state, doping effect on US attenuation 0-2522  
 KMnF<sub>3</sub>, dynamic scaling and US attenuation at structural phase transition 0-44260  
 K<sub>2</sub>Pt(CN)<sub>4</sub>Br<sub>3</sub>·3H<sub>2</sub>O, spin-lattice model for elastic anomalies 0-15179  
 Kr, liq., US attenuation and bulk viscosity 0-49304  
 (La,Gd)Al<sub>3</sub>, normal and supercond. state, US attenuation, freq. depend. and mechanisms 0-49992  
 LiCl in H<sub>2</sub>O, complexity investigation using US method 0-33326  
 Li<sub>2</sub>GeO<sub>3</sub>, acoustic props., intrinsic piezoeffect, US absorpt. coeffs. (*Russian*) 0-29692  
 N<sub>2</sub>, liquid, Brillouin scatt. obs., US vel. and absorpt. 0-45085  
 NaNO<sub>2</sub>, incommensurate-and-antiferroelectric phase transition, amplitude mode, ultrasonic study 0-39227  
 Nb<sub>3</sub>Sn, supercond., thin film, US attenuation of SAWs 0-49988  
 Nb<sub>2</sub>Zr<sub>80</sub>, supercond., US attenuation 0-44766  
 Ni film, damping and vel. of longit. elastic waves at 9.4 GHz 0-10596  
 NiCr<sub>2</sub>O<sub>4</sub>, acoustic props. rel. to cooperative Jahn Teller effect and structural phase transform 0-24538  
 Ni<sup>2+</sup>Fe<sub>0.75</sub><sup>3+</sup>V<sub>0.25</sub><sup>3+</sup>O<sub>4</sub>, acoustic props. rel. to cooperative Jahn Teller effect and structural phase transform 0-24538  
 O<sub>2</sub>, liquid, Brillouin scatt. obs., US vel. and absorpt. 0-45085  
 P, amorphous, US attenuation and sound vel. meas., 4.2 to 300K; 0-49308  
 PdSiCu, amorphous, US attenuation and vel. studies 0-19881  
 Rb<sub>2</sub>ZnCl<sub>4</sub>, US velocity and attenuation, around normal-incommensurate phase transition 0-40072  
 SO<sub>2</sub>, liq., vibr. relax., US absorpt. and vel. meas. 0-34147  
 Sb, dislocation internal friction changes due to high-amplitude US oscills. (*Russian*) 0-10556  
 Si, amorphous sputtered thin film, US anomalies, 0.5-300K 0-34145  
 SiO<sub>2</sub>, and SiO<sub>0.7</sub>, amorphous sputtered thin film, US anomalies, 0.5-300K 0-34145  
 V-Ti (42 at.%), mixed state, US attenuation meas. at 4.14K 0-15657  
 V<sub>2</sub>Si, US anomaly when cooled below martensitic and supercond. transition temps. 0-20354  
 YAG: rare earth metal, US absorpt. meas., relax. model 0-24539  
 ZnCl<sub>2</sub> in H<sub>2</sub>O, complexity investigation using US method 0-33326

**ultrasonic applications**

- see also biomedical ultrasonics; ultrasonic materials testing; ultrasonic welding*  
 acoustic holography system, Sonoscan using microprocessor 0-38184  
 acoustic imaging, electric coupling effects in transducer array 0-43587  
 air jets, free and constrained, acoustic emission, gas leak detection conditions 0-5895  
 biological surgery, severing corpus callosum in rats 0-26306  
 blood flowmeters, design considerations 0-23853  
 bubble detect. and meas. in liquids, blood appls. (*Japanese*) 0-1712  
 cinefilm cleaning system using focused ultrasonic energy source 0-31916  
 cleaning by chlorine solvents, US cavitation intensity measurement (*Polish*) 0-38464  
 colloid submicron particle size measurement, ultrasonically induced birefringence technique 0-30290  
 fluid flow meas. by contactless techniques (*Italian*) 0-53891  
 imaging techniques (*Japanese*) 0-19190  
 level detection appl. 0-27268  
 liquid cavitation technique for cleaning cinefilm 0-31918  
 liquid crystal film, imaging of US in air 0-38166  
 microbiology, status and problems of methods used 0-21592  
 mobility aid for blind people 0-56290  
 monitoring of local phase transitions during vinyl chloride polymerisation 0-33299  
 military appls., multilayered tape for perimeter warning device for combat troops 0-19200  
 photodetector metrological certification, using acoustooptical modulators 0-23727  
 pseudorandom signal-correlation system 0-43547  
 signal processing in ultrasonics, conf., London, England, Jan. 1980 0-33351  
 through-water diver communication system Wet-Phone, voice or switch operated, 31.5 KHz carrier, 1350 m range 0-38187  
 UNIPAN 545 thickness gauge, with digital readout 0-47019  
 vibration systems, appl. in power ultrasonics (*Chinese*) 0-43568  
 ZnO<sub>2</sub> powders, stabilised, for plasma spray-coatings 0-20869  
 Nd:glass laser with US modulated emission 0-48309

**ultrasonic delay lines**

- chirp transform processors using US strip dispersive delay lines, implementation 0-53577  
 piezoelectric vibrators, elec. steered line array, US probe characts. 0-35486  
 SAW, combined triple-transit and bulkwave suppression 0-53565  
 SAW, physical props. and communication signals processing applications and devices 0-38162  
 SAW and optical signal processing techniques compared 0-48173

**ultrasonic delay lines continued**

- SAW delay line filters, wideband, low insertion loss, VHF band 0-28398  
 SAW delay line signal processors using acousto-optic interactions, real time system 0-28384  
 SAW devices, appls. of amorphous magnetic-layers 0-28389  
 SAW dispersive delay lines, new cut of quartz for temperature stability 0-19185  
 shallow bulk acoustic wave delay line filters, narrowband and wideband implementations 0-28400  
 trimming using stroboscopic method of signal-to-time conversion 0-19191  
 two-phase PSK modulator employing SAW delay line, fundamental performance 0-33398

**ultrasonic devices**

- see also ultrasonic delay lines; ultrasonic transducers*  
 distance measuring device with decremental acquisition of the measuring results (*German*) 0-19199  
 flow meter for liquids (*Spanish*) 0-6181  
 fluid flow measurement 0-1710  
 image processing device status and prospects 0-48446  
 liquid-crystal film for US visualisation 0-5893  
 mobility aid for blind people 0-56290  
 planar reflector in interior/on surface of test objects, characts. (*German*) 0-43569  
 Splay-VM, automated US device for inspecting hollow extruded profiles 0-7747  
 thermometer, high temp., based on sound velocity temp. depend. 0-52202

**ultrasonic diffraction**

- caustics in non destructive evaluation, diffraction at crack like defects 0-43680  
 nonperiodic wave diffr. anal. (*French*) 0-48486  
 penny-shaped cracks in metals, theory and expt. 0-33267  
 surface wave diffraction, expt. and anal. 0-5898

**ultrasonic dispersion**

- liquid, weakly assoc., US wave reson. absorpt. 0-34141  
 Ag<sub>3</sub>SbS<sub>3</sub>, electron absorption and dispersion of ultrasound velocity 0-15197  
 Si, amorphous sputtered thin film, US anomalies, 0.5-300K 0-34145  
 SiO<sub>2</sub>, and SiO<sub>0.7</sub>, amorphous sputtered thin film, US anomalies, 0.5-300K 0-34145

**ultrasonic effects**

- air flow through capillary under action of ultrasound 0-6149  
 bioeffects of pulsed US 0-51155  
 bone regeneration, morphology, effect of US 0-41111  
 bubble layers in liquids, struct. of pressure pulses 0-38479  
 cavitation, production of pressure and light impulses (*French*) 0-33297  
 cavitation-induced capillary waves in US atomization 0-33328  
 holographic interferometry used in US field investigations, theoretical analysis of light intensity distrib. 0-32903  
 liquid dielectric breakdown influence of US excitation 0-15964  
 liquid He, subharmonic responses 0-33327  
 liquid light diffraction, Fresnel approx. 0-48135  
 liquid vibration 0-43559  
 magnon kinetic eqns. in parametric ultrasonically excited ferromagnets 0-44820  
 metals, erosion accompanying simultaneous action of laser emission and ultrasound (*Russian*) 0-7442  
 Mossbauer effect, ultrasonic excitation, phase effects 0-55004  
 plant root growth, cavitation as mechanism for effects 0-21489  
 platelet aggregation induced by US under specialised conditions in vitro 0-45963  
 polycapromamide, US degradation in H<sub>2</sub>SO<sub>4</sub> soln. 0-15191  
 protein synthesis in human fibroblasts in vitro, US stimulation, role of cavitation 0-8100  
 root meristem cells of Pisum sativum, increased G<sub>2</sub> duration after sonication obs. 0-56117  
 suspensions, changes in physical props. 0-23825  
 tumour irradiation with intense US, hamster 0-8099  
 US hardening kinetics rel. to dislocations 0-50644  
 Al, US hardening kinetics rel. to dislocations 0-50644  
 Al-Li (2.8 wt.%), ageing in US field, precip. hardening (*Russian*) 0-29968  
 BaTiO<sub>3</sub>-based nonpiezoelectric ceramic, acoustic convolution in paraelectric phase 0-6467  
 Bi<sub>95.6</sub>Mn<sub>4.4</sub>, magnetisation of ferromag. precipitates, effect of ultrasonic pulses 0-2121  
 Cu, US hardening kinetics rel. to dislocations 0-50644  
 Cu-Ti (3.5 wt.%), aged by US strain, struct. and props. (*Russian*) 0-21003  
 Fe, US oscillatory stress superimposition effects on deformation 0-35287  
 Fe-Si (3 wt.%), US oscillatory stress superimposition effects on deformation 0-35287  
 KCl, US plastic deform., dislocation struct. 0-19809  
 Mg, dislocation struct. after US deform. (*Russian*) 0-29027  
 Mg, US hardening kinetics rel. to dislocations 0-50644  
 MgSO<sub>4</sub>, soln., electrolytic cond. dispersion, 1-6 MHz, caused by US propagation. 0-44343  
 Ni, acoustic hardening, influence of US treatment temps. and material purity (*Russian*) 0-11656  
 Ni, electrical resistance in DC mag. field after ultrasonic deform. (*Russian*) 0-54671  
 Ni-Cr-Ti(Al), effect of ultrasound on crystallisation, dendritic structure, and plasticity (*Russian*) 0-11637  
 Zn, US hardening kinetics rel. to dislocations 0-50644

**ultrasonic equipment**

- acoustic lens-design with elliptic surfaces 0-48530  
 amplifier for directly driving solid-dielectric capacitance speakers 0-19186  
 array system, computer-controlled, acoustic beam steering and focusing, with variable frequency array transducers 0-38191  
 beamformer with programmable time delay and sum 0-53592  
 biomedical imaging system, CCD devices appl. in electronic focusing 0-56148  
 boxcar integrator/US recording unit using sample-and-hold circ., for student lab. 0-27083  
 combination probe for US flaw detect. 0-35492  
 computed tomography of breast, progress 0-51196  
 digitiser/processor for extraction of clinical parameters from Doppler-shift waveforms 0-36042  
 dynamic imaging, high resolution 0-17042  
 echo probes, flexible, and prospects for use in oncology 0-56147



**ultrasonic equipment continued**

- flowmeter, propagation time of acoustic signal 0-6175
- gating device, beam width, position and direction control 0-38192
- holography, US-field display device with transducer and LED linear arrays 0-23843
- LMFBR Na flow meas. using US flowmeter 0-32412
- mean frequency Doppler modulator performance, blood flow meas. appl. 0-45991
- pulse spectroscopy method, investigation apparatus 0-35483
- remote control circuit using US transducer 0-10097
- scanners, ceiling suspension 0-30815
- Splav-VM, automated US device for inspecting hollow extruded profiles 0-7747
- tissue analysis, comprehensive system 0-51189
- underwater, for biological object vel. measurement, design principles 0-19195
- UNIPAN 545 thickness gauge, with digital readout 0-47019
- US temp. profiling system for critical heat flux meas. of nuclear reactor fuel assembly 0-37032
- US velocity and damping coeff. meas. of polymers (French) 0-7723

**ultrasonic materials testing**

- acoustic emission, principles of technique and measuring instrums. 0-28375
- acoustic emission appl. 0-11854
- acoustic emission detection for small components production testing, review 0-16632
- acoustic emission techniques, improvement in noise immunity 0-21213
- acoustic microscopes, nondestructive material testing appls. 0-48537
- acoustic microscopy appl., scanning 0-16612
- annular array search units, potential appl. in conventional US testing systems 0-35446
- applications in medicine, seismology and communications 0-21198
- attenuation, of US main waves with distance 0-5859
- austenitic stainless steel weld metal, US propag. 0-45452
- axial resolution, of US testing by signal processing (German) 0-7736
- beam control, defect classification and reconstruct. by phased arrays (German) 0-35448
- bone, human, acoustic emission in restressing 0-3704
- caustics in non destructive evaluation, diffraction at crack like defects 0-43680
- combination probe for US flaw detect. 0-35492
- composite materials, fracture, elastic mismatch and interfacial bonding influence 0-40506
- concrete analyser, pulse velocity method 0-45472
- crack propagation, and prepack damage study with US attenuation 0-40656
- crack-like flaw identification and crack parameter determ. in US testing (German) 0-50794
- CrMoV, surface coating to prevent oxidation during high temp. AE 0-16539
- defect coordinate determ. by calibration of AE method 0-35473
- defect coordinates, in anisotropic cylindrical shell with aid of stress waves emission 0-3282
- Doppler effect, nonstationary, freq.-phase methods of investig., control of production processes 0-45464
- fatigue testing of different materials with equivalent vibration charact. 0-11847
- fault location, foreshortened projected distance concept (German) 0-16625
- ferrites, void, conc. and dimensions determ. by acoustic charact. 0-35472
- fibre reinforced composites, US diagnosis of elastic characts. and struct. parameters 0-40663
- fibre reinforced plastic laminates, US evaluation of hygrothermal effects 0-7730
- filled polymers, US study of internal damage, nonlinear elastic effects, theory 0-49307
- flaw detection, high temp. long duration US transducer tests 0-43586
- flaw detection in thin-sheet objects, based on variational method used in dynamics of irregular solid waveguides 0-5857
- flaw detector, automatic, for butt welds (Japanese) 0-25976
- flaws, size and shape meas. by US spectrum method 0-7745
- flaws, size and shape meas. method of ultrasonic spectrum pt.II 0-7746
- glass fibre reinforced plastic, filament wound tube, US defect detection 0-7734
- heterogeneous duplex grain structure in 304 austenitic stainless steel, US spectroscopy 0-30204
- holographs, for analysing methods of adjusting impedance inspection units 0-7744
- impedance method, variations, methods of treating information and adjusting apparatus 0-7743
- Inconel, cracks under pressure vessel cladding, detection, causes, danger 0-52760
- isotropic materials, third-order elastic moduli meas. using Rayleigh waves (Russian) 0-50786
- light optical imaging, of focused US field (German) 0-3275
- metallic materials, deformation process, stage-by-stage nature investigation using acoustic emission (Russian) 0-40434
- metals, coarse grained structure, US inspection, structural reverberation interference 0-45456
- metals, mechanical props., testing and modelling 0-25811
- microscopy, with microwave freq., determ. of mech. props. of materials 0-48535
- multiparameter system for investigating high-power US effects on metals 0-7742
- NDT probe array using 4 transducers 0-35499
- nuclear power plant system, optimisation with regard to design, materials and testing (German) 0-42739
- nuclear reactor pressure vessels, US pulses propag. by means of acoustic emission (German) 0-3274
- oxide coating, thermal sprayed, AE study of porosity 0-25927
- piezoelectric transducer, thick, operating as radiator or receiver, performance characts. 0-35484
- piezoelectric transducers, energy and spectral evaluations of broadband excitation 0-35485
- piezoelectric transducers, surface-driven, input impedance calc. 0-35493
- piezoelectric vibrators, elec. steered line array, US probe characts. 0-35486
- polycrystalline materials, freq. and grain size dependency of US attenuation 0-50783

**ultrasonic materials testing continued**

- polymeric materials, inelasticity degrees estimation, hysteresis friction model appl. rel. to US testing 0-3136
  - polymers, US velocities and damping coeff. meas. (French) 0-7723
  - polymers, using fast longitudinal and shear wave techniques 0-50793
  - pulse delay time calculation for testing of industrially produced substances (German) 0-3280
  - pulse echo techniques for locating flaws in metal components (French) 0-55613
  - pulse spectroscopy method, investigation apparatus 0-35483
  - pulse-echo systems, improved sensitivity using pseudo-random binary-code phase-modulated signals 0-38182
  - radial-bolt-hole cracks in mechanically fastened aircraft structs., measurement of size using Doppler shift 0-55597
  - reflection pattern interpretation, error analysis (German) 0-45470
  - refraction angle of sound waves produced by angle probe, temp. depend. 0-55618
  - rubber gasket inspection system, gas pipe appl. 0-30178
  - scanning laser acoustic microscope applications (German) 0-3271
  - sealed radioactive sources, US leak and surface contamination tests (Czech) 0-27846
  - separable combination scanner, macrostruct. inspection of rolled bars 0-45457
  - spherical voids, elastic wave scatt. at long wavelengths 0-48480
  - Splav-VM, automated US device for inspecting hollow extruded profiles 0-7747
  - steel, austenitic, optimum freq. for US testing (German) 0-30195
  - steel, austenitic stainless, pipe welds, US inspection pattern recognition reflector classification feasibility study 0-16615
  - steel, austenitic stainless, US fatigue meas. 0-40489
  - steel, austenitic welds, US longitudinal wave examination 0-50784
  - steel, C, EM excitation of US 0-33412
  - steel, inclusion cleanliness, US meas. 0-25978
  - steel, phase conversion kinetics, exam. using ultrasonic method, apparatus design 0-21203
  - steel, plain C, type 304 and type 316 stainless, fatigue damage indicators, non-destructive 0-25932
  - steel, plastic deform. effect on third-order elastic moduli, dislocation anharmonism (Russian) 0-50786
  - steel, rail, AE use for mech. tests 0-35467
  - steel, stainless, cracks under pressure vessel cladding, detection, causes, danger 0-52760
  - steel, stainless austenitic welds, time domain approach to crack location and sizing 0-50781
  - steel, strength, acoustic monitoring 0-35479
  - steel, temp. depend. of elastic, moduli US obs. (Japanese) 0-25750
  - steel 20, deformation process, stage-by-stage nature investigation using acoustic emission (Russian) 0-40434
  - steel pressure vessel plates, PISC trials result 0-52746
  - steel products, hot thick, US inspection system 0-40661
  - stell, austenitic stainless, deformation process, stage-by-stage nature investigation using acoustic emission (Russian) 0-40434
  - stress measurement, calibration expt. results (German) 0-53725
  - surface defects in metals estimation, Rayleigh wave scattering technique (French) 0-55612
  - surface wave scatt. from elliptical cracks for failure prediction 0-55608
  - techniques for engineers, interpretation of reflection patterns in tube thickness meas. (German) 0-35451
  - thermoelastic expansion flexible acoustic probe 0-16618
  - transducer performance, theoretical anal. 0-30176
  - visualisation of US propag. in solids, for NDT 0-22424
  - weld joints, austenitic, practical appl. of US testing 0-40655
  - weld monitoring, in-process, with acoustic emission 0-16620
  - Ag, granular thin film, adhesion measurement 0-50807
  - Al alloys, fatigue, microcrack development, acoustic SHG study 0-35440
  - Al, surface wave scatt. from elliptical cracks for failure prediction 0-55608
  - Al<sub>2</sub>O<sub>3</sub>, crack detection caused by thermal shock, AE technique (Japanese) 0-21248
  - C fibre reinforced plastic, deform. and failure using AE method (Russian) 0-40630
  - C fibres, durability, elastic props. and struct., heat treatment temp. effect, US meas. methods 0-40446
  - M-1Cu, deformation process, stage-by-stage nature investigation using acoustic emission (Russian) 0-40434
  - GaAs, during deformation, acoustic emission rel. to cracks, dislocations 0-35441
  - MgO and MgO-dolomite, crack detection caused by thermal shock, AE technique (Japanese) 0-21248
  - Nb-H system, temp.-stimulated acoustic emission, hydride precip. 0-3044
  - Ni, electrical resistance in DC mag. field after ultrasonic deform. (Russian) 0-54671
  - Si<sub>3</sub>N<sub>4</sub>, hot pressed, surface wave scatt. from elliptical cracks for failure prediction 0-55608
- ultrasonic measurement**
- see also *ultrasonic velocity measurement*
  - aortic haemodynamics meas. in humans using US pulsed Doppler transoesophageal method 0-30808
  - arc-welding seam defectoscope (Russian) 0-43564
  - biological object vel. measurement, underwater, design principles of instrums. 0-19195
  - biomedical crown rump length meas., comparison of methods 0-45992
  - blood flow, quantitative meas. by pulsed Doppler technique 0-45990
  - blood flow echography using Doppler techniques (French) 0-26303
  - blood flow velocity profiles, US MTI meas. 0-36033
  - composite torsional quartz transducer for shear US measurements of aqueous liquids 0-53599
  - distance measuring device with decremental acquisition of the measuring results (German) 0-19199
  - echography for medical diagnosis (French) 0-26305
  - field intensity meas. using wideband piezoelectric convertors (Russian) 0-38209
  - field meas. by optical holography 0-14532
  - flaw detection in metal components by pulse echo techniques (French) 0-55613
  - flow measurement, microcomputer-controlled 0-24111
  - flowmeter, 240 Clampitron, applicability study 0-24108
  - flowmeter, Danfoss, using electronic unit and piezoelectric transducers 0-6172
  - level detection 0-27268



**ultrasonic measurement continued**

- LMFBR Na flow meas. using US flowmeter 0-32412
- nuclear reactor steam generator duplex tubing 0-32379
- optical-acoustic probing of heterogeneous condensed media 0-38211
- single transducer swept frequency ultrasonic reflection measurements 0-14534
- surface characterisation meas. of randomly rough surfaces by US backscatter at normal incidence (*French*) 0-52165
- surface defects in metals estimation, Rayleigh wave scattering technique (*French*) 0-55612
- tissue characterisation, US propag. parameter meas. 0-45953
- transcutaneous blood flow measurements using pseudorandom noise Doppler system 0-36035
- US Doppler spectragrams refreshed display and haemodynamic parameter meas. 0-41152
- vortices in wind tunnel expts. meas. using US pulses 0-10334
- UF<sub>6</sub> vibrational relaxation, ultrasonic meas. in UF<sub>6</sub>-Ar-N<sub>2</sub> mixtures 0-1050

**ultrasonic paramagnetic resonance** *see acoustic paramagnetic resonance***ultrasonic propagation**

- see also ultrasonic diffraction; ultrasonic dispersion; ultrasonic reflection; ultrasonic refraction; ultrasonic relaxation; ultrasonic scattering; ultrasonic transmission*
- biological tissue, phase and amplitude fluctuations 0-8097
- breast tissue, US ref. index and attenuation images 0-17036
- N-n-butoxybenzylidene-n-butylaniline, US propag. near nematic-smectic A transition, mag. field effect 0-39266
- cloud of isotropic scatterers, air bubbles in water appl. (*French*) 0-53507
- Doppler effect, nonstationary, freq.-phase methods of investig., control of production processes 0-45464
- human tissue, transmission of US beams, focusing and attenuation studies 0-45948
- liquids with vapour bubbles 0-33661
- liquids with very low US propag. velocities for use in biomedical optical computer 0-28392
- marine sediments, penetration as function of physico-mech. characts. (*French*) 0-33324
- metals, anomalous sound propag. by cond. electrons 0-11048
- mixtures and suspensions, flow rate meas., ultrasound propagation and scatt. approach 0-43806
- multiple nomogram for US propag. calcs. 0-28371
- nonlinear US fields in air, numerical representation, microphone signal example (*French*) 0-53521
- nonlinearity in free progressive waves at 20 kHz 0-33394
- rotation of US plane of polarisation under ESR saturation conditions 0-29123
- Schaaffs' molecular-kinetic theory of propag. in liquids, temp. and pressure changes of 'collision factor' 0-19143
- skeletal muscle fibre orientation, US attenuation meas. 0-30763
- solid layer-liquid system 0-31522
- steel, austenitic welds, US longitudinal wave examination 0-50784
- steel, stainless austenitic welds, time domain approach to crack location and sizing 0-50781
- superconductor, nonequilib., hypersound enhancement (*Russian*) 0-34552
- thermoelastic material, deformed isotropic, thermal effect on acoustoelasticity 0-33276
- tibial bones, of highly trained athletes phys. stress effect type as measured by US techniques 0-16992
- tissue, mammalian, survey of US vel. and attenuation data 0-46744
- tissue characterisation, US propag. parameter meas. 0-45953
- tissue characterisation, US propag. props. 0-45950
- visualisation of US propag. in solids, for NDT 0-22424
- C fibres, durability, elastic props. and struct., heat treatment temp. effect, US meas. methods 0-40446
- KMgF<sub>3</sub>, elastic moduli, press. and temp. depend., US technique 0-6453
- LiNbO<sub>3</sub>, crystals, elec. field influence on hypersonic wave propag. 0-44668
- LiTaO<sub>3</sub>, crystals, elec. field influence on hypersonic wave propag. 0-44668
- PdZr, amorphous, supercond., US props. 0-44765

**ultrasonic radiation** *see ultrasonic waves***ultrasonic reflection**

- liquid-solid interface, nonspecular refl. near longit. crit. angle 0-48483
- liver, estimating acoustic attenuation coeff. slope from reflected US signals 0-5876
- longitudinal wave, conversion into transverse wave by reflection from boundary of half space 0-5860
- planar reflector in interior/on surface of test objects, characts. (*German*) 0-43569
- pulse-echo systems, improved sensitivity using pseudo-random binary-code phase-modulated signals 0-38182
- single transducer swept frequency ultrasonic reflection measurements 0-14534
- Hg, liq., sound vel. near metal-nonmetal transition, up to 1600°C and 2000 kg/cm<sup>2</sup> 0-39222

**ultrasonic refraction**

- angle probe produced waves, temp. depend. 0-55618
- attenuation, of US main waves with distance 0-5859
- breast tissue, US ref. index and attenuation images 0-17036
- breast tissue characterisation in vivo by US TOF computed tomography 0-51186
- tomography, refractive index field reconstruction for strongly refractive asymmetric fields 0-4760

**ultrasonic relaxation**

- acoustic wave absorption processes in atmosphere 0-53531
- benzene-similar liquids, 10 to 1300 MHz 0-39229
- chlorocyclohexane 0-24540
- deep ocean LF attenuation data, review 0-33318
- glass filled solids, ultrasonic absorpt., scatt., velocity and attenuation 0-44262
- heterocyclic liquids, 10 to 1300 MHz 0-39229
- liquid, weakly assoc., US wave reson. absorpt. 0-34141
- MBBA/EBBA binary liquid crystal mixture, US absorpt. and vel. dispersion, phase transition and alignment effects (*Korean*) 0-29121
- methanol, ethanol, aqueous mixtures (*French*) 0-6468
- micellar solutions, US absorpt. 0-45571
- polyethylene, glass filled solids, ultrasonic absorpt., scatt., velocity and attenuation 0-44262
- polystyrene, monosubstituted, US relaxation, dynamics of mol. chains 0-29124
- polystyrene, soln., macromol. dynamics, us relax. 0-19882

**ultrasonic relaxation continued**

- 2,4,6,8-tetraphenylnonane soln., macromol. dynamics, us relax. 0-19882
- thiophene, US and hypersonic investigations of vibrational relaxation 0-33377
- vinyl-series polymer solutions, longitudinal US waves absorption 0-15192
- Al, lattice resistance stress, Bordoni relax., microdeform. and US attenuation results 0-25747
- CdCl<sub>2</sub>, aq. solns., sound absorpt. and relax. phenomena 0-49311
- GaAs:Cr<sup>2+</sup>, dynamic Jahn-Teller effect, relaxation time for reorientation 0-6798
- <sup>3</sup>He, liquid, fluctuation contrib. to sound vel. and damping above superfluid transition temp. 0-15324
- LiCl in H<sub>2</sub>O, complexity investigation using US method 0-33326
- LiNO<sub>3</sub> in N,N-dimethylacetamide, Raman, IR and US relaxation studies 0-50315
- LiSCN in N,N-dimethylacetamide, Raman, IR and US relaxation studies 0-50315
- NH<sub>4</sub>Cl, λ-type phase transition, hypersonic study using Brillouin scatt. 0-34165
- NaNO<sub>3</sub> in N,N-dimethylacetamide, Raman, IR and US relaxation studies 0-50315
- NaSCN in N,N-dimethylacetamide, Raman, IR and US relaxation studies 0-50315
- YAG: rare earth metal, US absorpt. meas., relax. model 0-24539
- Zn single crystal, US flow detection in dislocation relaxation investigations 0-29122
- ZnCl<sub>2</sub> in H<sub>2</sub>O, complexity investigation using US method 0-33326

**ultrasonic scattering**

- A-mode echo computer spectral anal. 0-51193
- animal tissues, freshly excised, attenuation and backscatt. obs. 0-51148
- backscatter of short US pulses by solid elastic cylinders at large ka 0-43502
- backscattered wave minima for solid metal cylinder immersed in water (*French*) 0-53510
- backscattering in water due to elastic cylinder, short pulse backscatter (*French*) 0-53511
- blood, US backscattering, haematocrit and erythrocyte aggregation depend. 0-45961
- blood, US scattering, theoretical study 0-51147
- bone, cancellous, US attenuation and dispersion 0-51149
- cardiac pressure noninvasive US measurement, scatt. from encapsulated bubbles 0-36048
- caustics in non destructive evaluation, diffraction at crack like defects 0-43680
- cloud of isotropic scatterers, air bubbles in water appl. (*French*) 0-53507
- glass filled solids, ultrasonic absorpt., scatt., velocity and attenuation 0-44262
- heart and liver, quantitative meas. 0-45959
- liver, US backscatter from human tissue, depend. of freq. and protein/lipid content 0-45960
- lung surface US tissue signature 0-45957
- mixtures and suspensions, flow rate meas., ultrasound propagation and scatt. approach 0-43806
- ocean turbulence, small-scale, study by acoustic scatt. method 0-26540
- polycrystal, US scatt. by grains 0-2122
- polycrystalline materials, freq. and grain size dependency of US attenuation 0-50783
- polyethylene, glass filled solids, ultrasonic absorpt., scatt., velocity and attenuation 0-44262
- randomly rough surface backscatter anal., autocorrelation theory (*French*) 0-53508
- Schlieren observations of short US pulses scattered from elastic cylinders (*French*) 0-53500
- spherical voids, elastic wave scatt. at long wavelengths 0-48480
- surface characterisation meas. of randomly rough surfaces by US backscatter at normal incidence (*French*) 0-52165
- tissue characterisation by angle scan and freq.-swept scatt. technique 0-45958
- tissue US backscatter and attenuation distrib. mapping, digital reconstruction 0-51188
- tissues, fixed and unfixed, US propagation, backscattering coeffs. and speech determ. 0-41109
- underwater sound, volume scattering strengths and zooplankton distributions at acoustic frequencies between 0.5 and 3 MHz 0-33317
- volume scattering at 25 kHz in presence of temp. discontinuity layer 0-38157

**ultrasonic transducers**

- acoustooptic Bragg deflector, wide-band guided wave, using tilted-finger chirp transducer 0-14440
- annular array search units, potential appl. in conventional US testing systems 0-35446
- arrays, electric coupling effects in acoustic imaging 0-43587
- bandpass filters with quarter wave reflections, design 0-19183
- blood velocimeters, US transesophageal meas. of human haemodynamic parameters 0-41146
- bolt-clamped Langevin type transducer, effect of surface conditions on performance (*Japanese*) 0-48543
- broad band clinical transducers, pulse echo beam profiles through attenuating and non attenuating media 0-45945
- broadband fluid loaded US transducers, design 0-19202
- calibration by measuring total nearfield force, theoretical results 0-33400
- ceramic transducer, spatially-bounded US wave response 0-48542
- composite torsional quartz transducer for shear US measurements of aqueous liquids 0-53599
- cylindrical tubes, high-intensity US radiators (*Japanese*) 0-33404
- dynamic focusing transducer design for diagnostic image quality improvement 0-41155
- electronically scanned US diagnostic systems, electromechanical coupling coeff. for plank-shaped transducers 0-33383
- electrostrictive material for transducers, proposal of method for evaluation 0-38208
- farfield angular radiation pattern generated from arrayed piezoelectric transducers using finite element anal. 0-33401
- field intensity meas. using wideband piezoelectric convertors (*Russian*) 0-38209
- finite SAW transducer, surface charge density and elec. field distrib., moment method 0-23857
- flow detector, automatic, for butt welds (*Japanese*) 0-25976
- flowmeter, 240 Clampitron, applicability study 0-24108



**ultrasonic transducers continued**

- flowmeter, Danfoss, using electronic unit and piezoelectric transducers 0-6172
- flowmeters, petroleum and similar fluids 0-43804
- focusing device with IDT on thin piezoelectric plate 0-1398
- focusing transducers 0-33410
- HF, lumped bandpass filter equiv. ccts., quarter-wave matching characts. 0-1397
- integrated optical effect produced by US fields, study using light diffraction technique 0-23848
- interdigital transducer, book contrib. 0-1400
- interdigital transducer models for accurate design implementation of SAW transversal filters 0-28396
- level detection appl. 0-27268
- LF sandwich transducers for underwater acoustics analogy between fluid and solid horns 0-38213
- longitudinal wave, for US inspection of hot thick steel products 0-40661
- materials and adhesives, high temp. long duration tests 0-43586
- medical imaging, modelling (*French*) 0-26302
- mixed matrix representation of interdigital transducers 0-19184
- military appls., multilayered tape for perimeter warning device for combat troops 0-19200
- multilayer electroacoustic transducer containing active layers electrically connected in parallel 0-5902
- NDT probe array using 4 transducers 0-35499
- parametric, for high-resolution sonar 0-14539
- performance, theoretical anal., material testing appl. 0-30176
- piezoelectric, US energy meas. for echography 0-36044
- piezoelectric transducer, thick, operating as radiator or receiver, performance characts. 0-35484
- piezoelectric transducers, energy and spectral evaluations of broadband excitation 0-35485
- piezoelectric transducers, surface-driven, input impedance calc. 0-35493
- polyvinylidene fluoride, US transducers, dielec. and acoustic losses 0-48541
- pulsed fields radiated by thick piezoelectric discs immersed in petrol, expt. study (*French*) 0-53512
- quartz acoustic bulk wave resonators using AT-cut crystals, tolerance effects 0-53601
- reciprocity calibration of acoustic emission transducers 0-28401
- reciprocity calibration of arbitrarily terminated transducers 0-53574
- reciprocity technique for estimating the diffuse-field sensitivity of piezoelectric transducers 0-48538
- remote control circuit using US transducer 0-10097
- response dependence on fluid layer coupling (*French*) 0-43580
- SAW filters, low insertion loss, using multiphased unidirectional transducers 0-28397
- SAW IDT, electrode charge distrib. as element factor, anal. 0-1396
- SAW Lamb wave transducer with three operation modes, communication system appls. 0-43583
- SAW transducer with capacitive electrode weighting, band-pass filters 0-48544
- slotted transducer arrays with matched backings for underwater imaging 0-38214
- spherical arrays, reconstruction of three dimens. US reflectivity images 0-38203
- surface skimming bulk waves, excitation and detection on rotated Y-cut quartz 0-43492
- thin film interdigital transducers for SAW devices at GHz freqs. form. by electron beam lithography 0-4702
- tracking focusing annular array transducer (*French*) 0-26301
- underwater, parabolic reflector as nearfield calibration device 0-48528
- underwater acoustical compliance element, elastic problem of flattened cylinder type 0-33309
- underwater acoustical compliance tube for sound projectors, stress and deformation analysis 0-33310
- US inclined probe, construction improvements 0-33411
- wide-band, transmission, and reception of short US pulses 0-10099
- Y-Z LiNbO<sub>3</sub>, radiation patterns of bulk acoustic modes from finite interdigital transducer 0-43491
- ZnO piezoelectric film US transducers obtained by DC diode sputtering, dielec. breakdown props. 0-40066

**ultrasonic transmission**

- transkull transmission of axisymm. focused US beams, 0.5 to 1 MHz 0-51184
- velocity and damping of ultrasound, in CHCl<sub>3</sub> and C<sub>2</sub>H<sub>5</sub>OH and mixtures of these 0-29120
- Hg, liq., sound vel. near metal-nonmetal transition, up to 1600°C and 2000 kg/cm<sup>2</sup> 0-39222

**ultrasonic velocity***see also ultrasonic dispersion*

- acetic acid-acetone mixture, physical parameters 0-2716
- adamantane, elastic props., press. depend. rel. to intermol. forces 0-54297
- aortic wall, canine, speed of 10 MHz sound, effects of temp., storage, formalin soaking 0-56112
- aqueous solutions of acetamide, dimethyl urea,  $\beta$ -alanine interferometric obs. 0-19878
- benzene-tetrahydrofuran, soln., excess thermodynamic props. and interactions, US vel. and density meas. 0-39288
- blood, canine, US attenuation and speed, rel. to packed cell vol., 37°C 0-41106
- bone, cancellous, US attenuation and dispersion 0-51149
- bone, human cortical, US properties and microtexture 0-51144
- brain, normal and abnormal, attenuation, vel. and impedance 0-45955
- butanol-methylethyl ketone, soln., excess thermodynamic props. and interactions, US vel. and density meas. 0-39288
- carbon tetrachloride, US vel., 265-435K 0-6464
- computerised tomography, var. of acoustic speed with temp. in excised human tissues 0-51150
- concrete, US wave propag. and microcracking (*French*) 0-39225
- cubic single crystal misorientation angle determ. by US speed meas. 0-54315
- p-dioxane, aq. soln., excess molar heat capacities, 298.15K, US vel. obs. 0-6523
- fibre reinforced composite, ultrasonic vibrs. propagation velocity, dependence on composites elastic props. 0-5975
- glass filled solids, ultrasonic absorpt., scatt., velocity and attenuation 0-44262
- glass with frozen structure, viscous flow, valence configuration flow theory 0-39335
- isobutyric acid-water, crit. mixture, conc. fluctuation mean relax. time, US absorpt. and vel. meas 0-29163
- kaersutite, sound vels. and anisotropy, rel. to upper mantle seismic struct. 0-26501
- liquid, Rao's acoustical constant, temp. depend., from C<sub>1</sub>-parameter 0-6462
- MBBA/EBBA binary liquid crystal mixture, US absorpt. and vel. dispersion, phase transition and alignment effects (*Korean*) 0-29121
- methane, liquid, Brillouin scatt. obs., US vel. and absorpt. 0-45085
- methylethyl ketone-butanol, soln., excess thermodynamic props. and interactions, US vel. and density meas. 0-39288
- mixtures and suspensions, flow rate meas., ultrasound propagation and scatt. approach 0-43806
- myocardium, acoustic microscopic anal. 0-45995
- nitrobenzene-n-heptane, crit. mixture, conc. fluctuation mean relax. time, US absorpt. and vel. meas 0-29163
- nitroethane-isooctane, crit. mixture, conc. fluctuation mean relax. time, US absorpt. and vel. meas 0-29163
- poly(4-methyl pentene-1), US props., glass transition, Gruneisen parameters 0-54316
- poly-4-methylpentene-1, elastic parameters, US velocity meas. at 2.1-240K 0-40415
- polyethylene, glass filled solids, ultrasonic absorpt., scatt., velocity and attenuation 0-44262
- propagation in austenitic stainless steel weld metal, effect of anisotropy 0-45452
- quartz, crystal growth in fluoride environment, growth features and props. 0-6373
- rare earth metals, elastic props., connection with electron struct. (*Russian*) 0-19895
- sandstone elastic wave velocity, function of moisture content 0-56459
- Schaaffs' molecular-kinetic theory of propag. in liquids, temp. and pressure changes of 'collision factor' 0-19143
- steel, stainless austenitic welds, time domain approach to crack location and sizing 0-50781
- steel, stainless type 304, elastic const. variability, US vel. meas. 0-55446
- tetrahydrofuran-benzene, soln., excess thermodynamic props. and interactions, US vel. and density meas. 0-39288
- thermoelastic material, deformed isotropic, thermal effect on propag. vels. 0-33276
- tissue, mammalian, survey of US vel. and attenuation data 0-46744
- tissue, mammalian, US attenuation and speed determ. as function of temp. 0-41108
- tissue, soft, temp. depend., rel. to temp. distrib. monitoring 0-45994
- tissues, fixed and unfixed, US propagation, backscattering coeffs. and speech determ. 0-41109
- tourmaline, elastic const. by US phase-comparison method 0-2108
- US velocity rel. to mineral content 0-45962
- water, speed determ. over wide range of pressure and temp. 0-23821
- water-ethanol(methanol) mixtures, nonlinear acoustic coeff. meas., 0-50°C (*French*) 0-34142
- Ag film, damping and vel. of longit. elastic waves at 9.4 GHz 0-10596
- Ag<sub>5</sub>SbS<sub>6</sub>, electron absorption and dispersion of ultrasound velocity 0-15197
- Al-Mg solid solns., decomposition studied by ultrasonic meas. of elastic props. 0-35184
- $\beta$ -Al<sub>2</sub>O<sub>3</sub>-Na<sub>2</sub>O, non-stoichiometric, amorphous, US attenuation and velocity 0-39228
- As, amorphous, US attenuation and sound vel. meas., 4.2 to 300K; 0-49308
- As<sub>2</sub>S<sub>3</sub>(Se<sub>3</sub>) glasses, elastic moduli, hydrostatic press. effect, US wave vel. meas. 0-34115
- Au film, damping and vel. of longit. elastic waves at 9.4 GHz 0-10596
- B fibre reinforced Al, orthotropic elastic stiffness const., US vel. meas. 0-49289
- B<sub>2</sub>O<sub>3</sub>, amorphous, acoustic props. at 20 GHz, Brillouin scatt., 3-300K 0-24536
- Ba I-Ba II phase boundary, Ba I fusion curve peak at high press. (*Russian*) 0-2165
- CHCl<sub>3</sub> and C<sub>2</sub>H<sub>5</sub>OH and mixtures, velocity and damping of ultrasound 0-29120
- CO, liquid, Brillouin scatt. obs., US vel. and absorpt. 0-45085
- Cr film, damping and vel. of longit. elastic waves at 9.4 GHz 0-10596
- CsH<sub>2</sub>AsO<sub>4</sub>, elastic props., photoelasticity near ferroelectric phase transition 0-29107
- Cu film, damping and vel. of longit. elastic waves at 9.4 GHz 0-10596
- Cu, HF ultrasound, viscous and relax. components of dislocation attenuation 0-15196
- Fe<sup>2+</sup>Fe<sub>0.2</sub><sup>3+</sup>Cr<sub>1.8</sub><sup>3+</sup>O<sub>4</sub>, acoustic props. rel. to cooperative Jahn Teller effect and structural phase transform 0-24538
- <sup>3</sup>He, liquid, fluctuation contrib. to sound vel. and damping above superfluid transition temp. 0-15324
- <sup>4</sup>He, superfluid, phonon dispersion 0-10722
- In, film, damping and vel. of longit. elastic waves at 9.4 GHz 0-10596
- In, US velocity dispersion in external mag. field 0-20446
- In-Pb alloys, elastic const. of three phases, acoustic mode softening from US vel. meas. 0-30006
- K<sub>2</sub>Mn<sub>2</sub>(SO<sub>4</sub>)<sub>3</sub>, elastic props. using piezoelec. reson. and US vel. meas. 0-15180
- N<sub>2</sub>, liquid, Brillouin scatt. obs., US vel. and absorpt. 0-45085
- NH<sub>4</sub>BrCl<sub>1-x</sub>, cryst., order-disorder phase transitions, US investig. 0-6378
- (NH<sub>4</sub>)<sub>2</sub>(1-x)Rb<sub>2x</sub>SO<sub>4</sub>, mixed crystal, dielectric and US meas. of ferroelec. phase transition (*Japanese*) 0-7305
- NaNO<sub>2</sub>, incommensurate-and-antiferroelectric phase transition, amplitude mode, ultrasonic study 0-39227
- Ni film, damping and vel. of longit. elastic waves at 9.4 GHz 0-10596
- NiCr<sub>2</sub>O<sub>4</sub>, acoustic props. rel. to cooperative Jahn Teller effect and structural phase transform 0-24538
- Ni<sup>2+</sup>Fe<sub>0.75</sub><sup>3+</sup>V<sub>1.25</sub><sup>3+</sup>O<sub>4</sub>, acoustic props. rel. to cooperative Jahn Teller effect and structural phase transform 0-24538
- O<sub>2</sub>, liquid, Brillouin scatt. obs., US vel. and absorpt. 0-45085
- P, amorphous, US attenuation and sound vel. meas., 4.2 to 300K; 0-49308
- PbI<sub>2</sub>, cubic, elastic const., hydrostatic press. effect, US vel. meas. 0-49292
- PdSiCu, amorphous, US attenuation and vel. studies 0-19881
- RbHSO<sub>4</sub>, acoustic and dielectric props. near phase transition 0-55053
- Rb<sub>2</sub>ZnCl<sub>4</sub>, US velocity and attenuation, around normal-incommensurate phase transition 0-40072



**ultrasonic velocity continued**

- SO<sub>2</sub>, liq., vibr. relax., US absorpt. and vel. meas. 0-34147  
 Se, vitreous, elastic coeffs. about glass transition temp. US study (*French*) 0-19865  
 SiO<sub>2</sub>, vitreous, hypersound velocity meas. from Brillouin scatt. freq. 0-27349  
 Tb, magnetic phase diagram, US meas. of elastic const. 0-15721  
 Tb<sub>0.3</sub>Dy<sub>0.7</sub>Fe<sub>2</sub>, sound velocity mag. field and temp. depend. elastic moduli calcs. 0-39839  
 UAl<sub>2</sub>, elastic consts., temp. and mag. field depend. 0-55450

**ultrasonic velocity measurement**

- binary liquid mixtures of aromatic amines with carbon tetrachloride, theoretical evaluation 0-39224  
 Brillouin scattering frequency high-precision meas., rel. to hypersound velocity meas. 0-27349  
 cyclohexane+n-heptyl alcohol 0-38200  
 digital US vel. meter using freq. counter 0-38202  
 ethyl methyl ketone+cyclohexane, measurements for determination of excess props. 0-37910  
 ethyl methyl ketone+n-butanol, measurements for determination of excess props. 0-37910  
 liquids, high-accuracy differential meas. in different liquids 0-5889  
 liquids, US vel. meas. method for elastic const. determ. w.r.t. temp. and pressure 0-15177  
 liquids with very low US propag. velocities for use in biomedical optical computer 0-28392  
 picrite, calculation of Gruneisen parameter and specific heat from measurements 0-41436  
 polymers, US velocities and damping coeff. meas. (*French*) 0-7723  
 pulse echo method, minicomputer program control (*Japanese*) 0-53587  
 sing-around meter, IC 0-38198  
 solids, with allowance for statistical characts. of bonding layers 0-5894  
 sonic interface detection for multiproduct liquid transportation by pipeline, developments 0-33382  
 ternary organic liquid mixtures 0-38201  
 tetrachloromethane+n-heptyl alcohol 0-38200  
 tissue, meas. device 0-45993  
 Hg, liq., sound vel. near metal-nonmetal transition, up to 1600°C and 2000 kg/cm<sup>2</sup> 0-39222  
 LiCl in H<sub>2</sub>O, complexity investigation using US method 0-33326  
 NH<sub>4</sub>Cl,  $\lambda$ -type phase transition, hypersonic study using Brillouin scatt. 0-34165  
 Pb<sub>0.97</sub>La<sub>0.02</sub>(Zr<sub>0.92</sub>Ti<sub>0.08</sub>)O<sub>3</sub>, ferroelec. ceramic, stress effects 0-2119  
 Pb<sub>0.99</sub>Nb<sub>0.01</sub>(Zr<sub>0.95</sub>Ti<sub>0.05</sub>)O<sub>3</sub>, ferroelec. ceramic, stress effects 0-2119  
 ZnCl<sub>2</sub> in H<sub>2</sub>O, complexity investigation using US method 0-33326

**ultrasonic wave propagation** *see ultrasonic propagation***ultrasonic waves**

- see also surface acoustic waves; ultrasonic propagation*  
 distortion of ultrasound beams in tissue and tissue-equivalent media 0-45945  
 integrated optical effect produced by US fields, study using light diffraction technique 0-23848  
 liquids, photoelastic visualisation 0-28374  
 propagation in austenitic stainless steel weld metal, effect of anisotropy 0-45452  
 pulsed fields radiated by thick piezoelectric discs immersed in petrol, expt. study (*French*) 0-53512  
 SAW, nonlinear interaction in 2-6 MHz range (*French*) 0-33296

**ultrasonic welding**

- microcontacting in thin metallic layers (*German*) 0-55624  
 UV radiation effects on welded joints and substrate surface 0-37008

**ultrasonics**

- see also acousto-optical effects; ultrasonic applications; ultrasonic devices; ultrasonic equipment; ultrasonic waves*  
 internal losses in metals subjected to high intensity US flexural vibrations 0-6460

**ultraviolet astronomical observations**

- OB-type stars, O VI obs. in stellar winds 0-8630  
 0406+121, optical spectra 4950-7950 Å, of possible BL Lacertae object 0-51895  
 RT Andromedae, eclipsing binary, three-colour photoelectric obs. and improved ephemeris 0-22043  
 RT Andromedae, light curve anal. of short period eclipsing binary 0-46603  
 ET Andromedae (HR 8861), Ap star, light vars. and period 0-46571  
 AE Aquarii, cataclysmic variable, rapid light oscils. rel. to white dwarf oblique rotator model 0-36634  
 $\alpha$  Aquarii, chromospheric event detect. from UV spectrum obs. 0-31299  
 U Aquarii, R Coronae Borealis star, extraordinary comp. rel. to unusual s-processing event 0-17588  
 R Aquarii, UV obs. of hot component 0-56854  
 387 Aquitania, slow spinning asteroid with rot. period of nearly one day, photometric evidence 0-17529  
 56 Arietis, spectrophotometry of Ap star, continuum features vars. 0-36638  
 Be stars, photometric behaviour, UV excess, emission indices, galactic distrib. 0-36637  
 776 Berbericia, slow spinning asteroid with rot. period of nearly one day, photometric evidence 0-17529  
 $\alpha$  Bootis, search for Ti II 3080 Å multiplet emission 0-51769  
 $\xi$  Bootis A, active dwarf star, chromospheric emission lines obs. 0-12762  
 $\zeta$  33, 98, 184.1 and 218, rotation axes 0-26997  
 $\alpha$  Camelopardalis (O9.5 Ia), stellar wind terminal vel. short time changes from UV spectrum 0-36625  
 38 Cancri,  $\delta$  Scuti star, UV photometric obs. of variability 0-22021  
 49 Cancri, spectrophotometry of Ap star, continuum features vars. 0-36638  
 $\alpha$  Canis Majoris (Sirius B), spectral energy distrib. 0-8629  
 $\beta$  Canis Majoris stars, ANS UV photometry 0-26871  
 $\beta$  Canis Majoris stars, UV flux obs., basic data obtained with TD-1A satellite 0-51783  
 AG Carinae, luminous star in symmetric nebulae, IUE low-dispersion spectrum 0-46560  
 Cassiopeia A supernova remnant, abundance inhomogeneities 0-12797  
 $\gamma$  Cassiopeiae, Be star, polarisation rapid vars. 0-22022  
 RZ Cassiopeiae, eclipsing binary, spectroscopic orbit 0-22040  
 $\kappa$  Cassiopeiae, effective temp. radius, mass loss and luminosity 0-51748  
 $\gamma$  Cassiopeiae, N I interstellar absorption in  $\gamma$  Cassiopeiae direction, UV obs. 0-51823  
 cataclysmic variables, visual continuum flux distrib. 0-36636  
 ultraviolet astronomical observations continued  
 proxima=V645 Centauri, dMe flare star, quiescent corona, transition region, and chromosphere obs. 0-56850  
 BV Centauri, dwarf nova, identification as spectroscopic binary 0-51775  
 V436 Centauri, dwarf nova, photometry during superoutburst (May 1978) 0-46570  
 $\alpha$  Centauri A and B, IUE spectra and transition region models 0-46543  
 central stars of planetary nebulae, UV spectral obs. from TD-1 satellite 0-31300  
 U Cephei, eclipsing binary, gas stream effects in UV spectrum, IUE obs. 0-26898  
 VV Cephei system, distant, in Puppis, spectral classification, UV photometry and polarimetry 0-51810  
 $\kappa$  Ceti, IUE obs. of far UV spectra of G-type dwarf 0-56831  
 $\sigma$  Ceti AB, IUE obs. of UV spectrum 0-22027  
 Comet Arend-Roland (1957 III), visible and UV spectra anal. (*Chinese*) 0-12709  
 Comet Kobayashi-Berger-Milon (1975 IX), Lyman- $\alpha$  obs. 0-4301  
 comet West (1976 VI), emission bands and continuum flux heliocentric depend. 0-36575  
 Comet West (1976 VI), Lyman  $\alpha$  isophotes 0-46485  
 cool stars, Mg II flux profiles and chromospheric radiative loss rates 0-36611  
 CPD-26°389, central star of NGC 1360, radial vel. obs. 0-4350  
 SS Cygni, dwarf nova, spectrophotometry rel. to accretion disc models in eruption and at min. light 0-36635  
 P Cygni, effective temp. radius, mass loss and luminosity 0-51748  
 P Cygni, extreme B-type supergiant, UV spectroscopy 0-22004  
 P Cygni, high resolution UV spectrum obs. 0-26873  
 32 Cygni, IUE obs. and effects of B-type star within late-type supergiant upper chromosphere 0-22036  
 V382 Cygni, IUE spectra of massive close binary 0-8659  
 V832=59 Cygni, mass-losing Be star, changes in UV spectrum 0-46561  
 57 Cygni, spectroscopic binary, search for systematic radial vel. anomalies 0-17617  
 CH Cygni, symbiotic star, rapid and slow light vars. 0-51792  
 59=V832 Cygni, variable mass flux from spectroscopic obs. 0-41840  
 V1500 Cygni (Nova 1975), visible and UV spectra and light curve 0-12771  
 V1668 Cygni (Nova 1978), linear polarisation obs. 0-26875  
 V1668 Cygni (Nova 1978), UV light curve 0-46565  
 Cygnus OB2 number 12, spectral classification and membership of association 0-51760  
 Cygnus X-1, UV shot noise upper limit 0-4458  
 Cygnus X-2, rapid UV flux vars., IUE obs. 0-12833  
 degenerate star candidates, photoelectric and spectroscopic obs. 0-12763  
 Deimos, spectral evidence for carbonaceous chondrite surface comp. 0-41754  
 HR Delphini, UV spectrum, stellar wind 0-26880  
 $\delta$  Delphini stars in Michigan Spectral Catalogue, uvby $\beta$  photometry rel. to spectral types 0-4377  
 diffuse cosmic far UV background, rocket obs. 0-46708  
 diffuse cosmic UV background, spectrum 0-17696  
 S Doradus (HD 35343), luminous LMC supergiant, long time baseline VBLUW photometry 0-22007  
 S Doradus (HD 35343), luminous LMC supergiant, long time baseline VBLUW photometry 0-36630  
 30 Doradus central object (HD 38268), interstellar and nebular lines obs. 0-51839  
 CR Draconis, UV Ceti variable, flares colour behaviour 0-22020  
 dwarf novae, spectra (*Russian*) 0-8638  
 dwarf novae, spectrophotometry, 1250-7500 Å region 0-46577  
 early type stars, 206-287 nm UV spectra of Ap, Bp, Be, Bn and shell stars 0-51776  
 early type stars, 'normal', with anomalous mid UV spectra 0-26857  
 early type stars, mid UV spectra obs. 0-21995  
 early type stars, normal, near UV line blocking depend. on spectral type and luminosity 0-36619  
 early-type stars, Copernicus UV obs., of He I lines 0-41825  
 faint early-type stars in neighbourhood of H II region RCW 38, UV photometry 0-4352  
 ESO 012-G21, Seyfert 1 galaxy, spectrum, redshift, UV photometry and X-ray identification 0-8695  
 ESO 113-IG 45 (=Fairall 9), Seyfert galaxy, spectroscopic and multiaperture photometric obs. 0-31362  
 247 Eukrate, UV photometry, light curve and rot. period 0-21942  
 Feike 86, UV high-resolution spectrum 0-41834  
 flare stars in Orion Nebula region, new objects and repeated outbursts 0-56852  
 G200-39, hot hybrid white dwarf, spectroscopic obs. 0-26852  
 G292.0+1.8, abundance anomalies, radial vels., possible Crab-like SNR 0-46628  
 G292.0+1.8, young supernova remnant, high vel. material obs. 0-22064  
 G-type dwarf stars, far UV Si emission line analysis 0-56829  
 galactic G-type supergiants, UV photometry 0-41824  
 galactic high-latitude regions, balloon-borne UV survey 0-41891  
 galaxies, irregulars and blue compacts, chemical comp. and evolution from spectrophotometry 0-36711  
 galaxies with UV continuum, photoelectric UVBR photometry (*Russian*) 0-36721  
 Ganymede, stellar occultation obs. by Voyager 1 rel. to exospheric atmosphere 0-26792  
 GCl 0422-213, distant globular cluster in Eridanus, preliminary photometry and spectroscopy 0-17624  
 globular cluster giant stars, blanketing differences meas. 0-4345  
 HD 149499 B, IUE obs. of hottest white dwarf 0-41828  
 HD 15570, Of/WN7 spectral classification problem 0-51786  
 HD 190603, effective temp. radius, mass loss and luminosity 0-51748  
 HD 192163, 191765, Wolf-Rayet stars, optical interstellar spectra obs. 0-17640  
 HD 193793, Wolf-Rayet star, photometric evidence for C-rich dust cloud 0-26861  
 HD 221568, Ap star, light var. period 0-56856  
 HD 33579, 35343, HDE 286757, 269006, most luminous LMC supergiants, long time baseline VBLUW photometry 0-22007  
 HD 33579, HD 35343 (S Doradus), HDE 268757, HDE 269006, most luminous LMC supergiants, long time baseline VBLUW photometry 0-36630  
 HD 3980, late Ap star, photometric and mag. variability obs. 0-56845  
 HD 51480, shell star, spectroscopic obs., atmospheric struct. and distance 0-31305



## ultraviolet astronomical observations continued

- HD 64740, He rich star, UV spectral vars. 0-22016  
 HD 94033 ultra short period cepheid, obs. 0-22024  
 HDE 245770, possible counterpart of variable X-ray source A 0535+26, line and continuum vars. 0-17600  
 AC Herculis, RV Tauri star, UVB obs. 0-56857  
 u Herculis, synthetic light curve soln. of OAO-2 UV light curves 0-4399  
 high-velocity stars, southern, radial vels. 0-21988  
 high-velocity stars, southern, UVB colours 0-21989  
 hot white dwarfs, EUV flux interstellar absorpt., local clumpiness factor determ. 0-36627  
 HR 4665, spectroscopy of bright long-period RS Canum Venaticorum system 0-36665  
 HR 9049, (HD 224113), eclipsing spectroscopic binary star, period determ. 0-46609  
 RW Hydrae, UV obs. of hot component 0-56854  
 IC 3568, planetary nebula, struct. and internal extinction 0-31338  
 International Ultraviolet Explorer, orbiting telescope, 1978 observations (French) 0-8540  
 interstellar abundance and depletion models for B, V, Cr, and Co 0-46630  
 interstellar lines towards Cepheus OB2 association, anal. 0-22052  
 interstellar low mass dust clouds in solar vicinity, photometric survey results 0-36512  
 interstellar matter towards Orion OB1 assoc. stars  $\epsilon$  Orionis and  $\pi^5$  Orionis, Copernicus obs. 0-22050  
 Io, evidence of SO<sub>2</sub> from UV obs. 0-36561  
 Io plasma torus, Voyager 1 EUV spectrum obs. 0-26792  
 IUE, first year of obs., conference, London, England (1979 April 4 to 6) 0-51960  
 IUE satellite, observing experience 0-36476  
 Jupiter, Lyman  $\alpha$  emission var. with solar cycle 0-41759  
 Jupiter, O<sup>+</sup> forbidden emission detect. in inner magnetosphere 0-51687  
 Jupiter, upper atmosphere temperature, Voyager 1 meas. 0-17536  
 Jupiter, Voyager 1 EUV obs. 0-26792  
 Jupiter spectrum, obs. from 1500 to 2000 Å with IUE 0-56752  
 EV Lacertae, UV Ceti variable, flares colour behaviour 0-22020  
 late-type stars, search for Ti II 3080 Å multiplet emission 0-51769  
 $\rho$  Leonis, effective temp. radius, mass loss and luminosity 0-51748  
 AD Leonis, UV Ceti variable, flares colour behaviour 0-22020  
 LMC, stellar photoelectric UVB photometry (German) 0-21932  
 LMC interstellar extinction, visible and UV obs. 0-51877  
 loose stellar clusterings in southern Milky Way, continued photometric studies 0-36679  
 LS I +61°303, radio variable Be star, UV spectrum, stellar models 0-26879  
 luminous stars in M31 0-36622  
 luminous stars in symmetric nebulae, IUE low-dispersion spectra 0-46560  
 $\alpha$  Lyrae (Vega), Copernicus UV obs. of C II and Si II lines 0-8627  
 $\alpha$  Lyrae (Vega), spectral anal. from Copernicus 0-26856  
 RR Lyrae variables in globular cluster NGC 6121 (M4), UVB photometry 0-22018  
 M33, UV integrated magnitudes of spiral galaxy 0-31368  
 M83, H II regions spectral characts. and chemical abundances 0-56927  
 M87 jet knots, polarisation and spectroscopic props. 0-12817  
 Markarian 501, UV and X-ray obs. of BL Lacertae-type object 0-36717  
 Markovian 297, IUE UV spectra of clumpy irregular galaxy 0-26981  
 Melotte 66, oldest open cluster, colour-magnitude diagram rel. to age 0-17621  
 9 Metis, UVB photometry, light curve and rot. period 0-21942  
 19 Monocerotis,  $\beta$  Canis Majoris variable, photometric obs. 0-4379  
 V616 Monocerotis (A 0620-00), UVB photometry 0-56846  
 MXB 1837+05 (Serpens X-1), detect. of optical burst coincident with X-ray burst 0-27013  
 NAB 0137-01, quasar, UVB photometry and brightness vars. 0-56967  
 NGC 1261, globular cluster, colour-magnitude diagram 0-17623  
 NGC 2110, Seyfert 2 X-ray galaxy, optical studies 0-22071  
 NGC 2264, open cluster, reddening, blanketing and metallicity from spectroscopic obs. 0-26916  
 NGC 2420, old disc cluster, photometry and spectra rel. to stars chemical comp. 0-46620  
 NGC 300, NGC 1365, southern galaxies, H II regions comp. 0-4441  
 NGC 3532, southern open cluster, UVB photometric study 0-46621  
 NGC 4151, Seyfert galaxy, for UV line profiles 0-22083  
 NGC 520, Irr II galaxy, new photographic and spectroscopic obs. 0-41889  
 NGC 6144, globular cluster, and neighbouring region, photometric obs. 0-51816  
 NGC 6528, metal-rich globular cluster, colour-magnitude diagram from UVB photometry 0-4406  
 NGC 6822, new compact H II regions discovery 0-51854  
 NGC 7023, refl. nebula, surface brightness study 0-56903  
 novaklike object in Vulpecula, UVB photometry (1979 August 6 to September 20) 0-8644  
 O-type stars in open cluster IC 1805, C IV UV reson. line P Cygni profiles 0-31296  
 OB-type stars in SA 98, UVB photoelectric meas. 0-46535  
 UZ Octantis, W Ursae Majoris system, UVB light curves 0-22042  
 U Ophiuchi, massive eclipsing binary star, spectrophotometry 0-26900  
 OQ 172, quasar, H<sub>2</sub> lines in absorpt. spectrum 0-36734  
 Orion nebula, C and Mg abundances from UV spectrum 0-41882  
 Orion Nebula peripheral regions, spectrum obs. rel. to element depletion and ionisation 0-36686  
 $\beta$  Orionis, mass loss and shell, IUE and balloon UV obs. 0-51765  
 $\lambda$  Orionis, obs. of UV radiation scattered by interstellar dust 0-56918  
 EQ Pegasi, active dwarf binary star, chromospheric emission lines obs. 0-12762  
 AU Pegasi, binary Type II cepheid, photometric and spectroscopic study 0-26866  
 AG Persei, massive eclipsing binary star, spectrophotometry 0-26900  
 21 Persei, spectrophotometry of Ap star, continuum features vars. 0-36638  
 PKS 1157+014, spectral obs., of QSO with no L $\alpha$  emission 0-31384  
 PKS 2155, BL Lacertae object, UV flux meas. by IUE 0-12833  
 planetary nebula IC 418, search for absorpt. in CO fourth positive system 0-46647  
 planetary nebula in irregular galaxy NGC 6822, spectrophotometry and He, N, O and Ne abundances 0-41867  
 planetary nebulae, low excitation, of small ang. size, spectral studies 0-17646

## ultraviolet astronomical observations continued

- Pleione (28 Tauri), envelope behaviour in 1976, spectroscopic obs. 0-8636  
 Pleione (28 Tauri), metallic-line shell spectrum anal., (1973-1976) 0-8637  
 R Puppis (HD 62058), G-type supergiant, UVB photometry and variability confirmation 0-41824  
 Q 0932+501, bright quasar with broad absorption features 0-46697  
 Q 2240.9-3702, Q 2238.9-4115, optically selected QSOs with broad-lined absorpt. systems spectra 0-4456  
 QSO candidates, spectroscopic obs., identifications 0-31385  
 QSOs, high-redshift, Image Dissector Scanner (IDS) spectrometry and redshifts 0-22111  
 QSOs of small and intermediate emission redshift, absorpt. lines homogeneous survey results 0-31218  
 quasar, strong emission line, with redshift  $z=0.189$ , spectrum and photometry 0-8710  
 quasar emission lines 0-27009  
 quasars, low-red shift, photoelectric UVB photometry (French) 0-51904  
 quasars, Mg II 2798 Å and H $\beta$  emission, line profiles 0-12807  
 quasars in region of NGC 1629 companion galaxy, spectra and redshifts 0-56965  
 quasars of Michigan-Tololo survey, spectrophotometry 0-22105  
 radio galaxies, broad-line Mg II 2798 Å and H $\beta$  emission, line profiles 0-12807  
 SA 133 field near galactic centre, three-colour stellar photometry (German) 0-36618  
 HM Sagittae, emission-line star, UVB photometry and spectral obs. in (1978) (Russian) 0-36648  
 HM Sagittae, emission-line star, polarimetry, (1977 to 1978) (Russian) 0-36649  
 WZ Sagittae, recurrent nova, spectroscopic obs. during 1978 outburst 0-26862  
 WZ Sagittae, recurrent nova, spectroscopic study during 1978 outburst 0-56849  
 XZ Sagittarii, Algol system, UVB photometric investigation 0-22041  
 $\mu$  Sagittarii, binary star, B8 star eclipse obs. during (June 1979) 0-4401  
 V356 Sagittarii, massive eclipsing binary star, spectrophotometry 0-26900  
 MV Sagittarii, R Coronae Borealis variable, brightness decline obs. and UVB photometry 0-8641  
 Saturn, rings, four colour phase curves, analysis 0-4295  
 Saturn globe and rings, optical reflectance polarimetry and interpretations for B-ring 0-31248  
 $\alpha$  Scorpii, circumstellar absorption lines in UV spectrum 0-51804  
 $\zeta^1$  Scorpii, extreme B1 supergiant, IUE obs. of line spectrum and continuum energy distrib. 0-17583  
 $\zeta^1$  Scorpii, extreme B1 supergiant, UV reson. lines obs. 0-4349  
 $\zeta^1$  Scorpii, extreme B-type supergiant, UV spectroscopy 0-22004  
 V861 Scorpii (OAO 1653-40?), simultaneous UV and X-ray obs. 0-17616  
 Seyfert galaxies, Mg II 2798 Å and H $\beta$  emission, line profiles 0-12807  
 solar active regions and X-ray bright points, birthplaces 0-12739  
 solar atmosphere, C III 1909 Å and Si III 1892 Å emission lines, echelle obs. 0-31277  
 solar flare 0-26829  
 solar flares, EUV and hard X-ray sources relationship 0-46512  
 solar flares, Fe XXI 1354 Å obs. from Skylab rel. to ionisation equilib. calcs. 0-21956  
 solar photosphere, UV continuum high resolution photographic obs. 0-17565  
 solar prominence, EUV limb spectra, Skylab obs. 0-12717  
 solar prominence, EUV spectrum rel. to horizontal temp. gradient meas. and prominence condensation 0-26832  
 solar quiescent prominences, middle Balmer decrement meas. 0-12737  
 solar surge, EUV limb spectra obs. from Skylab 0-17560  
 solar transition zone, energy balance and press. for network and active region features 0-21957  
 southern peculiar emission-line stars, observational data rel. to mass ejection 0-41843  
 spiral galaxies nuclei, spectra and stellar population 0-56926  
 stars, UV chromospheric and transition-layer emission 0-56823  
 stars, young, in galactic anticentre direction, photometry and spectra rel. to outer Galaxy struct. 0-22079  
 stellar coronae, evidence for existence from X-ray and UV obs. 0-12756  
 stellar coronae, IUE search 0-4233  
 stellar photoelectric UVB sequences, in fields of eight low-red shift quasars (French) 0-51904  
 Sun, 1973 August 14 loop prominence, XUV emission and density 0-56807  
 Sun, active region coronal loops, gyroresonance absorption evidence 0-56792  
 Sun, chromosphere-corona transition region, OSO 8 UV obs. of optically thick region 0-56788  
 Sun, coronal holes, EUV and radio spectrum 0-56802  
 Sun, relative chemical abundances in different solar regions 0-46518  
 Sun, supergranulation structure in coronal holes 0-51729  
 Sun, transition-zone plasmas, electron densities and mass motions in flares 0-56804  
 Sun, UV radiation, ferrioxalate actinometer meas. 0-41731  
 supergiants, C IV resonance lines in B- and early A-type objects 0-46550  
 supernovae stellar remnants, spectroscopic search 0-26890  
 87 Sylvia, UVB photometry, light curve and rot. period 0-21942  
 $\lambda$  Tauri, massive eclipsing binary star, spectrophotometry 0-26900  
 $\alpha$  Tauri, search for Ti II 3080 Å multiplet emission 0-51769  
 V471 Tauri, white dwarf eclipsing binary, IUE UV spectra 0-26912  
 V711 Tauri (HR 1099), Lyman  $\alpha$  H I and D I interstellar absorption 0-8658  
 RV Tauri and yellow semiregular variables, photometric investigations 0-26865  
 Tautenburg objective prism survey objects, high-resolution spectra and redshifts 0-4436  
 Triton, diameter and reflectance, spectral and radiometric obs. 0-17546  
 47 Tucanae, globular cluster, photometry and spectra rel. to stars chemical comp. 0-46620  
 4 U 2129+47 optical counterpart, spectrum and photometry rel. to 0-17693  
 AW Ursae Majoris, light curve anal. of contact binary 0-56875  
 Venus, cloud images from Pioneer orbiter 0-46432  
 Venus, cloud structure, high-contrast UV detail 0-51682  
 Venus, Pioneer nephelometer expts. results 0-46430



**ultraviolet astronomical observations continued**

- Venus, regional polarization, 1950-77 obs. 0-8570
- Venus, rotation of upper atmosphere (*French*) 0-36534
- Venus, ultraviolet photometry and cloud struct., Venera obs. 0-56738
- Venus, UV markings, Venera 9 cloud top data analysis 0-17521
- Venus cloud cover, obs. by Venera 9 orbiter 0-51680
- Venus clouds, UV absorbers, Pioneer data 0-46433
- Vesta, UV photometry and lightcurve 0-36546
- Vulpecula OB2 stars, photometry and spectra rel. to membership of 67 day Cepheid S Vulpeculae 0-41831
- NQ Vulpeculae (Nova 1976), UV and visual spectra analysis (*Chinese*) 0-12770
- white dwarfs in open clusters, obs. rel. to progenitor stars upper mass limit 0-51738
- Wolf-Rayet stars, ANS UV spectrophotometric obs. 0-22023
- yellow semiregular and RV Tauri variables, photometric investigations 0-26865
- B II 1362 Å, interstellar line detect. in front of  $\kappa$  Orionis 0-51841
- H deficient and He weak stars, uvby photometry, variability 0-46579
- H II regions in Perseus arm, spectrophotometry and reassessment of galactic abundance gradients 0-22055
- HgMn stars, spectrophotometry 0-26867

**ultraviolet astronomy**

- see also *ultraviolet sources (astronomical)*
- diffuse cosmic UV background, spectrum 0-17696
- echelle spectrograph, high-resolution, for far UV and visible astronomy, design and performance 0-26744
- electrographic image detectors, development, and applications in UV astronomy and scientific research 0-43465
- electrographic instrumentation for ultraviolet imaging and spectrography 0-46399
- EUV solar line emission weakening short of 912 Å wavelength 0-21962
- EUV spectrograph with single toroidal grating, stigmatic performance 0-36498
- Fabry-Perot scanning interferometer with piezoelec. spacers, appl. to solar UV spectrum 0-12678
- FAUST instruments, high focal ratio telescope for UV imagery 0-41724
- He II 304 Å line redshifted to 1450 Å in far UV background 0-41893
- image converter-intensifier detector for interference spectroscopy in balloon UV 0-56707
- interstellar clouds, diffuse UV radiation penetration 0-56901
- interstellar grains and molecules, UV obs. from Spacelab 0-41871
- IUE, search for stellar coronae 0-4233
- IUE satellite, observing experience 0-36476
- measurement of UV radiation, accurate techniques 0-47103
- OSO-8 UV spectrometers, computer-controlled mission operations 0-41723
- primaeval galaxies, model emission spectra 0-46655
- QSOs, dust opacity and photoionization in far UV 0-46696
- solar UV vars. rel. to climatic changes 0-26607
- spectroscopy, fabrication of transmission gratings 0-14490
- Sun, N III and O IV intersystem multiplets as density indicators for solar plasmas 0-31264
- Ultraviolet Spectrometer and Polarimeter on Solar Maximum Mission 0-51661
- D<sub>2</sub> gas discharge lamp as UV continuum source, space appls. 0-36505
- O I isoelectronic sequence, excited level populations, line intensity ratios, solar corona appl. 0-32637

**ultraviolet communication** see *optical communication***ultraviolet detectors**

- biological application, UV meas. 0-35963
- calorimeter, pulse gas, for vacuum UV rad. meas. 0-251
- electrographic instrumentation for ultraviolet imaging and spectrography 0-46399
- ferrioxalate actinometer for solar UV radiation meas. 0-41731
- liquid chromatograph for homogeneous mixture analysis 0-16757
- measurement of UV radiation, accurate techniques 0-47103
- microcomputer controlled UV ozone calibrator 0-13149
- solar UV meas. and physics 0-41784
- spatial imaging detector system for pulsed plasma extreme ultraviolet diagnostics 0-33821
- standards, at Australian Nat. Meas. Lab. 0-31704
- Zn<sub>3</sub>P<sub>2</sub>, UV photoconductive detectors 0-4766
- CaSO<sub>4</sub>:Tm intrinsic thermoluminescence stability for UV dosimetry 0-12262
- Zn-In-S ultraviolet detector (*Russian*) 0-18014

**ultraviolet lamps** see *lamps***ultraviolet radiometry** see *photometry***ultraviolet sources** see *light sources***ultraviolet sources (astronomical)**

- accreting magnetic degenerate dwarfs, X-ray and UV emission 0-41826
- Cygnus X-2, rapid UV flux vars., IUE obs. 0-12833
- diffuse cosmic far UV background, rocket obs. 0-46708
- Feige 86, UV high-resolution spectrum 0-41834
- HD 192273, high latitude EUV source, low-mass binary 0-4353
- RU Lupi, T Tauri star, for UV radiation rel. to chromosphere, corona and X-ray emission (*Russian*) 0-51770
- NGC 4151, Seyfert galaxy, for UV line profiles 0-22083
- NGC 7023, refl. nebula, far UV brightness rel. to HD 200775 reddening and dust albedo and scatt. 0-51832
- PKS 2155, BL Lacertae object, UV flux meas. by IUE 0-12833
- stars in high-latitude regions, balloon-borne UV survey 0-41891

**ultraviolet spectra of inorganic solids** see *visible and ultraviolet spectra of inorganic solids***Umklapp process**

- dielectric material, phonon thermal conductivity, Umklapp process, comparison with LiF data 0-39367
- electron gas, 1-D, 2-D Coulomb gas, and 2-D epitaxial monolayer problems, family of mappings 0-34346
- Fermi one dimensional gas with long range potential, renormalisation group, exchange, Umklapp interactions 0-2351
- one-dimensional metal, cond., electron-electron scatt. 0-10957
- superconductivity, high-temp. electron-hole 0-2512
- two-dimensional Wigner-crystal-liquid-surface system, eigenmodes and instability of charged liq. surface 0-10896
- Al, positron annihilation, angular distrib., Umklapp effects (*French*) 0-50454
- Al, positron annihilation studies using high-density proportional chambers 0-25478

**Umklapp process continued**

- C<sub>6</sub>Cs, intercalation cpd., theory of order-disorder phase transitions 0-19908
- Cu, positron annihilation studies using high-density proportional chambers 0-25478
- K, thermomagnetic and thermoelectric properties, phonon scatt. processes 0-29390
- K<sub>2</sub>Pt(CN)<sub>4</sub>, quasi-one-dimens. Peierls system, phonon dispersion and neutron scatt., calc. 0-24550
- TaSe<sub>2</sub> (2H), optical absorpt., band struct., plasmons, and CDW 0-45104
- TaSe<sub>2</sub> (2H), plasmon behaviour at charge density wave onset 0-10900

**uncertainty principle** see *indeterminancy***underground cables**

- oil-cooled, laminar friction factor and heat transfer 0-10247

**underwater acoustics** see *underwater sound***underwater cables** see *submarine cables***underwater sound**

- see also *hydrophones; oceanography; sonar*
- 3-layer waveguide, wave numbers and phase difference between components of sound field 0-38144
- acoustic line array operation in water layer 0-5866
- acoustical compliance element, elastic problem of flattened cylinder type 0-33309
- acoustical compliance tube for sound projectors, stress and deformation analysis 0-33310
- ambient noise depth-dependence models and their relation to low-frequency attenuation 0-43514
- amplitude fluctuations due to temp. microstructure 0-19140
- basic principles and problems 0-53536
- beam pattern side lobes, significance in fluid flow measurement 0-19136
- Benthic Untethered Multipurpose Platform for underwater acoustic TV 0-46319
- biological object vel. measurement, design principles of instrums. 0-19195
- broadside vertical array in shallow water, comments on array gain 0-19138
- broadside vertical array in shallow water, reply to comments on array gain 0-19139
- composite compliant baffle anal., comments 0-48482
- deep ocean LF attenuation data review 0-33318
- deep towed seismic profiling system, multichannel hydrophone array, sub-bottom oceanic structure study appl. 0-26550
- differential Doppler shift estimation 0-19162
- directional spectral spreading in randomly inhomogeneous media 0-19133
- explosion generation of sound wave pulse, nonlinear region 0-56493
- explosion of detonating gas with high initial bulk energy density 0-5867
- explosions in shallow water, determination of acoustic source levels 0-19131
- explosive shock waves, formulation of weak shock soln. 0-10070
- explosive wave profile transformation, time constant derivation 0-48485
- fish stock count by acoustic target strength meas. of individual fish, comparative anal. 0-19129
- fish target strength functions, model for averaging 0-43512
- flexural wave transmission across line inhomogeneity on plate in liquid, radiation of sound 0-38159
- fluctuating ocean, computations of strength and diffraction parameters 0-33320
- fundamental and second harmonic pressures meas. in field of circular piston source 0-33322
- generalised wave theory applied to propagation of sound in deep water (*French*) 0-53505
- geophone and hydrophone recordings in Californian offshore sediment 0-46192
- Green's function field soln. in plane multilayered medium, theoretical and numerical 0-33314
- high-resolution ocean subbottom survey data analysis model 0-46211
- hydrophone shadowing by seamounts 0-33308
- infrasonic field structure in shallow sea, machine expt. 0-14512
- Inverted Echo Sounder for ocean thermal structural variations and currents 0-46312
- LF sandwich transducers, analogy between fluid and solid horns 0-38213
- low-freq. absorption in seawater, borate-complex relaxation 0-36304
- low-frequency absorption contour chart for Atlantic, Indian and Pacific Oceans 0-36303
- magnetostriuctive transducer at air-water surface, effect of spherical scatterer on radiation reactance 0-48531
- magnetostriuctive underwater sound transducers, use of rare earth alloys 0-19204
- marine particulate plume density and distrib., acoustic assessment 0-45843
- marine sediments, saturated, nonlinear parameter 0-19132
- marine sediments and rocks, ratio of compressional wave vel. to shear wave vel. and Poisson's ratios 0-12404
- midocean environment, fluctuations in reciprocal acoustic transmission 0-10069
- mode interactions in isovelocity ocean of uniformly varying depth 0-33321
- multielement array underwater acoustic instrumentation 0-43571
- multilayered media, layer-indexed acoustic reflection model 0-43517
- multipath interference nulls in long-range, low-frequency acoustic propagation by normal modes 0-33315
- nearfield measurement system for computing farfield radiation characts. of transducers 0-10101
- noise radiated by incompressible boundary-layer transition 0-33319
- nonacoustic noise interference in measurements of infrasonic ambient noise 0-19135
- nonlinear reflection of short impulsive waves at water surface 0-33298
- North Pacific, variation of vertical directionality of noise with depth 0-19130
- ocean acoustic background noise, detection of sinusoids 0-33347
- ocean acoustic tomography, for large scale monitoring 0-4119
- ocean bed carbonate sediments, acoustic stratigraphy 0-21709
- ocean bottom, influence of range dependence on adiabatic approximation 0-10066
- ocean bottom, sloping, effects of tidally varying sound speed on propag. 0-10062
- ocean bottom plane-wave reflection loss model including sediment rigidity 0-33311
- ocean channel, deep, analysis of acoustical effects of receiver and source motions at short ranges 0-10063



**underwater sound continued**

- ocean cyclonic eddies, influence on short-range acoustic transmission 0-33316
- ocean environment, range dependent, examination of multipath processes within context of adiabatic mode theory 0-19134
- ocean internal waves, acoustic reverberation data 0-41562
- ocean sediments, experimental studies of attenuation 0-10067
- ocean surface characteristics affecting acoustic scatt. 0-46194
- oceanic finestructure effects on acoustic transmission, numerical simulation 0-43511
- optical generation of sound in liquid half-space bounded by solid layer 0-38158
- N.Pacific mesoscale phenomena, oceanographic model and acoustic survey comparison 0-46195
- S.Pacific Ocean, acoustic cross-section (Project Kiwi One) 0-36330
- N.Pacific Ocean, west, depth, var. of temp., salinity and sound vel. meridional gradients 0-51429
- parabolic reflector as nearfield calibration device for transducers 0-48528
- parabolic wave theories and applications 0-51436
- partially random sonobuoy array directivity index analysis 0-43518
- passive coherence processing sonars, near-field performance 0-33346
- penetration of marine sediments as function of physico-mech. characts. (French) 0-33324
- plane wave propag. in ocean, fluctuations of arrival angle at line array 0-43515
- propagation in shallow water expts. for long range communication systems 0-33323
- pulse compression system, signal processing methods 0-56630
- reflection from sea bottom with linearly increasing sound speed 0-33312
- resonance theory of acoustic waves interacting with an elastic plate 0-33268
- scattering of boundary wave generated by grazing incidence at slightly rough rigid surface 0-10064
- scattering of spherical pulses by slightly rough surfaces 0-10065
- sea explosion waves, comparison of empirical and theoretical laws of parameter variation 0-36325
- sediment classification by ocean subbottom acoustic Q meas. 0-46168
- sediments, penetration of highly directional acoustic beams 0-14511
- shallow water prop., beam forming and freq. dependence of mode identification 0-28373
- ship noise, source level model for propeller blade rate radiation 0-43513
- ships, acoustical determination of course speed and lateral drift 0-5892
- signal coherence limits in random ocean environment 0-46193
- slotted transducer arrays with matched backings for underwater imaging 0-38214
- sonar performance, incoherent and coherent processing against echo fading in shallow water 0-19142
- sonomagnetic pulses from underwater explosions and implusions 0-43510
- source location in random dispersive media using generalised reduction methods 0-43509
- source power spectrum measurement in shallow water 0-19141
- spherical targets, dynamics of acoustic resonance scattering appl. to gas bubbles in fluids 0-10068
- surface duct propag., influence of submerged duct 0-5865
- surface duct propagation model based on radiation transport eqn. 0-46196
- through-water diver communication system Wet-Phone, voice or switch operated, 31.5 KHz carrier, 1350 m range 0-38187
- towed arrays, hydroacoustic sources of locally generated sound, hose material 0-23822
- towed arrays, hydrodynamics 0-23823
- transducer, ceramic, spatially-bounded US wave response 0-48542
- ultrasound speed determ. over wide range of pressure and temp. 0-23821
- undersea acoustic signal coherence fluctuations 0-46191
- undersea platform location by acoustic signature processing 0-43519
- upper ocean, spatial variability 0-51435
- US backscattered wave minima for solid metal cylinder immersed in water (French) 0-53510
- US backscattering by elastic cylinders in water (French) 0-53511
- US focusing device with IDT on thin piezoelectric plate 0-1398
- US propag. in water with air bubbles (French) 0-53507
- US pulse transmission and reception by wide-band transducers 0-10099
- US waves in liquids, photoelastic visualisation 0-28374
- VLF wind-generated noise produced by turbulent pressure fluctuations in atmosphere near ocean surface 0-19137
- volume scattering at 25 kHz in presence of temp. discontinuity layer 0-38157
- volume scattering strengths and zooplankton distributions at acoustic frequencies between 0.5 and 3 MHz 0-33317
- wave direction-finding by full-aperture beam forming delay line 0-48527
- wave eqn. derivation for inhomogeneous ocean 0-33313
- wideband acoustic characterisation method for fish schools and long-range propag. channels 0-43551

**undulator radiation**

- electron relativistic beam in synchrotron, ang. spread of vel. using undulator radiation electron 0-14021
- hard, in dispersive medium, in dipole approx. 0-23608
- review 0-9794
- shortwave coherent undulator radiation, classical theory 0-23195

**unified field theories**

see also *supergravity; Weinberg model*

- (1+1) dimensional model field, fermion-boson correspondence, Klein transformation 0-42379
- Abelian and non-Abelian gauge theories, mass generation, renormalisation, chiral and unified theories 0-4871
- astronomical bodies, mag. field, cosmological interpretation 0-46714
- attempts at unification, general review 0-13250
- baryon decay effective lagrangian flavour struct. and renormalisation, grand unification 0-27447
- baryon nonconservation in grand unified theories, rel. to Universe isotropy and homogeneity 0-22125
- baryon number nonconservation limits, grand unified theory nucleon decay modes 0-411
- baryon- and lepton-nonconserving processes in grand unified theories 0-13253
- Big Bang primordial fluctuations and Universe smoothness in grand unified theories 0-56987
- Bonnor transform. extension 0-31643
- Borel multipliers for the Bondi-Metzner-Sachs group 0-18088

**unified field theories continued**

- boson field operator constructed from even number of fermion field operators 0-27416
- Brans-Dicke theory, generalised static EM fields 0-12972
- causal theory, removal of Einstein's objections to quantum theory, unification 0-31572
- classical non-Abelian gauge theories in the space of reference frames 0-31977
- Clifford algebra based unified theory for quarks and leptons 0-47228
- conference, quarks and leptons as fundamental particles, Schlaming, Austria, (Feb.-Mar. 1978) 0-17709
- conformal electrodynamics in Einstein spacetime 0-31644
- cosmological baryon asymmetry origin, unification mass 0-31398
- cosmological baryon production, kinematical constraints for heavy boson decay 0-51932
- D-type nondiverging and nontwisting electrovac soln. with  $\lambda$  0-115
- de Sitter gauge invariance based unified field theory 0-22255
- Dirac particle creation in Einstein-Cartan-Sciama-Kibble theory 0-4622
- $E_7$  grand unification using  $SU(3) \times (U(1))^3$  gauge group, neutral currents 0-27444
- $E_8$  group, branching rules, Kronecker, products 0-27438
- $E(6)$  grand unified theories, one loop renormalisation effects, stepwise symmetry breaking 0-32058
- early big bang, asymptotic freedom, rel. to cosmic microwave background isotropy 0-46712
- effective potential for spontaneously broken gauge theories and gauge hierarchies 0-18080
- Einstein's theories extended, book 0-22164
- Einstein's unified field eqns., strength 0-52103
- Einstein and the quantum theory, review 0-22337
- Einstein theory, Faraday's EM induction prop. 0-117
- Einstein-Maxwell eqn., static electrovac soln. 0-31642
- Einstein-Maxwell eqns., algebraically special space-times with nontwisting rays 0-42114
- Einstein-Maxwell eqns., Robinson, Schild and Strauss soln. 0-46901
- Einstein-Maxwell eqns., static stationary solns. 0-4617
- Einstein-Maxwell eqns. with axial symmetry, exact solns. 0-118
- Einstein-Maxwell equations: gauge formulation and solutions for radiating bodies (German) 0-27194
- Einstein-Maxwell equations, charged solution, type-G 0-46904
- Einstein-Maxwell non-static field eqn. solns. 0-42128
- Einstein-Maxwell space-times, infinitesimal holonomy group structure, Lie algebra 0-12976
- Einstein-Maxwell stationary eqns., symmetries 0-31627
- Einstein-Maxwell stationary field eqns. 0-31626
- Einstein-Yang-Mills system in six dimensions, static solution 0-8883
- Einstein's unified field theory, electric cylindrically symmetric solns. 0-22254
- electrodynamics and gravitation, closed theory 0-52445
- elementary particle physics, information from astronomical observations 0-51935
- EM and gravitational field unification, development attempts (Norwegian) 0-4615
- EM and weak interaction unification, bearing of Weinberg model and gauge invariance (German) 0-32054
- exceptional groups, patterns of symmetry breaking 0-42356
- fermion mass, unified gauge model based on  $E_6$  0-32053
- fine structure constant, estimate in unified theories with unstable proton 0-9133
- Finzi's nonsymmetric theory, plane wave solns. 0-8885
- gauge hierarchies, book contrib. 0-42384
- gauge hierarchy in presence of discrete symmetry,  $U(1)_L \times U(1)_R$  and  $SU(2)_L \times SU(2)_R \times U(1)$  0-9094
- gauge model, weak interactions of leptons and quarks 0-22556
- general relativity, quantum field theory, vierbein formalism 0-22263
- grand unified theories, baryon asymmetry of the Universe,  $SO(10)$  model 0-4619
- gravitation, gauge formulations, relationship to Riemannian holonomy struct. 0-42131
- gravitation, gauge theory, special relativistic limit 0-22256
- gravitational field theory, ten-dimensional manifold of local inertial reference frames 0-46903
- hadron spectroscopy, quark models and  $SU(5)$  grand unification scheme 0-4958
- Higgs bosons, masses, gauge hierarchies,  $SU_3$  model 0-47236
- historical contributions (Hungarian) 0-46900
- history of gravitational and unified theories, book contrib. 0-22259
- horizontal-quantum-flavour-dynamics approach to the fermion mass spectrum in  $[SU(2) \times U(1)]_{WS} \times U(1)$  gauge 0-52474
- isotopic spin sources, motion, gauge theories 0-12977
- Jordans 5-D unified theory of gravitation, Ehlers-Harrison type transform 0-8882
- Kaluza-Klein bundle, unified theory 0-37153
- mass scales, alternatives to  $SU(5)$  0-27441
- massless boson, unified nonlinear theory 0-376
- mixing angle and proton lifetime, two-loop corrections 0-13249
- monopole solutions for strong gravity coupled to  $SO(3)$  gauge fields 0-4621
- neutrino, Maxwell, and scalar fields in the cylindrical magnetic or plasma universe 0-120
- neutrino-generated static space-times 0-52107
- non Abelian gauge theories, relation between fields and pot. 0-22529
- nonlinear Heisenberg-Klein-Gordon equation, localised solns. in flat Schwarzschild space-time 0-4620
- nonlinear realizations of compact and noncompact gauge groups, grand unification 0-47183
- nonlinear wave propagation in relativistic continuum mechanics 0-22203
- nucleon decay operator anal., superunified theories selection rules 0-13302
- $O(10)$  theory of strong, weak and EM interactions, masses and mixing 0-13248
- observability differences between classical EM and gravitational gauge fields 0-36925
- partial unification of strong, weak and EM interactions, B-meson decay 0-18106
- Pati-Salam neutral vector gluons, possible expt. search in  $e^+e^-$  collisions 0-37202
- Peres space-time, generalised, algebraic props. and solns. 0-106
- phenomenological ideas toward a field theory of matter, unification of EM and gravity fields 0-378



**unified field theories continued**

precocious chiral grand unification based on  $SU(8)_L \times SU(8)_R$  semi-simple gauge group (*Russian*) 0-42382  
 proton decay, confirmation of unification of forces, book contrib. 0-42383  
 proton half life, Dirac approach to large number coincidences 0-27501  
 quantum field theory, lattice-limit definition of functional integrals 0-27396  
 quarks and leptons, high energy and nuclear physics interface 0-41974  
 quartz resonator, large mag. field effect on rate of time 0-27195  
 riemannian-Maxwellian invertible structures in general relativity 0-4618  
 $SO_{10}$  hierarchical breaking and neutrino masses 0-22550  
 $SO(10)$ , p decay modes 0-13301  
 $SO(10)$  grand unified theories, one loop renormalisation effects, stepwise symmetry breaking 0-32058  
 $SO(10)$  grand unified theory, breaking scheme and neutrino mass 0-47230  
 spontaneous CP nonconservation in theories with more than four quarks 0-47212  
 standard weak-EM gauge model, six-quark phenomenology and Grand Unification 0-37204  
 static coupled zero-mass and source-free EM fields, generalised Laplace eqn. 0-52102  
 stationary charged C-metric 0-17849  
 strong gravity contrib. to nucleonic axial-vector form factor in  $SU(3)$  0-4902  
 strong gravity with torsion and the Cabibbo angle 0-4913  
 $(SU_3 \times U_1) \times S_4$  flavour dynamics, flavour number bound, n quark and n lepton generations unification 0-4907  
 $SU_4$  gauge model of weak and EM interactions, u- and d-quark masses 0-13254  
 $SU_5$  theory, superheavy particles, decoupling at low momenta 0-52431  
 $SU_2(2) \times SU_R(2) \times U(1) \times [SU(3) \times SU(3)]_C$  gauge model, chiral colour symmetry breaking 0-47234  
 $SU(2)_L \times (T_3)_R \times U(1)_Y$  gauge unified model, neutral current interactions, ed and  $\nu$  scatt. 0-18107  
 $SU(2)_L \times SU(2)_R \times U(1)$  gauge with permutation symmetry, quark mass and Cabibbo angles 0-47232  
 $SU(2)_L \times U(1)$ , natural flavour conservation of Higgs couplings and Cabibbo mixing conflict 0-37200  
 $SU(2)_L \otimes SU(2)_R \otimes U(1)$  calculability, fermion mass matrix and CP invariance violation 0-13252  
 $SU(2)_L \otimes U(1)$  theory, CP violation and Cabibbo angle 0-52447  
 $SU(2)$ , unification of isospin and hypercharge, electroweak interactions of leptons 0-27439  
 $SU(2) \times SU(1) \times SU(3)$  unifying mass scales without intermediate schiral colour symmetry 0-22555  
 $SU(2) \times U(1)$  unified theory, symmetry and renormalisation 0-22551  
 $SU(2) \times U(1) \times G$  expanded gauge models of neutral currents, propagator momentum transfer 0-47237  
 $SU(2) \times U(1) \times U(1)$  model, Cabibbo angle and Higgs coupling strangeness conservation 0-47233  
 $SU(2) \times U(1)$  gauge theories, successes and current issues 0-18064  
 $SU(2) \times U(1)$  gauge theory of weak, EM and dual EM interactions 0-52448  
 $SU(2) \times U(1)$  scheme, CP violation parametrization, quark n-doublet weak interaction (*Russian*) 0-13231  
 $SU(2) \otimes U(1)$  gauge models of weak and electromagnetic interactions and the  $\mu e$  universality (*Russian*) 0-13257  
 $SU(3)_C$  gauge symmetry, unification of fundamental forces in nature, elementary particle constituents, review 0-27448  
 $SU(3)$  gauge model of weak and EM interactions, Weinberg angle, Han-Nambu quarks 0-52452  
 $SU(4)_C \times SU(4)_L$  synthesis of strong, weak, and electromagnetic interactions 0-13255  
 $SU(5)$ , p decay modes 0-13301  
 $SU(5)$  and  $SO(10)$  grand unified theories, fermion and Higgs boson mass bounds 0-9134  
 $SU(5)$  grand unification, fermion mass and Higgs representations 0-27446  
 $SU(5)$  grand unification, nucleon lifetime, bag model calc. 0-52450  
 $SU(5)$  grand unification, strong CP violation, quark-lepton mass ratio 0-32057  
 $SU(5)$  grand unification embedding in  $SU(N)$ ,  $SU(9)$  theory, flavour unification 0-32059  
 $SU(5)$  grand unified theories, proton decay, flavour mixing effects 0-377  
 $SU(5)$  grand unified theory, flavour number limit from fermion mass higher order corrections 0-4904  
 $SU(6)$  grand unification model, hierarchy of symmetry breakings and neutral currents 0-52446  
 $SU(6)$  grand unified theories, one loop renormalisation effects, stepwise symmetry breaking 0-32058  
 $SU(7)$  grand unified theory with heavy colour 0-42380  
 $SU(9)$  grand unification of flavor with three generations 0-13251  
 $SU(N)$  grand unification with several quark-lepton generations 0-27443  
 $SU(N)$  unification of extra strong interactions, no-go theorem 0-32056  
 $SU(s)$  grand unification, neutrino mass and oscillations, B-L nonconservation 0-52449  
 superconductivity and elementary particles theory, review 0-4911  
 supergravity and unification of laws of physics (*Polish*) 0-36926  
 superheavy magnetic monopoles, cosmological prod. in grand unified models 0-8884  
 supersymmetry, physico-geometrical comments, unified field theories and supergravity, gauge transformations 0-364  
 superunified theories in superspace 0-8886  
 $U(1) \times SU(2)$  unified gauge field theories, field function  $O(4)$  invariance 0-37201  
 unified description of quarks and leptons using colour and flavour degrees of freedom 0-27445  
 unified model for atomic parity violation and neutral currents in gauge theories 0-4912  
 universal supersymmetry and its need for grand unification theories 0-13230  
 Universe and microcosm, gravitational-inertial field theory 0-8721  
 vertical-horizontal symmetric minimal grand-unification 0-47229  
 very early Universe, nonequilibrium, grand unified particle interactions, baryon number violating bosons 0-36752  
 very early Universe, phase transitions and mag. monopole prod., grand unification 0-51934  
 weak and EM interaction unification with strong interactions following  $\tau$  and T, book contrib. 0-47235

**unified field theories continued**

Weyl-Dirac theory with torsion 0-52106  
 Z-boson and two-boson models, neutral current phenomena,  $\mu$ -e universality 0-18109  
 $e^+e^- \rightarrow l^+l^-$  via many-vector boson exchange, cross sections from unified models 0-22597  
 $eN$  interactions, parity nonconservation,  $SU(2)_L \times SU(2)_R \times U(1)$  gauge model anal., Z boson decay widths 0-47302  
 P decay, baryon number-lepton number conservation or violation, grand unification implications 0-27425  
 $\theta$  vector particles, calibration interaction macroscopic confinement radius (*Russian*) 0-47257  
 T, quixotic interpretation as QQ bound state 0-13280  
 Z-mass prediction as test of standard model 0-47239

**unijunction transistors**  
 negative resistance as phase transition, critical exponents (*French*) 0-49746  
 transition critical exponents, negative resistance phenomena 0-44713

**unimolecular layers** see *monolayers*

**uninterruptible power supply** see *emergency power supply*

**units (measurement)**  
 see also *constants; dimensions; measurement; nomenclature and symbols*  
 angular, ambiguity of status 0-8951  
 COMECON standard ST SEV 1052-78 for establishing units of physical quantities 0-42189  
 definitions, of units, standards and measurement methods (*French*) 0-27264  
 electromagnetism, dimensions and symmetry considerations, duality transformations 0-28139  
 health physics quantities and units 0-8193  
 International Bureau of Weights and Measures, 1978 activities and news 0-188  
 magnetism teaching w.r.t. chemistry, guide to units 0-12871  
 mass, force and weight, relationship 0-27273  
 pressure unit, optimum metric, for thermodynamic standard state 0-8950  
 radioactivity, definitions and interrelations 0-17914  
 SI system, need for periodic recalibration of laboratory equipment 0-31705  
 SI units, conventions and practices, physics teacher's viewpoint 0-36968  
 SI units, group props., dimensionality 0-17746  
 SI units, group props. 0-17745  
 SI units, rationalisation and need for approximation to SI 0-36969  
 standard for unification within COMECON framework 0-42187  
 thermodynamics, SI units (*Croatian*) 0-189

**universe** see *cosmology*

**universe models** see *cosmology*

**unwinding** see *winding (process)*

**upper atmosphere**  
 see also *exosphere; ionosphere; magnetosphere; mesosphere; radiation belts; thermosphere*  
 aerospace environment, upper atmosphere and solar-terrestrial relations, book 0-8466  
 artificial aurora, optical emission excited by electron ejection from rocket 0-51592  
 auroral X-rays, balloon obs. in Canada rel. to X-ray illuminating regions determ. 0-31156  
 coupling between neutral and ionized atmosphere, NATO conf. proceedings (Spand, Norway, 1977 April 12-22) 0-27036  
 density derivation from near-circular satellite orbits, effect of temp. diurnal var. 0-21867  
 density models rel. to drag on artificial satellites 0-17428  
 electron beam injection into neutral gas, laboratory study 0-54004  
 electrostatic V-shocks in auroral plasma, approximate equipotentials 0-21870  
 gas clouds released at satellite orbital velocity, dynamics expts. 0-14748  
 gas releases, collisionless-diffusive flow transition 0-12577  
 geocorona, rocket borne resonant absorption spectrometer and photometer for He obs. 0-4155  
 gravity waves propag. through critical layer 0-51591  
 ion chemistry, ion+mol., rate consts., in situ ion comp. meas. 0-31154  
 ionization inhomogeneities advected neutral gas motions, geomag. field effects 0-26677  
 meteor trail, maximum ionization height detect. method 0-8487  
 meteor trail diffusion, radio refl. determination 0-46329  
 meteor trails, scattered radio waves trapping by ionospheric ducts 0-4172  
 neutral composition variations at F-region heights, meas. from incoherent scatt. and nightglow obs. (*Portuguese*) 0-41584  
 neutral wind gradients, meteor radar obs. 0-41575  
 nightglow O I 5577 Å line, intensity var., related to solar tides (*Russian*) 0-12585  
 O I nocturnal 6300 Å luminesc., profiles from incoherent scatt. radar and photometry (*Portuguese*) 0-41591  
 positron annihilation line at 511 keV, balloon obs. 0-41582  
 radiometers characts. assessment, statistical analysis of time-dependent series (*Russian*) 0-56777  
 relativistic electron beam localisation, stabilising effects (*Russian*) 0-21868  
 rotational rate and winds, determ. from China 2 rocket (1971-18B) orbit 0-4231  
 rotational vel. from Interkosmos 10 inclination var. analysis 0-41693  
 solar flare X-rays, atmosphere reflected fluxes rel. to flare spectrum beyond 200 keV 0-51710  
 temperature, turbulence and  $N_2$  composition, 95-150 km altitude, 1967-75 obs. 0-51588  
 UV radiation sources, modelling 0-1288  
 visual observations from space 0-21825  
 wind, obs. by radio meteor drift, 80-100 km altitude over Adelaide 0-46328  
 wind and temperature measurement, laboratory discharge lamp source appl. 0-4148  
 wind determination by meteor track movement (*French*) 0-51589  
 wind observed at solar eclipse, 80-100 km altitude 0-46327  
 winds of 95 km altitude, meteor obs. at 45°N 0-46330  
 zonal winds at 95 km altitude, correl. with radar meteor echo rates 0-56775  
 $N_2$  vibrational level distrib. in upper atmos., theory 0-41576  
 O, UV photoionisation cross-section calc., 304 and 584 Å 0-43015  
 O<sub>3</sub> content of atmos. rel. to solar activity 0-41488



## uranium

see also nuclei with .....  
 see also fission of uranium  
 abundance in Precambrian basement, W.Canada, petrologic and tectonic controls 0-17257  
 adsorption of water and O<sub>2</sub>, XPS study 0-7473  
 advanced high U-density reduced-enrichment plate-type fuel development for test and research reactors 0-23101  
 atom, laser fluoresc. spectroscopy using pulse hollow cathode lamp 0-27973  
 atom, sputtered, absorpt. spectra in hollow cathode glow discharge 0-32643  
 atom and ions, shell energy struct., SCF calc. by Dirac-Fock-Slater method 0-52877  
 blood, U conc. meas. 0-21532  
 breeder reactors, current status in Europe 0-27796  
 charge density wave, first order transition 0-10664  
 conference, natural fission reactors, Paris, France, 1977 0-17716  
 content anomaly of sediment under Galapagos hydrothermal mounds 0-56434  
 core and valence band spectra, XPS obs. 0-50530  
 core fuel elements, of A-1 reactor, volume growth (Czech) 0-27745  
 development possibilities of energy resources, review (German) 0-21355  
 educational module, nature and exploration in US sandstone deposits 0-36799  
 electron stopping power, continuous slowing down approx., range difference for 0.2 to 10 MeV electrons 0-39187  
 electronic band struct. and props. 0-10861  
 enrichment induction in test and research reactors, US program 0-22949  
 enrichment methods, efficiencies and costs (Dutch) 0-37634  
 enrichment plants, 1979 status (French) 0-807  
 exploration in developing countries, facts and trends 0-16764  
 exploration of the Oklo natural fission reactors, review (French) 0-21753  
 explosively clad uranium targets 0-18737  
 exposure standards for U mining 0-46055  
 extraction from seawater, feasibility 0-37564  
 extraction from seawater using composite absorbents, Ti(IV)-Fe(II) oxide 0-24730  
 extraction from seawater using magnetic adsorbents 0-37563  
 extraction from seawater using Ti based composite hydrous oxides (Japanese) 0-804  
 fission reactors, integral experiments for testing Th and <sup>233</sup>U data 0-27707  
 fuel cycle, supply, enrichment and irradiated fuel reprocessing developments (French) 0-18565  
 fuel supplies security up to year 2000 (French) 0-3480  
 geological exploration, LANDSAT data merged with geol. and geophysics data 0-56651  
 gravimetric titration, automated, determ. of U in safeguard materials 0-622  
 heat capacity, from 80 to 1000K of high purity metallic sample 0-34201  
 HTR fuel cycle program in the Federal Republic of Germany 0-644  
 HTR fuel of low/medium enrichment 0-645  
 in situ leach mining, environmental considerations rel. to water quality 0-3543  
 isotope separation and ratios, neutron irradiation of natural U in Japan Material Testing Reactor (Japanese) 0-52730  
 isotope separation appl. to nucl. fuel cycle, teaching module 0-36805  
 isotope separation by Redox chromatography 0-37565  
 isotope separation processes, w.r.t. economics, reliability and safety (French) 0-806  
 isotopes, in soil, determination using alpha-spectrometry 0-45601  
 isotopic depletion curves at Oklo natural fission reactor (French) 0-21759  
 leaching, design criteria for criticality safety of dissolution vessel 0-13772  
 liquid, electronic density of states, shock vaporization technique 0-29300  
 lunar drill sample, neutron activation and radiochemical anal. (German) 0-51673  
 migration, and trapping of D in U and UO<sub>2</sub> during D<sup>+</sup> implantation 0-34243  
 mineral deposits, organization in Mouana, Gabon district (French) 0-21741  
 miners, chromosome aberrations as biological dose-response indicator 0-17019  
 mining, CEA and Cogema activities (French) 0-626  
 mining, processing and transportation, in Western US, impact 0-45621  
 mining, radioactive mining waste disposal (Dutch) 0-21418  
 natural fission reactors, parametric study of criticality conditions (French) 0-21768  
 natural fission reactors, requirements for formation, search for new examples 0-21772  
 neutron criticality, solid angle computations using computer code 0-13726  
 neutron spectra in fast neutron systems using <sup>6</sup>Li sandwich counter 0-27884  
 nondestructive assay of mixed samples using neutron activation anal. 0-18423  
 nuclear fuel, burn-up, chemical separation, ion exchange 0-42746  
 oceanic crust abundance, heat flow implications, basalt fission track anal. 0-8287  
 Oklo fossil nuclear reactors, ion analysis exam. of U grains and gangue (French) 0-21758  
 Oklo natural fission reactor, computer calc. of neutron balance and flux distrib. (French) 0-21767  
 Oklo natural fission reactor, dating from U-Pb isotopic data 0-21763  
 Oklo natural fission reactor, eval. of neutron temp. from <sup>176</sup>Lu/<sup>175</sup>Lu and <sup>156</sup>Gd/<sup>155</sup>Gd isotopic ratios (French) 0-21766  
 Oklo natural fission reactor, isotopic anal. of rare earth metals (French) 0-21761  
 Oklo natural fission reactor, radioactive dating from Pb and Th meas. (French) 0-21762  
 Oklo natural fission reactor, Ru isotopic anal. (French) 0-21765  
 Oklo natural fission reactors, formation, propagation and control, review (French) 0-21774  
 Oklo natural fission reactors, geology, review (French) 0-21770  
 Oklo natural fission reactors, geophysical eval. of U distrib., topography, sedimentology and structure (French) 0-21755  
 Oklo natural fission reactors, migration in core sample, appl. to dating of reactions (French) 0-21760  
 Oklo natural fission reactors, migration paths for radioactive products 0-21773

## uranium continued

Oklo natural fission reactors, review of French geological research (French) 0-21744  
 Oklo natural fission reactors, U radiometric meas. and isotopic anal. (French) 0-21754  
 Oklo natural fission reactors geological environment, tectonic anal., petrography, geochemistry (French) 0-21742  
 Oklo natural reactors, control and propag. of nuclear reactions, thermal effects (French) 0-21769  
 Oklo natural reactors, data on stability and remobilisation, summary (French) 0-21771  
 Oklo natural reactors, mining, geology and tectonics (French) 0-21743  
 Oklo natural reactors, review of mineralogical and petrographic studies at Strasbourg (French) 0-21745  
 ore, Ru isotopic anal. 0-21764  
 ore at Oklo, appl. of Ep-pH diagrams to problems of retention and migration of fissionogenic elements 0-21757  
 ore dating from meas. of <sup>238</sup>U and Ru conc. 0-21863  
 ores treatment, in France and African countries (French) 0-805  
 photoneutron yields released by incident electrons, improved calc. 0-27630  
 PIXE elemental anal. at  $\mu\text{g g}^{-1}$  levels in ore samples 0-55758  
 plate-type research and test reactors, near-term reduced enrichment conversions 0-22951  
 powder, hydriding kinetics, 13.3 and 26.6 kPa, 50-250°C 0-16725  
 production in New Mexico, constraints 0-42843  
 radioactivity of thermal and mineral springs in Slovenia 0-7963  
 rolling texture formation, computer simulation in HCP and orthorhombic metals 0-3095  
 sand grains containing high <sup>238</sup>U and <sup>232</sup>Th concentrations, enhanced natural radiation exposure (German) 0-51018  
 soil, U and Ac series nuclides radioactive disequilibrium 0-4014  
 solubility in the Oklo reactor 0-21756  
 solubility of O<sub>2</sub>, and composition of lower phase boundary of UO<sub>2</sub> at 1950K 0-49366  
 specific heat, Debye temp. for  $\alpha$ -U 0-15258  
 spraypainting of deposits for nuclear measurements 0-18736  
 tailings management, economic impact on nuclear fuel cycle 0-18494  
 target, microwave laser irradiation, plasma form., inhibited electron thermal cond., laser intensity threshold Z-depend. 0-48928  
 thermionic spacecraft reactors with <sup>233</sup>U as fuel, reflector drums as control mechanism 0-47686  
 urine analysis by delayed neutrons 0-26331  
 vacancy formation and phase transformations by positron annihilation 0-49215  
 in water samples, conc. determ. by fission track registration technique 0-12565  
 world resources, effect on development of nuclear power 0-55826  
 $\alpha$ -particle detectors, two layer proportional counter for measuring U content in solid-waste mats. (Russian) 0-27904  
 $\alpha$  disintegration, liquid scintillation counting 0-27873  
 BaF<sub>2</sub>:U, absorption band spectra following neutron irradiation 0-29763  
 BaF<sub>2</sub>:U, neutron irradiation, absorpt. band attributed to F<sub>2</sub><sup>-</sup> centres 0-7380  
 CaF<sub>2</sub>:U, charge conversion of U<sup>3+</sup>, ESR spectra 0-7150  
 CaF<sub>2</sub>:U, U<sup>5+</sup> centres, nonoctahedral symmetry 0-11266  
 CaF<sub>2</sub>:U<sup>4+</sup>, EPR hyperfine struct. 0-15781  
 LaCl<sub>3</sub>:U<sup>3+</sup> (5F<sub>3</sub>), polarised absorption spectra and energy levels 0-16063  
 ThBr<sub>4</sub>:U<sup>4+</sup>, absorpt. spectrum, zero phonon line (French) 0-11443  
 $\alpha$ -U, orthorhombic, computer simulation of rolling texture formation 0-3095  
 U-SbO<sub>3</sub> catalyst, dynamic measurements of electrical conductivity during adsorption and catalysis 0-13096  
 U+H<sup>+</sup>, L X-ray production cross sections, 0.3-1.8 MeV, expt. rel. to PWBA prediction 0-53115  
 U+H<sup>+</sup>(D<sup>+</sup>), L-subshell vacancy production, Coulomb deflection effects 0-9711  
 U+U, K-shell ionisation, classical relativistic trajectory method appl., 1, 10 GeV/n 0-43129  
 U<sup>+</sup>+U(U<sup>+</sup>)(U<sup>2+</sup>), elastic scatt. in plasma, interaction pots. and momentum transfer 0-38534  
 UI, absorption line shape change, pulsed hollow cathode source (French) 0-47927  
<sup>233</sup>U, enhanced fuel prod. using Th-Li hybrid reactor blanket with UO<sub>2</sub> multipliers 0-13810  
<sup>233</sup>U-<sup>235</sup>U fuel, nondestructive isotopic meas. using fission neutron counting 0-32385  
<sup>234</sup>U-<sup>230</sup>Th-<sup>226</sup>Ra, superposition soln. of transport of decay chain through sorbing medium 0-37500  
<sup>234</sup>U-<sup>230</sup>Th-<sup>226</sup>Ra decay chain, hydrogeological migration anal. 0-37501  
<sup>235</sup>U, conc. in UO<sub>2</sub>(NO<sub>3</sub>)<sub>2</sub> aq. soln., pulsed NMR determination 0-2658  
<sup>235</sup>U, nondestructive determ. of content in fuel elements using passive gamma ray spectrometry 0-18418  
<sup>235</sup>U/<sup>238</sup>U ratio, non-destructive field meas. for geophysical prospecting 0-21862  
<sup>235</sup>U-mica, solid state nuclear track detector, neutron response 0-27876  
<sup>238</sup>U, conc. in Florida phosphate materials 0-30615  
<sup>238</sup>U, neutron spectra for fusion + hybrid reactor materials 0-23142  
<sup>238</sup>U vapour, hollow-cathode generator, energetic yield 0-47724  
<sup>238</sup>U/<sup>232</sup>Th comparative breeding potential in LMFBR blankets 0-22948  
 U(Pd<sup>2+</sup>) + molecule, collisional relax. of <sup>3</sup>K<sub>3</sub><sup>0</sup> and <sup>3</sup>L<sub>7</sub><sup>0</sup> states, laser-induced fluoresc. obs. 0-52925  
 U(g)+nC(graphite)→UC<sub>n</sub>(g) (n=1 to 6), enthalpy changes 0-7842  
 U(n,X), Japan Material Testing Reactor, U and Pu isolation and isotopic ratios (Japanese) 0-52730

## uranium alloys

(Np<sub>1-x</sub>U<sub>x</sub>)Fe, Mossbauer spectra, magnetism and hyperfine interactions 0-20529  
 U-Al, storage of unirradiated fuel in borated concrete, criticality safety anal. 0-13608  
 $\alpha$ -U-Mo, dil., electronic properties depend. on 2<sup>1</sup>/<sub>2</sub>-th order phase transition under high press. (Russian) 0-11128  
 U-UNi<sub>2</sub>-UCO<sub>2</sub>, system, phase equilibria, lattice constants (German) 0-50598  
 U-ZrH low enrichment fuel for TRIGA and plate-type reactors 0-22950  
 UAl<sub>2</sub>, elastic consts., temp. and mag. field depend. 0-55450  
 UAl<sub>2</sub>, high field, high press. mag. props. 0-11172  
 UAl<sub>2</sub>, inelastic neutron scatt. 0-11165  
 UAl<sub>2</sub>, transport props., susceptibility and sp. ht. 0-11174  
 U(Co<sub>x</sub>Ni<sub>1-x</sub>)<sub>2</sub>, cryst. struct. and mag. props. at 4.2K 0-54175



## uranium alloys continued

- UCu<sub>5</sub>, core and valence band spectra, XPS obs. 0-50530  
 UFe<sub>2</sub>, Mossbauer diff., combination type maxima, hyperfine interactions on nuclei 0-25263  
 UFe<sub>2</sub>, nonstoichiometry effects on Curie temp., susceptibility obs. 0-25131  
 UGa<sub>2</sub>, mag. and magnetoelastic props. 0-15775  
 UHf prep. from uranyl ion using two-compartment electrolyser 0-802  
 UIr<sub>2</sub>X<sub>2</sub> (X=Si,Ge), cryst. struct. 0-1964  
 UNi<sub>5</sub>, core and valence band spectra, XPS obs. 0-50530  
 UNi<sub>5</sub>Cu<sub>4.5</sub>, core and valence band spectra, XPS obs. 0-50530  
 UNi<sub>5-5.5</sub>Cu<sub>x</sub>, NMR and press. effects 0-25230  
 U<sub>3</sub>Ni<sub>4</sub>Si<sub>4</sub>, X-ray cryst. struct. determ. 0-33931  
 UPb<sub>3</sub>, crystal field energy levels, magnetisation and susceptibility, neutron spectra obs. 0-50064  
 UPd<sub>3</sub>, crystalline elec. field studies using neutron inelastic scatt. at NRCN 0-10931  
 UPt, valence bands, XPS spectra 0-50520  
 U<sub>3</sub>Si, crystalline elec. field studies using neutron inelastic scatt. at NRCN 0-10931  
 USn<sub>3</sub>, crystalline elec. field studies using neutron inelastic scatt. at NRCN 0-10931  
 USn<sub>3</sub>, inelastic neutron scatt. 0-11165  
 U<sub>1-x</sub>Th<sub>x</sub>Al<sub>2</sub>, mag. susceptibility, low temp. depend. 0-11173

## uranium compounds

- see also uranium alloys  
 / 0-2987  
 tetragonal compounds, mag. props. 0-15704  
 (U, Pu)O<sub>2</sub> fuel, remote fabrication experience in FRG 0-13753  
 UC<sub>2</sub>O<sub>3</sub>, fissile fuel, SiC-fission product reaction kinetics in thermal gradient 0-47570  
 uranyl salts, cryst., multiphonon relax. 0-15208  
 AgUO<sub>2</sub>(NO<sub>3</sub>)<sub>3</sub>, fluoresc. decay rates, temp. depend. 0-25429  
 AmO<sub>2</sub>UO<sub>2</sub>, target possibilities for waste incineration, simulation study 0-32419  
 CC UF<sub>6</sub> conversion to UO<sub>2</sub>, reactor fuels, review 0-23099  
 (CH<sub>3</sub>)<sub>4</sub>NiUO<sub>2</sub>(NO<sub>3</sub>)<sub>4</sub>, fluoresc. decay rates, temp. depend. 0-25429  
 Ca<sub>2</sub>Cu(UO<sub>2</sub>)(CO<sub>3</sub>)<sub>4</sub>·6H<sub>2</sub>O, voglite, cryst. and powder diff. data 0-24421  
 CoU<sub>2</sub>S<sub>5</sub>, mag. struct. and props. 0-11166  
 CsUO<sub>2</sub>(NO<sub>3</sub>)<sub>3</sub>, <sup>15</sup>N isotope shifts in electronic spectrum, internal mode identification 0-55098  
 CsUO<sub>2</sub>(NO<sub>3</sub>)<sub>3</sub>, fluoresc. decay rates, temp. depend. 0-25429  
 Cu-U-O system, equilib. relationships (German) 0-35163  
 KUO<sub>2</sub>(NO<sub>3</sub>)<sub>3</sub>, fluoresc. decay rates, temp. depend. 0-25429  
 K<sub>2</sub>UO<sub>2</sub>(NO<sub>3</sub>)<sub>4</sub>, fluoresc. decay rates, temp. depend. 0-25429  
 K<sub>2</sub>[(UO<sub>2</sub>)<sub>3</sub>F<sub>6</sub>·H<sub>2</sub>O]·3H<sub>2</sub>O, cryst. struct. (French) 0-49193  
 Li<sub>2</sub>UO<sub>2</sub>F<sub>2</sub>, 0 ≤ x ≤ 2, use in electrochemical batteries 0-50858  
 Mg, U<sub>1-x</sub>O<sub>2-x</sub>, thermodynamic props., EMF meas. 0-29187  
 NH<sub>4</sub>UO<sub>2</sub>(NO<sub>3</sub>)<sub>3</sub>, fluoresc. decay rates, temp. depend. 0-25429  
 NdP-UP solid soln., cryst. field parameters 0-10927  
 RbUO<sub>2</sub>(NO<sub>3</sub>)<sub>3</sub>, fluoresc. decay rates, temp. depend. 0-25429  
 (Th,U)<sub>2</sub>, chemical form of solid fission product simulating high burnup 0-616  
 (Th,U)O<sub>2</sub> microspheres, fabrication 0-801  
 Th<sub>3</sub>As<sub>5</sub>-U<sub>3</sub>As<sub>4</sub> solid soln., electronic props. 0-34469  
 (U,Pu)O<sub>2</sub>, LMFBR fuel pin lattices, calcs. of k<sub>eff</sub> valves 0-13569  
 (U, Pu)C, LMFBR carbide fuel cladding damage anal. at TREAT 0-13602  
 (U,Pu)C, self-diffusion meas. 0-6544  
 (U,Pu)N, self-diffusion meas. 0-6544  
 (U,Pu)O<sub>2</sub>, FBR fuel cycle, review 0-47682  
 (U,Pu)O<sub>2</sub>, FBR fuel pellets, gel-supported precipitation conversion and prep. 0-813  
 (U,Pu)O<sub>2</sub>, FBR fuel pellet fabrication, control of O<sub>2</sub>-to-metal ratio 0-13760  
 (U,Pu)O<sub>2</sub>, FBR fuel pin thermal design, effect of fuel stoichiometry 0-18570  
 (U,Pu)O<sub>2</sub> fuel, criticality control, critical mass meas., fission rate distrib. by solid state dosimetry 0-13723  
 (U,Pu)O<sub>2</sub> fuel performance, effect of O<sub>2</sub>-metal ratio 0-13762  
 (U,Pu)O<sub>2</sub> fuel-cladding chemical interaction, effect of O<sub>2</sub>-metal ratio 0-13763  
 (U,Pu)O<sub>2</sub> GCFR fuel behaviour, effect of O<sub>2</sub>-metal ratio 0-18569  
 (U,Pu)O<sub>2</sub> LWR high burnup fuels, remote fabrication and performances 0-13755  
 (U,Pu)O<sub>2</sub>, neutron activation determ. of O<sub>2</sub> coeff. 0-37457  
 (U,Pu)O<sub>2</sub>, oxidation rates 0-37557  
 (U,Pu)O<sub>2</sub> powder, FBR fuel prep. by Au/PuC coprecipitation process 0-814  
 (U,Th)O<sub>2</sub> fuel pellet fabrication using gel microspheres 0-42844  
 (U,Th)O<sub>2</sub> fuel rods, analytical stressing in hot cell 0-18566  
 (U,Th)O<sub>2</sub>, γ-active pellet fuels fabrication, conceptual design of remotely operated plant 0-32340  
 U complex, bis-hexafluoroacetylacetonate uranyl tetrahydrofuran, laser-induced dissociation 0-53071  
 U complexes, UT<sub>3</sub> and UTCl<sub>4</sub> (T=tropolone), synthesis, cryst. struct. parameters 0-33945  
 U<sup>3+</sup>, U<sup>4+</sup>, shielding factors, cryst. field effects 0-10926  
 U-ZrH fission reactor fuel options for TRIGA Mk.III 0-5235  
 UAs, anisotropic susceptibility 0-7087  
 UAs, magnetic struct. in high mag. fields, neutron diff. study 0-34597  
 UAs, magnetisation, ferrimag. spin struct. 0-7088  
 UAs, NaCl struct., band struct. 0-6714  
 UAs, sp. ht. meas., 5-300K, mag. transition obs. 0-50101  
 UAs, U 4f ESCA spectra 0-16148  
 U<sub>3</sub>As<sub>4</sub>, mag. anisotropy, magnetisation meas. 0-50085  
 U<sub>3</sub>As<sub>4</sub>, magnetisation in strong fields, 4.2 to 200K anisotropy and exchange forces 0-54886  
 UBi, NaCl struct., band struct. 0-6714  
 UC 0-15046  
 UC FBR fuel fabrication by reaction sintering of UO<sub>2</sub> and UC<sub>2</sub> 0-812  
 UC, low temp. reactor irradiation 0-39168  
 UC, temp. depend. of Gruneisen parameter and lattice vibr. freq., between 298 to 2500K 0-29142  
 UC<sub>2</sub>O<sub>3</sub>, sample prep. method importance in O determ. (Japanese) 0-23100  
 UC/PuC, grain boundary energy to surface energy ratio, as determ. from pore geometry 0-34291  
 UC<sub>1±x</sub>, C diffusion 0-49428

## uranium compounds continued

- UC<sub>2</sub>, fissile fuel, SiC-fission product reaction kinetics in thermal gradient 0-47570  
 UC<sub>2</sub>, fission fuel, HTGR TRISO, SiC-fission product reaction under isothermal conditions 0-42744  
 UC<sub>n</sub> (n=1 to 6), formation and atomization energies by high temp. mass spectrometry 0-7842  
 UC<sub>2</sub>O<sub>3</sub>, fission fuel, HTGR TRISO, SiC-fission product reaction under isothermal conditions 0-42744  
 UD<sub>3</sub>, crystalline elec. field studies using neutron inelastic scatt. at NRCN 0-10931  
 UD<sub>3</sub>, dissociation, isotope effect 0-26174  
 β-UD<sub>3</sub>, electronic props., metallic character 0-6693  
 UF<sub>4</sub>, 5f element fluoride bond length-strength anal. 0-54166  
 UF<sub>4</sub>, crystalline elec. field studies using neutron inelastic scatt. at NRCN 0-10931  
 UF<sub>4</sub> matrix with <sup>235m</sup>U isomer, conversion process electron role in valence band (Russian) 0-13416  
 UF<sub>5</sub>, electronic struct. calc. 0-6716  
 UF<sub>5</sub>, electronic struct. and geometry, ab initio calcs. using relativistic ECP 0-32606  
 UF<sub>6</sub>, negative surface ionisation investigation using sensitive detector and pressure gauge 0-31781  
 UF<sub>6</sub>, non-equilibr. condensation calcs. for laser isotope separation 0-10132  
 UF<sub>6</sub>, photophysical props., laser study 0-28040  
 UF<sub>6</sub>, room temp., IR absorpt. obs., isotope shift of fund. band and combination bands, freq. depend. 0-23421  
 UF<sub>6</sub>, UV photophysics, energy balance through quantum efficiency meas. 0-9634  
 UF<sub>6</sub> vibrational relaxation, ultrasonic meas. in UF<sub>6</sub>-Ar-N<sub>2</sub> mixtures 0-1050  
 UF<sub>6</sub>-graphite intercalation cpds., prep. and props. 0-40686  
 UF<sub>6</sub>-H<sub>2</sub>, near UV and visible excitation, quantum yield from photodissociation 0-35549  
 UF<sub>6</sub>+SiH<sub>4</sub>, photoinduced reaction in low temp. SiH<sub>4</sub> matrix 0-30256  
 UGe<sub>3</sub>, induced magnetisation density and f-d bonding, polarised neutron diff. study 0-50063  
 UGe<sub>3</sub>, magnetisation density, neutron scatt. meas. 0-50038  
 UH<sub>3</sub>, dissociation, isotope effect 0-26174  
 UH<sub>6</sub>, Dirac-Fock one-centre expt. calc. 0-5485  
 UI<sub>3</sub>, alkali metal halide system, prep. 0-50568  
 UN, density of states calc. 0-6715  
 UN, electronic struct., relativistic energy band struct. calc. 0-34354  
 UN, mag. inelastic scatt. 0-7079  
 UN, mag. susceptibility under press. 0-7086  
 UN, NaCl struct., band struct. 0-6714  
 UN, temp. depend. of Gruneisen parameter and lattice vibr. freq., between 298 to 2500K 0-29142  
 UN, U 4f ESCA spectra 0-16148  
 (UN)<sub>6</sub><sup>15+</sup>, electronic struct., variational Xα cluster calc. 0-39499  
 UO, fission reactor fuel, suitability of spent fuel shipping casks 0-27757  
 UO, nuclear oxide fuel anal., coulometry, emission anal., chromatography, X-ray anal. 0-18420  
 UO, spectroscopic data rel. to thermodynamic functions 0-34208  
 UO<sub>2</sub>, (110), (100), and (111) surfaces, struct. study using He<sup>+</sup> ion scatt. spectroscopy 0-40206  
 UO<sub>2</sub> and (U, Pu)O<sub>2</sub> nuclear oxide fuels, vapour pressure meas. for fast reactor safety anal. by laser techniques to 5000K 0-13591  
 UO<sub>2</sub> BWR fuel rod design to remedy fuel-cladding interactions 0-42766  
 UO<sub>2</sub>, boundary heat transfer from volumetrically boiling pools following LMFBR HCDA 0-47654  
 UO<sub>2</sub> ceramic fuel fabrication, simulation of thermal processes by emanation thermal anal. 0-811  
 UO<sub>2</sub>, comp. of lower phase boundary at 1950K 0-49366  
 UO<sub>2</sub>, contact conductivity between core and cladding, statistical processing of experimental data 0-5238  
 UO<sub>2</sub>, cryst. growth by chem. transport 0-16166  
 UO<sub>2</sub>, crystalline elec. field studies using neutron inelastic scatt. at NRCN 0-10931  
 UO<sub>2</sub>, cumulative diffusional release of fission product gases from an equivalent sphere, generalised anal. 0-47569  
 UO<sub>2</sub>, D migration and trapping during D<sup>+</sup> implantation 0-34243  
 UO<sub>2</sub>, desintering of unstructured UO<sub>2</sub> fuel during film boiling testing, grain boundary separation 0-22997  
 UO<sub>2</sub>, diffusion mobility of gas bubbles 0-39357  
 UO<sub>2</sub>, electronic struct. contribs. to excess enthalpy at 3000K and in liq. phase 0-15265  
 UO<sub>2</sub>, electronic struct. and Coulomb correl. energy, XPS and bremsstrahlung spectra 0-55272  
 UO<sub>2</sub> equiaxed grain growth modelling 0-13589  
 UO<sub>2</sub> fuel, dynamic intragranular fission gas behaviour model, DIGRAS computer code 0-32345  
 UO<sub>2</sub> fuel fabrication by the AUC powder process 0-13744  
 UO<sub>2</sub> fuel melting and Zircaloy cladding thermal failure during LWR PCM transient 0-42834  
 UO<sub>2</sub> fuel pellet, bending strength, fabrication and microstruct. effect 0-2986  
 UO<sub>2</sub> fuel pellet fabrication using gel microspheres 0-42844  
 UO<sub>2</sub>, irradiated fuel, unstable fission product release 0-617  
 UO<sub>2</sub>, isolated rod, exptl. and calculated resonance integrals 0-22986  
 UO<sub>2</sub>, LWR fuel, microstruct. and chemical props. of powder and pellet 0-629  
 UO<sub>2</sub>, LWR fuel, prep. and advantages of CAMEL, a sheeted fuel of UO<sub>2</sub> pellets 0-630  
 UO<sub>2</sub>, liquid, reactor safety research, laser experiments (German) 0-42787  
 UO<sub>2</sub>, low-enriched HTR fuel, performance data review 0-42780  
 UO<sub>2</sub>, mag. ordering lattice internal rearrangement transition, theory 0-20402  
 UO<sub>2</sub>, micropore sintering, irradiated below 1100°C, in Winfrith SGHWR 0-5255  
 UO<sub>2</sub>, microwave heating in nuclear fuel preparation 0-37556  
 UO<sub>2</sub>, mobility of intergranular gas bubbles 0-15310  
 UO<sub>2</sub>, molten fuel debris, 1-D penetration into concrete following FBR HCDA 0-47640  
 UO<sub>2</sub>, molten fuel radial motion during a LWR high temp. transient 0-42833  
 UO<sub>2</sub>, nuclear fuel, eqn. of state and thermodynamic props. 0-13592  
 UO<sub>2</sub>, oxidation rates 0-37557  
 UO<sub>2</sub> pellet reactor fuel rods, fission gas release in high burnup range 0-635



## uranium compounds continued

- $\text{UO}_2$  pellet surfaces,  $\beta\text{-UO}_{2.33}$  formation in air at 229 to 275°C, X-ray diff. study 0-35362  
 $\text{UO}_2$  pellets-graphite-Zircaloy cladding, evaluation of graphite lubrication 0-32342  
 $\text{UO}_2$  phase, thermodynamic props. 0-13594  
 $\text{UO}_2$  powder, sintering effect of compaction 0-20874  
 $\text{UO}_2$  powder, temp. depend. of atomic thermal displacements, Rietveld profile-refinement procedure 0-49190  
 $\text{UO}_2$  pyrocarbon-coated HTR fuel particles, fast neutron influence on fission product transport 0-42777  
 $\text{UO}_2$  reactor fuel, high burnup performance in LWR 0-634  
 $\text{UO}_2$  reanal. of neutron diff. data 0-15084  
 $\text{UO}_2$ , SiC coated, small surface area determ. by Kr adsorption 0-44429  
 $\text{UO}_2$ , sintered, production by gel calcination and drying, thermal anal. (Czech) 0-45260  
 $\text{UO}_2$  spectral emissivity meas. up to 3800K 0-24625  
 $\text{UO}_2$ , spectroscopic data rel. to thermodynamic functions 0-34208  
 $\text{UO}_2$ , surface props. of low index faces, calc. 0-6604  
 $\text{UO}_2$ , thermal and transport props., electronic contrib. 0-15432  
 $\text{UO}_2$ , unstructured fuel, intergranular fracture during film boiling 0-3169  
 $\text{UO}_2$  vapour, saturated, thermodynamic state and gas kinetic relaxation to 5000K 0-13593  
 $\text{UO}_2$  vapour press. meas. up to 5000K, appl. of laser pulse heating 0-52230  
 $\text{UO}_2$  volume boiling pools, meas. and calc. of average void fraction for LMFBR HCDA anal. 0-47653  
 $\text{UO}_2$ , Zircaloy sheathed, CEA expt. on transient behaviour (French) 0-18417  
 $\text{UO}_2^{+}$ , precipitation reaction in KSCN 0-26040  
 $\text{UO}_2\cdot\text{Cr}_2\text{O}_3$ , fission gas release and swelling 0-47567  
 $\text{UO}_2\cdot\text{Nb}_2\text{O}_5$ , additions on elec. cond. 0-49712  
 $\text{UO}_2/\text{Gd}_2\text{O}_3$ , grain boundary energy to surface energy ratio, pore geometry 0-34291  
 $\text{UO}_2/\text{PuO}_2$ , grain boundary energy to surface energy ratio, pore geometry 0-34291  
 $\text{UO}_2\cdot 20\text{CeO}_2$  mixed powder, X-ray and microprobe exam. of homogenisation 0-25609  
 $\text{UO}_2\cdot\text{UC}_2\cdot\text{C}$ , HTGR fuel microspheres, carbothermic conversion process 0-42845  
 $\text{UO}_2\cdot\text{UC}_2\cdot\text{C}$  microspheres, carbothermic prep., rate-controlling preps. 0-45257  
 $\text{UO}_2$ -Zircaloy fuel element behaviour in PWR power plants 0-631  
 $\text{UO}_2$ -zircaloy-4, reaction kinetics at high temps.,  $\text{O}_2$  diffusion 0-16667  
 $\text{UO}_2 + \text{ZrC}$ , high temp. reactions 0-3320  
 $\text{UO}_2^{2+} + \text{UO}_2\text{NO}_3^{+}$ , ground and excited state interaction, struct., thermodynamic functions, photochemistry obs. 0-32779  
 $\text{UO}_3$ , microwave heating in nuclear fuel preparation 0-37556  
 $\text{UO}_3$ , spectroscopic data rel. to thermodynamic functions 0-34208  
 $\text{UO}_6$ , electronic struct., discrete variation and scatt. wave  $X_\alpha$  methods 0-917  
 $(\text{UO}_6)^{12-}$ ,  $(\text{UO}_6)^{10-}$ , electronic struct., variational Xalpha cluster calc. 0-39499  
 $\text{U}_3\text{O}_8$ , microwave heating in nuclear fuel preparation 0-37556  
 $\text{U}_3\text{O}_8$ , oxidation rates 0-37557  
 $\text{U}_3\text{O}_8\cdot\text{Y}_2\text{O}_3(\text{Sc}_2\text{O}_3)$ , solid soln. electrode, high temp. electrochem. appl. 0-6828  
 $\text{UO}_2\text{Br}_2$ , high temp. enthalpy increments and thermodynamic functions 0-29189  
 $\text{UO}_2\text{Cl}_2$ , high temp. enthalpy increments and thermodynamic functions 0-29189  
 $\text{UO}_2\text{F}_2$ , high temp. enthalpy increments and thermodynamic functions 0-29189  
 $\text{U}(\text{OH})_2\text{SO}_4$ , mag. susceptibility, heat capacity anomalies at 21K 0-11151  
 $\text{UO}_2(\text{NO}_3)_2$ , aq. soln., pulsed NMR relax. time,  $^{235}\text{U}$  enrichment depend. 0-2658  
 $\text{UO}_2(\text{NO}_3)_2$  complexes, IR spectra, normal coordinate anal., vibr. assignments, force consts. and ligation effects 0-9608  
 $\text{UO}_2(\text{NO}_3)_2$  highly enriched soln. with  $\text{Cd}(\text{NO}_3)_4\cdot 4\text{H}_2\text{O}$  neutron poison, criticality expts. 0-13724  
 $\text{UO}_2(\text{NO}_3)_2$ , secondary criticality control, use of chlorinated PVC piping 0-13607  
 $(\text{UO}_2\text{NO}_3)^{+}_{\text{aq}} + \text{UO}_2^{2+}$ , ground and excited state interaction, struct., thermodynamic functions, photochemistry obs. 0-32779  
 $(\text{UO}_2)_2[\text{SiO}_4](\text{H}_2\text{O})_3$ , synthetic soddyite cryst. struct., powder photographs 0-39050  
 $\text{UO}_2\cdot\text{HCONH}_2\cdot 0.5\text{H}_2\text{O}$ , prep., cryst. struct. and charact 0-29010  
UP, anisotropic susceptibility 0-7087  
UP, NaCl struct., band struct. 0-6714  
UP, U 4f ESCA spectra 0-16148  
UP, vol. changes at mag. transitions 0-7107  
 $\text{U}_x\text{Pb}_{1-x}\text{Mo}_{0.6+y}\text{S}_8$ , sputtered supercond. props. 0-50019  
 $(\text{U}_x\text{Pu})\text{O}_2 + x$ ,  $\text{O}_2$  chem. diffusion (French) 0-49427  
US, density of states calc. 0-6715  
US, ferromag., AC mag. susceptibility at high press. 0-7085  
US, ferromagnet, electronic structure, reflectivity (German) 0-49567  
US, NaCl struct., band struct. 0-6714  
US, optical props. and electronic struct. 0-25410  
US, optical reflectivity and electronic density of states 0-16053  
US, photoelectron energy distrib. and spin polarisation, electronic and mag. props. 0-16146  
US, spin polarisation and magnetism, photoelectron study 0-40219  
US, U 4f ESCA spectra 0-16148  
 $(\text{UO}_6)^{10-}$ , electronic struct., variational Xalpha cluster calc. 0-39499  
USb, anisotropic susceptibility 0-7087  
USb, NaCl struct., band struct. 0-6714  
USb, neutron inelastic scatt. from collective excitation 0-7080  
USb, neutron inelastic scatt. meas., phonon spectra, mag. response, anisotropy 0-50065  
USb, reflectivity spectrum, band struct. 0-736  
USb, UPS and XPS, surface oxidation 0-7465  
 $\text{USb}_2$ , single crystal growth, structural perfection 0-15024  
 $\text{USb}_{0.8}\text{Te}_{0.2}$ , magnetisation and neutron meas., mag. moments 0-15703  
 $\text{USb}_{0.9}\text{Te}_{0.1}$ , multiaxial mag. structure 0-15696  
 $\text{USb}_{1-x}\text{Te}_x$ , mag. struct. and mag. phase diagram, neutron diff. study 0-50059  
USc, optical reflectivity and electronic density of states 0-16053  
USc, photoelectron energy distrib. and spin polarisation, electronic and mag. props. 0-16146

## uranium compounds continued

- USE, spin polarisation and magnetism, photoelectron study 0-40219  
 $\text{U}_3\text{Si}$ , crystalline elec. field studies using neutron inelastic scatt. at NRCN 0-10931  
UTe, critical mag. fluctuations near  $T_c$  0-7122  
UTe, magnetisation and neutron meas., mag. moments 0-15703  
UTe, photoelectron energy distrib. and spin polarisation, electronic and mag. props. 0-16146  
UTe, spin polarisation and magnetism, photoelectron study 0-40219  
 $\text{UTeSb}_{1-x}$ , photoemission, densities of states 0-16147  
 $(\text{U}_x\text{Th}_{1-x})\text{Sb}$ , magnetisation, U valence change 0-7089  
 $(\text{U}_{0.3}\text{Y}_{0.7})\text{O}_{2-x}$ , ionic cond. 0-6828  
UZrH low enrichment fuels, test programs and analysis 0-9398  
 $\text{UO}_2(\text{NO}_3)_2$ ,  $a=233$ , 235, slab tanks for criticality control, neutron multiplication calc. 0-13606  
 $^{233}\text{U}$  fuels for HTGR, remote fabrication 0-13752  
 $(^{233}\text{U}, \text{Th})\text{O}_2$  fuels for HTGR, remote fabrication 0-13752  
 $(^{233}\text{U}, \text{Th})\text{O}_2$  pellet-type fuels for CANDU reactors, remote fabrication plant design 0-13751  
 $^{235}\text{UF}_6$  enrichment equipment, running-belt and rotary-disc concentrators, transient Knudsen diffusion 0-32421

## Uranus

- e ring, precession 0-26804  
atmosphere, IR radiation, review 0-8568  
clouds, particle comp. 0-31253  
decimetric radio obs., brightness temp. 0-46474  
disk structure in 7300 Å methane band 0-17544  
IR spectrum from 0.8 to 2.75 microns, obs. 0-21946  
lunar occultation obs., 1977 February 10, radius, limb darkening and polar brightening at 6900 Å 0-17545  
magnetic field origin 0-36564  
microwave radiometry and interferometry 0-56766  
Oberon, near IR spectra and JHK photometry, mass and dia. measurement 0-56761  
orbital perturbations by Pluto, representation (French) 0-26724  
ring system, origin and location of narrow rings 0-56764  
rings, as volatile material in satellite orbits, model 0-26807  
rings and regular satellite system formation 0-41746  
rotation period, effects of seeing on reflected spectrum 0-46479  
rotation period, spectroscopic determ. 0-51691  
structure and magnetic field, theory using two-layer model 0-4298  
Titania, near IR spectra and JHK photometry, mass and dia. measurement 0-56761  
Umbriel, near IR spectra and JHK photometry, mass and dia. reassessment 0-56761  
upper atmosphere, mean temp. and temp. vars. 0-46477  
upper atmosphere, struct. from SAO 158687 occultation obs. 0-17547

## urban planning see town and country planning

## utility programs

- bWR servicing and refueling improvement program 0-9390

## u.v. astronomy see ultraviolet astronomy

## u.v. detectors see ultraviolet detectors

## V-centres

- see also H-centres  
alkali halide, hole capture kinetics, influence of autolocalised and zone holes (Russian) 0-54714  
alkali halide crystal, defect formation in thermal equilibrium state of self-localised exciton 0-44205  
a-As<sub>2</sub>Se<sub>3</sub> chalcogenide glass, influence of thermally induced defects on transport props. 0-49766  
a-As<sub>2</sub>Se<sub>3</sub> film, metallic impurity effect on transport props. 0-49963  
BaO, electronic struct. of V<sup>-</sup> and related centres 0-2355  
CaO, electronic struct. of V<sup>-</sup> and related centres 0-2355  
CsI:Na, self-trapped exciton emission polarisation 0-49607  
GaP:Fe(Cr), photo-ESR of annealed crystals 0-15795  
KBr, efficiency of V<sub>k</sub><sup>-</sup> and Ag<sup>0</sup>-centres generation (Russian) 0-39080  
KBr, pulse radiolysis of metastable interstitial centre of high temp. 0-20658  
KBr, V- and X-centres accumulation (Russian) 0-54228  
KBr:Ti excitation in fund. absorpt. region, luminesc. and thermolum. 0-50433  
KBr(Cl), X-ray irradi., tunnelling recomb. luminesc. 0-2873  
KCl (Br) crystals, thermally stimulated luminescence accompanying recombination of V<sub>F</sub> and F centres 0-55201  
KCl, thermal annealing of F, V<sub>2</sub><sup>-</sup>, V<sub>3</sub><sup>-</sup> centres (Russian) 0-54229  
KCl, V- and X-centres accumulation (Russian) 0-54228  
KCl:Ag(In)(Ti), excitation in fund. absorpt. region, luminesc. and thermolum. 0-50433  
KCl:Ti, hole capture kinetics, influence of autolocalised and zone holes (Russian) 0-54714  
KI:Ti, electron-hole and V<sub>k</sub>-Ti recomb., TSC and thermolum. study (French) 0-34461  
KI:Ti, excitation in fund. absorpt. region, luminesc. and thermolum. 0-50433  
LiF, V<sub>1</sub> centre (F<sub>3</sub><sup>2-</sup>) identification, ESR spectrum anal. 0-7164  
MgO, single crystal, thermal and optical stimulation processes of V-centres (Japanese) 0-11485  
NaCl, emission of Cl atoms during V<sub>k</sub> centre decomposition 0-10578  
NaCl, V- and X-centres accumulation (Russian) 0-54228  
NaCl:Ag, excitation in fund. absorpt. region, luminesc. and thermolum. 0-50433  
NaI:Ti, scintillation excitation mechanism 0-2857  
RbBr (I), optical absorpt. centre formation time meas. 0-40081  
RbBr, suprapure, thermolum. glow and emission studies at room temp. 0-7423  
SrO, electronic struct. of V<sup>-</sup> and related centres 0-2355  
SrTiO<sub>3</sub>, EPR of Fe<sup>3+</sup>-V<sub>O</sub> centre, above T<sub>c</sub> 0-39870

V<sub>H</sub>-centres see H-centres

## V-VI semiconductors see semiconductor materials

## vacancies (crystal)

- see also Frenkel defects; impurity-vacancy interactions; Schottky defects; vacancy condensation loops; vacancy-dislocation interactions  
alkali metals, vacancy formation energy calcs., electron density functional method 0-19801  
amorphous solids, vacancies and vacancy clusters, stability under relaxation 0-15005  
binary alloys, ordered, self-diffusion kinetics 0-10698  
α-brasses, cold worked, atomic diffusion kinetics to stacking faults, Laplace transformation method 0-19977



## vacancies (crystal) continued

concentration of vacancies in crystal in temp. gradient, kinetic anal. 0-49217  
 condensed media, low-temp. particle transport theory, impurity electron transfer 0-19974  
 covalent semiconductors, vacancy screening, dielec. const., exchange correl. pot., Thomas-Fermi description 0-44528  
 crystallites with two and three vacancies, models, topological approach 0-44202  
 crystals, with diamond struct., vacancy formation energy rel. to plastic state transition temp. (*Russian*) 0-19795  
 diamond, natural, subthreshold defect formation due to electron irradi., cathodoluminescence study (*Russian*) 0-45152  
 dielectric, dipolar point defects, studied by ITC 0-6405  
 electron solid, two-dimens., defects and implications for melting 0-39076  
 film, microporosity described in terms of vacancies and voids 0-24769  
 fission reactor materials, point defect nucleation and growth, rate theory model for simultaneous clustering 0-13604  
 fusion of metals, vacancy theory 0-44299  
 fusion reactor first wall material, mobile He inclusion in void swelling rate theory model 0-34069  
 fusion reactor metals, irradiated, defect cluster nucleation, He injection effect 0-34091  
 gas behaviour in closed porosity body, exam. 0-24642  
 grain boundary Gibbs thermodynamics anal., interaction with vacancies (*Russian*) 0-2034  
 grain boundary migration vacancy generation, and drag force 0-15090  
 graphite, neutron irradiation, electron transport, annealing study 0-39165  
 graphite vacancy and substitutional impurities, moderately-large-embedded-cluster approach 0-49663  
 ice surface layer, viscosity, from thermal contraction meas., 0 to  $-50^{\circ}\text{C}$  0-49469  
 III-V oxide interface state and Schottky barrier form., unified mechanism 0-44724  
 inert gas crystals, Monte Carlo calc. of conc. of lattice vacancies, method of overlapping distribts. 0-39077  
 inert gases, solid, long-range many-body interaction and monovacancy heat of form. 0-38996  
 ionic crystals, imperfect, positron stabilisation 0-40182  
 ionic electret behaviour, ionic thermoconductivity technique 0-7274  
 layered transition metal dichalcogenide, diffuse intensity contours in electron diff. patterns, struct. interpretation 0-38878  
 metal, FCC, props. of vacancies and divacancies 0-10545  
 metal, FCC, small vacancy clusters, structures and energies, computer simulation 0-39073  
 metal, FCC, vacancy migration near twin boundaries and stacking faults 0-39075  
 metal halide intercalated graphite, acceptor sites 0-49218  
 metals, FCC, pair potentials calc., appl. to point defect props. 0-19798  
 metals, heat capacity near melting point, vacancy mechanism of melting 0-10641  
 metals, irradiation induced swelling, bias factor 0-2062  
 metals, noble, dilute alloys, solute vacancy binding energy, Dingle temp. 0-49177  
 metals, point defect relaxation volumes, dipole tensors and Kanzaki forces 0-54222  
 nonlinear diffusion 0-39338  
 nonmetallic crystals, collapse of tracks formed by fission fragments 0-24510  
 oxide, defect struct., nonstoichiometry and elec. cond., pentavalent oxide dopant effect 0-24442  
 point defect production in irradiation, swelling, cascade diffusion theory 0-34044  
 polycrystalline materials, diffusion-controlled stress rupture 0-3186  
 polyethylene, cryst., transverse deform. and transverse movement of defects 0-38958  
 polyethylene, crystalline, steric struct. modelling of end defects 0-6371  
 positron trapping rate into vacancy clusters in metals 0-2890  
 precipitate hardened material, intergranular cavity growth inhibition 0-50677  
 radiation blistering, interpretation based on radiation stimulated vacancy migration 0-49265  
 radiation damage cascades, stochastic theory of particle transport 0-54291  
 rare earth metals, heat capacity near melting pt., vacancy mechanism of melting 0-15221  
 rare earth zirconate,  $\text{R}_2\text{Zr}_2\text{O}_7$ , Raman spectra, anion disorder characterization 0-25358  
 semiconductor, bulk evaporation, injection of nonequilibrium vacancies 0-39273  
 semiconductors, dangling-bond states theory 0-24840  
 semiconductors, Watkins-type radiation defects, low temp. form. mechanism 0-15153  
 semiconductors, Z 0-19799  
 small particles, cause of reduction in lattice spacing (*Russian*) 0-38967  
 solid electrolyte dielectric permeability, phase transition to superionic state (*Russian*) 0-49403  
 solid electrolyte with structural disorder, current flow mechanism 0-19982  
 solids, vacancy migration vol. 0-10701  
 steel, stainless, void swelling, Si point defect trapping, interstitial loop growth rate temp. depend. obs. 0-49270  
 succinonitrile, defects in plastic phase, positron annihilation obs. 0-11504  
 tetrahedrally coordinated covalent semiconductor point defects, multiple scatt. X $\alpha$  model 0-54636  
 topological approach to vacancy modelling 0-10543  
 void sink strength depend. on mutual recombination, point defect loss to fixed sinks 0-33995  
 zinc blende type ionic semiconductors, vacancies, bound state energy level calcs., tight binding approx. 0-44694  
 Ag, injection of vacancies by electrochem. etching at high temp. (*German*) 0-49219  
 Ag-Fe, dil., ion implanted, phase comp., Mossbauer study 0-7244  
 Ag-Zn, vacancy prod. rate by displacement cascades, anelastic meas. during neutron irradi. 0-19794  
 AgCl: CdCl $_2$ , point defect model, free energy and radial distrib. functions 0-44201  
 Al, empirical pot. methods, use of Wedepohl pot., vacancy form energy 0-39230  
 Al, high purity, neutron irradiated, void annealing kinetics 0-44234

## vacancies (crystal) continued

Al, positron annihilation, effects of quenching, annealing and neutron irradi. 0-20732  
 Al, positron annihilation with high-momentum core electrons, vacancies study 0-25481  
 Al, quenched, irradiated, and quenched plus irradiated, grain boundary hardening 0-3162  
 Al, quenched, muon $^{+}$  trapping at vacancies, compared with positron annihilation 0-15937  
 Al, single vacancy formation energy calc., SCF-LCGO modified solid state scatt. theory 0-54637  
 Al, vacancy distribution, interbonding atoms, heat peaks in scattered cascades (*Russian*) 0-39169  
 Al- $^{57}\text{Co}$ , implanted, Mossbauer effect obs. of annealing 0-39126  
 Al-Co, defect structs. introduced by electron irradi., Mossbauer study 0-7239  
 Al-Cu-Sn, ageing process, effect of Sn atoms,  $^{119}\text{Sn}$  Mossbauer spectra obs. 0-7598  
 Al-Mg $_2$ Si (1 wt.%), precipitation reactions, vacancy formation 0-11652  
 Al-Sn alloys, heat treatment effect on  $^{119}\text{Sn}$  Mossbauer spectrum 0-7228  
 Al,Ga $_{1-x}$ As:N, ion implantation, in situ annealing photoluminesc. obs. 0-10567  
 $\alpha\text{-Al}_2\text{O}_3$ , crystal defects from X-ray irradiation, F-centres, X-ray luminesc. obs. 0-55176  
 $\text{Al}_2\text{O}_3$ , defect microstructure due to ion bombardment, TEM study 0-34100  
 $\alpha\text{-Al}_2\text{O}_3\text{:Er(Cr)}$ , crystal defects from X-ray irradiation, F-centres, X-ray luminesc. obs. 0-55176  
 Ar crystal, Monte Carlo calc. of conc. of lattice vacancies, method of overlapping distribts. 0-39077  
 Ar, vacancy, electronic structure, Green's function theory 0-39525  
 Au, electron irradiated, interstitials and their clusters, diffuse X-ray scatt. study 0-33997  
 Au films, (111), sputtering in high voltage electron microscope 0-35027  
 Au quenched single crysts., vacancies, diffuse scatt. and resist. obs. 0-33994  
 Au, thin foil, growth of stacking fault tetrahedra 0-19815  
 Au-Ag, radiation damage and diffusion 0-24645  
 Au-Cu, dil., electron irradiated, interstitials and their clusters, diffuse X-ray scatt. study 0-33997  
 Au-Fe, dil., ion implanted, phase comp., Mossbauer study 0-7244  
 BaTiO $_3$ :X(X=Cr, Mn, Fe, Co, Ni, Zn, Ga), annealed in H $_2$  and O $_2$ , valence change in phase stability 0-20600  
 Bi $_{1-x}$ Sr $_x$ O $_{1.5-x/2}$  vacancy-type solid soln., anionic cond. (*French*) 0-49407  
 C, vacancy, tight-binding calc. 0-24844  
 CaF $_2$ , phonon resonances associated with vacancy 0-19893  
 CaF $_2$ :Na, vacancy motion activation vol., complex dielec. const. meas. 0-39356  
 CaF $_2$ :O $_2^{-}$ , OH $^{-}$ , ion incorporation by reaction with surrounding atm. 0-55143  
 CdS, deep level IR luminescence, origin 0-20704  
 CdS, polycrystalline evaporated layers, donor and trap densities 0-20213  
 CdSe film, vac. deposited, elec. resist. and surface changes by laser annealing 0-2491  
 CdTe:Cl, LPE from CdCl $_2$  soln., elec. props., defects 0-39689  
 CdTe:P, annealing induced lattice defects, TEM obs. 0-2010  
 CeO $_2$ :S, acceptor properties of S, free electron concentrations 0-34395  
 Co, FCC, self-diffusion and isotope effect, influence of mag. order-disorder transition 0-29205  
 Co, phase transformations and vacancy form. by positron annihilation 0-2155  
 Co-Ga  $\beta'$  quenched single crystals, annealing-out of point defects 0-55426  
 CoM $_2$ O $_{4+x}$  (M=Rh,Mn), anomalous  $^{57}\text{Fe}^m$  charge states, Mossbauer study 0-40017  
 CoO, electrotransport 0-2196  
 CoO, Mossbauer lines, quadrupole splitting due to defects 0-2670  
 Cr, thermal vacancies, energy of form. and conc. 0-29014  
 CsCl:Fe, defect struct., Mossbauer spectra and X-ray diff. obs. 0-7237  
 CsCl-type crystal, cation vacancies migration energies 0-2192  
 Cu, Ar $^{+}$  ion irradiated, defects study by electron microscopy (*German*) 0-2087  
 Cu crystal, cohesion and vacancy form., electron statistical model 0-54169  
 Cu, positron annihilation with high-momentum core electrons, vacancies study 0-25481  
 Cu, radiation damage and diffusion 0-24645  
 Cu, vacancy, lattice vibrs., reson. and localised modes 0-39236  
 Cu-Au, vacancies and divacancies, quenching effects and elec. resist. meas. 0-39072  
 Cu-Fe, dil., ion implanted, phase comp., Mossbauer study 0-7244  
 Cu-Ge, dil., point defect props., density functional approach 0-29013  
 Cu-Ni, annealing effect on oxidation kinetics, reduction in vacancy level 0-50760  
 CuCl, defect and impurity bands, lattice consts. 0-54638  
 Cu $_0$ .In $_2$ .Se $_4$ , transition state and domain struct. by electron microscopy and diff. studies 0-15095  
 Cu $_{2-x}$ Se, electrical activity of Cu vacancies 0-39606  
 Cu $_{2-x}$ Te, electrical activity of Cu vacancies 0-39606  
 D NaCl:Fe, defect struct., Mossbauer spectra and X-ray diff. obs. 0-7237  
 DyCoO $_3$ , anomalous  $^{57}\text{Fe}^m$  charge states, Mossbauer study 0-40017  
 Er $_2$ O $_3$ , pure and HfO $_2$ -doped polycryst., Er self-diffusion 0-29207  
 EuCoO $_3$ , anomalous  $^{57}\text{Fe}^m$  charge states, Mossbauer study 0-40017  
 EuSe, annealed, AC conductivity and dielectric anomaly 0-34445  
 EuSe, polarisability of shallow donors, permittivity meas. 0-24833  
 Fe, BCC, void nucleation following electron irradi. 0-29054  
 Fe, defect trapping of ion implanted D, depth profile, diffusion eqn. calcs. 0-2047  
 $\alpha\text{-Fe}$ , irradiation induced void swelling, Cr additions effect 0-55408  
 Fe, phase transformations and vacancy form. by positron annihilation 0-2155  
 Fe, point defect estimation from specific heat and volume in plastically deformed pure metals (*Russian*) 0-54223  
 $\alpha\text{-Fe}$ , vacancy, lattice vibrs., reson. and localised modes 0-39236  
 Fe, vacancy mobility determ., HVEM expts. 0-33993  
 Fe-Cr, irradiation induced void swelling, Cr additions effect 0-55408  
 Fe $_{50}$ Co $_{50}$ , neutron irradiation, close pair recombination (*French*) 0-39162  
 Fe $_{49}$ Co $_{49}$ V $_2$ , neutron irradiation, close pair recombination (*French*) 0-39162



**vacancies (crystal) continued**

- ( $\text{Fe}^{2+}\text{Fe}_{2-x}^{3+}\text{M}_x^{3+}\text{O}_4^{2-}$  ( $\text{M}^{3+}=\text{Al}^{3+}$ ,  $\text{Cr}^{3+}$ ), oxidation to  $\gamma$  lacunar spinels, rate law vs.  $\text{O}_2$  press. 0-50849  
 $\text{Fe}_{1-x}\text{O}$ , wustite, struct. at high temp., neutron diff. (*French*) 0-1982  
 $\text{Fe}_2\text{O}_3$ , based  $\gamma$  defective spinels, elec. cond. behaviour during transform. to  $\alpha$  rhombohedral phases (*French*) 0-49354  
 $\text{Fe}_3\text{Si}_2$ , polytypism, Fe diffusion near antiferromag. to ferrimag. transition 0-44830  
 $\text{Fe}_{(1+x)}\text{Ti}_{2(1+x)}\text{S}_4$  non-stoichiometric cpds., vacancy-cation distrib., Mossbauer spectra 0-15900  
GaAs, electron and neutron irradi., defect clusters 0-2077  
GaAs, electron-irrad., deep-level defect anal. using  $2\gamma$  positron annihilation and IR absorption spectra 0-16120  
GaAs, surface, vacancies, bound state energy level calcs., tight binding approx. 0-44694  
GaAs:Ge, ion-implanted, photoluminesc., deep emission centres 0-34965  
GaAs:Sn, implantation, annealing, impurity-defect struct., Mossbauer study 0-54269  
GaP, internal friction due to reorientation of Ga divacancies, calc. 0-2116  
GaP:Fe, heat treated, EPR spectra, struct. defects 0-7158  
GaP:Fe(Cr), photo-ESR of annealed crystals 0-15795  
GaSb and alloys, struct. defect, photoluminesc. 0-25459  
GaSb, sputtered films, on GaAs, growth, Hall effect, impurity levels 0-20334  
Ge, vacancy, tight-binding calc. 0-24844  
 $^3\text{He}$ - $^4\text{He}$ , solid soln., struct. of vacancies 0-2242  
 $\text{HfO}_2\text{:Er}_2\text{O}_3(\text{Y}_2\text{O}_3)(\text{Eu}_2\text{O}_3)$ , elastic props., sonic reson. meas. 0-7612  
HgTe, vacancy mech. of desorption of Hg droplets 0-39070  
In, vacancy formation and activation volume, macroscopic model 0-54221  
 $\text{In}_2\text{Te}_3$ -type semiconductor, mechanism of electrically inactive impurities 0-24834  
Ir (111), ( $\sqrt{3}\times\sqrt{3}$ ) $30^\circ$  S overlayer struct., LEED obs. 0-15365  
KBr, proton irradi., divacancies, positron capture, ionic cond. and TSC study 0-54289  
KBr: $\text{Cl}^-$ , diffusion traps for divalent ions, dielectric loss and ionic thermocurrent techniques 0-6566  
KCl, thermal annealing of  $\text{F}$ ,  $\text{V}_2$ ,  $\text{V}_3$ -centres (*Russian*) 0-54229  
KCl, vacancy complex formation and binding energies in zeroth approx. 0-24441  
KCl: $\text{H}^-$ , diffusion traps for divalent ions, dielectric loss and ionic thermocurrent techniques 0-6566  
KCl:Pb, light induced ionic polarisation 0-7264  
KCl:Pb $^{2+}$ , low temp. sp. ht. 0-2178  
KCl(Br)(I) with alkali and halogen impurities, colour centre deformation induced nonradiative decay 0-7387  
 $\text{KNbO}_3$ , elec. and thermoelec. props., influence of O defects 0-29401  
(La,Gd)Al $_2$ , normal and supercond. state, US attenuation, freq. depend. and mechanisms 0-49992  
La-Co-O system, stability of ternary phases, nonstoichiometry 0-24434  
 $\text{LaCoO}_3\text{:Ca}(\text{Sr})$ , anomalous  $^{57}\text{Fe}^m$  charge states, Mossbauer study 0-40017  
 $\beta$ -Li-Al, lattice parameters, density, defect struct. 0-24440  
LiCl:Fe, defect struct., Mossbauer spectra and X-ray diff. obs. 0-7237  
LiF:Mg, X-ray irradi., trapping processes, Z-centres and dipoles, two models 0-49222  
MnZn ferrite, Ti substituted, vacancy contents and phase equilibria 0-29012  
Mo, BCC, void nucleation following electron irradi. 0-29054  
Mo, positron annihilation and vacancy formation 0-16119  
NaCl, electronic structure calculation, CNDO semi-empirical methods (*Russian*) 0-10909  
NaCl, thermal expansion meas. after X-ray irradi., F-centre bleaching 0-44338  
NaCl, vacancy complex formation and binding energies in zeroth approx. 0-24441  
NaCl, X-ray irradi., vacancy conc., thermal expansion meas. 0-6431  
NaCl:Mn $^{2+}$ , CN $^-$ , EPR spectrum rel. to Mn $^{2+}$ -vacancy-CN $^-$  complex 0-54942  
NaCl:Sr, dimer and trimer aggregate formation by NMR, ionic cond. and dielectric losses 0-15094  
NaF:Ca, migration enthalpy and entropy, TSC obs. 0-54716  
 $\text{Na}_x\text{In}_x\text{Sn}_{1-x}\text{S}_2$ , intercalation-substitution compounds, NMR study 0-44952  
 $\text{NaNO}_3$ , dielec. loss anal., Debye type loss peaks 0-50260  
 $\text{NaNbO}_3$ , elec. and thermoelec. props., influence of O defects 0-29401  
 $\text{NaNbO}_3$ -based ferroelec. solid solns., morphotropic transitions and elec. props., enhanced vacancy conc. 0-55048  
Nb, BCC, void nucleation following electron irradi. 0-29054  
Nb, defect annealing in 7 MeV-irrad. samples, positron annihilation obs. 0-24497  
Nb, positron annihilation and vacancy formation 0-16119  
Nb, positron trapping and annihilation at vacancies 0-29823  
NbC, electronic struct. of vacancies, effect on supercond. transition temp. 0-29347  
NbC, valence band XPS meas., comparison with X-ray emission spectra and band struct. spectral calcs. 0-50535  
NbC,  $x=0.868$ , 0.834, 0.766, self-diffusion of  $^{14}\text{C}$  0-29206  
 $\text{Nb}_3\text{Sn}$ , A-15 struct. Nb based superconductors, irradi. type influence on radiation defects 0-15093  
Ne, vacancy, electronic structure, Green's function theory 0-39525  
Ni, H diffusion, trapping and mobility near vacancies, dislocations and cracks 0-49426  
Ni, mass transport parameters, lattice defect effects under laser pulse action (*Ukrainian*) 0-6537  
Ni, phase transformations and vacancy form. by positron annihilation 0-2155  
Ni, point defect estimation from specific heat and volume in plastically deformed pure metals (*Russian*) 0-54223  
 $\beta_2$ -Ni-Al, elastic const., supersaturated thermal vacancy effects 0-54298  
Ni-Co-Cr-Al-Ti-Mo superalloy IN738, casting porosity removal using hydrostatic press. sintering 0-55322  
Ni-Ge, defect-solute interactions and radiation-induced segregation 0-25705  
Ni-Si, defect-solute interactions and radiation-induced segregation 0-25705  
NiAl, thermal defects, dilatometric study (*Japanese*) 0-15092  
 $\text{Ni}_{0.5-x}\text{Co}_x\text{Zn}_{0.5}\text{Fe}_2\text{O}_4$  ferrosilical solid solutions, cryst. lattice defects and props. 0-19796

**vacancies (crystal) continued**

- $\text{Ni}_{1-x}\text{Fe}_x^{2+}\text{Fe}_{2-x}^{3+}\text{Vac}_x\text{O}_4^{2-}$  (Vac=cation vacancy), solid solns., cryst. lattice imperfections 0-39069  
 $\text{Ni}_5\text{Mo}_2\text{Fe}$ ,  $\text{O}_2$  effect on secondary recrystallisation and mag. props. 0-35201  
NiO, stress appl. high temp. creep and point defects, creep rate obs. 0-49297  
Pb-Tl, vacancies, positron capture, function of Tl concentration (*German*) 0-49213  
Pb-Tl alloys, positron trapping in vacancies, varying concentration effects (*German*) 0-25477  
 $\text{PbTiO}_3\text{-La}_2\text{O}_3\text{-3TiO}_2$ , struct. and dielec. props. 0-54200  
Pt, interstitial thermal conversion study by elec. cond. meas. 0-15096  
Pt wire, single vacancy form., activation energy meas. 0-49212  
 $\text{Sc}_2\text{O}_3$ , polycryst., form. conditions of anion vacancies, phase comp. 0-54220  
Si (111) surface reconstruction, milk-stool model, quantum chem. ab initio calc. 0-49477  
Si, CW laser annealed, defect luminesc. 0-50388  
Si, defect formation kinetics during charged particle irradi. 0-29096  
Si, dislocation free, C and O impurity clouds, heat treatment influence on light scatt. 0-6427  
Si, divacancies due to proton irradi., IR absorpt., annealing effects 0-20673  
Si, divacancies orientation induced by IR light, EPR spectra 0-25209  
Si, electron irradi., two-vacancy defect EPR 0-29619  
n-Si, gamma ray irradi., impurity composition influence on recombination centre formation 0-6872  
Si implanted layers, interaction of defects and impurities stimulated by induced ionisation, ESR 0-11270  
Si, Jahn-Teller distorted vacancy, electronic struct. 0-10869  
Si, localised defect, self consistent Green's function calc. 0-10919  
Si, nearly perfect crystals., point defect aggregates, high resolution diffuse X-ray scattering study 0-49211  
n-Si neutron and electron irradi., isochronous annealing influence on edge absorpt. 0-11449  
Si, neutron irradi., small angle neutron scatt. meas. 0-29073  
Si, neutron transmutation doping, at. displacement effects 0-19852  
Si, point defects, multiple scatt.  $\alpha$  model 0-54636  
Si, point defects, negative-U props. 0-49660  
Si, positively charged divacancy photoionisation cross section by photocapacitance meas. 0-6901  
Si, proton irradi., efficiency of form. and nature of defects, Hall meas. 0-6444  
Si, reconstructed surface physics, review 0-10766  
Si, Schottky barrier structs., proton bombarded, defect states 0-29356  
Si, vacancies and interstitials 0-29015  
Si, vacancy, possible Anderson negative-U system 0-2358  
Si, vacancy, self consistent Green's function method 0-24843  
Si, vacancy, self-consistent electronic states 0-29354  
Si, vacancy, tight-binding calc. 0-24844  
Si, vacancy electronic struct., self-consistent Koster-Slater method 0-10920  
Si, vacancy screening, dielec. const., exchange correl. pot., Thomas-Fermi description 0-44528  
Si:As, displacement effect beam energy depend., vacancy trapping 0-33996  
Si:B, implanted, effectiveness of charged vacancies in diffusion 0-34239  
Si:B(P), proton enhanced diffusion, vacancies diffusion length 0-29226  
a-Si:H, spin defect and recombination influence on electronic transport 0-50409  
Si:In, electron irradi., Hall effect meas. 0-2401  
Si:P(As)(B)-SiO $_2$  interface oxidation kinetics, high doping levels, experiment 0-11828  
Si:P(B), high temp. impurity diffusion via vacancies and self-interstitials 0-24667  
Si-SiO $_2$  interface oxidation kinetics, high doping levels, theory 0-11827  
Sn, vacancy formation and activation volume, macroscopic model 0-54221  
Sn-Bi, eutectic, superplastic anisotropy (*German*) 0-25808  
Ta, positron annihilation and vacancy formation 0-16119  
Ta, positron trapping and annihilation at vacancies 0-29823  
 $\text{Ta}_2\text{O}_5$ , anodic film, thermally stimulated exo-electron emission 0-11546  
Ti, point defect estimation from specific heat and volume in plastically deformed pure metals (*Russian*) 0-54223  
 $\text{TiC}_{1-x}$ , substoichiometric, electronic density of states 0-2319  
TiO $_2$  (rutile), (001) and (110) faces, UPS and LEED obs. 0-45206  
TiO $_2$ -S, acceptor properties of S, free electron concentrations 0-34395  
TiO $_2$ :V(Cr)(Mn)(Fe), impurity levels, photocurrent and ESR meas. 0-29346  
TiO $_{2-x}$ , reduced, cond. between elec. props. in equil. at 1100°C and after quenching, defects role (*French*) 0-44582  
U, vacancy formation and phase transformation by positron annihilation 0-49215  
V, positron annihilation and vacancy formation 0-16119  
 $\text{VC}_x\text{O}_y$ , conc. depend., of unit cell filling degree 0-54199  
VN, electronic struct. of vacancies, effect on supercond. transition temp. 0-29347  
VO $_x$ , defect struct., local ionic arrangements in disordered phase 0-10532  
W, implantation effects of  $^{133}\text{Xe}$ , annealing behaviour, Mossbauer study 0-40011  
W, ion irradiated, defect clusters obs. 0-2089  
W, positron annihilation and vacancy formation 0-16119  
W, positron trapping and annihilation at vacancies 0-29823  
W, vacancies, quenching and recovery invest., resist. and TEM study 0-39074  
YCo $_3$ , anomalous  $^{57}\text{Fe}^m$  charge states, Mossbauer study 0-40017  
YIG:B,Pb, IR spectrum, localised modes, rel. to impurities and O vacancies 0-50377  
ZnS:Ag, TSC and induced impurity photoconductivity, existence of two electron trapping centres 0-44655  
ZnTe:Al,Cl, photolum., complex acceptor, ionization energy 0-20693  
Zr-base alloys, annealed specimens, irradiation growth 0-49276  
 $\text{ZrO}_2\text{:Y}_2\text{O}_3$ , low-temp. specific heat, oxygen vacancy effects 0-49376

**vacancy condensation loops**

see also *prismatic dislocations*

- fusion reactor metals and alloys, microvoid form., gaseous impurity atom effects, positron annihilation study 0-49275  
metals, FCC, small vacancy clusters, structures and energies, computer simulation 0-39073



**vacancy condensation loops continued**

- metals, irradiation-induced creep, transient stage, vacancy loop contrib. (Russian) 0-29115  
 void swelling rate, vacancy dislocation loop effect 0-2084  
 $\text{Cu}_{90}\text{Pd}_{10}$ ,  $\text{Cu}^+$  ( $\text{Au}^+$ ) ion-bombarded, displacement cascades and disorder zones, TEM studies 0-15167  
 $\text{Fe:Yb(Au)}$ , radiation-damage evolution, influence on lattice-location meas. 0-6426  
 $\text{Fe}_3\text{Al}$ ,  $\text{Cu}^+$  ( $\text{Au}^+$ ) ion-bombarded 0-15167  
 $\text{Pt}^{18}\text{Hf}$ , interaction of implanted impurity with radiation induced lattice defects, TDPAC meas. 0-24494

**vacancy-dislocation interactions**

- Nimonic PE16, He injected, bubble-void transitions in Ni ion bombard. 0-34095  
 $\text{Al-Cu}$  (96.5, 3.5 wt.%), characts. of disappearance of excess vacancies on dislocations 0-33991  
 $\text{Co-Ni}$ , deformed and isochronally annealed, positron lifetimes, annihilation at dislocation trapped monovacancy 0-55221  
 $\text{Ge}$ , defect form. under radiation-accelerated diffusion conditions 0-19854  
 $\text{NaCl}$ , moving dislocations, interaction with defects, elec. effects meas. in plastic deformation (Hungarian) 0-10572  
 $\text{Si}$ , defect form. under radiation-accelerated diffusion conditions 0-19854  
 $\text{Te}$ , electron irradi., mobility increase due to defect prod. 0-24501

**vacuum apparatus**

- includes apparatus for producing, maintaining and handling vacuum per se  
 see also vacuum gauges; vacuum pumps; vacuum techniques  
 capacitive displacement system for UHV operation 0-31737  
 cavity of rotating He cryostat, centrifugal field rel. to residual press. 0-42232  
 compensating work holder for coating two sides of substrate uniformly 0-22372  
 coupler, for connection of H-flanges (Japanese) 0-13083  
 differential Burnett apparatus, virial coeff. meas. at various temps. 0-22373  
 electronograph cryogenic trap construction 0-31766  
 feedthroughs, coaxial and multipin, cryogenic performance 0-8995  
 furnace system for heat treatment, ultrahigh vacuum conditions 0-52222  
 heated vacuum monochromator for 40-280 nm spectroscopy 0-33176  
 history and development 0-31775  
 leak detector, sparking, using semiconductor switching diodes 0-31774  
 low energy ion scattering spectroscopy, UHV apparatus (Japanese) 0-20746  
 magnetic safety valve 0-8966  
 manometric tube with vacuum valve 0-47066  
 metal-seal valve for high radiation use in high vacuum 0-233  
 monochromator low-temp. attachment construction and optics 0-31764  
 NUMATRON project test accumulation ring, vacuum system (Japanese) 0-18724  
 O-ring, for ultrahigh vacuum, heat cycle test of stainless hollow (Japanese) 0-13084  
 seal, for rotary motion 0-31772  
 seals, Cu-ceramic, metallisation process 0-37046  
 toroidal vacuum chamber, large, elastomer seal 0-27315  
 UHV bakeable vacuum chamber, use of Al alloy (Japanese) 0-52248  
 UHV microbalance, with ion gun, absolute meas. of sputtering yield (Japanese) 0-17951  
 UPS ultrahigh vacuum apparatus, appl. to clean and gas covered  $\text{Si(III)}$  surfaces (Japanese) 0-37125  
 vacuum-arc plasma extracted ion precipitation unit 0-35106  
 Cu vacuum gaskets, basic problems 0-47064  
 TiN film as protective coating for vacuum deposition chamber, Auger electron spectroscopy study 0-25922

**vacuum control**

- vapour pressure temperature estimation method in ultra high vacuum range (Chinese) 0-232

**vacuum deposited coatings**

- amorphous, vac. evaporated, doping, transport and optical props. 0-49715  
 antireflection coatings, thickness monitoring during deposition 0-19114  
 copper phthalocyanine, thermal behaviour (Japanese) 0-24753  
 dielectric film, electron beam produced pore form. mechanism, statistical model (Russian) 0-6667  
 intrinsic stress determ. by cantilevered plate method, substrate bending 0-54571  
 microporosity and absorptivity in vacuo meas. apparatus 0-9053  
 optical, improved film quality, progress in vacuum generation and deposition technology 0-35101  
 Permalloy film, multi- and single-layer, reson. curves subjected to tangential mag. reversals (Russian) 0-50195  
 p-terphenyl oriented layers, charge carrier transport, hopping model 0-2506  
 rare earth element sulphides, condensates, struct. and optical transmittance 0-20727  
 reference fission foils preparation by fluoride deposition, characterisation 0-23218  
 refractory metal films, evaporated, optical props., rel. to struct. 0-55211  
 resistive foils, manufacture and props. of multicomponent alloys (Polish) 0-35131  
 TTT film, hopping cond. AC and DC meas. and EPR 0-11111  
 vacuum deposited film, as first wall material, sputtering yield mea. (Japanese) 0-25513  
 Ag, defect density and activation energy depend. on deposition rate 0-29294  
 Ag film, in situ struct. determ. by internal stress meas. 0-54569  
 Ag, internal stress and its depend. on gas adsorption 0-6683  
 Ag, on Cu, ion-induced intermixing 0-15420  
 Ag, on evaporated AgBr layers, growth mechanism 0-35095  
 Ag, vac. deposition of oriented coating on doped alkali halide substrate 0-2303  
 Ag vacuum deposited coating on glass, strength 0-55505  
 Al, condensed film, phase and struct. nonuniformity (Russian) 0-54536  
 Al film, vacuum evaporation growth, impurity presence, effects (Hungarian) 0-7495  
 Al, vacuum condensate, struct. and mech. props. depend. on deposition conditions 0-15417  
 Al vacuum deposited coating on glass, strength 0-55505  
 Al-Cu thin films, microstruct. rel. to electromigration 0-44355  
 $\text{As}_2\text{S}_3$ , amorphous film waveguide and grating coupler 0-53448  
 $\text{As}_2\text{S}_3$  film, selective etching characts. obs. (Russian) 0-3207

**vacuum deposited coatings continued**

- $\text{As}_2\text{S}_3$ , single-layer vac. antirefl. coatings for near IR spectral region 0-33099  
 $\text{As}_2\text{S}_3$  thin films, vacuum deposited on Ge and PbS, sealing props. and TEM 0-35097  
 $\text{As}_2\text{S}_3$ , vapour-deposited, pure and doped, hole mobility 0-49728  
 $\text{As}_2\text{Se}_3$ , amorphous, hole emission defect states 0-49759  
 Au, discontinuous, evaporated on C and  $\text{SiO}_2$ , struct. and elec. cond. 0-39686  
 Au fine particles, morphological features using TEM weak-beam dark-field technique 0-15410  
 Au, internal stress and its depend. on gas adsorption 0-6683  
 Au, on Cu, ion-induced intermixing 0-15420  
 Au vacuum deposited coating on glass, strength 0-55505  
 Au/Sn, microstructure and texture, TEM obs. 0-39481  
 Au-Cu-Cr, deposited on glass or Si substrate, X-ray microanalysis (French) 0-50902  
 $\text{BaCl}_2$ , non-cryst., very-low-freq. inelastic light scatt. 0-25367  
 $\text{BaFCl}$ , non-cryst., very-low-freq. inelastic light scatt. 0-25367  
 Bi film, evaporated, lattice distortion spectrum, elec. resistance temp. variation 0-54806  
 Bi-Sb alloy, amorphous nature, AC and DC cond. and Hall coeff. obs. 0-11114  
 $\text{Bi}_2\text{O}_3$  films, dielec. props., 90 to 298K, freq. range 0.1 to 10 kHz, ageing effect 0-55036  
 $\text{Bi}_2\text{O}_3$ , thermally grown, I-V characts., current controlled neg. resist. 0-15637  
 C, amorphous, density meas., microcrystalline model of struct. 0-2313  
 C, amorphous, diamond-like 3-fold coord. 0-50323  
 C, amorphous, struct. and semicond. props. and heterojunction form. with single cryst. Si 0-25002  
 C, diamond-like, ion deposited, hardness and mech. stability 0-2314  
 C, diamond-like, ion-plated, electron energy loss spectra characterisation 0-2308  
 C, graphitisation, electrn microscopy 0-40265  
 Ca films, thin and ultrathin, struct. and photoemission meas. 0-11538  
 Cd, HCP, microstruct., X-ray obs. 0-10827  
 $\text{CdIn}_2\text{S}_4$ , growth, struct., optical and photoelectronic props. 0-10831  
 $\text{CdS}$ , polycryst., optical spectra, 0.5-6.5 eV 0-55212  
 $\text{CdS:Ag}$ , recrystn. by  $\text{H}_2\text{S}$  heat treatment 0-34328  
 $\text{CdS:Cu(Cl)}$ , thin layer, electron pulse induced cond. relax. 0-2501  
 $\text{CdS:In}$ , flash evaporated, prep. and elec. props. 0-20792  
 $\text{CdS:Se}_{-x}$ , flash evaporated, prep. and elec. props. 0-20792  
 $\text{CdS:Se}_{-x}$ , photosensitive films, prep., props., and use for photodetectors 0-55298  
 $\text{CdS(Se)(Te)}$ , growth and struct., HEED obs. 0-29292  
 $\text{CdSe}$ , electrical resist. and surface changes by laser annealing 0-2491  
 $\text{CdTe-Te}$  film, prep. by combined hot-wall-flash evaporation method, and characterisation 0-55296  
 $\text{CdTe}_{-x}\text{Se}_x$ , solid solution films, prep., struct., and photocond. 0-54541  
 Co film, columnar struct. depend. on degree of texture 0-54567  
 Co film, texture and columnar struct. 0-54566  
 Cr vacuum deposited coating on glass, strength 0-55505  
 Cr-Si, for resistor manufacture, residual gas atmosphere analysis (German) 0-6681  
 Cu, adsorption and desorption of water vapour, relative humidity effects 0-49505  
 Cu alloy vacuum condensed films, alloying addition influence on electro-physical props., elec. cond. (Russian) 0-34529  
 Cu film, in situ struct. determ. by internal stress meas. 0-54569  
 Cu vacuum coating on steel substrate, influence of precipitation conditions on porosity (Russian) 0-54578  
 Cu, vacuum condensate, struct. and mech. props. depend. on deposition conditions 0-15417  
 Cu vapour deposited mirror on SiC substrate, pulsed laser damage characts. 0-48314  
 Cu-Al, vacuum condensate, struct. and mech. props. depend. on deposition conditions 0-15417  
 $\text{CuInSe}_2$ , evaporation source temp. effect, on comp. 0-39478  
 $\text{Cu}_{-x}\text{S}$ , ordering process, electron diffr. study 0-39477  
 $\text{Cu}_2\text{S}$  evaporated thin films, composition, prep. and characts. 0-25569  
 Eu chelate, fluoresc. lifetime, depend. on optical environment 0-9630  
 Eu complex, benzoyltrifluoro-acetone-chelate, refr. index determ. of fluoresc. films 0-40175  
 Fe, evaporated at oblique incidence, optical and mag. anisotropies 0-7134  
 Fe, on Au (111), interaction layer formation mechanism 0-54559  
 Fe, thermally evaporated, contamination effects obs. 0-49545  
 $\text{Fe-Al}$ , dil., NMR spin echo, rel. to struct. inhomogeneities (Russian) 0-29644  
 $\text{Fe-Co}$ , dil., NMR spin echo, rel. to struct. inhomogeneities (Russian) 0-29644  
 $\text{Fe-Gd}$  amorphous film, struct. and mag. props. 0-20439  
 Fe-refractory compound, dispersion strengthened, thick vacuum condensate, control of struct. and mech. props. 0-16324  
 $\text{Fe-Si}$  amorphous film, struct. and crystallisation, Mossbauer study 0-11300  
 $\text{Fe}_2\text{O}_3$ , thermally evaporated, contamination effects obs. 0-49545  
 $\text{FeSb}$  solid solution, supersaturated, mag. hyperfine field, Mossbauer study 0-44961  
 $\text{GaSb}$  films, amorphous and cryst., vac. evaporated, Elec. cond. thermolec. power and optical absorpt. 0-2504  
 $\text{GdCo}$  film structure, dependent on substrate type (Russian) 0-24747  
 $\text{GdFe}$  film structure, dependent on substrate type (Russian) 0-24747  
 Ge, amorphous, density meas., microcrystalline model of struct. 0-2313  
 Ge, amorphous, non-destructive density meas. 0-6680  
 Ge amorphous film, O depth profiling by SIMS 0-39480  
 Ge amorphous film, ultra high vac. prep., DC elec. cond. 0-49721  
 Ge, on Si(111), solid phase heteroepitaxy 0-6670  
 Ge-metal films codeposited, amorphous and polycryst., struct. and elec. props. 0-24766  
 $\text{GeO}$ , optical props., rel. to possible appl. in holography 0-29816  
 $\text{GeS}$  film, between  $\text{Al(Zn)(Sn)}$  electrodes, Schottky and Poole-Frenkel cond. mechanisms 0-54799  
 $\text{GeTe}$ , electro-reflectance meas. 0-11496  
 $\text{GeTe}$  films, elec. props. and struct., influence of annealing and condensation conditions 0-15388  
 $\text{HgTe}$ , electrical props., 78-420K 0-11119  
 In film, vacuum evaporation growth, impurity presence, effects (Hungarian) 0-7495  
 In particles, grown in ultra-high vac. on KCl substrates, struct. and orientation 0-10814



**vacuum deposited coatings continued**

- InSb films on LiNbO<sub>3</sub>, prep. and props. 0-35093  
 Ir, CO adsorption, IR refl.-absorpt. spectroscopy 0-34925  
 K<sub>2</sub>S<sub>3</sub>, condensates, struct. and optical transmittance 0-20727  
 LaB<sub>6</sub>, prep. by electron beam evaporation, and optical and elec. props. 0-20793  
 LiF, polycrystalline and single-cryst., comparative study of phonons by electron spectroscopy 0-25505  
 LiF(Cl)(Br) film, electron emission under metastable He and Ne atom impact 0-20747  
 Mg and Mg-Fe films, defect energy distrib., elec. resist. meas. during annealing 0-54808  
 MgF<sub>2</sub>, destruction props. obs., suitability for integrated optics assessment (*Slovak*) 0-33224  
 Mn, contact to p-Si, barrier height 0-34510  
 Mn-SiO cermet films, DC and AC resist. 0-54804  
 Mn-SiO cermet films, elec. resist., annealing behaviour 0-54803  
 MoC coatings, produced by plasma flux deposition in vacuum, exam. (*Russian*) 0-11567  
 Na, for expendable filter in VUV, use and preparation technique 0-33193  
 Na<sub>2</sub>AlF<sub>6</sub>, electron bombard. effect on secondary electron emission, Auger peak shifts 0-2903  
 NaF(Cl) film, electron emission under metastable He and Ne atom impact 0-20747  
 Nb, superconducting, deposition parameter effects on crit. temp. 0-2514  
 Nd<sub>0.35</sub>Co<sub>0.65</sub>, vacuum evaporated, magnetisation ripple struct., TEM and defocused Lorentz microscopy 0-7136  
 Ni, few atomic layers thick, transition from Pauli paramag. to band ferro-mag. 0-44885  
 Ni film, layer mode growth on Fe (001) surface, AES study 0-49540  
 Ni film, multi- and single-layer, reson. curves subjected to tangential mag. reversals (*Russian*) 0-50195  
 Ni, ultrathin film, field effect meas., influence of CO adsorption 0-11108  
 Ni-Al films, evaporated, grain size and microstruct. 0-15423  
 Ni-Al<sub>2</sub>O<sub>3</sub>(ZrO<sub>2</sub>), dispersion strengthened, thick vacuum condensate, control of struct. and mech. props. 0-16324  
 Ni-Co films, electron-beam evaporated, magnetoresist. anisotropy, deposition temp. effect 0-34528  
 Ni-ZrO<sub>2</sub>, electron-beam-evaporated condensate, cold deform. and annealing effects on microstruct. 0-16331  
 NiSe, phase transformation, electron microscope studies 0-2302  
 Pb, vapour deposited FCC, normal and oblique incidences, microstructure, X-ray diffr. study 0-20048  
 PbF<sub>2</sub>, antireflection coating deposition technique, 2.87  $\mu$ m laser damage threshold 0-33264  
 $\beta$ -PbF<sub>2</sub> film between metal electrodes, vac. evaporated, AC study of elec. props. 0-2207  
 PbS, optical and phys. props. 0-2315  
 Pb<sub>1-x</sub>Sn<sub>x</sub>Te heterojunction lasers, instantaneous vacuum evaporation growth, threshold current density 0-5759  
 Pd, on Si, ion-induced intermixing 0-15420  
 Pd, resistivity and thermoelec. power, annealing effects 0-39684  
 Pd-Ag, deposited on glass or Si substrate, X-ray microanalysis (*French*) 0-50902  
 PrB<sub>6</sub>, prep. by electron beam evaporation, and optical and elec. props. 0-20793  
 Pt evaporated film, optical props. meas. in VUV, 220 to 150 Å 0-45159  
 Pt, on Au, crit. thickness of pseudomorphic film growth, substrate size depend. (*Russian*) 0-29286  
 Pt, on Si, ion-induced intermixing 0-15420  
 Sb, amorphous film on glass substrate, effect of substrate temp. on crystallisation 0-39468  
 Sb<sub>2</sub>Te<sub>3</sub>-Sb<sub>2</sub>Se<sub>3</sub> thin layers, struct., phase comp., and elec. cond. 0-15389  
 Se, amorphous, density meas., microcrystalline model of struct. 0-2313  
 Se, amorphous, vac. deposition on polymer substrates, use of temp. gradient vac. coating device 0-35099  
 Se, amorphous electrophotographic layers, resolution parameters 0-31926  
 Si amorphous film, vacuum deposited, microscopic voids, gas absorpt., crystn. study 0-49534  
 Si and Si:H amorphous films, porosity and oxidation of evap., sputtered and plasma-deposited films 0-10838  
 Si:H amorphous films for solar cells, optical and elec. props. of RF glow discharge deposited films 0-54576  
 Si:Li(Na)(K)(F)(Cl), amorphous, implantation effects on elec. props. 0-49716  
 SiO<sub>2</sub>, amorphous, density meas., microcrystalline model of struct. 0-2313  
 SiO film, vacuum evaporation on NaCl single cryst., IR absorption spectra 0-35098  
 SiO<sub>2</sub>, single-layer vac. antirefl. coatings for near IR spectral region 0-33099  
 SiO<sub>2</sub> thin films, comparison of RI and IR spectra 0-11497  
 SiO<sub>2</sub>, powder and vac. deposited, amorphous struct., X-ray diffr. meas. 0-1931  
 SmB<sub>6</sub>, prep. by electron beam evaporation, and optical and elec. props. 0-20793  
 Sn film, effect of rate of deposition on supercond. props. and struct. 0-2954  
 SnO<sub>2</sub>-Si solar cells, electron-beam deposited, struct., photovolt. props. 0-50956  
 SnTe, electro-reflectance meas. 0-11496  
 SnCl<sub>2</sub>, non-cryst., very-low-freq. inelastic light scatt. 0-25367  
 Te, amorphous, phonon-assisted hopping cond. 0-2392  
 Te coating of PbTe surfaces, struct. and junction characts. 0-50743  
 Ti-Al alloy film, evaporated, anodisation characts. obs. (*Polish*) 0-55574  
 TiH<sub>4</sub> film, kinetics of H<sub>2</sub> interaction 0-6620  
 TiN, synthesis using enhanced reactive evaporation 0-2953  
 TiO<sub>2</sub>, amorphous, struct. and crystn., TEM obs. 0-2291  
 TiO<sub>2</sub>, destruction props. obs., suitability for integrated optics assessment (*Slovak*) 0-33224  
 TiI<sub>2</sub>-PbF<sub>2</sub> graded-index film coating technique and results 0-33265  
 WO<sub>3</sub>, amorphous, density meas., microcrystalline model of struct. 0-2313  
 WO<sub>3</sub>, amorphous, struct. and crystn., TEM obs. 0-2291  
 WO<sub>3</sub> film, evaporated, mech. of elec. cond. 0-44747  
 WO<sub>3</sub> films, electron struct. changes during electrocoloration, XPS obs. 0-40217  
 ZnF<sub>2</sub>:Mn, thin films, electroluminescence, brightness voltage characts. hysteresis 0-20709  
 ZnS, destruction props. obs., suitability for integrated optics assessment (*Slovak*) 0-33224

**vacuum deposited coatings continued**

- ZnS films prepared by thermal evaporation in vac., nature of defects 0-10835  
 ZnS, ZnS-CeF<sub>3</sub>, single-layer vac. antirefl. coatings for near IR spectral region 0-33099  
 ZnS:Tb<sup>3+</sup>, NdF<sub>3</sub> film, electrolum. energy transfer 0-2861  
 ZnTe film preparation and props. using single-source method (*Japanese*) 0-6664  
 ZnTe films, grown on glass using atomic layer evaporation 0-44453

**vacuum deposited thin films** *see vacuum deposited coatings***vacuum deposition**

- used for EVAPORATED layer production in vacuum*  
*see also electron beam deposition*  
 actinide target prep. for synthesis of transactinide elements 0-23206  
 closed field sputtering equipment 0-50556  
 cold light production by high vacuum deposition of multilayer interference coatings (*German*) 0-53486  
 cryogenic thin film ultrahigh-vacuum evaporation/sputtering apparatus 0-20790  
 di-butyl-sebacate, HV evaporation, mass transfer in evaporating space (*Japanese*) 0-50558  
 discrete-pulse evaporation, films of substances with complicated composition production 0-50557  
 double-layer antireflection coatings for plastic lenses, evaporation coating process 0-14491  
 electric arc deposition of coatings using extracted ion precipitation unit 0-35106  
 HV, mass transfer in evaporating space (*Japanese*) 0-50558  
 IR multilayer interference filter manufacture, supposed longwave limit 0-9989  
 isotope target preparation by laser beam evaporation techniques 0-18735  
 metallic thin film, early stage obs. using microbalance technique and electron microscopy (*Japanese*) 0-54554  
 metallurgical coatings, vapour deposition processes in vac. 0-35430  
 optical coatings, improved film quality, progress in vacuum generation and deposition technology 0-35101  
 quartz crystal thickness sensor isotope target preparation 0-17923  
 rare earth films, prep., struct., and props., general review 0-54556  
 Re-sputtering and implanting sputtered atoms during deposition 0-16137  
 substrate bending during thin film evaporation due to temp. difference between substrate faces 0-54571  
 substrate temp. meas. by laser beam 0-20794  
 targets manufacture, Al<sub>2</sub>O<sub>3</sub>, by powder metallurgy (*German*) 0-11586  
 thin film composition gradient production 0-55295  
 vacuum deposited film, as first wall material, sputtering yield mea. (*Japanese*) 0-25513  
 Ag, film, condensate obtained in electric field, anisotropy of elec. props. 0-44743  
 Ag, on evaporated AgBr layers, growth mechanism 0-35095  
 Al, film, condensate obtained in electric field, anisotropy of elec. props. 0-44743  
 Al thin films, vacuum deposited, crystal growth in presence of O<sub>2</sub> and Ni 0-15409  
 As<sub>2</sub>S<sub>3</sub> thin films, vacuum deposited on Ge and PbS, sealing props. and TEM 0-35097  
 Au, vac. deposited thin film, Auger spectroscopy 0-2952  
<sup>10</sup>B self supporting target preparation up to 500  $\mu$ g/cm<sup>2</sup> 0-18745  
<sup>11</sup>B self supporting target preparation up to 500  $\mu$ g/cm<sup>2</sup> 0-18745  
 Bi film deposition by vacuum evaporation on NaNO<sub>3</sub> single cryst. cleavage 0-35091  
 Ca, nuclear target preparation 0-23224  
 Cd films, nucleation and growth, props. 0-29878  
 CdS<sub>x</sub>Se<sub>1-x</sub> photosensitive films, prep., props., and use for photodetectors 0-55298  
 CdTe-Te film, prep. by combined hot-wall-flash evaporation method, and characterisation 0-55296  
 Cr-Si coatings, for resistor manufacture, residual gas atmosphere analysis (*German*) 0-6681  
 Cu, vac. deposited thin film, Auger spectroscopy 0-2952  
 Cu+Fe+Cd, nuclear target preparation by evaporation and rolling 0-23224  
 Cu+Fe+Sn, nuclear target preparation by evaporation and rolling 0-23224  
 Cu<sub>2</sub>S evaporated thin films, composition, prep. and characts. 0-25569  
 FeSb alloy films, vapour-deposited, formation of metastable phase 0-44437  
 Ge<sub>15</sub>Te<sub>85</sub>X<sub>4</sub> amorphous semicond. switches, fabrication technology (*German*) 0-7493  
 HgTe thin film Hall sensor fabrication 0-2951  
 In<sub>2</sub>O<sub>3</sub> transparent conductive coating production 0-35092  
 Li, nuclear target preparation 0-23224  
 MgF<sub>2</sub>-ZnS multilayers, high vacuum deposition for cold light mirror prod. (*German*) 0-53486  
 Ni foil, crystal struct. as function of substrate temp. during deposition 0-18742  
 PbSe films, synthesis characts. 0-35094  
 PbTe-ZrO<sub>2</sub> (SiO<sub>2</sub>), epitaxial MIS struct., fabrication and elec. props. 0-2472  
 Pt foil, crystal struct. as function of substrate temp. during deposition 0-18742  
 Se, amorphous, vac. deposition on polymer substrates, use of temp. gradient vac. coating device 0-35099  
 SeS gas, thermodynamic props., quadrupole mass filter study 0-16716  
 Si, solid-state epitaxial growth of amorphous layer 0-10803  
 SiO film, vacuum evaporation on NaCl single cryst., IR absorption spectra 0-35098  
 SnO<sub>2</sub> thin film gas sensor, prep. 0-39691  
 Te textured thin films, prep., high solar absorptivity by multiples refl. 0-11568  
 Ti-Al-V (6.4 wt.%) alloy foil, substrate temp. effect on struct. 0-7497  
 ZnS, epitaxial growth, appl. to electronic devices, review (*Japanese*) 0-55281  
 ZnS films prepared by thermal evaporation in vac., nature of defects 0-10835  
 ZnTe film preparation and props. using single-source method (*Japanese*) 0-6664



**vacuum gauges**

- see also *barometers; ionisation gauges; manometers; vacuum measurement*  
 absolute pressure vacuum gauges, testing and calibration automation 0-22378  
 Bayard-Alpert gauge, modulated, reverse X-ray currents (*Japanese*) 0-13087  
 bimetallic, temperature difference type (*Japanese*) 0-13089  
 calibration, by static method 0-52258  
 calibration using simple volume ratio method 0-31780  
 control of pumping process, 'Pirani', 'Penning' and ionisation gauges (*Czech*) 0-52256  
 Pirani type, dimension- and gas-dependence of characteristics (*Japanese*) 0-13086  
 Pirani type, with TaN thin films (*Japanese*) 0-52257  
 three grid modulated Bayard-Alpert gauge (*Japanese*) 0-13088

**vacuum measurement**

- see also *vacuum gauges*  
 control of pumping process and vacuum apparatus (*Czech*) 0-52256  
 differential membrane manometer 0-31777  
 magnetic discharge manometric converter 0-31779  
 Pirani type vacuum gauge, with TaN thin films (*Japanese*) 0-52257  
 pulsed pressure meas., using piezoelectric pick-up 0-31778  
 ultra-high vacuum, total pressure meas. 0-31782  
 vapour pressure temperature estimation method in ultra high vacuum range (*Chinese*) 0-232

**vacuum polarisation** see *quantum electrodynamics***vacuum pumps**

- see also *cryopumping; diffusion pumps; ion pumps*  
 crystal units, vacuum system for cleaning and cold welding (*Polish*) 0-31776  
 ELMO-G quiet running vacuum pumps and compressors for plant noise reduction 0-5872  
 miniaturised turbo-molecular pump, for space appl. (*French*) 0-42234  
 orbitron ion-getter, small non-cooled and low power consumption 0-52532  
 pumping down curve,  $P(t)$ , rel. to adsorption isotherm (*Japanese*) 0-52249  
 Roots pumps, mechanical booster pump, clean vacuum, reduction of oil backstreaming (*French*) 0-17954  
 rotary, vacuum use of perfluoro polyether as pump fluid 0-52251  
 summary of new laboratory pumps 0-22375  
 turbo molecular pump, performance for  $H_2$  (*Japanese*) 0-13085  
 turbomolecular pump, miniaturized for space appl. 0-52254  
 water content meas. and display with AF3 0-22376  
 Ti sublimation pump, pre-cleaned, atomically clean surface environment, confirmation using field electron emission 0-52250

**vacuum sintering** see *sintering***vacuum techniques**

- includes *techniques for producing, maintaining and handling vacuum per se*  
 see also *cryopumping; getters*  
 atomically clean surface environment, confirmation using field electron emission 0-52250  
 differential Burnett apparatus, virial coeff. meas. at various temps. 0-22373  
 discharge, cathode spot, models analysis 0-19636  
 discharge, cathode spot parameters, existence diagram method applic. 0-24276  
 evacuated tubular solar collector integration with LiBr absorption cooling systems 0-3493  
 extraction device with mass spectrum analyser for determ. of gas-forming admixtures in metals 0-22371  
 high pressure preparation lock for surface analysis in ultrahigh vacuum chamber (*German*) 0-52261  
 ion accelerator, atomic collision processes rel. to vacuum system, review 0-54290  
 leak detection, ultrasensitive 0-47065  
 leak detection using liquid spray 0-234  
 low energy ion scattering spectroscopy, UHV apparatus (*Japanese*) 0-20746  
 metal hollow O-ring seal, for UHV and cryogenic use (*Japanese*) 0-22374  
 metals and alloys, fatigue behaviour, vacuum effect, review 0-35309  
 Monte Carlo analysis of backscattering and sputtering in vacuum systems 0-235  
 outgassing, effect of ambient and other pretreatment 0-17953  
 pressure vessel, effects of method of return to atm. press. (*French*) 0-42233  
 pulsed high voltage measurement using 2 MV resistive voltage divider 0-31803  
 pumping down curve,  $P(t)$ , rel. to adsorption isotherm (*Japanese*) 0-52249  
 reactor defective fuel detection using vac. slipping technique 0-9389  
 seal with thermomechanical drive of Ti-Ni 0-31773  
 SEM and Auger electron spectroscopy, vacuum improvement technique 0-27381  
 steel, stainless type 304, radiation induced outgassing 0-624  
 transition metals processing technology and appl. (*Hungarian*) 0-55318  
 UPS ultrahigh vacuum apparatus, appl. to clean and gas covered Si(III) surfaces (*Japanese*) 0-37125  
 $N_2$  supply, liquid, to vacuum installations 0-31762

**vacuum tubes**

- see also *diodes; tetrodes; triodes*  
 HV vacuum accelerator tube, microparticle obs. 0-864

**valence bands**

- adsorbed atom on solid surface, photoemission from valence band, surface plasmon emission, model Hamiltonian calcs. 0-50525  
 alkali graphite intercalation compound, evidence for alkali-like cond. bands 0-45201  
 alkali graphite intercalation compounds, evidence for alkali-like conduction band, UPS study 0-45208  
 alkali graphite intercalation cpds., selection rules and restricted valence band self-convolution for KVV Auger transition 0-29832  
 Cain model, two-band, dispersion and iso-energy surfaces of valence and conduction bands (*Russian*) 0-24783  
 core and valence electron enhancement factors from positron annihilation-correlation curves 0-25479  
 covalent semiconductor, valence band calc. using many-electron theory 0-15434

**valence bands continued**

- degenerate semiconductors, heavy hole-phonon bound states for valence band with degeneracy point (*Russian*) 0-15461  
 diamond, natural, free exciton luminesc. line shape 0-40165  
 diamond, valence band calc. using many-electron theory 0-15434  
 (ethylene), mol. crystals, quantum theory, mol. tight binding method calcs. 0-49572  
 ferromagnetic semiconductors, dielectric function depend. on magnetisation, light absorpt. coeff. (*Russian*) 0-15467  
 (formamide), mol. crystals, quantum theory, mol. tight binding method calcs. 0-49572  
 gapless semiconductor valence band in mag. field 0-49600  
 graphite, Compton profiles, momentum densities, comparison with glassy C 0-2895  
 molecular crystal, band structure, excitonic processes, trap distrib. 0-6720  
 molecules, valence and core photoionisation, spectral lines, many body effects 0-47853  
 MOS structure, p-channel, effect of isotropic stress on Si valence band struct., press. transducer appl. 0-25011  
 organic molecular crystals, photoemission, book contrib. 0-16158  
 passive layer, on Fe electrode, semiconductor model, appl. to electrochem. reactions, review 0-26022  
 photoelectron spectroscopy of solids, review 0-55263  
 photoemission in solids, book 0-12860  
 polyacetylene, band struct. valence Hamiltonian minimal STO-3G basis calc., nonempirical model pot. 0-54596  
 polyethylene, band struct. valence Hamiltonian minimal STO-3G basis calc., nonempirical model pot. 0-54596  
 polyethylene film, soln.-cast, low energy electron scatt. obs. of band struct. 0-16131  
 pyrene, band structure, excitonic processes, trap distrib. 0-6720  
 rare earths, and their alloys and cpds., photoemission, rel. to electronic struct., book contrib. 0-16157  
 semiconductor, Wannier excitons, fine structure, lineshape and dispersion, review 0-44520  
 semiconductor thin films, degenerate one-valley and many-valley, photo-galvanic effect calcs. 0-34487  
 semiconductors, photoelectron spectra and band struct., book contrib. 0-16155  
 simple metals, photoemission theory, book contrib. 0-16159  
 transition metal clusters, particle size rel. to bulk metallic props. 0-44490  
 transition metal compounds, valence band struct., X-ray spectroscopic study 0-29319  
 transition metal monosulphides of first-row, XPS and UV PES 0-20760  
 transition metals, and their alloys and cpds., photoelectron energy distrib. curves, rel. to band struct., book contrib. 0-16156  
 AgI, superionic conductor, density of valence states, photoelectron spectra meas. 0-25523  
 Ar, solid gaseous, valence and inner shell excitonic band struct. 0-6735  
 Ar, vacancy, electronic structure, Green's function theory 0-39525  
 Ar, valence electron distrib., pseudopotential calcs. 0-2335  
 As-Se amorphous film, density of upper valence band states, annealing effects, UPS obs. 0-29845  
 As-Se chalcogenide glass, optical const. photoinduced changes mechanism 0-7321  
 $As_2(Se,Te)_3$  glasses, X-ray absorption and photoelectron spectroscopy study 0-7463  
 Au-Cs(Mg)(Rb)(Zn), charge transfer, Mossbauer effect  $^{197}Au$  isomer shifts, XPS valence-band spectra 0-2676  
 Au-Si interface, valence band and core levels, Si diffusion, alloy form., photoelectron spectra obs. 0-45205  
 BP,  $As_{1-x}$  system, electron struct. and interatomic interactions, X-ray spectroscopy 0-20736  
 $BaTiO_3$ , undoped and Cu doped,  $\Gamma_{15}$  phonon freezing, electronic instability, LCAO calc. 0-25318  
 Be, HCP metals, K-emission valence bands, structure and bonding 0-7438  
 C, amorphous, inelastic electron scatt., valence electron contrib. 0-55240  
 C, glassy, Compton profiles, momentum densities, comparison with graphite 0-2895  
 $Cd_3As_2$ , valence band struct., optical absorpt. meas. 0-50293  
 $CdGa_2Se_4$ , struct. of valence band, photocond. and reflection spectra meas. 0-6719  
 $CdI_2(Br_2)(Cl_2)$ , dielec. function and band struct., EELS meas. 0-40195  
 $CdIn_2S_4$ , electronic states, sensitivity to cryst. struct., UPS study 0-45209  
 CdS, band structure calcs. by modified orthogonalised plane wave (MOPW) method 0-54609  
 $CdS:F(Cl)$ , shallow donors electronic Raman scatt., reson. enhancement 0-45068  
 Cu film, valence bands, XPS excited by Zr  $M\zeta$  radiation 0-40236  
 Cu, valence band splitting, X-ray K-emission spectroscopy 0-40189  
 Cu-Zr, metallic glasses, valence band struct. investigation 0-11533  
 CuCl, UPS meas., electronic struct. 0-50529  
 CuCl, XPS and Auger spectroscopy, elec. struct. 0-29852  
 $EuCu_2Si_2$ , valence fluctuation and temp. depend. of Cu nuclear quadrupole interaction 0-15818  
 Fe-B amorphous alloys, valence band spectrum, XPS study 0-50534  
 Fe-Ni alloys, electronic struct., XPS study 0-29842  
 FeO, valence band XPS and UPS, LCAO-MO calcs. 0-45197  
 FeSb<sub>2</sub>, quasi-magnetic semicond., mag. susceptibility 0-39757  
 GaAs, angle-resolved photoemission and valence band dispersions 0-7469  
 GaAs, surface states, band struct. by discontinuous potential method 0-20276  
 p-GaAs: Cd, (110) cleaved surface, defect-induced surface states 0-6925  
 GaAs-Ge structure, electronic struct., ang.-resolved photoemission obs. 0-49881  
 GaP (110), electronic surface states, initial steps of  $O_2$  chemisorption 0-49844  
 GaP, cleaved (110) surface, electron surface props. 0-11067  
 GaP-liq.  $NH_3$  soln. junctions, elec. characts. (*French*) 0-2460  
 $GaS_{1-x}Se_x$ , wavefunction symm. and binding energies, synchrotron radiation photoemission spectroscopy 0-50532  
 Ge, ion implanted, cond. and valence bands study by X-ray bremsstrahlung and photoelectron spectra 0-2360  
 Ge uniaxially deformed, cyclotron resonance of RF field heated hot holes, (*Russian*) 0-44925  
 Ge-rare earth alloys, nature of chemical interaction, X-ray emission, absorpt. and photoelectron study (*Russian*) 0-55261  
 (HCN), mol. crystals, quantum theory, mol. tight binding method calcs. 0-49572



**valence bands continued**

- Hg, valence band spectra by PES study 0-4822  
 p-InSb, stress induced k-linear terms in band struct. 0-49595  
 InSe, spin orbit split off valence bands, exciton transitions, Hopfield's quasicubic model, visible absorpt. spectrum 0-50370  
 LaB<sub>6</sub>, valence band dispersions, angle-resolved photoemission 0-11536  
 LiC<sub>6</sub>, intercalated, charge-transfer and non-rigid-band effects 0-44496  
 Mg, HCP metals, K-emission valence bands, structure and bonding 0-7438  
 MgO, single crystal, thermal and optical stimulation processes of V-centres (*Japanese*) 0-11485  
 MgO, valence electron distrib., pseudopotential calcs. 0-2335  
 NaCl, valence electron distrib., pseudopotential calcs. 0-2335  
 NaCl-type crystals, donor levels due to dislocations, calc. 0-6771  
 Nb-Zr-C (0.1, 0.01 wt.%) plastic deform. influence on electronic state of Nb atoms 0-40463  
 NbC, valence band XPS meas., comparison with X-ray emission spectra and band struct. spectral calcs. 0-50535  
 Ne, vacancy, electronic structure, Green's function theory 0-39525  
 Ni, chemisorptive binding of O, CNDO calc. of potential energy curves (*German*) 0-44431  
 Ni films, HCP and amorphous, RF sputtered, O<sub>2</sub> incorporation, ESCA obs. 0-10832  
 Ni, valence-band photoemission spectra, self-energy corrections effect 0-11534  
 p-PbS, struct. of valence band, transport processes study 0-20081  
 PbS, temp. effects on valence bands, UPS study 0-11537  
 PbSe, temp. effects on valence bands, UPS study 0-11537  
 Pb<sub>0.8</sub>Sn<sub>0.18</sub>Te, thermomagnetic, thermoelectric props., valence band struct. (*Russian*) 0-54724  
 Pd-Zr, metallic glasses, valence band struct. investigation 0-11533  
 Se, trigonal, luminesc. identification of indirect transition 0-55189  
 Si, amorphous, position of Fermi level, spectroscopic and transport determ. 0-6706  
 Si, clean and gas (O<sub>2</sub> and H<sub>2</sub>O) covered surface, appl. of UPS ultrahigh vacuum apparatus (*Japanese*) 0-37125  
 Si, core and valence electron excitations, AES, chemical shift and line shape 0-2365  
 Si, electronic struct., non-spherical local pseudopotential calcs. 0-39496  
 p-Si, high ohmic material, deep level investigation, vacuum growth (*Russian*) 0-54654  
 p-Si, interband transitions, contrib. to conductivity at submillimetre wavelengths 0-34473  
 Si, valence bands, XPS excited by Zr M $\gamma$  radiation 0-40236  
 Si:F(H), amorphous, electronic struct., orthogonalised LCAO calc. 0-44486  
 Si-H, amorphous film, in situ prepared, photoemission studies 0-35060  
 Si<sub>2</sub>H<sub>12</sub> cluster, Si valence band Auger spectrum, cluster approach, comparison with experimental spectrum 0-40191  
 Si<sub>3</sub>N<sub>4</sub> amorphous film, CVD, core and valence electron excitations, low energy electron loss spectroscopy and AES 0-2365  
 SiO<sub>2</sub> amorphous film, thermal, core and valence electron excitations, low energy electron loss spectroscopy and AES 0-2365  
 SnO<sub>2</sub>, electronic struct. and densities of states, tight-binding calcs. 0-15447  
 SrTiO<sub>3</sub> semicond. electrode, electrochem., photoelectrochem. props. 0-3352  
 Te, intervalence band absorption, press. and defects influence 0-55149  
 Te, opt. props. under high press., band struct. transform. 0-55112  
 Te, trigonal, self-consistent ground state, X $\alpha$  calcs. 0-54604  
 Te, uniaxially stressed, submm. cyclotron reson., deform. pots. and k.p. coeffs. 0-54606  
 Te, valence band struct. under press., spin-orbit splitting, intraband absorpt. spectra 0-2330  
 ThPt, valence bands, XPS spectra 0-50520  
 Ti (0001), valence band struct. and chemisorption, XPS and UPS study 0-35062  
 TiO<sub>2</sub>, clusters, surface electron struct. and defect states, DV-X $\alpha$  calc. 0-20268  
 TiS<sub>2</sub>, valence density of states 0-44465  
 U, core and valence band spectra, XPS obs. 0-50530  
 UCu<sub>5</sub>, core and valence band spectra, XPS obs. 0-50530  
 $\beta$ -UD<sub>3</sub>, electronic props., metallic character 0-6693  
 UNi<sub>5</sub>, core and valence band spectra, XPS obs. 0-50530  
 UNi<sub>0.5</sub>Cu<sub>4.5</sub>, core and valence band spectra, XPS obs. 0-50530  
 UPt, valence bands, XPS spectra 0-50520  
 V oxides, XPS and AES study, electron correl. effects, semicond.-metal transition 0-7467  
 V<sub>2</sub>O<sub>5</sub>, high-temp. phase transition, resistivity, valence photoelectron spectra 0-49357  
 YbCu<sub>2</sub>Si<sub>2</sub>, valence fluctuation and temp. depend. of Cu nuclear quadrupole interaction 0-15818  
 Zn, HCP metals, K-emission valence bands, structure and bonding 0-7438  
 ZnS, band structure calcs. by modified orthogonalised plane wave (MOPW) method 0-54609  
 ZnTe, valence band parameters and free exciton reduced mass, free exciton magnetorefectance 0-45046  
 ZrS<sub>2</sub>, valence density of states 0-44465

**valence bond calculations** *see VB calculations***valency**

- actinides, valence fluctuation model, physical prop. response 0-6791  
 borides, proposed classification 0-19741  
 epoxy resins, correlation between valence energies and low temp. flexibility 0-25815  
 inorganic complexes, chem. bonding, quantum mech. ideas development and use 0-12878  
 inorganic complexes, chem. bonding, quantum mech. ideas development and use 0-12879  
 polyethylene, correlation between valence energies and low temp. flexibility 0-25815  
 rare earth intermetallics, valence, coordination no., polyhedral at. vols. 0-19742  
 rare earth metals, 4f level energy position relative to Fermi energy 0-6764  
 rare earth metals, elastic props., connection with electron struct. (*Russian*) 0-19895  
 rare earths, valency, ionicity and electronic config. 0-18775  
 TCNQ, charge transfer complexes, changes in valence electronic structure 0-7477

**valency continued**

- transition elements, 3d, ESR for valency assessment, appl. to ceramics and glass industries (*German*) 0-34757  
 Al matrix, capture radius of impurities 0-20110  
 As<sub>2</sub>S<sub>3</sub>, amorphous, time resolved spectroscopy of valence alternation pair luminesc. 0-50400  
 BaTiO<sub>3</sub>:X (X=Cr, Mn, Fe, Co, Ni, Zn, Ga), annealed in H<sub>2</sub> and O<sub>2</sub>, valence change in phase stability 0-20600  
 CaF<sub>2</sub>:Eu, oxidation and reduction of Eu, EPR and optical studies 0-25199  
 CeRu<sub>2</sub>, H absorption induced Ce valence change, mag. and supercond. props. 0-50042  
 CrO<sub>2</sub>, valence states of Cr, XPS obs. 0-40216  
 In<sub>2</sub>Te<sub>3</sub>-type semiconductor, mechanism of electrically inactive impurities 0-24834  
 LaRu<sub>2</sub>, H absorption induced Ce valence change, mag. and supercond. props. 0-50042  
 LiNbO<sub>3</sub>:Fe, impurity valence state charge on X-ray irradi., Mossbauer meas. 0-7235  
 Li<sub>1-x</sub>V<sub>x</sub>FeS<sub>2</sub>, intercalated battery cathode material, Mossbauer studies 0-44984  
 NbAs<sub>3</sub>, magnetic props., 4.2 to 77K, Mossbauer study 0-39937  
<sup>6</sup>S state ions, overlap and covalency contrib. to zero field splitting, LCAO-MO calc. 0-24850  
 Si<sub>3</sub>N<sub>4</sub>, CVD, chem. bond nature, Compton scatt. expts. 0-49539  
 Sm, XPS, electronic struct. determ. for surface 0-20765  
 TbCrO<sub>4</sub>, valence states of Cr, XPS obs. 0-40216  
 (U,Th)<sub>1-x</sub>Sb, magnetisation, U valence change 0-7089  
 YbB<sub>12</sub>, valence state and mag. props. 0-50031  
 YbNi<sub>2</sub>-YbCu<sub>2</sub> system, valency state, Yb behaviour (*French*) 0-45277  
 YbPd-YbAg-ZZ (*French*) 0-45277  
 YbPt-YbAu system, valency state, Yb behaviour (*French*) 0-45277

**valve voltmeters** *see voltmeters***valves**

- see also diaphragms*  
 1300 MW nuclear reactor steam isolating valve blowdown tests (*German*) 0-22967  
 Bjork-Shiley aortic prosthesis, in vitro vel. meas. using laser-Doppler anemometer 0-17196  
 BWR containment, influence of safety relief valve discharge loads 0-42793  
 emergency cold valve, operating in He II 0-22367  
 gas thermometry, constant volume valve design 0-4711  
 hybrid field-effect liquid crystal light valve, sensitometry control 0-23788  
 magnetic safety valve 0-8966  
 metal-seal valve for high radiation use in high vacuum 0-233  
 plasma chromatograph/mass spectrometer column overload prevention valve 0-16748  
 shock tubes, use of fast-acting valves, shock wave formation 0-24052  
 vacuum, mounted on pressure pickup 0-47066

**valves (electronic)** *see electron tubes***Van Allen radiation** *see radiation belts***Van Allen radiation belts** *see radiation belts***Van de Graaff accelerators**

- bunched beams, transport, second order aberrations 0-52801  
 heavy ion facility, target production 0-23213  
 Heidelberg postaccelerator for heavy ions, design criteria and experience 0-18722  
 HV vacuum accelerator tube, microparticle obs. 0-864  
 injection to linear accelerator, beam dynamics, computer simulation 0-13989  
 neutron primary beam and shielding radiation quality and absorbed dose obs. 0-12281  
 As ion prod. in 2 MV Van de Graaff 0-14031  
<sup>14</sup>C dating technique using cyclotrons, or Van de Graaff as mass spectrometer 0-5414  
 Se ion prod. in 2 MV Van de Graaff 0-14031

**Van de Graaff generators**

- neutron detection and neutron reaction cross-sections, Van de Graaff generator and cyclotron facility 0-47805  
 neutron experiments, Braunschweig accelerator facility, data acquisition and anal. 0-47806

**Van der Pol oscillators** *see relaxation oscillators***Van der Waals forces**

- adatom interaction with solid substrate, effect of mechanical stress on chem. pot. 0-10784  
 adsorption, gas on solid substrate, Van der Waals model 0-29271  
 alkali halide crystal, Gruisen parameter, vol. depend. anal. 0-2135  
 alkali metal halides, crystal properties, cohesive energy, bulk modulus and press. depend., interionic force model 0-15035  
 n-alkanes, liq. mixtures, thermodynamics 0-55700  
 aromatic five-membered heterocyclic ring system, covalent radii determ. method 0-23332  
 bounds on van der Waals coeffs., oscillator strength sum rules 0-27941  
 cluster, gas phase, vibr. predissoc., rel. to matrix isolated O<sub>2</sub> multiphonon vibr. relax. 0-18861  
 collision anisotropy and spectral line impact contour (*Russian*) 0-52942  
 DNA conformation, influence of intermol. interactions 0-16900  
 ethylene dimer, CO<sub>2</sub> laser induced photodissoc., pulsed mol. beam obs., van der Waals bond 0-9660  
 fluid, classical one-dimens. Lennard-Jones type, eqn. of state 0-24562  
 fluid, inhomogeneous, free-energy theory 0-10751  
 gas, thermodynamic props. review 0-31694  
 hadrons, Yang-Mills pots., Van der Waals force and fermion motion 0-52465  
 intermolecular energies calculation from delocalised pictures, artifacts and elimination 0-18899  
 ionic crystals, evaluation of photoelastic consts. 0-50297  
 laser-induced atom-atom collision line shape 0-9691  
 liquid-vapour interface, surface tension-compressibility relation 0-44397  
 molecules, pot. functions, level spacings and thermodynamic props. 0-14185  
 multipole long-range interaction coeffs., two- and three-body van der Waals interactions 0-37847  
 net repulsive van der Waals forces between different particles, macromolecular, or biological cells in liqs., appls. 0-34274  
 neutral particles interaction pot. with surfaces (*Russian*) 0-6937  
 polyatomic molecule, crit. consts. evaluation from intermol. force consts. 0-37844



**Van der Waals forces continued**

- quantum mechanical system dynamic polarisability, van der Waals constants 0-46867  
 real gas thermodynamics, Van der Waals model approach 0-38515  
 semiconductor, donor van der Waals interactions, spectral lineshapes 0-11450  
 soft-sphere mixture viscosity, nonequilibrium dynamics 0-19680  
 sphere and half-space, van der Waals attraction energy 0-16735  
 tetracene-Kr(Xe), intramolecular intersystem crossing in supersonic beam, external heavy atom effect 0-14167  
 tetrazine-Ar, van der Waals bond, nonstatistical vibr. energy distrib., photochemical reaction effects 0-30255  
 TTF-TCNQ, organic metal, Van der Waals donor stacking 0-15037  
 Ag (110), CN<sup>-</sup> chemisorbed, Raman scatt. 0-45075  
 Ar-O<sub>2</sub>, Van der Waals complex, struct. and props., RF and microwave obs. 0-32704  
 Ar<sub>2</sub>, accurate ab initio calc. of intermol. energy 0-18899  
 GaAs, donor van der Waals interactions, spectral lineshapes 0-11450  
 H+He, H Balmer- $\alpha$  fine-struct. line shift and broadening 0-37783  
 (H<sub>2</sub>)<sub>2</sub>, (D<sub>2</sub>)<sub>2</sub>, (HD)<sub>2</sub> and H<sub>2</sub>-D<sub>2</sub>, Van der Waals complexes, mol. symmetry 0-42963  
 HeI<sub>2</sub>, Van der Waals mol. vibr. predissoc. anharmonicity effects 0-52971  
 He(2s<sup>1</sup>S, 2<sup>3</sup>S)+Ne(Ar)(Kr)(Xe), Van der Waals forces, one-electron model pot. calcs. 0-14094  
 Hg 6<sup>1</sup>S<sub>0</sub>-Hg 6<sup>1</sup>P<sub>1</sub>, Van der Waals term in interaction, blue satellite line (French) 0-37848  
 I<sub>2</sub>Ne, He, van der Waals complexes photodissoc. 0-50864  
 I<sub>2</sub>\*He, vibrational predissociation, van der Waals molecules, vibration-translation scaling theory 0-43135  
 KRHCl, van der Waals complexes, struct., RF and microwave spectra, isotope effects 0-37806  
 N<sub>2</sub>O, pure and in mixtures, electron attachment near 1 atm., microcave cond. meas. 0-1063  
 NaO<sub>2</sub>, physical mechanisms of phase transitions 0-6381  
 Se, vitreous, elastic coeffs. about glass transition temp. US study (French) 0-19865

**Van der Waals molecules see quasimolecules****vanadium**

see also nuclei with .....

- band effective mass, Animalu TMMP theory 0-29312  
 blistering after Ar<sup>+</sup> ion bombard., irradi. mode effect 0-39176  
 charged particle prod. cross sections for 14 MeV neutrons, Ti, V, Cr, Mn 0-42648  
 deoxidation of Fe by V, phase equilibrium with V<sub>2</sub>O<sub>3</sub> (Russian) 0-16275  
 determ. by atomic absorption, using low temp. flames 0-30307  
 diffusion characteristics in Ag, 1051 to 1220K 0-15308  
 elastic constants in pure and hydrogenated crystals, effect of pressure 0-7614  
 elastic properties, at high temp. 0-30007  
 electrotransport of H(D) at high H concs. 0-34246  
 film, electron beam evaporator for in situ deposition studies in UHV electron microscope 0-40264  
 film, evaporated, optical props., rel. to struct. 0-55211  
 film, resist. supercond. transition 0-25033  
 fluxural oscillations in longitudinal mag. field, sound attenuation, magnetoelasticity (Russian) 0-54844  
 foil, electron energy loss spectra 0-7452  
 foil, rolling procedures 0-23225  
 fusion reactor first wall material, cyclic deform. tests 0-30074  
 impurity defect interaction influence on radiation hardening and embrittlement 0-35199  
 impurity in Al nuclear reactor fuel tubes, proton activation determ. 0-27741  
 interatomic pair potential, phonon spectra 0-33927  
 internal friction, low temp., H<sub>2</sub> effects 0-40419  
 interstellar abundance and depletion models 0-46630  
 ion implanted with 2 MeV He under pulsed conditions, microstructure obs. 0-29088  
 magnetic susceptibility, orbital, calc. 0-7075  
 muon trapping, Knight shift, rel. to H interstitials 0-50247  
 neutron low energy interaction cross sections, gravitational spectrometer meas. 0-24521  
 oxidised in air during laser irradiation, switching effect (Russian) 0-24977  
 plasticity and strength change in temp. range 20 to 1000°C, impurity effects 0-35235  
 positron annihilation and vacancy formation 0-16119  
 purification and plastic props. 0-25810  
 secondary ion emission, normalised energy spectra from Hg<sup>+</sup> impact, anomalous behaviour 0-45193  
 strain hardening, screw dislocations and microtwinning (Russian) 0-29971  
 superconducting, spin fluctuations effect on T<sub>c</sub>, from sp. ht. and mag. suscept. 0-7030  
 superconducting transition temperature, ab initio calc. 0-25036  
 surface, particle valence by neutrons 0-25493  
 twin and stacking fault energies calc. 0-2038  
 XPS and AES study, electron correl. effects 0-7467  
 Al determination, Fe and Al alloys, in presence of V (Polish) 0-35605  
 $\alpha$ -Al<sub>2</sub>O<sub>3</sub>:Cr(Ti)(V), impurities effect on thermoluminesc. 0-40170  
 $\alpha$ -Al<sub>2</sub>O<sub>3</sub>:V<sup>3+</sup>, local deform. due to uniaxial stress 0-34140  
 $\alpha$ -Al<sub>2</sub>O<sub>3</sub>:V<sup>3+</sup>, magnetocaloric effect in high magnetic fields 0-25140  
 $\alpha$ -Al<sub>2</sub>O<sub>3</sub>:V<sup>3+</sup>, stress-induced linear dichroism in <sup>3</sup>A<sub>2</sub>(<sup>3</sup>T<sub>1</sub>)→<sup>3</sup>T<sub>2</sub> transition, Jahn-Teller effect 0-34884  
 Be-Li-V, phase diagram, metallurgical aspects for fusion blanket use 0-32467  
 CaO:V<sup>3+</sup> orbital triplet, intermediate Jahn-Teller effect, APR 0-34758  
 H solubility, and diffusivity around room temp. 0-29225  
 KCl:V<sup>2+</sup>, EPR spectra above 300K 0-34765  
 KZnF<sub>3</sub>:V<sup>2+</sup>, calc. of t<sub>2g</sub> antibonding mol. orbital in [VF<sub>6</sub>]<sup>4-</sup>, rel. to ESR 0-50174  
 MgO:V<sup>2+</sup>, <sup>4</sup>A<sub>2g</sub>→<sup>4</sup>T<sub>2g</sub> spectra, new expt. results 0-11441  
 NaCl:V<sup>2+</sup>, EPR spectra above 300K 0-34765  
 NaCl:V<sup>2+</sup>, elec. field effect on Z-like centres spectrum 0-2802  
 Ni-V system, interdiffusion, kinetics of phase growth (Russian) 0-29230  
 SrTiO<sub>3</sub>:V, Jahn-Teller impurity, V<sup>4+</sup> EPR 0-29608  
 TiO<sub>2</sub>:V, impurity levels, photocurrent and ESR meas. 0-29346  
 (V,Ti)C+Ni cermet, binder grain size 0-44401  
 V thin film-amorphous Si interface, V silicide formation, backscattering diffraction meas. 0-2285

**vanadium continued**

- V XII, level struct. and predicted intercombination lines 0-14098  
 V:N, ion bombard., void form. 0-34097  
 V:O, neutron irradi., void form., 673-1073K 0-29066  
 V/Al-Al<sub>2</sub>O<sub>3</sub>-Pb tunnel junction, superconducting transition, critical currents, Josephson effect (Russian) 0-29507  
 V<sup>2+</sup>F<sup>-</sup>, V<sup>2+</sup>F<sup>-</sup>V<sup>2+</sup>  $\pi$ -electron systems, transferred hyperfine interaction, HF calc. 0-24859  
 ZnSiF<sub>6</sub>·6H<sub>2</sub>O:V<sup>2+</sup>, spin-lattice relax. at normal and high press. 0-2632  
 Zr<sub>2</sub>-SiC-C-V, refractory cermet hot pressing and oxidation resist. 0-3231

**vanadium alloys**

see also vanadium compounds

- fusion reactor first wall and blanket material, props. for struct. appl. 0-30071  
 fusion reactor first-wall and blanket material, mech. props. 0-34074  
 fusion reactor materials, He and simultaneous damage production simulation 0-32480  
 fusion reactor materials, performance and economics 0-32433  
 low-alloy, strength and ductility at high temp. and different strain rates 0-16401  
 Permdur 49, ordered and disordered, clean mild wear 0-16508  
 steel, alloy, V-W-Mo-Cr, exam. of carbide transformation 0-16299  
 steel, alloy, W-Mo-Cr-V, blanks welded to steel 45, optimal high temp. tempering 0-16351  
 steel, austenitic stainless, biphasic, ferritic, ageing and thermomech. treatment effects on struct. and props. 0-35226  
 steel, Cr, carbide form. depend. on Mn, Cr, V additions, cementite stabilisation, microstruct. (Russian) 0-55399  
 steel, Cr-Mo-V, austenite to bainite transformation under cooling conditions, effect on creep 0-3033  
 steel, Cr-Mo-V, biaxial cyclic deformation behaviour 0-16431  
 steel, Cr-Mo-V, high temp. main steam pipe, residual stresses in butt welds 0-21059  
 steel, Cr-Mo-V, high temp. steam pipe weld, defect distrib. and growth 0-25979  
 steel, Cr-Mo-V, stress rupture strength at high temps. (German) 0-40474  
 steel, Cr-Mo-V-W, crack-growth and thermal-mech. fatigue 0-21072  
 steel, Cr-Ni-Mo-V, magnetic induction, struct. dependence (Czech) 0-50141  
 steel, Cr-Ni-Mo-V, Mossbauer austenitometry and mag. props. 0-40003  
 steel, Cr-W-V-Mo (3.9 to 4.5, 1.5 to 2, 0.9 to 1.2, 3.9 to 4.4 wt.%), heat resistant, type 8Kh4M4V2F1-Sh, mech. props. 0-16464  
 steel, fine grained C-Mn-V-Al-N, relationship between ferrite and austenite grain size 0-3001  
 steel, HSLA, V effect on mech. props. (Korean) 0-29987  
 steel, low-alloy, V effect on mech. props. 0-35312  
 steel, medium C, microalloying with V and Ti, effect on hardness and structure 0-11750  
 steel, Nb-Va microalloyed, mech. props. (French) 0-35252  
 steel, Si-Cr-Mo-W-V (2.4,1.3,2 wt.%), heat treatment and props. 0-16349  
 steel, V, carbide eutectic presence, solidification and struct. 0-50624  
 Au<sub>4</sub>V single crystal, ordered, mag. props., domain models 0-39770  
 B<sub>2</sub>C-V, contact reaction with liq. Ni 0-55707  
 Co-V, solid and liq., mag. susceptibility and electronic struct. 0-39738  
 Co-V (10 to 23 wt.%) system, phase constitution, X-ray and elec. resist. meas. 0-3007  
 Co-V (20.7 wt.%), cryst. struct., electron and X-ray diffr. study 0-44172  
 Co-Vc (12 wt.%), directionally solidified eutectic, oxidation 0-11821  
 Cr-Co-V alloys, dil., elec. resist. min. 0-54680  
 Cr-V, dil., mag. susceptibility, 77 to 400K (Russian) 0-50066  
 Cr-V-B-V system, fatigue strength and fatigue fracture at 20 and 1100°C, SEM study 0-3194  
 Cr<sub>1-x</sub>V<sub>x</sub>, nucl. spin relax., spin fluctuation effect 0-34811  
 Cu-V-Si, two-step supercond. transition 0-34539  
 (Fe, Co, Ni)<sub>3</sub>V, control of ordered struct. and ductility 0-21029  
 (Fe,Ni,Co)<sub>3</sub>V, long-range ordered alloy for fusion reactor appl. 0-32481  
 Fe-Co-V, ordered and disordered, dynamic ageing (French) 0-16355  
 Fe-Co-V, plastic flow, order-disorder transform. effect on creep, traction and relaxation (French) 0-35180  
 Fe-Co-V, Vicalloy, magnetisation reversal by stretching and twisting 0-34733  
 Fe-Co-V (33, 33 at.%), BCC  $\beta$  phase, high temp. creep, existence of master curve 0-55473  
 Fe-Co-V wire for high-speed matrix printers, wear resistivity obs. (Japanese) 0-55540  
 Fe-HI (Si) (Ti) (V), molten, gaseous O<sub>2</sub> absorption 0-11836  
 Fe-Mn-V-C austenitic steel, discontinuous precipitation, morphological changes 0-3078  
 Fe-Ni-Co-V, effects on fusion reactor neutronics performance 0-47705  
 Fe-Ni-V, concentration ferromag. antiferromag. phase transition and mag. state diagram. (Russian) 0-20401  
 Fe-O-V melts, phase equilib. (Russian) 0-16273  
 Fe-Sb-V, dil., interactions and precip., Mossbauer study 0-39997  
 Fe-V, BCC, ferromag., high-field susceptibility 0-7083  
 Fe-V, dil., local mag. moments, polarised neutron elastic diffuse scatt. 0-50088  
 Fe-V, order-disorder transition and  $\sigma$ -phase form. 0-7555  
 Fe-V, unlimited component solubility, intercrystallite internal adsorption (Russian) 0-39294  
 Fe-V-C, austenite to ferrite+precipitate reaction, TEM/STEM study 0-3075  
 Fe-V-C (0.3, 0.05 wt.%), interphase precipitation obs. in assoc. with Widmanstätten ferrite lateral growth 0-40365  
 Fe-VC-WC(TiC), sintering, densification 0-25615  
 Fe<sub>40</sub>Co<sub>40</sub>V<sub>20</sub>, neutron irradiation, close pair recombination (French) 0-39162  
 (Fe<sub>1-x</sub>V<sub>x</sub>)<sub>3</sub>Ge, magnetic and X-ray studies 0-1966  
 Hf-V foil, rapidly quenched and heat treated, supercond. props. 0-54852  
 HfV<sub>2</sub>, C-15 struct., phase transitions, elec. cond., crystal lattice parameters (Russian) 0-54826  
 HfV, latent heat of structural transform. 0-24589  
 Mn-V-Mo-C master alloys, development for low alloyed PM steel 0-50576  
 Mo-V-C, hot-worked, substructural hardening and high-temp. strength (Russian) 0-25731  
 Nb-V, negative muon Coulomb capture ratio and Lyman series intensities 0-14255  
 Nb-V oxidation in air, rate determining process (Russian) 0-21170  
 Nb-V-(Cr), oxidation resist., Cr and V effects (Russian) 0-40585



## vanadium alloys continued

- Ni-V, solid and liq., mag. susceptibility and electronic struct. 0-39738  
 Ni-V system, interdiffusion, kinetics of phase growth (*Russian*) 0-29230  
 $\text{Ni}_3\text{Mn}_2\text{V}_{1-x}\text{Sn}$ , mag. hyperfine fields,  $^{119}\text{Sn}$  Mossbauer spectra study 0-55003  
 Pd-V, alloy and bilayer, silicide form. solid phase reaction with Si 0-6568  
 $\text{Pd}_{82-x}\text{V}_{18-x}\text{Si}_{18}$ , metallic glasses, effect of press. on elec. resist. 0-6805  
 Ti-6Al-4V, stress distrib. for steady axisymmetric extrusion 0-3103  
 Ti-Al-Mo-V, crack resistance in chloride soln., electrochem. protection, polarization effect 0-55589  
 Ti-Al-V, (6.4 wt %), fracture mode, tearing topography surface fracture 0-7670  
 Ti-Al-V, (6.4 wt.%), single and dual ion irradiat., microstruct. studies 0-29077  
 Ti-Al-V, alloy 685, fatigue life, creep and dynamic strain ageing effect, 25 to 400°C (*French*) 0-45384  
 Ti-Al-V, containing 0-6000 ppm  $^3\text{He}$ , sensitivity of tensile props. 0-39197  
 Ti-Al-V, impact strength anisotropy, influence of texture (*Russian*) 0-20952  
 Ti-Al-V, irradi. induced creep 0-39163  
 Ti-Al-V, rolled, elastic stiffness and Bauschinger effect accompanying anisotropic hardening (*Russian*) 0-40435  
 Ti-Al-V, VT6 alloy, butt welded joints, electron beam welding conditions effecting interstitial impurities distribution 0-39136  
 Ti-Al-V (4.7, 2 wt.%) pseudo alpha alloy, laminar struct. singularities,  $\beta$  to  $\alpha$  transformation (*Russian*) 0-7552  
 Ti-Al-V (6, 4 wt.%), corrosion resist. in marine environments (*French*) 0-50767  
 Ti-Al-V (6, 4 wt.%), dynamic crit. stress intensity vs. crack vel. 0-2115  
 Ti-Al-V (6, 4 wt.%), friction characts. improvement by  $\text{O}_2$  dissolution and controlled surface hardening (*French*) 0-45401  
 Ti-Al-V (6, 4 wt.%), gust spectrum fatigue crack propag. 0-21105  
 Ti-Al-V (6, 4 wt.%), improvement of props. by ion implantation 0-16601  
 Ti-Al-V (6, 4 wt.%), repassivation and pitting corrosion 0-30143  
 Ti-Al-V (6, 4 wt.%), temp. distrib. for steady axisymmetric extrusion 0-11670  
 Ti-Al-V (6, 4 wt.%), temp. distrib. for steady axisymmetric extrusion numerical results 0-11671  
 Ti-Al-V (6, 4 wt.%), type IMI 318, internal friction study of martensitic transformations 0-7573  
 Ti-Al-V (6, 4 wt.%), type IMI 318, stability of martensitic phases 0-7574  
 Ti-Al-V (6, 4 wt.%) slow crack growth in air and fracture toughness, H content effect (*French*) 0-45385  
 Ti-Al-V (6.4 wt %), superplasticity, effect of temp. 0-7639  
 Ti-Al-V (6.4 wt.%),  $\alpha/\beta$  interface phase influence on tensile props. 0-30034  
 Ti-Al-V (6.4 wt.%), D profiles after  $\text{D}_3^+$  implantation 0-37581  
 Ti-Al-V (6.4 wt.%), D trapping in fusion reactor materials, temp. dependence 0-37577  
 Ti-Al-V (6.4 wt.%), fretting fatigue behaviour of temps. up to 600°C 0-21104  
 Ti-Al-V (6.4 wt.%), high temp. fretting fatigue, fatigue and fretting wear 0-3197  
 Ti-Al-V (6.4 wt.%), phase transformation after hydrogenation 0-7560  
 Ti-Al-V (6.4 wt.%), quenched, struct. and age hardening rel. to treatment temp. 0-11657  
 Ti-Al-V (6.4 wt.%), strongly textured, influence of crystallographic orientation on tensile behaviour 0-7633  
 Ti-Al-V (6.4 wt.%), to H effect on fracture props. and microstruct. 0-40512  
 Ti-Al-V (6.4 wt.%) alloy foil, substrate temp. effect on struct. 0-7497  
 Ti-Al-V (6.4 wt.%) for TiC reactively sputtered coatings, adherence, XPES and wear study 0-25565  
 Ti-Al-V-Sn (6, 6, 2 wt.%) weldments, heat treated, transangular fracture 0-40524  
 Ti-Al-V-Sn (6, 6, 2 wt.%), fatigue crack growth, cyclic freq. and microstruct. influence 0-55515  
 Ti-Al-V-Sn (6.6, 2 wt.%),  $\alpha$ - $\beta$  type 662, fusion zone fracture behaviour in weldments 0-30093  
 Ti-Al-V-Sn (6.6, 2 wt.%), depend. of  $K_{\text{ISCC}}$  on loading rate and crack orientation 0-45427  
 Ti-Al-V-Sn (6.6, 2 wt.%) solid metal embrittlement by Cd, Ag and Au 0-16551  
 Ti-Al-V(Sn) alloys, plastic deformation and fracture characts. at low temps. (*Russian*) 0-7624  
 Ti-V, elastic moduli, comparison with paramagnetic Cr, V-Cr, rel. to bandstructure 0-7615  
 $\alpha$ -Ti-V, Mossbauer spectra, metastable  $\beta$ - and  $\omega$ -phases 0-20556  
 Ti-V-Cr, electron-lifetime effects on props. 0-10951  
 Ti-V-Cr, type Ti-15-333, irradi. induced creep 0-39163  
 Ti-V-Cr-Al (13, 11, 3 wt.%), stress corrosion cracking in methanolic solutions 0-50752  
 Ti-V-Mo-Cr system,  $\beta$ -phase stability 0-55353  
 V/H, heat capacity and supercond. between 1.5 and 16K 0-2521  
 V-Al, band struct. and density of states, KKR method and X-ray meas. 0-10863  
 V-Al, conduction band states, X-ray spectra obs. (*Russian*) 0-29317  
 V-based ternary solutions, containing H, thermodynamics 0-19961  
 V-Cr, elastic moduli, comparison with paramag. Cr, Ti-V, rel. to bandstructure 0-7615  
 V-Cr (15 wt.%), radiation-induced solute segregation 0-29086  
 V-Cr-H system, electronic sp. ht. 0-49378  
 V-D $_{0.015}$ , enrichment of D during the ion bombardment 0-54288  
 V-Fe,  $^{51}\text{V}$  Mossbauer spectra, diffusion mechanism of Fe 0-15292  
 V-Fe, force constant change with pressure, relative Mossbauer fraction 0-34163  
 V-H, BCC, quasimolecular Jahn-Teller reson. states 0-44550  
 V-H, effect of neutron irradiat. on electrical resistance, magnetic susceptibility 0-29063  
 V-H, electron work function, 300 to 600 degrees C, contact potential difference meas. 0-29462  
 V-H, fusion reactor first wall material, cyclic deform. tests 0-30074  
 V-H rods, twisting effect, anelastic deviations on thermal cycling 0-21043  
 V-H(D), metallographic and thermal differential anal., potential for H energy storage appls. 0-45281  
 V-Mn, equiatomic, ordering kinetics and antiphase domain coarsening 0-7559

## vanadium alloys continued

- V-Nb(Ti)(Zr)(Cr)(Mo)(Fe)(Cu), H solubility and diffusivity around room temp. 0-29225  
 V-Ni, ion bombard., void form. 0-34097  
 V-Ni-Mo, structure in alloy crystallisation region, peritectic equilibria (*Russian*) 0-50622  
 V-Pd, H mobility and solubility, appearance pot. spectra obs. 0-55231  
 V-Si, strengthening by internal oxidation 0-55424  
 V-Si, struct. and supercond., Cu influence 0-50592  
 V-Sn(Al)(Ga)(Ge)(Si)-C, phase equilib. and supercond. 0-50593  
 V-Ta (5 wt.%), strain hardening, screw dislocations and microtwinning (*Russian*) 0-29971  
 V-Ti, and V-Ti-Be(Zr), 4 MeV  $\text{Ni}^{++}$  irradiat., He gas bubble form. 0-29085  
 V-Ti (42 at.%), mixed state, US attenuation meas. at 4.14K 0-15657  
 V-Ti, strengthening by internal oxidation 0-55424  
 V-Zr-C-Y alloy weld metal, hardening phase precipitates examination, TEM appl. 0-7576  
 VBe $_{12}$ , coated limiters, first wall protection 0-32483  
 VBe $_{12}$  coating, erosion rates under  $\text{H}^+$  ion bombard., fusion reactor appls. 0-39179  
 $(\text{V}_{1-x}\text{Cr}_x)_3\text{Si}$ , mag. susceptibility, 4.2 to 320K, density of states model 0-7035  
 $\text{V}_{3-x}\text{Cr}_x\text{Si}$ ,  $x=0$  to 3, struct., supercond. and mag. props. 0-1962  
 $\text{V}_{1-x}\text{Fe}_x$ , low temp. sp. ht. and mag. props. 0-2548  
 $\text{V}_{1-x}\text{Fe}_x\text{H}_x$ , low temp. sp. ht. and mag. props. 0-2548  
 $\text{V}_{1-x}\text{Ga}_x$ , A-15 cpds., nucl. mag. relax. in normal and supercond. state 0-49993  
 $\text{V}_3\text{Ga}$ , high-current A-15 microcomposite material 0-44781  
 $\text{V}_3\text{Ga}$ , multifilament superconductor, pulsed mag. field losses and critical current densities 0-54853  
 $\text{V}_3\text{Ga}$  superconducting composite, bronze process, metallurgy 0-3004  
 $\text{V}_3\text{Ga}$  superconducting tape, stress effect on critical current (*Japanese*) 0-50020  
 $\text{V}_3\text{Ga}$ -Cu, high-current A-15 microcomposite material 0-44781  
 $\text{V}_3\text{Ge}$ , A-15 cpds., nucl. mag. relax. in normal and supercond. state 0-49993  
 $\text{V}_3\text{Ge}$ , anisotropic thermal vibrations, lattice const. X-ray study 0-34164  
 $\text{V}_3\text{Ge}$ , superconducting A-15 type compounds, transition temp., radii ratio and structure (*Chinese*) 0-44752  
 $\text{V}_{1-x}\text{Pt}_x$ , A-15 cpds., nucl. mag. relax. in normal and supercond. state 0-49993  
 $\text{V}_{1-x}\text{Si}_x$ , A-15 cpds., nucl. mag. relax. in normal and supercond. state 0-49993  
 $\text{V}_3\text{Si}$ , d-spacing fluctuations above Martensitic phase transition 0-7570  
 $\text{V}_3\text{Si}$ , electrical resistivity, saturating contrib. from electron-phonon interactions 0-2376  
 $\text{V}_3\text{Si}$ , Fermi surface determ. by positron annihilation 0-2326  
 $\text{V}_3\text{Si}$ , ion irradiated, influence on struct., resist., and supercond. transition temp. 0-54823  
 $\text{V}_3\text{Si}$ , NMR meas. near struct. transform. (*Russian*) 0-44942  
 $\text{V}_3\text{Si}$ , NMR of  $^{51}\text{V}$  above and below 21K struct. transition (*Russian*) 0-34796  
 $\text{V}_3\text{Si}$ , normal, mixed and supercond. state, specific heat meas., thermodynamic and superconducting props. 0-49987  
 $\text{V}_3\text{Si}$ , plastic deform. effect on supercond. props. 0-29500  
 $\text{V}_3\text{Si}$ , single crystals, supercond. tunnel characts. 0-7044  
 $\text{V}_3\text{Si}$ , superconducting, optical props. and electron-phonon interactions 0-2510  
 $\text{V}_3\text{Si}$ , superconducting thin films, energy gaps from tunnelling meas. 0-25050  
 $\text{V}_3\text{Si}$ , thermal expansion, 20-300°C, using differential push-rod dilatometer 0-39320  
 $\text{V}_3\text{Si}$ , US anomaly when cooled below martensitic and supercond. transition temps. 0-20354  
 $\text{V}_3(\text{Si}_{1-x}\text{C}_x)$ , bulk, effect of C on supercond. transition temps. and microstructure 0-54824  
 $\text{V}_2\text{Zr}(\text{Hf})$ , struct. transform. at low temp., X-ray diff. anal. (*Russian*) 0-45298  
 Zr-Al-V, H sorption props. for H storage, influence of Al 0-45794  
 Zr-V foil, rapidly quenched and heat treated, supercond. props. 0-54852  
 Zr-V-H, synthesis at high H pressure exam. of props. 0-29924  
 $\text{Zr}_x\text{Hf}_{1-x}\text{V}_2$ , polycrystalline superconductor, resist. and mag. susceptibility, transition temp., temp. depend. 0-25113  
 $\text{ZrV}_2$ , C-15 struct., phase transitions, elec. cond., crystal lattice parameters (*Russian*) 0-54826  
 $\text{ZrV}_2$ , latent heat of structural transform. 0-24589  
 $\text{ZrV}_2\text{D}_{4.5}$ , deuterated cubic Laves phase, D atom distrib., neutron diff. anal. 0-29006

## vanadium compounds

- see also vanadium alloys  
 gadolinium vanadium sulphate hexahydrate, singlet ground state system, low temp. mag. props. 0-44843  
 oxides, FTIRs thermochromic materials, colour and visual contrast 0-33100  
 oxides, XPS and AES study, electron correl. effects, semicond.-metal transition 0-7467  
 oxides mixture, thermochromic material, appl. to laser beam indicator/visualiser 0-9976  
 phthalocyanide, thermal stability obs., by DTA (*German*) 0-11945  
 potassium oxalate,  $\text{VO}^{2+}$  EPR spectra 0-39858  
 potassium oxalate monohydrate:  $\text{VO}^{2+}$  cryst., IR absorpt. 0-55134  
 refractory carbides, borides and nitrides, wetting by and interactions with liq. metals 0-54473  
 vanadyl bisacetylacetonate, polarised X-ray absorption and double refraction 0-50459  
 $\text{BaO-K}_2\text{O-VO}_2\text{-SiO}_2$ , glass, elec. cond. rel. to ion polarisability, polarons 0-49729  
 $\text{BaO-La}_{0.6}\text{O-VO}_2\text{-SiO}_2$ , glass, elec. cond. rel. to ion polarisability, polarons 0-49729  
 $\text{BaVSe}_3$ , one-dimensional, struct. and mag. props. 0-28993  
 $\beta'\text{-Cu}_2\text{V}_2\text{O}_5$ , mag. and spectroscopic study, semiconductor to metal transition 0-2628  
 $\text{Ca}_{2x}\text{Bi}_{1-2x}\text{Fe}_{5-x-y}\text{V}_x\text{In}_y\text{O}_{12}$ , ferromagnetic relax. meas., 4.2-300K 0-44923  
 $\text{CsVl}_3$ , Mossbauer spectra, struct., electronic and mag. props. 0-15908  
 $\text{CuO-V}_2\text{O}_5\text{-P}_2\text{O}_5$  glass, elec. cond. and switching (*Japanese*) 0-34492  
 $\alpha\text{-Cu}_2\text{V}_2\text{O}_5$ , EPR and mag. susceptibility meas. 0-2627  
 $\text{Cu}_3\text{VS}_4$ , Raman active modes 0-11414



## vanadium compounds continued

- Fe<sub>2</sub>V<sub>2</sub>O<sub>7</sub> solid solutions, specific heat near semiconductor-metal transition 0-24612  
 K<sub>2</sub>O-V<sub>2</sub>O<sub>5</sub>-Al<sub>2</sub>O<sub>3</sub> melt, soln. of Al<sub>2</sub>O<sub>3</sub> single crystal 0-20910  
 Li<sub>2</sub>O-V<sub>2</sub>O<sub>5</sub>-Al<sub>2</sub>O<sub>3</sub> melt, soln. of Al<sub>2</sub>O<sub>3</sub> single crystal 0-20910  
 Li<sub>2</sub>V<sub>1-x</sub>Fe<sub>x</sub>S<sub>2</sub>, intercalated battery cathode material, Mossbauer studies 0-44984  
 Li<sub>2</sub>V<sub>2</sub>O<sub>7</sub> (0.1 < x < 1.0), phase relationship in ambient temperature system 0-20912  
 β-Li<sub>2</sub>V<sub>2</sub>O<sub>7</sub>-y bronzes, thermodynamic props. by coulometric titration 0-34209  
 (NH<sub>4</sub>)<sub>2</sub>SO<sub>4</sub>·VO<sub>2</sub><sup>+</sup>, EPR spectrum, temp. depend. 110-300K 0-11249  
 Na<sub>2</sub>O-V<sub>2</sub>O<sub>5</sub>-Al<sub>2</sub>O<sub>3</sub> melt, soln. of Al<sub>2</sub>O<sub>3</sub> single crystal 0-20910  
 Na<sub>2</sub>O-V<sub>2</sub>O<sub>5</sub>-(VO<sub>2</sub>)<sub>2</sub>-V<sub>2</sub>O<sub>5</sub>, phase comp. and equil. 0-35172  
 Na<sub>2</sub>VS<sub>2</sub>(Se<sub>2</sub>), intercalation compounds, phys. props. 0-44179  
 Na<sub>2</sub>V<sub>2</sub>Ti<sub>6</sub>O<sub>16</sub>, characterisation and mag. props., 90-800K, Na<sub>x</sub>Ti<sub>6</sub>O<sub>8</sub> bronze isotypes (French) 0-39735  
 Nb<sub>0.47</sub>V<sub>0.13</sub>Se<sub>2</sub>(4Hb), stacking layer study, appl. of convergent beam electron diff. 0-39116  
 TeO<sub>2</sub>-V<sub>2</sub>O<sub>5</sub> glass threshold devices, reversible monopolar switching 0-2434  
 (Ti<sub>1-x</sub>V<sub>x</sub>)C, activated reactive evaporation deposited films, annealing study, microstructure 0-24762  
 TiC-VC, mag. susceptibility, elec. cond. and thermoelec. props. 0-50033  
 (Ti<sub>0.9</sub>V<sub>0.1</sub>)<sub>2</sub>O<sub>3</sub>, spin glass, dynamic mag. susceptibility meas. 0-39792  
 (Ti<sub>1-x</sub>V<sub>x</sub>)<sub>2</sub>O<sub>7</sub>, order-disorder and metal-insulator transition theory 0-24802  
 (Ti<sub>1-x</sub>V<sub>x</sub>)<sub>2</sub>O<sub>3</sub>, spin-glass props., 0.05-300K 0-25149  
 (Ti<sub>1-x</sub>V<sub>x</sub>)<sub>2</sub>O<sub>7</sub>, elec. cond. and phase diagram near metal-insulator transition 0-11054  
 (Ti<sub>1-x</sub>V<sub>x</sub>)<sub>2</sub>O<sub>7</sub>, metal-insulator transitions, EPR, elec. and mag. props. 0-2336  
 (Ti<sub>1-x</sub>V<sub>x</sub>)<sub>2</sub>O<sub>7</sub>, order-disorder and metal-insulator transitions 0-39504  
 V<sub>0.99</sub>V<sub>0.01</sub>Se<sub>2</sub>, negative magnetoresist. and nonlinear cond. 0-44617  
 V complex, VOCL [Co(cyclopentadienyl)<sub>2</sub>]<sub>0.16</sub>, synthesis and struct. 0-44176  
 V complex, triaminomethyl vanadium sulphate hexahydrate, S=1 ground state, mag. props. in external field 0-11157  
 V-H, effect of neutron irradiation on electrical resistance, magnetic susceptibility 0-29063  
 V-H, electron work function, 300 to 600 degrees C, contact potential difference meas. 0-29462  
 V-H, exam. of electron structure 0-29306  
 V-O system β phase BCT, X-ray diff. study of additional scatt. effect (Russian) 0-10537  
 VBe<sub>2</sub>, plasma-sprayed coatings on Cu and stainless steel, fusion reactor appl. 0-18619  
 VC, soft X-ray emission, excitation pot. spectra, excited level binding energy 0-35009  
 VC-Ni, fracture mode determination, using Auger electron spectroscopy 0-7680  
 VC, coating, C steel vanadisation by CVD 0-44454  
 VC<sub>2</sub>N<sub>2</sub>, superstructure induced by ageing, neutron diff. obs. (Russian) 0-49195  
 VC<sub>2</sub>O<sub>3</sub>, conc. depend., of unit cell filling degree 0-54199  
 VCl<sub>4</sub>, liq., struct. factor, mol. dynamics calc. 0-38898  
 VCl<sub>4</sub>(Br<sub>4</sub>), vibronic systems, degenerate ground states, statistical sums, thermodynamic func. calcs. 0-27997  
 VD, struts. phase diagrams, morphologies, prep. methods, book contrib. 0-25675  
 V<sub>2</sub>D, ordered, distortion-induced superstruct. modulation, from X-ray scatt. 0-49186  
 V<sub>0.986</sub>Fe<sub>0.014</sub>O<sub>2</sub>, metal-insulator phase transition, effect of hydrostatic press. 0-6725  
 V<sub>1-x</sub>Fe<sub>x</sub>O<sub>2-xF<sub>2</sub></sub>, 0 < x < 0.2, phase diagrams, <sup>57</sup>Fe-Mossbauer spectra, X-ray diff. studies (German) 0-29663  
 V<sub>1-x</sub>Fe<sub>x</sub>O<sub>2-xF<sub>2</sub></sub>, 0 < x < 0.20, magnetic susceptibility and electron cond. (German) 0-39754  
 VH, struts. phase diagrams, morphologies, prep. methods, book contrib. 0-25675  
 VH<sub>0.51</sub>, optic modes study by neutron spectroscopy 0-19891  
 VH<sub>0.55</sub>, ultra-high vacuum cleavage, H<sub>2</sub> desorption 0-54514  
 V<sub>1</sub>, antiferromag., zone-boundary phonon Raman scattering, modulation of exchange interaction 0-11386  
 V<sub>1</sub>, antiferromagnet, phonon Raman scatt. from spin superstructures 0-16030  
 V<sub>1</sub>, lattice dynamics and ionic charge 0-10615  
 VN, electronic struct. of vacancies, effect on supercond. transition temp. 0-29347  
 VN, interatomic interactions from XPS 0-49171  
 VN, soft X-ray emission, excitation pot. spectra, excited level binding energy 0-35009  
 VN-CrN solid solutions, thermal cond., Lorentz number 0-15317  
 VN<sub>0.74</sub> and VN<sub>0.89</sub>, low-temp. specific heat and superconducting critical temp. meas., density of states 0-54835  
 β-V<sub>2</sub>N, neutron powder profile-refinement cryst. struct. determ. 0-15060  
 (V<sub>1-x</sub>Nb<sub>x</sub>)<sub>2</sub>C, C ordering formation of varieties 0-38968  
 V<sub>1/3</sub>NbS<sub>2</sub>, Hall coefficient and resistivity 0-39610  
 V<sub>1/3</sub>NbS<sub>2</sub>, magnetic susceptibility, function of temp. 0-39756  
 V<sub>0.5</sub>NbSe<sub>2</sub>, cryst. struct., metallic cond., mag. and phys. props. (French) 0-33956  
 VO, energy band struct. and density of states (Russian) 0-44493  
 VO<sub>2</sub><sup>+</sup>, EPR in solids, review 0-11254  
 VO<sub>2</sub>, absorbing film parameters determ. by ellipsometry 0-254  
 VO<sub>2</sub>, cylindrical specimen, thermal switching 0-44679  
 VO<sub>2</sub>, film, visualisation of microwave and IR radiation 0-5839  
 VO<sub>2</sub> film as holographic recording medium, diff. efficiency 0-28180  
 VO<sub>2</sub>, metal-insulator transitions, effect of isotopic substitution 0-2337  
 VO<sub>2</sub>, nonstoichiometry influence on electron struct. and metal-insulator phase transition 0-44507  
 VO<sub>2</sub> single cryst. film, ion-irrad., 'splitting' of semicond.-metal transition 0-11053  
 VO<sub>2</sub>, single crystal and polycrystalline, synthesis and resist. near metal-semicond. phase-transition 0-44680  
 VO<sub>2</sub>, switching effect, temp. depend. 0-20259  
 VO<sub>2</sub> thin film semiconductor-metal transition applications 0-49835  
 VO<sub>2</sub> variable-reflectance mirror for CO<sub>2</sub>-N<sub>2</sub>-He 10.6 μm scan laser 0-38026  
 VO<sub>2</sub>-CrNbO<sub>4</sub>, solid solns., synthesis and phase diagram 0-35171  
 VO<sub>2</sub>+Er<sub>2</sub>O<sub>3</sub>, high-pressure reaction, cryst. struct. and mag. props. of ErVO<sub>3</sub> 0-19773

## vanadium compounds continued

- VO<sub>2</sub>, defect struct., local ionic arrangements in disordered phase 0-10532  
 V<sub>13</sub>O<sub>24</sub> long-period Magneli phase as product of V<sub>6</sub>O<sub>11</sub>-V<sub>7</sub>O<sub>13</sub> periodic microsyntactic intergrowth 0-50618  
 V<sub>2</sub>O<sub>3</sub>, metal-insulator transitions, effect of isotopic substitution 0-2337  
 V<sub>2</sub>O<sub>3</sub>, phase equilibrium with Fe deoxidized by V (Russian) 0-16275  
 V<sub>2</sub>O<sub>3</sub>-H<sub>2</sub>, interaction with surface, quantum chemical study 0-45549  
 V<sub>2</sub>O<sub>3</sub>+x, 0 ≤ x ≤ 0.08, mag. and elec. props. 0-49833  
 V<sub>2</sub>O<sub>3</sub>, (001) surface modification, during catalytic oxidation of propene (French) 0-45557  
 V<sub>2</sub>O<sub>3</sub> amorphous films, CVD prep., structural characts. 0-49114  
 V<sub>2</sub>O<sub>3</sub> crystal, photoinduced threshold switching in VO<sub>2</sub> channel 0-29450  
 V<sub>2</sub>O<sub>3</sub> film, amorphous, CVD prep. method 0-55299  
 V<sub>2</sub>O<sub>3</sub> film, amorphous, thickness, density and refr. index determ. from reflectance interference spectra 0-55206  
 V<sub>2</sub>O<sub>3</sub>, quadrupole broadening in <sup>51</sup>V NMR spectrum 0-20469  
 V<sub>2</sub>O<sub>3</sub> single cryt. microhardness and anisotropy of mech. props. (French) 0-50713  
 V<sub>2</sub>O<sub>3</sub>, thermoelec. props., 500-1500K 0-29423  
 V<sub>2</sub>O<sub>3</sub>:Na(Li), pure and doped, elec. cond. and thermoelec. power meas. 0-10987  
 V<sub>2</sub>O<sub>3</sub>-BaO-K<sub>2</sub>O-ZnO glasses, elec. props. and struct. 0-15547  
 V<sub>2</sub>O<sub>3</sub>-Ge, elec. props., molecular deposition method 0-34525  
 V<sub>2</sub>O<sub>3</sub>-MoO<sub>3</sub> solid solns., small polaron cond., elec. resist. and thermoelec. power meas. 0-34447  
 V<sub>2</sub>O<sub>3</sub>-P<sub>2</sub>O<sub>5</sub> (70-30), electrical cond. and thermoelectric meas., Au-glass-Au sandwich 0-29403  
 V<sub>2</sub>O<sub>3</sub>, high-temp. phase transition, resistivity, valence photoelectron spectra 0-49357  
 V<sub>2</sub>O<sub>3</sub>, metal-insulator transitions, effect of isotopic substitution 0-2337  
 V<sub>2</sub>O<sub>3</sub>, spin order, one-dimensional, Neel transition 0-39799  
 V<sub>2</sub>O<sub>7</sub>, microscopic mag. props., NMR 0-7177  
 V<sub>2</sub>O<sub>9</sub>, metal-insulator phase transition temp. depend. on press. 0-29327  
 V<sub>6</sub>O<sub>11</sub>, metal-insulator phase transition temp. depend. on press. 0-29327  
 V<sub>6</sub>O<sub>13</sub>, optical props. in metallic and semicond. phase 0-40135  
 V<sub>6</sub>O<sub>2n-1</sub> (3 ≤ n ≤ 9), Magneli phases, mag. susceptibilities at low temp. 0-20389  
 V<sub>6</sub>O<sub>2n-1</sub>, insulating Magneli phases, mag. susceptibility and sp. ht. meas. 0-34604  
 VOPO<sub>4</sub>, prep. of cryst. from H<sub>3</sub>PO<sub>4</sub> and V<sub>2</sub>O<sub>5</sub> 0-35068  
 (VO)<sub>2</sub>P<sub>2</sub>O<sub>7</sub>, cryst. struct. determ. 0-15081  
 VOSO<sub>4</sub>·6H<sub>2</sub>O, single-cryst. X-ray diff. struct. determ. (French) 0-39021  
 VO(tartrate)<sub>2</sub> complex, EPR study of VO<sup>2+</sup> ions in Rochelle salt crystal 0-34762  
 VS through V<sub>3</sub>S<sub>4</sub>, nonstoichiometric, phase relations and thermodynamics 0-29188  
 VS<sub>2</sub> (1T), electronic struct. using nonspherical cryst. pot. 0-44498  
 VS<sub>2</sub>, non-stoichiometric phase, physico-chemical props. 0-29532  
 V<sub>2</sub>S<sub>3</sub>, enthalpy and specific heat, temp. depend. 0-54406  
 V<sub>2</sub>S<sub>8</sub>, non-stoichiometric phase, physico-chemical props. 0-29532  
 V<sub>2</sub>S<sub>8</sub>, paramag. cryst., struct. factors using polarised neutron diff. 0-15691  
 VS<sub>2</sub>(Se<sub>2</sub>), and alkali metal intercalates, phys. props. 0-44179  
 VSB<sub>2</sub>, free-energy, heat and entropy of formation, 430-600°C (Ukrainian) 0-7837  
 VSe<sub>2</sub> (1T), electronic struct. using nonspherical cryst. pot. 0-44498  
 VSe<sub>2</sub>, angle-resolved UPS, Fermi surface determ. 0-55257  
 VSi<sub>2</sub>, form. from solid phase reaction between Si and Pd-V 0-6568  
 (V<sub>1-x</sub>Ta<sub>x</sub>)<sub>2</sub>C, C ordering formation of varieties 0-38968  
 V<sub>1/3</sub>TaS<sub>2</sub>, Hall coefficient and resistivity 0-39610  
 V<sub>1/3</sub>TaS<sub>2</sub>, magnetic susceptibility, function of temp. 0-39756  
 (V<sub>1-x</sub>Ti<sub>x</sub>)Ge, pseudobinary A15 compound, supercond. transition temp. 0-49970  
 (V<sub>1-x</sub>Ti<sub>x</sub>)<sub>2</sub>O<sub>3</sub>:Fe, metallic antiferromagnetism, Mossbauer spectra 0-15881  
 V<sub>2</sub>WO<sub>6</sub>, magnetic structure, stability of mag. modes, neutron diffraction study (French) 0-39744  
 Va<sub>2</sub>D, neutron diff. meas. of disorder-order phase transitions 0-29947  
 ZnCs<sub>2</sub>(SO<sub>4</sub>)<sub>2</sub>·6H<sub>2</sub>O:VO<sup>2+</sup>, optical absorpt. spectra obs. 0-40146  
 ZrV<sub>2</sub>D<sub>4</sub>, deuterated cubic Laves phase, D atom distrib., neutron diff. anal. 0-29006

## vanadium phosphate semiconductor glasses see amorphous semiconductors

## vaporisation

- see also boiling; evaporation; heat of vaporisation; sublimation  
 alkali halides, sputtering, thermal effects, review 0-35033  
 binary mixtures, hydrostatic and external field effect, anal. 0-19929  
 comet nuclei, vaporisation effects on light curves and life times 0-56772  
 droplet convection vaporization with unsteady heat transfer in circulating liq. phase 0-53771  
 droplet interactions, vaporisation effects 0-24106  
 droplets, atomized, polydisperse system, nonisothermal vaporisation, algorithm for calc. vaporisation parameters 0-48782  
 fluid, combustion, vaporisation and heat transfer under elec. field 0-7798  
 free energy change, classroom example for teaching thermodynamics 0-42010  
 fuel-coolant interactions in a shock tube geometry 0-13660  
 glass melt, high-temp. transpiration apparatus 0-52231  
 high melting particle heating, melting and vaporisation in hot gas 0-6201  
 high temperature vapours, phase transitions, equations of state, appl. of laser pulse heating 0-52230  
 Leidenfrost phenomena, spheroidal state min. wall temp., total vaporisation times 0-38246  
 liquid mixtures, superheat limits, homogeneous vapour nucleation 0-38247  
 liquid vaporisation, radiation induced, spinodal singularity manifestation 0-2152  
 mass and heat exchange in high temp. gas, Sherman eqn. calcs. (Russian) 0-39270  
 metal, partial pressure meas. (Japanese) 0-34179  
 metallic particle, surface tension depend. on size, vaporisation time (Russian) 0-34290  
 metals, erosion accompanying simultaneous action of laser emission and ultrasound (Russian) 0-7442  
 multidroplet system, condensation-evaporation by kinetic theory 0-7873  
 nonisotropic systems near liquid-vapour critical point, similarity hypothesis, gravitational effects 0-17913  
 oxides, sputtering, thermal effects, review 0-35033  
 particles, vaporisation calc. taking account of rarefaction of medium (Russian) 0-24575



**vapourisation continued**

- particles in nonisothermal plasma jet, trajectory and temp. calcs. (*Russian*) 0-7514
- rare earth halides, prep. and props., book contrib. 0-54211
- rock vaporising to elements, meteorite impact study 0-36583
- superheated liquids, vapour generation in steady flashing flow, appl. to fission reactor LOCA anal. 0-23004
- vapour pressure measurement, effusion method, review 0-51995
- volatile highly thermally conductive spherical drop, theory of diffusio-phoresis 0-14784
- water droplet, explosive vapourisation on 10.6  $\mu\text{m}$  radiation exposure, inhomogeneous internal heat evolution 0-29162
- Bi, vapour, optical activity, Faraday effect, parity nonconservation, mag. transitions (*Russian*) 0-55070
- Cs, vapourisation by laser impact for production of atomic beam pulses 0-37123
- GaAs vapourisation during laser annealing 0-25495
- Hg, in NAA from samples and standards (*Russian*) 0-41128
- Hg<sub>1-x</sub>Cd<sub>x</sub>Te, vapourisation under Knudsen effusion conditions 0-2154
- K<sub>2</sub>O<sub>2</sub>, thermodynamic props. 0-29184
- K<sub>2</sub>SO<sub>4</sub>, mass spectrum obs. of vapourisation, vapour comp. and press., transition and form. heats 0-19933
- LaCrO<sub>3</sub>, vaporization in oxidizing atmos. 0-24579
- Li-LiH two-phase equil. system, vaporis. diagram at high temps. 0-19926
- NaCl, interpolational eqn. of state with allowance for melting, vaporis., dissoc. and ionis. processes 0-24566
- NaCl, thermodynamic equil. vapourisation, transpiration mass spectrometry 0-52356
- Na<sub>2</sub>O-SiO<sub>2</sub> glass, influence of p(O<sub>2</sub>) on Na vaporisation at 1345°C 0-6502
- Na<sub>2</sub>SO<sub>4</sub>, thermodynamic equil. vapourisation, transpiration mass spectrometry 0-52356
- Sb<sub>2</sub>Se<sub>3</sub> solid, vaporization, thermodynamic props. of molecules formed 0-11943
- SiO<sub>2</sub>, vapourisation in steam atmosphere 0-44306
- SmF<sub>3</sub>, sublimation, Knudsen effusion method 0-6508
- TiO, high temp. thermodynamics, vaporisation, and pressures over 0-10685
- TiS, vapourisation chemistry and thermodynamics, computer-automated simultaneous Knudsen-torsion effusion 0-48837
- UO<sub>2</sub> phase, thermodynamic props. 0-13594
- W, heat resistant particles in low temp. Ar plasma, heating, melting, vapourisation (*Russian*) 0-40384
- ZnO, from defective spinel powders, in vac. 0-16675
- ZrI<sub>4</sub>, thermodynamics of vaporisation from substoichiometric solid Zr iodides 0-3393
- ZrO<sub>2</sub>, substoichiometric, thermodynamic props. at lower phase boundary 0-29185
- vaporising** *see* **vaporisation**
- vapour density** *see* **density of gases**
- vapour deposited coatings**  
*see also* **CVD coatings**; **plasma deposited coatings**; **sputtered coatings**; **vacuum deposited coatings**
- adhesion measurement methods 0-50822
- diamond-based, fabrication and wear resist. 0-40576
- dichloride 2,4'-bis (trimethylammonium-acetamide)-benzal-fluorene, thin layers, behaviour in electric field (*Rumanian*) 0-35108
- ion-beam-activated vacuum deposition, struct. and props. of deposits 0-15422
- laser deposited dielectric thin films, optical and struct. props. 0-7506
- magnetic anisotropy rel. to columnar microstruct., calc. 0-39822
- manganin thin film microtransducers for elastohydrodynamic lubrication studies 0-37048
- metal vapour condensate, anisotropy in electric field 0-15624
- metallurgical coatings, conf., San Diego, USA (23-27 Apr., 1979) 0-12848
- microporosity described in terms of vacancies and voids 0-24769
- naphthalene, microcryst. and evaporated film, excimer emission 0-2823
- rare earth-transition metal alloy magnetic thin films, influence of gaseous phase on mag. props. (*Polish*) 0-39820
- Ag, evaporated, chemisorption effects on reflectance and elec. resist. 0-11495
- Ag film, ion plated, on AT-cut quartz crystal, crystallographic structure obs. 0-2280
- Ag, on Cu, defects and their effect on props. 0-39474
- AgBr, evaporated layers, use as registrating system (*Bulgarian*) 0-52344
- Al cathodes for He-Ne lasers, performance improvement by Cu addition 0-5748
- Al, on NaCl, defects and their effect on props. 0-39474
- Al-Al<sub>2</sub>O<sub>3</sub>-GaAs MOS struct., mol. beam reaction growth of Al<sub>2</sub>O<sub>3</sub> film, C-V characts. 0-11095
- Al-Cu (1 to 10 wt.%), vapour deposited films, ion scattering spectrometry characterisation 0-15386
- Al-Ni with multiple layer plasma coating, exam. of cohesion strength (*Russian*) 0-7714
- Al-SiO<sub>2</sub>-Al evaporated film anomalous dielectric dispersion under high DC field 0-15620
- As<sub>2</sub>S<sub>3</sub>, amorphous, elec. cond. mech. obs. (*Japanese*) 0-11028
- Au, ion plated, defect growth structs., SEM obs. 0-24768
- B film growth by phys. vapour deposition 0-16200
- B-transition metal thin films, amorphous to cryst. transformation 0-7563
- C, transparent and hard insulating layer, struct. and props. 0-10830
- Co, on Ni-Cr type alloys, surface pretreatment to attain pore-free aluminised coatings 0-40612
- Cr film, vapour deposited on low temp. KCl substrates, struct. obs. 0-10826
- Cr-NdAlO<sub>3</sub>, dielectric films, phase composition and structure 0-39464
- Cu alloy solid solution condensed films, influence of alloying components on phase composition and lattice spacing (*Russian*) 0-20047
- Cu, ion plated, defect growth structs., SEM obs. 0-24768
- Er-diphthalocyanine complex, electrochromism (*Japanese*) 0-20611
- GaAs layers, from gas phase, impurity influence on growth micromechanism 0-45237
- GdFe homogeneous amorphous films, compensation point switching, magneto-optical Kerr signal anal. 0-15726
- H<sub>2</sub>WO<sub>4</sub> films, proton diffusion coeffs. 0-6548
- HfN on stainless steel, activated reactive evaporated coatings, high rate deposition, microhardness 0-25580
- In<sub>2</sub>O<sub>3</sub>, transparent heat mirror formation by ion plating on ambient temp. substrates and props. 0-25578

**vapour deposited coatings continued**

- NdAlO<sub>3</sub>, dielectric films, phase composition and structure 0-39464
- PbSe films, synthesis and growth 0-45236
- PbTe 0-45236
- Pt ion plating on  $\alpha+\beta$  Ti alloy Ti-6242, creep property improvement 0-16408
- Pt, on Ir and W, defects and their effect on props. 0-39474
- (SN)<sub>n</sub>\* radicals polymerisation to (SN)<sub>x</sub> in thin films, optical spectra 0-16656
- Se, gas-evaporated, selective absorpt. characts. and emissivity 0-50998
- Te, gas-evaporated, selective absorpt. characts. and emissivity 0-50998
- (Ti,V)C, activated reactive evaporation deposited films, annealing study, microstructure 0-24762
- Ti-Pt-Au, nonalloyed ohmic contacts to n-GaAs by pulse-electron beam annealed Se implants 0-2466
- TiC, activated reactive evaporation deposited films, annealing study, microstructure 0-24762
- TiN film as protective coating for vacuum deposition chamber, Auger electron spectroscopy study 0-25922
- TiN layers formation, on steel substrate, microhardness and structure obs. (*Hungarian*) 0-2965
- TiN, reactive ion plating with auxiliary discharge deposition conditions influence on film props. 0-20801
- TiN-Ti<sub>3</sub>N<sub>2</sub>, activated reactive evaporation formed deposits, microstructure, transformation depend. on depositing conditions 0-24761
- V<sub>2</sub>O<sub>5</sub> film, amorphous, thickness, density and refr. index determ. from reflectance interference spectra 0-55206
- W-Al<sub>2</sub>O<sub>3</sub> cermet films, oxide evaporation deposited on Mo, Ti, Al<sub>2</sub>O<sub>3</sub> substrates, struct., props. 0-25581
- ZnO film, prep. by reactive ionized cluster beam deposition, and characterisation 0-10829
- vapour deposited thin films** *see* **vapour deposited coatings**
- vapour deposition**  
*see also* **chemical vapour deposition**; **crystal growth from vapour**; **electron beam deposition**; **ion plating**; **plasma deposition**; **sputtering**; **vacuum deposition**
- ceramics coating by physical vapour deposition processes (*Japanese*) 0-55306
- dichloride 2,4'-bis (trimethylammonium-acetamide)-benzal-fluorene, thin layers, behaviour in electric field (*Rumanian*) 0-35108
- ion evaporation techniques based on the electron beam evaporation source only 0-16203
- ionized-cluster beam and reactive ionized-cluster beam deposition, new developments 0-16202
- metallurgical coatings, conf., San Diego, USA (23-27 Apr., 1979) 0-12848
- optical fibre, low-loss high-numerical-aperture, fabrication by vapour-phase axial deposition 0-1315
- overlay coatings for turbine parts, physical vapour deposition techniques, economic evaluation 0-35429
- saturation cluster density in vapour deposited thin films, general formula 0-15408
- surface treatment, ionic deposition and electron bombardment industrial equipment, pollution control (*French*) 0-7699
- thin film deposition technique, review (*Japanese*) 0-35107
- VAD optical fibre cables, characts. 0-43461
- VAD optical fibres for transmission system field trial 0-43462
- Al-Cu alloy, deposition from RF induction source, onto laminated polyimide substrates and characterisation 0-16535
- CdTe film, low-resist., prep. by multi-source evaporation method, and characterisation 0-25582
- Cr, film, defects and mechanical stability, different deposition methods (*Bulgarian*) 0-44438
- Cr, on O treated polystyrene, microscopic interactions 0-3407
- Es film, preparation and characterisation 0-15405
- GaAs, prep. of thin films by ionised-cluster beam deposition (*Japanese*) 0-25576
- HfN on stainless steel, activated reactive evaporated coatings, high rate deposition, microhardness 0-25580
- InSb, prep. of thin films by ionised-cluster beam deposition (*Japanese*) 0-25576
- MnBi, ionized-cluster beam and reactive ionized-cluster beam deposition 0-16202
- Ni, on O-treated polystyrene, microscopic interactions 0-3407
- Ni, thin film, growth on Au (001) substrates (*French*) 0-44446
- PbSe films, synthesis and growth 0-45236
- PbTe 0-45236
- SiO<sub>2</sub>-GeO<sub>2</sub> optical fibre fabrication, 21.2 km graded-index VAD fibre with low loss and wide bandwidth 0-53414
- SiO<sub>2</sub>-P<sub>2</sub>O<sub>5</sub> cladding vapour-phase axial deposition fibres at 1.3  $\mu\text{m}$  and 1.6  $\mu\text{m}$  0-9996
- TiN film as protective coating for vacuum deposition chamber, Auger electron spectroscopy study 0-25922
- TiN, reactive ion plating with auxiliary discharge deposition conditions influence on film props. 0-20801
- W-Al<sub>2</sub>O<sub>3</sub> cermet films, oxide evaporation deposited on Mo, Ti, Al<sub>2</sub>O<sub>3</sub> substrates, struct., props. 0-25581
- ZnO film, prep. by reactive ionized cluster beam deposition, and characterisation 0-10829
- vapour-liquid transformations** *see* **liquid-vapour transformations**
- vapour phase epitaxial growth**  
*see also* **molecular beam epitaxial growth**
- chemoepitaxial nucleation during reaction diffusion, thermodynamic anal. (*Russian*) 0-15394
- deep level studies, growth by time difference method at controlled vapour pressure 0-39522
- dielectric films, low temp. epitaxy in laser sputtering 0-34335
- growth processes, in-situ obs. (*Japanese*) 0-35104
- heteroepitaxial surface morphologies and misalignments (*Japanese*) 0-15411
- III-V semiconductors, p-n heterostructures, epitaxial growth techniques, appl. to optoelectronics, review 0-54770
- III-V semiconductors, VPE by metalorganic CVD (*Japanese*) 0-50562
- impurity profile computer-aided control 0-2962
- ionized-cluster beam and reactive ionized-cluster beam deposition, new developments 0-16202
- microscopic mechanism of film growth from non-condensed phases, kinetic anal. 0-54565
- monocrystalline film, from gaseous phase, gasdynamic and heat transfer processes (*Russian*) 0-55301



## vapour phase epitaxial growth continued

- rare earth garnets, prep. and props. book contrib. 0-44193  
 reactive closed-space vapour transport, simplified theory 0-15396  
 reproductive epitaxy, exam. 0-55303  
 semiconductor epitaxial groove and tunnel growth mechanism 0-10804  
 Ag epitaxial growth, cluster mobilities, in-situ electron microscopes obs. 0-15407  
 Ag film, epitaxial growth on isolated Au patches covered with amorphous C layer 0-40270  
 Ag film, ion plated on AT-cut quartz crystal, crystallographic structure obs. 0-2280  
 Ag, growth on electron bombard. NaCl(111) surfaces, RHEED and AES 0-15419  
 Ag, vac. deposition of oriented coating on doped alkali halide substrate 0-2303  
 Ag/Si (111), metastable 2D condensations, epitaxy, growth modes, exp. techniques, book contrib. 0-49558  
 Al<sub>1-x</sub>Ga<sub>x</sub>As-GaAs, CW 300k quantum-well heterojunction laser, optical and injection pumping operation 0-5735  
 Al<sub>1-x</sub>Ga<sub>x</sub>As-GaAs, heterojunction, interface width, AES obs. 0-20290  
 Al<sub>1-x</sub>Ga<sub>x</sub>As-GaAs DH lasers, metalorganic CVD growth and performance characts. 0-53312  
 Al<sub>1-x</sub>Ga<sub>x</sub>As-GaAs heterostruct. lasers, metalorganic CVD 0-23692  
 Al<sub>1-x</sub>Ga<sub>x</sub>As-GaAs multiple-quantum-well injection lasers grown by metal-organic CVD, room temp. continuous operation 0-1218  
 Au epitaxial growth, cluster mobilities, in-situ electron microscopes obs. 0-15407  
 Bi film deposition by vacuum evaporation on NaNO<sub>3</sub> single cryst. cleavage 0-35091  
 CdS, grown by vac. evaporation on Si 0-25567  
 CdS heterojunction solar cells by CVD method 0-45685  
 CdS-CdTe double layers on various GaAs surfaces, morphology and crystallography 0-34326  
 CdS(Se)(Te), condensation from gas phase of controlled comp., and props. 0-54562  
 CdTe epitaxial films, on CdS substrate, closed-tube vapour growth 0-55302  
 CdTe epitaxial films, surface morphology, layer and spiral growth 0-10823  
 CdTe-PbTe(InSb) superlattices, laser deposition of multilayer heteroepitaxial structs. 0-44450  
 Cd<sub>1-x</sub>Zn<sub>x</sub>S-p-GaAs heterojunctions, elec. and photovolt. props. rel. to growth technique 0-29466  
 Cu/Ag (111), metastable 2D condensations, epitaxy, growth modes, exp. techniques, book contrib. 0-49558  
 CuGaTe<sub>2</sub> films deposited on GaAs substrates by flash evaporation, struct. and elec. cond. 0-24755  
 CuInS<sub>2</sub>, epitaxial thin film on GaAs, exam. of growth, electrical props. 0-24754  
 Fe, on W tip, depositing direction depend. 0-10812  
 Fe/Cu (100), metastable 2D condensations, epitaxy, growth modes, exp. techniques, book contrib. 0-49558  
 Ga<sub>1-x</sub>Al<sub>x</sub>As VPE layers, X-ray diff. 0-29296  
 GaAs, epitaxial, Si and Ge doping 0-24470  
 GaAs, epitaxial deposition, growth kinetics (*French*) 0-2961  
 GaAs epitaxial growth, in GaAs-AsCl<sub>3</sub>-H<sub>2</sub> system, elec. field effect 0-2306  
 GaAs, epitaxial layer, micron and submicron vap. phase growth, for FET 0-11577  
 GaAs epitaxial layer high power Gunn diode development and fabrication 0-16199  
 GaAs, influence of growth parameters, AsCl<sub>3</sub> transport method 0-29881  
 GaAs ribbons from Ga-AsCl<sub>3</sub>-H<sub>2</sub> epitaxy 0-7498  
 GaAs, selective in situ vapour etch of substrate and growth 0-2958  
 GaAs substrates, out-diffusion of Cr 0-10708  
 GaAs using organometallic method, deep trap levels 0-10923  
 GaAs, VPE, incorporation of deep levels, effects of growth conditions 0-20111  
 p-GaAs, VPE growth and characterisation, doping levels 0-10841  
 GaAs, VPE growth on {110} cryst. plane 0-10840  
 GaAs, VPE in CVD systems, anisotropic phenomena 0-54563  
 GaAs, VPE layer growth with abrupt doping profile 0-24746  
 GaAs, VPE layer props. control using boundary layer characts. 0-50561  
 GaAs VPE layers, elec. props., semi-insulating substrates effect 0-11123  
 GaAs VPE layers for FET devices, impurity characterisation 0-29491  
 GaAs, vapour phase epitaxial appl. to hyperabrupt varactor fabrication 0-29288  
 n-GaAs vapour phase epitaxial film electrophysical props. rel. to growth temp. (*Russian*) 0-49961  
 GaAs:Si(Te)(S), vapour phase epitaxial grown layers, photoluminesc. and emission spectra 0-29774  
 n-GaAs:Sn, VPE growth, reactor design 0-2956  
 GaAsP epitaxial film, composition self modulation, defect struct. 0-34331  
 GaAsP, VPE, lattice forbidden band composition depend. (*Hungarian*) 0-6669  
 GaAs<sub>1-x</sub>Sb<sub>x</sub>, organometallic VPE, use of trimethyl As and trimethyl Sb 0-45238  
 Ga<sub>1-x</sub>In<sub>x</sub>As organometallic VPE, use of trimethyl As and trimethyl Sb 0-45238  
 Ga<sub>1-x</sub>In<sub>x</sub>As, VPE growth, thermodynamic anal. 0-2933  
 GaInAsP, VPE growth and props. 0-16194  
 GaN:Al, VPE grown, luminesc. and elec. props. depend. on doping conc., bound excitons 0-20688  
 GaN:Zn, VPE growth, photoluminesc. rel. to doping conditions 0-55159  
 GaP:N, epitaxial layers, N concentration determination by two independent methods 0-39142  
 GaSb, CVD using organometallics, epitaxial growth 0-29879  
 Ge, polycrystalline epitaxial film, exam. of growth kinetics and props. 0-55304  
 HgSe/CdSe lattice-matched heterostructs. as Schottky barriers, CVD epitaxial growth and elec. props. 0-49877  
 HgTe, VPE growth control by EM irradi. (*Russian*) 0-34338  
 In epitaxial growth, cluster mobilities, in-situ electron microscopes obs. 0-15407  
 InAs, organometallic VPE growth on InAs and GaSb 0-16193  
 InAs<sub>1-x</sub>Sb<sub>x</sub>, organometallic VPE growth on InAs 0-45233  
 InGaAs, lattice-matched VPE on (100) InP, photodiode appl. 0-35102  
 InGaAs on (100) InP substrate, VPE 0-40267  
 In<sub>1-x</sub>Ga<sub>x</sub>As, VPE on (100), (111)A, and (111)B InP substrates 0-15382  
 InGaAsP/InP DH, vapour phase growth by dual-growth-chamber method 0-50559

## vapour phase epitaxial growth continued

- In<sub>1-x</sub>Ga<sub>x</sub>P LEDs and electron-beam-pumped lasers 0-2281  
 In<sub>1-x</sub>Ga<sub>x</sub>P<sub>1-y</sub>As<sub>y</sub> LEDs and electron-beam-pumped lasers 0-2281  
 InP, organometallic growth by cracking of In(C<sub>2</sub>H<sub>5</sub>)<sub>3</sub> and PH<sub>3</sub> 0-11575  
 InP VPE, In-H<sub>2</sub>-PCl<sub>3</sub> chemistry 0-11549  
 InP, VPE layer props. control using boundary layer characts. 0-50561  
 InP VPE with new metallorganic compound 0-55278  
 p-InP:Zn, vapour grown, prep. and props. 0-54268  
 InSb-PbTe(CdTe) superlattices, laser deposition of multilayer heteroepitaxial structs. 0-44450  
 MnBi, ionized-cluster beam and reactive ionized-cluster beam deposition 0-16202  
 NaCl (001) substrate, preferential epitaxy of evaporated films induced by electron bombard. or elec. field 0-10824  
 Ni, epitaxial growth, on NiO(100), by low pressure hydrogen reduction (*French*) 0-11578  
 PbSe, epitaxial growth, cluster mobilities, in-situ electron microscopes obs. 0-15407  
 Pb<sub>1-x</sub>Sn<sub>x</sub>Te:In epitaxial layers, growth, elec. props., and luminesc. 0-54542  
 PbTe, and Pb<sub>1-x</sub>Sn<sub>x</sub>Te, VPE growth control by EM irradi. (*Russian*) 0-34338  
 PbTe-CdTe(InSb) superlattices, laser deposition of multilayer heteroepitaxial structs. 0-44450  
 Pd, epitaxial growth, cluster mobilities, in-situ electron microscopes obs. 0-15407  
 Pd/W (110), metastable 2D condensations, epitaxy, growth modes, exp. techniques, book contrib. 0-49558  
 Si, autoepitaxy, displacement of microrelief 0-2307  
 Si beam epitaxy for epitaxial film growth and p-n junction formation in high vacuum 0-16187  
 Si, CVD on SiO<sub>2</sub> and Si<sub>3</sub>N<sub>4</sub>, SEM study (*Dutch*) 0-2960  
 Si, epitaxial film growth on Si(111) and sapphire (1102), simultaneous RHEED/AES study 0-10833  
 Si, epitaxial growth, adsorbed layer model for autodoping mech. 0-7505  
 Si epitaxial interface migration, theory and expt. test 0-29290  
 Si epitaxial layer growth in vacuum, Ar, Xe ion bombardment effect 0-39463  
 Si, growth processes, in-situ obs. (*Japanese*) 0-35104  
 Si heteroepitaxial films on sapphire, vac. deposited, struct. and elec. props. 0-15390  
 Si, heteroepitaxial growth using SiH<sub>4</sub> in H<sub>2</sub>-He atm. 0-20049  
 Si homo-epitaxial deposition, deposition techniques 0-7501  
 Si layer growth by CVD on Sn-coated background (*Dutch*) 0-7502  
 Si, reduced pressure, advances 0-40242  
 Si thin autoepitaxial layers low temp. growth mechanism in SiCl<sub>4</sub>-H<sub>2</sub> system 0-20795  
 Si, VPE layer props. control using boundary layer characts. 0-50561  
 Si:P, doping element incorporation, temp. depend. in CVD epitaxy 0-45234  
 SiC, appl. for solid state devices (*Japanese*) 0-11579  
 SiC, epitaxial film, effect of impurities on polymorphism during growth 0-15414  
 SiC, epitaxial growth by sublimation sandwich method, effect of impurities 0-25568  
 SiC, epitaxial growth by direct synthesis in vacuum 0-40262  
 SiC epitaxial layer growth from sublimation in vac., kinetics 0-20791  
 SiC:Al epitaxial layers, growth, Al distrib. and solubility 0-15391  
 Ta epitaxial layers, formation conditions influence on struct. (*Russian*) 0-20045  
 Te film, on electron irradi. KBr, epitaxial growth and surface coverage 0-10825  
 Ti, oxide film form. during thermal treatment, morphological and struct. study (*French*) 0-50766  
 TiO<sub>2</sub>, evaporated films, epitaxial growth on NaCl, electron microscopy obs. 0-10822  
 W-Os system films, condensation temp., conc., and phase comp. effect on struct. and props. (*Russian*) 0-24749  
 ZnO film, prep. by reactive ionized cluster beam deposition, and characterisation 0-10829  
 ZnS, epitaxial growth, appl. to electronic devices, review (*Japanese*) 0-55281  
 ZnS(Se), growth kinetics on CaF<sub>2</sub> by vapour phase transport (*French*) 0-54572  
 ZnSe epitaxial layers, prep. by chem. transport reactions 0-16192  
 ZnTe film preparation and props., by single-source vacuum deposition method (*Japanese*) 0-6664
- vapour pressure**  
 see also humidity; vaporisation  
 associated one-component unsaturated vapour, press., composition changes, eqns. (*Russian*) 0-55696  
 carbonyl in benzene, evaporation, vapour press. determ. from gaseous diffusion coeff. 0-10654  
 curves for pure substances in terms of conic sections 0-44304  
 graphite intercalation compounds, coherency strains and staging 0-44167  
 hydrocarbons, heavy liq., vapour press. and enthalpies of vaporisation by group-contrib. method 0-40726  
 hydrogen, and isotopic forms, cryogenic data relevant to mag. fusion energy 0-8746  
 Kelvin equation, effect of surface tension on vapour pressure, derivation 0-2248  
 liquid vaporisation, radiation induced, spinodal singularity manifestation 0-2152  
 liquid-liquid-ideal vap., isothermal condition, 3-phase equil. line special point (*Russian*) 0-54345  
 liquid-vapour equilibrium, azeotropic props. meas., differential tensimetric titration appl. (*Russian*) 0-54363  
 magnetic solids, surface rate processes and vapour press. 0-34182  
 polyphenyl ether in benzene, evaporation, vapour press. determ. from gaseous diffusion coeff. 0-10654  
 polyurethanes, vapour press. of solvent above swollen crosslinked networks rel. to rubber elasticity theory 0-45536  
 temperature estimation method in ultra high vacuum range (*Chinese*) 0-232  
 tetrachloroisophthalonitrile, vapour press. by effusion method, solid phase eqn. of state 0-49350  
 tetrafluoromethane, vap. press., triple pt. to 173K 0-6522  
 (Ag, Ti, Ca)NO<sub>3</sub>, aqueous solutions, meas. 0-6504  
 Ag, heat pipe meas. of corrosion and vapour press. 0-23878  
 Al-Mg alloys, vapour press. temp. depend., 1104 to 1637K 0-24576



**vapour pressure continued**

- Al-Zn, liq. solutions, thermodynamic properties (*Polish*) 0-49380  
 Am, vap. press., 1200-1600K, heats of vap. and La mixing 0-15232  
 Ar, phase transition, anharmonic cryst.-gas transition 0-6510  
 Au, heat pipe meas. of corrosion and vapour press. 0-23878  
 BaB<sub>6</sub> powder, surface struct. effects on thermionic emission characts. and vapour pressure (*Japanese*) 0-50506  
 Ca<sub>2</sub>, new ground state, photolum. obs. vibr. const., dissoci. energy 0-5576  
 CdSe, partial press. meas. by optical absorption 0-15234  
 CdTe, partial press. meas. by optical absorption 0-15234  
<sup>249</sup>Cf, vapour pressure, thermodynamic functions 0-6509  
 Cl<sub>2</sub>, 206 to 270K and 334 to 417K 0-19931  
 Cu, heat pipe meas. of corrosion and vapour press. 0-23878  
 CuCl<sub>2</sub>-water solution, Nd-glass laser radiation induced vaporisation, press. history 0-2153  
 Fe-Ni-Cr system, absolute partial pressures and chem. activities of component metals 0-50600  
 G<sub>2</sub>-B<sub>2</sub>O<sub>3</sub> melt, thermodynamic props. from mass spectroscopy 0-39318  
 Ga, heat pipe meas. of corrosion and vapour press. 0-23878  
 GaN, thermodynamic anal. of prep. methods 0-55328  
 Ga<sub>2</sub>Se<sub>3</sub>, evaporation, thermodynamic props. 0-54365  
 Ge, heat pipe meas. of corrosion and vapour press. 0-23878  
<sup>3</sup>He-<sup>4</sup>He mixture, transport props. near superfluid transition and tricritical point 0-29242  
<sup>4</sup>He films adsorbed on graphite, transition temp., entropies, internal energies and heats of desorption, vapour press. meas. 0-2238  
 In, heat pipe meas. of corrosion and vapour press. 0-23878  
 K<sub>2</sub>SO<sub>4</sub>, mass spectrum obs. of vaporisation, vapour comp. and press., transition and form. heats 0-19933  
 Li-Pb, thermodynamic study using Knudsen effusion mass spectrometry 0-24578  
 NH<sub>3</sub>, isotope effect, relevance to isotope exchange reaction calcs. 0-39272  
 NbO<sub>2</sub>, phase comp. on heating 2000-4000K 0-21267  
 Pb(Zr,Ti)O<sub>3</sub>, thermodynamic properties and formation data 0-29939  
 Pu vapour pressure determ. 1724 to 2219K by Knudsen effusion technique 0-654  
 PuO<sub>2</sub> nuclear fuel, eqn. of state and thermodynamic props. 0-13592  
 Sb, vaporisation behaviour, transpiration and boiling temp. studies 0-29161  
 SmF<sub>3</sub>, vaporisation, sublimation, Knudsen effusion method 0-6508  
 Sn, heat pipe meas. of corrosion and vapour press. 0-23878  
 Sn-S system, use of boiling points to investigate vapour pressure 0-54361  
 Ti-Ir alloys, Ti-rich, thermodynamic study at high temp. using Knudsen cell mass spectrometry 0-45539  
 TiO, high temp. thermodynamics, vaporisation, and pressures over 0-10685  
 TiS, vaporisation chemistry and thermodynamics, computer-automated simultaneous Knudsen-torsion effusion 0-48837  
 TiCl(Cl<sub>2</sub>), vap. press. and thermodynamics 0-6503  
 UO<sub>2</sub> nuclear fuel, eqn. of state and thermodynamic props. 0-13592  
 UO<sub>2</sub>, vapour press. meas. up to 5000K, appl. of laser pulse heating 0-52230  
 ZnSO<sub>4</sub>·7H<sub>2</sub>O, meas. of water physically adsorbed rel. to water of crystallisation (*Japanese*) 0-6622

**vapour pressure measurement**

- effusion method, review 0-51995  
 heat pipe, gas controlled, for meas. thermophysical props. 0-23878  
 high temperature vapours, phase transitions, equations of state, appl. of laser pulse heating 0-52230  
 metallic vapour, partial pressure meas. (*Japanese*) 0-34179  
 partial vapour pressure, determ. for volatile component by static method 0-37150  
 temperature estimation method in ultra high vacuum range (*Chinese*) 0-232  
 thermo-balance method for expts. under controlled vapour press. 0-47021  
 thermometric barometer for remote locations and data buoys 0-46300  
 torsion-effusion method, automatic data acquisition 0-52188  
 Fe-Ni-Cr system, absolute partial pressures and chem. activities of component metals 0-50600  
 H<sub>2</sub>SO<sub>4</sub>, partial press. meas. with tunable diode laser (*German*) 0-43361  
 Sn, SVP measurement by line absorpt. method in atomic absorpt. spectroscopy of SnI 0-55747  
 UO<sub>2</sub>, and (U, Pu)O<sub>2</sub> nuclear oxide fuels, vapour pressure meas. for fast reactor safety anal. by laser techniques to 5000K 0-13591  
 UO<sub>2</sub>, liquid, reactor safety research, laser experiments (*German*) 0-42787

**vapour-solid transformations** *see solid-vapour transformations***varactors**

- GaAs FET amplifier, varactor-tuned, for UHF SQUID magnetometer 0-31814  
 hyperabrupt, fabrication from vapour phase epitaxial GaAs 0-29288  
 hyperabrupt junction, C-V index, junction parameters depend. 0-49876

**variable-frequency oscillators**

- see also swept-frequency oscillators*  
 digital controlled acoustic beam steering and focusing 0-38191

**variable stars**

- see also eclipsing binary stars*  
 2A 0526-328 optical candidate, high speed optical photometry 0-51917  
 2A 1052+606, X-ray and optical variability of RS CVn star 0-31331  
 adiabatic non-radial oscillations with moderate or large l, theory 0-56819  
 AE 1, He-rich variable, spectroscopy and photometry 0-41836  
 λ Andromedae, high-press. transition region in model chromosphere 0-26847  
 ET Andromedae (HR 8861), Ap star, light vars. and period 0-46571  
 AE Aquarii, cataclysmic variable, rapid light oscils. rel. to white dwarf oblique rotator model 0-36634  
 U Aquarii, R Coronae Borealis star, extraordinary comp. rel. to unusual s-processing event 0-17588  
 R Aquarii, UVRI polarimetric obs., orbital motion effect (*Russian*) 0-36646  
 R Aquarii, UV obs. of hot component 0-56854  
 U Aquilae, Cepheid variable, detect. as long-period binary by radial vel. spectrometer 0-51667  
 BD+61° 1211 (2A 1052+606), RS Canum Venaticorum binary star, spectroscopic obs. 0-36663  
 Be stars, variability search, 1971-8 photometric obs. 0-36650  
 UZ Bootis, cataclysmic variable similar to WZ Sagittae, outburst characts. 0-17596

**variable stars continued**

- Z Camelopardalis, dwarf nova, photometric obs. and light curve (1973-77) 0-56853  
 53 Camelopardalis, photometric vars. 0-4367  
 SS Camelopardalis, UVB photometry and light curve soln. for eclipsing RS Canum Venaticorum binary 0-41854  
 38 Cancri, δ Scuti star, UVB photometric obs. of variability 0-22021  
 VY Canis Majoris, OH/IR star, 1612 MHz OH maser multibaseline VLBI obs. 0-12766  
 β Canis Majoris stars, ANS UV photometry 0-26871  
 β Canis Majoris stars, UV flux obs., basic data obtained with TD-1A satellite 0-51783  
 Y Canum Venaticorum, C star, IR spectrum between 1.2 and 30 microns 0-46544  
 AM Canum Venaticorum, orbital period increase 0-12765  
 RS Canum Venaticorum systems, candidate list for southern HD stars 0-4395  
 RS Canum Venaticorum systems, X-ray obs. and coronal model development 0-56873  
 η Carinae, high-resolution IR radiation maps of homunculus, spectral and spatial distrib. 0-12767  
 η Carinae, location in H II region (NGC 3372) 0-4383  
 AG Carinae, luminous star in symmetric nebulae, IUE low-dispersion spectrum 0-46560  
 η Carinae, silicate grains size distrib. in Homunculus Nebula 0-4382  
 ν Carinae, X-ray emission obs. from star and surrounding nebula 0-26876  
 γ Cassiopeiae, Be star, polarisation rapid vars. 0-22022  
 SU and TU Cassiopeiae, short-period Cepheids, photometry and spectra rel. to radius anomalies 0-26864  
 V509 Cassiopeiae (HR 8752), emission-line spectrum rapid changes 0-36645  
 cataclysmic binaries, evolution and origin 0-56885  
 cataclysmic binary formation through common envelope evolution 0-8651  
 cataclysmic variables, emission lines from accretion discs 0-51774  
 cataclysmic variables, role of accretion disks (*Polish*) 0-26739  
 cataclysmic variables, visual continuum flux distrib. 0-36636  
 V553 Centauri, C rich Cepheid, C and N abundances 0-4378  
 proxima=V645 Centauri, dMe flare star, quiescent corona, transition region, and chromosphere obs. 0-56850  
 BV Centauri, dwarf nova, identification as spectroscopic binary 0-51775  
 V436 Centauri, dwarf nova, photometry during superoutburst (May 1978) 0-46570  
 δ Cephei, H $\alpha$  radial vel. behaviour 0-51788  
 DI Cephei, spectrum vars. in T Tauri star 0-8628  
 β Cephei stars, effective temps., ang. diameters, distances and linear radii 0-17584  
 β Cephei stars, mid UV spectra obs. 0-21995  
 β Cephei stars, nonradial oscils., linear nonadiabatic analysis 0-56836  
 δ Cephei stars, parallaxes and distance scale, max. likelihood technique 0-51746  
 Cepheid instability strip 0-56833  
 Cepheid pulsation period variability and convective efficiency 0-26885  
 Cepheid variables, mag. fields effects on pulsational behaviour 0-31302  
 Cepheid variables kinematics, appl. to galactic spiral structure parameters derivation 0-17665  
 cepheids, double mode, in northern hemisphere, search using existing obs. 0-8634  
 Cepheids, double-mode, freq. anal. 0-31308  
 Cepheids, double-mode, Wesselink radii 0-31311  
 Cepheids, enhanced He abundance effects on visible spectra 0-12759  
 Cepheids, He enrichment effects in atm., models 0-26884  
 Cepheids, multimode, two-zone models, resonances 0-36641  
 classical Cepheids, nonvariable supergiants and bright giants, spectrophotometric comparison 0-56837  
 Cepheids, short-period, radial vels., BVRI photometry, radii 0-31309  
 Cepheids in Magellanic Clouds, extrinsic model of anomalies 0-4361  
 WX Ceti, cataclysmic variable similar to WZ Sagittae, outburst characts. 0-17596  
 o Ceti, SiO maser variability at 86 GHz 0-41839  
 o Ceti AB, IUE obs. of UV spectrum 0-22027  
 ω Ceti stars, Sio J=1-0  $\nu$ =1 and 2 masers relative intensity and vel. 0-4339  
 ZZ Ceti stars search, photometric obs. of apparently quiescent stars 0-22005  
 ZZ Ceti white dwarfs, implications of seismological theory for non-radial oscils. periods 0-17577  
 Circinus X-1, radio flare phenomena Dec. 1979 and Jan. 1980 obs. 0-36731  
 comparison stars near OJ287 and ON325, variability, period determ. 0-26882  
 R Coronae Borealis in quiet state, spectral energy distrib. (*Russian*) 0-51781  
 β Crucis, β Canis Majoris star, photometric obs. 0-17595  
 SS Cygni, colour variations during dwarf nova outbursts 0-46576  
 SS Cygni, dwarf nova, soft X-ray pulsation obs. 0-46563  
 SS Cygni, dwarf nova, spectrophotometry rel. to accretion disc models in eruption and at min. light 0-36635  
 P Cygni, effective temp. radius, mass loss and luminosity 0-51748  
 P Cygni, extreme B-type supergiant, UV spectroscopy 0-22004  
 V1057 Cygni, FU Orionis star, IR spectroscopy with contact-type image tube 0-17587  
 P Cygni, high resolution UV spectrum obs. 0-26873  
 V1016 Cygni, image-tube spectrograms 0-8639  
 V832-59 Cygni, mass-losing Be star, changes in UV spectrum 0-46561  
 V1016 Cygni, new spectroscopic obs., simultaneous presence of increasing excitation and cool features 0-26874  
 V1057 Cygni, OH obs. 0-36629  
 NML=V1489 Cygni, OH/IR star, 1612 MHz OH maser multibaseline VLBI obs. 0-12766  
 CH Cygni, symbiotic star, rapid and slow light vars. 0-51792  
 V832-59 Cygni, variable mass flux from spectroscopic obs. 0-41840  
 V1357 Cygni (Cygnus X-1), no long-term light vars. (1928-77) 0-41861  
 V1341 Cygni (Cygnus X-2), IUE obs. of rapid UV flux vars. 0-12833  
 V1341 Cygni (Cygnus X-2), shortest optical variability (*Russian*) 0-17695  
 V1500 Cygni (Nova 1975), H $\alpha$  and H $\beta$  emission line vars. 0-4389  
 V1500 Cygni (Nova 1975), light curve for 1975 Aug.-1977 July period 0-4372  
 V1500 Cygni (Nova 1975), radio emission from expanding shell 0-26868



## variable stars continued

- V1500 Cygni (Nova 1975), review of development (*French*) 0-17598  
 V1500 Cygni (Nova 1975), visible and UV spectra and light curve 0-12771  
 V1668 Cygni (Nova 1978), linear polarisation obs. 0-26875  
 V1668 Cygni (Nova 1978), photoelec. photometry, rapid flickering 0-36640  
 V 1668 Cygni (Nova 1978), spectral development 0-51789  
 V1668 Cygni (Nova 1978), UVB light curve 0-46565  
 Cygnus OB2 number 12, spectral classification and membership of association 0-51760  
 HR Delphini, UV spectrum, stellar wind 0-26880  
 HR Delphini (Nova 1967), cataclysmic binary spectrum 0-4359  
 HR Delphini (Nova 1967), emission lines at nebular stage (*Russian*) 0-17597  
 HR Delphini (Nova 1967), photoionisation models, binary system evolution 0-17590  
 HR Delphini (Nova 1967), physical conditions of different regions of envelope 0-4369  
 HR Delphini (Nova 1967), radio emission from expanding shell 0-26868  
 HR Delphini (Nova 1967), spectra, line identification, radial vels. 0-17594  
 $\delta$  Delphini stars in Michigan Spectral Catalogue, uvby $\beta$  photometry rel. to spectral types 0-4377  
 S Doradus (HD 35343), luminous LMC supergiant, long time baseline VBLUW photometry 0-22007  
 S Doradus (HD 35343), luminous LMC supergiant, long time baseline VBLUW photometry 0-36630  
 BY Draconis, prototype spotted flare star, pre-main-sequence nature 0-36633  
 CR Draconis, UV Ceti variable, flares colour behaviour 0-22020  
 BY Draconis stars, rot. vels. rel. to pre-main sequence evolutionary stage 0-51767  
 dwarf Cepheids evolutionary stage, anal. and conclusions 0-46562  
 dwarf novae, HEAO-A2 soft X-ray survey during optical outburst 0-46574  
 dwarf novae, quasi-periodic oscills. and nonradial pulsations of accretion disks 0-46568  
 dwarf novae, spectra (*Russian*) 0-8638  
 eclipsing variable stars, Fourier analysis of light curves, error anal. in freq. domain 0-31214  
 eclipsing variable stars with extended atmospheres, Fourier anal. of light curves 0-46604  
 emission-line stars in galactic cluster NGC 663, emission line variability 0-4363  
 eruptive variable stars, IR spectra rel. to grains props. 0-26943  
 flare stars, flare data reduction and interpretation, interactive method (*Italian*) 0-8552  
 flare stars, model chromospheres, Balmer-line profiles 0-46558  
 flare stars, source of galactic cosmic rays, hypothesis 0-46559  
 flare stars in Orion Nebula region, new objects and repeated outbursts 0-56852  
 flare stars in solar neighbourhood, physical parameters 0-51777  
 galactic G-type supergiants, UVB photometry 0-41824  
 HD 15165,  $\sigma$  Scuti type star in BDS 1269 visual binary system 0-4397  
 HD 184927, He variable star, spectroscopic props. 0-51790  
 HD 193793, Wolf-Rayet star, circumstellar dust form. episode 0-31301  
 HD 193793, Wolf-Rayet star, photometric evidence for C-rich dust cloud 0-26861  
 HD 221568, Ap star, light var. period 0-56856  
 HD 31908, freq. analysis of  $\delta$  Delphini star 0-46581  
 HD 33579, HD 35343 (S Doradus), HDE 268757, HDE 269006, most luminous LMC supergiants, long time baseline VBLUW photometry 0-36630  
 HD 3980, late Ap star, photometric and mag. variability obs. 0-56845  
 HD 64740, He rich star, UV spectral vars. 0-22016  
 HD 80383, UVB photometry of  $\delta$  Cephei type star 0-36644  
 HD 8781, freq. anal. of low-amplitude  $\delta$  Scuti star 0-46575  
 HD 94033 ultra short period cepheid, obs. 0-22024  
 HDE 245770, possible counterpart of variable X-ray source A 0535+26, line and continuum vars. 0-17600  
 HDE 326333, new  $\beta$  Canis Majoris star, photometric obs. 0-17595  
 AC Herculis, curve-of-growth analysis of RV Tauri variable 0-22026  
 AC Herculis, RV Tauri star, UVB obs. 0-56857  
 AM Herculis (4U 1813+50), rapid light variability obs. (*Russian*) 0-8662  
 HZ Herculis (Hercules X-1), optical pulsations rel. to accretion disc/mag field interaction (*Russian*) 0-51799  
 DQ Herculis (Nova 1934), high time resolution spectrophotometry 0-22017  
 DQ Herculis (Nova 1934), short-period oscills. modulation and pulsed emission lines asymmetry interpretation 0-22044  
 V533 Herculis (Nova 1963), 63 sec. oscill., UVB photometry 0-17592  
 HR 1217, Ap star, spectrum and light vars. relationship 0-26878  
 HR 432, 515 and 8006,  $\delta$  Scuti stars, spectrographic obs. 0-36639  
 HR 9070, Be star, spectral vars. obs. 0-12773  
 Hubble-Sandage variables, mass accretion model 0-26877  
 W Hydrae, long-period variable, suspected Zeeman splitting in OH masers 0-36632  
 RW Hydrae, UV obs. of hot component 0-56854  
 VW Hydri, cataclysmic variable, light curve superhumps model 0-4381  
 VW Hydri, colour variations during dwarf nova outbursts 0-46576  
 IRC+10216, spatial spectra from 2.2 to 20 microns, deviations from spherical symmetry 0-41911  
 K1082, in globular cluster M15, suspected ultrashort period variable star 0-26883  
 12 Lacertae, nonradial oscills. of  $\beta$  Cephei type star 0-4366  
 DD=12 Lacertae, obs. study of secular var. and pulsational stability 0-41833  
 EV Lacertae, UV Ceti variable, flares colour behaviour 0-22020  
 late-type stars, O-rich, 16 to 39 micron spectroscopy 0-22002  
 R Leonis, IR atomic line spectrum of Mira variable 0-46557  
 R Leonis, SiO maser variability at 86 GHz of Mira variable 0-41839  
 AD Leonis, UV Ceti variable, flares colour behaviour 0-22020  
 AD Leonis, X-ray emission from flares, HEAO 1 obs. 0-41837  
 long period, system constitution (*Russian*) 0-36651  
 LS I +61°303, radio variable Be star, UV spectrum, stellar models 0-26879  
 $\alpha, \gamma$  Lupi,  $\beta$  Canis Majoris stars, photometric obs. 0-17595  
 RU Lupi, T Tauri star, chromosphere and corona parameters and expected X-ray fluxes (*Russian*) 0-51770

## variable stars continued

- RR Lyrae pulsators as He indicators in globular clusters 0-51778  
 RR Lyrae star in globular cluster NGC 6717, photometric investigation 0-46624  
 RR Lyrae stars, effective temp. and colour, metallicity effects 0-56841  
 RR Lyrae stars, inconsistency in local mixing-length convection theory 0-26841  
 RR Lyrae stars, parallaxes and distance scale, max. likelihood technique 0-51746  
 RR Lyrae stars, period-luminosity-colour relations, metallicity effects 0-56842  
 RR Lyrae stars in globular cluster NGC 1216, photometry rel. to cluster distance 0-17623  
 RR Lyrae stars in Microscopium, VBLUW photometry and proposed intergalactic dust cloud 0-56851  
 RR Lyrae stars models, radial pulsations 0-26863  
 RR Lyrae variables, three-dimensional motion 0-12754  
 RR Lyrae variables in globular cluster NGC 6121 (M4), UVB photometry 0-22018  
 in M3, globular cluster, proper motions and membership status 0-8665  
 M-type Miras, IR photometry 0-41823  
 AT Microscopii, X-ray emission from flares, HEAO 1 obs. 0-41837  
 Mira stars, OH main lines, IR pumping 0-46632  
 Mira variables, envelope pulsational instability rel. to planetary nebula form. 0-26928  
 Mira variables, OH maser sources, accurate position meas. 0-46646  
 Mira variables, SiO 86.2 GHz masers polarisation props. 0-4449  
 Mira variables, statistical anal. of galactic concentration (*German*) 0-4390  
 Mira variables around globular clusters, freq. distrib., cluster membership 0-36676  
 Mira variables kinematics towards galactic centre 0-46578  
 Mira-type, Tc in late-type stars, spectral analysis 0-8623  
 Miras, angular dia. in near IR, 2-5  $\mu$ m speckle interferometry 0-27010  
 V493 Monoceros, C star, discovery in two-micron objects survey 0-8555  
 19 Monocerotis,  $\beta$  Canis Majoris variable, photometric obs. 0-4379  
 1 Monocerotis,  $\delta$  Scuti star, oscillation modes from photoelectric radial vels. and BVRI photometry 0-51787  
 V616 Monocerotis (A 0620-00), UVB photometry 0-56846  
 NGC 2287, open cluster, spectral classification of brightest stars 0-26919  
 NGC 6913 galactic cluster, photoelec. photometry of brighter stars, variability obs. 0-46625  
 in NGC 6934, globular cluster, variable stars photometry 0-56891  
 nonradial pulsation hypothesis with simulated line profile vars. 0-8618  
 Nova Serpentis 1978, IR photometry 0-4365  
 Nova Vulpeculae 1979, slow nova, pre-maximum light curve 0-4364  
 novallike object in Vulpecula, UVB photometry (1979 August 6 to September 20) 0-8644  
 V380 Orionis, B8-A2e star, assoc. interstellar CH emission obs. 0-51856  
 FU Orionis, IR spectroscopy with contact-type image tube 0-17587  
 U Orionis, Mira variable, relation between 1612 MHz flare and light curve 0-56844  
 FU Orionis mechanism 0-51763  
 YY Orionis stars in Orion population, UVB photometry of young emission-line objects 0-46552  
 YY Orionis stars line profiles, spectral line form. in axisymmetric moving envelopes 0-41813  
 EQ Pegasi, active dwarf binary star, chromospheric emission lines obs. 0-12762  
 AU Pegasi, binary Type II cepheid, photometric and spectroscopic study 0-26866  
 period determination, maximum entropy method accuracy 0-56712  
 53 Persei, nonradial mode identification 0-8632  
 53 Persei, nonradial pulsator, light var. rel. to line profile changes 0-4362  
 b Persei, UVB photometry and spectroscopic study of ellipsoidal variable 0-36666  
 SX Phoenicis, evolutionary stage of RRs star 0-46583  
 physical and eclipsing variable stars, review of surveys and obs. 0-12772  
 BX Puppis, cataclysmic variable, possible member of Hyades-like cluster (NGC 2482) 0-31289  
 R Puppis (HD 62058), G-type supergiant, UVB photometry and variability confirmation 0-41824  
 radial and nonradial stellar oscills. effect on light, colour and vel. vars. 0-31310  
 HM Sagittae, emission-line star, UVB photometry and spectral obs. in (1978) (*Russian*) 0-36648  
 WZ Sagittae, cataclysmic variable, light curve superhumps model 0-4381  
 HM Sagittae, emission-line star, polarimetry, (1977 to 1978) (*Russian*) 0-36649  
 HM Sagittae, new spectroscopic obs., simultaneous presence of increasing excitation and cool features 0-26874  
 WZ Sagittae, recurrent nova, spectroscopic obs. during 1978 outburst 0-26862  
 WZ Sagittae, recurrent nova, spectroscopic study during 1978 outburst 0-56849  
 HM Sagittae, variable emission object, spectrophotometry 0-17599  
 AQ Sagittarii, C star, ang. dia. from lunar occultation meas. 0-22008  
 MV Sagittarii, R Coronae Borealis variable, brightness decline obs. and UVB photometry 0-8641  
 RY Sagittarii, spectra near min. light 0-36642  
 $\delta$  Scuti variables, photometric search of Hyades cluster 0-36677  
 semi-regular variables, SiO 86.2 GHz masers polarisation props. 0-4449  
 RT Serpentis (Nova 1909), spectrum in 1964, 1975 and (1978) 0-46566  
 FH Serpentis (Nova 1970), radio emission from expanding shell 0-26868  
 spotted stars, spot sizes 0-41812  
 SS 433, 10 GHz variability and thermal radio emission hypothesis 0-31307  
 SS 433, 1979 May-June radio flare, 3.24 GHz obs. 0-46567  
 SS 433, 6.55 day periodicity in emission line wavelengths 0-51784  
 SS 433, binary star model including mag. white dwarf 0-4385  
 SS 433, discrepancy between optical and radio positions 0-31303  
 SS 433, early-type binary model 0-56843  
 SS 433, enormous periodic Doppler shifts obs. 0-17593  
 SS 433, H I absorption obs. and distance 0-56848  
 SS 433, IR and visible obs., IR excess and emission processes 0-4387  
 SS 433, IR energy distrib. obs. 0-31312  
 SS 433, IR light curves from BVJHK photometry, period and ephemeris 0-8642  
 SS 433, IR spectral obs., reddening and emission 0-4388



## variable stars continued

- SS 433, light minimum epoch and period 0-26886  
 SS 433, mass accel. and collimation mechanisms 0-4368  
 SS 433, mass loss rates and lifetime from W50 optical filaments 0-12804  
 SS 433, nature and evolutionary state (*Russian*) 0-36647  
 SS 433, Of star orbited by neutron star, model 0-22025  
 SS 433, photometry, 1979 July to October, and 6.5 day period identification 0-8643  
 SS 433, radio jet discovery 0-31381  
 SS 433, short term H $\alpha$  central intensity increases 0-4375  
 SS 433, spectroscopic obs. and probable binary nature 0-51780  
 SS 433, VLBI detect. and ang. struct. 0-31304  
 SS 433 (W50), assoc. optical supernova remnant discovery 0-56916  
 SS 433 as veiled pulsar 0-41842  
 SS 433 model, precessing jets in ultra-close binary system 0-4384  
 Stepanyan's star found to be eclipsing binary, possibly cataclysmic 0-51806  
 Stephenson-Sanduleak 433, 1.2-2.5  $\mu$ m spectroscopy, photometry and polarimetry 0-41838  
 Stephenson-Sanduleak 433, Thomson scatt. lines in spectrum, relativistic gas motions 0-22019  
 symbiotic stars, magnetic field generation by close binary interaction 0-26903  
 symbiotic stars, obs. of unidentified bands at 6830 and 7088  $\text{\AA}$  0-46573  
 symbiotic stars, survey at 1612 MHz 0-12774  
 V711 Tauri, change in nature of light curve, and flare, 1979 October to December 0-26906  
 SU Tauri, emission lines at min. and BV photoelectric photometry 0-8640  
 DR Tauri, pre-main-sequence star, brightening, 1970 to 1979, and historical light curve 0-31297  
 RR Tauri, rapid periodicity, photometric investigations 0-26853  
 V711 Tauri (HR 1099), Lyman  $\alpha$  H I and D I interstellar absorption 0-8658  
 BU Tauri (Pleione), envelope behaviour in 1976, spectroscopic obs. 0-8636  
 BU Tauri (Pleione), metallic-line shell spectrum anal., (1973-1976) 0-8637  
 RV Tauri and yellow semiregular variables, photometric investigations 0-26865  
 T Tauri stars, effects of D burning on early evolution and outbursts 0-51736  
 T Tauri stars, role of accretion disks (*Polish*) 0-26739  
 T Tauri stars assoc. with Taurus-Auriga dark clouds, proper motions 0-41821  
 T Tauri stars atmospheres, sphere and low chromosphere model 0-36623  
 T Tauri stars in Orion population UVB photometry of young emission-line objects 0-46552  
 U Trianguli Australis, UBVRi obs. of beat Cepheid, pulsation energy changes 0-4360  
 4 U 2129+47 optical counterpart, spectrum and photometry rel. to 0-17693  
 SU Ursae Majoris, probable 1980 March super outburst 0-51785  
 $\gamma$  Ursae Minoris, high dispersion spectroscopy 0-41853  
 AH Velorum, radius, delta luminosity and pulsation mode of  $\delta$  Cepheid 0-46572  
 $\alpha$  Virginis,  $\beta$  Cephei type pulsation characts. 0-56835  
 XX Virginis, field Population II Cepheid, absolute mag. 0-41832  
 AR Virginis, RR Lyrae variable, photographic photometry and mean light curve (*Russian*) 0-12769  
 S Vulpeculae, 67 day Cepheid, case for membership in (Vulpecula OB2) 0-41831  
 21 Vulpeculae, new luminous long period  $\delta$  Scuti star, photometry 0-31306  
 BW Vulpeculae, V photometry, light curve, quadratic ephemeris 0-26881  
 NQ Vulpeculae (Nova 1976), UV and visual spectra analysis (*Chinese*) 0-12770  
 yellow semiregular and RV Tauri variables, photometric investigations 0-26865  
 young stars, circumstellar mols. 0-22013  
 ZB 33, RR Lyrae type star, light curve study (*Chinese*) 0-8633  
 SS Cygni, soft X-ray emission detect. during optical outburst 0-46574  
 U Geminorum, soft X-ray emission detect. during optical outburst 0-46574  
 H deficient and He weak stars, uvby photometry, variability 0-46579  
 H $\alpha$ -emission stars in Perseus OB1 assoc. region 0-56855

## variational calculus see variational techniques

## variational techniques

- adsorption system surface properties variational calcs., binding energy, Lang model 0-29279  
 alkali metal ion, with filled shell, dipole polarisability 0-9501  
 alloys, dilute mag., local moment formation, nonequivalent orbitals model 0-11164  
 amorphous Heisenberg ferromagnet, variational cluster method 0-39728  
 analytic radial orbitals, optimisation on variational parameters 0-42941  
 anharmonic oscillator, computation of energy eigenvalues of Hamiltonian 0-12925  
 apodizing filters for optimum Sparrow resolution in coherent systems with annular aperture 0-53435  
 atom, bound state quantum fluctuations and variational method, relativistic HF calc. with radiative effects 0-42918  
 atom, dynamic multipole polarisability, hydrodynamic model, variational approximations 0-23340  
 atomic correlation energies calc., Wilson's scaling parameter evaluation 0-5486  
 atomic independent particle pots. comparison 0-52846  
 atomic resonance theory, appl. to two-level at. S autoionising states 0-23329  
 band structure, generalised APW method using variational expression 0-6695  
 beams, thin walls, stress-strain state determ., method of segments 0-28424  
 bending, plates, bilinear and biquadratic quadrilaterals, variational principles, numerical convergence 0-48576  
 bending of thin plates, finite element anal., variational principle, simplified modified potential energy technique 0-52029  
 bimetal rolling, calc. of strains by variational method (*Polish*) 0-45323  
 Bose system, Jastrow wavefunction, hypernetted chain method 0-17866  
 buckling, stability anal. of rectangular plates, complementary energy method 0-48611  
 variational techniques continued  
 catastrophes and bifurcations in variational problems 0-8789  
 classical systems with non-integrable constraints, quantisation 0-36901  
 complementary variational principles for Maxwell's equations 0-32876  
 complex eigenfrequencies 0-28631  
 compressible finitely conducting rotating fluid in mag. field, Rayleigh-Taylor instability 0-10228  
 conductivity of inhomogeneous media with macroscopic inclusions 0-49685  
 conservation equation, numerical soln. by variational approach, mass transfer problem appl. (*French*) 0-19317  
 continuous medium and grav. field, eqns. of state from variational method 0-42122  
 cosmology, Newtonian, generalised Clebsch representation for velocity field of fluid, variational formulation 0-51930  
 covalent semiconductor, valence band calc. using many-electron theory 0-15434  
 covalent semiconductors, electronic struct. of localised defects, review 0-44535  
 creeping flow in closed cylindrical cavity, numerical calculation 0-16976  
 critical exponents in three dimensions, derivation from  $\phi^4$  field theory with Gaussian propagator 0-4686  
 crystal band struct., variational cellular method, electronic struct. calcs. 0-54591  
 cylindrical shell, buckling, combined action of axial compression and internal pressure 0-28447  
 degenerate semiconductors, ionised impurity scattering cross-section, variational calc. 0-20180  
 degenerate semiconductors, longitudinal thermo-EMF in quantising mag. field, scatt. mechanism (*Russian*) 0-24960  
 diamond and sphalerite type crystals, with spin-orbit interaction, indirect exciton energy levels 0-24804  
 diamond semiconductors, electronic structure, self consistent local description 0-20067  
 diatomic molecules, Stark effect variational and perturbational calcs. 0-1022  
 diffusion-controlled defect recombination, quasi-steady radius, tunnelling and elastic interaction (*Russian*) 0-10908  
 Dirichlet forms, construction of stochastic processes 0-8921  
 disordered systems, density of states, variational method 0-49565  
 elastic design problems, optimality, iterative solutions, finite element analysis and variational method 0-23887  
 elastic incompressible body, contact problems involving forces and moments, rigid punch problems 0-53719  
 elastic-plastic torsion, variational inequality concept, finite element anal. 0-23907  
 elasticity, local effects and energy methods (*Chinese*) 0-42060  
 elastodynamics, time harmonic, pointwise variational principle for mixed boundary value problems 0-31510  
 electric conductance and resistance, anisotropic body of arbitrary geometry 0-32865  
 electrodynamics and electrostatic problems, solns. 0-1105  
 electron correlation, variational description, loop driven graphical unitary group approach,  $\text{SO}_2(2'A')$  appl. 0-47903  
 electron gas, two-dimensional, variational approach to ground state, CDW instability 0-39517  
 electrostatic problems in presence of linear and isotropic quadrupole matter (*German*) 0-37924  
 exciton-phonon coupling, variational solns. 0-10601  
 excitonic molecules, binding energy, variational calc. 0-10891  
 exterior linear elliptic problem, numerical method, appl. to 2-dimens. wave resistance 0-28485  
 Fermi system, Jastrow wavefunction, hypernetted chain method 0-17866  
 field theory, Lie-Backlund operators props. from variational derivatives 0-37159  
 finite medium freezing (melting), variational anal., radiation and convection effects 0-38244  
 finite sample, mag. rearrangements near surface 0-11240  
 functional integral method appl. to classical and quantum spin models 0-15676  
 Gel'fand-Levitan equations with comparison measures and comparison potentials 0-12931  
 general relativistic phenomenological theory 0-2518  
 geometrical nonlinear shell theory, dual extremum and complementary stationary principles 0-4526  
 gravitational eqns. of Bianchi identity type vac. 0-4599  
 hadrons, string state, WKB-like wave functional and path-dependent phase factor, colour flux 0-52481  
 halogen ion, with filled shell, dipole polarisability 0-9501  
 Hamiltons principle appl. to large deformation and flow problems 0-48600  
 heat conduction, Biot variational eqn. generalisation 0-43591  
 hot atom chemistry, general variational principles 0-11941  
 hydrocarbons, mol. Raman intensities calcs. 0-52993  
 hypervirial theorems and symmetry, optimal variational wave function 0-17841  
 incompatible basis functions in boundary value problems, limitations of simplified variational principles 0-48587  
 inert gas atom, two-photon excitations; interelectron correlation 0-957  
 intermediate valence, three-site, six-electron model, variational calc. 0-20126  
 intermolecular forces, ab initio calcs. applicability and accuracy 0-18898  
 invariant tori and cantori, variational principles 0-37666  
 ion+atom collisions, asymmetric, polarisation and binding of inner-shell electrons, recoil in close encounters 0-18915  
 ion+electron scatt., static exchange approx. Schwinger variational principle, photoionisation cross section 0-43192  
 ionic crystal, simple, high temp. dynamics, var. approach 0-29130  
 Ising, 2- and 3-dimens. antiferromag. lattices, appl. of Kadanoff's variational approx. 0-2583  
 Ising model, free energy, variational calc. for 3 dimens. system 0-42167  
 jellium metal, surfaces props., statistical calc. 0-24987  
 kinetic theory, projection and variational methods 0-6189  
 Langmuir soliton solns. with high nonlinearities, energy principle 0-24156  
 Lennard-Jones gas, second virial coeff. calc. using equilib. Wigner distrib. function variational principle 0-4685  
 linear elastic half space, frictional unloading problem 0-33542  
 linear filter matrix, variational principle; functional max. value 0-27243  
 linear molecules, dispersion forces calcs. 0-9675



## variational techniques continued

- linear structures, complex, eigenvalues numerical bracketing (*French*) 0-42053  
 linear transport relaxation equations, matrices, variational principle 0-17785  
 liquid metal flow in curved channels, transversely applied mag. field 0-14829  
 lubrication, hydrodynamic, free boundary problem including surface tension 0-19542  
 magnetic thin films, charged domain walls, variational method calc. 0-11235  
 magnetisation curve analytic functions, numerical parameter calc., variational methods appl. (*Russian*) 0-14267  
 measurable selection theorem (*French*) 0-42045  
 metal, Ziman's variational expression for resistivity, use 0-15494  
 molecular vibrational wave functions, semiclassical Gaussian basis set method 0-9583  
 molecules, two criteria for labelling approx. treatments as fully quantal ones 0-23289  
 negative ion, singly-charged Thomas-Fermi-Amaldi eqn., approx. variational soln. 0-52870  
 neutron second order transport eqn., variational formulation and projectional methods 0-164  
 neutron streaming along fusion reactor ducts, perturbation and variational corrections 0-23143  
 neutron transport, contribution Monte Carlo technique, variational derivation 0-5194  
 neutron transport equation, perturbation method to estimate functionals 0-27698  
 nonconservative circulatory systems, variational formulation 0-48584  
 nuclear matter, finite temperature props., variational theory, effective mass 0-5084  
 nuclear matter, wave functions, correlation operators, review 0-22748  
 nuclear reactors, fission gas behaviour, calc. of diffusive flow to spherical boundary 0-47574  
 one component plasma fluid, derivation of eqn. of state in strong coupling 0-33741  
 optical absorption spectrum of  $D^-$  centre in strong magnetic field 0-20670  
 optimal rod and shell shape determ. using variational principle 0-5929  
 orbit-orbit interaction, new tensor expansion, matrix and graphical forms 0-14064  
 partially random sonobuoy array directivity index analysis 0-43518  
 path integrals and lower bounds for density matrices 0-138  
 perturbation theory, variational methods, evaluation of second-order matrix elements 0-12936  
 plasma, laser-irradiated, Langmuir soliton generation at crit. density 0-6267  
 plasma MHD, numerical simulation, variational approach 0-28625  
 plates, isoparametric finite elements, variational formulation of plate equilibrium problem (*French*) 0-43608  
 polaron effects on excitons 0-24811  
 polarons, Fröhlich, mean field theory, phase transitions 0-34371  
 polarons, strong coupling theory, variational approach 0-54621  
 position space LCAO wave function, momentum space variation approx., many centre integrals 0-27926  
 potential scatt., variational methods calcs., comparison of convergence 0-52043  
 potential scattering, refined Born approx. 0-77  
 power-law fluid, two-stream mixing along flat plate, variational solns. 0-53817  
 quantum liquids and crystals, computer modelling 0-54472  
 radiative transfer albedo problem in inhomogeneous isotropically scatt. atmospheres 0-36398  
 random Ising model, variational principle for distrib. function in the Bethe approx. 0-15674  
 rigid punch problems, forces and moments by reciprocal variational techniques 0-23967  
 rocket propulsion using nuclear reactor, optimisation problem, calculus of variation 0-27694  
 rod, naturally twisted curvilinear, asymptotic variational method anal. (*Russian*) 0-38251  
 rotating stars, normal modes, general variational principle 0-12750  
 rotating stars, perturb. and stability, eigenvectors and variational principle 0-46537  
 S-wave phaseshifts bounds, least norm variational principle tests, appl. to  $H+e(e^+)$  0-5619  
 sandwich system, near transition temp., proximity effect and Josephson current 0-7039  
 scalar field, modified stationary action principle, field eqns. for perfect fluid (*French*) 0-52076  
 scene principal vector analysis by multiple spatial filtering 0-48179  
 Schwinger variational principle, appl. to electron-mol. ion scatt. 0-48086  
 Schwinger variational principle for dynamic susceptibilities 0-4639  
 semiconductor, impurity ion pot., nonlinear Poisson eqn. soln., var. principles 0-29350  
 shell, circular cylindrical with varying wall thickness, creep buckling, variational methods 0-14595  
 shell, conical, stress distrib. near hole, orthotropy effect 0-43630  
 shell, ribbed conical, subjected to harmonic load, forced vibrations 0-43658  
 shell, spherical, subjected to external pressure, matching conditions 0-1447  
 Singer polymal tempering methods 0-52845  
 solitary Rossby waves, atmospheric, variational principle 0-56539  
 soliton perturbations, variational calcs. 0-46825  
 spatial curved bars, kinematic elements of mechanisms, movement equations 0-46809  
 spatially periodic convective flow, stability and fluctuations 0-19394  
 spectral shifts, variational study, relativistic aspects (*French*) 0-21909  
 spin glass, quantum effects 0-2581  
 spin glass binary mixture at  $T=0$ , energy and variational props. 0-39794  
 stability of spinning liquid-filled solid bodies 0-43609  
 Stark effect, perturbation and variation treatments, appl. to  $H(1s)$  reson. 0-14105  
 stress anal., direct and variational principles rel. to approx. techniques 0-28420  
 structural element design calc. under creep conditions 0-48598  
 superconductivity, general relativistic phenomenological theory 0-2518  
 superconductor tunnelling system, approx. Hamiltonian (*Chinese*) 0-44768

## variational techniques continued

- supergravity, self-duality in superspace, functional anal. 0-46902  
 symmetry-adapted Wannier functions, variational procedure 0-2323  
 TDMF phase, unique implication of variational principle 0-27583  
 thermorigid dielectrics, nonlinear thermodynamic theory 0-10149  
 three-body systems, number of bound states and Efimov's effect 0-31536  
 three-dimensional gasdynamic flows, variational principle in Euler description, vortex conservation 0-48731  
 transition metal complexes, discrete variational  $X\alpha$  cluster calcs. 0-15444  
 transition state theory, absolute rate theory and variational formulations, Porter Karplus pot. surface 0-16642  
 transition state theory generalisations 0-26002  
 transition state theory generalisations 0-26003  
 transversally nonhomogeneous waveguide EM wave propagation, using variational methods (*Czech*) 0-33155  
 triangular Ising lattice, anal. of Kadanoff lower-bound renormalisation-group, approx. 0-8930  
 turbomachine airfoil cascades, variational and dual extremum principles for aerodynamic problems (*Chinese*) 0-43729  
 viscoelastic solid, linear quasi-static theory, variational and minimum principles 0-10157  
 viscoelasticity, linear theory (*Japanese*) 0-48599  
 voids, sink strength of random array, steady-state diffusion problem, variational technique 0-49266  
 X-ray dose mean value of specific energy, variational meas. 0-12276  
 $C_3$ , Renner effect, vibronic levels and wavefunctions, ab initio variational method 0-14127  
 CO, electronic struct., binding energy and interatomic distance, SCF variational cellular calc. 0-9498  
 CuCl, energy bands and effective mass 0-10859  
 GaP, scatt. mech., mobility tensor 0-6826  
 Ge, acceptor ground state, stress effects 0-34385  
 P-Ge, acceptor wavefunctions in spherical approx. and piezoresist. 0-29405  
 H, condensed, spin-aligned, props. from variational calcs. 0-4637  
 H, electron scatt., equivalent exchange pots., algebraic variational method, 2p-2p and 2s-2p transitions 0-18931  
 H, spin-polarised atom, binding to free surface of liq.  $^4\text{He}$  0-34277  
 $H^-$ , bound states in mag. field, binding anal., variational calcs. 0-42940  
 H-like ion+H, two-body dispersion interaction, freq. depend. multipole polarisability, variational calc. 0-37758  
 $H_2$ ,  $X\alpha$  theory appls. approximations 0-9510  
 $H_2^+$ , high ( $10^9$  G) mag. fields, dissociation energy, electron binding energy and equilib. separation 0-52910  
 $H_2+H_2$ , dispersion forces calcs. 0-9675  
 He, bound states in mag. field, binding anal., variational calcs. 0-42940  
 He, double photoionisation calcs., variational method 0-37734  
 He, isoelectronic sequence, 2S states, analytic wave function 0-9525  
 He, isoelectronic series, ground state specific mass shift, HF variation perturbation calc. 0-47889  
 He, isoelectronic sequence, triply excited bound state, variational calc. 0-9526  
 He+He(Li), intermol. forces, ab initio VB calc. using nonorthogonal basis set 0-23490  
 $^3\text{He}$ ,  $^4\text{He}$  few atom mixed mols., binding energy, size, particle distrib. 0-32864  
 $^4\text{He}$  superlattices on graphite, ground-state energy, variational calc. 0-24710  
 $\text{MoO}_6^{6-}$ , electronic struct., discrete variation and scatt. wave  $X_\alpha$  methods 0-917  
 $\text{N}_2$ , electronic struct., binding energy and interatomic distance, SCF variational cellular calc. 0-9498  
 $\text{N}_2$ ,  $X\alpha$  theory appls. approximations 0-9510  
 $\text{N}_2+\text{N}_2$ , dispersion forces calcs. 0-9675  
 Na, variational cellular method, electronic struct. calcs. 0-54591  
 Ne, atomic struct. calc., symmetry adapted pair functions, Rayleigh Schrodinger HF variational perturbation theory 0-42944  
 Ni,  $X\alpha$  theory appls. approximations 0-9510  
 $\beta'$ -NiAl, self consistent embedded cluster model for Fe, Co, Ni mag. impurities 0-2549  
 Si-SiO<sub>2</sub>, n-type inversion layer, theory of impurity-shifted intersubband transitions 0-20324  
 TiO<sub>2</sub>, clusters, surface electron struct. and defect states, DV- $X\alpha$  calc. 0-20268  
 $\text{UO}_6^{6-}$ , electronic struct., discrete variation and scatt. wave  $X_\alpha$  methods 0-917  
 $(\text{UO}_2)_n^{12-}$ , electronic struct., variational  $X\alpha$  cluster calc. 0-39499  
 $(\text{UX}_3)_n^{n-}$ ,  $X=\text{N},\text{O},\text{S}$ , electronic struct., variational  $X\alpha$  cluster calc. 0-39499  
 $\text{WO}_6^{6-}$ , electronic struct., discrete variation and scatt. wave  $X_\alpha$  methods 0-917

## varistors

- Si, bicrystals, grain boundary states and varistor characts. 0-24829  
 ZnO, statistics and grain size effects on breakdown characts. 0-34010  
 ZnO-based, grain-boundary segregation, thin film X-ray spectroscopy obs. 0-35185

## varnish

- shellac, electrical cond. mechanisms, Schottky and Poole-Frenkel processes and work function 0-29402

## Vavilov-Cherenkov radiation see Cherenkov radiation

## VB calculations

- actinide compounds, BOA valence bonding with f-character 0-6790  
 benzene, noncrossing and degeneracy in Hubbard models 0-14096  
 cyclobutadiene, noncrossing and degeneracy in Hubbard models 0-14096  
 electrostatic isopotential maps for large biomolecules, STO transferable bond calc. 0-3571  
 extended correlated electronic systems, charge transfer transitions 0-29362  
 extended lattice VB theory, long range order spin pairing 0-52136  
 geminal product approx., optimisation of molecular wavefunction 0-37733  
 honeycomb extended lattice VB theory, long range order spin pairing 0-52136  
 narrow band conductors, valence bond theory 0-24777  
 polyacetylene, band struct. valence Hamiltonian minimal STO-3G basis calc., nonempirical model pot. 0-54596  
 polyethylene, band struct. valence Hamiltonian minimal STO-3G basis calc., nonempirical model pot. 0-54596  
 subtilisin charge-relay system, electrostatic pot. map, STO transferable bond calc. 0-3571



**VB calculations continued**

- surfaces and interfaces, quantum chemical calc. methods 0-49849  
 XY<sub>4</sub> molecules of D<sub>2d</sub> symmetry, G, F and  $\Sigma$  matrices (*French*) 0-970  
 $\alpha$ -Al<sub>2</sub>O<sub>3</sub>, IR intensities, valence-band dynamic and electrooptic models 0-34906  
 FNO, four electron three centre bonding units, ab initio valence bond calcs. four electron three centre bonding units, ab initio valence bond calcs. 0-27949  
 GaAs (110), reconstruction and oxidation initial stages, ab initio calc. 0-49473  
 HF<sub>2</sub><sup>-</sup>, four electron three centre bonding units, ab initio valence bond calcs. 0-27949  
 HNO, four electron three centre bonding units, ab initio valence bond calcs. 0-27949  
 He+He(Li), intermol. forces, ab initio VB calc. using nonorthogonal basis set 0-23490  
 LiNO, four electron three centre bonding units, ab initio valence bond calcs. 0-27949  
 LiON, four electron three centre bonding units, ab initio valence bond calcs. 0-27949

**vector diagrams** *see* **vectors****vector meson dominance model**

- charged pseudoscalar meson photoprod. from H and D with 16 GeV linearly polarised photons 0-13318  
 generalized vector dominance, photon-hadron interaction anal., review, book contrib. 0-47265  
 hadron EM interactions, review 0-412  
 hadron photoproduction, diffractive high energy processes, review, book contrib. 0-47309  
 meson resonances, strong and EM decays, particle mixing and meson pole dominance 0-18127  
 nuclear shadowing of electromagnetic processes, vector dominance model anal., review, book contrib. 0-47266  
 photons, effect of large intermediate masses in hadron-mediated photon-nucleus interaction 0-27625  
 T' (10040) as an I=1 vector meson resonance 0-47241  
 D meson decay, SU<sub>4</sub> 20-plet dominance model, inclusive branching ratios 0-13299  
 $\eta \rightarrow \gamma\gamma$ , radiative widths,  $\delta$  and S\* background, SU(3) and VDM anal. 0-419  
 $\eta' \rightarrow \rho\gamma$ , radiative widths,  $\delta$  and S\* background, SU(3) and VDM anal. 0-419  
 F<sup>+</sup> decay, SU<sub>4</sub> 20-plet dominance model, inclusive branching ratios 0-13299  
 $\gamma p$  cross-section observed increase, jets as source, QCD and vector-meson dominance model 0-22620  
 $p\gamma$ , one-gluon exchange, quark loop contrib. to photon total cross sections 0-4999  
 $\tau \rightarrow \pi\mu\nu$ , decay width and form factor calc. using vector dominance hypothesis (*Russian*) 0-47271

**vector mesons** *see* **meson resonances****vectors**

- arbitrary moving magnetic dipole, EM field calc. (*Russian*) 0-9772  
 elliptic polarisation, Stokes parameters, vector trihedron, optical element evaluation 0-53209  
 Feynman diagrams, dimensionally regularised, symbolic evaluation, quantum gravity application 0-13259  
 first integrals and symmetries, geometrical obtention 0-22535  
 palaeomagnetism, Zijderfeld vector diagrams use in multicomponent magnetisation studies 0-17420  
 precession theory, vector-matrix notation 0-51642  
 teaching acceleration and velocity, racetrack game 0-31458

**vehicles**

- see also electric vehicles; locomotives; road vehicles; space vehicles*  
 coherent optical processor for vehicle tracking and identification using laser diode light sources 0-37957  
 flywheels, performance of retainerless bearings for vehicular energy storage apps. 0-30567  
 H-fuelled passenger bus, design 0-40924  
 Stirling engine powered total energy system for recreational vehicle apps. 0-30538  
 H cryogenic storage and refuelling for automobiles 0-30604  
 H fuel, survey of liquid hydrogen container technology for highway vehicle fuel system applications 0-30607  
 H storage by metal hydrides for automotive propulsion 0-40922  
 H<sub>2</sub> fuelled vehicles, design and engine modifications with Fe-Ti hydride storage 0-40925  
 H<sub>2</sub>-powered, high temp. hydrides for H storage 0-45793

**velocity**

- see also acoustic wave velocity; ion mobility; light velocity*  
 galaxies, bright, nearby, vel. field and Local Group peculiar motion rel. to Virgo cluster 0-36699  
 interstellar shocks, post-shock gas temp., density and vel. profiles, analytical results 0-56911  
 laser velocimeter, appl. to aerodynamics, operating principle (*Spanish*) 0-53902  
 planetesimal population, equilib. vels. 0-31219  
 spiral galaxies bulges, vel. dispersions meas. 0-26965  
 teaching acceleration and velocity, racetrack game 0-31458  
 wind velocity gust factors, analytical expression and wind tunnel simulation 0-31107

**velocity analyzers** *see* **particle separators****velocity measurement**

- see also acoustic wave velocity measurement; anemometers; angular velocity measurement; flow measurement; flowmeters; laser velocimeters; light velocity measurement; stroscopes*  
 air stream, subsonic, using laser Doppler interferometer system, errors analysis (*Russian*) 0-27336  
 aircraft velocity and altitude measurements using a tunable diode laser 0-13042  
 airflow using wind-speed measuring instrums., calibration using low-vel. facility 0-1718  
 annular flow, vel. distrib., expt. determ. 0-38510  
 biological objects underwater, design principles of US instrums. 0-19195  
 Björk-Shiley aortic prosthesis, in vitro vel. meas. using laser-Doppler anemometer 0-17196  
 blood flow echography using Doppler techniques (*French*) 0-26303  
 blood velocimeters, US transesophageal meas. of human haemodynamic parameters 0-41146

**velocity measurement continued**

- bubbles, measurements using RF probe 0-6177  
 channel, 2-dimens. rectangular, vel. profiles and fluctuations, laser Doppler anemometry 0-53864  
 contactless, of running strips of bands, transit time determ. by pick-up (*German*) 0-14862  
 correlator, Malvern, based on photon correlation and laser scattering spectroscopy, development and appl. 0-5741  
 cross-wind velocity meas., interference fringe visibility and spacing, atmospheric turbulence effects 0-51572  
 dielectric flows, EM method for flowrate and velocity meas. 0-53893  
 fission reactor control rod drop damping and velocity meas. instrumentation (*German*) 0-5248  
 flowpath velocity meas., semiconductor hot element anemometer 0-48823  
 freely sinking probe horizontal velocity meas. interpretation 0-46321  
 Gulf of Alaska SeaSat Experiment 14.6 GHz scatterometer surface wind obs. 0-46200  
 internal combustion engine, measurement of pulsating temp. and vel. using US flowmeter 0-1704  
 internal contraction engine, highly loaded, exhaust gases temp. and velocity meas. using two thermometer method (*German*) 0-31754  
 ion beam, fast, meas. using Doppler shift method 0-9083  
 laser Doppler anemometer measurements, bias correction 0-24114  
 laser Doppler velocimeter for meas. of specified velocity vector 0-47040  
 microwaves non-conventional appl. survey (*Italian*) 0-13093  
 ocean sediment free-fall penetrometer with Doppler telemetry 0-46320  
 on-axis velocity component measurement with laser velocimeters 0-19526  
 particle velocity distrib. meas. by holography 0-5705  
 SeaSat scanning multichannel microwave radiometer 0-46248  
 ships, acoustical determination of course speed and lateral drift 0-5892  
 simple linearised hot wire anemometer, performance characs. 0-53904  
 speech production process, articulatory characteristics of tongue and jaw point movements in connected sounds of Japanese 0-26243  
 spherical particle velocity and size meas., crossed-beam light scatt. interferometry 0-47011  
 US transducers for medical imaging (*French*) 0-26302  
 velocimeter for fluctuating temp. and vel. meas. in combustion field 0-14856  
 wind meter, digital 0-207  
 wind velocity, remote meas. using video equipment for pollution monitoring (*French*) 0-7990  
 xerographic cascade flow, carrier bead velocity distribution meas. probe 0-47136

**velocity meters** *see* **velocity measurement****velocity microphones** *see* **microphones****velocity-modulation tubes**

No entries

**velocity spectrometers** *see* **mass spectrometers****Veneziano model** $\pi^-p \rightarrow \psi n$ , generalised Veneziano models 0-22638**ventilating** *see* **ventilation****ventilation***see also air conditioning*

- fan systems and energy 0-6145  
 louvres, sound transmission loss for various louver geometries 0-45839  
 nuclear fuel reprocessing plant ventilation control 0-5318  
 particle accelerators, radiation exposure 0-5350

**ventilators** *see* **ventilation****Venus**

- astrometric radar meas. in 1977, results 0-17522  
 atmosphere, 0 to 200 km, physical parameters from Pioneer Venus mission (*French*) 0-46421  
 atmosphere, chemical composition deduced from twilight glow obs. 0-56739  
 atmosphere, composition and structure, Pioneer results 0-46230  
 atmosphere, cyclic and diurnal vars. in thermosphere and exosphere 0-51683  
 atmosphere, IR radiation absorpt. induced by press., mol. collision between CO<sub>2</sub>, N<sub>2</sub>, O<sub>2</sub> (*Russian*) 0-56600  
 atmosphere, model from radio, radar and occultation obs. 0-46420  
 atmosphere, net radiation meas. by Pioneer small probe 0-46435  
 atmosphere, neutral gas comp., diurnal vars. 0-46427  
 atmosphere, photoelectrons caused by solar photons of less than 80 Å 0-56744  
 atmosphere, radiative transfer, line form. level 0-17487  
 atmosphere, radiative transfer of solar radiation, model based on Venera 10 data (*Russian*) 0-12698  
 atmosphere, role of gaseous S<sub>2</sub>, S<sub>3</sub>, S<sub>4</sub> and H<sub>2</sub>S<sub>n</sub> 0-17518  
 atmosphere, scattered solar radiation, day sky spectrum, Venera meas. 0-56573  
 atmosphere, scattering coeff. from Venera 9 and 10 photometry 0-8572  
 atmosphere, struct. and comp. from refl. sunlight polarisation calc. and obs. 0-36533  
 atmosphere, sunlight absorption 0-46434  
 atmosphere, temp., cloud structure and dynamics from IR remote sensing 0-46429  
 atmosphere, thermal contrast from Pioneer probe data 0-46229  
 atmosphere, thermal radiative transfer, numerical modelling 0-8574  
 atmosphere, upper, temp. and dynamics from Pioneer Orbiter IR radiometer meas. 0-26766  
 atmosphere turbulence from Pioneer multiprobe radio scintillations 0-46437  
 atmospheric precipitation, props. and possibilities of detect. 0-56741  
 bow shock, depend. on solar wind strength 0-41748  
 bow shock, Pioneer magnetometer obs. 0-36535  
 bow shock observations, 4th Dec. 1978 0-41747  
 cloud cover, obs. by Venera 9 orbiter 0-51680  
 cloud microstructure 0-46431  
 cloud optical properties and atmos. layered struct. 0-51681  
 cloud structure, high-contrast UV detail 0-51682  
 clouds, UV absorbers, Pioneer data 0-46433  
 clouds spectropolarimetry, lines equivalent widths information content 0-31215  
 dayside ion densities 0-46444  
 dust ring possibility from Venera 9 and 10 spectroscopy 0-8573  
 electron obs. and ion flows, Pioneer orbiter plasma analyzer expt. 0-46448  
 exosphere, hot hydrogen origin 0-36536



## Venus continued

- gas comp. meas., implications for origin of planetary atmospheres 0-51678
- gravitational spectrum, determ. from Pioneer Venus orbiter tracking 0-41744
- gravity field from Pioneer tracking 0-46439
- hothouse theory of recent cosmological catastrophe 0-41749
- impact cratering and tectonic activity, evidence from radar obs. 0-46426
- infrared spectra near superior conjunction, CO<sub>2</sub> bands 0-56740
- ionosphere, CO<sub>2</sub> and CO electron vibr. cooling rates 0-41750
- ionosphere, daytime, two-freq. radio transillumination data using Venera-9, 10 probes 0-21936
- ionosphere, diurnal ion comp. vars., Pioneer orbiter meas. 0-46440
- ionosphere, ion comp., photochemical and thermal diffusion control 0-46445
- ionosphere, thermal structure and energy influx 0-46443
- ionosphere, whistler mode wave absorption 0-46446
- IR radiometer on Pioneer Venus orbiter 0-36469
- lightning discharges in atmosphere, frequency of occurrence 0-56743
- lithosphere global TRM in presence of central dipole field, theory 0-31223
- magnet field, nightside Pioneer magnetometer obs. 0-46447
- magnetic field and magnetosphere 0-56737
- magnetic tail formed by solar wind interaction 0-51679
- nightside ionosphere, electron temp. and density models 0-46442
- nightside ionosphere, formation process, ionization, mixing ratios 0-41751
- nightside ionosphere, Pioneer orbiter radio occultations 0-46441
- Pioneer gas chromatograph analyses, laboratory simulation 0-46362
- Pioneer rephelometer expts. results 0-46430
- Pioneer Venus results, surface and atmosphere 0-17523
- radar observation of surface relief, soil and atmos. 0-36537
- radar studies of Venusian surface using refraction attenuation 0-4280
- regional polarization, 1950-77 obs. 0-8570
- rotation, possible dynamical evolution since formation 0-56742
- rotation axis, free wobble damping time 0-17516
- solar wind interaction 0-41687
- spin evolution 0-46423
- stratosphere, large-scale turbulence, model 0-12699
- sulphur chemical cycles, involving S, sulphite, sulphide and sulphate 0-50837
- surface, Venera 9 and 10 landers, visible radiation 0-46425
- surface features, Pioneer orbiter topographic and surface imaging 0-46438
- surface panoramas at Venera landing sites, contrasts and relief 0-8571
- surface rocks, mineral composition prediction 0-17519
- tectonics, comparison with Earth and Mars 0-26767
- thermal radiometry by Venera 9 and 10 of cloud tops 0-46424
- thermosphere, acoustic-gravity waves 0-17520
- thermosphere during daytime, nitrogen chemistry 0-17517
- tidal theory and torque balance 0-46422
- ultraviolet photometry and cloud struct., Venera obs. 0-56738
- upper atmosphere, rotation (French) 0-36534
- UV cloud images from Pioneer orbiter 0-46432
- UV markings, Venera 9 cloud top data analysis 0-17521
- UV nightglow and thermospheric circulation 0-46428
- Venus Orbital Imaging Radar (VOIR), stereo side-looking radar accuracy anal. 0-56646
- winds, retrograde zonal movement below clouds 0-46436
- Ar isotope abundances in Venus thermosphere, upper limits 0-4281
- <sup>36</sup>Ar excess in Venus atmosphere, implications for Venus accretion 0-12700
- NO production by lightning in clouds, odd N chem. reactions 0-26768
- O<sub>2</sub>( $\Delta$ ) airglow and nightglow emission 0-17515

Verdet constant *see Faraday effect*Verneuil process *see crystal growth from melt*

## vertex functions

- see also elementary particle interactions; elementary particle theory; quantum field theory of interactions*
- gauge invariance in non-Abelian gauge theories, triple-gluon vertex 0-42326
- quarkonia states, heavy, strong decay into other heavy flavours, and triple-gluon vertex 0-47279
- Reggeon vertices and finite mass sum rule, bootstrap eqn., dual resonance model 0-13292
- Wess-Zumino model, massive, dimensional regularisation, supersymmetry 0-27398
- $\Delta_{33}$  energy region, electroproduction, simple-pole model,  $\gamma N \Delta_{33}$  vertex 0-22625
- $\pi NN$  form factor,  $\Delta(1236)$  contrib., calc. 0-22609

## vibrating bodies

- see also elastic waves; pendulums; piezoelectric oscillations; vibrations*
- 2D finite amplitude acoustic waves radiating from flat plate in arbitrary periodic vibrations 0-33283
- acoustic emissions during flexion (French) 0-48625
- acoustic generation by vibrating bodies in homentropic potential flow at low Mach number 0-23826
- acoustomechanical characts. of laminated first-order transducers 0-14537
- aerial camera stabilised mounts, calc. of parameters 0-9059
- aerofoil stall flutter with acoustic flow control 0-23991
- aircraft engine inlet guide vanes, acoustic fatigue due to intake flow distortions 0-53542
- annular plates elastically restrained against rotation along edges, transverse vibrs. 0-38312
- annular radial-mode concentrators, calc. 0-5869
- antisymmetric laminated plates, finite element analysis 0-53683
- arbitrarily shaped membrane with point supports 0-23937
- attenuation of resilient mounts and dampers under actively vibrating machines 0-14514
- automobile whip antenna, first overtone vibrational mode obs. 0-17747
- bar, curved, in-plane vibrs., shear deform. and rotatory inertia effects 0-43646
- bar, thin curvilinear elastic; natural freq. of vibr. optimisation (Russian) 0-19266
- base excited cantilever beam, whirling motion, comments 0-48488
- base excited system with Coulomb and viscous friction, response determ. 0-19269
- beam, multiplicity of solns. of inverse problem 0-28462
- beam, optimum distrib. of additive damping 0-38310
- beam, rotating slender, bending vibrs., Galekin method anal. 0-1465
- beam on nonlinear spring support, random vibr. 0-33515

## vibrating bodies continued

- beam with heavy tip mass, freq. eqn. 0-43657
- beam with moving load, numerical anal. of vibration 0-23943
- beam with nonlinear elastic constraints, transverse vibr. 0-38309
- beams, eqn. of motion of large amplitude vibration of beams (Japanese) 0-33511
- beams, linearly tapered, transverse vibr. 0-48627
- beams, non-linear vibrations, stability analysis method 0-53686
- beams, optimal design, iterative procedure 0-1457
- beams, radiation efficiencies, flexural vibration 0-53541
- beams of variable thickness layers, free transverse vibrations 0-23940
- bluff structures, aerodynamic mechanism of torsional flutter 0-53689
- building structure, estimation of structural system parameters from ambient vibrations 0-28456
- cantilever strips with inserts, damping characts. 0-38315
- circular cantilevered rod in nominally axial flow, effect of trailing end geometry 0-28455
- circular ring segment, damped, test vs. theory for forced vibr. 0-38326
- circular rings on radial supports, free vibration 0-23946
- circular sandwich plates, free asymmetric vibr. 0-1459
- circular tubes subjected to liquid cross flow, dynamic responses 0-53693
- clusters of flexible cylinders in axial flow, dynamics 0-28460
- composite cylindrical shell, torsional vibr. in mag. field 0-48624
- composite materials elastic characts. by vibr. tests and discrete conservative model calcs. (French) 0-45337
- composite panel under fluid loading, reflection and free wave props. 0-14603
- conservative discrete-continuous system, free vibration (Russian) 0-23950
- convex polygonal membrane, two dimensional Helmholtz eqn. soln. 0-19271
- curved bars, in-plane vibrations of connecting system 0-43647
- curved bars, out-of-plane vibrations of connecting system 0-43648
- cylinder, acoustic surface intensity measurements for determination of machine noise 0-43577
- cylindrical sleeves, non-linear forced vibrs. (German) 0-53698
- damped 3-layer plates, finite element analysis of harmonic response 0-53691
- damped continuous systems, forced vibrations, Galerkin and Hamilton-Ritz methods 0-53684
- discrete-continuous system, vibrations 0-23951
- elastic plates, vibration and sound transmission due to a spherical sound wave (Japanese) 0-33330
- elastic-plastic oscillators under random excitation 0-28458
- external disturbance transformation into boundary layer waves 0-28523
- flexible rods, stability under follower forces 0-19273
- floating gyroscope with vibrating base, perturbing moments (Russian) 0-40
- free circular plate, vibration under non-conservative edge loading 0-23948
- gear systems, analysis of vibratory excitation, tooth error representations 0-33506
- grid in viscous medium, damping, basis for electrostatic viscometer 0-38308
- heated plates with two opposite edges simply supported 0-38314
- infinite elastic bar, induced oscills., normal and associated wave propagation 0-5980
- integrally stiffened skew plates on irregularly spaced elastic supports, free vibration and transient forced response 0-14604
- isolation of vibration, survey of use and characterization 0-19144
- isotropic elastic circular plate, flexural vibrs., Mindlin's theory 0-43650
- laminated structures, of viscoelastic and elastic layers, damping mechanism analysis (Japanese) 0-5968
- laminates, fibre-reinforced, optimum design under natural frequency restraints 0-53688
- limaçon-shaped membrane, approx. expression for fundamental frequency 0-53695
- lumped parameter beam models, transient response 0-19270
- magnetoelastic strange attractor, chaotic type non-periodic motions 0-23945
- mechanical networks and applications (Japanese) 0-10072
- membrane and plate, functionals method for lateral vibr. freqs. determ. (Japanese) 0-12918
- membrane with rigid centre, free axisymmetric oscillations (Russian) 0-38302
- Mindlin annular plate of varying thickness, steady state response 0-48626
- Mindlin-Goodman method of solving problems with time-dependent boundary conditions, comments 0-53694
- moving strip, transverse vibrations 0-28459
- musical acoustics wave motion experiment, phase vel. meas. using spring 0-8762
- noise radiation from vibrating machine systems, prediction by analytical method 0-43521
- non-circular plates, fundamental freq. estimation, comments 0-23942
- one-dimensional linear oscillator impacting under harmonic excitation, steady-state response 0-53690
- orthotropic plate on elastic foundation, force vibration 0-53682
- oscillator with dry friction, forced vibrs., response random process treatment (Russian) 0-36841
- piezoelectric plate, thickness vibrations, natural freq. spectrum 0-15979
- plate, bending vibrations and acoustic pressure (Russian) 0-23949
- plate, clamped, with multi-holes, free vibr. freq. and modes (Japanese) 0-53697
- plate, thick, vibration anal. using Mindlin plate elements 0-38305
- plate, thin flat, transverse vibrs., eqns. of motion, kinematic elements (French) 0-5977
- plate, thin harmonically vibrating, improved extended field method numerical results 0-36833
- plate having circular inside edge and cornered outside edge consisting of arcs 0-33507
- plate thin harmonically vibrating, extended field method free vibration solns. 0-38311
- plate under impact of elastic sphere, radiation of transient sound 0-38168
- plates, circular, free transverse vibration, axisymmetric, Hamiltons energy principle 0-53679
- plates, pre-stressed, 3-D problems, basis systems of homogeneous solns. (Ukrainian) 0-10177
- plates, rectangular with parabolically varying thickness, nonlinear vibrs. 0-19267



**vibrating bodies continued**

plates, sandwich, rectangular, singly curved, with clamped boundaries, iterative calc., using Kantorovich method (*Japanese*) 0-5970

plates, thin, converged stress solns. by extended field method 0-38306

plates, vibration response using general Dirac delta function method to loads along arbitrarily closed lines 0-23938

plates of arbitrary shape, new analytical approach 0-53692

point-driven elastic plate, influence of shear, rotary inertia and longitudinal vibrs. on acoustic emission 0-5871

polar orthotropic annular discs, vibration anal. 0-23941

polar-orthotropic sector plates, free vibrations 0-53687

polygonal plates, analysis of doubly connected problem 0-33508

prestressed non-uniform cantilever cylindrical shells, axisymmetric vibration 0-14605

quartz crystal flexure bars and tuning forks, frequency-temp. characts. 0-5971

$\alpha$ -quartz plates vibrating in thickness, doubly rotated, zero polarizing effect 0-55038

radiation of plane circular source, nonlinear solutions (*French*) 0-33280

record player tone arm resonant frequencies and their avoidance (*Japanese*) 0-33329

rectangular plate, supported at arbitrary number of points 0-23947

rectangular plate, thin elastic, resting on nonlinear elastic foundation, vibration and stability for large deformation 0-53696

rectangular plate of variable thickness, approximate strain energy expression 0-38317

rectangular plate with in-plane forces, vibration anal. by finite strip method 0-14607

rectangular plate with nonuniform thickness, forced vibrations 0-14606

rectangular plates of linearly varying thickness, analysis of lower modes of vibration 0-33502

reinforced annular circular plates, axisymmetric vibrations with impulsive loads 0-23939

resonance testing of complex structs., first-order formulation 0-28457

resonance theory of acoustic waves interacting with an elastic plate 0-33268

response analysis of a vibrational system of multi degrees of freedom subjected to an arbitrary force 0-12912

rigid sphere in elastic medium, effect of random compressional waves 0-53681

rod, cantilever, constrained end, transverse vibrs., energy dissipation 0-19278

rod with varying elasticity clamped at one end, forced vibr. 0-43653

rotating cantilever with offset rod, natural freqs. 0-28454

rotating deformable elastic disc, vibr. stress anal. (*Russian*) 0-19265

rotating flexible rods at transitional parameter values, vibr. and buckling, off-clampings 0-1464

rotating machinery diagnostics, signal extraction and filtering 0-23840

rotating non-uniform disc, spline interpolation technique for calculation of free vibration 0-43656

saws, control of vibrations through thermal tensioning 0-48516

shallow cylindrical panel, on nonlinear elastic foundation, nonlinear vibrations 0-53680

shell, cylindrical, dynamic instability due to attached mass (*Ukrainian*) 0-38297

shell, cylindrical, free vibrs., asymptotic integration solns. (*Russian*) 0-1463

shell, cylindrical, thin, tentative equation for vibrational analysis 0-5969

shell, cylindrical in supersonic flow, vibration, finite element anal. 0-5973

shell, elastic, containing ideal fluid, anharmonic vibr. 0-5978

shell, filled with compressible liq., internal press. effect on free oscill. freq. (*Russian*) 0-23934

shell, orthotropic, axisymmetric vibrs. in mag. field, asymptotic solns. 0-2620

shell, with negative curvature, free vibr. calc. (*Russian*) 0-23936

shell segments and non-axisymmetric shells, free vibration analysis using isoparametric finite elements 0-23944

shells, orthotropic, cylindrical, axial pressure wave effects 0-10183

shells, thin stiffened reinforced, stability and vibrs. 0-14610

sound field attenuation of diverse sources in plate by means of surface corrugations 0-14515

sound field calculation (*Japanese*) 0-48493

sound wave diffraction by hollow elastic cylinder in partial annular layer of finite thickness 0-14506

storage ring, feedback-stabilised, resonator wall instability caused by ponderomotive forces 0-5418

stranded wire helical spring, general axial response 0-33453

string, acceleration discontinuity propagation due to solid friction (*French*) 0-22196

string, harmonic waves, introduced through Fourier synthesis, for teaching 0-27080

structural foundations, excitation by seismic surface wave 0-10182

surfaces, procedure for measuring sound intensity near vibrating surface 0-53580

tapered orthotropic plates having thermal gradient, natural freqs. 0-53685

tensioned bar with initial curvature, parametric excitation 0-43654

thin circular membrane, forced symmetric vibrs. 0-10181

thin I-shaped plates, exptl. determ. of transverse vibration modes 0-28474

thin plate dynamics, elastic asymptotic anal. of boundary and initial conditions 0-43640

thin walled tank containing compressible liq., vibr. anal. (*Russian*) 0-1462

torsional vibrators, design by computer optimisation (*Japanese*) 0-33405

tubes with inclined terminal nozzle, stability boundaries for flow induced vibrations 0-19512

tuning fork, longit. vibr. mode 0-38

tuning forks, electrically driven, Melde's experiment apparatus 0-42022

unhomogeneous bars, normal mode response, stress anal. by boundary operator method 0-19239

viscoelastic beam, constrained, flexural vibrating, response to random excitation of white noise and turbulent boundary layer type 0-53671

viscoelastic shells, axisymm., transient vibrations 0-10179

viscoelastic spring rod, vibration heating, amplitude depend. (*Ukrainian*) 0-38301

wind-induced bending torsional galloping vibration of rigid body, minimal wind velocity determ. 0-48623

AI rod, measurement of small amplitude vibrations using multiple-beam interferometer 0-4759

**vibration control**

see also damping

damping, polymeric coatings 0-10178

dynamic balancing, influence coefficient method, balancing of rigid rotors 0-53724

electrodynamic vibration test beds, feedback signals for correcting characteristics 0-53543

gyrosystem, optical methods (*Russian*) 0-8983

legal remedies for noise and vibration problems 0-10084

modal anal., digital simulation (*French*) 0-42216

optical equipment, precision, insulation against vibration using springs and viscoelastic substances (*German*) 0-17986

survey of use and characterization of vibration isolation 0-19144

**vibration measurement**

see also seismometers

acousto-optical fibre interferometer for reflective surface motion meas. 0-13127

automatic system for simulating and analyzing wide-band random vibrations 0-53730

automatic testing of vibration installations, certification results processing 0-22336

calibration of devices, ring comparison meas. of equipment (*German*) 0-52189

dynamic balancing, influence coefficient method, balancing of rigid rotors 0-53724

electrodynamic vibration test beds, feedback signals for correcting characteristics 0-53543

errors evaluation, due to pulse signals 0-23972

gas turbine rotor, contactless system (*Russian*) 0-8982

gyroscope rotor, scanning laser based detector (*Russian*) 0-22351

gyrosystem, optical methods (*Russian*) 0-8983

holographic interferometry, general shift reference 0-1150

hydrodynamic instabilities in heated channel, identification using appl. of vibration signals 0-28500

in-plane, real time speckle interferometry meas. with aid of liq. cryst. light valve 0-53734

introduction, as diagnostic and monitoring technique 0-37025

laser Doppler vibr. meas. system using bispectral anal. 0-38357

long tow-wire complex vibration obs. and empirical drag law 0-46309

machine testing and dynamic balancing 0-23971

mechanical, in precision units, testing by real-time holography (*German*) 0-38366

microtremor, laser interferometer, He-Ne laser (*Japanese*) 0-9025

modal anal., digital simulation (*French*) 0-42216

motion picture apparatus vibration meas. by holographic interferometry (*Russian*) 0-37112

nuclear power plant equipment vibrations caused by flow, indirect meas. methods (*Hungarian*) 0-18453

piezoceramic accelerometers and associated instrumentation for vibration meas. 0-10073

piezoelectric transducer, HF vibration measurement using time-average electronic speckle pattern interferometry system 0-37966

piezoelectric transducer systems, noise suppression and prevention for shock and vibration meas. 0-22353

power spectrum estimation using maximum entropy method, data analysis appl. 0-37006

random vibration simulator, practical realisation 0-53732

rough surface small vibrs., light scatt. meas. 0-1494

simulating system optimisation, rel. to efficiency and cost 0-53728

simulating system optimisation 0-53729

simulator design, optimisation 0-53731

small amplitude, using multiple-beam interferometer 0-4759

soil surfaces using vibration pickup, horizontal resonant freqs. 0-10102

speckle method for meas. mechanical translations ( $10^{-11}$  to  $10^{-3}$  m) (*German*) 0-17924

structural dynamics analyser development, microcomputer-based 0-53733

thin I-shaped plates, exptl. determ. of transverse vibration modes 0-28474

train induced ground vibration, measurement and analysis 0-48494

**vibrational states in disordered systems**

acetone, liq., C-C stretching mode relax., Fermi reson. influence 0-25352

acetonitrile, in liq. phase, Ramon band profiles, calc. using IR intensities 0-2741

alkali metal tetrafluoroborates, intramol. force fields and mean vibr. amplitudes 0-2743

amorphous metals, electron-phonon coupling const. and Eliashberg function 0-39567

amorphous solid, phonon scatt. by density fluctuations and thermal cond. 0-10626

amorphous solids, low-energy excitations of phonons, magnons, electrons rel. to struct. factor 0-44488

amorphous tetrahedrally coord. solids, bond charge model 0-49108

p-bromochlorobenzene, vibr. relax., Raman active phonons temp. depend. 0-29139

CBOOA, isotropic, nematic, smectic-A phases, Brillouin scatt. 0-11421

condensed H-containing media, cold neutron total section data interpretation 0-33857

1,1-cyclobutane dicarboxylic acids and K salts, IR and Raman vibr. spectra (*French*) 0-2758

p-dichlorobenzene, vibr. relax., Raman active phonons temp. depend. 0-29139

2,2-dinitropropane- $d_0$ (- $d_5$ ), phase polymorphism, vibrational assignments, IR and Raman study 0-16031

ethane, liq., correl. function modelling, third order memory function method 0-7339

glass, tunnelling systems, intrinsic elec. dipole moment, coherent elec. echo obs. 0-29705

glass-forming polymer, paramag. spin-lattice interactions 0-7149

glasses, thermal cond. rel. to diffusion process due to phonon-defect interaction 0-34259

hexafluorobenzene-benzene, liq., mol. interactions, IR and Raman line-shape obs. 0-28907

ice, IV, 4000-400  $\text{cm}^{-1}$  IR spectra, H-bonding and assignments, orientational disorder 0-16022

IR continua, phonon theory for obs. of vibr. modes 0-5800

liquids, picosecond laser techniques for obs. of vibr. modes 0-6480

local modes in disordered crystals, two-time Green's functions 0-6480

$\alpha,\omega$ -methoxy-poly(ethylene oxide) effect of swelling on longitudinal acoustic mode 0-29739



**vibrational states in disordered systems continued**

- molecular pair, fluoresc. depolarisation, using stochastic Liouville eqn. with radiative terms 0-16074  
 naphthalene, melting of rotational degrees of freedom near cryst.-liq. transition 0-54352  
 nylon, H-bridge interactions, far IR spectra study 0-11374  
 one-dimensional system, phase fluctuations, disorder, nonlinearity 0-54331  
 phonon-like excitations, dispersion and damping 0-49331  
 phosphate glasses, cation-site interactions, IR and Raman spectroscopy 0-2744  
 poly-1,6-di-p-toluenesulphonyloxy-2,4-hexadiyne, thermal polymerisation, Raman spectra 0-35531  
 polyacetylene, doped and neutral, resonance Raman scatt. 0-55107  
 polyalkenamers, longitudinal accordion mode, low frequency Raman spectroscopy 0-25369  
 polyethylene, H bonding effects on skeletal optical and longitudinal acoustical modes 0-34914  
 polyethylene, solid, IR spectra, interference distortion of  $73\text{ cm}^{-1}$  absorpt. line 0-11375  
 polyethylene oxide, cryst., lowest laser Raman active accordion oscillations, elastic moduli effect 0-29734  
 polymer glass, sp.ht. discontinuity at glass transition 0-19954  
 polystyrene and model cpds., conformational struct. influence on normal modes of benzene ring, Raman study 0-14144  
 polysulphur nitride, Kohn anomalies in phonon dispersion 0-24555  
 polytetrahydrofuran, H bonding effects on skeletal optical and longitudinal acoustical modes 0-34914  
 quartz glass, spectral absorpt., 3000-4000K 0-25401  
 Raman scattering cross section for LF spectrum study 0-25363  
 rigid molecules, dil. soln. in decalin, mean librational freqs. 0-6479  
 semiclassical model of vibr. energy relax. in simple liqs. and compressed fluids 0-33865  
 semiconductors, disordered, phonon-assisted interband optical absorption 0-34947  
 spectra, IR and Raman, of disordered solids, analytical models 0-7336  
 tetrabromomethane, in disordered phases, IR active mode Raman line shape, dipole-dipole interaction 0-9603  
 tetrafluoromethane, in disordered phases, IR active mode Raman line shape, dipole-dipole interaction 0-9603  
 tetramethylsilane, liq., electron drift vel. saturation, skeletal vibr. 0-34451  
 thermal conductivity, Callaway eqn., phonon scatt. in highly disordered systems 0-20000  
 time dependent spectral transfer, Monte Carlo calc. 0-11464  
 toluene sulphonate diacetylene polymer, vibr. modes, strain depend. using Raman spectra 0-20626  
 water-carbon tetrachloride soln., fundamental  $\text{H}_2\text{O}$  IR spectrum, liq. struct. 0-23419  
 ( $\text{AgI}$ ), ( $\text{Ag}_2\text{O} \cdot \text{B}_2\text{O}_3$ )<sub>1-x</sub> glass, ionic cond. and disorder modes 0-39344  
 As, amorphous, vibr. excitations at defect sites, IR and Raman spectra calc. 0-49329  
 As, amorphous, vibrational excitations of defect sites 0-49332  
 As-S, glass, IR vibr. spectra, optical characts. calc. 0-40119  
 As-S glasses, resonance Raman scatt. 0-50325  
 As<sub>2</sub>O<sub>3</sub>, vitreous, local struct. and vibrational spectra 0-55091  
 As<sub>2-x</sub>S<sub>3+x</sub>, hydrogenated chalcogenide glasses, prep. by plasma decomposition 0-49735  
 As<sub>2-x</sub>Se<sub>3+x</sub>, hydrogenated chalcogenide glasses, prep. by plasma decomposition 0-49735  
 B<sub>2</sub>O<sub>3</sub> glass, struct. and phonon spectra 0-50324  
 B<sub>2</sub>O<sub>3</sub>-SiO<sub>2</sub> glass film, CVD, differential IR studies 0-55213  
 BaCl<sub>2</sub>, non-crystalline film, disorder-induced Raman scatt. 0-11387  
 BaFCl, non-crystalline film, disorder-induced Raman scatt. 0-11387  
 C, amorphous, diamond-like 3-fold coord. 0-50323  
 CS<sub>2</sub>, liq., props. from allowed light scatt. spectra 0-25364  
 CdS<sub>1-x</sub>Se<sub>x</sub> mixed crystals, free excitons, disorder effects 0-34365  
 Cs-Graphite, interaction ordered and disordered cpd., Raman spectra 0-11393  
 Cu<sub>46</sub>Zr<sub>54</sub>, metallic glass, dynamical struct. factor and freq. distrib. meas. 0-54136  
 GaAs<sub>1-x</sub>H<sub>x</sub>, amorphous, vib. props., Raman and IR meas. 0-50322  
 Ge, amorphous, electronic struct., far infrared absorption 0-45051  
 Ge amorphous film, high freq. phonon scatt. 0-49328  
 GeO<sub>2</sub>, glassy high freq. vibr. bands, central force model 0-49330  
 GeS<sub>2</sub>, glassy, high freq. vibr. bands, central force model 0-49330  
 H<sub>2</sub>, vibr. population relax. in gas and fluid 0-29775  
 HCl, liq., IR spectral intensity and Raman cross-section meas. 0-2742  
 HClO<sub>4</sub>-H<sub>2</sub>O, aq. soln., IR and Raman spectra, conc. depend. (Russian) 0-53002  
 He, liquid, charged surface vibrations in metal approx. (Russian) 0-10718  
 NH<sub>4</sub>Br and NH<sub>4</sub>I, Raman scatt., 1 bar-7 kbar, 86-295 K 0-34909  
 Na, liquid, entropy calc. using phonon theory of liquids 0-39310  
 Na<sub>2</sub>S-GeS<sub>2</sub> system, glass formation, struct. and ionic conduction 0-54138  
 O<sub>2</sub>, liq., stimulated Raman scatt., vibr.-translational relax. rate, schlieren technique meas. 0-9955  
 P, amorphous, red, far IR absorpt. spectra 0-34923  
 P, amorphous, vibrational excitations of defect sites 0-49332  
 P, amorphous red, Raman scattering 0-11416  
 PH<sub>3</sub>, liq. and solid, Raman spectra, vibr. correl. functions, rot. motions 0-55087  
 PHD<sub>2</sub>, vibr. dephasing in liq. and solid PD<sub>3</sub>, calcs. 0-19884  
 P<sub>2</sub>O<sub>5</sub>, glassy, high freq. vibr. bands, central force model 0-49330  
 Pd-Si-Fe amorphous alloy, Mossbauer spectra, struct. and bonding 0-7224  
 PdZr, amorphous, supercond., US props. 0-44765  
 SO<sub>2</sub> liquid, short range orientation effects, vibr. Raman spectra 0-2759  
 Sb, amorphous, vibrational excitations of defect sites 0-49332  
 Se, amorphous and liq. states, Raman scatt. meas. 0-50328  
 Se, trigonal, vitreous and red amorphous, phonon density of states comparison 0-54329  
 Si, amorphous, electronic struct., far infrared absorption 0-45051  
 Si:F, amorphous, pure and doped, vibr. excitations at defect sites, IR and Raman spectra calc. 0-49329  
 Si:H, amorphous, Brillouin scattering from acoustic bulk and surface waves 0-11425  
 SiO amorphous film, high freq. phonon scatt. 0-49328  
 SiO<sub>2</sub>, amorphous, intrinsic surface phonons, Raman scatt. and IR refl. 0-24728

**vibrational states in disordered systems continued**

- SiO<sub>2</sub> and SiO<sub>2</sub>-B<sub>2</sub>O<sub>3</sub> glasses, struct. and phonon spectra 0-50324  
 SiO<sub>2</sub> glass, IR spectral emissivity and absorpt. coeff. at 600 to 1700K 0-16018  
 SiO<sub>2</sub> glass, phonon scatt.,  $>10^2$  GHz, by supercond. junction spectrosc. 0-10625  
 SiO<sub>2</sub>, vitreous, multiphonon IR absorpt. 0-25381  
 SrCl<sub>2</sub>, non-crystalline film, disorder-induced Raman scatt. 0-11387  
 Te, amorphous, Rayleigh scatt. of Mossbauer radn., lattice dynamics 0-15845
- vibrations**  
*see also lattice dynamics; molecular vibration; vibrating bodies*  
 acoustic noise propagation models, railway lines 0-48500  
 aeroelastic vibr. elimination, optimal control method 0-33514  
 aeroelasticity in separation streamline flow 0-5979  
 air column resonance spectra, meas. using basic lab. apparatus 0-41998  
 ambient vibrations of building struct., estimation of structural system parameters using exploratory-confirmatory analysis 0-28456  
 asymmetric elastic medium, electrically conducting, magneto-thermo-elastic waves anal. 0-15772  
 beam, clamped, hinged, sudden change of boundary conditions, support failure vibrs. (German) 0-1456  
 beam, nonuniform, sectionalization and averaging method for calc. natural freq. and normal modes (Chinese) 0-43643  
 beam, two-span, with curved initial path contour, transverse vibrs. 0-38324  
 beam-like lattice trusses, numerical analysis, shear deformation 0-14566  
 beamlike dynamic vibration absorbers, anal. 0-53539  
 branched systems, single-junction, analysis using Rayleigh-Kohn and Newton Raphson methods 0-52035  
 cavity-backed panel anal. for sound transmission in air (French) 0-38164  
 circular disk resonators in vicinity of thickness resonance, vibration mode anal. 0-48634  
 classical string problem, constants of motion 0-27113  
 classical string problem, evolution eqn. 0-27114  
 complex moduli derived from vibrations of Timoshenko beam 0-38163  
 composite materials, rational bonding of structures, fracture resistance 0-5990  
 curved tube bank vibration in turbulent transverse water flow (Russian) 0-33678  
 cylinder, torsional vibr. superposed on finitely deformed state 0-19263  
 cylindrical shell with liquid, resonance frequencies determ. 0-43661  
 cylindrical shells, correlation between vibration and buckling 0-28463  
 cylindrical shells of viscoelastic material, natural transverse vibrations 0-43660  
 droplets, forced vibr., Raman scatt. obs. 0-34929  
 duration effects on human comfort and task proficiency 0-26247  
 dynamic stabilization of multiphase media subjected to vibrations under low gravitation conditions 0-7511  
 earthquake response of nonlinear plates 0-13955  
 effect of noise and vibration on human beings, summary of symposium, Southampton Univ. (Dec. 1978) 0-35958  
 effectiveness rating of vibration-absorbing coatings 0-5870  
 elastic, numerical characts. determ. (Russian) 0-38181  
 elastic cylinder, end resonance under axisymmetric vibr. (Ukrainian) 0-23932  
 elastic cylindrical resonator in liquid filled cavity (Russian) 0-38303  
 elastic half-bounded medium, unidimensional deformation under vibr. loading (Ukrainian) 0-5933  
 electrorheological suspension flow, vibr. effect (Russian) 0-53877  
 engine structure vibrations, transmission path and dynamic behavior, background and static tests 0-43520  
 engine structure vibrations, transmission path and dynamic behavior, motoring tests 0-48487  
 finite orthotropic cylinder with penny-shaped crack, transient response under torsion 0-48640  
 fission reactors, flow-induced structural vibrations anal. 0-42795  
 flexural, radiation efficiencies of beams 0-53541  
 floor, nature and effect on precision, machinery, isolation methods 0-43522  
 flowmeter, float-area-type, jumping instabilities of float 0-14855  
 fluid and structural dynamics, transient 3-D potential flow problems, SING-S 0-48668  
 Fokker-Planck eqn. eigenfunction expansion soln. extension, first order system 0-31668  
 forced, lower bound on forcing amplitude for stability, third order non-linear system 0-52013  
 forced, orthotropic plate on elastic foundation 0-53682  
 fractal resonators, mode distribution 0-8782  
 Green function expansion into eigenfunction set 0-22205  
 gyroscope, forced vibrations, shock absorber selection parameters 0-43659  
 harmonic oscillations of single degree of freedom systems 0-33516  
 impact vibrations, steady, of body having hysteresis collision characteristics 0-14602  
 internal losses in metals subjected to high intensity US flexural vibrations 0-6460  
 isolation, fluid-saturated porous solids 0-53726  
 linear lumped-parameter systems, synthesis with prescribed mode shape 0-23881  
 liquid, in vessel, vibr. amplitude determ., structural damping and surface tension applied to stress anal. 0-19417  
 magnetic repelling force system, with cylindrical rare-earth magnets (Japanese) 0-4744  
 membrane, fundamental free eigenvalue, lower bounds 0-38319  
 Mindlin-Goodman method of solving problems with time-dependent boundary conditions, comments 0-53694  
 multi-degree of freedom mechanical systems, antiresonances (Chinese) 0-42049  
 nonlinear mechanical systems, periodic vibr. 0-33513  
 nonlinear mechanical systems with time optional condition 0-31492  
 nonlinear oscillators, normal modes, uncoupling and stability 0-27115  
 nonlinear system with stops, viscous-Coulomb damping influence 0-36842  
 nonlinear systems, vibrations under space-time stochastic loads 0-33524  
 nonlinear two-degree-of-freedom system, internally resonanced, forced vibrs. 0-36838  
 nonlinear vibr. eqns., modified stroboscopic method for approx. determination of periodic solns. 0-38313  
 nonlinear vibration decoupling using canonical transformation (German) 0-28451



**vibrations continued**

- nonsymmetric vibrations of piezoelectric ceramic rings polarized along the thickness 0-7299
- orthotropic elliptical plate with similar hole, free vibration 0-43649
- oscillator, linear, excitation by stationary random force (*Russian*) 0-27116
- particle vibrational movement under impulse perturbation of an inclined plane (*Russian*) 0-17791
- pipng systems under seismic excitation, modal anal. 0-33512
- plate, thin, thermally stressed, vibrations 0-48628
- plate excitation, difference of structure-borne-sound levels in point excitation and large area excitation (*German*) 0-53538
- plate on eccentric annular elastic support, transverse vibr. 0-14601
- plate with hole, rigidly clamped, natural vibrs. 0-33520
- plates, annular, of variable thickness, natural vibr. eigenfreq. Mindlin eqn. integration 0-38318
- plates, rectangular, stability and vibrations (*Chinese*) 0-43644
- plates, thin circular, modal anal. of transient asymmetric response 0-23931
- plates, thin elastic, large amplitude vibrs. by conformal transformation method 0-19262
- plates, uniform circular, with free edge, natural modes and freqs. 0-48638
- plates at elevated temp., vibr. and buckling, fundamental freq. 0-23935
- power ultrasonic applications of vibration systems (*Chinese*) 0-43568
- pulsed excitation of flexural modes in infinite plates 0-38167
- PWR power plant flow pressure fluctuations as vibration source, relationships (*Hungarian*) 0-47685
- railway ground noise, underground systems 0-48490
- railway tunnels, structure-borne sound levels and spectra 0-48499
- random compressional waves, effect on rigid sphere in elastic medium 0-53681
- random vibration analysis, correlation function (*Chinese*) 0-43645
- reduced model theory, hydrodynamical approach for vel. autocorrelation functions 0-27135
- resonant nonlinear vibrations, continuous system, undamped case 0-28450
- resonant nonlinear vibrations, continuous systems, damped and transient behaviour 0-33504
- response analysis of a vibrational system of multi degrees of freedom subjected to an arbitrary force 0-12912
- road traffic noise, effect of structure-borne tunnel vibrations on buildings 0-48492
- road vehicles, digital modal analysis system 0-38173
- rod, cantilever, constrained end, transverse vibrs., energy dissipation 0-19278
- rod, short elastic, in viscous liquid axial flow, stability and transverse oscillations 0-33521
- shell, cylindrical, fibre reinforced, fluid conveying, vibr. characts., flow effects 0-14600
- shell, cylindrical, optimal natural freq. vibrs., rib eccentricity influence 0-38325
- shell, multilayer composite, optimisation, buckling under stability and vibr. conditions (*Russian*) 0-53667
- shell, ribbed conical, subjected to harmonic load, forced vibrations 0-43658
- shell, spherical, with rigidly clamped edges, Poisson ratio influence on natural vibrs. 0-33523
- shell, thin cylindrical, stiffened with viscoelastic rings, vibr. damping characts. 0-28452
- shell, thin elastic, containing liquid, free vibrs. (*Russian*) 0-33505
- shell and surface rigidity, pseudobending, vibrs. and stability loss (*Russian*) 0-33470
- shells, applicability limits for approx. theories (*Ukrainian*) 0-23933
- shells, circular cylindrical, wide band random axisymmetric vibrs. 0-48637
- shells, flexible shallow elastic-plastic, natural vibrs. and buckling 0-33519
- shells, thin stiffened reinforced, stability and vibrs. 0-14610
- sound radiation, critical freq. of flat plates in dense fluids (*German*) 0-38165
- steel, low C, absolute dimensions effect on logarithmic decrement of torsional vibrs. 0-3150
- Sturm-Liouville system with discontinuous coeffs., direct soln. for vibr. and heat conduction 0-23930
- teaching, Newtonian motion anal. using micro-computer simulations (*Japanese*) 0-31462
- thick circular rings, T or I cross section, in-plane vibrs. 0-48639
- thin walled sphere in contact with elastic or acoustic media, interior dynamics 0-5981
- Timoshenko arcs with variable cross section, in-plane vibr. 0-28453
- train generated ground vibrations, propagation and wayside effects 0-48489
- train induced ground vibration, propagation pathway prediction 0-48491
- turbomachinery for central power stations, review of vibration and noise 0-23835
- two channel drive dynamics with differential wave mechanism (*Russian*) 0-28449
- two-mass system, free vibrs., damping factor optimisation (*Russian*) 0-42
- unstaggered tube bank vibration induced by viscous liquid flow (*Russian*) 0-33677
- unsteady aerodynamic modelling for arbitrary motions 0-19433
- violin G-string, resonant response and excitation of wolf-note 0-53540
- viscous incompressible liquid, vibrational displacement, wave mechanism 0-43777
- water boiling, vibr. effect on heat transfer crisis 0-33423
- wedge region with mixed boundary conditions, elasticity theory, dynamic problems soln. 0-43641

**vibrations, crystal lattice** see *lattice dynamics*

**vibrations, molecular** see *molecular vibration*

**vibrations of crystal lattices** see *lattice dynamics*

**vibrometers** see *vibration measurement*

**vibronic states of molecules** see *molecular vibronic states*

**video recording**

- airborne passenger entertainment, dual language Super 8 mm sound system 0-4785
- chalcogenide films, laser-beam recordings by thermal creation of holes 0-35010
- cinematography, development and introduction of TV facilities (*Russian*) 0-22465
- disc information retrieval by optical readout 0-43284
- disk pit geometry, control, optical techniques 0-5775

**video recording continued**

- holographic colour video memories, recording and playback technique 0-9833
- laser engineering and appls., conf., Washington, USA (May-June 1979) 0-1216
- medical laser video recorder 0-36065
- vapour pressure measurement, torsion-effusion method, automatic data acquisition 0-52188
- VLB1, Japanese domestic system, recording signal generator (*Japanese*) 0-21924
- AlGaAs high-power constricted DH diode laser, for optical recording 0-43351

**video signals**

- remote sensing, image transformation and coding in conventional colours via electron system 0-4117
- seawater transmission props. for underwater laser communication 0-33069
- X-ray image convertor with video signal output 0-36125

**videotext** see *viewdata*

**vidicons** see *television camera tubes*

**viewdata**

- Prestel viewdata system, introduction 0-42013

**viewing screens** see *screens (display)*

**virial coefficients** see *equations of state*

**virtuons (virtual phonons)** see *phonons*

**viscoelasticity**

- see also *creep; internal friction; stress relaxation*
- anisotropic layer, nonstationary torsional waves problem (*Russian*) 0-53678
- aqueous liquids, shear US meas. with composite torsional quartz transducer 0-53599
- bars with nonlinear characteristics, stability 0-10174
- beam, constrained, flexural vibrating, response to random excitation of white noise and turbulent boundary layer type 0-53671
- bimolecular lecithin membranes, artificial, rheological and viscoelastic props. 0-26252
- blood, rheological parameters for viscosity, viscoelasticity and thixotropy 0-16963
- blood rheology, clinical changes in peripheral vascular disease and smokers 0-16965
- bronchial elasticity and air flow, mathematical anal. 0-45942
- buried impulsive load, effect on viscoelastic layer on elastic half-space 0-28428
- cell suspensions, stability to small disturbances in circular Couette flow 0-56099
- cellulose esters, plasticiser effects on mech. and dielec. relax. 0-40047
- circular plates, thermoviscoelastic anal. of a thermorheologically simple material 0-10161
- complex moduli derived from vibrations of Timoshenko beam 0-38163
- composite semi-infinite rod, wave propagation 0-10180
- conference, computational methods in nonlinear problems in mechanics and engineering, Austin, Texas, USA (March 1979) 0-51945
- cortical bone, wet, non-linear constitutive eqn. of viscoelastic props. 0-30754
- cortical bone, wet, torsional and biaxial viscoelastic props. obs. 0-30752
- cortical bone, wet, viscoelastic props., relax. mechs. 0-30753
- crack propagation in linear viscoelastic medium 0-53700
- cracked linear viscoelastic solid, dynamic anal. by finite element method 0-53706
- creep meas. of rotating disks 0-38360
- cylinder, hollow, nonlinear viscoelastic material, dynamic pressure loading 0-38289
- cylindrical shells of viscoelastic material, natural transverse vibrations 0-43660
- deformation taking into account influence of accumulated defects 0-19252
- p-p'-dibutyl-azoxybenzene, DIBAB, light scatt. studies (*Dutch*) 0-33885
- die swell problems, viscoelastic fluid flow, collocation and Galerkin finite element anal. 0-14751
- differential eqn. method approximation, for solving dynamic viscoelastic problems 0-14585
- dipolar dumbbells in a viscoelastic Oldroyd liquid, dilute soln., electric field effect on rheological behaviour 0-6009
- drag reduction of an oscillating flat plate with an interface film 0-10268
- dynamic response of viscoelastic halfspace, complex moduli concept 0-23902
- dynamical problems, approx. soln. of integral eqns. 0-10164
- Earth, free oscillations attenuation theory 0-21652
- elastic adhesion problems, rel. to linear fracture mechanics (*French*) 0-14617
- elastomeric network, finite linear viscoelastic theory, time-depend. deform. behaviour 0-38292
- entangled monodisperse polymers kinetic network model for nonlinear viscoelastic flow props. 0-28538
- epichlorohydrin/bisphenol A epoxy polymer concrete, viscoelastic props. 0-45340
- epoxy resin, Cl-containing, relation between static and dynamic deform. characts. 0-3137
- epoxy resin, heat generated by fatigue (*Spanish*) 0-11736
- epoxy resin, meas. of glass transition temp., linear viscoelasticity 0-29157
- epoxy resin, time-temp. superposition of creep data, linear viscoelastic props. 0-30045
- fibre reinforced composite, fibre geometry and filler vol. influence on fracture stresses 0-45397
- fibre reinforced composites, viscoelastic thermal shrinkage stresses 0-38287
- fibre reinforced materials, therm. stresses in unit cell 0-10160
- fluid flow in fixed geometry, collocation and Galerkin finite element methods 0-14750
- fluid theories based on left Cauchy-Green tensor history 0-4534
- fluid under flow through tubes 0-14753
- fluids, heat transfer at low Deborah numbers, rheological effects 0-19445
- generalised thermorheologically simple porous materials, thermomechanical theory of viscoelasticity 0-33479
- half-space, dynamic indentation and impact by axisymmetric rigid body, iterative method anal. 0-14626
- heterogeneous or anisotropic bodies, error estimation in viscoelastic problem soln., using method of approx. 0-19253



## viscoelasticity continued

- high mol. wt. polymer melts, viscoelastic props., relaxation and retardation spectra 0-19310  
 homogeneous viscoelastic mixtures, speed of sound 0-33272  
 hydrodynamic stability of structurally viscous medium, effect of elastic factor 0-19303  
 incompressible liquid oscills. in variable cross section viscoelastic tube due to pulsating press. 0-31519  
 incompressible simple fluid with fading memory, stability 0-43741  
 inhomogeneous bodies, deformation under quasistatic loading 0-14587  
 inhomogeneous viscoelastic body, effective props. 0-19256  
 instantaneous moduli, determ. from long-term static test results 0-38286  
 integro-differential viscoelasticity dynamics 0-14586  
 laminar shells, with viscoelastic binder, stability 0-10165  
 layered medium, transient wave propagation normal to layering 0-53676  
 linear solids, stress/strain tensor eqns. (*French*) 0-53656  
 linear theory solns. by model  $\gamma$ -irradiation, polarisation-optical method 0-33485  
 liquid, flow through porous channel, free and forced convection effects 0-53861  
 liquid, heat transfer in rot. flow, suction and injection effects 0-33596  
 liquid layer, electrohydrodynamic instability 0-14832  
 liquids, relation between viscoelasticity and shear-thinning behaviour 0-19307  
 liquids, viscoelastic props. meas. using torsion resonator, 20-1200 KHz (*Russian*) 0-52196  
 low-frequency fluctuation, dissipation and relaxation properties 0-39661  
 LPDE melt, tensile stress overshoot in uniaxial extension, single integral constitutive eqn. 0-1507  
 magnetothermoviscoelastic waves reflection at semi-infinite solid boundary 0-48633  
 mammalian DNA, rat obs. 0-8078  
 mixed protein phospholipid films, viscoelastic behaviour and Marangoni effect 0-3602  
 monolayer, viscoelastic, of apoprotein, dynamic surface potentials 0-3603  
 non-ageing materials, quasi-constant operators in viscoelasticity theory (*Russian*) 0-53650  
 non-homogeneous, Lagrange equations and Galerkin method, boundary value problems 0-53654  
 non-linear model, constitutive equation testing with free. vol. relax. spectrum 0-6011  
 non-Newtonian liquid, convective stability, energy method 0-38455  
 non-Newtonian liquids, resist. to tensile stress 0-1505  
 nonlinear, stress relaxation, Volterra integral equation, numerical analysis 0-53646  
 nonlinear functional relations and superposition principles 0-42065  
 nonlinear strain waves in viscoelastic rod (*Russian*) 0-1460  
 nonlinear viscoelastic wave of very small amplitude (*French*) 0-8803  
 nonlinear viscoelasticity, a method of successive approxs., based on non-linear correspondence principle 0-5953  
 nonlinear viscoelasticity, bifurcation and uniqueness, Hadamard stability 0-43621  
 nonlinear viscoelasticity, convergence of successive approx. method with integral transforms 0-19255  
 optimal strain paths in linear viscoelasticity 0-5956  
 periodically layered medium, wave propag. normal to layering, viscoelastic analogy 0-48636  
 pitch and coke-pitch disperse system 0-1500  
 plane interface between two viscoelastic superposed cond. fluids, instability in mag. field 0-1694  
 plastics, nonlinear viscoelastic anisotropic, creep 0-35249  
 plates and shells, viscoelastic, flexible, thermomech. behaviour during cyclic loading 0-33478  
 plates at elevated temp., vibr. and buckling, fundamental freq. 0-23935  
 PMMA, laser damage mechanism rel. to viscoelastic props. 0-55233  
 PMMA, partial draining of low-molecular weight polymers with flexible chains 0-23592  
 PMMA, viscoelastic props. in plastic zone, cooling rate effect 0-40418  
 PMMA fracture toughness, flame-retardant additive effect obs. 0-16470  
 Poiseuille flow of viscoelastic fluid between eccentric cylinders 0-1652  
 poly(ethylene oxide), partial draining of low-molecular weight polymers with flexible chains 0-23592  
 polyacrylonitrile-dimethylformamide soln., viscoelasticity and shear modulus meas. (*German*) 0-38374  
 polyalkaneimide, mech. and thermophys. props. at liq. He temps. 0-3117  
 polyamide-polyoxirane copolymers, mechanical properties evaluated 0-11700  
 polybutadiene, linear and star branched, rheology 0-23977  
 polycarbonate, viscoelastic props. in plastic zone, cooling rate effect 0-40418  
 polycrystalline materials, high temp. creep, role of grain boundary sliding 0-34128  
 polyester-polyurethane semi-interpenetrating networks, mech. props., morphology 0-45362  
 polyether ester-PVC blends, annealed, dynamic mechanical and sonic velocity behaviour 0-25740  
 polyethylene, fatigue, fractographic study 0-30101  
 polyethylene, fatigue crack growth charact. 0-30100  
 polyethylene, partial draining of low-molecular weight polymers with flexible chains 0-23592  
 polyethylene melts, low-density, viscosity and viscoelasticity, filler effect 0-10222  
 polyethylene oxide, aq. soln., mech. props. in parallel superposed flows, geometric effects 0-19448  
 polyisobutylene solution in cetane, hyperelasticity, filler effect 0-10223  
 polymer, fatigue, fractographic study 0-30101  
 polymer, fatigue crack growth charact. 0-30100  
 polymer, high-modulus, behaviour in solid state, nonlinear irreversible thermodynamics approach 0-44154  
 polymer melt, particulate mixing, fluid dynamics, rheological and energetic considerations 0-43686  
 polymer melts, elongational properties, microscopic stretch history 0-23981  
 polymer melts, flowing, irreversibility assumption of network disentanglement, effects on elastic recoil predictions 0-6006  
 polymer melts, meas. of elongation props. with universal extensional rheometer 0-6004  
 polymer melts, quasistatic bulk strength meas., specially built apparatus 0-7737  
 polymer network, crosslinks and trapped entanglements, two-network model 0-38962

## viscoelasticity continued

- polymer network, Riemann's metric degeneration to graph metric demonstration, chain entanglement problems 0-38963  
 polymer network formation, relaxational props. variation 0-38961  
 polymer network in solution, free energy of deform. 0-38900  
 polymer viscoelasticity and strength characterisation, advanced light scatt. techniques 0-11857  
 polymeric materials, inelasticity degrees estimation, hysteresis friction model appl. rel. to US testing 0-3136  
 polymeric systems, fluid, rheology, characterised by mol. int. distrib., review 0-1504  
 polymeric systems, supported on inert substrates, dynamic thermomech. study 0-55623  
 polymers, and their solns., dynamic storage and loss compliances determ. from creep data 0-5948  
 polymers, entangled, ternary blends of monodisperse homopolymers, viscoelastic props. 0-19301  
 polymers, fluid, harmonic distortions, under nonlinear periodic deform. 0-28482  
 polymers, fraction exponential function use for viscoelastic behaviour (*Russian*) 0-53652  
 polymers, viscoelastic, deform., depth of polymerisation 0-40414  
 polymers with periodic deform., longitudinal flow 0-6008  
 polystyrene, partial draining of low-molecular weight polymers with flexible chains 0-23592  
 polystyrene, swollen network in benzene, pendent chains, influence on thermodynamic and viscoelastic props. 0-28481  
 polystyrene amorphous film, cyclically fatigued, molecular behaviour 0-35310  
 polystyrene melt, linear viscoelastic props. influence of molecular wt. distrib. 0-19309  
 polystyrene melts, stresses and birefringence in intermittent shear flows 0-19308  
 polyurethane, filled, relation between static and dynamic deform. characts. 0-3137  
 polyvinyl acetate, partial draining of low-molecular weight polymers with flexible chains 0-23592  
 porous bodies, stresses induced by drying, elastoviscoplastic model, finite element anal. 0-23904  
 prefluorinated polymer, DuPont Krytox 143-AB, viscoelastic and dielectric props. 0-1503  
 PVC, plasticised, fatigue, fractographic study 0-30101  
 PVC, plasticised, fatigue crack growth charact. 0-30100  
 Rayleigh problem, similarity soln. for totally automorphous model (*German*) 0-28426  
 red cell membrane, temp. dependence of viscoelastic recovery 0-40979  
 rheonomic viscoelastic materials, under prolonged loading, failure hypothesis 0-3180  
 rigid ellipsoidal particles in external field, dil. suspension, rheological eqns. (*Ukrainian*) 0-48661  
 rod, conical, nonlinear viscoelastic materials, soln. using generalised correspondence principle 0-38288  
 rod, forced longitudinal oscillations, thermomechanical coupling effect 0-19274  
 rod, shock rel. to hard obstacle (*Russian*) 0-23911  
 rubber, network, highly swollen, long time dynamics 0-38291  
 rubber, network entanglement contrib. 0-39203  
 rubber network elasticity, mol. theory 0-38290  
 rubbers, swollen, low-freq. dynamics, optical and mech. props. 0-43626  
 SH waves due to shearing-stress discontinuity in viscoelastic half-space, displacement 0-56405  
 shell, thin cylindrical, stiffened with viscoelastic rings, vibr. damping characts. 0-28452  
 shells, axisymm., transient vibrations 0-10179  
 simple liquids, collective motion 0-24329  
 skeletal muscle mechanical props. and model, contractile force depend. (*Japanese*) 0-56091  
 skin components, rheological props. under compressive load 0-35945  
 skin rheological behaviour, expt. results and struct. model 0-16968  
 solid, linear quasi-static theory, variational and minimum principles 0-10157  
 solid viscoelastic body, motion relative to centre of mass (*Russian*) 0-53649  
 spherical particle, free-fall rate in immobile liq. 0-19302  
 spine, intervertebral disc material, human, viscoelastic response obs. 0-51141  
 spring rod, vibration heating, amplitude depend. (*Ukrainian*) 0-38301  
 stability problems 0-27133  
 steel ingot, state of viscoelasticoplastic stress deformation, in process of solidification (*Russian*) 0-45295  
 stratified material, compressed, stress determ. (*Rumanian*) 0-28434  
 strength and stability of viscoelastic structures, method of solving integral eqns. used 0-10167  
 stress field for half-space in randomly varying temp. field (*Ukrainian*) 0-33467  
 stress-strain behaviour, mathematical simulation for viscoelastic material (*German*) 0-1442  
 stress/strain relationships, fluctuations 0-17802  
 strip, flat, stationary bending plane determ., under moving load (*German*) 0-1446  
 structure damping for noise control, evaluation of viscoelastic props. 0-43632  
 styrene-acrylonitrile copolymer, amorphous, rubbery state, nonequil. tensile deform., effects of temp. and strain 0-40442  
 styrene-butadiene block copolymers, in dil. soln., extrapolation methods for intrinsic viscosity 0-24636  
 styrene/MMA copolymers, struct. and rheology 0-1444  
 subcritical growth of cracks in thin viscoelastic plates 0-28465  
 surface waves on standard linear viscoelastic solid 0-28461  
 synovial fluid, normal and pathological 0-16966  
 technical fabrics, viscoelastic compliance, appl. of stress-time analogy method 0-1497  
 tetrafluoroethylene-vinylidene fluoride mixture, in epoxide-diphenylene propane resin, exam. of temp. depend. of stress relaxation, viscoelasticity 0-11688  
 thermoplastic elastomers, crosslinked by secondary valence interactions, elasticity and processing, crosslinking behaviour 0-40320  
 thermoviscoelastic media, dynamical problems, Volterra method generalisation 0-33481  
 thermoviscoelastic transient responses, stability and accuracy of finite element solns. 0-5951



**viscoelasticity continued**

- thermoviscoelastic-plastic materials, constitutive reln. 0-58  
 thermoviscoelasticity, heat liberation effect in deformable linear medium 0-33484  
 thermoviscoelasticity, linear bound, minimum principle (*Ukrainian*) 0-33468  
 thin walled systems, stability (*Russian*) 0-1452  
 transitional flow of viscoelastic medium, lag time eval. 0-38371  
 triblock copolymer, model for rheology 0-23979  
 tube, porous, nonlinear viscoelastic materials, soln. using generalised correspondence principle 0-38288  
 two-layered beam, vibrational analysis, with unconstrained viscoelastic layer damping (*Japanese*) 0-5968  
 variational and minimum principle applications (*Japanese*) 0-48599  
 viscoelastic fluid, flow anal. between 2-D surfaces subject to normal high freq. oscillations 0-16493  
 vitreous humour, human, in vivo obs. 0-56077  
 wave propagation, nonperiodic, in compressible elastico-viscous fluid 0-43724  
 wedge, plane, nonlinear viscoelastic materials, soln. using generalised correspondence principle 0-38288  
 Al-SiC fibre reinforced materials, therm. stresses in unit cell 0-10160  
 C fibre reinforced epoxy resin, transverse creep compliance, time and temp. depend. (*Japanese*) 0-45358  
 C paste, viscoelastic props., depend. on coke grain size 0-1501  
 CaCO<sub>3</sub> filled polymer melts, viscous props. 0-19311  
 Si<sub>3</sub>N<sub>4</sub>-MgO, compressive creep, source of viscoelastic effect 0-50675  
 YIG, phonon viscosity effect on dislocation motion 0-24450

**viscometers**

see also viscosity measurement

- aperiodic industrial for non-Newtonian fluid (*Russian*) 0-53897  
 electrostatic, development based on investigation of damping of vibrating grid in viscous medium 0-38308  
 Rankine-type capillary viscometer, for gases (*Japanese*) 0-14859  
 rotational viscometer, non-Newtonian fluid viscosity measurement 0-19529  
 spinning drop interfacial viscometer, liquid-gas interface, surface viscosity meas. 0-44395  
 vibrating, for measurement of viscosity of slurries, assessment 0-28586  
 viscometric data from Brookfield RVT viscometer, conversion to shear stress-shear rate relationship 0-1495

**viscoplasticity** see plasticity**viscosimeters** see viscometers**viscosity**

see also electroviscous effect; internal friction; viscosity of gases; viscosity of liquids

- acoustic field in stratified media of variable viscosity, Green's functions 0-4545  
 acoustic wave propagation in isotropic viscous weakly compressible medium, eqn. limits problem (*French*) 0-8808  
 aerodynamics, high Reynolds number, global approach and coupling approach 0-48742  
 approximate viscosity matrix, differential-difference representation 0-31518  
 B<sub>2</sub>O<sub>3</sub>-SiO<sub>2</sub> glass, surface flattening kinetics by sinusoidal profile decay method (*Japanese*) 0-34284  
 biomembrane fluidity, influence on activity of bound enzymes, book contrib. 0-30688  
 convection rates of viscous fluid, Earth upper mantle and continental drift appl. (*Russian*) 0-1581  
 cylinder, circular, wake of steady flow at different Reynolds numbers 0-38416  
 dipolar dumbbells in a viscoelastic Oldroyd liquid, dilute soln., electric field effect on rheological behaviour 0-6009  
 dislocation segments, pinned, effects of viscosity on quantum motion (*Russian*) 0-44207  
 ferroelectric narrow walls, steady-state motion 0-11356  
 gas flows, selfgravitating, thermodynamic processes and radiation, numerical method 0-14848  
 glass, flat, dependence of creep, viscosity on cooling intensity, during quenching 0-20964  
 glass, solidification kinetic eqn., derivation from heat transfer and viscosity eqns. 0-25679  
 glass with frozen structure, viscous flow, valence configuration flow theory 0-39335  
 gravity waves, non-uniform free surface, superficial viscosity and tension (*French*) 0-48728  
 ice surface layer, viscosity, from thermal contraction meas., 0 to -50°C 0-49469  
 incompressible turbulence, statistical investigation of eddy viscosity 0-14675  
 intracellular membrane microviscosity, rat liver and hepatoma 27 0-30675  
 Invar N36 melt, cast metal struct. depend. on heat treatment, subgrain struct. (*Russian*) 0-40343  
 LPDE melt, tensile stress overshoot in uniaxial extension, single integral constitutive eqn. 0-1507  
 lubricant, shear rheological behaviour at high press. 0-35342  
 micropolar fluid drop in viscous fluid, flow, stream functions, velocities, spins, drag 0-53821  
 minerals, effect of viscosity on release adiabatic meas. 0-51388  
 Navier-Stokes eqn. discontinuities, appl. of distributions (*French*) 0-6022  
 ocean, vertical eddy viscosity effects on Rossby and Eady waves 0-51404  
 optical waveguides, inhomogeneous glass sintering, self stresses producing bulk flow 0-14448  
 overthrust faulting, model of const. thickness overthrust on visco-plastic sole 0-51378  
 oxides at high temperatures, crystalline and non-crystalline, surface mass transport mechanisms obs. (*Japanese*) 0-54479  
 photoemulsions, gels, coloured component addition, struct. form., dynamic shear modulus, viscosity meas. (*Russian*) 0-7871  
 PMMA, solvent cast, surface characts., chromatographic study 0-20020  
 polybutadiene, hydrogenation 0-26008  
 polybutadiene rubber, modified with oligoester acrylate, plastic-elastic and rheological props. (*German*) 0-19871  
 polymer melts, rheological props., effects of hydrostatic press. 0-48663  
 polymer solutions, dilute and moderately concentrated, intrinsic viscosity 0-48753  
 porous medium immiscible viscous displacement, stability anal. 0-48799  
 second virial viscosity coefficient, temp. depend. 0-19543

**viscosity continued**

- silicate glasses, viscosity-temp. relation 0-2187  
 slow viscous flow due to motion of sphere on axis of circular cone 0-14654  
 sludge, cohesive, dynamic props. (*Japanese*) 0-45580  
 stars, rigidly rotating, secular instabilities due to viscosity 0-4342  
 stars, rigidly rotating, secular instabilities in general relativity due to viscosity 0-4341  
 statistical mechanics, response theory for systems nonlinearly displaced from equilibrium, graphical approach 0-22285  
 steel, austenitic Mn-Ni ageing, alloying element influence on struct. and mechanical props. (*Russian*) 0-35256  
 steel, martensitic low C, development and props. (*Russian*) 0-20933  
 Stokes flow, attached and free eddies 0-48679  
 suspensions, heavily filled, viscosity relations 0-48776  
 turbulent viscosity in stellar convection zones, effect of rot. 0-36612  
 ultrasound resonance absorption by moving dislocation 0-54318  
 vinyl alcohol-vinyl acetate copolymers, mol. architecture and physicochem. props. 0-44103  
 BaGeO<sub>3</sub>-(0.25MgF<sub>2</sub>·0.75YF<sub>3</sub>)-Ga<sub>2</sub>O<sub>3</sub> glass, synthesis and props. 0-25648  
 Co<sub>2</sub>Ge<sub>3</sub>, solid and liquid, physicochemical props. and structure 0-39548  
 Fe<sub>40</sub>Ni<sub>40</sub>P<sub>14</sub>B<sub>6</sub> metallic glass, isothermal viscosity and crystn. 0-49395  
 H plasma, viscosity calcs. (*Russian*) 0-53953  
 K<sub>2</sub>O-Al<sub>2</sub>O<sub>3</sub>-P<sub>2</sub>O<sub>5</sub> glass, low-temp. viscosity 0-39198  
 LiF-NaPO<sub>3</sub>-MeF<sub>x</sub> (Me=Mg, Ca, Al) glasses, IR spectroscopy study 0-16042  
 Na<sub>2</sub>O-Al<sub>2</sub>O<sub>3</sub>-P<sub>2</sub>O<sub>5</sub> glass, low-temp. viscosity 0-39198  
 Ni<sub>2</sub>Ge<sub>3</sub>, solid and liquid, physicochemical props. and structure 0-39548  
 PbO containing crystal glasses, viscosity, effects of Li<sub>2</sub>O, BaO, ZnO, MgO and SrO 0-19973  
 PbO containing crystal glass, viscosity-temp. depend., glass transition, and softening point 0-24637  
 PbO-SiO<sub>2</sub>, surface flattening kinetics by sinusoidal profile decay method (*Japanese*) 0-34284  
 SiO<sub>2</sub>, vitreous, heat treatment effect on viscosity and struct. 0-19714  
 SiO<sub>2</sub>-Al<sub>2</sub>O<sub>3</sub>-CaO-MgO-Na<sub>2</sub>O-K<sub>2</sub>O effect of partial substitution of Na<sub>2</sub>O by K<sub>2</sub>O, on crystallisation 0-10499  
 TiN, thermoplastic slips, viscosity, thixotropy, dilatance determs. 0-25633  
 ZnB<sub>2</sub>O<sub>4</sub>-MF<sub>2</sub> (M=Mg, Ca, Sr, Ba) glass system, physicochem. props. 0-34877

**viscosity measurement**

see also viscometers

- flow injection analyser, microprocessor-based 0-33713  
 gas, Rankine-type capillary viscometer (*Japanese*) 0-14859  
 non-Newtonian, aperiodic industrial viscometer (*Russian*) 0-53897  
 oxide melts, at 1000 to 1750°C, methods survey (*Slovak*) 0-47079  
 polymers, conc. solns. in volatile solvents, high temps., method for viscosity meas. 0-19535  
 rolling bottle device, for measuring flow of liqs. and powders 0-6174  
 rotational viscometer, non-Newtonian fluid viscosity measurement 0-19529  
 slurries using vibrating viscometers, assessment 0-28586  
 viscometric data from Brookfield RVT viscometer, conversion to shear stress-shear rate relationship 0-1495  
 Fe-Al liquid alloys, apparatus for viscosity meas. (*Czech*) 0-29103  
 Hg vapour, viscosity and thermal cond. meas., data anal., 694-1054K 0-19545  
 Hg vapours, vibr. disc method, 620-800K 0-19530

**viscosity of gases**

- atmospheric wave propag., viscous diffusion, heat loss damping mechanism 0-56516  
 n-butane-N<sub>2</sub>(CO<sub>2</sub>) mixtures, viscosity, diffusion coeffs. 0-1722  
 critical fluids, non-Newtonian effect and normal stress effect 0-49396  
 dilute gas mixtures, transport props., calc. prog. 0-10342  
 ethane-CO<sub>2</sub>(N<sub>2</sub>)(SF<sub>6</sub>)(tetrafluoromethane) mixtures, viscosity, diffusion coeffs. 0-1722  
 fluids at evaluated pressures 0-2191  
 gas flow, through ultrafine capillaries 0-6151  
 low-pressure gas discharge, mean free path and viscosity, mag. field effects 0-24282  
 nonlinear shear viscosity in steady Couette flow 0-28588  
 nonstationary viscous flow of thermally conductive gas around semi-infinite plate, numerical anal. 0-6104  
 propane-N<sub>2</sub>(CO<sub>2</sub>) mixtures, viscosity, diffusion coeffs. 0-1722  
 spinning drop interfacial viscometer, liquid-gas interface, surface viscosity meas. 0-44395  
 steam, low and moderate density, compressibility factor and viscosity coeff. eqn. 0-33722  
 symmetric top molecules, viscosity and thermal cond. under simultaneous elec. and mag. field 0-6188  
 viscous gas flow, subsonic and supersonic, simplified Navier-Stokes eqns. 0-31520  
 water, vap., averaged potential for complex polar fluids 0-48833  
 Ar and Ar-NH<sub>3</sub> mixtures, viscosity under press., density depend. and mol. assoc. 0-1727  
 Ar<sub>2</sub>, interatomic potential single parameter 0-48059  
 CO<sub>2</sub>, viscosity, density expansion near critical temp. 0-53909  
 CO<sub>2</sub>, viscosity meas. at low temps. 0-6193  
 He, dense gas, transport eqns., shear viscosity and acoustic vel., quasi-particle kinetic eqn. calcs. 0-53906  
 He+Ar, interatomic pot. well depth, SPFD pot., diffusion, viscosity and second virial coeff. 0-5599  
 Hg vapour, viscosity and thermal cond. meas., data anal., 694-1054K 0-19545  
 Hg vapours, viscosity meas. by vibr. disc method, 620-800K 0-19530  
 N<sub>2</sub>O, viscosity meas. at low temps. 0-6193  
 Na, vapour, viscosity meas., 1101-1186K, 0.2-0.8 bar 0-1723  
 SF<sub>6</sub>, viscosity meas. at low temps. 0-6193

**viscosity of liquids**

see also lubrication

- acetic acid-acetone mixture, physical parameters 0-2716  
 Al-Si (2.4 wt.%), liq. fluidity, solid-liq. coexisting zone (*Japanese*) 0-15175  
 alcohols, assoc. liq., viscous props. 0-2186  
 alcohols, H-bond system, liq., high-press. effect 0-49080  
 alkali, chlorides, aqueous solns., high precision viscosity meas. 0-10695  
 N-alkylpyridium halides, molten, and mixtures with AlCl<sub>3</sub>, density, elec. cond. and viscosity meas. 0-24630  
 alloy, binary liq., viscosity coeffs. by Enskog theory 0-1920



## viscosity of liquids continued

- binary liquid systems, apolar-apolar and polar-apolar, significant structure theory, appl. 0-1909  
 binary polymeric mixtures, soln. viscosities meas. 0-54423  
 blood, rheological parameters for viscosity, viscoelasticity and thixotropy 0-16963  
 blood oscillatory flow, Fahraeus-Lindqvist effect 0-3668  
 blood plasma, reduced viscosity in joggers rel. to non-joggers 0-16967  
 blood rheology, clinical changes in peripheral vascular disease and smokers 0-16965  
 blood viscosity and red cell aggregation under near-zero gravity 0-3660  
 blood viscosity factors and functions, clinical appls. 0-3664  
 butadiene-acrylonitrile copolymer liquid, viscosity (*Japanese*) 0-39334  
 2-chloro-p-nitroaniline, in benzene soln., dipole moment from solute relax. time-solvent viscosity relation 0-37905  
 classical simple liq., long-time anomalies suppression, Ar(Rb) appls. 0-24339  
 coolants and index matching media for Nd:glass laser systems 0-33015  
 critical fluids, non-Newtonian effect and normal stress effect 0-49396  
 dense one-component systems, low-temp., kinetic phenomena, shear viscosity (*Russian*) 0-10694  
 DOBAMBC, chiral smectic C-phase ferroelectric liq. crystal film, classical X-Y system, props. 0-44123  
 dye laser, pulsed, light polarisation, solvent viscosity effect 0-32977  
 elastohydrodynamic contact, rheological model 0-33544  
 electrolyte mixtures in aq. soln., viscosity contrib. coeffs. (*German*) 0-15287  
 (ethylene-co-vinyl alcohol)-g-ethylene oxide graft copolymers, sol. behaviour 0-19682  
 Fermi liquid viscosity in finite geometry 0-24702  
 fluids at evaluated pressures 0-2191  
 gelatin gels, coloured component addition, struct. form., dynamic shear modulus, viscosity meas. (*Russian*) 0-7871  
 glass devitrification, heat treatment parameters determ. from viscosity changes (*Polish*) 0-40404  
 glass transition rel. to press. depend. of viscosity 0-34171  
 glass-forming, viscous flow and valence config. theory 0-14756  
 glass-forming melts, window, glass-transition temps. from viscosity temp. depend. 0-34113  
 hyaluronate solns., cooperative phase transitions, review 0-45850  
 isobutyric acid and water, shear viscosity of critical mixture, amplitude ratios 0-2188  
 liquid theories, validity, agreement with pertinent experimental fact 0-38881  
 liquid-glass transition, free volume approach, thermodynamic behaviour 0-1940  
 macromolecule liquid, translational friction coeffs. of rigid, symm. top mols. 0-6003  
 metals, calc. using microinhomogeneous struct. model (*Russian*) 0-15284  
 methane-Ar, cryogenic fluid mixture, transport phenomena, shear viscosity (*Russian*) 0-29198  
 methylcyclohexane, dense liq., self-diffusion and viscosity 0-15278  
 microemulsions, aerosol OT, inhomogeneous interior, fluoresc. and polarisation decay probes 0-50891  
 microemulsions, phase diagram and homogeneity gap, light scatt. and viscosity meas. 0-16736  
 mixture, of dense simple fluids, bulk viscosity, hard spheres appl. 0-14982  
 molecules, spheroid-cylindrical, dynamics in dilute soln. 0-44090  
 mucus mechanical props. rel. to mucociliary transport, effect of pharmacologic interventions 0-3663  
 3-nitro-o-anisidine, in benzene soln., dipole moment from solute relax. time-solvent viscosity relation 0-37905  
 nitrobenzene, in acetone-isopropanol soln., Rayleigh scatt. and viscosity 0-5550  
 non-linear model, constitutive equation testing with free. vol. relax. spectrum 0-6011  
 non-Newtonian liquids, Rayleigh classical equation generalisation 0-19444  
 p-phenitidine, in benzene soln., dipole moment from solute relax. time-solvent viscosity relation 0-37905  
 polar molecule/nonpolar solvent, dielec. relax. computation from viscosity data 0-11330  
 poly(aminiophosphate)s, mol. wts., and cond. studies 0-14264  
 poly-N-benzamide, lyotropic liq. crystals, viscosity anisotropy 0-10693  
 polyacrylamide solutions, viscous behaviour 0-2185  
 polyamide mixtures, thermodynamically incompatible, composition-prop. relationship (*Russian*) 0-7872  
 polyazomethines, dil. soln. props. 0-19972  
 polybutadiene, hydrogenated, linear and star branched, melt rheology 0-23978  
 polyelectrolytes, translating, electrolyte friction theory 0-29194  
 polyethylene, foam growth, thermomech. anal. 0-3416  
 polyethylene, linear, melt rheology 0-23976  
 polyethylene, low density melts, temp. depend. of the elongational behaviour 0-6012  
 polyethylene melts, low-density, viscosity and viscoelasticity, filler effect 0-10222  
 polyisobutylene solutions, viscous behaviour 0-2185  
 polymer melt, polydispersity, estimation from rheological data 0-6535  
 polymer solns., dilute, Hartree self-consistent field analysis 0-5648  
 polymer solution, dilute, chain mol. dynamics and transport processes 0-14989  
 polymer solution, intrinsic viscosity, mol. wt. and temp. dependence 0-34222  
 polymer solutions in nematic liquids, dilute 0-29199  
 polymer solutions viscosity rel. to mol. mass (*Russian*) 0-2190  
 polymeric solutions, viscous behaviour 0-2185  
 polymers, conc. solns. in volatile solvents, high temps., method for viscosity meas. 0-19535  
 polymers solns., cooperative phase transitions, review 0-45850  
 polymers with periodic deform., longitudinal flow 0-6008  
 polymethine cyanine dyes, viscosity depend. fluoresc. lifetime using synchronously operated ps streak camera 0-28041  
 polyoxymethylene-copolyamide mixtures, melt rheological props., extrudate microstruct. (*Russian*) 0-7530  
 polypropylene sulphide in athermal solvent, viscosity-temp. coeffs. 0-39333  
 polystyrene melt, carbon-black filled, rheological study 0-48665  
 polystyrene solutions, viscous behaviour 0-2185

## viscosity of liquids continued

- polystyrene-co-divinylbenzene microgels in dimethylformamide, diffusion coeff., viscosity and mol. wt. meas. 0-30286  
 polystyrene-mineral oil mixture, viscosity and normal stress coeff. 0-44349  
 PVC, plasticised, foam growth, thermomech. anal. 0-3416  
 PVC plastisols, high resin level, rheological behaviour, discontinuous viscosity 0-23980  
 semiquantum liquids, viscosity and heat cond. temp. depend. (*Russian*) 0-34260  
 sodium tetraborate glass, melt, temp. depend. of high viscosity property (*Russian*) 0-39336  
 soft spheres binary mixtures, equilib. and non-equilib. radial distrib. functions 0-49074  
 soft-sphere mixture viscosity, nonequilibrium mol. dynamics 0-19680  
 spinning drop interfacial viscometer, liquid-gas interface, surface viscosity meas. 0-44395  
 spirobenzopyran copolymer photochromic soln., photoviscosity effect 0-6536  
 styrene divinylbenzene, viscosity meas. during radical copolymerisation 0-3344  
 styrene-butadiene block copolymers, in dil. soln., extrapolation methods for intrinsic viscosity 0-24636  
 suspension, dil., of spherical particles in non-Newtonian liq., rheological behaviour 0-24058  
 tetraalkylammonium bromide soln., conductance and viscosity, temp. and concentration depend. 0-6531  
 tetrabutylammonium iodide, in aq. proline soln., elec. conductance investigation 0-10692  
 tetramethylammonium iodide, in aq. proline soln., elec. conductance investigation 0-10692  
 viscoelastic fluid, flow anal. between 2-D surfaces subject to normal high freq. oscillations 0-16493  
 viscoelastic non-Newtonian liquids, resist. to tensile stress 0-1505  
 water, multiparameter viscosity-temp. eqns. analysis 0-15283  
 water, nonfreezing thin interlayer between ice column and quartz capillary 0-54475  
 water viscosity changes close to quartz surface, fine capillary calcs. 0-54422  
 water viscosity changes effect on electrokinetic phenomena in capillaries 0-53867  
 Widom-Rowlinson hard-sphere mixture model, transport props. 0-14981  
 xanthane, dilute solns., viscosity rel. to temp., shear rate (*French*) 0-39332  
 Al alloys, liquid, kinematic viscosity temp. depend., porosity, H solubility, supercooling (*Russian*) 0-54425  
 Al, liquid, kinematic viscosity temp. depend., porosity, H solubility, supercooling (*Russian*) 0-54425  
 Al soap solutions, viscous behaviour 0-2185  
 Ar, dense fluid, viscosity, gaussian memory function approach 0-28904  
 Ar, kinetic phenomena, shear viscosity (*Russian*) 0-10694  
 BaPO<sub>3</sub>-F-Al<sub>2</sub>O<sub>3</sub>-B<sub>2</sub>O<sub>3</sub> glasses, viscosity in the softening region and crystn. range 0-29105  
 Bi<sub>2</sub>O<sub>3</sub>-SiO<sub>2</sub>-(GeO<sub>2</sub>), metastable phases form., crystn. conditions, melt viscosity and density effects 0-35167  
 CO<sub>2</sub>, viscosity near liquid-vapour transition point 0-2189  
 CaO-SiO<sub>2</sub>-MnO molten mixtures, struct. and phys. props. (*French*) 0-24635  
 CdCl<sub>2</sub>, aq. solns., sound absorpt. and relax. phenomena 0-49311  
 Co(II)-containing aq. electrolyte soln., nucl. mag. relax., hydration shell (*Russian*) 0-54966  
 Cr-Ge liquid and amorphous alloys, struct. props., cond., viscosity, surface tension (*Russian*) 0-54119  
 Cs, liquid, neutron diff. struct. anal., density and viscosity temp. depend. 0-6352  
 Cu tripolyphosphate complexes, electrolyte development for direct deposition of Cu 0-45246  
 D<sub>2</sub>O, assoc. liq., viscous props. 0-2186  
 Fe melt, oscillating viscometer viscosity meas. (*Czech*) 0-29103  
 Fe-Si (0-6 wt.%) melts, viscosity (*Russian*) 0-15285  
 FeO-Fe<sub>2</sub>O<sub>3</sub>-SiO<sub>2</sub> system, molten, struct. by high temp. X-ray diff. 0-49084  
 Fe<sub>2</sub>O<sub>3</sub>, flocculated suspension in ethylene glycol, intrinsic viscosity rel. to shear rate 0-1502  
 Fr, properties from melting point to 7500K, prediction (*Russian*) 0-44296  
 H<sub>2</sub>O, assoc. liq., viscous props. 0-2186  
 H<sub>2</sub>PO<sub>4</sub>-H<sub>2</sub>O, superviscous and glass, relax., <sup>111</sup>Cd TDPAC obs. 0-15831  
<sup>3</sup>He, superfluid, A-phase, viscosity tensor, generalised paramagnon model 0-39379  
<sup>3</sup>He, superfluid, dynamic orbital effects, US propag. and viscosity, book contrib. 0-2235  
<sup>3</sup>He-<sup>4</sup>He, liquid mixture, second sound, quantised vortex creation at contractions, excitation model 0-44383  
<sup>3</sup>He-<sup>4</sup>He, viscosity behaviour props. (*Russian*) 0-44382  
<sup>4</sup>He, liquid (*Russian*) 0-44382  
<sup>4</sup>He, superfluid, viscosity props. depend. on oscill. freq. 0-6576  
<sup>4</sup>He, superfluid, viscosity and thermal conductivity (*Russian*) 0-10720  
 Hf complex, Hf-EDTA 0-34837  
 HfOCl<sub>2</sub>, aqueous solns., rotational diffusion, TDPAC study 0-34837  
 Hg, liquid, ferromag., containing Fe particles, time depend. magnetisation 0-44877  
 KCl solution, nonfreezing thin interlayer between ice column and quartz capillary 0-54475  
 Kr, liq., US attenuation and bulk viscosity 0-49304  
 LiBr soln., conductance and viscosity, temp. and concentration depend. 0-6531  
 MnCl<sub>2</sub>-tetra-n-butylammonium halide melts, density, elec. cond., and viscosity 0-24631  
 NH<sub>4</sub>Br soln., conductance and viscosity, temp. and concentration depend. 0-6531  
 Ni-Al, diffusion coeff. differences, rotating-disc determ. 0-39330  
 Pb<sub>2</sub>Se<sub>2-x</sub> melts, viscosity and radial distrib. function for stoichiometric and peritectic comp. 0-1916  
 Ti<sub>2</sub>Te<sub>3</sub>, exam. of electrical props., in solid, liquid state 0-54686  
 YIG, garnet, high temp. solns., shear viscosity meas., rel. to LPE 0-10697  
 Zn-Cd liquid/Fe-Ni-Al mag. powder, effective viscosity of composites (*Russian*) 0-54424  
 ZnCl<sub>2</sub>-MCl (M=Li,Na,K,Cs), melt, viscosity meas. by oscillating cylinder method (*Japanese*) 0-10696



**visibility**

see also atmospheric optics; brightness; light transmission

- acetylene smoke particles, agglomerated, optical extinction meas. at 0.5145 and 10.6  $\mu\text{m}$  0-48155  
 astronomical observatories, dome seeing theory 0-12657  
 definition, confirmation using marine optics data 0-23633  
 grating, sine-wave, average-luminance surround effect 0-51092  
 interference fringe visibility and spacing, atmospheric turbulence effects 0-51572  
 Kitt Peak National Observatory, probability of clear daytime skies 0-12512  
 nephelometer visual range estimates, contrast brightness theory, operational theory 0-8424  
 pollution effects over SW United States, historical database 0-21424  
 Sacramento Peak Observatory night sky conditions, cloud cover, seeing and precipitable water 0-51653  
 transparent film on absorbing substrate, optimum angle of incidence for monochromatic interference 0-43254

**visible and ultraviolet spectra of inorganic solids**

- actinide compounds, spectroscopic techniques for electronic props. meas. 0-11427  
 alkali halides, absorption spectra, freq. and temp. depend. of vibr. bands 0-2787  
 alkali halides, doped, optical absorption and MCD spectra, Gaussian quadrature calc. 0-7367  
 alkali halides,  $F_A$ -centre optical absorpt., estimate using symmetry-adapted wave functions 0-11448  
 alkali lime germanosilicate glasses, optical absorpt. of transition metal impurities 0-2784  
 bimetallic cluster, photoselective bimetallic aggregation, review 0-53182  
 biotites, optical absorpt. bands 0-7371  
 borate glass: Ni, absorption spectra, mag. props., coordination behaviour (German) 0-40147  
 caesium uranyl propionate, low temp. absorpt., luminesc. spectra, intermol. interactions 0-2830  
 CdS film, polycryst., optical spectra, 0.5-6.5 eV 0-55212  
 chalcogenide glass films, photostructural changes, photodarkening 0-49121  
 $D^-$  centre in strong magnetic fields, optical absorpt. spectrum 0-20670  
 diamond: Sb, ion implanted, defect study using optical absorpt. and EPR 0-24480  
 diamond, GR1 and UV band, fine struct. 0-20678  
 diamond, optical absorption and luminesc. spectra, review 0-2848  
 diamond, optical absorption lines, GR4 and GR8, effect of uniaxial stress 0-34956  
 diamond, role of electron-hole interaction in optical spectra, review 0-45113  
 diamond, UV absorpt. produced by substitutional  $N_2$  pairs 0-29770  
 dielectric crystal, phase transitions, laser spectrometry, use of diamond anvil devices (Japanese) 0-49362  
 F-centre optical absorption bandshape calc. for transition to state with Jahn-Teller and spin orbit couplings 0-55135  
 Gd, optical conductivity meas., 0.5-3.1 eV (Russian) 0-45100  
 glass, coloured, toughening process, spectral characts. 0-43416  
 glass, multicomponent Schott, proton-induced colouring 0-9974  
 glass, photochromatic, induced colour by optical/thermal treatment 0-34954  
 glass, photochromic, spectral characts. control 0-16073  
 glass fibre waveguide,  $\gamma$ -irrad., reversible optical bleaching of induced absorpt. 0-14462  
 gradient index material models and exptl. verification 0-16002  
 graphite intercalation compounds, band struct. model, dynamical dielec. function, reflectivity 0-34348  
 graphite-alkali metal intercalation cpds., electronic props. 0-45202  
 II-VI semiconductor, two-photon and two-step absorption of light 0-7389  
 II-VI semiconductors, zinc blende and wurtzite struct., two photon spectra, quantitative investigation 0-50373  
 inorganic molecular crystals, metal complexes electronic spectra and intermolecular interactions 0-55137  
 IV-VI semiconductors, two photon spectra, quantitative investigation 0-50373  
 manganese aluminosilicate glass, insulating spin glass, exchange dipole optical transition 0-40136  
 metaphosphate glasses,  $n(M_2O.P_2O_5).(1-x)Y_2O_3.xTb_2O_3.3P_2O_5$ ,  $M=Li, Na, K$ , excitation and emission spectra 0-40150  
 microcrystals on C foil, size distrib. from electron micrograph obs., UV absorpt. spectra obs. 0-55121  
 $NH_4Al(SO_4)_2.12H_2O:MnO_4^-$ , visible and UV absorpt. spectra interpretation 0-45116  
 phosphate glass: Ni, absorption spectra, mag. props., coordination behaviour (German) 0-40147  
 polarised electronic absorption spectrum at 300 and 77K, phys. chem. lab. expt. 0-17774  
 quartz glass, spectral absorpt., 3000-4000K 0-25401  
 rare earth complexes, formation and props., book contrib. 0-43204  
 rare earth element sulphides, condensates, struct. and optical transmittance 0-20727  
 rare earth oxides, binary, struct. and props., book contrib. 0-45292  
 rare earth titanates, pseudoperovskite struct., nonlinear spectral and luminesc. characts. 0-29771  
 refractory metal films, evaporated, optical props., rel. to struct. 0-55211  
 rocks from Cr-rich areas, visible and near IR spectra, remote sensing appls. 0-4000  
 rubidium uranyl propionate, low temp. absorpt., luminesc. spectra, intermol. interactions 0-2830  
 ruby,  $Cr^{3+}$  ion doped, R-line region, absorpt. spectrum, dispersion rel. to mag. field 0-2732  
 ruby, optical free induction decay modulation and absorpt. line struct. due to superhyperfine interaction 0-33091  
 sapphire, 14.8 MeV neutron damaged, optical vibronic absorption spectra 0-50384  
 sapphire, synthetic and natural, optical spectra comparison and identification 0-40138  
 semiconducting films, exciton polariton attenuation, spatial dispersion effect 0-20097  
 semiconductors, magnetic, electron spectrum, light absorpt. spectrum, calcs. 0-2793  
 silicate Fe activated glass, diffraction trating recording by UV laser 0-5842  
 sodium uranyl acetate (deuteroacetate) 0-2830

**visible and ultraviolet spectra of inorganic solids continued**

- solid-liquid transition, optical reflectance spectra 0-24569  
 solids, XUV photoabsorpt. spectra, at. effects 0-2785  
 $TTT_2(I_3)_{1+x}$ , physical props., elec., mag. and optical meas. 0-24908  
 Ag, electroreflectance spectroscopy, longitudinal surface plasmons 0-40137  
 Ag film, evaporated, chemisorption effects on reflectance and elec. resist. 0-11495  
 Ag, single cryst. electrodes, electroreflectance obs. in aqueous solns. 0-25342  
 Ag-Al<sub>2</sub>O<sub>3</sub>-Au structure, electrorefl. meas. (French) 0-50366  
 AgCl photochromic glass, additional absorpt. spectrum, ellipsoidal model of colour centres 0-40142  
 $\beta$ -AgI (4H), visible spectra, reflected light phase and amplitude, exciton resonance 0-45110  
 $\beta$ -AgI thin film, exciton spectrum 0-55216  
 Al<sub>0.9</sub>Ga<sub>0.1</sub>As, press. coeff. of direct band gap from optical absorpt. meas. 0-11430  
 Al<sub>0.9</sub>Ga<sub>0.1</sub>As-GaAs, CW 300k quantum-well heterojunction laser, optical and injection pumping operation 0-5735  
 AlNH<sub>4</sub>(SO<sub>4</sub>)<sub>2</sub>·Cr<sup>3+</sup>, optical spectral, crystal field, spin orbit and exciton interactions 0-34958  
 $\alpha$ -Al<sub>2</sub>O<sub>3</sub>, additively coloured single crystal, luminescence (Russian) 0-55169  
 $\alpha$ -Al<sub>2</sub>O<sub>3</sub>, crystal defects from X-ray irradiation, F-centres, X-ray luminesc. obs. 0-55176  
 $\alpha$ -Al<sub>2</sub>O<sub>3</sub>:Co,H, Co and proton ENDOR, IR and optical spectra charge compensator nature and defect struct. 0-44956  
 Al<sub>2</sub>O<sub>3</sub>:Cr<sup>3+</sup>, shock compression, absorpt. spectra 0-20675  
 $\alpha$ -Al<sub>2</sub>O<sub>3</sub>:Er(Cr), crystal defects from X-ray irradiation, F-centres, X-ray luminesc. obs. 0-55176  
 Al<sub>2</sub>O<sub>3</sub>:Ni anodised films, electrolytically coloured, spectrally selective surface 0-11490  
 As-S glasses, acousto-induced structural changes, optical props. 0-49122  
 As<sub>2</sub>S<sub>3</sub> glass, press. effect on optical props. 0-50363  
 As<sub>2</sub>S<sub>3</sub> amorphous film, photoinduced changes in optical props. 0-50445  
 As<sub>2</sub>S<sub>3</sub> chalcogenide glass thin films, absorption in range of large optical densities (Russian) 0-11428  
 As<sub>2</sub>S<sub>3</sub>-Te<sub>x</sub>, ternary chalcogenide glassy system, optical absorpt., mag. susceptibility and AC cond. meas. 0-55125  
 As<sub>2</sub>Se<sub>3</sub>, amorphous, time resolved meas. of photoinduced optical absorpt. and photocond. 0-49807  
 As<sub>2</sub>Se<sub>3</sub>, lone-pair semiconductor, defect chemistry 0-25421  
 B:H amorphous CVD films, IR, visible, and near UV optical props. 0-50442  
 B<sub>12</sub>C<sub>x</sub>, phonon energies and electronic props., x depend., refl. spectra and thermoelec. power meas. 0-16052  
 BaF<sub>2</sub>, undoped and U-doped, neutron irrad., absorpt. band attributed to F<sub>2</sub>-centres 0-7380  
 BaF<sub>2</sub>:Pr<sup>3+</sup>, wavelength and temp.-modulated UV absorpt. 0-2799  
 BaF<sub>2</sub>:U, absorption band spectra following neutron irrad. 0-29763  
 BaFCl crystals, F-centres, X- and  $\gamma$ -irradiation, thermoluminescence and optical absorption spectra 0-45155  
 BaO, logarithmic derivative reflectance spectra 0-11429  
 (Be, Al)B<sub>12</sub>, wide-gap semicond., elec. cond., refl. and absorpt. spectra 0-20188  
 Bi<sub>2</sub>Ge<sub>2</sub>O<sub>12</sub> crystals, doped with Dy<sup>3+</sup>, Ho<sup>3+</sup>, Er<sup>3+</sup>, Tm<sup>3+</sup>, Yb<sup>3+</sup>, growth, spectral and laser props. 0-45115  
 Bi<sub>2</sub>Ge<sub>2</sub>O<sub>12</sub>:Nd<sup>3+</sup> and Bi<sub>2</sub>Si<sub>3</sub>O<sub>12</sub>:Nd<sup>3+</sup> crystals, absorpt. and luminesc. spectra, 4.2-300K 0-34957  
 BiI<sub>3</sub>, layered compound, exciton spectra, surface and stacking fault effects 0-40134  
 Bi<sub>2</sub>SiO<sub>20</sub>, visible and UV refl. and absorpt. spectra 0-34950  
 $\beta$ -Cu<sub>2</sub>V<sub>2</sub>O<sub>5</sub>, mag. and spectroscopic study, semiconductor to metal transition 0-2628  
 Cu<sub>2</sub>O high press. phase transforms, optical and X-ray studies 0-44313  
 CaF<sub>2</sub>:CaO, optical scatt., absorpt. at 205 nm 0-20669  
 CaF<sub>2</sub>:Ce<sup>3+</sup>, absorpt. peaks in the lowest 4f-5d band, effect of conc. 0-2798  
 CaF<sub>2</sub>:Dy crystal with M centre, antiresonance line, mag. field effect 0-55138  
 CaF<sub>2</sub>:Eu, oxidation and reduction of Eu, EPR and optical studies 0-25199  
 CaF<sub>2</sub>:Ho<sup>3+</sup>, site-selective spectroscopy 0-29791  
 CaF<sub>2</sub>:Na, single cryst., X-irrad., optical absorpt. and thermoluminesc. 0-34952  
 CaF<sub>2</sub>:Pr<sup>3+</sup>, wavelength and temp.-modulated UV absorpt. 0-2799  
 CaF<sub>2</sub>:Tb, spectra of radn.-induced defect form. 0-2801  
 CaSO<sub>4</sub> phosphors:Ce(Eu)(Dy)(Tm), gamma-irradiated valency conversions in rare-earth ions 0-55198  
 CaY<sub>2</sub>Mg<sub>2</sub>Ge<sub>2</sub>O<sub>12</sub>:Nd<sup>3+</sup>, optical absorpt. and fluoresc. intensities 0-29793  
 Cd<sub>1-x</sub>Mn<sub>x</sub>Te, exchange interaction, magneto-optical spectra 0-25348  
 CdCr<sub>2</sub>Se<sub>4</sub>, magnetic red shift origin, specular reflectivity, band struct. 0-40127  
 CdF<sub>2</sub>:Eu, role of solution and precipitation phenomena on ITC spectra 0-7265  
 CdGa<sub>2</sub>Se<sub>4</sub>, struct. of valence band, photocond. and reflection spectra meas. 0-6719  
 CdGa<sub>2</sub>Se<sub>4</sub>, thermorefectance and visible absorpt. spectra, energy gap, cryst. field splitting 0-34945  
 Cd,Hg<sub>1-x</sub>Te, band struct. and optical props. 0-15450  
 CdIn<sub>2</sub>S<sub>4</sub> film, vac. deposited, growth, struct., optical and photoelectronic props. 0-10831  
 CdIn<sub>2</sub>S<sub>4</sub>, photoconducting semiconductors, fundamental absorption edge 0-40130  
 Cd<sub>1-x</sub>Mn<sub>x</sub>Te mixed crystals, excitonic magnetoabsorption 0-40095  
 CdO-GeO<sub>2</sub>:TiO<sub>2</sub> photochromic glass for optical information retention media 0-33108  
 CdO-SnO<sub>2</sub> film, DC reactively sputtered, transparent electrode props., optimum sputtering conditions 0-11116  
 CdO-SnO<sub>2</sub> film, prep. by RF sputtering, elec. cond. and transparency 0-7492  
 CdPS<sub>3</sub>, layered, organometallic intercalates, X-ray diff., optical absorpt. and mag. props. 0-45103  
 CdS, A<sub>n-1</sub>-exciton, reflectance and thermorefectance spectra, spatial dispersion and angle of incidence effects 0-25409  
 CdS active surface, exciton stimulated emission and superradiance refl. spectra, props. 0-25411  
 CdS, exciton optical and luminescence spectra characts. near dislocation slip bands 0-45111



## visible and ultraviolet spectra of inorganic solids continued

- CdS, excitonic mol. transitions, optical gain and induced absorpt. spectra 0-11438  
 CdS, excitonic polariton reflectance, B-exciton and k-linear term 0-7369  
 CdS films, electrolessly deposited, annealing effect on optical spectra 0-2884  
 CdS, high intensity excited, exciton reflection spectra, reflection struct. 0-20692  
 CdS, influence of Lamb US waves on exciton spectra (*Russian*) 0-7374  
 CdS:Cu(In), two-photon and two-step absorption of light 0-7389  
 CdS:Li film, chemical bath deposited, photocond. and optical props. 0-2426  
 CdS:Li film, optical props. 0-2886  
 CdSe epitaxial layers, on GaP-CdS substrates, absorption and electroabsorption 0-40178  
 CdSe, excitonic mol. transitions, optical gain and induced absorpt. spectra 0-11438  
 CdSe, high intensity excited, exciton reflection spectra, reflection struct. 0-20692  
 CdSiP<sub>2</sub>, reflectance spectra at 300K 0-25407  
 CdTe film, low-resist., prep. by multi-source evaporation method, and characterisation 0-25582  
 CdTe, oscillatory magnetoabsorpt. spectra 0-40096  
 CdTe, spatial dispersion rel. to exciton reflection spectra (*Russian*) 0-40126  
 CdTe, time-resolved spectra, carrier relax. time, phonon lifetime 0-11433  
 CdTe:Fe(Ni), luminesc. and refl. spectra, high temp. annealing effects 0-24472  
 CdTe-Te film, prep. by combined hot-wall-flash evaporation method, and characterisation 0-55296  
 Co<sub>1-x</sub>Fe<sub>x</sub>Si, elec. and optical props. 0-49740  
 CoO-MgO-Cr<sub>2</sub>O<sub>3</sub>-Fe<sub>2</sub>O<sub>3</sub>-TiO<sub>2</sub>, form. and colour of spinel solid soln. (*Japanese*) 0-16059  
 Cr<sub>2</sub>O<sub>3</sub>/γ-Fe<sub>2</sub>O<sub>3</sub>/Pt electrode, two layer oxide surface film anal. by modulation spectroscopy (*Japanese*) 0-11491  
 Cs, UV absorpt. spectra 0-2780  
 CsBr, temp. depend. of Cs colloids absorption bands 0-40145  
 Cs<sub>2</sub>CrCl<sub>6</sub>, thermo-optical spectroscopy, detection by mirage effect 0-47116  
 CsCuCl<sub>3</sub>, cryst., gyrotropy, anomalous dispersion curves 0-2719  
 CsF, F-centre optical absorption bandshape calc. for transition to state with Jahn-Teller and spin orbit couplings 0-55135  
 CsFeS<sub>2</sub>, crystal ligand field theory, band assignment, absorpt. spectra study 0-20657  
 CsI, temp. depend. of Cs colloids absorption bands 0-40145  
 Cs<sub>2</sub>NaTmCl<sub>6</sub>, UV absorpt. spectra, mag. circular dichroism spectra, vibr. obs. 0-29758  
 Cs<sub>2</sub>O-Ag photocathode, light absorption and photoemission 0-50510  
 Cs<sub>2</sub>O-B<sub>2</sub>O<sub>3</sub>:Ti<sup>3+</sup>(Pb<sup>2+</sup>)(Bi<sup>3+</sup>) glass, optical basicity, variation with probe ion and comp. 0-2800  
 CsPbBr<sub>3</sub>, electronic and optical props. 0-25414  
 CsPbCl<sub>3</sub>, electronic and optical props. 0-25414  
 CsPbCl<sub>3</sub>Br<sub>1-x</sub>, optical meas., LCAO band scheme 0-25437  
 Cu complex, catena-μ-isothiocyanato-(N'-pyridyl)methylene-N'-salicyloylhydrazinato-NN'O copper (II), EPR and visible spectra 0-5566  
 Cu complex with L-phenylalanine amino acid, ESR spectra and magnetic susceptibility measurement 0-34761  
 Cu halides two photon spectra, quantitative investigation 0-50373  
 Cu, single cryst. electrodes, electroreflectance obs. in aqueous solns. 0-25342  
 Cu-Ni, optical absorption and photoemission spectra 0-45216  
 CuBr, biexciton two-photon absorpt. 0-11432  
 CuBr, exciton absorpt. band shape, dielectric const. real part derivatives (*Russian*) 0-25413  
 CuBr, P exciton fine struct. 0-20091  
 CuBr(Cl)(I), energy bands, relativistic KKR method, UV absorpt. spectra 0-39501  
 CuCl, biexciton two-photon absorpt. 0-11432  
 CuCl, optical absorption under press. 0-34949  
 CuCl, two-photon absorpt. and luminesc., biexcitons 0-11434  
 CuFeS<sub>2</sub>, single crystal, optical reflectivity spectrum 0-40129  
 CuGaTe<sub>2</sub>, elec. and optical props. 0-6829  
 Cu<sub>2</sub>O, energy band interactions under uniaxial compression 0-25412  
 Cu<sub>2</sub>O, even-parity excitons assignment, from two-photon spectrum 0-6731  
 Cu<sub>2</sub>O, sample thickness depend. of exciton polariton absorption coeff. 0-34941  
 Cu<sub>2</sub>S, polycryst. thin films, struct., optical and elect. props. for solar energy appl. 0-10837  
 DyIG, magneto-optical absorption, near IR 0-40094  
 EsCl<sub>3</sub>(Br)<sub>3</sub>(I)<sub>3</sub>, prep., characterisation and decay of Es(II) 0-16727  
 EuO<sub>1-x</sub> films, Faraday effect dispersion rel. to electronic struct., visible and IR spectra 0-45162  
 EuS films, ferromag., optical spectra and light scatt. from spin waves 0-16116  
 Eu<sub>1-x</sub>Sr<sub>x</sub>S, exciton refl. spectra 0-2782  
 (Fe, Ti) silicate glasses, optical absorption and Mossbauer spectra 0-55136  
 Fe, interband optical conductivity, self energy correction 0-2792  
 Fe-Cr, passivation films, modulation spectroscopy study 0-3244  
 FeBO<sub>3</sub>, mag. linear dichroism and absorpt. spectra, Jahn-Teller effect 0-54662  
 Fe<sub>2</sub>O<sub>3</sub>, haematite, anal. of refl. spectrum by Kramers-Kronig relations 0-16058  
 Fe<sub>2</sub>O<sub>3</sub>, magnetite, charge carriers, optical props. 0-34874  
 GaAs, amorphous sputtered films, hydrogenated, photoinduced optical absorpt. 0-50362  
 GaAs, CC Ga-3d-excitation, high resolution reflectivity down to 15K 0-25415  
 GaAs, donor van der Waals interactions, spectral lineshapes 0-11450  
 GaAs epitaxial layers, polariton wave packet propag. in exciton reson. 0-2345  
 GaAs, exchange interaction, analytical and nonanalytical parts, from polariton spectra in mag. fields 0-50367  
 GaAs, optical absorption spectrum dynamics using sub-ps. optical pulses 0-11431  
 GaAs, time-resolved spectra, carrier relax. time, phonon lifetime 0-11433  
 GaAs:Cr, luminescence and absorption spectra, temp. depend. of fine structure 0-6779  
 GaAs:O, annealing effects, optical absorpt. and I-V characts. 0-29037

## visible and ultraviolet spectra of inorganic solids continued

- n-GaAs-Ga<sub>1-x</sub>Al<sub>x</sub>As, superlattice, subband struct. and optical spectra, self-consistent calc. 0-15443  
 GaAs<sub>1-x</sub>P<sub>x</sub>, electron irradi., radiation defects annealing 0-29059  
 GaN:Zn, VPE grown, optical cross sections, photoluminesc. and optical absorpt. meas. 0-55160  
 GaP, electron irradi., radiation defects annealing 0-29059  
 GaP:Cu, elec. and optical props., rel. to doping and heat treatment 0-16056  
 GaS, reflectivity from 4 to 32 eV, Kramers-Kronig anal. 0-34943  
 GaSb films, amorphous and cryst., vac. evaporated, Elec. cond. thermoelec. power and optical absorpt. 0-2504  
 GaSe, electron-phonon interaction and optical props. 0-34942  
 GaSe, excitation spectra and structural props., X-ray Laue diagrams and optical transmission (*French*) 0-50358  
 GaSe, exciton-phonon bound state, photocond. and visible absorpt. spectra obs. 0-50369  
 GaSe excitonic spectra fine struct., reflection and transmission spectra (*Russian*) 0-55126  
 GaSe, optical excitation, excitonic spectra, stimulated luminesc. 0-40132  
 GaSe, reflectivity from 4 to 32 eV, Kramers-Kronig anal. 0-34943  
 GaTe, exciton polariton effect on absorpt. edge, absorpt. and refl. spectra, 4.2 to 300K 0-20664  
 GaTe, exciton polariton effect on absorpt. edge, thickness depend. of absorpt. 0-20665  
 GaTe, excitonic absorpt. edge, transmission and refl. meas. 0-40133  
 Gd-La alloy, optical freq. cond. in 0.5-3.1 eV range, paramag.-ferromag. transition 0-29761  
 GdAlO<sub>3</sub>:Er<sup>3+</sup>, <sup>4</sup>S<sub>3/2</sub> to <sup>4</sup>I<sub>9/2</sub> transition laser action, optical and luminescence spectra 0-16082  
 Gd<sub>3</sub>Ga<sub>2</sub>O<sub>7</sub>:Nd<sup>3+</sup>, optical absorpt. and fluoresc. intensities 0-29793  
 Ge, amorphous sputtered films, hydrogenated, photoinduced optical absorpt. 0-50362  
 Ge-S-Ga(In) system glasses, photoinduced changes 0-24365  
 Ge-Se, amorphous, photocond., photo-induced ESR, optical edge shift 0-49809  
 GeFe<sub>2</sub>O<sub>4</sub>, single crystals, elec. and mag. props, optical absorpt. spectra 0-54719  
 GeO film, optical props., rel. to possible appl. in holography 0-29816  
 GeS<sub>2</sub> glass, melt quenched, reversible photostructural change, optical transmission spectra obs. 0-45109  
 Ge<sub>20</sub>Sb<sub>25</sub>S<sub>55</sub> glasses, optical props., absorption edge temp. depend. 0-2789  
 GeSe, single crystal, optical absorption 0-25383  
 GeSe<sub>2</sub>, amorphous film, laser induced light absorpt. oscillation, exciton model 0-50446  
 GeSe<sub>2</sub>, amorphous film, photocond., photo-induced ESR, optical edge shift 0-49809  
 Ge(111)2X1, oxide layer, surface states detect optical reflectivity obs. 0-50368  
 Hg<sub>0.75</sub>Cd<sub>0.25</sub>Te, single crystal, reflection spectra 0-40140  
 Hg<sub>0.75</sub>Cd<sub>0.25</sub>Te, thermoref. spectra, effect of excitons on E<sub>1</sub> and E<sub>1</sub>+Δ<sub>1</sub> structs. 0-16057  
 Hg<sub>1-x</sub>Cd<sub>x</sub>Te, two-photon absorpt. spectra 0-20660  
 α-HgS, cinnabar, reson. Raman effect and luminesc. meas. 0-50338  
 Ho<sub>2</sub>O<sub>3</sub>, photoacoustic spectra using Helmholtz reson. cells 0-9048  
 In<sub>0.9</sub>Ga<sub>0.1</sub>As, epitaxial solid soln. film, spectral depend. of transparency, absorpt. spectra calcs. 0-45161  
 In<sub>0.9</sub>Ga<sub>0.1</sub>Se single crystals, exciton absorption spectra 0-20663  
 InN film, specular reflection spectra, lattice parameters 0-7428  
 InP, exchange interaction, analytical and nonanalytical parts, from polariton spectra in mag. fields 0-50367  
 InP, reflection spectra, optical functions, exciton peaks (*Russian*) 0-50372  
 InP:Fe, Hall and resistivity meas., optical absorpt. 0-10990  
 InSb, film, E<sub>0</sub>, E<sub>1</sub> absorption edge size quantisation, optical and electroreflectance spectra 0-34998  
 InSb, two-photon absorpt. spectra 0-20660  
 InSb-CdTe solid solns., electroreflectance spectra, Brillouin zone transitions 0-7330  
 γ-InSe, fundamental absorpt. edge 0-2781  
 InSe, optical props. from 2-25 eV 0-29760  
 InSe, reflectivity and low energy absorption 0-34944  
 InSe, reflectivity from 4 to 32 eV, Kramers-Kronig anal. 0-34943  
 InSe, spin orbit split off valence bands, exciton transitions, Hopfield's quasibound model, visible absorpt. spectrum 0-50370  
 In<sub>2</sub>Te<sub>3</sub> film thermal deposition, transmission spectra and elec. cond. (*Russian*) 0-49555  
 K, UV absorpt. spectra 0-2780  
 KAl(SO<sub>4</sub>)<sub>2</sub>·12H<sub>2</sub>O:MnO<sub>4</sub><sup>-</sup>, visible and UV absorpt. spectra interpretation 0-45116  
 KBr, efficiency of V<sub>K</sub>- and Ag<sup>0</sup>-centres generation (*Russian*) 0-39080  
 KBr, electron irradiated, defect accumulation kinetics of low temps. 0-10577  
 KBr, pulse radiolysis of metastable interstitial centre of high temp. 0-20658  
 KBr:Ag, optical absorpt. spectra interpretation mol. orbital scheme 0-20671  
 KBr:In<sup>3+</sup>, B-band, optical absorpt. and mag. circular dichroism calcs. 0-29765  
 KBr:In<sup>3+</sup>, optical absorption and MCD spectra, Gaussian quadrature calc. 0-7367  
 KBr:Na(Rb)(Cs), microcrystalline powders, isothermal decay of colour centres 0-2804  
 KCl, photo-induced F-centres, hologram recording 0-28174  
 KCl, thermal and photothermal conversion of colour centres, after high-dose electronic interaction (*Russian*) 0-39156  
 KCl:Ag, optical absorpt. spectra interpretation mol. orbital scheme 0-20671  
 KCl:Ba(Sr), Z-centre, luminesc. and absorpt. spectra obs. 0-49221  
 KCl:Ca(Ba)(Mg)(Sr), microcrystalline powders role of Z centres in stabilising coloration, optical absorption 0-54227  
 KCl:Eu<sup>2+</sup>, lattice defect equilib. optical absorpt. and cond. studies 0-29767  
 KCl:Pr<sup>3+</sup>(Sm<sup>3+</sup>), absorption spectra at 4.2 K, anal. 0-7378  
 KCl:SnCl<sub>2</sub>, X-ray irradi., polarised luminesc. and EPR study of Sn<sup>3+</sup> centres 0-39868  
 KCl:Ti<sup>3+</sup> cryst., A band, mag. field effect 0-34897  
 KCl:Ti<sup>2+</sup>, optical absorpt. spectra interpretation mol. orbital scheme 0-20671  
 KCl-KH, F- and U-centre redistrib. at end of proton tracks, microspectrophotometric anal. 0-10583



## visible and ultraviolet spectra of inorganic solids continued

- KCl-Mg, thermolum. of Z-centre, optical absorpt. 0-55203  
 KClO<sub>3</sub>Br<sub>2</sub>:Ca, X-ray irr., Z<sub>1</sub>-centres, thermoluminesc. and optical absorpt. meas. 0-16108  
 KCl(Br)(I) with alkali and halogen impurities, colour centre deformation induced nonradiative decay 0-7387  
 KCl(Br)(I):Eu<sup>2+</sup>, single cryst. optical absorpt. spectra 0-45117  
 KF, F<sub>2</sub><sup>+</sup>-centre excited-state absorption spectrum, rel. to H<sub>2</sub><sup>+</sup> model 0-16066  
 KF(Br)(Cl)(I), K<sup>+</sup>3p core excitons, refl. spectra study, low temp. 0-29759  
 KFeS<sub>3</sub>, crystal ligand field theory, band assignment, absorpt. spectra study 0-20657  
 KI, piezo-optical study of excitons 0-16055  
 KI, quenched, absorpt. and emission spectra, α-centres 0-11442  
 KI: Pb<sup>2+</sup>, UV absorpt. and mag. circular dichroism spectra 0-25418  
 KNdP<sub>4</sub>O<sub>12</sub>, laser emission cross sections, fluorescence spectra, radiative lifetimes, quantum efficiency 0-23694  
 K<sub>2</sub>O-BaO-SiO<sub>2</sub>:Nd<sup>3+</sup> glasses, absorption and fluoresc. spectra, density 0-25417  
 KZnF<sub>3</sub>:Ni<sup>2+</sup>, Mn<sup>2+</sup>, interference transition electric dipole mechanism 0-34896  
 K<sub>2</sub>S<sub>3</sub>, condensates, struct. and optical transmittance 0-20727  
 La compounds, plasma light reflection by free charge carriers 0-11403  
 La<sub>2</sub>Be<sub>2</sub>O<sub>7</sub>:Nd<sup>3+</sup>, optical absorpt. and fluoresc. intensities 0-29793  
 LaCl<sub>3</sub>:U<sup>3+</sup>(5f<sup>3</sup>), polarised absorption spectra and energy levels 0-16063  
 LaF<sub>3</sub>:Pr<sup>3+</sup>, optical transition, spin decoupling and magic angle line narrowing 0-28286  
 LaF<sub>3</sub>:Pr<sup>3+</sup>, ultrahigh resolution photon echo spectroscopy 0-28285  
 LaF<sub>3</sub>:Pr(Nd)(Sm)(Eu)(Gd)(Dy)(Ho)(Er)(Tm), cryst. field anal. of triply ionised ion spectra 0-2796  
 LiBr:Cu<sup>2+</sup>(Ni<sup>2+</sup>)(Co<sup>2+</sup>)(Fe<sup>2+</sup>)(Mn<sup>2+</sup>), optical absorpt., charge transfer spectra 0-2797  
 LiCl:Cu<sup>2+</sup>(Ni<sup>2+</sup>)(Co<sup>2+</sup>)(Fe<sup>2+</sup>)(Mn<sup>2+</sup>), optical absorpt., charge transfer spectra 0-2797  
 LiF, TLD-100, trapping centres, optical absorpt. spectra defect and thermolum. mechanism models 0-50436  
 LiF:Mg,Ti crystals, Z<sub>2</sub>-centres, correlation of thermoluminescence and optical absorption 0-45154  
 LiF:OH crystals, X-irradiated, H centres formation and annealing 0-54226  
 Li<sub>0.5</sub>Fe<sub>2</sub>O<sub>4</sub>, magneto-optical spectra, polar Kerr rotation, dielectric tensor elements spectra 0-40091  
 Lil crystal, irradiated at low temps., optical absorption spectra 0-45123  
 Lil:Ti, absorpt. spectrum obs. 0-50378  
 LiNbO<sub>3</sub>:Cu<sup>2+</sup>, EPR and optical spectra 0-20453  
 LiNdP<sub>4</sub>O<sub>12</sub>, laser emission cross sections, fluorescence spectra, radiative lifetimes, quantum efficiency 0-23694  
 Li<sub>2</sub>O-B<sub>2</sub>O<sub>3</sub>:Ti<sup>3+</sup>(Pb<sup>2+</sup>)(Bi<sup>3+</sup>) glass, optical basicity, variation with probe ion and comp. 0-2800  
 LiSO<sub>4</sub>H<sub>2</sub>O:Cr<sup>3+</sup>, single cryst., EPR and optical absorpt. spectra 0-39855  
 LuAlO<sub>3</sub>:Er<sup>3+</sup>, <sup>4</sup>S<sub>3/2</sub> to <sup>4</sup>I<sub>9/2</sub> transition laser action, optical and luminescence spectra 0-16082  
 (Mg, Fe)SiO<sub>3</sub>, orthopyroxenes, cation distrib., electronic and Mossbauer spectra 0-7370  
 MgF<sub>2</sub>:Co<sup>2+</sup>(Mn<sup>2+</sup>), Coulomb and exchange interaction consts. optical spectra line assignment, new technique 0-45124  
 Mg(NH<sub>4</sub>)<sub>2</sub>(SO<sub>4</sub>)<sub>2</sub>·6H<sub>2</sub>O:Cr<sub>2</sub>O<sub>7</sub><sup>2-</sup>, optical absorption study, Cr<sub>2</sub>O<sub>7</sub><sup>2-</sup> and CrO<sub>4</sub><sup>3-</sup> centres 0-55128  
 Mn ferrites, Fe-excess, charge carriers, optical props. 0-34874  
 MnAs<sub>0.88</sub>P<sub>0.12</sub>, excitonic absorpt., derivative refl. spectra 0-25406  
 MnAu<sub>2</sub>, helical antiferromagnetic compound, optical props. and electronic struct., visible and IR obs. (French) 0-45101  
 Mn<sub>2</sub>Fe<sub>3</sub>-O<sub>4</sub>, optical props. 0-20606  
 (Mo, V<sub>1-x</sub>)<sub>2</sub>O<sub>5</sub>, mag. and spectroscopic investigation 0-25206  
 Na, UV absorpt. spectra 0-2780  
 Na-Fe fluorophosphate glass, Mossbauer study, mag. and optical props. 0-16065  
 NaBr:Ag<sup>+</sup>, UV absorption bands, temp. depend. 0-20672  
 NaBrO<sub>3</sub>, dispersion of Faraday effect 0-2731  
 NaCl, absorpt. spectra, influence of elec. field 0-2794  
 NaCl crystals irr. by high electron doses, annealing, colour centre prod., absorpt. spectra study 0-2074  
 NaCl:Ag, absorpt. spectra, influence of elec. field 0-2794  
 NaCl:Ca, Z<sub>1</sub> centre thermoluminescence study 0-16109  
 NaCl:Eu<sup>2+</sup>, single cryst. optical absorpt. spectra 0-45117  
 NaCl:Pr<sup>3+</sup>(Sm<sup>3+</sup>), absorption spectra at 4.2 K, anal. 0-7378  
 NaCl:V<sup>2+</sup>, elec. field effect on Z-like centres spectrum 0-2802  
 NaClO<sub>4</sub>, dispersion of Faraday effect 0-2731  
 NaF film on ZnSe plate, absorption coeff. ATR spectroscopy 0-35000  
 NaF: Mn<sup>2+</sup>, VUV absorpt. spectrum and EPR 0-55142  
 Na<sub>2</sub>MoO<sub>4</sub>(S<sub>4</sub>)(Se<sub>4</sub>) crystals, charge transfer spectra of MoX<sub>4</sub><sup>2-</sup> complexes 0-54658  
 NaNdP<sub>4</sub>O<sub>12</sub>, laser emission cross sections, fluorescence spectra, radiative lifetimes, quantum efficiency 0-23694  
 Na<sub>2</sub>O-B<sub>2</sub>O<sub>3</sub>:Au glasses, Au solubility, oxidation state and opt. absorpt. 0-44321  
 Na<sub>2</sub>O-B<sub>2</sub>O<sub>3</sub>:Cu<sup>2+</sup>+ZZ 0-34760  
 Na<sub>2</sub>O-BaO-SiO<sub>2</sub>:Nd<sup>3+</sup> glasses, absorption and fluoresc. spectra, density 0-25417  
 Na<sub>2</sub>O-CaO-SiO<sub>2</sub> glass, electronic struct. and optical props. 0-2790  
 Na<sub>2</sub>O-SiO<sub>2</sub> glass, electronic struct. and optical props. 0-2790  
 Na<sub>2</sub>WO<sub>3</sub>, metallic, optical and electronic props. 0-24398  
 Nd<sub>2</sub>(MoO<sub>4</sub>)<sub>3</sub>, thermo-optical spectroscopy, detection by mirage effect 0-47116  
 Ni, interband optical conductivity, self energy correction 0-2792  
 Ni, optical consts., influence of temp. and relation to bandstruct. 0-25403  
 Ni, optical spectrum, anomalous temp. depend. around T<sub>c</sub>, band struct. 0-40128  
 Ni-pigmented anodic Al<sub>2</sub>O<sub>3</sub>, for selective absorpt. of solar energy, optical and struct. props. 0-55892  
 Ni(H<sub>2</sub>V)<sub>2</sub>(H<sub>2</sub>O)<sub>2</sub>, synthesis and characterisation (French) 0-45225  
 PbBr<sub>2</sub>, red luminesc., absorpt. spectra 0-2831  
 PbCl<sub>2</sub>:NaCl, trapped exciton states, absorption spectra 0-50383  
 PbI<sub>2</sub> crystals, exciton condensation, excitation and luminesc. study 0-55182  
 PbI<sub>2</sub>, exciton absorpt. band shape, dielectric const. real part derivatives (Russian) 0-25413  
 PbI<sub>2</sub>, excitons in spatially dispersive medium, absorption theory 0-54618

## visible and ultraviolet spectra of inorganic solids continued

- PbI<sub>2</sub>, layered compound, exciton spectra, surface and stacking fault effects 0-40134  
 PbI<sub>2</sub>, visible exciton spectrum, exciton-phonon interactions, dielectric const. and oscill. strengths 0-25405  
 PbI<sub>2</sub>:KI, trapped exciton states, absorption spectra 0-50383  
 PbO-B<sub>2</sub>O<sub>3</sub>:Cu<sup>2+</sup>, glasses, ESR and optical absorpt. 0-34760  
 PbO-SiO<sub>2</sub> glass, electronic struct. and optical props. 0-2791  
 PbSe<sub>0.5</sub>S<sub>0.5</sub>, valence band struct., absorpt. spectra, elec. props. 0-44505  
 PbTe very thin epitaxial films, transmission and refl. spectra, 1 to 5 eV 0-7430  
 Pdl<sub>n</sub>, refractive index, reflectivity and band struct., APW calcs. 0-40139  
 Pr compounds, plasma light reflection by free charge carriers 0-11403  
 Pr(OH)<sub>3</sub>, low temp. heat capacity, thermophys. props. optical spectra, anal. of Schottky contributions, review 0-24611  
 Pt evaporated film, optical props. meas. in VUV, 220 to 150 Å 0-45159  
 PtO<sub>2</sub>, sputtered film, optical props. under H<sub>2</sub> reduction 0-20728  
 Rb, UV absorpt. spectra 0-2780  
 RbCl:Eu<sup>2+</sup>, tetragonal sites, spin Hamiltonian parameters, EPR and UV absorpt. spectra obs. 0-50177  
 RbCl(Br):Eu<sup>2+</sup>, single cryst. optical absorpt. spectra 0-45117  
 RbFeS<sub>3</sub>, crystal ligand field theory, band assignment, absorpt. spectra study 0-20657  
 Rb<sub>2</sub>MnCl<sub>4</sub>, layer antiferromag., optical absorpt., temp. and mag. field depend. 0-20661  
 Sbl<sub>3</sub>, layered compound, exciton spectra, surface and stacking fault effects 0-40134  
 Si, amorphous, doping and absorption edge 0-29042  
 Si, amorphous, photostructural changes, photodarkening 0-49121  
 Si amorphous film, film, glow discharge deposited, refl. spectra and dielec. function 0-50360  
 Si, amorphous sputtered films, hydrogenated, photoinduced optical absorpt. 0-50362  
 Si, CVD prepared solar thermal absorber, temp. variation of absorpt. edge 0-12028  
 Si, continuum-exciton effect in optical spectrum 0-25416  
 Si, free carrier and interband absorpt. at 1.06 μm, temp. depend. 0-2783  
 Si, glow discharge amorphous film, reflectance and transmittance (Japanese) 0-34995  
 Si, glow discharge deposited, optical spectra, reflectance, dielectric function and oscillator strength 0-11492  
 Si, ion irr., temp. and dose depend. of defect profiles 0-29097  
 Si, role of electron-hole interaction in optical spectra, review 0-45113  
 Si, surface roughness evaluation by UV refl. 0-39393  
 Si:H amorphous film, prop. by glow discharge deposition, and plasma parameter effects on props. 0-45240  
 Si:H amorphous films, photoinduced optical absorpt. and photocond. 0-50361  
 Si:H(B)(P), amorphous, UV absorpt. spectra 0-25420  
 SiC(6H), ion-implanted, laser-induced recrystallization and defects 0-44221  
 SiN<sub>x</sub> film, plasma deposited, comp. and characterisation, optical and elec. props. 0-15401  
 SiO<sub>2</sub> glass, electronic struct. and optical props. 0-2790  
 Si(111)2X1, oxide layer, surface states detec., optical reflectivity obs. 0-50368  
 (Sn)<sub>x</sub>, superconducting polymer, elec. cond., heat capacity and optical props. 0-7028  
 SnS<sub>2</sub>(Se<sub>2</sub>), optical transitions from d core levels 0-45105  
 SrF<sub>2</sub>:Pr<sup>3+</sup>, wavelength and temp.-modulated UV absorpt. 0-2799  
 SrO, logarithmic derivative reflectance spectra 0-11429  
 SrO, luminesc. band edge, 4-6.5 eV, optical absorpt., photoluminesc., cathodoluminescence, photocond. obs. 0-50411  
 SrO:Ni, optical absorption spectra in visible and near IR region 0-45119  
 SrTiO<sub>3</sub>, energy band struct., two-photon absorption spectra study 0-15453  
 TaSe<sub>2</sub> (2H), optical absorpt., band struct., plasmons, and CDW 0-45104  
 Tb complex, in Cs<sub>2</sub>NaTbCl<sub>6</sub>, f-f transitions, mag. dipole intensities, vibronic coupling model 0-25404  
 Te, valence band struct. under press., spin-orbit splitting, intraband absorpt. spectra 0-2330  
 TeO<sub>2</sub>, paratellurite, optical absorpt. and refl. spectra, 80-500K, optical consts. determ. 0-50359  
 Th, optical reflectivity 0-16054  
 ThBr<sub>4</sub>:U<sup>4+</sup>, absorpt. spectrum, zero phonon line (French) 0-11443  
 Ti, clean and oxidised surfaces, refl., 2-25 eV 0-55123  
 Ti-Ni, martensite transform. B2-B19', optical props. and electron struct. (Russian) 0-34878  
 TiO<sub>2</sub>, metal-semicond. transition, refl. spectra study 0-10880  
 TiCl<sub>3</sub>, role of electron-hole interaction in optical spectra, review 0-45113  
 TiGaS<sub>2</sub>Se<sub>2(1-x)</sub>, solid soln., fundamental optical absorpt. edge 0-25408  
 TmCrO<sub>3</sub>, optical-absorption spectra of Tm<sup>3+</sup> 0-20662  
 US, ferromagnet, electronic structure, reflectivity (German) 0-49567  
 US, optical props. and electronic struct. 0-25410  
 USb, reflectivity spectrum, band struct. 0-7368  
 Use (s) 0-16053  
 VO<sub>2</sub>, nonstoichiometry influence on electron struct. and metal-insulator phase transition 0-44507  
 V<sub>2</sub>O<sub>5</sub> film, amorphous, thickness, density and refr. index determ. from reflectance interference spectra 0-55206  
 V<sub>2</sub>O<sub>5</sub>, optical props. in metallic and semicond. phase 0-40135  
 W, chemisorbed H, surface cond. and intrinsic surface states, surface refl. spectra 0-15378  
 W-Fe spin glass, optical props. and electronic states 0-20412  
 Xe, crystalline, polarization effects, reflectivity, absorpt., and resonant luminesc. spectra calcs. 0-20095  
 YA-O<sub>3</sub>:Er<sup>3+</sup>, pulsed laser action, <sup>4</sup>S<sub>3/2</sub> to <sup>4</sup>I<sub>9/2</sub> transition laser action, optical and luminescence spectra 0-16082  
 YAlO<sub>3</sub>:Pr<sup>3+</sup>, ultrahigh resolution photon echo spectroscopy 0-28285  
 YIG, magneto-optical spectra, polar Kerr rotation, dielectric tensor elements spectra 0-40091  
 YIG, pure and Ga-substituted diffuse refl. and thermorefl. spectra near Curie point 0-40131  
 Y<sub>2</sub>O<sub>3</sub> sintered pieces, optical transmittance 0-40561  
 Zn<sub>0.1</sub>Cd<sub>0.9</sub>S, two-photon and two-step absorption of light 0-7389  
 ZnCs<sub>2</sub>(SO<sub>4</sub>)<sub>2</sub>·6H<sub>2</sub>O:VO<sup>2+</sup>, optical absorpt. spectra obs. 0-40146  
 ZnIn<sub>2</sub>S<sub>4</sub>, III(a) polytype, absorpt. spectrum tail changes due to microstructures 0-2788  
 ZnO, excitonic mol. transitions, optical gain and induced absorpt. spectra 0-11438  
 ZnO-B<sub>2</sub>O<sub>3</sub>:Cu<sup>2+</sup>, glasses, ESR and optical absorpt. 0-34760



# visible and ultraviolet spectra of inorganic solids continued

- Zn<sub>3</sub>P<sub>2</sub> bulk and thin film, UV reflectivity spectra, photovoltaic effects, optical consts. 0-25472
- Zn<sub>3</sub>P<sub>2</sub>, direct and indirect optical transitions, metal-Zn<sub>3</sub>P<sub>2</sub> contact photovoltage response 0-25402
- Zn<sub>3</sub>P<sub>2</sub>, single crystal, growth, electronic and device props. 0-25551
- ZnS:Mn<sup>2+</sup>, T<sub>2</sub> level, Zeeman splittings, Jahn-Teller effect 0-40141
- ZnSe crystal, exciton reflection spectra, control of exciton-free surface layer thickness 0-7373
- ZnSe, two-photon and two-step absorption of light 0-7389
- ZnSe:Cu, discovery of bound exciton, electroabsorption 0-45038
- ZnTe, refined, undoped, Cu acceptor, optical absorption and photoluminesc. meas. 0-34970
- ZnTe, reflectivity meas., double beam wavelength modulated technique (Korean) 0-50365
- ZnTe:Cr(Mn)(Fe), exciton refl. spectra 0-2806
- ZnTe:P, pure and doped, electron and exciton excited states of neutral donor 0-34393
- ZrS<sub>3</sub>, thermomodulated reflectivity and transmission 0-50357

# visible astronomical observations

- 13 Egeria, occultation of SAO 92603, photoelectric obs. rel. to minor planet possible satellite 0-46460
- 0406+121, optical spectra 4950-7950 Å, of possible BL Lacertae object 0-51895
- 0957+561 A, B, twin QSOs, spectroscopic obs. with multiple-mirror telescope 0-12827
- 0957+561A and B, twin QSOs, direct imaging rel. to gravit. lens interpretation 0-17686
- 1947 XC=1979 XA, positions, UVB photometry and ephemeris continuation 0-31233
- 1947 XC=1979 XA, precise positions, 1979 December 18 to 1980 January 5 0-31238
- 1979 VA, discovery of fast-moving asteroid 0-12703
- 1979 VA, precise positions, (1979 November 15 to 16) 0-26776
- 1979 VA, precise posns., and rotation period from UVB photometry 0-17534
- 1979 VA, precise posns., elements and ephemeris (1979 Nov.-1980 Jan.) 0-26777
- 1979 XA, fast-moving asteroidal object in Aries, discovery 0-26771
- 1979 XA, precise posns. (1979 Dec. 15 and 19) 0-31235
- 1979 XA (=1947 XC), discovery and precise positions (1979 December 13 to 15) 0-26774
- 1979 XB, precise positions, (1979 December 11 to 15) 0-46458
- 1979 XB, very fast-moving asteroidal object in Eridanus-Fornax, discovery and positions 0-26772
- 1979 YA, discovery and approx. posn. (1979 December 16) 0-26775
- 1979 YA, posn. for 1979 Dec. 20 and comet-like appearance 0-31234
- 1980 AA, discovery of fast-moving object in Gemini 0-41756
- 1980 AA, precise positions, 1980 January 16, orbital elements and ephemeris 0-36556
- β Canis Majoris star, photometric obs. 0-17595
- 2A 0311-227, complex emission line structure of spectroscopic binary 0-51915
- 2A 0311-227, high-speed photometry of AM Herculis-type binary 0-41912
- 2A 0526-328, high speed optical photometry 0-51917
- 2A 0526-328, optical photometry of assoc. star 0-22120
- 2 A 1052+606, X-ray and optical variability of RS CVn star 0-31331
- Abell 1831, statistical and photometric study of cluster of galaxies 0-51885
- Abell 30, Abell 78, planetary nebulae, unusual central struct. 0-51855
- ADS 4299, 8048 and 9352, parallaxes and masses for visual binaries 0-4402
- AE 1, He-rich variable, spectroscopy and photometry 0-41836
- RT Andromedae, eclipsing binary, three-colour photoelectric obs. and improved ephemeris 0-22043
- RT Andromedae, light curve anal. of short period eclipsing binary 0-46603
- σ Andromedae, rapid spectral line variability disproved 0-8625
- ET Andromedae (HR 8861), Ap star, light vars. and period 0-46571
- α Aquarii, Ca II K-line profile obs. rel. to chromospheric event 0-31299
- AE Aquarii, cataclysmic variable, rapid light oscills. rel. to white dwarf oblique rotator model 0-36634
- U Aquarii, R Coronae Borealis star, extraordinary comp. rel. to unusual s-processing event 0-17588
- R Aquarii, UVRI polarimetric obs., orbital motion effect (Russian) 0-36646
- U Aquilae, Cepheid variable, detect. as long-period binary by radial vel. spectrometer 0-51667
- 387 Aquitania, slow spinning asteroid with rot. period of nearly one day, photometric evidence 0-17529
- Arakelian 120, Seyfert 1 galaxy, UVB photometry, brightness and colour vars., models 0-26983
- 56 Arietis, spectrophotometry of Ap star, continuum features vars. 0-36638
- asteroid, 1980 AA, position Jan 20-22 1980 and ephemeris until Feb. 21st 0-31239
- asteroid, 1980 AA, rot. period observed photometrically 0-36558
- asteroid satellites, discovery from occultations of stars 0-4286
- asteroids, Crimean obs. (1963-76) (Russian) 0-46456
- asteroids, FK4 equinox corrections from meridian obs. 0-8519
- asteroids, light curve survey of faint objects 0-4283
- asteroids, Minor Planet Circulars, 3094 precise posns. 0-31241
- asteroids, Minor Planet Circulars 4937-5016, 3390 precise posns. 0-8580
- asteroids, Minor planet circulars 5017-5066, 669 precise posns. 0-17533
- asteroids, Minor Planet Circulars 5137-5188, 2067 precise posns. 0-46459
- asteroids, Palomar planet-crossing asteroid survey, 1973-1978 period 0-36539
- asteroids, rotation rates, pole positions and shapes 0-17531
- asteroids, Saratov obs. (1974 April-Oct.) (Russian) 0-46457
- asteroids, topocentric positions for 11 objects (Sept. 1977-Oct. 1978) (German) 0-46453
- atmospheric turbulence effects on optical and IR image form. (French) 0-46257
- IU Aurigae, eclipsing binary, two-colour photometry rel. to presence of third body 0-36669
- α Aurigae (Capella), orbital motion determ. using phase effect detect. at CERGA stellar interferometer (French) 0-36508
- B2 1308+326, optical and IR variability during 1978 outburst 0-51888

# visible astronomical observations continued

- BDS 1269, visual binary, metal abundances and characts. of components 0-4397
- Be stars, photometric behaviour, UV excess, emission indices, galactic distrib. 0-36637
- 776 Berbericia, slow spinning asteroid with rot. period of nearly one day, photometric evidence 0-17529
- binary galaxies, radial vels. and masses of 44 pairs 0-26990
- blue star in SNR 1006, spectral features and UVB photoelectric meas. 0-41830
- α Bootis, comparison of predicted and observed spectral energy distrib. 0-46546
- i Bootis, light curve and period vars. of W Ursae Majoris type star 0-4398
- SS Bootis, UVB obs. and Fourier anal., eclipsing RS Canum Venaticorum binary 0-17613
- α Bootis (Arcturus), spectral line asymmetry meas. rel. to Sun 0-51753
- Brno fireball (1977 Sept. 14), photographic data 0-41771
- 3C 286, quasar, optical absorpt. lines detect., redshift 0-4454
- 3C 33, 98, 184.1 and 218, rotation axes 0-26997
- 3C 345, optical spectrum variability 0-8709
- C- and M-type stars near globular cluster NGC 419 in SMC, cluster membership 0-26921
- Z Camelopardalis, dwarf nova, photometric obs. and light curve (1973-77) 0-56853
- 53 Camelopardalis, photometric vars. 0-4367
- α Camelopardalis (O9.5 Ia), variable Hα P Cygni profile 0-41818
- 38 Cancrī, δ Scuti star, UVB photometric obs. of variability 0-22021
- 49 Cancrī, spectrophotometry of Ap star, continuum features vars. 0-36638
- Canis Major R1, anomalous diffuse bands 0-51820
- α Canis Majoris (Sirius), Ca II K line high resolution profile obs. 0-56830
- RS Canum Venaticorum, intrinsic linear polarization of eclipsing binary 0-4394
- AM Canum Venaticorum, orbital period increase 0-12765
- Carina spiral feature, photometry and spectra rel. to stars and interstellar dust distrib. 0-51871
- θ Carinae, radial vel. of chemically-peculiar B-type star 0-8635
- Cassiopeia A supernova remnant, abundance inhomogeneities 0-12797
- γ Cassiopeiae, Be star, polarisation rapid vars. 0-22022
- RZ Cassiopeiae, eclipsing binary, spectroscopic orbit 0-22040
- AZ Cassiopeiae, long-period eclipsing system, photoelectric obs. 0-46608
- SU and TU Cassiopeiae, short-period Cepheids, photometry and spectra rel. to radius anomalies 0-26864
- 6 Cassiopeiae, spectroscopic obs. of supergiant star, equivalent widths, microturbulence and radial vel. 0-22006
- cataclysmic variables, visual continuum flux distrib. 0-36636
- V553 Centauri, C rich Cepheid, spectrum and photometry rel. to C and N abundances 0-4378
- BV Centauri, dwarf nova, identification as spectroscopic binary 0-51775
- V436 Centauri, dwarf nova, photometry during superoutburst (May 1978) 0-46570
- ω Centauri region, faint filamentary nebulosity obs. near globular cluster 0-56914
- EM Cephei, B-type eclipsing binary system, investigation of period and min. 0-17614
- δ Cephei, Hα radial vel. behaviour 0-51788
- U Cephei, period changes in 1972-7 interval 0-8657
- XY Cephei, photoelec. elements of semidetached binary system 0-31327
- DI Cephei, spectrum vars. in T Tauri star 0-8628
- VV Cephei, UVB obs. 0-17611
- 17=ξ Cephei A, speckle interferometry, visual orbital elements 0-56874
- VV Cephei system, distant, in Puppis, spectral classification, UVB photometry and polarimetry 0-51810
- Cepheid variable stars, short-period, radial vels., BVRI photometry, radii 0-31309
- classical Cepheids, nonvariable supergiants and bright giants, spectrophotometric comparison 0-56837
- ZZ Ceti stars search, photometric obs. of apparently quiescent stars 0-22005
- cluster of galaxies 0122-688, spectrographic obs., redshift 0-41906
- clusters of galaxies, radial number-density distrib. 0-8697
- Comet, Bradfield (1979), precise positions (1979 December 28 to 30) 0-31255
- Comet Arend-Roland (1957 III), visible and UV spectra anal. (Chinese) 0-12709
- Comet Bowell (1980b), discovery posns., elements and ephemeris 0-51695
- Comet Bowell (1980b), precise posn. and orbital evolution 0-56770
- Comet Bradfield (1979), 1980 March 4 magnitude and coma diameter 0-51696
- Comet Bradfield (1979), discovery posns. (1979 December) 0-31254
- Comet Bradfield (1979), obs. of precise position in 1980, 8th to 22nd Jan. 0-36572
- Comet Bradfield (1979), photographic obs. in 1980 23-4 Jan. 0-36574
- Comet Bradfield (1979), posns., elements and ephemeris (1980 Jan. 5-26) 0-31256
- Comet Bradfield (1979), precise props., orbital element and ephemeris (1979 Dec.-1980 Feb.) 0-26813
- Comet Bradfield (1979), spectra and visual obs. (1980 Jan.-Feb.) 0-41768
- Comet Bradfield (1979), visual obs. (1979 February 8 to 20) 0-46489
- Comet Kohler (1977 XIV), precise positions (1977 Oct.) (German) 0-46453
- Comet Kohler (1977 XIV), precise positions for 1977 Sept.-Dec. from photographic obs. 0-4302
- Comet Kohoutek (1973 XII), visible spectra, band intensity var., electrospectrophotometric meas. 0-8588
- Comet Meier (1978 XXI), photoelectric BV photometry rel. to opposition effect 0-31258
- Comet Meier (1979i), precise positions (1979 September 22 to 28) 0-4306
- comet Meier (1979i) total visual mag. estimates (1979 Sept.-Oct.) 0-8590
- comet West (1976 VI), emission bands and continuum flux heliocentric depend. 0-36575
- Comet West (1976 VI), polarisation of head 0-8587
- Comet West (1976 VI), spectrophotometry, emission bands and lines obs. 0-56768



## visible astronomical observations continued

- comets, Minor Planet Circulars, 42 precise posns. for eight objects 0-31241
- comets, Minor Planet Circulars 4937-5016, 122 precise posns. for 16 comets 0-8580
- comets, Minor planet circulars 5017-5066, 42 precise posns. for 11 objects 0-17533
- comets, Minor Planet Circulars 5137-5188, 41 precise posns. for seven objects 0-46459
- comets, precise posns. in 1974-6 period 0-46494
- comparison stars near OJ287 and ON325, variability, period determ. 0-26882
- cool stars, Ti isotopic abundance ratios 0-26840
- $\epsilon$  Coronae Austrinae, polarimetric obs. of eclipsing binary 0-56888
- R Coronae Borealis in quiet state, spectral energy distrib. (*Russian*) 0-51781
- CPD-26°389, central star of NGC 1360, radial vel. obs. 0-4350
- $\beta$  Crucis,  $\beta$  Canis Majoris star, photometric obs. 0-17595
- CTB 80, peculiar supernova remnant, central radio source optical and H I obs. 0-56896
- 65 Cybele, occultation of AGK3+19°599, 1979 October 17, obs. 0-31237
- SS Cygni, colour variations during dwarf nova outbursts 0-46576
- SS Cygni, dwarf nova, spectrophotometry rel. to accretion disc models in eruption and at min. light 0-36635
- V1016 Cygni, image-tube spectrograms 0-8639
- $\alpha$  Cygni, radial vel. and line profile vars. in supergiant 0-22010
- 57 Cygni, spectroscopic binary, search for systematic radial vel. anomalies 0-17617
- CH Cygni, symbiotic star, rapid and slow light vars. 0-51792
- 59=V832 Cygni, variable mass flux from spectroscopic obs. 0-41840
- $\beta$  Cygni, visual obs. of brighter component close companion 0-8663
- V1357 Cygni (Cygnus X-1), no long-term light vars. (1928-77) 0-41861
- V1341 Cygni (Cygnus X-2), shortest optical variability (*Russian*) 0-17695
- V1500 Cygni (Nova 1975), H $\alpha$  and H $\beta$  emission line vars. 0-4389
- V1500 Cygni (Nova 1975), light curve for 1975 Aug.-1977 July period 0-4372
- V1500 Cygni (Nova 1975), visible and UV spectra and light curve 0-12771
- V1668 Cygni (Nova 1978), linear polarisation obs. 0-26875
- V1668 Cygni (Nova 1978), photoelec. photometry, rapid flickering 0-36640
- V 1668 Cygni (Nova 1978), spectral development 0-51789
- V1668 Cygni (Nova 1978), UVB light curve 0-46565
- Cygnus Loop, radial distrib. of Fe X and XIV forbidden line emission 0-51828
- Cygnus OB2 number 12, spectral classification and membership of association 0-51760
- degenerate star candidates, photoelectric and spectroscopic obs. 0-12763
- Deimos, spectral evidence for carbonaceous chondrite surface comp. 0-41754
- HR Delphini (Nova 1967), cataclysmic binary spectrum 0-4359
- HR Delphini (Nova 1967), emission lines at nebular stage (*Russian*) 0-17597
- HR Delphini (Nova 1967), spectra, line identification, radial vel. obs. 0-17594
- $\delta$  Delphini stars in Michigan Spectral Catalogue, uvby $\beta$  photometry rel. to spectral types 0-4377
- diffuse interstellar line at 6284 Å, obs. and relation to interstellar reddening 0-51843
- S Doradus (HD 35343), luminous LMC supergiant, long time baseline VBLUW photometry 0-22007
- S Doradus (HD 35343), luminous LMC supergiant, long time baseline VBLUW photometry 0-36630
- 30 Doradus central object (HD 38268), interstellar and nebular lines obs. 0-51839
- 30 Doradus direction, unique interstellar Ca II K-line profile obs. 0-51850
- 30 Doradus nebula, in LMC, interstellar Ca II and Na I obs. 0-46643
- double galaxies, observational data on well-defined sample 0-17674
- double stars, Lick obs. of 254 pairs 0-8660
- double stars, measures of 120 visual pairs 0-56878
- double stars, obs. with Herstmoucheux 28-inch refractor, (1963-1970) 0-41863
- WW Draconis, RS Canum Venaticorum type star, two-colour photoelectric lightcurves and elements 0-46606
- BY Draconis, spotted flare star, spectra and photometry rel. to pre-main-sequence nature 0-36633
- CR Draconis, UV Ceti variable, flares colour behaviour 0-22020
- dwarf nova outbursts, colour vars. 0-46576
- dwarf novae, spectra (*Russian*) 0-8638
- dwarf novae, spectrophotometry, 1250-7500 Å region 0-46577
- early-type stars, northern intermediate galactic latit., H $\beta$  photometry, rel. to galactic struct. 0-36631
- faint early-type stars in neighbourhood of H II region RCW 38, UVB photometry 0-4352
- elliptical galaxies, photometric data on twists 0-56932
- 182 Elsa, photoelec. light curve and rot. period of asteroid 0-56750
- emission nebulae, first obs. with optical multichannel analysis of Sao Paulo University 0-26743
- emission-line stars in galactic cluster NGC 663, spectroscopic obs. 0-4363
- Enceladus, near IR spectra and JHK photometry 0-56761
- $\gamma$  Equulei, magnetic field obs. of Ap-star 0-51782
- WX Eridani light curves, period, orbital elements of eclipsing binary 0-26902
- ESO 012-G21, Seyfert 1 galaxy, spectrum, redshift, UVB photometry and X-ray identification 0-8695
- ESO 113-IG 45 (=Fairall 9), Seyfert galaxy, spectroscopic and multiaperture photometric obs. 0-31362
- 247 Eukrate, UVB photometry, light curve and rot. period 0-21942
- extragalactic radiosources, optically violent variables, monitoring of long-term vars. 0-31376
- faint blue stars in high galactic latit., search of PSS fields near South Galactic Pole 0-46415
- faint proper-motion stars, spectra and photometry to very low luminosity degenerates deficiency 0-17575
- FK4 star coord. improvements using Ni2 astrolabe obs. (*German*) 0-26719
- FK4 supplementary stars, right ascensions obs., definitive results 0-17473

## visible astronomical observations continued

- Fornax dwarf elliptical galaxy, giant branch colour-magnitude diagram 0-4431
- Fornax galaxy, very red giant stars discovery 0-51768
- G200-39, hot hybrid white dwarf, spectroscopic obs. 0-26852
- G292.0+1.8, abundance anomalies, radial vel., possible Crab-like SNR 0-46628
- G292.0+1.8, young supernova remnant, high vel. material obs. 0-22064
- G339.2-0.4, supernova remnant or planetary nebula, radio and optical obs. 0-22104
- G and K-type giant stars, Li abundances 0-41819
- galactic centre field, planetary nebulae and Wolf-Rayet stars identifications 0-8674
- galactic G-type supergiants, UVB photometry 0-41824
- galactic H $\alpha$  background emission, high spatial and spectral resolution pictures 0-56897
- galaxies, apparent luminosity function to 21st magnitude 0-31350
- galaxies, counts up to 25th apparent magnitude (*Russian*) 0-51879
- galaxies, elliptical and S0, absorpt.-line strengths 0-4430
- galaxies, faint, number magnitude counts 0-26976
- galaxies, interacting, luminosities and diameters 0-17677
- galaxies, irregulars and blue compacts, chemical comp. and evolution from spectrophotometry 0-36711
- galaxies, optical redshifts 0-56936
- galaxies, radial vel. for 42 southern objects 0-41902
- galaxies, redshifts for 196 bright objects 0-46661
- galaxies with radio jets, H $\alpha$  and 450 nm obs. 0-51889
- galaxies with UV continuum, photoelectric UVBR photometry (*Russian*) 0-36721
- galaxies with UV excess, spectra and morphology of 58 objects 0-26968
- galaxy redshifts survey, data reduction techniques 0-22074
- Galilean satellites, orbits from numerical integration (*French*) 0-26779
- GCl 0422-213, distant globular cluster in Eridanus, preliminary photometry and spectroscopy 0-17624
- Geminids, flux in 1974, magnitude ratio and mass index 0-4307
- GK-type dwarf stars, Mg H lines obs. rel. to Mg isotopic abundances 0-51757
- globular cluster giant stars, blanketing differences meas. 0-4345
- globular clusters, in M31, luminosity distrib. 0-36708
- globular clusters, NGC 6440, 6541, 7099, surface brightness, star density and colour profiles 0-12783
- GX304-1 (4U 1258-61), shell spectrum of optical counterpart 0-46582
- H 0544-665, optical candidate for LMC X-ray source 0-36737
- H 2155-304, highly luminous BL Lacertae object, spectral obs. 0-4459
- H-H 7 and 11, spectrophotometry of very low-excitation objects 0-46549
- HD 11579, spectroscopic binary orbit from photoelectric radial vel. obs. 0-41862
- HD 14969, IAU radial-velocity standard star, orbit from photoelectric radial vel. obs. 0-56884
- HD 153919 (3U 1700-37), further spectroscopic obs. 0-4358
- HD 170899, possible halo population giant star 0-26859
- HD 175742, spectroscopic binary, orbit determ. with CORAVEL photoelectric radial vel. spectrometer (*French*) 0-36671
- HD 184927, He variable star, spectroscopic props. 0-51790
- HD 192163, 191765, Wolf-Rayet stars, optical interstellar spectra obs. 0-17640
- HD 193077, probable single WN 5 star with absorption lines 0-56834
- HD 193793, Wolf-Rayet star, photometric evidence for C-rich dust cloud 0-26861
- HD 197406, Wolf-Rayet spectroscopic binary, radial vel. and orbital elements 0-51812
- HD 221568, Ap star, light var. period 0-56856
- HD 2343, spectroscopic binary, orbit from photoelectric radial vel. obs. 0-8656
- HD 31908, freq. analysis of  $\delta$  Delphini star 0-46581
- HD 33579, 35343, HDE 286757, 269006, most luminous LMC supergiants, long time baseline VBLUW photometry 0-22007
- HD 33579, HD 35343 (S Doradus), HDE 268757, HDE 269006, most luminous LMC supergiants, long time baseline VBLUW photometry 0-36630
- HD 38268, in 30 Doradus, unique interstellar Ca II K-line profile obs. 0-51850
- HD 3980, late Ap star, photometric and mag. variability obs. 0-56845
- HD 4174, peculiar M-giant, magnetic field 0-8631
- HD 50896, WN5 star, variable emission-line spectrum obs. 0-51791
- HD 51480, shell star, spectroscopic obs., atmospheric struct. and distance 0-31305
- HD 63791, probable metal-poor halo G-type giant field star 0-26859
- HD 80383, UVB photometry of  $\beta$  Cephei type star 0-36644
- HD 8781, freq. anal. of low-amplitude  $\delta$  Scuti star 0-46575
- HD 94033 ultra short period cepheid, obs. 0-22024
- HD 96953, spectroscopic binary orbit from photoelectric radial vel. obs. 0-56887
- HDE 226868 (Cygnus X-1), H $\alpha$  emission in (1977) 0-51919
- HDE 245770, possible counterpart of variable X-ray source A 0535+26, line and continuum vars. 0-17600
- HDE 326333, new  $\beta$  Canis Majoris star, photometric obs. 0-17595
- Herbig-Haro object 1 exciting star, identification as T Tauri star 0-17633
- Herbig-Haro object 24, emission/reflection nature 0-41829
- Hercules supercluster, basic redshift data 0-36725
- Hercules supercluster, evidence for intracluster medium 0-22092
- Hercules X-1 (HZ Herculis), coordinated optical and X-ray pulsations obs. 0-51909
- AC Herculis, curve-of-growth analysis of RV Tauri variable 0-22026
- AC Herculis, RV Tauri star, UVB obs. 0-56857
- AM Herculis (4U 1813+50), rapid light variability obs. (*Russian*) 0-8662
- high-velocity stars, southern, radial vel. obs. 0-21988
- high-velocity stars, southern, UVB colours 0-21989
- HR7922, B-type spectroscopic binary, orbital soln. 0-26910
- HR8891, B-type spectroscopic binary, orbital soln. 0-26910
- HR 1217, Ap star, spectrum and light vars. relationship 0-26878
- HR 2081, double-lined spectroscopic binary, radial vel. orbit and min. masses 0-51811
- HR 432, 515 and 8006,  $\delta$  Scuti stars, spectrographic obs. 0-36639
- HR 4665, spectroscopy of bright long-period RS Canum Venaticorum system 0-36665
- HR 5161, spectroscopic binary star, radial vel. orbit 0-12781



## visible astronomical observations continued

- HR 8752 (V509 Cassiopeiae), emission-line spectrum rapid changes 0-36645  
 HR 9049, (HD 224113), eclipsing spectroscopic binary star, period determ. 0-46609  
 HR 9070, Be star, spectral vars. obs. 0-12773  
 Hyades cluster, possible members BVRI photometry 0-51821  
 Hyades cluster, shape and luminosity distrib. 0-17622  
 EX Hydrae, 2:3 period ratio in light curve 0-46580  
 VW Hydri, colour variations during dwarf nova outbursts 0-46576  
 Hyperion, near IR spectra and JHK photometry 0-56761  
 IAU Radial Velocity Standard stars, radial vels. meas. (*French*) 0-51743  
 IC 1318 nebular complex in Cygnus X region, light extinction 0-51835  
 IC 1795 (W3), N II forbidden line unusual profiles over giant H II region 0-46645  
 IC 342, Scl galaxy, discovery of companion 0-36712  
 IC 3568, planetary nebula, struct. and internal extinction 0-31338  
 IC 4329A, Seyfert galaxy, photographic photometry and optical spectrum 0-36706  
 IC 5152, low-luminosity barred galaxy, struct., rot. curve and redshift 0-56950  
 interstellar absorption lines of Na I, K I, Ca II, in stellar spectra rel. to galactic gas distrib. 0-26963  
 interstellar lines towards Cepheus OB2 association, anal. 0-22052  
 interstellar low mass dust clouds in solar vicinity, photometric survey results 0-36512  
 interstellar matter towards Orion OB1 assoc. stars  $\epsilon$  Orionis and  $\pi^5$  Orionis, Copernicus obs. 0-22050  
 85 Io, astrometric obs., 1865-1977, and definitive orbit 0-4284  
 Io, currently active volcanism discovery 0-26789  
 Io, IR refl. spectra, 2.8-5.2  $\mu$ m 0-56756  
 Juno, occultation of AGK3 +0°1022, obs. 0-26773  
 Juno, occultation of AGK3 +0°1022 re-analyzed 0-41757  
 Jupiter, Galilean satellites, 1975-6 astrometric obs. 0-4288  
 Jupiter, ground-based imaging rel. to Pioneer and Voyager cloud configurations interpretation 0-26787  
 Jupiter, near IR spectral albedo 0-31242  
 Jupiter, NH<sub>3</sub>, spatial distrib. from optical band strengths and curves of growth 0-46386  
 Jupiter, ring system, Voyager 2 obs. 0-12707  
 Jupiter, spectrophotometry in 0.6 to 1.1  $\mu$ m region, Jovian atmosphere optical parameters latit. vars. 0-46468  
 Jupiter, Voyager 1 photographic obs. of atmosphere ring and major satellites 0-26788  
 Jupiter and Galilean satellites, positions obtained in 1978 at ESO-La Silla (*French*) 0-21943  
 Jupiter faint satellites, astrometric obs. during 1976 to 1977 opposition 0-26778  
 Jupiter Galilean satellites, Amalthea, Voyager 1 results 0-4293  
 Jupiter magnetosphere, S II obs. rel. to S plasma discontinuities 0-4291  
 K1082, in globular cluster M15, suspected ultrashort period variable star 0-26883  
 K-type giant stars at South Galactic Pole, DDO photometry rel. to CN anomalies and distances 0-8622  
 22 Kalliope, pole coordinates from photoelectric photometry 0-31230  
 Kepler's SNR, distance from interstellar absorption determ. 0-46651  
 Kottamia Observatory site, seasonal atm. extinction due to aerosol 0-46253  
 EV Lacertae, UV Ceti variable, flares colour behaviour 0-22020  
 BL Lacertae type objects, southern, optical monitoring 0-56969  
 late type stars, Ca II H and K lines and nearby continuum photoelectric calibration 0-36617  
 late-type stars photometry, photoelectric MgH+MgB index meas. 0-12753  
 AD Leonis, UV Ceti variable, flares colour behaviour 0-22020  
 LMC, dynamics of giant interstellar shells from line profiles 0-46674  
 LMC, stellar photoelectric UVB photometry (*German*) 0-21932  
 LMC interstellar extinction, visible and UV obs. 0-51877  
 loose stellar clusterings in southern Milky Way, continued photometric studies 0-36679  
 luminous obscured galaxy assoc. with G127.11+0.54, optical spectroscopy and photometry 0-31371  
 luminous stars in M31 0-36622  
 lunar mare grounds relative spectral reflectivity 0-12695  
 lunar surface features mapping at Kottamia obs. 0-12691  
 Lynds 134, optical extinction and surface brightness obs. of dark nebula 0-17627  
 Lynds 1778/1780, optical extinction and surface brightness obs. of dark nebula 0-17627  
 $\beta$  Lyrae, narrow-band photometry in (1971) 0-46605  
 RR Lyrae star in globular cluster NGC 6717, photometric investigation 0-46624  
 RR Lyrae variables in globular cluster NGC 6121 (M4), UVB photometry 0-22018  
 M22, comparison with  $\omega$  Centauri, spectroscopic evidence 0-46617  
 M31, semistellar nucleus, possible M-dwarf enrichment 0-51862  
 M31 nuclear bulge, rotational vels. meas. 0-41888  
 M33, emission regions catalogue 0-46416  
 M33, warped optical plane obs. 0-56944  
 M36, photographic obs., mass, radius, central density, stellar vels. of open cluster (*German*) 0-31333  
 M43, small diffuse nebulae in Orion complex, optical linear polarization map 0-46644  
 M81, enigmatic dark lines identified as galactic high latit. nebulosity 0-56947  
 M82, surface photometry and gross struct. of irregular galaxy 0-31367  
 M83, H II regions spectral characts. and chemical abundances 0-56927  
 M87, emission-line filaments and active accreting nucleus in giant elliptical galaxy 0-56931  
 M87 jet, radiation from knots rel. to model (*Russian*) 0-36719  
 M87 jet knots, polarisation and spectroscopic props. 0-12817  
 Markarian galaxies in poor cluster ZwCl 1122.3+6317, radial vels. 0-26989  
 Markaryan 372, H $\beta$  profile of Seyfert galaxy 0-26972  
 Mars, atmosphere opacity, 1977 obs. from Viking 0-41753  
 MC2(3) radio sources, optical positions from Palomar Sky Survey 0-31375  
 Me, globular cluster, stellar proper motions, membership and cluster internal motions 0-8665  
 Melotte 66, oldest open cluster, colour-magnitude diagram rel. to age 0-17621

## visible astronomical observations continued

- 18 Melpomene, occultation of SAO 114159, secondary extinction event obs. rel. to 1978 (18) 1, possible satellite 0-56749  
 Mercury, regolith containing Fe<sup>2+</sup>, refl. spectra, 0.65-2.5  $\mu$ m 0-56736  
 metal-poor dwarfs, Fe/H abundances from red spectra of nine objects 0-51751  
 meteor counts, test for registration independence 0-8594  
 meteors, photographic altitudes 0-8593  
 9 Metis, pole coordinates from photoelectric photometry 0-31230  
 9 Metis, UVB photometry, light curve and rot. period 0-21942  
 9 Metis occultation of SAO 80950, Guianan obs. 0-31236  
 MKW 3s, poor galaxy cluster, redshifts obs. rel. to cD galaxy extended X-ray emission 0-51884  
 Monoceros OB2 association, evidence for supernova-induced star form. 0-31334  
 19 Monocerotis,  $\beta$  Canis Majoris variable, photometric obs. 0-4379  
 1 Monocerotis,  $\delta$  Scuti star, oscillation modes from photoelectric radial vels. and BVRI photometry 0-51787  
 V616 Monocerotis (A 0620-00), UVB photometry 0-56846  
 Moon, photometric and polarimetric obs., 1976 April to 1977 December 0-51677  
 Moon, selenodetic coord. system based on Kazan heliometric obs. (*Russian, English*) 0-41738  
 MWC 349, IR source optical identification with reddened high-luminosity star 0-56971  
 MXB 1837+05 (Serpens X-1), detect. of optical burst coincident with X-ray burst 0-27013  
 NAB 0137-01, quasar, UVB photometry and brightness vars. 0-56967  
 Neptune, rot. period determ. and effects of seeing on reflected spectrum 0-46479  
 NGC 1068, Seyfert galaxy, forbidden O III lines high-resolution profile 0-46665  
 NGC 1087 and 1090, surface B photometry and mass distrib. in spiral galaxies 0-46676  
 NGC 1261, globular cluster, colour-magnitude diagram 0-17623  
 NGC 1275, photometric and spectrum vars. 0-22075  
 NGC 1275 as pair of interacting galaxies, spectra and structure 0-26969  
 NGC 1365 and 1386, IR and optical props. of emission-line galaxies 0-51867  
 NGC 1566, Sbc galaxy, spectrophotometry of nucleus and nine H II regions 0-51824  
 NGC 1868 in LMC, BV photometry of metal-poor intermediate-age cluster 0-51814  
 NGC 1999, electronographic imaging polarimetry obs. of reflection nebula 0-26964  
 NGC 2264, N II forbidden line unusual profiles over giant H II region 0-46645  
 NGC 2264, open cluster, reddening, blanketing and metallicity from spectroscopic obs. 0-26916  
 NGC 2420, old disc cluster, photometry and spectra rel. to stars chemical comp. 0-46620  
 NGC 2477, photographic obs., mass, radius, central density, stellar vels. of open cluster (*German*) 0-31333  
 NGC 2639 companion galaxy, redshift and assoc. UV excess objects 0-56965  
 NGC 300, NGC 1365, southern galaxies, H II regions comp. 0-4441  
 NGC 3115, lenticular galaxy, photometry and struct. 0-36707  
 NGC 3372, H II region, forbidden O III emission obs. rel. to  $\eta$  Carinae location 0-4383  
 NGC 3379, elliptical galaxy as luminosity distrib. standard 0-22073  
 NGC 3532, southern open cluster, UVB photometric study 0-46621  
 NGC 4321 (M100), interstellar Na I and Ca II absorption in supernova spectrum 0-51847  
 NGC 4472 and 5846, luminous giant ellipticals, B-V colour appl. 0-51865  
 NGC 4593, Seyfert galaxy, spectrophotometry 0-51878  
 NGC 4755, southern open cluster, Balmer line photoelectric photometry 0-56892  
 NGC 5128 (Centaurus A), globular clusters deficiency 0-26986  
 NGC 5128 (Centaurus A), high-resolution spectroscopy and tubelike model of dust band 0-56945  
 NGC 5128 (Centaurus A), struct. and evolution from photographic and spectroscopic obs. 0-4429  
 NGC 5128 (Centaurus A), image tube spectrograms 0-41892  
 NGC 520, Irr II galaxy, new photographic and spectroscopic obs. 0-41889  
 NGC 604, giant H II region in M33, SNRs rel. to content of high mass stars 0-31340  
 NGC 612, rotation of lenticular radio galaxy 0-51874  
 NGC 6144, globular cluster, and neighbouring region, photometric obs. 0-51816  
 NGC 6166, cD galaxy, B-V profiles 0-51865  
 NGC 6240, unusual radio galaxy, radio and optical, obs. 0-4440  
 NGC 6251, radio galaxy, CCD photometry rel. to central supermassive object 0-26966  
 NGC 650/1, planetary nebula, emission line profiles and internal kinematics 0-17639  
 NGC 6528, metal-rich globular cluster, colour-magnitude diagram from UVB photometry 0-4406  
 NGC 6611, young open cluster, UVB magnitudes and colours, reddening, distance, luminosity 0-31332  
 NGC 6717, globular cluster, colour-magnitude diagram, distance and metallicity 0-46624  
 NGC 6822, new compact H II regions discovery 0-51854  
 NGC 6823, UVB photometry and spectra, extinction study of young open cluster 0-4407  
 NGC 6872, remarkably large barred spiral galaxy 0-31358  
 NGC 6902, H I rich southern supergiant spiral galaxy, optical studies 0-8680  
 NGC 6913 galactic cluster, photoelec. photometry of brighter stars, variability obs. 0-46625  
 NGC 7023, refl. nebula, surface brightness study 0-56903  
 NGC 7027, planetary nebula, struct. from electronographic obs. 0-12789  
 NGC 772, galaxy, false companions identified as refl. nebulosities (*Russian*) 0-36723  
 NGC 7793, late-type galaxy, ionized gas phys. conditions and mass-luminosity distrib. 0-26967  
 North America and Pelican Nebular Complex, struct., visual extinction map 0-22063  
 northern FK4 stars, radial vel. meas. 0-26848



## visible astronomical observations continued

- nova in Sagittarius, discovery of probable declining nova (1978 March) 0-4376
- Nova Vulpeculae 1979, slow nova, pre-maximum light curve 0-4364
- novaleike object in Vulpecula, UVB photometry (1979 August 6 to September 20) 0-8644
- 44 Nysa, pole coordinates from photoelectric photometry 0-31230
- OB-type stars in SA 98, UVB photometric meas. 0-46535
- Oberon, near IR spectra and JHK photometry, mass and dia. measurement 0-56761
- UZ Octantis, W Ursae Majoris system, UVB light curves 0-22042
- OJ 287, BL Lacertae object, case for synchronous optical-radio outbursts 0-8679
- 171 Ophelia, binary asteroid evidence from light curve 0-4287
- U Ophiuchi, massive eclipsing binary star, spectrophotometry 0-26900
- † Ophiuchi, spectral vars. related to rot. 0-22000
- OQ 172, quasar, H<sub>2</sub> lines in absorpt. spectrum 0-36734
- Orion Nebula, fine-struct. lines obs. and elemental abundances 0-4410
- Orion Nebula peripheral regions, spectrum obs. rel. to element depletion and ionisation 0-36686
- 49 Pales, binary asteroid evidence from light curve 0-4287
- AU Pegasi, binary Type II cepheid, photometric and spectroscopic study 0-26866
- BX Pegasi, photoelectric photometry of totally eclipsing W Ursae Majoris systems, 1978 Oct. to Nov. (Chinese) 0-31330
- θ Pegasi, rapid spectral line variability disproved 0-8625
- 118 Peitho, rot. period and light curve from photoelectric obs. 0-46454
- Periodic Comet Ashbrook-Jackson (1978 XIV), precise positions (German) 0-46453
- Periodic Comet Ashbrook-Jackson (1978 XIV), precise posns. (1978 April) (French) 0-41767
- Periodic Comet Ashbrook-Jackson (1978 XIV) 0-31258
- Periodic Comet Forbes (1980a), recovery obs. and corrected ephemeris 0-46490
- Periodic Comet Halley, rotation period from halo diameter meas. 0-51694
- Periodic Comet Reinmuth 1 (1979j), recovery obs. 0-8589
- Periodic Comet Schwassmann-Wachmann 1, appearance and total magnitude (1979) December 0-36571
- Periodic Comet Schwassmann-Wachmann 1, coma obs. (1979 October 31) 0-8591
- Periodic Comet Schwassmann-Wachmann 1, obs. on 21st and 22nd Jan. 1980 of coma dimensions 0-36573
- Periodic Comet Schwassmann-Wachmann 2 (1979k), recovery posns. and ephemeris 0-26811
- Periodic Comet Tempel 2, optical spectrophotometry at 3 AU distance, albedo, nucleus radius 0-26814
- φ Persei, binary Be star, He II emission obs. rel. to components masses 0-12768
- AG Persei, massive eclipsing binary star, spectrophotometry 0-26900
- 53 Persei, nonradial mode identification 0-8632
- 53 Persei, nonradical pulsator, light var. rel. to line profile changes 0-4362
- 21 Persei, spectrophotometry of Ap star, continuum features vars. 0-36638
- X Persei (3U 0352+30), simultaneous X-ray and ground-based optical obs. 0-17591
- β Persei (Algol), orbital inclination and masses determ. from speckle interferometry 0-36668
- γ Persei cluster, stellar membership determ. by proper motion meas. 0-56890
- Perseid meteor shower, television obs. 0-4309
- PHL 957, quasar, upper limits on Lyman α halo 0-51907
- Phoebe, near IR spectra and JHK photometry 0-56761
- photographic obs., mass, radius, central density, stellar vels. of open cluster (German) 0-31333
- photosphere faculae intensity, centre to limb var. 0-21967
- PKS 0548-322, surface photometry of X-ray emitting BL Lacertae object 0-22069
- PKS 0736+01, optical spectrum variability 0-8709
- PKS 1157+014, spectral obs., of QSO with no L<sub>α</sub> emission 0-31384
- planetary nebula in irregular galaxy NGC 6822, spectrophotometry and He, N, O and Ne abundances 0-41867
- planetary nebulae, absolute flux densities for emission lines in 6000-11000 Å range rel. to physical parameters 0-51857
- planetary nebulae, low excitation, of small ang. size, spectral studies 0-17646
- planetary nebulae kinematics, radial vel. meas. 0-46633
- Pleione (28 Tauri), envelope behaviour in 1976, spectroscopic obs. 0-8636
- Pleione (28 Tauri), metallic-line shell spectrum anal., (1973-1976) 0-8637
- Pluto, diameter meas. by speckle interferometry 0-41763
- Pluto, geocentric positions for the 1974-8 period 0-46478
- 308 Polyo, photoelectric lightcurves and rotation period 0-46455
- Praesepe, photometry in BVRI colours 0-26917
- 790 Pretoria, C-type asteroid, light vars. obs. and rot. period 0-21941
- Przybylski's star (HD 101065), β photometry and period determ. 0-41835
- PSR 0531+21, Crab pulsar, optical light curve changes in 1970-7 period 0-36654
- PSR 0833-45, Vela pulsar, optical pulse profile 0-46593
- R Puppis (HD 62058), G-type supergiant, UVB photometry and variability confirmation 0-41824
- Q 0932+501, bright quasar with broad absorption features 0-46697
- Q 0957+561, double quasar, intervening galaxy obs. rel. to gravit. lens hypothesis 0-27005
- Q 2240.9-3702, Q 2238.9-4115, optically selected QSOs with broad-lined absorpt. systems spectra 0-4456
- QSO 1038+528 A,D, close pair of radio-emitting quasi-stellar objects, radio and optical obs. 0-51902
- QSO candidates, spectroscopic obs., identifications 0-31385
- QSO candidates and radio galaxies, optical spectroscopy 0-56966
- QSOs, compact group in Leo 0-27006
- QSOs, high-redshift, Image Dissector Scanner (IDS) spectrometry and redshifts 0-22111
- QSOs of small and intermediate emission redshift, absorpt. lines homogeneous survey results 0-31218
- quasars, magnitude estimation from Palomar Sky Survey prints 0-36510
- quasar, strong emission line, with redshift z=0.189, spectrum and photometry 0-8710

## visible astronomical observations continued

- quasars, low-red shift, photoelectric UVB photometry (French) 0-51904
- quasars, Mg II 2798 Å and H<sub>β</sub> emission, line profiles 0-12807
- quasars, southern, optical monitoring 0-56969
- quasars, spectral characts. of three high redshift objects 0-4455
- quasars, spectral props. of 85 objects from spectrophotometry 0-51897
- quasars in region of NGC 1629 companion galaxy, spectra and redshifts 0-56965
- quasars of Michigan-Tololo survey, spectrophotometry 0-22105
- radio galaxies, broad-line Mg II 2798 Å and H<sub>β</sub> emission, line profiles 0-12807
- radiogalaxies, faint southern objects, identification and spectrophotometry 0-56935
- red and nebulous objects in dark clouds, survey, catalogue of 150 objects 0-56904
- rich galaxy cluster 0004.8-3450, bri photometry 0-46685
- Rst 4036, red-dwarf binary star, orbital period and total mass 0-12780
- S0 galaxies, luminosity distrib. perpendicular to plane of discs rel. to struct. and origin 0-36705
- S-type stars, revised spectral classification system in red 0-46541
- SA 133 field near galactic centre, three-colour stellar photometry (German) 0-36618
- HM Sagittae, emission-line star, UVB photometry and spectral obs. in (1978) (Russian) 0-36648
- HM Sagittae, emission-line star, polarimetry, (1977 to 1978) (Russian) 0-36649
- WZ Sagittae, recurrent nova, spectroscopic obs. during 1978 outburst 0-26862
- WZ Sagittae, recurrent nova, spectroscopic study during 1978 outburst 0-56849
- XZ Sagittarii, Algol system, UVB photometric investigation 0-22041
- μ Sagittarii, binary star, obs. of eclipse of unseen companion 0-4401
- AQ Sagittarii, C star, ang. dia. from lunar occultation meas. 0-22008
- V356 Sagittarii, massive eclipsing binary star, spectrophotometry 0-26900
- MV Sagittarii, R Coronae Borealis variable, brightness decline obs. and UVB photometry 0-8641
- RY Sagittarii, spectra near min. light 0-36642
- Santiago astrolabe observations from 1972 to 1976, results 0-46363
- Saturn, 1979 S 3, discovery of possible satellite 0-26802
- Saturn, F-ring and new satellite, Pioneer II discoveries 0-8585
- Saturn, near IR spectral albedo 0-31242
- Saturn, outer ring and five possible new satellites discovery 0-46472
- Saturn, outer ring search, 1979 November obs. 0-17543
- Saturn, rings, four colour phase curves, analysis 0-4295
- Saturn, rings, International Planetary Patrol obs. and data reduction 0-4294
- Saturn globe and rings, optical reflectance polarimetry and interpretations for B-ring 0-31248
- Saturn innermost satellites, separations and times of elongation, (1980 February 29 to March 18) 0-56762
- Saturn ring system, optical polarimetry during 1979 opposition 0-36570
- δ Scuti variables, photometric search of Hyades cluster 0-36677
- Seyfert galaxies, Mg II 2798 Å and H<sub>β</sub> emission, line profiles 0-12807
- Seyferts in 12th list of galaxies with UV continuum (Russian) 0-17659
- Sharpless 235A, optical, radio and IR obs. of H II region 0-4415
- SIMS, C and SC stars, new discoveries on southern, red-sensitive objective-prism plates 0-36511
- 140 Siwa, C-type asteroid, light vars. obs. 0-21941
- SN 1972e in NGC 5253, spectrum 0-41844
- SN in NGC 1199, mag. 17 object, 1979 Sept. obs. 0-41846
- SN in NGC 3733, discovery of mag. 15 supernova (1980 March 17) 0-51793
- SN in NGC 5854, discovery of mag. 15 Type I supernova (1980 March 20) 0-51793
- solar active region, 1978 April to May, morphological features (Chinese) 0-8613
- solar corona, colours during eclipse and dust composition 0-51730
- solar coronal structure overlying type III burst producing active region, Skylab obs. 0-21976
- solar eclipse, 1973 June 30, spectroscopic obs. by Dutch expedition 0-8614
- solar eclipse, 1973 June 30, spectroscopic obs. by Dutch expedition 0-8615
- solar eclipse of 1979, February 26, an illustrated record from N.American obs. 0-4328
- solar Fe I line spectrum, photosphere Fe abundance determ. (Russian) 0-12720
- solar filaments disparitions brusques, evidence for role of mag. field (Russian) 0-51726
- solar flares, microwave and optical emissions comparison 0-31284
- solar granulation, dark dot form. in cell 0-31274
- solar H<sub>α</sub> post-flare loops dynamics, 1973 July 29 flare 0-31286
- solar photospheric granulation, speckle interferometric obs. (French) 0-46523
- solar photospheric oscillations depth depend. 0-31275
- solar prominence model based on spectral obs. 0-31287
- solar velocity fields, large-scale, from Doppler line shift obs. 0-12730
- southern metal-poor stars, UVBRI photometry and UV excesses 0-56828
- southern peculiar emission-line stars, observational data rel. to mass ejection 0-41843
- Southern Sky Survey, role of European Southern Observatory 0-12658
- spiral galaxies, optical surface photometry rel. to local mass-to-light ratio 0-31361
- spiral galaxies, rot. direction determ. by means of edge-on systems (Russian) 0-36722
- spiral galaxies bulges, vel. dispersions meas. 0-26965
- spiral galaxies nuclei, spectra and stellar population 0-56926
- spiral galaxies studied at Westerbork, optical surface photometry 0-17655
- SS 433, discrepancy between optical and radio positions 0-31303
- SS 433, enormous periodic Doppler shifts obs. 0-17593
- SS 433, IR and visible obs., IR excess and emission processes 0-4387
- SS 433, IR light curves from BVJHK photometry, period and ephemeris 0-8642
- SS 433, light minimum epoch and period 0-26886
- SS 433, photometry, 1979 July to October, and 6.5 day period identification 0-8643
- SS 433, radio and optical positions coincidence 0-56840
- SS 433, short term H<sub>α</sub> central intensity increases 0-4375
- SS 433, spectroscopic obs. and probable binary nature 0-51780



## visible astronomical observations continued

- star pair latitude obs. anal., mean pole position calc. 0-21892  
 stars, 313 nearly low galactic latitude objects, linear polarization meas. 0-46641  
 stars, young, in galactic anticentre direction, photometry and spectra rel. to outer Galaxy struct. 0-22079  
 stars in dust clouds with bright nebulosities 0-56893  
 stars with planets, astrometric photoelectric detection obs. 0-56882  
 stellar iris diaphragm photometry, nonuniform background correction 0-12680  
 stellar photoelectric UBV sequences, in fields of eight low-red shift quasars (*French*) 0-51904  
 stellar photometry, extinction oscills. caused by atmospheric disturbances 0-56606  
 Stepanyan's star, spectrophotometric and photometric obs., 228-min period 0-56883  
 Stepanyan's star found to be eclipsing binary, possibly cataclysmic 0-51806  
 Stephenson-Sanduleak 433, Thomson scatt. lines in spectrum, relativistic gas motions 0-22019  
 Sun, 1978 May 7 events, radio, optical and geophysical manifestations (*French*) 0-8611  
 Sun, blue continuum flares and D3 preflare shell obs. 0-51709  
 Sun, coronal oscillations above active region, Fe XIV spectra obs. 0-41794  
 Sun, granule fragmentation, morphological study in Ca II K-line 0-56799  
 Sun, H $\alpha$ -flares rel. to radio bursts and sunspots 0-41803  
 Sun, light absorption in photospheric layers, eclipse limb darkening obs. (*French*) 0-8612  
 Sun, limb emission lines near Ca II H and K and spatial intensity vars. 0-51720  
 Sun, spectral line asymmetries, radial movement effects 0-41792  
 Sun, structure from global studies of 5-min. oscills. 0-26838  
 sunspot chromosphere, radial vel. and brightness oscills. regimes (*Russian*) 0-51727  
 sunspot groups, small pores proper motion meas. 0-12733  
 sunspot magnetic fields higher rot. rate at photosphere, Doppler meas. 0-46516  
 sunspot moats, lifetimes from magnetograph obs. 0-21966  
 sunspot umbral brightening assoc. with two-ribbon flare 0-41804  
 sunspot umbral dots, improved obs. 0-26831  
 sunspots, Wilson effect (*Chinese*) 0-12721  
 supergiant elliptical galaxies nuclei, CCD photometry rel. to supermassive object in (NGC 6251) 0-26966  
 supernova in ESO 153-G27, discovery and magnitudes (1979 August 19 to October 15) 0-26892  
 supernova remnants, galactic, new optical obs. 0-17636  
 supernova remnants in M33, catalogue and spectroscopic survey 0-41734  
 supernovae in anonymous galaxies, three new discoveries 0-46589  
 supernovae stellar remnants, spectroscopic search 0-26890  
 87 Sylvia, UBV photometry, light curve and rot. period 0-21942  
 symbiotic stars, obs. of unidentified bands at 6830 and 7088 Å 0-46573  
 V711 Tauri, change in nature of light curve, and flare, 1979 October to December 0-26906  
 SU Tauri, emission lines at min. and BV photoelectric photometry 0-8640  
 $\lambda$  Tauri, massive eclipsing binary star, spectrophotometry 0-26900  
 V471 Tauri, period var. and light curves of eclipsing binary system 0-22038  
 DR Tauri, pre-main-sequence star, brightening, 1970 to 1979, and historical light curve 0-31297  
 RV Tauri and yellow semiregular variables, photometric investigations 0-26865  
 Tautenburg objective prism survey objects, high-resolution spectra and redshifts 0-4436  
 88 Thise, photoelectric light curves and rotation 0-17528  
 Titan (Saturn VI) eclipse, 1979 December 20, photometric obs. 0-31250  
 Titania, near IR spectra and JHK photometry, mass and dia. measurement 0-56761  
 Tokyo Astronomical Obs., Time and Latitude Bulletins (Jan-Mch. 1978) 0-17476  
 Tokyo Astronomical Obs., Time and Latitude Bulletins (July-Sept. 1978) 0-4239  
 Triton, diameter and reflectance, spectral and radiometric obs. 0-17546  
 47 Tucanae, globular cluster, photometry and spectra rel. to stars chemical comp. 0-46620  
 Tycho SNR spectrum, model of optical emission from fast shock wave 0-46631  
 4U 1626-67, 7.7-second X-ray pulsar, simultaneous X-ray and optical obs. 0-51914  
 4U 1626-67, light pulses from optical counterpart 0-51916  
 4 U 2129+47 optical counterpart, spectrum and photometry rel. to 0-17693  
 Umbriel, near IR spectra and JHK photometry, mass and dia. reassessment 0-56761  
 Uranus, disk structure in 7300 methane band 0-17544  
 Uranus, lunar occultation, 1977 February 10, radius, limb darkening and polar brightening at 6900 Å 0-17545  
 Uranus, rot. period determ. and effect of seeing on reflected spectrum 0-46479  
 Uranus, rot. period spectroscopic determ. 0-51691  
 Uranus occultation of SAO 158687, obs. rel. to upper atmosphere mean temp. and temp. vars. 0-46477  
 Uranus upper atmosphere, struct. from SAO 158687 occultation obs. 0-17547  
 AW Ursae Majoris, light curve anal. of contact binary 0-56875  
 SU Ursae Majoris, probable 1980 March super outburst 0-51785  
 $\gamma$  Ursae Minoris, high dispersion spectroscopy 0-41853  
 variable stars in globular cluster NGC 6934, photometry 0-56891  
 AH Velorum, radius, delta luminosity and pulsation mode of  $\delta$  Cepheid 0-46572  
 Venus, atmospheric, scattering coeff. from Venera 9 and 10 photometry 0-8572  
 Venus, atmospheric net radiation meas. by Pioneer small probe 0-46435  
 Venus, atmospheric struct. and comp. from refl. sunlight polarisation calc. and obs. 0-36533  
 Venus, cloud optical properties and atmos. layered struct. 0-51681  
 Venus, dust ring possibility from Venera 9 and 10 spectroscopy 0-8573  
 Venus, infrared spectra near superior conjunction, CO<sub>2</sub> bands 0-56740

## visible astronomical observations continued

- Venus, nightside ionosphere, formation process, ionization, mixing ratios 0-41751  
 Venus, Pioneer nephelometer expts. results 0-46430  
 Venus, regional polarization, 1950-77 obs. 0-8570  
 Venus, sunlight absorption in atmosphere, Pioneer radiometer meas. 0-46434  
 Venus atmosphere, scattered solar radiation, day sky spectrum, Venera meas. 0-56573  
 Venus surface, Venera 9 and 10 landers, visible radiation 0-46425  
 Vesta, UBV photometry and lightcurve 0-36546  
 78 Virginis, magnetic Ap star, high resolution polarisation obs. inside spectral lines 0-51772  
 AR Virginis, RR Lyrae variable, photographic photometry and mean light curve (*Russian*) 0-12769  
 visual double stars, photographic meas. of position angles and separations 0-26909  
 Vulpecula OB2 stars, photometry and spectra rel. to membership of 67 day Cepheid S Vulpeculae 0-41831  
 21 Vulpeculae, new luminous long period  $\delta$  Scuti star, photometry 0-31306  
 BW Vulpeculae, V photometry, light curve, quadratic ephemeris 0-26881  
 NQ Vulpeculae (Nova 1976), UV and visual spectra analysis (*Chinese*) 0-12770  
 VV 5-32-63/64 in Abell 1775, supermassive double galaxy, radial vels. 0-8693  
 W50, supernova remnant, optical filaments spectra rel. to SS 433 mass loss rates and lifetime 0-12804  
 W50, supernova remnant, spectrum of optical nebulosity 0-51851  
 W50 (SS 433), supernova remnant, optical filamentary nebulosity discovery 0-56916  
 white dwarfs in open clusters, obs. rel. to progenitor stars upper mass limit 0-51738  
 Wolf 922, nearby red dwarf, evidence for low-mass unseen companion 0-51809  
 Wolf-Rayet stars in galactic-centre field, new discoveries from spectroscopic obs. 0-8674  
 Wolf-Rayet stars in LMC, new discoveries, positions, spectra and magnitudes 0-46569  
 X-ray bursters, 1980 plans for simultaneous optical/X-ray obs. 0-8716  
 X-ray bursters, spectroscopic study of optical counterparts 0-46699  
 yellow semiregular and RV Tauri variables, photometric investigations 0-26865  
 Yerkes poor cluster members, reshifts 0-51858  
 ZB 33, RR Lyrae type star, light curve study (*Chinese*) 0-8633  
 zodiacal light surface brightness meas. by AE-C satellite 0-17548  
 VII Zw 421 and II Zw 67, spectrophotometry of S0 galaxies 0-51866  
 $\mu$  Draconis (ADS 10345), radial vel. var. from spectra in visible 0-17612  
 1228, nearby red dwarf, evidence for low-mass unseen companion 0-51809  
 C stars in Cygnus, new discoveries and BV photometry 0-46551  
 C<sub>2</sub> absorption bands in stellar spectra, 876 nm obs. 0-12805  
 Ca II H and K lines in F0 to M2-type stars, high resolution absolute flux profiles 0-26842  
 Fe III in astronomical sources, multiplet table 0-41732  
 H deficient and He weak stars, uvby photometry, variability 0-46579  
 H II regions in Perseus arm, spectrophotometry and reassessment of galactic abundance gradients 0-22055  
 H $\alpha$  emission stars, optical scanner data 0-56827  
 H $\alpha$ -emission stars in Perseus OB1 assoc. region 0-56855  
 HgMn stars, spectrophotometry 0-26867

## vision

- see also colour vision; eye; vision defects; visual perception  
 accessory optic projections upon oculomotor nuclei and vestibulocerebellum 0-3643  
 accessory optic system in the rat 0-21470  
 accommodation in infants, photorefractive study 0-56028  
 acoustic seeing aid for blind (*Polish*) 0-8215  
 acuity, infant, underestimation as near threshold gratings are not preferentially fixated, expt. obs. 0-56053  
 acuity asymmetry in opposed semi meridians (*French*) 0-16936  
 acuity charts, suitable illumination sources 0-12079  
 annular artificial pupils, props. 0-41356  
 axon-bearing horizontal cells, teleost retina, functionality obs. 0-51084  
 bathoproducts of rhodopsin, isorhodopsin I, and isorhodopsin II 0-51088  
 binocular interactions, role in development in cat 0-12117  
 binocular summation and the binocularity of cat visual cortex 0-16946  
 binocularity and stereopsis in the evolution of vertebrate vision 0-12144  
 biomedical stimulus device for characterizing temporal MTFs in man 0-51204  
 blink reflex, peripheral electrical stimulation inhibitory effect, abolition by naloxone (*French*) 0-35880  
 cataractous lens, optical transmission at 430 nm and blue field entoptoscopy 0-45883  
 cerebral potential sources location for visual field impairment assessment in humans 0-30922  
 chromatic response of human eye, Karhunen-Loeve analysis of landscape multispectral data 0-48164  
 compensatory eye movements to miniature rotations, rabbit, retinal image stability implications 0-45890  
 complex pattern discrimination, learning by young kittens, expt. obs. 0-56049  
 complex shaped objects, visual resolution and recognition, vibr. influence (*Russian*) 0-45909  
 compound eye, Dipteran, small signal phototransduction 0-35882  
 computed tomography of the visual pathways 0-56178  
 conference, Houston, USA, (March 1977) 0-8736  
 contact lenses, thickness definition 0-46094  
 contingent negative variation and accuracy of time estimation. A study on cats 0-26216  
 contrast evoked potential, invariance with retinal illuminance changes 0-51085  
 contrast sensitivity rel. to stimulus onset and image motion 0-16938  
 contrast threshold response of human eye based on Tiffany data anal. 0-51093  
 cortex area 19 cells, cat, classification by connectivity and photic responsiveness 0-35886  
 cortical effects of early visual experience 0-12119  
 cortical electrical phosphene props. 0-12112  
 cortical orientation selectivity, of partially visually deprived cats 0-26230



## vision continued

cortical slow negative waves following non-paired auditory and visual stimuli 0-3650  
 crayfish, coding and decoding of steady state information by patterned pulse trains 0-12105  
 critical duration changes during dark adaptation 0-51094  
 diabetic blindness prevention with ophthalmic photography 0-16920  
 EEG, operant conditioning of brain steady potential shifts in man 0-21466  
 EEG, pattern stimulated pots., dipole localisation 0-26235  
 EEG, pattern-evoked potentials and nerve conduction vel. in family with adrenoleucodystrophy 0-45875  
 EEG photic flash response, quantitative approach 0-30923  
 electro oculography, computerised diagnostic system 0-21566  
 energy uptake in the first step of visual excitation 0-30724  
 epilepsy, photosensitive, role of pattern in TV viewing 0-26214  
 epiphysis, frog, characts. of slow pots. 0-56029  
 ERG, human corneal, frequency domain anal. 0-45888  
 ERG, rabbit, dynamic light-dark adaptation 0-35887  
 ERG, suprafusion, theoretical retinal anal. 0-56020  
 ERG, Wiener kernels and freq. response functions, human retina, obs. 0-45887  
 ERG B-wave of ground squirrel, spectral components 0-51082  
 ERG photostimulus calibration by standard photometer and photodiode 0-8222  
 ergo-ophthalmology and ergo-optometry (*Italian*) 0-26223  
 evoked cortical responses, monocular study 0-3640  
 evoked potential, nonstationary EEG, anal. using max. entropy method 0-26397  
 evoked potential, theoretical investigations and clinical appl. 0-26234  
 evoked potential analysis (*Japanese*) 0-12090  
 evoked potential rel. to sensory discrimination task 0-3645  
 evoked potential waveform, effects of head support (*Japanese*) 0-3642  
 evoked potentials, amplitude and degree of event-related desynchronisation 0-12087  
 evoked potentials, average, microprocessor-based system for studying 0-56150  
 evoked potentials, n-hexane induced changes, ERG of industrial workers 0-45886  
 evoked potentials, recording and evaluation procedure for neurophysiology and medical diagnostics (*German*) 0-26404  
 evoked potentials, steady-state, effects of meridional variation 0-56033  
 evoked potentials, use in intracranial pressure estimation 0-26398  
 evoked potentials, use in pediatric diagnosis 0-26407  
 evoked potentials in monkeys 0-45885  
 evoked response, multiplexing system for multichannel signal averaging 0-36165  
 evoked response meas. using versatile pattern-reversal stimulator 0-17177  
 evoked response to sinusoidal gratings, latency obs. 0-16933  
 evoked scalp pot., random within-set design for sampling 0-3842  
 evoked-response data acquisition system, specification and design 0-56165  
 external geniculate body, metric of space of description of images 0-30716  
 extrafoveal spectral sensitivity during dark adaptation 0-45896  
 eye movement research, data collection using on-line computers 0-41329  
 eye torsion in response to tilted visual stimulus 0-45891  
 fixation disparity rel. to rapid prism adaption 0-16929  
 fixation stability observations, proprioceptive information and autokinesis considerations 0-51086  
 flicker fusion phenomena, expt. studies of random neural nets 0-12077  
 foveal vision central mechanisms, monkey 0-12108  
 glare source position and BCD brightness relationships under uniform field brightness, expt. (*Japanese*) 0-35889  
 gloss appearance by means of moire patterns, connection to binocular vision (*German*) 0-52300  
 grating, sine-wave, average-luminance surround effect 0-51092  
 grating, free scanning, production of patterned retinal exposure obs. 0-56034  
 guided locomotion, psychophysical evidence for neural mechanism sensitive to flow patterns 0-51107  
 human visual system, transient characteristic using masking experiments 0-41009  
 inhomogeneous model predictions, detect. of local, extended spatial stimuli 0-45894  
 insect visual neurones, sexual differences 0-41010  
 IR nonlinear perception in 800-1355 nm range 0-12123  
 IR recording retinoscope for accommodation monitoring 0-36055  
 laser low-level prolonged exposure effects on visual function 0-3714  
 laser scanned visual displays, pulsed light data extrapolation 0-3713  
 lateral geniculate nucleus, monkey, cell size changes in undeprived laminae after monocular closure 0-16927  
 lateral geniculate nucleus in cat, struct. of identified X and Y cells 0-26231  
 lateral geniculate nucleus of cat, periodic stimulation, neural activity transient persistence 0-56021  
 lateral geniculate nucleus postnatal development in humans 0-12114  
 lens, human and calf, light scatt. and reversible cataracts 0-56019  
 lens accommodation, interpositus neuron control obs. 0-21469  
 light adaption in a normal and a rod monochromat, psychophysical and VEP increment obs. 0-16939  
 light sources, psychophysical luminous efficiency (*Polish*) 0-33110  
 masking-induced sensitivity changes in Limulus photoreceptors 0-41024  
 microcomputer-controlled visual stimulator for eye movement and visual evoked pots. study 0-41350  
 mobility aid for blind people based on US sensing 0-56290  
 molecular mechanism for initial process of visual excitation 0-51089  
 monocular occlusion, alternating, effects on cat visual cortex 0-16932  
 motion and vision, stabilised spatio-temporal threshold surface 0-16926  
 motor systems, eye and hand, optimal response in pointing at visual target 0-56079  
 multiple sclerosis diagnosis using cerebral evoked response and optokinetics 0-36183  
 nervous activity monitoring in *Drosophila* by [<sup>3</sup>H]deoxyglucose 0-56024  
 neural information processing, primate visual system appl. 0-30722  
 neural network dynamical response, effect of boundaries, Limulus retina 0-30717  
 neuron-discharges in eye movements 0-12099  
 ocular peripheral saccades, latency obs. 0-12089  
 ocular physiology review 0-56023

## vision continued

ophthalmic lenses, thin, chemtempered, static load strength testing 0-5812  
 ophthalmology and vision research, appl. of lasers, holography 0-12210  
 optic nerve fibre arrangement in cat, non-retinotopic 0-30720  
 optic tectum, pigeon, single cell spatial- and temporal-freq. selectivity 0-41016  
 optic tectum, pigeon, single-neuron responses to moving sine-wave gratings 0-41015  
 optic tract fibers, cat, Markov properties of nonstationary spike trains 0-51077  
 optical line spread width judgement, merits of Gaussian moment 0-16924  
 optical scan system for encoding and tabulation of visually scored sleep data 0-8197  
 optokinetic reactions in man elicited by localised retinal motion stimuli 0-45889  
 optokinetic stimulation device, expt. and clinical appls. 0-3844  
 optometry, future of public and community health 0-12084  
 optometry as remediation and education 0-12082  
 optometry opportunities, trends in higher education and health 0-8756  
 optical line spread width judgement, merits of Gaussian moment 0-16923  
 pattern evoked pots., implicit time in infants, spatial vision maturation index 0-16928  
 pattern reversal generator for visually evoked responses studies 0-46004  
 pattern-evoked potential, modifications rel. to stimulated part of visual field 0-26225  
 peripheral critical flicker frequency 0-41039  
 phase selectivity of spatial frequency channels 0-45895  
 phasic pupillary light reflex and visual evokes potentials, simultaneous anal. 0-26226  
 photic sensitivity of macaque monkey and pulvinar neurons 0-12106  
 photoconvertible pigment states and excitation, prolonged depolarising afterpot., blowfly 0-8060  
 photomicrography, low-power critical focusing 0-13165  
 photon counting microspectrophotometer for study of single vertebrate photoreceptor cells 0-12323  
 photopigment and receptor props. in *Drosophila* compound eye and ocellar receptors 0-8063  
 photopigment rapid conversions in blowfly visual sense cells, effect on receptor pot., pupillary response 0-8062  
 photoreceptor, barnacle, conditioning light effect modification by metarhodopsin absorpt. of light 0-8064  
 photoreceptor, barnacle, effects on prolonged depolarising afterpot. of Mn<sup>2+</sup>, Ca<sup>2+</sup> 0-8051  
 photoreceptor, barnacle, props. of on-transient of intracellular response 0-8052  
 photoreceptor, barnacle, upper limit on translational diffusion of visual pigment 0-8053  
 photoreceptor sensitivity increase following light illumination, frog expts. 0-51095  
 photoreceptor transduction, determ. of pigment transition or state coupled to excitation 0-8054  
 photostable pigments, function in fly photoreceptors 0-8058  
 physical and biological sciences, conf., Japan (Mar. 1979) 0-17714  
 polarised light detection by humans 0-16934  
 preferred orientation, variability due to methodology 0-56032  
 primary visual cortex, orientation selectivity development models, normally and dark reared kittens 0-41007  
 primary visual cortex orientation selectivity development kinetics, normally and dark reared kittens 0-41006  
 primate, subdivisions and interconnections 0-12110  
 psychophysical evidence for sustained and transient channels in the monkey visual system 0-35896  
 psychophysical functions in fish with respecified retinotectal connections 0-12152  
 psychophysiological techniques applied to aircraft design and other operational problems 0-26384  
 pupil diameter of observer's eye, effect of electron-optical convertor screen luminance 0-35890  
 pupillary escape, positive off-diagonal kernels as correlates of dynamic process 0-26229  
 pupillary system, human, same-signed 1st and 2nd -degree kernels 0-26228  
 pursuit after-nystagmus 0-41018  
 reading through pinholes, for teaching 0-17765  
 receptive field props. of neurones in visual cortex of cat 0-26227  
 research, the place of the library 0-30711  
 research laboratory, clinically oriented, tasks and goals 0-12083  
 response properties of fly visual systems 0-41021  
 retina photoreceptor membrane, light and GTP-regulated GTPase interaction 0-45897  
 retinal chromophore transition dipole moment, orientational changes obs. 0-41023  
 retinal diffusion and eye optics quality, OTF and light scatt. characterisation 0-41004  
 retinal ganglion cell response props. in Siamese cat 0-12115  
 retinal ganglion cells, responses to stationary and moving stimuli 0-51080  
 retinal ganglion cells of a tree shrew, definition of neural response and incremental sensitivity 0-41011  
 retinal horizontal cells, nonlinear characts. of spatial summation in receptive field, model 0-26232  
 retinal image stabilisation 0-12088  
 retinal L-type horizontal cells, dynamic interaction in receptive field 0-26233  
 retinal model, layered visual processing 0-16925  
 retinal neurons, catfish, spatiotemporal testing and modelling 0-41005  
 retinal receptor directional sensitivity, flicker effects 0-8057  
 retinal response, expected waiting time 0-51091  
 retino-suprachiasmatic tract, evidence for in the rat 0-21471  
 retinoscopy, near and cycloplegic, in early primary schoolchildren 0-8047  
 retinoscopy artefact in rat and rabbit eyes, origin at retina/vitreous interface obs. 0-51075  
 retinotectal pathway, uncrossed, development rel. to plasticity studies, rat 0-56025  
 retinotectal projection development, Gierer-Meinhardt eqns. appl. 0-56022  
 retinotectal projection development, mathematical model (*Japanese*) 0-21467  
 rhodopsin, photo- and thermo-bleaching rel. to heterogeneity problem 0-41114  
 rhodopsin, vertebrate, chromophore orientation obs. 0-40959



## vision continued

- rhodopsin, visual pigment, mag. anisotropy estimation 0-51137
- rhodopsin and its photoproducts, directional absorpt. props. obs. 0-51090
- rod ERG, human, dark-adapted a-wave response function obs. 0-56036
- rod outer segments, spread of activation and desensitisation 0-35881
- rod-cone interaction, spatial patterns 0-16930
- rod-cone interrelationships at light onset and offset 0-41022
- saccade-related unit activity in monkey superior colliculus 0-12101
- saccadic eye movement, accompanying pots. 0-12102
- saccadic eye-movement system, processing of direction and magnitude obs. 0-56035
- saccadic system, anal. by double step stimuli 0-41014
- shutter control system, rapid cycling, for expts. 0-41358
- spatial contrast sensitivity in albino and pigmented rats, behavioural obs. 0-41013
- spatial localisation during pursuit eye movements 0-51081
- spatial vision, psychophysical investigation, normal and reeler mutant mouse obs. 0-41032
- speckle movement in laser refraction 0-41001
- spectrally-opponent responses in ground squirrel optic nerve 0-35883
- Stiles-Crawford function, specification of directionality 0-45907
- stimulus onsets and offsets, response of visual mechanisms 0-16937
- striate neurons in area 17 of Siamese cats, response props. 0-12116
- superior colliculus and its sensory inputs, primate 0-12100
- threshold, transient increase due to combined changes in propagation direction and polarisation plane 0-51096
- threshold spatial vision, sensitivities to complex gratings and aperiodic stimuli 0-35888
- tracking, target vel. signals in vermal Purkinje cells, monkey obs. 0-56026
- transduction in photoreceptors with bistable pigments, prolonged depolarising afterpot. obs. 0-8050
- ventral photoreceptors, Limulus, excitation by photons and fluoride ions 0-8065
- vestibular nystagmus, Alexander's law model 0-35878
- visual field plotting using eye movement response 0-8045
- visual pigment, steady-state composition in rainbow trout 0-51097
- visual pigment chromophores, models, spectroscopic and photochemical studies 0-30723
- visual pigment processes and prolonged pupillary responses in insect photoreceptor cells 0-8061
- visual pigment regeneration studies, use of [ $^{15}\text{H}$ ]all-trans-retinal tracer 0-41357
- Visual pigment systems, implications of bistability 0-8059
- visual pigments, conf., Florence, Italy (Sep. 1978) 0-4468
- visual pigments, resonance Raman studies of the primary photochemical event 0-41020
- visual Wulst retinotopic organisation in nocturnal and diurnal raptors 0-12098
- working position illumination, factors affecting good vision and efficiency (*Spanish*) 0-3638

## vision defects

- see also contact lenses*
- 100-Hue response, scotopic axis 0-26236
- accommodation orthoptics, objective assessment of dynamic insufficiency 0-45884
- acuity deterioration in acquired colour vision deficiencies 0-56040
- amblyopia, acuity and contour interactions across the visual field, expt. obs. 0-56038
- amblyopia, visual acuity and contrast sensitivity rel. to stimulated region of the retina 0-45893
- amblyopia, visual development in humans, animal models 0-12118
- ametropia, expt. obs. of speckle motion in laser refraction 0-45879
- aniseikonia, eikonic lens design for minus prescriptions 0-46095
- anisometropia, artificially induced, effect on separable binocular processes 0-45906
- astigmatism, acuity development in normal and astigmatic infants 0-12151
- astigmatism of oblique rays and TiO glass lenses (*Italian*) 0-56278
- brain damage patients, 'extinguished field' information processing 0-30728
- chromatic aberration, effect of yellow ocular filter, fish eye 0-8046
- colour, exchange threshold method of anal. in humans 0-12129
- colour blindness and opponent-colours theory 0-12133
- colour defects, X-chrom lens (*Italian*) 0-17186
- colour vision, normal and dichromatic, vector model 0-51099
- constant esotropia with anomalous correspondence, home visual therapy 0-8207
- contact lens, soft, base curve radius selection, sagittal depth considerations 0-46096
- dark adaptation, normal and pathological data-distinguished by dark adapter 0-41019
- divergence excess, prevalence and management 0-35877
- ergo-ophthalmology and ergo-optometry (*Italian*) 0-26223
- exotropia, intermittent, of divergence excess type, panoramic viewing, visual acuity and anomalous retinal correspondence 0-51076
- extinction photometry, entoptical scatter, model 0-51087
- eye strain and chromatic asthenopia rel. to affectations of optic pathways (*Italian*) 0-56041
- Friedmann quantitative analyser for study of posterior pole disease (*Italian*) 0-17172
- fusional amplitude deterioration in diabetic people 0-26224
- glaucoma, optic disc changes meas. using retinal stereophotogrammetry 0-3757
- Haidinger's brushes, recent explanation and their clinical use 0-45880
- Hudson-Stahl line of the cornea, prevalence obs. 0-35876
- lateral geniculate nucleus in dark-reared cats, Y cell loss without cell size changes 0-3644
- meridional amblyopia 0-12150
- myopia, corrected and uncorrected, effect of pupil size on visual acuity 0-45882
- myopia, Prentice Memorial Lecture [optometry] 0-27089
- myopia, spherical error of refraction, statistical anal. of biological theory 0-45881
- myopia incidence changes following classroom environment changes 0-12080
- nystagmus, congenital, orientational detect. modification obs. 0-56039
- primary glaucoma etiopathogenesis 0-12086
- pseudophakic patients, binocularity evaluation 0-51106

## vision defects continued

- refraction meridional differences and illum. depend., sharpness and recognition thresholds of defocused targets 0-16922
- refractive error measurement by Ophthalmotron, cycloplegia effect 0-41002
- refractive keratoplasty, theory and computations of optical modification to cornea 0-35875
- retinal degeneration, hereditary, cone inputs to ganglion cells 0-8056
- scotopic axis in 100-Hue response of congenital defectives under high press. Na illum. 0-16940
- soft contact lenses, future developments 0-12310
- spheroidal degeneration of cornea and conjunctiva, pathology 0-12085
- strabismic amblyopia in infants 0-30715
- strabismus and amblyopia, eye movement analysis by computerised ocular motility test system 0-41299
- stress, functional consequences, annotated bibliography 0-26222
- therapy of strabismus, amblyopia and learning disorders, rel. to visual deprivation studies 0-12081
- time-varying response anomalies 0-16935
- tritanomaly detection, optimisation of a Rayleigh-type equation 0-56044
- visual cortex, altered connections in Siamese cat 0-12091
- visual auroras** *see aurora*
- visual perception**
  - acuity development in normal and astigmatic infants 0-12151
  - analyser space-frequency filter harmonisation with statistics of images 0-30726
  - apparent vernier offset, acuity obs. 0-16949
  - asynchronous gratings summation obs. 0-35901
  - auditory-visual perception of speech with reduced optical clarity 0-35919
  - binocular depth discrimination, spatio-temporal aspects, Mach-Dvorak effect 0-12149
  - binocular vision, effect on separable processes of artificially induced anisometropia 0-45906
  - binocular vision, fusional vergence eye movements rel. to fixation disparity 0-56031
  - binocularity evaluation of pseudophakic patients 0-51106
  - brain damage patient, 'extinguished field' information processing 0-30728
  - brightness increase effect due to direction of light polarisation 0-41041
  - Broca-Sulzer effect, combined temporal and spatial unified model 0-35893
  - changing size perception, effect of object size 0-51108
  - chromatic input to stereopsis, calcs. 0-16948
  - colour, exchange threshold method of anal. in humans 0-12129
  - colour vision perception in Greek literature 0-22184
  - complex shaped objects, visual resolution and recognition, vibr. influence (*Russian*) 0-45909
  - constancy limits, colour, and colour perception 0-41025
  - contrast, edge-induced, Crack-O'Brien effect 0-35894
  - contrast perception, suprathreshold response obs. 0-30729
  - contrast sensation, stimulus contrast obs. 0-41040
  - contrast sensitivity, orientation anisotropy in rhesus monkey, behavioural study 0-45912
  - contrast thresholds versus border enhancement, sensitivity to retinal defocus 0-30725
  - critical flicker fusion in normal and binocularly deprived cats 0-35898
  - cross-modal and intramodal matching tests, tape construction method 0-41334
  - depth perception by motion, instability 0-35895
  - depth perception from spatial freq. difference 0-41033
  - EEG contingent negative variation rebound effect, visual and auditory stimuli 0-3648
  - egocentric distance, oculomotor rel. to motion parallax cues 0-45914
  - experience neural correlates in single units of cat visual and somatosensory cortex 0-12120
  - extrafoveally perceived displacement, illusory reversal 0-56048
  - eye movement amplitudes, information used by the perceptual and oculomotor systems 0-35885
  - eye movement role in hand movement control 0-26237
  - Fechner-Benham colour effect, hue reversal following white light adaption 0-51112
  - field size utilised by human visual system, static and dynamic conditions 0-12135
  - fields, computer appls. 0-45892
  - figure-ground discrimination by relative movement, fly appl. 0-56046
  - form vision, role of geniculocortical system, behavioral anal., cat 0-12137
  - generation and display of visual stimuli, psychology experiments, microprocessor based system 0-41328
  - grating acuity of the wild European rabbit 0-35900
  - gratings, coloured, perceived duration, interocular effects of adaption 0-56051
  - grouping, new approach 0-12142
  - hallucination patterns, mathematical theory of neuronal activity 0-35892
  - hue change with eccentricity, rod and cone contribs. 0-45904
  - hue change with rod intrusion during dark-adaptation 0-51104
  - illusions and visual functions 0-12143
  - illusory movement perception obs. 0-21473
  - image matching with the eye, effects of pictorial noise 0-51113
  - lateralisation effect in reading Chinese characters. 0-30727
  - light adaptation in cone photoreceptors, dark glasses model 0-12122
  - masking independent of both separation and spatial frequency 0-16947
  - matching information to brain, problems 0-51114
  - microcomputer controlled haploscope for binocular experiments 0-46091
  - mirror symmetry detection in random dot displays, versatility and absolute efficiency 0-16944
  - monocular space perception and visual stability, math. model 0-45910
  - motion in depth, information processing 0-21474
  - motion perception, form in formation is necessary 0-16950
  - motion perception rel. to smooth pursuit eye movements 0-3649
  - motion smear 0-56047
  - movement detection, upper-velocity threshold 0-8067
  - Necker cube perceptual reversal, absence of accommodation 0-41037
  - opponent chromatic mechanisms predict hue naming 0-12132
  - opponent-colours theory and colour blindness 0-12133
  - optical instrument image evaluation by multitarget array detection 0-1362
  - optical system quantitative tolerance specification and standard development 0-48384
  - optical system specification and test procedures 0-48385
  - orientation discrimination 0-12141
  - pattern detection, absolute efficiency, humans 0-12138



**visual perception continued**

- pattern discrimination, phase-dependent interaction of widely separated spatial freqs. 0-45913  
 patterns, drifting contrast, electronic device for generation 0-26421  
 perspective distortion in photography, eye as simple lens 0-17734  
 psychophysical function, harmonisation of Fechner and Stevens 0-8068  
 psychophysiological function of the human eye (*Czech*) 0-21472  
 Pulfrich effect study device, versatile, multi-input 0-8221  
 radiographic image formation, perceptual eval. of phys. parameters, computer-simulated images 0-41222  
 radiography, computed, contrast-detail-dose evaluation 0-41221  
 radiography, detection of bars and discs in quantum noise [radiography] 0-41042  
 resolution and contour interaction in the fovea and periphery 0-51109  
 retina, significance of antidromic potentiation and induced activity 0-12092  
 simulation and image realism, seminar, San Diego, USA (Aug. 1978) 0-3639  
 size constancy, failure below half a degree 0-45911  
 size constancy, visual angle constancy of subjective checkerboard pattern 0-16945  
 spatial filtering constrained by biological data 0-30731  
 spatial frequency, perceived shift at orientations orthogonal to adapting gratings 0-51110  
 spatial frequency channel interactions in human visual system 0-12140  
 spatial organisation of human visual system at detect. threshold, status of research 0-12139  
 spatial vision, cat 0-12136  
 speckle motion in laser refraction, apparent speed obs. 0-45879  
 speech, visual vowel and diphthong perception from two horizontal viewing angles 0-35923  
 speechreading, visual perception of syllables and sentences, age effects 0-16943  
 stereopsis, absolute thresholds as meas. by crossed and uncrossed disparities 0-45908  
 stereopsis, contrast disparity obs. 0-41034  
 stereopsis, obs. of independent channels for different extents of spatial pooling 0-56052  
 stereopsis, orientation and position disparities 0-12145  
 stereopsis, synkinetic interaction of convergence accommodation and accommodation convergence 0-51111  
 stereopsis in monkeys using random dot stereograms, effect of viewing duration 0-41038  
 stereopsis mechanisms 0-12148  
 stereoscope vergence, convergence and divergence independence obs. 0-30714  
 stereoscopic depth channels for position and for motion 0-12146  
 stereoscopic depth perception, underlying neural mechanisms in visual cortex of cat 0-12147  
 stimulus effect on surrounding visual space, induction field effect (*Japanese*) 0-8066  
 stimulus subjective offset and total persistence obs. 0-56056  
 texture similarity judgments, spatial frequency bases 0-30730  
 tilt effect due to viewing large, patterned rotating field 0-41035  
 tilt illusion and tilt aftereffect, linear summation 0-35897  
 time frequency response of visual analyser and linearity eval. (*Russian*) 0-41031  
 two movement directions of intermingled dot fields, mutual repulsion 0-56050  
 vertical fusional vergence ranges of the rhesus monkey 0-35899  
 waterfall illusion in an insect visual system, expt. obs 0-56055

**visualisation, particle track** *see particle track visualisation***vitreous state**

*see also electron energy states of amorphous solids; glass; glass transition*

- alkali metal polyphosphates, vitreous IR spectra 0-16043  
 alkaline glassy state, aq., density determ., radiation chem. 0-42197  
 ceramic suspension, rheological properties, effect of grainy filler ceramic suspensions 0-43685  
 ceramics, glassy phase, struct. study through electron-beam induced ionisation effects, HVEM obs 0-14978  
 decalin, liq. and glass mol. motion, kinematic and electrodynamic solns. 0-25293  
 dielectric relaxation, theory, appl. of derived dielec. loss formula 0-50262  
 diffusion of radical-ion pairs, spatial distrib., electron spin echo obs. 0-29622  
 electron trap relaxation model, for glassy polar matrix 0-15470  
 ethanol glass, trapped and solvated electrons produced in presence of applied electric field 0-7379  
 glass-forming systems, structure (*Russian*) 0-38925  
 glass-forming systems, structure and thermodynamics (*German*) 0-38924  
 glycerol, cryst. and glassy states, sp.ht. 0-2176  
 ionicity and coordination, tight binding calcs. 0-49129  
 liquids, glass-forming, viscous flow and valence config. theory 0-14756  
 lunar regolith fine fraction, Luna-24 slow positron probe 0-26762  
 mathematical models of disordered systems, book 0-1878  
 methanol glass solvated electrons, EPR, <sup>1</sup>H spin flip satellites, geometrical model 0-7146  
 2-methyltetrahydrofuran-methanol mixed glasses, annealed,  $\gamma$ -ray produced electrons transfer from IR to bisible traps 0-11440  
 microscopic theory 0-44137  
 molecular fluoresc., phosphoresc., and ODMR line narrowing in solids 0-43084  
 nylon 6, oriented glassy, mol. wt. influence on cryst. rate 0-44156  
 organic glass, electron-cation recombination; charge distrib. simulation and luminesc. kinetics 0-2855  
 PET, glassy polymer, local struct. determ. 0-33904  
 PMMA, glassy, photoelasticity 0-45034  
 polyacrylonitrile glassy polymer, energetics of gas sorption 0-29270  
 polycarbonate, glassy polymer, energetics of gas sorption 0-29270  
 polyethylene terephthalate, glassy, energetics of CO<sub>2</sub> sorption 0-29270  
 polymer, glassy, sheets and spheres, gel diffusion with discontinuous swelling 0-44354  
 polymer, isobaric vol. and enthalpy recovery, transparent multiparameter theory 0-24375  
 polymer, solvent osmotic stresses, prediction of Case II transport kinetics 0-26049  
 polymer glasses, aged, enthalpic state determ. by scanning calorimetry 0-6528  
 polymers, vitreous, quasibrittle fracture 0-21094

**vitreous state continued**

- polypropene-alt-1,4-butadiene and hydrogenated derivative, mol. relaxations in glassy state 0-53177  
 polystyrene, glassy, light scattering, quenching effect 0-20649  
 polystyrene, glassy state, relax., free vol. fluctuations effect 0-19722  
 polystyrene, sorption of organic vapours, glassy-state relaxation induction and meas. 0-44415  
 polystyrene-b-isoprene and hydrogenated derivative, mol. relaxations in glassy state 0-53177  
 PVC, sorption of organic vapours, glassy-state relaxation induction and meas. 0-44415  
 quartz, irradiated, fused, crystalline, absorpt. spectra, colour centres 0-7384  
 real liquids, quenched to glassy state, struct., one dims. Ising model appl. 0-54134  
 silicate glaze, diffusion of Sn(IV) 0-49417  
 styrene-isoprene triblock copolymer, mol. relax. in glassy state 0-53177  
 tektites and natural glasses, Mossbauer anal. 0-21952  
 o-terphenyl, dipolar solutes, reorientational motions, dielectric relax. below glass transition 0-19706  
 As<sub>2</sub>O<sub>3</sub>, glassy, intermediate range order from polarised features of Raman spectrum 0-49113  
 As<sub>2</sub>O<sub>3</sub>, vitreous, local struct. and vibrational spectra 0-55091  
 B<sub>2</sub>O<sub>3</sub>, glassy, influence of annealing on transition region 0-44145  
 B<sub>2</sub>O<sub>3</sub>-K<sub>2</sub>O-Na<sub>2</sub>O-Rb<sub>2</sub>O-Cs<sub>2</sub>O glass, small angle X-ray scatt. exam. of struct. 0-38922  
 C, glassy and fibrous, density of states, magnetoresistance theory appl. 0-44620  
 Ca(NO<sub>3</sub>)<sub>2</sub>-H<sub>2</sub>O system, induction period supercooling depend. meas. 0-19918  
 Co enamel, vitreous, objective colour evaluation, rel. to firing parameters (*Czech*) 0-42252  
 Co-Si interface, metal-semiconductor transition, rel. to first compound nucleation 0-24771  
 D<sub>2</sub>, solid, quadrupolar glass ordering NMR adsorption line shapes 0-7178  
 GaCl<sub>3</sub>, Raman spectral differences from liquid to glassy state, ionic equilib. interpretation 0-20619  
 GeO<sub>2</sub>, glassy high freq. vibr. bands, central force model 0-49330  
 GeO<sub>2</sub>, structural analysis, using fluorescence excitation (*German*) 0-38923  
 H<sub>2</sub>, solid quadrupolar glass, relax. time and low temp. sp.ht., computer simulations 0-49377  
 H<sub>3</sub>PO<sub>4</sub>-H<sub>2</sub>O, superviscous and glass, relax., <sup>111</sup>Cd TDPAC obs. 0-15831  
 (Li,Na,K) (Nb,Ta)O<sub>3</sub>, pseudo-binary and ternary systems quenched metastable glassy and cryst. phases 0-29935  
 LiNbO<sub>3</sub>:Cr<sup>3+</sup> glass, roller quenched, crystn. kinetics 0-44143  
 MoF<sub>6</sub>, mol. and electronic struct., vitreous, liq., and tetrameric states, <sup>19</sup>F NMR obs., mol. mobility 0-34787  
 NaClO<sub>4</sub>, aq. glass, formation of trapped H-atoms and electrons on X-irrad. 0-35559  
 Pb ceramic glaze, Cu<sup>2+</sup> doped, Pb<sup>2+</sup> release 0-49101  
 Se, elastic coeffs. about glass transition temp. US study (*French*) 0-19865  
 Se, glassy, pure and K-doped, photolum. and optically induced ESR 0-50398  
 Se, trigonal, vitreous and red amorphous, phonon density of states comparison 0-54329  
 Se, vitreous, darkened films, thermal and optical bleaching, light transmission obs. 0-50447  
 SiO<sub>2</sub>, effect of high-dose X-rays and reactor radiation 0-19838  
 SiO<sub>2</sub>, fused, ion beam induced luminescence 0-40166  
 SiO<sub>2</sub>, fused, structural analysis, using fluorescence excitation (*German*) 0-38923  
 SiO<sub>2</sub>, glass, <sup>29</sup>Si hyperfine struct. of E' centre, microwave saturation props. 0-7165  
 SiO<sub>2</sub>, impurity C determ. by isotopic spectral method 0-26093  
 SiO<sub>2</sub>, intrinsic surface phonons, Raman scatt. and IR refl. 0-24728  
 SiO<sub>2</sub>, irrad., EPR of Al E' centres 0-11268  
 SiO<sub>2</sub>, low temp. thermal props. and intrinsic defects 0-29057  
 SiO<sub>2</sub>, multiphonon IR absorpt. 0-25381  
 SiO<sub>2</sub>, resist. to NaOH 0-21143  
 SiO<sub>2</sub>, struct. and phonon spectra 0-50324  
 SiO<sub>2</sub>, vitreous, heat treatment effect on viscosity and struct. 0-19714  
 SiO<sub>2</sub>, vitreous, intrinsic radiation defects, nonbridging O 0-19837  
 SiO<sub>2</sub>, vitreous, non-bridging O centre, optical props. and energetic struct. 0-34976  
 SiO<sub>2</sub>, vitreous, Raman active defects, thermal equilibration 0-55092  
 SiO<sub>2</sub>, vitreous film on Si, defect struct. comparison with crystalline SiO<sub>2</sub> and Si-O bond nature 0-54557  
 SiO<sub>2</sub>, vitreous films on Si, channel and network defects 0-54142  
 SiO<sub>2</sub>:Fe, absorption spectra and structural state of Fe<sup>3+</sup> ion 0-16071  
 SiO<sub>2</sub>:Nd<sup>3+</sup> films, cathodoluminesc. 0-20717  
 SiO<sub>2</sub>-based glassy layers, passivating Cu at 500°C 0-3246  
 Sn (IV) in glassy aq. soln., Mossbauer spectra 0-15894  
 TeO<sub>2</sub>, structure simulation of some tellurite and chalcogenide glasses quasi-crystalline structural diffusion method (*Russian*) 0-54147  
 TeO<sub>2</sub>-NaCl-(NaBr), condition diagram, thermographic obs. (*Russian*) 0-55377  
 YIG, amorphous, ionic glass, hard-sphere random-packing model 0-24369  
 ZrSiO<sub>4</sub>, heavy ion irrad., metamict zircon form. 0-2088

**vitrification**

- ceramics, consisting of quartz, feldspar, and kaolin, compaction press. during firing effects 0-29909  
 chalcogenide melts, glass form. regions calc. using empirical theory of glass form. 0-33894  
 epoxy resin, cure history effect on dynamic mech. props. 0-54356  
 fission products solutions at Marcoule, description and hot operation results 0-5270  
 fluoride systems, fundamental condition for glass formation 0-44135  
 glass, structure, influence of thermal history (*German*) 0-38930  
 glass forming and props. 0-19717  
 Lennard-Jones liquid, mol. dynamics studies of glass form. 0-38896  
 liquid-glass transition, free volume approach, thermodynamic behaviour 0-1940  
 nonmetallic compounds, type A<sub>2</sub>B<sub>3</sub>, glass form. from melt 0-44140  
 polyester-organic solvent mixtures, phase diagrams, eutectic props., devitrification, crystn. (*French*) 0-3015



**vitrification continued**

- Purex solvent extracting system, monitoring and control instrumentation 0-37566
- radioactive liquid waste, thermal decomp. of Harvest feed slurries 0-52757
- radioactive waste conversion to glass, exptl. joule-heated ceramic melter 0-18471
- thermosetting materials, formation and props., phase diagram and torsion pendulum anal. 0-55381
- As-S, amorphous, glass transition and specific heat, intermolecular bond saturation 0-15011
- As-Se, amorphous, glass transition and specific heat, intermolecular bond saturation 0-15011
- B<sub>2</sub>S<sub>3</sub>-Ti<sub>2</sub>S system, phase diagram and verification 0-35165
- Cu<sub>56</sub>Zr<sub>44</sub> metallic glass, devitrification and its effect on mech. props. 0-33893
- Fe<sub>78</sub>Mo<sub>2</sub>B<sub>20</sub> glass, thermal expansion, glass transform. and crystn. temps. 0-2183
- Fe<sub>3</sub>Ni<sub>36</sub>Cr<sub>14</sub>P<sub>12</sub>B<sub>6</sub> glass, thermal expansion, glass transform. and crystn. temps. 0-2183
- Fe<sub>40</sub>Ni<sub>40</sub>P<sub>14</sub>B<sub>6</sub> glass, thermal expansion, glass transform. and crystn. temps. 0-2183
- Ge-S-Se system, glass-forming, struct. and props. 0-19713
- Ge-S-Te system, glass forming 0-19718
- LaF<sub>3</sub>-BaF<sub>2</sub>-ZrF<sub>4</sub>(-MF), M=Na, Li, glassy transition, refr. index, density and molar refr. 0-1937
- Nb<sub>40</sub>Ni<sub>40</sub>, amorphous, pair distrib. function, temp. depend., rel. to glass transition 0-24368
- P-S, amorphous, glass transition and specific heat, intermolecular bond saturation 0-15011
- P-Se, amorphous, glass transition and specific heat, intermolecular bond saturation 0-15011
- SiO<sub>2</sub> fused powder, difference between white and black silica, devitrification rates 0-28918
- SiO<sub>2</sub>-(TiO<sub>2</sub>) glass prep., melting (*Polish*) 0-40316
- SnSe-GeSe<sub>2</sub>-As<sub>2</sub>Se<sub>3</sub> glasses, vitrification region and elec. cond. 0-15008
- TiO<sub>2</sub>-Ti<sub>2</sub>O<sub>3</sub>-P<sub>2</sub>O<sub>5</sub> glass form., struct. and elec. props. 0-44592
- Tl-Ge-S system, glass forming 0-19716

**Vlasov equation**

- Bernstein modes in electron cyclotron heating of Tokamak, Vlasov dispersion eqn. 0-33809
- crystal thermodynamics in statistical theory, density Fourier coeffs., stress tensor, internal energy 0-13025
- cubic crystals, temp. series in statistical theory 0-17895
- cyclotrons resonance maser, Vlasov-Maxwell eqns., guided wave field theory 0-14309
- dispersion eqn. from linearised Vlasov eqn. with local approx. for laser produced plasma instabilities 0-38687
- dispersion function for anisotropic longitudinal waves 0-14891
- electron gas with external mag. field, Vlasovs equation with mollified density 0-1756
- electrostatic ion cyclotron electron drift instability anal. using linear Vlasov dispersion reln. 0-1780
- electrostatic Vlasov turbulence, iterative soln. 0-10375
- high freq. rad. field in turbulent plasma 0-38648
- hot nonuniform magnetised plasma wave propag. theory, Vlasov eqn. perturbation expansion 0-33768
- ion beam with rotational and axial motion, thermal equilibrium props. 0-53934
- Langmuir wave evolution, three dimensional kinetic model, Vlasov eqn. calcs. 0-43923
- laser-fusion regime, plasma transport, extension of Braginskii system of fluid equations 0-53935
- linearised form of Vlasov plasma, optimal control 0-53920
- non-linear transport equations: Properties deduced through transformation groups 0-4680
- plasma, coherent four-wave scatt., appl. to plasma diagnostics 0-28681
- plasma, renormalised Vlasov turbulence 0-19579
- plasma sheath, integro-differential eqns., nonlinear, nonlocal, soln. formalism 0-43936
- relativistic electron beam, Vlasov eqn. in plasma medium 0-14910
- screw-pinch configs., collisionless, hybrid-kinetic stability props. of high-beta plasmas 0-43871
- sharp boundary Vlasov-fluid screw pinch, free and forced m=0 oscillations 0-38636
- stochastic equations of motion for plasma particles 0-38551
- theta pinch, rigidly rotating, Vlasov fluid stability 0-28794
- Bi, Bernstein waves, electrostatic wave dispersion relation in mag. field 0-34471

**V<sub>2</sub>O<sub>5</sub>-P<sub>2</sub>O<sub>5</sub> semiconducting glasses see amorphous semiconductors****vocoders**

- see also speech synthesis
- C-CD discrete Fourier transform processors for channel vocoder 0-53568
- deaf speech and hearing aids, vocoders, frequency lowering and lipreading cues 0-12309
- digital, optimization by exploiting human auditory masking 0-33356
- digitizers for present day and for mid 1980s, practical implementation 0-33357
- tactual vocoder, max. information transmission, time-invariant stimulation (*Japanese*) 0-41317

**voice see speech****voice coders see vocoders****voice communication**

- sub-band coding with adaptive bit allocation 0-28386
- through-water diver communication system Wet-Phone, voice or switch operated, 31.5 KHz carrier, 1350 m range 0-38187
- transmission channel quality determining physical method 0-33369

**voids (solid)**

- α-brass, metallographic and fractographic study of void formation during creep 0-16449
- cavity growth, creep mechanisms, independent and sequential 0-55480
- cavity size distrib. functions evolution, numerical study for 1 MeV electrons 0-2072
- defect clusters, nucleation and growth due to energetic particle radiation, chemical rate reaction theory, computer program 0-49263
- ductile metals, spontaneous void growth in elastic and elastic/plastic media 0-48567
- epoxy treeing breakdown, slit model 0-15970
- ferrites, void, conc. and dimensions determ. by acoustic charact. 0-35472
- ferromagnet containing void, Gibbs free energy, numerical calc. 0-29597

**voids (solid) continued**

- film, microporosity described in terms of vacancies and voids 0-24769
- fission reactor materials, void swelling calculations using FACSIMILE VSI 0-42782
- fluorene, γ-irrad., void form. 0-2068
- fusion materials, heavy ion irradiation, swelling theory 0-34090
- fusion reactor first wall material, mobile He inclusion in void swelling rate theory model 0-34069
- fusion reactor metals, irradiated, defect cluster nucleation, He injection effect 0-34091
- fusion reactor metals and alloys, microvoid form., gaseous impurity atom effects, positron annihilation study 0-49275
- gas bubbles in solids, simultaneous hetero- and homogeneous nucleation model 0-2066
- graphite nucleation, role of pre-heat treatments (*Japanese*) 0-35220
- growth, defect theory and processes, review 0-2009
- Hastelloy C-4, loaded at high temp., useful life 0-40523
- ion bombardment, electron microscopical anal. of surface effects and volume defects, review (*Rumanian*) 0-29093
- ion exchange resins, macroporous rapid method of rating total void volume 0-21208
- irradiation effects, void nucleation, swelling, creep, rate eqns. 0-49274
- Kevlar 29 and 49, aramid fibres, microvoid obs. 0-38960
- lenticular, thermal gradient migration 0-2216
- metal, effects of large scale voids on thermal magnetoresist. 0-10946
- metal, trapping of H, book contrib. 0-24491
- metal ductile fracture, void growth stress/strain relations (*French*) 0-19280
- metals, irradiation induced swelling, bias factor 0-2062
- metals, radiation effects on elasticity and elastic moduli, yield stress 0-2078
- Nimonic PE16, He injected, bubble-void transitions in Ni ion bombard. 0-34095
- nuclear fuel, transport phenomena under severe temp. gradient 0-615
- point defect production in irradiation, swelling, cascade diffusion theory 0-34044
- polycrystals, intergranular void stability during diffusion growth (*Russian*) 0-10540
- polyethylene, ultrahigh modulus, drawing temp. effect on void form. and modulus 0-35241
- polyethylene insulation of HV cables, water-treeing, environmental stress cracking phenomenon of elec. origin 0-40575
- polystyrene filament, melt spun, struct. and mech. props., effect of drawing, twisting, annealing, untwisting 0-45331
- precipitate hardened material, intergranular cavity growth inhibition 0-50677
- pulsed radiation effect on void growth and swelling 0-34043
- radiation effects, sink strength of random array of voids, steady-state diffusion problem, variational technique 0-49266
- reactor fuel element defects, loss of cladding tightness, anal. of fuel element exploitation (*Czech*) 0-52736
- refractory fusion reactor materials, neutron irrad., microstruct., voids, nucleation TEM study 0-29065
- SEM of sintered materials, qualitative and quantitative study of voids 0-16212
- spherical voids, elastic wave scatt. at long wavelengths 0-48480
- steel, alloy, forgings, H precipitation kinetics, diffusion to voids, effect on shattercrack formation 0-16344
- steel, austenitic, annealed, Ni ion bombardment, swelling temp. depend. effect of He implantation 0-29080
- steel, austenitic, gas implantation effects, fusion reactor first wall damage simulation 0-29079
- steel, austenitic, tempering cavity condensation (*French*) 0-55442
- steel, austenitic, type En58B, martensite formation and reversion, effect on void swelling 0-11641
- steel, austenitic, type M316, martensite formation and reversion, effect on void swelling 0-11641
- steel, austenitic stainless, type 316, irradiated with 46.5 MeV Ni<sup>6+</sup> ions, soluble C effect on void swelling and low dose dislocation structs. 0-49280
- steel, austenitic stainless FV548, neutron irradiated, Si-rich phase occurrence of M<sub>6</sub>C phase 0-15156
- steel, austenitic type 316, continuous gas generation effects in neutron and simulation environments 0-34068
- steel, Cr-Ni (18%, 12(8)%), martensite formation and reversion, effect on void swelling 0-11641
- steel, ferritic, void swelling during irradiation, suppression mechanisms 0-6441
- steel, ferritic alloy and martensitic stainless, void swelling response after fast reactor irradiation 0-6437
- steel, nonmetallic inclusion, effect on hot ductility 0-29999
- steel, Si, electron irrad. in HVEM, void swelling, Si role 0-54285
- steel, stainless, depth distrib. of swelling, TEM exam. 0-15165
- steel, stainless, He effects on microstruct. in ion-irrad. 0-29078
- steel, stainless, He ion bombard., in situ electron microscope examination 0-34094
- steel, stainless, laser fusion reactor first wall, void growth charact. 0-34042
- steel, stainless, type 316, neutron irrad., Ni ion bombard. effects of injected interstitials on void volume 0-34092
- steel, stainless, void swelling, Si point defect trapping, interstitial loop growth rate temp. depend. obs. 0-49270
- steel, stainless, void swelling obs., under HV electron microscope (*Japanese*) 0-54218
- steel, type FV548, 1 MeV electron irradiated, influence of pre-injected He on void nucleation and growth 0-34054
- superconducting composites, Kirkendall void elimination by solution anneals 0-7520
- swelling rate, vacancy dislocation loop effect 0-2084
- TEM contrast of void arrays in crystals 0-14975
- TEM observation of cavities, review of techniques 0-14974
- thermoplastics, structural changes during deformation, rel. to impact resistance 0-25800
- void sink strength depend. on mutual recombination, point defect loss to fixed sinks 0-33995
- Ag thin films, deposited by cathodic sputtering using high-resolution electron microscopy, voids obs. 0-49557
- Al, high purity, neutron irradiated, void annealing kinetics 0-44234
- Al-SiO<sub>2</sub>-Si, void form. in Al interconnection lines at Si-SiO<sub>2</sub> boundaries 0-2476
- n-Al<sub>0.9</sub>Ga<sub>0.1</sub>As, Au-based ohmic contacts TEM obs. 0-34509



**voids (solid)** continued

- Au, epitaxial film, on NaCl substrate, electrotransport inferred from void growth rate (*German*) 0-10699  
 Au film, effect of high DC density stressing on pre-existing voids 0-24770  
 CaF<sub>2</sub>, fine-grained, forging and bulk optical props. 0-33103  
 CdTe:P, annealing induced lattice defects, TEM obs. 0-2010  
 Co-Ga  $\beta'$  quenched single crystals, annealing-out of point defects 0-55426  
 Cu alloy, superplastic, microscopic examination of internal void formation 0-16383  
 Fe, BCC, void nucleation following electron irradi. 0-29054  
 $\alpha$ -Fe, irradiation induced void swelling, Cr additions effect 0-55408  
 $\alpha$ -Fe, void swelling during irradiation, suppression mechanisms 0-6441  
 $\alpha$ -Fe, void swelling response after fast reactor irradiation 0-6437  
 Fe-Cr, irradiation induced void swelling, Cr additions effect 0-55408  
 Fe-Ni-Cr, pulsed HVEM irradi., effect on microstruct. evolution 0-34053  
 Ge, amorphous, pure and H doped, voids, atom probe FIM 0-49107  
 H assisted cracking, mechanisms, review 0-50721  
 InSb, ion implanted, efficient void form., TEM obs. 0-44237  
 LiF, radiation induced voids, formation on dislocations 0-15159  
 Mo, BCC, void nucleation following electron irradi. 0-29054  
 Mo, microstruct., swelling induced by ion bombard., He injection effects 0-29083  
 Mo, neutron irradiated, void swelling and shrinkage, TEM study 0-34079  
 Mo tips, film coated characterisation by atom probe FIM, atomic clusters, voids 0-33863  
 Mo-Ti-Zr (0.5, 0.1 wt.%), neutron irradiated, void swelling and shrinkage, TEM study 0-34079  
 Mo-Zr, heavy ion irradiated, void swelling, phase instability 0-29084  
 Nb, BCC, void nucleation following electron irradi. 0-29054  
 Ni, cavity evolution in 500 keV <sup>4</sup>He<sup>+</sup> irradi. 0-29082  
 Ni, void swelling rates in self-ion irradi. sample 0-29081  
 Ni-Co-Cr-Al-Y, plasma-arc-sprayed, metallurgical characts. and oxidation behaviour 0-40618  
 Ni-Si, proton irradi.,  $\gamma'$  precipitation, early stages 0-34096  
 PbS film, vac. deposited, optical and phys. props. 0-2315  
 Si, amorphous, hydrogenated, small angle X-ray scatt., void distrib. 0-15087  
 Si-H, amorphous, random network model 0-1932  
 V, purification and plastic props. 0-25810  
 V:N, ion bombard., void form. 0-34097  
 V:O, neutron irradi., void form., 673-1073K 0-29066  
 V-Ni, ion bombard., void form. 0-34097  
 W, ion irradiated, defect clusters obs. 0-2089  
 W-Mo, vapour deposited, long-term strength and thermocyclic creep 0-16405  
 Zn-Al (22 at.%) eutectic, superplastic, microscopic examination of internal void formation 0-16383  
 Zr-base alloys, annealed specimens, irradiation growth 0-49276

**Voigt effect** *see magneto-optical effects*

**volatilisation** *see vaporisation*

**volcanology**

- 1923 to 1957, volcanic eruptions effects on atmospheric transmission, Smithsonian Astrophysical Observatory meas. 0-17374  
 Afar region plate tectonics, seismic and volcanic evidence 0-21700  
 Aleutian subduction zone seismicity, volcano-trench separation, rel. to great thrust-type earthquakes 0-21655  
 alkali basalts, Nd, Sr isotope geochemistry rel. to metasomatically veined mantle heterogeneities 0-56420  
 andesites, Andean region, petrogenetic composition variations 0-8313  
 Antarctic Peninsula igneous rocks, transverse geochemical vars. rel. to calc-alkaline magmas genesis 0-56466  
 Asal-Ghoubbet rift zone, Afar, 1978-9 geodetic survey after seismo-volcanic activity 0-46164  
 ash generated by ignimbrite/sea water explosions 0-26480  
 Azores, K-Ar age of oldest volcanics, volcanic history 0-46158  
 basalt glasses from FAMOUS area, Mid-Atlantic Ridge, regional var. and petrogenesis 0-31041  
 basalt petrogenesis, role of dynamic partial melting 0-46179  
 basaltic pillars, in collapsed lava pools on deep ocean floor 0-3991  
 Belgium, possible volcanic anomalies 0-21691  
 Campanian tuff ash layer (Y-5) in E.Mediterranean, age, origin and volcanology 0-56444  
 clinopyroxenes from deep-sea basalts, statistical anal. of chemistry 0-41437  
 deep-sea basalts, He and Xe as measure of magmatic differentiation 0-31040  
 Denchai Basalt, N.Thailand, paleomagnetism, age and geochemistry 0-41421  
 dust loading of atmos., 1923-54, pyrheliometric and circumsolar sky radiation obs. 0-46240  
 Eifel fields, pliocene and quaternary volcanic phases, K/Ar age determ. 0-46160  
 eruption clouds in Guatemala, atmospheric studies 0-41505  
 eruptions clusters, as course of abrupt palaeoclimatic events 0-51531  
 SW.Ethiopia, dating of volcanic and rifting history 0-51369  
 Etna, activity and implications 0-31017  
 Etna volcano, shallow geological struct. by elec. sounding 0-41419  
 external ballistics of volcanic eruptions 0-46159  
 Fishguard Volcanic Group, SW.Wales, rhyodacitic pillow lava and isolated-pillow breccia 0-12389  
 Galapagos Rift at 86°W, regional morphological and struct. anal. 0-26491  
 Galapagos Rift at 86°W, sealed topography and magmatic episodes 0-21681  
 Galapagos Rift at 86°W, volcanism struct. and evolution of rift valley 0-21707  
 Geronimo lavas from Quaternary in S.E. Arizona 0-8303  
 E Greenland, struct. of coastal dyke swarm and assoc. plutonic intrusions 0-56467  
 Iceland Krafla, activity history 0-21694  
 ignimbrites with low aspect ratio, characts. 0-41423  
 ionospheric plasma disturbance due to earthquakes and volcanic eruptions 0-36453  
 Kamchutka, tectonic tilt meas. rel. to volcanic activity 0-3984  
 Kauai shield-building volcanism, age and Hawaiian Island chain volcanism linear migration 0-36281  
 KBS Tuff, E.Turkana, Kenya, K-Ar age estimate 0-56433

**volcanology** continued

- KBS Tuff, N.Kenya, fission track age and assoc. hominid remains 0-56432  
 Kilauea fumaroles, He/CO<sub>2</sub> ratios as premonitors of volcanic activity 0-26482  
 kimberlite pipes, exploration geophysics appl. 0-51393  
 komatiite-derived tholeiites in Proterozoic of New Quebec 0-8305  
 lava flows of Mt. Etna, partial self-reversal and NRM 0-46126  
 lava lakes of Kilauea, Hawaii rel. to mantle magma 0-26483  
 Lesser Antilles island arc, palaeomagnetic and geochronological survey 0-8265  
 magma migration beneath ocean ridge mantle convection 0-12366  
 magma series erupted in different marine tectonic settings, trace element anal. 0-21667  
 magmas, influence of volatile components 0-41418  
 magmatic rocks, anchieutectic comp. 0-12381  
 magnetic spherules in Arctic Ocean sediments, volcanic origin from Ti content 0-26488  
 Makaopuhi lava lake, Hawaii, influence of augite on plagioclase fractionation 0-12390  
 Malartic Group, Abitibi, Archaean volcanism, petrography and geochemistry of lavas 0-17258  
 mantle plume, fluid-dynamic model of ascending flow 0-12370  
 Marcus-Necker Ridge, volcanic rocks comp. and stages of development 0-36282  
 lower metadiabase from Michigan Basin basement, alkaline affinities from petrological study 0-4009  
 mid-ocean ridge basalts, density var. rel. to magma mixing and primitive lavas scarcity 0-56460  
 mud volcano in Trinidad, gravity anomaly model 0-56442  
 Nazca group volcanic rocks, Peru, volcanic history 0-12357  
 Neogene explosive volcanicity, temperature and glaciation 0-26481  
 oceanic basins, volcanic evolution of marginal and interarc basins 0-8271  
 oceanic lithosphere flexure and uplifted atolls, comment 0-26486  
 Oshima Island, Japan, anomalous secular variation, rel. to earthquake or volcanicity (*Japanese*) 0-41369  
 Oshima Volcano, Japan, elec. resist. changes and 1978 Jan. 14 earthquake (*Japanese*) 0-46132  
 Oshima Volcano seismic activity prior to Jan. 1978 Izu-Oshima-kinkai earthquake (*Japanese*) 0-46138  
 E.Pacific Rise, hydrothermal vents on seabed issuing H<sub>2</sub> and methane 0-41422  
 E.Pacific Rise, struct. of crust, volcanism periodicity and magma flow 0-17243  
 E.Pacific Rise, young cratered volcanoes pairs 0-12374  
 Papua New Guinea, Late Cainozoic geotectonics and volcanism 0-51372  
 Pinacate volcanic field, Mexico, cinder cone struct. and eruptions 0-56443  
 Piton de la Fournaise volcano, SE.Reunion Island, gravity survey (*French*) 0-56334  
 Late Pleistocene tephra in South Island, New Zealand, identification and significance 0-8306  
 Poas volcano, pyroclastic sulphur eruption, Costa Rica 0-51370  
 Proterozoic anorogenic magmatism, rel. to analogous apparent polar wander loops 0-56360  
 pyroclastic flow deposits, utilisation 0-12365  
 Roberts Arm Group, Newfoundland, age rel. to phases of volcanism 0-12354  
 Roccamonfina volcano, Roman comagmatic region, Italy., potassic igneous rocks O isotope geochemistry 0-41420  
 Soufriere eruption, April-June 1979 activity 0-21693  
 stratosphere chemistry, quantity of injected sulphur and halogens 0-51474  
 Tambora, Indonesia, 1816 eruption rel. to year without summer (New England, 1816) 0-4089  
 tephra deposits, dating of ancient events 0-36283  
 Turkish-Iranian Plateau, post-collisional tectonics, comparison with Tibet 0-3986  
 Y-5 ash layer in E.Mediterranean, age, origin and volcanology 0-56444  
 Yellowstone Park hot spot, volcanic and tectonic evolution 0-56472  
<sup>13</sup>C/<sup>12</sup>C ratio in magmatic gases of Afar ridge volcanism 0-21732  
<sup>34</sup>S/<sup>32</sup>S ratio in magmatic gases of Afar ridge volcanism 0-21732
- volt-ampere meters**  
*see also power measurement; wattmeters*  
 No entries
- Volta effect** *see contact potential*
- voltage** *see electric potential*
- voltage comparators** *see comparators (circuits)*
- voltage control**  
 storage ring, feedback-stabilised, resonator wall instability caused by ponderomotive forces 0-5418
- voltage-controlled oscillators** *see variable-frequency oscillators*
- voltage controllers** *see voltage regulators*
- voltage distribution**  
*see also electric breakdown; surface discharges; transients*  
 chloroform HV polarisation and space charge obs. (*Russian*) 0-25277  
 methylene chloride HV polarisation and space charge obs. (*Russian*) 0-25277
- voltage dividers**  
*see also potentiometers*  
 2 MV resistive voltage divider for measurement of pulsed voltages in vacuum 0-31803  
 inductive, calibration methods comparison, between 10 kHz and 100 kHz 0-13100
- voltage drop** *see electric potential*
- voltage measurement**  
*see also potentiometers; voltmeters*  
 AC, matching measurement sensing method to application 0-47072  
 AC, small, combined meter checking 0-13057  
 arcs parameters determ., natural fluctuations of voltage and emitted light correlation (*French*) 0-19654  
 automotive distributor, arc initiating processes, EM radiation reduction 0-19665  
 calibration service in 0.1 to 10 Hz range using AC voltmeter/calibrator 0-22385  
 data logger, 16-channel with multiplexing, and voltage pulse measurement 0-42203  
 digital panel meters, noise resist and CMRR improvement, power source interference elimination 0-211



**voltage measurement continued**  
 divider calibration, inductive, between 10 kHz and 100 kHz, international comparison of calibration methods 0-13100  
 nitrobenzene, temp. depend. of electro-optic Kerr coeff. 0-2725  
 pulsed high voltages in vacuum using 2 MV resistive voltage divider 0-31803  
 ratios, in two-bridge gas analyser 0-50907  
 RMS measurement, error estimation in voltmeters 0-22381  
 semiconductor, current and voltage fluctuation determ. by noise spectral density meas. 0-15577  
 tree root potential meas. electrode earthing method (*Russian*) 0-26420

**voltage reference diodes** *see avalanche diodes; Zener diodes*

**voltage regulation** *see voltage control*

**voltage regulator diodes** *see avalanche diodes; Zener diodes*

**voltage regulators**  
*see also voltage control*  
 commutable source of reference voltages in ionospheric plasma probe meas. 0-31192

**voltage stabilizers** *see voltage regulators*

**voltage transients** *see transients*

**voltammetry (chemical analysis)**  
*see also polarography*  
 bipotentiostat of simplified design 0-35589  
 chronocoulometry, square root of time mark generator using TTL digital ccts. 0-35588  
 chronopotentiometry, programmed current, electrode process followed by chem. reaction 0-35595  
 cyclic voltammograms at spherical electrodes, switching pot., drop size effects, digital simulation technique 0-40766  
 electrode reaction, number of electrons involved determ. method 0-35596  
 linear sweep anodic stripping voltammetry, recursive estimation evaluation 0-26067  
 linear sweep voltammetry, charge transfer, diffusion control 0-45583  
 liquid chromatography, use of electrochemical detection methods 0-50906  
 phase selective anodic stripping voltammetry, review 0-40788  
 Cu-rare earth oxide-Y composite coatings, oxide and Y effect on coating precipitation 0-55554  
 Li/SOCl<sub>2</sub> primary cell, cyclic voltammetric and coulometric obs. of SOCl<sub>2</sub> reduction 0-30440  
 Pb-H<sub>2</sub>SO<sub>4</sub> cells, Sb alloying effect on solid Pb electrochemical properties 0-55668  
 Y<sub>2</sub>Ti<sub>2</sub>O<sub>7</sub>, precipitation from oxalates, carbonates, exam. 0-55641  
 ZnO:Cu, point defects, electrochem. characterisation 0-35599

**voltmeters**  
*see also digital voltmeters; potentiometers*  
 AC voltages, small, combined meter checking 0-13057  
 checking using UPMA-3, extension of meas. limits 0-13058  
 DC microvoltmeter based on modem 0-31798  
 DC nanovoltmeter based on modem 0-31797  
 error estimation and use 0-22381  
 frequency error determination over wide range 0-4734  
 frequency measurement applications (*French*) 0-22331  
 kilovoltmeter for X-ray equipment 0-13191  
 LF millivoltmeter, range 0-100 mV at frequencies from 20 to 100 KHz (*Spanish*) 0-13060  
 millivoltmeter, instantaneous peak value response, biomedical appls. 0-42208  
 SQUID, DC, circuits, optimisation 0-13056

**volume control**  
 circulatory assist apparatus, stabilisation of gas vol. in pneumatic transmission unit 0-3863

**volume diffusion** *see diffusion in solids*

**volume measurement**  
 body organ volume determination by US scanning 0-17034  
 flow, CW NMR to determining volume fractions and flow rates of component mixtures 0-33710  
 US bladder volume sensor, pocket-size 0-36034

**vortex flow** *see vortices*

**vortex flow (superconductivity)** *see flux flow*

**vortex lattice pinning** *see flux pinning*

**vortex state (superconductivity)** *see mixed state*

**vortex structure (superconductivity)** *see flux-line lattice*

**vortices** *see vortices*

**vortices**  
*see also cavitation; turbulence*  
 aerodynamics, discrete vortices method and multidimensional singular integral eqns. theory 0-19421  
 aerofoil, oscillating, viscous incompressible flow, finite element anal. 0-38427  
 airships, vortex filament-shock front interference, vortex dissipation 0-10253  
 atmosphere, oscill. model of action centres, vortices interactions (*Russian*) 0-4075  
 atmosphere large-scale eddy transports, linear parameterisation 0-17361  
 atmospheric, potential vorticity conservation by finite difference eqns. in generalised vertical coordinates 0-26576  
 body-propeller combination, numerical soln. including swirl and data comparisons 0-19407  
 boiling, mechanism model based on rotating vortex model with spatial heating 0-14694  
 breakdown flowfields, spectral characts. in water 0-19408  
 buoyancy induced flow over inclined heated porous surface, vortex instability 0-33601  
 bursting phenomenon in bounded turbulent shear flow, streamwise vortices 0-1600  
 cavity, square, 2-D, recirculating flow of incompressible fluid, large Re, convergence of finite-difference schemes 0-33611  
 cavity flow, columnar vortices 0-24037  
 circular cylinder, turbulent crossflow in vortex zone 0-10252  
 combustion chamber, acoustic mode excitation by vortex shedding 0-19150  
 concentration interface in turbulent mixing layer, visual growth 0-38392  
 convective diffusion problems, finite element solns., Navier-Stokes eqns. 0-1583  
 convergence, vortex methods for Euler's equations 0-33614  
 cosmology, early evolutionary stages of universe spatially inhomogeneous models (*Russian*) 0-4467

**vortices continued**  
 counter gradient flow downstream of two different diameter cylinders (*French*) 0-43693  
 cyclone centre location using kinematical determinant 0-56535  
 cyclone-anticyclone couplets, vorticity budget 0-8391  
 cylinder, circular, wake of steady flow at different Reynolds numbers 0-38416  
 cylinder, forced convective heat transfer, sound wave effects 0-43699  
 cylinder wakes, vortex periodicity criterion, separated flow region 0-19399  
 definition problems, proposal based on pathlines, book contrib. 0-1605  
 detached flow round thin wings, vortex struct. 0-38421  
 developed flow in curved channels, vortex formation (*German*) 0-1689  
 dual jet discharged into rectangular duct, flow and heat transfer 0-43751  
 duct wall cavities, heated bottom surface, forced convection heat transfer 0-6048  
 edge interaction, low frequency component generation mechanisms 0-53795  
 enclosed rotating cone with superimposed throughflow, frictional resistance, Taylor vortices effects 0-43717  
 Euler equation in two dimens., numerical approx. (*French*) 0-48715  
 external disturbance transformation into boundary layer waves 0-28523  
 flow separation experiments, galloping and vortex induced oscillations 0-43750  
 flow through porous media, eddy motion characts. 0-6136  
 fluid mechanics, mathematical introduction, book 0-66  
 fluid with constant vorticity, motion in singly-connected region, Kirchhoff's elliptical vortex 0-6067  
 formation from downdraught in rotating environment, appl. to cloud. mech. 0-8399  
 formation in mixing layer downstream of a separation in near wake of body (*French*) 0-48716  
 forward facing step, neutrally stable atmospheric flow, shear layer, separation, vortices 0-48685  
 free vortices behind stationary wing as energy source for wind turbines 0-40820  
 furrowed channels with pulsatile flow, observed flow patterns, separation and vortices 0-33673  
 gas turbine annular vortex shedding acoustic resonance analysis (*Japanese*) 0-14526  
 Giffing propeller operation characts. by computer aided numerical anal. 0-6068  
 Gortler vortices, high value eigenstates, stability diagrams, book contrib. 0-1606  
 Gortler vortices in the nonlinear region, book contrib. 0-1607  
 Gross Pitaevskii eqn., generalised solns. 0-49437  
 heart valves, blood flow, vortex-grid method 0-41105  
 Helmholtz instability of vortex sheet, effect of background vorticity (*Japanese*) 0-10254  
 Helmholtz's vortex eqn., Cauchy problem, diff. approx. soln. (*German*) 0-1608  
 high gradient magnetic separation at moderate Reynolds number 0-38500  
 hurricane surge potentials over SE. Louisiana, forecast model 0-46216  
 hurricanes, interaction between symmetric mean vortex and shearing steering current rel. to spiral bands excitation 0-56538  
 hydromagnetic stability of a vortex sheet in compressible, perfectly conducting fluids 0-14831  
 impulsively started circular cylinder, initial flow, separation, vortices, wakes and boundary layers 0-19401  
 impulsively started flow about circular cylinder, two-dimens. vortex shedding, inviscid model 0-19400  
 inhomogeneous turbulent flow scale characts., vortex struct. relationship 0-53754  
 interactions, book contrib., review 0-19410  
 inviscid, 3-dimens. incompressible flow, spontaneous singularity, Taylor-Green vortex 0-48720  
 inviscid barotropic vorticity eqn., soln. by finite difference, finite element and pseudospectral method 0-43687  
 isotropic turbulence, conditional flow struct., anal. 0-19335  
 Jupiter, vortices buoyancy rel. to atmosphere differential rot. 0-46467  
 Karman vortex air flow system (*Japanese*) 0-38417  
 laminar boundary-layer flows with swirl and large suction 0-1519  
 Maxwell toroidal vortex, analogs and extensions 0-28510  
 mesoscale eddies in mid-ocean, simulated dynamic balances, model 0-26525  
 MHD shear inviscid flow, vortex sheet stability 0-28571  
 MINI-OTEC ocean thermal energy conversion plant test 0-45727  
 multiple fluid in three dimensions, vortex theory 0-14709  
 Navier-Stokes equation, operator version, convection propagation and convected curl operators, Lie algebra 0-46812  
 noise generated by an eddy (*French*) 0-19363  
 nominally planar turbulent boundary layer, spanwise nonuniformity and vortices 0-53762  
 ocean, topographically trapped vortex on Norwegian continental shelf 0-31046  
 ocean currents, synoptic-scale, numerical model 0-12424  
 oceanic eddy formation in Somali Current, wind effects 0-26523  
 particle flow behaviour in branching vessels models, vortices in 90° T-junctions 0-16971  
 phase space quantisation of interacting vortices in two dimensions 0-4634  
 pinning in nucleopores, effect on second sound resonators 0-49439  
 pipe-jet system in crossflow, turbulent vortex shedding modes 0-10274  
 plane incompressible perfect fluid, equilibrium states, Euler equation 0-53791  
 plane mixing layer, two-point LDV meas., vorticity distrib. 0-38506  
 plasma generator arc chamber, hydrodynamic struct. 0-1817  
 plates, flat, rotating stratified flow, boundary layers 0-53793  
 quantum fluids, vortex formation and dynamics, Magnus force (*Russian*) 0-10719  
 rectangular cavities, end effects, vortex flow and wall jet 0-10309  
 rollup and pairing, energetics 0-38419  
 rotating Bernoulli surfaces in compressible inviscid flow, vorticity transport 0-19403  
 rotating fluid, vortices formation near reson. for elastoid-inertia waves 0-12473  
 Saturn, vortices buoyancy rel. to atmosphere differential rot. 0-46467  
 separated flows, upwind and central difference schemes 0-28539  
 separating laminar boundary layer, horseshoe vortex 0-19405



**vortices continued**

- shaped edge cylinders in oscillatory flow, separation and vortex shedding forces 0-53825
- shear stress determination, in laminar and Taylor vortex flows, using flush-mounted hot film probe 0-28486
- sink-vortex flow in compressible medium, book contrib. (*German*) 0-1603
- sound diffraction by perforated screen, low Mach number grazing flow 0-53805
- spiral vortex flow characteristics at high Taylor numbers 0-1598
- stable solutions for vortex systems 0-33613
- stratified flow, Coriolis force blocking attenuation, wakes, baroclinic vorticity and boundary layers 0-6129
- stratified rotating fluid, mass transfer between layers causing vortex 0-12401
- streamwise vortex separation and stability (*German*) 0-6069
- streets, stability on curved surface with reflection symmetry 0-46810
- sub and transonic flow over wing, flow separation, vortex struct., shock wave shape (*French*) 0-14733
- superfluid rot. speedups accompanying ang. deceleration 0-10738
- swirling jet from vortex filament, Navier-Stokes eqn. soln. 0-38470
- Taylor vortex flow, effect on development length in concentric annuli 0-1597
- Taylor-Couette flows at very high Taylor number, marginal instability 0-1599
- three-dimensional gasdynamic flows, variational principle in Euler description, vortex conservation 0-48731
- tornado flowfield struct., laboratory expts. 0-56566
- tornado life cycle, photographic sequence 0-41537
- turbomachinery ring chamber, oscillatory behaviour of confined ring vortex 0-6075
- turbulent flow simulation with three-dimens. vortex in cell method 0-19330
- turbulent jets, vortex-street structure 0-10280
- turbulent mixing layer, numerical simulation via vortex dynamics 0-19362
- turbulent mixing layer description from transient vortex flow results 0-1533
- turbulent pressure fluctuations on jets, long range effects, book contrib. 0-1663
- two dimensional convective transport, vorticity at wall with suction, finite difference representation 0-10255
- unsteady airfoil stall in laminar boundary layer, water tunnel visualisations 0-53745
- unsteady flow, vorticity meas. technique and data acquisition 0-19525
- unsteady separated flow, aerodynamic characts., vorticity field 0-38457
- US meas. of vortices in wind tunnel expts. 0-10334
- V-grooved rotating cylinders, vortex motions and mixing performance 0-43714
- velocity of circular vortex ring with thin elliptical core 0-48719
- viscous flow, time-dependent, integral representation approach to simulation 0-38375
- viscous fluid, vortex dipoles 0-48718
- viscous gas flow, subsonic and supersonic, simplified Navier-Stokes eqns. 0-31520
- vortex ring core, turbulence struct. 0-33615
- wake vortices, interactions and water tank obs. (*Japanese*) 0-28514
- wake vortices of axisymmetrical bodies, vortex-pair obs. (*Japanese*) 0-28513
- wind energy generator system, tornado-type, latent heat from moist air, effect on vortex 0-30365
- He, film, Brownian motion, boundary layers and quantised vortex prod. 0-6579
- He film, jump in superfluid density 0-44387
- He II, superfluid, rotating with vortices, defect hydrodynamics (*Russian*) 0-49445
- He II superfluid, turbulence during rotation, critical lengths 0-49443
- <sup>3</sup>He, superfluid A-phase, new phase-transfer decay mechanism for persistent currents 0-6586
- <sup>3</sup>He, superfluid A-phase, rotating, vortex lattice detectability 0-29240
- <sup>3</sup>He-HeII solutions, van der Waals molecular dimers (<sup>3</sup>He)<sub>2</sub>, bound states (*Russian*) 0-49454
- <sup>4</sup>He, isotopically pure superfluid, vortex nucleation 0-44378
- <sup>4</sup>He, liq., Venturi level differences 0-24698
- <sup>4</sup>He, liquid, second sound, quantised vortex creation at constrictions, excitation model 0-44383
- <sup>4</sup>He, rotating superfluid, vortex patterns and energies 0-6578
- <sup>4</sup>He, superfluid, pressurised, vortex nucleation by neg. ions, thermal roton influence 0-10721
- <sup>4</sup>He, superfluid, rotating, Tkachenko waves 0-39376
- <sup>4</sup>He, superfluid rot. film, melting of two-dimensional vortex lattices 0-2539
- <sup>4</sup>He, superfluid turbulence, vel. and temp. depend. from thermal resist. meas. 0-20003
- rotating system, equilibrium Onsager-Feynman vortex lattice <sup>4</sup>He, superfluid, rotating system, equilibrium Onsager-Feynman vortex lattice (*Russian*) 0-29234

**vulcanisation**

- glass fibre reinforced poly- and vinyl ester thermoset moulding, cure cycle effect on mech. props. 0-45369
- polyester-polyurethane interpenetrating polymeric network glues, props. 0-16640

**waiting line theory** *see queueing theory***wakes**

- arbitrary body, unsteady separated inviscid incompressible flow, numerical soln. 0-28509
- asymptotic, supersonic, 2-dimens. turbulent wakes, fully developed mean flow criteria 0-14706
- axisymmetric transonic turbulent base pressures 0-19425
- blunt body, boundary and wake, supersonic viscous gas flow, numerical soln. 0-38441
- blunt cone hypersonic and supersonic flow, near wake Reynolds number effects, interferometric obs. 0-43733
- body of revolution, low-drag, thick axisymmetric turbulent boundary layer and near wake 0-19352
- cavitation erosion intensity in hydrodynamic wakes (*Russian*) 0-53790
- channel height effect on nearcritical flow past circular cylinder, pressure distrib. in wake 0-14818
- circular cylinder near wake in turbulent crossflow, expt. techniques 0-14705

**wakes continued**

- circular cylinder with tripping wires, heat transfer, flow and wakes (*German*) 0-1589
- counter gradient flow downstream of two different diameter cylinders (*French*) 0-43693
- cylinder, circular, wake of steady flow at different Reynolds numbers 0-38416
- cylinder, circular with boundary layer suction, wake changes 0-53785
- cylinder, forced convective heat transfer, sound wave effects 0-43699
- cylinder, heated, turbulent temp. and thermal flux characts. using four-wire probe 0-19541
- cylinder wakes, vortex periodicity criterion, separated flow region 0-19399
- cylinders placed in turbulent plane mixing layer, time-averaged aerodynamic forces 0-28524
- flame holders, two-, three-dimensional, wake struct. 0-53786
- fluid flow and heat transfer around two circular cylinders of different diameters in cross flow 0-14687
- fluidised beds, three-phase, containing fine/light solids, contraction or expansion 0-28557
- galactic wake turbulence, rel. to head-tail radio sources form. 0-36703
- gasdynamic laser nozzle wake, flowfield props. boundary layers 0-24027
- heated flat plate plane wake, intermittency in free turbulent shear flows 0-19348
- hypersonic wake, excitation temp. meas. by atomic spectral line relative intensities 0-43732
- impulsively started circular cylinder, initial flow, separation, vortices, wakes and boundary layers 0-19401
- jet, two-dimensional turbulent, in moving stream, preferential entrainment 0-1660
- laminar boundary layer induced wake behind cylinder attached to plate 0-43712
- large eddies in wake and turbulent boundary layer, vel. fluctuations 0-24036
- main eddies of recirculating zone induced by impulsively started cylinder, origin (*French*) 0-53784
- momentumless wakes, similarity and decay laws 0-53789
- near-wake phenomena, with and without external compression, axial and radial air injection effects 0-10273
- non-Newtonian power law fluid, laminar far wake flow 0-53824
- nonlinear stern wave production in pot. flow past flat bottomed body 0-38425
- Oseen velocity distributions in the wake of a flat plate 0-53788
- particles in a fluid, convective diffusion and mass transfer, wakes, chemical reactions 0-38394
- pipe-jet system in crossflow, turbulent vortex shedding modes 0-10274
- slightly heated cylinder, turbulent wake, conditional sampling study, turbulence struct. 0-6063
- spectrally local disturbance evolution in grid generated nearly isotropic turbulence 0-48681
- steady transonic flow past aerofoil, viscous effects, prediction model 0-14732
- stochastic self-oscillations and turbulence, review 0-4537
- stratified flow, Coriolis force blocking attenuation, wakes, baroclinic vorticity and boundary layers 0-6129
- stratified flow, wakes, book contrib., review 0-19473
- stratified fluid in channel, wake collapse in the thermocline and internal solitary waves 0-53787
- submersion of a body into a fluid (*Ukrainian*) 0-33610
- subsonic base pressure fluctuations on axisymmetric blunt-based body, Mach no. depend. 0-19423
- subsonic bluff body wakes, measurement of fluctuating pressures 0-10249
- supersonic jet, nonsteady interaction with barrier, math. model of oscillatory cycle 0-19462
- symmetrical airfoil, transonic flow, inviscid and turbulent flow props., wake 0-48736
- symmetrical wake calc., two-dimens. laminar and turbulent flows 0-14707
- thermal convection in step wake with pulsating jet (*French*) 0-10240
- turbulent boundary layer with separated flow, integral method 0-1547
- turbulent separating boundary layer, subsonic, integral prediction method 0-1623
- turbulent skin friction at subsonic and supersonic speeds, wake component influence 0-19340
- turbulent wake of axial flow turbomachinery rotor blades, numerical anal. 0-1596
- typhoon Tess wake vertical struct. in upper layer of Pacific Ocean 0-26538
- unsteady quasiperiodic flows, self-synchronising Schlieren flow visualisation, near wake 0-19527
- vortex breakdown flowfields, spectral characts. in water 0-19408
- vortices, interactions and water tank obs. (*Japanese*) 0-28514
- vortices formation in mixing layer downstream of a separation in near wake of body (*French*) 0-48716
- vortices of axisymmetrical bodies, vortex-pair obs. (*Japanese*) 0-28513
- wall jet, 3-dimens., surface layer props. computation 0-1667

**Walsh functions**

- see also encoding; filtering and prediction theory; signal processing*
- fast Walsh transform configuration program derivation, appl. to seismic data processing (*Chinese*) 0-21853
- optical processing, performance of generalized two-dimensional linear transforms 0-9824
- surface texture assessment 0-36995

**Wannier functions**

- Bravais-lattice operator in one band of solid 0-10519
- diamond semiconductors, electronic structure, self consistent local description 0-20067
- ferromagnet, itinerant electron, surface spin waves, tight-binding Hubbard model 0-39763
- generalized lattice representations using generalized Bloch and Wannier functions 0-22300
- impurity electron level position depend. on interaction with bands, Wannier representation calcs. 0-54653
- lattice, deformable, local and global stabilities of electron 0-54620
- polar semiconductor, exciton, energies, oscillator strengths, and phonon side bands 0-44512
- polyacetylene, bond length alternation and energy gap, intermediate exciton formalism 0-29305
- semiconductor, Wannier excitons, fine structure, lineshape and dispersion, review 0-44520



**Wannier functions continued**

- semiconductors, Fourier transformed X-ray Compton profiles 0-35004
- spatially dispersive media, optical boundary value problem 0-45024
- symmetry-adapted Wannier functions, variational procedure 0-2323
- Ar, valence electron distrib., pseudopotential calcs. 0-2335
- CdS, Wannier exciton and Wannier-exciton-ionised-donor complex, binding energies of lowest excited states 0-34363
- InSe, energy band structure, chem. bond polarity, photoemission, semi\*-n-pirical tight binding method 0-44504
- MgO, valence electron distrib., pseudopotential calcs. 0-2335
- NaCl, valence electron distrib., pseudopotential calcs. 0-2335
- TiCl(Br), Wannier exciton-ionised donor complexes, binding energy calc. 0-49609

**warning systems** *see alarm systems***waste disposal**

- see also radioactive waste*
- atactic polypropylene waste, pyrolytic conversion to fuel oil 0-35627
- deep ocean sediment thermal conductivity meas. platform rel. to nuclear waste storage 0-46175
- fibre-optic glass manufacture using polypropylene sump pumps 0-14410
- fission product waste solidification, high-level, for final storage (*German*) 0-22958
- fluid radioactive waste, processing plant for long-term storage rel. to ocean dumping 0-5279
- fluidised bed containing biomass, expansion 0-14803
- geologic repositories, characteristics for radioactive waste acceptance criteria 0-18486
- geologic repositories for commercial nuclear waste, feasibility study of basalt formations 0-18479
- geologic repositories for nuclear waste isolation 0-18584
- geologic repositories for radwaste, feasibility study of granite formations, Stripa, Sweden 0-18481
- geologic repositories for radwaste, US Earth Science Technical Plan 0-18482
- geologic repositories of radioactive waste, US Geological Survey Program [for nuclear waste geologic repositories] 0-22989
- geologic repository for nuclear waste at Nevada Test Site 0-18480
- geologic repository for radioactive waste, status report on Waste Isolation Pilot Plant 0-18478
- geological disposal of high-level radwaste, chemical factors controlling environmental actinide sorption 0-13713
- geological long-term disposal of high-level radwaste, Sweden 0-13712
- high-level radioactive waste management 0-37470
- immobilised nuclear waste, disposal centre conceptual design 0-52774
- industrial use of sink-and-float test (*Japanese*) 0-55948
- Iranian solar town conceptual development 0-35645
- liquids, flash point meas. for safe disposal 0-47051
- LWR spent-fuel processing and packaging options, for disposal in geologic repository 0-18485
- metallurgical, with heavy metal ions, influence on flotation of PbSO<sub>4</sub> with sodium hexadecyl sulphate (*Japanese*) 0-55701
- nuclear fuel reprocessing, radioactive waste elimination by nuclear transmutation (*Spanish*) 0-5298
- nuclear fuel reprocessing in West Germany, case against suspension (*German*) 0-32418
- nuclear power stations, fuel circuit review, radioactive conditioned waste final storage (*German*) 0-799
- nuclear waste constituents, stabilisation in Portland cement 0-13630
- particle accelerator decommissioning, radioactive waste management 0-18720
- polymers, synthetic, radiative degradation, chem., phys., environmental, technological effects, review 0-40948
- radioactive, cask concepts for spent-fuel storage 0-5284
- radioactive, geochemical aspects of radionuclide migration from waste repositories 0-13711
- radioactive, in mines, Dutch policy (*Dutch*) 0-671
- radioactive, oceanic and geological, environmental impact assessment (*Japanese*) 0-9346
- radioactive, reprocessing of irradiated fuels, French and European policies (*French*) 0-809
- radioactive low-level waste, industrial processes for treatment and storage 0-5280
- radioactive waste, decision anal. 0-18488
- radioactive waste, geologic repository, site search and qualification process 0-18474
- radioactive waste, leach-migration experiments to determine the mobility of radionuclides in geologic media 0-18487
- radioactive waste, pool systems for spent-fuel interim storage facilities 0-5283
- radioactive waste, thermomech. impact around rock salt borehole 0-5278
- radioactive waste by incineration in shaft furnaces (*German*) 0-47584
- radioactive waste by Julich incineration process (*German*) 0-47583
- radioactive waste disposal criteria proposals by EPA and NRDC, review 0-18484
- radioactive waste disposal following decommissioning of nuclear facilities (*French*) 0-13736
- radioactive waste geologic repositories, computer anal. of long-term radiation hazards 0-18483
- radioactive waste management practices in selected European countries 0-37471
- radioactive waste processing, consequences of separation of long-lived  $\alpha$ -emitters (*Czech*) 0-5251
- radioactive waste repository, shale investig. and vermiculite role 0-32354
- radioactive wastes, disposal in sea 0-37472
- radwaste, operation of a pilot solid waste incinerator 0-22990
- residual waste treatment technology, review 0-40932
- society effects of nuclear power developments 0-47590
- spent LWR fuel storage in Pacific Basin at Palmyra Island, decision making methods 0-27763
- thermal analysis of irradiated nuclear fuel transport flasks 0-5281
- transuranic nuclear waste management, evaluation of alternatives 0-18490
- water disinfection and oxidation, ClO<sub>2</sub> appl. 0-12032
- U mining, U refining and decay processes, radioactive mining waste disposal (*Dutch*) 0-21418

**water**

- see also groundwater; heavy water; hydroxonium ion; ice; moisture; seawater; steam*
- $\alpha$ -particle stopping power and straggling in water and tissue-equivalent liquid 0-23274

**water continued**

- absorption by rigid foamed polyurethanes, effect of cellular struct. 0-39416
- acetonitrile-water mixture, electrolyte transfer, thermodynamic props. 0-3395
- action potentials in single axons, effects of hyperbaric air and hydrostatic press. 0-56007
- adsorbed layer, polymolecular, on quartz surface, IR absorption spectra 0-9595
- adsorbed layer on NaCl surface, absorpt. and thickness meas. 0-16001
- adsorbed layers on Pt(100), bonding, electron energy loss spectra 0-34311
- adsorbed multilayers on quartz, surface forces 0-6597
- adsorbed on kaolinite, vol. expansion, lattice deform. 0-45555
- adsorption, detection of OH groups for adsorption centres in plant tissues, dielectric relaxation (*Japanese*) 0-7999
- adsorption, O<sub>2</sub>-induced and reaction with other adsorbates on Ag(110) 0-55714
- adsorption, on ZnSO<sub>4</sub>·7H<sub>2</sub>O, meas. of water physically adsorbed rel. to water of crystallisation (*Japanese*) 0-6622
- adsorption anomaly in SnO<sub>2</sub>, effects of cryst. growth of solid 0-10779
- adsorption on Cu (100) surface, EELS study 0-2260
- adsorption on Fe, Co, Ni, Pt, Cu, and Au films, work function changes 0-44705
- adsorption on GaAs(110) surface, UPS study 0-6632
- adsorption on GaAs (110), surface photovolt. spectroscopy 0-49499
- adsorption on MgO during  $\alpha$ -irrad., thermostimulated surface cond. obs. 0-34499
- adsorption on plasma deposited a-Si:H, effect on cond. 0-49749
- adsorption on Pt, reaction between H<sub>2</sub> and adsorbed O 0-49514
- adsorption on pure Co surfaces, decomp. phenomena (*German*) 0-26054
- adsorption on U, XPS study 0-7473
- adsorption on SiO<sub>2</sub>·Co(II), coord. lifetime, surface effect, NMR obs. 0-34299
- aerosol, propagation of intense radiation at 10.6  $\mu$ m 0-5692
- aerosol with fine droplets, laser radiation intensity fluctuations at 630 nm 0-4109
- alkaline electrolysis, chrysotile asbestos corrosion in KOH, effect of SiO<sub>2</sub><sup>2-</sup> on electrode overvoltages 0-30433
- amplified spontaneous emission in spherical and disk-shaped laser media 0-1177
- atmosphere, precipitable water meas. as Sacramento Peak Observatory 0-51653
- atmosphere precipitation, D-<sup>18</sup>O relationship global climatic interpretation 0-17331
- boiling, free-convection, critical heat flux density 0-48691
- boiling, subcooled and low quality flow film, at atmospheric pressure 0-32324
- boiling in Laval nozzles, discharge and dynamic characteristics 0-19470
- catalytic surface activity, LaNi<sub>3</sub> surface segregation (*German*) 0-51008
- cavitation due to ultrasound, radn. force balance method 0-24063
- central force model, appl. to mol. dynamics simulation of NaCl aq. soln. 0-49077
- chemical analysis, review 0-7877
- chemisorption, on Si (111) surface, appl. of UPS ultra high vacuum apparatus (*Japanese*) 0-37125
- chemisorption on Si (111) 7 $\times$ 7 surface 0-10792
- chloroplast, mag. relax. of water protons and state of water photo-dissociation system 0-51133
- clouds, liquid water and ice contents rel. to radiative props. parameterisation 0-56601
- clusters, struct. and props. 0-39304
- comet nuclei, water dominated, vaporisation rel. to lifetimes and orbits 0-56772
- Compton profile, electronic energy calc. 0-37822
- computer simulation, intermolecular potentials 0-38890
- condensation onto ice, deposition coeffs. 0-6507
- condensed multilayers, electron bombard. effects, AES line-shape anal., XPS, and desorption meas. 0-7450
- critical mixture of water and isobutyric acid, shear viscosity, amplitude ratios 0-2188
- decomposition H production by thermochemical and thermoelectrochemical cycles 0-26029
- density, meas. of small difference by elastic vibrator method (*Japanese*) 0-27272
- desorption rate, effects of method of return to atm. press. for pressure vessel (*French*) 0-42233
- diffusion const. in presence of large background gradients, modified pulsed gradient technique 0-31831
- diffusion in wheat grain endosperm tissue, <sup>1</sup>H NMR obs. 0-8001
- dimer, intermolecular pot. functions from ab initio calcs. 0-5473
- dimer, meteorological implications 0-8418
- dimer config., vib.-rot. band intensities, rel. to 8-13  $\mu$ m atmospheric extinction 0-9610
- dimers, and H<sub>2</sub>O·Ne, excited, first order interaction energy, ab initio calc. 0-32598
- p-dioxane-water system, excess molar heat capacities, 298.15K, US vel. obs. 0-6523
- dissociation by polynaphthoquinone-SO<sub>2</sub>-I<sub>2</sub> system for H<sub>2</sub> prod. 0-16825
- dissociation by S-I cycle for thermochem. prep. of H<sub>2</sub> 0-16823
- dissociation by Sb-I-Ca process for thermochem. prod. of H<sub>2</sub> 0-16824
- dissociation on Pt(111), identification of adsorbed OH species 0-49509
- dissociation using solar energy for H prod. 0-30597
- DNA interaction, single and double helix DNA 0-30646
- droplet, explosive vaporisation on 10.6  $\mu$ m radiation exposure, inhomogeneous internal heat evolution 0-29162
- droplet, IR emissivity 0-36394
- droplet conc. and size determ. from cloud liquid water content and extinction meas. 0-51579
- droplet/ice crystal clouds, angular depolarisation and multiple scattering of polarised laser light 0-41549
- droplet/ice crystal clouds, angular scattering of polarised laser light 0-41548
- droplets, initiation of optical breakdown in air 0-10352
- drops in PMMA, effect of drop size on contact angle 0-2245
- drops on HV overhead power lines, expt. 0-33851
- electrification during laminar flow in metal pipe 0-6954
- electrokinetic and rheological parameters in single capillary 0-10220
- electrolysis, H thermochemical prod. using H<sub>2</sub>SO<sub>4</sub>-SO<sub>2</sub> cycle, electrochem. aspects 0-35776



## water continued

electrolysis, S cycle H prod. process, laboratory prod. model and electrolyser development 0-30602  
 electrolysis at Hg cathode,  $H^+(D^+)$  discharge activation energies in  $H_2O(D_2O)$  0-40707  
 electrolysis at high temp. for H prod. 0-30439  
 electrolytic decomposition in acid molten electrolytes at 220 to 320°C for H prod. 0-45769  
 electron attachment to  $O_2$  and  $H_2O$  in flames, kinetics 0-3349  
 electron degraded 1 keV energy spectra in water vapour and C foil 0-9474  
 electron elastic and inelastic interactions with liq. water 0-9477  
 electron slowing down in water, spatial correlation of energy deposition events 0-9473  
 electron slowing down spectra in X and  $\gamma$  irradiated water 0-12197  
 electron stopping power, continuous slowing down approx., range difference for 0.2 to 10 MeV electrons 0-39187  
 electron track end effects in water 0-11932  
 electron transport simulation in liq. water, appl. to microdosimetry and radiobiology (*French*) 0-12202  
 enthalpy of ionisation, meas. by reaction-solution rotating-bomb calorimeter 0-4717  
 equation of state, between 350 and 1000°C (0 to 10 GPa) and between 100 to 350°C (200 MPa to melting curve) 0-15214  
 equations of state in uniform and two-phase states, thermodynamic model interpolation 0-24565  
 ethanol-benzene-water- $(NH_4)_2SO_4$ , liq. mixture, near tricrit. pt., light scatt. and sum rules 0-34933  
 evaporation, surface cooling, apparent evaporation coeff. 0-2148  
 film, between muscovite sheets, permittivity change meas. method, 20-70°C 0-55009  
 flat plate multiple pass solar collector using aqueous optical properties 0-7957  
 flow through circular pipe, pulsed NMR study 0-28566  
 flow with air contents, partially- and super-cavitating hydrofoils in cascade, analysis method (*Japanese*) 0-14763  
 free surface, metastable effects associated with press. pulse refl. 0-6463  
 Freon-12 and water, flow boiling crisis in horizontal tubes, fluid-to-fluid modelling 0-48785  
 freshwater, precipitation processes, study by particle site anal. 0-50883  
 gamma-ray buildup factors 0-27822  
 glass-transition temperature, crystn. temp., and dielec. const. 0-15229  
 gravity wave, steady, numerical soln. using Riemann Hilbert method 0-33618  
 heavy charged particle/water interaction, dose distrib. due to electrons, delta rays 0-13937  
 hydration of surfactant micelles,  $H_2O$  penetration 0-45572  
 hydrophobic interaction, of two Xe atoms, mean force determ. 0-54114  
 interface with Bi electrode, halide ion adsorption parameters, zero charge pot. conc. depend. 0-40706  
 interface with fatty acid solid monolayer, model 0-54505  
 interstellar  $H_2O$ , 183 GHz line emission obs. 0-41869  
 interstellar  $H_2O$ , abundance and column density in post-shock gas 0-56911  
 interstellar  $H_2O$  maser features, high-velocity, in  $W3(OH)$ , obs. 0-31339  
 interstellar  $H_2O$  maser in Orion A, giant outburst 0-8703  
 intracellular water, effect of paramag. impurities on proton spin-lattice relax. 0-51134  
 ion-water interactions, survey of diff. studies 0-24347  
 Ising lattice model with directional bonding, renormalisation group study 0-28894  
 isobutyric acid-water, crit. mixture, conc. fluctuation mean relax. time, US absorpt. and vel. meas 0-29163  
 jet streaming, planar and cylindrical, instabilities rel. to glassy alloy casting 0-35129  
 kidney, tissue water freezing study,  $^1H$  NMR obs. 0-8027  
 laser backscattering from turbid mixtures 0-1129  
 laser spectroscopy using an optothermal receiver 0-37810  
 laser-induced ionisation, quantum yield, temp. and wavelength depend. 0-11924  
 liquid, and glycerin soln., heat transfer in oscillating liquid-filled cylinders 0-10117  
 liquid, critical heat flux of saturated natural convection boiling with heating from below 0-10114  
 liquid, far IR optical consts. meas. with optically pumped laser 0-40082  
 liquid, H bond distrib., Monte Carlo simulation calcs. 0-54106  
 liquid, Monte Carlo-Metropolis computer simulation, convergence characts. 0-10485  
 liquid, pulsed electric field applied to sharp point, prebreakdown field 0-6308  
 liquid, struct. relax. time in 2-state model, 0-100°C 0-1914  
 liquid, viscous props. 0-2186  
 liquid, visible absorpt. meas., pulsed dye laser optoacoustic spectroscopy 0-11426  
 liquid interface, mol. orientation and surface pot. at 4°C 0-15339  
 liquid intermol. force model, used to compare Monte Carlo and mol. dynamics calc. methods 0-14984  
 liquid layer beneath ice crust on Europa, model 0-26780  
 liquid mixtures, with methanol(ethanol)(acetic acid), Verdet const., pulsed mag. field meas. 0-16012  
 liquid structure, Monte Carlo studies, review 0-54101  
 lithium perfluoro-octanoate-water, liquid crystal,  $^{19}F$  multipulse NMR obs. 0-34795  
 in magmas, influence on physical props. and comp. 0-41418  
 mammalian cells, NMR relax. time meas. of bulk water 0-21454  
 metals determ., in water and organic materials, flameless atomic absorpt. spectrometry with wire loop atomiser 0-45586  
 in meteorites, low temp. condensation rel. to H and O isotope study 0-36518  
 methanol- $H_2O$  mixture, evaporating droplets in air, temp. modelling (*German*) 0-2243  
 MHD free convection flow past infinite porous plate 0-33703  
 microwave absorption by biological material, role of water 0-17004  
 mobility, sorption by epoxy resin, low resolution PMR method 0-11276  
 molecular dynamics, computer simulation, intermolecular potentials 0-38890  
 molecular ion,  $H_2O^+$ , sub-Doppler laser spectroscopy using fast ion beams 0-9655  
 molecule,  $4\nu_2$  band, hot vap., Fourier transform spectrum, rot. consts. 0-32712

## water continued

molecule, and  $P_2O$ ,  $T_2O$ , inertia defects and dipole moments by kinetic consts. method 0-928  
 molecule, bonding electron pairs, size and shape parameters, Gaussian basis set MO calcs. 0-27935  
 molecule, dipole properties and dispersion energies additivity, using atoms and small mol. models 0-53091  
 molecule, electron pair interactions calcs. 0-23298  
 molecule, electron propagator theory for mol. electron binding energies and photoionis. intensities 0-47848  
 molecule, energy levels, triat. large amplitude vibrs. model appl. 0-23392  
 molecule, ESCA and soft X-ray emission, vibr. excitation 0-23433  
 molecule, ground state correlation energy, diagrammatic perturbation theory 0-18774  
 molecule, ground state props., coupled cluster and MBPT methods appl. 0-47881  
 molecule, H bonding, electronic struct., geometries, moments, dimerisation energies, charge distrib., pseudopotential calcs. 0-27942  
 molecule, homeomorphism, structural, between nuclear pot. and electronic charge density 0-42968  
 molecule, in  $D_2O$  ice I<sub>h</sub>, decoupled vibr. spectra 0-52984  
 molecule, KLL Auger electron spectrum, semi-internal correl. 0-48038  
 molecule, many body perturbation theory fourth order calc. of correl. energy 0-14087  
 molecule, nuclear spin-spin coupling consts., finite perturbation-CI calcs. 0-5563  
 molecule, photoassisted decomposition at room temp. with activated C over Pt/TiO<sub>2</sub> 0-55703  
 molecule, polarisability tensor components, virial theorem calcs. 0-53087  
 molecule, relaxation by IR and microwave coherent transients 0-28092  
 molecule, self assoc., intermolecular interactions, matrix isolation vibr. spectra obs. Raman and IR spectra 0-52995  
 molecule, semi-empirical INDO calc. of electronic struct. 0-32611  
 molecule, shape as function of O-H separation 0-43203  
 molecule, slow electron scatt., rigid mol. model with exchange and polarisation 0-43194  
 molecule, vapour, mol. association entropy and enthalpy, thermal cond. meas. 0-7777  
 molecule, vibr. motion, local- vs. normal-mode description 0-5521  
 molecule ground state ionis. pots., generalized MO theory 0-52907  
 molecules in biological systems, relax. rel. to vol., pulse NMR obs. 0-40960  
 Monte Carlo simulation 0-54113  
 muscle, mouse,  $^1H$  NMR anal. above and below freezing 0-56073  
 muscle water, frog, varied mag. field, multiple-pulse and magic-angle spinning  $^1H$  NMR obs. 0-51135  
 muscle water, study of spin-lattice and spin-spin relax. times of  $^1H$ ,  $^2H$ , and  $^{17}O$  0-21443  
 n-state configurational excitation model, diagnostic thermodynamic props. 0-10481  
 NMR studies of water in biological systems 0-3886  
 oil-water interface, electroadsorption and electrocapillarity 0-44393  
 optical props. of Lake Ontario coastal waters 0-36337  
 photoassisted oxidation at TiO<sub>2</sub>:Be electrodes 0-30502  
 photocatalysis on TiO<sub>2</sub> using solid C, appl. to H prod. 0-26150  
 photodesorption from TiO<sub>2</sub>, pulsed-laser-dynamic-mass-spectrometer study 0-35568  
 photoelectrochem. H prod. using hybrid electrodes 0-45775  
 photoelectrolytic H prod., recent advances, review 0-45774  
 photolysis, for H fuel prod. (*French*) 0-55776  
 photolysis, for photoelectrochem.  $H_2$  production using solar energy and Zn(Mg)(Cr)(Ni) phthalocyanine dyes (*French*) 0-55936  
 photolysis for H prod., using fission pumped gas lasers 0-45810  
 polarisation model, appl. to hydrated  $Li^+$ , review 0-54115  
 prebreakdown stage fundamental characts., calc. (*Russian*) 0-49019  
 precipitable water amounts meas. using integrated absorption in atmospheric 1.38 $\mu m$  band 0-4108  
 proton beam dosimetry, miniature Si dosimeter 0-47733  
 pulsed NMR studies of biological water 0-35930  
 pumping, by means of flat solar energy collectors (*French*) 0-55902  
 pyrex- $H_2O$  system, electrokinetic coeff. determ. from sedimentation pot. 0-3365  
 pyridine- $H_2O$ , bonding, double quadrupole reson. obs. 0-32749  
 pyrolysis, computer thermodynamic anal. and optimisation of thermochem. cycles for H prod. 0-45766  
 pyrolysis, for H prod., development of two new thermochem. cycles at ORNL 0-35780  
 pyrolysis, for H prod., optimum temp. conditions utilizing HTGR nuclear heat 0-35781  
 pyrolysis, for thermochem.  $H_2$  prod. 0-55928  
 pyrolysis, H prod. using the Mark 13 process, status report 0-30606  
 pyrolysis by Mg-I cycle for thermochem. H prod. 0-35786  
 pyrolysis by S-I cycle for H prod. 0-35769  
 pyrolysis for H prod., equilibrium effects in high press. prod. 0-35775  
 pyrolysis for H prod., HBr decomposition using  $FeBr_2$  and  $Fe_3O_4$  0-35778  
 pyrolysis for H prod. using S-I cycle 0-35770  
 pyrolysis using Br-Ca-Fe cycles for H production 0-35784  
 pyrolysis using S-cycles for H prod. thermochem. anal. of energy balance 0-35779  
 quark affinity to water molecule, centre expansion SCF calcs. 0-43213  
 radial distribution functions, for liqs. and amorphous substances, analytical computation method 0-24301  
 radiolysis,  $O(^3P)$  atom yield 0-35556  
 saturated water vapour pressure standardization 0-26596  
 seasonal reservoir, optimal releases, deterministic case 0-8362  
 self diffusion in frog muscle 0-8037  
 self-diffusion coeff., pressure and temp. depend. meas. by proton spin echo 0-39328  
 simulated water, cooperative effects importance 0-28906  
 skin stratum corneum, human, linear meas. of water content using microwave probe 0-21518  
 snow, water content meas., calorimetric method (*Japanese*) 0-31142  
 sodium decanoate-n-decanol-water system, lamellar G-phase, orientational-order, EPR investigation 0-24355  
 soil-water system,  $\gamma$ -ray transmission studies, calibration 0-26629  
 solar photochemical decomposition for  $H_2$  prod. 0-16822  
 solar-heated water system for a photographic processing laboratory 0-40837  
 solvated electrons, optical absorpt. spectra, temp., isotope effects 0-55124  
 solvated electrons, optical spectra and model potentials 0-30318



## water continued

sorbed on DNA, temp. anomaly, IR spectroscopic obs. 0-51046  
 sorption and desorption on DNA and lysozyme, thermal-stimulated press. and thermogravimetric anal. 0-8008  
 sorption in polysiloxane dizwitterionomers 0-49506  
 sorption into polysiloxane dizwitterionomers, effect on dielec., mech. relax. 0-50261  
 ST2 solution, hydrophobic hydration around apolar species pair, Monte Carlo simulation 0-6336  
 ST2 solution of nonpolar spheres, hydrophobic interaction Monte Carlo simulation 0-6335  
 structure and props., minimal basis set description 0-6347  
 supercooled, polychromatic correlated site percolation 0-22296  
 surface energy, electrostatic contrib. 0-20014  
 surface tension and energy, Fowler model 0-10754  
 surfactant-water liquid crystal phases, review 0-28913  
 thermal conductivity equation, 0 to 800°C, triple pt. press. to 1000 bars, crit. region 0-39364  
 thermochemical decomposition, based on  $\text{CeTiO}_3$  for  $\text{H}_2$  prod. 0-55929  
 thermochemical decomposition by Ce-Cl cycle for H production 0-35783  
 thermochemical decomposition for H prod., impact of thermal burdens and kinetics 0-35787  
 thermochemical decomposition for H prod. using S-Br cycle, development of lab-scale plant 0-35774  
 thermochemical decomposition using General Atomic S-I cycle for H prod. 0-55941  
 thermochemical H production using  $\text{SO}_2$ - $\text{I}_2$  water splitting cycle 0-30600  
 thermochemical water-splitting cycles based on Ce and alkaline earth phosphates for  $\text{H}_2$  prod. 0-55945  
 thermodynamic props., computer programme calcs. (French) 0-54409  
 tritiated, inhalation hazard from open containers 0-8240  
 tritium in rabbits after ingestion of freeze-dried tritiated food and tritiated water 0-21549  
 underwater spark discharge, vapour-gas cavities generation and space-time evolution characts. 0-19650  
 unsteady heat transfer to water at supercritical press. 0-48692  
 unsteady transient heat transfer with phase transitions 0-48693  
 vapourisation, latent heat, student expt. 0-27081  
 vapour, 2-D laminar boundary layer 0-19492  
 vapour, absorpt. lines at ruby laser wavelengths, saturation effect 0-4098  
 vapour, absorption spectrum,  $\text{LiF F}_2^+$ -centre laser intracavity spectroscopy appl. 0-32999  
 vapour, adsorption on Cu and  $\text{Cu}_2\text{O}$  and desorption, relative humidity effects 0-49505  
 vapour, adsorption on Ge films, IR spectra 0-6628  
 vapour, adsorption on  $\text{SnO}_2$ , desorpt. and cond. meas. 0-10790  
 vapour, anal. of skin evaporimeter performance 0-56256  
 vapour, averaged potential for complex polar fluids 0-48833  
 vapour, chemisorption on TiC (001) surface, change in work function 0-29461  
 vapour, continuous detection during thermal decomposition reacts. 0-3440  
 vapour, effect on contact resist. of  $\text{ZnO:NiO-Li}_2\text{O}$  n-p heterojunction 0-34506  
 vapour, far IR absorpt. coeffs. by  $\text{H}_2\text{O}$  laser meas. 0-9599  
 vapour, ionis. coeffs. and dissociative electron attachment 0-43833  
 vapour, IR absorpt. spectrum, contrib. by molecular clusters 0-9598  
 vapour, line shape functions in absorpt. coeff. calc. 0-9600  
 vapour, low density flow temp. and density meas. by submillimetre spectroscopy 0-43816  
 vapour, photoinduced nucleation expt. 0-2149  
 vapour, radiation absorption capacity 0-14873  
 vapour, wet, boundary layer in compressible flow 0-10295  
 vapour and HCN mixtures, adsorption by activated and impregnated C 0-39412  
 vapour channel, atmospheric transmission function, cloudless radiances 0-46256  
 vapour continuum absorpt., 4.5-5.0  $\mu\text{m}$  0-36395  
 vapour electron stopping power and energy degradation 0-23276  
 vapour etching of GaAs, rate 0-16519  
 vapour images from Meteosat, comparison to tropical steamline analyses 0-8384  
 vapour line 724 nm differential absorption lidar at 724 nm water vapour 0-17384  
 viscosity, multiparameter viscosity-temp. eqns. analysis 0-15283  
 viscosity changes close to quartz surface, fine capillary calcs. 0-54422  
 viscosity changes effect on electrokinetic phenomena in capillaries 0-53867  
 water-carbon tetrachloride soln., fundamental  $\text{H}_2\text{O}$  IR spectrum, liq. struct. 0-23419  
 water-ethanol mixture, nonlinear acoustic coeff. meas., 0-50°C (French) 0-34142  
 water-isobutyric acid, crit. mixture 0-24601  
 water-isobutyric acid (2,6-lutidine) mixtures, critically quenched, phase separation and coalescence 0-24581  
 water-isobutyric acid mixture, heat of transport, crit. exponent 0-15277  
 water-methanol (n-propanol), binary mixtures, nucleation 0-44305  
 water-methanol mixture, nonlinear acoustic coeff. meas., 0-50°C (French) 0-34142  
 weirs and flumes for flow measurement, book 0-1717  
 yeast cell membrane, water transport study, pulse NMR obs. 0-40981  
 $\text{CO}_2$ - $\text{O}_2$ - $\text{H}_2\text{O}$ , photodissoc. and photodetachment of negative ions 0-14182  
 $\text{D}_2\text{O-H}_2\text{O-HDO}$ , gaseous mixture, absorpt. meas. by Michelson inclined mirror interferometer, high spectral resolution 0-9023  
 $\text{EuCl}_3\text{-NaPO}_3\text{-H}_2\text{O}$  system, Eu polyphosphates form. at 0°C 0-35515  
 Fe, influence of acid  $\text{Na}_3\text{PO}_4$  soln. in tap water as a corrosion inhibitor 0-45424  
 Fe- $\text{H}_2\text{O}$  laminated radiation shield, fast neutron transport 0-13931  
 H production, thermochem.  $\text{H}_2\text{O}$  decomposition using S compounds, feasibility anal. 0-35768  
 HCl-KCl- $\text{H}_2\text{O}$  mixed electrolyte solns., elec. transport 0-3355  
 $\text{HClO}_4\text{-H}_2\text{O}$ , aq. soln., IR and Raman spectra, conc. depend. (Russian) 0-53002  
 HDO, interactions with myosin, intermolecular spin diffusion study 0-18951  
 $\text{H}_2\text{O}^+$ , pot. energy surface from  $\text{O}^+ + \text{H}_2$  reaction 0-47922  
 $\text{H}_2\text{O}^+$ , states geometries, electronic vibr. coupling consts. HF calcs., comparison with Xalpha calcs. 0-27946  
 $\text{H}_2\text{O-CsCl-1-glycerol-1-octanoate}$ ,  $\text{Cs}^+\text{H}_2\text{O}$  interaction in lamellar phase, NMR quadrupole splitting and chemical shift 0-50209

## water continued

$\text{H}_2\text{O}$ -formaldehyde complex, IR spectrum in solid Ar,  $\text{N}_2$  matrix 0-43042  
 $\text{H}_2\text{O-H}_2$  cooling in supersonic nozzle, submillimetre wave generation 0-48229  
 $\text{H}_2\text{O-H}_2\text{S}$  complexes, equilib. config., H-bond energies and electron densities, CNDO/2 method 0-14084  
 $\text{H}_2\text{O-HF}$ , H-bonded complex, cubic force consts. calcs. 0-47868  
 $\text{H}_2\text{O-HNO}_3\text{-NO}_2$  clusters, gas phase, thermodynamic quantities, mass spectra obs. 0-50875  
 $\text{H}_2\text{O}$ -trifluoroacetic acid, molecular dynamics simulation of chemical reactions in solution 0-40673  
 $\text{H}_2\text{O} + \text{Ar}^+$ , thermal-energy charge transfer,  $\text{H}_2\text{O}^+$  product internal and kinetic energy 0-16654  
 $\text{H}_2\text{O} + \text{Cl}_2\text{O} = \text{HOCl}$ , equilib. const., Fourier transform IR determ. 0-7765  
 $\text{H}_2\text{O} + \text{H}_2\text{O}(\text{F}^-)(\text{CH}_4)$ , interaction energy calc. using minimal basis sets 0-9678  
 $\text{H}_2\text{O} + \text{H}_2\text{O}(\text{Na}^+)(\text{K}^+)(\text{NH}_4^+)$ , supermolecule calcs. with additive procedure, intermolecular interactions and binding energy 0-52880  
 $\text{H}_2\text{O} + \text{OH}$ , mean collision cross sections from microwave spectroscopy 0-1046  
 $\text{H}_2\text{O} + \text{OH}(\text{A}^2\Sigma^+)$ , quenching rates and fluoresc. efficiency, rel. to atmosphere 0-14199  
 $\text{H}_2\text{O} + \text{O}(\text{D})$ , direct reaction in flow system 0-3333  
 $\text{H}_2\text{O} + \text{O}(2\text{D}_2)$ , collisional deactivation meas., 295K, rel. to atmospheric processes 0-16663  
 HOD, IR spectra in  $\text{D}_2\text{O}$ , combination vibr. 0-9609  
 $\text{H}_2\text{O}(\text{ads}) + \text{H}(\text{ads}) \rightarrow \text{OH} + \text{H}_2(\text{g})$ ,  $\text{H}_2$  formation mechanism 0-6628  
 $\text{K}_2\text{O-Ga}_2\text{O}_3\text{-P}_2\text{O}_5\text{-H}_2\text{O}$ , reactions, 150-500°C 0-35514  
 $(\text{NH}_4)_2\text{SO}_4$ -ethanol-benzene-water, liq. mixture, near tricrit. pt., thermodynamic model and sun rules 0-34196  
 $\text{N}_2\text{O}_4\text{-NO-H}_2\text{O}$ , distrib. coeff. for  $\text{N}_2\text{O}_4$  on liquid-vapour equil. (Russian) 0-55699  
 $^{13}\text{N}$  species formed by proton irradiation of water 0-45532  
 $\text{NaCl-KCl}(\text{MgCl}_2)\text{-H}_2\text{O}$  mixed electrolyte solns., elec. transport 0-3355  
 THO, prediction of flux from air to plant leaves 0-26381  
 U conc. determ. by fission track registration technique 0-12565  
 $^{133}\text{Xe}$  solubility coefficients in water, saline, dog blood and organs 0-56331

## water boilers see boilers

## water conditioning see water treatment

## water cooling towers see cooling towers

## water pollution

see also water pollution detection and control  
 Bantry Bay, Ireland, oil spill from tanker Betelgeuse, initial effects 0-3540  
 biological material analysis, As and Hg determ. by neutron activation anal. 0-36216  
 Chesapeake Bay pollution, data importance 0-3544  
 Clyde Sea Area, Scotland,  $^{134}\text{Cs}$  and  $^{137}\text{Cs}$  contamination, water and sediment tracer species 0-3541  
 Cochin backwater, India, estuarine water, particulate heavy metal content 0-7964  
 convection-diffusion equation, 1-D, finite elements method, weighted residuals 0-53775  
 Cs accumulation in muscle tissue of marine fishes 0-35797  
 dredger spoil, dumping ground obs., motion of fine particles with current 0-17287  
 estuarine salt marsh, micro-organisms and trace metals 0-55950  
 filtration parameters of polluting miscible fluids through porous aquiferous phreatic media 0-53855  
 geothermal energy, environmental problems, air and water pollution, subsidence, induced seismicity, blowouts, noise, review 0-55797  
 Great Lakes, toxic substances 0-55949  
 groundwater from geologic repositories, computer anal. of long-term radiation hazards 0-18483  
 heavy metals, content in water and sediments in reservoir reservoir supplying major mining centre 0-30617  
 in situ leach mining, environmental considerations rel. to water quality 0-3543  
 marine pollution, dynamically passive impurity propag. in sea surface layer 0-31063  
 migration obs. near South Carolina coastal front 0-45831  
 mirex in lake Ontario sediments, circulation simulation 0-26556  
 Netherlands, chlorophenols in surface waters, 1976-7 obs. 0-16858  
 nuclear power stations, long term radioactivity values, meas. in marine life (Spanish) 0-7962  
 ocean data collection 0-3545  
 ocean dumping of high level radioactive waste 0-32376  
 ocean floor hot spring created by drill hole 0-55951  
 ocean subsurface oil-rich layer at 200 metres, obs. in Caribbean and N. Atlantic 0-56498  
 oil slick burning in Arctic, adverse atm. effects during clearing of spills 0-16875  
 organic pollutants, influence of detergents on hydrosolubility and suspension (French) 0-7961  
 Ottawa River, multidisciplinary research project on pollution 0-21421  
 Passaic River, New Jersey, nitrification, historical and expt. investigation 0-7968  
 Perch Lake Basin, Ontario, hydrological and geochemical studies conference, Chalk River, 1978 April 25 to 26 0-51955  
 phosphate facility, evaluation of  $^{226}\text{Ra}$  and  $^{222}\text{Rn}$  concs. in nearby water 0-45827  
 Puget Sound, oil migration, mixed Lagrangian-Eulerian model 0-45830  
 quality indices, statistical anal. 0-8368  
 radioactive, use of box model method (Japanese) 0-9346  
 radioactive waste, computer anal. of relative potential hazards 0-21422  
 radioisotope environmental dispersion models, evaluation of uncertainties 0-46074  
 river systems, water quality models, Monte-Carlo anal. 0-8367  
 undersea resources and related topics, world-wide survey 0-35622  
 NE.United States, soil Al leaching by acid precip. in high-elevation watersheds 0-12442  
 Venice lagoon, effect on contaminant residence time of modified tide regime 0-12431  
 CO, radioactive and stable, determ. in marine biological materials 0-36157  
 Cu, rate of loss and speciation in lakewater 0-7967  
 Hg concentrations in seawater,  $^{203}\text{Hg}$  tracer and  $^{75}\text{Se}$  tracer 0-21420



**water pollution continued**

Hg in Gulf Stream 0-7965

<sup>238</sup>Pu<sup>4+</sup>, <sup>238</sup>Pu<sup>6+</sup>, <sup>239</sup>Pu<sup>4+</sup>, <sup>239</sup>Pu<sup>6+</sup>, alga uptake rel. to isotope and oxidation state 0-30692<sup>239</sup>Pu, <sup>240</sup>Pu, concs. in fish and seawater from Kwajalein Atoll 0-26380

Ra, assessment of quantities in North Carolina drinking water supplies 0-45826

Se concentration in seawater, <sup>75</sup>Se tracer and <sup>203</sup>Hg tracer 0-21420T concentration in natural waters of N. Italy (*Italian*) 0-40933**water pollution detection and control***see also water treatment*

activated sludge control parameter, oxygen uptake rate 0-35798

Arctic oil spillage response techniques 0-46204

benzo(a)pyrene, determ. in water using spectrofluorimetry 0-7997

biological nitrification systems, control strategy 0-35799

capillary gas chromatography of chlorophenols in surface waters 0-16858

chronic radioactive release assessment, models and computer codes 0-13710

continuous oil-in-water meas. by towed fluorometer 0-45846

dinitrotoluene isomers, occurrence and determ. in seawater 0-7966

dissolved O<sub>2</sub> in water, automatic analyser (*Japanese*) 0-35812electrochemical porous flow-through electrodes, mass and charge transfer and cell design (*French*) 0-16697

environmental monitoring instruments 0-45825

fluidised bed containing biomass, expansion 0-14803

fluorometric dye meas. background variation expts. 0-45844

fluorometric techniques and instrumentation 0-45845

groundwater, chemical pollutants convective dispersion reln. 0-16855

groundwater contamination, Holt County, Nebraska, USA 0-12033

groundwater system, transport of chain decaying radionuclides 0-51019

Gulf of La Napoule in France, pollution abatement attempt, results from dredgings 0-16857

high-level liquid waste, damage to organic extractant in positioning process 0-9345

industrial surface treatment water residues (*French*) 0-16528

instrumental photon activation analysis of lyophilized seawater, multielement conc. of heavy-metal contaminants 0-16892

lake quality monitoring, multirate Landsat data extraction program 0-17299

marine particulate plume density and distrib., acoustic assessment 0-45843

modular system for monitoring of temp., pH, dissolved acids, turbidity and colour (*German*) 0-26186

multielement instrument neutron-activation analysis, ecology appl. 0-40946

ocean acid waste dump, particulate Fe mapping 0-56497

ocean surface wind wave related turbulence meas. by impeller current meter array 0-46301

organochlorine, pesticide residual levels, pollution in Sathiar reservoir water, mud and organisms 0-45828

organonitrogen wastes 0-35796

organophosphorus pesticide residual levels, pollution in Sathiar reservoir water, mud and organisms 0-45828

pelagic tar ocean distribution and surface circulation 0-16856

plastic ocean distribution and surface circulation 0-16856

potentiostatic measurements for pollutants analysis in waste waters (*German*) 0-26185radioactive tracing of hydrological pollutants (*French*) 0-7995

radionuclide sorption from shallow land disposal of low level radioactive waste 0-16851

Raman spectroscopy, tonic organic substances detection 0-30616

regional water pollution control, energy anal. 0-26180

river pollution, dynamic behaviour of distributed systems (*Dutch*) 0-3542sea area surveillance using side looking airborne radar system (*Dutch*) 0-12560silt double-labelling technique for radioactive tracing of physico-chemical behaviour of Zn (OH)<sub>2</sub> (*French*) 0-7994

systems analysis appl. 0-26182

total organic carbon measurements for industrial water and wastewater 0-26071

waste water disinfection and oxidation, ClO<sub>2</sub> appl. 0-12032waste water of sulphate cellulose prod., radiation treatment (*Russian*) 0-55688

wastewater treatment, distributed digital processing and closed loop computer control 0-45824

As conc. meas., column chromatography versus flameless atomic absorption spectrophotometry 0-55969

Cd determ. in drinking water by graphite furnace at absorpt. anal. 0-55733

Hg flux meas. in South Atlantic Bight 0-4046

I<sup>-</sup>, anal. in groundwater by X-ray fluorescence spectrometry 0-45829<sup>54</sup>Mg, removal from waste water by oxine-impregnated activated charcoal 0-9344<sup>90</sup>Sr and T in N. Pacific surface water during 1974, conc. meas. 0-26181

T concentration reduction for aquifer 0-21423

Zn and Cu levels in Belfast Lough 0-3539

**water purification** *see water treatment***water supply***see also dams*

Galal Badra Basin, Iraq, water deficit 0-26565

hot water supply using solar collectors (*Dutch*) 0-7954

reservoir supplying major mining centre, water and sediments heavy metals content 0-30617

river basin water resource, Pareto region, stochastic multicriterial problem in control 0-4055

storage reservoir analysis, mass-curve techniques, systems and perspective 0-8457

**water treatment***see also desalination*

biological wastewater treatment system using photosynthetic energy conversion 0-30510

dissolved O<sub>2</sub> in rivers, reliability parameter in probabilistic programming models 0-26179electrochemical porous flow-through electrodes, mass and charge transfer and cell design (*French*) 0-16697

fluidised bed containing biomass, expansion 0-14803

high-level liquid waste, damage to organic extractant in positioning process 0-9345

industrial wastes, Mg recovering, use of sink-and-float test (*Japanese*) 0-55948**water treatment continued**

ion chromatography appl., on-stream, impact on energy conservation 0-55737

ion-exchange wash water recycling system, photographic processing laboratory appl. 0-42277

municipal wastewater treatment plants, mathematical modelling of electrical energy consumption and heating requirements 0-26194

solar photodecomposition, redox reaction thermodynamics 0-35697

wastewater treatment, distributed digital processing and closed loop computer control 0-45824

water distillation using basin-type solar stills, use of wood charcoal beds 0-7924

wind powered brackish water purification by electrodialysis and reverse osmosis 0-35630

ClO<sub>2</sub> appl., waste water disinfection and oxidation 0-12032<sup>54</sup>Mg, removal from waste water by oxine-impregnated activated charcoal 0-9344**watthour meters***see also power measurement*

No entries

**wattmeters***see also power measurement; volt-ampere meters*analogue, appl. for specific core loss meas. or elec. steel sheets (*German*) 0-13099

battery self-discharge process assessment by microcalorimetry 0-30935

defibrillator energy meters, traceable calibration methods 0-30928

digital, for compact electronic equipment 0-209

heat receivers with moving heat carrier, freq. characts. 0-4733

**wave equations***see also Dirac equation; Schrodinger equation*

Backlund transform. derivation in inverse scatt. formalism 0-8810

Benjamin-Ono eqn., conservation laws 0-31524

Benjamin-Ono equation, Backlund transform. and conservation laws 0-4540

Benjamin-Ono equation, internal wave solitons, linear stability 0-53802

Benjamin-Ono equation, meromorphic solutions 0-31980

Benney's long wave eqns., Hamiltonian formalism 0-31525

Benney's long wave equations, conservation laws and Lax representation 0-14719

bilinear soliton equations, method of constructing generalised soliton solns. 0-4541

Boussinesq type eqn., reduction to modified Hirota eqn. 0-8804

Burgers equation, relationship to differential stochastic eqn. 0-36869

catastrophe theory, anal. of wavefront dislocations 0-8812

linear Chapman-Enskog procedure, evolution equations of hydrodynamic variables 0-49075

completeness value for eigenfunctions of second order differential eqns. 0-31564

conference, nonlinear problems in theoretical physics, Jaca, Gain 1978 0-4478

continuously stratified liquid, linear wave theory, internal wave operator solution 0-43759

deep water gravity waves, two-dimens. nonlinear wave eqn., exact envelope soliton solns. 0-43725

difference method for extended stability range 0-4538

dynamic stability of solitons and general nonlinear wave phenomena (*German*) 0-4544

electron spin equations of motion in external field 0-18102

electronic wavefunctions in a space of constant curvature 0-5466

evolutionary problems, error anal. of finite difference, finite element and spectral methods 0-46815

field statistical moments in medium with large-scale inhomogeneities 0-37953

finite-band solutions to the duality equation on S<sup>4</sup> and two-dimensional relativistically invariant systems 0-42349

fluids of finite depth, exact one- and two-periodic wave solns. 0-53797

fluids of finite depth, N-soliton soln. of higher order wave eqn. 0-48724

free Klein Gordon fields, conservation laws 0-340

Gel'fand-Levitan equations with comparison measures and comparison potentials 0-12931

generalised sine-Gordon eqn., Backlund transformation, nonlinear  $\sigma$  model 0-4844

Green function expansion into eigenfunction set 0-22205

harmonic oscillators, vibr.-vibr. energy transfer, perturbed wave eqn. soln. 0-1051

hidden symmetries in dynamical systems 0-37168

higher order Benjamin-Ono equation, N-soliton and N-periodic wave solns. 0-12915

integral transform groups for differential operators from Lie algebras 0-4887

internal waves with finite fluid depth, inverse scatt. problem, Backlund transformation 0-31517

invariant bedding, numerical solution of drift wave equations 0-10374

Jaulent-Miodek family of nonlinear evolution eqns., Hamiltonian formulation 0-31511

Kadomtsev-Petviashvili eqn., appl. of variation of action method of one field solitons 0-331

Kadomtsev-Petviashvili eqn., asymptotic behaviour of solns. (two-dimensional Korteweg-de Vries eqn.) 0-52036

KdV eqn., particular N-soliton soln. 0-31971

Klein-Gordon eqn. with step nonlinearity, jetlike solutions 0-17813

Klein-Gordon particles, massless bound state, Coulomb potential 0-37188

Klein-Gordon particles in deep square wells 0-31982

Korteweg de Vries modified eqn., solitary wave solns. 0-46818

Korteweg-de Vries, cylindrical eqn., soln. asymptotic behaviour 0-31526

Korteweg-de Vries, Hirota and inverse spectral methods 0-71

Korteweg-de Vries eqn., Fourier expansion soln. 0-46814

Korteweg-de Vries eqn., quasi-solitary wave soln. 0-70

Korteweg-de Vries eqn., slowly varying solitary wave solns. 0-72

Korteweg-de Vries eqn., weak dissipation effect on two soliton soln. 0-27143

Korteweg-de Vries eqns., nonresonant mode coupling 0-27142

Korteweg-de Vries eqns., perturbed solns. and soliton production 0-42074

Korteweg-de Vries equation, modified, N-soliton soln., matrix trace method 0-36871

Korteweg-de Vries equation, numerical methods of solution, difference and transform schemes, accuracy 0-46833

Korteweg-de Vries equation, soliton soln. using matrix trace 0-36870

Korteweg-de Vries equation, solns. for slowly decreasing boundary conditions 0-36872



## wave equations continued

- Korteweg-de Vries equations, N-soliton soln., functional integral representation 0-4542  
 Korteweg-de Vries (Burgers) nonlinear long waves, mathematical modelling 0-8791  
 light rays, commutator relation of ray operators and wave equation, relation 0-36877  
 linear waves, asymptotic behaviour and wave patterns construction (*Czech*) 0-69  
 local spin- $1/2$  wave equations and harmonic confinement 0-4926  
 meromorphic solutions of nonlinear partial differential equations and many-particle completely integrable systems 0-31523  
 modified Korteweg-de Vries eqn., N-soliton solns. 0-36876  
 modified Korteweg-de Vries solitary wave in a slowly varying medium 0-36873  
 non-Abelian gauge group theory, relationship with solitons 0-4549  
 nonlinear, soliton solutions, inverse scattering method 0-12919  
 nonlinear, soliton solutions and their applications 0-8813  
 nonlinear evolution equation, exact two-periodic wave soln. 0-12914  
 nonlinear evolution equations, integrable, inverse scatt. method 0-12913  
 nonlinear field equations, scattering theory 0-4882  
 nonlinear hydrodynamical eqn. of Kaup, periodic and N-soliton solns. (*French*) 0-31521  
 nonlinear long waves, mathematical modelling 0-8791  
 nonlinear media, Poincare normal form method 0-36875  
 nonlinear Schrodinger equation solns., recurrent motion in continuum dynamical systems 0-22235  
 nonlinear transmission line, solitary waves 0-4543  
 nonrelativistic limits for Klein-Gordon and Dirac eqn. 0-330  
 ocean random gravity wave mathematical representation 0-46198  
 off energy two body t-matrix in the R-matrix theory (*Russian*) 0-22780  
 phase memory, necessary conditions 0-22206  
 plane wave solns., rel. to const.-identity 3-dimens. wave 0-17749  
 polycrystal, US scatt. by grains 0-2122  
 progressive waves in dissipative media, long range ray theory (*French*) 0-42070  
 rotating plane-fronted waves and their Poincare-invariant differential geometry 0-332  
 sine-Gordon eqn. separable solutions in terms of Painleve transcendent 0-52037  
 sine-Gordon equation, two soliton solutions, breather solution 0-12945  
 sine-Gordon field theory Coulomb gas equivalence, classical gas with logarithmic pot. 0-4850  
 sine-Gordon perturbed equation, soliton mass formulae 0-22200  
 sine-Gordon supersymmetric eqn., inverse scatt. 0-47165  
 singular hypersurfaces, asymptotic regularisation as alternative to distrib. 0-36923  
 Smoluchowski equation in presence of hydrodynamic interactions, Chapman-Enskog method 0-46979  
 soliton formation, mth order parametric interaction, using Klein-Gordon eqns. 0-12917  
 solitons amplification in modified Korteweg-de Vries eqn. 0-27145  
 spectral transform, nonlinear discrete evolution equations 0-4553  
 spectral transform and nonlinear evolution equations 0-4551  
 spectral transforms, nonlinear evolution equations 0-4552  
 superposition of solitons from same nonlinear differential eqns. 0-67  
 transversely inhomogeneous slab, modal wave propag. with gain or loss variations 0-48122  
 travelling waves, memory effects in random walk process 0-27232  
 vector wave equation, depolarisation term anal. 0-8814  
 He, superfluid B phase, spin wave breathers, double sine-Gordon equations 0-15329

## wave functions

- see also orbital calculation methods  
 alkali halide, polarisation energy for core states 0-10903  
 alkali halides,  $F_A$ -centre optical absorpt., estimate using symmetry-adapted wave functions 0-11448  
 analytic radial orbitals, optimisation on variational parameters 0-42941  
 atom Breit interaction between electrons, calc. angular coeffs., computer program 0-18779  
 atom scattering by corrugated potential wall, appl. to diff. by cryst. surface 0-42104  
 atomic collisions, quasiclassical theory, transition between spatially degenerate levels 0-43150  
 atomic model potentials soluble in closed form 0-23287  
 atoms, singly excited states, oscillator strengths, ab initio calcs. 0-920  
 Bose system, Jastrow wavefunction, hypernetted chain method 0-17866  
 catastrophe and fractal regimes in random waves 0-8811  
 catastrophe and stochasticity in semiclassical quantum mechanics 0-8861  
 catastrophe theory, anal. of wavefront dislocations 0-8812  
 CI methods for improving unrestricted Hartree-Fock spin densities 0-32617  
 cluster expansion, electron correlations, SAC and SAC CI calcs. 0-18802  
 cluster expansion electron correlations, SAC and SAC CI theories 0-18801  
 commutation symmetry for system of identical particles (*Russian*) 0-12944  
 confining potentials, peculiar prop. of wavefunctions 0-46863  
 curved space-time quantum stochastic processes, covariant Kolmogorov-Klein-Fock eqn. 0-18083  
 dechannelling (aligned-to-random beam transition), WKB approx. 0-34109  
 deuteron wave functions, relativistic 0-22595  
 Dirac particles, massless bound state, Coulomb potential 0-37189  
 electronic system, props. without antisymmetrisation 0-32586  
 Fermi system, Jastrow wavefunction, hypernetted chain method 0-17866  
 field wavefunction, analytic properties in optics 0-1138  
 hadrons and their constituents, wave-particle quality 0-9136  
 HF subsystems, long range induction and dispersion interactions 0-53092  
 highly charged ion,  $1s^2 2s^2 2p^3 3d$  configuration, energy spectra in relativistic approx. 0-14082  
 hydrazones, protonation energy and basic strength 0-37719  
 hypervirial theorems and symmetry, optimal variational wave function 0-17841  
 inert gas atom, photoionis. cross sections of excited levels, quantum defect method calcs. 0-37795  
 inhomogeneous Airy function,  $Gi(3)$  and  $Hi(3)$  0-43259  
 inhomogeneous electron gas at jellium surface, exchange energy 0-10901  
 local multigaussian FSGO one-determinant wave functions, energy gradient expression 0-23282

## wave functions continued

- localised electrons, single particle wave function random field calcs. (*Russian*) 0-34397  
 logarithmic perturbation expansions, appl. to H in multipole field 0-37720  
 matrix elements of  $\delta(r_1)$ , approx. wavefunction 0-47860  
 MCSCF method improvement 0-52857  
 molecular ab initio CI pot. curves, mol. wavefunctions and vibr. freqs. comparison of methods 0-27956  
 molecular vibrational wave functions, semiclassical Gaussian basis set method 0-9583  
 molecule, polar, electron scatt. symmetry 0-32834  
 moving electron in field of two Coulombic ions fixed in space, rel. to  $H_2^+$  line spectrum 0-42083  
 multidimensional systems, semiclassical calc. of bound states 0-963  
 nuclear matter, variational techniques, review 0-22748  
 off-energy-shell generalisation 0-18257  
 one-dimensional particle-in-the-box problem, perturbation theory illustration using champagne bottle situation 0-36816  
 optical absorption spectrum of  $D^-$  centre in strong magnetic field 0-20670  
 perturbation theory, variational methods, evaluation of second-order matrix elements 0-12936  
 phonons, coupled rotational band approach, zero-rank operators 0-47341  
 point charge model approach to intermol. interaction coeffs. 0-18897  
 point charge model approach to mol. elec. polarisability 0-18797  
 polar molecule, excited state MCSCF wave functions, BeO appl. 0-47916  
 polyatomic molecule, vibr. struct. of electronic spectra, FORTRAN programs 0-32699  
 position space LCAO wave function, momentum space variation approx., many centre integrals 0-27926  
 prolate spheroidal radial function of third kind, asymptotic formula 0-42077  
 quantum bundles, group actions, relationship to group representations 0-17837  
 quantum dynamics semiclassical approximation 0-12927  
 quantum mechanical particle in random potential, inverse participation ratio in  $2+e$  dims. 0-36908  
 quantum system, jarring and corresponding stimulated transitions 0-17839  
 quantum transition concept in undergrad. courses, explanation of photon creation and absorpt. 0-36807  
 radial integrals calc. in Coulomb approx., use of semiclassical wavefunctions 0-43025  
 relativistic effects in central field approximation, RELAC method and use 0-9520  
 rotated coordinate method use, rel. to stabilisation method 0-37845  
 Saito potential, off-energy-shell unitarity 0-18207  
 Schrodinger equation, new type, evolution of wave function with respect to position 0-27178  
 Schrodinger wave functions at pot. discontinuities, continuity conditions, for teaching 0-27077  
 shell model matrix elements, two-body, by Taylor-series method 0-32212  
 Siegert wavefunctions, partial widths calcs. 0-5507  
 stationary state, standing de Broglie wave, Aharonov-Bohm effect 0-22228  
 superfluid model, isotopic invariance and pairing energies 0-22687  
 symmetry breaking, wave function choice, effect on predictions, DKP formalism view 0-9120  
 transition metal ion, superposition of quasidegenerate configurations, principal quantum number  $N=3$  0-14079  
 two-nucleon reduced widths in symmetric two-centre shell model 0-32213  
 two-particle collective excitations, energy and wave function calcs. 0-20098  
 valence nucleons, muonic atom analysis 0-27530  
 Wigner's  $(2n+1)$  rule in MBPT 0-42095  
 e+atom wavefunction by solving coupled second order integro-differential equations, computer programs 0-18924  
 e+ion wavefunction by solving coupled second order integro-differential equations, computer programs 0-18924  
 Ar XV, wavefunctions and oscill. strengths, CI calcs. 0-23317  
 C, optical oscillator strengths, independent particle model, excited state wave functions, LS coupling and Born approx. 0-32674  
 C<sub>3</sub>, Renner effect, vibronic levels and wavefunctions, ab initio variational method 0-14127  
 Ca XVII, wavefunctions and oscill. strengths, CI calcs. 0-23317  
 Cu-like ions, E1 transitions, wavelengths, oscillator strengths and transition probabilities, data tables 0-37780  
 Fe XXII, allowed transition CI wave functions, oscill. strengths and transition probabilities 0-32664  
 Fe XXIII, wavefunctions and oscill. strengths, CI calcs. 0-23317  
 n-GaAs-Ga<sub>1-x</sub>Al<sub>x</sub>As, superlattice, subband struct. and optical spectra, self-consistent calc. 0-15443  
 P-Ge, acceptor wavefunctions in spherical approx. and piezoresist. 0-29405  
 H atom, variations, quantum theory calcs., generator coord. calcs. 0-41987  
 H<sub>2</sub>, polarisabilities, higher, static, calc., wave-function quality depend. 0-18814  
 H<sub>2</sub><sup>+</sup>, exponentially small part of wave function (*Russian*) 0-9497  
 HF, Auger spectra, correl. effects, energies and wavefunctions, ab initio CI calc. 0-14125  
 He,  $1s^2$  ground state piecewise polynomial CI natural radial orbitals wave functions 0-18805  
 He, exchange and correlation pots., density functional theory 0-52848  
 He ground state, Hylleraas six parameter wave function, minimisation method 0-27925  
 He, isoelectronic sequence,  $2S$  states, analytic wave function 0-9525  
 HeH<sup>+</sup>, excited states, variable screening models, natural spin orbital analysis of wave functions 0-37747  
<sup>4</sup>He, liquid, condensed phase, long-range order of one- and two-body density matrices 0-10726  
<sup>4</sup>He system, O<sup>+</sup> states, microscopic wave function 0-463  
 K, Pauli susceptibility and Knight shift meas., electron wave functions 0-44937  
 LiH, one electron props., X $\alpha$  multiple scattering wave functions 0-42945  
 LiNC type molecules, Born-Oppenheimer approx. applicability 0-32603  
 Mg IX, wavefunctions and oscill. strengths, CI calcs. 0-23317  
 Na isoelectronic series, wave functions and effective pots. of valence electron 0-47873



**wave functions continued**

- Ne, Auger spectra, correl. effects, energies and wavefunctions, ab initio CI calc. 0-14125  
 Ne II, III, and IV ground state, photoionis. cross sections, close coupling calcs. 0-5513  
 S-IV, P-, D-, S-states, oscillator strengths, transition strengths, CI calcs. 0-922  
 Si IV radial wave functions of discrete spectrum calcs., dipole and quadrupole polarisation 0-5476  
 Si isoelectronic sequence, CI calcs. of oscillator strengths, L-S framework 0-14089  
 Si XI, wavefunctions and oscill. strengths, CI calcs. 0-23317  
<sup>A</sup>Zr, A=90, 92 and 94, charge densities and single-particle structure 0-9224

**wave mechanics**

- see also wave equations; wave functions*  
 bispectrum and nonlinear wave coupling for three-wave coupling 0-52038  
 de Broglie wave packet for a simple stationary state 0-17810  
 group velocity, four-dimensional 0-17814  
 origin, pedagogical approach (*Portuguese*) 0-22166  
 Schrodinger's route to wave mechanics 0-17783  
 sine-Gordon equation, two soliton solutions, breather solution 0-12945  
 wave-packet motion in Eckart and quadratic pots., appl. to H interstitials in transition metals 0-52067

**wave power generation**

- ball screw type wave power generator, design, eqns. of motion, digital simulation 0-35632  
 Coriolis ocean turbine energy system status 0-45628  
 efficiency meas. and optimisation 0-21370  
 electrochemical gas concentration cells for the conversion of ocean wave energy 0-40821  
 energy exchanger in advanced power cycle systems 0-35633  
 energy potential of ocean surface waves, currents and tides as renewable energy sources 0-30371  
 energy resources and technologies, Conf., Chicago, IL, USA, Nov. (1978) 0-23123  
 hydroelectric potential of the Zaire River, specifications and cost estimates of proposed plants 0-30375  
 ocean swell and wave energy conversion system, feasibility 0-55795  
 ocean wave energy conversion techniques and subsystems 0-45627  
 offshore float device, prototype design and expt. results 0-26107  
 small scale generators, design criteria and wave characts. 0-55796  
 submerged sphere as an absorber of wave power 0-26108  
 weatherproof submersible ocean wave energy convertor 0-45626

**wave propagation**

- see also acoustic wave propagation; electromagnetic wave propagation*  
 acoustic field in stratified media of variable viscosity, Green's functions 0-4545  
 arteries, pulse wave propag., initial stresses and muscle activity effects 0-12172  
 atmosphere stationary planetary waves, propag. in longit.-depend. basic wind flow (*German*) 0-56526  
 atmospheres, wave propag. with high radiation pressure 0-26729  
 bimaterial interface, wave propagation in non-uniform motion of displacement discontinuities 0-19264  
 bodies with initial stresses, elastic wave propag., review 0-38323  
 classical mechanics, logical drawbacks 0-17799  
 composite semi-infinite rod, wave propagation 0-10180  
 compressional and shear waves in saturated rock during water-steam transition 0-30995  
 constant Q-wave propagation and attenuation 0-30996  
 continuously stratified liquid, linear wave theory, internal wave operator solution 0-43759  
 diffraction problem, non-homogeneous media, non-stationary problem 0-22211  
 diffraction stationary problem in non-homogeneous media 0-68  
 dissipative and/or dispersive systems, perturbative and reductive method (*French*) 0-36868  
 elastic half-plane, wave propagation for non-uniform motion of displacement discontinuities 0-1478  
 elastic short waves grazing incidence on slender cavity 0-5983  
 elastico-viscous fluid, compressible, nonperiodic wave propag. 0-43724  
 elastodynamic diffraction, two-dimens., by cracks, matched asymptotic expansions 0-1468  
 elliptical cavity, wave diffraction 0-38320  
 explosive instability upon interaction of localized and nonlocalized waves 0-31530  
 fibre reinforced composites, ultrasonic vibrs. propagation velocity, dependence on composites elastic props. 0-5975  
 fluid-structural interactions, one-dimensional networks, MULTIFLEX code 0-13535  
 frictional attenuation, amplitude depend., rocks appl. 0-31034  
 granular material, finite amplitude 1-D pulses 0-43642  
 gravitational waves, dispersion in cold matter 0-12967  
 Green function expansion into eigenfunction set 0-22205  
 group velocity, W.R. Hamilton's investigation 0-17815  
 Helmholtz's reciprocity theorem, invalidity for scalar wave field propag. 0-31527  
 hidden symmetries in dynamical systems 0-37168  
 hydromagnetic waves in high  $\beta$  plasmas, propag. and damping 0-17482  
 ideal elastic fibre-reinforced slab, dynamic flexural deformations, flexural wave propag. 0-33510  
 incompressible liquid oscills. in variable cross section viscoelastic tube due to pulsating press. 0-31519  
 infinite elastic bar, induced oscills., normal and associated wave propagation 0-5980  
 interplanetary two-fluid shock waves propag., model 0-26711  
 inverse problem, finite difference method calcs. 0-17809  
 ionospheric ions and electrons, collision cross-section 0-26666  
 Kadomtsev-Pyatiashvili eqn., asymptotic behaviour of solns. (two-dimensional Korteweg-de Vries eqn.) 0-52036  
 laminated composites, mechanics of homogenisation and random evolutions 0-28423  
 linear waves, asymptotic behaviour and wave patterns construction (*Czech*) 0-69  
 longitudinal wave scattering by sphere-like bodies of revolution (*Ukrainian*) 0-22202  
 MHD waves, vertically propagating, in isothermal atm. with horizontal mag. field 0-6162

**wave propagation continued**

- molecular dynamics method in statistical physics, longitudinal and shear waves, dense systems, review 0-18895  
 multiply scattering medium, intensity fluctuation spectra, theory 0-46819  
 neutron wave propagation in couple core Argonaut reactors 0-27752  
 nonlinear aftereffect medium, longitudinal one-dimens. wave propagation 0-5974  
 nonlinear dispersive wave ensemble asymptotic dynamical eqns. 0-4547  
 nonlinear elastic dispersive media, interaction of solitary waves (*Russian*) 0-42076  
 nonlinear wave propagation in relativistic continuum mechanics 0-22203  
 nonlinear wave theory 0-36874  
 nuclear matter, elongated soliton type wave solutions, finite amplitude wave propagation (*Russian*) 0-13397  
 parabolic wave theories and applications 0-51436  
 periodically layered medium, wave propag. normal to layering, viscoelastic analogy 0-48636  
 phase-space projection identities for diffraction catastrophes 0-27162  
 planning plate with high speed in regular waves, pitching and heaving (*Chinese*) 0-43721  
 polarisation state of waves, theory 0-56525  
 polarised radiation transport theory, charact. eqn. 0-4678  
 progressive waves in dissipative media, long range ray theory (*French*) 0-42070  
 radiation problems transport eqns., using Wigner distribution 0-168  
 reaction-diffusion systems with explicit traveling wave and transient solutions 0-22207  
 relativistic thermo-viscous fluid dynamics, heat conduction and wave propag. 0-24107  
 seismic data migration, collocation formulation of wave equation migration 0-4126  
 seismic S<sub>v</sub> waves, propag. through Bering Sea and NW.Pacific Ocean 0-51346  
 seismic wave attenuation in partially saturated rocks 0-3997  
 SH waves refl. and refr. at plane boundary 0-12339  
 shallow seas, nonlinear stationary internal and surface waves propag. 0-17292  
 shell, cylindrical, Rayleigh wave propag. using elasticity theory (*Russian*) 0-38307  
 shell, orthotropic cylindrical, interacting with a fluid, nonaxisymmetric elastic wave propag. 0-33518  
 shock wave dispersion on plane layer (*Russian*) 0-33628  
 shock waves in isotropic elastic space 0-28448  
 shock waves in optically thin grey atmosphere 0-53810  
 solitary wave propagation in 3-dimensional lattice 0-8929  
 Sommerfeld's diffraction problem 0-12916  
 stellar collapse, adiabatic hydrodynamics and shock wave propag. 0-56861  
 stratified fluid, modified finite depth fluid eqn., exact N-soliton soln. 0-28517  
 sunspot umbral flashes and overstable magnetoacoustic modes 0-12734  
 tsunami simulation, Hawaii, open boundary reflection interference 0-17232  
 tsunamis propagation, finite difference simulation, book contrib. 0-3956  
 two-dimensional periodic plates, free wave propagation 0-19268  
 Van der Pol oscillators, diffusion-coupled active medium, nonlinear waves 0-4546  
 water wave propag. over circular shoal, parabolic eqn. method 0-14717  
 wave propagation in a random medium, statistical properties (*French*) 0-52040  
 wave scattering, second order approx. in planar linear sheet 0-17812  
 weak discontinuities evolution law for hyperbolic quasilinear systems 0-4548  
 weak spherical shock waves, propagation from arbitrary piston motions 0-22204
- wave scattering** *see scattering*
- waveform analysis**  
*see also spectral analysis*  
 neutron spin-echo integral transform spectroscopy 0-4748  
 seismic exploration, technique and processing, book 0-51975  
 volume holograms, coupled wave analysis, effect of second order derivatives 0-53232
- wavefront-reconstruction imaging** *see holography*
- waveguide antennas**  
 active-passive array for plasma wave excitation 0-48911
- waveguide connectors** *see waveguide couplers*
- waveguide couplers**  
*see also directional couplers*  
 optical fibre coupling techniques (*German*) 0-28330  
 RF coupling loops, transmission line approx. 0-28672
- waveguide joints** *see waveguide couplers*
- waveguide junctions** *see waveguide couplers*
- waveguide theory**  
*see also guided electromagnetic wave propagation; optical waveguide theory*  
 acoustic, Bleustein-Gulyaev waveguides with gratings, anal. 0-1391  
 charged filament moving in iris-loaded plane waveguide EM radiation 0-23609  
 cylindrical inhomogeneity in homogeneous medium of infinite extent, guided EM field numerical computation 0-14274  
 dielectric screened three-layer waveguide, cut-off characteristics and modal inversion screened three-layer waveguide, cut-off characteristics and modal inversion 0-1303  
 discrete modes of a system subject to an inhomogeneous, high-frequency force 0-43237  
 electron beam in circ. waveguide electrostatic instability in rippled magnetic field 0-19588  
 enclosed dielectric microstrip, analysis of losses, Schelkunoff method (*Spanish*) 0-45005  
 H<sub>10</sub> mode scatt., in rectangular waveguide, by cylinder with longitudinal slot 0-43238  
 Huygens' principle and equivalence principles 0-1106  
 inhomogeneous circular waveguide, asymptotic eigenvalues 0-53442  
 multilayer lossless dielectric loaded waveguide, transient field distribution 0-23604  
 nonlinear lower-hybrid waveguide in plasma, stability 0-19578  
 open-ended, finite element method for unbounded field problems 0-23600  
 planar, bounds on soln. of Helmholtz equation 0-14507



**waveguide theory continued**

- RF plasma heating, effect of wall corrugations on lower hybrid wave spectrum 0-33787
- scattering and mode conversions by circular cylinder, slab waveguide guided modes 0-9791
- TM mode-conversion at terminator for anisotropic ionosphere, param. study (*German*) 0-46333
- transversally nonhomogeneous waveguide EM wave propagation, using variational methods (*Czech*) 0-33155

**waveguides**

- see also *acoustic waveguides; circular waveguides; dielectric-loaded waveguides; dielectric waveguides; optical waveguides; plasma filled waveguides; rectangular waveguides*
- acoustic wave propagation as guided modes, parabolic approx. 0-43506
- Earth mantle, seismic  $S_p$  waves propag. through Bering Sea and NW-Pacific Ocean 0-51346
- electron beam, relativistic, high-current, in microwave linear accelerator, transient behaviour 0-32541
- electron waves in plane periodic system, linear theory 0-48130
- ferrite ring, 2000 NN type, self-accel. caused by high-current electron beam interruption 0-4809
- Gaussian-beam launcher for microwave exposure studies, dielectric hemisphere-loaded scalar horn 0-12206
- microwave discharge, supersonic flow in waveguide, electron densities, possible laser 0-38842
- microwave system for chronic exposure of small animals 0-56318
- open-ended waveguide probe/appliator combination (*French*) 0-3820
- space-time processing of acoustic signals in waveguides 0-5878
- tropospheric, numerical comparison of ray method and normal wave method 0-21858
- $\text{CO}_2/\text{N}_2\text{O}$  waveguide laser design 0-33025

**wavemeters**

- see also *frequency meters*
- fringe-counting wavemeter, based on compact spherical interferometer 0-42255
- interferometer, two-channel, based on prismatic dividers, energy factor analysis, using model of coupled multi-terminal networks (*Russian*) 0-52302
- laser beam interferometric wavelength measurements through post-detection signal processing 0-42254

**waves**

- see also *charge density waves; elastic waves; electromagnetic waves; gravitational waves; gravity waves; liquid waves; magnetohydrodynamic waves; magnetostatic waves; ocean waves; oscillations; plasma waves; spin density waves; spin waves; surface waves (fluid); wave propagation*
- aerodynamic noise from wave-turbulence interaction 0-14679
- asymmetrical fluid, thermoconvection wave propagation, microinertial and couple stress effect 0-19446
- atmosphere, solitary Rossby waves theory 0-56539
- atmosphere planetary waves, tropospheric-stratospheric interaction during stratospheric warming event 0-4074
- atmosphere unstable baroclinic waves, downstream and upstream development 0-56540
- baroclinic finite amplitude instabilities, book contrib., review 0-19328
- Benjamin-Ono equations, two-parameter Miura transform. 0-14720
- Benney's long wave eqns., Hamiltonian formalism 0-31525
- Benney's long wave equations, conservation laws and Lax representation 0-14719
- bisppectrum and nonlinear wave coupling for three-wave coupling 0-52038
- collisional drift waves, nonlinear evolution, bifurcations to chaotic state 0-14666
- computational fluid mechanics, book 0-1517
- density waves in M33, evidence from H I distrib. and spiral struct. 0-56948
- diffusive instabilities in rotating elec. conducting compressible layers 0-38379
- dynamo action associated with random waves in a rotating stratified fluid 0-33687
- eddy heat fluxes and temp. variances in baroclinic waves, weakly nonlinear theory 0-8390
- energy transport by waves without spatial damping, dissipative media 0-31531
- flame, laminar long wave stability, EHD problem anal. 0-53866
- flood wave propagation in channel (*Italian*) 0-28564
- fluid mechanics, mathematical introduction, book 0-66
- free shear layer in viscous critical layer regime, nonlinear stability 0-33576
- galactic density waves, excitation at Lindblad and corotation resons. by external potential 0-22072
- gas system entropy waves dissipation, power plant appl. 0-19395
- gaseous density waves in barred spiral galaxies, steady-state gas-dynamical study 0-12819
- gradually varying channel, solitary wave evolution, KdV eqn. soln. 0-24040
- gravitating disc, rotating, nonlinear stability theory 0-17488
- high subsonic nozzle flows, pressure waves from convection of temp. disturbances 0-6125
- hurricanes, spiral bands excitation by interaction between symmetric mean vortex and shearing steering current 0-56538
- hydrostatic mountain waves, terrain shape effects for stratified fluid 0-21804
- incompressible viscous liquids, dynamic anal. 0-48729
- internal wave motion in a periodic stratification 0-1672
- irrotational waves at the limit of breaking (*Italian*) 0-24039
- Lee waves classical theory, asymptotic approx., upper boundary condition role 0-12472
- linear waves, asymptotic behaviour and wave patterns construction (*Czech*) 0-69
- linearly stratified fluid, gravitational collapse of mixed region 0-33653
- mixed fluid, nonlinear internal wave formation from gravitational collapse 0-33619
- modified Benjamin-Ono eqn., N-periodic wave and N-soliton solns. 0-28518
- non-rotational waves at the limit of breaking (*Italian*) 0-24038
- paraffin wax, solar energy storage heat transfer characts. 0-55921
- plane wave growth eqn. in polytropic heat cond. relativistic fluid (*French*) 0-28580
- planetary waves, vertical propag. rel. to lower ionosphere VLF transmission disturbances 0-8485
- polythermal glaciers, flow, surface wave anal. 0-46210

**waves continued**

- relativistic hydrodynamics, thermal waves and growth eqn. (*French*) 0-28579
- relaxing gas flow, discontinuity growth 0-28525
- resonance tube, oscillation excitation from supersonic jet (*Japanese*) 0-24116
- resonant interaction of long and short waves, envelope pulse solitons and breather state 0-1616
- roll-wave stability on thin laminar flow down inclined plane wall 0-28488
- Rossby wave interactions and stability in rot. two-layer fluid on  $\beta$ -plane 0-10257
- Rossby waves in rotating annulus, laboratory and theoretical study (*Russian*) 0-19509
- Schwarzschild black hole stationary spherical accretion flow, travelling wave perturbations 0-51800
- shell, elastic, containing ideal fluid, anharmonic vibr. 0-5978
- short cylindrical channel, laminar axisymmetric nonstationary viscous gas flow, oscillations 0-38495
- solar corona, slow waves rel. to slowly moving disturbances in X-ray corona 0-21971
- solitary Rossby waves in two-layer system, theory 0-17293
- stratified fluid in channel, wake collapse in the thermocline and internal solitary waves 0-53787
- stratified fluid of finite depth, exact multi-soliton soln. for nonlinear waves 0-22199
- subsonic turbulent jet, entry zone flow wave struct., eddies 0-14773
- supersonic underexpanded jets, discharging into opposing supersonic stream, wave structure anal. 0-19461
- thermoconvective waves in a conducting and radiating fluid 0-19415
- thermoconvective waves in stratified compressible fluid, stability criterion contradiction 0-19414
- thin body in nonsteady longitudinal motion, wave resistance in finite depth liquid 0-33616
- transient gas flows with vibr. relaxation, acceleration wave growth and decay 0-1610
- transient thermal convection in horizontal rectangular spaces heated from below, waves 0-1566
- trapped nonlinear waves near sonic type singularity 0-24041
- turbulent gas flows in channels with high freq. press. oscillations, heat transfer 0-24024
- two-layered flow, internal waves at interface, statistical props. (*Japanese*) 0-1673
- viscous incompressible liquid, vibrational displacement, wave mechanism 0-43777
- waving plate, external flow of perfect fluid, pressure field (*French*) 0-38426

**waxes**

- carnauba wax, electret states, role of crystallites 0-2686
- carnauba wax, polarised, simultaneous variation of dielec. const. and discharge current, room temp. to beyond melting point 0-11314
- carnauba wax, thermoelectret, lattice parameter changes at elevated temps. 0-29674
- carnauba wax and rosin thermal electret, elec. charge studied by TSC 0-7286
- carnauba wax electrets, residual strain and crystal size of orienting crystallites and their effect on charge behaviour 0-11319
- carnauba wax thermoelectret, charge behaviour 0-7276
- Fischer-Tropsch wax, NMR investigation 0-7186
- impurity in polyethylene film electrets, influence on polarisation props. (*French*) 0-44999
- wax-graphite composite, specific capacitance, temp. and grain size depend. 0-50286

**waxing see polishing****weak ferromagnetism**

- see also *canted spin arrangements; Morin temperature*
- dialkylammonium copper tetrachloride, ferromagnetic layer compound, magnetostatic mode excitation 0-29538
- high-frequency props. of weak ferromagnets and antiferromagnets, singularities (*Russian*) 0-50196
- orthoferrites, single ion anisotropy contrib. 0-25126
- soft phonons and mag. phase transitions 0-54889
- $\text{CoCo}_3$ , antiferromagnetic reson. and two-magnon absorpt. (*Russian*) 0-29627
- $\text{DyFe}_{0.999}\text{Co}_{0.002}\text{O}_3$ , orthoferrite, domain struct. near mag. transitions 0-2599
- $\text{ErCrO}_3$ , magnetisation, NMR freq. temps. depend. weak ferromagnetic-antiferromagnetic spin reorientation transition 0-29631
- $\text{ErFeO}_3$ , high freq. props. in ordering region of spin system, antiferromag. reson. study (*Russian*) 0-2644
- Fe base amorphous alloys, Invar and Elinvar characts. 0-29592
- $\text{Fe}_2\text{O}_3$ , hematite, transverse galvanomag. parity effects anisotropy (*Russian*) 0-49770
- $\alpha\text{-Fe}_2\text{O}_3\text{:Al}^{3+}(\text{Ga}^{3+})(\text{Cr}^{3+})(\text{In}^{3+})$ , substitution effect on Morin transition, neutron diff. study 0-44827
- $\text{Fe}_2\text{Pd}_{2-x}\text{Si}_{18}$  metallic glass, mag. phase diagram, weak ferromagnet-spin glass transition 0-54893
- $\text{GdCrO}_3$ , EPR linewidth, Neel point to 700K 0-39849
- $\text{GdSn}_2$ , Neel temp., hydrostatic press. depend. 0-29549
- $(\text{Ge,Pb})_{1-x}\text{Mn}_x\text{Te}$ , mag. and elec. props. meas. 0-29534
- $\text{Ho}_{0.5}\text{Dy}_{0.5}\text{FeO}_3$  orthoferrite, domain wall struct., stability conditions, Morin transition, anisotropy const. 0-34684
- $\text{KMnF}_3$ , soft phonons and mag. phase transitions 0-54889
- $\text{NdSn}_3$ , Neel temp., hydrostatic press. depend. 0-29549
- $\text{Pd-Mn}$ , Curie temp. and magnetisation, vol. depend. 0-34629
- $\text{PrSn}_3$ , Neel temp., hydrostatic press. depend. 0-29549
- $\text{RbFeF}_3$ , Mossbauer spectra, mag. phases 0-15878
- $\text{RbNi}_2\text{Mn}_{1-x}\text{F}_3$ , powder, mag. props. 0-2560
- UPT, valence bands, XPS spectra 0-50520
- $\text{YCrO}_3$ , EPR linewidth, Neel point to 700K 0-39849
- $\text{YCrO}_3$ , magnetisation, NMR freq. temps. depend. weak ferromagnetic-antiferromagnetic spin reorientation transition 0-29631
- $\text{YFeO}_3$ , weak ferromagnet, domain wall motion and velocity (*Russian*) 0-54917
- $\text{YFeO}_3\text{:Co}^{2+}$ , single ion anisotropy contrib. 0-25126
- $\text{Zr(Fe,Al)}_2$ , weak itinerant ferromag., mag. anisotropy effects on mag. isotherms 0-11187



weak interactions, elementary particle *see elementary particle weak interactions*

## wear

*see also abrasion; hardness*

abrasive wear mechanism, grit size effect 0-16501  
 antifriction materials, device for wear testing 0-21223  
 arc electrodes, heat exchanges obs., dependence on electrode material and cooling conditions (*French*) 0-19655  
 asbestos-reinforced friction materials, wear and thermal processes 0-40559  
 bearing materials, rolling, steel, WC and  $\text{Si}_3\text{N}_4$ , effects of high temperature operation 0-21124  
 belt grinding, struct. transformations 0-30169  
 brass, abrasive wear, critical grit size effect (*Japanese*) 0-11783  
 brass rings, sliding against mild steel, prow formation processes (*Japanese*) 0-35336  
 bronze, Al, wear on 13% Cr steel in presence of aviation fuel 0-11781  
 cavitation erosion intensity in hydrodynamic wakes (*Russian*) 0-53790  
 ceramics, erosion in high temp. steam and H atmosphere 0-35334  
 continuous recording of wear of specimens on friction machine 0-55604  
 curved pipe carrying gas particle mixture, erosion 0-16498  
 cutting fluids testing rel. to tool wear, thin layer activation technique 0-55619  
 delamination wear, macroscopic effects 0-35343  
 die wear during wire drawing, review 0-30113  
 dressing effect on grinding performance, review 0-16502  
 EM sensor window materials, particulate erosion 0-38080  
 epoxy resin, filled, wear props., SEM obs. 0-16500  
 erosion damage due to cavitation, expt. studies in plasticine 0-1490  
 erosivity and mechanoluminescence (*German*) 0-25873  
 fracture mechanics appl. to wear 0-11792  
 fretting effect on fatigue 0-16482  
 fretting fatigue cracks 0-35345  
 frictional heating and oxidation theory 0-44255  
 hard-facing alloy, assessment method 0-15186  
 Inconel 718, high temp. fretting fatigue, fatigue and fretting wear 0-3197  
 lubricant evaluation, using four ball friction machine 0-25951  
 lubricated contacts, adhesive wear 0-16491  
 machine tool wear resistance, accelerated testing (*Russian*) 0-40543  
 materials selection for wear resistance 0-21120  
 mechanical treatment in aq. salt soln., material transport rel. to wear 0-16506  
 metal, cavitation erosion resist., increase by case hardening, possible mechanism 0-11845  
 metal, coated abrasive belt grinding, relation between wear of grain cutting edge and material removal 0-16507  
 metal, erosion by high speed particles, temp. effects 0-40556  
 metal, soft film, initial wear rate 0-11795  
 metals, antiwear action of Zn di-n-butyl phosphate 0-11782  
 metals, friction and wear rel. to comp., struct. and props., review 0-25872  
 metals, ion-implanted, friction and wear, review 0-40555  
 Mossbauer spectroscopy appl. to friction, lubrication and wear studies 0-40547  
 nonferrous metals, unlubricated wear data 0-16510  
 optical surface shaping, contact problem soln. 0-33260  
 palliative treatments for fretting fatigue, review 0-21126  
 Permalloy, magnetic head wear resistance and surface charact. against magnetic tape (*Japanese*) 0-35335  
 Permendur 49, ordered and disordered, clean mild wear 0-16508  
 PTFE, combined rotating and linear motion effects on wear 0-3201  
 plant condition monitoring in nuclear power generating industry, review 0-47612  
 polyethylene: ( $\text{Dy}_2\text{O}_3$ ), mech. props. and transfer to steel surfaces 0-16496  
 polyethylene, ultra high mol. wt., knee prosthesis, in vivo wear props. 0-17204  
 polymer endoprosthetic joint, fatigue life 0-40521  
 polymer viscoelasticity and strength characterisation, advanced light scatt. techniques 0-11857  
 polymers, wear in thermally stressed state 0-3202  
 polyphenylquinoxalines, graphite filled, behaviour during friction 0-40553  
 powders, ultra fine prod. by rotating friction mill, mechanism in initial wear region (*Japanese*) 0-25589  
 PTFE+metal, fluoride prod., DSC and XPS anal., rel. to polymer wear 0-11889  
 PTFE-metal interaction, X-ray photoelectron spectroscopy obs. 0-11788  
 Rebinder effect rel. to wear, chemomechanical interaction 0-21121  
 rubber, graphite filled, performance assessed against steel structures under water lubrication conditions 0-21123  
 rubber mixtures, device for determining wear 0-21226  
 Sendust alloy, magnetic head wear resistance and surface characts. against mag. tape (*Japanese*) 0-35335  
 signature response, for friction and wear 0-40541  
 Sital, microcrystalline glass, exam. of frictional props. under end-end rubbing 0-16488  
 slide calipers, bench for production testing of wear resistance 0-8959  
 sliding wear test apparatus, design and statistical evaluation, polymeric restoratives evaluation 0-21237  
 steady, mechanism anal. by fatigue theory as stochastic process 0-11789  
 steel, alloy, electroslog remelting effect, an impact-abrasive wear resistance 0-55541  
 steel, austenitic, martensitic transform. effect on hardening kinetics and fracture resist. of friction surface of 45Kh12G8 and 110G13 (*Russian*) 0-50727  
 steel, austenitic stainless, fretting wear in air and  $\text{CO}_2$  at elevated temps. 0-21119  
 steel, C, 45, surface wearing ability, surface finishing method and running-in effects 0-11794  
 steel, C, austempered, exam. of running in and wear 0-16485  
 steel, C, erosion-corrosion in aq.  $\text{H}_2\text{S}$  soln. up to  $120^\circ\text{C}$ , 1.6 MPa press. 0-21155  
 steel, C, induction hardened, surface durability, optimum case depth 0-30137  
 steel, C, spinning machine ring, increasing wear resist. by boriding 0-21115  
 steel, C, wear of Cr, Zn protective coatings, exam. using nuclear radiation excited X-ray fluorescence 0-21206  
 steel, C and Cr, surface damage during friction, struct. effect 0-35339

## wear continued

steel, Cr-Ni-Nb, LKh16N4B, high temp. frictional characts. 0-21118  
 steel, eutectoid, wear due to impulsive friction, device for exam. 0-25957  
 steel, gas boronized, sliding wear charact. 0-16499  
 steel, HSLA, V effect on mech. props. (*Korean*) 0-29987  
 steel, punch, for blanking tools, method of wear resist. determ. 0-55600  
 steel, scoring and scuffing on lubricated sliding surfaces, Mossbauer study 0-7690  
 steel, Si-Cr-Mo-W-V (2,4,1,3,2 wt.%), heat treatment and props. 0-16349  
 steel, stainless, cavitation-erosion in fresh water, electron microscope and electrochem. study 0-55580  
 steel, stainless, improvement of props. by ion implantation 0-16601  
 steel, surface wearing ability, finished surface direction effect on wearing ability 0-11793  
 steel, tool, improvement of props. by ion implantation 0-16601  
 steel, W-Mo, tool, hydrostatic extrusion and tempering, wear resistance effect 0-50728  
 steel, wear resist., mech. props. and struct. effects 0-35338  
 steel, wear resistance during abrasive wear, comp. and struct. effects 0-35337  
 steel gas nitrosulphurising, S25C, wear property 0-50729  
 superficial plastic deformations by particles (*French*) 0-40540  
 surface coatings, materials conservation and optimum tribological performance 0-34130  
 surface damage, plastic deformation cause in fatigue, wear, fretting and rolling fatigue 0-40537  
 surface texture assessment, Walsh function method 0-36995  
 Teflon-4, gamma irradi., wear resistance and antifriction props. 0-7691  
 temperatures reached during sliding 0-16505  
 test specimen, metallographic technique 0-35496  
 theory, metallography of worn surfaces 0-35346  
 Tokamak, recycling and surface erosion processes 0-33805  
 tribological system and wear factors, worn vol., load and sliding distance calc. 0-21122  
 vacuum metallised surfaces, protection by clear coatings 0-35392  
 wire for high-speed matrix printers (*Japanese*) 0-55540  
 wood chip refiners, cavitation effects in two-phase flow 0-35348  
 Al alloy 7075-T7351, fretting fatigue crack form. 0-35344  
 Al alloys, impact wear, microstruct. effect 0-11791  
 Al, cavitation erosion considering bubble collapse and pulse height spectra 0-16503  
 Al, soft, type 1100-0, erosion tests in cavitating venturi 0-35347  
 Au film, ion plated, defect growth structs., SEM obs., and effect on mech. props. 0-24768  
 BN, cubic, sintering technology and cutting performance of tools 0-29919  
 Co-Cr-Mo alloy shoulder prosthesis, wear and fatigue tests 0-26415  
 Cr-Ti/MgO-NbC(TaC) dispersion-strengthened, high temp. wear and oxidation resist. 0-25877  
 Cr-Ti/NbC(TaC) dispersion-strengthened, high temp. wear and oxidation resist. 0-25877  
 $\text{Cr}_3\text{C}_2$ , plasma sprayed wear resistance coating, exam. of wear behaviour 20 to  $1000^\circ\text{C}$  0-16487  
 $\text{Cr}_3\text{C}_2$ -Ni, friction and wear, 20- $1000^\circ\text{C}$  0-30112  
 Cu against Pyrex glass, steady wear mechanism, expt. study to confirm theoretical anal. 0-45404  
 Cu film, ion plated, defect growth structs., SEM obs., and effect on mech. props. 0-24768  
 Cu-Sn-P (5, 1-5 wt.%), effect of P on friction and wear characts. 0-16494  
 Fe alloy granule reinforced Cu M2 wear resistance in rubbing with lubrication 0-16490  
 Fe alloy granule reinforced Cu, friction in vacuum 0-25880  
 Fe and Fe-C, (0.8 wt.%), sintered, hot forging and chemothermal treatment, effect on wear resistance 0-25606  
 Fe and Fe-Cr alloys, friction behaviour in oxygen, development of wear-protective oxides and influence on sliding friction 0-30111  
 Fe, cast, nitrided, wear resistance (*Korean*) 0-21178  
 Fe, ductile, with different secondary struct., abrasive wear (*German*) 0-25871  
 Fe-Cu-Ni-Cr $_3$ C $_2$ -C based sintered friction material, wear, surface geometry and struct. effects 0-25875  
 Fe-glass porous material, wear resist. under dry friction 0-25876  
 Fe-P-S composite sintered bearing materials manufacture, wear intensities 0-20881  
 $\text{Fe}_2\text{O}_3$ , plasma sputtered coatings, oxide dissociation, coating props., struct. and composition (*Russian*) 0-54577  
 HfC-HfB $_2$  alloys, wear in vacuum, role of boride phase 0-21113  
 Mo sintered composite,  $\text{MoS}_2$  containing, friction and wear props. 0-11786  
 $\text{Mo}_2\text{B}_3$ -based alloys, mech. props., rel. to appl. as electrodes in electros-park machining 0-21174  
 $\text{MoS}_2$ , self-propag. high-temp. synthesis, props. 0-2975  
 NbC, deformation behaviour during rubbing in wide temp. range 0-16486  
 Ni-Cr (20 wt.%), high temp. frictional characts. 0-21118  
 Ni-Cr (20 wt.%) alloy LNKh, room-temp. friction characts. 0-25874  
 Pb ion plated soft film, initial wear rate 0-11795  
 SiC, single cryst., friction and wear behaviour in sliding contact with various metals 0-21112  
 SiC single crystal, friction and fracture in contact with itself and Ti 0-11780  
 $\beta$ -SiC/Si abrasive resistant material, prep. and props. 0-20878  
 Sn, ion plated soft film, initial wear rate 0-11795  
 Ti-Al-V (6,4 wt.%), fretting fatigue behaviour of temps. up to  $600^\circ\text{C}$  0-21104  
 Ti-Al-V (6,4 wt.%), high temp. fretting fatigue, fatigue and fretting wear 0-3197  
 TiC, deformation behaviour during rubbing in wide temp. range 0-16486  
 TiC reactively sputtered coatings on Ni-Cr-Mo-Ti (19,11,3 wt.%), adherence, XPES and wear study 0-25565  
 TiC-TiB $_3$ , friction characts., comp. depend., 20- $1000^\circ\text{C}$  0-3203  
 TiC-TiB $_2$ , strength and antifriction props. over wider range of concs. 0-50673  
 TiC-TiB $_3$  alloys, composition effect on surface layer rupture at various temps. 0-25879  
 TiC-TiB $_3$  alloys, wear in vacuum, role of boride phase 0-21113  
 $\text{W}_2\text{B}_5$ -based alloys, mech. props., rel. to appl. as electrodes in electros-park machining 0-21174  
 WC, deformation behaviour during rubbing in wide temp. range 0-16486



**wear continued**

- WC-Co alloy, hard metal, resistance of cavitation erosion (*Japanese*) 0-16575
- WS<sub>2</sub>, self-propag. high-temp. synthesis, wear props. 0-2975
- Zr alloys, wear due to fretting and periodic impacting 0-16509
- ZrC-ZrB<sub>2</sub>, friction characts., comp. depend., 20-1400°C 0-3203
- ZrC-ZrB<sub>2</sub>, strength and antifriction props. over wider range of concs. 0-50673
- ZrC-ZrB<sub>2</sub> alloys, wear in vacuum, role of boride phase 0-21113

**wear, abrasive** *see abrasion***wear resistant coatings**

- bituminous surfaces, review of aggregate selection criteria for improved wear and skid resist. 0-7689
- cemented carbide ion plating, high-speed steel tools, cost and cutting performance 0-30174
- clear, protection of sputtered metal layers 0-35392
- cutting tool coating by cubic BN reactive vapour deposition 0-40545
- diamond-based, fabrication and wear resist. 0-40576
- Fe, cast, high Cr, hardfacing of roll, wear resistance and thermal durability 0-7686
- fretting corrosion control using coatings and surface treatments 0-35368
- glazes with improved abrasion resistance (*German*) 0-11798
- hard coating deposition by sputtering 0-40544
- ion implantation, surface treatment process in production engineering 0-34028
- materials selection, relation between materials properties and wear 0-21120
- Nichrome-silicate glass-CaF<sub>2</sub> multicomponent self-lubricating coating, prep. by plasma spraying, and props. 0-40604
- palliative treatments for fretting fatigue, review 0-21126
- Permalloy, solid boring for mag. head appl., wear resist. and microhardness 0-21172
- photographic migration images, liquid developed, fixing and abrasion resistance 0-4792
- plasma spraying technique appl. (*Japanese*) 0-55558
- silica hard coating for magnetic surfaces 0-7715
- silica-alumina hard coating for magnetic surfaces 0-7715
- surface coatings, materials conservation and optimum tribological performance 0-34130
- BN-based, fabrication and wear resist. 0-40576
- Be-B, ion implanted surface hardened layer on Be 0-16604
- Cr electroplated steel, laser treatment 0-21191
- Cr<sub>3</sub>C<sub>2</sub> (Cr<sub>7</sub>C<sub>3</sub>) based coatings, detonation deposited, wear resist., 20-1000°C 0-11843
- Cr<sub>3</sub>C<sub>2</sub>, plasma sprayed wear resistance coating, exam. of wear behaviour 20 to 1000°C 0-16487
- Cr<sub>3</sub>C<sub>2</sub>-Cr-Ni-Mo wear resistant coating prep. by laser beam melting, and props. 0-40607
- Cr<sub>2</sub>O<sub>3</sub>, RF sputtered coating for wear appls., on Inconel X-750 foil, prep. and props. 0-40605
- Fe and Fe-Cr alloys, friction behaviour in oxygen, development of wear-protective oxides and influence on sliding friction 0-30111
- Mn<sub>3</sub>(PO<sub>4</sub>)<sub>2</sub> coating on steel, wear resistant appl. 0-16609
- Mo flame sprayed coatings, comp., microstruct. and mech. props. 0-16598
- MoS<sub>2</sub>, RF sputtered layers with variable stoichiometry, lubrication props. 0-40557
- MoS<sub>2</sub>, RF sputtered lubricant, wear life, sputtering parameter effects 0-40558
- Ni coating, heat treated, as plated, electrochemical study of corrosive wear 0-16536
- Ni coating, self lubricating containing oxides, carbides and borides on steel 0-21189
- Ni-Cr-Fe-Si-B wear-resist. and corrosion-resist. coatings by furnace melting 0-35428
- Ni-SiC coating, heat treated, as plated, electrochemical study of corrosive wear 0-16536
- TiB<sub>2</sub>, on WC-Co alloy cutting plates, hardness and struct. 0-21175
- TiC layers, on steel and cemented carbides, load-bearing capacities 0-40606
- TiCN overlay coating on stainless steel, Ti or Al, effect on physico-mechanical and wear props. 0-40603
- WC-Co (15 wt.%), alloy VK15 coating on Ti-Al, detonation sprayed, antifriction props. 0-21188
- WC-Co (15 wt.%), detonation sprayed on Cr-Ni steel with automatic powder feed 0-25558
- WC-Co particles electrophoretic deposition, on metal surfaces (*German*) 0-2969

**weather** *see meteorology***webs (membranes)** *see membranes***weighers** *see balances***weighing**

- accuracy class increase, using several standard weights of equivalent mass (*Rumanian*) 0-47022
- automatic, Russian balances types 900VN and 959DN, accuracy improvement 0-52166
- balance, microprocessor based, capabilities 0-13067
- British trade weights and measures activities 0-27267
- dynamic weighing method using transducer 0-17926
- industrial weighing, gyroscope appl. 0-42217
- liquid density measurement, displacement sphere method (*German*) 0-52168
- load cell pattern approval, France 0-42199
- mass, force and weight, relationship and measurement of weight 0-27273
- oxide melts, specific weight determ. at 1000 to 1750°C, methods survey (*Slovak*) 0-47079
- single-pan analytical balances, liquid density meas. using solid density standards (*German*) 0-52167
- substance amount measurement and dosage determ. 0-31717
- thermogravimetric system for investigating gas-metal reactions at elevated temps. 0-229
- torsion balance, sat up by welding fused quartz rods and fibres (*Japanese*) 0-31738
- weights and measures, conference, Washington (1978) 0-27260

**weighing machines** *see balances***weight, atomic** *see atomic mass***weight, molecular** *see molecular weight***weight indicators** *see balances***weight measurement** *see weighing***weightlessness experiments** *see zero gravity experiments***Weinberg model**

- $\Delta I=1/2$  dominated weak decays of strange hadrons, Weinberg-Salam scheme 0-27499
- $\Delta S=1$  nonleptonic weak decays,  $\Delta I=1/2$  rule, quark models and current algebra 0-47282
- antiquark sea role in determ. of  $\sin^2\theta_W$  from total neutron cross sections (*Russian*) 0-4910
- Callan-Symanzik and Weinberg equations: frame dependence of fixed points 0-4838
- chiral unified gauge model based on nonlinear chiral hadron Lagrangian 0-42378
- divergence cancellations, in Weinberg-Salam model 0-32052
- duality invariance, simple gauge theories including EM-type fields with sources 0-27440
- dynamical Higgs mechanism, weak  $\Delta I=1/2$  rule, sum rules, heavy quarks and leptons 0-27442
- electric charge, critical value in classical model (*Russian*) 0-13256
- electro-weak interactions concept and Weinberg-Salam model verification (*Czech*) 0-22549
- EM and weak interaction unification, bearing of Weinberg model and gauge invariance (*German*) 0-32054
- grand unification E<sub>8</sub> theory, Weinberg-Salam model reproduction (*Russian*) 0-4909
- hadronic matter, Pomeron and critical temp. 0-22566
- Han-Nambu and SUB quark models, modified, appl. to Weinberg-Salam unified gauge model 0-22562
- Higgs bosons, photoproduction 0-22558
- Higgs bosons, Weinberg model, input mass scale 0-22554
- high energy neutrino physics, recent expt. results 0-4982
- inclusive lepton pair prod., P violation, quark-parton model in Weinberg-Salam theory, QCD 0-37217
- Lee-Weinberg model of weak and EM interactions, string-like solns., vortices 0-47231
- lepton mixing matrix, sequential Weinberg-Salam theory, CP conservation 0-47238
- leptonic interaction gauge model in SU<sub>3</sub> with 30° Weinberg angle 0-4903
- minimal anomaly-free electroweak model for several generations 0-4906
- neutral currents, flavour-changing, Weinberg-Salam model 0-22553
- non leptonic hyperon decay amplitudes, calc. without arbitrary parameters 0-13300
- non-Abelian gauge theories, local covariant operator formation, quark confinement 0-47190
- nucleon weak interaction pots. in the Weinberg-Salam model (*Russian*) 0-13258
- parity violating neutral currents, radiative corrections, Weinberg-Salam and left-right symmetric models 0-52451
- quark mass, current, induced isospin violations 0-32069
- quark masses from Weinberg-Salam model renormalisation group eqns. 0-42377
- quark-lepton correspondence, multigeneration SU(2)<sub>L</sub>×U(2)-based model 0-22584
- quarks, flavour number determination using Higgs scalar particle 0-13288
- spontaneous symmetry breaking dynamics 0-32060
- Sterman-Weinberg formula for quark jets and gluon jets, leading log version, master equation 0-22552
- SU(2), unification of isospin and hypercharge, electroweak interactions of leptons 0-27439
- unified theories, mass scales, alternatives to SU(5) 0-27441
- Weinberg-Salam model, gauge ambiguity effects 0-4908
- Yang-Mills theory, Higgs particle 0-4905
- zero-fermion modes in models with spontaneous symmetry-breaking 0-18105
- $e^+e^- \rightarrow e^+e^-$ , Bhabha scatt. one loop radiative corrections in Weinberg model 0-13310
- $e^+e^- \rightarrow \mu^+\mu^-$ , 40-200 GeV, cross section, one loop corrections in Weinberg model 0-18139
- $e^+e^- \rightarrow \mu^+\mu^-X$ , possible Higgs boson detection in missing mass plot 0-4977
- $e^+e^- \rightarrow W^+W^-$ , polarisation amplitudes 0-42484
- $e^+e^- \rightarrow W^+W^-$ , radiative, corrections in Weinberg model 0-52512
- $e^+e^- \rightarrow Z^0\gamma \rightarrow \mu^+\mu^- \gamma$ , Weinberg model anal. of Z<sup>0</sup> decay ang. distrib. 0-47275
- $e^+e^- \rightarrow ZZ$ , polarisation amplitudes 0-42484
- ep, high Q<sup>2</sup>, QCD corrections to parity-violating asymmetries 0-22618
- $\gamma N \rightarrow l^+l^- X$ , pol.  $\gamma$ , neutral current effect, Weinberg-Salam model calcs., p violation 0-5000
- $\gamma N \rightarrow l^+l^- X$ , polarisation effects on P-violating asymmetry in Weinberg-Salam model 0-32055
- K→3 $\pi$ , CP violation, current algebra anal., six quark Weinberg-Salam model 0-47281
- $\mu$  magnetic moment, weak coupling contribution, Weinberg-Salam model 0-22607
- $\mu$  to e<sup>+</sup> conversion in nuclei, mediation by Majorana lepton 0-22547
- np→d $\gamma$  radiative capture, relativistic effects, parity violation, Weinberg-Salam model (*Russian*) 0-32120
- $\nu$  neutral current couplings and  $\nu e^-$  weak neutral current coupling constraint, fermionic assignments 0-4915
- $\nu_e(\bar{\nu}_e)e$ , charged and neutral current interference, test of Weinberg-Salam model 0-42385
- $\nu n \rightarrow \nu n \pi^+$ , neutral current induced one-pion production, Weinberg-Salam structure 0-52454
- $\nu n \rightarrow \nu p \pi^+$ , neutral current induced one-pion production, Weinberg-Salam structure 0-52454
- $\nu p \rightarrow \nu p \pi^+$ , neutral current induced one-pion production, Weinberg-Salam structure 0-52454
- $\nu p \rightarrow \nu p \pi^0$ , neutral current induced one-pion production, Weinberg-Salam structure 0-52454
- $\Omega^-$  nonleptonic decay branching ratios from Weinberg-Salam and MIT bag models 0-37261
- pN, dilepton production by pol. protons, parity violating, asymmetry, Weinberg-Salam calcs. 0-42488
- pp, hadronic jets, possible intermediate bosons 0-18149
- pp and pp collision, intermediate vector boson production 0-9186
- pp(p) $\rightarrow W^\pm(Z^0)X$ , QCD perturbation theory struct. function predictions 0-42505



**Weinberg model continued**

$W^{+0}$  bosons, lowest order g-2 Weinberg-Salam model, Feynman diagrams 0-47291  
 $Z^0 \rightarrow H^0 + \nu + \bar{\nu}$ , leptonic decay into light Higgs boson, grand unification test 0-42381

**Weissenberg cameras** see cameras; X-ray crystallography apparatus**welding**

see also electric welding; electron beam welding; laser beam welding; ultrasonic welding  
 alloys, variable composition, errors in deriving empirical relationships using accelerated methods 0-25980  
 bimetal rolling, calc. of strains by variational method (Polish) 0-45323  
 bimetallic welded joints, heterogeneous, metallographic anal., etchings and etching regimes 0-40635  
 Br.AZhNMts 7-2.5-1.5-9 bronze, Mg-Al, type, fatigue and stress corrosion cracking, welding effects 0-3233  
 butt joints, calc. of temp. field for nonideal thermal contact (Russian) 0-10121  
 crystal units, vacuum system for cleaning and cold welding (Polish) 0-31776  
 fatigue strength of welds 0-3179  
 fission reactor pressure vessel and circuit development, conf. report 0-47541  
 flaws detection, by acoustic emission monitoring, with aid of microcomputer 0-11866  
 irradiated fuel rods, in-cell welding techniques 0-22956  
 metal, welded joints, pore formation mechanism evaluation, rel. to solidification 0-3017  
 monitoring in-process, with acoustic emission 0-16620  
 noble-metal tubes, cold-weld sealing 0-41556  
 steel, austenitic, high-temp. crack resist., B and Mo influence (Russian) 0-16435  
 steel, austenitic stainless, ferritic, single phase ferritic solidification in welds, exam. 0-7546  
 steel, austenitic stainless, welds, exam. of austenitic solidification mode 0-7545  
 steel, brittle fracture resistance, welding and heat treatment effects 0-50723  
 steel, C, cold rolled sheet, spot welded joints, static fracture appearance 0-55538  
 steel, H effect on weldability 0-50720  
 steel, low alloy, welded joints, cracking during heat treatment 0-7724  
 steel, low alloy type 14Kh2GMR, high strength, welded joint, impact toughness, welding thermal cycle and tempering effects 0-3157  
 steel, maraging, 18 Ni, welded joints ageing props. obs. (Japanese) 0-40401  
 strain measurements, transient longitudinal strain changes 0-16332  
 ultrasonic flaw detector, automatic, for butt welds (Japanese) 0-25976  
 Al foil, alloying additions (Si, Mg, Y, Se, Sc) effect, on tensile strength, weldability 0-55475  
 Al plates with air gap, temp. field for microplasma welding of edge joints (Russian) 0-7755  
 Al-Mg-Zn, granulated, degassing atm. effect on mech. props. of semi-finished products 0-7720  
 Cu, diffusion welding, tensile fracture strength (Japanese) 0-7663  
 Zr-Nb (2.5 wt.%), transforms. during annealing of welded joint, after thermal cycling (Russian) 0-29984

**welding electrodes**

bimetallic electrodes for plasma torches, Cu to W joining methods 0-24266

**Wentzel-Kramers-Brillouin calculations** see WKB calculations**Wertheim effect** see Wiedemann effect**wetting**

adhesion, of liq. to solid surface, contact angle rel. to dielectric constant 0-10741  
 cladding, three-regions rewetting model with decay heat generation and inlet subcooling 0-22965  
 contact angle, ionic crystal surfaces 0-10746  
 contact reaction between graphite and electrolytic Mn, Co, Ni and Fe 0-15342  
 cooling wave on hot surface, development, method of weighted residuals 0-27767  
 electrode, wetproofed, pore filling degree with electrolyte and liq. reactant 0-40702  
 evaporating menisci of wetting fluids 0-29248  
 Freon-113 vapour environment, rewetting of hot surfaces, two-phase high pressure flow simulation 0-32358  
 glass, surface props. and contact angle after treatment with glow discharge and heating 0-21139  
 horizontal surface, silicone oil drop spreading 0-2250  
 ice, rel. to particle engulfment, theoretical model 0-54351  
 imbibition equation, similarity solutions, wetting abilities of immiscible fluids 0-43773  
 immiscible liquids, binary system, wetting hypothesis, validity, Antonow's rule appl. (French) 0-49462  
 irrigating films, laminar, entry zone length for vertical plate wetting 0-53742  
 low melting, metals, on Cu surface, spreading kinetics 0-10742  
 maximum speed of wetting, experimental results 0-29253  
 metal supported crystallites, wetting in sintering and redispersion 0-24751  
 pendant drop, glass spheres attachment, wetting perimeter 0-2251  
 poly(vinyl pyrrolidone), silicone grafted, for contact lenses, surface props. and stability of thin tear film 0-17194  
 polyethylene, linear, melt props. correl. with chain length distrib. (Russian) 0-37920  
 polymer, adhesion phenomena and influence of various factors, work of adhesion (Polish) 0-3292  
 polymer, wetted by insulating liq., under elec. field, charge transport and absorpt. 0-6534  
 polystyrene melts, wetting kinetics for spreading of viscous sessile drops 0-15338  
 powder-water-oil system, cohesion of powder particles with water, rheological prop. (Japanese) 0-14647  
 refractory carbides, borides and nitrides, wetting by and interactions with liq. metals 0-54473  
 size effect accompanying wetting (Russian) 0-6596  
 solid surface roughness, effects on wetting, expt. study 0-34275  
 static drop on inclined plate, shape, finite element method anal. 0-29245

**wetting continued**

viscous liquid creeping on surface, asymptote to free surface and vel. depend. of contact angle 0-6600  
 wetting tension depend. on meniscus curvature, adjacent liquid film disjoining press. isotherm 0-2247  
 Ag clusters on Si substrates, opt. spectra investig. of struct. (German) 0-25492  
 Al alloys, contamination, automated nondestructive inspection 0-16629  
 $B_4C$ -Ti(V)(Cr), contact reaction with liq. Ni 0-55707  
 Cd, spreadability on Cu and brass plates (Japanese) 0-29252  
 Cu, corrosion and wetting in presence of thiol reagents 0-11822  
 Fe-C (graphite), adhesion and wettability of graphite (Russian) 0-20008  
 $\gamma$ -Fe $_2$ O $_3$ , densified, rheological and mag. props. 0-44873  
 Na, heat pipe meas. with gas plug containment up to 720°C 0-23878  
 NaCl-LiCl mixed crystals, Au decoration study of solid-melt interface, phase separation 0-15026  
 Na $_2$ O-B $_2$ O $_3$  glass, wetting and adherence on Au 0-24714  
 Pd-C (graphite), adhesion and wettability of graphite (Russian) 0-20008  
 Pt-C (graphite), adhesion and wettability of graphite (Russian) 0-20008  
 Rh-C (graphite), adhesion and wettability of graphite (Russian) 0-20008  
 Sn-Pb solder on Cu plate, spreadability, effect of fluoride and iodide addition to ZnCl $_2$  flux (Japanese) 0-29251  
 TiC-Ni powder compact, wetting problems in sintering 0-11596  
 W surface wetting by liquid Cu depend. on preliminary surface treatment (Russian) 0-35388

**whiskers (crystal)**

CdSe whiskers, growth in H $_2$  0-15425  
 elastic strains producing device, at He temperatures in magnetic field 0-50788  
 mechanical properties, method for investigating in complex stressed state 0-3264  
 metal whisker point contact junctions, tunnelling and rectification characteristics. 0-6955  
 steel fibres, polycrystalline, Mossbauer spectroscopy 0-44959  
 Bi, electron transition on simple extension, elec. resist. and magnetoresist. meas. (Russian) 0-29422  
 Bi wire, elastically bent, elec. resist. in mag. field 0-44568  
 CaSO $_4$ , growth on CaF crystal. face etched in H $_2$ SO $_4$ , etch pit morphology 0-6408  
 Cr, crystal growth incorporated with field electron emission 0-44458  
 Fe, elastically and plastically deformed, mag. domain structs. 0-15752  
 Fe, mag. anisotropy, magnetisation and temp. depend. near T $_c$  0-39766  
 Fe whisker growth, on wustite, Wagner's mechanism 0-10847  
 Fe whiskers, dynamics of mag. freq. response near Curie point 0-34648  
 Fe whiskers, magnetisation in small mag. fields, investigation using Kerr magneto-optic effect 0-2603  
 Fe, whiskers, polycrystn., Mossbauer study 0-20571  
 GaP ribbon waveguide, vapour-grown, phase-matched SHG 0-48339  
 Ge, whisker growth from vapour phase 0-15426  
 KBr, whiskers, F-centre accumulation and track effects due to X-ray irradi. 0-39484  
 KCl, whiskers, F-centre accumulation and track effects due to X-ray irradi. 0-39484  
 Mo, crystal growth incorporated with field electron emission 0-44458  
 NaCl, plastic deformation influence on shape recovery effects 0-6684  
 NaCl whiskers, plastification in elec. field (Russian) 0-21010  
 Si, (111) oriented, FIM and atom-probe FIM obs. 0-10473  
 Si, amorphous whisker growth characts. by SiH $_4$  thermal decomposition 0-34342  
 Si whisker field desorption ion source, Cu, Sn, Ag, Te, Cd and Sb isotope abundance ratios 0-11975  
 Si:Au(P)(B) whiskers, impurity inhomogeneity 0-39145  
 Sn wire, elastically bent, elec. resist. in mag. field 0-44568  
 W, crystal growth incorporated with field electron emission 0-44458  
 W-Ni, MBM diode, resist. depend. of detected signals 0-2482  
 Zn wire, elastically bent, elec. resist. in mag. field 0-44568

**whistlers**

see also ionospheric electromagnetic wave propagation; magnetospheric electromagnetic wave propagation  
 Cerenkov interaction between obliquely propagating whistler wave and electron beam, computer simulation 0-43937  
 damping near electron gyrofreq. due to cold-plasma injection, rel. to magnetosphere 0-28659  
 dispersion measurement using five channels phase-locked loop discriminator (Japanese) 0-31143  
 Dowden-Alcock approximation, generalisation and comparison with Bernard approximation 0-51607  
 Earth-ionosphere waveguide propagation effect on polarisation and arrival angles 0-36457  
 electron interacting with whistler in magnetosphere 0-46349  
 electrostatic noise damping by warm auroral electrons 0-41668  
 excitation of high-frequency waves with mixed polarization by streaming energetic electrons 0-1773  
 ionosphere propagation, equatorial anomaly affecting ground reception 0-51601  
 Jupiter magnetosphere, discrete whistlers obs. by (Voyager 1) 0-26795  
 Jupiter magnetosphere, electron pitch-angle diffusion by whistler mode waves near Io plasma torus 0-4290  
 Jupiter magnetosphere, Io plasma injection rel. to whistler mode waves and Jovian diffuse aurora 0-4289  
 large amplitude oscillation by high power microwaves 0-43913  
 magnetosphere, parallel elec. field effect on whistler mode instability 0-26700  
 magnetosphere examination of VLF whistler pulse analysis 0-17441  
 magnetosphere meas. of occurrence rate of whistlers during geomagnetic storms 0-12621  
 magnetosphere whistlers, meas. via remote unmanned ELF/VLF geomagnetometer receiver in Antarctica 0-21854  
 measurement with microprocessor control (Japanese) 0-31144  
 monochromatic whistler wave, nonlinear evolution in nonuniform mag. 0-43912  
 nature, types and observations, review 0-36458  
 parallel electric field affecting thermal damping 0-41663  
 plasma, parametric decay of non-ducted whistler-mode signal 0-6239  
 plasma, whistler wave trapping in density crest 0-53984  
 plasmasphere, horiz. inhomogeneities, whistler obs. 0-4168  
 precursor whistler mode plasma turbulence formation in parallel shock waves 0-24172  
 propagation in narrow density trough 0-38629  
 review 0-46348



**whistlers continued**

- scattering, nonlinear, by lower hybrid and ion Bernstein modes 0-43929
- spectral-temporal analysis, digital methods 0-4175
- substorm electric fields in plasmasphere, model based on whistler data 0-41661
- super whistler, theory and anal. 0-26688
- VLF direction-finding techniques comparison for determ. whistlers exit point at ionosphere 0-26631
- VLF subionospheric propag., whistler-induced anomalies 0-26668
- wave modulation, nonlinear theory 0-26686
- whistler propagation times eqn., inversion via spectral expansion 0-8495

**white dwarfs**

- 2A 0311-227, complex emission line structure of spectroscopic binary 0-51915
- 2A 0311-227, high-speed photometry of AM Herculis-type binary 0-41912
- accreting compact object in binary system, magnetosphere theory, X-ray sources 0-46394
- accreting magnetic degenerate dwarfs, X-ray and UV emission 0-41826
- AE Aquarii, cataclysmic variable, rapid light oscills. rel. to white dwarf oblique rotator model 0-36634
- atmospheres chem. evolution, diffusion and accretion 0-36628
- $\alpha$  Canis Majoris (Sirius B), spectral energy distrib. 0-8629
- $\alpha$  Canis Majoris B (Sirius B), minimum flux H coronal model rel. to X-ray emission 0-8626
- $\alpha$  Ceti AB, IUE obs. of UV spectrum 0-22027
- ZZ Ceti stars search, photometric obs. of apparently quiescent stars 0-22005
- Z Chamaeleontis, cataclysmic binary, masses radii, and mass exchange rel. to gravit. radiation 0-4386
- cluster white dwarfs, numbers rel. to progenitor stars upper mass limit 0-51738
- cyclotron self-absorption in accretion columns of magnetic degenerate stars, X-ray sources appl. 0-12760
- Cygnus X-2 as spherically accreting nonmagnetic degenerate dwarf 0-46703
- DB-type white dwarfs, model atmospheres 0-51761
- degenerate star candidates, photoelectric and spectroscopic obs. 0-12763
- degenerate stars with H atmospheres, props. rel. to theoretical models 0-17576
- formation rate in globular clusters 0-4346
- G200-39, hot hybrid white dwarf, spectroscopic obs. 0-26852
- gamma ray bursts from magnetic white dwarfs, model (*Chinese*) 0-12831
- HD 149499 B, IUE obs. of hottest white dwarf 0-41828
- heavy ion diffusion in envelopes 0-51754
- AM Herculis type binaries, cyclotron self-absorption in accretion columns of magnetic degenerate stars 0-12760
- hot white dwarfs, EUV flux interstellar absorpt., local clumpiness factor determ. 0-36627
- magnetic white dwarfs spectra, cyclotron absorpt. features theory 0-4351
- mass accretion onto massive white dwarfs, rel. to thermonuclear runaways 0-41822
- mass distribution, rel. to stellar mass loss rates and galactic evolution models 0-46548
- nonradial oscillations of slowly rotating models 0-4348
- rapidly rotating, oscills., numerical calc. 0-46554
- relativistic degenerate electron plasma, dielectric response in mag. field, plasma oscillations 0-54022
- secular instabilities of rigidly rotating stars in general relativity, theoretical formalism 0-4341
- secular instabilities of rigidly rotating stars in general relativity, numerical results 0-4342
- seismology, effects of crystalline core on nonradial oscills. freqs. 0-17577
- SS 433, binary star model including mag. white dwarf 0-4385
- SS 433, ultra-close black hole-degenerate dwarf binary system model 0-4384
- supercritical accretion discs winds struct. and appearance, numerical models 0-21984
- surface accretion of interstellar matter 0-51734
- V471 Tauri, white dwarf eclipsing binary, IUE UV spectra 0-26912
- triple close approaches effect on stellar system evolution, one-parameter family appl. 0-17618
- two-colour diagram, calcs. rel. to white dwarfs masses and radii 0-46547
- uvby photometry of 112 southern objects 0-8624
- very low luminosity degenerates, deficiency from faint proper-motion stars obs. 0-17575
- VV Puppis, 3470 Å emission as cyclotron line 0-36673
- C-O dwarf, H and He burning in degenerate envelope (*Russian*) 0-17585
- C<sub>2</sub> (4670 Å band) stars, evolutionary status 0-4355
- H, He white dwarf atmospheres, minimum-flux coronal models 0-8626
- He shell burning, thermal pulses in accreting white dwarf 0-22009

**white noise**

- attenuated white noise statistical gravity model 0-30977
- coherence improvement in anal. by use of repeated random sequence generator 0-36203
- film grain noise, spectral density estimation, in electron microscopy (*French*) 0-9075
- Markovian integro-differential master eqns., Langevin description 0-31676
- viscoelastic beam, constrained, flexural vibrating, response to random excitation of white noise and turbulent boundary layer type 0-53671

**Widmanstatten structure**

- steel, austenitic stainless, ferritic, single phase ferritic solidification in welds, exam. 0-7546
- steel, hypoeutectoid, fracture toughness, effect of Widmanstatten ferrite 0-35315
- Cu-Ti (4 wt.%), isothermal transformation, electron and optical microscopy obs. of microstructure 0-16307
- Fe-Cu-Ni (2, 5 wt.%), interphase precipitation obs. in assoc. with Widmanstatten ferrite lateral growth 0-40365
- Fe-V-C (0.3, 0.05 wt.%), interphase precipitation obs. in assoc. with Widmanstatten ferrite lateral growth 0-40365
- $\alpha+\beta$ Ti alloys, colony size effect on fatigue crack growth on Widmanstatten struct. 0-30094
- $\alpha$ - $\beta$ Ti alloys, high strength, heat-treated weldments, intergranular fracture 0-21097
- Ti-Al-V-Sn (6, 6, 2 wt.%) weldments, heat treated, transangular fracture 0-40524

**Wiedemann effect**

- Fe<sub>40</sub>Ni<sub>40</sub>P<sub>14</sub>B<sub>6</sub>, amorphous ribbon, influence of torsion on mag. props. 0-7138

**Wiedemann-Franz law** *see* Lorenz number**Wien effect**

- No entries

**Wigner coefficients** *see* Clebsch-Gordan coefficients**Wigner crystal**

- conductivity of cryst. on liq. He surface (*Russian*) 0-6594
- electron gas, classical and two-dimens., self-diffusion theory 0-141
- lattice quantum oscills. in mag. field, specific heat, mag. moments (*Russian*) 0-49636
- TCNQ, generalised Wigner lattices and band motion effects 0-24815
- TCNQ salt, MEM(TCNQ)<sub>2</sub>, phase transition electronic struct. interpretation 0-24781
- TCNQ salt, NMP-TCNQ, electronic struct., SCF calc., total energy polarisation effects 0-15469
- TTF-TCNQ, antiferroelectric ordering of TCNQ ion elec. polarisation 0-20598
- two-dimensional crystal in magnetic field 0-2350
- two-dimensional Wigner-crystal-liquid-surface system, eigenmodes and instability of charged liq. surface 0-10896
- $\alpha$ -AgI, superionic conductor, struct. and dynamics, two-dimens. mol. dynamics model 0-49413
- HgCdTe, Magneto transport anomalies at low carrier densities, Wigner crystallisation 0-20222
- PbSnTe, Magneto transport anomalies at low carrier densities, Wigner crystallisation 0-20222
- PbTe, Magneto transport anomalies at low carrier densities, Wigner crystallisation 0-20222
- SmB<sub>6</sub>, valence fluctuating state, sp. ht. 0-20127

**Wigner effect** *see* radiation effects**Wigner lattice** *see* Wigner crystal**Wilson cloud chambers** *see* cloud chambers**wind**

- acoustic radar method for wind measurement (*Chinese*) 0-46290
- aeolian sedimentation on Earth and Mars, comparisons 0-31042
- aerodynamic drag of sea surface, role of high freq. gravity waves 0-26536
- aircraft meteorograph, design, appls., accuracy (*Chinese*) 0-17387
- Apennine valley day breezes, Parma, Italy 0-26589
- Arctic Basin, ice movements, external factors 0-26541
- NE Atlantic circulation, climate and oceanic var., Little Ice Age 0-8422
- auroral NO densities, horizontal winds effects 0-26656
- beaufort scale data, conversion to wind vel. study (*German*) 0-8407
- Beaufort Sea Coast, Alaska, sea breeze processes 0-41485
- Benguela Current, wind regime rel. to anomalously high waves region 0-51434
- boundary layer, obstacle in weakly stratified flow, upstream influence, theory 0-56527
- boundary layer, stratified and oscillating, driven by surface temp. grad. 0-51515
- upland Britain, wind chill 0-41546
- Chesapeake Bay, atm. forcing effect on subtidal sea level var. 0-26530
- Chinook effects on Calgary air quality 0-16876
- cloud motion wind data, meas. improvement 0-8386
- cloud-motion winds derivation, Meteosat image data 0-46270
- coastal zone, local thermal wind-field disturbances freq. statistical forecasting 0-36371
- cross-wind velocity meas., interference fringe visibility and spacing, atmospheric turbulence effects 0-51572
- crosswind profiles, remote sensing using correlation slope method 0-31131
- cyclones, ring of max. wind, centre location using kinematical determinant 0-56535
- direction fluctuation statistics and lateral dispersion 0-56577
- divergence theorem for wind velocity (*Spanish*) 0-36376
- Doppler radar data analysis 0-41564
- Doppler-radar techniques for wind meas. 0-26645
- downdraught caused by nimbostratus rainfall evaporation, numerical anal. 0-8400
- Earth annual wobble, affected by wind stressed sea level 0-36221
- effect on ocean currents, regression coeffs. and bottom stress anal. 0-8320
- effect on winter 1975 circulation in Chesapeake Bay 0-36313
- energy transfer to near-inertial ocean waves, calc. 0-4017
- SW England and S.Wales, gale force winds and blizzard (1978 February 18 to 19) 0-12507
- erosive action on sub-Antarctic Marion Island 0-31093
- F-region at night time, negative correl. of wind to elec. field 0-41603
- flow field determination, comparison of interpolation methods for sparse data 0-51575
- flow over isolated hill of moderate slope 0-12515
- forcing effect on infinite  $\beta$ -plane ocean model 0-4031
- Great Britain, northerly gales of (1978 January 11 to 12) 0-12508
- ground level and geostrophic frequency distribution, topographic influence 0-17346
- ground surface roughness change, affecting air flow characts. 0-51501
- Gulf of Alaska, SeaSat scanning multichannel microwave radiometer results 0-46248
- N.Gulf of Alaska, wind stress rel. to coastal flow meas. by drogued drift buoys 0-51431
- Gulf of Alaska SeaSat Experiment 14.6 GHz scatterometer surface wind obs. 0-46200
- Gulf of Genova, effect of low freq. winds on sea level and currents 0-8322
- W.Gulf of Maine, wind rel. to gulf winter circulation 0-51430
- HAPP investigation for high-altitude platform operation feasibility 0-17369
- heat transfer of boundary layer with ocean, reef effects, AMTEX 1975 obs. 0-26567
- high-altitude wind measurement, radiowave drifts technique 0-31137
- hill affecting turbulent diffusion from point source in stratified flow 0-56505
- hurricane model-ocean model integration, mutual response 0-4032
- hurricane sea surface wind speed, L-band radar backscatt. obs. 0-56561
- hurricanes, interaction between symmetric mean vortex and shearing steering current rel. to spiral bands excitation 0-56538



## wind continued

India, November 1977 Andhra Pradesh cyclone and associated storm surge 0-51499  
 Indian Ocean, sea levels in western equatorial region rel. to tides, meteorology and ocean circulation 0-4018  
 industrial aerodynamics, conference, Aachen 0-17712  
 intertropical convergence zone cloud cluster, wind field behaviour 0-17322  
 ionosphere, equatorial, zero and maximal vel. contours rel. to mid-latit. absorpt. 0-12597  
 ionosphere EM wave absorpt. rel. to wind and temp. struct., winter 1975/6 obs. 0-36438  
 Iowa, wind-aligned drainage in loess 0-41467  
 jet stream, different, theory 0-46242  
 katabatic wind model, hydraulic approach 0-17321  
 katabatic wind observations 0-56587  
 Kuroshio current, wind-stress curl. rel. to surface vel. vars. in East China Sea, (1956-75) (*Chinese*) 0-31049  
 Lagrangian and Eulerian fluctuations 0-41519  
 land and sea breeze simulation along complex coastline 0-36364  
 longitude dependent wind flow, stationary planetary waves propag. theory (*German*) 0-56526  
 marine surface wind, numerical prediction (*Chinese*) 0-46212  
 measurement, continuous, using VHF Doppler radar, preliminary results 0-8444  
 measurement by tethered aerodynamically lifting anemometer for WTG siting 0-48830  
 measurement with propeller vane devices, dynamic props. 0-31138  
 mesosphere, winds and waves over Jicamarca, 1974 May 23-24 VHF radar obs. 0-12497  
 meteor region winds at 45°N latitude, 95 km altitude 0-46330  
 meteor wind data, tidal winds and poleward momentum transport 0-12581  
 meteor zone, wind height struct. by statistical method (*French*) 0-51589  
 meter, digital, speed and direction indication 0-207  
 mountain waves and severe downslope windstorms, theory 0-56551  
 ocean, advective mixed-layer model with imposed surface heating and wind stress 0-12395  
 ocean, wind field variability relationship with internal waves 0-31052  
 ocean, wind long-term fluctuations rel. to ocean nonlinear coastal and equatorial jets 0-51427  
 ocean, wind-driven flow in zonal channel with stratification and bottom topography 0-51402  
 ocean circulation driven by wind, finite element anal. 0-56487  
 ocean current flow at planetary boundary layer, wind induced, temp. profiles, model 0-26526  
 ocean surface, microwave emission at 37 GHz, wind effects 0-12414  
 ocean surface microwave emissivity, model of wind roughening 0-46184  
 ocean surface wind obs., SeaSat scatterometer/scanning radiometer/altimeter comparison 0-46249  
 ocean surface wind wave related turbulence meas. by impeller current meter array 0-46301  
 ocean wave prediction using parametrical wind-sea model 0-17272  
 ocean wind wave elevation sensor array system 0-46322  
 oceanic boundary layer, effect on pack ice drift, model 0-26528  
 oceanic eddy formation in Somali Current, wind effects 0-26523  
 overdetermined windfinding systems, error anal. 0-17399  
 N.Pacific Ocean, tropical, wind forcing of annual Rossby wave 0-51421  
 Paradip Coast, India, surface wind directions rel. to wave characts. 0-41450  
 pressure distribution variations in geostrophic wind 0-17348  
 radar detection of wind shear, for airport use 0-51565  
 radar determination of winds at sea 0-26644  
 radioactive dust captured by wind from Earth's surface, radioactive fallout (*Russian*) 0-16869  
 radiotheodolite windfinding system of USA National Weather Service 0-17379  
 remote probing by line-of-sight MM wave and optical methods, spatial filtering concepts 0-36426  
 remote sensing from Earth orbit using microwave technique 0-41573  
 rocket sounding methods since World War II 0-17398  
 rough surface affecting momentum transfer of flow 0-51511  
 Sahel rainfall 1975-6, D, T and <sup>18</sup>O evidence and regional winds (*French*) 0-21809  
 sand barrier beach shoreline accumulative section, protective dune ridge morphodynamics (*Russian*) 0-36287  
 sand barrier beach shoreline transit section, protective dune ridge morphodynamics (*Russian*) 0-36286  
 sea state, surface wave prediction model for varying wind fields 0-12408  
 sea surface wind-driven flow 0-46187  
 shearing instability mechanism model, effect of horizontal differencing 0-26578  
 sand grain surface texture rel. to wind vel. conditions 0-41443  
 speed, interannual and monthly vars. 0-51490  
 speed, rel. to maximum sensible heat flux in stable boundary layer 0-17345  
 speed and direction prediction, statistical analysis of ground wind vector 0-17347  
 speed anomaly in surface layer in Po Valley 0-17313  
 speed from Geos 3 data 0-4079  
 speed limits to work under hot environments for clothed men 0-8030  
 speed meas. from orbit using lidar system 0-4114  
 sporadic-E layer, electron density explained by wind shear acting on metallic ions 0-46338  
 St. Louis, urban-rural wind differences, tower meas. 0-51487  
 stability classification schemes applied to non-homogeneous terrain coastal region 0-8379  
 storm turbulence, characts. near top of spruce forest 0-17349  
 stratified flow around three-dimens. barrier 0-48769  
 stratosphere, wind monitoring using Concorde-generated infrasound 0-51492  
 stratosphere and mesosphere winds, 20-80 km 1975/6 obs. of W.Europe 0-36359  
 summer monsoon circulation aspects 0-8413  
 surface ocean current response, quadratic and linear laws 0-26529  
 surface speed over drifting pack ice from surface weather charts 0-41476  
 surface wind, algorithm for wind speeds using Geos 3 measurements 0-4078  
 surface wind speed data, appl. to hourly mixing depths estimation 0-51482  
 synoptic windfinding, satellite imagery of cloud drift 0-17397

## wind continued

synoptic windfinding technique, Loran and VLF nav aids used with radio-sondes 0-17392  
 synoptic windfinding using Omega VLF nav aid, atmos. radiowave propag. 0-17309  
 synoptic windfinding using tropical constant-level balloon system 0-17395  
 thermosphere, ion-drag effects 0-17432  
 thermosphere, nighttime, winds rel. to neutral atmosphere parameters var. (*Portuguese*) 0-41584  
 thermosphere and exosphere, neutral temperature and winds, geomag. disturbances effects 0-26658  
 thermosphere circulation, seasonal and solar cycle variation 0-56661  
 thermosphere neutral wind, midlatitude meas. during ALADDIN programme 0-31153  
 thermosphere neutral winds, tidal modes rel. to low latit. dynamo currents seasonal vars. 0-8479  
 tornado flowfield struct., laboratory expts. 0-56566  
 tornado vortex, barotropic instability theory 0-51458  
 transverse vel., remote meas. using laser Doppler velocimeter 0-4115  
 tropical stratopause, 2-day oscill. of meridional wind 0-56557  
 troposphere, N.Hemisphere wintertime disturbance, transient disturbance 0-51459  
 troposphere, variance spectrum over E.Europe 0-8397  
 turbulence structure over water in high wind 0-12502  
 typhoon prediction by barotropic primitive equation model using splines (*Chinese*) 0-4063  
 typhoon Tess wake vertical struct. in upper layer of Pacific Ocean 0-26538  
 upper atmosphere, winds determ. from China 2 rocket (1971-18B) orbit 0-4231  
 upper atmosphere neutral wind gradients, meteor radar obs. 0-41575  
 upper atmosphere wind, solar eclipse obs. at 80-100 km altitude 0-46327  
 upper atmosphere wind and temperature meas., laboratory discharge lamp source appl. 0-4148  
 upper atmosphere winds observed by radio meteor drift, 80-100 km altitude 0-46328  
 valley ventilation by cross winds 0-48771  
 velocity, remote meas. using video equipment for pollution monitoring (*French*) 0-7990  
 velocity gust factors, analytical expression and wind tunnel simulation 0-31107  
 velocity sensors, crossed hot-film anemometers, compensating for non-ideal geometry 0-31122  
 wave tank, microscopic and macroscopic surface structs. growth and decay rates 0-48726  
 weather maps, for present weather, wind, and ceiling, examples, forecasting use (*German*) 0-4081  
 Weddell Sea drift ice, pushed north by barrier winds 0-26514  
 zonal winds at 95 km altitude, correl. with radar meteor echo rates 0-56775  
 O<sub>3</sub> affected by sea breeze, Wallops Island, Virginia 0-51473

## wind energy see wind power

## wind power

anemometer, low level wind meas. for WTG siting 0-48830  
 assessment of wind energy systems in a utility framework 0-30369  
 availability, analysis of the potential of wind energy conversion systems 0-30363  
 brackish water purification by electrodialysis and reverse osmosis, wind powered-processing 0-35630  
 conference, London, 21 Nov. 1979 0-55790  
 desalination appl. reverse osmosis, expt. installations (*French*) 0-55807  
 design and development of small systems at 1-2 kW, 8 kW and 40 kW 0-55784  
 development as alternative energy source, c.f. nuclear power, book 0-45624  
 developments and improvements, energy data at Danish stations (*Norwegian*) 0-30364  
 electrolysis of brine using wind energy 0-30368  
 energy output analysis of small scale generation systems using local climatological data 0-55787  
 energy resources, overall view (*French*) 0-40804  
 fluid dynamic aspects, turbulence, review 0-7909  
 flywheel system for storage and conversion of energy from wind turbine 0-30572  
 Hawaii, wind and insolation as alternative energy resources 0-45623  
 Iran, rural electrification program utilising wind power 0-55789  
 Ireland, assessment of actual wind power availability 0-21366  
 limits to wind power utilization 0-7908  
 MOD-2 wind turbine system, 300 ft diam. 2.5 kW, development program 0-35631  
 offshore wind energy systems for the UK 0-55794  
 plant design in MW range 0-55788  
 Prince Edward Island, evaluation of system worth to electrical grid 0-50932  
 pumps, development programme 0-55792  
 renewable energy sources, Rumania (*Rumanian*) 0-35639  
 review of the US Wind Energy Programme 0-50929  
 solar photovoltaic-wind hybrid alternative energy system 0-30409  
 tornado-type generator system, latent heat from moist air, effect on vortex 0-30365  
 turbines, bicycle rotors for vertical axis wind turbines, design and performance 0-30367  
 United Nations energy program for solar and wind energy appls. 0-3496  
 urban development of small-scale wind power systems in New York City 0-55786  
 utilisation, machine dynamics, geometry, economics and social acceptance 0-45625  
 vertical axis wind turbine, operation and anal. 0-30366  
 Weibull wind speed distrib. parameters, estimation using Weibull prob. paper and percentile estimators 0-50931  
 wind turbines, rotational dynamics, eval. of turbine response to wind speed changes 0-55785  
 windmill arrays, wind-power conversion limits, simple formulas 0-3485  
 windmill for use in irrigation, with horizontal axis sail 0-21368  
 windmill using sail-type Savonius rotor, low-cost water pumping appl. 0-21367  
 windmills in closely spaced arrays, performance 0-40819  
 windpump ITDG development program, for small-scale manufacture and use in under-developed arid regions 0-26106



**wind power plants**

- assessment of wind energy systems in a utility framework 0-30369
- control and stabilization of the DOE/NASA Mod-1 two megawatt wind turbine generator 0-30370
- Cretan windmills, high rate energy extraction from low speed winds 0-30362
- design and development as alternative energy source, c.f. nuclear power, book 0-45624
- design of plant in MW range 0-55788
- developments and improvements, energy data at Danish stations (*Norwegian*) 0-30364
- electricity production, in Denmark from 1900 to 1950 0-16778
- energy accumulators appl., flywheel, stationary, economic assessment (*German*) 0-35757
- high temperature storage for a wind energy system 0-55920
- MOD-2 wind turbine system, 300 ft diam. 2.5 kW, development program 0-35631
- review of the US Wind Energy Programme, MOD-1 and MOD-2 machines 0-50929
- small scale wind energy systems, design characts. and appls. 0-55791
- turbine generator system, optimum selection 0-40818
- urban development of small-scale wind power systems in New York City 0-55786
- utilisation, solar energy model anal. to 2010 (*German*) 0-26109
- windmills in closely spaced arrays, performance 0-40819

**wind tunnels**

- 3-D laser Doppler velocimeter 0-10331
- airport fencing for air pollution reduction, wind-tunnel expt. (*Japanese*) 0-12034
- atmospheric motion simulation, wind tunnel characts. review (*Italian*) 0-4156
- cascade deviation, prediction and measurement 0-24049
- channel height effect on nearcritical flow past circular cylinder 0-14818
- digital data filtering in continuous wind tunnels 0-10336
- dynamic force balance, two-component, for mounted flying insects 0-22350
- flow separation experiments, galloping and vortex induced oscillations 0-43750
- graupel formation and growth, cloud simulation 0-17324
- hypersonic wind tunnel, flow core relative area, nozzle similitude ratios 0-48747
- IR camera for separated flow regions diagnosis in wind tunnels 0-10335
- low-Reynolds-number turbulent boundary layers 0-1556
- open cct., exptl. procedures to improve characts. (*Japanese*) 0-19528
- test program for determining effect of spin on boundary-layer transition at Mach numbers 5 and 8 on 9-deg. cone configurations 0-14864
- transonic flow simulation by tracking and blowing (*German*) 0-6081
- unsteady aerodynamics research, data acquisition using minicomputer 0-10337
- vortices in wind tunnel expts. meas. using US pulses 0-10334

**wind turbines**

- bicycle rotors for vertical axis wind turbines, design and performance 0-30367
- control and stabilization of the DOE/NASA Mod-1 two megawatt wind turbine generator 0-30370
- Darrieus wind turbine system, parametric performance analysis by digital simulation 0-40817
- design and development of small systems at 1-2 kW, 8 kW and 40 kW 0-55784
- fluid dynamic aspects, turbulence, review 0-7909
- flywheel system for storage and conversion of energy from wind turbine 0-30572
- free vortices behind stationary wing as energy source 0-40820
- generator system, optimum selection 0-40818
- MOD-2 wind turbine system, 300 ft diam. 2.5 kW, development program 0-35631
- offshore wind energy systems for the UK 0-55794
- reciprocating water pump, stroke adjusting mechanism for rotor speed control 0-50930
- review of the US Wind Energy Programme, MOD-1 and MOD-2 machines 0-50929
- rotational dynamics, eval. of turbine response to wind speed changes 0-55785
- UK field measurements collaboration [wind turbines] 0-55793
- vertical axis wind turbine, operation and anal. 0-30366
- windmill arrays, wind-power conversion limits, simple formulas 0-3485

**winding (process)**

- fibre reinforced composites, zonal winding pattern analysis, thin spherical shells 0-38253

**wires (electric)**

- see also conductors (electric)*
- aging process investigation natural and accelerated, Cu wire leads with Sn60Pb coating appl. (*Polish*) 0-35231
- die wear during wire drawing, review 0-30113
- metal wire and bar NDT, electrical and EM methods 0-11865
- steel-Al bimetallic wire for overhead lines, manufacturing methods 0-16247
- Al, eddy current effects on NMR 0-2645
- Cu, growth of diffusion layer in Sn coatings due to ageing effect (*Polish*) 0-34227
- Cu/SbF<sub>3</sub> intercalated graphite/Cu composite wires, elec. cond. 0-44687
- Pd-Ag microwires, electrical resistance, influence of gaseous environment in heat treatment (*Russian*) 0-20146

**wiring diagrams *see circuit diagrams*****WKB calculations**

- $\phi^4$  system, metastable state, decay rate calc. 0-22301
- atom-surface scatt., inelastic, energy transfer and sticking coeff., classical and quantum treatments 0-40209
- bound states, semiclassical, in one-dimension, perturbation formalism 0-12937
- collisionless drift wave in Vlasov plasma, nonlocal anal. 0-43910
- complex potential energy surface systems, nonradiative processes, WKB calcs. 0-45133
- cosmological particle production 0-27023
- dechanneling (aligned-to-random beam transition), WKB approx. 0-34109
- diffusion in bistable potential, systematic WKB treatment 0-46975
- distorted crystal, X-ray intensity mode oscills., two wave WKB approx. calcs. 0-28876
- gravitational waves dispersion in cold matter 0-12967

**WKB calculations continued**

- hadrons, string state, WKB-like wave functional and path-dependent phase factor, colour flux 0-52481
- heavy ion scattering cross-sections, WKB calcs., unphysical reflection phenomena 0-27656
- inhomogeneous circular waveguide, asymptotic eigenvalues 0-53442
- laser-assisted inelastic collisions, impulse approximation theory and other short wavelength approximations 0-18904
- lattice quantum theory; WKB approx. 0-32009
- lower hybrid wave, linear amplification and absorption 0-28673
- lower hybrid waves, ray trajectory and ion absorpt. in Tokamak 0-28667
- metal-semiconductor-metal junction, tunnelling phenomena in terms of exact method and WKB approx. 0-20329
- optical fibre, power-law refractive index profile, scalar modal eigenvalues and group delays 0-28322
- optical step-index fibres with microbending, bandwidth 0-23775
- phase memory, necessary conditions 0-22206
- pseudo-first-order phase transitions in one dimension 0-22270
- quarkonium, quantum mechanical applications, masses and leptonic widths of  $\psi$  and  $T$  0-27484
- quartic oscillator, semi-classical expansion 0-31592
- radial integrals calc. in Coulomb approx., use of semiclassical wavefunctions 0-43025
- Robertson-Walker universe, pair-creation of particles 0-22265
- soliton free energies calcs., WKB approx. failure 0-42073
- stochastic diffusion in a periodic potential 0-12994
- meso-tetraphenylporphine, potential parameters of H migration tunnel rates calcs. 0-5600
- Tokamak machines, Vlasov plasmas, geometrical optics approach, Tokamak appl. 0-14902
- WKB five term approx. 0-31569
- ArBr, pot. curves, population distrib. and chemiluminesc. for B(1/2) and C(3/2) electronic states 0-45509
- KI:Ti<sup>+</sup>, A<sub>T</sub> emission, mag. circular polarisation, WKB approx. for non-radiative transition rate 0-55180
- KI:Ti, A<sub>T</sub> emission, linear polarisation, appl. of semi-classical WKB formalism 0-45134
- KrF\*, oscillatory bound-free emission spectra, semiclassical anal. method 0-7799
- U<sup>+</sup>+U(U<sup>+</sup>)(U<sup>2+</sup>), elastic scatt. in plasma, interaction pots. and momentum transfer 0-38534

**wolfram *see tungsten*****wood**

- balsa, cryogenic insulation, exam. of strength specifications, props. 0-25819
- boiler fuel, sawdust waste of timber mills (*German*) 0-40805
- combustion in heating plants, calorific values (*German*) 0-40815
- cutting, stress distrib. and frictional coeff. at tool-chip interface, specific gravity effect (*Japanese*) 0-1492
- dimensional stabilisation, with 2-hydroxyethyl methacrylate and MMA (*Japanese*) 0-7532
- dimensional stability, and hygroscopicity, with ethylene glycol and isocyanate (*Japanese*) 0-2982
- gasification using fluidized bed wood gasifier 0-30348
- prestrain effect on dynamic modulus of elasticity and attenuation coeff. in nonconducting materials 0-29110
- screw, effects of crest and pilot hole in withdrawal resist. (*Japanese*) 0-3290
- softwoods, flow paths (*Japanese*) 0-3288
- softwoods, transverse Poisson's ratio and Young's modulus (*Japanese*) 0-2111
- stud walls, rel. between maximum compressive load and width (*Japanese*) 0-3124
- timber, determ. of critical Rice integral (*French*) 0-16412
- timber butt-joint, with metal plate connectors, rotating bending fatigue (*Japanese*) 0-3175
- tree form energy plantations, woodchip transport and handling 0-30327
- tree rings, reconstruction of climate vars. since (1602) 0-51528
- waterlogged woods, props., conservation problems (*Japanese*) 0-3289
- <sup>13</sup>C record in tree rings, vars. in N.hemisphere trees during last 150 years 0-17363

**wood processing**

- see also paper industry*
- polysaccharide components dissolved into chlorite liquor according to the variation of treating conditions (*Japanese*) 0-3291
- timber dryer, forced-air, for tropical latitudes, solar heating appl. 0-21384
- waste, fuel gas production, gasifier design and construction 0-7895

**word processing**

- semantically accessible communication aid development trends 0-8218

**work function**

- see also electron emission; Schottky effect*
- adsorption system surface properties variational calcs., binding energy, Lang model 0-29279
- high-current multirod cathode, influence of absorption effects on characts. 0-20756
- jellium metal, surfaces props., statistical calc. 0-24987
- metal, surface dipole barrier, semi-empirical calc. 0-39659
- metal, surface energies and work function, simple analytic model 0-49862
- metal, with terraced surface, calc. 0-6950
- metal surface, influence of submonolayer films on props., calc. (*Russian*) 0-2273
- metal-insulator interface, catalytic reactions studied by work function meas. 0-55711
- metal-metal contacts, use as prevention H escape from metals 0-24595
- metallic and nonmetallic solids, Fermi energies 0-2451
- metallic granules, electron work function interrelation with granule size 0-39660
- metallic thin films electrostatic interaction of charges with metal surface in size-quantised film 0-24996
- rare earth element submonolayer films, electronic phase transitions, heat of absorption 0-24736
- refractory metals, work function, ionising radiation effects meas. method 0-6951
- semiconductor substrate, work function rel. to AES (*French*) 0-50479
- semiconductor-metal boundary, Schottky barrier form., chem. mechanisms 0-49869
- thermionic electron emission from surface with adsorbed atom islands 0-7462



**work function continued**

Ag, adsorption on W, substrate temp. effect on relation between work function and coverage, FEM obs. 0-2272  
 Al-SiO<sub>2</sub>-Si system with reactively sputtered SiO<sub>2</sub>, work functions difference 0-6987  
 Au film, work function changes upon water contamination 0-44705  
 Ca films, thin and ultrathin, vac. deposited, struct. and photoemission meas. 0-11538  
 Co film, work function changes upon water contamination 0-44705  
 Co, pure surfaces, adsorpt. of water and decomp. (*German*) 0-26054  
 Cr (100), adsorption of O<sub>2</sub> and initial oxidation at room temp. 0-20034  
 Cu (100) surface, interaction with O<sub>2</sub>, AES, EELS, LEED and work function studies 0-24731  
 Cu (111), Cs adsorption system, electronic surface band energy 0-2443  
 Cu film, work function changes upon water contamination 0-44705  
 Cu(110), adsorption of O<sub>2</sub> and its reaction with CO 0-15373  
 Eu<sub>1-x</sub>La<sub>x</sub>Al<sub>2</sub>, binding energy and workfunction charges using XPS 0-33928  
 Fe (100), adsorption of Br<sub>2</sub>, AES, LEED, work function, and thermal desorption study 0-15375  
 Fe (100), adsorption of carbon tetrachloride, AES, LEED, work function, and thermal desorption study 0-15376  
 Fe (100), adsorption of I<sub>2</sub>, AES, LEED, thermal desorption, and work function study 0-15374  
 Fe (100), adsorption of tetrabromomethane, AES, LEED, work function, and thermal desorption meas. 0-39422  
 Fe (111) surface, S segregation, LEED, AES and work function changes 0-15350  
 Fe film, work function changes upon water contamination 0-44705  
 GaAs (110), clean, cleaved, surface states, work function meas. 0-49847  
 GaAs, MBE (001) layers, work function meas. 0-49870  
 GaAs-metal Schottky barrier height rel. to chem. reactivity 0-25008  
 GaSe-metal Schottky barrier height rel. to chem. reactivity 0-25008  
 GaSb surface, temp. depend of work function (*French*) 0-6949  
 Ge, bound exciton complexes, density functional calc. 0-10890  
 He, liquid dielec. breakdown voltages, depend. on work function of cathode surface 0-2695  
 HgSe/CdSe lattice-matched heterostructs. as Schottky barriers, CVD epitaxial growth and elec. props. 0-49877  
 Ir, with adsorbed Xe, 5p photoemission, local surface struct. influence 0-2920  
 (La, Y, Sc)B<sub>6</sub> solid solns. electron work function, thermal emission technique 0-20755  
 LaB<sub>6</sub> (100) surface, O<sub>2</sub> adsorption, UPS and LEED study 0-49519  
 LaB<sub>6</sub>, adsorption on Ta 0-20039  
 LaB<sub>6</sub>, high temp. interaction with O<sub>2</sub>, AES and mass desorption expts. 0-7698  
 LaB<sub>6</sub> single crystal needles, thermal field emitted electron total energy distribution spread 0-45218  
 LaB<sub>6</sub>, synthesis and props. (*Japanese*) 0-40255  
 MgO, adsorption of Cs and Li, AES, LEED, work function, and secondary electron emission meas. 0-44407  
 Mo (100), adsorption of O<sub>2</sub>, AES, LEED, work function, and desorption meas. 0-6654  
 Mo (110), of Cs and O<sub>2</sub>, common adsorption, work function and thermal stability by contact pot. method 0-44427  
 Mo, (112) face, Sr submonolayer adsorption 0-2271  
 Mo (112) surface adsorption of Li film, LEED and contact pot. method 0-10794  
 Mo-TiC(ZrC)(HfC), thermionic emission, surface structural characts. after prolonged use, work function variation 0-20758  
 Mo(001), H chemisorbed, self-consistent electron struct. 0-44693  
 Na<sub>2</sub>AlF<sub>6</sub> film, evaporated, electron bombard. effect on secondary electron emission, Auger peak shifts 0-2903  
 Na<sub>2</sub>WO<sub>3</sub>, x=0.6 and 0.8, surface characts. 0-39392  
 Nb-H, electron work function, 300 to 600 degrees C, contact potential difference meas. 0-29462  
 Nb-Mo-Ti-Zr-C, work function temp. and phase depend. (*Russian*) 0-2449  
 Ni (100), adsorption of CO, EELS and concomitant surface anal. 0-7453  
 Ni (110), chemisorption of O<sub>2</sub> and initial oxidation, AES, EELS, and work function meas. 0-54523  
 Ni (111), chemisorption geometry of H, LEED, thermal desorption, and work function meas. 0-39433  
 Ni film, work function changes upon water contamination 0-44705  
 Ni monolayer and submonolayer films, on ZnO, UPS study 0-7472  
 Pd-Pt, with adsorbed Xe, 5p photoemission, local surface struct. influence 0-2920  
 Pd-TiO<sub>2</sub> Schottky barrier, work function depend. on adsorbed species 0-54782  
 Pd-ZnO Schottky-barrier diode, H<sub>2</sub> sensitivity 0-11085  
 Pd(110) surface, adsorption of Xe, work function study 0-6633  
 Pt, adsorption of water, H<sub>2</sub> and reaction between H<sub>2</sub> and adsorbed O 0-49514  
 Pt film, work function changes upon water contamination 0-44705  
 Re, thermionic work function of low index planes 0-55255  
 Ru, with adsorbed Xe, 5p photoemission, local surface struct. influence 0-2920  
 Si, electron-hole drops, thermodynamical parameter determ. from luminescence data 0-2845  
 p-Si-SiO<sub>2</sub> system, C-V meas. using Au/Hg probe, work function difference between probe and Si 0-2450  
 Ta autocathode, influence of electric field and heating on work 0-7478  
 Ta, photo field emission spectroscopy of band structure by He-Ne laser irradi. 0-55276  
 Ta-H, electron work function, 300 to 600 degrees C, contact potential difference meas. 0-29462  
 Ti (0001) film, with adsorbed H (1×1) monolayer, electronic struct., surface geometry 0-54750  
 Ti, interaction with O<sub>2</sub>, resist. and work function changes obs. 0-45431  
 TiC (001) surface, change in work function with chemisorption of O<sub>2</sub> and H<sub>2</sub>O 0-29461  
 TiO<sub>2</sub>, (100) surfaces, ionisation of sputtered-atomic particles 0-20750  
 V-H, electron work function, 300 to 600 degrees C, contact potential difference meas. 0-29462  
 W (100), adsorption of CO, thermal desorption and work function meas. 0-29273  
 W (100), adsorption of Zr, AES, LEED, thermal desorption, and work function meas. 0-39444  
 W (100), coadsorption of Zr and O<sub>2</sub> at high temp. 0-6653

**work function continued**

W (100), reconstruction in presence of O half monolayer, struct. props. 0-44421  
 W (110), (112), of Cs and O<sub>2</sub>, common adsorption, work function and thermal stability by contact pot. method 0-44427  
 W (110), codeposition of Cs and O, Cs<sub>2</sub>O form. 0-44425  
 W (110), Fowler-Nordheim studies 0-34501  
 W (110), oxygenated and oxidised, Cs absorption 0-44424  
 W (110) and (100), adsorption of Xe and coadsorption with O, work function and thermal desorption meas. 0-39448  
 W, ion induced secondary electron emission, probe for adsorbed O 0-55251  
 W-Ti, Ti addition effect on heat resistance and radiative props. (*Russian*) 0-25515  
 W-TiC(ZrC)(HfC), thermionic emission, surface structural characts. after prolonged use, work function variation 0-20758  
 W-Zr, Zr addition effect on heat resistance and radiative props. (*Russian*) 0-25515  
 W-Zr-C, Zr and C addition effect on heat resistance and radiative props. (*Russian*) 0-25515  
 ZnS-metal Schottky barrier height rel. to chem. reactivity 0-25008  
 ZnSe-metal Schottky barrier height rel. to chem. reactivity 0-25008

**work hardening**

*see also cold working*  
 alloy, space lattice types A<sub>1</sub>, A<sub>2</sub> and A<sub>3</sub>, strain hardening function (*German*) 0-20955  
 alloys, hot plastic strain, stress-strain-time dependences (*Russian*) 0-40430  
 α-β brass, two phase bicrystal, deform. and fracture at 450K 0-16409  
 ceramic nuclear fuels, mech. props. at compressive deformation 0-651  
 cubic single crystals, hardness meas. by spherical indentation 0-16622  
 deformable solids, fracture and hardening kinetics 0-35210  
 dislocations model, compatibility with transient and steady state creep (*Italian*) 0-33487  
 elastic-plastic models, integration algorithms 0-5959  
 elastoplastic strip or half-plane under moving load, residual stresses and plastic zones 0-53645  
 electrotechnical steel, quality significance on energy and materials savings in magnetic circuits (*Czech*) 0-20947  
 forming limit curve for bending processes 0-7627  
 isotropic strain hardening theory (*Russian*) 0-38279  
 kinematic hardening models, use in multi-axial cyclic plasticity 0-25717  
 metal, anisotropic, description of history dependent plastic flow behaviour 0-11732  
 metal, FCC or BCC, dislocation annihilation during tensile and cyclic deform. and limits of dislocation densities 0-34007  
 metal, space lattice types A<sub>1</sub>, A<sub>2</sub> and A<sub>3</sub>, strain hardening function (*German*) 0-20955  
 metals, FCC, yield threshold at 4.2K, effect on strain-hardening curve (*Russian*) 0-50671  
 metals and alloys, yield criterion, rheological interpretation (*Russian*) 0-21014  
 microstrains distrib. in macroinhomogeneous fields (*Russian*) 0-21018  
 oxides, interaction between point defects and dislocations, cryst. plasticity 0-15149  
 perforated plates, finite element elasto-plastic anal. 0-10168  
 plastic constitutive equations with work hardening (*Japanese*) 0-25718  
 polyethylene, high density, hydrostatic extrusion behaviour 0-50649  
 steel, anisotropic sheet, strain hardening, stress state depend. 0-55421  
 steel, austenite hot deformation influence on phase transformations 0-7606  
 steel, austenitic stainless, 08Kh18N10T, hot-worked precipitation kinetics and struct. of dispersed phases, Ti effect 0-29964  
 steel, austenitic stainless, types 304L and 316L, work-hardened, electrochem. and corrosion behaviour in acid solns. 0-50757  
 steel, austenitic-martensitic, phase comp., struct. and mech. props. 0-29974  
 steel, C, deformation strength and strain rate depend. under plain strain state (*Japanese*) 0-30028  
 steel, C, strain ageing and fatigue limit 0-40378  
 steel, C content effect on annealing texture, plastic anisotropy and mechanical props. 0-29976  
 steel, Cr-Mo (2.25, 1 wt.%), strain hardening shakedown load during bending 0-20958  
 steel, deform. resist., softening effects, analytical depend. calcs. (*Russian*) 0-49293  
 steel, deformed eutectoid C<sub>2</sub> back stress decrease on annealing and H embrittlement 0-20981  
 steel, grain boundary strengthening mechanism 0-35207  
 steel, high Si dual-phase, mech. props and microstruct. anal. 0-40444  
 steel, low alloy structural, type 30KhGSA, effect of thermomech. treatment on strength, fracture toughness and fatigue props. 0-11676  
 steel, low C, instability obs. by large strain compression 0-35253  
 steel, low C, low cycle fatigue props. with variable strain ranges (*Czech*) 0-45390  
 steel, low C, stress-controlled and strain-controlled tests, S/N curves comparison (*German*) 0-40476  
 steel, low or medium alloy, work hardening effect on martensitic transform. cond. (*French*) 0-16329  
 steel, low-alloy, props. with nitride and Cu hardening at low temps. (*Russian*) 0-40372  
 steel, mild, annealed, plastic flow under proportional and non-proportional straining 0-40465  
 steel, sheet, rapid test for props. assessment 0-40650  
 steel, stainless, wire, cold drawing 0-50650  
 steel, stainless type 304 L, mech. behaviour under constant stress associated with cyclic strain 0-25767  
 steel, stress relaxation, short-term, creep and strain hardening (*Russian*) 0-30005  
 steel, TRIP, warm extrusion, process control and tensile props. 0-16338  
 steel, type 28Kh3SNMVA, strain hardened martensite, resist. to tempering, exam. 0-16348  
 steel, ultrahigh strength, monotonic and cyclic stress strain curves 0-35268  
 steel fatigue in surface active media, adsorption facilitation mech. 0-55586  
 steel fibre reinforced concrete, tensile strength and ultimate strain (*Polish*) 0-21027  
 steels, heat-treated, nature of high sensitivity to stress raisers 0-21051



**work hardening continued**

- steels, hot plastic strain, stress-strain-time dependences (*Russian*) 0-40430  
 stress/strain relation, rate and temp. depend., analytic formulation 0-40466  
 tensile creep and early failure, model 0-15185  
 torsional strain curves plotting 0-40638  
 Tresca type plastic material, simple shear deform. with combined work hardening (*Japanese*) 0-35206  
 Al, deformed, thermal recovery, microstruct. and stress-strain relations 0-16325  
 Al, polycrystalline, acoustic emission energy release, grain size and flow stress depend. 0-11722  
 Al-alloys, precipitation hardening, effect on dynamic strain ageing and jerky flow 0-20945  
 Al-CuAl<sub>3</sub> eutectic, heat treatment and interlamellar spacing effect on tensile deformation 0-29979  
 Al-Mg<sub>2</sub>Si(1.42 wt.%), aged, dislocation structs. caused by plastic deformation 0-25786  
 Al-rare earth alloys, granules, rolling to form foil, exam. 0-20825  
 Al-Si crystals, work hardened, softening and creep rates on annealing 0-11663  
 CaF<sub>2</sub>, plastic deform, work hardening regions, TEM obs. 0-3140  
 Cu alloys, strain hardened, struct. factor effect on stress relaxation (*Russian*) 0-25748  
 Cu-Ni-Sn (10, 6 wt.%), temp. depend of yield stress and work hardening 0-21026  
 Fe, quenched-in hydrogen, yield stress decrease of prestrained specimens 0-16454  
 $\alpha$ -Fe, single crystals, work hardening (*German*) 0-50652  
 LiF single crystals, glide band sources, work hardening 0-34126  
 MgO, compressive stress-strain behaviour at high temps. 0-25774  
 Mo, single crystals, work hardening and softening in cyclic strain 0-20957  
 Mo-V-C, hot-worked, substructural hardening and high-temp. strength (*Russian*) 0-25731  
 NbC, deformation behaviour during rubbing in wide temp. range 0-16486  
 Nb<sub>3</sub>Sn fatigue effects in unidirectional composites, computer simulated model 0-35289  
 Ni, lattice defects, formation kinetics, work hardening and resistivity study (*Russian*) 0-10557  
 Ni-alloys, precipitation hardening, effect on dynamic strain ageing and jerky flow 0-20945  
 Ni<sub>3</sub>Fe, nondislocation origin friction stress in alloys, deformation hardening 0-21050  
 Ni<sub>3</sub>Fe, single crystals, long range order degree influence on strain hardening (*Russian*) 0-11660  
 Pb, work hardening, and recovery rates during steady state deformation, temp. and stress effect 0-45319  
 Pb-In (5%), supercond. mobile dislocation density, instantaneous flux change meas. 0-15670  
 Pd<sub>77</sub>Cu<sub>16</sub>Si<sub>7</sub>, metallic glass wire, cold drawing 0-50650  
 Sn plate, rapid test for props. assessment 0-40650  
 Ti, dynamic annealing, effect on dynamic strain ageing phenomena 0-7594  
 Ti-Al-Mo(Cr)(Fe), thermomechanical treatment effect on mech. props., strengthening mechanisms 0-55441  
 TiC, deformation behaviour during rubbing in wide temp. range 0-16486  
 V, strain hardening, screw dislocations and microtwinning (*Russian*) 0-29971  
 V-Ta (5 wt.%), strain hardening, screw dislocations and microtwinning (*Russian*) 0-29971  
 WC, deformation behaviour during rubbing in wide temp. range 0-16486  
 Zn, strengthening by electroplastic strain, surfactant effect (*Russian*) 0-20953  
 Zn-Al (10,22,50wt.%), low temp. mech. props. plastic deformation, glissile dislocation nucleation (*Russian*) 0-11695

workers see personnel

wrapping see packaging

Wratten filters see optical filters

X<sup>0</sup> meson resonances see eta meson resonances**X-ray absorption**

see also X-ray absorption spectra

- azimuthal scanning method, allowance for X-ray absorpt. in single-crystal diffractometry 0-38874  
 biological X-ray microanalysis 0-41349  
 characteristic absorption, study using diffractometer DRON-2.0 0-20733  
 computerised tomographic scan evaluation, partial vol. phenomenon effects on linear attenuation coeffs. 0-41176  
 HTR, pyrocarbon coated fuel, C density determ. by X-ray absorpt. 0-5301  
 intense scatterers, at low angles, absorpt. correction and normalisation of X-ray small angle scattering data 0-19671  
 mass absorption coeffs., meas. using X-ray diffractometers and fluoresc. spectrometers 0-18063  
 medical equipment, physical characts. of radiation 0-26334  
 radiography, dose distribution description by X-ray quality monitoring (*German*) 0-41251  
 stopping power, cavity theory verification by ionisation chamber 0-9476  
 X-ray filter assembly for fluorescence measurements of X-ray absorption fine structure 0-31961  
 Mn, extended X-ray finestruct. obs. 0-25482  
 NbO<sub>2</sub>, rutile phase, energy levels, momentum density, and Compton profile, embedded cluster model 0-50453  
 Se, X-ray sensitivity, induced photocurrents, xeroradiographic meas., pair creation energy 0-22490
- X-ray absorption spectra**  
 actinide compounds, spectroscopic techniques for electronic props. meas. 0-11427  
 adsorbates, photoexcitation theory rel. to angle-resolved UPS and surface EXAFS 0-39426  
 amorphous solids, inorganic, struct., review 0-15004  
 atom Breit interaction between electrons, calc. angular coeffs., computer program 0-18779  
 book on X-ray spectroscopy 0-2899  
 computerised tomography, noise factor of a polyenergetic X-ray beam 0-56204  
 diamond:Ni, synthetic, X-ray absorpt. fine structure study of impurities 0-55133  
 dynamical calculations 0-55227

**X-ray absorption spectra continued**

- EXAFS, and complementary techniques, muon spin rotation and Mossbauer spectroscopy 0-39912  
 EXAFS in photoelectron yield spectra 0-16123  
 glass, struct. determ. using EXAFS 0-45169  
 graphite intercalates with K, staging classical model variations, EXAFS results 0-45166  
 Invar, X-ray K-absorpt. spectra, depend. on composition and temp. changes (*Russian*) 0-55226  
 metallic glass, bulk and surface properties, review 0-44147  
 metals, X-ray spectra, final state pot., one-electron theory 0-55230  
 non-crystalline materials of low atomic number, X-ray Raman edge extended modulation for struct. study 0-49111  
 plasmas, laser produced, as X-ray source for extended X-ray absorption fine-structure spectroscopy 0-320  
 polyacetylene:AsF<sub>6</sub>, X-ray absorpt. meas. of mol. struct., orientation and charge transfer 0-25486  
 polyacetylene, doping with AsF<sub>5</sub>, mechanism, effect on elec. cond. and spectra 0-24473  
 rare earth alloys, RCo<sub>5</sub>, X-ray absorpt. spectra, electronic struct. 0-16122  
 rare earth germanides, X-ray emission, absorption and photoelectron spectra (*Russian*) 0-11509  
 superionic conductors, EXAFS studies of struct. and cond. process, book contrib. 0-25485  
 surface characterisation, physical methods, review (*French*) 0-7889  
 transition metal germanides, X-ray emission, absorption and photoelectron spectra (*Russian*) 0-11509  
 vanadyl bisacetylacetonate, polarised X-ray absorption and double refraction 0-50459  
 Al, chemisorption of O, O-Al and O-O bond lengths, surface extended X-ray absorpt. fine struct. 0-29267  
 Al, many-body response in X-ray absorption, emission and photoemission spectra 0-16124  
 Al, soft X-ray emission and absorpt. edges, self-absorpt. studies 0-40183  
 Al, X-ray absorpt. and emission edges, one-electron and many-body effects 0-25484  
 Al-Cu alloys, dil., EXAFS spectra 0-2898  
 AlF<sub>3</sub>, L<sub>2,3</sub> fine struct. of XAS 0-11508  
 Al<sub>2</sub>O<sub>3</sub>, monolayer, core excitons and inner well resonances in surface soft X-ray absorpt. spectra 0-40187  
 As, X-ray K absorpt. edge, effective ionic charge and bonding schemes 0-29827  
 As<sub>2</sub>O<sub>3</sub> crystalline and amorphous, EXAFS study of struct. 0-19776  
 As<sub>2</sub>(Se,Te)<sub>3</sub> glasses, X-ray absorption and photoelectron spectroscopy study 0-7463  
 B, amorphous, X-ray Raman edge extended modulation for struct. study 0-49111  
 Be, soft X-ray emission and absorpt. edges, self-absorpt. studies 0-40183  
 Br<sub>2</sub>, extended X-ray absorption fine struct. amplitude attenuation, rel. to XPS satellites 0-37821  
 CO, K-absorpt. spectra, reson. obs., near fine struct. 0-37817  
 Co and its cpds., X-ray K-absorpt. edge shifts, plasmon energies correlation 0-20734  
 Co complex, Co-thiourea compounds, X-ray K-absorpt. edge, effective nuclear charge 0-35006  
 Co complexes, EXAFS obs. 0-998  
 Co compounds, X-ray K-absorpt. edge, effective nuclear charge 0-35006  
 Cr and its cpds., X-ray K-absorpt. edge shifts, plasmon energies correlation 0-20734  
 Cu and its cpds., X-ray K-absorpt. edge shifts, plasmon energies correlation 0-20734  
 Cu complexes, EXAFS obs. 0-998  
 Cu, EXAFS Debye-Waller factors 0-45168  
 Cu film, EXAFS meas. by total refl. 0-55228  
 Cu, thermal disorder, EXAFS determ. 0-45167  
 CuI, superionic cond., EXAFS study 0-50462  
 DyCo<sub>5</sub>, X-ray absorpt. edge shifts 0-25483  
 Fe, EXAFS Debye-Waller factors 0-45168  
 Fe, far fine struct., multiple scatt. terms contrib. 0-40184  
 Fe, X-ray K-absorpt. spectra, depend. on composition and temp. changes (*Russian*) 0-55226  
 Fe-Cu (75 ppm), internal oxidation, local struct. determ. by EXAFS 0-25916  
 Ga, X-ray K absorpt. edge, effective ionic charge and bonding schemes 0-29827  
 GaAs (110), O chemisorption, surface EXAFS meas. 0-50460  
 GaAs amorphous film, EXAFS, optical and elec. props. 0-49547  
 GaAs, X-ray K absorpt. edge, effective ionic charge and bonding schemes 0-29827  
 GaP amorphous film, EXAFS, optical and elec. props. 0-49547  
 Gd, X-ray absorpt. edge, plasmon excitation 0-7437  
 GdCo<sub>3</sub>, X-ray absorpt. edge shifts 0-25483  
 Ge-Ni, amorphous, struct., EXAFS study 0-49110  
 Ge-rare earth alloys, nature of chemical interaction, X-ray emission, absorpt. and photoelectron study (*Russian*) 0-55261  
 GeF<sub>4</sub> (GeCl<sub>4</sub>), X-ray absorpt. spectra struct. 0-37819  
 I<sub>2</sub>, adsorbed on Ag(111), Cu(111), and Cu(110), surface EXAFS study 0-40186  
 K, soft X-ray emission and absorpt. edges, self-absorpt. studies 0-40183  
 Li, X-ray absorpt. and emission edges, one-electron and many-body effects 0-25484  
 Mg, soft X-ray emission and absorpt. edges, self-absorpt. studies 0-40183  
 Mg, X-ray absorpt. and emission edges, one-electron and many-body effects 0-25484  
 (MgAl<sub>2</sub>O<sub>4</sub>)<sub>x</sub>(AMn<sub>2</sub>O<sub>4</sub>)<sub>1-x</sub>, A=Mg,Mn,Zn,Cd, 0<x<1, mixed oxide spinels, chemical shifts of Mn K-absorpt. edge 0-29828  
 N<sub>2</sub>, K-absorpt. spectra, reson. obs., near fine struct. 0-37817  
 Na, impurities and photoexcited ions 0-39523  
 Na, X-ray absorpt. and emission edges, one-electron and many-body effects 0-25484  
 Nb<sub>0.5</sub>Mo<sub>0.5</sub>, soft X-ray spectra, theoretical considerations 0-11511  
 NbSe<sub>2</sub> intercalated with Rb, EXAFS 0-2897  
 NbSe<sub>2</sub>, intercalated with Rb, EXAFS meas. 0-40185  
 NdO, mag. props., lattice const., and X-ray absorpt. spectra 0-44798  
 Ni and its cpds., X-ray K-absorpt. edge shifts, plasmon energies correlation 0-20734  
 Ni, M<sub>2,3</sub> edge, temp. depend. 0-50463  
 Ni, X-ray K-absorpt. spectra, depend. on composition and temp. changes (*Russian*) 0-55226  
 $\beta$ -Ni-Al, X-ray absorpt. spectra meas., Fermi level location 0-35005



**X-ray absorption spectra continued**

- NiCl<sub>2</sub>, aq. soln., Ni<sup>2+</sup> coordination from extended X-ray absorption fine struct. 0-1913  
 PrO<sub>3</sub>, mag. props., lattice consts., and X-ray absorpt. spectra 0-44798  
 Pt, EXAFS Debye-Waller factors 0-45168  
 (SN), Br, X-ray absorpt. meas. of mol. struct., orientation and charge transfer 0-25486  
 Sc-[Co,Ni,Cu]-Ga, phase equilibria, diagrams of state, X-ray, microstructural study (*Russian*) 0-55356  
 Si (111), chemisorbed O<sub>2</sub> bonding geometry, electron yield EXAFS meas. 0-50461  
 SiF<sub>4</sub>, (SiCl<sub>4</sub>), (SiBr<sub>4</sub>), X-ray absorpt. spectra struct. 0-37819  
 SiO<sub>2</sub> monolayer, core excitons and inner well resonances in surface soft X-ray absorpt. spectra 0-40187  
 Si(111), surface density of states from soft X-ray absorpt. spectra 0-40187  
 SmO, mag. props., lattice consts., and X-ray absorpt. spectra 0-44798  
 TbCo<sub>3</sub>, X-ray absorpt. edge shifts 0-25483  
 Zn and its cpds., X-ray K-absorpt. edge shifts, plasmon energies correlation 0-20734

**X-ray analysis**

see also *electron probe analysis; X-ray chemical analysis; X-ray crystallography; X-ray diffraction examination of materials; X-ray spectroscopy*

- human body components, anal. by X-rays, developments 0-3810  
 molecules, electron distrib., ab initio anal. 0-47866  
 optimised energy dispersive X-ray microanalysis 0-4811  
 scanning electron probe microanalyser, development of x-ray microanalysis 0-37139  
 SEM, cryogenic stage for sample preparation for X-ray microanalysis 0-42306  
 soft X-ray analysers for pulsed-source emissions 0-31957  
 Al coated steel, porosity evaluation, micro X-ray spectral anal. (*Russian*) 0-35389

**X-ray apparatus**

see also *biomedical equipment; X-ray crystallography apparatus; X-ray monochromators; X-ray spectrometers; X-ray tubes*

- biological sample analysis, nanosec. X-ray diffr. pattern techniques 0-26429  
 biological specimen microscopy, flash X-ray method 0-51310  
 biomedical scanners, fast, incomplete scan geometries 0-26330  
 camera for structural anal., high temp. system, for examining liquid metals 0-25950  
 cinematographic systems for ballistics diagnosis 0-13194  
 computerised tomography, dynamic spatial reconstructor, high temporal resolution scanner 0-51235  
 diagnostic apparatus optimal operating conditions 0-30847  
 diagnostic equipment, method and algorithm for adjusting 0-30852  
 diagnostic sets, operation of optical centring systems 0-30831  
 dose compensation filter design using megavoltage radiography 0-3785  
 Einstein X-ray observatory, HEAO-2, results to date 0-56692  
 electronic radiography, computerised, for early detect. of vascular disease 0-41226  
 electrophotetic X-ray imager, self-contained instant display erasable 0-22491  
 electroradiographic image laser readout 0-41225  
 external beam therapy, 4 MeV linear accelerator, dosimetric aspects 0-17140  
 generators, acceptable latitudes in the specifications 0-37137  
 image intensifier performance, image quality, and development trends 0-36124  
 image intensifiers, quantum noise meas. 0-46033  
 image magnification technique 0-18054  
 kilovoltmeter for X-ray equipment 0-13191  
 kymography, motion picture apparatus 0-30851  
 mammographic imaging, historical review in terms of image quality and reduced radiation dose 0-41229  
 mammography, detective quantum efficiency anal. of electrostatic imaging and screen-film imaging 0-41232  
 mammography techniques comparison, in vitro studies of breast microcalcification detectability 0-41230  
 mammography with magnification and grids: detail visibility and dose measurements 0-41231  
 medical equipment, physical characts. of radiation 0-26334  
 penetrometer for measuring peak kilovoltage of dental X-ray sets 0-41171  
 phase analysis, using DRON-1 diffractometer 0-22489  
 photofluorographic camera with electro-optical image intensifier 0-36128  
 pinhole camera, hole size required for no distortion 0-46028  
 portable stress analyser using position-sensitive scintillation detector 0-13190  
 radiographic CaWO<sub>4</sub> intensifying screen, meas. of X-ray induced light photons emitted 0-41218  
 radiographic contrast improvement using fore-and-aft rotating aperture wheel device 0-41227  
 radiographic phantoms for testing X-ray imaging performance 0-51229  
 radiographical subtraction device for daily practice and vascular procedures 0-36090  
 radiography, micro-dose system 0-51233  
 radiography equipment, idealised, for routine chest exams., specifications and requirements 0-46034  
 radiography screen-film combination selection 0-46047  
 radiotherapy high energy X-ray machines, effect on tumour cure rate 0-36067  
 rapid process frame-by-frame registration 0-47159  
 Roentgen-video computed tomography for 3D dynamic imaging by heart lungs and circulation 0-17112  
 RUM-20 apparatus, obs. on improving roentgenogram quality 0-30850  
 screen-film system evaluation, intensity vs. time scale sensitometry 0-41219  
 screen-film system evaluation, sensitometric method 0-41220  
 transmission grating for X-ray diffr. into orders, efficiency 0-47157  
 tuneable polarisers using multiple Bragg reflections in grooved crystals 0-315

**X-ray applications**

- see also *radiation therapy; radiography*  
 biological X-ray microanalysis 0-41349  
 cerebral tissue perfusion rate determ. from <sup>15</sup>O activity decay after photon activation 0-26341  
 human body components, anal. by X-rays, developments 0-3810

**X-ray applications continued**

- microscopy of biological specimens, flash X-ray method 0-51310  
 muscle contraction kinetics obs., time-resolved diffraction diagrams recording with aid of computer (*Japanese*) 0-56291  
 neutron activation anal. with X-ray registration, reduction of background using mag. field 0-16738  
 patient diagnosis, equipment development trends (*German*) 0-3751  
 photographs, determ. of structural and quantum granularity 0-35477  
 residual stress, X-ray evaluation, treatments for nonlinear distribns., review 0-25966  
 scanning electron probe microanalyser, development of x-ray microanalysis 0-37139  
 steel, austenitic, X-ray elasticity constants (*German*) 0-30004  
 steel, ferritic-pearlitic, X-ray elasticity constants (*German*) 0-30004  
 steel, hardened, X-ray elasticity constants (*German*) 0-30004  
 stress anal., using position-sensitive proportional counter 0-1498  
 stress anal. of strongly fluorescing specimen 0-1499  
 stress measurement, error caused by side declining angle of counter scanning plane (*Chinese*) 0-52373  
 stress measurement method, appl. to practical materials (*Japanese*) 0-52379  
 tensometric measurements, reliability (*Czech*) 0-27382  
 α-β-Ti alloys, stress anal. of strongly fluorescing specimen 0-1499

**X-ray astronomical observations**

see also *X-ray sources (astronomical)*

- 2A 0526-328, location and identification with blue emission line star 0-22118  
 A 0535+26, transient X-ray source, flare obs. by (Prognoz 6) (*Russian*) 0-51920  
 2A 1052+606, location and identification with late type emission line star (SAO 015338) 0-22118  
 2 A 1052+606, X-ray and optical variability of RS CVn star 0-31331  
 Abell clusters of galaxies, X-ray survey, HEAO 1 1-10 keV obs. 0-51882  
 α Aurigae (Capella), X-ray line emission obs., corona models 0-26905  
 AWM 4, poor galaxy cluster, extended X-ray emission detect. surrounding cD galaxy (NGC 6051) 0-51884  
 background radiation isotropy, 2-18 keV energy range 0-46709  
 bursting radio sources, search for 2-60 keV emission 0-17679  
 3C 273, X-ray spectrum, 2-60 keV 0-12824  
 3C 58, supernova remnant, soft X-ray flux upper limits 0-56915  
 RS Canum Venaticorum systems, X-ray obs. and coronal model development 0-56873  
 ν Carinae, X-ray emission obs. from star and surrounding nebula 0-26876  
 Cassiopeia A, SNR, high-resolution X-ray obs., struct., expansion phase, mass 0-26960  
 Cassiopeia A, SNR, X-ray spectrum, line emission obs. 0-26961  
 proxima=V645 Centauri, dMe flare star, quiescent corona, transition region, and chromosphere obs. 0-56850  
 Centaurus A, X-ray struct., radio-lobe energy source evidence 0-26978  
 Centaurus X-3, search for X-ray polarization 0-4457  
 VW Cephei, W Ursae Majoris star, identification with faint X-ray source 0-51913  
 CG 176-7, 189+1 and 195+4, X-ray emission associated with γ-ray source 0-31393  
 Circinus X-1 and Cygnus X-1, time variability comparison 0-56974  
 clusters of galaxies, large-scale X-ray struct. 0-8700  
 clusters of galaxies, search for extended hot gas halos in Perseus, Virgo and Coma clusters 0-56953  
 clusters of galaxies, X-ray spectra and relationship to other cluster props. 0-22093  
 σ Coronae Borealis (HD 146361), spectroscopic binary, soft, X-ray obs. with (HEAO-1) 0-56886  
 Crab Nebula, X-ray line emission, balloon-borne obs. 0-41884  
 SS Cygni, dwarf nova, soft X-ray pulsation obs. 0-46563  
 Cygnus Loop, supernova remnant, imaging X-ray obs., temp. struct. 0-41876  
 Cygnus OB2 association (VI Cygni), soft X-ray emission sources discovery 0-26918  
 Cygnus X-1, extended-bandwidth X-ray obs. 0-17689  
 Cygnus X-1, X-2 and X-3, long-term-studies with Ariel 5 All-Sky Monitor (ASM) 0-17688  
 Cygnus X-1, X-ray flux time variability struct. (*Russian*) 0-51921  
 Cygnus X-1 and Circinus X-1, time variability comparison 0-56974  
 Cygnus X-2, 3-8 keV obs. of possible degenerate dwarf 0-46703  
 Cygnus X-3, 4.8 hour modulation period change disproved 0-8713  
 Cygnus X-3, 50-400 keV obs., power law spectrum 0-41913  
 Cygnus X-3, hard X-ray spectrum obs. 0-31388  
 diffuse X-ray background, spectrum from 3 to 50 keV 0-41916  
 dwarf novae, HEAO-A2 soft X-ray survey during optical outburst 0-46574  
 Einstein X-ray observatory, HEAO-2, results to date 0-56692  
 FXP 0520-66, flaring X-ray pulsar in Dorado, Venera 11 and 12 obs. 0-27018  
 galaxy clusters, structure and evolution 0-26994  
 galaxy clusters, X-ray spectra 0-26996  
 galaxy clusters at cosmological distances, X-ray emission detect. 0-26993  
 galaxy rich clusters and superclusters, and clusters extended halos, X-ray emission search 0-26988  
 H 1538-32, new extended soft X-ray source detect., possible old supernova remnant 0-51912  
 hard X-ray sources discovered by HEAO A-2 expt. 0-17690  
 HB 3, supernova remnant, soft X-ray obs. 0-56915  
 HB 9, soft X-ray emission obs. from old SNR 0-36697  
 HD 77581 (4U 0900-40), apsidal motion test of eclipsing binary 0-51908  
 Hercules supercluster, evidence for intracluster medium 0-22092  
 Hercules X-1, search for X-ray polarization 0-4457  
 Hercules X-1 (HZ Herculis), coordinated optical and X-ray pulsations obs. 0-51909  
 high-sensitivity X-ray survey, discrete source contrib. to extragalactic background 0-27016  
 IC 3575, peculiar galaxy possibly 4U 1232+07, HEAO 1 obs. 0-12832  
 BL Lacertae objects, high-energy X-ray obs. 0-31353  
 AD Leonis, X-ray emission from flares, HEAO 1 obs. 0-41837  
 LMC, SNRs identification from Einstein Obs. X-ray meas. 0-26980  
 LMC, X-ray survey using HEAO 1 scanning modulation collimator 0-17648  
 Lupus flare source, Ariel 5 ASM obs. (1979 October 25) 0-8715  
 M31, X-ray sources, obs. 0-26979



**X-ray astronomical observations continued**

- M87, high-resolution X-ray spectroscopy, O VIII emission line detect. 0-26977
- Markarian 501, UV and X-ray obs. of BL Lacertae-type object 0-36717
- MCG 8-11-11, Seyfert galaxy, hard X-ray emission detect. 0-46660
- AT Microscopii, X-ray emission from flares, HEAO 1 obs. 0-41837
- MKW 3s, poor galaxy cluster, extended X-ray emission detect. surrounding cD galaxy (NGC 5920) 0-51884
- MXB 1728-34, type I X-ray burst obs. by (HEAO-1) 0-17692
- MXB 1730-335, new mode of X-ray bursts 0-41915
- MXB 1730-335 (Rapid Burster), steady X-ray emission obs. 0-22119
- MXB 1837+05 (Serpens X-1), detect. of optical burst coincident with X-ray burst 0-27013
- N49 SNR in LMC, X-ray obs. of gamma-burst field 0-27019
- NGC 4151, Seyfert galaxy, hard X-ray emission detect. 0-46660
- NGC 4410a/b, interacting pair, possible HEAO 1 obs. 0-12832
- NGC 5506, Seyfert 2 galaxy, detect. of flare in X-ray emission 0-17656
- OAO 1653-40 area, 38.22 second X-ray pulsations discovery 0-27014
- $\rho$  Ophiuchi dark cloud region, soft X-ray obs. 0-26947
- Orion Nebula, low-luminosity X-ray sources obs., assoc. with star form. 0-26959
- X Persei (3U 0352+30), simultaneous X-ray and ground-based optical obs. 0-17591
- PKS 0548-322, BL Lacertae object, X-ray spectrum 0-17654
- quasars, X-ray properties from Einstein Observatory obs. 0-27004
- Sagittarius, Ariel V obs. of X-ray nova (1979 October-November) 0-12834
- V861 Scorpii (OAO 1653-40?), simultaneous UV and X-ray obs. 0-17616
- Scorpius X-1, high energy X-ray obs. with Ariel V 0-17694
- Seyfert 1 galaxies, HEAO 1 scanning modulation collimator, obs. 0-51859
- Seyfert 1 X-ray emitting galaxies, HEAO 1 spectra 0-51860
- SNRs, electron-ion equilib. and ionization nonequilib., X-ray evidence 0-41879
- solar active regions and X-ray bright points, birthplaces 0-12739
- solar active regions height struct., X-ray obs., OSO-8 limb crossing obs. 0-31280
- solar corona, interconnecting loops sudden brightenings morphology 0-21972
- solar coronal X-ray bright point and small active region fine struct. rapid vars. 0-12741
- solar flare second-stage X-ray emission, spectrum beyond 200 keV 0-51710
- solar flare X-ray spectra, laboratory reproduction in region of Fe XXV-XXVI reson. lines 0-18819
- solar flares, EUV and hard X-ray sources relationship 0-46512
- solar flares, hard X-ray polarization 0-41787
- solar flares, high-resolution X-ray spectra obs. 0-26837
- solar flares, particle acceleration, X-ray and gamma-ray obs. 0-31265
- solar flares X-ray spectra, Fe XXIV-XXV lines wavelengths in 1.85-1.87 Å region 0-21973
- solar impulsive X-ray burst from coronal source, obs. 0-26836
- solar multiply impulsive bursts, hard X-ray and microwave spectral evolution 0-26828
- solar X-ray active regions temp. and emission measure rel. to coronal mag. fields 0-12745
- solar X-ray bright points, obs. rel. to globally variability in solar mag. flux emergence 0-51716
- solar X-ray bright points, short-term temporal vars. 0-12740
- solar X-ray flares, Skylab obs. rel. to physical parameter profiles 0-17561
- spectroscopic binaries, single-line, nature of secondary stars from X-ray obs. 0-31329
- stellar coronae, evidence for existence from X-ray and UV obs. 0-12756
- stellar X-ray sources at high galactic latit., location with HEAO 1 scanning modulation collimator 0-22118
- Sun, 1973 August 14 loop prominence, XUV emission and density 0-56807
- Sun, active region coronal loops, gyroresonance absorption evidence 0-56792
- Sun, slowly moving disturbances obs. in X-ray corona 0-21971
- Sun, soft X-ray bursts, statistical distrib. 0-26839
- Sun, X-ray photometry from Prognostic satellites 0-17462
- supernovae, extragalactic, X-ray bursts search using HEAO-1 satellite 0-46585
- Tycho's SNR, HEAO 1 obs. and structure study 0-51842
- Tycho supernova remnant, Type I SNR, elemental abundances from X-ray spectrum 0-46635
- Tycho supernova remnant, X-ray line emission obs. 0-46636
- 4U 0041+32, hard X-ray outburst, 1970 obs. 0-56976
- 4U 0115+63, absorption line in pulsed hard X-ray spectrum, HEAO 1 obs. 0-27017
- 4U 1206+39 (NGC 4151), hard X-ray variability of Seyfert galaxy 0-17647
- 4U 1232+07, HEAO 1 obs 0-12832
- 4U 1249-28, location and identification with dwarf nova EX Hydrae 0-22118
- 4U 1626-67, 7.7-second X-ray pulsar, simultaneous X-ray and optical obs. 0-51914
- 4U 1702-36, Scorpius X-1 like source, high energy X-ray obs. with Ariel V 0-17694
- 4U 1907+09, X-ray flare obs. during 1980 Jan. period 0-41914
- 4U 2129+47, position and optical identification, evidence for X-ray heating and binary period 0-17693
- 4U 2129+47, X-ray light curve and binary model 0-46704
- Vela supernova remnant, X-ray maps 0-51838
- Virgo cluster, X-ray obs. of galaxies, rel. to dynamical evolution 0-26995
- weak X-ray sources, ANS meas. 0-46701
- X-ray bursters, 1980 plans for simultaneous optical/X-ray obs. 0-8716
- SS Cygni, soft X-ray emission detect. during optical outburst 0-46574
- U Geminorum, soft X-ray emission detect. during optical outburst 0-46574

**X-ray astronomy**

see also X-ray sources (astronomical)

- conference proc. (Innsbruck, 1978 May 29-June 10) 0-36775
- dielectronic recombination spectra, appls. in astronomy 0-46391
- emission lines from Seyfert galaxies and QSOs, hard X-ray effects 0-26974

**X-ray astronomy continued**

- gas scintillation spectrometer for X-ray astronomy, performance characteristics 0-56709
- Hard X-Ray Burst Spectrometer on Solar Maximum Mission 0-51658
- Hard X-ray Imaging Spectrometer on Solar Maximum Mission 0-51659
- HEAO-2, X-ray telescope description, obs. and sources 0-12643
- High Energy Astrophysics Division of Am. Astron. Soc., meeting (Cambridge, MA, 28-30 Jan. 1980) 0-36761
- imaging system, real-time, for solar coronal X-ray obs. from sounding rockets 0-41725
- interstellar gas heating and ionization by X-ray photoelectrons 0-46383
- pulse shape analysers for phoswich detectors in space borne hard X-ray expts. 0-36501
- soft X-ray polychromator for Solar Maximum Mission 0-51660
- solar X-ray photometer on Prognostic satellites, description and meas. method 0-17462
- solar X-ray spectrometer and imager, Space Shuttle 0-17495
- spectroscopy, fabrication of transmission gratings 0-14490
- telescope, appl. of lobster eye optical configuration 0-17491
- X-ray bursters, 1980 plans for simultaneous optical/X-ray obs. 0-8716
- Mg XII, resonance line, atomic parameters calc. for dielectronic satellite lines 0-42983

X-ray characteristic temperature see Debye temperature

**X-ray chemical analysis**

- see also electron probe analysis; X-ray diffraction examination of materials; X-ray fluorescence analysis
- advances, techniques and instrumentation, conference, Denver, USA (Aug. 1978) 0-3447
- air particulate deposits, particle-induced X-ray emission anal., 2 MeV protons 0-45833
- anodic oxide superficial layer, X-ray emission spectrometry and ion back-scattering (French) 0-49482
- biological material, X-ray microanalysis, graphite grids 0-8232
- broadband X-ray excitation, quasi-fundamental correction methods 0-321
- cast Fe, grey and ductile, subsurface defects, SEM and EDAX study 0-44400
- computerised control of powder diffractometer 0-3453
- electrically conductive coating influence on X-ray microanalysis accuracy 0-11988
- electron beam particulate analysis of air samples 0-40785
- electron microprobes and scanning electron microscopy, conf., Orsay, France, Dec. (1978) 0-11979
- electron probe, feldspar minerals from Mt. Rokko 0-31038
- electron spectroscopy, for bulk and surface microscopy and microanal. 0-52367
- elemental analyser, diffractometer based 0-318
- elemental analysis by means of X-ray attenuation measurements 0-50912
- energy dispersive X-ray diffraction method, annotated bibliography (1968-78) 0-36794
- forensic materials anal., problems influencing sample handling 0-3448
- gall bladder stones, human, X-ray anal. 0-36081
- grain boundary segregation, X-ray spectral analysis method, for element distrib. determination 0-21337
- Guinier camera projects, microcomputer automation 0-3454
- Inconel 625, nitriding in N<sub>2</sub>-H<sub>2</sub> glow discharge 0-16590
- kidney stones, human, X-ray anal. 0-36081
- light elements, principles of quantitative microanal. (French) 0-11980
- minimum depth electron probe X-ray microanalysis for determining S content of human hair surface 0-22500
- multiphase unknowns, identification by computer methods and quality of X-ray powder data 0-3452
- mussel trace element monitoring appl. 0-30954
- pigments of Minoan painted pottery, XRF-XRD analysis method 0-35586
- PIXE analysis, MX-ray correction factors calcs., internal standard methods 0-45614
- powders, spray drying to minimize preferred orientation 0-3098
- PVC, chlorinated, X-ray photoelectron spectra investig. 0-3469
- qualitative, with automated X-ray spectrometer 0-22497
- quantitative, of solid phases (German) 0-3446
- radioactive materials, X-ray diffr. studies 0-3450
- refractories, castable, X-ray powder diffr. meas. of phase composition, and flexural strength 0-3449
- scanning electron microscope appl., energy dispersive vs. wavelength dispersive concepts 0-16739
- small particles, characterisation and microanal. by STEM combined with other techniques 0-50901
- spectra analysis, energy-dispersive, with aid of computer 0-3433
- steel, austenitic, Cr-Ni, nonmetallic inclusions modification using rare earth metals (Russian) 0-40369
- steel, austenitic, Cr-Ni-Mn-V, X-ray anal. of carbide phases formed during ageing (Russian) 0-20936
- steel, austenitic, non-oxidising, B and by secondary ion emission and X-ray microanal. (French) 0-11985
- steel, austenitic stainless, X-ray microanalysis of C (French) 0-11981
- steel, austenitic stainless FV548, neutron irradiated, Si-rich phase occurrence of M<sub>6</sub>C phase 0-15156
- steel, commercial alloy ferritic, meas. of alloy and impurity elemental distrib. using STEM 0-35601
- steel, stainless, ferritic, passivity in 1N HCl, X-ray photo-electron spectroscopic study 0-11817
- surface and bulk microanalysis, electron spectroscopy apparatus (French) 0-47151
- thin foils, chem. anal. by electron microscopy (French) 0-50899
- trace element transport meas. during haemodialysis by PIXE 0-36102
- ultramicroanalysis, single grain oscillating crystal method (Chinese) 0-21332
- X-ray phase analysis, rapid phase anal. methods, using DRON-1 diffractometer 0-22489
- Al brass condenser tubes, XPS study of protective layers 0-35383
- Au-Cu-Cr, thin layer, deposited on glass or Si substrate, X-ray microanalysis (French) 0-50902
- CdTe, trace anal. by heavy ion induced X-ray emission and SIMS 0-55755
- Cs-Sn alloy, peritectic reactions, phase diagram (Russian) 0-40784
- Es compounds, X-ray powder diffr. 0-2002
- <sup>59</sup>Fe/<sup>55</sup>Fe activity ratio of blood, meas. using semicond. detector 0-17062
- GdCl<sub>3</sub>·6H<sub>2</sub>O, thermal decomp., X-ray emission luminesc. (Japanese) 0-55763
- LiBO<sub>2</sub>-In<sub>2</sub>O<sub>3</sub>, phase composition, mag. props, elec. cond. 0-55365



**X-ray chemical analysis continued**

- Ni<sub>3</sub>Al-Ti(Cr)(Fe)(Zr)(Mo)(W), powder, X-ray spectral analysis exam. 0-16239  
 Pb content in blood, PIXE determination 0-51228  
 Pd-Ag, thin layer, deposited on glass or Si substrate, X-ray microanalysis (French) 0-50902  
 Si(Li) detectors, escape peak losses 0-27383  
 SiO<sub>2</sub>-base cores, for superalloys, high temp. characterisation 0-10640

**X-ray crystallography**

- For results of structure analysis see crystal atomic structure  
 see also X-ray crystallography apparatus; X-ray crystallography calculation methods; X-ray crystallography technique  
 anomalous X-ray scattering 0-54075  
 atom form factors of different atomic models, fitting theoretical struct. factors by varied temp. factors 0-1882  
 coherent scattering by crystal, photon model 0-24309  
 deformation density approach to cryst. orbital calc., transferable integrals, X-ray crystallographic meas. 0-38993  
 diffraction lines distorted profile, determ. of maxima positions 0-24307  
 diffraction topography, introduction (Chinese) 0-1883  
 disordered crystals, 2H to 6H solid state transformation, deformation mechanism, X-ray diffraction study 0-33921  
 disordered crystals, 2H to 6H solid state transformation, layer displacement, X-ray diffraction study 0-33920  
 energy-dispersive diffractometry meas. on large crystals, expts. on GaAs 0-1888  
 high energy resolution X-ray spectroscopy, review 0-14959  
 imperfect crystals, asymmetric limits of X-ray scattering in Bragg case 0-33853  
 integrated intensities, in secondary extinction theory 0-49043  
 Laue patterns, cylindrical, flat transmission or flat back-reflection Laue photographs, calc. of crystal orientation 0-19670  
 Laue patterns and stereographic projections, Laue back-reflection techniques, plot program PLOMAC 0-19669  
 phase analysis, quantitative, methods of mixing 0-24317  
 polarisation states, of dynamically diffr. X-ray beams in Laue case 0-28878  
 polycrystalline material, substitutionally disordered, domain size rel. to diffr. 0-28871  
 polycrystalline materials, size and angular spread of coherently reflecting regions, X-ray microdiffraction method 0-24311  
 powder diffraction data, American Crystallographic Association recommendations for standardisation (Czech) 0-24306  
 powder patterns for tetragonal and hexagonal polycrystalline materials, improved indexing method 0-24312  
 quartz, bent perfect crystal, diffractational focusing, X-ray spectroscopy (Russian) 0-54076  
 scattering factors of ions in crystals, Watson sphere model, Hartree Fock Roothan method 0-49046  
 semiconductor, Bragg X-ray diffr. in elastically bent cryst. 0-24310  
 spectral instability of four wave coplanar X-ray diffr. (Russian) 0-33855  
 superlattice, 1D, kinematic and dynamic X-ray diffr. 0-33854  
 superlattices, one- and two-dimens., possibility of X-ray and electron diffr. struct. determ. 0-54560  
 theory (Chinese) 0-44072  
 thin films,  $1 \sim \sin^2 x/x^2$  intensity eqn. verification (German) 0-19668  
 two-crystal system with non-diffracting zone, X-ray interferogram fine struct. 0-1887  
 X-ray interferometer, temp. gradient influence on fringe pattern 0-1896  
 Si, elastically bent crystal, with large strain gradient, X-ray diffraction study 0-44073

**X-ray crystallography apparatus**

- see also goniometers; X-ray diffractometers; X-ray monochromators  
 automatic scanning system for multiple-sample Guinier X-ray powder diffraction films 0-22492  
 Buerger precession camera, diffuse X-ray scatt. meas. (Japanese) 0-49049  
 capacitance-based micropositioning system for X-ray rocking curve measurements 0-205  
 cryostat, liq. He, for collection of 3-dimensional X-ray intensity data down to 20K 0-22369  
 double focusing X-ray camera, use with synchrotron radiation 0-313  
 high-pressure energy dispersive X-ray diffr., miniature piston-cylinder apparatus 0-38870  
 hot microdeformation, and simultaneous X-ray topography apparatus (French) 0-38871  
 position sensitive detector for fast X-ray powder diffr. 0-319  
 powder diffraction, computer automation 0-1899  
 rotation camera data, empirical method correction for absorpt. and decay effects 0-14962  
 shielding arrangement, for diffr. equipment 0-849  
 topogram visualisation raster tube with shoot-through target 0-31956  
 two crystal spectrometer, small angle X-ray scatt. obs. 0-54077

**X-ray crystallography calculation methods**

- absorbing perfect crystal, temp. depend. of X-ray reflection intensity near absorpt. edge 0-1889  
 absorption, in single-crystal diffractometry, calc. program 0-38874  
 absorption correction, and normalisation of X-ray small angle scattering data for materials producing intense scattering at extremely low angles 0-19671  
 Bond method, of meas. lattice parameters, asymmetric Bragg reflections appl. 0-38861  
 Bragg reflections, ang. positions calcs. by computer program 0-38863  
 broadening errors, in deconvoluted X-ray diffr. line profiles 0-38862  
 centrosymmetric electron density distributions, direct determ. by maximising integrated cube of electron density 0-10453  
 computer simulation, of X-ray traverse topographs, on basis of Green function method 0-49044  
 crystal structure analysis, separation of unknown parameters 0-28869  
 crystallites, curved with layer shifts, diffracted intensities 0-28879  
 diamond, directional Compton profiles, X-ray scattering factors and 1-electron density matrix 0-10458  
 diffraction-profile Fourier analysis, determ. of microstruct. parameters 0-49042  
 direct methods, survey as number and kind of solved acentric equal atom structs. 0-38865  
 direct procedures, triplet and quartet rels. 0-24305  
 disordered crystals, 1D, structure in formation from diffuse reflexions (German) 0-10459

**X-ray crystallography calculation methods continued**

- distorted crystal, X-ray intensity mode oscils., two wave WKB approx. calcs. 0-28876  
 Gauss-Seidel least-square refinement, procedure with rigid-group and parameter restraint capabilities 0-10455  
 haemoglobin, sickling deer type III, macromol. struct. refinement by restrained least-squares and interactive graphics 0-28870  
 integrated intensities, from a noncentrosymmetric cryst. near absorpt. edge, thermal vibr. effect 0-1884  
 integrated intensities, in secondary extinction theory 0-49043  
 lattice parameter determ. by X-ray multiple diffr. study, analytical and graphical methods (Russian) 0-10460  
 LCAO calculation, of temp. effects on X-ray scattering factors of crystals. 0-10454  
 line profile analysis, in theory of fine structures 0-33852  
 multiphase X-ray scatterers, randomness in two- and three-phase systems 0-19667  
 orientationally disordered structures, orientation and position correlations of a mol. 0-14966  
 orientationally disordered structures, positive definiteness of orientational distrib. functions 0-14958  
 oscillation method, for cryst. with large unit-cells, determ. of relevant parameters 0-14961  
 particle-size distribution functions, determ. from SAS data by indirect transformation method 0-38860  
 phase extension, and refinement 0-14963  
 polycrystalline material, substitutionally disordered, domain size rel. to diffr. 0-28871  
 powder diffraction data, search-match system 0-28874  
 powder least-squares program, POWLS 0-1892  
 powder technique, trial struct. generating program for determ. of crystal struct. 0-28881  
 preferred orientation, in tetragonal powders, X-ray intensity corrections 0-1880  
 primary extinction, for cylindrical finite crystals. 0-24300  
 programmable calculator use for students in crystallographic comput. 0-36811  
 protein structures, Fourier refinement 0-51037  
 proteins, minimisation of functions of many variables appl. to X-ray struct. anal. 0-3589  
 radial autocorrelation function, significance in X-ray diffr. patterns 0-51048  
 radial distrib. anal., computer program 0-28875  
 radial distribution functions, for liqs. and amorphous substances, analytical computation method 0-24301  
 radial distribution functions, quasi-crystalline model 0-1879  
 reciprocal squares of lattice parameters, determ. by solving linear eqns. (German) 0-10452  
 rotation camera data, empirical method correction for absorpt. and decay effects 0-14962  
 saddle point method, for SAXS anal., error reduction 0-38868  
 segment description, of unique set of reflections to data collection and data reduction 0-1881  
 short-range order parameters, AC-BD, X-ray diffr. determ. 0-38875  
 single-crystal diffractometry, peak searching, crystal setting and determining automatic cell constants 0-6319  
 SIR program, use of negative quartets 0-24304  
 small angle scatt. depend. on divergence (French) 0-49045  
 small angle scattering, curve anal., by triaxial body models using graphic display model 0-28873  
 small angle X-ray scatt., slit height smearing correction prog. 0-10456  
 small angle X-ray scatt., slit height smearing correction prog. 0-10457  
 spherical crystals, mean path length of X-rays weighted by absorpt. 0-28877  
 spherical X-ray wave, dynamic diffr. theory, numerical results 0-38867  
 STRUKTURA, program system for cryst. struct. investigations 0-44071  
 superlattice, 1D, kinematic and dynamic X-ray diffr. 0-33854  
 tetragonal powders, X-ray intensity corrections for preferred orientation 0-1880  
 Vavilov-Cerenkov parametric effect, to use in cryst. struct. investigation 0-1895  
 Ge, directional Compton profiles, X-ray scattering factors and 1-electron density matrix 0-10458  
 LiH crystals, temp. effects on X-ray scattering factors in LCAO calcs. 0-10454  
 Si, directional Compton profiles, X-ray scattering factors and 1-electron density matrix 0-10458  
 Ti-S system, nonstoichiometric, containing stacking faults, X-ray diffr. intensity distrib. calc. 0-28872  
 ZnS, cubic crystals, having substitutional elastic distortion centres, diffuse X-ray scattering 0-24302

**X-ray crystallography technique**

- azimuthal scanning method, allowance for X-ray absorpt. in single-crystal diffractometry 0-38874  
 crystal centering, and diffractometer alignment errors calcs., appl. to high pressure crystallography 0-22494  
 diffuse X-ray scatt. meas. by stationary use of Buerger precession camera (Japanese) 0-49049  
 dislocation image in X-ray plane wave topography, computer simulation 0-54234  
 disordered crystals, 1D, structure in formation from diffuse reflexions (German) 0-10459  
 energy dispersive X-ray diffraction method, annotated bibliography (1968-78) 0-36794  
 extended deformation fields, X-ray diffr. meas. method sensitivity 0-28880  
 grain boundary thickness, meas. using X-ray techniques 0-34011  
 high angle double crystal diffractometry, improvement for meas. temp. depend. of lattice constants, pt.I 0-1890  
 high angle double crystal diffractometry, temp. depend. of lattice constants, pt.II 0-1891  
 lattice deformations, determ. by pendellosung X-ray fringes 0-54078  
 microcrystal size meas. 0-38872  
 multiple scattering, secondary reflections and their interference 0-33856  
 oscillation camera data, processing and post-refinement 0-24316  
 oscillation method, for cryst. with large unit-cells, determ. of relevant parameters 0-14961  
 powder, Guinier camera, film densitometry and pattern search-match procedures appls. 0-3454  
 powder diffraction data, search-match system 0-28874



**X-ray crystallography technique continued**

- proteins, minimisation of functions of many variables appl. to X-ray struct. anal. 0-3589  
 quantitative structural studies by means of the energy-dispersive method with X-rays from a storage ring 0-24314  
 randomised X-ray powder diffraction patterns, adjustable sample holder 0-6317  
 Rietveld profile refinement method, anal. 0-24315  
 rotation camera data, empirical method correction for absorpt. and decay effects 0-14962  
 sample preparation methods, survey 0-1898  
 silicate mineral, identification and asbestiform varieties, electron optical and X-ray techniques 0-8446  
 single-crystal plates deformations meas., using four-crystal X-ray spectrometer 0-49048  
 synchrotron radiation source for electronic states and struct. anal. (Chinese) 0-44075  
 texture topography (German) 0-1894  
 textures materials, residual stress evaluation by X-rays (German) 0-40670  
 topograph recording, of large cryst. slices, geometrical conditions 0-38869  
 Vavilov-Cerenkov parametric effect, to use in cryst. struct. investigation 0-1895  
 white radiation methods using synchrotron sources 0-44076  
 Cu, single crystal sintering model evaluation, Kossel interference and digital graphic simulation appl. (German) 0-2980

**X-ray detection and measurement**

- see also *X-ray spectrometers*  
 CAMAC, 2-D anal. of spectroscopic data, electronics 0-5460  
 computerised tomography, effective photon energy and linearity meas. 0-30841  
 computerised tomography, software balancing of multiple detectors during CT scanning 0-46026  
 crystal spectrograph with active readout 0-4826  
 dose mean value of specific energy, variational meas. 0-12276  
 dosimetry, appl. of cavity theory 0-13947  
 fluorescence spectra, detector response function approach in least squares anal. 0-11989  
 free air chamber for X-ray exposure standardisation at high quantum energies 0-14053  
 gas scintillation counter, for high count rate X-ray detection 0-14052  
 gas scintillation drift counter for fast X-ray detection 0-888  
 gas-filled electroluminescent detector for soft X-rays, constr. and characts. 0-32569  
 lightning, thermoluminescent dosimetry measurement of radiation 0-36361  
 metal screen-film detector MTF at megavoltage X-ray energies 0-30868  
 metal screen-film detectors, radiographic contrast obs. 0-30866  
 muscle contraction, time-resolved X-ray diff., data-collection system (Japanese) 0-46108  
 orthovoltage X-ray therapy, TLD dose intercomparison 0-12272  
 photographic film response to 25 MV X-rays, sensitometric curves, relative dosimetry 0-52376  
 position-sensitive detector incorporating self-scanning Si photodiode array 0-52831  
 position-sensitive scintillation detector for portable stress analyser 0-13190  
 primary standard for determination of absorbed dose in water for X-rays generated at potentials of 7.5 to 30 kV 0-5354  
 radiography, diagnostic, X-ray spectra determ., high intensity 0-41217  
 radiography beam characteristic time vars. meas. using solid state devices 0-46048  
 radiotherapy, high-energy accelerators, mixed photon-neutron field meas. 0-51267  
 thickness measurement, determ. by continuum integration 0-31713  
 transitional emission detector, electron identification in cosmic ray background, X-ray detection study 0-4213  
 ultrasoft X-ray burst fluence, using fast, large-signal, free-standing foil bolometer 0-4770  
 X-ray fluorescence anal. by total reflection (German) 0-30314  
 Bi<sub>12</sub>SiO<sub>20</sub> photoelectret, in optical processing and X,  $\gamma$  ray imaging 0-23764  
 CaSO<sub>4</sub>:Dy Teflon TLD discs, metal filters for compnesation of photon energy depend. 0-30901  
 CdS monocrystalline sputtered X-ray transducer characteristics (Russian) 0-47162  
 CdTe detectors, X-ray fluorescence escape peaks in X-ray spectra 0-9448  
 Se, X-ray sensitivity, induced photocurrents, xeroradiographic meas., pair creation energy 0-22490  
 Si-Li surface-barrier detectors for electron and soft X-ray spectrometry 0-882  
 Si(Li) detector response function approach in least squares anal. of X-ray fluorescence spectra 0-11989  
 Si(Li) detector system, discrepancies in X-ray excitation efficiencies 0-9450  
 Si(Li) detectors, escape peak losses 0-27383  
 Si(Li) photopeak efficiency meas., 0.52-8.04 keV 0-27889  
 Si(Li) X-ray detector, efficiency calibration in 1.5 to 60 keV energy range 0-47823  
 Si(Li) X-ray spectrometer, development, and interdisciplinary appl. (Hungarian) 0-18056  
 X-ray dosimetry, intercomparison and standardisation 0-12270

**X-ray diffraction**

- see also *X-ray crystallography*; *X-ray diffraction examination of materials*; *X-ray diffractometers*; *X-ray scattering*  
 synchronous nonlinear interaction between waves on Bragg diff. in media with periodic struct. (Russian) 0-14399  
 time resolved, muscle contraction kinetics obs., appl., with aid of computer (Japanese) 0-56291

**X-ray diffraction examination of liquids**

- see also *liquid structure*  
 alkali chlorides, aq. soln., ion-solvent and solvent-solvent interactions, X-ray obs. 0-44107  
 cholesteryl methyl carbonate, liq. cryst., low-ang. X-ray diff. obs., solid and liq. 0-49093  
 industrial wastes, Mg recovering, use of sink-and-float test (Japanese) 0-55948  
 ion-water interactions, survey of diff. studies 0-24347  
 ionic liquids, struct. determ., summer school lecture series 0-6349

**X-ray diffraction examination of liquids continued**

- lyotropic mesophase, mag.-oriented, X-ray diff. obs. 0-1921  
 lyotropic nematic liquid crystals, mag. susceptibility, mol. aggregation meas. 0-19690  
 4-nitrophenyl-4'-alkoxybenzoates, incommensurate smectic A phase 0-10647  
 4-n-octyloxybenzoyloxy-4'-cyanostilbene, re-entrant polymorphism, nematic-smectic A-nematic-smectic A, X-ray study 0-34172  
 organic liquid, simple, struct. exam. and scatt. data interpret. 0-54096  
 4-pentylphenyl-4'-benzoyloxybenzoate/TBBA system, smectic A<sub>1</sub>-smectic A<sub>2</sub> transition, X-ray diff. obs. 0-44303  
 polyisobutene solns., X-ray scatt., Kratky cone collimation 0-19681  
 polyisocyanides, solns., struct. and acidification 0-19915  
 polystyrene-polyisoprene two-block copolymer soln., conformation, small angle neutron scattering, X-ray diffraction, review (Rumanian) 0-6348  
 radial distribution functions, method of reducing termination errors 0-24332  
 TBPA, liq. cryst., smectic F phase, X-ray diff. obs. 0-44122  
 AlCl<sub>3</sub>, aq. solns., order phenomena, X-ray diff. obs. 0-1915  
 AlPO<sub>4</sub>, high temp. behaviour up to liq. state, phase relations, X-ray diff. and therm. anal. study (French) 0-10660  
 CaCl<sub>2</sub>·6H<sub>2</sub>O, liq., structural order 0-33871  
 Co melt, struct. charact. time depend. in X-ray studies (Russian) 0-24350  
 Fe, liq., short-range order struct., O impurity influence (Russian) 0-38901  
 Fe-C melt structure, X-ray diff. study (Russian) 0-19685  
 Fe-Co melt, volumetric characts., molar volume conc. depend. density (Russian) 0-33873  
 FeCl<sub>3</sub>, solns. and hydrated melts, complexes form., X-ray diff. obs. 0-24342  
 Hg, liquid structure, X-ray diff. obs., 173-473K 0-14997  
 Hg-K, liquid, structure factors, X-ray scatt. (Japanese) 0-54122  
 Hg-Na, liquid, structure factors, X-ray scatt. (Japanese) 0-54122  
 K<sub>2</sub>SO<sub>4</sub>, molten, struct. analysis using X-ray scatt., correl. with cryst. struct. 0-10486  
 Mg-Bi melt; X-ray and neutron diff., conc. depend., correl. number and nearest neighbours 0-49091  
 Ni melt, struct. charact. time depend. in X-ray studies (Russian) 0-24350  
 SbCl<sub>3</sub>, liquid, neutron X-ray diffraction pattern and models 0-38893

**X-ray diffraction examination of materials**

- for results of crystal structural analysis see *crystal atomic structure*  
 see also *X-ray chemical analysis*; *X-ray diffraction examination of liquids*; *X-ray diffraction examination of microstructure*; *X-ray diffraction examination of molecular structure*  
 actinide pnictides, single cryst. and film growth by CVD 0-16165  
 adamantane, Ising, diffuse scatt., hard-core correl., weak-graph method 0-49137  
 adamantine ceramic, structural, thermophysical and electrophysical props. 0-6918  
 Ag-Cu fibre composites, highly deformed, lattice defects, X-ray interference lines anal. 0-10559  
 p-alkoxy-phenyl-p-acryloyloxy benzoate polymers, mesomorphic struct. 0-38905  
 alloys, concentrated, local atomic arrangements, associated with ordering, review 0-50632  
 amorphous alloy, and metastable phases, cryst. kinetics, review (Japanese) 0-38912  
 amphiphilic-polymer liquid crystal, NaCl conc. influence on struct., X-ray diff. study 0-44126  
 andalusite, shock-loaded, deform. 0-19873  
 aniline-HBr, ferroelasticity, orthorhombic to monoclinic phase transition, X-ray scatt. 0-39276  
 astigmatic X-rays, diaphragm for investigating materials by this method 0-25935  
 biological sample analysis, nanosec. X-ray diff. pattern techniques 0-26429  
 biological structural determinations using synchrotron X-rays 0-46112  
 biomembrane struct. parameters determ. method 0-30948  
 $\alpha$ - $\beta$ -brass, two phase biccrys., deform. and fracture at 150K 0-16388  
 $\alpha$ -brasses, cold worked, atomic diffusion kinetics to stacking faults, Laplace transformation method 0-19977  
 caesium propanoate, solid state transitions and melting process, diff. and conductometric meas. 0-10670  
 carnauba wax, thermoelectret, lattice parameter changes at elevated temps. 0-29674  
 carnauba wax electrets, residual strain and crystal size of orienting crystallites and their effect on charge behaviour 0-11319  
 carnauba wax thermoelectret, charge behaviour 0-7276  
 ceramics, local atomic arrangements, associated with ordering, review 0-50632  
 Ceylon graphite, randomised X-ray powder diffraction patterns, adjustable sample holder 0-6317  
 Cu<sub>1-x</sub>Mo<sub>x</sub>S<sub>8</sub>, superconducting state, triclinic struct., X-ray powder diff. anal. 0-6388  
 DL-cysteine, phase transition obs. at 10°C (French) 0-49355  
 diamond (113), scattering factor, Bragg reflection Pendellosung interference study 0-1885  
 ferrite spinel films, LPE growth and props., SIMS, X-ray diff., and spin wave reson. obs. 0-34323  
 ferrite spinels, normal and inverse, solid state chem. expts. for students 0-36815  
 2-fluoronaphthalene, disordered form, thermal expansion, neutron and X-ray diff. study 0-24621  
 gall bladder stones, human, X-ray anal. 0-36081  
 gem stones, synthetic prep. X-ray studies for optimum conditions of heat treatment 0-45263  
 glass, struct. determ. using EXAFS 0-45169  
 graphite intercalation compound C<sub>24</sub>K, order-disorder transition, X-ray study 0-33922  
 graphite intercalation compounds, low energy optical transitions, refl. spectra, and X-ray diff. 0-25371  
 graphite intercalation compounds, X-ray struct. factor meas. applications 0-54207  
 graphite-like materials, orientation, exam. of preferred functions 0-1945  
 high energy resolution X-ray spectroscopy, review 0-14959  
 Inconel 600, PWR primary corrosion products 0-13578  
 Invar, magnetic and thermal anomalies 0-34603  
 kidney stones, human, X-ray anal. 0-36081



**X-ray diffraction examination of materials continued**

- liquid crystals, struct. and optical props., neutron and X-ray diffr. obs. 0-24323
- lunar regolith particles in Earth's atmosphere, variation in chemical composition in surface layers (*Ukrainian*) 0-12685
- metallic glass, bulk and surface properties, review 0-44147
- metals and alloys, crystn. process, X-ray fluoroscopic obs. 0-50620
- meteorite Zaisho, Japanese pallasite, mineralogical and petrographical study 0-46509
- mixes, ordered, characterisation 0-16215
- multiphase unknowns, identification by computer methods and quality of X-ray powder data 0-3452
- NMP-TCNQ, X-ray diffuse scatt., and cond. study 0-49701
- nylon 6, oriented glassy, mol. wt. influence on cryst. rate 0-44156
- Nylon-6, shish-kebab struct., obtained from quiescent soln. by self seeding 0-15017
- Nylon-6 fibre, crystal struct., WAXS obs. 0-15015
- obsidian, Lipari and Teotihuacan origin, Mossbauer, magnetisation, X-ray diffr. and fluoresc. study 0-46173
- one-dimens. ionic conductor, modulation and incommensurability 0-19980
- order-disorder structures, X-ray powder patterns features 0-38864
- orientationally disordered cryst., diffuse scatt., hard-core correl., weak-graph method 0-49137
- perlite, low temp., processes occurring during firing 0-11607
- Permalloy RF sputtered films, struct.-sensitive mag. props. 0-34705
- PET fibres, amorphous, exam. of birefringence 0-11360
- $\alpha$ -phenazine, multiple scattering, secondary reflections and their interference 0-33856
- piperidine solution of  $\text{PbI}_2$ , crystn. of intercalation cryst. 0-16170
- PMMA, atactic, elastic strain detection by X-ray scatt. 0-25751
- poly( $\gamma$ -n-amylyl L-glutamate), crystal transition, X-ray diffr. exam. of structure 0-24374
- poly( $\gamma$ -n-butyl L-glutamate), crystal transition, X-ray diffr. exam. of structure 0-24374
- poly( $\gamma$ -n-ethyl L-glutamata), crystal transition, X-ray diffr. exam. of structure 0-24374
- poly( $\gamma$ -n-propyl L-glutamate), crystal transition, X-ray diffr. exam. of structure 0-24374
- poly(tetramethylene terephthalate), struct., X-ray obs. 0-19725
- poly(vinylidene fluoride) films, piezoelec. response depend. on phase I vol. fraction 0-20593
- poly(vinylidene fluoride) films, poled, piezoelec. activity and field-induced cryst. struct. transitions 0-20592
- $\beta$ -poly(vinylidene fluoride) films, single cryst. orientation, piezoelec. 0-20591
- polyacrylonitrile, copolymerisation with poly-2-hydroxyethyl methacrylate rel. to crystallinity 0-38935
- polyacrylonitrile, single cryst. formation, during soln. polymerisation, struct. determ. 0-38938
- polyamide blends, formation by injection moulding, structs. (*Russian*) 0-44155
- polybutene-1 film, deform. mechanism, rheo-optical meas. 0-21041
- polybutene-1 film, tubular-extended, anal. of orientational and form birefringence 0-29712
- polycrystalline materials, size and angular spread of coherently reflecting regions, X-ray microdiffraction method 0-24311
- polycrystals, single phase, stress strain relations by X-ray diffraction (*Russian*) 0-5999
- polyesters, thermotropic, quiescent crystn. 0-38937
- polyethylene, crystn. under high pressure 0-38946
- polyethylene, doubly oriented, low density, deformation and structure, exam. 0-11705
- polyethylene, fibrillar, high mol. wt., oriented crystallisation, heat treatment effect (*Japanese*) 0-25738
- polyethylene, high- and low-density, crystallinity degree, comparative obs. (*Polish*) 0-1943
- polyethylene, linear, crystallised from melt, effect of crystallisation time on density, mech. props., X-ray scattering 0-25680
- polyethylene, linear, glass transition temp. 0-15225
- polyethylene, low density,  $\alpha$  mgch. dispersion in relation to spherulite deform. mech. 0-25781
- polyethylene, nascent, electron microscope study 0-38940
- polyethylene, solid-state extruded, exam. of props. 0-11669
- polyethylene, ultra-high-strength filaments, soln. spun/drawn, mech. and thermal props. 0-40440
- polyethylene crystal, longitudinal growth in flowing soln., melting of continuous fibrillar crystal 0-19917
- polyethylene fibres, high density, ultra oriented, physical, mech. props. 0-25649
- polyethylene fibril, high mol. wt., high melting point crystal (*Japanese*) 0-38954
- polyethylene terephthalate-co-isophthalate, gelation and crystallization 0-24377
- polyethyleneterephthalate, crystallised from thin layer melts, temp. depend. of morphology 0-54149
- polyhexamethylene adipamide, calorimetric, X-ray and IR study 0-10512
- polyimides, DFOFP and DFOB, X-diffr. exam. of structure and elasticity 0-6370
- polyisobutylene fibres, stretched, crystn. kinetic study using synchrotron radiation 0-33909
- polymers, diffuse boundary thicknesses, determ. by small angle X-ray scattering 0-38947
- polymers, Fourier anal. of X-ray diffr. patterns 0-15016
- polyoxymethylene, drawn, extra meridional reflections 0-24376
- polyoxymethylene, ultrahigh modulus oriented, exam. of true crystal modulus, from -150 to 20°C 0-11687
- polyoxymethylenes, determ. of crystalline fraction from X-ray diffraction 0-44150
- polysiloxane dizwitterionomers, morphology, ionic aggregation 0-49130
- polystyrene, isotactic, orientation of remaining amorphous chains during crystallisation 0-10506
- polystyrene amorphous film, cyclically fatigued, molecular behaviour 0-35310
- polystyrene filament, melt spun, struct. and mech. props., effect of drawing, twisting, annealing, untwisting 0-45331
- polyvinylidene fluoride, struct. study, piezoelec. and pyroelec. props. 0-7300
- polyvinylidene fluoride, X-ray high press. study 0-6369
- polyvinylidene fluoride film, uniaxially stretched and corona poled, piezoelec. meas. 0-25311

**X-ray diffraction examination of materials continued**

- potassium oxalate, anhydrous, phase II, vibr. spectra and cryst. struct. 0-34901
- powder specific surface, X-ray determ. method 0-47012
- proteins, globular, crystalline, intermol. interactions, denaturation, DSC and X-ray diffr. obs. 0-16897
- PVC, rigid, microdomains, small angle X-ray scattering study 0-28930
- PVDF, film, polymorphism induced by poling and annealing 0-24372
- $\gamma$ -quartz, reaction, with NaCl-KCl melt, exam. of struct., IR absorption spectra 0-55706
- quartz c-axis orientation in Saxony Granulites, petrofabric anal. by optical and X-ray diffr. studies 0-21740
- quartz plates, acoustic reson. vibr., Berg-Barrett X-ray diffr. method 0-40063
- radiation induced defects, review (*Japanese*) 0-15152
- radioactive materials, X-ray diffr. studies 0-3450
- rare earth oxyphosphates,  $x \text{Ln}_2\text{O}_3 \cdot y \text{P}_2\text{O}_5$ , synthesis, characterisation and thermal stability 0-16256
- refractories, castable, X-ray powder diffr. meas. of phase composition, and flexural strength 0-3449
- refractory metal films, evaporated, optical props., rel. to struct. 0-55211
- roll surface damage eval. by X-ray diffr. technique (*Japanese*) 0-25892
- rubidium propanoate, solid state transitions and melting process, diffr. and conductometric meas. 0-10670
- Sialon, prep. and charact. of ultrafine powders 0-11604
- SiAlON X-phase, X-ray diffr. data 0-49198
- silicate mineral, identification and asbestiform varieties, election optical and X-ray techniques 0-8446
- silk fibroin films, conformational changes induced by water immersion 0-10498
- slurries, solids content determ. by X-ray scatt. 0-3467
- small particles, cause of reduction in lattice spacing (*Russian*) 0-38967
- steel, alloy, type Kh16N11M3, struct. changes during thermocyclic working, dislocation struct. (*Russian*) 0-54243
- steel, alloy type 25KhN3MFA, tempering of bainitic structure 0-20983
- steel, austenitic stainless, Ni-alloyed,  $\text{Cr}_2\text{N}$  precipitation, interface struct. and morphology 0-11644
- steel, C, failure mechanisms in impact fatigue 0-40493
- steel, Cr ferritic stainless, meas. of alloy and impurity elemental distrib. using STEM 0-35601
- steel, Cr-Mn, metastable constitution diagram and phase transforms. (*Russian*) 0-50590
- steel, Cr-Mo low alloy ferritic, meas. of alloy and impurity elemental distrib. using STEM 0-35601
- steel, heat treated high strength, X-ray diffr. anal. of residual stress 0-3200
- steel, low C fatigued, appl. of microbeam X-ray technique to plastic zone size evaluation 0-3199
- steel, martensitic, age hardening with Cu, Nb additions, exam. of hardness 0-7681
- steel, mild, AISI 1009 and 1018, corrosion incipient processes in hypersaline geothermal brine at 90°C 0-50753
- steel, Mo and Cr-Mo, X-ray elasticity constants at high specimen temp. (*German*) 0-35239
- steel, plain C, type 304 and type 316 stainless, fatigue damage indicators, non-destructive 0-25932
- steel, Si-Cr-Mo-W-V (2.4,1.3,2 wt.%), heat treatment and props. 0-16349
- steel, stainless, austenitic,  $\text{H}_2$  induced transformation obs. (*Japanese*) 0-11640
- steel, stainless, PWR primary corrosion products 0-13578
- steel, stainless type 316,  $\text{M}_{23}\text{C}_6$  carbide precipitation, intermetallic phases, X-ray diffr. study 0-7586
- steel, W-Mo, types R6M5 and R6M5K5, decarburising layer evaluation 0-21164
- steels, high-purity and commercially based, containing 10 wt.%W or 5 wt.%Mo, tempering behaviour 0-7600
- stress meas., residual, use of position sensitive proportional counter (*Japanese*) 0-11853
- succinonitrile, plastic, diffuse scatt., hard-core correl., weak-graph method 0-49137
- $\text{TaS}_2$ , amine intercalation, water effects, X-ray diffr. meas. 0-44178
- TCNQ complexes with ferrocenes, charge transfer type, struct. and mag. props. 0-24439
- TCNQ salt,  $(\text{NMe}_3\text{H})(\text{I})(\text{TCNQ})$ , one-dimens. semicond. with metal-like cond. 0-24909
- TCNQ salt,  $(\text{TSeF})_x(\text{TTF})_{1-x}\text{-TCNQ}$ , struct., elec. and mag. props., review 0-20158
- TCNQ salt,  $\text{TSeF-TCNQ}$ , Peierls transition and CDW ordering, X-ray study 0-20101
- Teflon foils, cryst. struct. and texture changes due to polarisation process (*Polish*) 0-35209
- textured sheet metals, X-ray diffr. anal. 0-6316
- thermoplastics, structural changes during deformation, rel. to impact resistance 0-25800
- thin foils, chem. anal. by electron microscopy (*French*) 0-50899
- torbermorite study by X-ray line profile anal. (*Japanese*) 0-33984
- transuranic chalcogenides and pnictides, prep. and cryst. chem. 0-16255
- TSeF-TCNQ, Kohn anomaly of metallic state, X-ray diffuse scatt. meas. 0-19887
- TTF-Cu bis-dithiolene, dimer, mol. displacements at 4.2K 0-10539
- VPE, growth processes, in-situ obs. (*Japanese*) 0-35104
- YIG, hot spraying to give fine, free flowing, sinterable powder 0-20865
- Zircaloy, PWR primary corrosion products 0-13578
- Ag, Debye temperature correlations at high temp. 0-15210
- Ag/Al thin film couples, diffusional alloying, Kiessig X-ray interf. obs. 0-10713
- Ag-Al, short-range order, X-ray and electron diffr. study 0-54173
- Ag-CdO cermets, coprecipitated carbonates and hydroxides, physicochem. props. 0-25706
- Ag-Ga(In) thin film couples, room temp. interactions, X-ray powder patterns 0-2220
- Ag-Ge-S glasses, X-ray determ. of struct. (*Japanese*) 0-10501
- Ag-Sn (6(8.2)(11) wt.%), splat-quenched, X-ray line broadening 0-40397
- AgI solid electrolyte  $\alpha$ -phase stabilisation 0-29209
- $\alpha$ -AgI, superionic phase, struct., X-ray scatt. anal. 0-28983
- B-AgI, X-ray diffuse scattering 0-14964
- $\text{Ag}_3\text{SI}$ , superionic cond., phase transition and cryst. structs., sp. ht., neutron and X-ray diffr. obs. 0-10662
- $\beta$ -AgSbS<sub>2</sub>, phase transitions, electrophysical props. 0-44316
- $\text{AgZr}_2(\text{PO}_4)_3$  system, phase charact. at different temps. 0-29936



## X-ray diffraction examination of materials continued

- Al crystal, lattice rotation during tensile deform., X-ray diffr. meas. 0-49231
- Al, fast neutron irradiated, struct. of defect cascades, diffuse X-ray scatt. study 0-39167
- Al, pure, hydroextrudates, incomplete axial orientation (*Russian*) 0-20949
- Al-alloy, type 2024, fatigue life prediction, X-ray diffr. method 0-25837
- Al-alloy plates, type VAD23, thermomech. parameters effect on struct. and props. 0-20988
- Al-Cu-Zn system, solid-phase reactions, phase diagram 0-50603
- Al-Ge (100) interfaces, MBE prep. and geometrical struct., total refl. X-ray diffr. study 0-49531
- Al-Mg, ageing process, effects of Ag additions and pressure (*Russian*) 0-45321
- Al-W(Mo)(Nb), struct. and props. of alloys obtained from granules 0-50717
- Al-Zn (15 at.%), structural changes during post ageing between 125°C to 215°C 0-40399
- Al-Zn (15 at.%), supersaturated alloy, growth and decomposition kinetics 0-29965
- Al-Zn-Mg (4.5, 2 to 3 at.%) solid state reactions by interrupted continuous heating 0-25737
- Al-Zn-Mg (4.5 at.%, 2 or 3 at.%), decomposition behaviour during continuous cooling, XAS and TEM examination 0-16264
- Al-Zn-Mg (4.5 at.%, 2 to 3 at.%), decomp. behaviour during continuous heating 0-29922
- Al<sub>30</sub>As<sub>40</sub>Te<sub>40</sub>, amorphous alloy, radial distribution function anal., X-ray diffr. (*Spanish*) 0-28915
- Al<sub>4</sub>C<sub>3</sub>3Be<sub>2</sub>C, X-ray diffr. and TEM study 0-14973
- AlN, X-ray diffuse scattering 0-14964
- Al<sub>2</sub>O<sub>3</sub>, hot pressing, microstruct., texture 0-40299
- Al<sub>2</sub>O<sub>3</sub>-Cr<sub>2</sub>O<sub>3</sub>, solid soln., thermal expansion anisotropy, lattice const. 0-54411
- Al<sub>2</sub>O<sub>3</sub>-Dy<sub>2</sub>O<sub>3</sub>, phase diagram at high temps. (*Japanese*) 0-50619
- Al<sub>2</sub>O<sub>3</sub>-Ga<sub>2</sub>O<sub>3</sub> system, phase diagram at high temp. (*Japanese*) 0-45290
- Al<sub>2</sub>O<sub>3</sub>-glass mixture, microstructural changes and shrinkage during sintering 0-25640
- Al<sub>2</sub>O<sub>3</sub>-Na<sub>2</sub>O,  $\beta$  and  $\beta''$  phases, formation by solid state reaction between NaAlO<sub>2</sub> and  $\gamma$ -Al<sub>2</sub>O<sub>3</sub> 0-29912
- Al<sub>2</sub>O<sub>3</sub>-SiO<sub>2</sub> system, andalusite and kyanite powders, shock induced transformations 0-45301
- AlPO<sub>4</sub>, high temp. behaviour up to liq. state, phase relations, X-ray diffr. and therm. anal. study (*French*) 0-10660
- Al<sub>4</sub>Si<sub>2</sub>C<sub>5</sub>, synthesis, X-ray diffraction pattern, lattice constants 0-50581
- Am, high press. form, cryst. struct., X-ray diffr. obs. up to 14 GPa 0-24399
- AsF<sub>3</sub> intercalation with graphite and benzenoid systems, EPR, NMR and X-ray diffr. obs. 0-19775
- As<sub>2-x</sub>S<sub>3+x</sub>, hydrogenated chalcogenide glasses, prep. by plasma decomposition 0-49735
- As<sub>2-x</sub>Se<sub>3+x</sub>, hydrogenated chalcogenide glasses, prep. by plasma decomposition 0-49735
- Au film, interface reaction with n-type Ga<sub>0.7</sub>Al<sub>0.3</sub>As and GaAs 0-39482
- Au-Fe-Ni layer coating, Fe and Ni conc. meas. by X-ray diffr. (*German, English*) 0-34330
- Au-Zn, (55 to 88 at.%), equil. diagram, X-ray diffr. obs. 0-25660
- Au<sub>3</sub>Cd, order-disorder phase transform., X-ray diffr. anal. (*Russian*) 0-45297
- B dispersed fractionated powder, struct. obs. 0-19703
- B films, prep. by H reduction of BCl<sub>3</sub>, struct. and hardness 0-54543
- B pellets preparation from powder, high-pressure testing appl. 0-50569
- B<sub>2</sub>C, melting and phase homogeneity range 0-20911
- BN, structural changes occurring during shock compression in presence of H<sub>2</sub>O 0-16301
- B<sub>2</sub>O<sub>3</sub>-K<sub>2</sub>O-Na<sub>2</sub>O-Rb<sub>2</sub>O-Cs<sub>2</sub>O glass, small angle X-ray scatt. exam. of struct. 0-38922
- B<sub>2</sub>S<sub>3</sub>-TiS<sub>3</sub> system, phase diagram and verification 0-35165
- B<sub>2</sub>Se<sub>3</sub>-Ti<sub>2</sub>Se<sub>3</sub> system, phase diagram 0-35165
- Ba<sub>2</sub>Co<sub>2</sub>Ni<sub>2-2</sub>Fe<sub>2</sub>O<sub>7</sub>, mechanically oriented, topotactic prod. technique, mag. props. 0-35140
- BaO-Fe<sub>2</sub>O<sub>3</sub>-B<sub>2</sub>O<sub>3</sub> glass, splat cooled, low temp. micromagnetism 0-34660
- BaS, press. induced phase transform., X-ray diffr. study 0-39283
- BaS-CaS:Cu phosphors, X-ray diffr. and fluoresc. spectra 0-40148
- Ba<sub>2</sub>SiAl<sub>10</sub>O<sub>20</sub>, Ce<sup>4+</sup> activated, X-ray diffr. and luminesc. props. 0-49199
- BaSi<sub>2-x</sub>Ge<sub>x</sub>, solid solution with type SrSi<sub>2</sub> struct., lattice parameters at high press. 0-54203
- (Ba,Sr)<sub>1-x</sub>SO<sub>4</sub>:Eu mixed crystal series, X-ray diffr. study of miscibility 0-2168
- Ba<sub>0.15</sub>VO<sub>2</sub>, electrical cond., thermo-EMF, and lattice const. 0-54685
- Be, core electron distribution, X-ray diffr. and  $\gamma$ -ray Compton profile obs. 0-1958
- Bi foil, splat quenched, preferred orientation 0-40381
- Bi<sub>24</sub>CoO<sub>37</sub>, in Bi<sub>2</sub>O<sub>3</sub>-CoO system, X-ray diffr., thermal anal. and metallography obs. 0-24598
- Bi<sub>2</sub>GeO<sub>20</sub>, X-ray sensitive ceramic, sintering 0-25621
- BiH(PO<sub>3</sub>)<sub>4</sub>, condensed, thermal behaviour and IR spectra 0-19912
- Bi<sub>2</sub>O<sub>3</sub>-AlPO<sub>4</sub>, phase equil. 0-35168
- Bi<sub>2</sub>O<sub>3</sub>-CoO system, X-ray diffr., thermal anal. and metallography obs. 0-24598
- BiPO<sub>4</sub>, condensed, thermal behaviour and IR spectra 0-19912
- Bi<sub>2</sub>Sn<sub>2</sub>O<sub>7</sub>, polymorphic phase transition, X-ray, DSC, SHG, dielec. and optical obs. 0-44163
- Bi<sub>2</sub>Te<sub>3</sub> single crystals, melt grown; structural perfection 0-15101
- Bi<sub>2</sub>W<sub>2</sub>O<sub>9</sub>-BiVO<sub>4</sub>, solid soln., X-ray diffr. study 0-2001
- C fibres, fibril dimension estimation, using lubricostatic structural models 0-54171
- C, graphitisation, cooperative accelerating effect of CaCO<sub>3</sub> and N<sub>2</sub> 0-55429
- C microneedles, grown on W wires under intense elec. fields, X-ray diffr. and AES 0-54580
- C, non-graphitic, two-dimensional X-ray reflections, anal. 0-24308
- C, structure change, during thermal ordering, radiation disordering 0-54283
- CC Al-Zn-Mg (4.5,1(2)(3) at.%), decomposition during ageing, preageing and cooling rate influence 0-20938
- CU<sub>2</sub>O high press. phase transforms, optical and X-ray studies 0-44313
- CaF<sub>2</sub>, etching in H<sub>2</sub>SO<sub>4</sub>, etch pit morphology and CaSO<sub>4</sub> growth 0-6408
- CaO, produced from CaCO<sub>3</sub> powder decomp. in vac. and in CO<sub>2</sub> 0-45255
- CaO-P<sub>2</sub>O<sub>5</sub>-H<sub>2</sub>O system, phase diagram at 200°C 0-45286

## X-ray diffraction examination of materials continued

- Ca<sub>3</sub>(PO<sub>4</sub>)<sub>2</sub>OH, prep. from sulphate, X-ray diffr. and IR spectrosc. 0-28993
- CaSO<sub>4</sub>, thermal expan., 22-1000°C 0-6530
- Ca<sub>0.15</sub>VO<sub>2</sub>, electrical cond., thermo-EMF, and lattice const. 0-54685
- Cd foil, splat quenched, preferred orientation 0-40381
- CdGeAs<sub>2</sub>, amorphous, thermal gradient expts., recrystn. 0-55438
- Cd<sub>65</sub>Hg<sub>35</sub> and Cd<sub>55</sub>Hg<sub>45</sub>, X-ray study of cryst. struct. and thermal expansion 0-24405
- CdI<sub>2</sub> crystals, growth conditions effect on polytypism, X-ray diffr. study 0-28942
- CdI<sub>2</sub>, hexagonal-rhombohedral polytypic transformation, electron diffr. and X-ray diffr. obs. 0-49163
- CdIn<sub>2</sub>S<sub>4</sub> film, vac. deposited, growth, struct., optical and photoelectronic props. 0-10831
- CdPS<sub>3</sub>, layered, organometallic intercalates, X-ray diffr., optical absorpt. and mag. props. 0-45103
- CdS, X-ray diffuse scattering 0-14964
- CdS:In, flash evaporated films, struct. anal. 0-20792
- CdS:Se<sub>1-x</sub>, flash evaporated films, struct. anal. 0-20792
- CdSe film, vac. deposited, elec. resist. and surface changes by laser annealing 0-2491
- CdSe, X-ray diffuse scattering 0-14964
- CdTe<sub>1-x</sub>Se<sub>x</sub>, solid solution films, prep., struct., and photocond. 0-54541
- Ce-Co-Al (0-33.3 at.% Ce), isothermal section, X-ray study (*Ukrainian*) 0-39002
- Ce-Pr powder, DHCP $\rightleftharpoons$ FCC transition, X-ray, DTA and resistivity studies 0-50629
- CeNiC<sub>2</sub>, struct. determ. using X-ray diffraction (*Ukrainian*) 0-33949
- CeO<sub>2</sub>, plasma deposition of crystals, and their characterisation 0-20800
- CeRu<sub>2</sub>, H absorption induced Ce valence change, mag. and supercond. props. 0-50042
- Ce<sub>2</sub>Si<sub>2</sub>O<sub>7</sub>N<sub>2</sub>, lattice const., X-ray diffr. anal. 0-28986
- CrAs(N)(P)(S)(Sb)(Se)(Te), lattice const., X-ray diffr. study 0-33953
- (Co,Fe)<sub>0.75</sub>B<sub>0.25</sub> metallic glasses, annealed, equil. crystalline phases 0-3019
- Co, corrosion in Ar-SO<sub>2</sub> atmospheres, scale struct. obs. (*Japanese*) 0-55568
- Co evaporated film, X-ray diffr. study 0-6663
- Co ferrite, growth on fine acicular  $\gamma$ -Fe<sub>2</sub>O<sub>3</sub> particles 0-29871
- Co film, evaporated, texture and columnar struct. 0-54566
- Co film, on Si substrate, laser irradi., cellular struct. and silicide form. 0-10710
- Co-Al, band struct. and density of states, KKR method and X-ray meas. 0-10863
- Co-Ni-Cr-Nb, effect of Fe addition on precipitation behaviour 0-29962
- Co-V (10 to 23 wt.%) system, phase constitution, X-ray and elec. resist. meas. 0-3007
- CoO-MgO-Cr<sub>2</sub>O<sub>3</sub>-Fe<sub>2</sub>O<sub>3</sub>-TiO<sub>2</sub>, form. and colour of spinel solid soln. (*Japanese*) 0-16059
- CoTe<sub>2</sub>-GeTe<sub>2</sub>, phase diagram, from thermal, X-ray, microstructural analyses 0-55367
- Co<sub>0.83</sub>[Pt(C<sub>2</sub>O<sub>4</sub>)<sub>2</sub>].6H<sub>2</sub>O, quasi-one-dimens. conductor, Peierls distortion and superlattice, X-ray study 0-29397
- Cr, interaction with dense stream of N ions, metallography, microhardness, specific volume (*Russian*) 0-15169
- Cr-Al, band struct. and density of states, KKR method and X-ray meas. 0-10863
- Cr-Ge liquid and amorphous alloys, struct. props., cond., viscosity, surface tension (*Russian*) 0-54119
- Cr-Mo-N system, at high-pressure, temp., X-ray anal., phase diagram 0-50607
- Cr-SiO films, sputtered, elec. and struct. props. 0-39694
- CrS<sub>2</sub>Te<sub>x</sub> (x=0 to 0.2), magnetic props. study 0-11194
- CrSe<sub>2</sub>, layered, phys. and elec. props. 0-44594
- CsCl, twin form. by compressive stress during phase transform. 0-49358
- CsCl:Fe, defect struct., Mossbauer spectra and X-ray diffr. obs. 0-7237
- CsFeF<sub>4</sub>, struct. phase transition at 250K 0-10663
- Cs<sub>2</sub>Ni<sub>3</sub>(F<sub>2</sub>O<sub>7</sub>)<sub>2</sub>.nH<sub>2</sub>O, thermal dehydration 0-35513
- Cs<sub>2</sub>PbCl<sub>3</sub>, lattice thermal expansion, X-ray powder technique 0-19965
- Cs<sub>2</sub>PbCu(NO<sub>3</sub>)<sub>6</sub>, one-dimensional stacking order 0-28941
- CsSnX<sub>3(5/6)</sub> (X=Cl, Br, I), single cryst. gel growth, X-ray diffr. study 0-29870
- CsVF<sub>4</sub>, structural phase transitions above room temp. 0-29167
- Cu crystals, floating zone method growth, X-ray diffr. study of preferred growth 0-7490
- Cu-Al system, high temp. lattice parameters by X-ray diffr. 0-28950
- Cu-Al-Ni, long period martensite phases, X-ray diffr. obs. 0-7571
- Cu-Al-Ni (13.8, 7.9 wt.%), cooling rates effect on internal friction (*Japanese*) 0-39217
- Cu-Ni alloys 706 and 715, corrosion in flowing sea water, dissolved sulfide effect 0-35379
- Cu-Ni-Be-(Al) (30,0.5,(0.2-2) wt.%), Al addition effect on grain boundary reaction (*Japanese*) 0-54254
- CuCl, optical microscop. and elec. resist. studies at high press. 0-11051
- CuCr<sub>2</sub>Se<sub>4</sub>, crystal growth from melt, exam. of props. 0-55283
- CuI solid electrolyte  $\alpha$ -phase stabilisation 0-29209
- Cu<sub>2</sub>O-CuO-MoO<sub>3</sub>, subsolidus phase diagram, mag. props. 0-50615
- Cu<sub>2</sub>S, polycryst. thin films, struct., optical and elec. props. for solar energy appl. 0-10837
- Cu<sub>2</sub>SbS<sub>3</sub>, skinnerite, polymorphism, X-ray diffr. and NQR meas. 0-49165
- D NaCl:Fe, defect struct., Mossbauer spectra and X-ray diffr. obs. 0-7237
- Dy<sub>2</sub>Ni<sub>2</sub>B<sub>2</sub>, struct., space groups, X-ray study (*Ukrainian*) 0-39029
- Er(Fe<sub>1-x</sub>Co<sub>x</sub>)<sub>3</sub>, spin reorientation, easy axis of magnetisation 0-25144
- Er<sub>2</sub>Ga<sub>3</sub>Ni<sub>2.5</sub>, struct. determ. by X-ray powder method (*Ukrainian*) 0-39001
- ErRh<sub>4</sub>B<sub>4</sub>, film, sputter deposition and low temp. props. 0-2948
- Es compounds, X-ray powder diffr. 0-2002
- EuC<sub>6</sub>, intercalation cpd. with graphite, synthesis and struct. 0-44184
- Eu<sub>2</sub>(PO<sub>4</sub>)<sub>2</sub>OH, prep. from sulphate, X-ray diffr. and IR spectrosc. 0-29893
- Fe, Armco, borided surface layers, Mossbauer and metallographic anal. 0-50769
- Fe complex, FeOCl[(ethyltetramethylcyclopentadienyl)<sub>2</sub>Fe]<sub>0.16</sub> synthesis and struct. 0-44176
- Fe complex, iron 4,7-(CH<sub>3</sub>)<sub>2</sub>-(1,10-phenanthroline)<sub>2</sub>(NCS)<sub>2</sub>, spin state transition, X-ray and Mossbauer obs. 0-7195



## X-ray diffraction examination of materials continued

- Fe, ductile, with different secondary struct., abrasive wear (*German*) 0-25871  
 Fe electrodeposited foils, microstruct., internal stress and mech. props. 0-20807  
 Fe film, thermally evaporated, contamination effects obs. 0-49545  
 Fe, interaction with dense stream of N ions, metallography, microhardness, specific volume (*Russian*) 0-15169  
 Fe, oxidised aerosoled ultrafine particles, X-ray and Mossbauer examination 0-21183  
 $\alpha$ -Fe, textured, residual stress evaluation by X-rays (*German*) 0-40670  
 Fe/Fe-Cr composite powder, X-ray diffr. exam. of densification during rolling 0-40289  
 Fe/ZrB<sub>2</sub>, metal-like cpd. form. in diffusion layer during solid phase saturation 0-19994  
 Fe-Al, band struct. and density of states, KKR method and X-ray meas. 0-10863  
 Fe-C, liquid, C content effect on short-range order struct., X-ray diffr. obs. 0-6351  
 Fe-Cr alloys and Fe, lattice parameters, 293 to 1273K,  $\alpha$  to  $\gamma$  phase transform., X-ray diffr. exam. (*Russian*) 0-50625  
 Fe-Mn (15(24)(30)wt.%), high hydrostatic pressure influence on stress-strain curve 0-25805  
 Fe-Mn-Ti alloys, austenitic, precipitation strengthened 0-25714  
 Fe-Ni (30 wt.%), Ni segregation singularities during dendrito-cellular solidification (*Russian*) 0-7542  
 Fe-Ni alloys, mag. state of austenite and  $\gamma$ - $\alpha$  transform. (*Russian*) 0-40350  
 Fe-Ni electrodeposit, sectional analyses and impurities (*Japanese*) 0-21350  
 Fe-Ni superstructure in metal particles in chondrites 0-12713  
 Fe-Ni-Cr, Elinvlar, struct. and mag. props., singularities during tempering (*Russian*) 0-50627  
 Fe-Ni-Mo (16.4, 8.1 wt.%), effect of substituting Mo by W during ageing 0-29991  
 Fe-Zn, crystallographic relations by X-ray diffr. 0-24408  
 Fe-Zn, phase diagram, DTA, EDAX, X-ray diffr. study 0-50602  
 Fe<sub>80</sub>B<sub>20</sub>, amorphous to cryst. transform. 0-34188  
 Fe<sub>2</sub>Cu<sub>1-x</sub>Cr<sub>2x</sub>Se<sub>4</sub>, crystallographic and image props. 0-39049  
 (Fe<sub>90-x</sub>Ni<sub>x</sub>)<sub>100-y</sub>B<sub>y</sub>, metallic glass, embrittlement and crystn. 0-7685  
 Fe<sub>2</sub>O<sub>3</sub>, plasma sputtered coatings, oxide dissociation, coating props., struct. and composition (*Russian*) 0-54577  
 $\alpha$ -Fe<sub>2</sub>O<sub>3</sub>-Li<sub>2</sub>O, structural and thermal phase behaviour from mag., spectral and thermal studies 0-2673  
 Fe<sub>2</sub>O<sub>3</sub>-PbO-B<sub>2</sub>O<sub>3</sub> glass, X-ray and electron microscope studies, mag. and Mossbauer effect meas. 0-28919  
 Fe<sub>3</sub>O<sub>4</sub>, magnetite, phase transition, X-ray diffr. meas. 0-15238  
 Fe<sub>3</sub>O<sub>4</sub> powder, oxidation to  $\gamma$ -Fe<sub>2</sub>O<sub>3</sub>, coercivity changes 0-44864  
 Fe<sub>2</sub>O<sub>3</sub> film, thermally evaporated, contamination effects obs. 0-49545  
 $\delta$ -FeO(OH) and its solid solns. synthesis, X-ray diffr. and TEM studies 0-28891  
 FeOOH, crystal growth in FeSO<sub>4</sub> solution with NaOH or NH<sub>4</sub>OH as precipitant, phase diagrams (*Chinese*) 0-44158  
 20Fe<sub>2</sub>O<sub>3</sub>.80[3B<sub>2</sub>O<sub>3</sub>(1-x)PbO.xGeO<sub>2</sub>] glass, phys. props. 0-49119  
 Fe<sub>25</sub>Pd<sub>75</sub>Au<sub>25</sub>, atomic ordering influence on mag. props. and elec. resistance (*Russian*) 0-7551  
 FeS<sub>2</sub>, oxidation, Mossbauer spectroscopic and magnetokinetic studies, 400-500°C 0-44880  
 (Fe<sub>1-x</sub>V<sub>x</sub>)<sub>2</sub>Ge, magnetic and X-ray studies 0-1966  
 Ga-Ni-R, (R=Dy, Ho, Er, Tm, Lu), struct. determ. by X-ray powder method (*Ukrainian*) 0-39001  
 Ga<sub>1-x</sub>Al<sub>x</sub>As VPE layers, X-ray diffr. 0-29296  
 Ga<sub>1-x</sub>Al<sub>x</sub>As-GaAs heterojunctions grown by metallorganic CVD 0-15599  
 GaAs, anomalous scattering factors determ. near absorpt. edges, by one-intensity-ratio method 0-1888  
 GaAs, temp. depend. of X-ray reflection intensity near absorpt. edge 0-1889  
 GaAs:Sn, proton implantation and annealing behaviour (*Chinese*) 0-44224  
 GaAs-Al interface, struct. study by X-ray total-external-refl.-Bragg diffr. 0-34321  
 (Ga<sub>1-x</sub>In<sub>x</sub>)<sub>2</sub>Se<sub>3</sub>, 1 $\geq$ x $\geq$ 0, phases, lattice parameters and thermal expansion between room temp. and melting point 0-39031  
 GaP, As<sub>1-x</sub>-GaAs one dimens. superlattice, possibility of X-ray and electron diffr. struct. determ. 0-54560  
 GaS, lattice dynamics parameters, X-ray diffr. study (*Russian*) 0-29146  
 GaSe, lattice dynamics parameters, X-ray diffr. study (*Russian*) 0-29146  
 GdCl<sub>3</sub>.6H<sub>2</sub>O, X-ray emission luminesc. (*Japanese*) 0-55763  
 Gd<sub>3</sub>Ga<sub>2</sub>O<sub>12</sub> crystal growth from melt, X-ray topography meas. (*Hungarian*) 0-11556  
 Gd<sub>3</sub>Ga<sub>2</sub>O<sub>12</sub>, high energy heavy ion irradi., lattice strain 0-49278  
 GdH<sub>2</sub>O<sub>2</sub>, electrical resistance anomalies at high pressures 0-29381  
 Ge, cross-slip of single dissociated screw dislocations, double etching and X-ray topography studies 0-15104  
 Ge, lattice parameter determ. by X-ray multiple diffr. study (*Russian*) 0-10460  
 Ge, polycrystalline epitaxial film, exam. of growth kinetics and props. 0-55304  
 Ge-Si, solid phase heteroepitaxy 0-6670  
 Ge<sub>1-x</sub>H<sub>x</sub>, amorphous, atomic struct., X-ray study 0-49106  
 GeSe, amorphous, pair distrib. function, anomalous X-ray scatt. 0-49126  
 Ge<sub>2</sub>Se<sub>3</sub>, amorphous, X-ray diffr. and local order modelling 0-49125  
 Hf-C-N-O-H, solid solns. of H, exam. of props. 0-29172  
 HfB<sub>2</sub>, oxidation in O<sub>2</sub> atmosphere, exam. 0-11814  
 HfO<sub>2</sub>, plasma deposition of crystals and their characterisation 0-20800  
 Hg<sub>1-x</sub>Cd<sub>x</sub>Te, LPE growth and characterisation 0-50565  
 InAs<sub>1-x</sub>Sb<sub>x</sub>, organometallic VPE growth on InAs 0-45233  
 In<sub>90</sub>Ga<sub>10</sub>As<sub>93</sub>P<sub>0.7</sub>, short-range order parameters, X-ray diffr. determ. 0-38875  
 InSb:Se, exam. of defects in crystal 0-6423  
 $\alpha$ -In<sub>2</sub>Se<sub>3</sub>, X-ray diffr. line broadening 0-49047  
 Ir<sub>2</sub>Cr<sub>3</sub>, yield stress and saturation magnetisation 0-16389  
 K-rare earth double sulphates, K<sub>6+3n</sub>R<sub>4-n</sub>(SO<sub>4</sub>)<sub>9</sub>, (n $\approx$ 0.4), cryst. struct. 0-28985  
 KBr, additively dyed, amplitude-phase holograms (*Russian*) 0-1152  
 KClO<sub>4</sub>, cryst. growth from gelatin gels, exam. of growth and morphology 0-7488  
 KCoF<sub>3</sub>, lattice parameter temp. depend., phase transitions and thermal expansion coeff. 0-1988  
 K<sub>2</sub>Cr<sub>2</sub>O<sub>7</sub>, polymorphic behavior, depend. on thermal and prep. history 0-34184

## X-ray diffraction examination of materials continued

- KMnF<sub>3</sub>, lattice parameter temp. depend., phase transitions and thermal expansion coeff. 0-1988  
 KMn<sub>0.9</sub>M<sub>0.1</sub>F<sub>3</sub>, (M=Co,Ni), lattice parameter temp. depend., phase transitions and thermal expansion coeff. 0-1988  
 KNiF<sub>3</sub>, lattice parameter temp. depend., phase transitions and thermal expansion coeff. 0-1988  
 K<sub>2</sub>Ni<sub>3</sub>(P<sub>2</sub>O<sub>7</sub>)<sub>2</sub>.nH<sub>2</sub>O, thermal dehydration 0-35513  
 K<sub>2</sub>O-B<sub>2</sub>O<sub>3</sub>-Fe<sub>2</sub>O<sub>3</sub> glasses, nonbridging O formation, Mossbauer spectroscopy 0-55001  
 K<sub>2</sub>O.SiO<sub>2</sub> glass, X-ray diffr. (*Japanese*) 0-19720  
 LaH<sub>2.98</sub>, electrical resistance anomalies at high pressures 0-29381  
 LaNiC<sub>2</sub>, struct. determ. using X-ray diffraction (*Ukrainian*) 0-33949  
 LaOF-LaF<sub>3</sub>, high pressure phase transitions 0-55368  
 LaRu<sub>2</sub>, H absorption induced Ce valence change, mag. and supercond. props. 0-50042  
 LiAl<sub>2</sub>O<sub>6</sub>, ordered single cryst., struct. determ. (*French*) 0-15074  
 LiCl:Fe, defect struct., Mossbauer spectra and X-ray diffr. obs. 0-7237  
 LiF, single crystal, neutron and gamma irradiation, SEM and Bragg profile anal. 0-15158  
 LiF-AlF<sub>3</sub>-Na<sub>3</sub>AlF<sub>6</sub>-Al<sub>2</sub>O<sub>3</sub> system, phase equilibrium, X-ray diffr., DTA, quenching, optical microscopy study 0-50610  
 LiF-Al(PO<sub>3</sub>)<sub>3</sub> glass, phase decomp., X-ray diffr. and IR spectra study 0-30003  
 LiNH<sub>4</sub>SO<sub>4</sub>, ferroelectric phase transition, lattice parameters and thermal expansion coeffs. 0-40074  
 LiNbO<sub>3</sub>:Na<sup>+</sup>(Co<sup>2+</sup>,Zr<sup>4+</sup>) films, LPE growth from Li<sub>2</sub>O-V<sub>2</sub>O<sub>5</sub> flux, X-ray and acoustic characterisation 0-15383  
 LiNdP<sub>4</sub>O<sub>12</sub>, grown by top seeded pulling technique, possible laser material 0-25542  
 Li<sub>2</sub>O-Al<sub>2</sub>O<sub>3</sub>(Ga<sub>2</sub>O<sub>3</sub>)(Bi<sub>2</sub>O<sub>3</sub>), quenched glasses, crystn. and ionic cond. 0-33899  
 Li<sub>2</sub>O-SiO<sub>2</sub> glasses, crystn. kinetics from amorphous X-ray scattering study 0-38919  
 LiTi, substituted ferrite, cation distribution, Mossbauer, X-ray, neutron diffr. study 0-28975  
 Li<sub>2</sub>TiS<sub>2</sub>, electrochemically intercalated, ion ordering, X-ray diffr. meas. 0-44177  
 Li<sub>2</sub>V<sub>2</sub>O<sub>8</sub> (0.1<x<1.0), phase relationship in ambient temperature system 0-20912  
 Li<sub>2</sub>WO<sub>4</sub>, type II polymorph. crys. struct. determ. 0-15073  
 LiZn, substituted ferrite, cation distribution, Mossbauer, X-ray, neutron diffr. study 0-28975  
 Lu<sub>4</sub>Si<sub>2</sub>O<sub>7</sub>N<sub>2</sub>, lattice const., X-ray diffr. anal. 0-28986  
 M<sub>1-x</sub>Sr<sub>x</sub>Si<sub>3</sub> (M=Ca, Eu, Ba), solid solution with type SrSi<sub>2</sub> struct., lattice parameters at high press. 0-54203  
 MgCu<sub>2-x</sub>Ni<sub>x</sub>, X-ray and neutron diffr. investigation of Laves phases of MgCu<sub>2</sub>-type (*German*) 0-15050  
 MgCu<sub>2-x</sub>Zn<sub>x</sub>, X-ray and neutron diffr. investigation of Laves phases of MgCu<sub>2</sub>-type (*German*) 0-15050  
 Mg(NO<sub>3</sub>)<sub>2</sub>.6H<sub>2</sub>O, crystal structure changes due to substitution of Mg<sup>2+</sup> by Co<sup>2+</sup> or Ni<sup>2+</sup> (*German*) 0-24428  
 MgNi<sub>2-x</sub>Zn<sub>x</sub>, X-ray and neutron diffr. investigation of Laves phases of MgCu<sub>2</sub>-type (*German*) 0-15050  
 MgO, hot-pressed, elasticity props. of polycrystals and single crystals 0-54301  
 MgO, lattice defects, calcination temp. effect 0-15091  
 MgO, solid solubility of Sc<sub>2</sub>O<sub>3</sub>, Al<sub>2</sub>O<sub>3</sub>, Cr<sub>2</sub>O<sub>3</sub>, SiO<sub>2</sub> and ZrO<sub>2</sub> 0-15247  
 MgO-Al<sub>2</sub>O<sub>3</sub>-SiO<sub>2</sub>:ZrO<sub>2</sub>, TiO<sub>2</sub>, glass, phase separation (*German*) 0-38932  
 Mn-Al-C, ferromag., transform., kinetics 0-34627  
 Mn-Si (62.5 to 63.8 wt.%), phase anal. and cryst. struct. (*Japanese*) 0-15049  
 Mo film, on Si substrates, laser irradi., cellular struct. and silicide form. 0-10710  
 Mo, thin film fabrication for photothermal solar converters 0-11573  
 Mo-Mn powder mixture, X-ray diffr. exam. of reaction between Mo and Mn, during sintering 0-16242  
 (Mo<sub>0.6</sub>Ru<sub>0.4</sub>)<sub>82</sub>B<sub>18</sub>, supercond. metallic glass, neutron irradi. effects 0-29060  
 MoS<sub>3</sub>, amorphous struct., X-ray radial distrib. anal. and XPS 0-49115  
 MoSe<sub>2</sub>, coating, on Mo, support annealing influence on orientation, texture and hardness (*Russian*) 0-20961  
 (NH<sub>4</sub>)<sub>2</sub>H(SO<sub>4</sub>)<sub>2</sub>, successive phase transitions, dilatometric and X-ray expts. 0-11348  
 $\alpha$ -NH<sub>4</sub>HgCl<sub>3</sub>, thermal expansion, lattice constants between 302 and 364K 0-15268  
 (NH<sub>4</sub>)<sub>2</sub>Ni<sub>3</sub>(P<sub>2</sub>O<sub>7</sub>)<sub>2</sub>.nH<sub>2</sub>O, thermal dehydration 0-35513  
 NaCN, diffuse scatt., hard-core correl., weak-graph method 0-49137  
 NaCl-KCl melt, reaction with Li<sub>2</sub>O-2SiO<sub>2</sub> X-ray, IR exam. 0-55706  
 NaF-YF<sub>3</sub> system, fusibility diagram, quasibinary section of NaF-YF<sub>3</sub>-YOF system characts. 0-55371  
 NaNO<sub>2</sub>, ferroelec., electron distrib., X-ray and neutron diffraction study 0-24411  
 NaNO<sub>2</sub>(NO<sub>3</sub>), linear compressibility to 27 kbar, X-ray diffr. obs. 0-34125  
 NaNbO<sub>3</sub>-based ferroelec. solid solns., morphotropic transitions and elec. props., enhanced vacancy conc. 0-55048  
 Na<sub>2</sub>Ni<sub>3</sub>(P<sub>2</sub>O<sub>7</sub>)<sub>2</sub>.nH<sub>2</sub>O, thermal dehydration 0-35513  
 Na<sub>2</sub>O-GeO<sub>2</sub> glass, X-ray diffr. study of Ge coordination number 0-10503  
 Na<sub>2</sub>O-NaF-CaO.ZnO<sub>1-x</sub>Al<sub>2</sub>O<sub>3</sub>-SiO<sub>2</sub>, opal glasses, strength, surface composition 0-30066  
 Na<sub>2</sub>O.y(Al<sub>1-x</sub>Fe<sub>x</sub>)<sub>2</sub>O<sub>3-m</sub>,  $\beta$ -Al<sub>2</sub>O<sub>3</sub> phase stability, lattice constants 0-45283  
 Na<sub>2</sub>TiS<sub>2</sub>, electrochemically intercalated, ion ordering, X-ray diffr. meas. 0-44177  
 Na<sub>3</sub>Zr<sub>2</sub>Si<sub>2</sub>PO<sub>12</sub>, NASICON, phase transition, X-ray diffr., ionic cond. and sp. ht. meas. 0-19979  
 Nb CVD coatings on graphite, grain struct. depend. on temp. 0-25574  
 Nb film on Si, Ar ion bombard., NbSi<sub>2</sub> form. 0-10709  
 Nb-C-N-O-H, solid solns. of H, exam. of props. 0-29172  
 Nb-Ga-Fe ternary system, phase equilib. at 1000°C, supercond. transition temp. 0-35158  
 Nb-Ge, supercond. A-15 phase, supercond. transition temp. after ion implantation 0-49972  
 Nb-Ge-Cu, phase equilib. and supercond. props. (*Russian*) 0-40332  
 Nb-Ge-Si film, CVD, struct., comp., stability and homogeneity 0-15421  
 Nb-Ni glasses, struct. factor temp. depend. 0-28920  
 Nb-Sn(Al)(Ga)(Ge)(Si)-C, phase equilib. and supercond. 0-50593  
 NbC, deformation behaviour during rubbing in wide temp. range 0-16486



## X-ray diffraction examination of materials continued

- Nb<sub>3</sub>Ge supercond. thin films, He- and Ar-irradiated, X-ray diffr. studies 0-29503
- Nb<sub>3</sub>Ge superconducting film, Nb<sub>3</sub>Ge<sub>3</sub> and NbO content, X-ray diffr. obs. 0-2515
- Nd-Ni-Al, isothermal section, 600°C, X-ray struct. anal. (*Ukrainian*) 0-33929
- Nd(Ga,Cr)<sub>2</sub>(BO<sub>3</sub>)<sub>4</sub>, cryst. growth by LPE, Nd<sup>3+</sup> fluorescence, lattice constants 0-29883
- Nd<sub>2</sub>Pr<sub>2</sub>Sm<sub>2</sub>Co<sub>2</sub>, permanent magnets, coercive force, low-temp. annealing influence (*Russian*) 0-39812
- NdTiO<sub>3</sub>, physicochem. props. 0-25625
- (Ni,Cr)<sub>2</sub>Py, layer formed on phosphidation of Ni-Cr alloy in P vapour, 700°C 0-25906
- Ni, dislocation structure parameter determ. due to plastic deformation (*Russian*) 0-54242
- Ni electrodeposits, struct., electrolyte anions influence 0-20056
- Ni-Al, band struct. and density of states, KKR method and X-ray meas. 0-10863
- Ni-C-Ce, overmodification (*Russian*) 0-40432
- Ni-Fe-Nb-Al(-Mo), wear resisting mag. head material, mag. props. and struct. 0-35350
- Ni-Nb alloys, oxidation at high temp., high energy ion backscattering anal. (*Japanese*) 0-35405
- Ni-P, amorphous electrodeposited alloys, phase-separation (*Japanese*) 0-54140
- Ni-Ta-Al system, phase equilibria and diagram, electron probe, X-ray diffr. anal. 0-29927
- Ni-Ti (1.6, 7.64 wt.%), monophasic high temp. scaling, metallography study 0-21159
- Ni-W sintered powder pressings, intermetallic phases (*Russian*) 0-55349
- Ni<sub>6</sub>B<sub>34</sub>, morphological, structural and phys. props. (*French*) 0-44444
- Ni<sub>2</sub>Fe<sub>2</sub>Cr<sub>1-x-y</sub> films, struct., mag. props., and corrosion resist. 0-34706
- NiO, lattice parameters, microstrains, non-stoichiometry, comparison between mosaic microcrysts. and quasi-perfect single microcrysts. 0-24414
- NiO:Cr, effect of Cr additives on structure parameters (*Bulgarian*) 0-44319
- Ni<sub>1-x</sub>S, metal-semimetal transition, lattice dynamics and thermodynamic props. 0-29324
- Ni<sub>62</sub>Ti<sub>38</sub>Zr<sub>9</sub>, amorphous, H-sorption, X-ray and DSC obs. 0-49526
- Ni<sub>64</sub>Zr<sub>36</sub>, amorphous and cryst., H-sorption, X-ray and DSC obs. 0-49526
- O<sub>2</sub>, solid, transformation charact. and orientation relations 0-33917
- PLZT ceramics, ferroelectric and struct. transitions, crystallographic, thermal, and dielec. anal. 0-29693
- 2PbFe<sub>1/2</sub>Nb<sub>1/2</sub>O<sub>3</sub>-Pb<sub>2</sub>FeReO<sub>6</sub>, comp., struct., dielec. and mag. props. 0-2704
- 2PbFe<sub>1/2</sub>Ta<sub>1/2</sub>O<sub>3</sub>-Ba<sub>2</sub>FeReO<sub>6</sub>, comp., struct., dielec. and mag. props. 0-2704
- 2PbFe<sub>1/2</sub>Ta<sub>1/2</sub>O<sub>3</sub>-Pb<sub>2</sub>FeReO<sub>6</sub>, comp., struct., dielec. and mag. props. 0-2704
- Pb<sub>3</sub>(PO<sub>4</sub>)<sub>3</sub>OH, prep. from sulphate, X-ray diffr. and IR spectrosc. 0-29893
- PbS film, soln. grown on Si, struct. and comp. of heterojunction 0-54530
- PbS, oxidation, PbSO<sub>4</sub> distrib. in products (*Polish*) 0-25883
- PbSe, X-ray diffr. exam. of struct., and luminescence props. 0-55209
- Pb<sub>1-x</sub>Sn<sub>x</sub>Te:In epitaxial layers, growth, elec. props., and luminesc. 0-54542
- Pb<sub>3</sub>TaMnO<sub>6</sub>, reaction of form. from oxides, ferroder. props. 0-55326
- PbTe, crystallite size in epitaxial layers by X-ray diffraction rocking curves 0-20052
- Pb(Ti, Zr)O<sub>3</sub>, piezoelectric-ferroelectric ceramic, polarisation processes, X-ray obs. 0-34847
- PbTiO<sub>3</sub>, X-ray interference intensity temp. depend., lattice ion vibr. (*Russian*) 0-20601
- PbTiO<sub>3</sub>-La<sub>2</sub>O<sub>3</sub>-3TiO<sub>2</sub>, struct. and dielec. props. 0-54200
- PbTiO<sub>3</sub>-PbZrO<sub>3</sub>-based multicomponent ferroelec. solid solns., morphotropic transitions and comp.-temp. phase diagrams 0-55047
- Pb(Zr,Ti)O<sub>3</sub> ceramic, X-ray investigation before and after polarisation (*Chinese*) 0-2712
- Pb(Zr,Ti)O<sub>3</sub> thin film, ferroelec., fabrication by RF sputtering (*Japanese*) 0-25560
- PbZrO<sub>3</sub>, phase transitions, X-ray, dielec., and thermal anal. 0-45020
- 1-xPbZrO<sub>3</sub>-xPbScO<sub>3</sub>-Nb<sub>2</sub>O<sub>5</sub>, 0≤x≤1, phase transitions, X-ray, dielec., and thermal anal. 0-45020
- Pb(Zr,Ti<sub>1-x</sub>)O<sub>3</sub> films, ion beam deposition, struct., dielec. and ferroelec. props. 0-20788
- PbZrO<sub>3</sub>, X-ray interference intensity temp. depend., lattice ion vibr. (*Russian*) 0-20601
- Pd film, on Si substrate, laser irradi., cellular struct. and silicide form. 0-10710
- Pd film on Si, Xe ion beam induced form. of PdSi 0-10800
- Pd-V, alloy and bilayer, silicide form. solid phase reaction with Si 0-6568
- Pd-Zn, L<sub>10</sub> type intermetallic phase, X-ray diffr. study of lattice compression 0-49182
- Pd<sub>2</sub>MnIn<sub>1-x</sub>Sb<sub>x</sub>, Heusler alloy, mag. order obs. 0-29528
- Pd<sub>80</sub>Si<sub>20</sub>, amorphous, structural changes with neutron irradi., X-ray scatt. obs. 0-33898
- PrNiC<sub>2</sub>, struct. determ. using X-ray diffraction (*Ukrainian*) 0-33949
- Pr(OH)<sub>3</sub>, thermal decomposition, exam. 0-55640
- Pr<sub>2</sub>Si<sub>2</sub>O<sub>7</sub>, X-ray diffr. anal. 0-28986
- Pt chain compounds, one dimens. conductors, Fermi wavevector determ., X-ray scatt. obs. 0-44187
- RbCaF<sub>3</sub>, cubic to tetragonal phase transform., X-ray, neutron, Mossbauer diffr. study 0-49360
- Rb<sub>4</sub>Cu<sub>16</sub>I<sub>13</sub> in CuCl-CuI-RbCl system, high Cu ion cond. solid electrolyte, elec. props. and powder X-ray diffr. anal. 0-15295
- RbHSeO<sub>4</sub>, ferroelec. phase transition, X-ray study 0-7309
- RbLiSO<sub>4</sub>, successive struct. transitions, X-ray diffr. 0-10521
- Rb<sub>2</sub>Ni<sub>3</sub>(P<sub>2</sub>O<sub>7</sub>)<sub>2</sub>·nH<sub>2</sub>O, thermal dehydration 0-35513
- RbSnX<sub>3(5/6)</sub> (X=Cl, Br, I), single cryst. gel growth, X-ray diffr. study 0-29870
- RuS<sub>2</sub>, amorphous, prep. at ambient temp., magnetic structure 0-35119
- (SN)<sub>x</sub>\* radicals polymerisation to (SN)<sub>x</sub> in thin films, optical spectra 0-16656
- Sc-Rh-Si system, partial phase diagram, X-ray diffr. and microprobe anal. 0-25659
- Se film, noncryst., ageing and crystn. obs., tentative struct. model 0-2295
- Se, monoclinic to trigonal conversion, thermodynamic stability and associated investigations. 0-24592

## X-ray diffraction examination of materials continued

- (Se)<sub>x</sub>, crystn. and melting 0-40241
- Si, cross-slip of single dissociated screw dislocations, double etching and X-ray topography studies 0-15104
- Si, crystalline struct. and lattice imperfections 0-24398
- Si, Czochralski-grown, oxide precip. form. process 0-49364
- Si films, polycryst., glow discharge deposited below 250°C, struct. and morphology 0-49535
- Si, lattice parameter determ. by X-ray multiple diffr. study (*Russian*) 0-10460
- Si, local mechanical defects, annealing and effect on autoepitaxial growth (*Russian*) 0-7701
- Si, precipitation of O, 1000°C TEM, IR absorpt. and X-ray studies 0-34194
- Si, transmission topograph recording, of large cryst. slices, geometrical conditions 0-38869
- Si wafer, heat treatment behaviour of microdefects and residual impurities, X-ray diffr. and IR absorpt. study 0-49214
- Si:Au(P)(B) whiskers, impurity inhomogeneity 0-39145
- Si:B, inhomogeneous surface layer, diffusion and implanted, X-ray rocking curves 0-6603
- Si:B ion implanted, X-ray topographical images at different absorption conditions 0-2052
- Si:Ge B, strain compensation, X-ray Bragg reflexion 0-39137
- Si/Pd-W, contact reactions, backscattering, X-ray diffr. meas. 0-20040
- Si-H, amorphous, struct. and press. induced transition 0-44131
- SiC coating on Mo, CVD and stability under thermal cycle conditions 0-7500
- SiC coatings for first-wall candidate materials by RF sputtering 0-25563
- SiC coatings for HTR nuclear fuels, characterisation by small-angle X-ray scatt. 0-44451
- SiC, further polytypes discovered using Laue diffraction (*Chinese*) 0-10535
- SiC, high period polytype at interface of two interacting spirals 0-20041
- SiC, X-ray diffuse scattering 0-14964
- SiC-2H, structure parameters and polarity, X-ray diffr. meas. 0-19781
- Si<sub>1-x</sub>H<sub>x</sub>, amorphous, atomic struct., X-ray study 0-49106
- Si<sub>3</sub>N<sub>4</sub>, consolidation by hot isostatic pressing 0-11605
- SiO<sub>2</sub>-Al<sub>2</sub>O<sub>3</sub>-Fe<sub>2</sub>O<sub>3</sub>-CaO, basalt glass ceramics, crystallite form. due to heat treatment 0-38917
- SiO<sub>2</sub>-base cores, for superalloys, high temp. characterisation 0-10640
- SiO<sub>2</sub>-Li<sub>2</sub>O-K<sub>2</sub>O-ZnO glass ceramic, prep., phase transformations and physical props. 0-45299
- SiO<sub>2</sub>-Na<sub>2</sub>O-CaO glass, phase separation characts., melting atmosphere effect 0-44141
- SiO<sub>2</sub>, powder and vac. deposited, amorphous struct., X-ray diffr. meas. 0-1931
- Sm(-Pr)-Co, sintered, cryst. phases (*Russian*) 0-39004
- SmF, vapourisation, sublimation, Knudsen effusion method 0-6508
- SmH<sub>2</sub> [x=2.78, 2.85, 2.91], electrical resistance anomalies at high pressures 0-29381
- Sm<sub>2</sub>La<sub>1-x</sub>B<sub>6</sub>, solid solns., exam. of structure, elec. props. 0-39290
- Sn<sub>1-x</sub>Sn<sub>x</sub>F<sub>2</sub> system, phase diagram construct. (*French*) 0-50605
- SnO chlorination, Mossbauer and X-ray phase anal. 0-21266
- SnO<sub>2</sub>-Si solar cells, electron-beam deposited, struct., photovolt. props. 0-50956
- Sn<sub>2</sub>Ti<sub>(1-x)</sub>O<sub>2</sub>, solid soln., thermal reaction with V(V), Cr(III), Cr(VI), Mn(II), Fe(III), Co(II), Ni(II), Cu(II), Sb(III) 0-16674
- Sr<sub>5</sub>(PO<sub>4</sub>)<sub>3</sub>OH, prep. from sulphate, X-ray diffr. and IR spectrosc. 0-29893
- Sr<sub>3</sub>SiAl<sub>10</sub>O<sub>20</sub>, Ce<sup>3+</sup> activated, X-ray diffr. and luminesc. props. 0-49199
- Sr<sub>0.15</sub>VO<sub>2</sub>, electrical cond., thermo-EMF, and lattice consts. 0-54685
- Ta epitaxial layers, formation conditions influence on struct. (*Russian*) 0-20045
- TaC<sub>x</sub>, solubility of H, X-ray diffr. exam. 0-44318
- Ta<sub>2</sub>C<sub>x</sub>, solubility of H, X-ray diffr. exam. 0-44318
- Ta<sub>2</sub>C<sub>x</sub>O<sub>y</sub>, solubility of H, X-ray diffr. exam. 0-44318
- TaSe<sub>2</sub>, 1T and 2H superstruct., cryst. struct. using X-ray diffr. 0-39044
- TaSe<sub>2</sub>, 4Hb polytype, CWD induced atomic shifts 0-39045
- TbCo<sub>2</sub>, rhombohedral distortion at low temp. 0-34743
- Tc<sub>2</sub>Si<sub>2</sub>, (x=78.87, y=22.13), amorphous, struct., X-ray diffr. study 0-6362
- ThO<sub>2</sub>, plasma deposition of crystals, and their characterisation 0-20800
- Ti alloy, BT22 quenched from 850-1200°C, X-ray study of structure (*Ukrainian*) 0-24402
- Ti complex, TiOCl[Co(cyclopentadienyl)<sub>2</sub>]<sub>0.16</sub>, synthesis and struct. 0-44176
- Ti-Al film, struct. and elec. props. 0-7002
- Ti-C-N-O-H, solid solns. of H, exam. of props. 0-29172
- Ti-Cu thin films, oxidation kinetics in air at 100 to 300°C, meas. 0-40590
- Ti-H, deposited on carriers, synthesis, structure and catalytic props. 0-29890
- Ti-Mo-Fe (3, 0.13 at.%), metastable phases, Mossbauer study 0-7243
- Ti-Permalloy films, interdiffusion, Auger anal. and X-ray diffr. obs., degradation of mag. props. 0-34251
- Ti-Si cosputtered films, silicide form., X-ray diffr. and resist. study 0-54546
- Ti-Si film thin film interaction, metallisation, X-ray diffr. and sheet resist. 0-54442
- TiC coating thickness meas. using X-ray diffr. 0-21243
- TiC, deformation behaviour during rubbing in wide temp. range 0-16486
- TiC-B, struct. and mech. props. 0-55461
- TiCl<sub>4</sub>-MgCl<sub>2</sub>, high activity catalyst for polyethylene, struct. and mechanism investig. 0-11951
- TiN, synthesised in SHF discharge plasma, exam. of props. (*Russian*) 0-7524
- TiN-Ti<sub>2</sub>N, activated reactive evaporation formed deposits, microstructure, transformation depend. on depositing conditions 0-24761
- TiN<sub>x</sub> film, reactively sputtered in Ar-N<sub>2</sub> atm., elec. and struct. props. 0-15636
- Tl-Bi system, phase transitions near Tl<sub>3</sub>Bi, elec. props. meas. 0-35181
- Tl-Pb-S system, phase diagram quasibinary Tl<sub>3</sub>S-PbS section obs. 0-55372
- TlBr-Tl, KRS-5, periodic strain anisotropy, optical and X-ray diffr. study 0-54167
- TlGaSe<sub>2</sub>-TiGaSe<sub>2</sub>, phase and composition-property diagrams 0-55366
- TlInS<sub>2</sub>-TlInSe<sub>2</sub>, phase and composition-property diagrams 0-55366
- Tl<sub>2</sub>S-SnS, phase equilibria exam. 0-55369
- Tm<sub>4</sub>Si<sub>2</sub>O<sub>7</sub>N<sub>2</sub>, lattice consts., X-ray diffr. anal. 0-28986



**X-ray diffraction examination of materials continued**

- U-UNi<sub>2</sub>-UCo<sub>2</sub>, system, phase equilibria, lattice constants (*German*) 0-50598  
 UO<sub>2</sub> pellet surfaces,  $\beta$ -UO<sub>2.33</sub> formation in air at 229 to 275°C, X-ray diffr. study 0-35362  
 UO<sub>2</sub>-20CeO<sub>2</sub> mixed powder, X-ray and microprobe exam. of homogenisation 0-25609  
 UO<sub>2</sub>-UC<sub>2</sub>-C microspheres, carbothermic prep., rate-controlling preps. 0-45257  
 USb<sub>2</sub>, single crystal growth, structural perfection 0-15024  
 V complex, VOCL [Co(cyclopentadienyl)]<sub>2</sub>, synthesis and struct. 0-44176  
 V-Al, band struct. and density of states, KKR method and X-ray meas. 0-10863  
 V-Mn, equiatomic, ordering kinetics and antiphase domain coarsening 0-7559  
 V-Sn(Al)(Ga)(Ge)(Si)-C, phase equil. and supercond. 0-50593  
 V<sub>3-x</sub>Cr<sub>x</sub>Si, x=0 to 3, struct., supercond. and mag. props. 0-1962  
 VO<sub>2</sub>, defect struct., local ionic arrangements in disordered phase 0-10532  
 V<sub>2</sub>O<sub>5</sub>, high-temp. phase transition, resistivity, valence photoelectron spectra 0-49357  
 VS<sub>2</sub>, non-stoichiometric phase, physico-chemical props. 0-29532  
 V<sub>2</sub>S<sub>3</sub>, non-stoichiometric phase, physico-chemical props. 0-29532  
 V<sub>2</sub>S<sub>3</sub>, paramag. cryst., struct. factors using polarised neutron diffr. 0-15691  
 V<sub>2</sub>Si, d-spacing fluctuations above Martensitic phase transition 0-7570  
 V<sub>2</sub>Zr(Hf), struct. transform. at low temp., X-ray diffr. anal. (*Russian*) 0-45298  
 W-Hf-C, phase equil. 0-55348  
 W-Ru based refractory transition metal-metalloid glass, struct. 0-1938  
 WC, deformation behaviour during rubbing in wide temp. range 0-16486  
 WC-Co powder, prep. by direct carburisation of WO<sub>3</sub> in presence of CO<sub>2</sub> 0-50573  
 WS<sub>2</sub>, amorphous struct., X-ray radial distrib. anal. and XPS 0-49115  
 (Y,Sm,Lu,Cu)<sub>3</sub>(Fe,Ge)<sub>2</sub>O<sub>12</sub>, ion implanted, hard bubble suppression 0-11238  
 YAG, production of densely sintered ceramic, exam. of recrystallisation during sintering 0-11609  
 YIG and Ga-substituted YIG, high energy heavy ion irradi., lattice strain 0-49278  
 YNi<sub>2</sub>, amorphous alloy, at. struct. 0-19704  
 YOF-YF<sub>3</sub>, high pressure phase transitions 0-55368  
 YbC<sub>6</sub>, intercalation cpd. with graphite, synthesis and struct. 0-44184  
 Zn foil, sput. quenched, preferred orientation 0-40381  
 Zn-Al, unidirectional eutectic, FCC phase, preferred orientation 0-29973  
 ZnFe<sub>2</sub>O<sub>4</sub>-Fe<sub>2</sub>O<sub>3</sub> solid solns., form. of  $\alpha$ -Fe<sub>2</sub>O<sub>3</sub> during oxidation 0-25889  
 ZnIn<sub>2</sub>S<sub>4</sub>, III(a) polytype, absorpt. spectrum tail changes due to microstructures 0-2788  
 ZnO fibre reinforced elastomer, X-ray diffr. exam. of filamentary crystal distrib. 0-7738  
 ZnO, structure parameters and polarity, X-ray diffr. meas. 0-19781  
 ZnO, X-ray diffuse scattering 0-14964  
 ZnS, X-ray diffuse scattering 0-14964  
 ZnTe films, grown on glass using atomic layer evaporation 0-44453  
 ZnTe, polymorphism at elevated temp., elec. resist. and X-ray diffr. under press. 0-49359  
 Zr-C-N-O-H, solid solns. of H, exam. of props. 0-29172  
 Zr-H, deposited on carriers, synthesis, structure and catalytic props. 0-29890  
 ZrB<sub>2</sub>, oxidation in O<sub>2</sub> atmosphere, exam. 0-11814  
 ZrO<sub>2</sub> gels, calcination 0-11964  
 ZrO<sub>2</sub>, plasma deposition of crystals and their characterisation 0-20800  
 ZrO<sub>2</sub>, stabilised, fabrication by hot petroleum drying method, X-ray diffr. and thermal anal. study 0-40297  
 ZrO<sub>2</sub>-Nd<sub>2</sub>O<sub>3</sub>(Sm<sub>2</sub>O<sub>3</sub>)(Dy<sub>2</sub>O<sub>3</sub>) eutectic, unidirectional solidification, microstruct. and crystallographic characterization 0-35176  
 ZrO<sub>2</sub>-SiO<sub>2</sub>- $\alpha$ -Al<sub>2</sub>O<sub>3</sub> mixed powders, solid state reactions 0-40337  
 ZrSiO<sub>4</sub>, synthesis, influence of rare-earth additives on props. 0-20868

**X-ray diffraction examination of microstructure**

- see also crystal microstructure*  
 aluminosilicate glass, phase separated, phase characterization by STEM and X-ray microanal. 0-50643  
 $\alpha$ - $\beta$  brass, cold-rolled, energy dispersive X-ray diffr. studies 0-40379  
 carnauba wax, electret states, role of crystallites 0-2686  
 ceramics acid-resistant, based on Artemov clay and obsidian 0-20852  
 crystallite, cylindrical, layer disorder, X-ray diffr. intensity effect 0-39113  
 crystallite dimensions determ. using synchrotron radiation X-ray diffr. photographs 0-24313  
 crystallites, curved, cluster with layer shift, X-ray diffr. intensities 0-39114  
 crystallites, with step displacement, particle sizes and distortion determ. (*German*) 0-14960  
 diamond, synchrotron electron beam damage, study by optical, cathodoluminesc. and X-ray topography 0-39155  
 diamond, synthetic grits, crystal morphology of cyclic twins 0-2037  
 dislocation outcrop, extra equal-thickness fringes obs. with X-ray plane wave 0-39084  
 epitaxial thin films, structural characterisation 0-3451  
 heteroepitaxial surface morphologies and misalignments (*Japanese*) 0-15411  
 II-VI semiconductors, lattice defects, X-ray diffr. and electron microscopic study 0-15088  
 Invar N36 melt, cast metal struct. depend. on heat treatment, subgrain struct. (*Russian*) 0-40343  
 Kevlar 29 and 49, aramid fibres, microvoid obs. 0-38960  
 microcrack enlargement in heterogeneous materials, conc. criterion 0-11769  
 nuclear track detectors, microcrystallite nucleation and detection threshold 0-890  
 Nylon-6, injection moulded, struct. and morphology 0-38949  
 poly(vinylidene fluoride) orientation, solid state deformation by coextrusion 0-40394  
 polyethylene, oriented, shear strain, effect on struct., props. (*Russian*) 0-7656  
 polyvinylidene fluoride, poling process effect on fine struct. 0-7285  
 polyvinylidene fluoride, polycryst. ferroelec., microstruct., piezoelec. and pyroelec. props. 0-7303  
 quartz, crystal growth in fluoride environment, growth features and props. 0-6373

**X-ray diffraction examination of microstructure continued**

- quartz, defects growth, study by X-ray diffr. topography (*French*) 0-39095  
 steel, alloy, type 11Kh18M, eutectic carbide composition change due to heating 0-16353  
 steel, alloy, type ST.5, structural and phase changes after high temp. heating (*Russian*) 0-55439  
 steel, alloy, V-W-Mo-Cr, exam. of carbide transformation 0-16299  
 steel, austenitic, Cr-Ni-Mn-V, X-ray anal. of carbide phases formed during ageing (*Russian*) 0-20936  
 steel, austenitic Cr-Mn, M<sub>23</sub>C<sub>6</sub> carbide precipitates comp., heat and thermomech. treatment influence (*Russian*) 0-40361  
 steel, austenitic stainless, ferritic, single phase ferritic solidification in welds, exam. 0-7546  
 steel, austenitic stainless, welds, exam. of austenitic solidification mode 0-7545  
 steel, austenite-martensitic, struct. changes during plastic deform., mutual influence of phases (*Russian*) 0-30015  
 steel, C, transform. kinetics, heat cond. and elastic-plastic stresses during quenching (*Japanese*) 0-25688  
 steel, C and alloy, nitriding, effect on struct. and internal stresses 0-30162  
 steel, cast structural, heat treatment and mech. working influence on mech. props. (*Russian*) 0-40392  
 steel, Cr and Ni-Cr, cyclic re-austenitizing 0-35222  
 steel, low alloy, low C grain boundary proeutectoid ferrite formation, direct obs. method 0-3074  
 steel, martensitic, low C without Ni, for deep-well sucker rods, corrosion fatigue 0-55588  
 steel, medium C, microalloying with V and Ti, effect on hardness and structure 0-11750  
 steel, medium C 0-11752  
 steel, mild, plastic deform. around fatigue cracks, X-ray microbeam and recrystn. studies 0-35258  
 steel, NC6, cementite network separation, kinetics (*Polish*) 0-25698  
 steel, stainless, alloyed with C, magnetron-sputtered, microstruct., and cryst.-amorphous transition 0-19719  
 steel, tool, W-Mo, heat treatment effect on props. 0-50656  
 steel, type 1Kh17N2, white zone formation and props. during friction in vac. (*Russian*) 0-40542  
 steel fibre reinforced Mg, fibre-matrix interfacial reactions 0-20043  
 swirl defects in single crystals. 0-44200  
 textured material, X-ray quantitative phase anal. (*Chinese*) 0-21195  
 wide-angle analysis, plastic deformation appl., alloys behaviour obs. (*German*) 0-3283  
 Zircaloy-4, microstrain and particle size meas. by Warren-Averbach method 0-55420  
 3PbO.GeO<sub>2</sub>, X-ray and electron diffr. exam. (*German*) 0-11632  
 Ag film, ion plated on AT-cut quartz crystal 0-2280  
 Al, and Al-Cu(Pb) dil. alloys, pulsed ruby laser irradi., noncryst. phase form 0-35012  
 Al, defects formed during cryst. growth or by plastic deform., X-ray transmission topography obs. (*Russian*) 0-25761  
 Al-Ag alloy mirror for use as solar reflector, co-sputtering 0-20789  
 Al-Cu(Zn, Ag, Mg, Si), intermediate precipitates, stability, X-ray, elec. resist. and hardness study 0-3063  
 Al-Li (10 at.%), struct. changes on annealing, 25-500°C, Li atoms role 0-35183  
 Al-Si, deformed, local lattice rotations at second phase particles 0-25709  
 Al-silicide-Si systems with CoSi<sub>2</sub>, Pt, Ni<sub>3</sub>-Si, and MoSi<sub>2</sub> as silicide, diffusion, compound form., and microstructure 0-34253  
 Al-Zn alloy, metastable phases formed at 200°C, room temp. stability 0-16315  
 Al-Zn-Mg, Guinier-Preston zones, comp. and contrib. to elec. resist. 0-16316  
 Al-Zn-Mg (4.8, 1.2 wt.%), quenched, Guinier Preston zones formation 0-45273  
 Al-Zn-Mg alloys, extra-resistivity of coherent precipitates calc. using X-ray small angle scattering intensities 0-3050  
 AlN, prep. and charact. of ultrafine powders 0-2983  
 Au bicrystal, grain boundary thickness, meas. using X-ray techniques 0-34011  
 Au, electron irradiated, interstitials and their clusters, diffuse X-ray scatt. study 0-33997  
 Au quenched single crystals, vacancies, diffuse scatt. and resist. obs. 0-33994  
 Au-Cu, dil., electron irradiated, interstitials and their clusters, diffuse X-ray scatt. study 0-33997  
 B fibre reinforced Mg, fibre-matrix interfacial reactions 0-20043  
 BN, polycryst. cubic, props. 0-21013  
 BN powder, wurtzite sphalerite struct. phase transition, effect on substruct. 0-25690  
 BaTiO<sub>3</sub>-CeO<sub>2</sub> liquid immiscibility region, X-ray diffr. anal. 0-50611  
 Ba<sub>3</sub>(VO<sub>4</sub>)<sub>2</sub>, determination of enthalpies of formation, from heats of solution 0-2182  
 Bi<sub>4</sub>Ti<sub>3</sub>O<sub>12</sub> ceramics, ferroelectric, hot-forged, grain orientation and dielectric props. 0-40076  
 Cd, vacuum evaporated film, HCP, microstruct., X-ray obs. 0-10827  
 Cd,Hg<sub>1-x</sub>Te, correlation between structural and chemical inhomogeneity (*Russian*) 0-49484  
 CdS-CdTe double layers on various GaAs surfaces, morphology and crystallography 0-34326  
 CdTe, single cryst. sublimation growth, X-ray topographic characterisation 0-29866  
 CdTe-ZnS ternary mutual system, phase diagram 0-20904  
 Ce, cold working, deform. induced struct. effects 0-25719  
 Co film, evaporated, columnar struct. depend. on degree of texture 0-54567  
 Co-Ge-Te system, phase equil. 0-20908  
 Cr bronze Sn, recrystn. props., hot rolling, annealing, polygonisation (*Russian*) 0-55419  
 Cr, CVD on Ni, reaction mechanism, growth rate and struct. obs. 0-39476  
 Cr-NdAlO<sub>3</sub>, dielectric films, phase composition and structure 0-39464  
 Cu plates, thin, dislocation-dislocation interaction inducing cross-slip, X-ray topographic anal. 0-49233  
 $\beta$ -Cu-Al martensite, stacking order, disorder anal. by continuous Fourier transformation of diffracted intensities 0-39115  
 Cu-Ga porous solid formed by shock compression 0-29905  
 Cu-Ge single cryst. containing heavily faulted regions, X-ray diffr. profiles 0-24462



**X-ray diffraction examination of microstructure continued**

- Cu-Ni, sintered, props. and degree of nonhomogeneity 0-20848  
 Cu-SiO<sub>2</sub>, deformed, lattice rotations at second phase particles 0-25709  
 Cu-Sn (25 wt.%), liq., struct. from thermodynamic and diffr. studies 0-6350  
 Cu-Zn-Sn (24-34, 1.0 wt.%), cold-worked microstruct., X-ray diffr. obs. 0-3088  
 Cu<sub>0.5</sub>Fe<sub>0.5</sub>O<sub>4</sub>, ferrite, determination of specific heat at 298-800K 0-2579  
 Cu-S-Ti-S system, phase diagram 0-20906  
 Fe, Armco, inter- and intragranular sulphidation 0-55570  
 Fe, pure, initial grain boundaries effect on cold-rolling and annealing textures (Japanese) 0-35205  
 Fe-Mn-C, anomalous changes in austenite and martensite lattice parameters 0-50636  
 Fe-Si single crystals, interaction of {110} 90° walls with lattice imperfections 0-39807  
 FeGe<sub>2</sub>, single cryst. perfection depend. on growth rate and direction 0-55284  
 Ga<sub>2</sub>In<sub>1-x</sub>P<sub>x</sub>As<sub>1-y</sub>, 111-A and 111-B faces, defect struct., etching and X-ray diffr. obs. 0-2026  
 GaSe, excitation spectra and structural props., X-ray Laue diagrams and optical transmission (French) 0-50358  
 GdCrO<sub>3</sub>-GdAlO<sub>3</sub> solid solutions 0-20887  
 Gd<sub>2</sub>Ga<sub>2</sub>O<sub>12</sub>, planar defects, X-ray topography obs. (French) 0-2008  
 Ge, hot microdeformation and simultaneous X-ray topography apparatus (French) 0-38871  
 Ge-As, supersaturated solid soln., dislocation form. during thermocyclic treatment (Russian) 0-3057  
 GeTe-MnTe, heat treatment effect on struct., elec. props. 0-54725  
 Hf-Ni(Cu)-Ge, alloys, phase diagrams and cryst. struct. (Russian) 0-25658  
 HgCr<sub>2</sub>Se<sub>4</sub>-Cd, precipitations during growth by chem. transport method 0-55409  
 InP, and InP<sub>1-x</sub>As<sub>x</sub>, 111-A and 111-B faces, defect struct., etching and X-ray diffr. obs. 0-2026  
 KCl:TiCl<sub>3</sub> lattice defects, X-ray line profile obs. 0-24455  
 K<sub>2</sub>Hf<sub>2</sub>O<sub>7</sub> acid, exam. of thermal decomposition 0-55638  
 K<sub>2</sub>O-Fe<sub>2</sub>O<sub>3</sub>-SiO<sub>2</sub>, subsolidus sector of phase diagram, X-ray obs. 0-40335  
 K<sub>2</sub>O<sub>4</sub>TiO<sub>2</sub>, new fibrous phase 0-20917  
 (Li<sub>2</sub>Na<sub>2</sub>K<sub>2</sub>)(Nb,Ta)O<sub>3</sub>, pseudo-binary and ternary systems quenched metastable glassy and cryst. phases 0-29935  
 Mg-Y-Al alloys, phase equilib. (Russian) 0-20890  
 Mg-Y-Cd, phase equilibria and mech. props. (Russian) 0-20894  
 Mg<sub>3</sub>(VO<sub>4</sub>)<sub>2</sub>, determination of enthalpies of formation, from heats of solution 0-2182  
 Mo, dislocation structure inhomogeneity in electromachining crater zone (Russian) 0-16326  
 Mo, fracture and crack propag. tested in tension along [001] axis (Russian) 0-50697  
 Nb, plastically deformed single crystal, foil, damage free prep. for TEM and X-ray topography (German, English) 0-30200  
 NdAlO<sub>3</sub>, dielectric films, phase composition and structure 0-39464  
 Ni/Au-Ge/GaAs contact system, alloying behaviour, microprobe AES and X-ray diffr. 0-54548  
 Ni-Fe-Nb (Mo), magnetic alloy, TEM and X-ray obs. (Chinese) 0-24401  
 Ni<sub>65</sub>Mo<sub>35</sub>Fe, O<sub>2</sub> effect on secondary recrystallisation and mag. props. 0-35201  
 Pb films, vapour deposited FCC, normal and oblique incidences, microstructure, X-ray diffr. study 0-20048  
 Pb<sub>3</sub>Ge<sub>2</sub>O<sub>7</sub>, dielectric thin film, obtained by sedimentation, exam. of dielectric props. and structure 0-2282  
 Re-Cu-Al phase diagram, X-ray structural and microscopic anal. (Russian) 0-20895  
 Se-[Co,Ni,Cu]-Ga, phase equilibria, diagrams of state, X-ray, microstructural study (Russian) 0-55356  
 Si, amorphous, hydrogenated, small angle X-ray scatt., void distrib. 0-15087  
 Si, Bragg diffraction from crystals, Mo K<sub>α</sub> radiation polarisation 0-1893  
 Si, edge dislocation, crystal surface interception, X-ray diffr. obs. in Bragg case 0-49228  
 Si, elastically bent crystal, with large strain gradient, X-ray diffraction study 0-44073  
 Si, mechanical strength, origin of difference in Czochralski grown and float-zone-grown cryst. 0-44212  
 Si, microdefects, diffuse X-ray scatt. obs. 0-34014  
 Si, near (111) surface, dislocation movement at annealed scratches, X-ray topography obs. 0-2029  
 Si, nearly perfect crystals, point defect aggregates, high resolution diffuse X-ray scattering study 0-49211  
 Si, snowflake defect due to annealing in H at 1000°C, X-ray topography study (Chinese) 0-49227  
 Si, thermally induced microdefect form., C and O role 0-11439  
 Si:Cu extinction of X-ray topographic images of Cu precipitates 0-45310  
 Si-Al-O-N, mullite like cpd. comp., EPMA, X-ray and chem. anal. obs. (Japanese) 0-35175  
 Si-Al-O-N sintered ceramic, microstruct., phase composition and transformation mech. mech. props. 0-40309  
 Si-Li(Au)(Cu), diffusion-induced defects, X-ray triple cryst. diffraction 0-2213  
 SiC crystals, 2H to 6H solid-state transformation, X-ray diffraction study 0-28943  
 SiC(6H), ion-implanted, laser-induced recrystallization and defects 0-44221  
 Si<sub>3</sub>N<sub>4</sub>, prep. and charact. of ultrafine powders 0-2983  
 Si<sub>3</sub>N<sub>4</sub>(MgO+Al<sub>2</sub>O<sub>3</sub>)(Y<sub>2</sub>O<sub>3</sub>), hot-pressed and sintered, microstruct. and impurity distrib. 0-49261  
 Si<sub>3</sub>N<sub>4</sub>-AlN-Al<sub>2</sub>O<sub>3</sub>-SiO<sub>2</sub>-Y<sub>2</sub>O<sub>3</sub>, phase equilibrium study by X-ray diffr. and optical microscopy 0-50614  
 Si<sub>3</sub>N<sub>4</sub>-SiO<sub>2</sub>-ZrN-ZrO<sub>2</sub>, X-ray diffr. phase anal. and reactions Si<sub>3</sub>N<sub>4</sub>+ZrO<sub>2</sub>, SiO<sub>2</sub>+ZrN 0-50613  
 SiO<sub>2</sub>-CaO-ZnO-B<sub>2</sub>O<sub>3</sub>-Na<sub>2</sub>O-SrO effect on crystallisation 0-54135  
 SiO<sub>2</sub>-Na<sub>2</sub>O-CaO (13, 11 wt.%) glass, phase separation, SiO<sub>2</sub> purity effect 0-44144  
 SiO<sub>2</sub>-Na<sub>2</sub>O-CaO-MgO-Al<sub>2</sub>O<sub>3</sub> charge, silicate formation during heating 0-55342  
 SmCO<sub>5</sub>, based permanent magnets, props. and cryst. orientation (Russian) 0-20431  
 Sn, X-ray diffraction study of thermal motion of atoms in β-Sn 0-39243  
 Sr<sub>3</sub>(VO<sub>4</sub>)<sub>2</sub>, determination of enthalpies of formation, from heats of solution 0-2182

**X-ray diffraction examination of microstructure continued**

- Ta-O supersaturated solid solution, precipitation processes, hardness change meas. 0-25712  
 Th-Fe (20 to 70 at.%), amorphous alloy, electrical resistivity and thermal stability 0-33901  
 Ti-Al-V (6.4 wt.%), phase transformation after hydrogenation 0-7560  
 Ti-Cr-Zr, martensite formation, chemical composition effect 0-50634  
 Ti-Nb-Al, decomposition during isothermal annealing 0-25653  
 Ti-Nb-Zr (35, 3 wt.%), martensitic  $\tau$  phase, X-ray diffr. obs. 0-16300  
 Ti-TiC-TiN system, phases 0-20905  
 Ti-Zr-W-(Al) alloys, phase struct. and props. (Russian) 0-16270  
 V-Ni-Mo, structure in alloy crystallisation region, peritectic equilibria (Russian) 0-50622  
 V-O system  $\beta$  phase BCT, X-ray diffr. study of additional scatt. effect (Russian) 0-10537  
 Y<sub>2</sub>Ti<sub>2</sub>O<sub>7</sub>, precipitation from oxalates, carbonates, exam. 0-55641  
 YbCr<sub>1-x</sub>Al<sub>x</sub>O<sub>3</sub> solid solutions 0-20887  
 Zn-Sn-Hg, diagram of state, melting temp., peritectic and eutectic phases (Russian) 0-55350  
 ZnS:Mn, dopant conc. effect on stacking fault energy 0-2041  
 ZnTe film, prepared by single-source vacuum deposition method (Japanese) 0-6664  
 Zn<sub>3</sub>(VO<sub>4</sub>)<sub>2</sub>, determination of enthalpies of formation, from heats of solution 0-2182  
 $\alpha$ -Zr monocrystal perfection using Berg method and diffractometer with omega device (French) 0-2035  
 Zr-Al (14 wt.%), transformation sequence from Zr-Al martensite to Zr<sub>3</sub>Al phase 0-3027  
 ZrO<sub>2</sub>-SiO<sub>2</sub> (11 to 13 wt.%), X-ray phase anal. 0-35195

**X-ray diffraction examination of molecular structure**

see also molecular configurations

- biological structural determinations using synchrotron X-rays 0-46112  
 dibromomaleic acid thioanhydride, mol. and cryst. structs., X-ray obs. (German) 0-44199  
 diiodomaleic acid thioanhydride, mol. and cryst. structs., X-ray obs. (German) 0-44199  
 epoxide compound, polymerisation in non-uniform magnetic field, exam. of structural changes 0-7791  
 myelin lattice swelling kinetics study 0-21436  
 polyoma virion and capsid crystal structures 0-8011  
 Schiff's base compounds, double axis, Siamese Twin type liq. crystals, thermal and X-ray obs. 0-39312  
 TCNQ complex with 5-phenyl-[1-thiol]-3-selenol-2-thione, charge-transfer salt, cryst. and mol. struct. 0-33986  
 transition metal complexes, mol. dissymmetry, book 0-27057

**X-ray diffractometers**

- angle and energy-dispersive diffractometry system, design, operation and appls. 0-47163  
 autoclave attachment for Philips instrum. 0-31959  
 automated powder diffractometer, computerised control 0-3453  
 characteristic absorption of X-rays, diffractometer study 0-20733  
 crystal centering, and diffractometer alignment errors calcs., appl. to high pressure crystallography 0-22494  
 elemental analyser, diffractometer based 0-318  
 Enraf-Nonius CAD-4 diffractometer, mechanical design, computer control and system performance 0-24318  
 four-circle, solid-state detector, for white X-ray diff. work (Japanese) 0-1897  
 four-circle diffractometers, simple methods of aligning with crystal reflections 0-22493  
 high angle double crystal diffractometry, improvement for meas. temp. depend. of lattice constants, pt.I 0-1890  
 high angle double crystal diffractometry, temp. depend. of lattice constants, pt.II 0-1891  
 HZG 4/A universal instrument, applic. versatility of basic software 0-52375  
 laser thermonuclear fusion, shell target parameters meas. using X-ray schlieren method 0-14942  
 low-temperature X-ray diffractometer for work with actinide metals and compounds 0-316  
 microcomputer controlled system 0-317  
 monitor arrangements (German) 0-52374  
 Philips PW 1100, used for crystal struct. research at high pressure 0-38873  
 Picker FACS-I diffractometer, microprocessor-controlled optical incremental angle encoder system 0-18058  
 polythermal attachment for powder diffractometers to allow operations in range -150 to +900°C 0-311  
 scanning block modernisation by scaler adjustment 0-31958  
 single-crystal diffractometry, peak searching, crystal setting and determining automatic cell constants 0-6319  
 slit unit, for PW1100, computer controlled 0-37135  
 X-ray powder diffractometer, APD3600, file searching techniques 0-24319

**X-ray effects**

see also biological effects of X-rays

- alkali borate binary glass, energy storage behaviour studied by thermoluminesc. 0-50432  
 alkali halides, <sup>14</sup>N impurities, molecular point defects, EPR isotropic hyperfine triplets 0-2636  
 dielectric, surface vac. breakdown by ultrasoft X-rays 0-43989  
 doped-silica optical fibres, nuclear radiation effects 0-33172  
 dulcitol, X-irrad., 4.2K, electron traps, alkoxy hyperfine coupling, ENDOR obs. 0-50863  
 imidazole, EPR study of H exchange 0-40718  
 insulating materials, high energy radiation effects 0-19835  
 N-acetyl-L-leucine, single crystals, X-ray induced free radicals 0-45525  
 polyethylene, high density, carrier trapping, X-ray induced TSC 0-11005  
 $\alpha$ -quartz, hydrogenic trapped hole species, EPR studies 0-44915  
 radiography, rare-earth screens, effect of P X-rays 0-30867  
 silicate glasses, effect of high-dose X-rays and reactor radiation 0-19838  
 sorbitol, X-irrad., 4.2K, electron traps, alkoxy hyperfine coupling, ENDOR obs. 0-50863  
 TGS X-irradiated, paramag. relax, spin-echo study 0-7168  
 TTF-TCNQ, X-ray irrad., transverse cond. 0-6432  
 xylitol, X-irrad., 4.2K, electron traps, alkoxy hyperfine coupling, ENDOR obs. 0-50863  
 $\alpha$ -Al<sub>2</sub>O<sub>3</sub>, crystal defects from X-ray irradiation, F-centres, X-ray luminesc. obs. 0-55176



## X-ray effects continued

- $\alpha$ -Al<sub>2</sub>O<sub>3</sub>:Er(Cr), crystal defects from X-ray irradiation, F-centres, X-ray luminesc. obs. 0-55176  
 $\beta$ -Al<sub>2</sub>O<sub>3</sub>:K<sub>2</sub>O(Na<sub>2</sub>O)(H<sub>3</sub>O<sup>+</sup>), ESR of paramag. defects in cond. planes 0-29617  
 BaFCl crystals, F-centres, X- and  $\gamma$ -irradiation, thermoluminescence and optical absorption spectra 0-45155  
 BaSO<sub>4</sub>, X-ray irradi., electron and holes traps, g-factors, ESR obs. 0-50183  
 BaTiO<sub>3</sub>, ferroelectric semicond. anomalous photovoltaic effect due to ionising radiation 0-29437  
 CaF<sub>2</sub>:Na, single cryst., X-irrad., optical absorpt. and thermoluminesc. 0-34952  
 Ca(OH)<sub>2</sub>:Ni<sup>2+</sup> single cryst., X-irrad., Ni<sup>+</sup> EPR, g-factors and point-charge model 0-2626  
 CaS:Tb,Eu phosphors, fluoresc. spectra under X-ray excitation 0-16083  
 Cd(ClO<sub>4</sub>)<sub>2</sub>, irradiated single crystal, ESR and annealing, trapped defect centre 0-55141  
 CdS single crystals, Roentgenoluminescence, exciton interactions (*Russian*) 0-2853  
 Co melt, struct. charact. time depend. in X-ray studies (*Russian*) 0-24350  
 CsBr:Cu<sup>+</sup>, X-ray irradi., thermoluminesc. 0-16107  
 CsCl:Cu<sup>+</sup>, X-ray irradi., thermoluminesc. 0-16107  
 H<sub>2</sub>SO<sub>4</sub>, frozen soln., EPR of trapped H-atoms produced by UV and X-irrad. 0-3369  
 KBr, excitation of thermolum. near liq. He temp. 0-40171  
 KBr, whiskers, F-centre accumulation and track effects due to X-ray irradi. 0-39484  
 KBr, X-irrad., F-centre role in thermoluminescence 0-20720  
 KBr(Cl), X-ray irradi., tunnelling recomb. luminesc. 0-2873  
 KCl (Br) crystals, thermally stimulated luminescence accompanying recombination of V<sub>F</sub> and F centres 0-55201  
 KCl, whiskers, F-centre accumulation and track effects due to X-ray irradi. 0-39484  
 KCl:Ga(In), ESR of impurity centres, impurity optical absorpt. bands 0-29618  
 KCl:SnCl<sub>2</sub>, X-ray irradi., polarised luminesc. and EPR study of Sn<sup>3+</sup> centres 0-39868  
 KCl:Sr, thermally pre-treated, glow curves 0-25470  
 KCl-Ba, X-ray irradi. cryst., thermoluminescence spectra 0-20719  
 KCl<sub>0.5</sub>Br<sub>0.5</sub>:Ca, X-ray irradi., Z<sub>1</sub>-centres, thermoluminesc. and optical absorpt. meas. 0-16108  
 KClO<sub>4</sub>, X-irrad. induced paramag. defects, ESR study 0-24493  
 K<sub>2</sub>Cr<sub>2</sub>O<sub>7</sub> single crystals, X-irrad., EPR spectra 0-2638  
 KI(Br), X-irradiated cryst., luminesc. during press. release 0-20722  
 K<sub>2</sub>SO<sub>4</sub>:(NH<sub>4</sub>)<sub>2</sub>SO<sub>4</sub>, X-irrad., EPR of NH<sub>3</sub><sup>+</sup> 0-11272  
 LiD:Mg<sup>2+</sup>, X-irrad., dielec. loss 0-55024  
 LiF, X-irradiated cryst., luminesc. during press. release 0-20722  
 LiF:Mg, X-ray irradi., trapping processes, Z-centres and dipoles, two models 0-49222  
 LiF:OH crystals, X-irradiated, H centres formation and annealing 0-54226  
 LiNbO<sub>3</sub> crystals, polaron character of colour centres produced by X-rays 0-2013  
 LiNbO<sub>3</sub>:Fe, impurity valence state charge on X-ray irradi., Mossbauer meas. 0-7235  
 LiNbO<sub>3</sub>:Fe, X-ray and  $\gamma$ -ray irradiation effects on Fe charge state, Mossbauer study 0-40013  
 Li<sub>2</sub>O-LiCl-B<sub>2</sub>O<sub>3</sub> system, fast Li<sup>+</sup> ion vitreous superconductors, EPR study (*French*) 0-11269  
 Mg(NH<sub>4</sub>)<sub>2</sub>(SO<sub>4</sub>)<sub>2</sub>·6H<sub>2</sub>O:Cr<sub>2</sub>O<sub>7</sub><sup>2-</sup>, optical absorption study, Cr<sub>2</sub>O<sub>7</sub><sup>2-</sup> and CrO<sub>4</sub><sup>3-</sup> centres 0-55128  
 MgO, single crystal, thermal and optical stimulation processes of V-centres (*Japanese*) 0-11485  
 NaBr-U-centre containing cryst., X-ray radiation induced cation vacancy generation 0-39078  
 NaCl crystals with dipole O colour centres, radiation colouring and holographic recording 0-48187  
 NaCl, irradiated, at 80K, thermolum. processes 0-34990  
 NaCl, thermal expansion meas. after X-ray irradi., F-centre bleaching 0-44338  
 NaCl, X-ray irradi., vacancy conc., thermal expansion meas. 0-6431  
 NaCl:Ca, Z<sub>1</sub> centre thermoluminescence study 0-16109  
 NaCl:Ga(In), ESR of impurity centres, impurity optical absorpt. bands 0-29618  
 NaCl:O<sup>2-</sup>, X-ray irradi., defect generation during radiolysis 0-7831  
 NaClO<sub>4</sub>, aq. glass, formation of trapped H-atoms and electrons 0-35559  
 NaClO<sub>4</sub>, frozen soln., EPR of trapped H-atoms produced by UV and X-irrad. 0-3369  
 NaOH, frozen soln., EPR of trapped H-atoms produced by UV and X-irrad. 0-3369  
 Ni melt, struct. charact. time depend. in X-ray studies (*Russian*) 0-24350  
 SbSI, ferroelectric semicond. anomalous photovoltaic effect due to ionising radiation 0-29437  
 Se, electroconductivity (*Russian*) 0-15519

## X-ray emission spectra

- see also appearance potential spectra; conversion electron spectra  
 actinide compounds, spectroscopic techniques for electronic props. meas. 0-11427  
 actinides, K X-ray energies, natural widths and intensities 0-37768  
 air/glass interface, ns. grazing discharge, X-ray emission 0-33846  
 atom, electron impact ionisation, characteristic X-radiation ang. distrib. obs. 0-1069  
 atom, K <sub>$\alpha$</sub> /K <sub>$\beta$</sub>  ratio for X-ray transitions in collisions 0-27972  
 atom, K <sub>$\alpha$</sub> /K <sub>$\beta$</sub>  X-ray intensity ratio, depend upon energy of incident proton 0-47934  
 atom, multielectron, correlated transitions in decay of two inner-shell vacancies 0-37799  
 atom, transition array and energy level distrib. variance, Mo VX-XIV appl. 0-37767  
 atom Breit interaction between electrons, calc. angular coeffs., computer program 0-18779  
 atoms, Z=46-54, L<sub>7,2,3</sub> emission spectra, breadth, dynamical effects 0-32645  
 book on X-ray spectroscopy 0-2899  
 dielectronic recombination spectra, appls. in astronomy 0-46391  
 dynamical calculations 0-55227

## X-ray emission spectra continued

- fluorescence spectra, energy dispersive, least-squares anal., detector response function approach 0-3457  
 fluorescence spectra, resolution by weighted least squares computer program 0-3459  
 fourth-row elements, Pd to Xe, XPS, XES, dynamical effects 0-52924  
 hard X-ray energy and flux meas. for 50 keV to 10 MeV range 0-48992  
 ion-surface impact, MO X-ray spectra, recoil effects 0-25510  
 K <sub>$\beta$</sub> /K <sub>$\alpha$</sub>  X-ray intensity ratio used to obtain efficiency curve of planar Ge(Li) detector 0-880  
 K <sub>$\beta$</sub> /K <sub>$\alpha$</sub>  rel. intensity obs., 33 $\leq$ Z $\leq$ 57 0-32665  
 K level X-ray lines, relative transition probability 0-935  
 K-satellites, screening effect 0-999  
 K-spectra, origin of low-energy satellites,  $\alpha$ -region 0-55229  
 metals, X-ray spectra, final state pot., one-electron theory 0-55230  
 Mg, K X-ray emission spectra, double plasmon high energy satellite 0-11510  
 molecular X-ray transitions in heavy ion-atom collisions 0-43170  
 muonic atoms, X-ray vacuum corrections, nuclear moments, transitions and deformation parameters 0-37912  
 muonic X-ray intensities in low-Z elements and their hydrides 0-9761  
 muonic X-rays, formation and expts. 0-43215  
 neutron induced X-ray atomic excitation 0-23510  
 nuclear K-X-ray satellites, Z=50-83, by  $\alpha$ -bombard, 17.5-22.5 MeV 0-42984  
 pionic atom, X-ray intensity, at. no. variation, Z=5-90 0-43212  
 plasma XUV transition Doppler broadening suppression, collisional-radiative model 0-19614  
 polyethylene, X-ray emission spectra of CO<sub>2</sub> laser-irrad. targets, nonlinear processes 0-33793  
 radiography, diagnostic, X-ray spectra determ., high intensity 0-41217  
 rare earth germanides, X-ray emission, absorption and photoelectron spectra (*Russian*) 0-11509  
 simple metals, effect of core hole on X-ray emission spectra 0-20737  
 target, ion beam heated, soft X-ray and VUV spectra 0-2907  
 techniques and spectral interpretation, rel. to XPS, book contrib. 0-11514  
 theory, techniques, and appl., book 0-8748  
 thin films, thickness meas. anal. characterisation using proton-induced X-ray emission 0-35618  
 Tokamak plasma confinement systems, soft X-ray meas. 0-48959  
 transition metal, many-config. approx. in X-ray and electronic spectra interpret. 0-32615  
 transition metal carbonitrides, carbides and oxynitrides, electronic struct., theoretical approach 0-54584  
 transition metal compounds, chem. shifts of X-ray emission K-lines of transition elements, free-atom approx. applic. 0-11513  
 transition metal compounds, valence band struct., X-ray spectroscopic study 0-29319  
 transition metal germanides, X-ray emission, absorption and photoelectron spectra (*Russian*) 0-11509  
 transition metals, 3d, electron impact excited soft X-ray spectra, resonances and many body effects 0-50468  
 Z=8-50 kaonic atoms, X-rays, strong interaction effects 0-9763  
 ZnO-based varistor, grain-boundary segregation, thin film X-ray spectroscopy obs. 0-35185  
 Zr, X-ray emission spectrum, K-satellites 0-40188  
 $\mu^{\pm}$  spin rotation,  $\mu$  relaxation and repolarisation, muonic X-rays 0-42644  
 $\mu$ Xe muonic atoms, vanishing muon transfer effect 0-9765  
 Ag, X-ray prod. by 5 MeV/amu deuterons (oxygen ions), projectile Z depend. 0-42982  
 Al coated glass microballoon targets for laser implosion expt., search for shell disintegration 0-33792  
 Al, many-body response in X-ray absorption, emission and photoemission spectra 0-16124  
 Al, soft X-ray emission and absorpt. edges, self-absorpt. studies 0-40183  
 Al, X-ray absorpt. and emission edges, one-electron and many-body effects 0-25484  
 Al, X-ray emission spectra of CO<sub>2</sub> laser-irrad. targets, nonlinear processes 0-33793  
 Al-Cu, disordered, electron energy struct. and X-ray emission bands, average t-matrix approx. (*Russian*) 0-24779  
 Ar, free ats. electron bombard., subsequent X-radiation ang. distrib. 0-53144  
 Ar<sup>15+</sup> and Ar<sup>16+</sup>, beam-foil obs. of lifetimes of metastable states 0-14116  
 Ar+Ar low energy collisions, K X-ray excitation, impact parameter depend. 0-23539  
 Ar+N ion, K $\alpha$  X-ray satellites prod. 0-9541  
 As, L-shell soft X-ray emission spectra, oscillator strengths 0-32651  
<sup>33</sup>As, origin of high and low freq. K-satellites in X-ray emission spectra 0-50466  
 Au+H<sup>+</sup>, L X-ray production cross sections, 0.3-1.8 MeV, expt. rel. to PWBA prediction 0-53115  
 Au+H<sup>+</sup> ionisation, induced L-shell alignment 0-32813  
 BP<sub>x</sub>As<sub>1-x</sub> system, electron struct. and interatomic interactions, X-ray spectroscopy 0-20736  
 Be, HCP metals, K-emission valence bands, structure and bonding 0-7438  
 Be, soft X-ray emission and absorpt. edges, self-absorpt. studies 0-40183  
 BeO, X-ray emission spectra, double plasmon high energy satellites 0-29829  
 Bi+H<sup>+</sup>, L X-ray production cross sections, 0.3-1.8 MeV, expt. rel. to PWBA prediction 0-53115  
 Br, L-shell soft X-ray emission spectra, oscillator strengths 0-32651  
 C, pionic X-ray intensities in graphite 0-32858  
 C-bearing gases, K-shell X-ray yields, proton-induced, chem. effects 0-37820  
 CH<sub>2</sub>(CD<sub>2</sub>), pionic X-ray intensities in polyethylene(-d<sub>n</sub>) 0-32858  
 CO<sub>2</sub><sup>-</sup>, molecular orbital anal., anisotropic X-ray emission obs. of components 0-18786  
<sup>44</sup>Ca, A=40, 42-44, 48, pionic X-rays, strong interaction and isotope shifts,  $\pi$ -nuclear optical pot. 0-53169  
 CdO-Bi<sub>2</sub>O<sub>3</sub>:Al<sub>2</sub>O<sub>3</sub>, glass formation and IR transmission (*Japanese*) 0-54146  
 CdTe, trace anal. by heavy ion induced X-ray emission and SIMS 0-55755  
 Co,  $\alpha$  and  $\beta$  phases, L<sub>111</sub> emission bands (*Russian*) 0-25491  
 Co, K <sub>$\beta$</sub>  X-ray emission spectra, low energy plasmon satellites 0-19560  
 Cr, X-ray prod. by 5 MeV/amu deuterons (oxygen ions), projectile Z depend. 0-42982



**X-ray emission spectra continued**

- Cr, O<sub>2</sub>, low energy X-ray emission satellite, unpaired electron and plasmon effects 0-35007
- Cu, K $\beta_{1,3}$  X-ray emission spectra, low energy plasmon satellites 0-19560
- Cu, L-shell soft X-ray emission spectra, oscillator strengths 0-32651
- Cu, valence band splitting, X-ray K-emission spectroscopy 0-40189
- Cu, X-ray prod. by 5 MeV/amu deuterons (oxygen ions), projectile Z depend. 0-42982
- <sup>64</sup>Cu  $\beta^-$  and  $\beta^+$ -decays, K-shell ionisation probabilities, X-ray spectra 0-42592
- Dy+H<sup>+</sup> ionisation, induced L-shell alignment 0-32813
- <sup>160</sup>Dy anomalous  $\gamma$ -L X-ray directional correlations from <sup>160</sup>Tb decay 0-52610
- <sup>152</sup>Eu, X-ray emission probabilities per decay 0-14027
- F<sup>+</sup>+He, 10 to 40 MeV, F<sup>6+</sup> K-vacancy production, role of excitation 0-37859
- Fe alloys, ion-implanted, depth profile and diffusion coeff., X-ray emission study 0-54277
- Fe F<sub>2</sub> (Fe F<sub>3</sub>), electronic struct., binding energy, X-ray emission and photoelectron spectra obs. 0-35008
- Fe X, 3p<sup>4</sup>s levels, population processes 0-47926
- Fe, X-ray prod. by 5 MeV/amu deuterons (oxygen ions), projectile Z depend. 0-42982
- Fe-Al, X-ray emission spectra 0-25489
- Fe+I, Fe K- $\alpha$  X-ray emission, high-resolution meas. 0-37871
- Ga, L-shell soft X-ray emission spectra, oscillator strengths 0-32651
- <sup>31</sup>Ga, origin of high and low freq. K-satellites in X-ray emission spectra 0-50466
- GdCl<sub>3</sub>·6H<sub>2</sub>O, thermal decomp., X-ray emission luminesc. (Japanese) 0-55763
- Ge-rare earth alloys, nature of chemical interaction, X-ray emission, absorpt. and photoelectron study (Russian) 0-55261
- <sup>32</sup>Ge, origin of high and low freq. K-satellites in X-ray emission spectra 0-50466
- H<sub>2</sub>O, ESCA and soft X-ray emission, vibr. excitation 0-23433
- He, electron impact excitation rel. to photon interactions 0-27985
- He<sup>+</sup> Lamb-shift measurement by the quenching-radiation anisotropy method 0-18824
- Hf+H<sup>+</sup> (He<sup>+</sup>), L-subshell ionisation cross section, branching ratios, fluorescence yield, Coster-Kronig factors 0-43166
- H<sup>+</sup> (spin polarised)+atom, inner-shell ionis., subsequent radiation ang. distrib. 0-53114
- In, X-ray prod. by 5 MeV/amu deuterons (oxygen ions), projectile Z depend. 0-42982
- K, soft X-ray emission and absorpt. edges, self-absorpt. studies 0-40183
- Kr, free ats. electron bombard., subsequent X-radiation ang. distrib. 0-53144
- La, electron impact excited soft X-ray spectra, resonances and many body effects 0-50468
- La, X-ray reson. emission, appearance pot. and charact. electron energy loss spectra 0-16126
- Li, X-ray absorpt. and emission edges, one-electron and many-body effects 0-25484
- Mg, HCP metals, K-emission valence bands, structure and bonding 0-7438
- Mg I, Mg II autoionisation state radiative decay (Russian) 0-5509
- Mg, K $\alpha_1$  and K $\alpha_2$  wavelengths 0-50464
- Mg, soft X-ray emission and absorpt. edges, self-absorpt. studies 0-40183
- Mg, X-ray absorpt. and emission edges, one-electron and many-body effects 0-25484
- Mg XII, resonance line, atomic parameters calc. for dielectronic satellite lines 0-42983
- Mg<sup>2+</sup>, beam-foil excited, spin orbit-forbidden X-ray transition obs. 0-23537
- Mo, X-ray M $\zeta$  energy, revised values 0-14102
- Mo+Nb, K-shell vacancy prod., impact parameter depend. 0-14225
- MoS<sub>2</sub>, struct., XES and XPS obs. 0-43105
- <sup>A</sup>Mo,  $\Lambda=92, 94-98, 100$ , muonic atom X-ray transitions, nuclear charge radii 0-27545
- NH<sub>3</sub>, ESCA and soft X-ray emission, vibr. excitation 0-23433
- Na compounds, muonic X-ray intensities, Lyman series 0-23578
- Na, impurities and photoexcited ions 0-39523
- Na, K $\alpha_1$  and K $\alpha_2$  wavelengths 0-50464
- Na, X-ray absorpt. and emission edges, one-electron and many-body effects 0-25484
- Na, X-ray emission spectra, double plasmon high energy satellites 0-29829
- Na<sub>2</sub>O(K<sub>2</sub>O)-P<sub>2</sub>O<sub>5</sub> glasses, P K-band X-ray emission spectra, state anal. 0-40190
- Nb, X-ray M $\zeta$  energy, revised values 0-14102
- Nb XXXIX and XL, X-ray spectrum weak line detection 0-5497
- Nb-V, negative muon Coulomb capture ratio and Lyman series intensities 0-14255
- Nb-Zr-C (0.1, 0.01 wt.%) plastic deform. influence on electronic state of Nb atoms 0-40463
- Nb+Nb, selected MO X-ray coincidence with separated at. K X-rays 0-43148
- Nb<sub>3</sub>Ga(So)(Ir)(Pt)(Au), X-ray M<sub>IV,V</sub> emission bands (Russian) 0-45170
- Nb<sub>0.5</sub>Mo<sub>0.5</sub>, soft X-ray spectra, theoretical considerations 0-11511
- NbO<sub>2</sub>, rutile phase, energy levels, momentum density, and Compton profile, embedded cluster model 0-50453
- Nb<sub>3</sub>(Sn-Al) system, X-ray spectroscopic studies of electronic struct. of A15 cpds. 0-2900
- Ne+heavy ion, few-electron states prod. K X-rays obs. 0-9718
- Ni+Ni, continuum X-ray radiation, collision broadening 0-9539
- Ni+Ni<sup>+</sup>, with nuclear sticking, molecular orbital and compounds nucleus X-ray emission 0-1048
- O, K $\alpha$  spectrum, intensity of high energy peak as function of oxide layer thickness 0-936
- <sup>185</sup>Os, muonic resonance spectra, deduced isomer shifts and electric moments 0-18948
- P allotropic modifications, muonic X-ray intensities, computer analysis 0-23577
- P, muonic allotropes muonic Roentgen intensities (German) 0-53168
- PH<sub>3</sub>, K-fluoresc. obs. of electronic struct. 0-37818
- <sup>31</sup>P, muonic, 3d-2p X-ray transition 0-9764
- Pb, X-ray emission spectra of CO<sub>2</sub> laser-irrad. targets, nonlinear processes 0-33793
- Pb+Pb K-MO spectrum, impact parameter depend. 0-5613
- PbO-Bi<sub>2</sub>O<sub>3</sub>-Al<sub>2</sub>O<sub>3</sub>, glass formation and IR transmission (Japanese) 0-54146

**X-ray emission spectra continued**

- Pt, laser produced plasma, Ni-like X-ray spectrum 0-43983
- Rb, L-shell soft X-ray emission spectra, oscillator strengths 0-32651
- S adsorption in coal, content meas., using X-ray radiometric analysis 0-26077
- <sup>113</sup>Sb mean nuclear lifetime from X-ray spectrum in <sup>112</sup>Sn(p,p') 0-9267
- Se allotropic modifications, muonic X-ray intensities, computer analysis 0-23577
- Se, K-emission satellites, HF and LF, origin 0-50465
- Se, muonic allotropes, muonic Roentgen intensities (German) 0-53168
- Si, in laser-irradiated glass shell plasma, electron density and temp. diagnostics (Chinese) 0-38718
- Si ions, multiply-charged, beam-foil obs. of 1s2p<sup>3</sup>P, lifetime 0-14114
- Si, relativistic electron channelling spectra 10-130 keV 0-24516
- SiO<sub>2</sub>, amorphous and  $\alpha$ -cristobalite cryst., band struct., photoelectron and X-ray spectra interpret. 0-24787
- SiX<sub>4</sub> (X=Cl,H,F), chemical shifts, relax., X-ray spectra, SCF Xalpha calcs. 0-27928
- Sm, X-ray prod. by 5 MeV/amu deuterons (oxygen ions), projectile Z depend. 0-42982
- Sr, L-shell soft X-ray emission spectra, oscillator strengths 0-32651
- Ta+H<sup>+</sup> (He<sup>+</sup>), L-subshell ionisation cross section, branching ratios, fluorescence yield, Coster-Kronig factors 0-43166
- Ti+He<sup>2+</sup> (C<sup>4+</sup>)(O<sup>5+</sup>)(N<sup>4+</sup>)(N<sup>5+</sup>) atom-ion collisions, ratio of single K-shell ionisation cross section to double K-shell ionisation cross section 0-53119
- TiC, soft X-ray emission, excitation pot. spectra, excited level binding energy 0-35009
- TiF<sub>2</sub>, TiF<sub>4</sub>, X-ray emission, core level chem. shift calcs. 0-53010
- TiH<sub>4</sub>, X-ray emission, core level chem. shift calcs. 0-53010
- TiH<sub>3</sub>F, X-ray emission, core level chem. shift calcs. 0-53010
- TiN, soft X-ray emission, excitation pot. spectra, excited level binding energy 0-35009
- <sup>A</sup>Ti,  $\Lambda=46, 48, 50$ , pionic X-rays, strong interaction and isotope shifts,  $\pi$ -nuclear optical pot. 0-53169
- U+H<sup>+</sup>, L X-ray production cross sections, 0.3-1.8 MeV, expt. rel. to PWBA prediction 0-53115
- V, atom and ions, shell energy struct., SCF calc. by Dirac-Fock-Slater method 0-52877
- VC, soft X-ray emission, excitation pot. spectra, excited level binding energy 0-35009
- VN, soft X-ray emission, excitation pot. spectra, excited level binding energy 0-35009
- W+H<sup>+</sup> (He<sup>+</sup>), L-subshell ionisation cross section, branching ratios, fluorescence yield, Coster-Kronig factors 0-43166
- Xe compounds, Xe chemical and isomer shifts, electron valence struct. (Russian) 0-53056
- Xe, free ats. electron bombard., subsequent X-radiation ang. distrib. 0-53144
- Xe+H<sup>+</sup>, ionisation, induced L-shell alignment 0-32813
- Y, X-ray M $\zeta$  energy, revised values 0-14102
- YOF, electronic struct. calcs. from XPS and X-ray emission spectra 0-35056
- Yb+Yb<sup>+</sup>, with nuclear sticking, molecular orbital and compounds nucleus X-ray emission 0-1048
- <sup>172</sup>Yb, muonic resonance spectra, deduced isomer shifts and electric moments 0-18948
- Zn, HCP metals, K-emission valence bands, structure and bonding 0-7438
- Zn, L-shell soft X-ray emission spectra, oscillator strengths 0-32651
- <sup>30</sup>Zn, electron bombardment, K $\alpha$  satellites 0-47932
- Zr, X-ray M $\zeta$  energy, revised values 0-14102
- Zr XII, energy level system, spectrum obs. 70 to 630 Å 0-37766
- ZrH<sub>x</sub> (x=1.55, 1.7), synthesis and electron structure 0-29889
- ZrN<sub>x</sub>H<sub>x</sub> (y=0.81 or 0.84, x=0.19 or 0.16) synthesis and electron structure 0-29889

**X-ray fluorescence analysis**

- advances, techniques and instrumentation, conference, Denver, USA (Aug. 1978) 0-3447
- anodic oxide superficial layer, X-ray emission spectrometry and ion back-scattering (French) 0-49482
- background determination by simple check ratios 0-3435
- biological X-ray microanalysis 0-41349
- components mutual effect, exam. by calibration method during analysis 0-21339
- computer operating system for X-ray diffr., fluoresc. anal. and electron microprobe anal. 0-322
- data interpretation, online system using multivariate statistical anal. and pattern recognition 0-3461
- empirical influence coefficient methods, review 0-3455
- energy-dispersive, using X-ray tubes in combination with secondary targets, spectrometer optimisation 0-30316
- epitaxial thin films, chemical structure 0-3451
- EXAFS, detection with X-ray filter assembly 0-31961
- external standard variant method, construction of analytical curve 0-21338
- glass, structural analysis, using fluorescence excitation (German) 0-38923
- high intensity polarised X-rays, excitation, improved X-ray fluoresc. capabilities 0-3468
- intensity due to photoelectrons, calc. 0-26075
- intensity measurements in X-ray fluorescence analysis 0-16759
- intensity-concentration modelling in energy dispersive systems 0-3464
- interactive regression anal., computer program 0-3463
- joint inflammation, radioisotope X-ray fluoresc. technique obs. 0-56184
- least squares anal., detector response function approach 0-11989
- mass absorption coeffs., meas. using X-ray diffractometers and fluoresc. spectrometers 0-18063
- matrix correction, computer program (German) 0-3427
- matrix correction methods using scattered radiation 0-3456
- matrix effects, reduction by Monte Carlo, fundamental parameters method 0-3460
- metal compounds on microfilters, X-ray fluoresc. spectrometry anal. 0-30315
- Monte Carlo simulation, inter-element effects determ. 0-26080
- multielement apparatus using semiconductor detector and X-ray tube 0-22488
- observation limit, relationship with atomic number 0-18057
- pigments of Minoan painted pottery, XRF-XRD analysis method 0-35586



**X-ray fluorescence analysis continued**

- radioisotope X-ray fluoresc. analysis of trace elements in biological specimens 0-12240  
 Schartz's inequality applic. to equiv. wavelength variation analysis (*French*) 0-50894  
 secondary excitation correction 0-30317  
 simultaneous determ. of three elements 0-40786  
 slurries, solids content determ. by X-ray scatt. 0-3467  
 spectra, energy dispersive, least-squares anal., detector response function approach 0-3457  
 spectra, resolution by weighted least squares computer program 0-3459  
 spectrometer system, PW1400, microprocessor controlled (*German*) 0-16758  
 spectrometry, single and multielement anal., optimum excitation conditions, automated determ. 0-323  
 steel, C, wear of Cr, Zn protective coatings, exam. using nuclear radiation excited X-ray fluorescence 0-21206  
 steel, carbon content in surface layers and in bulk 0-3466  
 steel, galvanised coatings, thickness meas. using X-ray fluorescence radiation, apparatus design 0-21202  
 steel, mild, AISI 1009 and 1018, corrosion incipient processes in hypersaline geothermal brine at 90°C 0-50753  
 steel, stainless, 300 and 400 series, quantitative anal. 0-3465  
 steel, standard, energy dispersive X-ray fluoresc. spectrometry, computer directed optimisation 0-45585  
 steels, stainless and low-alloy, X-ray fluorescence anal., matrix corrections, minicomputer program 0-3458  
 surface and bulk microanalysis, electron spectroscopy apparatus (*French*) 0-47151  
 thickness meas. of Au and Ni layers on Cu substrates simultaneously 0-13041  
 thin film calibration standards 0-22496  
 total reflection X-ray fluorescence analysis (*German*) 0-30314  
 trace elements in light element matrices, direct determ. using incoherent scattered radiation as internal standard 0-11970  
 wavelength dispersive X-ray fluorescence analysis, rel. to energy dispersive X-ray fluorescence anal. 0-7885  
 Al alloys, energy dispersive X-ray fluoresc. spectrometry, computer directed optimisation 0-45585  
 Cr-Mo-N system, at high-pressure, temp., X-ray anal., phase diagram 0-50607  
 Fe<sub>3</sub>O<sub>4</sub>-FeAl<sub>2</sub>O<sub>4</sub>-FeTiO<sub>3</sub> titaniferous magnetite, chlorination, 1273 to 2273K 0-55752  
 I<sup>-</sup> anal. in groundwater by X-ray fluorescence spectrometry 0-45829  
 K<sub>2</sub>O-TiO<sub>2</sub>-SiO<sub>2</sub> glass, Si-O bonding, SiK $\beta$  X-ray fluorescence and IR spectra 0-10500  
 Mn, Pb and V in waste water, coprecipitation method (*Japanese*) 0-21333  
 Na<sub>2</sub>O-TiO<sub>2</sub>-SiO<sub>2</sub> glass, Si-O bonding, SiK $\beta$  X-ray fluorescence and IR spectra 0-10500  
 S meter, model XA-300, for laboratory use 0-26085  
 Si(Li) gas cooled detector for in situ XFA spectrometer 0-18055  
 ZnSe:Ga,As, characts. of simultaneous incorporation, by Mn<sup>2+</sup> ESR and X-ray fluoresc. anal. 0-34017

**X-ray fluorimetry** *see* X-ray fluorescence analysis**X-ray lasers**

- amplification by ion accel. in plasma by steady state fields 0-28187  
 coherent X-ray generation from CO<sub>2</sub> laser backscattered relativistic electron beam 0-53252  
 Li laser, 207 Å, proposal for construction 0-43324

**X-ray monochromators**

- fixed wavelength, with removable Soller collimators 0-6318  
 monolithic crystal monochromators for synchrotron radiation with order sorting and polarizing properties 0-31963

**X-ray photoeffect** *see* X-ray photoelectron spectra**X-ray photoelectron spectra**

- actinide compounds, spectroscopic techniques for electronic props. meas. 0-11427  
 actinides, XPS, many-electron effects, comparison with rare earths 0-7466  
 adsorbed atoms and molecules XPS, many-body effects 0-55266  
 analytical potential, book contrib. 0-16761  
 atom, Ti 5d XPS comparison with TII 0-43099  
 book on X-ray spectroscopy 0-2899  
 bremsstrahlung-induced Auger peaks 0-45199  
 cobalt stearate, monomolecular layer, electron escape depth, XPS (*Japanese*) 0-11532  
 core level ligand field splittings 0-43106  
 crystals, electron spectroscopy, book 0-36786  
 difluoroethylenes, plasma polymerisation, ESCA characterisation of polymers 0-21283  
 dimethyl ether, condensed multilayers, electron bombard. effects, AES line-shape anal., XPS, and desorption meas. 0-7450  
 dynamical calculations 0-55227  
 electron spectroscopy, for bulk and surface microscopy and microanal. 0-52367  
 electronic levels, appl. of XPS (*French*) 0-45200  
 EXAFS in photoelectron yield spectra 0-16123  
 fluorides, meas. (*Japanese*) 0-16154  
 fourth-row elements, Pd to Xe, XPS, XES, dynamical effects 0-52924  
 germanates, meas. (*Japanese*) 0-16154  
 graphite plate sample holders 0-11972  
 graphite-alkali metal intercalation cpds., electronic props. 0-45202  
 graphite-SbF<sub>6</sub>(Cl<sub>4</sub>) intercalation compounds, compacts, elec. resistivity, C fluorination 0-34493  
 Incoloy 600 and 800, surface film in hot conc. NaOH, XPS study 0-11824  
 lunar regolite, Fe reduction on heating in vacuum, XPS spectra 0-41740  
 metal, ultrasoft XPS, plasmon satellite intensity 0-35058  
 metal halide intercalated graphite, acceptor site, XPS study 0-49218  
 metal-InP contacts, intermediate adsorbed layer effect on electronic props. 0-39674  
 metallic glass, bulk and surface properties, review 0-44147  
 metalloporphyrin, Z-ray photoelectron spectra satellites 0-5582  
 condensed multilayers, electron bombard. effects, AES line-shape anal., XPS, and desorption meas. 0-7450  
 mixed valence inorganic compounds with inequivalent atoms, XPS 0-2918  
 molecules or clusters, interpretation of data from Mossbauer, ESR, susceptibility, optical and XPS meas. 0-37825  
 nitrides, meas. (*Japanese*) 0-16154  
 p-nitroaniline, binding energy, XPS obs. 0-37833  
 organo-tin polymer films, glow discharge prep., comp. determ. by XPS and AES 0-35109  
 passivation films, on Sn plate, lacquer adhesion, ESCA exam. of constitution and effects 0-40776  
 Permalloy films, oxidation effects on atmospheric corrosion, AES, XPS and ion sputtering anal. 0-11829  
 Permalloy-Rh, film, influence of Rh on corrosion resist. and mag. props. 0-3235  
 polyacetylene:AsF<sub>6</sub>, thermal decomp. kinetics, elec. cond., ESCA and mass spectra 0-50830  
 polymer films on Au, ESCA, sample charging phenomena 0-20764  
 polystyrene, O treated, interaction with vapour-deposited Cr and Ni atoms 0-3407  
 polysulphur nitride:bromine, struct. and phase transition 0-24382  
 primary and secondary yields using low-energy monochromatic X-rays, standard surfaces 0-35053  
 PTFE+metal, fluoride prod., DSC and XPS anal., rel. to polymer wear 0-11889  
 PVC, chlorinated, X-ray photoelectron spectra investig. 0-3469  
 rare earth compound, valence fluctuation type, replicate core level XPS probe 0-25521  
 rare earth germanides, X-ray emission, absorption and photoelectron spectra (*Russian*) 0-11509  
 rare earth metals, electronic structure rel. to valence, chem. bonding 0-54601  
 rare earth metals, XPS and bremsstrahlung isochromat spectra of f<sup>n+1</sup>, f<sup>n-1</sup> states 0-40220  
 rare earth mixed valence compounds, spin dynamics, mag. neutron scatt., Mossbauer effect, XPS studies 0-39786  
 rare earth oxides, electronic structure rel. to valence, chem. bonding 0-54601  
 relative intensities, elastic scatt. in solid effect on free path and ang. distrib. 0-11531  
 rubber-brass interface, adhesion failure, XPS study 0-40671  
 silicates, core-level XPS peak intensity ratio ang. variations rel. to surface anal. and chemisorption 0-40225  
 simple metals, photoemission theory, book contrib. 0-16159  
 solid-state effects in XPS 0-55264  
 spectroscopy resolution with Mg K $\alpha$  radiation 0-18888  
 steel, galvanised, with paint coating, adhesion failure, XPS study 0-40671  
 steel, stainless, ferritic, passivity in 1N HCl, X-ray photo-electron spectroscopic study 0-11817  
 steel, stainless, surface treatment, X-ray photoelectron spectrosc. study 0-50764  
 steel, stainless, type 430, Ni<sup>+</sup>-implanted, struct., comp. and electrochem. anal. of surface alloy 0-16603  
 steels, free-machining, fractography and X-ray photoelectron spectroscopy 0-7673  
 surface (100), atomic struct., angle-resolved XPS, LEED and ISS investigation 0-10765  
 surface characterisation, physical methods, review (*French*) 0-7889  
 surface problems, in materials science and technology, conference, Gothenburg, Sweden, June 1979 0-51950  
 systems Ni ions anal. by ESCA (*Japanese*) 0-40787  
 thin film, and surface anal., modern methods 0-54486  
 transition metal borides, silicides and germanides, binding energies from X-ray photoelectron spectra 0-49170  
 transition metal borides, XPS meas. and chem. bond 0-20761  
 transition metal clusters, particle size rel. to bulk metallic props. 0-44490  
 transition metal compounds, valence band struct., X-ray spectroscopic study 0-29319  
 transition metal germanides, X-ray emission, absorption and photoelectron spectra (*Russian*) 0-11509  
 transition metal monosulphides of first-row, XPES and UV PES 0-20760  
 water, condensed multilayers, electron bombard. effects, AES line-shape anal., XPS, and desorption meas. 0-7450  
 Ag, adsorption and surface reaction of formic acid 0-40741  
 Ag, contact material, contamination layer thickness, resist., ESCA study (*German*) 0-55561  
 Ag, photoemission spectra and total primary yields for exploding wire radiator source 0-32773  
 Ag-Cu (10 wt.%), contact material, contamination layer thickness, resist., ESCA study (*German*) 0-55561  
 Ag-Pb (30 wt.%), contact material, contamination layer thickness, resist., ESCA study (*German*) 0-55561  
 Al, anodic behaviour in NO<sub>3</sub><sup>-</sup>/Cl<sup>-</sup> solns., electrochemical and XPS meas. 0-16694  
 Al brass condenser tubes, XPS study of protective layers 0-35383  
 Al, many-body response in X-ray absorption, emission and photoemission spectra 0-16124  
 AlN, interatomic interactions from XPS 0-49171  
 Al<sub>2</sub>O<sub>3</sub>, dense, exposed to steam, influence of Ca migration on strength reduction 0-11797  
 Ar, photoionisation, Auger processes, decay lifetime, line shift, profile, X-ray photoelectron spectra 0-37798  
 As<sub>2</sub>O<sub>3</sub> crystalline and amorphous, EXAFS study of struct. 0-19776  
 As<sub>2</sub>(Se,Te)<sub>3</sub> glasses, X-ray absorption and photoelectron spectroscopy study 0-7463  
 Au surface electronic structure, XPS study 0-55259  
 Au, XPS, electronic struct. 0-7464  
 Au-Cs(Mg)(Rb)(Zn), charge transfer, Mossbauer effect <sup>197</sup>Au isomer shifts, XPS valence-band spectra 0-2676  
 AuSn, XPS, electronic struct. 0-7464  
 BN, interatomic interactions from XPS 0-49171  
 B<sub>2</sub>O<sub>3</sub>, chem. bonding, electronic struct., ESCA, Auger, and SIMS spectra 0-50512  
 Ba, electron-correlation satellites, selective reson. enhancement 0-9569  
 Ba, XPS, in BaS and BaSO<sub>4</sub> 0-43104  
 BaTiO<sub>3</sub>, electronic props., SCF-MS-X $\alpha$  calc. 0-54607  
 BaTiO<sub>3</sub>, XPS satellite spectra, mol. orbital study 0-43100  
 Bi, XPS, electronic struct. 0-7464  
 Br<sub>2</sub>, extended X-ray absorption fine struct. amplitude attenuation, rel. to XPS satellites 0-37821  
 C, photoemission spectra and total primary yields for exploding wire radiator source 0-32773



## X-ray photoelectron spectra continued

- C<sub>6</sub>FeCl<sub>3</sub> intercalation compound, charge transfer, acceptor sites, XPS study 0-49218  
 CO, hydrogenation on Fe foil, AES and XPS study 0-7858  
 Cd, AES and XPS, vapour-metal electron energy shifts 0-16142  
 Cd<sub>0.6</sub>Mn<sub>0.4</sub>Te crystals, Mn(3d<sup>5</sup>) band, photoemission evidence 0-11535  
 γ-Ce, photoelectron spectra, 4f level position 0-25519  
 Co<sub>3</sub>B, crystalline, photoemission and electronic struct. 0-2926  
 Co<sub>78</sub>P<sub>14</sub>B<sub>8</sub>, amorphous, photoemission and electronic struct. 0-2926  
 Cr film, reversal etching in gas plasma, reaction mechanism, AES and XPS obs. 0-16564  
 Cr/polymer interface, electronic struct., XPS study 0-45204  
 CrO<sub>2</sub>, valence states of Cr, XPS obs. 0-40216  
 Cr<sub>2</sub>O<sub>3</sub>, electronic struct. study by XPS 0-25518  
 Cu (001), adsorbed O c(2×2), surface geometry determ. by deep-core-level XPS 0-40224  
 Cu (111), hydroxylation and dehydroxylation, XPS obs. 0-7850  
 Cu, adsorption and surface reaction of formic acid 0-40741  
 Cu, chem. aspects of corrosion inhibition by benzotriazole 0-16545  
 Cu film, valence bands, XPS excited by Zr M<sub>γ</sub> radiation 0-40236  
 Cu, surface, d-band narrowing, obs. using angle-resolved XPS 0-11062  
 Cu, surface film of 2-mercaptobenzothiazole and 2-mercaptobenzimidazole, XPS and X-ray induced Auger spectra obs. 0-40600  
 Cu/polymer interface, electronic struct., XPS study 0-45204  
 Cu-Sn-P (5, 1-5 wt.%), effect of P on friction and wear characts. 0-16494  
 Cu-Zr, metallic glasses, valence band struct. investigation 0-11533  
 CuCl, XPS and Auger spectroscopy, elec. struct. 0-29852  
 Cu(111) frequency depend. photoelectric surface state cross section periodic oscils., PES study 0-50522  
 ErH<sub>3</sub>, synchrotron XPS obs., rel. to theory for metal dihydrides 0-55275  
 Eu<sub>2</sub>La<sub>1-x</sub>Al<sub>2</sub>, binding energy and workfunction charges using XPES 0-33928  
 Fe, adsorption and surface reaction of formic acid 0-40741  
 Fe base amorphous alloys, alloying element role in improving corrosion resist., ESCA study 0-50754  
 Fe F<sub>2</sub> (Fe F<sub>3</sub>), electronic struct., binding energy, X-ray emission and photoelectron spectra obs. 0-35008  
 Fe oxides, interatomic interaction by XPS 0-7474  
 Fe-B amorphous alloys, valence band spectrum, XPS study 0-50534  
 Fe-Ni alloys, electronic struct., XPS study 0-29842  
 FeB and Fe<sub>2</sub>B, multiplet splitting of ESCA Fe 3s core levels 0-29847  
 Fe<sub>30</sub>B<sub>70</sub>, metallic glass, high-resolution XPS study, electronic state struct. 0-29846  
 Fe<sub>37</sub>Ni<sub>36</sub>Cr<sub>14</sub>P<sub>12</sub>B<sub>6</sub>, metallic glass, high-resolution XPS study, electronic state struct. 0-29846  
 Fe<sub>40</sub>Ni<sub>40</sub>P<sub>14</sub>B<sub>6</sub>, metallic glass, high-resolution XPS study, electronic state struct. 0-29846  
 FeO, valence band XPS and UPS, LCAO-MO calcs. 0-45197  
 Fe<sub>1-x</sub>O, surface struct., XPS study 0-20759  
 GaAs (110), adsorption of O<sub>2</sub>, oxide form., XPS/UPS study 0-49497  
 GaAs (110), coadsorption of Cs and O<sub>2</sub>, initial oxidation, soft XPS obs. 0-10793  
 GaAs (110), initial oxidation, XPS and AES study 0-11542  
 GaAs (110), with ultrathin Al and Cs overlayers, O<sub>2</sub> adsorption, comparative studies 0-50740  
 GaAs (110) surfaces, ordered and disordered, O<sub>2</sub> adsorption, XPS meas. 0-49498  
 GaAs, anodic oxide layers, chem. depth profiles, XPS determ. 0-3222  
 GaAs film, RF sputtered, ESCA, surface chemistry suitability for photo-volt. appl. 0-7476  
 GaAs, LMTO self consistent band struct. calc. 0-20078  
 GaAs oxide films, anodically and thermally grown, XPS study 0-16141  
 GaAs surface states obs. by XPS 0-50515  
 GaAs, surface states XPS 0-25528  
 GaAs-oxide interfaces, local atomic and electronic struct., high resolution XPS 0-49927  
 GaN, interatomic interactions from XPS 0-49171  
 GaP (110), initial oxidation, XPS and AES study 0-11542  
 Ge, inelastic mean free path in 700 to 1200 eV range, bulk method 0-20763  
 Ge, ion implanted, cond. and valence bands study by X-ray bremsstrahlung and photoelectron spectra 0-2360  
 Ge-rare earth alloys, nature of chemical interaction, X-ray emission, absorpt. and photoelectron study (*Russian*) 0-55261  
 H<sub>2</sub>BO<sub>3</sub>, chem. bonding, electronic struct., ESCA, Auger, and SIMS spectra 0-50512  
 Hg-As-S system glasses, photoelectron X-ray spectroscopy study 0-29858  
 In film, oxidation, XPS excited by Zr M<sub>γ</sub> radiation 0-40236  
 In film, oxidized polycrystalline, spectra obtained from combined XPES and SIMS investigation of surface 0-52377  
 In film, RF plasma oxidised, surface analysis using ESCA 0-50742  
 InSb (110), initial oxidation, XPS and AES study 0-11542  
 K<sub>2</sub>FeO<sub>4</sub>, XPS of hexavalent iron binding energies calcs. 0-43013  
 KNbO<sub>3</sub>, electronic props., SCF-MS-Xα calc. 0-54607  
 KTaO<sub>3</sub>, electronic props., SCF-MS-Xα calc. 0-54607  
 LaB<sub>6</sub>, surface (100), atomic struct., angle-resolved XPS, LEED and ISS investigation 0-10765  
 LaB<sub>6</sub>, synthesis and props., review (*Japanese*) 0-40255  
 LaCo<sub>2</sub>N<sub>2</sub>, formation by N<sub>2</sub> absorpt. by LaCo<sub>2</sub> 0-24599  
 La<sub>1-x</sub>M<sub>x</sub>CrO<sub>3</sub>, M=Mg, Sr, electronic struct. study by XPS 0-25518  
 La<sub>2</sub>O<sub>3</sub>, electronic struct. study by XPS 0-25518  
 Li electrode, in lithium perchlorate-propylene carbonate solution, surface anal. (*French*) 0-50859  
 LiBrO<sub>3</sub>, radiation damage, XPS obs. 0-29844  
 LiClO<sub>4</sub>, radiation damage, XPS obs. 0-29844  
 LiIO<sub>4</sub>, radiation damage, XPS obs. 0-29844  
 LuH<sub>2</sub>, synchrotron XPS obs., rel. to theory for metal dihydrides 0-55275  
 Mg, plasmon-loss intensities in XPS, EELS and Auger spectra 0-10902  
 MoN, interatomic interactions from XPS 0-49171  
 MoS<sub>2</sub>, struct., XES and XPS obs. 0-43105  
 MoS<sub>3</sub>, amorphous struct., X-ray radial distrib. anal. and XPS 0-49115  
 NaClO<sub>3</sub>, radiation damage, XPS obs. 0-29844  
 Na<sub>2</sub>O-P<sub>2</sub>O<sub>5</sub> glass, XPS quantitative struct. anal. 0-2917  
 Na<sub>2</sub>O-SiO<sub>2</sub>-NiO systems Ni ions anal. by ESCA (*Japanese*) 0-40787  
 Nb, oxide growth and oxide coatings, XPS and AES studies 0-50765  
 NbC, valence band XPS meas., comparison with X-ray emission spectra and band struct. spectral calcs. 0-50535  
 NbN, interatomic interactions from XPS 0-49171

## X-ray photoelectron spectra continued

- Ni (001), adsorbed CO c(2×2), surface geometry determ. by deep-core-level XPS 0-40224  
 Ni (001)/CO(O) system, adsorbate geometries determ. from final state scattering in X-ray photoemission 0-54488  
 Ni, Ar ion implantation 1S<sub>1/2</sub>O, 1S<sub>1/2</sub>t and 2P<sub>3/2</sub>Ni states 0-16149  
 Ni, bound hole pairs, XPS study, satellite peaks 0-40218  
 Ni films, HCP and amorphous, RF sputtered, O<sub>2</sub> incorporation, ESCA obs. 0-10832  
 Ni intermetallics and oxide, interatomic interaction by XPS 0-7474  
 Ni, surface, d-band narrowing, obs. using angle-resolved XPS 0-11062  
 Ni/polymer interface, electronic struct., XPS study 0-45204  
 Ni-Pd surfaces, electrochem. passive film form. and comp. determ. by SEM, SIMS, XPS 0-39401  
 NiO:C, surface charge, O(1s), C(1s) and Ni(2p) XPS 0-45196  
 P, amorphous, stability in air, XPS study, comparison with cryst. polymorphs 0-25517  
 Pb, inelastic mean free path in 700 to 1200 eV range, bulk method 0-20763  
 PbInAu film, RF plasma oxidised, surface analysis using ESCA 0-50742  
 Pd, XPS, electronic struct. 0-7464  
 Pd-Zr, metallic glasses, valence band struct. investigation 0-11533  
 PdO, electronic struct., XPS and UPS study 0-35061  
 PdSb, XPS, electronic struct. 0-7464  
 Pd<sub>80</sub>Si<sub>20</sub> metallic glass, high-resolution XPS study, electronic state struct. 0-29846  
 Pt oxidation, XPS spectra study 0-3254  
 Pt, XPS, electronic struct. 0-7464  
 Pt-Cu, ESCA study 0-2923  
 Pt-Cu, surface composition, XPS (*Portuguese*) 0-24722  
 Pt-Cu alloys, ESCA determ. of electronic struct. 0-34352  
 Pt-SrTiO<sub>3</sub> (100) interface, Auger and photoemission studies, relax. and chem. shift effects 0-54749  
 PtBi, XPS, electronic struct. 0-7464  
 PtCl<sub>2</sub><sup>2-</sup>, electronic struct., SCF Xα ESCA spectrum assignment 0-23339  
 Pt(IV), reduction to Pt(II), X-ray irradi., Ar ion bombardment, XPS obs. 0-35573  
 Ru (001), adsorption of NO, KPS, UPS, and X-ray AES meas. 0-6655  
 S, XPS, in BaS and BaSO<sub>4</sub> 0-43104  
 Sb, XPS, electronic struct. 0-7464  
 SeH<sub>2</sub>, synchrotron XPS obs., rel. to theory for metal dihydrides 0-55275  
 Si (111), chemisorbed O<sub>2</sub> electronic struct. tight-binding calc., XPS and UPS meas. 0-49845  
 Si, dry etching induced surface contamination, SIMS, AES, and XPS obs. 0-11810  
 Si KLL Auger peaks, bremsstrahlung-induced 0-45199  
 Si, semi-insulating polycrystalline CVD layers, AES and XPS characterisation 0-16129  
 Si, valence bands, XPS excited by Zr M<sub>γ</sub> radiation 0-40236  
 Si-SiO<sub>2</sub>, bonding at (111) interface, stoichiometry and kinetics, synchrotron radiation photoemission spectroscopy 0-24744  
 Si-SiO<sub>2</sub> interface, local at. struct., XPS obs. 0-20042  
 Si-SiO<sub>2</sub> interface study by XPS 0-50507  
 Si-SiO<sub>2</sub> interfaces, local atomic and electronic struct., high resolution XPS 0-49927  
 Si-SiO<sub>2</sub> interfacial transition layer thickness, XPS obs. 0-11540  
 Si+NH<sub>3</sub>, surface nitride form., XPS excited by Zr M<sub>γ</sub> radiation 0-40236  
 SiN, interatomic interactions from XPS 0-49171  
 SiO<sub>2</sub>, amorphous, local at. struct., XPS obs. 0-20042  
 SiO<sub>2</sub>, dry etching induced surface contamination, SIMS, AES, and XPS obs. 0-11810  
 SiO<sub>2</sub> film, thermally grown, thickness, XPS obs. 0-11540  
 SiO<sub>2</sub>/InP film/substrate system, interface formation during CVD, modelling 0-24764  
 SiON/GaAs film/substrate system, interface formation during CVD, modelling 0-24764  
 Sm surface, electron spectroscopy of 4f energy shift 0-2925  
 Sm surface electronic structure, XPS study 0-55259  
 Sm, XPS, electronic struct. determ. for surface 0-20765  
 Sn, inelastic mean free path in 700 to 1200 eV range, bulk method 0-20763  
 Sn plate surface, ion-bombardment conditions effect on chem. profile 0-54287  
 Sn, XPS, electronic struct. 0-7464  
 TbCrO<sub>4</sub>, valence states of Cr, XPS obs. 0-40216  
 Te coating of PbTe surfaces, struct. and junction characts. 0-50743  
 Th, adsorption of O<sub>2</sub>, XPS study 0-7473  
 Th, XPS of 5p level, screening and configuration interaction effects 0-54633  
 ThPt, valence bands, XPS spectra 0-50520  
 Ti (0001), valence band struct. and chemisorption, XPS and UPS study 0-35062  
 Ti, nitriding, ESCA study (*Japanese*) 0-11833  
 Ti-H, deposited on carriers, synthesis, structure and catalytic props. 0-29890  
 Ti-Ni, electron phase transition XPS, optical spectra and mag. susceptibility meas. 0-19943  
 TiC reactively sputtered coatings on Ni-Cr-Mo-Ti (19,11,3 wt.%), adherence, XPES and wear study 0-25565  
 TiC sputtered coatings on Ti-Al-V (6,4 wt.%), adherence, XPES and wear study 0-25565  
 TiC, refractory layers on steel surfaces, ESCA obs. 0-39471  
 TiN, interatomic interactions from XPS 0-49171  
 TiO<sub>2</sub>, clean and hydrated, surface sites, XPS 0-35052  
 TiO<sub>2</sub>, XPS satellite spectra, mol. orbital study 0-43100  
 TiO<sub>2</sub>:Cu, anodic, effect of Cu on optical props., rel. to possible appl. in solar energy conversion 0-16115  
 TiL, Ti 5d XPS comparison with Ti L 0-43099  
 TiL, XPS and UPS study of phase transforms. 0-45210  
 U, adsorption of water and O<sub>2</sub>, XPS study 0-7473  
 U, core and valence band spectra, XPS obs. 0-50530  
 UAs, U 4f ESCA spectra 0-16148  
 UCu<sub>5</sub>, core and valence band spectra, XPS obs. 0-50530  
 β-UD<sub>3</sub>, electronic props., metallic character 0-6693  
 UN, U 4f ESCA spectra 0-16148  
 UNi<sub>3</sub>, core and valence band spectra, XPS obs. 0-50530  
 UNi<sub>0.5</sub>Cu<sub>4.5</sub>, core and valence band spectra, XPS obs. 0-50530  
 UO<sub>2</sub>, electronic struct. and Coulomb correl. energy, XPS and bremsstrahlung spectra 0-55272



**X-ray photoelectron spectra continued**

- UP, U 4f ESCA spectra 0-16148  
 UPt, valence bands, XPS spectra 0-50520  
 US, U 4f ESCA spectra 0-16148  
 USB, UPS and XPS, surface oxidation 0-7465  
 V oxides, XPS and AES study, electron correl. effects, semicond.-metal transition 0-7467  
 VN, intratomic interactions from XPS 0-49171  
 V<sub>2</sub>O<sub>5</sub>, (001) surface modification, during catalytic oxidation of propene (French) 0-45557  
 V<sub>2</sub>O<sub>5</sub>, high-temp. phase transition, resistivity, valence photoelectron spectra 0-49357  
 WC-Co hard alloys, machined with polycryst. superhard materials, surface struct. using X-ray photoelectron spectroscopy 0-25919  
 WO<sub>3</sub> films, electron struct. changes during electrocoloration, XPS obs. 0-40217  
 WS<sub>3</sub>, amorphous struct., X-ray radial distrib. anal. and XPS 0-49115  
 YH, synchrotron XPS obs., rel. to theory for metal dihydrides 0-55275  
 YOFe, electronic struct. calcs. from XPS and X-ray emission spectra 0-35056  
 Yb, 4f levels, hole lifetime and chemical shift, UHV study 0-20762  
 YbAu, surface electronic structure, XPS study 0-55259  
 Zn, AES and XPS, vapour-metal electron energy shifts 0-16142  
 ZnTe films, grown on glass using atomic layer evaporation 0-44453  
 Zr-H, deposited on carriers, synthesis, structure and catalytic props. 0-29890  
 ZrH<sub>2</sub>, synchrotron XPS obs., rel. to theory for metal dihydrides 0-55275

**X-ray production**

see also *X-ray tubes*

- biological sample analysis, nanosec. X-ray diffr. pattern techniques 0-26429  
 high power microsecond electron beam, soft X-ray prod. 0-52378  
 plasmas, laser produced, as X-ray source for synchrotron radiation research and microradiography 0-320  
 rotary anode X-ray generators, comparison of characteristics of X-ray and  $\gamma$ -ray sources 0-14030  
 synchrotron radiation source, book contrib. 0-5421

**X-ray protection** see radiation protection**X-ray reflection**

- crystal defect observation by X-ray reflection topography (Chinese) 0-44074  
 rough surface, X-ray total external refl. 0-2896  
 Takagi-Taupin equations, boundary conditions in numerical integration, appl. to Bragg and Laue cases 0-1886  
 X-ray fluorescence anal. by total reflection (German) 0-30314  
 BaTiO<sub>3</sub>, pot. functions of ions 0-19885

**X-ray scattering**

see also *Compton effect*; *X-ray diffraction*

- anomalous X-ray scattering 0-54075  
 anomalous scattering factors 0-9540  
 crystal, coherent scatt., photon model 0-24309  
 disordered multicomponent solid solutions conc. fluctuation waves, microscopic theory 0-44327  
 distorted crystal, X-ray intensity mode oscills., two wave WKB approx. calcs. 0-28876  
 DNA, circular superhelical, X-ray scatt. calcs. 0-56109  
 fluorescence, matrix correction methods using scattered radiation 0-3456  
 graphite, X-ray scatt. from small particles at zero k 0-11505  
 graphite, X-ray spectrum in region of Raman band 0-7436  
 Hercules X-1, reson. Compton cyclotron scatt. rel. to cyclotron line form. 0-8711  
 photon resonance scattering by relativistically channelled electrons, enhancement coeff. 0-39190  
 plasma scattering, influence of electron exchange energy 0-50458  
 rotating aperture wheel device for radiographic contrast improvement 0-56202  
 spectroscopy, book 0-2899  
 TTF-SCN, quasi one-dimens. conductor, CDW phase transform., X-ray scatt. study 0-24594  
 Al-Zn, age hardenable precipitation and dissolution, positron annihilation and X-ray scatt. 0-16314  
 Al-Zn, isothermal preprecipitation, small angle X-ray scatt. expts. 0-35186  
 NbSe<sub>3</sub>, quasi one-dimens. conductor, CDW phase transform., X-ray scatt. study 0-24594

**X-ray sources (astronomical)**

see also *X-ray astronomical observations*

- 2A 0311-227, complex emission line structure of spectroscopic binary 0-51915  
 2A 0311-227, high-speed photometry of AM Herculis-type binary 0-41912  
 2A 0526-328, high speed optical photometry 0-51917  
 2A 0526-328, location and identification with blue emission line star 0-22118  
 2A 0526-328, optical photometry of assoc. star 0-22120  
 A 0535+26, transient source, possible RR Tauri relationship 0-26853  
 A 0535+26, transient X-ray source, flare obs. by (Prognoz 6) (Russian) 0-51920  
 A 0535+26, variable source, line and continuum vars. of possible optical counterpart (HDE 245770) 0-17600  
 2A 1052+606, location and identification with late type emission line star (SAO 015338) 0-22118  
 2A 1052+606, X-ray and optical variability of RS CVn star 0-31331  
 2A 1052+606 (BD+61°1211), RS Canum Venaticorum binary star, spectroscopic obs. 0-36663  
 Abell 2256, X-ray cluster of galaxies, radio props. 0-36726  
 Abell clusters of galaxies, X-ray survey, HEAO 1 1-10 keV obs. 0-51882  
 accreting compact object in binary system, magnetosphere theory, X-ray sources 0-46394  
 accreting magnetic degenerate dwarfs, X-ray and UV emission 0-41826  
 accretion discs, structure in mag. field, MHD eqns. approach 0-8714  
 accretion disks, theoretical review (Polish) 0-26739  
 Ariel 0620-00 (V616 Monocerotis), UVB photometry 0-56846  
 AWM 4, poor galaxy cluster, extended X-ray emission detect. surrounding cD galaxy (NGC 6051) 0-51884  
 background radiation isotropy, 2-18 keV energy range 0-46709  
 binary star systems, Roche lobe formation 0-41858  
 binary X-ray sources light and velocity curves simultaneous solution, eccentric orbit generalisation 0-36664  
 black hole accretion discs, Lightman-Eardley instabilities rel. to disc thickening 0-31324  
 black hole candidates (Czech) 0-31325  
 black holes, electron-positron pair production in hot unsaturated Compton accretion models 0-36658  
 black holes, high-freq. EM waves propag. through magnetised plasma in curved space time 0-48894  
 black holes, theory, of rapid X-ray variability and dying pulse trains 0-56872  
 black holes, X-ray radiation polarisation features 0-46700  
 burst sources, appl. of sinking filaments model of accretion onto magnetised neutron stars 0-51798  
 burst sources, neutron star thermonuclear runaway model 0-22032  
 burst sources, obs. and models (Danish) 0-12830  
 bursters, models 0-4460  
 bursters, radius and mass, general relativistic effects 0-8712  
 bursters, spectroscopic study of optical counterparts 0-46699  
 3C 273, quasar, second-order Compton interpretation of X-rays and  $\gamma$ -radiation 0-22106  
 $\alpha$  Canis Majoris B (Sirius B), minimum flux H coronal model rel. to X-ray emission 0-8626  
 RS Canum Venaticorum systems, candidate list for southern HD stars 0-4395  
 RS Canum Venaticorum systems, X-ray obs. and coronal model development 0-56873  
 $\nu$  Carinae, X-ray emission obs. from star and surrounding nebula 0-26876  
 catalogue of 517 objects 0-56720  
 proxima=V645 Centauri, dMe flare star, quiescent corona, transition region, and chromosphere obs. 0-56850  
 Centaurus A (NGC 5128), slowly varying flux component, 22 GHz confirmation 0-56939  
 Centaurus X-3, search for X-ray polarization 0-4457  
 Centaurus X-3, stellar wind vel. change during transition 0-12829  
 VW Cephei, W Ursae Majoris star, identification with faint X-ray source 0-51913  
 CG 176-7, 189+1 and 195+4, X-ray emission associated with  $\gamma$ -ray source 0-31393  
 Circinus X-1, radio flare phenomena Dec. 1979 and Jan. 1980 obs. 0-36731  
 Circinus X-1 and Cygnus X-1, time variability comparison 0-56974  
 clusters of galaxies, implications of galactic coronae model for intracluster medium origin 0-31355  
 clusters of galaxies, intracluster hot gas temp. and entropy 0-17660  
 clusters of galaxies, large-scale X-ray struct. 0-8700  
 clusters of galaxies, radial vel. dispersions 0-8696  
 clusters of galaxies, search for extended hot gas halos in Perseus, Virgo and Coma clusters 0-56953  
 clusters of galaxies, X-ray spectra and relationship to other cluster props. 0-22093  
 compact source, intensities from stellar wind flow past compact object 0-22116  
 compact X-ray sources, spectra form. 0-22115  
 Comptonization of X-rays by low-temp. electrons, Monte Carlo calc. 0-12653  
 $\sigma$  Coronae Borealis (H 1613+33), spectroscopic binary, soft, X-ray obs. with (HEAO-1) 0-56886  
 Crab Nebula, optical and X-ray surface brightness from supernova remnant physical theory supernova 0-51834  
 cyclotron self-absorption in accretion columns of magnetic degenerate stars, X-ray sources appl. 0-12760  
 SS Cygni, dwarf nova, soft X-ray pulsation obs. 0-46563  
 Cygnus OB2 association (VI Cygni), soft X-ray emission sources discovery 0-26918  
 Cygnus X-1, (Cygnus X-1), in optical counterpart V1357 Cygni 0-41861  
 Cygnus X-1, evidence for new variability in hard X-ray emission 0-27011  
 Cygnus X-1, extended-bandwidth X-ray obs. 0-17689  
 Cygnus X-1, inverse Compton model 0-51918  
 Cygnus X-1, model of neutron star surrounded by massive disc 0-36736  
 Cygnus X-1, UV shot noise upper limit 0-4458  
 Cygnus X-1, X-2 and X-3, long-term-studies with Ariel 5 All-Sky Monitor (ASM) 0-17688  
 Cygnus X-1, X-ray flux time variability struct. (Russian) 0-51921  
 Cygnus X-1 (HDE 226868), accretion disk size 0-51910  
 Cygnus X-1 (HDE 226868), H $\alpha$  emission in (1977) 0-51919  
 Cygnus X-1 and Circinus X-1, time variability comparison 0-56974  
 Cygnus X-2, rapid UV flux vars., IUE obs. 0-12833  
 Cygnus X-2 (V1341 Cygni), shortest optical variability (Russian) 0-17695  
 Cygnus X-2 as spherically accreting nonmagnetic degenerate dwarf 0-46703  
 Cygnus X-3, 4.8 hour modulation period change disproved 0-8713  
 Cygnus X-3, 50-400 keV obs., power law spectrum 0-41913  
 Cygnus X-3, efficient particle acceleration 0-31391  
 Cygnus X-3, hard X-ray spectrum obs. 0-31388  
 diffuse X-ray background, spectrum from 3 to 50 keV 0-41916  
 discrete source model for cosmic X-ray background, search for correl. with light of galaxies 0-56977  
 EXP 0520-66, flaring X-ray pulsar, recurrent gamma-ray bursts obs. (Russian) 0-36741  
 FXP 0520-66, flaring X-ray pulsar in Dorado, Venera 11 and 12 obs. 0-27018  
 galactic bulge X-ray sources, black hole and orbital disk model 0-17691  
 galaxies, primeval, appearance in X- and  $\gamma$ -ray regions, contrib. to background rad. 0-8692  
 galaxies, X-ray luminosity limit of nearby normals 0-4443  
 galaxies active nuclei, models of unsaturated Compton accretion discs around supermassive black holes 0-22033  
 galaxy cluster relaxation effect on intergalactic gas and X-ray emission 0-46684  
 galaxy clusters, X-ray spectra 0-26996  
 galaxy rich clusters and superclusters, and clusters extended halos, X-ray emission search 0-26988  
 globular clusters, gas content upper limits rel. to X-ray emission 0-22047  
 GX304-1 (4U 1258-61), shell spectrum of optical counterpart 0-46582  
 H1122-59 (G292.0+1.8), young supernova remnant, high vel. material obs. 0-22064  
 H2155-304 (PKS 2155-304), newly discovered BL Lacertae object, X-ray and optical props. 0-36702



**X-ray sources (astronomical) continued**

- H 0544-665, optical candidate for LMC X-ray source 0-36737  
 H 1538-32, new extended soft X-ray source detect., possible old supernova remnant 0-51912  
 H 2155-304, highly luminous BL Lacertae object, spectral obs. 0-4459  
 hard X-ray sources discovered by HEAO A-2 expt. 0-17690  
 HB 3, supernova remnant, soft X-ray obs. 0-56915  
 Hercules X-1, cyclotron line form. by reson. Compton cyclotron scatt. 0-8711  
 Hercules X-1, cyclotron self-absorpt. in accretion column of mag. degenerate star 0-12760  
 Hercules X-1, precessing twisted accretion disks 0-56973  
 Hercules X-1, search for X-ray polarization 0-4457  
 Hercules X-1 (HZ Hercules), 70 day period refuted 0-56975  
 Hercules X-1 (HZ Herculis), coordinated optical and X-ray pulsations obs. 0-51909  
 Hercules X-1 (HZ Herculis), optical pulsations rel. to accretion disc/mag field interaction (*Russian*) 0-51799  
 Hercules X-1 (HZ Herculis), periodic mass transfer rel. to X-ray light curve 0-51911  
 AM Herculis type binaries, cyclotron self-absorption in accretion columns of magnetic degenerate stars 0-12760  
 High Energy Astrophysics Division of Am. Astron. Soc., meeting (Cambridge, MA, 28-30 Jan. 1980) 0-36761  
 high-sensitivity X-ray survey, discrete source contrib. to extragalactic background 0-27016  
 information sources for neutron star, dense matter and gravitational collapse physics 0-36657  
 inverse Compton reflection, time-depend. theory, X-ray sources appl. 0-12652  
 BL Lacertae objects, high-energy X-ray obs. 0-31353  
 LMC, X-ray survey using HEAO 1 scanning modulation collimator 0-17648  
 LMC N 49, X-ray source 0525.9-66.1, gamma-ray burst obs. (*Russian*) 0-36739  
 LMC X-1 region (MC76 and 77), 2 cm obs. 0-51875  
 Loop I, X-ray features, SNR model 0-22066  
 RU Lupi,  $\tau$  Tauri star, chromosphere and corona parameters and expected X-ray fluxes (*Russian*) 0-51770  
 Lupus flare source, Ariel 5 ASM obs. (1979 October 25) 0-8715  
 M31, X-ray sources, obs. 0-26979  
 M87, central giant galaxy in Virgo cluster, excess X-ray emission 0-41907  
 magnetoactive plasma, cyclotron absorption effects 0-8533  
 massive X-ray binaries, evolution of optical components 0-41857  
 MKW 3s, poor galaxy cluster, extended X-ray emission detect. surrounding cD galaxy (NGC 5920) 0-51884  
 MXB 1728-34, type I X-ray burst obs. by (HEAO-1) 0-17692  
 MXB 1730-335, 2.2  $\mu$ m flashes from X-ray rapid burster 0-46706  
 MXB 1730-335, 4100 MHz obs. of microwave bursting pattern 0-46705  
 MXB 1730-335, new mode of X-ray bursts 0-41915  
 MXB 1730-335, Rapid Burster, IR bursts detect. confirmation 0-27020  
 MXB 1730-335 (Rapid Burster), steady X-ray emission obs. 0-22119  
 MXB 1837+05 (Serpens X-1), detect. of optical burst coincident with X-ray burst 0-27013  
 neutron star, thermal X-ray emission 0-41849  
 neutron stars, highly magnetised, thermal radiation 0-56869  
 neutron stars surface radiation, detectability rel. to cooling and heating processes 0-31323  
 NGC 1275, central giant galaxy in Perseus cluster, excess X-ray emission 0-41907  
 NGC 2110, Seyfert 2 X-ray galaxy, optical studies 0-22071  
 NGC 5506, Seyfert 2 galaxy, detect. of flare in X-ray emission 0-17656  
 non-thermal sources, constraints rel. to X-ray background synthesis constraints rel. to X-ray background synthesis 0-27021  
 NP 0532, Crab pulsar, X-ray and gamma-ray radiation 0-41885  
 OAO 1653-40 area, 38.22 second X-ray pulsations discovery 0-27014  
 OAO 1653-40 (V861 Scorpii?), simultaneous UV and X-ray obs. 0-17616  
 OAO 1653-40 (V861 Scorpii), near IR obs. of single line spectroscopic binary 0-8652  
 optical spectrum of high temp. gas, emission line formation (*Russian*) 0-36740  
 X Persei (3U 0352+30), simultaneous X-ray and ground-based optical obs. 0-17591  
 PKS 0548-322, BL Lacertae object, X-ray spectrum 0-17654  
 PKS 0548-322, surface photometry of X-ray emitting BL Lacertae object 0-22069  
 PKS 2155, BL Lacertae object, UV flux meas. by IUE 0-12833  
 pulsating X-ray sources, period changes due to rot. mag. neutron stars accretion torques 0-31320  
 pulsating X-ray sources, strongly magnetised plasma collisional relax. of ion beam 0-33785  
 pulsating X-ray sources spectra, possible vacuum signature 0-27015  
 Puppis A, X-ray and Fe XIV 5303 Å emission 0-26962  
 QSO 0241+622, nearby X-ray quasar, extended radio emission search 0-31382  
 quasars, models of unsaturated Compton accretion discs around supermassive black holes 0-22033  
 quasars and active galactic nuclei, magnetic flare model, magnetised accretion disc around massive black hole 0-22113  
 Sagittarius, Ariel V obs. of X-ray nova (1979 October-November) 0-12834  
 Scorpius X-1, high energy X-ray obs. with Ariel V 0-17694  
 Seyfert 1 galaxies, HEAO 1 scanning modulation collimator, obs. 0-51859  
 Seyfert 1 galaxy nuclei, luminosity function and implications for X-ray background 0-8682  
 Seyfert 1 X-ray emitting galaxies, HEAO 1 spectra 0-51860  
 spherically symmetric accretion flows, stability anal., X-ray sources appl. 0-46387  
 SS 433, 10 GHz variability and thermal radio emission hypothesis 0-31307  
 SS 433, 1979 May-June radio flare, 3.24 GHz obs. 0-46567  
 SS 433, 6.55 day periodicity in emission line wavelengths 0-51784  
 SS 433, binary star model including mag. white dwarf 0-4385  
 SS 433, discrepancy between optical and radio positions 0-31303  
 SS 433, early-type binary model 0-56843  
 SS 433, enormous periodic Doppler shifts obs. 0-17593  
 SS 433, evidence for association with supernova remnant (W50) 0-51851

**X-ray sources (astronomical) continued**

- SS 433, H I absorption obs. and distance 0-56848  
 SS 433, IR and visible obs., IR excess and emission processes 0-4387  
 SS 433, IR energy distrib. obs. 0-31312  
 SS 433, IR light curves from BV1JHK photometry, period and ephemeris 0-8642  
 SS 433, IR spectral obs., reddening and emission 0-4388  
 SS 433, light minimum epoch and period 0-26886  
 SS 433, mass accel. and collimation mechanisms 0-4368  
 SS 433, mass loss rates and lifetime from W50 optical filaments 0-12804  
 SS 433, nature and evolutionary state (*Russian*) 0-36647  
 SS 433, Of star orbited by neutron star, model 0-22025  
 SS 433, photometry, 1979 July to October, and 6.5 day period identification 0-8643  
 SS 433, radio and optical positions coincidence 0-56840  
 SS 433, radio jet discovery 0-31381  
 SS 433, short term H $\alpha$  central intensity increases 0-4375  
 SS 433, spectroscopic obs. and probable binary nature 0-51780  
 SS 433, VLBI detect. and ang. struct. 0-31304  
 SS 433 (W50), assoc. optical supernova remnant discovery 0-56916  
 SS 433 as veiled pulsar 0-41842  
 SS 433 model, precessing jets in ultra-close binary system 0-4384  
 stellar coronae, evidence for existence from X-ray and UV obs. 0-12756  
 stellar X-ray sources at high galactic latit., location with HEAO 1 scanning modulation collimator 0-22118  
 Stephenson-Sanduleak 433, 1.2-2.5  $\mu$ m spectroscopy, photometry and polarimetry 0-41838  
 Stephenson-Sanduleak 433, Thomson scatt. lines in spectrum, relativistic gas motions 0-22019  
 subcritically accreting black holes, model for X-ray sources in globular cluster cores and X-ray burster sources 0-12779  
 supercritical accretion discs winds struct. and appearance, numerical models 0-21984  
 supernova  $\gamma$ - and X-rays, recorded by Antarctic ice NO $_3^-$  content 0-31314  
 supernovae, extragalactic, X-ray bursts search using HEAO-1 satellite 0-46585  
 supernovae, type II, nonequib. processes in evolution 0-46586  
 V711 Tauri (HR 1099), Lyman  $\alpha$  H I and D I interstellar absorption 0-8658  
 turbulent disc  $\alpha\omega$  dynamo theory for mag. field generation 0-46663  
 Tycho supernova remnant, Type I SNR, elemental abundances from X-ray spectrum 0-46635  
 Tycho supernova remnant, X-ray line emission obs. 0-46636  
 4U 0041+32, hard X-ray outburst, 1970 obs. 0-56976  
 3 U 0055-79, possible identification with Seyfert 1 galaxy (ESO 012-G21) 0-8695  
 4 U 0115+63, absorption line in pulsed hard X-ray spectrum, HEAO 1 obs. 0-27017  
 4U 0115+63 transient near G126.2+1.6 SNR 0-8668  
 4 U 0900-40 (HD 17581), apsidal motion test 0-51908  
 4 U 1206+39 (NGC 4151), hard X-ray variability of Seyfert galaxy 0-17647  
 4U 1232+07, HEAO 1 obs. 0-12832  
 4U 1249-28, location and identification with dwarf nova EX Hydrae 0-22118  
 4U 1626-67, 7.7-second X-ray pulsar, simultaneous X-ray and optical obs. 0-51914  
 4U 1626-67, light pulses from optical counterpart 0-51916  
 3U 1700-37 (HD 153919), further spectroscopic obs. 0-4358  
 4U 1702-36, Scorpius X-1 like source, high energy X-ray obs. with Ariel V 0-17694  
 4U 1813+50 (AM Herculis), rapid light variability obs. (*Russian*) 0-8662  
 4U 1907+09, X-ray flare obs. during 1980 Jan. period 0-41914  
 4 U 2129+47, position and optical identification, evidence for X-ray heating and binary period 0-17693  
 4U 2129+47, X-ray light curve and binary model 0-46704  
 AN Ursae Majoris, soft X-ray flux detected 0-4400  
 Vela supernova remnant, X-ray maps 0-51838  
 VV Puppis, 3470 Å emission as cyclotron line 0-36673  
 weak X-ray sources, ANS meas. 0-46701  
 X-ray bursters, 1980 plans for simultaneous optical/X-ray obs. 0-8716

**X-ray spectra**

- see also X-ray absorption spectra; X-ray chemical analysis; X-ray emission spectra  
 energy dispersive, computer-aided analysis 0-3433  
 Al, condensed film, phase and struct. nonuniformity (*Russian*) 0-54536  
 Ca ions, dielectronic recombination excitation in solar X-ray lines 0-51725  
 CdTe detectors, X-ray fluorescence escape peaks in X-ray spectra 0-9448  
 Co(VIII), resonance transitions, classification 0-42985  
 Cs $^{+}$  formation during electron-ion collisions, ultrasoft X-ray spectroscopic study (*Russian*) 0-43193  
 Cu,  $K\beta_{1,2}$  intensity distribution, line strength calcs., single vacancy scheme 0-32650  
 Cu(X), resonance transitions, classification 0-42985  
 Fe XXIV, XXV, line wavelengths in 1.85 to 1.87 Å region in solar flare X-ray spectra 0-21973  
 Fe XXV-XXVI resonance lines region, laboratory reproduction of solar flare X-ray spectra 0-18819  
 Mo XXXIII, XXXIV, XXXV, transition identification X-ray spectra 0-32648  
 NaNO $_3$ , fine structure changes on interaction with weak shock waves (*Russian*) 0-54313  
 Nb XXXII, XXXIII, XXXIV, transition identification X-ray spectra 0-32648  
 $^{107}\text{Pd}$ , K-electron capture decay, double K-shell vacancy creation 0-22773  
 Rb $^{2+}$  formation during electron-ion collisions, ultrasoft X-ray spectroscopic study (*Russian*) 0-43193  
 YbB $_2$ , valence state and mag. props. 0-50031  
 Zr XXXI, XXXII, XXXIII, transition identification X-ray spectra 0-32648

**X-ray spectrometers**

- see also X-ray crystallography apparatus  
 APS, soft X-ray, with Al foil in front of photocathode (*Japanese*) 0-13193  
 automated, qualitative anal. 0-22497  
 crystal spectrograph with active readout 0-4826  
 dispersive crystal spectrometers, geometric accuracy (*Chinese*) 0-22495



**X-ray spectrometers continued**

- fluorescence spectrometer system, PW1400, microprocessor controlled (German) 0-16758  
 four-crystal, single-crystal plates deformation meas. 0-49048  
 gas scintillation counter, for high count rate X-ray detection 0-14052  
 gas scintillation spectrometer for X-ray astronomy, performance characteristics 0-56709  
 grazing incidence, crossed optics 0-314  
 grazing incidence spectrometer, 10 m, for soft X-ray mol. appls. 0-18062  
 Hard X-Ray Burst Spectrometer on Solar Maximum Mission 0-51658  
 Hard X-ray Imaging Spectrometer on Solar Maximum Mission 0-51659  
 metal compounds on microfilters, X-ray fluoresc. spectrometry anal. 0-30315  
 optimisation, for energy-dispersive XFA using X-ray tubes in combination with secondary targets 0-30316  
 steel, standard, energy dispersive X-ray fluoresc. spectrometry, computer directed optimisation 0-45585  
 thermostatic control, Diapazon temperature variator 0-47160  
 threshold-potential, based on Auger electron solid surfaces meas. appl. 0-52365  
 two crystal, small angle scattering obs. 0-54077  
 wavelength dispersive X-ray fluorescence analysis, rel. to energy dispersive X-ray fluorescence anal. 0-7885  
 Al alloys, energy dispersive X-ray fluoresc. spectrometry, computer directed optimisation 0-45585  
 CdTe detectors, use in spectrometers, physical and electronic factors (Czech) 0-23259  
 Si-Li surface-barrier detectors for electron and soft X-ray spectrometry 0-882  
 Si(Li) detector system, discrepancies in X-ray excitation efficiencies 0-9450  
 Si(Li) detector window of aluminised mylar for X-ray fluorescence meas. 0-27894  
 Si(Li) gas cooled detector for in situ XFA spectrometer 0-18055  
 Si(Li) photopeak efficiency meas., 0.52-8.04 keV 0-27889  
 Si(Li) X-ray detector, efficiency calibration in 1.5 to 60 keV energy range 0-47823  
 Si(Li) X-ray spectrometer, development, and interdisciplinary appl. (Hungarian) 0-18056

**X-ray spectroscopy**

- see also appearance potential spectroscopy; X-ray crystallography; X-ray diffraction; X-ray spectra*  
 aerosol sampling, chemical heterogeneity revealed by X-ray photoelectron spectroscopy 0-55970  
 broadband X-ray excitation, quasi-fundamental correction methods 0-321  
 CAMAC, 2-D anal. of spectroscopic data, electronics 0-5460  
 data interpretation, online system using multivariate statistical anal. and pattern recognition 0-3461  
 energy dispersive X-ray diffraction method, annotated bibliography (1968-78) 0-36794  
 fluorescence spectrometry, single and multielement anal., optimum excitation conditions, automated determ. 0-323  
 focusing X-ray spectrograph for laser fusion expts. 0-31962  
 gas-filled electroluminescent detector for soft X-rays, constr. and characts. 0-32569  
 heterostructures, effect of primary electrons scattering on results of X-ray spectral microanal. 0-20735  
 high energy resolution X-ray spectroscopy, review 0-14959  
 microcomputer automatic control of double-crystal X-ray spectrometer (Polish) 0-32563  
 Mossbauer gamma-X-ray coincidence meas. 0-14041  
 mussel trace element monitoring appl. 0-30954  
 photoelectron, combination with SIMS for surface studies 0-52377  
 solid state spectroscopy using synchrotron radiation, book contrib. 0-7375  
 synchrotron radiation spectroscopy instrumentation and appls., book contrib. 0-4782  
 time resolved spectroscopy with synchrotron radiation 0-31902  
 Cu, valence band splitting, X-ray K-emission spectroscopy 0-40189  
 Hg-As-S system glasses, photoelectron X-ray spectroscopy study 0-29858  
 HgI<sub>2</sub> thin sections with Peltier-cooled preamplification for X-ray spectrosc. 0-324  
 ZrO<sub>2</sub>-SiO<sub>2</sub>- $\alpha$ -Al<sub>2</sub>O<sub>3</sub> mixed powders, solid state reactions 0-40337

**X-ray transport** *see photon transport theory***X-ray tubes**

- biomedical, target angle and inferential kilovoltage meas. 0-30843  
 current fall-off during an exposure, investigation and explanation 0-56203  
 fluorescent X-ray intensifying screen, efficiency determ., standard method 0-37140  
 image convertor with video signal output 0-36125  
 performance characteristic rel. to radiologic image quality 0-17125  
 radiography, diagnostic, X-ray spectra determ., high intensity 0-41217  
 rapid process recording using type RTR-1 tube 0-9080  
 technological and philosophical changes over a decade 0-37136  
 Tel-X-Ometer apparatus for educational demonstrations 0-8763  
 topogram visualisation raster tube with shoot-through target 0-31956  
 TV chain MTF and image quality determ. factors 0-36126

**X-rays**

- see also cosmic ray X-rays; photons*  
 demonstration using Tel-X-Ometer apparatus 0-8763  
 Rontgen's discovery of X-rays, accidents role in scientific enterprise 0-4502  
 T-10 Tokamak, plasma X-ray emission 0-28840

**X-Y model**

- anisotropic, quasi-one-dimens. system, with spin Peierls phase transition, tricritical point 0-25142  
 DOBAMBC, chiral smectic C-phase ferroelectric liq. crystal film, classical X-Y system, props. 0-44123  
 double scaling limit of one-dimens. XY model in monodromy preserving deformation theory 0-47194  
 FCC lattice, phase transitions of fully frustrated models 0-29517  
 frustrated two-dimensional planar model, spin-spin correl. 0-11212  
 frustration effect in  $s=1/2$  XY and Heisenberg models 0-15677  
 frustration network, phase transitions 0-2596  
 gauge theory analogue, 4-D self-dual gauge model, phases and transitions 0-27399  
 high-temperature representation of anisotropic rotator, XY and Heisenberg models for dimensions  $D \geq 2$  0-11146  
 isotropic, alternating, homogeneous, time and frequency depend. correlation functions 0-36953

**X-Y model continued**

- lattice spin systems, matching conditions for crit. props., group struct. of block transforms 0-22305  
 meron and meron pair analogs in XY model 0-32010  
 Migdal-like approximation, quantum spin systems 0-34649  
 one dimensional spin-1/2 XY model, finite temp. transverse autocorrelation function 0-50024  
 one particle reduced density matrix of impenetrable bosons in one dimension at zero temperature 0-17863  
 order parameter, fluctuation, high temp. series expansion, simple hypercubic and face-centred hypercubic lattices, spin 1/2 0-50098  
 phase transition in 2D Coulomb gas, sine-Gordon theory and XY model, renormalisation group anal. 0-36950  
 phase transitions in quantum X-Y and Heisenberg models 0-25141  
 planar spin two-dimens. model, mag. correlation function, self-consistent calc. 0-29563  
 quantum one-dimensional model, renormalisation group method anal. 0-17887  
 second order Green's function theory 0-54913  
 spin glass, quantum, frustration, 2-D lattice, functional integration technique (French) 0-39789  
 spin Peierls transition, gap eqns. 0-24801  
 spin wave theory of spin 1/2 X-Y model 0-7068  
 spin-1/2 XY model, thermodynamic quantities, high-temp. series expansions anal. 0-7067  
 TMMC, XY-Ising crossover transition, quasi-elastic neutron scatt. obs. 0-44826  
 two-dimensional, physical realisation, surface reconstruction 0-15351  
 two-dimensional spin system on square lattice, exact duality-decimation transform. 0-17890  
 zero temperature crit. behaviour in transverse mag. field 0-29555  
 CsMnF<sub>3</sub>, mag. phase boundaries, XY to Ising crossover, virtual bicritical point 0-50095  
 Cu-Mn, spin glass, meas. of order parameter 0-34642

**Xalpha calculations**

- atomic independent particle pots. comparison 0-52846  
 atomic multiplet struct. obtained from HF, statistical exchange and local spin density approx. 0-32619  
 cyclobutane, MS-X $\alpha$ -MT study 0-52906  
 diatomic molecules of 1st row, total X $\alpha$  energy, LCAO calc., rel. to local density models 0-32607  
 ethylene cation, state geometries, electronic vibr. coupling consts., HF calcs., comparison with Xalpha calcs. 0-27946  
 interface modelling, X $\alpha$ -scatt. wave cluster approach 0-49851  
 molecular multicentre potential, X $\alpha$  scattered waves method and Schrodinger eqn. soln. 0-37740  
 tetrahedrally coordinated covalent semiconductor point defects, multiple scatt. X $\alpha$  model 0-54636  
 transition metal clusters, particle size rel. to bulk metallic props. 0-44490  
 transition metal complexes, discrete variational X $\alpha$  cluster calcs. 0-15444  
 [Re<sub>2</sub>Cl<sub>8</sub>]<sup>2-</sup>, spectral assignment, metal-metal bonds, SCF X $\alpha$  SW calcs., relativistic corrections 0-53006  
 Ar, solid, lattice dynamics calc. using energy band theory 0-49320  
 BaTiO<sub>3</sub>, electronic props., SCF-MS-X $\alpha$  calc. 0-54607  
 CrCl<sub>4</sub>, ligand field states, multiple scatt. Xalpha calcs. 0-47891  
 Cu, chemisorption of O, S, Se, NO and O<sub>2</sub>, discrete variational X $\alpha$  cluster method 0-29264  
 F<sub>2</sub>, LCAO-GTO X $\alpha$  calc., rel. to other LCAO calcs. 0-52871  
 F<sub>2</sub>, MSX $\alpha$  calc., partial wave expansion, binding energy and orbital energy 0-37738  
 GaAs:Cr, impurity electron states by X $\alpha$  scattered wave cluster method, electron-electron interactions 0-6767  
 GaAs:O, electronic struct., multiple-scatt. X $\alpha$  mol. cluster model 0-15445  
 H<sub>2</sub>, ground state, pot. curves, MTX $\alpha_R$  method 0-5482  
 H<sub>2</sub>, X $\alpha$  theory appls. approximations 0-9510  
 H<sub>2</sub><sup>+</sup>, SCF multiple scatt. calc. 0-916  
 H<sub>2</sub>O<sup>+</sup>, states geometries, electronic vibr. coupling consts. HF calcs., comparison with Xalpha calcs. 0-27946  
 KC<sub>8</sub>, intercalated graphite, electronic and cryst. struct. 0-44472  
 KNbO<sub>3</sub>, electronic props., SCF-MS-X $\alpha$  calc. 0-54607  
 KTaO<sub>3</sub>, electronic props., SCF-MS-X $\alpha$  calc. 0-54607  
 Li<sub>2</sub>Br<sub>2</sub>, UPS of dimeric mol., expt. and X $\alpha$  calc. 0-9640  
 Li<sub>2</sub>Cl<sub>2</sub>, UPS of dimeric mol., expt. and X $\alpha$  calc. 0-9640  
 Li<sub>2</sub>F<sub>2</sub>, UPS of dimeric mol., expt. and X $\alpha$  calc. 0-9640  
 LiH, ground state, pot. curves, MTX $\alpha_R$  method 0-5482  
 LiH, one electron props., X $\alpha$  multiple scattering wave functions 0-42945  
 Li<sub>2</sub>I<sub>2</sub>, UPS of dimeric mol., expt. and X $\alpha$  calc. 0-9640  
 MoO<sub>4</sub><sup>6-</sup>, electronic struct., discrete variation and scatt. wave X $\alpha$  methods 0-917  
 N<sub>2</sub>, MSX $\alpha$  calc., partial wave expansion, binding energy and orbital energy 0-37738  
 N<sub>2</sub>, X $\alpha$  theory appls. approximations 0-9510  
 Na-Li, liq., Knight shift calc. by multiple scatt. X $\alpha$  method 0-54961  
 Na<sub>3</sub>(Al<sub>2</sub>Si<sub>2</sub>O<sub>7</sub>)Cl<sub>3</sub>, sodalite, electronic struct. of F-centre 0-2356  
 NaCl, electronic struct., SCF cryst. cluster model 0-24792  
 NaH, ground state, pot. curves, MTX $\alpha_R$  method 0-5482  
 Na<sub>2</sub>MoO<sub>4</sub>(S<sub>4</sub>)(Se<sub>4</sub>) crystals, charge transfer spectra of MoX<sub>4</sub><sup>2-</sup> complexes 0-54658  
 Ne, solid, lattice dynamics calc. using energy band theory 0-49320  
 Ni, chemisorption of O, S, Se, NO and O<sub>2</sub>, discrete variational X $\alpha$  cluster method 0-29264  
 Ni, X $\alpha$  theory appls. approximations 0-9510  
 Ni(CO)<sub>4</sub>, bonding, shakeup energies, and shakeup intensities for photoelectron spectra 0-50528  
 Ni<sub>3</sub>Ti, electronic struct., X $\alpha$  calc., photoelectron and AES spectra 0-20769  
 O<sub>2</sub>, MSX $\alpha$  calc., partial wave expansion, binding energy and orbital energy 0-37738  
 PbS, first-principles calc. of eqn. of states 0-49649  
 PtCl<sub>4</sub><sup>2-</sup>, electronic struct., SCF Xalpha ESCA spectrum assignment 0-23339  
 PtCl<sub>2</sub>(NH<sub>3</sub>)<sub>2</sub>, cis- and trans-isomers, electronic struct., SCF-X $\alpha$  study 0-18795  
 Re<sub>2</sub>Cl<sub>9</sub> metal cluster complexes, He(I) photoelectron spectrum, SCC DV X $\alpha$  calcs., Re<sub>2</sub>Cl<sub>8</sub><sup>2-</sup> comparison 0-28063  
 ScP, electronic struct., self-consistent Hedin-Lundqvist and X $\alpha$  APW calcs. 0-29322  
 SeP, energy band struct., exchange-correl. pot. effects, APW calcs. 0-29321  
 Si, amorphous, hydrogenated, electronic struct., SCF X $\alpha$  calc. 0-49580



**Xalpa calculations continued**

- SiX<sub>4</sub> (X=Cl,H,F), chemical shifts, relax., X-ray spectra, SCF Xalpa calcs. 0-27928  
 SrTiO<sub>3</sub> (100) surface electronic structure, DV-X $\alpha$  cluster method 0-39646  
 Te, trigonal, self-consistent ground state 0-54604  
 Ti<sub>2</sub>, electronic structure of five and ten atom chains SCF-X $\alpha$ -SW calcs. 0-5483  
 TiH, electronic structure of five and ten atom chains SCF-X $\alpha$ -SW calcs. 0-5483  
 TiO<sub>2</sub>, clusters, surface electron struct. and defect states, DV-X $\alpha$  calc. 0-20268  
 UO<sub>6</sub><sup>6-</sup>, electronic struct., discrete variation and scatt. wave X $\alpha$  methods 0-917  
 (UO<sub>6</sub>)<sup>12-</sup>, electronic struct., variational Xalpa cluster calc. 0-39499  
 US, optical props. and electronic struct. 0-25410  
 (UX)<sub>n</sub><sup>n-</sup>, X=N,O,S, electronic struct., variational Xalpa cluster calc. 0-39499  
 WO<sub>6</sub><sup>6-</sup>, electronic struct., discrete variation and scatt. wave X $\alpha$  methods 0-917  
 YOF, electronic struct. calcs. from XPS and X-ray emission spectra 0-35056

**xenon**

see also nuclei with .....

- adsorbed layer of Ag, lateral compression effects calc. 0-6641  
 adsorbed layers on Pd-Pt, Ir, and Ru, 5p photoemission, local surface struct. influence 0-2920  
 adsorbed on Pd (110), anomalous 5p photoemission 0-7471  
 adsorption and coadsorption with O on W, work function and thermal desorption meas. 0-39448  
 adsorption on Ag(111), structural and thermodynamic studies 0-6640  
 adsorption on graphite, substrate deform. meas. 0-54520  
 adsorption on Ir (100), local surface struct., UPS study 0-39429  
 adsorption on Pd(110) surface, AES, UPS, LEED, work function, flash desorption 0-6633  
 afterglow, radiative and collisional deexcitation of reson. states, absorpt. and emission obs. 0-38742  
 arc, wall-stabilised, dynamic analysis, radiation transport 0-44066  
 atom, 5s $\rightarrow$ ep photoelectron ang. distrib. near Cooper minimum 0-18834  
 atom, elastic electron scatt., 2-300 eV, ang. distrib. 0-43179  
 atom, elastic positron scatt., phaseshifts and elastic, diffusion and annihilation cross section 0-53134  
 atom, elastically scattered electrons spin polarisation 5-300 eV, 30-120° 0-23548  
 atom, electron ionisation and excitation coeffs. in low E/N region 0-48090  
 atom, electron scattering, elastic, low-energy, polarised-orbital calcs. 0-37882  
 atom, g-factors meas. by optical pumping and mag. reson. 0-14246  
 atom, independent particle pots. comparison 0-52846  
 atom, ns $\rightarrow$ ep photoelectrons, spin polarisation 0-37792  
 atom, outer shell photoionisation, relativistic RPA calcs. 0-9571  
 atom, photoelectron studies of 5p branching ratio 0-37793  
 atom, plane polarised VUV irradi., emitted photoelectron polarisation, ang. depend. 0-47952  
 atom, relativistic Hartree-Fock calcs. using spherical Gaussian basis sets 0-32595  
 atom, s-p transitions, Stark consts. and oscill. strengths, shock tube meas. 0-18822  
 atom, scatt. from Pt(111), direct inelastic scatt. with trapping-desorption scatt., vel. and ang. distrib. 0-16140  
 atom, XPS and XES, dynamical effects 0-52924  
 atoms, free, electron bombard., subsequent X-radiation ang. distrib. 0-53144  
 condensed electron beam excited, exciton radiative lifetimes 0-6727  
 cryogenic distillation from gaseous effluents in nucl. fuel reprocessing 0-5309  
 crystalline, polariton effects, reflectivity, absorpt., and resonant luminesc. spectra calcs. 0-20095  
 crystallite on Be substrate, crystallite dimensions determ. using synchrotron radiation X-ray diffr. photographs 0-24313  
 deep-sea basalts, He and Xe as measure of magmatic differentiation 0-31040  
 diffusion, sorption, solubility, permeation in polyvinyltrimethylsilane (*Russian*) 0-6564  
 diffusion and solubility in PTFE 0-6561  
 discharge, Blumlein-type transverse fast, voltage meas discharges (electric) 0-19642  
 discharge, pulsed, visible line afterglow emission obs., excimer form. 0-38754  
 discharge lamps, large, electrode temp. meas. by photographic method (*Russian*) 0-47057  
 discharges, electrodeless, UHF in waveguide rel. to DC characts. 0-38762  
 electrical conductivity beyond critical point, intermediate density between gas plasma and solid (*Russian*) 0-20265  
 electron scattering, Ramsauer effect enhancement in mag. field 0-53137  
 excimer laser, high-power repetitive, tunable, VUV 0-5758  
 excimers and excimer lasers 0-48217  
 excitation by low energy electrons, IR spectra obs. 0-27974  
 high power pulse gas discharges development, photographic obs. 0-14954  
 HTGR, large pebble bed, Xe oscillations detection 0-22988  
 inner electron energy characteristics, validity of Hartree-Fock-Pauli approx. 0-42957  
 IR lasers pumped by U fission fragments 0-28198  
 isotope separation, HF stationary discharge, travelling mag. field, barodiffusion separation 0-44049  
 lamp, ultrahigh-pressure, Soviet-made DKSSH lamp spectral characts., in pulsed regime 0-48371  
 laser induced gas breakdown threshold at 1.06 micron 0-28594  
 lattice heat capacity, thermal vibrations, Lindeman parameter, lattice dynamic model (*Russian*) 0-29141  
 liquid, electron mobility, role of shallow traps 0-34440  
 liquid, recomb. and self-trapped exciton luminesc., free electron dynamics, excited states 0-25463  
 liquid, struct. factor calc., perturbation treatment using Lennard Jones (6, 12) pot. 0-10483  
 liquid and solid,  $\gamma$ -irrad., average energy expended per ion pair (*Russian*) 0-5438  
 monolayer adsorption on Ag (111), statistical mech. 0-34306

**xenon continued**

- oscillation suppression, reactor system reciprocity props. 0-27773  
 physisorbed monolayer on graphite, dynamical and thermal props. 0-34292  
 physisorption on W (100), Lennard-Jones model, mol. dynamics study 0-34308  
 plasma, electron energy distrib. function, Coulomb collision effects 0-38532  
 plasma, photodetonation and supersonic radiation wave propag. (*Russian*) 0-10385  
 plasma, shock-heated, dense, continuum radiation and optical transmittance diagnostics 0-24202  
 plasma, shock-heated, high-density, elec. cond. 0-38557  
 plasma column in flashtube, characts. and parameters 0-54053  
 plasma shock front, elementary processes 0-19581  
 poisoning transient anal. in fission reactors using XESAMO code (*Spanish*) 0-52749  
 power reactor parameter identification in Xe oscillation model using maximum likelihood method 0-18466  
 prebreakdown elec. cond. of nearly saturated Xe vapour 0-48841  
 precursors, associative ionisation and photoionisation, relative contrib., electron density prediction 0-43858  
 probe for radiation contamination monitoring 0-27826  
 PWR, Xe-induced spatial flux transient, anal. and control, parameter identification 0-18441  
 scintigraphy, estimation of regional ventilatory clearance 0-30854  
 shock wave, strong, piston struct. and gas distrib. 0-10265  
 solid, self-trapped exciton emission bands 0-20697  
 solution, mean force of two atoms dissolved in water 0-54114  
 sorption, diffusion, solubility in polyvinyltrimethylsilane rel. to temp. (*Russian*) 0-6565  
 tetracene-Kr(Xe), intramol. intersystem crossing in supersonic beam, external heavy atom effect 0-14167  
 thermal conductivity, Lennard-Jones (12-6) pot. parameters calcs. 0-28591  
 united atom rare gas spectra analogy with mol. Rydberg states 0-32700  
 $\mu$ Xe muonic atoms, vanishing muon transfer effect 0-9765  
<sup>133</sup>Xe custom trapping and holding system for animal research, design and evaluation 0-30950  
 Ar-Xe, low-threshold nuclear pumped laser, generation characts. 0-19018  
 Ar-Xe-NF<sub>3</sub>, mixture in XeF laser, discharge stabilised by short-pulse electron beam 0-14358  
 Ar-Xe-tetrachloromethane, self-sustained electrophotoionised discharge in compressed gas 0-38003  
 He-Ne-Xe, ion laser transitions, hollow cathode excitation 0-1184  
 He-Xe, ion laser transitions, hollow cathode excitation 0-1184  
 He-Xe, low-threshold nuclear pumped laser, generation characts. 0-19018  
 He-Xe optical amplifier, high gain coeff., noise characts. 0-43365  
 He-Xe optical amplifier, striation form. for DC discharge plasma, noise anal. 0-43366  
 He-Xe recombination lasers, CO<sub>2</sub> laser-produced plasma-initiated 0-48286  
 He-Xe-F<sub>2</sub> mixture, pulsed avalanche discharge at high gas press., homogeneous form. conditions 0-49027  
 Hg-Xe film, random mixtures, superconducting transition temp. and metal-nonmetal transition 0-29498  
 Kr-Xe-F<sub>2</sub> excimer laser, kinetics of excimer formation 0-14328  
 KrCl\*+Xe, substitution efficiency during excitation in transverse AC electric discharge 0-50850  
 N<sub>2</sub>-Kr-Xe, liquefaction, retention of <sup>85</sup>Kr from fission exhaust gases, separation technique (*German*) 0-27753  
 Na+Xe, nonreson. two-photon absorpt., 4s excited states and pot. energy curves, close coupled eqns. 0-48068  
 O<sub>2</sub>-<sup>85</sup>Kr-Xe, liquefaction, retention of <sup>85</sup>Kr from fission exhaust gases, separation technique (*German*) 0-27753  
 Ti-Xe, electric discharge excitation of Ti in high-press. Xe 0-49025  
 W-Xe, attachment of mobile particles to non-saturable traps 0-39418  
 Xe II, radiative lifetimes, beam-foil spectroscopy 0-18825  
 Xe III, 5s<sup>2</sup>5p<sup>1</sup>(<sup>4</sup>S)nl levels, ionis. pot., from spectral data 0-47920  
 Xe IV laser excited by long current pulse discharge, double-pulsed output 0-37993  
 Xe, in gas discharge, collisional excitation, radiation lifetimes, macroscopic alignment obs. 0-33734  
 Xe prod. cross sections with protons of 320-590 MeV, nuclear medicine appl. 0-36133  
 Xe VII, VUV line classifications and energy levels in triplet system 0-37763  
 Xe VIII, beam-foil lifetime meas., cascading problem 0-14249  
 Xe VIII, one-electron spectrum in theta pinch discharge, line identification 0-32640  
 Xe<sup>2+</sup>, energy level radiative lifetimes using 1-5 MeV ions 0-47947  
 Xe<sup>24+</sup>, impact on highly-ionised Ne target, selective target electron capture effects 0-14202  
 Xe: <sup>57</sup>Co, solid, ion implantation for rare gas matrix isolation, Mossbauer spectroscopy study 0-54271  
 Xe-<sup>3</sup>He plasma, plasma parameters determ. 0-54047  
 Xe-He source, intensity fluctuations of amplified spontaneous emission at 3.51  $\mu$ m 0-32957  
 Xe-He(Ne), gas mixture, element and isotope separation in impulse plasma centrifuge (*Russian*) 0-38725  
 Xe-I dating of silicate and troilite in Fe meteorites group IAB 0-17554  
 Xe-Kr, gas, diffusion coeffs. meas., 350-1200K 0-14869  
 Xe-methane, mol. relax., optoacoustic reson. meas. 0-27351  
 Xe-Xe(Kr), glory structure in total cross section, crossed supersonic atomic beam, n(X)-6 potential 0-48060  
 Xe+ inert gas, Xe three level system, collisional transfers, disalignment cross section 0-53098  
 Xe+C<sub>2</sub>H<sub>4</sub> liquid mixtures, intermol. forces effect on phase diagram and excess props., perturbation theory 0-39287  
 Xe+Cs, Cs spectral line profile and absorpt. transitions 0-47944  
 Xe+Cs, shift, halfwidth, satellite and absorpt line in square-well pot. 0-42993  
 Xe+H, simultaneous ionisation investig. 0-32815  
 Xe+H<sup>+</sup>, electron capture, charge-state distrib. 0-32814  
 Xe+H<sup>+</sup> ionisation, induced L-shell alignment 0-32813  
 Xe+HCl, infrared line shape, rotational lines, influence of collision duration 0-43110  
 Xe+HCl(HBr), liquid mixtures, intermol. forces effect on phase diagram and excess props., perturbation theory 0-39287  
 Xe+He(2<sup>2</sup>S,2<sup>2</sup>S'), Van der Waals forces, one-electron model pot. calcs. 0-14094



**xenon continued**

- Xe<sup>+</sup> ion ( $1 \leq Z_1 \leq 90$ ), 2.5-400 keV, 1-6°, effective interat. pots. 0-23492  
 Xe+K, K 5<sup>2</sup>P level broadening and collisional relax., quantal, semiclassical and expt. comparison 0-18903  
 Xe+K, photon emission polarisation anal., coincidence studies 0-5614  
 Xe+NO, angle depend. intermolecular pot., crossed beams study 0-9682  
 Xe+O(<sup>1</sup>D), inelastic collisions, spin-orbit coupling 0-5605  
 Xe<sup>+</sup>+Xe, quasi-resonant charge transfer at thermal energies 0-48082  
 Xe<sup>2+</sup>+H<sub>2</sub>(N<sub>2</sub>(O<sub>2</sub>) (inert gas), charge transfer reaction rate consts. 0-7779  
 Xe<sub>2</sub>, e-beam excited, 193 nm absorpt. studies 0-43323  
 Xe<sub>2</sub>, electron beam excited, 193 nm absorpt. meas. rel. to 172 nm laser pulse termination 0-28200  
 Xe<sub>2</sub>, excimer laser action in coaxial field emission diode, comparison with Ar<sub>2</sub>, Kr<sub>2</sub> 0-28201  
 Xe<sub>2</sub>, laser performance for atm. press. and microsecond electron beam excitation 0-28199  
 Xe<sub>2</sub>, performance as photolytic driver at low electron beam excitation rates 0-32963  
 Xe<sub>2</sub><sup>+</sup>, A<sup>2</sup> $\Sigma_{1/2u}^+$  → D<sup>2</sup> $\Sigma_{1/2g}^+$  system, theoretical absorption spectrum 0-32734  
 Xe<sub>2</sub><sup>+</sup> excimer form. in pulsed discharge, visible emission obs. 0-38754  
 XeF\*(B), nuclear pumped laser, buffer effects 0-37617  
<sup>131</sup>Xe+Rb, spin-exchange cross section, <sup>131</sup>Xe nucl. spin relax. obs. 0-37868  
<sup>133</sup>Xe air contamination, meas. technique 0-41255  
<sup>133</sup>Xe, probability distrib. for release in PWR steam generator tube rupture 0-13668  
<sup>133</sup>Xe retention in hepatic steatosis rel. to biopsy 0-17069  
<sup>133</sup>Xe solubility coefficients in water, saline, dog blood and organs 0-56331  
<sup>133</sup>Xe washout rel. to single-breath imaging for ventilation abnormalities detect. 0-41183  
<sup>133</sup>Xe/<sup>133</sup>Cs, implanted in various hosts, isomer shift values, Mossbauer spectra 0-7240  
<sup>136</sup>Xe 7p[3/2]<sub>1</sub> level, cascade alignment in discharge 0-44057  
 Xe<sup>+</sup>(7s<sup>2</sup>P<sub>1/2,3/2</sub>), charge exchange excitation in Ne-Xe glow discharge 0-38857

**xenon compounds**

- chemical and isomer shifts, electron valence struct. (*Russian*) 0-53056  
 ArXe, continuous VUV emission spectrum 0-43066  
 XeBr, emission and form. kinetics, sequential two-photon absorpt. expt. 0-32767  
 XeBr laser, energy decrease mechanism 0-28243  
 XeCl 0-53323  
 XeCl avalanche discharge laser, D and B state coupling, population depletion 0-28214  
 XeCl discharge laser, energy characts. 0-48228  
 XeCl, energy curves and transition moments 0-28210  
 XeCl, excimers and excimer lasers 0-48217  
 XeCl high specific power long-pulse supersonic flow laser at 308 nm 0-48221  
 XeCl laser, closed cycle characts. 0-33030  
 XeCl laser, closed cycle flow type, operating characts. 0-43349  
 XeCl laser, discharge excited, preionisation technique 0-23714  
 XeCl laser, discharge stabilisation with 50 nsec electron beam 0-23716  
 XeCl laser, electron beam, beam-stabilized discharge and fast discharge excitations 0-28204  
 XeCl laser pulse backward Raman compression in Pb vapour 0-19068  
 XeCl molecule excited by electron beam, stimulated emission obs. 0-32966  
 XeCl, relax. and quenching rate consts., emission spectra modelling 0-28211  
 XeCl UV preionised simple compact laser, elec. and gain characts. 0-28206  
 XeCl\*+Kr, substitution efficiency during excitation in transverse AC electric discharge 0-50850  
 XeF, (B,C) state prod. and kinetics, XeF<sub>2</sub> photolysis with VUV radiation 0-32975  
 XeF, B and C-state kinetics with self-sustained discharge pumping 0-28212  
 XeF, broadband emission origin 0-38007  
 XeF, discharge excited laser operation at elevated temps., transitions, output power 0-43359  
 XeF, electron beam pumped laser, gain, fluoresc. and laser output at 351, 488 nm 0-28215  
 XeF electron beam pumped laser, energy, time and spectral characts. 0-38005  
 XeF, electron impact deexcitation, low energy cross-sections and rate consts. 0-1071  
 XeF, electron impact deexcitation cross sections and rate consts. calcs. 0-32848  
 XeF, electron quenching rate consts. meas. by fluoresc. anal., laser implications 0-32969  
 XeF, energy curves and transition moments 0-28210  
 XeF excimer laser, self-sustained discharge pumping 0-28219  
 XeF, excimer laser pumped dye laser (*Chinese*) 0-1234  
 XeF, ground state dissoc. vibr. equilibrium 0-9652  
 XeF, high-intensity short pulse generation, oscillator-optical gate-amplifier system 0-38038  
 XeF laser, C-A blue-green, multipass amplification and tuning 0-43346  
 XeF laser, closed cycle characts. 0-33030  
 XeF laser, closed cycle flow type, operating characts. 0-43349  
 XeF laser, efficient operating conditions with electron beam stabilisation 0-38006  
 XeF laser, electron beam, beam-stabilized discharge and fast discharge excitations 0-28204  
 XeF laser, electron beam excited, gain measurements using amplified spontaneous emission 0-37986  
 XeF laser, temp. depend. absorpt. processes in Ne-Xe-NF<sub>3</sub> mixtures 0-1188  
 XeF laser, UV preionised discharge pumped, 10 kHz repetition rate 0-33029  
 XeF, laser action on C→A transition, pumping mechanisms, kinetics and efficiencies 0-32967  
 XeF laser using Ar-Xe-NF<sub>3</sub> mixture, discharge stabilised by short-pulse electron beam 0-14358  
 XeF laser using XeF<sub>2</sub> photodissociation, fluoresc. and laser performance 0-32976

**xenon compounds continued**

- XeF laser wavelength transient absorpt. in electron beam excited inert gases 0-32644  
 XeF linac-excited gas mixture, UV fluoresc. meas. 0-28216  
 XeF molecule formed by XeF<sub>2</sub> photodissociation, laser action due to bound-free C(3/2)-A(3/2) transition 0-14334  
 XeF pumped Tm:LiYF<sub>4</sub> excimer excited storage laser 0-33003  
 XeF, relax. and quenching rate consts., emission spectra modelling 0-28211  
 XeF, supersonic expansion jet, B-X system rot. and vibr. anal., isotope intervals, fluoresc. spectra 0-14174  
 XeF<sub>2</sub>, photodissoc. yield in solid Xe and Kr, time-resolved photolum. excitation obs. 0-3372  
 XeF<sub>2</sub> photodissociation forming XeF, laser action due to bound-free C(3/2)-A(3/2) transition 0-14334  
 XeF<sub>2</sub> photodissociation for XeF laser 0-32976  
 XeF<sub>2</sub> photolysis with VUV radiation, XeF (B,C) state prod. and kinetics 0-32975  
 XeF\*, broadband emission origin 0-28202  
 XeF\* gas-discharge excimer laser, kinetics 0-48226  
 XeF\* laser system, trimer form. rates 0-50831  
 XeO, luminesc. meas. of O(<sup>1</sup>S) absolute quantum yield in photolysis of CO<sub>2</sub>, N<sub>2</sub>O 0-35561  
 XeO photochemical laser, energy characts., kinetic model of physicochem. processes 0-28228  
 XeO<sup>+</sup>, X<sup>2</sup> $\Sigma^-$  state, pot. energy curves and correl. effects, elastic scatt. cross sections 0-23502  
 XeS, photoluminesc. in rare gas matrices 0-5568

**xerography** see *electrophotography*; *reproduction (copying)*

**xeroradiography** see *electrophotography*

**XPS** see *X-ray photoelectron spectra*

**Yang-Mills theory**

- $\sigma$  model representation as a spontaneous violation (*Russian*) 0-13220  
 Abelian field configurations, instability 0-344  
 asymptotic freedom in the infinite-momentum frame, SU(N) Yang-Mills theory renormalisation 0-22519  
 asymptotic scattering states of colored classical particles 0-397  
 asymptotically free models and the G<sub>2</sub>-group 0-18072  
 asymptotically non-free Yang-Mills theory, IR divergences 0-37166  
 axially symmetric multi-instanton solutions generated by conformal mappings in SU(2) Yang-Mills field 0-42337  
 Backlund transforms and symmetries of Yang eqns. 0-52393  
 bag and multimeron solutions of the classical Yang-Mills equation 0-4853  
 Belavin Yang-Mills pseudoparticle soln., metric representation, isotropic Universe relation 0-27404  
 Cauchy problem for the Yang-Mills equations 0-13206  
 classical eqns., singular pots. and analytic regularisation 0-334  
 classical field theory geometrisation, applied to Yang-Mills field theory 0-46841  
 classical SU(2) Yang-Mills field, ignorable variables extraction from Hamiltonian 0-328  
 classical SU(2) Yang-Mills field eqns., periodic solns. in Minkowski spacetime 0-4854  
 colour spin and path ordered phase factor, path integrals 0-4932  
 conformal properties of fields 0-32024  
 conserved quantities in classical theories 0-350  
 Coulomb solution of Yang-Mills eqns. with external sources 0-27407  
 dense and dilute instanton-anti-instanton pair configurations 0-52424  
 dual strings, interaction, correspondence between gauge group and dual model 0-42432  
 Dyson equations, Ward identities, and the infrared behavior of Yang Mills theories 0-42353  
 effective potential in intense fields, gauge non-fixing calc. 0-52397  
 Einstein-Maxwell and Einstein-Yang-Mills space-times, infinitesimal homonomy group structure 0-12976  
 Einstein-Yang-Mills system in six dimensions, static solution 0-8883  
 elliptic function methods 0-4829  
 Euclidean functional determinant, bounds 0-32019  
 Euclidean lattice Yang-Mills theory in two spacetime dimensions (*German*) 0-37157  
 Feynman diagram theory, finite, analogy with space-time approach 0-52400  
 Feynman path integrals, conference, Marseille, France, 1978 0-31422  
 finite local gauge transformation 0-31968  
 finite-band solutions to the duality equation on S<sup>4</sup> and two-dimensional relativistically invariant systems 0-42349  
 formal linearisation of eqns. 0-335  
 gauge dependence in the Yang-Mills S matrix 0-351  
 gauge invariant S-matrix elements with Yang-Mills SU(2) instantons and anti-instanton 0-22511  
 general Taub-NUT-De Sitter metric, self-dual Yang-Mills soln. of gravity 0-46946  
 generalised Einstein eqn., field eqn. for EM field and Yang-Mills instantons 0-8872  
 geometrical gauge conditions, nonexistence results 0-47166  
 geometrical setting for Yang-Mills type gauge fields, review 0-32014  
 gravity theory bases on internal translation group 0-42134  
 hadronic matter, Pomeron and critical temp. 0-22566  
 hadrons, Yang-Mills pots., Van der Waals force and fermion motion 0-52465  
 high energy meson elastic scatt. amplitude, leading term approx. in SU(2) Yang-Mills theory 0-5017  
 higher-derivative theory, ghost problem 0-31970  
 instability of constant Yang-Mills fields 0-343  
 instantaneous Coulomb interaction in SU(2) Yang-Mills QCD 0-396  
 instantaneous Coulomb interaction in SU(2) Yang-Mills QCD 0-22574  
 instanton gas, bag-to-vacuum phase transition, mean field approx. 0-9097  
 instanton solutions to reduced eqns., F=F review 0-32021  
 instantons and merons in Euclidean space solns. (*Russian*) 0-42344  
 inverse scatt. in higher dimensions 0-47165  
 IR divergences and zero mass limit 0-32025  
 isotopic spin sources, motion, gauge theories 0-12977  
 k-instantons in Sp(1) Yang-Mills theory, calculation method 0-13223  
 lattice gauge theories, comparison with gauge groups SU(2) and Z<sub>2</sub> 0-31966  
 lattice gauge theory, Gaussian transformation into string field theory 0-32003  
 Lienard-Wiechert type of solution in SU(2) 0-4879  
 line space construction of non-self-dual Yang-Mills fields 0-9103



**Yang-Mills theory continued**

- linear field equations on self-dual spaces 0-42328
- magnetic monopoles, non-Abelian, stability analysis, Yang-Mills equations 0-31987
- magnetic monopoles in the presence of quark sources 0-13213
- massive, appl. of path integrals to non-perturbative study 0-32020
- Maxwell eqns., null solns., generalised to Yang-Mills theory 0-27388
- mesons, deformations and spectral props. 0-13203
- monopole system, equivalence with Yang-Mills field, 't Hooft monopolar solution 0-9084
- non-Abelian gauge theories, local covariant operator formation, quark confinement 0-47190
- non-perturbative quantum field theory, lattice renormalisation construction 0-9098
- nonAbelian, nonlinear Yang-Mills field eqns., self-duality, helicity, coherent states 0-31988
- O(2) symmetric connections in an SU(2) Yang-Mills theory 0-4839
- O(4) Yang-Mills, Higgs system, topologically stable solns. 0-52382
- over-critical point source 0-4846
- potential determination from field strength 0-32011
- Prasad-Sommerfield dyon (monopole) soln. of SU(2) Yang-Mills field with Higgs multiplet 0-339
- quantisation without fixing gauge 0-13207
- quantised topological charge, implications of zero field tensor 0-31983
- quantum scattering by external metrics and Yang-Mills potentials 0-31535
- quark field quantum fluctuation computation in arbitrary Yang-Mills instanton background 0-13268
- relativistic string model generalisation in geometrical approach, Yang-Mills approx. 0-383
- renormalisation of theory developed around instanton 0-32027
- rotating plane-fronted waves and their Poincare-invariant differential geometry 0-332
- S-matrix for interaction of gravitational and Yang-Mills fields 0-42315
- self dual SU(N) Yang-Mills fields, nonlocal continuity eqns. 0-9096
- self-dual Yang Mills fields in Minkowski space 0-18078
- Sikivie-Weiss magnetic dipole soln. 0-22523
- six-dimensional approach to Weinberg-Salam model, Higgs particle 0-4905
- stability and bifurcation in Yang-Mills theory 0-52417
- stability and gap phenomena 0-18073
- stability of solitons, Poincare stability, gauge theories, nonlinear Schrödinger equation 0-4881
- SU(2), Yang-Mills field eqn. configurations in curved spacetimes 0-18076
- SU(2) colour Yang-Mills theory, quark source charge screening, confinement 0-22565
- SU(2) Yang-Mills eqns., classical solns. 0-4875
- supergravity, gauge group and geometry 0-8888
- temporal gauge struct. by Feynman propagation kernel 0-37162
- U(N) lattice Yang-Mills theory, Schwinger-Dyson eqns., string model equivalence 0-4855
- vacuum wave functional calc. 0-13212
- vertex functions, triple-gluon, gauge invariance in non-Abelian gauge theories 0-42326
- zeta-function regularization and multi-instanton determinants 0-13215

**yield point**

see also *yield strength; yield stress*

- concrete slabs, subjected to biaxial moments, optimum design of steel bars reinforcement, using analytical and graphical methods 0-50664
- elastic springback in beams and plates, bending 0-38256
- glass fibre reinforced plastics, relation between matrix vol. changes and mech. props. 0-11715
- metal-H systems, anelastic and plastic props., review 0-49298
- metals, FCC, yield threshold at 4.2K, effect on strain-hardening curve (Russian) 0-50671
- Ni alloy KhN45Yu, strength properties, dispersity of struct. effect 0-55486
- oxides, interaction between point defects and dislocations, cryst. plasticity 0-15149
- plates, rectangular, hinge-supported, eccentrically applied, ultimate point load, kinematic solutions 0-53638
- polycarbonate of bisphenol A, neck form. and propaga., strain anal. 0-16376
- polyethylene, linear, crystallised from melt, effect of crystallisation time on density, mech. props., X-ray scattering 0-25680
- polyisobutylene, undiluted, mol. wt. influence on creep behaviour 0-45370
- polyolefins, plastic flow, yield limit rel. to press. (Russian) 0-7657
- PVC, stress relaxation in macrodeformation range 0-16370
- steel, austenitic stainless Kh18N10T, strength properties, dispersity of struct. effect 0-55486
- steel, correlation links between mech. props. controlled rolling effect 0-35234
- steel, Cr-Mo (2.25, 1 wt.%), strain hardening shakedown load during bending 0-20958
- steel, Cr-Mo-Ni-Nb, Nb effect on mech. props. (German) 0-30012
- steel, for pressure tanks, yield point influence on brittle fracture, tensile strength (German) 0-40539
- steel, low-alloy, props. with nitride and Cu hardening at low temps. (Russian) 0-40372
- steel, low-C, fully pearlitic, struct. and mech. characts. rel. to cooling conditions (French) 0-40425
- steel, mild, AC effect on fatigue and static props. 0-45372
- steel, mild, yield point, effect of neutron irradi. and N<sub>2</sub> conc. 0-45365
- steel, Ni-Cr-Mo, quenched and tempered, notched bar tensile tests (German) 0-35247
- steel, stainless type 03Kh13AG19, deformation temp. influence on dislocation struct (Russian) 0-11698
- Ag, yield point, temp. depend., 2 to 300K (Russian) 0-45346
- Al, polycrystalline, acoustic emission energy release, grain size and flow stress depend. 0-11722
- Cu-Be alloy props. obs., dependence on heat treatment (Czech) 0-55448
- Fe, cast, thermal treatment influence on mechanical props. (German) 0-29980
- Fe, quenched-in hydrogen, yield stress decrease of prestrained specimens 0-16454
- $\alpha$ -Fe, yield point behaviour for extremely inhomogeneous deformation (German) 0-55453

**yield point continued**

- $\alpha$ -Fe, yield point behaviour in homogeneous plastic deformation (German) 0-35248
- KCl, US plastic deform., dislocation struct. 0-19809
- Mo, mechanical props. and dislocation struct., mag. field effect 0-54935
- Mo-V-C, hot-worked, substructural hardening and high-temp. strength (Russian) 0-25731
- NaCl, dislocation struct. of slip bands, hydrostatic press. effect 0-54249
- NaCl:Ca<sup>2+</sup> crystals, influence of dipoles and dipole complexes on yield point 0-39208
- Nb, mechanical props. and dislocation struct., mag. field effect 0-54935
- Ni, deformation in const. mag. field, 4.2K (Russian) 0-29591
- Ni, yield point, effect of alloying elements (Russian) 0-50670
- SbS<sub>2</sub>Se<sub>1-x</sub> layer elec. and ferroelec. props., mech. stress effects (Russian) 0-50279
- Ti, commercial, creep behaviour, 25 to 400°C, role of impurities and/or alloying elements (French) 0-45354

**yield strength**

- alloys, two-phase, coarse microstructs., structural approach to yield strength 0-7634
- butt joint, tensile bond strength, effect of aspect ratio 0-50823
- composites, unidirectional, micromech. prediction of initial yield surfaces 0-25777
- heat-resistant alloys, installation for mech. tests under superplasticity conditions 0-55603
- metal mechanical property effects on frictional behaviour 0-55548
- metals, determ. of yield strength 0-25937
- microstruct. and tensile props. 0-34077
- notch-tip geometry, influence on stress and strain distrib. 0-33535
- plastic constitutive equations with work hardening (Japanese) 0-25718
- poly(2,6-dimethyl-1,4-phenylene oxide)/poly(styrene-co-p-chlorostyrene) blends, tensile props. modelling 0-19868
- polycarbonate, plastic insulation for cryogenic power cable, exam. of dielectric, tensile props. 0-25823
- polyester (Mylar), plastic insulation for cryogenic power cable, exam. of dielectric, tensile props. 0-25823
- polyethylene (Dy<sub>2</sub>O<sub>3</sub>), mech. props. and transfer to steel surfaces 0-16496
- polyethylene, plastic insulation for cryogenic power cable, exam. of dielectric, tensile props. 0-25823
- polypropylene, oriented, compressive elastic modulus and yield strength 0-16385
- polypropylene, plastic insulation for cryogenic power cable, exam. of dielectric, tensile props. 0-25823
- polysulphone, plastic insulation for cryogenic power cable, exam. of dielectric, tensile props. 0-25823
- reinforced concrete containment model behaviour under thermal gradients and internal pressure 0-42837
- sludge, cohesive, dynamic props. (Japanese) 0-45580
- solid solution hardening, statistical behaviour analysis, with aid of computer (Japanese) 0-11658
- spinodal alloys characterisation techniques, props. and appls., review 0-50588
- steel, austenitic stainless, biphasic, ferritic, ageing and thermomech. treatment effects on struct. and props. 0-35226
- steel, austenitic stainless, mech. props. correl. methodology development for fusion environments 0-29068
- steel, austenitic stainless, type 321S12, fatigue cycling in R=-1 loadings 0-35317
- steel, duplex ferrite-martensite, microstructure resistance optimisation 0-40482
- steel, high speed type M-50 and 18-4-1, fracture and fatigue 0-16457
- steel, HSLA, V effect on mech. props. (Korean) 0-29987
- steel, low-C martensitic, Ni addition influence on toughness and ductile-brittle transition 0-30099
- steel, maraging, influence of microstructure, strain rate and temp., on tensile props. 0-11733
- steel, microalloyed, precipitation effect on microstruct. and mech. props. (French) 0-25708
- steel, Mn-Cr-Mo, Mn-V-Mo, high-strength heat-treatable sintered 0-50575
- steel, Mn-Si, St 52-3, cleavage fracture toughness, temperature and notch sharpness influence (German) 0-35291
- steel, Mn-Si, St 52-3, fracture toughness determ. from yield strength and cleavage fracture strength (German) 0-35292
- steel, Mn-Te, structural, brittle fracture resistance, Ti addition effect (Czech) 0-45392
- steel, Nb-Va microalloyed, mech. props. (French) 0-35252
- steel, Ni-Cr-Mo, cleavage fracture toughness, temperature and notch sharpness influence (German) 0-35291
- steel, Ni-Cr-Mo, fracture toughness determ. from yield strength and cleavage fracture strength (German) 0-35292
- steel, sheet, rapid test for props. assessment 0-40650
- steel, statistical treatment of experimental data 0-53644
- steel, strength, acoustic monitoring 0-35479
- steel, tempered, high strength, internal stresses and mech. props. 0-3200
- steel, Ti, hot-rolled, inhomogeneity of mech. props. (Chinese) 0-55455
- steel/Cu bimetallic pipe, determ. of yield, tensile strength 0-25771
- wire in torsion, installation for automated determination of yield strength 0-21221
- Zircaloy-2, effect of simulated fission products on elongation fractography and metallography 0-649
- Zircaloy-4 tubes, texture influence on anal. of thermoelastic/plastic anisotropy and initial yielding 0-35260
- Al alloy 6061-T6, yielding of tubing under dynamic biaxial loading 0-16377
- Al-Cu-Mg, type 2036, deformation at ageing temp., effect on struct. and props. 0-7605
- BaF<sub>2</sub>, formation and growth of oxidation centres result of O<sup>2-</sup> diffusion 0-7706
- C evaporated films, nucl. appl. 0-23214
- Cu-Zr-(Cr), powder metallurgical alloys, thermomech. treatment effect on props. 0-50660
- CaF<sub>2</sub>, press forged, mech. and optical props. 0-38079
- Cu, polycryst., grain size and high-temp. yield strength 0-7641
- Cu-BeCo (1.85, 0.29 wt.%), type CA172 (TH04), strengthened by spinodal decomp., stress relax. in bending 0-7616
- Cu-Ti-Fe (0.7, 0.9 wt.%) film, dispersion-strengthened, form. by high rate magnetron/plasmatron sputtering, and props. 0-25715
- Fe, sintered, strength and elongation, rel. to density 0-30047



**yield strength continued**

- Fe-Mn (up to 8 wt.%), microstructure, mech. props. and fracture (*Japanese*) 0-35304  
 Fe-Mn-Ti alloys, austenitic, precipitation strengthened 0-25714  
 Fe-Ni heterogeneous alloys, ferrite, martensite and austenite phase distrib., effect on mech. props. 0-45363  
 LiF mech. and optical props. rel. to forging conditions 0-33101  
 LiF, press forged, mech. and optical props. 0-38079  
 Mo alloys, fusion reactor first wall and blanket material, props. for struct. appl. 0-30071  
 Mo-Mn alloy, plasticity, fracture, strength depend. on C content (*Russian*) 0-35257  
 Nb alloys, fusion reactor first wall and blanket material, props. for struct. appl. 0-30071  
 Nb, neutron irradi., microstruct. and tensile props. 0-34077  
 Nb-low alloys, strength and ductility at high temp. and different strain rates 0-16401  
 Nb<sub>3</sub>Sn fatigue effects in unidirectional composites, computer simulated model 0-35289  
 Ni, neutron irradi., microstruct. and tensile props. 0-34077  
 Ni-Cr-Mn-Fe-Nb (20,3,3,2,5 wt.%), short-range order effects on tensile behaviour 0-25793  
 Ni<sub>3</sub>Al-B, L1<sub>1</sub> type intermetallic cpd. room temp. ductility improvement by B addition (*Japanese*) 0-35263  
 Pb-(Au) (0.1 and 0.2 wt.%), single crystals, yield strength depend. at 77K on Av conc. 0-55479  
 Sn plate, rapid test for props. assessment 0-40650  
 $\alpha$ - $\beta$ Ti alloys, high strength, heat-treated weldments, intergranular fracture 0-21097  
 Ti-Al-H, H effect on mech. props. and lattice constants 0-21036  
 Ti-Al-V (6.4 wt.%),  $\alpha/\beta$  interface phase influence on tensile props. 0-30034  
 Ti-Al-V (6.4 wt.%), strongly textured, influence of crystallographic orientation on tensile behaviour 0-7633  
 V alloys, fusion reactor first wall and blanket material, props. for struct. appl. 0-30071  
 V-low alloys, strength and ductility at high temp. and different strain rates 0-16401  
 W, with different microstructs., temp. depend. of yield strength 0-16404

**yield stress**

see also *yield point; yield strength*

- alkaline silicate glass, surface layers, plasticity and microcrack formation, electron microscopy (*German*) 0-40469  
 brass, M63, yield stress decrease in compression, rel. to previous elongation (*Polish*) 0-50665  
 $\alpha$ - $\beta$  brass, two phase bicrystal, deform. and fracture at 450K 0-16409  
 ceramic nuclear fuels, mech. props. at compressive deformation 0-651  
 crack tips, yielding on inclined planes 0-33525  
 deformation behaviour contrib. in rod drawing (*German*) 0-11684  
 epoxy resin systems, synthesis review, phys. and mech. props. at low temps. 0-25650  
 epoxy resins, correlation between valence energies and low temp. flexibility 0-25815  
 ionic crystals, structurally modulated, elasticity and its limits, yielding and melting 0-49295  
 iron, pure, tensile deformation behaviour under high pressure (*Japanese*) 0-16381  
 metal, BCC, polycrystalline aggregate, prediction of plastic props., deformation by {111} pencil glide 0-11731  
 metals, radiation effects on elasticity and elastic moduli, yield stress 0-2078  
 metals and alloys, yield criterion, rheological interpretation (*Russian*) 0-21014  
 microstruct. and tensile props. 0-34077  
 non-Newtonian fluids, rheological props., pressure induced change of yield stress 0-53736  
 Nylon 6, injection moulded, yield stress and fracture toughness 0-38951  
 olivine, hardness var. with temp., rel. to polycryst. yield stress 0-26500  
 orthotropic strip, stress intensity factors and crack opening displacements 0-53710  
 plastic flow in thick-walled cylindrical shell, non-homogeneity effect, numerical calc. 0-19248  
 plasticised cellulose acetate sheet, post-yield fracture 0-25859  
 polyethylene, correlation between valence energies and low temp. flexibility 0-25815  
 polyethylene, solid-state extruded, exam. of props. 0-11669  
 polystyrene melt, carbon-black filled, rheological study 0-48665  
 porous metal, yield stress variation during cold deformation 0-16395  
 steel, brass clad plate/roll bonded Ni clad, fatigue crack growth behaviour 0-40484  
 steel, C, deformation strength and strain rate depend. under plain strain state (*Japanese*) 0-30028  
 steel, Cr (13 wt.%), sintered, organometallic complex addition effects on mech. props. 0-25595  
 steel, Cu-Zn, brass clad, fatigue crack growth behaviour 0-40484  
 steel, low C, plastic deformation by pencil glide,  $r$ -values and yield loci 0-7654  
 steel, low-C martensitic, Ni addition influence on toughness and ductile-brittle transition 0-30099  
 steel, mild, tensile deformation, behaviour under high pressure (*Japanese*) 0-16381  
 steel, Mn-Mo-Ni-Cr, bainitic, microstructures and mechanical properties (*French*) 0-16362  
 steel, Nb, controlled-rolled into ferrite temp. range, soln. temp. and rolling effects 0-11678  
 steel, stainless, neutron irradiation effect on low cycle fatigue and tensile props. at 298K 0-30059  
 steel, structural, grain size depend. of yield stress in homogeneous deformation range (*German*) 0-30013  
 steel, ultrahigh strength, monotonic and cyclic stress strain curves 0-35268  
 steel, V containing dual-phase, yielding and strain ageing, early stages 0-25794  
 steels, C, quenched and tempered, struct.-prop. relationships 0-7599  
 steels, structural St 37-2, cleavage fracture, report 0-25868  
 stress/strain relation, rate and temp. depend., analytic formulation 0-40466  
 Tresca type plastic material, simple shear deform. with combined work hardening (*Japanese*) 0-35206

**yield stress continued**

- trigonal monocrystals, classes 3 and  $\bar{3}$ , elastic potential and yield condition (*Russian*) 0-29108  
 trigonal monocrystals, classes 3 and  $\bar{3}$ , plastic potential and yield stress (*Russian*) 0-29109  
 Zircaloy-2, neutron irradiated, inhomogeneous deformation behaviour 0-50679  
 Zircaloy-4,  $\beta$ -transformed, flow stress and dynamic strain ageing 0-3101  
 Al-Cu-Zr (6, 0.4 wt.%), superplastic deformation characts. 0-16387  
 Al-CuAl<sub>3</sub> eutectic, heat treatment and interlamellar spacing effect on tensile deformation 0-29979  
 Al-Zn-Mg-Cu, age hardened, effect of strain rate, temp. and environment on ductility 0-45368  
 C-fibre reinforced epoxy resin, laminated struct. mech. props. 0-50672  
 Cu, M1E, yield stress decrease in compression, rel. to previous elongation (*Polish*) 0-50665  
 Cu, pure, dynamic stress strain relations in combined tension and torsion, testing device 0-21197  
 Cu-Al, two-phase Cu-rich alloy, influence of microstruct. on stress-strain behaviour 0-7631  
 Cu-Ni-Sn (10, 6 wt.%), temp. depend. of yield stress and work hardening 0-21026  
 Cu<sub>3</sub>Au, dislocation slip band mobility, critical stress 0-2032  
 Fe electrodeposited foils, microstruct., internal stress and mech. props. 0-20807  
 Fe, high purity single crystals, thermally activated slip deformation between 4.2 and 300K 0-25801  
 Fe, Luder's band form. high speed camera obs. 0-16410  
 Fe single crystals, size effect on slip deformation ability at very low temps. 0-21049  
 Fe-Cu alloy, effect of  $\epsilon$ -Cu phase on strain ageing (*Japanese*) 0-7582  
 Ir<sub>2</sub>Cr, yield stress and saturation magnetisation 0-16389  
 KCl:Pb, lead aggregation effect on yield stress, incoherent precipitates, solubility determ. method 0-50645  
 MgO, compressive stress-strain behaviour at high temps. 0-25774  
 Mo, neutron irradiated, radiation softening and hardening 0-34083  
 Mo-Ti-Zr, alloy TZM, polycrystalline, anal. of elastic anisotropy and microyielding 0-30050  
 NaCl+Pb, Pb aggregation effect on yield stress, incoherent precipitates, solubility determ. method 0-50645  
 Nb, neutron irradi., microstruct. and tensile props. 0-34077  
 Ni, neutron irradi., microstruct. and tensile props. 0-34077  
 Ni<sub>2</sub> (Al, Nb) single crystals, orientation and temp. depend. of yield stress 0-25791  
 Ni<sub>49</sub>Fe<sub>29</sub>P<sub>14</sub>B<sub>6</sub>Si<sub>2</sub> glass, flow and failure 0-40438  
 Pb-(Au) (0.1 and 0.2 wt.%), single crystals, yield strength depend. at 77K on Av conc. 0-55479  
 Ti, dynamic annealing, effect on dynamic strain ageing phenomena 0-7594  
 Zr-Al (8.0 wt.%), tensile props. and fracture toughness after fast neutron irradiation 0-3198

**yielding** see *plastic deformation***Young's modulus**

- biomembrane elasto-viscous properties determined from bilayer meas. 0-30671  
 bone anisotropy, fibre-reinforced composite model 0-35944  
 column, non-uniformly compressed, optimal shape and non-homogeneity 0-10145  
 1,6-dicarbazolyl hexadiene, solid-state polymerisation, monomer to polymer phase transformations 0-38948  
 epoxy impregnated superconducting composites, mech. props., strain effect at 4K 0-25822  
 glass fibre reinforced epoxy resin, dynamic Young's modulus and internal friction 0-25754  
 glass fibre reinforced plastics, heat treatment and heating temp. effect on Young's modulus 0-35233  
 insulating thin films, Young's modulus measurement by micromechanics 0-33548  
 isotropic materials, Young's modulus determ., kinematic excitation of resonance oscillations 0-25958  
 measurement using automated Marx's composite oscillator method 0-37151  
 metallic glasses, amorphous, Young's modulus, using impulse induced resonance method 0-30008  
 metallic glasses, small samples, Young's modulus meas. by impulse induced resonance technique 0-40411  
 metals, radiation effects on elasticity and elastic moduli, yield stress 0-2078  
 optical waveguide blanks, thermal and elastic stresses in a cylinder 0-14447  
 PAN fibres, neutron irradiated, struct. and props. (*Russian*) 0-25763  
 photopolymer, biaxial stress-strain test 0-40417  
 plastic, glass-reinforced bottoms with a filler, rigidity 0-15183  
 poly(2,6-dimethyl-1,4-phenylene oxide)/poly(styrene-co-p-chlorostyrene) blends, tensile props. modelling 0-19868  
 poly-4-methylpentene-1, elastic parameters, US velocity meas. at 2.1-240K 0-40415  
 polyethylene, linear, crystallised from melt, effect of crystallisation time on density, mech. props., X-ray scattering 0-25680  
 polyethylene, of low density, determ. of avoiding of tensile cracks (*German*) 0-19874  
 polyethylene, oriented chain-extended, Young's modulus, fracture and compression behavior 0-11747  
 polyethylene, ultra-high modulus, drawing behaviour, effect of drawing temp. 0-35232  
 polyethylene, ultra-high-strength filaments, soln. spun/drawn, mech. and thermal props. 0-40440  
 polyethylene filaments, ultrahigh-strength, from soln. spinning and hot drawing 0-45268  
 polymer, semicryst., and filled, elastic modulus, strength, rel. to crystallite shape 0-45335  
 polymers, anal. of mechanics of solid phase extrusion 0-39204  
 polyoxymethylene, ultrahigh modulus oriented, exam. of true crystal modulus, from -150 to 20°C 0-11687  
 polypropylene rods, prep. by die-drawing 0-45327  
 polystyrene, amorphous, failure in methanol and ambient air 0-3165  
 rock, mech. props. rel. to cooling (*Japanese*) 0-31036  
 softwoods, transverse Poisson's ratio and Young's modulus (*Japanese*) 0-2111



**Young's modulus continued**

- steel, austenitic, age-hardening kinetics, study by resistivity, Young's modulus and internal friction (*Czech*) 0-29970
- steel, stainless type 304, elastic const. variability, US vel. meas. 0-55446
- surface layers and microvolumes, physical and mechanical props., continuous indentation calcs. (*Russian*) 0-40629
- viscoelasticity, instantaneous moduli, determ. from long-term static test results 0-38286
- Al-Fe<sub>3</sub>Mo<sub>2</sub>B<sub>20</sub> wire composite, mech. props. 0-40441
- Al-Zn-Mg plasma sputtered, mech. props. rel. to heat treatment (*Russian*) 0-40387
- Al<sub>2</sub>O<sub>3</sub> ceramics, elastic props. meas. in 100 to 300°C range 0-55445
- As<sub>2</sub>S<sub>3</sub> glass fibre, elongation, force depend., deviations from linearity 0-45334
- B fibre reinforced Al, dynamic Young's modulus and internal friction 0-25754
- B fibre reinforced epoxy, dynamic Young's modulus and internal friction 0-25754
- B, C, mech. and thermal props. 0-21083
- B<sub>2</sub>O<sub>3</sub> glass fibre, elongation, force depend., deviations from linearity 0-45334
- B<sub>2</sub>O<sub>3</sub> mech. and thermal props. 0-21083
- C fibre reinforced C, processing, room temp. mech. props., and low temp. expansion 0-25820
- C fibre reinforced epoxy, dynamic Young's modulus and internal friction 0-25754
- C fibres, durability, elastic props. and struct., heat treatment temp. effect, US meas. methods 0-40446
- C-fibre reinforced epoxy resin, laminated structs. mech. props. 0-50672
- Co, internal friction anomalies in spin reorientation temp. range (*Russian*) 0-49299
- Co-Fe, internal friction anomalies in spin reorientation temp. range (*Russian*) 0-49299
- Co-powder, isostatic compaction, mech. and elec. props. (*French*) 0-40285
- Cu wires, electrolytic, Young's modulus, working temp. effects 0-50667
- Cu-Al-Ni (13.8, 7.9 wt.%), cooling rates effect on internal friction (*Japanese*) 0-39217
- Cu-Be alloy props. obs., dependence on heat treatment (*Czech*) 0-55448
- Cu-Fe<sub>3</sub>Mo<sub>2</sub>B<sub>20</sub> wire composite, mech. props. 0-40441
- Fe base amorphous alloys, Invar and Elinvar characts. 0-29592
- Fe-B-Si amorphous ribbons, effect of annealing conditions on magneto-mechanical props. 0-34740
- Fe-Cr-B, amorphous, Elinvar and Invar charact. (*Japanese*) 0-11832
- GeO<sub>2</sub> glass fibre, elongation, force depend., deviations from linearity 0-45334
- MnBi, mictomag. alloys, elastic props. (*Russian*) 0-7141
- Mo-Ti-Zr alloy TZM, polycrystalline, anal. of elastic anisotropy and microyielding 0-30050
- Nb<sub>0.55</sub>Ir<sub>0.45</sub> metallic glass, Young's modulus meas. by impulse induced resonance technique 0-40411
- Ni powders, stereological appl. in study of compacting process, elec. and mech. props. (*French*) 0-40286
- (Ni<sub>1-x</sub>Cu<sub>x</sub>)Ti, martensitic, shape memory effect kinetics and thermodynamics 0-3021
- NiTi, martensitic, shape memory effect kinetics and thermodynamics 0-3021
- PbO-B<sub>2</sub>O<sub>3</sub>-ZnO solder glass, with admixtures, crystallisation and thermal expansion 0-24364
- Se, vitreous, elastic coeffs. about glass transition temp. US study (*French*) 0-19865
- SiB<sub>4</sub>, mech. and thermal props. 0-21083
- SiO<sub>2</sub> glass fibre, elongation, force depend., deviations from linearity 0-45334
- SiO<sub>2</sub>B<sub>2</sub>O<sub>3</sub>-K<sub>2</sub>O-Al<sub>2</sub>O<sub>3</sub>-As<sub>2</sub>O<sub>3</sub> glass fibres containing metallic granules, tensile strength, Young's modulus, DC conductivity 0-30023
- Ti<sub>0.60</sub>Ni<sub>0.40</sub> metallic glass, Young's modulus meas. by impulse induced resonance technique 0-40411
- W<sub>2</sub>C and WC, plastic deform. under bending, 800-2200°C (*French*) 0-55482
- Zr<sub>0.35</sub>Cu<sub>0.65</sub> metallic glass, Young's modulus meas. by impulse induced resonance technique 0-40411

**ytterbium**

- see also nuclei with .....
- atom, autoionisation and Auger decay, collective excitation effect 0-43008
- atom, isomers and hyperfine struct., selective detection through Rydberg states 0-52903
- electron and positron multiple scatt. 0-15171
- FCC phase, low temp. mag. props., impurity effects 0-20387
- hole lifetime and chemical shift of 4f-levels, XPS study 0-20762
- phosphate glass:Yb<sup>3+</sup>, excitation migration in inhomogeneous line profile, energy gap depend. 0-7407
- photoemission, valence-charge-induced Fano reson. 0-55267
- structural and electronic changes under 200 kbar press. and above 0-24588
- BaY<sub>2</sub>Fe<sub>2</sub>Yb<sup>3+</sup> ESR spectra and spin-lattice relax. 0-11263
- Bi<sub>2</sub>Ge<sub>2</sub>O<sub>12</sub>:Yb<sup>3+</sup> crystal growth, spectral and laser props. 0-45115
- CaWO<sub>4</sub>:Yb<sup>3+</sup> phase relaxation electron spin echo spectra 0-29613
- CaWO<sub>4</sub>:Yb<sup>3+</sup> phase relax. time rel. to g-factor anisotropy, electron spin echo obs. 0-29615
- DyAlO<sub>3</sub>:Yb<sup>3+</sup>, Mossbauer relax. 0-15875
- Er<sup>3+</sup>:Yb<sup>3+</sup> in liq. media, luminesc. cooperative sensitisation 0-2827
- Fe:Yb(Au), radiation-damage evolution, influence on lattice-location meas. 0-6426
- H, and He, stopping powers meas. 0-42904
- HoAlO<sub>3</sub>:Yb<sup>3+</sup>, Mossbauer relax. 0-15875
- LiYF<sub>4</sub>:Yb<sup>3+</sup>, ESR, nonlinear effect of elec. field 0-2635
- Na<sub>2</sub>O-B<sub>2</sub>O<sub>3</sub>-SiO<sub>2</sub>:Yb(Tb), luminesc. cooperative processes, glass struct. and comp. effect 0-16101
- Na<sub>2</sub>Sc<sub>2</sub>V<sub>2</sub>O<sub>12</sub>:Yb<sup>3+</sup>, EPR of Yb<sup>3+</sup> in octahedral sites 0-54948
- Tb<sup>3+</sup>:Yb<sup>3+</sup> in liq. media, luminesc. cooperative sensitisation 0-2827
- TbAlO<sub>3</sub>:Yb<sup>3+</sup>, Mossbauer relax. 0-15875
- YAlO<sub>3</sub>:Yb<sup>3+</sup>, absorption and luminescence spectra, electron-phonon resonances, Stark splitting (*Russian*) 0-20674
- YF<sub>3</sub>:Yb,Er, limit efficiency of transformation of IR to visible radiation 0-29784
- Yb<sup>3+</sup>, in soln., non-radiative transitions as Forster's energy transfer to solvent vibrations 0-1014
- Yb-glass, luminesc., low temp. energy transfer 0-2837

**ytterbium continued**

- Yb+Yb<sup>+</sup>, with nuclear sticking, molecular orbital and compounds nucleus X-ray emission 0-1048
- <sup>171</sup>Yb, A=170,171,173, 6s6p <sup>1</sup>P<sub>1</sub>-6s<sup>2</sup> <sup>1</sup>S<sub>0</sub> transition, spectrosc., isotope shifts and hyperfine structure 0-23368
- <sup>172</sup>Yb, muonic resonance spectra, deduced isomer shifts and electric moments 0-18948
- ytterbium alloys**
- CePd<sub>2</sub>-Yb, dil., EPR 0-25201
- Mg-Yb, dil., Kondo scatt. from Yb, low temp. elec. resist. meas. 0-44578
- Tb-Yb, mag. ordering temps., susceptibility meas. 0-25136
- Yb-Al, valence changes during autoionisation and Auger electron emission 0-50475
- Yb-Eu alloys, mag. ordering, magnetisation meas. 0-7081
- YbAl<sub>2</sub>-Gd(Er)(Dy)(Nd), dil., EPR and mag. susceptibility 0-15797
- YbAu<sub>2</sub>, surface electronic structure, XPS study 0-55259
- YbCu<sub>2</sub>Si<sub>2</sub>, valence fluctuation and temp. depend. of Cu nuclear quadrupole interaction 0-15818
- YbFe<sub>2</sub>, Curie temp., elec. quadrupole couplings, Mossbauer study 0-39949
- YbFe<sub>2</sub>, preparation and mag. props. 0-25259
- YbNi<sub>2</sub>-YbCu<sub>2</sub> system, valency state, Yb behaviour (*French*) 0-45277
- YbPd-YbAg system, valency state, Yb behaviour (*French*) 0-45277
- YbPt-YbAu system, valency state, Yb behaviour (*French*) 0-45277

**ytterbium compounds**

## see also ytterbium alloys

- mixed valence compounds, charge dominated fluctuation props. comparison, mag. moments and ordering 0-54659
- Kb<sub>2</sub>S<sub>3</sub>, condensates, struct. and optical transmittance 0-20727
- NaYb(WO<sub>4</sub>)<sub>2</sub>, thermal expansion, X-ray determ. 0-39323
- (Y, Gd, Yb, Bi)<sub>3</sub>(Fe, Al)<sub>5</sub>O<sub>12</sub> epitaxial film, domain wall motion and oscill. 0-2616
- (YEuYbCa)<sub>3</sub>(FeGe)<sub>5</sub>O<sub>12</sub>, garnet film, isolated straight stripe domain, dynamic behaviour 0-39809
- (YEuYbCa)<sub>3</sub>(GeFe)<sub>5</sub>O<sub>12</sub> bubble film with ion-implanted layer, FMR study 0-2643
- (YGdYbBi)<sub>3</sub>(FeAl)<sub>5</sub>O<sub>12</sub> epitaxial film, diffuse domain wall, bubble domain expansion 0-25170
- YbB<sub>12</sub>, valence state and mag. props. 0-50031
- YbB<sub>4</sub>, mag. and elec. props., metallic character 0-20386
- YbB<sub>6</sub>, <sup>11</sup>B nucl. quadrupole interaction, NMR meas. 0-2660
- YbB<sub>6</sub>, growth by soln. method, struct. and mech. props. 0-16168
- YbB<sub>6</sub>-C<sub>x</sub>, pure and doped, mag. and transport props. 0-54689
- YbBe<sub>13</sub>, mag. props. and EPR meas. 0-11175
- YbC<sub>6</sub>, intercalation cpd. with graphite, synthesis and struct. 0-44184
- Yb(ClO<sub>4</sub>)<sub>3</sub>, osmotic coeffs. 0-45556
- YbCl<sub>3</sub>·6H<sub>2</sub>O, paramag. relax., Mossbauer spectra 0-20536
- YbCr<sub>1-x</sub>Al<sub>x</sub>O<sub>3</sub> solid solutions 0-20887
- YbF<sub>3</sub>-alkali fluoride binary liquid mixtures, thermochemistry 0-45538
- YbH<sup>+</sup>, YbH<sub>2</sub>, relativistic (non-relativistic) HF one-centre expansion calcs. 0-52908
- YbNbO<sub>4</sub>-CaWO<sub>4</sub>, phase transitions of fergusonite-scheelite (*French*) 0-19942
- YbPO<sub>4</sub>, IR and Raman spectra 0-34904
- YbP<sub>2</sub>O<sub>4</sub> and Yb<sub>9</sub>Tb<sub>10</sub>P<sub>2</sub>O<sub>4</sub>, IR absorpt. and luminesc. spectra 0-55079
- Yb(P<sub>2</sub>O<sub>7</sub>)<sub>2</sub>, X-ray struct. characts. 0-54202
- YbS<sub>1.387</sub>, magnetic and thermal props. 0-34586
- YbSb, forbidden band gap and electrotransfer parameters 0-39497
- Yb<sub>2</sub>(SeO<sub>4</sub>)<sub>3</sub>·8H<sub>2</sub>O, thermal decomp. and IR spectra 0-3319

**yttrium**

## see also nuclei with .....

- de Haas-van Alphen effect, Fermi surface 0-15435
- elastic consts., 4 to 300K 0-39200
- electron and positron multiple scatt. 0-15171
- film, ion plating deposition system using electron beam evaporation (*French*) 0-20802
- magnetic and elec. props., 100 to 900K (*Russian*) 0-25077
- X-ray M<sub>2</sub> energy, revised values 0-14102
- Cu-rare earth oxide-Y composite coatings, oxide and Y effect on coating precipitation 0-55554
- <sup>90</sup>Y, spectrum and energy levels 0-32639
- <sup>90</sup>Y, appl. to cancer therapy of liver 0-17098
- <sup>91</sup>Y, removal rate in lower stratosphere, seasonal vars. 0-55957

**yttrium alloys**

## see also yttrium compounds

- Al-Y foil, alloying effect on strength characts. and weldability 0-55475
- Au-Y, dil., Friedel d-reson. scatt. and elec. resists. 0-44566
- Co-Cr-Al-Y, low temp. hot corrosion, Na<sub>2</sub>SO<sub>4</sub>-induced, mechanism, burner rig tests 0-40610
- Co-Cr-Al-Y protective coating for combustion turbines, hot corrosion evaluation 0-40608
- Co<sub>35</sub>Y<sub>65</sub>, metallic glass, internal friction peaks 0-25753
- Cr-Y-B-Y system, fatigue strength and fatigue fracture at 20 and 1100°C, SEM study 0-3194
- Dy<sub>0.9</sub>Y<sub>0.1</sub>Al<sub>2</sub>, hyperfine field, NMR spectra 0-15811
- (Er<sub>1-x</sub>Y<sub>x</sub>)Al<sub>2</sub>, cryst. field splitting, inelastic neutron scatt. data 0-44551
- Er<sub>2</sub>Y<sub>1-x</sub>Al<sub>2</sub>, mag. props. meas. and neutron diff. data 0-7126
- Er<sub>2</sub>Y<sub>1-x</sub>Cu, antiferromagnetic, mag. and resist. behaviour 0-34412
- Fe, cast, influence of Y and Sb on microhardness and lattice spacing of ferrite (*Russian*) 0-19748
- Fe, cast, Y effect on struct. 0-29967
- Fe-Cr-Al-Y, high temp. corrosion depend. on Y, oxidation, stress growth (*Russian*) 0-40588
- Fe-Cr-Al-Y, oxide grain morphology and growth mechanism 0-3239
- Fe-Cr-Al(-Y), isothermal oxidation behaviour at 1200°C, SEM 0-50755
- Fe-Cr-Al(-Y), thermal cycling influence on oxidation behaviour at 1200°C, SEM 0-50756
- Gd-Y, Kaufman approach to calc. of intra-rare earth phase diagrams 0-25657
- Gd<sub>1-x</sub>Y<sub>x</sub>, Mossbauer spectra, hyperfine interactions 0-15923
- Gd<sub>2</sub>Y<sub>1-x</sub>Al<sub>2</sub> (x<0.05), Hall effect measurements 0-44569
- Ho<sub>2</sub>Y<sub>1-x</sub>(Fe<sub>0.1</sub>Co<sub>0.9</sub>)<sub>2</sub>, <sup>57</sup>Fe hyperfine interaction, mag. props., Mossbauer study 0-39951
- Mg-Mg<sub>17</sub>Y<sub>13</sub>, high temp. hydrides for vehicular H storage 0-45793
- Mg-Y-Al alloys, phase equilib. (*Russian*) 0-20890
- Mg-Y-Cd, phase equilibria and mech. props. (*Russian*) 0-20894
- Mg-Y-Zn alloys, phase equilib. (*Russian*) 0-16271
- Mg-Y-Zn-Nd-Cd alloys, influence of Zr addition on struct. and mech. props. (*Russian*) 0-40370



## yttrium alloys continued

- Mn-Y-Zn-Cd alloy phase equilibria, plastic deformation, microhardness (Russian) 0-40334  
 Mn<sub>2</sub>Y<sub>2</sub>D<sub>2</sub>, D atom location, neutron diffr. study (French) 0-24426  
 Ni-Co-Cr-Al-Y, plasma-arc-sprayed, metallurgical characts. and oxidation behaviour 0-40618  
 Ni-Co-Cr-Al-Y protective coating for combustion turbines, hot corrosion evaluation 0-40608  
 Ni-Cr-Al-Y/ZrO<sub>2</sub>-Y<sub>2</sub>O<sub>3</sub>, NASA two-layer thermal barrier coating, for gas turbine engines, test results 0-40617  
 (NiCo)-Cr-Al-Y/ZrO<sub>2</sub>-Y<sub>2</sub>O<sub>3</sub> plasma sprayed ceramic coating for turbine engine components 0-40616  
 Tb-Y, mag. anisotropy, contrib. from single-ion cryst. anisotropy and anisotropic exchange (Russian) 0-29546  
 Tb-Y, mag. ordering temps., susceptibility meas. 0-25136  
 Tb<sub>1-x</sub>Y<sub>x</sub>Co<sub>0.1+x</sub>, exchange interactions and magnetocrystalline anisotropy 0-34618  
 Tb<sub>1-x</sub>Sb<sub>x</sub>, elec. resist., cryst. field and exchange interaction contribs. 0-39556  
 V-Zr-C-Y alloy weld metal, hardening phase precipitates examination, TEM appl. 0-7576  
 Y-Co, ferromagnet, first and second order transitions 0-34631  
 Y-Gd, de Haas-van Alphen effect, Fermi surface 0-15435  
 Y-Gd spin glass, sp. ht., 0.3-10K 0-25145  
 Y-Si melts, enthalpy of formation and dissolution, microinhomogeneous struct., interatomic interactions (Russian) 0-34206  
 YAl<sub>2</sub>-Er, dil., EPR, Er<sup>3+</sup>T<sub>2</sub> ground state 0-15798  
 YAl<sub>2</sub>-Er(Dy)(Bd), dil., EPR and mag. susceptibility 0-15797  
 Y(Co<sub>1-x</sub>Cu<sub>x</sub>)<sub>2</sub>, neutron diffr., thermal exspn. (French) 0-19749  
 Y(Co<sub>1-x</sub>Cu<sub>x</sub>)<sub>2</sub>, neutron diffraction study (Chinese) 0-39000  
 Y(Co<sub>1-x</sub>Ni<sub>x</sub>)<sub>2</sub>, mag. heterogeneities and coercive force, neutron scatt. study 0-2553  
 Y(Co<sub>1-x</sub>Ni<sub>x</sub>)<sub>2</sub>, spontaneous magnetisation mag. anisotropy, spin reorientation transformation (Russian) 0-7082  
 Y<sub>1-x</sub>Er<sub>x</sub>, dil., cryst. field interactions, neutron scatt. spectra 0-50048  
 Y<sub>1-x</sub>Er<sub>x</sub>Al<sub>2</sub>, paramag. anisotropy 0-39737  
 YFe<sub>2</sub>, amorphous concentrated spin glass, susceptibility, Mossbauer and neutron scatt. meas. 0-39783  
 YFe<sub>2</sub>, ferromagnetic cpds., mean field exchange const., Stoner itinerant model calcs. 0-50084  
 Y(FeAl<sub>1-x</sub>)<sub>2</sub>, Mossbauer spectra and mag. props. 0-39950  
 Y(Fe<sub>0.022</sub>Co<sub>0.978</sub>)<sub>2</sub>, ferromag. relax. model, Mossbauer spectra 0-15853  
 Y(FeCo<sub>1-x</sub>)<sub>2</sub>, Mossbauer effect at 78 and 300K, <sup>57</sup>Fe hyperfine fields 0-2677  
 Y(Fe<sub>1-x</sub>Ir<sub>x</sub>)<sub>2</sub>, magnetisation, mag. hyperfine field 0-20531  
 Y(Fe<sub>1-x</sub>Mn<sub>x</sub>)<sub>2</sub>, mag. order onset 0-25135  
 Y(Fe<sub>1-x</sub>Mn<sub>x</sub>)<sub>2</sub>, Mossbauer spectra and mag. props. 0-39952  
 Y<sub>6</sub>(Fe<sub>1-x</sub>Mn<sub>x</sub>)<sub>23</sub>, struct. and mag. props. 0-25083  
 Y(FeRh<sub>1-x</sub>)<sub>2</sub>, mag. props., Mossbauer spectra 0-25108  
 Y(FeTi<sub>1-x</sub>)<sub>2</sub>, Mossbauer spectra, mag. props. 0-20563  
 Y<sub>1-x</sub>Gd<sub>x</sub>Co<sub>2</sub>, exchange interactions and magnetocrystalline anisotropy 0-34618  
 (Y<sub>1-x</sub>Gd<sub>x</sub>)Co<sub>2</sub>, spin echo NMR of mag. states 0-7190  
 YM<sub>2</sub>Al<sub>8</sub> (M=Cr, Mn, Fe, Cu), magnetism and hyperfine interactions 0-25256  
 Y<sub>6</sub>Mn<sub>23</sub>, magnetic moments, magnetisation 0-25094  
 Y<sub>1-x</sub>Nd<sub>x</sub>Co<sub>2</sub>, exchange interactions and magnetocrystalline anisotropy 0-34618  
 YNi<sub>2</sub>, amorphous alloy, at. struct. 0-19704  
 YNi<sub>3</sub>, loss of ferromagnetism after H<sub>2</sub> absorpt., Pauli paramag. props. 0-34588  
 Y<sub>2</sub>Ni<sub>1-x</sub>, amorphous, high press. magnetisation and Curie temp. 0-20442  
 Y<sub>1-x</sub>Tb<sub>x</sub>Co<sub>2</sub>, spontaneous magnetisation anisotropy, spin reorientation transforms. (Russian) 0-7082  
 Y<sub>1-x</sub>Th<sub>x</sub>Fe<sub>3</sub> system, elec. resist. meas., 77-300K 0-34413

## yttrium compounds

## see also yttrium alloys

- metaphosphate glasses, n(M<sub>2</sub>O.P<sub>2</sub>O<sub>5</sub>).(1-x)Y<sub>2</sub>O<sub>3</sub>.xTb<sub>2</sub>O<sub>3</sub>.3P<sub>2</sub>O<sub>5</sub>, M=Li, Na, K, excitation and emission spectra 0-40150  
 plasma sprayed ceramic coating for turbine engine components 0-40616  
 YAG crystals, EPR spectra of V<sup>2+</sup> ions, ion energy levels 0-7157  
 YIG, hot spraying to give fine, free flowing, sinterable powder 0-20865  
 YIG, thermal cond. at low temps. 0-2222  
 Al<sub>2</sub>O<sub>3</sub>-Y<sub>2</sub>O<sub>3</sub> ceramics, corrosion protective W coating 0-35367  
 BaGeO<sub>3</sub>-(0.25MgF<sub>2</sub>.0.75YF<sub>3</sub>)-Ga<sub>2</sub>O<sub>3</sub> glass, synthesis and props. 0-25648  
 BaY<sub>2</sub>F<sub>6</sub>Nd<sup>3+</sup>(Ho<sup>3+</sup>)(Yb<sup>3+</sup>), ESR spectra and spin-lattice relax. 0-11263  
 CaS-Y<sub>2</sub>S<sub>3</sub> (1 wt.%), solid electrolyte, elec. cond. under low partial pressures of S (Japanese) 0-49409  
 CaY<sub>2</sub>Mg<sub>2</sub>Ge<sub>2</sub>O<sub>12</sub>Nd<sup>3+</sup>, optical absorpt. and fluoresc. intensities 0-29793  
 Er<sub>2</sub>Y<sub>3-x</sub>Fe<sub>2</sub>O<sub>12</sub>, garnet, mag. anisotropy and magnetostriction 0-11189  
 Er<sub>2</sub>Y<sub>1-x</sub>Rh<sub>2</sub>B<sub>4</sub>, supercond. phase transitions, recentering temp. to normal ferromag. state 0-7024  
 EuGaYIG:Cr, epitaxial garnet film, interaction pot. of domain walls with localised stress fields 0-44889  
 Eu<sub>2</sub>Y<sub>1-x</sub>Ga<sub>2</sub>Fe<sub>3</sub>O<sub>12</sub>, epitaxial garnet films, props. at compensation points 0-39823  
 EuYIG:Sn, growth from PbO-B<sub>2</sub>O<sub>3</sub> based flux, prop. depend. on Pb content 0-39824  
 HfO<sub>2</sub>-Y<sub>2</sub>O<sub>3</sub>, elastic props., sonic reson. meas. 0-7612  
 Ho-YIG, magnetic props. in strong fields at low temp., Ising approx. calcs. (Russian) 0-54920  
 Ho<sub>2</sub>Y<sub>1-x</sub>Sb<sub>x</sub>, mag. props. 0-34634  
 (La, Y, Sc)B<sub>6</sub> solid solns. electron work function, thermal emission technique 0-20755  
 La<sub>2</sub>O<sub>3</sub>-Y<sub>2</sub>O<sub>3</sub>-Al<sub>2</sub>O<sub>3</sub>-SiO<sub>2</sub>, coloration by transition metal oxides, absorpt. bands (Japanese) 0-55148  
 LiTb<sub>0.5</sub>Y<sub>0.5</sub>F<sub>4</sub>, mag. susceptibility, dilution effect on critical behaviour of dipolar uniaxial ferromagnet 0-34635  
 LiYF<sub>4</sub>:Ce, tunable UV laser at 325, 309 nm, KrF laser excitation 0-38022  
 LiYF<sub>4</sub>:Pr<sup>3+</sup>, spectroscopic determ. of ground config. energy levels 0-34969  
 LiYF<sub>4</sub>:Tm, XeF pumped, excimer excited storage laser 0-33003  
 LiYF<sub>4</sub>:HO<sup>3+</sup>, 1.392, 1.673 and 3.914  $\mu$ m stimulated emission, laser cascades 0-9886  
 Mn<sub>2</sub>Y<sub>2</sub>D<sub>2</sub>, D atom location, neutron diffr. study (French) 0-24426  
 NaF-YF<sub>3</sub> system, fusibility diagram, quasibinary section of NaF-YF<sub>3</sub>-YOF system characts. 0-55371  
 Nd:YAG, solid-state formation 0-35121

## yttrium compounds continued

- Si<sub>3</sub>N<sub>4</sub>-(MgO+Al<sub>2</sub>O<sub>3</sub>)(Y<sub>2</sub>O<sub>3</sub>), hot-pressed and sintered, microstruct. and impurity distrib. 0-49261  
 Si<sub>3</sub>N<sub>4</sub>-AlN-Al<sub>2</sub>O<sub>3</sub>-SiO<sub>2</sub>-Y<sub>2</sub>O<sub>3</sub>, phase equilibrium study by X-ray diffr. and optical microscopy 0-50614  
 Si<sub>3</sub>N<sub>4</sub>-SiC-Y<sub>2</sub>O<sub>3</sub>, reactively sintered, microstruct. and strength 0-25631  
 Si<sub>3</sub>N<sub>4</sub>-Y<sub>2</sub>O<sub>3</sub>, hot pressed, sintered, microstruct., flexural strength and fractographic anal. 0-40293  
 Si<sub>3</sub>N<sub>4</sub>-Y<sub>2</sub>O<sub>3</sub>, hot-pressed, oxidation kinetics 0-16520  
 Si<sub>3</sub>N<sub>4</sub>-Y<sub>2</sub>O<sub>3</sub> ceramic, thermal degradation, C impurity effect 0-50708  
 Si<sub>3</sub>N<sub>4</sub>-Y<sub>2</sub>O<sub>3</sub> prepared by hot press, cryst. struct. 0-10534  
 (SmYCa)<sub>2</sub>(FeGe)<sub>2</sub>O<sub>12</sub> epitaxial layer, growth kinetics and struct. as functions of cryst. lattice parameter mismatch 0-6677  
 Sm<sub>0.25</sub>Y<sub>0.75</sub>S, phonon anomalies and electron-lattice coupling 0-39490  
 Sm<sub>0.75</sub>Y<sub>0.25</sub>S, intermediate valence compound, phonon investigation by neutron scatt. 0-6476  
 Sm<sub>0.75</sub>Y<sub>0.25</sub>S, mixed valence, phonon dispersion theory 0-34153  
 Sm<sub>0.76</sub>Y<sub>0.24</sub>S, induced magnetic form factor, polarised neutron studies 0-25078  
 Tm<sub>2</sub>Y<sub>1-x</sub>Se, Kondo effect, Van Vleck behaviour 0-25085  
 U<sub>3</sub>O<sub>8</sub>-Y<sub>2</sub>O<sub>3</sub>, solid soln. electrode, high temp. electrochem. appl. 0-6828  
 (U<sub>0.5</sub>Y<sub>0.5</sub>)O<sub>2-x</sub>, ionic cond. 0-6828  
 (Y, Gd, Yb, Bi)<sub>3</sub>(Fe, Al)<sub>2</sub>O<sub>12</sub> epitaxial film, domain wall motion and oscill. 0-2616  
 (Y,Gd)BO<sub>3</sub>:Eu<sup>3+</sup>, phosphor, vac. UV excitation spectra, appl. to gas discharge display 0-2816  
 (Y,La)B<sub>6</sub>, superconducting transition temps., impurity effects 0-20341  
 (Y,Sm,Lu,Ca)<sub>3</sub>(Fe,Ge)<sub>2</sub>O<sub>12</sub> bubble magnetic garnet film, LPE grown, props., CaCO<sub>3</sub>/GeO<sub>2</sub> molar ratio influence 0-50152  
 (Y,Sm,Lu,Cu)<sub>3</sub>(Fe,Ge)<sub>2</sub>O<sub>12</sub>, ion implanted, hard bubble suppression 0-11238  
 (Y,Sm,Lu,Tm,Ca)<sub>3</sub>(Fe,Ge)<sub>2</sub>O<sub>12</sub>, epitaxial garnet film, temp. depend. mag. props. 0-39825  
 (Y,Sm)<sub>3</sub>(Fe,Ge)<sub>2</sub>O<sub>12</sub>, garnet LPE films, growth rate anisotropy 0-54558  
 (Y,Sm)<sub>3</sub>(Ga,Fe)<sub>2</sub>O<sub>12</sub>/(Eu,Er)<sub>3</sub>(Ga,Fe)<sub>2</sub>O<sub>12</sub> double-layer self-biasing garnet films, dynamic behaviour of domain walls 0-34722  
 Y-H, exam. of electron structure 0-29306  
 Y-H system, solid soln. phase, wide-line PMR 0-25226  
 Y-Si-Al-O-N glass, prep. and props. 0-25647  
 YA-O<sub>3</sub>:Er<sup>3+</sup>, pulsed laser action, <sup>4</sup>S<sub>3/2</sub> to <sup>4</sup>I<sub>9/2</sub> transition laser action, optical and luminescence spectra 0-16082  
 YAG brittleness anisotropy, microcrack formation due to surface treatment 0-40526  
 YAG crystal with rare earth ion impurities, active medium reson. pumping method for Nd laser freq. conversion 0-1206  
 YAG, high-resolution many beam lattice image anal. 0-14979  
 YAG, production of densely sintered ceramic, exam. of recrystallisation during sintering 0-11609  
 YAG single crystal growth, by vertical directed crystn., thermal characts. 0-2944  
 YAG:Ce phosphors, luminesc. efficiency, prep. and dopant effects 0-45151  
 YAG:Ce<sup>3+</sup>, photoluminescence excitation energy, crystal field and temp. effects 0-11460  
 YAG:Ce<sup>3+</sup>, scintillation detector, in SEM, electro-optical props. 0-52819  
 YAG:Ce<sup>3+</sup>(Eu<sup>3+</sup>)(Gd<sup>3+</sup>)(Tb<sup>3+</sup>), cathodoluminesc. efficiency rel. to activator conc. 0-11479  
 YAG:Cr<sup>3+</sup> 0-2740  
 YAG:Eu<sup>3+</sup>, reson. fluoresc. spectra, showing multiple Eu<sup>3+</sup> sites 0-2812  
 YAG:Nd garnet, heat capacity and thermal diffusivity meas. 0-19956  
 YAG:Nd laser pulses, mutual exchanges with plasma (German) 0-48918  
 YAG:rare earth metal, US absorpt. meas., relax. model 0-24539  
 YAl<sub>3</sub>(BO<sub>3</sub>)<sub>4</sub>, and (Y,Er)Al<sub>3</sub>(BO<sub>3</sub>)<sub>4</sub>, crystallisation and growth characts., density and composition 0-35080  
 YAl<sub>3</sub>(BO<sub>3</sub>)<sub>4</sub>, crystallisation from solution in a melt, solvent composition 0-38976  
 YAl<sub>3</sub>(BO<sub>3</sub>)<sub>4</sub>-NdAl<sub>3</sub>(BO<sub>3</sub>)<sub>4</sub>, substitution of Nd for Y in YAl<sub>3</sub>(BO<sub>3</sub>)<sub>4</sub>, exam. 0-11551  
 Y<sub>3</sub>(Al<sub>1-x</sub>Ga<sub>x</sub>)<sub>2</sub>O<sub>12</sub>:Nd<sup>3+</sup>, time-resolved site-selection spectroscopy, energy transfer 0-2814  
 YAlO<sub>3</sub>, rare earth doped, intra- and inter-ionic multiphonon transitions 0-34973  
 YAlO<sub>3</sub>:Pr<sup>3+</sup>, ultrahigh resolution photon echo spectroscopy 0-28285  
 YAlO<sub>3</sub>:Yb<sup>3+</sup>, absorption and luminescence spectra, electron-phonon resonances, Stark splitting (Russian) 0-20674  
 YB<sub>12</sub>, mag. susceptibility, 90-1200K 0-50032  
 (YBiSmCa)<sub>3</sub>(FeGe)<sub>2</sub>O<sub>12</sub> epitaxial layer, growth kinetics and struct. as functions of cryst. lattice parameter mismatch 0-6677  
 Y<sub>3-x</sub>Ca<sub>x</sub>(Fe<sub>2-x</sub>Sn<sub>x</sub>)<sub>2</sub>Fe<sub>2</sub>O<sub>12</sub>, Mossbauer spectra, Sn hyperfine mag. field 0-15893  
 YCoO<sub>3</sub>, anomalous <sup>57</sup>Fe charge states, Mossbauer study 0-40017  
 YCrO<sub>3</sub>, EPR linewidth, Neel point to 700K 0-39849  
 YCrO<sub>3</sub>, magnetisation, NMR freq. temps. depend. weak ferromagnetic-antiferromagnetic spin reorientation transition 0-29631  
 YCrO<sub>3</sub>-MgCr<sub>2</sub>O<sub>4</sub> sintered ceramics, elec. cond. 0-24927  
 Y<sub>2</sub>Cr<sub>2</sub>O<sub>7</sub>, Y<sub>2</sub>Mn<sub>2</sub>O<sub>7</sub>, pyrochlore type, synthesis and physical props. 0-33963  
 YEuLuCaGe garnets, 7  $\mu$ m-period bubble devices 0-44887  
 YEuLuGa garnets, 7  $\mu$ m-period bubble devices 0-44887  
 YEuTmCaGe garnets, 7  $\mu$ m-period bubble devices 0-44887  
 (YEuTm)<sub>3</sub>(FeGa)<sub>2</sub>O<sub>12</sub> film, dynamic props. of bubble domains by high speed photography 0-15771  
 (YEuTm)<sub>3</sub>(FeGa)<sub>2</sub>O<sub>12</sub> garnet film, bubble domain steady state motion on a circle 0-29589  
 YEuTmGa garnet bubble film, dynamic diffuse wall deform. 0-54927  
 YEuTmGa garnets, 7  $\mu$ m-period bubble devices 0-44887  
 (YEuYbCa)<sub>3</sub>(GeFe)<sub>2</sub>O<sub>12</sub> garnet film, isolated straight stripe domain, dynamic behaviour 0-39809  
 (YEuYbCa)<sub>3</sub>(GeFe)<sub>2</sub>O<sub>12</sub> bubble film with ion-implanted layer, FMR study 0-2643  
 YF<sub>3</sub>, mol. const., kinetic const. and L-approx. methods 0-18839  
 YF<sub>3</sub>:Nd, Ce, energy transfer between 5d electronic states 0-2808  
 YF<sub>3</sub>:Tm, Nd, energy transfer between 5d electronic states 0-2808  
 YF<sub>3</sub>:Yb,Er, limit efficiency of transformation of IR to visible radiation 0-29784  
 YF<sub>3</sub>-alkali fluoride binary liquid mixtures, thermochemistry 0-45538  
 YFe<sub>3</sub>(BO<sub>3</sub>)<sub>4</sub>, solubility in Bi<sub>2</sub>O<sub>3</sub>-B<sub>2</sub>O<sub>3</sub> melt and crystallisation 0-19736  
 Y<sub>2</sub>Fe<sub>2-x</sub>Ga<sub>2</sub>O<sub>12</sub> garnet, spin wave parametric excitation threshold anisotropy in second region 0-29542  
 Y<sub>3</sub>Fe<sub>2-x</sub>Ga<sub>2</sub>O<sub>12</sub>, garnet, magnetically inequivalent positions of cations in external mag. field 0-11307



## yttrium compounds continued

- Y<sub>3</sub>Fe<sub>5-x</sub>Ga<sub>x</sub>O<sub>12</sub>, substituted garnet, floating zone grown, FMR line width, saturation magnetisation 0-29626  
 YFeO<sub>3</sub>, weak ferromagnet, domain wall motion and velocity (*Russian*) 0-54917  
 YFeO<sub>3</sub>:Co<sup>2+</sup>, weak ferromagnetism, single ion anisotropy contrib. 0-25126  
 YFe<sub>2</sub>O<sub>4</sub>, low temp. phase transitions and mag. props. 0-7106  
 YFe<sub>2</sub>O<sub>4</sub>, Mossbauer spectra of <sup>51</sup>Fe in antiferromag. and paramag. states 0-15834  
 YFe<sub>2</sub>O<sub>4</sub>, two-dimensional spin ordering, neutron diffr. study 0-29530  
 Y<sub>10</sub>Ga<sub>3</sub>Co<sub>7</sub>, X-ray cryst. struct. determ. 0-33977  
 Y<sub>3-x</sub>Gd<sub>x</sub>Fe<sub>5-y</sub>Al<sub>y</sub>O<sub>12</sub>, solid solns., IR absorpt. spectra, physical props. 0-55082  
 Y<sub>3-x</sub>Gd<sub>x</sub>Fe<sub>5</sub>O<sub>12</sub>, mag. phase diagrams, mag. transitions, exchange interaction (*Russian*) 0-54896  
 Y<sub>3-x</sub>Gd<sub>x</sub>Fe<sub>5</sub>O<sub>12</sub>, solid solns., IR absorpt. spectra, physical props. 0-55082  
 (Y<sub>2</sub>Gd)(GaFe)<sub>2</sub>O<sub>12</sub> epitaxial film, nonlinear magnetoelastic effects (*French*) 0-34745  
 Y<sub>1-x</sub>Gd<sub>x</sub>Rh<sub>2</sub>B<sub>4</sub>, mag. supercond., anomalous temp. depend. of upper crit. fields 0-29510  
 Y<sub>1-x</sub>Gd<sub>x</sub>Rh<sub>2</sub>B<sub>4</sub>, supercond., phase diagrams and upper crit. fields 0-2531  
 (Y<sub>2</sub>GdYbBi)<sub>3</sub>(FeAl)<sub>2</sub>O<sub>12</sub> epitaxial film, diffuse domain wall, bubble domain expansion 0-25170  
 (Y<sub>2</sub>GdYbBi)<sub>3</sub>(FeAl)<sub>2</sub>O<sub>12</sub> epitaxial film, 360° domain walls with periodically distrib. Bloch lines 0-7127  
 YH<sub>1.92</sub>, <sup>2</sup>Σ state, Dirac-Fock one-centre calcs. 0-23301  
 YH<sub>1.92</sub>, tensile strength and creep 0-55459  
 YH<sub>2</sub>, electronic struct., photoelectron spectra study 0-50527  
 YH<sub>2</sub>, self-consistent energy bands, KKR method with Hedin-Lundqvist approx. 0-49593  
 YH<sub>2</sub>, synchrotron XPS obs., rel. to theory for metal dihydrides 0-55275  
 YH<sub>3</sub> (x=1.92 to 1.98), magnetic and elec. props., 100 to 900K (*Russian*) 0-25077  
 YIG, amorphous, ionic glass, hard-sphere random-packing model 0-24369  
 YIG and Ga-substituted YIG, high energy heavy ion irradi., lattice strain 0-49278  
 YIG bubble films, light scatt. from spin waves, hysteresis meas. by Voigt effect 0-15770  
 YIG dielectric layered struct., magnetostatic bulk wave steering 0-25166  
 YIG, dilute, magnetoacoustic surface wave excitation by RF field on Bloch walls 0-25178  
 YIG, distrib. of easy magnetisation axes near edge dislocation (*Russian*) 0-44891  
 YIG, domain boundary nuclear spin echo excitation, NMR domain freq. capture effect (*Russian*) 0-44955  
 YIG, double layer struct., LPE growth from molybdate and Pb borate fluxes 0-39827  
 YIG epitaxial films, substituted, floating bubble domains, effect of structural stratification 0-2615  
 YIG ferromagnetic film, quasi surface spin wave giant oscills. (*Russian*) 0-15767  
 YIG, ferromagnetic resonance and magnetostatic waves in inhomogeneous internal field (*Russian*) 0-54954  
 YIG film, dielec. layered struct., magnetostatic bulk wave power flow and energy distrib. 0-34610  
 YIG film, magnetostatic surface wave propag. in nonuniform mag. field, anal. 0-20437  
 YIG film, magnetostatic surface and forward volume wave oblique incident at shallow groove 0-34704  
 YIG film tangentially magnetised, magnetostatic surface wave excitation 0-29586  
 YIG film-dielectric layer-conductor struct., magnetostatic bulk wave propag. dispersion relations 0-54925  
 YIG, garnet, high temp. solns., shear viscosity meas., rel. to LPE 0-10697  
 YIG, hyperfine parameters, Huckel theory calc. 0-39542  
 YIG, MCD meas. by retardation modulation technique 0-16014  
 YIG, magnetised in raised cosine profile magnetostatic surface wave propag. 0-2567  
 YIG, magneto-optical spectra, polar Kerr rotation, dielectric tensor elements spectra 0-40091  
 YIG octa- and tetra-sublattices, anisotropy of effective mag. field at <sup>57</sup>Fe (*Russian*) 0-10929  
 YIG periodic film layer, magnetostatic surface wave propag. 0-2607  
 YIG, phonon viscosity effect on dislocation motion 0-24450  
 YIG, polarised neutron expts., extinction models 0-24322  
 YIG, polariser neutron study of covalency effects 0-2552  
 YIG, pure and Ga-substituted diffuse refl. and thermoeffl. spectra near Curie point 0-40131  
 YIG, Si substituted, spin reorientation, Mossbauer spectroscopy obs. 0-44989  
 YIG slab, partially magnetised, expt. obs. of group delay of magnetostatic waves 0-7100  
 YIG, spin and magnetoelastic waves on longit. mag. pumping, optical obs. (*Russian*) 0-29727  
 YIG, subsidiary absorpt. spin-wave instability threshold, anomalous struct. 0-34776  
 YIG substrates, magnetoelastic surface waves, magnetostatic reson. anal. 0-20441  
 YIG, thermorefectance spectra 0-20616  
 YIG:Bi,Pb, IR spectrum, localised modes, rel. to impurities and O vacancies 0-50377  
 YIG:Ca eddy current damping 0-39876  
 YIG:Si(Ge), Fe<sup>2+</sup> spectroscopic props., nontrigonal cryst. field effects 0-44553  
 YIG-rare earth garnet solid solutions, magnetisation temp. depend. calcs. 0-20388  
 YIr<sub>2</sub>B<sub>4</sub>, NdCo<sub>2</sub>B<sub>4</sub> type struct., mag. behaviour 0-20375  
 YLiF<sub>4</sub>, rare earth doped, intra- and inter-ionic multiphonon transitions 0-34973  
 Y<sub>2</sub>Lu<sub>1-x</sub>Ir<sub>x</sub>B<sub>4</sub>, supercond., magnetism and metastability 0-29501  
 (Y<sub>2</sub>Lu<sub>1-x</sub>)<sub>2</sub>V<sub>2</sub>O<sub>7</sub> semiconducting ferromag. pyrochlore, mag. props. 0-29547  
 YMnO<sub>3</sub>, solid phase synthesis mechanism 0-21268  
 Y<sub>2</sub>MoO<sub>6</sub>, cryst. struct., IR spectra, elec. and mag. props. 0-33954  
 YNO<sub>3</sub>(Se<sub>2</sub>O<sub>3</sub>).3H<sub>2</sub>O, X-ray cryst. struct. determ. 0-1972  
 Y<sub>2</sub>O<sub>3</sub>, electron irradi., dislocations (*French*) 0-2076  
 Y<sub>2</sub>O<sub>3</sub> fused single crystals, struct. 0-19804  
 Y<sub>2</sub>O<sub>3</sub> laser coating, UV damage obs. 0-33056

## yttrium compounds continued

- Y<sub>2</sub>O<sub>3</sub> powder, active, sintering 0-20870  
 Y<sub>2</sub>O<sub>3</sub> sintered pieces, optical transmittance 0-40561  
 Y<sub>2</sub>O<sub>3</sub> stabilized ZrO<sub>2</sub> heat-resistant granular artifacts, procedure for making 0-35148  
 Y<sub>2</sub>O<sub>3</sub>, synthesis at high-pressure and temp., supercond. 0-2513  
 Y<sub>2</sub>O<sub>3</sub> transparent ceramic, transmittance, grain size and dopant effects (*Japanese*) 0-19083  
 Y<sub>2</sub>O<sub>3</sub>:HfO<sub>2</sub>, elec. cond. and O ion mobility 0-34490  
 Y<sub>2</sub>O<sub>3</sub>-2Y<sub>2</sub>O<sub>3</sub>-Al<sub>2</sub>O<sub>3</sub> two-phase refractory, fracture 0-21080  
 YOF, electronic struct. calcs. from XPS and X-ray emission spectra 0-35056  
 YOF-YF<sub>3</sub>, high pressure phase transitions 0-55368  
 Y<sub>2</sub>O<sub>3</sub>:S:Eu phosphor, luminescence saturation effects due to N<sub>2</sub> laser and cathode-ray excitation 0-40151  
 Y<sub>2</sub>O<sub>3</sub>:S:Tb<sup>3+</sup> (Eu<sup>3+</sup>) temp. and viscosity depend. of colour coords. 0-40149  
 Y(PO<sub>3</sub>)<sub>2</sub>, vitreous, microhardness 0-25864  
 YPO<sub>4</sub>, cryst., IR spectra, complex anions internal vibr. resonance splitting 0-34907  
 YPO<sub>4</sub> phosphor, ionisation of capture centres, thermolum. spectra 0-11487  
 Y<sub>2</sub>Pb<sub>1-x</sub>Mo<sub>0.5+y</sub>S<sub>8</sub>, sputtered supercond. props. 0-50019  
 Y(ReO<sub>3</sub>)<sub>3</sub>.4H<sub>2</sub>O, <sup>187</sup>Re HQR freq. temp. depend. 0-25245  
 YRh<sub>2</sub>B<sub>4</sub>, NMR and sp. ht. in supercond. and mag. ordered phases 0-7037  
 YRh<sub>2</sub>B<sub>4</sub>, supercond., anomalous cond.-electron polaris. 0-25047  
 YS, electronic instability and phonon softening, APW calc. 0-29323  
 YS, phonon anomalies and electron-lattice coupling 0-39490  
 δ-Y<sub>2</sub>S<sub>3</sub>:Nd<sup>3+</sup>, spectroscopic props. from absorpt., photoluminesc. and excitation spectra 0-34968  
 Y<sub>2</sub>(SeO<sub>4</sub>)<sub>3</sub>.8H<sub>2</sub>O, thermal decomp. and IR spectra 0-3319  
 Y<sub>1.65</sub>Sm<sub>0.21</sub>Lu<sub>0.27</sub>Cu<sub>0.9</sub>Ge<sub>0.9</sub>Fe<sub>4.1</sub>O<sub>12</sub>, implanted bubble garnet, anisotropy profile, FMR study 0-7103  
 YSmCaFeGe, mag. garnet films, segregation of Ca and Ge in LPE growth 0-29959  
 (YSmCaLu)<sub>3</sub>(FeGe)<sub>2</sub>O<sub>12</sub>, bubble film inhomogeneity, spin wave reson. meas. 0-44439  
 (YSm)<sub>3</sub>(FeGa)<sub>2</sub>O<sub>12</sub> film, LPE on Gd<sub>3</sub>Ga<sub>5</sub>O<sub>12</sub>, interface processes, horizontal dipping obs. 0-49552  
 (YSmLuCa)<sub>3</sub>(FeGe)<sub>2</sub>O<sub>12</sub>, double layer struct., LPE growth from molybdate and Pb borate fluxes 0-39827  
 (YSmLuCa)<sub>3</sub>(FeGe)<sub>2</sub>O<sub>12</sub>, bubble material, dynamic characterisation, comparison between transport and FMR methods 0-39833  
 YSmLuCaGe garnets, 7 μm-period bubble devices 0-44887  
 (YSmLu)<sub>3</sub>(FeGaSe)<sub>2</sub>O<sub>12</sub>, submicron mag. bubble garnet 0-54929  
 YSmLuGa garnets, 7 μm-period bubble devices 0-44887  
 YSmTmCaGe garnets, 7 μm-period bubble devices 0-44887  
 YSmTmGa garnets, 7 μm-period bubble devices 0-44887  
 Y<sub>2</sub>Ti<sub>2</sub>O<sub>7</sub>, precipitation from oxalates, carbonates, exam. 0-55641  
 YVO<sub>4</sub> phosphor, ionisation of capture centres, thermolum. spectra 0-11487  
 YVO<sub>4</sub>, soft X-ray APS study of empty electron states, VO<sub>4</sub><sup>3-</sup> cluster model 0-25488  
 Y<sub>2</sub>V<sub>10</sub>O<sub>28</sub>.24H<sub>2</sub>O, X-ray cryst. struct. anal. 0-39060  
 Y<sub>2</sub>(V<sub>4/3</sub>W<sub>2/3</sub>)<sub>2</sub>O<sub>7</sub> pyrochlore, synthesis and elec. props. 0-29914  
 Y<sub>6</sub>WO<sub>12</sub>:ZrO<sub>2</sub>(MgO)(CeO)(SrO)(BaO), polycryst., elec. cond., 800-7400°C 0-15517  
 ZrO<sub>2</sub>:Y<sub>2</sub>O<sub>3</sub>, low-temp. specific heat, oxygen vacancy effects 0-49376  
 ZrO<sub>2</sub>-Y<sub>2</sub>O<sub>3</sub> powder, prep. for plasma spheroidisation, sputter drying (*Russian*) 0-55324  
 ZrO<sub>2</sub>-Y<sub>2</sub>O<sub>3</sub> superionic cond. cell, complex impedance 0-10702  
 ZrO<sub>2</sub>-Y<sub>2</sub>O<sub>3</sub>/Ni sputtered multilayered ceramic/metal coatings, props. 0-40620  
 ZrO<sub>2</sub>-Y<sub>2</sub>O<sub>3</sub>/(Cr-Ni) sputtered multilayered ceramic/metal coatings, props. 0-40620  
 ZrO<sub>2</sub>:Y<sub>2</sub>O<sub>3</sub>/Ni-Cr-Al-Y, NASA two-layer thermal barrier coating, for gas turbine engines, test results 0-40617  
**Yukawa potential** see meson field theory; nuclear forces  
**Z-centres**  
 KCl:Ba(Sr), Z-centre, luminesc. and absorpt. spectra obs. 0-49221  
 KCl:Ca(Ba)(Mg)(Sr), microcrystalline powders, role of Z-centres in stabilizing coloration 0-54227  
 KCl:Sr, thermally pre-treated, glow curves 0-25470  
 KCl:Sr, triplet state of F<sub>2</sub>-centres, ESR spectra 0-29616  
 KCl:Mg, thermolum. of Z-centre, optical absorpt. 0-55203  
 KCl<sub>0.5</sub>Br<sub>0.5</sub>:Ca, X-ray irradi., Z<sub>1</sub>-centres, thermoluminesc. and optical absorpt. meas. 0-16108  
 LiF:Mg, X-ray irradi., trapping processes, Z-centres and dipoles, two models 0-49222  
 LiF:Mg,Ti crystals, Z<sub>1</sub>-centres, correlation of thermoluminescence and optical absorption 0-45154  
 NaCl:Ca, Z<sub>1</sub> centre thermoluminescence study 0-16109  
 NaCl:V<sup>2+</sup>, elec. field effect on Z-like centres spectrum 0-2802  
**Z pinch** see pinch effect  
**Z transforms**  
 sonar beamforming by CCD scan conversion for SAW chirp-Z transform 0-43552  
**Zeeman effect**  
 see also atomic spectra; Hanle effect; spectral line breadth  
<sup>3</sup>He-<sup>2</sup>Ne stabilised transverse Zeeman laser, tuning characts., freq. fluctuation 0-48273  
 alkali halides, spin lattice relax. and g-shift 0-15799  
 atomic absorption spectrosc. anal. curve shapes 0-22437  
 atomic absorption spectroscopy, Zeeman effect, appls. (*Japanese*) 0-35600  
 atomic RF spectroscopy, nonlinear and parametric effects, review 0-18816  
 atomic spectra and radiative transitions, book 0-22159  
 6-chloro 2,4-dimethoxypyrimidine, <sup>35</sup>Cl NQR, Zeeman effect 0-18874  
 collisional excitation transfer in high mag. fields, theory 0-9688  
 3-cyanopyridine, NQR Zeeman obs., crystal packing 0-54978  
 V1057 Cygni, OH line Zeeman splitting and stellar mag. field 0-36629  
 p-dichlorobenzene, <sup>35</sup>Cl powder Zeeman NQR, injection and phase locked NQR spectrometer 0-54979  
 3,5-dichloronitrobenzene, NQR line, Zeeman effect 0-28034  
 4,6-dichloropyrimidine, <sup>35</sup>Cl NQR, Zeeman effect 0-18874  
 ferroelectric semiconductor, magnetic field influence, ferroelectric transitions 0-55049  
 formyl radical, laser mag. reson. spectrum at 5.3 micron 0-47981



**Zeeman effect continued**

ground state Zeeman splittings, reson. Raman spectra and mag.-optical activity 0-5579  
 highly excited atoms, review of recent expts. 0-23325  
 W Hydrae, long-period variable, suspected Zeeman splitting in OH masers 0-36632  
 laser gyro, Zeeman, beat-note sensitivity 0-53340  
 laser modes selection, expts. with He-Ne laser (*Russian*) 0-1251  
 laser or amplifier, Zeeman systems, bistability and intensity fluctuations 0-53254  
 nuclear resonance scattering of gamma rays, line inversion 0-39919  
 palladium porphyrin, in n-alkane crystal, Zeeman and crystal field effects, absorpt. vibr. anal. 0-7372  
 perchloro-3-cyclopentenone,  $^{35}\text{Cl}$  NQR Zeeman obs. 0-54981  
 polycrystalline samples,  $^{14}\text{N}$  NQR, Zeeman effect, second-order theory 0-20503  
 porphyrins orientation in n-alkane Shpolskii hosts, spectra 0-48035  
 quadrupole spin echo envelope EFG tensor axisymmetry in mag. field 0-20497  
 $\alpha$ -quartz, hydrogenic trapped hole species, EPR studies 0-44915  
 ring laser, four-mode operation 0-19053  
 ring Zeeman laser, interaction of modes characterized by orthogonal circular polarizations 0-48306  
 ruby,  $\text{Cr}^{3+}$  ion doped, R-line region, absorpt. spectrum, dispersion rel. to mag. field 0-2732  
 ruby, double electron-nuclear resonance at  $\text{Cr}^{3+}$  B1, B2 absorpt. lines, optical detection (*Russian*) 0-7194  
 ruby, optically excited, diffusion of bottlenecked  $29\text{ cm}^{-1}$  phonons 0-6472  
 ruby, optically induced two-phonon processes connecting  $^2\text{E}$  states 0-25443  
 ruby, phonon bottleneck of direct decay within  $\tilde{\text{E}}(^2\text{E})$  state, optical detection 0-10608  
 spin  $3/2$  nuclei, Zeeman NQR powder spectra 0-20502  
 Stark splitting, optical dynamic, Zeeman degeneracy 0-37774  
 Sun, magnetosensitive line contours in active regions (*Russian*) 0-51718  
 sunspot penumbrae, line shifts and asymmetries 0-51715  
 tetrahedral four spin  $1/2$  systems, Zeeman and tunnel system reson., coupled and uncoupled relax. 0-50214  
 travelling-wave Zeeman gas laser operating at high radiation intensities, theory 0-9912  
 $\text{Ag}_3\text{AsS}_3$ , proustite, structural changes in low temp. phase transition, NQR study 0-19935  
 Bk, emission spectrum, 2540-9800 Å, electrodeless lamp source 0-27970  
 $\text{CO}_2$  IR Zeeman spectra utilizing copropag. wave reson., diamag. shift obs. 0-53055  
 $\text{CaSnCl}_6$ , Cl NQR anomalous temp. depend., crystal struct. and phase transitions 0-54977  
 $\text{Cs}$ ,  $7\text{P}_{3/2}$ - $6\text{S}_{1/2}$  transition, photon-echo quantum beats obs. 0-23373  
 $\text{Cs}_2\text{SiF}_6$ ,  $\text{Mn}^{2+}$ , Jahn-Teller effect in  $^4\text{T}_{2g}$  state, Zeeman meas. 0-29367  
 $\text{CuBr}_4^{2-}$ , ground state Zeeman splittings, reson. Raman spectra and mag.-optical activity 0-5579  
 $\text{Cu(I)}$  complexes, cuprous halide triphenylphosphines, NQR, Zeeman effect 0-54980  
 $\text{Dy}_2\text{O}_3\text{SO}_4$ , magnetic struct. in antiferromag. and ferrimag. states 0-15695  
 Ga, ground-state hyperfine struct., differential Stark effect 0-42990  
 GaAs, trace element conc. meas. by Zeeman atomic absorpt. spectroscopy 0-29046  
 $\text{GaCl}_3$ , cryst. struct., Zeeman split fine struct. lines, FT NQR obs. 0-54982  
 Ge, excitation spectra of shallow acceptors, Zeeman effect, expt. 0-7381  
 H, dispersion relations 0-27978  
 H, spin-aligned atoms, theoretical props., expt. prep. 0-42969  
 H-like atom, fine struct. and HFS levels, Zeeman effect, relativistic corrections 0-37776  
 He-Ne ring laser, influence of pressure on Zeeman effect 0-19056  
 He-Ne ring laser, operating well above lasing threshold Zeeman effect 0-33039  
 He-Ne stabilised transverse Zeeman laser, light source for optical meas. 0-48272  
 $\text{Hg } 6^3\text{P}_1$  collisional transfer rate between m-sublevels mag. field depend. 0-32802  
 $\text{HgCl}_2$ ,  $^{35}\text{Cl}$  powder Zeeman NQR, injection and phase locked NQR spectrometer 0-54979  
 $^{181}\text{Hg}^{\text{m}}$  and  $^{186\text{m}-191\text{m}}\text{Hg}$ , nucl. spins, on-line quantum beat spectrosc. determ. 0-9562  
 $\text{Hg}(6^3\text{P}_1) + \text{Hg}(6^1\text{S}_0)$ , collisional excitation transfer in high mag. fields, fluoresc. obs. 0-9689  
 $\text{Ho}_2\text{O}_3\text{SO}_4$ , magnetic struct. in antiferromag. and ferrimag. states 0-15695  
 $\text{IrCl}_6^{2-}$ , ground state Zeeman splittings, reson. Raman spectra and mag.-optical activity 0-5579  
 $\text{K}$ ,  $4^3\text{P}_{1/2}$  resonance substrate, disorientation cross-section, Zeeman scanning obs. 0-42988  
 $\text{KCl:PO}_2^-$ , triplet state, level anticrossing and pseudonuclear Zeeman effect, microwave ODIMR 0-39896  
 $\text{KMgF}_2\text{:Ni}$ , Ni-Ni pair optical spectra 0-45042  
 $\text{LaCl}_3\text{:Pr}^{3+}$ , Zeeman second-order effects, fluoresc. line narrowing technique 0-16103  
 $\text{LaF}_3\text{:Pr}^{3+}$ , optical line narrowing by nuclear spin decoupling, photon echo meas. 0-48353  
 $\text{La}_{1-x}\text{Tb}_x\text{Ag}(\text{Sn}_3)(\text{Al}_2)$ , paramag. anisotropy of  $\text{Tb}^{3+}$  in cubic cryst. field 0-15687  
 NO, intracavity Zeeman modulation detect., passive Q-switching, CO IR laser obs. 0-9597  
 Na D<sub>1</sub> line profile, Zeeman scanning 0-47928  
 $\text{Na}_3\text{Pr}(\text{C}_4\text{H}_4\text{O}_3)_3 \cdot 2\text{NaClO}_4 \cdot 6\text{H}_2\text{O}$ , single cryst., forbidden  $\text{A}_1 \rightarrow \text{A}_1$  transition, mag. field induced intensification 0-50302  
 $\text{Na}(3^3\text{P}) + \text{Na}(3^2\text{S}_{1/2})$ , collisional excitation transfer, pot. symm. rules and cond. function 0-9690  
 Ne, fine struct. obs. by beam-gas spectroscopy, level crossing resonances 0-9719  
 OH, interstellar, new main line maser obs. with probable Zeeman pattern 0-56908  
 $\text{Pb}_3(\text{PO}_4)_2\text{:Gd}^{3+}(\text{Eu}^{2+})$ , EPR spectra of  $\alpha$ - and  $\beta$ -phases 0-11261  
 $\text{Pr}^{3+}$  aquo ion spectra, MCD of  $^3\text{P}_0 \rightarrow ^3\text{H}_4$  transition 0-7331  
 $\text{Rb}_2\text{MnCl}_4$  layer antiferromag., optical absorpt., temp. and mag. field depend. 0-20661  
 SO, and isotopic forms,  $\text{X}^3\Sigma^-$  state,  $\text{CO}_2$  laser mag. reson. spectroscopy 0-9602

**Zeeman effect continued**

$\text{SbCl}_3$ , cryst. struct., Zeeman split fine struct. lines, FT NQR obs. 0-54982  
 $\text{Si:P}^+$ , Zeeman energy transfer at surface layer 0-11247  
 $\text{SiC}$ , (6H), radiation damaged, luminesc. 0-25462  
 $\text{SiO}_2$ , glass, irradi., EPR of Al  $\text{E}_1'$  centres 0-11268  
 Sm, coherent ground state transients, beat meas. 0-948  
 $\text{Xe}^+$  inert gas, Xe three level system, collisional transfers, disalignment cross section 0-53098  
 $\text{YIG:Si(Ge)}$ ,  $\text{Fe}^{2+}$  spectroscopic props., nontrigonal cryst. field effects 0-44553  
 $\text{ZnS:Mn}^{2+}$ ,  $^4\text{T}_2$  level, Zeeman splittings, Jahn-Teller effect 0-40141

**Zener breakdown see Zener effect****Zener diodes**

No entries

**Zener effect**

see also Zener diodes

No entries

**Zener relaxation**

Al-Ag, precipitation study by internal friction (*French*) 0-35190  
 $\alpha$ -CuNiZn alloys, Zener-relaxation effect 0-3121

**zero gravity experiments**

Atmospheric Cloud Physics Laboratory on Space Shuttle, image dissector for size and position of statically suspended particles 0-26616  
 Atmospheric Cloud Physics Laboratory on Spacelab 0-4090  
 biorheology 0-3659  
 blood viscosity and red cell aggregation under near-zero gravity 0-3660  
 bubble thermal migration, internal heat transport effects in weightless liquids 0-24075  
 cardiovascular system, early adaption to simulated zero gravity 0-3827  
 composite materials preparation under microgravity conditions, stability during melting, thermal soak, solidification (*German*) 0-7521  
 dynamic stabilization of multiphase media subjected to vibrations under low gravitation conditions 0-7511  
 flow processes in microgravity environments 0-1720  
 glass technology, optical and magnetic materials (*German*) 0-40317  
 haemorheology in near zero gravity environment 0-3661  
 relativity experiments, control requirements 0-8896  
 superconductivity, space applications 0-41694  
 $\text{Al}_2\text{O}_3$ , Czochralski bulk flow, in microgravity, digital simulation 0-28934  
 $\text{CBr}_4$ , low gravity solidification, bubble behaviour 0-15219  
 Ge-Sb glasses, microgravity effect on recryst., optical and elec. props. 0-49127  
 $^4\text{He}$ , superfluid film 0-54464  
 Mn-Bi alloy, melting and solidification under microgravity, mag. props. (*German*) 0-45296

**zero sound**

see also liquid helium sound propagation

exciton dielectric type system with doping, low freq. excitations (*Russian*) 0-15459**zeros see poles and zeros****zeta-potential see electrokinetic effects****zinc**

see also nuclei with .....

adiabatic to sudden regime transition for  $\text{M}_3\text{M}_4\text{M}_5(^1\text{G})$  Auger excitation 0-45176  
 AES and XPS, vapour-metal electron energy shifts 0-16142  
 atom, and  $\text{Zn}^{2+}$ , excitations, comparison of gas-phase, plasma, sputtering and beam-foil 0-32820  
 atom, electron bombardment,  $\text{K}\alpha$  satellites 0-47932  
 atom, excited states, collisional quenching cross sections and exit channels, fluoresc. quenching obs. 0-18919  
 atom, L-shell soft X-ray emission spectra, oscillator strengths 0-32651  
 atomic vibr. and fermion behaviour of HCP metals 0-6474  
 Auger effect,  $\text{K}-\text{M}^2$  radiative, low energy satellites meas. 0-45174  
 basal dislocation-prismatic dislocation ring interactions by method of moments (*Russian*) 0-10550  
 bicrystal, (1010) tilt, misorientation depend. of grain boundary sliding 0-15119  
 bicrystals, galvanomagnetic phenomena at common boundary, electric field potential distribution (*Russian*) 0-29388  
 bicrystals, grain boundary slip in deform. 0-34008  
 coating on steel, cold rolling influence on struct. and deform. of diffusional layer (*Russian*) 0-55465  
 cold rolling texture development 0-25720  
 comparison with conventional Leclanche cells 0-35660  
 compressive strength of polycryst., temp. and strain rate effects 0-16616  
 corrosion in HCl under forced convection 0-35426  
 corrosion inhibition by n-decylamine, synergistic effect of halide ions 0-11819  
 corrosion inhibition by surface active substances 0-40589  
 corrosion rate monitoring, automatic, in near-neutral soln., using a micro-computer 0-50749  
 crystal growth, Bridgman method (*Japanese*) 0-40252  
 determ., in seawater, graphite furnace atomic absorption spectroscopy 0-40768  
 determ. in water and organic materials, flameless atomic absorpt. spectrometry with wire loop atomiser 0-45586  
 diffusion in  $\text{GaInAsP-InP}$  planar stripe lasers, sputtered  $\text{SiO}_2$  diffusion mask 0-48249  
 diffusion in  $\text{In}_{1-x}\text{Ga}_x\text{As}$ , diffusion coeff. and surface conc. 0-39122  
 diffusion in ion implanted GaAs, profiles 0-24681  
 dust,  $\text{O}_2$  determ. by 14 MeV neutron activation anal. (*Japanese*) 0-11977  
 electrodeposited, residual stresses, effect of triacetylpyridine and polyethylene glycol additives to  $\text{NH}_4\text{Cl}$  electrolytes 0-21190  
 electrodeposited coatings, residual stress diagrams 0-16588  
 electrodes, porous, concentration changes during cycling 0-35666  
 electron irradi. effect on electrolum., defects form. and quenching obs. 0-55194  
 estuarine river water, particulate heavy metal content, Cochran backwater, India 0-7964  
 extractive metallurgy, developments, review 0-20820  
 foil, splat quenched, preferred orientation 0-40381  
 grain boundaries, activationless motion, group co-operative transition mechanism 0-2039  
 grain boundary diffusion in Al, nonvacancy mechanism (*Russian*) 0-24669  
 HCP, lattice dynamics, local pseudopotential approach, dielectric functions 0-34151



## zinc continued

HCP metals, K-emission valence bands, structure and bonding 0-7438  
 HCP structure, selection rule, electron momentum distrib. rel. to positron annihilation 0-39495  
 ion etching, dispersion coeff. determ. (*German*) 0-40597  
 isomer shift values of implanted  $^{133}\text{Xe}/^{133}\text{Cs}$ , Mossbauer spectra 0-7240  
 liquid, surface tension, temp. depend. (*Russian*) 0-15336  
 liquid, viscosity calc. using microinhomogeneous struct. model (*Russian*) 0-15284  
 Mossbauer spectra, quadrupole interaction 0-7206  
 neutron irradiated, recovery of c-axis spacing and elec. resist. 0-34081  
 phonon density of states determ. from heat capacity (*Russian*) 0-29131  
 phosphidation in P vapour, kinetics and associated diffusion coeffs. 0-3405  
 pollution levels in Belfast Lough 0-3539  
 polycrystals, deformation, grain sizes effect at room temp. (*Czech*) 0-45359  
 polycrystals with axial texture, heterogeneity of props. (*Russian*) 0-29192  
 polyethylene/Cu(Zn) adhesion, role of surface topography 0-35500  
 protective coating on C steel, durability obs. using nuclear radiation excited X-ray fluoresc. 0-21206  
 rolling texture formation, computer simulation in HCP and orthorhombic metals 0-3095  
 skin lesion Mn, Cu and Zn conc. meas. by neutron activation 0-17063  
 slip, density of basal dislocations, rel. to deforming stress, 1.5-300K (*Russian*) 0-29028  
 stacking faults, plastic deformation, due to laser beam irradi. (*Russian*) 0-15121  
 steel, Zn coated strips, plastic deform. influence on struct. and quality (*Russian*) 0-40377  
 stopping power for 6.75 MeV protons 0-34107  
 strength of single crystals, temp. and strain rate effects 0-16373  
 strengthening by electroplastic strain, surfactant effect (*Russian*) 0-20953  
 substrate for polystyrene film, electrode effect on carrier injection, TSC, I-V characts. 0-34463  
 superconducting transition temp., perturbative corrections, direct and indirect ladder diagrams 0-49979  
 thermal neutron cross sections, in single crystals 0-19672  
 thermal sprayed coating on steel substrate, cavitation and corrosion resist. in sea water 0-35427  
 thermally stimulated exo-electron emission 0-11547  
 twin boundaries, computer simulation 0-39109  
 US hardening kinetics rel. to dislocations 0-50644  
 wire, elastically bent, elec. resist. in mag. field 0-44568  
 X-ray K-absorpt. edge shifts, plasmon energies correlation 0-20734  
 zone melting by electron beam, isotope fractionation enhancement 0-45229  
 $\text{Al}_2\text{Ga}_{1-x}\text{Sb}_x\text{Zn}$ , impurity diffusion, p-n junction depth 0-24678  
 $\text{BaTiO}_3\text{:Zn}$ , annealed in  $\text{H}_2$  and  $\text{O}_2$ , valence change in phase stability 0-20600  
 Cu-Zn heterocontacts, microcontact spectra (*Russian*) 0-34502  
 $\text{Fe}_3\text{O}_4\text{:Zn}^{2+}$ , Verwey transition 0-6513  
 GaAlAs:Zn recombination radiation drift, charge carrier photon induced drift in varigap semicond. 0-50418  
 GaAs:Cr, Zn, shallow impurity implantation, elec. props. after annealing 0-24465  
 GaAs:Cr:Zn, implanted, doping profiles after laser annealing, elec. props. 0-2058  
 GaAs:Zn, diffusion during LPE, impurity gradients and annealing effects 0-29882  
 GaAs:Zn, diffusion of Zn by two-temp. method, LED fabrication 0-49416  
 GaAs:Zn, heavily doped, photolum. obs., above gap 0-29796  
 p-GaAs:Zn, luminescent, ion doped MBE growth 0-44436  
 p-GaAs:Zn, Raman scatt. by LO phonon-plasmon coupled modes, wave vector non-conservation 0-16033  
 n-GaAs:Zn, VPE, deep-level transient spectroscopy 0-34383  
 GaAs:Zn ion implanted ionic alloy, electrophysical props., annealing 0-39133  
 GaN:Zn, VPE grown, optical cross sections, photoluminesc. and optical absorpt. meas. 0-55160  
 GaN:Zn, VPE growth, photoluminesc. rel. to doping conditions 0-55159  
 GaP:Zn, doping from gas phase during LPE 0-55312  
 GaP:Zn, implanted, elec. profiling using anodic oxidation in N-methylacetamide 0-54690  
 GaP:Zn, luminesc., acceptor-bound multiple excitons 0-11476  
 GaP:Zn, Sn doped epitaxial layers, Hall const., hole mobility and conc. 0-15143  
 GaP:Zn,S, donor-acceptor pair luminesc., excitation spectroscopy 0-25440  
 He-Zn hollow cathode laser discharge, comparison with He-ZnCl<sub>2</sub> discharge 0-28203  
 He-Zn II laser, 0.4924  $\mu\text{m}$  oscill. spectra meas. using scanning interferometer (*Japanese*) 0-9864  
 InAs:Zn,S(Se), solubility and donor-acceptor interaction 0-54263  
 p-InP:Zn, vapour grown, prep. and props. 0-54268  
 liquid, polyvalent, electrical resistivity by harmonic model potential 0-54668  
 NaCl:NaF:Zn<sup>2+</sup>, point defects, ionic thermal current and optical meas. 0-6403  
 Ni electrochem. deposition on Zn surfaces 0-29885  
 Si:Zn, photoionisation of deep impurity levels 0-34386  
 Si:Zn, reson. characts. of impedance near excitation threshold of recomb. waves 0-20301  
 Si:Zn, surface characterised by negative electrochemical pot., electronic props. 0-44695  
 Si:Zn p-n junction diode, computer-aided study of carrier lifetimes 0-24999  
 Zn, elec. field gradient at  $^{111}\text{Cd}$ , effects of high press., TDPAC meas. 0-25266  
 Zn I, absorpt. spectra, line and total absorpt. comparison 0-11991  
 Zn I, relative populations in arc, sputtering and gas phase collisions 0-934  
 Zn II, lifetime extraction from beam-foil decay curves 0-14107  
 Zn XXII, 2p-4d and 2p-4s transition arrays, wavelengths and oscillator strengths 0-47933  
 Zn<sup>2+</sup> binding to nucleic acid bases, ab initio SCF (pseudopot.) calcs. 0-12052  
 Zn<sup>2+</sup>, <sup>1</sup>P and <sup>3</sup>P energy levels, relativistic RPA calc. 0-47913  
 Zn-GeS-Zn system, Schottky and Poole-Frenkel cond. mechanisms 0-54799

## zinc continued

Zn-H<sub>2</sub>(He)(Ar) mixtures, binary diffusion coefficients, 1 atm., 720-1120K 0-1725  
 Zn-pore electrodes and cells, operation 0-26126  
 Zn-Sb diffusion couple, layer growth of ZnSb phase at high press., elec. meas. 0-2218  
 Zn<sup>+</sup>-He, positive column laser discharge, upper and lower state densities, Penning collision 0-32964  
 Zn+H<sup>+</sup>, K-shell ionisation calcs. 0-23534  
 Zn+H<sup>+</sup>, K-shell ionisation cross-sections calcs. 0-43165  
 Zn+N<sub>2</sub>, A<sup>3</sup> $\Sigma_u^+$  state, vibr. excitation 0-1054  
 Zn+Se,  $\pi^-$  capture, radioactivity meas. 0-47831  
 Zn<sup>+</sup>+He(Ne)(Ar), 1-500 keV, Zn<sup>+</sup> excitation, reson.-line emission and polaris. 0-18911  
 Zn<sup>+</sup>+He(Ne)(Ar), Zn<sup>+</sup> collision-induced alignment, reson.-line emission polaris. obs. 0-18912  
 Zn<sup>2+</sup>+H, electron capture by slow ions, pseudo-crossing 0-43176  
 Zn<sub>2</sub>, quenching and predissociation, possible excimer laser 0-32770  
 ZnI, II, excited states, radiative lifetimes, multi-channel delayed-coincidence method 0-32669  
<sup>64</sup>Zn isotope, fractionation during zone recrystn. 0-2946  
<sup>65</sup>Zn, uptake of gamma-emitting activation products in plants 0-30614  
<sup>67</sup>Zn, <sup>3</sup>D, <sup>1</sup>D, <sup>3</sup>P<sub>1</sub> and <sup>1</sup>P<sub>1</sub> levels, quadrupole coupling consts. 0-23434

**zinc alloys**  
*see also brass; zinc compounds*  
 binary substitutional solutions, thermodynamics 0-44337  
 brazing, flux adhesion, and spreading coefficient 0-15379  
 positron annihilation expts., electronic struct. and Fermi surface studies 0-54594  
 rare earth alloys, RZn<sub>12</sub>, mag. struct. and interactions 0-25092  
 steel, galvanized, Fe-Zn phases, Mossbauer study 0-50233  
 Ag-Zn, negative muon capture ratios 0-55007  
 Ag-Zn, vacancy prod. rate by displacement cascades, anelastic meas. during neutron irradi. 0-19794  
 Ag-Zn (2 to 12 wt.%) containing several metals, internal oxidation (*Japanese*) 0-16570  
 Ag-Zn (50 at.%), BCC  $\beta$  phase, high temp. creep, existence of master curve 0-55473  
 Al-Cu-Zn system, solid-phase reactions, phase diagram 0-50603  
 Al-Mg-Zn, granulated, degassing atm. effect on mech. props. of semifinished products 0-7720  
 Al-Mg-Zn, O<sub>2</sub><sup>+</sup> ion bombard., SIMS and photon emission spectra, local thermodynamic equilb. model 0-20751  
 Al-Mg-Zn alloy 7179-T651, reduced ductility under tensile after exposure to water 0-11835  
 Al-Mg-Zn alloys, liq./solid phase equilibria determ. (*German*) 0-50601  
 Al-Zn, age hardenable precipitation and dissolution, positron annihilation and X-ray scatt. 0-16314  
 Al-Zn, binary metallic melt, deviation from the Kopp law, specific heat (*Russian*) 0-39305  
 Al-Zn, comparison between very-slow-neutron transmission and small-angle neutron scatt. expts. 0-19677  
 Al-Zn, G.P. zone form., temp. limit 0-16317  
 Al-Zn, interdiffusion meas. by elec. resist. 0-49433  
 Al-Zn, isothermal preprecipitation, small angle X-ray scatt. expts. 0-35186  
 Al-Zn, liq. solutions, thermodynamic properties (*Polish*) 0-49380  
 Al-Zn, metastable phases formed at 200°C, room temp. stability 0-16315  
 Al-Zn (10 at.%), short-range order parameter calc. in pseudopot. approx. (*Russian*) 0-49183  
 Al-Zn (10 wt.%), ageing behaviour, calorimetric study 0-45328  
 Al-Zn (15 at.%), structural changes during post ageing between 125°C to 215°C 0-40399  
 Al-Zn (15 at.%), supersaturated alloy, growth and decomposition kinetics 0-29965  
 Al-Zn (15 wt.%), calorimetric ageing study 0-45330  
 Al-Zn (20 (30) (35) (40) (60) at.%), effect of UTS on cyclic creep strength (*Korean*) 0-25778  
 Al-Zn (3.9 wt.%), single crystals, fatigued age-hardenable, dislocation structure (*German*) 0-54247  
 Al-Zn (40(50)(65) wt.%), deformed, free energy changes in process of discontinuous precipitation 0-3054  
 Al-Zn (40(50)(65) wt.%), plastic deform. effect on discontinuous precipitation 0-3053  
 Al-Zn alloys, recrystallisation and superplasticity, HVEM straining 0-39207  
 Al-Zn alloys, spinodally decomposing, resistivity behaviour 0-45271  
 Al-Zn-Cu-Mg (V95T1), subcritical crack growth under static plane stress 0-55528  
 Al-Zn-Mg, acoustic emission meas. during tensile testing, reproducibility of results 0-50782  
 Al-Zn-Mg, decomp. kinetics and ageing mechanism (*Russian*) 0-45269  
 Al-Zn-Mg, Guinier-Preston zones, comp. and contrib. to elec. resist. 0-16316  
 Al-Zn-Mg, plastic deform. influence on structural transform. and mechanical props. (*Russian*) 0-7623  
 Al-Zn-Mg, polygonized struct. in extrusions, thermal stability and mech. props. 0-50659  
 Al-Zn-Mg, stress conversion cracking based on micromech. surface reactions 0-7716  
 Al-Zn-Mg, type 7075, strain rate effects on H embrittlement 0-3190  
 Al-Zn-Mg, welded section stress in rolled plate edges, mechanical surface treatment and environment effects 0-21193  
 Al-Zn-Mg (2.1, 1.3 wt.%), single crystals, fatigued age-hardenable, dislocation structure (*German*) 0-54247  
 Al-Zn-Mg (4.5, 2 to 3 at.%) solid state reactions by interrupted continuous heating 0-25737  
 Al-Zn-Mg (4.5 at.%, 2 or 3 at.%), decomposition behaviour during continuous cooling, XSAS and TEM examination 0-16264  
 Al-Zn-Mg (4.5 at.%, 2 to 3 at.%), decomp. behaviour during continuous heating 0-29922  
 Al-Zn-Mg (4.8, 1.2 wt.%), quenched, Guinier Preston zones formation 0-45273  
 Al-Zn-Mg (5.9, 2.9 wt.%), ageing effects on microstruct. 0-16306  
 Al-Zn-Mg (6.3 wt.%), hydrogen embrittlement and trapping 0-55490  
 Al-Zn-Mg alloys, extra-resistivity of coherent precipitates calc. using X-ray small angle scattering intensities 0-3050  
 Al-Zn-Mg alloys stress corrosion 0-35395  
 Al-Zn-Mg plasma sputtered, mech. props. rel. to heat treatment (*Russian*) 0-40387



## zinc alloys continued

- Al-Zn-Mg powder, selected-area electron diffr. ring patterns 0-50642  
 Al-Zn-Mg-B fibre reinforced composite, packet rolling, thermodeform. process parameters (*Russian*) 0-55433  
 Al-Zn-Mg-Co, crazing tendency (*Russian*) 0-30068  
 Al-Zn-Mg-Cu, age hardened, effect of strain rate, temp. and environment on ductility 0-45368  
 Al-Zn-Mg-Cu, type 7075, microstruct. role in hydrogen assisted fracture 0-30091  
 Al-Zn-Mg-Cu (6.76, 2.37, 1.80 wt.%), cyclic SCC in salt water (*Japanese*) 0-45435  
 Al-Zn-Mg-Cu age-hardened alloys, fatigue crack propagation rel. to grain size in vac. and NaCl soln. 0-16538  
 Al-Zn-Mg-Cu-Co (6.5, 2.5, 1.5, 0.4 wt.%), fatigue crack propag. 0-55521  
 Al-Zn-Mg-Cu-Co-Fe-Si, powder alloy, fatigue crack tip plasticity, from load interactions 0-21066  
 Al-Zn-Mg-(Zr) alloy, microstruct. effect on fatigue crack growth 0-3164  
 Au-Ni-Cu-Zn, white gold, metallographic struct., heat treatment and plastic working effect 0-40403  
 Au-Zn, (55 to 88 at.%), equilib. diagram, X-ray diffr. obs. 0-25660  
 Au-Zn, charge transfer, Mossbauer effect <sup>197</sup>Au isomer shifts, XPS valence-band spectra 0-2676  
 Au-Zn, liq., thermodynamic props. (*German*) 0-49386  
 Bi-Zn, alloy absolute thermoEMF temp. and conc. depend. (*Russian*) 0-39561  
 Bi-Zn, liquid, interstitial index, definition and variation with temp. (*French*) 0-2011  
 CC Al-Zn-Mg (4.5,1(2)(3) at.%), decomposition during ageing, preageing and cooling rate influence 0-20938  
 Cd-Zn, binary metallic melt, deviation from the Kopp law, specific heat (*Russian*) 0-39305  
 Cd-Zn single crystals, crit. resolved shear stress at low temps. 0-3138  
 CeZn, cryst. field and exchange effects, inelastic neutron scatt. study 0-24855  
 Cu-Ni-Zn, diffusion couples, zero-flux planes and flux reversals 0-15313  
 Cu-Ni-Zn system, tie lines in a two phase region 0-24404  
 Cu-O-Zn dilute liquid alloy, Zn-O interaction parameter 0-55694  
 Cu-Zn, charge transfer, core-electron binding-energy shift 0-2676  
 Cu-Zn, cold worked solid solution, flow stress and activation volume 0-16393  
 Cu-Zn, optical composition modulation spectra, dielec. const. var., Fermi surface and electronic level shifts 0-6707  
 Cu-Zn, thermally stimulated exo-electron emission 0-11547  
 Cu-Zn (50 at.%), BCC  $\beta$  phase, high temp. creep, existence of master curve 0-55473  
 $\beta$ -Cu-Zn-Al, diffr. effects., obs. and interpretation of extra maxima 0-44173  
 Cu-Zn-Al, martensitic phase transformation effect on low cycle fatigue behaviour 0-7666  
 Cu-Zn-Al, memory alloy wire and ribbon reversible martensitic transformation, ageing effect, review 0-7564  
 Cu-Zn-Al, single cryst., stress induced martensitic transformation 0-45308  
 Cu-Zn-Al (19.5, 6.35 wt.%), martensitic, static stresses influences on damping behaviour 0-10594  
 $\beta$ -Cu-Zn-Al (27.5, 4.0 wt.%), strain induced martensite, exam. of structure, microstructure 0-7648  
 Cu-Zn-Ga(Al), martensites, internally faulted, shape memory mechanism 0-30010  
 Cu-Zn-Sn (24-34, 1.0 wt.%), cold-worked microstruct., X-ray diffr. obs. 0-3088  
 $\beta$ -Cu-Zn (47.4 wt.%), heat content between 300.05 and T (T from 400 to 1000K) drop calorimetry (*French*) 0-10682  
 $\alpha$ -CuNiZn alloys, Zener-relaxation effect 0-3121  
 Cu<sub>2</sub>Zn<sub>1-x</sub>, disordered alloy, muffin-tin model, electronic struct. and density of states calc. 0-29302  
 Fe-Zn, crystallographic relations by X-ray diffr. 0-24408  
 Fe-Zn, phase diagram, DTA, EDAX, X-ray diffr. study 0-50602  
 Fe-Zn intermetallics, initial stages of form. (*Russian*) 0-20889  
 HoZn, magnetic excitations 0-25115  
 Mg-Al-Zn (9wt.%Al), sand cast, preferred orientation and mechanical props. (*Japanese*) 0-20979  
 Mg-Y-Zn alloys, phase equil. (*Russian*) 0-16271  
 Mg-Y-Zn-Nd-Cd alloys, influence of Zr addition on struct. and mech. props. (*Russian*) 0-40370  
 MgCu<sub>2-x</sub>Ni<sub>x</sub>, X-ray and neutron diffr. investigation of Laves phases of MgCu<sub>2</sub>-type (*German*) 0-15050  
 MgNi<sub>2-x</sub>Zn<sub>x</sub>, X-ray and neutron diffr. investigation of Laves phases of MgCu<sub>2</sub>-type (*German*) 0-15050  
 Mn-Y-Zn-Cd alloy, phase equilibria, plastic deformation, microhardness (*Russian*) 0-40334  
 Mn-Zn ferrite single crystals, mech. polishing effect on mag. props. (*Japanese*) 0-16569  
 $\alpha$ -Ni-Zn, solid soln. diffusion annealing effect (*Japanese*) 0-34255  
 Ni-Zn-Mn-Fe spinel, crystn. from soln. in melt 0-2945  
 Pd-Zn, L1<sub>0</sub> type intermetallic phase, X-ray diffr. study of lattice compression 0-49182  
 Sn-Zn melts, plasticising action in deform. hardening of medium C steel 0-55415  
 TbZn, ferromag., elec. resist., just below crit. temp., effect of mag. domains 0-39557  
 TbZn, ferromag. transition, transport coeffs. critical behaviour 0-15498  
 TmZn, quadrupolar phase transitions, magnetoelastic and quadrupolar coupling const. 0-15744  
 Zn-Al, unidirectional eutectic, FCC phase, preferred orientation 0-29973  
 Zn-Al (10.22,50wt.%), low temp. mech. props. plastic deformation, glissile dislocation nucleation (*Russian*) 0-11695  
 Zn-Al (15 wt.%), thermal sprayed coating on steel substrate, cavitation and corrosion resist. in sea water 0-35427  
 Zn-Al (22 at.%) eutectic, superplastic, microscopic examination of internal void formation 0-16383  
 Zn-Al (22 wt.%), positron diffusion and trapping at grain boundaries 0-39157  
 Zn-Al (22 wt.%) superplastic alloy, cavitation and neck form. 0-30022  
 Zn-Al eutectic alloy, uni-directionally solidified, damping capacity (*Japanese*) 0-16364  
 Zn-Al eutectoid alloy sheets, creep bulging 0-1439  
 Zn-Al superplastic eutectoid alloy, low strain rate behaviour 0-40458  
 Zn-Al-Cu (18, 4 wt.%), plastic deform. at room temp., superplastic props., tensile strength (*Czech*) 0-45360

## zinc alloys continued

- Zn-Cd liquid/Fe-Ni-Al mag. powder, effective viscosity of composites (*Russian*) 0-54424  
 Zn-Mn(Cr), dil. mag. anisotropy, Hartree-Fock calcs. 0-11162  
 Zn-Mn(Cr), dil., mag. anisotropy below 1K, low field magnetisation meas. 0-20382  
 Zn-Pb(Bi), liquid, surface tension, size effect (*French*) 0-15341  
 Zn-Sn, binary metallic melt, deviation from the Kopp law, specific heat (*Russian*) 0-39305  
 Zn-Sn-Hg, diagram of state, melting temp., peritectic and eutectic phases (*Russian*) 0-55350  
 Zn-Ti, environmental factors affecting pitting corrosion potential in NaOH solns. 0-45423  
 ZnAl (18.75 wt.%), supercooling phase  $\beta$  break up kinetics (*Polish*) 0-25654  
 Zr<sub>1-x</sub>Nb<sub>x</sub>Zn<sub>2</sub>, microscopic mag. props., NMR investigation 0-15807  
 ZrZn<sub>2</sub>, phonon contrib. to Stoner enhancement factor, ferromag. and possible superconductivity 0-25070  
 ZrZn<sub>2</sub><sup>57</sup>Fe mag. props. from Mossbauer effect obs. (*Japanese*) 0-15933

## zinc compounds

see also zinc alloys

- alkylammonium zinc tetrachloride cpds., high temp. phase transitions 0-54372  
 chalcogenides, film, on NaCl, preferential epitaxy induced by electron bombard. or elec. field 0-10824  
 chalcopyrites, refr. index dispersion 0-55057  
 elbaites, Zn-Fe,  $\gamma$ -irradiated, Mossbauer study 0-44990  
 manganese zinc formate dihydrate, two-dimens. antiferromag., anomalous crit. phenomena, neutron scatt. and PMR obs. 0-50104  
 metal-ZnO-SiO<sub>2</sub>-Si structures, charge injection 0-49919  
 tetramethylammonium tetrachlorozincate, ferroelec., incommensurate-commensurate transition, neutron scatt. study 0-40073  
 tetramethylammonium tetrachlorozincate, low temp. phases, superstruct., X-ray study 0-39065  
 tetramethylammonium zinc tetrachloride, <sup>13</sup>C NMR and PMR study of incommensurate phase transition 0-34863  
 zinc blende type crystals, internal displacements 0-34127  
 zinc stearate lubricant, admixed, effect on Fe sintered compact, shrinkage and mech. props. 0-45402  
 zinc stearate lubricant effect on Fe powder compact, apparent density, mixing, and friction 0-45403  
 Zn<sub>3</sub>P<sub>2</sub>, UV photoconductive detectors 0-4766  
 ZnS single crystals, O content determ. by fast neutron activation anal. 0-15142  
 Ba<sub>2</sub>Co<sub>2</sub>Zn<sub>2-x</sub>Fe<sub>2-x</sub>O<sub>22</sub>, mechanically oriented, topotactic prod. technique, mag. props. 0-35140  
 BaO-K<sub>2</sub>O-Na<sub>2</sub>O-ZnO-SiO<sub>2</sub>, corrosion and microhardness, effect of detergents 0-16518  
 CdSb-ZnSb, crystallisation characts., phase diagram 0-55383  
 CdTe-ZnS system, phase diagram and solid solubility 0-20909  
 CdTe-ZnS ternary mutual system, phase diagram 0-20904  
 Cd<sub>1-x</sub>Zn<sub>x</sub>S/Cu<sub>2</sub>S thin film heterojunction solar cells, operational charact. 0-45687  
 Cd<sub>1-x</sub>Zn<sub>x</sub>S-p-GaAs heterojunctions, elec. and photovolt. props. rel. to growth technique 0-29466  
 Co<sub>1-x</sub>Zn<sub>x</sub>Fe<sub>2(1-y)}</sub>Cr<sub>2</sub>O<sub>4</sub> spinels, solid solns., struct. 0-19764  
 CsZnCl<sub>2</sub>:Cu<sup>2+</sup>, electron spin echo, 35 GHz 0-13113  
 Cu<sup>2+</sup> ions influence on PbSO<sub>4</sub> flotation, with sodium hexadecyl sulphate, metallurgical waste treatment appl. (*Japanese*) 0-55701  
 (CuInTe<sub>2</sub>)<sub>1-x</sub>(ZnTe)<sub>x</sub>, phase diagram and cryst. growth of CuZn<sub>2</sub>InTe from ZnCl<sub>2</sub> flux 0-16287  
 CuO-ZnO-Fe<sub>2</sub>O<sub>3</sub>, sintered ferrite, preparation, mag. susceptibility, DC resistivity 0-34598  
 Cu<sub>2</sub>S-Zn<sub>2</sub>Cd<sub>1-x</sub>, heterojunction, composition meas. near interface using aqueous ion-exchange 0-29465  
 (Cu<sub>2</sub>SnS<sub>3</sub>)<sub>2</sub>(3ZnS)<sub>1-x</sub>, diamond-type semiconductor, Mossbauer spectrum of <sup>119</sup>Sn 0-44991  
 Cu<sub>2</sub>Zn<sub>1-x</sub>SiF<sub>6</sub>H<sub>6</sub>O, heat capacities and thermodynamic props., 14 to 300K, cooperative Jahn-Teller transition 0-21314  
 (GaAs)<sub>1-x</sub>(ZnSe)<sub>x</sub> single crystal, visible cathodoluminesc. spectra 0-20716  
 p-(GaAs)<sub>1-x</sub>(ZnSe)<sub>x</sub>-nn<sup>+</sup>.GaAs, avalanche heterojunctions, inverse branch of volt ampere characts. (*Russian*) 0-6974  
 Ge-ZnSe, (100) interface, electronic struct. calc. 0-49861  
 He-ZnCl<sub>2</sub> hollow cathode laser discharge, comparison with He-Zn discharge 0-28203  
 In<sub>2-x</sub>Sn<sub>x</sub>O<sub>3-y</sub>-ZnS:Mn thin film structure, surface morphology and electro-optical props. (*Russian*) 0-49554  
 K<sub>2</sub>O-PbO-ZnO-B<sub>2</sub>O<sub>3</sub>-SiO<sub>2</sub>, corrosion and microhardness, effect of detergents 0-16518  
 KZnF<sub>3</sub>:Ni<sup>2+</sup>, Mn<sup>2+</sup>, interference transition electric dipole mechanism 0-34896  
 LiZn ferrite, Mossbauer study, relax. and supertransferred hyperfine fields 0-39941  
 LiZn, substituted ferrite, cation distribution, Mossbauer, X-ray, neutron diffr. study 0-28975  
 MgF<sub>2</sub>-ZnS multilayers, high vacuum deposition for cold light mirror prod. (*German*) 0-53486  
 MgMnZn ferrite, ultrafine powder, prod. by cryochemical, freeze drying, spray drying or soln. techniques 0-55336  
 MgO-ZnO-Fe<sub>2</sub>O<sub>3</sub>, sintered ferrite, preparation, mag. susceptibility, DC resistivity 0-34598  
 Mn-Zn ferrosilicates, carrier transfer phenomena 0-54727  
 MnZn ferrite, combined Bridgman-zone levelling cryst. growth technique 0-35076  
 MnZn ferrite, mag. anisotropy, effect on recording head characts. 0-39765  
 MnZn ferrite, mag. loss accommodation depend. on freq. and amplitude of mag. field (*Russian*) 0-34686  
 MnZn ferrite, mag. permeability accommodation depend. on mag. field (*Russian*) 0-34685  
 MnZn ferrite, O<sub>2</sub> stoichiometry effect on fracture 0-25826  
 MnZn ferrite, Ti substituted, vacancy contents and phase equilibria 0-29012  
 MnZn ferrite, wall topography change induced by external press. 0-34734  
 MnZn ferrite fabricated by hot isostatic pressing, recording head appl. 0-35139  
 MnZn ferrites, elec. cond. mechanism in paramag. and ferrimag. phases 0-15524



## zinc compounds continued

- MnZn, pressing powders, spray dried, pressing behaviour and props. 0-11617  
 MnZn soft ferrites, commercial grade, microstruct. rel. to mag. props. 0-34009  
 MnZn-ferroferrites, sintered, microstruct., TEM study (*Dutch*) 0-2036  
 Ni-Zn ferrite, grain size depend. of grain boundary sliding (*Japanese*) 0-15120  
 Ni-Zn ferrites 600 NN and M450 NNI, Curie point radiative shift due to neutron irradi. (*Russian*) 0-39775  
 Ni<sub>0.5-x</sub>Co<sub>x</sub>Zn<sub>0.5</sub>Fe<sub>2</sub>O<sub>4</sub> ferrosilical solid solutions, cryst. lattice defects and props. 0-19796  
 NiO-ZnO, solid solution, exam. of mechanism and kinetics of reaction with Fe<sub>2</sub>O<sub>3</sub>, ferrite formation 0-3309  
 NiZn ferrite, wall topography change induced by external press. 0-34734  
 Ni<sub>0.38</sub>Zn<sub>0.62</sub>Fe<sub>2</sub>O<sub>4</sub>, preparation, Mossbauer study 0-50231  
 Ni<sub>1-x</sub>Zn<sub>x</sub>Fe<sub>2</sub>O<sub>4</sub>, catalytic oxidation of CO, mag. props., kinetic parameters and composition depend. 0-16723  
 Ni<sub>x</sub>Zn<sub>1-x</sub>Fe<sub>2</sub>O<sub>4</sub>, crystal growth from BaO-B<sub>2</sub>O<sub>3</sub>-ZnO-NiO-Fe<sub>2</sub>O<sub>3</sub> melt, exam. of crystal props. 0-40249  
 PbO-B<sub>2</sub>O<sub>3</sub>-SiO<sub>2</sub>-Al<sub>2</sub>O<sub>3</sub>-ZnO-CuO-Bi<sub>2</sub>O<sub>3</sub> solder glass, crystallisation prevention by Cu addition 0-11654  
 PbO-B<sub>2</sub>O<sub>3</sub>-ZnO solder glass, with admixtures, crystallisation and thermal expansion 0-24364  
 PbTe-ZrO<sub>2</sub> (SiO<sub>2</sub>), epitaxial MIS struct., fabrication and elec. props. 0-2472  
 SiO<sub>2</sub>-CaO-ZnO-B<sub>2</sub>O<sub>3</sub>-Na<sub>2</sub>O-S, SrO effect on crystallisation 0-54135  
 SiO<sub>2</sub>-Li<sub>2</sub>O-K<sub>2</sub>O-ZnO-P<sub>2</sub>O<sub>5</sub>, glass ceramic, phase changes and crystn. processes 0-7562  
 SiO<sub>2</sub>-Li<sub>2</sub>O-K<sub>2</sub>O-ZnO glass ceramic, prep., phase transformations and physical props. 0-45299  
 SiO<sub>2</sub>-ZnO-Na<sub>2</sub>O-Li<sub>2</sub>O, glass-ceramic coating, optimisation of props. by selective oxide action 0-55552  
 Sn<sub>2</sub>Li<sub>1.6</sub>Sn<sub>1.6</sub>O<sub>8</sub>, four layer hexagonal close packing, cryst. struct. determ. (*French*) 0-28999  
 SnO<sub>2</sub>-ZnS:Mn thin film structure, surface morphology and electro-optical props. (*Russian*) 0-49554  
 V<sub>2</sub>O<sub>5</sub>-BaO-K<sub>2</sub>O-ZnO glasses, elect. props. and struct. 0-15547  
 (Zn,Cd)S:Cu,Al, luminesc. efficiency deterioration due to surface oxidation by (NH<sub>4</sub>)<sub>2</sub>Cr<sub>2</sub>O<sub>7</sub> thermal decomp. 0-29810  
 Zn (OH)<sub>2</sub>, physico-chemical behaviour in Garonne-Gironde river estuary system, radioactive tracing (*French*) 0-7994  
 Zn complex, Zn(l-sparteine)Cl<sub>2</sub>, IR circular dichroism spectra, vibr.-electronic interaction 0-55074  
 Zn diethyldithiocarbamates, use in liquid-liquid extraction of corrosion and fission products 0-18459  
 Zn-Fe-O ferrite system, thermodynamic stability, dissociation and phase relations (*Japanese*) 0-55378  
 Zn-In-S ultraviolet detector (*Russian*) 0-18014  
 Zn<sup>2+</sup>-Cl<sup>-</sup> system, ion exchange, complex form. studied using radiotracer, effect of macroelectrolyte cation 0-16659  
 Zn<sup>2+</sup>-H<sub>2</sub>O clusters, solvation, Monte Carlo simulation 0-44102  
 ZnAl<sub>2</sub>O<sub>4</sub>:Cr<sup>3+</sup>, Raman effect to probe dynamical processes of Cr<sup>3+</sup> photoexcited states 0-2740  
 Zn<sub>3</sub>As<sub>2</sub>, optical band-gap, absorption meas. 0-25372  
 Zn<sub>3</sub>As<sub>2</sub>-ZnSe(ZnTe) solid solutions, single cryst., phase equilib. and props. 0-16283  
 ZnBr<sub>2</sub>, <sup>61</sup>Br NQR line width obs. 0-50219  
 ZnC<sub>2</sub>O<sub>4</sub>·2H<sub>2</sub>O, crystn. kinetics by precipitation 0-50884  
 ZnCdS:(Cu+Ag) binder layer for electrophotography 0-4797  
 ZnCdS:Ag, phosphor screen, electron beam excited, light ang. distrib., modulation transfer function 0-45150  
 ZnCdS:Ag screen, electron beam excited, light emission spectra 0-25466  
 Zn<sub>0</sub>Cd<sub>0.95</sub>S, two-photon and two-step absorption of light 0-7389  
 Zn<sub>x</sub>Cd<sub>1-x</sub>S, bound-exciton lines, compositional fluctuation-induced broadening 0-2846  
 Zn<sub>x</sub>Cd<sub>1-x</sub>S, film, single-thermal-source form. 0-2492  
 Zn<sub>x</sub>Cd<sub>1-x</sub>S, resonance Raman scatt. involving exciton complexes 0-16039  
 Zn<sub>x</sub>Cd<sub>1-x</sub>S:Cu, photoluminescence 0-29783  
 Zn<sub>x</sub>Cd<sub>1-x</sub>S:Cu crystallophosphors, spectra of IR electrophotographic sensitivity (*Russian*) 0-50423  
 Zn<sub>x</sub>Cd<sub>1-x</sub>S/GaAs heterojunction solar cells, meas. of minority carrier diffusion length 0-26158  
 ZnCl<sub>2</sub>, hydrocracking densities, relativistic effect 0-42928  
 ZnCl<sub>2</sub>, deformation of solvent refined coal for petroleum prod. 0-30333  
 ZnCl<sub>2</sub> in H<sub>2</sub>O, complexity investigation using US method 0-33326  
 ZnCl<sub>2</sub>, steam hydrolysis, for thermochem. H prod. using ZnSe cycle 0-35782  
 ZnCl<sub>2</sub>-MCl (M=Li,Na,K,Cs), melt, viscosity meas. by oscillating cylinder method (*Japanese*) 0-10696  
 ZnCl<sub>2</sub>-oil system, simulation of steel-slag, macrophotographic method of diagnosing disperse system 0-25952  
 Zn(ClO<sub>3</sub>)<sub>2</sub>·2H<sub>2</sub>O, X-ray cryst. struct. determ. 0-19759  
 Zn<sub>x</sub>Cu<sub>1-x</sub>Fe<sub>2</sub>O<sub>4</sub>, Cu, Zn substituted magnetite, domain wall resonance, mag. props. 0-15756  
 Zn<sub>0.7</sub>Co(Ni)<sub>0.3</sub>O. 1.1Al<sub>2</sub>O<sub>3</sub> powders, ZnO vaporisation from 0-16675  
 ZnCrFeO<sub>4</sub>, ferrite spinel, unsupported and SiO<sub>2</sub> supported, structural and catalytic studies 0-44191  
 ZnCr<sub>2</sub>Se<sub>4</sub>, Mn, paramagnetic, giant cubic anisotropy 0-7073  
 ZnCs<sub>2</sub>(SO<sub>4</sub>)<sub>2</sub>·6H<sub>2</sub>O:VO<sup>2+</sup>, optical absorpt. spectra obs. 0-40146  
 ZnF<sub>2</sub>, 93.3 keV Mossbauer transition in <sup>67</sup>Zn, isomer shifts 0-39978  
 ZnF<sub>2</sub>, electronic structure of outermost levels, UPS study 0-7468  
 ZnF<sub>2</sub> powder, preferred orientation, X-ray intensity corrections 0-1880  
 ZnF<sub>2</sub>:Mn, thin films, electroluminescence, brightness voltage characs. hysteresis 0-20709  
 ZnFeO<sub>4</sub>, ferrite spinel, structural and catalytic studies 0-44191  
 ZnFe<sub>2</sub>O<sub>4</sub>, heat capacity investigation of dopant effects on mag. disordering temp. 0-25143  
 ZnFe<sub>2</sub>O<sub>4</sub>-Fe<sub>2</sub>O<sub>4</sub> solid solns., form. of α-Fe<sub>2</sub>O<sub>4</sub> during oxidation 0-25889  
 Zn<sub>2</sub>Fe<sub>2</sub>O<sub>4</sub>, heat capacity investigation of dopant effects on mag. disordering temp. 0-25143  
 ZnGa<sub>2</sub>O<sub>4</sub>:Fe<sup>3+</sup> (Mn<sup>2+</sup>), EPR, spin Hamiltonian parameters 0-25195  
 ZnGeO<sub>2</sub>, HP phase transform. 0-19941  
 ZnGeP<sub>2</sub>, birefringence, effects on hydrostatic pressure and temp. 0-45033  
 ZnH<sup>+</sup>, ZnH<sub>2</sub>, relativistic (non-relativistic) HF one-centre expansion calcs. 0-52908  
 Zn(HSeO<sub>3</sub>)<sub>2</sub>·2H<sub>2</sub>O, neutron diffr. cryst. struct. determ. 0-33983  
 Zn<sub>x</sub>Hg<sub>1-x</sub>Se, band struct. from Shubnikov de Haas effect and hydrostatic press. meas. 0-49599  
 Zn<sub>x</sub>Hg<sub>1-x</sub>Se, galvanomagnetic effects, Shubnikov-de Haas oscill. determ. of band struct. 0-6884

## zinc compounds continued

- Zn<sub>x</sub>Hg<sub>1-x</sub>Te, vacancy mech. of desorption of Hg droplets 0-39070  
 ZnIn<sub>2</sub>S<sub>4</sub>, cond. and valence band states, photoemission study 0-35054  
 ZnIn<sub>2</sub>S<sub>4</sub>, electronic props. of polytypic forms, pseudopot. calc. 0-38997  
 ZnIn<sub>2</sub>S<sub>4</sub>, III(a) polytype, absorpt. spectrum tail changes due to microstructures 0-2788  
 ZnIn<sub>2</sub>S<sub>4</sub> single cryst., intense radiation effect on optical transmission, absorpt. saturation 0-53385  
 ZnIn<sub>2</sub>S<sub>4</sub> switching investigation, negative resistance state instability, resistivity transitions 0-6920  
 Zn<sub>1-x</sub>Mg<sub>x</sub>Te alloys, high purity, metallurgical and analytical methods of prep. 0-40247  
 Zn<sub>1-x</sub>Mg<sub>x</sub>Te alloys, luminesc. and elec. props. 0-2813  
 ZnMn<sub>1-x</sub>Cr<sub>x</sub>FeO<sub>4</sub>, Mossbauer effect, quadrupole splitting 0-29664  
 (ZnMn<sub>2</sub>O<sub>4</sub>)<sub>1-x</sub>(MgAl<sub>2</sub>O<sub>4</sub>)<sub>x</sub>, 0<x<1, mixed oxide spinels, chemical shifts of Mn K-absorpt. edge 0-29828  
 Zn(Mo<sub>2</sub>Re<sub>2</sub>)S<sub>8</sub>, synthesis and electrical props. of mixed tetrahedral cluster phases 0-2971  
 ZnMoS<sub>8</sub>, mixed Chevrel phases, crystallography 0-39038  
 Zn<sub>1-x</sub>Ni<sub>x</sub>Fe<sub>2</sub>O<sub>4</sub>, heat treatment and sintering effect on porosity 0-25610  
 Zn<sub>0.91</sub>Ni<sub>0.09</sub>Fe<sub>2</sub>O<sub>4</sub>, Mossbauer spectra, mag. hyperfine struct. 0-15877  
 ZnO, 93.3 keV Mossbauer transition in <sup>67</sup>Zn, isomer shifts 0-39978  
 ZnO absorbers, <sup>67</sup>Zn isomer shift 0-39920  
 ZnO, accumulation layer, ESR and NMR studies of adsorbed H<sub>2</sub> (*Japanese*) 0-50186  
 ZnO additive for celsian ceramics, props. obs. (*Bulgarian*) 0-50579  
 ZnO, adsorption of Br<sub>2</sub> and I<sub>2</sub>, γ-irrad. induced centres 0-54513  
 ZnO, biexciton levels, luminescence-assisted two-photon spectra 0-29795  
 ZnO ceramic, nonohmic, drift phenomena of capacitance and current 0-39587  
 ZnO, chemical effect, influence on stopping power 0-47830  
 ZnO crystals, adsorbed dye laser, charge transfer, field effect and spectrally sensitised photocond. meas. 0-49815  
 ZnO crystals, SEM study (*German*) 0-33860  
 ZnO, dye adsorption, contact pot. difference 0-27365  
 ZnO, effect on props. of PbO containing cryst. glass 0-24637  
 ZnO, effect on viscosity of PbO containing crystal glasses 0-19973  
 ZnO, elec. cond. and oxidation kinetics of Zn in O<sub>2</sub>-CO<sub>2</sub>-SO<sub>2</sub> gas mixture 0-34448  
 ZnO, electric field dependence of photoconductivity (*Russian*) 0-49821  
 ZnO, electron irradi. damage, orientation depend. 0-2075  
 ZnO epitaxial film, ionized-cluster beam and reactive ionized-cluster beam deposition, cathodolum. characterisation 0-16202  
 ZnO epitaxial film on Al<sub>2</sub>O<sub>3</sub> substrate, recombination radiation in intense single photon excitation 0-7410  
 ZnO, excited states of bound excitons, photoluminesc. obs. 0-44513  
 ZnO, excitonic mol. transitions, optical gain and induced absorpt. spectra 0-11438  
 ZnO fibre reinforced elastomer, X-ray diffr. exam. of filamentary crystal distrib. 0-7738  
 ZnO film, prep. by reactive ionized cluster beam deposition, and characterisation 0-10829  
 ZnO, film for solar cell appl. structural, optical and elec. props. 0-2294  
 ZnO, growth rate, sublimation rate and etching behaviour along polar axis 0-24387  
 ZnO layers, electrophotographic processes 0-4802  
 ZnO, multiparticle exciton complexes, luminesc. spectra (*Russian*) 0-16090  
 ZnO, photodesorption of CO<sub>2</sub>, pulsed-laser-dynamic-mass-spectrometer study 0-35568  
 ZnO, piezoelec. films produced by gas transport reaction, US excitation efficiency 0-2700  
 ZnO, plasmochemical synthesis, oxidised from metals, exam. of props. 0-2984  
 ZnO, polar semiconductor, electron-hole liquid, electron-phonon interactions 0-6739  
 ZnO, polariton dispersion, IR reflection spectroscopy 0-11415  
 ZnO powders, electron-beam-induced desorption, phase-sensitive detection 0-54502  
 ZnO powders, UV luminesc. spectral distrib., comparison with single crystals, excitons role 0-55167  
 ZnO single cryst., UV laser, electron beam excited 0-53304  
 ZnO sintered electrode, for dye-sensitive solar photocell 0-16816  
 ZnO, small crystal, surface phonon modes, IR transmission spectra 0-11398  
 ZnO, structure parameters and polarity, X-ray diffr. meas. 0-19781  
 ZnO substrate, for Ni films, band bending, UPS study 0-7472  
 ZnO, surface phonon-phonon coupling (surface plasmons) 0-54497  
 ZnO thin film SAW devices, for HF range (*Japanese*) 0-53598  
 ZnO, two photon spectra, quantitative investigation temp. depend. 0-50373  
 ZnO, two-photon-excitation, tunable laser emission, luminesc. processes 0-55127  
 ZnO vaporisation from defective spinel powders, in vac. 0-16675  
 ZnO varistors, statistics and grain size effects on breakdown characs. 0-34010  
 ZnO, X-ray diffuse scattering 0-14964  
 ZnO:<sup>31</sup>P<sup>+</sup> implanted nonlinear resistor production and characteristics (*Russian*) 0-49252  
 ZnO-B<sub>2</sub>O<sub>3</sub>:Cu<sup>2+</sup>, glasses, ESR and optical absorpt. 0-34760  
 ZnO-based ceramic microstructure and nonlinear props., B diffusion effects (*Russian*) 0-49423  
 ZnO-based varistor, grain-boundary segregation, thin film X-ray spectroscopy obs. 0-35185  
 ZnO-Bi<sub>2</sub>O<sub>3</sub>-CoO-MnO-Sb<sub>2</sub>O<sub>3</sub> (97.5, 0.5, 0.5, 1.0 mole%), exam. of elec. props. at different annealing temps. 0-3099  
 ZnO-GeO<sub>2</sub>-MnO-B<sub>2</sub>O<sub>3</sub> wideband cathodoluminescent phosphor 0-55196  
 ZnO-NiO-Li<sub>2</sub>O n-p heterojunction, contact resist., effects of water vapour 0-34506  
 ZnO-Pd Schottky-barrier diode, H<sub>2</sub> sensitivity 0-11085  
 ZnO-SiO<sub>2</sub> system, struct. and phase comp. of luminescent Zn orthosilicate 0-19951  
 ZnO-TeO<sub>2</sub>, cryst. chem. study, X-ray diffr. powder data (*French*) 0-15080  
 ZnO-Ti transparent type MIS solar cells 0-45662  
 Zn<sub>2</sub>(BO<sub>3</sub>)<sub>2</sub>:Tb, phosphoresc. study (*Spanish*) 0-16105  
 α-ZnP<sub>2</sub>, local centre parameters, photoelectron transition scheme, recomb. process anal. 0-44654  
 ZnP<sub>2</sub>, second-order vibr. spectra and dispersion of phonon branches 0-25376  
 ZnP<sub>2</sub>, sublimation 0-34181



## zinc compounds continued

- ZnP<sub>2</sub> tetragonal crystals, light scatt. by optic phonons 0-55116  
 ZnP<sub>2</sub>:As, local vibrs. of impurity ions, Raman study 0-29745  
 Zn<sub>3</sub>P<sub>2</sub> bulk and thin film, UV reflectivity spectra, photovoltaic effects, optical consts. 0-25472  
 Zn<sub>3</sub>P<sub>2</sub>, direct and indirect optical transitions, metal-Zn<sub>3</sub>P<sub>2</sub> contact photo-voltage response 0-25402  
 Zn<sub>3</sub>P<sub>2</sub>, single crystal, growth, electronic and device props. 0-25551  
 Zn<sub>3</sub>P<sub>2</sub>, stoichiometry deviation from phase diagram 0-35164  
 Zn(PO<sub>3</sub>)<sub>2</sub>, vitreous, microhardness 0-25864  
 Zn(S,Se), large single crystals, vapour growth and defect characterisation 0-25540  
 ZnS 0-35096  
 ZnS, <sup>57</sup>Co gamma source, time depend. Mossbauer spectra 0-50245  
 ZnS, 93.3 keV Mossbauer transition in <sup>67</sup>Zn, isomer shifts 0-39978  
 ZnS, antireflection coating, 100 ns pulsed laser damage at 2.7 and 3.8  $\mu$ m 0-33057  
 ZnS antireflection coatings on solar cells 0-43414  
 ZnS, band structure calcs. by modified orthogonalised plane wave (MOPW) method 0-54609  
 ZnS, Bridgeman growth under pressure, macroscopic inclusions and defects 0-45226  
 ZnS CVD IR material specifications 0-48364  
 ZnS CVD window, IR lattice absorption, phonon assignments and image spoiling 0-33104  
 ZnS, clean surface, AES and LEED exam. 0-10762  
 ZnS, cubic, IR-active phonons obs. 0-55084  
 ZnS, cubic crystals, having substitutional elastic distortion centres, diffuse X-ray scattering 0-24302  
 ZnS, electroluminescent emission, UV excitation after effects 0-45144  
 ZnS, epitaxial growth, appl. to electronic devices, review (*Japanese*) 0-55281  
 ZnS epitaxial layers, growth kinetics on CaF<sub>2</sub> by vapour phase transport (*French*) 0-54572  
 ZnS, excited phosphor, IR stimulation and quenching of luminesc., review (*Russian*) 0-11455  
 ZnS film production, for luminophors, method and apparatus (*Bulgarian*) 0-7499  
 ZnS films prepared by thermal evaporation in vac., nature of defects 0-10835  
 ZnS, gas, identification by high-temp. mass spectrometry 0-45593  
 ZnS, growth rate, sublimation rate and etching behaviour along polar axis 0-24387  
 ZnS, inhomogeneous interface laser mirror coatings 0-1252  
 ZnS, large single crystals, vapour growth and defect characterisation 0-25540  
 ZnS, laser irradiated, in-depth and surface temp. meas. by Moire-Schlieren technique 0-53392  
 ZnS layer, spectrophotometer-type filters of highest possible performance, 2.5-40  $\mu$ m 0-14438  
 ZnS, luminescence of M-centre 0-29779  
 ZnS, phosphor, voltage and temp. dependence of pre-breakdown electroluminescence 0-45147  
 ZnS, phosphor, voltage depend. of electrolum. brightness 0-45148  
 ZnS, second order Raman scatt., lattice dynamical calc. and expt. 0-25370  
 ZnS single cryst., UV laser, electron beam excited 0-53304  
 ZnS, single crystals, excited by laser beam and elec. field, streamer luminesc. and photolum. obs. 0-34986  
 ZnS, time differentiated Mossbauer spectra from <sup>57</sup>Co impurities, relaxation processes (*Russian*) 0-34834  
 ZnS, wurtzite, ZnO solubility, 1444-1240°C 0-15248  
 ZnS, X-ray diffuse scattering 0-14964  
 ZnS, ZnS-CeF<sub>3</sub>, single-layer vac. antirefl. coatings for near IR spectral region 0-33099  
 ZnS:Ag, luminesc. efficiency deterioration due to surface oxidation by (NH<sub>4</sub>)<sub>2</sub>Cr<sub>2</sub>O<sub>7</sub> thermal decomp. 0-29810  
 ZnS:Ag, phosphor, luminesc. of surface glow centres 0-29782  
 ZnS:Ag, single crystal, ionisation mechanism of field trapping centres 0-45156  
 ZnS:Ag, TSC and induced impurity photoconductivity, existence of two electron trapping centres 0-44655  
 ZnS:Ag,Cl, embedded in H<sub>2</sub>BO<sub>3</sub>-glass matrix, blue electrolum. 0-55195  
 ZnS:Al,Cu(Ag) phosphors, luminesc. excitation spectra and exciton struct. 0-55164  
 ZnS:Al(Te) phosphors, luminesc. excitation spectra and exciton struct. 0-55165  
 ZnS:Cl, shape of self-activated cathodoluminesc. band 0-34987  
 ZnS:Co Mossbauer source, Fe<sup>2+</sup> abnormal populations and vibronic props. 0-15912  
 ZnS:Cr<sup>2+</sup>, Cr<sup>2+</sup> <sup>5</sup>T<sub>2</sub> and <sup>5</sup>E states, Jahn-Teller effect calcs. 0-39539  
 ZnS:Cr<sup>2+</sup>, photoionisation, lattice relaxation energy 0-6778  
 ZnS:Cu crystallophosphors, spectra of IR electrophotographic sensitivity (*Russian*) 0-50423  
 ZnS:Er<sup>3+</sup>, ion-implanted, annealing, cathodolum. obs. 0-2868  
 ZnS:Fe, luminesc. and ESR investigations 0-2822  
 ZnS:Fe<sup>2+</sup>, relax. meas. from Mossbauer absorber and source expts. 0-39956  
 ZnS:Fe<sup>2+</sup>, spin-lattice relax., expt. evidence for optical phonons 0-20451  
 ZnS:Mn, dopant conc. effect on stacking fault energy 0-2041  
 ZnS:Mn, self-activated and Mn<sup>2+</sup> emission, high press. action 0-16093  
 ZnS:Mn AC thin film electrolum. device, filament behaviour 0-20712  
 ZnS:Mn co-deposited electrolum. thin film device, phys. and elec. characterisation 0-20713  
 ZnS:Mn Schottky diodes, reverse-biased, electroluminescence, hot electron impact excitations 0-25005  
 ZnS:Mn<sup>2+</sup>, <sup>4</sup>T<sub>2</sub> level, Zeeman splittings, Jahn-Teller effect 0-40141  
 ZnS:Mn<sup>2+</sup>, spin-lattice relaxation, EPR, optical phonons 0-39852  
 ZnS:Mn<sup>2+</sup> phosphors, luminesc. excitation spectra and exciton struct. 0-55164  
 ZnS:Ne, implanted single crystals, photolum. and bombardment effect, thermolum. curve obs. 0-55166  
 ZnS:Pb phosphor, ionisation mechanism of field trapping centres 0-45156  
 ZnS:Tb<sup>3+</sup>, NdF<sub>3</sub> film, vac. deposited, electrolum. energy transfer 0-2861  
 ZnS:TbF<sub>3</sub> film between semicond. Y<sub>2</sub>O<sub>3</sub> layers, bright green electrolum. 0-2859  
 ZnS-CdS, equimolar solid soln. formation kinetics 0-39289  
 ZnS-CdS films, prep. by atomisation 0-16176  
 ZnS-CdS:Ag, Ni luminophor, temp. sensitive, biological effects of micro-waves determ. appl. 0-36186  
 ZnS-GaAs solar cell structs., photolum. props. 0-50958

## zinc compounds continued

- ZnS-metal interface, metal-induced chem. reactions and surface states 0-20311  
 ZnS-metal interface in MIM struct., photoexcitation level assignment (*French*) 0-15622  
 ZnS-metal Schottky barrier height rel. to chem. reactivity 0-25008  
 ZnS-MnS-CuInS<sub>2</sub>, subsolidus equilib., phase diagrams 0-3016  
 ZnS-Na<sub>2</sub>O-K<sub>2</sub>O-SiO<sub>2</sub>, form. using electric furnace, furnace design 0-11620  
 ZnS-SrF, multilayer dielec. coatings, radiation breakdown and microinhomogeneities 0-7294  
 ZnSO<sub>4</sub>.7H<sub>2</sub>O, meas. of water physically adsorbed rel. to water of crystallisation (*Japanese*) 0-6622  
 ZnS(Se), reaction with Sn chalcogenides, thermodynamic anal. 0-40728  
 ZnS(Se):Mn<sup>2+</sup>, <sup>4</sup>E levels, orbit-lattice interaction and Jahn Teller effect 0-24860  
 ZnS,Se<sub>1-x</sub>, epitaxial film on CaF<sub>2</sub>, comp. and temp. depend. of fund. band gap 0-11115  
 ZnS,Se<sub>1-x</sub>, VPE, characterisation of defect centres by photoelectronic meas. 0-10914  
 ZnS(Se)(Te):Co<sup>2+</sup>, IR luminesc. quenching, Co<sup>2+</sup> level position, ionisation energy 0-16079  
 ZnSb, enthalpy of formation (*Russian*) 0-35564  
 ZnSb, epitaxial films, growing conditions effect on elec. cond., thermo-EMF 0-39687  
 ZnSb, layer growth in Zn-Sb diffusion couple at high press., elec. meas. 0-2218  
 ZnSe, 93.3 keV Mossbauer transition in <sup>67</sup>Zn, isomer shifts 0-39978  
 ZnSe, Bridgeman growth under pressure, macroscopic inclusions and defects 0-45226  
 ZnSe CVD IR material specifications 0-48364  
 ZnSe, clean and oxidised surfaces, surface states, low-energy EELS study 0-11522  
 ZnSe coatings on CaF<sub>2</sub> laser windows, photoacoustic spectroscopy 0-33052  
 ZnSe, cryst., elec. cond., dislocation motion effects 0-54710  
 ZnSe crystal, exciton reflection spectra, control of exciton-free surface layer thickness 0-7373  
 ZnSe crystal, refr. index temp. increments meas. 0-33098  
 n-ZnSe crystals, electron scatt. mechanisms, high mobility 0-34433  
 ZnSe, cubic monocrystal, electron-phonon interaction, low temp. luminesc. (*Russian*) 0-25451  
 ZnSe, electronic structure, self consistent local description 0-20067  
 ZnSe epitaxial layers, prep. by chem. transport reactions 0-16192  
 ZnSe epitaxial layers, growth kinetics on CaF<sub>2</sub> by vapour phase transport (*French*) 0-54572  
 ZnSe, film, hopping cond. 0-2499  
 ZnSe, Gudden-Pohl effect, release of electrons from traps 0-45149  
 ZnSe, inhomogeneous interface laser mirror coatings 0-1252  
 ZnSe, ionisation energy of H-like impurities 0-20120  
 ZnSe, laser irradiated, in-depth and surface temp. meas. by Moire-Schlieren technique 0-53392  
 ZnSe laser window photoacoustic spectroscopy 0-33052  
 ZnSe, lattice vibration, thermal expansion and pressure effect 0-39233  
 n-ZnSe, long persistent cond. relax. and frozen cond. 0-54735  
 ZnSe, moments of phonon spectra from specific heats 0-15203  
 ZnSe, polar semicond., radiative recomb., electron-phonon interaction effects, calc. 0-49631  
 ZnSe, relaxation processes in Raman scattering and exciton luminescence under resonant excitation 0-25386  
 ZnSe, second order Raman scatt., lattice dynamical calc. and expt. 0-25370  
 ZnSe single cryst. for LED, heat treatment effects on elec. props. 0-29406  
 ZnSe thermochem. cycle for H prod., chemical and process design studies 0-35782  
 ZnSe, two-photon and two-step absorption of light 0-7389  
 ZnSe:Cr, piezodichroism due to reorientation of Jahn-Teller centres 0-11363  
 ZnSe:Cr<sup>2+</sup>, Cr<sup>2+</sup> <sup>5</sup>T<sub>2</sub> and <sup>5</sup>E states, Jahn-Teller effect calcs. 0-39539  
 ZnSe:Cr<sup>2+</sup>, photoionisation, lattice relaxation energy 0-6778  
 ZnSe:Cu, deep energy levels 0-6774  
 ZnSe:Cu, discovery of bound exciton, electroabsorption 0-45038  
 ZnSe:Cu, I ceramic, injection electroluminesc. of p-n microjunctions 0-40163  
 ZnSe:Ga,As, characts. of simultaneous incorporation, by Mn<sup>2+</sup> ESR and X-ray fluoresc. anal. 0-34017  
 ZnSe:Ga(As), edge luminesc. 0-20699  
 ZnSeI/aqueous electrolyte junction, electrochem. behaviour in dark and under illum. 0-25003  
 ZnSe:In films, MBE growth, doping effect on photoluminesc. 0-10818  
 ZnSe:Li(Na)(Ga) doped and pure cryst., donor-acceptor bands 0-11465  
 ZnSe:Ni, evidence for exciton binding at Ni impurity sites, photolum. excitation spectrum 0-45135  
 ZnSe-GaAs narrow junction lasers 0-43334  
 ZnSe-Ge (100) interface, electronic struct. calc., scattering theoretic approach 0-6940  
 ZnSe-metal Schottky barrier height rel. to chem. reactivity 0-25008  
 (ZnSe)<sub>1-x</sub>(GaAs)<sub>x</sub> solid solns., photoluminescence spectra 0-40159  
 ZnSiAs<sub>2</sub>, birefringence, effects on hydrostatic pressure and temp. 0-45033  
 ZnSiF<sub>6</sub>.6H<sub>2</sub>O:Mn<sup>2+</sup>, ESR spectrum, effect of uniaxial compression 0-29609  
 ZnSiF<sub>6</sub>.6H<sub>2</sub>O, spin-phonon interaction between Ni<sup>2+</sup> ions, phonon bottleneck effects, splitting parameters (*Russian*) 0-15796  
 ZnSiF<sub>6</sub>.6H<sub>2</sub>O:V<sup>2+</sup>, spin-lattice relax. at normal and high press. 0-2632  
 ZnSiO<sub>3</sub>, HP phase transform. 0-19941  
 Zn<sub>2</sub>SiO<sub>4</sub>:Mn film, electron beam depth-dose functions, cathodoluminesc. 0-2867  
 Zn<sub>2</sub>SiO<sub>4</sub>:Mn phosphor, efficiency enhancement by AlPO<sub>4</sub> substitution 0-11452  
 Zn<sub>4</sub>Si<sub>2</sub>O<sub>7</sub>(OH)<sub>2</sub>.H<sub>2</sub>O, hemimorphite, phase-angle determ. by anomalous X-ray scattering with 4-circle SSD diffractometer 0-49188  
 ZnSiP<sub>2</sub>, birefringence, effects on hydrostatic pressure and temp. 0-45033  
 ZnSiP<sub>2</sub>, crystal growth, DTA obs. of Sn-Zn-ZnSiP<sub>2</sub> phase diagram 0-24394  
 ZnSiP<sub>2</sub>, pseudodirect chalcopyrite semicond., electronic band struct. 0-20079  
 ZnSiP<sub>2</sub>, reflectance spectra at 300K 0-25407  
 ZnSiP<sub>2</sub>-In Schottky diode, photovoltaic spectra 0-2423



**zinc compounds continued**

- ZnTe, relaxation processes in Raman scattering and exciton luminescence under resonant excitation 0-25386  
 ZnTe, 93.3 keV Mossbauer transition in  $^{67}\text{Zn}$ , isomer shifts 0-39978  
 ZnTe (110) surface struct. determ. by LEED, UPS, and EPR 0-49475  
 ZnTe, clean and oxidised surfaces, surface states, low-energy EELS study 0-11522  
 ZnTe crystals, secondary radiation polarization and relaxation of optical excitation 0-11399  
 ZnTe, dominant acceptors, annealing and quenching 0-24463  
 ZnTe, effects of Zn anneals in 400-550°C range on acceptor conc. 0-10571  
 ZnTe, elec., SEM and TEM studies of impurity segregation during long annealing 0-30001  
 ZnTe, electron-phonon coupling, donor-acceptor pairs selective excitation 0-11475  
 ZnTe, extrinsic luminesc., bands, temp. injection level, and freq. depend. 0-20714  
 ZnTe film preparation and props., by single-source vacuum deposition method (*Japanese*) 0-6664  
 ZnTe films, grown on glass using atomic layer evaporation 0-44453  
 ZnTe, gas, identification by high-temp. mass spectrometry 0-45593  
 ZnTe, lattice vibration, thermal expansion and pressure effect 0-39233  
 ZnTe, luminesc., donor-acceptor-pair excitation spectroscopy 0-25456  
 ZnTe, luminescence spectra struct. surface and volume polaritons (*Russian*) 0-16089  
 ZnTe, moments of phonon spectra from specific heats 0-15203  
 ZnTe, nonlinear magnetoelec. susceptibility, three-dimens. model 0-39845  
 ZnTe, photoinduced dielec. loss and capacitance changes, rel. to space charge polarisation 0-2417  
 ZnTe, polymorphism at elevated temp., elec. resist. and X-ray diffr. under press. 0-49359  
 ZnTe, real structure effect on luminescence and absorption spectra, dislocations 0-16085  
 ZnTe, refined, undoped, Cu acceptor, optical absorption and photoluminesc. meas. 0-34970  
 ZnTe, reflectivity meas., double beam wavelength modulated technique (*Korean*) 0-50365  
 ZnTe, resonance Raman scatt. at high excitation levels (*Russian*) 0-55109  
 ZnTe, second order Raman scatt., lattice dynamical calc. and expt. 0-25370  
 ZnTe, TEM obs. of precipitates, shape of Te solidus line 0-25703  
 ZnTe thin film, model for off-on transition 0-54742  
 ZnTe, unalloyed, photoluminesc., mechanism of radiative transitions 0-50405  
 ZnTe, undoped, electroreflectance of fundamental edge, exciton levels (*Japanese*) 0-20612  
 ZnTe, valence band parameters and free exciton reduced mass, free exciton magnetorefectance 0-45046  
 ZnTe:Ag, doped during growth and by diffusion, defect form. 0-15129  
 ZnTe:Ag, real structure effect on luminescence and absorption spectra, dislocations 0-16085  
 ZnTe:Al,Cl, photolum., complex acceptor, ionization energy 0-20693  
 ZnTe:As(Li), donor-acceptor pair excitation and recomb., photoluminesc. obs. 0-20691  
 ZnTe:Cr $^{2+}$ , Cr $^{2+}$   $^5\text{T}_2$  and  $^5\text{E}$  states, Jahn-Teller effect calcs. 0-39539  
 ZnTe:Cr(Mn)(Fe), exciton refl. spectra 0-2806  
 ZnTe:Cu, precipitates, electron microscopic investigation 0-45312  
 ZnTe:Cu, red centre, electric and optical props. 0-20239  
 ZnTe:Li, diffusion investigation by SEM and TEM 0-10706  
 ZnTe:Li, impurity segregation during short annealing and quenching, SEM, TEM and elec. meas. 0-10676  
 ZnTe:Li, Li in Te precipitates, diffusion during thermal anneal 0-39358  
 ZnTe:Mn, ordering mechanism 0-2572  
 ZnTe:P, pure and doped, electron and exciton excited states of neutral donor 0-34393  
 (ZnTe) $_{1-x}$ (ZnSe) $_x$ , diamond-type semiconductor, Mossbauer spectra, quadrupole interaction of  $^{125}\text{Te}$  0-44992  
 ZnTe:Se $_{1-x}$ , Raman phonon spectra, resonance interaction effect 0-25375  
 ZnTiO $_3$ , HP phase transform. 0-19941  
 ZnU $_2$ nH $_2$ O, cryst. struct. (*German*) 0-1987  
 Zn $_3$ (VO $_4$ ) $_2$ , determination of enthalpies of formation, from heats of solution 0-2182  
 Zn $^{2+}$ .CO $_2$ .H $_2$ O clusters, solvation, Monte Carlo simulation 0-44102  
 Zns, vacuum deposited, destruction props. obs., suitability for integrated optics assessment (*Slovak*) 0-33224

**zirconium**

- see also nuclei with .....  
 adsorption on W (100), AES, LEED, thermal desorption, and work function meas. 0-39444  
 alloying addition in Mg-Y-Zn-Nd-Cd alloy, influence on struct. and mech. props. (*Russian*) 0-40370  
 annealed, high-temp., kinetics (*Russian*) 0-21166  
 BCC, phonon vibr., pseudopot. method 0-15204  
 cast iron-steel mixture, interaction of Zr, formation reaction thermodynamics (*Russian*) 0-55645  
 coadsorption with O $_2$  on W (100) 0-6653  
 de Haas-van Alphen studies in high mag. fields, Fermi surface model 0-6702  
 deuteron irradiated, 10 keV, retention and precipitation 0-34099  
 diffusion and solubility of H in  $\beta$ -Zr, above 1000°C and below  $1 \times 10^{-4}$  mm Hg (*Russian*) 0-24671  
 electrochemical pitting in alkaline chloride soln., H $_2$  evolution and anodic disintegration 0-16553  
 embrittlement in I $_2$ , environmental purity effect 0-30149  
 integral emittance, during high temp. heating and oxidation (*Russian*) 0-39327  
 magnetic form factor, field-induced, polarised neutron scatt. meas. 0-50044  
 monocrystal perfection using Berg method and diffractometer with omega device for  $\alpha$ -phase (*French*) 0-2035  
 nuclear fuel element sheathing, reliability, including hydration process, probabilistic model (*Russian*) 0-52742  
 nuclear steam superheating, design tests of Zr channels 0-5211  
 $\beta$ - $\alpha$  phase transformation, cooling rate effects 0-7565  
 point defect migration into dislocation loops, finite difference calc. 0-54225  
 polycrystals with axial texture, heterogeneity of props. (*Russian*) 0-29192

**zirconium continued**

- proton irradiation, 10 to 16 MeV, isochronal annealing meas. 0-2083  
 proton irradiation, 10 to 16 MeV, resistivity changes 0-2082  
 RF sputter deposition, ion bombardment and ion implantation 0-25564  
 rolling texture formation, computer simulation in HCP and orthorhombic metals 0-3095  
 surface structure, (0001) face, HCP phase, LEED study 0-20017  
 vacuum technology appl., melt processing and appl. (*Hungarian*) 0-55318  
 X-ray emission spectrum, K-satellites 0-40188  
 X-ray M $_2^s$  energy, revised values 0-14102  
 Zn-salt, molten system, separation of Hf and Zr 0-11884  
 H terminal solid solubility, in  $\alpha$ -Zr, optical metallographic study 0-34195  
 LiNbO $_3$ :Co $^{2+}$ , Zr $^{4+}$  films, LPE growth from Li $_2$ O-V $_2$ O $_5$  flux, X-ray and acoustic characterisation 0-15383  
 NbSe $_3$ :Zr, dopant effect on supercond. transition temp. rel. to CDW 0-39699  
 Si $_3$ N $_4$ /Zr laminates, metal to ceramic joints, adherence props. 0-45386  
 T diffusion coeff. deter. 0-15306  
 $\beta$ -Zr, Cr diffusion rates in temp. range 914 to 1240°C 0-15304  
 $\alpha$ -Zr, electrolytic polishing optimal condition determ. from anodic impedance meas. (*French*) 0-3250  
 $\alpha$ -Zr, grain-boundary sliding component in high temp. fatigue 0-50706  
 $\alpha$ -Zr, some stress change expts. on creep 0-3125  
 Zr XII, energy level system, spectrum obs. 70 to 630 Å 0-37766  
 Zr XXXI, XXXII, XXXIII, transition identification X-ray spectra 0-32648  
 Zr+H $^+$ , K-shell ionisation cross-section determ. 0-48077

**zirconium alloys**

## see also zirconium compounds

- embrittlement in I $_2$ , environmental purity effect 0-30149  
 $\beta$ - $\alpha$  phase transformation, cooling rate effects 0-7565  
 plasma-sprayed thermal barrier coatings, evaluation 0-40619  
 steel, stainless, oxidation effect of Zr 0-35394  
 wear due to fretting and periodic impacting 0-16509  
 Zircaloy, design and performance evaluation of All-Zircaloy fuel assemblies for PWR 0-13560  
 Zircaloy, H absorption, Sn(Fe)(Cr)(Ni) effect 0-49527  
 Zircaloy, PWR primary corrosion products 0-13578  
 Zircaloy clad UO $_2$  fuel elements, irradi. effects 0-666  
 Zircaloy cladding, stress corrosion cracking due to I and Cs redistrib. in LWR fuel rods 0-32343  
 Zircaloy cladding, stresses due to pellet cladding interaction 0-42762  
 Zircaloy cladding ballooning, analytical model for transient gas flow in LWR 0-18499  
 Zircaloy cladding thermal failure and UO $_2$  fuel melting during LWR PCM transient 0-42834  
 Zircaloy claddings, PWR fuel assemblies, LOCA behaviour in multirod burst tests 0-27739  
 Zircaloy fuel cladding, azimuthal temp. distrib. during LOCA 0-662  
 Zircaloy fuel claddings, multirod burst tests following PWR LOCA 0-777  
 Zircaloy oxidation, improved evaluation model 0-32349  
 Zircaloy PWR fuel cladding, balloon deformation during LOCA 0-659  
 Zircaloy reactor fuel cladding tubes, high temp. deformation model with nonlinear temps. 0-661  
 Zircaloy sheathed UO $_2$  combustibles, CEA expt. on transient behaviour (*French*) 0-18417  
 Zircaloy tubing, I $_2$  stress corrosion cracking, pellet cladding interaction mechanism (*German*) 0-16565  
 Zircaloy-2, cold worked, temp. cycling effects on irradiation growth 0-2079  
 Zircaloy-2, effect of simulated fission products on elongation fractography and metallography 0-649  
 Zircaloy-2, effects of simulated fission products on mechanical props. 0-52740  
 Zircaloy-2, electrochemical pitting in alkaline chloride soln., H $_2$  evolution and anodic disintegration 0-16553  
 Zircaloy-2, I $_2$  stress corrosion cracking, Cs $_2$ O and Cs influence, in- and out-of-pile 0-3252  
 Zircaloy-2, iodine environment, plane strain tension test 0-22944  
 Zircaloy-2, neutron irradiated, inhomogeneous deformation behaviour 0-50679  
 Zircaloy-2, tritium diffusion 0-32341  
 Zircaloy-2 and -4, (c) component dislocations from TEM contrast expts. 0-6412  
 Zircaloy-2 claddings, oxidation reaction kinetics in steam environment in temp. range 1273-1673K 0-35401  
 Zircaloy-4,  $\beta$ -transformed, flow stress and dynamic strain ageing 0-3101  
 Zircaloy-4, anomalous oxide growth during transient temp. oxidation 0-50773  
 Zircaloy-4, CANDU irradi. fuel bundles storage, long-term stability investigation 0-13774  
 Zircaloy-4, heat treatment in SiO $_2$  capsules, vapour transport of Zr and Si 0-55437  
 Zircaloy-4, in-pile PWR creep meas., comparative eval. of 10 creep correl. 0-652  
 Zircaloy-4, microstrain and particle size meas. by Warren-Averbach method 0-55420  
 Zircaloy-4, oxidation in steam, 900-1500°C, kinetics 0-3241  
 Zircaloy-4, tensional stress cycling 0-3168  
 Zircaloy-4 cladding rubes, burst strain and stress corrosion cracking, I influence 0-3248  
 Zircaloy-4 fuel cladding axial deform. in PWR LOCA 0-13585  
 Zircaloy-4 tubes, texture influence on anal. of thermoelastic/plastic anisotropy and initial yielding 0-35260  
 Zircaloy-O $_2$  phase diagram 0-3003  
 Zircaloy-UO $_2$  fuel rods, eddy-current testing of claddings using encircling and probe coils 0-21245  
 Zircaloy-Z, thermal diffusion of H, numerical soln. with computer (*Korean*) 0-19989  
 Al-Cu-Zr, superplastic alloy Supral, solidification and recrystallisation 0-7550  
 Al-Cu-Zr (6, 0.4 wt.%), superplastic flow activation energy 0-11701  
 Al-Cu-Zr (6, 0.4 wt.%), superplastic deformation characts. 0-16387  
 Al-Zn-Mg-(Zr) alloy, microstruct. effect on fatigue crack growth 0-3164  
 Al-Zr, simultaneous recrystallisation and precipitation (*French*) 0-16313  
 Au-Zr, dil., Friedel-d-reson. scatt. and elec. resists. 0-44566  
 Cu-Zr-(Cr), powder metallurgical alloys, thermomech. treatment effect on props. 0-50660



## zirconium alloys continued

- Co-Zr, dil., mag. annealing effect, depend. of uniaxial mag. anisotropy on Zr conc. 0-39772
- Co-Zr-Er alloys, mag. annealing effect, effect of Er on induced uniaxial mag. anisotropy 0-39771
- Cu-Zr, metallic glasses, valence band struct. investigation 0-11533
- Cu-Zr alloys, isothermal transformation diagram 0-20902
- Cu<sub>46</sub>Zr<sub>54</sub>, devitrification effect on mech. props. 0-30082
- Cu<sub>46</sub>Zr<sub>54</sub>, metallic glass, dynamical struct. factor and freq. distrib. meas. 0-54136
- Cu<sub>50</sub>Zr<sub>50</sub>, metallic glass, internal friction peaks 0-25753
- Cu<sub>56</sub>Zr<sub>44</sub>, metallic glass, devitrification and its effect on mech. props. 0-33893
- Cu<sub>60</sub>Zr<sub>40</sub>, amorphous powder, production using gas-water atomisation unit 0-7518
- Cu<sub>60</sub>Zr<sub>40</sub>, metallic glass, composition, mech. props., simulation 0-49117
- Mo-Ti-Zr, alloy TZM, polycrystalline, anal. of elastic anisotropy and microyielding 0-30050
- Mo-Ti-Zr, D trapping in fusion reactor materials, temp. dependence 0-37577
- Mo-Ti-Zr, fusion reactor first wall material, compatibility with impure He 0-32469
- Mo-Ti-Zr (0.5, 0.1 wt.%), neutron irradiated, void swelling and shrinkage, TEM study 0-34079
- Mo-Ti-Zr (0.5, 0.7 wt.%) alloy TZM, props. and appl. (German) 0-21040
- Mo-Zr, heavy ion irradiated, void swelling, phase instability 0-29084
- Mo-Zr-B, neutron irradi. at 780-1080°C, porosity, hardening and embrittlement (Russian) 0-29062
- Mo-Zr-B, porosity and mech. props. after neutron bombard., 780-1080°C (Russian) 0-24502
- Nb-Mo-Ti-Zr-C, work function temp. and phase depend. (Russian) 0-2449
- Nb-Ti-Zr, superconducting wire, coil simulation meas. of losses and instabilities 0-37050
- Nb-W-Mo-Zr, long-term strength props., vac. level effect 0-55484
- Nb-W-Mo-Zr-C, strength and ductility, prolonged high-temp. soaking effect 0-55483
- Nb-W-Zr-Ta, long-term strength props., vac. level effect 0-55484
- Nb-Zn-N alloys, Zr-N complex formation, internal friction temp. depend. (Russian) 0-54311
- Nb-Zr, acoustic phonon anomalies and superstructure, neutron inelastic scatt. meas. 0-19892
- Nb-Zr, fusion reactor first wall materials, compatibility with impure He 0-32469
- Nb-Zr, nitriding, diffusive saturation, lattice spacing and activation coeffs. (Russian) 0-21168
- Nb-Zr (1 at.%), annealed, TEM study of ion implanted irregular He bubbles 0-15164
- Nb-Zr (1 wt.%), fusion reactor blanket struct. material, low cycle fatigue behaviour 0-30073
- Nb-Zr (1.5 wt.%) alloy, field ion microscopy investigation, surface struct. 0-45220
- Nb-Zr-C, plastic deform. and annealing, dislocation struct. (Russian) 0-20951
- Nb-Zr-C (0.1, 0.01 wt.%) plastic deform. influence on electronic state of Nb atoms 0-40463
- Nb<sub>0.75</sub>Zr<sub>0.25</sub>, effect of force constant, disorder on Eliashberg function 0-29504
- Nb<sub>20</sub>Zr<sub>80</sub>, supercond., US attenuation 0-44766
- (Nb<sub>0.99</sub>Zr<sub>0.01</sub>)<sub>1-x</sub>Ge<sub>x</sub>, supercond., mag. field props. 0-54822
- Ni-ZrB<sub>2</sub>, powders, densification by hot pressing 0-25604
- Ni<sub>3</sub>Al-Zr, powder, X-ray spectral analysis exam. 0-16239
- Ni<sub>62</sub>Ti<sub>38</sub>Zr<sub>90</sub>, amorphous, H-sorption, X-ray and DSC obs. 0-49526
- Ni<sub>100-x</sub>Zr<sub>x</sub> (x=34-40) metallic glass, cryst., isothermal annealing behaviour 0-6367
- Ni<sub>64</sub>Zr<sub>36</sub>, amorphous and cryst., H-sorption, X-ray and DSC obs. 0-49526
- Pd-Zr, metallic glasses, valence band struct. investigation 0-11533
- PdZr, amorphous, supercond., US props. 0-44765
- SiC fibre reinforced Ti, effect of Al, Zr and Mo alloying additions on reaction rate of Ti with fibres 0-16249
- Sm-Co-Cu-Fe-Zr, reversible changes in coercive force and struct. state during heat treatment 400-800°C (Russian) 0-29574
- TZM, fatigue and threshold behaviour under high cycle fatigue 0-40487
- Ti-Al-Mo-Cr-Fe, distrib. of Sn, Zr between phases, temp effect. 0-55357
- Ti-Al-Mo-Zr SiC fibre reinforced composites, matrix selection (Russian) 0-35192
- Ti-Al-Mo-Zr-Si (6.6, 3.3, 1.8, 0.3 wt.%) SiC fibrous composite, component interaction kinetics (Russian) 0-55364
- Ti-Al-Sn-Zr-Mo (6.2, 4.6 wt.%),  $\alpha$ - $\beta$  type 6246, fusion zone fracture behaviour in weldments 0-30093
- Ti-Al-Sn-Zr-Mo alloy, Ti-6242,  $\alpha$ + $\beta$ , creep property improvement by Pt ion plating 0-16408
- Ti-Al-Sn-Zr-Mo-Si (6, 2, 4, 2, 0.1 wt.%), effect of elevated temperature and environment on fatigue crack growth 0-40486
- Ti-Al-V (6, 4 wt.%) cylinders, residual stresses introduced by quenching elastoplastic anal. (French) 0-45355
- Ti-Al-Zr alloy, TA6Zr5D, structural evolution during continuous cooling at different rates (French) 0-45300
- Ti-Al-Zr-Mo alloy 685, phase at  $\alpha/\beta$  interface (French) 0-25661
- Ti-Bc-Zr, coupled phase diagrams and thermochemical descriptions 0-25656
- Ti-Cr-Zr, martensite formation, chemical composition effect 0-50634
- Ti-Mo-Zr-Sn (11.5, 6, 4.5 wt.%), metastable beta III phase, recrystallization and grain growth 0-3091
- Ti-Nb-Zr (35, 3 wt.%), martensitic  $\tau$  phase, X-ray diffr. obs. 0-16300
- Ti-Zr-Cr-Mn/LaNi<sub>5</sub> hydriding alloy mixtures for H energy storage 0-45788
- $\alpha$ -Ti-Zr-W, effect of W impurity on mech. props. 0-16392
- Ti-Zr-W-(Al), phase struct. and props. (Russian) 0-16270
- Ti(Zr,Hf)-Gd-B system, phase equilib. 0-11629
- U-Zr low enrichment fuel for TRIGA and plate-type reactors 0-22950
- UO<sub>2</sub> pellets-graphite-Zircaloy cladding, evaluation of graphite lubrication 0-32342
- UO<sub>2</sub>-Zircaloy fuel element behaviour in PWR power plants 0-631
- UO<sub>2</sub>-zircaloy-4, reaction kinetics at high temps., O<sub>2</sub> diffusion 0-16667
- V-Ti-Zr, 4 MeV Ni<sup>++</sup> irradi., He gas bubble form. 0-29085
- V-Zr, strengthening by internal oxidation 0-55424
- V-Zr-C-Y alloy weld metal, hardening phase precipitates examination, TEM appl. 0-7576

## zirconium alloys continued

- V<sub>2</sub>Zr, struct. transform. at low temp., X-ray diffr. anal. (Russian) 0-45298
- W-Cu-Zr exam. of mech. props. as function of temp., composition, and oxidation props. 0-16472
- W-Zr, Zr addition effect on heat resistance and radiative props. (Russian) 0-25515
- W-Zr-C, Zr and C addition effect on heat resistance and radiative props. (Russian) 0-25515
- Zircaloy, I<sub>2</sub> stress corrosion cracking, temp. and stress depend., threshold press. determ. 0-16595
- Zr-Al (14 wt.%), transformation sequence from Zr-Al martensite to Zr<sub>3</sub>Al phase 0-3027
- Zr-Al (8.0 wt.%), tensile props. and fracture toughness after fast neutron irradiation 0-3198
- Zr-Al-Cr H sorption props. for H storage, influence of Al 0-45794
- Zr-Al-V, H sorption props. for H storage, influence of Al 0-45794
- Zr-Al-(Fe,Co), H sorption props. for H storage, influence of Al 0-45794
- Zr-Al(8.6 wt.%), neutron irradiated, irradiation growth and recovery, annealing 0-15162
- Zr-B, abrasive props. 0-16489
- Zr-base alloys, annealed specimens, irradiation growth 0-49276
- Zr-Be, coupled phase diagrams and thermochemical descriptions 0-25656
- Zr-Be, metallic glass form. and props. 0-16219
- Zr-Cr-B system, self-propagating high temp. synthesis, crystallochemical and mech. props. 0-20861
- Zr-Cu (1.6 wt.%), near eutectoid, active eutectoid decomposition ageing and quenching effects 0-2993
- Zr-Fe, Mossbauer spectra parameters of Zr<sub>2</sub>Fe particles (Russian) 0-29654
- Zr-Fe-Cu-W, Mossbauer spectra parameters of Zr<sub>2</sub>Fe particles (Russian) 0-29654
- Zr-H, diffusion in hydride phase, exam. 0-29204
- Zr-H, effect of neutron irradi. on electrical resistance, magnetic susceptibility 0-29063
- Zr-Hf, dil., <sup>178</sup>Hf Mossbauer transition, electric quadrupole interaction 0-39928
- Zr-Hf (2.2 wt.%), oxidation kinetics in flowing CO<sub>2</sub>, 873 to 1173K 0-16596
- Zr-Hf-ZZ (Russian) 0-39551
- Zr-Hf(2.2 wt.%), oxidation kinetics in flowing CO<sub>2</sub> at high temp. 0-47575
- Zr-M-H (M=V, Cr, Mn, Fe, Co, Ni), synthesis at high pressure, props 0-29924
- Zr-Mo(Co)(Fe)(Cu)(Ni-Cu)-H, catalytic props. 0-30274
- Zr-Nb (20 wt.%),  $\omega$ -phase form., diffuse Mossbauer scatt. 0-25324
- Zr-Nb (2.25 wt.%), oxidation kinetics in flowing CO<sub>2</sub>, 873 to 1173K 0-16596
- Zr-Nb (2.5 wt.%), crack resistance, influence of ZrH<sub>x</sub> fracture toughness 0-16444
- Zr-Nb (2.5 wt.%), hydride induced crack growth, effect of stress, temp. and H<sub>2</sub> content 0-3178
- Zr-Nb (2.5 wt.%), superplastic and strain rate depend. plastic flow, 873 to 1373K 0-30052
- Zr-Nb (2.5 wt.%), transforms. during annealing of welded joint, after thermal cycling (Russian) 0-29984
- Zr-Nb-Ga, phase equilibria 800°C (Ukrainian) 0-35157
- Zr-Nb-Sn (3.1 wt.%), corrosion resist. depend. on mech. and heat treatments 0-653
- Zr-Nb-Sn (3.0, 1.0 wt.%), oxidation kinetics in flowing CO<sub>2</sub>, 873 to 1173K 0-16596
- Zr-Nb-Sn(3 wt.%, 1 wt.%), oxidation kinetics in flowing CO<sub>2</sub> at high temp. 0-47575
- Zr-Nb(2.5 wt.%), oxidation kinetics in flowing CO<sub>2</sub> at high temp. 0-47575
- Zr-Ni, diffusion of H<sub>2</sub>, 900 to 1080°C (Korean) 0-19988
- Zr-Ni, surface layer, segregation of ferromag. Ni, magnetooptic investigation 0-2256
- Zr-Ni-Cu-H, catalytic activity, exam. by conversion of toluene, and bicyclic aromatic hydrocarbons 0-30276
- Zr-Ni-H, catalytic activity, exam. by conversion of toluene, and bicyclic aromatic hydrocarbons 0-30276
- Zr-Ni-H<sub>2</sub>(x=2.8 to 3), surface layer, segregation of ferromag. Ni, magnetooptic investigation 0-2256
- Zr-Sc-Ga, phase equilibria 800°C (Ukrainian) 0-35157
- Zr-Sn, grain-boundary migration during fatigue at 600 to 775°C 0-16443
- Zr-Ti, alloy, mag. susceptibility, elec. cond., Hall conc. thermoEMF conc. depend. (Russian) 0-39551
- Zr-V foil, rapidly quenched and heat treated, supercond. props. 0-54852
- Zr<sub>3</sub>Al, neutron irradi. effect on tensile props. 0-3156
- Zr<sub>3</sub>Al, tensile props., surface preparation depend. 0-3155
- Zr<sub>3</sub>Be<sub>1-x</sub> noncrystalline alloy, phonon-electron scatt., superconducting temp. 0-54330
- Zr-W (75 wt.%) eutectic refractory alloys, smelting in suspended states, components distrib. (Russian) 0-19913
- ZrC-ZrB<sub>2</sub>, friction characts., comp. depend., 20-1400°C 0-3203
- ZrC-ZrB<sub>2</sub>, wear in vacuum, role of boride phase 0-21113
- Zr<sub>0.35</sub>Cu<sub>0.65</sub> metallic glass, Young's modulus meas. by impulse induced resonance technique 0-40411
- (Zr<sub>1-x</sub>Er<sub>x</sub>)<sub>3</sub>Rh, amorphous, influence of mag. ordering on supercond. props. 0-29511
- Zr(Fe,Al)<sub>2</sub>, weak itinerant ferromag., mag. anisotropy effects on mag. isotherms 0-11187
- ZrFe<sub>2</sub>, lattice dynamics, Mossbauer spectra 0-19888
- ZrFe<sub>2</sub>, Mossbauer diffr., combination type maxima, hyperfine interactions on nuclei 0-25263
- Zr(Fe<sub>1-x</sub>Al<sub>x</sub>)<sub>2</sub>, transition region, spin glass or long range mag. order 0-44841
- Zr(Fe<sub>1-x</sub>Co<sub>x</sub>)<sub>2</sub>, magnetovolume effects, thermal expansion and forced vol. magnetostriction meas. 0-29595
- Zr(Fe<sub>1-x</sub>Co<sub>x</sub>)<sub>2</sub>, micromagnetism 0-15863
- Zr(Fe<sub>1-x</sub>Co<sub>x</sub>)<sub>2</sub>, transition region, spin glass or long range mag. order 0-44841
- Zr<sub>2</sub>Hf<sub>1-x</sub>V<sub>x</sub>, polycrystalline superconductor, resist. and mag. susceptibility, transition temp., temp. depend. 0-25113
- (Zr<sub>1-x</sub>Nb<sub>x</sub>)Fe<sub>2</sub>, magnetovolume effects and Invar characters 0-15773
- Zr<sub>1-x</sub>Nb<sub>x</sub>Zn<sub>2</sub>, microscopic mag. props., NMR investigation 0-15807
- ZrNi, surface segregation of Ni, influence on catalytic activity 0-30275
- ZrV<sub>2</sub>, C-15 struct., phase transitions, elec. cond., crystal lattice parameters (Russian) 0-54826



**zirconium alloys continued**

- ZrV<sub>2</sub>, latent heat of structural transform. 0-24589  
 ZrV<sub>2</sub>D<sub>4.5</sub>, deuterated cubic Laves phase, D atom distrib., neutron diff. anal. 0-29006  
 ZrZn<sub>3</sub>, phonon contrib. to Stoner enhancement factor, ferromag. and possible superconductivity 0-25070  
 ZrZn<sub>2</sub>, <sup>51</sup>Fe mag. props. from Mossbauer effect obs. (*Japanese*) 0-15933

**zirconium compounds**

see also *zirconium alloys*

- MgO-ZrO<sub>2</sub>, ceramic reinforced with filamentary crystals, mech. and thermal props. 0-45262  
 refractory carbides, borides and nitrides, wetting by and interactions with liq. metals 0-54473  
 tetrahalides of Gp.IV elements, M-X bond flexibility, by compliance scheme 0-37805  
 Zircaloy-2, deformation and fracture behaviour, uniaxial tension test in I<sub>2</sub> environment 0-13580  
 Zircon ceramic, exam. of development and fabrication 0-11608  
 ZrO<sub>0.98</sub>, porosity influence on high temp. creep. (*Russian*) 0-25764  
 ZrO<sub>2</sub>, high temperature interactions with Re 0-16665  
 ZrO<sub>2</sub>, powders, stabilised, for plasma spray-coatings 0-20869  
 AgZr<sub>2</sub>(PO<sub>4</sub>)<sub>3</sub> system, phase charact. at different temps. 0-29936  
 Al<sub>2</sub>O<sub>3</sub>-Mo (20 wt.%) cermet, ZrO<sub>2</sub> crystal-addition effect on thermal fatigue resistance 0-40528  
 Al<sub>2</sub>O<sub>3</sub>-ZrSiO<sub>4</sub> mixture, reaction sintering, correlation between densification and reaction 0-29911  
 Ca-Mg-Zr combustion sensor, pipe-form ceramics appl. (*Japanese*) 0-55761  
 CaO-MgO-ZrO<sub>2</sub>-SiO<sub>2</sub> refractories, phase diagram 0-11634  
 Fe/ZrB<sub>2</sub>, metal-like cpd. form. in diffusion layer during solid phase saturation 0-19994  
 Fe-ZrB<sub>2</sub>, dispersion strengthened, thick vacuum condensate, control of struct. and mech. props. 0-16324  
 Fe-ZrO<sub>2</sub>, dispersion strengthened, thick vacuum condensate, control of struct. and mech. props. 0-16324  
 Fe-ZrO<sub>2</sub> granular film, interface props., Mossbauer spectroscopy 0-34336  
 Fe-ZrO<sub>2</sub> granular films, superparamag., Mossbauer effect 0-7131  
 K<sub>4</sub>Zr<sub>2</sub>O<sub>7</sub>, cryst. struct., X-ray study 0-33957  
 LaF<sub>3</sub>-BaF<sub>2</sub>-ZrF<sub>4</sub>(-MF), M=Na, Li, glassy transition, refr. index, density and molar refr. 0-1937  
 MgO-Al<sub>2</sub>O<sub>3</sub>-SiO<sub>2</sub>: ZrO<sub>2</sub>, TiO<sub>2</sub>, glass, phase separation (*German*) 0-38932  
 Na<sub>2</sub>O-Al<sub>2</sub>O<sub>3</sub>-ZrO<sub>2</sub>-SiO<sub>2</sub> glass, chemical stability in NaOH and Na<sub>2</sub>CO<sub>3</sub> solns. 0-16532  
 Na<sub>2</sub>O-SnO<sub>2</sub>-ZrO<sub>2</sub>-SiO<sub>2</sub> glass, chemical stability in NaOH and Na<sub>2</sub>CO<sub>3</sub> solns. 0-16532  
 Na<sub>2</sub>O-ZrO<sub>2</sub>-SiO<sub>2</sub> glass, treated with 2 N solns. of NaCO<sub>3</sub> and NaOH, surface layer comp. 0-35366  
 Na<sub>1+x</sub>Zr<sub>2-x</sub>In<sub>3</sub>(PO<sub>4</sub>)<sub>3</sub>, three-dimens. solid soln., comp. depend. of ionic cond. (*French*) 0-34230  
 Na<sub>2</sub>ZrSiO<sub>3</sub>, scintillation props., excited by  $\alpha$  particles 0-29809  
 Ni-ZrO<sub>2</sub>, dispersion strengthened, thick vacuum condensate, control of struct. and mech. props. 0-16324  
 Ni-ZrO<sub>2</sub>, electron-beam-evaporated condensate, cold deform. and annealing effects on microstruct. 0-16331  
 POCl<sub>3</sub>-ZrCl<sub>4</sub>, splitting of Sm<sup>3+</sup> near IR absorpt. bands 0-2750  
 Pb(Zr, Ti)O<sub>3</sub> internal struct., prep. effect, ionic shadowing obs. (*Polish*) 0-11612  
 Pb(Zr,Ti)O<sub>3</sub> polycrystalline ceramic, fracture and strength, surface treatment effects 0-11704  
 Si-Al-Zr-O-N, calc. of phase diagrams from data set 0-55362  
 Si<sub>3</sub>N<sub>4</sub>-SiO<sub>2</sub>-ZrN-ZrO<sub>2</sub>, X-ray diff. phase anal. and reactions  
 Si<sub>3</sub>N<sub>4</sub>+ZrO<sub>2</sub>, SiO<sub>2</sub>+ZrN 0-50613  
 SiO<sub>2</sub>-ZrO<sub>2</sub>-Al<sub>2</sub>O<sub>3</sub>-CaO-Na<sub>2</sub>O-K<sub>2</sub>O-Li<sub>2</sub>O, chemical resistant glass for glass fibres 0-21128  
 SiO<sub>2</sub>-ZrO<sub>2</sub>-Li<sub>2</sub>O-Na<sub>2</sub>O based crystallisable glasses composition and properties 0-50731  
 (Ti,Zr)B<sub>2</sub> on graphite, CVD coatings, hardness meas., SEM study 0-24760  
 TiC-ZrC, mag. susceptibility, elec. cond. and thermoelec. props. 0-50033  
 TiC-ZrC, solid soln., conc. and temp. dependence of props. 0-39736  
 TiO<sub>2</sub>-ZrO<sub>2</sub>, submicron powders, vapour phase production from TiCl<sub>4</sub>-ZrCl<sub>4</sub>-O<sub>2</sub> system 0-40301  
 U-ZrH fission reactor fuel options for TRIGA Mk.III 0-5235  
 Y<sub>2</sub>WO<sub>6</sub>:ZrO<sub>2</sub>(MgO)(CeO)(SrO)(BaO), polycryst., elec. cond., 800-7400°C 0-15517  
 Zr-C-N-O-H, solid solns. of H, exam. of props. 0-29172  
 Zr-H, deposited on carriers, synthesis, structure and catalytic props. 0-29890  
 Zr-H, diffusion in hydride phase, exam. 0-29204  
 Zr-H, effect of neutron irradi. on electrical resistance, magnetic susceptibility 0-29063  
 Zr-H, exam. of electron structure 0-29306  
 Zr-H, tensile strength and creep 0-55459  
 Zr-M-B systems (M=Rh,Ir), phase equilib. and cryst. structs. 0-15072  
 Zr-Ni-H, surface segregation of Ni, influence on catalytic activity 0-30275  
 ZrB<sub>2</sub>, electric arc melting prep. and oxidation props. 0-20860  
 ZrB<sub>2</sub>, impurity content, effect of synthesis conditions 0-21344  
 ZrB<sub>2</sub>, oxidation in O<sub>2</sub>, atmosphere, exam. 0-11814  
 ZrB<sub>2</sub> powders, synthesis and impurities 0-55329  
 ZrB<sub>2</sub>, reactions with Ti-Al-Cr-Mo alloy VT3-1 0-16585  
 ZrB<sub>2</sub>-SiC-C(-V)(-Nb), refractory cermet, hot pressing and oxidation resist. 0-3231  
 ZrBr, electronic struct., self-consistent and non-self-consistent band calcs. 0-44499  
 ZrC CVD coated fuel particles, diffusion of <sup>137</sup>Cs, <sup>90</sup>Sr and <sup>144</sup>Ce 0-13582  
 ZrC crystals, electron energy spectra 0-49568  
 ZrC powders, synthesis and impurities 0-55329  
 ZrC powders produced by various methods, impurities 0-11615  
 ZrC, reactions with Ti-Al-Cr-Mo alloy VT3-1 0-16585  
 ZrC single crystals, synthesis and impurities 0-55329  
 ZrC, true heat capacity meas. by pulse method 0-19953  
 ZrC-W(Mo), thermionic emission, surface structural characts. after prolonged use, work function variation 0-20758  
 ZrC-ZrB<sub>2</sub>, strength and antifractionation props. over wider range of concs. 0-50673  
 ZrC+CeO<sub>2</sub>(UO<sub>2</sub>)(SrO), high temp. reactions 0-3320  
 ZrC<sub>0.91</sub>, sintered, strength charact. effect of struct. and substruct. 0-16260

**zirconium compounds continued**

- ZrCl<sub>4</sub>, electronic struct., self-consistent and non-self-consistent band calcs. 0-44499  
 ZrCl<sub>4</sub> reaction with POCl<sub>3</sub> in O<sub>2</sub>, for ZrP<sub>2</sub>O<sub>7</sub> prep. 0-21272  
 ZrClH, <sup>1</sup>H NMR shielding anisotropy 0-20466  
 ZrD, electrodes with externally ignited vacuum arc source of D<sup>+</sup> ions 0-33845  
 ZrF<sub>4</sub>, mol. struct. and vibr. freqs., gaseous electron diff. obs. 0-32836  
 ZrH<sub>2</sub>, non-secular part of nucl. dipolar broadening detected by  $\mu^+$  zero-field spin relaxation 0-7250  
 ZrH<sub>2</sub>, synchrotron XPS obs., rel. to theory for metal dihydrides 0-55275  
 ZrH<sub>2</sub>, fracture toughness, influence on crack resistance of Zr alloys 0-16444  
 ZrH<sub>2</sub> (x=1.55, 1.7), synthesis and electron structure 0-29889  
 ZrH<sub>2</sub>, self-diffusion of T<sub>1</sub>, autoradiographic study, energy of soln. in H sublattice (*Russian*) 0-2194  
 ZrH<sub>2</sub>:Er (x=1.5 and 1.85), Mossbauer spectra 0-20527  
 Zr(HPO<sub>4</sub>)<sub>2</sub>, amorphous, crystalline, enthalpy of formation 0-6518  
 ZrI<sub>4</sub>, thermodynamics of vaporisation from substoichiometric solid Zr iodides 0-3393  
 ZrN, RF sputter deposition, ion bombardment and ion implantation 0-25564  
 ZrN-Al<sub>2</sub>O<sub>3</sub>, sintering reaction thermodynamics 0-2989  
 ZrN-Mo, cermet, sintering reaction thermodynamics 0-2989  
 ZrN+SiO<sub>2</sub>, X-ray diff. phase anal. of reaction products 0-50613  
 ZrN<sub>2</sub>H<sub>4</sub> (y=0.81 or 0.84, x=0.19 or 0.16) synthesis and electron structure 0-29889  
 ZrO, B<sup>II</sup> state radiative lifetimes, transition rates and oscillator strengths, reson. fluoresc. decay 0-28053  
 ZrO bands, integrated intensity meas. and effective vibr. temp. 0-43111  
 ZrO corrosion layer, specimen preparation for TEM by ion beam thinning (*German, English*) 0-11861  
 ZrO spectrum, new <sup>3</sup>II-<sup>2</sup> $\Delta$  system identification 0-23414  
 ZrO, X(<sup>1</sup> $\Sigma$ ) state, vibrational IR spectrum using microwave powered molecular source, rotational analysis 0-9596  
 ZrO<sup>+</sup> spectrum, <sup>3</sup>II-<sup>2</sup> $\Sigma$  system identification 0-23413  
 ZrO<sub>2</sub>, baddeleyite, high-press. phase transform., Earth mantle appl. 0-8296  
 ZrO<sub>2</sub>, CW CO<sub>2</sub> laser deposited dielect. thin film, optical and struct. props. 0-7506  
 ZrO<sub>2</sub>, cell electrolysis of H<sub>2</sub>O at 800° to 1000°C (*French*) 0-26024  
 ZrO<sub>2</sub> ceramics, microstruct. and props., monoclinic to tetragonal transition 0-3035  
 ZrO<sub>2</sub> gels, calcination 0-11964  
 ZrO<sub>2</sub>, isoelec. points, effect of pH on electrophoretic mobility 0-35548  
 ZrO<sub>2</sub> laser coating, UV damage obs. 0-33056  
 ZrO<sub>2</sub> particles, influence of ionic treatment on formation of Al coatings (*Russian*) 0-50552  
 ZrO<sub>2</sub>, plasma deposition of crystals and their characterisation 0-20800  
 ZrO<sub>2</sub> products from granules, props., prep. method effect 0-25628  
 ZrO<sub>2</sub> refractories, elec. cond. variation, gas flow effect 0-39581  
 ZrO<sub>2</sub> refractories, high-temp. induced porosity increase 0-35146  
 ZrO<sub>2</sub>, solid solubility in MgO 0-15247  
 ZrO<sub>2</sub>, stabilised, fabrication by hot petroleum drying method, X-ray diff. and thermal anal. study 0-40297  
 ZrO<sub>2</sub>, stabilized porous refractory, mech. strength 0-35322  
 ZrO<sub>2</sub>, substoichiometric, thermodynamic props. at lower phase boundary 0-29185  
 ZrO<sub>2</sub>, tetragonal to monoclinic phase transf. by ball-milling 0-25687  
 ZrO<sub>2</sub>, thin film coated sample, absorptive laser damage analysis by Weibull distrib. 0-33061  
 ZrO<sub>2</sub>, transformation toughened, localised impact damage 0-7665  
 ZrO<sub>2</sub>, Y<sub>2</sub>O<sub>3</sub> stabilized, heat-resistant granular artifacts, procedure for making 0-35148  
 ZrO<sub>2</sub>:CaO, polycrystalline, grain boundary enhanced interdiffusion, flux density eqn. 0-29220  
 ZrO<sub>2</sub>:Cu, point defects, electrochem. characterisation 0-35599  
 ZrO<sub>2</sub>:Y<sub>2</sub>O<sub>3</sub>, low-temp. specific heat, oxygen vacancy effects 0-49376  
 ZrO<sub>2</sub>-Al<sub>2</sub>O<sub>3</sub>-SiO<sub>2</sub> fusion cast ceramics, crystn., microstructures rel. to conditions 0-11638  
 ZrO<sub>2</sub>-HfO<sub>2</sub>, monoclinic solid soln., ceramic prep. and use 0-55338  
 ZrO<sub>2</sub>-Nd<sub>2</sub>O<sub>3</sub>(Sm<sub>2</sub>O<sub>3</sub>)(Dy<sub>2</sub>O<sub>3</sub>) eutectic, unidirectional solidification, microstruct. and crystallographic characterization 0-35176  
 ZrO<sub>2</sub>-SiO<sub>2</sub> (11 to 13 wt.%), X-ray phase anal. 0-35195  
 ZrO<sub>2</sub>-SiO<sub>2</sub> powder mixture for optical glass polishing 0-28367  
 ZrO<sub>2</sub>-Y<sub>2</sub>O<sub>3</sub> powder, prep. for plasma spheroidisation, sputter drying (*Russian*) 0-55324  
 ZrO<sub>2</sub>-Y<sub>2</sub>O<sub>3</sub> superionic cond. cell, complex impedance 0-10702  
 ZrO<sub>2</sub>-Y<sub>2</sub>O<sub>3</sub>/Ni sputtered multilayered ceramic/metal coatings, props. 0-40620  
 ZrO<sub>2</sub>-Y<sub>2</sub>O<sub>3</sub>/(Cr-Ni) sputtered multilayered ceramic/metal coatings, props. 0-40620  
 ZrO<sub>2</sub>-Y<sub>2</sub>O<sub>3</sub>/(NiCo)-Cr-Al-Y plasma sprayed ceramic coating for turbine engine components 0-40616  
 ZrO<sub>2</sub>+Si<sub>3</sub>N<sub>4</sub>, X-ray diff. phase anal. of reaction products 0-50613  
 ZrO<sub>2</sub>-Y<sub>2</sub>O<sub>3</sub>/Ni-Cr-Al-Y, NASA two-layer thermal barrier coating, for gas turbine engines, test results 0-40617  
 ZrO<sub>2</sub>-SiO<sub>2</sub>-Al<sub>2</sub>O<sub>3</sub> mixed powders, solid state reactions 0-40337  
 Zr<sub>11</sub>Os<sub>4</sub>, cubic struct. type described by cluster concept, X-ray determ. 0-33933  
 ZrP<sub>2</sub>O<sub>7</sub>, prep. from ZrCl<sub>4</sub> reaction with POCl<sub>3</sub> via O<sub>2</sub> 0-21272  
 ZrS<sub>2</sub>, valence density of states 0-44465  
 ZrS<sub>3</sub>, phonon study of chemical bonding 0-20645  
 ZrS<sub>3</sub>, quasi one-dimens., optical phonon anisotropy, IR spectra study 0-40112  
 ZrS<sub>3</sub>, Raman spectra and cryst. symm. 0-34922  
 ZrS<sub>3</sub> synthesis 0-35142  
 ZrS<sub>3</sub>, thermomodulated reflectivity and transmission 0-50357  
 ZrS<sub>2</sub>Cs<sub>0.37</sub>, lamellar cpd., gas absorpt. 0-44418  
 ZrSe<sub>3</sub>, long wavelength optical phonons, Raman scatt. and IR refl. 0-34921  
 ZrSe<sub>3</sub>, phonon study of chemical bonding 0-20645  
 ZrSe<sub>3</sub>, quasi one-dimens., optical phonon anisotropy, IR spectra study 0-40112  
 ZrSi<sub>2</sub>, self-propag. high-temp. synthesis 0-2988  
 ZrSiO<sub>4</sub>, heavy ion irradi., metamict zircon form. 0-2088  
 ZrSiO<sub>4</sub>, single cryst. growth from soln. in melt, solvent system selection 0-55285  
 ZrSiO<sub>4</sub>, synthesis, influence of rare-earth additives on props. 0-20868  
 ZrSiO<sub>4</sub>, zircon, high-press. phase transform., Earth mantle appl. 0-8296



**zirconium compounds continued**

ZrSiO<sub>4</sub>, zircon, resonance splitting of internal vibr. freq. of complex anion 0-55080

ZrSiO<sub>4</sub>-Al<sub>2</sub>O<sub>3</sub> system, particle rearrangement kinetics due to densification 0-25626

ZrTe<sub>3</sub>, phonon study of chemical bonding 0-20645

**zodiacal light**

see also sky brightness

charged dust particles, motion in interplanetary space 0-4299

surface brightness meas. by AE-C satellite 0-17548

**zonal heating** see atmospheric thermodynamics**zone melting**

concentration profile during zone melting, radiometric determ., slot method (*Czech*) 0-55289

high melting pt. cpds., single cryst. growth (*Japanese*) 0-16175

refractory metal, heat treatment and zone melting installation 0-20959

semiconductor growth, process parameters influence on radial scatter of resist. 0-16174

B, electron beam non-crucible zone remelting prep., anal. of gaseous impurities 0-20785

β-B, electron beam zone melting growth, crystn. and defect form. 0-15020

B, physical characterisation (*French*) 0-16189

Cr, floating zone-melting prep., activation anal. 0-29875

Ga<sub>1-x</sub>In<sub>x</sub>Sb, temp. gradient zone melting 0-50550

LaB<sub>6</sub>, synthesis and props., review (*Japanese*) 0-40255

MnZn ferrite, combined Bridgman-zone levelling cryst. growth technique 0-35076

Mo, doped, surface tension driven flow in electron beam floating zone expts. 0-19731

Ni single crystal, preferred growth direction in floating zone method 0-25555

Si, crystal growth conditions effect, on microdefect distrib. 0-50549

n-Si, dislocation free, process induced cryst. defects 0-24392

Si, floating zone structural perfection changes by high temp. treatment, dendrites, dislocation interactions 0-29049

Si, growth conditions rel. to cryst. struct. perfection (*Russian*) 0-38971

Si, swirl defects A-type as source of dislocation generation on macroscopic scale 0-25554

<sup>119</sup>Sn isotope, fractionation during zone recrystn. 0-2946

Y<sub>3</sub>Fe<sub>5-x</sub>Ga<sub>x</sub>O<sub>12</sub>, substituted garnet, floating zone grown, FMR line width, saturation magnetisation 0-29626

Zn, zone melting by electron beam, isotope fractionation enhancement 0-45229

<sup>64</sup>Zn isotope, fractionation during zone recrystn. 0-2946

**zone plates (optical)** see optical zone plates**zone refining**

CdAs<sub>2</sub>, thermoelec. props., anisotropy 0-34470

Cr, floating zone-refining, activation anal. 0-29875

Cu crystals, floating zone method growth, X-ray diffr. study of preferred growth 0-7490

Si, monocryst. plates, purification by thermal diffusion, impurity migration anal. 0-25553

W, zonal electronic purification, mass spectra of contaminants (*Polish*) 0-25552

**zoology**

2.45 GHz irradiation effect on rat digestive transit (*French*) 0-3723

915 MHz prenatal irradiation effect on rat foetal and postnatal development 0-3722

animals, small, nose-only inhalation exposures to <sup>106</sup>RuO<sub>4</sub>, system 0-41346

Aplysia, restoration of transmission in synapses inactivated by habituation 0-56009

bird skulls, struct. anal. using mammography techniques 0-36209

conference, Tokyo, Japan (June 1979) 0-31412

lizard jaw action, mechanical significance of streptostyly 0-51143

locust, proprioceptors with central cell bodies 0-51132

pigeon magnetic field sensing capability 0-56076

rat brain ATP, ADP and AMP levels after 2.45 GHz whole-body irradiation 0-3718

rat EEG activity depression by 2.45 GHz whole-body irradiation 0-3720

rat sleep patterns under chronic low-power microwave irradiation (*French*) 0-3716

turtle retina, chromaticity horizontal cells, synapse mechanisms 0-51079

whale biothermal mathematical model 0-12059

wildlife biotelemetry, reviews 0-30966

**zoosemiotics** see biocommunications**Zr** see zirconium







ABSTRACTS AND CURRENT PAPERS JOURNALS

SUBSCRIPTION PRICES

	USA \$	UK £	ROW £	JAPAN ¥
<b>PHYSICS ABSTRACTS</b>				
Paper or Microfiche.....	920	365	470	343,100
Paper and Microfiche.....	1380	547	705	514,650
2nd and subsequent copies.....	480	250	250	182,500
<b>ELECTRICAL &amp; ELECTRONICS ABSTRACTS</b>				
Paper or Microfiche.....	680	310	375	273,700
Paper and Microfiche.....	1020	465	562	410,550
<b>COMPUTER &amp; CONTROL ABSTRACTS</b>				
Paper or Microfiche.....	395	190	240	175,200
Paper and Microfiche.....	592	285	360	262,800
<b>PA/EEA/CCA COMBINED SUBSCRIPTION</b>				
Paper or Microfiche.....	1790	760	970	708,100
Paper and Microfiche.....	2685	1140	1455	1,062,150
<b>EEA/CCA COMBINED SUBSCRIPTION</b>				
Paper or Microfiche.....	960	445	560	408,800
Paper and Microfiche.....	1440	667	840	613,200
<b>CURRENT PAPERS IN PHYSICS</b>				
Member rate.....	50	25	25	—
Non-Member rate.....	115	65	65	47,400
<b>CURRENT PAPERS IN ELECTRICAL &amp; ELECTRONICS ENGINEERING</b>				
Member rate.....	45	25	25	—
Non-Member rate.....	98	54	54	39,400
<b>CURRENT PAPERS ON COMPUTERS &amp; CONTROL</b>				
Member rate.....	45	25	25	—
Non-Member rate.....	98	54	54	39,400
<b>KEY ABSTRACTS</b>				
Member rate*.....	25	12	12	—
Non-Member rate.....	45	20	20	14,600
<b>KEY ABSTRACTS</b>				
EMI/PMI PER SECTION—Member.....	40	12	12	—
Non-Member rate.....	55	25	25	18,200
COMBINED.....	—	40	40	29,200

\*The Key Abstracts Member rate is available to Members of the IEE and IEEE only.

CUMULATIVE INDEXES

Cumulative indexes are available for *Physics Abstracts*, *Electrical & Electronics Abstracts* and *Computer & Control Abstracts*, for both authors and subjects. These cumulations generally cover a period of four years, with the exception of *Computer & Control Abstracts* where the initial volume covered the period 1966-68. The table below shows the prices and periods for the two types of cumulative index.

	PHYSICS ABSTRACTS		ELECTRICAL & ELECTRONICS ABSTRACTS		COMPUTER & CONTROL ABSTRACTS	
	Subject	Author	Subject	Author	Subject	Author
	£	£	£	£	£	£
1955-59	20	20	15	20	—	—
1960-64	40	17	20	12	—	—
1965-68	63	25	35	20	—	—
1969-72	—	—	72	64	48	30
1973-76	600	300	250	150	150	75
1966-68	—	—	—	—	15	

For US\$ and Yen prices please contact the appropriate address below

ORDERING PROCEDURE

THE AMERICAS

North (including Canada), Central and South

All orders from the above areas, and orders from members of Institute of Electrical and Electronics Engineers Inc. anywhere in the world, should be sent to Fulfillment Manager, Institute of Electrical & Electronics Engineers Inc., 445 Hoes Lane, Piscataway, N.J. 08854, USA.

日本のお客様にご案内申し上げます

日本国内に於ける INSPEC の購入価格はすべて円建てとなっております。また刊行物はすべて航空便で配達されます。INSPEC 刊行物の価格、その他についてのお問い合わせは最寄の洋書取扱専門店または輸入総代理店(株)ユー・エス・エシアテック・カンパニー 〒105 東京都港区新橋1-13-12、TEL 03 (502) 6471 までご連絡ください。

REMAINDER OF THE WORLD

All remaining subscriptions should be sent to INSPEC Marketing Department, P O Box 26, Hitchin, Herts SG5 7RS, England. Telephone Hitchin 53331, Telex 825962, Telegrams IEE G.

OTHER INSPEC SERVICES

SDI

(Selective Dissemination of Information.) This is a service individually tailored to the requirements and interests of the engineer or research worker. Details of information relevant to the interest profile of the individual subscriber are selected from the data being processed for the INSPEC database. Information is dispatched weekly on 150 mm x 100 mm (6" x 4") cards.

TOPICS

This is an SDI service based on standard profiles. There are over 70 subjects covering high-activity areas of research and development. This is an inexpensive card service designed to alert engineers and researchers to the availability of literature within their subject area.

MAGNETIC TAPES

Tapes containing all the information included in the INSPEC publications are issued twice monthly. They enable the larger research and development organisations to produce their own internal information and current-awareness services.



articles from  
literature you  
do not hold ?

# **BOSTON SPA**

**Can help you**

**Over 43000 current periodicals available\***

Most of the papers listed in INSPEC services  
are held at the British Library Lending Division (BLLD)

**REQUESTS DEALT WITH IN 48 HOURS\***

Write for further information to:

The Director General  
The British Library Lending Division  
Boston Spa  
Wetherby  
West Yorkshire LS23 7BQ  
England

\*Photocopies of papers are available for research or private study to organisations in the UK registered as users of the BLLD. Where individuals in the UK do not belong to an organisation registered with the BLLD they should apply via their public library. In case of difficulty please contact the BLLD.

All requests from outside the UK should be made via the BLLD Overseas Photocopy Service.